Applied Ecology and Environmental Research

International Scientific Journal

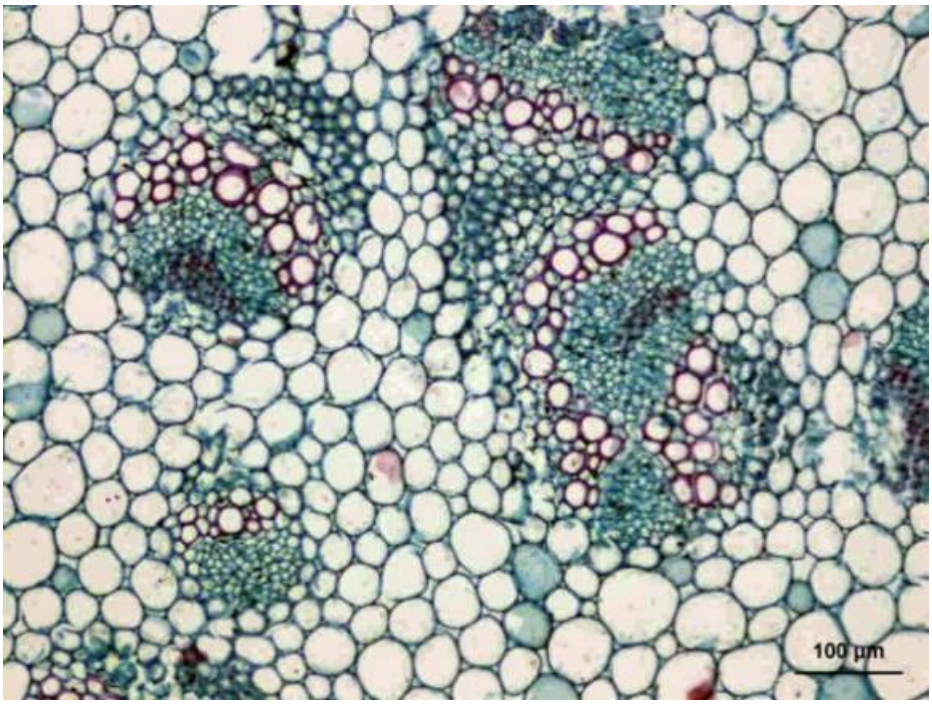

VOLUME 17 * NUMBER 6 * 2019

http://www.aloki.hu
ISSN 1589 1623 / ISSN 1785 0037
DOI: http://dx.doi.org/10.15666/aeer

GLEMOK – NOVEL METHOD FOR CATCHMENT MOISTURE DETERMINATION USING HIGH-RESOLUTION SOIL MAP

BAZIAK, B.* – GĄDEK, W. – SZCZEPANEK, R.

Department of Water Engineering and Water Management of the Cracow University of Technology, Cracow, Poland

**Corresponding author*
e-mail: beata.baziak@iigw.pk.edu.pl

(Received 8th Jan 2019; accepted 13th Jun 2019)

Abstract. One of the crucial elements having a direct impact on rainfall-runoff transformation is soil moisture of the catchment. Moisture conditions can be expressed by physical catchment descriptors, like PROPWET or FLATWET. Their values are represented by ratio between time when the soil is wet and analysed period, using wet-dry threshold R_g. The wet-dry threshold is based on climatic data and is constant for the PROPWET (R_g=6 mm) and for FLATWET (R_g=8.5 mm). The purpose of the present publication is to define a descriptor suitable for any area in Europe. The authors propose novel descriptor (GLEMOK) using additionally physical soil properties. Public SoilGrids250m soil database was applied, which served to develop a high-resolution soil map and pF curves. For the Raba river catchment (research area) the R_g. threshold is equal 11.5 mm. The GLEMOK descriptor for this research area has proportionally larger values than the other two, which is closer to real water regime in this region of Poland. The novel descriptor GLEMOK using physical soil properties is more universal compared to PROPWET and FLATWET. Use of the global SolidGrids250m soil database enables implementation of this method in any area in Europe.
Keywords: *PROPWET, FLATWET, SMD, SoilGrids250m, database, wet-dry threshold*

Introduction

So far, in hydrology, the problem of forecasting flow characteristics has been solved using mathematical modelling for which unambiguous procedures have not been determined (O'Connor, 2014). In United Kingdom, a methodology has been developed for the needs of engineering practice, which has been called design hydrology (Reed, 1999; Faulkner, 1999; Robson and Reed, 1999; Houghton-Carr, 1999; Bayliss, 1999). In design hydrology, the physical catchment descriptors (PCDs) play a fundamental role (Bayliss, 1999; Mills et al., 2014) in quantitative and qualitative description of the given catchment. Based on these descriptors, hydrological characteristics used in the design, management and analysis of changes taking place in the catchment can be determined. PCDs can be divided into three groups:

- **fixed** – related to the topography, orography and hydrography of the catchment, including for instance the catchment area, the river network density, the watercourse slope, etc.
- **variable** – representing spatial development of the catchment, for instance forest land cover, urbanization, length of watercourses under anthropopressure, etc.
- **process-related** – for instance, moisture conditions of the catchment, surface retention, flood attenuation by channels and lakes, urbanization pressure on the outflow, etc.

Process descriptors form the foundations for the development of formulas that allow linking engineering hydrology with dynamic hydrology, which until now has been used

http://www.aloki.hu ● ISSN 1589 1623 (Print) ● ISSN 1785 0037 (Online)
DOI: http://dx.doi.org/10.15666/aeer/1706_1266712681

in mathematical hydrological modelling. Such a combination provides the opportunity to extend the scope of its applicability to new areas, related for instance to determining the impact of climate change on hydrological characteristics (Apel et al., 2006; Vrijling et al., 1998; Zeleňáková et al., 2017) or to the impact of urbanized areas on flood risk (Zevenbergen et al., 2011).

Among the descriptors used around the world to define the dynamics of the transformation of rainfall (precipitation) into runoff, two are particularly noteworthy in terms of describing the watercourse supply. These are the PROPWET and BFI descriptors (Bayliss, 1999; Reed, 2007; Mills, 2014), which determine what part of the precipitation is transformed into runoff in the form of surface or subsurface runoff. The PROPWET descriptor is determined from the soil moisture deficit (SMD) (Hubbard et al., 2007), using the Hybrid Soil Moisture Deficit Model (Allen et al., 1998; Reed, 2007). SMD is calculated as follows:

$$SMD_t = SMD_{t-1} - Rain + ET_a - Drain \quad \text{(Eq.1)}$$

where:

- SMD_t, SMD_{t-1} – the SMDs on day t and day t-1 respectively (mm).
- *Rain* - the daily precipitation (mm d^{-1}).
- ET_a - the daily actual evapotranspiration for a reference grass crop (mm d^{-1}).
- *Drain* - the amount of water drained daily by percolation and/or overland flow (mm d^{-1}).

Climatic data used to determine the SMD include: atmospheric precipitation, temperature and air humidity, wind speed, and net radiation (Narasimhan and Srinivasan, 2005). Atmospheric precipitation is divided into effective precipitation and soil retention (*Figure 1*).

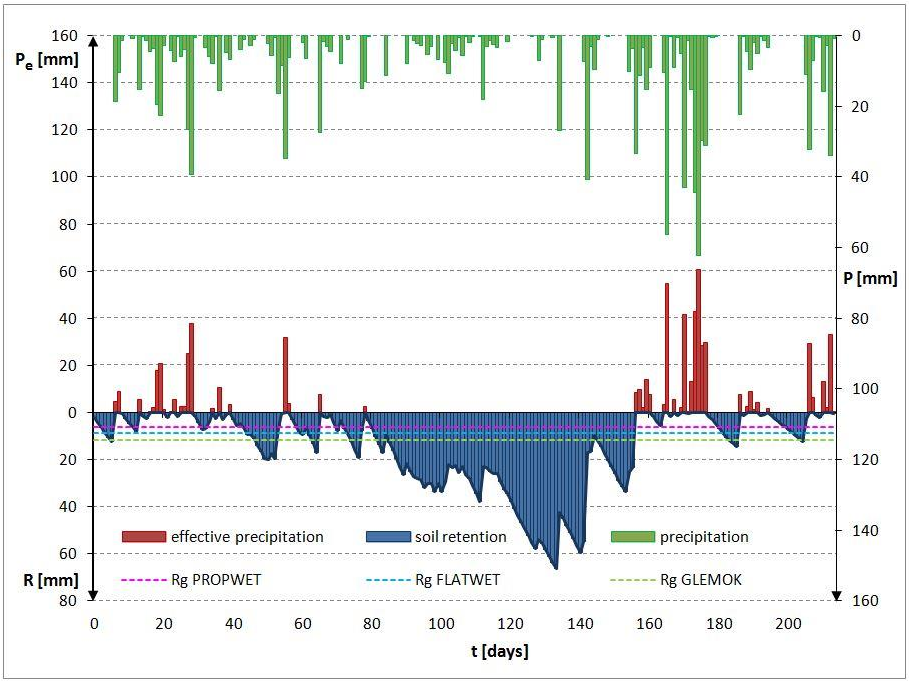

Figure 1. *Division of atmospheric precipitation into surface runoff and soil retention using the SMD*

http://www.aloki.hu ● ISSN 1589 1623 (Print) ● ISSN 1785 0037 (Online)
DOI: http://dx.doi.org/10.15666/aeer/1706_1266712681

The soil moisture deficit assumes only positive values and represents soil retention *R*. In the case of precipitation exceeding the soil retention, excess precipitation flows down as surface runoff, and the *SMD* is set to 0 value. Increase in the *SMD* humidity deficit means soil drying, whereas the reduction of its value means the replenishment of water in soil by precipitation. The values of the *SMD* which are lower than the threshold values, presented in the form of dashed lines (*Figure 1*), denote wet soil. Dry soil is represented by values greater than the threshold values, in which case water is available only for plants.

Based on the SMD the PROPWET descriptor was designated. It represents the share of time in which the soil remains wet compared to the whole of the analysed period. For this purpose, it is necessary to determine the threshold of soil division R_g, into wet soil and dry soil. The search for the threshold between wet and dry soil is carried out in the optimization process. For a given threshold value (for instance R_g=2.5 mm) for all climate stations, the share of time during which the soil remains wet is calculated ($PROPWET_{2.5}$). The next step is to determine the differences between the calculated $PROPWET_{2.5}$ values for all pairs of climate stations. On this basis, the average value of these differences is calculated for a given threshold (2.5 mm). The threshold is determined for the assumed objective function, which is the maximum of the average differences. The threshold is chosen to maximise the inter-site variation in PROPWET across all gauged sites. For the United Kingdom R_g=6 mm (Reed, 2007), for the Ireland R_g=8.5 mm (Schulte et al., 2005), thus PROPWET descriptor has been renamed to FLATWET and is used only in Ireland (*Figure 1*).

FLATWET and PROPWET descriptors were developed for United Kingdom and Ireland, which according to the Köppen-Geiger division (Kottek et al., 2006) lies in the same climate zone as Poland (Cfb – warm temperate climate, fully humid, warm summer). The amplitude of air temperature changes throughout the year in Poland is greater than in the United Kingdom, resulting in four seasons. When estimating the values of these descriptors, the winter period poses a problem when the ground is frozen, and the precipitation occurs in the form of snow. This involves the growing season, which in Poland is between April and October (Olszewski and Żmudzka, 2000). Then the catchment's behaviour is completely different than in the growing season. In contrast to British Isles, the number of days with Tmin <0˚C ranges from less than 100 days on the Baltic coast to over 140 days in the east of Poland (Kejna et al., 2009). This causes freezing of the soil, which is associated with a change in water conduction properties. Under such conditions, the permeable soil becomes impermeable, sublimation or evaporation occurs without transpiration, and the precipitation occurs in solid form (snow). The outflow from the catchment in this period comes mainly from groundwater, whereas the surface runoff from the melting snow (thaw or snow-melt). For this reason, for the territory of Poland, the winter period should be omitted in the calculations related to establishing the threshold between wet and dry soil.

The purpose of the present publication is to define a descriptor that will take into account the moisture conditions of the catchment, suitable for any area in Europe. The authors propose the GLEMOK descriptor, specifying the share of time during which the soil remains wet, based on the PROPWET descriptor elaborated in United Kingdom and FLATWET descriptor used in Ireland. However, during the development of the descriptor, the winter period have been eliminated from the calculations, therefore the principle of the descriptor's determination had to be changed in relation to the original model.

http://www.aloki.hu ● ISSN 1589 1623 (Print) ● ISSN 1785 0037 (Online)
DOI: http://dx.doi.org/10.15666/aeer/1706_1266712681

Determination of the threshold between wet and dry soil should be carried out for the area of Poland in a different way than for the PROPWET or FLATWET. For the latter two descriptors, the threshold is determined for climatic data from the whole calendar year. The very idea of PROPWET and FLATWET originates from dynamic hydrology, in which the issues related to the process of infiltration form the basis for solving the set of equations for the rainfall-runoff transformation (Eagleson, 1970; Ozga-Zielińska et al., 2002). One of the characteristics describing the physical properties of soil is the pF curve (*Eq. 2*), which illustrates the relationship between soil water content Θ and soil matric potential h_s affecting water molecules in soil (*Figure 2*).

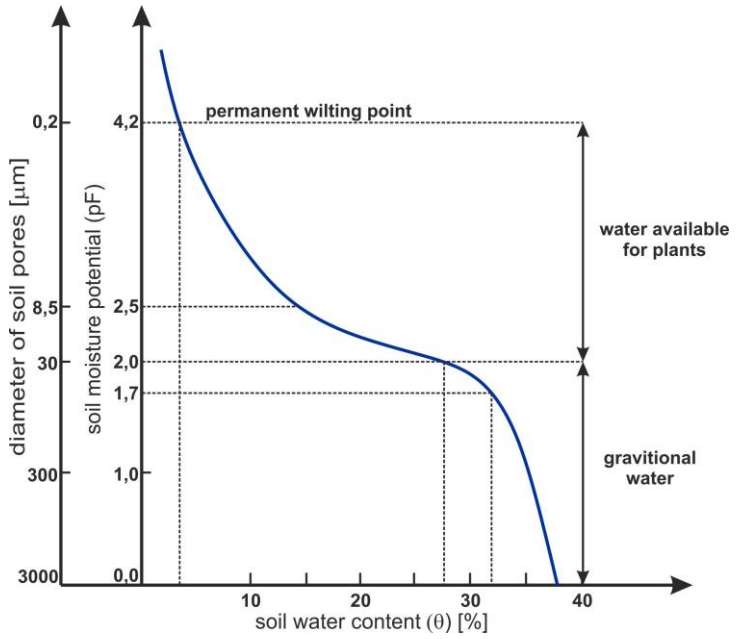

Figure 2. *Sample pF curve of the soil*

$$pF = log\ (-h_s) \qquad \text{(Eq.2)}$$

where:

h_s – soil matric potential (suction pressure) (cm).

On the basis of the pF curve, it is possible to determine points, which determine the state of soil moisture. These are:

- h_s = *-50 cm (pF = 1.7)* – from the value of h_s = *-50 cm* to the value of h_s = *0 cm* water in the soil moves mainly due to gravity (force of attraction) and it is assumed that this water is not available for plants, but it takes part in the direct supply of watercourses.

- h_s = *-100 cm (pF = 2.0)* – from the value of h_s = *-100 cm* to the value of h_s =*-50 cm* water moves mainly under the influence of gravity, and the process of evapotranspiration begins.

- h_s = *-300 cm (pF = 2.5)* – water is readily available for plants, and with lower values of suction pressure, the evapotranspiration process is gradually reduced.

- h_s = *- 15,000 cm (pF = 4.2)* is the point of permanent wilting of plants, and at this point evapotranspiration disappears.

http://www.aloki.hu ● ISSN 1589 1623 (Print) ● ISSN 1785 0037 (Online)
DOI: http://dx.doi.org/10.15666/aeer/1706_1266712681

In 1986, Driessen proposed the equation describing pF curves for soils (*Eq. 3*), according to the European classification:

$$\theta(h_s) = \theta_s e^{-\mu[ln(-h_s)]^2} \quad \text{(Eq.3)}$$

where:

- Θ_s – maximum volumetric humidity ($cm^3\ cm^{-3}$).
- μ – parameter dependent on the type of the soil (cm^{-2}).

Soil classification can be made using the grain size information, which is described in the Feret's diagram shown in *Figure 3*.

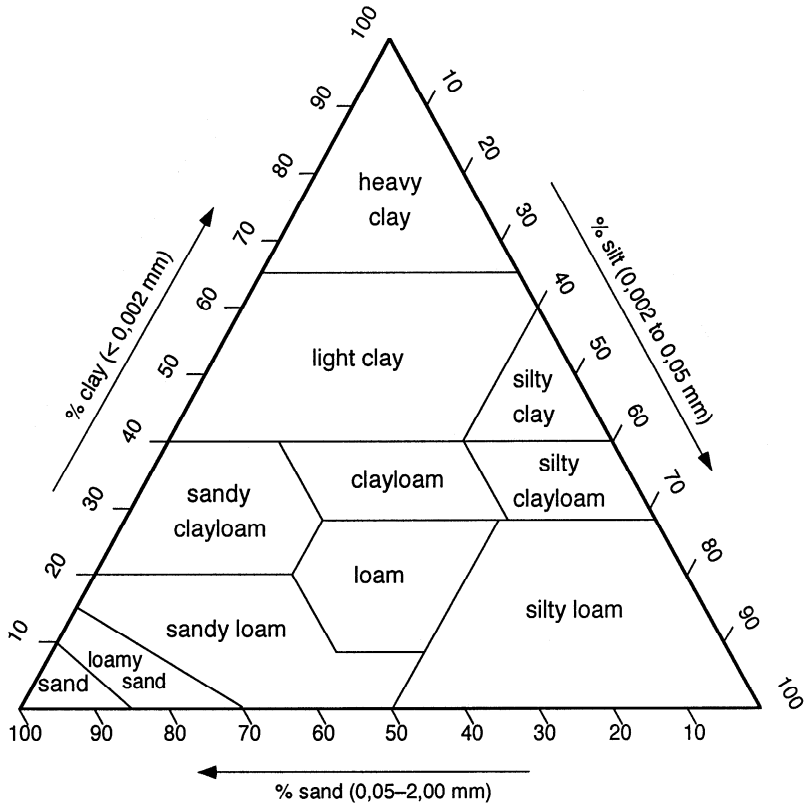

Figure 3. *Feret's diagram according to the European classification of soils (Dreissen, 1986)*

Materials and methods

The area and data under study

The Raba river catchment had been adopted as the study area. Raba river is a right-bank tributary of the Vistula river. It is about 132 km long and covers an area of 1537.1 km^2, flowing through three hydrological regions. The largest part of the catchment is located in the Carpathian zone, representing the mountainous terrain. The remaining part is located in the upland area, whereas the estuary part represents the lowlands. The average elevation of the catchment is about 500 m above sea level. The highest point of the catchment is Turbacz mountain, at 1310 m above sea level, and the lowest is 180 m above sea level, at the point where Raba enters the Vistula river.

http://www.aloki.hu ● ISSN 1589 1623 (Print) ● ISSN 1785 0037 (Online)
DOI: http://dx.doi.org/10.15666/aeer/1706_1266712681

Within the Raba river catchment 9 water gauges were used in calculation, 7 of them located upstream water reservoir in Dobczyce. *Figure 4* shows sub-catchments for particular water gauges.

The values of the mean annual precipitation from the summer half-year, for all computational cross-sections, are presented in *Table 1*.

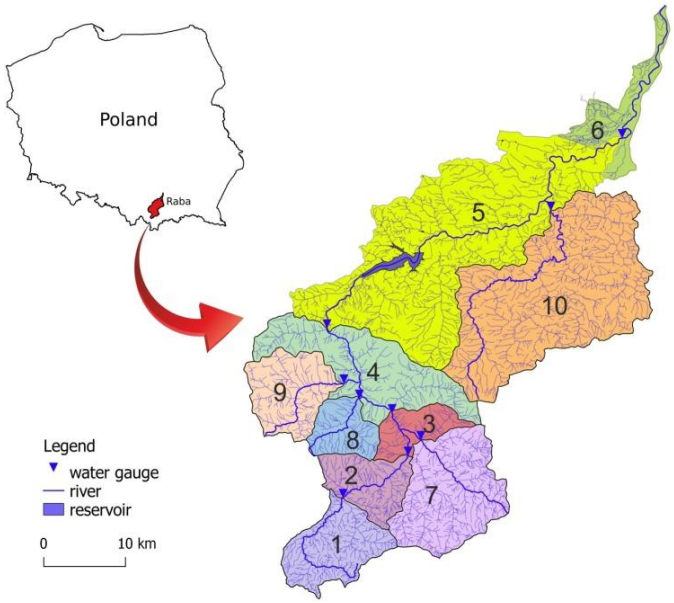

Figure 4. *Location of water gauges in the catchment of Raba river, in accordance with Table 1*

Table 1. *Values of mean annual precipitation from the summer half-year, for computational cross-sections of Raba river catchment*

No.	River	Gauge station	Mean rainfall in the summer half-year [mm]
1	RABA	Rabka	568
2		Mszana Dolna	550
3		Kasinka Mała	540
4		Stróża	533
5		Proszówki	519
6		Outlet to Wisła	514
7	MSZANKA	Mszana Dolna	534
8	LUBIEŃKA	Lubień	525
9	KRZCZONÓWKA	Krzczonów	525
10	STRADOMKA	Stradomka	508

The calculations were carried out for the PROPWET, FLATWET and GLEMOK descriptors, for a 30-year measurement data series from April 1 to October 31 in the years 1983-2012. For each descriptor, the appropriate wet-dry threshold was accepted. Climatic data, including atmospheric precipitation in the years 1983-2006, comes from the station in Stróża, run by the Hydrology Department of the Institute of Engineering and Water Management of the Cracow University of Technology, whereas the data for the period 2007-2012 was obtained from the climate station of the IMGW PIB in Dobczyce. Small distance between Stróża and Dobczyce stations (15 km) with the same

http://www.aloki.hu ● ISSN 1589 1623 (Print) ● ISSN 1785 0037 (Online)
DOI: http://dx.doi.org/10.15666/aeer/1706_1266712681

measurement conditions (standard Hellmann rain gauge) enabled merge of data from those two series (Noone et al., 2016). The non-parametric Mann-Whitney-Wilcoxon test for yearly precipitation, with resulting p=0.001 at significance level α=0.05, confirmed hypothesis on series homogeneity (Yue and Wang, 2002). The spatial distribution of atmospheric precipitation and field evaporation for the whole catchment was elaborated on the basis of rainfall maps and evapotranspiration index for grass, published by IMGW PIB in the "Hydrological Atlas of Poland" (IMGW, 1987).

In order to determine the type of soils, raster layers of soil granulometry were used, derived from the SoilGrids250m project (Hengl et al., 2017). Soil grain size is available in the form of three fractions (sandy, loamy and silty), for seven depths in the soil profile (0, 5, 15, 30, 60, 100 and 200 cm).

SoilGrids250m database (https://soilgrids.org) is one of the few global soil information resources, making it possible to determine the type of soil in any area of the globe, with a spatial resolution of about 250 m (Hengl et al., 2017). The sources of data for the development of this database included:

- Approximately 150 000 soil profiles.
- Expert profiles for non-monitored areas.
- 158 satellite products, including MODIS land products, SRTM DEM, as well as climatic and lithological data, etc.
- Machine learning algorithms.

The data are available to the public in the form of raster layers on a free-of-charge license basis (ODbL - Open Database License).

Methodology

Using the Feret's diagram (*Figure 3*) and the grain size information for selected depths (0, 5, 15 and 30 cm), the type of soil was determined. This was accomplished by developed application (https://gitlab.com/OpenHydrology/soil-map), using the Python 3.7 programming language, with rasterio and python-ternary packages (Harper et al., 2015). Raster layers with a spatial resolution of 250 m from SoilGrids250m project were used as input data. For the processing and visualization of the spatial data QGIS 2.18 software was used (Sherman, 2014).

As a result, a high-resolution raster map of soils for the area of Poland was generated (*Figure 5*). This map was used to determine the threshold between wet and dry soil for the GLEMOK descriptor, which is determined for each soil individually. The name of this new descriptor is abbreviation of "wet soil" term (Polish: GLEba MOKra). Precipitation events causes the soil became moist, so descriptor value should exceed relative number of days with precipitation. Relative number of days with precipitation can be calculated as ratio between average number of days with precipitation and growing season lengths.

This is a different approach than in the PROPWET and FLATWET descriptors, where the threshold value is determined arbitrarily, by using optimization methods. When determining the wet-dry threshold in the GLEMOK descriptor, pF curves were applied that characterize the properties of a given soil type, as presented in *Table 2*.

Procedure for calculating the GLEMOK descriptor:

1. Based on climatic data, the soil moisture deficit SMD in the catchment, up to the gauge cross-section, is determined.
2. Based on the soil map, the average value of the wet-dry threshold R_g is determined (*Table 3*) according to the following ratio:

http://www.aloki.hu ● ISSN 1589 1623 (Print) ● ISSN 1785 0037 (Online)
DOI: http://dx.doi.org/10.15666/aeer/1706_1266712681

$$\boldsymbol{R_g} = \frac{\sum_{i=1}^{n}(\boldsymbol{R_g^i} \cdot \boldsymbol{A_g^i})}{\sum_{i=1}^{n} \boldsymbol{A_g^i}} \quad \text{(Eq.4)}$$

where:

$\boldsymbol{R_g^i}$ – threshold between wet and dry soil, for a particular type of soil *i* (mm).

$\boldsymbol{A_g^i}$ – area occupied by a particular type of soil *i* (km^2).

n – number of soil types in the catchment (-).

3. Based on the soil moisture deficit and the calculated average wet-dry threshold R_g (*Eq. 4*), the time during which the soil remains wet is calculated.
4. The value of the GLEMOK descriptor is defined as the ratio of time during which the soil remains wet to the considered measurement period.

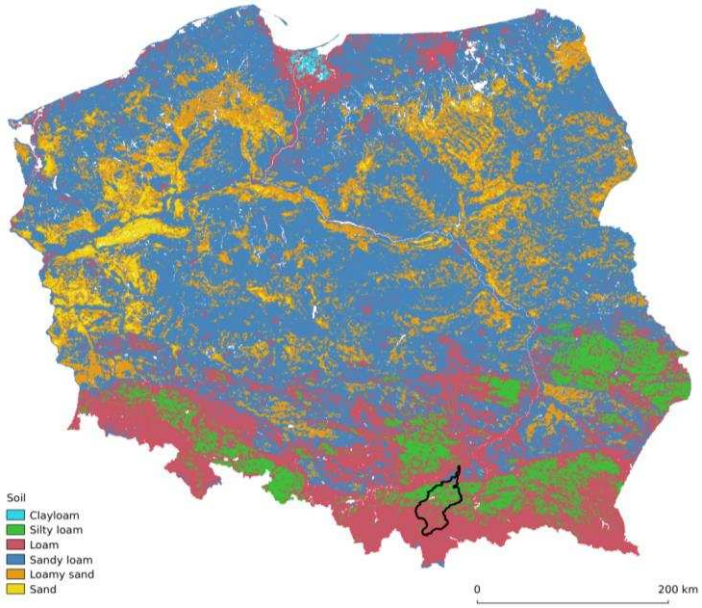

Figure 5. *Classification of soils for the area of Poland, based on granulometric data from the SoilGrids250m project (https://soilgrids.org). Raba catchment is outlined*

Table 2. *Values of maximum volumetric humidity Θ_s, parameter μ (Driessen, 1986) and volumetric humidity Θ for suction pressure pF=1.7 and pF=2.0*

Type of the soil	Θ_s [cm^3/cm^3]	μ [cm^{-2}]	Θ(pF=1.7) [cm^3/cm^3]	Θ(pF=2.0) [cm^3/cm^3]
coarse sand	0.395	0.1000	0.085	0.047
fine sand	0.364	0.0288	0.234	0.198
loamy sand	0.439	0.0330	0.265	0.218
fine loamy sand	0.504	0.0207	0.367	0.325
silty loam	0.509	0.0185	0.383	0.344
loam	0.503	0.0180	0.382	0.343
loess loam	0.455	0.0169	0.351	0.318
sandy clay loam	0.432	0.0096	0.373	0.352
silty clay loam	0.475	0.0105	0.404	0.380
clay loam	0.445	0.0058	0.407	0.393
light clay	0.453	0.0085	0.398	0.378
silty clay	0.507	0.0065	0.459	0.442
heavy clay	0.54	0.0042	0.506	0.494
peat (variable)	0.863	0.0112	0.727	0.681

http://www.aloki.hu ● ISSN 1589 1623 (Print) ● ISSN 1785 0037 (Online)
DOI: http://dx.doi.org/10.15666/aeer/1706_1266712681

Table 3. *Values of the SMD threshold determining the division into wet and dry soil R_g, for the specified soils with the thickness of 0.30 m*

Type of soil	R_g [mm]
sand	11.2
loamy sand	14.1
fine loamy sand	12.7
silty loam	11.9
loam	11.5
loess loam	10.0
sandy clay loam	6.2
silty clay loam	7.3
clay loam	4.1
light clay	5.8
silty clay	5.2
heavy clay	3.7
peat (variable)	14.0

Results

Relative number of days with precipitation, calculated as ratio between average number of days with precipitation and growing season lengths, for Raba river catchment equals 0.458.

Four soil maps for individual soil depth layers according to SoilGrids250m: 0, 5, 15, 30 cm were developed for the Raba river catchment. Differences observed in soil classification for the elaborated maps did not exceeded 1%. Therefore, in order to determine the wet-dry threshold R_g, an average value from four soil layers.

On the basis of the developed soil map (*Figure 5*), the values of the wet-dry threshold R_g were calculated. The wet-dry thresholds for the GLEMOK descriptor were determined for all sub-catchments (up to the water gauge, and the outflow to the Vistula river). For most of these sub-catchments, the calculated value of the threshold between wet and dry soil R_g is set at 11.5 mm. The following constitute an exception: catchment of the Stradomka river up to the Stradomka cross-section, where R_g=11.7 mm and the Raba river catchment up to the Proszówki cross-section, where R_g=11.6 mm (*Table 4*). For the whole area of Poland R_g=9.1 mm. Raster maps of soils/Rg for Poland can be downloaded from project web page (https://gitlab.com/OpenHydrology/soil-map).

Table 4. *Values of the threshold between wet and dry soil for the GLEMOK descriptor for the Raba river catchment*

No.	River	Gauge station	A [km^2]	R_g [mm]
1	RABA	Rabka	91.8	11.5
2		Mszana Dolna	157.2	11.5
3		Kasinka Mała	353.2	11.5
4		Stróża	643.7	11.5
5		Proszówki	1471.8	11.6
6		outflow to Wisła	1537.1	11.5
7	MSZANKA	Mszana Dolna	151.5	11.5
8	LUBIEŃKA	Lubień	47.8	11.5
9	KRZCZONÓWKA	Krzczonów	87.3	11.5
10	STRADOMKA	Stradomka	362.9	11.7

http://www.aloki.hu ● ISSN 1589 1623 (Print) ● ISSN 1785 0037 (Online)
DOI: http://dx.doi.org/10.15666/aeer/1706_1266712681

It was found that for the catchment of the Raba river up to the Proszówki water gauge, the increase in the R_g value from 11.5 mm to 11.6 mm does not affect the GLEMOK value, whereas for the Stradomka river catchment up to the Stradomka section, the GLEMOK value increases by 0.002. This is considered a slight increase, and it has been assumed that in the whole Raba river catchment, the value determining the threshold between wet and dry soil can be set at $R_g = 11.5$ *mm*. *Table 5* presents the values of the calculated PCDs: PROPWET, FLATWET and GLEMOK, for individual sub-catchments of the Raba river.

Table 5. *Values of the PROPWET, FLATWET and GLEMOK descriptors in the Raba river catchment, determined for the period of 1983-2012, and for the adopted fixed threshold between wet and dry soil (the subscript of the descriptor)*

No.	River	Gauge station	A [km^2]	PROPWET$_{6.0}$ [-]	FLATWET$_{8.5}$ [-]	GLEMOK$_{11.5}$ [-]
1	RABA	Rabka	91.8	0.354	0.441	0.535
2		Mszana Dolna	157.2	0.352	0.427	0.514
3		Kasinka Mała	353.2	0.338	0.413	0.505
4		Stróża	643.7	0.326	0.406	0.486
5		Proszówki	1471.8	0.254	0.310	0.366
6		outlet to Wisła	1537.1	0.263	0.312	0.411
7	MSZANKA	Mszana Dolna	151.5	0.329	0.408	0.495
8	LUBIEŃKA	Lubień	47.8	0.326	0.404	0.491
9	KRZCZONÓWKA	Krzczonów	87.3	0.319	0.394	0.477
10	STRADOMKA	Stradomka	362.9	0.178	0.225	0.308

Based on the obtained results, a comparison was made between PROPWET, FLATWET and GLEMOK descriptors for all sub-catchments, determining absolute and relative changes. The relative increment in the GLEMOK value in relation to the PROPWET and FLATWET was calculated based on the following formula:

$$FLAT_{GLE} = \frac{GLE-FLAT}{FLAT}100 \; and \; PROP_{GLE} = \frac{GLE-PROP}{PROP} \qquad \text{(Eq.5)}$$

where:

- $FLAT_{GLE}$ ($PROP_{GLE}$) – increment of the GLEMOK$_{11.5}$ descriptor compared to FLATWET$_{8,5}$ or PROPWET$_{6.0}$.
- *GLE* – value of the GLEMOK$_{11.5}$ descriptor (-)].
- *FLAT* (*PROP*) – value of the FLATWET$_{8.5}$ descriptor or the PROPWET$_{6.0}$ descriptor (-).

The variability of the analysed descriptors is related to the topography of the area (*Figure 6*). The highest values of all descriptors can be observed in the upper (southern) parts of the Raba river catchment. Descriptors changes are visible, clearly dividing the catchment into two parts: mountains and uplands (*Figure 6*). The lowest values of all descriptors were obtained for the Stradomka river catchment, up to the Stradomka cross-section. This is probably due to the fact that there are lower precipitation heights in this catchment (*Table 1*) than in the remaining area, hence the relative increase in the value of the GLEMOK, as compared to PROPWET value, exceeds 70%.

http://www.aloki.hu ● ISSN 1589 1623 (Print) ● ISSN 1785 0037 (Online)
DOI: http://dx.doi.org/10.15666/aeer/1706_1266712681

Table 6. *The absolute and the relative increment of the GLEMOK descriptor value compared to the value of the PROPWET and FLATWET descriptors*

No.	River	Gauge station	$FLAT_{GLE}$		$PROP_{GLE}$	
			[-]	[%]	[-]	[%]
1	RABA	Rabka	0.094	21.3	0.181	51.0
2		Mszana Dolna	0.087	20.3	0.162	46.0
3		Kasinka Mała	0.092	22.2	0.167	49.3
4		Stróża	0.080	19.7	0.160	48.9
5		Proszówki	0.056	18.2	0.113	44.5
6		outlet to Wisła	0.099	31.6	0.148	56.3
7	MSZANKA	Mszana Dolna	0.087	21.3	0.167	50.7
8	LUBIEŃKA	Lubień	0.087	21.5	0.164	50.4
9	KRZCZONÓWKA	Krzczonów	0.082	20.8	0.157	49.3
10	STRADOMKA	Stradomka	0.082	36.5	0.129	**72.4**

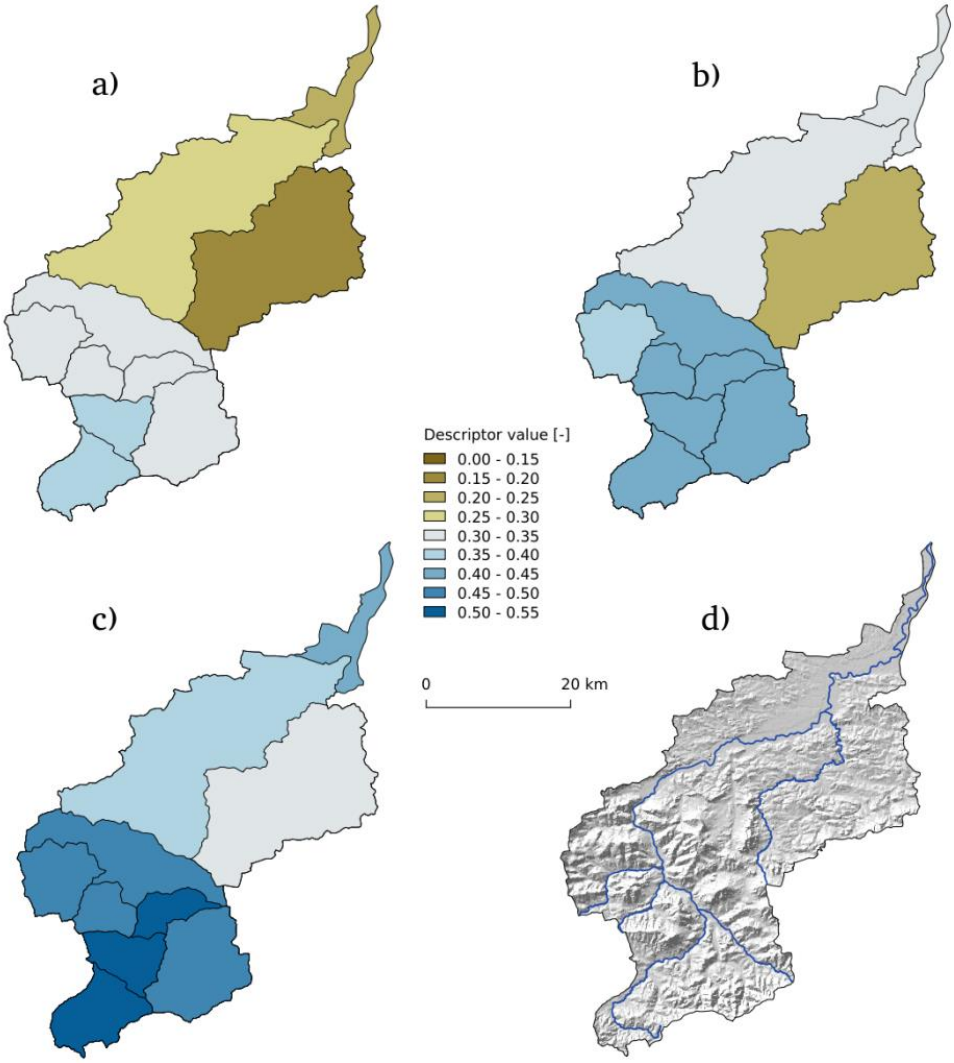

Figure 6. *Spatial variability for the sub-catchments of the Raba river catchment, according to: a) PROWET, b) FLATWET, c) GLEMOK; d) topography of the Raba river catchment*

http://www.aloki.hu ● ISSN 1589 1623 (Print) ● ISSN 1785 0037 (Online)
DOI: http://dx.doi.org/10.15666/aeer/1706_1266712681

Discussion

In the PROPWET and FLATWET descriptors calculation method, the wet-dry threshold R_g is determined using statistical analysis, as constant value for the whole area in analysed period. According to authors of PROPWET for Ireland "the choice of wet-dry threshold is rather arbitrary" (Reed, 2007).

The assumption that the threshold is constant in time and space, means that the ratio between precipitation and evaporation is maintained. When this ratio changes, the value of the wet-dry threshold R_g must be updated (Bayliss and Morris, 1999). These changes may be caused, among others by the climate change. The maximum daily precipitation changes have been documented in the studied area (Kundzewicz et al., 2005; Młyński et al., 2018) so direct implementation of PROPWET and FLATWET in Poland would be impractical.

The PROPWET values in the United Kingdom ranges from 0.51 to 0.75. Despite the high variability of the PROPWET value, one wet-dry threshold value R_g=6 mm was adopted (Reed, 2007). The wet-dry PROPWET threshold for the Ireland 8.5 mm was obtained. As a result, a new FLATWET descriptor was created with values from 0.55 to 0.74, referring only to the area of Ireland (Mills et al., 2014). Thus the various wet-dry threshold values for the PROPWET descriptors in the United Kingdom and FLATWET in Ireland indicate their regional nature. High descriptors values for relatively low R_g can be caused by higher precipitation for British Isles compared to Poland. Implementation of PROPWET and FLATWET descriptors in other area would required wet-dry threshold R_g determination for long-term data series from several climatologic stations.

To check regional nature and spatial variability of descriptors, the Raba river catchment (A=1537 km^2) with its sub-catchments was selected as research area.

Since the descriptors refer to the soil moisture condition, the parameter considering the soil type should be taken into account in the calculation process. The soil types are variable in space and soil data are available worldwide. The adopted method for determining the soil type, based on the physical soil parameters from the SoilGrids250m database (Hengl et al., 2017), enables the universal use of the GLEMOK descriptor. Value of this descriptor is based on the unambiguous determination of wet-dry threshold R_g, from type of soil and pF curves.

The wet-dry threshold R_g in Poland ranges from 6.2 to 14.1 mm with the average value 9.1 mm. For Raba river catchment the variability of R_g is small - maximum difference equals 0.2 mm (*Table 4*). It has been shown that even in such a small area compared to Ireland or United Kingdom, there is spatial variability in the values of the PROPWET, FLATWET and GLEMOK descriptors (*Figure 6*). The values are: for the PROPWET - from 0.178 to 0.354, for the FLATWET - from 0.225 to 0.441, and for the GLEMOK - from 0.308 to 0.535 (*Table 5*). Descriptors values should correspond to number of days with precipitation. For longer precipitation period descriptors values should be higher. It corresponds to wet soil conditions, when river supply comes mainly from surface and sub-surface runoff. In the remaining period, dry soil represents river supply only from groundwater.

The average number of days with precipitation in the analysed period is 98 per growing season in the Raba river catchment. The precipitation indicator determining the number of precipitation days for the growing season (214 days) equals 0.458. Therefore, it would be expected that the values of these descriptors will not be lower than the precipitation indicator. For the analysed area of Raba river catchment, this assumption

http://www.aloki.hu ● ISSN 1589 1623 (Print) ● ISSN 1785 0037 (Online)
DOI: http://dx.doi.org/10.15666/aeer/1706_1266712681

for PROPWET and FLATWET descriptors is not fulfilled - in both cases the values are lower than the precipitation indicator. However, precipitation indicator is in the range of GLEMOK descriptor values. Taking into account the physical soil properties (like in GLEMOK) results are more reliable.

Low values of PROPWET and FLATWET descriptors in the Raba river catchment imply that groundwater is the main source of water supply, which is not true.

The spatial variability of all three descriptors reflects the character of spatial variability of precipitation and evapotranspiration. The difference between GLEMOK and the other two descriptors is based on a different method of determining the wet-dry threshold R_g. Only GLEMOK descriptor includes local physical soil properties.

According to the authors, determining the value of the threshold R_g on the basis of physical properties of soils and the pF curve is more justified than statistical methods used to determine the PROPWET and FLATWET descriptors.

Conclusion

The wet-dry threshold R_g is a key parameter in determination of all three descriptors – PROPWET, FLATWET, GLEMOK. Calculation of wet-dry threshold value in PROPWET (R_g=6.0) and FLATWET (R_g=8.5) is based on meteorological records, which are combined into averaged value over whole research area. In GLEMOK descriptor this value (R_g=11.5 for the Raba river catchment, R_g=9.1 for Poland) is calculated from spatial distribution of meteorological records but additional information on soil types is provided. Difference in R_g values between British Isles and Poland is result of both climate and soil type.

Relative difference of the GLEMOK value in relation to the PROPWET is about 50%, whereas compared to the FLATWET, it is about 20% (Figure 6).

The GLEMOK descriptor better adopts runoff values comparing to those expected from the other two descriptors. Direct implementation of PROPWET or FLATWET for the area of Poland would cause unreliable water regime which is based on groundwater supply.

Direct implementation of PROPWET and FLATWET to locations outside British Isles requires long-term series of meteorological data from several stations. Implementation of GLEMOK is possible with data from just single meteorological station. It is a great advantage of proposed GLEMOK method.

The new method using the GLEMOK descriptor is more universal compared to PROPWET and FLATWET. Use of the global SolidGrids250m soil database enables implementation of this method in any area in Europe.

REFERENCES

[1] Allen, R. G., Pereira, L. S., Raes, D., Smith, M. (1998): Crop evapotranspiration (guidelines for computing crop water requirements). – FAO Irrigation and Drainage Paper 56.

[2] Apel, H., Thieken, A. H., Merz, B., Blöschl, G. (2006): A Probabilistic Modelling System For Assessing Flood Risks. – Natural Hazards 38: 295-308.

[3] Bayliss, A. C. (1999): Catchment descriptors. – Volume 5 of the Flood Estimation Handbook. Center for Ecology & Hydrology.

http://www.aloki.hu ● ISSN 1589 1623 (Print) ● ISSN 1785 0037 (Online)
DOI: http://dx.doi.org/10.15666/aeer/1706_1266712681

[4] Bayliss, A. C., Morris, S. E. (1999): Climate and soils. – Chapter 5 of FEH Vol. 5 Catchment descriptors. IH, Wallingford: 27-38.
[5] Driessen, P. M. (1986): The water balance of soil. – In: van Keulen, H., Wolf, J. (eds.) Modeling of agricultural production: weather, soils and crops. Simulation Monographs. Pudoc, Wageningen: 76-116.
[6] Eagleson, P. (1970): Dynamic Hydrology – McGraw-Hill.
[7] Faulkner, D. (1999): Rainfall frequency estimation. – Volume 2 of the Flood Estimation Handbook. Center for Ecology & Hydrology.
[8] Harper, M., Weinstein, B., Simon, C., Morgan, W., Knight, V., Swanson-Hysell, N., Evans, M., Anglo, S., Greco, M., Zuidhof, G. (2015): Python-ternary: ternary Plots in Python. – Zenodo. 10.5281/zenodo.34938.
[9] Hengl, T., Mendes de Jesus, J., Heuvelink, G. B. M., Ruiperez Gonzalez, M., Kilibarda, M., Blagotić, A., Shangguan, W., Wright, M. N., Geng, X., Bauer-Marschallinger, B., Guevara, M. A., Vargas, R., MacMillan, R. A., Batjes, N. H., Leenaars, J. G. B., Ribeiro, E., Wheeler, I., Mantel, S., Kempen, B. (2017): SoilGrids250m: Global gridded soil information based on machine learning. – PLoS ONE 12(2): e0169748. https://doi.org/10.1371/journal.pone.0169748.
[10] Houghton-Carr, H. (1999): Restatement and application of the Flood Studies Report rainfall-runoff method. – Volume 4 of the Flood Estimation Handbook. Center for Ecology & Hydrology.
[11] Hubbard, K. G., You, J., Hunt, E. D. (2007): Development of the Soil Moisture Index to Quantify Agricultural Drought and Its "User Friendliness" in Severity-Area-Duration Assessment. – Journal of Hydrometeorology 9: 660-676.
[12] IMGW (1987): Atlas hydrologiczny Polski. – tom I (The hydrological Atlas of Poland - vol. I).
[13] Kejna, M., Araźny, A., Maszewski, R., Przybylak, R., Uscka-Kowalkowska, J., Vizi, Z. (2009): Daily minimum and maximum air temperature in Poland in the years 1951–2005. – Bulletin of Geography. Physical Geography Series 2(1): 35-56.
[14] Kottek, M., Grieser, J., Beck, C., Rudolf, B., Rubel, F. (2006): World map of the Köppen-Geiger climate classification updated. – Meteorologische Zeitschrift 15(3): 259-263.
[15] Kundzewicz, Z. W., Ulbrich, U., Brücher, T., Graczyk, D., Krüger, A., Leckebusch, G. C., Menzel, L., Pińskwar, I., Radziejewski, M., Szwed, M. (2005): Summer floods in Central Europe - climate change track? – Nat. Hazards 36(1/2): 165-189. DOI: 10.1007/s11069-004-4547-6.
[16] Mills, P., Nicholson, O., Reed, D. (2014): Flood Studies Update, Technical Research Report. Vol. IV. Physical Catchment Descriptors. – Based on research reports by Compass Informatics. DWRconsult and OPW.
[17] Młyński, D., Cebulska, M., Wałęga, A. (2018): Trends, Variability, and Seasonality of Maximum Annual Daily Precipitation in the Upper Vistula Basin, Poland. – Atmosphere 9: 313. doi:10.3390/atmos9080313.
[18] Narasimhan, B., Srinivasan, R. (2005): Development and evaluation of Soil Moisture Deficit Index (SMDI) and Evapotranspiration Deficit Index (ETDI) for agricultural drought monitoring. – Agricultural and Forest Meteorology 133(1): 69-88.
[19] Noone, S., Murphy, C., Coll, J., Matthews, T., Mullan, D., Wilby, R. L., Walsh, S. (2016): Homogenization and analysis of an expanded long-term monthly rainfall network for the Island of Ireland (1850–2010). – International Journal of Climatology 36(8): 2837-2853.
[20] O'Connor, K., Goswami, M., Faulkner, D. (2014): Flood Studies Update. – Technical Research Report, Volume III, Hydrograph Analysis, pp 186.
[21] Olszewski, K., Żmudzka, E. (2000): Variability of the vegetative period in Poland. – Miscellanea Geographica 9.1: 59-70.

http://www.aloki.hu ● ISSN 1589 1623 (Print) ● ISSN 1785 0037 (Online)
DOI: http://dx.doi.org/10.15666/aeer/1706_1266712681

[22] Ozga-Zielińska, M., Gądek, W., Książyński, K., Nachlik, E., Szczepanek, R. (2002): Mathematical Model Of Rainfall-Runoff Transformation - WISTOO. – In: Singh, V. P., Frevert, D. K. (eds.) Mathematical Models Of Large Watershed Hydrology. Water Resources Publications, LLC, Littleton, Colorado: 811-860.
[23] Reed, D. (1999): Overview. – Volume 1 of the Flood Estimation Handbook. Center for Ecology & Hydrology.
[24] Reed, D. (2007): Flood Studies Update Work-Package 5.4. Report to OPW. PROPWET for Ireland: A dimensionless index of typical catchment wetness. – Wallingford.
[25] Robson, A., Reed, D. (1999): Statistical procedures for flood frequency estimation. – Volume 3 of the Flood Estimation Handbook. Center for Ecology & Hydrology.
[26] Schulte, R. P. O., Diamond, J., Finkele, K., Holden, N. M., Brereton, A. J. (2005): Predicting the Soil Moisture Conditions of Irish Grasslands. – Irish Journal of Agricultural Research 44: 95-110.
[27] Sherman, G. (2014): The PyQGIS Programmer's Guide Extending QGIS 2.x with Python. – Locate Press LLC.
[28] Vrijling, J. K., Van Hengel, W., Houben, R. J. (1998): Acceptable Risk As A Basis For Design. – Reliability Engineering And System Saferty 59: 141-150.
[29] Yue, S., Wang, C. (2002): The influence of serial correlation on the Mann–Whitney test for detecting a shift in median. – Advances in Water Resources 25(3): 325-333.
[30] Zeleňáková, M., Gaňová, L., Purcz, P., Horský, M. (2017): Mitigation of the Adverse Consequences of Floods for Human Life. – Infrastructure, and the Environment, Natural Hazards Review 18(4).
[31] Zevenbergen, C., Cashman, A., Evelpidou, N., Pasche, E., Garvin, S., Ashley, R. (2011): Urban Flood Management. – CRC Press London.

http://www.aloki.hu ● ISSN 1589 1623 (Print) ● ISSN 1785 0037 (Online)
DOI: http://dx.doi.org/10.15666/aeer/1706_1266712681

EVALUATION OF PHYTOTOXIC POTENTIAL OF SELECTED PLANTS AGAINST WEEDS

ANWAR, T.[1*] – ILYAS, N.[1] – QURESHI, R.[1] – QURESHI, H.[1,2] – GILANI, N.[3] – KHAN, S.[4] – KHAN, S. A.[5] – FATIMAH, H.[6] – WASEEM, M.[6] – MAQSOOD, M.[1]

[1]*Department of Botany, Pir Mehr Ali Shah Arid Agriculture University, Murree Road, Shamsabad, Rawalpindi-46300 Punjab, Pakistan*

[2]*Department of Botany, Government Post Graduate College (Women), Sub-Campus University of Gujrat, Satellite Town, Rawalpindi-46300, Punjab, Pakistan*

[3]*Department of Zoology, Pir Mehr Ali Shah Arid Agriculture University, Murree Road, Shamsabad, Rawalpindi-46300, Punjab, Pakistan*

[4]*Department of Environmental Sciences, Gomal University, Dera Ismail Khan-29050, Khyber Pakhtunkhwa, Pakistan*

[5]*Department of Earth and Environmental Sciences, Bahria University, Islamabad Campus, Shangrilla Road, Sector E-8, Islamabad-44000, Pakistan*

[6]*Department of Biology, Allama Iqbal Open University, H-8, Islamabad-44000, Pakistan*

**Corresponding author*
e-mail: drtauseefanwar@gmail.com; phone: +92-33-3686-0562

(Received ; 27th Feb 2019; accepted 10th Apr 2019)

Abstract. Huge amounts of synthetic chemical herbicides are used to manage weeds. Heavy doses of synthetic chemicals for weed control are encouraging herbicidal resistance in weeds, risking human health and environment. Natural compounds, known as "bio herbicides" are environmentally safe herbicides, based on compounds produced by living organisms. The study was aimed to evaluate allelopathic activity of leaf powder of *Rhazya stricta, Pinus roxburghii, Carica papaya* and *Lantana camara* against selected weeds viz. *Phalaris minor, Avena fatua, Chenopodium album, Euphorbia helioscopia* and *Rumex dentatus* on 0.75 (w/v) agar, soil and filter paper at concentration of 10 and 50 mg leaf powder. Germination percentage (%), radicle length (cm) and plumule length (cm) were parameters to assess allelopathic potential. The STATISTIX 9 software was used to analyse data. Based on results, it was concluded that selected plants possesses potential inhibitory effects. Detailed analysis is required to establish allelopathic potential and onward application to be used as phytoherbicide.
Keywords: *factors affecting wheat production, weed infestation, harms of synthetic compounds, natural herbicides, growth retardation*

Introduction

Food security depends upon a sustainable agricultural production and higher levels of yield. It may also enable the agricultural sector less vulnerable to the threat of climate change (Shah et al., 2016). Agriculture is the backbone of Pakistan's economy. This sector gave 20.9% of the Gross Domestic Product (GDP) for the fiscal year 2014-15. Moreover, agriculture is a source of income for 43.5% of the village population of the country. Wheat (*Triticum aestivum* L.) is one of the most important cereal crops of the world. Its role is quite important in the provision of human

http://www.aloki.hu ● ISSN 1589 1623 (Print) ● ISSN 1785 0037 (Online)
DOI: http://dx.doi.org/10.15666/aeer/1706_1268312696

nutrition. Wheat caters to about 73% of the caloric portion of a common person's average diet. Its contents include starch (59-89%), protein (10-15.4%), fat (1.4-2.1%), inorganic ions (1.3-2.2%) and vitamins E and B-complex (Rueda-Ayala et al., 2011). As the world is progressively converting into a global village, globalization and market connectivity are presenting new hindrances in growth and development. The average annual production of wheat is quite low in Pakistan in comparison to other agricultural economies. There might be two ways for increasing wheat production: either by adding more area in cultivation or increasing its production per hectare. The first option is not practicable due to other essential crops, limited availability of the irrigation water occupation of the fertile soils by expanding cities. In this case, wheat production in Pakistan can only be increased by getting higher production per hectare. This can be obtained by efficient agricultural methods. There are many factors, which cause hindrance in wheat production, such as delayed sowing, less amount of fertilizers, water shortage, non-availability of better seed, diseases and dry periods.

Weed infestation is a serious threat to wheat production caused lowering wheat yield. If weeds management strategies are not devised, greater production losses in wheat yield can take place (Khan et al., 2016). It has been shown that wheat farmers are offering very little time and attention to the weed management practices, consequently, 15 to 25% wheat grain losses occur. Weeds are, at large, in causing annual damage of about 10% in agricultural yields globally (Cavero et al., 2011). In Pakistan, weeds cause 45% loss in wheat production (Anwar et al., 2016). In Pakistan, however, annual economic loss, due to weeds in agricultural production is estimated around 18.2 billion dollars. Including, 3-6 billion dollars spent on weeds control methods. There are around 30 different weed species generally found in the wheat crop, becoming the sources of losses. As the smaller farmers lack related tact and necessary resources, it becomes quite impossible to remove these weeds from the cultivated field. Weed harms most of the crops and grain. Moreover, it remains as a perennial problem in Pakistan's agriculture sector (Mubarik et al., 2015). According to an estimate, grain produce in Pakistan can be enhanced by up to 41% if weeds are managed properly. The controlling weeds through traditional methods is time consuming, weather hinged and exhibit more labour cost. While modern weed control techniques have not been up to the mark in solving this problem (Arafat et al., 2015).

Synthetic chemicals are in wider use for controlling weeds. These chemicals may enhance crop production, but concurrently these may have a negative effect on the environment as well as upon human health. In addition to these, the heading up of synthetic herbicides resistant weeds is another major area of concern. Excessive use of herbicides for controlling weeds during the last few years is becoming one of the noteworthy ecological and environmental threats for the world. Herbicide remnants in crops, soil and underground water which causes an evolution of various resistant weed biotypes, and linked health threats are some of the huge dangers that scientists are facing these days in devising various weed management techniques. Due to the negative effect of using synthetic chemicals, one may highly be in demand the new classes of chemicals, especially, biodegradable products such as those originating from plants, which have the potential of getting developed as herbicides (Aryakia et al., 2015). Allelopathy is a natural and eco-friendly technique. This strategy might be one of the very efficient tools for weed management and thereby increasing crop production (Kamran et al., 2017). Natural herbicides obtained from allelopathic

http://www.aloki.hu ● ISSN 1589 1623 (Print) ● ISSN 1785 0037 (Online)
DOI: http://dx.doi.org/10.15666/aeer/1706_1268312696

plants can help in reducing usage of synthetic herbicides for weed control. Consequently, these may cause less pollution, better agricultural products as well as alleviate human health concerns. The most commonly available allelochemicals are cinnamic and benzoic acids, alkaloids, flavonoids, phenolics, glucosionates and various terpenes. These compounds are called as phytotoxic (Khan et al., 2014).

R. stricta, belongs to family Apocynaceae. It is poisonous perennial evergreen shrub of desert and possess tannins, triterpenes, glycosides, volatile bases and alkaloids (Ebid, 2016). *L. camara* belongs to family Verbenaceae, possess phenolic, alkaloids and aromatic compounds (Dobhal et al., 2010). *C. papaya* belongs to family Caricaceae. It possess organic acids, alkaloids, tannins and flavonoids (Canini et al., 2007). *P. roxburghii* belongs to family Pinaceae. Pinus needles possess phytochemicals like isopimaric acid, abietic acid, friedelin, car-3-ene, α-pinene, β-pinene, Longifolene, β- sitosterol, cetyl alcohol (Zafar et al., 2010).

Keeping all this in view, the present study was performed to evaluate *Rhazya stricta* Decne, *Lantana camara* L., *Carica papaya* L. and *Pinus roxburghii* Sarg., for their allelopathic activity against major weeds viz. *Phalaris minor, Avena fatua*, *Chenopodium album*, *Euphorbia helioscopia* and *Rumex dentatus*.

Materials and methods

Allelopathic potential of leaves of selected plants viz., *R. stricta*, *P. roxburgii, C. papaya*, *L. camara* was evaluated. Fresh leaves (~400 gm) for each species were collected (73°02' E longitude and 33°36' N latitude) during March-April, 2018. Collected plant material was washed under running tap water and dried at 30 °C in laboratory that was crushed using heavy duty blender to make fine powder (mesh size 2 mm) and preserved in air tight plastic zip lock bags (Ramsumair et al., 2014; Anwar et al., 2016). Seeds of test weeds viz. *Phalaris minor, Avena fatua, Chenopodium album, Euphorbia helioscopia* and *Rumex dentatus* were procured from the Barani Agricultural Research Institute (BARI), Pakistan. Seeds were surface sterilized by 2% solution of Sodium hypochlorite (NaOCl) (Biljana and Kragujevac, 2015). The sandwich method was followed by Fujii et al. (2003, 2004). Five ml of 0.75 percent (w/v) agar (Nalge Nunc Intl., Roskilde, Denmark, gelling temperature 30-31 °C) was poured in each well of the six-welled (10 cm^2 area per well) multi-dish plastic plate. The agar solution was left for solidification. Leaf powder of each test species @ 10 and 50 mg were placed in suitable wells of the plate and were roofed by a thin layer of 0.75 percent (w/v) agar. After solidification, 10 seeds of each test species were placed on agar gel in each well of the plate. The multi-well plastic plates were then wrapped with the plastic tape and incubated in the growth chamber (NTS Model MI-25S) at room temperature for 15 days. In the control treatment, only agar gel without dried leaves powder was used as a seed bed for test species seeds. Each treatment was replicated five times. The same procedure was repeated to screen phytoxic activity of plants using soil (25 gm/petri dish) and filter paper (Whatman filter paper 1) as medium (*Fig. 1*). Germination percentages (%), lengths of radicle and plumule (cm) for each test species were calculated by comparing with control (Anwar et al., 2017). The statistical analysis was carried out using STATISTIX 9 and means were separated by Fisher's protected LSD test (Nekonam et al., 2014).

http://www.aloki.hu ● ISSN 1589 1623 (Print) ● ISSN 1785 0037 (Online)
DOI: http://dx.doi.org/10.15666/aeer/1706_1268312696

Figure 1. *Test species seeds in petri dishes ready to be incubated (treated with plant powder and wrapped in aluminium foil)*

Results and discussion

Allelopathic potential of R. stricta

The data revealed that *R. dentatus, C. album* and *P. minor* showed 31%, 28% and 25% seed germination inhibition respectively as compared to control on filter paper, whereas, no significant effect on seed germination percentage of *A. fatua* and *E. Helioscopia* was observed. *R. dentatus*, *C. album* and *P. minor* showed 41%, 38%, and 33% germination inhibition respectively as compared to control in *R. stricta* leaf powder applied into soil. The results declared that maximum (98%) germination was shown by *A. fatua* and *E. Helioscopia* while minimum germination was noted for *R. dentatus* i.e. 69% and 59% on filter paper and soil, respectively. Highest germination reduction was noted for *R. dentatus* (35%), followed by *P. minor* (31%) and *C. album* (30%) at 10 mg conc. Similarly, the highest germination reduction was noted for *R. dentatus* (37%), followed by *P. minor* (32%) and *C. album* (30%) at 50 mg conc. The statistical data concluded that minimum germination was noted for *R. dentatus* i.e. 65% and 63% at 10 mg and at 50 mg conc., respectively. The statistics also recommended that with the increase of concentration, the inhibitory effect was progressively increased for *R. dentatus, C. album* and *P. minor* (*Table 1a*).

The data revealed that *R. dentatus* (41%) and *A. fatua* (38%) exhibited radicle length inhibition in *R. stricta* leaf powder on filter paper, whereas, no significant effect on radicle length of *P. minor, E. helioscopia* and *C. album* showing resistance to dry powder. It is also clear from the result that *R. dentatus* (49%) and *A. fatua* (46%) showed and radicle length inhibition respectively as compared to control in powder applied into soil. The results also declared that maximum (98%) radicle length was noted for *P. minor, E. helioscopia* and *C. album.* In the present study, it was demonstrated that minimum radicle length was noted for *R. dentatus* i.e. 59% and 51% on filter paper and soil, respectively. The experimental results of the current study indicated on agar the highest radicle length reduction was noted for *A. fatua* (40%), followed by *R. dentatus* (39%) at 10 mg conc. Similarly, the highest radicle length reduction was noted for *R. dentatus* (47%), followed by *A. fatua* (46%) at 50 mg conc. The statistical data concluded that minimum radicle length was noted for *A. fatua* i.e. 53% and *R. dentatus* i.e. 60% at 10 mg and at 50 mg conc., respectively (*Table 1b*).

The data revealed that *A. fatua* (32%) and *R. dentatus* (31%) exhibited significant plumule length inhibition in *R. stricta* leaf powder on filter paper, whereas, no

http://www.aloki.hu ● ISSN 1589 1623 (Print) ● ISSN 1785 0037 (Online)
DOI: http://dx.doi.org/10.15666/aeer/1706_1268312696

significant effect on plumule length of *P. minor, E. helioscopia* and *C. album* showing resistance to dry powder. It is also clear from the result that *R. dentatus* (34%) and *A. fatua* (33%) showed and plumule length inhibition respectively as compared to control in powder applied into soil. The results also declared that maximum (98%) plumule length was noted for *P. minor, E. helioscopia* and *C. album.* The results of the current study indicated on agar highest plumule length reduction was noted for *A. fatua* (30%) and *R. dentatus* (28%) at 10 mg conc. Similarly, highest plumule length reduction was noted for followed by *R. dentatus* (32%) and *A. fatua* (31%) at 50 mg concentration (*Table 1c*).

It was noted that maximum germination was observed for *A. fatua* and *E. helioscopia*. While minimum germination noticed for *C. album*. The maximum radicle length was noted for *P. minor, E. helioscopia* and *C. album*. While minimum radicle length was noted for *R. dentatus*. The data revealed that the maximum plumule length was observed for *P. minor, E. helioscopia* and *C. album*. Inderjit and Duke (2003) studied the effect of allelochemicals from the leaf powder of *R. stricta* on the weed species. The findings of current study were in accordance with that of Hussain et al. (2011) who noted similar allelopathic effects by other plants. Batish et al. (2002) observed phytotoxicity of *R. stricta* might be due to allelochemicals leached from its leaves in natural environment.

Table 1. *Allelopathic potential of R. stricta leaf powder against tested species on filter paper, soil and agar (a) germination percentage (b) radicle length (c) plumule length*

(a) Germination percentage		***A. fatua***	***R. dentatus***	***P. minor***	***E. helioscopia***	***C. album***
Filter paper	10 mg	83	61	62	84	58
	Control	85	89	83	86	81
Soil	50 mg	84	53	56	85	51
	Control	86	90	84	87	82
Agar	10 mg	85	58	59	84	57
	50 mg	84	56	58	83	56
	Control	86	89	85	85	80
(b) Radicle length (cm)		***A. fatua***	***R. dentatus***	***P. minor***	***E. helioscopia***	***C. album***
Filter paper	10 mg	5.59	5.46	8.14	7.52	9.16
	Control	9.12	9.19	8.29	7.93	9.29
Soil	50 mg	5.04	4.69	8.22	7.26	9.13
	Control	9.31	9.21	8.39	7.33	9.32
Agar	10 mg	5.56	5.75	8.42	7.65	9.84
	50 mg	5.02	5.01	8.31	7.32	9.64
	Control	9.24	9.43	8.54	7.91	9.93
(a) Plumule length (cm)		***A. fatua***	***R. dentatus***	***P. minor***	***E. helioscopia***	***C. album***
Filter paper	10 mg	5.76	6.25	8.09	9.02	7.19
	Control	8.45	9.12	8.13	9.12	7.45
Soil	50 mg	5.41	5.99	8.89	9.2	7.64
	Control	8.07	9.1	8.95	9.32	7.92
Agar	10 mg	5.94	6.46	8.78	9.22	7.69
	50 mg	5.85	6.13	8.68	9.11	7.51
	Control	8.49	9.03	8.96	9.33	7.85

http://www.aloki.hu ● ISSN 1589 1623 (Print) ● ISSN 1785 0037 (Online)
DOI: http://dx.doi.org/10.15666/aeer/1706_1268312696

Allelopathic potential of L. camara

The data revealed that *A. fatua* (60%)*, R. dentatus* (58%), *P. minor* (54%) and *E. helioscopia* (53%) possessed significant germination in *L. camara* leaf powder on filter paper, whereas, no significant effect on germination of *C. album* showing resistance to dry powder. It is also clear from the result that *E. helioscopia* (65%)*, P. minor* (64%)*, A. fatua* (64%) and *R. dentatus* (61%) showed inhibition respectively as compared to control in powder applied into soil. The results also declared that maximum (95%) germination was noted for *C. album.* In the present study, it was demonstrated that minimum germination was noted for *A. fatua* (40%) and *E. helioscopia* (35%) on filter paper and soil, respectively. The experimental results of the current study indicated on agar the highest germination reduction was noted for *E. helioscopia* (59%), followed by *P. minor* (58%), *R. dentatus* (56%) and *A. fatua* (56%) at 10 mg conc. Similarly, the highest germination reduction was noted for *E. helioscopia* (63%), followed by *P. minor* (62%), *A. fatua* (60%) and *R. dentatus* (59%) at 50 mg conc. The statistical data concluded that minimum germination was noted for *E. helioscopia* i.e. 41% and 37% at 10 mg and at 50 mg conc., respectively. The statistics also recommended that with the increase of concentration, the inhibitory effect was progressively increased for *E. helioscopia, P. minor, A. fatua* and *R. dentatus*. The statistical results recommended that the germination percentage *C. album* were completely resistant to dry powder (*Table 2a*).

The data revealed that *C. album*, *P. minor* and *A. fatua* showing 52%, 5% and 50% radicle length inhibition respectively as compared to control in *L. camara* leaf powder on filter paper, whereas, no significant effect on radicle length of *R. dentatus* and *E. helioscopia* showing resistance to dry powder. It is also clear from the result that *C. album, P. minor* and *A. fatua* showed 55%, 53% and 52% radicle length inhibition respectively as compared to control in powder applied into soil. The results also declared that maximum (98%) radicle length was noted for *R. dentatus* and *E. helioscopia.* In the present study, it was demonstrated that minimum radicle length was noted for *C. album* i.e. 48% and 45% on filter paper and soil, respectively. The results of the current study indicated on agar the highest radicle length reduction was noted for *P. minor* (36%), followed by *A. fatua* (33%) and *C. album* (32%) at 10 mg conc. Similarly, the highest radicle length reduction was noted for *C. album* (53%), followed by *P. minor* (51%) *A. fatua* (50%) at 50 mg conc. The statistical data concluded that minimum radicle length was noted for *P. minor* (64%) and *C. album* (37%) at 10 mg and at 50 mg conc., respectively (*Table 2b*).

The data revealed that *E. helioscopia*, *C. album*, *R. dentatus* and *A. fatua* showing 54%, 53%, 51% and 50% plumule length inhibition respectively as compared to control in *L. camara* leaf powder on filter paper, whereas, no significant effect on plumule length of *P. minor* showing resistance to dry powder. It is also clear from the result that *E. helioscopia, C. album, A. fatua* and *R. dentatus* showed 64%, 61%, 59% and 56% plumule length inhibition respectively as compared to control in powder applied into soil. The results also declared that maximum (98%) plumule length was noted for *P. minor.* In the present study, it was demonstrated that minimum plumule length was noted for *E. helioscopia* i.e. 46% and 36% on filter paper and soil, respectively. The experimental results of the current study indicated on agar the highest plumule length reduction was noted for *R. dentatus* (43%), followed by *E. helioscopia* (42%), *C. album* (42%) and *A. fatua* (37%) at 10 mg conc. Similarly, the highest plumule length reduction was noted for *C. album* (59%), followed by *E. helioscopia* (57%), *A. fatua*

http://www.aloki.hu ● ISSN 1589 1623 (Print) ● ISSN 1785 0037 (Online)
DOI: http://dx.doi.org/10.15666/aeer/1706_1268312696

(56%) and *R. dentatus* (55%) at 50 mg conc. The statistical data concluded that minimum plumule length was noted for *R. dentatus* (67%) and *C. album* (41%) at 10 mg and at 50 mg conc., respectively (*Table 2c*).

Table 2. *Allelopathic potential of L. camara leaf powder against tested species on filter paper, soil and agar (a) germination percentage (b) radicle length (c) plumule length*

(a) Germination percentage (%)		***A. fatua***	***R. dentatus***	***P. minor***	***E. helioscopia***	***C. album***
Filter paper	10 mg	34	37	39	43	80
	Control	80	89	85	91	83
Soil	50 mg	29	35	31	32	81
	Control	81	90	86	92	84
Agar	10 mg	36	40	36	38	83
	50 mg	33	37	33	34	81
	Control	82	91	86	93	85
(b) Radicle length (cm)		***A. fatua***	***R. dentatus***	***P. minor***	***E. helioscopia***	***C. album***
Filter paper	10 mg	4.58	7.91	4.01	9.1	4.41
	Control	9.11	7.98	8.19	9.2	9.21
Soil	50 mg	4.36	7.94	3.86	9.3	4.26
	Control	9.13	8	8.21	9.4	9.41
Agar	10 mg	6.12	8.2	5.25	9.4	6.57
	50 mg	4.61	8.19	4.07	9.2	4.51
	Control	9.15	8.21	8.23	9.6	9.62
(c) Plumule length (cm)		***A. fatua***	***R. dentatus***	***P. minor***	***E. helioscopia***	***C. album***
Filter paper	10 mg	3.98	4.61	10.1	3.29	4.59
	Control	8.01	9.48	10.2	7.09	9.71
Soil	50 mg	3.26	3.94	10.3	3.26	3.86
	Control	8.03	9	10.4	9.01	10.01
Agar	10 mg	5.02	5.2	10.4	4.15	5.87
	50 mg	3.51	4.19	10.2	3.06	4.21
	Control	8.05	9.21	10.6	7.13	10.2

It was detected that maximum germination was observed for *C. album*. The analysis further indicated that minimum germination was noted for *A. fatua* and *E. helioscopia* on filter paper and soil being most sensitive to *L. camara* leaf powder. It was detected that maximum radicle length was observed for *R. dentatus* and *E. helioscopia*. The analysis further indicated that minimum radicle length was noted for *C. album* showed being most sensitive to *L. camara* leaf powder. It was detected that maximum plumule length was observed for *P. minor.* The analysis further indicated that minimum plumule length was noted for *E. helioscopia* showed being most sensitive among all the test species. The leaf powder of *L. camara* had inhibitory potential on germination, radicle and plumule length of radish and lettuce (Qiaoying et al., 2009). The leaf powder of *L. camara* suppressed the seed germination and plumule elongation of *P. hysterophorus* (Mishra and Singh, 2012). Das et al. (2012) also noticed inhibition linked with the production of allelochemicals from the *L. camara* leaves that inhibit growth of adjacent

http://www.aloki.hu ● ISSN 1589 1623 (Print) ● ISSN 1785 0037 (Online)
DOI: http://dx.doi.org/10.15666/aeer/1706_1268312696

plants by outcompeting for soil nutrients and altering micro environment by forming dense thickets. Allelopathy is a form of plant interference that can significantly influence ecosystem and agro ecosystem dynamics (Michelangelo et al., 2016).

Allelopathic potential of C. papaya

The data revealed that *A. fatua, P. minor* and *E. helioscopia* showing 39%, 38% and 33% germination inhibition respectively as compared to control in *C. papaya* leaf powder on filter paper, whereas, no significant effect on germination of *R. dentatus* and *C. album* showing resistance to dry powder. It is also clear from the result that *E. helioscopia, P. minor* and *A. fatua* showed 51%, 49% and 47% germination inhibition respectively as compared to control in powder applied into soil. The results also declared that maximum (98%) germination was noted for *R. dentatus* and *C. album.* In the present study, it was demonstrated that minimum germination was noted for *A. fatua* (61%) and *E. helioscopia* (49%) on filter paper and soil, respectively. The experimental results of the current study indicated on agar the highest germination reduction was noted for *P. minor* (41%), followed by *A. fatua* (38%) and *E. helioscopia* (36%) at 10 mg conc. Similarly, the highest germination reduction was noted for *A. fatua* (51%), followed by *P. minor* (49%) and *E. helioscopia* (47%) at 50 mg conc. The statistical data concluded that minimum germination was noted for *P. minor* (59%) and *A. fatua* (49%) at 10 mg and at 50 mg conc., respectively. The statistics also recommended that with the increase of concentration, the inhibitory effect was progressively increased for *A. fatua, P. minor* and *E. helioscopia*. The statistical results recommended that the germination *R. dentatus* and *C. album* were completely resistant (*Table 3a*).

The data revealed that *P. minor* and *R. dentatus* showing 51%, 41% and 30% radicle length inhibition respectively as compared to control in *C. papaya* leaf powder on filter paper, whereas, no significant effect on radicle length of *C. album, A. fatua* and *E. helioscopia* showing resistance to dry powder. It is also clear from the result that*, R. dentatus* and *P. minor* showed 55%, 41% and 35% radicle length inhibition respectively as compared to control in powder applied into soil. The results also declared that maximum (98%) radicle length was noted for *C. album, A. fatua* and *E. helioscopia.* The experimental results of the current study indicated on agar the highest radicle length reduction was noted for *P. minor* (35%) and *R. dentatus* (31%) at 10 mg conc. Similarly, the highest radicle length reduction was noted for *P. minor* (45%) and *R. dentatus* (42%) at 50 mg concentration (*Table 3b*).

The data revealed that *P. minor* (31%) and *C. album* (30%) showing plumule length inhibition as compared to control in *C. papaya* leaf powder on filter paper, whereas, no significant effect on plumule length of *A. fatua, R. dentatus* and *E. helioscopia* showing resistance to dry powder. It is also clear from the result that *C. album* and *P. minor* showed 45% and 33% plumule length inhibition respectively as compared to control in powder applied into soil. The results also declared that maximum (96%) plumule length was noted for *A. fatua, R. dentatus* and *E. helioscopia.* In the present study, it was demonstrated that minimum plumule length was noted for *P. minor* (69%) and *C. album* (55%) on filter paper and soil, respectively. The experimental results of the current study indicated on agar the highest plumule length reduction was noted for *C. album* (41%), followed by *P. minor* (30%) at 10 mg conc. Similarly, the highest plumule length reduction was noted for *C. album* (50%), followed by *P. minor* (43%) at 50 mg conc. The statistical data concluded that minimum plumule length was noted for *C. album* i.e. 59% and 50% at 10 mg and at 50 mg conc., respectively (*Table 3c*).

http://www.aloki.hu ● ISSN 1589 1623 (Print) ● ISSN 1785 0037 (Online)
DOI: http://dx.doi.org/10.15666/aeer/1706_1268312696

Table 3. *Allelopathic potential of C. papaya leaf powder against tested species on filter paper, soil and agar (a) germination percentage (b) radicle length (c) plumule length*

(a) Germination percentage (%)		***A. fatua***	***R. dentatus***	***P. minor***	***E. helioscopia***	***C. album***
Filter paper	10 mg	54	69	49	51	81
	Control	89	71	79	76	84
Soil	50 mg	48	70	41	39	82
	Control	91	73	81	79	86
Agar	10 mg	57	74	49	52	88
	50 mg	46	72	42	43	86
	Control	93	75	83	81	89
(b) Radicle length (cm)		***A. fatua***	***R. dentatus***	***P. minor***	***E. helioscopia***	***C. album***
Filter paper	10 mg	8.23	4.92	4.32	8.15	7.33
	Control	8.34	7.07	7.27	8.37	7.45
Soil	50 mg	8.32	4.28	4.9	8.38	7.54
	Control	8.56	7.23	7.59	8.58	7.68
Agar	10 mg	8.65	5.19	5.15	8.34	7.49
	50 mg	8.64	4.38	4.36	8.56	7.67
	Control	8.67	7.49	7.87	8.86	7.83
(c) Plumule length (cm)		***A. fatua***	***R. dentatus***	***P. minor***	***E. helioscopia***	***C. album***
Filter paper	10 mg	7.99	7.17	5.6	7.21	5.8
	Control	8.01	7.19	8.17	7.35	8.31
Soil	50 mg	8.09	7.24	5.44	7.46	4.46
	Control	8.12	7.38	8.12	7.59	8.07
Agar	10 mg	8.23	7.43	5.86	7.83	4.72
	50 mg	8.21	7.41	4.75	7.81	4.06
	Control	8.25	7.45	8.39	7.85	8.06

It was detected that maximum germination was observed for *R. dentatus* and *C. album*. The analysis further indicated that minimum germination was noted for *A. fatua* and *E. helioscopia* on filter paper and soil, being most sensitive to *C. papaya* leaf powder. It was detected that maximum radicle length was observed for *C. album, A. fatua* and *E. helioscopia*. Similar, results were obtained in bioassays with lettuce seeds (Gherardi and Valio, 1976; Chow and Lin, 1991) and by Reyes et al. (1980) with cucumber seeds. Chow and Lin (1991) used extracts of papaya, which showed that there is a higher concentration of inhibitors in the sarcotesta, canceling the germination of lettuce seeds, which had already been observed by Gherardi and Valio (1976). They excluded the possibility that the germination inhibitor present in the sarcophagus of papaya seeds was abscisic acid, stating that such inhibitors are phenolic in nature.

Allelopathic potential of P. roxburghii

The data revealed that *C. album* and *A. fatua* showing 52%, 47% and 44% germination inhibition respectively as compared to control in *P. roxburghii* needles

http://www.aloki.hu ● ISSN 1589 1623 (Print) ● ISSN 1785 0037 (Online)
DOI: http://dx.doi.org/10.15666/aeer/1706_1268312696

powder on filter paper while on soil *C. album* and *A. fatua* showing 55%, 48% and 46% germination inhibition, whereas, no significant effect on germination of *R. dentatus, P. minor* and *E. helioscopia* showing resistance to dry powder. The results also declared that maximum (97%) germination was noted for *R. dentatus, P. minor* and *E. helioscopia.* The experimental results of the current study indicated on agar the highest germination reduction was noted for *C. album* (36%) and *A. fatua* (35%) at 10 mg conc. Similarly, the highest germination reduction was noted for *C. album* (48%) and *A. fatua* (43%) at 50 mg conc. The statistics also recommended that with the increase of concentration, the inhibitory effect was progressively increased for *C. album* and *A. fatua*. The statistical results recommended that the germination of *P. minor, E. helioscopia* and *R. dentatus* were completely resistant to dry powder (*Table 4a*).

The data revealed that *C. album* and *R. dentatus* showing 35% and 32% radicle length inhibition respectively as compared to control in *P. roxburghii* needles powder on filter paper, whereas, no significant effect on radicle length of *A. fatua, P. minor* and *E. helioscopia* showing resistance to dry powder. It is also clear from the result that *C. album* and *R. dentatus* showed 45% and 42% radicle length inhibition respectively as compared to control in powder applied into soil. The results also declared that maximum (96%) radicle length was noted for *A. fatua, P. minor* and *E. helioscopia.* In the present study, it was demonstrated that minimum radicle length was noted for *C. album* i.e. 65% and 55% on filter paper and soil, respectively. The experimental results of the current study indicated on agar the highest radicle length reduction was noted for *R. dentatus* (35%), followed by *C. album* (34%) at 10 mg conc. Similarly, the highest radicle length reduction was noted for *R. dentatus* (41%), followed by *C. album* (36%) at 50 mg conc. The statistical data concluded that minimum radicle length was noted for *R. dentatus* i.e. 65% and 59% at 10 mg and at 50 mg conc., respectively (*Table 4b*).

The data revealed that *A. fatua* (39%) and *R. dentatus* (37%) showing plumule length inhibition respectively as compared to control in *P. roxburghii* needles powder on filter paper, whereas, no significant effect on plumule length of *C. album*, *E. helioscopia* and *P. minor* showing resistance to dry powder. It is also clear from the result that *R. dentatus* (49%) and *A. fatua* (46%) showed and plumule length inhibition respectively as compared to control in powder applied into soil. The results also declared that maximum (95%) plumule length was noted for *C. album*, *E. helioscopia* and *P. minor.* In the present study, it was demonstrated that minimum plumule length was noted for *A. fatua* (61%) and *R. dentatus* (51%) on filter paper and soil, respectively. The results of the current study indicated on agar the highest plumule length reduction was noted for *R. dentatus* (42%), followed by *A. fatua* (40%) at 10 mg conc. Similarly, the highest plumule length reduction was noted for *R. dentatus* (49%), followed by *A. fatua* (44%) at 50 mg conc. The statistical data concluded that minimum plumule length was noted for *R. dentatus* measuring 68% and 61% at 10 mg and at 50 mg conc., respectively (*Table 4c*). The data attained from statistical analysis revealed that maximum germination was observed for *R. dentatus, P. minor* and *E. helioscopia.* The data attained from statistical analysis revealed that maximum radicle length was observed for *A. fatua, P. minor* and *E. helioscopia*. In the present study it was demonstrated that radicle length was noted for *C. album*. It was noted that maximum plumule length was observed for *C. album*, *E. helioscopia* and *P. minor.* In the present study it was demonstrated that minimum plumule length was noted for *A. fatua* and *R. dentatus* on filter and soil respectively. Blum (1998) observed that *P. divaricata* and *P. resinosa* needles leachates suggestively checked seedling growth and germination of *Epilobium*

http://www.aloki.hu ● ISSN 1589 1623 (Print) ● ISSN 1785 0037 (Online)
DOI: http://dx.doi.org/10.15666/aeer/1706_1268312696

angustifolium, Agropyron repens and *Phleum pretense. The* seedling growth of *Lepidium virginicum* was significantly checked by *P. roxburghii* needles (Williams and Hoagland, 1982). The mechanism of retardation on the seedling growth produced by phytochemicals checked cell elongation and division (Node et al., 2003). Similarly, *P. densiflora* cones have high biological activity against select plant species (Lee and Monsi, 1963).

Table 4. *Allelopathic potential of P. roxburghii needles powder against tested species on filter paper, soil and agar (a) germination percentage (b) radicle length (c) plumule length*

(a) Germination percentage (%)		***A. fatua***	***R. dentatus***	***P. minor***	***E. helioscopia***	***C. album***
Filter paper	10 mg	44	86	74	83	48
	Control	78	88	79	84	91
Soil	50 mg	43	87	80	85	45
	Control	80	90	81	86	93
Agar	10 mg	54	93	82	88	60
	50 mg	47	91	80	86	49
	Control	83	93	83	89	95
(b) Radicle length (cm)		***A. fatua***	***R. dentatus***	***P. minor***	***E. helioscopia***	***C. album***
Filter paper	10 mg	7.21	5.63	8.6	7.23	5.98
	Control	7.29	8.23	8.82	7.33	9.15
Soil	50 mg	7.46	4.91	8.54	7.41	5.09
	Control	7.68	8.4	8.93	7.56	9.23
Agar	10 mg	7.54	5.71	8.85	7.46	6.15
	50 mg	7.41	5.25	8.63	7.39	5.93
	Control	7.89	8.83	8.99	7.78	9.31
(c) Plumule length (cm)		***A. fatua***	***R. dentatus***	***P. minor***	***E. helioscopia***	***C. album***
Filter paper	10 mg	5.8	5.91	8.15	9.19	8.28
	Control	9.48	9.44	8.27	9.25	8.4
Soil	50 mg	4.95	4.85	8.56	9.52	8.49
	Control	9.09	9.6	8.68	9.62	8.68
Agar	10 mg	5.82	5.72	8.9	9.8	8.82
	50 mg	5.38	5.05	8.92	9.82	8.81
	Control	9.69	9.86	8.95	9.84	8.87

Some recent studies indicating the phytotoxic/allelopathic effect of weeds include Parthenium hysterophorus (Saranya et al., 2019), Brassica napus (Rodriguez et al., 2016), Raphanus raphanistrum (Ali, 2016) and Ageratum conyzoides (Kumar et al., 2018). All these studies indicate the release of phototoxic chemicals. Based on this, studies were further extended to explore the impact of selected species, as they possessed greater phytotoxicity on the emergence and growth of weed plants in wheat crop.

http://www.aloki.hu ● ISSN 1589 1623 (Print) ● ISSN 1785 0037 (Online)
DOI: http://dx.doi.org/10.15666/aeer/1706_1268312696

Conclusions

Present results indicated that water leachates from leaves of selected plants at higher concentrations reduce the seed germination, radicle and plumule length of weeds associated with the wheat crop. Results provided evidence about herbicidal potential of tested plant species viz. *L. camara*, *P. roxburghhii* and *C. Papaya* against weeds of wheat crop (*Avena fatua, Phalaris minor, Chenopodium album* and *Rumex dentatus*) while *R. stricta* was proved non-promising in the case as it affected growth parameters of wheat as well. Since *L. camara*, *P. roxburghhii* and *C. Papaya* inhibited growth of weeds without affecting wheat, the study seems effective than the other ones published in previous literature. Further work is, however, recommended to appraise the potential inhibitory effects of allelochemicals from the these plants in field.

REFERENCES

[1] Ali, K. A. (2016): Allelopathic potential of radish (*Raphanus sativus* L.) on germination and growth of some crop and weed plants. – Int. J. Biosci. 9: 394-403.
[2] Anwar, T., Khalid, S., Saeed, M., Mazhar, R., Qureshi, H., Rashid, M. (2016): Allelopathic interference of leaf powder and aqueous extracts of hostile weed: *Parthenium hysterophorus* (Asteraceae). – Sci. Int. 4: 86-93.
[3] Anwar, T., Khalid, S., Panni, M. K., Qureshi, H., Rashid, M. (2017): Allelopathic effect of Euphorbia helioscopia on *Avena fatua, Rumex dentatus, Helianthus annuus, Zea mays* and *Triticum aestivum*. – Pak. J. Weed Sci. Res. 23: 165-177.
[4] Arafat, Y., Khalid, S., Lin, W., Fang, C., Sadia, S., Ali, N., Azeem, S. J. (2015): Allelopathic evaluation of selected plants extract against broad and narrow leaves weeds and their associated crops. – Acad. J. Agric. Res. 3: 226-234.
[5] Aryakia, E., Naghavi, M. R., Farahmand, Z., Fazeli, S. A. H. S. (2015): Evaluating allelopathic effects of some plant species in tissue culture media as an accurate method for selection of tolerant plant and screening of bioherbicides. – J. Agr. Sci. Tech. 17: 1011-1023.
[6] Batish, D. R., Singh, H. P., Kohli, R. K., Saxena, D. B., Kaur, S. (2002): Allelopathic effect of parthenium against two weedy species, *Avena fatua* and *Bidens pilosa*. – Environ. Exp. Bot. 47: 149-155.
[7] Biljana, M. B., Kragujevac, D. Z. J. (2015): Allelopathic relations of selected cereal and vegetable species during seed germination and seedling growth. – J. Sci. 37: 135-142.
[8] Blum, U. (1998): Effects of microbial utilization of phenolic acids and their phenolic acid breakdown products on allelopathic interactions. – J. Chem. Ecol. 24: 685-708.
[9] Canini, A., Alesiani, D., Arcangelo, G., Tagliatesta, P. (2007): Gas chromatography-mass spectrometry analysis of phenolic compounds from *Carica papaya* L. leaf. – J. Food Compos. Anal. 20: 584-590.
[10] Cavero, J., Zaragoza, C., Cirujeda, A., Anzalone, A., Faci, J. M., Blanco, O. (2011): Selectivity and weed control efficacy of some herbicides applied to sprinkler irrigated rice (*Oryza sativa* L.). – Spanish J. Agric. Res. 9: 597-605.
[11] Chow, Y. J., Lin, C. H. (1991): p-Hydroxybenzoic acid the major phenolic germination inhibitor of papaya seed. – Seed Sci. Techn., Zürich 19: 167-174.
[12] Das, C. R., Mondal, N. K., Aditya, P., Datta, J. K., Banerjee, A., Das, K. (2012): Allelopathic potentialities of leachates of leaf litter of some selected tree species on gram seeds under laboratory conditions. – Asian. J. Exp. Biol. Sci. 3: 59-65.
[13] Dobhal, P. K., Kohli, R. K., Batish, D. R. (2010): Evaluation of impact of *Lantana camara* L. invasion on four major woody shrubs along Nayar river of Pauri Garhwal in Himalaya. – Int. J. Biodivers. Conserv. 2: 166-172.

http://www.aloki.hu ● ISSN 1589 1623 (Print) ● ISSN 1785 0037 (Online)
DOI: http://dx.doi.org/10.15666/aeer/1706_1268312696

[14] Ebid, A. I. (2016): Allelopathic effect of three wild species on seed germination and seedling growth of Vicia faba, Hordeum vulgare and *Triticum aestivum*. – J. Agric. Ecol. Res. Int. 6: 1-7.
[15] Fujii, Y., Parvez, S. S., Parvez, M. M., Ohmae, Y., Iida, O. (2003): Screening of 239 medicinal plant species for allelopathic activity using sandwich method. – Weed Biol. Manag. 3: 233-241.
[16] Fujii, Y., Shibuya, T., Nakatani, K., Itani, T., Hiradate, S., Parvez, M. M. (2004): Assessment method for allelopathic effect from leaf litter leachates. – Weed Biol. Manag. 4: 19-23.
[17] Gherardi, E. I., Valio, F. M. (1976): Occurrence of promoting and inhibitory substances in the seed arils of *Carica papaya* L. – J. Hortic. Sci. 51: 1-14.
[18] Hussain, M. I., González, L., Reigosa, M. J. (2011): Allelopathic potential of *Acacia melanoxylon* on the germination and root growth of native species. – Weed Biol. Manag. 11: 18-28.
[19] Inderjit and Duke, S. O. (2003): Eco physiological aspects of allelopathy. – Planta 217: 529-539.
[20] Kamran, M., Raza, A., Ali, Q., Ali, H. H., Chattha, M. S. (2017): Investigating the influence of fertilizer and allelopathic water extracts on maize and associated weeds. – Pak. J. Weed Sci. Res. 23: 361-378.
[21] Khan, I., Ali, Z., Khan, M. I., Hussain, Z., Khan, I. A., Waqas, M., Khan, R., Khan, S. (2014): Allelopathic effects of some weeds on chickpea crop. – Pak. J. Weed Sci. Res. 20: 207-211.
[22] Khan, R., Khan, M. A., Shah, S., Uddin, S., Ali, S., Ilyas, M. (2016): Bioherbicidal potential of plant extracts against weeds of wheat crop under agro-climatic conditions of Peshawar-Pakistan. – Pak. J. Weed Sci. Res. 22: 285-294.
[23] Lee, I. K., Monsi, M. (1963): Ecological studies on *Pinus densiflora* forest 1. Effects of plant substances on the floristic composition of the undergrowth. – Bet. Mag. Tokyo 76: 400-413.
[24] Michelangelo, M. T., Vidal, R. A., Junior, A. A. B., Bittencourt, H. V. H., Filho, S. S. (2016): Allelopathy: driving mechanisms governing its activity in agriculture. – J. Plant Interact. 1: 53-60.
[25] Mishra, A., Singh, R. (2012): Allelopathic effect of Lantana camara extract of different parts on seed germination of *Parthenium hysterophorus,* L. – Int. J. Plant Sci. 5: 74-75.
[26] Mubarik, S., Khan, K., Memon, R. A., Shaheen, G., Hashmatulla (2015): Allelopathic effects of important weeds on germination and growth of maize (*Zea mays* L.). – Pak. J. Weed Sci. Res. 21: 181-180.
[27] Nekonam, M. S., Kraimmojeni, H., Sharifnabi, B., Razmjoo, J., Amini, H., Bahrami, F. (2014): Assessment of some medicinal plants for their allelopathic potential against redroot pigweed (*Amaranthus retroflexus*). – J. Plant Prot. Res. 54: 90-95.
[28] Node, M., Yokotani, K. T., Suzuki, T., Kosemura, S., Hirata, H., Hirata, K., Hasegawa, K. (2003). Allelopathy of pinecone in Japanese red pine tree (*Pinus densiflora* Sieb. et Zucc.). – Weed Biol. Manag. 3: 111-116.
[29] Qiaoying, Z., Shaolin, P., Yunchun, Z. (2009): Allelopathic potential of reproductive organs of exotic weed *Lantana camara*. – Allelopathy J. 23: 213-220.
[30] Ramsumair, A., Mlambo, V., Lallo, C. H. O. (2014): Effect of drying method on the chemical composition of leaves from four tropical tree species. – Trop. Agric. (Trinidad) 91: 179-186.
[31] Reyes, M. N., Perez, A., Cuevas, J. (1980): Detecting endogenous growth regulators on the sarcotesta, sclerotesta, endosperm and embryo by paper chromatography on fresh and old papaya seeds. – J. Agri. Uni. Puerto Rico 64: 167-172.
[32] Rodriguez, D., Casagrande, G., Carmona-Galindo, V. D. (2016): Effects of black mustard allelopathy on the fitness and life history strategies of buffalo gourd in southern California. – Bios 87(3): 98-103.

http://www.aloki.hu ● ISSN 1589 1623 (Print) ● ISSN 1785 0037 (Online)
DOI: http://dx.doi.org/10.15666/aeer/1706_1268312696

[33] Rueda-Ayala, V. P., Rasmussen, J., Gerhards, R., Fournaise, N. E. (2011): The influence of post-emergence weed harrowing on selectivity, crop recovery and crop yield in different growth stages of winter wheat. – Weed Res. 51: 478-488.
[34] Saranya, M., Rangaraj, T., Ragavan, T., Amutha, R. (2019): Allelopathic Potential of *Parthenium hysterophorus* and *Tridax procumbens* aqueous leaf extracts on weed control and growth of Blackgram (*Vigna mungo* L.). – Int. J. Agric. Sci. 11: 7697-7700.
[35] Shah, S. H., Khan, E. A., Shah, H., Ahmed, N., Khan, J., Sadozai, G. U. (2016): Allelopathic sorghum water extract helps to improve yield of sunflower (*Helianthus annuus,* L.) – Pak. J. Bot. 48: 1197-1202.
[36] Williams, R. D., Hoagland, R. E. (1982): The effects of naturally occurring phenolic compounds on seed germination. – Weed Sci. 30: 206-212.
[37] Zafar, I., Fatima, A., Khan, S. J., Rehman, Z., Mehmud, S. (2010): GC-MS studies of needles essential oil of *Pinus roxburghii* and their antimicrobial activity from Pakistan. – Electr. J. Environ. Agric. Food Chem. 9: 468-473.

http://www.aloki.hu ● ISSN 1589 1623 (Print) ● ISSN 1785 0037 (Online)
DOI: http://dx.doi.org/10.15666/aeer/1706_1268312696

NUTRITIONAL AND PHYTOCHEMICAL SCREENING OF WILD FRUIT OF *BERBERIS BALUCHISTANICA* – AN ENDEMIC SPECIES TO PAKISTAN

RAHIM, B. Z.[1] – QURESHI, R.[2*] – TAREEN, R. B.[1] – SHAZMEEN[2]

[1]*Department of Botany, Baluchistan University, 87500 Quetta, Baluchistan, Pakistan*

[2]*Department of Botany, Pir Mehr Ali Shah Arid Agriculture University Murree Road, Shamsabad, 46300 Rawalpindi, Punjab, Pakistan*

**Corresponding author*
e-mail: rahmatullahq@yahoo.com, rahmatullahq@uaar.edu.pk

(Received 29th Mar 2019; accepted 2nd Jul 2019)

Abstract. *Berberis baluchistanica* Ahrendt is an endemic species to Pakistan belonged to Berberidaceae family. Its ripened fruit is collected by the natives and consumed as wild fruit. The present study aimed at evaluating nutritional and phytochemical potential of wild fruits of *B. baluchistanica*. The proximate analysis revealed that the fruit possessed highest proportion of dry matter (92%), followed by crude fibre (35%), moisture content (8%), crude protein (7%) and crude fat (6.3%), while total ash percentage was the least (3.5%). Mineral analysis indicated that iron (Fe) was found in the highest quantity (3.835%), followed by zinc (1.039%), copper (0.851%), manganese (0.764%), potassium (0.101%), while the sodium was in least amount. This study further determined five major phytochemical compounds such as alkaloids, flavonoids, phenols, tannins and saponins trough six solvent extracts. Alkaloids were detected by all solvents, except the aqueous extract. Phenols and tannins were detected by three solvent extracts. Flavonoids were isolated by two solvent extracts, while, saponins were only detected by the aqueous extract. Based on results, it can be concluded that the investigated fruit has great potential owing to substantial quantity of essential nutrients, minerals and phytochemicals and requires further detailed investigation prior to commercial production and introduction in the market.
Keywords: *commercial production, essential nutrients, mineral analysis, phytochemical compounds, solvent extracts*

Introduction

It is an established fact that use of fruits may improve the rate of human health Nwachukwu et al. (2010). Fruits provide nutrients including minerals, vitamins, antioxidants, polyphenols, etc. (Sher et al., 2003). Furthermore, fruits and vegetables possess fairly low calories, high dietary fibre and beneficial to human health (Khalil et al., 2013). These further aid in maintaining healthy weight and decrease the risk of numerous persistent illness Nwachukwu et al. (2010), like cardiovascular disorders, diabetes cancers, etc.

Pakistan has moderate diversity in ecological zones having range of plants. Since majority of the human population is residing in rural areas, so they are facing food insecurity and malnutrition. According to Chakraborty and Newton (2007), if the food with high nutritive value is safe, accessible, affordable and available for the reasonable population can form food security. During certain period of time, several food crops may turn into limited and expensive either during planting season or famine particularly for low income earners. Such consequences experience malnutrition and poor health. Owing to such issues, scientists are looking into screening the wild edible fruit which may have latent to balance staple food.

http://www.aloki.hu ● ISSN 1589 1623 (Print) ● ISSN 1785 0037 (Online)
DOI: http://dx.doi.org/10.15666/aeer/1706_1269712707

Berberis baluchistanica Ahrendt, locally known as *Tor Zaralag* (Pashto) is an endemic to Pakistan belonged to Berberidaceae family. It is evergreen shrub up to 3 m tall with red to red-brown stem (*Fig. 1*). Leaves are thick, rigid, sub-orbicular to obovate-oblong, sessile to sub-sessile Flowers are approximately 7-10 mm across, yellow. Fruits are berries with ovoid to suborbicular shaped, dark red turned to black and pruinose blue. Its ripened fruit is collected by the natives and consumed as wild fruit. The decoction of roots has been reported in treating cough, infection and internal injury of human being as well animals (Ghafoor, 2002). Previously Abbasi et al. (2013) carried out antioxidant potential of leaves of *Berberis baluchistanica*. The present study aimed at evaluating nutritional, phytochemical and antioxidant potential of wild fruits of *B. baluchistanica*.

Figure 1. *The habit of Berberis baluchistanica*

http://www.aloki.hu ● ISSN 1589 1623 (Print) ● ISSN 1785 0037 (Online)
DOI: http://dx.doi.org/10.15666/aeer/1706_1269712707

Materials and methods

Location and area

Ziarat district is located at 30° 22′ 51 N and 67° 43′ 37 E at an altitude of 2453 m (8050 ft) in the north Balochistan province, Pakistan (*Fig. 2*). Khilafat Hills are the highest peak with an altitude of 11.400 ft (3.475 m) in Ziarat district. Ziarat District has the highest Human Development Index of all districts in Balochistan (District Profile Ziarat, 1997). This district is famous for its antique and splendid juniper forest which spreads over 126,000 acres and is the second largest in the world. Some of the trees are almost 4,000 years old (Anonymous, 2019).

Climate

The climate of the study area is mostly dry temperate characterized by excessive cold during the winter season and refreshingly cool and pleasant in summer. Snow mostly falls during December to March. Mean annual precipitation is about 282 mm/year, mainly received during winter in the form of snow. Some showers also occur in July and August. Temperature extremes are characteristics feature of the area with mean maximum temperature of 28 °C recorded in July and August and mean minimum temperature of -9 °C in January. The highest average relative humidity (67%) was recorded in December, while the lowest (23%) in October (Ahmed et al., 1990).

Collection and identification of plant material

The ripened fruits (1 kg) of *Berberis baluchistanica* Ahrendt were collected from the growing localities of Ziarat, Baluchistan during September to October, 2017 (*Table 1*). One set of voucher specimens of the species were prepared and identified by Dr. Rasool Bakhsh Tareen, Department of Botany, University of Baluchistan, Quetta. The determined specimens were deposited in the herbarium of Baluchistan University for record.

Table 1. *Collection of fruits and plant specimens of B. baluchistanica from different growing localities of District Ziarat, Balochistan, Pakistan*

S. No.	Locality	Longitude	Latitude	Elevation (m)
1	Ahmadun	30° 29′ 07.58″	67° 22′ 48.35″	2100
2	Zargi	30° 30′ 12.99″	67° 41′ 18.99″	2350
3	Zezri	30° 19′ 40.00″	67° 42′ 00.00″	2500

Ethnobotanical investigation

The traditional knowledge of *Berberis baluchistanica* was collected by using semi-structured questionnaire following the work of Qureshi (2004) and Qureshi and Bhatti (2008). Regular field trips were arranged in order to collect information about the folk knowledge of plants.

Proximate and mineral analysis

The proximate analysis was carried out from the dried powdered sample by using standard method (AOAC, 2005). The powdered samples were analyzed for proteins, fat,

http://www.aloki.hu ● ISSN 1589 1623 (Print) ● ISSN 1785 0037 (Online)
DOI: http://dx.doi.org/10.15666/aeer/1706_1269712707

carbohydrates, moisture and ash. The mineral composition was analyzed by using Atomic Absorption Spectrophotometer (Agilent Technologies Model No. 200 series) in the department of Botany, Pir Mehr Ali Shah Arid Agriculture University, Rawalpindi, Pakistan. For statistical analysis, standard error was determined from the triplicates readings.

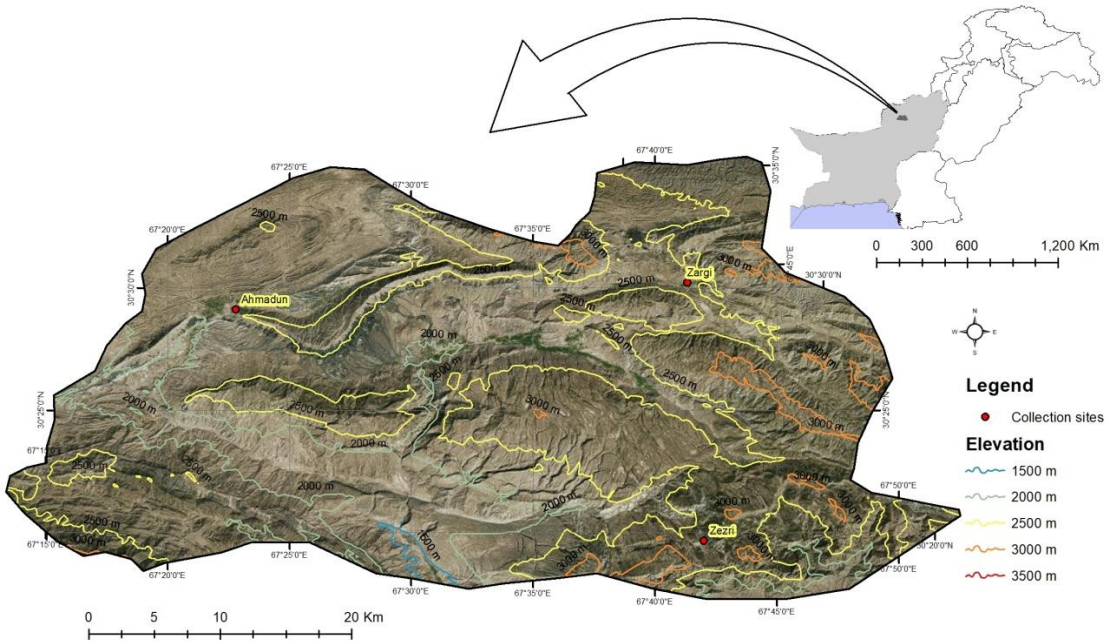

Figure 2. *Location map of the study area and collection sites of the plant material*

Preparation of fruit extract

The collected fruits were thoroughly rinsed with tap water and dried under shade. These were powdered to fine powder (80 mesh) by using grinder (Model No. MX1100XT21CE) and preserved in airtight bottle and kept in refrigerator. The powder was soaked in six solvents such as acetone, aqueous, Ethyl acetate, methanol, n-hexane and petroleum ether. The same was then shaken at 37 °C for 24 h. The same were subsequently sieved using Whatman filter paper (No. l) and then concentrated on reduced pressure at 40 °C by employing rotary evaporator (Rahim et al., 2013). These extracts were used the phytochemicals screening.

Determination of yield extracts

The crude extracts yield percentage was carried out by using following formula after Dellavalle et al. (2011) and Rahim et al. (2013):

$$Yield\ \% = \frac{\text{Weight of lyophilized extract}}{\text{Weight of dried fruit}} \times 100 \qquad \text{(Eq.1)}$$

Assay for phytochemicals screening

The chemical assays were carried out from six different solvents based fruit extracts of the *Berberis baluchistanica* by using standard protocols for the detection of phytochemicals after Egwaikhide and Gimba (2007).

http://www.aloki.hu ● ISSN 1589 1623 (Print) ● ISSN 1785 0037 (Online)
DOI: http://dx.doi.org/10.15666/aeer/1706_1269712707

Analysis for alkaloids

The 0.2 mg fruit extract was warmed in 2% sulphuric acid for 2 min. The filtrate was mixed in few drops of Dragendorff's reagent**.** The appearance of orange red precipitate confirmed the presence of alkaloids (Egwaikhide and Gimba, 2007; Rahim et al., 2013).

Analysis for tannins

A small quantity of fruit extract was liquefied in water and heated on water bath. Then it was filtered and few drops of ferric chloride were poured in it. The emergence of dark green colour revealed the occurrence of tannins in the sample (Egwaikhide and Gimba, 2007).

Analysis for saponins

The 0.2 g extract was forcefully shaken in 5 ml of distilled water and boiled. The occurrence of bubble supposed to the presence of saponins (Egwaikhide and Gimba, 2007).

Analysis for flavonoids

The 0.2 g fruit extract was combined with diluted sodium hydroxide and few drops of hydrochloric acid were poured in it. This solution converted first into yellow colour and then colourless within few minutes. Such reactions indicated the presence of flavonoids in the test sample (Egwaikhide and Gimba, 2007).

Analysis for phenolic compounds

This test has two parts. In first part, 50 mg of each solvent extract was added with 5 ml distilled water and vigorously shaken for a minute. Then, five drops of 5% ferric chloride solution were supplemented. This mixture was resulted into dark green colour known as ferric chloride test. In the other test, 300 ml of distilled water were added to 50 mg of each solvent extract and shaken for a while. Then 3 ml of 10% lead acetate were poured. The appearance of white precipitates in the resultant mixture showed the presence of phenolic compounds (Munazir et al., 2015).

Results

Traditional uses

The leaves and branches are dried and made into powder and is then dusted upon the injury and wounds to heal. Once sheep of hill was fired and after some time that sheep was observed under shadow of *Berberis baluchistanica* with repaired injury revealing that the injury was repaired by eating of the leaves of this plant. Wild fruits are collected by the local communities and eaten as nutritional as well as iron supplement.

Extract yield

Different solvent based extracts showed range of ratios in terms of extract yield and quantity (*Fig. 3*). The maximum amount of the extract yield was obtained by methanol (12.95%). It was followed by water (6.7%), ethyl acetate (1.8%), acetone (1.15%), while n-hexane and petroleum ether yielded less quantity (*Fig. 3*).

http://www.aloki.hu ● ISSN 1589 1623 (Print) ● ISSN 1785 0037 (Online)
DOI: http://dx.doi.org/10.15666/aeer/1706_1269712707

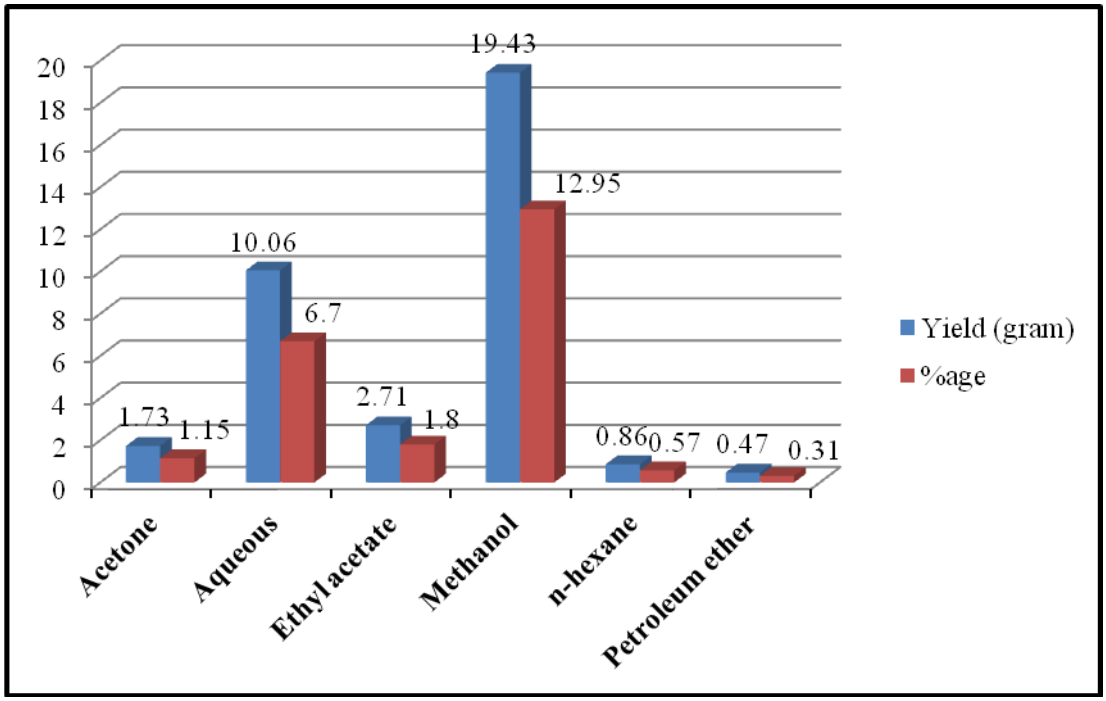

Figure 3. *Yielding potential of various solvent based extracts from B. baluchistanica*

Proximate and mineral composition

The proximate analysis of wild fruits of *Berberis baluchistanica* (Berberidaceae) was carried out and the data is provided in *Figure 4*. The data showed that the fruit possesses the highest proportion of dry matter (92%), followed by crude fibre (35%), moisture content (8%), crude protein (7%), crude fat (6.3%), while total ash percentage was the least (3.5%). It is apprising that the fruit retains an appreciable amount of all the beneficial elements. Iron (Fe) was found in the highest quantity (3.835%), followed by zinc (1.039%), copper (0.851%), manganese (0.764%), potassium (0.101%), while the sodium was in lesser amount (0.009%). The Na/K ratio was found as 0.089 in the fruit (*Fig. 5*).

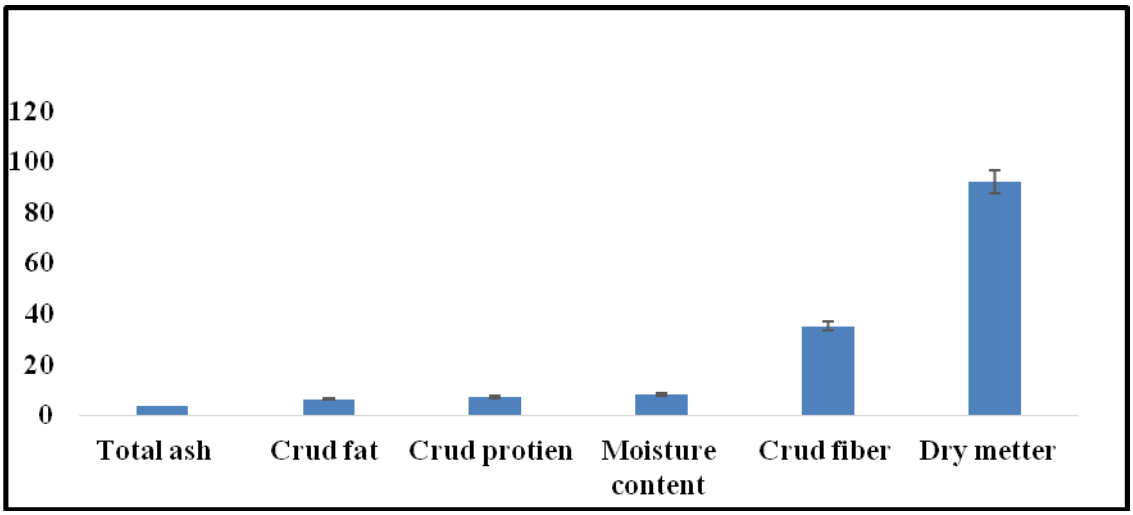

Figure 4. *Graphical presentation of proximate analysis of B. baluchistanica*

http://www.aloki.hu ● ISSN 1589 1623 (Print) ● ISSN 1785 0037 (Online)
DOI: http://dx.doi.org/10.15666/aeer/1706_1269712707

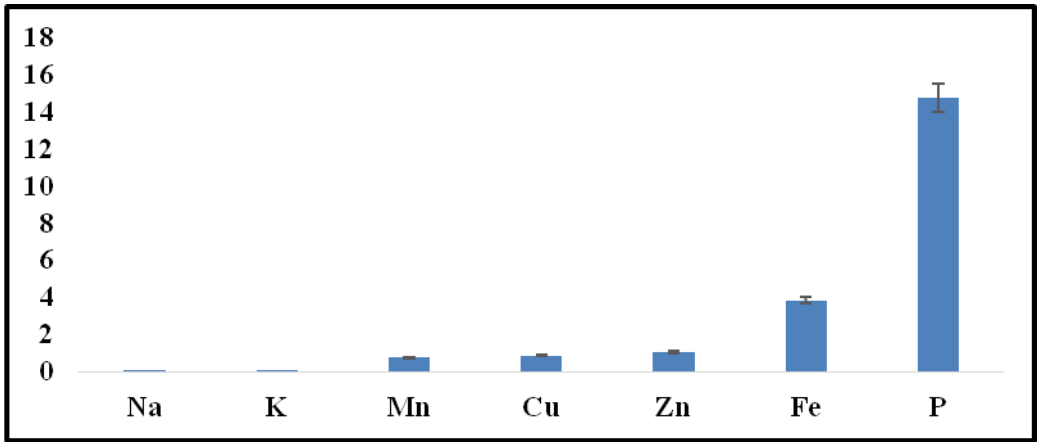

Figure 5. *Graphical presentation of mineral analysis of B. baluchistanica*

Qualitative phytochemical screening

The fruits of *Berberis baluchistanica* were screened for five major phytochemical classes namely alkaloids, flavonoids, phenols, saponins and tannins from six polarity based solvent extracts such as acetone, aqueous, ethyl acetate, methanol, n-hexane and petroleum ether. All the tested phytochemical classes were detected by various solvent extracts. Results of screening have been tabulated and shown in *Figure 6*.

In all, acetone and petroleum ether detected three groups of phytochemicals, while rest of the solvents such as aqueous, ethyl acetate, methanol and n-hexane screened two phytochemicals (*Fig. 6*). Alkaloids were detected by all solvents, except the aqueous extract. Saponins were only detected by the aqueous extract. Tannins were detected by three solvent extracts such as acetone, aqueous and ethyl acetate. The phenols were isolated by three solvent extracts like acetone, methanol and petroleum ether. In the case of flavonoids, it was detected by both the non-polar solvents i.e. n-hexane and petroleum ether.

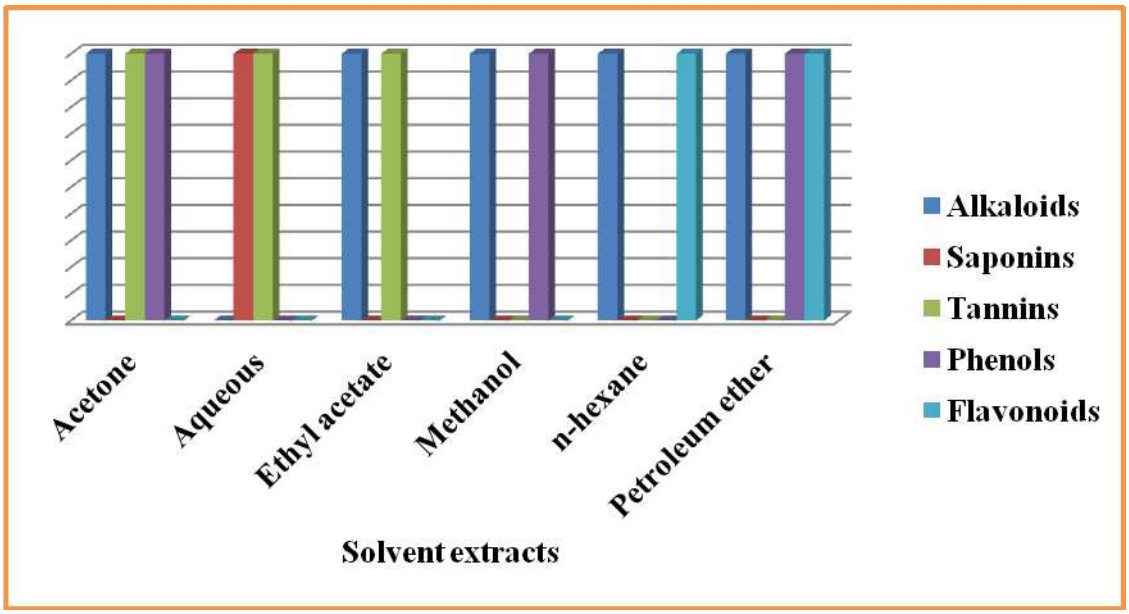

Figure 6. *Phytochemical screening of Berberis baluchistanica solvent extracts*

http://www.aloki.hu ● ISSN 1589 1623 (Print) ● ISSN 1785 0037 (Online)
DOI: http://dx.doi.org/10.15666/aeer/1706_1269712707

Discussion

Due to food insecurity issues, indigenous wild fruits may alleviate nutrition deficiency especially in the case Pakistan being developing country. In order to test this hypothesis, the present research work was undertaken to investigate nutritional composition and phytochemical screening of wild fruit of *Berberis baluchistanica*.

The proximate and mineral analyses were carried out by employing the methodology of the Association of Official Analytical Chemists (AOAC, 2005). The results are shown in *Table 1*. It is apprising that the fruit retains an appreciable amount of nutritional and beneficial elements. The data showed that the fruit possesses the highest proportion of dry matter (92%), followed by crude fibre (35%), moisture content (8%), crude protein (7%), crude fat (6.3%) and ash content.

Protein is a vital to diet and deficient of it results in causing various diseases. Foods over its 12% calorific values obtained from proteins are considered good source from plants (Pearson, 1976). This study revealed that wild fruit of *Berberis baluchistanica* possessed good amount of protein. The species possessed values higher than the reported species by Abbasi (2013) such as *Prunus domestica, Grewia optiva, Juglans regia, Morus nigra*, etc. The fruit is also contained 6.3% crude fat from *Berberis baluchistanica* which would be a good source of lipids.

The crude fibre contents were richly found in the fruits of *Berberis baluchistanica* (35%). According to Ishida et al. (2000), taking fibre regularly can lower the jeopardy of cardiovascular disease including hypertension and diabetes as well as colon and breast cancer. The present results clearly indicated that the investigated wild fruits possessed higher values of dietary fibres that can mitigate human malnutrition.

It is worthwhile to mention that the moisture content was comparatively low in the tested fruit which may be due to drier conditions of soils. *B. baluchistanica* is growing in harsh climatic conditions such as poor in soil nutrition and less availability of moisture in hilly areas. Such conditions resulted in retaining lesser amount of moisture contents. It is evident from the results that the moisture content of the investigate fruit is low contrasting to that of *Xylopia aethiopia* (16.04) reported by Abolaji et al. (2007) and *Acalypha hispida* (11.91) by Iniaghe et al. (2009). Such results indicate that low moisture content is excellent for the long-term safeguarding from spoilage.

The ash content shows the presence of mineral contents in plant samples (Mammen et al., 2010). The fruits of *B. baluchistanica* possessed 3.5% total ash content (*Table 1*). Abbasi (2013) reported low values of ash contents from traditional fruits. Summarizing the results of proximate analysis, it is evident from the results that the investigated wild fruit possess nutritional component and can be used a good source nutrition. According to the literature, the values of proximate composition of the evaluated wild fruits were either higher or at par with the previous studies (Imran et al., 2007, 2010). The variations in values might be due to varied climates, soils, seasonal collection, nutrients uptake by plant species, etc.

Iron (Fe) was found in the highest quantity (3.835%), followed by zinc (1.039%), copper (0.851%), manganese (0.764%), potassium (0.101%), while the sodium was in lesser amount (0.009%). Our results far high as reported by Gani et al. (2018) who showed the data of various important fruits such as cherry. According to Davis et al. (2004), the mineral contents may be lower due to change of cultivars chosen for yield, rapid growth, pest resistance, herbivore resistance, etc. They are also in opinion that soil types and climate may also affect nutrient composition in food plants.

http://www.aloki.hu ● ISSN 1589 1623 (Print) ● ISSN 1785 0037 (Online)
DOI: http://dx.doi.org/10.15666/aeer/1706_1269712707

This study was carried out to screen chief phytochemicals such as alkaloids, flavonoids, phenols, saponins and tannins from six polarity based solvent extracts of wild fruits of *Berberis baluchistanica*. The selected phytochemicals were detected by various solvent extracts (*Fig. 6*). Alkaloids were detected by all solvents, except the aqueous extract. All these phytochemicals are well known to have curative properties (Rabe, 2000). Among them, alkaloids are accounted as the chief therapeutic agent (Njoku and Akumefula, 2007).

Flavonoids are group of natural antioxidants which play an important role in combating the jeopardy of deteriorating cells (Okwu and Okwu, 2004). Plants may produce these compounds to mitigate microbial infection (Dixon et al., 1983). The present study detected flavonoids from n-hexane and petroleum ether. This is the important and copious group of phytochemicals present in many medicinal plants (Singh et al., 2007) which is responsible in reducing carcinogenic development, possesses anticancer and antimicrobial (Okwu, 2004; Lewis and Elvin-Lewis, 1995) and anti-inflammatory activities (Cushnie and Lamb, 2005).

From this study, tannins were detected by acetone, aqueous and ethyl acetate. This group is believed to hold anti-diarrheal, anti-fungal, anti-hemorrhoidal and anti-oxidant properties (Asquith and Butter, 1986). Besides, this compound possesses a bitter principle of drinks and foods (Chikezie et al., 2008).

The present study revealed the presence of saponins which was detected by the aqueous extract only. These secondary metabolites hold anti-inflammatory effect (Just et al., 1998) and also responsible in coagulating red blood cells that include development of foams in water solutions, haemolytic activity, cholesterol binding properties and bitterness (Trease and Evans, 1985; Lewis and Elvin-Lewis, 1995; Okwu, 2004).

Conclusion

This study revealed that the wild fruits of *B. baluchistanica* hold substantial quantity of essential nutrients such as protein, fibre, carbohydrates, fats, iron, zinc, copper, manganese, potassium and various important phytochemicals. This fruit is locally consumed by the natives and requires further investigation prior to commercial production and introduction in the market. Such kind of fruit supplement will help to meet the dietary requirement and improve the malnutrition problem in the country. Besides, presence of various secondary metabolites in the fruit also requires thorough investigation which may be used as plant based antimicrobial and antioxidant molecules.

Acknowledgement. This paper is extracted from the PhD dissertation of the first author.

REFERENCES

[1] Abbasi, M. A., Naqvi, S. S. H., Rehman, A. U., Tareen, R. B. (2013): *Berberis baluchistanica*: Assessment of natural antioxidants to reprieve from oxidative stress. – International Research Journal of Pharmacy 4(5): 101-105.

[2] Abolaji, O. A., Adebayo, A. H., Odesanmi, O. S. (2007): Nutritional qualities of three medicinal plant parts (*Xylopia aethiopica, Blighia sapida* and *Parinari polyandra*)

http://www.aloki.hu ● ISSN 1589 1623 (Print) ● ISSN 1785 0037 (Online)
DOI: http://dx.doi.org/10.15666/aeer/1706_1269712707

commonly used by pregnant women in the western part of Nigeria. – Pakistan Journal of Nutrition 6(6): 665-668.

[3] Ahmed, M., Naqui, E., Wang, E. L. M. (1990): Present state of juniper in Roadhmullazi forest of Baluchistan, Pakistan. – Pak. J. For. 227-236.

[4] Anonymous (2019): Ziarat-Government of Balochistan. – https://www.balochistan.gov.pk/index.php?option=com_content&view=article&id=816&Itemid=1102 (date of access: 25.05.2019).

[5] AOAC (2005): Official Method of Analysis. 18th Ed. – Association of Officiating Analytical Chemists, Washington DC.

[6] Asquith, T. N., Butter, L. G. (1986): Interaction of condensed tannins with selected proteins. – Phytochem. 25(7): 1591-1593.

[7] Chakraborty, S., Newton, A. C. (2011): Climate change, plant diseases and food security: an overview. – Plant Pathology 60: 2-14.

[8] Chikezie, P. C., Agomuo, E. N., Amadi, B. A. (2008): Biochemistry: Practical Research Method. A Fundamental Approach. Vol. 2. – Mega Soft Publishers, Owerri, pp. 51-53.

[9] Cushnie, T. P., Lamb, A. J. (2005): Antimicrobial activity of flavonoids. – Int. J. Antimicrob. Agents 26(5): 343-356.

[10] Davis, D. R., Epp, M. D., Riordan, H. D. (2004): Changes in USDA food composition data for 43 garden crops, 1950 to 1999. – Journal of the American College of Nutrition 23(6): 669-682.

[11] Dellavalle, P. D., Cabrera, A., Alem, D., Larrañaga, P., Ferreira, F., Rizza, M. D. (2011): Antifungal activity of medicinal plant extracts against phytopathogenic fungus *Alternaria* spp. – Chilean Journal of Agricultural Research 71(2): 231-239.

[12] Dixon, R. A., Dey, P. M., Lamb, C. J. (1983): Phytoalexins: enzymology and molecular biology. – Adv. Enzymol. 55: 1-69.

[13] Egwaikhide, I., Gimba, C. E. (2007): Analysis of phytochemical content and antimicrobial activity of *Plectranthus glandulosis* whole plant. – Middle-East Journal of Scientific Research 2(3-4): 135-138.

[14] Gani, M., Jabeen, A., Majeed, D., Mir, S. A., Dar, B. N. (2018): Proximate composition, mineral analysis and antioxidant capacity of indigenous fruits and vegetables from temperate region of Indian Himalayas. – Journal of Food Measurement and Characterization 12: 1011-1019.

[15] Imran, M., Talpur, F. N., Jan, M. I., Khan, A., Khan, I. (2007): Analysis of nutritional component of some wild edible plant. – Journal of Chemical Society of Pakistan 29(5): 500-508.

[16] Imran, M., Khan, H., Shah, M., Khan, R., Khan, F. (2010): Chemical composition and antioxidant activity of certain *Morus* species. – Journal of Zhejiang University - Science B (Biomedicine & Biotechnology) 11(12): 973-980.

[17] Iniaghe, O. M., Malomo, S. O., Adebayo, J. D. (2009): Proximate composition and phytochemical constituents of leaves of some *Acalypha* species. – Journal of Nutrition 8(3): 256-258.

[18] Ishida, H., Suzuno, H., Sugiyama, N., Innami, S. Todokoro, T. (2000): National evaluation of chemical component of leaves stalks and stem of sweet potatoes. *Ipomea batata* Poir. – Food Chemistry 68: 359-367.

[19] Khalil, A. T., Khan, I., Ahmad, K., Khan, Y. A., Khan, M., Khan, M. J. (2013): Synergistic antibacterial effect of honey and *Herba Ocimi Basilici* against some bacterial pathogens. – Journal of Traditional Chinese Medicine 33: 810-814.

[20] Lewis, W. H., Elvin-Lewis, M. (1995): Medical Botany: Plants Affecting Mans Health. – John Wiley Interscience, New York.

[21] Mammen, D., Daniel, M., Sanert. (2010): Variations in values of proximate analysis in *Aerva lanata* Juss ex Schultes, *Hedyotis corymbosa* (L.) Lam. and *Leptadenia reticulata* (Retz.) W. & A. – International Journal of Pharma and Bio Sciences 1(4): 629-636.

http://www.aloki.hu ● ISSN 1589 1623 (Print) ● ISSN 1785 0037 (Online)
DOI: http://dx.doi.org/10.15666/aeer/1706_1269712707

[22] Munazir, M., Qureshi, R., Munir, M. (2015): Preliminary phytochemical screening of roots and aerial parts of *Leptadenia pyrotechnica*. – Pakistan Journal of Botany 47(2): 659-664.
[23] Njoku, P. C., Akumefula, M. I. (2007): Phytochemical and nutrient evaluation of *Spondias mombin* leaves. – Pakistan Journal of Nutrition 6(6): 613-615.
[24] Nwachukwu, C. U., Umeh, C. N., Kalu, I. G., Okere, S., Nwoko, M. C. (2010): Identification and traditional uses of some common medicinal plants in Ezinihitte Mbaise L. G. A., of Imo State, Nigeria. – Report and Opinion 2(6): 1-8.
[25] Okwu, D. E. (2004): Phytochemicals and vitamin content of indigenous species of southeastern Nigeria. – J. Sustain. Agric. Environ. 6(1): 30-37.
[26] Okwu, D. E., Okwu, M. E. 2004. Chemical composition of *Spondias mombin* Linn. plant parts. – J. Sustain. Agric. Environ. 6(2): 140-147.
[27] Pearson, J. (1976): Determination of Phytic Acid and Phosphorus Content of Biological Materials. – Cambridge University Press, London.
[28] Rabe, T. S. J. (2000): Isolation of antimicrobial sesquiterpenoid from *Warbugie salutarius*. – Journal of Ethnopharmacology 93: 171-174.
[29] Rahim, G., Qureshi, R., Arshad, M., Gulfraz, M. (2013): Phytochemical analysis and antioxidant properties of *Teucrium stocksianum* flower from Malakand Division, Pakistan. – International Journal of Agriculture & Biology 15(2): 377-381.
[30] Sher, H., Midrarullah, Khan, A. U., Hussain, F., Ahmad, S. (2003): Medicinal plants of Udigram, District Swat, Pakistan. – Pakistan Journal of Forestry 53(1): 65-74.
[31] Singh, R., Singh, S. K., Arora, S. (2007): Evaluation of antioxidant potential of ethyl acetate extract/fractions of *Acacia auriculiformis.* – Food Chem. Toxicol. 45(7): 1216-23.
[32] Trease, G. E., Evans, W. C. (1985): Pharmacognosy. 12th Ed. – English Language Books Society, Bailliere Tindall.

http://www.aloki.hu ● ISSN 1589 1623 (Print) ● ISSN 1785 0037 (Online)
DOI: http://dx.doi.org/10.15666/aeer/1706_1269712707

ANT FAUNA OF ANNUAL AND PERENNIAL CROPS

JEŠOVNIK, A.[1,2,3*] – BLAŽEVIĆ, I.[4] – LEMIĆ, D.[4] – PAJAČ ŽIVKOVIĆ, I.[4*]

[1]*Ministry of environment and energy, Radnička cesta 80/7, 10000 Zagreb, Croatia*

[2]*Croatian Myrmecological Society, Gortanova 14, 10000 Zagreb, Croatia*

[3]*National Museum of Natural History, Smithsonian Institution, Department of Entomology Washington, District of Columbia, United States of America*

[4]*University of Zagreb, Department of Agricultural Zoology Svetošimunska cesta 25, 10000 Zagreb, Croatia*

[*]*Corresponding authors*
e-mail: ana.mrav@gmail.com (Ana Ješovnik), ipajac@agr.hr (Ivana Pajač Živković)

(Received 15th Apr 2019; accepted 4th Jul 2019)

Abstract. Ants (Hymenoptera: Formicidae) are a diverse and abundant part of soil fauna with the ability to maintain and restore soil quality and to increase crop yields in agroecosystems. Some ant species are sensitive to land management, which makes them good bioindicators of soil function in land use management and conservation throughout the world. In Croatia, ants are understudied and they were never sampled on agricultural crops. In this study, we used pitfall traps to collect ants on three different land use types: annual crops, perennial crops, and semi-natural habitats. We found 12 ant species, out of which one species, *Tetramorium atratulum* (Schenck, 1852), is a new record for Croatia. We observed significantly lower ant abundance on annual crops than on both perennial crops and semi-natural habitats. Similarly, ant richness and diversity were lowest on annual crops, although this difference was not statistically significant. Our results contribute to the increasing evidence that intensive agricultural practices, particularly soil tillage, are detrimental to the arthropod diversity. The transition to sustainable agriculture will require utilizing the ecosystem services of naturally occurring insects, such as ants.
Keywords: *Formicidae, Tetramorium atratulum, sustainable agriculture, CAP, bioindicators, reduced tillage*

Introduction

Agricultural intensification across Europe has a severe impact on the environment, mainly through pesticide and nitrate pollution, soil erosion, loss of habitats, and simplification of animal and plant communities, all of which leads to the decline and extinction of wildlife (Skinner et al., 1997; Stoate et al., 2001; Schweiger et al., 2005; German et al., 2017). With additional pressures of human population growth and climate change (Piao et al., 2010; Myers et al., 2014) the intensive, industrial-scale crop production has become unsustainable, and the need is recognized for a transition to agroecological farming systems. Traditional farming, organic farming, and conservation agriculture all tend to govern management by ecological principles, to decrease the environmental impact, and to increase the nutritional value of the produced food (Hobbs et al., 2008; Reganold and Wachter, 2016; German et al., 2017). One of the important goals of agroecology is the efficient utilization of ecosystem services of naturally occurring organisms, in particular insects and other invertebrates (Lavelle et al., 2006). This includes using diversity and abundance of soil fauna as indicators of soil quality, integrated pest management, and incorporating agricultural practices that support the

http://www.aloki.hu ● ISSN 1589 1623 (Print) ● ISSN 1785 0037 (Online)
DOI: http://dx.doi.org/10.15666/aeer/1706_1270912722

biodiversity of soil organisms, which are crucial for soil health (Power, 2010; Sanabria et al., 2014; Furlan et al., 2017).

Ants (Hymenoptera: fam. Formicidae) are ubiquitous, diverse, and dominant terrestrial insects (Holldobler and Wilson, 1990). Majority of ant species nest in soil, and have a well-documented impact on its biological, physical, and chemical properties (Stadler et al., 2006; Frouz and Jilková, 2008; Dorn, 2014; Farji-Brener and Werenkraut, 2017). By creating micropores ants aerate the soil and increase its water absorption, bring in minerals and nutrients (Lobry De Bruyn, 1999; Evans et al., 2011), improve soil fertility (Farji-Brener and Werenkraut, 2017), and ant nests are an important resource for other organisms. The vicinity of ant nests has 30 fold higher density of microarthropods, five-fold higher density of protozoa, and significantly higher mineralization rates (Lobry De Bruyn, 1999; Wagner et al., 2004). Large-scale exclusion experiments on ants in agricultural systems show that ants have a positive net influence (up to 50%) on crop yield, as they increase soil porosity and moisture; nitrogen, carbon and phosphorus content, microorganism biomass, and decrease pest populations (Evans et al., 2011; Wielgoss et al., 2013; Gras et al., 2016; Shukla et al., 2016).

Additionally, ants can be used as bioindicators of soil quality in land management (Read and Andersen, 2000; Andersen et al., 2002; Sanabria et al., 2014). Ants, in general, respond rapidly to environmental changes, they are abundant and easy to sample, and some species have specific ecological requirements (Dufrêne and Legendre, 1997; Lobry De Bruyn, 1999; Underwood and Fisher, 2006; Sanabria et al., 2014). The practice of using ants as tools in land management is more common in tropical and subtropical than in temperate agroecosystems (Dufrêne and Legendre, 1997; Lobry De Bruyn, 1999; Underwood and Fisher, 2006; Sanabria et al., 2014). Several studies in Europe show potential for using ants in land management. In Italy and France ants were good bioindicators of organic farming (Masoni et al., 2017) and environmentally safe soil amendment treatments (Castracani et al., 2015), as well as a useful tool in conservation, e.g. as indicators of restoration processes (Ottonetti et al., 2006).

Ant research has been relatively neglected in Croatia (Bračko, 2006). The national ant survey was never conducted, and collections focus on a series of small scale inventory studies in protected areas (Ješovnik et al., 2011; Ješovnik and Pečarevič, 2018). Ants were never investigated in the context of agricultural habitats in Croatia, unlike other arthropods, e.g., carabid beetles (Lemić et al., 2016, 2017; Pajač Živković et al., 2016). In this study, we investigate ant fauna associated with agricultural habitats in Croatia, determine which species are associated with intensive agriculture, and test whether ant species richness, abundance, diversity, and community composition differ between annual and perennial crops. We predict that agricultural intensity would negatively affect the abundance, richness, and diversity of ants.

Materials and methods

Study site and data collection

We conducted the fieldwork in Zagreb, Croatia (45°49′N 15°59′E, altitude 145 meters), on experimental fields of Faculty of Agriculture and surrounding semi-natural habitats. Zagreb has a temperate continental climate modified by the maritime influence of the Mediterranean and under the local influence of Mount Medvednica (Zaninović et al., 2008). Based on the last comprehensive review of Croatian ants Zagreb has 23 ant species (Bračko, 2006).

http://www.aloki.hu ● ISSN 1589 1623 (Print) ● ISSN 1785 0037 (Online)
DOI: http://dx.doi.org/10.15666/aeer/1706_1270912722

We sampled ants on three plots per each land use type (nine plots total): on annual crops (potato, soy, corn), perennial crops (two apple orchards and vineyard), and on non-agricultural habitats as a control (three semi-natural habitats: meadow, meadow next to the forest edge, park-forest). Each plot was 25 x 11 meters in size. The annual crop fields were the most intensive agricultural management regime in our study, with standard and deep soil tillage and pre-planting soil preparation in autumn. The perennial plots represented the intermediate management regime, with no tillage or any other mechanical soil manipulation, and with mowing as only cultivation technique. Both annual and perennial crops had a variable degree of fertilization and insecticide use (details in *Table 1*). Sampled semi-natural habitats had no soil management regime, no fertilizer was used, and the mowing was the only cultivation regime. Semi-natural habitats were chosen to represent the gradation from open to closed habitats, and to be as natural as possible considering their location in the urban area. All plots were located on the University of Agriculture campus or adjacent to it (*Fig. 1*).

Table 1. *Study plots (Zagreb, Croatia). T – Tillage, F – Fertilizer, I – Insecticide*

Plot	Land use	Habitat	T	F	I	Latitude	Longitude
P1	control	meadow	–	–	–	45.826548	16.029084
P2	control	meadow	–	–	–	45.828077	16.028118
P3	control	park forest	–	–	–	45.826011	16.030004
V1	perennial	orchard	–	yes	yes	45.828628	16.029201
V2	perennial	orchard	–	–	–	45.826138	16.028996
VL	perennial	vineyard	–	yes	–	45.827507	16.028881
KR	annual	potato field	standard	yes	yes	45.829358	16.034092
KU	annual	corn field	deep	yes	–	45.827378	16.034005
SO	annual	soy field	standard	yes	–	45.825106	16.032288

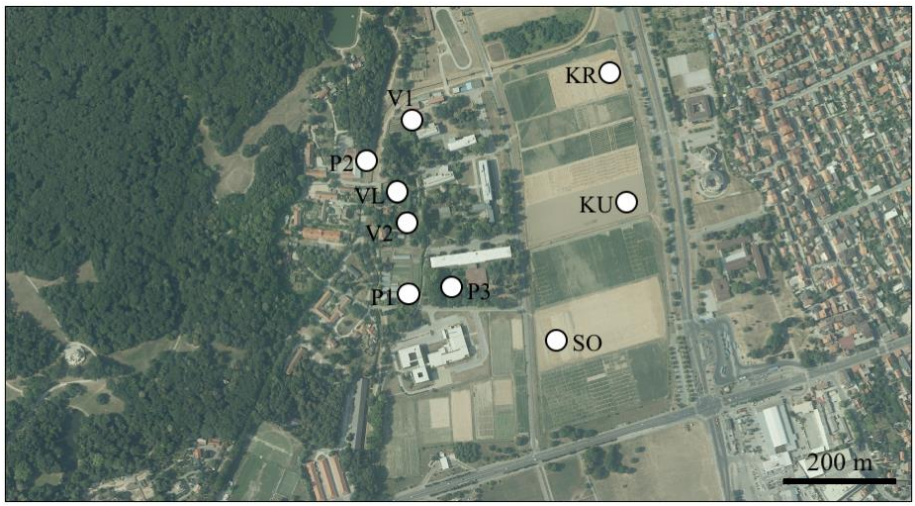

Figure 1. *Map with localities of sampling plots (P1, P2, P3 – control; V1, V2, VL – perennial; KR, KU, SO – annual plots) in Zagreb, Croatia*

We sampled ants using pitfall traps (100 mL container, 6 cm diameter), which are the standard sampling technique of ground-nesting ants (Agosti et al., 2000). We set up 10 pitfall traps per plot, five in each of two parallel rows, with a 4-meter distance between the individual traps, and a minimum of 4.5 m distance from the plot edge. Pitfall traps

http://www.aloki.hu ● ISSN 1589 1623 (Print) ● ISSN 1785 0037 (Online)
DOI: http://dx.doi.org/10.15666/aeer/1706_1270912722

were filled with 20–25 mL of the mixture of 90% ethanol, water, glycerol, and detergent. The traps were active for 48 hours, from 12–14 July 2018, after which they were collected, labeled, and ants were sorted into 90% ethanol. The 48-hour period of trapping is recommended as a standard protocol for the efficient estimate of abundance, occurrence, and community composition of ants (Agosti et al., 2000; Borgelt and New, 2006), and it is frequently used in similar studies (Castracani and Mori, 2006; Ribas et al., 2011; Frizzo and Vasconcelos, 2013).

Data processing and analyses

We identified collected ants to the species level using taxonomical keys (Agosti and Collingwood, 1987; Seifert, 2007; Wagner et al., 2017) and online resources (antweb.org). Specimens were counted, and at least one representative of each species was pinned and deposited in Croatian myrmecological society collection (HMD, Zagreb, Croatia). Map of the sampling plots was prepared in ESRI GIS ArcMap 10.1 software.

We calculated descriptive statistics, ant species richness (S), diversity (Shannon-Weiner's index, H' and Fisher's alpha), and abundance (individual counts per species) for each plot and each land use type. We conducted a one-way analysis of variance (ANOVA) on log-transformed data to compare the effect of agricultural intensity on ant richness, abundance, and diversity in our studied land use types (annual, perennial, and control habitat). When the results of ANOVA were significant, we ran the post hoc Tukey test to calculate the significant difference between individual groups (annual-control, annual-perennial, control-perennial). To investigate the differences in ant community assemblages between the land use types we used non-parametric multidimensional scaling (NMDS) based on pairwise distance (Bray-Curtis dissimilarity) using ant abundance data. We ran all of the analyses and created plots in R program language (R Development Core Team, 2014), using packages vegan, ape, picante, and psych. The custom R code we used is available online from https://github.com/anajesovnik/AgriAnt.

Results

Comparison of ant communities of different agricultural intensity

We collected a total of nine ant species in semi-natural habitats, eight on perennial crops, and six species on annual crops. The differences in ant abundances show a similar trend, with 175 individuals collected on semi-natural habitat, 158 on perennial, and 34 on annual crops (*Table 2, Fig. 2*).

Table 2. *Mean (± standard deviation) ant species richness, abundance, and diversity*

Land use	Richness	Abundance	Diversity (H')
control	5.67 (± 0.58)	58.33 (± 13.65)	1.3 (± 0.13)
perennial	4.67 (±1.53)	52.67 (± 13.65)	1.21 (± 0.3)
annual	2.33 (±1.15)	11.33 (± 9.24)	0.57 (± 0.52)

Ant abundance on plots with different agricultural intensity was statistically significantly different (ANOVA $F_{(2,6)}$=13.58, p=0.00593). The post hoc Tukey test found a significant difference in ant abundance between the annual and control (p=0.008) and annual and perennial groups (p=0.01). In contrast, ant richness and ant diversity (Fisher's Alpha) were not significantly different between different land use

http://www.aloki.hu ● ISSN 1589 1623 (Print) ● ISSN 1785 0037 (Online)
DOI: http://dx.doi.org/10.15666/aeer/1706_1270912722

plots (richness: ANOVA $F_{(2,6)}$=4.53, p=0.0631; diversity: ANOVA $F_{(2,6)}$=0.568, p=0.594), although they showed the same trend: both richness and diversity were decreasing with the increase in agricultural intensification (*Table 3*). The results of the NMDS analysis (stress value: 0.08, R^2=0.993) show an overlap of ant communities of different land use types (*Fig. 3*), with no clear clustering of plots based on land use type. One of the annual crop plots (potato field) grouped closer to natural and perennial plots.

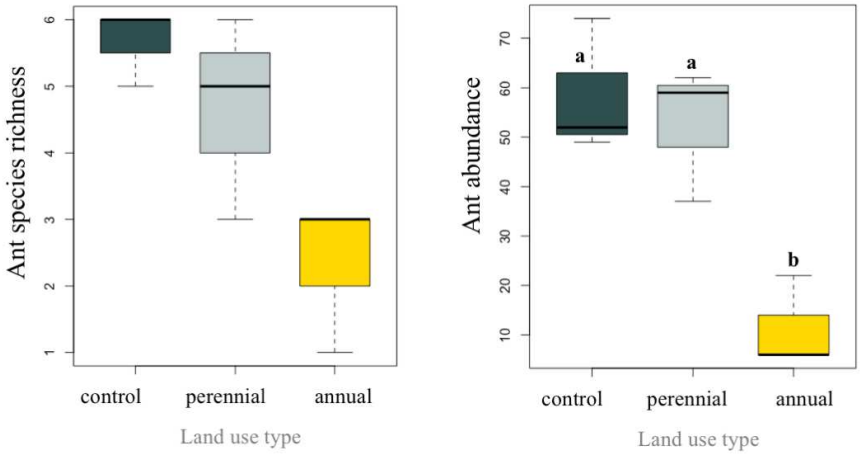

Figure 2. *Ant richness and abundance across different land use types. Significant level for post hoc test was 0.05*

Table 3. *Ant species abundance per plot replicates in different land use types. Species names are followed by the index to species' image in Figure 4*

Species	control			perennial			annual		
	P1	P2	P3	V1	V2	VL	KR	KU	SO
Ponera coarctata 4h	–	–	–	–	1	–	–	–	–
Aphaenogaster subterranea 4f	–	–	21	–	3	–	–	–	–
Myrmica scabrinodis 4e	1	–	4	–	8	–	–	–	–
Solenopsis fugax 4d	30	14	3	6	5	2	–	–	3
Tetramorium caespitum 4b	–	7	–	24	–	17	16	–	2
Tetramorium semilaeve 4g	–	3	–	–	–	–	–	–	–
Tetramorium atratulum 4k	–	–	–	–	–	–	1	–	–
Formica cunicularia 4a	2	10	5	7	20	18	5	–	–
Lasius myops 4i	–	–	–	2	–	–	–	–	1
Lasius niger 4c	8	37	19	23	22	–	–	6	–
Polyergus rufescens 4l	1	3	–	–	–	–	–	–	–
Tapinoma erraticum 4j	7	–	–	–	–	–	–	–	–
Total richness	6	6	5	5	6	3	3	1	3
Total abundance	49	74	52	62	59	37	22	6	6

The composition of ant communities

During this study, we collected 367 ants, belonging to 12 species within four ant subfamilies and nine genera (*Table 3, Fig. 4*). Eight of the species (*Formica cunicularia* Latreille, 1798; *Lasius myops* Forel, 1894; *Ponera coarctata* (Latreille, 1802); *Tetramorium semilaeve* André, 1883; *Aphaenogaster subterranea* (Latreille, 1798); *Myrmica scabrinodis* Nylander, 1846; *Solenopsis fugax* (Latreille, 1798)) are first

http://www.aloki.hu ● ISSN 1589 1623 (Print) ● ISSN 1785 0037 (Online)
DOI: http://dx.doi.org/10.15666/aeer/1706_1270912722

records for Zagreb, which reflects the lack of myrmecological investigations, rather than surprising discoveries. One species, a rare workerless social parasite, *Tetramorium atratulum* (Schenck, 1852), is a new record for Croatia as well. We collected a single queen of this species, on one of the annual crop plots (potato field).

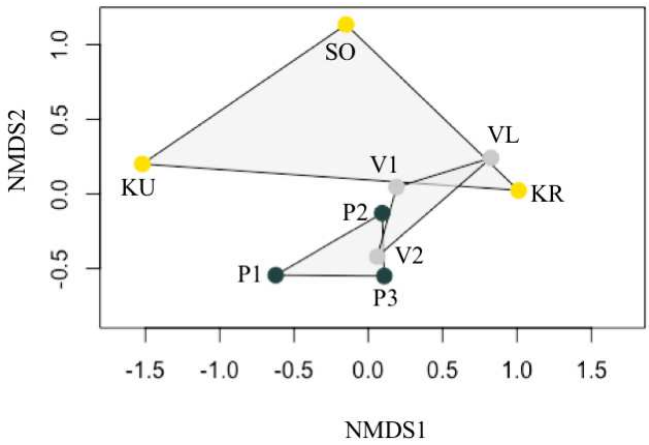

Figure 3. *Non-metric multidimensional scaling of ant community assemblages. The circles represent the position of the individual plots in the ordination space, labeled with plot codes (Table 1) and color-coded according to land use (blue- control, grey- perennial, yellow-annual)*

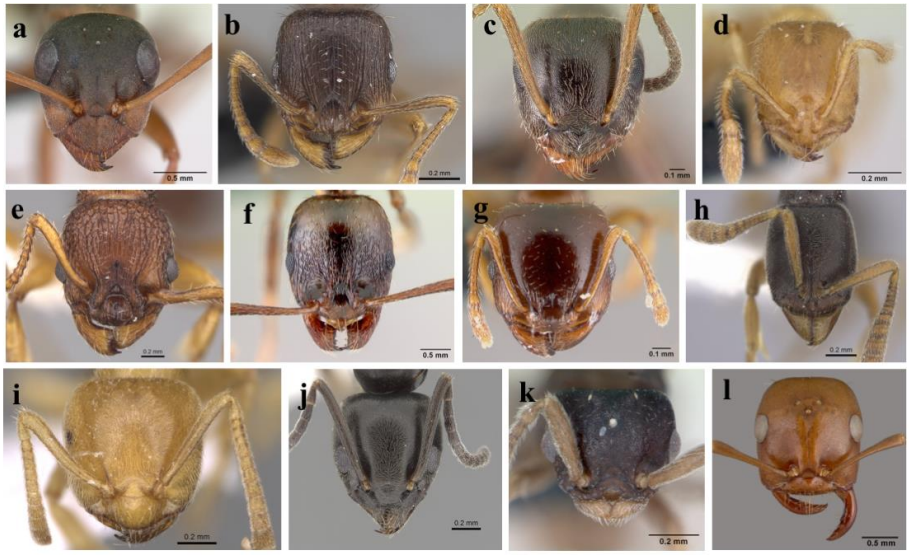

Figure 4. *Images (head, frontal view) of sampled ant species.* ***a*** *Formica cunicularia (photo: antweb.org, CASENT0173175);* ***b*** *Tetramorium caespitum (photo: antweb.org, Flavia Esteves, CASENT0919632);* ***c*** *Lasius niger (source: antweb.org, photo by Erin Prado, CASENT0179897);* ***d*** *Solenopsis fugax (photo: antweb.org, CASENT0173147),* ***e*** *Myrmica scabrinodis (photo: antweb.org, Wade Lee, CASENT0922795);* ***f*** *Aphaenogaster subterranea (photo: antweb.org, Erin Prado, CASENT0179934);* ***g*** *Tetramorium semilaeve (photo: antweb.org, Erin Prado, CASENT0008637);* ***h*** *Ponera coarctata (photo: antweb.org, Will Ericson, CASENT0249225);* ***i*** *Lasius myops (photo: antweb.org, Shannon Hartman, CASENT0906073);* ***j*** *Tapinoma erraticum (photo: antweb.org, Shannon Hartman, CASENT0249760);* ***k*** *Tetramorium atratulum (photo: antweb.org, CASENT0173077);* ***l*** *Polyergus rufescens (photo: antweb.org, CASENT0010688)*

http://www.aloki.hu ● ISSN 1589 1623 (Print) ● ISSN 1785 0037 (Online)
DOI: http://dx.doi.org/10.15666/aeer/1706_1270912722

The most represented subfamilies were Myrmicinae (6 species) and Formicinae (4 species), while Ponerinae and Dolichoderinae were both represented by a single species. The species with the highest abundance was *Lasius niger* (Linnaeus, 1758) (31% of total ants collected, 115 individuals), which was present on all three land use types, and on 6 out of 9 plots. Three other species were present on all land use types and had a high abundance: *Solenopsis fugax* (17% of total ants collected, 63 individuals), *Tetramorium caespitum* (Linnaeus, 1758) (18%, 66 individuals), and *Formica cunicularia* (18%, 67 individuals).

Discussion

Effect of agricultural intensity on the ant fauna

Results of our study show that agricultural practices associated with annual crops significantly decrease ant abundance. In contrast, the perennial crops support ant abundance slightly lower but similar to those in semi-natural habitats. Although no significant difference was found in the ant richness and diversity between the different land use types the plots with high agricultural intensity have the lowest ant richness and diversity. The community composition showed no clear separation by land use type, and most plots were dominated by the four common, generalist species. Our sample size was relatively small, so some of the observed results are likely to change with a larger data set. However, our results are concordant with previous findings that intensive agriculture has a negative impact on arthropod abundance and diversity (Sánchez-Bayo and Wyckhuys, 2019).

In particular, the decline of ants and other soil invertebrates has been associated with conventional tillage (Radford et al., 1995; Wilson-Rummenie et al., 1999; Sharley et al., 2008; Fernandes et al., 2018; Hevia et al., 2019), use of insecticides (Sánchez-Bayo and Wyckhuys, 2019), lack of nesting habitats due to habitat simplification, and changes in soil temperature and moisture (Kaspari et al., 2000; Armbrecht, 2004; Sanders et al., 2007; Graham et al., 2009; van Oudenhove et al., 2011). How strongly these different factors influence ant communities is not straightforward. For example, ant communities in olive orchards in Spain are found to be most affected by tillage practices (Hevia et al., 2019), while ant communities in French vineyards are strongly correlated with pesticide use (Masoni et al., 2017). The combination of those factors (soil disturbance by tillage, pesticide use, and habitat simplification) decreases the diversity and abundance of ants, which in turn changes the ecological balance of soil fauna and physical and chemical properties of soil.

Our study design does not allow us to test the influence of individual factors, such as insecticide and fertilizer use, because they both varied across the two agricultural land use systems. However, we hypothesize that the soil disturbance caused by tillage, which was conducted on annual plots only, and which was the most substantial difference in agricultural practice between annual and perennial plots, was the strongest individual factor that influenced ant richness, abundance, and diversity. Conventional tillage includes mechanical plowing, which causes physical disturbance of soil structure and soil biota, and causes water loss and erosion (Faulkner, 1943; Stinner, 2002). In contrast, conservation tillage practices do not include ploughing and retain a minimum of 30% cover of crop residue on the soil surface. Consequently, conservation tillage reduces soil erosion and water loss and supports diverse beneficial soil fauna (Blevins and Frye, 1993; Radford et al., 1995; Wilson-Rummenie et al., 1999; Stinner, 2002; Li,

http://www.aloki.hu ● ISSN 1589 1623 (Print) ● ISSN 1785 0037 (Online)
DOI: http://dx.doi.org/10.15666/aeer/1706_1270912722

2018). The other likely factor that influenced ant fauna in our study is severe habitat homogenization in annual plots and consequently reduced resource availability. A future study that would manipulate the individual treatments, e.g. tillage only, needs to be conducted to determine the relative effects of these factors.

Research such as our study can provide scientific evidence for changes in future policies. In particular, we hope conservation tillage will gain support in both research and practice in Croatia in the near future. Knowing how land practices affect insect communities is especially important in the context of the coming changes in Common Agricultural Policy (CAP), one of the core EU policies. Historically, CAP was production oriented and promoted agricultural intensification. Since reform in 2013, it also addresses the environmental issues through the cross-compliance system, although this was recognized as a weak attempt by the conservation sector (Pe'er et al., 2014). Cross-compliance defines a set of rules for farmers in order to receive the subsidies, and some of them require practices that reduce soil erosion or enhance plant and animal biodiversity. In the future CAP reform, for the 2021-2027 period, currently under negotiations, three out of nine objectives are the environment or climate change oriented, and preserving carbon rich soils will be one of the new obligations (European Commission, 2018). The CAP provides a framework for national rural development policies in EU member states. In Croatia, cross-compliance legislation is in force since 2013 (Ministry of Agriculture, 2013), and the future CAP will certainly initiate its changes. Ideally, the new legislation should regulate conventional tillage, or at least publish the set of guidelines that emphasize the benefits of conservation tillage.

The ant fauna of agricultural habitats

The ant fauna of agricultural habitats in Zagreb is similar to ant fauna described in previous studies of open, disturbed, urban, and agricultural habitats (Seifert, 2007; Slipinski et al., 2012; Castracani et al., 2015; Masoni et al., 2017). It is composed of opportunistic, thermophilic, and disturbance-tolerant species such as *T. caespitum*, *F. cunicularia*, *L. niger* (Collingwood, 1979; Seifert, 2018). Most of the collected species have generalist diets but are primarily predators and scavengers (e.g., *S. fugax*, *P. coarctata*, *T. caespitum*). Predator diversity is a crucial natural mechanism for prevention of pest outbreaks, and ants are known to decrease pest populations by direct predation, chemically deterring pests, and by causing pests to drop from the plants (Way and Khoo, 1992; Perfecto and Snelling, 1995; Schmitz et al., 2000). In contrast, some ant species can be harmful by farming herbivorous insects (e.g., aphids and scale insects), but considering the number of beneficial effects, the net impact is shown to increase crop yield (Wielgoss et al., 2013).

All species collected in this study are primarily soil nesting, and their nest size varies from around 30 (*P. coarctata*) to 10 000 workers (*S. fugax*). However, the majority of collected species have colonies of several hundred to 2000 workers (Taylor, 1967; Collingwood, 1979; Seifert and Schultz, 2009; Seifert, 2018). Soil nesting ant species contribute to maintaining and restoring soil quality (Lobry De Bruyn, 1999; Dorn, 2014; Sanabria et al., 2014). In particular, the impact of soil activities has been studied in two of the collected species. Studies in the USA found that *L. niger* move 885 kg of soil per hectare per year (Talbot, 1953; Lobry De Bruyn, 1999), *F. cunicularia* in China increases soil organic matter, total and available nitrogen, phosphorous, and potassium, electrical conductivity, and water content (Chen and Li, 2012).

http://www.aloki.hu ● ISSN 1589 1623 (Print) ● ISSN 1785 0037 (Online)
DOI: http://dx.doi.org/10.15666/aeer/1706_1270912722

We sampled a rarely collected *Polyergus rufescens* on two plots: control plot (P2, meadow at the forest edge) and the perennial crop plot (V2, apple orchard). This is the only European species of genus *Polyergus* (Mori et al., 1991; Trager, 2013) and it is an obligate parasite of ant genus *Formica* (Castracani et al., 2008; Mori et al., 2010). Because of their specific life history ant species from genus *Polyergus* are of high conservation value (Social Insects Specialist Group, 1996; Trager, 2013). This species was last reported for Zagreb more than 70 years ago (Vogrin, 1955). Its host in the studied habitats is most likely *Formica cunicularia,* a common host of this species in Central Europe (Trager, 2013).

Another surprising find is obscure *Tetramorium atratulum*, inquiline social parasite, for the first time found in Croatia. This is a West Palearctic species that takes permanent residence in the nests of its host, mostly *Tetramorium caespitum*. Worker caste of *T. atratulum* is entirely missing, which is considered the extreme form of social parasitism in ants (Crawley, 1912; Buschinger, 2009; Seifert, 2018). Because of its complex life cycle, restricted gene flow, and low population size, this species is listed as Vulnerable (VU) on IUCN Red List (Social Insects Specialist Group, 1996). In our study area, the most likely host of this species is *Tetramorium caespitum,* one of the four most abundant ants in our study, and the most abundant species on the plot where *T. atratulum* queen was collected.

Conclusion and recommendation for future study

Our study has two main outcomes. First, it shows that ants have the potential for use as tools in agricultural management in Croatia, thanks to their abundance and sensitivity to land use. Second, it shows the importance of future studies in agricultural habitats, as they hold some of the vulnerable species important for insect conservation. Future research of ants of agricultural land in Croatia should identify the particular ecological and physiological factors that support a diverse and abundant ant community. This was previously investigated in other countries (Armbrecht, 2004; Frizzo and Vasconcelos, 2013), but needs to be tested in regionally specific environmental conditions. For example, future studies should compare the ant communities of different levels of tillage (no-tillage, reduced, standard and deep), in different regions of Croatia. Knowing which agricultural practices are detrimental or beneficial to ants can inform sustainable management planning and increase crop yields (Evans et al., 2011; Wielgoss et al., 2013; Gras et al., 2016; Shukla et al., 2016). Another important direction for future research is identifying the ant species that can be bioindicators of soil quality and of High Nature Value (HNV) farming, like those already successfully developed for other regions (Perfecto and Snelling, 1995; Philpott and Ambrecht, 2006; Sanabria et al., 2014). This would require a comparative study of ants and physical and biochemical soil properties, across land use gradient. Ants are thermophilic, and successful in dry climates, unlike some other taxa important for soil quality (e.g., earthworms). Considering the effects of climate change, which among other hazards predict increased drought and higher temperatures (Myles et al., 2018), the development of ants as a tool for sustainable farming is urgently needed in Croatia.

Acknowledgments. Three anonymous reviewers provided comments and suggestions that improved this manuscript. We are indebted to Tanja Mihinjač, Marko Rajković, and Josip Živković for their help with fieldwork. Ivana Ilijaš was available for useful discussions about CAP and cross-compliance. Jelena

http://www.aloki.hu ● ISSN 1589 1623 (Print) ● ISSN 1785 0037 (Online)
DOI: http://dx.doi.org/10.15666/aeer/1706_1270912722

Bujan provided statistical advice, commented on the manuscript, and helped with lists. This study would not be possible if ants are not such interesting and resilient organisms that provide perpetual research inspiration.

REFERENCES

[1] Agosti, D., Collingwood, C. A. (1987): A provisional list of the Balkan with a list to the worker caste. II. Key to the worker caste, including the European species without the Iberian. – Mitteilungen der Schweizerischen Entomologischen Gesellschaft 60: 261-293.
[2] Agosti, D., Majer, J. D., Alonso, L. E., Schultz, T. R. (2000): Ants: Standard methods for measuring and monitoring biodiversity. – Smithsonian Institution Press.
[3] Andersen, A. N., Hoffmann, B. D., Müller, W. J., Griffiths, A. D. (2002): Using ants as bioindicators in land management: Simplifying assessment of ant community responses. – Journal of Applied Ecology 39: 8-17.
[4] Armbrecht, I. (2004): Enigmatic biodiversity correlations: ant diversity responds to diverse resources. – Science 304: 284-286.
[5] Blevins, R. L., Frye, W. W. (1993): Conservation tillage: An ecological approach to soil management. – Advances in Agronomy (USA).
[6] Borgelt, A., New, T. R. (2006): Pitfall trapping for ants (Hymenoptera, Formicidae) in mesic Australia: what is the best trapping period? – Journal of Insect Conservation 10: 75-77.
[7] Bračko, G. (2006): Review of the ant fauna (Hymenoptera: Formicidae) of Croatia. – Acta Entomologica Slovenica 14: 131-156.
[8] Buschinger, A. (2009): Social parasitism among ants: A review (Hymenoptera: Formicidae). – Myrmecological News 12: 219-235.
[9] Castracani, C., Maienza, A., Grasso, D. A., Genesio, L., Malcevschi, A., Miglietta, F., Vaccari, F. P., Mori, A. (2015): Biochar-macrofauna interplay: Searching for new bioindicators. – Science of the Total Environment 536: 449-456.
[10] Castracani, C., Mori, A. (2006): The role of permanent grasslands on ant community structure: ants (Hymenoptera: Formicidae) as ecological indicators in the agro-ecosystems of the Taro River Regional Park (Italy). – Myrmecologische Nachrichten 9: 47-54.
[11] Castracani, C., Tamarri, V., Grasso, D. A., Le Moli, F., Palla, G., Millar, J. G., Francke, W., Mori, A. (2008): Chemical communication in mating behaviour of the slave-making ant *Polyergus rufescens* (Hymenoptera, Formicidae): 3-ethyl-4-methylpentanol as a critical component of the queen sex pheromone. – Insectes Sociaux 55: 137-143.
[12] Chen, Y.-W., Li, X.-R. (2012): Spatio-temporal distribution of nests and influence of ant (*Formica cunicularia* Lat.) activity on soil property and seed bank after revegetation in the Tengger desert. – Arid Land Research and Management 26: 365-378.
[13] Collingwood, C. A. (1979): The Formicidae (Hymenoptera) of Fennoscandia and Denmark. – Scandinavian Science Press 8: 1-174.
[14] Crawley, W. C. (1912): *Anergates atratulus*, Schenk., a British ant, and the acceptance of a queen by *Tetramorium caespitum*, L. – Entomologist's Record and Journal of Variation 24: 218-219.
[15] Dorn, R. I. (2014): Ants as a powerful biotic agent of olivine and plagioclase dissolution. – Geology 42: 771-774.
[16] Dufrêne, M., Legendre, P. (1997): Species assemblages and indicator species: The need for a flexible asymmetrical approach. – Ecological Monographs 67: 345-366.
[17] European Commission (2018): EU Budget: the Common Agricultural Policy beyond 2020.
[18] Evans, T. A., Dawes, T. Z., Ward, P. R., Lo, N. (2011): Ants and termites increase crop yield in a dry climate. – Nature Communications 2: 262.

http://www.aloki.hu ● ISSN 1589 1623 (Print) ● ISSN 1785 0037 (Online)
DOI: http://dx.doi.org/10.15666/aeer/1706_1270912722

[19] Farji-Brener, A. G., Werenkraut, V. (2017): The effects of ant nests on soil fertility and plant performance: a meta-analysis. – Journal of Animal Ecology 86: 866-877.
[20] Faulkner, E. H. (1943): Plowman's folly. – LWW 56(5): 1-394.
[21] Fernandes, W. D., Lange, D., Pereira, J. M., Raizer, J. (2018): Ant community in neotropical agrosystems: A four-year study in conventional and no-tillage systems. – Sociobiology 65: 130-137.
[22] Frizzo, T. L. M., Vasconcelos, H. L. (2013): The potential role of scattered trees for ant conservation in an agriculturally dominated neotropical landscape. – Biotropica 45: 644-651.
[23] Frouz, J., Jilková, V. (2008): The effect of ants on soil properties and processes (Hymenoptera: Formicidae). – Myrmecological News 11: 191-199.
[24] Furlan, L., Vasileiadis, V. P., Chiarini, F., Huiting, H., Leskovšek, R., Razinger, J., Holb, I. J., Sartori, E., Urek, G., Verschwele, A., Benvegnù, I., Sattin, M. (2017): Risk assessment of soil-pest damage to grain maize in Europe within the framework of Integrated Pest Management. – Crop Protection 97: 52-59.
[25] German, R. N., Thompson, C. E., Benton, T. G. (2017): Relationships among multiple aspects of agriculture's environmental impact and productivity: a meta-analysis to guide sustainable agriculture. – Biological Reviews 92: 716-738.
[26] Graham, J. H., Krzysik, A. J., Kovacic, D. A., Duda, J. J., Freeman, D. C., Emlen, J. M., Zak, J. C., Long, W. R., Wallace, M. P., Chamberlin-Graham, C., Nutter, J. P., Balbach, H. E. (2009): Species richness, equitability, and abundance of ants in disturbed landscapes. – Ecological Indicators 9: 866-877.
[27] Gras, P., Tscharntke, T., Maas, B., Tjoa, A., Hafsah, A., Clough, Y. (2016): How ants, birds and bats affect crop yield along shade gradients in tropical cacao agroforestry. – Journal of Applied Ecology 53: 953-963.
[28] Hevia, V., Ortega, J., Azcárate, F. M., López, C. A., González, J. A. (2019): Exploring the effect of soil management intensity on taxonomic and functional diversity of ants in Mediterranean olive groves. – Agricultural and Forest Entomology 21: 109-118.
[29] Hobbs, P. R., Sayre, K., Gupta, R. (2008): The role of conservation agriculture in sustainable agriculture. – Philosophical Transactions of the Royal Society B: Biological Sciences 363: 543-555.
[30] Holldobler, B., Wilson, E. O. (1990): The Ants. – Springer-Verlag Berlin Heidelberg.
[31] Ješovnik, A., Bujan, J., Bračko, G. (2011): One genus and three species of ants (Hymenopter: Formicidae) new for Croatia. – Entomologia Croatica 15: 113-122.
[32] Ješovnik, A., Pečarevič, M. (2018): The importance of invertebrates in conservation: the case of the ants. – Book of Abstracts of the 13th Croatian Biological Congress: 126-127.
[33] Kaspari, M., O'Donnell, S., Kercher, J. R. (2000): Energy, density, and constraints to species richness: ant assemblages along a productivity gradient. – The American Naturalist 155: 280-293.
[34] Lavelle, P., Decaëns, T., Aubert, M., Barot, S., Blouin, M., Bureau, F., Margerie, P., Mora, P., Rossi, J. P. (2006): Soil invertebrates and ecosystem services. – European Journal of Soil Biology 42: 3-15.
[35] Lemić, D., Čačija, M., Virić Gašparić, H., Drmić, Z., Bažok, R., Pajač Živković, I. (2017): The ground beetle (Coleoptera: Carabidae) community in an intensively managed agricultural landscape. – Applied Ecology and Environmental Research 15: 661-674.
[36] Lemić, D., Virić Gašparić, H., Petrak, I., Graša, Ž., Bažok, R. (2016): Utjecaj četverogodišnjeg plodoreda na obnovu korisne faune člankonožaca površinskog sloja tla. – Journal of Central European Agriculture 17: 1346-1359.
[37] Li, J. (2018): Analysis of soil fertility and biological changes under long-term conservation tillage. – Asian agricultural research 10: 62-65.
[38] Lobry De Bruyn, L. A. (1999): Ants as bioindicators of soil function in rural environments. – Agriculture, Ecosystems and Environment 74: 425-441.

http://www.aloki.hu ● ISSN 1589 1623 (Print) ● ISSN 1785 0037 (Online)
DOI: http://dx.doi.org/10.15666/aeer/1706_1270912722

[39] Masoni, A., Frizzi, F., Brühl, C., Zocchi, N., Palchetti, E., Chelazzi, G., Santini, G. (2017): Management matters: A comparison of ant assemblages in organic and conventional vineyards. – Agriculture, Ecosystems & Environment 246: 175-183.
[40] Ministry of Agriculture (2018): Regulation on cross-compliance. – Official Gazette 32/2013, 45/2016, 26/2018, 84/2018.
[41] Mori, A., Grasso, D. A., Le Moli, F. (1991): Notes on the biology of the slave-making ant *Polyergus rufescens* Latr. (Hymenoptera Formicidae) in the field. – Ethology Ecology & Evolution 3: 81-85.
[42] Mori, A., Grasso, D. A., Moli, F. (2010): Eco-ethological study on raiding behaviour of the European Amazon ant, *Polyergus rufescens* Latr. (Hymenoptera: Formicidae). – Ethology 88: 46-62.
[43] Myers, S. S., Zanobetti, A., Kloog, I., Huybers, P., Leakey, A. D. B., Bloom, A. J., Carlisle, E., Dietterich, L. H., Fitzgerald, G., Hasegawa, T., Holbrook, N. M., Nelson, R. L., Ottman, M. J., Raboy, V., Sakai, H., Sartor, K. A., Schwartz, J., Seneweera, S., Tausz, M., Usui, Y. (2014): Increasing CO2 threatens human nutrition. – Nature 510: 139-142.
[44] Myles, A., Mustafa, B., Yang, C., de Coninck, H. (2018): Global Warming of 1.5°C. Summary for Policymakers. – IPPC.
[45] Ottonetti, L., Tucci, L., Santini, G. (2006): Recolonization patterns of ants in a rehabilitated lignite mine in Central Italy: Potential for the use of Mediterranean ants as indicators of restoration processes. – Restoration Ecology 14: 60-66.
[46] Pajač Živković, I., Barić, B., Kos, T., Suda, H., Jemrić, T., Fruk, M., Lemić, D. (2016): The ground beetle fauna (Coleoptera) of apple orchard in Croatia. – Agriculturae Conspectus Scientificus 81: 103-107.
[47] Pe'er, G., Dicks, L. V., Visconti, P., Arlettaz, R., Baldi, A., Benton, T. G., Collins, S., Dieterich, M., Gregory, R. D., Hartig, F., Henle, K., Hobson, P. R., Kleijn, D., Neumann, R. K., Robijns, T., Schmidt, J., Shwartz, A., Sutherland, W. J., Turbe, A., Wulf, F., Scott, A. V. (2014): EU agricultural reform fails on biodiversity. – Science 344: 1090-1092.
[48] Perfecto, I., Snelling, R. (1995): Biodiversity and the transformation of a tropical agroecosystem: Ants in coffee plantations. – Ecological Applications 5: 1084-1097.
[49] Philpott, S. M., Ambrecht, I. (2006): Biodiversity in tropical agroforests and the ecological role of ants and ant diversity in predatory function. – Ecological Entomology 31: 369-377.
[50] Piao, S., Ciais, P., Huang, Y., Shen, Z., Peng, S., Li, J., Zhou, L., Liu, H., Ma, Y., Ding, Y., Friedlingstein, P., Liu, C., Tan, K., Yu, Y., Zhang, T., Fang, J. (2010): The impacts of climate change on water resources and agriculture in China. – Nature 467: 43-51.
[51] Power, A. G. (2010): Ecosystem services and agriculture: tradeoffs and synergies. – Philosophical Transactions of the Royal Society B: Biological Sciences 365: 2959-2971.
[52] R Development Core Team (2014): R: A language and environment for statistical computing. – R Foundation for Statistical Computing, Vienna, Austria.
[53] Radford, B., Key, A., Robertson, L., Thomas, G. (1995): Conservation tillage increases in soil water storage, soil animal populations, grain yield, and response to fertiliser in the semi-arid subtropics. – Australian Journal of Experimental Agriculture 35: 223.
[54] Read, J. L., Andersen, A. N. (2000): The value of ants as early warning bioindicators: responses to pulsed cattle grazing at an Australian arid zone locality. – Journal of Arid Environments 45: 231-251.
[55] Reganold, J. P., Wachter, J. M. (2016): Organic agriculture in the twenty-first century. – Nature Plants 2: 15221.
[56] Ribas, C. R., Schmidt, F. A., Solar, R. R., Campos, R. B., Valentim, C. L., Schoereder, J. H. (2012): Ants as indicators of the success of rehabilitation efforts in deposits of gold mining tailings. – Restoration Ecology 20(6): 712-720.
[57] Sanabria, C., Lavelle, P., Fonte, S. J. (2014): Ants as indicators of soil-based ecosystem services in agroecosystems of the Colombian Llanos. – Applied Soil Ecology 84: 24-30.

http://www.aloki.hu ● ISSN 1589 1623 (Print) ● ISSN 1785 0037 (Online)
DOI: http://dx.doi.org/10.15666/aeer/1706_1270912722

[58] Sánchez-Bayo, F., Wyckhuys, K. A. G. (2019): Worldwide decline of the entomofauna: A review of its drivers. – Biological Conservation 232: 8-27.
[59] Sanders, N. J., Lessard, J. P., Fitzpatrick, M. C., Dunn, R. R. (2007): Temperature, but not productivity or geometry, predicts elevational diversity gradients in ants across spatial grains. – Global Ecology and Biogeography 16: 640-649.
[60] Schmitz, O. J., Hambäck, P. A., Beckerman, A. P. (2000): Trophic cascades in terrestrial systems: A review of the effects of carnivore removals on plants. – The American Naturalist 155(2): 141-153.
[61] Schweiger, O., Maelfait, J. P., Van Wingerden, W., Hendrickx, F., Billeter, R., Speelmans, M., Augenstein, I., Aukema, B., Aviron, S., Bailey, D., Bukacek, R., Burel, F., Diekotter, T., Dirksen, J., Frenzel, M., Herzog, F., Liira, J., Roubalova, M., Bugter, R. (2005): Quantifying the impact of environmental factors on arthropod communities in agricultural landscapes across organizational levels and spatial scales. – Journal of Applied Ecology 42: 1129-1139.
[62] Seifert, B. (2007): Die Ameisen Mittel- und Nordeuropas. – Lutra Verlags- und Vertriebsgesellschaft.
[63] Seifert, B. (2018): The ants of central and northern Europe. – Lutra Verlags und Vertriebsgesellschaft.
[64] Seifert, B., Schultz, R. (2009): A taxonomic revision of the *Formica rufibarbis* Fabricius, 1793 group (Hymenoptera: Formicidae). – Myrmecological News 12: 255-272.
[65] Sharley, D. J., Hoffmann, A. A., Thomson, L. J. (2008): The effects of soil tillage on beneficial invertebrates within the vineyard. – Agricultural and Forest Entomology 10: 233-243.
[66] Shukla, R. K., Singh, H., Rastogi, N. (2016): How effective are disturbance – tolerant, agroecosystem – nesting ant species in improving soil fertility and crop yield? – Applied Soil Ecology 108: 156-164.
[67] Skinner, J. A., Lewis, K. A., Bardon, K. S., Tucker, P., Catt, J. A., Chambers, B. J. (1997): An overview of the environmental impact of agriculture in the U.K. – Journal of Environmental Management 50: 111-128.
[68] Slipinski, P., Zmihorski, M., Czezhowski, W. (2012): Species diversity and nestedness of ant assemblages in an urban environment. – European Journal of Entomology 109: 197-206.
[69] Social Insects Specialist Group (1996): The IUCN Red List of Threatened Species.
[70] Stadler, B., Schramm, A., Kalbitz, K. (2006): Ant-mediated effects on spruce litter decomposition, solution chemistry, and microbial activity. – Soil Biology and Biochemistry 38: 561-572.
[71] Stinner, B. (2002): Arthropods and other invertebrates in conservation-tillage agriculture. – Annual Review of Entomology 35: 299-318.
[72] Stoate, C., Boatman, N., Borralho, R., Carvalho, C. R., de Snoo, G. R., Eden, P. (2001): Ecological impacts of arable intensification in Europe. – Journal of Environmental Management 63: 337-365.
[73] Talbot, M. (1953): Ants of an old-field community on the Edwin S. George Reserve, Livingston County, Michigan. – Contributions to Laboratory of Vertebrate Biology, University of Michigan 69: 1-9.
[74] Taylor, R. W. (1967): A monographic revision of the ant genus *Ponera* Latreille (Hymenoptera: Formicidae). – Pacific Insects Monographs 13: 1-112.
[75] Trager, J. C. (2013): Global revision of the dulotic ant genus *Polyergus* (Hymenoptera: Formicidae, Formicini). – Zootaxa 3722: 501-548.
[76] Underwood, E. C., Fisher, B. L. (2006): The role of ants in conservation monitoring: If, when, and how. – Biological Conservation 132: 166-182.
[77] Van Oudenhove, L., Billoir, E., Boulay, R., Bernstein, C., Cerdá, X. (2011): Temperature limits trail following behaviour through pheromone decay in ants. – Naturwissenschaften 98: 1009-1017.

http://www.aloki.hu ● ISSN 1589 1623 (Print) ● ISSN 1785 0037 (Online)
DOI: http://dx.doi.org/10.15666/aeer/1706_1270912722

[78] Vogrin, V. (1955): Prilog fauni Hymenoptera - Aculeata Jugoslavije. – Zaštita Bilja 31: 1-74.
[79] Wagner, D., Jones, J. B., Gordon, D. M. (2004): Development of harvester ant colonies alters soil chemistry. – Soil Biology and Biochemistry 36: 797-804.
[80] Wagner, H. C., Arthofer, W., Seifert, B., Muster, C., Steiner, F. M., Schlick-Steiner, B. C., (2017): Light at the end of the tunnel: Integrative taxonomy delimits cryptic species in the *Tetramorium caespitum* complex (Hymenoptera: Formicidae). – Myrmecological News 25: 95-129.
[81] Way, M. J., Khoo, K. C. (1992): Role of ants in pest management. – Annual Review of Entomology 37: 479-503.
[82] Wielgoss, A., Tscharntke, T., Rumede, A., Fiala, B., Seidel, H., Shahabuddin, S., Clough, Y. (2013): Interaction complexity matters: disentangling services and disservices of ant communities driving yield in tropical agroecosystems. – Proceedings of the Royal Society B: Biological Sciences 281.
[83] Wilson-Rummenie, A. C., Radford, B. J., Robertson, L. N., Simpson, G. B., Bell, K. L. (1999): Reduced tillage increases population density of soil macrofauna in a semiarid environment in Central Queensland. – Environmental Entomology 28: 163-172.
[84] Zaninović, K., Gajić-Capka, M., Perčec Tadić, M. (2008): Klimatski atlas Hrvatske / Climate atlas of Croatia 1961-1990, 1971-2000. – Državni hidrometeorološki zavod.

http://www.aloki.hu ● ISSN 1589 1623 (Print) ● ISSN 1785 0037 (Online)
DOI: http://dx.doi.org/10.15666/aeer/1706_1270912722

THE CONVENTIONAL METHOD OF RAINWATER COLLECTION AND THE ION-EXCHANGE RESIN METHOD IN MONITORING THE NITROGEN DEPOSITION FROM THROUGH FALL

WANG, G.[1] – HAN, L.[2*] – TANG, X. Y.[1] – YANG, Y.[2]

[1]*Institute of Plateau Meteorology, China Meteorological Administration /Heavy Rain and Drought - Flood Disasters in Plateau and Basin Key Laboratory of Sichuan Province, Chengdu 610072, China*

[2]*Chengdu University of Information Technology, Chengdu 610225, China*

[*]*Corresponding author*
e-mail: hanlin@cuit.edu.cn

(Received 22nd Apr 2019; accepted 11th Jul 2019)

Abstract. Concerns are on the rise over the impact of atmospheric nitrogen (N) deposition on forest ecosystems in the tropical and subtropical areas. This study used the conventional rainwater collection method and the ion-exchange resin (IER) method to measure through fall N deposition over time in the Picea abies forests in the Tibet Plateau. The results were compared, and their applicability in determining the atmospheric N deposition was analyzed. The results indicated a strong correlation between the IER method and the conventional method in determining the NH_4^+-N and NO_3^--N content (R^2=0.47 and R^2=0.75, P<0.001). However, the NH_4^+-N content measured with the IER method was generally lower, while the NO_3^--N was generally higher. The total mineral N deposition in through fall measured with both methods was about the same. Therefore, we can use the IER method instead of the conventional method for determining the total inorganic N deposition in forests at the Tibet Plateau.
Keywords: *Tibet Plateau, forest ecosystems, atmospheric nitrogen deposition, NH_4^+-N content, NO_3^--N content*

Introduction

From 1860 to 2000, the nitrogen (N) discharged into the atmosphere had increased from 15 Tg N a^{-1} to 165 Tg N a^{-1} due to human activities (Chen, 2007). Rainwater penetration is an important factor that keeps the nutrient balance of forest ecosystems, directly affecting the distribution of soil moisture and recycling of nutrients (Carly-Moses, 2004). Therefore, a quantitative assessment of N sediment in penetration rainwater is key in monitoring atmospheric N sediment received by the forest ecosystem, and also necessary for understanding the feedback mechanism of the forest ecosystem for atmospheric N sediment (Thimonier, 1998).

Rainwater penetration has strong spatial heterogeneity and will be influenced by various factors such as the altitude, landform, vegetation type and edge effect (Du et al., 2008; Parker et al., 2009; Schmidt et al., 2010). The conventional rainwater collection method used to observe the N sediment flux is labor intensive and largely limited by the sampling point distribution. The functional group of the ion-exchange resin (IER) can dissociate some cations or anions, while absorbing other original cations or anions in the solution, so the NO_3^- in the rainwater can be fixed on functional groups that have positive charges in the resin, and NH_4^+ can be fixed on functional groups that have negative charges in the resin, which keeps them more stable. With this approach, there

http://www.aloki.hu ● ISSN 1589 1623 (Print) ● ISSN 1785 0037 (Online)
DOI: http://dx.doi.org/10.15666/aeer/1706_1272312729

will be no need for rainwater collection. Instead, regularly replacing the IER will be enough to obtain the atmospheric N sediment. The IER method has been widely used globally to monitor rainwater N sediment (Simkin et al., 2004; Klopatek et al., 2006; Verburg et al., 2009).

Currently in China, anion exchange resins are widely used in the N cycle to measure soil N (Bo et al., 2001; Fang et al., 2004; Yang et al., 2005; Li, 2005). Wang et al. (2010) used the IER method to monitor the sediment of ammonium N and nitrate N in the different functional zones in Changchun. Wenping et al. (2010) focused on the man-made ecological forest in Qianyanzhou, compared the IER method and the conventional rainwater collection method, and determined the dynamic difference of N sediment in forest penetrated rainwater.

Due to a high average altitude of over 4000 meters, challenging transportation and working conditions, situ data from Tibet Plateau have been scarce. This study intended to establish the linear regression equation between the conventional and the IER methods for experimental data. The IER method is more suitable for collection in remote areas or in winter as the sampling is easier and less frequent.

This study took the Picea abies forest as the research object, used the conventional rainwater collection method and the IER method at the same time to monitor the change of rainwater N in forests of different temperate zones and the main factors influencing the N content. By comparing the two methods, the feasibility of the IER method in analyzing wet sediment of atmospheric N was determined, and the applicability of the IER method to determine N sediment flux of forest rainwater in Tibet Plateau was discussed.

Materials and methods

Overview of the studied area

The experimental plot of this study is located in the standard woodland (29°46'N, 94°44'E) of the South-East Tibetan Plateau Station for integrated observation and research of alpine environment of Chinese Academy of Sciences near Lulang town, Nyingchi district, Tibet Autonomous Region, which is flat and 3200 meters above sea level. Nyingchi district has the typical tropical humid and semi-humid climate that is affected by warm currents of the Indian Ocean and the Pacific Ocean. Dry and windy in spring, cool and foggy in autumn, it has a warm short summer and a sunny, cold, and long winter, and features a short frost-free period (about 170 days throughout the year) and a long frozen period. The average annual temperature is 7-16°C; the annual average rainfall ranges from 600 to 800 mm, and the 92.4% of the rainfall concentrates during the growing season.

In the studied area, the vegetation type is coniferous Picea abies forest in Tibetan Plateau, forest type is mature virgin forest, dominant tree species have more than 100 years of average age, the main tree species include: Abies georgei var. smithii, Picea likiangenses var. linzhiensis, Pinus yunnanensis and Pinus densata. The soil in this area is dark brown forest soil.

Sample collection and analysis

Rainwater samples were collected with self-made rain collectors, which consist of a funnel and a collecting bottle. 16 collectors were evenly placed around the experimental

http://www.aloki.hu ● ISSN 1589 1623 (Print) ● ISSN 1785 0037 (Online)
DOI: http://dx.doi.org/10.15666/aeer/1706_1272312729

area, and 2-3 times of irregular sampling monthly were performed from May to October in 2012 (a total of 8 times of sampling in the year) based on the change of seasonal rainfall intensity. In addition, a resin bag was placed beside each rainwater collector (a nylon bag, which contains 20 g of anion and cation resin, respectively, is horizontally placed in the PVC tube). Resin samples were taken when sampling the rainwater. The atmospheric N sediment content in two samples were then determined respectively.

This study chose the anion exchange resin 717 and the cation exchange resin 732 produced by Sinopharm Chemical Reagent Co., Ltd (Shanghai). The PVC tubes beside each precipitation collector had a diameter of 7.5 cm and a height of 5 cm. After each collection, new resin bags which with the same producing method would be placed in the PVC tubes to monitor the N content.

Calculation and statistical analysis

The NH_4^+-N and NO_3^--N content in rainfall and resin samples can be determined using the colorimetric method (Kim, 1995).

The units of N sediment fluxes of different forms and resin mineral N flux are mg N m^{-2}. The average values and standard error have been calculated. The correlated coefficient of atmospheric N wet sediment has been regressively analyzed and calculated with the SPSS.

Results

Changes of the N wet sediment flux of the coniferous Picea abies forest in Tibetan Plateau

Figure 1 shows the N wet sediment flux of different forms from May to October in 2012, and indicates that atmospheric N wet sediment flux changes with the seasons, with the highest flux in summer and low flux after the fall.

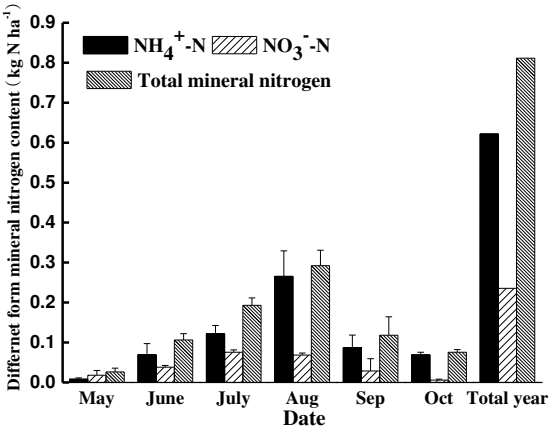

Figure 1. *Seasonal change of mineral N content of different forms in forest penetrated rainwater*

In 2012, $NH4_+^-$-N, NO_3^--N and total mineral N in atmospheric wet sediment amount of the coniferous Picea abies forest in Tibetan Plateau were 6.22, 2.36 and 8.58 kg N ha^{-1} yr^{-1}, and ammonium N accounts for about 77% of the mineral N. A significant positive

http://www.aloki.hu ● ISSN 1589 1623 (Print) ● ISSN 1785 0037 (Online)
DOI: http://dx.doi.org/10.15666/aeer/1706_1272312729

correlation has been found between the $NH4_+^-$-N (y_1) and NO_3^--N (y_2) mineral N sediment in rainfall and the monthly average temperature(°C) (x, unit: mm), $y_1 = 0.02x - 0.12$ ($R^2 = 0.41$, n = 6, $P < 0.01$), $y_2 = 0.01x - 0.06$ ($R^2 = 0.73$, n = 6, $P < 0.01$), and between NO_3^--N (y2) and the monthly average rainfall (x, unit: mm), $y_2 = 0.0006x - 0.0023$ ($R^2 = 0.5$, n = 6, $P < 0.01$). However, the correlation is weaker between $NH4_+^-$-N and the monthly rainfall ($R^2 = 0.08$).

Comparison between the IER method and the conventional rainwater collection method

The purpose of this study is to compare the IER method and the conventional rainwater collection method in determining mineral N wet sediment flux in the woodland. Depending on the result, the IER method may be considered for use in uninhabited areas in winter (for example, the Tibetan Plateau woodlands) instead of the conventional rainwater collection method.

From *Figure 2* and *Figure 3*, a relatively strong correlation can be observed between the IER method and the conventional method for determining mineral nitrogen in wet sediment flux in the coniferous Picea abies forest ($R^2 \geq 0.46$, $P < 0.001$), but the NH4+-N measured using the IER method is generally lower, while the NO_3^--N is generally higher. The total mineral N deposition in through fall measured with both methods is about the same (*Figure 3*).

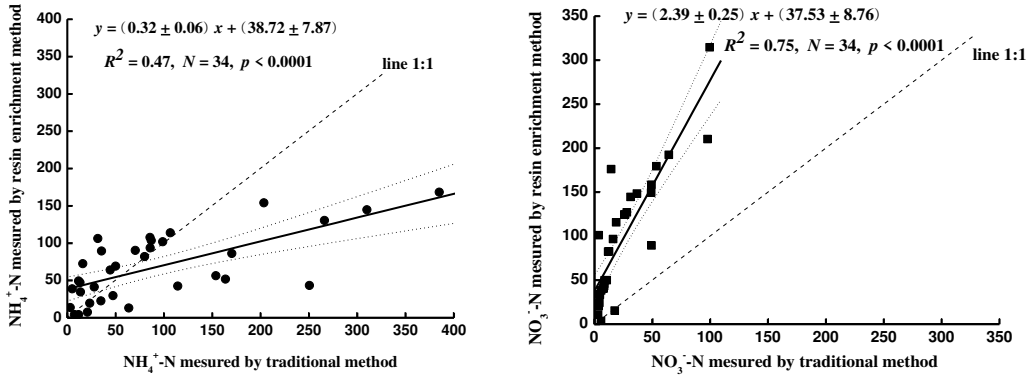

Figure 2. *Comparison between the IER method and the conventional rainwater collection method in determining $NH4_+^-$-N and NO_3^--N in wet sediment flux. The dotted line is 95% of upper*

Discussion

N deposition flux characteristics and influencing factors

The N sediment flux was higher in late summer and early autumn and began to decline in autumn and winter in southern China (Jianfen et al., 2005; Du et al., 2008). March, in particular, witnesses larger N sediment, in which NH_4^+-N takes up 64.6% of the mineral N sediment (Du et al., 2008). Results of this study are similar with that of Berger et al. (2008). Berger et al. (2008) measured the mineral N wet sediment in an Australian forest, which was lower than the mineral N wet sediment of forests in Germany and southern China.

http://www.aloki.hu ● ISSN 1589 1623 (Print) ● ISSN 1785 0037 (Online)
DOI: http://dx.doi.org/10.15666/aeer/1706_1272312729

Berger et al. (2008) measured that mineral N wet sediment of the conifer and broadleaf forest in central Australian was 9.1-16.6 kg N $ha^{-1}yr^{-1}$, and the sediment amount was mainly influenced by rainfall. Stephan (2001) observed obvious seasonal changes of soluble organic N sediment contained in the rainwater of forests in southern Germany, and found a significantly positive correlation between the soluble organic N and the temperature (R^2 = 0.58). Fang et al. (2004) also found a significantly positive correlation between the atmospheric N deposition and the annual precipitation, when measuring the N deposition in through fall in 14 forests in southern China using the IER method (R^2 = 0.49).

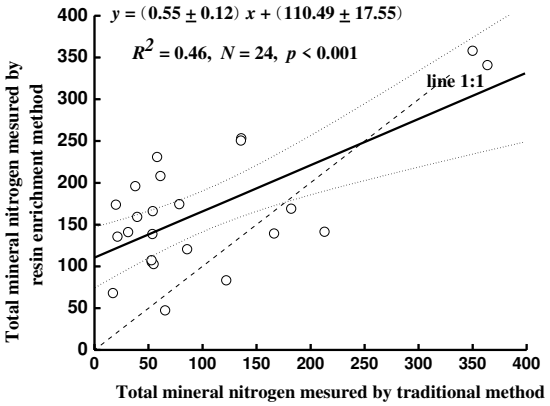

Figure 3. *Comparison between the IER method and the conventional rainwater collection method in determining total mineral N in wet sediment flux. The dotted line is 95% of upper*

Differences of results and applicability of the IER method and the rainwater collection method

The line 1:1 in *Figures 2 and 3* shows that the NO_3^--N content measured with the IER method is generally higher, and the possible reason might be that the conventional method collects samples 2-3 times a month according to the intensity of rainfall, while the IER method collects only 1 to 2 times a month. During the long sampling period, ammonium N converts into nitrate N, leading to a higher nitrate N value in the IER method (Xu et al., 2009). However, the NH_4^+-N content measured with the IER method is generally lower, because the current speed might be too fast in ion resin column with high precipitation intensity, which does not allow for complete exchange between the ammonium N and the ion resin (Wenping et al., 2010). In addition, with the increase of rainfall, the atmospheric N deposition increases (Berger et al., 2008).

Wenping et al. (2010) also found that the mineral N deposition measured with the conventional method is higher in the coniferous forest. This may be caused by the conversion of the organic N into mineral N facilitated by microbes during the longer sampling time with higher precipitation intensity. Fang's research (Fang et al., 2004) results show that due to reduced precipitation in winter (October to February), the dry deposition of atmospheric N on the canopy would increase, and then fall down to the ground in wet sedimentation due to spring rain, which explains why the N content is significantly higher after the first rain of spring than other seasons.

http://www.aloki.hu ● ISSN 1589 1623 (Print) ● ISSN 1785 0037 (Online)
DOI: http://dx.doi.org/10.15666/aeer/1706_1272312729

In addition, previous studies seldom considered the living environment outside the forest or collect resin samples monthly. However, sufficient lighting and evaporation for resin surface may lead to underestimated N sediment when using the IER method.

Therefore, in an uninhabited area (such as the Tibet Plateau), the IER method may be used, instead of the conventional method, in the forest zone and the growing season to determine the N sediment flux in atmosphere, while in the living environment outside the forest or in winter, the sampling frequency of the IER method may be increased to monthly or half-monthly.

Conclusions

A strong correlation has been found between the IER method and the conventional rainwater collection method in determining the NH_4^+-N and NO_3^--N content ($R^2 = 0.47$ and $R^2 = 0.75$, $P < 0.001$). However, the NH_4^+-N content measured with the IER method is generally lower, while the NO_3^--N is generally higher. The total mineral N deposition in through fall measured with both methods is about the same. Therefore, we can use the IER method instead of the conventional method for determining the total inorganic N deposition in forest at the Tibet Plateau.

There is a correlation between atmospheric nitrogen deposition, soil nitrogen transformation, and nitrogen leaching. Atmospheric nitrogen deposition can also influence the mineralization and nitrification rate of forest soil nitrogen which can lead to woodland nitrogen loss and nitrogen storage change. China is the third largest nitrogen deposition concentration area in the world. But there is a lack of research on comprehensive assessment of the effects of deposition of different forms of nitrogen, different forest types, and different climatic factors on net mineralization flux of soil nitrogen.

Acknowledgements. This research was financially supported by Dr. Yongjie Wang, Boqing Xu and Jinlong Chang of the Southeast Mountain Environment Comprehensive observation station of Chinese Academy of Sciences assisted with sample collection and analysis. Thanks also to employees of the Institute of Tibetan Plateau Research Chinese Academy of Sciences for assistance and cooperation in the experiments. This research was supported by the National Natural Science Foundation of China (41105101 and 41405043).

REFERENCES

[1] Berger, T. W., Untersteiner, H., Schume, H., Jost, G. (2008): Through fall fluxes in a secondary spruce (Picea abies), a beech (Fagus sylvatica) and a mixed spruce-beech stand. – J. Forest Ecology and Management 255: 605-618.

[2] Bo, S., Han, X., Qu, C., Huang, J. (2001): Net nitrogen mineralization and nitrification in one pure fine (Pinus tabulaeformis) forest and one pine-oak mixed forest in Dongling Mountainous region. – J. Acta Phytoecologica Sinica 25(2): 195-203.

[3] Carly-Moses, D. E. (2004): Through fall, stem flow, and canopy interception loss fluxes in a semiarid Sierra Madre Oriental matorral community. – J. Journal of Arid Environments 58(2): 182-202.

[4] Chen, X. Y., Jan, M. (2007): Indicators for nitrogen status and leaching in subtropical forest ecosystems, South China. – J. Biogeochemistry 82: 165-180.

http://www.aloki.hu ● ISSN 1589 1623 (Print) ● ISSN 1785 0037 (Online)
DOI: http://dx.doi.org/10.15666/aeer/1706_1272312729

[5] Du, C., Zeng, G., Zhang, G., Tang, L., Li, X., Huang, D., Huang, L., Jiang, Y. (2008): Input-output budgets for inorganic nitrogen under acid rain in a subtropical evergreen mixed forest in central-south China. – J. Water, Air & Soil pollution 1(4): 171-181.
[6] Fang, Y. T., Mo, J. M., Gundersen, P., Zhou, G. Y., Li, D. J. (2004): Nitrogen transformations in forest soils and its responses to atmospheric nitrogen deposition: a review. – J. Acta Ecologica Sinica 24(7): 1523-1531.
[7] Glatzel, S., Stahr, K. (2001): Methane and nitrous oxide exchange in differently fertilised grassland in southern Germany. – J. Plant and soil 231(1): 21-35.
[8] Jianfen, G., Yusheng, Y., Guangshui, C., Peng, L. (2005): Dissolved organic carbon and nitrogen in precipitation, through fall and stem flow from Schima superba and Cunninghamia lanceolata plantations in subtropical China. – J. Journal of Forestry Research 16: 19-22.
[9] Kim, H. T. (1995): Soil Sampling, Preparation and Analysis. – M. New York: Marcel Dekker.
[10] Klopatek, J. M., Barry, M. J., Johnson, D. W. (2006): Potential canopy interception of nitrogen in the Pacific Northwest, USA. – J. Forest Ecology and Management 234: 344-354.
[11] Li, M. R., Sha, L. Q. (2005): Soil nitrogen mineralization under different land use patterns in Xishuangbanna. – J. Chinese Journal of Applied Ecology 16(1): 54-58.
[12] Parker, B. R., Schindler, D. W., Beaty, K. G., Stainton, M. P., Kasian, S. E. M. (2009): Long-term change in climate, stream flow, and nutrient budgets for first-order catchment at the experimental Lake Area (Ontario, Canada). – J. Canadian Journal of Fisheries & Aquatic Sciences 66: 1848-1863.
[13] Schmidt, B. H. M., Wang, C. P., Chang, S. C., Matzner, E. (2010): High precipitation causes large fluxes of dissolved organic carbon and nitrogen in a subtropical montane Chamaecyparis forest in Taiwan. – J. Biogeochemistry 101: 243-256.
[14] Simkin, S. M., Lewis, D. N., Weathers, K. C., Lovett, G. M., Schwarz, K. (2004): Determination of sulfate, nitrate, and chloride in through fall using Ion-exchange resins. – J. Water, Air, and Soil Pollution 153: 343-354.
[15] Thimonier, A. (1998): Measurement of atmospheric deposition under forest canopies: Some recommendation for equipment and sampling design. – J. Environmentental Monitoring and Assessment 52(3): 353-387.
[16] Verburg, P. S. J., Johnson, D. W., Schorran, D. E., Wallace, L. L., Luo, Y., Arnone, J. A. I. (2009): Impacts of an anomalously warm year on soil nitrogen availability in experimentally manipulated intact tall grass prairie ecosystems. – J. Global Change Biology 15: 888-900.
[17] Wang, D. X., Zhao, P. S., Zhang, Y. X. (2010): Monitoring atmospheric nitrogen deposition in Changchun using ion exchange resin columns method. – J. Research of Environmental Sciences 23(8): 1013-1018.
[18] Wenping, S., Guirui, Y., Huajun, F., Yunfen, L. (2010): Determination of nitrogen deposition in through fall using ion-exchange resins: A field test in planted coniferous forest ecosystem at Qianyanzhou. – Acta Ecologica Sinica 30(24): 6872-6880.
[19] Xu, X., Han, L., Luo, X., Liu, Z., Han, S. (2009): Effects of nitrogen addition on dissolved N_2O and CO_2, dissolved organic matter, and inorganic nitrogen in soil solution under a temperate old-growth forest. – J. Geoderma 151(3-4): 370-377.
[20] Yang, X., Dong, Y., Yuchun, Q. I., Geng, Y., Liu, L. (2005): Soil net nitrogen mineralization in an aneulolepidium chinensisi grassland, inner Mongolia. – J. Progress in geography 24(2): 30-37.

http://www.aloki.hu ● ISSN 1589 1623 (Print) ● ISSN 1785 0037 (Online)
DOI: http://dx.doi.org/10.15666/aeer/1706_1272312729

POWER REQUIREMENT FOR SOWING PATTERNS ON TWO FALLOW LANDS UNDER WHEAT PRODUCTION

KHURSHID, F. F.[1] – SEDEEQ, A. M. A.[2*]

[1]*College of Agricultural Sciences, University of Sulaimani, Sulaimani, Iraq*
(e-mail: fawzy.khurshid@univsul.edu.iq; phone: +964-770-144-2400)

[2]*College of Agriculture and Forestry, University of Mosul, Mosul, Iraq*

**Corresponding author*
e-mail: arkanma.agri.col@uomosul.edu.iq; phone: +964-770-162-2813

(Received 22nd Apr 2019; accepted 20th Aug 2019)

Abstract. An experiment related to wheat cultivation was conducted at south of Sulaimani province, Kurdistan region- Iraq during autumn in 2016-2017. Completely Randomized Block Design was applied with split-split plot arrangement, and the experiment was conducted on two fallow lands, the first land was plowed in the spring and the other remained unplowed, two different sowing modes with rotary seed broadcaster were used, namely conventional and overlapped prose lines, and two similar sets of tillage systems were chosen for the study. The averages were compared by using Duncan's test. The coefficients of variance (CV) for overlapped and conventional seed spreading were 9.2% and 48.4%, respectively. The spring-plowed fallow land proved to obtain significantly different values compared to the unplowed land, which were higher by 51.9%, 48.5%, 47.1%, 26.9%, 31.6%, 6.7% and 30.1% for fuel consumption, draft, power losses due to slippage, working time, energy utilization, wheat yield and total cost, respectively. The average results for overlapped seed broadcasting were higher than those of the conventional manner by: 0.8%, 0.3% 1%, 0%, 3.3%, 6.7% and 14.5%. The lowest values were resulted from applying: MB plus seed distributor plus MB, while, the maximum yield was given by applying: cultivator plus seed distributor plus cultivator.
Keywords: *land type, fuel consumption, cultivator, spreading modes*

Introduction

Cereal crops are considered to have a fundamental importance in human life. They have had an essential role in the past. Cereal crops are the mainstay of food supply and the development of the world's people at all times. In Kurdistan region- Iraq, the availability of suitable agricultural land, labour, abundance of water and adequate climate for the cultivation of many of the strategic crops are regarded as the ingredients of successful agricultural operations. Wheat and barley are special crops which help to strengthen and install the status of the agricultural sector in a stable level position to provide a durable and robust economy of the region.

The total arable land area in Kurdistan region- Iraq, was 968468.48 ha, 664771.5 ha of wheat farms that produce 1019481 tons, and constituted 34% of Sulaymani area. Sowing patterns employed by farmers vary considerably from area to area. The vast majority of the farmers spread their seeds by broadcaster machines after preparing the field in different ways to avoid costs. In addition to fallow rotation few farmers who owned large farms drilled their seeds. Of course, production is noteworthy various in quantity and quality.

The main objective of tillage is to prepare the soil or the seedbed where the plants can easily grow. The crop rotation system, which consists of wheat-fallow, is widely applied in the Kurdistan Region, as is the case in other places in semi-dense and dry

http://www.aloki.hu ● ISSN 1589 1623 (Print) ● ISSN 1785 0037 (Online)
DOI: http://dx.doi.org/10.15666/aeer/1706_1273112751

areas, even in some rain-fed areas. Aims of fallow are to maximize soil water storage through improved water capacity, reduce evaporation; maximize plant nutrient availability; and minimize soil erosion risk (Greb, 1979).

Zengin and Ocakoglu (2013) found that the plowing (stubble fallow method) was more effective than the other methods in terms of high grain yield and yield components. Yield increase of ~50% was observed in both years when compared to the minimum tillage (stubble fallow method) when they studied the effect of different tillage patterns and fallow methods (minimum tillage/stubble fallow, plowing/stubble fallow and plowing/non-stubble Fallow) on wheat yield, and yield components.

Tillage methods have different tillage depths and ability to change soil physical and chemical properties that affect the crop yield and quality (Strudley et al., 2008). Farmers have begun to apply reduced and no-tillage management practices for production of grain in their fallow lands instead of conventional tillage systems. The main reasons for this idea of less tillage are reduced fuel and labour costs, lowered soil erosion, and enhanced water conservation. The growth in soil water decreases some of the hazard in semiarid and arid farming lands (Broder et al., 1984). Even though overall national yield data of wheat crop mention that it is increasing slowly. However, feasibility is declining due to soil fertility decline, weed problem, disease and insects, labour and power scarcity, and the high cost of inputs (Asheesh et al., 2017).

In general, wheat production in large areas will depend upon mechanized production systems efficiently used and managed. Special attention should be given during the selection of the appropriate machine for proper land preparation and suitable sowing methods for high and profitable crop yield (Mergani, 2006). Askari and Khalifahamzehghasem (2013), pointed out that the needed force to pull the Moldboard plow (16.30 kN) is about five times larger than the needed force of field cultivator (3.49 kN), which correlates with the data estimation that obtained from ASABE, 2016, that is 19.55 kN and 3.82 kN respectively.

Botta et al. (2006) and Kahloon et al. (2012) reported that, the maximum economic benefit of the farmers reduced when fuel consumption increased, so that tillage equipment was used in cultivating of wheat. As a principle, in general it can be said that one pass for planting compared to two or extra tillage implementations means fewer hours on a tractor operation, fewer labour hours to pay and may reduce production costs or more acres to farm. Çarman et al. (2013) mentioned that, currently, the search for alternative economic methods for tillage is an inevitable consequence of the high cost of energy spent on conventional tillage, on the other hand, conservation tillage means any plowing or planting method that leaves crop residues covering the field by at least 30% after seeding practice. Erosion in such soils is reduced by at least 50% compared to the fallow soil.

Hanna (2016) showed that the highest value of effective field capacity (A/hr) was recorded by the fertilizer spreader compared to other machines which were 4.1, 6.8, 14.4, 5.1 and 20.4 for Moaldboard plow, Chisel Plow, Field cultivator, Grain drill and Fertilizer spreader respectively. Mckyes (1985) defined energy efficiency as the number of cubic meters of soil raised by plows for each megajoule of consumed energy. This efficiency is affected by several factors, the most important of which is the depth of tillage. Muhsin (2017) mentioned that the energy utilization efficiency and the plowed soil volume rate increased by 34.30% and 87.38% when the plowing depth increased from 10 to 30 cm, respectively.

http://www.aloki.hu ● ISSN 1589 1623 (Print) ● ISSN 1785 0037 (Online)
DOI: http://dx.doi.org/10.15666/aeer/1706_1273112751

Bai et al. (2008) recommended that the absence of suitable machinery and the trepidation of a reduction of yield make it difficult for farmers to adopt an attitude towards the idea of reducing traffic. By minimizing the machines traffic, the bulk density in the 0–0.15 m of the soil layer was reduced, the total porosity in the 0–0.60 m soil layer was increased, better available water content and best saturated hydraulic conductivity were characteristic compared with the traditional mouldboard tillage treatment

In early American history, wheat was sown broadcast. Broadcasting has been observed to reduce plant establishment as seeds are said to be lost to pests and unsuitable weather conditions. Thus, high seed rates have been recommended when seeds are broadcast in order to compensate for seed loss. Presently in America almost all wheat is drilled. The main reason given for drilling wheat was better germination, which resulted in higher stands compared to broadcasting. Though favored crop incorporation and crop yield have been reported when wheat is planted by seed drill compared to other sowing patterns, however, wheat drilling is a costly technology regarding labor requirements for drilling or machinery employed in seed drilling. Thus, seed broadcasting is common in farmers' plots. It was observed, seed broadcasting even when followed by harrowing or raking does not bring seed in ideal contact with the soil for sufficient water uptake (Oyewole et al., 2001).

Broadcasting is the process of random spreading of seed on the surface of seedbeds at controlled rates. Hassann et al. (2009) studied the effect of different field plot area on wheat planting machinery performance. The results showed that it is important to notice that seed drill planter allowed a saving in wheat seeds of 26% compared with the seed spreader. Wuest et al. (1999) showed that, distinct technique of seeding and seed-soil contact had strong influence time to germination. Lan et al. (1999) confirmed that uniformity for seed spaces is important for crops because it has an influential role in crop production. There are a lot of environmental and economic reasons for using more accurate broadcasters as a device of reducing undesirable environmental effects (Sanaeifar and Sheihkdavoodi, 2012). The relevance of soil and its physiological effects on plants had not been specified perfectly yet, but it was estimated that unfavorable effects of non-uniformity of broadcasting would economically lose a considerable amount of money (Svensson, 1990). The basic performance parameter of a broadcaster is uniformity of spreading over a wide range of situations, this parameter determines the quality of broadcasting, if the broadcasting is suitable the quality will improve better (Speelman, 1979). To help avoid unregularly stands, the equipment should be driven close enough to overlap the previous spread pass to guarantee regular seed distribution (Zewdu, 2008).

All seed broadcaster operators in the region follow the conventional method to spread Wheat granules. The traditional method means spreading granules without overlapping broadcast applications, even the operators leave untreated areas, or sometimes the overlapping of the broadcasting curve may be within a distance not exceeding 2 m, the reason is the operator use visual oversight to the tractor wheel traces, also he often depends on his guessing and skill to achieve parallel swaths in the field. All this results in a heterogeneous distribution of seeds over the field surface. Of course, the production become uneven in quantity and quality from place to place in the field.

Even after all spreader adjustments obtainable have been tested, the distribution shape from a broadcaster is not adequately uniform. A common recommendation in many books and technical papers was mentioned to solve the problem of non-

http://www.aloki.hu ● ISSN 1589 1623 (Print) ● ISSN 1785 0037 (Online)
DOI: http://dx.doi.org/10.15666/aeer/1706_1273112751

uniformity of the granular by making rate of application for half and cover the field twice at perpendicular angles (Colvin and Turner, 1980). But, also this technique is not the best manner to solve this problem (Parish, 1999). Effective overlap (30 to 50%) between adjacent passes is absolutely necessary to overcome this uneven distribution shape (UMass Extension, 2011).

Broadcasting not only requires higher seed rate but also results in lower plant population, whereas drill sowing method is recommended because of its uniform seed distribution and sowing at the desired depth, which usually results in higher germination and uniform stand. A key factor in the highest wheat production is the understanding of early crop establishment. Beside other agronomic factors seed rate and sowing method are major factors which determine the crop vigour and ultimate yield (Soomro et al., 2009)

It is known that the conventional mode for wheat sowing by seed spreader lead to distribute the wheat grains in a heterogeneous shape that leave places on the soil surface without seeds or light coverage, while other areas are covered with grain intensively which increases the competition between plants to obtain the necessary energy sources for appropriate growth, in addition the negative effects of irregular distribution of seeds results in the loss of a lot of money (Svensson, 1990). Therefore, the variation in the distribution of seeds on the soil surface and uneven emergence, depth and stands often result in lower production (Herbek and Lee, 2009). On the other hand, following the overlapping pattern for scattered lines by seed broadcaster is the best solution to the disadvantages of the uneven seed distribution that mentioned by Zewdu (2008).

It can be said, most farmers tend to raise their seeding rates when they used spinning disc type broadcaster. Higher seeding rates normally only lead to more seed costs and produce excessive plant populations. While bad stands as a result of poor seeding rate that prosed by broadcaster typically result in variation in soil–seed contact, seed scattered and seeding depth, predation of seed on the soil surface by birds, insects and mice in addition to high dense weed population that compete for available moisture (Brennan and Leap, 2014; Houk, 2009).

An effective technique to ensure improvement of the uniformity is to cut both the application rate and the swath width to half while preserving parallel swaths (Parish, 1986). For further explanation of half-width method, spread curve overlap of 100% is commonly needed to obtain uniform coverage. That mean, if the spread pattern width is 10 m wide, then a 100% overlap will result in a 5-m swath spacing width.

Generally, most farmers sowed own wheat by spinning disc type seed spreader by conventional mode after preparing the soil by variance tillage systems, which varies from place to another in the region, in terms of the type of machines used and the number of mechanical operations in order to get a quick profit through reducing time, effort and spent money, without taking into account the recommendations and the basis of the management of agricultural operations when using the machines with the right method. Here, the objective of this study was extracted.

The objective of this study is to evaluate the economic feasibility and relative profitability of various combinations of two sowing patterns for wheat crop in two different prepared fallow lands after introducing the advanced technique (overlapping manner) for wheat sowing by granules broadcaster machine at acceptable cost and energy consumption and comparing the results with those in conventional manner in order to improve wheat production through increasing the productivity per unit area.

http://www.aloki.hu ● ISSN 1589 1623 (Print) ● ISSN 1785 0037 (Online)
DOI: http://dx.doi.org/10.15666/aeer/1706_1273112751

Materials and methods

This study was carried out under rainfed conditions during the growing seasons at Experimental Farms of the College of Agricultural Sciences, University of Sulaimani at Bakrajo located in the southwest of Sulaimani province, Kurdistan region- Iraq (Latitude: 35° 33' N; Longitude 45° 27' E at an altitude of approximately 830 m). In this region, the climate is rainy and cloudy in winters, rainy in springs, hot and dry in summers, the information on agro-climatic conditions is given in *Table 1.* The physical properties of the soil of the experimental field were examined in the Soil and Water Department laboratories at the College of Agricultural Sciences *Table 2*.

Table 1. *Agro-climatic conditions at the Bakrajo Experimental Station for three cultivation seasons*

Season				Months							Total
		Oct.	Nov.	Dec.	Jan.	Feb.	Mar.	Apr.	May	Jun.	
				Precipitation (mm)							
2014-2015		43.2	151.6	128.6	100.0	65.0	98.4	25.8	19.8	0.0	632.3
2014-2016		114.2	197.2	75.8	110.6	76.2	171.8	57.6	12.2	0.0	830.8
2016-2017		13.7	44.5	149.4	59.2	96.5	111.5	54.5	20.0	0.0	566.7
				Air temperature (°C)							
2014-2015	Max.	35.3	13.9	12.6	16.9	20.1	23.0	33.2	37.6	34.2	
	Min.	9.2	6.9	2.5	-2.5	0.5	3.4	5.4	11.4	14.6	
2015-2016	Max.	34.4	13.3	12.1	16.6	19.8	22.0	32.2	36.9	34.1	
	Min.	9.1	6.1	2.2	-3.2	0.2	3.2	5.0	11.2	15.4	
2016-2017	Max.	32.7	24.3	18.0	15.8	30.1	24.8	32.4	39.2	37.6	
	Min.	8.7	8.0	-2.9	1.8	-2.5	1.2	2.8	14.4	15.4	

Table 2. *Soil physical properties of the experimental area to depth (20 cm)*

Sand ($g.kg^{-1}$)	Silt ($g.kg^{-1}$)	Clay ($g.kg^{-1}$)	Texture (P.S.D)	PH	S.W.C (%)	O.M ($g.kg^{-1}$)	Bulk density ($g/cm^{3)}$	Penetration (Kpa)
48.5	449.8	501.7	Silty clay	7.44	16	21.02	1.32	1370.5

Field experiment

For wheat cultivation, the year fallow system is one of the most common manners followed by growers as crop rotation in Iraqi-Kurdistan's large rain fed region. Therefore, two fallow lands were selected for conducting current research, the first fallow land as (F1) was plowed one time at the spring of 2016 at a depth of 0.25 m, while the second fallow land as (F2), was left in a resting stage without conducting any mechanical operation until the time of research. Adopting the overlapping ratios of 30% to 50% for prose lines of seed spreader was necessary to achieve acceptable values of the coefficient of variance (C.V.) (be as close to zero as possible). Values up to 15% are acceptable, but once the CV goes above 20% a crop and financial loss will happen (Forristal and Teagasc, 2017).

http://www.aloki.hu ● ISSN 1589 1623 (Print) ● ISSN 1785 0037 (Online)
DOI: http://dx.doi.org/10.15666/aeer/1706_1273112751

Two sets of sowing patterns were selected for the current experiment, the sowing of wheat seeds was applied by following the conventional mode of seed scattering and the intertwined mode of prose lines. Each set was consisting of the following patterns:

1. Soil tillage by moldboard plow one pass plus sowing with seed broadcaster and covering the seeds by moldboard plow one pass as (T1).
2. Soil tillage by moldboard plow one pass plus sowing with seed broadcaster plus covering the seeds by field cultivator one pass as (T2).
3. Soil tillage by field cultivator one pass plus sowing with seed broadcaster plus covering the seeds by field cultivator one pass as (T3).
4. Sowing with seed broadcaster plus covering the seeds by moldboard plow one pass as (T4).
5. Sowing with seed broadcaster plus covering the seeds by cultivator one pass as (T5).

Therefore, the number of sowing patterns becomes ten, five of them conducted by conventional sowing mode (farmers practice) and five patterns applied by adopting the overlapping mode of seed prose lines, as illustrated in *Table 3*. The experiment was carried out in a randomized plot design with a split-split plot arrangement by placing the condition of the fallow lands (F1 and F2) in the main plots, the sowing modes (conventional and overlapped) were placed in sub plots and each sowing pattern represented plot as explained in *Table 3*, each plot was replicated three times. The preceding crop in the season of 2014-2015 was winter wheat for both fallow lands. The experiment was conducted in the second decade of November 2016 when the soil moisture was approximately 16% for both lands. The sowing by overlapping mode was carried out by adopting the mode that Parish (1999) and UMass Extension (2000) recommended by cutting each of the delivery rate and swath width to half while maintaining parallel swaths by applying: right-on-right, left-on-left overlapping with back-and-forth traffic system as shown in *Figure 1*.

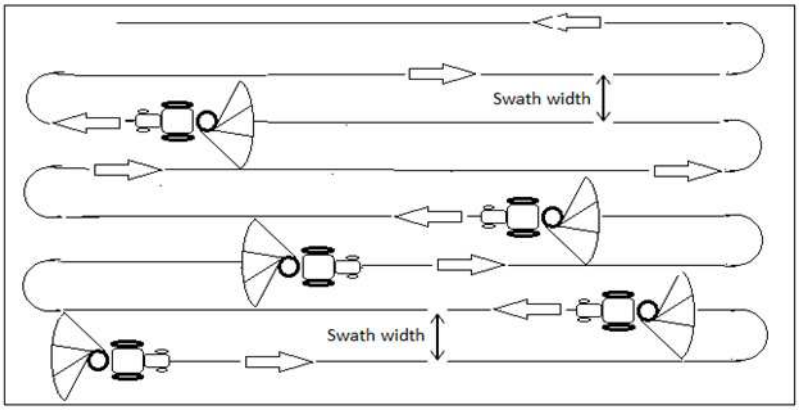

Figure 1. *Half-width method and half rate application (a right-on-right) and (a left-on-left) overlap manner*

Calibration

Centrifugal type broadcaster which used for this experiment had the following features: tractor mounted with P.T.O shaft driven at 540 rpm, hopper capacity of 0.8 m^3,

http://www.aloki.hu ● ISSN 1589 1623 (Print) ● ISSN 1785 0037 (Online)
DOI: http://dx.doi.org/10.15666/aeer/1706_1273112751

single spinning disc and height of the spinning disc from the ground was 1.1 m during operation. *Table 4* shows the main features of the machines used in the present study. The seed broadcaster was calibrated for traditional sowing on rate 200 Kg/ha (5000000 kernel/ha) a day before the study considering wind speed less than 8 km/h. According to ASAE S341.2 (1999) and as followed by Sanaeifar and Sheikhdavoodi (2012), the calibration test begun by putting twenty collecting trays 1 × 1m (each had partitions barriers) for granules in a row with equal distances to the longitudinal center line of the tractor in symmetric shape.

Table 3. *Layout of the study method for the three factors (fallow lands, sowing manners and sowing patterns)*

	Prose mode by seed spreader	Operat. code	Soil management by machines								Total no. of operat.
			Tillage operation			Seeding operation		Seed covering operation			
			Type of plow	Depth cm	Pass	Type of machine	Pass	Type of machine	Depth cm	Pass	
Spring plowed fallow land (F1)	Conventional (without overlap)	F1T1	Moldboard	25	1	Seed broadcaster	1	Moldboard	25	1	4
		F1T2	Moldboard	25	1	Seed broadcaster	1	Cultivator	15	1	4
		F1T3	Cultivator	15	1	Seed broadcaster	1	Cultivator	15	1	4
		F1T4	------		---	Seed broadcaster	1	Moldboard	25	1	3
		F1T5	------		---	Seed broadcaster	1	Cultivator	15	1	3
	Advanced technique with overlap	F1T1	Moldboard	25	1	Seed broadcaster	2	Moldboard	25	1	5
		F1T2	Moldboard	25	1	Seed broadcaster	2	Cultivator	15	1	5
		F1T3	Cultivator	15	1	Seed broadcaster	2	Cultivator	15	1	5
		F1T4	------		---	Seed broadcaster	2	Moldboard	25	1	4
		F1T5	------		---	Seed broadcaster	2	Cultivator	15	1	4
Fallow land without spring plowed (F2)	Conventional (without overlap)	F2T1	Moldboard	25	1	Seed broadcaster	1	Moldboard	25	1	3
		F2T2	Moldboard	25	1	Seed broadcaster	1	Cultivator	15	1	3
		F2T3	Cultivator	15	1	Seed broadcaster	1	Cultivator	15	1	3
		F2T4	------		---	Seed broadcaster	1	Moldboard	25	1	2
		F2T5	------		---	Seed broadcaster	1	Cultivator	15	1	2
	Advanced technique with overlap	F2T1	Moldboard	25	1	Seed broadcaster	2	Moldboard	25	1	4
		F2T2	Moldboard	25	1	Seed broadcaster	2	Cultivator	15	1	4
		F2T3	Cultivator	15	1	Seed broadcaster	2	Cultivator	15	1	4
		F2T4	------		---	Seed broadcaster	2	Moldboard	25	1	3
		F2T5	------		---	Seed broadcaster	2	Cultivator	15	1	3

http://www.aloki.hu ● ISSN 1589 1623 (Print) ● ISSN 1785 0037 (Online)
DOI: http://dx.doi.org/10.15666/aeer/1706_1273112751

Table 4. *Main features for all machines participated in the experiment*

Tractor/equipment	Mod.	Weight Kg	Working width m	Specification	Type	Linkage with tractor
Tractor (56 kW)	ITM/Iran	2812	-----	4-stroke-direct injection	4WD	------
Mouldboard plow	Unlu/Turkey	330	O.85	3 furrow	General purpose MB	Mounted
Cultivator	Unlu/Turkey	240	2	9 vertical spring tines	Duck feet	Mounted
Seed broadcaster	Solano/Spain	68	16	500 Lt/hopper	Mono disc	Mounted

In accordance with Clark and Evans (1954) both the tractor and the spreader were put in a stable state and spreading begun 30 m before trays row and continued to 40 m after trays row. The calibrating tests were repeated three times at the same tractor forward speed 7.1 Km/h. The collected seeds in each tray were recorded and weighed in order to determine the quantity and the uniformity of seeds distributed within the field. The collected seeds from each tray were put in a tube as represented in *Figure 2*. This calibration result is consistent with which confirmed by UMass Extension (2011) that, in centrifugal type broadcasters, material distributed in a fan like pattern that the intensive rates applied to the center of the spreader path while the application rates reduce to left and right of center and seems like a bell shape curve with distance of the scattered.

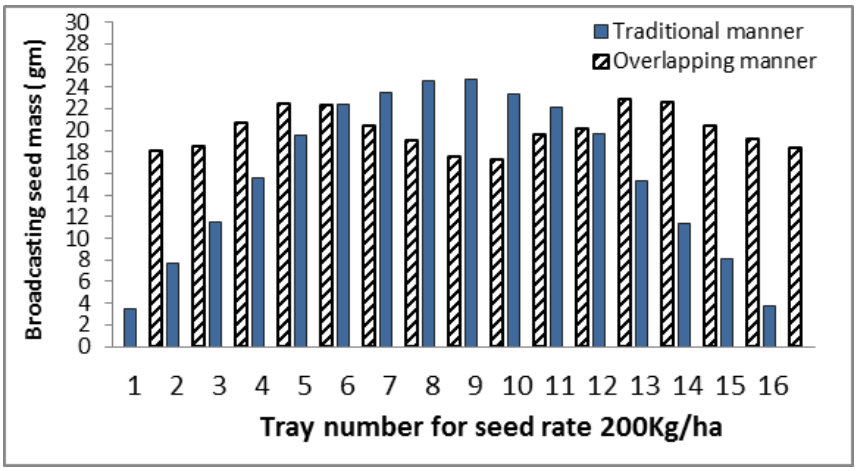

Figure 2. *Pattern of seed amounts distribution in each tray after broadcaster calibration on the seed rate of 200 Kg/ha*

To apply the advanced technique half-width method and half rate application for the seed broadcaster as overlap sowing mode in this study, another calibration was conducted in the same manner as the previously applied method that followed for sowing rate (200 Kg/ha) but this time for the rate of 100 Kg/ha (2500000 kernal/ha). This calibration started by the layout of 16 trays (the working width for the seed broadcaster as shown in *Fig. 2*) on a line perpendicular to the direction of tractor travel.

http://www.aloki.hu ● ISSN 1589 1623 (Print) ● ISSN 1785 0037 (Online)
DOI: http://dx.doi.org/10.15666/aeer/1706_1273112751

After achieving the correct amount of seeds per hectare, the "progressive" application method conducted in alternate directions, back and forth, as mentioned before and as illustrated in *Figure 1*. This method was replicated several times. The results were very satisfactory in terms of the homogenous distribution of seeds and quantity.

Selected forward speed for any tillage or covering operation in this experiment was 7.1 Km/h. The recorded data when the fallow land was plowed in spring by moaldboard were: the drawbar force was 11.526 KN on 25 cm depth at a forward speed of 7.05 Km/h at 15% soil moisture. These values have been used and added to the relevant equations to measure the studied parameters. Necessary information for all machinery contributed in the study had given in *Table 4* and *Figure 3*. The averages resulted from ANOVA analyses were compared by using Duncan's test.

Seed broadcaster | Moldboard plow | Field cultivator

Figure 3. *Machines used in the study*

Studied indicators

Since the machines used in this research include a heterogeneous working width, the calculation of the studied indicators was carried out on 1 m of machine width so as to avoid bias in favour of a specific treatment and to show the results more clearly and accurately. After measuring the results for each operation within each sowing pattern the total was calculated and adopted.

The coefficient of variance (C.V)

The percentage of mean value is the standard deviation in the form of a relative scale of dispersion. The following formula was used by Laghari et al. (2014) to measure the coefficient of variance:

$$CV\% = \frac{100 \times Sd}{\bar{x}} \qquad \text{(Eq.1)}$$

$$sd = \sqrt{\frac{1}{n} \sum_{i=1}^{n} (xi - \bar{x})^2} \qquad \text{(Eq.2)}$$

where:
CV = coefficient of variation
Sd = standard deviation
Xi = value of an individual observation
$\bar{x}$ = mean value of all observations

http://www.aloki.hu ● ISSN 1589 1623 (Print) ● ISSN 1785 0037 (Online)
DOI: http://dx.doi.org/10.15666/aeer/1706_1273112751

Total fuel consumption (L/ha).m^{-1}

The fuel consumption was measured according to the standard method followed by observing the fuel needed for traveling 40 m long distance for completing each sowing pattern using a graduated cylinder which was directly attached to the fuel tank as Sümer et al. (2010) suggested.

Total draft force (KN/m)

Total draft force was measured by using mechanical dynamometer Dillon type (10000 Kg) for each plot.

Total power bar losses due to slippage (KW/m)

It was found as the same equation followed by (Abdullah and Ghazwan, 2014).

$$PFT\,(KW) = \frac{(FT \times (VT - VP) \div 3.6)}{W} \qquad \text{(Eq.3)}$$

where:
PFT: drawbar power lost by slippage (KW/m)
VT: theoretical speed (Km/h).

Working time (H/Ha)/m

It is measured as mentioned by Moitzi (2013), Firas et al. (2016) and ASABE Standards (2016) by using the following formula:

$$WT = \frac{1}{\mathrm{C_{theo}}} \qquad \text{(Eq.4)}$$

$$\mathrm{C_{theo}} = \frac{W \times V_{avg} \times 0.1}{\mathrm{m}} \qquad \text{(Eq.5)}$$

where:
WT: time required for completing any Mechanical operation (H/Ha)/m
C_{theo}: field capacity (Ha/h)
V_{avg}: practical speed (Km/h)

Energy utilization efficiency (η) (m^3/Mj)

Measured by the equation that McKyes (1985), Muhsin (2017) and Abdullah and Ghazwan (2014) followed:

$$SR = \frac{F}{\mathrm{A}} \qquad \text{(Eq.6)}$$

$$A = \frac{Bp}{\mathrm{Dp}} \qquad \text{(Eq.7)}$$

http://www.aloki.hu ● ISSN 1589 1623 (Print) ● ISSN 1785 0037 (Online)
DOI: http://dx.doi.org/10.15666/aeer/1706_1273112751

where:
η: energy efficiency (M^3/Mj)
SR: the amount of force used by the shears on the unit area
F: force
A: area
Bp: working width
Dp: working Depth
m: unit of length (m)

Wheat yield (Kg/Ha)

For each plot, the yield was harvested by using thresher.

Total cost for each sowing pattern (T.C)

The total cost of any agricultural pattern was calculated separately on costs associated only with mechanical repair and maintenance, as well as fuel, lubricants and labour wages.

Results

The coefficient of variance (C.V):

Based on *Table 5*, the calculated result of the coefficient of variance (C.V) of seeding by traditional distribution was very high 48.4%, indicating that homogeneity of distribution was very bad compared to the intertwined mode of grain distribution which gave 9.2% of variance, because, the lower the coefficient of variation, the better the distribution.

Table 5. *The coefficient of variance (C.V) for spreading uniformity for the samples of seeds collected for each traditional and overlapping prose*

Sowing manner	Collecting trays number (working width of the spreader)																C.V %
	Right side scattering								Left side scattering								
	1	2	3	4	5	6	7	8	9	10	11	12	13	14	15	16	
CM	4.1	9.1	13.2	20.3	24.2	27.6	29.8	31.3	31.9	29.5	27.9	24.6	20.7	12.9	9.4	4.5	48.4
OM	18.1	18.6	20.7	22.5	22.4	20.5	19.1	17.6	17.4	19.7	20.2	22.9	20.7	20.5	19.2	18.4	9.2

CM- conventional mode, OM- overlapping mode

Effect of fallow land condition

As seen in *Table 6*, the fallow land condition clearly affected all studied parameters. The best averages were resulted by conducting mechanical operations on spring-plowed fallow land by: 23.80 (L/ha)/m, 11.22 kN/m, 2.72 kW/m and 5.29 (Hr/ha)/m for total fuel consumption, total draft need, power loss due to slippage and total time required respectively. These results differ from non-plowed land at spring with an increase of: 51.9%, 28.7%, 47.1% and 26.9% respectively. On the other hand, the fallow land that was non-plowed at spring, gave the highest averages compared to that plowed type land with percentages of 31.6% and 3.2% for both total energy utilization efficiency and total wheat production, respectively. The total cost spent on sowing the plowed fallow land at

http://www.aloki.hu ● ISSN 1589 1623 (Print) ● ISSN 1785 0037 (Online)
DOI: http://dx.doi.org/10.15666/aeer/1706_1273112751

spring was 8.56 USD/ha, which exceeds the cost spent on non-plowed land at spring by 30.2%.

Table 6. *Effect of fallow land condition on power requirements, total yield and total cost spent*

Fallow land condition	Tot. F.C (L/ha/)/m	Tot. draft kN/m	Tot. SDHp kW/m	Tot. W.t (Hr/ha)/m	Tot. E.U.E M^3/MJ/m*	Tot. wheat yield Kg/ha	Tot. cost USD/ha
F1	49.45 a	21.77 a	5.14 a	7.24 a	89.07 a	2809.36 a	8.56
F2	23.80 b	11.22 b	2.72 b	5.29 b	60.92 b	2620.78 b	5.98

*Means with similar letters in each row or column are non-significant at the 5% level (Duncan's test)

Effect of sowing mode

From the results of *Table 7*, the sowing method had no effect on most measured characteristics except for total energy utilized efficiency. The given results from conventional sowing method were 36.47 (L/ha)/m, 16.52 kN/m, 3.91 kW/m, 6.26 (Hr/ha)/m, 73.72 (M^3/MJ)/m and 2721.10 Kg/ha for the parameters total fuel consumption, total draft force, total power loss due to slippage, total working time, total energy utilization efficiency and total wheat yield, respectively. As well as, the averages from applying overlapped sowing mode were 36.78 (L/ha)/m, 16.47 kN/m, 3.95 kW/m, 6.26 (Hr/ha)/m, 76.27 (M^3/MJ)/m and 2809.10 Kg/ha for the studied indicators, respectively.

As observed in *Table 7* the reduction percent of values obtained from using conventional manner were: 0.8%, 1% and 0% for total fuel consumption, total power loss due to slippage and total working time. However, the value of the draft force resulted by using overlapping method decreased at a time when it was supposed to increase. The values of the averages resulted from using sowing manners are too close to each other, and the difference between them can be considered as the amount of power spent for applying the second travel of the seed spreader in overlapped method during conducting the half-swath width and half-seed application rate. It can be said, the amount of power consumed by the seed distributor is too small compared to that consumed by other machines used for tillage operation, especially, the moldboard plow. Therefore, in practice, the amount of power consumed by the seed distributor can melt between the relatively large variations in the frequency of power values consumed by tillage machines due to the difference of the two fallow land conditions. The highest proportion of energy used to complete the agricultural process is consumed by the plows (Larson and Clyma,1995).

Table 7. *Effect of sowing manner on power requirements, total yield and total cost spent*

Sowing modes	Tot. F.C (L/ha/)/m	Tot. draft kN/m	Tot. SDHp kW/m	Tot. W.t (Hr/ha)/m	Tot. E.U.E (M^3/MJ)/m*	Tot. wheat yield Kg/ha*	Tot. cost USD/ha
Conventional	36.47 a	16.52 a	3.91 a	6.26 a	73.72 b	2621.08 a	6.70
Overlapped	36.78 a	16.47 a	3.95 a	6.26 a	76.27 a	2809.06 b	7.84

*Means with similar letters in each row or column are non-significant at the 5% level (Duncan's test)

http://www.aloki.hu ● ISSN 1589 1623 (Print) ● ISSN 1785 0037 (Online)
DOI: http://dx.doi.org/10.15666/aeer/1706_1273112751

The highest amount of total energy utilization efficiency was73.72 (M^3/MJ)/m when conventional spreading applied, with an increase of 3.3% than in other applications. The total wheat production was 2809.06 Kg/ha when 7.84 USD/ha spent for applying overlapping mode of seed spreading with an increase of 7.17% than the yield resulted from using conventional method.

Effect of sowing patterns

The results in *Table 8* illustrate the averages of parameters studied that were affected by applying different sowing patterns. The lowest amounts for total fuel consumption, total draft force used, total power loss due to slippage and total working time were found by treating T5 pattern, which gave 20.33 (L/ha)/m, 9.37 kN/m, 2.08 kW/m and 5.05 (Hr/ha)/m respectively, with percent of 63.2%, 62%, 65.2% and 29.2% less than averages resulted from T1 treat. The draft force of Mouldboard plow was 78.6% more than the force needed to pull field cultivator. The reason of this increase is due to the variance of the resistance force of each machine during soil preparation which depends on many factors as Keller (2004) mentioned the draft requirement for each plow dependent on implement parameters; plowing depth, forward speed and soil strength.

As well as, the highest amount of total energy utilization efficiency and total wheat yield were 122.66 (M^3/MJ)/m and 2904.80 Kg/ha, respectively which resulted by applying the T3 system. While, the lowest amounts were: 73.1% and 13.9% less than the averages obtained by using T4 pattern. The lowest cost noted to complete sowing operation was 5.54 USD/ha spent on conducting T5 operation with a reduction of 38.6% than the highest cost which spent for conduct T1 treatment.

Table 8. *Effect of sowing patterns on studied power indicators, total yield and total cost*

Sowing patterns	Tot. F.C (L/ha/)/m	Tot. Draft kN/m	Tot. SDHp kW/m	Tot. W.t (Hr/ha)/m	Tot. E.U.E (M^3/MJ)/m*	Total wheat yield Kg/ha*	Total cost USD/ha
T1	55.28 a	24.68 a	5.98 a	7.13 a	66.81 c	2706.88 ab	9.02
T2	43.41 b	19.68 b	4.79 b	7.04 b	98.23 b	2877.95 a	8.17
T3	26.56 d	11.52 d	2.34 d	6.93 c	122.66 a	2904.75 a	7.28
T4	37.54 c	17.21 c	4.46 c	5.17 d	32.98 e	2500.68 b	6.34
T5	20.33 e	9.37 e	2.08 e	5.05 e	54.30 d	2585.10 b	5.54

*Means with similar letters in each row or column are non-significant at the 5% level (Duncan's test)

Effect of the fallow land condition and sowing modes interactive

The data are shown in *Table 9* indicate that there is a clear effect of the interaction between soil type and agricultural ethics on most of the characteristics involved. The averages produced by applying both traditional and overlapping seeding method for each of the studied parameters did not differ in either of the two fallow lands. Lower values were observed in the case of conducting conventional broadcasting on the non-spring plowed fallow land for fuel consumption, total draft, total power loss due to slippage and total working time were: 23.66 (L/ha)/m, 11.16 kN/m, 2.70 kW/m, 5.29 (Hr/ha)/m, 59.92 (M^3/MJ)/m and 59.92 (M^3/MJ)/m, respectively, with a reduction of 52.3%, 48.7%, 47.8%, 26.9% and 33.9% compared to the highest values resulted from overlapped spreading on spring plowed land. The increases of energy consumed are due to the fact of using extra tillage operation by moldboard at spring, The energy and draft

http://www.aloki.hu ● ISSN 1589 1623 (Print) ● ISSN 1785 0037 (Online)
DOI: http://dx.doi.org/10.15666/aeer/1706_1273112751

used for spring tillage at fallow land were more than in the case of only autumn plowing (Raper et al., 2000).

On the other hand, the interaction of studied factors had no effect on total wheat yield; the highest yield obtained was 2943.90 Kg/ha when the modern technique of seed scattering was adopted on the spring plowed land with total cost of 9.16 USD/ha. While, the minimum yield recorded was 2674.30 Kg/ha. The lowest spent cost appeared was 5.45 USD/ha when the sowing operation was done by applying a conventional mode on the non-plowed land at spring.

Table 9. *Effect of fallow land condition and sowing modes on studied power indicators, total yield and total cost*

Fallow land condition	Sowing mode	Tot. F.C (L/ha/)/m	Tot. draft kN/m	Tot. SDHp kW/m	Tot. W.t (Hr/ha)/m	Tot. E.U.E (M^3/MJ)/m*	Total wheat yield Kg/ha*	Total cost USD/ha
F1	Convent.	49.28 a	21.77 a	5.12 a	7.24 a	87.52 a	2674.86 a	7.96
	Overlap	49.62 a	21.77 a	5.17 a	7.24 a	90.61 a	2943.86 a	9.16
F2	Convent.	23.66 b	11.16 b	2.70 b	5.29 b	59.92 b	2567.30 a	5.45
	Overlap	23.93 b	11.27 b	2.74 b	5.29 b	61.93 b	2674.26 a	6.52

Effect of the interaction between fallow land condition and sowing patterns

Based on the results seen in *Table 10*, the interaction between the fallow lands condition and sowing pattern significantly affected all indicators included in the study. The lowest values for total fuel consumption, total draft, total power loss due to slippage and total working time by applying T5 operation either on F1T5 or on F2T5, were: 33.01 (L/ha)/m, 25.72 kN/m, 3.49 kW/m and 6.04 (Hr/ha)/m respectively, with: 51.5%, 49.4%, 50.2% and 25.4% less than the highest values obtained by applying T1 operation on each fallow land condition. While, the highest amount of total energy utilization efficiency was 138.74 (M^3/MJ)/m which was obtained from using F1T3 or F2T3 with an increase of approximately 67% than the amount resulted from using F1T4 or F2T4. The maximum total wheat production was 2977.82 Kg/ha obtained when F2T3 treatment was conducted, but, the minimum yield observed was 2473.18 Kg/ha by applying F1T4 treatment. The lowest cost was 4.17 USD/ha spent to complete the sowing operation of F2T5 by 60.3% less than the highest cost spent on using F1T1 treatment.

Effect of the interaction between sowing modes and sowing patterns

Table 11 refers to the significant effect of the interaction between sowing modes and sowing patterns on studied power indicators and total yield of wheat. The lowest values noticed for fuel consumption, total draft, total power loss due to slippage and total working time when the conventional sowing operation interacted with T5 treatment were 20.15 (L/ha)/m, 9.35 kN/m, 2.07 kW/m and 5.05 (Hr/ha)/m, respectively, the highest values were obtained by applying overlapped technique of seed spreading with T1 operation, that is 55.45 (L/ha)/m, 24.75 kN/m, 5.96 kW/m and 7.13 (Hr/ha)/m. The highest amount for total energy utilization efficiency was 125.43 (M^3/MJ)/m, observed at the interaction of overlapped sowing technique with T3 treatment by more than four times the average obtained by the interaction of T4 and overlapped seeding mode.

http://www.aloki.hu ● ISSN 1589 1623 (Print) ● ISSN 1785 0037 (Online)
DOI: http://dx.doi.org/10.15666/aeer/1706_1273112751

On the other hand, the maximum wheat production was 3097.50 Kg/ha, given by the interaction of T3 pattern and overlapped sowing technique. The lowest amount of wheat production was 2437.50 Kg/ha resulted from the interaction of T4 with conventional seeding mode. The lowest spent cost was recorded by applying T5 operation with conventional sowing method by a reduction of 39.4% than the cost spent to complete T1 treatment with conventional sowing.

Table 10. *Effect of the interaction between fallow land condition and sowing patterns on studied power indicators, total yield and total cost*

Fallow land condition	Sowing patterns	Tot. F.C (L/ha/)/m	Tot. draft kN/m	Tot. SDHp kW/m	Tot. W.t (Hr/ha)/m	Tot. E.U.E (M^3/MJ)/m*	Total wheat yield Kg/ha*	Total cost USD/ha
F1	T1	68.01 a	50.83 a	7.01 a	8.10 a	79.80 c	2782.75 ab	10.51
	T2	56.59 b	42.44 b	5.89 b	8.01 b	114.58 b	2991.10 a	9.44
	T3	39.54 d	29.59 d	3.69 d	7.90 c	138.52 a	2996.05 a	8.40
	T4	50.11 c	38.19 c	5.62 c	6.16 d	44.91 e	2581.65 ab	7.53
	T5	33.01 e	25.73 e	3.49 e	6.04 e	67.34 d	2695.25 ab	6.91
F2	T1	68.00 a	50.96 a	6.90 a	8.10 a	79.46 c	2631.00 ab	7.53
	T2	56.59 b	42.56 b	5.80 b	8.01 b	114.81 b	2764.80 ab	6.91
	T3	39.55 d	29.70 d	3.65 d	7.90 c	138.74 a	2813.45 ab	6.16
	T4	50.10 c	38.20 c	5.60 c	6.16 d	44.96 e	2419.70 b	5.16
	T5	33.01 e	25.72 e	3.49 e	6.04 e	67.39 d	2474.95 b	4.17

*Means with similar letters in each row or column are non-significant at the 5% level (Duncan's test)

Table 11. *Effect of the interaction between sowing manner and sowing patterns on studied power indicators, total yield, and total cost*

Sowing modes	Sowing patterns	Tot. F.C (L/ha/)/m	Tot. draft kN/m	Tot. SDHp kW/m	Tot. W.t (Hr/ha)/m	Tot. E.U.E (M^3/MJ)/m*	Total wheat yield Kg/ha*	Total cost USD/ha
Convent	T1	55.11 a	24.61 a	6.00 a	7.13 a	66.57 e	2591.30 abc	8.31
	T2	43.23 b	19.66 b	4.74 b	7.04 b	94.83 d	2847.50 abc	7.62
	T3	26.48 d	11.53 d	2.33 d	6.93 c	119.89 b	2712.00 abc	6.81
	T4	37.38 c	17.19 c	4.40 c	5.17 d	33.01 g	2437.50 c	5.74
	T5	20.15 e	9.35 e	2.07 e	5.05 e	54.31 f	2517.10 bc	5.04
Overlap	T1	55.45 a	24.75 a	5.96 a	7.13 a	67.05 e	2822.45 abc	9.74
	T2	43.59 b	19.71 b	4.85 b	7.04 b	101.64 c	2908.40 abc	8.73
	T3	26.64 d	11.52 d	2.35 d	6.93 c	125.43 a	3097.50 a	7.75
	T4	37.70 c	17.22 c	4.51 c	5.17 d	32.95 g	2563.85 bc	6.95
	T5	20.50 e	9.40 e	2.09 e	5.05 e	54.28 f	2653.10 abc	6.04

Effect of interaction between fallow land condition, sowing modes and sowing patterns

The averages of most of the characteristics shown in *Table 12* were significantly affected by the interaction of the studied factors, where, the highest values were

http://www.aloki.hu ● ISSN 1589 1623 (Print) ● ISSN 1785 0037 (Online)
DOI: http://dx.doi.org/10.15666/aeer/1706_1273112751

recorded from the interaction of F1, overlapped spreading and T1 operation, that is 68.19 (L/ha)/m, 29.64 kN/m, 7.02 kW/m and 8.10 (Hr/ha)/m for studied power indicators: total fuel consumption, total draft, total power loss due to slippage and total working time respectively, with an increase of 89%, 87.6%, 90.6% and 49.8% compared to the lowest values obtained from F1, overlapped sowing manner and T1 operation interaction. The highest amount of total energy utilization efficiency and total wheat yield were 141.57 (M^3/MJ)/m and 3235.00 Kg/ha resulted from applying F1, overlapped seeding mode and the T3 interaction. While, the lowest amount for both indicators were 21.05 (M^3/MJ)/m and 2399.50 Kg/ha respectively, which were observed when F2, conventional seeding mode and the T4 interacted. The lowest total cost was spent for conducting F2, conventional seed prosing and T5 operation interaction resulted in 3.71 USD/ha, which was less by 67.3% than the highest cost which spent for completing F1, overlapped spreading manner and T1 treatment interaction.

Table 12. *Effect of interaction between fallow land condition, sowing modes and sowing patterns on studied power indicators, total yield and total cost*

Fallow land cond.	Sowing mode	Sowing pattern	Tot. F.C (L/ha/)/m	Tot. draft kN/m	Tot. SDHp kW/m	Tot. W.t (Hr/ha)/m	Tot. E.U.E (M^3/MJ)/m*	Total wheat yield Kg/ha*	Total cost USD/ha
F1	Convent	**T1**	67.84 a	29.63 a	7.01 a	8.09 a	79.42 d	2631.80 bc	9.68
		T2	56.40 b	24.75 b	5.85 bc	8.01 b	110.60 c	2913.50 abc	8.87
		T3	39.38 e	17.03 e	3.68 fg	7.90 c	135.47 a	2757.10 abc	7.93
		T4	49.95 c	22.44 c	5.57 d	6.15 d	44.96 g	2475.50 bc	6.93
		T5	32.82 f	15.00 f	3.48 gh	6.04 e	67.17 e	2596.40 bc	6.37
	Overlap	**T1**	68.19 a	29.64 a	7.02 a	8.10 a	80.57 d	2933.70 abc	11.34
		T2	56.78 b	24.75 b	5.94 b	8.01 b	118.56 b	3068.70 abc	10.00
		T3	39.71 e	17.02 e	3.71 f	7.90 c	141.57 a	3235.00 ab	8.87
		T4	50.26 c	22.44 c	5.68 cd	6.16 d	44.85 g	2687.80 abc	8.13
		T5	33.19 f	15.00 f	3.49 gh	6.04 e	67.51 e	2794.10 abc	7.45
F2	Convent	**T1**	42.38 d	19.59 d	4.98 e	6.16 d	53.72 f	2550.80 bc	6.93
		T2	30.07 g	14.57 f	3.62 fg	6.07 e	79.05 d	2781.50 abc	6.37
		T3	13.58 i	6.02 h	0.99 j	5.96 f	104.31 c	2666.90 bc	5.68
		T4	24.81 h	11.94 g	3.23 i	4.18 g	21.05 h	2399.50 c	4.55
		T5	7.49 j	3.69 i	0.66 k	4.07 h	41.45 g	2437.80 c	3.71
	Overlap	**T1**	42.71 d	19.86 d	4.90 e	6.16 d	53.53 f	2711.20 abc	8.13
		T2	30.40 g	14.67 f	3.75 f	6.07 e	84.72 d	2748.10 abc	7.45
		T3	13.58 i	6.02 h	1.00 j	5.96 f	109.29 c	2960.00 abc	6.63
		T4	25.14 h	12.01 g	3.34 hi	4.19 g	21.06 h	2439.90 c	5.76
		T5	7.82 j	3.80 i	0.69 k	4.06 h	41.05 g	2512.10 bc	4.63

*Means with similar letters in each row or column are non-significant at the 5% level (Duncan's test)

Discussion

From Table 5

The high percentage of coefficients of variance obtained from the traditional method of grain dispersion is due to the poor distribution of grains by rotatory type spreader as referred by most relevant research (Laghari et al., 2014). The reason of the variance may be that in centrifuge type of spreader, the grain is scattered by centrifugal force

http://www.aloki.hu ● ISSN 1589 1623 (Print) ● ISSN 1785 0037 (Online)
DOI: http://dx.doi.org/10.15666/aeer/1706_1273112751

which pushes those falling seeds out in all directions and far away from the center of the rotation, except the side behind the driver, where they fall on the ground near the distribution center which causes an increase in the number of grains compared to places far from the center. This fact is consistent with what was confirmed by Sanaeifar and Sheikhdavoodi (2012). While, the C.V values resulting from the use of the overlap method were much better, which serves as an evidence of the good distribution of seeds that affect the equal growth opportunities between plants and increase production (Herbek and Lee, 2009).

Table 6

The large difference between the results obtained from the two land types is due to the added values from plowing by MB at spring. These results encourage farmers to leave their fallow land in unplowed condition, to reduce input costs with less effort, they (the farmers) don't know, that spending extra few dollars (2.58 USD/ha) will generate more money by selling the difference of the yield results from the two lands types. This is confirmed by Moitzi (2013).

Table 7

Although there is no significant effect of sowing mode on the studied indicators, however, there are slight differences observed in their averages. In fact, these differences represent the value of the second traffic of the broadcaster during applying the overlapped technique of prose lines as observed in fuel consumption, power losses due to slippage and total cost of 1.14 USD/ha, which led to increase the wheat production by 3.1%. The increase in the yield was due to the homogenous distribution of the seeds, which has led to equal access for food sources, this is confirmed by Herbek and Lee (2009).

Results presented in Table 8

The reasons of the increases in the total amounts measured by using T1 treatment for most indicators compared to other treatments, is due to the large variation of soil resistance force towards differences of number of passes, operation depths and equipment shears as mentioned in *Table 3*. Therefore, farmers tend to apply a few tillage practices than conventional tillage to reduce the energy requirements associated with a low cost, as confirmed by Kumar et al. (2013).

The obtained wheat production by applying T3 pattern was more by: 11%, 13.9%, 0.9%, and 6.8% than applying T5, T4, T2 and T1 treatments, respectively. The reason of these variations of wheat yield is due to the suitable management of the soil which mean available seed-soil contact, which affects positively the soil physical and chemical properties in comparison to other practices, as mentioned by Strudley et al. (2008).

Table 9

As noticed from the averages, the interaction between the fallow land condition and sowing modes had a clear effect, at a time when the seeding manner had no effect on the measured characteristics, as illustrated in *Tables 9* and *8*. That means the effect of the fallow land condition is much greater than that of the sowing technique.

http://www.aloki.hu ● ISSN 1589 1623 (Print) ● ISSN 1785 0037 (Online)
DOI: http://dx.doi.org/10.15666/aeer/1706_1273112751

Table 10

Applying minimum mechanical operation on each of spring plowed fallow land and non-plowed fallow land at spring gives minimum power consumption with lower cost in comparison to applying other tillage systems, which was also pointed by Broder et al. (1984) and Çarman et al. (2013).

Table 11

The lowest power needs and cost spent can be resulted by conducting T5 treatment with conventional sowing mode. The apparent variation in each sowing pattern in term of the number of operations, operation depth and difference of machines typically used in each agricultural process are the main reasons for the large variances between averages obtained from the overlapped factors, this is what Muazu et al. (2015) pointed out.

Table 12

The lowest power measurements and total cost need to be achieved by applying the sowing practice T5 with conventional or overlapped spreading technique on the unplowed fallow land at spring compared to the highest values resulted from using T1 operation on spring plowed fallow land. The reason for these wide variations is due to the differences in a number of operations applied, machine types and tillage depths.

In the spring, plowing operation killed a high percentage of weeds and insects, made the soil softer in terms of energy consumption and a more suitable environment was created for seed growth at the fall season than in the case of unplowed fallow land. The reduced tillage (T3), leaves more coverage of plant residues than using conventional tillage (Botta et al., 2006 and Kahloon et al., 2012). Also, the application of the overlapped seeding method was appropriate in obtaining the highest wheat production, This is consistent with what Mergani (2006) has indicated. Therefore, the growers must apply reduced tillage (T3) to minimize soil stress and to increase the yield.

Conclusion

The results obtained from the experiment can lead to the following conclusions

Applying sowing patterns on unplowed fallow land at spring gives lower power requirements and costs spent on wheat production as compared to spring-plowed fallow land cultivation, except, the total yield becomes less. Adoption of the overlapped mode of seed distribution by the broadcaster is better than applying the conventional technique to obtain high wheat production, despite the increased energy consumption and the slight increase in costs.

The lowest power consumption can occur by using conventional sowing plus field cultivator for covering the distributed seeds, and the highest power needs are occurred by excessive tillage. The recommendation is to apply reduced tillage with field cultivator for both tillage and seeds covering operations which results in the highest wheat production with acceptable cost and energy consumed. The effect of the fallow land condition is much greater than that of the sowing technique factor on the studied characteristics. Reducing a number of traffic reduces power spent and total cost.

http://www.aloki.hu ● ISSN 1589 1623 (Print) ● ISSN 1785 0037 (Online)
DOI: http://dx.doi.org/10.15666/aeer/1706_1273112751

Exploiting a spring-plowed fallow land by conventional tillage is more expensive than applying reduced tillage system on unplowed fallow land at spring.

For future experiments the followings are suggested:

1. Using other sowing patterns which include other implements for soil tilling and covering the seeds which may give good results affect the plant growth. For example, Chisel plow plus disc harrow or, rototiller plus field cultivator.

2. Comparing the performance of twin disc type seed spreader with mono disc type through the coefficient of variance measurement which is an important factor for increasing the crop production.

3. We recommend testing further experiments on the uniformity of the seeds distribution on the soil by using both seed drill and broadcaster with overlapped lines mode and comparing the results.

4. Taking into account using different speeds and heights of the rotating disc from the ground and the forward speeds of the tractor, which are important factors affecting the ratio of the uniformity of seed spreading.

5. Studying the effect of the number of machines passes on the soil compaction and its reflection on roots, seed germination, plant growth and total yield.

REFERENCES

[1] Abdullah, A. A., Ghazwan, A. D. (2014): Studying locally made Mouldboard plow shares performance and its effect on some power requirements and plowing criteria. – Mesopotamia J. of Agric. 42 (1):14-20.

[2] ASABE Standard (2016): Annual International Meeting, Paper No. 162461746. – ASABE, St. Joseph, MI, pp. 1-18. DOI: 10.13031/aim.20162461746.

[3] ASAE Standards (1999): S341.2. Procedure for Measuring Distribution Uniformity and Calibrating Granular Broadcast Spreaders. 46th Ed. – ASAE, St. Joseph, MI.

[4] Asheesh, M., Vikas, K., Saurabh, S., Amit, K. (2017): Performance evaluation of strip-till seed drill for wheat. – International Journal of Scientific & Engineering Research 8(7): 2229-5518.

[5] Askari, M., Khalifahamzehghasem, S. (2013): Draft force inputs for primary and secondary tillage implements in a clay loam soil. – World Applied Sciences Journal 21(12): 1789-1794.

[6] Bai, Y., Chen, F., Li, H., Chen, H., He, J., Wang, Q., Gong, Y. (2008): Traffic and tillage effects on wheat production on the Loess Plateau of China: 2. Soil physical properties. – Soil Research 46(8): 652-658.

[7] Bashir, M. A., Dawelbeit, M. I., Eltom, M. O., Tanakamaru, H. (2015): Performance of different tillage implements and their effects on sorghum and maize grown in Gezira Vertisols, Sudan. – International Journal of Scientific & Technology Research 4(4): 237-242.

[8] Botta, G. F., Jorajuria, D., Rosatto, H., Ferrero, C. (2006): Light tractor traffic frequency on soil compaction in the Rolling Pampa region of Argentina. – Soil and Tillage Research 86(1): 9-14.

[9] Brennan, E. B., Leap, J. E. (2014): A comparison of drill and broadcast methods for establishing cover crops on beds. – Hortscience 49(4): 441-447.

[10] Broder, M. W., Doran, J. W., Peterson, G. A., Fenster, C. R. (1984): Fallow tillage influence on spring populations of soil nitrifiers, denitrifiers, and available nitrogen. – Soil Sci. Soc. Am. J. 48: 1060-1067.

http://www.aloki.hu ● ISSN 1589 1623 (Print) ● ISSN 1785 0037 (Online)
DOI: http://dx.doi.org/10.15666/aeer/1706_1273112751

[11] Çarman, K., Marakoğlu, T., Gür, K. (2013): Alternative tillage and direct seeding systems on wheat production in Middle Anatolia. – 2013 International Conference on Agriculture and Biotechnology, Kuala Lumpur.
[12] Clark, P. J., Evans, F. C. (1954): Distance to nearest neighbors as a measure of spatial relationships in population. – Ecology 35(3): 445-453.
[13] Colvin, T. S., Turner, J. H. (1980): Applying Pesticides. – AAVIM, Athens, GA.
[14] Firas, S., Matthew, J., Benjamin, R., Levi, J. (2016): The performance of farm tractors as reported by CAN-BUS measures. – An ASABE Meeting Presentation, Paper Number: 162461746. DOI: 10.13031/aim.20162461746.
[15] Forristal, D., Teagasc, O. P. (2017): Precise application of fertiliser. The Irish Agriculture and Food Development Authority, FAI meeting, Technical Bulletin Series No. 3. – http://www.fertilizer-assoc.ie/publications/technical-bulletins/.
[16] Greb, B. W. 1979: Reducing drought effects on croplands in the west central Great Plains. – Info. Bull. No. 420, U. S. Dept. Agric, Washington, DC.
[17] Hanna, M. (2016): Estimating the field capacity of farm machines. – Ag Decision Maker Information Files. 8. http://lib.dr.iastate.edu/pubs_agdm/8.
[18] Hassann, M. M., Khater, I. M., YŞar, B. (2009): Effect of field size on mechanical wheat seeder performance in reclaimed lands of Egypt. – Tarım Makinaları Bilimi Dergisi 5(1): 45-51.
[19] Herbek, J., Lee, C. (2009): A Comprehensive Guide to Wheat Management in Kentucky. – University of Kentucky College of Agriculture, Lexington, and Kentucky State University, Frankfort.
[20] Houk, M. J. (2009): Conservation planting methods for native and introduced species. – Plant Materials Technical Note No. 14. United States Department of Agriculture Natural Resources Conservation Service. http://www.nrcs.usda. gov/ Internet /FSE_PLANTMATERIALS/publications/lapmctn9048.pdf (accessed 24 February 2014).
[21] Kahloon, M. H., Iqbal, M. F., Farooq, M., Ali, L., Fiaz, M., Ahmad, I. (2012): A comparison of conservation technologies and traditional techniques for the sowing of wheat. – J. Anim. Plant Sci. 22(3): 827-830.
[22] Keller, T. (2004): Soil compaction and soil tillage - studies in agricultural soil mechanics. – Ph. D. thesis at the Swedish University of Agric. Sciences, Uppsala.
[23] Laghari, M., Laghari, N., Shah, A. R., Chandio, F. A. (2014): Calibration and performance of tractor mounted rotary fertilizer spreader. – International Journal of Advanced Research 2(4): 839-846.
[24] Kumar, V., Saharawat, Y. S., Gathala, M. K., Jat, A. S., Singh, S. K., Chaudhary, N., Jat, M. L. (2013): Effect of different tillage and seeding methods on energy use efficiency and productivity of wheat in the Indo-Gangetic Plains. – Field Crops Research 142: 1-8.
[25] Lan, Y., Kocher, M. F., Smith, J. A. (1999): Opto-electronic sensor system for laboratory measurement of planter seed spacing with small seeds. – Journal of Agricultural Engineering Research 72(2): 119-127.
[26] Larson, D. L., Clyma, H. E. (1995): Electro-osmosis effectiveness in reducing tillage draft force and energy forces. – Transactions of ASAE 38: 1281-1288.
[27] McKyes, E. (1985): Soil Cutting and Tillage. 1st. Ed. – Elsevier, Amsterdam.
[28] Mergani, S. (2006): Evaluation of some land preparation and sowing methods for wheat production in a northern state (Dongola area) Sudan. – Thesis, Department of Agricultural Engineering, Faculty of Agriculture, University of Khartoum.
[29] Moitzi, G., Szalay, T., Schüller, M., Wagentristl, H., Refenner, K., Weingartmann, H., Liebhard, P., Boxberger, J., Gronauer, A. (2013): Effects of tillage systems and mechanization on work time, fuel and energy consumption for cereal cropping in Austria. – Agric Eng Int: CIGR Journal 15(4): 94-101.
[30] Muazu, A., Yahya, A., Ishak, W. I. W., Khairunniza-Bejo, S. (2015): Analysis of fuel consumption and carbon dioxide emission in direct seeding wetland rice cultivation

http://www.aloki.hu ● ISSN 1589 1623 (Print) ● ISSN 1785 0037 (Online)
DOI: http://dx.doi.org/10.15666/aeer/1706_1273112751

systems in Malaysia. – Research Journal of Applied Sciences, Engineering and Technology 11(3): 281-292.
[31] Muhsin, S. J. (2017): Determination of energy requirements, plowed soil volume rate and soil pulverization ratio of chisel plow under various operating conditions. – Basrah Journal of Agricultural Sciences 30(1): 73-84.
[32] Oyewole, C. I., Magaji, M. D., Falaki, M. (2001): Effects of sowing method and rodent control on plant establishment, growth and grain yield of two varieties of wheat (Triticum aestivum L.). – J. Agric. Environ. 2(2): 233-241.
[33] Parish, L. R. (1999b): Granular Spreaders: Selection, Calibration, Testing and Use. – Louisiana Agricultural Experiment Station, Louisiana State University.
[34] Parish, R. L. (1986): Evaluation of two methods of fertilizer spreader pattern correction. – Transactions of the ASAE 29(2): 370-373.
[35] Raper, R. L., Reeves, D. W., Burmester, C. H., Schwab, E. B. (2000): Tillage depth, tillage timing, and cover crop effects on cotton yield, soil strength, and tillage energy requirements. – Applied Engineering in Agriculture 16(4): 379.
[36] Sanaeifar, A., Sheikhdavoodi, M. J. (2012): Evaluating of broadcasting uniformity of centrifugal and oscillating granular broadcasters. – Research Journal of Applied Sciences, Engineering and Technology 4(15): 2460-2468.
[37] Soomro, U. A., Rahman, M. U., Odhano, E. A., Gul, S., Tareen, A. Q. (2009): Effects of sowing method and seed rate on growth and yield of wheat (Triticum aestivum). – World Journal of Agricultural Sciences 5(2): 159-162.
[38] Speelman, L. (1979): Features of a Reciprocating Spout Broadcaster in the Process of Granular Fertilizer Application. – H Veenman & Zonen, Wageningen.
[39] Strudley, M. W., Green, T. R., Ascough, J. C. (2008): Tillage effects on soil hydraulic properties in space and time. – Soil Tillage Res. 99: 4-48.
[40] Sumer, S. K., Kocabiyik, H., Say, S. M., Cicek, G. (2010): Comparisons of 540 and 540e PTO operations in tractors thr laboratory tests. – Bulgarian Journal of Agricultural Science 16(4): 526-533.
[41] Svensson, J. E. T. (1990): Pneumatic Fertilizer Spreaders. A Review of the Literature. – Technical Report. Dept. of Energy and Technology, Uppsala.
[42] UMass Extension (2011): Rotary Spreader Calibration Procedures. – Center for Agriculture, United States Department of Agriculture, Washington.
[43] Wuest, S., Albrecht, B. S. L., Skirvin, K. W. (1999): Vapor transport vs. seed-soil contact in wheat germination. – Agronomy Journal 91: 783-787.
[44] Zengin, M., Ocakoğlu, F. (2013): Effects of different tillage and fallow methods on Wheat yield and soil quality. – Romanian Agricultural Research 30: 191-198.
[45] Zewdu, A. D. (2008): Simulation of Tef seed broadcasting. – Agricultural Engineering International: CIGR Journal 10: 1-14.

http://www.aloki.hu ● ISSN 1589 1623 (Print) ● ISSN 1785 0037 (Online)
DOI: http://dx.doi.org/10.15666/aeer/1706_1273112751

EFFICACY OF POSTEMERGENCE HERBICIDES FOR CONTROLLING CURLED DOCK (*RUMEX CRISPUS* L.) IN WHEAT CROPS

IQBAL, M. F.[1,3] – SHAD, G. M.[2] – FENG, Y. L.[1*] – LIU, M. C.[1] – WANG, S.[1] – LU, X. R.[1] – IQBAL, Z.[4] – TARIQ, M.[5]

[1]*College of Bioscience and Biotechnology, Shenyang Agricultural University No. 120 Dongling Road, Shenyang, Liaoning Province 110866, China*

[2]*Department of Pest Warning and Quality Control of Pesticides, Gujrat, Pakistan*

[3]*Department of Agriculture, Adaptive Research Station Sialkot, Punjab-Pakistan*

[4]*University of Veterinary and Animal Sciences, Sub-campus, Narowal, Punjab, Pakistan*

[5]*Department of Entomology, PMAS-Arid Agriculture University, Rawalpindi, Pakistan*

**Corresponding author*
e-mail: yl_feng@tom.com; phone: +86-24-8848-7163; fax: +86-24-8849-2799

(Received 29th Apr 2019; accepted 11th Jul 2019)

Abstract. Curled dock (*Rumex crispus* L.) is a common perennial toxic weed species in wheat crop. To our knowledge, this is the distinctive scientific study proposed to evaluate the efficacy of four new chemical combinations of herbicides viz. Starane-M @ 750 ml ha^{-1}; Clean Wave @ 800 ml ha^{-1}; Broad-X @ 875 ml ha^{-1} and Allymax @ 35 g ha^{-1} sprayed as foliar application in wheat crop. These applications conducted with control treatment for proper comparison. Results illustrated that broad-X afforded highly significant ($P < 0.001$) potential for controlling this weed resulting in strong positive R^2 (0.84) with RMSE (0.69 & 0.80) compared to clean wave proved the evidence for model fitness. Significant ($P < 0.01$) mortality of curled dock catalyzed by mist spraying of broad-X (91.16%; 91.55%) conferred better control efficacy 30 days after treatment. Significant ($P < 0.001$) increase in yield (33.29%) was observed as a consequent of spraying broad-X followed by clean wave (29.63%) herbicides. The interaction of leaf area (cm^2) with herbicides correlated as predicted, which indicated that manual quantification method is suitable. The productivity increased significantly by spraying broad-X (33.29%) and clean wave (29.63%) compared to control. According to our findings, the new chemical herbicides obtained a high potential for controlling this invasive weed in wheat crops.
Keywords: *broadleaves weed, mortality, quantification, weed yield interaction, Gujrat, Punjab, Pakistan*

Introduction

Being a significant bellicose weed, curled dock (*Rumex crispus* L.) belongs to Polygonaceae family, native to South-East Asia (Schuster et al., 2015) and now has become a severe problem in irrigated wheat ecosystems in Gujrat, Punjab-Pakistan. *Rumex obtusifolius* is another species of this family present in arable soils (Marshall et al., 2003); however, broadleaf dock (*R. dentatus*) density was present in different locations of Dera Ismail Khan (Marwat et al., 2013). Weed competition has become a significant discretion in limiting the yield of any crop (Siddiqui and Bajwa, 2010). Weeds fight with the crop for the place, fluorescence, moisture, nutrient and reduce the yield (Shehzad et al., 2013). Weeds can infest any ecosystems; therefore, researchers focus on how to weed diversity affect crop yield (Davis et al., 2009).

http://www.aloki.hu ● ISSN 1589 1623 (Print) ● ISSN 1785 0037 (Online)
DOI: http://dx.doi.org/10.15666/aeer/1706_1275312767

Herbicide resistance created many problems (Délye et al., 2013a) in response to its numerous applications across many years (Moss et al., 2019). Herbicide resistance alleles create pleiotropic effects on a weed's life cycle (Délye et al., 2013b). The rising figure of resistant weed biotypes is a critical fear for agriculture as no new herbicide mode of action has been marketed for over 30 years (Duke, 2012; Westwood et al., 2018).

Further, as pointed out that the effectiveness of herbicides depends upon the proper time of application, dose and selectivity of herbicides (Steckel et al., 1997), high weeds intensity and competition cause maximum reduction in yield (Chaudhry et al., 2008; Dalley et al., 2006). Weeds account for a significant 37-50% reduction in yield (Nayyar et al., 1994; Waheed et al., 2009) among them curled dock is a significant pest of many agriculture crops that not only reduce and also spoil the quality of the produce. Its control measures are ineffective in most of the plants due to the taproot system (Zaller, 2004a, b). High weeds intensity and competition with crops affected negatively reducing the yield of wheat crops (Dalley et al., 2006).

The weed infestations suppress the quality and quantity of crops; directly effects on economic and increasing the chance of spreading diseases (Marwat et al., 2008). Ecological surveys carried out in different areas of Pakistan revealed that curled dock seeds are prolific (Qureshi et al., 2009). Curled dock germinated from seed but also regenerate from the underground part of roots (Zaller, 2004b; Zimdahl, 2018).

The negligence factor considered a vital role responsible for weed infestation; hence, there is a dire need to develop effective management policies. However, researchers would focus on intensity, competition between weed ecosystem and appropriate application of proper new chemical herbicides are essential factors in determining the yield losses. The researchers would adopt better weed management strategies (WMS) for controlling this invasive weed in the ecosystem of Pakistan (*Fig. 1*).

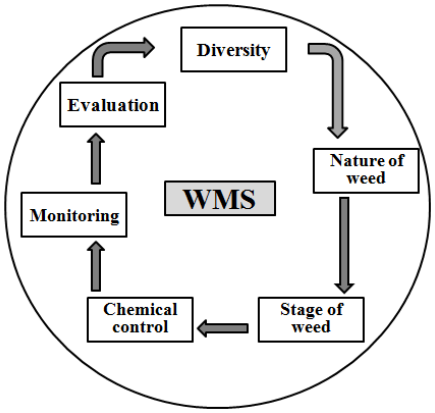

Figure 1. *Weed management strategies (WMS) for controlling curled dock*

The experiment suggested that the habitat of curled dock is annual present at roadsides, near the bank of ponds and non-cropped areas. In the arable areas, invasive weeds easily controlled by herbicides compared to agricultural lands (Crone et al., 2009). Nevertheless, in the present scenario curled dock (*Rumex crispus* L.) species shifted from non-cropped fellow lands to wheat crops, which creates alarming situations for researchers. This distinctive study aimed to screen out the best one herbicide for effective weed control, ensure better management and ultimately increasing the yield of

http://www.aloki.hu ● ISSN 1589 1623 (Print) ● ISSN 1785 0037 (Online)
DOI: http://dx.doi.org/10.15666/aeer/1706_1275312767

the wheat crops. The hypothesis integrated that curled dock could control by foliar application of a mixture of two herbicides except one. Due to its hard phenotypic nature, new chemical combinations of herbicides tested for examining its better management. To sum up, the overall study planned to evaluate the response of new combinations of chemicals available in the market of Punjab, Pakistan. These chemicals sprayed to control curled dock according to its maximum abundance in wheat crops selected after extensive survey at different locations at Gujrat, Punjab-Pakistan during two consecutive years.

Materials and methods

Study sites

Table 1 shows two years of study designed after extensive field survey in Gujranwala division in order to evaluate the efficacy of four newly introduced combinations of herbicides for controlling Curled dock in wheat crop compared to control.

Table 1. *List of herbicides used in the study*

Chemical name	Trade name	Rate (g ai ha^{-1})	Chemical family	Dose (ml ha^{-1})
Control	Control	-	-	-
Fluroxypyr + MCPA	Starane-M	239 + 956	Phenoxy acetic acid	750
Fluroxypyr + Aminopyralid + MCPA	Clean Wave	350 + 25 + 956	Phenoxy acetic acid	800
Fluroxypyr + Clopyralid + MCPA	Broad-X	199.75 + 300 + 799.25	Pyridine carboxylic acid	875
Metsulfuron + Tribenuron	Allymax	357.5 + 357.5	Sulfonylurea	35 g

g = gram, ai = active ingredient, ha^{-1} = per hectare, ml = millilitre

The authors selected different sites in two villages of Tehsil Gujrat and Kharian in our experiments where the maximum abundance of this toxic weed recorded in wheat crops during 2015-16 and 2016-17 (*Fig. 2*).

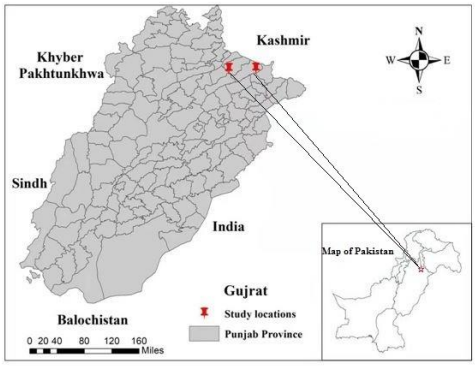

Figure 2. *ArcGIS map showing experimental sites in District Gujrat, Punjab-Pakistan*

http://www.aloki.hu ● ISSN 1589 1623 (Print) ● ISSN 1785 0037 (Online)
DOI: http://dx.doi.org/10.15666/aeer/1706_1275312767

Experimental outline

The trial was exhibited by randomized complete block design (RCBD) with three replications having the net plot size for all treatments were 65 × 60 m, but for each treatment, the area designed was 13 × 20 m. Each plot or block was separated clearly by making paths (Dalga et al., 2014), and the experiment repeated in time, keeping in view the abundance of the curled dock. The wheat variety Faisalabad-2008 was cultivated in well-prepared soil using seed @ 125 kg ha^{-1} collected from Punjab Seed Corporation, Gujranwala. Di-ammonium Phosphate (DAP) 125 kg ha^{-1} and K_2O (SOP) @ 62 kg ha^{-1} were applied as a basal dose after planking by drilling method on last week of November each year. The wheat crops irrigated 30 days after cultivation and urea broadcasted uniformly in the field @ 125 kg ha^{-1}.

Foliar application

Herbicides sprayed at proper moist conditions with manually operated Knapsack hand sprayer with required spray and volume of water kept up to 300 L ha^{-1} using T-Jet nozzle with a droplet size of 225 µm and a fine mist of 2 PSI 45 days after sowing.

Data collection

The data collected randomly by quadratic ring using the diagonal method at three different locations in each treatment. The total populations of curled dock recorded before foliar application from each block/treatment. The wheat crop visited fifteen (15) days after applications, counted weed populations, and the same procedure adopted at the interval of 30 days each year, however, the experimental field monitored throughout the growing season. The mortality (%) of weed calculated (Alvi et al., 2004).

Leaf area measurement

Leaves from each treatment collected randomly for leaf area determination. These leaves placed on a white rectangular sketch of the whiteboard, calculated the leaf length (cm) and a maximum width of the leaf and multiplied by a constant value, i.e. 0.75 (Montgomery, 1911; Ahmad et al., 2015; Aldesuquy et al., 2014).

Root length measurement

At the time of harvesting, the root length (cm) of different treated plots calculated by measuring tape. The stems removed from the top portion of roots by a knife of each randomly selected plant. The total root length area from top to bottom measured compared to control (*Fig. 3*).

Figure 3. *Comparison of treated with control roots of curled dock*

http://www.aloki.hu ● ISSN 1589 1623 (Print) ● ISSN 1785 0037 (Online)
DOI: http://dx.doi.org/10.15666/aeer/1706_1275312767

Collection of yield data

At the time of harvesting of wheat crops, yields recorded randomly from three positions of each treatment with 1 m^2 quadratic rings. Wheat plants were then removed manually by sickles from these rings and harvested these with mini thresher and assessed grain yield (Scursoni et al., 2011).

Statistical analysis

The data anatomized statistically by analysis of variance in Duncan's Multiple Range test with $P > 0.05$ level of probability. The analysis performed by SPSS 13.0 (Inc.) software and interaction between the observed and predicted variables by using R package, version 3.5.2. (MuMin, 2018) moreover, graphical representations were framed on Sigma-Plot 10 software (Iqbal et al., 2018).

Model validation

The coefficient of determination relationship conceded out for developing the model for leaf area versus herbicide treatments and comparison of R^2 and RMSE. This model was set out to determine the effectiveness of leaf area (cm^2), and root length (cm) ultimately provide the information concerning model fitness of how far away the fitted line is from the reference line. The researchers previously exposed how condensed or scattered the observed values are around the fitted line, which alternatively revealed about the validity and model fitness (Hossain et al., 2017). RMSE used to evaluate the performance of the model in the curled dock: chemical herbicides (Debaeke et al., 1997; Ahmed et al., 2019).

Results

Effect of herbicides on mortality

The effect of herbicides on mortality of curled dock (30 DAS) progression and analysis of variance resulted year wise comparison stated highly significant ($P < 0.01$) mortality (91.16%) by Broad-X with standard deviation (SD = 1.69), coefficient of variance (CV = 13.11) and standard error (SE = 4.788) after comparison with mean values by Duncan Multiple Range test. Clean wave followed this herbicidal treatment with statistically significant ($P < 0.05$) mortality (84.05%) with SD = 1.64 accordingly followed by Starane-M (79.92%), however, the lowest mortality was recorded by Allymax (61.21%) compared to control treatment during 2015-16 (*Table 2*).

The current research confirms the remarkable mortality of weed after the application of Broad-X (91.55%) with a probability value ($P < 0.01$) along with the SD (0.70) followed by clean wave (82.01%); Starane-M (77.86%). Allymax produced the lowest mortality (60.47%) compared to control treatment during 2016-17 (*Table 2*).

On the other hand, after 15 DAS (days of spray) mortality (70.84%) investigated by the application of Broad-X with SD = 3.84 differed statistically ($P < 0.05$) with clean wave (59.94%) along with rest of the treatments during 2016-17. In case of Broad-X (72.93%) and clean wave (63.52%) do not differ statistically from each other, but broad-X differed with Starane-M (56.57%) and other treatments during 2015-16 (*Table 2*).

http://www.aloki.hu ● ISSN 1589 1623 (Print) ● ISSN 1785 0037 (Online)
DOI: http://dx.doi.org/10.15666/aeer/1706_1275312767

Table 2. *Effect of different herbicides on mortality percentage during 2015-16 and 2016-17*

Herbicides treatments	Mortality (%) 2015-16		Mortality (%) 2016-17	
	15 DAS	30 DAS	15 DAS	30 DAS
Control	0.000 ± 0.00^{d}	0.000 ± 0.00^{c}	0.000 ± 0.00^{d}	0.000 ± 0.00^{c}
Starane-M	56.57 ± 3.80^{b}	79.92 ± 4.41^{ab}	50.24 ± 1.74^{c}	77.86 ± 4.33^{ab}
Clean wave	63.52 ± 3.08^{ab}	84.05 ± 1.64^{a*}	59.94 ± 2.36^{b}	82.01 ± 1.59^{ab}
Broad-X	72.93 ± 4.25^{a*}	91.16 ± 1.69^{a**}	70.84 ± 3.62^{a*}	91.55 ± 0.70^{a**}
Allymax	48.73 ± 0.59^{c}	61.21 ± 17.85^{b}	44.40 ± 2.44^{c}	60.47 ± 20.21^{b}
ANOVA				
C.V.	6.06	13.11	5.22	14.88
S. E.	1.6795	4.788	1.36	5.35

DAS = days after spraying; t ha^{-1} = ton per hectare. The same letters do not differ statistically from each other at 5% significance level. C. V. = Coefficient of Variance; mean ± SD (Standard Deviation). Maximum (SD) means the sample of weed population was collected in the field conditions having maximum weed population in a replication

The curled dock leaf area displayed a steep asymptotic decrease using different new chemical herbicides compared to before spraying. However the evaluations of leaf area versus herbicides measured quantitatively recorded strong positive coefficient of determination $R^2 = 0.94$ and $R^2 = 0.93$, 15 and 30 days after treatment comparable before herbicide application as depicted (*Fig. 4*).

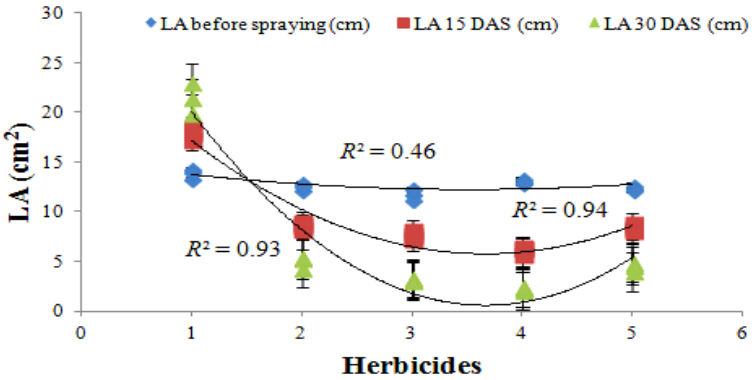

Figure 4. *Power relation of leaf area with different herbicides used in the experiment (1 = control, 2 = Starane-M, 3 = Clean wave, 4 = Broad X, 5 = Allymax) after 15, 30 days during 2015-2016, LA = Leaf area, R^2 = Coefficient of determination, DAS = days after spraying, cm^2 = centimeter square*

In wheat crop, all herbicide treatments had a similar influence shown by the mild asymptotic upright curve on leaf area development compared to before foliar application with $R^2 = 0.40$ (*Fig. 5*). The recorded leaf area 15 and 30 days after foliar application of broad-X performed maximum outcome on the weed followed by clean wave herbicides indicated that broad-X herbicide was most effective and potential for controlling this invasive weed. The power relation in wheat crop performed better coefficient of determination ($R^2 = 0.93$, $R^2 = 0.88$) indicated the evolution of observed leaf area recorded highly significant ($P < 0.01$) relationship with the progression of predicted leaf area during 2016-17 (*Fig. 5*).

http://www.aloki.hu ● ISSN 1589 1623 (Print) ● ISSN 1785 0037 (Online)
DOI: http://dx.doi.org/10.15666/aeer/1706_1275312767

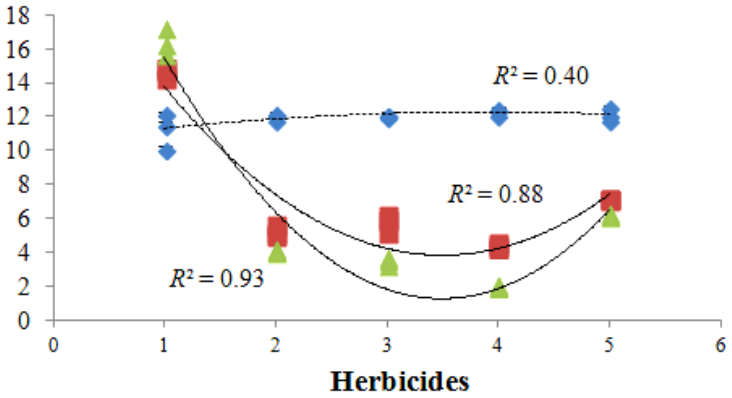

Figure 5. *Power relationship of leaf area with herbicide treatments (1 = control, 2 = Starane-M, 3 = Clean wave, 4 = Broad X, 5 = Allymax) used at 15, 30 days after spraying herbicides during 2016-17, R^2 = Coefficient of determination*

Response of herbicides with root damage (%)

The response of foliar herbicidal treatments performed statistically non-significant ($P > 0.05$) reduction in root damage (%), however highly significant ($P < 0.001$) responses were investigated by broad-X (97.15 ± 0.03%; 98.25 ± 1.08%) mean ± sd and (97.15 ± 0.017%; 98.25 ± 0.0626%) on mortality of curled dock during both seasons (*Fig. 6*).

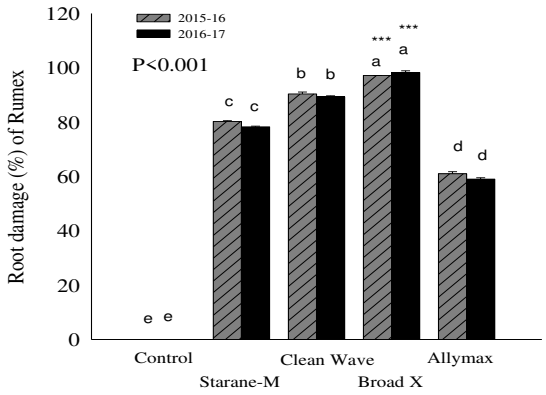

Figure 6. *Efficacy of new chemistry foliar herbicides used for controlling curled dock and herbicides influence on root damage (%) during 2015-16 & 2016-17. The means having the same lettering do not differ statistically from each other. *** indicated difference among treatments of herbicides with root damage (%) is highly significant*

Model validation performance of R^2

The polynomial relationship during both years for all treatments performed comparable arc trends, ensuring a decline after full ground cover. The R^2 for root length (0.93 and 0.88) were found statistically significant ($P < 0.001$) strong positive relationship in regards to observed and predicted root length (RL) during both the years

http://www.aloki.hu ● ISSN 1589 1623 (Print) ● ISSN 1785 0037 (Online)
DOI: http://dx.doi.org/10.15666/aeer/1706_1275312767

(*Fig. 7*) which indicated the best relation between two years resulting in the better fitting of the model.

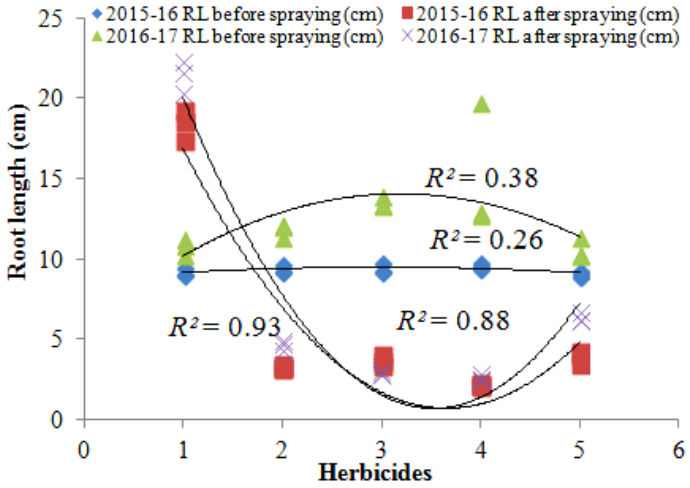

Figure 7. *Efficacy of different herbicides on root length (cm) of the curled dock during 2015-16 & 2016-17. Whereas power relation Root Length with herbicides (1 = control, 2 = Starane-M, 3 = Clean wave, 4 = Broad X, 5 = Allymax), R^2 = Coefficient of determination; RL = Root length, cm = centimeter*

Impact of herbicides on yield

Significant ($P < 0.001$) yield (3.43 t ha^{-1}) recorded by foliar application of Broad-X herbicides in a wheat crop with standard deviation (0.04); standard error (0.027) and coefficient of variance (1.71) during the first year 2015-16. Broad-X produced highly significant ($P < 0.001$) yield (3.69 t ha^{-1}) with (sd = 0.09) and se = 0.035 compared to rest of the herbicides during 2016-17. Year-wise accumulation by ANOVA also stated highly significant yield (CV = 1.97), however significant increase in yield produced by Broad-X (33.29%) followed by clean wave (29.63%) over control treatment (*Table 3*).

Table 3. *Co-efficient of determination (R^2) showing the effect of different herbicides on yield (t ha^{-1})*

Herbicides treatments	Yield (t ha^{-1})		R^2	RMSE	
	2015-16	2016-17		2015-16	2016-17
Control	2.420^{e}	2.327^{e}	0.72	0.67	0.81
Starane-M	2.920^{c}	3.067^{c}	0.72	0.58	0.81
Clean wave	3.297^{b**}	3.447^{b**}	0.83	0.67	0.75
Broad-X	3.433^{a***}	3.693^{a***}	0.84	0.69	0.80
Allymax	2.693^{d}	2.800^{d}	0.71	0.33	0.47

** P < 0.01; ***P < 0.001. The same letters do not differ statistically from each other. R^2 – Coefficient of determination; RMSE – root mean square error; t = tones; ha^{-1} = per hectare

Model validation performance for RMSE

Maximum yield was recorded by foliar application of Broad-X with a strong positive coefficient of determination R^2 (0.84) and RMSE (0.69 and 0.80). These results based on

http://www.aloki.hu ● ISSN 1589 1623 (Print) ● ISSN 1785 0037 (Online)
DOI: http://dx.doi.org/10.15666/aeer/1706_1275312767

highly signified accurate conclusions when comparing focused treatments in both years. The polynomial relation for all herbicides for corresponding years also exposed a linear arc pattern which strung with an initial linear stage followed by maximum asymptotic trend at the growth stage by R^2 (0.83) with RMSE (0.67 and 0.75) also indicated the best relationship that specified the method accuracy (*Table 3*).

Interaction of yield (t ha^{-1}) with mortality (%)

In *Table 4,* maximum interaction in yield (t ha^{-1}) with mortality (%) of curled dock 15 and 30 days after spraying conferred highly significant ($P < 0.0001$) performance during 2015-16 at Kharian. The interaction of yield versus herbicides 15 days after treatment and interaction of this with 30 days proved highly significant ($P < 0.0001$) mortality (%) that showed better performance during 2016-17. However, yield recorded significant ($P < 0.05$) interaction with mortality of curled dock 30 days after treatment (*Table 4*).

Table 4. *Analysis of variance of factors affecting yield (t ha^{-1}) interaction with mortality 15, 30 days after spraying postemergence herbicides*

Effect	D.f.	SS	MS	F	P
(a) Yield (t ha^{-1}) during 2015-16					
M15	1	7.221	7.221	849.99	< 0.0001
M30	1	0.186	0.186	21.86	< 0.0001
M15 x M30	1	0.938	0.938	110.40	< 0.0001
Residuals	41	0.348	0.008		
(b) Yield (t ha^{-1}) during 2016-17					
M15	1	4.898	4.898	619.406	< 0.0001
M30	1	0.023	0.023	2.953	< 0.05
M15 x M30	1	1.144	1.144	144.647	< 0.0001
Residuals	41	0.324	0.008		

M15, M30 = Mortality after 15, 30 days of spray; the level of significance was $P > 0.05$, $P < 0.0001$***; $P < 0.001$**; $P < 0.01$*; $P < 0.05$; D.f. = degree of freedom; SS = Sum of square; MS = Mean square; F and P values. DAS = days after spraying; t = tones; ha^{-1} = per hectare

Discussion

Curled dock (*Rumex crispus* L.) is a common perennial (Ulber, 2010) invasive weed species in wheat crop. This weed characterized by high ecological plasticity and ability to spread in the wheat crop from non-cropped vicinity. Due to its high exotic potential, this weed becomes most economically important and creates many problems in irrigated wheat ecosystems. This invasive weed species can control easily in the non-cropped area, but this weed shifted into the wheat fields. No doubt, curled dock populations scattered in some areas of District Gujrat (Tehsil Kharian and Gujrat) in patches.

Broad-leaved dock is a common and troublesome grassland weed with a wide geographic distribution. In conventional farming, Curled dock managed by selective herbicides, however in an organic farming destructive method is the best option (van Evert et al., 2011) but it is laborious in large scale.

The studied chemicals (*Table 1*) disrupt hormone balance; protein syntheses in the curled dock and cause a variety of plant growth abnormalities. Cleave wave act as a growth regulator is synthetic auxin's (Yerkes et al., 2014) travel equally upward and

http://www.aloki.hu ● ISSN 1589 1623 (Print) ● ISSN 1785 0037 (Online)
DOI: http://dx.doi.org/10.15666/aeer/1706_1275312767

downward inside the phloem to the growing points of the shoots and roots. Many herbicides in phenoxy acetic acids group are effective on perennial and annual broadleaf weeds (Gunsolus and Curran, 1999). Allymax selectively inhibits broad leaves by acetolactate syntheses ALS due to its systemic action. This herbicide belongs to sulfonylurea (SU) one of the most critical classes of herbicides worldwide. It is well known for its eco-friendly, extremely low toxicity towards mammals (Li et al., 2012). These are selective herbicides that kill dicots, sensitive to auxinic herbicides include abnormal growth, senescence, and plant death without affecting monocots (Song, 2014).

Weed management is significantly principal activity on agricultural and non-agricultural lands but faced with many types of challenges. There is a need to adopt broad-spectrum new approaches for its management strategies (Liebman et al., 2016; Calado et al., 2010). Therefore, critical challenges for invasive weed supervision comprised territory wise obstacle of weed emergence and expansion of cost-effective strategies would adopt for the control of invader (Buckley and Han, 2014) including biological control agents.

The response of foliar herbicide on mortality of curled dock performed highly significant ($P < 0.001$) responses by the application of Broad-X which is the combination of three herbicides (97.15 $\pm$ 0.03%; 98.25 $\pm$ 1.08%), i.e. (mean $\pm$ sd) and (97.15 $\pm$ 0.017%; 98.25 $\pm$ 0.0626%), i.e. (mean $\pm$ se) have a more significant potential for controlling curled dock under irrigated system of Gujrat (*Table 2*). The experimental effect was in agreement to Cheema et al. (2006) who described that the use of broad-leaved herbicides controlled maximum Chenopodium album. Curled dock controlled by Propanil herbicide (Price and Kelton, 2013) however, common sorrel (*Rumex acetosa*) species were susceptible to postemergence MCPA (Marshall et al., 2003) in wheat crops.

The study results were also in agreement with (Usman et al., 2010), who illustrated that 2,4-dichlorophenoxy acetic acid was effective for the better management of broadleaf dock (*Rumex dentatus*) in wheat crops. The previously described results against broadleaf dock were reported by (Naseer-ud-Din et al., 2011) that 2,4-dichlorophenoxy acetic acid (Bromoxynil + MCPA @ 0.49 kg a.i ha^{-1}) gave better performance compared to Pyroxasulfone @ 0.15 kg a.i ha^{-1} against Indian dock/broadleaved dock (*R. dentatus*) species in wheat crops during 2008-2009. These results are following the researchers who reported that the broadleaf dock (*R. dentatus*) having an identical family was controlled inadequately with 2,4-D. while, halauxifen + florasulam used @ 12.76 g; metsulfuron 4 g and etsulfuron + carfentrazone @ 4+20 g a.i ha^{-1} provided absolute control (Chhokar et al., 2015).

Isoproturon sprayed @ 1080 g a.i ha^{-1} reduced the density of Indian dock significantly (Shehzad et al., 2012).

The researchers reported that herbicides are most effective for controlling curled dock in their field experiments (Humphreys et al., 1999; Benvenuti et al., 2001; Eekeren et al., 2006). Maximum mortality investigated by Sulfosulfuran + Metsulfuran (92.27%) followed by Metsulfuran (81.69%) against this invasive weed after 30 days of spraying herbicides (Singh et al., 2017). Results of this and previous studies indicated that 2,4-DB (Butyrac 200) and Asulam @ 1.5 lb a.i $acre^{-1}$ (Asulox) provide better control efficacy against the dock in red clover field (Roerig et al., 2015).

The toxic effect of herbicides inhibited the growth of plants resulted in plant death. Scientists reported that herbicides killed weeds up to 90.5-94.1% after fifteen days of spraying; however, 100% mortality investigated after 21 days of foliar application

http://www.aloki.hu ● ISSN 1589 1623 (Print) ● ISSN 1785 0037 (Online)
DOI: http://dx.doi.org/10.15666/aeer/1706_1275312767

(Dimitrova and Marinov-Serafimov, 2008). Different doses of sulfosulfuron controlled weeds up to 98.7% (Paswan et al., 2017). Premix application of sulfosulfuron and metsulfuron methyl used @ 30 + 2 g ha^{-1} at 60 DAS was recorded highest mortality (%) compared to control treatment. Clodinofop + Metsulfuron methyl @ 60 + 4 g ai ha^{-1} was exercised by (91.75%) control followed by Sulfosulfuron @ 25 g ha^{-1} (87.60%) and Isoproturon + 2,4-D @ 1000 + 400 g ai ha^{-1} (87.42%) in the wheat crop after 90 days of post emergence application (Choudhary et al., 2016).

The studied leaf area of curled dock exhibited a steep declining curvature using different herbicides, which was comparable with low asymptotic development before spraying. The stable positive coefficient of determination developed in both of the seasons compared to control treatment (*Figs. 4* and *5*). Experimental findings correlate with previously reported work that leaf area measured exposed excellent performance $R^2 = 0.88$ and RMSE = 0.96. These results are conformity to (Ahmad et al., 2015) who reported $R^2 = 0.59$ in wheat crops by destructive method compared to non-destructive. The broadleaf dock (*R. dentatus*) controlled significantly by using different treatments; however, the effect of the relationship between crop succession and weed control treatments was significant (Fakkar and El-Dakkak, 2015).

Statistically yield (3.43 t ha^{-1}) recorded by foliar application of Broad-X herbicides in a wheat crop. The results of this study confirmed with (Malekian et al., 2013; Steckel et al., 1997) who recorded foliar spray of metsulfuron-methyl + sulfosulfuron @ 36g.a.i.ha^{-1} effectively controlled annual weed resulting in the highest yield of the wheat crops. Scientists previously revealed that severe infestation of weed plants in wheat crops resulting in 18-73% reduction in grain yield (Pandey et al., 2006). The researchers also described in their experiments that the mixture of Metsulfuran and Sulfosulfuron performed more efficient control with their foliar application resulting higher yield of crops (Singh et al., 2011). The model of density inhibition exposed effectively against the broadleaved dock; however its density reduced up to 69-88%, and wheat yield was enhanced up to 22-48% compared to control treatment by the application of Atlantis 3.6WG @ 14.4 g a.i ha^{-1} (Khaliq et al., 2011).

The invasive weed deteriorates the quality of grain by creating hindrance in cultural practices, i.e. fertilizer application and irrigation (Memon et al., 2003). The yield reduced up to 20-30% by the attack of broad-leaved weeds in wheat crop (Ashok et al., 2006). Due to the hard nature and invasiveness of curled dock, effective combinations of herbicides recommended for its better management.

Conclusion

Based on our knowledge, this is an exclusive comparative study in which the author used an applied combination of herbicides already present in the market having two and or three chemicals for controlling curled dock in wheat crops. These results screened out Broad-X herbicide performed better against the curled dock followed by Clean Wave in wheat crops. According to the above analysis and findings, the farmers in this region advised using these postemergence herbicides for controlling this toxic weed in ordered to obtain higher yield. We encouraged researchers to explore the mode of action, resistance mechanism of these herbicides and to find out suitable biological control agents (BCA's) against this toxic weed in future.

http://www.aloki.hu ● ISSN 1589 1623 (Print) ● ISSN 1785 0037 (Online)
DOI: http://dx.doi.org/10.15666/aeer/1706_1275312767

Acknowledgements. This study was supported by the National Key R&D Program of China (2017YFC1200101), the National Natural Science Foundation of China (31470575, 31670545 and 31971557).

Conflict of interests. All authors declare no conflict of interests.

Ethical approval. This research was two years field experiments to check out the efficacy of post emergence herbicides against this invasive weed (curled dock) which can consider a risk to the wheat growers in future.

REFERENCES

[1] Ahmad, S., Ali, H., Ur Rehman, A., Khan, R. J. Z., Ahmad, W., Fatima, Z., Abbas, G., Irfan, M., Ali, H., Khan, M. A. (2015): Measuring leaf area of winter cereals by different techniques: a comparison. – Pak. J. Life Soc. Sci 13: 117-125.

[2] Ahmed, M., Ji, M., Qin, P., Gu, Z., Liu, Y., Sikandar, A., Iqbal, M. F., Javeed, A. (2019): Phytochemical screening, total phenolic and flavonoids contents and antioxidant activities of *Citrullus colocynthis* L. and *Cannabis sativa* L. – Applied Ecology and Environmental Research 17: 6961-6979.

[3] Aldesuquy, H., Baka, Z., Mickky, B. (2014): Kinetin and spermine mediated induction of salt tolerance in wheat plants: Leaf area, photosynthesis and chloroplast ultrastructure of flag leaf at ear emergence. – Egyptian Journal of Basic and Applied Sciences 1: 77-87.

[4] Alvi, S. M., Sanaullah, C., Ali, M. A. (2004): Evaluation of some herbicides for the control of weeds in wheat crop. – Pak. J. Life Soc. Sci 2: 24-27.

[5] Ashok, K., Malik, R. K., Hasija, R. C. (2006): Efficacy of metribuzin alone and as tank mixture with different herbicides against weeds in wheat. – Environment and Ecology 245: 1046-1049.

[6] Benvenuti, S., Macchia, M., Miele, S. (2001): Light, temperature and burial depth effects on *Rumex obtusifolius* seed germination and emergence. – Weed Research 41: 177-186.

[7] Buckley, Y. M., Han, Y. (2014): Managing the side effects of invasion control. – Science 344: 975-976.

[8] Calado, J. M. G., Basch, G., de Carvalho, M. (2010): Weed management in no-till winter wheat (*Triticum aestivum* L.). – Crop Protection 29: 1-6.

[9] Chaudhry, S., Hussain, M., Ali, M. A., Iqbal, J. (2008): Efficacy and economics of mixing of narrow and broad leaved herbicides for weed control in Wheat. – Journal of Agricultural Research 46: 355-360.

[10] Cheema, M. S., Akhtar, M., Iqbal, M. S. (2006): Performance of different herbicides in wheat under irrigated conditions of Southern Punjab, Pakistan. – Pakistan Journal of Weed Science Research 12: 53-59.

[11] Chhokar, R. S., Sharma, R. K., Gill, S. C., Meena, R. P. (2015): Herbicides for broad-leaved weeds management in wheat. – Indian J. Weed Sci 47: 353-361.

[12] Choudhary, D., Singh, P. K., Chopra, N. K., Rana, S. C. (2016): Effect of herbicides and herbicide mixtures on weeds in wheat. – Indian Journal of Agricultural Research 50: 107-112.

[13] Crone, E. E., Marler, M., Pearson, D. E. (2009): Non-target effects of broadleaf herbicide on a native perennial forb: a demographic framework for assessing and minimizing impacts. – Journal of Applied Ecology 46: 673-682.

[14] Dalga, D., Sharma, J. J., Tana, T. (2014): Growth and yield of bread wheat (*Triticum aestivum* L.) as influenced by row spacing and weeding frequency in Southern Ethiopia. – Scientia 8: 19-30.

[15] Dalley, C. D., Bernards, M. L., Kells, J. J. (2006): Effect of weed removal timing and row spacing on soil moisture in Corn (*Zea mays*). – Weed Technology 20: 399-409.

http://www.aloki.hu ● ISSN 1589 1623 (Print) ● ISSN 1785 0037 (Online)
DOI: http://dx.doi.org/10.15666/aeer/1706_1275312767

[16] Davis, A. S., Hall, J. C., Jasieniuk, M., Locke, M. A., Luschei, E. C., Mortensen, D. A., Riechers, D. E., Smith, R. G., Sterling, T. M., Westwood, J. H. (2009): Weed science research and funding: a call to action. – Weed Science 57: 442-448.
[17] Debaeke, P., Caussanel, J. P., Kiniry, J. R., Kafiz, B., Mondragon, G. (1997): Modelling crop: weed interactions in wheat with ALMANAC. – Weed Research 37: 325-341.
[18] Délye, C., Jasieniuk, M., Le Corre, V. (2013a): Deciphering the evolution of herbicide resistance in weeds. – Trends in Genetics 29: 649-658.
[19] Délye, C., Menchari, Y., Michel, S., Cadet, É., Le Corre, V. (2013b): A new insight into arable weed adaptive evolution: mutations endowing herbicide resistance also affect germination dynamics and seedling emergence. – Annals of Botany 111: 681-691.
[20] Dimitrova, T., Marinov-Serafimov, P. (2008): Chemical control of curled dock (*Rumex crispus* L.) and other weeds in noncropped areas. – Pestic. Phytomed. (Belgrade) 23: 123-126.
[21] Duke, S. O. (2012): Why have no new herbicide modes of action appeared in recent years? – Pest Management Science 68: 505-512.
[22] Eekeren, V. N., Fehér, L., Smeding, F., Prins, U., Jansonius, P. (2006): Controlling broad-leaved dock (*Rumex obtusifolius*) in grass clover mixtures. – Sustainable Grassland 11: 391-393.
[23] Fakkar, A. A. O., El-Dakkak, A. A. A. (2015): Effect of crop sequence and weed control treatments on weeds and pea crop productivity. – Annals of Agricultural Sciences 60: 157-168.
[24] Gunsolus, J. L., Curran, W. S. (1999): Herbicide mode of action and injury symptoms. – Order 612: 625-8173.
[25] Hossain, S. A. A. M., Wang, L., Chen, T., Li, Z. (2017): Leaf area index assessment for tomato and cucumber growing period under different water treatments. – Plant, Soil and Environment 63: 461-467.
[26] Humphreys, J., Jansen, T., Culleton, N., MacNaeidhe, F. S., Storey, T. (1999): Soil potassium supply and *Rumex obtusifolius* and *Rumex crispus* abundance in silage and grazed grassland swards. – Weed Research (Oxford) 39: 1-13.
[27] Iqbal, M., Hussain, M. M., ur Rehman, K., Shah, M., Iqbal, M. F., Hussain, M., Iqbal, Z. Aatika, S. (2018): Evaluation of new chemistry insecticides for controlling invasive pest in citrus orchard. – International Journal of Advance Research in Biological Sciences 5: 100-105.
[28] Khaliq, A., Matloob, A., Tanveer, A., Areeb, A., Aslam, F., Abbas, N. (2011): Reduced doses of a sulfonylurea herbicide for weed management in wheat fields of Punjab, Pakistan. – Chilean Journal of Agricultural Research 71: 424.
[29] Li, Z.-M., Ma, Y., Guddat, L., Cheng, P.-Q., Wang, J.-G., Pang, S. S., Dong, Y.-H., Lai, C.-M., Wang, L.-X., Jia, G.-F., Li, Y.-H., Wang, S.-H., Liu, J., Zhao, W.-G., Wang, B.-L. (2012): The structure–activity relationship in herbicidal monosubstituted sulfonylureas. – Pest Management Science 68: 618-628.
[30] Liebman, M., Baraibar, B., Buckley, Y., Childs, D., Christensen, S., Cousens, R., Eizenberg, H., Heijting, S., Loddo, D., Merotto, A. (2016): Ecologically sustainable weed management: How do we get from proof-of-concept to adoption? – Ecological Applications 26: 1352-1369.
[31] Malekian, B., Ghadiri, H., Kazemeini, S. A., Edalat, M. (2013): Evaluation of sulfosulfuron, metsulfuron-methyl plus sulfosulfuron, mesosulfuron-methyl plus iodosulfuron-methyl and iodosulfuron plus mesosulfuron herbicides in winter Wheat (*Triticum aestivum* L.). – J. Biol. Environ. Sci 7: 177-182.
[32] Marshall, E. J. P., Brown, V. K., Boatman, N. D., Lutman, P. J. W., Squire, G. R., Ward, L. K. (2003): The role of weeds in supporting biological diversity within crop fields. – Weed Research 43: 77-89.

http://www.aloki.hu ● ISSN 1589 1623 (Print) ● ISSN 1785 0037 (Online)
DOI: http://dx.doi.org/10.15666/aeer/1706_1275312767

[33] Marwat, K. B., Muhammad, S., Zahid, H., Bakhtiar, G., Haroon ur, R. (2008): Study of various herbicides for weed control in wheat under irrigated conditions. – Pakistan Journal of Weed Science Research 14: 1-8.
[34] Marwat, S. K., Usman, K., Khan, N., Khan, M. U., Khan, E. A., Khan, M. A., ur Rehman, A. (2013): Weeds of wheat crop and their control strategies in dera Ismail khan district, Khyber Pakhtun Khwa, Pakistan. – American Journal of Plant Sciences 4: 66.
[35] Memon, R., Raza Bhatti, G., Khalid, S. (2003): Weed diversity of wheat crop in Khairpur District, Sindh. – Pakistan Journal of Weed Science Research 9(1-2): 99-103.
[36] Montgomery, E. G. (1911): Correlation studies in corn. – Neb. Agric. Exp. Stn. Annu. Rep 24: 108-159.
[37] Moss, S., Ulber, L., Den Hoed, I. (2019): A herbicide resistance risk matrix. – Crop protection 115: 13-19.
[38] MuMin, B. K. (2018): Multi-model inference. – R package version 1.15. 6.
[39] Naseer-ud-Din, G., Shehzad, M., Nasrullah, H. M. (2011): Efficacy of various pre and postemergence herbicides to control weeds in wheat. – Pakistan Journal of Agricultural Sciences 48: 185-190.
[40] Nayyar, M. M., Shafi, M., Mahmood, T., Randhwa, A. M. (1994): Effect of herbicides on monocot weeds in wheat. – Journal of Agriculture Research 32: 149-155.
[41] Pandey, A. K., Gopinath, K. A., Gupta, H. S. (2006): Evaluation of sulfosulfuron and metribuzin for weed control in irrigated wheat (*Triticum aestivum* L.). – Indian Journal of Agronomy 51: 135-138.
[42] Paswan, A. K., Mandal, D., Kumar, J., Kumar, R. (2017): Influence of weed management practices on productivity of wheat (*Triticum aestivum* L.) under Middle Indo-Gangetic Plains of Eastern India. – International Journal of Current Microbiology and Applied Sciences 6: 2486-2491.
[43] Price, A. J., Kelton, J. A. (2013): Integrating Herbicides in a High-Residue Cover Crop Setting. – In: Price, A., Kleton, J. (eds.) Herbicides. Current Research and Case Studies in Use. IntechOpen, London.
[44] Qureshi, R., Waheed, A., Arshad, M. (2009): Weed communities of wheat crop in District Toba Tek Singh, Pakistan. – Pakistan Journal of Botany 41: 239-245.
[45] Roerig, K. C., Anderson, N. P., Hulting, A. G., Curtis, D. W., Mallory-Smith, C. A. (2015): Evaluation of Asulam and 2, 4-DB Crop Safety and Dock Control in Red Clover Grown for Seed. – Seed Production Research at Oregon State University, CrS 152.
[46] Schuster, T. M., Reveal, J. L., Bayly, M. J., Kron, K. A. (2015): An updated molecular phylogeny of Polygonoideae (Polygonaceae): Relationships of *Oxygonum*, *Pteroxygonum*, and *Rumex*, and a new circumscription of Koenigia. – Taxon 64: 1188-1208.
[47] Scursoni, J. A., Martín, A., Catanzaro, M. P., Quiroga, J., Goldar, F. (2011): Evaluation of postemergence herbicides for the control of wild oat (*Avena fatua* L.) in wheat and barley in Argentina. – Crop Protection 30: 18-23.
[48] Shehzad, M., Tanveer, A., Ayub, M., Mubeen, K., Ibrahim, M., Qadir, I., Sarwar, N. (2013): Effect of weed-crop competition on growth and yield of Garden Cress. – Sarhad Journal of Agriculture 29: 79-82.
[49] Shehzad, M. A., Nadeem, M. A., Sarwar, M. A., Naseer-ud-Din, G. M., Ilahi, F. (2012): Comparative efficacy of different postemergence herbicides in wheat (*Triticum aestivum* L.). – Pak. J. Agri. Sci 49: 27-34.
[50] Siddiqui, I., Bajwa, R. (2010): Effect of six problematic weeds on growth and yield of wheat. – Pak. J. Bot 42: 2461-2471.
[51] Singh, A. K., Kumar, R., Singh, A. K., Singh, N. K., Kumari, A. (2011): Performance of sulfosulfuron against weeds in irrigated wheat (*Triticum aestivum* L.). – CAB Abstracts Environment and Ecology 29: 831-833.

http://www.aloki.hu ● ISSN 1589 1623 (Print) ● ISSN 1785 0037 (Online)
DOI: http://dx.doi.org/10.15666/aeer/1706_1275312767

[52] Singh, S., Singh, A. K., Yadav, A., Harikesh, S. (2017): Assess the effect of different combinations of herbicides on weed population and economic feasibility of treatments in late sown wheat crop. – Journal of Pharmacognosy and Phytochemistry 5: 648-651.
[53] Song, Y. (2014): Insight into the mode of action of 2, 4-dichlorophenoxyacetic acid (2, 4-D) as an herbicide. – Journal of Integrative Plant Biology 56: 106-113.
[54] Steckel, G. J., Wax, L. M., Simmons, F. W., Phillips, W. H. (1997): Glufosinate efficacy on annual weeds is influenced by rate and growth stage. – Weed Technology 11: 484-488.
[55] Ulber, L. (2010): Weed species diversity in cropping systems: management and conservation strategies. – .
[56] Usman, K., Khalil, S. K., Khan, A. Z., Khalil, I. H., Khan, M. A. (2010): Tillage and herbicides impact on weed control and wheat yield under rice–wheat cropping system in Northwestern Pakistan. – Soil and Tillage Research 110: 101-107.
[57] van Evert, F. K., Samsom, J., Polder, G., Vijn, M., Dooren, H. J. v., Lamaker, A., van der Heijden, G. W. A. M., Kempenaar, C., van der Zalm, T., Lotz, L. A. P. (2011): A robot to detect and control broad-leaved dock (*Rumex obtusifolius* L.) in grassland. – Journal of Field Robotics 28: 264-277.
[58] Waheed, A., Qureshi, R., Jakhar, G. S., Tareen, H. (2009): Weed community dynamics in wheat crop of District Rahim Yar Khan, Pakistan. – Pakistan Journal of Botany 41: 247-254.
[59] Westwood, J. H., Charudattan, R., Duke, S. O., Fennimore, S. A., Marrone, P., Slaughter, D. C., Swanton, C., Zollinger, R. (2018): Weed management in 2050: Perspectives on the future of weed science. – Weed Science 66: 275-285.
[60] Yerkes, C. N., Mann, R. K., Satchivi, N. M., Schmitzer, P. R. (2014): Herbicidal compositions comprising 4-amino-3-chloro-5-fluoro-6-(4-chloro-2-fluoro-3-methoxyphenyl) pyridine-2-carboxylic acid or a derivative thereof and synthetic auxin herbicides. – Google Patents.
[61] Zaller, J. G. (2004a): Ecology and non-chemical control of *Rumex crispus* and *R. obtusifolius* (Polygonaceae): A review. – Weed Research 44: 414-432.
[62] Zaller, J. G. (2004b): Competitive ability of *Rumex obtusifolius* against native grassland species: above- and belowground allocation of biomass and nutrients. – Journal of Plant Diseases and Protection 19: 345-351.
[63] Zimdahl, R. L. (2018): Fundamentals of Weed Science. – Academic Press, San Diego.

http://www.aloki.hu ● ISSN 1589 1623 (Print) ● ISSN 1785 0037 (Online)
DOI: http://dx.doi.org/10.15666/aeer/1706_1275312767

VULNERABILITY AND LIVELIHOOD RESILIENCE IN THE FACE OF NATURAL DISASTER: A CRITICAL CONCEPTUAL REVIEW

SARKER, M. N. I.[1] – CAO, Q.[1,2] – WU, M.[1*] – HOSSIN, M. A.[3] – ALAM, G. M. M.[4] – SHOUSE, R. C.[1]

[1]*School of Public Administration, Sichuan University, Chengdu 610065, China*

[2]*School of Economics and Management, Hubei MinZu University, Enshi 445000, China*

[3]*Department of Information Management and E-commerce, University of Electronic Science and Technology of China, Chengdu, China*

[4]*Faculty of Agricultural Economics and Rural Development, Bangabandhu Sheikh Mujibur Rahman Agricultural University, Gazipur, Bangladesh*

**Corresponding author*
e-mail: wuminhelen@163.com

(Received 3rd May 2019; accepted 1st Jul 2019)

Abstract. The concepts of vulnerability and resilience are gaining popularity in the development literature but still lack conceptual integration with the theory and practices of livelihood dynamics. However, the livelihood system of a community is a key element of the social system which may frequently be disrupted by the ecological, financial, natural and human-made vulnerability. Therefore, the purpose of this study is to clarify the concept of vulnerability and resilience in the perspective of livelihoods in a climate vulnerable context. It also addresses the methodological gaps through translation of theory from existing literature. This study argues that vulnerability and livelihood resilience are inversely related. It recommends some indicators and pillars for a better understanding of the vulnerability and livelihood resilience drawing from assorted literature through analysing the concept from various dimensions. The study will be helpful in understanding the livelihood dynamics and its assessment in the perspective of vulnerability and resilience.
Keywords: *environmental management, security, climate change, adaptive capacity, environmental risk*

Introduction

Vulnerability of people to possible natural hazards was impossible to measure before 1990s due to a lack of data availability, appropriate scales, and appropriate measurement approaches. Though according to Janssen (2006), the word 'vulnerability' appeared about 939 times in 2286 publications of disaster literatures in the last 30 years. Vulnerability to natural disasters is a combined effect of nature, environment, society, financial condition and community sensitivity. It is characterized by the susceptibility to be victimized or disrupted by natural disasters. Natural disasters, particularly climate change is a global concern and a daunting challenge for humanity since time immemorial. Natural disasters affect the livelihood of people of developing countries lacking in resources the most. So, natural disaster is one of the major causes of vulnerability (Dyakov, 2013; Garamvölgyi, 2013; Jamali et al., 2018; Sarker et al., 2019). The devastation of natural disasters occur in ways such as gradually changing average temperature, humidity and other environmental factors, increasing annual and seasonal climatic conditions, gradually increasing the frequency of hazardous events and the speed at which catastrophe factors are changing (Tompkins and Adger, 2004; IPCC, 2014; Omotoso et al., 2018; Nistor et al., 2018; Akhtar et al., 2019).

http://www.aloki.hu ● ISSN 1589 1623 (Print) ● ISSN 1785 0037 (Online)
DOI: http://dx.doi.org/10.15666/aeer/1706_1276912785

Vulnerability is the ability of people, organization, and societies to withstand the adverse effects of stressors (Ajibade et al., 2013; Lee, 2014; Hoa, 2019; Terin, 2019). Most of the cases, the socio-ecological vulnerability of the people is the same across the globe. People usually faces three vulnerability components viz. exposure, sensitivity and adaptive capacity (Cutter et al., 2003; Fatemi et al., 2017). Comprehensive vulnerability analysis requires a specific context for better understanding. Vulnerability analysis should be done to find out the root causes and provide a suggestion for tackling adverse effect. Resilience is a concept which has been applied to research and practice in every possible field from science to sociology, nursing (Ho et al., 2012), medicine (Garcia-Dia et al., 2013), psychology, business and public administration. It is a process of "bounce back" or "returning to form" (Weldegebriel and Amphune, 2017). Livelihood resilience is the ability of an individual, group, or community to bounce back to anticipating livelihood challenges, reducing the effect of vulnerabilities, recovering effects from past and present vulnerabilities, and thriving even in a difficult livelihood environment (Gwimbi, 2009). This study is going to assess the status of livelihood resilience of riverine island dwellers and recommend some measures for improving their livelihood resilience.

The word 'resilience' originates from Latin word *resilio* that means 'to jump back' (Manyena, 2006). Walker and Salt (2012) have claimed that 'resilience' originated from ecological research where Holling (1973) sought to differentiate between an ecological system that persists in a condition of equilibrium or stability, and response of dynamic systems when they are stressed and move from this equilibrium. A resiliency perspective is an understanding of a system's adaptive capacity. For livelihood systems, the four pillars of this perspective relate to activities and processes allowing for effectively (a) *anticipating* livelihood challenges and potential for surprises (b) *minimizing* the impact of present vulnerabilities (c) *recovering* from the impact of past as well as present vulnerabilities and (d) *thriving* from a complex livelihood situation (Gwimbi, 2009).

Livelihood resilience is a top policy concept in development context research which emerging from various disciplines (Tanner et al., 2015). It actually focuses the ability of a community to bounce back to normal condition i.e. previous conditions after suffering shocks. Resilience is a process which tackles a wide range of shocks, vulnerability, and stress like vulnerable livelihood, food insecurity, social protection, disasters and social conflicts (Zebrowski, 2013). United Nations (2013) has already declared resilience as an important agenda for working as part of an integrated and comprehensive approach to assessing and addressing factors that undermine communities' and countries' resilience, including climate risk, environmental sustainability and social inequalities or exclusion. Natural disaster particularly climate change is a global concern and worst challenges for humanity from the ancient period. The main effect of natural disasters is on the livelihood of the resource poor people of developing countries.

Some studies have already been done on resilience in the psychology literature, climate change literature, engineering literature and social sciences (Dyakov, 2013; Garamvölgyi, 2013; Jamali et al., 2018; Alam et al., 2018; Sarker et al., 2019). Most of them focus on ecological analysis and few of them explain clearly about the concept of vulnerability and resilience in the perspective of a society which resulted to fill the connection with livelihood dynamics. Therefore, this study attempts to fill the research gap by addressing this issue through an extensive review of the literature. This study also intends to add the methodological implication for understanding and measuring the livelihood vulnerability of a community with the clarification of the concept. It also provides a new lens of the suitability and superiority of resilient livelihood thinking over sustainable livelihood framework (SLF)

http://www.aloki.hu ● ISSN 1589 1623 (Print) ● ISSN 1785 0037 (Online)
DOI: http://dx.doi.org/10.15666/aeer/1706_1276912785

by exploring the weakness of SLF and adding solution for achieving livelihood resilience in a disaster vulnerability context. Though the term "resilience" is gaining popularity in the literature irrespective of the disciplines and livelihood research, the meaningful integration of the concept through proper translation from theories to action is really challenging. The concept of vulnerability and resilience is focused on the mainstream literatures such as climate change (Adger, 1999; Alam et al., 2018); disaster management (Shah et al., 2018; Adger, 2005), urban management (Sarker et al., 2019), nursing and engineering management (Fox-Lent and Linkov, 2018). But some researchers used the concepts for social-ecological system literature (Chaffin and Scown, 2018; Adger, 2005). The present study focuses the concept in the perspective of the socio-ecological system which is a better fit to livelihood system.

The rest of the paper is organized as section 2 deals with the methodology, section 3 describes the result of the study, section 4 deals with discussion focusing resilience and resilience concept emphasizing livelihood through developing a conceptual framework and final section concludes the article.

Methodology

Research design

A systematic literature review has been conducted for obtaining research objectives. An extensive desk literature review has been done for obtaining recent literature (from 2005 to 2018). Concept analysis has been done to clarify the resilience concept and validate the concept through filed data. A case study (as part of the author's PhD study) also has been done to validate the conceptual framework through assessing the vulnerability of disaster-prone community.

Search strategy

This study emphasizes the resilience concept in the multidisciplinary aspects. An extensive literature search has been done on some renowned databases like web of science, engineering village, and Scopus databases by using keywords such as "resilience, resilient, vulnerability, capacity" (*Appendix A*).

Inclusion criteria

The literature search is guided by two criteria; first, the study must focus on vulnerability and resilience; and second, livelihood is the main concern of the study. Livelihood resilience focused and peer reviewed articles have been considered for the time from 2005 to 2018 which focuses on human population. The focal points of the study are to identify the important definitive research on vulnerability and livelihood resilience, and the trend of the modification and integration of the concept and meaning of resilience to other discipline and its potential implication to the society.

Exclusion criteria

This study excludes the journal articles which have no full text, duplication and published in other languages than English. It also excludes the articles in which content does not cover the concept of resilience and disaster vulnerability context.

http://www.aloki.hu ● ISSN 1589 1623 (Print) ● ISSN 1785 0037 (Online)
DOI: http://dx.doi.org/10.15666/aeer/1706_1276912785

Review results

Preferred Reporting Items for Systematic Review and Meta-Analysis (PRISMA) guidelines has been followed in a systematic literature review (Moher et al., 2009). The review search has been done by following several steps; first, 575 documents are identified with 19 from references (*Fig. 1*). After removing the duplicates, 254 documents have been selected by abstract screening. Then 116 documents have been excluded due to lack of full text, irrelevant, not focusing on livelihood resilience. Finally, 29 documents have been selected from journal articles, books, book chapters, and working papers (*Appendix B*). The checklist of the Reporting of Observational Studies in Epidemiology (STROBE) is also followed for qualitative document selection (Vandenbroucke et al., 2007). This review has been conducted from December 2018 to January 2019. A conceptual model has been developed for livelihood resilience.

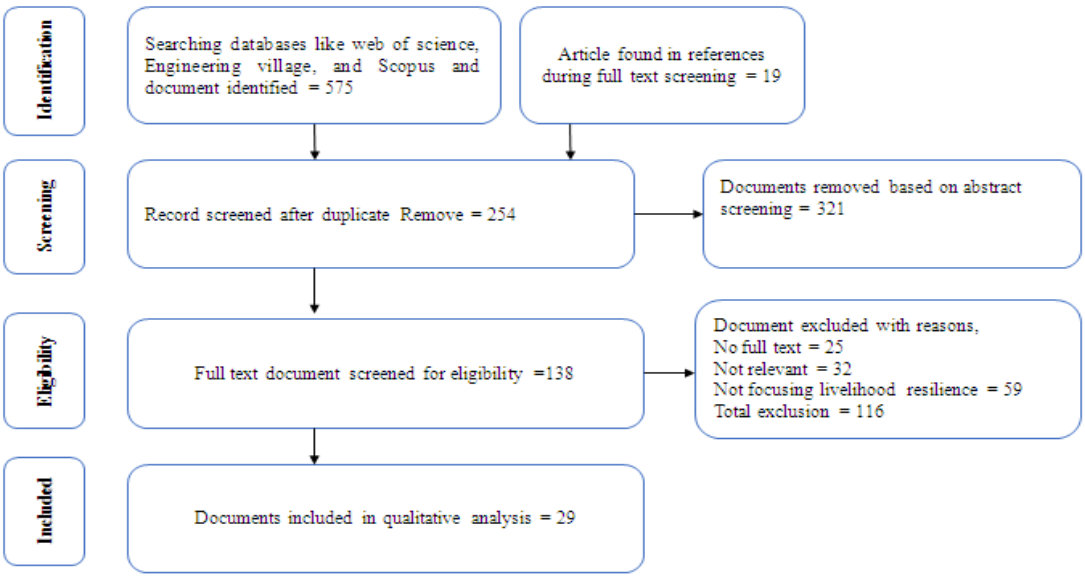

Figure 1. *PRISMA selection for qualitative study*

Discussion

The findings of this study have been presented into two following sub-sections; the first section deals with vulnerability and second section deals with livelihood resilience.

Vulnerability

The concept of vulnerability

The major characteristics of vulnerability are its dynamic nature that influences people's social and biophysical processes (IPCC, 2014). Significant attention is needed from the researchers and policymakers to develop successful adaptation strategies. Citizens of developing countries are highly vulnerable due to low income and dependency on agriculture (UNDP, 2008). These burdens should spark exploration of potential adaptive capacities for resource poor communities. People's susceptibility to the impact vulnerability of natural hazards are increasing to almost all spheres of life like social physical, human, financial, and natural dimensions. Though the effect of

http://www.aloki.hu ● ISSN 1589 1623 (Print) ● ISSN 1785 0037 (Online)
DOI: http://dx.doi.org/10.15666/aeer/1706_1276912785

natural hazards may be occasional, seasonal or year-round, the extent of exposure varies across communities.

Rural livelihood is highly dependent on climatic variability as its dependence on agriculture. Livelihood vulnerability means the susceptibility of livelihood system of stressors. Since the livelihood system of a community comprises natural, human, social, physical and financial capitals that mean it solely depends on the socio-ecological system. According to DasGupta and Shaw (2015), rural livelihood is adversely affected by the effect of climate change. Abid et al. (2016) mention that rural livelihood is dependent on a complex system of institutional, biophysical, financial and political condition of the community. Livelihood vulnerability actually focuses the exposure, sensitivity as well as adaptive capacity of an individual's livelihood or a community's livelihood in the face of natural disasters.

Dimensions of vulnerability

The major three components of livelihood vulnerability are exposure, sensitivity and adaptive capacity (*Fig. 2*). Exposure addresses the extent of a system facing varying climate conditions. It generally focuses the condition of an individual or community during facing variable climatic situations. It shows the frequency, and extent of loss in terms of livelihood capitals. Sensitivity means the degree of a system which addresses how sensitive to the variable climatic conditions. It generally focuses the reaction of an individual or community during facing changing climatic situations. It also shows the frequency, and sensitiveness in terms of livelihood capitals. Adaptive capacity is the ability of a system to withstand against the stressors and shocks. It emphasizes the ability of an individual or a society to tackle or control the situation which occurs during natural hazards.

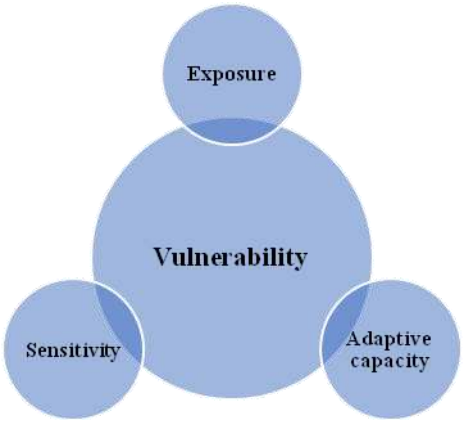

Figure 2. *The major elements of vulnerability in a socio-ecological system*

Vulnerability of the people of developing countries is almost similar all over the world such as flooding, riverbank erosion, drought, storm, cyclone, crop and livestock diseases infestation. Paavola (2008) conducted a study on livelihood vulnerability of Tanzanian farmers and reported that agricultural farming-based livelihood is highly vulnerable to climatic variability. Livelihood system is varied from community to community such as livelihood of the people of rural Burkin Faso is solely dependent crop cultivation, livestock and agroforestry and they suffer from seasonal food

http://www.aloki.hu ● ISSN 1589 1623 (Print) ● ISSN 1785 0037 (Online)
DOI: http://dx.doi.org/10.15666/aeer/1706_1276912785

insecurity due to climatic variability (Addisu et al., 2016). Jacobi conducted a study on the livelihood of the fish farming community in Kenya and reported that climatic variability was the main drivers of vulnerability to the community. Beckford and Rhiney (2016) assess the vulnerability of a community living in north eastern St Vincent and concluded that the main driver of poverty was livelihood vulnerability caused by environmental variability and globalization. Climate change is one of the main drivers of livelihood vulnerability of the people of coastal areas especially natural resources dependent people. Chinwendu et al. (2017) conducted a study on household vulnerability and adaptation to climate change in Kaduna river basin in Nigeria and reported that livelihood vulnerability was varied from village to village of riverbank community due to varies of sensitivity to risk, uncertainty and limited access to natural resources and institutional capacity. Antwi et al. (2015) assessed the community vulnerability of a flood prone community in Ghana and mentioned that climate induced disasters make the people vulnerable in terms of socio-ecological, financial and political aspects.

Natural disasters are the outcome of interaction among hazard and stake, living and non-living and fixed and moving elements which causes human, economic, environmental, socio-political losses and cultural crisis in people's livelihood. Most of the rural communities have faced vulnerabilities in terms of various livelihood capitals such as social, political, financial and natural assets due to dynamic changes of environment in Zimbabwe (Nyamwanza, 2012). Wilson (2014) conducted a study on livelihood vulnerability and politics of adaptation in Alaska and reported that subsistence livelihood of the people was highly vulnerable due to climate change impact which could be minimized through developing context specific adaptation strategies. Literature across the world shows that changing climate is the main driver of livelihood vulnerability which affects almost all aspects of human life.

Livelihood resilience

The concept of livelihood resilience

Livelihood is a way of living which is comprised of the capabilities, assets, and activities. Livelihood resilience is the ability of a people or a community to sustain and retain livelihood opportunities in a stress situation which caused by the disturbances of social-ecological system, political system, and financial reasons. Resilience is a set of behaviors that stimulate social transformation and empower a group of people or social system (Earvolino-Ramirez, 2007; Gaillard, 2010; Jorgenson et al., 2010; Scholz et al., 2012). Livelihood resilience integrates livelihood system with resilience in a way where people are the main actors in the adaptation practices. The environmental factors are responsible for hampering the livelihood system of resource poor and vulnerable people to conduct their daily life (Adger, 1999). It thus requires an in-depth investigation of how climatic factors influence the livelihoods of people. Though sustainable livelihood framework is developed for the use of international agencies for poverty alleviation through improving livelihood assets, it adds a new dimension for livelihood research especially for the livelihoods which associated with the vulnerability, shocks, and stress of social and ecological systems (Vogel et al., 2007; Zebrowski, 2013). Importantly, people are the central concern of livelihood thinking where ecological factors, social and political factors, market, technology and resources are the associated factors related to livelihood (Panthi et al., 2016).

http://www.aloki.hu ● ISSN 1589 1623 (Print) ● ISSN 1785 0037 (Online)
DOI: http://dx.doi.org/10.15666/aeer/1706_1276912785

Livelihood resilience however, stimulates the capacities of an individual, community or administrative system to respond to the challenges, risks, stressors and disturbances. It also enables people to perceive the risks and uncertainties of social-ecological systems and to take anticipatory actions to tackle the adverse situation. An ideal resilience system requires natural resources, information and access to physical, economic and logistic assets for developing the system against the disturbances of the environment. Livelihood resilience also integrates social networks with human rights for resilience thinking. Both human rights and social network are essential elements of social system to develop the capacity of the system against any adverse situation.

Livelihood resilience thinking from sustainable livelihood framework

The present study borrows the concept of ecological resilience for livelihood inquiry for better explanation of livelihood resilience in the disaster vulnerability context. The other concept of resilience is indirectly related to livelihood system because of its relation to the changing climate, stress and shocks as well as physical infrastructure, social and economic system and institutional responses. Since ecological system is completely different from livelihood system, this study considers all related dimensions of social and ecological systems for better integration of livelihood inquiry to resilience. A sustainable livelihood approach is followed to assess the livelihood pattern which consists of the analysis in the context of people's livelihood. This approach confirms Sen's (1981) classic focus entitlement, Long's (1984) action oriented approach, and Chambers and Conway's (1992) seminal paper on sustainable livelihood. Sustainable livelihood approach is a well-accepted approach which has emerged in 1990s for assessing the livelihood system and strategies in the face of natural disasters and vulnerability of rural people. According to sustainable livelihood approach (following Chambers and Conway, 1992; Scoones, 1998), livelihood is a set of physical and social assets, and actions for living as well as it can be sustainable in such a condition when it is able to cope with and retain from risk, uncertainty and stress through enhancing capabilities and without hampering the natural resources.

The sustainable livelihood approach considers demographic, socio-economic, political and ecological context of people's life and access to social, economic, physical, natural and human capitals as well as institutional aspects for ensuring people's access and control over assets. Various scholars developed some analytical framework by using the diagrammatic checklist developed by Scoones (1998) such as vulnerability framework by Moser (1998), capitals and capability framework of Bebbington (1999) and micro-policy analytical framework by Ellis (2000). Using the principles of sustainable livelihood framework, some renowned organization already developed their operational SLF such as Cooperative for Assistance and Relief Everywhere (CARE), Department for International Development (DFID), Oxfam and the United Nations Development Program (UNDP). Since various organization developed their livelihood analysis framework in the light of SLF, this study only considers SLF for guiding own research direction.

There is an increasing trend of using the sustainable livelihood framework in assessing vulnerability, risk, uncertainty and livelihood literatures (for example, Can et al., 2013; Amos, et al., 2015; Addisu et al., 2016; Alam, 2016; Bhuiyan et al., 2017) all over the world. Sustainable livelihood framework (SLF) is a basis of rural vulnerability studies irrespective of the country (for example Li et al., 2018; Pandey et al., 2017). Theoretically, the sustainable livelihood framework (SLF) is developed to deal with

http://www.aloki.hu ● ISSN 1589 1623 (Print) ● ISSN 1785 0037 (Online)
DOI: http://dx.doi.org/10.15666/aeer/1706_1276912785

condition where the poor perform as 'strategic managers' in transferring the livelihoods outcomes, through a set of livelihood activities in accordance with the entitlements and access to resources, as decided by the conditions of institutional contexts (Moser, 1998). The sustainable frameworks point to assets as central concern which is mainly affected by the environmental stressors. Livelihood strategies and institutional process are the driver for transforming the vulnerable context to sustainable livelihood. Livelihood strategies are the strategies taken by the people for maintaining their livelihood and institutional process is responsible for translating the assets and strategies into action for making desirable and sustainable changes in people's livelihood. The major livelihood strategies of rural people are agricultural practices, diversification of livelihood, and migration (Ellis, 2008).

The SLF approach may be explained in three ways; first, framework for short-term livelihood trajectories; second, a way of development activities; and third, outline of overall development. In the livelihood related literature, the SLF was possibly envisioned as the earlier; as "a diagram to organize ideas into manageable categories, to identify entry points and critical processes, and assist with prioritizing catalysts for change that can improve people's livelihoods" (Ellis, 2000).

Strength of sustainable livelihood framework

Vulnerability assessment requires understanding of the SLF in terms of its strengths and weakness for building a concrete method of assessment (Pandey et al., 2017). Due to its strength, it is well accepted all over the world for livelihood assessment. The main strengths of SLF are focusing people-centeredness, people's capabilities and holisticness. First, SLF is people-centered approach which focuses people's realities, strengths and compromises to others. It emphasizes local complexities and realities for analyzing the issues in a better way. Second, SLF analyzes people's capabilities and strengths which is necessary for overcoming risk, uncertainty and livelihood insecurity (Ekblom, 2012). Third, SLF is a holistic in nature in terms of its recognition to multiple strategies, actors and outcomes where people's livelihood is connected. So, it is applicable to assess the dynamics of livelihood vulnerability of char dwellers in Bangladesh. Sustainable livelihood framework has broad aspects of inquiry covering vulnerability, shocks, risks, assets, institutional response, strategies of livelihood and outcomes which may be a toolkit for livelihood analysis. According to Clark and Carney (2008), SLF is a key analytical tool to assess and understand various aspects of the livelihood of people.

Weakness of sustainable livelihood framework

Though SLF is well accepted by various scholar but it is still criticized due to ignoring or avoiding some important issues. The main limitation of SLF is its inability to address the social, political, and institutional aspects (Scoones, 2009). It actually avoids focusing the role of structures, acting process, and institutions rather emphasizing assets and activities of household though the assets are not neutral due to its inclusion and exclusion nature (Antwi et al., 2015). SLF generally assess the livelihood status at household level which is a key to local context but less concentration to connect with national and global level. Livelihood vulnerability analysis requires an emphasize on a connection with institutional levels for better integration with the institutional capital irrespective of micro or macro level

http://www.aloki.hu ● ISSN 1589 1623 (Print) ● ISSN 1785 0037 (Online)
DOI: http://dx.doi.org/10.15666/aeer/1706_1276912785

perspectives. An importance on institutional process and political economy focusing structural forces is necessary to assess the dynamic of rural livelihoods and resilience (Scoones, 2009) but present form of SLF cannot meet this issue. Besides the term "sustainable," a core term of SLF, has not been properly focused in terms of variable local context (Bhattacharjee and Behera, 2018).

SLF cannot provide the answers to some quires such as 'sustainable to what and for whom' whose reality to be addressed? (Chambers and Conway, 1992) which are very much important in dynamic vulnerability context. According to Longley and Maxwell (2013), SLF is very much developed and applicable only for reducing poverty in relatively stable context. One of the major weak points of SLF is how to address sustainability in the dynamic vulnerability context where livelihood assets are recurrently hampered with environmental factors. SLF is basically outcome-based approach which cannot address the related process and capacities. It focuses only on short-term dynamics rather than long term which reduce the ability to address the dynamic vulnerability context of livelihood.

From sustainable livelihoods to resilient livelihoods thinking

This study attempts to develop a framework for addressing the weakness of SLF and assess the dynamic context of vulnerability and livelihood through including elements of adaptive, absorptive and transformative capacity. Resilience thinking is the advanced option of livelihood vulnerability assessment following SLF but addressing all weakness of SFL. This study adopted SLF for operationalization of the perspective of resiliency using the useful idea from SLF for better understanding the dynamic vulnerable context. The transformation from sustainable livelihood to resilient livelihood is summarized and presented in *Table 1*.

Table 1. *Summarizing main aspects on shifts from sustainable to resilient livelihoods thinking (Source: adapted after Nyamwanza, 2012)*

Sustainable livelihoods thinking	Resilient livelihoods thinking
Sustainability	Resiliency by adaptive, absorptive and transformative capacity
Assets	Institutions and assets
Linking household and geographical/spatial scales	Linking institution, community, household and temporal scales
Coping and short-term dynamics	Both coping and adapting – however focusing more on long-term adaptation dynamics
Outcome-oriented	Process-oriented

It is well established that the core ideas of sustainable livelihood framework form the central position of the analysis of dynamic vulnerability context. In this study, resilient livelihood thinking is focused on using the useful ideas from sustainable livelihoods for better understanding the dynamics of changing vulnerability context. The resiliency perspective as advanced in this work builds on the strengths of this thinking, blending it with new ideas in taking livelihood analysis forward – from thinking about 'sustainable' livelihoods to 'resilient' livelihoods. Ideas from Scoones's (1998) 'diagrammatic checklist' and Ellis's (2000) livelihoods framework were used in the adapted framework to guide analysis. This is because while showing general interrelationships and

http://www.aloki.hu ● ISSN 1589 1623 (Print) ● ISSN 1785 0037 (Online)
DOI: http://dx.doi.org/10.15666/aeer/1706_1276912785

connections, these scholars' presentations provide room for re-arranging ideas and infusing new ones as they seem less rigidly formulated to show particular linear or contextual patterns. *Table 1* summarizes the major aspects vis-à-vis shifts from sustainable livelihoods to resilient livelihood thinking as raised in various discussions in this work so far.

The conceptual framework (*Fig. 3*) has been developed by following 'diagrammatic checklist' of Scoones (1998), livelihood framework of Ellis (2000) and livelihood framework for resilience of Nyamwanza (2012). This selection is due to the flexibility of their framework to include element, re-arranging ideas and developing new one for context specific livelihood analysis. The conceptual framework focuses vulnerability context (flood, drought, riverbank erosion, cyclones, shocks, and risks), livelihood assets (human, natural, social, physical and financial assets), institutions (household, community, sub-national, and national level), adaptive strategies (livelihood strategies), various capacities (adaptive, absorptive, and transformative capacity) and outcome related livelihood.

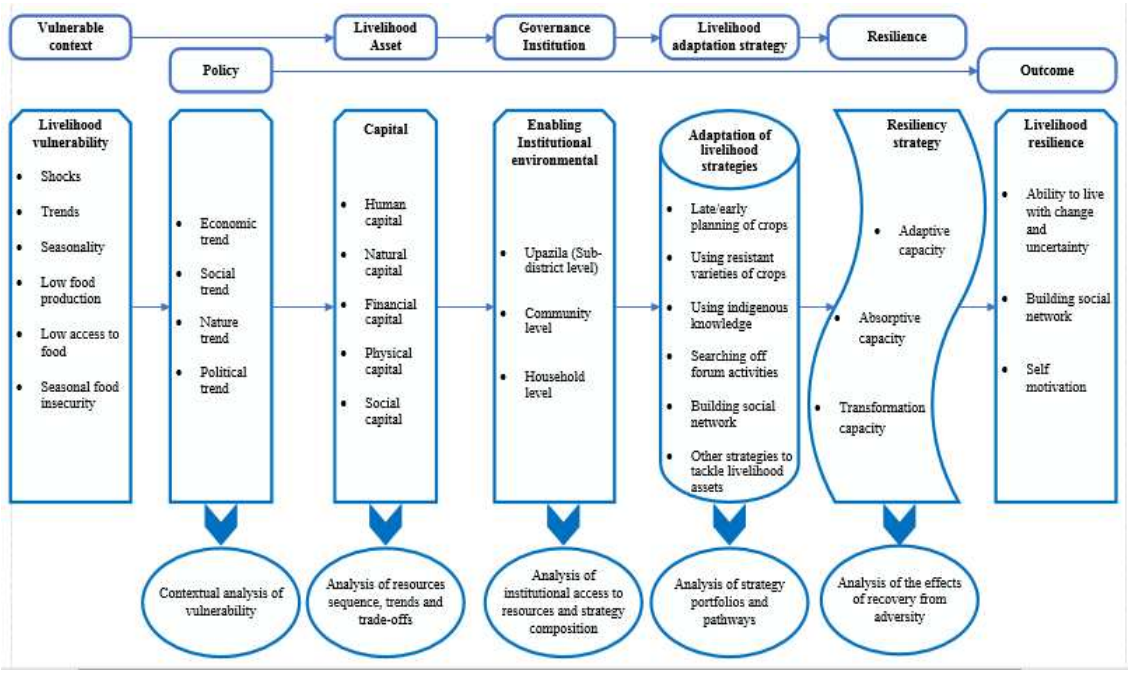

Figure 3. *Adapted livelihood framework for resilience (Source: adapted after Scoones, 1998; Ellis, 2000; Nyamwanza, 2012)*

The framework will be applicable to analyze the vulnerability of any community especially who are facing the adverse of climate change. It will help to interpret the factors responsible for livelihood vulnerability, and the positive effect of policy measures and livelihood assets to overcome the vulnerable condition. It also provides the direction of how government institution can solve and improve the vulnerability context and which level is most suitable for government intervention. This framework might be useful for its adaptation strategies for improving livelihood condition in a vulnerability context. It also focuses how resilience capacities developed and work in a vulnerable livelihood context for obtaining a self-motivation, strong social network and ability to live with uncertainty.

http://www.aloki.hu ● ISSN 1589 1623 (Print) ● ISSN 1785 0037 (Online)
DOI: http://dx.doi.org/10.15666/aeer/1706_1276912785

Conclusion

The concept of livelihood resilience is relatively new in natural disaster vulnerability context. This study attempts to clarify the livelihood resilience concept from the perspective of climate change vulnerability and natural disasters. It analyzes the resilience concept by focusing on various dimensions of vulnerability and resilience. It also integrates the livelihood system to the resilience concept successfully through analyzing more related existing literature of the renowned databases. This study reveals that vulnerability is a function of exposure, sensitivity and adaptive capacity of a system in which exposure and sensitivity are positively related to vulnerability while adaptive capacity is negatively related. Similarly, livelihood resilience is a function of the adaptive, absorptive and transformative capacity of livelihood system which enables people to sustain and retain livelihood opportunities in stress events caused by natural disasters. Livelihood capitals (e.g. social, natural, human, physical and financial capital) help to enhance the capacity of the people in the face of climate change vulnerability. This study also interprets the development of resilient livelihood thinking from traditional sustainable livelihood framework which is suffering from various weaknesses. This study argues that livelihood resilience is more advanced and suitable approach to address disaster related vulnerability issues. This study further argues that resilience livelihood framework and related indicators will help to assess the vulnerability of a socio-ecological system and to take proper measure to improve livelihood resilience of any vulnerable people, group or community. The study suggests conducting in-depth empirical study on livelihood resilience assessment in the natural disaster prone vulnerability context using specific indicators developed in this study for future research.

Acknowledgements. This article is funded by Management Science and National Governance Disciplines Platform of Sichuan University, Sichuan University Innovation Spark Project (No.2018hhs-21), Sichuan University Central University Basic Scientific Research Project (No.skqx201501).

REFERENCES

[1] Abid, M., Schilling, J., Scheffran, J., Zulfiqar, F. (2016): Climate change vulnerability, adaptation and risk perceptions at farm level in Punjab, Pakistan. – Science of the Total Environment 547: 447-460. https://doi.org/10.1016/j.scitotenv.2015.11.125.

[2] Addisu, L. S., Olutayo, O. A., Sulaiman, H., Rao, P. (2016a): Assessing climate change impacts in the Lake Tana Sub-Basin, Ethiopia using livelihood vulnerability approach. – Journal of Earth Science Climatic Change 7(9): https://doi.org/10.4172/2157-7617.1000368.

[3] Addisu, S., Fissha, G., Gediff, B., Asmelash, Y. (2016a): Perception and adaptation models of climate change by the rural people of lake Tana Sub-Basin, Ethiopia. – Environmental Systems Research 5(1): 7. https://doi.org/10.1186/s40068-016-0059-0.

[4] Adger, W. N. (1999): Social vulnerability to climate change and extremes in coastal Vietnam. – World Development 27(2): 249-269. https://doi.org/10.1016/S0305-750X(98)00136-3.

[5] Adger, W. N. (2005): Social-ecological resilience to coastal disasters. – Science 309(5737): 1036-1039. https://doi.org/10.1126/science.1112122.

[6] Ajibade, I., McBean, G., Bezner-Kerr, R. (2013): Urban flooding in Lagos, Nigeria: patterns of vulnerability and resilience among women. – Global Environmental Change 23(6): 1714-1725. https://doi.org/10.1016/j.gloenvcha.2013.08.009.

http://www.aloki.hu ● ISSN 1589 1623 (Print) ● ISSN 1785 0037 (Online)
DOI: http://dx.doi.org/10.15666/aeer/1706_1276912785

[7] Akhtar, N., Saqib, Z., Khan, M. I., Martin, M. A., Atif, S. B., Zaman, M. H. (2019): A bibliometric analysis of contemporary research regarding industrial symbiosis: a path towards urban environmental resilience. – Applied Ecology and Environmental Research 17(1): 1159-1221. https://doi.org/10.15666/aeer/1701_11591221.

[8] Alam, G. M. M. (2016): An assessment of the livelihood vulnerability of the riverbank erosion hazard and its impact on food security for rural households in Bangladesh. – PhD Dissertation, University of Southern Queensland, Toowoomba, Australia.

[9] Alam, G. M. M., Alam, K., Mushtaq, S., Filho, W. L. (2018): How do climate change and associated hazards impact on the resilience of riparian rural communities in Bangladesh? Policy implications for livelihood development. – Environmental Science Policy 84: 7-18. https://doi.org/10.1016/j.envsci.2018.02.012.

[10] Amos, E., Akpan, U., Ogunjobi, K. (2015): Households' perception and livelihood vulnerability to climate change in a coastal area of Akwa Ibom State, Nigeria. – Environment, Development and Sustainability 17(4): 887-908. https://doi.org/10.1007/s10668-014-9580-3.

[11] Antwi, E. K., Boakye-Danquah, J., Barima Owusu, A., Loh, S. K., Mensah, R., Boafo, Y. A., Apronti, P. T. (2015): Community vulnerability assessment index for flood prone savannah agro-ecological zone: a case study of Wa West District, Ghana. – Weather and Climate Extremes 10: 56-69. https://doi.org/10.1016/j.wace.2015.10.008.

[12] Bebbington, A. (1999): Capitals and capabilities: A Framework for Analyzing Peasant Viability, Rural Livelihoods and Poverty. – World Development 27(12): 2021-2044. https://doi.org/10.1016/S0305-750X(99)00104-7.

[13] Beckford, C. L., Rhiney, K. (2016): Globalization, Agriculture and Food in the Caribbean. – In: Beckford, C. L., Rhiney, K. (eds.) Globalization, Agriculture and Food in the Caribbean: Climate Change, Gender and Geography. Palgrave Macmillan, London. https://doi.org/10.1057/978-1-137-53837-6.

[14] Bhattacharjee, K., Behera, B. (2018): Determinants of household vulnerability and adaptation to floods: empirical evidence from the Indian State of West Bengal. – International Journal of Disaster Risk Reduction 31: 758-769. https://doi.org/10.1016/j.ijdrr.2018.07.017.

[15] Bhuiyan, M. A. H., Islam, S. M. D.-U., Azam, G. (2017): Exploring impacts and livelihood vulnerability of riverbank erosion hazard among rural household along the river Padma of Bangladesh. – Environmental Systems Research 6(1): 25. https://doi.org/10.1186/s40068-017-0102-9.

[16] Can, N. D., Tu, V. H., Hoanh, C. T. (2013): Application of livelihood vulnerability index to assess risks from flood vulnerability and climate variability—a case study in the Mekong Delta of Vietnam. – Journal of Environmental Science and Engineering 2: 476-486.

[17] Chaffin, B. C., Scown, M. (2018): Social-ecological resilience and geomorphic systems. – Geomorphology 305: 221-230. https://doi.org/10.1016/j.geomorph.2017.09.038.

[18] Chambers, R., Conway, G. R. (1992): Sustainable Rural Livelihoods: Practical Concepts for the 21st Century. – Institute of Development Studies, UK.

[19] Chinwendu, O. G., Sadiku, S. O. E., Okhimamhe, A. O., Eichie, J. (2017): Households vulnerability and adaptation to climate variability induced water stress on downstream Kaduna River Basin. – American Journal of Climate Change 6(02): 247-267. https://doi.org/10.4236/ajcc.2017.62013.

[20] Clarke, J., Carney, D. (2008): Sustainable livelihoods approaches - what have we learned? – Background paper for ESRC Livelihoods Seminar, Institute of Development Studies, Brighton. https://doi.org/10.3362/0262-8104.2002.002.

[21] Cutter, S. L., Boruff, B. J., Shirley, W. L. (2003): Social vulnerability to environmental hazards. – Social Science Quarterly 84(2): 242-261. https://doi.org/10.1111/1540-6237.8402002.

http://www.aloki.hu ● ISSN 1589 1623 (Print) ● ISSN 1785 0037 (Online)
DOI: http://dx.doi.org/10.15666/aeer/1706_1276912785

[22] DasGupta, R., Shaw, R. (2015): An indicator based approach to assess coastal communities' resilience against climate related disasters in Indian Sundarbans. – Journal of Coastal Conservation 19(1): 85-101. https://doi.org/10.1007/s11852-014-0369-1.
[23] Dyakov, N. (2013): Alien species invasion and diversity of riparian forest according to environmental gradients and disturbance regime. – Applied Ecology and Environmental Research 11(2): 249-272. https://doi.org/10.15666/aeer/1102_249272.
[24] Earvolino-Ramirez, M. (2007): Resilience: a concept analysis. – Nursing Forum 42(2): 73-82. https://doi.org/10.1111/j.1744-6198.2007.00070.x.
[25] Ekblom, A. (2012): Livelihood security, vulnerability and resilience: a historical analysis of Chibuene, Southern Mozambique. – Ambio 41(5): 479-489. https://doi.org/10.1007/s13280-012-0286-1.
[26] Ellis, F. (2000): Rural Livelihoods and Diversity in Developing Countries. – Oxford University Press, Oxford, pp. 1-256.
[27] Ellis, F. (2008): The determinants of rural livelihood diversification in developing countries. – Journal of Agricultural Economics 51(2): 289-302. https://doi.org/10.1111/j.1477-9552.2000.tb01229.x.
[28] Fatemi, F., Ardalan, A., Aguirre, B., Mansouri, N., Mohammadfam, I. (2017): Social vulnerability indicators in disasters: findings from a systematic review. – International Journal of Disaster Risk Reduction 22: 219-227. https://doi.org/10.1016/j.ijdrr.2016.09.006.
[29] Fox-Lent, C., Linkov, I. (2018): Resilience matrix for comprehensive urban resilience planning. – Lecture Notes in Energy 65: 29-47. https://doi.org/10.1007/978-3-319-75798-8_2.
[30] Gaillard, J. C. (2010): Vulnerability, capacity and resilience: perspectives for climate and development policy. – Journal of International Development 22(2): 218-232. https://doi.org/10.1002/jid.1675.
[31] Garamvölgyi, Á. (2013): Impacts of climate change on vegetation distribution no. 1 -- climate change induced vegetation shifts in the palearctic region. – Applied Ecology and Environmental Research 11(1): 79-122. https://doi.org/10.15666/aeer/1101_079122.
[32] Garcia-Dia, M. J., DiNapoli, J. M., Garcia-Ona, L., Jakubowski, R., O'Flaherty, D. (2013): Concept analysis: resilience. – Archives of Psychiatric Nursing 27(6): 264-270. https://doi.org/10.1016/j.apnu.2013.07.003.
[33] Gwimbi, P. (2009): Linking rural community livelihoods to resilience building in flood risk reduction in Zimbabwe. – Jàmbá: Journal of Disaster Risk Studies 2(1): 71-89. https://doi.org/10.4102/jamba.v2i1.16.
[34] Ho, H. Y., Lee, Y. L., Hu, W. Y. (2012): Elder resilience: a concept analysis. – Journal of Nursing 59(2): 88-92. https://doi.org/10.1111/j.1744-6198.2007.00070.x.
[35] Hoa, A. X. (2019): Advancing smallholders' sustainable livelihood through linkages among stakeholders in the Cassava (Manihot Esculenta Crantz) value chain: the case of Dak Lak province, Vietnam. – Applied Ecology and Environmental Research 17(2): 5193-5217. https://doi.org/10.15666/aeer/1702_51935217.
[36] Holling, C. S. (1973): Resilience and stability of ecological systems. – Annual Review of Ecology and Systematics 4(1): 1-23. https://doi.org/10.1146/annurev.es.04.110173.000245.
[37] Sarker, M. N. I., Wu, M., Shouse, R. C., Ma, C. (2019): Administrative Resilience and Adaptive Capacity of Administrative System: A Critical Conceptual Review. – In: Xu, J. et al. (ed.) Lecture Notes on Multidisciplinary Industrial Engineering. Springer, Switzerland, pp. 1-13. https://doi.org/10.1007/978-3-030-21255-1_55.
[38] IPCC (2014): Climate change 2014: Impacts, adaptation and vulnerability. Fifth assessment report. – In: Intergovernmental Panel on Climate Change. – Cambridge University Press, Cambridge, UK.

http://www.aloki.hu ● ISSN 1589 1623 (Print) ● ISSN 1785 0037 (Online)
DOI: http://dx.doi.org/10.15666/aeer/1706_1276912785

[39] Jamali, A. A., Zarekia, S., Randhir, T. O. (2018): Risk assessment of sand dune disaster in relation to geomorphic properties and vulnerability in the Saduq-Yazd Erg. – Applied Ecology and Environmental Research 16(1): 579-590. https://doi.org/10.15666/aeer/1601_579590.

[40] Janssen, M. A., Schoon, M. L., Ke, W., Börner, K. (2006): Scholarly networks on resilience, vulnerability and adaptation within the human dimensions of global environmental change. – Global Environmental Change 16(3): 240-252. https://doi.org/10.1016/j.gloenvcha.2006.04.001.

[41] Jorgenson, M. T., Romanovsky, V., Harden, J., Shur, Y., O'Donnell, J., Schuur, E. A. G., … Marchenko, S. (2010): Resilience and vulnerability of permafrost to climate change. – Canadian Journal of Forest Research 40(7): 1219-1236. https://doi.org/10.1139/X10-060.

[42] Lee, Y. J. (2014): Social vulnerability indicators as a sustainable planning tool. – Environmental Impact Assessment Review 44: 31-42. https://doi.org/10.1016/j.eiar.2013.08.002.

[43] Li, C., Wang, M., Song, Y. (2018): Vulnerability and livelihood restoration of landless households after land acquisition: evidence from peri-urban China. – Habitat International 79: 109-115. https://doi.org/10.1016/j.habitatint.2018.08.003.

[44] Long, N. (1984): Family and Work in Rural Societies-Perspectives on Non-Wage Labour. – Tavistock, London.

[45] Longley, C., Maxwell, D. (2013): Livelihoods, Chronic conflict and humanitarian response: a synthesis of current practice (No. 182). – ODI Working Paper, London SE3 7JD, UK.

[46] Manyena, S. B. (2006): Rural local authorities and disaster resilience in Zimbabwe. – Disaster Prevention and Management: An International Journal 15(5): 810-820. https://doi.org/10.1108/09653560610712757.

[47] Moher, D., Liberati, A., Tetzlaff, J., Altman, D. G., Altman, D., Antes, G., … Tugwell, P. (2009): Preferred reporting items for systematic reviews and meta-analyses: the PRISMA statement. – PLoS Medicine 6(7): 1-5. https://doi.org/10.1371/journal.pmed.1000097.

[48] Moser, C. O. N. (1998): The asset vulnerability framework: reassessing urban poverty reduction strategies. – World Development 26(1): 1-19. https://doi.org/10.1016/S0305-750X(97)10015-8.

[49] Nistor, M. M., Nicula, A. S., Cervi, F., Man, T. C., Irimuş, I. A., Surdu, I. (2018): Groundwater vulnerability GIS models in the Carpathian mountains under climate and land cover changes. – Applied Ecology and Environmental Research 16(4): 5095-5116. https://doi.org/10.15666/aeer/1604_50955116.

[50] Nyamwanza, A. M. (2012): Resiliency and Livelihoods Inquiry in Dynamic Vulnerability Contexts: Insights from Northern Zimbabwe. – The University of Manchester, UK.

[51] Omotoso, A. B., Daud, A. S., Adebayo, R. A., Omotayo, A. O. (2018): Socioeconomic determinants of rural households'food crop production in Ogun state, Nigeria. – Applied Ecology and Environmental Research 16(3): 3627-3635. https://doi.org/10.15666/aeer/1603_36273635.

[52] Paavola, J. (2008): Livelihoods, vulnerability and adaptation to climate change in Morogoro, Tanzania. – Environmental Science Policy 11(7): 642-654. https://doi.org/10.1016/j.envsci.2008.06.002.

[53] Pandey, R., Jha, S. K., Alatalo, J. M., Archie, K. M., Gupta, A. K. (2017): Sustainable livelihood framework-based indicators for assessing climate change vulnerability and adaptation for Himalayan communities. – Ecological Indicators 79: 338-346. https://doi.org/10.1016/j.ecolind.2017.03.047.

[54] Panthi, J., Aryal, S., Dahal, P., Bhandari, P., Krakauer, N. Y., Pandey, V. P. (2016): Livelihood vulnerability approach to assessing climate change impacts on mixed agro-

http://www.aloki.hu ● ISSN 1589 1623 (Print) ● ISSN 1785 0037 (Online)
DOI: http://dx.doi.org/10.15666/aeer/1706_1276912785

livestock smallholders around the Gandaki River Basin in Nepal. – Regional Environmental Change 16(4): 1121-1132. https://doi.org/10.1007/s10113-015-0833-y.
[55] Sarker, M. N. I., Wu, M., Alam, G. M. M., Shouse, R. C. (2019): Livelihood vulnerability of riverine-island dwellers in the face of natural disasters in Bangladesh. – Sustainability 11(6): 1623. https://doi.org/10.3390/su11061623.
[56] Scholz, R. W., Blumer, Y. B., Brand, F. S. (2012): Risk, vulnerability, robustness, and resilience from a decision-theoretic perspective. – Journal of Risk Research 15(3): 313-330. https://doi.org/10.1080/13669877.2011.634522.
[57] Scoones, I. (1998): Sustainable rural livelihoods: a framework for analysis. – IDS Working Paper (No. 72). https://doi.org/10.1057/palgrave.development.1110037.
[58] Scoones, I. (2009): Livelihoods perspectives and rural development. – The Journal of Peasant Studies 36(1): 37-41. https://doi.org/10.1080/03066150902820503.
[59] Sen, A. (1981): Poverty and Famines. – Clarendon Press, Oxford, UK. https://doi.org/10.1086/451432.
[60] Shah, A. A., Ye, J., Abid, M., Khan, J., Amir, S. M. (2018): Flood hazards: household vulnerability and resilience in disaster-prone districts of Khyber Pakhtunkhwa province, Pakistan. – Natural Hazards 93(1): 147-165. https://doi.org/10.1007/s11069-018-3293-0.
[61] Tanner, T., Lewis, D., Wrathall, D., Bronen, R., Cradock-Henry, N., Huq, S., … Thomalla, F. (2015): Livelihood resilience in the face of climate change. – Nature Climate Change 5(1): 23-26. https://doi.org/10.1038/nclimate2431.
[62] Terin, M. (2019): Determining factors in food away from home expenditure of Turkish households. – Applied Ecology and Environmental Research 17(2): 3441-3455. https://doi.org/10.15666/aeer/1702_34413455.
[63] Tompkins, E. L., Adger, W. N. (2004): Does adaptive management of natural resources enhance resilience to climate change? – Ecology and Society 9(2): 1-14. https://doi.org/10.5751/ES-00667-090210.
[64] UNDP (2008): Human Development Reports 2007/8. – In: Fighting Climate Change: Human Solidarity in a Divided World. United Nations Development Programme. Kluwer Academic Publishers, Dordrecht, pp. 1-115.
[65] United Nations (2013): United Nations Plan of Action on Disaster Risk Reduction for Resilience. – United Nations System, Chief Executives Board for Coordination, USA, pp-6-8.
[66] Vandenbroucke, J. P., Von Elm, E., Altman, D. G., Gøtzsche, P. C., Mulrow, C. D., Pocock, S. J., … Egger, M. (2007): Strengthening the reporting of observational studies in epidemiology (STROBE): explanation and elaboration. – PLoS Medicine 4(10): 1628-1654. https://doi.org/10.1371/journal.pmed.0040297.
[67] Vogel, C., Moser, S. C., Kasperson, R. E., Dabelko, G. D. (2007): Linking vulnerability, adaptation, and resilience science to practice: pathways, players, and partnerships. – Global Environmental Change 17(3-4): 349-364. https://doi.org/10.1016/j.gloenvcha.2007.05.002.
[68] Walker, B., Salt, D. (2012): Practicing Resilience in Different Ways. – In: Walker, B., Salt, D. (eds.) Resilience Practice. Island Press/Center for Resource Economics, Washington, DC, pp. 145-167. https://doi.org/10.5822/978-1-61091-231-0_9.
[69] Weldegebriel, Z. B., Amphune, B. E. (2017): Livelihood resilience in the face of recurring floods: an empirical evidence from Northwest Ethiopia. – Geoenvironmental Disasters 4(1): 10. https://doi.org/10.1186/s40677-017-0074-0.
[70] Wilson, N. J. (2014): The politics of adaptation: subsistence livelihoods and vulnerability to climate change in the Koyukon Athabascan Village of Ruby, Alaska. – Human Ecology 42(1): 87-101. https://doi.org/10.1007/s10745-013-9619-3.
[71] Zebrowski, C. (2013): The nature of resilience. – Resilience 1(3): 159-173. https://doi.org/10.1080/21693293.2013.804672.

http://www.aloki.hu ● ISSN 1589 1623 (Print) ● ISSN 1785 0037 (Online)
DOI: http://dx.doi.org/10.15666/aeer/1706_1276912785

APPENDIX

Appendix A

The following search strategies have been followed

Web of science:	TS = (resilien* AND vul)
Engineering village:	resilience AND vulnerability ---- > climate change ---- > disaster
Scopus:	(TITLE-ABS-KEY (resilience AND vulnerability)) AND (livelihood AND resilience) AND (LIMIT-TO (DOCTYPE , “ar”) OR LIMIT-TO (DOCTYPE , “cp”) OR LIMIT-TO (DOCTYPE , “ch”) OR LIMIT-TO (DOCTYPE , “ip”) OR LIMIT-TO (DOCTYPE , “bk”)) AND (LIMIT-TO (SUBJAREA , “SOCI”)) AND (LIMIT-TO (LANGUAGE , “English”))

Appendix B

The following articles have been selected for the systematic literature review due to more relevancy

Sl no.	Researcher	Title	Method	Sources/journal
1	Adger (1999)	Social Vulnerability to Climate Change and Extremes in Coastal Vietnam	Quantitative	World Development
2	Kleine et al. (2003)	Resilience to natural hazards: How useful is this concept?	Critical review	Environmental Hazards
3	Adger (2005)	Social-Ecological Resilience to Coastal Disasters	Quantitative	Science
4	Adger (2006)	Vulnerability	Quantitative	Global Environmental Change
5	Thomalla et al. (2006)	Reducing hazard vulnerability: towards a common approach between disaster risk reduction and climate adaptation	Quantitative	Disasters
6	Earvolino-Ramirez (2007)	Resilience: A Concept Analysis	Critical review	Nursing Forum
7	Vogel et al. (2007)	Linking vulnerability, adaptation, and resilience science to practice: Pathways, players, and partnerships	Quantitative	Global Environmental Change
8	Paavola (2008)	Livelihoods, vulnerability and adaptation to climate change in Morogoro, Tanzania	Quantitative	Environmental Science Policy
9	Gwimbi (2009)	Linking rural community livelihoods to resilience building in flood risk reduction in Zimbabwe	Quantitative	Jamba: Journal of Disaster Risk Studies
10	Alinovi et al. (2010)	Measuring Household Resilience to Food Insecurity: Application to Palestinian Households	Quantitative	Agricultural Survey Methods
11	Gaillard (2010)	Vulnerability, capacity and resilience: Perspectives for climate and development policy	Quantitative	Journal of International Development
12	Jorgenson et al. (2010)	Resilience and vulnerability of permafrost to climate change	Quantitative	Canadian Journal of Forest Research
13	Scholz et al. (2012)	Risk, vulnerability, robustness, and resilience from a decision-theoretic perspective	Quantitative	Journal of Risk Research
14	Can et al. (2013)	Application of Livelihood Vulnerability Index to Assess Risks from Flood Vulnerability and Climate Variability—A Case Study in the Mekong Delta of Vietnam	Quantitative	Journal of Environmental Science and Engineering

http://www.aloki.hu ● ISSN 1589 1623 (Print) ● ISSN 1785 0037 (Online)
DOI: http://dx.doi.org/10.15666/aeer/1706_1276912785

15	Ekblom (2012)	Livelihood Security, Vulnerability and Resilience: A Historical Analysis of Chibuene, Southern Mozambique	Critical review	Ambio
16	Zebrowski (2013)	The nature of resilience	Critical review	Resilience
17	Ajibade et al. (2013)	Urban flooding in Lagos, Nigeria: Patterns of vulnerability and resilience among women	Quantitative	Global Environmental Change
18	Fatemi et al. (2017)	Social vulnerability indicators in disasters: Findings from a systematic review	Qualitative	International Journal of Disaster Risk Reduction
19	Abid et al. (2016)	Climate change vulnerability, adaptation and risk perceptions at farm level in Punjab, Pakistan	Quantitative	Science of The Total Environment
20	Tanner et al. (2015)	Livelihood resilience in the face of climate change	Critical review	Nature Climate Change
21	Lee (2014)	Social vulnerability indicators as a sustainable planning tool	Quantitative	Environmental Impact Assessment Review
22	Pandey et al. (2017)	Sustainable livelihood framework-based indicators for assessing climate change vulnerability and adaptation for Himalayan communities	Quantitative	Ecological Indicators
23	Panthi et al. (2016)	Livelihood vulnerability approach to assessing climate change impacts on mixed agro-livestock smallholders around the Gandaki River Basin in Nepal	Quantitative	Regional Environmental Change
24	Shaw et al. (2016)	Building Community Resiliency	Quantitative	Urban Disasters and Resilience in Asia
25	Weldegebriel and Amphune (2017)	Livelihood resilience in the face of recurring floods: an empirical evidence from Northwest Ethiopia	Quantitative	Geoenvironmental Disasters,
26	Bhuiyan et al. (2017)	Exploring impacts and livelihood vulnerability of riverbank erosion hazard among rural household along the river Padma of Bangladesh	Quantitative	Environmental Systems Research
27	Alam et al. (2018)	How do climate change and associated hazards impact on the resilience of riparian rural communities in Bangladesh? Policy implications for livelihood development	Quantitative	Environmental Science and Policy
28	Chaffin and Scown (2018)	Social-ecological resilience and geomorphic systems	Quantitative	Geomorphology
29	Bhattacharjee and Behera (2018)	Determinants of household vulnerability and adaptation to floods: Empirical evidence from the Indian State of West Bengal	Quantitative	International Journal of Disaster Risk Reduction

http://www.aloki.hu ● ISSN 1589 1623 (Print) ● ISSN 1785 0037 (Online)
DOI: http://dx.doi.org/10.15666/aeer/1706_1276912785

THE EFFECT OF AFFORESTATION ON BIODIVERSITY IN MALATYA, TURKEY

MUTLU, B.

Hakkari Forest Management Directorate, Hakkari, Turkey
(e-mail: basrimutlu44@hotmail.com; phone: +90-438-211-6224/+90-530-347-9860)

(Received 3rd May 2019; accepted 20th Aug 2019)

Abstract. Since 1960s, the Tepehan (Turkey) region had long been suffering from serious soil erosion. Therefore, large-scale afforestation with mainly coniferous species has continued during the past decades in order to control soil erosion and it has yielded quite successful results. However, since it has been unknown how afforestation influences biodiversity so far this study investigated it. Braun–Blanquette method was used to select a plot in each stratum which represents the vegetation characteristic of the whole area of the forest and to assess vegetation parameters. The results of the survey show that 77 species belonging to 58 genera were recorded in different layers including 7 trees, 4 shrubs and 66 herbs in the study area. Diversity index was used for measuring biological diversity and was found consistently and significantly greater in native Quercus forests than in exotic coniferous plantation forests. These results show that afforestation has a negative influence on species diversity. Therefore, it is recommended to develop strategies for biodiversity conservation in afforestation work in the country to maintain habitats and minimize loss of native species.
Keywords: *afforestation, biodiversity, biodiversity index, vegetation*

Introduction

For 5 to 6 thousand years in our world the delicate balance between soil, vegetation and water has been disturbed in natural environments as a consequence of the removal or destruction of natural vegetation for various reasons. Especially wrong land use with deforestation and erosion in sensitive ecosystems where semi-arid and arid climatic conditions dominated caused the loss of soil and the disappearance of plant species. Afforestation activities have an important role in re-equilibrating the degraded ecosystem as well as reducing the effects of some global disasters and fighting erosion. However, the impact of afforestation with single or several of exotic coniferous species has been discussed without much consideration of the ecological characteristics of the forests.

Whereas some afforestation efforts are believed to harm ecosystem biodiversity and interfere with biodiversity conservation goals (Cao et al., 2009; Calvino-Cassela et al., 2012; Pourbabaei et al., 2012), a large number of studies in many countries has shown that the plantation of forests can provide habitat for a wide range of native forest plants, animals, and fungi and can support a diverse array of native understorey plants (Barbaro et al., 2005; Carnus et al., 2006; Brockerhoff et al., 2008; Juying et al., 2017).

Usually, the used species show rapid growth instead of natural species in afforestation to control soil erosion, accelerate vegetation restoration, and improve ecological environments in Turkey and quite successful results have been obtained. However, the positive/negative impact of afforestation on biodiversity is not discussed so much in Turkey. Whereas it is important to identify the effects of afforestation on biodiversity and the functioning of ecosystems. Biodiversity has been shown to play a key role at all levels of the ecosystem service hierarchy (Mace et al., 2012; Gao et al., 2014). Therefore, the importance of measuring biodiversity increased.

http://www.aloki.hu ● ISSN 1589 1623 (Print) ● ISSN 1785 0037 (Online)
DOI: http://dx.doi.org/10.15666/aeer/1706_1278712798

Various diversity indices are used to measure biodiversity. Diversity index is a statistical method which is planned to evaluate the variety of a data group consisting of different types of components. Such as number of existing species (Richness), equal distribution of individuals (Evenness) and total number of existing individuals. Any changes in any of these three features are effectively used to identify changes in a population (Mısır et al., 2018).

The study area Tepehan (Malatya-Turkey) is on the southeastern Taurus Mountains where Davis describes in terms of floristic as medium, few or never worked and where studies suggest that the work should be done at a local level and in detail and had long been suffering from serious soil erosion since 1960s. So large-scale afforestation with mainly coniferous species has continued during the past decades in order to control soil erosion and quite successful results has been obtained. However, it has unknown how afforestation influences biodiversity so far. So in this study both inventories have been carried out and the influence of afforestation on the vegetation was assessed by using biodiversity indices.

Materials and methods

Study area

Study was conducted in Tepehan located at 38° 11’ 45.3” N and 38° 52’ 8.1” E. The first afforestation and erosion control works started here in Malatya in 1962.

In Tepehan and its surrounding, Puturge metamorphic consisting of gneiss, micaschist and amphibolite dominate the terrain. These are the oldest formations in the region and they form the foundation (*Fig. 1*).

Figure 1. *The location of the study area*

http://www.aloki.hu ● ISSN 1589 1623 (Print) ● ISSN 1785 0037 (Online)
DOI: http://dx.doi.org/10.15666/aeer/1706_1278712798

Climate

The climate data of the Puturge Forest Station, which is the nearest meteorological station to the research area, are given in *Table 1*.

Table 1. *2017-2018 data of Puturge forest meteorological station (MGM, 2019)*

Meteorological data	Period	MONTHS											
		Jan.	Feb.	Mar.	Apr.	May.	Jun.	July	Aug.	Sep.	Oct.	Nov.	Dec.
Total rainfall (mm = kg÷m²)	2	72.7	24.75	53.6	57.95	117.3	25.25	3	1.55	6.3	42.65	51.6	32.4
Maximum rainfall (mm = kg÷m²)	2	22.9	12.95	15.75	22.3	35.8	10.4	1.8	0.55	4.6	20.15	13.9	12.15
Avarage temperature (°C)	2	-1.85	0.8	6.05	10.1	13.6	19.3	24.25	24.7	21	12.6	5.6	2
Maximum temperature (°C)	2	6.15	10.55	16.65	21.5	25.35	32.3	34.6	34.4	31.4	23.25	15.95	9.8
Minimum temperature (°C)	2	-9.85	-8.05	-4.25	-2.2	5.6	8.05	12.75	14.75	10.35	1.8	-5.05	-6.1
Average wind speed (m÷sn)	2	2.3	2.6	3.2	3.15	2.6	2.8	3.15	2.95	2.45	2.4	1.85	2.25

Table 1 is to show that the average annual temperature is 11.51 °C, the annual rainfall is 489.05 mm and the average annual relative humidity is 47.01%. In terms of temperature regime, it is a summer season of 4-months between June and September, a winter season of about 4.5-months between November and late March and the spring and fall seasons of about 1.5-2-months.

According to the WALTER method, ombrotermik climate (precipitation-temperature) diagrams of Puturge was seen (*Fig. 2*).

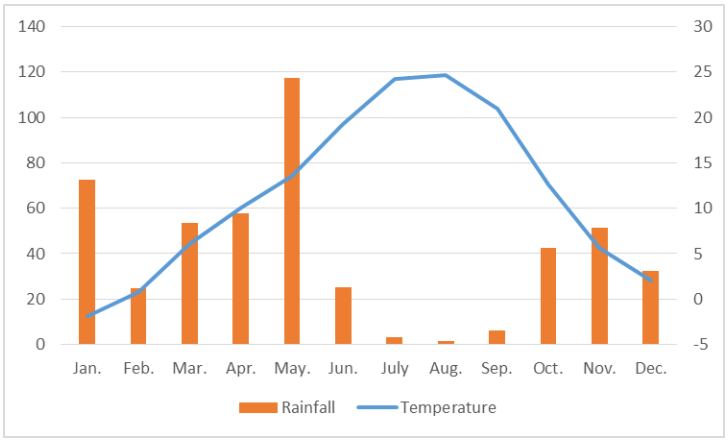

Figure 2. *Ombrotermik climate (precipitation-temperature) diagrams of Puturge*

Figure 2 shows that a drought period of four months has been from the end of May to the end of November.

Vegetation

According to Davis (1965-1988), the research area is located at the B7 Iranian-Turonian floristic region that is characterized with dwarf trees, grasses and meadow at a high rate although the number of tree species that is relatively few. Walter (1976) described the zonal vegetation as climate zone "Temperate arid- Step forest Zone", and Zohary (1973) classified it as "Persian xenophile Quercus brantii forest". These dry forests, which are generally pure oak communities constituted a narrow rung among Hakkâri, Malatya and Kahramanmaraş where the spreading of the oak-juniper forests

http://www.aloki.hu ● ISSN 1589 1623 (Print) ● ISSN 1785 0037 (Online)
DOI: http://dx.doi.org/10.15666/aeer/1706_1278712798

continued on the slopes of the west and central Taurus (Louis, 1939; Mayer and Aksoy, 1998).

The current vegetation of the research area consists of oak-bush communities, steppe communities with secondary characters created along with the anthropogenic influences for years, pine and cedar communities established with afforestation in 1962 (*Fig. 3*).

Figure 3. *A view of the vegetation of the study area*

Vegetation sampling

Sample plots were randomly selected in the field and Braun–Blanquette method was used to select a plot in each stratum which represents the vegetation characteristic of the whole area of the forest and vegetation studies was carried out in 9 plots of 20×20 m during periods of optimum development of the vegetation in 2018 (*Table 2*).

Table 2. *Geographical locations of the plots*

No	Name of plant community	Geographical location (WGS 84)	Altitude (m)
1	Pinus nigra afforestation area (Pn1)	477151-4220072	1500
2	Native Quercus sp. forest (Q1)	477164-4220086	1500
3	Pinus nigra afforestation area (Pn2)	475820-4220064	1510
4	Native Quercus sp. forest (Q2)	475799-4220076	1515
5	Pinus sylvestris afforestation area (Ps1)	478215-4219536	1575
6	Cedrus libani afforestation area (C1)	479417-4218245	1540
7	Mixed forest (M1)	477067-4222421	1280
8	Pinus nigra afforestation area (Pn3)	477670-4222935	1190
9	Native Quercus sp. forest (Q3)	477696-4222942	1200

The limit value of vegetation cover was determined according to Scamoni (1963) and showed *Table 3* (Aksoy, 1978).

Table 3. *Limit values of vegetation layer according to Scamoni (1963)*

> 5 m	T tree layer
50 cm – 5 m	S shrub layer
< 50 cm	H herb layer

http://www.aloki.hu ● ISSN 1589 1623 (Print) ● ISSN 1785 0037 (Online)
DOI: http://dx.doi.org/10.15666/aeer/1706_1278712798

According to Braun–Blanquette, the abundance-cover (density) scale is:
r: One species, the cover condition is ambiguous,
+: Species abundant, but cover is weak, cover is 1-5%,
1: Species abundant, but cover grade weak, cover 5-25%,
2: Species cover is between 25-50%,
3: Species cover is between 50-75%,
4: Species cover is between 75-100%.

Measuring plant diversity

There are some common diversity indexes. However, Shannon-Wiener index are most widely used for measuring biological diversity. When used species richness and species evenness together, the diversity of the community can be expressed and compared to other communities.

To calculate vegetation profiles, Braun–Blanquette scores were transformed to relative cover (r: 0.01; +: 0.02; 1: 0.04; 2: 0.15; 3: 0.375; 4: 0.625; 5:0.875) prior to analysis (Fontaine et al., 2007).

Species richness

Species richness is the actual number of species present in a community (Atlas, 1984; Patrick, 1949):

$$D = S$$

where D = species richness, S = number of species in the community.

Shannon-Wiener index

Shannon-Weiner diversity index (H') was calculated (Shannon and Weaver, 1949) as:

$$H' = -\sum_{i=1}^{s} P_i \, In \, Pi$$

where S = total number of species, Pi (Ni/N) = proportional abundance of species i, In Pi = the natural logarithm of the proportional abundance of species i. Values of H' can range from 0 to 5.

Species evenness

From the formula above we obtain Shannon evenness index J (Pielou, 1966) as

$$J = \frac{H'}{\ln S}$$

where J: Pielou Regularity Index, H: Shannon-Weaner Diversity Index, S: Number of species, J ranges from 0 to 1.

http://www.aloki.hu ● ISSN 1589 1623 (Print) ● ISSN 1785 0037 (Online)
DOI: http://dx.doi.org/10.15666/aeer/1706_1278712798

Results

Vegetation analysis

9 samples were established and 77 species belonging to 58 genera were recorded in the study area in different layers including 7 trees (T), 4 shrubs (S) and 66 herbs (H) (*Table 4*). Within the study area, there were important differences between exotic coniferous plantations and native species plots with respect to structural development. Exotic coniferous plantations had significantly greater numbers of planted tree species, higher stem density and crown cover, greater mean tree heights and stem diameters than native Quercus. On the other hand, the plant community in Quercus forest varied in structure and composition among sites due to physiographic and anthropogenic pressures. The density of grasses in the native forest is clearly a reflection of favourable light conditions. Species richness and species diversity correlated negatively with crown cover.

Table 4. *Vegetation analysis*

Plot area no		**Pnk1**	**Q1**	**Pn2**	**Q2**	**Ps1**	**C1**	**M1**	**Pn3**	**Q3**	**EXISTENCE**
Area (m²)		400	400	400	400	400	400	400	400	400	
Altitude (m)		1500	1500	1510	1515	1575	1540	1280	1190	1200	
Cover of layer											
T Layer (%)		70	30	80	25	80	70	60	90	40	
S Layer (%)		10	30	3	30	-	5	15	10	50	
H Layer (%)		10	90	15	95	15	30	60	10	80	
Vegetation height											
Tree layer (m)		8-10	6.-8	16-18	6	20	12	12-15	12	6	
Shrub layer (m)		3	3	2.5	3	-	2.5	2.5	3	3	
Herb layer (cm)		30	50	40	50	30	50	30	10	50	
Distinguishing taxa											
T	Pinus nigra	3	.	4	1	.	.	2	4	.	5
T	Quercus cerris	2	2	+	.	.	.	1	.	2	5
T	Cedrus libani	1	.	.	.	.	4	3	1	.	4
T	Quercus infectoria subsp. boissieri	.	1	.	2	.	.	.	.	2	3
T	Robinia pseudoacacia	.	.	.	1	.	.	.	2	1	3
T	Quercus libani	.	r	.	.	.	.	.	.	+	2
T	Pinus sylvesteris	.	.	1	.	5	.	.	.	.	2
S	Quercus cerris	1	2	.	1	.	.	1	.	3	5
S	Quercus infectoria subsp. boissieri	.	2	.	2	.	.	1	.	2	4
S	Crataegus aronia subsp. aronia	.	.	1	1	.	1	1	.	.	4
S	Pinus nigra	1	.	.	.	.	.	1	.	.	2
S	Rosa canina	.	.	.	r	.	.	1	.	.	2
S	Cedrus libani	.	.	.	.	.	.	.	1	.	1
S	Quercus libani	.	.	.	.	.	.	.	.	1	1
S	Crataegus monogyna subsp monogyna	.	.	.	.	.	.	+	.	.	1

http://www.aloki.hu ● ISSN 1589 1623 (Print) ● ISSN 1785 0037 (Online)
DOI: http://dx.doi.org/10.15666/aeer/1706_1278712798

S	Robinia pseudoacacia	.	.	.	r	.	.	.	.	.	1
S	Colutea cilica	.	.	.	.	.	.	.	.	r	1
H	Poa bulbosa	2	1	2	3	1	2	2	1	2	9
H	Lotus gebelia var. gebelia	1	2	1	2	+	+	1	.	.	7
H	Muscari comosum	+	2	1	2	.	2	.	r	1	7
H	Trifolium arvense var. arvense	1	5	1	3	.	1	3	.	1	7
H	Ziziphora capitata	1	1	1	1	.	.	+	.	1	6
H	Trifolium boissieri	1	2	.	4	.	1	3	.	2	6
H	Astragalus sp.	.	1	.	1	+	+	1	.	1	6
H	Pilosella piloselloides	.	r	.	1	+	+	1	+	.	6
H	Rumex acetellosa	.	.	.	1	1	.	1	1	1	5
H	Hypericum scabrum	1	1	+	2	.	.	.	.	1	5
H	Trifolium pilulare	.	r	.	2	.	.	2	2	4	5
H	Astragalus altanii	+	1	.	1	+	.	.	.	1	5
H	Bunium paucifolium var. brevipes	.	r	+	1	+	+	.	.	.	5
H	Lotus gebelia	.	1	.	.	.	+	.	2	1	4
H	Astragalus cephalotes var. brevicalyx	+	.	.	.	+	.	1	.	2	4
H	Achillea bieberstenii	.	+	.	2	+	.	1	.	.	4
H	Tragopogon longistris subsp. longistris	.	+	.	1	+	.	.	.	1	4
H	Phlomis kurdica	.	r	.	1	.	r	1	.	.	4
H	Galium spurium subsp. ibecinum	.	+	+	+	.	.	.	+	.	4
H	Ranunculus cuneatus	1	.	1	.	2	1	.	.	.	4
H	Pinus nigra	1	.	1	+	.	.	.	.	.	3
H	Senecio vernalis	+	.	+	.	+	.	.	.	.	3
H	Arenaria serpylifolia	.	.	1	.	.	1	.	.	1	3
H	Alyssum szowotsii	.	1	.	.	+	.	.	.	1	3
H	Astragalus angustifolius subsp anatolicus	.	.	.	.	+	.	.	+	1	3
H	Cerastium dicthomum subsp. dicthomum	.	.	.	.	.	+	.	+	1	3
H	Crepis cf. alpina	.	.	.	.	.	+	.	+	1	3
H	Helichrysum armenium subsp. araxinum	.	.	.	1	.	+	1	.	.	3
H	Geranium tuberosum	.	.	+	.	r	+	.	.	.	3
H	Lactuca serriola	.	+	.	+	.	.	.	+	.	3
H	Onosma sericeum	.	+	.	1	.	.	+	.	.	3
H	Quercus cerris	+	.	+	.	.	.	.	+	.	3
H	Veronica bozakmanii	.	.	+	.	+	+	.	.	.	3
H	Anthemis sp.	.	1	.	.	.	.	.	.	1	2
H	Torilis leptophylla	.	.	.	.	.	r	.	.	1	2
H	Crataegus aronia var. aronia	.	.	+	.	.	r	.	.	.	2

http://www.aloki.hu ● ISSN 1589 1623 (Print) ● ISSN 1785 0037 (Online)
DOI: http://dx.doi.org/10.15666/aeer/1706_1278712798

H	Myosotis stricta	.	.	.	1	.	+	.	.	.	2
H	Sanguisorba minor subsp muricata	.	.	.	1	.	+	.	.	.	2
H	Leontodon asper var. setulosus	.	.	.	+	.	.	.	.	+	2
H	Vicia sativa subsp. nigra var. nigra	.	1	.	1	.	.	.	.	.	2
H	Vicia cracca subsp. stenophylla	.	.	.	.	r	.	.	.	2	2
H	Viola occulta	.	.	.	.	r	+	.	.	.	2
H	Bromus japonica	.	.	.	1	.	.	.	.	1	2
H	Cedrus libani	.	.	.	.	.	1	+	.	.	2
H	Tripleurospermum oreades var oreades	.	.	+	+	.	.	.	.	.	2
H	Verbascum sp.	.	.	.	.	.	.	+	.	+	2

Single repetition taxa: Picnomon acarna +, Bromus tectorum + (Pn3), Teucrium polium +, Papaver dubium +, Briza humilis +, Cerastium dicthomum subsp. inflatum +, Cyanus depressa +, Trifolium purpureum + (Q3), Myosotis refracta +, Valerianella coronata + (Q2), Crupina crupinastrum +, Euphorbia cf. macroclada +, Eryngium campestre var. virens +, Salvia multicaulis +, Opopanax hispidus +, Taeniatherum caput-medusae subsp. crinitum 1(2) (M1), Lecokia cretica +, Ophrys frigida r (Pn2), Geranium rotundifolium r, Crepis sancta +, Centaurea virgata +, Potentilla argentea +, Erysimum kotschyii + (C1), Cnicus benedictus subsp. benedictus r (Q1)

Biodiversity measurement

The sample which were the highest in species richness were also found to have the highest species diversity or Shannon-Wiener Index value (*Table 5*).

Table 5. *Biodiversity measurement in sampling plots*

Sampling plots no.	**Pn1**	**Q1**	**Pn2**	**Q2**	**Ps1**	**C1**	**M1**	**Pn3**	**Q3**
Shannon-Wiener Index (H')	2.27	2.47	2.29	3.01	1.69	2.46	2.88	2.02	3.08
Species richness	15	26	21	35	20	27	28	17	36
Species evenness	0.84	0.76	0.75	0.85	0.57	0.75	0.86	0.71	0.86

Species diversity

Results show that Q3 plot has the highest plant diversity as compared to other plots, followed by Q2 and M1 plots as the second and third most diverse respectively. Ps1 plot was the least diverse among all 9 plots (*Table 5*). Shannon-Weiner diversity index was 62% greater in native Quercus forest than in exotic coniferous plantations (pine and cedar) areas as a diversity index of 2.85 and 1.79 for the native Quercus forest and afforested areas was registered consecutively.

Species richness

It shows that Q3 plot has the highest plant diversity as compared to other plots, followed by Q2 and M1 plots as the second and third richest, respectively. Pn1 plot was the least rich (*Table 5*). Species richness was higher in native afforested areas than in

http://www.aloki.hu ● ISSN 1589 1623 (Print) ● ISSN 1785 0037 (Online)
DOI: http://dx.doi.org/10.15666/aeer/1706_1278712798

afforested areas, where average species richness was 32.3 in native and mixed areas compared to 21.3 in exotic coniferous plantations (pine and cedar) areas.

Species evenness

It shows that Q3 plot has the highest as compared to other plots, followed by M1 and Q2 plots as the second and third most even, respectively. Ps1 plot was the least even (*Table 5*). We can see from our results that evenness in the native Quercus forest are much higher than in plantation area. But some samples with the most species (highest species richness) and species diversity did not have the highest species evenness.

Discussion and conclusion

Since the Şiro River Basin is risky in terms of erosion, studies were started in 1962 to protect soil in the basin to prevent the arrival of sediment to the Karakaya Dam. Soil conservation and afforestation activities have been achieved and it has been observed that sediment in the dam basin has been largely prevented. And in order to improve the distorted coppices in Tepehan, more regular and highly productive forests were created in terms of establishment characteristics as a result of plantation of oak seeds and afforestation of open and gradient areas.

However, the pine afforestation in this area can be anticipated for possible negative effects): (i) in pine plantations the dense and thick layer of needle litter represent a serious risk for uncontrolled, severe wildfires (*Fig. 4*); (ii) the change of the structure of these afforested heathlands means the loss of this dense scrubland vegetation type for its associated fauna; (iii) Leaves of quercus sp. constitute part of the diet of goats and sheep (*Fig. 5*). They are among the less resistant woody species in pine-tree stands and individuals lose foliage and are, subsequently, no longer valuable as food source for goats and sheep. This not only means an actual loss of resources, but also implies an increase of browsing by these large herbivores on adjacent open heathland stands, which would have negative consequences if that increase exceeded the heathland's carrying capacity (Andrés and Ojeda, 2002) and (iv) biological adaptation disorders such as resistance to biotic and abiotic pests.

Figure 4. *A view of the pine afforestation in the research area*

http://www.aloki.hu ● ISSN 1589 1623 (Print) ● ISSN 1785 0037 (Online)
DOI: http://dx.doi.org/10.15666/aeer/1706_1278712798

Figure 5. *A view of the Quercus tree and shrub in the research area*

The general conclusion from the case studies clearly indicates that afforestation affects species richness of different functional groups in different ways. Especially the number of species of vascular plants is negatively affected by afforestation. Shade tolerant plant groups had replaced the original heathland communities.

On the other hand, this study shows that the species diversity (Shannon-Wiener index, H') followed very similar correlation for species richness, however, for species evenness it did not. All the same, diversity index was found consistently and significantly greater in native Quercus forests than exotic coniferous plantations forest. This result is in line with the findings of a number of research studies where the negative effects of afforestation on species diversity was highlighted (Andrés and Ojeda, 2002; Pourbabaei et al., 2012). Because species richness of vascular plants is affected by exotic coniferous species. This difference is mainly due to the amount of light which reaches the forest floor. Similarly, understorey biomass is related to the amount of light. So shade tolerant plant groups replace the original heathland communities. Namely, there is a negative correlation between tree coverage and grass density in afforestation areas. As the coverage of the tree layer increases, the degree of coverage of the shrub and grass decreases and the coverage of the shrub layer increases, the degree of coverage of the grass decreases. This situation has a negative effect on vegetation composition and species diversity. The number of endemic taxa decreased in subsamples under coniferous species compared to native broadleaved forests.

Another important finding of this study was that high species richness did not always indicate plant density. In other words, forests with a greater number of species were found to have less tree density were also found to have more shrub and grass density as compared to forests with low species richness in similar area size.

While the afforestation results appear favourable to stop erosion, it is very important to develop strategies for the conservation of biodiversity in afforestation. New forests must be designed in such a way that they conform to the other elements and the character of the landscape. With exotic and monocultural plant species, full coveraged and sharp, straight borders should be avoided. It is also important to maintain open areas within the forest, which will be largely successful in creating a dynamic and sustainable environment in terms of biodiversity in the arid and semi-arid region.

http://www.aloki.hu ● ISSN 1589 1623 (Print) ● ISSN 1785 0037 (Online)
DOI: http://dx.doi.org/10.15666/aeer/1706_1278712798

REFERENCES

[1] Aksoy, H. (1978): Research on forest societies and their silvicultural characteristics in Karabük-Büyükdüz Research Forest. – İ.Ü. Yayın No: 2332, O.F. Yayın No: 237, İstanbul.
[2] Andrés, C., Ojeda, F. (2002): Effects of afforestation with pines on woody plant diversity of Mediterranean heathlands in southern Spain. – Biodiversity and Conservation 11: 1511-1520.
[3] Atlas, R., M. (1984): Diversity of microbial communities. – Adv. Microb. Ecol 7: 1-47.
[4] Barbaro, L., Pontcharraud, L., Vetillard, F., Guyon, D., Jactel, H. (2005): Comparative responses of bird, carabid, and spider assemblages to stand and landscape diversity in maritime pine plantation forests. – Ecoscience 12: 110-121. DOI: 10.2980/i1195-6860-12-1-110.1.
[5] Brockerhoff, E. G. et al. (2008): Plantation Forests and Biodiversity: Oxymoron or Opportunity? – Springer, Dordrecht.
[6] Calvino-Cansela, M., Rubido-Bará, M., van Etten, E. J. B. (2012): Do eucalypt plantations provide habitat for native forest biodiversity? – Forest Ecology and Management 270: 153-162.
[7] Cao, S., Chen, L., Xinxiao, Y. (2009): Impact of China's Grain for Green Project on the landscape of vulnerable arid and semi-arid agricultural regions: a case study in northern Shaanxi Province. – Journal of Applied Ecology 46: 536-5.
[8] Carnus, J. M., Parrotta, J., Brockerhoff, E., Arbez, M., Jactel, H., Kremer, A., Lamb, D., Herve, M., O'Hara, K., Walters, B. (2006): Planted forests and biodiversity. – Journal of Forestry 104: 65-77.
[9] Davis, P. H. (1965-1988): Flora of Turkey and the East Aegean Islands. Vol. 1-10. – Edinburgh University, Yayınları.
[10] Fontaine, M., Aerts, R., Özkan, K., Mert, A., Gülsoy, S., Süel, H., Waelkens, M., Muys, B. (2007): Elevation and exposition rather than soil types determine communities and site suitability in Mediterranean mountain forests of southern Anatolia, Turkey. – Forest Ecology and Management 247: 18-25.
[11] Gao, T., Hedblom, M., Emilsson, T., Nielsen, A. B. (2014): The role of forest stand structure as biodiversity indicator. – Forest Ecology and Management 330: 82-93.
[12] Juying, J., Ning, W., Yanfeng, J., Dongli, W. (2017): Influence of afforestation on the species diversity of the soil seed bank and understory vegetation in the hill-gullied Loess Plateau, China. – Int J Environ Res Public Health 14(10): 1285. DOI: 10.3390/ijerph14101285.
[13] Louis, H. (1939): Das natürliche Pflanzenkleid Anatoliens. – Geographische Abhandlungen, 3. Reihe, Heft 12, Stuttgart.
[14] Mace, G. M., Norris, K., Fitter, A. H. (2012): Biodiversity and ecosystem services: A multilayered relationship. – Trends in Ecology and Evolution 27(1): 19-26.
[15] Mayer, H., Aksoy, H. (1998): Forests of Turkey. – T. C. Orman Bakanlığı, Batı Karadeniz Ormancılık Araştırma Enstitüsü Müdürlüğü, Abant İzzet Baysal Üniversitesi Basımevi, Bolu.
[16] Mısır, N., Satıroglu, S., Mısır, M. (2018): Estimation of biodiversity of eastern Black Sea mixed forests in Turkey. – Anadolu, J. of Aari 28(1): 23-29.
[17] MGM (2013): Puturge Forest Weather Station Data. – MGM, Ankara.
[18] Patrick, R. (1949): A proposed biological measure of stream conditions, based on a survey of the Conestoga Basin, Lancester Country, Pennsylvania. – Proc. Acad. Nat. Sci. Phila. 101: 277-341.
[19] Pielou, E. C. (1966): The measurement of diversity in different types of biological collections. – J. Theoret. Biol. 13: 131-144.

http://www.aloki.hu ● ISSN 1589 1623 (Print) ● ISSN 1785 0037 (Online)
DOI: http://dx.doi.org/10.15666/aeer/1706_1278712798

[20] Pourbabaei, H., Asgari, F., Reif, A., Abedi, R. (2012): Effect of plantations on plant species diversity in the Darabkola, Mazandaran Province, North of Iran. – Biodiversitas 13: 72-78.
[21] Shannon, C. E., Weaver, W. (1949): The Mathematical Theory of Communication. – University of Ilinois Press, Urbana, IL.
[22] Walter, H. (1962): Vegetation Structure of Anatolia. – Çev. Selman USLU, İstanbul Üniversitesi, Yayınları, Nr. 944; Orman Fakültesi Yayın Nr. 80.
[23] Zohary, M. (1973): Geobotanical Foundations of the Middle East. Volumes 1 & 2. – Gustav Fischer Verlag, Stuttgart; Swets & Zeitlinger, Amsterdam.

http://www.aloki.hu ● ISSN 1589 1623 (Print) ● ISSN 1785 0037 (Online)
DOI: http://dx.doi.org/10.15666/aeer/1706_1278712798

DISCOVERY OF THE ACONITE (*ACONITUM UMBROSUM* (KORSH.) KOM) EVOLVEMENT STRUCTURE FROM DICOTYLEDON TO A MONOCOTYLEDON

MA, Y.[1#] – GAO, T.[1#] – MA, Y.[2] – ZHANG, L.[3] – LI, Y.[1] – LU, J.[1*] – YOU, J.[1*]

[1]*College of Life Sciences, North East Normal University, Changchun 130024, China*

[2]*School of Botany Sciences, Jilin University, Changchun 130028, China*

[3]*College of College of Pharmacy, Tonghua Normal University, Tonghua 134002, China*

[#]*These authors have contributed equally to this work*

**Corresponding authors*
e-mail: jingmlu@163.com

(Received 6th May 2019; accepted 20th Aug 2019)

Abstract. An optical microscope technique and paraffin method was used to conduct an anatomical study on the stems and leaves of *Aconitum umbrosum* (Korsh.) Kom. (Ranunculaceae). The results showed that the stem had scattered vascular bundles, without the intrafascicular cambium. The leaf epidermis possessed pseudo-bulliform cells. The mesophyll had no distinction between palisade tissue and spongy tissue. The leaves developed multiple vascular bundles of parallel leaf veins, which had the structural characteristics of monocotyledons.
The microscopic structure of the stems and leaves of *A. umbrosum*, a living fossil, were analyzed as part of an attempt to confirm the evolution of plants from dicotyledons to monocots; this study contributes to the completion of the theory of evolution as seen in the Takhtajan and Cronquist systems.
Keywords: *vascular bundles, vascular cylinder, bifacial leaf, isolateral leaf, mesophyll*

Introduction

The genus *Aconitum* has about 350 species worldwide, and is widely distributed in temperate regions of the Northern Hemisphere. About 200 species of *Aconitum* occur in China, many of which are distributed in Northeast China. In 2019, Qin et al. through ITS sequence analysis and secondary structure prediction of 9 species of aconitum, combined with data from the public database, established a molecular method for identification of plant species of aconitum, laying a foundation for subsequent studies on authentic medicinal materials in Qinghai-Tibet Plateau (Qin et al., 2019). Li (2018) applied optical microscope and scanning electron microscope to study the phytological identification of 33 species of liliaceae belonging to 15 genera in Changbai Mountains, and summarized, sorted out and classified the phytological identification results with mathematical statistics. Tian et al. (2017) summarized aconitum plants of ranunculaceae in Qinling area from several aspects including distribution, active components, resource utilization and application of active components. Wu (2015) studied the identification and systematic evolution of epigenetic phytoliths of 17 genera of ranunculaceae, providing first-hand microscopic evidence of external morphology and internal anatomical structure. Gao (2014) described the genetic polymorphism of 7 species of aconitum from Xinjiang.

Li et al.'s (2019a), research results: WVBF and CFA may have potential synergetic effects on the target genes of certain diseases such as inflammation, cancer and diabetes.

http://www.aloki.hu ● ISSN 1589 1623 (Print) ● ISSN 1785 0037 (Online)
DOI: http://dx.doi.org/10.15666/aeer/1706_1279912806

Li et al. (2019b) proved a preparation of two Actinomycetes plays a role in the biocontrol of root diseases and growth promotion of A. carmichaelii by inhibiting pathogen growth and shaping the rhizosphere microbiota. Xionb et al. (2019) studied the chemical constituents of the aboveground parts of aconitum in the genus ranunculaceae. Results a total of 16 compounds were isolated from dried stems and leaves of monkshood with methanol percolation. Li and Feng (1990) studied the abnormal structure of root duct group of aconite. According to Wu and Zhao (2011) there are about 200 species of aconitum in China, of which about 76 species can be used for medicinal purposes. Most aconitum medicinal plants are root tubers and roots, most of which have the effect of dispelling wind and dehumidifying, warming meridians and relieving pain, among which alkaloids are the main active ingredients. Xu and Dong (2009) investigated some plant resources of aconite in north China, and believed that aconite plants could be used for cut flowers, potted flowers and flower borders in gardens and had high ornamental value. Tamura et al. (1993): Dicotyledons: Magnoliid, Hamameliid and Caryophyllid.

However, there is no systematic evolutionary structure study of aconitum. This research will make efforts and contributions in this field.

Materials and methods

A. umbrosum specimens were collected in the tundra zones of Changbai Mountain in Jilin, China (*Map 1*). 100 samples of plant experimental materials were collected.

Permanent slides were then made as follows. First, the paraffin method was used to preserve 10-μm-thick slices (Li, 2018). Then, the slices were dehydrated by alcohol, clarified by dimethylbenzene, dyed with safranine fast green, sealed in neutral gum and observed using an Eclipse 80 microscope. Microscopic photographs were taken (Wu, 2005).

Map 1. *Map of Changbai Mountain*

http://www.aloki.hu ● ISSN 1589 1623 (Print) ● ISSN 1785 0037 (Online)
DOI: http://dx.doi.org/10.15666/aeer/1706_1279912806

Results

Stem anatomical structure of A. umbrosum

The cross section of the stems of *A. umbrosum* was nearly round. The epidermis was composed of a single layer of tightly packed cells. Scattered heterocysts were observed, with stoma rarely seen on the epidermis (*Fig. 1*). In the epidermis, the epidermal cells of the external tangential wall had an average width of 2–3 μm. The cortex was divided into exodermis, and into parenchyma cells of the cortex and endodermis. The thickened part of the corners of the epidermis was approximately 110 μm thick. The intercellular spaces were not developed and there was an obvious thickening of the Casparian band in the endodermis. The stem had no obvious pith cell (*Fig. 2*).

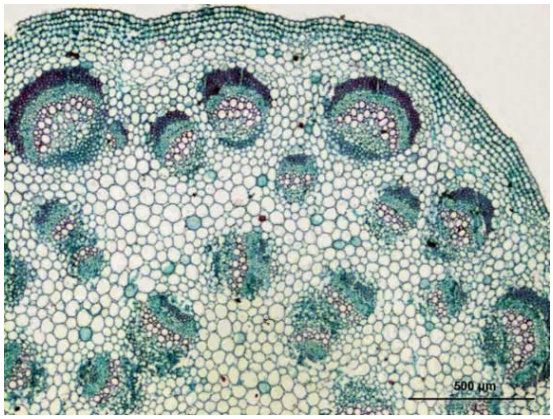

Figure 1. *Cross section of stems, with somewhat scattered atactostele*

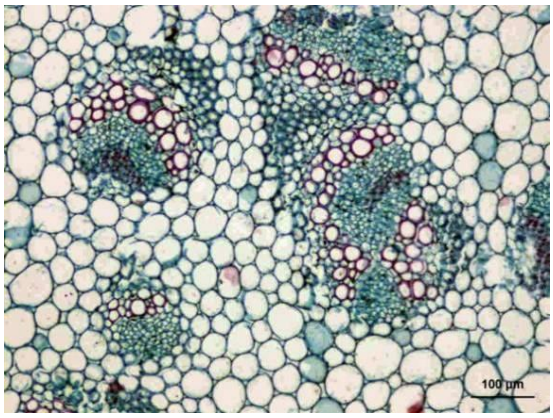

Figure 2. *Cross section of stems, abnormal vascular bundles*

Each stem had more than 40 vascular bundles distributed in the parenchyma tissues; bundles were either large or small in size and scattered in a disorderly fashion. The vascular bundles had obvious external contours. The vascular bundle sheath was formed by the outermost layer surrounded by sclerenchyma tissue (*Figs. 3* and *4*). The phloem were well-developed, composed of sieve tubes, companion cells, phloem parenchyma cells and phloem fibers. The xylem matured from the inside toward the outside. No vascular cambium was present in the bundles.

http://www.aloki.hu ● ISSN 1589 1623 (Print) ● ISSN 1785 0037 (Online)
DOI: http://dx.doi.org/10.15666/aeer/1706_1279912806

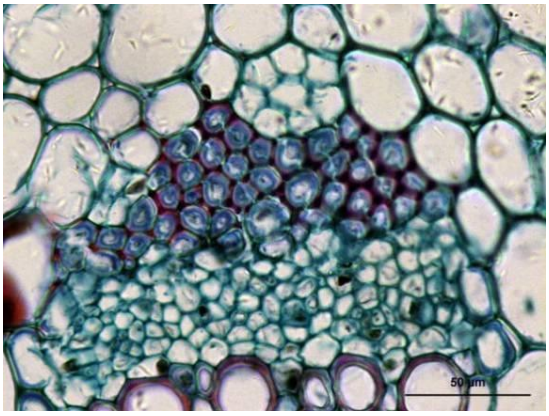

Figure 3. *Cross section of stems, phloem and phloem fibers*

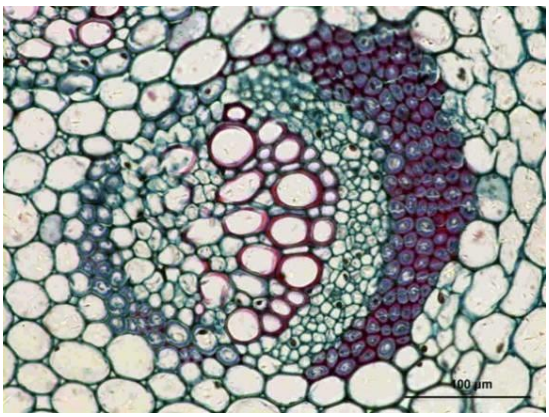

Figure 4. *Cross section of stems, lack of intrafascicular cambium in vascular bundles*

Leaf anatomical structure of A. umbrosum

The adaxial and abaxial epidermis was both composed of a single layer of tightly aligned cells. The epidermal cells varied in size with two or three large scattered heterocysts. The cuticle of the external tangential walls of the adaxial epidermis was more than 5 μm thick. Stomata were densely distributed on the abaxial epidermis. There was no distinction between the palisade tissues and spongy tissues in the mesophyll, which had the structure of an isobilateral leaf. Cells had abundant chloroplasts and well-developed aerenchymas (*Fig. 5* and *6*).

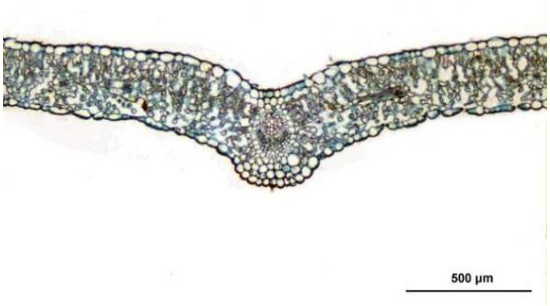

Figure 5. *Cross section of a leaf, epidermis of blade, mesophyll and structure of a leaf vein*

http://www.aloki.hu ● ISSN 1589 1623 (Print) ● ISSN 1785 0037 (Online)
DOI: http://dx.doi.org/10.15666/aeer/1706_1279912806

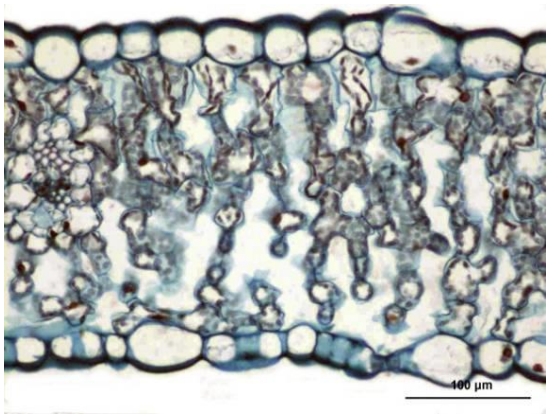

Figure 6. *Cross section of a leaf, structure of an isobilateral leaf*

The cross section of the main vein of the leaf was 400 μm × 450 μm. The leaf was 297 μm thick. The main vein was not well developed and had few mechanical tissues. The capillaries were mostly composed of small parallel vascular bundles. The main vein was composed of phloem and xylem, without intrafascicular cambium. A layer of the vascular bundle sheath was composed of parenchyma cells that had developed around the main vein (*Fig. 7*). At maturity, the xylem was neither aligned on the inside nor the outside. Instead, it was aggregated in a disorderly fashion to form a special type of leaf vein. This type of vein was completely different from the structure of leaf veins of typical dicots (*Fig. 8*).

Discussion

The stele of the vascular plants includes protostele, siphonostele, dictyostele, eustele and atactostele, etc. (Liu, 2008). The protostele is the most primitive, while the atactostele is well-developed in monocots.

The scattered vascular bundles in the stems of *A. umbrosum* look similar to the atactostele of monocots. However, the atactostele of monocots has large centripetal vascular bundles and small centrifugal vascular bundles. However, the centripetal vascular bundles were small in *A. umbrosum* while the centrifugal ones were large. The abnormal vascular bundles for *A. umbrosum* can be called scattered atactostele-like bundles. The scattered atactostele-like bundles provide strong evidence of the evolution of *A. umbrosum* from dicot to monocot, which also verified the viewpoint proposed by Tamura (1964) that the Ranales represent a living ancestor of the monocots.

The vascular bundles in the stem of *A. umbrosum* had sheaths composed of sclerenchyma, with a structure similar to that of the vascular bundle sheaths in the stem of monocots. The vascular bundles in the stem had no intrafascicular cambium, which is the same as the closed vascular bundles of monocots.

The scattered distribution of vascular bundles, the vascular bundle sheath of sclerenchyma and the lack of intrafascicular cambium are typical structures of monocots. The same structures were found in this investigation in the stems of a dicot (*A. umbrosum*) for the first time.

The epidermal cells on the top of the leaves of *A. umbrosum* had obvious heterocysts with a structure similar to that of bulliform cells in the adaxial epidermis of monocots. This structure provided microscopic proof for the evolution of dicots from Ranales to

http://www.aloki.hu ● ISSN 1589 1623 (Print) ● ISSN 1785 0037 (Online)
DOI: http://dx.doi.org/10.15666/aeer/1706_1279912806

monocots. The leaves of dicots are typically net-veined, while those of monocots have parallel veins. The structure of the pseudo-parallel veins of *A. umbrosum* is not like the netted veins of dicots. Instead, they are extremely similar to the parallel vein of monocots.

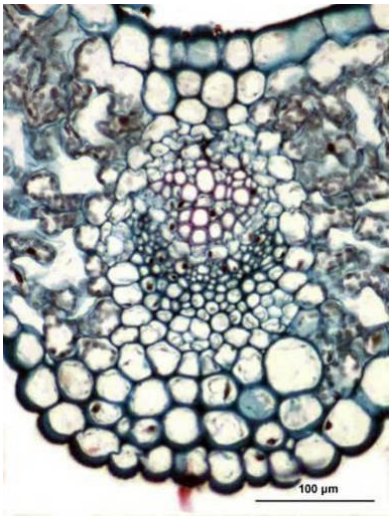

Figure 7. *Vascular bundle sheath of a leaf, main vein composed of parenchyma cells*

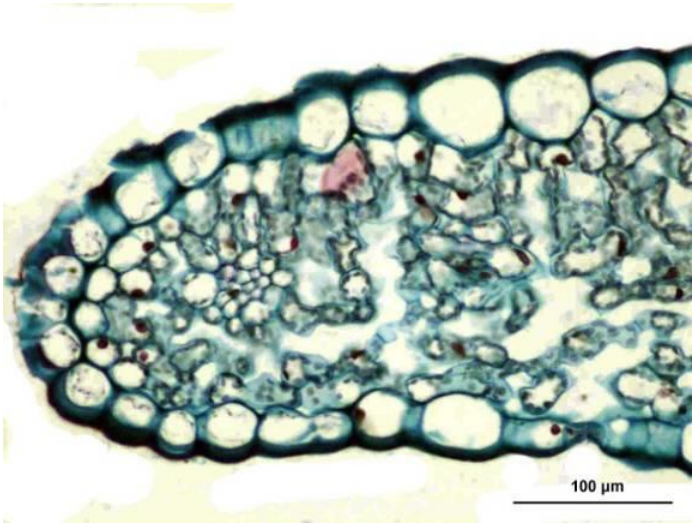

Figure 8. *Cross section of a leaf, bulliform cells and heterocysts*

No distinction can be seen between the palisade tissues and spongy tissues of the mesophyll of *A. umbrosum*, similar to those of the mesophyll of monocots which evolved into the structure of isobilateral leaf. There were multiple vascular bundles with small parallel leaf veins in the mesophyll in *A. umbrosum*; it can be considered to be a transitional type from the leaf veins of dicots (*A. umbrosum*) to those of monocots.

There was no intrafascicular cambium in the vascular bundles of the leaf veins, which conformed to the leaf structure of monocots. The mesophyll was not differentiated. The guard cells of the leaf stoma appeared to be transitional from the semilune type to the dumb-bell type. This type of structure has not been reported in

http://www.aloki.hu ● ISSN 1589 1623 (Print) ● ISSN 1785 0037 (Online)
DOI: http://dx.doi.org/10.15666/aeer/1706_1279912806

dicots. This was the first time that the leaf of a dicot (*A. umbrosum*) was found to have a structure similar to that of monocots.

The anatomical structures of the stems and leaves of *A. umbrosum* provide microscopic proof that the study of the systematic evolution of *A. umbrosum* (*Aconitum,* Ranunculaceae) could prove useful. It also supplemented and improved the Takhtajan and the Cronquist systems of classification. Anatomical studies on the roots of *A. umbrosum* still need to be completed and discussed.

The evolutionary investigation in this article proves that the dicot (*A. umbrosum*) is a living fossil exhibiting the evolution from dicot to monocot.

This paper supports the idea of the evolution from dicotyledons of ranunculaceae to monocotyledons of liliaceae proposed by Tamura et al. (1993) that is, liliaceae originated from ranunculaceae.

Conclusion

The stem had scattered vascular bundles, without the intrafascicular cambium. The leaf epidermis possessed pseudo-bulliform cells. The mesophyll had no distinction between palisade tissue and spongy tissue. The leaves developed multiple vascular bundles of parallel leaf veins, which had the structural characteristics of monocotyledons. The microscopic structure of the stems and leaves of *A. umbrosum*, a living fossil, were analyzed as part of an attempt to confirm the evolution of plants from dicotyledons to monocots; this study contributes to the completion of the theory of evolution as seen in the Takhtajan and Cronquist systems.

This paper has obtained the first-hand experimental evidence of the evolution of dicotyledon into monocotyledon plants.

Today, we sincerely suggest that colleagues continue to carry out the structural experimental research of plant system evolution. The anatomical experiments will provide more powerful evidence of evolutionary structure for the study of plant system evolution.

Acknowledgements. This work was financially supported by The number of the national key research and development program of the 13th five-year plan, approval number: 2017YFC0803803; Project of ministry of public security, approval number:1510697607 and Changchun “double ten” science and technology project, approval number: 17SS026.

Conflicts of interests. The authors declare no conflict of interests.

REFERENCES

[1] Gao, F. C. (2014): ISSR Analysis of Genetic Polymorphism of 7 Aconite Species in Xinjiang. – Xinjiang Medical University, Xinjiang.

[2] Li, J., Liu, G., Ihsan, A., Yi, X. J., Wang, D. G., Cheng, H., Muhammad, A., Huang, X. J. (2019a): Effects of veratrilla baillonii extract on hepatic gene expression profiles in response to aconitum brachypodum-induced liver toxicity in mice. – Frontiers in Pharmacology. DOI: 10.3389/fphar.2019.00568.

[3] Li, M., Feng, Y. X. (1990): Abnormal structure of aconitum root vessel group. – Journal of Integrative Plant Biology 9: 670-673 + 742.

[4] Li, Y. (2018): Phytological identification and phylogenetic structure of some liliaceae plants. – Doctoral Dissertation, Northeast Normal University.

http://www.aloki.hu ● ISSN 1589 1623 (Print) ● ISSN 1785 0037 (Online)
DOI: http://dx.doi.org/10.15666/aeer/1706_1279912806

[5] Li, Y. L., Guo, Q., He, F., Li, Y. Z., Xue, Q. H., Lai, H. X. (2019b): Biocontrol of root diseases and growth promotion of the tuberous plant Aconitum carmichaelii induced by actinomycetes are related to shifts in the rhizosphere microbiota. – Microbial Ecology. DOI: 10.1007/s00248-019-01388-6.
[6] Qin, R., Zhang, D. D., Liu, H., Wu, Z. H., Zhang, J. J., Han, D., Wang, J. (2019): Sequence and structural characteristics of ITS barcodes of aconitum. – Journal of Southwest University for Nationalities (Natural Science Edition) 45(02): 134-145.
[7] Tamura, M., Ranunculaceae, A., Kubitzki, K., Rohwcr, J. G., Bittrich, V. (1993): The Families and Genera of Vascular Plants. Vol. 11. Flowering Plants. Dicotyledons: Magnoliid, Hamameliid and Caryophyllid. – Springer, Berlin.
[8] Tian, W., Zhou, T. H. (2017): Research progress of aconitum resources in Qinling area. – Guangdong Chemical Industry 44(12): 155-156.
[9] Wu, C., Zhao, J. (2011): Research progress of aconitum in China. – Journal of Xinjiang Medical University 34(10): 1153-1157.
[10] Wu, D. M. (2015): Identification and systematic evolution of epigenetic phytoliths in 17 genera of ranunculaceae. – Doctoral Dissertation, Northeast Normal University.
[11] Xiong, J., Liu, W. Y., He, D., Zhang, L., Yang, C. K., Luo, Q. P., Liu, J., Shen, Y. (2019b): Study on diterpene alkaloids from overground parts of Aconitum chinensis. – Chinese Herbal Medicine 50(10): 2279-2284 (in Chinese with English abstract).
[12] Xu, S., Dong, B. Y. (2009): Investigation on plant resources of aconitum in North China. – Jiangsu Agric SCI (06): 421-425.

http://www.aloki.hu ● ISSN 1589 1623 (Print) ● ISSN 1785 0037 (Online)
DOI: http://dx.doi.org/10.15666/aeer/1706_1279912806

PHOTOSYNTHETIC PHYSIOLOGICAL CHARACTERISTICS OF FOUR MEDICINAL PLANTS

MA, Y.[1,2] – DING, Y.[3] – LU, J.[1*]

[1]*School of Life Sciences, Northeast Normal University, Changchun 130024, China*

[2]*College of Landscape Architecture, Changchun University, Changchun 130012, China*

[3]*College of Art and Design, Jilin Jianzhu University, Changchun 130118, China*

**Corresponding author*
e-mail: ahappyday9217@126.com

(Received 9th May 2019; accepted 16th Jul 2019)

Abstract. The objective of this research was the study of research on the photosynthetic characteristics of four kinds of medicinal plants, to provide a reliable reference for the high quality cultivation of these four plants. Methods: the four kinds of medicinal plants were as the experimental materials. The photosynthetic rate, chlorophyll content, carotenoid content and photosynthesis of four medicinal plants were determined. The effects of net photosynthetic rate on photosynthetic effective radiation were studied, and the water use efficiency and transpiration rate were calculated. Results: through the comparison of net photosynthetic rate, it can be seen that the average photosynthetic rate, chlorophyll content and carotene content of the four medicinal plants are very different in the growing season. Conclusion: *Platycodon grandiflorum* has a wide range of adaptability to light intensity. It can not only utilize intense light efficiently, but also has shade tolerance. It is suggested to be cultivated in an intense light environment; *North Atractylodes* has high light utilization rate, but poor shade tolerance, it is suitable for cultivation in direct sunlight environment; *Carthamustinctorious* and *Menthahaplocalyx*has have strong shade tolerance, but are not resistant to intense light, and can adopt intercropping.
Keywords: *medicinal plants, photosynthetic rate, content of photosynthetic pigment, physiological and ecological factors, water use efficiency*

Introduction

Traditional Chinese medicine is an important weapon in the prevention and treatment of diseases in Chinese traditional medicine. It has been playing an important role in protecting health. Medicinal plants contain bioactive ingredients, is used for special economic crops and anticorrosion treatment (Kannan et al., 2018). As an important industrial raw material, it can be processed into drugs, pesticides and veterinary drugs (Qadir et al., 2018; Khosravi et al., 2018). China is the country with the largest species of medicinal plants in the world, and has a long history of cultivation. Because medicinal plants are natural, stable, with little toxic and side effects, they have the unique advantages that Western medicine does not have. Modern people are increasingly turning their attention from synthetic chemicals to natural medicines, and hoping to reduce the incidence of drug-induced diseases (Liu et al., 2014).

With the vigorous development of the pharmaceutical industry, the establishment of plant research institutes has been established (Kim et al., 2018; Allahdadi et al., 2018). The production of Chinese herbal medicines has reached an unprecedented level from the variety and scale (Zhu et al., 2014). Unlike the field crop production, the economic characters such as yield and quality of Chinese herbal medicines are not easy to control, and their adaptability is poor. Moreover, because of the "absolute heterogeneity" of

http://www.aloki.hu ● ISSN 1589 1623 (Print) ● ISSN 1785 0037 (Online)
DOI: http://dx.doi.org/10.15666/aeer/1706_1280712826

natural plants, the quality evaluation of Chinese herbal medicines is more difficult. Therefore, it is of great theoretical and practical significance (Huang et al., 2016) to study the fertility laws and various physiological characteristics of traditional Chinese medicine. At present, standardized construction of traditional Chinese medicine production bases, breeding and utilization of germplasm resources and excellent varieties, and pesticide residues and heavy metals are all actively studied. However, there are few reports about the relationship between photosynthetic performance and diurnal variation of photosynthesis and ecological factors, especially the research on main limiting factors and physiological characteristics of photosynthesis in different medicinal plants.

Photosynthesis is the process of transforming inorganic matter into organic matter and converting light energy into chemical energy. It is the basis of plant matter production (Lee et al., 2016). Photosynthetic rate determines the ability of photosynthesis, and is the key to the formation of plant biomass. The photosynthetic rate increases with the increase of light intensity in a certain range.

In this study, for further understanding of medicinal plant photosynthesis and physiological changes, the photosynthetic and physiological characteristics and environmental factors of four kinds of medicinal plants (*Platycodon grandiflorum*, *North Atractylodes*, *Carthamustinctorious* and *Menthahaplocalyx*) are determined and analyzed, and the diurnal changes of net photosynthetic rate and the content of photosynthetic pigments (Chlorophyll a, b, and carotenoid) were measured. Through light saturation point, light compensation point and photosynthetic pigment content, the shade tolerance and photosynthetic capacity were determined, the response of net photosynthetic rate to photosynthetically active radiation was discussed, the transpiration rate and water use efficiency were calculated as well as the physiological effects of ecological factors on the diurnal variation of net photosynthetic rate. The photosynthetic and physiological characteristics of these four medicinal plants are further studied to provide experimental basis for the creation of the cultivation environment which is beneficial to improve its photosynthesis.

Materials and methods

Materials

Brief introduction of materials

Platycodon grandiflorum: a perennial herb of the family Platycodon, and it grows in the shrubs region of less than 2100 m above sea level. It has the effects of relieving sore throat, and eliminating phlegm, etc. (Kim et al., 2016; Wanget al., 2015). *Platycodon grandiflorum* is not only a kind of resource plant but also a kind of economic plant for medicine and food. As shown in *Figure 1* of *Platycodon grandiflorum*.

North Atractylodes: is a perennial herb of family Compositae, mainly divided into the North Atractylodes and the South Atractylodes. The North Atractylodes is mainly distributed in the north of China. It grows on the dry slopes of 300-900 m above sea level, with sparse broad-leaved forests or coniferous broad-leaved mixed forests (Gao et al., 2017; Shen et al., 2017). The site is the main use of Atractylodes rhizome, with eliminating heat and removing sweat, digestion and other effects, so the treatment used to ease bloating, diarrhea and edema disease, night blindness, rheumatism and diabetes and so on. As shown in *Figure 2* of *North Atractylodes*.

http://www.aloki.hu ● ISSN 1589 1623 (Print) ● ISSN 1785 0037 (Online)
DOI: http://dx.doi.org/10.15666/aeer/1706_1280712826

Figure 1. *Platycodon grandiflorum*

Figure 2. *North Atractylodes*

Carthamustinctorious: is an annual herbaceous plant of family Compositae. It has special fragrance, warm and spicy taste, it has the effects of activating blood circulation, removing blood stasis, dysmenorrhea and relieving pain. It also has the effects of anti-inflammatory, improving myocardial blood supply, anti-aging and protecting liver. Safflower yellow is also a natural quality food pigment and dyestuff. As shown in *Figure 3* of *Carthamustinctorious*.

Figure 3. *Carthamustinctorious*

Menthahaplocalyx: is a perennial herb of the family Lamiaceae. Mint can grow in a region of less than 2100 m above sea level. It has the function of evacuating the wind and heat, clearing the head, and regulating the flow of vital energy and remove obstruction to it and relieving depression. It is good for preventing and curing cholesterol calculus, and has a role in central nervous system and digestive system. It is

http://www.aloki.hu ● ISSN 1589 1623 (Print) ● ISSN 1785 0037 (Online)
DOI: http://dx.doi.org/10.15666/aeer/1706_1280712826

mainly for treating wind heat and common cold, headache and stuffiness, throat swelling and pain, rubella and itching. As shown in *Figure 4* of *Menthahaplocalyx*.

Figure 4. *Menthahaplocalyx*

Experimental materials

Study area survey: the test was carried out in the agricultural science and technology demonstration base of Tongzhou District Agricultural Technology Extension Station in Beijing. This area is a continental monsoon climate zone, the annual average temperature is 11.3 °C, the annual rainfall is 620 mm, and the annual sunshine is 2730 h. The soil fertility is medium, and the texture is medium loam.

Experimental materials: *Platycodon grandiflorum*: in mid-April, the seeds of *Platycodon grandiflorum*, which were full of maturity, were seeded after germination in early May, the line spacing was 20 cm × 20 cm, and the routine field management measures were adopted. *North Atractylodes*: was collected from the Dabie Mountains in Hubei Province, which was identified by the Institute of traditional Chinese medicine of Hubei province. At the end of the March, *Carthamustinctorious*, *Menthahaplocalyx* were sowed in the experimental base, soil preparation, fertilizing, weeding, ridging and field management were carried out according to agronomic measures of common origin.

Methods

Determination of photosynthetic rate of leaves

From each cultivated plant population, a number of leaves were selected to accept the natural solar radiation. The gas exchange measurement (Nie et al., 2014) was carried out by a portable optical gas analysis system (LI-6400, Li-CorInc, Lincoln NE, USA). The control of the environmental factors in the leaf chamber was 20 °C, the concentration of the gas source CO_2 was $350\ \mu mol\ \ CO_2^{\circ} mol^{-1}$, and the light flux density (PFD) was $1000\ \mu mol\ \ photo\ ns^{\circ} m^{-2\circ} s^{-1}$. The experiment was carried out on all sunny days and repeated 5~6 times.

The calculation of the quantum efficiency (AQY) of the leaves shows a linear regression of the net photosynthetic rate (P_n) between $0 \sim 200 \mu mol\ \ photo\ ns^{\circ} m^{-2\circ} s^{-1}$ in the response curve to PFD, and the regression equation is obtained.

$$P_n = R_d + AQY \times PFD \qquad \text{(Eq.1)}$$

http://www.aloki.hu ● ISSN 1589 1623 (Print) ● ISSN 1785 0037 (Online)
DOI: http://dx.doi.org/10.15666/aeer/1706_1280712826

when $P_n = 0$, PFD is the optical compensation point Φ_i for photosynthesis. Where, R_d is the rate of dark respiration.

The calculation of the carboxylation efficiency of the leaves was linear regression on the $0 \sim 200\ \mu mol\ CO_2^{\circ} mol^{-1}$ point in the C_i curve of the intercellular CO_2 concentration by P_n, and the regression equation was obtained.

$$P_n = R_p + CE \times C_i \quad \text{(Eq.2)}$$

when $P_n = 0$, C_i is the CO_2 compensation point Γ of photosynthesis. R_p is the rate of respiration in the light, and CE is the carboxylation efficiency. As dark breathing is very small, the rate of CO_2 release can be approximated as the rate of photorespiration.

Determination of chlorophyll content

The leaves of the mature leaves with the diameter of 0.7 cm were collected from 30 mature leaves. The leaves were divided into 3 groups. They were immersed in the extract of 10 ml 80% acetone. The sample bottle was tightly sealed, and it was colorless under low temperature. When the concentration of leaf green was detected, the concentration of chlorophyll was obtained by detecting the light intensity of the fluorescence (Ribeiro-Filho et al., 2014). Portable optical gas analysis system is designed based on the principle that different gases have selective absorption of light. It is often used to detect carbon monoxide, carbon dioxide and other gases. The formula for calculating the fluorescence intensity is:

$$F = kQI_0\left(1 - e^{-\varepsilon cb}\right) \quad \text{(Eq.3)}$$

in *Equation 3:* k is a constant; Q is the fluorescence efficiency; I_0 is the laser light intensity; c is the concentration of chlorophyll a; b is the light path for the test sample; ε is the molar absorbing coefficient.

In the way of logarithmic calculation, the formula is arranged and the logarithm is obtained.

$$C = A - B\log\left(D - F\right) \quad \text{(Eq.4)}$$

where $A = \frac{2.3}{\varepsilon b}\log kQI_0$, $B = \frac{2.3}{\varepsilon b}$, $D = kQI_0$.

A, B, D in *Equation 4* are constant. When the sample of the fluorescence is determined, ε, k, Q, and I_0 are constant. Therefore, by measuring the fluorescence intensity of chlorophyll a emitted from cells, it can determine the concentration chlorophyll a and the fluorescence intensity of chlorophyll b to determine the concentration of chlorophyll b.

Determination of carotenoid content

The mixture of ethanol: acetone as 1:1 was used to extract 24 h in the dark, then be measured by UV-2001 ultraviolet spectrophotometer. And then the carotenoid content was calculated according to *Equation 5*.

http://www.aloki.hu ● ISSN 1589 1623 (Print) ● ISSN 1785 0037 (Online)
DOI: http://dx.doi.org/10.15666/aeer/1706_1280712826

$$C_x = (1000D_{470} - 2.05C_a - 114.8C_b)/245 \quad \text{(Eq.5)}$$

D_{470} is the absorbance at the wavelength of 470 nm. Pigment content = (pigment concentration× extract volume) / fresh weight of leaves.

Response of net photosynthetic rate to photosynthetically active radiation ($P_n - PAR$)

Using the red and blue light source, the light quantum flux density (PFD) in the Li-6400 portable photosynthetic system were 0, 400, 800, 1200, 1600, 2000, 2400 $\mu mol \cdot m^{-2} \cdot s^{-1}$, respectively. The temperature was 27 °C and the concentration of CO_2 is set by CO_2 injection system to 390 $\mu mol \cdot mol^{-1}$, which was actually $390 \pm 10 \mu mol \cdot mol^{-1}$. The response of the net photosynthetic rate to the photosynthetic effective radiation was measured by the non-right angled hyperbolic model.

$$P_n = \frac{aI = P_{\max} - \sqrt{(aI + P_{\max})^2 - 4akIP_{\max}}}{2k} - R_d \quad \text{(Eq.6)}$$

According to the light response equation, the simulated photosynthetic response curve was estimated, the light compensation point (LCP) and the optical saturation point (LSP) were calculated. That is to say, when the P_n reaches a certain level of $P_{\max}$, the I value was obtained, and the light saturation point was estimated (Shen et al., 2016). The value of I is used to estimate optical compensation point with P_n at 0. In *Equation 6*, P_n is the net photosynthetic rate ($\mu mol \cdot m^{-2} \cdot s^{-1}$), a is the use efficiency of optical quantum, I is the light flux density ($\mu mol \cdot m^{-2} \cdot s^{-1}$), $P_{\max}$ is the maximum total photosynthetic rate ($\mu mol \cdot m^{-2} \cdot s^{-1}$), R_d is dark respiration efficiency ($\mu mol \cdot m^{-2} \cdot s^{-1}$), and k reflects the degree of curvature of the photosynthesis curve.

Determination of photosynthesis and ecophysiological factors

Li-6400 portable photosynthesis measurement system produced by LI-COR Company was used. The net photosynthetic rate (P_n) of plant leaves was measured under natural condition. The time interval was 8:00–18:00, every 2 h was measured once, five values were recorded each time, and the average value was recorded. Li-6400 portable photosynthesis measurement system also recorded physiological and ecological factors such as temperature (T_a), relative humidity (RH), photosynthetically active radiation (PAR), stomatal conductance (G_s) and transpiration rate E, etc. (Ding et al., 2015).

Water use efficiency

Water use efficiency (WUE) = net photosynthesis rate * 44 / transpiration rate * 18, unit: $mgCO_2 / gH_2O$.

Results

The *Figure 5* is the leaves' photosynthetic rate comparison chart of four species of medicinal plants during the whole growth period. The *Figure 6* is a daily change map of

http://www.aloki.hu ● ISSN 1589 1623 (Print) ● ISSN 1785 0037 (Online)
DOI: http://dx.doi.org/10.15666/aeer/1706_1280712826

the environment factor. The *Figure 7* is the effect of net photosynthetic rate on photosynthetically active radiation.

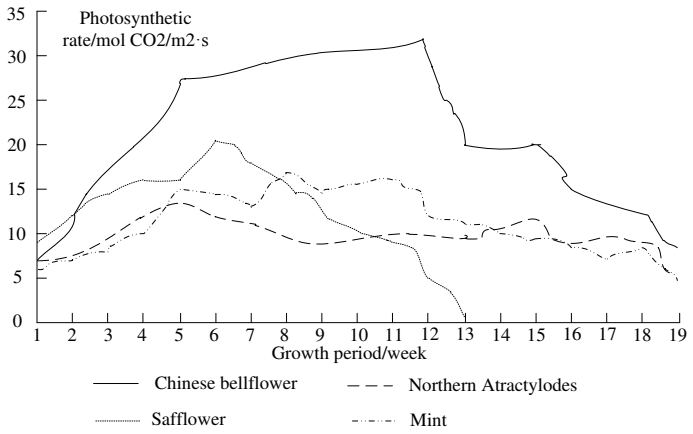

Figure 5. *Contrast diagram of photosynthetic rate of leaves at full growth stage*

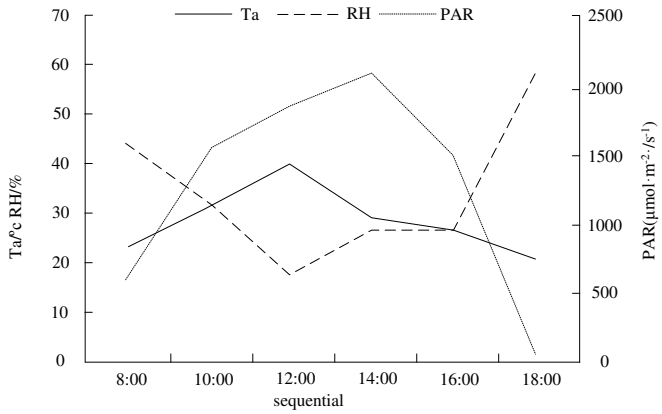

Figure 6. *Diurnal variation of environmental factors*

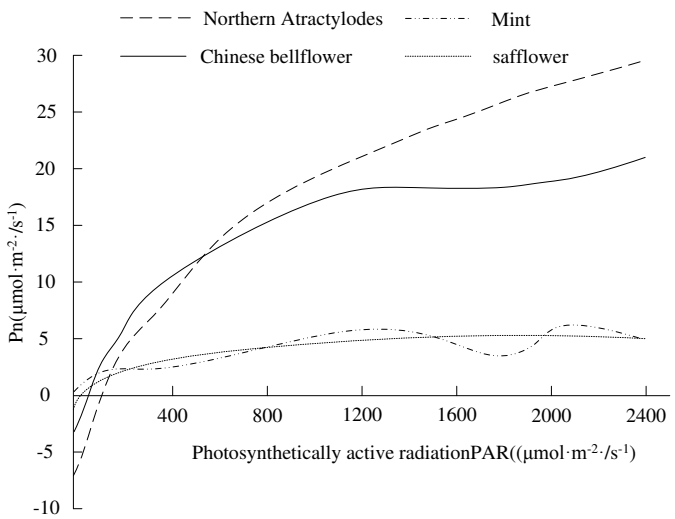

Figure 7. *Effect of net photosynthetic rate on photosynthetically active radiation*

http://www.aloki.hu ● ISSN 1589 1623 (Print) ● ISSN 1785 0037 (Online)
DOI: http://dx.doi.org/10.15666/aeer/1706_1280712826

Table 1 is the photosynthetic parameters of four medicinal plants. *Table 2* is the content of photosynthetic pigments in four medicinal plants. *Table 3* is the path analysis between the main factors affecting the net photosynthetic rate.

Table 1. *Photosynthetic parameters of 4 medicinal plants*

Medicinal plant	LCP (μmol·m^{-2} s^{-1})	LSP (μmol·m^{-2} s^{-1})	Pmax (μmol·m^{-2} s^{-1})
Platycodon grandiflorum	45 ± 6.03 b	1052 ± 113.16 b	21.8 ± 2.02 b
North Atractylodes	106 ± 10.97 a	1558 ± 162.97 a	29.7 ± 2.86 a
Carthamustinctorious	38 ± 6.56 b	307 ± 42.67 c	5.8 ± 0.76 c
Menthahaplocalyx	7 ± 1.53 c	261 ± 12.17 c	5.0 ± 0.53 c

The difference between the different letters in the same column is significant ($p < 0.05$), the same below

Table 2. *Content of photosynthetic pigments in 4 medicinal plants*

Medicinal plant	Chlorophyll (mg·g^{-1})	Carotenoid (mg·g^{-1})	Chlorophyll a/b
Platycodon grandiflorum	1.769 ± 0.021 2 b	0.342 ± 0.016 4 b	2.880 ± 0.007 0 b
North Atractylodes	1.085 ± 0.032 1 c	0.204 ± 0.015 1 c	3.189 ± 0.402 0 a
Carthamustinctorious	1.919 ± 0.061 7 a	0.417 ± 0.020 4 a	2.861 ± 0.086 3 b
Menthahaplocalyx	1.701 ± 0.102 1 b	0.396 ± 0.017 8 a	2.471 ± 0.073 2 c

Table 3. *Path analysis between the main factors affecting the net photosynthetic rate*

Medicinal plant	Influence factor	Direct action	Indirect effect of Ta	Indirect effect of RH	Indirect effect of PAR	Indirect effect of Gs	Total effect	Decision coefficient
Platycodon grandiflorum	Ta	-0.247 2		-0.001 6	0.225 2	0.020 1	0.178 5	-0.149 380
	RH	0.001 7	0.220 8		-0.230 7	-0.271 1	-0.279 3	-0.000 950
	PAR	0.368 7	-0.150 9	-0.001 1		0.436 0	0.652 7**	0.345 357
	Gs	0.810 3	-0.061 6	-0.000 6	0.198 4		0.946 5**	0.877 275
North Atractylodes	Ta	-0.000 8		-0.108 1	0.244 4	0.104 9	0.240 4	-0.000 390
	RH	0.121 1	0.000 8		-0.232 5	-0.200 4	-0.311 0	-0.090 010
	PAR	0.333 9	-0.000 6	-0.084 3		0.502 5	0.751 5**	0.390 402
	Gs	0.793 8	-0.000 1	-0.030 6	0.211 4		0.974 5**	0.917 012
Carthamustinctorious	Ta	-0.064 2		-0.134 4	0.092 8	-0.130 8	-0.236 6	0.026 247
	RH	0.154 7	0.055 7		-0.061 9	-0.104 2	0.044 3	-0.010 180
	PAR	0.142 5	-0.041 8	-0.067 1		0.255 8	0.289 4	0.062 163
	Gs	0.942 9	0.008 9	-0.017 1	0..38 7		0.973 4**	0.946 522
Menthahaplocalyx	Ta	-2.669 7		1.328 0	0.883 1	0.092 6	-0.366 0	-5.173 310
	RH	-1.504 3	2.357 0		-0.624 9	-0.031 0	0.196 8	-2.854 550
	PAR	1.371 3	-1.719 4	0.685 5		-0.036 5	0.300 9	-1.054 840
	Gs	-0.235 1	1.052 0	-0.198 2	0.212 8		0.831 5**	-0.446 230

Figure 8 is the diurnal variation of the stomatal conductance and net photosynthetic rate. *Figure 9* is a seasonal change in net photosynthetic rate.

Table 4 is the changes of transpiration rate (unit: mg/g FW) of *Platycodon grandiflorum* and *North Atractylodes* in the whole growth period. *Table 5* is the changes of transpiration rate (unit: mg/g FW) of *Carthamustinctorious* and *Menthahaplocalyx* in the whole growth period. *Table 6* is the water use efficiency of *Platycodon*

http://www.aloki.hu ● ISSN 1589 1623 (Print) ● ISSN 1785 0037 (Online)
DOI: http://dx.doi.org/10.15666/aeer/1706_1280712826

grandiflorum and *North Atractylodes* in the whole growth period (unit $mgCO_2 / gH_2O$). *Table 7* is the water use efficiency of *Carthamustinctorious* and *Menthahaplocalyx* in the whole growth period (unit $mgCO_2 / gH_2O$).

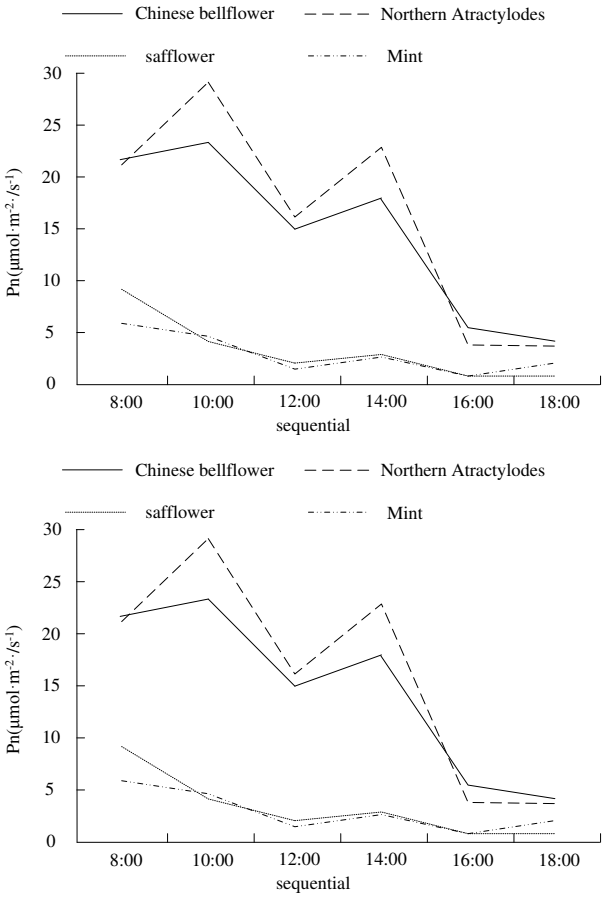

Figure 8. *Diurnal variation of stomatal conductance and net photosynthetic rate*

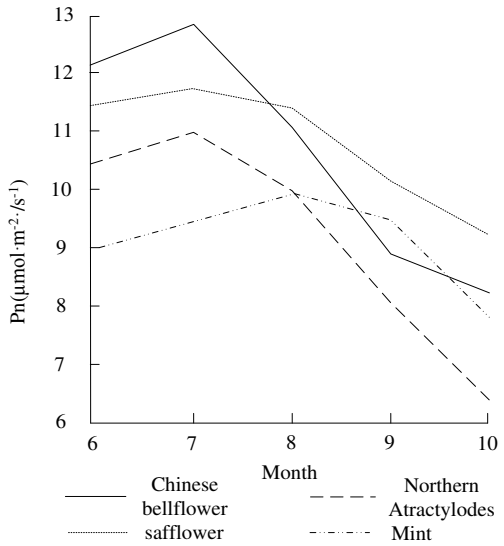

Figure 9. *Seasonal variation of net photosynthetic rate*

http://www.aloki.hu ● ISSN 1589 1623 (Print) ● ISSN 1785 0037 (Online)
DOI: http://dx.doi.org/10.15666/aeer/1706_1280712826

Table 4. *Change of transpiration rate of Platycodon grandiflorum and North Atractylodes during the whole growth period*

Platycodon grandiflorum			***North Atractylodes***		
Period of birth	**Date**	**Transpiration rate/g•m^{-2}•h^{-1}**	**Period of birth**	**Date**	**Transpiration rate/g•m^{-2}•h^{-1}**
Seedling stage	05-10	1.50	Seedling stage	05-10	2.06
	05-24	1.66		05-17	2.04
	06-07	2.27		05-24	2.86
Rosette stage	06-14	4.02	Florescence	06-10	3.81
	06-22	3.42		06-22	3.06
	07-07	3.09		07-01	2.41
Florescence	07-25	2.43	Fruit	07-13	2.33
	08-05	2.54		07-19	2.33
	08-16	1.81		07-25	2.29
Fruit	08-31	1.52	Bulking period of tuber	08-05	2.78
	09-10	1.27		08-16	2.90
	09-26	1.28		08-31	2.74
			Tuber weight gain period	09-10	2.04
				09-25	1.63

Table 5. *The change of transpiration rate in the whole growth period of Carthamustinctorious and Menthahaplocalyx*

Carthamustinctorious			***Menthahaplocalyx***		
Period of birth	**Date**	**Transpiration rate/g•m^{-2}•h^{-1}**	**Period of birth**	**Date**	**Transpiration rate/g•m^{-2}•h^{-1}**
Rosette stage	5.10	1.52	Seedling stage	5.10	1.43
	5.17	2.66		5.17	2.12
	5.24	2.37		5.24	2.65
Branching period	6.1	2.97	Branching period	6.7	2.81
	6.7	3.13		6.14	2.40
	6.14	3.43		6.22	2.99
Florescence	6.22	2.75	Florescence	7.7	2.91
	7.1	2.32		7.19	2.90
	7.13	1.59		7.25	2.44
Fruit	7.19	1.63	Fruit	8.5	2.39
	7.25	0.20		8.16	2.09
				8.31	1.92

http://www.aloki.hu ● ISSN 1589 1623 (Print) ● ISSN 1785 0037 (Online)
DOI: http://dx.doi.org/10.15666/aeer/1706_1280712826

Table 6. *Water use efficiency of Platycodon grandiflorum and North Atractylodes at full growth stage*

Platycodon grandiflorum			***North Atractylodes***		
Period of birth	**Date**	**WUE (g/kg)**	**Period of birth**	**Date**	**WUE (g/kg)**
Seedling stage	5.10	11.37	Seedling stage	5.10	2.06
	5.17	10.63		5.17	2.04
	5.24	8.93		5.24	2.86
Rosette stage	6.1	11.35	Florescence	6.11	3.81
	6.7	16.82		6.22	3.06
	6.14	12.49		7.1	2.41
Florescence	7.20	13.38	Fruit	7.13	2.33
	8.15	12.96		7.19	2.33
	9.5	12.91		7.25	2.29
Fruit	9.10	10.56	Bulking period of tuber	8.5	2.78
	9.17	9.81		8.16	2.90
	9.25	8.02		8.31	2.74
			Tuber weight gain period	9.10	2.04
				9.25	1.63

Table 7. *Water use efficiency of the full growth period of Carthamustinctorious and Menthahaplocalyx*

Carthamustinctorious			***Menthahaplocalyx***		
Period of birth	**Date**	**WUE**	**Period of birth**	**Date**	**WUE**
Rosette stage	5.10	12.39	Seedling stage	5.10	11.29
	5.17	11.66		5.17	10.02
	5.24	14.84		5.24	8.92
Branching period	6.1	12.88	Branching period	6.07	11.54
	6.7	12.78		6.14	15.96
	6.14	13.79		6.22	11.90
Florescence	6.22	15.89	Florescence	7.7	13.03
	7.1	16.45		7.19	12.86
	7.13	16.92		7.25	12.98
Fruit	7.19	11.56	Fruit	8.5	11.90
	7.25	7.57		8.16	10.49
	7.31	5.42		8.31	8.95

http://www.aloki.hu ● ISSN 1589 1623 (Print) ● ISSN 1785 0037 (Online)
DOI: http://dx.doi.org/10.15666/aeer/1706_1280712826

Data analysis

The following results are derived from the experiments in the previous section.

Comparison of photosynthetic rate in whole growth period

From *Figure 5,* we can see that in the whole growth period, the net photosynthetic rate of medicinal plants propagated by seeds showed a single peak curve: that is, the seedling stage is low, and the net photosynthetic rate increases with the expansion of vegetative body. When it reached high in the period of flower and fruit, it was gradually reduced; while the change curve of net photosynthetic rate of the medical plants propagated by rhizome showed bimodal curve. This is because the physiological and biochemical characteristics of medicinal plants are also different. Therefore, there are some differences in net photosynthetic rate.

The seasonal variation of net photosynthetic rate

Figure 9 showed that plant leaves had matured in June, and the photosynthetic rate of the four medicinal plants began to rise, and the maximum of the growth season was reached about July. With the change of season, photosynthetic rate began to decrease. In October, photosynthetically active radiation and air temperature decreased, leaves began to senescence, physiological activity decreased, and photosynthetic rate decreased to the minimum value in growing season. In addition, four kinds of medicinal plant photosynthetic rate in the growing season was significantly higher than that at the end of the growing season, this was because the higher leaf physiological activity of plant growth season (Chen et al., 2015). But with the leaf senescence and seasonal variation of environmental factors, the physiological activity of leaves decreased, the efficiency of photosynthetic apparatus declined, and the ability of assimilating CO_2 decreased, which showed that the photosynthetic rate of all plants decreased.

Diurnal changes of environmental factors

The environmental factors that affect plant photosynthesis include temperature, moisture, photosynthetic effective radiation, etc. The changes of temperature (T_a), relative humidity (RH) and photosynthetically active radiation (PAR) in the test day were shown in *Figure 6*.

In one day, the change of three environmental factors showed a single peak. PAR increased from $589\ \mu mol \cdot m^{-2} \cdot s^{-1}$ to $1989\ \mu mol \cdot m^{-2} \cdot s^{-1}$ in 8:00-14:00, and then dropped to a minimum at 18:00, only $91\ \mu mol \cdot m^{-2} \cdot s^{-1}$. T_a was mainly affected by PAR (r = 0899**), the largest was at 12:00, as 40.9 °C, and to 22.3 °C at 18:00. RH and PAR was significantly negatively correlated with T_a ($p < 0.01$). The correlation coefficient r_1 and r_2 were -0.945**.-0.941**, respectively.

Diurnal variation of stomatal conductance (G_s) and net photosynthetic rate (P_n)

It can be clearly seen from *Figure 8* that the changes of G_s and P_n of *Platycodon grandiflorum* and *North Atractylodes* were typical bimodal curve in one day, and the first peak > the second peak. This is due to the low light intensity and low temperature in the morning. At about 10:00, it reached the first peak, at this time PAR was $1161\ \mu mol \cdot m^{-2} \cdot s^{-1}$, and T_a was 32 °C. At about 12:00, *Platycodon grandiflorum* and *North*

http://www.aloki.hu ● ISSN 1589 1623 (Print) ● ISSN 1785 0037 (Online)
DOI: http://dx.doi.org/10.15666/aeer/1706_1280712826

Atractylodes were in the "noon break" state of photosynthesis, G_s decreased, and P_n decreased. At about 14:00, G_s and P_n reached second peak. G_s and P_n of *Carthamustinctorious* and *Menthahaplocalyx* were the largest at 8:00, and they were at a lower level since then, and there was no obvious "noon break" phenomenon.

The daily change of net photosynthetic rate of *Platycodon Platycodon* and *North Atractylodes* was bimodal curve, and the "noon break" phenomenon of photosynthesis appeared. This is a kind of beneficial ecological adaptation and self-regulation mechanism for the hot summer in the plant.

The relationship between the diurnal variation of net photosynthetic rate (P_n) and ecophysiological factors

The path analysis results of P_n and eco physiological factors (*Table 3*) showed that P_n and PAR of *Platycodon grandiflorum* and *North Atractylodes* was significantly positively correlated with G_s, but without correlation of RH and T_a. P_n of *Carthamustinctorious* and *Menthahaplocalyx* were positively correlated with G_s, not related to RH and PAR, but negatively correlated with T_a. According to the physiological and ecological factors, the decision coefficient P_n of the four medicinal plants in a day showed that the determinants that affected the diurnal variation of *Platycodon grandiflorum* and *North Atractylodes* were PAR and G_s, and PAR was the main determining factor. Limiting factors were T_a and RH, where T_a was a major limiting factor for the diurnal variation of *Carthamustinctorious* P_n, and the limiting effect of T_a and RH on *North Atractylodes* P_n was small. G_s was the main determinants of the diurnal variation of *Carthamustinctorious*, T_a and PAR also had certain promoting effect on P_n, but the effect was very small; RH was a limiting factor of diurnal variation of *Carthamustinctorious* P_n. T_a, RH, PAR and G_s were the limiting factors of the diurnal variation of *Menthahaplocalyx* P_n, and T_a of them were the most important limiting factor.

Comparison of photosynthetic parameters

The light compensation point (LCP), the light saturation point (LSP) and the maximum net photosynthetic rate can directly reflect the tolerance and photosynthetic capacity of plants. The low LCP of plants means that plants have strong ability to use weak light. The low LSP showed that the photosynthetic rate of plants increased rapidly with the increase of light quantum density, and quickly reached the maximum efficiency. Therefore, lower LCP and LSP enable plants to maximize photosynthetic capacity under low light density and maximize their photosynthesis under light limitation, thereby enhancing the accumulation of organic matter and meeting their energy needs for survival and growth.

It can be seen from the light response of P_n (*Fig. 7*) that the order of respiration rate of four medicinal plants were: *Menthahaplocalyx* < *Carthamustinctorious* < *Platycodon grandiflorum* < *North Atractylodes*. In the PAR range of $0 \sim 100 \mu mol \cdot m^{-2} \cdot s^{-1}$, the P_n and PAR of four kinds of medicinal plants was closed tothe linear relationship. The P_n of *Menthahaplocalyx* in the range wasthe maximum and that of *North Atractylodes* was the minimum. P_n of *Carthamustinctorious* and *Menthahaplocalyx* increased slowly in

http://www.aloki.hu ● ISSN 1589 1623 (Print) ● ISSN 1785 0037 (Online)
DOI: http://dx.doi.org/10.15666/aeer/1706_1280712826

that PAR was $100 \sim 300\ \mu mol \cdot m^{-2} \cdot s^{-1}$ and reached saturation, and then tended to be stable after $300\ \mu mol \cdot m^{-2} \cdot s^{-1}$. P_n of *Platycodon grandiflorum* and *North Atractylodes* increased rapidly in that PAR was $100 \sim 1000 \mu mol \cdot m^{-2} \cdot s^{-1}$, and closed to saturation in about $1000 \mu mol \cdot m^{-2} \cdot s^{-1}$ and $1600 \mu mol \cdot m^{-2} \cdot s^{-1}$. The light compensation curve (LCP), light saturation point (LSP) and maximum net photosynthetic rate of the four medicinal plants were estimated according to the fitting equation of light response curve, shown in *Table 3*.

The results showed that the LCP, LSP and the maximum net photosynthetic rate of the *North Atractylodes* were significantly higher than those of the other 3 medicinal plants, indicating that they had strong ability to use intense light and high photosynthetic capacity under intense light, and $106 \mu mol \cdot m^{-2} \cdot s^{-1}$ of LCP showed their shade tolerance. The LCP of *Carthamustinctorious* and *Menthahaplocalyx* was lower than that of the *North Atractylodes*, indicating that they had high ability to use weak light and strong shade tolerance. The LCP of *Platycodon grandiflorum* was close to *Carthamustinctorious*, while LSP was higher, and has a higher maximum net photosynthetic rate, indicating that its photosynthesis was effective and its adaptability to light was the largest. The maximum net photosynthetic rate of *Carthamustinctorious* and *Menthahaplocalyx* was significantly lower than that of *Platycodon grandiflorum* and *North Atractylodes*, while *Platycodon grandiflorum* was lower than that of *North Atractylodes*.

Water use efficiency in the production of photosynthetic substances in medicinal plants

It can be seen from *Tables 6* and *7* that in the 4 medicinal plants, except the *North Atractylodes*, the remaining plants have a common characteristic in the water use efficiency, that is, the single peak curve changes in the whole growth period.

Differences between species in water use efficiency: Although the change of water use efficiency during the growth period is a single peak curve, for different plant species, water use efficiency has the characteristics of species, mainly in the following areas:

Firstly, the comparison of the whole growth period, *Platycodon Grandiflorum* has the highest water use efficiency of $15.62 \sim 23.22\ mgCO_2 / gH_2O$, followed by *Carthamustinctorious*, *Menthahaplocalyx*, and the lowest is the *North Atractylodes*.

Secondly, the period of highest water use efficiency has interspecific difference: *Platycodon grandiflorum*, *Carthamustinctorious* and *Menthahaplocalyx* propagated by seeds is at flowering stage, while the *North Atractylodes* propagated by vegetative is in accumulation stage.

Thirdly, the water use efficiency of *Platycodon grandiflorum* is relatively stable during the whole growth period, that is, there is little difference in the growth period. For example, the water use efficiency of *Platycodon grandiflorum* at different growth stages was 7.21%-11.63% compared with the water use efficiency of the whole growth period, while the differences in the three other medicinal plants was more than 50%.

Change of transpiration rate of medicinal plants in the whole growth period

Transpiration is the process of loss of water from the surface of the living plant (mainly leaves) in the state of water vapor into the atmosphere. It is different from the

http://www.aloki.hu ● ISSN 1589 1623 (Print) ● ISSN 1785 0037 (Online)
DOI: http://dx.doi.org/10.15666/aeer/1706_1280712826

evaporation process of physics. Transpiration is not only influenced by environmental conditions, but also regulated and controlled by the plant itself, so it is a complex physiological process.

Transpiration is of great importance to plants, providing the main motive force for the plant to absorb and transport water, and also to lose the water. Photosynthesis is a way for plants to produce organic matter by means of light energy. It is often related to the importance of plant growth and crop yield.

The results of *Tables 4* and *5* showed that the change of transpiration rate of different medicinal plants was similar to that of their net photosynthetic rate.。 The total change trend of transpiration rate in the whole growth period of the medicinal plants propagated by seeds showed a single peak curve: that is, the seedling stage was low, and transpiration rate gradually increased with the continuous expansion of the vegetative body. After reaching the highest level, it gradually reduced to the lowest in the late growth stage, and the transpiration rate of *Platycodon grandiflorum* varied greatly, While the *North Atractylodes*, which propagated with rhizomes and tubers, showed the bimodal curve.

There are some differences between the transpiration rates of medicinal plants: the *Platycodon grandiflorum* has the maximum transpiration rate, especially in the branching stage and the early flowering stage, between $2.43 \sim 4.02\ m\ mol\ \mathrm{H_2}O / \mathrm{m}^2 / s$, followed by *Carthamustinctorious* and *Menthahaplocalyx*, and the lowest is Atractylodis sinensis. The changes of the whole growth period of the Atractylodis sinensis is more stable.

Discussion

Photosynthesis is the process of green plant uses visible light energy to synthetize the carbon dioxide and hydration to become carbohydrate (usually glucose) through the chloroplast, and release oxygen (Zhu et al., 2016). The reaction equation of photosynthesis is: $6CO_2 + 12H_2O \xrightarrow[\text{Chloroplast}]{\text{Luminous energy}} C_6H_{12}O_6 + 6O_2 + 6H_2O$. Net photosynthetic rate is closely related to its own factors, such as chlorophyll content, leaf thickness and leaf maturity. It is also affected by light intensity, air temperature, air relative humidity and soil water content (Schwinghamer et al., 2015).

Analysis of photosynthetic rate during the whole growth period

Among the four studied medicinal plants, *Platycodon grandiflorum* should be C4 plant and the other three species of medicinal plants are C3 plants. In each growth period, the net photosynthetic rate of *Platycodon grandiflorum* was significantly higher than that of *North Atractylodes*, *Carthamustinctorious*, *Menthahaplocalyx* cultivated in the same medicine Park. This is due to the C4 pathway of *Platycodon grandiflorum*, which has a fixed CO_2, and the source of energy is continuously supplied and fully utilized by CO_2, so it has a higher net photosynthetic rate (Schwinghamer et al., 2015).

The results showed that the photosynthetic rate of *Carthamustinctorious* and *Menthahaplocalyx* was slightly lower than that of *North Atractylodes* in the early stage of growth, while in the middle growth stage, it was significantly higher than that of *North Atractylodes*. The reason may be related to the difference of propagation mode (Peng et al., 2015): rhizome was used as propagating material for North Atractylodes, and soon entered fast growing stage, which showed strong photosynthetic ability. In

http://www.aloki.hu ● ISSN 1589 1623 (Print) ● ISSN 1785 0037 (Online)
DOI: http://dx.doi.org/10.15666/aeer/1706_1280712826

addition, the time when the *North Atractylodes* entered the flowering and fruiting stage was earlier than that of *Carthamustinctorious* and *Menthahaplocalyx*, and there was a strong physiological bank.

In the middle growth period, the rapid growth of *Carthamustinctorious* and *Menthahaplocalyx* needs large amounts of organic material for the vegetative growth (Almeida et al., 2014), and although Atractylodes sinensis at this time also began to rapid growth of vegetative, because the strain was smaller and the consumption of organic substances were also relatively less. The net photosynthetic rate of the former is not high.

The difference in the medicinal parts was different: rhizome was the storage location of *North Atractylodes*, and it had swelling and nutrient accumulation in the late growth stage (Kjaer et al., 2014), thus showing another peak of net photosynthetic rate.

The seasonal variation of net photosynthetic rate is discussed

In June to July, the ability of *Platycodon grandiflorum*root, *Carthamustinctorious* and *North Atractylodes* to use high temperature and high light intensity was obviously better than that of *Menthahaplocalyx*; In August and September, the photosynthetic capacity of *Menthahaplocalyx* increased slightly, indicating that *Menthahaplocalyx* could make use of relatively low light and temperature conditions more effectively. The photosynthetic rate of the *North Atractylodes* was the lowest in September and October, indicating that its ability to use relatively low light and temperature conditions was the lowest in four medicinal plants. The results showed that in the growing season, the order of average photosynthetic rate of four species of medicinal plants was: *Platycodon grandiflorum* > *Carthamustinctorious* > *Menthahaplocalyx* > *North Atractylodes*.

The diurnal variations of stomatal conductance and net photosynthetic rate are discussed

The plant self-factors that cause the net photosynthetic rate of plant leaves decreased at noon including stomatal and non-stomatal factors. At noon, in the field, the intense light, high temperature, low humidity and other environmental factors caused by plant stomatal closures, CO_2 was blocked to enter into the leaves and photosynthesis decreased, while non-stomatal factor was because the temperature was too high, resulting in a decline in net photosynthesis in mesophyll cells. In addition, under high light intensity for a long time, light inhibition and photorespiration can also lead to a decrease in net photosynthetic rate at noon. The response of P_n from *Platycodon grandiflorum* and *North Atractylodes* to PAR showed that *Platycodon grandiflorum* and *North Atractylodes* still had high P_n (above 19.5 and 26, $26.6\ \mu\text{mol}\cdot\text{m}^{-2}\cdot\text{s}^{-1}$) under intense light (above $1800\ \mu\text{mol}\cdot\text{m}^{-2}\cdot\text{s}^{-1}$), so photoinhibition and photorespiration were not the factors limiting P_n at this time. At 12:00, RH dropped to the lowest point of the day, and G_s was also lower than 10:00 and 14: 00, so the stomatal factor was one of the reasons for the low net photosynthetic rate at this time. In addition, T_a reached 40.9 °C at this time. Previous studies found that the optimum activation temperature for the key enzyme of Rubisco in photosynthesis was at 25~30 °C, its activity directly affects the photosynthetic rate. When the leaf temperature is too high, it will affect the activities of some related enzymes in the body, which is not conducive to the photosynthesis.

http://www.aloki.hu ● ISSN 1589 1623 (Print) ● ISSN 1785 0037 (Online)
DOI: http://dx.doi.org/10.15666/aeer/1706_1280712826

Therefore, the decline of P_n in the two plants is also caused by the decrease of the non-stomatal factors, the activity of the carboxycarboxylase of mesophyll cells.

The net photosynthetic rate of *Carthamustinctorious* and *Menthahaplocalyx* had a diurnal variation. The maximum net photosynthetic rate of the two plants was $9.1\mu mol \cdot m^{-2} \cdot s^{-1}$ and $5.8\ \mu mol \cdot m^{-2} \cdot s^{-1}$ respectively. After that, the net photosynthetic rate declined rapidly, which was similar to the results of the diurnal variation of the photosynthesis by Zhang Jingguang, et al. In the response of the P_n of the two plants to the PAR, the P_n decreased at PAR > $1400\ \mu mol \cdot m^{-2} \cdot s^{-1}$, indicating that the photoinhibition might have occurred under the intense light. The correlation analysis between diurnal variation of photosynthesis and physiological and ecological factors showed that G_s is the main influence factor of *Carthamustinctorious* P_n, while G_s of the *Carthamustinctorious* is low in a day, so stomatal limitation is a cause of low P_n in the daytime. It is believed that high temperature and intense light cause the potential activity of the active center and the primary light conversion efficiency decreasing, which hindered the photosynthetic electron transport. It is the limiting factor of photosynthesis (Zhang et al., 2015).

Content of photosynthetic pigment

The pigment that absorbs light in photosynthesis is called photosynthetic pigment, and there are two main types in higher plants: chlorophyll (including chlorophyll a, b) and carotenoids. The color of the leaves is mainly a comprehensive representation of the proportion of green chlorophyll and yellow carotenoid. The chlorophyll a/b of the leaves of the common sun plants is about $3:1$, and the chlorophyll a/b of the shade plants is $2:3:1$. The relative increase of chlorophyll b content may make more effective use of the blue violet light in the leaching light. So the chlorophyll b has the name of the chromophore system. The chlorophyll content of plants depends not only on site conditions, but also on the characteristics of plant species, and determines the ability of plants to absorb and convert light energy (Li et al., 2016).

The content of chlorophyll is also related to the resistance of plants to the shade. The chlorophyll content of *Platycodon grandiflorum* and *Menthahaplocalyx* had not significantly different, but the LSP and the maximum net photosynthetic rate of *Platycodon grandiflorum* were significantly higher than that of *Menthahaplocalyx*. The chlorophyll content of the *North Atractylodes* was significantly lower than that of *Platycodon grandiflorum*, but LSP was significantly higher than that of *Platycodon grandiflorum*, and the maximum net photosynthetic rate of them had no significant difference. The results showed that the content of chlorophyll was not directly related to LSP and the maximum net photosynthetic rate. The LCP of *Platycodon grandiflorum*, *Carthamustinctorious* and *Menthahaplocalyx* were lower than that of the *North Atractylodes*, so does the chlorophyll a/b value, but the content of chlorophyll and carotenoid was higher than that of the *North Atractylodes*, this may be because the plants with high chlorophyll content have weak absorption ability of light, it has better resistance to shade. In addition, it was found that low chlorophyll a/b value increased the absorption of far red light. Therefore, plants with low chlorophyll a/b value also had higher photosynthetic activity under low intensity of light.

In the experiment, the chlorophyll content of *Carthamustinctorious* was the highest in the four medicinal plants, followed by *Platycodon grandiflorum* and

http://www.aloki.hu ● ISSN 1589 1623 (Print) ● ISSN 1785 0037 (Online)
DOI: http://dx.doi.org/10.15666/aeer/1706_1280712826

Menthahaplocalyx, and that of *North Atractylodes* was the lowest. However, the content of chlorophyll a/b of *North Atractylodes*'s is the highest, followed by *Platycodon grandiflorum* and *Carthamustinctorious*, and that of *Menthahaplocalyx* leaves is the lowest. *Carthamustinctorious* and *Menthahaplocalyx* in four medicinal plants have the highest carotenoid content.

Conclusions

With the continuous progress of the social development and the accelerated process of industrialization, agriculture and green land area is decreased. The study of Photosynthetic Physiology plays a very important role in the selection of germplasm resources, the rational allocation of planting environment and the increase of yield in medicinal plants (Niakan et al., 2015). According to the first two chapters, we can further understand their photosynthetic and physiological characteristics by studying and discussing four kinds of medicinal plants of *Platycodon grandiflorum*, *Atractylodis sinensis*, *Carthamustinctorious* and *Menthahaplocalyx*.

The Atractylodis sinensis has high utilization rate of intense light, but it belongs to the light plant, and has poor shade tolerance. Thus, it should be cultivated in the environment of direct sunlight enough to increase the yield. *Carthamustinctorious* and *Menthahaplocalyx* are shade loving plants, but they are not resistant to intense light. The cultivation environment outside the forest is easy to inhibit their photosynthesis. Therefore, the intercropping way of forest and medical plants can be adopted. *Platycodon grandiflorum* has great adaptability to light intensity. It can not only efficiently use intense light but also have a characteristic of certain shade tolerance. If it wants to increase photosynthetic rate and increase yield, it is recommended to cultivate it in an intense light environment.

In the future research stage, the ecological characteristics of the same species of medicinal plants in different growing areas will be studied in depth, so as to provide more theoretical support for the development and utilization of medicinal plants.

Acknowledgements. This work was supported by Jilin Science and Technology Development Plan Project - Demonstration of Large Scale Breeding and Cultivation Techniques of Chinese Medicinal Herbs, such as Parasenecio firmus (Komar.) Y. L. Chen and Platycodon grandiflorus (Jacq.) A. DC., Changbai Mountain (No. 20170307027YY).

REFERENCES

[1] Allahdadi, M. N., Li, C. (2018): Numerical simulation of Louisiana shelf circulation under Hurricane Katrina. – Journal of Coastal Research 34(1): 67-80.
[2] Almeida, A. A. F., Gomes, F. P., Araujo, R. P. (2014): Leaf gas exchange in species of the Theobroma, genus. – Photosynthetica 52(1): 16-21.
[3] Chen, G., Chen, B., Gao, S. (2015): Parallel simulation model for plant growth by integrating morphology and physiology. – Computer Simulation 32(8): 404-408.
[4] Ding, H., Yin, Q., Wan, G. (2015): Solubilization of menthol by platycodin D in aqueous solution: an integrated study of classical experiments and dissipative particle dynamics simulation. – International Journal of Pharmaceutics 480(2): 143-51.

http://www.aloki.hu ● ISSN 1589 1623 (Print) ● ISSN 1785 0037 (Online)
DOI: http://dx.doi.org/10.15666/aeer/1706_1280712826

[5] Gao, W., Baig, A. Q., Ali, H., Sajjad, W., Farahani, M. R. (2017): Margin based ontology sparse vector learning algorithm and applied in biology science. – Saudi Journal of Biological Sciences 24(1): 132-138.
[6] Huang, Y. H., Jung, D. W., Lee, O. H. (2016): Fermented Platycodon grandiflorum extract inhibits lipid accumulation in 3T3-L1 adipocytes and high-fat diet-induced obese mice. – Journal of Medicinal Food 19(11): 1004.
[7] Kannan, P., Jithinraj, P., Natesan, M. (2018): Multiphasic inhibition of mild steel corrosion in H2S gas environment. – Arabian Journal of Chemistry 11(3): 388-404.
[8] Khosravi, A., Koury, R. N. N., Machado, L., Pabon, J. J. G. (2018): Prediction of hourly solar radiation in Abu Musa Island using machine learning algorithms. – Journal of Cleaner Production 176: 63-75.
[9] Kim, E. B., Nam, Y. H., Kang, T. H. (2016): Anti-diabetic activity of flavonoids isolated from the aerial parts of Platycodon grandiflorum in zebrafish, a model of type 2 diabetes. – Planta Medica 81(S 01): S1.
[10] Kim, N. Y., Jeon, E. J., Jung, S. H., Ahn, S. J., Park, M. A., Seo, J. S. (2018): Gene expression profiling and expression analysis of freshwater shrimp (Neocaridina denticulata denticulata) using expressed sequence tags and short-term exposure to copper. – Journal of Environmental Biology 39(1): 51-57.
[11] Kjaer, K. H., Clausen, M. R., Sundekilde, U. K. (2014): Photoperiodic variations induce shifts in the leaf metabolic profile of Chrysanthemum morifolium. – Functional Plant Biology 41(12): 1310-1322.
[12] Lee, N. K., Nyakudya, E., Jeong, Y. (2016): Bioconversion of platycodon Grandiflorum saponins by the platycodin D-converting microorganism, yeast Cyberlindnera Fabianii. – Journal of Food Biochemistry 40(3): 358-365.
[13] Li, Z., Bai, W., Zhang, L. (2016): Increased water supply promotes photosynthesis, C/N ratio, and plantamajoside accumulation in the medicinal plant Plantago depressa, Willd. – Photosynthetica 54(4): 1-9.
[14] Liu, M., Xu, Z., Guo, S. (2014): Evaluation of leaf morphology, structure and biochemical substance of balloon flower (Platycodon grandiflorum, (Jacq.) A. DC.) plantlets in vitro, under different light spectra. – Scientia Horticulturae 174(1): 112-118.
[15] Niakan, M., Mahjoob, S. R., Ghorbanli, M. (2015): Effect of exogenous putrescine on growth, photosynthesis and alkaloid compounds of Datura (Daturastramonium L.) in response to salinity stress under hydroponic conditions. – Journal of the Electrochemical Society 159(10): A1682-A1689.
[16] Nie, C., Liu, R., Li, S. (2014): Assessment of Platycodon grandiflorum germplasm resources from northern Anhui province based on ISSR analysis. – Molecular Biology Reports 41(12): 8195-201.
[17] Peng, H., Zhang, F., Jiang, J. (2015): Identification of quantitative trait loci for branching traits of spray cut chrysanthemum. – Euphytica 202(3): 385-392.
[18] Qadir, M. I., Mushtaq, H., Mobeen, T. (2018): In-silico study of potential carboxylic acid derivatives as D-glutamate ligase inhibitors in Salmonella typhi. – Kuwait Journal of Science 45(1): 100-107.
[19] Ribeiro-Filho, J., Leite, F. C., Costa, H. F. (2014): Curine inhibits mast cell-dependent responses in mice. – Journal of Ethnopharmacology 155(2): 1118-1124.
[20] Schwinghamer, T., Souleimanov, A., Dutilleul, P. (2015): The plant growth regulator lipo-chitooligosaccharide (LCO) enhances the germination of canola (Brassicanapus, [L.]). – Journal of Plant Growth Regulation 34(1): 183-195.
[21] Shen, W., Guan, Y., Wang, J. (2016): A polysaccharide from pumpkin induces apoptosis of HepG2 cells by activation of mitochondrial pathway. – Tumor Biology 37(4): 5239-5245.
[22] Shen, Y., Mi, W., Zhang, Z. (2017): A positioning lockholes of container corner castings method based on image recognition. – Polish Maritime Research 24(SI): 95-101.

http://www.aloki.hu ● ISSN 1589 1623 (Print) ● ISSN 1785 0037 (Online)
DOI: http://dx.doi.org/10.15666/aeer/1706_1280712826

[23] Wang, Y., Lu, B. H., Yang, L. N. (2015): First report of Fusarium armeniacum causing stem and root rot on Platycodon grandiflorus in Jilin Province, China. – Plant Disease 99(11): 150603065432001.
[24] Zhang, L. X., Guo, Q. S., Chang, Q. S. (2015): Chloroplast ultrastructure, photosynthesis and accumulation of secondary metabolites in Glechoma longituba, in response to irradiance. – Photosynthetica 53(1): 144-153.
[25] Zhu, L. X., Liu, D. (2014): Effects of different phosphorus applications on growth and platycodin content of Balloon Flower, (Platycodon grandiflorum). – Scientia Horticulturae 178(178): 8-13.
[26] Zhu, L. X., Zhang, W. J. (2016): Effects of controlled-release urea combined with conventional urea on nitrogen uptake, root yield, and quality of Platycodon grandiflorum. – Journal of Plant Nutrition 40(5): 662-672.

http://www.aloki.hu ● ISSN 1589 1623 (Print) ● ISSN 1785 0037 (Online)
DOI: http://dx.doi.org/10.15666/aeer/1706_1280712826

A SIMULATION STUDY OF THE APPROPRIATE BULK DENSITY AND DEPTH OF THE PLOW LAYER IN A SOYBEAN (*GLYCINE MAX* (L.) MERR) FIELD OF THE NORTHEAST BLACK SOIL REGION OF CHINA

KANG, S. – YU, L. – GONG, Z. P.*

College of Agriculture, Northeast Agricultural University, Harbin 150030, China

**Corresponding author*
e-mail: gzpyx2004@163.com

(Received 9th May 2019; accepted 20th Aug 2019)

Abstract. We studied the different patterns of nutrient accumulation, root-shoot ratio, and yield of soybean plants observed in response to the changes in the soil bulk density and plow depth; this was achieved by adopting the frame-planting method and taking two soybean varieties, Jiyu 79 (JY79) and Heinong 44 (HN44), as the test materials. The results showed that soybean dry matter; the accumulation of nitrogen (N), phosphorous (P), and potassium (K); and the yield had a single-peak curve change at the bulk density of 1.00 g/cm^3-1.45 g/cm^3, with the most appropriate soybean growth and yield observed at the bulk density of 1.15 g/cm^3-1.30 g/cm^3. Soybean dry matter; N, P, and K accumulation; and yield with the increase in plow depth, with the 30 cm plow depth being the optimal plow depth for the soybean field. The root-shoot ratio of the soybean plants was relatively high during the early growth period and decreased with the progression of the growth. In the R_1 stage, the root-shoot ratio showed a "V"-shaped change with the increase in bulk density in the plow layer, with the smallest root-shoot ratio occurring under the treatment with the bulk density of 1.30 g/cm^3; in the R_5 and R_8 stages, the root-shoot ratio was not significantly affected when the bulk density in the plow layer was between 1.00 g/cm^3 and 1.30 g/cm^3, but the root-shoot ratio significantly increased under the treatment with the bulk density of 1.45 g/cm^3. In the R_1 stage, no significant difference existed in the root-shoot ratio between the treatments with plow depths of 0-20 cm, and their root-shoot ratios were higher than those under the treatment with plow depths of 30 and 40 cm; in the R_5 and R_8 stages, no significant difference existed in the root-shoot ratio between the 10 to 40 cm plow depths.
Keywords: *bulk density, plow depth, soybean, nutrient accumulation, yield, root-shoot ratio*

Introduction

The average soil bulk density of China's terrestrial ecosystems is 1.32 g/cm^3. Soil bulk density increases with the depth of the soil layer (Chai and He, 2016) and has a significant effect on the soil water content characteristics (Blouin et al., 2004; Zhong et al., 2016). Soil bulk density also affects the soil microbial community structure (Kaiser et al., 1991) and physiological characteristics (Williams and Rice, 2007), thereby affecting the physiological and biochemical indicators and dry matter accumulation in crops (Assaeed et al., 1990; Siczek et al., 2013). Buttery et al. (1998) found that when bulk density increased from 1.2 g/cm^3 to 1.5 g/cm^3 in clay loam and 1.6 g/cm^3 in sandy loam, the soybean dry matter and root weight decreased significantly (Nunes et al., 2015a); the increased bulk density also reduced the number of pea root nodules and the root nodule dry weight, as well as the nitrogen (N) fixation enzyme activities and total N content (Siczek and Lipiec, 2011; Siczek et al., 2013).

Soil bulk density is an important indicator of soil physical properties. Excessive bulk density results in a decrease in the number of large pores in the soil, an increase in the soil compaction, and a decrease in the gas exchange rate (Kaiser et al., 1991).

http://www.aloki.hu ● ISSN 1589 1623 (Print) ● ISSN 1785 0037 (Online)
DOI: http://dx.doi.org/10.15666/aeer/1706_1282712842

Differences in soil compactness can have a significant impact on the growth and penetration of the crop roots (Colombi and Walter, 2016; Maganti et al., 2005). Siczek et al. (2015) found that the root number, root dry weight, root length, and root vigor of the crops all decreased with the increase in bulk density and that the increase in soil bulk density interfered with the growth of the pea roots and plants, leading to thicker roots and thus to less uptake of nutrients. Bengough et al. (1994) found that when soil bulk density was increased from 0.85 g/cm^3 to 1.40 g/cm^3, the growth rate of the pea roots was significantly reduced, and when the root growth encountered an increased resistance, the pea root elongation rate was decreased by 50% within half an hour; after the resistance was removed, the root growth rate increased slightly. The responses of the different crops to soil compactness are basically the same. Rosolem et al. (1998) studied the effect of soil compaction on the growth of cotton roots and showed that when the soil strength reached 2.5 MPa, the cotton roots would no longer grow. Freitas et al. (1999) disclosed that when the compaction of the soil increases, the morphology pattern of the lateral roots of maize also changes correspondingly, developing a thicker root diameter, a greater number of lateral roots and root hairs, and changing their direction of growth (Barley, 1962; Goss and Russell, 1980). Iijima et al. (1991) found that an excessive soil bulk density in the lower soil layers would inhibit growth in rice roots and corn roots, which in turn would promote the formation of lateral roots in the upper layer; this finding indicates that the growth of roots in different soil layers exhibits certain compensation effects. The results of previous studies in our laboratory showed that the effect of the soil bulk density on the N content and accumulation amount in soybean exhibits a parabolic change in trend, with soils that are too loose or too tight soil being unfavorable (Zhang et al., 2017). Johnson et al. (1989) found that the compaction in the 0 to 30 cm surface soil layer reduced the soybean yield by 15%, but the compaction of subsoil below the 30 cm layer had little effect on soybean yield. Gaultney et al. (1980) reported that the compaction of soil at lower layers can significantly affect the growth and final yield of corn. Bushamuka and Zobel (1998) argued that when the soil layer bulk density was 1.6 g/cm^3, the corn root system could not penetrate. However, Stypa et al. (1987) claimed that bulk density threshold in the soil layer for corn root growth could reach 1.8 g/cm^3. Increasing the subsoiling depth can effectively reduce the soil bulk density in the lower layers (Wang et al., 2015), which essentially increases the plow depth and increases the crop yield (Nunes et al., 2015b). Qi et al. (2015) conducted a subsoiling test under the same regional conditions, and the results showed that the resistance of the subsoiling blade increased in a quadratic curve as the subsoiling depth increased in the subsoiling operation. The above studies show that crop growth and yield have an appropriate range of bulk density and depth in the plow layer (Gayosso-Moralesl et al., 2017; Gomez-Lopez et al., 2018; Ufuk Kasim and Kasim, 2017; Vicente-Molina et al., 2018). When the bulk density in the plow layer is greater than the appropriate bulk density, the soil should be loosened; when the bulk density is too loose, the soil should be compacted. The tillage depth should be within the range of the appropriate plow depth, whereas tilling too deep would increase the cost and would not achieve the effect of increasing production (Fu and Liu, 2017; Peng et al., 2017).

The Northeast black soil region in China is the main soybean-producing area in China. The appropriate ranges of bulk density and plow depth in the plow layer in this region have not been determined by systematic study. In this study, the frame-planting method was used to simulate different bulk densities and plow depths to study their

http://www.aloki.hu ● ISSN 1589 1623 (Print) ● ISSN 1785 0037 (Online)
DOI: http://dx.doi.org/10.15666/aeer/1706_1282712842

effects on the growth and yield of the soybeans, thereby providing a theoretical basis for determining the appropriate bulk density and plow depth in the plow layer of the soybean field and providing a reference for scientific farming of field soybeans.

Materials and methods

Test materials

The experiment was conducted using the frame-planting method in the research field of the college of Agriculture, Northeast Agricultural University, China, in 2016. The round frame was made from a PVC circular tube (with an inner diameter of 20 cm, a height of 45 cm, and no bottom); 40 cm of the soil was packed, and the upper frame extended to 5 cm above the soil layer. The test soil was taken from the maize field and was of the black soil type (with a soil specific gravity of 2.65). Soil organic matter was 32.49 g/kg, available N was 65.01 mg/kg, available phosphorus (P) was 60.53 mg/kg, and available potassium (K) was 192.45 mg/kg. Soybean varieties included the Jiyu 79 (JY79) and Heinong 44 (HN44). The fertilizer application rate included 0.47 g (150 kg/hm^2) of diammonium hydrogen phosphate (P_2O_5: 46%) per frame and 0.24 g (75 kg/hm^2) of potassium sulfate (K_2O: 54%) per frame.

Experimental design

The soil density of the 20 to 30 cm soil layer of farmland in the black soil region was approximately 1.43 g/cm^3 (Zhao et al., 2010). The maximum value of the soil bulk density in this study was set as 1.45 g/cm^3.

Bulk density treatment: Four bulk density levels, including 1.00 g/cm^3, 1.15 g/cm^3, 1.30 g/cm^3, and 1.45 g/cm^3, were established and respectively denoted by B1.00, B1.15, B1.30, and B1.45. For each bulk density treatment, 30 frames were included, for a total of 120 frames in this study. The method was applied as follows: by measuring the soil water content, the weight of the soil 40 cm high in the frame was calculated, and a jack was used to compact the test soil in the round frame according to the different bulk density settings.

Plow depth treatment: The test soil within the round frame was divided into two layers (upper and lower layers) for simulation; that is, the upper layer was taken as the plow layer, and the lower layer was the layer below the plow layer. The soil bulk density in the plow layer was uniformly set to be 1.15 g/cm^3, and the soil bulk density in the layer below the plow layer was uniformly set to be 1.45 g/cm^3. Five plow depths were included, which were 0 cm, 10 cm, 20 cm, 30 cm, and 40 cm, respectively, and these depths were denoted as D0, D10, D20, D30, and D40, respectively. For each plow depth treatment, 30 frames were included, for a total of 150 frames. Specifically, for D0, the bulk density of the 40 cm of soil within the round frame was uniformly set as 1.45 g/cm^3; for D10, the bulk density of the upper 10 cm soil layer within the frame was set as 1.15 g/cm^3, and the bulk density of the lower 30 cm soil layer was set as 1.45 g/cm^3; for D20, the bulk density of the upper 20 cm soil layer within the round frame was set as 1.15 g/cm^3, and the bulk density of the lower 20 cm soil layer was set as 1.45 g/cm^3; for D30, the bulk density of the upper 30 cm soil layer with the round frame was set as 1.15 g/cm^3, and the bulk density of the lower 10 cm soil layer was set as 1.45 g/cm^3; and for D40, the 40 cm

http://www.aloki.hu ● ISSN 1589 1623 (Print) ● ISSN 1785 0037 (Online)
DOI: http://dx.doi.org/10.15666/aeer/1706_1282712842

soil bulk density in the round frame was uniformly set as 1.15 g/cm^3. A jack was used to first compact the soil below the plow layer and then to compact the upper soil.

For sowing, the soil within the frame was watered to saturation, and then, four seeds were sown in hills and covered with 3 cm of soil; after seedling emergence, final thinning of the seedlings was conducted, with two plants being retained per frame.

Sampling and nutrient determination

Sampling methods: Samples were taken at the R_1 (incipient flowering stage), R_5 (granule stage), and R_8 (maturity stage). During sampling, the aboveground part of the soybean plant was removed at the cotyledon trace, and the roots were rinsed with clean water. The various parts were respectively placed in different envelopes, which were subjected to fixation at 105 °C for 30 min and oven drying at 65 °C; samples were weighed for determination of the nutrient contents.

Nutrient determination: Plant N and P contents, respectively, were measured by using $CuSO_4$ and K_2SO_4 as catalysts, and after digestion of the sample with concentrated H_2SO_4, the N was measured by the Kjeldahl method, and the P was measured by the molybdenum antimony anti-colorimetric method. Following digestion of the sample by the concentrated H_2SO_4, the K content in the plants was determined by the flame spectrophotometry method by using hydrogen peroxide as a catalyst.

The accumulated amounts of N, P, and K were determined, respectively, by multiplying the corresponding N, P, and K content by the dry matter amount.

Results and analysis

Effects of soil bulk density and plow layer on soybean nutrient accumulation

Effect of soil bulk density on soybean nutrient accumulation

Table 1 shows the dynamics of the dry matter accumulation and the accumulation of the N, P, and K in soybean plants under the different soil bulk density conditions. As show in *Table 1*, under the four bulk density levels, the dry matter and the N, P, and K accumulation amounts of the two test soybean varieties increased with the progression of the growth stages. The dry matter and the N, P, and K accumulation amounts for the two test varieties under the various soil bulk density treatments showed a descending order of B1.30 > B1.15 > B1.00 > B1.45, showing a single-peak curve with the increase in soil bulk density. Specifically, in the R_1 stage, the dry matter and K accumulation amounts for the two varieties, as well as the N accumulation amount for JY79, were not significantly different between the B1.30 and B1.15 treatments; in the R_5 stage, the dry matter and the K accumulation amounts for the two test soybean varieties, as well as the N accumulation amount for HN44, were not significantly different between the B1.30 and B1.15 treatments; and in the R_8 stage, the P accumulation amounts for the two test soybean varieties were not significantly different between the B1.30 and B1.15 treatments. In the other stages, the B1.30 treatment showed significantly higher nutrient accumulation than the other treatments.

http://www.aloki.hu ● ISSN 1589 1623 (Print) ● ISSN 1785 0037 (Online)
DOI: http://dx.doi.org/10.15666/aeer/1706_1282712842

Table 1. *Effect of soil bulk density on soybean nutrient accumulation*

Variety	Period	Dispose	Dry matter quantity (g·case^{-1})	Nitrogen accumulation (mg·case^{-1})	Phosphorus accumulation (mg·case^{-1})	Potassium accumulation (mg·case^{-1})
JY79	R_1	B1.00	12.4 ± 0.20b	353.2 ± 5.83b	46.8 ± 0.78c	206.7 ± 3.41b
		B1.15	15.9 ± 0.30a	548.4 ± 9.64a	61.5 ± 0.80b	268.9 ± 3.72a
		B1.30	15.8 ± 0.32a	551.5 ± 11.3a	67.4 ± 1.37a	277.9 ± 5.67a
		B1.45	5.8 ± 0.12c	144.7 ± 3.23c	21.0 ± 0.44d	89.0 ± 1.84c
		Mean	12.5	399.5	38.7	210.6
	R_5	B1.00	63.5 ± 0.98b	2058.3 ± 31.41c	166.8 ± 2.52c	763.3 ± 10.87b
		B1.15	68.9 ± 1.57ab	2428.1 ± 51.39b	203.3 ± 3.91b	939.6 ± 18.41a
		B1.30	74.4 ± 1.64a	2689.3 ± 58.67a	215.7 ± 4.72a	985.1 ± 19.1a
		B1.45	16.4 ± 0.80c	453.0 ± 21.99d	42.0 ± 1.99d	174.2 ± 8.05c
		Mean	41.6	1899.7	157.0	715.6
	R_8	B1.00	145.4 ± 0.78c	4783.1 ± 29.83c	412.4 ± 2.75b	1636.2 ± 11.22c
		B1.15	168.0 ± 2.49b	6024.9 ± 100.98b	539.2 ± 14.11a	2084.9 ± 35.35b
		B1.30	181.5 ± 1.16a	6313.8 ± 17.66a	539.7 ± 5.65a	2225.2 ± 44.12a
		B1.45	42.9 ± 1.66d	1303.4 ± 28.26d	117.8 ± 1.78c	448.8 ± 8.07d
		Mean	134.5	4606.3	402.3	1598.8
HN44	R_1	B1.00	13.1 ± 0.44b	402.0 ± 13.06c	42.2 ± 1.33c	189.3 ± 6.59b
		B1.15	14.0 ± 0.19ab	453.7 ± 5.60b	47.8 ± 0.59b	218.1 ± 3.52a
		B1.30	14.7 ± 0.15a	497.5 ± 4.12a	51.4 ± 0.44a	222.3 ± 2.32a
		B1.45	6.0 ± 0.16c	143.8 ± 3.86d	21.4 ± 0.57d	78.4 ± 2.12c
		Mean	12.0	374.3	40.7	177.0
	R_5	B1.00	80.8 ± 1.58b	2418.3 ± 45.40b	215.9 ± 4.22c	1001.3 ± 20.89b
		B1.15	86.4 ± 1.83ab	2744.0 ± 65.22a	234.5 ± 5.11b	1117.5 ± 23.45a
		B1.30	89.1 ± 1.36a	2834.0 ± 43.50a	251.9 ± 3.56a	1173.8 ± 13.44a
		B1.45	27.0 ± 0.48c	704.9 ± 14.81c	79.0 ± 1.58d	338.6 ± 7.60c
		Mean	70.8	2175.3	147.8	907.8
	R_8	B1.00	135.0 ± 1.34b	4012.5 ± 36.23c	370.1 ± 2.87b	1559.2 ± 14.66b
		B1.15	144.5 ± 2.27b	4486.7 ± 61.97b	409.1 ± 4.91a	1684.3 ± 26.59b
		B1.30	165.0 ± 4.35a	5006.7 ± 180.56a	436.9 ± 18.90a	1895.7 ± 71.88a
		B1.45	40.6 ± 0.96c	1101.0 ± 18.31d	110.3 ± 1.56c	438.3 ± 7.84c
		Mean	121.3	3751.7	331.6	1394.4

Vertical comparison, 5% significant level

Effect of plow depth and soil bulk density on soybean nutrient accumulation

Table 2 shows the changes in the dry matter and the N, P, and K accumulation amounts of soybean plants under the different plow depths. From *Table 2*, under the five plow depths, the dry matter and NPK accumulation amounts of the two test varieties increased as the growth stage progressed and increased as the plow depth increased. Specifically, in the R_1 stage, the dry matter amount and the N accumulation amount of the two varieties showed a descending order of D40 > D30 > D20 > D10 > D0, and significant difference existed among the various treatments. The P accumulation amounts of the two varieties showed a descending order of D30 > D40 > D20 > D10 > D0; for JY79, significant differences existed among the various treatments and for HN44; and the P accumulation amount under D30 showed no significant difference from that under D40 but was significantly higher than those under

http://www.aloki.hu ● ISSN 1589 1623 (Print) ● ISSN 1785 0037 (Online)
DOI: http://dx.doi.org/10.15666/aeer/1706_1282712842

the other treatments. The K accumulation amounts of the two varieties were different because JY79 showed a descending order of D40 > D30 > D20 > D10 > D0, whereas HN44 showed a descending order of D30 > D40 > D20 > D10 > D0; for the two varieties, the P accumulation amount under D40 showed no significant difference from that under D30 but was significantly higher than those under the other treatments. In the R_5 stage, the dry matter and the N, P, K accumulation amounts for the two test soybean varieties showed a descending order of D40 > D30 > D20 > D10 > D0, and significant differences existed among the various treatments. In the R_8 stage, for JY79, the dry matter and the N and K accumulation amounts showed a descending order of D40 > D30 > D20 > D10 > D0, with significant differences existing among the various treatments; the P accumulation amount showed a descending order of D30 > D40 > D20 > D10 > D0, and the P accumulation amount under D30 showed no significant difference from that accumulation under D40 but was significantly higher than those under the other treatments. For HN44, the dry matter and the N, P, and K accumulation amounts showed a descending order of D30 > D40 > D20 > D10 > D0, and the dry matter and K accumulation amounts under D30 showed no significant difference from those under D40 but showed significant differences from those amounts under the other treatments.

Effects of soil bulk density and plow depth on the root weight and root-shoot ratio in soybean

Effect of soil bulk density on the root weight and root-shoot ratio in soybean

Table 3 shows the dynamic changes of the root weight and root-shoot ratio under the different soil bulk densities. As shown in *Table 3*, the root weights of the two test soybean varieties showed a single-peak curve with the increase of bulk density in the growth process, but differences existed in the changes of the root weight in the different stages among the various treatments. In the R_1 and R_5 stages, both varieties had the highest root weights at the bulk density of B1.15. In the R_1 stage, for HN44, the root weight under the B1.15 treatment showed no significant difference from that under the B1.30 treatments but was significantly higher than those under the other treatments. In the R_5 stage, for JY79, the root weight under the B1.15 treatment showed no significant difference from that under the B1.30 treatment but was significantly higher than those under the other treatments; however, for HN44, the root weight under the B1.15 treatment showed no significant difference from those under the B1.00 and B1.30 treatments but was significantly higher than that under the B1.45 treatment. In the R_8 stage, both varieties had the highest root weights at the bulk density of B1.30. Specifically, for JY79, the root weight under the B1.30 treatment showed no significant difference from that under the B1.15 treatment but was significantly higher than those under the other treatments; for HN44, the differences in the root weight between B1.30 and the other treatments all reached the level of significance. The effect of the soil bulk density on the root-shoot ratio of the soybean plants showed that the two test varieties showed a consistent pattern. In the R_1 stage, the root-shoot ratio of the soybean showed a trend in a "V"-shaped curve with the increase in the soil bulk density; the root-shoot ratio under B1.30 was the lowest and showed significant differences from those under the other treatments; and the root-shoot ratio under B1.15 showed no significant difference from that under B1.00 but was significantly lower than that under B1.45. In the R_5 and R_8 stages, the root-shoot ratio showed a consistent pattern: the ratio under

http://www.aloki.hu ● ISSN 1589 1623 (Print) ● ISSN 1785 0037 (Online)
DOI: http://dx.doi.org/10.15666/aeer/1706_1282712842

B1.30 showed no significant difference from those under B1.15 and B1.00 but was significantly lower than those under the B1.45 treatment. These results showed that the soil bulk density had a great influence on the root-shoot ratio in the early growth period, but the soil bulk density had no significant effect when it was 1.00 g/cm^3-1.30 g/cm^3 during the mid-to-late period; in contrast, when the soil bulk density reached 1.45 g/cm^3, the root-shoot ratio increased significantly.

Table 2. *Effect of plow depth and soil bulk density on soybean nutrient accumulation*

Variety	Period	Dispose	Dry matter quantity (g·case^{-1})	Nitrogen accumulation (mg·case^{-1})	Phosphorus accumulation (mg·case^{-1})	Potassium accumulation (mg·case^{-1})
JY79	R_1	D0	5.8 ± 0.15d	144.7 ± 3.23e	21.0 ± 0.44e	89.0 ± 1.84d
		D10	7.0 ± 0.19d	204.5 ± 5.11d	27.2 ± 0.71d	123.0 ± 3.42c
		D20	9.6 ± 0.43c	314.7 ± 13.98c	40.8 ± 1.78c	178.0 ± 8.11b
		D30	14.3 ± 0.07b	484.9 ± 3.65b	65.8 ± 0.41a	261.9 ± 1.43a
		D40	15.9 ± 0.30a	548.4 ± 9.64a	61.5 ± 0.80b	268.9 ± 3.72a
		Mean	10.5	339.4	43.3	184.2
	R_5	D0	16.4 ± 0.80e	453.0 ± 21.99e	42.0 ± 1.99e	174.2 ± 8.05e
		D10	29.9 ± 0.10d	840.5 ± 26.92d	83.6 ± 2.64d	379.6 ± 12.63d
		D20	50.3 ± 1.32c	1547.6 ± 38.72c	143.2 ± 3.77c	671.7 ± 17.55c
		D30	58.4 ± 1.01b	1976.6 ± 31.90b	174.4 ± 2.88b	793.8 ± 13.26b
		D40	68.9 ± 1.57a	2428.1 ± 51.39a	203.3 ± 3.91a	939.6 ± 18.41a
		Mean	41.8	1449.2	129.3	591.8
	R_8	D0	42.9 ± 1.66e	1303.4 ± 28.26e	117.8 ± 1.78d	448.8 ± 8.07e
		D10	68.8 ± 3.05d	2450.1 ± 115.33d	248.6 ± 13.20c	832.3 ± 39.58d
		D20	106.6 ± 1.71c	3719.4 ± 39.70c	371.7 ± 3.67b	1186.6 ± 13.36c
		D30	144.5 ± 1.55b	5411.6 ± 59.57b	543.1 ± 6.19a	1726.5 ± 20.06b
		D40	168.0 ± 2.49a	6024.9 ± 100.98a	539.2 ± 14.11a	2084.9 ± 35.35a
		Mean	106.2	3781.9	364.1	1175.8
HN44	R_1	D0	6.0 ± 0.16d	143.8 ± 3.86e	21.4 ± 0.57d	78.4 ± 2.12d
		D10	6.7 ± 0.14d	176.4 ± 4.02d	24.5 ± 0.51c	107.9 ± 2.45c
		D20	9.7 ± 0.22c	293.4 ± 8.30c	38.3 ± 0.99b	169.6 ± 3.64b
		D30	12.4 ± 0.39b	384.4 ± 11.56b	49.0 ± 1.52a	221.1 ± 7.01a
		D40	14.0 ± 0.29a	453.7 ± 5.60a	47.8 ± 0.59a	218.1 ± 3.52a
		Mean	9.8	290.3	36.2	159.0
	R_5	D0	27.0 ± 0.48e	704.9 ± 14.81e	79.0 ± 1.58e	338.6 ± 7.60e
		D10	33.3 ± 0.81d	976.2 ± 22.97d	100.1 ± 2.54d	424.9 ± 12.79d
		D20	41.3 ± 0.63c	1233.4 ± 13.16c	122.0 ± 1.68c	530.7 ± 5.97c
		D30	69.5 ± 0.99b	1985.1 ± 41.53b	216.9 ± 3.45b	905.3 ± 15.72b
		D40	86.4 ± 1.83a	2744.0 ± 65.22a	234.5 ± 5.11a	1117.5 ± 23.45a
		Mean	51.5	1528.7	150.5	663.4
	R_8	D0	40.6 ± 0.96d	1101.0 ± 18.31e	110.3 ± 1.56e	438.3 ± 7.84d
		D10	48.6 ± 0.90c	1441.0 ± 31.90d	148.6 ± 3.58d	520.6 ± 11.58c
		D20	114.5 ± 0.93b	3647.2 ± 37.22c	388.0 ± 4.78c	1310.9 ± 15.42b
		D30	147.3 ± 1.07a	4815.2 ± 29.54a	501.9 ± 3.46a	1723.4 ± 14.78a
		D40	144.5 ± 2.27a	4486.7 ± 61.97b	409.1 ± 4.91b	1684.3 ± 26.59a
		Mean	99.1	3098.2	291.6	1135.5

Vertical comparison, 5% significant level

http://www.aloki.hu ● ISSN 1589 1623 (Print) ● ISSN 1785 0037 (Online)
DOI: http://dx.doi.org/10.15666/aeer/1706_1282712842

Table 3. *Changes in the root weight and root-shoot ratio under the various soil bulk densities*

Period	Dispose	JY79		HN44	
		Root weight ($g \cdot case^{-1}$)	Root-shoot ratio	Root weight ($g \cdot case^{-1}$)	Root-shoot ratio
R_1	B1.00	2.9 ± 0.06b	0.30 ± 0.003b	2.6 ± 0.11b	0.26 ± 0.010b
	B1.15	3.5 ± 0.06a	0.28 ± 0.004b	3.0 ± 0.03a	0.27 ± 0.006b
	B1.30	2.9 ± 0.06b	0.22 ± 0.003c	2.8 ± 0.06ab	0.24 ± 0.003c
	B1.45	1.5 ± 0.06c	0.35 ± 0.010a	1.6 ± 0.04c	0.36 ± 0.001a
	Mean	2.5	0.29	2.2	0.28
R_5	B1.00	7.5 ± 0.15b	0.13 ± 0.003b	11.2 ± 0.34a	0.16 ± 0.006b
	B1.15	8.4 ± 0.16a	0.14 ± 0.001b	11.4 ± 0.18a	0.15 ± 0.003b
	B1.30	8.2 ± 0.05a	0.12 ± 0.003b	10.8 ± 0.18a	0.14 ± 0.001b
	B1.45	3.5 ± 0.14c	0.28 ± 0.015a	5.3 ± 0.19b	0.25 ± 0.017a
	Mean	5.9	0.17	7.2	0.18
R_8	B1.00	7.8 ± 0.19b	0.06 ± 0.003b	8.7 ± 0.26b	0.07 ± 0.001b
	B1.15	8.6 ± 0.14a	0.05 ± 0.003b	9.3 ± 0.33b	0.07 ± 0.003b
	B1.30	8.8 ± 0.25a	0.05 ± 0.001b	10.5 ± 0.42a	0.07 ± 0.003b
	B1.45	2.8 ± 0.14c	0.07 ± 0.001a	3.3 ± 0.13c	0.09 ± 0.003a
	Mean	4.9	0.06	6.6	0.08

Vertical comparison, 5% significant level

Effect of plow depth on the root weight and root-shoot ratio in the soybean

Table 4 shows the changes in the root weight and root-shoot ratio under the different plow depths. As shown in *Table 4*, the root weights of the two soybean varieties during the growth process also increased as the plow depth increased. In the R_1 stage, for JY79, no significant difference existed in the root weight between D40 and D30, but the root weights under these two treatments were significantly higher than those under the other treatments; for HN44, the root weight under D40 was significantly higher than those under the other treatments. In the R_5 stage, the root weights for the two soybean varieties under D40 were significantly higher than those under the other treatments. In the R_8 stage, for JY79, the root weight under D40 was significantly higher than those under the other treatments; for HN44, the maximum root weight was observed under D30, with the D30 root weight showing no significant difference from the weight under D40 but showing a significantly higher root weight than those under the other treatments. In addition, in terms of the effect of the plow depth on the root-shoot ratio of soybean plants, the two test varieties showed a consistent pattern because both showed a decreasing trend with the increase in plow depth. In the R_1 stage, for JY79, no significant difference existed in the root-shoot ratio under D0, D20, and D30, but these ratios were significantly higher than those under D30 and D40; no significant difference existed between those ratios under D30 and D40. For HN44, no significant difference existed between D0 and D10, but their root-shoot ratios were significantly higher than those under D20, D30, and D40, with no significant difference existing among D20, D30, and D40. In the R_5 stage, the two varieties showed a consistent pattern in that the root-shoot ratio under D0 was significantly higher than those under D10, D20, D30, and D40, with no significant difference existing between the latter four treatments. In the R_8

http://www.aloki.hu ● ISSN 1589 1623 (Print) ● ISSN 1785 0037 (Online)
DOI: http://dx.doi.org/10.15666/aeer/1706_1282712842

stage, for JY79, the root-shoot ratio under D0 was significantly different from those under the other treatments, with no significant difference observed among those under the D10, D20, D30, and D40 treatments; for HN44, the root-shoot ratio under D0 showed no significant difference from that under D10 but was significantly higher than those ratios under the other treatments, with no significant difference existing among those ratios under the D20, D30, and D40 treatments.

Table 4. *Changes in root weight and root-shoot ratio under the various plow layers*

Period	Dispose	JY79		HN44	
		Root weight ($g \cdot case^{-1}$)	Root-shoot ratio	Root weight ($g \cdot case^{-1}$)	Root-shoot ratio
R_1	D0	1.55 ± 0.05d	0.35 ± 0.009a	1.58 ± 0.04e	0.36 ± 0.001a
	D10	1.82 ± 0.04c	0.34 ± 0.006a	1.83 ± 0.06d	0.38 ± 0.020a
	D20	2.56 ± 0.13b	0.34 ± 0.019a	2.17 ± 0.02c	0.29 ± 0.012b
	D30	3.32 ± 0.05a	0.30 ± 0.008b	2.53 ± 0.1b	0.26 ± 0.003b
	D40	3.47 ± 0.06a	0.28 ± 0.004b	2.97 ± 0.03a	0.27 ± 0.006b
	Mean	2.69	0.32	2.51	0.31
R_5	D0	3.54 ± 0.14d	0.28 ± 0.015a	5.3 ± 0.19c	0.25 ± 0.017a
	D10	3.85 ± 0.09d	0.15 ± 0.003b	4.97 ± 0.11c	0.18 ± 0.009b
	D20	6.24 ± 0.18c	0.14 ± 0.001b	5.45 ± 0.2c	0.15 ± 0.006b
	D30	7.59 ± 0.21b	0.15 ± 0.006b	9.05 ± 0.24b	0.15 ± 0.006b
	D40	8.36 ± 0.16a	0.14 ± 0.001b	11.43 ± 0.18a	0.15 ± 0.003b
	Mean	6.90	0.17	9.67	0.18
R_8	D0	2.77 ± 0.14d	0.07 ± 0.001a	3.28 ± 0.13c	0.09 ± 0.003a
	D10	2.78 ± 0.03d	0.04 ± 0.001b	3.68 ± 0.24c	0.08 ± 0.007a
	D20	4.71 ± 0.38c	0.05 ± 0.003b	7.37 ± 0.27b	0.07 ± 0.001b
	D30	5.86 ± 0.13b	0.04 ± 0.001b	9.49 ± 0.51a	0.07 ± 0.003b
	D40	8.55 ± 0.14a	0.05 ± 0.003b	9.25 ± 0.33a	0.07 ± 0.003b
	Mean	6.97	0.05	7.92	0.08

Vertical comparison, 5% significant level

Effects of the soil bulk density and plow depth on soybean yield

Effect of the soil bulk density on the soybean yield

As shown in *Table 5*, the plant height, node number, grain number, 100-seed weight, and yield in the soybeans all showed a single-peak curve with the increase in the soil bulk density, with maximum values observed under the B1.30 treatment and minimum values observed under the B1.45 treatment. The plant heights of the two varieties both showed a descending order of B1.30 > B1.15 > B1.00 > B1.45. Specifically, the plant heights of JY79 under the B1.30 and B1.15 treatments showed no significant difference and were significantly higher than that under other treatments; the plant height of HN44 under B1.30 was significantly different from that under the other bulk density treatments. The node number of JY79 showed a descending order of B1.30 > B1.15 > B1.00 > B1.45, with no significant difference existing between B1.30 and B1.15; the node number of HN44 showed a descending order of B1.30 > B1.00 > B1.15 > B1.45, with B1.30 being significantly different from the other

http://www.aloki.hu ● ISSN 1589 1623 (Print) ● ISSN 1785 0037 (Online)
DOI: http://dx.doi.org/10.15666/aeer/1706_1282712842

bulk density treatments. The grain numbers of the two varieties both showed a descending order of B1.30 > B1.15 > B1.00 > B1.45. Specifically, the grain numbers of JY79 under B1.30 and B1.15 showed no significant difference and were significantly higher than those under the other treatments, and the grain number of HN44 under B1.30 was significantly different from the grain numbers under the other bulk density treatments. The 100-seed weights of the two varieties showed a descending order of B1.30 > B1.15 > B1.00 > B1.45; the 100-seed weight under B1.30 showed no significant difference from those under B1.15 and B1.00 but was significantly higher than that under the B1.45 treatment. The yields of the two varieties showed a descending order of B1.30 > B1.15 > B1.00 > B1.45, and except for the yields of HN44 under B1.00 and B1.15 showing no significant difference, the yields under the other treatments were significantly different. The results from the SPSS regression analysis show that for the two soybean varieties, the best-fitting equation between the yield and soil bulk density is cubic: for JY79, the equation is $y = -448.923x^3 + 799.66x^2 - 292.617$ ($R^2 = 0.946$), and the highest yield was achieved at the bulk density of 1.19 g/cm^3 out of the 1.00 g/cm^3-1.45 g/cm^3 range; for HN44, the equation is $y = -315.164x^3 + 554.203x^2 - 184.55$ ($R^2 = 0.899$), with the yield being the greatest at 1.17 g/cm^3. No significant difference existed in the optimal soil bulk density between the two varieties.

Table 5. *Yield components and morphology indexes under the different soil bulk densities*

Variety	Dispose	Height (cm)	Node number (nodes·plant^{-1})	Grain number (grains·plant^{-1})	100-seed weight (g)	Yield (g·case^{-1})
JY79	B1.00	70.6 ± 0.70b	14.2 ± 0.44b	189.2 ± 0.93b	18.3 ± 0.06ab	69.2 ± 0.56c
	B1.15	81.8 ± 1.27a	15.3 ± 0.33ab	214.7 ± 4.91ab	19.7 ± 0.52a	84.7 ± 0.28b
	B1.30	84.2 ± 2.23a	16.3 ± 0.44a	228.0 ± 12.50a	19.8 ± 0.86a	90.0 ± 1.52a
	B1.45	46.6 ± 0.73c	12.3 ± 0.33c	62.2 ± 0.60c	16.4 ± 0.29b	20.4 ± 0.16d
HN44	B1.00	76.6 ± 1.67b	15.2 ± 0.17b	160.0 ± 4.78b	20.7 ± 0.35a	66.3 ± 0.92b
	B1.15	78.0 ± 1.67b	14.8 ± 0.16b	169.3 ± 3.38b	20.7 ± 0.23a	70.2 ± 0.88b
	B1.30	89.1 ± 0.46a	16.2 ± 0.20a	188.0 ± 4.19a	20.9 ± 0.18a	78.5 ± 1.30a
	B1.45	43.6 ± 1.93c	12.3 ± 0.33c	52.5 ± 1.76c	19.2 ± 0.40b	20.2 ± 1.02c

Vertical comparison, 5% significant level

Effect of plow depth on soybean yield

Table 6 shows that with the increase in plow depth, the plant height, grain number, 100-seed weight, and yield showed increasing trends. The plant height of JY79 showed a descending order of D40 > D30 > D20 > D10 > D0; D40 showed no significant difference from D30 but showed significant differences from other various treatments. The plant height of HN44 showed a descending order of D30 > D40 > D20 > D10 > D0; D30 was significantly higher than other treatments, and D20 was not significantly different from D40 but was significantly higher than D10 and D0 treatments. The node number of JY79 showed a descending order of D40 > D20 > D30 > D10 > D0; no significant differences existed among D40, D20, and D30, among D30, D20, and D10, and between D10 and D0. The node number of HN44 showed a descending order of D30 > D40 > D20 > D0 > D10, and no significant difference existed among these treatments. The grain number of JY79 showed a descending order of D40 > D30 > D20 > D10 > D0, with no significant difference existing between D40 and

http://www.aloki.hu ● ISSN 1589 1623 (Print) ● ISSN 1785 0037 (Online)
DOI: http://dx.doi.org/10.15666/aeer/1706_1282712842

D30; the grain number of HN44 showed a descending order of D30 > D40 > D20 > D10 > D0, with no significant difference existing between D30 and D40. The 100-seed weight of JY79 showed a descending order of D40 > D30 > D20 > D10 > D0; D40 showed no significant difference between D30 and D20 but was significantly higher than D0 and D10; the 100-seed weight of HN44 showed a descending order of D30 > D20 > D10 > D40 > D0, with D30 showing no significant difference from D20 but being significantly higher than the other treatments. The yield of JY79 showed a descending order of D40 > D30 > D20 > D10 > D0; D40 showed no significant difference from D30, and D40 and the yield for D30 was significantly higher than with the other treatments. The yield of HN44 showed a descending order of D30 > D40 > D20 > D10 > D0, and D30 was significantly different from the other plow depth treatments. SPSS regression analysis showed that, for the two soybean varieties, the best-fitting equation between yield and plow depth is cubic: for JY79, the equation is $y = -0.001x^3 + 0.078x^2 + 0.677x + 18.438$ ($R^2 = 0.985$), and 30-40 cm is the optimal plow depth range within the 0 to 40 cm plow range; for HN44, the equation is $y = -0.005x^3 + 0.244x^2 - 1.376x + 16.95$ ($R^2 = 0.987$), with the yield being the highest at 29.4 cm, and 27.9-30.9 cm is the optimal plow depth range in the 0 to 40 cm plow range.

Table 6. *Soybean yield components and morphology indexes under the different plow depth treatments*

Variety	Dispose	Height (cm)	Node number (nodes·plant^{-1})	Grain number (grains·plant^{-1})	100-seed weight (g)	Yield (g·case^{-1})
JY79	D0	46.6 ± 0.73d	12.3 ± 0.33c	62.2 ± 3.60d	16.4 ± 0.28c	20.4 ± 0.36d
	D10	61.5 ± 0.62c	12.7 ± 0.44bc	102.0 ± 5.48c	18.6 ± 0.07bc	37.7 ± 1.78c
	D20	73.1 ± 2.73b	14.5 ± 0.57ab	141.7 ± 2.94b	19.3 ± 0.43ab	54.7 ± 0.34b
	D30	78.1 ± 1.99ab	14.3 ± 0.33ab	189.5 ± 4.73a	21.0 ± 0.74a	79.5 ± 2.08a
	D40	81.8 ± 1.27a	15.3 ± 0.33a	201.3 ± 8.41a	21.3 ± 0.69a	84.7 ± 0.28a
HN44	D0	43.6 ± 1.93c	12.3 ± 0.33a	52.5 ± 2.75c	19.2 ± 0.40c	20.2 ± 1.02d
	D10	50.8 ± 1.52c	12.2 ± 0.33a	55.5 ± 2.60c	21.4 ± 0.06b	23.8 ± 0.76d
	D20	76.2 ± 2.39b	13.0 ± 0.76a	138.8 ± 1.72b	22.9 ± 0.20a	63.5 ± 2.28c
	D30	89.0 ± 1.51a	14.8 ± 0.83a	172.0 ± 1.44a	23.4 ± 0.21a	80.4 ± 1.20a
	D40	78.0 ± 1.67b	14.2 ± 0.85a	169.3 ± 3.38a	20.7 ± 0.41b	70.2 ± 0.88b

Vertical comparison, 5% significant level

Discussion

Appropriate soil bulk density for soybean field

Soil bulk density is an important factor affecting soil porosity (Kaiser et al., 1991), and changes in soil bulk density cause changes in soil moisture characteristics. The changes in soil bulk density do not affect soil composition, but rather multiple soil physical indicators. The increase of soil bulk density causes significantly decreased saturated hydraulic conductivity, infiltration rate, and water diffusivity, thereby affecting crop growth and yield. A soil compaction test by Assaeed et al. (1990) found that when the bulk density was increased from 1.03 g/cm^3 to 1.51 g/cm^3, the barley yield was reduced by 29%; when the bulk density was increased from 1.49 g/cm^3 to 1.75 g/cm^3, the yields of barley, corn, and peas decreased by 29%, 33%, and 14%,

http://www.aloki.hu ● ISSN 1589 1623 (Print) ● ISSN 1785 0037 (Online)
DOI: http://dx.doi.org/10.15666/aeer/1706_1282712842

respectively; when the bulk density was increased from 1.35 g/cm^3 to 1.58 g/cm^3, the yield of peas decreased by 25%. Zhang et al. (2017) studied the relation between the N uptake and accumulation in soybean and the soil bulk density, and found that the impact of soil bulk density on soybean yield exhibited a single-peak curve, with the optimal bulk density being 1.23 g/cm^3-1.31 g/cm^3. In this experiment, the dry matter; N, P, and K accumulation; and the yield of soybeans showed a single-peak curve change when soil bulk density had the range of 1.00 g/cm^3-1.45 g/cm^3, with the optimal bulk density being 1.30 g/cm^3. The experiment shows that the yields of the two test soybean varieties at the soil bulk density of 1.30 g/cm^3 increased, respectively, by 6.3%, 30.2%, and 341.4% and by 11.8%, 18.4%, and 289.3%, respectively, compared to their yields at bulk densities of 1.15 g/cm^3, 1.00 g/cm^3, and 1.45 g/cm^3. The difference in yield was small between the bulk densities of 1.30 g/cm^3 and 1.15 g/cm^3, and 1.15 g/cm^3 – 1.30 g/cm^3 could be considered the appropriate range of bulk density for soybean growth. Therefore, when the bulk density is lower than 1.15 g/cm^3, the soil needs to be compacted properly, and when the bulk density is higher than 1.30 g/cm^3, the soil needs to be cultivated and loosened.

Significant differences exist in the soil bulk density under the different tillage measures, and as the soil bulk density increases, the number of pea root nodules and the dry weight of the root nodule, as well as the N-fixation enzyme activities and the total N content, would increase accordingly (Siczek and Lipiec, 2011; Siczek et al., 2013). Buttery et al. (1998) also found that in the clay loam, when the soil bulk density was increased from 1.2 g/cm^3 to 1.5 g/cm^3, the dry matter amount and the root weight of the soybean declined by 76.7% and 68.2%, respectively; in sandy loam, when the soil bulk density was increased from 1.2 g/cm^3 to 1.6 g/cm^3, the dry matter amount and the root weight of the soybean were reduced by 70.5% and 48.1%, respectively. In this study, the soybean root weight also showed a single-peak curve trend with the increase in the soil bulk density. Specifically, the maximum values for the two test varieties in the R_1 and R_5 stages occurred under the treatment with the bulk density of 1.15 g/cm^3, and the maximum value in the R_8 stage occurred under the treatment with the bulk density of 1.30 g/cm^3. When the bulk density was increased to 1.45 g/cm^3, the root weight was decreased significantly, which agreed with the findings of Buttery et al. (1998).

The increase in soil bulk density obstructs the growth of crop roots and of plants and results in thickened roots and poor nutrient uptake, leading to changes in crop root-shoot ratio. The root-shoot ratio of the soybean can indicate the distribution of the dry matter in the root and aboveground parts. Bengough et al. (1994) argued that when the soil bulk density increased from 0.85 g/cm^3 to 1.40 g/cm^3, the growth rate of the pea roots declined significantly; when the root growth resistance increased, the root elongation rate in the pea decreased by 50% within half an hour, and upon the removal of the resistance, the root growth rate increased slightly. In this experiment, the root-shoot ratios of the two test soybean varieties were high during the early growth period and decreased with the progression of the growth stages. The change of soil bulk density did not alter the pattern of gradual decrease in the root-shoot ratio during the progression of the soybean growth stages. However, a significant difference occurred in the root-shoot ratio among the different bulk density treatments. In the R_1 stage, the root-shoot ratio showed a "V"-pattern change with the increase of soil bulk density and reached its minimum value at the soil bulk density of 1.30 g/cm^3. The root-shoot ratios in the R_5 and R_8 stages showed no significant

http://www.aloki.hu ● ISSN 1589 1623 (Print) ● ISSN 1785 0037 (Online)
DOI: http://dx.doi.org/10.15666/aeer/1706_1282712842

difference among the treatments with the soil bulk densities of 1.00 g/cm^3, 1.15 g/cm^3, and 1.30 g/cm^3, but the ratios were significantly lower than those observed under the treatment with the soil bulk density of 1.45 g/cm^3. Notably, the treatment with the soil bulk density of 1.30 g/cm^3 was the most conducive to the growth of soybean, with the dry matter and the N, P, and K accumulation amounts being the highest when the root-shoot ratio was the smallest and the treatment with the soil bulk density of 1.45 g/cm^3 being the most unfavorable to the growth of soybean when the root-shoot ratio was the highest. These results indicate that when the soil bulk density was too high, root growth was hindered, and soybean plants had to allot more dry matter to the root system, resulting in an increase in the root-shoot ratio. When the soil was too loose (i.e., the bulk density was too low), bulk density only had a significant influence on the root-shoot ratio in the early soybean growth period; in contrast, excessive bulk density had a significant impact on the entire growth period.

Appropriate plow depth for the soybean field

Increased tillage and subsoiling depth can effectively reduce the soil bulk density in the lower layer and increase the plow depth, promoting crop growth and yield increase. Wang et al. (2015) conducted a comparative study between subsoiling of 30 cm, rotary tillage of 10 cm, and no-till treatments, and they found that the bulk density in the 20 to 30 cm soil layer under the subsoiling treatment decreased by 10.3% compared with that under the rotary tillage and no-till treatments; under the subsoiling treatment, the dry matter in the corn showed an increase, and the yield was 8.9% and 10.6% higher, respectively, than that under rotary tillage and no-tillage. Johnson et al. (1989) found that with a plow depth of 0-30 cm, the yield of crops gradually would increase with the increase of plow depth and would not increase significantly below the plow depth of 30 cm. Gaultney et al. (1980) noted that the soil compaction of the lower soil layers can significantly affect the growth and final yield of corn. Increasing the subsoiling depth can effectively reduce the soil bulk density in the lower soil layers (Wang et al., 2015), and with the increase in plow depth, the crop yield also increases (Nunes et al., 2015b). In this experiment, the dry matter and the N, P, and K accumulation amounts of plants increased as the growth stage progressed. Among the two test soybean varieties, for JY79, the accumulation of dry matter and of N, P, and K and yield during the three sampling periods showed an increasing trend with the increase in plow depth, with the maximum values occurring under the 40 cm plow depth treatment (albeit, no significant difference in yield existed between the 30 cm and 40 cm plow depth treatments). For HN44, the dry matter, the N, P, and K accumulation amounts, and the yield in the R_8 stage all had a single-peak curve, with the maximum value occurring under the 30 cm plow depth treatment.

Increased plow depth promotes soybean root growth toward the lower soil layers. In this experiment, the root weights of the two test soybean varieties showed an increasing trend with the increase of plow depth in the three sampling periods, but the root-shoot ratio decreased with the increase of growth stage and plow depth. Plow depth had a large impact on the root-shoot ratio during the early soybean growth period but had a small impact during the late growth period. In the R_1 stage, no significant difference was observed in the root-shoot ratio between the 0 to 10 cm plow depths, but the root-shoot ratios for these two depths were significantly higher than those for the 30 cm and 40 cm plow depths, whereas no significant difference existed between the 30 cm and the 40 cm plow depths. In the R_5 and R_8 stages, only

http://www.aloki.hu ● ISSN 1589 1623 (Print) ● ISSN 1785 0037 (Online)
DOI: http://dx.doi.org/10.15666/aeer/1706_1282712842

the 0 cm treatment had a relatively large root-shoot ratio, and no significant difference existed among the other depths. The above results showed that increasing the plow depth promotes the growth of aboveground parts of soybean and underground root systems, and it also promotes the distribution of nutrients toward the aboveground parts.

According to Qi et al. (2015), traction resistance in subsoiling increases quadratically with depth, with the subsoiling depths of 10 cm, 20 cm, 30 cm, and 40 cm showing resistance values of 0.42 kN, 0.85 kN, 2.56 kN, and 5.49 kN, respectively. In this test, the average yield of the two test soybean varieties showed an increase of 92.2% in yield when the plow depth was increased from 10 cm to 20 cm and an increase of 35.3% in yield when the plow depth was increased from 20 cm to 30 cm. When the plow depth increased from 30 cm to 40 cm, JY79 showed an increase in yield of 6.5% but without a significant difference; HN44 did not show an increase in yield. When the plow depth was greater than 30 cm, the increase in soybean yield was not significant, but the traction resistance during field preparation increased greatly, resulting in a significant increase in the operating costs. Therefore, a plow depth of 30 cm for soybean field setting is appropriate.

Conclusions

(1) Soybean dry matter; N, P, and K accumulation amounts; and yield exhibited a single-peak curve change when the bulk density reach a range of 1.00 g/cm^3-1.45 g/cm^3, with 1.15 g/cm^3-1.30 g/cm^3 being the appropriate ranges for soybean growth and yield formation. The soybean dry matter; the N, P, and K accumulation amounts; and the yield increased with the increase in plow depth. When the plow depth increased from 30 cm to 40 cm, the two test soybean varieties did not show a significant increase in yield, and the 30 cm plow depth could thus be determined to be the appropriate plow depth for the soybean field.

(2) The root-shoot ratio of the soybean plants was higher at the early growth period and decreased as growth progressed; the changes in bulk density and plow depth in the plow layer had a greater impact on the root-shoot ratio in the early soybean growth period, but they did not alter the pattern where the root-shoot ratio gradually decreased during the growth of the soybean. In the R_1 stage, the root-shoot ratio exhibited a "V"-shaped trend for change as the bulk density in the plow layer increased, with the minimum root-shoot ratio occurring under the 1.30 g/cm^3 treatment; in the R_5 and R_8 stages, the root-shoot ratio was not significantly affected when the bulk density in the plow layer was 1.00 g/cm^3-1.30 g/cm^3, but the root-shoot ratio significantly increased under the 1.45 g/cm^3 treatment. In the R_1 stage, no significant difference was observed in the root-shoot ratio between the 0 to 20 cm plow depth treatments, and their root-shoot ratios were higher than those under the treatments with the 30 cm and 40 cm plow depths; in the R_5 and R_8 stages, the root-shoot ratio was not significantly different between the 10 to 40 cm plow depth treatments.

Acknowledgements. The National Key Research and Development Program of China (2016YFD0300803); the Applied Technology Research and Development Program of Heilongjiang Province (GA16B401).

http://www.aloki.hu ● ISSN 1589 1623 (Print) ● ISSN 1785 0037 (Online)
DOI: http://dx.doi.org/10.15666/aeer/1706_1282712842

REFERENCES

[1] Assaeed, A. M., Mcgowan, M., Hebblethwaite, P. D., Brereton, J. C. (1990): Effect of soil compaction on growth, yield, and light interception of selected crops. – Annals of Applied Biology 117: 653-666.
[2] Barley, K. P. (1962): The effects of mechanical stress on the growth of roots. – Journal of Experimental Botany 2: 175-185.
[3] Bengough, A. G., Mackenzie, C. J., Elangwe, H. E. (1994): Biophysics of the growth responses of pea roots to changes in penetration resistance. – Plant and Soil 167: 135-141.
[4] Blouin, V., Schmidt, M., Bulmer, C., Krzic, M. (2004): Soil compaction and water content effects on lodgepole pine seedling growth in British Columbia. – SuperSoil 2004: 3rd Australian New Zealand Soils Conference, 5-9 December 2004, University of Sydney.
[5] Bushamuka, V. N., Zobel, R. W. (1998): Differential genotypic and root type penetration of compacted soil layers. – Crop Science 38: 776-781.
[6] Buttery, B. R., Tan, C. S., Drury, C. F., Park, S. J., Armstrong, R. J., Park, K. Y. (1998): The effects of soil compaction, soil moisture and soil type on growth and nodulation of soybean and common bean. – Revue Canadienne De Phytotechnie 78: 571-576.
[7] Chai, H., He, N. P. (2016): Evaluation of soil bulk density in Chinese terrestrial ecosystems for determination of soil carbon storage on a regional scale. – Acta Ecologica Sinica 36(13): 1-7.
[8] Colombi, T., Walter, A. (2016): Root responses of triticale and soybean to soil compaction in the field are reproducible under controlled conditions. – Functional Plant Biology 43(2): 114-128.
[9] Freitas, P. L. D., Zobel, R. W., Synder, V. A. (1999): Corn root growth in soil columns with artificially constructed aggregates. – Crop Science 39: 725-730.
[10] Fu, H., Liu, X. (2017): A study on the impact of environmental education on individuals' behaviors concerning recycled water reuse. – Eurasia Journal of Mathematics Science and Technology Education 13(10): 6715-6724.
[11] Gaultney, L., Krutz, G. W., Steinhardt, G. C., Liljedahl, J. B. (1980): Effects of subsoil compaction on corn yield in Indiana. – ASAE Paper 25.
[12] Gayosso-Moralesl, M. A., Nandini, S., Martinez-Jeronimo, F. F., Sarma, S. S. S. (2017): Effect of organic and inorganic turbidity on the zooplankton community structure of a shallow waterbody in Central Mexico (Lake Xochimilco, Mexico). – Journal of Environmental Biology. 38(6SI): 1183-1196.
[13] Gomez-Lopez, V. M., Buitrago, M. E., Tapia, M. S., Martinez-Yepez, A. (2018): Effect of ultrasonication on sensory and chemical stability of passion fruit juice during refrigerated storage. – Emirates Journal of Food and Agriculture 30(1): 85-89.
[14] Goss, M. J., Russell, R. S. (1980): Effects of mechanical impedance on root growth in barley (Hordeum vulgare L.) III. Observations on the mechanism of response. – Journal of Experimental Botany 31: 577-588.
[15] Iijima, M., Kono, Y., Yamauchi, A., Pardales Jr, J. R. (1991): Effects of soil compaction on the development of rice and maize root systems. – Environmental and Experimental Botany 31(3): 333-342.
[16] Johnson, J. F., Voorhees, W. B., Nelson, W. W., Randall, G. W. (1989): Soybean growth and yield as affected by surface and subsoil compaction. – Agronomy Journal 81: 973-979.
[17] Kaiser, E. A., Heisler, C., Walenzik, G., Heinemeyer, O. (1991): Effects of soil compaction on development of microbial biomass, soil fauna (Collembola), denitrification and mineralization in an arable soil. – Mitteilungen der Deutschen Bodenkundlichen Gesellschaft 110: 385-388.

http://www.aloki.hu ● ISSN 1589 1623 (Print) ● ISSN 1785 0037 (Online)
DOI: http://dx.doi.org/10.15666/aeer/1706_1282712842

[18] Maganti, M., Weaver, S., Downs, M. (2005): Responses of spreading orach (Atriplex patula) and common lambsquarters (Chenopodium album) to soil compaction, drought, and waterlogging. – Weed Science 53: 90-96.
[19] Nunes, M. R., Denardin, J. E., Pauletto, E. A., Faganello, A., Pinto, L. F. S. (2015a): Effect of soil chiseling on soil structure and root growth for a clayey soil under no-tillage. – Geoderma s 259-260: 149-155.
[20] Nunes, M. R., Denardin, J. E., Pauletto, E. A., Faganello, A., Pinto, L. F. S. (2015b): Mitigation of clayey soil compaction managed under no-tillage. – Soil and Tillage Research 148: 119-126.
[21] Peng, W., Ge, S., Ebadi, A. G., Hisoriev, H., Esfahani, M. J. (2017): Syngas production by catalytic co-gasification of coal-biomass blends in a circulating fluidized bed gasifier. – Journal of Cleaner Production 168: 1513-1517.
[22] Qi, G. Y., Liu, L., Zhao, Y. Z., Gong, Z. P., Yang, Y. Q., Yang, Y. (2015): Effects of subsoiler's penetrating depth and spade shape on traction resistance. – Journal of Agricultural Mechanization Research 2015(11).
[23] Rosolem, C. A., Schiochet, M. A., Souza, L. S., Whitacker, J. P. T. (1998): Root growth and cotton nutrition as affected by liming and soil compaction. – Communications in Soil Science and Plant Analysis 29: 169-177.
[24] Siczek, A., Lipiec, J. (2011): Soybean nodulation and nitrogen fixation in response to soil compaction and surface straw mulching. – Soil and Tillage Research 114: 50-56.
[25] Siczek, A., Lipiec, J., Wielbo, J., Szarlip, P., Kidaj, D. (2013): Pea growth and symbiotic activity response to Nod factors (lipo-chitooligosaccharides) and soil compaction. – Applied Soil Ecology 72: 181-186.
[26] Siczek, A., Horn, R., Lipiec, J., Usowicz, B., Łukowski, M. (2015): Effects of soil deformation and surface mulching on soil physical properties and soybean response related to weather conditions. – Soil and Tillage Research 153: 175-184.
[27] Stypa, M., Nunez-Barrios, A., Barry, D. A., Miller, M. H., Mitchell, W. A., Stypa, M., Nunez-Barrios, A., Barry, D. A., Miller, M. H., Mitchell, W. A. (1987): Effects of subsoil bulk density, nutrient availability and soil moisture on corn root growth in the field. – Canadian Journal of Soil Science 67: 293-308.
[28] Ufuk Kasim, M., Kasim, R. (2017): Yellowing of fresh-cut spinach (Spinacia oleracea L.) Leaves delayed by UV-B applications. – Information Processing in Agriculture 4(3): 214-219.
[29] Vicente-Molina, M. A., Fernandez-Sainz, A., Izagirre-Olaizola, J. (2018): Does gender make a difference in pro-environmental behavior? The case of the Basque Country University students. – Journal of Cleaner Production 176: 89-98.
[30] Wang, X., Zhou, B., Sun, X., Yue, Y., Ma, W., Zhao, M. (2015): Soil tillage management affects maize grain yield by regulating spatial distribution coordination of roots, soil moisture and nitrogen status. – PloS One 10: e0129231.
[31] Williams, M. A., Rice, C. W. (2007): Seven years of enhanced water availability influences the physiological, structural, and functional attributes of a soil microbial community. – Applied Soil Ecology 35: 535-545.
[32] Zhang, X. T., Cao, L. W., Lv, S. C., Chen, G. X., Wang, Y. J., Yu, S. H., Gong, Z. P. (2017): Effects of bulk density on nitrogen absorption and yield of soybean on black soil. – Crops 2017: 132-137.
[33] Zhao, Z., Huang, Y., Ma, C., Gong, Z., Yang, Y., Song, Q., Dong, S., Zhang, L. (2010): Effects of tillage practices on soybean field soil moisture and soil bulk density. – Journal of Agricultural Mechanization Research 2010(7): 181-184.

http://www.aloki.hu ● ISSN 1589 1623 (Print) ● ISSN 1785 0037 (Online)
DOI: http://dx.doi.org/10.15666/aeer/1706_1282712842

CHANGES IN PB, CR AND CU CONCENTRATIONS IN SOME BIOINDICATORS DEPENDING ON TRAFFIC DENSITY ON THE BASIS OF SPECIES AND ORGANS

SEVIK, H.[1] – CETIN, M.[2*] – OZTURK, A.[3] – OZEL, H. B.[4] – PINAR, B.[5]

[1]*Department of Environmental Engineering, Faculty of Engineering and Architecture, Kastamonu University, Kastamonu, Turkey*

[2]*Department of Landscape Architecture, Faculty of Engineering and Architecture, Kastamonu University, Kastamonu, Turkey*

[3]*Department of Forest Engineering, Faculty of Forestry, Kastamonu University, Kastamonu, Turkey*

[4]*Department of Forest Engineering, Faculty of Forestry, Bartin University, Bartin, Turkey*

[5]*Deparment of Sustainable Agriculture and Natural Plant Resources, Institute of Science, Kastamonu University, Kastamonu, Turkey*

**Corresponding author*
e-mail: mcetin@kastamonu.edu.tr; phone: +90-366-280-2920; fax: +90-366-280-2900

(Received 11th May 2019; accepted 28th Aug 2019)

Abstract. The growing population and industrialization is causing air pollution. In some cities pollution has reached to a point where it is threatening human lives. Pollution has become one of the biggest issues of today's world. Pollutants are produced by exhaust gases, car wheels, and vehicles. Heavy metals (HM) are one of the major culprits that cause air pollution. This is due to the fact that HM can exist in the environment for a long time without deterioration, and their concentration in the atmosphere is ever-growing. They also tend to bioaccumulate. Therefore, determining HM concentration levels is crucial in terms of identifying risk zones and levels. Bioindicators are the most important determinants that can indicate the change in the concentration of HM in the atmosphere. This study aims to monitor the changes in Pb, Cr and Cu concentrations in the leaves, seeds and branches of cherry plum (Prunus ceracifera), horse chestnut (Aesculus hippocastanum), Tilia (Tilia tomentosa), European ash (Fraxinus excelsior) and Norway maple (Acer platanoides) species, which can be used for monitoring the traffic-induced HM concentration. We observed that the concentration of all the elements increased according to the traffic density, this is especially visible in the case of Pb and Cr.
Keywords: *heavy metal, biomonitoring, pollution, landscape plant, plant species, vehicle, urban road*

Introduction

The increasing number of people living in urban centers in addition to the increase in the world population in recent years has brought along many problems with it. This process causes the destruction of nature, pollution of air, water and soil, as well as the deterioration of the ecological balance (Cetin, 2015a; Cetin et al., 2017a, b, 2018a, b, c, d, e, 2019a, b; Yucedag et al., 2019; Bozdogan Sert et al., 2019; Cetin 2019; Varol et al., 2019a, b). Air pollution is one of the most serious problems of today (Aricak et al., 2019; Kaya, 2009; Kaya et al., 2009, 2018; Yucedag and Kaya, 2016, 2017; Yucedag et al., 2018; Bozdogan Sert et al., 2019; Cetin, 2019; Sevik et al., 2019a, b, c). In fact, it is stated that approximately 6.5 million people die every year due to air pollution (Cetin, 2015a; Cetin et al., 2018a; Cetin et al., 2019a, b; Cetin, 2019). Even in Turkey, where

http://www.aloki.hu ● ISSN 1589 1623 (Print) ● ISSN 1785 0037 (Online)
DOI: http://dx.doi.org/10.15666/aeer/1706_1284312857

air is considered to be quite clean compared to many other countries, 29 thousand people lost their lives in 2016 due to air pollution (Cetin, 2015a, b, c; Cetin et al., 2019a, b, 2018c, d, e).

Since heavy metals tend to bioaccumulate, and they may be toxic even in low concentrations, they are of particular importance among the air pollution culprits. Although micronutrients such as Mn, Zn, Cr, Cu, Fe and Ni are necessary for living organisms, including plants, higher levels of them can have detrimental effects. Metals such as Hg, Cd, As and Pb have serious toxic effects on organisms even at low levels (Shahid et al., 2017). Many studies were conducted on heavy metals due to the importance of the subject (Turkyilmaz et al., 2018a, b; Sevik et al., 2019a; Akarsu et al., 2019; Bozdogan Sert et al., 2019; Jawed and Abo Aisha, 2019).

Plants are often used as bioindicators in monitoring heavy metal concentrations. However, different heavy metals accumulate at different levels in different plant species and organs. For this reason, it is necessary to determine which plant organs have what levels of heavy metal accumulation, so they can be used as bioindicators. In this study, we aim to determine the traffic-induced changes of Pb, Cr and Cu concentrations in the leaves, seeds and branches of four different plant species.

Materials and methods

Materials

The study was conducted in the Kastamonu town center. Kastamonu town center is built within a valley as a general view, and it is where the traffic is the densest. Within the scope of the study, the samples were collected from the areas with dense traffic, with low density traffic, and with almost no traffic as well as the areas with no roadway within 50 m vicinity (*Fig. 1*).

Figure 1. *Study region, traffic intensity, and sampling points*

Kastamonu town center, where the samples are collected from within the scope of the study, with dense traffic is an area where a 4-lane highway passes through with 2 lanes on

http://www.aloki.hu ● ISSN 1589 1623 (Print) ● ISSN 1785 0037 (Online)
DOI: http://dx.doi.org/10.15666/aeer/1706_1284312857

each direction. In this area, the traffic is generally dense during the day. The areas with low-density traffic are en route to the main road but outside the town center where the traffic is flowing. Taskopru and Inebolu routes were selected as the areas with low-density traffic. There is a two-lane road in this area, the traffic is flowing and the traffic density is quite low compared to the town center. Kastamonu University campus area was selected as the area with no traffic, and the points, where there was no roadway found within 50 m vicinity, were selected from the campus area, and samples were collected from those points.

Within the scope of the study, samples were collected from cherry plum (Prunus ceracifera), horse chestnut (Aesculus hippocastanum), tilia (Tilia tomentosa), European ash (Fraxinus excelsior) and Norway maple (Acer platanoides) plant species, which are often used in landscaping works. The samples were taken from last year's shoots, namely the one-year-old parts. Seeds of horse chestnut were used as the seed, whereas the seeds of tilia, European ash and Norway maple were used together with their coat and wings. However, the fruit flesh of cherry plum was used together with the peel. The samples were collected at the end of vegetation season of 2017, in August, and were brought to the lab after being packed and labelled.

Method

The measurements of heavy metal analyses were made in 2018. The samples, which were taken to the lab after being collected and labelled, were subjected to a separation process by being laid on the cardboards. The leaves, branches and seeds were separated and grouped. Then the branches were broken to enable them to dry thoroughly, and the seeds were crushed. The crushing of the seeds was carried out using marble pieces, and no metal tool was used during this process. The prepared samples were placed in glass settle plates and they were re-labelled. The fruit flesh of plum fruits was separated from the seed and was taken into glass settle plates and labelled. The samples prepared in such way were kept waiting for 15 days to be come air-dried, and the lab was ventilated every day throughout this process.

The air dried samples were made fully dried in a drying-oven at 45 °C for a week. In the next step, the plant samples were pulverised into powder and each weighing 0.5 g, powdered samples were placed in tubes designed for microwave. 10 mL of 65% HNO3 was added onto the samples. Fume cupboard was used during this process. The prepared samples were then burned at 280 PSI pressure and 180 °C in the microwave device for a period of 20 min. The tubes were removed from the microwave after the process was completed and left to cool down. The cooled samples were filled in until they reached 50 ml by adding deionized water. The prepared samples were read on the ICP-OES device at proper wavelengths after being filtered through the filter paper.

The data obtained were analyzed by using SPSS package program, and variance analysis was applied to the data. Homogeneous groups were obtained by applying Duncan test to the values with differences at 95% of confidence level statistically. The data obtained were interpreted after being simplified and tabulated.

Results

Change of Cr concentration depending on traffic density

Changes in Cr concentration of study samples were determined in the areas with no traffic, with low-density traffic and with dense traffic, and variance analysis and Duncan

http://www.aloki.hu ● ISSN 1589 1623 (Print) ● ISSN 1785 0037 (Online)
DOI: http://dx.doi.org/10.15666/aeer/1706_1284312857

test were applied to the data obtained. The mean values, F value and significance level obtained as a result of variance analysis, and homogeneous groups formed as a result of Duncan test are given in *Table 1*.

Table 1. *Concentrations of Cr in plants and organelles in different vehicle flow paths*

Species	Organ	Traffic density			F value
		No traffic	Low-density traffic	Dense traffic	
Cherry plum	Leaf	987.3 a	1470.3 b	1487.3 b	1217.820***
	Seed	1611.3 a	2283.0 b	2671.3 c	36.114***
	Branch	1069.6 a	1247.3 b	1827.6 c	334.763***
Horse chestnut	Leaf	2303.0 a	2357.0 b	7046.6 c	35179.582***
	Seed	443.3 a	653.0 b	910.6 c	24.926**
	Branch	721.6 a	1002.0 b	1635.6 c	87.183***
Tilia	Leaf	1058.9 a	1518.6 b	2148.9 c	1388.556***
	Seed	1051.9 a	1509.0 b	2134.9 c	103.211***
	Branch	706.6 a	825.3 b	996.3 c	149.214***
European ash	Leaf	548.5 a	1538.6 b	3538.4 c	11660.581***
	Seed	626.3 a	996.1 b	1366.0 c	363.166***
	Branch	476.6 a	733.6 b	1003.0 c	213.453***
Norway maple	Leaf	1174.3 a	1310.3 a	1739.6 b	54.594***
	Seed	951.0 a	992.6 a	1776.3 b	794.866***
	Branch	759.3 a	871.0 b	1001.3 c	21.065**

**Significant at 0.01 level. ***Significant at 0.001 level. The letters a, b, c, etc. mean according to Duncan test results show that the group is located. It is statistically different from the values contained in different groups, starting with the letter a the numerical value grows

As a result of the variance analysis conducted, it was determined that the traffic-induced change in Cr concentration in all organs was statistically significant at minimum of 95% confidence level. When the mean values and the groups formed as a result of Duncan test are examined, it is seen that in all organs, the values obtained in the areas with no traffic are in the first homogeneous group, whereas the values obtained in the areas with dense traffic are in the last one. Therefore, we can surmise that the Cr concentration correlatively increases with traffic density

When the values are examined, we can observe that Cr concentration varies between the areas with no traffic and the areas with dense traffic in the same organs, as well as between different organs of the same species and the same organs of different species. The highest difference due to traffic density was determined in European ash leaves, and the value of 548.5 ppb in areas with no traffic increased up to 3538.4 ppb in areas with dense traffic, thus increasing by 6.5 times.

Change of Pb concentration depending on traffic density

Pb is one of the heavy metals most associated with traffic density. Within the scope of the study, the change in Pb concentration was determined for each factor, separately, and the mean values, F value and significance level obtained as a result of variance analysis, and the homogeneous groups formed as a result of the Duncan test are given in *Table 2*.

http://www.aloki.hu ● ISSN 1589 1623 (Print) ● ISSN 1785 0037 (Online)
DOI: http://dx.doi.org/10.15666/aeer/1706_1284312857

Table 2. *Concentrations of Pb in plants and organelles in different vehicle flow paths*

Species	Organ	Traffic density			F value
		No traffic	Low-density traffic	Dense traffic	
Cherry plum	Leaf	718.1 a	928.9 b	1432.2 c	367.932***
	Seed	605.3	1464.3	6801.0	1.654 ns
	Branch	1412.0 a	1565.3 b	2500.3 c	281.616***
Horse chestnut	Leaf	960.0 a	1209.3 b	2329.6 c	528.478***
	Seed	39.6 a	324.0 b	781.3 c	26.795**
	Branch	160.6 a	241.6 a	611.3 b	10.697*
Tilia	Leaf	769.0 a	934.0 b	1062.2 c	25.680**
	Seed	737.6 a	894.0 ab	1018.7 b	5.958*
	Branch	364.3	208.6	149.3	1.680 ns
European ash	Leaf	405.8 a	1112.2 b	2848.2 c	6723.160***
	Seed	165.9	202.3	238.7	4.078 ns
	Branch	603.6 a	727.3 a	1386.6 b	15.781**
Norway maple	Leaf	377.0 a	504.6 b	798.6 c	304.785***
	Seed	49.3 a	347.0 b	520.6 c	379.738***
	Branch	83.3 a	224.3 a	403.6 b	14.639**

*Significant at 0.05 level. **Significant at 0.01 level. ***Significant at 0.001 level. The letters a, b, c, etc. means according to Duncan test results; show that the group is located. It is statistically different from the values contained in different groups, starting with the letter a numerical value grows

When the change of Pb concentration depending on the traffic density was examined, it was determined that the change of Pb concentration was statistically significant at a minimum of 95% confidence level in all the samples, except cherry plum and European ash seeds and tilia branches. When the mean values and homogenous groups formed as a result of Duncan test are examined, it can be observed that Pb concentration also correlatively increases with traffic density. As a result of the Duncan test, in all organs the values obtained in the areas with no traffic were in the first homogenous groups, whereas the values obtained in the areas with dense traffic were in the last one. When all values are examined, it is seen that the lowest value of 39.6 ppb is obtained in the horse chestnut seeds in the areas with no traffic, and the highest value of 6801 ppb is obtained in cherry plum seeds in the areas with dense traffic.

When the traffic-induced changes in the organs are examined, the ratio of the values obtained in the areas with dense traffic to the values obtained in the areas with no traffic is found to be lowest in the tilia seeds (approximately 1.38 times), and the highest ratio is found in the horse chestnut seeds (approximately 19.7 times).

Change of Cu concentration depending on traffic density

Changes in Cu concentration of study samples were determined in the areas with no traffic, with low-density traffic and with dense traffic, and variance analysis and Duncan test were applied to the data obtained. Afterwards, the mean values, F value and significance level obtained as a result of variance analysis, and homogeneous groups formed as a result of Duncan test are given in *Table 3*.

http://www.aloki.hu ● ISSN 1589 1623 (Print) ● ISSN 1785 0037 (Online)
DOI: http://dx.doi.org/10.15666/aeer/1706_1284312857

Table 3. *Concentrations of Cu in plants and organelles in different vehicle flow paths*

Species	Organ	Traffic density			F value
		No traffic	Low-density traffic	Dense traffic	
Cherry plum	Leaf	4.4 c	0.6 a	1.6 b	5310.500***
	Seed	5.0 a	5.3 a	45.3 b	31.705**
	Branch	1.0 a	9.2 b	13.4 c	6339.353***
Horse chestnut	Leaf	6.1 b	1.6 a	20.6 c	13329.150***
	Seed	0.3 a	0.8 a	2.9 b	70.408***
	Branch	3.2 a	7.7 b	8.7 c	146.478***
Tilia	Leaf	0.5 a	0.6 b	11.3 c	9368.455***
	Seed	13.4 a	16.6 a	286.5 b	140.116***
	Branch	6.2 b	6.2 b	2.4 a	228.071***
European ash	Leaf	7.5 a	10.5 b	36.9 c	117657.167***
	Seed	8.0 a	8.6 b	9.2 c	25.528**
	Branch	5.6 b	0.4 a	16.6 c	3122.898***
Norway maple	Leaf	3.3 a	3.5 a	7.1 b	831.267***
	Seed	14.4 a	17.3 b	20.0 c	492.818***
	Branch	4.8 a	7.9 b	11.6 c	807.474***

**Significant at 0.01 level. ***Significant at 0.001 level. The letters a, b, c, etc. mean according to Duncan test results show that the group is located. It is statistically different from the values contained in different groups, starting with the letter a the numerical value grows

When the change of Cu concentration depending on the traffic density is examined, it is seen that the traffic-induced change is statistically significant at a minimum of 95% confidence level in all organs, and that the Cu concentration correlatively increases together with the traffic density in general. While in 11 out of 15 study organs, the areas with no traffic were determined to be in the first homogeneous group, in 13 of them, the areas with dense traffic were in the last homogeneous group.

All in all, Cu concentration increases correlatively with traffic density in 11 out of 15 organs. While the minimum Cu concentration value of 0.3 ppm was obtained in the horse chestnut seeds in areas with no traffic, the highest value of 286.5 was obtained in Tilia seeds in the areas with dense traffic. However, other than this value, the maximum value was found to be 45.3 ppm.

Discussion

The study results showed that the elements subjected to study changed significantly on the basis of species. While the highest values of the metals other than Cu metal were obtained from the cherry plum, it was determined that the European ash was found in the first homogeneous group in all the metals. It was found that the concentrations of the metals subjected to study significantly varied among the species, and that sometimes the said difference was more than five times among the species.

In the studies carried out to date, it was found that the heavy metal concentration changed significantly on the basis of species. In his study, Mossi (2018) states that the difference between species is approximately twice more in Pb, which has a toxic effect even at low doses, approximately 2.75 times in Cr, which is one of carcinogenic

http://www.aloki.hu ● ISSN 1589 1623 (Print) ● ISSN 1785 0037 (Online)
DOI: http://dx.doi.org/10.15666/aeer/1706_1284312857

elements, and more than 5 times in Cu with toxic effects. Saleh (2018) states that the difference between species is more than 5 times in Cu, and even more than 24 times in Cd.

In the studies conducted, it is found that heavy metal concentrations change significantly on the basis of species, which means that different heavy metals are retained by different plants more intensely (Turkyilmaz et al., 2018a, b, c, d, 2019; Sevik et al., 2019a). This situation is primarily associated with the anatomical structure of the plant (Mossi, 2018; Saleh, 2018). The heavy metal intake of leaves varies depending on some factors such as the physical and chemical properties of the metals, their forms, morphology of the leaves, surface area, plant habitus next to the surface texture, heavy metals exposure time, environmental conditions and gas exchange (Beckett et al., 2000; Shahid et al., 2017; Turkyilmaz et al., 2018a, c; Sevik et al., 2019a; Mossi, 2018).

Within the scope of the study, it is found that heavy metal concentrations can change significantly on the basis of organs. However, the more important result is that the heavy metal concentrations in organs on the basis of species are different. For example, while the highest concentrations in Pb and Cr, which were some of the most important elements, were obtained in the seeds of P. ceracifera in the areas with dense traffic, they were obtained in the leaves of other species. However, the highest concentrations in Cu in the areas with dense traffic were obtained in the seeds of P. cerasifera, T. tomentosa and A. platanoides, while they were obtained in the leaves of A. hippocastanum and F. excelsior.

The change of heavy metal concentrations on the basis of organs became the subject of many studies as well. Mossi (2018) found organ differences between the leaf and branch organs, while Turkyilmaz et al. (2018d) and Turkyilmaz (2019) found it between bark and wood organs, Erdem (2018) and Sevik et al. (2019a) between leaf, seed and branch organs, and Elfantazi et al. (2018a, b) between the leaf and branch organs. Also in these studies, the heavy metal concentrations were found to be changing significantly on the basis of organ.

The main aim of the study is to determine the change of the elements subjected to the study depending on the traffic density. As a result of the study, it was determined that the concentrations of Pb and Cr elements correlatively increased with the traffic density in all organs of all species subjected to study, and the concentration of Cu element correlatively increased with traffic density in 11 out of 15 organs. Industrial and traffic activities are regarded as the most important sources of heavy metal pollution (Martley et al., 2004; Shahid et al., 2017; Erdem, 2018). In the studies conducted, it was found that the heavy metal concentrations in the plant organs changed significantly depending on the traffic density (Assirey et al., 2015; Galal et al., 2015; Saleh, 2018; Turkyilmaz et al., 2018a, b; Mossi, 2018; Sevik et al., 2019a; Akarsu et al., 2019; Jawed and Abo Aisha, 2019).

Cr, one of the heavy metals subjected to study, is one of the most toxic heavy metals in terms of potential toxicities and exposure to living organisms (Shahid et al., 2015, 2017). When taken into the human body through respiration, as it may cause nasal discharge, nasal bleedings, itching and perforation in upper respiratory tract it may also cause people, who are allergic to chromium, to get asthma attacks (Asri and Sonmez, 2006). As for plants, it is toxic for many high plants at the level of 100 mg/kg dry matter (Asri and Sonmez, 2006). Non-essential metals such as Cr are able to enter the plant leaves through leaf transfer (Shahid et al., 2017).

http://www.aloki.hu ● ISSN 1589 1623 (Print) ● ISSN 1785 0037 (Online)
DOI: http://dx.doi.org/10.15666/aeer/1706_1284312857

Within the scope of the study, it was found that Cr concentration ranged between 443.3 ppb and 7046.6 ppb. It was determined that the Cr concentration changed significantly depending on the traffic density, for example in the European ash leaves, and that the difference between the areas with no traffic and the areas with dense traffic was approximately 6.5 times.

Similar results were obtained in many studies conducted. Turkyilmaz et al. (2018b) reported that the Cr concentration was 16.595 ppm in the areas with no traffic, and that it increased up to 23.716 ppm in the areas with dense traffic. Sawidis et al. (2011) reported that the Cr concentration in the control group of Platanus orientalis leaves was 0.227 µg/g in Salzburg, 0.404 µg/g in Belgrade and 0.558 µg/g in Thessaloniki, while in polluted areas it increased up to 0.388 µg/g in Salzburg, 0.472 µg/g in Belgrade and 0.621 µg/g in Thessaloniki.

Pb, another element of the study, is of particular importance among heavy metals. Pb, which is widely used in industrial and agricultural activities, and thus is a common element, is a heavy metal which is emitted to the atmosphere as a metal or compound, and it is toxic in any case. Pb is one of the heavy metals that damages the ecological system most through human activities (Mossi, 2018; Erdem, 2018; Pinar, 2019).

Pb takes place near the top among the metals causing environmental pollution as well as being an important metal for people for many years (Mossi, 2018). Lead may be present more than normal levels especially in vegetable and food of animal origin grown in areas close to the town center and industrial zones (Kahvecioglu et al., 2007; França et al., 2017). In addition to these, lead-containing gasoline is an important resource as well (Pinar, 2019). Therefore, there are many studies available documenting the relationship between Pb and traffic density (Qing et al., 2015; Lei et al., 2015; Assirey et al., 2015; Galal et al., 2015; Begum et al., 2017).

Within the scope of the study, the Pb concentration was found to be ranging between 39.6 ppb and 6801 ppb. Aksoy and Sahin (1999) found that the average Pb concentration in the unwashed leaves of E. angustifolia was 180.21 µgg-1 in industrial zones, 75.82 µgg-1 by the roadside, 50.56 µgg-1 in the town centre, 30.45 µgg-1 close to the town, and 16.81 µgg-1 in rural areas. Tam et al. (1987) found that the Pb concentration in the Bauhina varigeata leaves in Hon Kong was 12 µg g-1 in the unwashed leaves of the control group, while it was as high as 276 µg g-1 in the unwashed leaves by the roadside. Celik et al. (2005) reported that the average Pb content in Robinia pseudoacacia L. in Denizli province was 180.85 µgg-1 in the samples collected from the industrial zone, 336.55 µgg-1 in the samples collected from the urban roadsides, 74.86 µgg-1 in the samples collected from outside the town center and 34.26 µg g-1 in the samples collected from rural areas.

As a result of the study, the Cu concentration was found to be ranging between 0.3 ppm and 286.5 ppm and increased with traffic density, in general. Cu is quite an important element due to its involvement in enzyme activation, carbohydrate and lipid metabolisms within the plant body (Asri and Sonmez, 2006). Although different plant species need different amounts of copper, it is a highly toxic metal. Some effects of copper poisoning can be regarded as tissue damage, deterioration of roots and darkening of plant colour. Other effects are ion loss in the stem cells due to deterioration of membrane permeability and DNA damage due to deterioration of photosynthesis process (Okcu et al., 2009). Even though copper is an essential trace element for human and animal metabolism, acute copper intoxication may cause abdominal pain, nausea, vomiting and diarrhoea (Asri and Sonmez, 2006). Low levels of copper ion intake may

http://www.aloki.hu ● ISSN 1589 1623 (Print) ● ISSN 1785 0037 (Online)
DOI: http://dx.doi.org/10.15666/aeer/1706_1284312857

cause liver cirrhosis, Wilson's disease, systemic rheumatic diseases and kidney diseases, while high levels of copper ion intake may cause leukaemia (Hayta, 2006).

For this reason, many studies have been conducted on the determination of copper concentration in plants and its correlation with traffic density (Turkyilmaz et al., 2018a, b; Erdem, 2018; Mossi, 2018; Ozel, 2019). Turkyilmaz et al. (2018b) reports that the Cu concentration changes depending on the traffic density, and that Cu concentration, which is 69.615 ppb in areas with no traffic, increases up to 110.441 ppb in areas with dense traffic. Suzuki et al. (2009) states that Cu concentration in Rhododendron pulchrum leaves in Okayama, Japan goes up to 22.22 mg kg-1, while Demirayak et al. (2011) state that the average Cu concentration in M. grandiflora leaves in Samsun province is around 35 ppm. Li et al. (2007) reports that Cu concentration in the leaves of Sophora japonica L. is higher in individuals by the roadside than individuals in the parks.

The studies conducted show that heavy metal concentrations are at different levels in plant species and organs depending on the traffic density. There are different reasons of this situation. First of all, traffic-induced heavy metal pollution in the atmosphere increases. This because the car wheels, vehicles, vehicle wear and exhaust gases in the urban areas cause heavy metals to be emitted into air (Zhuang et al., 2009; Schreck et al., 2012; Shahid et al., 2017; Turkyilmaz et al., 2018a). However, after emission into the atmosphere, heavy metals can be carried for miles away with the help of wind. In fact, studies conducted show that many heavy metals, especially Pb, can be carried far from their source (Uzu et al., 2009; Schreck et al., 2012; Shahid et al., 2017; Mossi, 2018). After the heavy metals are mixed into the atmosphere, the accumulation process within the plant is also very complex and under the influence of many factors. This process is primarily related to the structure of plant organs and heavy metals (Mossi, 2018; Erdem, 2018; Sevik et al., 2019a).

Accumulation of heavy metals within the plant body is closely related to environmental conditions as well. Heavy metals can be carried far from the source with the help of wind. Apart from this, environmental conditions have direct influence on the plant metabolism, and the entry of heavy metals into the plant structure is different within this process. It is also stated that there is a significant relationship between the entrance of heavy metals into the plant body and the air humidity and precipitation, in particular (Uzu et al., 2009; Schreck et al., 2012; Shahid et al., 2017; Mossi, 2018; Turkyilmaz et al., 2018a, b, c, d, 2019).

There are also some factors that are likely to affect the heavy metal concentration. For instance, the change in heavy metal concentration depending on the plant species was shown in this study as well as in others (Sevik et al., 2019a, b, c; Saleh, 2018; Erdem, 2018). However, heavy metal concentrations may be expected to be at different levels in the sub-types, forms, varieties and origins of plants. Likewise, many studies show that many phenological, morphological and anatomical structures vary according to these characteristics. In this case, it is inevitable for the plant metabolism to change and this situation to affect the heavy metal absorption (Sevik et al., 2012; Mossi, 2018).

The heavy metal absorption in plants is closely related to plant metabolism (Speak et al., 2012; Shahid et al., 2017). Therefore, it is possible for many factors, which affect the plant metabolism significantly such as the plant's stress level, (Sevik and Cetin, 2015; Sevik and Karaca, 2016), plant origin (Sevik et al., 2019a, c), chlorophyll content (Sevik et al., 2013; Cetin, 2017; Zeren et al., 2017; Zeren Çetin et al., 2018) and genetic

http://www.aloki.hu ● ISSN 1589 1623 (Print) ● ISSN 1785 0037 (Online)
DOI: http://dx.doi.org/10.15666/aeer/1706_1284312857

structure (Sevik, 2012), to affect heavy metal absorption, and hence heavy metal concentration in plants.

As a consequence, the change in heavy metal concentration in plants is the result of a complex mechanism due to the interaction of many factors (Mossi, 2018). However, the studies are not sufficient to gain a clear understanding of this mechanism, and thus to clearly reveal the factors affecting the change of heavy metal concentration. For this reason, studies on this subject should be increasingly continued and diversified.

Conclusions

Air pollution is one of the most important problems of today's world. Air pollution has gained a particular importance with the increase in the consciousness level in this field along with the population density in town centers, and many studies have been carried out to solve this important problem. Increasing green spaces is considered as one of the most effective methods among the solution proposals. The studies conducted showed that green spaces and the plants used in such spaces decreased the air pollution of all types and levels (Cetin et al., 2017a, b).

Plants can reduce air pollution significantly. However, the impacts of different species on different pollution factors are also at different levels. Although a large number of plant species have been the subject of studies to date, these studies are not at a sufficient level yet. There is no information on the heavy metal accumulation potentials of many plant species. However, great differences were determined between the heavy metal accumulating potentials of plant species in the studies conducted. For this reason, it is necessary to use the species, which have not been subjected to any study, in similar studies and to identify the plants, which are to be more effective in both monitoring and reducing the heavy metal pollution. Therefore, it can be recommended to continue and diversify similar studies.

One of the important results of the study is that some heavy metal concentrations are very high, especially in the seeds. For instance, heavy metal concentrations were found to be quite high in the seed of cherry plum. This shows that it can be highly risky to consume the plants grown in areas with high level of heavy metal concentration such as industrial zones and urban centers as food. However, the number of studies on this subject is not quite sufficient yet. Priority should also be given to the studies on this subject.

REFERENCES

[1] Akarsu, H., Zeren Çetin, İ., Jawed, A. A., Abo Aisha, A. E. S., Cesur, A., Keskin, R. (2019): Changes of some heavy metal concentrations based on organic and traffic density in Fraxinus excelsior L.. – International Journal of Engineering, Design and Technology 1(1): 24-30.

[2] Aksoy, A., Sahin, U. (1999): Elaeagnus angustifolia L. as a biomonitor of heavy metal pollution. – Turkish Journal of Botany 23: 83-87.

[3] Aricak, B., Cetin, M., Erdem, R., Sevik, H., Cometen, H. (2019): The change of some heavy metal concentrations in Scotch pine (Pinus sylvestris) depending on traffic density, organelle and washing. – Applied Ecology and Environmental Research 17(3): 6723-6734.

[4] Asri, F. Ö., Sonmez, S. (2006): Effects of heavy metal toxicity on plant metabolism. – Derim, Journal of West Mediterranean Agricultural Institute 23(2): 36-45 (in Turkish).

http://www.aloki.hu ● ISSN 1589 1623 (Print) ● ISSN 1785 0037 (Online)
DOI: http://dx.doi.org/10.15666/aeer/1706_1284312857

[5] Assirey, E., Al-Qodah, Z., Al-Ahmadi, M. (2015): Impact of traffic density on roadside pollution by some heavy metal ions in Madinah city, Kingdom of Saudi Arabia. – Asian Journal of Chemistry 27(10): 3770-3776.
[6] Beckett, K. P., Freer-Smith, P. H., Taylor, G. (2000): The capture of particulate pollution by trees at five contrasting urban sites. – Arboricultural Journal 24(2-3): 209-230.
[7] Begum, H. A., Hamayun, M., Zaman, K., Shinwari, Z. K., Hussain, A. N. W. A. R. (2017): Heavy metal analysis in frequently consumable medicinal plants of Khyber Paktunkhwa, Pakistan. – Pak J Bot 49(3): 1155-1160.
[8] Bozdogan Sert, E., Turkmen, M., Cetin, M. (2019): Heavy metal accumulation in rosemary leaves and stems exposed to traffic-related pollution near Adana-İskenderun Highway (Hatay, Turkey). – Environmental Monitoring and Assessment 191: 553. https://rd.springer.com/article/10.1007/s10661-019-7714-7
[9] Celik, A., Kartal, A. A., Kaska, Y. (2005): Determining the heavy metal pollution in Denizli Turkey) by using Robinia pseudoacacia L. – Environment International 31: 105-112.
[10] Cetin, M. (2015a): Determining the bioclimatic comfort in Kastamonu City. – Environmental Monitoring and Assessment 187(10): 640. http://link.springer.com/article/10.1007%2Fs10661-015-4861-3.
[11] Cetin, M. (2015b): Evaluation of the sustainable tourism potential of a protected area for landscape planning: a case study of the ancient city of Pompeipolis in Kastamonu. – International Journal of Sustainable Development & World Ecology 22(6): 490-495. http://www.tandfonline.com/doi/abs/10.1080/13504509.2015.1081651?src=recsys&journalCode=tsdw20.
[12] Cetin, M. (2015c): Using GIS analysis to assess urban green space in terms of accessibility: case study in Kutahya. – International Journal of Sustainable Development & World Ecology 22(5) 420-424. http://www.tandfonline.com/doi/abs/10.1080/13504509.2015.1061066?journalCode=tsdw20.
[13] Cetin, M. (2017): Change in amount of chlorophyll in some interior ornamental plants. – Kastamonu University Journal of Engineering and Sciences 3(1): 11-19. http://dergipark.gov.tr/download/issue-file/5600.
[14] Cetin, M., Sevik, H., Isinkaralar, K. (2017a): Changes in the particulate matter and CO_2 concentrations based on the time and weather conditions: the case of Kastamonu. – Oxidation Communications 40(1-II): 477-485.
[15] Cetin, M., Sevik, H., Saat, A. (2017b): Indoor air quality: the samples of Safranbolu Bulak Mencilis Cave. – Fresenius Environmental Bulletin 26(10): 5965-5970. http://www.prt-parlar.de/download_feb_2017/.
[16] Cetin, M., Onac, A. K., Sevik, H., Canturk, U., Akpinar, H. (2018a): Chronicles and geoheritage of the ancient Roman city of Pompeiopolis: a landscape plan. – Arabian Journal of Geosciences 11(24): 798. DOI: 10.1007/s12517-018-4170-6. https://link.springer.com/article/10.1007/s12517-018-4170-6.
[17] Cetin, M., Sevik, H., Yigit, N. (2018b): Climate type-related changes in the leaf micromorphological characters of certain landscape plants. – Environmental Monitoring and Assessment 190(7): 404. https://doi.org/10.1007/s10661-018-6783-3.
[18] Cetin, M., Sevik, H., Yigit, N., Ozel, H. B., Aricak, B., Varol, T. (2018c): The variable of leaf micromorphogical characters on grown in distinct climate conditions in some landscape plants. – Fresenius Environmental Bulletin 27(5): 3206-3211.
[19] Cetin, M., Zeren, I., Sevik, H., Cakir, C., Akpinar, H. (2018d): A study on the determination of the natural park's sustainable tourism potential. – Environmental Monitoring and Assessment 190(3): 167. https://doi.org/10.1007/s10661-018-6534-5.
[20] Cetin, M., Sevik, H., Canturk, U., Cakir, C. (2018e): Evaluation of the recreational potential of Kutahya Urban Forest. – Fresenius Environmental Bulletin 27(5): 2629-2634.

http://www.aloki.hu ● ISSN 1589 1623 (Print) ● ISSN 1785 0037 (Online)
DOI: http://dx.doi.org/10.15666/aeer/1706_1284312857

[21] Cetin, M., Kalayci Onac, A., Sevik, H., Sen, B. (2019a): Temporal and regional change of some air pollution parameters in Bursa. – Air Quality, Atmosphere & Health 12(3): 311-316. https://doi.org/10.1007/s11869-018-00657-6.

[22] Cetin, M., Adiguzel, F., Gungor, S., Kaya, E., Sancar, M. S. (2019b): Evaluation of thermal climatic region areas in terms of building density in urban management and planning for Burdur, Turkey. – Air Quality Atmosphere & Health 12 (9): 1103-1112. https://link.springer.com/content/pdf/10.1007%2Fs11869-019-00727-3.pdf

[23] Cetin, M. (2019): The effect of urban planning on urban formations determining bioclimatic comfort area's effect using satellitia imagines on air quality: a case study of Bursa city. –Air Quality, Atmosphere & Health 2019: 1-13. Doi: 10.1007/s11869-019-00742-4. https://rd.springer.com/article/10.1007/s11869-019-00742-4

[24] Demirayak, A., Kutbay, H. G., Kilic, D., Bilgin, A., Huseyinova, R. (2011): Heavy metal accumulation in some natural and exotic plants in Samsun City. – Ekoloji 20(79): 1-11.

[25] Elfantazi, M. F. M., Aricak, B., Baba, F. A. M. (2018a): Changes in concentration of some heavy metals in leaves and branches of acer pseudoplatanus due to traffic density. – International Journal of Trend in Research and Development 5(2): 704-707.

[26] Elfantazi, M. F. M., Aricak, B., Ozer Genc, C. (2018b): Concentrations in Morus Alba L. leaves and branches due to traffic density. – International Journal of Current Research 10(05): 68904-68907.

[27] Erdem, T. (2018): The change of heavy metal concentrations in some plants due to species, organelles and traffic densities. – Master Thesis. Kastamonu University, Institute of Science, Department of Forest Engineering, Kastamonu, Turkey.

[28] França, F. C., Albuuerque, A. M., Almeida, A. C., Silveira, P. B., Crescêncio Filho, A., Hazin, C. A., Honorato, E. V. (2017): Heavy metals deposited in the culture of lettuce (Lactuca sativa L.) by the influence of vehicular traffic in Pernambuco, Brazil. – Food Chemistry 215: 171-176.

[29] Galal, T. M., Shehata, H. S. (2015): Bioaccumulation and translocation of heavy metals by Plantago major L. grown in contaminated soils under the effect of traffic pollution. – Ecological Indicators 48: 244-251.

[30] Hayta, A. B. (2006): the palce and importance of the family in the prevention of environmental pollution. – Ahi Evran University Journal of Kirsehir Faculty of Education 7(2): 359-376 (in Turkish).

[31] Jawed, A. A., Abo Aisha, A. E. S. (2019): Usability of horse chestnut (Aesculus hippocastanum L.) as Biomonitor for monitoring some heavy metal concentrations caused by traffic. – International Journal of Engineering, Design and Technology 1(1): 16-23.

[32] Kahvecioglu, Ö., Kartal, G., Güven, A., Timur, S. (2007): Environmental effects of metals-I. – www.metalurji.org.tr/dergi/dergi136/d136_4753.pdf (accessed on 19.04.2019).

[33] Kaya, L. G. (2009): Assessing forests and lands with carbon storage and sequestration amount by trees in the State of Delaware, USA. – Scientific Research and Essays 4(10): 1100-1108.

[34] Kaya, L. G., Cetin, M., Doygun, H. (2009): A holistic approach in analyzing the landscape potential: Porsuk Dam Lake and its environs, Turkey. – Fresenius Environmental Bulletin 18(8): 1525-153.

[35] Kaya, L. G., Kaynakci-Elinc, Z., Yucedag, C., Cetin, M. (2018): Environmental outdoor plant preferences: a practical approach for choosing outdoor plants in urban or suburban residential areas in Antalya, Turkey. – Fresenius Environmental Bulletin 27(12): 7945-7952.

[36] Lei, J., Hasi, E., Sun, Y. (2015): Assessing the Influence of Different Road Traffic on Heavy Metal Accumulation in Rural Roadside Surface Soils of the Eastern Ordos Plateau Grassland in China. – In: Aswathanarayana, U. (ed.) Water Resources and Environment. CRC Press, Boca Raton, FL, pp. 247-252.

http://www.aloki.hu ● ISSN 1589 1623 (Print) ● ISSN 1785 0037 (Online)
DOI: http://dx.doi.org/10.15666/aeer/1706_1284312857

[37] Li, F. R., Kang, L. F., Gao, X. Q., Hua, W., Yang, F. W., Hei, W. L. (2007): Traffic-related heavy metal accumulation in soils and plants in Northwest China. – Soil & Sediment Contamination 165): 473-484.
[38] Martley, E., Gulson, B., Pfeifer, H. R. (2004): Metal concentrations in soils around the copper smelter and surrounding industrial complex of Port Kembla, NSW, Australia. – Science of the Total Environment 325: 113-127.
[39] Mossi, M. M. M. (2018): Determination of heavy metal accumulation in some shrub formed landscape plants. – PhD Thesis. Kastamonu University, Institute of Science, Department of Forest Engineering, Kastamonu, Turkey.
[40] Okcu, M., Tozlu, E., Kumlay, A. M., Pehluvan, M. (2009): Effects of heavy metals on plants. – Alınteri Journal 17: 14-26 (in Turkish).
[41] Ozel, S. (2019): The variation of heavy metal accumulation in some fruit tree organelles due to traffic density. – MsC Thesis. Kastamonu University, Institute of Science, Kastamonu, Turkey.
[42] Pinar, P. (2019): The variation of heavy metal accumulation in some landscape plants due to traffic density. – MsC Thesis. Kastamonu University Institute of Science, Kastamonu, Turkey.
[43] Qing, X., Yutong, Z., Shenggao, L. (2015): Assessment of heavy metal pollution and human health risk in urban soils of steel industrial city (Anshan), Liaoning, Northeast China. – Ecotoxicology and Environmental Safety 120: 377-385.
[44] Saleh, E. A. A. (2018): Determination of heavy metal accumulation in some landscape plants. – Ph.D. Thesis. Kastamonu University, Institute of Science, Department of Forest Engineering.
[45] Sawidis, T., Breuste, J., Mitrovic, M., Pavlovic, P., Tsigaridas, K. (2011): Trees as bioindicator of heavy metal pollution in three European cities. – Environmental Pollution 159: 3560-3570.
[46] Schreck, E., Foucault, Y., Sarret, G., Sobanska, S., Cécillon, L., Castrec, R. M., Uzu Dumat, C. (2012): Metal and metalloid foliar uptake by various plant species exposed to atmospheric industrial fallout: mechanisms involved for lead. – Science of the Total Environment 427-428: 253-262.
[47] Sevik, H. (2012): Variation in seedling morphology of Turkish fir (Abies nordmanniana subsp. bornmulleriana Mattf). – African Journal of Biotechnology 11(23): 6389-6395.
[48] Sevik, H., Cetin, M. (2015): Effects of water stress on seed germination for select landscape plants. – Polish Journal of Environmental Studies 24(2): 689-69.
[49] Sevik, H., Karaca, U. (2016): Determining the resistances of some plant species to frost stress through ion leakage method. – Fresenius Environmental Bulletin 25(8): 2745-2750.
[50] Sevik, H., Guney, D., Karakas, H., Aktar, G. (2012): Change to amount of chlorophyll on leaves depend on insolation in some landscape plants. – International Journal of Environmental Sciences 3(3): 1057-1064.
[51] Sevik, H., Karakas, H., Karaca, U. (2013): Color - chlorophyll relationship of some indoor ornamental plant. – International Journal of Engineering Science & Research Technology 2(7): 1706-1712.
[52] Sevik, H., Ozel, H. B., Cetin, M., Özel, H. U., Erdem, T. (2019a): Determination of changes in heavy metal accumulation depending on plant species, plant organism, and traffic density in some landscape plants. – Air Quality, Atmosphere & Health 12(2): 189-195. https://doi.org/10.1007/s11869-018-0641-x.
[53] Sevik, H., Cetin, M., Ozturk, A., Yigit, N., Karakus, O. (2019b): Changes in micromorphological characters of Platanus orientalis L. leaves in Turkey. – Applied Ecology and Environmental Research 17(3): 5909-5921. http://dx.doi.org/10.15666/aeer/1703_59095921.
[54] Sevik, H., Cetin, M., Ozel, H. B., Pinar B. (2019c): Determining toxic metal concentration changes in landscaping plants based on some factors. Air Quality

http://www.aloki.hu ● ISSN 1589 1623 (Print) ● ISSN 1785 0037 (Online)
DOI: http://dx.doi.org/10.15666/aeer/1706_1284312857

Atmosphere & Health 12(8): 983-991. https://doi.org/10.1007/s11869-019-00717-5, https://link.springer.com/content/pdf/10.1007%2Fs11869-019-00717-5.pdf

[55] Shahid, M., Khalid, S., Abbas, G., Shahid, N., Nadeem, M., Sabir, M., Aslam, M., Dumat, C. (2015): Heavy Metal Stress and Crop Productivity. – In: Hakeem, K. R. (ed.) Crop Production and Global Environmental Issues. Springer International Publishing, Switzerland, pp. 1-25.

[56] Shahid, M., Dumat, C., Khalida, S., Schreck, E., Xiong, T., Nabeel, N. K. (2017): Foliar heavy metal uptake, toxicity and detoxification in plants: a comparison of foliar and root metal uptake. – Journal of Hazardous Materials 325: 36-58.

[57] Speak, A., Rothwell, J., Lindley, S., Smith, C. (2012): Urban particulate pollution reduction by four species of green roof vegetation in a UK city. – Atmospheric Environment 61: 283-293.

[58] Suzuki, K., Yabuki, T., Ono, Y. (2009): Roadside Rhododendron pulchrum leaves as bioindicators of heavy metal pollution in traffic areas of Okayama, Japan. – Environmental Monitoring and Assessment 149: 133-141.

[59] Tam, N. F. Y., Liu, W. K., Wang, M. H., Wong, Y. S. (1987): Heavy metal pollution in roadside, urban parks and gardens in Hong Kong. – Science of the Total Environment 59: 325-328.

[60] Turkyilmaz, A., Sevik, H., Cetin, M. (2018a): The use of perennial needles as biomonitors for recently accumulated heavy metals. – Landscape and Ecological Engineering 14(1): 115-120. https://doi.org/10.1007/s11355-017-0335-9.

[61] Turkyilmaz, A., Sevik, H., Cetin, M., Ahmaida Saleh. E. A. (2018b): Changes in heavy metal accumulation depending on traffic density in some landscape plants. – Polish Journal of Environmental Studies 27(5): 2277-2284. https://doi. org/10.15244/pjoes/78620.

[62] Turkyilmaz, A., Sevik, H., Isinkaralar, K., Cetin, M. (2018c): Using Acer platanoides annual rings to monitor the amount of heavy metals accumulated in air. – Environmental Monitoring and Assessment 190(10): 578. https://doi.org/ 10.1007/s10661-018-6956-0.

[63] Turkyilmaz, A., Cetin, M., Sevik, H., Isinkaralar, K., Ahmaida Saleh, E. A. (2018d): Variation of heavy metal accumulation in certain landscaping plants due to traffic density. – Environment, Development and Sustainability. 1-14. https://doi.org/10.1007/s10668-018-0296-7.

[64] Turkyilmaz, A., Sevik, H., Isinkaralar, K., Cetin, M. (2019): Use of tree rings as a bioindicator to observe atmospheric heavy metal deposition. – Environmental Science and Pollution Research 26(5): 5122-5130. https://doi.org/10.1007/s11356-018-3962-2.

[65] Uzu, G., Sobanska, S., Aliouane, Y., Pradere, P., Dumat, C. (2009): Study of lead phytoavailability for atmospheric industrial micronic and sub-micronic particles in relation with lead speciation. – Environmental Pollution 157(4): 1178-1185.

[66] Varol, T., Gormus, S., Cengiz, S., Ozel, H. B., Cetin, M. (2019a): Determining potential planting areas in urban regions. – Environmental Monitoring and Assessment 191(3): 157. DOI: 10.1007/s10661-019-7299-1.

[67] Varol, T., Ertuğrul, M., Özel, H. B., Emir, T., Çetin, M. (2019b): The effects of rill erosion on unpaved forest road. – Applied Ecology and Environmental Research 17(1): 825-839. http://www.aloki.hu/indvol17_1.htm.

[68] Yucedag, C., Kaya, L. G. (2016): Effects of air pollutants on plants. – Mehmet Akif Ersoy University Journal of the Institute of Science and Technology 7(1): 67-74 (in Turkish).

[69] Yucedag, C., Kaya, L. G. (2017): Recreational Trend and Demands of People in Isparta-Turkey. – In: Arapgirlioglu, H., Atik, A., Elliott, R. L., Turgeon, E. (eds.) Researches on Science and Art in 21 st Century Turkey. Chap. 104. Gece Publishing, Ankara.

[70] Yucedag, C., Kaya, L. G., Cetin, M. (2018): Identifying and assessing environmental awareness of hotel and restaurant employees' attitudes in the Amasra District of Bartin. –

http://www.aloki.hu ● ISSN 1589 1623 (Print) ● ISSN 1785 0037 (Online)
DOI: http://dx.doi.org/10.15666/aeer/1706_1284312857

Environmental Monitoring and Assessment 190(2): 60. https://doi.org/10.1007/s10661-017-6456-7.

[71] Yucedag, C., Ozel, H. B., Cetin, M., Sevik, H. (2019): Variability in morphological traits of seedlings from five Euonymus japonicus cultivars. – Environmental Monitoring and Assessment 191(5): 285. DOI: 10.1007/s10661-019-7464-6.

[72] Zeren, I., Cantürk, U., Yaşar. M. O. (2017): Change of chlorophyll quantity in some landscaping plants. – Journal of Bartin Faculty of Forestry 19(2): 174-182.

[73] Zeren Çetin, İ., Cesur, A., Keskin, R., Akarsu, H. (2018): Variation of chlorophyll content in some landscape plants: a case study of Samsun. – Kastamonu University Journal of Engineering and Sciences 4(1): 1-10 (in Turkish). https://dergipark.org.tr/download/article-file/609695.

[74] Zhuang, P., McBride, M. B., Xia, H., Li, N., Li, Z. (2009): Health risk from heavy metals via consumption of food crops in the vicinity of Dabaoshan mine, South China. – Science of the Total Environment 407: 1551-1561.

http://www.aloki.hu ● ISSN 1589 1623 (Print) ● ISSN 1785 0037 (Online)
DOI: http://dx.doi.org/10.15666/aeer/1706_1284312857

VARITATION OF STOMATAL CHARACTERISTICS IN BROAD LEAVED SPECIES BASED ON HABITAT

YIGIT, N.[1] – CETIN, M.[2*] – OZTURK, A.[1] – SEVIK, H.[3] – CETIN, S.[4]

[1]*Department of Forest Engineering, Faculty of Forestry, Kastamonu University, Kastamonu, Turkey*

[2]*Department of Landscape Architecture, Faculty of Engineering and Architecture, Kastamonu University, Kastamonu, Turkey*

[3]*Department of Environmental Engineering, Faculty of Engineering and Architecture, Kastamonu University, Kastamonu, Turkey*

[4]*Department of Landscape Architecture, Faculty of Architecture, Adiyaman University, Adiyaman, Turkey*

**Corresponding author*
e-mail: mcetin@kastamonu.edu.tr; phone: +90-366-280-2920; fax: +90-366-280-2900

(Received 13th May 2019; accepted 28th Aug 2019)

Abstract. This research aims to find the habitat-dependent variation of micromorphological characteristics in the leaves of *Fraxinus excelsior* (European ash), *Platanus orientalis* (Plane tree) and *Tilia tomentosa* (Silver lime) collected from 6 different cities of different climates. The leaves were collected in Turkey in the cities of Rize, Samsun, İzmir, Antalya, Sivas, and Ankara. Samsun and Rize fall under the Black Sea climate region, Ankara and Sivas under the continental climate, whereas Antalya and İzmir enjoy a Mediterranean climate. Using scanning electron microscopy (SEM) to highlight the visible morphological characteristics of the plant, we hoped to uncover how stress affects the micro-morphological properties of the plant but does not affect its vital functions. Leaf epidermis images were obtained with SEM and stoma width (μm), length (μm), pore width (μm), pore length (μm), and density (in an area of 1 mm^2) measurements were obtained using Image J (https://imagej.net) software. A Duncan test and variance analysis were performed via SPSS® (IBM Analytics) and the habitat-dependent change of these characteristics was evaluated statistically. Accordingly, we determined that the stomatal characteristics varied depending on the habitat, but trees were affected differently by climate conditions. The micromorphological characteristics on the leaves depending on growth conditions were also investigated.

Keywords: *cities, various climates, micromorphlogy, SEM, landscape plants, Fraxinus excelsior, Platanus orientalis, Tilia tomentosa*

Introduction

Parallel to the increasing rate of urbanization, destruction of green areas around the world has led to an inevitable and undesirable consequence. Along with increasing urbanization, today's modern individuals with increasing incomes and consciousness have begun to realize the importance of green spaces, and as a result, landscape architecture projects have become an integral part of modern life (Sevik and Cetin, 2016; Sevik et al., 2016; Bozdogan Sert et al., 2019; Cetin et al., 2019; Cetin 2019). Landscape studies gain value in proportion to the plant variety used in the design, and the use of uncommon plants in the design process makes the designs even more valuable. This approach has resulted in growing plants in areas that differ from their natural habitats. So much so that although Turkey is located in a region dominated by three main climate types, similar plants have begun to be grown in all three of the

http://www.aloki.hu ● ISSN 1589 1623 (Print) ● ISSN 1785 0037 (Online)
DOI: http://dx.doi.org/10.15666/aeer/1706_1285912868

climate zones. A frequently encountered issue in landscaping is that plant species are often faced with stress factors due to being grown in areas outside their natural habitats. In addition to the visible morphological characteristics of the plant, stress influences not only the micromorphological features of the plant that are not visible to the naked eye but also their vital functions (Cetin et al., 2017; Cetin et al., 2019; Cetin 2019). However, since the number of researches in this field is insufficient, the level of information on the subject is limited. In fact, the changes that occur on the micromorphological level in plants depending on different growth environments and habitats may provide useful insights in many areas including the stress level to which the plant is exposed, its ability to adapt to the growth environment, and the effect of climatic factors on phenotype (Cetin, 2016; Sevik et al., 2017; Sevik et al., 2019; Cetin et al., 2019; Cetin 2019; Bozdogan Sert et al., 2019).

In landscaping, plants used outside the natural distribution areas often do not show their performance in natural habitats, do not reflect their forms in the natural distribution area, and often remain alone with stress factors. These stress factors affect the plant's visible morphological features as well as micromorphological features that are not visible to the eye. If we can determine how these changes at the micro level change in relation to the climate parameters, we can have a lot of ideas from plant stress levels to adaptation levels. However, in order to determine how these changes in micromorphological characteristics should be interpreted, it is necessary to first determine the conditions under which these changes take shape.

The scope of this research was to find the variation of some micromorphological characteristics according to climate type in *Fraxinus excelsior* L. (European ash), *Platanus orientalis* L. (Plane tree) and *Tilia tomentosa* Moench (silver lime) plants grown in various regions of Turkey dominated by different climate types. The hypothesis of the study: Micromorphological characteristics of individuals grown in regions dominated by different climate properties are shaped depending on climate type.

Material and methods

This work was conducted on the leaves of *Fraxinus excelsior, Platanus orientalis*, and *Tilia tomentosa* species. Among these species, *Fraxinus excelsior* is generally found in Caucasia, North and South Europe. In our country, its general spreading zone is Northern Anatolia, but it also grows naturally in Hatay. It grows naturally between an elevation of 900-2100 m on the edges of creeks and in mixed forests with deciduous and coniferous leaves, but it is also used in landscaping in nearly the whole of Europe. *Platanus orientalis* naturally grows in Southeast Europe and Western Asia, and nearly in all regions in our country on banks of streams, riversides, at the bottom of valleys, and on leaky and gravelly slopes up to an elevation of 1100 m from sea level. It is commonly preferred in landscaping as a dust and noise barrier, and widely used in parks and gardens as an alle tree. The natural habitat of *Tilia tomentosa* species in the world consists of Southeast Europe and Western Asia. In our country, it grows naturally in the deciduous forests of Western and Northern Anatolia between the elevations of 400-1500 m, but it is also widely used in landscaping thanks to its drought-tolerant characteristic and being an alle tree (Kaya et al., 2009).

Leaf samples of the determined species were collected from individuals in Turkey in the cities of Rize, Samsun, İzmir, Antalya, Sivas, and Ankara (*Fig. 1* and *Table 1*). The patterns were collected from individuals used in landscape architecture arrangements in

http://www.aloki.hu ● ISSN 1589 1623 (Print) ● ISSN 1785 0037 (Online)
DOI: http://dx.doi.org/10.15666/aeer/1706_1285912868

centers of city. Among these cities, Samsun and Rize are located in a region where Black Sea climate type is dominant, Ankara and Sivas are located in a region where Continental climate type is dominant, and Antalya and İzmir are located in a region where Mediterranean climate type is dominant. Ten leaves were sampled form five trees of each species. Although these cities are located in regions where a certain climate type is dominant, there is a great variability between their climatic data (*Table 2*).

Mature leaf specimens collected during the vegetation season (25 August 2017) were pressed and dried, brought to the laboratory and tested under the electron microscope. Scaled images were obtained of the leaf blade abaxial surface near the midvein using scanning electron microscopy (SEM) and transposed into .jpeg photos for use with ImageJ software. SPSS® (IBM Analytics), analysis of variance (ANOVA) and a Duncan's test were used to evaluate measurements of stoma width (SW), stoma length (SL), stoma pore width (PW), stoma pore length (PL), and stomatal density (across 1 mm^2, SDEN) were evaluated potential statistically significant relationships between the selected characteristics (*Fig. 2*).

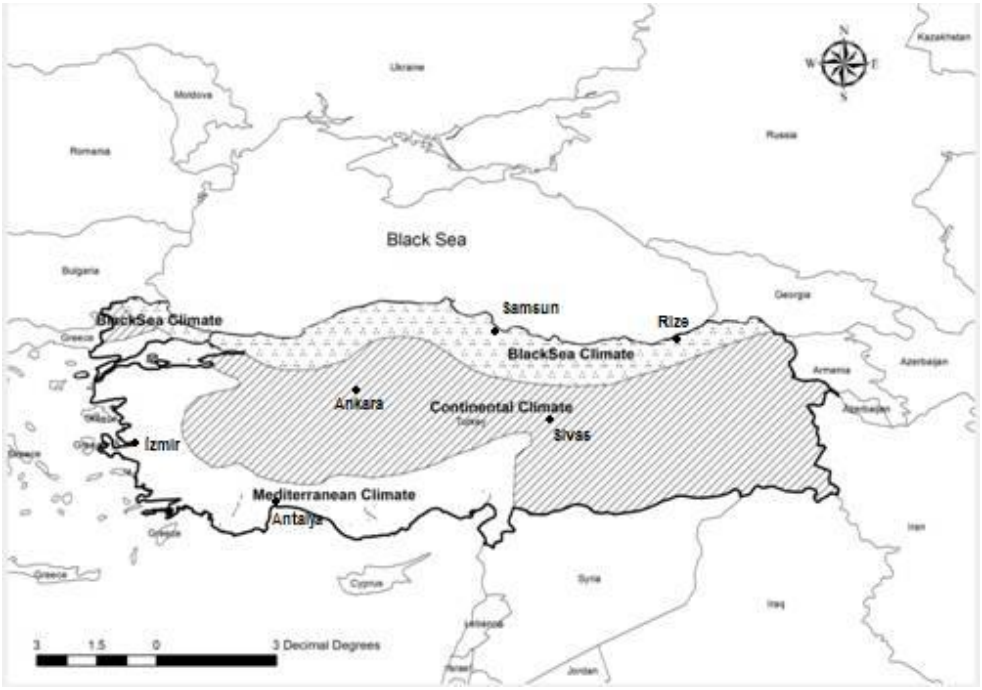

Figure 1. *A map indicating the location of each city in Turkey*

Table 1. *Giving the GPS coordinates of the sampling sites*

Cities	**Coordinates DMS (degrees, minutes, seconds) Latitude N – Longitude E**
Rize	41° 01' 34.22" N – 40° 31' 02.34" E
Samsun	41° 16' 49.77" N – 36° 20' 16.14" E
İzmir	38° 25' 05.72" N – 27° 08' 59.84" E
Antalya	36° 53' 49.81" N – 30° 42' 46.70" E
Sivas	39° 45' 05.84" N – 37° 00' 53.45" E
Ankara	39° 56' 19.13" N – 32° 51' 40.11" E

http://www.aloki.hu ● ISSN 1589 1623 (Print) ● ISSN 1785 0037 (Online)
DOI: http://dx.doi.org/10.15666/aeer/1706_1285912868

Table 2. *Some climatic data of cities where leaf samples were collected*

Annual average values	Antalya	İzmir	Rize	Samsun	Ankara	Sivas
	(Mediterranean climate type)		(Black Sea climate type)		(Continental climate type)	
Average temperature (°C)	18.6	17.8	14.3	14.5	11.9	8.9
Highest average temperature (°C)	24.1	22.6	18.0	18.2	17.8	15.3
Lowest average temperature (°C)	13.7	13.4	11.1	11.0	6.2	2.8
Avg. sunshine duration (hours/month)	100.3	94.5	49.4	61.0	80.3	80.5
Average number of rainy days	75.1	77.7	172.5	135.6	102.3	112.5
Total rainfall (mm/yr)	1066.9	695.9	2304.1	717.5	387.2	429.2
Highest temperature (°C)	45.0	43.0	38.2	39.0	41.0	40.0
Lowest temperature (°C)	-4.6	-8.2	-7.0	-9.8	-24.9	-34.6

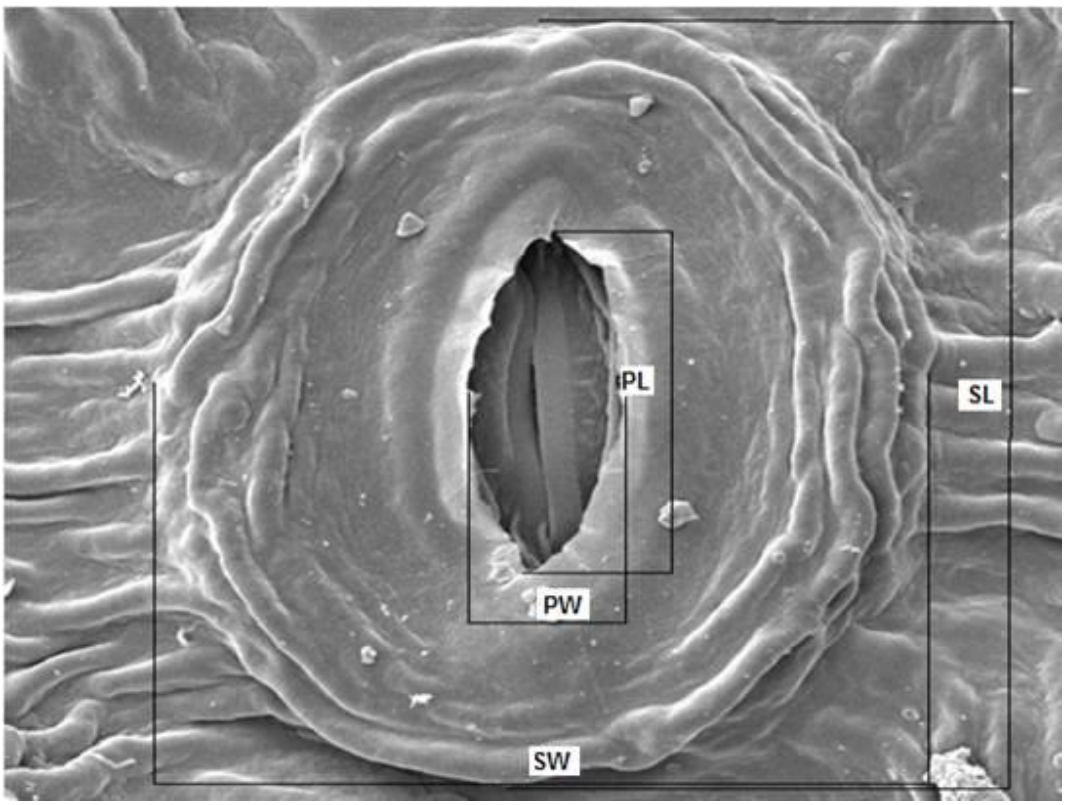

Figure 2. *SEM images the representation of the stoma with the width, length, etc. showing exactly where measurements were taken*

Data obtained on the micromorphological characteristics were evaluated with SPSS package software, and Duncan test and variance analysis were applied to these data. In

http://www.aloki.hu ● ISSN 1589 1623 (Print) ● ISSN 1785 0037 (Online)
DOI: http://dx.doi.org/10.15666/aeer/1706_1285912868

addition, correlation analysis was performed on the data with the help of SPSS package software in order to determine whether there is a statistically significant relationship between the micromorphological characteristics to be studied.

Results

City based average values of micromorphological characteristics investigated and the results of the Duncan test and variance analysis applied to these data are presented (*Table 3*).

Table 3. *Variation in leaf micromorphological characteristics based on habitat with species and places responding differently to climatic conditions*

Species	City	SL	SW	PL	PW	SDEN
Fraxinus excelsior	Ankara	25.77 ab	19.05 b	12.57 b	6.18 bc	132 a
	Antalya	26.75 b	19.61 bc	14.93 c	5.12 abc	164 b
	Samsun	23.06 a	15.67 a	9.86 a	3.97 a	179 b
	İzmir	30.00 c	22.13 c	13.24 bc	6.51 c	262 c
	Rize	33.92 d	21.90 c	19.65 d	8.49 d	509 d
	Sivas	24.99 ab	20.82 bc	12.40 b	4.59 ab	717 e
	F value	14.674***	8.160***	23.380***	8.418***	928.934***
Platanus orientalis	Ankara	31.96 cd	25.06 c	11.59 a	4.01 b	312 d
	Antalya	25.92 b	21.58 b	16.12 b	4.13 b	267 c
	Samsun	34.86 d	30.44 d	14.12 b	5.93 c	145 b
	İzmir	27.52 b	22.54 bc	14.18 b	6.85 d	97 a
	Rize	15.72 a	10.53 a	9.96 a	2.24 a	309 d
	Sivas	30.88 c	24.86 c	13.99 b	5.76 c	145 b
	F value	41.110***	39.842***	8.059***	25.710***	294.646***
Tilia tomentosa	Ankara	18.89 c	13.40 bc	10.57 a	4.23 a	121 c
	Antalya	15.18 a	11.95 b	10.51 a	3.53 a	145 d
	Samsun	16.01 ab	14.54 bc	9.76 a	3.67 a	113 c
	İzmir	14.36 a	9.36 a	11.26 a	3.38 a	176 e
	Rize	17.92 c	15.07 c	10.94 a	3.82 a	29 a
	Sivas	17.54 bc	13.97 bc	10.73 a	4.35 a	72 b
	F value	7.870***	6.582***	1.826 ns	1.441 ns	124.119***

SL, stoma length; SW, stoma width; PL, stoma pore length; PW, stoma pore width; SDEN, stomatal density across 1 mm^2. Values with same letter were not significantly different according to a Duncan test. ***Statistically significant at the $p < 0.001$ level of probability
Each value is the average value of 50 leaves, of which 5 are individual leaves

When the results of the study were examined; it was determined that among the three species studies, only *Tilia tomentosa* did not demonstrate any statistically significant difference between the cities in terms of pore characteristics. All other species showed statistically significant differences among the values obtained from different cities in all characteristics studied at a confidence level of 95%. For *Fraxinus excelsior*, the lowest values except for SDEN were obtained in Samsun, and the significantly higher values were obtained in Rize. For SDEN, the lowest values were obtained in Ankara, and

http://www.aloki.hu ● ISSN 1589 1623 (Print) ● ISSN 1785 0037 (Online)
DOI: http://dx.doi.org/10.15666/aeer/1706_1285912868

significantly higher values were obtained in Sivas. For *Platanus orientalis*, the lowest values except for SDEN were obtained in Rize, and the significantly higher values were obtained in Samsun. For SDEN, the lowest values were obtained in İzmir, and significantly higher values were obtained in Ankara and Rize. In addition, the highest PW value was obtained in Izmir. For *Tilia tomentosa*, the values obtained in İzmir were in the last homogeneous group for SDEN, while they were in the first homogeneous group for all other characteristics; conversely, the values obtained in Rize were the lowest values for SDEN, whereas the values were in the last homogeneous groups for other characteristics.

According to the results, we concluded that each species give different reactions to climatic demands. For example, while the lowest values for characteristics other than SDEN were obtained in samples collected from Rize for *Platanus orientalis*, for *Tilia tomentosa* and *Fraxinus excelsior,* the significantly higher values for characteristics other than SDEN were obtained in samples collected from Rize. Similarly, for *Fraxinus excelsior*, the lowest values for all characteristics except SDEN were obtained in Samsun, while the significantly higher values for *Platanus orientalis* for all characteristics except SDEN were obtained in Samsun. This is the case with most of the characteristics.

Different values were also obtained in the same species for samples gathered from cities located in the same climate zone. For example, in *Fraxinus excelsior*, the lowest values in all characteristics except SDEN were obtained in Samsun and the significantly higher values were obtained in Rize. In fact, Rize and Samsun are located in areas dominated by the same climate type. A similar situation was also observed in *Platanus orientalis*.

In order to determine the direction and magnitude of the relationships of the studied characteristics with each other, a correlation analysis was applied to the data and the results of this analysis in *Table 4* are given.

Table 4. *Relevance of the species characters in relation to the level of each other*

	SW	**PL**	**PW**	**SDEN**
SL	0.887**	0.711**	0.688**	0.300**
SW		0.551**	0.554**	0.205**
PL			0.726**	0.300**
PW				0.152

Weak correlation (0.10-0.29); moderate correlation (0.30-0.49); strong correlation (0.5-1.0). **Statistically significant at the $p < 0.01$ level of probability

According to correlation analysis results, it was determined that there is a statistically significant relationship between all characteristics except PW and SDEN. According to Cohen (1988), the relationship between two variables is weak if the value of the correlation coefficient is between 0.10 and 0.29, moderate if it is between 0.30 and 0.49, and strong if it is between 0.50 and 1.0. When we take a look at the level of relationship between the characteristics accordingly, we see that there is a weak or moderate relationship between SDEN and other characteristics. While there is a strong relationship between other characteristics, it was found that the strongest relationships were between STL and SW (0.887), and PL and PW (0.726).

http://www.aloki.hu ● ISSN 1589 1623 (Print) ● ISSN 1785 0037 (Online)
DOI: http://dx.doi.org/10.15666/aeer/1706_1285912868

Discussion

Plants have positive effects such as reducing air and noise pollution in the environments they are in. In addition to these positive effects, they also perform many functions such as reducing wind speed, being an economic resource, and supporting wild life (Kaya et al., 2009; Guney et al., 2016, 2017; Sevik et al., 2016; Cetin and Sevik, 2016; Cetin et al., 2019; Cetin 2019). Used and grown for various purposes in urban centers today, plants are accepted as an indicator of quality and liveability in urban life (Cetin, 2015, 2016; Cetin et al., 2017; Cetin et al., 2019; Cetin 2019).

Plants are living organisms, and fulfilling these functions depends primarily on being grown in areas where optimum climatic and edaphic factors are present for them. Otherwise, plants are exposed to stress conditions, and cannot properly fulfill the functions expected from them. It is therefore a very important matter to determine whether plants are exposed to stress conditions in their growth environment. In landscaping studies, plants are usually exposed to stress factors, depending on whether the plants are used outside their natural habitats. These stress conditions are known to affect the morphological characteristics of the plant. Studies have shown that plant morphological characteristics are influenced by many stress factors such as light (Cetin, 2016; Guney et al., 2016; Cetin et al., 2017), salt stress (Romero-Aranda et al., 2001), and water stress (Ferris et al., 1996). Therefore, it is quite possible that stomatal characteristics are also affected by environmental conditions and especially stress factors (Banon et al., 2004).

Stomata are the most important organelles in terms of leaf activity. Water evaporates from the leaf and stomata control the entry of CO_2 (Xu and Zhou, 2008). The number and size of stomata are significantly affected by environmental factors (Pearce et al., 2006; Galmés et al., 2007; Xu and Zhou, 2008). It has been pointed out in many studies that stoma density, in particular, is affected by environmental conditions and stress factors (Dunlap and Stettler, 2001; Guerfel et al., 2009; Bosabalidis and Kofidis, 2002).

There were significant differences in values obtained in different cities under the same climatic conditions. For example, for *Fraxinus excelsior,* the lowest values for all characteristics except SDEN were obtained in Samsun, while the significantly higher values were obtained in Rize. In fact, both of these cities are located in a region dominated by the Black Sea climate type. This suggests that microecological conditions may have more impact on leaf micromorphological characteristics. It is known that phenotypic character is the result of the interaction between genetics and the environment, and is shaped by the influence of many environmental factors (Sevik and Cetin, 2015) as well as genetic factors (Yigit et al., 2016). Therefore, genetic and microenvironmental conditions may be more effective on stomatal characteristics.

This situation also explains the fact that species can respond differently to the same climate conditions. As a matter of fact, it has been determined in the study that species do react differently to the same climate type. For example, for *Platanus orientalis*, the lowest values for all characteristics except SDEN were obtained in samples collected from Rize, whereas for *Tilia tomentosa* and *Fraxinus excelsior* the significantly higher values were obtained in samples collected from Rize. This can be explained by the fact that genetic structures of these species are different and therefore they are affected differently from the same climatic type.

It is known that morphological characteristics vary among species depending on many factors, especially origin. Researches have also demonstrated that micromorphological characteristics vary considerably among species (Maiti et al., 2016;

http://www.aloki.hu ● ISSN 1589 1623 (Print) ● ISSN 1785 0037 (Online)
DOI: http://dx.doi.org/10.15666/aeer/1706_1285912868

Galmés et al., 2007). In this case, it is not surprising that different origins of the same species respond differently to the conditions of the growth environment and also to stress factors. As a matter of fact, similar results have been obtained in various studies (Yigit et al., 2016; Sevik and Cetin, 2016; Bozdogan Sert et al., 2019; Sevik et al., 2019).

The correlation analyses performed in this study noted significant relationships between stomatal characteristics as was previously described by Cetin et al. (2017).

Conclusions

The variation of micromorphological characteristics detected on the leaves depending on growth conditions was investigated in this study. Scanning electron microscopy provides very high zoom levels thanks to high-resolution imaging techniques. Therefore, it is possible to obtain morphological, structural and elemental information from plants under these high zoom levels. The data obtained this way has the potential of being used in many areas such as determination of plant stress level, genetic variation studies, and determination of optimal plant growth conditions. However, in order for these characteristics to be effectively used in these specified areas, similar studies need to be replicated and diversified in different areas. The data in this study indicated a distinct morphological shift in size as trees are exposed to drier conditions, an indication that localized adaptation responses to stress can be observed using measurements. In particular, the studies to be done in natural populations where microclimatic conditions and human effects are absent or limited can provide much more reliable data.

REFERENCES

[1] Banon, S., Fernandez, J. A., Franco, J. A., Torrecillas, A., Alarcón, J. J., Sánchez-Blanco, M. J. (2004): Effects of water stress and night temperature preconditioning on water relations and morphological and anatomical changes of Lotus creticus plants. – Scientia Horticulture 101(3): 333-342. https://doi.org/10.1016/j.scienta.2003.11.007.

[2] Bosabalidis, A. M., Kofidis, G. (2002): Comparative effects of drought stress on leaf anatomy of two olive cultivars. – Plant Science 163(2): 375-379. https://doi.org/10.1016/S0168-9452(02)00135-8.

[3] Bozdogan Sert, E., Turkmen, M., Cetin, M. (2019): Heavy metal accumulation in rosemary leaves and stems exposed to traffic-related pollution near Adana-İskenderun Highway (Hatay, Turkey). – Environmental Monitoring and Assessment 191: 553. https://rd.springer.com/article/10.1007/s10661-019-7714-7

[4] Cetin, M. (2015): Evaluation of the sustainable tourism potential of a protected area for landscape planning: a case study of the ancient city of Pompeipolis in Kastamonu. – International Journal of Sustainable Development & World Ecology 22(6): 490-495. https://doi.org/10.1080/13504509.2015.1081651.

[5] Cetin, M. (2016): Changes in the amount of chlorophyll in some plants of landscape studies. – Kastamonu University Journal of Forestry Faculty 16(1): 239-245. http://dergipark.ulakbim.gov.tr/kastorman/article/view/5000176824/5000167063.

[6] Cetin, M., Sevik, H. (2016): Evaluating the recreation potential of Ilgaz Mountain National Park in Turkey. – Environmental Monitoring and Assessment 188(1): 52. https://doi.org/10.1007/s10661-015-5064-7.

http://www.aloki.hu ● ISSN 1589 1623 (Print) ● ISSN 1785 0037 (Online)
DOI: http://dx.doi.org/10.15666/aeer/1706_1285912868

[7] Cetin, M., Sevik, H., Saat, A. (2017): Indoor air quality: the samples of Safranbolu Bulak Mencilis Cave. – Fresenius Environmental Bulletin 26(10): 5965-5970.
[8] Cetin, M., Adiguzel, F., Gungor, S., Kaya, E., Sancar, M. S. (2019): Evaluation of thermal climatic region areas in terms of building density in urban management and planning for Burdur, Turkey. – Air Quality Atmosphere & Health 12 (9): 1103-1112. https://link.springer.com/content/pdf/10.1007%2Fs11869-019-00727-3.pdf
[9] Cetin, M. (2019): The effect of urban planning on urban formations determining bioclimatic comfort area's effect using satellitia imagines on air quality: a case study of Bursa city. – Air Quality, Atmosphere & Health 2019: 1-13. https://doi.org/10.1007/s11869-019-00742-4. https://rd.springer.com/article/10.1007/s11869-019-00742-4
[10] Dunlap, J. M., Stettler, R. F. (2001): Variation in leaf epidermal and stomatal traits of Populus trichocarpa from two transects across the Washington Cascades. – Canadian Journal of Botany 79(5): 528-536. https://doi.org/10.1139/b01-029.
[11] Ferris, R., Nijs, I., Beaeghe, T., Impens, I. (1996): Elevated CO_2 and temperature have different effects on leaf anatomy of perennial ryegrass in spring and summer. – Annals of Botany 78: 489-497. https://doi.org/10.1006/anbo.1996.0146.
[12] Galmés, J., Flexas, J., Savé, R., Medrano, H. (2007): Water relations and stomatal characteristics of Mediterranean plants with different growth forms and leaf habits: responses to water stress and recovery. – Plant and Soil 290(1): 139-155. https://doi.org/10.1007/s11104-006-9148-6.
[13] Guerfel, M., Baccouri, O., Boujnah, D., Chaïbi, W., Zarrouk, M. (2009): Impacts of water stress on gas exchange, water relations, chlorophyll content and leaf structure in the two main Tunisian olive (Olea europaea L.) cultivars. – Scientia Horticulture 119(3): 257-263. https://doi.org/10.1016/j.scienta.2008.08.006.
[14] Guney, K., Cetin, M., Sevik, H., Guney, K. B. (2016): Influence of germination percentage and morphological properties of some hormones practice on Lilium martagon L. seeds. – Oxidation Communications 39(1-II): 466-474.
[15] Guney, K., Cetin, M., Guney, K. B., Melekoglu, A. (2017): The effects of some hormones applications on Lilium martagon L. germination and morphological characters. – Polish Journal of Environmental Studies 26(6): 2533-2538. http://www.pjoes.com/pdf/26.6/Pol.J.Environ.Stud.Vol.26.No.6.2533-2538.pdf.
[16] Kaya, L. G., Cetin, M., Doygun, H. (2009): A holistic approach in analyzing the landscape potential: Porsuk Dam Lake and its environs, Turkey. – Fresenius Environmental Bulletin 18(8): 1525-1533.
[17] Maiti, R., Rodríguez, H. G., Rodríguez, P. C., Balboa, J. G., Moncivais, M., Tijerina, H. A. D., Kumari, A. (2016): Leaf surface anatomy in some woody plants from northeastern Mexico. – Pakistan Journal of Botany 48(5): 1825-1831. https://www.pakbs.org/pjbot/PDFs/48(5)/09.pdf.
[18] Pearce, D. W., Millard, S., Bray, D. F., Rood, S. B. (2006): Stomatal characteristics of riparian poplar species in a semi-arid environment. – Tree Physiology 26(2): 211-218. https://doi.org/10.1093/treephys/26.2.211.
[19] Romero-Aranda, R., Soria, T., Cuartero, J. (2001): Tomato plant-water uptake and plant-water relationships under saline growth conditions. – Plant Sci 160(2): 265-272. https://doi.org/10.1016/S0168-9452(00)00388-5.
[20] Sevik, H., Cetin, M. (2015): Effects of water stress on seed germination for select landscape plants. – Polish Journal of Environmental Studies 24(2): 689-693. http://www.pjoes.com/pdf/24.2/Pol.J.Environ.Stud.Vol.24.No.2.689-693.pdf.
[21] Sevik, H., Cetin, M. (2016): Evaluation of topiary applications and problems: a case study of Kastamonu. – International Journal of Multidisciplinary Thought 05(05): 45-50.
[22] Sevik, H., Cetin, M., Kapucu, O. (2016): Effect of light on young structures of Turkish Fir (Abies nordmanniana subsp. bornmulleriana). – Oxidation Communications 39(1-II): 485-492.

http://www.aloki.hu ● ISSN 1589 1623 (Print) ● ISSN 1785 0037 (Online)
DOI: http://dx.doi.org/10.15666/aeer/1706_1285912868

[23] Sevik, H., Cetin, M., Kapucu, O., Aricak, B., Canturk, U. (2017): Effects of light on morphologic and stomatal characteristics of Turkish fir needles (Abies nordmanniana subsp. Bornmulleriana Mattf.). – Fresenius Environmental Bulletin 26(11): 6579-6587.
[24] Sevik, H., Cetin, M., Ozel, H. B., Pinar B. (2019): Determining toxic metal concentration changes in landscaping plants based on some factors. Air Quality Atmosphere & Health 12(8): 983-991. https://link.springer.com/content/pdf/10.1007%2Fs11869-019-00717-5.pdf
[25] Xu, Z., Zhou, G. (2008): Responses of leaf stomatal density to water status and its relationship with photosynthesis in a grass. – J Exp Bot 59(12): 3317-3325. https://doi.org/10.1093/jxb/ern185.
[26] Yigit, N., Sevik, H., Cetin, M., Kaya, N. (2016): Determination of the effect of drought stress on the seed germination in some plant species. – In: Rahman, I. M. M., Begum, Z. A., Hasegawa, H. (eds.) Water Stress in Plants. Chap. 3. InTech, Rijeka, pp. 43-62.

http://www.aloki.hu ● ISSN 1589 1623 (Print) ● ISSN 1785 0037 (Online)
DOI: http://dx.doi.org/10.15666/aeer/1706_1285912868

CHARACTERIZATION AND ANTIBACTERIAL ACTIVITY OF SILVER NANOPARTICLES BIOSYNTHESIZED USING (*INDIGOFERA OBLONGIFOLIA*) LEAVES EXTRACT

SALMEN, S. H.* – ALWHIBI, M. S. – ALHARBI, S. A.

Department of Botany and Microbiology, College of Science, King Saud University, P. O. Box 2455, Riyadh 11451, Saudi Arabia

**Corresponding author*
e-mail: ssalmen@ksu.eda.sa

(Received 13th May 2019; accepted 28th Aug 2019)

Abstract. Here, we describe the novel biosynthesis of silver nanoparticles (AgNPs) using the extract of *Indigofera oblongifolia* (Hasr) leaves. The synthesized AgNPs were confirmed and characterized using ultraviolet–visible spectrophotometry, Fourier transform infrared spectroscopy (FTIR), energy dispersive spectroscopy (EDS), scanning electron microscopy (SEM), and transmission electron microscopy (TEM). An extreme absorption was detected at a wavelength near 400 nm after the formation of AgNPs. FTIR determined the extract biomolecules responsible for the reduction of the synthesized AgNPs. An EDS signal at 3 keV confirmed the presence of the Ag signal using surface plasmon resonance. SEM and TEM revealed the generally circular shape of AgNPs with sizes ranging from 8 nm to 25 nm (average particle size 15 nm). The antibacterial activity of AgNPs was pronounced for all bacteria studied.
Keywords: *nanoparticles, I. oblongifolia, biosynthesis, bacteria, biotechnology*

Introduction

Nanoparticles (NPs) play significant roles in biotechnology and pharmaceutical industries (Vijayakumar et al., 2013). The physical, biological, and chemical characterization of manufactured NPs is one of the fastest growing areas of science. The biosynthesis of NPs using plants (Peter et al., 2013, 2015; Deenadayalan et al., 2014), bacteria (Husseiny et al., 2006; El-Shanshoury et al., 2011), and fungi (Ingle et al., 2009; Neveen-Mohamed, 2014) has been described.

Interest has grown concerning the use of silver (Ag) NPs, which are inexpensive, safe, and ecologically-friendly. Recent studies have successfully biosynthesized AgNPs using plant components including the *Eriobotrya japonica* (Thunb.) leaf extract (Yu et al., 2019), cowpea (*Vigna sp*. L) seed extract (Mohammadi et al., 2016), *Pandanus odorifer* leaf extract (Hussain et al., 2019), *Ribes nigrum* fruit extract (Dobrucka et al., 2018), *Rosmarinus officinalis* leaf extract (Ghaedi et al., 2015), *Terminaliachebula* leaf extract (Chandra et al., 2016), and *Diospyros paniculata* root extract (Hanumanta et al., 2016). *Indigofera oblongifolia* is a perennial shrub that belongs to the family Fabaceae. It grows throughout Asia and Africa (Abdel and Ahmed, 2016). It is commonly known as Hasr in the South of Saudi Arabia and Yemen. As a traditional medicine, the leaves of this plant are used to treat some diseases due to their analgesic and anti-inflammatory activities. Moreover, in Saudi Arabia, *I. oblongifolia* is cultured in regions with a high occurrence of malaria, such as Nagran and Jazan (Nzila, 2013). The plant contains indigoferic acid and indigin as the fatty acid esters of hydroxy (E)-cinnamic acid and alkylated xanthenes, respectively, and also 3-hydroxybenzoic acid and β-sitosterol (Sharif et al., 2005).

http://www.aloki.hu ● ISSN 1589 1623 (Print) ● ISSN 1785 0037 (Online)
DOI: http://dx.doi.org/10.15666/aeer/1706_1286912876

To our knowledge, this is the first study to examine the use of the extract of *I. oblongifolia* (Hasr) leaves for the biosynthesis of AgNPs. AgNPs biosynthesized as such were characterized using different physical techniques that included ultraviolet (UV)–visible spectrophotometry, Fourier transform infrared (FTIR) spectroscopy, energy dispersive X-ray spectroscopy (EDS), scanning electron microscopy (SEM), and transmission electron microscopy (TEM). Finally, the antibacterial activity of the biosynthesized NPs against select gram-negative and gram-positive bacteria was studied.

Materials and methods

Plant material and preparation of extract

I. oblongifolia leaves were collected from Shabwah, South of Yemen. The plant was verified by the staff of the Herbarium, Department of Botany and Microbiology, King Saud University. Fresh leaves of *I. oblongifolia* were rinsed thoroughly numerous times using distilled water and allowed to completely air-dry in the dark. The powder prepared from the dried leaves (10 g) was placed in 100 mL deionized water and boiled for 10 min with stirring. The liquid extract was filtered using Whatman No. 1 filter paper. The residual extract was stored at 4 °C until processed.

Biosynthesis of AgNPs

Ten milliliters of the aqueous plant extract was mixed with 100 mL of 0.01 mM aqueous solution of silver nitrate ($AgNO_3$) with constantly stirring for 5 min at 25 °C. The resulting mixture was maintained undisturbed until the neutral solution changed to a brown color. Then, the molecules were by centrifugation at 13,000 rpm for 20 min. Finally, the obtained AgNPs were dried in oven at 40 °C for 2 h prior to characterization of AgNPs.

Characterization of AgNPs

UV–Visible spectroscopy

The formation of AgNPs in suspension was monitored using UV–Visible spectroscopy of the solution at wavelengths ranging from 300 to 800 nm using an Ultrospec 2100 Pro UV/visible spectrophotometer (Biochrom, UK).

FTIR spectroscopy

FTIR spectroscopy was performed to screen for functional groups in the phytoconstituents in the synthesized AgNPs and aqueous extract of *I. oblongifolia*. FTIR spectra were obtained by scanning from 400 to 4,000 cm^{-1}.

SEM and EDS

SEM used a model JSM-6380 LA microscope (JEOL, Japan). EDS was done using an Altima IV device (Regaku, Japan).

TEM

TEM examination of AgNP size, shape, and morphology was performed using a JEM-1011 microscope (JEOL).

http://www.aloki.hu ● ISSN 1589 1623 (Print) ● ISSN 1785 0037 (Online)
DOI: http://dx.doi.org/10.15666/aeer/1706_1286912876

Antibacterial studies

Bacteria

The bacteria were obtained from the Microbiology Laboratory of the College of Science, King Saud University. The gram-positive bacteria examined were *Staphylococcus aureus* (29213 ATCC), *Bacillus subtilis*, and *Streptococcus pyogenes*. The gram-negative bacteria examined were *Escherichia* coli (25922 ATCC) and *Salmonella typhimurium* (14028 ATCC). All bacteria were inoculated on nutrient agar (Sigma–Aldrich, Munich, Germany) and incubated at 37 °C for 24 h.

Antibacterial activities

The antibacterial activity of the synthesized AgNPs was studied using the agar well diffusion technique (Valodkar et al., 2011). Petri plates containing 20 ml Mueller Hinton Agar medium (Sigma–Aldrich) were inoculated with each bacterium to obtain a lawn of growth. Wells 6 mm in diameter were cut into the medium using a sterile agar borer. Then, synthesized nanoparticles (100 µl) were added to each well, and the plates were incubated at 37 °C for 24 h. Inhibition of growth was evident as a clear zone around the well. The control used was distilled water.

Statistical analysis

The results of antibacterial activity were expressed as the mean ± standard deviation (SD), and all experiments were performed in triplicate. The statistical results were calculated by one-way analysis using the SPSS statistical software (SPSS Inc., USA), A P-value < 0.05 indicated statistical significance.

Results and discussion

Biosynthesis of AgNPs and their visible spectrum

Immediately after mixing the *I. oblongifolia* extract with an $AgNO_3$ solution, a dark brown color developed. The color change indicated the formation of AgNPs, which was confirmed by the UV–Visible absorption spectrum (*Fig. 1*). UV–Visible spectroscopy has been used to investigate the shape and size of AgNPs in aqueous solution (Ranjit et al., 2013) and provided primary evidence for the formation of AgNPs (Nanda and Saravanan, 2013). Presently, the biosynthesized mixture was evaluated at wavelengths ranging from 200 to 800 nm; the highest peak absorption was observed at 400 nm as a result of AgNP formation.

FTIR

FTIR was used to confirm the presence of biocompounds in the extract of *I. oblongifolia* that were responsible for the formation of AgNPs. *Figure 2A* and *B* depict the FTIR spectra of the *I. oblongifolia* extract and AgNPs. The extreme band at 3,413 cm^{-1} in the *I. oblongifolia* extract was attributed to the O–H stretching band of phenols and alcohols (Preeti and Mausumi, 2013), which shifted to 3,433 cm^{-1} after reduction of the synthesized AgNPs as a result of protein binding. The other bands at 2917 and 1448 cm^{-1} in *I. oblongifolia* extract corresponded to C-H (alkane) and C-N (aromatic amines), respectively, which were absent from the FTIR spectrum of AgNPs. A second intense peak was observed at 1,614 cm^{-1} in the *I. oblongifolia* extract. It

http://www.aloki.hu ● ISSN 1589 1623 (Print) ● ISSN 1785 0037 (Online)
DOI: http://dx.doi.org/10.15666/aeer/1706_1286912876

changed to 1596 cm^{-1} with the formation of AgNPs, signifying the presence of carbonyl (C–O) stretching vibrations. The findings indicate that effective groups like phenols, alcohols, alkane, and aromatic amines present in the extract of *I. oblongifolia* may be responsible for the bioreduction of silver into AgNPs.

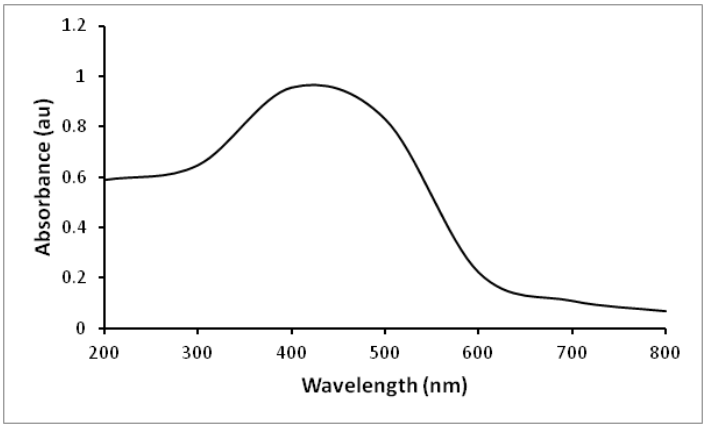

Figure 1. *UV–Visible spectrum for the reaction of the I. oblongifolia extract with the $AgNO_3$ solution*

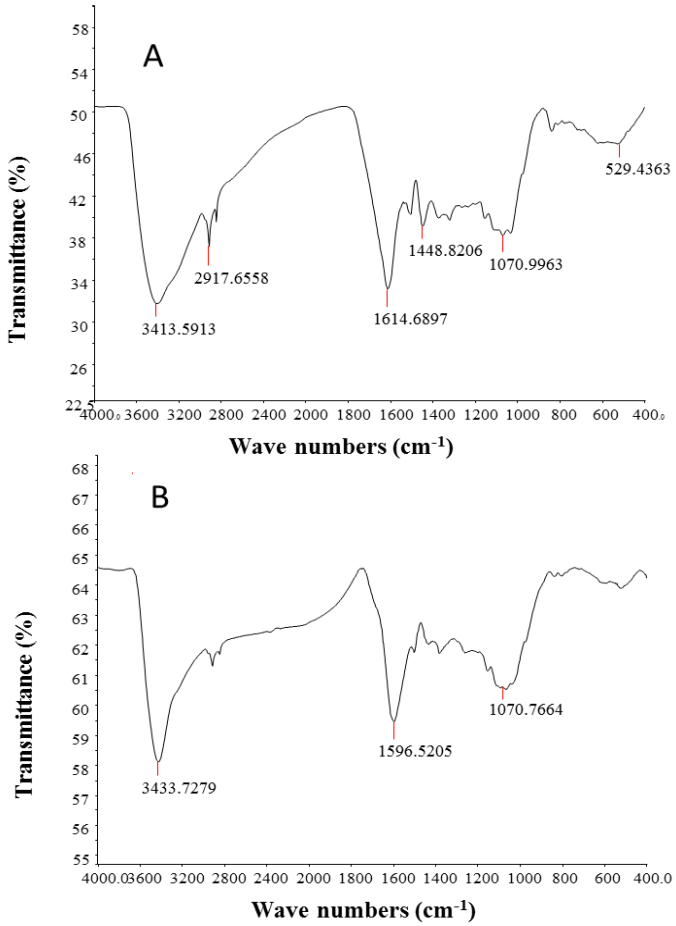

Figure 2. *FTIR spectra of the I. oblongifolia extract (A) and AgNPs produced using the I. oblongifolia leaf extract (B)*

http://www.aloki.hu ● ISSN 1589 1623 (Print) ● ISSN 1785 0037 (Online)
DOI: http://dx.doi.org/10.15666/aeer/1706_1286912876

SEM and EDS analyses

SEM of the biosynthesized AgNPs revealed various sizes of the irregularly formed AgNPs (*Fig. 3*). Clusters of AgNPs were evident in some images, which can be associated with the aggregation of NPs during the sample synthesis. The EDS spectra of AgNPs for study of elemental composition of the silver particles are presented in *Figure 3* and displayed strong signals in the silver region at 3 keV. An exemplary absorption peak of AgNPs at approximately 3 keV was reported using surface plasmon resonance (Nadagouda et al., 2011; Khan et al., 2014). EDS analysis revealed the existence of silver (68.94%). The appearance of chlorine and oxygen signals in the image may be due to X-ray emissions from the proteins present in the plant extract.

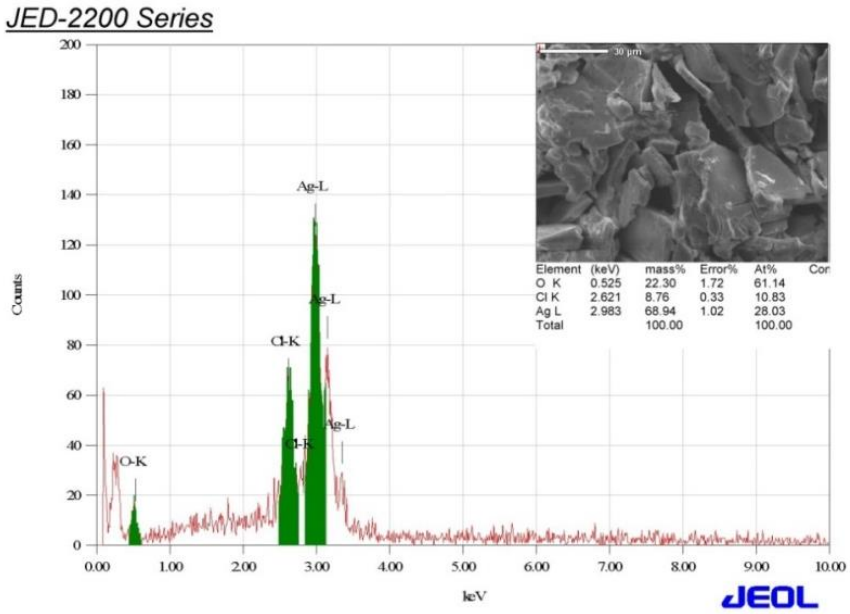

Figure 3. *SEM image and EDS of AgNPs synthesized using I. oblongifolia leaf extract*

TEM

TEM was performed to observe the morphology and sizes of the AgNPs. A representative image is presented in *Figure 4*. The AgNPs were extremely stable, smooth, and circular. The NPs ranged in size from 8 nm to 25 nm with an average particle size of 15 nm. No accumulation of AgNPs was observed.

Antibacterial activity

The growth inhibition caused by the AgNPs biosynthesized using the *I. oblongifolia* extract against representative gram-positive and -negative bacteria are presented in *Table 1*. The growth of all the bacteria was impeded, however, *E. coli* and *B. subtilis* were most sensitive to the inhibitory effect of the AgNPs, showing larger zones of growth inhibition compared to those of *S. aureus, S. typhimurium*, and *S. pyogenes*. As anticipated, growth was not inhibited for the control. These findings are consistent with those of other studies demonstrating the preparation of AgNPs with potent antibacterial and anti-fungal activities using plants extracts (Puiso et al., 2014; Ismail et al, 2017; Khalil et al., 2017; Matinise, et al., 2018; Premkumara et al,. 2018).

http://www.aloki.hu ● ISSN 1589 1623 (Print) ● ISSN 1785 0037 (Online)
DOI: http://dx.doi.org/10.15666/aeer/1706_1286912876

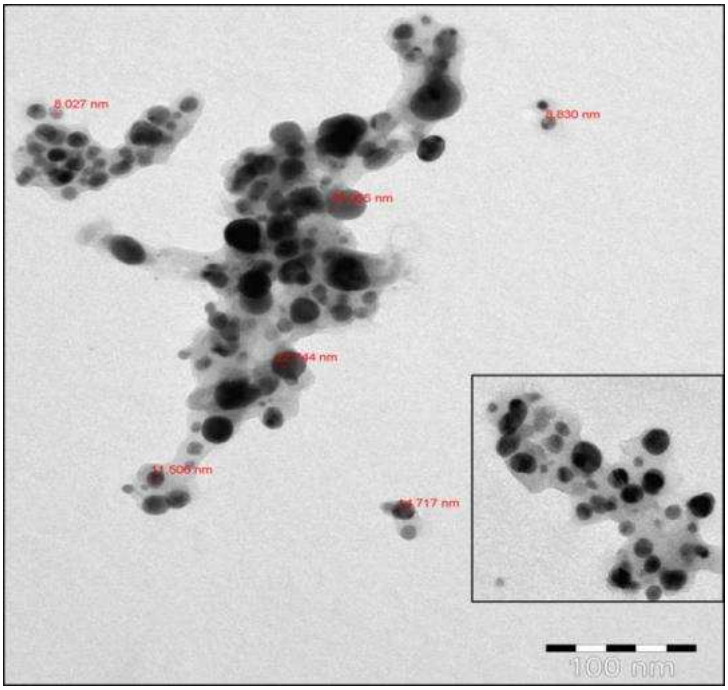

Figure 4. *TEM image of AgNPs synthesized using I. oblongifolia leaf extract*

Table 1. *Antibacterial activity of silver nanoparticles (AgNPs) against representative gram-positive and gram-negative bacteria*

Name of bacteria	Inhibition zone (mm)	
	AgNPs	Control
Staphylococcus aureus	13.5 ± 0.5*	0 ± 0.0
Bacillus subtilis	15.3 ± 0.5	0 ± 0.0
Streptococcus pyogenes	11 ± 0.0	0 ± 0.0
Escherichia coli	17 ± 1.15	0 ± 0.0
Salmonella typhimurium	13 ± 0.0	0 ± 0.0

*Results are shown as mean ± SD

Conclusions

This is the first description of the biosynthesis of AgNPs using the extract of *I. oblongifolia* leaves. The method is rapid, simple, eco-friendly, and safe. UV–Visible spectrophotometry, FTIR spectroscopy, EDS, SEM, and TEM confirmed the production of AgNPs. The success of the *I. oblongifolia* leaf extract to synthesize AgNPs is very promising for the eco-friendly and sustainable production of nanomaterials. The potency of the antibacterial activity of the AgNPs synthesized in this study was evident, and the results of this study are in agreement with those of other recent studies regarding the use of plant extracts for the synthesis of nanoparticles.

Acknowledgments. This project was supported by Researchers Supporting Project number (RSP-2019/5) King Saud University, Riyadh, Saudi Arabia.

http://www.aloki.hu ● ISSN 1589 1623 (Print) ● ISSN 1785 0037 (Online)
DOI: http://dx.doi.org/10.15666/aeer/1706_1286912876

REFERENCES

[1] Abdel, M., Ahmed, E. (2016): *Indigofera oblongifolia* prevents lead acetate-induced hepatotoxicity, oxidative stress, fibrosis and apoptosis in rats. – PloS One 11(7): 1–18.

[2] Chandra, S. E., Krishna Rao, K. V., Madhusudana Rao, K. (2016): Bio-synthesis and characterization of silver nanoparticles using *Terminalia chebula* leaf extract and evaluation of its antimicrobial potential. – Mater. Let. 174: 129–133.

[3] Deenadayalan, A. K., Palanichamy, V., Selvaraj, M. R. (2014): Green synthesis of silver nanoparticles using *Alternanthera dentata* leaf extract at room temperature and their antimicrobial activity. – Spectrochimica Acta Part A. 127: 168–171.

[4] Dobrucka, R., Kaczmarek, M., Dlugaszewska, J. (2018): Cytotoxic and antimicrobial effect of biosynthesized silver nanoparticles using the fruit extract of Ribes nigrum. – Adv. Nat. Sci. Nanosci. Nanotechnol. 9: 025015.

[5] El-Shanshoury, A. E. R., El Silk, S. E., Ebeid, M. E. (2011): Extracellular biosynthesis of silver nanoparticles using *Escherichia coli* ATCC 8739, *Bacillus subtilis* ATCC 6633, and *Streptococcus thermophilus* ESh1 and their antimicrobial activities. – ISRN Nanotechnol. #385480. http://dx.doi.org/10.5402/2011/385480.

[6] Ghaedi, M., Yousefinejad, M., Safarpoor, M., Khafria, H.Z, Purkaitc, M. K. (2015): *Rosmarinus officinalis* leaf extract mediated green synthesis of silver nanoparticles and investigation of its antimicrobial properties. – J. Industr. Eng. Chem. 31: 167–172.

[7] Hanumanta Rao, N., Lakshmidevi, N., Pammi, S. N., Kollu, P., Ganapaty, S., Lakshmi, P. (2016): Green synthesis of silver nanoparticles using methanolic root extracts of *Diospyros paniculata* and their antimicrobial activities. – Mater. Sci. Eng. C. 62: 553–557.

[8] Hussain, A., Alajmi, M. F., Khan, M. A., Pervez, S. A., Ahmed, F, Amir. S., Husain, F. M., Khan, M. S., Shaik, G. M., Hassan, I, Rais, A., Khanand Md. Rehman, T. (2019): Biosynthesized silver nanoparticle (AgNP) from *Pandanus odorifer* leaf extract exhibits anti-metastasis and anti-biofilm potentials. – Front. Microbiol. 10: 8.

[9] Husseiny, M. I., Aziz, M. A. E., Badr, Y., Mahmoud, M. A. (2006): Biosynthesis of gold nanoparticles using *Pseudomonas aeruginosa*. – Spectrochim Acta Part A. 67: 1003–1006.

[10] Ingle, A., Rai, M., Gade, A., Bawaskar, M. (2009): Fusarium solani: a novel biological agent for the extracellular synthesis of silver nanoparticles. – J. Nanoparticle Res. 11: 2079–2085.

[11] Ismail, E., Khenfouch, M., Dhlamini, M., Dube, S., Maaza, M. (2017): Green palladium and palladium oxide nanoparticles synthesized via *Aspalathus linearis* natural extract. – J. Alloys Comp. 695: 3632–3638.

[12] Khalil, T. A., Ovais, M., Ullah, I., Ali, M., Shinwari, Z. K., Maaza, M. (2017): Physical properties, biological applications and biocompatibility studies on biosynthesized single phase cobalt oxide (CO_3O_4) nanoparticles via *Sageretia thea* (Osbeck). – Arabian J. Chem. http://dx.doi.org/10.1016/j.arabjc.2017.07.

[13] Khan, M., Khan, S. T., Khan, M., Adil, S. F., Musarrat, J., Al-Khedhairy, A. A., Al-Warthan, A., Siddiqui, M. R., Alkhathlan, H. Z. (2014): Antibacterial properties of silver nanoparticles synthesized using *Pulicaria glutinosa* plant extract as a green bioreductant. – Int. J. Nanomed. 9: 3551–3565.

[14] Matinise, N., Kaviyarasu, K., Mongwaketsi, N., Khamlich, S., Maaza, M. (2018): Green synthesis of novel zinc iron oxide ($ZnFe_2O_4$) nanocomposite via *Moringa oleifera* natural extract for electrochemical applications. – Appl. Surf. Sci. 446: 66–73.

[15] Mohammadi, S., Pourseyedi, S., Amini, A. (2016): Green synthesis of silver nanoparticles with a long lasting stability using colloidal solution of cowpea seeds (*Vigna* sp. L). – J. Environ. Chem. Engin. 4: 2023–2032.

[16] Nadagouda, M. N., Speth, T. F., Varma, R. S. (2011): Microwave-assisted green synthesis of silver nanostructures. – Acc. Chem. Res. 44(7): 469–478.

http://www.aloki.hu ● ISSN 1589 1623 (Print) ● ISSN 1785 0037 (Online)
DOI: http://dx.doi.org/10.15666/aeer/1706_1286912876

[17] Nanda, A., Saravanan, M. (2013): Biosynthesis of silver nanoparticles from *Staphylococcus aureus* and its antimicrobial activity against MRSA and MRSE. – Nanomed. Nanotechnol. Biol. Med. 1: 452–456.
[18] Neveen-Mohamed, K. (2014): Biogenic silver nanoparticles by *Aspergillus terreus* as a powerful nanoweapon against Aspergillus fumigates. – Afr. J. Microbiol. Res. 7: 5645–5651.
[19] Nzila, A., Al-Zahrani, I. (2013): Drugs for the treatment of malaria in the Kingdom of Saudi Arabia. – Saudi Med. J. 34: 569–578.
[20] Peter, L., Silambarasan, S., Abraham, J. (2013): Ecofriendly synthesis of silver nanoparticles from commercially available plant powders and their antibacterial properties. – Scientia Iranica 20: 1049–1054.
[21] Peter, L., Sivagnanam, S., Abraham, J. (2015): Synthesis of silver nanoparticles using plants extract and analysis of their antimicrobial property. – J. Saudi. Chem. Soc. 19: 311–317.
[22] Preeti, D., Mausumi, M. (2013): In-vitro free radical scavenging activity of biosynthesized gold and silver nanoparticles using *Prunus armeniaca* (apricot) fruit extract. – J. Nanopart. Res. 15(1): 1366.
[23] Premkumara, J., Sudhakara, T., Dhakala, A., Shresthaa, J. B., Krishnakumara, S., Balashanmugamb, P. (2018): Synthesis of silver nanoparticles (AgNPs) from cinnamon against bacterial pathogens. – Biocatal. Agric. Biotechnol. 15: 311–316.
[24] Puiso, J., EJonkuviene, D., Macioniene, I., Salomskiene, J., Jasutiene, I., Kondrotas, R. (2014): Biosynthesis of silver nanoparticles using lingonberry and cranberry juices and their antimicrobial activity. – Colloids Surf. B. Biointerfaces 121: 214–221.
[25] Ranjit, K, Baquee, A. A. (2013): Nanoparticle: an overview of preparation, characterization and application. – Int. Res. J. Pharm. 4: 4–9.
[26] Sharif, A., Ahmed, E., Malik, A., Riaz, N., Afza, N., Nawaz, S. A., Arshad, M., Shah, M. R., Choudhary M. I. (2005): Lipoxygenase inhibitory constituents from *Indigofera oblongifolia*. – Arch. Pharm. Res. 28: 761–764.
[27] Valodkar, M., Nagar, P. S., Jadeja, R. N., Thounaojam, M. C., Devkar, R. V., Thakore, S. (2011): Euphorbiaceae latex induced green synthesis of non-cytotoxic metallic nanoparticle solutions: a rational approach to antimicrobial applications. – Colloids Surf. A. Physicochem. Eng. Asp. 384: 337–344.
[28] Vijayakumar, M., Priya, K., Nancy, F. T., Noorlidaha, A., Ahmeda, A. B. A. (2013): Biosynthesis, characterization and anti-bacterial effect of plant-mediated silver nanoparticles using *Artemisia nilagirica*. – Ind. Crops Prod. 41: 235–240.
[29] Yu, C., Tang, J., Liu, X., Ren, X., Zhen, M., Wang, L. (2019). Green biosynthesis of silver nanoparticles using *Eriobotrya japonica* (Thunb.) leaf extract for reductive catalysis. – Materials 12: 189. DOI: 10.3390/ma12010189.

http://www.aloki.hu ● ISSN 1589 1623 (Print) ● ISSN 1785 0037 (Online)
DOI: http://dx.doi.org/10.15666/aeer/1706_1286912876

IN VITRO EFFECT OF METALLIC SILVER NANOPARTICLES (AgNPs): A NOVEL APPROACH TOWARD THE FEASIBLE PRODUCTION OF BIOMASS AND NATURAL ANTIOXIDANTS IN PEARL MILLET (*PENNISETUM GLAUCUM* L.)

KHAN, I.[1,3#] – RAZA, M. A.[2#] – AWAN, S. A.[3#] – KHALID, M. H. B.[4#] – RAJA, N. I.[3] – MIN, S.[1] – ZHANG, A.[1] – NAEEM, M.[2] – MERAJ, T. A.[2] – IQBAL, N.[2] – ZHANG, X.[1] – HUANG, L.[1*]

[1]*Department of Grassland Science, Sichuan Agricultural University, Chengdu, 611130, China*

[2]*College of Agronomy, Sichuan Agricultural University, Chengdu 611130, China*

[3]*Department of Botany, PMAS - Arid Agriculture University, Rawalpindi 46000, Pakistan*

[4]*Maize Research Institute, Sichuan Agricultural University, Chengdu 611130, China*

**Corresponding author*
e-mail: huanglinkai@sicau.edu.cn; phone: +86-187-8357-5058

[#]*These authors contributed equally to this work*

(Received 18th May 2019; accepted 28th Aug 2019)

Abstract. Nanotechnology has become a revolutionary science over the past few decades with the potential for positive environmental, health and constructive effects. Nanoparticles (NPs) can be applied almost in every field of science, including the agricultural sector, and attaining great importance in current years. In the present study, Silver nanoparticles (AgNPs) were applied *in vitro* to examine their effects on economically important crop, pearl millet (*P. glaucum* L.*)* grown on MS basal medium supplemented with variable concentrations (T1 = control, T2 = 20 ppm, T3 = 40 ppm, T4 = 60 ppm and T5 = 80 ppm). Effects of AgNPs were assessed by analysing the seed germination, seedlings growth and biochemical profile of pearl millet, which were significantly affected ($p \leq 0.05$) and observed to be superior under T3 of AgNPs. The highest seed germination, seedling vigour index, root length, shoot length and biomass accumulation were achieved under T3 as compared to other treatments. Antioxidant enzymatic activity, Proline content, Catalase (CAT), Superoxide dismutase (SOD), Peroxidase (POD) including total flavonoids and total phenolic contents were also determined. AgNPs under (T5), inhibited the seed germination and seedlings growth and negatively influenced the biochemical profile by decreasing biomass accumulation. High doses of AgNPs proved to be a stressor and produced more ROS and toxicity, whereas it was indicated that AgNPs at suitable ratio minimized the production of ROS and stabilized the existing mechanisms of plantlets by increasing their growth and biomass production.
Keywords: *agriculture, constructive, germination, biochemical, accumulation*

Introduction

The world human's population is predicted to reach 9 billion by 2050, from the point of the current 7.4 billion (Hakeem, 2015). Current agricultural practices will not meet the expected demand for food due to the decrease in crop production by various factors, including inefficient means of fertilizers, industrial pollution, insecticides, heavy metals and climatic stresses (Hakeem, 2015). The agriculture sector is a significant contributor of greenhouse gases (CO_2, NO) due to overuse of mineral fertilizers, which emitted about 12% of total greenhouse gases (Hakeem, 2015). A rapid increase in population, depletion of natural resources and climatic issues are the key elements which create pressure on the environment to use chemical fertilizers for projected demand for food

http://www.aloki.hu ● ISSN 1589 1623 (Print) ● ISSN 1785 0037 (Online)
DOI: http://dx.doi.org/10.15666/aeer/1706_1287712892

(Mittal and Mittal, 2013). Demand for environmentally safe agricultural products is growing up with increasing technological advancement. Application of mineral fertilizers and pesticides causes serious intimidations to the environment, resulting in more production of unhealthy food products. For example, the application of nitrogen fertilizers generates the nitrous oxide, which is a greenhouse gas (Vejan et al., 2016). Long term use of mineral fertilizers has resulted in a reduction of soil organic matter leading to acidification of soil and causing severe threats to the survival of plants (Patra et al., 2016). Consequently, excessive use of fertilizers to get more production can result in damaging effects such as pollution, leaching, destruction of friendly insects and micro-organisms which ultimately reduction in soil fertility (Hazra and Das, 2014).

In recent eras, most of the research work has been focused on exploring the effects of nanoparticles (NPs) on plants, including other living organisms (Austin et al., 2016). NPs characterizes significant physiochemical properties and are extensively being used in physics, chemistry, agricultural science, environmental and medicinal field (Majdalawieh et al., 2014; Tripathi et al., 2017) but their interactions with plant metabolism is still needed more attention to exploring on large scale. The application of nanotechnology in agriculture reduces the environmental risks along with high production of agronomical crops (Chaudhuri and Malodia, 2017). In agriculture, metal-based development of NPs such as copper (Cu), iron (Fe), silver (Ag), zinc (Zn) and titanium dioxide (TiO2) has great potential to produce alternative nano fertilizers for crop improvement. Among these, silver nanoparticles (AgNPs) possess more positive effects on the plant's growth and development at suitable concentrations which depend on the size and distribution of AgNPs (Yasur and Rani, 2013).

Several agricultural concerns related to crop production under stress conditions have been elevated and improved by using AgNPs due to their diverse range of chemical and physical properties. Antifungal, antibacterial and antimicrobial properties of AgNPs provide a supreme edge to the farmer for the synthesis and utilization of nano fertilizers that may lessen the cost of agronomic production and enhance sustainable agriculture. Furthermore, AgNPs are cheaper, less toxic and environment-friendly, resulting in more constructive effects on crop yield and production by enhancing seed germination rate, increased seedling growth, i.e. root and shoot length and chlorophyll contents (Rafi and Ramezanian, 2013). Different plant species (e.g. *Phaseolus vulgaris, Zea mays* and *Lycopersicon esculentum)* have been exposed to a various dosage of AgNPs, resulted in a significant increase in plant total biomass, lower oxidative stress, increased flavonoid contents and high level of total phenolic contents (Berahmand et al., 2012). AgNPs have been applied with fungicide by seed priming, which enhanced the root length, shoot length and total biomass at lower concentrations while high levels of dosage reduced morphological profile at germination stage in plants. In order to know the beneficial facets of nanotechnology applied to agriculture, penetration, accumulation and transport of NPs should be investigated, which are unexplored yet (Parveen and Rao, 2015). Among the best methods of AgNPs application, foliar spray is demonstrated as most exceptional for agronomic viewpoint as plant leaves may able to intake essential elements more proficiently than roots which are directly in contact with leaf surfaces due to high magnetic properties of AgNPs as compared to other NPs (Chaudhuri and Malodia, 2017; Thakkar et al., 2010).

Pennisetum is the rich genus of Poaceae family. It comprises approximately 140 species that grow under various environmental conditions all over the world (Zhou et al., 2018). *P. glaucum* is one of the premium and important food crops which occupy

http://www.aloki.hu ● ISSN 1589 1623 (Print) ● ISSN 1785 0037 (Online)
DOI: http://dx.doi.org/10.15666/aeer/1706_1287712892

the sixth rank in the world with the substantial cultivated area (60%) in Africa and (35%) in Asia. It covers about half of the total global production of millets and is utilized as a staple food, source of protein for human beings and fodder for livestock (Basavaraj et al., 2010; Wang et al., 2018; Zhou et al., 2019b). Seedling stage of plants is susceptible to different types of stresses, which leads to significant loss of crop production in the agriculture system while NPs enhance the germination potential (Parveen and Rao, 2015). Some evidence has shown the excellent effects of phenolic compounds to minimize the risk of non-communicable diseases (NCD) caused by nutritional imbalance and protection against oxidative stress within the human body (Okarter and Liu, 2010).

AgNPs are now widely used in various fields, including agronomic crop production and revealed as stress-reducing agents; however, more research work is still needed to be known that how AgNPs affect antioxidant enzyme essay. The principal objective of recent research work is to explore the influence of AgNPs on seed germination, seedlings growth and biochemical profile in *P. glaucum,* which is still unexplored. To our best knowledge, this is the first report on the biochemical profiling of *in vitro* germinated *P. glaucum* seedlings under different concentrations of AgNPs.

Materials and methods

Plant material and sterilization

Seeds of *Pennisetum glaucum* (L.) R. Br. were obtained from the key laboratory of Grassland Science, Sichuan Agricultural University, China and used as an explant for this experiment. Seeds were well washed with simple tap water and dipped in ethanol for 30 min. Then sterilized in 0.1% mercuric chloride ($HgCl_2$) for 4 minutes and rinsed with autoclaved distilled water.

Seed germination experiment

The experiment was carried out in the key laboratory of Grassland Science, Sichuan Agricultural University, China. In this experiment, synthesized silver nanoparticles (AgNPs) were obtained from NANOCS (Nanocs lnc. New York, NY 10001, USA), manufactured according to > 0.75A520 units/m having 100 nm sizes (solution form). Firstly, the dilution of nanoparticles was taken out by using a stock solution. Five different types of treatments of AgNPs (T1 = control, T2 = 20 ppm, T3 = 40 ppm, T4 = 60 ppm and T5 = 80 ppm) were applied to MS medium. Sterilized seeds were inoculated in the conical flasks having MS solid medium and allowed them to germinate under controlled laboratory conditions at the temperature of 30 ± 5 °C (Hussain et al., 2017). Seed germination was experiential in 4-5 days and data were collected after ten days of germination. The experiment was repeated in twice, and data were taken out in triplicate.

Germination parameters

Germination frequency percentage

Seeds were considered as germinated when radical has taken out from the seed coat (Hussain et al., 2017).

http://www.aloki.hu ● ISSN 1589 1623 (Print) ● ISSN 1785 0037 (Online)
DOI: http://dx.doi.org/10.15666/aeer/1706_1287712892

Germination frequency = No. of seeds germinated × 100 / total no. of seeds

Shoot and root morphology

Length of shoot and root was measured in cm and compared by using a bar chart.

Seedling vigour index (SVI)

This was calculated by using the method of Ushahra and Malik (2013) and expressed as:

SVI = [root length + shoot length] × germination percentage

Biochemical profiling

DPPH activity

For the estimation of antioxidant activity, a protocol described by Abbasi et al. (2010) was used for DPPH (2, 2-diphenyl-1-picrylhydrazyl) free radical scavenging assay (FRSA). 10 mg of dried plant samples were dissolved in 4 ml methanol and then mixed with 0.5 ml of DPPH solution. The mixture was gently vortexed for fifteen seconds and placed at room temperature for 30 min. Final results were concluded when the sample absorbance was checked by spectrophotometer at 517 nm. FRSA was calculated and expressed as:

DPPH discoloration %age = 100 x ($1-A_s/A_b$)

A_s: Absorbance of the solution with extract addition. A_b: Absorbance of the solution without extract addition.

Proline contents

Proline contents were measured according to Bates et al. (1973), 0.5 g of plant samples were homogenized by pestle and mortar in 5 ml of 3% sulphosalycylic acid. 2 ml of ninhydrin reagent and 2 ml of glacial acetic acid were added to the test tube having 2 ml of extract. The mixture was placed in a water bath and boiled at 100 °C for 30 min. 6 ml of toluene was added to a reaction mixture after cooling and transferred to separating funnel. Thoroughly mixing resulted separation of the chromophore with toluene and absorbance was measured at 520 nm by using a spectrophotometer DU-730 (Beck Man Coulter Inc., USA)

Antioxidant enzyme extracts were prepared by using mortar and pestle. Plant samples (1 g) were homogenized with 10 ml of extraction buffer containing (50 mM potassium (K)-phosphate buffer with 1% polyvinyl polypyrrolidone at pH 7). The mixture was centrifuged at 15,0000 g for 30 min at 4 °C and supernatant was used for Antioxidant enzyme activity (Ullah et al., 2015).

Superoxide dismutase (SOD)

One of the methods described by Ullah et al. (2015) with some improvements was used to measure the SOD activity. 1 ml of the reaction mixture was composed of 1 millimolar (mM) EDTA, 130 millimolar methionine, 0.05 molar phosphate buffer (pH 7) 0.02 millimolar riboflavin and 0.75 millimolar nitroblue tetrazoliums (NBT). The

http://www.aloki.hu ● ISSN 1589 1623 (Print) ● ISSN 1785 0037 (Online)
DOI: http://dx.doi.org/10.15666/aeer/1706_1287712892

reaction mixture was placed under the fluorescent light for 7 min and absorbance was measured at 560 nm using spectrophotometer DU-730 (Beck Man Coulter Inc., USA). By using the Lambert-Beer law equation, SOD activity was calculated:

$$A = \varepsilon LC$$

A: absorbance, ε: extinction coefficient, L: length of each wall, C: concentration of enzymes.

Catalases and peroxidases activity

The protocol of Aebi (1984) was used with some modifications to determine the catalase activity. Enzyme extract (0.5 ml) was added to 3 ml of reaction solution (50 mM phosphate buffer, pH 7.0 and 30% w/v H_2O_2). The catalase activity was examined at the decrease of absorbance at 240 nm using spectrophotometer DU-730 (Beck Man Coulter Inc., USA). The estimation of peroxidase activity was measured by following the method of Chance and Maehly (1955). 3 ml of reaction solution containing (20 mM guaiacol, ten mM phosphate buffer and ten mM H_2O_2) was mixed with 0.5 ml of enzyme extract (heated in a water bath at 45 °C for 5 min before mixing). Increase in absorbance was measured at 470 nm using spectrophotometer DU-730 (Beck Man Coulter Inc., USA) due to the formation of tetraguaiacol (Klapheck et al., 1990).

Estimation of total phenolic content (TPC)

For TPC estimation, 0.75 ml of Folin–Ciocalteu reagent was added to 100 µl plant extract, gently mixed and placed them at 22 °C for 5 min. 0.75 ml of Na_2CO_3 solution was then added to the mixture and kept at 22 °C for 90 min. Final results were concluded by checking sample absorbance at 725 nm at UV/Vis-DAD spectrophotometer (UV-2250, Kyoto, Japan) (Velioglu et al., 1998).

Estimation of total flavonoids content (TFC)

For the estimation of TFC, $AICI_3$-$NaNO_2$-NaOH reaction complex was used according to the protocol given by Lopez-Contreras et al. (2015). 0.2 ml of extract was added to 3.5 ml of distilled water. Furthermore, (0.15 ml) 5% $NaNO_2$, (0.15 ml) 10% $AlCl_3$ and (1 ml) 1 M NaOH were added to mixture by equal 5 min time intervals each and placed it at room temperature for 15 mins. Reaction absorbance was measured at 510 nm by using UV/Vis-DAD spectrophotometer (UV-2250, Kyoto, Japan).

Statistical analysis

All the data were analysed by using Statistical software (version 7.0; StatSoft). Significance was determined via one-way analysis of variance. Values are presented as mean ± standard error (SD) from three independent biological replicates. A comparison of the means (control + treatments) was confirmed by Duncan's multiple range test at $p < 0.05$.

http://www.aloki.hu ● ISSN 1589 1623 (Print) ● ISSN 1785 0037 (Online)
DOI: http://dx.doi.org/10.15666/aeer/1706_1287712892

Results

Silver nanoparticles and germination percentage

In the recent study we have explored the *in vitro* phytotoxic and beneficial aspects of synthesized metallic silver nanoparticles (AgNPs) in *Pennisetum glaucum* (L.), AgNPs were purchased from China which possessed the size of 100 nm (*Fig. 1A)*. AgNPs did not show any adverse effect on seed living mechanism. Interestingly, AgNPs have boosted the seed germination in *P. glaucum* (L.) as compared to non-treated. The enhancement in seed germination has been assessed as dispersed AgNPs could create 'nanoholes' in the seed coats and make their entry easier to seeds via seed coat, resulting in enhanced germination conditions, slow and slight release of silver ion (Ag^+) could be a second primary reason for Ag-nanoparticles to have no deleterious effects on germination of *P. glaucum* (L.) seeds at optimal concentrations.

Moreover, the maximum seeds germination percentage (99%) was recorded in T3 of AgNPs *(Fig. 1B)*. This was observed as the appropriately applied ratio of AgNPs, which resulted in enhanced germination of seeds *in vitro* and possible to utilize in the agricultural system for better crop production. This may elucidate, at the optimal range of applied AgNPs, seeds germination was not altered harmfully so AgNPs could be used as conventional fungicides to protect the seeds against fungi and reduce environmental sways of fungicides as well as lower the cost of agricultural production.

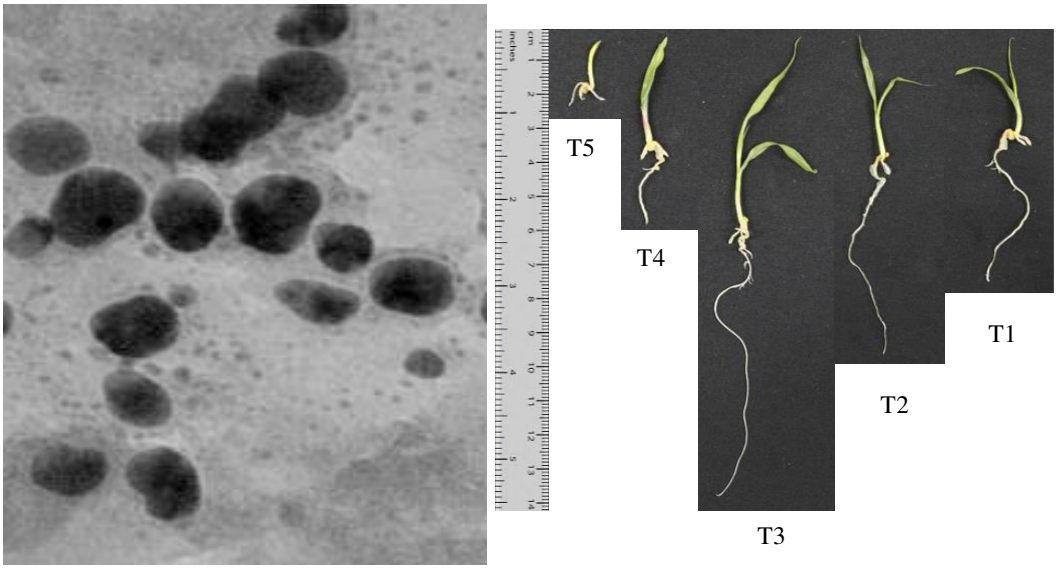

Figure 1. *(A) Transmission electron microscopy (TEM) images of metallic silver nanoparticles having size of 100 nm. (B) Effect of different treatments (T1 = 0 ppm, T2 = 20 ppm, T3 = 40 ppm, T4 = 60 ppm and T5 = 80 ppm) of metallic silver nanoparticles (AgNPs) on growth of Pennisetum galucum (L.) seedlings. Each seedling represented an experimental unit*

The *Figure 2A* and *B* indicate that seed germination percentage and seed vigour index affected by various treatments of AgNPs. Germination percentage at control (T1) and T3 was 92% and 99% respectively while in comparison with T5, it was strongly reduced to 66%. These results revealed that AgNPs application at T3 sharply boosted the germination potential by increasing emergence speed of radical and plumule in *P.*

http://www.aloki.hu ● ISSN 1589 1623 (Print) ● ISSN 1785 0037 (Online)
DOI: http://dx.doi.org/10.15666/aeer/1706_1287712892

glaucum (L.) seeds on MS solid media. Though the emergence response of seeds was dependent on applied concentration in T5, a noticeable reduction in germination was observed.

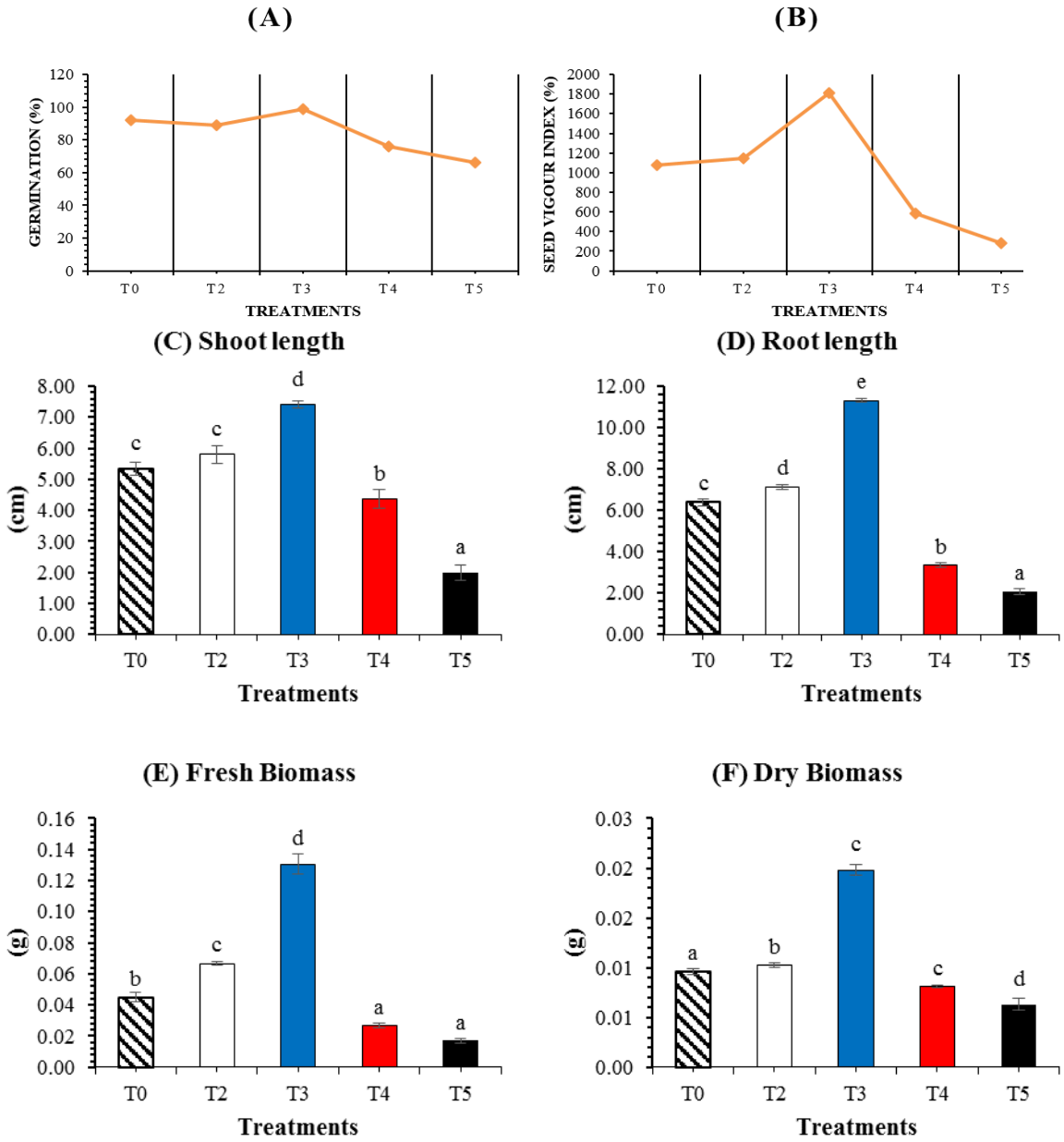

Figure 2. *The response of seed germination and seedling growth treated with AgNPs (A) Seed germination potential, (B) Seed vigour index, (C) Shoot length (D) Root length (E) Fresh biomass (F) Dry biomass. Values are the average of three repetitions. Means (n = 3) and standard errors (±) were calculated by analysis of variance (one-way). A comparison of the means (control + treatments) was confirmed by Duncan's multiple range test at p < 0.05*

Morphological parameters and total biomass

Under T5, root length, shoot length and seedling vigour index (SVI) were significantly reduced, as shown in *Figure 2*. In case of seedlings growth, the length was

http://www.aloki.hu ● ISSN 1589 1623 (Print) ● ISSN 1785 0037 (Online)
DOI: http://dx.doi.org/10.15666/aeer/1706_1287712892

enhanced up to 76.5% and 38.8% in root and shoot respectively in T3 which showed best results as compared to control while rapidly reduced as concentrations of nanoparticles increased or decreased. It was noticed that higher concentrations of AgNPs had a deleterious effect on plantlets, resulting in a significant reduction in root and shoot length and SVI. Consequently, the fresh and dry biomass were dependent on better seedling growth. In comparison with control, fresh and dry biomass were enhanced (190.1%) and (106.2%) respectively in T3 and readily decreased to 163.2% and 52.38% at high doses (T5) (*Fig. 2E, F*). The highest reduction in biomass could be due to more accumulation of ions released from nanoparticles, which reduced the availability of nutrients to seedlings for growth at higher doses (Hussain et al., 2017).

Antioxidant activity

DPPH radical scavenging assay

DPPH (2, 2-diphenyl-1-picrylhydrazyl) free radical scavenging activity of plantlets treated with AgNPs is presented in *Figure 3*. AgNPs suspension significantly influenced the DPPH activity in *P. glaucum* (L.). The highest DPPH activity (26%) was recorded in the plantlets which were exposed to T5 while others showed less. In contrast with others, T3 had reduced the antioxidant activity (9%) even then control (13%), revealed less production of ROS at this concentration which was advantageous for plant metabolisms and successful growth (Zhou et al., 2019a) as found in *Figure 3*.

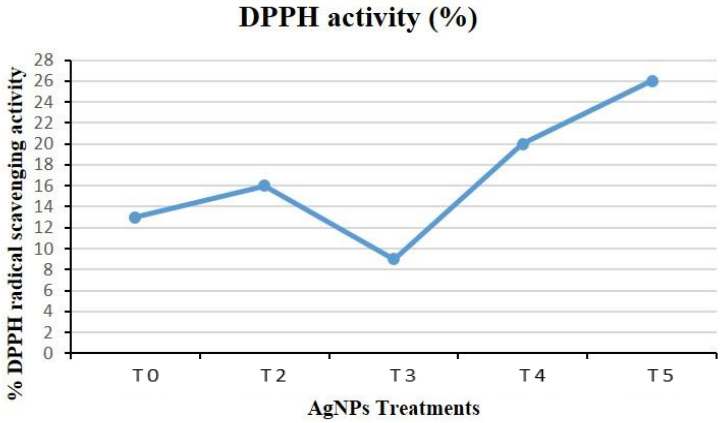

Figure 3. *Percentage DPPH radical scavenging activity of P glaucum L. against different treatments of metallic silver nanoparticles (AgNPs)*

Proline and superoxide dismutase (SOD) activity

Proline contents and SOD activity also have been evaluated in the present investigation, as shown in *Figure 4A, B*. Proline contents were relatively less (1.12 ± 0.0152 µg/mg) in the seedlings treated with T3 as compared all other treatments, including control (1.17 ± 0.0264 µg/mg). However, the highest value (2.15 ± 0.435 µg/mg) was found at T5, which reflected the stressed conditions faced by plantlets. By increasing the AgNPs doses, SOD activity tends to become more and highest at T5 (0.048 ± 0.0043 µmol/mg) and lower at T3 (0.031 ± 0.0020 µmol/mg). Stress could be a critical factor which enhanced the Proline and SOD activity (Mohamed et al., 2017).

http://www.aloki.hu ● ISSN 1589 1623 (Print) ● ISSN 1785 0037 (Online)
DOI: http://dx.doi.org/10.15666/aeer/1706_1287712892

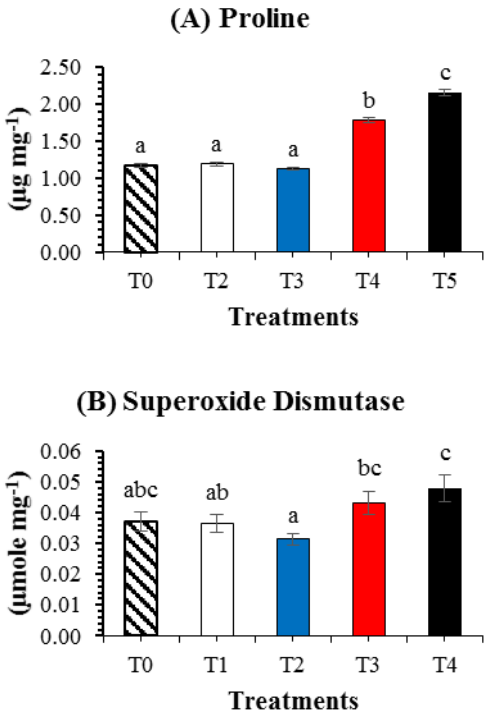

Figure 4. *Antioxidant enzyme activity in P glaucum L. seedlings treated with AgNPs. (A) Proline content. (B) Superoxide dismutase (SOD) activity. Values are the average of three repetitions. Means (n = 3), and standard errors (±) were calculated by analysis of variance (one-way). A comparison of the means (control + treatments) was confirmed by Duncan's multiple range test at p < 0.05*

Catalases (CAT) and peroxidases (POD) activity

Our results showed a negative relationship between CAT and POD activity as seen in *Figure 5A, B*, at higher dose (T5) more POD activity (1.03 ± 0.723 µg/g) was recorded, however POD activity was significantly decreased to 101.9% and 68.8% in T3 and T1 respectively, which strongly reflected the consistent and sustainable living mechanism of plantlets whereas, more POD activity resulted in more stress on plantlets. The CAT activity was seemed to be higher (141 ± 2.081 mg/g) in T3 and lower as the dosage increased from T3. However, lowest CAT activity (100 ± 3.833 mg/g) was recorded in the plantlets treated with T5, at this concentration plantlets were observed in stress condition which could be due to more production of ROS. Furthermore, CAT is found in peroxisome (Alberts et al., 2002) so, AgNPs at the suitable ratio may cause more production of catalases that provide longevity to plantlets under different environmental settings.

Total phenolic contents (TPC) and total flavonoids contents (TFC)

Total phenolic contents in the seedlings which treated in T3 were comparatively more (0.56 ± 0.0152 µg/mg) than control and T2, as shown in *Figure 5D*. On the contradictory, there were significant effects ($p \leq 0.01$) in the phenolic compound's accumulation since the rise in doses from T3 to T5, declined in the accumulation of total phenolic contents (12.1%) and (35.2%) under T4 and T5 respectively when compared with T1. These results indicated that seedlings exposed to higher doses of

http://www.aloki.hu ● ISSN 1589 1623 (Print) ● ISSN 1785 0037 (Online)
DOI: http://dx.doi.org/10.15666/aeer/1706_1287712892

AgNPs faced more stress by which they accumulated less phenolic compounds because a high dosage of AgNPs acted as a stressor and inhibited the accrual of TPC.

Unlike phenolic compounds, the flavonoid contents were higher as the concentrations of AgNPs increased from T2 to T5 as in *Figure 5C*. Total flavonoid contents were significantly enhanced to 0.58 ± 0.0233 µg/mg under T3 than T1, resulting from the proper entry of nanoparticles into seeds at the time of germination which provided signals to emerging seedlings by which these could cope with different environmental settings. Therefore, significant differences have been recorded at high doses of AgNPs when compared with T3. A higher concentration of nanoparticles produced more TFC (0.76 ± 0.055 µg/mg), but a significant reduction in seedling growth was observed.

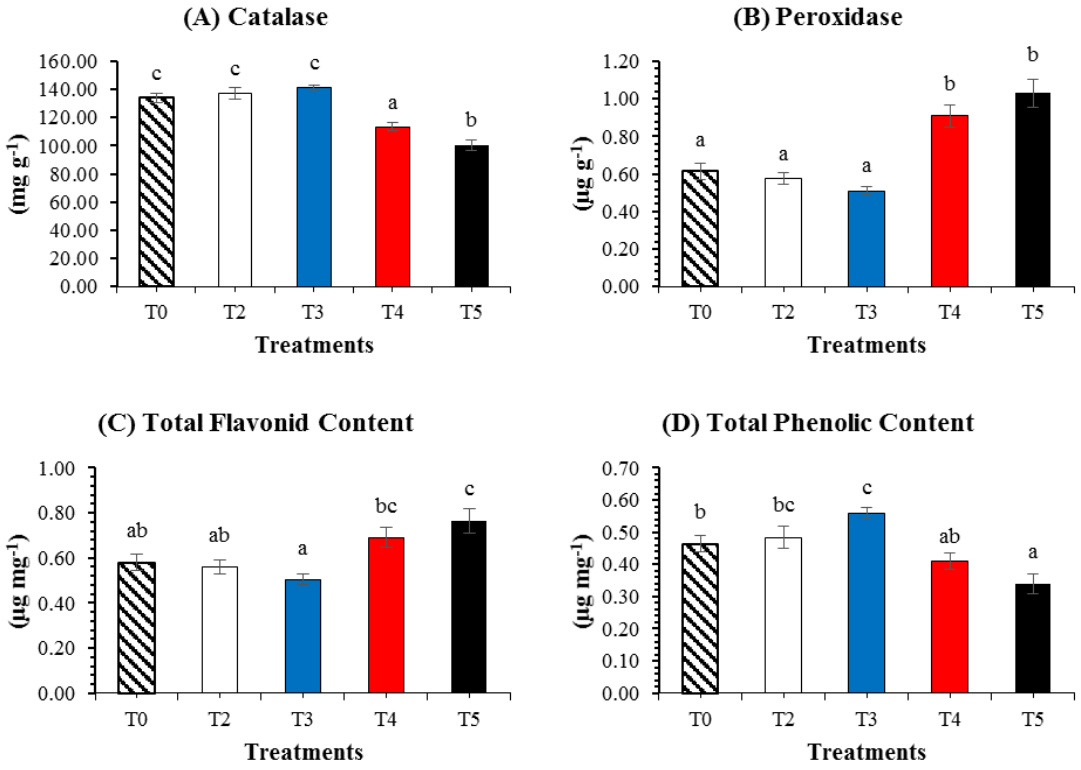

Figure 5. *Antioxidant enzyme activity and phenolic content in Pennisetum galucum L. seedlings treated with AgNPs. (A) Catalase (CAT) activity, (B) Peroxidase (POD) activity, (C) Total flavonoid content (TFC) (D) Total phenolic content (TPC). Values are the average of three repetitions. Means (n = 3) and standard errors (±) were calculated by analysis of variance (one-way). A comparison of the means (control + treatments) was confirmed by Duncan's multiple range test at $p < 0.05$*

Discussion

Results of recent research work disclosed that suitable concentrations of AgNPs significantly enhanced the seed germination, growth attributes and improved the biochemical profile of *P. glaucum* (L.) while high dosage acted as a stressor or toxic to plants at germination stage and reduced the total biomass. Study of the toxicity of nanomaterial is the nanotoxicology, which is dependent on their sizes, shapes and effects because nanoparticles have distinctive properties. Although toxicity mechanism

http://www.aloki.hu ● ISSN 1589 1623 (Print) ● ISSN 1785 0037 (Online)
DOI: http://dx.doi.org/10.15666/aeer/1706_1287712892

of nanoparticles is still unknown nonetheless, it would depend upon the nanomaterials chemical composition, chemical structure, sizes and surface area. Two major key factors can be the cause of toxicity (1) release of more toxic ions and (2) stress due to size, shape or surface of nanomaterial. NPs bearing small sizes have more surface area, so these are more toxic (Parveen and Rao, 2015). In case of metallic nanoparticles (MNP), small-sized CuNPs have been observed more toxic on two plant species wheat (*Triticum aestivum*) and mung bean (*Phaseolus radiatus*) by reducing seedling growth than other MNPs (Lee et al., 2008). However, High emergence percentage of root and shoot from seeds is triggered by the positive role of plant hormones. Nanoparticles were entered to seeds successfully and filled the space between permeable membrane which enhanced the biosynthesis of hormones especially auxins and gibberellins to degrade seed reserves resulted from increased seed germination and seedling growth (El-Kereti et al., 2013; van Dongen et al., 2003).

It was observed in our findings that maximum germination percentage and seedling growth were attained at T3, this range could be a suitable for rapid entry of AgNPs and positive acceleration of seed metabolism for the enhancement of seedling growth as shown in *Figure 1B*. Kumari et al. (2011) reported that AgNPs influenced the cell division process of plant and caused cell enlargement, where they interfered with plant components in plant systems and translocated from stem to leaves. Interestingly, lower concentrations of AgNPs were seemed to be useful to increase the seed vigour and seedlings growth and had no deleterious effects to cell division process and seedlings growth in kinnow (Hussain et al., 2018). High dosage of AgNPs inhibited or reduced the seed germination, decreased seedlings growth, chlorophyll contents, and plant biomass in *Hordeum vulgare* and *Spirodela polyrhiza* which strongly affirm our recent findings in case of *P. glaucum* (L.). Besides, AgNPs possess antiviral, antifungal, antibacterial properties and can be utilized as potent fungicides due to their strengthening shielding role against fungi and enhanced germination frequency as described by Karimi et al. (2012), who reported the better germination potential and seedling growth from the seeds, coated with a suitable concentration of AgNPs solution compared with fungicides coated seeds. Same results for growth parameters were investigated by Hussain et al. (2017), who achieved 98.6% germination vigour which was about 7% better than control and 22% more seedling growth compared with control in Artemisia under suitable concentrations (30 mg/L) of AgNPs. Study of AgNPs on rice (*Oryza sativa*) seedlings also have been examined, and results revealed, as a dosage of NPs increased from 60 mg/L all the growth attributes including seed germination, root length, shoot length, leaf length, leaf area and biomass readily decreased (Mirzajani et al., 2013). Total biomass reduction in wheat (*Triticum aestivum*) and *(Pennisetum glaucum)* under high concentrations of AgNPs was also reported by Mohamed et al. (2017) and Khan et al. (2019). Reduction in total biomass (fresh and dry) accumulation due to the high amount of AgNPs has been shown in *Figure 2*. We have applied AgNPs to *P. glaucum* on MS basal medium while most of the above described findings were achieved in soil experiments in which other plant species have been experienced, but all these strongly affirm our best germination results under suitable concentrations and poor results under the high ratio of NPs as in *Figure 1B*.

In the present study, ranges of AgNPs above T3 negatively affected the root and shoot growth, alternatively increased the antioxidant activity, total flavonoids and proline contents. Likewise, under stressed conditions, *Triticum aestivum* increased MDA contents and H_2O_2 level resulting in increased antioxidant activity to cope with

http://www.aloki.hu ● ISSN 1589 1623 (Print) ● ISSN 1785 0037 (Online)
DOI: http://dx.doi.org/10.15666/aeer/1706_1287712892

the stress for better survival of plant (Mohamed et al., 2017). A higher concentration of AgNPs led to more production of ROS and such behaviour caused the blockage of electron transfer that induced the oxidative stress (Zou et al., 2016). It was in support of our findings, as shown in *Figure 3* that more the DPPH activity at the maximum NPs concentration. A similar report was described by García-López et al. (2018), in the case of ZnNPs, increased DPPH activity was recorded at high concentrations in *Capsicum annuuam*. Proline, as a multifunctional amino acid triggered the plant growth through signalling mechanism, upregulated and accumulated in a large amount under stressed conditions and optimal under normal growth settings (Yang et al., 2009). Our results demonstrated that a high level of proline was observed in T5 while lower at T3 than T1 that is associated with the above findings and presented in *Figure 4*. Our results indicated healthy and progressive plants growth under an ideal range of NPs (T3) by minimizing proline contents less than control because plants enhance the endogenous proline level when suffered from more stress (Szabados and Savoure, 2010).

Furthermore, we have observed that changes in morphology and accumulation of secondary metabolites with greater efficacy under high ranges of AgNPs resulted in oxidative stress in *P. glaucum* (L.). More ROS lead to more antioxidant production, which was previously reported by Sewelam et al. (2016) as ZnNPs applied to plants in higher concentrations. Our results exhibited increased SOD and POD activities at higher AgNPs ranges than T1. This reflects the development of a well-defined antioxidant defensive mechanism to cope with stress (Gill and Tuteja, 2010). However, the optimum range of NPs (T3) showed less SOD and POD activity and in plantlets instead of control which indicated a small amount of ROS production by decreasing cell damage risk due to NPs and enhanced the plant growth. According to present research work, this optimal concentration of NPs could be used under stress condition for the inhibition of ROS production. Our findings are associated with Parry et al. (1994), who reported more production of antioxidants under stress condition which mitigated the biosynthesis of the enzymes that produce ROS, and provides tolerance to plants for their better survival. AgNPs at 75 mg/L, have increased the SOD and POD activities in tomato plants (Parry et al., 1994) and this has reaffirmed our present findings.

In another investigation, AgNPs at higher ratio decreased the CAT activity than control in mustard seedlings, but comparatively less reduction was observed (Vishwakarma et al., 2017). However, in the present study higher CAT activity was observed at T3 while significant reduction recorded at T5 as presented in *Figure 5* which might be due to interactions of silver nanoparticles with proteins found in lipid bilayer and cytosol; thereby changing the proteins configuration resulting destruction of antioxidant defensive systems (McShan et al., 2014). Our findings are not in line with Krishnaraj et al. (2012) who have described less CAT activity in *Bacopa monnieri* under suitable concentrations of AgNPs. Variations in responses by different plant species have been reported by researchers whereas, the enhanced activity of CAT indicating that it plays important role to scavenge the ROS and decreases the ROS production with greater efficacy (Hayashi et al., 2013; Sneha et al., 2014).

Our findings revealed that seedlings under T3 exhibited higher TPC while lower in T5 as compared with T1 however these results are different from the previous researchers (Zaka et al., 2016) who have described increased TPC in *Eruca sativa* under stressed conditions along with AgNPs application. The main reason could be that high NPs ratio causes discrete changes in the proteome and interfere with cell signalling (Saptarshi et al., 2013) while on the other hand, a linear expression was observed in

http://www.aloki.hu ● ISSN 1589 1623 (Print) ● ISSN 1785 0037 (Online)
DOI: http://dx.doi.org/10.15666/aeer/1706_1287712892

TFC. TFC were showing a significant progressive response in all treatments of AgNPs than control, reflecting improved plant growth with reduced toxic effects. In order to assess the TFC, (García-López et al., 2018) examined high TFC contents under high ZnNPs concentrations. Overall, our results are the pioneer for the evaluation of advantageous and phytotoxic effects of AgNPs in *Pennisetum glaucum* by stabilizing the biochemical profile and serve as guidelines for crop producer to use AgNPs instead of fungicides to get high production at low cost. Previously, the antioxidant mechanism of *P. glaucum* under AgNPs application was unknown, but recent findings will provide a particular direction to other researchers to explore genetic and molecular mechanisms for the action of AgNPs in plants.

Conclusions

This study concluded that AgNPs showed different responses to germination, seedlings growth and antioxidant activity under variable concentrations in pearl millet (*P. glaucum* L.*)*. The optimum concentration of AgNPs (T3) significantly increased all the growth parameters and improved the biochemical profile as compared to other treatments. Seedlings exposed to higher doses of AgNPs showed a reduction in growth and more toxicity. Desirable secondary metabolites may be produced in plants by inducing the changes in physiological and biochemical processes with the help of nanoparticles. High doses of AgNPs seemed like a stressor and caused significant reduction in biomass. It is confirmed that higher doses of NPs are toxic to plants, even in stressed conditions (salt, drought, heat, etc.). Moreover, AgNPs at suitable concentrations can be used as a fertilizer for better crop production and fungicides to produce safe food. Shortly, this preliminary study warrants a comprehensive work to understand the toxicity of NPs at a genetic level and molecular mechanisms against undesirable molecules (free radicals) for better crop production under different environmental conditions.

Acknowledgements. Imran Khan's thanks, to Loving Parents and Brothers for their prayers and guidance, to Associate Professor Dr Muhammad Arshad for his expert advice throughout this challenging research project. This research was funded by the Modern Agro-industry Technology Research System (CARS-34) and the Sichuan Province Breeding Research grant (2016NYZ0039) and Modern Agricultural Industry System Sichuan Forage Innovation Team.

Author contributions. I.K. generated the data. All authors analysed, examined, and evaluated the data. The manuscript was written by I.K., M.A.R., S.A.A., and M.H.B.K. Statistical analysis was done by I.K. and N.I. R. New art work was completed by I.K., T.A.M. and M.N. Review was done by H.L. and N.I.R. X.Z. helped in the final revision and editing.

Conflict of interests. The authors declare that there is no conflict of interests.

REFERENCES

[1] Abbasi, B. H., Khan, M. A., Mahmood, T., Ahmad, M., Chaudhary, M. F., Khan, M. A. (2010): Shoot regeneration and free-radical scavenging activity in Silybum marianum L. – Plant Cell, Tissue and Organ Culture (PCTOC) 101: 371-376.

[2] Aebi, H. (1984): Catalase *in Vitro*. – In: Slater, T. F. (ed.) Methods in Enzymology. Vol. 105. Elsevier, New York, pp. 121-126.

http://www.aloki.hu ● ISSN 1589 1623 (Print) ● ISSN 1785 0037 (Online)
DOI: http://dx.doi.org/10.15666/aeer/1706_1287712892

[3] Alberts, B., Johnson, A., Lewis, J., Raff, M., Roberts, K., Walter, P. (2002): The shape and Structure of Proteins. – In: Alberts, B. et al. (eds.) Molecular Biology of the Cell. 4th Ed. Garland Science, New York.
[4] Austin, C. A., Hinkley, G. K. (2016): Distribution and accumulation of 10 nm silver nanoparticles in maternal tissues and visceral yolk sac of pregnant mice, and a potential effect on embryo growth. – Nanotoxicology 10: 654-661.
[5] Basavaraj, G., Rao, P. P., Bhagavatula, S., Ahmed, W. (2010): Availability and utilization of pearl millet in India. – SAT eJournal 8: 1-6.
[6] Bates, L. S., Waldren, R. P., Teare, I. (1973): Rapid determination of free proline for water-stress studies. – Plant and Soil 39: 205-207.
[7] Berahmand, A. A., Panahi, A. G., Sahabi, H., Feizi, H., Moghaddam, P. R., Shahtahmassebi, N., Fotovat, A., Karimpour, H., Gallehgir, O. (2012): Effects silver nanoparticles and magnetic field on growth of fodder maize (Zea mays L.). – Biological Trace Element Research 149: 419-424.
[8] Chance, B., Maehly, A. (1955): Assay of Catalases and Peroxidases. – In: Glick, D. (ed.) Methods of Biochemical Analysis. Vol. 1. Interscience Publishers, Inc., New York.
[9] Chaudhuri, S. K., Malodia, L. (2017): Biosynthesis of zinc oxide nanoparticles using leaf extract of Calotropis gigantea: characterization and its evaluation on tree seedling growth in nursery stage. – Applied Nanoscience 7: 501-512.
[10] El-Kereti, M, A., El-feky, S. A., Khater, M. S., Osman, Y. A., El-sherbini, E. S. A. (2013): ZnO nano fertilizer and He Ne laser irradiation for promoting growth and yield of sweet basil plant. – Recent Patents on Food, Nutrition & Agriculture 5: 169-181.
[11] García-López, J., Zavala-García, F., Olivares-Sáenz, E., Lira-Saldívar, R., Díaz Barriga-Castro, E., Ruiz-Torres, N., Ramos-Cortez, E., Vázquez-Alvarado, R., Niño-Medina, G. (2018): Zinc oxide nanoparticles boosts phenolic compounds and antioxidant activity of Capsicum annuum L. during germination. – Agronomy 8: 215.
[12] Gill, S. S., Tuteja, N. (2010): Reactive oxygen species and antioxidant machinery in abiotic stress tolerance in crop plants. – Plant physiology and biochemistry 48: 909-930.
[13] Hakeem, K. R. (2015): Crop Production and Global Environmental Issues. – Springer, Switzerland.
[14] Hayashi, Y., Miclaus, T., Scavenius, C., Kwiatkowska, K., Sobota, A., Engelmann, P., Scott-Fordsmand, J. J., Enghild, J. J., Sutherland, D. S. (2013): Species differences take shape at nanoparticles: protein corona made of the native repertoire assists cellular interaction. – Environmental Science & Technology 47: 14367-14375.
[15] Hazra, G., Das, T. (2014): A review on controlled release advanced glassy fertilizer. – Global J. Sci. Front. Res 14: 33-43.
[16] Hussain, M., Raja, N. I., Iqbal, M., Sabir, S., Yasmeen, F. (2017): *In vitro* seed germination and biochemical profiling of Artemisia absinthium exposed to various metallic nanoparticles. – 3 Biotech 7: 101.
[17] Hussain, M., Raja, N. I., Naz, F., Iqbal, M., Aslam, S. (2018): Green synthesis and characterisation of silver nanoparticles and their effects on antimicrobial efficacy and biochemical profiling in Citrus reticulata. – IET Nanobiotechnology 12: 514-519.
[18] Karimi, N., Minaei, S., Almassi, M., Shahverdi, A. (2012): Application of silver nano-particles for protection of seeds in different soils. – African Journal of Agricultural Research 7: 1863-1869.
[19] Khan, I., Raza, M. A., Khalid, M. H. B., Awan, S. A., Raja, N. I., Zhang, X., Huang, L. (2019): Physiological and biochemical responses of pearl millet (Pennisetum glaucum L.) seedlings exposed to silver nitrate (AgNO3) and silver nanoparticles (AgNPs). – International Journal of Environmental Research and Public Health 16(13): 2261.
[20] Klapheck, S., Zimmer, I., Cosse, H. (1990): Scavenging of hydrogen peroxide in the endosperm of Ricinus communis by ascorbate peroxidase. – Plant and Cell Physiology 31: 1005-1013.

http://www.aloki.hu ● ISSN 1589 1623 (Print) ● ISSN 1785 0037 (Online)
DOI: http://dx.doi.org/10.15666/aeer/1706_1287712892

[21] Krishnaraj, C., Jagan, E., Ramachandran, R., Abirami, S., Mohan, N., Kalaichelvan, P. (2012): Effect of biologically synthesized silver nanoparticles on Bacopa monnieri (Linn.) Wettst. plant growth metabolism. – Process Biochemistry 47: 651-658.
[22] Kumari, M., Khan, S. S., Pakrashi, S., Mukherjee, A., Chandrasekaran, N. (2011): Cytogenetic and genotoxic effects of zinc oxide nanoparticles on root cells of Allium cepa. – Journal of Hazardous Materials 190: 613-621.
[23] Lee, W. M., An, Y. J., Yoon, H., Kweon, H. S. (2008): Toxicity and bioavailability of copper nanoparticles to the terrestrial plants mung bean (Phaseolus radiatus) and wheat (Triticum aestivum): plant agar test for water-insoluble nanoparticles. – Environmental Toxicology and Chemistry 27: 1915-1921.
[24] Lopez-Contreras, J. J., Zavala-Garcia, F., Urias-Orona, V., Martinez-Avila, G. C. G., Rojas, R., Guillermo, N. M. (2015): Chromatic, phenolic and antioxidant properties of Sorghum bicolor genotypes. – Notulae Botanicae Horti Agrobotanici Cluj-Napoca 43: 366-370.
[25] Majdalawieh, A., Kanan, M. C., El-Kadri, O., Kanan, S. M. (2014): Recent advances in gold and silver nanoparticles: synthesis and applications. – Journal of Nanoscience and Nanotechnology 14: 4757-4780.
[26] McShan, D., Ray, P. C., Yu, H. (2014): Molecular toxicity mechanism of nanosilver. – Journal of Food and Drug Analysis 22: 116-127.
[27] Mirzajani, F., Askari, H., Hamzelou, S., Farzaneh, M., Ghassempour, A. (2013) Effect of silver nanoparticles on Oryza sativa L. and its rhizosphere bacteria. – Ecotoxicology and Environmental Safety 88: 48-54.
[28] Mittal, R., Mittal, C. G. (2013): Impact of population explosion on environment. – The Nat. J. 1: 1-5.
[29] Mohamed, A. K. S., Qayyum, M. F., Abdel-Hadi, A. M., Rehman, R. A., Ali, S., Rizwan, M. (2017) Interactive effect of salinity and silver nanoparticles on photosynthetic and biochemical parameters of wheat. – Archives of Agronomy and Soil Science 63: 1736-1747.
[30] Okarter, N., Liu, R. H. (2010): Health benefits of whole grain phytochemicals. – Critical Reviews in Food Science and Nutrition 50: 193-208.
[31] Parry, A. D., Tiller, S. A., Edwards, R. (1994): The effects of heavy metals and root immersion on isoflavonoid metabolism in alfalfa (Medicago sativa L.). – Plant Physiology 106: 195-202.
[32] Parveen, A., Rao, S. (2015): Effect of nanosilver on seed germination and seedling growth in Pennisetum glaucum. – Journal of Cluster Science 26: 693-701.
[33] Patra, S., Mishra, P., Mahapatra, S., Mithun, S. (2016): Modelling impacts of chemical fertilizer on agricultural production: a case study on Hooghly district, West Bengal, India. – Modeling Earth Systems and Environment 2: 1-11.
[34] Rafi, Z. N., Ramezanian, A. (2013): Vase life of cut rose cultivars 'Avalanche' and 'Fiesta' as affected by Nano-Silver and S-carvone treatments. – South African Journal of Botany 86: 68-72.
[35] Saptarshi, S. R., Duschl, A., Lopata, A. L. (2013): Interaction of nanoparticles with proteins: relation to bio-reactivity of the nanoparticle. – Journal of Nanobiotechnology 11: 26.
[36] Sewelam, N., Kazan, K., Schenk, P. M. (2016): Global plant stress signaling: reactive oxygen species at the cross-road. – Frontiers in Plant Science 7: 187.
[37] Sneha, S., Rishi, A., Chandra, S. (2014): Effect of short term salt stress on chlorophyll content, protein and activities of catalase and ascorbate peroxidase enzymes in pearl millet. – Am. J. Plant Physiol 9: 32-37.
[38] Szabados, L., Savoure, A. (2010): Proline: a multifunctional amino acid. – Trends in Plant Science 15: 89-97.
[39] Thakkar, K. N., Mhatre, S. S., Parikh, R. Y. (2010): Biological synthesis of metallic nanoparticles. – Nanomedicine: Nanotechnology, Biology and Medicine 6: 257-262.

http://www.aloki.hu ● ISSN 1589 1623 (Print) ● ISSN 1785 0037 (Online)
DOI: http://dx.doi.org/10.15666/aeer/1706_1287712892

[40] Tripathi, D. K., Mishra, R. K. (2017) Nitric oxide ameliorates zinc oxide nanoparticles phytotoxicity in wheat seedlings: implication of the ascorbate-glutathione cycle. – Frontiers in Plant Science 8: 1.
[41] Ullah, N., Haq, I. U., Safdar, N., Mirza, B. (2015): Physiological and biochemical mechanisms of allelopathy mediated by the allelochemical extracts of Phytolacca latbenia (Moq.) H. Walter. – Toxicology and Industrial Health 31: 931-937.
[42] Ushahra, J., Malik, C. (2013): Putrescine and ascorbic acid mediated enhancement in growth and antioxidant status of Eruca sativa varieties. – CIB Tech J Biotechnol 2: 53-64.
[43] van Dongen, J. T., Ammerlaan, A. M., Wouterlood, M., van Aelst, A. C., Borstlap, A. C. (2003): Structure of the developing pea seed coat and the post-phloem transport pathway of nutrients. – Annals of Botany 91: 729-737.
[44] Vejan, P., Abdullah, R., Khadiran, T., Ismail, S., Nasrulhaq, Boyce, A. (2016): Role of plant growth promoting rhizobacteria in agricultural sustainability—a review. – Molecules 21: 573.
[45] Velioglu, Y., Mazza, G., Gao, L., Oomah, B. (1998): Antioxidant activity and total phenolics in selected fruits, vegetables, and grain products. – Journal of Agricultural and Food Chemistry 46: 4113-4117.
[46] Vishwakarma, K., Upadhyay, N. (2017) Abscisic acid signaling and abiotic stress tolerance in plants: a review on current knowledge and future prospects. – Frontiers in Plant Science 8: 161.
[47] Wang, C., Yan, H., Li, J., Zhou, S., Liu, T., Zhang, X., Huang, L. (2018): Genome survey sequencing of purple elephant grass (Pennisetum purpureum Schum 'Zise') and identification of its SSR markers. – Molecular Breeding 38(7): 94.
[48] Yang, S. L., Lan, S. S., Gong, M. (2009): Hydrogen peroxide-induced proline and metabolic pathway of its accumulation in maize seedlings. – Journal of Plant Physiology 166: 1694-1699.
[49] Yasur, J., Rani, P. U. (2013): Environmental effects of nanosilver: impact on castor seed germination, seedling growth, and plant physiology. – Environmental Science and Pollution Research 20: 8636-8648.
[50] Zaka, M., Abbasi, B. H., Rahman, L. U., Shah, A., Zia, M. (2016): Synthesis and characterisation of metal nanoparticles and their effects on seed germination and seedling growth in commercially important Eruca sativa. – IET Nanobiotechnology 10: 134-140.
[51] Zhou, S., Wang, C., Frazier, T. P., Yan, H., Chen, P., Chen, Z., Yan, Y. (2018): The first Illumina-based de novo transcriptome analysis and molecular marker development in Napier grass (Pennisetum purpureum). – Molecular Breeding 38(7): 95.
[52] Zhou, S., Chen, J., Lai, Y., Yin, G., Chen, P., Pennerman, K. K., Wang, C. (2019a): Integrative analysis of metabolome and transcriptome reveals anthocyanins biosynthesis regulation in grass species Pennisetum purpureum. – Industrial Crops and Products 138: 111470.
[53] Zhou, S., Wang, C., Yin, G., Zhang, Y., Shen, X., Pennerman, K. K., Ren, S. (2019b): Phylogenetics and diversity analysis of Pennisetum species using Hemarthria EST-SSR markers. – Grassland Science 65(1): 13-22.
[54] Zou, X., Li, P., Huang, Q., Zhang, H. (2016): The different response mechanisms of Wolffia globosa: light-induced silver nanoparticle toxicity. – Aquatic Toxicology 176: 97-105.

http://www.aloki.hu ● ISSN 1589 1623 (Print) ● ISSN 1785 0037 (Online)
DOI: http://dx.doi.org/10.15666/aeer/1706_1287712892

OXIDATIVE STRESS AND GENETIC DIFFERENTIATION IN EXPERIMENTAL TILAPIA FISH EXPOSED TO HEAVY METALS IN A RESERVOIR NEAR A MUNICIPAL LANDFILL

KAMOLLERD, C.[1,2] – SENAPHAN, K.[1,2] – TENGJAROENKUL, B.[1,2] – MONKHEANG, P.[1,3] – NEERATANAPHAN, L.[1,3*]

[1]*Research Group on Toxic Substances in Livestock and Aquatic Animals, Khon Kaen University, Khon Kaen, Thailand*

[2]*Faculty of Veterinary Medicine, Khon Kaen University, Khon Kaen, Thailand*

[3]*Faculty of Science, Khon Kaen University, Khon Kaen, Thailand*

**Corresponding author*
e-mail: hlamya@kku.ac.th

(Received 18th May 2019; accepted 28th Aug 2019)

Abstract. This study aimed to investigate the concentrations of Cd, Cr and Pb in the water and sediment, and to compare the concentrations of these metals in fish muscles, the levels of plasma oxidative stress biomarkers (malondialdehyde and protein carbonyl) and the genetic differentiation between experimental tilapia fish from the contaminated reservoir near municipal landfill and the reference area after chronic exposure to the metals. The concentrations of Cd, Cr and Pb in the water exceeded the Thailand water quality standard, whereas the concentration of Cd in the sediment exceeded the Thailand soil quality standard. The concentrations of these metals in fish muscles were below Thailand food quality standard. In comparison to the reference fish, the fish in the landfill reservoir revealed a significant increase in malondialdehyde and protein carbonyl ($p < 0.05$). The dendrogram results demonstrated values of genetic similarity for the fish from the reference and the landfill areas at 0.84-0.94 and 0.65-0.97, respectively, implying that the values of genetic differentiation as a consequence of genotoxicity of the fish from the landfill were greater than those of the fish from the reference area. The results indicate that chronic heavy metal exposure could induce oxidative stress and genotoxicity of tilapia fish in the reservoir near municipal landfill.

Keywords: *oxidative stress, genetic differentiation, heavy metal, tilapia fish, municipal landfill*

Introduction

In the past few decades, industrial, commercial and urban communities have continuously and rapidly grown in Khon Kaen Province, Thailand (PCD, 2014). This growth has inevitably been accompanied by rapid increases in municipal and industrial solid wastes. Due to poor management of landfill waste, toxic leachate that can spread heavy metals and other toxic substances around the landfill environment is present (Papadimitriou and Loumbourdis, 2003). The major heavy metals found in the Khon Kaen municipal landfill were cadmium (Cd), chromium (Cr), lead (Pb) and arsenic (As) (Sarun, 2004; Sriuttha et al., 2017; Intamat et al., 2017). Sriuttha et al. (2017) demonstrated that concentrations of Cd, Cr and Pb in the water and sediment near the municipal landfill were as not detected, 0.016 ± 0.009, 0.009 ± 0.0006 mg/L and 0.47 ± 0.23, 19.91 ± 0.96, 5.40 ± 0.13 mg/kg, respectively, while Intamat et al. (2017) determined that As values in the water, sediment and tilapia fish in the landfill environment were 0.006 ± 0.002, 1.08 ± 0.64 and 0.16 ± 0.16 mg/kg, respectively. From previous reports, these toxic metals can always spread from hazardous waste such as

http://www.aloki.hu ● ISSN 1589 1623 (Print) ● ISSN 1785 0037 (Online)
DOI: http://dx.doi.org/10.15666/aeer/1706_1289312907

batteries, light bulbs, chemical containers and lubricants, into leachate and surrounding reservoirs (Oost et al., 2003; ATSDR, 2007), and can be taken up and accumulate in aquatic organisms, including fish (Luoma and Rainbow, 2008). Intamat et al. (2017) revealed that the As concentrations in *Oreochromis niloticus*, *Barbonymus gonionotus, Rasbora tornieri* and *Anabas testudineus* exceeded Thailand food quality standards. Sriuttha et al. (2017) found that the Cd concentrations in *O. niloticus* and *B. gonionotus* exceeded the limit of International standard for fish, additionally the Cr concentration in *R. tornieri* and *A. testudineus* exceeded the International standard, and the Pb concentration in all four fish species exceeded the International standards. Fish that inhabit heavy metal-contaminated reservoirs generally take in toxic metals by absorbing metals through their skin, gills and alimentary tracts (Kamunde et al., 2002; Papadimitriou and Loumbourdis, 2003; Robinson et al., 2003) and can demonstrate biomagnification, and these contaminated fish can result in health risks to consumers (Godt et al., 2006).

Several research studies have demonstrated that heavy metals can cause an imbalance between the production and reduction of free radical species, i.e., causing oxidative stress in fish (Livingstone, 2003; Sevcikova et al., 2011). The free radicals can attack protein and lipid molecules to induce oxidative stress products as well as cause negative consequences such as increases in malondialdehyde and protein carbonyl as well as fragmentation of deoxyribonucleic acid (DNA) (Castano and Becerril, 2004; Talas et al., 2008; Velma and Tchounwou, 2013; Vilela et al., 2018). Recently, the amount and diversified species of oxidative stress products have been considered biomarkers for environmental monitoring indices in terms of both status and situation of aquatic ecosystems (Skorbiłowicz, 2009; Burlibasa and Gavrila, 2011; Webb, 2011; Authman et al., 2015). The consequences of oxidative stress from toxic metals to aquatic animals have been reported, but information on their effects on fish with either acute or chronic exposure time in landfill ecosystems is limited. Therefore, the objectives of this study were to investigate heavy metal accumulation in a landfill reservoir, and to compare oxidative stress biomarkers as well as genetic differentiation between the experimental tilapia fish (*Oreochromis niloticus*) from the contaminated reservoir near municipal landfill and the reference area after chronic exposure to the metals.

Materials and methods

Study site

The study site was a reservoir located approximately 100 meters from the municipal landfill, Maung District, Khon Kaen Province, Thailand at latitude 16°35’41.30”N and longitude 102°48’12.11”E (*Fig. 1*). Geographic coordinate is UTM 48Q N 1,835,718 E 266,085 at a height of 200 m from the sea level.

Fish and experimental design

Juvenile tilapia fish at an average weight of 10.3 grams were reared at a density of 20 fish/m^2 in 2 × 2 m floating cages in the reservoir that received metal-contaminated leachate from the Khon Kaen municipal landfill. The experimental fish were randomly allocated into 2 treatments (reference and landfill) with 3 replications of each treatment, and they were fed a commercial pellet diet (Charoen Pokphan Co., Thailand) at 10%

http://www.aloki.hu ● ISSN 1589 1623 (Print) ● ISSN 1785 0037 (Online)
DOI: http://dx.doi.org/10.15666/aeer/1706_1289312907

w/w, 3 times/day for 4 months during April-July 2018 simulating the length of the tilapia production as in general practice. At the end of the experiment, fish muscles were measured for heavy metal accumulation, blood was collected from the caudal vessels for the plasma oxidative stress test, and the gills and livers were excised for the DNA study and genetic differentiation analysis. The control fish were collected from the Khon Kaen Inland Fisheries Research and Development Center, Thailand. Aquaculture in the Department of Fisheries is non-affected heavy metal contamination which has control of contamination for human food. Therefore, the control fish of this study is expected to not receive heavy metals.

Figure 1. *Overview of the municipal landfill and the location of the contaminated reservoir*

Water quality parameters

Temperature, dissolved oxygen, pH, total dissolved solids and electro-conductivity were measured at the sampling site using digital mobile meters. Total ammonia nitrogen was measured using the titration method (APHA, 2005) (*Table 1*).

Table 1. *Methods used for analyses of water quality parameters*

Water quality parameters	Analysis methods
Temperature	Thermometer
Dissolved oxygen	DO meter, model 966, Mettler Toledo
pH	pH meter, model EcoScan pH 5, Eutech
Total dissolved solid	Total dissolved solid, model CH-8603, Mettler Toledo
Electro-conductivity	EC meter, model CH-8603, Mettler Toledo
Total ammonia nitrogen	Titration method

Heavy metal measurements

The water samples were acidified in the field by adding concentrated nitric acid until the pH was less than 2, the sediment samples were wrapped in aluminum foil to prevent oxidation, and the live fish were put into oxygenated plastic bags. All collected samples

http://www.aloki.hu ● ISSN 1589 1623 (Print) ● ISSN 1785 0037 (Online)
DOI: http://dx.doi.org/10.15666/aeer/1706_1289312907

were digested following EPA method 6010, and the Cd, Cr and Pb concentrations were analyzed using inductively coupled plasma optical emission spectrometry (ICP-OES) (Chand and Prasad, 2013; Neeratanaphan et al., 2017). The detection limits of each analyzed element were as follows: Cd and Cr: 0.001 mg/kg and Pb: 0.005 mg/kg. The ICP-OES wavelengths for the Cd, Cr and Pb analyses were set to 188.979, 226.502 and 267.716 nm, respectively.

The analysis of blanks and quality control standards was performed after every 10th sample. The concentrations of the elements in the procedural blanks were typically < 5% of the mean analyzed concentrations for all the heavy metals. Replicate analyses and standard reference materials were used to guarantee the precision and accuracy of the measurements for all elements. The results were found not to deviate by more than 2% of the certified values, indicating the accuracy of the analysis (APHA, 2005). The heavy metal recovery values were calculated by acceptance criteria in the range of 85-115% (USEPA, 2000). The results were 90-100% of the acceptable values and considered accurate.

Oxidative stress biomarkers

After being reared for 4 months in the landfill reservoir, the blood plasma of the experimental fish were collected at the reservoir site to determine malondialdehyde (MDA) by measuring thiobarbituric acid reactive substances (Luangaram et al., 2007; Nakmareong et al., 2011) and to measure protein carbonyl (PC) by its reaction with 2,4-dinitrophenylhydrazine (Reznick and Packer, 1994; Nakmareong et al., 2011). For the genotoxicity study, DNA from the livers and gills of the fish were extracted and amplified by 46 inter-simple sequence repeats (ISSR) primers (*Table 2*) in a PCR thermal cycler (Flex Cycler^2, Analytikjena) (Tengjaroenkul et al., 2018). Each DNA band was evaluated and recorded as the following diallelic characters as present = 1 and absent = 0. All of the bands were imported to construct dendrogram by the NTSYSpc 2.1 program (Rohlf, 2009) for analysis of genetic differentiation as a consequence of genotoxicity.

Statistical analyses

Statistical analyses of the oxidative stress biomarkers in experimental and control fish were analysed using the Mann-Whitney U-test. The genetic differentiation was analyzed to construct dendrogram by the NTSYSpc 2.1 program (Rohlf, 2009). All of the statistical tests were conducted at a 95% confidence level.

Results and discussion

Water quality parameters

The water quality parameters of the reference and the landfill reservoir water samples after 4 months of the experiment are shown in *Table 3*.

Water quality describes conditions of water medium and its related suitability to sustainably support aquatic ecosystems as well as public health. Low water quality could influence the stress, metabolism, health, reproduction, genetics and biodiversity of fish (Jezierka and Witeska, 2001; Buet et al., 2006; Da Rocha et al., 2009). In this study, the water quality parameters from both the reference and the landfill reservoirs were within the Thailand standard concentration limits for surface water sources (Ip et

http://www.aloki.hu ● ISSN 1589 1623 (Print) ● ISSN 1785 0037 (Online)
DOI: http://dx.doi.org/10.15666/aeer/1706_1289312907

al., 2001; PCD, 2014); therefore, plasma oxidative stress and genotoxicity biomarkers in long-term experimental tilapia tended to have fewer effects from the water quality parameters in both areas.

Heavy metal concentrations

The heavy metal concentrations in the water, sediment and fish muscles from the reservoir near the municipal landfill are shown in *Table 4*.

Table 2. *The 24 successful primer sequences for ISSR fingerprinting*

Primer	Nucleotide sequences	Total bands	Monomorphic band	Polymorphic band
P1	AGAGAGAGAGAGAGAGG	127	7	10
P3	CTCTCTCTCTCTCTCTGC	100	3	12
P4	CACACACACACAAC	54	4	5
P5	CACACACACACAGT	101	3	11
P6	CACACACACACAAG	77	4	9
P7	CACACACACACAGG	127	7	11
P8	GAGAGAGAGAGAGG	102	7	6
P10	GAGAGAGAGAGACC	126	3	17
P11	GTGTGTGTGTGTCC	51	4	3
P12	CACCACCACGC	119	6	9
P13	GAGGAGGAGGC	117	7	8
P14	CTCCTCCTCGC	111	3	14
P15	GTGGTGGTGGC	116	8	8
P16	ACTGACTGACTGACTG	113	8	7
P17	GACAGACAGACAGACA	81	2	13
I1	CTCTCTCTCTCTCTCTTG	99	2	15
I2	AGAGAGAGAGAGAGCTGCT	127	7	9
A4	AGAGAGAGAGAGAGAA	118	6	14
A5	AGAGAGAGAGAGAGAGC	142	10	7
A6	AGAGAGAGAGAGAGAGT	114	4	18
A11	AGAGAGAGAGAGAGAAA	108	3	13
A12	AGAGAGAGAGAGAGAAC	126	8	9
A13	AGAGAGAGAGAGAGAAG	118	9	7
A14	AGAGAGAGAGAGAGAAT	88	3	10
	Total	2,562	128	245

Table 3. *Water quality parameters (temperature, dissolved oxygen, pH, total dissolved solids, electro-conductivity and total ammonia nitrogen) of the reference and the landfill reservoir*

Samples	Parameters					
	Temperature (°C)	DO (mg/L)	pH	TDS (mg/L)	EC ($\mu Sm^{-1}/s$)	NH_3-N (mg/L)
Reference reservoir	25.96 ± 0.55	5.31 ± 0.76	7.02 ± 0.02	0.44 ± 0.03	304.33 ± 7.37	0.72 ± 0.04
Landfill reservoir	26.18 ± 0.53	4.79 ± 0.44	6.72 ± 0.07	0.57 ± 0.03	452.67 ± 17.51	0.94 ± 0.04

DO = dissolved oxygen; TDS = total dissolved solids; EC = electro-conductivity; NH_3-N = total ammonia nitrogen; n (numbers of measured individuals) = 3

http://www.aloki.hu ● ISSN 1589 1623 (Print) ● ISSN 1785 0037 (Online)
DOI: http://dx.doi.org/10.15666/aeer/1706_1289312907

Table 4. *Heavy metal concentrations in the water, sediment and fish muscles from the landfill reservoir (mean and standard deviation; n = 9)*

Samples	Individual number	Cd	Cr	Pb
Water (mg/L)	9	0.66 ± 0.32	16.73 ± 1.32	17.85 ± 4.28
Standard (mg/L)		0.005[a]	0.05[a]	0.05[a]
Sediment (mg/kg)	9	2.60 ± 2.07	33.82 ± 7.79	16.61 ± 9.47
Standard (mg/kg)		1[b]	100[b]	100[b]
Fish muscle (mg/kg)	9	0.02 ± 0.01	1.22 ± 0.29	0.10 ± 0.02
Standard (mg/kg)		0.5[c]	2[c]	0.5[c]

[a]Water quality standards for surface water sources, Pollution Control Department, Ministry of Natural Resources and Environment, Thailand (PCD, 1994)
[b]Soil quality standard, Pollution Control Department, Ministry of Natural Resources and Environment, Thailand (PCD, 2004)
[c]Thailand food quality standards, Ministry of Public Health, Thailand (Ministry of Public Health, 2003)

The concentrations of Cd, Cr and Pb in the water exceeded the Thailand water quality standards for surface water sources (PCD, 1994), whereas the concentration of Cd exceeded the Thailand soil quality standard (PCD, 2014). The concentrations of the metals in the fish muscles were below those of Thailand food quality standards (Ministry of Public Health, 2003). Waste segregation and management in the Khon Kaen municipal landfill were not appropriate, resulting in the disposal of municipal waste and hazardous waste, which can be potential sources of heavy metal exposure in fish (Sarun, 2004). As in other polluted areas, heavy metal contamination in the Khon Kaen landfill leachate can lead to metal accumulation in the soil and sediment of the reservoir, and can then be absorbed and accumulated into aquatic plants and animals (Luoma and Rainbow, 2008). These bioaccumulation processes were identified by the studies of Promsid (2014): and Intamat et al. (2017): who found heavy metal accumulation in plants and animals in the reservoir, especially emerged plants (*Limnocharis flava*, *Diplasum esculentum* and *Nymphea lotus*) and aquatic animals such as *Monopterus albus*, *Clarias batrachus* and *Channa striata*. Intamat et al. (2017) revealed that As in *Oreochromis niloticus*, *Barbonymus gonionotus, Rasbora tornieri* and *Anabas testudineus* exceeded the Thailand food quality standard. Sriuttha et al. (2017) found that the Cd concentration in *O. niloticus* and *B. gonionotus* exceeded the limit in the International standards for fish (FAO, USA), whereas the Cr concentration in *R. tornieri* and *A. testudineus* exceeded the limits in the International standards, and the Pb concentration in four fish species exceeded the limit in the International standards. Furthermore, this study investigated the Cd, Cr and Pb concentrations in the tilapia as the major commercialized fish consumed throughout local communities in Khon Kaen Province. Generally, tilapia fish culture in Thailand of 4 months was the model condition that simulated the practice. As the experimental tilapia fish had a relatively long exposure period of 4 months, they could continuously accumulate heavy metals from water and sediments into their organs (Chen and Liao, 2004; Cumberlidge, 2009; Abdulali et al., 2013; Abdel-mohsien and Mahmoud, 2015). This continuous accumulation in the tilapias occurs probably because they have a large body size and surface area with the contaminated environment. In accordance with several reports, chronic exposure of Cd, Cr and Pb to experimental tilapia fish may lead to stress, metabolic changes, physical damage and hematological, hepatological, and immunological alterations (Mishra and Mohanty, 2008; Paul et al., 2014; Pereira et al.,

http://www.aloki.hu ● ISSN 1589 1623 (Print) ● ISSN 1785 0037 (Online)
DOI: http://dx.doi.org/10.15666/aeer/1706_1289312907

2016). Furthermore, after consumption, a fish that has accumulated heavy metals can do harm to humans in surrounding communities by causing detrimental diseases and disorders related to these metals (Godt et al., 2006; Tiwari et al., 2011). In general, the levels and potential of risk from the accumulated metals in the fish in the landfill reservoir to consumer health depend on several factors, including speciation, dose, time and toxicokinetics of the heavy metals contained in the exposed animals (Abu-Daabes et al., 2013; Wachirawongsakorn and Sangyoka, 2013).

Oxidative stress biomarkers

Malondialdehyde

Levels of plasma MDA in the tilapia fish are shown in *Figure 2*. In comparison with the reference fish, the fish from the reservoir near the Khon Kaen municipal landfill demonstrated a significant increase in plasma MDA ($p < 0.05$).

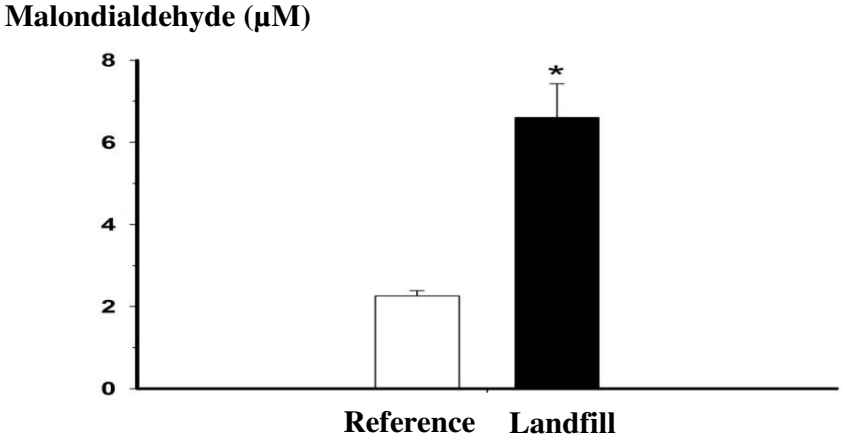

Figure 2. *The levels of plasma malondialdehyde in both treatments of the Nile tilapia fish. Values are expressed as the mean ± SEM of 10 fish. *p < 0.05 compared with the reference fish*

Contaminated landfill leachate as well as reservoir water and sediments usually contain complex mixtures of heavy metals capable of accumulating in aquatic organisms (Luoma and Rainbow, 2008). Heavy metals can induce reactive oxygen and nitrogen species, i.e., causing oxidative stress or free radical overload in aquatic organisms, including fish (Sevcikova et al., 2011). Assessments of oxidative damage in fish can directly reflect metal exposure in an aquatic environment, which could affect the health of the creatures (Livingstone, 2003). Contaminated heavy metals in living fish generally interact with nuclear proteins, lipid molecules and nuclear nucleic acids, resulting increases in MDA and PC and fragmentation of DNA strands (Livingstone, 2003; Sevcikova et al., 2011).

MDA is one of the lipid peroxidation products derived from oxidative attacks on cell membrane phospholipids and circulating lipids, and its increased level directly involves the degree of oxidative damage induced by the contaminants, including heavy metals (Banerjee et al., 1999; Ercal et al., 2001). A measure of MDA content provides the relative consequence of the potential for pollutants to cause oxidative injury (Vlahogianni et al., 2007; Calapoglu et al., 2017). In this study, a significant increase in plasma MDA concentration was found in the tilapia fish, indicating that the presence of heavy metals could cause oxidative stress as well as negative effects on cell homeostasis such as protein

http://www.aloki.hu ● ISSN 1589 1623 (Print) ● ISSN 1785 0037 (Online)
DOI: http://dx.doi.org/10.15666/aeer/1706_1289312907

metabolism, glutathione pathways and mitochondrial functions. Several other reports revealed similar results related to increases MDA in fish, including killifish, mullet, flounder, catfish and stickleback, after exposure to pollutants (Bakanskas et al., 2004; Ferreira et al., 2005; Farombi et al., 2007; Sanchez et al., 2007; Bayir et al., 2011).

Protein carbonyl

The levels of plasma PC in the tilapia fish are shown in *Figure 3*. In comparison with the reference fish, the fish from the reservoir near the landfill area demonstrated a significant increase in plasma PC ($p < 0.05$).

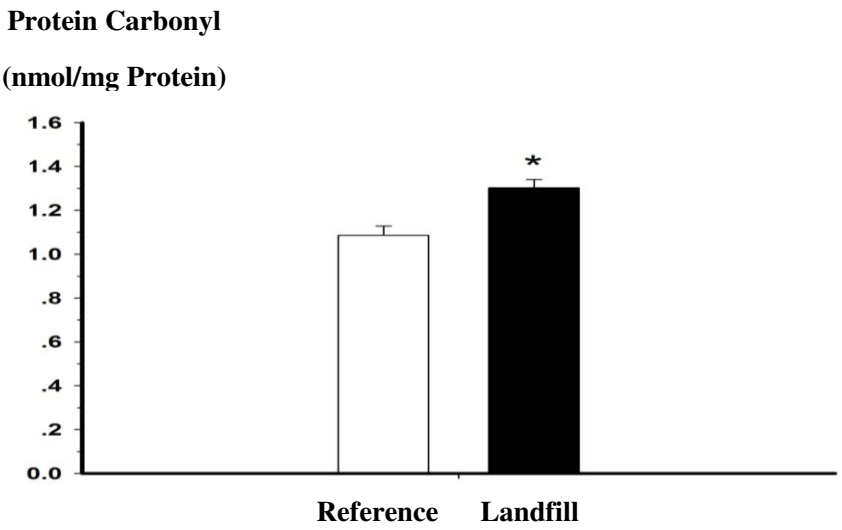

Figure 3. *The levels of plasma protein carbonyl in both groups of the Nile tilapia fish. Values are expressed as the mean ± SEM of 10 fish. * $p < 0.05$ as compared with the reference fish*

PC formation can occur as a result of oxidative stress, and has been shown as a number of tissue lesions and disease issues (Requena et al., 2003). An increase in the number of carbonyl groups correlates well with protein damage caused by oxidative stress; therefore, PC can be a distinctive marker to induce the degradation of enzymes, to change amino acid structures and to alter protein functions (Grune, 2000; Parvez and Raisuddin, 2005; Dalle-Donne et al., 2006; Craig et al., 2007). In accordance with previous reports, the elevated level of PC in the Nile tilapia from the landfill reservoir could suggest that metal pollutants may cause protein damage as a consequence of oxidative stress. Furthermore, the significant increase in oxidative stress biomarkers in tilapia fish may be associated with a low resistance to pollution in this fish. To present, responses to oxidative stress in fish have been recorded differently according to habitat and feeding behavior of fish as well as concentrations and types of the pollutants (Giulio et al., 1993; Wilhelm, 1996; Hebert et al., 2008).

DNA

The 24 ISSR primers were successfully applied to generate 2,562 total bands with 375 characteristics, including 128 similar band profiles and 245 different band profiles. The dendrogram separated tilapia fish into two clusters corresponding to their studied areas. The genetic similarity values of the fish in the contaminated reservoir near municipal

http://www.aloki.hu ● ISSN 1589 1623 (Print) ● ISSN 1785 0037 (Online)
DOI: http://dx.doi.org/10.15666/aeer/1706_1289312907

landfill (Fish No. 2.1, 2.2, 2.3, 2.4 and 2.5) ranged from 0.65 to 0.97, and the values for the fish from the reference area (Fish No. 1.1, 1.2, 1.3, 1.4 and 1.5) (*Table 5; Figs. 4–5*) ranged from 0.84 to 0.94.

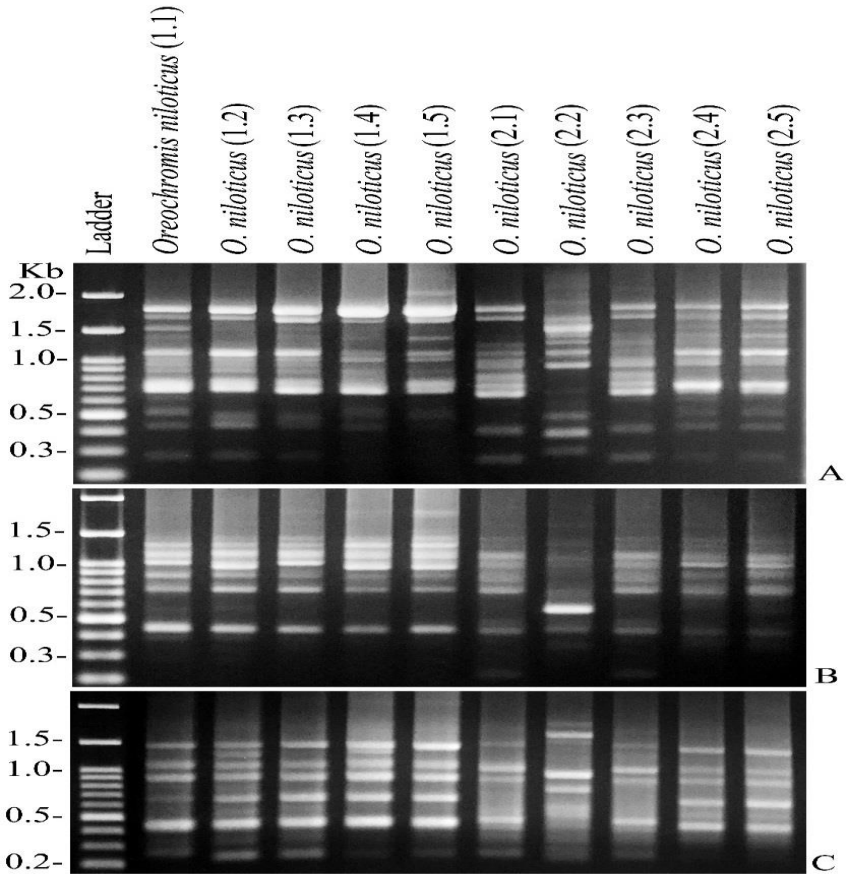

Figure 4. *Examples of ISSR fingerprints from the reference fish (1.1, 1.2, 1.3, 1.4, and 1.5) and the contaminated reservoir near a municipal landfill (2.1, 2.2, 2.3, 2.4, and 2.5) from the specific primers TGACCCCTCC (a), GTAGACGAGC (b) and TGTCTGGGTG (c) showing monomorphic bands*

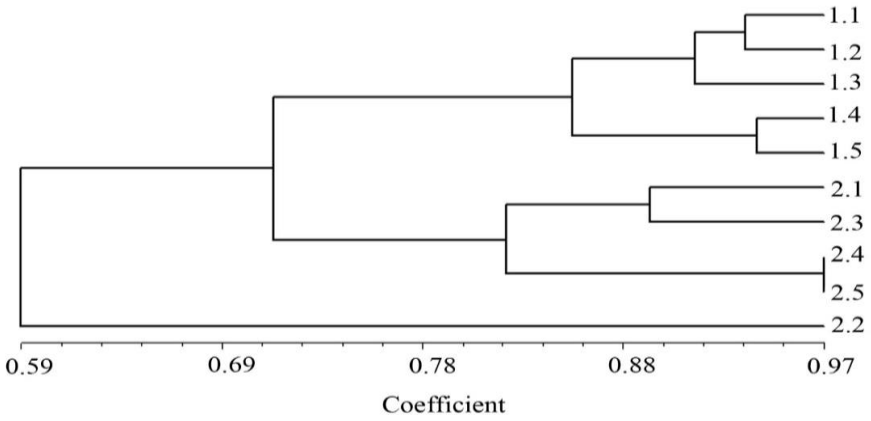

Figure 5. *The dendrogram constructed from 24 ISSR primers by the NTSYSpc 2.1 program showing the genetic relationships of the tilapia fish from the reference area and the contaminated reservoir near a municipal landfill*

http://www.aloki.hu ● ISSN 1589 1623 (Print) ● ISSN 1785 0037 (Online)
DOI: http://dx.doi.org/10.15666/aeer/1706_1289312907

Table 5. *Values of genetic similarity between the tilapia fish from the reference and the contaminated reservoir near municipal landfill using NTSYSpc 2.1 program*

Fish No.	1.1	1.2	1.3	1.4	1.5	2.1	2.2	2.3	2.4	2.5
1.1	1.00									
1.2	0.94	1.00								
1.3	0.92	0.90	1.00							
1.4	0.84	0.86	0.87	1.00						
1.5	0.85	0.84	0.87	0.94	1.00					
2.1	0.72	0.73	0.71	0.68	0.69	1.00				
2.2	0.55	0.57	0.53	0.52	0.52	0.65	1.00			
2.3	0.73	0.73	0.73	0.68	0.69	0.89	0.66	1.00		
2.4	0.73	0.74	0.71	0.67	0.67	0.80	0.65	0.84	1.00	
2.5	0.75	0.75	0.72	0.68	0.68	0.80	0.66	0.84	0.97	1.00

The results from the dendrogram analyses separated the tilapia into two clusters corresponding to their studied areas. The genetic differentiation in tilapia fish revealed a positive correlation with Cd, Cr and Pb concentrations accumulated in the fish body. The genetic differentiation in the fish from the contaminated reservoir near the landfill was greater than that of the fish from the reference area. These findings suggested that the metal accumulations in the landfill fish could affect the genetic toxicity in term of the molecular nucleic acid profile. In contaminated environments, heavy metal exposure could demonstrate DNA damage in fish as single and double strand breakages, alterations in DNA repair processes, oxidation of nucleic bases and DNA-protein crosslinks (Wood et al., 2001; Monserrat et al., 2007; Vilela et al., 2018). When heavy metals enter the cell membrane, they generally induce diversified genotoxicity through several mechanisms. For example, Cd can induce oxidative stress, DNA damage, point mutations, mutagenesis, deletions, ploidy changes, substitutions and oxidization in gene bases (Waalkes, 2003; Castano and Becerril, 2004; Suhartono et al., 2013). Cr exposure demonstrated micronucleus appearance, Cr-DNA adducts, DNA strand breakage, protein-Cr-DNA adducts and modification of the DNA nitrogenous base, leading to neoplastic growth in fish (Teles et al., 2005; Wise et al., 2008; Arunachalam et al., 2013; Velma and Tchounwou, 2013). Pb can induce oxidative damage, mitogenesis, alteration in gene transcription, carcinogenic events involved in DNA damage and several other indirect genotoxic changes (Silbergeld, 2003). Furthermore, the loss of DNA structural or functional integrity in exposed organisms can initiate deleterious effects at both the individual and population levels, especially through impaired growth or reproduction (Bolognesi and Hayashi, 2011; Mustafa et al., 2012; Ngamniyom, 2012). Furthermore, experimental tilapia fish could be a potential bioindicator for genotoxicity in aquatic ecosystems. In addition, local communities around the municipal landfill should increase their awareness, and enhance environmental management to reduce the risks to human health from consuming the heavy metals accumulated in the fish from the landfill reservoir.

Conclusion

The concentrations of Cd, Cr and Pb in *O. niloticus* after chronic exposure to heavy metals in a reservoir near municipal landfill for 4 months were below Thailand food

http://www.aloki.hu ● ISSN 1589 1623 (Print) ● ISSN 1785 0037 (Online)
DOI: http://dx.doi.org/10.15666/aeer/1706_1289312907

quality standard for these metals. In comparison to the fish in the reference area, the fish in the landfill area demonstrated a significant increase in MDA and PC with a relatively greater genetic differentiation. The results of the study demonstrate that heavy metals potentially induce oxidative stress and genetic alteration in the tilapia fish in the reservoir near the municipal landfill. Future researches should be comparative study oxidative stress in the other aquatic animals in this area.

Acknowledgements. This research was supported by Khon Kaen University under the Incubation Researcher Project and the Research Group on Toxic Substances in Livestock and Aquatic Animals, Khon Kaen University, Thailand**.**

REFERENCES

[1] Abdel-mohsien, H., Mahmoud, M. (2015): Accumulation of some heavy metals in *Oreochromis niloticus* from the Nile in Egypt: potential hazards to fish and consumers. – Journal of Environmental Protection 6(9): 1003-1013.

[2] Abdulali, T., Shuhaimi-Othman, M., Ahmad, A. K. (2013): Assessment of heavy metals in tilapia fish (*Oreochromis niloticus*) from the Langat River and engineering lake in Bangi, Malaysia, and evaluation of the health risk from tilapia consumption. – Ecotoxicology and Environmental Safety 93: 45-51.

[3] Abu-Daabes, M., Qdais, H. A., Alsyouri, H. (2013): Assessment of heavy metals and organics in municipal solid waste leachates from landfills with different ages in Jordan. – Journal of Environmental Protection 4: 344-352.

[4] Agency for Toxic Substances and Disease Registry (ATSDR) (2007): Toxicological Profile for Lead. – Agency for Toxic Substances and Disease Registry, Washington DC.

[5] American Public Health Association (APHA) (2005): Standard Methods for the Examination of Water and Wastewater. 21st Ed.– American Public Health Association, Washington DC.

[6] Arunachalam, K. D., Annamalai, S. K., KuruvaIn, J. K. (2013): In-vivo evaluation of hexavalent chromium induced DNA damage by alkaline comet assay and oxidative stress in *Catla catla*. – American Journal of Environmental Sciences 9(6): 470-482.

[7] Authman, M. M. N., Zaki, M. S., Khallaf, E. A., Abbas, H. H. (2015): Use of fish as bio-indicator of the effects of heavy metals pollution. – Journal of Aquaculture Research and Development 6: 328.

[8] Bacanskas, L. R., Whitaker, J., Di, Giulio, R. T. (2004): Oxidative stress in two populations of killifish (*Fundulus heteroclitus*) with differing contaminant exposure histories. – Marine Environmental Research 58(2): 597-601.

[9] Banerjee, B. D., Seth, V., Bhattacharya, A., Pasha, S. T., Chakraborty, A. K. (1999): Biochemical effects of some pesticides on lipid peroxidation and free-radical scavengers. – Toxicology Letters 107: 33-47.

[10] Bayir, A., Bayir, M., Sirkecioğlu, A. N., Aras, N. M., Haliloğlu, H. İ., Aksakal, E., Güneş, M., Aras, N. M. (2011): Influence of season on antioxidant defense systems of *Silurus glanis* Linnaeus (Siluridae) and *Barbus capito* Güldenstädt (Cyprinidae). – Fresenius Environmental Bulletin 20(1): 3-11.

[11] Bolognesi, C., Hayashi, M. (2011): Micronucleus assay in aquatic animals. – Mutagenesis 26: 205-213.

[12] Buet, A., Banas, D., Vollaire, Y., Coulet, E., Roche, H. (2006): Biomarker responses in European eel (*Anguilla anguilla*) esposed to persistent organic pollutants. A field study in the Vaccares lagoon (Camargue, France). – Chemosphere 65: 1846-1858.

[13] Burlibasa, L., Gavrila, L. (2011): Amphibians as model organisms for study environmental genotoxicity. – Applied Ecology and Environmental Research 9(1): 1-15.

http://www.aloki.hu ● ISSN 1589 1623 (Print) ● ISSN 1785 0037 (Online)
DOI: http://dx.doi.org/10.15666/aeer/1706_1289312907

[14] Calapoglu, M., Sevinc, Z., Togany, V. A., Kalyoncu, H. (2017): Evaluation of oxidative stress and genotoxicity for environmental monitoring using farmed rainbow trout. – Fresenius Environmental Bulletin 26(12): 7105-7113.
[15] Castano, A., Becerril, C. (2004): *In vitro* assessment of DNA damage after short and long-term exposure to benzo (a) pyrene using RAPD and the RTG-2 fish cell line. – Mutation Research 552: 141-151.
[16] Chand, V., Prasad, S. (2013): ICP-OES assessment of heavy metal contamination in tropical marine sediments: A comparative study of two digestion techniques. – Microchemical 111: 53-56.
[17] Chen, B. C., Liao, C. M. (2004): Farmed tilapia *Oreochromis mossambicus* involved in transport and biouptake of arsenic in aquacultural ecosystems. – Aquaculture 242: 365-380.
[18] Cumberlidge, N., Ng, P. K. L., Yeo, D. C. J., Magalhaes, C., Campos, M. R., Alvarez, F., Naruse, T., Daniels, S. R., Esser, L. J., Attipoe, F. Y. K., Clotilde-Ba, F., Darwall, W., Mclvor, A., Baillie, J. E. M., Collen, B., Ram, M. (2009): Freshwater crabs and the biodiversity crisis importance, threats, status, and conservation challenges. – Biological Conservation 142: 665-1673.
[19] Craig, P. M., Wood, C. M., McClell, G. B. (2007): Oxidative stress response and gene expression with acute copper exposure in zebrafish (*Danio rerio*). – American Journal of Physiology-Regulatory, Integrative and Comparative Physiology 293: 1882-1892.
[20] Da Rocha, A. M., Salomao de Freitas, D. P., Burns, M., Vieira, J. P., de la Torre, F. R., Monserrat, J. M. (2009): Seasonal and organ variation in antioxidant capacity, detoxifying competence and oxidative damage in freshwater and estuarine fishes from southern Brazil. – Comparative Biochemistry and Physiology 150: 512-520.
[21] Dalle-Donne, I., Aldini, G., Carini, M., Colombo, R., Rossi, R., Milzani, A. (2006): Protein carbonylation, cellular dysfunction, and disease progression. – Journal of Cellular and Molecular Medicine 10(2): 389-406.
[22] Ercal, N., Gurer-Orhan, H., Aykin-Burns, N. (2001): Toxic metals and oxidative stress part I: mechanisms involved in metal-induced oxidative damage. – Current Topics in Medicinal Chemistry 1: 529-539.
[23] Farombi, E. O., Adelowo, O. A., Ajimoko, Y. R. (2007): Biomarkers of oxidative stress and heavy metal levels as indicators of environmental pollution in African Catfish (*Clarias gariepinus*) from Nigeria Ogun River. – International Journal of Environmental Research and Public Health 4(2): 158-165.
[24] Ferreira, M., Moradas-Ferreira, P., ReisHenriques, M. A. (2005): Oxidative stress biomarkers in two resident species, mullet (*Mugil cephalus*) and flounder (*Platichthys flesus*), from a polluted site in River Douro Estuary, Portugal. – Aquatic Toxicology 71(1): 39-48.
[25] Giulio, R. T. D., Habig, C., Gallagher, E. P. (1993): Effects of black rock harbor sediments on indices of biotransformation, oxidative stress, and DNA integrity in channel catfish. – Aquatic Toxicology 26: 1-22.
[26] Grune, T. (2000): Oxidative stress, aging and the proteasomal system. – Biogerontology 1(1): 31-40.
[27] Godt, J., Scheigig, F., Grosse-Siestrup, C., Esche, V., Brandenburg, P., Reich, A., Groneberg, D. A. (2006): The toxicity of cadmium and resulting hazards for human health. – Journal of Occupational Medicine and Toxicology 1: 22.
[28] Hebert, N., Gagne, F., Cejka, P., Cyr, D., Marcogliese, D. J., Blaise, C., Pellerin, J., Fournier, M. (2008): The effects of a primary-treated municipal effluent on the immune system of rainbow trout (*Oncorhynchus mykiss*): exposure duration and contribution of suspended particles. – Comparative Biochemistry and Physiology Part C: Comparative Pharmacology 148(3): 258-264.

http://www.aloki.hu ● ISSN 1589 1623 (Print) ● ISSN 1785 0037 (Online)
DOI: http://dx.doi.org/10.15666/aeer/1706_1289312907

[29] Intamat, S., Buasriyot, P., Sriuttha, M., Tengjaroenkul, B., Neeratanaphan, L. (2017): Bioaccumulation of arsenic in aquatic plants and animals near a municipal landfill. – International Journal of Environmental Studies 74(2): 303-314.
[30] Ip, Y. K., Chew, S. F., Randall, D. J. (2001): Ammonia Toxicity, Tolerance and Excretion. – In: Hoar, W. S., Randall, D. J., Farrell, A. P. (eds.) Fish Physiology, Vol. 20. Nitrogen Excretion. Academic Press, San Diego, CA. pp. 109-148.
[31] Jezierska, B., Witeska, M. (2001): Metal toxicity to fish. – Reviews in Fish Biology and Fisheries 11(3): 279-279.
[32] Kamunde, C., Grosell, M., Higgs, D., Wood, C. M. (2002): Copper metabolism in actively growing rain bow trout (*Oncorhynchus mykiss*): Interactions between dietary and waterbone copper uptake. – Journal of Experimental Biology 205: 279-290.
[33] Livingstone, D. (2003): Oxidative stress in aquatic organism in relation to pollution and agriculture. – Revue de Medecine Veterinaire 154: 427-430.
[34] Luangaram, S., Kukongviriyapan, U., Pakdeechote, P., Kukongviriyapan, V., Pannangpetch, P. (2007): Protective effects of quercetin against phenylhydrazine-induced vascular dysfunction and oxidative stress in rats. – Food and Chemical Toxicology 45: 448-455.
[35] Luoma, S., Rainbow, P. (2008): Sources and Cycles of Trace Metals. In: Metal Contamination in Aquatic Environments: Science and Lateral Management. – Cambridge University Press, Cambridge.
[36] Ministry of Public Health (2003): Standard of Contaminants in Food. – Notification of the Ministry of Public Health No. 273/2, Bangkok, Thailand.
[37] Mishra, A. K., Mohanty, B. (2008): Acute toxicity impacts of hexavalent chromium on behavior and histopathology of gill, kidney and liver of the freshwater fish, *Channa punctatus* (Bloch). – Environmental Toxicology and Pharmacology 26: 136-141.
[38] Monserrat, J. M., Martinez, P. E., Geracitano, L., Amado, L. L., Martins, C., Pinho, G. L. L., Chaves, I. S., Cravo, M. F., Ventura-Lima. J., Biachini, A. (2007): Pollution biomarkers in estuarine animals: Critical review and new perspectives. – Comparative Biochemistry and Physiology Part C: Toxicology Pharmacology 146(1-2): 221-234.
[39] Mustafa, S., Widodo, M. A., Kristianto, Y. (2012): Albumin and zinc content of snakehead fish (*Channa striata*) extract and its role in health. – International Journal of Science and Technology 1: 1-18.
[40] Nakmareong, S., Kukongviriyapan, U., Pakdeechote, P., Donpunha, W., Kukongviriyapan, V., Kongyingyoes, B., Sompamit, K., Phisalaphong, C. (2011): Antioxidant and vascular protective effects of curcumin and tetrahydrocurcumin in rats with L-NAME-induced hypertension. – Naunyn-Schmiedeberg's Archives of Pharmacology 383: 519-529.
[41] Neeratanaphan, L., Khamlerd, C., Chowrong, S., Intamat, S., Sriuttha, M., Tengjaroenkul, B. (2017): Cytotoxic assessment of flying barb fish (*Esomus metallicus*) from a gold mine area with heavy metal contamination. – International Journal of Environmental Studies 74(4): 613-624.
[42] Ngamniyom, A. (2012): Thai ricefish: a potential bio-indicator specis for monitoring freshwater environment pollutions. – Srinakharinwirot Science Journal 28: 207-218.
[43] Oost, R., Beyer, J., Vermeulem, N. P. E. (2003): Fish bioaccumulation and biomarkers in environmental risk assessment: a review. – Environmental Toxicology and Pharmacology 13: 57-149.
[44] Papadimitriou, E. P., Loumbourdis, N. S. (2003): Copper kinetics and hepatic metallothionein levels in the frog *Rana ridibunda*, after exposure to $CuCl_2$. – Biometals 16(2): 271-277.
[45] Parvez, S., Raisuddin, S. (2005): Protein carbonyls: novel biomarkers of exposure to oxidative stress-inducing pesticides in freshwater fish *Channa punctata* (Bloch). – Environmental Toxicology and Pharmacology 20: 112-117.

http://www.aloki.hu ● ISSN 1589 1623 (Print) ● ISSN 1785 0037 (Online)
DOI: http://dx.doi.org/10.15666/aeer/1706_1289312907

[46] Paul, N., Chakraborty, S., Sengupta, M. (2014): Lead toxicity on non-specific immune mechanisms of freshwater fish *Channa punctatus*. – Aquatic Toxicology 152: 105-112.
[47] Pereira, L. S., Ribas, J. L. C., Vicari, T. (2016): Effects of ecologically relevant concentrations of cadmium in a fresh water fish. – Ecotoxicology and Environmental Safety 130: 29-36.
[48] Pollution Control Department (PCD) (1994): Surface Water Quality Standards. – Notification of the National Environmental Board; No. 8, Ministry of Natural Resources and Environment, Bangkok, Thailand.
[49] Pollution Control Department (PCD) (2004): Soil Quality Standards for Habitat and Agriculture. – Notification of the National Environmental Board; No. 25, Ministry of Natural Resources and Environment, Bangkok, Thailand.
[50] Pollution Control Department (PCD) (2014): Thailand State of Pollution Report 2014. – Pollution Control Department, Ministry of Natural Resources, Bangkok, Thailand.
[51] Promsid, P. (2014): Chromosomal aberration assessment of fish in reservoir affected by leachate in municipal landfill. – Master Thesis in Department of Environmental Science, Graduate School, Khon Kaen University, Thailand.
[52] Requena, J. R., Levine, R. L., Stadtman, E. R. (2003): Recent advances in the analysis of oxidized proteins. – Amino Acids 25: 221-226.
[53] Reznick, A. Z., Packer, L. (1994): Oxidative damage to proteins: spectrophotometric method for carbonyl assay. – Methods in Enzymology 233: 357-363.
[54] Robinson, B., Duwig, C., Bolan, N., Kannathasan, M., Saravanan, A. (2003): Up take of arsenic by New Zealand watercress (*Lepidium sativum*). – Science of the Total Environment 301: 67-73.
[55] Rohlf, F. J. (2009): NTSYSpc: Numerical Taxonomy and Multivariate Analysis Version 2.2. – Applied Biostatistics Inc., New York.
[56] Sanchez, W., Ait-Aissa, S., Palluel, O., Ditche, J. M., Porcher, J. M. (2007): Preliminary investigation of multi-biomarker responses in three-spined stickleback (*Gasterosteus aculeatus* L.) sampled in contaminated streams. – Ecotoxicology 16(2): 279-287.
[57] Sarun, K. (2004): Analysis of hazardous waste stream in Khon Kaen metropolitan municipality. – Master Thesis in Environmental Engineering, Graduate School, Khon Kaen University, Thailand.
[58] Sevcikova, M., Modra, H., Slaninova, A., Svobodova, Z. (2011): Metals as a cause of oxidative stress in fish: a review. – Veterinarni Medicina 56: 537-546.
[59] Silbergeld, E. K. (2003): Facilitative mechanisms of lead as a carcinogen. – Mutation Research 533(1-2): 121-133.
[60] Skorbiłowicz, E. (2009): Aquatic plants as bioindicators of contamination of upper Narew river and some of its tributaries with heavy metals. – Environmental Protection Engineering 35(1): 65-77.
[61] Sriuttha, M., Tengjaroenkul, B., Intamat, S., Phoonaploy, U., Thanomsangad, P., Neeratanaphan, L. (2017): Cadmium, chromium and lead accumulation in aquatic plants and animals from a municipal landfill. – Human and Ecological Risk Assessment 23(2): 350-363.
[62] Suhartono, E., Triawanti, Yunanto, A., Firdaus, R. T., Iskandar. (2013): Chronic cadmium hepatooxidative in rats: treatment with haruan fish (*Channa striata*) extract. – APCBEE Procedia 5: 441-445.
[63] Talas, Z. S., Orun, I., Ozdemir, I., Erdogan, K., Alkan, A., Yilmaz, I. (2008): Antioxidative role of selenium against the toxic effect of heavy metals (Cd^{+2}, Cr^{+3}) on liver of rainbow trout (*Oncorhynchus mykiss*, Walbaum 1792). – Fish Physiology and Biochemistry 34(3): 217-222.
[64] Teles, M., Pacheco, M., Santos, M. A. (2005): Physiological and genetic responses of European eel (*Anguilla anguilla* L.) to short-term chromium or copper exposure-influence of pre-exposure to a PAH-Like compound. – Environmental Toxicology 20(1): 92-99.

http://www.aloki.hu ● ISSN 1589 1623 (Print) ● ISSN 1785 0037 (Online)
DOI: http://dx.doi.org/10.15666/aeer/1706_1289312907

[65] Tengjaroenkul, B., Intamat, S., Thanomsangad, P., Phoonaploy, U., Neeratanaphan, L. (2018): Cytotoxic effect of sodium arsenite on the Nile tilapia (*Oreoshromis niloticus*) in vivo. – International Journal of Environmental Studies 75(4): 580-591.
[66] Tiwari, K. K., Singh, N. K., Patel, M. P. (2011): Metal contamination of soil and translocation in vegetables growing under industrial wastewater irrigated agricultural field of Vadodara, Gujarat, India. – Ecotoxicology and Environmental *S*afety 74: 1670-1677.
[67] US Environmental Protection Agency (USEPA) (2000): Bioaccumulation Testing and Interpretation for the Purpose of Sediment Quality Assessment. – Bioaccumulation Analysis Workgroup, US Environmental Protection Agency, Washington, DC.
[68] Velma, V., Tchounwou, P. B. (2013): Oxidative stress and DNA damage induced by chromium in liver and kidney of goldfish, *Carassius aurata*. – Biomarker Insights 8(8): 43-51.
[69] Vilela, C. L. S., Bassin, J. P., Peixoto, R. S. (2018): Water contamination by endocrine disruptors: Impacts, microbiological aspects and trends for environmental protection. – Environmental Pollution 235: 546-559.
[70] Vlahogianni, T., Dassenakis, M., Scoullos, M. J., Valavanidis, A. (2007): Integrated use of biomarkers (superoxide dismutase, catalase and lipid peroxidation) in mussels *Mytilus galloprovincialis* for assessing heavy metals pollution in coastal areas from the Saronikos Gulf of Greece. – Marine Pollution Bulletin 54: 1361-1371.
[71] Waalkes, M. P. (2003): Cadmium carcinogenesis. – Mutation Research 533: 107-120.
[72] Wachirawongsakorn, P., Sangyoka, S. (2013): Assessment of heavy metal distribution in soil and groundwater surrounding municipal solid waste dump site in Nai Muang Sub-District Administrative Organization, Amphur Phichai, Uttaradit. – Naresuan University Journal: Science and Technology 10(1): 18-29.
[73] Webb, D. (2011): Freshwater shrimp (*Palaemonetes australis*) as a potential bioindicator of crustacean health. – Environmental Monitoring and Assessment 178(1-4): 537-544.
[74] Wilhelm, F. D. (1996): Fish antioxidant defences -a comparative approach. – Brazilian Journal of Medical and Biological Research 29: 1735-1742.
[75] Wise, S. S., Holmes, A. L., Wish, J. P. (2008): Hexavalent chromium-induced DNA damage and repair mechanisms. – Reviews on Environmental Health 23(1): 39-57.
[76] Wood, R. D., Mitchell, M., Srouros, J., Lindahi, T. (2001): Human DNA repair genes. – Science 291: 1284-1289.

http://www.aloki.hu ● ISSN 1589 1623 (Print) ● ISSN 1785 0037 (Online)
DOI: http://dx.doi.org/10.15666/aeer/1706_1289312907

CONTRIBUTION OF LIVESTOCK TO CO_2 EMISSION IN D-8 (DEVELOPING-8) COUNTRIES: AN EMPIRICAL ANALYSE OF PANEL DATA

DOĞAN, H. G.[1*] – SAÇLI, Y.[2]

[1]*Department of Agricultural Economics, Agricultural Faculty, Kırşehir Ahi Evran University, Kırşehir, Turkey*

[2]*The Department of Strategy and Budget, Presidency of the Republic of Turkey, Ankara, Turkey*

**Corresponding author*
e-mail: hg.dogan@ahievran.edu.tr

(Received 20th May 2019; accepted 28th Aug 2019)

Abstract. Climate change makes itself perceivable day by day. Therefore, the determination of the factors that cause climate change and the effects of these are studied increasingly nowadays. Considering the global scale, it is seen as an effective way for countries to reduce the impacts of climate change and to act together in adaptation efforts. Therefore, regional and non-regional collaborations are important in this struggle. The aim of this study is to reveal the relationships between livestock activity and Carbon Dioxide (CO_2) emissions in Developing-8 (D-8) countries, an economic co-operation organization, with panel data analysis. In this study, the effect of the cattle, sheep and poultry stock of D-8 countries between 1990 and 2017 on CO_2 emissions was investigated with the Autoregressive Distributed Lag (ARDL) model. As a result, there was a statistically significant positive correlation between the stock number of cattle and poultry and the CO_2 emissions in general, although there was no statistically significant relationship with the breeding of sheep. The effect of animal husbandry activities on climate change is important because of their contribution to CO_2 emissions. In the processes involving materials such as enteric fermentation, animal originated fertilizer, animal waste, it is thought that the political/regulatory arrangements that will eliminate such factors can be made for producers in the micro-scale and for the agricultural sector in the macro scale.
Keywords: *climate change, livestock production, D-8 countries, ARDL model, CO_2 emission*

Introduction

Global warming due to climate change is at the top of today's most important problems. A lot of research has been done on the future effects of global warming (FAO, 2015; Riphah, 2015; Seneviratne et al., 2016; Özdemir et al., 2017; Prasad et al., 2017; Chena et al., 2018; Doğan and Kan, 2018; Iddrisu and Peker, 2018; Doğan and Kan, 2019; Qadir et al., 2019) and its effects are felt day by day. Many scenarios have been developed for this. In this regard, there is a common consensus for many countries around the world: the countries with the highest greenhouse gas emissions should have more duties. Scientists point out that, by the first quarter of the 21st century, the carbon dioxide content in the atmosphere increased by 40% and the methane gas content by 150% compared to the years when the industrial revolution began (Euronews, 2015). China and the United States are the most prominent countries in terms of greenhouse gas emissions, while they are followed by countries such as AB-27, India, Russia, Japan and Brazil (The World Bank, 2019a).

There are also studies on the impact of the sectors on greenhouse gas emissions as the main factor of global warming (Bayar and Bahrend; 1994; Pekin, 2006; FAO, 2015; Riphah, 2015; Doğan and Kan, 2018; Kanat and Keskin, 2018; EPA, 2019;

http://www.aloki.hu ● ISSN 1589 1623 (Print) ● ISSN 1785 0037 (Online)
DOI: http://dx.doi.org/10.15666/aeer/1706_1290912919

Peker et al.; 2019; PSU, 2019), and the impact of each sector is different. Agriculture is an important sector that impacts climate change, also being affected by itself, because it affects the global flow of greenhouse gases. Greenhouse gases such as CO_2, CH_4, and N_2O are counted among the causes of climate change as a result of agricultural activities (energy consumption, plant and animal production, fertilization, pesticide use, etc.) (Houghton, 2003; Akalın, 2014). Agricultural activities are reported to be responsible for about 20% of the growing greenhouse gases in the world (Pathak and Wasmann, 2007). The activities of agriculture, such as the destruction of forests to transform the agricultural field, also greatly increase greenhouse gas emissions. The destruction of forest lands is considered to be responsible for 10% to 30% of the carbon dioxide released into the atmosphere. Therefore, it is the second biggest source of greenhouse gas emissions into the atmosphere after fossil fuel combustion (Harvey et al., 2010). The second important greenhouse gas originating from agricultural activities is methane. Rice cultivation is blamed for more than 40% of global methane emissions. Farm animals account for 15% of global methane emissions. Ruminants (cattle, sheep, goats, camels, and buffalo) digest grass and cellulose. In this way, they release methane into the air. The world's cattle number accounts for about 75% of the methane emissions of total farm animals (IPCC, 2007). However, since methane gas life is considerably lower than that of CO2 gas, CO2 emissions are generally emphasized in research.

The measures to prevent global climate change, as well as, the adaptation strategies for possible adverse effects constitute the main framework of this struggle. In the world, each country is creating its own strategy against adverse effects of climate change, and these strategies sometimes turn into a common struggle with regional integrations or national integrations. The provision of governance collaboration in the fight against climate change (mitigation, adaptation, and resilience) is one of the most important phases (Peker et al., 2019). Therefore, in regional integrations based on economic co-operation, the issues of combating climate change need to be more involved and the increase of collaborations is necessary.

The D-8 organization (Developing 8), which was established to act as a partner in the global system based on economic cooperation, consists of 8 countries (Bangladesh, Indonesia, Iran, Malaysia, Egypt, Nigeria, Pakistan, Turkey). Its foundations were laid in October 1996 at the invitation of Prof. Dr. Necmettin Erbakan, the former Prime Minister of the Republic of Turkey, at the "Cooperation in Development Conference" organized in Istanbul with the participation of representatives of those countries. After a series of preparatory meetings following the Cooperation in Development Conference on October 22, 1996, the establishment of the D-8 was formally announced at "the Summit of the Heads of State and Government" organized in Istanbul on June 15, 1997 (Istanbul Declaration). The purpose of the D-8 is to increase trade and co-operation between the Member States. The aim of launching the D-8 initiative is to create and diversify new opportunities in trade relations between 8 countries representing a large economic potential, various sources, a wide population and geographical area, and to increase participation in the decision making process at international level, to provide better life conditions, to improve economic co-operation around concrete joint projects and to strengthen the situation of developing countries in the world economy. Agriculture and food safety, renewable energy resources, industry, transportation, tourism are some of the main issues that are expected to be cooperated (D-8 OEC, 2019a).

http://www.aloki.hu ● ISSN 1589 1623 (Print) ● ISSN 1785 0037 (Online)
DOI: http://dx.doi.org/10.15666/aeer/1706_1290912919

The D-8 has established a common platform for advocating the rights of developing countries against developed countries, especially in the World Trade Organization (WTO) decisions, with the goal of targeting more global partnerships than regional integration. In addition, this common platform has played an important role in protecting the rights of countries in determining the measures and responsibilities of the countries on the global CO_2 emissions causing climate change. For the first time, at the Malaysia-Kuala Lumpur Declaration in 2008, it was reported as follows: *"Recognizing the adverse impacts of global warming and climate change on development, we reaffirm our commitment to enhance cooperation in climate change negotiations following the Bali Roadmap to support the adaptation efforts of the developing countries, especially those of the least developed and the low-lying coastal countries and uphold the principle of common but differentiated responsibilities in mitigation of the emission of greenhouse gases"* (D-8 OEC, 2019b). In the 2012 Islamabad declaration, it was noted that the effects of climate change in sustainable and inclusive development should have also been considered (D-8 OEC, 2019c). The development of joint adaptation strategies against the impacts of climate change and need to be working to reduce the adverse effects, which may arise primarily from global warming, on the people of the D-8 countries were reported again in the 2017 Istanbul Declaration (D-8 OEC, 2019d).

It is clearly seen that climate change threatens human welfare and agricultural production, considering that nearly 2.5 billion people in developing countries earn their lives from agriculture. The D-8 countries constitute 13.94% of the world's agricultural production (465.7 billion $) (the World Bank, 2019b) according to 2017 data, and 6.20% of the world's CO_2 emissions according to 2014 data (The World Bank, 2019a). According to the data of 2016, the gross production value of beef is examined as $258,084,093 in Bangladesh, $2,636,059,545 in Egypt, $3,428,638,282 in Indonesia, $1,845,763,741 in Iran, $68,611,219 in Malaysia, $559,357,239 in Nigeria, $2,608,695,845, and also $6,217,254,585 in Turkey. The gross production value of mutton is $ 9,036,936 in Bangladesh, $490,525,023 in Egypt, $275,071,662 in Indonesia, $1,044,326,227 in Iran, $146,262 in Malaysia, $265,000,401 in Nigeria $328 274 105 in Pakistan and $2,173,555,064 in Turkey. Poultry gross production value is $228,811,476 in Bangladesh, $1,775,763,964 in Egypt, $ 6,918,959,386 in Indonesia, $8,275,937,537 in Iran, $280,193,375 in Malaysia, and $252,579,138 in Nigeria, $2,529,530,629 in Pakistan and also $3,943,021,371 in Turkey. Looking at the CO_2 emissions of the 8 countries that constitute the D-8, it is seen to be less than China, the United States, the EU-28 and India, which are countries and/or regional unions that are releasing the most CO_2 emissions in the world. Despite this, combating climate change continue to be a common share of global economic partnerships.

In this study, the effects of the animal stock numbers in D-8 countries on CO_2 emissions were investigated by using the panel data set, and for the D-8 meeting to be done thereafter, policy proposals have been attempted to develop measures for the prevention and adaptation of climate change.

Materials and methods

In the study, the relationship of CO_2 emission (kt) with cattle, sheep, and poultry stock numbers in D-8 countries was investigated. The variables and units are presented in *Table 1*.

http://www.aloki.hu ● ISSN 1589 1623 (Print) ● ISSN 1785 0037 (Online)
DOI: http://dx.doi.org/10.15666/aeer/1706_1290912919

Table 1. *Variables, abbreviations and units used in research*

Variable names	Symbols	Units	Data sources
Carbon dioxide emission	CO_2	kt	World Bank, FAO
Cattle stock	C	Head	World Bank, FAO
Sheep stock	S	Head	World Bank, FAO
Poultry stock	P	Head	World Bank, FAO

Some econometric models have been utilized with the help of panel data set in examining the variables and relations between countries. The research covers the years between 1990 and 2017. Eight countries, called D-8, constitute the research area. These countries are Bangladesh, Indonesia, Iran, Malaysia, Egypt, Nigeria, Pakistan, and Turkey. The research is based on two fundamental analyses. The data evaluated in full logarithmic form was analyzed by the unit root test and ARDL. Descriptive information for tests can be expressed as follows.

Unit root test (ADF)

The unit root tests have several fractions, which are proposed by researchers in the literature (Maddala and Wu, 1999; Kao and Chiang, 2000; Hadri, 2000; Choi, 2001; Levin et al., 2002; Im et al., 2003). This study uses Levin, Lin, Chu (LLC) and Im, Peseran, Shin (IPS) unit root tests based on the Augmented Dickey Fuller (ADF) test statistic. Basic equality for unit root tests based on ADF principles can be expressed as follows:

$$\Delta lnX_{it} = \beta_i lnX_{it-1} + \sum_{j=1}^{n} \theta_{ij} \Delta lnX_{it-j} + e_{it} \quad \text{(Eq.1)}$$

Autoregressive distributed lag (ARDL)

In the literature, the Engle-Granger (1987) models based on error term and Johansen (1988) and Johansen and Jesilius (1990) models based on the system approach (Altıntaş, 2013) are often used in cointegration tests. However, in order for these methods to be valid, all variables must be stationary at level I(1) and not stationary at the level I(0) (Peseran et al., 2001). The ARDL boundary test approach allows for co-integration testing with non-stationary series at the same level (Pesaran and Shin, 1995; Pesaran et al., 2001). The advantage of the ARDL approach is that it is possible to test the cointegration without considering the degree of integration of variables. There are three important points to be considered in the method. I- The boundary test procedure is easy and, unlike multivariate co-integration methods of Johansen and Juselius (1990), it is possible to verify co-integration after lag lengths are determined. II- Unlike the co-integration techniques of Johansen and Juselius (1990), the boundary test procedure does not require preliminary testing of the variables included in the unit root test model. The boundary test can be applied, regardless of whether I (0) and I (1) or all of them are mutually co-integrated at the same level except when the series in the model is at the level I (2), I (0) and I (1). III-Boundary testing is very effective for small or limited sample size.

ARDL notations adapted to the research were expressed in *Equations 2–5:*

http://www.aloki.hu ● ISSN 1589 1623 (Print) ● ISSN 1785 0037 (Online)
DOI: http://dx.doi.org/10.15666/aeer/1706_1290912919

$$\Delta \ln CO2 = \beta_0 + \sum_{i=1}^{m} \beta_{1i} \Delta \ln CO2_{t-i} + \sum_{i=0}^{m} \beta_{2i} \Delta \ln C_{t-i} + \sum_{i=0}^{m} \beta_{3i} \Delta \ln S_{t-i} + \sum_{i=0}^{m} \beta_{4i} \Delta \ln P_{t-i} + a1 \ln CO2_{t-1} + a2 \ln C_{t-1} + a3 \ln S_{t-1} + a4 \ln P_{t-1} + u_t \quad \text{(Eq.2)}$$

$$\Delta \ln C = \beta_0 + \sum_{i=1}^{m} \beta_{1i} \Delta \ln C_{t-i} + \sum_{i=0}^{m} \beta_{2i} \Delta \ln CO2_{t-i} + \sum_{i=0}^{m} \beta_{3i} \Delta \ln S_{t-i} + \sum_{i=0}^{m} \beta_{4i} \Delta \ln P_{t-i} + a1 \ln CO2_{t-1} + a2 \ln C_{t-1} + a3 \ln S_{t-1} + a4 \ln P_{t-1} + u_t \quad \text{(Eq.3)}$$

$$\Delta \ln S = \beta_0 + \sum_{i=1}^{m} \beta_{1i} \Delta \ln S_{t-i} + \sum_{i=0}^{m} \beta_{2i} \Delta \ln CO2_{t-i} + \sum_{i=0}^{m} \beta_{3i} \Delta \ln C_{t-i} + \sum_{i=0}^{m} \beta_{4i} \Delta \ln P_{t-i} + a1 \ln CO2_{t-1} + a2 \ln C_{t-1} + a3 \ln S_{t-1} + a4 \ln P_{t-1} + u_t \quad \text{(Eq.4)}$$

$$\Delta \ln P = \beta_0 + \sum_{i=1}^{m} \beta_{1i} \Delta \ln P_{t-i} + \sum_{i=0}^{m} \beta_{2i} \Delta \ln CO2_{t-i} + \sum_{i=0}^{m} \beta_{3i} \Delta \ln S_{t-i} + \sum_{i=0}^{m} \beta_{4i} \Delta \ln C_{t-i} + a1 \ln CO2_{t-1} + a2 \ln C_{t-1} + a3 \ln S_{t-1} + a4 \ln P_{t-1} + u_t \quad \text{(Eq.5)}$$

In *Equations 2–5,* however, Δ refers to the difference processor, and m refers to the lag length. Information criteria such as AIC, SC, FPE, and HQ are utilized for determining the lag length. The lag length, which provides the smallest critical value, is determined as the model's lag length. Until reaching the model without autocorrelation, the process is resumed by passing the next lag value, for example, the first smallest value, the second smallest, etc. In Equations 2-3-4-5, H_0 hypothesis expressing that there is no co-integration between variables is formed as H_0: a1 = a2 = a3 = a4, the alternative hypothesis that mentions the existence of co-integration is formed as H_1: a1≠a2≠ a3≠ a4.

Results and discussion

Regional partnerships increase the capacity of countries to economically collaborate in the process of globalization, which is a great advantage for developing adaptability to global challenges. In these challenges, global climate change is the first of the most talked and debated issues nowadays. The factors that cause global climate change and the solution proposals against it require efforts to create an international policy outside of national policy creation. The struggle with this problem is only possible with collaboration (Peker et al., 2019).

The D-8 organization, which is an important step in regional, economic and social partnership, has an important potential in agriculture. In terms of total agricultural production, it produces 13.94% of the world's agricultural production according to 2017 data (465.7 billion $) (The World Bank, 2019b), constitutes the 8.75% of the world's bovine existence, 21.55% of chicken existence, 25.06% of goat existence, and 13.98% of sheep existence (FAOSTAT, 2019). As seen from *Figure 1,* Pakistan is the leading country for the cattle stock numbers between D-8 countries. Nigeria, Pakistan, Iran, and Bangladesh are the leading countries for the sheep stock numbers. Also, Indonesia and Iran are the leading countries for poultry stock numbers.

http://www.aloki.hu ● ISSN 1589 1623 (Print) ● ISSN 1785 0037 (Online)
DOI: http://dx.doi.org/10.15666/aeer/1706_1290912919

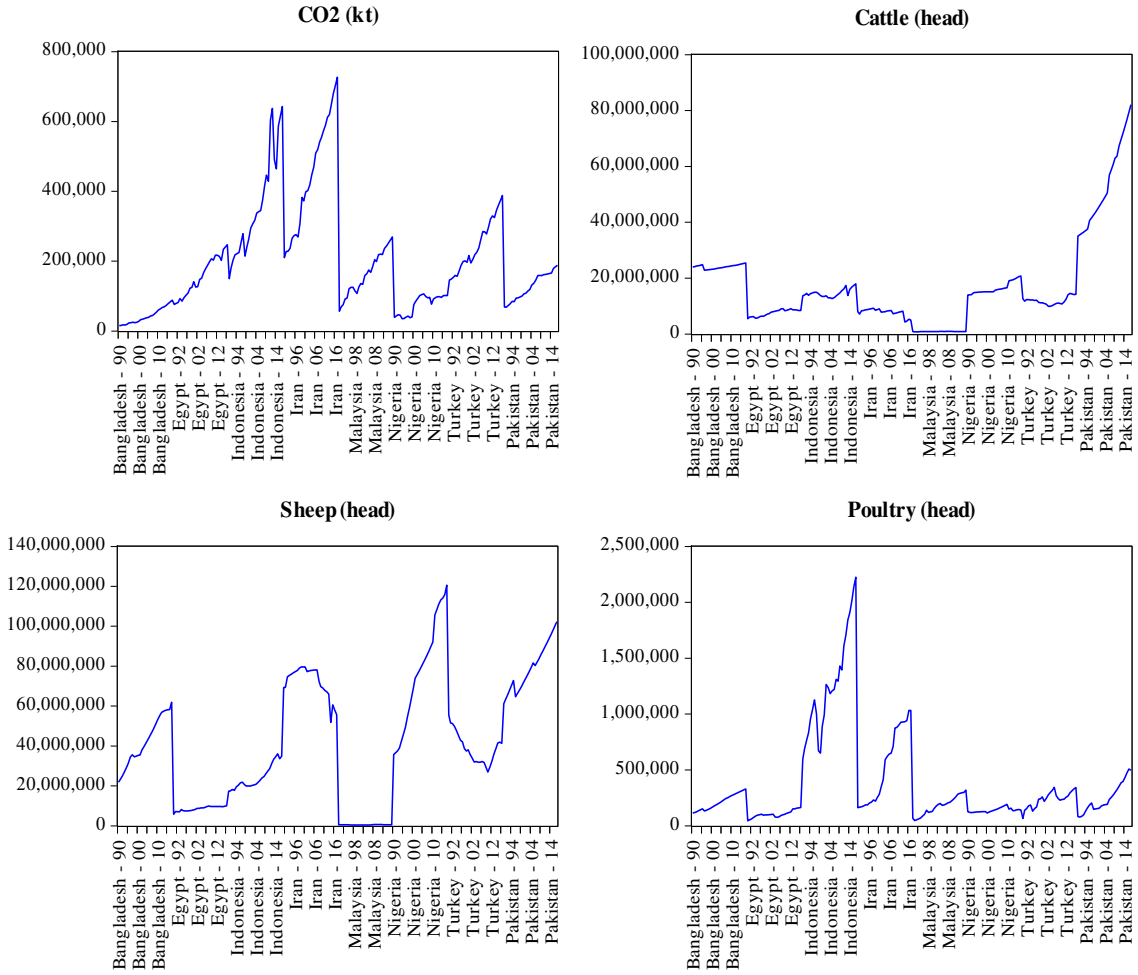

Figure 1. *CO_2 emission, cattle stock, sheep stock and poultry stock of D-8 countries by 1990-2017 years*

In econometric forecasts, the stationary of time series is important. Granger and Newbold (1974) showed that working with non-stationary time series might cause a false regression problem. In the study, if the results of the Levin, Lin, Chu, and Im, Peseran, Shin unit root test are examined, they can be seen as stationary in both Intercept and Intercept + Trend models. The unit root test results of the variables used in the study are given in *Table 2*.

Table 2. *Unit root test results*

Variables	Levin, Lin, Chu Test				Im, Peseran, Shin Test			
	Individual intercept		Individual intercept and trend		Individual intercept		Individual intercept and trend	
	Level	Dif.	Level	Dif.	Level	Dif.	Level	Dif.
$lnCO_2$	-2.4404*	-13.2348*	-2.1050**	-11.7832*	1.2650	-12.7269*	-2.2506**	-11.5971*
LnC	1.3652	-11.8788*	0.2041	-8.0473*	2.3058	-10.9181*	1.5564	-7.9102*
LnS	-1.8772**	6.4899*	0.0415	-5.0677*	1.3060	6.7918*	1.0787	-6.9924*
lnP	-0.8249	-7.3930*	1.5670	-1.5855**	1.1393	-9.6590*	0.1938	-6.6021*

*, **, *** are 1%, 5%, 10% significant, respectively

http://www.aloki.hu ● ISSN 1589 1623 (Print) ● ISSN 1785 0037 (Online)
DOI: http://dx.doi.org/10.15666/aeer/1706_1290912919

In this study, the long run effects of bovine, sheep and poultry stock factors on CO_2 emissions were quantitatively determined, and they could be said to be in interaction with each other. However, in order to interpret the direction and severity of these interactions, ARDL analysis was performed and the results were shown in *Table 3*. *Table 3* shows that the contribution of cattle and poultry to CO_2 emissions in the long run in D-8 countries were positive and statistically significant, whereas the contribution of sheep stock was positive but statistically insignificant at 95% confidence level.

Table 3. *Results of ARDL estimators in a long and short run*

Long run equation			
Selected model: ARDL(4, 4, 4, 4)			
Variable	**Coefficient**	**Std. error**	**t-statistic**
lnC	1.6359	0.1186	13.7932*
lnS	0.0976	0.0894	1.0915
lnP	1.2047	0.0499	24.1101*
Short run equation			
Variable	**Coefficient**	**Std. error**	**t-statistic**
COINTEQ01	-0.02307	0.1433	-0.1609
D(LNCO2(-1))	-0.3779	0.1711	-2.2079**
D(LNCO2(-2))	-0.4184	0.1714	-2.4404**
D(LNCO2(-3))	-0.2962	0.1623	-1.8244***
D(LNC)	0.7301	0.8016	0.9108
D(LNC(-1))	-0.1592	1.0014	-0.1589
D(LNC(-2))	-0.9467	1.0094	-0.9378
D(LNC(-3))	-1.0718	0.7809	-1.3725
D(LNS)	-0.3897	0.5941	-0.6559
D(LNS(-1))	0.5907	0.4012	1.4723
D(LNS(-2))	-0.2341	0.4971	-0.4710
D(LNS(-3))	-0.2574	0.3911	-0.6580
D(LNP)	-0.5942	0.5123	-1.1598
D(LNP(-1))	-0.5277	0.3280	-1.6085
D(LNP(-2))	0.0977	0.2301	0.4246
D(LNP(-3))	0.0566	0.2277	0.2488
C	-0.3253	4.5388	-0.0716
Mean dependent var	0.0044	S.D. dependent var	0.0857
S.E. of regression	0.0628	Akaike info criterion	-2.5490
Sum squared resid	0.3362	Schwarz criterion	-0.4320
Log likelihood	424.49	Hannan-Quinn criterion	-1.6945

*,**,*** are 1%, 5%, 10% significant, respectively

In evaluating the emergence of this situation, it is necessary to consider firstly the relationship between animals and global warming. When animal husbandry activities are evaluated in terms of global warming, two kinds of effects, direct and indirect, occur. Methane, one of the most important causes of global warming, primarily creates greenhouse gas effects, while the CO_2 effect is second-degree important. The heat-capture capacity of methane in the atmosphere is 21 times higher than CO_2, and its life

http://www.aloki.hu ● ISSN 1589 1623 (Print) ● ISSN 1785 0037 (Online)
DOI: http://dx.doi.org/10.15666/aeer/1706_1290912919

is shorter than other gases (Naqvi and Sejian, 2011). Methane gas is emerging as a result of the storage of fertilizers of animals, especially ruminant animals, and related activities (Sherlock et al., 2002). Ruminants are defined by their structures with a special digestive system. In this way, ruminants are an important methane producer with the greenhouse gases they produce as a result of their comfortable digestion of low-quality cellulose-rich materials. In fact, animals produce very small amounts of methane individually. For example, a cattle produces approximately 80-110 kg of methane per year. At this point, however, the main reason for the responsibility of ruminants is their numbers worldwide rather than the amount of gas they produce. This situation results in a significant contribution to emissions (Koyuncu and Akgün, 2017). From here, the presence of animals itself directly contributes to global warming as a factor.

The indirect effect of animal stock on global warming is sourced from the need for energy in the production of animal foods that are a need for human. The energy requirement used in the feeding chain produces 10% of total CO_2 emissions. The most important source of the resulting CO_2 emissions is animal production and it is said to be equivalent to 9% of total emissions (Clarke, 2001). The source of the resulting emission is not directly the animal itself, but the CO_2 generated by the energy used in feed production, fertilizer processing, product processing, and transport has a significant share (Anonymous, 2012). According to the 2017 data, per capita CO2 levels in D-8 countries were 553.74 kg in Bangladesh, 2564.37 kg in Egypt, 2428.09 kg in Indonesia, 9006.33 kg in Iran, 8651, 53 kg in Malaysia, 532, 98 kg in Nigeria, in Turkey, and 905.88 kg in Pakistan (World Bank, 2019).

In the D-8 countries, because of the fact that sheep breeding is mostly based on pasture, less energy is consumed for the production of feed plants required for these animals than for other animal groups. This could lead to no statistically significant contribution of the sheep stock to the CO_2 emissions in the analysis. In addition, corn production from feed plants, which has a significant share in cattle and poultry production, requires a significant amount of nitrogenous fertilizer (HSUS, 2008). In response to this imperative, the nitrogenous soil pollutes water and air at a significant level. According to FAOSTAT data of 2017, D-8 countries are among the major corn producing countries in the world, especially Indonesian is sixth in corn production worldwide. Indonesia, Nigeria, Egypt, Turkey, and Pakistan, respectively, are among the first 22 countries in the production of corn. D-8 countries have 7.75% (15.3 million ha) of the world corn production area and realize 5.41% of production (61.4 million tons) (FAOSTAT, 2019).

Conclusion

The contribution of direct agricultural production to climate change is lower compared to other sectors, and it plays an important role to meet the basic needs of humanity. In the process of adaptation to climate change, it will be wrong to consider both the vegetable and animal part of the agricultural production separately and to make the planning in direction to that. The result of the study reveals that the indirect effects of livestock activity can be effective in CO_2 emissions as much as livestock numbers. Although the animal husbandry has a direct share in global warming, the role of unconscious input use in the production of feed crops, and the role of animal products processing industry, especially corn for animal feeding, are more important for climate change. Nowadays, it is emphasized that national country policies are not sufficient

http://www.aloki.hu ● ISSN 1589 1623 (Print) ● ISSN 1785 0037 (Online)
DOI: http://dx.doi.org/10.15666/aeer/1706_1290912919

alone and that it is more effective to act together in the struggle and adaptation of climate change. It is important that the D-8 countries, which have an important agricultural share in the world, should meet and act on common denominators in economic cooperation as well as climate change. In this context, working together not only in livestock but in all aspects of agriculture will have an impact on the development of more effective policies in terms of mitigation and adaptation of climate change impacts. Global climate change can be directly and indirectly influenced by the quality and quantity of feed given to animals, feeding strategies, seasonal availability of pastures, genetic studies, number of animals and animal health. Accordingly, some recommendations such as the correct setting of the sowing dates of the feed sources, the right practices for shelter air conditioning, the right approaches to pest and disease control (monitoring, crop rotation, diversity, etc.), the more efficient use of water, soil management and the selection of animals from the right breeds according to the region/conditions could be evaluated.

REFERENCES

[1] Akalın, M. (2014): The climate change impacts on agriculture: adaptation and mitigation strategies for these impacts. – Journal of Hitit University Social Science 2: 351-357 (in Turkish).
[2] Altıntaş, H. (2013): The relationship between oil prices, export and real exchange rate in turkey: bounds testing approach and analysis of dynamic causality. – International Management Journal of Economics and Business Administration 9(19): 1-30 (in Turkish).
[3] Anonymous (2012): The Impact of Livestock Agriculture on Climate Change. – Agricultural Greenhouse Gas Research Centre, New Zealand.
[4] Bayar, A. B., Bahrend, H. (1994): Global Environmental Problems. – Özkan Printing Press Matbaası, Ankara (in Turkish).
[5] Chena, S., Zhi-Honga, J., Wei-Lina, C., Li, L., (2018): Changes in temperature extremes over China under 1.5 °C and 2 °C global warming targets. – Advances in Climate Change Research 9: 120-129.
[6] Choi, I. (2001): Unit root tests for panel data. – J Int Money Financ 20: 249-72.
[7] Clarke, J. (2001): Potential management practices and technologies to reduce nitrous oxide, methane and carbon dioxide emissions from New Zealand agriculture. – http://www.maf.govt.nz/mafnet/rural-nz/sustainable-resource-use/climate/green-house-gas-migration/ghg-mitigation.pdf.
[8] D-8 OEC (D-8 Organisation for Economic Cooperation) (2019a): Brief history of D-8. – http://developing8.org/about-d-8/brief-history-of-d-8/.
[9] D-8 OEC (D-8 Organisation for Economic Cooperation) (2019b): 2008-Kuala Lumpur-Malaysia Declaration. – http://developing8.org/image/DocumentandResouce/9026795.pdf.
[10] D-8 OEC (D-8 Organisation for Economic Cooperation) (2019c): 2012-Islamabad-Pakistan Declaration. – http://developing8.org/report/islamabad-declaration/.
[11] D-8 OEC (D-8 Organisation for Economic Cooperation) (2019c): 2017-Istanbul-Turkey Declaration. – http://developing8.org/report/istanbul-declaration-2017/.
[12] Doğan, H. G., Kan, A. (2019). The effect of precipitation and temperature on wheat yield in Turkey: a panel FMOLS and panel VECM approach. – Environment, Development and Sustainability 21(1): 447-460.
[13] Doğan, H. G., Kan, M., (2018): The nexus of CO2 emission, population, agricultural area size, GDP and energy use in Turkey. – Fresen. Environ. Bull. 27(10): 6812-6823.

http://www.aloki.hu ● ISSN 1589 1623 (Print) ● ISSN 1785 0037 (Online)
DOI: http://dx.doi.org/10.15666/aeer/1706_1290912919

[14] Engle, F., Granger, R., Clive, W. J. (1987): Cointegration and error correction: representation, estimation and testing. – Econometrica 55: 251-276.
[15] Euronews (2015): Green house gasses explained. – https://www.euronews.com/2015/06/26/green-house-gasses-explained.
[16] EPA (United States Environmental Protection Agency) (2019): Sources of greenhouse gas emissions. – https://www.epa.gov/ghgemissions/sources-greenhouse-gas-emissions.
[17] FAO (2015): Estimating greenhouse gas emissions in agriculture. A manual to address data requirements for developing countries. – http://www.fao.org/3/a-i4260e.pdf.
[18] FAOSTAT (2019): Live animals data-2017. – http://www.fao.org/faostat/en/#data/QA.
[19] Hadri, K. (2000): Testing for stationarity in heterogeneous panel data. – Econometric Journal 3: 148-161.
[20] Harvey, A., Matthews, E., Sarma, D. (2010): The Global Methane Cycle. – NASA Goddard Institute for Space Studies. http://icp.giss.nasa.gov/education/methane/intro/cycle.html.
[21] Houghton, R. A. (2003): Why are estimates of the terrestrial carbon balance so different. – Global Change Biology 9: 500-509.
[22] Iddrisu, A. M., Peker, K. (2018): Assessment of technology for climate change adaptation in Sub-Saharan Africa. – J. Glob. Innov. Agric. Soc. Sci. 6(4): 101-114.
[23] Im, K. S., Pesaran, M. H., Shin, Y. (2003): Testing for unit roots in heterogeneous panels. – J Econom 115: 53-74.
[24] IPCC (2007): IPCC, fourth assessment report. Working Group III report "Mitigation of climate change". Chapter 8: Agriculture. – https://www.ipcc.ch/site/assets/uploads/2018/02/ar4-wg3-chapter8-1.pdf.
[25] Johansen, S. (1988): Statistical analysis of cointegration vectors. – Journal of Economic Dynamics and Control 12(1): 231-54.
[26] Johansen, S., Juselıus, K. (1990): Maximum likelihood estimation and inference on cointegration with application to the demand for money. – Oxford Bulletin of Economics and Statistics 52: 169-210.
[27] Kanat, Z., Keskin, A. (2018): Studies on climate change in the world and current situation in Turkey. – Atatürk Univ., J. of the Agricultural Faculty 49(1): 67-78.
[28] Kao, C., Chiang, M. H. (2000): On the estimation and inference of a cointegrated regression in panel data. – Adv Econom 15: 179-222.
[29] Koyuncu, M., Akgün, H., (2017): Interaction between livestock and global climate change. – Journal of Agricultural Faculty of Uludag University 32(1): 151-164.
[30] Levin, A., Lin, C. F., Chu, C. (2002): Unit root tests in panel data: asymptotic and finite sample properties. – J Econom108: 1-24.
[31] Maddala, G. S., Wu, S. A. (1999): comparative study of unit root tests with panel data and a new simple test. – Oxf Bull Econ Stat 61: 631-52.
[32] Naqvi, S. M. K., Sejian, V. (2011): Global climate change: role of livestock. – Asian Journal of Agricultural Sciences 3: 19-25.
[33] Özdemir, F., Küçükçongar, M., Arısoy, R. Z., Öztürk, E., Önder, M., Kan, M., Kınacı, İ., Yılmaz, T., Yorgancılar, M., Şahin, M. (2017): Determination of Drought Perception and Socio-Economic Impact in Kop Region of Turkey. Project Report. – Turkish Republic Ministry of Food Agriculture and Livestock, Ministry of Development, KOP Regional Development Administration.
[34] Pathak, H., Wassmann, R. (2007): Introducing greenhouse gas mitigation as a development objective in rice-based agriculture: I. Generation of technical coefficients. – Agricultural Systems 94: 807-825.
[35] Peker, K., Kan, M., Nadeem, M. (2019): Corporate governance of climate change adaptation. – J. Glob. Innov. Agric. Soc. Sci. 7(1): 1-5.
[36] Pekin, M. A., (2006): Greenhouse gas emissions produced by transportation sector. – MSc. Thesis. Istanbul Technical University, Institute of Science and Technology, Istanbul.

http://www.aloki.hu ● ISSN 1589 1623 (Print) ● ISSN 1785 0037 (Online)
DOI: http://dx.doi.org/10.15666/aeer/1706_1290912919

[37] Pesaran, H., Shin, Y. (1995): An Autoregressive Distributed Lag Modelling Approach to Cointegration Analysis. – In: Strom, S., Holly, A., Diamond, A. (eds.). Centennial Volume of Ranger Frisch. Cambridge University Press, Cambridge.
[38] Pesaran, H., Shin, Y., Smith, R. J. (2001): Bound testing approaches to the analysis of long run relationship. – Journal of Applied Econometrics 16(3): 289-326.
[39] PSU (The Pennsylvania State University) (2019): Current Emissions by Sector: Industry, Agriculture, and Forestry. – In: College of Earth and Mineral Sciences, The Pennsylvania State University E-Education (eds.) METEO 469: From Meteorology to Mitigation: Understanding Global Warming. https://www.e-education.psu.edu/meteo469/node/227.
[40] Prasad, P. V. V., Thomas, J. M. G., Narayanan, S. (2017): Global Warming Effects. – In: Thomas, B., Murray, B. G., Murphy, D. J. (eds.) Encyclopedia of Applied Plant Sciences. Second Ed. Academic Press, Amsterdam, pp: 289-299.
[41] Qadir, T., Akhtar, K., Ahmad, A., Shaoor, A., Saqib, M., Hussain, S., Rafiq, M. (2019): Wheat production under changing climate: consequences of environmental vulnerabilities on different abiotic and biotic stresses. – J. Glob. Innov. Agric. Soc. Sci. 7(1): 7-17.
[42] Riphah, U. S., (2015): Global warming: causes, effects and solutions. – Durreesamin Journal 1(4): 1-7.
[43] Seneviratne, S. I., Donat, M. G., Pitman, A. J. et al. (2016): Allowable CO_2 emissions based on regional and impact-related climate targets. – Nature 529(7587): 477e483.
[44] Sherlock, R. R., Sommer, S. G., Khan, R. Z., Wood, C. W., Guertal, E. A., Freney, J. R., Dawson, C. O., Cameron, K. C. (2002): Ammonia, methane and nitrous oxide emission from pig slurry applied to a pasture in New Zeeland. – Journal Environmental Quality 31: 1491-1501.
[45] The World Bank (2019a): 2014 year CO_2 emissions (kt) data. – https://data.worldbank.org/indicator/EN.ATM.CO2E.KT.
[46] The World Bank (2019b): 2017 year agriculture, forestry, and fishing, value added (current US$) data. – https://data.worldbank.org/indicator/NV.AGR.TOTL.ZS.

http://www.aloki.hu ● ISSN 1589 1623 (Print) ● ISSN 1785 0037 (Online)
DOI: http://dx.doi.org/10.15666/aeer/1706_1290912919

ASSESSMENT OF VALUE FOR CULTIVATION AND USE (VCU) TRIAL DATA BY GGE-BIPLOT ANALYSIS IN BREAD WHEAT (*TRITICUM AESTIVUM* L.)

AKTAS, B.

Variety Registration and Seed Certification Center, Ankara, Turkey
(e-mail: bekir_aktas@yahoo.com; phone: +90-538-433-6374; fax: +90-312-315-0901)

(Received 21st May 2019; accepted 10th Sep 2019)

Abstract. The study was carried out with 17 bread wheat (*Triticum aestivum* L.) genotypes in 7 different environments under rain-fed conditions of the Thrace region in Turkey during 2014-2015 and 2015-2016 growing seasons. Value for cultivation and use (VCU) trial data on yield and quality traits (1000-kernel weight, test weight, protein content, Zeleny sedimentation and alveograph energy value) of bread wheat genotypes were assessed through GGE-biplot analysis. Variance analysis revealed significant genotype (G) × environment (E) interaction (GEI). GGE-biplot analysis explained 79.18% of total variation. Environment-focused assessments revealed 3 mega-environments (ME). E7 (Luleburgaz-2016) was identified as the best representative of all environments and had the greatest separation power among the genotypes. According to the average environment coordinate (AEC), of the genotypes with high PC1 (Principal component) scores, the ones with a PC2 score close to 0.0 were identified as the most stable genotypes. G15, G14, G10 and G13 were the closest genotypes to AEC apsis and they had high PC1 scores. Biplot graphs were generated for 5 quality traits and stabilities of genotypes were put forth based on their positions with respect to AEC. In VCU trials, 5 control cultivars were also used and the average of control cultivars (AC) was generated. AC-focused comparisons of the genotypes were performed. It was concluded based on the present findings that GGE-biplot analysis facilitated the assessments of VCU trial data on yield and quality traits.
Keywords: *genotype × environment interaction, grain yield, quality, stability, multi-environment trials*

Introduction

Wheat is among the leading agricultural products of Turkey with optimal available ecological conditions for its culture. Since the country is composed of different agro-ecological zones, breeders are directed to select appropriate genotypes for these zones or regions. Therefore, variety registration trials for wheat are conducted regionally. In the variety breeding efforts, selection criteria vary based on climate, soil, diseases and pests of the region. In other words, varieties developed by breeders in accordance with their regional adaptation capacities are tested in official registration trials.

In VCU trials, Thrace and Southern Marmara constituting the Marmara region are taken into consideration under different categories due to the different environmental conditions of these two zones. The Thrace region has the second greatest annual precipitation after the Black Sea region according to long-term climate data (TSMS, 2018).

In VCU trials, candidate varieties are compared to control cultivars. The registration committee assesses the candidate varieties for yield, quality, resistance to diseases and economic value and then the ones equivalent to or better than the control cultivars are registered (RTMAF, 2008). Widely cultivated and accepted varieties by both the farmers and the industry are used as the control varieties in VCU trials. The VCU trials are conducted during at least two growing seasons and in at least 3 locations in each growing season. The varieties are grouped according to their performance using several statistical analyses. However, genotypes may have different responses to varying

http://www.aloki.hu ● ISSN 1589 1623 (Print) ● ISSN 1785 0037 (Online)
DOI: http://dx.doi.org/10.15666/aeer/1706_1292112936

environmental conditions. Genotype by environment interaction (GEI) is a phenotypic outcome of interaction between genotype and environment (Gebru et al., 2011). The phenotypic effects manifest themselves in yield, quality, diseases or the other attributes. Plant breeders consider phenotypic characteristics of the genotypes in different environments while selecting genotypes under the existence of GEI. In VCU trials, variety register experts assess the performance of candidate varieties in different environments. Although regional adaptation is taken into consideration in wheat VCU trials of Turkey, each region is divided into sub-regions or zones with different ecologies.

The significance of GEI is attempted to be revealed through variance analysis and different statistical parameters have been developed to elucidate response of genotypes to different environmental conditions. In the present study, GGE-Biplot method developed by Gabriel (1971) to assess G and GEI in multi-environment and multi-genotype trials was used. Biplot analysis facilitates a visual presentation of data. The method separates environments into mega environments based on genotype performances and points out which genotype is better in which environment (Yan et al., 2000). Biplot analysis also allows the user to compare the genotypes and environments and to estimate ideal genotypes for each environment, thus facilitate the assessment of VCU trials. For bread wheat, previous researchers used biplot analysis to assess yield (Kaya et al., 2006; Tulu and Wondimu, 2019), quality (Aktas et al., 2017) and disease data (Akcura et al., 2017). Xu et al. (2017) pointed out the significance of superior cultivars in cultivar registration system and indicated that quality should also be taken into consideration besides the yield levels in cotton. Researchers convert environment into a trait in GGE-biplot analysis and assessed candidate cultivars through GT-Biplot (Genotype by trait) by scaling all traits. GGE-Biplot analysis was used to assess cotton genotypes (Farias et al., 2016), maize genotypes (Oyekunle et al., 2017), barley genotypes (Solonechnyi et al., 2015) and potato genotypes (Flis et al., 2014).

The supports provided for certified seeds have brought about significant developments in the seed industry of Turkey. The number of varieties brought from abroad and applied for registration increased significantly. The majority of these varieties are Europe-originated ones and applied for registration in irrigated or rain-fed conditions of Thrace and Central Anatolia regions. It is quite significant to test candidate varieties together with control cultivars in different environments and to assess the trial outcomes together. Recent climate extremities increased the significance of variety stability. Put forth of response of candidate varieties to poor and ideal environmental conditions through VCU trials will facilitate the decision of the registration committee.

This study was conducted with 17 bread wheat genotypes at 7 different environments under rain-fed conditions of Thrace region in 2014-2015 and 2015-2016 growing seasons to assess genotype-environment interactions for grain yield and some quality traits through variety registration trials.

Materials and methods

Present experiments were conducted with 17 bread wheat genotypes at 7 different environments of the Thrace region in 2014-2015 and 2015-2016 growing seasons in randomized blocks design with 4 replications. Growing seasons and locations are provided in *Table 1* and locations are also shown on the map (*Fig. 1*). 12 bread wheat

http://www.aloki.hu ● ISSN 1589 1623 (Print) ● ISSN 1785 0037 (Online)
DOI: http://dx.doi.org/10.15666/aeer/1706_1292112936

genotypes (Energo, Yigit, Maya, Asli, Huseyinbey, Dunaviya, Pannonia, Misiia Odes'ka, Rebelde, Nomade, Os Jelena and Duru 17) and 5 control cultivars (Gelibolu, Kate A-1, Selimiye, Pehlivan, Krasunia odes'ka) were the plant material of the study. Experiments were set up on 9 m long plots with 6 rows in each plot spaced 17.0 cm apart. Sowing was performed with a 6-row grain drill as to have 500 seeds per m^2 arranged based on thousand-seed weight of the varieties. To each plot, 200 kg ha^{-1} composed fertilizer (20-20-0) was applied at sowing, 150 kg ha^{-1} urea (46%) was applied in February and 180 kg ha^{-1} ammonium nitrate (26%) was applied in April. Harvest was performed in the last week of June with a plot combine harvester. Side effects were omitted from the plots and harvest area 8 m^2 was used in assessments.

Table 1. *Genotypes and experimental locations*

Code	Genotype	Origin of genotype	Code	Growing season	Location
G1*	Gelibolu	Edirne-Turkey	E1	2014-2015	Kesan
G2*	Kate A-1	Bulgaria	E2	2015-2016	Kesan
G3*	Selimiye	Edirne-Turkey	E3	2014-2015	Edirne
G4*	Pehlivan	Edirne-Turkey	E4	2015-2016	Edirne
G5*	Krasunia odes'ka	Ukraine	E5	2014-2015	Tekirdag
G6	Energo	Austria	E6	2015-2016	Tekirdag
G7	Yigit	Kesan-Turkey	E7	2015-2016	Luleburgaz
G8	Maya	Tekirdag-Turkey			
G9	Asli	Austria			
G10	Huseyinbey	Tekirdag-Turkey			
G11	Dunaviya	Bulgaria			
G12	Pannonia	Serbia			
G13	Misiia Odes'ka	Ukraine			
G14	Rebelde	Italy			
G15	Nomade	Italy			
G16	Os Jelena	Croatia			
G17	Duru 17	Croatia			

*Control cultivars

Figure 1. *The view of experimental locations on the map*

http://www.aloki.hu ● ISSN 1589 1623 (Print) ● ISSN 1785 0037 (Online)
DOI: http://dx.doi.org/10.15666/aeer/1706_1292112936

Quality criteria such as 1000-kernel weight, test weight, protein content, Zeleny sedimentation and alveograph energy values were determined. For 1000-kernel weight, 4 × 100 kernels were randomly selected. They were then weighed to calculate 1000-kernel weight. Results were expressed in dry matter. Hectoliter or test weight was determined in accordance with Uluoz (1965). Protein content was determined in accordance with ICC 105/2 method and results were expressed in dry matter (ICC, 2002a). Zeleny sedimentation analysis was performed in accordance with ICC 116-1 method (ICC, 2002b) and alveograph analysis was performed in accordance with AACC 54.50 (AACC, 2000).

Monthly precipitation and average temperatures of the experimental locations for growing seasons are provided in *Table 2*. In the first growing season, total precipitations were greater than the long-term averages in Edirne, Luleburgaz and Tekirdag locations and lower than long-term averages in Kesan location. In the second growing season, all locations, except for Edirne, had total precipitations lower than the long-term averages. With regard to total monthly precipitations, deviations were observed from the long-term averages in both experimental years. In general, monthly average temperatures were greater than the long-term averages in all locations. Especially in the second growing season, average temperatures were quite greater than both the first growing season and the long-term averages.

Since the locations were not same to each growing season, statistical analyses for yield and quality parameters were performed through assuming each location as an environment. For grain yield, a combined variance analysis over the environments was performed. The GGE biplot method was used to identify genotype-environment interactions for yield and quality parameters. GenStat (Genstat, 2009) statistical analysis software was used for GGE-Biplot analysis.

Results and discussion

Grain yield

Results of combined variance analysis over the environments for grain yields are provided in *Table 3*. According to variance analysis, G, E and GEI were found to be significant ($p < 0.01$). The coefficient of variation was calculated as 8.96%.

The mean yields of bread wheat genotypes over 7 environments are given in *Table 4*. The highest yield was obtained from E1 (Kesan-2015) environment and the lowest yield was obtained from E4 (Edirne-2016) environment. Considering the results obtained from all environments, the genotype G15 (Nomade) had the greatest grain yield. G14, G10, G9 and G13 were in the same statistical group with G15. With regard to grain yield of G15 in different environments, it gave the highest yields in E4, E6 and E7 environments. However, for grain yield performance, G15 was ranked as 14^{th} in E1 and 13^{th} in E3 environment. Considering the grain yields of the other genotypes, they exhibited more or less different performances in different environments.

GGE-biplot analysis was able to explain 79.18% of GGE-induced variation in the grain yields of 17 bread wheat genotypes tested at 7 different environments. In the environment-focused model, GGE ratio was 62.50% over PC1 axis and 16.68% over PC2 axis. Also, in the environment-focused GGE-biplot graph, all of the environments had positive PC1 values and such a case indicate the existence of non-crossover GEI (*Fig. 2*). For PC2, environments had either negative or positive values. With regard to PC2, environments indicated the existence of crossover GEI. The vector lengths from

http://www.aloki.hu ● ISSN 1589 1623 (Print) ● ISSN 1785 0037 (Online)
DOI: http://dx.doi.org/10.15666/aeer/1706_1292112936

the biplot origin and the angles between the vectors of the environments were different. Vector lengths of the environments indicate the separation power among the genotypes (Yan and Kang, 2003). The angles between the vectors reveal significant information for comparison of the environments. Lower angles between the vectors indicate increasing similarity between the environments and closer response of genotypes in those environments (Yan, 2001). Obtuse angle between E1 (Kesan-2015) and E5 (Tekirdag-2015) vectors indicate that the performance of environments or genotypes was not similar. On the other hand, acute angles between E2, E3, E4, E6 and E7 vectors indicated that these environments were placed in the same mega-environment (*Fig. 3*). E1 and E5 constituted the other 2 mega-environments.

Table 2. *Monthly precipitation (mm) and average temperature (°C) data for the experimental years and locations*

	Precipitation (mm)											
	Edirne			**Tekirdag**			**Kesan**			**Luleburgaz***		
Months	**A**	**B**	**C**	**A**	**B**	**C**	**A**	**B**	**C**	**A**	**B**	**C**
September	105.0	29.5	37.2	92.2	34.9	33.6	121.4	63.0	34.0	4.8	35.0	34.2
October	121.8	52.6	57.7	131.0	83.7	62.4	59.2	97.2	58.0	89.9	80.4	54.4
November	43.2	26.2	68.1	35.2	48.5	75.4	22.4	26.2	84.0	64.6	31.9	66.1
December	111.3	0.3	70.0	80.3	0.6	81.5	93.4	3.0	102.0	116.3	0	70.6
January	42.2	114.8	66.7	49.4	70.7	68.8	56.4	85.0	81.0	98.7	97.2	61.9
February	68.6	89.2	52.0	90.3	68.4	54.1	58.8	77.0	72.0	36.1	91.4	51.0
March	67.8	54.8	51.6	29.4	30.6	54.4	59.8	23.6	69.0	43.5	20.9	46.6
April	44.4	116.1	47.2	60.1	22.9	40.9	69.8	28.8	51.0	67.1	46.0	45.6
May	45.2	81.4	53.3	32.0	28.4	36.7	9.0	45.4	40.0	24.2	50.6	49.4
June	31.0	10.2	46.5	58.4	35.0	37.9	42.8	40.4	36.0	67.9	26.2	47.4
Total	680.5	575.1	550.3	658.3	423.7	545.7	593.0	489.6	627.0	613.1	479.6	527.2
	Average temperature (°C)											
	Edirne			**Tekirdag**			**Kesan**			**Luleburgaz***		
Months	**A**	**B**	**C**	**A**	**B**	**C**	**A**	**B**	**C**	**A**	**B**	**C**
September	20.9	24.0	19.9	20.7	22.7	20.0	18.9	24.8	19.6	18.6	22.1	19.3
October	15.4	15.6	14.2	15.6	16.5	15.4	13.8	14.1	14.4	13.1	14.7	13.9
November	9.3	13.5	9.1	11.2	13.8	11.0	9.7	22.8	9.9	8.0	12.7	9.1
December	6.6	5.5	4.6	9.3	7.3	7.1	7.3	4.8	6.0	6.8	5.5	5.0
January	3.8	2.8	2.7	5.8	5.6	4.7	5.1	3.7	3.7	4.0	3.5	2.9
February	6.4	9.8	4.5	6.5	9.6	5.4	6.5	8.5	5.1	5.3	9.2	4.2
March	9.0	10.2	7.6	8.5	10.4	7.3	8.9	9.7	7.5	7.6	9.4	7.0
April	13.1	15.5	12.9	11.4	11.4	11.8	9.4	16.5	12.3	10.9	15.1	12.1
May	20.4	17.4	18.1	18.2	17.9	16.8	17.7	18.1	16.9	18.7	17.0	17.3
June	22.5	23.9	22.4	21.3	23.6	21.3	21.5	22.9	21.1	21.0	23.3	21.6
Means	12.7	13.8	11.6	12.9	13.9	12.1	11.9	14.6	11.7	11.4	13.3	11.2

A: 2014-2015 growing season, B: 2015-2016 growing season, C: Long-term average
*Kirklareli central station data

http://www.aloki.hu ● ISSN 1589 1623 (Print) ● ISSN 1785 0037 (Online)
DOI: http://dx.doi.org/10.15666/aeer/1706_1292112936

Table 3. *Results of combined variance analysis for grain yield*

Source of variation	Degrees of freedom (DF)	Sum of squares (SS)	Mean square (MS)	F
Replication	21	17.482	0.832**	2.36
Environment	6	155.852	25975**	73.74
Genotype	16	133.270	8329**	23.65
Genotype × Environment	96	85.926	0.895**	2.54
Error	336	118.361	0.352	
Corrected total	475	510.891		
CV (%): 8.96				

**Significant at 0.01 probability level

Table 4. *Mean yield of 17 bread wheat genotypes tested across 7 environments (t ha^{-1})*

Genotypes	Environments[3]							Mean[2]
	E1	E2	E3	E4	E5	E6	E7	
Gelibolu[1]	7.875	6.568	6.926	5.280	5.840	6.572	6.900	6.566 c-f
Kate A-1[1]	7.430	5.256	5.852	4.514	5.971	5.765	5.927	5.816 g
Selimiye[1]	6.924	4.342	5.569	4.047	6.246	5.916	5.993	5.577 g
Pehlivan[1]	6.542	5.204	5.659	3.887	6.081	5.886	6.414	5.667 g
Krasunia odes'ka[1]	7.765	6.812	6.524	6.372	6.191	6.772	7.357	6.827 bc
Energo	7.224	6.602	6.705	4.767	6.928	5.615	6.397	6.320 f
Yigit	7.827	6.093	6.932	5.468	5.793	6.302	6.985	6.486 def
Maya	7.936	6.641	6.422	5.792	5.728	6.510	7.393	6.632 cde
Asli	7.410	7.526	7.463	5.220	7.861	6.954	7.718	7.164 a
Huseyinbey	7.301	7.887	7.819	5.999	6.904	7.028	7.304	7.177 a
Dunaviya	7.450	6.690	6.582	6.176	6.788	6.236	6.420	6.620 c-f
Pannonia	8.076	7.095	6.253	5.555	6.017	6.806	7.357	6.737 cde
Misiia Odes'ka	7.565	7.517	6.990	6.012	6.961	7.438	7.371	7.122 ab
Rebelde	7.749	7.817	7.025	5.901	7.794	7.342	7.667	7.328 a
Nomade	7.285	7.784	6.296	6.937	7.189	7.850	8.082	7.346 a
Os Jelena	7.304	6.215	6.593	5.579	5.856	7.070	6.441	6.437 ef
Duru 17	7.957	6.504	6.869	5.227	6.701	7.202	7.081	6.791 cd
Mean	7.507	6.621	6.616	5.455	6.520	6.662	6.989	6.624

[1]Control cultivars
[2]Least Significant Difference (LSD) of genotypes: 0.312 (for alpha 0.05)
[3]Codes of environments are given in *Table 1*

For the assessment of multi-environment trials, initially mega-environments were determined to explain which-won-where model. Polygon view of GGE-biplot is an efficient means of data assessment (Yan and Kang, 2003; Yan, 2014). A polygon view is generated through connecting genotype pointers furthest located from the biplot origin and called as a vertex (*Fig. 3*). Eight orthogonal rays were drawn from the biplot origin to polygon sides or side extensions. In this way, 8 sectors were generated including environments and genotypes. Vertex genotypes are considered as the best genotype of that sector and the genotypes between the vertex genotype and the biplot

http://www.aloki.hu ● ISSN 1589 1623 (Print) ● ISSN 1785 0037 (Online)
DOI: http://dx.doi.org/10.15666/aeer/1706_1292112936

origin were considered as less sensitive. Despite 8 sectors were generated with the rays drawn, there were 3 mega-environments (ME) in the biplot graph. E1 (Kesan-2015) constituted ME-1; E2 (Kesan-2016), E3 (Edirne-2015), E4 (Edirne-2016), E6 (Tekirdag-2016) and E7 (Luleburgaz-2016) constituted ME-2 and E5 (Tekirdag-2015) constituted ME-3. G12 (Pannonia) and G8 (Maya) were identified as vertex genotypes of ME-1, G15 (Nomade) was the vertex genotype of ME-2 and G9 (Asli) was identified as the vertex genotype of ME-3.

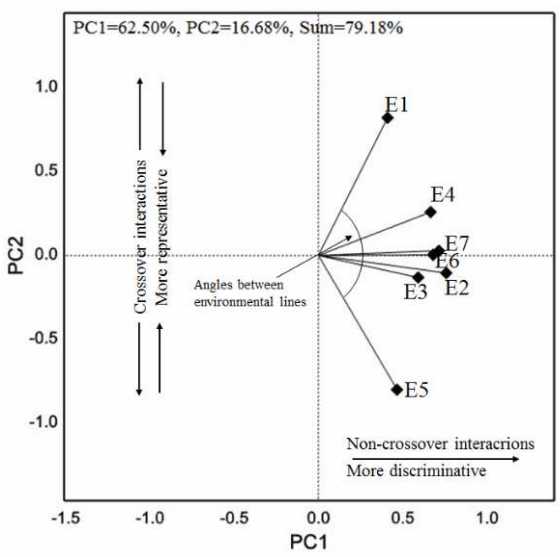

Figure 2. *The vector view of the GGE biplot among the trial environments. Abbreviations of environments are given in Table 1*

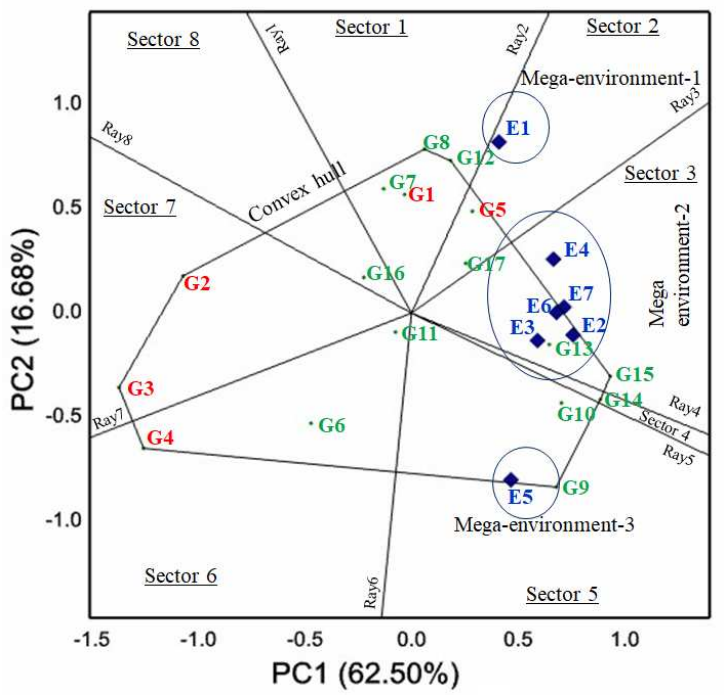

Figure 3. *The polygon view of the GGE biplot based on pattern for 17 bread wheat genotypes and trial environments. Codes of environments and genotypes are given in Table 1*

http://www.aloki.hu ● ISSN 1589 1623 (Print) ● ISSN 1785 0037 (Online)
DOI: http://dx.doi.org/10.15666/aeer/1706_1292112936

In *Figure 4,* the average environment coordinate (AEC) connecting average environment point representing the entire environments to biplot origin was drawn. In this way, the apsis of AEC was formed. The ordinate of AEC passes through the biplot origin and is orthogonal to AEC apsis (Yan and Kang, 2003). The arrow on AEC apsis shows the direction from the lower genotype effect to the higher genotype effect. AEC ordinate expresses bi-directional effect and indicates decreasing stability as moved away from the AEC apsis (Yan, 2001; Yan, 2002). From the ordinate of AEC to high performance along the AEC apsis, genotypes were respectively ordered as G8, G12, G17, G5, G13, G9, G10, G14 and G15. The other genotypes were left below the average. Considering the distances of genotypes (vector lengths) between AEC ordinate and average from the AEC apsis, it was observed that G13 was the closest cultivar to AEC apsis. The genotypes of G15, G14, G10 and G13 with high PC1 values and relatively shorter vector lengths to AEC apsis were expressed as stable genotypes. Although G9, G12 and G8 were above the average, they placed furthest to AEC apsis. In other words, although these cultivars were above the average, they were not able to exhibit stable performance in changing environments, thus they were considered as less stable cultivars. G11 was the closest cultivar to biplot origin, thus exhibited the least reaction to changing environments.

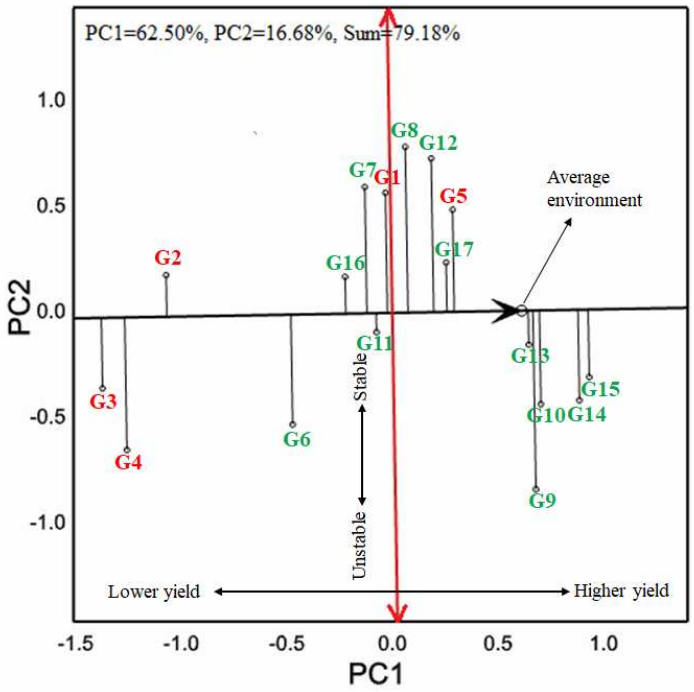

Figure 4. *The view of the distribution according to AEC of 17 bread wheat genotypes. Codes of genotypes are given in Table 1*

From a different perspective, assessments were made based on the ideal genotype in *Figure 5a*. The innermost circle represents the ideal genotype and the other circles represent the distance of other genotypes to the ideal genotype circle. G15 placed on the border of the innermost circle. G14, G10 and G13 were close to the ideal genotype region. Gradually increasing circle diameters indicate the way to undesirable genotypes region.

http://www.aloki.hu ● ISSN 1589 1623 (Print) ● ISSN 1785 0037 (Online)
DOI: http://dx.doi.org/10.15666/aeer/1706_1292112936

As it was in ideal genotype-focused assessments in *Figure 5a,* the environment-focused assessments are presented in *Figure 5b*. The environment E7 (Luleburgaz-2016) placed closest to the ideal environment center. Thus, E7 was considered as the best representative of all environments and thus had the greatest power of separation for genotypes. E1 and E5 were placed furthest from the ideal environment circle. These two environments constituted separately the ME-1 and ME-3 as presented in *Figure 3*.

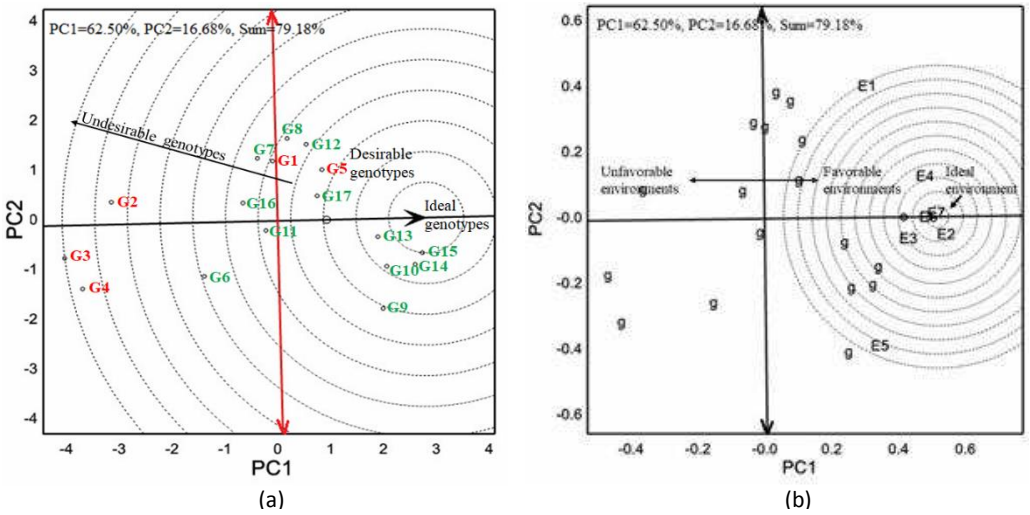

Figure 5. *(a) Comparison of 17 bread wheat genotypes with the ideal genotype. (b) Comparison of test environments with the ideal environment. Codes of environments and genotypes are given in Table 1*

Quality traits

The 1000-kernel weights, test weights, protein contents, Zeleny sedimentation and alveograph energy values of 17 bread wheat genotypes tested at 7 different environments are provided in *Table 5*. The variance analysis revealed significant differences ($p \leq 0.01$) in the quality traits between genotypes. The biplot graphs were generated separately for each quality trait. In VCU trials, candidate varieties are compared with the control varieties in terms of performance and adaptability. For quality criteria, the average of control cultivars (AC) was generated over the average of G1, G2, G3, G4 and G5 accepted as the control cultivars in each environment and candidate varieties were assessed on biplot over AC values.

Thousand-kernel weight

Regarding 1000-kernel weight, the genotypes G7, G10, G13, G11, G5, G1, G3, G6 and G4 gave PC1 values above the AEC ordinate (*Fig. 6a*). Among them, G4 had the greatest average 1000-kernel weight with the greatest vector length to AEC apsis. G7 and G8 were quite close to biplot origin, thus they were considered as the least sensitive to the environment. Of the genotypes with positive PC1 scores, except for G4 and G10, the others had close vector lengths to AEC. When the 1000-kernel weights were assessed over AC values, it was observed that G6 was the only genotype with a value greater than AC (*Fig. 6b*). Except for G6, all the other genotypes had values lower than AC. G14 had the lowest 1000-kernel weight, thus placed furthest to AEC and

http://www.aloki.hu ● ISSN 1589 1623 (Print) ● ISSN 1785 0037 (Online)
DOI: http://dx.doi.org/10.15666/aeer/1706_1292112936

considered as the least stable variety (*Fig. 6a*). The 1000-kernel weight is a significant yield parameter and greatly influenced by the genotype and environment (Mut et al., 2005). Besides being a yield component, it also reveals significant information about the flour yield (Aydogan and Soylu, 2017). With the GGE-biplot analysis on 1000-kernel weights, 79.75% of GGE-induced variation was explained.

Table 5. *Mean and standard deviation of some quality characteristics of 17 bread wheat genotypes tested across 7 environments*[1]

Genotypes	1000 Kernel weight (g)	Test weight (kg)	Protein content (%)	Zeleny sedimentation (ml)	Alveograph energy value (10^{-4} Joule)
Gelibolu[2]	35.5 (2.7)	79.1 (1.5)	12.6 (0.8)	45.1 (13.0)	253.1 (43.2)
Kate A-1[2]	33.4 (3.1)	78.3 (1.7)	13.8 (1.1)	40.3 (16.5)	178.6 (27.0)
Selimiye[2]	35.7 (1.8)	79.5 (1.6)	13.2 (1.1)	45.4 (17.5)	206.9 (45.0)
Pehlivan[2]	39.8 (4.1)	79.2 (1.4)	12.8 (0.7)	35.4 (14.9)	164.9 (42.1)
Krasunia odes'ka[2]	35.4 (2.2)	78.1 (1.3)	13.1 (0.5)	57.4 (12.1)	254.6 (44.9)
Energo	36.4 (2.5)	79.4 (1.1)	15.5 (1.1)	55.1 (11.5)	282.6 (71.6)
Yigit	34.4 (3.4)	76.8 (1.6)	13.6 (1.0)	39.1 (8.9)	199.6 (47.2)
Maya	34.1 (2.1)	76.9 (1.7)	12.1 (0.7)	38.9 (9.3)	169.0 (34.0)
Asli	33.8 (3.7)	78.8 (2.0)	13.6 (0.6)	52.6 (12.3)	266.7 (34.8)
Huseyinbey	35.3 (3.6)	76.7 (1.9)	12.7 (0.7)	43.3 (12.6)	186.6 (26.8)
Dunaviya	35.4 (2.3)	78.3 (1.0)	13.1 (0.7)	54.3 (12.9)	229.7 (39.8)
Pannonia	33.8 (3.9)	78.3 (2.2)	13.5 (1.1)	49.1 (17.4)	245.1 (59.2)
Misiia Odes'ka	35.3 (3.6)	77.7 (1.7)	12.4 (0.9)	48.1 (13.6)	221.0 (37.6)
Rebelde	28.3 (5.1)	79.0 (1.7)	14.9 (0.6)	63.7 (9.9)	267.4 (81.3)
Nomade	32.6 (2.6)	76.0 (1.6)	13.4 (0.8)	49.7 (13.8)	180.0 (50.0)
Os Jelena	31.3 (1.7)	80.2 (1.9)	13.3 (0.6)	52.3 (12.8)	249.7 (42.0)
Duru 17	32.1 (2.7)	77.2 (1.6)	13.9 (0.6)	48.3 (11.9)	253.9 (74.2)
Mean	34.27	78.21	13.37	48.13	224.08
LSD	2.21**	1.02**	0.69**	5.95**	43.87**

[1]The values in brackets indicate the standard deviation
[2]Control cultivars
**Significant at 0.01 probability level

Test weight

The genotypes of G2, G12, G11, G9, G14, G1, G4, G6, G3 and G16 had high PC1 values greater than the average on the test weight's biplot graph (*Fig. 7a*). Since G4 was placed over the AEC apsis indicates it was considered as the most stable genotype. Although G16, G3 and G6 had greater PC1 scores, they had the longest vector lengths to AEC apsis. The G15 with the greatest PC1 score for grain yield had the least PC1 score and a PC2 score of 0.0 for test weight. Besides having the least test weight, G15 proved such a trait in all environments. With regard to control cultivar-focused GGE-biplot, the AC axis had a greater PC1 score than the AEC axis (*Fig. 7b*). Such a case indicated that average of control cultivar was greater than the average of environments. Test weight is a physical analysis like 1000-kernel weight and reveals information about the shape, size and density of kernels (Bulut, 2012; Aktas et al., 2017).

http://www.aloki.hu ● ISSN 1589 1623 (Print) ● ISSN 1785 0037 (Online)
DOI: http://dx.doi.org/10.15666/aeer/1706_1292112936

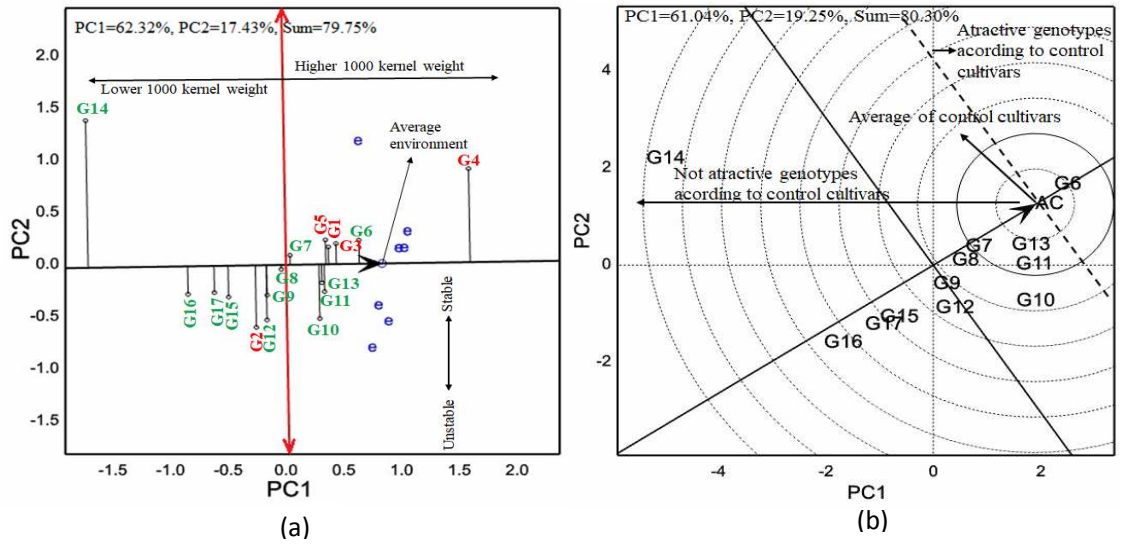

Figure 6. *(a) The view of the distribution of 1000 kernel weight of 17 bread wheat genotypes according to AEC. (b) Comparison of 12 bread wheat genotypes in terms of 1000 kernel weight with the average of control cultivars (AC). Codes of genotypes are given in Table 1*

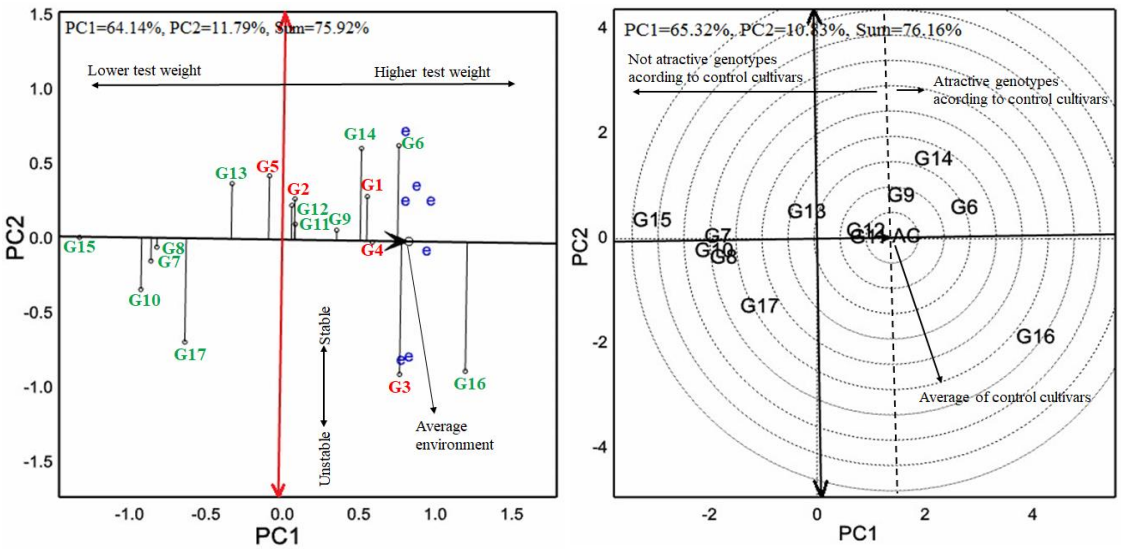

Figure 7. *(a) The view of the distribution of test weight of 17 bread wheat genotypes according to AEC. (b) Comparison of 12 bread wheat genotypes in terms of test weight with the average of control cultivars (AC). Codes of genotypes are given in Table 1*

Protein content

When evaluating genotypes from the aspect of protein content, G7, G12, G9, G2, G17, G14 and G6 had high PC1 scores over the averages (*Fig. 8a*). Since G9 was placed on AEC apsis, it was considered as the most stable genotype. The G6 was the most prominent genotype since it had the greatest PC1 score and was placed as the second closest genotype to the AEC axis after G9. The G14 had the second greatest PC1 score after G6, but it had a high vector length to AEC. In *Figure 8b,* biplot graphs were

http://www.aloki.hu ● ISSN 1589 1623 (Print) ● ISSN 1785 0037 (Online)
DOI: http://dx.doi.org/10.15666/aeer/1706_1292112936

generated through reversing PC1 and PC2 axes. When the assessments were done through comparisons with the control cultivars, it was observed that G10, G13 and G8 were placed behind the AC axis, in other words, they had lower protein contents than the control cultivars. The other genotypes had protein contents of above AC. Protein content is a significant quality trait for bread wheat and greatly influenced by the genotype and environment (Kahraman et al., 2017). Keceli et al. (2017) reported significant positive correlations between protein content and the other significant quality attributes.

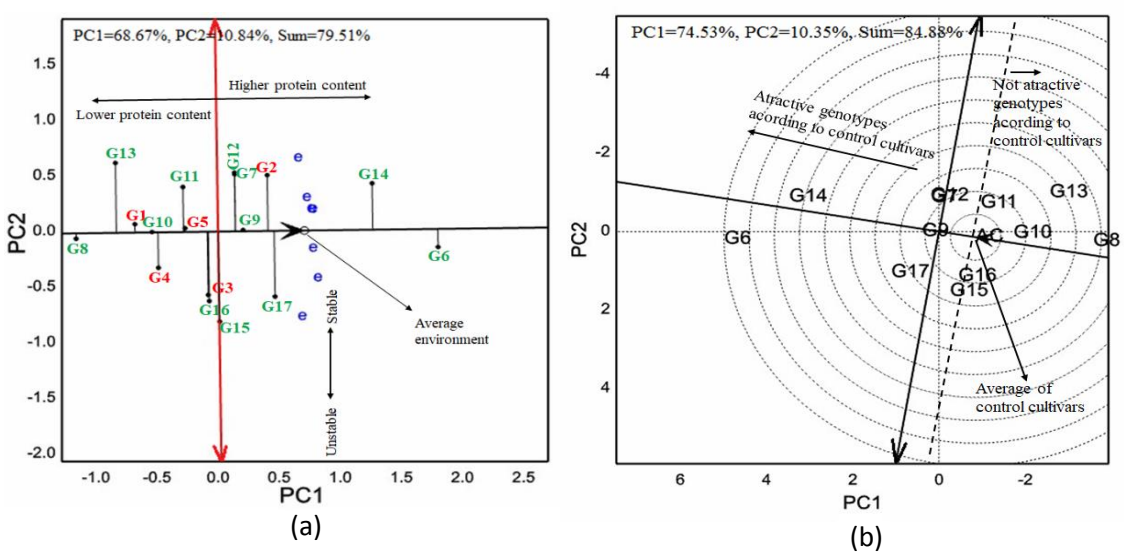

Figure 8. *(a) The view of the distribution of protein content of 17 bread wheat genotypes according to AEC. (b) Comparison of 12 bread wheat genotypes in terms of protein content with the average of control cultivars (AC). Codes of genotypes are given in Table 1*

Zeleny sedimentation and alveograph energy value

With regard to Zeleny sedimentation, G13, G15, G12, G16, G9, G11, G6, G5 and G14 were placed over the average (*Fig. 9a*). G13, G9, G11, G6 and G5 were the closest genotypes to the AEC axis. G14 had the greatest sedimentation score and a high vector length to AEC. G7, G8, G1, G2 and G3 with negative PC1 scores were placed furthest to AEC. These genotypes were behind the average of environments and quite sensitive to the environment. The G17 on biplot origin was considered as the least sensitive genotype to changing environments. When the Zeleny sedimentation values of the genotypes were compared with the values of control cultivars, it was observed that the majority of them had scores of above the AC (*Fig. 9b*). In *Figure 9b,* PC1 and PC2 axes were reversed. G10, G7 and G8 had scores of below AC. Zeleny sedimentation is considered as an indicator of protein quality and high values are desired in bread wheat (Sahin et al., 2017; Aydogan and Soylu, 2017).

Alveograph energy values yield significant information about the bread-making quality of the flour (Aydogan et al., 2012). The genotypes of G11, G16, G17, G12, G1, G5, G14, G9 and G6 had greater values than the average and thus had high PC1 scores, but their vector lengths to AEC were quite different (*Fig. 10a*). G6 had the greatest alveograph energy value. G14 had the greatest vector length to the AEC axis. As it was

http://www.aloki.hu ● ISSN 1589 1623 (Print) ● ISSN 1785 0037 (Online)
DOI: http://dx.doi.org/10.15666/aeer/1706_1292112936

in protein content, the majority of the varieties had values over the AC axis (*Fig. 10b*). G7, G8, G10 and G15 had lower values than the control cultivars. The other genotypes were above the AC.

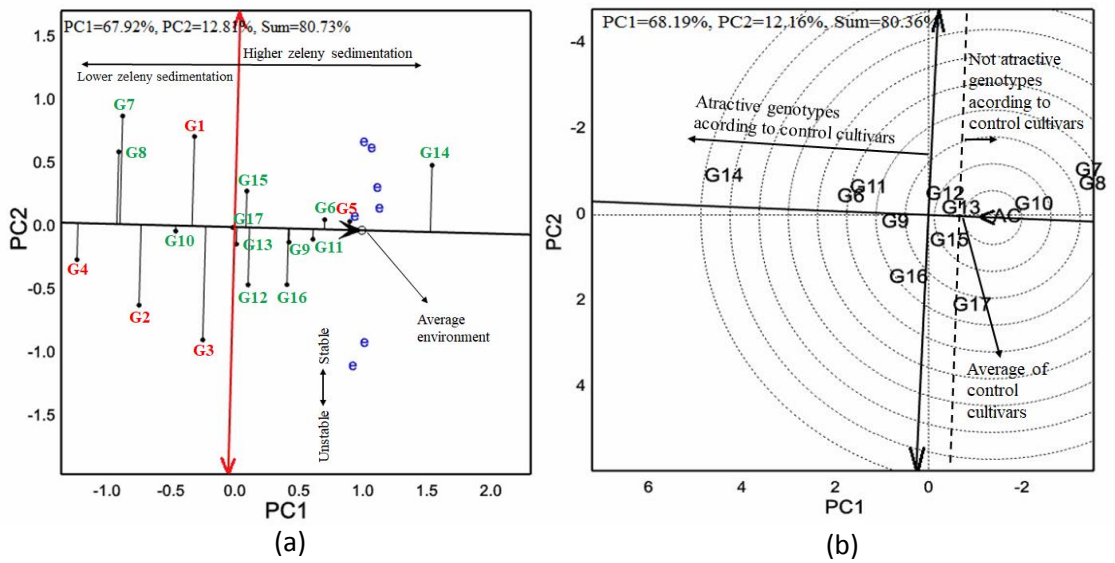

Figure 9. *(a) The view of the distribution of Zeleny sedimentation of 17 bread wheat genotypes according to AEC. (b) Comparison of 12 bread wheat genotypes in terms of Zeleny sedimentation with the AC. Codes of genotypes are given in Table 1*

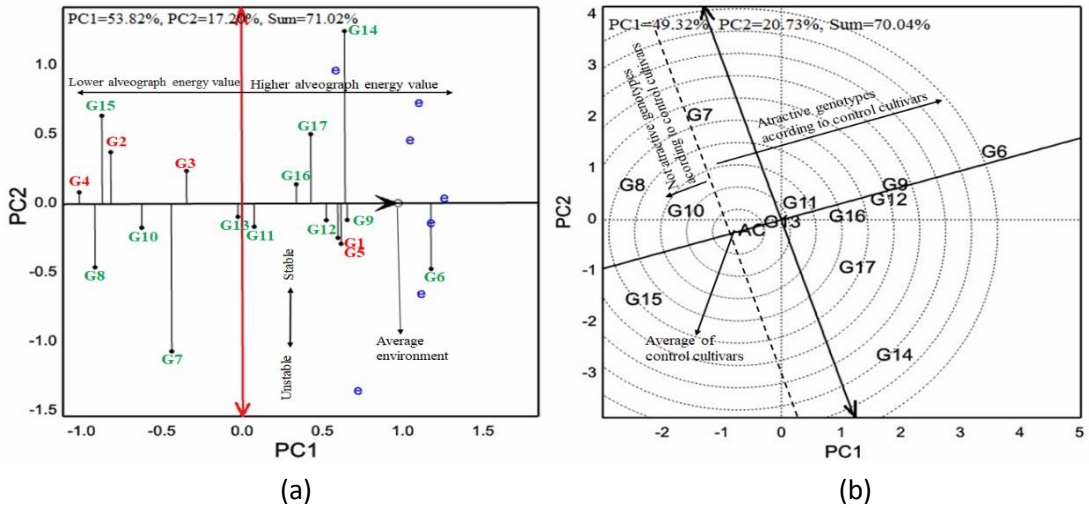

Figure 10. *(a) The view of the distribution of alveograph energy value of 17 bread wheat genotypes according to AEC. (b) Comparison of 12 bread wheat genotypes in terms of alveograph energy value with the AC. Codes of genotypes are given in Table 1*

Conclusion

A general assessment on grain yields revealed that control cultivars (Gelibolu, Kate A-1, Selimiye, Pehlivan, Krasunia odes'ka) had lower values than the average and the other genotypes had close to or greater values than the average. With regard to physical

http://www.aloki.hu ● ISSN 1589 1623 (Print) ● ISSN 1785 0037 (Online)
DOI: http://dx.doi.org/10.15666/aeer/1706_1292112936

quality traits (1000-kernel weight and test weight), control cultivars had greater values and genotypes exhibited different performances for the other quality traits. In this study, genotypes with quite high performance for both yield and quality traits were identified. Genotype responses to different environments and their stabilities in different environments were put forth.

The majority of Turkish agricultural lands are used in wheat culture. In recent years, several varieties were brought to Turkey from different countries and they were subjected to VCU trials. Although VCU trials are conducted for wheat based on regional adaptation capacities, climate parameters exhibited great variations from the long-term averages in recent years with the impacts of global warming. Wheat culture is practiced commonly under rain-fed conditions in Turkey, thus changes in environmental conditions play a significant role in the production. Genotype responses to changing environmental conditions with regard to yield, quality, diseases and other agricultural traits should be identified and registration reports should be prepared accordingly. Thrace region of Turkey is among the regions with the greatest number of varieties coming from abroad. Thus, the present study was conducted with 17 bread wheat varieties at 7 different environments of the Thrace region. Present findings revealed that GGE-biplot analysis could reliably be used in VCU trials for yield and quality traits. Grouping of experimental environments based on genotype responses, put forth of which-won-where model visually on graph and comparisons of environments and genotypes yielded quite significant assessments for the VCU trial reports.

Performance of registration experiments for new cultivars developed through long-term breeding programs is a significant issue for both breeders and growers. Grain yield is the most significant criterion for bread wheat in Turkey. Despite the satisfactory levels in grain yields, quality then became a dominant criterion in recent years. High stability in quality attributes besides high stability in grain yields will have great contributions to widespread of new cultivars.

REFERENCES

[1] AACC (2000): American Association of Cereal Chemists, Approved Methods of the AACC. 10th Ed. Method No: 54-50. – The Association, St. Paul, MN.

[2] Akcura, M., Akan, K., Hocaoglu, O. (2017): Biplot analysis of leaf rust resistance in pure lines selected from eastern Anatolian bread wheat landraces of Turkey. – Turkish Journal Field Crops 22(2): 227-234.

[3] Aktas, H., Erdemci, I., Karaman, M., Kendal, E., Tekdal, S. (2017): Evaluation grain yield and some quality traits of winter bread wheat genotypes using GGE-biplot analysis. – Tr. J. Nature Sci. 6(1): 43-51.

[4] Aydogan, S., Akcacik, A. G., Sahin, M., Kaya, Y., Koc, H., Gorgulu, M. N., Ekici, M. (2012): Determination of the relations between rheological properties of wheat flour which measured with alveograph, farinograph and mixograph. – Suleyman Demirel Un. Faculty of Agriculture Journal 7(1): 74-82.

[5] Aydogan, S., Soylu, S. (2017): Determination of yield, yield components and some quality properties of bread wheat varieties. – Journal of Field Crops Central Research Institute 26(1): 24-30.

[6] Bulut, S. (2012): Quality in bread wheat. – Journal of Erciyes University Institute of Natural and Applied Science 28(5): 441-446.

http://www.aloki.hu ● ISSN 1589 1623 (Print) ● ISSN 1785 0037 (Online)
DOI: http://dx.doi.org/10.15666/aeer/1706_1292112936

[7] Farias, F. J. C., Carvalho, L. P., Silva Filho, J. L., Teodoro, P. E. (2016): Biplot analysis of phenotypic stability in upland cotton genotypes in Mato Grosso. – Genetics and Molecular Research 15(2): gmr.15028009.
[8] Flis, B., Domanski, L., Zimnoch-Guzowska, E., Polgar, Z., Pousa, S. A., Pawlak, A. (2014): Stability analysis of agronomic traits in potato cultivars of different origin. – Am. J. Potato Res. 91: 404-413.
[9] Gabriel, K. R. (1971): The biplot graphic display of matrices with application to principal component analysis. – Biometrika 58: 453467.
[10] Gebru, H., Hailemariam, A., Belay, T. (2011): Genotype by environment interaction and grain yield stability of early maturing bread wheat (*Triticum aestivum* L.) genotypes in the drought prone areas of Tigray region, northern Ethiopia. – Ethiopian Journal of Science and Technology 2(1): 51-57.
[11] GenStat (2009): GenStat for Windows (12th Ed.) Introduction. – VSN International, Hemel Hempstead.
[12] ICC (2002a): Determination of Crude Protein in Cereals and Cereal Products for Food and Feed. Standard No: 105/2. – International Association for Cereal Science and Technology (ICC), Vienna.
[13] ICC (2002b): Standard Methods of International Association for Cereal Science and Technology. – ICC-Vienna.
[14] Kahraman, T., Ozturk, I., Avci, R., Aktas, H. (2017): The Effects of Genotype x environment ınteraction on some quality assessments in bread wheat (*T. aestivum* L.). – Journal of Central Research Institute for Field Crops 26(Special Issue): 15-22.
[15] Kaya, Y., Akcura, M., Taner, S. (2006): GGE-Biplot analysis of multi-environment yield trials in bread wheat. – Turkish Journal of Agriculture & Forestry 30: 325-337.
[16] Keceli, A., Evlice, A. K., Pehlivan, A., Sanal, T., Karaca, K., Kulen, S., Subasi, A. S., Salantur, A. (2017): Investigation of the relationship between Zeleny sedimentation analysis and other quality parameters in bread wheat (*Triticum aestivum* L.). – KSU J. Nat. Sci. 20(Special Issue): 292-296.
[17] Mut, Z., Aydın, N., Ozcan, H., Bayramoglu, H. O. (2005): Determination of yield and some quality traits of bread wheat (*Triticum aestivum* L.) genotypes in the Middle Black Sea Region. – GOU Journal of Faculty of Agriculture 22(2): 85-93.
[18] Oyekunle, M., Haruna, A., Badu-Apraku, B., Usman, I. S., Mani, H., Ado, S. G., Olaoye, G., Obeng-Antwi, K., Abdulmalik, R. O., Ahmed, H. O. (2017): Assessment of early-maturing maize hybrids and testing sites using GGE biplot analysis. – Crop Sci. 57: 2942-2950.
[19] RTMAF (2008): Regulation on Registration of Plant Varieties. – Republic of Turkey Ministry of Agriculture and Forestry, Official Newspaper, Date 13.01.2008, No: 26755.
[20] Sahin, M., Akcacik, A. G., Aydogan, S., Hamzaoglu, S., Demir, B., Yakisir, E. (2017): Investigation of the relationship between zeleny sedimentation and yield and some quality traits in winter bread wheat varieties. – J. of Bahri Dagdas Crop Research 6(1): 10-21.
[21] Solonechnyi, P., Vasko, N., Naumov, A., Solonechnaya, O., Vazhenina, O., Bondareva, O., Logvinenko, Y. (2015): GGE biplot analysis of genotype by environment interaction of spring barley varieties. – Zemdirbyste-Agriculture 102(4): 431-436.
[22] TSMS (2018): Rainfall Assessment Report. – The Turkish State Meteorological Service, Ankara.
[23] Tulu, L., Wondimu, A. (2019): Adaptability and yield stability of bread wheat (*Triticum aestivum*) varieties studied using GGE-biplot analysis in the highland environments of South-western Ethiopia. – African Journal of Plant Science 13(6): 153-162.
[24] Uluoz, M. (1965): Wheat, Flour and Bread Analysis Methods. – Ege University Faculty of Agriculture Publications, Izmir, Publication number: 57.

http://www.aloki.hu ● ISSN 1589 1623 (Print) ● ISSN 1785 0037 (Online)
DOI: http://dx.doi.org/10.15666/aeer/1706_1292112936

[25] Xu, N., Fok, M., Li, J., Yang, X., Yan, W. (2017): Optimization of cotton variety registration criteria aided with a genotype-by-trait biplot analysis. – Scientific Reports 7(1): 17237.
[26] Yan, W. (2001): GGE-biplot - a Windows application for graphical analysis of multi-environment trial data and other types of two way data. – Agron. J. 93: 1111-1118.
[27] Yan, W. (2002): Singular-value partitioning in biplot analysis of multienvironment trial data. – Agron. J. 94: 990-996.
[28] Yan, W. (2014): Crop Variety Trials: Data Management and Analysis. – Wiley-Blackwell, Hoboken, NJ.
[29] Yan, W., Hunt, L. A., Sheng, Q., Szlavnics, Z. (2000): Cultivar evaluation and mega-environment investigation based on the GGE biplot. – Crop Sci. 40: 597-605.
[30] Yan, W., Kang, M. S. (2003): GGE-Biplot Analysis: A Graphical Tool for Breeders, Geneticists and Agronomists. – CRD Press, Boca Raton.

http://www.aloki.hu ● ISSN 1589 1623 (Print) ● ISSN 1785 0037 (Online)
DOI: http://dx.doi.org/10.15666/aeer/1706_1292112936

PROPERTIES OF A PHTHALATE ESTERS HYDROLASE FROM *ARTHROBACTER* SP. ZJUTW AND COMPARISON OF ITS TRANSESTERIFICATION AND ESTER HYDROLYSIS ABILITY

QIU, L. – ZHANG, H. – YIN, X. – LIU, T. – WU, S.*

College of Biotechnology and Bioengineering, Zhejiang University of Technology, Hangzhou 310032, China

**Corresponding author*
e-mail: wujan28@zjut.edu.cn

(Received 22nd May 2019; accepted 28th Aug 2019)

Abstract. Microbial degradation is suggested to be the principal mechanism for removing Phthalate esters (PAEs) from the environment. PAEs esterase is one of key enzymes in the degradation pathway. In this study, a phthalate esters hydrolase gene, *pehA*, that displays good alkali stability, is cloned from *Arthrobacter* sp. ZJUTW and characterized. The enzyme showed a monomeric structure with a molecular mass of approximately 26.17 kDa and pI of 4.42. Its optimal pH and temperature were pH 10.0 and 50 °C, respectively. The enzyme was stable in a pH ranging from 8.0 to 10.0. In addition, the ester hydrolysis and transesterification catalytic ability of the esterase were compared through high performance liquid chromatography (HPLC) and Gas Chromatography-Mass Spectrometer (GC-MS). When performing the ester hydrolysis function, PehA has the catalytic ability to hydrolyze two ester bonds at the same time. The kinetic parameters of transesterification and ester hydrolysis conditions showed that the catalytic efficiency of transesterification is significantly higher than that of ester hydrolysis, and PehA preferentially catalyzed transesterification with PAEs and methanol as a substrate. This is the first report on the comparison of transesterification and ester hydrolysis ability of the PAEs esterase.
Keywords: *PehA, gene cloning, endocrine disrupting chemicals, degradation, purification*

Introduction

Phthalate esters (PAEs) are important synthetic organic compounds used as plasticizers in the industrial production of plastics. However, PAEs have become dangerous pollutants in environmental samples in recent years as endocrine disrupting chemicals which influence the genitals. Among rats and adult men, researches have shown that phthalate exposure increased DNA damage in sperm, induced hepatocellular tumors and in some cases reproductive toxicity (Fatoki and Ogunfowokan, 1993; Wang et al., 2004). Some of the PAEs including dimethyl phthalate (DMP), di-n-butyl phthalate (DBP), and di-n-octyl phthalate (DOP) have been listed as priority pollutants by the China National Environmental Monitoring Center (Fenner et al., 2013) and the US Environmental Protection Agency (Xu et al., 2005).

Since the photolysis and chemical hydrolysis rates of phthalate esters are very slow, microbial degradation is suggested to be the principal mechanism for removing PAEs from the environment. In recent years, some microorganisms have been reported to be capable of PAE degradation, these include *Gordonia* sp. (Jin et al., 2012), *Pseudomonas* sp. (Wang et al., 2003), *Arthrobacter* sp. (Wang et al., 2012), *Rhodococcus* sp. (Jin et al., 2010), *Camelimonas* sp. (Chen et al., 2014), *Pelotomaculum* and *Desulfotomaculum* species (Qiu et al., 2004). Numerous studies have demonstrated the microbial biodegradation pathways of phthalate esters. The metabolism of phthalate esters is initiated in bacteria by their hydrolysis converting them into mono-phthalate esters,

http://www.aloki.hu ● ISSN 1589 1623 (Print) ● ISSN 1785 0037 (Online)
DOI: http://dx.doi.org/10.15666/aeer/1706_1293712949

which are further degraded by ester-hydrolysis to phthalate (PA). PA is further metabolized in aerobic bacteria by two different dioxygenase-initiated pathways through the common intermediate, protocatechuate (3,4-dihydroxybenzoate). Protocatechuate is further degraded into organic acids through either ortho- or meta-cleavage pathway by ring cleavage enzymes, which eventually converted them into CO_2 and H_2O through Krebs cycle (Eaton, 2001; Stingley et al., 2004; Ren et al., 2018).

Hydrolysis of the ester bond is a common key initial step in the microbial degradation of PAEs. PAEs esterase is one of key enzymes in the degradation pathway. However, only a few enzymes involved in this reaction have been reported. These enzymes include dimethyl terephthalate (DMT) esterase from *Fusarium* sp. DMT-5-3 (Luo et al., 2012), two distinct PAE hydrolases in *Micrococcus* sp. YGJ1 (Akita et al., 2001; Maruyama et al., 2005), mono-2-ethylhexyl phthalate hydrolase from *Gordonia* sp. P8219 (Nishioka et al., 2006; Iwata et al., 2016), ester hydrolase PatE from *Rhodococcus jostii* RHA1 (Hara et al.,2010), DBP hydrolase CarEW from *Bacillus* sp. K91 (Ding et al.,2015), DBP hydrolase from *Acinetobacter* sp. M673 (Wu et al., 2013), and Esterase EstB and EstG from *Sphingobium* sp. SM42 (Whangsuk et al., 2015). The esterase can either cleave the ester bond by ester hydrolysis or transesterify with alcohols. Previous studies have only reported the ester hydrolysis catalytic ability of PAEs esterase, but not explored its transesterification ability. Due to the complex composition of pollutants in the environment, it is possible that both alcohols and PAEs exist simultaneously. It is necessary to explore the transesterification of microorganisms and their esterases.

The PAEs esterase play important roles in the decontamination of PAEs. Studying the catalytic mechanism and recombinant expression of PAEs esterase can help improve the efficiency of PAEs pollutants treatment. In this paper, we described a basophilic enzyme from *Arthrobacter* sp. ZJUTW isolated from sludge of the river of Hangzhou city. This enzyme displayed specific hydrolase activity toward PAEs. The experimental data from HPLC and GC-MS led us to compare the ester hydrolysis and transesterification catalytic ability of the esterase.

Materials and methods

Strains and reagents

Arthrobacter sp. ZJUTW was isolated from sludge in Shangtang River of Hangzhou City, using dibutyl phthalate as sole carbon and energy source. The strain was deposited at the China Center for Type Culture Collection (CCTCC) under the accession number CCTCC M2012246.

DMP, diethyl phthalate (DEP), DBP, di (2-ethylhexyl) phthalate (DEHP) were purchased from Sinopharm Chemical Reagent Co., Ltd, all were > 98% pure. HPLC-grade methanol was purchased from Tianjin Siyou Fine Chemicals Co., Ltd. (Tianjin, China). Nickel-NTA agarose and pET28a expression kit were purchased from Shanghai Sangon Biological Engineering Technology Co., Ltd. (Shanghai, China). Other chemicals were analytical-reagent grade, and were purchased locally.

Genome sequencing and sequence analysis

Genomic DNA of *Arthrobacter* sp. ZJUTW was extracted using a genomic DNA isolation kit by Dalian Takara Biomedical Technology Co., Ltd (Dalian, China).

http://www.aloki.hu ● ISSN 1589 1623 (Print) ● ISSN 1785 0037 (Online)
DOI: http://dx.doi.org/10.15666/aeer/1706_1293712949

Genome sequencing was performed by Zhejiang Tianke Biological Technology Co., Ltd. (Zhejiang, China) using Illumina Hiseq 2000 Sequencing platform, and a partial genomic sequence was obtained. Oligonucleotide primers were synthesized by Shanghai Sangon Biological Engineering Technology and Services Co., Ltd. (Shanghai, China). The full-length salicylate esterase gene *pehA* was revealed based on the prediction of ORFs from the partial genomic sequence by the Glimmer 3.02 (http://www.cbcb.umd.edu/software/glimmer/). Putative functions were inferred using the Basic Local Alignment Search Tool (BLAST) (http://blast.ncbi.nlm.nih.gov/Blast.cgi). Protein similarity search and alignment were performed using the data from CLUSTAL W (Thompson et al., 1994). The signal sequence for peptide cleavage in the amino acid sequences of *pehA* was predicted using SignalP 4.0 (www.cbs.dtu.dk/services/Signal P) (Petersen et al., 2011). ESPript output was used to render the analysis of multiple sequence alignment (Gouet et al., 1999). The neighbor-joining method in the molecular evolutionary genetic analysis software package MEGA (version 6.0) was used to construct a phylogenetic tree. The theoretical molecular mass and isoelectric point of the deduced *pehA* protein sequence was calculated using the Compute pI/Mw tool on the ExPASy proteomics server (available at http://ex pasy.org/tools/p itool.html).

Expression and purification of recombinant PehA

The *pehA* gene was amplified by primers P1 (forward): 5'-CGCGGATCCATGGAGATCGTACTGGTGCA-3' and P1 (reverse): 5'-CCCAAGCTTCCA GTCCTGTTAGGCAATGAC-3'. Initial activation of the *Taq* DNA polymerase was performed for 5 min at 94 °C, followed by 32 cycles as follows: 94 °C for 45 s, then 55 °C for 45 s, 72 °C for 90 s, followed by a final extension at 72 °C for 10 min. Then following the manufacturer's instructions, the expression of *pehA* gene was performed using the *pET*28a expression kit. The PCR product was ligated to the *pET*28a vector and introduced into *E. coli* BL21 (DE3) cells. Positive colonies were picked and grown in Luria-Bertani (LB) at 37 °C in the presence of 50 μg/ml of kanamycin to an OD600 of 0.6. The culture was then induced with 1.0 mM IPTG and grown at 22 °C with shaking at 180 rpm for 18 h. The cells were harvested, re- suspended in 20 mM potassium phosphate buffer (pH 8.0), and disrupted by sonication. After centrifugation at 12,000 × g at 4 °C for 15 min, the supernatant was collected and further purified by a 2 ml volume of NTA-Ni^{2+} agarose following the manufacturer's instructions. The following purification was then performed by size exclusion chromatography on a Q Sepharose XL 10/30 column (Amersham Bioscience) equilibrated with 20 mM sodium phosphate buffer (pH 8.0) at a flow rate of 1.0 ml min. The purified recombinant PehA was examined using sodium salt-polyacrylamide gel electrophoresis (SDS-PAGE). The protein concentration was quantified using the Bradford procedure with bovine serum albumin as a standard.

Assay of enzyme activity

Enzyme activity was quantified at 40°C, with 120 uL of 10 mM ρ-nitrophenyl butyrate (ρ-NPC4) substrates, 1.68ml of 50 mM phosphate buffer (pH 8.0), and 200 μl of the purified PehA. Blank reactions were performed with every measurement to subtract appropriate values for non-enzymatic hydrolysis of the substrate. The production of ρ-nitrophenol (ρ-NP) was monitored in triplicate every minute for 5 min

http://www.aloki.hu ● ISSN 1589 1623 (Print) ● ISSN 1785 0037 (Online)
DOI: http://dx.doi.org/10.15666/aeer/1706_1293712949

at 405 nm. One unit of esterase activity was defined as the amount of enzyme that produced 1 μmol ρ-NP in 1 min under the assay conditions

Properties of the PehA

The effect of pH and temperature on enzyme activity and stability was measured on ρ-NPC4 ester substrates for relative activity, which was expressed as a percentage of the initial activity. The optimum pH was determined by measuring the activity at 40 °C over the pH region 3.0-11.0. The stability at different pH (5.0-10.0) was determined after incubating the enzyme for 30 min and by measuring the relative activity at 40 °C and pH 8.0. The optimum temperature was determined by assaying the enzyme activity at various temperatures (30-70 °C) for 20 min in 0.02 mol/l potassium phosphate buffer (pH 8.0). The thermostability was determined by measuring the remaining activity at 30 °C and pH8.0, after incubation of the purified esterase between 30 and 70 °C and pH 8.0 for 30 min.

The effect of different potential inhibitors or activators (metal ions and organic solvents) on the enzyme activity was also determined by measuring the relative activity using a standard assay with ρ-NPC4 as the substrate. The reaction system was 120 μL of 10 mM ρ-NPC4 ester substrates, 1.68 ml of 50 mM phosphate buffer (pH 8.0), 200 μl of the purified PehA, and a final concentration of 1.0 mM of different metal or a final concentration of 1.0% (volume to volume ratio) of organic solvent. The enzyme was preincubated at 40 °C for 5 min. The remaining activity was assayed was described. The activity assayed in the absence of inhibitors or activators was defined as the control.

Comparison of transesterification and ester hydrolysis ability

For comparing the transesterification and ester hydrolysis ability of PehA, the enzyme kinetic constants were determined by measuring the initial rate of enzymic reaction for DBP, DEP and DMP, which were firstly dissolved in methanol and dimethyl sulfoxide (DMSO), respectively. Parametric identification of maximum velocity (V_{max}) and Michaelis-Menten constants (K_m) was used from the equation for initial reaction velocity. The recombinant PehA assays were performed in 50 mM Tris-HCl buffer (pH 8.0) with 10 mM of DBP, DEP or DMP (firstly dissolved in methanol and DMSO, respectively) at 40 °C for 10 min. The substrate amount was then determined by HPLC/MS analysis. The substrate-free assay system was also used as blank simultaneously. Kinetic values were calculated from nonlinear regression data analysis against various substrate concentrations.

HPLC and GC-MS analytical methods

The mixture of enzymatic degradation was extracted with equal volume dichloromethane, then the extract was evaporated, and the residue was dissolved in 1 ml methanol. The amount of remaining substrate was determined by HPLC (Agilent 1260 series, USA) equipped with a Diamonsil-C18 column (4.6 mm × 250 mm × 5 μm; Dikma Technologies Inc, China). A mixture of methanol and H_2O (90:10 by volume) was used as the mobile phase at a flow rate of 1.0 ml min^{-1}. The UV detector wavelength was 235 nm and the sampling quantity was 20 μl.

After collecting the HPLC peaks separately, enzymatic degradation products were identified using a Hewlett Packard 6890N gas chromatograph (Hewlett Packard, USA) equipped with an Agilent 5975C mass selective detector (Agilent, USA). The column

http://www.aloki.hu ● ISSN 1589 1623 (Print) ● ISSN 1785 0037 (Online)
DOI: http://dx.doi.org/10.15666/aeer/1706_1293712949

used was a HP-5MS (30 m × 250 m × 0.25 m) capillary column. The temperature program consisted of 1 min hold at 60 °C, an increase to 220 °C at 30 °C min^{-1}, and 2 min hold, an increase to 250 °C at 5 °C min^{-1}, and 2 min hold, an increase to 280 °C at 5 °C min^{-1}, and 3 min hold. The injection volume was 1 μl and the carrier gas was helium (1.0 ml min^{-1}). The mass spectrometer was operated at an electron ionization energy of 70 eV. Instrumental library searches, comparison with available authentic compounds, and mass fragmentation pattern were used to identify the degradation products.

Statistical analysis methodology

Each treatment in the experiment was performed in triplicates. Software Origin 8.0 was used to draw the figures with error bars. Data are expressed as the mean ± standard deviation (SD).

Results and discussion

Sequence analysis of PehA

A gene annotated as "salicylate esterase" with a 723-long ORF that encoded 240 amino acid proteins was found and we named it as *pehA*. No signal sequence was found. Sequence alignment revealed that amino acid sequence of *pehA* was 100% sequence identity to alpha/beta hydrolase from *Gordonia* QH-11 (*Fig. 1*), which was not reported about catalytic ability of PAEs. In addition, these sequences all contain the typical catalytic triad composed of Ser75-Glu194-His221 and the consensus motif (Gly-X-Ser-X-Gly) around the active-site serine (*Fig. 2*). Some PAEs esterases sequences were retrieved and compared with known representative esterases' sequences of eight families (Ren et al., 2018). The catalytic triad containing Ser, Glu (or Asp), and His was widely reported in families IV, V, and VII. Most enzymes in family V possess the typical α/β-hydrolase fold with a catalytic triad (Arpigny and Jaeger, 1999), and existed basic amino acid (H and R) in GX1SX2GG motif, suggesting PehA belongs to the family V. The sequence similarities and conservation of typical catalytic triads suggest that these enzymes may have a number of important common functions that were conserved during the course of evolution.

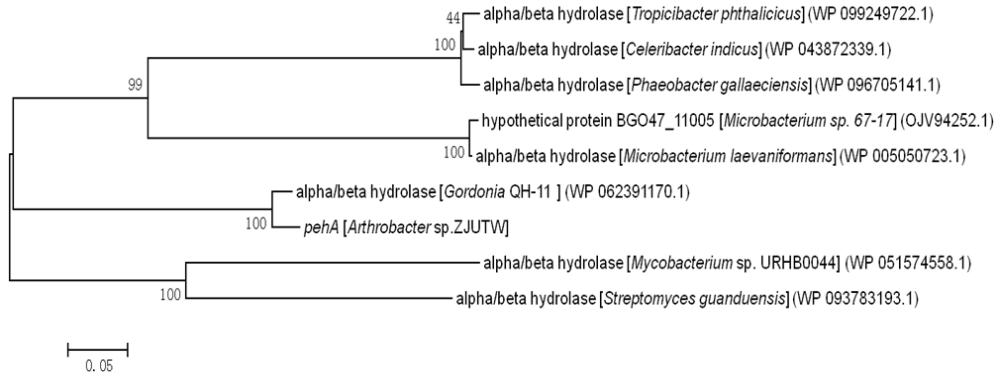

Figure 1. *Neighbor-joining tree of esterases. Protein sequences were aligned using the built-in CLUSTAL W (default parameters), the tree was built using the neighbor-joining method with default parameters and 1000 bootstrap replications*

http://www.aloki.hu ● ISSN 1589 1623 (Print) ● ISSN 1785 0037 (Online)
DOI: http://dx.doi.org/10.15666/aeer/1706_1293712949

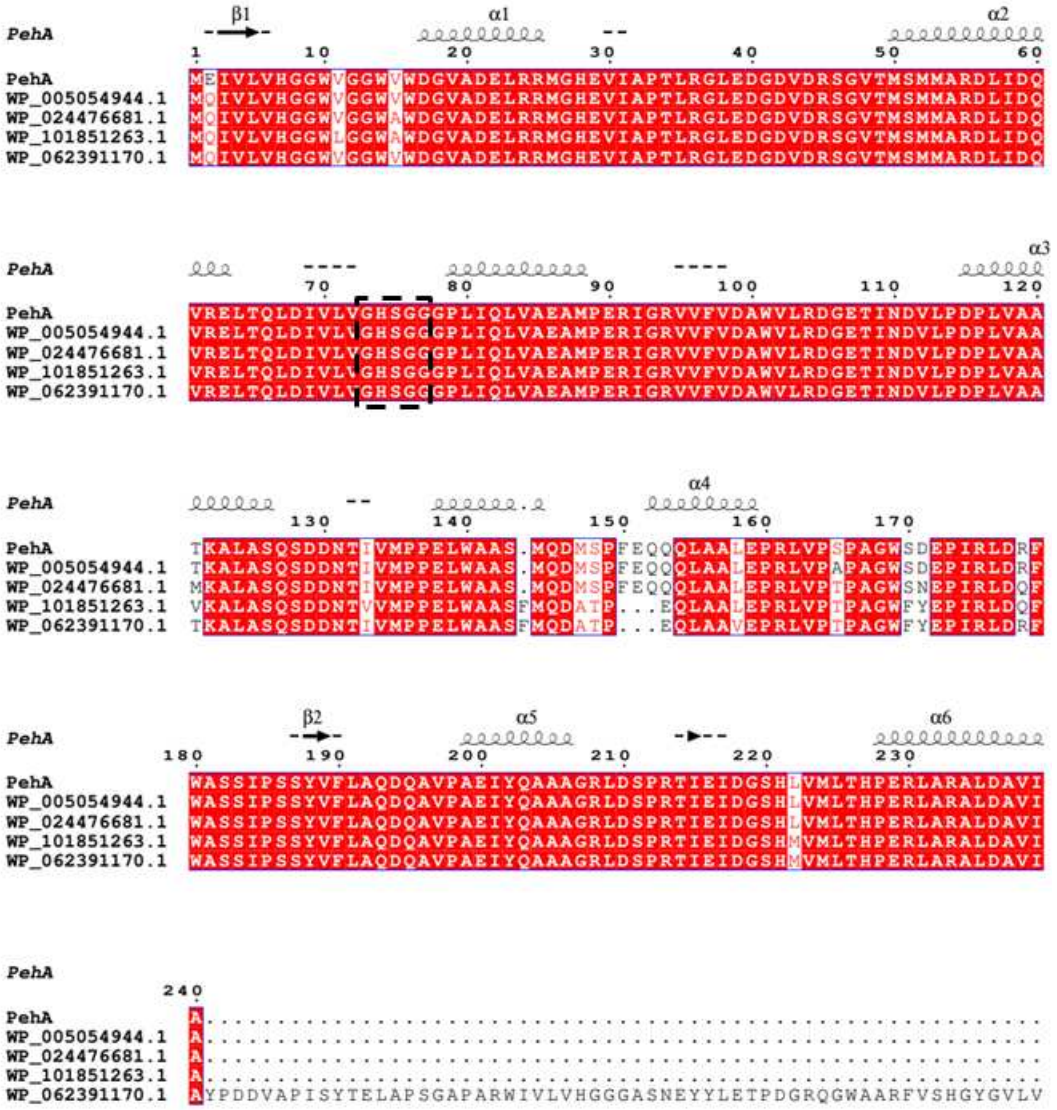

Figure 2. *Protein sequences alignment between PehA and homologs from the carboxylesterase family. ESPript outputs obtained with the sequences from the SWISSPROPT databank and alignment with CLUSTAL W. Sequences are grouped according to similarity. WP_005054944.1 from alpha/beta hydrolase of Microbacterium; WP_024476681.1 from alpha/beta hydrolase of Actinobacteria; WP_101851263.1 from alpha/beta hydrolase of Kocuria flava; WP_062391170.1 from alpha/beta hydrolase of Gordonia phthalatica. A conserved pentapeptide (GXSXG), containing the serine residue of the catalytic triad, was framed by a dotted box. Symbols above blocks of sequences represent the secondary structure, springs represent helices, and arrows represent β-strands*

Enzyme cloning, overexpression and purification

To investigate the biochemical properties of the enzyme, the *pehA* gene was expressed in the *pET*-28a vector as a 6 × His tagged fusion protein and induced with 1 mM IPTG or without IPTG at 20 °C for 18 h. The crude enzyme extracted from recombinant *E. coli* BL21 cells was purified using Ni^{2+}-NTA metal-chelating affinity chromatography and analyzed by SDS–PAGE. As shown in *Figure 3* (lane 3), one band corresponded in size to the calculated molecular mass of PehA was detected

http://www.aloki.hu ● ISSN 1589 1623 (Print) ● ISSN 1785 0037 (Online)
DOI: http://dx.doi.org/10.15666/aeer/1706_1293712949

(26.17 kDa). The band was absent in the control lane from the *E. coli* BL21 cells induced without IPTG (*Fig. 3,* lane 1). The isoelectric point (pI) was 4.42.

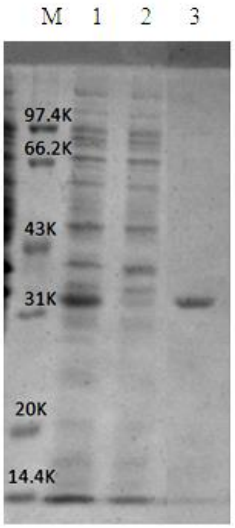

Figure 3. *Analysis of the protein expressed in E. coli BL21 cells following purification on a 12% SDS- PAGE. Lane M, protein molecular marker; Lane 1, after induction with 1 mM IPTG and grown at 20 °C for 18 h; Lane 2, before induction with IPTG; and Lane 3, purified recombinant PehA (molecular weight without histidine tag is 26.17 kDa)*

Effect of pH and temperature on enzyme activity and stability

The effect of pH on PehA activity was determined using ρ-NPC4 as the substrate at 40 °C with pH values ranging from 4.0 to 11.0. Optimum activity was observed at pH 10.0, with approximately no activity at pH 4.0 (*Fig. 4A*). The pH stability analysis revealed that the enzyme was very stable at pH 7.0- 10.0, retaining more than 70% of the original activity after pre-incubation at the given pH range for 60 min. However, PehA only maintained 41% and 32% of its activity at pH 6.0 and 11.0, respectively, after incubation for 60 min.

The effect of temperature on PehA activity was investigated using ρ-NPC4 as the substrate at pH 7.0 with the temperature ranging from 30 to 70 °C. Optimum activity was observed at 50 °C. When the temperature rises above 50 °C, the enzyme activity drops sharply. The temperature stability of PehA was examined by measuring its residual activity after incubating the purified enzyme for 0.5 h from 30 to 70 °C. PehA retained approximately 95%, 99%, 86% of its activity after incubation for 0.5 h at 30, 40 and 50 °C respectively. However, the enzyme was unstable above 70 °C, and retained approximately 33% of activity (*Fig. 4B*).

Effect of metal ions and organic solvents on enzyme activity

The effect of different metal ions on PehA activity was examined by addition of each metal ion into the reaction mixture at a final concentration of 1.0 mM. The results are presented in *Table 1*. Ni^{2+}, had a moderately inhibitory effect (86.2% residual activity); Mg^{2+}, K^{+}, Zn^{2+}, Ba^{2+}, Al^{3+} and Li^{+} had no apparent effect on enzyme activity; whereas Co^{2+}, Cu^{2+} and Mn^{2+} activated PehA, and Fe^{3+} strongly activated PehA with residual activities of 163%.

http://www.aloki.hu ● ISSN 1589 1623 (Print) ● ISSN 1785 0037 (Online)
DOI: http://dx.doi.org/10.15666/aeer/1706_1293712949

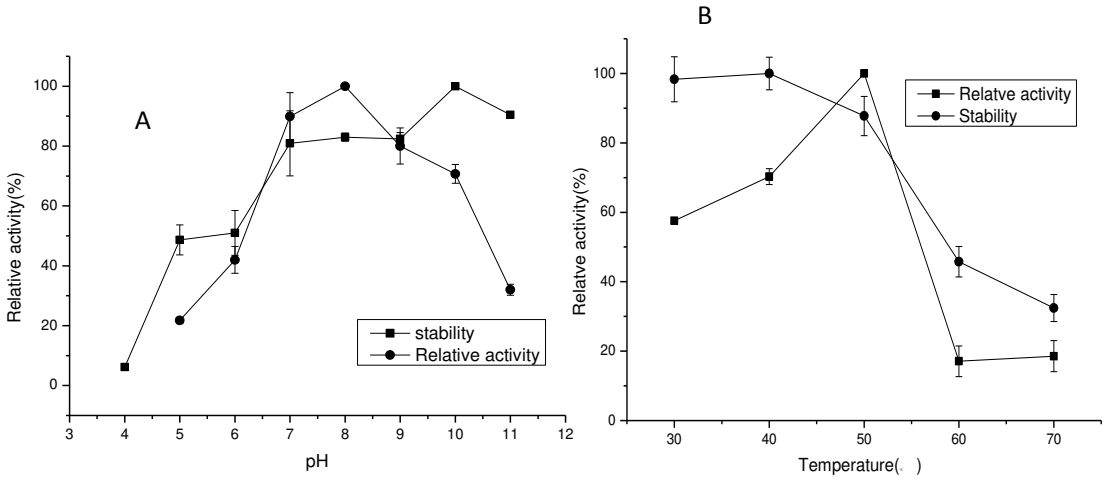

Figure 4. *Effect of temperature and pH on PehA activity and stability. Relative activity of purified PehA was determined at different pH (A) or temperatures (B) using ρ-NP butyrate (ρ-NPC4) as the substrate at 405 nm. Remaining enzyme activity was measured at 40 °C and pH 8.0 after incubating purified PehA at different temperatures (B) or pH for 60 min*

Table 1. *Effect of various metal ions and organic solvents on enzyme activity*

Metal ions/organic solvents	Concentration	Relative activity (%)
control	0 mmol/L	100
Ni^{2+}	1 mmol/L	86.2 ± 3.78
Mg^{2+}	1 mmol/L	98.0 ± 6.24
Co^{2+}	1 mmol/L	109.3 ± 3.21
Ba^{2+}	1 mmol/L	105.4 ± 2.61
Zn^{2+}	1 mmol/L	105.0 ± 7.43
Ca^{2+}	1 mmol/L	112.3 ± 6.37
Cu^{2+}	1 mmol/L	117.6 ± 4.45
Mn^{2+}	1 mmol/L	123.0 ± 3.54
Fe^{3+}	1 mmol/L	163.1 ± 4.59
K^{+}	1 mmol/L	107.3 ± 2.15
Al^{3+}	1 mmol/L	101.2 ± 2.07
Methanol	1%V/V	107.4 ± 7.74
Ethanol	1%V/V	109.9 ± 8.21
Acetone	1%V/V	105.5 ± 1.88
DMSO	1%V/V	97.4 ± 0.81
Formaldehyde	1%V/V	22.3 ± 1.33
Acetonitrile	1%V/V	93.8 ± 21.97
Trichloromethane	1%V/V	60.3 ± 2.87
Tween 80	1%V/V	80.5 ± 8.91

Organic solvents such as Formaldehyde (1%) strongly inhibited PehA (22.3% residual activity), and Trichloromethane (1%) and Tween 80 (1%) exhibited moderate

http://www.aloki.hu ● ISSN 1589 1623 (Print) ● ISSN 1785 0037 (Online)
DOI: http://dx.doi.org/10.15666/aeer/1706_1293712949

inhibitory effects (approximately 60.3% and 80.5%, respectively). Acetonitrile (1%) and DMSO (1%) had little inhibitory effect on the enzyme activity (97.4% and 93.8% residual activities, respectively), whereas methanol (1%), ethanol (1%), and acetone (1%) little activated PehA with residual activities of 107.4%, 109.9% and 105.5%, respectively.

Comparison of transesterification and ester hydrolysis ability of PehA

Break of the ester bond is a common key initial step in the microbial degradation of phthalate esters. Esterase has two kinds of catalytic reactions involved transesterification and Ester hydrolysis to execute the Initial degradation step. To explore the catalytic ability for transesterification and Ester hydrolysis of PehA, The products of the reaction catalyzed were identified by HPLC and GC-MS. In the reaction system containing methanol, butyl methyl phthalate (BMP) was detected (*Figs. 5A* and *6A, B*), indicating that in this system, PehA exchanged a methyl group on methanol with butyl group of DBP through a transesterification reaction. In the reaction system containing no methanol (DBP dissolved in DMSO), PA was detected (*Figs. 5B* and *6C*), and mono-butyl phthalate (MBP) was not detected, indicating that the esterase hydrolyzes two ester bonds simultaneously by ester hydrolysis to produce PA. However, in most of the previous reports, the initial step in the degradation of PAEs is that esterase hydrolyzes one ester bond to produce a monoester, then monoesterase hydrolyze another ester bond to form PA, suggesting that PehA has the catalytic ability to hydrolyze two ester bonds at the same time. Kcat/Km is one of the specificity constants of the enzyme, and can represent the specificity of the same enzyme for several substrates that compete with each other. The Kcat/Km ratio is a measure of the priority of different substrates, and the substrate with the larger Kcat/Km ratio is the preferred target for the enzyme. The kinetic parameters of different substrates were determined at pH 8.0 and 40 °C using the purified recombinant PehA (*Table 2*). After comparing the ester hydrolysis and transesterification catalytic kinetic constants of several PAEs, the results showed that the ester hydrolysis catalytic activity of esterase was significantly stronger than that of transesterification. In *Table 2,* the Kcat/Km values of DEP (containing methanol) and DEP (no methanol) as substrates are 41.02 and 0.47, respectively, and that of DBP (containing methanol) and DBP (no methanol) are 8.95 and 0.213, respectively, indicating that the catalytic efficiency of transesterification is significantly higher than that of ester hydrolysis in the presence of methanol, and PehA preferentially catalyzed transesterification with PAEs and methanol as a substrate. In addition, PehA exhibited strong catalytic ability for DBP and DEP, weak catalytic ability for DMP, and no catalytic ability for DEHP. This result suggested that PehA might have an ester chain length-dependence of PAEs. The kinetic parameters of some PAEs hydrolase are reported, the Kcat/Km values of DBP as substrates are 0.109 s^{-1} μM^{-1} (Ding et al., 2015), 0.07 s^{-1} μM^{-1} (Jiao et al., 2013) and 10.11 s^{-1} μM^{-1} (Wu et al., 2013), respectively, but all these data could only be measured at the condition of hydrolyzation. There is no report on the kinetic parameters of transesterification of these PAEs esterase. Some studies have reported that microorganisms can degrade PAEs through the ester conversion reaction process (Cartwright et al., 2000; Amir et al., 2005; Okamoto et al., 2011), but did not separate the esterases from these strains. To our knowledge, this is the first report on the comparison of transesterification and ester hydrolysis ability of PAEs esterase, and can help to further understand the degradation mechanism of PAEs by microbial.

http://www.aloki.hu ● ISSN 1589 1623 (Print) ● ISSN 1785 0037 (Online)
DOI: http://dx.doi.org/10.15666/aeer/1706_1293712949

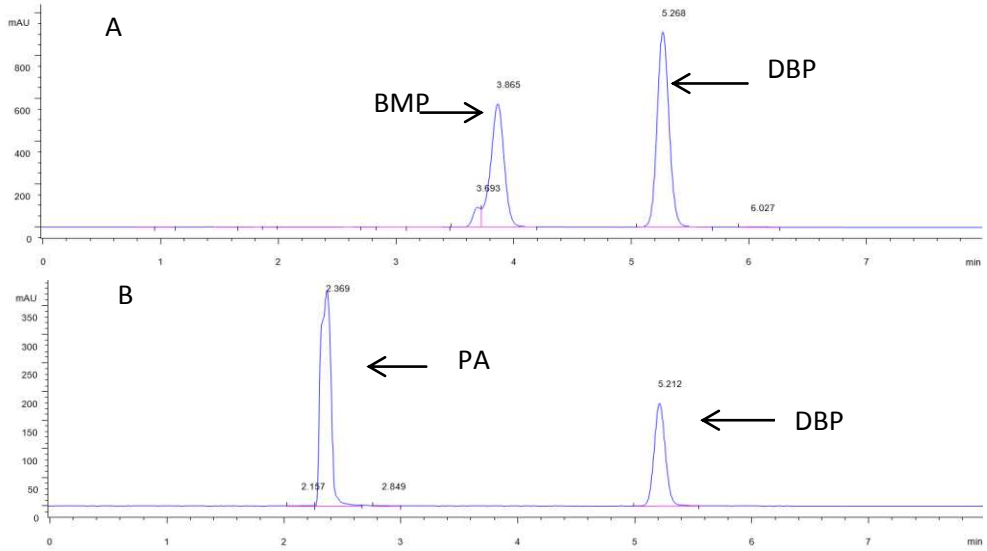

Figure 5. *The results of HPLC analyses of enzymatic products. (A) The results of DBP dissolved in methanol as a substrate after incubation with PehA. (B) The results of DBP dissolved in DMSO as a substrate after incubation with PehA*

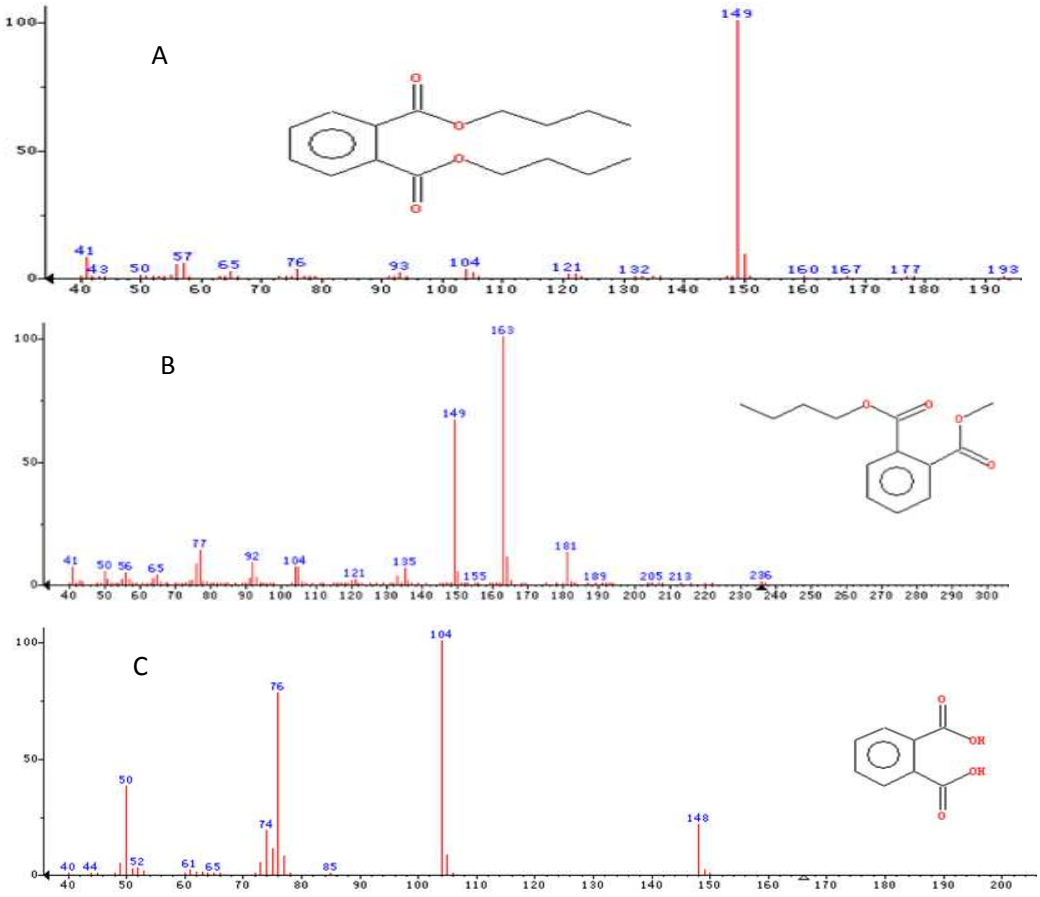

Figure 6. *GC-MS analysis of products identified in the PehA catalyzed reaction. (A) Mass spectrometry of peak time of 5.212 min and 5.268 min by HPLC in Figure 5. (B) Mass spectrometry of peak time of 3.865 min by HPLC in Figure 5. (C) Mass spectrometry of peak time of 2.369 min by HPLC in Figure 5*

http://www.aloki.hu ● ISSN 1589 1623 (Print) ● ISSN 1785 0037 (Online)
DOI: http://dx.doi.org/10.15666/aeer/1706_1293712949

Table 2. *Kinetic parameters of the recombinant PehA on different substrates at pH 8.0 and 40 °C*

Substrate	Vmax (mmol/min·mg)	Km (mmol/l)	Kcat(/s)	Kcat/Km (l/s·mmol)
DEP (dissolved in methanol)	41.17 ± 1.32	0.44 ± 0.03	17.9 ± 1.44	41.02
DBP (dissolved in methanol)	54.90 ± 1.87	2.67 ± 0.02	23.8 ± 0.94	8.95
DMP (dissolved in methanol)	0.239 ± 0.01	10.79 ± 0.72	0.104 ± 0.01	0.0096
DEP (dissolved in DMSO)	373.02 ± 11.42	347.6 ± 9.35	162.2 ± 6.58	0.470
DBP (dissolved in DMSO)	319.11 ± 22.06	472.5 ± 13.18	100.64 ± 8.36	0.213
DMP (dissolved in DMSO)	1.032 ± 0.02	1288 ± 20.07	3.56 ± 0.4	0.00276

Conclusions

In this study, the *pehA* gene efficiently degraded several PAEs such as DBP, DEP and DMP, was cloned from *Arthrobacter* sp. ZJUTW and heterologously expressed in *Escherichia coli* BL21 using the *pET28a* expression system. The enzyme showed a monomeric structure with a molecular mass of approximately 26.17 kDa and pI of 4.42. The enzyme exhibited maximal activity at pH 10.0 and 50 °C, The enzyme was better stable within the pH range from 8.0 to 10.0. HPLC and GC-MS were employed to detect the catalytic ability of PehA. The results showed that this enzyme has two catalytic functions: transesterification and Ester hydrolysis. When performing the ester hydrolysis function, it has the catalytic ability to hydrolyze two ester bonds at the same time. Through comparing the kinetic parameters of transesterification and ester hydrolysis conditions, we found that the catalytic efficiency of transesterification is significantly higher than that of ester hydrolysis, and PehA preferentially catalyzed transesterification with PAEs and methanol as a substrate. The PAEs esterase play important roles in the decontamination of PAEs, the production of such recombinant enzyme can probably provide efficient biocatalysts at low costs for environmental protection purposes.

Acknowledgments. This study was supported by the Zhejiang Provincial Natural Science Foundation of China under Grant No. LY15C010002, for that the authors are grateful.

REFERENCES

[1] Akita, K., Naitou, C., Maruyama, K. (2001): Purification and characterization of an esterase from *Micrococcus* sp. YGJ1 hydrolyzing phthalate esters. – Bioscience Biotechnology and Biochemistry 65: 1680-1683.

[2] Amir, S., Hafidi, M., Merlina, G., Hamdi, H., Jouraiphy, A., El Gharous, M., Revel, J. C. (2005): Fate of phthalic acid esters during composting of both lagooning and activated sludges. – Process Biochemistry 40(6): 2183-2190.

[3] Arpigny, J. L., Jaeger, K. E. (1999): Bacterial lipolytic enzymes: classification and properties. – Biochemical Journal 343(1): 177-183.

[4] Cartwright, C. D., Owen, S. A., Thompson, I. P., Burns, R. G. (2000): Biodegradation of diethyl phthalate in soil by a novel pathway. – Fems Microbiology Letters 186(1): 27-34.

[5] Chen, X. P., Xu, S. S., Tan, T. F., Lee, S. T., Cheng, S. H., Lee, F., Xu, S., Ho, K. C. (2014): Toxicity and estrogenic endocrine disrupting activity of phthalates and their

http://www.aloki.hu ● ISSN 1589 1623 (Print) ● ISSN 1785 0037 (Online)
DOI: http://dx.doi.org/10.15666/aeer/1706_1293712949

mixtures. – International Journal of Environmental Research and Public Health 11: 3156-3168.

[6] Ding, J. M., Wang, C. F., Xie, Z. R., Li, J. J., Yang, Y. J., Mu, Y. L., Tang, X. H., Xu, B., Zhou, J. P., Huang, Z. X. (2015): Properties of a Newly Identified Esterase from *Bacillus* sp. K91 and Its Novel Function in Diisobutyl Phthalate Degradation. – PLoS One 10: e0119216.

[7] Eaton, R. W. (2001): Plasmid-encoded phthalate catabolic pathway in *Arthrobacter keyseri* 12B. – Journal of Bacteriology 183: 3689-3703.

[8] Fatoki, O. S., Ogunfowokan, A. O. (1993): Determination of phthalate ester plasticizers in the aquatic environment of southwestern Nigeria. – Environment International 19: 619-623.

[9] Fenner, K., Canonica, S., Wackett, L. P., Elsner, M. (2013): Evaluating pesticide degradation in the environment: blind spots and emerging opportunities. – Science 341: 752-758.

[10] Gouet, P., Courcelle, E., Stuart, D. I., Metoz, F. (1999): ESPript: analysis of multiple sequence alignments in Post-Script. – Bioinformatics 15: 305-308.

[11] Hara, H., Stewart, G. R., Mohn, W. W. (2010): Involvement of a novel ABC transporter and monoalkyl phthalate ester hydrolase in phthalate ester catabolism by *Rhodococcus jostii* RHA1. – Applied and Environmental Microbiology 76: 1516-1523.

[12] Iwata, M., Imaoka, T., Nishiyama, T., Fujii, T. (2016): Re-characterization of mono-2-ethylhexyl phthalate hydrolase belonging to the serine hydrolase family. – Journal of Bioscience and Bioengineering 122: 140-145.

[13] Jiao, Y., Chen, X., Wang, X., Liao, X., Xiao, L., Miao, A., Wu, J., Yang, L. (2013): Identification and characterization of a cold-active phthalate esters hydrolase by screening a meta genomic library derived from biofilms of a wastewater treatment plant. – PLoS One 8(10): e75977.

[14] Jin, D., Bai, Z., Chang, D., Hoefel, D., Jin, B., Wang, P., Wei, D., Zhuang, G. (2012): Biodegradation of di-n-butyl phthalate by an isolated *Gordonia* sp. strain QH-11: Genetic identification and degradation kinetics. – Journal of Hazardous Materials 221-222: 80-85.

[15] Jin, D. C., Liang, R. X., Dai, Q. Y., Zhang, R. Y., Wu, X. L., Chao, W. L. (2010): Biodegradation of di-n-butyl phthalate by *Rhodococcus* sp. JDC-11 and molecular detection of 3,4-phthalate dioxygenase gene. – Journal of Microbiology and Biotechnology 20: 1440-1445.

[16] Luo, Z. H., Wu, Y. R., Chow, R. K. K., Luo, J. J., Gu, J. D., Vrijmoed, L. L. P. (2012): Purification and characterization of an intracellular esterase from a *Fusarium* species capable of degrading dimethyl terephthalate. – Process Biochemistry 47: 687-693.

[17] Maruyama, K., Akita, K., Naitou, C., Yoshida, M., Kitamura, T. (2005): Purification and characterization of an esterase hydrolyzing monoalkyl phthalates from *Micrococcus* sp. YGJ1. – Journal of Biochemistry 137: 27-32.

[18] Nishioka T., Iwata M., Imaoka T., Mutoh, M., Fujii, T. (2006): A mono-2-ethylhexyl phthalate hydrolase from a *Gordonia* sp. that is able to dissimilate di-2-ethylhexyl phthalate. – Applied and Environmental Microbiology 72: 2394-2399.

[19] Okamoto, Y., Toda, C., Ueda, K., Hashizume, K., Kojima, N. (2011): Transesterification in the microbial degradation of phthalate esters. – Journal of Health Science 57(3): 293-299.

[20] Petersen, T. N., Brunak, S., von Heijne, G., Nielsen, H. (2011): SignalP 4.0: discriminating signal peptides from transmembrane regions. – Nature Methods 8: 785-786.

[21] Qiu, Y. L., Sekiguchi, Y., Imachi, H., Kamagata, Y., Tseng, I. C., Cheng, S. S., Akiyoshi, O., Hideki, H. (2004): Identification and isolation of anaerobic, syntrophic phthalate isomer-degrading microbes from methanogenic sludges treating wastewater from terephthalate manufacturing. – Applied and Environmental Microbiology 70: 1617-1626.

http://www.aloki.hu ● ISSN 1589 1623 (Print) ● ISSN 1785 0037 (Online)
DOI: http://dx.doi.org/10.15666/aeer/1706_1293712949

[22] Ren, L., Lin, Z., Liu, H., Hu, H. (2018): Bacteria-mediated phthalic acid esters degradation and related molecular mechanisms. – Applied Microbiology and Biotechnology 102: 1085-1096.
[23] Stingley, R. L., Brezna, B., Khan, A. A., Cerniglia, C. E. (2004): Novel organization of genes in a phthalate degradation operon of *Mycobacterium vanbaalenii* PYR-1. – Microbiology 150: 2749-2761.
[24] Thompson, J. D., Higgins, D. G., Gibson, T. J. (1994): CLUSTAL W: improving the sensitivity of progressive multiple sequence alignment through sequence weighting, position-specific gap penalties and weight matrix choice. – Nucleic Acids Research 22: 4673-4680.
[25] Xu, X., Li, H., Gu, J. D. (2005): Biodegradation of an endocrine-disrupting chemical di-n-butyl phthalate ester by *Pseudomonas fluorescens* B-1. – International Biodeterioration & Biodegradation 55: 9-15.
[26] Wang, Y., Fan, Y., Gu, J. D. (2003): Microbial degradation of the endocrine-disrupting chemicals phthalic acid and dimethyl phthalate ester under aerobic conditions. – Bulletin of Environmental Contamination and Toxicology 71: 810-818.
[27] Wang, Y., Miao, B., Hou, D., Wu, X., Peng, B. (2012): Biodegradation of di-n-butyl phthalate and expression of the 3,4-phthalate dioxygenase gene in *Arthrobacter* sp. ZH2 strain. – Process Biochemistry 47: 936-940.
[28] Wang, Y. Y., Fan, Y. Z., Gu, J. D. (2004): Dimetbyl phtbalate ester degradation by two planktonic and immobilized bacterial consortia. – International Biodeterioration & Biodegradation 53: 93-101.
[29] Whangsuk, W., Sungkeeree, P., Nakasiri, M., Thiengmag, S., Mongkolsuk, S., Loprasert, S. (2015): Two endocrine disrupting dibutyl phthalate degrading esterases and their compensatory gene expression in *Sphingobium* sp. SM42. – International Biodeterioration & Biodegradation 99: 45-54.
[30] Wu, J., Liao, X., Yu, F., Wei, Z., Yang, L. (2013): Cloning of a dibutyl phthalate hydrolase gene from *Acinetobacter* sp. Strain M673 and functional analysis of its expression product in *Escherichia coli*. – Applied Microbiology and Biotechnology 97: 2483-2491.

http://www.aloki.hu ● ISSN 1589 1623 (Print) ● ISSN 1785 0037 (Online)
DOI: http://dx.doi.org/10.15666/aeer/1706_1293712949

STUDY ON THE AEROBIC MICROBE POPULATION DYNAMICS OF BULKING SLUDGE IN WASTEWATER TREATMENT

WANG, S.[1,2] – XIAO, X. L.[1*] – CHENG, S. G.[1,2] – LAI, F.[1] – QIAO, X. R.[3]

[1]*School of Environmental Science and Engineering, Shaanxi University of Science and Technology, Xi'an 710021, China*

[2]*National Demonstration Center for Experimental Light Chemistry Engineering Education, Shaanxi University of Science & Technology, Xi'an 710021, China*

[3]*School of Arts and Sciences, Shaanxi University of Science and Technology, Xi'an 710021, China*

**Corresponding author*
e-mail: xxl0108@163.com, phone: + 86-136-3680-8617

(Received 22nd May 2019; accepted 28th Aug 2019)

Abstract. Activated sludge process is one of the most common methods in wastewater treatment, however, bulking sludge is nerve-wracking during the actual treatment. In this study, Polymerase chain reaction-denaturing gradient gel electrophoresis (PCR-DGGE) was employed to study the diversity of the micro-organisms of the untreated sludge and bulking sludge in the biological wastewater treatment. Simultaneously, microbe species and dominant microflora of the untreated sludge and the bulking sludge were analyzed. This paper provides a reliable theoretical basis to the prevention and control of the bulking of the activated sludge. The results indicate that the bulking of the activated sludge is mainly caused by the change of microbe population.
Keywords: *PCR-DGGE, the diversity of microbe, bulking sludge, filamentous, dominant microflora*

Introduction

The activated sludge treatment is an aerobic biological treatment. Under the aerobic condition, the organic matter in the wastewater is decomposed into inorganic materials, so as to purify the wastewater (Shao et al., 2005). Sludge bulking is a frequent and serious problem in plants using activated sludge, and the causes are fairly complex. Many researchers have studied this issue. The over-growth of many filamentous bacteria may cause the bulking problem (Henze et al., 2008). Simultaneously, theoretical studies on the overgrowth of the filamentous bacteria have also progressed (Eikelboom et al., 1975; Sezgin et al., 1980). The causes of sludge bulking can be divided into two types: the first is caused by the rapid multiplication of the filamentous bacteria in the activated sludge; and the other is caused by a large accumulation of highly viscous substances produced by bacterial colloid (Qin et al., 1989; Ma et al., 2012). In recent years, the metabolic diversity and genetic adaptability of microbes in sludge have been studied. Denaturing gradient gel electrophoresis (DGGE) fingerprint results indicated a shift in bacterial community composition during the granulation of aerobic granules, which was confirmed by 16SrRNA gene sequencing (Aqeel et al., 2015). Real-time quantitative polymerase chain reaction (qPCR) was used to study the abundance and community structure of ammonia-oxidizing bacteria in the activated sludge taken from different geographic

http://www.aloki.hu ● ISSN 1589 1623 (Print) ● ISSN 1785 0037 (Online)
DOI: http://dx.doi.org/10.15666/aeer/1706_1295112958

regions in China (He et al., 2018). The abundance of filamentous morphotypes and floc-formers able to store biopolymers were analysed by PCR-DGGE and 16S amplicon sequencing (Meunier et al., 2016). With the development of modern molecular biotechnology such as DNA extraction, it is possible to analyze the diversity of microbial species and heredity (Li et al., 2015; Jiang et al., 2014).

In this study, PCR-DGGE was employed to study the micro-biodiversity of the untreated sludge and the bulking sludge. The species and dominant microflora of microbes in the two kinds of sludge were compared, and the causes of sludge bulking were found, which provides a reliable perspective for solving the problem.

Materials and methods

Materials

The experiment material was collected from the acclimated sludge and filamentous bulking sludge in a wastewater treatment plant Xi'an, China.

Methods

PCR-DGGE include preparation of sample DNA, PCR amplification and denaturing gradient gel electrophoresis (Sun et al., 2009).

(1) Preparation of sample DNA

Bacteria acquired through Centrifuge collection were dissolved in 5mL extraction buffer (100 mM Tris·Cl, 100 mM EDTA-Na2, 200 mM NaCl, 2% CTAB, pH 8.0) and were shaken at 37 °C for 30min. 0.75 mL 20% SDS was added in the solution above then water bathed it at 65 °C for 1 h. The supernatant was collected by centrifugation at 12000 rpm for 10 min. The volume (the same as the supernatant) of the mixture of phenol, Chloroform and Isoamyl alcohol, the ratio of which are 25:24:1, was extracted twice, 0.3 M of NaAC (pH 5.2) and ethyl alcohol which was twice as the volume as the extracted solution were added, and precipitated for 1 h at ambient temperature. After centrifugation (12000 rpm, 20 min) at 4 °C, the precipitate was collected and rinsed twice with 70% ethanol, then dried and dissolved in 50 μl TE.

(2) PCR amplification

PCR amplification primers used are F357(5'-CGCCCGCCGCGCCCCGCGCCCGGCCCGCCGCCCCCGCCCCCCTACGGGAGGCAGCAG -3') and R518(5'- ATT ACC GCGGCTGCT GG -3') from bacteria 16SrDNA V3 Highly variable region for the analysis of the diversity of the bacteria in the activated sludge. PCR amplification primers used fungus NS1(GTAGTCATATGCTTGTCTC) and Fung-GC(GC-ATTCCCCGTTACCCGTTG) for the analysis of the fungal diversity.

(3) Denaturing gradient gel electrophoresis (DGGE)

D-Code Universal Mutation Detection System (Bio-Rad) was used for the DGGE of the PCR products.

http://www.aloki.hu ● ISSN 1589 1623 (Print) ● ISSN 1785 0037 (Online)
DOI: http://dx.doi.org/10.15666/aeer/1706_1295112958

Results and discussion

Analysis of the bacteria diversity of the untreated activated and bulking sludge

After DGGE analysis and sequencing, the gene sequence was compared with the NCBI database, and the results of the main bacteria identification in the untreated sludge and bulking sludge were shown in *Tables 1,2* and *Figures 1,2*.

Table 1. *Identified bacteria species in the untreated sludge*

Stripe number	Clone number	V3 region	Bacteria species generic name
1	> 8.15XDG123-1-M13-	194bp	*Zoogloea sp.*
2	> 8.20XDG123-3-M13-	194bp	*Sterolibacterium sp.*
3	> 8.15XDG123-4-M13-	194bp	*Uncultured bacterium*
4	> 8.15XDG123-5-M13-	194bp	*Pseudomonas sp.*
5	> 8.15XDG123-8-M13-	194bp	*Legionella pneumophila*
6	> 8.15XDG123-9-M13-	193bp	*Uncultured bacterium*
7	> 8.15XDG123-10-M13-	194bp	*Uncultured Aquabacterium sp.*
8	> 8.15XDG123-12-M13-	187bp	*Uncultured bacterium*
9	> 8.15XDG123-15-M13-	174bp	*Agrococcus lahaulensis*
10	> 8.15XDG123-18-M13-	194bp	*Uncultured Alcaligenes sp.*

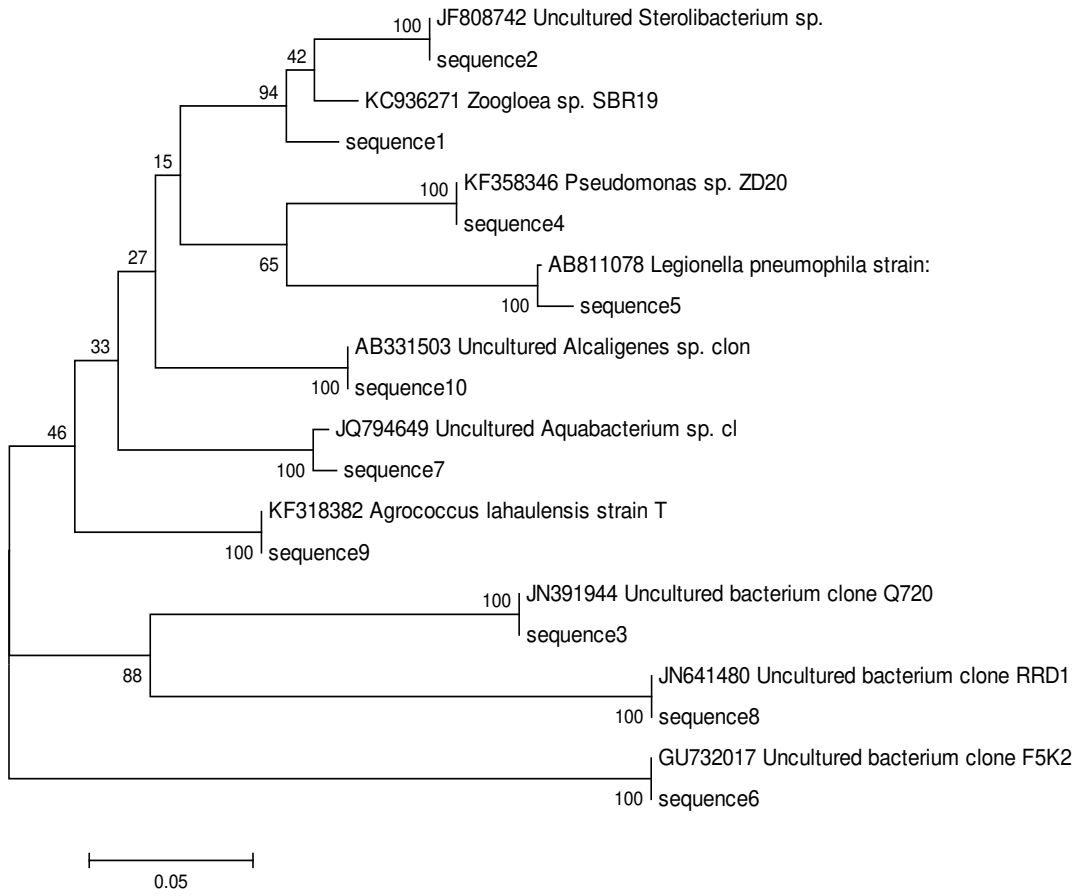

Figure 1. *Phylogenetic tree of the bacteria in the untreated sludge*

http://www.aloki.hu ● ISSN 1589 1623 (Print) ● ISSN 1785 0037 (Online)
DOI: http://dx.doi.org/10.15666/aeer/1706_1295112958

Most bacteria in the untreated sludge belong to proteobacteria (including *α-proteobacteria*、*β-proteobacteria* and *γ-proteobacteria*) (*Table 1*) and showed a close genetic relationship. Sequence 2, 1, 4, 5, 10, 7 stand for the dominant microfloras in the activated sludge. Moreover, the bacteria represented by sequence 3, 8, 6 were not artificially cultivated and classified, and they also showed a close genetic relationship. The microbe community of the activated sludge is formed together with the same 9 microbes (Wang et al., 2015).

Significant reduction in the total number of the dominant bacteria in the bulking sludge is showed from 10 species in the untreated sludge to 6 species (*Table 2*) after the treatment and the microbial community changed greatly.

The strains represented by sequence 2~5 (*Fig. 2*) are in accordance with the four strains represented by sequence 5, 6, 8, 10 in the untreated sludge. Two strains of bacteria represented by sequence 1 and sequence 6 are new in the bulking sludge. Strains represented by sequence 1 and sequence 6 highly similar to the *Anaerolineaceae* and *Collinsella aerofaciens*, respectively.

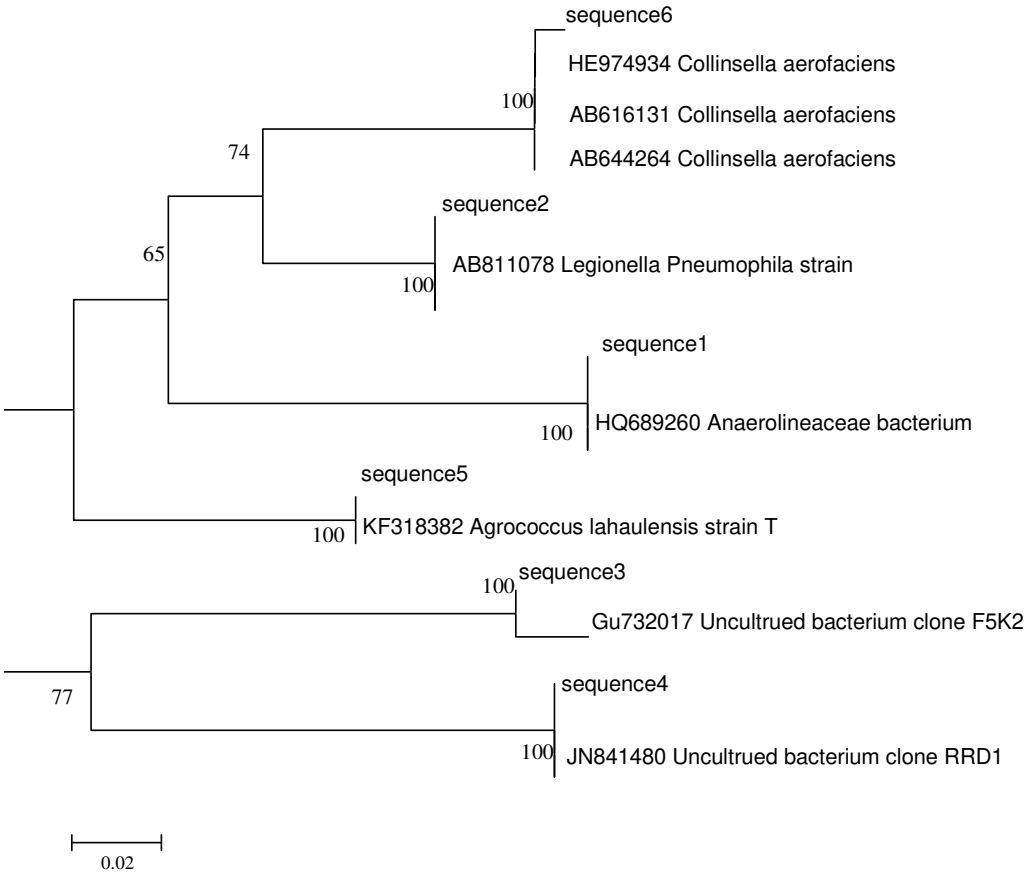

Figure 2. *Phylogenetic tree of the bacteria in the bulking sludge*

Table 2. *Identified bacteria species in the bulking sludge*

Stripe number	Clone number	V3 region	Bacteria species
1	> 7.11XD1512-2(DG50-X-4)M13-	169bp	*Anaerolineaceae*
2	> 7.11XD1513-1(DG50-X-5)M13-	194bp	*Legionella pneumophila*
3	> 7.18XD1514-2(DG50-X-6)M13-	193bp	*Uncultured bacterium*

http://www.aloki.hu ● ISSN 1589 1623 (Print) ● ISSN 1785 0037 (Online)
DOI: http://dx.doi.org/10.15666/aeer/1706_1295112958

4	> 7.11XD1515-1(DG50-X-7)M13-	187bp	*Uncultured bacterium*
5	> 7.11XD1517-2(DG50-X-9)M13-	174bp	*Agrococcus lahaulensis*
6	> 7.11XD1518-3(DG50-X-10)M13-	170bp	*Collinsella aerofaciens*

Analysis of fungus diversity of the bulking sludge

After DGGE analysis and sequencing, the gene sequences were compared with the sequences in the NCBI database, and the main funguses in the bulking sludge were shown in *Table 3*.

Table 3. *Identified funguses in the bulking sludge*

Stripe number	Clone number	V3 region	*Fungus* species
1	> 7.24XD1534-6(DG50-Z-2)M13-	349bp	*Uncultured eukaryote*
2	> 7.24XD1535-1(DG50-Z-3)M13-	349bp	*Saccharomyces cerevisiae*
3	> 8.16XD1631-2(DG50-Z-4)M13-	347bp	*Unculture alveolate*
4	> 8.16XD1632-1(DG50-Z-5)M13-	346bp	*Hanseniaspora guilliermondii*
5	> 8.16XD1633-1(DG50-Z-8)M13-	337bp	*Uncultured eukaryote*

The bulking sludge contains five kinds of funguses (*Table 3*), besides bacteria, they constitute the microbial community of the sludge, and are a part of the dominant microflora in the bulking sludge. The genus can be identified by cloning V3 conservative regions. The result is shown in *Figure 3*.

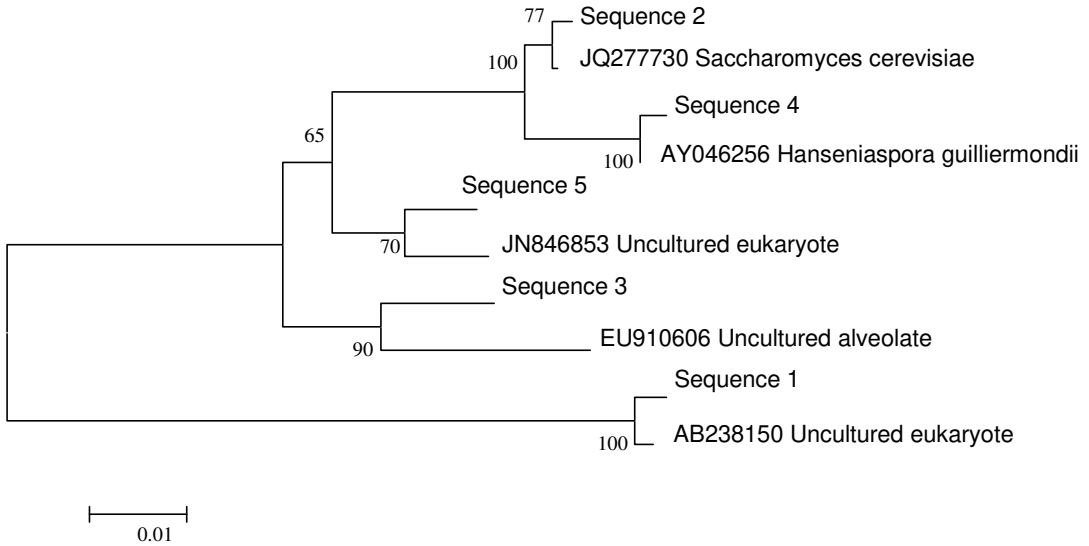

Figure 3. *Phylogenetic tree of the funguses of in the bulking sludge*

From *Figure 3,* the funguses represented by sequence 1, 3 and 5 are not artificially cultivated strains. The two fungus strains represented by sequence 2 and sequence 4 were closely related to *Saccharomyces cerevisiae* and *Hanseniaspora guilliermondii* in the evolutionary relations. So the two funguses were identified as *Saccharomyces cerevisiae* and *Hanseniaspora guilliermondii.*

http://www.aloki.hu ● ISSN 1589 1623 (Print) ● ISSN 1785 0037 (Online)
DOI: http://dx.doi.org/10.15666/aeer/1706_1295112958

Analysis of the root causes of sludge bulking

(1) Changes of bacterial composition of non-treated and bulking sludge

From the results of DGGE analysis in *Figure 4,* it can be seen that bacterial composition changed greatly after sludge bulking, showing a decrease of bacterial species and the change of the amount of the dominant microflora. The microflora represented by sequence1 in the untreated sludge are *Zoogloea sp*. Under natural conditions, the *Zoogloea sp*. produces capsule that not only directly affects the growth and reproduction of the bacteria but also the living environment of the bacteria. Bacteria can improve the poor living environment with its capsule property, and prevent the phagocytosis and utilization by some bad cell tissue. And on the surface of some specific bacteria cells, it showed a strong specificified of attack and defense capability (Wang, 2016). Microfloras which are commonly used microbes in sewage treatment cluster in the common bacteria colloid, so that the sludge has a good gel-flocculation structure and sedimentation property (Zhong et al., 2010). The disappearance of *Zoogloea sp*. in the sludge is the direct cause of sludge bulking.

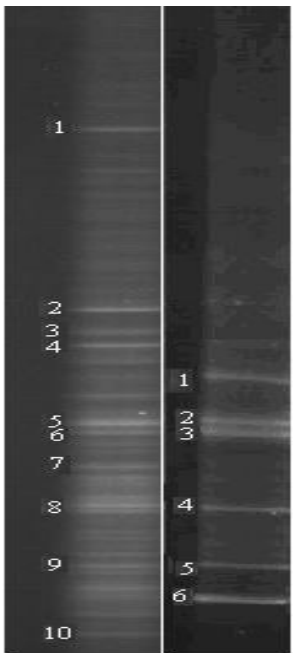

Figure 4. *Bacteria domains in the untreated sludge and bulking sludge*

(2) Changes of funguses composition of the untreated and bulking sludge

As can be seen from the DGGE bands in *Figure 5,* the fungus bands in the untreated sludge are few and unclear, indicating that the types and amounts of the funguses contained in the untreated sludge are small but the bulking sludge contains five kinds of fungi whose species and quantity are much more than the untreated sludge. Thus, the multiplication of fungi has changed the nutritional composition of the environment, absorbing a large number of nutrients, directly affect the growth of the bacteria such as *Zoogloea sp*. Thereby, the change of the composition of the microbe microfloras in the sludge, as well as the destruction of the flocs structure of the sludge lead to the sludge bulking.

http://www.aloki.hu ● ISSN 1589 1623 (Print) ● ISSN 1785 0037 (Online)
DOI: http://dx.doi.org/10.15666/aeer/1706_1295112958

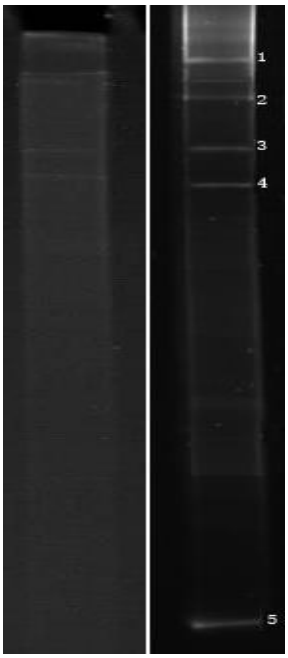

Figure 5. *Fungus domains in the untreated sludge and bulking sludge*

Conclusion

From the analysis of the diverse microbes of untreated sludge and bulking sludge, it is seen that sludge bulking is mainly caused by the change of microbe microfloras.

(1) The sludge bulks because the microfloras in it changed greatly, the main signs are the decrease of the bacterial species and the dominant flora changes. Under natural conditions, *Zoogloea sp*. in the untreated sludge flora has the property of producing capsule and the bacteria which are the common microbes in wastewater treatment cluster in the common bacteria colloid, so that the sludge has a good gel-flocculation structure and sedimentation property. The disappearance of *Zoogloea sp*. is one of the direct causes of sludge bulking.

(2) DGGE analysis of the untreated sludge showed that only a very small amount of fungi were present in the activated sludge, which indicates that the activated sludge mainly consisted of bacteria, but five kinds of filamentous fungi (most of which have hyphae) in the bulking sludge were detected with the same method. The mass growth of these filamentous fungi has replaced the predominant bacteria such as *Zoogloea sp*. in the activated sludge, therefore, the destruction of the gel-flocculation structure of the sludge eventually leads to the filamentous fungus sludge bulking.

In the future studies, the changes of carbon source, nitrogen source and inorganic salts in sludge before and after bulking should be systematically analyzed. Combined with the study of microfloras changes and strain metabolism, the mechanism of change would be deeply revealed, which would lay a theoretical foundation for controlling the sludge bulking.

Acknowledgements. The authors are grateful for the financial support from Technical Innovation Guidance Project of Shaanxi Province(2019CGXNG-039), Shaanxi Science and Technology Plan Project (2018SF-377), Open Project Program of National Experimental Demonstration Center for Experimental Light Chemical Engineering (2018QGSJ02-04, (Shaanxi University of Science and Technology), Science and Technology project of Xi' an (2017068CG/RC031 (SXKD002).

http://www.aloki.hu ● ISSN 1589 1623 (Print) ● ISSN 1785 0037 (Online)
DOI: http://dx.doi.org/10.15666/aeer/1706_1295112958

REFERENCES

[1] Aqeel, H., Basuvaraj, M., Hall, M. (2015): Microbial dynamics and properties of aerobic granules developed in a laboratory-scale sequencing batch reactor with an intermediate filamentous bulking stage. – Environmental Biotechnology 100(1): 447-460.
[2] Eikelboom, D. H. (1975): Filamentous organism observed in activated sludge. – Wat. Res 6: 148-154.
[3] He, R. J., Zhao, D. Y., Xu, H. M. (2018): Abundance and community structure of ammonia-oxidizing bacteria in activated sludge from different geographic regions in China. – Water Science & Technology 77(6): 1698-1705.
[4] Henze, M., van Loosdrecht, M. C. M., Ekama, G. A., Brdjanovic, D. (2008): Biological Wastewater Treatment: Principles, Modelling and Design. – IWA Publishing, London.
[5] Jiang, Y. X. (2014): Analysis of community structure of sludge microbes based on molecular biology technology. – Master's thesis, Beijing University of Chemical Technology.
[6] Li, S., Zhang, L., Qiu, Y. L. (2015): Study on microbial diversity of sludge in rural biogas digester. – Life Science Research 4: 321-327.
[7] Ma, J. M., Li, D., Wu, D. (2012): Study on filamentous sludge bulking in A/O phosphorus removal process. – China Water and Wastewater 28(7): 38-42.
[8] Meunier, C., Henriet, O., Schoonbroodt, B. (2016): Influence of feeding pattern and hydraulic selection pressure to control filamentous bulking in biological treatment of dairy wastewaters. – Bioresource Technology 221: 300-309.
[9] Qin, L. Y. (1989): Biological Treatment of Wastewater. – Tongji University Press, Tongji, pp. 197-199.
[10] Sezgin, M., Jenkins, D., Palm, J. C. (1980): Floc size, Filament length and settling properties of prototype activated sludge plants. – Wat. Res. 11(12): 68-73.
[11] Shao, Q. X. (2005): Characteristics and effects of main microbial groups in activated sludge. – Shanxi Architecture 4: 30.
[12] Sun, J. (2009): Application of denaturing gradient gel electrophoresis in the identification of microalgae and the study of phytoplankton community structure. – PhD thesis, Ocean University of China.
[13] Wang, T., Liu, L. L., Zhang, K. Q. (2015): Effect of fertilizer irrigation on soil ammonia oxidizing microorganisms. – Journal of Agriculture Environment Science 34(9): 1737-1746.
[14] Wang, Z. (2016): Changes of the core polysaccharide structure of E. coli lipopolysaccharide molecule effect on cell membrane and intracellular metabolism. – PhD thesis, University of Jiangnan, China.
[15] Zhong, S. G. (2010): Singular integral equations on the real axis with solutions having singularities of higher order. – Acta Mathematica Scientia 25: 1093-1099.

http://www.aloki.hu ● ISSN 1589 1623 (Print) ● ISSN 1785 0037 (Online)
DOI: http://dx.doi.org/10.15666/aeer/1706_1295112958

ESTIMATION OF COUNTY ECOLOGICAL CIVILIZATION CONSTRUCTION LEVEL IN SICHUAN PROVINCE BASED ON IMPROVED ECOLOGICAL FOOTPRINT MODEL

WANG, X. Y.[1] – XIE, Z. Y.[1*] – MA, Y.[2]

[1]*Faculty of School of Economics and Management, North China University of Technology*
No. 5 Jinyuanzhuang Road, Shijingshan District, Beijing, China

[2]*Department of Management and Engineering, Beihang University*
No. 37 Xueyuan Road, Haidian District, 100191 Beijing, China

**Corresponding author*
e-mail: 867917280@qq.com; phone: +86-185-0019-1013

(Received 22nd May 2019; accepted 28th Aug 2019)

Abstract. The construction of ecological civilization is an important part of the cause of socialism with Chinese characteristics. It concerns the well-being of the people, the future of the nation, the goal of "two hundred years" and the realization of the Chinese dream of great rejuvenation of the nation. County is the basic unit of ecological civilization construction in China. The construction of county ecological civilization is of great significance to that on the national scale. Therefore, how to accurately calculate the level of county ecological civilization construction has become a significant subject. Based on the general situation of Sichuan Province, this paper uses a large number of county data collected from Sichuan Province to calculate the county ecological footprint of Sichuan Province through the improved ecological footprint model. The ecological footprint model is revised based on NPP by GIS technology, which makes the calculation result more accurate and scientifically evaluates the level of County Ecological Civilization Construction in Sichuan Province.
Keywords: *net primary productivity, ecological deficit, NPP, equilibrium factor, yield factor*

Introduction

First of all, due to the characteristics of simple population composition and small area, county governments have a better understanding of the situation within the scope of management, which is more useful in the process of ecological civilization construction. Secondly, for the counties which are at the key position of implementing national policies, the task of ecological civilization construction is more specific, the space of play is broader, and it is easier to find problems in policy formulation and implementation and solve them timely and accurately. Thirdly, the county level is closer to the grassroots level and the masses, and promoting the construction of county ecological civilization will help making policies more precise to benefit the vast majority of the people. It can be seen that the county ecological civilization construction is the basic unit of the national ecological civilization construction, and is the key and foundation of the ecological civilization construction. Therefore, how to accurately calculate the level of county ecological civilization construction has become a significant subject. Based on the general situation of Sichuan Province, this study uses county data collected in here to measure the county ecological footprint of Sichuan Province through the improved ecological footprint model to measure the level of County Ecological Civilization Construction in Sichuan Province. In the process of

http://www.aloki.hu ● ISSN 1589 1623 (Print) ● ISSN 1785 0037 (Online)
DOI: http://dx.doi.org/10.15666/aeer/1706_1295912971

using the ecological footprint model, the ecological footprint model is modified based on NPP by GIS technology, which makes the calculation result more accurate.

Literature review

Many studies have been made on the construction of ecological civilization at home and abroad, which mainly concentrates on the concept and connotation, evaluation methods and technical means of ecological civilization construction.

In terms of the concept and connotation of ecological civilization construction: The concepts in this regard have not been unified. Morrison (1995) put forward the concept of "ecological civilization" in 1995. Foreign researches on this concept are mainly based on the ecological study of civilization. Arnason (1998) studied the relationship between Japanese civilization and Marine ecology, and expounded the characteristics of Japanese civilization from the ecological perspective. Quinilley (2011) analyzed the spatial dimensions needed to ensure the development of ecological civilization based on the spatial attributes of ecological environment. Scholar Alakbarov (2015) started with the ecological civilization of Azerbaijani, and studied the impact of human resource development, increasing fixed assets, innovation strategy on ecological knowledge, as well as the relationship between these related issues. In 1987, the ecologist Ye (1987) first applied the concept of ecological civilization. He believed that ecological civilization means that human beings can benefit from nature and return to nature. After the 18th National Congress, both academia and government departments at all levels have expounded their understanding of ecological civilization from many perspectives. Qin et al. (2015) have subdivided the concept of ecological civilization into two dimensions, one is the history of human development, the other is the real social system, corresponding to the broad sense and narrow sense of ecological civilization.

As for the evaluation methods of ecological civilization construction, the main methods include ecological footprint method, real development index method and index system method. Mikuliqi et al. (2016) applied the ecological footprint method in the analysis of cement industry. The research results show that the industry has invested a lot of raw materials in time, but the level of energy utilization has not changed significantly. Bartocci et al. (2016) studied the environmental problems of Sagrantino and Grechetto by using carbon footprint, ecological footprint and water footprint methods respectively. Ferreira et al. (2016) introduced the life cycle assessment theory into the ecological footprint assessment system. Sziget et al. (2016) takes Hungary as the research object to analyze the changes of ecological footprint density in that country in recent years. The ISEW index proposed by scholar H. Daly, that is, the economic welfare index of sustainable development, can be used to replace GDP. Verhofstadt et al. (2016) studies the integration of personal welfare and ecological footprint. Qian et al. (1990) and others used the method of quantitative and qualitative integration to study the giant system. Because in the face of such a huge system, only by building a comprehensive index system, can it be more accurate quantitative research. After this method was put forward, Kong et al. (2016), Ma et al. (2017), Xing (2016) and other Tongdu all applied the index system method to give the corresponding evaluation to the construction of ecological civilization.

As far as the technical means of evaluating the construction of ecological civilization are concerned, in foreign countries, the work of evaluating the construction of ecological civilization can be traced back to the 1960s at the earliest, but only in the

http://www.aloki.hu ● ISSN 1589 1623 (Print) ● ISSN 1785 0037 (Online)
DOI: http://dx.doi.org/10.15666/aeer/1706_1295912971

1970s did it enter the stage of development. Based on this, Remote Sensing (RS), Geographic Information System (GIS) and landscape ecology were developed, and the corresponding ecological evaluation was carried out through them. Lee and Wong (2001) believe that landscape quality and ecological value are closely related. Through GIS and land use data, he evaluated the landscape and ecological value of the analysis area. Based on these results, corresponding management policies are formulated. Smith et al. (1999) used remote sensing, mapping and statistical techniques to analyze the level of land use in the region. Based on remote sensing monitoring data, Espejel (1987), analyzed the ecological status and sustainability of the monitoring area, and constructed different land use conditions in the analysis process. Scholar Reid et al. (2000), based on GIS technology, evaluates the effects of land use and land cover on ecosystem. Tang (2014) took Pengshan County as the research object, and analyzed its defects in the construction of ecological civilization. Lu et al. (2015) based on the space-time comprehensive measurement model and sustainable development evaluation index system, and then according to the technology of gravity center displacement, AHP and GIS, take many districts and counties in Liaoning Province as the research object, and adopt the comprehensive measurement model to study their sustainable development. Liu et al. (2017) are evaluating the sustainable development of Jiangxi Province. Wang and Ren (2018) took Yulin area as the research object, and made a comprehensive evaluation and analysis of the ecological security of the area through remote sensing and GIS technology, and compiled an evaluation index system for the area.

There are many methods to measure the level of regional ecological civilization construction, but the evaluation of the level of regional ecological civilization construction from the county perspective is relatively less. There are many studies on the evaluation of ecological footprint method, but most of them can not improve their inherent defects. The improvement of Ecological Footprint Based on NPP method is relatively rare. This paper studies the integration of improved ecological footprint model and GIS technology, and effectively improves the accuracy of evaluation.

Method selection and data source

Method selection

In 1992, W. Rees from Canada first proposed the ecological footprint model, which was improved by M. Wackemagel. The model is an important research tool. It introduces the concept of ecological space size and maps the natural capital consumption and the ecological services supported by natural systems to evaluate the sustainability of human activities. The core of the theory is “bio-production area”. With the help of ecological footprint analysis tools, the overall calculation results can be simplified, and the natural capital supply and demand information of the calculated area can be more vividly mapped. However, the ecological footprint model also has some shortcomings, mainly in the following aspects: firstly, the lack of dynamic. Only real-time ecological information can be analyzed, which belongs to a typical static analysis. When calculating the related ecological land area, a definite time is needed. Secondly, the assumption of spatial mutuality is flawed. In this footprint theory, the hypothesis of land spatial exclusion is put forward. However, this hypothesis obviously has defects, that is, land itself has various and replaceable attributes, which divides the whole system. Thirdly, the comparability and reality of equilibrium factors and yield factors

http://www.aloki.hu ● ISSN 1589 1623 (Print) ● ISSN 1785 0037 (Online)
DOI: http://dx.doi.org/10.15666/aeer/1706_1295912971

are difficult to coordinate. Based on the concept of global hectare ecological footprint, it is difficult to get close to the actual situation of the study area, and when calculating the ecological carrying capacity of cultivated land, construction land is usually equated with cultivated land, which invisibly increases the cultivated land area, and the corresponding calculation results will naturally become larger. Because the ecological footprint model has some defects and shortcomings, this study introduced the concept of time series to analyze the economic, natural and social changes of different time nodes. In addition, the parameters used in the traditional footprint model are based on the global perspective, which is lack of accuracy for the study of Sichuan. Therefore, the concept of Net Primary Productivity (NPP) is introduced to make the footprint model play a greater role.

Data sources

This study focuses on the county-level administrative regions of Sichuan Province. However, due to the sparse land, weak industrial, forestry, fishery and agricultural foundations, the calculation results of ecological footprint in Western Sichuan alpine Tibetan area and Liangshan Yi area are significantly lower than those in other areas, considering the availability of statistical data in some years. This study does not include 48 districts and counties under the jurisdiction of Ganzi Tibetan Autonomous Prefecture, Aba Qiang Autonomous Prefecture and Liangshan Yi Autonomous Prefecture. Therefore, this study selected 135 districts and counties in Sichuan Province (excluding alpine Tibetan areas in Western Sichuan and Liangshan Yi areas in large and small). The data are from Sichuan Yearbook, Sichuan Statistical Yearbook, Sichuan Statistical Bulletin of National Economic and Social Development and statistical yearbooks of cities at all levels in Sichuan Province from 2007 to 2016.

In this study, the ecological footprint of Sichuan counties mainly includes the consumption of bio-resources and fossil energy. According to the consumption of bio-resources in Sichuan Province, it mainly includes grain, oil, raw hemp, sugar, tobacco leaves, beef, mutton, rabbit meat, aquatic products, tea, garden fruits, etc. Energy consumption mainly includes Coal, gasoline, kerosene, diesel and natural gas, as shown in *Table 1*.

Table 1. *The indicator of county ecological footprint accounts*

Ecosystem consumption types	Land type	Account index
Biological resources account	Cultivated land	Food, oil crops, raw hemp, sugar, tobacco leaves, vegetables, medicinal materials
	Woodland	Garden fruits and tea
	Grassland	Pork, beef, mutton, rabbit, milk, eggs, honey, cocoon
	Waters	Aquatic product
Fossil energy account	Fossil fuel	Coal, gasoline, kerosene, diesel and natural gas
	Building land	Electric power

In addition, this study uses MOD17A3 data provided by the National Aeronautics and Space Administration (NASA). The fitting model is BIOME-BGC with a spatial resolution of 1 km. Modis Reprojection Tool (MRT) software provided by NASA is used to process the image mosaic and re-projection. Then ALBERS isoproduct projection is selected to remove outliers and other operations to process the MODIS data, and then NPP value is obtained. ArcGIS 10.2 software is used to clip global

http://www.aloki.hu ● ISSN 1589 1623 (Print) ● ISSN 1785 0037 (Online)
DOI: http://dx.doi.org/10.15666/aeer/1706_1295912971

MODIS data with the help of Sichuan geographic information vector map. The result is shown in *Figure 1.* In *Figure 1,* the data of 2006, 2009, 2012 and 2015 are shown respectively. Through the analysis of the above chart can find that the NPP value from east to West shows a decreasing trend, mostly 500-750 gC M 2 a 1. In a word, the low altitude is higher than the high altitude. The land in this province is classified according to the types of resources on the way, and overlapped with the map after cutting. Then the corresponding NPP mean values and corresponding areas of six types of land in Sichuan Province are calculated.

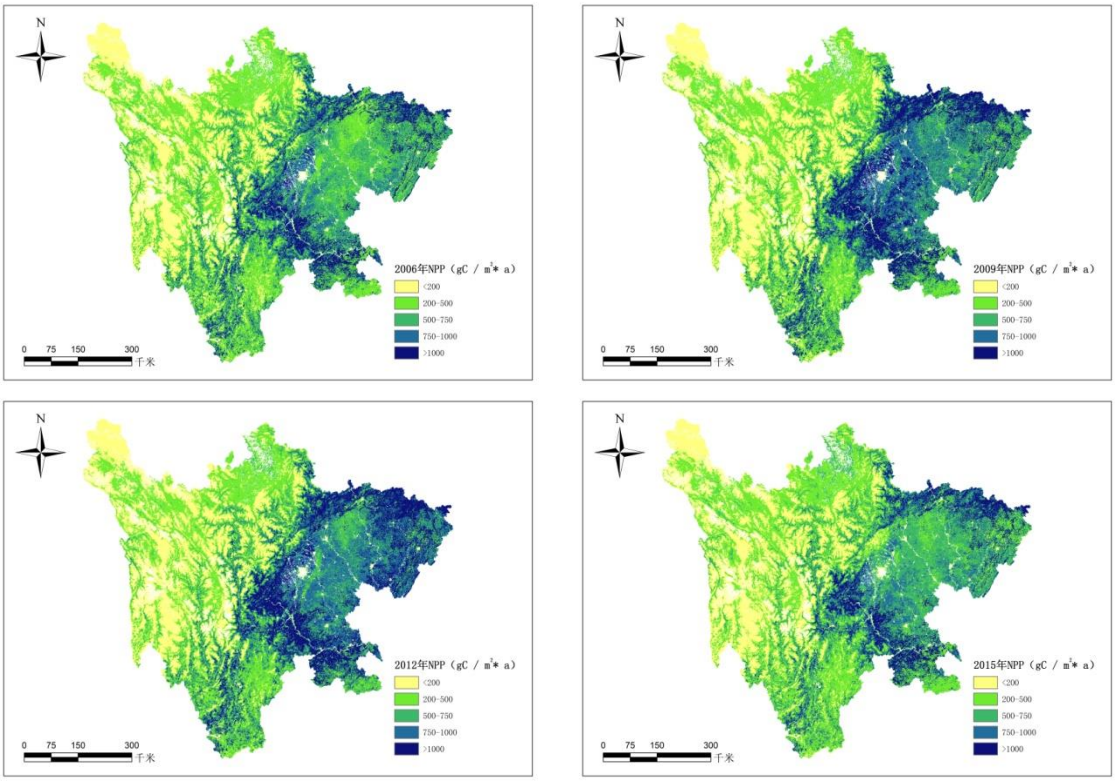

Figure 1. *Vegetation NPP spatial distribution of Sichuan Province on 2006, 2009, 2012 and 2015*

Adjustment of yield factor and equilibrium factor

This study applied the concept of "provincial hectare" to study the county ecological footprint of Sichuan Province. The basis of this province's hectare model is still the ecological footprint model. When calculating the output and equilibrium factors of Sichuan Province, the average productivity of the province is used. Equilibrium factors of related types of land are the ratio of their average productivity to other types of average productivity. The so-called yield factor is the ratio of the average productivity of the related types of land in a region to that of the same kind of land in a province. Bio productivity can be expressed by NPP. After removing self-consuming oxygen, green plants produce organic matter per unit time and area, which is called NPP. Therefore, it can be used to express the productivity of plants, and also to show the productivity of different land types, and then more accurately obtain the development level of the study area. NPP in this region needs to calculate NPP value of water area, woodland,

http://www.aloki.hu ● ISSN 1589 1623 (Print) ● ISSN 1785 0037 (Online)
DOI: http://dx.doi.org/10.15666/aeer/1706_1295912971

grassland and cultivated land, and the corresponding area, then weighted sum, the corresponding formula is as follows:

$$\overline{NPP} = \frac{\sum_j \left(A_j \times NPP_j\right)}{\sum_j A_j} \quad \text{(Eq.1)}$$

In *Equation 1:* the area of various land types (m2).

The formulas for calculating the four types of land equilibrium factors of cultivated land, woodland, grassland and water area in China are as follows:

$$r_j = \frac{NPP_j}{\overline{NPP}} \quad \text{(Eq.2)}$$

In *Equation 2:* It is the average NPP of the land type j (gC/m2.a) and the average NPP of the land type (gC/m2.a).

The formulas for calculating the yield factors of cultivated land, woodland, grassland and water area in Sichuan Province are as follows:

$$y_i = \frac{NPP_j^{'}}{\overline{NPP_j}} \quad \text{(Eq.3)}$$

In *Equation 3:* NPP' is the average NPP (gC/m2.a) of all kinds of land types in Sichuan Province and the average NPP (gC/m2.a) of all kinds of land types in China.

Model calculation

Measuring ecological footprint

There are six main types of bio-productive area: fossil energy land, construction land, grassland, cultivated forest land, cultivated land and water area. Different types of bio-productive land have different ecological productivity, so it is necessary to introduce the equilibrium factor to calculate the bio-productive area with the world average productivity, so that different types of bio-productive land can be transformed into equivalent ecological productivity and the total ecological footprint can be calculated. Similarly, when calculating the ecological carrying capacity, it is necessary to introduce yield factors to convert the land area of the same ecological productivity in different countries or regions into comparable area. The calculation formula is as follows:

$$EF = N \times ef = N \times \sum \left(r_j \times A_j\right) = N \times \sum \left(r_j \times \left(c_j / p_j\right)\right) \quad \text{(Eq.4)}$$

In *Equation 4, EF* represents the total ecological footprint of a region. *N* is the total population. *ef* represents the per capita ecological footprint. r_j is the equilibrium factor. A_j is the ecological productive land area per capita converted from type j. c_j is

http://www.aloki.hu ● ISSN 1589 1623 (Print) ● ISSN 1785 0037 (Online)
DOI: http://dx.doi.org/10.15666/aeer/1706_1295912971

the type i per capita consumption. p_j is the average production capacity of species j. j is productive land.

Estimation of ecological carrying capacity

Eco-carrying capacity, also known as biological carrying capacity, refers to the maximum amount of resources and wastes that can be supplied and digested without harming the ecosystem and on the basis of complete productivity and function.

$$EC = N \times ec = N \times \sum a_j \times r_j \times y_j \quad \text{(Eq.5)}$$

In *Equation 5,* EC is the total ecological carrying capacity of the region. N is the total population. ec is the per capita ecological carrying capacity. a_j is per capita Eco-productive land area. r_j is the equilibrium factor. y_j is the yield factor.

Estimating the ecological deficit

The ecological surplus/deficit is determined by comparing the size of EF and EC. When $EF - EC > 0$, there will be an ecological deficit; on the contrary, when $EF - EC < 0$, there will be an ecological surplus. By comparing the size of EF and EC, the sustainability of social development can be judged. Shengzhi deficit indicates that the human load in the region exceeds its ecological capacity. To meet the consumption demand under the existing living standard, the region either consumes its own natural capital to make up for the shortage of energy supply, or imports the lack of resources from outside the region to make up for the shortage of supply. Its development mode is in an unsustainable state. On the contrary, the ecological surplus indicates that the production and consumption patterns in the region are sustainable, and the human load in the region is within its ecological capacity, and its development pattern is in a sustainable state. The calculation formula is as follows:

$$ed = ec - ef \quad \text{(Eq.6)}$$

In *Equation 6:* ed is the per capita ecological deficit, when $ed < 0$, it is the ecological deficit, when $ed > 0$, it is the ecological surplus, ef is the per capita ecological footprint, ec is the per capita ecological carrying capacity.

Empirical results

Calculations of equilibrium factor and yield factor

By calculating *Equations 1–3,* the equilibrium factors and yield factors of various land types in Sichuan Province from 2006 to 2015 are obtained, as shown in *Tables 2* and *3*. *Tables 2* and *3* show only the land equilibrium factors and yield factors in 2006, 2009, 2012 and 2015 as follows.

The values of yield factor and equilibrium factor in the improved ecological footprint model are taken from the values in *Tables 2* and *3*.

http://www.aloki.hu ● ISSN 1589 1623 (Print) ● ISSN 1785 0037 (Online)
DOI: http://dx.doi.org/10.15666/aeer/1706_1295912971

Table 2. *Balance factors for land types in major years in Sichuan Province*

Land type	2006	2009	2012	2015
Grassland	0.563	0.582	0.599	0.619
Cultivated land	1.518	1.515	1.487	1.461
Fossil energy	0.898	0.898	0.898	0.898
Building land	1.518	1.515	1.498	1.461
Woodland	1.083	1.062	1.065	1.069
Waters	1.167	1.187	1.155	1.103

Table 3. *Output factors of land types in major years in Sichuan Province*

Land type	2006	2009	2012	2015
Grassland	1.824	1.813	1.762	1.742
Cultivated land	1.688	1.598	1.498	1.357
Building land	1.688	1.586	1.505	1.357
Woodland	0.727	0.752	0.729	0.681
Waters	1.557	1.520	1.408	1.270

Calculation results of ecological footprint

The average ecological footprint, ecological carrying capacity and ecological deficit per capita of 135 county-level administrative units in Sichuan Province were calculated by improved ecological footprint model. Calculate the ecological footprint according to *Equation 4*. Limited to the length of the article, only selected in 2006, 2000, 2009, 2012 and 2015 to show the ecological footprint per capita, ecological carrying capacity per capita and total ecological deficit per capita of 135 counties and districts in Sichuan Province in the main years. The counties and districts with the first-fifth and 131-135 indicators are shown in *Tables 4* and *5,* respectively.

Table 4. *Counties Ranking 1-5 on per capita ecological footprint of major years in Sichuan*

Ranking	1		2		3		4		5	
Year	County	Value	County	Value	County	Value	County	Value	County	Value
2006	Renshou	28.14	Anyue	27.87	Santai	22.09	Yuechi	19.64	Zhong jiang	18.92
2009	Anyue	30.86	Renshou	30.03	Santai	25.11	Zhong jiang	23.33	Rong	20.28
2012	Renshou	34.69	Anyue	33.30	Yuechi	30.99	Zhong jiang	28.47	Santai	27.74
2015	Renshou	36.14	Anyue	35.87	Yuechi	35.31	Santai	34.85	Lu	33.17

Table 5. *Counties ranking 131-135 on per capita ecological footprint of major years in Sichuan*

Ranking	131		132		133		134		135	
Year	County	Value	County	Value	County	Value	County	Value	County	Value
2006	Cangxi	2.98	Yilong	2.58	Luojiang	2.45	Qionglai	2.05	Wusheng	1.73
2009	Yu cheng	3.04	Cangxi	2.85	Yilong	2.43	Wan yuan	2.33	Wusheng	1.87
2012	Ming shan	3.42	Wan yuan	2.63	Qionglai	2.38	Yilong	2.05	Wusheng	1.68
2015	Yu cheng	3.94	Cuiping	3.82	Wanyuan	2.87	Yilong	2.08	Wusheng	1.76

http://www.aloki.hu ● ISSN 1589 1623 (Print) ● ISSN 1785 0037 (Online)
DOI: http://dx.doi.org/10.15666/aeer/1706_1295912971

Tables 4 and *5* show the per capita ecological footprint of counties in Sichuan Province in the main years. From the table, it can be seen intuitively that the top five and the last five counties in the per capita ecological footprint have great differences in numerical value. Especially in 2012, the per capita ecological footprint of Renshou County ranked first reached 30.86, 20.65 times that of Wusheng County ranked 135. Secondly, from the perspective of trend, from 2006 to 2015, the per capita ecological footprint of counties in Sichuan Province shows an increasing trend year by year. Especially in the period of 2012-2015, the growth rate accelerated significantly. Thirdly, by analyzing the counties with large per capita ecological footprint can find that most of the counties with high ranking, such as Renshou County, Anyue County, Santai County, Luxian County and Zhongjiang County, are the main producing areas of agricultural products in the province and have a large population base.

Calculation results of ecological carrying capacity

According to *Equation 5,* the ecological carrying capacity is calculated. The results are shown in *Tables 6* and *7*.

Table 6. *Counties ranking 1-5 on per capita ecological capacity of major years in Sichuan*

Ranking	**1**		**2**		**3**		**4**		**5**	
Year	County	Value	County	Value	County	Value	County	Value	County	Value
2006	Mabian	1.23	Pingwu	1.21	Qing chuan	1.15	Wang cang	1.02	Ebian	1.01
2009	Pingwu	1.21	Mabian	1.20	Qing chuan	1.13	Wan yuan	1.03	Wangcang	1.00
2012	Mabian	1.21	Pingwu	1.19	Qing chuan	1.08	Wang cang	1.04	Wanyuan	0.96
2015	Mabian	1.19	Qingchuan	1.00	Wang cang	0.99	Pingwu	1.15	Baoxing	0.93

Table 7. *Counties ranking 131-135 on per capita ecological capacity of major years in Sichuan*

Ranking	**131**		**132**		**133**		**134**		**135**	
Year	County	Value	County	Value	County	Value	County	Value	County	Value
2006	Shuang liu	0.15	Dazhu	0.12	Xuanhan	0.11	Weiyuan	0.10	Qu	0.08
2009	Shuang liu	0.13	Xuanhan	0.12	Dazhu	0.11	Weiyuan	0.10	Qu	0.09
2012	Shuang liu	0.12	Dazhu	0.11	Xuanhan	0.10	Qu	0.08	Weiyuan	0.07
2015	Shuang liu	0.12	Dazhu	0.10	Xuanhan	0.09	Qu	0.06	Weiyuan	0.05

Tables 6 and *7* show the main years in Sichuan province county per capita ecological carrying case, can be seen from the table, the per capita ecological carrying capacity in 2006-2015, there is no significant change, but in the top five and five districts after from the numerical difference is bigger, especially in 2012, the number one cause of Mabian County per capita ecological carrying capacity is 1.21, 23.8 times is ranked 135th in Weiyuan. Secondly, in terms of trend, unlike the per capita ecological footprint, the per capita ecological carrying capacity of counties in Sichuan Province does not generally show a decreasing trend year by year, and the per capita ecological carrying capacity of some districts and counties has increased. Thirdly, by analyzing the counties with larger per capita ecological carrying capacity in Sichuan Province will find that Mabian County, Pingwu County, Qingchuan County, Wancang County, Wanyuan County, Baoxing County and Ebian County are the key ecological functional counties in

http://www.aloki.hu ● ISSN 1589 1623 (Print) ● ISSN 1785 0037 (Online)
DOI: http://dx.doi.org/10.15666/aeer/1706_1295912971

Sichuan Province, with the distribution of national-level nature reserves such as Dafeng Ding, Xuebaoding, Wang Lang, Tangjiahe, Micang Mountain, Huacalyx Mountain, Beepupa Village, Heizhugou Valley, Jiajinshan and so on. Domestic forest park, under the improved ecological footprint algorithm based on NPP, has a certain role in improving the ecological carrying capacity of the region.

Calculation results of ecological deficit

According to *Equation 6,* the ecological deficit is calculated. The results are shown in *Tables 8* and *9.*

Table 8. *Counties ranking 1-5 on per capita ecological deficit of major years in Sichuan*

Ranking	1		2		3		4		5	
Year	County	Value	County	Value	County	Value	County	Value	County	Value
2006	Renshou	27.56	Anyue	27.20	Santai	21.50	Yuechi	19.18	Zhong jiang	18.38
2009	Anyue	30.21	Renshou	29.46	Santai	24.55	Zhong jiang	22.72	Rong	19.67
2012	Renshou	34.01	Anyue	32.70	Yuechi	30.33	Zhong jiang	27.89	Santai	27.12
2015	Renshou	35.56	Anyue	35.27	Yuechi	34.73	Santai	34.24	Lu	32.58

Table 9. *Counties ranking 131-135 on per capita ecological deficit of major years in Sichuan*

Ranking	131		132		133		134		135	
Year	County	Value	County	Value	County	Value	County	Value	County	Value
2006	Cangxi	2.27	Yilong	1.88	Luo jiang	1.77	Qionglai	1.35	Wusheng	1.01
2009	Yucheng	2.33	Cangxi	2.16	Yilong	1.70	Wan yuan	1.60	Wusheng	1.10
2012	Ming shan	2.71	Wan yuan	1.90	Qionglai	1.66	Yilong	1.31	Wusheng	0.98
2015	Yucheng	3.23	Cuiping	3.18	Wan yuan	2.17	Yilong	1.33	Wusheng	1.06

Tables 8 and *9* show the per capita ecological deficit of counties in Sichuan Province in the main years. As mentioned above, the per capita ecological deficit is the difference between the per capita ecological footprint and the per capita ecological carrying capacity. However, from the calculation results, the difference between the per capita ecological carrying capacity and the per capita ecological footprint in Sichuan Province is very large. The ranking of the per capita ecological deficit is basically the same as that of the per capita ecological footprint. The ecological footprint of each county in Sichuan Province is far greater than that of the ecological carrying capacity.

The result of comprehensive evaluation shows that the per capita standard can reduce the error caused by population differences and make the calculation more reliable. It is feasible to evaluate the ecological footprint, ecological carrying capacity and ecological deficit based on the improved ecological footprint model. The evaluation shows that the ecological environment carrying capacity of the districts and counties in Sichuan Province is generally good, but there are great differences among the districts and counties, which are different from Shi et al. (2013). Agriculture, industrialization and fishery, represented by arable land, construction land and water area, are the core elements to evaluate the ecological carrying capacity. Industrialization is the root cause of the increase in energy and consumption, which is partly consistent with the conclusions of Zhao et al. (2008). The development of construction industry promotes

http://www.aloki.hu ● ISSN 1589 1623 (Print) ● ISSN 1785 0037 (Online)
DOI: http://dx.doi.org/10.15666/aeer/1706_1295912971

the transfer of rural surplus labor force, but also provides convenient conditions for industrial transformation and upgrading.

Conclusion

Because of the traditional ecological footprint model has certain defects, this article through the use of software and the MRT ArcGIS10.2 software of 1:100000 in Sichuan in 2006-2015 data of land use (geographic conditions monitoring cloud platform) and MOD17A3 data for Mosaic and projection, eliminate outliers, multiplied by the scale factor, the MODIS data into NPP actual value, represented the biological productivity of land with a NPP, improve the ecological footprint model of production factor and the equilibrium factor in order to closer to the actual of Sichuan province. Through the improvement of the ecological footprint model 135 counties of Sichuan province county per capita ecological footprint in 2006-2015, the per capita ecological carrying capacity and ecological deficit per capita, the results can be seen that all present in the study area of ecological deficit and increased year by year, the overall ecological environment extremely safe state for a long time, the development of sustainability. But at the same time, after 2012 because many counties began to emphasize the importance of ecological civilization construction in the development of county economy, the trend of high-speed growth of ecological footprint in some counties has not only been curbed, but also a trend of decreasing ecological footprint. For regions with too large ecological footprint, it is necessary to establish and improve the evaluation mechanism reflecting the requirements of ecological civilization, incorporate the construction of ecological civilization into the evaluation index system of county-level government's economic and social development performance objectives, increase the weight of assessment, and strengthen the constraints of indicators. a differentiated performance appraisal system will be implemented, explore the preparation of balance sheets for natural resources, and conduct outgoing audits of natural resources assets and environmental responsibilities for leading cadres. This also requires that Sichuan counties and districts in the formulation of county economic development strategy can not blindly compare, like great success, but need to take full account of their ecological conditions, in accordance with their own county conditions, so as to adapt to local conditions.

In future research, we should make full use of remote sensing technology, strengthen early warning of regional ecological carrying capacity, and provide scientific guarantee services for national county development policies to ensure sustainable development of regional ecology.

Acknowledgements. The authors acknowledge Research Start-up Funds of North China University of Technology (110051360002); Basic Scientific Research Project of the Beijing Municipal Education Commission in 2018 (110052971921).

REFERENCES

[1] Alakbarov, U., Lawrence, J. E. (2015): Towards ecological civilization: ideas from Azerbaijan. – Journal of Human Resource and Sustainability Studies 3(3): 93.
[2] Arnason, R. (1998): Ecological fisheries management using individual transferable share quotas. – Ecological Applications 8(sp1): S151-S159.

http://www.aloki.hu ● ISSN 1589 1623 (Print) ● ISSN 1785 0037 (Online)
DOI: http://dx.doi.org/10.15666/aeer/1706_1295912971

[3] Bartocci, P., Fantozzi, P., Fantozzi, F. (2017): Environmental impact of Sagrantino and Grechetto grapes cultivation for wine and vinegar production in central Italy. – Journal of Cleaner Production 140: 569-580.
[4] Espejel, I. (1987): A phytogeographical analysis of coastal vegetation in the Yucatan Peninsula. – Journal of Biogeography 14(6): 499-519.
[5] Ferreira, V. L., Torregrosa-López, J. I., Capuz-Rizo, S. F. (2016): Use of life cycle assessment methodology in the analysis of ecological footprint assessment results to evaluate the environmental performance of universities. – Journal of Cleaner Production. DOI: 10.1016/j.jclepro.2016.05.046.
[6] Kong, L., Liu, W., Zhang, L. (2016): Study on the construction of evaluation index system of county ecological civilization construction - take Puer City as an example. – Forestry Economy 3: 30-33.
[7] Lee, J., Wong, D. W. (2001): Statistical Analysis with ArcView GIS. – John Wiley & Sons, New York.
[8] Liu, H., Yin, J., Chen, J., Chen, X. (2017): Sustainable development evaluation of Jiangxi Province based on ecological footprint. – Surveying and Mapping Science 5: 62-69.
[9] Lu, C., Zhang, L., Xue, B. (2015): Spatio-temporal comprehensive measurement of regional sustainable development in Liaoning Province. – Economic Geography 8: 32-39.
[10] Ma, Y., He, B., Ma, Z., Lin, Z., Luan, W. (2017): Study on the index system of county eco-civilization construction in agricultural and pastoral areas: taking Huocheng County of Xinjiang as an example. – Journal of Xinjiang University 1: 102-107.
[11] Mikulčić, H., Cabezas, H., Vujanović, M., Duić, N. (2016): Environmental assessment of different cement manufacturing processes based on emergy and ecological footprint analysis. – Journal of Cleaner Production 130: 213-221.
[12] Morrison, R. (1995): Ecological Democracy. – South End Press, Boston.
[13] Qian, X., Yu, J., Dai, R. (1990): A new field of science - open complex giant system and its methodology. – Journal of Nature 1: 3-10.
[14] Qin, H., Yuan, Z., Qin, J. (2015): Research progress in promoting ecological civilization in China. – Population Resources and Environment in China 2: 111-120.
[15] Quilley, S. (2011): Entropy, the anthroposphere and the ecology of civilization: an essay on the problem of 'liberalism in one village' in the long view. – The Sociological Review 59: 65-90.
[16] Reid, R. S., Kruska, R. L., Deichmann, U., Thornton, P. K., Leak, S. G. (2000): Human population growth and the extinction of the tsetse fly. – Agriculture, Ecosystems & Environment 77(3): 227-236.
[17] Shi, Y., Yin, C., Wang, H., et al. (2013): Research progress and prospect on urban comprehensive carrying capacity. – Geographical Research 32(1): 133-145.
[18] Smith, W., Meredith, T. C., Johns, T. (1999): Exploring methods for rapid assessment of woody vegetation in the Batemi Valley, North-central Tanzania. – Biodiversity & Conservation 8(4): 447-470.
[19] Szigeti, C., Toth, G., Szabo, D. R. (2017): Decoupling-shifts in ecological footprint intensity of nations in the last decade. – Ecological Indicators 72: 111-117.
[20] Tang, L. (2014): Research on Science and Technology Support in County Eco-civilization Construction. – Chengdu University of Technology, Chengdu.
[21] Verhofstadt, E., Van Ootegem, L., Defloor, B., Bleys, B. (2016): Linking individuals' ecological footprint to their subjective well-being. – Ecological Economics 127: 80-89.
[22] Wang, X. F., Ren, Z. (2008): Study on dynamic change of vegetation coverage in Yulin city based on RS and GIS. – Journal of Shaanxi Normal University (Natural Science Edition) 36(3): 1014.
[23] Xing, J. (2016): Study on the Path of Low-Carbon Economic Development in the Pilot Demonstration Area of County Ecological Civilization. – Shanxi University of Finance and Economics, Shanxi.

http://www.aloki.hu ● ISSN 1589 1623 (Print) ● ISSN 1785 0037 (Online)
DOI: http://dx.doi.org/10.15666/aeer/1706_1295912971

[24] Ye, Q. (1987): The era of true civilization has just begun. Professor Ye Qianji calls for "ecological civilization construction". – China Environment Daily 23: 3.
[25] Zhao, W., Li, J., Chen, Y. (2008): Changes of eco-capacity and ecological sustainability in the north Tian shan Mountains region: taking Fukang County as a case of study. – Acta Ecologica Sinica 28(9): 4363-4371.

http://www.aloki.hu ● ISSN 1589 1623 (Print) ● ISSN 1785 0037 (Online)
DOI: http://dx.doi.org/10.15666/aeer/1706_1295912971

PHOTOCATALYTIC DEGRADATION OF MULTIPLE CHLOROPHENOLS AS SIMULATED ENVIRONMENTAL POLLUTANTS IN $TiO_2/H_3PW_{12}O_{40}$/AG COMPOSITE FILM SYSTEM

LI, L.† – YANG, L.† – JIANG, L. Y. – WANG, Z. R. – WU, J. K. – LU, N.* – QU, J.*

School of Environment, Northeast Normal University, Changchun 130117, P. R. China

†These authors contributed equally.

**Corresponding authors*
e-mail: lun100@nenu.edu.cn (Lu, N.); Quj100@nenu.edu.cn (Qu, J.)

(Received 22nd May 2019; accepted 28th Aug 2019)

Abstract. Photocatalytic degradation of chlorophenols (CPs) has been attracting an increasing attention lately. In the paper, $TiO_2/H_3PW_{12}O_{40}$/Ag composite film was prepared by sol-gel method with programmed heating hydrothermal technology and spin coating technique to treat CPs. Direct photolysis of five CPs was performed according to the pseudo-first-order kinetics model, in which the photolysis rate of PCP was faster than that of the others under the simulated solar light. The results of mineralization indicated that the aromatic ring in PCP was difficult to be broken down via direct photolysis. By $TiO_2/H_3PW_{12}O_{40}$/Ag composite film, photocatalytic degradation efficiency elevated due to the enhancement of the quantum efficiency and visible-light absorption in comparison with direct photolysis as well as other reaction systems ($TiO_2/H_3PW_{12}O_{40}$ film and TiO_2 film), and the mineralization of PCP increased to 75.70%. The initial degradation rate (r_0) was in the following order as PCP (0.158 $mg \cdot L^{-1} \cdot min^{-1}$) > 4-CP (0.144 $mg \cdot L^{-1} \cdot min^{-1}$) > 2,4-DCP (0.014 $mg \cdot L^{-1} \cdot min^{-1}$) > 2,4,6-TCP (0.047 $mg \cdot L^{-1} \cdot min^{-1}$) > 2-CP (0.038 $mg \cdot L^{-1} \cdot min^{-1}$), confirming $TiO_2/H_3PW_{12}O_{40}$/Ag composite film as new catalyst to be more effective at removing for CPs.
Keywords: *direct photolysis, kinetics model, chlorine substituent, mineralization degree, degradation path*

Introduction

Chlorophenols (CPs) possess 19 homologues including mono-, di-, tri-, tetra-, and penta-chlorinated phenols, which have been widely used as pesticides, herbicides, fungicides, acaricides, and mold inhibitors (Olaniran et al., 2011; Garba et al., 2019; Yang et al., 2018; Guo et al., 2016). The position and quantity of chlorine substituent in CPs are closely correlated to their toxicity, e.g. ortho-substituted homologues are generally of lower toxicity than meta- and para-ones, and polychlorinated CPs are ascribed to increase hazardous effect for the organisms (Devillers et al., 1986; Du et al., 2016; Yu et al., 2019; Ge et al., 2017). CPs have been listed as priority pollutants by US EPA because of their adverse environmental effects, consequently, the disposal is currently one of the most serious environmental issues (Descorme et al., 2017). Photocatalytic degradation of CPs has been attracting an increasing attention lately, and numerous semiconductors have been investigated (Ku et al., 1996; Li et al., 2011; Gaya et al., 2009; Han et al., 2018; Al-Fahdi et al., 2019). TiO_2 is the most studied photocatalyst, however, the disadvantages including low quantum yield (approximately 0.14 at 365 nm) (Emeline et al., 2006), the limited solar light utilization (Meng et al., 2018), hindered its practical application.

In our previous work, an efficient plasmonic $TiO_2/H_3PW_{12}O_{40}$/Ag composite film was fabricated with an enhanced solar light photocatalytic activity due to the combined actions

http://www.aloki.hu ● ISSN 1589 1623 (Print) ● ISSN 1785 0037 (Online)
DOI: http://dx.doi.org/10.15666/aeer/1706_1297312983

of electrons-trapping via $H_3PW_{12}O_{40}$, visible-response induced by Ag, and Schottky-junction formed between TiO_2 and Ag (Lu et al., 2017). It has been documented that the chlorine positions in chlorophenol homologues act an important role in its photo-degradation kinetics (Hugül et al., 2000; Czaplicka et al., 2006). It is well known that ·OH is a very strong activator as well as ortho- and para-directing in electrophilic aromatic substitution (Antonaraki et al., 2002). Therefore, ·OH radical that was confirmed as the main role in $TiO_2/H_3PW_{12}O_{40}$/Ag reaction system (Lu et al., 2017) can directly attack the electron-rich positions in CPs molecules with a rapid degradation rate.

The current study is aimed to compare the removal efficiency and rate between direct photolysis and photocatalytic degradation of mono-, di-, tri- and penta-chlorophenols in TiO_2, $TiO_2/H_3PW_{12}O_{40}$, and $TiO_2/H_3PW_{12}O_{40}$/Ag systems. Moreover, the influence of chlorine substituent position and quantity on photocatalytic degradation in $TiO_2/H_3PW_{12}O_{40}$/Ag system was intensively investigated. The speculation of degradation path accompanied by mineralization degree analysis was discussed. This work would provide necessary information on the development of photocatalysis technique in practical application towards CPs wastewater treatment.

Material and methods

Reagents

The titanium tetraisopropoxide (TTIP, 98%) was purchased from Sigma-Aldrich Corporation. $H_3PW_{12}O_{40}$ (guaranteed reagent, GR), isopropanol (analytical purity, AR), $AgNO_3$ (AR), 2-CP (AR), 4-CP (AR), 2,4-CP (AR), 2,4,6-CP (AR) and PCP (AR) were purchased from China Pharmaceutical Group. Other chemicals were of reagent grade and applied without further purification. Double distilled water was utilized throughout the experimental procedures.

Catalyst preparation

The combining process of sol-gel-hydrothermal route and temperature programming was employed to fabricate $TiO_2/H_3PW_{12}O_{40}$/Ag composite film, which has been described in our previous study (Lu et al., 2017). The as-prepared film was confirmed with anatase phase TiO_2, the intact saturation Keggin structure, and metallic Ag inserted into the pore structures of $TiO_2/H_3PW_{12}O_{40}$, which enhanced the quantum efficiency, visible-light absorption and further improving in the photocatalytic performance.

Direct photolysis and photocatalytic experiment

2-chlorophenol (CP), 4-chlorophenol (4-CP), 2,4-dichlorophenol (2,4-DCP), 2,4,6-trichlorophenol (2,4,6-TCP), and pentachlorophenol (PCP) were selected as the targets, the corresponding molecular structures and detection conditions were listed in *Table 1*. The photocatalytic degradation of CPs was conducted in a home-made quartz photoreactor (*Fig. 1*) under the simulated solar light provided by a PLS-SXE300 Xe lamp (300 W, Beijing Trustech Co. Ltd., China) placing *ca.* 15 cm above the reactor. The lamp was equipped with cut filters to match solar light with wavelength of 320-780 nm, as well as light intensity of 200 mW/cm^2 measured by a radiometer (OPHIR, Newport, USA) (Lu et al., 2012). In the photocatalytic system, 2 pieces of coated films (Ag-$TiO_2/H_3PW_{12}O_{40}$ composite film, $TiO_2/H_3PW_{12}O_{40}$ composite film, or TiO_2 film) with a weight of *ca.* 5.0 mg were submerged in CPs solution (100 ml; 5 $mg \cdot L^{-1}$). Prior to

http://www.aloki.hu ● ISSN 1589 1623 (Print) ● ISSN 1785 0037 (Online)
DOI: http://dx.doi.org/10.15666/aeer/1706_1297312983

irradiation, the films were maintained in dark for 30 min to reach adsorption-desorption equilibrium of CPs. After irradiation, 2 mL CPs solution was sampled and analyzed at 30 min intervals. The experiments were carried out in triplicate. Direct photolysis were conducted in the same conditions without catalyst.

Table 1. *Molecular structures and detection conditions of CPs*

CPs	Molecular structures	Detection conditions HPLC equipped with Waters 2489 UV/visible detector and symmetry C18 (4.6 × 250 mm, particle size 5 μm)
2-CP	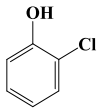	Mobile phase of acetonitrile (40%) and H_2O (60%, containing 0.1% acetic acid) at a flow rate of 0.7 ml·min^{-1} with a detection wavelength of 254 nm
4-CP	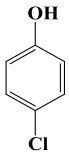	Mobile phase of acetonitrile (50%) and H_2O (50%, containing 1% acetic acid) at a flow rate of 1.0 ml·min^{-1} with a detection wavelength of 254 nm
2,4-DCP	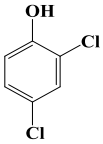	Mobile phase of methyl alcohol (80%) and H_2O (20%) at a flow rate of 1.0 ml·min^{-1} with a detection wavelength of 284 nm
2,4,6-TCP	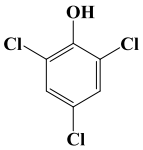	Mobile phase of methyl alcohol (80%) and H_2O (20%, containing 0.3% phosphoric acid) at a flow rate of 1.0 ml·min^{-1} with a detection wavelength of 210 nm
PCP	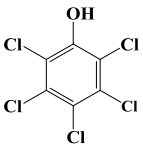	Mobile phase of methyl alcohol (90%) and H_2O (10%, containing 2.0% acetic acid) at a flow rate of 0.7 ml·min^{-1} with a detection wavelength of 254 nm

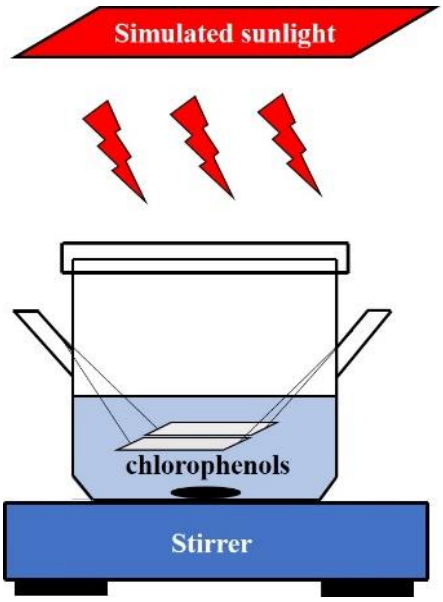

Figure 1. *Self-constructed quartz photoreactor*

http://www.aloki.hu ● ISSN 1589 1623 (Print) ● ISSN 1785 0037 (Online)
DOI: http://dx.doi.org/10.15666/aeer/1706_1297312983

Kinetics

Direct photolysis and photocatalytic degradation kinetics was accorded to simplified pseudo-first-order kinetics (Eq. 1) when the initial concentration of target compound was low.

$$ln\ (C_0/C_t) = K_{app} \cdot t + b \quad \text{(Eq.1)}$$

$$r_0 = K_{app} \cdot C_0 \quad \text{(Eq.2)}$$

in which K_{app} is the apparent constant; C_0 and C are initial and process concentration of the target compound, respectively; t is the reaction time; b is the intercept, R value was obtained by fitting with the least square method.

Statistical analysis

Statistical analysis and linear regression were conducted using SPSS 23.0 statistical software (SPSS Inc., Chicago, USA). The differences of K_{app} and r_0 were tested by one-way ANOVA, in which the comparisons were considered statistically significant, when $P < 0.05$.

Results

Direct photolysis and photocatalytic degradation

The direct photolysis of CPs under UV light was usually studied in many previous reports (Pandiyan et al., 2002; Hong et al., 2000); however, UV light only was around 4-5 percent in sunlight. In the current study, solar simulating irradiation was selected as light source, which was more similar to that of the practical proceeded under the natural sunlight. The results (*Fig. 2*) showed that PCP represented the highest direct photolysis rate as 90.95% after 240 min irradiation, followed by 4-CP (66.05%), 2,4-DCP (50.41%), 2,4,6-TCP (43.02%), and 2-CP (5.11%), which concluded most CPs could be direct photodegraded quickly except 2-CP.

In photocatalytic degradation system, the removal efficiency of CPs was increased obviously after adding the catalysts relative to direct photolysis (*Fig. 3*). By $TiO_2/H_3PW_{12}O_{40}$/Ag film, after 120 min irradiation, the photocatalytic degradation efficiency of 2-CP, 4-CP, 2,4-CP, 2,4,6-TCP, and PCP was 48.49%, 89.89%, 94.57%, 75.15%, and 90.50%, respectively. The degradation efficiency integrally elevated when irradiation time extended to 240 min, 4-CP, 2,4-CP and PCP was hardly completely degraded, while 90.22% of 2,4,6-TCP and 82.40% of 2-CP was degraded. All the values were higher than the attained degradation efficiency in $TiO_2/H_3PW_{12}O_{40}$ or TiO_2 film reaction systems.

Kinetics

By direct photolysis (*Fig. 4* and *Table 2*), the values of initial react rate (r_0) were in order as PCP (0.051 $mg \cdot L^{-1} \cdot min^{-1}$) > 4-CP (0.021 $mg \cdot L^{-1} \cdot min^{-1}$) > 2,4-DCP (0.014 $mg \cdot L^{-1} \cdot min^{-1}$) > 2,4,6-TCP (0.011 $mg \cdot L^{-1} \cdot min^{-1}$) > 2-CP (0.001 $mg \cdot L^{-1} \cdot min^{-1}$).

By photocatalytic degradation (*Fig. 5* and *Table 3*), kinetic study was conducted by selecting TiO_2 film, $TiO_2/H_3PW_{12}O_{40}$ film and $TiO_2/H_3PW_{12}O_{40}$/Ag film as the catalyst.

http://www.aloki.hu ● ISSN 1589 1623 (Print) ● ISSN 1785 0037 (Online)
DOI: http://dx.doi.org/10.15666/aeer/1706_1297312983

In $TiO_2/H_3PW_{12}O_{40}$/Ag composite film system, the values of initial react rate (r_0) were in order as PCP (0.158 $mg \cdot L^{-1} \cdot min^{-1}$) > 4-CP (0.144 $mg \cdot L^{-1} \cdot min^{-1}$) > 2,4-DCP (0.014 $mg \cdot L^{-1} \cdot min^{-1}$) > 2,4,6-TCP (0.047 $mg \cdot L^{-1} \cdot min^{-1}$) > 2-CP (0.038 $mg \cdot L^{-1} \cdot min^{-1}$), which was faster than that of $TiO_2/H_3PW_{12}O_{40}$ or TiO_2 film.

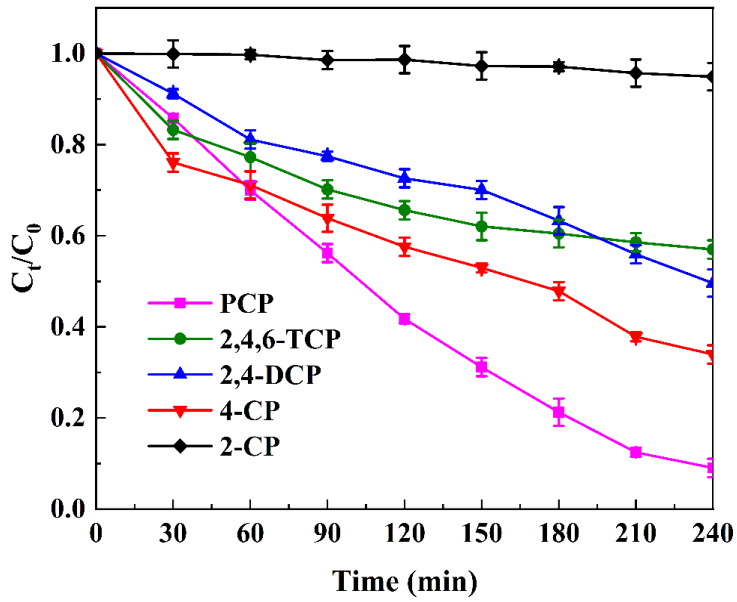

Figure 2. *Direct photolysis of CPs*

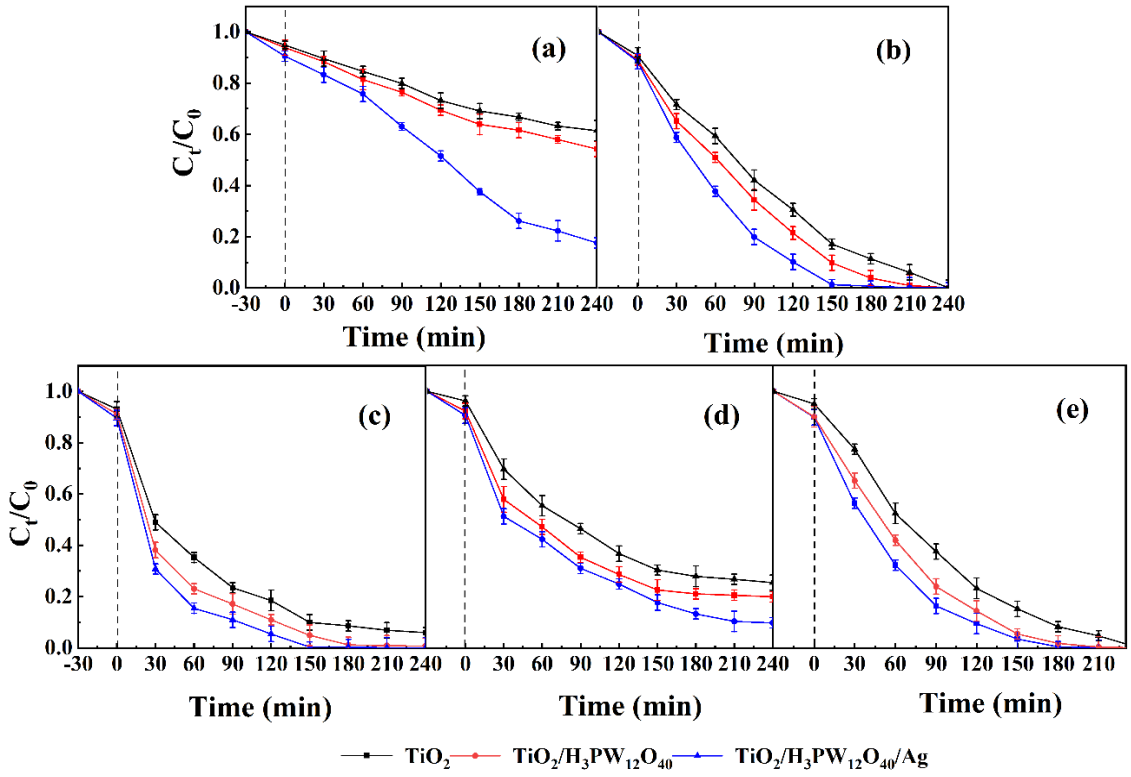

Figure 3. *Photocatalytic degradation of CPs by $TiO_2/H_3PW_{12}O_{40}$/Ag film, $TiO_2/H_3PW_{12}O_{40}$ film and TiO_2 film (a) 2-CP; (b) 4-CP; (c) 2,4-DCP; (d) 2,4,6-TCP; (e) PCP*

http://www.aloki.hu ● ISSN 1589 1623 (Print) ● ISSN 1785 0037 (Online)
DOI: http://dx.doi.org/10.15666/aeer/1706_1297312983

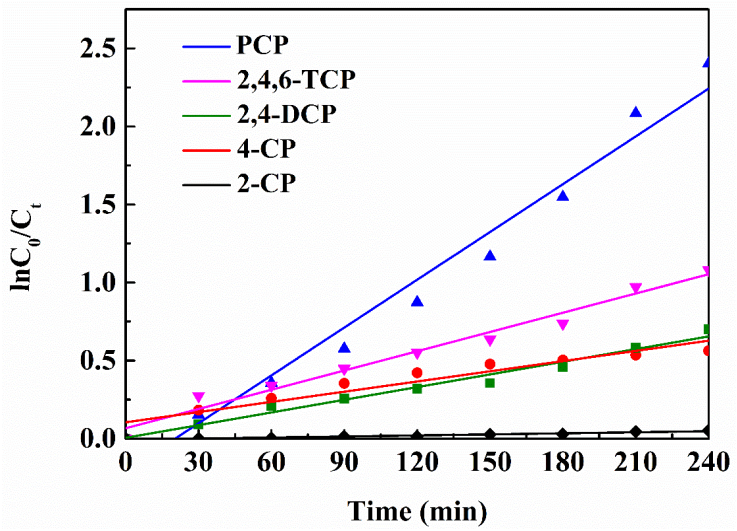

Figure 4. *Direct photolysis kinetics*

Table 2. *Direct photolysis kinetics*

CPs	Kinetic equation $ln(C_0/C) = K_{app}t$	Apparent constant K_{app} (min^{-1})	Initial rate r_0 ($mg \cdot L^{-1} \cdot min^{-1}$)	R
2-CP	y = 0.0002x – 0.0064	0.0002	0.001	0.9708
4-CP	y = 0.0041x + 0.0670	0.0041	0.021	0.9882
2,4-DCP	y = 0.0027x + 0.0058	0.0027	0.014	0.9895
2,4,6-TCP	y = 0.0022x + 0.1051	0.0022	0.011	0.9548
PCP	y = 0.0102x – 0.2070	0.0102	0.051	0.9855

Table 3. *Photocatalytic degradation kinetics*

Films	CPs	Kinetic equation $ln(C_0/C) = K_{app}t$	Apparent constant K_{app} (min^{-1})	Initial rate r_0 ($mg \cdot L^{-1} \cdot min^{-1}$)	R
TiO_2	2-CP	y = 0.0020x + 0.0410	0.0020	0.010	0.9892
	4-CP	y = 0.0129x – 0.0291	0.0129	0.065	0.9952
	2,4-DCP	y = 0.0116x + 0.2938	0.0116	0.058	0.9928
	2,4,6-TCP	y = 0.0056x + 0.1989	0.0056	0.028	0.9653
	PCP	y = 0.0146x-0.1851	0.0146	0.073	0.9928
$TiO_2/H_3PW_{12}O_{40}$	2-CP	y = 0.0025x + 0.0424	0.0025	0.013	0.9927
	4-CP	y = 0.0253x – 0.5083	0.0253	0.127	0.9695
	2,4-DCP	y = 0.0212x + 0.0697	0.0212	0.106	0.9841
	2,4,6-TCP	y = 0.0065x + 0.3175	0.0065	0.033	0.9454
	PCP	y = 0.0253x – 0.5083	0.0253	0.127	0.9695
$TiO_2/H_3PW_{12}O_{40}$/Ag	2-CP	y = 0.0075x – 0.1095	0.0075	0.038	0.9900
	4-CP	y = 0.0287x – 0.4627	0.0287	0.144	0.9665
	2,4-DCP	y = 0.0340x – 0.2204	0.0340	0.170	0.9828
	2,4,6-TCP	y = 0.0094x + 0.2502	0.0094	0.047	0.9862
	PCP	y = 0.0315x – 0.6207	0.0315	0.158	0.9657

http://www.aloki.hu ● ISSN 1589 1623 (Print) ● ISSN 1785 0037 (Online)
DOI: http://dx.doi.org/10.15666/aeer/1706_1297312983

Mineralization degree

The mineralization of PCP (20 $mg \cdot L^{-1}$) was evaluated by monitoring the changes of TOC in both direct photolysis and $TiO_2/H_3PW_{12}O_{40}$/Ag photocatalytic degradation system. Even though degradation rate of PCP was faster than that of other CPs in the two reaction systems, the mineralization degree of PCP was approximately 25.70% in direct photolysis, whereas it reached 75.70% in the photocatalytic reaction after 720 min (*Fig. 6*).

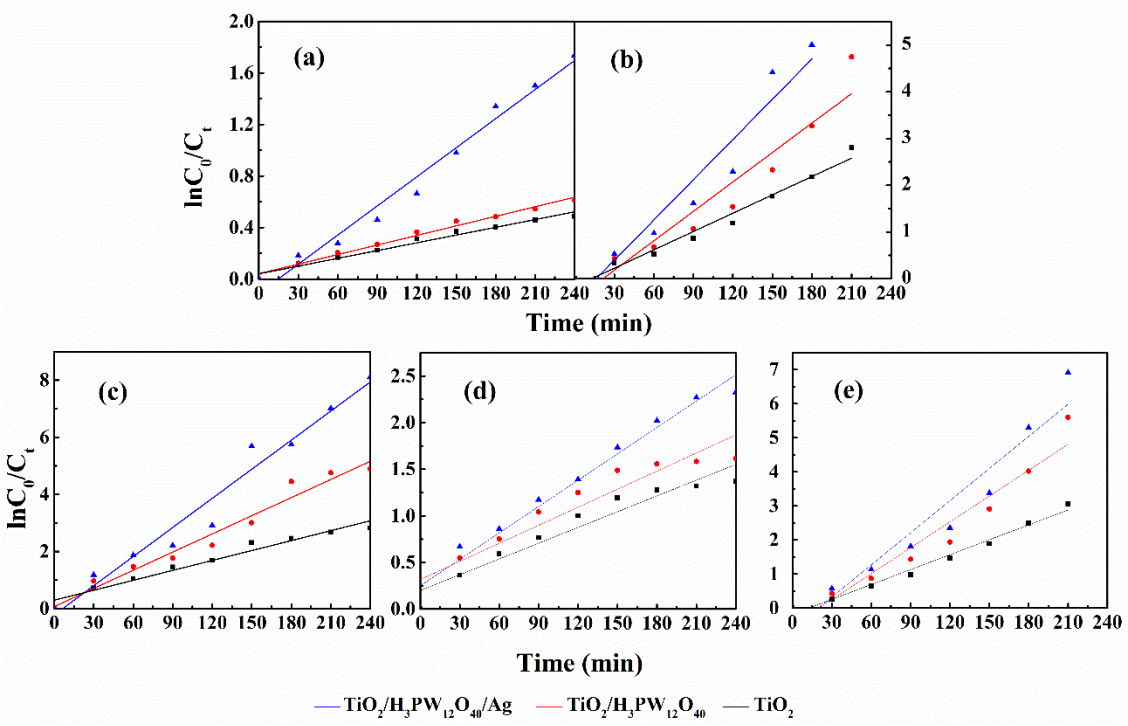

Figure 5. *Photocatalytic degradation kinetics*

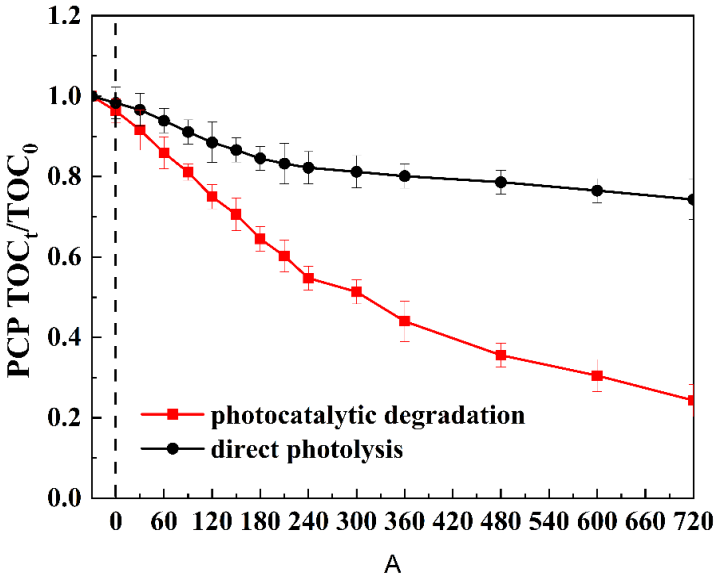

Figure 6. *TOC evolution of CPs*

http://www.aloki.hu ● ISSN 1589 1623 (Print) ● ISSN 1785 0037 (Online)
DOI: http://dx.doi.org/10.15666/aeer/1706_1297312983

Discussion

Based on the results of direct photolysis and photocatalytic degradation, it could be concluded as follow: firstly, all position was full by chlorine atoms in PCP molecule resulting in electron density decreased on the ring due to the electron withdrawing properties of Cl atoms, making the ring less favorable to electrophilic attack, so increased degradation rate (Kim et al., 2003); secondly, degradation of 2-CP was retarded due to the formation of intramolecular hydrogen bonding between OH and Cl (Yang et al., 2014); thirdly, the degradation rate order of 4-CP > 2,4-DCP > 2,4,6-TCP was attributed to the fact that the more chlorine substituent in *meta-* position, the stronger passivation generated among them (Sundstrom et al., 1989). Therefore, the direct photolysis and photocatalytic degradation was mainly controlled by the position and quantity of substituted chlorine atoms in CPs, which were in agreement with other reports (Ko et al., 2007; Yuan et al., 2005).

As-prepared $TiO_2/H_3PW_{12}O_{40}$/Ag film showed the excellent photocatalytic property, the results showed that K_{app} of as-prepared $TiO_2/H_3PW_{12}O_{40}$/Ag reaction system increased significantly in comparison with TiO_2 system ($P < 0.05$). Because $TiO_2/H_3PW_{12}O_{40}$/Ag reaction system delayed the recombination of holes and electrons pairs efficiently owing to the synergistic effects between the Keggin unit and TiO_2 and the generation of Schottky junction at the interface between Ag and TiO_2, meanwhile expanded the absorption of visible-light due to SPR effect (Lu et al., 2017). It is worth noting that only a limited amount of *ca.* 5.0 mg $TiO_2/H_3PW_{12}O_{40}$/Ag was used in the current system, the degradation rate under simulated solar light was considerable in comparison with that in other studies (*Table 4*) even if their experimental conditions showed more advantages including of strong ultraviolet as light source or large catalyst amount.

Table 4. *Photocatalytic degradation dynamics in other reports*

CPs	Co ($mg \cdot L^{-1}$)	Catalyst	Lamp	Initial rate r_0 ($mg \cdot L^{-1} \cdot min^{-1}$)	Reference
2-CP	10	TiO_2 ($2\ g \cdot L^{-1}$)	15 W black flue fluorescent	0.047	Ku et al., 1996
4-CP	20	TiO_2/AC-PC ($2.5\ g \cdot L^{-1}$)	125 W Hg lamp	6.733	Herrmann et al., 2002
2,4-DCP	20	TiO_2 ($0.1\ g \cdot L^{-1}$)	125 W Hg lamp	0.569	Jardim et al., 1997
2,4,6-TCP	100	α-Fe_2O_3 ($1.5\ g \cdot L^{-1}$)	Solar simulator	0.231	Bandara et al., 2001
PCP	170	TiO_2 ($0.1\ g \cdot L^{-1}$)	125 W Hg lamp	0.789	Jardim et al., 1997

In the mineralization study, the photon energy of simulated solar light can only destroy Cl-C of PCP molecule successively till producing the mono-chlorinated phenol but not powerful enough to break down the aromatic ring (Skurlatov et al., 1997). In photocatalytic degradation system, the complex effect of dichlorination, hydroxylation and ring-cleavage functioned in the removal of chlorophenols (Tang et al., 1996). The specific degradation path was shown in *Figure 7*.

http://www.aloki.hu ● ISSN 1589 1623 (Print) ● ISSN 1785 0037 (Online)
DOI: http://dx.doi.org/10.15666/aeer/1706_1297312983

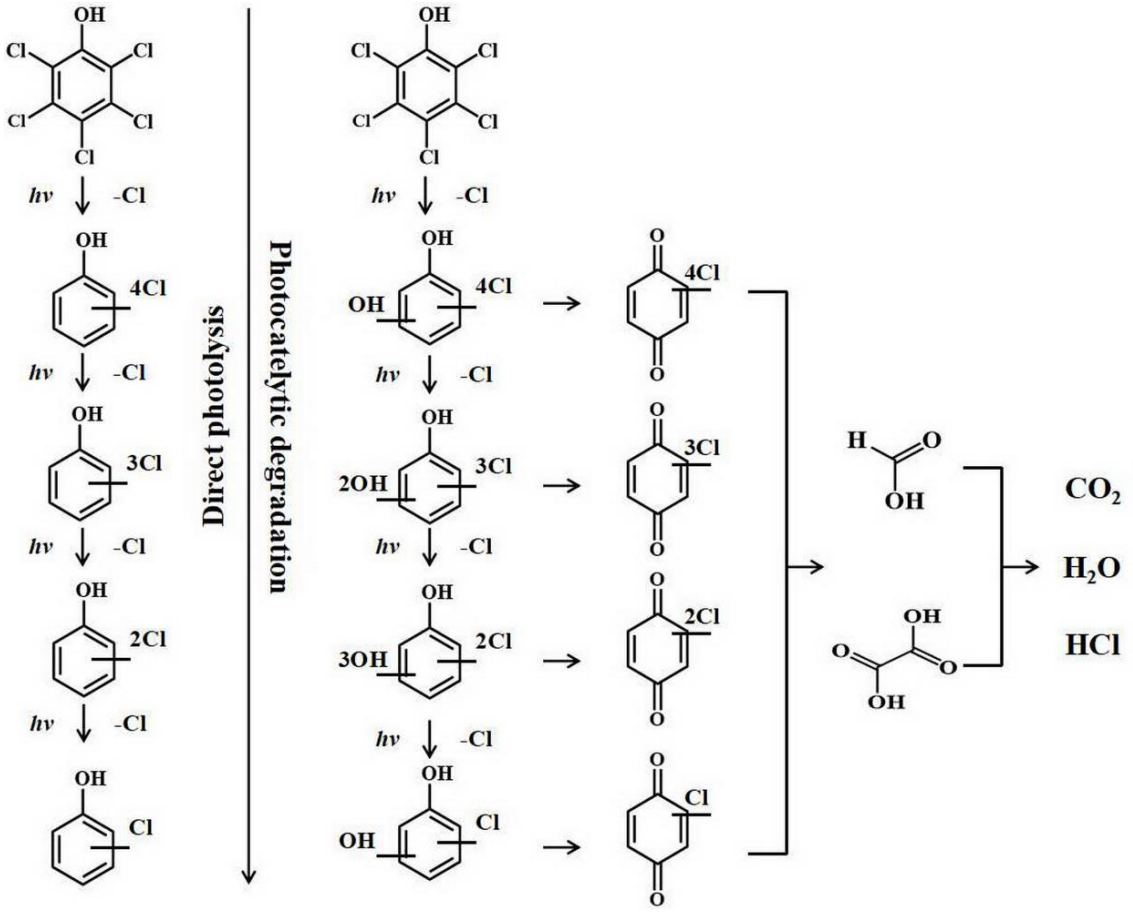

Figure 7. *Possible reaction pathway during photocatalytic degradation of PCP*

Conclusion

$TiO_2/H_3PW_{12}O_{40}$/Ag composite film as new photocatalyst represented an excellent removal efficiency towards CPs under the simulated sunlight relative to others photocatalytic system. The values of initial react rate (r_0) were in the order as PCP (0.158 $mg \cdot L^{-1} \cdot min^{-1}$) > 4-CP (0.144 $mg \cdot L^{-1} \cdot min^{-1}$) > 2,4-DCP (0.014 $mg \cdot L^{-1} \cdot min^{-1}$) > 2,4,6-TCP (0.047 $mg \cdot L^{-1} \cdot min^{-1}$) > 2-CP (0.038 $mg \cdot L^{-1} \cdot min^{-1}$) in the current system, which was related with chlorine substituent position and quantity in CPs molecules. Therein, PCP was highest degradation rate due to the decreased electron cloud density by full chlorine substituents in the phenolic ring, and 75.70% PCP (20 $mg \cdot L^{-1}$) could be mineralized after 720 min irradiation due to ·OH attack. This work will provide necessary information on the development of photocatalysis technique for chlorophenols wastewater treatment in practical application. Moreover, it can be predicted that other noble metal (Pt, Cu, et al) modified $TiO_2/H_3PW_{12}O_{40}$ will also show excellent photocatalytic performance, and the photoelectrocatalytic study of $TiO_2/H_3PW_{12}O_{40}$/Ag composite film is expected.

Acknowledgments. This work was financially supported by the National Natural Science Foundation of China (51408109); Changchun Science and Technology Project (18DY009).

http://www.aloki.hu ● ISSN 1589 1623 (Print) ● ISSN 1785 0037 (Online)
DOI: http://dx.doi.org/10.15666/aeer/1706_1297312983

REFERENCES

[1] Al-Fahdi, T., Marzouqi, F. A., Kuvarega, A. T., Mamba, B. B., Salma, M. Z., Kindy, A., Kim, Y. H., Selvaraj, R. (2019): Visible light active CdS@TiO_2 core-shell nanostructures for the photodegradation of chlorophenols. – Journal of Photochemistry and Photobiology A: Chemistry 374: 75-83.

[2] Antonaraki, S., Androulaki, E., Dimotikali, D., Hiskia, A. Papaconstantinou, E. (2002): Photolytic degradation of all chlorophenols with polyoxometallates and H_2O_2. – Journal of Photochemistry Photobiology A: Chemistry 148: 191-197.

[3] Bandara, J., Mielcazrski, J. A., Lopez, A., Kiwi, J. (2001): Sensitized degradation of chlorophenols on iron oxides induced by visible light. Comparison with titanium oxide. – Applied Catalysis B: Environmental 34: 321-333.

[4] Czaplicka, M. (2006): Photo-degradation of chlorophenols in the aqueous solution. – Journal of Hazardous Materials B134: 45-59.

[5] Descorme, C. (2017): Catalytic wastewater treatment: oxidation and reduction process. Recent studies on chlorophenols. – Catalysis Today 297: 324-334.

[6] Devillers, J., Chambon, P. (1986): Acute toxicity and QSAR of chlorophenols on *Daphnia magna*. – Bulletin of Environmental Contamination and Toxicology 37(4): 599-605.

[7] Du, P. H., Zhao, H., Li, H. T., Zhang, D., Huang, C. H., Deng, M. F., Liu, C. M., Cao, H. B. (2016): Transformation, products, and pathways of chlorophenols via electro-enzymatic catalysis: How to control toxic intermediate products. – Chemosphere 144: 1674-1681.

[8] Emeline, A. V., Zhang, X., Jin, M., Murakami, T., Fujishima, A. (2006): Application of a ‘‘Black Body” like reactor for measurements of quantum yields of photochemical reactions in heterogeneous systems. – Journal of Physical Chemistry C 110: 5259-5275.

[9] Garba, Z. N., Zhou, W. M., Lawan, I., Xiao, W., Zhang, M. X., Wang, L. W., Chen, L. H., Yuan, Z. H. (2019): An overview of chlorophenols as contaminants and their removal from waste water by adsorption: a review. – Journal of Environmental Management 241: 59-75.

[10] Gaya, U. I., Abdullah, A. H., Zainal, Z., Hussein, M. Z. (2009): Photocatalytic treatment of 4-chlorophenol in aqueous ZnO suspensions: intermediates, influence of dosage and inorganic anions. – Journal of Hazardous Materials 168: 57-63.

[11] Ge, T. T., Han, J. Y., Qi, Y. M., Gu, X. Y., Ma, L., Zhang, C., Naeem, S. J., Huang, D. J. (2017): The toxic effects of chlorophenols and associated mechanisms in fish. – Aquatic Toxicology 184: 78-93.

[12] Guo, J. Q., Wu, C. H., Lv, S. L., Lu, D. S., Feng, C., Qi, X. J., Liang, W. J., Chang, X. L., Xu, H., Wang, G. Q., Zhou, Z. J. (2016): Associations of prenatal exposure to five chlorophenols with adverse birth outcomes. – Environmental Pollution 214: 478-484.

[13] Han, A. J., Zhang, H. W., Lu, D., Sun, J. L., Chuah, G. K., Jaenicke, S. (2018): Efficient photodegradation of chlorophenols by BiOBr/$NaBiO_3$ heterojunctioned composites under visible light – Journal of Hazardous Materials 341: 83-92.

[14] Herrmann, J. M., Guilard, C., Disdier, J., Lehaut, C., Malato, S., Blanco, J. (2002): New industrial titania photocatalysts for the solar detoxification of water containing various pollutants. – Applied Catalysis B: Environmental 35: 281-294.

[15] Hong, J., Kim, D. G., Cheong, C., Jung, S. Y., Yoo, M. R., Kim, K. J., Kim, T. K., Park, Y. C. (2002): Identification of photolytical transformation products of pentachlorophenol in water. – Analytic Sciences 16: 621-626.

[16] Hugül, M., Apak, R., Demirci, S. (2000): Modeling the kinetics of UV/hydrogen peroxide oxidation of some mono-, di-, and trichlorophenols. – Journal of Hazardous Materials B77: 193-208.

http://www.aloki.hu ● ISSN 1589 1623 (Print) ● ISSN 1785 0037 (Online)
DOI: http://dx.doi.org/10.15666/aeer/1706_1297312983

[17] Jardim, W. F., Moraes, S. G., Takiyama, M. M. K. (1997): Photocatalytic degradation of aromatic chlorinated compounds using TiO_2: toxicity of intermediates. – Water Research 31: 1728-1732.
[18] Kim, Y. H., Carraway, E. R. (2003): Dechlorination of chlorinated phenols by zero valent zinc. – Journal Environmental Technology 24(12): 1455.
[19] Ko, S. O., Lee, D. H., Kim, Y. H. (2007): Kinetic studies of reductive dechlorination of chlorophenols with NI/FE bimetallic particles. – Environmental Technology 28: 583-594.
[20] Ku, Y., Leu, R. M., Lee, K. C. (1996): Decomposition of 2-chlorophenol in aqueous solution by UV irradiation with the presence of titanium dioxide. – Water Research 30(11): 2569-2578.
[21] Li, J. J., Hu, Y., Lü, W. H., Shi, L., Sun, Q., Zhou, Y. G., Xu, J. F., Wang, J., Shen, B. Z. (2011): Efficient oxidative degradation of 2-chlorophenol and 4-chlorophenol over supported CuO-based catalysts. – Journal of Natural Gas Chemistry 20: 493-497.
[22] Lu, N., Zhao, Y. H., Liu, H. B., Guo, Y. H., Yuan, X., Xu, H., Peng, H. F., Qin, H. W. (2012): Design of polyoxometalate-titania composite film ($H_3PW_{12}O_{40}/TiO_2$) for the degradation of an aqueous dye rhodamine B under the simulated sunlight irradiation. – Journal of Hazardous Materials 199-200: 1-8.
[23] Lu, N., Wang, Y. Q., Ning, S. Q., Zhao, W. J., Qian, M., Ma, Y., Wang, J., Fan, L. Y., Guan, J. N., Yuan, X. (2017): Design of plasmonic Ag-$TiO_2/H_3PW_{12}O_{40}$ composite film with enhanced sunlight photocatalytic activity towards o-chlorophenol degradation. – Scientific Reports 7: 17298-1-17.
[24] Meng, J., Xiong, X. Q., Zhang, X., Xu, Y. M. (2018): Improved photocatalytic degradation of chlorophenol over Pt/Bi_2WO_6 on addition of phosphate. – Applied Surface Science 439: 859-867.
[25] Olaniran, A. O., Igbinosa, E. O. (2011): Chlorophenols and other related derivatives of environmental concern: properties, distribution and microbial degradation process. – Chemosphere 83: 1297-1306.
[26] Pandiyan, T., Rivas, M., Martinez, J. O., Amezcua, G. B., Martinez-Carrillo, M. A. (2002): Comparison of methods for the photochemical degradation of chlorophenols. – Journal of Photochemistry Photobiology A: Chemistry 146: 149-155.
[27] Skurlatov, Y. I., Ernestova, L. S., Vichutinskaya, E. V., Samsonov, D. P., Semenova, I. V., Rod'ko, I. Y., Shvidky, V. O., Pervunina, R. I., Kemp, T. J. (1997): Photochemical transformation of polychlorinated phenols. – Journal of Photochemistry Photobiology A: Chemistry 107: 207-213.
[28] Sundstrom, D. W., Weir, B. A., Klei, H. E. (1989): Destruction of aromatic pollutants by UV light catalyzed oxidation with hydrogen peroxide. – Environmental Progress Banner 8: 6-11.
[29] Tang, W. Z., Huang, C. P. (1996): Effect of chlorine content of chlorinated phenols on their oxidation kinetics by Fenton's reagent. – Chemosphere 33: 1621-1635.
[30] Yang, J., Cui, S. H., Qiao, J. Q., Lian, H. Z. (2014): The photocatalytic dehalogenation of chlorophenols and bromophenols by cobalt doped nano TiO_2. – Journal of Molecular Catalysis A: Chemical 395: 42-51.
[31] Yang, K., Fu, Z. W., Cao, Y. F., Li, S. N., Du, Z., Sun, X. Y., Liu, Y. Z., Yang, K., Fang, Z. Z. (2018): New insights for risks of chlorophenols (CPs) exposure: Inhibition of UDP-glucuronosyltransferases (UGTs). – Chemosphere 206: 9-16.
[32] Yu, C., Wang, C., Lu, Z. B., Zhang, C., Dai, W., Yu, S. Q., Lin, S., Zhang, Q. (2019): The endocrine-disrupting potential of four chlorophenols by *in vitro* and *in silico* assay. – Chemosphere 218: 941-947.
[33] Yuan, S. H., Lu, X. H. (2005): Comparison treatment of various chlorophenols by electro-Fenton method: relationship between chlorine content and degradation. – Journal of Hazardous Materials 118: 85-92.

http://www.aloki.hu ● ISSN 1589 1623 (Print) ● ISSN 1785 0037 (Online)
DOI: http://dx.doi.org/10.15666/aeer/1706_1297312983

RESEARCH ON Cr^{6+} ADSORPTION OF MODIFIED CARBONIZED STRAW AND ITS MECHANISM DURING WASTEWATER TREATMENT BY RESPONSE SURFACE METHODOLOGY

ZENG, Y.G.[1*] – LI, W.Y.[1] – LUO, L.[2] – DU, T.T.[3] – YANG, P.[1] – XU, Q.[1] – LIU, J.J.[4] – SHEN, J.W.[1] – ZENG, Y.[1] – LI, X.[1] – CHEN, X.X.[1] – JIA, R.X.[1]

[1]*School of Architecture and Civil Engineering, Chengdu University, Chengdu 610106, China*

[2]*Post Office in Chengdu, Sichuan Province, Chengdu 610011, China*

[3]*School of Environment, Harbin Institute of Technology, Shenzhen 518055, China*

[4]*School of Mechanical Engineering, Chengdu University, Chengdu 610106, China*

**Corresponding author*
e-mail: 122054216@qq.com

(Received 22nd May 2019; accepted 28th Aug 2019)

Abstract. Heavy metal contaminated wastewater is difficult to treat, and trace amounts of heavy metals can produce toxic effects. In order to provide a more reliable basis for controlling heavy metal pollution, modified carbonized straw was used to adsorb Cr^{6+} in this study, and the optimal adsorption conditions and adsorption effects of Cr^{6+} were studied. Finally, the adsorption kinetics and adsorption activation thermodynamics were analyzed and studied. The results showed that the iodine adsorption value of carbonized wheat straw modified using $FeCl_2$ activation method was the highest at 1161.15 mg/g. The response surface method can be used to optimize the adsorption conditions of Cr^{6+} adsorbed by modified carbonized straw and predict the optimal conditions for Cr^{6+} adsorption. Experiments showed that the actual value was in agreement with the predicted value, indicating that the response surface methodology was feasible to optimize the adsorption of Cr^{6+} by modified carbonized straw. In the kinetic analysis, the Elovich equation could better describe the adsorption of Cr^{6+} by modified carbonized wheat straw, and its fitting degree exceeded 0.91. In the analysis of thermodynamic parameters, $\Delta H > 0$, $\Delta G < 0$, indicating that the adsorption of Cr^{6+} by modified wheat straw was a spontaneous endothermic process. During the adsorption process, $\Delta S > 0$, indicating that the adsorption of Cr^{6+} by modified carbonized wheat straw increased the disorder of the system.
Keywords: *modified carbonization straw, Cr^{6+}, response surface methodology, adsorption kinetics, heavy metal wastewater, heavy metal wastewater treatment, iodine adsorption value, agricultural waste*

Introduction

With the development of industry in China, heavy metal pollution has seriously endangered human health. In fact, heavy metal pollution is difficult to be degraded and removed by simple methods, and it tends to accumulate in organisms and produce toxic effects (Zhao, 2016). At present, the aggravation of heavy metal pollution poses a great threat to the healthy development of human beings and other organisms, and the treatment of heavy metal wastewater has become an urgent problem to be solved. Therefore, it is of great significance to analyze and study the treatment and disposal of heavy metal wastewater (Zeng, 2014a; Zeng and Li, 2014b).

China is a country of traditional agricultural production (Cao et al., 2012). At present, China's agricultural straw production is high. However, with the improvement of people's living standards, straw is no longer needed in daily life. Nowadays, most of

http://www.aloki.hu ● ISSN 1589 1623 (Print) ● ISSN 1785 0037 (Online)
DOI: http://dx.doi.org/10.15666/aeer/1706_1298512999

the straw is treated by incineration and disposal, and has not been reused (Sud et al., 2008), which not only wastes resources, but also brings more and more serious air pollution problems. Therefore, a large number of agricultural straws have not been properly utilized, and the conventional disposal methods have been unable to meet the current straw disposal requirements. In response to the call for building a resource-conserving and environment-friendly society, reusing these residues to dispose of waste is a good way to deal with agricultural waste (Ngah and Hanafiah, 2008). Straw is a biomass waste with high crude fiber content and low protein content (Zhu et al., 2010), which is difficult to be corroded, and it is not good to be directly returned to the field. However, the carbonized product of straw has good physicochemical properties, such as good combustibility, adsorption and low electrical resistance (Sun and Jiang, 2009), which can be used as fuels, soil conditioners and filling materials for electromagnetic shielding screen. Therefore, it is a feasible path to improve the comprehensive utilization rate of straw and carry out biochar utilization of straw and other biomass.

On the basis of the previous studies (Zeng et al., 2018), wheat, corn and paddy straw from farmland around Chengdu, Sichuan Province were carbonized to produce carbonized straw, which is used as activated carbon to study the best adsorption conditions and effects for Cr^{6+}, and the adsorption kinetics and thermodynamics of adsorption activation state were studied finally. In addition, this study evaluated the treatment of Cr^{6+} by modified carbonized straw, which is expected to provide some technical and theoretical support for the practical application of this method.

Materials and methods

Materials, reagents and instruments

The materials used in this experiment were waste wheat, corn, and rice straw produced by agriculture. Corn stalks were taken from Xihe Town, Longquanyi, Chengdu. Wheat straw and rice straw were taken from Huayang Town, Shuangliu, Chengdu.

The object of this experiment was a solution containing Cr^{6+}. The reagents used in the experiment were $ZnCl_2$, KOH, HCl, HNO_3, H_2SO_4, $K_2Cr_2O_7$, $FeCl_2$, I_2, KI, $Na_2S_2O_3$, soluble starch. All reagents were analytical pure. The equipments of the experiment include electrothermal constant temperature blast drying oven (DHG-9140A), visible light spectrophotometer (V-1200), water bath oscillator (HH-4), electronic analytical balance (ESJ120-4), pH meter (PHS-3C), constant temperature oscillator (THZ-032), electric stirrer (JJ-1), ultrasound instrument (KQ-50), high speed centrifuge (H1650R), universal electric furnace (BDW1-6), mesh screen (40 to 200 mesh).

Preparation of modified carbonized straw

In this paper, wheat, corn and rice straw were used as raw materials to prepare activated carbon by using chemical activation method, and the activator were zinc chloride, potassium hydroxide, concentrated sulfuric acid and ferrous chloride, the experimental scheme is shown in *Table 1* (Nu et al., 2017). First, distilled water was applied to clean three kinds of straws. Then straws were dried under the condition of 100 °C in the electrothermal constant temperature blast drying oven and cut into long strips of 3-4 cm. Next, the dried material was sealed with a foil paper and placed on a

http://www.aloki.hu ● ISSN 1589 1623 (Print) ● ISSN 1785 0037 (Online)
DOI: http://dx.doi.org/10.15666/aeer/1706_1298512999

universal electric furnace for 30 min (the temperature of wheat straw was 800 °C (Xiao et al., 2010), the temperature of corn straw was 600 °C (Chen et al., 2010), and the temperature of rice straw was 300 °C (Pinto et al., 2005), then the outer wrapped tin foil paper was removed, and the crude carbonized straw obtained after activation was ground and sieved (40 to 60 mesh). Next, the three sieved carbonized straws were mixed with $ZnCl_2$ (3 mol/L), KOH (3 mol/L), H_2SO_4 (37%) and $FeCl_2$ (2 mol/L) in a mass ratio of 1:3 in a 100 mL stoppered conical flask and closed it immediately, and then it was oscillated in the constant temperature oscillator (temperature: 25 °C, oscillation speed: 150 r/min, oscillation time: 120 min). At the end of the oscillation, solid modified carbonized straw was obtained by filtering the mixed liquor. Firstly, it was washed by 1:9 dilute hydrochloric acid solution (1 mol/L). Secondly, it was washed repeatedly with distilled water to neutral. Thirdly, it was dried to constant weight. After grinding, the activated carbon in 200-mesh was selected for use.

Table 1. *Experimental design of carbonized straw modification*

Number	Straw	Activator	Mass ratio (g:mL)	Temperature (°C)	Oscillation speed (r/min)	Oscillation time (min)
1	Wheat	$ZnCl_2$	1:3	25	150	120
2	Wheat	KOH	1:3	25	150	120
3	Wheat	H_2SO_4	1:3	25	150	120
4	Wheat	$FeCl_2$	1:3	25	150	120
5	Corn	$ZnCl_2$	1:3	25	150	120
6	Corn	KOH	1:3	25	150	120
7	Corn	H_2SO_4	1:3	25	150	120
8	Corn	$FeCl_2$	1:3	25	150	120
9	Rice	$ZnCl_2$	1:3	25	150	120
10	Rice	KOH	1:3	25	150	120
11	Rice	H_2SO_4	1:3	25	150	120
12	Rice	$FeCl_2$	1:3	25	150	120

Method for determining iodine value of modified carbonized straw

The iodine level is related to the adsorption capacity of activated carbon. It is generally believed that the higher the iodine value, the higher the porosity of activated carbon, which means the high adsorption capacity. In this experiment, the iodine value of modified carbonized straw was determined by national standard GB/T12496.8-2015 "Determination of iodine adsorption value by wood activated carbon experimental method" (Chen et al., 2007).

Drawing method of standard curve of Cr^{6+}

A certain concentration of Cr^{6+}-containing solution was configured with distilled water as a reference, and absorbance was measured at its maximum absorption wavelength (each sample was measured three times, averaged and recorded, n = 3). Taking 540 nm as the maximum absorption wavelength of Cr^{6+}, the concentration of the Cr^{6+}-containing solution respectively was 0 mg/L, 0.02 mg/L, 0.1 mg/L, 0.4 mg/L, and 0.8 mg/L. Then, the experiment was performed, the measured absorbance was taken as the ordinate, the concentration was taken as the abscissa, and the standard curve was drawn.

http://www.aloki.hu ● ISSN 1589 1623 (Print) ● ISSN 1785 0037 (Online)
DOI: http://dx.doi.org/10.15666/aeer/1706_1298512999

Configuration of Cr^{6+}-containing solution

First, the best grade pure potassium dichromate was weighed 1.4135 g and dissolved in water, and then the volume of solution reached at 500 mL by adding water. Therefore, the standard reserve solution containing Cr^{6+} 1.0 mg/mL was obtained. When the solution needs to be used, the standard reserve solution is absorbed with 1.0 mL nitric acid, and then a standard solution containing 100 mg/mL Cr^{6+} was obtained (Chen et al., 2010).

Response surface experiment of Cr^{6+}

The experiment used the Box-Behnken design to predict the optimal adsorption conditions and explore the interaction between the factors through Design Expert software (Hadjmohammadi et al., 2016). In this experiment, temperature (A), adsorption time (B), and adsorbent dosage (C) were used as independent variables, the removal rate of Cr^{6+} by activated carbon modified under different conditions as a response value, and then the adsorption performance of modified carbonized straw for adsorption of Cr^{6+} was optimized. The experimental design was shown in *Table 4*.

Adsorption kinetics

In this study, the first-order kinetic equation, the double-constant equation, and the Elovich equation were used to analyze the adsorption kinetics of the Cr^{6+}-containing solution by modified carbonized straw.

The linear expression of the first-order kinetic equation is as follows *Equation 1* (Takeshi et al., 2004). In the formula, C_t is the mass concentration at time t (mg/L), a and k are the kinetic constants, t is the adsorption time.

$$\ln C_t = \mathrm{a} - \mathrm{kt} \quad \text{(Eq.1)}$$

The double-constant equation is suitable for complex non-homogeneous diffusion processes, and the linear expression of which is as follows (*Eq. 2*) (Wu, 2015). In the formula, X is adsorption capacity (mg/g), a and k are the kinetic constants, t is the adsorption time.

$$\ln X = a + k\ln\mathrm{t} \quad \text{(Eq.2)}$$

The linear expression of the Elovich equation (Shi and Li, 2014) is as follows (Eq. 3). In the formula, X is adsorption capacity (mg/g), a and k are the kinetic constants, t is the adsorption time.

$$X = a + k\ln\mathrm{t} \quad \text{(Eq.3)}$$

Adsorption thermodynamics

Calculating the change of standard thermodynamic function based on experimental data of adsorption thermodynamics is an important part of adsorption thermodynamics research, which has theoretical and practical significance (McKay, 1984). In the adsorption process, the relationships between the thermodynamic functions ΔG, ΔH, ΔS and the adsorption partition coefficient K are as follows (*Eqs. 4–7*).

http://www.aloki.hu ● ISSN 1589 1623 (Print) ● ISSN 1785 0037 (Online)
DOI: http://dx.doi.org/10.15666/aeer/1706_1298512999

$$K = \frac{q_e}{C_e} \quad \text{(Eq.4)}$$

$$\Delta G = -RT \ln K \quad \text{(Eq.5)}$$

$$\Delta G = \Delta H - \mathrm{T}\Delta S \quad \text{(Eq.6)}$$

From the above formulas:

$$\ln K = \frac{\Delta S}{R} - \frac{\Delta H}{RT} \quad \text{(Eq.7)}$$

In the formulas, q_e is the equilibrium adsorption amount (mg/g), C_e is the mass concentration of adsorbate in solution during adsorption equilibrium (mg/L), T is the thermodynamic temperature (K), R is the gas constant (8.314 J/(mol·k)), K is the adsorption partition coefficient, ΔH is the change of adsorption enthalpy (kJ/mol), ΔS is the change of adsorption entropy (J/(mol K)), ΔG is adsorption free energy (kJ/mol).

Experimental results and analysis

Results of modified carbonized straw

The straw obtained after carbonization was dark black, and it had a brittle texture and was lighter in weight than raw materials. The activated carbonized straw was black powder after drying and grinding, and the straw components were shown in *Table 2*.

Table 2. *Component of straw*

Straw	Lignin	Crude fiber	Crude ash	Crude protein
Rice	6.3%	35.1%	19.4%	3.2%
Corn	4.6%	29.3%	7.0%	9.3%
Wheat	9.5%	43.6%	2.6%	2.6%

It could be seen from *Table 2* that the lignin content and crude fiber content of wheat straw were higher than those of rice straw and corn straw, and the pore structure of cellulose directly affected subsequent adsorption properties.

In the process of carbonization and modification, the average pore size of straw decreased, which made the total pore volume increase. At the same time, the non-microcrystalline carbon of the carbon structure was oxidized, which made the specific surface area larger, and the microcrystalline carbon was rearranged to make pores more stable. Therefore, the specific surface area of the modified carbonized straw was much higher than the specific surface area of the original straw. In fact, the increase in specific surface area increased the adsorption area of the adsorbent for heavy metals, and then the adsorption rate was increased (Zhong, 2011).

During the adsorption process, with the increase of temperature, raw materials were rapidly decomposed by heat, so C—OH, C—O—C, C—H and other groups in cellulose molecular structure were decomposed at 280~380 °C, and small amount of molecule fragments or groups were decomposed continuously when the temperature more than

http://www.aloki.hu ● ISSN 1589 1623 (Print) ● ISSN 1785 0037 (Online)
DOI: http://dx.doi.org/10.15666/aeer/1706_1298512999

380 °C. At the same time, carbon element was rearranged to form graphite microcrystalline (Zhu and Zhou, 2014).

Determination and analysis of iodine value of modified carbonized straw

Through the measurement experiment of iodine value, the iodine values of the experimental samples were shown in *Table 3*.

Table 3. *Iodine value of different modified carbonized straw*

Number	Carbonized straw	Modifier	Iodine value (mg/g)
1	Wheat	$ZnCl_2$	1005.32
2	Wheat	KOH	993.84
3	Wheat	H_2SO_4	994.86
4	Wheat	$FeCl_2$	1161.15
5	Corn	$ZnCl_2$	1072.23
6	Corn	KOH	1135.19
7	Corn	H_2SO_4	1101.27
8	Corn	$FeCl_2$	962.80
9	Rice	$ZnCl_2$	1021.13
10	Rice	KOH	993.87
11	Rice	H_2SO_4	937.04
12	Rice	$FeCl_2$	1007.25

In this study, different carbonized straws were modified by different modifiers, and the iodine adsorption value was used as an indicator to compare the adsorption capacity of different modified carbonized straws. After the four modifiers were applied separately, the adsorption capacity of the modified wheat straw was greater than that of corn and rice straw, which might be closely related to the content of crude fiber and lignin in wheat straw. In the experiment, the modified carbonized wheat straw with 2 mol/L $FeCl_2$ as modifier had the highest iodine adsorption value 1161.15 mg/g. Therefore, the subsequent adsorption experiments selected modified carbonized wheat straw as the main research object, which used 2 mol/L $FeCl_2$ as modifier.

Response surface analysis of Cr^{6+}

Based on single factor experiments and orthogonal experiments, this study used Design Expert software to design a response surface experimental scheme in Box-Behnken mode, and then used model analysis to predict the optimal adsorption conditions and the interaction between the factors. In the experiments, temperature (A), adsorption time (B), and dosage of adsorbent (C) were used as independent variables, and the removal rate of Cr^{6+} by activated carbon was used as the response value, and then the adsorption conditions for the adsorption of Cr^{6+} by modified carbonized straw were optimized. The experimental results were shown in *Table 4*.

The results of the *Table 4* were analyzed and modeled, and then the quadratic polynomial regression equations of temperature (A), adsorption time (B), adsorbent dosage (C), and Cr^{6+} adsorption rate R were obtained as follows (*Eq. 8*):

$$R = 98.20 + 1.66A + 0.57B + 0.51C - 0.010AB + 0.23AC + 0.22BC - 1.81A^2 - 0.69B^2 - 0.42C^2 \quad \text{(Eq.8)}$$

http://www.aloki.hu ● ISSN 1589 1623 (Print) ● ISSN 1785 0037 (Online)
DOI: http://dx.doi.org/10.15666/aeer/1706_1298512999

Table 4. *Results of response surface experiments*

Number	Condition			Response value-removal rate R (%)
	Temperature A (°C)	Time B (h)	Dosage C (g)	
1	25	2.5	2.4	98.17
2	25	2.5	2.4	98.45
3	35	3.5	2.4	98.28
4	25	3.5	3.6	98.23
5	15	3.5	2.4	94.18
6	15	2.5	3.6	95.16
7	25	2.5	2.4	98.12
8	25	2.5	2.4	98.68
9	35	2.5	3.6	98.14
10	15	1.5	2.4	93.09
11	25	3.5	1.2	97.14
12	35	1.5	2.4	97.23
13	25	1.5	1.2	96.38
14	25	2.5	2.4	97.88
15	35	2.5	1.2	96.31
16	15	2.5	1.2	94.24
17	25	1.5	3.6	96.53

The quadratic polynomial model and the results of various variance analyses were shown in *Table 5*, which could be used to judge the adaptability of the model to the study and lay the foundation for subsequent research.

Table 5. *Variance analysis of the model*

Resource	Quadratic sum	Degree of freedom	Mean square	F value	Prob > F	Significance
Model	44.91	9	4.99	18.48	0.0004	**
A-temperature	22.08	1	22.08	81.76	< 0.0001	**
B-time	2.59	1	2.59	9.58	0.0174	*
C-dosage	2.04	1	2.04	7.56	0.0286	*
AB	1.31	1	1.31	0.86	0.9704	Not significant
AC	0.21	1	0.21	0.77	0.4103	Not significant
BC	0.20	1	0.20	0.73	0.4201	Not significant
A^2	13.83	1	113.83	51.23	0.0002	**
B^2	2.02	1	2.02	7.48	0.0291	*
C^2	0.76	1	0.76	2.82	0.1372	Not significant
Residual	1.89	7	0.27			
Unfitting term	1.55	3	0.52	6.02	0.0577	Not significant
Pure error	0.34	4	0.086			
Total deviation	46.80	16				
R^2	0.9596	Adj R^2	0.9077	CV	0.54%	
Precision	12.354					

*Significant (P < 0.05), **highly significant (P < 0.01)

http://www.aloki.hu ● ISSN 1589 1623 (Print) ● ISSN 1785 0037 (Online)
DOI: http://dx.doi.org/10.15666/aeer/1706_1298512999

According to the *Table 5*, the P value of the model was 0.0004, and the unfitting term was 0.0577, which indicated that the model was not significant, but the regression was significant. The correlation coefficient (R2) was 0.9596, indicated that the fitting effect was better; the variation coefficient was 0.54%, indicated that the model had good reliability and accuracy. The precision indicated the ratio of signal to noise, which should normally be greater than 4. The precision of this experiment was 12.354, indicated that the model could appropriately reflect the experimental results (Han et al., 2018). In addition, correlation coefficient (R^2) and correction correlation coefficient (Adj R^2) showed that the fitting degree and correlation of the model were high, which indicated that the model could be used to predict the optimal adsorption conditions of Cr^{6+} on modified carbonized straw.

Effect of temperature and time on the adsorption rate of Cr^{6+}

In *Figure 1,* the left graph was a three-dimensional model of temperature, time, and chromium ion adsorption rate, and the right graph was the equal adsorption rate line for adsorption time and temperature. The shape of the equal adsorption rate line could reflect the strength of the interaction of the investigation factors. If it was circular, it meant that the interaction effect was not significant. However, if it was elliptical, it meant that the interaction effect was significant (Pang et al., 2017).

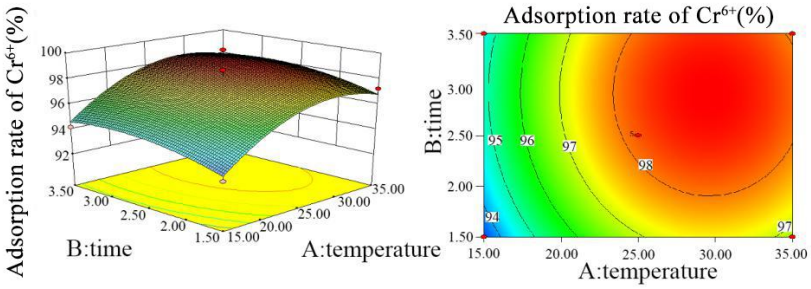

Figrue1. *Effect of temperature and time on the adsorption rate of Cr^{6+}*

As shown in *Figure 1,* the adsorption rate increased with the increase of temperature, indicated that heating was beneficial to the adsorption reaction. In addition, when the treatment time increased from 1.5 to 3.5 h, the adsorption rate increased first and then tended to be slow, indicated that the modified carbonized straw adsorbed Cr^{6+} rapidly first and then gradually reached adsorption equilibrium. According to *Table 5*, the P value of temperature (A) was < 0.0001, the P value of time (B) was 0.0174, and the P value of AB was 0.9704 > 0.05, indicated that the influence of factors A and B on the adsorption rate of Cr^{6+} had no interaction. According to the multiple quadratic regression equation obtained from the response surface, the coefficient of AB was -0.010, indicated that the interaction of the two factors had a negative effect on the result.

Effect of temperature and dosage on the adsorption rate of Cr^{6+}

As shown in *Figure 2,* the adsorption rate increased with increasing temperature, and a high adsorption rate could be achieved at 25 °C. And then the temperature continued to increase, but the adsorption rate increased slowly. Under the condition of constant temperature, the adsorption rate increased with the increase of dosage. However, when

http://www.aloki.hu ● ISSN 1589 1623 (Print) ● ISSN 1785 0037 (Online)
DOI: http://dx.doi.org/10.15666/aeer/1706_1298512999

the dosage reached 2.4 g, the adsorption rate increased very slowly. According to *Table 5*, the P value of temperature (A) was < 0.0001, the P value of dosage (C) was 0.0286, and the P value of AB was 0.4103 > 0.05, indicated that the influence of factors A and C on the adsorption rate of Cr^{6+} had no interaction. According to the multiple quadratic regression equation obtained from the response surface, the coefficient of AC was + 0.23, indicated that the interaction of the two factors had a positive effect on the result.

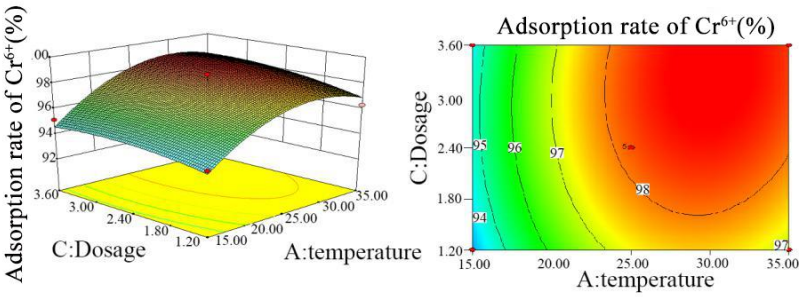

Figure 2. *Effect of temperature and dosage on the adsorption rate of* Cr^{6+}

The effect of time and dosage on the adsorption rate of Cr^{6+}

It could be seen from *Figure 3* that when the time was constant, the adsorption rate increased with the increase of the dosage, but when the dosage exceeded 2.4 g/L, the increase rate of the adsorption rate gradually decreased. At the same time, when the dosage was constant, the adsorption rate also increased with the time, and the growth rate was low. Theoretically, that was because the adsorbent rapidly adsorbed Cr^{6+} in the initial stage and had reached saturation in the later stage, so the adsorption rate did not increase significantly in the later stage. According to *Table 5*, the P value of time (B) was 0.0174, the P value of dosage (C) was 0.0286, and the P value of BC was 0.4201 > 0.05, indicated that the influence of factors B and C on the adsorption rate of Cr^{6+} had no interaction. According to the multiple quadratic regression equation obtained from the response surface, the coefficient of BC was + 0.22, indicated that the interaction of the two factors had a positive effect on the result.

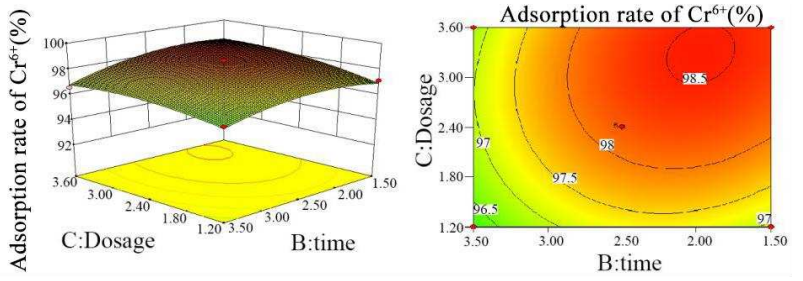

Figure 3. *Effect of time and dosage on the adsorption rate of* Cr^{6+}

The optimal solution was selected by response surface analysis

Further analysis was performed using the fitted multiple quadratic regression equation and Design-Expert 8.0.6 software. And the predicted values of the optimal values and optimal processing conditions were obtained within the experimental design

http://www.aloki.hu ● ISSN 1589 1623 (Print) ● ISSN 1785 0037 (Online)
DOI: http://dx.doi.org/10.15666/aeer/1706_1298512999

conditions. The optimal conditions for prediction were as follows: when the temperature was 30.12 °C, time was 3.05 h, the dosage was 3.45 g, the modified carbonized straw had the best adsorption effect on Cr^{6+}. And then it was proved that the actual and predicted values were well fitted, which indicated that it was feasible to optimize the modified carbonized straw to absorb Cr^{6+} by response surface method.

Adsorption kinetics of Cr^{6+} adsorbed by modified carbonized straw

The adsorption kinetics curves of different dosages (1.2 g/L, 2.4 g/L, 3.6 g/L) of carbonized wheat straw to 200 ml for 100 mg/L Cr^{6+} were shown in *Figure 4,* and the reaction conditions were as follows: temperature was 25 °C, pH was 9, oscillation speed was 250 r/min. The results showed that the larger the dosage of adsorbent, the smaller the adsorption capacity at equilibrium, and the time needed to reach adsorption equilibrium was close, which might be related to the concentration of Cr^{6+}. In addition, under different adsorbent dosages, the adsorbent exhibits similar adsorption kinetic behavior, and each curve could be divided into the following three stages: the dosage of 1.2 g/L was taken as an example. The slope of the first stage was very large, and the adsorption amount increased from 3.13 mg/g to 15.21 mg/g within 1.5 h, which might be caused by the Van der Waals' force between the adsorbent and the adsorbate, indicated that the adsorption process was a fast physical process (Gong, 2011). In the second stage, the adsorption amount increased from 15.21 mg/g to 16.34 mg/g within 0.5 h, which was slow. In the third stage, when the adsorption time was longer than 2 h, the adsorption amount reached equilibrium.

The data of *Figure 4* were fitted using the first-order kinetic equation, the double-constant equation, and the Elovich equation. The fitting results are presented in *Figures 5–7* and *Table 6*.

Table 6. *Fitting results of reaction rate equations under different dosages*

m (g/L)	First-order kinetic equation			Double-constant equation			Elovich equation		
	k_1	a	R^2	k_2	a	R^2	k_3	a	R^2
1.2	1.0457	4.5353	0.868	0.4701	2.2424	0.8732	5.4529	9.7438	0.9192
2.4	1.0877	4.390	0.8642	0.915	1.2643	0.9399	3.1211	4.4071	0.9123
3.6	1.0367	4.0728	0.8608	0.7668	0.8036	0.8946	2.2832	2.7421	0.9277

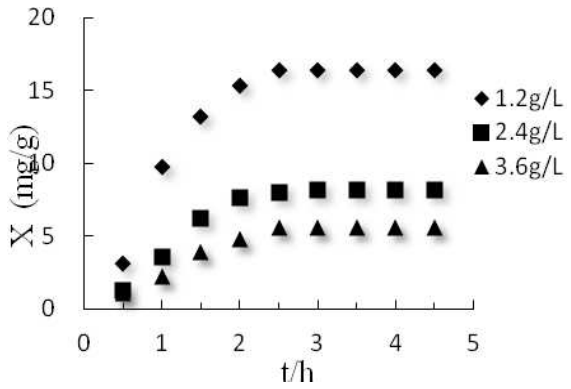

Figure 4. *Adsorption kinetic curves of different adsorbent dosages*

http://www.aloki.hu ● ISSN 1589 1623 (Print) ● ISSN 1785 0037 (Online)
DOI: http://dx.doi.org/10.15666/aeer/1706_1298512999

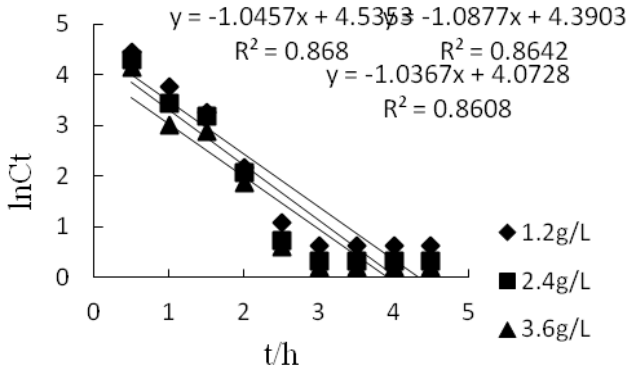

Figure 5. *First-order kinetic equation*

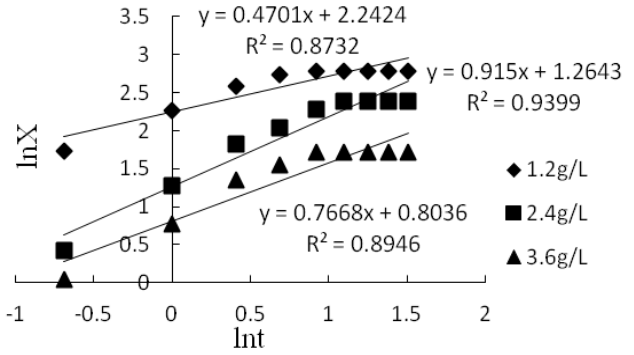

Figure 6. *Double-constant equation*

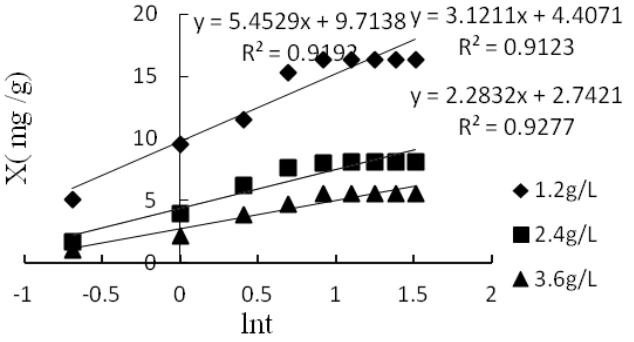

Figure 7. *Elovich equation*

It could be seen from *Table 6* that R^2 values of the first-order kinetic equation, the two-constant equation and the Elovich equation increase in turn, and R^2 values exceed 0.86. Therefore, the three kinetic equations could better fit the process of adsorbing Cr^{6+} by modified carbonized straw before the adsorption reaches equilibrium. However, Elovich equation had the highest fitting degree, and its R^2 was > 0.91, which indicated that the fitting effect of Elovich equation was the best, indicated that the fitting range of the first-order kinetic equation could not meet the process of adsorbing Cr^{6+} by modified carbonized straw. This might be due to the multiple effects of the modified carbonized straw on the adsorption of Cr^{6+}, rather than being limited to the first-order

http://www.aloki.hu ● ISSN 1589 1623 (Print) ● ISSN 1785 0037 (Online)
DOI: http://dx.doi.org/10.15666/aeer/1706_1298512999

kinetic range. In addition, the adsorption process was not a single adsorption mechanism, but a combination of interlayer cation exchange and surface complex adsorption, and it was also related to changes in structure and functional groups after straw modification (Li, 2015).

Thermodynamic analysis of Cr^{6+}

According to the thermodynamic experimental results of adsorption of Cr^{6+} by modified carbonized straw at different temperatures, the equilibrium partition coefficient K was obtained. lnK was used as the ordinate and 1/T was used as the abscissa to get a straight line, as shown in *Figure 8*. ΔS and ΔH could be calculated from the intercept and slope of the line respectively, and then ΔG was calculated. The calculation results were shown in *Table 7*.

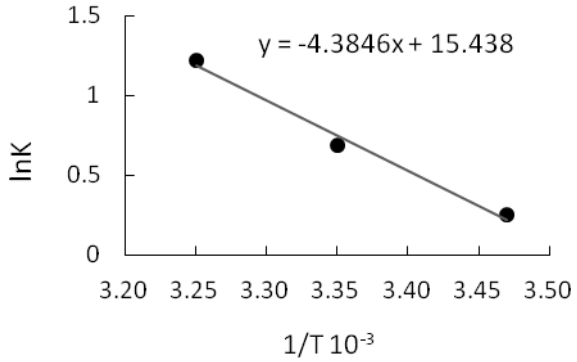

Figure 8. *lnK-1/T curve*

Table 7. *Thermodynamic parameters*

ΔS (J/mol·k)	ΔH (kJ/mol)	T (K)	ΔG (kJ/mol)
128.35	36.45	288	-0.51 kJ/mol
		298	-1.80 kJ/mol
		308	-3.08 kJ/mol

It could be seen from *Table 7* that ΔH > 0 in the adsorption process, indicated that the reaction process was an endothermic reaction, so the temperature rise was favorable for the adsorption process. ΔG could reflect the driving force of a reaction. It could be known from the above data that ΔG < 0 under the temperature conditions of 288 K, 298 K and 308 K, indicated that the adsorption of Cr^{6+} by modified carbonized straw was a spontaneous process. Therefore, chromium ions tended to spontaneously adsorb from the liquid body to the surface of the modified carbonized straw, and the spontaneity increased with the increase of temperature. In addition, ΔS > 0 indicated that the adsorption of Cr^{6+} by the modified carbonized straw increased the disorder of the system. According to the adsorption exchange theory, the adsorption of ions in the solution by the adsorbent was a process of entropy reduction. At the same time, the adsorbent would shrink and release part of the water molecules, which would increase the entropy of the system, and the combination of the two would increase the entropy of the system (Li, 2013).

http://www.aloki.hu ● ISSN 1589 1623 (Print) ● ISSN 1785 0037 (Online)
DOI: http://dx.doi.org/10.15666/aeer/1706_1298512999

Conclusions

In the experiment, different carbonized straws were modified by different modifiers, and the iodine adsorption value was used as an indicator to compare the adsorption capacity of different modified carbonized straws. It was found that the modified carbonized wheat straw with 2 mol/L $FeCl_2$ as modifier had the highest iodine adsorption value 1161.15 mg/g.

Response surface analysis showed that adsorption rate was taken as the response value, temperature, pH and dosage were taken as the factors, and the quadratic response surface regression model of chromium ion adsorption on modified carbonized straw was obtained. The model was significant, the unfitting term was not significant, and the fitting degree of the equation was high. Therefore, it was feasible to optimize the adsorption conditions of Cr^{6+} on modified carbonized straw by response surface methodology.

Using wheat straw as raw material, the modified carbonized straw prepared by $FeCl_2$ activation method could effectively absorb chromium ions. The Elovich equation, the double constant equation and the first-order kinetic equation could be well fitted to the process of adsorbing chromium ions by modified carbonized straw. However, Elovich equation had the highest fitting degree, and its R^2 was > 0.91, indicated that the fitting range of the first-order kinetic equation could not meet the process of adsorbing Cr^{6+} by modified carbonized straw. This might be due to the fact that the main form of adsorption of chromium ions by modified carbonized wheat straw was interlayer cation exchange and surface complex adsorption, rather than a single adsorption mechanism, and it was also related to changes in structure and functional groups after straw modification.

The adsorption of chromium ions by modified wheat straw was a spontaneous endothermic process, and the temperature rise was beneficial to the reaction. Moreover, in the adsorption process, $\Delta S > 0$ indicated that the adsorption of Cr^{6+} by the modified carbonized straw increased the disorder of the system. This might be due to the change in the surface structure of the modified carbonized straw after the adsorption of chromium ions by the modified carbonized straw, resulting in the increase of the disorder of adsorption system.

The results of this research could raise concerns over possible the comprehensive utilization of agricultural wastes and the treatment of heavy metal wastewater. The authors plan to further study the treatment of different types of heavy metal wastewater by other types of activated carbon under different conditions in the future.

Acknowledgements. This research was financed by the National Natural Science Foundation of China (No. 31600253), the Science and Technology Department Foundation of Sichuan Province (No. 2017JY0087), the Education Department Foundation of Sichuan Province (No. 18ZA0119), the Science and Technology Bureau Foundation of Chengdu (No. 2016-HM01-00004-SF), the Teaching Reform Project Foundation of Chengdu University (CDJGB2017050), the Meat Processing Key Laboratory Foundation of Sichuan Province (No.18-R-17) and the Excellence Project Foundation of Chengdu University (No. 82502&33111).

REFERENCES

[1] Cao, Y., Wang, X. Y., Meng, J., Gao, J. P., Lan, Y., Liu, B. (2012): Analysis of current status of straw utilization and its prospect of biocharging. – Crops 4: 9-12.

http://www.aloki.hu ● ISSN 1589 1623 (Print) ● ISSN 1785 0037 (Online)
DOI: http://dx.doi.org/10.15666/aeer/1706_1298512999

[2] Chen, S. H., Yue, Q. Y., Gao, B. Y., Xu, X. (2010): Equilibrium and kinetic adsorption study of the adsorptive removal of Cr(VI) using modified wheat residue. – Journal of Colloid and Interface Science 349: 256-264.
[3] Chen, W. F., Parette, R., Zou, J. Y., Cannon, F. S., Dempsey, B. A. (2007): Arsenic removal by iron-modified activated carbon. – Water Research 41(9): 1851-1858.
[4] Gong, J. H. (2011): Effect of sulfuric acid modification on adsorption performance of activated carbon. – Fujian Forestry Science and Technology 38(2): 103-106.
[5] Hadjmohammadi, M. R., Kiasari, Z. M., Nazari, S. S. S. J. (2016): Separation of some phenolic acids in micellar liquid chromatography using design of experiment-response surface methodology. – Journal of Analytical Chemistry 71(6): 610-616.
[6] Han, W., Lei, Z. C., Han, R. M., Zhang, Y. Y., Peng, Z. X. (2018): Optimization of phosphorus removal process in actual wastewater treatment plant by response surface methodology. – China Environmental Science 38(8): 2968-2973.
[7] Li, J. H. (2015): Activated modification of wheat straw charcoal and its nitrogen and phosphorus adsorption effects. – PhD Thesis, Chinese Academy of Agricultural Sciences, Beijing, pp. 34-35.
[8] Li, W. H. (2013): Preparation of sludge activated carbon and its adsorption properties for dyes. – PhD Thesis, Shandong University, Shandong, pp. 36-37.
[9] McKay, G. (1984): The adsorption of basic dye onto silica from aqueous solution-solid diffusion model. – Chemical Engineering Science 39(1): 129-138.
[10] Ngah, W. S. W., Hanafiah, M. A. K. M. (2008): Removal of heavy metal ions from wastewater by chemically modified plant wastes as adsorbents: a review. – Bioresourece Technology 99(10): 3935-3948.
[11] Nu, Y. L., Zhao, L. H., Chen, Q., Cao, K. (2017): Adsorption performance of modified corn stover for heavy metal copper ions. – Cleaning World 9: 13-19.
[12] Pang, C. L., Bai, L. J., Liu, L. (2017): Optimization of continuous closed circulating ammonia removal process response surface methodology. – Transactions of the Chinese Society of Agricultural Machinery 48(2): 288-293.
[13] Pinto, P. C., Evtuguin, D. V., Neto, C. P. (2005): Structure of hardwood glucuronoxylans: modification and impact on pulp retention during wood kraft pulpling. – Carbohydrate Polymers 60(4): 489-497.
[14] Shi, R., Li, Y. L. (2014): Preparation of activated carbon from corn stover and its adsorption kinetics. – Journal of Environmental Engineering 8(8): 3428-3432.
[15] Sud, D., Mahajan, G., Kaur, M. P. (2008): Agricultural waste material as potential adsorbent for sequestering heavy metal ions from aqueous solutions - a review. – Bioresource Technology 99(14): 6017-6027.
[16] Sun, K., Jiang, J. C. (2009): Research progress and development trend of activated carbon at home and abroad. – Forest Chemical 29(6): 98-103.
[17] Takeshi, K., Yujiro, W., Hirohisa, Y., Takashi, M. (2004): Sorption of phosphates on Al-pillared smectites and mica at acidic to neutral pH. – Applied Clay Science 25(3/4): 167-177.
[18] Wu, D. (2015): Soybean straw-based porous carbon material and its CO_2/CH_4 selective separation characteristics. – PhD Thesis, Fujian Normal University, Fujian, pp. 25-27.
[19] Xiao, G., Liu, J. C., Jin, B. S., Zuo, W., Wang, Q.(2010): Study on characteristics of high temperature carbonized coke in rice straw. – Journal of Combustion Science and Technology 16(1): 1-4.
[20] Zeng, Y. G. (2014): Research on absorbing heavy metal ions of landfill leachate by PAMPS. – Advanced Materials Research 955-959: 2192-2195.
[21] Zeng, Y. G., Li, L. (2014): Study on treatment of heavy metal ions of chemical wastewater by ion exchange resin. – Advanced Materials Research 955-959: 2230-2233.
[22] Zeng, Y. G., Li, W. Y., Wang, L. L., Du, T. T., Huang, J., Huang, Z. W., Wang, J., Tang, J. L., Wang, M. K., Wang, J. M., Jiang, C. Y., Yang, P. (2018): Study on the kinetics of

http://www.aloki.hu ● ISSN 1589 1623 (Print) ● ISSN 1785 0037 (Online)
DOI: http://dx.doi.org/10.15666/aeer/1706_1298512999

the adsorption of reactive brilliant red K-2BP onto modified soybean straw activated carbon. – Desalination and Water Treatment 125: 302-309.

[23] Zhao, Y. (2016): Harm of heavy metal wastewater pollution. – Jiangxi Chemical 3: 145-146.

[24] Zhong, Q. Q. (2011): Preparation of wheat chelating chelate sorbent and its adsorption properties for Cu(II) and Cr(VI). – PhD Thesis, Shandong University, Jinan.

[25] Zhu, J. L., He, X. F., Wang, Z. W., Li, Z. F., Lei, T. Y. (2010): Experimental study on pyrolysis of corn straw granules for carbon production. – Acta Energiae Solaris Sinica 31(7): 789-793.

[26] Zhu, Q. Q., Zhou. H. L. (2014): Structural changes of cellulose during carbonization and activation. – Journal of University of Science and Technology Beijing 36(11): 1545-1551.

http://www.aloki.hu ● ISSN 1589 1623 (Print) ● ISSN 1785 0037 (Online)
DOI: http://dx.doi.org/10.15666/aeer/1706_1298512999

STUDY ON THE ECOLOGICAL EFFICIENCY AND ITS TEMPORAL DYNAMIC EVOLUTION OF CHINA'S CRUISE TOURISM FROM THE PERSPECTIVE OF CARBON FOOTPRINT

YE, X.L.[1] – WANG, L.[1] – ZHU, Z.F.[2] – DU, J.[2] – SUN, R.H.[1*]

[1]*Department of Business Administration, School of Management, Shanghai University of Engineering Science, 333 Longteng Road, Songjiang District, Shanghai, China (e-mail: yexinliang@sues.edu.cn; phone/fax: +86-21-6787-4142)*

[2]*Jiuzhai Valley Scenic Area Administration, Zhangzha Town, Jiuzhaigou County, Aba Tibetan and Qiang Autonomous Prefecture, Sichuan Province, China (e-mail: 183796414@qq.com; ecojay@163.com; phone/fax: +86-83-7773-9753)*

**Corresponding author*
e-mail: sunruihong@sues.edu.cn

(Received 22nd May 2019; accepted 28th Aug 2019)

Abstract. China has grown rapidly to be Asian maximum cruise economic market (Green Book of Cruise Industry, 2018). To facilitate cruise economic growth and harmonious coexistence with ecological environment, this paper proposes a new perspective of the ecological efficiency and computes carbon footprint of the cruise tourism in China from 2009 to 2017. The results show a relatively low level of ecological efficiency in nearly nine years, the average ecological efficiency of cruise tourism is CNY 67.99/kg. In these nine years, ecological efficiency of cruise tourism within four years from 2011 to 2012 and from 2016 to 2017 is lower than the average and ecological efficiency within two years from 2009 to 2010 and from 2013 to 2015 is higher than the average, ecological efficiency within four years from 2013 to 2015 and 2017 is close to the average. Ecological efficiency has dropped continuously in 2011, but the overall carbon emissions and related carbon footprint of cruise tourism show the trend of rapid growth. It is necessary to explore a new way to develop cruise tourism, change the development mode of cruise tourism, rebuild a balance between industry booming and ecosystem by reducing resource consumption and pollution discharge, and further enhance ecological efficiency of cruise tourism.
Keywords: *cruise travel, ecological efficiency, carbon footprints, temporal evolution, China*

Introduction

As one of the fastest growing aspects of tourism, cruise tourism has become an industry power which cannot be ignored in driving the development of cruise ports and surrounding areas. Cruise tourism refers to trans-regional and transnational tourism activities, propelling industries relevant to ports with expansion of the cruise product market, logistics of cruise supplies, or even repair and maintenance of cruise ships. Cruise tourists and related spending can balance regional economic differences, even international balance of payments, and promote the prosperity of the local market. In 2006, international cruise lines began to enter Chinese market and start home port operation in China. It strongly boosts China cruise tourism market and constantly increases acceptance and engagement of tourists towards cruise tourism. China has become the largest Asian cruise tourist market and one of the fastest-growing cruise areas in the world. CCYIA's data shows 11 Chinese cruise terminals, including Shanghai and Tianjin, received totally 1,181 cruise ships in 2017, suggesting a year-on-year growth of 17%. In terms of cruise visitor reception, China received totally 4.954 million inbound and outbound tourists at 11 cruise terminals, suggesting a year-

http://www.aloki.hu ● ISSN 1589 1623 (Print) ● ISSN 1785 0037 (Online)
DOI: http://dx.doi.org/10.15666/aeer/1706_1300113013

on-year growth of 18%. China's cruise revenue in 2017 is CNY (Chinese Yuan) 8.92 billion, which is increased by 32.5%. As domestic coastal port cities have speeded up the development and investment on cruise industry, cruise development and construction and tourism activities will inevitably bring plenty of ecological and environmental challenges and problems, including coastal landscapes changes, loss of original ecological habitats, air pollution and environmental congestion when cruise ships are reaching and berthing at ports. Hence, how to reduce impacts of cruise ships on the ecological environment and realize sustainable development of cruise industry has become a high-profile issue in the industry and academic world. In this context, in order to protect ecological environment and achieve sustainable development of economy, this paper chooses the green and sustainable development of cruise economy as the aim and introduces the ecological efficiency index to evaluate the sustainable development status of cruise tourism by comparing ecological environmental loads with economic benefits, to explore a green development path for China cruise tourism, to propel the transformation and upgrading of the cruise tourism industrial structure and mode suitable for the marine ecosystem, and to improve ecological efficiency of cruise tourism.

Literature review

Despite considerable economic income brought by cruise development (Vina and Ford, 1999), the practical effect is affected by local economic development level and degree of integration in the global industrial chain, and thus cruise tourism's positive effect on local areas will be limited by local industrial structure, variety of products and reception capacity (Chase and Mckee, 2003; Chang et al., 2016; Sun and Hou, 2017). The areas where cruise ships pass through will be effected and suffer negative ecological impacts due to a great deal of waste coming from fuel consumption, energy use, food consumption, etc., which increases the ecological cost of local cruise tourism development and results in potential loss of cruise economic benefits (Chase and Mckee, 2003).

Scholar Erize (1987) showed concern over cruise ecological problems as early as 1980s, and Ritter and Schafer (1998) proposed that importance must be attached to marine pollution control with the rapid development of cruise tourism (Ritter and Schafer, 1998). On a basis of the life cycle theory, Johnson (2002) believes ecological problems and environmental pollution of cruise tourism is mainly caused by resource consumption and utilization, discharge of waste, infrastructure construction, passenger transport and logistics distribution (Johnson, 2002). In his point of view, cruise waste's impacts on environment include poor water quality (Lincoln et al., 2006), sea area pollution (Gibson et al., 2012), damage to coral reefs (Jones, 2007, 2011) and so forth. Along with global changes and climate warming in recent years, low-carbon emission reduction in cruise industry becomes a hot research topic. More empirical researches have been done on the sustainable development of cruise economy, including researches on economic, social and ecological impacts of cruise pollution (Miller et al., 2013; Murena et al., 2018), cruise energy efficiency (Lepistö et al., 2016), ecological cost (Carić, 2016), cruise's carbon emission (Howitt et al., 2010) and cruise ships' effects on public health and social costs, etc. (Chatzinikolaou et al., 2015; Mölders et al., 2013). Moreover, scholars also discuss the cruise ecological protection system and sustainable development mode in many ways. In spite of an increasing number of Chinese cruise

http://www.aloki.hu ● ISSN 1589 1623 (Print) ● ISSN 1785 0037 (Online)
DOI: http://dx.doi.org/10.15666/aeer/1706_1300113013

references, fewer references concern impacts of cruise tourism, especially in regard to negative environment impacts of cruise economy, sustainable development and green treatment (Sun and Hou, 2017). Therefore, the academic study in China tends to "take foreign documents for references" and be led by policies. In the context of outdated cruise environment monitoring and a lack of relevant data, domestic scholars focus on the review and reference (Xie, et al., 2010; Qiu, 2007; Sun and Hou, 2017) of foreign documents which concern practical experience and researches on ecological pollution of foreign cruise ships and foreign ecological protection, such as shore power experience (Wu and Shen, 2012), green port construction (Ye et al., 2017), construction of a port ecological protection system (Ren, et al., 2017), etc. On the other hand, domestic scholars conduct researches on the measurement of carbon emission in cruise industry (Li and Lv, 2016), pollution prevention and control for cruise ships (Wang and Huang, 2015) and so on.

In view of all mentioned above, the academic world agrees that cruise tourism must follow the principle of sustainable development, and carbon emission and energy consumption of cruise ships must be strictly limited under the threshold (Yao and Chen, 2016). Tourism refers to an energy intensive industry (Becken, 2008). As an index giving consideration to both ecology and economy, ecological efficiency can indicate how to balance economic development and ecological impacts. The tourism ecological efficiency theory provides an access to bi-effect (Dobers and Wolff, 1999), that is, when job opportunities are created in the new market, costs and tourism's negative effects on the environment are reduced at the same time (Holleran, 2008). In a word, the essence of ecological efficiency is to create the maximum economic value with the minimum ecological impact. As the ecological efficiency analysis is a kind of typical quantitative analysis, it has been taken seriously and applied (Holleran and Lehto, 2008; Su, 2014; Gössling et al., 2005) by scholars in evaluation and quantitative analysis of tourism and sustainable development of cruise ships, including ecological efficiency research based on emission inventory (Su, 2014) and research on ecological cost and ecological efficiency of cruise carbon footprint (Tichavska and Tovar, 2015). Though there are a great many Chinese and foreign researches on economic development and ecological pollution of cruise tourism at home and abroad, there are not sufficient ecological efficiency studies of how to balance economic development and ecological impacts of cruise tourism. The introduction of ecological efficiency to this paper helps analyze a balanced relationship between cruise tourism development and its ecological impact in a more profound way, discuss a coexistence mode of cruise economy and ecological environment, explore a harmonious and unified development mode for economy and ecology, seek for a way to promote ecological efficiency of cruise economy, and work out a cruise ecological pollution control system putting prevention first, paying attention to comprehensive treatment, and preventing and controlling pollution from the source.

Research method and design

Evaluation method for ecological efficiency

Evaluation methods of ecological efficiency mainly include the ratio method, index system method and model method (Yao and Chen, 2015; Peng et al., 2017). The ratio method makes sense by giving simple ratio values. The index system method, based on weight to express the relationship between environment and economy, may involve too much subjectivity. The model method mainly refers to the data envelopment analysis

http://www.aloki.hu ● ISSN 1589 1623 (Print) ● ISSN 1785 0037 (Online)
DOI: http://dx.doi.org/10.15666/aeer/1706_1300113013

model, ecological topological method and so forth. In use of this kind of method, it is necessary to define weight of different indexes for integrating them to a single numerical value. In this case, the weight may lose objectivity. For studies into ecological efficiency, ecological risks and energy consumption caused by tourism become the focus at the present time. According to Gössling, ecological efficiency of tourism indicates a ratio between the carbon dioxide emission equivalent and tourism revenue (Gössling et al., 2005, 2007). In view of this, this paper applies the ratio method to compute ecological efficiency of cruise tourism in China.

When referring to the ratio method, a generally accepted ecological efficiency calculation formula is the calculation model proposed by World Business Council for Sustainable Development (WBCSD):

$$EE = TR/CFT \quad \text{(Eq.1)}$$

In this formula, EE stands for ecological efficiency, which can be described as the result that the revenue of cruise industry removes its ecological impacts. TR stands for the revenue of cruise industry, here uses the cruise tourism revenue to demonstrate, and CFT stands for the ecological impact of cruise industry, here uses its carbon footprint to present. All variable values shall be assigned to the increment of a product or service or ecological impacts according to the nature of industry. The total amount of carbon footprint from cruise travel is selected as the index of ecological impacts of cruise tourism, while cruise tourism revenue is selected as the index to measure economic value of tourism.

Calculation formula for cruise carbon footprint and coefficient determination

a. Calculation of total carbon footprint from cruise travel

Caron footprint originates from the concept of "ecological footprint", refers to the land needed to absorb the carbon emission. But with the development of the carbon footprint theory, now it has almost been expressed as carbon dioxide equivalent. In this paper, carbon footprint from cruise travel is decided by the carbon emission from fuel consumption, solid waste and sewage discharge of cruise ships. The designed formula is as follows:

$$GCF = \sum_i G_i * CE_i \quad \text{(Eq.2)}$$

In *Equation 2,* GCF stands for total carbon footprint from cruise ships, "i" stands for energy and different types of waste and they are marine fuel oil, solid waste and sewage, G stands for amount of energy consumption or generated waste, and CE stands for response carbon emission coefficient.

b. Calculation of carbon emission of cruise fuel oil

In this paper, Wang (2015) is mainly used to calculate the carbon emissions of cruise ships. At the same time, according to the trend of large-scale cruise ships and the extension of berthing time in recent years, the specific values of the correlation coefficient are improved to make the calculation more scientific and reasonable. Based on the theme of low-carbon green development of Shanghai cruise port, Wang Bowen used this model to quantitatively and intuitively calculate specific carbon dioxide

http://www.aloki.hu ● ISSN 1589 1623 (Print) ● ISSN 1785 0037 (Online)
DOI: http://dx.doi.org/10.15666/aeer/1706_1300113013

emission data, quantitatively analyze the carbon emissions of cruise port, and provide guidance for the development of low-carbon green operation of cruise port. In addition, Li and Lu (2016) used the bottom-up dynamic method to calculate the emission of sulfur oxides and particulates from cruise ships, and the principle of the dynamic method is similar to the formula used in this paper.

The topic of this paper lies in carbon emission from cruise travel in China and thus the carbon footprint defined in this paper must be within Chinese territory. The main focus is carbon emission of cruise fuel oil consumed during the period from the moment when a cruise enters the sea of China to its docking to the moment when a cruise leaves the port to arrival of an open sea, namely, the carbon footprint during cruise ships' berthing. This paper believes carbon footprint during cruise ships' berthing is mainly related to the number of cruise ships moored to the port (see *Table 1*), the duration of berthing, etc. The calculation thought is to transfer the electrical load during cruise berthing to the amount of fuel consumed during berthing via engine fuel efficiency; and then calculate carbon footprint by using the carbon emission coefficient of fuel oil. The correlation values in the formula (e.g. W = 10.5 megawatt, Y = 200 g/kWh) are borrowed from the data in previous studies (Dong, 2017; Yang, 2013; Gui et al., 2017). The calculation formula for CO_2 pollutants generated from cruise ship is:

$$S = N \cdot W \cdot t \cdot Y \cdot \beta \cdot \eta \quad \text{(Eq.3)}$$

S is the total amount of CO_2 emission; N is the number of cruise ships moored to the port annually; N is electrical load for berthing, and W = 10.5 megawatt; t is the duration of cruise berthing, and t = 11.95 h (average value); Y is power consumed by diesel engine, and fuel consumption power of oil engine on the cruise is 200 g/kWh; β is the combustion carbon emission coefficient; HFO carbon emission factor is 3.114 kg CO_2/KG; η is the electrical grid power factor of cruise and η = 7.5.

Table 1. *Recommended discharge coefficient of cruise solid wastes. (Source: IPCC2006, General Principles for Calculation of the Comprehensive Energy Consumption (GBT 2589-2008))*

Fuel type	A		B		C = A×B	
	CO_2 emission original coefficient from *IPCC2006*		Heating value of China		Recommended emission coefficient	
	Original coefficient	Unit	Heating value	Unit of heating value	Numerical value	Unit
Solid waste	3.84E-04	Kg CO_2/Kcal	2,955	kcal/kg	1.13	KgCO_2/kg

The carbon emission coefficient of cruise fuel oil in this paper is in accordance with relevant Chinese regulations on marine fuel oil. In *Notice on Issuing the Implementation Plan for the Marine Air Pollutant Emission Control Area,* issued by Ministry of Transport of the People's Republic of China in 2018, it is specified that sea ships should consume marine fuel oil whose Sulphur content does not exceed 0.5%m/m since January 1, 2019 when they enter the emission control area. This means cruise ships consumed heavy oil before 2019. In this paper, the carbon emission coefficient of HFO and MGO are 3.114 kgCO_2/kg and 3.205 kgCO_2/kg, respectively.

http://www.aloki.hu ● ISSN 1589 1623 (Print) ● ISSN 1785 0037 (Online)
DOI: http://dx.doi.org/10.15666/aeer/1706_1300113013

c. Calculation of carbon footprint from solid waste of cruise ships

This paper borrows carbon emission original coefficients of different emission sources and different fuels from *IPCC2006*. The carbon emission original coefficient multiplied by the heating value equals to the recommended carbon emission coefficient of this type of fuel in China. For the heating value of solid waste, see the heating value of municipal solid waste, as shown in *Table 1*.

d. Calculation of carbon footprint of cruise solid waste

There is a lack of exact data about sewage carbon discharge domestically. For this reason, the sewage carbon discharge in this paper is replaced by the indirect carbon discharge of power consumption and use of PAM during sewage treatment. Power consumption and PAM consumption are two major indirect discharge sources from the sewage treatment plant. The carbon emission coefficient of power consumption varies greatly from 0.6 to 1.2 $kgCO_2/(kWh)$ with types of fuels used for local electricity generation. This paper cites the data of power supply emission intensity based on the national carbon market base value in 2015: 0.8066 $kgCO_2/kWh$. As the discharge coefficient of carbon consumed by PAM ranges from 20 to 30 $kgCO_2/kg$, this paper adopts the average value of 25 $kgCO_2/kg$. The statistical data in 2010 shows sewage per cubic meter consumes 0.24 kW electricity and 0.00076 kg PAM. The sewage carbon discharge coefficient formula in this paper is:

$$CE_{PW} = E_{PW} * CE_E + PAM_{PW} * CE_{PAW} \quad \text{(Eq.4)}$$

In *Equation 4*, PWCE stands for the sewage carbon discharge coefficient, Epw stands for electricity consumption for sewage treatment, CEE stands for power carbon discharge coefficient; PAMpw stands for the amount of PAM used for sewage treatment, and CEPAM stands for the carbon discharge coefficient of PAM. Upon calculation, the sewage carbon discharge coefficient is 0.212584 $kgCO_2/m^3$.

e. Discussion of uncertainty of the discharge coefficient

The carbon discharge original coefficient of energy in this paper are quoted from *IPCC2006*. For the combustion heating values of energy and waste, refer to national standard *General Principles for Calculation of the Comprehensive Energy Consumption* (GBT 2589-2008) released in 2008; average carbon emission per kilowatt hour in China (kg/kWh) is selected as the power carbon discharge coefficient used in the sewage carbon discharge calculation formula. Therefore, the coefficient uncertainty in this paper mainly comes from the regional differences domestically and there is a deviation from the actual carbon discharge coefficient.

Data collection

This paper collects data mainly from Annual Report on China's Cruise Industry (2016), Annual Report on China's Cruise Industry (2017), Annual Report on China's Cruise Industry (2018) and other relevant materials. Relevant coefficient values involved in carbon discharge calculation and the quantity of pollutants from tourists per day come from related studies as mentioned above. The quantity of pollutants per tourist is: 4 kg solid waste; 40 L black water; 340 L gray water; 10 L bilgy oily water;

http://www.aloki.hu ● ISSN 1589 1623 (Print) ● ISSN 1785 0037 (Online)
DOI: http://dx.doi.org/10.15666/aeer/1706_1300113013

0.16 kg toxic waste. The data on annual revenue in cruise tourism market from 2009 to 2017 comes from Annual Report on China's Cruise Industry (CCYIA, 2016), and the data on annul tourist reception in China cruise tourism industry and the data on the annual number of received cruise ships from 2009 to 2017 come from Annual Report on China's Cruise Industry (Wang, Ye, 2018), as shown in *Table 2*. The average value of cruise berthing durations in 2015, 2016 and 2017 is taken as the berthing duration.

Table 2. *Total number of cruise ships received by China, scale of the cruise tourism market and trading volume from 2009 to 2017. (Data source: Annual Report on China's Cruise Industry (2018), CCYIA)*

Year	2009	2010	2011	2012	2013	2014	2015	2016	2017
Cruise ships received by China (total number)	259	294	272	275	406	466	629	1,010	1,181
Trading volume of the cruise tourism market (100 million yuan)	19.7	23.8	7.1	11.8	26.2	33.5	45.3	60.8	82.3
Number of received cruise tourists (unit: 10,000 persons)	34.38	48.08	47.85	65.69	120.15	172.37	248	456.66	495.42

Research process and result analysis

Time evolution and characteristics of cruise carbon footprint

According to the data in *Table 2*, the carbon footprint of cruise ships received by China from 2009 to 2017 it obtained from *Equations 1* and *2*. *Table 3* shows values of annual and total carbon footprint of fuel oil, sewage and solid waste released by Chinese cruise ships from 2009 to 2017. Among three types of carbon footprint, solid waste, which is the most important source of carbon footprint, produces the largest carbon footprint load; fuel oil plays a secondary role, and carbon footprint from sewage occupies the smallest part.

Table 3. *Carbon footprints generated by cruise ships received in China from 2009 to 2017*

Carbon emission	2009	2010	2011	2012	2013	2014	2015	2016	2017
Cruise fuel oil	1516.03	1723.12	1594.17	1611.76	2379.54	2731.2	3686.53	5919.55	6921.77
Cruise sewage	7.04	9.84	9.80	13.43	24.60	35.3	50.78	93.5	101.4
Solid waste	404.03	565.04	562.33	771.99	1412	2025.69	2914.5	5366.67	5822.18
Total amount	1927.11	2298	2166.31	2379.20	3816.14	4792.18	6651.8	11379.72	12845.38

Table 3 lists carbon footprints from different sources and total amount of carbon emission. On this basis, this paper analyzes carbon emission composition and growth

http://www.aloki.hu ● ISSN 1589 1623 (Print) ● ISSN 1785 0037 (Online)
DOI: http://dx.doi.org/10.15666/aeer/1706_1300113013

change of China cruise tourism from 2009 to 2017, finds that cruise carbon emission shows a growing momentum when the number of cruise ships berthing in China increases (*Fig. 1*). The carbon emission from the fuel oil contributes the largest part to total emission. In respect to the growth rate of cruise carbon emission, the rate of fuel emission, solid waste carbon emission and overall carbon emission fluctuates greatly, and the fluctuation trend is similar.

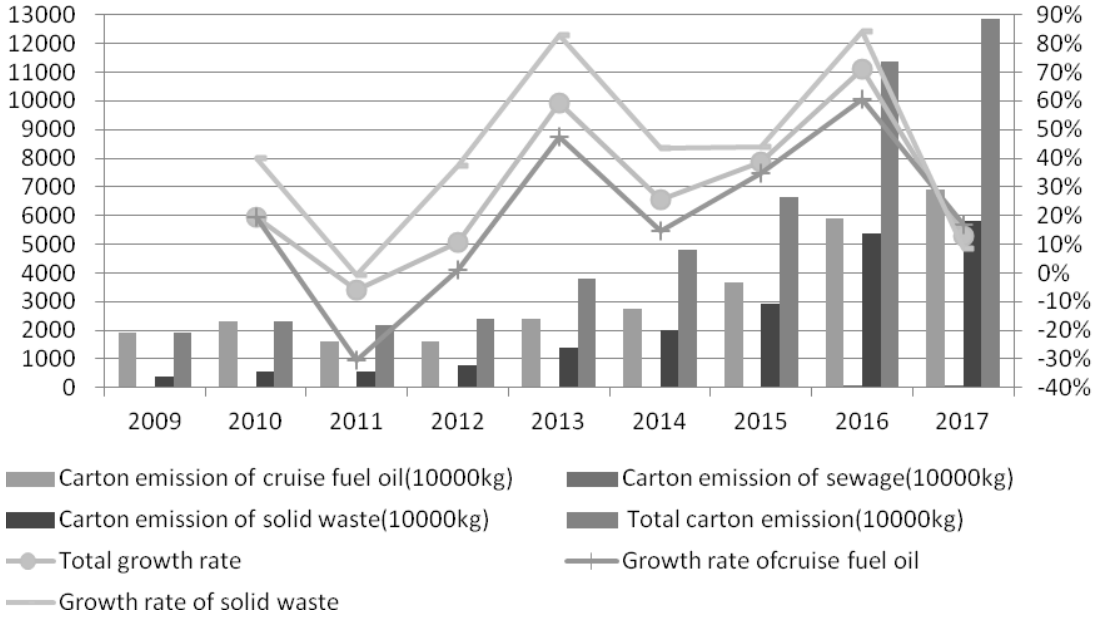

Figure 1. *Carbon footprints composition and growth change of China cruise tourism from 2009 to 2017*

Calculation of ecological efficiency of China cruise tourism

Table 4 shows the values of China's annual cruise revenue, total cruise carbon emission and ecological efficiency of cruise tourism from 2009 to 2017. These values are got by calculation according to the ratio of annual cruise travel revenue and total cruise carbon emission annually in *Equation 1*.

Table 4. *Ecological efficiency of China cruise tourism from 2009 to 2017*

	2009	**2010**	**2011**	**2012**	**2013**	**2014**	**2015**	**2016**	**2017**
Total carbon emission of cruise ships (10000 kg)	1927.11	2298.00	2166.31	2397.20	3816.14	4792.18	6651.80	11379.72	12845.38
Tourist revenue of cruise ships (10000 yuan)	197000	238000	71000	118000	262000	335000	453000	608000	823000
Ecological efficiency of cruise tourism	102.23	103.57	32.77	49.22	68.66	69.91	68.10	53.43	64.07

Figure 2 mainly reflects the ecological efficiency tendency of China cruise tourism over time from 2009 to 2017 and its average level. In these nine years, ecological

http://www.aloki.hu ● ISSN 1589 1623 (Print) ● ISSN 1785 0037 (Online)
DOI: http://dx.doi.org/10.15666/aeer/1706_1300113013

efficiency of China cruise tourism has generally declined, its numerical value is still low and the average value is merely CNY 67.99/kg. Hence, ecological efficiency of China cruise tourism needs to be improved essentially. In 2011, China's cruise tourist ecological efficiency was at a record low of CNY 32.77/kg. This is because Chinese tourist revenue in 2011 fell as historically low as CNY 710 million but cruise carbon emission of cruise ships did not decrease. From 2009 to 2017, the maximum value of cruise tourist ecological efficiency in China is CNY 103.57/kg.

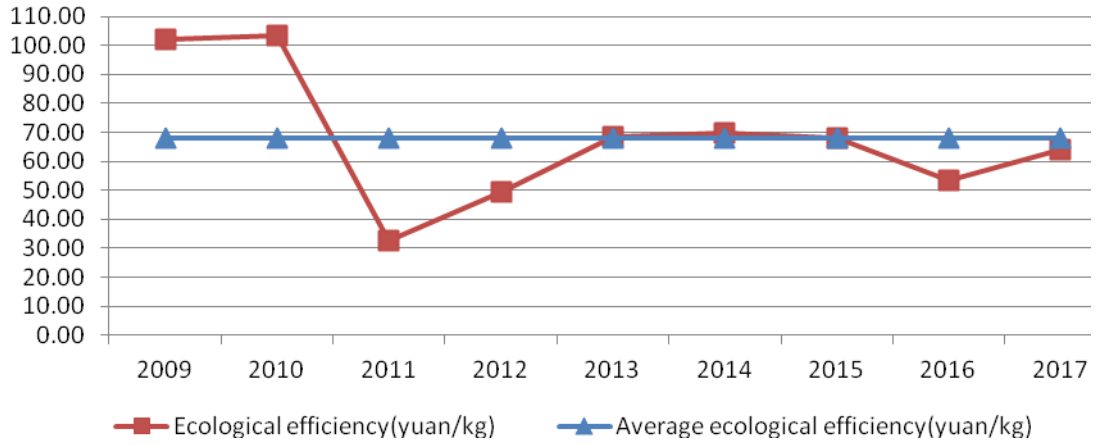

Figure 2. *Time evolution of China's cruise tourist ecological efficiency from 2009 to 2017*

Result analysis

Analysis on the time evolution characteristics of China cruise tourist ecological efficiency from 2009 to 2017

According to *Figure 2,* ecological efficiency of China cruise tourism shows an overall downtrend momentum from 2009 to 2017. The average tourist ecological efficiency is CNY 67.99/kg, namely, 1 kg pollutants are generated as soon as China cruise tourism earns CNY 67.99. In these nine years, the values of cruise tourist ecological efficiency from 2011 to 2012 and from 2016 to 2017 are lower than the average value and the values from 2009 to 2010 are higher than the average value and the values from 2015 to 2015 and 2017 are close to the average value. In 2011, China's cruise tourist ecological efficiency was at a record low of CNY 32.77/kg. This is because Chinese tourist revenue in 2011 fell as historically low as CNY 710 million, but cruise carbon emission of cruise ships did not decrease. In 2009-2017, cruise tourist ecological efficiency in China reached a record high of CNY 103.57/kg.

The overall ecological efficiency of China cruise tourism, which is still relatively low, does not benefit much from the continuously expansion of China's cruise tourist market. There are two root causes. The first one lies in low contribution of China cruise tourism to economy. International cruise lines play a leading role in global cruise industry and thus most economic benefit of cruise industry drains away. In this case, China benefits a little from the international cruise tourism. The second reason is a waste of resources and tourist spending. This is because China is still in the early stage of development to attract investment and expand size when the cruise market is moving eastward and the numbers of cruise tourists, cruise ships received in Chinese ports are growing; most cruise ships are used for outbound travel, featuring high mobility and

http://www.aloki.hu ● ISSN 1589 1623 (Print) ● ISSN 1785 0037 (Online)
DOI: http://dx.doi.org/10.15666/aeer/1706_1300113013

hidden environment pollution; due to a lack of relevant legal norms and backward maritime control, ecological problems caused by cruise travel have not been taken seriously and treated, and the ecological cost of cruise economy for development has not been taken into account.

Carbon footprint change of cruise tourism in China from 2009 to 2017

With the rapid development of China cruise tourism, the ever-growing numbers of cruise ships and cruise tourists lead to constant growth of cruise fuel consumption, solid waste, sewage discharge and tourist food consumption etc. In view of this, the total carbon footprint of cruise ships also rises. According to *Figure 1* and *Table 2*, carbon footprint of cruise solid waste shows a fast-growing momentum with the tourist development in China and this momentum becomes more obvious especially from 2011 to 2013. Furthermore, among the total carbon footprint of cruise ships, cruise fuel oils accounts for the largest proportion.

Conclusions and suggestions

On the basis of analysis above, the following points can be concluded: firstly, ecological efficiency of China's cruise tourism is still low and generally show a downward trend from 2009 to 2017 and the value of average ecological efficiency is merely CNY 67.99/kg. There's a lot of room for improvement. Secondly, accompanied by vigorous growth of tourists' reception and cruise ships' visits, cruise ships' impact on the environment from 2009 to 2017 becomes more serious. In particular, carbon emission of solid waste occupies the largest proportion and exerts the greatest impact on environment.

Owing to rapid expansion of China cruise tourism, the numbers of cruise ships berthing in ports and tourists are increasing quickly. Accordingly, resource occupancy and consumption, waste discharge and pollution brought by industrial expansion also become serious. All of this is challenging the sustainable development of areas around ports and sea areas. As a result, importance must be attached to ecological problems caused by cruise tourism and seek solutions. Firstly, it is suggested to re-examine China's cruise tourism development structure and industrial layout, promote the continuous upgrading and transformation of the cruise industry towards low-carbon, high efficiency and ecological protection, and build an ecologically-efficient cruise economic development model. Secondly, it is suggested to raise tourists' and the public's concerns over cruise lines, green ecology of ports and enterprises' ecological behaviors, and encourage tourists to convert consumption concept and use green products. In this way, it is available to reduce tourism consumption waste, control uncivilized ecological behaviors, and form a responsible consumption pattern of green tourism. Thirdly, it is suggested to promote intelligent transformation of cruise economy with the help of new technological revolution, and advocate construction of smart cruise, smart port and smart tourism; on the other hand, it is suggested to propel the use of shore power at ports, clean energy cruise ships, air filtration and sewage treatment to build a market-oriented green technology innovation system; finally, the national government and departments concerned should formulate specific and detailed legal rules of cruise travel to restrict behaviors of cruise passengers, cruise lines, cruise ships and support the green development of China cruise ships.

http://www.aloki.hu ● ISSN 1589 1623 (Print) ● ISSN 1785 0037 (Online)
DOI: http://dx.doi.org/10.15666/aeer/1706_1300113013

In future, China should explore actively the institutional assurance and operation mechanism. The first step is to make and perfect energy, ecological protection, economy, ocean, science and technology policies which can drive the green development of cruise ships, increase fiscal subsidies and policy support for clean energy, shore power technologies, energy conservation and ecological protection technologies, and perfect systems for coastal and marine ecological management and ecological management to build a policy system and a guidance mechanism for advocating clean production, low carbon emission and green development of cruise industry; the second step is to bring into full play the synergistic effect among climate change, energy conservation and ecological protection, new energy development, and ecological improvement, seek a stable and sustainable long-term capital investment operation mechanism, an efficient mechanism for transferring international low carbon ecological protection technologies and a public information platform to provide public mechanism guarantee for green development in terms of capital and technological information; the third step is to improve functions of maritime and coast guard departments for regulating marine ecosystem, clarify the supervision subject and personnel agency for coping with ecological environment problems caused by cruise ships, solidify cruise waste discharge and the sea area regulatory process, coordinate with relevant departments to take joint actions, and provide institutional safeguards for green regulators.

Acknowledgements. We are very grateful to express our special thanks to the grant of the National Social Science Foundation to the project study "Research on the development of domestic cruise tourism in China under the adjustment of supply structure" (No. 16BGL110), and the Ministry of Education to the youth planning project study "Research on the Environmental Externality and Green Governance Path of China's Cruise Industry from the Perspective of Ecological Economy" (No. 19YJC790117).

REFERENCES

[1] Becken, S. (2008): Developing indicators for managing tourism in the face of peak oil. – Tourism Management 29(4): 695-705.
[2] Carić, H. (2016): Challenges and prospects of valuation - cruise ship pollution case. – Journal of Cleaner Production 111: 487-498.
[3] Chang, Y. T., Park, H., Liu, S. M., et al. (2016): Economic impact of cruise industry using regional input-output analysis: a case study of Incheon. – Maritime Policy & Management 43(1): 1-18.
[4] Chase, G. L., Mckee, D. L. (2003): The economic impact of cruise tourism on Jamaica. – Journal of Tourism Studies 14(2): 16-22.
[5] Chatzinikolaou, S. D., Oikonomou, S. D., Ventikos, N. P. (2015): Health externalities of ship air pollution at port - Piraeus Port case study. – Transportation Research Part D Transport & Environment 40: 155-165.
[6] China Cruise & Yacht Industry Association, Hongkou District People's Government of Shanghai (2016): Annual Report on China's Cruise Industry (2015). – Shanghai International Shipping Institute, Shanghai.
[7] Dobers, P., Wolff, R. (1999): Eco-efficiency and dematerialization: scenarios for new industrial logics in recycling industries, automobile and household appliances. – Business Strategy & the Environment 8(1): 31-45.
[8] Dong, L. (2017): High-voltage shore power connection system and application of luxury cruise terminals. – Jiangsu Ship 34(2): 24-27.

http://www.aloki.hu ● ISSN 1589 1623 (Print) ● ISSN 1785 0037 (Online)
DOI: http://dx.doi.org/10.15666/aeer/1706_1300113013

[9] Erize, F. J. (1987): The impact of tourism on the Antarctic environment. – Environment International 13(1): 133-136.
[10] Gibson, P., Walters, C., Vogel, M., et al. (2012): Human Resource Management in the Cruise Industry. – In: Vogel, M. et al. (eds.) The Business and Management of Ocean Cruises. CABI, Wallingfrod, pp. 101-103.
[11] Gössling, S., Peeters, P., Ceron, J. P., et al. (2005): The eco-efficiency of tourism. – Ecological Economics 54(4): 417-434.
[12] Gössling, S., Broderick, J., Upham, P., et al. (2007): Voluntary carbon offsetting schemes for aviation: efficiency, credibility and sustainable tourism. – Journal of Sustainable Tourism 15(3): 223-248.
[13] Gui, S., Guo, Y., Gao, S., et al. (2017): Load analysis of power system of cruises in port. – Journal of Shanghai Maritime University 38(2): 61-65.
[14] Holleran, J. N. (2008): Sustainability in tourism destinations: exploring the boundaries of eco-efficiency and green communications. – Journal of Hospitality & Leisure Marketing 17(3-4): 373-394.
[15] Holleran, J. N., Lehto, X. Y. (2008): Sustainability in tourism destinations: exploring the boundaries of eco-efficiency and green communications. – Journal of Hospitality & Leisure Marketing 17(3-4): 373-394.
[16] Howitt, O. A., Revol, V. N., Smith, I. J., et al. (2010): Carbon emissions from international cruise ship passengers' travel to and from New Zealand. – Energy Policy 38(5): 2552-2560.
[17] Johnson, D. (2002): Environmentally sustainable cruise tourism: a reality check. – Marine Policy 26(4): 261-270.
[18] Jones, R. J. (2007) Chemical contamination of a coral reef by the grounding of a cruise ship in Bermuda. – Marine Pollution Bulletin 54(7): 905-911.
[19] Jones, R. J. (2011): Environmental effects of the cruise tourism boom: sediment resuspension from cruise ships and the possible effects of increased turbidity and sediment deposition on Corals (Bermuda). – Bulletin of Marine Science 87(3): 659.
[20] Lepistö, V., Lappalainen, J., Sillanpää, K., et al. (2016): Dynamic process simulation promotes energy efficient ship design. – Ocean Engineering 111: 43-55.
[21] Li, H., Lv, S. (2016): Environmental pollution measurement and control situation analysis of cruise travel - taking Shanghai Port as an example. – Ocean Development and Management 12: 32-38.
[22] Lincoln, C. L., Krause, C. B., George, K., et al. (2006): The significance of dilution in evaluating possible impacts of wastewater discharges from large cruise ships. – Marine Pollution Bulletin 52(6): 681-688.
[23] Miller, F. P., Vandome, A. F., Mcbrewster, J. (2013): Cruise ship pollution. – Alphascript Publishing.
[24] Mölders, N., Gende, S., Pirhalla, M. (2013): Assessment of cruise ship activity influences on emissions, air quality, and visibility in Glacier Bay National Park. – Atmospheric Pollution Research 4(4): 435-445.
[25] Murena, F., Mocerino, L., Quaranta, F., et al. (2018): Impact on air quality of cruise ship emissions in Naples, Italy. – Atmospheric Environment 187: 70-83.
[26] Peng, H., Zhang, J., Han, Y., et al. (2017): SBM-DEA model and empirical analysis of ecological efficiency measurement of tourism destinations. – Acta Ecologica Sinica 37(2): 628-638.
[27] Qiu, C. (2007): Anti-pollution thinking triggered by cruise economy boom. – Research on Waterborne Transportation 3: 54-56.
[28] Ren, C., Sun, R., Ye, X. (2017): Research prospect of environmental protection of cruise ports. – Journal of Shanghai University of Engineering Science 31(2): 166-173.
[29] Ritter, W., Schafer, C. (1998): Cruise-tourism. – Tourism Recreation Research 23(1): 65-71.

http://www.aloki.hu ● ISSN 1589 1623 (Print) ● ISSN 1785 0037 (Online)
DOI: http://dx.doi.org/10.15666/aeer/1706_1300113013

[30] Su, S. (2014): Ship emissions inventory, social cost and eco-efficiency in Shanghai Yangshan Port. – Atmospheric Environment 82(1): 288-297.
[31] Sun, X., Hou, Y. (2017): Summary of research on negative effect and responsibility of cruise travel. – Progress in Geography 36(5): 569-584.
[32] Tichavska, M., Tovar, B. (2015): Environmental cost and eco-efficiency from vessel emissions in Las Palmas Port,. –Transportation Research Part, E. 83(3): 126-140.
[33] Vina, L. L., Ford, J. (1999): Economic impact of proposed cruise ship business. – Annals of Tourism Research 26(1): 0-207.
[34] Wang, H., Ye, X. (2018): Annual Report on China's Cruise Industry (2018). – Social Sciences Academic Press, Beijing.
[35] Wang, J., Huang, J. (2015): Pollution prevention and control of cruise tourism at home and abroad under the model of circular economy and its Hainan enlightenment. – Journal of Green Science and Technology 10: 296-299.
[36] Wu, G., Shen, Y. (2012): Shore power design concept for large cruise terminals. – Port & Waterway Engineering 5: 74-76.
[37] Xie, F., Li, H., Li, D. (2010): Environmental pollution control mechanism of cruise based on full life cycle assessment and its countermeasures. – Marine Science Bulletin 6: 702-706.
[38] Yang, R. (2013): Research and standard construction on the technology of receiving shore power by cruises in port. – Port Engineering Technology 5: 30-34.
[39] Yao, Z., Chen, T. (2015): Tourism ecological efficiency model and its empirical study. – Chinese Journal of Population Resources and Environment 25(11): 113-120.
[40] Yao, Z., Chen, T. (2016): Research progress in tourist ecological efficiency. – Tourism Science 30(6): 74-91.
[41] Ye, X., Sun, R., Liu, M. (2017): Development situation of Green Cruise Port and its breakout path. – China Ship Survey 7: 60-63.

http://www.aloki.hu ● ISSN 1589 1623 (Print) ● ISSN 1785 0037 (Online)
DOI: http://dx.doi.org/10.15666/aeer/1706_1300113013

EFFECT OF CHEMICAL CORROSION ON THE PERMEABILITY OF ROCKS BELOW LANDFILLS AND ON THE MIGRATION OF POLLUTANTS

JIN, X.[1,2,3] – FENG, Y.[1,2,3*]

[1]*School of Civil Engineering, Chongqing University, Chongqing 400045, China*

[2]*Key Laboratory of New Technology for Construction of Cities in Mountain Area (Chongqing University), Ministry of Education, Chongqing 400045, China*

[3]*National Joint Engineering Research Center of Geohazards Prevention in the Reservoir Area (Chongqing), Chongqing 400045, China*
(phone: +86-189-8383-0834)

**Corresponding author*
e-mail: 727178971@qq.com; phone: + 86-83-9420-2720

(Received 23rd May 2019; accepted 2nd Sep 2019)

Abstract. Penetration of the landfill leachate during a tunnel excavation process has a certain impact on the properties of surrounding rocks, including their permeability. The present study was envisaged to analyze such changes by performing a comparative test on the rock specimens with or without being soaked in the landfill leachate. Furthermore, the groundwater flow and solute transport model were established. Tunnel drainage was conceptualized as a pumping well in the confined formation and the weighting factor for hydraulic conductivity coefficient was taken into consideration for specific regions in the model. Subsequently, the water level and the pollutant concentration distribution in these regions were analyzed. The results showed that the simulated groundwater levels on the south and north sides of the tunnel were higher than the original level. Fluctuation in the groundwater level caused by the tunnel drainage was significantly greater due to pumping well PW-1. Because of the soaking of the surrounding rocks in the landfill leachate, the hydraulic conductivity coefficients of these regions increased, which aggravated the downward penetration of the pollutants in the regions between the two tunnels.
Keywords: *groundwater flow simulation, solute transport simulation, surrounding rocks, hydraulic conductivity coefficient, tunnel excavation*

Introduction

Most municipal waste is disposed in the landfills in China (Zhan et al., 2014). Among these landfills, approximately 40% are devoid of a bottom liner system and leachate collection system (Du et al., 2009). Many scholars have studied the migration of the landfill leachate by simulation or experimental methods. In one such experiment a solute transport model was established with MT3D software, which simulated the migration process of Cr6 + leakage in the landfills and addressed the effects of different pollution control measures (Zhou et al., 2014). Han used the Visual MODFLOW software to study the longest distance travelled during the leakage of chloride ions from the landfill in the vertical direction (Han et al., 2014). A DRASTIC model and an MT3D model were further adopted to construct a vulnerability map of the groundwater of the Kinmen landfill (Liu et al., 2011). A three-dimensional solute transport model was established to study the changes in concentrations that found an increase of the sulfate concentrations due to the leaching of sulfate-rich waters from a landfill (Molinero and Samper, 2006)

http://www.aloki.hu ● ISSN 1589 1623 (Print) ● ISSN 1785 0037 (Online)
DOI: http://dx.doi.org/10.15666/aeer/1706_1301513033

Lin and Lee (2009) proposed that the process of constructing a tunnel caused huge disturbances in the surrounding rock, including its hydraulic conductivity coefficient and the distribution of the stress field. Currently, numerous analytical and semi-analytical models have been developed to predict the discharge rate per unit length of a tunnel. Tunnel discharge was estimated by simulating the rock as a statistically homogeneous stochastic continuum in two dimensions (Ando et al., 2003). The hydraulic conductivity coefficient and the vertical anisotropy of the studied area, including the tunnel disturbance zone, were incorporated into a simplified expression according to the empirical formula proposed by Ersoy (2013). However, the spatial distribution of the hydraulic conductivity is complex and was difficult to fully characterize (Jiang et al., 2010). Very few studies have focused on the effects on a tunnel below the landfill or on the erosion of the geological media by landfill leachate, which affects the hydraulic conductivity coefficient.

Penetration of the landfill leachate during the tunnel excavation process has a certain impact on the properties of the surrounding rocks, including the permeability of the surrounding rocks. In order to precisely capture the change in permeability of the surrounding rocks under excavation, a simulation is usually needed. Rock specimens obtained from tunnel excavation were processed into standard specimens, which were subsequently soaked in the landfill leachate. Finally, a comparative test was performed on the permeability of rock specimens among the soaked and not-soaked in the landfill leachate. The changes in the permeability of the surrounding rocks soaked in the prepared landfill leachate were characterized. Then, GMS software was used to establish the groundwater flow and solute transport model. Changes in hydraulic conductivity coefficients in the characteristic regions of the model were considered and the groundwater level and pollutant concentration distribution in these regions were analyzed.

Materials and methods

Working principles

Rock permeability test was divided into the *in-situ* test and the laboratory test. In-situ test was performed on site that accurately determined the permeability of the rock and soil mass. However, the in-situ test is time and money-consuming. Laboratory test is easily operable, controllable and reliable, and requires less investment in terms of money or labor resources. There are mainly two methods to test the soil permeability in laboratory, *viz.* the transient test and the static test.

In the static test, a certain level of penetration pressure is imposed on the two ends of the test specimen. The volume of the fluid penetrating into the rock specimen within a certain period of time is recorded. Then the permeability under this working condition is calculated according to the Darcy's law (Zimmerman et al., 2000; Brace et al., 1968). Static test is easier and more stable than the transient test and requires less time. Therefore, static test was performed in this study. *Equations 1* and *2* represent the working principle of the static test, where q is the flow rate (m^3/s); k is the permeability (m^2); A is the cross-sectional area of the specimen (m^2); dh is the pressure head (m); L is the length of the penetration path (m); γ_f is the fluid density, which is 1000 kg/m^3 for water; μ is the coefficient of dynamic viscosity of fluid (Pastoules et al., 1982).

http://www.aloki.hu ● ISSN 1589 1623 (Print) ● ISSN 1785 0037 (Online)
DOI: http://dx.doi.org/10.15666/aeer/1706_1301513033

$$q = -k\frac{\gamma_f}{\mu} \cdot \frac{dh}{dx} \cdot A \quad \text{(Eq.1)}$$

$$k = \frac{\mu LV}{A\Delta P\Delta t} \quad \text{(Eq.2)}$$

Test preparations

The purpose of the landfill leachate concentration test was to determine the pollutant concentration in the leachate that was used to immerse the rock specimens as well as the original landfill leachate concentration. *Figure 1* shows the picture of the sampling points at the No. 1 landfill BH-1. Samples were collected once per month from each of the landfills BH-1, BH-2 and BH-3. The GPS coordinates of BH-1, BH-2 and BH-3 were (30.644927, 104.359351), (30.648471, 104.362012) and (30.654969, 104.363600), respectively. The total number of sampling was 12, and the overall sampling duration was 1 year. The total nitrogen (TN) of the samples was determined by semi-micro Kjeldahl method. The oxidizing agent potassium permanganate ($KMnO_4$) was used for measuring chemical oxygen demand (COD). Ammonia nitrogen, chloride and sulfate ions were tested by titration. Subsequently, the pollutant concentrations were measured and processed statistically. *Table 1* shows the statistics of the field test results of landfill leachate for the concentrations of Cl^-, SO_4^{2-}, COD, TN, NH^{4+}-N and Ph at BH-1, BH-2 and BH-3, where Nu is the number of samples collected; Av is the mean and *Va* is the standard deviation of concentration. The unit of concentrations was *mg/L.*

Figure 1. *Picture of sampling points at BH-1*

http://www.aloki.hu ● ISSN 1589 1623 (Print) ● ISSN 1785 0037 (Online)
DOI: http://dx.doi.org/10.15666/aeer/1706_1301513033

Table 1. *Field test results of the landfill leachate (Feng et al., 2019)*

		Cl^-		SO_4^{2-}		COD		TN		NH_4^+-N		Ph	
	Nu	***Av***	***Va***	***Av***	***Va***	***Av***	***Va***	***Av***	***Va***	***Av***	***Va***	***Av***	***Va***
BH-1	12	3905	15877	5075	11145	3786	194919	1462	9604	839	8476	7.59	0.012
BH-2	12	3756	20649	5136	15129	3646	210261	1096	10479	756	5590	7.49	0.017
BH-3	12	4102	26358	4963	36289	4523	79645	1236	10491	563	4397	7.88	0.036

During tunnel excavation, the penetration of landfill leachate causes a certain impact on the surrounding rocks, and the influence on permeability of the surrounding rocks needs to be given a major consideration. In order to determine the changes in the permeability of the surrounding rocks after tunnel excavation, it is important to conduct the experiment by soaking the excavated and processed rock specimens in the landfill leachate. The measured concentration of landfill leachate used was used to prepare the experimental leachate. The mean of pollutant concentration at the sampling points of BH-1, BH-2 and BH-3 were taken and the leachate samples were prepared by mixing together the different ions in an appropriate proportion. Total nitrogen was defined as the sum of all inorganic and organic nitrogen, including the inorganic $NO^{3-,}$ NO^{2-} and NH_4^+ and organic proteins, amino acids and amines. However, the preparation of nitrogen-containing leachate was difficult, and the resulting solution exhibited a low stability. Therefore, nitrogen-containing leachate was not prepared. The prepared landfill leachate was mainly composed of COD, SO_4^{2-}, Cl^-, OH^- and NH_4^+, and the volume of the prepared solution was 2000 mL with Ph value of 8. Concentrations of each pollutant in the leachate are shown in *Table 2,* and the soaking time was 60 days (*Fig. 2*).

Table 2. *Concentrations of different pollutants in the prepared leachate*

Pollutant	**COD**	**SO_4^{2-}**	**Cl^-**	**NH_4^+**	**Ph**
Concentration (mg/L)	4000**	5000**	4000**	719**	8**

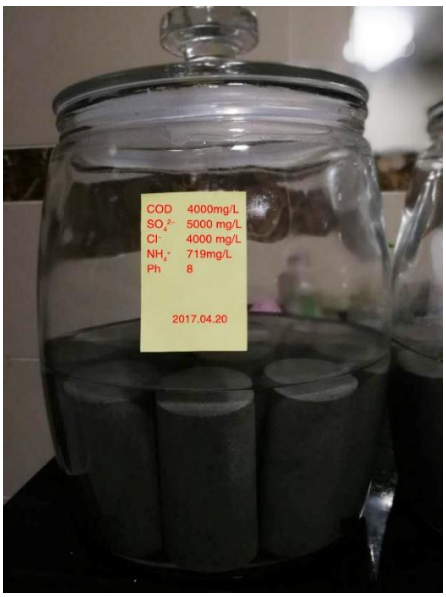

Figure 2. *Rock samples after soaking*

http://www.aloki.hu ● ISSN 1589 1623 (Print) ● ISSN 1785 0037 (Online)
DOI: http://dx.doi.org/10.15666/aeer/1706_1301513033

The rock specimens were taken out from the leachate and all specimens, with or without soaking, were numbered. Before the permeability test, all the specimens were first soaked in water. The specimens were subjected to vacuum pumping in a pressure vessel for 4 h, followed by dehumidification for another 4 h. Then the specimens were placed into distilled water for 16 h, so that the pores of the rock specimens were filled with water. Moreover, by soaking in water, the external leachate would not stay inside the rock specimens because the pores of the rock specimens were not completely filled with water, thus, impairing accuracy of the test. The permeability test was undertaken by using the TRIAXIAL CELL V 4.0 system, as shown in *Figure 3*. This system was composed of automatic confining pressure, axial pressure and interstitial fluid pressure servos. The system was suitable for temperature-hydraulic pressure-mechanic-chemistry multi-field coupling test for the geological materials such as rocks.

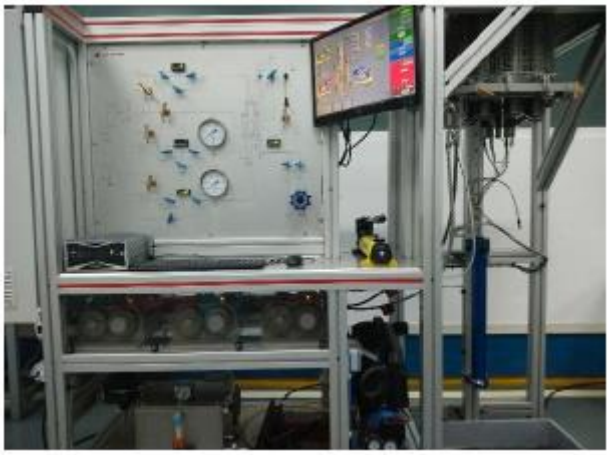

Figure 3. *Picture of TRIAXIAL CELL V 4.0*

Analysis of test results

The penetration pressure was set to 2 MPa in the test and the confining pressure test was 4 MPa and 10 M. In the meantime, two control groups were set up in order to analyze the influence of the landfill leachate on the permeability of the rock, *viz.* a group of test specimen not soaked in the leachate and a group of test specimen soaked in the leachate. The test results are displayed in *Figures 4* and *5*. Two types of curves are shown in the figure, the axial strain-deviatoric stress curve and axial-strain-permeability curve.

It can be seen that the rock permeability was closely related to the confining pressure. Under the penetration pressure of 2 MPa, the rock permeability decreased as with an increase in the confining pressure. Under a higher confining pressure, the micropores and microcracks inside the rock specimens were compressed or closed, leading to a reduction in the size of seepage radius and channels. As a result the permeability of the specimens decreased. For specimens with or without soaking, under the penetration pressure of 2 MPa, the maximum permeability occurred when the axial strain was 0.8101, before which the deviatoric stress decreased suddenly. When the confining pressure was 10 MPa and the penetration pressure was 2 MPa, a maximum permeability occurred where the axial strain was 0.9954 and 1.2788, before which the deviatoric stress decreased dramatically. The maximum permeability of the rock

http://www.aloki.hu ● ISSN 1589 1623 (Print) ● ISSN 1785 0037 (Online)
DOI: http://dx.doi.org/10.15666/aeer/1706_1301513033

specimens occurred after the peak strength, that is, after the fracture of specimens. When a macroscopic fracture plane was formed inside the specimen, this plane would become the preferential seepage channel, leading to a sudden increase in permeability. Mean values were taken of the difference in permeability in all specimens with or without being soaked. It was found that the permeability of the specimens soaked in leachate increased by 21% on average.

Numerical simulation

Numerical simulation

Feng et al. (2019) found that if no pollution sources or acid precipitation were identified in the study area, the peak concentration of sulfate ions in water samples collected from tunnels was 438 times that of the background concentration in January 2017. This indicated that the high concentration of sulfate ions in the tunnel was attributed to No. 1 landfill. Han et al. (2016) surveyed 32 scientific research papers on the pollution environment of landfills, and found that sulfate ions leaking from landfills not only pollute the groundwater but also corrode concrete. Chloride ions are relatively stable in the migration process. However, the migration distance is generally short and the sulfate ions will cause severe corrosion of the concrete in the tunnel. So sulfate ions were taken as the object of simulation in the model. Jamrah et al. (2008) proposed that the simulation results without considering the hydrochemical behaviors were very helpful for groundwater governance. Therefore, the hydrochemical behaviors were not considered in the model.

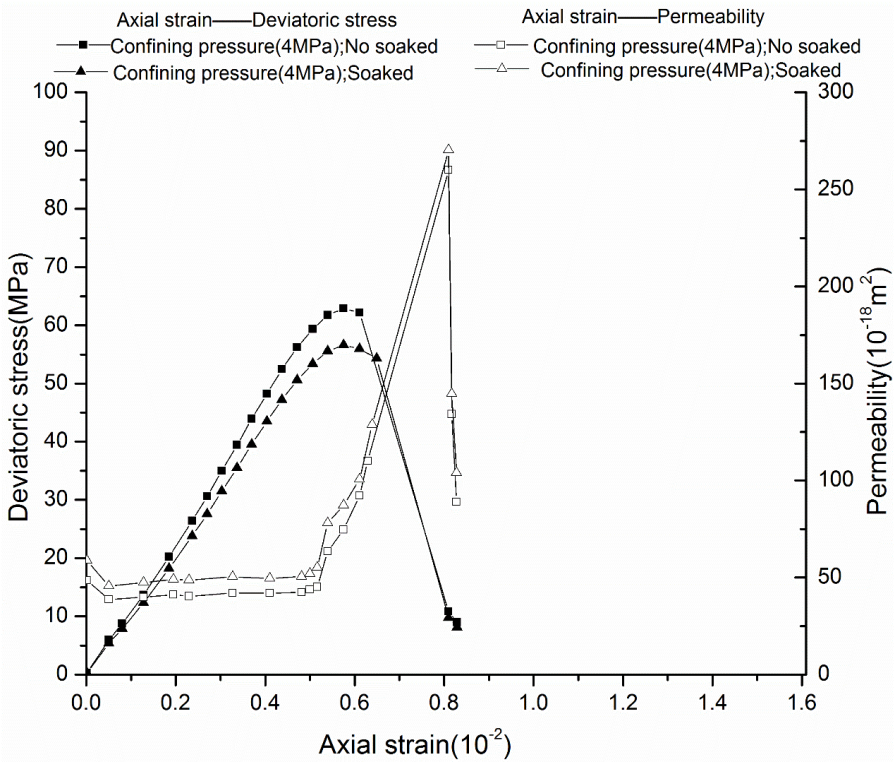

Figure 4. *Comparison of the axial strain-deviatoric stress curves and axial-strain-permeability curves in rock specimens soaked or not soaked under the confining pressure of 4 MPa and penetration pressure of 2 MPa*

http://www.aloki.hu ● ISSN 1589 1623 (Print) ● ISSN 1785 0037 (Online)
DOI: http://dx.doi.org/10.15666/aeer/1706_1301513033

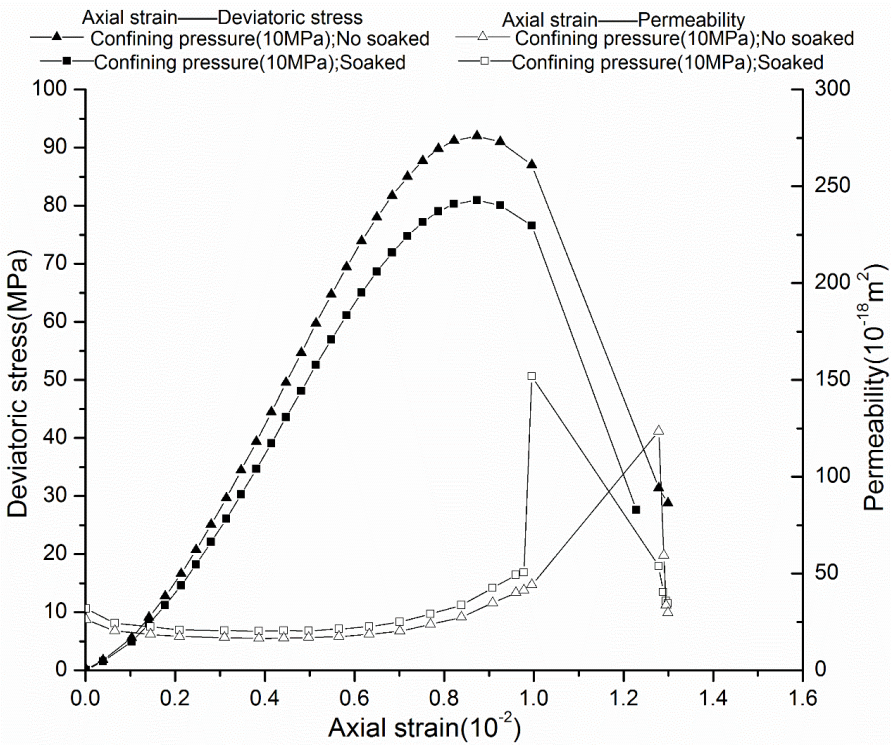

Figure 5. *Comparison of the axial strain-deviatoric stress curves and axial-strain-permeability curves in rock specimens soaked or not soaked under the confining pressure of 10 MPa and penetration pressure of 2 MPa*

The solute transport model (MT3D model) and groundwater flow model (MODFLOW model) in the study were established to simulate the solute transport and the groundwater flow, respectively (McDonald and Harbaugh, 1988; Zheng and Wang, 1999). Both the solute transport model and groundwater flow model were of the transient type. The time duration under simulation was from January 2015 to December 2030, for a total of stress periods. Configuration of the stress period was consistent with the changes in groundwater recharge, wherein, each month represented one stress period. Multiplier and time step were respectively set to 1.1 and 5. The boundary conditions, stress period and original conditions in MT3D model were consistent with those in MODFLOW model.

Original water level and boundary conditions

Feng et al. (2019) established a groundwater model in the study area, the boundary 4 in southwest and the boundary 2 in northeast were both conceptualized as the fixed head boundaries according to the measurements of the monitoring wells along the boundary 4 and boundary 2. Boundary 2 is set along the Shi fan Mountain and the head varied from 669.6 m to 672.0 m. The head on boundary 4 varied from 666.1 m to 667.3 m. Due to the presence of the impervious rocks, boundary 3 was set to the zero-flow boundary. Boundary 1 was set along a highway with roadbed, so it was also set as the zero-flow boundary. There were 4 intersections between the boundary 4 and the original water level, indicating that the head on the boundary 4 is reduced from ends to the middle. The boundary view is shown in *Figure 6*. The original water head is shown in *Figure 6*

http://www.aloki.hu ● ISSN 1589 1623 (Print) ● ISSN 1785 0037 (Online)
DOI: http://dx.doi.org/10.15666/aeer/1706_1301513033

and the groundwater generally flows from northeast to southwest. In addition, the values of the original head and the elevations of the layers were input in the MODFLOW and MT3D model and then interpolated to get a value for each cell of the models.

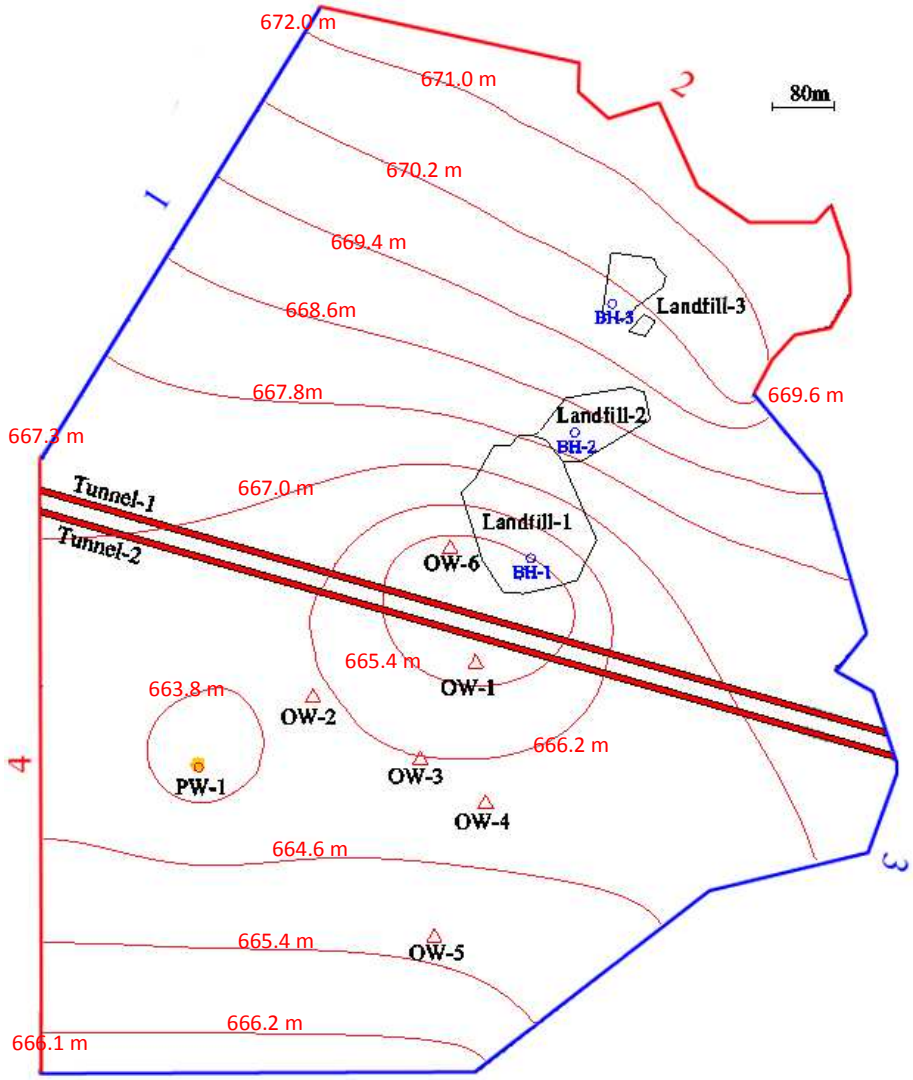

Figure 6. *Original water level in January 2014. Red circle and red triangles stand for the pumping well (PW-1) and six monitoring wells (OW-1, 2, 3, 4, 5, and 6), respectively. BH-3, 2, and 1 stand for the sampling points for Landfill-3, 2, and 1, respectively. Red boundary 4, 2 and the blue boundary 3, 1 stand for the fixed head boundary and zero-flow boundary, respectively*

Conceptualization of model

There was a very thin aquitard composed of silt in the stratum of the study area. The tunnel in the study area could be assumed to be inlaid in the thin aquitard, therefore the area of the location of the tunnels and the silt aquitard were conceptualized into the second layer. In addition, the layers from the bottom to the top were set to confined, convertible and unconfined, respectively. The layer 3 and layer 1 are composed of sandstone and argillaceous sandstone, respectively. The MODFLOW and MT3D model

http://www.aloki.hu ● ISSN 1589 1623 (Print) ● ISSN 1785 0037 (Online)
DOI: http://dx.doi.org/10.15666/aeer/1706_1301513033

for the studied area covered nearly 1.24 km^2 and consisted of 199 columns and 199 rows. The thickness of the first layer ranged from 24.5 m in the northeast to 10.8 m in the south. The thickness of the second layer was 0.1 m, beside that the tunnel area was 4.3 m to 4.6 m. The thickness of the third layer was 19 m. The drainage after tunnel excavation was generalized to the pumping well that was limited to the layer 2. The displacement of the four drainage points was 1700-2000 m^3/d. A spatial view of the MODFLOW and MT3D model is shown in *Figure 7*.

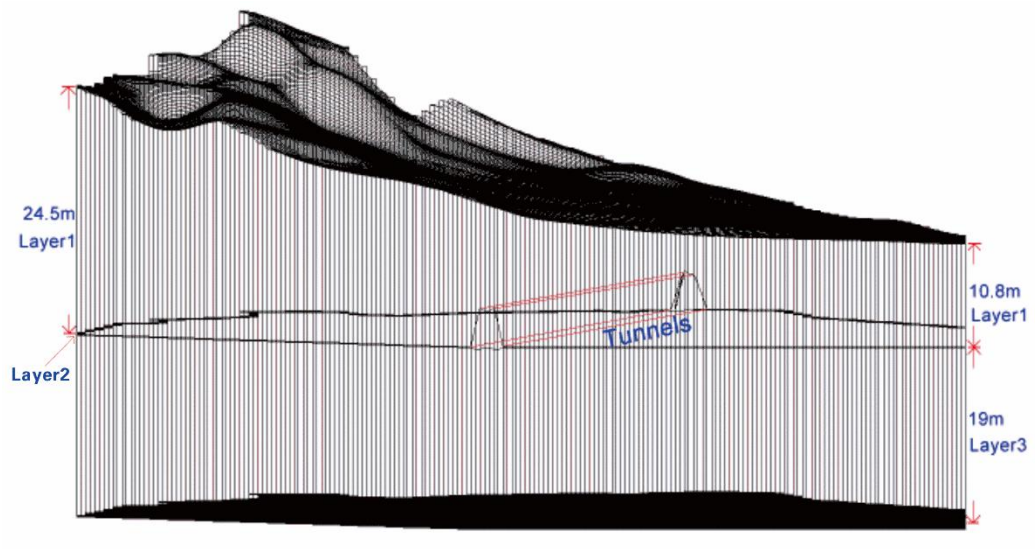

Figure 7. *Spatial view of the MODFLOW and MT3D model*

Parameter configuration

Groundwater recharge

The recharge values in the MODFLOW model were configured based on the monthly mean rainfall in Chengdu from 1970 to 2010. The recharge values and the amount of precipitation were represented by *Equation 3* (Huan et al., 2015).

$$Q_r = \lambda S_r \quad \text{(Eq.3)}$$

where the coefficient of recharge (λ) was consistently set to 0.19 from the precipitation (Feng et al., 2019); Q_r is the groundwater recharge (m/d) and S_r is the amount of precipitation. The recharge values and the average monthly precipitation are shown in *Table 3*.

Table 3. *Average monthly precipitation from 1970 to 2010 and recharge values. (Source: http://www.weather.com.cn/cityintro/101270101.shtml)*

Month	1	2	3	4	5	6	7	8	9	10	11	12
Precipitation (mm)	7.8	12.2	20.2	44.4	78.7	106.8	224.5	201.3	118.8	35.4	15.9	5.2
Recharge values (0.00001 m/d)	5.0	8.0	13.0	28.0	50.0	67.0	142.0	127.0	75.0	22.0	10.0	3.0

http://www.aloki.hu ● ISSN 1589 1623 (Print) ● ISSN 1785 0037 (Online)
DOI: http://dx.doi.org/10.15666/aeer/1706_1301513033

Hydrological parameters

The penetration coefficients in the first layer of the groundwater flow model were configured to vary in the range of 1.2~18.1 m/d. During model calibration for this layer, the range of parameter adjustment was directly set to 1.2~18.1 m/d. After correction, the horizontal penetration coefficient was 1.3 m/d. Following the general practice in the processing of penetration coefficients in hydrogeology, the vertical penetration coefficient was generally taken as one tenth of the horizontal penetration coefficient. Therefore, the vertical penetration coefficient was set to 0.13 m/d. After tunnel excavation began, the specific storage and specific yield of the first layer in the groundwater flow model were set to 0.00002 m^{-1} and 0.21, respectively. The configuration of the penetration coefficients in the second layer was more complex. The settings are displayed in *Figure 8,* where blue color represents the regions between the two tunnels, red color represents the tunnel under excavation, and white shows the ordinary region.

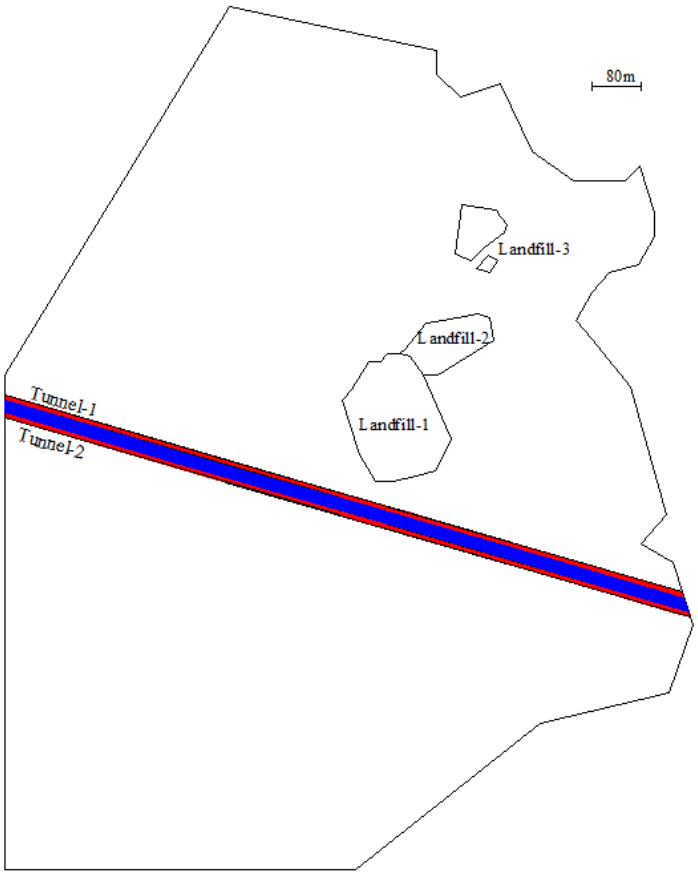

Figure 8. *Distribution of hydraulic conductivity coefficients of the second layer of model after tunnel excavation began*

The white region was silt, where the horizontal and vertical hydraulic conductivity coefficients were 0.005 m/d and 0.0005 m/d, respectively. Blue region was the argillaceous sandstone soaked in the leachate. For this region, the hydraulic conductivity coefficient was multiplied by the weighting factor of 1.21 that was obtained from the test. The horizontal and vertical hydraulic conductivity coefficients

http://www.aloki.hu ● ISSN 1589 1623 (Print) ● ISSN 1785 0037 (Online)
DOI: http://dx.doi.org/10.15666/aeer/1706_1301513033

were set to 1.5 m/d and 0.16 m/d, respectively. The specific storage and specific yield of the second layer in the groundwater flow model were set to 0.00002 m^{-1} and 0.08, respectively. The specific storage and specific yield of the third layer in the groundwater flow model were set to 3.6 m/d and 0.36 m/d, respectively. For the geological medium in this layer, the specific yield and specific storage were set to 0.21 and 0.00002 m^{-1}, respectively. *Table 4* shows the hydraulic conductivity coefficients, specific yield, specific storage and formation thickness of each layer in the groundwater flow model after the beginning of the tunnel excavation. According to the results of the field test, the original concentrations of sulfate ions at Landfill-1, Landfill-2 and Landfill-3 were all set to 5000 mg/L; the original concentrations of other grids were set to 0. The longitudinal dispersivity (m), transverse dispersivity (m), and vertical dispersivity (m) were set to 10 m, 1 m and 0.1 m, respectively. All the values were assigned using the earlier study done by Feng et al. (2019)

Table 4. *Hydraulic parameters of the three layers*

Layer number	Aquifer type	Specific yield	Specific storage (m^{-1})	K_x, K_y (m/d)	K_z (m/d)	Thickness (m)
1	Unconfined	0.21	0.00002	1.30	0.13	10.8-24.5
2	Convertible	0.08	0.00002	Blue: 1.50 White: 0.005 Red: 0.000009	Blue: 0.16 White: 0.0005 Red: 0.000009	0.10
3	Confined	0.21	0.00002	3.60	0.36	19.00

Calibration and validation of groundwater flow model

After the beginning of the tunnel excavation, the measured groundwater levels of observation wells in the study area in 2014 and 2015 were collected. The year of calibration and validation was 2014 and 2015, respectively. For calibration of the simulated and measured groundwater level, the hydraulic conductivity coefficients were varied. The simulated groundwater level was calibrated against the measured water levels of six observation wells from January 2014 to December 2015, until the simulation agreed well with the observation (Panagopoulos, 2012). Changes in the measured groundwater levels in the observation wells OW-1, OW-2, OW-3, OW-4, OW-5 and OW-6 and simulated values from the groundwater flow model during calibration (2014) and validation (2015) after the excavation began are shown in *Figure 9*. At the end of the calibration period of the groundwater flow model (December 2014), the maximum difference between simulated and measured groundwater level simultaneously occurred at OW-1, OW-2 and OW-3, the difference being 0.15 m; difference was 0.06 m at OW-4, 0.03 m at OW-5 and 0.01 m at OW-6. None of the difference at the end of the calibration period exceeded 0.2 m. At the end of the validation period of the groundwater flow model after the excavation began (December 2015), the maximum difference between the simulated and the measured groundwater level occurred at OW-1 was 0.14 m; the difference was 0.05 m at OW-2, 0.03 m at OW-3, 0.02 m at OW-4, 0.03 m at OW-5 and 0.02 m at OW-6. None of the difference at the end of the calibration period exceeded 0.15 m. On the whole, the difference at the end of the validation period of the model (December 2015) was smaller than that at the end of the calibration period of the model (December 2014), indicating that the parameter adjustment achieved a certain effect.

http://www.aloki.hu ● ISSN 1589 1623 (Print) ● ISSN 1785 0037 (Online)
DOI: http://dx.doi.org/10.15666/aeer/1706_1301513033

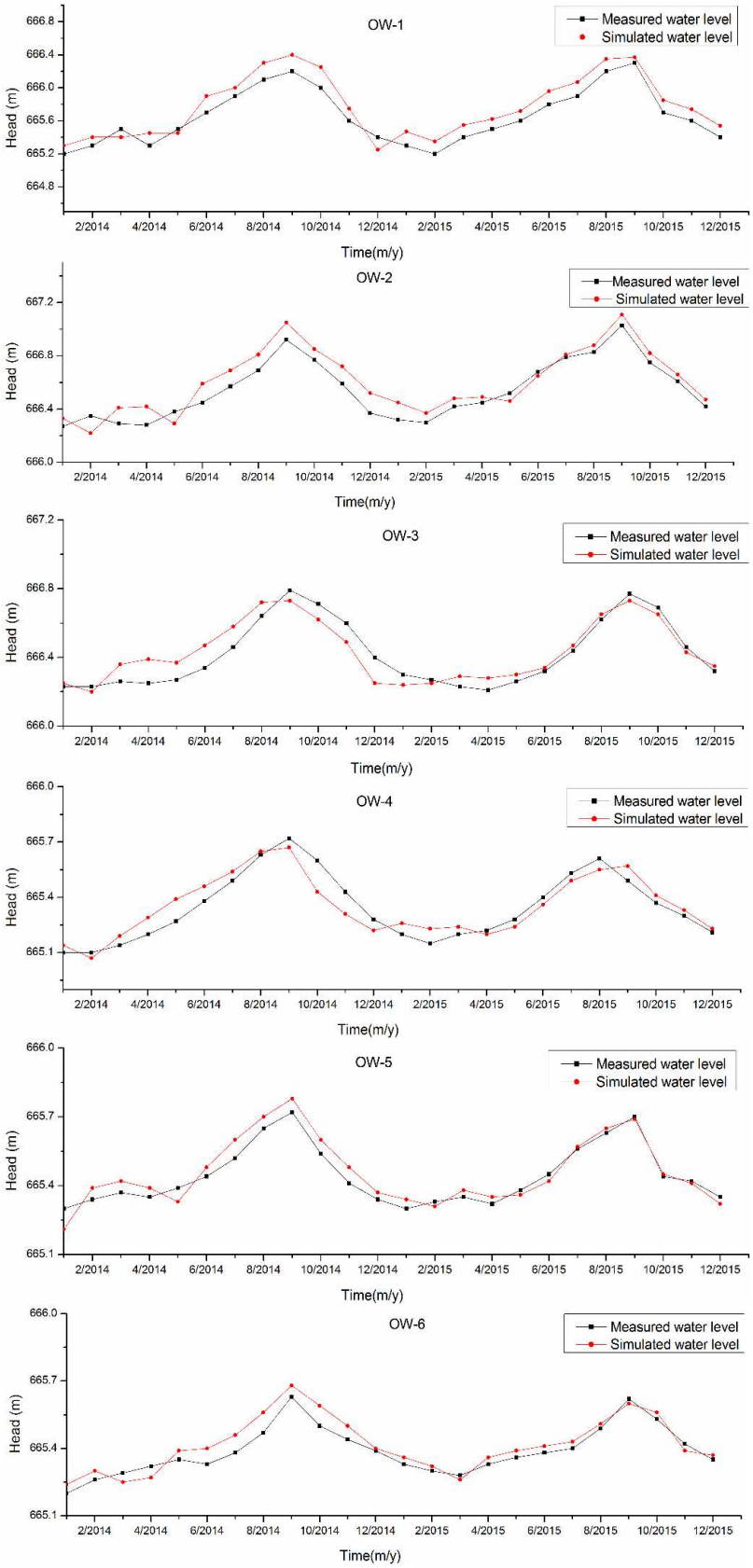

Figure 9. *Head changes in the simulation and measured water level of the OW-1, 2, 3, 4, 5, 6 observation well in the groundwater flow model after tunnel excavation in the calibration process (2014) and the verification process (2015)*

http://www.aloki.hu ● ISSN 1589 1623 (Print) ● ISSN 1785 0037 (Online)
DOI: http://dx.doi.org/10.15666/aeer/1706_1301513033

Simulation results

Groundwater flow simulation results

The simulated groundwater level in the first stress period after the validation of the groundwater flow model under tunnel excavation is shown in *Figure 10,* and the time was January 2016.

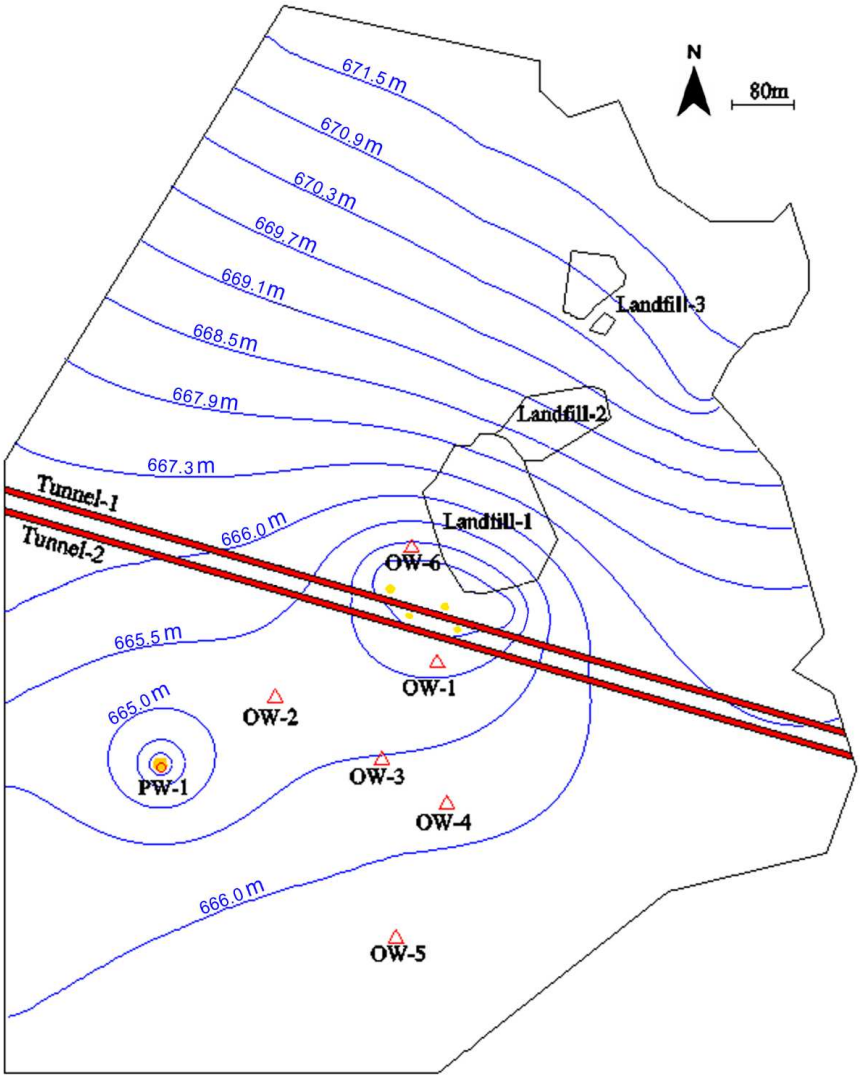

Figure 10. *Simulated groundwater level from the groundwater flow model in January 2016 after tunnel excavation began*

A precipitation funnel was formed near the middle section of the tunnel and PW-1. After the beginning of the tunnel excavation, four drainage sites were represented by small yellow circles. The amount of tunnel drainage varied within the range of 1700~2000 m^3/d. Tunnel drainage was conceptualized as a pumping well in a confined formation, which was the second layer. All the groundwater levels at the north and south sides of the tunnel in *Figure 10* were higher than the original groundwater level in *Figure 6,* and the water lines were denser. This indicated that the tunnel impeded the groundwater flow. Moreover, there was a large fluctuation in the simulated groundwater

http://www.aloki.hu ● ISSN 1589 1623 (Print) ● ISSN 1785 0037 (Online)
DOI: http://dx.doi.org/10.15666/aeer/1706_1301513033

level after the beginning of the tunnel excavation, which was attributed to the tunnel drainage. It was also found that the groundwater level showed greater fluctuations due to tunnel drainage than due to the pumping wells. Barrier to the groundwater flow and drainage due to the presence of tunnel decreased the pumping rate of PW-1.

Results of solute transport simulation

In the simulation of the solution transport under the tunnel excavation, it was necessary to import the results of groundwater flow simulation under excavation in advance. The solute transport model conceptualized three formations. However, while presenting the results of the transport of the pollutants, only the pollution plumes of the aquifer (first layer) and the convertible formation (second layer) are shown. *Figures 11* and *12* show the pollution plumes of the sulfate ions in the first layer (aquifer) of the solute transport model in December 2020 and December 2030, respectively.

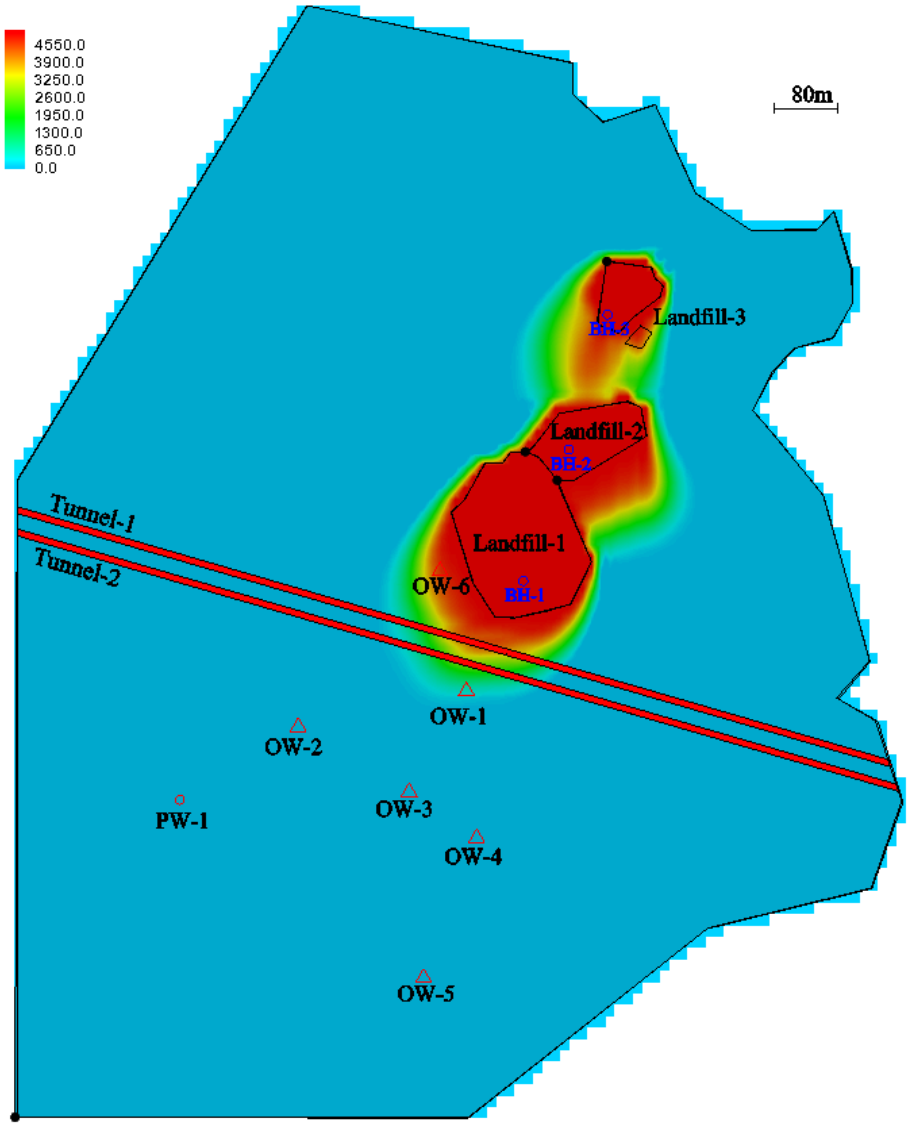

Figure 11. *Pollution plumes of sulfate ions in the aquifer (first layer) of the solute transport model under excavation in December 2020*

http://www.aloki.hu ● ISSN 1589 1623 (Print) ● ISSN 1785 0037 (Online)
DOI: http://dx.doi.org/10.15666/aeer/1706_1301513033

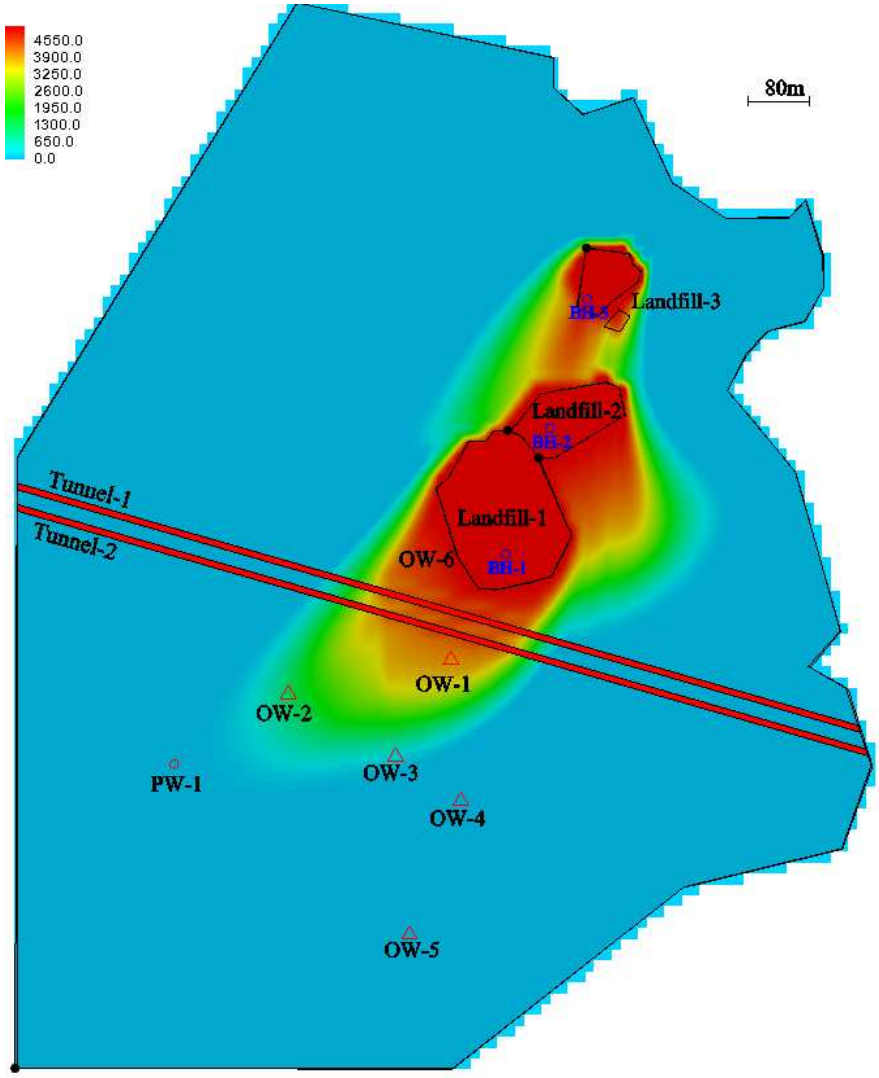

Figure 12. *Pollution plumes of sulfate ions in the aquifer (first layer) of the solute transport model under excavation in December 2030*

For the first layer, the pollution plumes just reached the OW-1 in December 2020. The concentrations of sulfate ions at OW-1 and OW-6 were 559 mg/L and 4115 mg/L, respectively. In December 2030, the plumes in the first layer completely covered OW-1, OW-2 and OW-6 and the transverse plumes just arrived at OW-3, while the vertical plumes had not yet arrived at PW-1. Observations at OW-1, OW-2, OW-3 and OW-6 indicated that the concentrations of sulfate ions were 3338 mg/L, 1872 mg/L, 440 mg/L and 4542 mg/L, respectively. *Table 5* shows the observed concentrations of the sulfate ions in the observation/pumping wells in the aquifer (first layer) of the solute transport model under tunnel excavation in December 2020 and December 2030, respectively.

Figures 13 and *14* show the pollution plumes of the sulfate ions in the second layer (convertible formation) of the solute transport model in December 2020 and December 2030, respectively. In practice, the shape of pollution plumes depends on several factors, including the groundwater flow rate, pressure head, distribution of hydraulic conductivity coefficients, and shape of the pollution source. A continuous leakage of landfill leachate represented a stable pollution source in the model. However, the

http://www.aloki.hu ● ISSN 1589 1623 (Print) ● ISSN 1785 0037 (Online)
DOI: http://dx.doi.org/10.15666/aeer/1706_1301513033

distribution features of the sulfate ions in the convertible formation were very different from those of the ordinary pollutants, and the reason was the irregular penetration path formed between the two tunnels. The hydraulic conductivity coefficients between the two tunnels increased due to the soaking of the surrounding rocks in the landfill leachate. As a result, the downward penetration of the sulfate ions from the first layer via the regions between the two tunnels was enhanced. In other words, the migration path of some the sulfate ions was indeed altered by the tunnel excavation. *Table 6* shows the observed concentrations of sulfate ions at the observation/pumping wells in the convertible formation (second layer) of the solute transport model under tunnel excavation in December 2020 and December 2030.

Table 5. *Comparison of sulfate ion concentrations in the aquifer (first layer) of the solute transport model under excavation between December 2020 and December 2030*

	Time of simulation	**Sulfate ion concentrations at the observation/pumping wells (mg/L)**						
		PW-1	**OW-1**	**OW-2**	**OW-3**	**OW-4**	**OW-5**	**OW-6**
Solute transport model (first layer) under tunnel excavation	December 2020	0**	559**	0**	0**	0**	0**	4115**
	December 2030	0**	3338**	1872**	440**	0**	0**	4542**

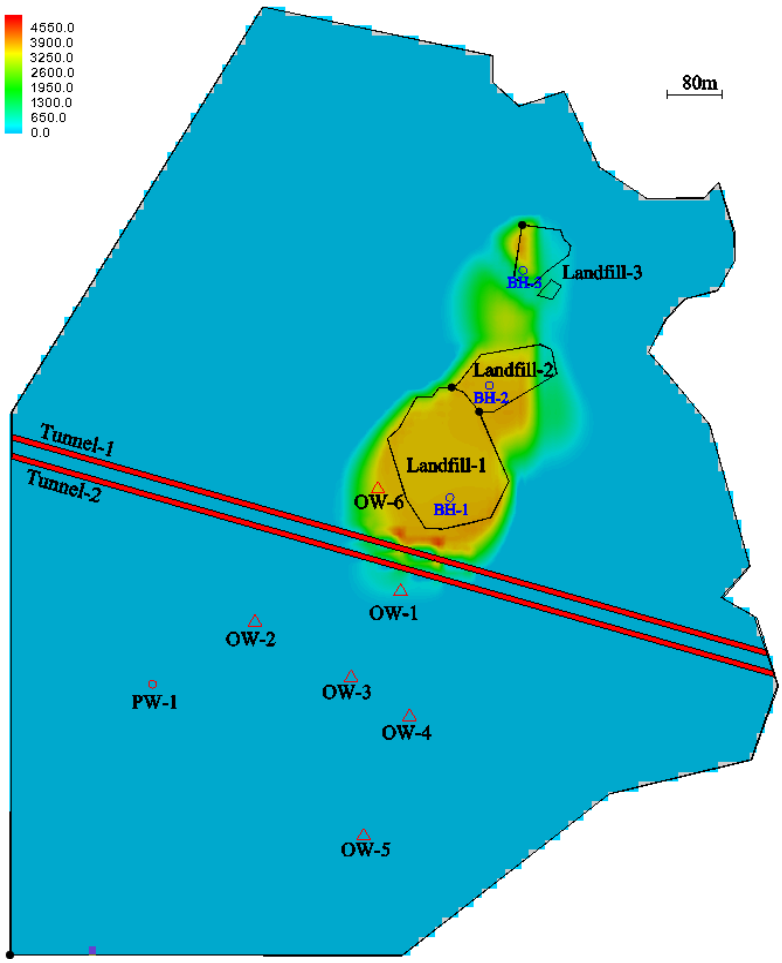

Figure 13. *Convertible formation (second layer) of the solute transport model under excavation. Pollution plumes of sulfate ions in December 2020*

http://www.aloki.hu ● ISSN 1589 1623 (Print) ● ISSN 1785 0037 (Online)
DOI: http://dx.doi.org/10.15666/aeer/1706_1301513033

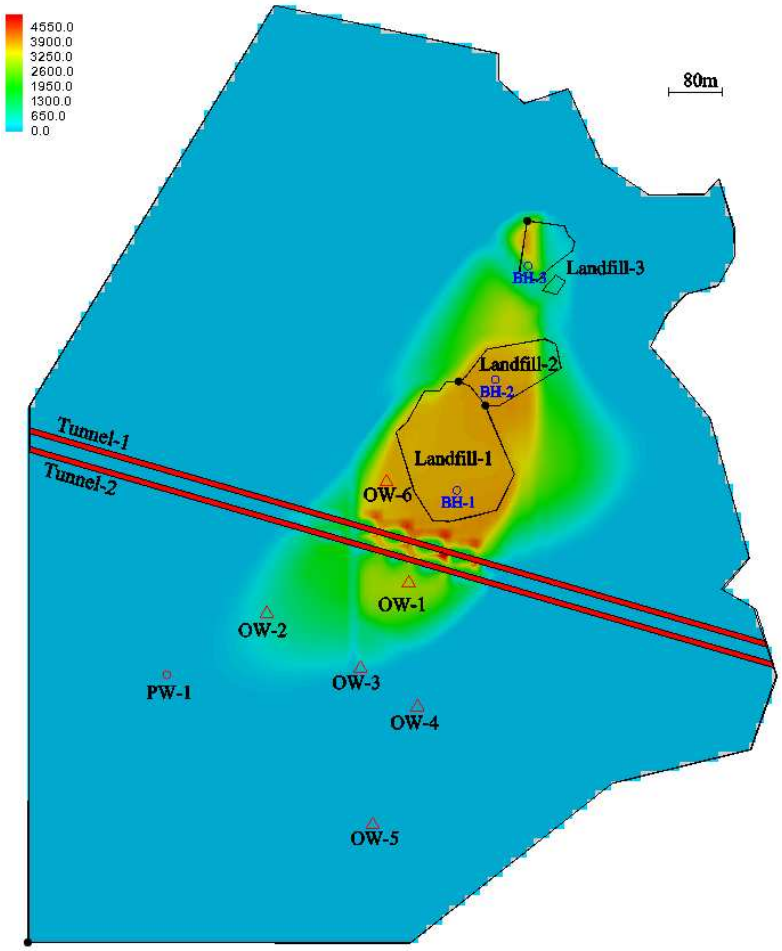

Figure 14. *Convertible formation (second layer) of the solute transport model under excavation. Pollution plumes of sulfate ions in December 2030*

Table 6. *Comparison of sulfate ion concentrations in the convertible formation (second layer) of the solute transport model under excavation between December 2020 and December 2030*

	Time of simulation	Sulfate ion concentrations at the observation/pumping wells (mg/L)						
		PW-1	OW-1	OW-2	OW-3	OW-4	OW-5	OW-6
Solute transport model (second layer) under tunnel excavation	December 2020	0**	559**	0**	0**	0**	0**	3146**
	December 2030	0**	2788**	578**	257**	0**	0**	3544**

Discussion and conclusion

(1) By comparing the test results, it was found that the confining pressure exhibited a greater impact on the overall trend of the permeability curve. This was also indicated by the shape of the permeability curve, since, the rate of variation at the increasing permeability stage decreased with the increase in the confining pressure. The maximum permeability of rock specimens occurred after the peak strength, that is, after the fracture of specimens. When a macroscopic fracture plane was formed inside the

http://www.aloki.hu ● ISSN 1589 1623 (Print) ● ISSN 1785 0037 (Online)
DOI: http://dx.doi.org/10.15666/aeer/1706_1301513033

specimen, this plane would become the preferential seepage channel, leading to a sudden increase in permeability. The mean values of the differences in the permeability between rock specimens with or without soaking were taken into consideration, after the beginning of the tunnel excavation under the same confining pressure and penetration pressure. On an average, it was found that the permeability of the specimens soaked in leachate was increased by 21%.

(2) Tunnel drainage in the model was conceptualized as a pumping well confined in the second layer. According to groundwater level simulation in January 2016, a precipitation funnel was formed near the middle segment of the tunnel and PW-1. Tunnel drainage in the model was conceptualized as a pumping well confined in the second layer. All the simulated groundwater levels in the north and south sides of the tunnel were higher than the original groundwater level, and the water lines were also denser. This indicated the barrier to the flow of the groundwater due to the presence of the tunnel. Moreover, there was large fluctuation in the simulated groundwater level after the beginning of the tunnel excavation, which was attributed to the tunnel drainage. It was also found that the groundwater level fluctuated more prominently due to the tunnel drainage, than due to the pumping wells. Furthermore, the presence of tunnel acts as a barrier to the groundwater flow and the drainage, thereby decreasing the pumping rate of PW-1.

(3) The distribution of the sulfate ion concentration in the second layer of model between the two tunnels showed an irregular pattern. The hydraulic conductivity coefficients between the two tunnels increased due to the soaking of surrounding rocks in the landfill leachate. As a result, the downward penetration of sulfate ions from the first layer via the regions between the two tunnels was enhanced. As the tunnel excavation accelerated the downward penetration of pollutants, this would lead to the pollution of deep groundwater. Therefore, the tunnel excavation area should not only pay attention to surface pollution, but also pay attention to underground pollution. In addition, it was necessary for the study area to conduct drilling sampling studies to support concentration simulation results.

REFERENCES

[1] Ando, K., Kostner, A., Neuman, S. P. (2003): Stochastic continuum modeling of flow and transport in a crystalline rock mass: Fanay-Augeres, France, revisited. – Hydrogeology Journal 11(5): 521-535.

[2] Brace, W. F., Walsh, J. B., Frangos, W. T. (1968): Permeability of granite under high pressure. – Journal of Geophysical Research 6(73): 2225-2236.

[3] Du, Y. J., Shen, S. L., Liu, S. Y., Hayashi, S. (2009): Contaminant mitigating performance of Chinese standard municipal solid waste landfill liner system. – Geotextiles and Geomembranes 27(3): 232-239.

[4] Ersoy, H., Bulut, F., Berkun, M. (2013): Landfill site requirements on the rock environment: A case study. – Engineering Geology 154(28): 20-35.

[5] Feng, Y. S., Jin, X. G. (2019): Studies on effects of traffic tunnels on the migration of the contaminants under landfill sites. – Environmental Science and Pollution Research 21(2): 1-17.

[6] Han, D. M., Tong, X. X., Currell, M. J., Gao, G. L., Jin, M. G., Tong, C. S. (2014): Evaluation of the impact of an uncontrolled landfill on surrounding groundwater quality, Zhoukou, China. – Journal of Geochemical Exploration 136: 24-39.

http://www.aloki.hu ● ISSN 1589 1623 (Print) ● ISSN 1785 0037 (Online)
DOI: http://dx.doi.org/10.15666/aeer/1706_1301513033

[7] Han, Z. Y., Ma, H. N., Shi, G. Z., He, L., Wei, L. Y., Shi, Q. Q. (2016): A review of groundwater contamination near municipal solid waste landfill sites in China. – Science of the Total Environment 569-570(1): 1255-1264.
[8] Huan, H., Wang, J. S., Lai, D. S., Teng, Y. G., Zhai, Y. Z. (2015): Assessment of well vulnerability for groundwater source protection based on a solute transport model: a case study from Jilin City, northeast China. – Hydrogeology Journal 23(3): 581-596.
[9] Jamrah, S., Al-Futaisi, A., Rajmohan, N., Al-Yaroubi, S. (2008): Assessment of groundwater vulnerability in the coastal region of Oman using DRASTIC index method in GIS environment. – Environmental Monitoring and Assessment 147(1): 125-138.
[10] Jiang, X. W., Wan, L., Yeh, T. C. J., Wang, X. S., Xu, L. (2010): Steady-state discharge into tunnels in formations with random variability and depth–decaying trend of hydraulic conductivity. – Journal of Hydrology 387(3-4): 320-327.
[11] Lin, H. L., Lee, C. H. (2009): An approach to assessing the hydraulic conductivity disturbance in fractured rocks around the Syueshan tunnel, Taiwan. – Tunnelling and Underground Space Technology 24(2): 222-230.
[12] Liu, C. W., Lin, C. N., Jiang, C. S., Ling, M. W., Tsai, J. W. (2011): Assessing nitrate contamination and its potential health risk to Kinmen residents. – Environmental Geochemistry and Health 33(5): 503-514.
[13] McDonald, M. G., Harbaugh, A. W. (1988): A modular three dimensional finite difference ground-water flow model. – Report in series Techniques of Water-Resources Investigations of US Geological Survey. Vol. 6. DOI: 10.3133/twri06A1.
[14] Molinero, J., Samper, J. (2006): Large-scale modeling of reactive solute transport in fracture zones of granitic bedrocks. – Journal of Contaminant Hydrology 82(3-4): 293-318.
[15] Panagopoulos, G. (2012): Application of MODFLOW for simulating groundwater flow in the Trifilia karst aquifer, Greece. – Environmental Earth Sciences 67(7): 1877-1889.
[16] Pastoules, M. G., Gripps, J. C. (1982): An investigation of the permeability of Yorkshire Chalk under differing pore water and confining pressure conditions. – Energy Sources 6(4): 321-334.
[17] Zhan, T. L. T., Guan, C., Xie, H. J., Chen, Y. M. (2014): Vertical migration of leachate pollutants in clayey soils beneath an uncontrolled landfill at Huainan, China: a field and theoretical investigation. – Science of the Total Environment 470: 290-298.
[18] Zheng, C., Wang, P. P. (1999): MT3DMS: A Modular Three Dimensional Multispecies Transport Model for Simulation of Advection, Dispersion, and Chemical Reactions of Contaminants in Groundwater Systems. Documentation and User's Guide. – US Army Corps of Engineers, Vicksburg, MS.
[19] Zhou, Y., Jiang, Y. H., An, D., Ma, Z. F., Xi, B. D., Yang, Y., Li, M. X., Hao, F. H., Lian, X. Y. (1999): Simulation on forecast and control for groundwater contamination of hazardous waste landfill. – Environmental Earth Sciences 72(10): 4097-4104.
[20] Zimmerman, R. W. (2000): Coupling in poroelasticity and thermoelasticity. – International Journal of Rock Mechanics & Mining Sciences 1(31): 79-81.

http://www.aloki.hu ● ISSN 1589 1623 (Print) ● ISSN 1785 0037 (Online)
DOI: http://dx.doi.org/10.15666/aeer/1706_1301513033

THE INTERRELATIONSHIPS OF CHILD UNDER-NUTRITION, ECOLOGICAL AND MATERNAL FACTORS: A CASE STUDY OF PAKISTAN BY USING COMPOSITE INDEX OF ANTHROPOMETRIC FAILURE

ASIF, M. A.[1*] – AKBAR, M.[1] – NOOR, F.[1] – SHERWANI, R. A. K.[2] – FAROOQ, M.[3]

[1]*Department of Mathematics and Statistics, Faculty of Basic and Applied Sciences, International Islamic University, 44000 Islamabad, Pakistan*

[2]*College of Statistical and Actuarial Sciences, University of the Punjab, Lahore, Pakistan*

[3]*Department of Statistics, University of Gujrat, Gujrat, Pakistan*

**Corresponding author*
e-mail: atta.msst18@iiu.edu.pk

(Received 23rd May 2019; accepted 28th Aug 2019)

Abstract. Under-nutrition is a serious health problem of developing countries, including Pakistan. Despite the implementation of a number of health strategies for the vulnerable population (especially children), the issue is still emerging and needs further investigation. The aim of this study was to investigate the role of various ecological and maternal factors responsible of children's nutritional health variations. By using Pakistan Demographic and Health Survey (PDHS) data, maternal factors were assessed as important factors of child under-nutrition. Multinomial nested logit regression and classification tree analysis were performed. A total of 1870 children of age < 5 years were included in the analysis and out of these 50.1% fall in the composite index of anthropometric failure (CIAF). Maternal education, mother's body mass index (BMI) and working status were among the significant factors while decision making autonomy remain insignificant. Maternal factors have significant impact on child health and use of CIAF as a measure of nutritional status is recommended for policy makers because of its capability to estimate the overall burden of under-nutrition.
Keywords: *child health, demographic and health survey, nested logit regression, wealth status, classification tree*

Introduction

Role of population's nutritional status is important in socio-economic development of a country. Adequate nutrition level for children's growth and development is imperative. Early years of life are of huge significance for mental as well as physical growth of a child. However, this age is regularly set apart by micronutrient inadequacies that meddle with ideal development. Moreover, children's of this age are powerless against the irresistible sicknesses such as diarrhea and acute respiratory infections (Final Report PDHS, 2012-2013). It is, therefore, considered as one of the important components of Sustainable Development Goals (SDGs) adopted by UN in 2015. A malnourished child is more likely to die from common illnesses such as malaria, measles, diarrhea and pneumonia (Chowdhury et al., 2016). Poor nutritional status increases the risk of infection, morbidity and mortality along with decline of mental development during the early years of child-hood (Endris et al., 2017). Hence, children are more vulnerable to under-nutrition. United Nations statistics show that 155 million children were stunted, 41 million were overweight and 52 million were wasted in 2016 (WHO, 2017). About 50% of these children live in the three south Asian countries, i.e.

http://www.aloki.hu ● ISSN 1589 1623 (Print) ● ISSN 1785 0037 (Online)
DOI: http://dx.doi.org/10.15666/aeer/1706_1303513055

Pakistan, India and Bangladesh (Achadi et al., 2016), and under-nutrition is one of the major challenges in these countries. Best nutritional status of the children is one of best indicators of their well-being (Poda et al., 2017). A bunch of factors, which can affect child under-nutrition, are considered by various studies. These factors comprise of health care services, maternal literacy, wealth status, maternal decision making autonomy etc. (Amugsi et al., 2014; Debnath and Bhattacharjee, 2016).

Maternal factors are considered as the most important factors for children's health (Vikram et al., 2012). Existing literature reveals that improved maternal education can positively affect child's health (Arooj et al., 2013). Numerous studies considered the role of maternal factors as well as other socio-economic and demographic factors for improvement of child under-nutrition in middle and low income countries (Poda et al., 2017; Debnath and Bhattacharjee, 2016; Krishna et al., 2017; Sarma et al., 2017; Rakotomanana et al., 2017; Altare et al., 2016; Alemayeha et al., 2015; Senbanjo et al., 2013; Anekwe and Kumar, 2012; Pradhan, 2010). Gender of the child, child, size at birth, maternal education, mother's BMI, wealth status, dietary diversity, mother's decision making autonomy and vaccination were among the most important factors affecting child under-nutrition in the above mention studies. However, some studies showed insignificant relationship between child under-nutrition and mother's BMI, mother's education, fathers educations as well as wealth status of household (Rahman, 2016; Sharma and Kader, 2013; Maïga, 2013).

Pakistan, with sixth largest country by population, is ranked at 124 out of 132 countries with 45% stunted children and 106 out of 130 countries with 11% prevalence of wasting among children (Raju and D'Souza, 2017). According to global nutritin report, only 0.7% of government expenditure is allocated for nutrition-sensitive interventions, which is less than other countries in the region such as Nepal and Bangladesh, with 3.1% and 2.1% allocations respectively (Achadi et al., 2016). It reveals worst conditions of child under-nutrition in Pakistan and government negligence. A number of studies have considered these issues and discuss various causes of child under-nutrition. For example Tariq et al. (2018) identified that mother's BMI, rural residence, parental education, poverty and type of toilet facility were the associated factors of child under-nutrition. A study explored that maternal health and child health were among the most significant factors associated with stunting and wasting (Achakzai and Khan, 2016). Wealth status was considered as important factor of child under-nutrition while maternal education was declared insignificant by a study (Khan and Raza, 2014). However, Mahmood et al. (2016) revealed that maternal education was a significant factor to improve child under-nutrition in Pakistan.

Most of the aforementioned studies applied logistic framework and child under-nutrition was measured through commonly used anthropometric indices named stunting, wasting and underweight. These measures however, describe different dimensions of under-nutrition and are overlapping. For instance, underweight is the composition of both wasting and stunting, but does not make a separation between them (Fentahun et al., 2016). Moreover, none of the conventional indices has capability to provide a comprehensive measure of under-nutrition in the population (Khan and Raza, 2014). Therefore, the use of single indicator, that must be able to capture the magnitude of nutritional status and identify the susceptible part in the population, is needed. Peter Svedberg, a development economist, proposed an important measure of child nutrition, known as composite index of anthropometric failure (CIAF) (Svedberg, 2000). A number of recent studies in the literature has used this proposed indicator for different

http://www.aloki.hu ● ISSN 1589 1623 (Print) ● ISSN 1785 0037 (Online)
DOI: http://dx.doi.org/10.15666/aeer/1706_1303513055

countries (Endris et al., 2017; Khan and Raza, 2014; Fentahun et al., 2016; Sen and Mondal, 2012; Ejaz and Azid, 2011; Das and Bose, 2011) and they have recommended this indicator as an alternative measure of under-nutrition.

Conventional measures of under-nutrition (stunting, wasting and underweight) are commonly used in the existing studies for Pakistan (Tariq et al., 2018; Arif et al., 2011; Mushtaq et al., 2011). Moreover, neither of these studies focused on ecological and maternal factors, solely, nor the exposure variables as well as control variables were selected under UNICEF conceptual framework to analyze child under-nutrition. Keeping in view these gaps the specific objectives of this study were: first, to check the role/importance of maternal factors, selected under UNICEF conceptual framework, on child under-nutrition. Second, to consider CIAF as an alternative measure of child under-nutrition instead of conventional measures using nationwide community health survey data.

Materials and methods

UNICEF conceptual framework and model specification

The analysis is performed under UNICEF conceptual framework that constitutes three levels of causes of under-nutrition; immediate, underlying and basic levels (UNICEF, 1990). This framework presents the general relationship between a set of variables and child nutritional level. The immediate level causes comprise of dietary intake and illness which are interlinked. If a child could not take nutritious food he/she may be attacked by infectious diseases due to illness. On the other hand, if a child falls ill then he/she may not be able to consume desired diet which in turn results into malnourishment. Whether a child is in danger of infectious disease or whether he/she gets insufficient food to consume, is the consequence of the underlying factors that are consider as the household causes of under-nutrition. According to the framework of household food security, maternal and child care and environmental factors are the main causes under this level. The causes at the third level of the framework are the basic causes which comprise of political, economic, genetic and socio-cultural factors.

Following the example of Akin et al. (1986) the specified econometric model of this study is based on discrete choice models. Derivation of discrete choice models is based on the hypothesis that the choice of an individual follows the maximization behavior of the random utility (Anye and Yene, 2016). The utility U_{ij} that ith child falling in the jth category of CIAF is given by:

$$U_{ij} = z_i'\alpha + x_{ij}'\beta_i + \varepsilon_{ij} \quad \text{(Eq.1)}$$

where U_{ij} stands for nutritional outcome of the ith child falling in the *j*th category of CIAF, z_i varies over upper nest alternatives and x_{ij}varies over both upper and lower nest alternatives.

Data source and construction of variables

Pakistan Demographic and Health Survey (PDHS) data, version 2012-13, is used for the analysis. Two stage sampling technique was used for the survey. At first stage 500 primary sampling units (248 urban and 252 rural) were selected by using probability proportional to size. At second stage systematic sampling technique was used to select

http://www.aloki.hu ● ISSN 1589 1623 (Print) ● ISSN 1785 0037 (Online)
DOI: http://dx.doi.org/10.15666/aeer/1706_1303513055

fixed no of household (28) from primary sampling units selected at first stage. A sample of 14,000 household was selected. Out of 14,569 eligible women, 13,558 were successfully interviewed from these selected households. These women contributed a total of 11,763 live born children within five years before the survey. However, the analysis in this study was limited to 1870 live born children of age 0-59 months (< 5 years) who have valid information about the anthropometric measures. Complete details about sampling procedure and data collection can be found elsewhere (Final Report PDHS 2012-2013).

Response variable

The response variable in this study is the new policy-relevant anthropometric indicator of under-nutrition known as CIAF. The proposed CIAF comprises seven anthropometric failure groups. A Child with height-for-age Z-score (HAZ), weight-for-height Z-score (WHZ) and weight-for-age Z-score (WAZ), below -2 standard deviations from the median of the WHO reference population, are considered to be stunted, wasted and underweight respectively (PDHS report, 2012-13). All these children were distributed into seven groups following Nandy et al., 2005. The details of groups are given in *Table 1*.

Table 1. *Different groups used for construction of response variable (CIAF)*

Group	Description	Wasting	Stunting	Underweight	N (%)
A	No failure	No	No	No	933(49.9)
B	Wasting only	Yes	No	No	70(3.7)
C	Wasting & Underweight	Yes	No	Yes	67(3.6)
D	Wasting, Stunting & Underweight	Yes	Yes	Yes	93(5.0)
E	Stunting & Underweight	No	Yes	Yes	305(16.3)
F	Stunting only	No	Yes	No	374(20.0)
Y	Underweight only	No	No	Yes	28(1.5)

Wasted children = 70 + 67 + 93 = 230 (12.3%); Stunted children = 93 + 305 + 374 = 772 (41.3%)
Underweight = 67 + 93 + 305 + 28 = 493 (26.4%); No of children fall in CIAF = 937 (50.1%)

Explanatory variables

A range of indicators were included in the analysis under different layers of UNICEF's conceptual framework. The data were extracted from the PDHS data and re-categorized (where necessary). These indicators include vaccination status (categorized as non-vaccinated, who did not receive a single dose of any of the prescribed vaccines, partially-vaccinated, who has receive at least one of the vaccine but not complete doses and fully-vaccinated, who received the complete dose of all vaccines), household wealth status was used as proxy for wealth index, given in the survey data, generated by applying principal component analysis on the factors of household ownership of assets (such as bicycle, motorcycle, car, radio, television, etc.) and characteristics of dwellings (such as roof material, main floor material, etc). The index was subsequently cut into quintiles as poorest, poorer, middle, richer and richest and we have re-categorize by merging poorest and poor to only poor and similarly by merging rich and riches and consider as rich only. In this way we have three categories for wealth status as poor, middle and rich. Type of toilet facility was categorized as poor quality, intermediate

http://www.aloki.hu ● ISSN 1589 1623 (Print) ● ISSN 1785 0037 (Online)
DOI: http://dx.doi.org/10.15666/aeer/1706_1303513055

quality and high quality following the method of (Fink et al., 2011). Maternal nutritional level was measured using the BMI (calculated as mother's weight in kilograms (kg) divided by her height in meters squared) and categorized as overweight (if $BMI \geq 25.0$), normal ($18.5 \leq BMI \leq 25.0$) and underweight (if $BMI \leq 18.5$). Mother's autonomy was based on four questions asked to the respondent regarding who take the decisions in the household about her own health care, large purchase, visit to family/relatives and the consumption of husband earnings. The possible answers were as follows: (i) Respondent alone, (ii) Respondent and husband/partner, (iii) Husband/partner alone, (iv) family elders and (v) others. A value of 1 was assigned if the answer was (i) or (ii) and 0 for (iii), (iv) or (v), for each question. These recoded values were then added to get a score ranging from 0 to 4. These scores were then categorized into three categories as: no-autonomy if the score value is 0, partial autonomy if the score value is 1, 2 or 3 and the full autonomy if she got a score 4. Different regions are presented in *Figure A1* and different categories of considered factors can be seen in *Table A1* in the *Appendix.*

Methodology of analysis

Analysis is conducted in three stages i.e. descriptive analysis, classification tree analysis and regression analysis based on multinomial nested logit modeling. Percentage distribution of explanatory variables and CIAF categories were explained at first stage. In order to find most effecting maternal factors and their inherent associations with CIAF, we consider a non-parametric techniques, known as classification tree (CT) formalized by (Breiman et al., 1984). It works as an exploratory procedure and select the exposure variables that are most important for analyzing the behaviour of response variable. The CT has tree like structure, where terminal nodes represent the CIAF categories. The initial node split the data into two subsets which are further split to second level partition. By default, Gini index is the splitting criteria used in CT (Pawloski and Kitsantas, 2008). An indicator split is known as best split if it observes relatively high value of homogeneity, measured through Gini impurity function, in the node. The impurity got maximized if all observations are equally distributed among different categories of the variable, which implies that at these nodes provides least interesting information. Gini index got minimized if all the observations belong to only one category of the variable which implies that this node provides most interesting information. The tree stops growing if the terminal nodes approach either of these two conditions (Jung et al., 2014).

For regression analysis *Equation 1* can be summarized by:

$$U_{ij} = V_{ij} + \varepsilon_{ij} \quad \text{(Eq.2)}$$

Here the term V_{ij} is the observable component of child under-nutrition (comprising of immediate, underlying and basic factors) and ε_{ij} is the unobservable random part. The probability of a child falling in category j is equal to the probability of such a category that yield a maximum level of utility for him, that is

$$P_{ij} = \Pr(U_{ij} > U_{ik}) \; ; \forall j \neq k \quad \text{(Eq.3)}$$

$$P_{ij} = \Pr(V_{ij} + \varepsilon_{ij} > V_{ik} + \varepsilon_{ik}) \; ; \forall j \neq k \quad \text{(Eq.4)}$$

http://www.aloki.hu ● ISSN 1589 1623 (Print) ● ISSN 1785 0037 (Online)
DOI: http://dx.doi.org/10.15666/aeer/1706_1303513055

$$P_{ij} = \Pr\left(V_{ij} - V_{ik} > \varepsilon_{ik} - \varepsilon_{ij}\right) ; \forall j \neq k \quad \text{(Eq.5)}$$

Since the econometric specification depends upon the hypothesis regarding the distributional form of the error term of *Equation 5*. If the error term is assumed to follow normal distribution, then the estimated model would be a probit model. Though a probit model relax the IIA property and is attractive; however, probit models are infeasible due to their computational difficulties (Ben-Akiva et al., 1985; Adhikari, 2011). An alternative way to model this type of phenomenon is that ε_{ij} is assumed to follow generalized extreme value (GEV) distribution. By assuming the GEV distribution, a closed form model can be estimated using maximum likelihood method. According to (McFadden, 1981) it produces multinomial logit model $P_{ij} = \exp\left(V_{ij}\right) / \sum_j \exp\left(V_{ij}\right)$. However, this specification may create a severe problem. Since multinomial logit model assumes that unobservable terms (ε_{ij}'s) are identically and independently distributed (IID) and the assumption of independence of irrelevant alternatives (IIA) is not violated. In our case, some of the categories of CIAF are likely to share the error terms and thus be correlated that may violate the IIA property. To circumvent this situation, a more generalized form of multinomial logit model is referred to as multinomial nested logit (MNL) model (McFadden, 1981) which relax IIA assumption (Anya and Yene, 2016). The use of MNL procedure implies that the under-nutrition categories can be organized into an understandable nesting structure. Consider that the nesting structure of the j alternatives can be seen in *Figure 1*.

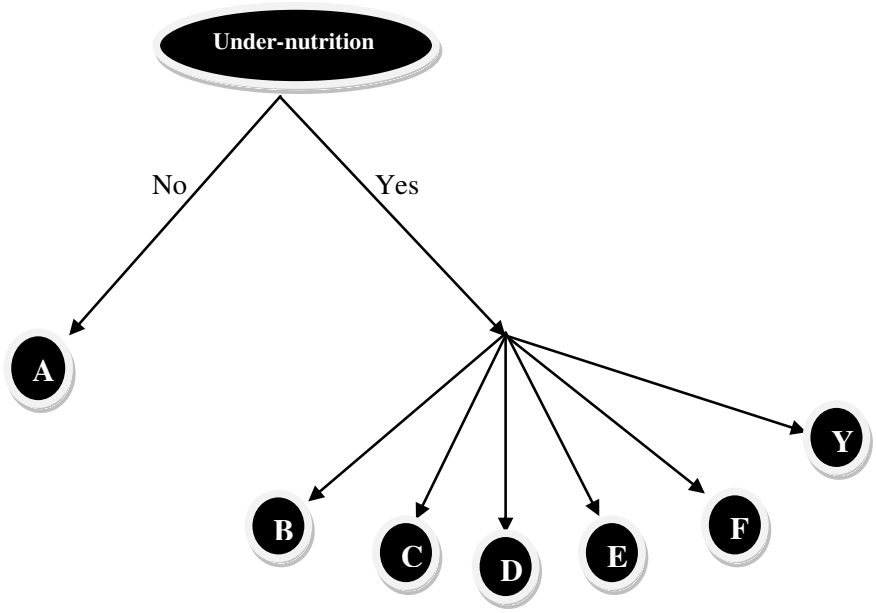

Figure 1. *Two-level nested structure of groups of CIAF*

A child may fall into one of the two categories (i. e. nourished or not-nourished) and if he/she fall in not-nourished category then he/she fall in one of the six categories of CIAF (i.e. B, C, D, E, F, Y). The probability that a child fall in category j given that he/she is malnourished is given by the equation:

$$P_{ij} = P_i * P_{j/i} \quad \text{(Eq.6)}$$

http://www.aloki.hu ● ISSN 1589 1623 (Print) ● ISSN 1785 0037 (Online)
DOI: http://dx.doi.org/10.15666/aeer/1706_1303513055

where $P_{j/i}$ is the conditional probability of falling in the jth category being in ith category of under-nutrition (i.e. at lower-nest) and P_i is the marginal probability of falling in ith alternative at upper-nest. Moreover,

$$P_i = \frac{\exp\,[z_i\alpha + \tau_i I_i]}{\sum_{i=1}^{I} \exp\,[z_i'\alpha + \tau_i I_i]} \quad \text{(Eq.7)}$$

$$P_{j/i} = \frac{\exp\,[x_{ij}\beta_{j/i}]}{\sum_{j=1}^{J} \exp\,[x_{ij}\beta_{j/i}]} \quad \text{(Eq.8)}$$

with $I_i = \ln\left(\sum_{j=1}^{J} \exp\left[x_{ij}\beta_{j/i}\right]\right)$. Here I_i is the inclusive value representing the maximum value of the attributes that determine the probability of a child falling in category$i$. $\tau_i$is the coefficient and its value must ranges from zero to one to be consistent with the NL derivation (McFadden, 1981). The NL model is estimated using full information maximum likelihood procedure. This method estimates the parameters in all stages simultaneously and produces consistent and efficient results (Hu and Donnell, 2010). Stata version 14 and Party-package of R were used for the regression analysis and classification trees respectively.

Results

Descriptive analysis

A total of 1870, children of age < 5 yrs were included in the analysis. Out of these children, about half (934 out of 1870) were female. According to the conventional indices of under-nutrition, 41.3% (772 out of 1870) were stunted, 12.3% (230 out of 1870) were wasted and 26.4% (493 out of 1870) were underweight among the studied sample. However, according to the CIAF, about 51% (937 out of 1870) of the children suffer from at least one of the groups (Group B-Y) and overall 49.9%(933 out of 1870) of the children fall in Group-A (i.e. without any failure). The highest prevalence of malnourishment was found to be in Group-F (20%: 374 out of 1870) followed by Group-E (16.3%: 305 out of 1870) while, Group-Y it was observed to be lowest with respect to malnourishment (1.5%: 28 out of 1870). Moreover, it was found to be approximately same in Group-B (3.7%: 70 out of 1870) and Group-C (3.6%: 67 out of 1870).

Majority of the mothers were uneducated (51.44%; 962 out of 1870) and have no autonomy (45.7%: 855 out of 1870) while, least of the women were underweight (12%: 225 out of 1870) among the studied sample. Prevalence of malnourished children among the poor and non-educated mothers remained high in failure groups E and F (23.3% & 25% for poor and 21.3% & 237% for non-educated mothers respectively). Moreover, percentage of undernourished children was lower in case of working mother (34.6%; 120 out of 347). Underweight mothers have high ratio of underweight and stunted children (i.e. Group-E: 29.3%; 66 out of 225). Six hundred and thirty six (34%: 636 out of 1870) children were resident of Punjab region followed by region Sindh (24%: 450 out of 1870). Percentage of nourished children stood high for Islamabad region (70.6%). About 40% (755 out of 1870) of the children belong to poor families (*Table 2*).

http://www.aloki.hu ● ISSN 1589 1623 (Print) ● ISSN 1785 0037 (Online)
DOI: http://dx.doi.org/10.15666/aeer/1706_1303513055

Table 2. *Percentage distribution of socio-economic and demographic factors of CIAF*

Variables	Total		Different categories of CIAF						
			A	B	C	D	E	F	Y
	f	%	%	%	%	%	%	%	%
Regions									
Punjab	636	34.0	55.8	2.8	3.5	3.9	15.4	17.0	1.5
Sindh	450	24.1	37.6	3.3	4.7	7.8	26.0	18.0	2.7
KPK	316	16.8	57.6	3.8	4.1	4.1	13.9	15.8	0.6
Blochistan	176	9.4	25.0	2.3	2.3	9.1	17.6	43.2	0.6
GB	172	9.3	57.2	6.4	2.3	1.2	5.8	27.2	0.0
Islamabad	119	6.4	70.6	8.4	2.5	1.7	4.2	10.1	2.5
Type of residence									
Urban	789	42.2	56.3	4.3	2.7	4.6	12.3	18.4	1.4
Rural	1081	57.8	45.2	3.3	4.3	5.2	19.2	21.2	1.6
Gender									
Male	936	50.1	48.1	3.8	3.9	5.8	17.0	19.9	1.5
Female	934	49.9	51.7	3.6	3.2	4.2	15.6	20.1	1.5
Wealth status									
Poor	755	40.4	35.6	2.9	4.1	7.7	23.3	25.0	1.3
Middle	363	19.4	50.1	5.2	4.4	2.5	14.3	21.2	2.3
Rich	752	40.2	64.1	3.9	2.7	3.4	10.2	14.4	1.3
Mother's education									
No education	962	51.4	38.6	3.3	4.5	7.2	21.3	23.7	1.5
Primary	311	16.6	48.9	5.1	2.6	2.9	18.3	19.3	2.9
Secondary	387	20.7	68.0	3.4	2.8	3.1	8.3	13.7	0.8
Higher and above	210	11.2	70.0	4.3	2.4	1.4	5.2	15.7	0.9
Vaccination									
Not vaccinated	178	9.5	35.4	5.1	3.9	7.3	20.2	27.5	0.6
Partially vaccinated	1094	58.5	48.8	4.1	3.5	4.8	17.5	19.5	1.8
Fully vaccinated	598	32.0	56.2	2.7	3.7	4.5	13.0	18.7	1.2
Working mother									
No	1523	81.4	53.4	3.8	3.6	4.5	14.4	19.0	1.3
Yes	347	18.6	34.6	3.5	3.5	7.2	24.5	24.5	2.3
Had diarrhea									
No	1430	76.5	51.0	3.6	2.8	4.3	16.5	20.4	1.4
Yes	440	23.5	46.4	4.1	6.1	7.0	15.7	18.9	1.8
Mother's BMI									
Normal	1098	58.7	47.8	4.1	3.3	4.9	17.7	20.5	1.7
Underweight	225	12.0	36.0	2.2	5.8	10.7	29.3	15.1	0.9
Overweight	547	29.3	59.8	3.7	3.3	2.7	8.2	21.0	1.3
Mother's autonomy									
No autonomy	855	45.7	47.6	3.4	3.9	5.3	17.1	21.2	1.6
Partial-autonomy	532	28.5	57.5	2.6	2.6	5.3	14.5	16.2	1.3
Full-autonomy	483	25.8	45.6	5.6	4.1	4.1	17.0	22.2	1.4
Toilet type									
High quality	1270	68.0	38.3	3.4	4.8	7.8	23.0	21.3	1.4
Medium quality	187	10.0	36.9	2.7	2.1	7.0	19.2	30.5	1.6
Poor quality	413	22.1	55.6	4.0	3.4	3.8	13.7	18.0	1.5
Sex of household head									
Male	1740	93.1	50.3	3.7	3.7	5.1	15.7	20.0	1.6
Female	130	6.9	44.6	4.6	2.3	3.9	24.6	20.0	0.0
Total	1870	100.0	49.9	3.7	3.6	5.0	16.3	20.0	1.5

http://www.aloki.hu ● ISSN 1589 1623 (Print) ● ISSN 1785 0037 (Online)
DOI: http://dx.doi.org/10.15666/aeer/1706_1303513055

Classification tree analysis

Two classification trees were constructed in our study. *Figure A2* (*Appendix*) demonstrates the first tree where mother's related variables (mother's education, mother's autonomy, mother's BMI, household wealth status and working status of mother) were considered. At the primary split the nutritional status of child is divided into two groups according to the mother's education (*one* is secondary and higher and the *other* is non-educated and primary). Subsequently node 2 is further divided according to the mother's BMI (underweight; normal and overweight) while, node 5 split into two groups according to wealth status (poor, middle and rich) while, node 6 and 9 are also split according to the mother's BMI (underweight; normal and overweight). There are total 11 nodes. There is higher percentage (about 20%; terminal node 3) of malnourished child with stunting and underweight (Group-F) whose mother has higher or secondary education with low BMI (underweight) while, about 70% of children are well nourished (Group-A) if the mother's nutritional level is better (i.e. she is normal or overweigh). Moreover, about 40% children (terminal node 8) belongs to mothers who either have primary education or non-educated, with lower BMI, are stunted and underweight (Group-E). Middle class or rich mothers with lower nutritional status have about 25% of the children with failure groups E and F (terminal node, 10). In the second tree (*Fig. A3* in the *Appendix*), impact of interactions of mother's schooling and working status on her child's nutritional level was presented. At the top, mother's education is divided into two groups (*one* is secondary and higher and the *other* is non-educated and primary). If the mother has secondary or higher education, about 70% of the children are with Group-A (i.e. well nourished; terminal node, 2) while, we move to node 3 if the mother has either primary- or no-education which further split mother's working status in two groups (yes and no). Node 4 showed that about 25% of the children prone to failure Groups E and F who belongs to working mothers with primary or no-education. However, if their mother is not working, the nutritional status of children of mothers having primary education is better than that of non-educated mothers (about 55% vs. 40%: terminal node 6 and 7).

Multinomial nested logit analysis

Associations of different groups of CIAF (Group B-Y) and various demographic and socio-economic factors, based on nested logit model, are shown in *Table 3* (Odd ratios and estimates with standard errors for upper nest) and *Table 4* (Odd ratios and estimates with standard errors for lower nest). The results at lower nest suggested that children, observed to have group C, D and E, were found a higher significant association with various exposure variables at that level. *Table 3* shows that inclusive value at lower nest was found to be 0.38 with p-value < 0.05, which suggests that shared unobservable are significantly present between different categories of CAIF (Group B-Y). According to the Wald-test the nesting structure is appropriate (Wald chi2 = 230.13, p-value < 0.001) while, likelihood ratio test for IIA property indicates that nested logit, is in fact, probably more convenient (chi2 (1) = 15.43, p-value < 0.001). The results and interpretations of variables at lower nest are briefly given below.

Effect of mother education: Mother education was found to be a highly significant factor of CIAF groups (Groups B-Y). Children of mothers with secondary education as compared to non-educated mothers were at about 50% lower risk to be lying in groups C, D, E and F (*Table 4*). However, this percentage fall down to 40% (OR = 0.61) for

http://www.aloki.hu ● ISSN 1589 1623 (Print) ● ISSN 1785 0037 (Online)
DOI: http://dx.doi.org/10.15666/aeer/1706_1303513055

group-B. If mother's education improved (higher and above), the nutritional level of children also improved. The results stated significantly lower odds for those children whose mothers have higher or above education. OR = 0.34, for group-D and OR = 0.40, for group-E). Moreover, mother's primary education does not show a significant association, implying that there exist no relative difference among the children of non educated mothers and those with primary education, regarding under-nutrition.

Effect of vaccination: The association of CIAF groups showed that vaccinated children were less likely to be malnourished as compared to non-vaccinated children. The odd values were significantly lower for the children of failure Group-B (OR = 0.55), Group-C (OR = 0.53), Group-D (OR = 0.57) and Group-Y (OR = 0.51). Those who were completely vaccinated have about 50% lower risk to fall in failure group-B (OR = 0.52) and Group-Y (OR = 0.50). However, the association of fully vaccinated children remained insignificant.

Effect of mother's Working Status: The impact of mother's working status was found to have higher effect on child under-nutrition. There were 36 percent more chances of falling in Group-F (OR = 1.36) and 31% more chance of lying in Group-F for the children of working mothers (OR = 1.31).

Effect of Diarrhea: Child who had diarrhea within two weeks prior to survey were found to have significantly higher odds for those suffering from wasting and underweight group (Group-C: OR = 1.48) and multiple failure group (Group-D: OR = 1.38).

Table 3. *Nested logit analysis of factors at upper nest*

Variables	OR	Estimate (SE)
Gender		
Male	1	
Female	0.83*	-0.19 (0.10)
Type of residence		
Urban	1	
Rural	0.99	-0.01 (0.12)
Region		
Punjab	1	
Sindh	1.80**	0.58 (0.14)
KPK	0.88	-0.12 (0.15)
Blochistan	3.17**	1.15 (0.22)
GB	0.77	-0.26 (0.20)
Islamabad	0.69	-0.37 (0.23)
Wealth status		
Poor	1	
Middle	0.70**	-0.35 (0.15)
Rich	0.51**	-0.67 (0.17)
Sex of household head		
Male	1	
Female	1.42*	0.35 (0.19)

Inclusive value = 0.39; P-value < 0.05; Wald chi2(88) = 230.13; P-value < 0.001; Log-likelihood = -2487.13; LR test for IIA: chi2(1) = 15.43; P-value < 0.001. N = 1870; OR: odd ratios; ** < .05, * < .10

http://www.aloki.hu ● ISSN 1589 1623 (Print) ● ISSN 1785 0037 (Online)
DOI: http://dx.doi.org/10.15666/aeer/1706_1303513055

Table 4. *Factors associated with different groups of CIAF at lower nest*

Variables	Group B		Group C		Group D		Group E		Group F		Group Y	
	OR	**Estimate (SE)**	**OR**	**Estimate (SE)**	**OR**	**Estimate (SE)**	**OR**	**Estimate (SE)**	**OR**	**Estimate (SE)**	**OR**	**Estimate (SE)**
Mother's education												
No education	Ref		Ref		Ref		Ref		Ref		Ref	
Primary	1.09	0.09 (0.19)	0.74	-0.29 (0.23)	0.69	-0.36 (0.24)	0.99	-0.01 (0.16)	0.94	-0.06 (0.15)	1.09	0.09 (0.22)
Secondary	0.61**	-0.50 (0.20)	0.49**	-0.71 (0.20)	0.46**	-0.78 (0.20)	0.49**	-0.72 (0.17)	0.55**	-0.60 (0.16)	0.43**	-0.85 (0.29)
Higher and above	0.67	-0.40 (0.28)	0.46**	-0.78 (0.27)	0.34**	-1.09 (0.33)	0.41**	-0.90 (0.24)	0.54**	-0.62 (0.21)	0.45**	-0.80 (0.35)
Vaccination												
Not vaccinated	Ref		Ref		Ref		Ref		Ref		Ref	
Partially vaccinated	0.56 **	-0.59 (0.27)	0.53**	-0.62 (0.28)	0.57**	-0.57 (0.26)	0.86	-0.15 (0.16)	0.86	-0.14 (0.15)	0.51**	-0.68 (0.32)
Fully vaccinated	0.52	-0.66 (0.36)	0.67	-0.40 (0.27)	0.73	-0.32 (0.25)	0.98	-0.01 (0.18)	1.04	0.04 (0.17)	0.5	-0.69 (0.40)
Working mother												
No	Ref		Ref		Ref		Ref		Ref		Ref	
Yes	1.14	0.13 (0.20)	1.07	0.07 (0.21)	1.28	0.25 (0.17)	1.36**	0.31 (0.15)	1.31**	0.27 (0.15)	1.42	0.35 (0.22)
Had diarrhea												
No	Ref		Ref		Ref		Ref		Ref		Ref	
Yes	1.17	0.16 (0.16)	1.48**	0.39 (0.16)	1.38**	0.32 (0.15)	1.15	0.15 (0.13)	1.16	0.15 (0.12)	1.15	0.14 (0.19)
Mother's BMI												
Normal	Ref		Ref		Ref		Ref		Ref		Ref	
Underweight	1.06	0.06 (0.28)	1.57**	0.46 (0.20)	1.73**	0.55 (0.19)	1.64**	0.49 (0.17)	1.24	0.21 (0.19)	0.92	-0.08 (0.38)
Overweight	0.82	-0.20 (0.16)	0.87	-0.14 (0.15)	0.74*	-0.39 (0.17)	0.74*	0.30 (0.15)	0.99	-0.01 (0.13)	0.72	-0.33 (0.21)
Mother's autonomy												
No autonomy	Ref		Ref		Ref		Ref		Ref		Ref	
Single autonomy	0.89	-0.11 (0.18)	0.87	-0.14 (0.18)	1.06	0.06 (0.15)	1.02	0.02 (0.14)	0.96	-0.04 (0.13)	0.85	- 0.16 (0.22)
Multiple autonomy	1.31*	0.27 (0.16)	1.09	0.09 (0.16)	0.02	0.02 (0.18)	1.16	0.16 (0.14)	1.22	0.20 (0.13)	0.91	-0.08 (0.24)
Toilet type												
High quality	Ref		Ref		Ref		Ref		Ref		Ref	
Medium quality	0.63	-0.45 (0.30)	0.58	-0.52 (0.33)	0.85	-0.16 (0.22)	0.9	-0.10 (0.20)	1.04	0.04 (0.20)	0.59	-0.53 (0.35)
Poor quality	0.79	-0.23 (0.21)	0.85	-0.15 (0.18)	0.92	-0.08 (0.17)	1.01	0.01 (0.14)	0.99	-0.01 (0.14)	0.64	-0.45 (0.30)

N = 1870; OR: odd ratios; ** < .05, * < .10; SE: standard error

http://www.aloki.hu ● ISSN 1589 1623 (Print) ● ISSN 1785 0037 (Online)
DOI: http://dx.doi.org/10.15666/aeer/1706_1303513055

Effect of Mother's BMI: Children of under-weight mother's were found to have significantly higher odds of falling in Group-C (OR = 1.57), Group-D (OR = 1.73) and Group-E (OR = 1.64). While, the children of overweight mother were less likely to be malnourished (OR = 0.74 for Group-D and OR = 0.74 for Group-E).

Mother's autonomy as well as toilet facility is among the important factors of UNICEF framework but their association could not found to be significant. We turn to the results and interpretation of variables at upper nest. A brief description is given below:

Effect of Gender: There were 17% lower chance of falling in under-nutrition for female child (OR = 0.87) as compared to the male child.

Effect of Wealth Status: Wealth status is among the important factors affecting child's nutritional status at upper nest. The children of middle class families were 30% (OR = 0.70) less likely to be malnourished while, rich children were at 49% at lower risk of under-nutrition as compared to poor children (OR = 0.51).

Regional Effects: Geographic location affects the health status of child. There were 80% (OR = 1.79) more chances of falling in under-nutrition for Sindhi child. However, the children of Baluchistan were three times more likely to fall in the anthropometric failure (OR = 3.17) as compared to the children of Punjab. There is no significant difference between KPK, GB and Islamabad regions as compared to Punjab with respect to child under-nutrition.

Type of Place of Residence: there exist no significant association between type of place of residence and child under-nutrition.

Sex of Household Head: children of female headed household were 42% more likely to be malnourished as compared to children of male headed households (OR = 1.42).

Discussion

Assessment of the nutritional status of children (of age < 5 yrs) plays an important role in developing countries, such as Pakistan, where the major part of population is malnourished (Sen and Mondal, 2012). According to the conventional measures, the prevalence of stunting, wasting and underweight remained 41.3%, 12.3% and 26.4% respectively among the studied sample, while the prevalence of under-nutrition was 51.1% using the CIAF. Based on the CIAF, the results of this study are higher as compared to other countries such as Ethiopia (Fentahun et al., 2016), while the position is little bit better than India (Dasgupta et al., 2015).

Classification trees may work as a useful alternative to the traditional statistical techniques such as logistic regression (Pawloski and Kitsantas, 2008). It is one of the data mining techniques that can identify subgroups in the data that share similar characteristics (Marshall, 2001) and display the results graphically which helps in understanding their interpretations. This display of classification tree can help in understanding how maternal factors interact to define and understand the importance of each variable examined. Moreover, some studies provide the comparison of classification trees with logistic regression models (Pawloski and Kitsantas, 2008; Kitsantas et al., 2007) and found that both methodologies provide comparable predictive performance. In this study, the classification trees revealed that mother's schooling is the most important factor among the maternal factor. The data also show that the children of educated (even primary) and healthy mothers living in household with middle or rich wealth status, were more likely to bear better nutritional status while, if

http://www.aloki.hu ● ISSN 1589 1623 (Print) ● ISSN 1785 0037 (Online)
DOI: http://dx.doi.org/10.15666/aeer/1706_1303513055

the mother's education is secondary or above the wealth status does not matter. Furthermore if mother has secondary or higher education then her work status does not affect her child's nutritional health. However, if she has either primary education or no-education then work status influence her child's nutritional level. Interestingly, mother's autonomy did not appear in the classification tree display (*Fig. B1*), suggesting that maternal autonomy may not play an important role for the prediction of poor nutritional status in our case. The results suggested by the tree structure also support the findings of nested logit model as well.

There exist a significant association between regions of residence and the nutritional status of children. Children of Balochistan region are at high risk of falling under-nutrition followed by region Sindh. Similar results were found in some other studies for Pakistan (Tariq et al., 2018). This may be due the cultural norms, seasonal food insecurity, poor health, and sanitation conditions. There are various aspects of gender discrimination in the literature. Some studies revealed that girls are at greater risk as compared to boys (Khan and Raza, 2014; Petrou and Kupek, 2010), while others demonstrated that male child is more likely to be undernourished (Alemayehu et al., 2015; Kandala et al., 2011). However, some studies showed no discrimination (Arif et al., 2011; Mushtaq et al., 2011). Our results showed that female children are less likely to be malnourished, which are in the line with different examinations on the planet (Poda et al., 2017; Altare et al., 2016; Hazarika, 2000). It may be due to the reason as female are less active and stay at home near food preparation. Another explanation may be that the economies like Pakistan, where women's role is important especially as agriculture labour; women's health is preferred (Akombi et al., 2017). A number of studies addressed that children of urban areas have better nutritional status than rural areas (Ejaz and Azid, 2011; Kandala et al., 2011; Hazarika, 2000). The results of this study uncovered no critical relationship amongst categories of CIAF and sort of place of home. Other studies have also showed the similar result (Poda et al., 2017; Rahman et al., 2015). The findings of this study also demonstrate that children of female headed households were more likely to prone in under nutrition. Commonly female headed households, in middle and low income countries, are those where child's mother is a widow or divorced. These households are generally poorer, own less and have lower access to good jobs which ultimately impact the health status of their residents. Similar results can be found elsewhere (Haidar and Kogi-Makau, 2009).

We examined how mothers 'decision making autonomy was associated with the likelihood of childhood under-nutrition. The finding suggests that mothers' sole decision-making as well as partial decision making was not associated with the likelihood of childhood under-nutrition. This result may suggest that child's nutritional status is not affected by who makes decisions in the household. There exist mixed results regarding mother's autonomy in empirical studies conducted in other countries. For example Deasi and Jhnson (2005) conducted a cross-country study for 12 developing countries, using DHS datasets, found that impact of mother's autonomy on height-for-age was positive for Mali and India however, negative association was found between child's nutrition and height for age in Haiti and Malawi. Non-significant results were also found in some studies (Kamiya et al., 2018).

Maternal education is one of the important factors of child health (Asif et al., 2017). There is an extensive literature supported the consequence that improved maternal education to be one of the protective measures of child's poor nutritional status (Alemayehu et al., 2015; Khan and Raza, 2014; Asena and Teni, 2015; Solanki et al.,

http://www.aloki.hu ● ISSN 1589 1623 (Print) ● ISSN 1785 0037 (Online)
DOI: http://dx.doi.org/10.15666/aeer/1706_1303513055

2014; Frongillo et al., 1997). Our study also showed that children of educated mothers (at least secondary) are less likely to fall in CIAF (in Categories B-Y). These results are consistent with other studies (Endris et al., 2017; Poda et al., 2017). An improvement in women's educational status may consider as a proxy for the increment in the household decision making autonomy which further act as a mediator for the relation between child's nutrition and mother's decision making autonomy (Akombi et al., 2017). Another way of explanation may be that an educated mother may get well pay jobs and more empowered in developing countries (Kandala et al., 2011) which positively affect the child's health ultimately. Thus, we may conclude that improved educational status of mother may consider as a protective measure of childhood under-nutrition.

In the present study we have evaluated the association between child's nutrition and mother's anthropometrics characteristic. Results indicated that maternal BMI was significantly associated with children nutritional status. Different Studies round the world showed that underweight mothers were more likely to have malnourished children as compared to normal or overweight mothers (Poda et al., 2017; Debnath and Bhattacharjee, 2016; Rahman et al., 2015; Tigga and Son, 2016; Ajslev et al., 2014; Fleten et al., 2012). This relationship also indicate and intergenerational transfer of socio-economic adversity and poor maternal health to child. Poverty may be another cause of low maternal BMI because poor mother are nutritionally deprived during early age which may not improve even after marriage. Moreover, social causes such early marriage, lack of birth spacing, and discrimination of food distribution in male dominant families may increase under-nutrition among mothers. The results of this study revealed that children of working mothers were more likely to prone under-nutrition. This may be due to the reasons: first, is that the working mothers have less time for care and feeding of their offspring. Second, generally the mothers of low-income families are less educated and engaged in informal work to earn a little money for the survival of their family. Moreover, such families lived in an unclear environment which adversely affects their health. Similar result can be found in the studies conducted for other countries (Toyama et al., 2001). Diarrhea is one of the important factors of child's death and illness in developing countries (Checkley et al., 2008) which may affect the child's health instantly. The findings of this study demonstrated that children with diarrhea were more likely to fall in Group-C and Group-D of CIAF. The reason behind might be that, diarrhea impact the child nutritional status indirectly as a child with diarrhea could not consume food properly and ultimately fall in undernourishment. Childhood vaccination may strengthen children's nutritional level and lead to a better childhood development in low and middle income countries, where 20% of children fewer than 5 years of age have low weight for age (underweight) and about 32% have low height for age (stunted). Childhood under-nutrition accounts for 35% of deaths worldwide among children of fewer than 5 years because it increases the risk of mortality due to infectious diseases (Anekwe and Kumar, 2012). The findings of our study showed that nutritional level can improve even if the child is partially immunized. Though the results for fully vaccinated children has been reported to be insignificant however this finding does not deny the importance of full vaccination for child's better nutritional status (Debnath and Bhattacharjee, 2016).

An association between household wealth status and child nutrition has been shown in several studies (Chowdhury et al., 2016; Poda et al., 2017). It is found that the children of middle class and rich families were less likely to fall in the CIAF. Other studies also demonstrated similar results (Chowdhury et al., 2016; Kandala et al., 2011;

http://www.aloki.hu ● ISSN 1589 1623 (Print) ● ISSN 1785 0037 (Online)
DOI: http://dx.doi.org/10.15666/aeer/1706_1303513055

Petrou and Kupek, 2010; Darteh et al., 2014). This is perhaps due to the reason that well off households may have better access to basic facilities such as good and nutritious food. On the other hand, children of poor SES are more likely to prone anthropometric failure due to insufficient intake, greater exposure to infection as well as lack of access to the basic needs (Hazarika, 2000). A study in Bangladesh has shown that parents of richer families are more likely to be educated than those from poor families, and thus have better access to food, allocate higher proportion of resources for children's welfare and improved standard of living (Sarma et al., 2017), which in turn gives better healthcare to the child. Another study investigating the interaction between SES and the mother's education in connection to child health, found that the impact of improved maternal education turned to be more protective for the children of rich families, while father's education works independently of SES and considered as protective element (Hatt and Waters, 2006).

Conclusion

A significant association among child under-nutrition and maternal factors in Pakistan underscore the requirement for sustained investment to highlight social factors and reproductive health. Our analysis has identified the most vital determinants influencing the child under-nutrition which may play a crucial role in the literature on the association of CIAF with socio-economic and demographic variables. There is need of interventions by the government in collaboration with non-governmental organizations, like USAID, for the improvement of children's nutritional level, especially in under-developed regions such as Blochistan and Sindh. The local governments representatives (Such as UC chairman, councilors etc.) in cooperation with civil society should work to frame child's nutritional level as a national development agenda. Steps should be taken to improve the maternal status in the society, especially the mother's education and her nutritional level. Such programmes should be launched that focus on increase in the women's role in the society, such as skilled education, well paid job opportunities and better health facilities. Moreover, the interventions for the improvement of household wealth status and the effective nutritional strategies (such as Benazir Income Support Programme (unconditional cash transfer for poverty reduction) and Health/Sehat cards (used for free or reduced-rate medical treatment issued by the government), over the long period, should be considered. However, for short run, maternal and child health programs as well as the provision of supplement food on subsidized rate may be useful for eradication of under-nutrition. The progress in preventive measures for infectious diseases, such as diarrhea, need attention of policy-makers to reduce child under-nutrition. Moreover, Lower maternal BMI needs attention in order to break the inter-generational existence of under-nutrition.

The use of CIAF as a measure nutritional status will serve to access more precise identification of nutritionally more vulnerable segments of population since, it has enough potential to improve the efficacy of different nutritional interventions by recognizing different failure groups (single, double and multiple) and also it gives an estimate of overall burden of under-nutrition. Therefore, further research on causes of malnutrition, taking CIAF as measure of malnutrition, is needed. Moreover, reproductive health care, maternal dietary pattern, access to information might be associated with children's nutritional status, therefore further studies should consider such maternal factors also, while investigating the causes of child under-nutrition.

http://www.aloki.hu ● ISSN 1589 1623 (Print) ● ISSN 1785 0037 (Online)
DOI: http://dx.doi.org/10.15666/aeer/1706_1303513055

Moreover, child's dietary pattern should be considered while exploring the causes of child under-nutrition.

Acknowledgments. The authors wish to thank measuredhs.com for giving access to Pakistan demographic and health survey data for 2012-13.

REFERENCES

[1] Achadi, E., Ahuja, A., Bendech, M. A., Bhutta, Z. A., De-Regil, L. M., Fanzo, J., … Kimani, E. (2016): Global Nutrition Report 2016: From Promise to Impact: Ending Under-Nutrition by 2030. – International Food Policy Research Institute (IFPRI), Washington, DC.

[2] Achakzai, P., Khan, R. (2016): Nutritional status and associated factors among children less than five years of age in Tehsil Zarghoon town, District Quetta, Baluchistan. – Journal of Ayub Medical College Abbottabad 28(1): 146-51.

[3] Adhikari, S. R. (2011): A methodological review of demand analysis: an example of health care services. – Economic Journal of Development Issues 13: 119-30.

[4] Ajslev, T. A., Ängquist, L., Silventoinen, K., Baker, J. L., Sørensen, T. I. (2014): Trends in parent-child correlations of childhood body mass index during the development of the obesity epidemic. – PLoS One 9(10): e109932.

[5] Akin, J. S., Griffin, C. C., Guilkey, D. K., Popkin, B. M. (1986): The demand for primary health care services in the Bicol region of the Philippines. – Economic Development and Cultural Change 34(4): 755-82.

[6] Akombi, B. J., Agho, K. E., Hall, J. J., Merom, D., Astell-Burt, T., Renzaho, A. M. (2017): Stunting and severe stunting among children under 5 years in Nigeria: a multilevel analysis. – BMC Pediatrics 17(1): 15.

[7] Alemayehu, M., Tinsae, F., Haileslassie, K., Seid, O., Gebregziabher, G., Yebyo, H. (2015): Under-nutrition status and associated factors in under-5 children, in Tigray, Northern Ethiopia. – Nutrition 31(7-8): 964-70.

[8] Altare, C., Delbiso, T. D., Mutwiri, G. M., Kopplow, R., Guha-Sapir, D. (2016): Factors associated with stunting among pre-school children in Southern highlands of Tanzania. – Journal of Tropical Pediatrics 62(5): 390-408.

[9] Amugsi, D. A., Mittelmark, M. B., Lartey, A., Matanda, D. J., Urke, H. B. (2014): Influence of childcare practices on nutritional status of Ghanaian children: a regression analysis of the Ghana Demographic and Health Surveys. – BMJ Open 4(11): e005340.

[10] Anekwe, T. D., Kumar, S. (2012): The effect of a vaccination program on child anthropometry: evidence from India's Universal Immunization Program. – Journal of Public Health 34(4): 489-97.

[11] Anya, S. B., Yene, A. (2016): The determinants of the choice of treatment of pregnant women in Cameroon. – Health Economics Review 6(1): 48.

[12] Arif, G. M., Nazir, S., Satti, M. N. and Farooq, S. (2012): Child malnutrition in Pakistan: trends and determinants. – Pak Inst Dev Econ 2012: 1-18.

[13] Arooj, S., Ali, S., Baber, N., Abbasi, A., Ali, M. (2013): Socioeconomic factors effecting polio vaccination in Pakistan. – Health 5(5): 892.

[14] Asif, A. M., Tahir, M. R., Arshad, I. A., (2017): Socioeconomic condition and prevalence of malaria fever in Pakistani children: findings from a community health survey. – Journal of Tropical Pediatrics 64(3): pp.189-194.

[15] Asena, T. F., Teni, D. A. (2015): Bayesian semi-parametric regression analysis of childhood under-nutrition in Gamo Gofa Zone: the social and economic impact of child under nutrition. – American Journal of Theoretical and Applied Statistics 4(4): 269-76.

http://www.aloki.hu ● ISSN 1589 1623 (Print) ● ISSN 1785 0037 (Online)
DOI: http://dx.doi.org/10.15666/aeer/1706_1303513055

[16] Ben-Akiva, M. E., Lerman, S. R., Lerman, S. R. (1985): Discrete choice analysis: theory and application to travel demand. – MIT Press, Cambridge, MA.
[17] Breiman, L., Friedman, J. H., Olshen, R., Stone, C. (1984): Classification and Regression Trees. – Wadsworth, California.
[18] Checkley, W., Buckley, G., Gilman, R. H., Assis, A. M., Guerrant, R. L., Morris, S. S., Mølbak, K., Valentiner-Branth, P., Lanata, C. F., Black, R. E., Childhood Malnutrition and Infection Network (2008): Multi-country analysis of the effects of diarrhoea on childhood stunting. – International Journal of Epidemiology 37(4): 816-830.
[19] Chowdhury, M. R., Rahman, M. S., Khan, M. M., Mondal, M. N., Rahman, M. M., Billah, B. (2016): Risk factors for child under-nutrition in Bangladesh: a multilevel analysis of a nationwide population-based survey. – The Journal of Pediatrics 172: 194-201.
[20] Darteh, E. K., Acquah, E., Kumi-Kyereme, A. (2014): Correlates of stunting among children in Ghana. – BMC Public Health 14(1): 504.
[21] Das, S., Bose, K. (2011): Assessment of nutritional status by anthropometric indices in Santal Tribal Children. – Journal of Life Sciences 3(2): 81-5.
[22] Dasgupta, A., Sahoo, S. K., Taraphdar, P., Preeti, P. S., Biswas, D., Kumar, A., Sarkar, I. (2015): Composite index of anthropometric failure and its important correlates: a study among under-5 children in a slum of Kolkata, West Bengal, India. – International Journal of Medical Science and Public Health 4(3): 414-20.
[23] Debnath, A., Bhattacharjee, N. (2016): Understanding under-nutrition of tribal children in India: the role of women's empowerment. – Ecology of Food and Nutrition 55(6): 508-27.
[24] Ejaz, A. K. R., Azid, T. (2011): Under-nutrition in primary school-age children: a case of urban and slum areas of Bahawalpur, Pakistan. – International Journal of Social Economics 38(9): 748-66.
[25] Endris N., Asefa, H., Dube, L. (2017): Prevalence of under-nutrition and associated factors among children in rural Ethiopia. – BioMed Research International. DOI: 10.1108/03068291111157221.
[26] Fentahun, N., Belachew, T., Lachat, C. (2016): Determinants and morbidities of multiple anthropometric deficits in southwest rural Ethiopia. – Nutrition 32(11-12): 1243-9.
[27] Final Report PDHS (2012-13): Pakistan Demographic and Health Survey. – https://dhsprogram.com/publications/publication-fr290-dhs-final-reports.cfm.
[28] Fink, G., Günther, I., Hill, K. (2011): The effect of water and sanitation on child health: evidence from the demographic and health surveys 1986-2007. – International Journal of Epidemiology 40(5): 1196-204.
[29] Fleten, C., Nystad, W., Stigum, H., Skjærven, R., Lawlor, D. A., Davey Smith, G., Næss, Ø. (2012): Parent-offspring body mass index associations in the Norwegian Mother and Child Cohort Study: a family-based approach to studying the role of the intrauterine environment in childhood adiposity. – American Journal of Epidemiology 176(2): 83-92.
[30] Frongillo Jr, E. A., de Onis, M., Hanson, K. M. (1997): Socioeconomic and demographic factors are associated with worldwide patterns of stunting and wasting of children. – The Journal of Nutrition 127(12): 2302-9.
[31] Haidar, J., Kogi-Makau, W. (2009): Gender differences in the household-headship and nutritional status of pre-school children. – East African Medical Journal 86(2): 69-73.
[32] Hatt, L. E., Waters, H. R. (2006): Determinants of child morbidity in Latin America: a pooled analysis of interactions between parental education and economic status. – Social Science & Medicine 62(2): 375-86.
[33] Hazarika, G. (2000): Gender differences in children's nutrition and access to health care in Pakistan. – The Journal of Development Studies 37(1): 73-92.
[34] Hu, W., Donnell, E. T. (2010): Median barrier crash severity: some new insights. – Accident Analysis & Prevention 42(6): 1697-704.

http://www.aloki.hu ● ISSN 1589 1623 (Print) ● ISSN 1785 0037 (Online)
DOI: http://dx.doi.org/10.15666/aeer/1706_1303513055

[35] Jung, S. H., Chen, Y., Ahn, H. (2014): Type I error control for tree classification. – Cancer Informatics 13: CIN-S16342.
[36] Kamiya, Y., Nomura, M., Ogino, H., Yoshikawa, K., Siengsounthone, L., Xangsayarath, P. (2018): Mothers' autonomy and childhood stunting: evidence from semi-urban communities in Lao PDR. – BMC Women's Health 18(1): 70.
[37] Kandala, N. B., Madungu, T. P., Emina, J. B., Nzita, K. P., Cappuccio, F. P. (2011): Under-nutrition among children under the age of five in the Democratic Republic of Congo (DRC): does geographic location matter? – BMC Public Health 11(1): 261.
[38] Khan, R. E., Raza, M. A. (2014): Child under-nutrition in developing economies: a case study of Bangladesh. – Quality & Quantity 48(3): 1389-408.
[39] Kitsantas, P., Moore, T. W., Sly, D. F. (2007): Using classification trees to profile adolescent smoking behaviors. – Addictive Behaviors 32(1): 9-23.
[40] Krishna, A., Mejía-Guevara, I., McGovern, M., Aguayo, V., Subramanian, S. V. (2017): Trends in inequalities in child stunting in South Asia. – Maternal & Child Nutrition e12517.
[41] Mahmood, S., Nadeem, S., Saif, T., Mannan, M., Arshad, U. (2016): Nutritional status and associated factors in under-five children of Rawalpindi. – Journal of Ayub Medical College Abbottabad 28(1): 67-71.
[42] Maïga, E. W. (2013): The impact of mother's education on child health and nutrition in developing countries: evidence from a natural experiment in Burkina Faso. – African Economic Conference 2013, 28-30 October, Johannesburg, South Africa.
[43] Marshall, R. J. (2001): The use of classification and regression trees in clinical epidemiology. – Journal of Clinical Epidemiology 54(6): 603-9.
[44] McFadden, D. (1981): Econometric Models of Probabilistic Choice. Structural Analysis of Discrete Data with Econometric Applications. – In: Manski, C., McFadden, D. (eds.) Structural Analysis of Discrete Data with Econometric Applications. MIT Press, Cambridge, pp. 198-272.
[45] Mushtaq, M. U., Gull, S., Khurshid, U., Shahid, U., Shad, M. A., Siddiqui, A. M. (2011): Prevalence and socio-demographic correlates of stunting and thinness among Pakistani primary school children. – BMC Public Health 11(1): 790.
[46] Nandy, S., Irving, M., Gordon, D., Subramanian, S. V., Smith, G. D. (2005): Poverty, child under-nutrition and morbidity: new evidence from India. – Bulletin of the World Health Organization 83: 210-6.
[47] Pawloski, L. R., Kitsantas, P. (2008): Classification tree analysis of stunting in Malian adolescent girls. – American Journal of Human Biology: The Official Journal of the Human Biology Association 20(3): 285-91.
[48] Petrou, S., Kupek, E. (2010): Poverty and childhood under-nutrition in developing countries: a multi-national cohort study. – Social Science & Medicine 71(7): 1366-73.
[49] Poda, G. G., Hsu, C. Y., Chao, J. C. (2017): Factors associated with under-nutrition among children < 5 years old in Burkina Faso: evidence from the Demographic and Health Surveys IV 2010. – International Journal for Quality in Health Care 29(7): 901-8.
[50] Pradhan, A. (2010): Factors associated with nutritional status of the under-five children. – Asian Journal of Medical Sciences 1(1): 6-8.
[51] Rahman, A. (2016): Significant risk factors for childhood under-nutrition: evidence from an Asian developing country. – Science Journal of Public Health 4(1-1): 16-27.
[52] Rahman, M. M., Saima, U., Goni, M. A. (2015): Impact of maternal household decision-making autonomy on child nutritional status in Bangladesh. – Asia Pacific Journal of Public Health 27(5): 509-20.
[53] Raju, D., D'Souza, R. (2017): Child Under-Nutrition in Pakistan: What Do We know? – The World Bank, Washington, DC.
[54] Rakotomanana, H., Gates, G. E., Hildebr, D., Stoecker, B. J. (2017): Determinants of stunting in children under 5 years in Madagascar. – Maternal & Child Nutrition 13(4): e12409.

http://www.aloki.hu ● ISSN 1589 1623 (Print) ● ISSN 1785 0037 (Online)
DOI: http://dx.doi.org/10.15666/aeer/1706_1303513055

[55] Sarma, H., Khan, J. R., Asaduzzaman, M., Uddin, F., Tarannum, S., Hasan, M. M., Rahman, A. S., Ahmed, T. (2017): Factors influencing the prevalence of stunting among children aged below five years in Bangladesh. – Food and Nutrition Bulletin 38(3): 291-301.
[56] Sen, J., Mondal, N. (2012): Socio-economic and demographic factors affecting the Composite Index of Anthropometric Failure (CIAF). – Annals OxF Human Biology 39(2): 129-36.
[57] Senbanjo, I. O., Olayiwola, I. O., Afolabi, W. A., Senbanjo, O. C. (2013): Maternal and child under-nutrition in rural and urban communities of Lagos state, Nigeria: the relationship and risk factors. – BMC Research Notes 6(1): 286.
[58] Sharma, A., Kader, M. (2013): Effect of women's decision-making autonomy on infant's birth weight in rural Bangladesh. – ISRN Pediatrics. DOI: 10.1155/2013/159542.
[59] Solanki, R., Patel, T., Shah, H., Singh, U. S. (2014): Measuring under-nutrition through z-scores and Composite Index of Anthropometric Failure (CIAF): a study among slum children in Ahmedabad City, Gujarat. – National Journal of Community Medicine 5(4): 434-9.
[60] Svedberg, P. (2000): Poverty and Under-Nutrition: Theory, Measurement, and Policy. – Clarendon Press, Oxford, UK.
[61] Tariq, J., Sajjad, A., Zakar, R., Zakar, M. Z., Fischer, F. (2018): Factors associated with under-nutrition in children under the age of two years: secondary data analysis based on the Pakistan Demographic and Health Survey 2012–2013. – Nutrients 10(6): 676.
[62] Tigga, P. L., Sen, J. (2016): Maternal body mass index is strongly associated with children-scores for height and BMI. – Journal of Anthropology. http://dx.doi.org/10.1155/2016/6538235.
[63] Toyama, N., Wakai, S., Nakamura, Y., Arifin, A. (2001): Mother's working status and nutritional status of children under the age of 5 in urban low-income community, Surabaya, Indonesia. – Journal of Tropical Pediatrics 47(3): 179-81.
[64] United Nations Children's Fund (1990): Strategy for Improved Nutrition of Children and Women in Developing Countries. A UNICEF Policy Review. – ERIC Clearinghouse, New York.
[65] Vikram, K., Vanneman, R., Desai, S. (2012): Linkages between maternal education and childhood immunization in India. – Social Science Medicine 75(2): 331-9.
[66] World Health Organization (2017): UNICEF-WHO-The World Bank: Joint Child Under-Nutrition Estimates. – https://www.who.int/nutgrowthdb/estimates/en.

APPENDIX

Table A1. *Descriptions of explanatory variables*

Variables	Categories (zero is the reference category)
Region	Punjab = 0, Sindh = 1, KPK = 2, Blochistan = 3, GB = 4, Islamabad = 5
Type of residence	Urban = 0, Rural = 1
Gender	Male = 0, Female = 1
Wealth status	Poor = 0, Middle = 1, Rich = 2
Mother's education	No-education = 0, Primary = 1, Secondary = 2, Higher & Above = 3
Working mother	No = 0, Yes = 1
Mother's BMI	Normal = 0, Underweight = 1, Overweight = 2
Mother's autonomy	No-autonomy = 0, Partial-autonomy = 1, Full-autonomy = 2
Diarrhea	No = 0, Yes = 1
Vaccination	Not-vaccinated = 0, Partially-vaccinated = 1, Fully-vaccinated = 2
Sex of household head	Male = 0, Female = 1
Type of toilet	High-quality = 0, Medium-quality = 1, poor-quality = 2

http://www.aloki.hu ● ISSN 1589 1623 (Print) ● ISSN 1785 0037 (Online)
DOI: http://dx.doi.org/10.15666/aeer/1706_1303513055

Figure A1. *Map showing different regions*

Figure A2. *Interactions for mother's education, wealth status and mother's body mass index*

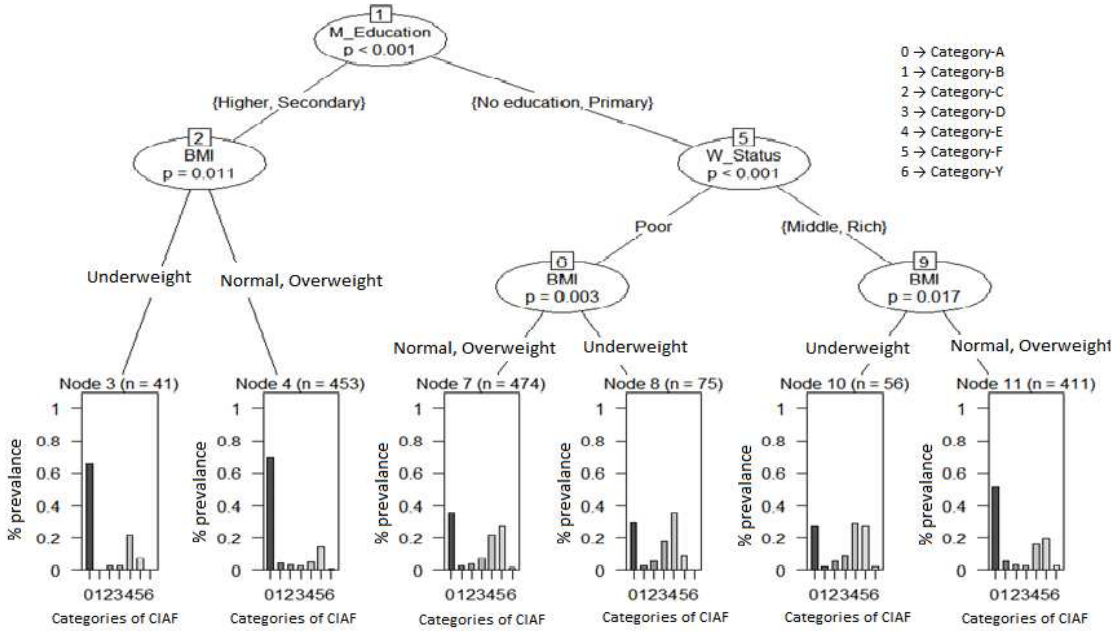

http://www.aloki.hu ● ISSN 1589 1623 (Print) ● ISSN 1785 0037 (Online)
DOI: http://dx.doi.org/10.15666/aeer/1706_1303513055

Figure A3. *Interactions for mother's education and mother's working status*

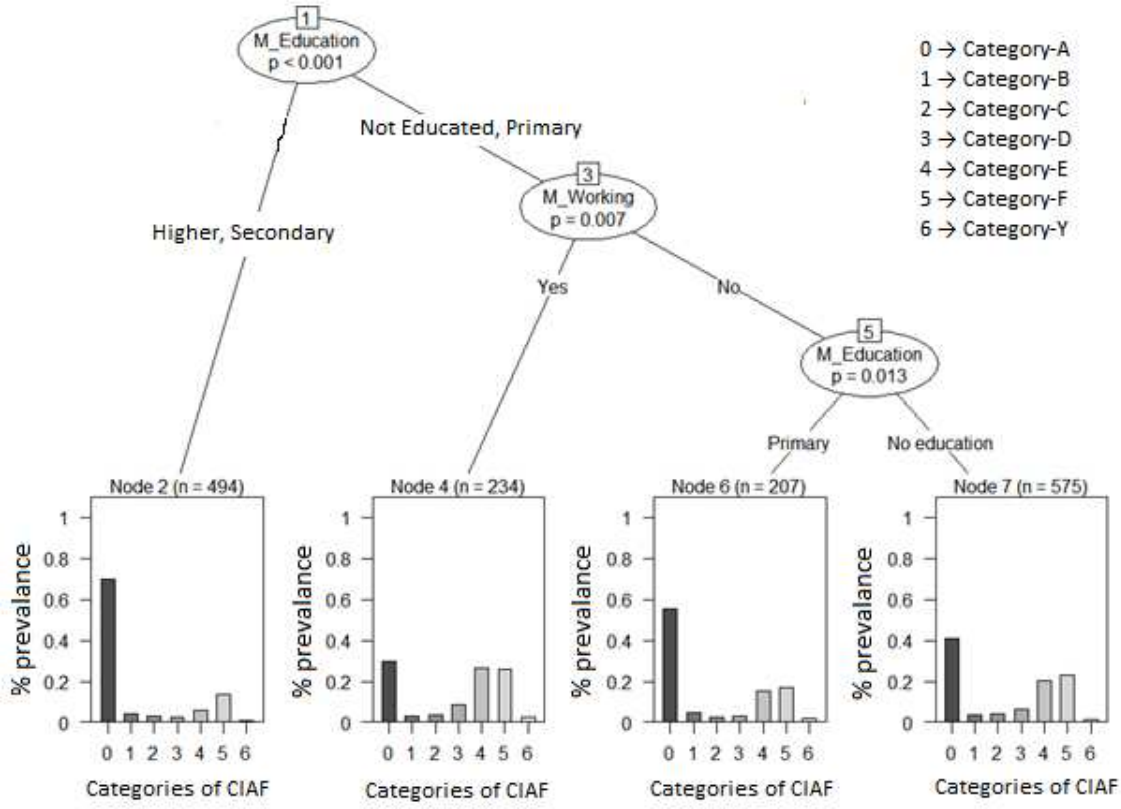

http://www.aloki.hu ● ISSN 1589 1623 (Print) ● ISSN 1785 0037 (Online)
DOI: http://dx.doi.org/10.15666/aeer/1706_1303513055

STUDY ON THE SPATIOTEMPORAL FEATURES AND EVOLUTION OF ALPINE NOMADIC SETTLEMENTS FROM THE PERSPECTIVE OF ECOLOGICAL WISDOM: CASE STUDY OF QIONGKUSHITAI VILLAGE IN XINJIANG, CHINA

MENG, F. L.[1,2] – HE, Y.[2*]

[1]*Shihezi University, School of Literature and Art, Shihe-zi 832003, Xinjiang, China*
No. 225, No. 31 Beishi Road, Shihezi City, Xinjiang, China
(e-mail: mengfuli2008@163.com; phone: +86-180-9598-3089)

[2]*HuaZhong University of Science And Technology, School of Architecture and Urban Planning*
Wuhan 430079, Hubei, China

[*]*Corresponding author*
e-mail: 330337342@qq.com; phone: +86-136-0713-9805

(Received 24th May 2019; accepted 3rd Sep 2019)

Abstract. Ecological wisdom in traditional nomadic societies is formed in the process of production, life and spiritual belief. Nomadic settlements are multidimensional cultural heritage and cultural landscape types in post-modern society. This research takes Qiongkushitai village as the research object, and referring to the research methods and achievements of human geography and temporal geography, this paper discusses the spatiotemporal features and evolution of the traditional nomadic settlements under the process of rapid urbanisation. Taking local wisdom as the breakthrough point, two characteristics of the traditional nomadic spatiotemporal picture are condensed: ① self-adaptability of nomadic spatiotemporal picture restricted by alpine resources, ② multi-level nesting law of nomadic spatiotemporal picture. By extracting the typical fragments on the spatiotemporal axis, this paper attempts to propose a periodic activity model on the multi-level spatiotemporal scale in the nomadic space and time trajectory. This paper explores the evolution mechanism of traditional nomadic settlements driven by national policies, individual demands, technology, and market. The results of this study can provide information for the study of resilience construction in the construction of ecological civilisations in alpine pastoral areas in Western China.
Keywords: *transhumance, adaptability of behavior, laws of nesting in multi-level space, ecological carrying capacity, conflict and acculturation*

Introduction

Ecological wisdom is a positive part of tradition in life and production,which shows recessive and dominant characteristics. It shows the recessive temporal and spatial order in time, but in form, it reflects the physical form or lifestyle reflected by the skills and values of regional cultural genes (Hills, 2009). The production and life patterns of the Kazakh settlements living in the high mountains can provide basic living security on the premise that nomadic data can be provided, although other dynamic factors restrict the strength and depth of their inheritance or continuation. However, this kind of livelihood method, which is rooted in the natural pastoral environment, will also show the trend that the one aspect wanes, the other waxes in the grassland ecosystem chain.

Xinjiang alpine nomadic settlement, as one of the important carriers of grassland man-land interaction, been concerned by the academic community and accumulated a wealth of academic achievements because of its special form. Through reviewing related research findings in recent years, reviewing, it mainly focuses on three aspects: (1) nomadic

http://www.aloki.hu ● ISSN 1589 1623 (Print) ● ISSN 1785 0037 (Online)
DOI: http://dx.doi.org/10.15666/aeer/1706_1305713073

settlement and its related Noumenon Research: study on the Ecological View, Environmental behavior of Nomadic settlement; (Cui, 2002; Chen, 2017), Archaeological Observation of Prehistoric Nomadic Industry of the Western Tianshan Mountains in Xinjiang (Jia, 2018), Climate change and the local environment affected human activities in Heihe River basin (Shi et al., 2019), the characteristics of temporal and spatial, and its formation Mechanism (Meng, 2017), focus on recently implemented projects in the sequence of sedentarisation programs, the so-called Nomadic settlement (Ptackova, 2011); (2) Diversification of research perspectives: the study of the historical evolution of nomadic settlements on archaeological perspective, the tourism resources development such as tourism management and other nomadic settlements (Han, 2013; Li and Yu, 2019), The production and lifestyle after settlement under cultural anthropology (Doumani et al., 2015), the change and evolution mechanism of national belief, etc. (Felr, 1994); (3) Study on Nested Scale of Nomadic Social Organizations: Grassland ecological restoration based on regional scale, regional mountain nomadic villages, etc. (Honeychurch, 2014; Chen, 2014), The Economy and Politics of Mountain Nomadism. Based on the above analysis, the research results of the nomadic spatio-temporal picture from the perspective of the ecological wisdoms are relatively few. The authors draw lessons from the research results of spatio-temporal behaviour of production and life in human geography and time geography. Taking Qiongkushitai village as an example, this paper makes a case study of Kazakh Alpine Nomadic Settlements in the Turks River Basin of Yili Prefecture and explores the ecological wisdom commonly found in traditional nomadic behaviour.

Based on a long-term field survey in the alpine pastoral areas of Yili Prefecture, Xinjiang, China, this paper explores the temporal and spatial characteristics of production, life and ecology of Kazakh herdsmen, who are the main body of traditional Alpine nomadic settlements. This paper attempts to explore the practical significance, cultural connotation, and the relationship between Kazakh traditional survival prospect and grassland ecology from the perspective of evolution mechanism driven by national policy, individual needs, technology, and market. The author hopes that other scholars will further explore the traditional nomadic society transformation period, herdsmen's modern living needs, and balance between human and natural ecology in pastoral areas, and provide some reference for the resilience building in the construction of ecological civilisations in pastoral areas in Western China.

Materials and Methods

In the process of rapid urbanisation, we should reflect on the practical value of ecological culture construction in traditional local wisdom. Each region is a local national badge (Crown, 2005). Ecological wisdom is one of the best symbols of regional cultural identification. Ecological wisdom is a stable structure and type inherited by a fixed group or region in the process of continuous reconstruction. It has the characteristics of self-discipline, local creation with the help of foreign knowledge, technology, formulation, and so on. The traditional Kazakh nomadic production, living in the exchange of material and energy with a grassland ecosystem, can achieve efficient coordination between resource utilisation and environmental conservation. Nomadic production is not only the result of adapting to nature but also the means of protecting nature to ensure the balanced utilisation of grassland and avoid the risk of natural disasters for herdsmen. The compensatory grassland ecological cycle mechanism, such as the roof-covering grassland model, compensation base ecological

http://www.aloki.hu ● ISSN 1589 1623 (Print) ● ISSN 1785 0037 (Online)
DOI: http://dx.doi.org/10.15666/aeer/1706_1305713073

mechanism, moderate migration and nomadism, is rooted in the ecological view and environmental behaviour in nomadic activities, which condenses their ecological wisdom to live with the grassland (Chen, 2019). Ecological wisdom in traditional nomadic society is formed in the process of production, life and spiritual belief. It is also a multi-dimensional cultural heritage and landscape type for post-nomadic society. Therefore, the protection and development of cultural memory and cultural sites in post-nomadic settlements have important theoretical and practical significance.

Constraint and adaptability of nomadic landscape

The spatial and temporal characteristics of alpine grassland are important factors for restricting and encouraging nomads' access to resources (energy or information) and the way of using them regionally. Spatio-temporal differences are the response of human beings to the optimal use of time, which is believed to eventually lead to the growth of reproduction. In the new Darwinian theory, "adaptation"should be attributed to "moderate exchange" of energy (Torrens et al., 2010), information and technology or "Spatio-temporal threshold mechanism" (Meng, 2017). Time in the nomadic society is like an invisible bond, through the nomadic production and life of different time scales, through the visible and invisible space mapping and connected in the same system, namely, the nomadic grassland system. High-quality grassland resources appear seasonally in nomadic alpine settlements, so the survival strategy of effective utilisation of time is determined by the limited time of obtaining resources, and the time segment or seasonal length of each year. In the one-year periodic-cycle of nomadism, the core variables, such as the duration of effective utilisation of resources, the seasonal differences in the spatial and temporal distribution of available resources, the concentration and dispersion of resources, etc. The seasonal transition of nomadic production must be carefully planned and organised to reflect the adaptability to space-time constraints.

Spatio-temporal trajectory, space-time picture

Spatio-temporal trajectory is the record sequence of the position and time of a moving object. As an important data type and information source (Yang, 2004; Gong et al., 2017) of spatio-temporal mapping, the spatio-temporal trajectory is the spatial appearance after different time overlaps in order in space. The spatial and temporal trajectory of grassland nomadism records Kazakh nomad stability, periodicity, regularity, the flexibility of nomadic behaviour, traffic logistics, and other information. The similarity and differences in characteristics of nomadic spatio-temporal trajectory data (nomadic time, linear space, behaviour node) were extracted under the typical space-time dimension, and the local ecological order in traditional nomadic behaviour was revealed. The recognition of typical regional characteristics was first reflected through a space and time picture.

The space and time picture is composed of recessive and explicit spatio-temporal order, behavioural pattern, materialised structure. The space-time picture is the sum of the material cultural landscape and the non-material cultural landscape formed under the same cultural or multi-cultural background. It is constructed by strong recognition symbols and is recognised and inherited. Local wisdom is transmitted to future generations through a concrete or visual form, and can also be regarded as the superposition and reproduction of spatio-temporal images through different historical periods.

http://www.aloki.hu ● ISSN 1589 1623 (Print) ● ISSN 1785 0037 (Online)
DOI: http://dx.doi.org/10.15666/aeer/1706_1305713073

Materials

The typical Nomadic Settlements in the Turks River Basin of Yili Prefecture in Xinjiang, China (*Figure 1*), were selected as the research subjects. The research area is located in western Xinjiang, and there are a large number of traditional nomadic settlements in the high mountain areas. The region has features of typical landforms: undulating mountains, river streams with vertical and horizontal water sources, open and flat terrace grasslands, and other features to provide a natural place for nomadic activities. The Qiongkushitai village is located in southern Tianshan on the western part of the Tianshan Mountains. Two sides around the Wusun mountain, the two sides of the peak mountain stretch, adjacent barriers. The region has a long history of nomads, it is rich in cultural relics, less affected by the urbanisation process, and the traditional nomadic production behaviour remains relatively intact.

Figure 1. *Sample Research Location Map . Drawn by author according to the official map of Xinjiang, China*

Historical evolution and general situation of Qiongkushitai Village

(1) Location factors of nomadic settlements. The Qiongkushitai Village is located in the town of Karadara, Tex County, Yili Kazakh Autonomous Prefecture (locally known as “Five townships”), 90 km from the town government. It is a typical traditional pastoral village. The village’s nomadic settlements are located within about 20 km of the Qiongkushitai River. Its territory is endowed with unique nomadic conditions: wide and flat terrain, warm climate, broad grassland, and suitable for farming and grazing.The village of Qiongkushitai has been a nomadic land for many ethnic groups since ancient times. Since the Western Han Dynasty, Wusun Ancient Road has been an important passageway connecting the north and south of Tianshan Mountains. A flat plateau between two streams provided a good place for business tours to stop here, hoard materials, and convert materials. It makes it possible to get together with the road.

http://www.aloki.hu ● ISSN 1589 1623 (Print) ● ISSN 1785 0037 (Online)
DOI: http://dx.doi.org/10.15666/aeer/1706_1305713073

(2) Livelihood elements of nomadic settlements. The total area of the village is 136 km², of which the total area of pastures is 84.7 km², of which 18.0 km² is winter pastures, 27.9 km² is summer pastures, 31.6 km² is spring pastures, and 7.2 km² is clipping pastures. There is a total of 303 households with a total population of 1737. At present, animal husbandry and tourism are dominated by 967 people engaged in animal husbandry and 770 part-time workers in the tourism service industry, accounting for 44.3% of the total population. The development and utilisation of tourism resources in famous historical and cultural villages at the national level have promoted a major adjustment of the economic structure of traditional animal husbandry in this village. At the same time, the living standard of herdsmen has greatly improved, with the average annual income of herdsmen reaching 12,700 Yuan (Economic Income Statistics of Qionkushitai Village, 2017), which is currently higher than that of other pastoral villages in the same region. The development of tourism resources in pastoral areas has become a hot pursuit in the past five years. Traditional nomadic settlement resources have become scarce and precious. Local cultural heritages in the nomadic landscape of Qiongkushitai village, such as log settlements, inhabited grasslands, Wusun Pastoral Road, and the three revolutionary historical sites, reflect the evolution of nomadic cultural landscape and the results of local wisdom in the process of development (*Figure 2*).

Research method

The main methods used in this study are historical literature analysis, and settlement landscape theory and method. Based on the field survey data of alpine pastoral areas and data such as Xinjiang Urban-Rural Construction Yearbook, Yili Pastoral Area Industry Long-term Development Planning Platform, Xinjiang Pastoral Area Urban-Rural Development Planning Implementation Guidelines. This study aimed at qualitative interviews with local nomads in a one-year nomadic cycle to obtain field data.The author analysed the space-time trajectory, internal characteristics, external expression and inheritance characteristics of nomadic cultural landscapes. The development of alpine nomadic settlements is a dynamic process. It is necessary to evaluate the regional characteristics and social structure in geography. The characteristics of nomadic cultural landscapes are identified and summarised by using ecological geography and economic research methods.

Results

Typical characteristics of traditional nomadic space-time landscape

The characteristics of nomadic production and life, such as social unit self-organisation, individual adaptability, time order, and nomadic spatial hierarchy , are the main factors that drive the dynamic space-time picture of nomadic life. Time factors, space factors, and social organisation factors determine the behaviour of the individual nomadic family as a unit and is restricted by nomadic ability (technical conditions, family labour force). The grass-roots organisation “Awule” provides the restriction effect and comprehensive guarantee of social authority, and optimises the combination of nomadic production activities of individual families and the conversion behaviour under the restriction of grassland resources under different seasonal elevation gradients. In the space-time, a social organisation unit shows a multi-layer nested human landscape picture.

http://www.aloki.hu ● ISSN 1589 1623 (Print) ● ISSN 1785 0037 (Online)
DOI: http://dx.doi.org/10.15666/aeer/1706_1305713073

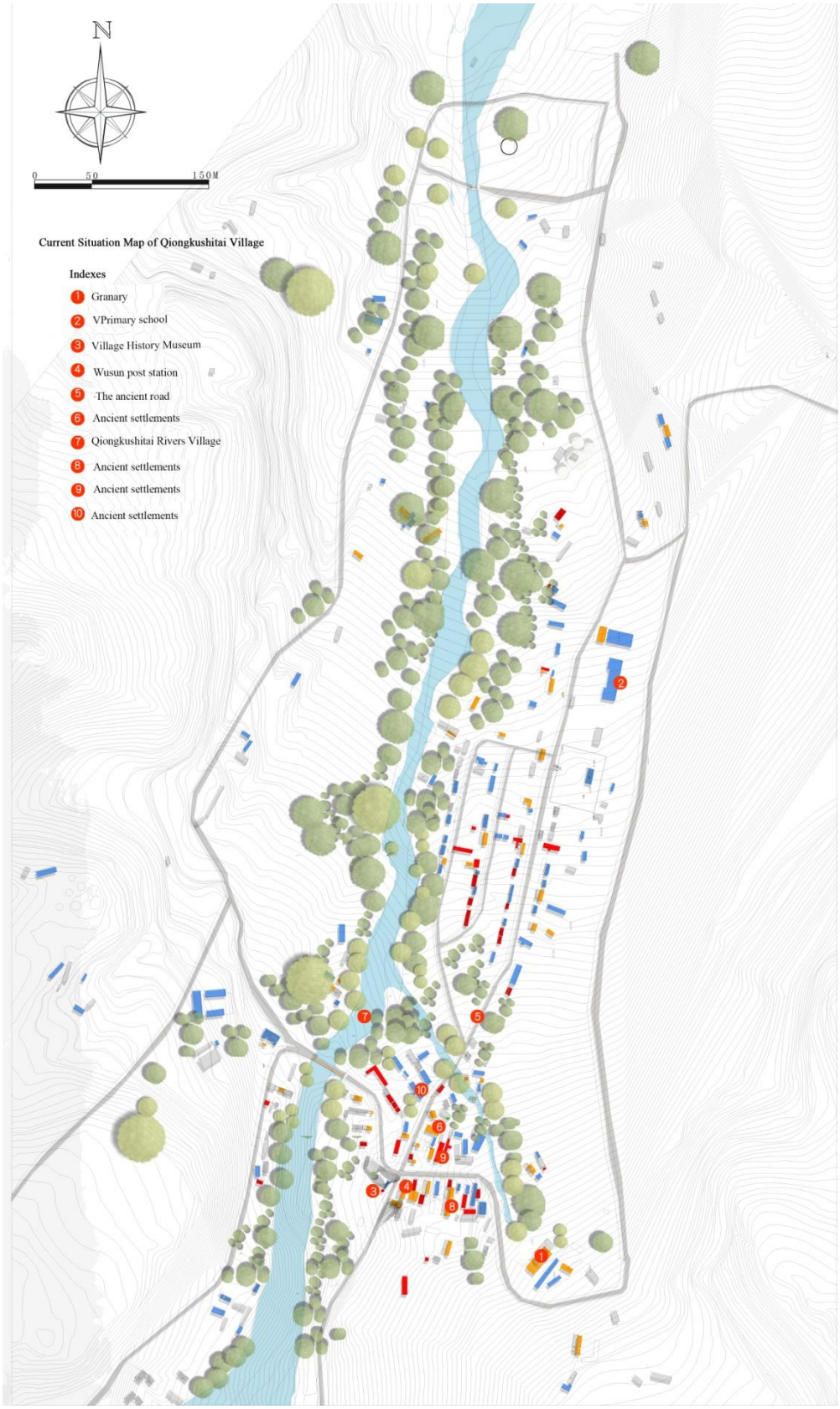

Figure 2. *Current Situation Map of Qiongkushitai Village. Self-drawn by author*

http://www.aloki.hu ● ISSN 1589 1623 (Print) ● ISSN 1785 0037 (Online)
DOI: http://dx.doi.org/10.15666/aeer/1706_1305713073

Adaptability of nomadic space-time picture under the restriction of resources

Mixed model of migration and fixed residence in nomadic space-time scene. The traditional nomadic settlement form is the minimum spatial scale and unit for nomads to engage in group production and life, and it is also the iconic element of nomadic space-time picture. The pasture and settlements show two spatial patterns of aggregation and dispersion in the nomadic complex space.The other is that pastures and residential space are very close. The main factors of the seasonal and elevation differences in the distribution of grassland resources, determine the aggregation and fragmentation of the spatial form of settlements. In the nomadic cycle of one year, the living space has obvious vertical zonality. The spatial characteristics of settlements reflect the interaction between human activities and the natural environment in the process of nomadic migration from the micro-scale. The living characteristics of QiongkuShitai Village are typical in the alpine pastoral areas of northern Xinjiang. The second-order flat area of the valley between the Wusun Ancient Road and the Qiongkushitai River is the first choice for the settlement. Its overall form is banded, local concentration, the courtyard is patchy, the building along the river and contour parallel to the horizontal expansion, but also perpendicular to the longitudinal continuation of the contour. The scattered distribution of residential groups corresponds with the characteristics of nomadic production.

Mobile residence under the adaptation of livelihood resources. In the process of periodic nomadic space-time picture, there are complete identifiable or identifiable nodes in nomadic adjacent time-space, and the residential space changes with the behaviour of the nomadic stage, which is the most typical. For example, when spring and autumn pastures migrate to winter pastures, the form of residence changes from “Haita” (temporary portable type of residential space) to “winter nest” (winter residence), and summer pastures-assembled felt houses for spring and autumn pastures. Portable features are suitable for long-distance transitional residences. Based on the period and frequency of building use, construction type and the degree of expenditure, residential forms can be divided into permanent type, stage type, and transition type.

The first choice of settlement location and the hierarchical selection mode of secondary dependency. Based on the analysis of the settlement layout and the shape of Qiongkushitai village, the relationship between settlement, grassland, and water source, the hierarchical selection model of nomadic settlement environment selection was put forward, which exists the first choice and the secondary dependency. The preferred land is usually flat valley, leeward, and riverside for water needs, especially in spring and autumn pastures, the attachment of water resources is stronger than summer pastures. Because of the high spatial distribution density of water resources in summer pastures and the short rainfall cycle in mountain areas, settlements are not necessarily built near the river, and usually have convenient commuting distance, which is also closely related to the quality of grassland resources.

Linear spatio-temporal presentation of nomadic spatio-temporal trajectory: transition track and pastoral space

Periodic transition is one of the core elements of the nomadic landscape, and it is also one of the symbols that nomadic space-time picture is strongly recognised. The track of nomadic space is jointly determined by three factors: the specific logic of the

http://www.aloki.hu ● ISSN 1589 1623 (Print) ● ISSN 1785 0037 (Online)
DOI: http://dx.doi.org/10.15666/aeer/1706_1305713073

spatial and temporal allocation of nomadic subjects and resources, the coherent time order, and the flexible nomadic behaviour.

(1) Stable and dynamic characteristics of nomadic spatio-temporal trajectory. The transitional pastoral path is the product of the nomadic spatio-temporal track. The migratory transition behaviour and the individual family each have the zonation and verticality of the spatial distribution of grassland resources, which determines the dynamics and stability of the nomadic spatio-temporal trajectory in which the nomadic herdsmen complete the periodic migration. Dynamics refers to a local strategy for nomads to deal with natural disasters in a short period of time. Stability refers to the maintenance of long-term effectiveness of high-quality grassland resources and the long-term stability of the selected and optimised linear space. The village of Qiongkushitai belongs to the alpine transition settlement, and the herdsmen have a certain time, order and route, so they have formed a transitional pastoral road with spatio-temporal order (Huang, 2013). Qiongkushitai pastoral road and the linear spatial scale is 110 km≤150 km. The characteristics of long transition route and strong stability; River valley meadow, Zhongshan grassland and alpine grassland are distributed at an average altitude of 1020 m≤2680 m. The long-span characteristics of grassland resources at elevation determine the dynamics of nomadic trajectory (*Figure 3*).

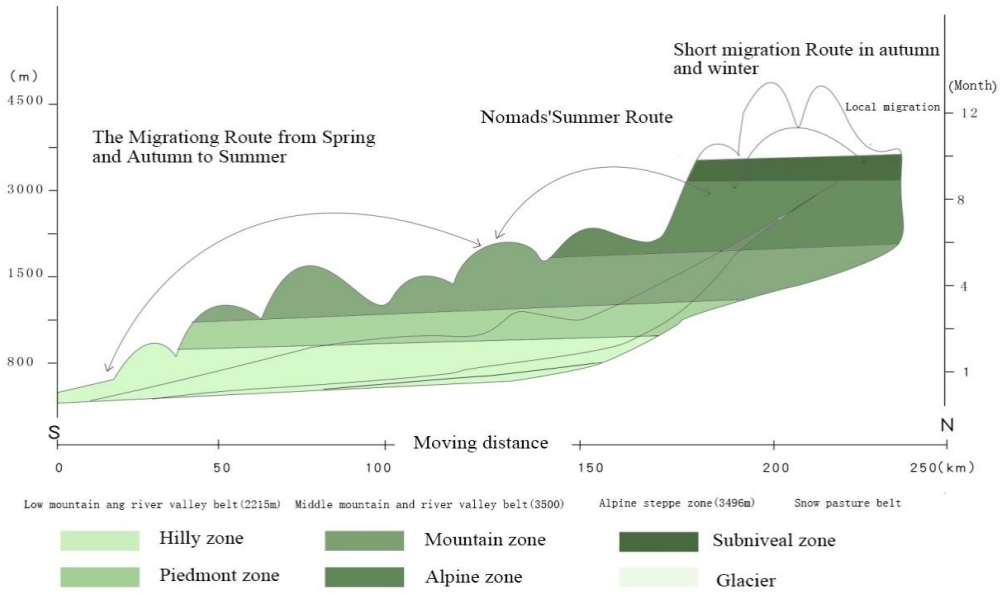

Figure 3. *The temporal and spatial trajectories of migration in the one year period of Nomadic settlement. Author redraws according to the illustration of "Transition and Modernity of Nomadic Society: Mountain Volume" (Center for Rural Environmentsocial studies, 2015)*

(2) Long-term "life path" and short-term "daily path" of nomadic spatio-temporal track.The construction of a nomadic path over long period is the representation of nomadic ecological strategy in time-space coordinates. The long-term migration strategy of alpine nomads has opened up a long-term "Life path" for their seasonal migration to summer pastures. It embodies the ecological values of the sustainable development of nomadic behaviour and ensures the possibility of the existence of nomadic picture for a long time.

http://www.aloki.hu ● ISSN 1589 1623 (Print) ● ISSN 1785 0037 (Online)
DOI: http://dx.doi.org/10.15666/aeer/1706_1305713073

To a large extent, nomadic individuals can flexibly adjust their nomadic behaviour and make strategic decisions on the basis of following their natural laws, which is specifically reflected in the dynamic characteristics of the“daily path”in a short period of time. The nomadic "daily path" with one year as the cycle, constitutes a long period of “life path” of nomadic production in alpine grasslands. The short period of "daily path" is the basic element of the inheritance of grassland production mode, which ensures the continuation of the long period of "life path". The short-term “daily path” promotes the existence of the long-term “life path”of nomadic activities. Each type of nomadic behaviour can find its place on the timeline of the "daily path" for a short period of time, and the nomadic activity per unit time presents a typical spatial or behavioural reflection on the “fragment order” (*Table 1*).The short-term nomadic track depicts the seasonal movement trends of nomads in the daily periods, such as the change of space place in spring, summer, autumn, and winter, the change of living space, and daily nomadic behaviour such as lambing, fattening, grabbing, captivity, stocking.

Table 1. *Space-time order of “daily track” in a short period. Self drawn by author*

Time order / Spatial order	1	2	3	4	5	6	7	8	9	10	11	12
Migration space		Winter ranch		Spring ranch		Summer ranch		Autumn ranch		Winter ranch		
Track of Daily Path												
Seasonal-felt Room Fixed Residence												
Everyday behaviour Node	Lambing Captivity.		Preliminary Transfer, Disease		Build houses, Catch fat, Shear wool, Repair horseshoe, etc.			Transition period Dismantling, Rransportation, etc.			Lambing Captivity	

Multi-level nesting law of nomadic space-time picture

Nomadic production and life are subject to regional resource conditions (the types of grassland resources and their advantages and disadvantages are distributed in time and space). The self-characteristics of nomadic production and life (the family is the unit + the group mutual aid mode of work) and other factors determine that the nomadic space-time picture shows the law of nesting at different levels. It is embodied in the nesting of the local order of the social unit and the nesting of the multi-level “centre-periphery” on the spatio-temporal scale of the relationship between man and land.

Local order nesting of social units: the organic combination of individual family and “awule” organization. “Local order nesting of activities” emphasises the relationship between human activities and the allocation of space-time resources needed for their

http://www.aloki.hu ● ISSN 1589 1623 (Print) ● ISSN 1785 0037 (Online)
DOI: http://dx.doi.org/10.15666/aeer/1706_1305713073

occurrence, implying the temporal arrangement and spatial combination of the resources needed behind human behaviour. Drawing lessons from its achievements, the interpretation of the grass-roots organisational order of nomadic society is helpful to explore the wisdom of building resilience in the construction of nomadic ecological civilisations. The grass-roots organisation of "Awule" is the builder of the grass-roots order in the traditional nomadic society. The stability of grass-roots social organisations depends on the ownership of the means of production, so each basic nomadic unit has its own territory, tribes have their own transfer routes, and customary law has a strong binding effect on life and production, to ensure the order of social organisations on a large scale.

The relationship between the nomadic family unit and "Awule" organisational behaviour is often inclusive and restricted. A series of activities of nomadic families aim at achieving individual goals: survival and nomadic activities are necessary to maintain survival on an individual scale. The goal of "Awule" organisational behaviour to maintain the basic order of nomadic society is to continue the fundamental activities of the existence and inheritance of such organisations and solidified into a symbolic organisational model. Nomadic individuals and organisations depend on each other and are reflected in the combination of nomadic behaviours. The nomadic space-time picture carries the activities of family, society, and nature. The temporal and spatial allocation of grassland resources and space is relatively regular in nomadic behaviour. It profoundly depicts the ecological process of the utilisation of regional resources by nomadic subjects under the influence of internal order.

Multi-level "center-sub-core-boundary" nested model of man-earth relationship on the spatio-temporal scale. The traditional settlement is not only the material support of human survival, but also the symbol of living space. The location of settlement integrates the basic elements of human survival mode and environmental choice (Han, 2008). Under the alpine nomadic production and lifestyle, the settlement environment follows the upward order of the vertical space of alpine grassland,medium alpine grassland, valley grassland, secondary grassland, and the diffusion law of successive circles in horizontal space. Nested model shows the relationship between human and land in Alpine nomadic ecological environment. This paper summarises the basic model of traditional man-land relationship in nomadic alpine settlements: horizontal multi-layer spatial nesting, and vertical upward "centre-sub-core-boundary" nesting model with grass migration. Through the settlement environment selection of Qiongkushitai village, the human-land relationship of nomads in the small watershed of Qiongkushitai River is re-examined. The multi-layer spatio-temporal nesting model of nomadic circle is a dynamic model which is used to deal with the complex nomadic ecosystem in balance and sustainability. For example, the location relationship between a family's multiple places of residence and grassland determines the man-land relationship model of settlement location.

Discussion

Conflict and Integration: the evolution of traditional nomadic space-time picture

The nomadic space-time picture is rooted in the space-time accumulation of specific natural conditions and human activities. It is reproduced through a series of time and space chain continuity such as a series of forms and activities in a specific alpine grassland space. Nomadic resources determine the type of production and mode of

http://www.aloki.hu ● ISSN 1589 1623 (Print) ● ISSN 1785 0037 (Online)
DOI: http://dx.doi.org/10.15666/aeer/1706_1305713073

production, while the nomadic mode of production determines the way of life and social organisation of nomads; lifestyle and social organisation form condense into grassland culture and art. The spatial layout of traditional nomadic production and life and the timing arrangement of production and life are deeply affected by industrial economic structure, family type, and technological innovation. When the traditional material space disappears (or the function is replaced), the nomadic picture may be presented in another way: the appearance of exhibition, fragmentation, and symbolization, then the grassland nomadic picture loses the vitality of expression and the path of inheritance.

The drive of national policy of settlement and pastoral settlement

Spatial compression and linear fracture of traditional nomadic spatio-temporal trajectory.

Functional displacement of the pastoral resources. "For nomadic animal husbandry, the key factor in its development lies not in possession of grassland, but more in the right of migration, only in the process of migration with the sun" (Han, 2003). Stable and continuous transition is the most essential feature of nomadic culture. When grassland resources are replaced by conversion paths are separated, conflicts between pastoral roads and modern roads overlap, nomadic production becomes settled captivity. As a result, the seasonal and spatial continuity of grassland nomadic space-time track is broken, the nomadic chain is fragmented, and the traditional nomadic picture shows fragmentation. The spatial evolution and utilisation pursuit of the production behaviour of the micro-subject is the main internal driving force for the emergence of the above situation.

Under the background of rapid urbanization, the traditional nomadic space is compressed, the nomadic trajectory is discontinuous. There are problems in the process of redistribution and use of grassland resources. Breaking the traditional model of resource allocation, the traditional model of life and production has been gradually dispelled, and the living form has moved to a fixed-point residence with the adjustment of production structure. The grassland boundary is fenced, the grassland resource type is single, the grassland space radius becomes smaller, and the controllable transition path is shortened. The people and cycles who undertake the transition are compressed (domestic work is replaced by employment, mechanised transfer, shortening the transition period), the surplus labour force begins to shift to other livelihoods, and grassland resources no longer carry the current multi-level demand. Captive cultivation, the replacement of resources in different places, and animal husbandry production have broken the barriers to the distribution of spatial resources, cross-regional grassland artificial planting and anti-ecological farmland grass which is one of the ways to solve forage resources.

Individual needs drive the elimination of local intelligence system in traditional pastoral society

The settlement of nomads is a profound process of social and cultural change. The settlement of nomads is a process of re-socialisation which differs greatly from their traditional social culture. Nomads will face, and inevitably experience, the problem of re-socialisation in the process of settlement. The traditional form of "Awule" and "family unit co-production", which exists in nomadic social organisations, has been replaced by "individual family type, modern employment production". Standardisation

http://www.aloki.hu ● ISSN 1589 1623 (Print) ● ISSN 1785 0037 (Online)
DOI: http://dx.doi.org/10.15666/aeer/1706_1305713073

and accuracy of time cost. The mechanised, long-distance, cross-regional fragmented transfer behaviour model promotes the local wisdom spread in the traditional transition field to be concentrated and dispelled, and the compression of time and space promotes the acceleration of the rhythm of time and the overcoming of the hindrance of time to space caused by it. The temporal and spatial constraints and incentives of nomadic daily life trajectory have been reduced. In order to better control the time cost, animal husbandry production promotes the standardisation of time cost: the quantification and accuracy of time in the nomadic process, but with the change of phenology, the time cost is controlled within a certain range. The precision of the cost of production and living commute is reflected in the evolution of residence: from a nomadic lifestyle to settlement, felt house, semi-settlement wooden house, settlement log building, mobile residence mode and semi-settlement residence that changes with the season, the ownership of grassland changes, evolution from mobile and semi-settled to permanent residence. In order to meet the current needs of life, herdsmen build so-called high-end living environments, but it destroys the balance of the grassland water system, vegetation, and biology. The grasslands with slopes were filled with raw soil foundations, and modern buildings were built on them. These buildings are incompatible with the original grassland environment (*Figure 4*).

Figure 4. *Driven by information, technology, and materials, it is possible to expand the living space. Photographed by author*

Qiongkushitai's settlement began construction in 2012. It was originally a traditional settlement and reserved feed land in the spring and winter seasons of the pastoral village. The scale of the settlement is larger than that in other areas. Apart from the first and second group of displaced herdsmen, some land (originally pasture) for other later settled herdsmen has been reserved. There are 87 settled herdsmen. The land composition of settlements is composed of public grassland and pasture of

http://www.aloki.hu ● ISSN 1589 1623 (Print) ● ISSN 1785 0037 (Online)
DOI: http://dx.doi.org/10.15666/aeer/1706_1305713073

herdsmen. In order to apply for settlements, the herdsmen need to take out three acre of land use rights to solve the land problem occupied by settlements. The settlement is facing the river, has convenient transportation, relatively open terrain, and good natural scenery. The water construction of the settlement is one of the projects of combining agriculture and animal husbandry, and developing pastoralists by settling down. The government hopes to develop tourism resources to solve the livelihood problems of some pastoralists after settling down. At present, it has attracted local herdsmen and some people from surrounding counties to settle and run tourism. In early 2017, the settler, Karze, transferred 56 acres of summer pasture and 15 acres of reserve pasture from his home. There is a steady income every year. At the same time, a Herdsman's Folk Tourist Inn has been built in the original settlements (not planned into the new settlements). Kalze has three children; two younger sons are in high school in Turks County. He and his daughter usually run their own camps together, and they are relatively wealthy. In the new settlement, Kalze has its own housing (herdsmen put out 60,000 yuan of construction funds, local government provides planning and other supporting facilities for the construction). When applying for settlement, the property rights of the housing belong to herdsmen, but no real estate certificate has been issued yet. For example, to protect herdsmen and social stability, settlements cannot be rented and sold out in principle, but there will be individual herdsmen to rent settlements to other people. The settled herdsmen have adapted to the present life, and the family economic structure has increased the additional income of the tertiary industry (pastoral transportation, tourism services, special breeding.) from the original pure income of animal husbandry production.

As a typical case, Qiongkushitai village is demonstrated in this area. Under the advocacy of governments at all levels, nomadic villages with tourism resources and convenient transportation conditions have begun a new round of “symbolic economy” rising, which repeats the upsurge of the urban symbolic economy. As famous villages and towns of history and culture, and as the main body of official protection law, their names will attract a large number of tourists. With the improvement of other factors, nomadic cultural resources, as an economic resource, enhance the income of local residents and also become a sign of local cultural tourism. The rise of symbolic economy is due to two reasons: one is the economic decline within the city relative to the suburbs. Cultural symbols play an important role in the process of the revival of the urban centre area. The other reason is the expansion of the investment field, and culture has become a new investment field. It has become a scarce resource for internal demand and external pursuit of dividends. Through the investigation of production and life in Qiongkushitai Village, it is concluded that the mode of production has changed after settlement.The traditional local wisdom heritage, agglomeration and decomposition, and the new life and production mode have become popular in pastoral areas (*Figure 5*).

Conflict and fusion: dynamic adjustment of nomadic picture induced by new technology

Technological change is a traditional factor of production for the sustainable and rapid development of settlements. Through the author's field investigation in the Tex River Basin, it is found that the application and popularisation of the new technology in the traditional pastoral areas is the main driving factor for the renewal or integration

http://www.aloki.hu ● ISSN 1589 1623 (Print) ● ISSN 1785 0037 (Online)
DOI: http://dx.doi.org/10.15666/aeer/1706_1305713073

of the traditional nomadic space-time picture, and it is also the inevitable result of social development. Extract t Three types of typical case descriptions:

(1) The innovation of production tools. The changes of transit vehicles: traditional horses, camels, flat cars vs horses and motor vehicles; innovation of weeding tools: traditional long handle sickle vs weeding mechanisation;

(2) Innovations of living facilities. The change of communication tools: horseback riding to transmit information vs modern mobile communication tools. The location of water resources and access to the reduced constraints: water-by-water living vs now long-distance across the space-time construction of water facilities. Comprehensive strategies to deal with disasters: local wisdom word of mouth vs rapid emergency system, mechanised long-distance commuting support.

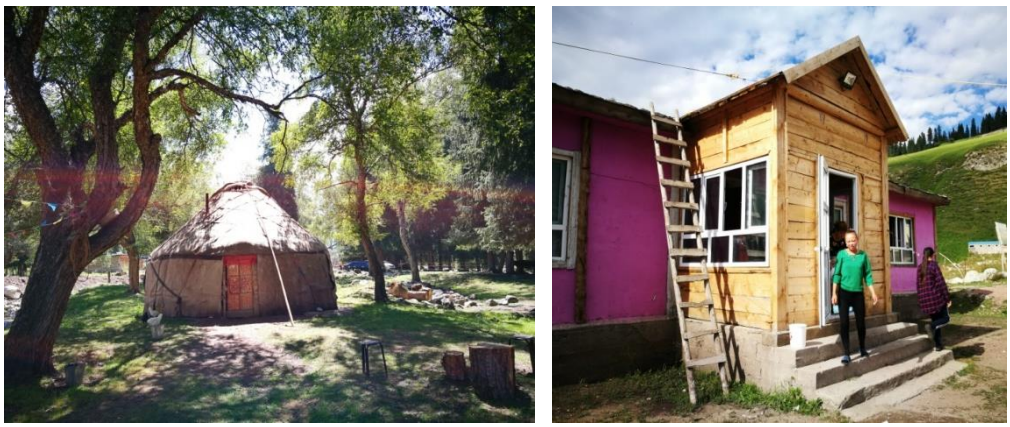

Figure 5. *Forms of Residence before and after Settlement. Photographed by author*

(3) Technology and Market Drive. Adjustment of nomadic landscape in the post-industrial era dynamic adjustment of nomadic space-time picture (cultural landscape). When the frequency of new technological innovation is accelerated, and the popularisation of application is high, the process of material production reflects the compression of space-time picture and the rapid change of spatio-temporal feeling. For example, the multi-level coverage of vehicles and roads has made it possible to explore potential sites for the spatial expansion of nomadic production. At that time, the boundary of space was broken through, and the cost of time was reduced to the lowest in geography and space. The acceleration of capital flow and exchange speed reconstructed the spatial picture of nomadic production and consumption. Post-modernist grassland nomadic cultural landscape, time and space experience is the result of the combination of various social resources. The traditional nomadic time and space picture has three possibilities: collage, reconstruction, and disintegration. Driven by external and internal forces, it has completely broken the rank, stability, and continuity of traditional time and nomadic space, and only the fragmentation of sporadic temporal and spatial characteristics has been retained and reconstructed in a single way. The segmented nomadic space-time picture is used as a display label and developed as a selling point (Harvey, 2003). The cultural tourism brand promotes the experience of this nomadic cultural landscape of a pastoral village by saying: return to the most primitive nomadic settlement: experience nomadic slow life here. It is not a real experience of grassland nomadic time and space, but an illusory experience

http://www.aloki.hu ● ISSN 1589 1623 (Print) ● ISSN 1785 0037 (Online)
DOI: http://dx.doi.org/10.15666/aeer/1706_1305713073

created by the collusion of capital and media to satisfy the strange experiences of tourists. We should understand the unique cultural landscape characteristics contained in different agricultural and cultural heritage and provide method support for the rational utilisation and protection of important agricultural, and cultural heritage in our country (Hu et al., 2018).

Conclusion

Based on the case study of Nomadic Settlements in the Turks River Basin, this paper puts forward two characteristics in the space-time landscape of nomadic alpine settlements: (1) the adaptability of nomadic space and time landscapes under the constraints of alpine grassland resources, and (2) multi-level nesting rule of nomadic space-time landscape. Nomads are passively adapted to regional resources in the process of nomadic production and life. However, the nomadic subjects dynamically adjust their nomadic behaviour according to their own conditions (population, technology, grassland resources), and form a multi-layer organic combination of mutual social organisations, periodic stability of nomadic space and time landscape, living scale and multi-point migration of space.

Driven by national policy, individual demand, technology, and market guidance, nomadic settlements in the process of urbanisation are out of order in production and life of traditional nomadic society, and their ecological carrying capacity is weakened due to the combined effects of external and internal forces such as policy implementation, modern technology, and market guidance. The short-term “daily path” of nomadic production and life characteristics will be decomposed or split, the long-term “life path” will disappear or be replaced by another form, and the “modern" nomadic landscape will be reconstructed. The reconstructed nomadic landscape is embodied in two aspects: (1) nomadic economy under the change of economic structure is no longer the core of family income. Herdsmen need to manage other economic types on the basis of traditional nomadic production to meet the needs of grassland resources, ecological deterioration, and improvement of living standards. For example, they are engaged in settled agricultural production, tourism, and non-agricultural production in cities, and (2) technology and market incentives, traditional natural nomadism to fixed-point non-organic pasture change. The practice of fixed-point industrialised captive farming production mode in traditional alpine pastoral areas has reduced the frequency and distance of transfer, weakened the constraints of grassland space-time resource allocation, weakened the original intimate relationship between nomads and livestock, water and grass, and gradually diluted or replaced the traditional alpine nomadic culture.

This article serves as a starting point for further research concerning the development and change of lifestyle for the nomads after settlement life and fixed grazing production. We should select samples with universality to ensure the validity of the universality of the research results. Due to the highly dispersed spatial pattern of nomadic alpine settlements and the constraints of researchers' energy and academic levels, it is hoped that comparative studies can be carried out in the latter part of the study to select sufficient samples within the geographical units of small watersheds to make up for the deficiencies in this study. Suggestions for future research would be to pay attention to the integration and adjustment of the old and new nomadic scenery in nomadic alpine settlements, retain the essence of the traditional, nomadic, and

http://www.aloki.hu ● ISSN 1589 1623 (Print) ● ISSN 1785 0037 (Online)
DOI: http://dx.doi.org/10.15666/aeer/1706_1305713073

humanistic landscape or the reconstruction of the new cultural landscape of the main components to meet the needs of the new era. The assessment of regional ecological environment carrying capacity of nomadic settlements should be paid attention to by scholars, and the research on the coordinated development of nomadic livelihood needs and ecological protection should be deepened to explore the theoretical and practical path suitable for the protection and development of traditional nomadic settlements.

Acknowledgements. This study benefited from the opinions of the reviewers and editors of the journal, and was supported by the National Social Science Foundation of China: "Study on Landscape Protection of Oasis Historic and Cultural Villages and Towns" (14G126) and "Study on the Cooperative Mechanism of Water Cultural Heritage Protection and Rural Revitalization in Xinjiang Section of the Silk Road" (19XMZ046).

REFERENCES

[1] Center for Rural Environmentsocial studies (2015): Transition and Modernity of Nomadic Society: Mountain Volume. – China Social Science Press, Bejing.
[2] Chen, X. J. (2014): Response and influence of grassland property rights change in Kazakh pastoral society - Taking Fuyun County of Altay, Xinjiang. – Journal of Xinjiang University (Philosophy, Humanities and Social Sciences Edition) 1: 62-67.
[3] Chen, X. J. (2017): Altai Mountain Nomads-Ecological Environment and Local Knowledge. – Social Science Literature Press, Beijing.
[4] Chen, X. J. (2019): Lost grassland sacredness: perspective of grassland ecology crisis. – Journal of Culture Vertical and Horizontal 2: 128-135.
[5] Crown, M. (2005): Cultural Geography. – Nanjing University Press, Nanjing.
[6] Cui, Y. (2002): Resocialization of nomadic settlements. – Journal of Xinjiang Normal University (Philosophy and Social Sciences Edition) 4: 76-82.
[7] Doumani, P. N., Frachetti, M. D., Beardmore, R., Schmaus, T. M., Spengler, R. N., Maryashev, A. N. (2015): Burial ritual, agriculture, and craft production among Bronze Age pastoralists at Tasbas. – Journal of Archaeological Research in Asia 2: 17-32.
[8] Felr, S. (1994): Drought, Nomadism, Grassland. – China Construction Industry Press, Beijing.
[9] Gong, X., Tao, P., Jia, S., Ming, L. (2011): Progress in spatiotemporal trajectory clustering. – Journal of Progress in Geographic Science 30(05): 522-528.
[10] Han, M. (2003): On the interaction between animal husbandry production and environment in northern China. – Journal of Geographical Research 1: 89-95.
[11] Han, M. (2008): Settlement Environment Selection and Human-Earth Relations in the West Liaohe River Basin since Holocene. – Journal of Geographic Studies 5: 118.
[12] Han, M. (2013): On the southward moving of agricultural technology and the economic center of ancient China by northern migrants. – Journal of Study of Chinese History 4: 117.
[13] Harvey, D. (2003): Study of the Origin of Cultural Change in the Post-modern Situation. – Beijing Commercial Press, Bejing.
[14] Hills, E. (2009): On Tradition. – Shanghai People's Press, Shanghai.
[15] Honeychurch, W. J. (2014): Alternative complexities: the archaeology of pastoral nomadic states. – Journal of Archaeological Research 4: 277-326.
[16] Hu, Z., Qingwen, M., Peilin, L. (2018): Exploration of Cultural Landscape Characteristics Recognition of Agricultural Cultural heritage. – Journal of Economic Geography 38(02): 187.

http://www.aloki.hu ● ISSN 1589 1623 (Print) ● ISSN 1785 0037 (Online)
DOI: http://dx.doi.org/10.15666/aeer/1706_1305713073

[17] Huang, S. Y. (2013): Pastoral inspection in alpine transition style: taking Turks County as an example. – Journal of Yili Normal University (Social Science Edition) 33(02): 27-35.
[18] Jia, W. M. (2018): Archaeological Observation of Prehistoric Nomadic Life: Analysis of Prehistoric Settlements in the Western Tian shan Mountains of Xinjiang. – Journal of Study of Western Regions 03: 63-75.
[19] Li, J., Yu, J. H. (2019): The change and adjustment of traditional culture of nomadic ethnic groups: a case study of Nadamu, Henan County, Qinghai Province. – Journal of Qinghai Social Sciences 2: 180-185.
[20] Meng, F. L. (2017): Study on spatial characteristics, types and causes of formation of historical and cultural villages and towns of oasis type in Xinjiang. – Guizhou Ethnic Studies 38(01): 95.
[21] Ptackova, J. (2011): Sedentarisation of Tibetan nomads in China: Implementation of the nomadic settlement project in the Tibetan Amdo area; Qinghai and Sichuan Provinces. – Journal of Pastoralism 9: 68-77.
[22] Shi, Z., Chen, T. T., Storozum, M. J., Liu, F. W. (2019): Environmental and social factors influencing the spatiotemporal variation of archaeological sites during the historical period in the Heihe River basin, northwest China. – Journal of Quaternary International 25: 34-42.
[23] Torrens, R., Hong, C., Yan, P. (2010): Time budget and hunting and collection techniques. – Journal of Southern Heritage 1: 147-153.
[24] Yang, N. (2004): Prospects for local knowledge, local sense and cross-regional research. – Journal of Tianjin Social Science 6: 119-125.

http://www.aloki.hu ● ISSN 1589 1623 (Print) ● ISSN 1785 0037 (Online)
DOI: http://dx.doi.org/10.15666/aeer/1706_1305713073

EFFICACY OF *EICHHORNIA CRASSIPES, PISTIA STRATIOTES* AND *NYMPHAEA LOTUS* IN THE BIOSORPTION OF NICKEL FROM REFINERY WASTEWATER

UGYA, A. Y.[1,2] – IMAM, T. S.[3] – HUA, X.[1] – MA, J.[1*]

[1]*College of New Energy and Environment, Jilin University, Changchun, China*

[2]*Department of Environmental Management, Kaduna State University, Kaduna State, Nigeria*

[3]*Department of Biological Sciences, Bayero University Kano, Kano State, Nigeria*

**Corresponding author*
e-mail: jincaima@jlu.edu.cn

(Received 24th May 2019; accepted 28th Aug 2019)

Abstract. The invasive nature of *Eichhornia crassipes, Pistia stratiotes*, and *Nymphaea lotus* is worrisome because they tend to dominate the economic and ecological region of the aquatic environment, hence the need for their eco-friendly utilization. This research is aimed at assessing the efficacy of *Eichhornia crassipes, Pistia stratiotes* and *Nymphaea lotus* as a low-cost absorbent for the biosorption of Nickel (Ni^{2+}) from refinery wastewater. Refinery wastewater was collected from the effluent point of Kaduna Refining and Petrochemical Company (KRPC). The selected macrophytes were characterized using Fourier transform infrared (FTIR) spectroscopy. Biosorption of Ni^{2+} from the wastewater and aqueous Ni^{2+} solution was performed under factors such as contact time, particle size, absorbent dosage, pH and Ni^{2+} concentration. The Langmuir equation and Freundlich isothermal were used in determining absorption equilibrium while pseudo-first and pseudo-second-order were used to determined adsorption kinetics. The result obtained shows that Ni^{2+} absorption by the selected macrophytes is greatly influenced by contact time, particle size, absorbent dosage, pH and Ni^{2+} concentration with high efficiency recorded in the removal of Ni^{2+} from refinery wastewater. Both Langmuir equation and Freundlich isothermal gives a nearly perfect fitting for adsorption of Ni^{2+} for all the selected macrophytes signifying favorable Ni^{2+} absorption. Pseudo-second-order kinetic model gives nearly perfect fitting than the pseudo second-order kinetic model signifying that adsorption of Ni^{2+} by the selected macrophytes is due to the physical and chemical reaction. The selected macrophyte can be effectively utilized as low-cost biosorbents for the removal of Ni^{2+} from Refinery wastewater.
Keywords: *Langmuir equation, adsorption kinetics, macrophytes, heavy metals, invasive species*

Introduction

Aquatic macrophytes are plants that can survive in or around water bodies (Osti et al., 2018). They are classified into four major groups namely emergent macrophyte, floating leaves macrophyte, submerged macrophyte and free-floating macrophyte (Bordoloi et al., 2015; Galal and Farahat, 2015; Pulzatto et al., 2018). The ability of *Eichhornia crassipes, Pistia stratiotes* and *Nymphaea lotus* to overtop ecological and economic zones of aquatic ecosystem is alarming due to the negative impact it causes on economic yield, human health and aquatic organisms (Lamb et al., 2016). These macrophytes hindered the penetration and flow of sunlight due to their ability to extend over water bodies (Ugya, 2015; Ma et al., 2019).

The control of *Eichhornia crassipes, Pistia stratiote* and *Nymphaea lotus* is necessary because of the macrophytes to interfere with water flow and sunlight penetration which is detrimental to flora and fauna inhabiting the habitat (Ugya et al., 2019a). Different control method has been used against these plants in the past but

http://www.aloki.hu ● ISSN 1589 1623 (Print) ● ISSN 1785 0037 (Online)
DOI: http://dx.doi.org/10.15666/aeer/1706_1307513087

recent research has focused on how to utilize the benefit associated with these plants (Lareo, 1981; Chen et al., 2012; Hanks et al., 2015).

The incessant discharge of heavy metal polluted water into the environment is worrisome due to their persistence nature and ability to accumulate in the food chain (Dudgeon et al., 2006; Lintern et al., 2016; Ugya and Imam, 2017; Liu et al., 2018). The menace associated with heavy metal pollution is endemic in developing countries where industries channel wastewater into nearby water bodies either untreated or not properly treated due to their proximity to these water bodies (Ugya et al., 2015; Desrosiers et al., 2019). The wastewater produced by oil refinery industries is rich in heavy metals particularly Ni^{2+} which pose serious toxicity at low-level exposure (Hughes et al., 2015; Ugya et al., 2019b). These heavy metal have been shown by many researchers to be associated with chronic and acute toxicological effects to man and detrimental to organisms such as algae, plants, micro-organisms and other vertebrate and invertebrate animals (Costa-Boeddeker et al., 2018; Wang et al., 2018; Xun et al., 2018; Ugya et al., 2019c). It is thereby paramount to treat wastewater before discharge (Zhang and Anadon, 2013; Tong and Elimelech, 2016).

A variety of techniques are available for the treatment of wastewater before discharging into water bodies, many of which have contributed in minimizing pollution resulting from chemical industries, but biosorption is gaining acceptance owing to the fact that most researchers have revealed the potentiality of some bio sorbents to effectively remediate wastewater with high heavy metal pollutants (Nahar et al., 2018; Ugya et al., 2019d). Biosorption is a remediation technology that depends on the mechanism of heavy metal accumulation by agricultural or biological adsorbents from an aqueous solution as a result of the binding site present on this bio sorbents (He and Chen, 2014; Ileri et al., 2014; Abdic et al., 2018). *Eichhornia crassipes, Pistia stratiote*, and *Nymphaea lotus* have been utilized by researchers such as in the biosorption of Cd, Pb, Cr, etc but little or no literature exists for the biosorption of Ni^{2+} from refinery wastewater. This study is aimed at assessing the efficacy of *Eichhornia crassipes, Pistia stratiote* and *Nymphaea lotus* as a low-cost absorbent for the biosorption of Ni^{2+} from refinery wastewater.

Materials and methods

Sample collection, authentication, and preparation

Eichhornia crassipes, Pistia stratiote, and *Nymphaea lotus* were collected at three different abandon pond of proximity located at Kinkinau, Ungwar Ma'azu, Kaduna South Local Government, Kaduna State, Nigeria. The macrophytes were handpicked with the aid of hand gloves, identified using relevant guides (Gusain and Suthar, 2017; Hanafiah et al., 2018) and authenticated in the herbarium of the Department of Botany, Ahmadu Bello University Zaria, Kaduna State, Nigeria and Department of Plant Biology, Bayero University Kano, Kano State, Nigeria (*Table 1*) (Ugya et al., 2019e). The macrophytes were cut into small pieces, washed twices with borehole water and once using distilled water and were dried in sunlight for 48 h. The macrophytes were grounded using a mechanical blender (Greenis, FGR-8840) and sieved accordingly to obtain Large (60 mm) and small (30 mm) particle sizes of *Eichhornia crassipes, Pistia stratiote*, and *Nymphaea lotus*. The macrophytes powders were stored separately in an airtight container before use. Refinery wastewater sample was collected from the effluent point of Kaduna Refining and Petrochemical Company (KRPC), which is in

http://www.aloki.hu ● ISSN 1589 1623 (Print) ● ISSN 1785 0037 (Online)
DOI: http://dx.doi.org/10.15666/aeer/1706_1307513087

Chikun Local Government, Kaduna State, Nigeria around latitude 10° 24' 36.18" N and longitude 7° 29' 17.37" E. The physicochemical and heavy metal characteristic of the wastewater was determined using standard method.

Table 1. *Test plants used for biosorption*

SN	Plants	Common name	Accession number
1	*Eichhornia crassipes*	Water Hyacinth	3268
2	*Pistia stratiotes*	Water Lettuce	1977
3	*Nymphaea lotus*	Water lily	BUKHAN0356

Sorbent characterization

The functional groups present in the treated and untreated *Eichhornia crassipes, Pistia stratiote* and *Nymphaea lotus* were determined using Fourier transform infrared (FTIR) spectroscopy (Rosales et al., 2016).

Effect of particle size and contact time on Ni^{2+} adsorption

The effect of contact time and particle size was determined by placing 2 g of *Eichhornia crassipes,* 0.5 g *Pistia stratiote* and 1 g *Nymphaea lotus* of two different particle sizes (30 mm (small size) and 60 mm (large size)) in separately in 250 ml containing 4.5 mg/l of Ni^{2+}. The mixture was shaken at 150 rpm using a magnetic shaker at a constant temperature of 25 °C. Each set of flasks were agitated for 20, 30, 40, 50 and 60 min, respectively (*Fig. 1*). The sample was then filtered and Ni^{2+} concentrations of the solution were determined using AAS techniques. Biosorption capacity was thus calculated using the mass balance formula below (Amer et al., 2015):

$$q = \frac{v(C_i - C_e)}{m} \quad \text{(Eq.1)}$$

where q (mg/g) is the adsorption capacity, C_i and Ce are the initial and final concentrations (mg/l) of Ni^{2+}, respectively, v (l) is the volume of aqueous and m is the weight (mass) of adsorbent (g).

Percentage removal was calculated using the formula:

$$q\%\ uptake\ = \frac{(C_0 - C_e)}{C_0} \cdot 100 \quad \text{(Eq.2)}$$

where C_0 and C_e are the initial and final concentrations (mg/l) of Ni^{2+} ions in the sample before and after shaking, respectively.

Effect of Ni^{2+} concentration on adsorption process

To 250 m/l of solution containing 10 mg/l, 20 mg/l, 30 mg/l, 40 mg/l, and 50 mg/l of Ni, 1 g of dried *Eichhornia crassipes,* 0.5 g *Pistia stratiote*, and 1 g *Nymphaea lotus* were added separately and the mixture was shaken at 150 rpm using a magnetic shaker at a temperature of 25 °C for 1 h. The sample was then filtered and Ni^{2+} concentrations of the solution were measured using AAS techniques. Ni^{2+} percentage reduction of Ni^{2+} was thus calculated using *Equation 2* (Kumar et al., 2018).

http://www.aloki.hu ● ISSN 1589 1623 (Print) ● ISSN 1785 0037 (Online)
DOI: http://dx.doi.org/10.15666/aeer/1706_1307513087

Figure 1. *Experimental setup during culture*

Effect of pH on Ni^{2+} adsorption process

The absorption ability of the macrophytes was compared at a pH of 2, 4, 6, 7, and 8 by placing 1 g of dried *Eichhornia crassipes,* 0.5 g *Pistia stratiote* and 1 g *Nymphaea lotus* in 250 ml each of the solution of Ni^{2+} at 4.5 mg/l and shaken at 150 rpm for 1 h using a magnetic stirrer at a constant temperature of 25 °C. The samples were filtered and the Ni^{2+} concentrations of the solution were determined using AAS technique. Ni^{2+} percentage removal was calculated using *Equation 2* (Kumar et al., 2018). The pH of the solution was adjusted using 0.01 N NaOH and HNO_3 (Salim et al., 2016).

Effect of absorbent dosage

The effect of adsorbent dosage was studied by placing 1 g, 2 g, 3 g, 4 g, and 5 g each of *Eichhornia crassipes,* 1 g, 2 g, 3 g, 4 g, and 5 g each *Nymphaea lotus* and 0.2 g, 0.4 g, 0.6 g, 0.8 g and 1 g of *Pistia stratiotes* where placed in to a solution 250 ml of solution containing 4.5 mg/l of Ni^{2+} and shaken at 150 rpm using a magnetic stirrer for 1 h at a constant temperature of 25 °C. The samples were filtered and the Ni^{2+} concentrations of the solution were determined using AAS technique. Ni^{2+} Percentage removal was calculated using *Equation 2* (Kumar et al., 2018).

Adsorption equilibrium study

Adsorption equilibrium study for Ni^{2+} using *Eichhornia crassipes, Pistia stratiote* and *Nymphaea lotus* was performed by placing 1g, 2g, 3g, 4g, and 5g of *Eichhornia crassipes,* 1 g, 2 g, 3 g, 4 g, and 5 g *Nymphaea lotus* and 0.2g, 0.4g, 0.6g, 0.8g and 1g of *Pistia stratiotes* in 5 mg/l, 10 mg/l, 15 mg/l, 20 mg/l and 25mg/l of Ni^{2+} and shake at using a magnetic stirrer at 150 rpm for 24 h at a constant temperature of 25 °C. The samples were filtered and the Ni^{2+} concentrations of the solution were determined using AAS technique. Langmuir and Freundlich isotherm models were thus determined using *Equations 3* and *5* (Manikandan et al., 2016).

Langmuir equation is represented below:

http://www.aloki.hu ● ISSN 1589 1623 (Print) ● ISSN 1785 0037 (Online)
DOI: http://dx.doi.org/10.15666/aeer/1706_1307513087

$$\frac{1}{q_x} = \frac{1}{b_i q_f} \cdot T_e + \frac{1}{q_f} \quad \text{(Eq.3)}$$

The equation above was adopted from Kumar et al. (2018), where T_e is equilibrium Ni^{2+} concentration in solution, q_f is maximum Ni^{2+} absorbed per unit weight of *Eichhornia crassipes, Pistia stratiote*, and *Nymphaea lotus*, b_i is affinity adsorbate. The value of q_f and b_i is determined from the slope and intercept. Z_l is the separation factor and is calculated using the formula below:

$$Z_l = \frac{1}{1 + b_i T_g} \quad \text{(Eq.4)}$$

where T_g is the initial concentration of Cr^{3+} and Pb^{2+} in the solution.

Freundlich Isotherm is represented below:

$$log(q_x) = log(K_f) + \frac{1}{r\ log\ T_e} \quad \text{(Eq.5)}$$

The equation was adopted from Wang et al. (2010), where K_f is *Freundlich* constant r is *Freundlich* coefficient, and K_f and r are determined by plotting a graph of q_x against T (Wang et al., 2010).

Adsorption kinetics

Adsorption kinetics is fundamental in describing the character of an absorbent. To ascertain the mechanism involved in the adsorption of Ni^{2+} by *Eichhornia crassipes, Pistia stratiote*, and *Nymphaea lotus*. Pseudo first-order and the pseudo second-order reaction was used (Ho and McKay, 1998).

The pseudo first-order is represented below:

$$log(q_i - q_t) = log\ (q_i) - \frac{K_i T}{2.303} \quad \text{(Eq.6)}$$

The pseudo second order is represented below:

$$\frac{T}{q_t} = \frac{1}{K_2 q_2} + \frac{T}{q_2} \quad \text{(Eq.7)}$$

Data treatment

Experiments were conducted in triplicate and data were analyzed statistically and presented as mean ± standard deviation as represented by error bar on figures. The Residual Sum of Squares (RSS) was determined for both adsorption kinetic and isotherm models to check error in model fittings. All analysis was done using BM SPSS statistics version 23

Results and discussion

Physicochemical and heavy metal characteristic of KRPC wastewater

The result represented in *Table 2* shows the heavy metal and physicochemical status of KRPC wastewater. Most of the parameters determine such as total suspended solid (TSS), electrical conductivity (EC) and hardness were within the permissible limit for

http://www.aloki.hu ● ISSN 1589 1623 (Print) ● ISSN 1785 0037 (Online)
DOI: http://dx.doi.org/10.15666/aeer/1706_1307513087

wastewater except for total dissolve solid (TDS), alkalinity and turbidity which were above the permissible limit as such indicate pollution resulting from organic and inorganic pollutants. Cu^{2+} and Ni^{2+} were within the permissible limit whereas Cd^{2+} was above the permissible limit and could pose a threat to aquatic organisms. Although, it has been reported that Ni^{2+} is an essential element needed for different biochemical and physiological pathways in biological systems, excess amount of Ni^{2+} could lead to cellular and tissue damage leading to a variety of disease. The detectable amount of Ni^{2+} in the wastewater was within the permissible limit of wastewater by WHO but this could still pose a treat to man and other aquatic organisms because of the persistence's nature of Ni^{2+} and subsequent bioaccumulation in the food chain (Tchounwou et al., 2012).

Table 2. *The physicochemical and heavy metal characteristic of KRPC wastewater*

SN	Parameter	Mean ± SD	WHO limit (2004)
1	pH	7.2 ± 0.75	6-9
2	Turbidity	15.4 ± 5.02	5
3	EC	65.5 ± 13.42	50-500
4	TDS	1219.50 ± 680.70	500
5	TSS	8.40 ± 6.40	30
6	Alkalinity	98.95 ± 43.57	50
7	Hardness	30.96 ± 17.23	500
8	Nitrate	2.07 ± 0.50	-
9	Chloride	33.28 ± 7.94	-
10	Ni^{2+}	0.54 ± 0.08	3.0
11	Cd^{2+}	0.09 ± 0.06	0.003
12	Cu^{2+}	1.77 ± 0.27	2.0

Mean ± SD are expressed in mg/l except for pH (no unit)

Characterization of biosorbent

The result obtains for the surface characterization of biosorbent using FTIR spectrum analysis (*Fig. 2*) shows that the functional group changes occur in the profile of *Eichhornia crassipes, Pistia stratiotes and Nymphaea lotus* following the absorption of Ni^{2+}. The peak at nearly 3500 cm^{-1} for untreated *Eichhornia crassipes, Pistia stratiotes, and Nymphaea lotus* represent the presence of OH^-group, this OH^-group has been stretched to Ni-OH bond in treated *Eichhornia crassipes, Pistia stratiotes, and Nymphaea lotus* as shown in *Figure 2*. The peak at nearly 1500 cm^{-1} shows the presence of CH_2 functional group in untreated *Eichhornia crassipes, Pistia stratiotes and Nymphaea lotus,* the stretching seen in the same peak for treated *Eichhornia crassipes, Pistia stratiotes and Nymphaea lotus* is attributed to the absorption of Ni^{2+}. The peak at nearly 3000 cm^{-1} for untreated *Eichhornia crassipes, Pistia stratiotes, and Nymphaea lotus* shows the presences of C-H functional group which stretches in the treated *Eichhornia crassipes, Pistia stratiotes and Nymphaea lotus* due to absorption of Ni^{2+} (Sujatha et al., 2013).

http://www.aloki.hu ● ISSN 1589 1623 (Print) ● ISSN 1785 0037 (Online)
DOI: http://dx.doi.org/10.15666/aeer/1706_1307513087

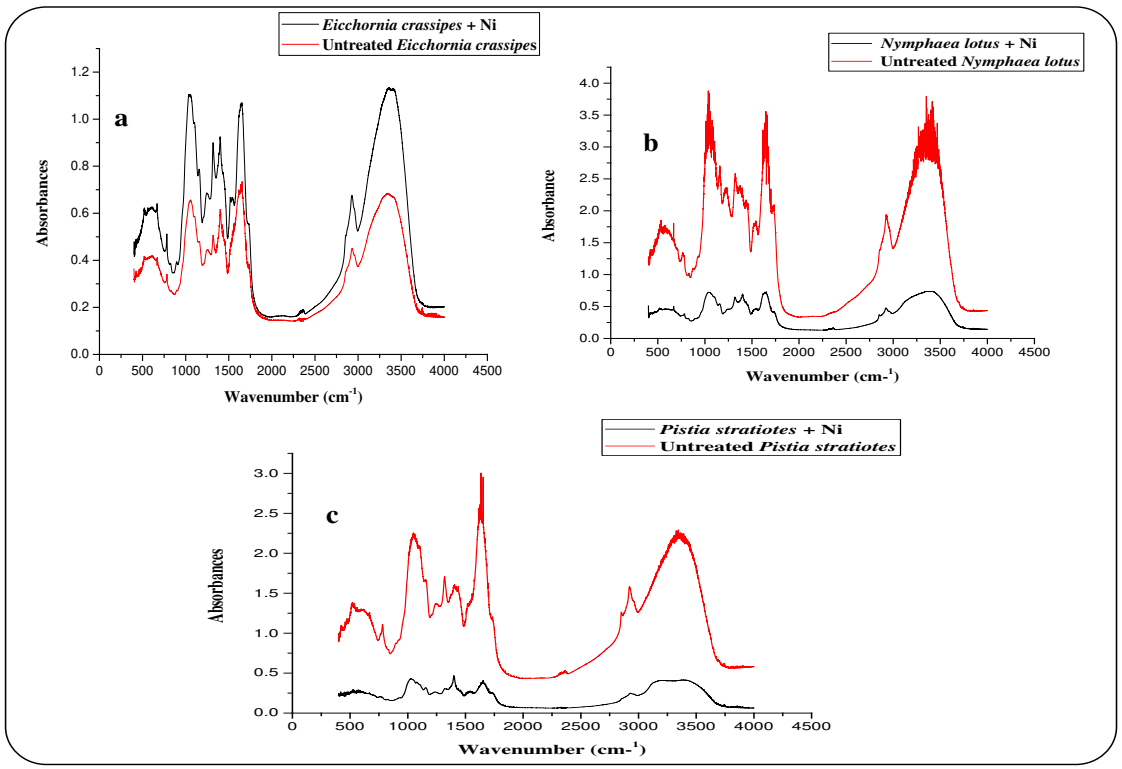

Figure 2. *FTIR of (a) Eichhornia crassipes (b) Nymphaea lotus and (c) Pistia stratiotes before and after treatment*

Effect of Ni^{2+} concentration and absorbent dosage on adsorption process

The result in *Figure 3a* shows that Ni^{2+} absorption by the macrophytes is strongly influenced by the change in Ni^{2+} concentration because significant difference exists between the absorption of Ni^{2+} by *Eichhornia crassipes, Pistia stratiotes and Nymphaea lotus* at Ni^{2+} concentration of 10 mg/l if compared to 20 mg/l, 30 mg/l, 40 mg/l, and 50 mg/l. This enhanced absorption of Ni ion at a concentration of 10 mg/l by the 3 absorbents is attributed to the fact that at the concentration of 10 mg/l the 3 absorbents have available binding sites to bind Ni^{2+} but these binding sites become saturated as metal ion increase (Feng et al., 2011). The result in *Figure 3b* shows that a significant difference exists in Ni^{2+} absorption for various dosages of *Eichhornia crassipes, Pistia stratiotes, and Nymphaea lotus.* These increasing trend of Ni^{2+} absorption with increasing dosage could be attributed to favorable pH of the solution and the fact that an increase in dosage of absorbent lead to increase of the maximum Ni^{2+} uptake due to availability of more binding site.

Effect of particle size, contact time and pH on Ni absorption

The result obtained shows higher reduction efficacy of Ni^{2+} from aqueous solution by biosorbent of larger size (60 mm) if compared to smaller sizes (30 mm) (*Fig. 4*). This significant differences could be attributed to the fact that the 60 mm biosorbent is porous as such have larger surfaces which permit increase Ni^{2+} absorption while 30 nm biosorbent is less porous as such have fewer surfaces whereas the absorption potential of a biosorbent depends on the number of surfaces of the biosorbent (Migahed et al.,

http://www.aloki.hu ● ISSN 1589 1623 (Print) ● ISSN 1785 0037 (Online)
DOI: http://dx.doi.org/10.15666/aeer/1706_1307513087

2017). The highest reduction efficacy of Ni^{2+} was recorded at a pH of 4 (*Fig. 5a*) this result could be attributed to the fact that the solubility of Ni is at pH 4 or the binding site of *Eichhornia crassipes, Pistia stratiotes and Nymphaea lotus* were activated at pH of 4. The result obtained in (*Fig. 5b*) shows that Ni^{2+} was effectively adsorbed by *Eichhornia crassipes, Pistia stratiotes, and Nymphaea lotus* at all the contact time when exposed to refinery wastewater, this could be attributed to the fact that binding is available via out the period of adsorbent exposure to Ni^{2+}. The availability of binding site via out the period of adsorbent exposure could be due to the fact that the competition of binding sites by Ni^{2+} is minimal even though other metals such as Cd^{2+}, Pb^{2+}, Cr^{3+}, etc were presences but the concentration is too low to cause competition for binding by the co-ions present (Nor, 1994).

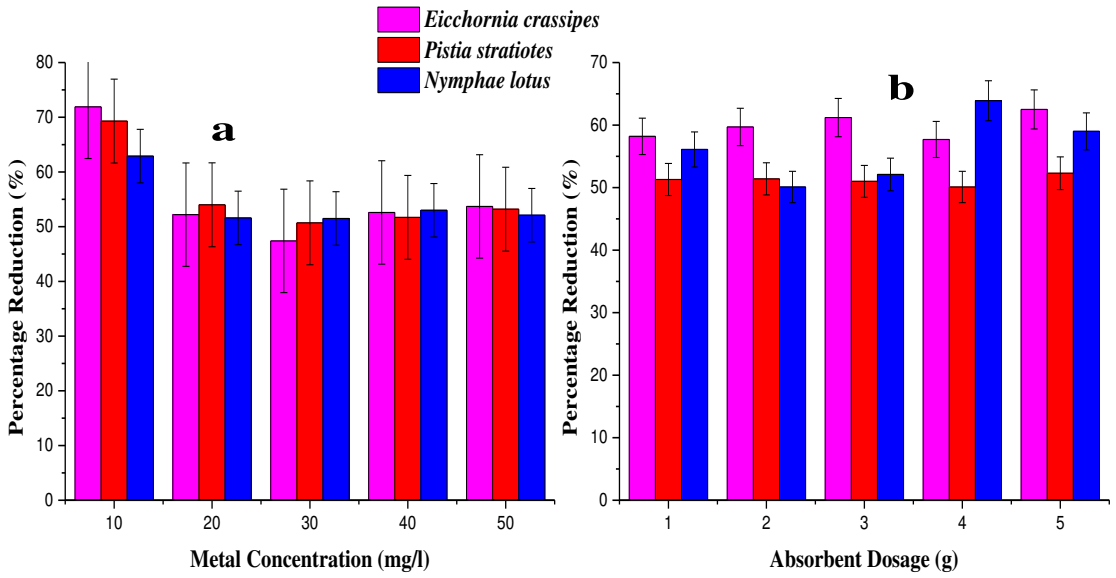

Figure 3. *Effect of absorbent dosage (a), metal concentration (b) on Ni biosorption*

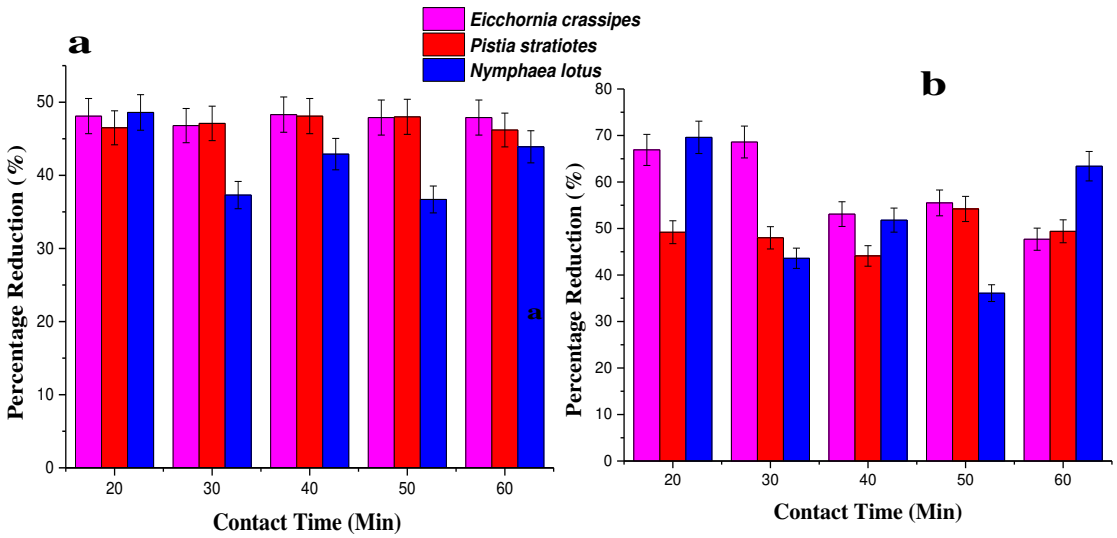

Figure 4. *Effect of contact time and particle size (a) small size (b) large size on the absorption of Ni*

http://www.aloki.hu ● ISSN 1589 1623 (Print) ● ISSN 1785 0037 (Online)
DOI: http://dx.doi.org/10.15666/aeer/1706_1307513087

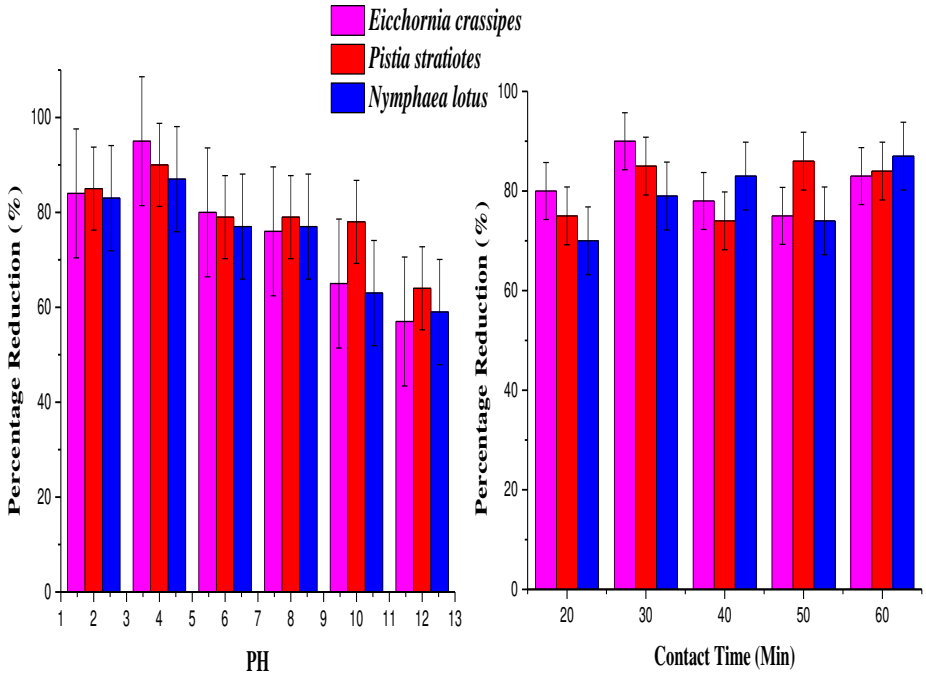

Figure 5. *(a) Effect of PH on Ni absorption from aqueous solution. (b) Effect of contact time on the Ni absorption from refinery wastewater*

Adsorption isotherms

The Langmuir model obtained gives a nearly perfect fitting for adsorption of Ni^{2+} for *Eichhornia crassipes* (0.9933) and *Pistia stratiotes* (0.9898) while poor-fitting was recorded for *Nymphaea lotus* (0.9311). Although it can be concluded that the adsorption of Ni^{2+} onto *Eichhornia crassipes, Pistia stratiotes, and Nymphaea lotus* correlated well with Langmuir equation with the relationship becoming more linear with R^2 value closer to 1 (Amer et al., 2015; Ugya et al., 2019c). The Freundlich model shows a nearly perfect fitting for absorption of Ni^{2+} for *Eichhornia crassipes* (0.9978), *Pistia stratiotes* (0.9885) and *Nymphaea lotus* (0.9753) with a high n value of (3.1) *Eichhornia crassipes*, (2.7) *Pistia stratiotes* and (2.3) *Nymphaea lotus* which are all within the range of 1-10 signifying favourable absorption of Ni^{2+} for *Eichhornia crassipes*, *Pistia stratiotes* and *Nymphaea lotus* (Rosales et al., 2016; Poonam et al., 2018).

Adsorption kinetics

The biosorption of Ni^{2+} by *Eichhornia crassipes, Pistia stratiotes*, and *Nymphaea lotus* was determined at various initial concentration and time interval for the understanding of biosorption mechanism (Manikandan et al., 2016). The result obtained shows that the Pseudo Second-order kinetic model gives nearly perfect fitting for *Eichhornia crassipes* (0.9194) and *Pistia stratiotes* (0.9645) but poor fitting for *Nymphaea lotus* (0.7329). The correlation coefficient shows that the absorption of Ni by *Eichhornia crassipes, Pistia stratiotes*, and *Nymphaea lotus* follows the pseudo second-order kinetic model because poor fittings of (0.7501) *Eichhornia crassipes,* (0.5678) *Pistia stratiotes* and (0.5404) *Nymphaea lotus* was obtained for pseudo-first order model. This result obtained signifies that that the absorption of Ni^{2+} to *Eichhornia crassipes, Pistia stratiotes* and *Nymphaea lotus* is due to chemical and physical reaction

http://www.aloki.hu ● ISSN 1589 1623 (Print) ● ISSN 1785 0037 (Online)
DOI: http://dx.doi.org/10.15666/aeer/1706_1307513087

of Ni^{2+} and the surface of *Eichhornia crassipes, Pistia stratiotes* and *Nymphaea lotus* which leads to the formation of bond between the valence electron and the negative surface charge of *Eichhornia crassipes, Pistia stratiotes* and *Nymphaea lotus* to attain an equilibrium state (Low et al., 1994).

Conclusion

The petrochemical refining industry is the world largest contributor of Ni^{2+} particularly in developing countries like Nigeria where wastewater containing Ni^{2+} is discharged into nearby water bodies without proper treatment due to low technologic know-how. It is thereby paramount for petrochemical refineries to utilize the availability of aquatic macrophytes as low-cost absorbents for further treatment of its wastewater before discharge since most industries are unwilling to establish a costly convectional treatment plant.

The comparison of the present study and other research as shown in *Table 3*, shows that although *Eicchornia crassipes* have the highest Ni^{2+} reduction efficiency both *Pistia stratiotes* and *Nymphaea lotus* can also be used effectively as biosorbents for the removal of Ni^{2+} from refinery wastewater.

Table 3. *Comparison of biosorption efficiency of Ni^{2+} by different macrophytes*

SN	Macrophytes	Heavy metal	Percentage reduction (%)	References
1	*Eichhornia crassipes*	Ni^{2+}	90	Present study
2	*Pistia stratiotes*	Ni^{2+}	87	Present study
3	*Nymphaea lotus*	Ni^{2+}	86	Present study
4	*Lemna minor*	Ni^{2+}	82	Axtell et al. (2003)
5	*Hydrilla verticillata*	Ni^{2+}	92	Mishra et al. (2016)
6	*Salvinia sp*	Ni^{2+}	71.4	Dhir and Kumar (2010)

Further investigation is needed on how to increase the efficiency of these macrophytes for the uptake of Ni^{2+}**.** More research needs to be done using more macrophytes such as *Salvinia sp, Azolla sp, Ludwigia sp,* etc to discover more novel eco-friendly cheap biosorbent for Ni^{2+} removal from wastewater.

Acknowledgments. The first author appreciates Petroleum Technology Development Fund (PTDF) Nigeria for providing the fund and enabling environment to carry out the research.

REFERENCES

[1] Abdic, S., Memic, M., Sabanovic, E., Sulejmanovic, J., Begic, S. (2018): Adsorptive removal of eight heavy metals from aqueous solution by unmodified and modified agricultural waste: tangerine peel. – International Journal of Environmental Science and Technology 15: 2511-2518.

[2] Amer, M. W., Ahmad, R. A., Awwad, A. M. (2015): Biosorption of Cu(II), Ni(II), Zn(II) and Pb(II) ions from aqueous solution by Sophora japonica pods powder. – International Journal of Industrial Chemistry 6: 67-75.

http://www.aloki.hu ● ISSN 1589 1623 (Print) ● ISSN 1785 0037 (Online)
DOI: http://dx.doi.org/10.15666/aeer/1706_1307513087

[3] Axtell, N. R., Sternberg, S. P. K., Claussen, K. (2003): Lead and nickel removal using Microspora and Lemna minor. – Bioresource Technology 89: 41-48.
[4] Bordoloi, S., Yamsani, S. K., Garg, A., Sreedeep, S., Borah, S. (2015): Study on the efficacy of harmful weed species Eicchornia crassipes for soil reinforcement. – Ecological Engineering 85: 218-222.
[5] Chen, H.-G., Peng, F., Zhang, Z.-Y., Zhang, L., Zhou, X.-D., Liu, H.-Q., Wang, W., Liu, G.-F., Xue, W.-D., Yan, S.-H., Xu, X.-F. (2012): Effects of engineered use of water hyacinths (Eicchornia crassipes) on the zooplankton community in Lake Taihu, China. – Ecological Engineering 38: 125-129.
[6] Costa-Boeddeker, S., Le Xuan, T., Hoelzmann, P., de Stigter, H. C., van Gaever, P., Hoang Duc, H., Schwalb, A. (2018): The hidden threat of heavy metal pollution in high sedimentation and highly dynamic environment: assessment of metal accumulation rates in the Thi Vai Estuary, Southern Vietnam. – Environmental Pollution 242: 348-356.
[7] Desrosiers, M., Usseglio-Polatera, P., Archaimbault, V., Larras, F., Methot, G., Pinel-Alloul, B. (2019): Assessing anthropogenic pressure in the St. Lawrence River using traits of benthic macroinvertebrates. – Science of the Total Environment 649: 233-246.
[8] Dhir, B., Kumar, R. (2010): Adsorption of heavy metals by Salvinia biomass and agricultural residues. – International Journal of Environmental Research 4: 427-432.
[9] Dudgeon, D., Arthington, A. H., Gessner, M. O., Kawabata, Z.-I., Knowler, D. J., Leveque, C., Naiman, R. J., Prieur-Richard, A.-H., Soto, D., Stiassny, M. L. J., Sullivan, C. A. (2006): Freshwater biodiversity: importance, threats, status and conservation challenges. – Biological Reviews 81: 163-182.
[10] Feng, N., Guo, X., Liang, S., Zhu, Y., Liu, J. (2011): Biosorption of heavy metals from aqueous solutions by chemically modified orange peel. – Journal of Hazardous Materials 185: 49-54.
[11] Galal, T. M., Farahat, E. A. (2015): The invasive macrophyte Pistia stratiotes, L. as a bioindicator for water pollution in Lake Mariut, Egypt. – Environmental Monitoring and Assessment 187. https://doi.org/10.1007/s10661-015-4941-4.
[12] Gusain, R., Suthar, S. (2017): Potential of aquatic weeds (Lemna gibba, Lemma minor, Pistia stratiotes and Eichhornia sp.) in biofuel production. – Process Safety and Environmental Protection 109: 233-241.
[13] Hanafiah, M. M., Mohamad, N. H. S. M., Abd Aziz, N. I. H. (2018): Salvinia molesta and Pistia stratiotes as phytoremediation agents in sewage wastewater treatment. – Sains Malaysiana 47: 1625-1634.
[14] Hanks, N. A., Caruso, J. A., Zhang, P. (2015): Assessing Pistia stratiotes for phytoremediation of silver nanoparticles and Ag(I) contaminated waters. – Journal of Environmental Management 164: 41-45.
[15] He, J., Chen, J. P. (2014): A comprehensive review on biosorption of heavy metals by algal biomass: Materials, performances, chemistry, and modeling simulation tools. – Bioresource Technology 160: 67-78.
[16] Ho, Y. S., McKay, G. (1998): A comparison of chemisorption kinetic models applied to pollutant removal on various sorbents. – Process Safety and Environmental Protection 76: 332-340.
[17] Hughes, D. J., Shimmield, T. M., Black, K. D., Howe, J. A. (2015): Ecological impacts of large-scale disposal of mining waste in the deep sea. – Scientific Reports 5: #9985.
[18] Ileri, O., Cay, S., Uyanik, A., Erdura, N. (2014): Removal of common heavy metals from aqueous solutions by waste Salvadora persica L. branches (Miswak). – International Journal of Environmental Research 8: 987-996.
[19] Kumar, K., Patavardhan, S. S., Lobo, S., Gonsalves, R. (2018): Equilibrium study of dried orange peel for its efficiency in removal of cupric ions from water. – International Journal of Phytoremediation 20: 593-598.

http://www.aloki.hu ● ISSN 1589 1623 (Print) ● ISSN 1785 0037 (Online)
DOI: http://dx.doi.org/10.15666/aeer/1706_1307513087

[20] Lamb, J. B., Wenger, A. S., Devlin, M. J., Ceccarelli, D. M., Williamson, D. H., Willis, B. L. (2016): Reserves as tools for alleviating impacts of marine disease. – Philos Trans R Soc Lond B Biol Sci 371. https://doi.org/10.1098/rstb.2015.0210.
[21] Lareo, L. (1981): Growth of the water hyacinth (Eichhornia crassipes (Mart) Solms Laubach) in the tropics. – Archivos Latinoamericanos de Nutricion 31: 758-765.
[22] Lintern, A., Leahy, P. J., Heijnis, H., Zawadzki, A., Gadd, P., Jacobsen, G., Deletic, A., McCarthy, D. T. (2016): Identifying heavy metal levels in historical flood water deposits using sediment cores. – Water Research 105: 34-46.
[23] Liu, M., Du, P., Yu, C., He, Y., Zhang, H., Sun, X., Lin, H., Luo, Y., Xie, H., Guo, J., Tong, Y., Zhang, Q., Chen, L., Zhang, W., Li, X., Wang, X. (2018): Increases of total mercury and methylmercury releases from municipal sewage into environment in China and implications. – Environmental Science & Technology 52: 124-134.
[24] Low, K. S., Lee, C. K., Tai, C. H. (1994): Biosorption of copper by water hyacinth roots. – Journal of Environmental Science and Health. Part A: Environmental Science and Engineering and Toxicology 29: 171-188.
[25] Ma, J., Ugya, Y. A., Isiyaku, A. U., Hua, X., Imam, T. S. (2019): Evaluation of Pistia stratiotes fractions as effective larvicide against Anopheles mosquitoes. – Artificial Cells, Nanomedicine, and Biotechnology 47: 945-950.
[26] Manikandan, N. A., Alemu, A. K., Goswami, L., Pakshirajan, K., Pugazhenthi, G. (2016): Waste litchi peels for Cr(VI) removal from synthetic wastewater in batch and continuous systems: sorbent characterization, regeneration and reuse study. – Journal of Environmental Engineering 142(9).
[27] Migahed, F., Abdelrazak, A., Fawzy, G. (2017): Batch and continuous removal of heavy metals from industrial effluents using microbial consortia. – International Journal of Environmental Science and Technology 14: 1169-1180.
[28] Mishra, A., Tripathi, B. D., Rai, A. K. (2016): Packed-bed column biosorption of chromium(VI) and nickel(II) onto Fenton modified Hydrilla verticillata dried biomass. – Ecotoxicology and Environmental Safety 132: 420-428.
[29] Nahar, K., Chowdhury, M. A. K., Chowdhury, M. A. H., Rahman, A., Mohiuddin, K. M. (2018): Heavy metals in handloom-dyeing effluents and their biosorption by agricultural byproducts. – Environmental Science and Pollution Research 25: 7954-7967.
[30] Nor, Y. M. (1994): Phenol removal by Eichhornia crassipes in the presence of trace metals. – Water Research 28: 1161-1166.
[31] Osti, J. A. S., Henares, M. N. P., Camargo, A. F. M. (2018): The efficiency of free-floating and emergent aquatic macrophytes in constructed wetlands for the treatment of a fishpond effluent. – Aquaculture Research 49: 3468-3476.
[32] Poonam, S., Bharti, K., Kumar, N. (2018): Kinetic study of lead (Pb^{2+}) removal from battery manufacturing wastewater using bagasse biochar as biosorbent. – Applied Water Science 8: 119. https://doi.org/10.1007/s13201-018-0765-z.
[33] Pulzatto, M. M., Lolis, L. A., Louback-Franco, N., Mormul, R. P. (2018): Herbivory on freshwater macrophytes from the perspective of biological invasions: a systematic review. – Aquatic Ecology 52: 297-309.
[34] Rosales, E., Meijide, I., Tavares, T., Pazos, M., Sanroman, M. A. (2016): Grapefruit peelings as a promising biosorbent for the removal of leather dyes and hexavalent chromium. – Process Safety and Environmental Protection 101: 61-71.
[35] Salim, R. M., Chowdhury, A. J. K., Rayathulhan, R., Yunus, K., Sarkar, M. Z. I. (2016): Biosorption of Pb and Cu from aqueous solution using banana peel powder. – Desalination and Water Treatment 57: 303-314.
[36] Sujatha, P., Kalarani, V., Kumar, B. N. (2013): Effective biosorption of nickel(II) from aqueous solutions using Trichoderma viride. – Journal of Chemistry 2013: 7.
[37] Tchounwou, P. B., Yedjou, C. G., Patlolla, A. K., Sutton, D. J. (2012): Heavy metal toxicity and the environment. – Experientia Supplementum 101: 133-164.

http://www.aloki.hu ● ISSN 1589 1623 (Print) ● ISSN 1785 0037 (Online)
DOI: http://dx.doi.org/10.15666/aeer/1706_1307513087

[38] Tong, T., Elimelech, M. (2016): The global rise of zero liquid discharge for wastewater management: drivers, technologies, and future directions. – Environmental Science & Technology 50: 6846-6855.
[39] Ugya, A. Y. (2015): The efficiency of Lemna minor L. in the phytoremediation of Romi Stream: a case study of Kaduna Refinery and Petrochemical Company polluted stream. – Journal of Applied Biology and Biotechnology 3: 11-14.
[40] Ugya, A. Y., Imam, T. S. (2017): Temporal heavy metals variation in vegetables sampled at Kasuwan Mata, Kaduna Metropolis, Nigeria. – Malaysia Journal of Sciences 36: 63-74.
[41] Ugya, A. Y., Imam, T. S., Tahir, S. M. (2015): The efficiency of Pistia stratiotes in the phytoremediation of Romi Stream. – International Journal of Health and Research 5: 492-497.
[42] Ugya, A.Y., Imam, T.S., Ma, J. (2019a) Mini-review on the Efficacy of the use of Macrophytes as Larvicide against Mosquitoes. – Journal of Applied Botany and Food Quality. Accepted Article.
[43] Ugya, A. Y., Ahmad, A. M., Adamu, I. H., Giwa, S. M., Imam, T. S. (2019b): Phytoextraction of heavy metals and risk associated with vegetables grown from soil irrigated with refinery wastewater. – Journal of Applied Biology and Biotechnology 7: 14-19.
[44] Ugya, A. Y., Hua, X., Agamuthu, P., Ma, J. (2019c): Molecular approach to uncover the function of bacteria in petrochemical refining wastewater: a mini review. – Applied Ecology and Environmental Research 17: 3645-3665.
[45] Ugya, A. Y., Hua, X., Ma, J. (2019d): Biosorption of Cr^{3+} and Pb^{2+} from tannery wastewater using combined fruit waste. – Applied Ecology and Environmental Research 17: 1773-1787.
[46] Ugya, A. Y., Hua, X., Ma, J. (2019e): Phytoremediation as a tool for the remediation of wastewater resulting from dyeing activities. – Applied Ecology and Environmental Research 17: 3723-3735.
[47] Wang, S., Yang, S., Jin, X., Liu, L., Wu, F. (2010): Use of low cost crop biological wastes for the removal of Nitrobenzene from water. – Desalination 264: 32-36.
[48] Wang, X., Meng, X., Ma, Y., Pu, X., Zhong, X. (2018): The prediction of combined toxicity of Cu-Ni for barley using an extended concentration addition model. – Environmental Pollution 242: 136-142.
[49] Xun, E., Zhang, Y., Zhao, J., Guo, J. (2018): Heavy metals in nectar modify behaviors of pollinators and nectar robbers: consequences for plant fitness. – Environmental Pollution 242: 1166-1175.
[50] Zhang, C., Anadon, L. D. (2013): Life cycle water use of energy production and its environmental impacts in China. – Environmental Science & Technology 47: 14459-14467.

http://www.aloki.hu ● ISSN 1589 1623 (Print) ● ISSN 1785 0037 (Online)
DOI: http://dx.doi.org/10.15666/aeer/1706_1307513087

EFFECT OF PLANT ANATOMY ON DETERMINATION OF IRRIGATION STRATEGY UNDER THE ECOLOGICAL CONDITIONS OF SOILLESS AGRICULTURE

TUYLU, G. İ.[1*] – TUYLU, M.[2]

[1]*Department of Agricultural Structures and Irrigation, Faculty of Agriculture, University of Harran, Şanlıurfa, Turkey*

[2]*Graduated from Department of Biology, Institute of Science, University of Süleyman Demirel, Isparta, Turkey*

**Corresponding author*
e-mail: gokhantuylu@harran.edu.tr

(Received 25th May 2019; accepted 9th Sep 2019)

Abstract. In the study, it was aimed to determine the optimum irrigation issue by examining the anatomical features of *Lycopersicon esculentum* Mill. cv. Ceren cultivated in perlite by different irrigation treatments. Irrigation strategies were created based on the amount of drainage water and different irrigation applications were performed by using the drip irrigation system. For anatomical examination, cross sections were taken from the samples of the root, stem and leaf by microtome and examined by light microscopy. Some tissues in the root, stem, and leaf under over-irrigation and limited irrigation conditions changed significantly. As a result, the condition created by reducing 25% of irrigation water was determined as the optimum irrigation issue in four different irrigation applications. The amount of drainage under optimum condition was 10% of the amount of irrigation water applied. The study will contribute to the researchers to optimize the ecological condition in terms of irrigation in greenhouse.
Keywords: *costs, plant histology, stress, tomato, water management*

Introduction

Soil and freshwater resources are within the guarantee of economic and social order in society. Limited land and freshwater resources in the world and in Turkey have been freely used by mankind for many years without any problems. However, later it was negatively affected by climate change and abuse of agricultural land. On the other hand, requirement for the crop product increased due to rapid increase of population. Greenhouse improvement has been developed in order to reduce or eliminate these negative effects (Tuylu et al., 2018).

Today vegetable production in Turkey is 28.4 10^6 ton and ranks 4th in the world (Yanmaz et al., 2015). Approximately 87% of vegetable production is open and 13% is under cover (61,000 ha). Tomato which is one of the vegetables cultivated in Turkey ranks 1st with the amount of 11.8 10^6 ton (Anonymous, 2015).

Today soil and soilless agriculture can be performed depending on the irrigation and crop production technologies developed in the greenhouse. Soilless agriculture is more productive than soil agriculture and its production cost is half of soil agriculture (Özkan, 2014). On the other hand, as a result of using geothermal water resources to heat greenhouse, the concept of geothermal greenhouse has started to develop in Turkey and greenhouse areas have increased where geothermal resources are available. Karaali, Şanlıurfa is a province where geothermal water is used for greenhouse heating and plant

http://www.aloki.hu ● ISSN 1589 1623 (Print) ● ISSN 1785 0037 (Online)
DOI: http://dx.doi.org/10.15666/aeer/1706_1308913104

production is performed by using high technology in modern greenhouse (Deliboran et al., 2013).

In the studies carried out in plant cultivation in greenhouses, 30-35% free drainage condition has been commonly used for the irrigation applications mentioned in Winsor and Shwarz (1990), Lieth (1996), and Öztekin et al. (2017). Irrigation applications are effective on anatomical, morphological, physiological, etc. features of plants. Plants try to survive by developing many reversible or irreversible responses to all biotic or abiotic environmental factors they perceive as stress effect (Korkmaz and Durmaz, 2017).

In this way the plants become compatible with the factors of their habitat by developing stress responses. The responses developed by the plants to adapt to stress conditions can be due to changes in physiological, morphological, anatomical, etc. features. In cultivation, irrigation is one of the important abiotic factor for creation of ecological request of plants. If the accurate irrigation strategy can not be determined, water stress or drought stress condition occurs when over-irrigation or limited irrigation is applied. It causes anatomical changes in the plant. The changes can occur in various tissues. For this reason, it was aimed to determine the optimum irrigation issue for the variety studied by examining anatomical features of the plants cultivated by applying different irrigation issues. The study will contribute to the producers to determine accurate irrigation strategy in greenhouse and also support the researchers for literature to optimize the ecological condition in terms of irrigation in greenhouse in the World.

Materials and methods

The workout was carried out in polycarbonate covered greenhouse in Harran University, Şanlıurfa, Turkey during the spring of 2016. Tomato (*Lycopersicon esculentum* Mill. cv. Ceren) was cultivated in perlite by using drip irrigation system (*Fig. 1*). Anatomical studies were performed in the laboratories at the Department of Biology in Ankara University, Ankara, Turkey.

Figure 1. *An appearance of cultivation area in the greenhouse*

Şanlıurfa is situated in the south eastern Anatolia, Turkey. The workout area is 465 above sea level and located between 37°08’ N latitude and 38° 46’ E longitude (Demirok and Tuylu, 2017).

http://www.aloki.hu ● ISSN 1589 1623 (Print) ● ISSN 1785 0037 (Online)
DOI: http://dx.doi.org/10.15666/aeer/1706_1308913104

Şanlıurfa has a climate feature that is hot and dry in summers and warm in winters. Some climate values measured in and outside the greenhouse for the year 2016 when the workout was carried out are presented in *Tables 1* and *2*, respectively.

Table 1. *Some climate parameters measured in greenhouse in 2016*

Months	Decades	Temperature* (°C)	Relative humidity* (%)
April	2	23.4	30.6
	3	24.3	28.0
May	1	23.8	33.1
	2	27.9	30.0
	3	26.1	31.6
June	1	29.9	28.7
	2	31.0	26.8
	3	35.3	28.3
July	1	35.4	27.1
	2	35.8	28.7
	3	35.4	28.3

*Measured at 14:00 pm

Table 2. *Average climate values of 2016 and 1985-2016 long years (LY) in research area (Anonymous, 2016)*

Climate parameters		Max. temperature (°C)	Min. temperature (°C)	Ort. Temperature (°C)	Relative humidity (%)	Wind speed (2 m s^{-1})	Hours of sunshine (h)
Months	Year						
April	2016	32.7	7.4	20.6	36.1	1.4	8.90
	LY	22.5	10.8	16.2	53.4	1.5	7.55
May	2016	35.0	10.7	23.2	38.3	1.9	10.20
	LY	29.7	19.7	21.9	39.4	1.7	9.70
June	2016	42.0	18.9	29.8	28.0	1.9	11.90
	LY	34.9	21.0	28.3	35.2	2.0	11.95
July	2016	43.0	20.9	33.0	25.4	1.9	12.40
	LY	37.4	25.7	33.4	29.1	1.9	12.00

The workout was created as with 3 replications according to the random parcels plant pattern. 8 plants were cultivated in each pot. 2 of 8 plants cultivated were separated as edge effect. The samples were randomly taken from the remaining 6 plants and were examined.

Perlite cultivation condition was created by filling perlite in white styrofoam pots with sizes of 100 × 20 × 20 cm and drainage holes at the bottom. The seedlings were planted as 135 × 25 cm or more row spacing (2.9 plants m^{-2}) (*Fig. 1*). The nutrient solution used were passed through the filter and water meter by taking from the 1 ton-reservoir with centrifugal pump and was given to the plants by means of four-outlet drip irrigation system set up on pressure-regulated dripper in the 8 L h^{-1} flow on lateral pipe

http://www.aloki.hu ● ISSN 1589 1623 (Print) ● ISSN 1785 0037 (Online)
DOI: http://dx.doi.org/10.15666/aeer/1706_1308913104

(Ø16). The workout design was performed according to the open feed system and the nutrient solution that was drained was not used again.

In the study, the irrigation issues were planned according to free drainage condition (Winsor and Shwarz, 1990; Lieth, 1996; Öztekin et al., 2017). The issues were created according to four different irrigation levels which were I_1, I_2, I_3, and I_4. I_1 was the issue allowed 20% drainage of irrigation water. I_2, I_3, and I_4 were planned by proportionally reducing the amount of irrigation water used in I_1 issue (25, 50, 75%, respectively).

Nutrient solution was modified by using Arnon and Hogland (Tuylu et al., 2018). Stock A and Stock B solutions were separately prepared (*Table 3*). Electrical conductivity (EC) of nutrient solution was measured as 2. 5 dS m^{-1} by EC meter and pH of nutrient solution was fixed at 5.8-6.5 by using nitric acid. In soilless agriculture EC of nutrient solution has to be kept at optimum level. While high electrical conductivity (EC) reduces the yield affecting number of fruit, the diameter of fruit and the thickness of pericarp negatively, it causes increase of parameters of quality such as titratable acidity and the amount of dry substance which is easily soluble in water reducing glucose and lycopene (Söylemez and Pakyürek, 2017).

Table 3. *The content of element in nutrient solution (mg l^{-1})*

Stock A										**Stock B**	
N	P	K	S	Mg	Mn	B	Cu	Zn	Mo	Ca	Fe
210	31	234	64	48	0.5	0.5	0.02	0.05	0.01	200	2.8

The samples of plants vegetatively and generatively grown were kept in alcohol 70% for anatomical studies (*Figs. 2* and *3*). Dehydration was applied to small pieces taken from the lower, middle, and upper parts of the root, stem and, leaf by means of different ethyl alcohol series. Then, they were saturated with paraffin. The samples were embedded in paraffin blocks to take cross sections. 8-10 µm thick cross sections from the root and the leaf and 20-30 µm thick cross sections from the stem were taken by microtome Leica SM 2000 R. The cross sections were stained by safranin-fast green (Tuylu et al., 2017; Tuylu, 2018a). They were examined by light microscope Leica 1000 and the results were photographed by digital camera Leica EC3.

Figure 2. *Morphological appearance of the roots grown in different irrigation areas. A: I_1, B: I_2, C: I_3, D: I_4*

http://www.aloki.hu ● ISSN 1589 1623 (Print) ● ISSN 1785 0037 (Online)
DOI: http://dx.doi.org/10.15666/aeer/1706_1308913104

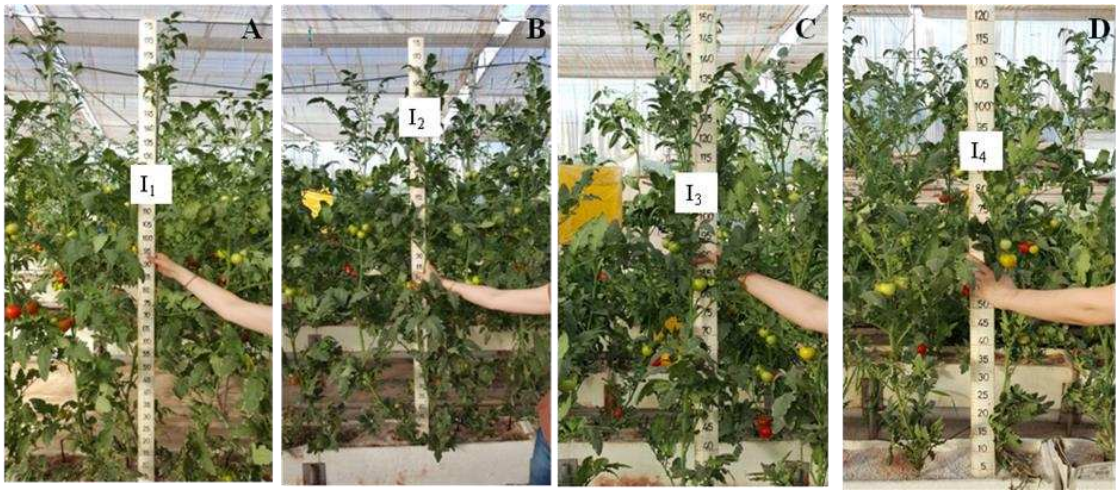

Figure 3. *Morphological appearance of the stems and leaves grown in different irrigation areas. A: I_1, B: I_2, C: I_3, D: I_4*

The photos are completely original. Biometric measurements were performed in some tissues by using Las v4.3 program. 3 groups in itself for each replication were created in the workout. The total number of cross sections taken from the plants and examined is 90 on 9 preparats for each replication and total 270 values of measurement were obtained by taking 3 from each section. The arithmetic mean of the values of measurements and mean standard error were calculated by using Microsoft Excel computer software and the results were anatomically expressed.

Results

Results for some anatomical features of the root, stem and leaf under different irrigation applications

Roots

The roots under all the conditions were formed by the cortex composed of wavy-walled cells surrounded by one-layered epidermis, one-layered endodermis, and one-layered pericycle. Prismatic crystals were observed (*Fig. 4*). Endodermis and pericycle were seen in some sections under I_2 and I_4 (*Figs. 5* and *6*). Both prismatic crystals and druz crystals were also seen under I_2. Prismatic crystals were regularly observed in parenchymatic cells around endodermis under I_3 (*Fig. 7*). Parenchymatic cells like a large air space in cortex were seen in some sections under I_4.

According to the biometric measurements performed in some tissues of the roots under four conditions; the thickness of cortex under I_3 and I_4 increased more than the one under I_2 ($p < 0.01$; $p < 0.05$; *respectively*). There was no significant change in the thickness of cortex under I_1 ($p > 0.05$). The diameter of xylem vessels narrowed under I_1, I_3, and I_4 ($p < 0.05$; $p < 0.01$; $p < 0.01$, *respectively*) more than the one under I_2 (*Fig. 8*). According to the results of the biometric measurements, the roots under the other issues underwent anatomical changes comparing to the ones under I_2 statistically and the I_2 condition was determined as optimum issue ($p < 0.01$: *highly significant,* $p < 0.05$: *significant,* $p > 0.05$: *no significant*).

http://www.aloki.hu ● ISSN 1589 1623 (Print) ● ISSN 1785 0037 (Online)
DOI: http://dx.doi.org/10.15666/aeer/1706_1308913104

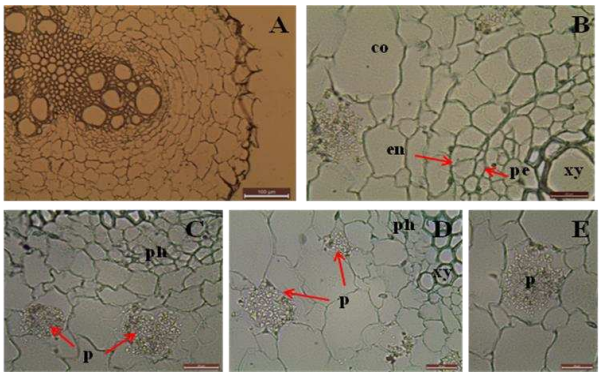

Figure 4. *The anatomy of the root cultivated under I_1 (cross section). A: general shape of root, bar = 100 µm, B: cortex (co), endodermis (en), pericycle (pe), xylem (xy), bar = 20 µm, C: phloem (ph), prismatic crystal (p), bar = 20 µm, D: phloem (ph), xylem (xy), prismatic crystal (p), bar = 20 µm, E: prismatic crystal (p), bar = 20 µm*

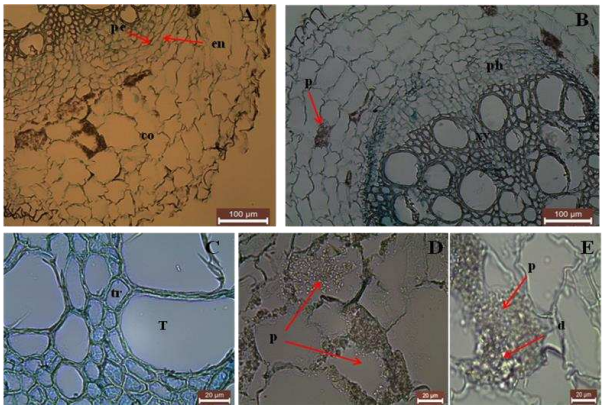

Figure 5. *The anatomy of the root cultivated under I_2 (cross section). A: cortex (co), endodermis (en), pericycle (pe), bar = 100 µm, B: phloem (ph), xylem (xy), prismatic crystal (p), bar = 100 µm, C: trachea (T), tracheid (tr), bar = 20 µm, D: prismatic crystal (p), bar = 20 µm, E: prismatic crystal (p), druz crystal (d), bar = 20 µm*

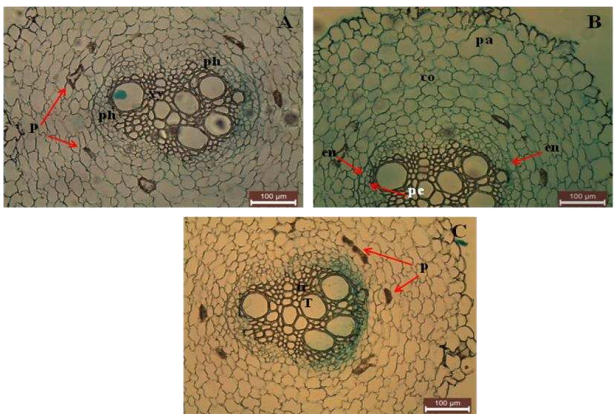

Figure 6. *The anatomy of the root cultivated under I_4 (cross section). A: phloem (ph), xylem (xy), prismatic crystal (p), bar = 100 µm, B: cortex (co), parenchymatic cell (pa), endodermis (en), pericycle (pe), bar = 100 µm, C: trachea (T), tracheid (tr), prismatic crystal (p), bar = 100 µm*

http://www.aloki.hu ● ISSN 1589 1623 (Print) ● ISSN 1785 0037 (Online)
DOI: http://dx.doi.org/10.15666/aeer/1706_1308913104

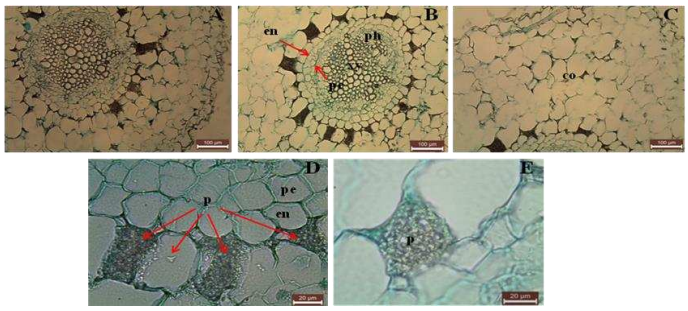

Figure 7. *The anatomy of the root cultivated under I_3 (cross section). A: general shape of root, bar = 100 µm, B: endodermis (en), pericycle (pe), phloem (ph), xylem (xy), bar = 100 µm, C: cortex (co), bar = 100 µm, D: endodermis (en), pericycle (pe), prismatic crystal (p), bar = 20 µm, E: prismatic crystal (p), bar = 20 µm*

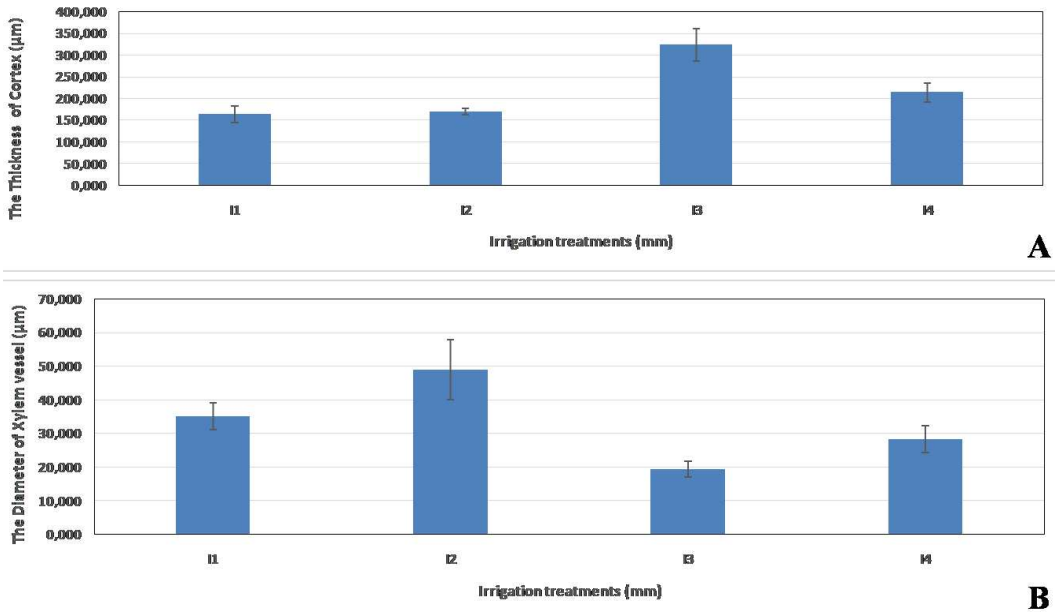

Figure 8. *Measurements of some tissues in roots of Ceren cv. under different irrigation treatment conditions. A. The relationship between irrigation treatments and thickness of cortex. B. The relationship between irrigation treatments and diameter of xylem vessel*

Stems

The stems under all the conditions were formed by one- layered epidermis, 1-2 layered chlorenchyma with large spaces between the cells, 4-5 layered collenchyma, 4-5 or 5-6 layered cortex. The pith was parenchymatic surrounded by bicollateral vascular bundles. 3-4 layered cambium and seconder xylem rays under I_1 and I_3 were observed (*Figs. 9* and *11*). The cambium was 4-5 layered under I_4 (*Fig. 12*). Sclerenchyma cells supported vascular bundles on both sides around phloems. All the stems had stomata, epidermal and glandular hairs. While prismatic crystals were generally observed, druz crystals were seen among prismatic crystals in some sections. Prismatic crystals in chlorenchyma under I_2, air spaces in chlorenchyma in some sections under I_4 and starch molecules under I_2, I_3, and I_4 were observed (*Figs. 10, 11* and *12*). Starch molecules were rarely seen under I_1.

http://www.aloki.hu ● ISSN 1589 1623 (Print) ● ISSN 1785 0037 (Online)
DOI: http://dx.doi.org/10.15666/aeer/1706_1308913104

According to the biometric measurements performed in some tissues of the stems under four conditions, cuticle thickened under I_1 and I_4 ($p < 0.01$; $p < 0.05$, *respectively*). It was not affected clearly under I_3 ($p > 0.05$). Epidermis did not change clearly under I_1 ($p > 0.05$), but it significantly thickened under I_3 and I_4 ($p < 0.05$). Cortex did not change clearly under I_1 and I_3 ($p > 0.05$), but it significantly thickened under I_4 ($p < 0.05$). Xylem vessel narrowed under I_1, I_3, and I_4 comparing to I_2 ($p < 0.05$; $p < 0.05$; $p < 0.01$, *respectively*) (*Fig. 13*). According to the results of the biometric measurements, the stems under the other issues underwent anatomical changes comparing to the ones under I_2 statistically and the I_2 condition was determined as optimum issue.

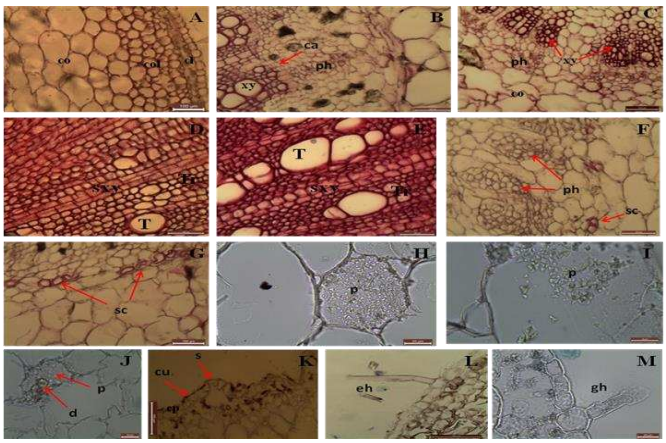

Figure 9. *The anatomy of the stem cultivated I_1 (cross section). A: chlorenchyma (cl), collenchyma (col), cortex (co), bar = 100 µm, B: phloem (ph), xylem (xy), cambium (ca), bar = 100 µm, C: cortex (co), phloem (ph), xylem (xy), bar = 100 µm, D: trachea (T), tracheid (tr), seconder xylem (sxy) bar = 100 µm, E: trachea (T), tracheid (tr), seconder xylem (sxy) bar = 100 µm, F: sclerenchyma (sc), phloem (ph), bar = 100 µm, G: sclerenchyma (sc), bar = 100 µm, H: prismatic crystal (p), bar = 20 µm, I: prismatic crystal (p), bar = 20 µm, J: prismatic crystal (p), druz crystal (d), bar = 20 µm, K: cuticle (cu), epidermis (ep), stomate (s), bar = 100 µm, L: epidermal hair (eh), bar = 100 µm, M: glandular hair (gh), bar = 20 µm*

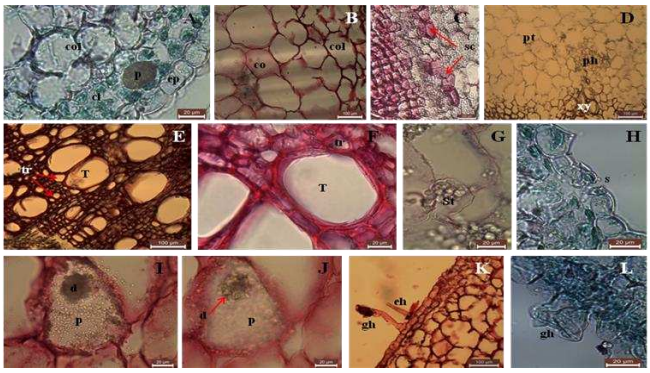

Figure 10. *The anatomy of the stem cultivated I_2 (cross section). A: epidermis (ep), chlorenchyma (cl), prismatic crystal (p), collenchyma (col), bar = 20 µm, B: collenchyma (col), cortex (co), bar = 100 µm, C: sclerenchyma (sc), bar = 100 µm, D: phloem (ph), xylem (xy), pith (pt), bar = 100 µm, E: trachea (T), tracheid (tr), bar = 100 µm, F: trachea (T), tracheid (tr), bar = 20 µm, G: starch (St), bar = 20 µm, H: stomate (s), bar = 20 µm, I: prismatic crystal (p), druz crystal (d), bar = 20 µm, J: prismatic crystal (p), druz crystal (d), bar = 20 µm, K: epidermal hair (ep), glandular hair (gh), bar = 100 µm, L: glandular hair (gh), bar = 20 µm*

http://www.aloki.hu ● ISSN 1589 1623 (Print) ● ISSN 1785 0037 (Online)
DOI: http://dx.doi.org/10.15666/aeer/1706_1308913104

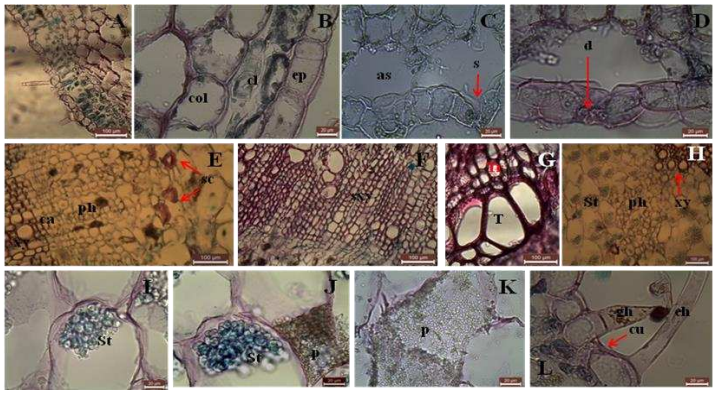

Figure 11. *The anatomy of the stem cultivated I_3 (cross section). A: general shape of some tissues, bar = 100 µm, B: epidermis (ep), chlorenchyma (cl), collenchyma (col), bar = 20 µm, C: stomate (s), air space (as), bar = 20 µm, D: druz crystal (d), bar = 20 µm, E: sclerenchyma (sc), phloem (ph), cambium (ca), xylem (xy), bar = 100 µm, F: seconder xylem (xy), bar = 100 µm, G: trachea (T), tracheid (tr), bar = 100 µm, H: phloem (ph), xylem (xy), starch (St), bar = 100µm, I: starch (St), bar = 20 µm, J: starch (St), prismatic crystal (p), bar = 20 µm, K: prismatic crystal (p), bar = 20 µm, L: epidermal hair (eh), glandular hair (gh), cuticle (cu), bar = 20 µm*

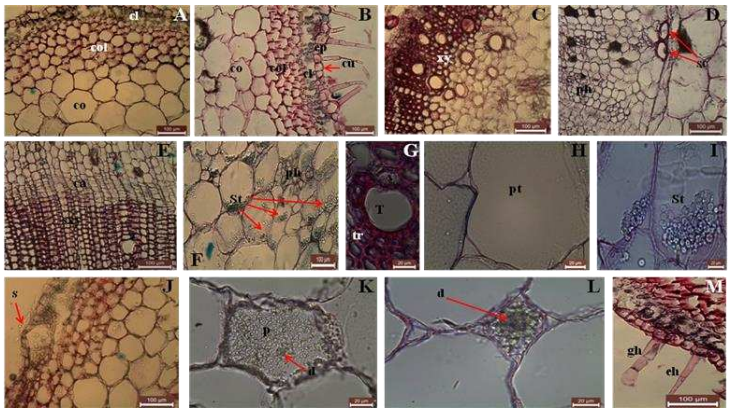

Figure 12. *The anatomy of the stem cultivated I_4 (cross section). A: chlorenchyma (cl), collenchyma (col), cortex (co), bar = 100 µm, B: cuticle (cu), epidermis (ep), chlorenchyma (cl), collenchyma (col), cortex (co), bar = 100 µm, C: xylem (xy), bar = 100 µm, D: sclerenchyma (sc), phloem (ph), bar = 100 µm, E: cambium (ca), seconder xylem (xy), bar = 100 µm, F: starch (St), phloem (ph), bar = 100 µm, G: trachea (T), tracheid (tr), bar = 20 µm, H: pith (pt), bar = 20 µm, I: starch (St), bar = 20 µm, J: stomate (s), bar = 100 µm, K: prismatic crystal (p), druz crystal (d), bar = 20 µm, L: druz crystal (d), bar = 20 µm, M: glandular hair (gh), epidermal hair (eh), bar = 100 µm*

Leaves

The leaves under all the conditions were bifacial and amphistomatic. Mesophyll was formed by one-layered palisade parenchyma with large spaces between the cells and 4-5 layered spongy parenchyma with large spaces between the cells under I_1 (*Fig. 14*). Palisade parenchyma was one-layered and spongy parenchyma was 2-3 layered under I_2 (*Fig. 15*). Mesophyll was formed by 2-3 layered palisade parenchyma generally rarely arranged by small cells and 3-4 layered spongy parenchyma with large spaces between

http://www.aloki.hu ● ISSN 1589 1623 (Print) ● ISSN 1785 0037 (Online)
DOI: http://dx.doi.org/10.15666/aeer/1706_1308913104

small cells under I_3 (*Fig. 16*). One-layered palisade parenchyma formed by long cylindirical cells and 3-4 layered spongy parenchyma with large spaces between the cells in mesophyll under I_4 were observed (*Fig. 17*). Druz crystals were observed among prismatic cyristals in mesophyll in some sections. Big vascular bundle was bicollateral. Small vascular bundles surrounded by bundle sheath were collateral and embedded in mesophyll. Epidermal and glandular hairs were observed under all the conditions. Glandular hairs were rarely seen under I_4.

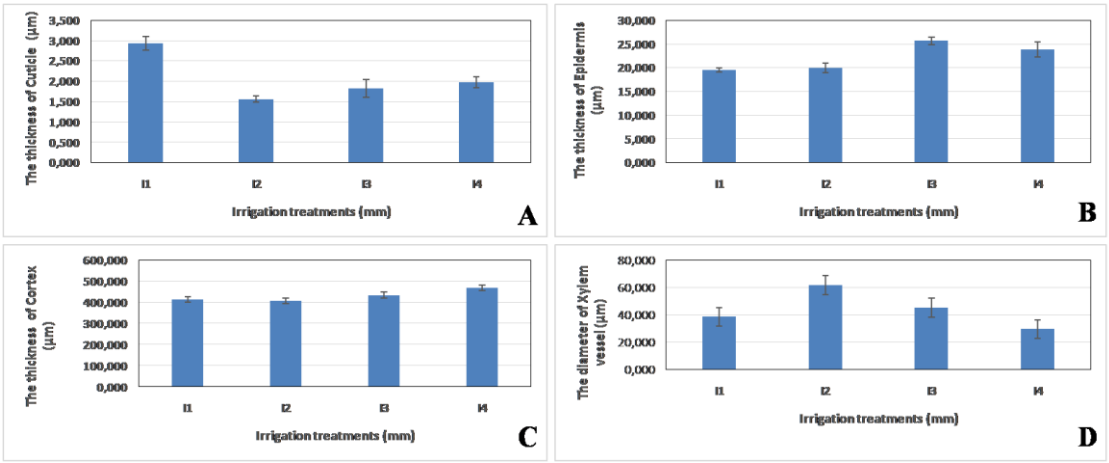

Figure 13. *Measurements of some tissues in stems of Ceren cv. under different irrigation treatment conditions. A. The relationship between irrigation treatments and thickness of cuticle, B. The relationship between irrigation treatments and thickness of epidermis, C. The relationship between irrigation treatments and thickness of cortex, D. The relationship between irrigation treatments and diameter of xylem vessel*

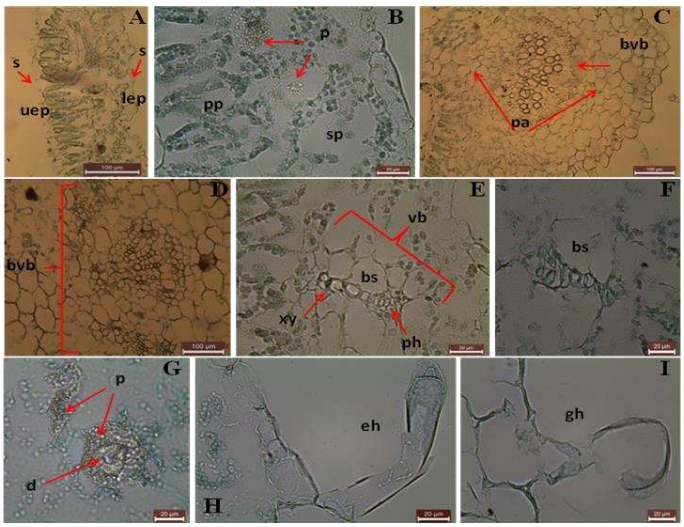

Figure 14. *The anatomy of the leaf cultivated I_1 (cross section). A: upper epidermis (uep), lower epidermis (lep), stomate (s), bar = 100 µm, B: palisade parenchyma (pp), spongy parenchyma (sp), prismatic crystal (p), bar = 20 µm, C: big vascular bundle (bvb), parenchymatic tissue (pa), bar = 100 µm, D: big vascular bundle (bvb), bar = 100 µm, E: vascular bundle (vb), bundle sheath (bs), xylem (xy), phloem (ph), bar = 20 µm, F: bundle sheath (bs), bar = 20 µm, G: prismatic crystal (p), druz crystal (d), bar = 20 µm, H: epidermal hair (eh), bar = 20 µm, I: glandular hair (gh), bar = 20 µm*

http://www.aloki.hu ● ISSN 1589 1623 (Print) ● ISSN 1785 0037 (Online)
DOI: http://dx.doi.org/10.15666/aeer/1706_1308913104

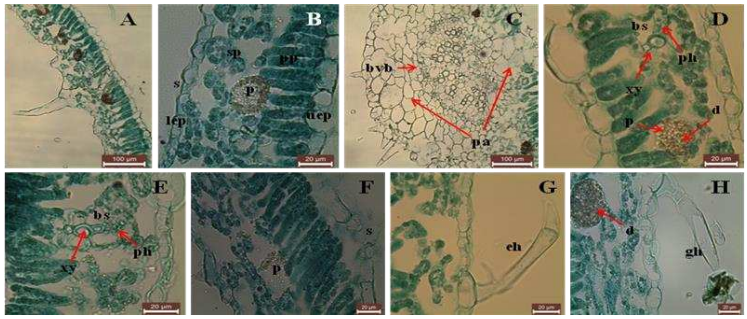

Figure 15. *The anatomy of the leaf cultivated I_2 (cross section). A: general shape of leaf, bar = 100 µm, B: upper epidermis (uep), lower epidermis (lep), stomate (s), palisade parenchyma (pp), spongy parenchyma (sp), prismatic crystal (p), bar = 20 µm, C: big vascular bundle (bvb), parenchymatic tissue (pa), bar = 100 µm, D: bundle sheath (bs), xylem (xy), phloem (ph), prismatic crystal (p), druz crystal (d), bar = 20 µm, E: bundle sheath (bs), xylem (xy), phloem (ph), bar = 20 µm, F: stomate (s), prismatic crystal (p), bar = 20 µm, G: epidermal hair (eh), bar = 20 µm, H: glandular hair (gh), druz crystal (d), bar = 20 µm*

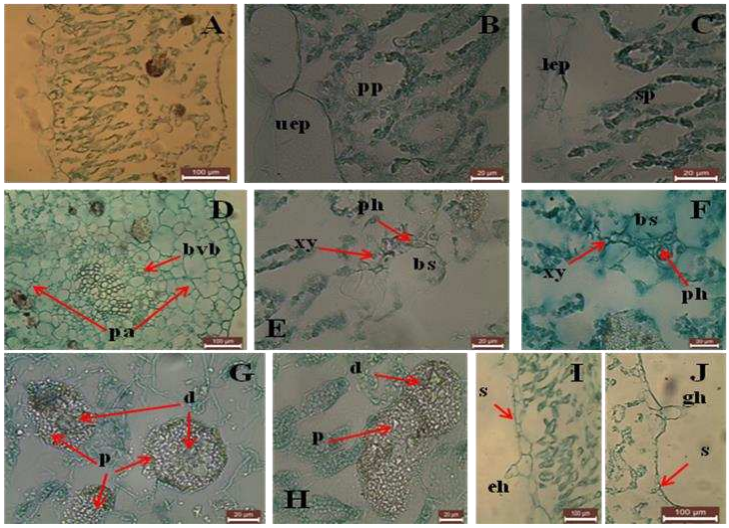

Figure 16. *The anatomy of the leaf cultivated I_3 (cross section). A: general shape of leaf, bar = 100 µm, B: upper epidermis (uep), palisade parenchyma (pp), bar = 20 µm, C: lower epidermis (lep), spongy parenchyma (sp), bar = 20 µm, D: big vascular bundle (bvb), parenchymatic tissue (pa), bar = 100 µm, E: bundle sheath (bs), xylem (xy), phloem (ph), bar = 20 µm, F: bundle sheath (bs), xylem (xy), phloem (ph), bar = 20 µm, G: prismatic crystal (p), druz crystal (d), bar = 20 µm, H: prismatic crystal (p), druz crystal (d), bar = 20 µm, I: stomate (s), epidermal hair (eh), bar = 100 µm, J: glandular hair (gh), stomate (s), bar = 100 µm*

According to the biometric measurements performed in some tissues of the leaves under four conditions; the thickness of cuticle decreased under I_1 ($p < 0.05$), but it did not change under I_3 and I_4 ($p > 0.05$). The thickness of upper epidermis was affected clearly under I_1, I_3, and I_4 ($p < 0.01$; $p < 0.01$; $p < 0.05$, *respectively*). The lower epidermis increased under I_1 ($p < 0.01$), but it did not change under I_3 and I_4 ($p > 0.05$). The width of mesophyll and the length of big vascular bundle increased under I_1, I_3, and I_4 ($p < 0.01$; $p < 0.01$; $p < 0.01$, *respectively*). The width of big vascular bundle

http://www.aloki.hu ● ISSN 1589 1623 (Print) ● ISSN 1785 0037 (Online)
DOI: http://dx.doi.org/10.15666/aeer/1706_1308913104

increased under I_1 and I_4 ($p < 0.01$; $p < 0.05$, *respectively*), but it decreased under I_3 ($p < 0.05$). The thickness of bundle sheath wall did not change clearly under I_1 and I_3 ($p > 0.05$), but it increased under I_4 ($p < 0.05$). The diameter of xylem vessel narrowed under I_3 and I_4 ($p < 0.05$; $p < 0.01$, *respectively*), but it did not change obviously under I_1 ($p > 0.05$). According to the results of the biometric measurements, the leaves under the other issues underwent anatomical changes statistically comparing to the ones under I_2 and the I_2 condition was determined as optimum issue (*Fig. 18*).

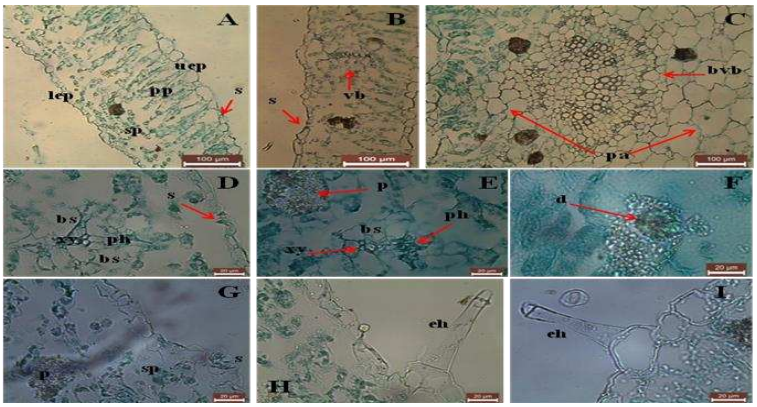

Figure 17. *The anatomy of the leaf cultivated I_4 (cross section). A: upper epidermis (uep), lower epidermis (lep), stomate (s), palisade parenchyma (pp), spongy parenchyma (sp), bar = 100 µm, B: stomate (s), vascular bundle (vb), bar = 100 µm, C: big vascular bundle (bvb), parenchymatic tissue (pa), bar = 100 µm, D: bundle sheath (bs), xylem (xy), phloem (ph), stomate (s), bar = 20 µm, E: bundle sheath (bs), xylem (xy), phloem (ph), prismatic crystal (p), bar = 20 µm, F: druz crystal (d), bar = 20 µm, G: stomate (s), spongy parenchyma (sp), prismatic crystal (p), bar = 20 µm, H: epidermal hair (eh), bar = 20 µm, I: epidermal hair (eh), bar = 20 µm*

Discussion

According to the results the anatomical features in the roots, stems and leaves in the issues analyzed are similar to the general anatomical features of Solanaceae family and *Lycopersicon esculentum* Mill. mentioned in Metcalfe and Chalk (1950), Rost (1996), Tuylu et al. (2018) and Tuylu (2018a). Abnormal changes in the development of basic tissues were not observed in the roots, stems and leaves in all the issues studied $I_{1\text{-}4}$. Structure and functions of all plant organs are affected by water stress (Sam et al., 2000). The tissues affected when the plant is applied by limited irrigation can be also affected by over-irrigation. The adaptation reactions of the tissues under over-irrigation or limited irrigation condition can be opposite or parallel to each other. In the study the I_1 issue was determined as over-irrigation. The comparison of the biometric measurements between the issues in the study and the results of the measurements of the tomato, Ceren cv. cultivated under hydroponic system and anatomically examined in Tuylu (2018a) contributed to determine I_1 issue as over-irrigation. The study mentioned was carried out in the same greenhouse, period and climate parameters. The stress- related anatomical changes were observed in the roots, stems and leaves of the plants cultivated under I_3 and I_4 issues determined as limited irrigation conditions comparing with the ones under I_2 issue determined as optimum condition.

http://www.aloki.hu ● ISSN 1589 1623 (Print) ● ISSN 1785 0037 (Online)
DOI: http://dx.doi.org/10.15666/aeer/1706_1308913104

When the results were evaluated for the root, the diameter of xylem vessels in the root in Ceren cv. narrowed in all the issues more than the one under optimum issue. It means that the diameter of xylem vessels anatomically reacted to water and drought stress conditions in the same way. The xylem vessels under I_1 condition in the study and the ones in Ceren cv. cultivated under hydrophonic culture in Tuylu (2018a) gave the same reactions. Similarly, Tuylu et al. (2018) figured out in the study on Malatya Kurucaova cv. that the xylem vessels in the root narrowed as a result of water stress under hydrophonic culture more than the ones under perlite condition well- irrigated. The xylem vessels in Malatya Kurucaova cv. and Ceren cv. gave reactions in parallel anatomically to stress resulting in over- irrigation.

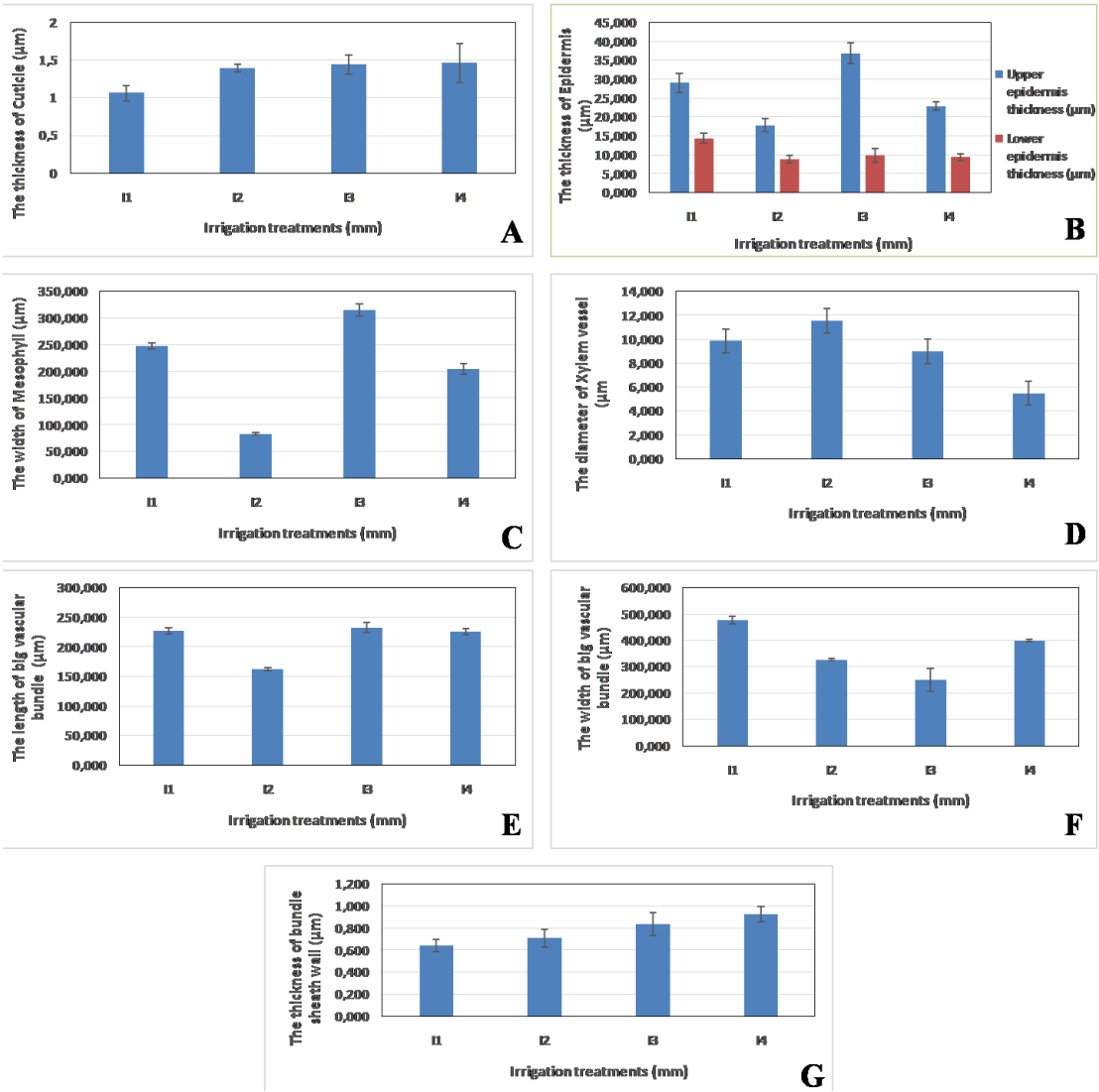

Figure 18. *Measurements of some tissues in leaves of Ceren cv. under different irrigation treatment conditions. A. The relationship between irrigation treatments and thickness of cuticle, B. The relationship between irrigation treatments and thickness of epidermis, C. The relationship between irrigation treatments and width of mesophyll, D. The relationship between irrigation treatments and diameter of xylem vessel, E. The relationship between irrigation treatments and length of big vascular bundle, F. The relationship between irrigation treatments and width of big vascular bundle, G. The relationship between irrigation treatments and thickness of bundle sheath wall*

http://www.aloki.hu ● ISSN 1589 1623 (Print) ● ISSN 1785 0037 (Online)
DOI: http://dx.doi.org/10.15666/aeer/1706_1308913104

When the results were evaluated for the stem, it was observed that cuticle and cortex thickened and the diameter of xylem vessel narrowed under I_1, I_3, and I_4 conditions comparing with I_2 condition. In the stem of Ceren cv. mentioned in Tuylu (2018a) the thickness of cuticle increased and the diameter of xylem vessel narrowed comparing with I_2 in the study. In the stem of Malatya Kurucaova cv. in Tuylu et al. (2018) it was stated that cuticle and epidermis thickened while cortex and xylem vessel narrowed under hydrophonic condition. It was clear that the thickness of cuticle and the diameter of xylem vessel anatomically changed in parallel in Ceren cv. and Malatya Kurucaova cultivated under hydrophonic condition and under over- irrigation and limited irrigation conditions in the present study.

When the results were evaluated for the leaf, it was obvious that upper and lower epidermis thickened under I_1, I_3, and I_4 conditions comparing to I_2 condition. Sam et al. (2000) studied the effects of water deficit on epidermis of leaf at preflowering stage in *Lycopersicon esculentum* Mill. cv. INCA9 and stated that water stress have slight effects on the width and the length of epidermis cells. Thus, it is understood that the plant also shows epidermal change under water stress as it shows under water deficit. In addition, in the present study, the width of mesophyll increased, the diameter of xylem vessel narrowed and the length of big vascular bundle increased. While the width of big vascular bundle increased under I_1 and I_4, it decreased under I_3. The thickness of bundle sheath wall increased as long as the amount of irrigation water reduced. Tuylu et al. (2018) introduced that midrib region widened and the width and the length of big vascular bundle increased in the leaf of Malatya Kurucaova cv. cultivated under hydrophonic condition as a result of water stress comparing to the ones under perlite condition. They stated that no clear change was observed in the other tissues measured. It was similar to the change observed in midrib region of the plant cultivated and exposed to over- irrigation under I_1 in the present study. A similar change in big vascular bundle was observed under particularly I_4 which was one of the limited irrigation issues. However; the fact that in the study the leaf under I_1 also showed anatomical changes in the other tissues comparing to the one under I_2 differed from Tuylu et al. (2018).

The fact that the thickness of upper epidermis and mesophyll increased and xylem narrowed in the leaf of Ceren cv. exposed to over- irrigation in Tuylu (2018a) was similar to the leaf under I_1 in the present study.

Tuylu (2018b) figured out that the thickness of cortex and the diameter of xylem vessel in the root, the diameter of xylem vessel in the stem and the thickness of cuticle, the thickness of upper epidermis, the number of stomate in the upper and the lower epidermis, the length and the width of bullate cell, the width of mesophyll, the diameter of xylem vessel, the distance of bundles, the thickness of midrib region, and the width of big vascular bundle in the leaf significantly changed under over- irrigation and limited irrigation in the study on the maize cultivar.

Conclusion

As a result, some tissues of Ceren cv. cultivated under perlite condition by applying different irrigation issues were anatomically examined and compared. When all the issues were compared according to the measurements performed in the root, stem and leaf, the tissues under I_1, I_3 and I_4 conditions showed anatomical changes due to drought and water stress comparing to I_2 condition.

http://www.aloki.hu ● ISSN 1589 1623 (Print) ● ISSN 1785 0037 (Online)
DOI: http://dx.doi.org/10.15666/aeer/1706_1308913104

Thus, the anatomical features analyzed pointed out that I_2 issue was optimum irrigation condition for the plant. It was the issue that 10% of irrigation solution was drained. The plants cultivated under over- irrigation (I_1) and limited irrigation (I_3, I_4) did not have a clear anatomical anomaly comparing to the ones cultivated under I_2. They underwent changes such as thickening or narrowing due to water and drought stress and they adapted to the conditions.

To determine the accurate irrigation strategy for the plant under irrigation applications some tissues of the root, stem and leaf can anatomically present if the plant was exposed to water stress or drought stress. In the study, it was figured out that the thickness of cortex under limited irrigation, and the diameter of xylem vessels under over- irrigation and limited irrigation in the root, the thickness of cuticle, and the diameter of xylem vessel under over- irrigation, and the thickness of cuticle, epidermis and cortex, and the diameter of xylem vessel under limited irrigation in the stem, the thickness of cuticle, the width of mesophyll, and upper and lower epidermis, the length and width of big vascular bundle under over- irrigation, and the thickness of upper epidermis, the width of mesophyll, the diameter of xylem vessel, the length and width of big vascular bundle, the thickness of bundle sheath wall under limited irrigation in the leaf significantly reacted anatomically. The optimum issue can be determined statistically in terms of importance levels by evaluating the measurements of these tissues.

According to the results of the study, it is suggested that the amount of drainage should be 10% in the irrigation applications in contrast to 30-35% drainage mentioned in Winsor and Shwarz (1990), Lieth (1996) and Öztekin et al. (2017). In other words, irrigation application should be performed by reducing 25% of irrigation water. It is suitable for the anatomical characteristics of the root, stem and leaf of tomato. In cultivation, not only saving up the cost of the nutrient solution in terms of its total cost but also supplying energy savings by reducing irrigation time will contribute considerably to the producer. In addition, researchers in the field should consider irrigation parameter to optimize the ecological condition in further studies.

Acknowledgements. This research did not receive any specific financially funding, but we thank to Harran University for equipments in greenhouse, and Ankara University for biology laboratories in Turkey for providing materials mentioned in the Materials and Methods to support the study.

Conflict of interests. The authors declare that there is no conflict of interests.

REFERENCES

[1] Anonymous (2015): Crop Production Statistics (Türkiye İstatistik Kurumu, Bitkisel Üretim İstatistikleri). – Turkish Statistical Institute, Ankara. http://www.tuik.gov.tr/bitkiselapp/bitkisel.zul (accessed on 14.04.2016).

[2] Anonymous (2016): Şanlıurfa Climate Values (Şanlıurfa iklim değerleri). – Regional Directorate of Meteorology Data Base (Meteoroloji Bölge Müdürlüğü Veri Tabanı), Şanlıurfa, Turkey. https://www.mgm.gov.tr/ (accessed on 19.03.2017).

[3] Deliboran, A., E., Gülle Sakin, E. D., Çoşkun, M. (2013): Evaluation of the some productivity characteristics of greenhouse soils at strict Karaali Şanlıurfa. – Soil-Water Journal 2(2): 1077-1084.

[4] Demirok, A., Tuylu, G. İ. (2017): Evaluation of planning and actual irrigation time scheduling for the maize (Zea mays L.) plant in Harran plain (Harran Ovası'nda Mısır

http://www.aloki.hu ● ISSN 1589 1623 (Print) ● ISSN 1785 0037 (Online)
DOI: http://dx.doi.org/10.15666/aeer/1706_1308913104

Bitkisi (*Zea mays* L.) için Planlanan ve Gerçekleşen Sulama Zamanı Programının Değerlendirilmesi). – Harran Journal of Agricultural and Food Science (Harran Tarım ve Gıda Bilimleri Dergisi) 21(1): 84-90.

[5] Korkmaz, H., Durmaz, A. (2017): Responses of plants to abiotic stress factors (Bitkilerin Abiyotik Stres Faktörlerine Verdiği Cevaplar). – GUFBED 7(2): 192-207.

[6] Lieth, J. H. (1996): Irrigation Systems. – In: Reed, D. W. (ed.) Water, Media and Nutrition for Greenhouse Crops. Ball Publishing Inc., Chicago, IL.

[7] Metcalfe, C. R., Chalk, L. (1950): Anatomy of the Dicotyledons. Vol. II. – Clarendon Press, Oxford, pp. 965-978.

[8] Özkan, Ş. (2014): Soilless agricultural production, current and future situation of soilless agricultural products in 2012-2013 cultivated in the Mediterranean region of Turkey. A Study on "tomato and strawberry" (Topraksız Tarım Üretimi, 2012-2013 Yıllarında Türkiye'nin Akdeniz Bölgesi'nde Gelişmekte Olan ''Topraksız'' Tarım Ürünlerinin Bugünkü Durumu ve Gelecekle İlgili Tahminler, Domates ve Çilek Üretimi Üzerine Bir Araştırma). – Yüksek Lisans Tezi, Giresun Üniversitesi Sosyal Bilimler Enstitüsü, Giresun.

[9] Öztekin, G. B., Tüzel, Y., Tüzel, İ. H. (2017): Effect of silicium on salt stress under soil less tomato cultivation in greenhouse (Serada topraksız domates yetiştiriciliğinde silisyumun tuz stresine etkisi). – Journal of Academical Agriculture (Akademik Ziraat Dergisi), Special Issue (Özel Sayı) 6: 243-256.

[10] Rost, T. L. (1996): Tomato Anatomy. – Section of Plant Biology Division of Biological Sciences, University of California, Davis. http://www-plb.ucdavis.edu/labs/rost/Tomato/tomhome.html (accessed on 17.10.2017).

[11] Sam, O., Jerez, E., Dell'Amico, J., Ruiz Sanchez, M. C. (2000): Water stress induced changes in anatomy of tomato leaf epidermis. – Biologia Plantarum 43(2): 275-277.

[12] Söylemez, S., Pakyürek, A. Y. (2017): Responses of rootstocks to nutrient induced high EC levels on yield and fruit quality of grafted tomato cultivars in greenhouse conditions. – Applied Ecology and Environmental Research 15(3): 759-770.

[13] Tuylu, M. (2018a): Examination of anatomical features of tomato (*Lycopersicon esculentum* Mill.) varieties cultivated under hydroponic system. – Applied Ecology and Environmental Research 16(3): 3381-3391.

[14] Tuylu, G. İ. (2018b): Effect of ecological conditions created by over- irrigation and limited irrigation on the anatomy of corn. – Applied Ecology and Environmental Research 16(6): 7619-7634.

[15] Tuylu, M., Büyükkartal, H. N., Akgül, G., Kalyoncu, H. (2017): Comparing stem and leaf anatomy of *Marrubium lutescens* Boiss. and *M. cephalanthum* Boiss. & Noë subsp. *akdaghicum* (*Lamiaceae*) (*Marrubium lutescens* Boiss. ve *M. cephalanthum* Boiss. & Noë subsp. *Akdaghicum* (Lamiaceae)' un Gövde veYaprak Özelliklerinin Anatomik Olarak Karşılaştırılması). – Süleyman Demirel Üniversitesi Fen Bilimleri Enstitüsü Dergisi 21(1): 113-117.

[16] Tuylu, M., Tuylu, G. İ., Söylemez, S., Büyükkartal, H. N. (2018): Comparing some anatomical features of tomato (*Lycopersicon esculentum* Mill. cv. Kurucaova) cultivated under perlit and hydroponic culture (Perlit ve Su Kültürü Ortamlarında Yetiştirilen Domates (*Lycopersicon esculentum* Mill. cv. Kurucaova) Bitkisinin Bazı Anatomik Özelliklerinin Karşılaştırılması). – Süleyman Demirel Üniversitesi Fen Bilimleri Enstitüsü Dergisi 22(2): 1104-1109.

[17] Winsor, G. W., Schwarz, M. (1990): Soilless Culture for Horticulture Crop Production. – FAO Plant Production and Protection, Paper 101, Rome.

[18] Yanmaz, R., Duman, İ., Yaralı, F., Demir, K., Sarıkamış, G., Sarı, N., Balkaya, A., Kaymak, H. Ç., Akan, S., Özalp, R. (2015): Changes in vegetable production and new research (Sebze Üretiminde Değişimler ve Yeni Arayışlar). – Turkey Agriculture Engineering VIII. Technique Congress (Türkiye Ziraat Mühendisliği VIII. Teknik Kongresi), Ankara, Turkey, 12-16 January, Proceeding Book-1 (Bildiriler Kitabı-1), pp. 579-605.

http://www.aloki.hu ● ISSN 1589 1623 (Print) ● ISSN 1785 0037 (Online)
DOI: http://dx.doi.org/10.15666/aeer/1706_1308913104

INTERACTION NETWORK OF *TaRHA2b* OF WHEAT *(TRITICUM AESTIVUM* L.*)* BASED ON HIGH-THROUGHPUT YEAST TWO-HYBRID SCREENING

LI, D. B.[#] – LYU, G. Z.[#] – JIANG, Y. M. – NIU, H. B. – WANG, X. – YIN, J.[*]

National Engineering Research Center for Wheat, State Key Laboratory of Wheat and Maize Crop Science, Collaborative Innovation Center of Henan Grain Crop, Henan Agricultural University, Zhengzhou 450002, China

**Corresponding author*
e-mail: xmzxyj@126.com; phone: +86-371-6355-8203

[#]These authors contributed equally to this work

(Received 26th May 2019; accepted 28th Aug 2019)

Abstract. To explore the signal transduction pathway that *TaRHA2b* gene is involved in regulating, yeast two-hybrid system was used to screen and identify proteins interacting with TaRHA2b. The homogenized cDNA library was constructed from the embryo of mixed barley. The decoy protein vector pGBKT7-*TaRHA2b* was constructed and transformed into yeast AH109 cells for self-activation detection. Candidate positive clones were screened by one to one yeast co-transfection, SD/-Leu/-Trp and SD/-Leu/-Trp/-Ade/-His medium screening and β-galactosidase chromogenic reaction. The in vitro co-transfection and GST-pull down experiments were used for further verification. The homogenized cDNA library of the barley embryos with titer of 1.2 10^6 cfu/ml and storage capacity of 1.1 10^6 was successfully constructed. The inserted fragment size was between 1000-3000 bp. The plasmids of the cDNA library were extracted and sequenced on a large scale, and 5000 plasmids were obtained. The decoy vector without self-activation function was successfully constructed. The x-gal filter paper of eighty-four hybrid clones showed strong blue color and forty-nine pieces of effective sequence information were obtained. Eight of them were selected for co-transfection verification. YTH2450 was selected for GST-pull down verification. The results showed that they were positive hybrid clones. TaRHA2b interacted with YTH2450 and other proteins. The information of above genes could be used for genetic improvement of crops, further improving the adaptability of crops to the environment.
Keywords: *preharvest sprouting, abscisic acid, cDNA library, self-activation, pull down assay*

Introduction

Preharvest sprouting (PHS) refers to the phenomenon of direct germination of grains on the ear in wet environment at the mature stage of wheat (*Triticum aestivum* L.). The negative effects of spike germination on wheat production are mainly reflected in decreasing yield, deteriorating quality and lower seed value. At present, the resistance of most wheat varieties to spike germination is not strong. The shortage of wheat resistance gene resources severely restricted the breeding and application of wheat varieties resistant to heading germination.

Cys-rich RING domain was identified for the first time in proteins encoded by *Really Interesting New Gene*. In *Arabidopsis thaliana* proteome, more than 5% of the predicted proteins (more than 1400 genes) are involved in ubiquitination/26S proteasome pathway (Smalle and Vierstra, 2004). Among these proteins, only a few encode E1 enzymes (two isoforms), 37 predicted proteasome components of E2, 26S, and other factors (such as deubiquitinase), while more than 1400 genes encode E3 ubiquitin ligases to participate in ubiquitination-dependent proteasome degradation pathways (Smalle and Vierstra,

http://www.aloki.hu ● ISSN 1589 1623 (Print) ● ISSN 1785 0037 (Online)
DOI: http://dx.doi.org/10.15666/aeer/1706_1310513124

2004). A variety of E3 ubiquitin ligases involve them in specific proteasome degradation pathways. Different binding of E2 and E3 can also increase the specificity of E3 in recognizing target proteins. Therefore, the diversity of E3 and the diversity of E3 binding with E2 can not only regulate different types of ubiquitination modification, but also specifically regulate target proteins.

The *AtRHA2b* gene of *Arabidopsis thaliana* encodes E3 ubiquitinated ligase. It plays an important role in ABA (abscisic acid) signal transduction and stress. Overexpression of *AtRHA2b* gene results in ABA-related phenotypes, such as ABA sensitivity at the stage of seed germination and seedlings (Li et al., 2011).

The *TaRHA2b* (Genbank: AEQ67396.1) gene, a Ring finger protein gene, was isolated from wheat by our team (Li et al., 2019). In previous studies, much work has been done on the *TaRHA2b* and *RsRHA2b* genes. The results showed that *TaRHA2b* gene may play an important role in seed dormancy during germination, which could be used to improve the PHS resistance of wheat. The genetic distance between radish and *Arabidopsis thaliana* is very small, so the function of radish *RsRHA2b* gene should be similar to that of *Arabidopsis thaliana AtRHA2b* gene. Compared to Zhengmai 9023, wheat lines transfected with *RsRHA2b* gene showed higher dormancy, PHS resistance and sensitivity to exogenous ABA. Meanwhile, under the treatment of 0.5 μM ABA and 5 μM ABA, the expression of ABA-related genes in transgenic lines was significantly higher than that in control Zhengmai 9023. The differences in nucleotide polymorphism sites of *RsRHA2b* gene resulted in differences in the three cleavage sites of *BstD102I, Cfr10I, and HpaII/MspI*. These results facilitate the exploration of the correlation between the *TaRHA2b* gene and wheat's increased PHS resistance ability and the development of molecular markers for PHS resistance.

The protein interaction network of RHA2b can be predicted by string software. This protein interaction network includes KIN1 (AT5G15960.1), ATDI8 (AT5G66400.1), AT5G12110 (AT5G12110.1), KUOX1 (AT5G07480.1), KUF1 (AT1G31350.1), AIRP1 (AT4G23450.2), SDIR1 (AT3G550.1), KEG (AT5G13530.1), AT5G58410.1 (AT5G58410.1) and ATC019 (AT1G52890.1). RHA2b is involved in the process of protein ubiquitination, cell protein metabolism and response to acid compounds. The regulatory network of a series of proteins interacting with RHA2b involves the processes of protein ubiquitination, cell protein metabolism, low temperature tolerance, and response to water loss, ABA, acidic compounds, oxygen-containing compounds and abiotic stress (Kurkela and Franck, 1990; Haynes et al., 2002; Sajan et al., 2007; Usadel et al., 2008; Jiang et al., 2009; Nelson et al., 2010; Robinson et al., 2010; Cho et al., 2011; Zheng et al., 2012; Stone, 2014).

The complexity of transcription factors determines the diversity of their functions. However, the specific signaling pathways and mechanisms involved in RHA2b are not very clear. What proteins can interact with it? Using TaRHA2b as bait and yeast two-hybrid technique to study the proteins interacting with TaRHA2b can lay a foundation for solving the above problems. Yeast two-hybrid technology has been widely used as an effective means to study protein interaction, providing a mature technology platform for the study of protein interaction and unknown proteins.

Fields and Song's yeast two-hybrid technique is a sensitive method for analyzing protein-protein interactions (Fields and Song, 1989). Although the system is closer to the natural conformation and function of the protein, but can not avoid the "false positive" problem. The self-activation detection of decoy protein is necessary for yeast two-hybrid experiment. If the decoy itself has self-activation function, then the

http://www.aloki.hu ● ISSN 1589 1623 (Print) ● ISSN 1785 0037 (Online)
DOI: http://dx.doi.org/10.15666/aeer/1706_1310513124

downstream reporter gene can be directly expressed, which makes no sense to use the decoy protein vector to screen the library.

In order to further understand the function of *TaRHA2b* and its mechanism of PHS resistance, some genes related to TaRHA2b were screened by yeast two-hybrid method. The present study can not only screen new stress-resistant genes, but also provide a theoretical basis for elucidating the mechanism of TaRHA2b-mediated PHS resistance.

Materials and methods

Construction and identification of homogeneous cDNA library

Wheat is hexaploid and its genome structure is too complex. Barley and wheat are both gramineous plants. The genetic distance between them is very small. Therefore, the interaction of TaRHA2b protein in barley can be studied first, and then the function of TaRHA2b in common wheat can be studied.

Preparation and purity detection of total RNA from barley (Hordeum vulgare L.) embryo

Barley seeds were treated with 5 μM ABA and distilled water, respectively. The seeds amount of each treatment was 50, and the sampling time was 0 h, 6 h, 12 h and 24 h. After the obtained materials were degerminated, mixed samples were prepared and total RNA was extracted using the RNAiso Plus Kit (Takara, Japan). Total RNA was determined by spectrophotometer at OD260/OD280 values. 1-2 μg RNA was treated with thermal denaturation (65 °C, 10 min). Then Agarose gel electrophoresis was used to detect the purity of RNA.

Synthesis of 1st strand and 2nd strand cDNA

The total RNA was taken as the template and the experimental steps were followed in the Creator Smart cDNA Library Construction Kit (Clontech, the United States). The electrophoresis on agarose gel was determined with 5 μL.

Homogenization

The obtained double-strand cDNA PCR was purified using the QIAquick PCR Purification Kit (Cat.No.28104, QIAGEN, Duesseldorf, Germany). Homogenization is performed according to trimmer-director kit (Cat#NK002, Evrogen, Moscow, Russia).

Purification, enzyme digestion, binding and library transformation of dscDNA

The dscDNA was purified using the QIAquick PCR Purification Kit. The purification of the ds cDNA was treated with *Sfi I* enzyme, 65 °C warm bath 2 h. The products were purified by CHROMA SPINTMTE-400 Column. Purified product was connected with pGADT7-Rec carrier, 16 °C, for the night. Connect the product to *E. coli* DH10B transformation, which was placed in the resistance of ammoniac benzyl LB tablet (15 cm in diameter) on 37 °C training for the night.

Identification of library

Observe and record the number of colony, then calculate its storage capacity. Thirty clones were randomly selected for PCR. The product was detected by agarose

http://www.aloki.hu ● ISSN 1589 1623 (Print) ● ISSN 1785 0037 (Online)
DOI: http://dx.doi.org/10.15666/aeer/1706_1310513124

gel electrophoresis, the recombination rate was calculated and the size of the inserted fragment was predicted.

Extraction, sequencing and bioinformatics analysis of cDNA library plasmids

2*96 monoclonal extraction templates were selected and sequenced with ABI3730. Positive sequencing was used. The sequence was analysed by BLAST. The NCBI and Swiss-Prot databases were used for bioinformatics.

Cloning of the wheat TaRHA2b gene

The seeds of wheat variety "Zhengmai 9023" were used for total RNA extraction. Total RNA was extracted with the Plus plant total RNA extraction kit (Tiangen Biotech (Beijing) Co., Ltd., Beijing, China). Fast Quant RT Kit (With gDNase) (Tiangen Biotech (Beijing) Co., Ltd., Beijing, China) was used to synthesize the first strand of DNA. The reverse transcription of wheat embryo DNA was used as template. Primers (*TaRHA2b*-F1 (Bait): 5'-GAATTCATGGGGTTCCCTGG-3', *TaRHA2b*-R1 (Bait): 5'-CTGCAGTCACCAAACGCGCGGGGGGGTGAG-3') were used for PCR amplification: 94 °C, 4min; 94 °C, 40s; 61 °C, 40s; 72 °C, 50s; 72 °C, 10min; 34 cycles. The length of the target fragment was 477 bp, and the target fragment was recovered by the gel recovery kit (Tiangen Biotech (Beijing) Co., Ltd., Beijing, China). The recovered product was linked to pMD-19T, transformed into *E. coli* DH5a and cultured overnight on ampicillin resistant LB plate 37 °C. Monoclones were selected and cultured in shaking bacteria. Plasmid DNA was extracted and identified by PCR.

Construction and self-activation detection of decoy protein vector

Screening of interacting proteins is done in accordance with Matchmaker™ Gold Yeast Two-Hybrid System User Manual (PT4084-1).

Construction of bait protein vector

Both pMD19-TaRHA2b and pGBKT7 vectors were digested by *EcoR I* and *PST I* at the same time, and the corresponding target fragments and linear pGBKT7 vectors were recovered. The recombinant vector pGBKT7-TaRHA2b was finally obtained and transformed into E. coli. Monoclones were selected and plasmids were extracted after shaking bacteria culture. The obtained plasmids were identified by enzyme digestion, and the rest were stored in a refrigerator at -80 °C with 50% glycerol.

Self-activation detection of bait carrier

Yeast strain AH109 was inverted cultured on YPDA plate at 30 °C. Yeast with diameters of 2-3 mm were selected and streaked on SD/-Trp, SD/-Leu, SD/-His and SD/-Ade media, respectively. The growth of yeast was recorded by inverted culture at 30 °C for 3-5 days. The bait vectors $pGBKT_7$-TaRHA2b and $pGADT_7$ were co-transfected into yeast AH109 competent state, and were separately delineated on SD/-Trp-Leu, SD/-Trp-Leu-His-Ade medium. The positive control group was co-transformed with $pGBKT_7$-53 and $pGADT_7$-T, while the negative control group was co-transformed with $pGBKT_7$-lam and $pGADT_7$-T. The growth of yeast was recorded after 3-4 days of inverted culture at 30 °C on all co-rotating plates.

http://www.aloki.hu ● ISSN 1589 1623 (Print) ● ISSN 1785 0037 (Online)
DOI: http://dx.doi.org/10.15666/aeer/1706_1310513124

Systematic high-throughput yeast two-hybrid assay

One-to-one transfection of bait plasmids and library plasmids into yeast competence

The bait vector pGBKT$_7$-TaRHA2b was transfected into yeast AH109 cells together with the library plasmid. The lines were drawn on SD/-Trp-Leu and SD/-Trp-Leu-His-Ade medium, respectively. At the same time, the yeasts transformed with pGBKT$_7$-53 and pGADT$_7$-T, pGBKT$_7$-lam and pGADT$_7$-T were used as positive control and negative control, respectively. The growth of yeast was observed and recorded after 3-4 days incubation at 30 °C.

Identification of yeast positive clones

The large-scale library plasmid and bait protein vector were co-transformed into yeast AH109 cells. The activity of beta-galactosidase co-transforming yeast colonies on SD/-Trp-Leu-His-Ade culture plate was detected by X-gal filter paper colorimetry. The colour reaction of yeast colonies was observed within 8 h.

Sequencing and analyzing the AD-ORF of positive candidates.

The plasmids corresponding to the yeast positive clones were sequenced. The obtained sequences were analyzed by bioinformatics. The NCBI and Swiss-Prot databases were used for bioinformatics.

The co-transfection verification

The barley DNA stored in laboratory was used as template and amplified with primers (*Table 1*). The amplification procedures were as follows: 94 °C, 5 min; 94 °C, 30 s; 57 °C, 30 s; 72 °C, 1 min 20 s; 72 °C, 10 min; 30 cycles. The size of the target fragment was 933 bp. After gel recovery, it was connected with pGEM-T and transformed into DH5a to extract plasmid. The above plasmids were digested by EcoRI/BamHI and pGADT$_7$-T by EcoRI/BamHI. The target fragment was linked with the digested pGADT$_7$-T vector by T4 ligase and transformed into DH5a. The plasmid was extracted and identified by PCR, and the corresponding candidate protein prey was finally obtained. The bait vector and prey vector co-transformed yeast were applied to SD/-Trp-Leu and SD/-Trp-Leu-His-Ade solid medium plates. Colony growth was observed after incubation for 2-4 day.

The GST-pull down verification

Cloning of YTH2450 gene and TaRHA2b gene

PGADT7-*YTH2450* was used as the template, and 59/60 primers were used for amplification. The amplification procedure was as follows: 94 °C, 5 min; 94 °C, 30 s; 60 °C, 30 s; 72 °C, 1 min 20 s; 72 °C, 10 min; 30 cycles. The size of the target fragment was 933 bp. It was linked with pGEM-T for *E. coli* transformation and plasmid extraction. Take pGBKT7-TaRHA2b as the template, The primers TaRHA2b-F1/R1 were used for amplification. Amplification procedure is as follows: 94 °C, 5 min; 94 °C, 30 s; 60 °C, 30 s; 72 °C, 45 s; 72 °C, 10 min; 30 cycles. The size of the target fragment was 477 bp. It was linked with pGEM-T for *E. coli* transformation and plasmid extraction. The primers used in the experiment are shown in *Table 2*. The design of all

http://www.aloki.hu ● ISSN 1589 1623 (Print) ● ISSN 1785 0037 (Online)
DOI: http://dx.doi.org/10.15666/aeer/1706_1310513124

primers is based on the homologous sequences obtained by bioinformatics analysis of the corresponding fragments.

Table 1. *Primers for the amplification of positive clones*

Number	Primer sequence (5'-3')	Amplified target fragment size
831	ACCAACAGGCAACAGAACAACCTACCG	*YTH2449*
832	CGTCTCAACTTCAAATCACAGCCCATAT	663bp
833	CTAGCTCGGGACCAGTGGGAGT	*YTH2450*
834	ACACTATTACAATTTGTCGGCAAGGAT	921bp
835	CCCGATTCCATCAGGAAAGCA	*YTH2456*
836	CGACGCGAGACACTGCAAAAC	594bp
837	TTGCTCGATCTGTTCAATTACGA	*YTH2457*
838	AGGAATGAATGGCTCGGCTA	1422bp
839	CAGTTGAGTGCTCGCTGCTC	*YTH2475*
842	CGTAAATATGTATGCCTGCTGCTAT	2028bp
841	GAGGGGCACAAGGAAGAAAT	*YTH2476*
844	AAAATGGCAAAGCTCGGTTA	699bp
843	GACGATCAAGCGATGGAAAGAAGT	*YTH2496*
846	GCAAGGCGGCCAGTAGGAAT	864bp
845	GCACGCACGAACACGCACAG	*YTH2708*
848	CGCAACATTTTAGAGTATCAGGACCATTA	1092bp

Table 2. *The primers for prokaryotic expression of positive clones*

Number	Primer sequence (5'-3')	Target produce
59	GGATCCATGGCGGATGCGAAG	*YTH2450*
60	GTCGACTTAAAGGCCGACAC	
TaRHA2b-F1	GCACGCACGAACACGCACAG	*TaRHA2b*
TaRHA2b-R1	CGCAACATTTTAGAGTATCAGGACCATTA	

Construction of prokaryotic expression vector

BamHI/SalI double enzyme digestion was performed on the plasmid pGEM-T-YTH2450. At the same time, *BamHI/SalI* double enzyme digestion was performed on the pMAL vector, and the target products were recovered after electrophoresis. The target fragment and the target vector were linked with T4 ligase, and the linked product was transformed into *E. coli*. The plasmid pMAL-YTH2450 was extracted. *BamH I/Xho I* double enzyme digestion was performed on the plasmid pGEMT-T-TaRHA2b. At the same time, the pLEICS vector was subjected to *BamH I/Xho I* double enzyme digestion, and the target products were recovered after electrophoresis detection. The target fragment and the target vector were linked with T4 ligase, and the linked product was transformed into *E. coli*. The plasmid pLEICS-TaRHA2b was extracted.

Induced expression and purification of fusion protein

Transfer 500 μL positive bacteria fluid to 10 ml LB liquid medium containing 50 μg/ml ampicillin, 37 °C for the night. Transfer 2 ml bacteria liquid to 50 ml LB

http://www.aloki.hu ● ISSN 1589 1623 (Print) ● ISSN 1785 0037 (Online)
DOI: http://dx.doi.org/10.15666/aeer/1706_1310513124

liquid medium containing 50 μg/ml ampicillin, 37 °C for the night. Take 1 ml bacteria liquid as a control, to add IPTG residual cultures to the final concentration of 0.3 mM, 37 °C to continue to develop. 1 ml of bacterial fluid was collected at different induction stages (1 h, 2 h, 3 h, 5 h). Centrifuge for 2 min, discard the supernatant, and suspend the cells with 100 L buffer solution. The samples were boiled in boiling water for 5 min, centrifuged for 1 min, and the cells were suspended with buffer solution. PAGE electrophoresis was performed on the obtained samples. Freeze thawing at room temperature, place on ice immediately, add 10-20 ml of bacterial lysate (PBS + l%Triton-100 + PMSF) for every 500 ml of medium, and mix well. Ultrasonic crushing on ice, open 2 s, stop 9 s, total 40-60 min. Until the lysate is sufficiently cool. 11000 rpm, 15 min, 4 °C on the centrifugal separation, -80 °C saved for later use.

GST (glutathione S-transferase) pull down

Three purified columns containing Glutathione sepharose 4B were balanced by adding a binding buffer (50 mM Tris-HCl, pH 7.4, 100 mM NaCl). The bacterial lysate was added by ultrasonic crushing and centrifugal filtration. Two of them were added with pLEICS-TaRHA2b to induce GST-TaRHA2b lysates in large quantities, while the other one was added with pLEICS to induce GST lysates in large quantities. Placed in 4 °C, horizontal oscillation apparatus, slow upside down with rights and cracking liquid contact with column material, promote the combination. After 2-4 h, discard the lysate and rinse 5-8 times with pre-cooled combined buffer. A large amount of pMAL-YTH2450 induced bacterial lysate (ultrasonic crushing, centrifugal filtration) was added to the GST-TaRHA2b column and the GST-bound column respectively. Also 4 °C, fluctuation slow oscillation 4 h, abandon cracking fluid, clean with combined buffer after 5-8 times, with the elution buffer (50 mM Tris HCl, pH 7.4, 10 mM NaCl, 10 mM reducing GSH) elution 3 purification column, collect samples for SDS-PAGE analysis.

Statistical analysis

The GraphPad Prism 8 was used for statistical analysis and drawing. For comparing results of different treatments, Variance analysis is followed by a post-hoc test in order to determine pairwise differences. Differences were considered significant for $P < 0.05$.

Results

Construction and identification of homogeneous cDNA library of barley embryos

When the prepared RNA was detected by spectrophotometer, the OD260/OD280 value was 2.03, which indicated that the purity of the RNA was very high. When RNA agarose gel electrophoresis, the brightness of the two bands of 28S and 18S is close to 2:1 (*Fig. 1A*). Normal proportion indicates that the integrity of the RNA is good. In summary, the prepared RNA can be further tested. The size of double-stranded DNA fragments was uniformly distributed in the range of 300-5000 bp by LD-PCR (*Fig. 1B*), with slightly high abundance gene bands.

The storage capacity of the plate is about 1200. The titer of the library was 1.2 10^6 cfu/ml and the storage capacity was 1.1 10^6. The results of colony PCR identification of randomly selected clones in the library showed that the size of inserted fragments in the

http://www.aloki.hu ● ISSN 1589 1623 (Print) ● ISSN 1785 0037 (Online)
DOI: http://dx.doi.org/10.15666/aeer/1706_1310513124

library ranged from 1000 to 3000 bp (*Fig. 1C*). The results showed that the library was of high quality and could be used in the follow-up yeast two-hybrid screening library.

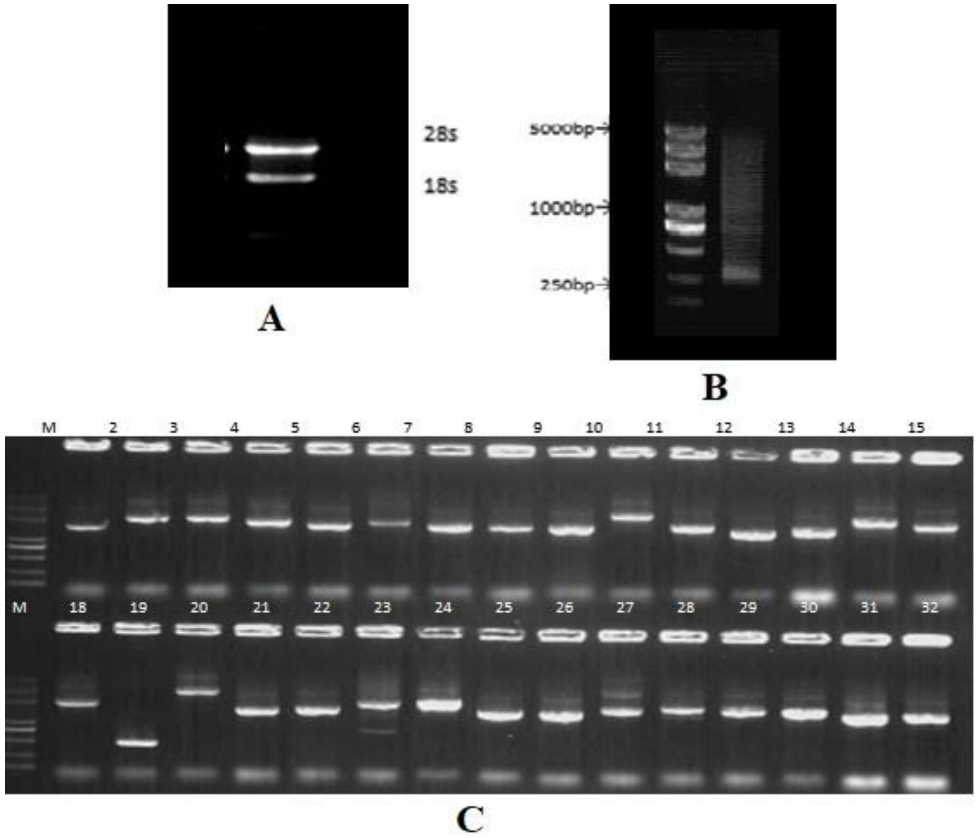

Figure 1. *Construction and identification of homogeneous cDNA library of barley embryos.* ***A*** *Detection of total DNA by 1.0% agorose;* ***B*** *The result of second cDNA ecletrophoresis. M: DL2, 000 plus marker, 1: the second Cdna;* ***C*** *The PCR identification of plasmid in the library. M: DL 2,000 plus marker, 2-32: the PCR products of the clonies*

Large-scale extraction, sequencing and bioinformatics analysis of library plasmids

The bacterial solution of barley cDNA library was amplified by PCR, and 5000 plasmids were finally extracted. Most of the amplified fragments are over 1000bp in size (*Fig. 2*). Considering the integrity of the DNA fragments, 120 plasmids with longer amplified fragments were selected and sequenced. Sequence data of 80 plasmids were obtained. A total of 71 genes were obtained after the duplication was removed (*Table 3*). The information about the sequences includes query coverage, percentage of identity, accession number, species and domain description. Information about 51 of these genes is known. Domain functions of some genes are related to Aldo/keto reductase family, EPSIN1, Zinc finger B-box type profile, Serine/Threonine, protein kinases active-site signature, AGD5, TPR repeat profile, NAF domain profile, AP2/ERF domain profile, Myb-type HTH DNA-binding domain profile, BARE-2, SAC9, Leucine-rich repeat profile, HEAT repeat profile, UBX domain profile, GRAS family profile, autophagy-related protein 7c (ATG7c), delta-1-pyrroline-5-carboxylate synthase, MO25-like protein and so on (*Table 3*). Information about 20 of these genes is unknown.

http://www.aloki.hu ● ISSN 1589 1623 (Print) ● ISSN 1785 0037 (Online)
DOI: http://dx.doi.org/10.15666/aeer/1706_1310513124

Stress-resistant genes mining is an important work in molecular breeding. The acquisition of these data lays a foundation for the discovery of genes.

Table 3. *Blast analysis of plasmid in library (from NCBI and Swiss-Prot databases). The symbol "-"indicates no matching information after blast analysis*

Number	Query coverage	Percentage of identity	Accession number	Species	Domain description
1	99%	98.73%	AK368673.1	*Hordeum vulgare*	*Aldo/keto reductase family*
4	90%	81%	MG560142.1	*Triticum aestivum*	*Fructose-1-6-bisphosphatase active site*
5	100%	99.87%	AK376197.1	*Hordeum vulgare*	Unknown
6	99%	100%	AK353866.1	*Hordeum vulgare*	*Trp-Asp (WD) repeats circular profile*
21	94%	97.19%	AK371436.1	*Hordeum vulgare*	*R3H domain profile*
23	99%	94.96%	AK248592.1	*Hordeum vulgare*	EPSIN1
24	94%	97.01%	AK355971.1	*Hordeum vulgare*	*Zinc finger B-box type profile*
26	82%	80.52%	AF474072.1	*Hordeum vulgare*	*Serine/Threonine protein kinases active-site signature*
27	100%	96.34%	AK372413.1	*Hordeum vulgare*	AGD5
29	95%	97.66%	AK371180.1	*Hordeum vulgare*	*TPR repeat profile*
30	95%	97.82%	AK359851.1	*Hordeum vulgare*	*NAF domain profile*
32	84%	80.08%	AB749310.1	*Triticum aestivum*	*AP2/ERF domain profile*
36	96%	97.09%	AK250324.1	*Hordeum vulgare*	Unknown
37	67%	95.24%	AK354512.1	*Hordeum vulgare*	Unknown
38	99%	95.39%	AM180263.1	*Hordeum vulgare*	*Myb-type HTH DNA-binding domain profile*
39	95%	96.70%	AK371597.1	*Hordeum vulgare*	*Armadillo/plakoglobin ARM repeat profile*
40	88%	95.04%	XM_020324227.1	*Aegilops tauschii*	Ras-group-related LRR protein 5-like
41	45%	94.92%	AK367111.1	*Hordeum vulgare*	Unknown
42	85%	84.37%	AJ279072.1	*Hordeum vulgare*	BARE-2
44	93%	97.63%	AK251198.1	*Hordeum vulgare*	Unknown
45	42%	99.36%	AK370277.1	*Hordeum vulgare*	Unknown

http://www.aloki.hu ● ISSN 1589 1623 (Print) ● ISSN 1785 0037 (Online)
DOI: http://dx.doi.org/10.15666/aeer/1706_1310513124

48	90%	98.92%	AK373080.1	*Hordeum vulgare*	*Type-1 KH domain profile*
49	68%	99.74%	AK357985.1	*Hordeum vulgare*	Unknown
50	64%	94.92%	AK252282.1	*Hordeum vulgare*	*Nucleolar GTP-binding protein 2*
51	99%	96.65%	AK365218.1	*Hordeum vulgare*	*Zinc-binding region signature*
53	99%	96.60%	AK365203.1	*Hordeum vulgare*	*Eukaryotic RNA Recognition Motif (RRM) profile*
55	98%	93.54%	AK447559.1	*Triticum aestivum*	*Putative DNA ligase 4-like (LOC100844955)*
57	76%	95.22%	AK365868.1	*Hordeum vulgare*	Unknown
58	99%	97.34%	AK364108.1	*Hordeum vulgare*	Unknown
59	27%	99.59%	AK371752.1	*Hordeum vulgare*	Beta-glucosidase BoGH3B-like
61	97%	92.31%	AB678347.1	*Hordeum vulgare*	Unknown
62	97%	97.00%	AK374311.1	*Hordeum vulgare*	Acyl-CoA-binding domain-containing protein
63	91%	91.80%	AP009567.1	*Hordeum vulgare*	*SPX domain profile*
64	98%	96.79%	AK358311.1	*Hordeum vulgare*	*AAA-protein family signature*
67	85%	96.98%	AK249586.1	*Hordeum vulgare*	Unknown
68	84%	92.81%	XM_020337903.1	*Aegilops tauschii*	*Solute carrier (Solcar) repeat profile*
69	56%	94.55%	AK360644.1	*Hordeum vulgare*	*Trp-Asp (WD) repeats circular profile*
70	85%	80.25%	AK370729.1	*Hordeum vulgare*	Unknown
73	99%	99.60%	AK357076.1	*Hordeum vulgare*	Mechanosensitive ion channel protein 10
74	99%	99.42%	AK252829.1	*Hordeum vulgare*	26S proteasome regulatory subunit 7A
75	99%	96.22%	XM_020340817.1	*Aegilops tauschii*	ABC transporter C family member 2
76	99%	99.02%	AK356202.1	*Hordeum vulgare*	Cycloeucalenol cycloisomerase
77	99%	98.77%	AK371292.1	*Hordeum vulgare*	Phosphatidylinositol 4-kinase gamma 6-like
78	91%	99.78%	AK356216.1	*Hordeum vulgare*	*DCUN1 domain profile*
79	99%	99.32%	AK372829.1	*Hordeum vulgare*	Unknown
80	98%	94.91%	AY268139.1	*Hordeum vulgare*	*Protein kinases ATP-binding region signature*

http://www.aloki.hu ● ISSN 1589 1623 (Print) ● ISSN 1785 0037 (Online)
DOI: http://dx.doi.org/10.15666/aeer/1706_1310513124

81	39%	95.96%	AK334556.1	*Triticum aestivum*	SAC9
83	99%	98.52%	AK250364.1	*Hordeum vulgare*	Unknown
84	98%	92.57%	MG560140.1	*Triticum aestivum*	Unknown
85	99%	97.33%	AP017301.1	*Hordeum vulgare*	*NADH dehydrogenase subunit 5 gene*
86	99%	96.78%	AK333961.1	*Triticum aestivum*	Unknown
88	99%	98.52%	AK365825.1	*Hordeum vulgare*	Unknown
89	91%	98.99%	AK364487.1	*Hordeum vulgare*	Unknown
90	97%	98.96%	AP017301.1	*Hordeum vulgare*	Mitochondrial DNA
91	79%	99.53%	AK355938.1	*Hordeum vulgare*	*RNA-binding protein Luc7-like 2*
92	99%	98.98%	AK362481.1	*Hordeum vulgare*	Signal recognition particle subunit SRP72
93	99%	98.74%	AK248376.1	*Hordeum vulgare*	Mitochondrial phosphate carrier protein 3
94	99%	83.66%	AP009567.1	*Hordeum vulgare*	*Leucine-rich repeat profile*
95	99%	99.24%	AK357387.1	*Hordeum vulgare*	*HEAT repeat profile*
96	99%	98.91%	AK364716.1	*Hordeum vulgare*	*UBX domain profile*
98	99%	97.81%	EF115541.1	*Hordeum vulgare*	*Ribosomal protein S12 signature*
100	99%	82.79%	AC256253.1	*Hordeum vulgare*	Unknown
102	99%	98.65%	AK359701.1	*Hordeum vulgare*	*GRAS family profile*
103	99%	99.41%	AK357819.1	*Hordeum vulgare*	*W2 domain profile*
104	99%	95.61%	KF294806.1	*Triticum aestivum*	Autophagy-related protein 7c (ATG7c)
108	72%	100%	AY552749.1	*Hordeum vulgare*	18S ribosomal RNA gene
111	94%	97.35%	AK251855.1	*Hordeum vulgare*	Delta-1-pyrroline-5-carboxylate synthase
113	99%	97.57%	AK248531.1	*Hordeum vulgare*	MO25-like protein
115	99%	95.72%	FM164415.1	*Hordeum vulgare*	HOX1
118	99%	94.87%	XM_020329084.1	*Aegilops tauschii*	*DBINO domain profile*
120	98%	99.12%	AK252011.1	*Hordeum vulgare*	Unknown

http://www.aloki.hu ● ISSN 1589 1623 (Print) ● ISSN 1785 0037 (Online)
DOI: http://dx.doi.org/10.15666/aeer/1706_1310513124

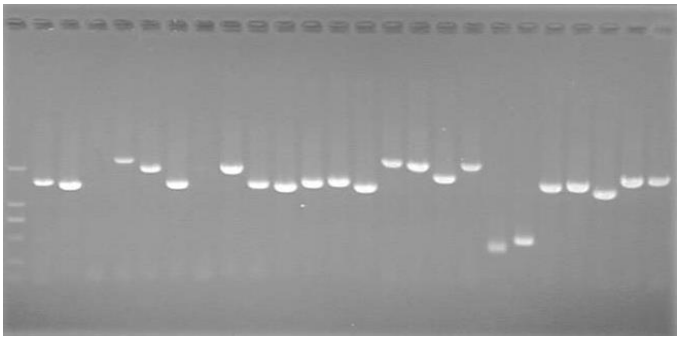

Figure 2. *The PCR results of liquid bacterial germ in the cDNA library*

Construction and self-activation detection of recombinant vector of decoy protein

RT-PCR was used to obtain a fragment size close to 500 bp, which was consistent with the expected fragment size (*Fig. 3A*). After sequencing, the size was confirmed to be 477 bp, which was found to be consistent with *TaRHA2b* gene sequence of wheat by sequence blast. The enzyme digestion results of decoy vector pGBKT7-*TaRHA2b* were shown in *Figure 3B*. After plasmid sequencing, sequence blast was compared and found to be consistent with the *TaRHA2b* gene sequence of wheat, indicating that *TaRHA2b* fragment was correctly integrated into the polyclonal site of pGBKT7 vector.

Yeast strains AH109 on SD/-Leu/-Trp/-Ade/-His medium did not grow after 3-5 d (*Fig. 3C*). This indicated that the yeast strain AH109 had no phenotypic mutation in the secondary culture. The experimental group, positive control group and negative control group grew on the SD/-Leu/-Trp medium (*Fig. 3D*). The positive control grew on the SD/-Leu/-Trp/-His/-Ade medium, but neither the experimental group nor the negative control grew on the SD/-Leu/-Trp/-His/-Ade medium (*Fig. 3E*). The results show that the decoy carrier pGBKT7-*TaRHA2b* has no self-activation function.

cDNA library was screened by decoy protein pGBKT7-RsRHA2b

A total of 1000 plasmids of a pair of transgenic yeast AH109 cells were tested (*Fig. 4A–C*), and the preliminary positive plasmids were 84 and 49 were effectively sequenced, all of which were analyzed by bioinformatics (*Table 4*). The information about the sequences includes query coverage, percentage of identity, accession number, species and domain description. The RHA2b interacting proteins include RGA, MYB, SF2, USP1, Lks2, Rp120, SBE starch branching enzyme, RPR44, TUDOR1, TEF1, auxin response factor 12, Hox-1, CBF9, TIP1, AP2/EREBP, MYB and ARF GTPase activator (*Table 4*).

The focus of the present research was plasmids in the following codes: 311, 611, 1065, 2433, 2437, 2438, 2443, 2449, 2450, 2456, 2457, 2475, 2476, 2496, 2708, 3019. In the process of in vitro and in vitro verification of yeast two-hybrid candidate proteins, 8 of them were finally selected, with codes 2449, 2450, 2456, 2457, 2475, 2476, 2496, 2708.

A pair of positive plasmids were co-transformation for in vitro validation

pGADT$_7$-*YTH2450* and pGBKT$_7$-*TaRHA2b* were co-transformed into yeast AH109 cells and then cultured on SD/–Trp–Leu–His–Ade medium for 3d (*Fig. 5*). The results showed that YTH2450 and RHA2b had a strong interaction.

http://www.aloki.hu ● ISSN 1589 1623 (Print) ● ISSN 1785 0037 (Online)
DOI: http://dx.doi.org/10.15666/aeer/1706_1310513124

The primers were designed according to the homologous sequences obtained by bioinformatics analysis of *YTH2450*. The obtained plasmid pMAL-*YTH2450* was sequenced. After bioinformatics analysis has determined that the fragment is correct, subsequent operations can be carried out. The final pMAL-*YTH2450* recombinant plasmid and its enzyme digestion identification results showed that it was correct (*Fig. 6A*). PCR was performed on the bacterial solution containing *pLEICS-TaRHA2b* plasmid, and the results were shown in *Figure 6B*. The size of the target fragment was consistent with the expectation. Sequencing was performed, bioinformatics analysis was performed to determine the correct fragment, and subsequent operations were carried out.

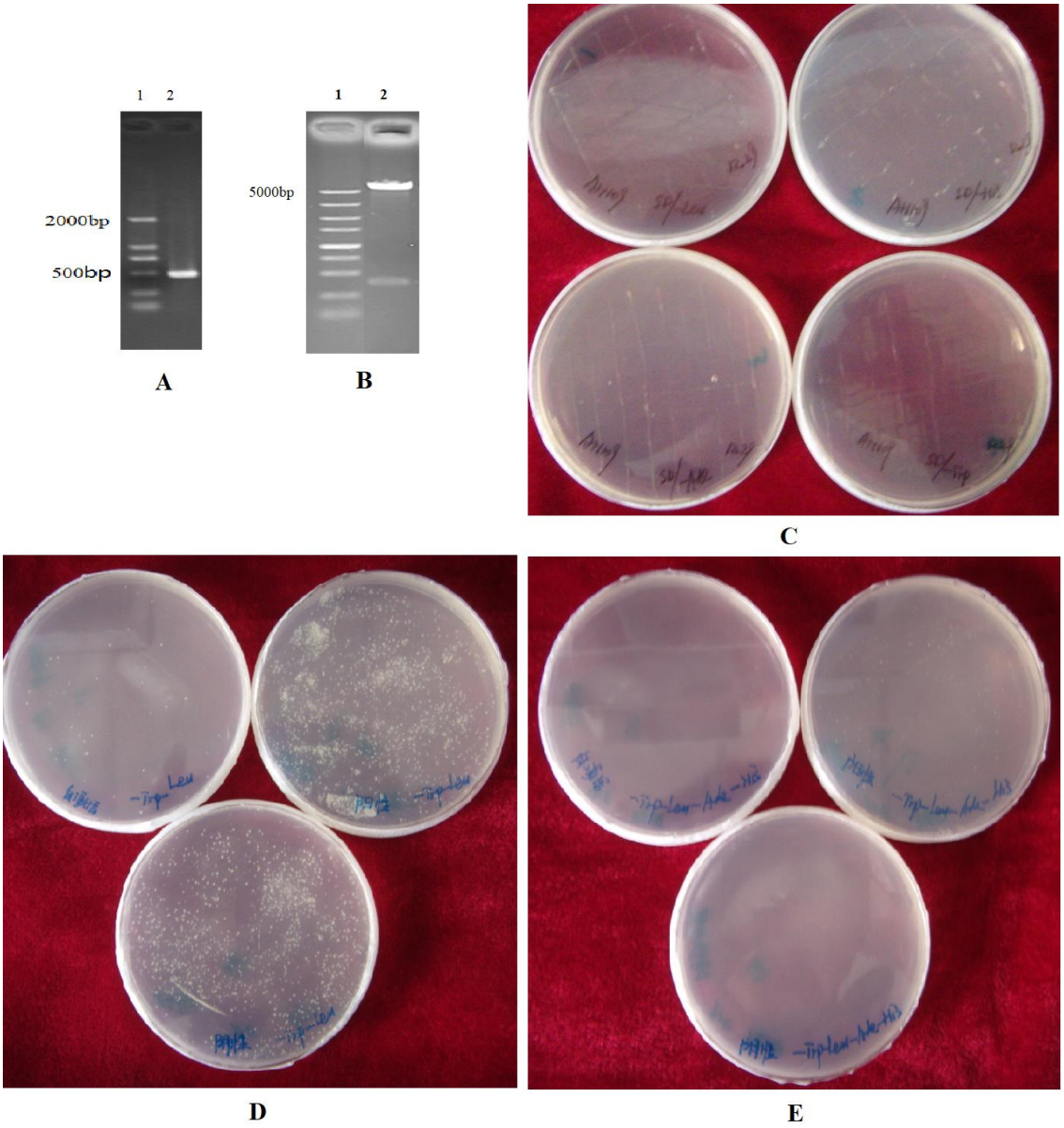

Figure 3. *Construction and self-activation detection of recombinant vector of decoy protein.* ***A*** *Clone of TaRHA2b gene, 1, Marker 2000; 2, the target fragment.* ***B*** *Enzyme digestion identification of pGBKT7-TaRHA2b, 1, Marker 5000; 2, the target fragment.* ***C*** *Growth of AH109 on each single defect medium.* ***D*** *The growth of the experimental group and the control group on SD/-Leu/-Trp medium.* ***E*** *The growth of the experimental group and the control group on SD/-Leu/-Trp/-His/-Ade medium*

http://www.aloki.hu ● ISSN 1589 1623 (Print) ● ISSN 1785 0037 (Online)
DOI: http://dx.doi.org/10.15666/aeer/1706_1310513124

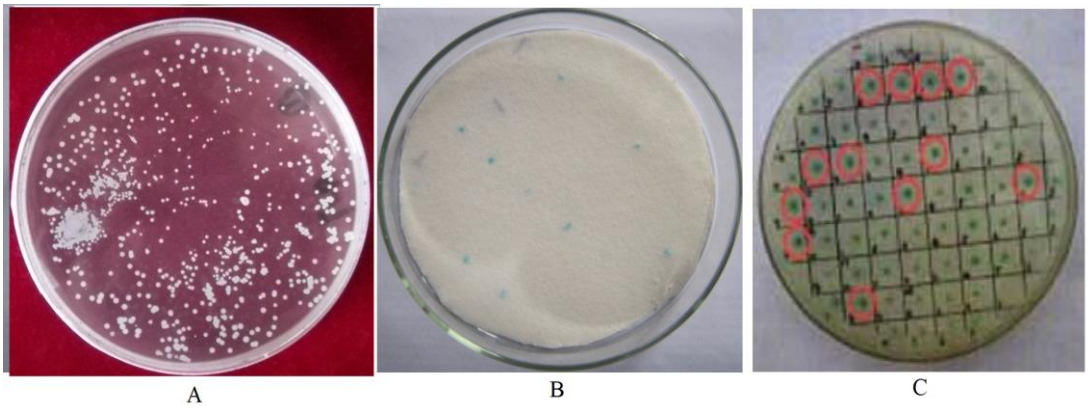

Figure 4. *cDNA library was screened by decoy protein pGBKT7-RsRHA2b.* ***A*** *The growth of co-transformation prey/bait AH109 on SD/-Leu/-Trp/-His/-Ade medium.* ***B*** *β-galactosidase color reaction of positive clones.* ***C*** *β-galactosidase color reaction of positive clones (circled with red lines)*

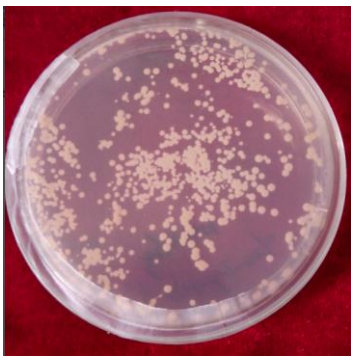

Figure 5. *The growth of co-transformation prey/bait AH109 in SD/-Leu/-Trp/-His/-Ade medium. pGADT$_7$-YTH2450 and pGBKT$_7$-TaRHA2b were co-transformed into yeast*

Table 4. *Blast analysis of positive plasmids (from NCBI and Swiss-Prot databases). The symbol "-"indicates no matching information after blast analysis*

Plasmid number	Barley			Wheat			Domain description
	Query coverage	Percentage of identity	Accession number	Query coverage	Percentage of identity	Accession number	
266	68%	78.80%	AK370200.1	91%	94.34%	AK455561.1	Mucin like protein
267	83%	99.89%	AK375235.1	-	-	-	NADH ubiquinone oxidoreductase subunit, NDUFA12
269	88%	99.22%	AK248821.1	-	-	-	RGA
271	52%	98.24%	AK372313.1	-	-	-	MYB
277	76%	94.49%	AY641412.1	69%	87.22%	KX447407.1	SF2, USP1
282	90%	99.19%	AK362421.1	24%	87.23%	MG560142.1	NADH dehydrogenase subunit 5
285	47%	78.10%	AC256251.1	-	-	-	Unknown
286	90%	92.41%	AB678347.1	18%	89.57%	CD903273.1	Lks2
291	89%	99.68%	AK370771.1	89%	96.88%	AK447925.1	Mechanosensitive ion channel protein
292	89%	99.03%	AK251731.1	89%	86.30%	AJ315040.1	18S rRNA gene (EST)
293	89%	99.34%	AK252316.1	89%	96.7%	BT009474.1	Rp120
302	67%	99.29%	AK355938.1	-	-	-	Putative RNA-binding protein Luc7-like 2-like
306	91%	99.25%	AK357819.1	91%	97.37%	JX978407.1	T16 eIF5-mimic protein (5MP) mRNA

http://www.aloki.hu ● ISSN 1589 1623 (Print) ● ISSN 1785 0037 (Online)
DOI: http://dx.doi.org/10.15666/aeer/1706_1310513124

311	90%	99.95%	FN179383.1	90%	98.53%	BT008928.1	SBE starch branching enzyme
594	89%	99.55%	AK359743.1	88%	90.78%	HE996524.1	PPR repeat family
611	90%	99.59%	AK363669.1	89%	95.74%	AK331993.1	Pyridine nucleotide-disulphide oxidoreductase
633	89%	88.96%	AF453665.1	-	-	-	Sukkula retrotransposon
1063	23%	97.49%	KC472759.1	76%	92.74%	AK333658.1	RPR44
1065	89%	99.37%	AK252316.1	89%	94.04%	AK453829.1	TUDOR1
1068	21%	80.66%	EU812563.1	21%	79.37%	AB201446.1	Rpg
1069	58%	98.71%	AK250775.1	40%	96.52%	AK336110.1	Dehydrogenase/reductase SDR family member 7-like
1072	90%	97.82%	AK357798.1	89%	93.48%	JN412070.1	60S ribosomal protein L5 mRNA
1078	88%	98.78%	AK250680.1	88%	95.96%	AK454722.1	TEF1
2433	64%	99.30%	AK372028.1	-	-	-	DDT domain protein
2436	88%	92.16%	AK249066.1	84%	83.64%	AK452430.1	Chitobiase/beta-hexosaminidase C-terminal domain
2437	78%	98.68%	AK358361.1	89%	95.15%	KY795022.1	Auxin response factor 12
2438	70%	92.90%	AK364219.1	84%	96.08%	AK332649.1	E3 UFM1-protein ligase 1 homolog
2443	89%	94.29%	DQ249273.1	88%	82.43%	EU660898.1	E3 UFM1-protein ligase 1 homolog
2449	89%	92.06%	FJ477091.1	89%	77.69%	FN564428.1	Hox-1
2450	89%	99.68%	AK357510.1	89%	96.50%	AK452889.1	2-oxoglutarate/malate translocator
2456	58%	98.57%	AK251632.1	39%	90.48%	GU452718.1	Rho-related protein from plants (Rop)-like
2457	91%	98.85%	KC912689.1	91%	97.39%	KC912694.1	PS II 43,44 kDa protein (psbC) mRNA
2461	79%	99.73%	AK366008.1	-	-	-	Cytochrome P450
2462	89%	94.56%	DQ445253.1	89%	78.15%	MG560140.1	CBF9
2463	89%	93.41%	FJ477091.1	89%	77.32%	FN564428.1	Hox1
2473	-	-	-	89%	82.37%	FN564429.1	Unknown
2475	86%	99.67%	AK362415.1	86%	96.42%	AK455067.1	NADB_Rossmann Superfamily
2476	90%	95.56%	AF254799.1	90%	82.55%	FN564431.1	TIP1, TIP2, Rar1
2486	91%	100%	NC_042692.1	91%	99.79%	MH051715.1	Ribosomal_L2_C
2487	90%	99.48%	AK371367.1	90%	96.90%	AK330835.1	Ribosomal_L10_P0
2495	89%	99.79%	AM055812.1	88%	92.48%	CJ834723.1	GPH_sucrose
2496	89%	99.68%	HQ647352.1	80%	84.63%	FJ560496.1	AP2/EREBP protein
2708	82%	99.6%	AK371673.1	-	-	-	MYB
3005	90%	98.30%	AK363781.1	90%	91.68%	AK331286.1	Lipase
3014	91%	99.59%	AK363781.1	91%	96.85%	AK331992.1	40S ribosomal protein S4 mRNA
3018	83%	96.89%	NC_043837.1	68%	96.89%	MK253668.1	Chloroplast
3019	90%	100%	AK364064.1	91%	95.15%	AK332298.1	SINT5
3039	91%	99.12%	AK370200.1	57%	93.57%	GU563378.1	ARF GTPase activator

The size of the expressed protein was about 75.0 KDa, which was consistent with the expected size of 75.0 KDa, indicating the successful expression of prokaryotic protein (*Fig. 6C*). The size of the expressed protein was about 63.0 KDa, which was consistent with the expected size of 63.0 KDa, indicating the successful expression of prokaryotic protein (*Fig. 6D*).

GST-*TaRHA2b* was fixed to Glutathione-Sepharose4B column and GST (inducing expression of empty vector pLEICS-14) was fixed as negative control. After repeated washing, SDS-PAGE analysis was performed. YTH2450 can bind specifically to GST-TaRHA2b (swim lane 1), but not to negative control GST (swim lane 2) (*Fig. 6E*). It indicates that there is an interaction between TaRHA2b and YTH2450 in vitro.

http://www.aloki.hu ● ISSN 1589 1623 (Print) ● ISSN 1785 0037 (Online)
DOI: http://dx.doi.org/10.15666/aeer/1706_1310513124

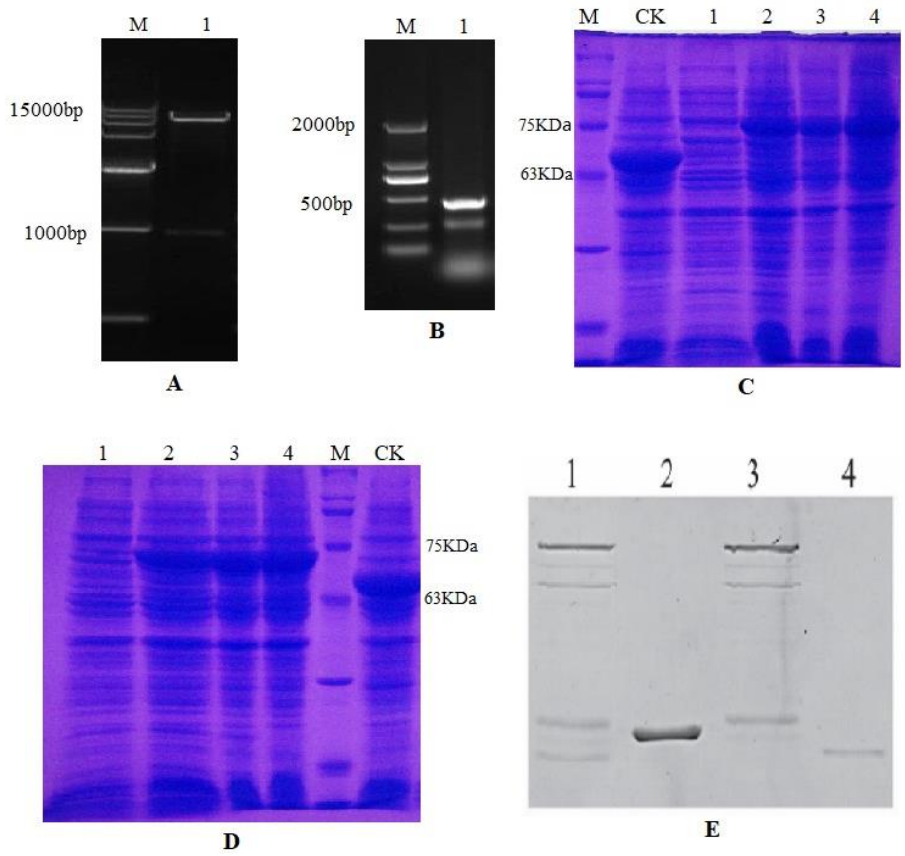

Figure 6. *GST-pull down validation.* ***A*** *Recombinant plasmid and enzyme digestion identification of pMAL-YTH2450. M: DL15000; 1: target product.* ***B*** *PCR results of BL21 containing pLEICS-TaRHA2b recombinant plasmid. M: DL2000, 1, the target fragment.* ***C*** *Prokaryotic expression of YTH2450. M: 11 kDa-245 kDa, CK, pMAL empty vector, 1-4, IPTG induction for 1 h,2 h,3 h and 5 h, respectively.* ***D*** *Prokaryotic expression of TaRHA2b. M: 11 kDa-245 kDa, CK, pMAL empty vector, 1-4, IPTG induction for 1 h,2 h,3 h and 5 h, respectively.* ***E*** *Pull-down assay of TaRHA2b and YTH2450. 1. pull down product of GST-TaRHA2b and YTH2450; 2. pull down product of GST and YTH2450; 3. GST-TaRHA2b for the pull down experiment; 4. the purified YTH2450*

Discussion

The development of cDNA library technology provides an important tool for functional genome research (Shao et al., 2009). At present, cDNA libraries are widely used in the research of model organisms and important crops, including tobacco, peanut and soybean (Ke et al., 2011; Cai et al., 2007). cDNA libraries provide information that reflects the level of gene expression at the RNA level. There are not many studies on the cDNA library of barley, and the construction of the cDNA library based on the embryo of barley treated by ABA treatment has not been studied. This project aims to explore the specific regulatory network of *TaRHA2b* gene in ABA signal transduction pathway and study the interaction between proteins. The yeast two-hybrid technique is the first choice. The construction of high-quality homogeneous cDNA library is the basis of subsequent experiments. Homogenization can ensure the existence of low-abundance mRNA as far as possible, which is necessary for the successful construction of cDNA library. In SMART technology, LD PCR method is adopted to obtain dscDNA, which

http://www.aloki.hu ● ISSN 1589 1623 (Print) ● ISSN 1785 0037 (Online)
DOI: http://dx.doi.org/10.15666/aeer/1706_1310513124

can obtain longer fragments as far as possible, fully reflecting the integrity of mRNA (Schuler, 1997; Wellenreuther et al., 2004). In this experiment, the homogeneous cDNA library was constructed with a capacity of 1.1 10^6. Random clone sequencing results showed that the fragment size was within the range of 1000-3000 bp. The storage capacity requirement of cDNA library is above 1.7 10^5 (Thanh et al., 2011). Only when this standard is reached, the low abundance mRNA can be well processed and the constructed library can be used for the yeast two-hybrid screening library experiment.

In the present study, the yeast AH109 was deficient in the synthesis ability of Leu, Trp, His and Ade. The synthesis of Leu and Trp was remedied when the plasmid was transformed into yeast. As for His, there is a possibility of background expression in yeast. However, it was found that AH109 could not grow in the SD/-His medium without 3-AT in the defect validation experiment on yeast. Therefore, 3-AT was not added in this experiment. In this experiment, the decoy vector pGBKT$_7$-TaRHA2b for yeast two-hybrid system was successfully constructed. The decoy vector can be expressed normally in yeast without toxicity. It is proved that it has no self-activation in the system.

Yeast two-hybrid screening consists of two methods. The first method was to screen AH109 by co-transposing decoy protein granules with ds cDNAs. Although this method is simple, the library can only be used once and it is difficult to screen the interacting proteins. The second was screened by conjugation of two inverters, including Y187 yeast inverter containing decoy protein and AH109 yeast inverter containing pGADT$_7$-Rec and ds-cDNAs. The operation of this method is complex. In this experiment, a pair of total transformed yeast AH109 was used. If positive interaction was confirmed, specific plasmids could be directly corresponding. The follow-up operation is more efficient.

Using the protein expressed by the limited PHS resistance gene *RHA2b* as bait, we screened some corresponding fragments of TaRHA2b-related proteins by yeast two-hybrid technology, which not only has important significance in searching for new PHS resistance genes, but also provides new information for studying the mechanism of TaRHA2b-mediated PHS resistance.

The interaction between TaRHA2b and interacting proteins was fully demonstrated by positive clones identification, sequencing, verification of the pair of repeated co-transformation and GST-pull down.

These conclusions lay a foundation for studying the interaction and mechanism of TaRHA2b/YTH2450, TaRHA2b/YTH2456 and TaRHA2b/YTH2476 in the stress tolerance pathway of wheat. The complex formed by yeast hybrid candidate proteins and TaRHA2b may act on different signal transduction pathways. Bioinformatics analysis showed that the function of YTH2450 may be malate/ketoglutarate transporter, the function of YTH2456 may be RACD protein, and the function of YTH2476 may be TIP1 protein.

TaRHA2b is a protein of the type of transcription factor positively regulated by ABA signal transduction, which is essentially an ubiquitinated ligase and mainly participates in the process of protein degradation in cells. RHA2b targeted MYB30 degradation to regulate ABA signal transduction (Zheng et al., 2018).

Ketoglutaric acid/malate transporter was involved in the tricarboxylic acid cycle. The present study showed a strong interaction between ketoglutarate/malate transporter and TaRHA2b. The process of ubiquitination involves the formation of multiple complexes and changes in energy metabolism. α-ketoglutarate carrier protein (OGCP), located on

http://www.aloki.hu ● ISSN 1589 1623 (Print) ● ISSN 1785 0037 (Online)
DOI: http://dx.doi.org/10.15666/aeer/1706_1310513124

mitochondria, encodes 314 amino acids and has the following important functions: scavenging endogenous oxygen free radicals in mitochondria and participating in cellular energy metabolism (De Palma et al., 2010; Regalado et al., 2013). These results indicated that the complex formed by ketoglutarate transporters and TaRHA2b could be involved in ABA signal transduction.

RAC/ROP involved in plant (ROP) family is related to small molecule G protein, which is a molecular switch of signal transduction in many cells, regulating the development process of cells and the response to the environment. RAC/ROP has three conformations, including an active GTP binding state, a transient free state, and a GDP bound state. In the active GTP binding state, RAC/ROP interacts with effector proteins to initiate downstream signaling (Haitina et al., 2006). These results indicate that the complex formed by RAC/ROP and TaRHA2b can activate the downstream signal and then play a role in a specific pathway.

TIP1 protein is a water channel protein, which can theoretically be expressed in all tissues, but the expression amount is not the same (Wudick et al., 2009). Therefore, in response to ABA, an abiotic stress, or in the climate where spikelet germination occurs, it is very likely that the complex formed by TIP1 and RHA2b participates in these regulatory pathways. These results lay a foundation for further study on the interaction and mechanism of TaRHA2b and protein-protein interaction in wheat stress resistance pathway.

Conclusion

The information of cDNA library lays a foundation for the discovery of stress resistance genes. TaRHA2b interact with YTH2450 and other proteins. The TaRHA2b interacting proteins could be used for genetic improvement of crops, further improving the adaptability of crops to the environment. The detailed regulatory mechanism mediated by TaRHA2b and interacting proteins needs to be further studied.

Acknowledgements. This work was supported by the "Twelfth Five-Year" National Science and Technology Projects in Rural Areas (2013BADD04B01-02) and Henan Science and Technology Project (162102110007).

Conflict of interests. The authors state no conflict of interests.

REFERENCES

[1] Cai, N., Huang, X., Zhuang, W. (2007): Construction and identification of a full-length cDNA library from peanut seeds. – Journal of Peanut Science 2: 1-6.

[2] Cho, S. K., Ryu, M. Y., Seo, D. H., Kang, B. G., Kim, W. T. (2011): The arabidopsis ring E3 ubiquitin ligase AtAIRP2 plays combinatory roles with AtAIRP1 in abscisic acid-mediated drought stress responses. – Plant Physiology 157: 2240-2257.

[3] De Palma, A., Prezioso, G., Spagnoletta, A., Genchi, G., Scalera, V. (2010): The oxoglutarate/malate carrier of rat brain mitochondria operates by a uniport exchange mechanism. – Journal of Bioenergetics and Biomembranes 42: 371-379.

[4] Fields, S., Song, O. (1989): A novel genetic system to detect proteinprotein interactions. – Nature 340: 245-246.

http://www.aloki.hu ● ISSN 1589 1623 (Print) ● ISSN 1785 0037 (Online)
DOI: http://dx.doi.org/10.15666/aeer/1706_1310513124

[5] Haitina, T., Lindblom, J., Renstrom, T., Fredriksson, R. (2006): Fourteen novel human members of mitochondrial solute carrier family 25 (SLC25) widely expressed in the central nervous system. – Genomics 88: 779-790.
[6] Haynes, C. M., Caldwell, S. R., Cooper, A. A. (2002): An HRD/DER-independent ER quality control mechanism involves Rsp5p-dependent ubiquitination and ER-Golgi transport. – Journal of Cell Biology 158: 91-102.
[7] Jiang, H., Li, H., Bu, Q., Li, C. (2009): The RHA2a-interacting proteins ANAC019 and ANAC055 may play a dual role in regulating ABA response and jasmonate response. – Plant Signaling & Behavior 4: 464-466.
[8] Ke, T., Dong, C.-H., Mao, H., Zhao, Y.-Z., Liu, H.-Y., Liu, S.-Y. (2011): Construction of a normalized full-length cDNA library of sesame developing seed by DSN and SMART™. – Agricultural Sciences in China 10: 1004-1009.
[9] Kurkela, S., Franck, M. (1990): Cloning and characterization of a cold-and ABA-inducible Arabidopsis gene. – Plant Molecular Biology 15: 137-144.
[10] Li, D., Lyu, G., Lyu, J., Niu, H., Wang, X., Jun, Y. (2019): Cloning and characterization of a wheat RING finger gene TaRHA2b whose expression is up-regulated by ABA treatment. – Applied Ecology and Environmental Research 17: 7495-7510.
[11] Li, H., Jiang, H., Bu, Q., Zhao, Q., Sun, J., Xie, Q., Li, C. (2011): The arabidopsis ring finger E3 ligase RHA2b acts additively with RHA2a in regulating abscisic acid signaling and drought response. – Plant Physiology 156: 550-563.
[12] Nelson, D. C., Flematti, G. R., Riseborough, J., Ghisalberti, E. L., Dixon, K. W., Smith, S. M. (2010): Karrikins enhance light responses during germination and seedling development in Arabidopsis thaliana. – Proceedings of the National Academy of Sciences of the United States of America 107: 7095-7100.
[13] Regalado, A., Pierri, C. L., Bitetto, M., Laera, V. L., Pimentel, C., Francisco, R., Passarinho, J., Chaves, M. M., Agrimi, G. (2013): Characterization of mitochondrial dicarboxylate/tricarboxylate transporters from grape berries. – Planta 237: 693-703.
[14] Robinson, T. J., Dinan, M. A., Dewhirst, M. W., Garciablanco, M. A., Pearson, J. L. (2010): SplicerAV: a tool for mining microarray expression data for changes in RNA processing. – BMC Bioinformatics 11: 108-108.
[15] Sajan, S. A., Warchol, M. E., Lovett, M. (2007): Toward a systems biology of mouse inner ear organogenesis: gene expression pathways, patterns and network analysis. – Genetics 177: 631-653.
[16] Schuler, G. D. (1997): Pieces of the puzzle: expressed sequence tags and the catalog of human genes. – Journal of Molecular Medicine 75: 694-698.
[17] Shao, Z., Cong, X., Yuan, J., Yang, G., Chen, Y., Pan, J., An, L. (2009): Construction and characterization of a cDNA library from head kidney of Japanese sea bass (Lateolabrax japonicus). – Molecular Biology Reports 36: 2031-2037.
[18] Smalle, J. A., Vierstra, R. D. (2004): The ubiquitin 26S proteasome proteolytic pathway. – Annual Review of Plant Biology 55: 555-590.
[19] Stone, S. L. (2014): The role of ubiquitin and the 26S proteasome in plant abiotic stress signaling. – Frontiers in Plant Science 5: 135-135.
[20] Thanh, T., Chi, V. T. Q., Abdullah, M. P., Omar, H., Noroozi, M., Ky, H., Napis, S. (2011): Construction of cDNA library and preliminary analysis of expressed sequence tags from green microalga Ankistrodesmus convolutus Corda. – Molecular Biology Reports 38: 177-182.
[21] Usadel, B., Blaesing, O. E., Gibon, Y., Retzlaff, K., Hoehne, M., Guenther, M., Stitt, M. (2008): Global transcript levels respond to small changes of the carbon status during progressive exhaustion of carbohydrates in arabidopsis rosettes. – Plant Physiology 146: 1834-1861.
[22] Wellenreuther, R., Schupp, I., Poustka, A., Wiemann, S. (2004): Smart amplification combined with cDNA size fractionation in order to obtain large full-length clones. – BMC Genomics 5: 36-36.

http://www.aloki.hu ● ISSN 1589 1623 (Print) ● ISSN 1785 0037 (Online)
DOI: http://dx.doi.org/10.15666/aeer/1706_1310513124

[23] Wudick, M. M., Luu, D., Maurel, C. (2009): A look inside: localization patterns and functions of intracellular plant aquaporins. – New Phytologist 184: 289-302.
[24] Zheng, Y., Schumaker, K. S., Guo, Y. (2012): Sumoylation of transcription factor MYB30 BY the small ubiquitin-like modifier E3 ligase Siz1 mediates abscisic acid response in arabidopsis thaliana. – Proceedings of the National Academy of Sciences of the United States of America 109: 12822-12827.
[25] Zheng, Y., Chen, Z., Ma, L., Liao, C. (2018): The ubiquitin E3 ligase RHA2b promotes degradation of MYB30 in abscisic acid signaling. – Plant Physiology 178: 428-440.

http://www.aloki.hu ● ISSN 1589 1623 (Print) ● ISSN 1785 0037 (Online)
DOI: http://dx.doi.org/10.15666/aeer/1706_1310513124

EFFECTS OF CADMIUM ON GROWTH AND THE UPTAKE OF CADMIUM AND MICRONUTRIENTS BY TOBACCO (*NICOTIANA TABACUM* L.) CULTIVARS

KINAY, A.[1*] – ERDEM, H.[2]

[1]*Department of Field Crops, Faculty of Agriculture, Gaziosmanpasa University, 60240 Tokat, Turkey*

[2]*Departement of Soil Science and Plant Nutrition, Faculty of Agriculture, Gaziosmanpasa University, 60240 Tokat, Turkey*

**Corresponding author*
e-mail: ahmetkinay@gmail.com; phone: + 90-356-252-1616/2117

(Received 28th May 2019; accepted 9th Sep 2019)

Abstract. Tobacco (*Nicotiana tabacum* L.) can accumulate higher concentrations of cadmium (Cd). However, genotypic differences of tobacco cultivars in Cd uptake and their responses to Cd toxicity have not been thoroughly investigated. This study was conducted to determine the resistance of four tobacco cultivars to Cd toxicity under greenhouse conditions. Four doses of Cd (0, 5, 10 and 20 mg kg^{-1} soil) were used to test the resistance of tobacco cultivars. Increasing the Cd applications significantly ($P < 0.01$) decreased the shoot dry matter yields of genotypes, while shoot Cd concentration and content significantly ($P < 0.01$) increased. The highest decrease in dry matter under the highest Cd (Cd20) treatment was in Özbaş (58.5% reduction), Birlik/124 (52.4% reduction) and Canik190/5 (51.1% reduction) cultivars, while the lowest decrease was in Xanthi/81 (44.6% reduction) cultivar. The amount of Cd removed from soil was significantly different among the tobacco cultivars. The highest Cd uptake was obtained in Cd20, while the lowest was in Xanthi/81 (395.2 µg Cd $plant^{-1}$) and Canik190/5 (232.6 µg Cd $plant^{-1}$) cultivars, respectively. The results revealed that Canik190/5 cultivar removes lower Cd compared to the other cultivars, whereas Cd uptake of Xanthi/81 cultivar is higher, thus is considered more resistant to Cd toxicity than other cultivars.
Keywords: *Nicotiana tabacum L., heavy metal, pollution, soil, yield*

Introduction

Cadmium (Cd), having a toxic effect on all living organisms, is one of the most dangerous heavy metal pollutants in the ecosystem (Mishra et al., 2019). The major sources of Cd in soils are geological parent material and inputs from human activities. Extraneous sources of cadmium are phosphorus fertilizers (54 to 58%), atmospheric storage (39 to 41%) and sewage sludge and farm manure applications (2 to 5%) (Cheng et al., 2014). The Cd uptake ratio of plants is high, due to its high-water solubility and mobility in soil compared to the other metals. Therefore, Cd is considered to be the most dangerous heavy metal accumulated in soils. The Cd causes many physiological changes due to changes in nitrogen and carbohydrate metabolism in plants. Cadmium inactivates the enzymes in -SH groups of proteins, closes stomata, causes water loss by transpiration and deterioration of chlorophyll biosynthesis (Sharma et al., 2019). The severity of heavy metal stress of plants varies depending on the environmental factors and the growth stage of plants (Stolt et al., 2003). The Cd resistance, uptake and transport of Cd in plant significantly vary among plant species. Grant et al. (1998) indicated that Cd concentrations of wheat, pea, maize and tobacco grown in the same solution culture were considerably different, and wheat contained lower Cd

http://www.aloki.hu ● ISSN 1589 1623 (Print) ● ISSN 1785 0037 (Online)
DOI: http://dx.doi.org/10.15666/aeer/1706_1312513134

concentration than the others. The magnitude of Cd accumulation and location of Cd in plants are major determinants of the plant resistance to Cd toxicity (Obata and Umebayashi, 1993; Quezada-Hinojosa et al., 2015). The responses of plant species and even between cultivars of a particular species to Cd toxicity considerably differ due to the prominent genetic variability among the different cultivars. The results reported by Erdem et al. (2012, 2017) for tobacco, Socha et al. (2015) for soybean, Wang et al. (2016) for maize, Zhang et al. (2002) for wheat and Zorrig et al. (2019) for lettuce clearly point out the effects of genetic variation in Cd uptake of plants. Several metal-tolerance mechanisms were introduced to explain the responses minimizing the adverse effects of heavy metal exposure. The Cd immobilization at the cell wall is the first prevention mechanism to prevent from excess Cd effect (Rizwan et al., 2016). Preventing the penetration of Cd into the cytosol, complexation of Cd with peptides or proteins to form phytochelatins and metallothioneins, compartmentalizing of Cd within vacuoles, and improving the antioxidative defense systems are major causes defined to explain the Cd detoxification in plants (Kirkham, 2006). Tobacco is one of the most common substances consumed for pleasure in the world. However, smoke of tobacco products is the most prevalent means of Cd reception of human, especially for smokers (Willers et al., 2005). Tobacco is known as an efficient Cd accumulator (Lugon-Moulin et al., 2004). Therefore, studies on investigating the effects of different Cd concentrations on Cd uptake of the commonly grown tobacco cultivars are needed. Determining the genetic variation of tobacco cultivars in Cd accumulation and uptake mechanisms are also important for the plant breeders. Research, particularly, focusing on metal uptake of international and local commercial tobacco cultivars used for tobacco products is missing.

This study was carried out to investigate the effects of different Cd concentrations on the growth of various tobacco cultivars, to determine the responses of tobacco cultivars in terms of Cd concentration and uptake, and to comprehend the interactions between Cd and Fe, Zn, Cu and Mn in tobacco plants.

Materials and methods

Materials

A pot experiment using Özbas, Canik190/5, Xanthi/81 and Birlik/124 tobacco cultivars was carried out at the greenhouse in Gaziosmanpasa University, Tokat, Turkey. Some characteristics of the genotypes used in the experiment are given in *Table 1.* The soil, used in the pot experiment was sandy loam, high in $CaCO_3$ content (11.8%), slightly alkaline in pH (8.01), low in organic matter content (0.89%) and Zn concentration (0.38 mg kg^{-1}), sufficient in Fe, Mn and Cu concentrations (6.65, 3.97 and 1.98 mg kg^{-1}), respectively), and low in Cd concentration (0.004 mg kg^{-1}).

Table 1. *Some characteristics of tobacco genotypes used in the experiment (Peksüslü, 1998)*

Genotypes	Flowering	Plant height (cm)	Number of leaves	Quality degree
Özbaş	Medium late	60-85	35-40	Medium
Canik190/5	Early	75-95	32-35	Medium
Xanthi/81	Medium late	65-105	30-32	High
Birlik/124	Medium late	85-125	40-44	High

http://www.aloki.hu ● ISSN 1589 1623 (Print) ● ISSN 1785 0037 (Online)
DOI: http://dx.doi.org/10.15666/aeer/1706_1312513134

Methods

Experiment

Greenhouse experiment was carried out in Field Research Centre of Tokat Gaziosmanpasa University located at 40°20'02.19"N latitude and 36°28'30.11"E longitude and 623 m above sea level, Tokat Province in middle Black Sea region of Turkey. The pot experiment was laid in a randomized plot design with three replications. Tobacco seedlings in a 4-leaf stage were transferred to the plastic pots filled with 2.75 kg sandy loam soil. Air-dried soil, prior to filling the pots, was homogeneously mixed with a fertilizer solution containing 250 mg N kg^{-1} soil as $Ca(NO_3)_2.4H_2O$, 100 mg P kg^{-1} soil as KH_2PO_4, 2.0 mg Fe kg^{-1} soil as Fe-EDTA and 2.0 mg Zn kg^{-1} soil as $ZnSO_4.7H_2O$. The treatments were control (Cd0), 5.0 (Cd5), 10 (Cd10) and 20 (Cd20) mg Cd kg^{-1}, and each treatment was replicated three times. The Cd was applied as a solution containing $3(CdSO_4).8H_2O$. Pots were watered as needed using deionized water. At 42 days after the transplanting of seedlings, leaves were harvested when the Cd toxicity symptoms (decline in growth and chlorosis in leaves) were observed (*Fig. 1*). The leaves were dried in an oven at 70 °C till constant weight. Dry weights (DW) of leaves were expressed as g DW of plants. Dried plant materials were powdered and then digested in a microwave oven using 2 ml of 35% H_2O_2 and 5 ml of 65% HNO_3. The Cd, Fe, Zn, Cu, and Mn concentrations were determined by inductively coupled plasma atomic emission spectroscopy (Varian Vista) (Bataglia et al., 1978). The Cd content of plant material was calculated by multiplying the dry weight of shoot by the concentration of Cd. The measurements of the metal concentrations were cross-checked by using the reference leaf samples of the National Institute of Standards and Technology (Gaithersburg, MD, USA).

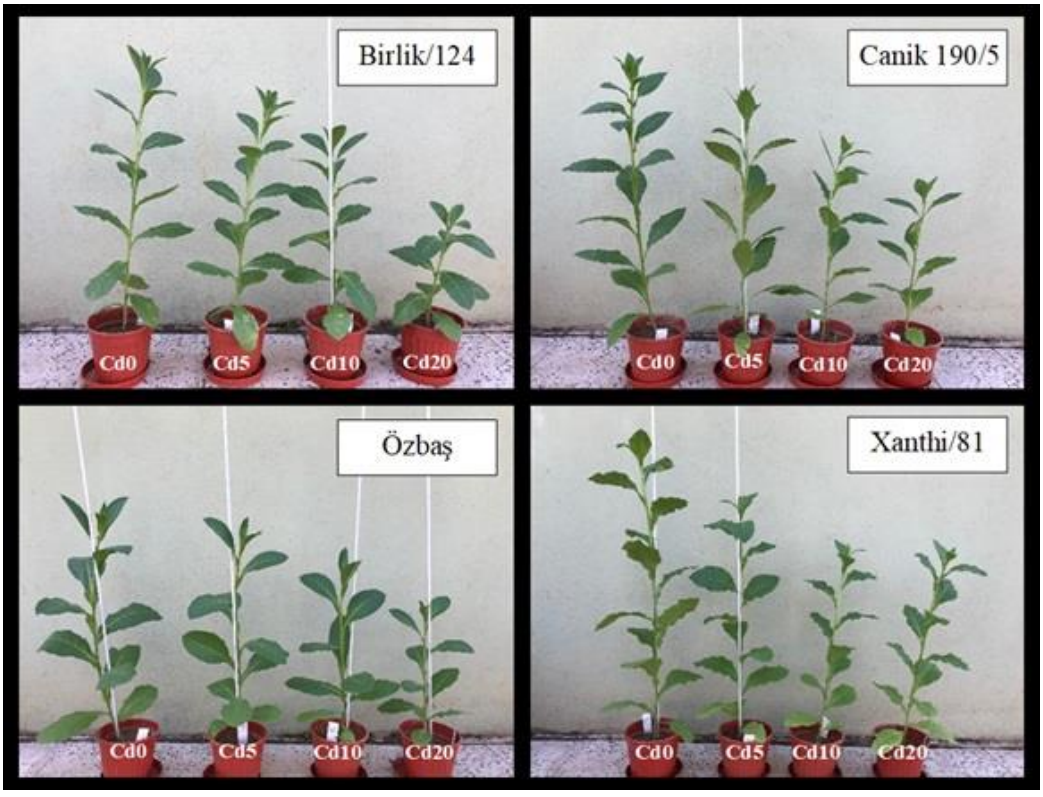

Figure 1. *Effects of increasing doses of cadmium on tobacco genotypes*

http://www.aloki.hu ● ISSN 1589 1623 (Print) ● ISSN 1785 0037 (Online)
DOI: http://dx.doi.org/10.15666/aeer/1706_1312513134

Statistical analyses

Analyses of variance (ANOVA) were performed to test the Cd dose effects on element concentrations and content of four different tobacco cultivars and on dry matter yield. The means were compared with Duncan's homogeneity test to determine whether the average concentrations and content of tobacco grown in the treated pots differed from those of tobacco grown in the control pots. The dose effect was considered significant when the P-value lower than 0.05. The statistical analyses were performed using the MSTAT-C statistical software.

Results and discussion

Effect of cadmium on shoot dry matter yield, Cd concentration and Cd content

The increasing Cd doses significantly ($P < 0.01$) reduced the shoot dry matter yield of four tobacco cultivars (*Table 2*). The highest decrease in dry matter yield with increasing Cd dose was observed in Özbaş, Birlik/124, and Canik190/5 cultivars respectively, and the lowest was in Xanthi/81 cultivar. The dry matter yield of Özbaş cultivar in control treatment (0 mg Cd kg^{-1}, Cd0) was 6.90 g $plant^{-1}$ which reduced to 2.87 g $plant^{-1}$ (58.5% reduction) with Cd20 application, whereas dry matter yield of Xanthi/81 cultivar was 7.63 g $plant^{-1}$ under Cd0 and decreased to 4.23 g of $plant^{-1}$ (44.6%) with Cd20 treatment (*Table 2*). The results of dry matter yield revealed that the Xanthi/81 is the least affected genotype from Cd toxicity. In a similar study conducted under greenhouse conditions testing five Cd doses (0, 100, 200 and 300 ppm) using 17 different tobacco cultivars, dry matter yields of cultivars significantly decreased with increasing Cd doses. However, the decrease in dry matter yield was significantly different among genotypes. The highest decrease in dry matter yield was reported in Connecticut (21% reduction), Drama (19% reduction), Myrodata Agryniou (18% reduction) and Katerini 53 (5% reduction) genotypes respectively, while the lowest decrease was obtained in Katerini 53 (5% reduction) and Argyroudis genotypes (Vasiliadou and Dordas, 2009).

Erdem et al. (2017) reported a significant decrease in dry matter yield of Xhanti 2A tobacco cultivar with increasing Cd doses (0, 10 and 20 mg Cd kg^{-1}). Dry matter yield in Cd20 (1.48 g of $plant^{-1}$) treatment was 47.5% lower compared to the control (2.82 g $plant^{-1}$). In another study conducted with maize, a significant decrease in shoot dry matter yield was reported with increasing Cd doses. The reduction in shoot dry matter yield was 11.9% with 10 mg Cd kg^{-1} and 23.5% with 20 mg Cd kg^{-1} treatment (Khurana and Jhanji, 2014). The decrease in dry matter yield with Cd treatment was attributed to the phytotoxic effect of Cd (Pereira et al., 2011). Cadmium toxicity negatively affects the photosynthesis of plants by inhibiting the activities of photosynthetic enzymes involved in Kalvin cycle and chlorophyll biosynthesis and consequently results in a decrease in dry matter yield (Sun et al., 2017).

Cadmium can be easily transferred to the green parts of plants following the taken up by roots. The mobility of Cd in soils is higher than other heavy metals (Mn, Zn, Mo and Se), thus can be easily taken up by many plant species (Moral et al., 2002). Therefore, a positive relationship was often reported between the increasing doses of Cd application and shoot Cd concentration and content. Shoot Cd concentrations and content of four tobacco cultivars were significantly ($P < 0.01$) increased with increasing Cd application to the soil (*Table 2*). The lowest shoot Cd concentration under Cd20 treatment was obtained for Canik190/5 (79.8 mg kg^{-1}) and the highest Cd concentration was for Özbaş (117.5 mg kg^{-1}) cultivars (*Table 2*).

http://www.aloki.hu ● ISSN 1589 1623 (Print) ● ISSN 1785 0037 (Online)
DOI: http://dx.doi.org/10.15666/aeer/1706_1312513134

Table 2. *The effects of increasing Cd doses on dry matter yield, shoot Cd concentration and content of four different tobacco cultivars*

Cultivar	Cd doses (mg kg^{-1})	Shoot dry matter** (g plant^{-1})	Decrease in shoot dry matter (%)	Shoot Cd concentration** (mg kg^{-1})	Shoot Cd content** (µg plant^{-1})
Özbaş	0	6,90^{a}	-	0,39^{d}	2,70^{c}
	5	4,97^{b}	27,9	47,6^{c}	237,3^{b}
	10	4,11^{bc}	40,5	65,0^{b}	260,0^{ab}
	20	2,87^{c}	58,5	117,5^{a}	337,3^{a}
	Average	**4,71^{B}**	**-**	**57,4^{B}**	**209,3^{AB}**
Canik190/5	0	5,99^{a}	-	0,34^{d}	2,05^{b}
	5	5,51^{ab}	8,0	42,9^{c}	238,5^{a}
	10	4,03^{bc}	32,7	55,4^{b}	222,7^{a}
	20	2,93^{c}	51,1	79,8^{a}	232, 6^{a}
	Average	**4,62^{B}**	**-**	**44,6^{D}**	**173,9^{B}**
Xanthi/81	0	7,63^{a}	-	0,35^{d}	2,62^{c}
	5	5,68^{b}	25,6	41,8^{c}	239,1^{b}
	10	4,37^{b}	42,7	71,2^{b}	310,6^{ab}
	20	4,23^{b}	44,6	93,4^{a}	395,2^{a}
	Average	**5,48^{A}**	**-**	**51,7^{C}**	**236,9^{A}**
Birlik/124	0	5,31^{a}	-	0,39^{d}	2,10^{c}
	5	4,71^{ab}	11,2	52,1^{c}	243,2^{b}
	10	3,69^{b}	30,5	84,8^{b}	312,9^{a}
	20	2,53^{c}	52,4	112,4^{a}	284,1^{a}
	Average	**4,06^{B}**	**-**	**62,4^{A}**	**210,6^{AB}**
Cultivar*Cd dose		**ns**		**	*

**p < 0.01, *p < 0.05, ns: non significant; small letters: differences in genotypes in terms of cadmium doses; capital letters: differences between genotypes

The Cd uptake and accumulation considerably differ between plant species and genotypes of the same species (Grant et al., 1998). The differences in Cd uptake and accumulation among plant species are considered as the main factors in determining plant tolerance to Cd toxicity (Obata and Umebayashi, 1993). The results indicated that the Cd uptake of plants significantly different between the cultivars used in the experiment. The highest Cd uptake (395.2 µg plant^{-1}) at Cd20 dose was in Xanthi/81 cultivar and the lowest was in Canik190/5 (232.6 µg plant^{-1}) (*Table 2*).

The results of shoot Cd concentration and content revealed that Cd uptake of Canik cultivar is lower than the other tobacco cultivars. On the other hand, the resistance level of Xanthi/81 cultivar to Cd toxicity is considered higher compared to the other three tobacco cultivars due to the lower decrease in dry matter yield and higher Cd uptake under the increased Cd application doses *(Table 2; Fig. 2)*. The Cd resistance of Xanthi/81 cultivar could be related to the detoxification of heavy metals. Similar to the finding of the current study, many studies have indicated that most of the plant species are capable of tolerating high Cd concentrations in soil (Mench et al., 1989; Cieśliński et al., 1998; Rizwan et al., 2016). Plants can build up tissue tolerance at different levels when exposed to high Cd concentration. Khan et al. (1984) reported that Cd accumulates in the cell wall, whereas Vazquez et al. (1992) reported that Cd accumulates in the vacuole in a study conducted with bean plants.

http://www.aloki.hu ● ISSN 1589 1623 (Print) ● ISSN 1785 0037 (Online)
DOI: http://dx.doi.org/10.15666/aeer/1706_1312513134

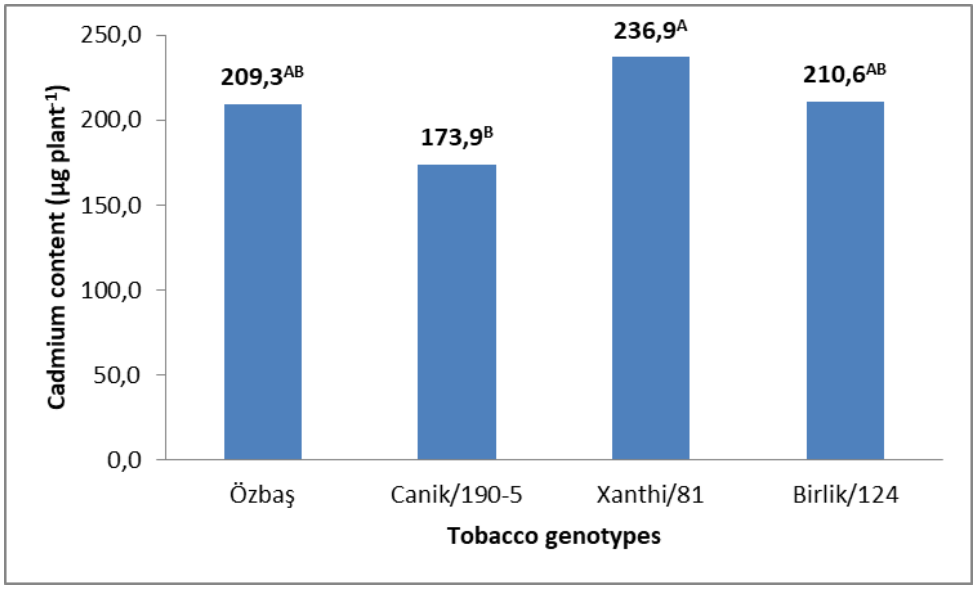

Figure 2. *Average cadmium content (µg Cd plant^{-1}) of tobacco genotypes*

Effect of cadmium on shoot Zn, Fe, Mn and Cu concentrations

Interaction of Cd with mineral nutrients (especially microelements) is an important effect of Cd toxicity in plants. The increasing Cd application dose to soil caused a decrease in the shoot Zn concentrations of 4 different tobacco varieties (*Table 3*). The decreases in shoot Zn concentration were insignificant for Canik190/5 and Birlik/124 cultivars, while it was significant ($P < 0.01$) for Özbaş and Xanthi/81 cultivars. The Zn concentration of Xanthi/81 cultivar under Cd0 dose was 108.2 mg kg^{-1}, which decreased to 74.5, 68.7 and 66.8 mg kg^{-1} at Cd5, Cd10, Cd20 doses, respectively. Vasiliadou and Dordas (2009) reported that increasing Cd application doses resulted in statistically significant reductions in shoot Zn concentrations (-0.542 ***) of 17 different tobacco cultivars. The decrease in Zn concentrations under increasing Cd doses may be linked to the antagonistic relationship between Cd and Zn. Higher Cd uptake of plants grown under Zn deficiency can be attributed to the competition of Cd and Zn, which have similar chemical properties, for absorption points on the membrane (Cakmak et al., 2000) and, increase in the membrane permeability (Cakmak and Marschner, 1988).

The shoot Fe concentrations of 4 different tobacco cultivars decreased with increasing Cd doses. The decrease was statistically significant in Canik190/5 while it was insignificant in the other three cultivars (*Table 3*). The Fe concentration of Canik190/5 cultivar was 64.8 mg kg^{-1} under control treatment, which decreased to 55.3, 54.8, and 57.4 mg kg^{-1} with Cd5, Cd10, and Cd20 treatments, respectively. Significant increases and decreases occurred in shoot Mn concentrations of the cultivars with Cd application. However, shoot Cu concentrations of all cultivars, particularly in the Cd10 and Cd20 treatments, decreased with Cd application (*Table 3*).

For example, shoot Cu concentration in Cd0 dose was 6.71 mg kg^{-1}, which decreased to 6.56 in Cd5, while increased to 28.7 and 25.9 mg kg^{-1} in Cd10 and Cd20 doses, respectively (*Table 3*). Erdem et al. (2012) reported that the increasing doses of Cd resulted in a statistically significant ($P < 0.05$) increase in shoot Cu concentration of tobacco plants. The results pointed out the importance of Cu absorption and/or translocation to the shoots, in contrast to the other essential micronutrients, under the

http://www.aloki.hu ● ISSN 1589 1623 (Print) ● ISSN 1785 0037 (Online)
DOI: http://dx.doi.org/10.15666/aeer/1706_1312513134

high concentration of Cd in the root zone. In addition, shoot Cu concentrations of all tobacco cultivars used in the experiment were not affected by Cd5 treatments, whereas Cd10 and Cd20 treatments significantly affected the shoot Cu concentrations. Ramos et al. (2002) reported that increasing doses of Cd caused a decrease in shoot Fe, Zn and Cu concentrations of lettuce plants grown under the water culture conditions, while an increase in Mn concentration. The results indicated a general decrease in the Zn, Fe and Mn concentrations of tobacco plants with increasing the doses Cd application to soils. This situation reveals that the most important cause of the decrease in ion uptake of plants grown under Cd stress is the prevention of root growth and development due to damage of plant roots under Cd toxicity (Rizvan et al., 2016).

Table 3. *The effects of increasing Cd doses on shoot Zn, Fe, Mn and Cu concentrations of 4 different tobacco cultivars*

Cultivar	Cd doses (mg kg^{-1})	Zn** (mg kg^{-1})	Fe** (mg kg^{-1})	Mn^{ns} (mg kg^{-1})	Cu** (mg kg^{-1})
Özbaş	0	82.5^{a}	71.8^{ns}	36.9	5.98^{b}
	5	65.9^{ab}	58.8 ^{ns}	41.0	6.26^{b}
	10	60.5^{b}	58.4 ^{ns}	41.3	29.5^{a}
	20	68.7^{ab}	62.1 ^{ns}	39.5	26.6^{a}
	Average	**69.4^{AB}**	**62.8^{AB}**	**39.7**	**17.1**
Canik190/5	0	85.2^{ns}	64.8^{a}	38.8	6.16^{b}
	5	73.3^{ns}	55.3^{b}	37.2	4.54^{b}
	10	62.8^{ns}	54.8^{b}	33.6	28.3^{a}
	20	60.3^{ns}	57.4^{ab}	34.5	27.7^{a}
	Average	**70.4^{AB}**	**58.1^{B}**	**36.0**	**16.7**
Xanthi/81	0	108.2^{a}	74.0^{ns}	38.8	4.92^{c}
	5	74.5^{b}	60.0^{ns}	34.2	3.92^{c}
	10	68.7^{b}	57.2^{ns}	39.1	28.7^{a}
	20	66.8^{b}	65.8^{ns}	36.5	23.6^{b}
	Average	**79.6^{A}**	**64.2^{AB}**	**37.1**	**15.30**
Birlik/124	0	66.9^{ns}	78.3^{ns}	39.6	6.71^{b}
	5	60.7^{ns}	59.0^{ns}	38.2	6.56^{b}
	10	52.9^{ns}	71.7^{ns}	35.5	28.7^{a}
	20	58.1^{ns}	72.9^{ns}	34.8	25.9^{a}
	Average	**59.7^{B}**	**70.5^{A}**	**37.0**	**17.0**
Cultivar x Cd dose		**ns**	**ns**	**ns**	**ns**

**p < 0.01, *p < 0.05, ns: non significant; small letters: differences in genotypes in terms of cadmium doses; capital letters: differences between genotypes

Conclusions

Cadmium pollution in soils is a worldwide serious problem for sustainable agriculture and human health (Dumat et al., 2019). This study presents novel information about the effects of toxic Cd doses on the growth of tobacco cultivars, the amount of Cd uptake from the soil, and uptake of microelements. Shoot dry matter yields of tobacco cultivars significant (P < 0.01) reduced with the increasing doses of

http://www.aloki.hu ● ISSN 1589 1623 (Print) ● ISSN 1785 0037 (Online)
DOI: http://dx.doi.org/10.15666/aeer/1706_1312513134

Cd application to soil. The greatest reduction has occurred in Özbaş, Birlik/124 and Canik190/5 cultivars, while the lowest was in Xanthi/81 cultivar. The Cd concentration and content of shoots significantly ($P < 0.01$) increased with the increase in Cd doses. The Xanthi/81 taken up the highest Cd concentration from soil under the highest Cd treatment (Cd20), while Canik190/5 cultivar removed lower Cd from soil compared to the other cultivars. The Cd treatments resulted in a decrease in shoot Zn and Fe concentrations of tobacco cultivars, while increases and decreases occurred for Mn concentrations. The Cu concentration of shoots significantly increased in Cd10 and Cd20 treatments. The results revealed that Canik190/5 cultivar uptakes lower Cd from the soil compared to the other three tobacco cultivars. In contrast, Xanthi/81 cultivar uptakes higher Cd from the soil, thus considered more resistant to Cd toxicity than other tobacco cultivars. The data obtained will contribute to the basic knowledge needed for further research on the genetic and biochemical basis of cadmium uptake of tobacco genotypes.

Conflict of interests. The authors have not declared any conflict of interests.

REFERENCES

[1] Bataglia, O. C., Teixeira, J. P. F., Furlani, P. R., Furlani, A. M. C., Gallo, J. R. (1978): Métodos de análise química de plantas. – IAC, Campinas.
[2] Cakmak, I., Marschner, H. (1988): Increase in membrane permeability and exudation in roots of zinc deficient plants. – J. Plant Physiol. 132(3): 356-361.
[3] Cakmak, I., Welch, R. M., Erenoğlu, B., Romheld,V., Norvell, W. A., Kochian, L. V. (2000): Influence of varied zinc supply on re-translocation of cadmium (^{109}Cd) and rubidium (^{86}Rb) applied on mature leaf of durum wheat seedlings. – Plant and Soil 219(1-2): 279-284.
[4] Cheng, K., Tian, H. Z., Zhao, D., Lu, L., Wang, Y., Chen, J., Huang, Z. (2014): Atmospheric emission inventory of cadmium from anthropogenic sources. – International Journal of Environmental Science and Technology 11(3): 605-616.
[5] Cieśliński, G., Van Rees, K. C. J., Szmigielska, A. M., Krishnamurti, G. S. R., Huang, P. M. (1998): Low-molecular-weight organic acids in rhizosphere soils of durum wheat and their effect on cadmium bioaccumulation. – Plant Soil 203(1): 109-117.
[6] Dumat, C., Pierart, A., Shahid, M., Khalid, S. (2019): Pollutants in urban agriculture. – Bioremediation of Agricultural Soils 100: 61.
[7] Erdem, H., Kınay, A., Ozturk, M., Tutus, Y. (2012): Effect of cadmium stress on growth and mineral composition of two tobacco cultivars. – Journal of Food, Agriculture & Environment 10(1): 965-969.
[8] Erdem, H., Kınay, A., Günal, E., Yaban, H., Tutuş, Y. (2017): The effects of biochar application on cadmium uptake of tobacco. – Carpathian Journal of Earth and Environmental Sciences 12(2): 447-456.
[9] Grant, C. A., Buckley, W. T., Bailey, L. D., Selles, F. (1998): Cadmium accumulation in crops. – Can. J. Plant Sci. 78(1): 1-17.
[10] Khan, D. H., Duckett, J. G., Frankland, B., Kirkham, J. B. (1984): An X-ray microanalytical study of the distribution of cadmium inroots of Zea mays L. – J. Plant Physiol. 115(1): 19-28.
[11] Khurana, M. P. S., Jhanji, S. (2014): Influence of cadmium on dry matter yield, micronutrient content and its uptake in some crops. – Journal of Environmental Biology 35(5): 865.

http://www.aloki.hu ● ISSN 1589 1623 (Print) ● ISSN 1785 0037 (Online)
DOI: http://dx.doi.org/10.15666/aeer/1706_1312513134

[12] Kirkham, M. B. (2006): Cadmium in plants on polluted soils. Effects of soil factors, hyperaccumulation, and amendments. – Geoderma 137(1-2): 19-32.
[13] Lugon-Moulin, N., Zhang, M., Gadani, F., Rossi, L., Koller, D., Krauss, M., Wanger, G. J. (2004): Critical review of the science and options for reducing cadmium in tobacco (*Nicotiana tabacum L.*) and other plants. – Adv. Agron. 83: 111-180.
[14] Mench, M., Tancogne, J., Gomez, A., Juste, C. (1989): Cadmium bioavailability to *Nicotiana tabacum L., Nicotiana rustica L., and Zea mays L.* grown in soil amended or not amended with cadmium nitrate. – Biology and fertility of soils 8(1): 48-53.
[15] Mishra, S., Bharagava, R. N., More, N., Yadav, A., Zainith, S., Mani, S., Chowdhary, P. (2019): Heavy Metal Contamination: An Alarming Threat to Environment and Human Health. – In: Sobti, R. C. et al. (eds.) Environmental Biotechnology: For Sustainable Future. Springer, Singapore, pp. 103-125.
[16] Moral, R., Cortés, A., Gomez, I., Mataix-Beneyto, J. (2002): Assessing changes in Cd phytoavailability to tomato in amended calcareous soils. – Bioresource Technology 85(1): 63-68.
[17] Obata, H., Umebayashi, M. (1993): Production of SH compounds in higher plants of different tolerance to Cd. – Plant and Soil 155(1): 533-536.
[18] Peksüslü, A. (1998): Morphological, physiological and biochemical properties of some tobacco types in İzmir-Bornova conditions. – PhD Thesis. Ege University Science Inst. Bornova, Izmir.
[19] Pereira, B. F. F., Rozane, D. E., Araújo, S. R., Barth, G., Queiroz, R. J. B., Nogueira, T. A. R. Malavolta, E. (2011): Cadmium availability and accumulation by lettuce and rice. – Revista Brasileira de Ciência do Solo 35(2): 645-654.
[20] Quezada-Hinojosa, R., Föllmi, K. B., Gillet, F., Matera, V. (2015): Cadmium accumulation in six common plant species associated with soils containing high geogenic cadmium concentrations at Le Gurnigel, Swiss Jura Mountains. – Catena 124: 85-96.
[21] Ramos, I., Esteban, E., Lucena, J. J., Gárate, A. (2002): Cadmium uptake and subcellular distribution in plants of *Lactuca sp*. Cd–Mn interaction. – Plant Sci. 162: 761-767.
[22] Rizwan, M., Ali, S., Adrees, M., Rizvi, H., Zia-ur-Rehman, M., Hannan, F., Ok, Y. S. (2016): Cadmium stress in rice: toxic effects, tolerance mechanisms, and management: a critical review. – Environmental Science and Pollution Research 23(18): 17859-17879.
[23] Sharma, A., Kumar, V., Shahzad, B., Ramakrishnan, M., Sidhu, G. P. S., Bali, A. S., Bakshi, P. (2019): Photosynthetic response of plants under different abiotic stresses: a review. – Journal of Plant Growth Regulation. https://doi.org/10.1007/s00344-019-10018-x.
[24] Socha, P., Bernstein, N., Rybanský, Ĺ., Mészáros, P., Gálusová, T., Spieß, N., Matušíková, I. (2015): Cd accumulation potential as a marker for heavy metal tolerance in soybean. – Israel Journal of Plant Sciences 62(3): 160-166.
[25] Stolt, J. P., Sneller, F. E. C., Bryngelsson, T., Lundborg, T., Schat, H. (2003): Phytochelatin and cadmium accumulation in wheat. – Environmental and Experimental Botany 49(1): 21-28.
[26] Sun, H., Wang, X., Shang, L., Zhou, Z., Wang, R. (2017): Cadmium accumulation and its effects on nutrient uptake and photosynthetic performance in cucumber (*Cucumis sativus L.*). – Philippine Agricultural Scientist (Philippines) 100(3): 263-270.
[27] Vasiliadou, S., Dordas, C. (2009): Increased concentration of soil cadmium affects on plant growth, dry matter accumulation, Cd, and Zn uptake of different tobacco cultivars (*Nicotiana tabacum L.*). – International Journal of Phytoremediation 11(2): 115-130.
[28] Vázquez, M. D., Poschenrieder, C. H., Barceld, Y. (1992): Cadmium in bean roots. – New Phytologist 120(2): 215-226.
[29] Wang, A., Wang, M., Liao, Q., He, X. (2016): Characterization of Cd translocation and accumulation in 19 maize cultivars grown on Cd-contaminated soil: implication of maize cultivar selection for minimal risk to human health and for phytoremediation. – Environmental Science and Pollution Research 23(6): 5410-5419.

http://www.aloki.hu ● ISSN 1589 1623 (Print) ● ISSN 1785 0037 (Online)
DOI: http://dx.doi.org/10.15666/aeer/1706_1312513134

[30] Willers, S., Gerhardsson, L., Lundh, T. (2005): Environmental tobacco smoke (ETS) exposure in children with asthma-relation between lead and cadmium and cotinine concentrations in urine. – Respir. Med. 99: 1521-1527.
[31] Zorrig, W., Cornu, J. Y., Maisonneuve, B., Rouached, A., Sarrobert, C., Shahzad, Z., Berthomieu, P. (2019): Genetic analysis of cadmium accumulation in lettuce (*Lactuca sativa*). – Plant Physiology and Biochemistry 136: 67-75.

http://www.aloki.hu ● ISSN 1589 1623 (Print) ● ISSN 1785 0037 (Online)
DOI: http://dx.doi.org/10.15666/aeer/1706_1312513134

MOLECULAR IDENTIFICATION OF CLINICAL MICROBES IN THALASSEMIA PATIENTS USING 16S rRNA GENE SEQUENCING

PISHTIWAN, A. H.* – KHADIJA, KH. M.

Department of Biology, College of Education, Salahaddin University-Erbil, Iraq

**Corresponding author*
e-mail: pishtiwan.hamad@su.edu.krd; phone: +964-750-462-6670

(Received 28th May 2019; accepted 2nd Sep 2019)

Abstract. Bacteria that are not identified by utilizing automated and manual systems can be identified precisely using 16S rRNA gene sequencing. It can also be used to characterize previously undescribed species. In the present study, the experiment entailed 16S rRNA sequencing of bacteria isolated from thalassemia patients in Erbil, Iraq. Samples were obtained from thalassemia patients from different sources. The bacteria were first identified by biochemical and Vitek method, and finally, the 16S rRNA of 78 clinical bacteria were amplified by PCR and sequenced. The results of the sequencing methods performed on the clinical bacteria identified the isolates as 5 genera and 7 species: *E. coli*, *P. aeruginosa*, *K. oxytoca*, *K. pneumoniae*, *M. morganii*, *E. fergusonii,* and *Pantoea sp*. The results show that the most common causative organism was *E. coli*, and the most common site of infection was found to be the urinary tract. The results demonstrated the significance of 16S rRNA sequencing in accurate identification bacteria and understanding the bacterial diversity. Given the advantages of 16S rRNA sequencing method including cost-effectiveness, availability, and convenience, and it would be worthwhile to integrate it into clinical practice in developing countries.
Keywords: *E. coli, microbial identification, VITEK 2, 16S rRNA gene, phylogenetic analysis*

Introduction

As a severe genetic blood disorder that results from a mutation in the globin gene, thalassemia causes excessive destruction of red blood cells. Its prevalence has been reported to be high among populations in Southeast Asia, Africa, and the Mediterranean region. Given the severity of its clinical presentation, thalassemia syndrome has been classified into 3 subgroups: thalassemia minor, thalassemia intermediate, and thalassemia major. Patients with thalassemia major have been the focus of most studies of bacterial infections (Vichinsky, 2005; Weatherall, 2012). According to the estimations, Beta-thalassemia afflicts more than 42000 newborns every year all over the world. If the patients are not treated, for example through blood transfusion, Beta-thalassemia major (TM) causes the infected children to die before they are 3 years old (Modell and Darlison, 2008).

As major complications and the second most frequently reported cause of mortality, infections have been referred to as the main cause of death in patients with thalassemia. A range of immune abnormalities, splenectomy, iron overload, and severe anaemia are the predisposing factors for infection in patients with thalassemia. *Yersinia enterocolitica* in western countries and *Klebsiella* spp in Asia have been introduced as the major causative organisms of bacterial infections in thalassaemic patients (Vento et al., 2006). The most common bacterial infections in thalassaemic patients are liver abscesses, septicaemia, soft tissue infection, biliary tract infection, and pneumonia, while the most frequently isolated bacteria are reported to be *Yersinia enterocolitica*, *Salmonella typhi*, *Streptococcus*

http://www.aloki.hu ● ISSN 1589 1623 (Print) ● ISSN 1785 0037 (Online)
DOI: http://dx.doi.org/10.15666/aeer/1706_1313513146

pneumoniae, *Escherichia coli*, *Klebsiella pneumoniae*, and other gram-negative bacteria (Aswapokee, 1988; Issaragrisil, 1988; Peng et al., 2000; Wanachiwanawin, 2000; Li et al., 2001; Chung et al., 2003; Wang et al., 2003). Yet, no studies have been carried out on bacterial infections in patients with thalassemia in the Kurdistan Region of Iraq.

Biochemical techniques and traditional culture are still the major methods in clinical microbiology laboratories to identify most pathogens. However, as technology has developed more than ever, many laboratories have adopted automated microbiology systems for the purpose of identifying pathogens. In recent years, there have been more reports on severe infections among patients. In most laboratories, the automated biochemical text platforms can be utilized to identify a number of clinical isolates from such patients. However, identifying some isolates is difficult through those platforms (Cheng et al., 2014). Currently, precise and fast identification of infectious agents is referred to as one of the main challenges for public health surveillance and clinical practice. Even the presence of a pathogen is usually vague in the setting of clinical syndromes like sepsis because causative agents are cultured in less than half of these cases (Martin et al., 2003), which leads to treating a large number of patients empirically. In addition, as indicated by several studies, patient outcomes, especially in the intensive care unit setting, can be significantly improved by appropriate, rapid, and adequate antibiotic treatments, moreover, it has been stated that patient mortality increases by 2 folds in the absence of such treatments (Iregui et al., 2002; Shorr et al., 2011). Therefore, molecular methods for bacterial identification are highly recommended.

Complete sequencing of the genome of some bacteria has been performed since automated DNA sequencing and polymerase chain reaction (PCR) were invented. As revealed by comparing the genomic sequences of bacterial species, the 16S ribosomal RNA (rRNA) gene is strongly conserved within a species and among species of the same genus; therefore, it can be utilized as a novel gold standard for specifying bacteria (Woo et al., 2000). The 16S rRNA gene sequences are very useful to study bacterial taxonomy and phylogeny. Over time, the function of the 16S rRNA gene has not changed despite the presence of the gene in almost all bacteria, often existing as a multigene family or operons, which suggests the fact that time is more accurately measured through random sequence changes, and the 16S rRNA gene (1500 bp) is large enough for informatic purposes (Patel, 2001). It has been stated that applying molecular approaches for clinical diagnosis has numerous advantages, including ease of specimen processing, speed, and sensitivity, over standard microbiological techniques. This has been proved to be useful to identify both fastidious, unusual and slow-growing bacteria and rare bacteria that have ambiguous profiles, which cannot be differentiated correctly by conventional methods (Sun et al., 2005; El Bakkali et al., 2013).

The present study was carried out in order to identify gram-negative bacteria in patients with thalassemia by employing 16S-rRNA gene sequencing and to compare 16S rRNA gene sequencing and non-16S based clinical methods (automated and phenotypic identification methods) regarding their identification accuracy.

Materials and methods

Clinical isolates

Specimens were retrieved form 160 thalassemia patients (85 females and 75 males) who referred to thalassemia center in Erbil province, Iraq. The records of total patients were reviewed, and bacterial infections were observed in 78 patients (48.75%). The 78

http://www.aloki.hu ● ISSN 1589 1623 (Print) ● ISSN 1785 0037 (Online)
DOI: http://dx.doi.org/10.15666/aeer/1706_1313513146

isolates were collected in various sources: urine cultures, buccal cavity specimens, ear specimens, and blood cultures over two years period from June 2016 to September 2018. In general, the isolates were represented the most common Gram-negative bacterial pathogens.

Culture-based and automated identification of clinical isolates

The isolates that were obtained from the thalassemia center had undergone culture and sub-culture on relevant selective media, which include MacConkey agar, Eosin methylene blue agar, Cetrimide agar and Xylose lysine deoxycholate. Afterwards, in order to provide a final culture-based identification, clinical microbiology laboratory protocols were utilized to test their biochemical profile (Collee et al., 1996; Atlas, 2010). Then, the isolates identified by automated microbiology system using the VITEK2 compact system (BioMerieux, France).

16S rRNA-based molecular identification of clinical isolates

The full length of 16S rRNA of all 78 bacterial strains was sequenced. From those 78 isolates, some bacteria had not been identified clearly by VITEK2 method or phenotypic methods. Therefore, 16S rRNA sequencing was utilized to identify the bacterial isolates with high confidence.

Genomic DNA preparation

Presto^{TM} Mini gDNA bacterial kit was used to isolate genomic DNA. The samples were stained with safe stain and run on 0.8% agarose gel. The presence of genomic bands in the gel was examined under UV light (*Fig. 1*). The DNA was stored at -20 °C until it was used for the PCR amplification.

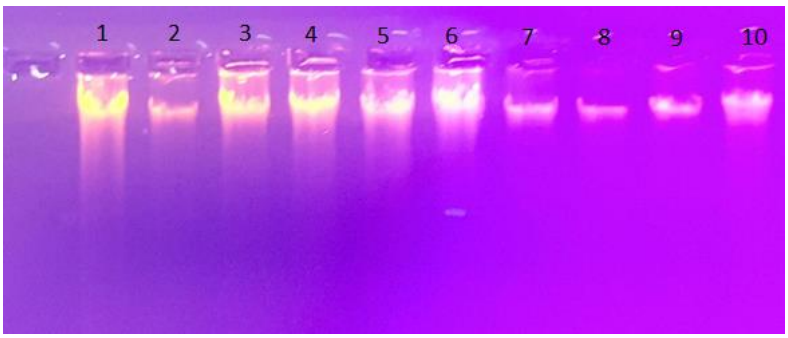

Figure 1. *Bacterial genome of 10 isolates in agarose gel electrophoresis*

Amplification of 16S gene

Universal primers 1492R (1) (5′- GGTTACCTTGTTACGACTT -3′) as reverse primer and 8F (5′- AGAGTTTGATCCTGGCTCAG -3′) as forward were used to carry out PCR for the amplification of the 16S rRNA gene (Turner et al., 1999). All reactions of PCR were conducted by utilizing 2 µl DNA template (density of 10 ng/µl), the Master Mix consisting of 3 mM $MgCl_2$, 0.2% Tween® 20, 20 mM Tris-HCl pH 8.5, $(NH_4)2S0_4$, 0.2 units/µl Ampliqon Taq DNA polymerase, 0.4 µM of each primer, and 0.4 mM of each dNTP. The conditions of PCR included primary denaturation at 95 °C

http://www.aloki.hu ● ISSN 1589 1623 (Print) ● ISSN 1785 0037 (Online)
DOI: http://dx.doi.org/10.15666/aeer/1706_1313513146

for 5 min, followed by 35 cycles at 95 °C for 45 s, at 55 °C for 45 s, and at 72 °C for 90 s, and a last extension at 72 °C for 6 min. After safe staining, the product of the reaction was visualized under UV light on a 1% agarose gel (Sambrook et al., 2001; *Fig. 2*). The PCR products were used for sequencing the 16S rRNA of all 78 bacterial isolates.

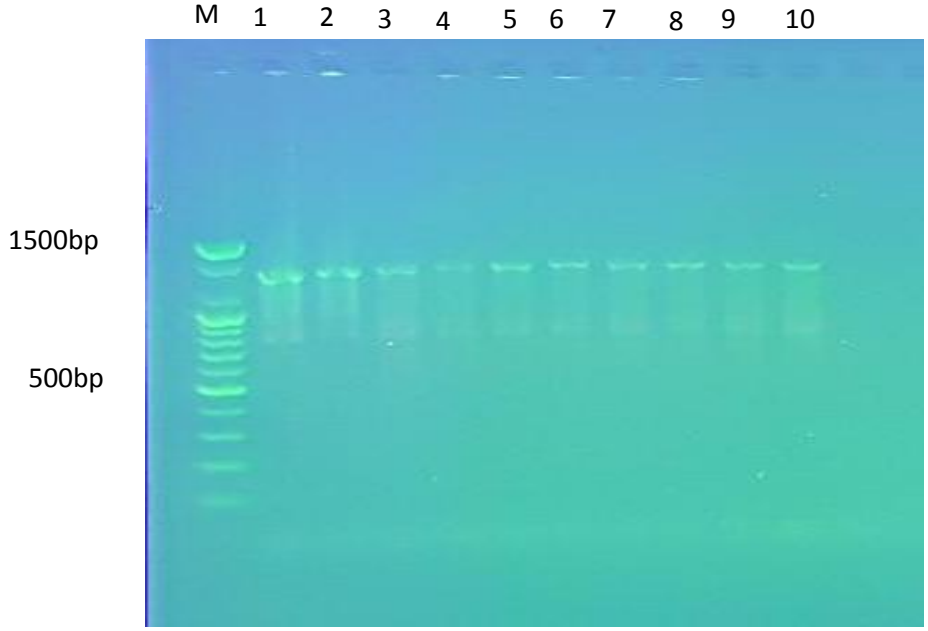

Figure 2. *Bacterial 16S rRNA PCR products in agarose gel electrophoresis*

Phylogenetic analysis and sequencing of 16S rRNA gene

The automated sequencer ABI 3100 with Big Dye Terminator Kit v. 3.1 was utilized to purify and sequence the amplified PCR products of microbial gene fragments at MACROGEN, Seoul, Korea. Primers 1391R (5'- GACGGGCGGTGTGTRCA -3') was used for sequencing (Turner et al., 1999). Sequencing was performed in only one direction since this is easy and inexpensive and phylogenic analysis is reported to be insensitive to quality of sequencing. As a result, the obtained sequences were compared with the database of NCBI via BLAST searches (http://blast.ncbi.nlm.nih.gov/Blast.cgi). In this comparison, sequences of type strains most closely related to the sequences of the isolates were searched. The sequences in the present study were only blasted against full genome sequences in NCBI database. For the phylogenetic analysis, the obtained sequences were aligned with Clustal W, and method based on the Jukes-Cantor model using the software MEGA and by the Maximum Likelihood, evolutionary distances were used to construct a phylogenetic tree (Kumar et al., 2016; Jukes and Cantor, 1969).

Results

In the current study, a total of 160 patients (85 females, 75 males) who referred to thalassemia center in Erbil, Iraq were examined, and 78 patients (48.75%) were found to suffer from bacterial infections. From these patients, 78 isolates were collected from

http://www.aloki.hu ● ISSN 1589 1623 (Print) ● ISSN 1785 0037 (Online)
DOI: http://dx.doi.org/10.15666/aeer/1706_1313513146

various sources: urine cultures, buccal cavity specimens, ear specimens, and blood cultures over a over two years period from June 2016 to September 2018. The isolates were initially been identified using either conventional (which is depend on cultural, morphological, and biochemical tests) or by automated microbiology system using the VITEK 2 compact system. These initial identities span 5 genera and 2 families, including a wide range of gram-negative rods. Among the 78 gram-negative isolates, 77 (98.7%) were members of Enterobacteriaceae and 1 (1.3%) members of Pseudomonadaceae.

Out of those 78 patients with infections, the most common causative organism was found to be *E. coli* (n = 48, 61.53%), followed by *K. pneumoniae* (n = 14, 17.94%), *M. morganii* (n = 11, 14.10%), *K. oxytoca* (n = 3, 3.84%), and *P. aeruginosa* and *Pantoea* sp. (n = 1, %1.28). Moreover, urinary tract infection was the most common site of infection (n = 61, 78.20%), followed by oral cavity infection (n = 10, 12.82%), ear otitis media (n = 5, 6.41%), and blood bacteremia (n = 2, 2.56%). *Tables 1* and *2* summarize the causative organisms, number of isolates, clinical identification method, and sites of infection in the 78 infected patients.

Table 1. *Clinical identity and techniques of identifying the isolates*

Clinical identity	Identification technique	Number of isolates (%)
Escherichia coli	Culture-based + VITEK 2 compact system	48 (61.53)
Klebsiella pneumonia	Culture-based + VITEK 2 compact system	14 (17.94)
Morganella morganii	VITEK 2 compact system	11 (14.10)
Klebsiella oxytoca	Culture-based + VITEK 2 compact system	3 (3.84)
Pseudomonas aeruginosa	Culture-based + VITEK 2 compact system	1 (1.28)
Pantoea species	VITEK 2 compact system	1 (1.28)

Table 2. *Sites of infection*

Site of infection, n (%)	Patients (n = 78)
Urine urinary tract infection	61 (78.20)
Oral cavity	10 (12.82)
Ear Otitis media	5 (6.41)
Blood Bacteremia	2 (2.56)

After isolates had initially been identified using either conventional or by automated microbiology system using the VITEK 2 compact system, the molecular method was used for isolate identification based on the sequence of 16S ribosomal RNA. The 16S rRNA gene was amplified and sequenced for each strain to confidently identify bacteria. Out of the 77 members of Enterobacteriaceae, 48 (62.3%) were confirmed as *E. coli* by conventional and automated microbiology system using the VITEK 2 compact system, whereas 16S rRNA sequencing method confirmed only 41 isolates as *E. coli*. Regarding the other Escherichia isolates, 5 out of the 48 tested isolates were sequenced successfully, but their sequences did not match with high similarity to any known bacterial deposited in NCBI database; therefore, they were called as unidentified bacteria since they had similarity with unknown cultured bacteria in the database.

http://www.aloki.hu ● ISSN 1589 1623 (Print) ● ISSN 1785 0037 (Online)
DOI: http://dx.doi.org/10.15666/aeer/1706_1313513146

Interestingly, the 2 *Escherichia* isolates without species ID were identified as *E. fergusonii* and *M. morganii* by 16S rRNA sequencing.

In general, the 16S rRNA gene is universal in bacteria, and so relationships can be measured among all bacteria. The comparison of the 16S rRNA gene sequences allows differentiation between organisms at the genus level across all major phyla of bacteria, in addition to classifying strains at multiple levels, including what we now call the species and subspecies level. The occasional exceptions to the usefulness of 16S rRNA gene sequencing usually relate to more than one well-known species having the same or very similar sequences.

Regarding *Klebsiella* species, among the 17 isolates, 14 isolates were confirmed as *Klebsiella pneumoniae* and 3 as *Klebsiella oxytoca* by conventional and automated microbiology system using the VITEK 2 compact system, while 16S rRNA sequencing method revealed 11 *K. pneumoniae* isolates and 4 *K. oxytoca* 4 isolates. Moreover, 11 member of non-lactose fermenter that identified by conventional and automated method as *Morganella morganii*, this ratio rose to 14 *M. morganii* by 16S rRNA sequencing method. One isolate that was identified by automated method as *Pantoea* species was confirmed by molecular method too. On the other hand, one members of Pseudomonadaceae was *Pseudomonas aeruginosa* that was identified by conventional and automated methods and confirmed by molecular methods.

Table 3 presents the results of comparing conventional and automated identification methods with the molecular approach is shown in. As shown in the table, 58 (74.35) out of 78 isolates were correctly identified.

Table 3. *Comparison between conventional and automated methods with the molecular approach*

Isolates	Clinical identification	
	Conventional and automated	**16S rRNA**
E. coli	48	41
K. pneumoniae	14	11
M. morganii	11	14
K. oxytoca	3	4
P. aeruginosa	1	1
Pantoea species	1	1
E. fergusonii	0	1
Unidentified	0	5
Total	78	78

Furthermore, the Neighbour-joining method was utilized to draw phylogenetic trees for 16S rRNA region. Moreover, MEGA (Molecular Evolutionary Genetics analysis) version 7.0 was employed to perform the molecular and phylogenetic evolutionary analyses. In addition, nucleotide BLAST was utilized to compare different sets of sequence databases and the 16S rRNA gene sequence of isolate. Bacterial identification was conducted using the annotated information for the sequence in the database of whole-genome sequences to which 16S rRNA aligns.

Phylogenetic tree of *E. coli* is presented in *Figure 3A,* which was drawn based on 1,548 conserved core gene clusters of 41 *E. coli* genomes. The phylogenetic trees

http://www.aloki.hu ● ISSN 1589 1623 (Print) ● ISSN 1785 0037 (Online)
DOI: http://dx.doi.org/10.15666/aeer/1706_1313513146

clearly indicate that there was an intra-species genetic distance of 0.010 between the individual isolates. As shown in *Figure 3B;* however, there was an intra-species genetic distance of 0.0020 between the individual isolates of the 11 *Klebsiella pneumoniae*. Moreover, in *Figure 3C,* an intra-species genetic distance of up to 0.020 was observed between the individual isolates of the *Morganella morganii*. Based on these findings, compared to *E. coli* and *Klebsiella pneumoniae*, *Morganella morganii* had a higher rate of evolution and the genetic variation.

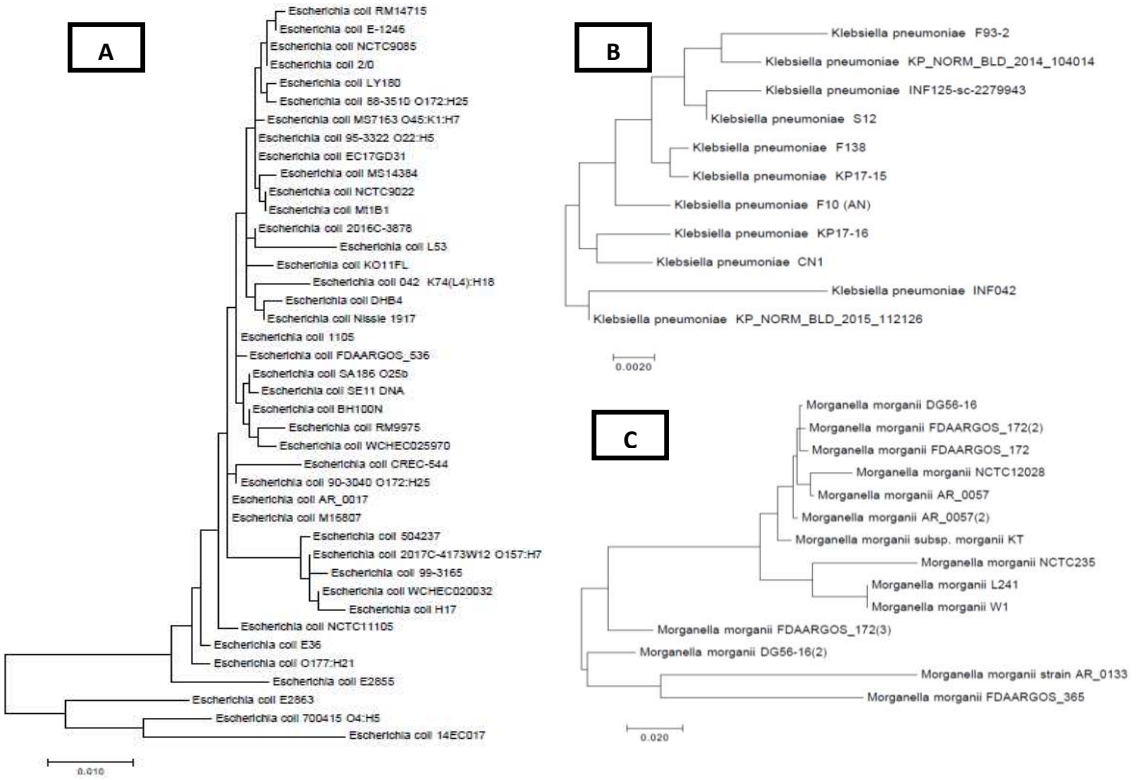

Figure 1. *Phylogenetic neighbor-joining trees of 16S rRNA amplified from the tested isolates of E coli (A), K. pneumoniae (B), and M. morganii (C)*

Discussion

Most of the isolates in the present study were identified by an automated microbiology system (i.e. BioMerieux VITEK 2 Compact) and conventional phenotypic method. However, the 16S rRNA gene was sequenced and amplified for each strain in order to identify the bacteria confidently. In scientific investigations and clinical practice, identification of bacterial species is frequently performed through sequence analysis of conserved "housekeeping" genes like the bacterial 16S rRNA (Clarridge, 2004; Petti et al., 2005). In fact, Bacterial identification traditionally achieved by carrying out labor-intensive and time-consuming, and the interests of identification genotypically are many including shorter time for results, higher reliability, sensitivity, and specificity (Jesumirhewe et al., 2016). To specify the phylogenetic characterization of prokaryotes such as archaea and bacteria, the16S rRNA gene sequence is utilized as the template in the latest bacteria identification manuals such as Bergey's Manual of Systematic Bacteriology which is widely used by microbiologists to identify and characterize bacteria (Werner et al., 2012).

http://www.aloki.hu ● ISSN 1589 1623 (Print) ● ISSN 1785 0037 (Online)
DOI: http://dx.doi.org/10.15666/aeer/1706_1313513146

In order to identify previous bacteria in clinical settings and amplify 16S rRNA, a set of universal reference primers were chosen based on previous clinical work and key reports. Moreover, previously conducted taxonomic studies have utilized sequence analysis of the 16S ribosomal RNA (rRNA) gene in order to identify bacterial species (Chakravorty et al., 2007).

Identifying typical clinical isolates through PCR and sequencing in the present study revealed the fact the consistency of this method with conventional laboratory methods. The desirable characteristics of this molecular identification method include: (1) cost-effectiveness: Given the low cost of developing the technology and information, the procedure is quite cost-effective; (2) accessibility: this procedure has a high level of accessibility because it is developed based on well-established methods and theories such as amplicon preparation through PCR, commercial sequencing, and Gene Bank verification); and (3) convenience: This procedure is quite convenient because it utilizes common techniques and methods of molecular biology including sequence analysis, commercial sequencing, electrophoresisand, PCR, and efficient one-step DNA extraction. Identifying microbes that are difficult to identify is conducted using molecular methods if laboratories do not have the required expertise to use other phenotypic identification methods (Cheng et al., 2014). Although 16S rRNA gene sequencing is frequently utilized in reference laboratories, the difficulty of interpreting 16S rRNA gene sequence results is one of the main limitations to its broader use. Marginal intra-species differences and significant inter-species differences in 16S rRNA gene sequences have a remarkable effect on utilizing 16S rRNA gene sequencing to identify bacteria. As a result, identifying the bacteria cannot be done with sufficient confidence through this technique when the same 16S rRNA gene sequence is share by two different bacterial species (Woo et al., 2009).

In the present study, sequencing was used to identify different bacteria. It was observed that sequence analysis had an excellent overall performance in distinguishing the bacterial isolates that were difficult to identify. Therefore, bacteria identification in clinical settings can be aided by the 16S rRNA sequencing as a supplement, particularly for organisms that are biochemically fastidious or deficient or poorly described. *Pantoea* is a difficult-to-identify bacterium. This bacterium can lead to development of infections in humans. It is also pathogenic to plants. However, different strains of Pantoea and their probable association with disease and hosts are poorly known, and it is difficult to identify Pantoea species. The biochemical heterogeneity of *Pantoea* makes it to be identified difficulty and due to similarities in phenotypic characteristics between *Pantoea* species and related Enterobacteriaceae. Currently, confident identification is not achieved routinely (Delétoile et al., 2009; Brady, 2013).

The advantage of 16S rRNA gene sequencing in clinical microbiology has been focused on in several studies. For example, Drancourt et al. (2000) carried out a study to compare 16S rRNA and phenotypic based identification techniques. For this purpose, they obtained 177 isolates, 81 of which were collected from medical clinical samples. Also, Bosshard et al. (2003) assessed the appropriateness of 16S rRNA for the identifying the clinical strains of aerobic gram-positive rods. Moreover, Spilker et al. (2004) examined 66 cystic fibrosis sputum isolates in order to check the agreement between the results identification of Pseudomonas species using phenotypic and 16S rRNA sequencing methods.

The present investigation, 78 infected patients were studied to figure out the causative organisms and sites of infection. It was observed that the most common

http://www.aloki.hu ● ISSN 1589 1623 (Print) ● ISSN 1785 0037 (Online)
DOI: http://dx.doi.org/10.15666/aeer/1706_1313513146

causative organism was *E. coli* that was identified in 41 cases, followed by *Morganella morganii* with 14 cases and *K. pneumoniae* with 11 cases. Moreover, the most common site of infection was identified to be urinary tract infection with 61 cases, followed by oral cavity infection with 10 cases.

The profile of pathogens in the series of the present study differed from those that were previously described for thalassaemia, such that *Escherichia coli* was the most common causative organism, followed by *Morganella morganii* in the second place and *Klebsiella* species in the third place. This finding is in line with those two studies that were conducted on Asian patients with thalassemia (Wang et al., 2003; Yapp et al., 2009). However, this finding is not in agreement with those of the studies conducted in Western countries, where the most common causative organism in thalassemia patients was found to be *Yersinia* species (Robins-Browne and Prpic, 1985; Abcarian and Demas, 1991).

In the present study, Escherichia coli species were found to be the most frequent organisms that cause infection in thalassemia, which can probably be contributed to the fact that there were a larger number of female patients than the males and that women develop urinary tract infections four times more frequently than males, and it is well known that *Escherichia coli* bacteria are responsible for most cases of urinary tract infection (UTI) (Sakamoto et al., 2018; Alperin et al., 2019).

In the present study, excess iron presence might be the reason for different spectrum of infections among the patients. Moreover, since iron plays a role in the growth of *Klebsiella* spp., high levels of ferritin seem to be a risk factor (Chung et al., 2003). Dissemination and replication of bacterial pathogens in which iron is used as a growth factor can be promoted by high levels of serum iron. Saturation of transferrin in iron overload makes labile iron available to bacteria. Iron overload changes the phagocytic and chemotactic properties of neutrophils, in turn leading to a decrease in their capability of killing invading pathogens. It also seems to change the function of T-cell. Moreover, immune effector mechanisms like immune cell proliferation iron, nitric oxide (NO) formation, or cytokine activities (interferon-c effector pathways towards macrophages) are also modulated by iron (Hoen, 1999; Weiss, 2002; Wiener, 2003). *Pseudomonas aeruginosa*, *Klebsiella* species (e.g., pneumoniae), and *Escherichia coli*, which are gram-negative, rod-shaped bacteria, frequently lead to infections and mortality in a splenic patients (Cappellini et al., 2014).

Conclusion

The results of the current study indicated that using DNA sequencing techniques to identify bacteria isolates, especially biochemically aberrant, rarely isolated, or poorly described strains, in clinical settings can lead to remarkable improvement in clinical microbiology. It was found that accurate identification and understanding of bacterial diversity across and within the group were fulfilled through 16S-rRNA gene sequencing. In addition, low cost and high accuracy are guaranteed by sequencing technologies which are effective and appropriate for small- and medium-sized microbiological laboratories. Furthermore, the results of the present study revealed that identification of all cases is possible through single-strand sequencing. By studying the isolates obtained from thalassemia patients in the present study, it was concluded that genetic methods can help to identify the pathogenic isolates, which will be further helpful in administering appropriate antibiotics and understanding the trend of

http://www.aloki.hu ● ISSN 1589 1623 (Print) ● ISSN 1785 0037 (Online)
DOI: http://dx.doi.org/10.15666/aeer/1706_1313513146

pathogens in various clinical samples. As figured out in the present study, the most common causative organisms were found to be *Escherichia coli*, followed by *Morganella morganii* While *Klebsiella pneumoniae* as the second and third most frequent causative organisms. It is recommended to depend on Multilocus Gene Sequencing for more rapid and accurate identification, especially for *Pantoea* typing in clinical samples due to its difficulty identification.

REFERENCES

[1] Abcarian, P. W., Demas, B. E. (1991): Systemic Yersinia enterocolitica infection associated with iron overload and deferoxamine therapy. – AJR. American Journal of Roentgenology 157: 773-775.
[2] Alperin, M., Burnett, L., Lukacz, E., Brubaker, L. (2019): The mysteries of menopause and urogynecologic health: clinical and scientific gaps. – Menopause 26: 103-111.
[3] Aswapokee, P. (1988): Severe infection in thalassemia: a prospective study. – Birth Defects 23: 521-526.
[4] Atlas, R. (2010): Handbook of Microbiological Media. 4th Ed. – ASM Press, Washington.
[5] Bosshard, P., Abels, S., Zbinden, R., Böttger, E., Altwegg, M. (2003): Ribosomal DNA sequencing for identification of aerobic gram-positive rods in the clinical laboratory (an 18-month evaluation). – Journal of Clinical Microbiology 41: 4134-4140.
[6] Brady, C. L. (2013): Taxonomic of Pantoea Associated with Bacterial Blight of Eucalyptus. – University of Pretoria, Hatfield.
[7] Cappellini, M., Cohen, A., Eleftheriou, A., Piga, A., Porter, J., Taher, A. (2014): Guidelines for the Clinical Management of Thalassaemia. – Thalassaemia International Federation (TIF), Strovolos, Cyprus.
[8] Chakravorty, S., Helb, D., Burday, M., Connell, N., Alland, D. (2007): A detailed analysis of 16S ribosomal RNA gene segments for the diagnosis of pathogenic bacteria. – Journal of Microbiological Methods 69: 330-339.
[9] Cheng, C., Sun, J., Zheng, F., Wu, K., Rui, Y. (2014): Molecular identification of clinical "difficult-to-identify" microbes from sequencing 16S ribosomal DNA and internal transcribed spacer 2. – Annals of Clinical Microbiology and Antimicrobials 13: 1.
[10] Chung, B. H., Ha, S. Y., Chan, G. C., Chiang, A., Lee, T. L., Ho, H. K., Lee, C. Y., Luk, C. W., Lau, Y. L. (2003): Klebsiella infection in patients with thalassemia. – Clinical Infectious Diseases 36: 575-579.
[11] Clarridge, J. E. (2004): Impact of 16S rRNA gene sequence analysis for identification of bacteria on clinical microbiology and infectious diseases. – Clinical Microbiology Reviews 17: 840-862.
[12] Collee, J. G., Miles, R. S., Watt, B. (1996): Tests for the Identification of Bacteria. – In: Collee, J. G., Fraser, A. G., Marmion, B. P., Simmons, A. (eds.) Mackie and McCartney Practical Medical Microbiology. 14th Ed. Churchill Livingstone, New York.
[13] Delétoile, A., Decré, D., Courant, S., Passet, V., Audo, J., Grimont, P., Arlet, G., Brisse, S. (2009): Phylogeny and identification of Pantoea species and typing of Pantoea agglomerans strains by multilocus gene sequencing. – Journal of Clinical Microbiology 47: 300-310.
[14] Drancourt, M., Bollet, C., Carlioz, A., Martelin, R., Gayral, J.-P., Raoult, D. (2000): 16S ribosomal DNA sequence analysis of a large collection of environmental and clinical unidentifiable bacterial isolates. – Journal of Clinical Microbiology 38: 3623-3630.
[15] El Bakkali, M., Chaoui, I., Zouhdi, M., Melloul, M., Arakrak, A., Elfahime, E., El Mzibri, M., Laglaoui, A. (2013): Comparison of the conventional technique and 16s

http://www.aloki.hu ● ISSN 1589 1623 (Print) ● ISSN 1785 0037 (Online)
DOI: http://dx.doi.org/10.15666/aeer/1706_1313513146

rDNA gene sequencing method in identification of clinical and hospital environmental isolates in Morocco. – African Journal of Microbiology Research 7: 5637-5644.

[16] Hoen, B. (1999): Iron and infection: clinical experience. – American Journal of Kidney Diseases 34: s30-s34.

[17] Iregui, M., Ward, S., Sherman, G., Fraser, V. J., Kollef, M. H. (2002): Clinical importance of delays in the initiation of appropriate antibiotic treatment for ventilator-associated pneumonia. – Chest 122: 262-268.

[18] Issaragrisil, S. (1988): Infection in thalassemia: a retrospective study of 1,018 patients with β-thalassemia/Hb E. – Birth Defects Orig Artic Ser 23: 505-511.

[19] Jesumirhewe, C., Ogunlowo, P. O., Olley, M., Springer, B., Allerberger, F., Ruppitsch, W. (2016): Accuracy of conventional identification methods used for Enterobacteriaceae isolates in three Nigerian hospitals. – PeerJ 4: e2511.

[20] Jukes, T. H., Cantor, C. R. (1969): Evolution of protein molecules. Mammalian protein – Metabolism 3: 132.

[21] Kumar, S., Stecher, G., Tamura, K. (2016): MEGA7: molecular evolutionary genetics analysis version 7.0 for bigger datasets. – Molecular Biology and Evolution 33: 1870-1874.

[22] Li, C. K., Shing, M. M. K., Chik, K. W., Lee, V., Pan, P. M. (2001): Klebsiella pneumoniae meningitis in thalassemia major patients. – Pediatric Hematology and Oncology 18: 229-232.

[23] Martin, G. S., Mannino, D. M., Eaton, S., Moss, M. (2003): The epidemiology of sepsis in the United States from 1979 through 2000. – New England Journal of Medicine 348: 1546-1554.

[24] Modell, B., Darlison, M. (2008): Global epidemiology of haemoglobin disorders and derived service indicators. – Bulletin of the World Health Organization 86: 480-487.

[25] Patel, J. B. (2001): 16S rRNA gene sequencing for bacterial pathogen identification in the clinical laboratory. – Molecular Diagnosis 6: 313-321.

[26] Peng, C.-T., Tsai, C.-H., Wang, J.-H., Chiu, C.-F., Chow, K.-C. (2000): Bacterial infection in patients with transfusion-dependent beta-thalassemia in central Taiwan. – Acta Paediatrica Taiwanica (Taiwan er ke yi xue hui za zhi) 41: 318-321.

[27] Petti, C., Polage, C., Schreckenberger, P. (2005): The role of 16S rRNA gene sequencing in identification of microorganisms misidentified by conventional methods. – Journal of Clinical Microbiology 43: 6123-6125.

[28] Robins-Browne, R., PRPIC, J. (1985): Effects of iron and desferrioxamine on infections with Yersinia enterocolitica. – Infection and Immunity 47: 774-779.

[29] Sakamoto, S., Miyazawa, K., Yasui, T., Iguchi, T., Fujita, M., Nishimatsu, H., Masaki, T., Hasegawa, T., Hibi, H., Arakawa, T. (2018): Chronological changes in the epidemiological characteristics of upper urinary tract urolithiasis in Japan. – International Journal of Urology 25: 373-378.

[30] Sambrook, J., Russell, D. W., Russell, D. W. (2001): Molecular Cloning: A Laboratory Manual. – Cold Spring Harbor Laboratory Press, New York.

[31] Shorr, A. F., Micek, S. T., Welch, E. C., Doherty, J. A., Reichley, R. M., Kollef, M. H. (2011): Inappropriate antibiotic therapy in Gram-negative sepsis increases hospital length of stay. – Critical Care Medicine 39: 46-51.

[32] Spilker, T., Coenye, T., Vandamme, P., Lipuma, J. J. (2004): PCR-based assay for differentiation of Pseudomonas aeruginosa from other Pseudomonas species recovered from cystic fibrosis patients. – Journal of Clinical Microbiology 42: 2074-2079.

[33] Sun, C.-P., Liao, J. C., Zhang, Y.-H., Gau, V., Mastali, M., Babbitt, J. T., Grundfest, W. S., Churchill, B. M., Mccabe, E. R., Haake, D. A. (2005): Rapid, species-specific detection of uropathogen 16S rDNA and rRNA at ambient temperature by dot-blot hybridization and an electrochemical sensor array. – Molecular Genetics and Metabolism 84: 90-99.

http://www.aloki.hu ● ISSN 1589 1623 (Print) ● ISSN 1785 0037 (Online)
DOI: http://dx.doi.org/10.15666/aeer/1706_1313513146

[34] Turner, S., Pryer, K. M., Miao, V. P., Palmer, J. D. (1999): Investigating deep phylogenetic relationships among cyanobacteria and plastids by small subunit rRNA sequence analysis 1. – Journal of Eukaryotic Microbiology 46: 327-338.
[35] Vento, S., Cainelli, F., Cesario, F. (2006): Infections and thalassaemia. – The Lancet Infectious Diseases 6: 226-233.
[36] Vichinsky, E. P. (2005): Changing patterns of thalassemia worldwide. – Annals of the New York Academy of Sciences 1054: 18-24.
[37] Wanachiwanawin, W. (2000): Infections in E/b-thalassaemia. – Journal of Pediatric Hematology Oncology 22: 581-587.
[38] Wang, S.-C., Lin, K.-H., Chern, J. P., Lu, M.-Y., Jou, S.-T., Lin, D.-T., Lin, K.-S. (2003): Severe bacterial infection in transfusion-dependent patients with thalassemia major. – Clinical Infectious Diseases 37: 984-988.
[39] Weatherall, D. J. (2012): The definition and epidemiology of non-transfusion-dependent thalassemia. – Blood Reviews 26: S3-S6.
[40] Weiss, G. (2002): Iron and immunity: a double-edged sword. – European Journal of Clinical Investigation 32: 70-78.
[41] Werner, J. J., Koren, O., Hugenholtz, P., Desantis, T. Z., Walters, W. A., Caporaso, J. G., Angenent, L. T., Knight, R., Ley, R. E. (2012): Impact of training sets on classification of high-throughput bacterial 16s rRNA gene surveys. – The ISME Journal 6: 94.
[42] Wiener, E. (2003): Impaired phagocyte antibacterial effector functions in β-thalassemia: a likely factor in the increased susceptibility to bacterial infections. – Hematology 8: 35-40.
[43] Woo, P., Leung, P., Leung, K., Yuen, K. (2000): Identification by 16S ribosomal RNA gene sequencing of an Enterobacteriaceae species from a bone marrow transplant recipient. – Molecular Pathology 53: 211-215.
[44] Woo, P. C., Teng, J. L., Wu, J. K., Leung, F. P., Tse, H., Fung, A. M., Lau, S. K., Yuen, K.-Y. (2009): Guidelines for interpretation of 16S rRNA gene sequence-based results for identification of medically important aerobic Gram-positive bacteria. – Journal of Medical Microbiology 58: 1030-1036.
Yapp, A. R., Lindemann, R., Gilroy, N., Gao, Z., MacIntyre, C. R. (2009): Infection outcomes in splenectomized patients with hemoglobinopathies in Australia. – International Journal of Infection Disease 13: 696-700.

http://www.aloki.hu ● ISSN 1589 1623 (Print) ● ISSN 1785 0037 (Online)
DOI: http://dx.doi.org/10.15666/aeer/1706_1313513146

MAPPING BUILT-UP AREAS USING TWO BAND RATIO ON LANDSAT IMAGERY OF ACCRA IN GHANA FROM 1980 TO 2017

TWUMASI, N. Y. D.[1,2*] – SHAO, Z.[1] – ALTAN, O.[3]

[1]*State Key Laboratory of Information Engineering in Surveying, Mapping and Remote Sensing, Wuhan University, 129 Luoyu Road, Wuhan 430079, China*
(e-mail: NanaTwumasi@whu.edu.cn; shaozhenfeng@whu.edu.cn; phone +86-158-2718-8114)

[2]*Civil Engineering Department, Wa Polytechnic, Box 553, Wa, Ghana*
(e-mail: bnydt45.ny@gmail.com; phone +233-024-943-9043)

[3]*Department of Geomatics, Istanbul Technical University, 36626 Istanbul, Turkey*
(e-mail: oaltan@itu.edu.tr; phone: +90-532-446-4409)

**Corresponding author*
e-mail: NanaTwumasi@whu.edu.cn; phone: + 86-131-7202-8873

(Received 28th May 2019; accepted 28th Aug 2019)

Abstract. Lack of historical land cover and urban growth governance structure makes spatial planning within the economic capitals of developing countries difficult. Monitoring urban built-up growth with in-situ methods is complicated. In this paper, long-term Landsat archive is utilised to map the built-up areas of Accra, the economic capital of Ghana, in Africa. Simple two band ratio and band combination is coupled with historic Google Earth imagery to monitor built-up dynamics from 1980-2017. A 10-year period was sub-divided into three parts each; early period, mid period and late period – for analysis. Maximum Likelihood classifier was used for the classification within the ENVI environment. The results show 11.90% as the highest and 4.63% as the lowest built-up growth rates between 2001-2005 and 1996-2000 respectively. Annual loss of non-built-up areas was 1.31%, and 48.57% over the entire study period. Water bodies lost 0.08% annually but 3.1% over the 37-year period. Highest and lowest overall accuracy were 87.18% and 81.31% respectively, with an average kappa coefficient of 0.7618. Gain in the built-up area was 1676.69 km^2 but non-built up areas lost 1576.10 km^2 while water bodies lost 100.60 km^2. Results will be of interest to spatial planners, policy makers and land administrators.
Keywords: *long term images, urbanization, band index, band combination, urban change rate, urban growth rate*

Introduction

Rapid urbanisation poses challenges to the United Nations sustainable goals (Giles-Corti et al., 2017), because challenges still exists in finding both temporal and spatial change information over a long period (Li et al., 2018). Ghana, like other developing countries face these challenges as well (The World Bank Group, 2015). However, there are very few studies done on the economic capitals, where most of the urbanisation takes place. These challenges are further worsened by low and sometimes non-availability of readily available long-term, urban growth governance structures, land cover maps, census data and high population projection ambiguity (Satterthwaite, 2010). Sometimes the data used is erroneous due to lack of size estimates and growth (Potts, 2012; Songsore, 2010). Gathering in-situ datasets to monitor urban growth in these countries is difficult, hence most developing countries like Ghana have turned to remote sensing for urban expansion studies and densification analysis (Potts, 2012). The use of long-term remote sensing datasets offers a full analysis which is believed to provide decision makers information for informed commitments on economic policy

http://www.aloki.hu ● ISSN 1589 1623 (Print) ● ISSN 1785 0037 (Online)
DOI: http://dx.doi.org/10.15666/aeer/1706_1314713168

drafting and spatial planning, to realise a translated impact of government economic policies, as there is a direct relation between population growth, urbanisation, infrastructure deficits and Gross Dometic Product (GDP).

A tentative attempt by (Osei et al., 2013) used only two-year imagery for the study on Accra, which is inadequate for an in-depth analysis. Previous studies have mapped the urban expansion extent and its monitoring for various applications using varied approaches; urbanisation and urban growth (Li and Yeh, 2000; Li, et al., 2015; Mohammady et al., 2013; Cobbinah and Niminga-Beka, 2017; Mu et al., 2006), urban expansion and urban sprawl (Angel et al., 2011; Yin et al., 2011; Ghosh et al., 2017), urban landcover change (Seto et al., 2000; Defries et al., 2010; Yang et al., 2014), all have used impervious surface extraction as a part for their study and analysis (Chester and Gibbons, 1996). A few have scrutinised spatial patterns of urban distribution and expansion with buffer zones in different directions (Li et al., 2016). Impervious Surface Areas (ISA) extraction, has mostly been done with high resolution imagery (HRI) due to accuracy issues. Spatial resolution becomes very important depending on the impervious characteristic under study (Sobrino et al., 2012).

Various studies (Guo et al., 2015; Yao et al., 2018; Sharma et al., 2016) and (Kuang et al., 2014), have proposed ISA extraction improvements using datasets such as Defense Meteorological Satellite Program-Operational Linescan System (DMSP-OLS), Quick Bird, Landsat, Visible Infrared Imaging Radiometer Suite-Day/Night Band (VIIRS-DNB), Moderate Resolution Imaging Spectroradiometer (MODIS), IKONOS and Advanced Spaceborne Thermal Emission and Reflection Radiometer (ASTER). In their proposed methods of multiresolution segmentation and canny algorithms, object layers were created first before extraction by spectrum, shape, size, texture, topology and context characteristics of the object. Noises were removed and the local singularity issue as well as the pepper and salt phenomenon were solved. However, the use of HRI and other data that are costly makes it difficult to replicate their methods especially over large regions in developing countries due to lack of research funds.

Again, the cost of HRI is a great challenge in Ghana which hinders urban studies research. These HRI also do not have the long-term advantage of more than two decades of data. This is a challenge for those involved in historical urban studies. As such urban feature extraction for analysis and planning sustainability is difficult. Landsat Thematic Mapper/Enhanced Thematic Mapper Plus/Operational Land Imager (TM/ETM + /OLI) data archive provide a solution to this hurdle, and are currently freely available with a global coverage. Most of these previous studies applied complex mathematical equations (Varshney and Rajesh, 2014) of spectral indices, sometimes combining two or more of these indices (Xiang et al., 2016), which are sometimes difficult to replicate. Also these applications were done on quite smaller areas and the effect of these methods is not fully appreciated over very large areas. Band ratios and band combinations can be useful in any scale of area for classification. Most important is the validating of the classification results or the algorithm. Long-term ground truth data is difficult to come by or in most cases impossible to acquire if it did not exist already. In this discussion we used the historical Google Earth (GE) map facility to obtain the ground truth. Landsat (4, 5, 7, and 8) imagery is used to extract the built-up areas for change dynamics analysis.

The main aims of this paper are; to do a built up analysis of the growth rate, growth change and the spatial area coverage of Greater Accra Region, the economic capital of Ghana, and, to provide a long-term base data for analysis in a long period spatial planning

http://www.aloki.hu ● ISSN 1589 1623 (Print) ● ISSN 1785 0037 (Online)
DOI: http://dx.doi.org/10.15666/aeer/1706_1314713168

for the Accra city planners. These examinations will be done using a two band ratio and Maximum Likelihood (ML) classifier. Most band ratio applications are coupled with multisource data, especially for lithological applications. In this study two band ratios solely applied to a single source data. Study is important because, analyses presented here can give an indication of the future impacts associated with urban built-up dynamics. Lessons drawn from happenings and the implemented solutions to them. For instance, most developed countries have turned to high rise buildings to solve the accommodation problem of the ever increasing urban population. These high rise buildings have caused an increase in surface temperatures at the heart of the cities (Giridharan, et al., 2004; J. Lu et al., 2007). Solutions to this problem have been suggested by (Kolokotroni et al., 2018). These lessons can inform the Ghana government not to commit the same mistakes of the advanced countries. This study is also vital for the development of sustainable policies to improve the adverse consequences of urbanization for sustainable urban development (Estoque and Murayama, 2015; Arsanjani et al., 2013).

Materials and methods

Study setting

The economic capital of most developing countries has similar traits. Most buildings within the Metropolitan are high rising and concentrated within the heart of the metropolis. This quick urban advancement comes with a constant congregation of population and an intense industrialisation (Senanayake et al., 2013) which has created its own environmental problems (Hettiarachchi et al., 2014). Most roads are paved, except some residential roads for newly developing estates. These characteristics are also observed in the study area. Accra had a population of 1.7 million as of 2010 (Ghana Statistical Service, 2014) and estimated to be 2.27 million by 2018. The total size area of Greater Accra Region is 3245 km^2, map of which is shown in *Figure 1*.

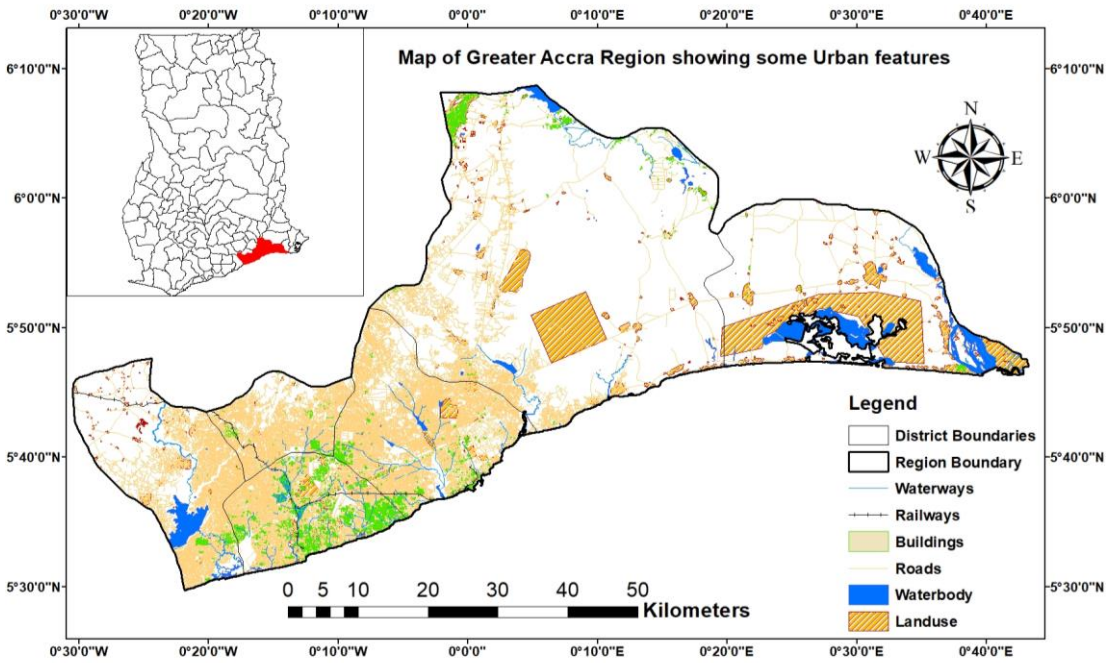

Figure 1. *Map of Greater Accra Region (insert: Ghana, study area shown in red)*

http://www.aloki.hu ● ISSN 1589 1623 (Print) ● ISSN 1785 0037 (Online)
DOI: http://dx.doi.org/10.15666/aeer/1706_1314713168

Dataset

We used Landsat imagery over a period of thirty-seven (37) years (1980–2017). However, one imagery before 1980 was obtained to provide a before-baseline comparison. The structure of Landsat Level-1 products ensures the provision of a steady annal of data quality to support time-series analyses and data "stacking", while controlling incessant improvement of the documentation and access to data as they are acquired. The images were obtained from the United States Geological Survey (USGS) website (https://earthexplorer.usgs.gov). Description of the Landsat imagery is given in *Table 1*. Although images were non-available for some years, it did not affect the objective since the study was not strictly an annual comparison. Those years with too much cloud cover were not used. Some excellent images were obtained though for these sensors, despite the scan line corrector failure of ETM+. The focal analysis tool was used to correct this. Although some spectral property may have been lost, it had insignificant influence on the quality of the work since mostly the combined bands were for visual interpretation and identification of the built-up areas. Image of 1972 has a size 170 km × 185 km and on path 207 and row 56. The rest all have size 170 km × 183 km and on path 93 and row 56.

Table 1. *Spectral descriptions of Landsat imagery and scenes*

Band name	**LS 1-5 MSS**	**LS 4-5 TM**	**LS 7 ETM +**	**LS 8 OLI**	**Pixel size (m)**	
Blue		B1 (0.45 - 0.52)	B1 (0.45 - 0.52)	B2 (0.45 - 0.51)	30	
Green	B1, B4 (0.5 - 0.6)	B2 (0.52 - 0.60)	B2 (0.52 - 0.60)	B3 (0.53 - 0.59)	30 (60 for MSS)	
Red	B2, B5 (0.6 - 0.7)	B3 (0.63 - 0.69)	B3 (0.63 - 0.69)	B1 (0.64 - 0.67)	30 (60 for MSS)	
NIR 1	B3, B6 (0.7 - 0.8)				60	
NIR	B4, B7 (0.8 - 1.1)	B4 (0.76 - 0.90)	B4 (0.77 - 0.90)	B5 (0.85 - 0.88)	30 (60 for MSS)	
SWIR 1		B5 (1.55 - 1.75)	B5 (1.55 - 1.75)	B6 (1.57 - 1.65)	30	
SWIR 2		B7 (2.08 - 2.35)	B7 (2.09 - 2.35)	B7 (2.11 - 2.29)	30	
	Other important information on dataset					
Number of bands used	4	6	6	6		
Radiometric bit	8	8	8	16		
Projection		UTM	UTM	UTM		
Ellipsoid	WGS 84	WGS 84	WGS 84	WGS 84		
	Latitude	**Longitude**	**Latitude**	**Longitude**	**Path**	**Row**
Accra	5.6037	-0.1870	811610.81 mE	619856.35 mN	193	56

In all cases the chosen bands (*Table 1*) were stacked together to provide a composite of all the good usable bands. Corresponding bands were chosen for the respective sensors. One key advantage for using this type of data is the possibility to detect a complete historical profile of urban growth, which is not easily discernible from stacked images with sparse satellite observations (Roy et al., 2014). We also used Google Earth (GE) from (https://earth.google.com) obtained around the same time of the acquisition date of the Landsat imagery for collecting ground truth to serve as training data. Google Earth provided historical records feature samples locations for five classes (i.e. vegetation, open bare land, roads, buildings and water). Bands were combined to visualise where these features are. Using visual interpretation these areas were digitised in GE and saved to shape-file in ArcGIS. For each digitised polygon, a point around the centre was taken and recorded in excel. These served as the ground truth and training

http://www.aloki.hu ● ISSN 1589 1623 (Print) ● ISSN 1785 0037 (Online)
DOI: http://dx.doi.org/10.15666/aeer/1706_1314713168

data for the classification. After the maximum likelihood supervised classification of five classes, a post-classification was done to regrouped into built-up areas (BUP), non-built up areas (NBUP) and water bodies (WB). Here, residential areas, commercial and industrial area are all classified as BUP. Agriculture, Plantation, Recreational Parks, Orchards and Forest are all classified as NBUP. Dams/Reservoirs, Ponds, River, Lakes, Stream are all classified as WB.

Procedure and approach

We used two band ratio and band combination to extract and classify features from the Landsat imagery. Developed indices serve as an indicator to analyse a particular type of land class during feature extraction and classification processes. In principle, indexing determines a ratio between the strongest (maximum) reflectance band and weakest (minimum) reflectance bands for the target feature. Then the normalised ratio of these two bands gives the highest contrast for the particular land type with minimum background noise. Landsat imagery that showed a significant presence of clouds was avoided. Conversely, Landsat images with less cloud cover outside the area of interest were included, which were subsequently imported into ERDAS Imagine for layer stacking. The focal analysis tool in ERDAS was applied to gap-fill the images that had stripes. The stacked images were later subsetted using shape-files of the study area. All the subset images were then moved to the ENVI environment for classification. The general procedure used is shown in *Figure 2*.

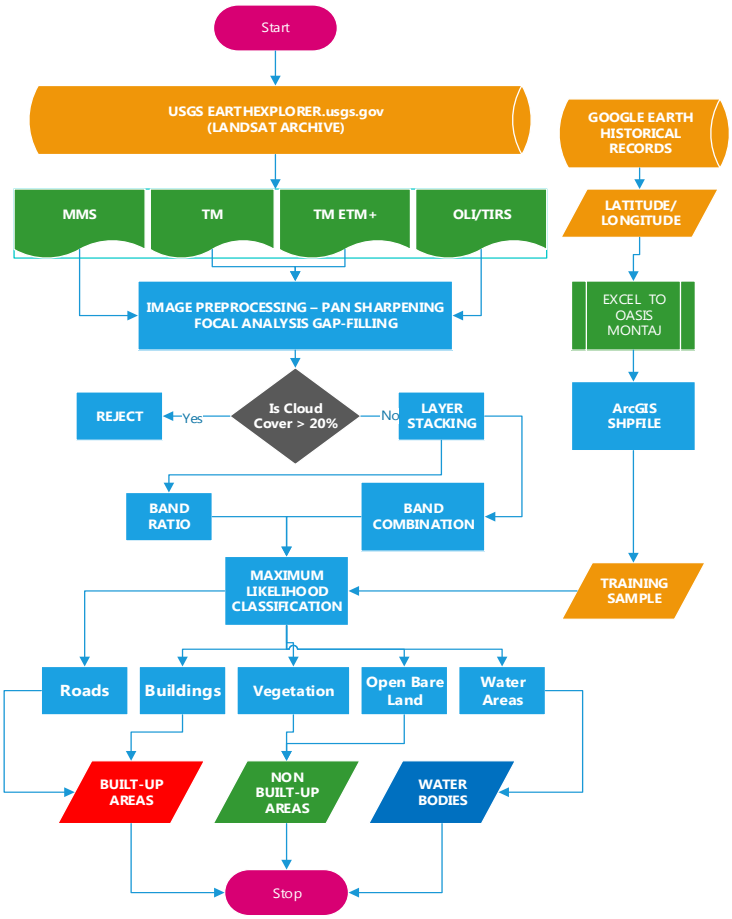

Figure 2. *Workflow procedure diagram*

http://www.aloki.hu ● ISSN 1589 1623 (Print) ● ISSN 1785 0037 (Online)
DOI: http://dx.doi.org/10.15666/aeer/1706_1314713168

Band combination

Band combination is an RGB composite that enhances the visual interpretation of the potential information content as shown in *Figure 3*. RGB composites for Landsat 8 differ from RGB composite obtained from Landsat 7 and Landsat 5 due to the difference in wavelength information for similar band in these images. For instance, a band combination of band 4, band 3 and band 2 create colour infrared (CIR) in Landsat 7 or Landsat 5, whereas the same resulting colour infrared in Landsat 8 is created using band 5, band 4 and band 3. Thus, it is imperative to choose a particular band combination dependent on the visual depiction of the preferred feature or phenomena. In this study, we created the following band combination to extract and classify features as described (*Fig. 3*):

- **Bands 7, 4, 2:** Urban areas appear in shades of magenta while vegetation appears light green. Light-green spots in the city specify grass-land cover like parks, golf courses, cemeteries**.**
- **Bands 4, 3, 2:** Deep red hues designate healthy vegetation while lighter reds show sparsely vegetated areas. Light blue shows densely populated urban areas.
- **Bands 4, 5, 3:** This blend offers further description of land-water boundaries and highlights subtle details not distinctively apparent in the visible bands**.** This combination exhibits moisture differences which are useful for soil and vegetation analysis.
- **Bands 5, 4, 3:** Healthy vegetation is bright green with soils as light purple, and mostly used for agricultural studies. It can also be applied in timber logging management.

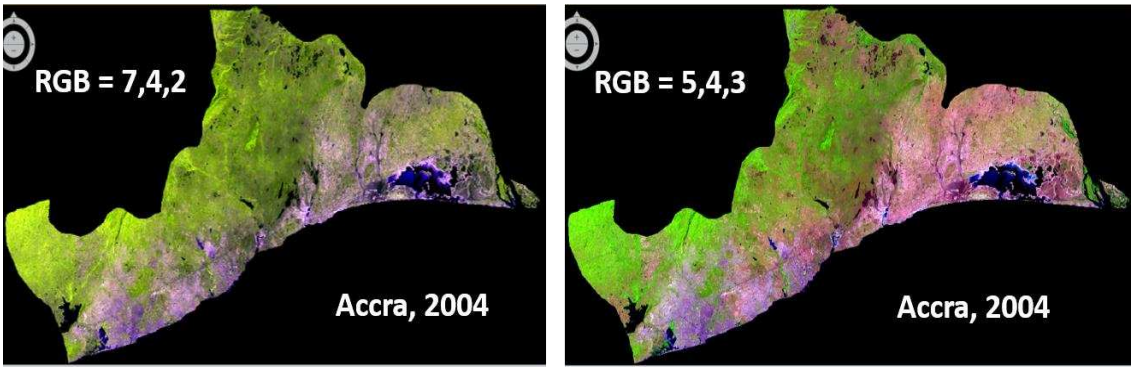

Figure 3. *Sample of some band combinations*

Band ratio

The Band Ratio (BR) technique has been applied before for geological interpretation as in (Inzana et al., 2003) and, for detecting mangrove forests as in (Rahman et al., 2013) among others. In these previous studies, band ratio images are evaluated based on their ability to discriminate the target feature (i.e. geologic units and structure; mangrove species). Generally, the illumination effect is removed in the spectral difference for any two-band ratio, in which the difference is the ratio. The illumination defines the magnitude of the DN received by satellite (Muniz et al., 2003). The principle is applied here to detect urban areas. In this study, the stacked images were loaded with

http://www.aloki.hu ● ISSN 1589 1623 (Print) ● ISSN 1785 0037 (Online)
DOI: http://dx.doi.org/10.15666/aeer/1706_1314713168

all the bands, however only the applicable RGB composites are loaded into the viewer for visual interpretation. The whole idea behind this method is to be able to confidently identify the targeted features (vegetation, open bare land, water areas, roads and buildings), on the displayed image to collect appropriate training sample features. Unique information with subtle spectral reflectance is provided by ratios for surface materials often difficult to detect in a standard image (Inzana et al., 2003). The following band ratios were applied to the respective targeted features.

- **Roads and buildings – (*Band 3/Band 5 and Band 3/Band 4*):** These sharply defined the urban area and barren land. They enhance barren lands, street patterns, highways in the urban areas and urban built-up or paved areas. Urban and built-up areas appear as brighter tone and forests, water body and croplands appear darker.
- **Open bare land – (*Band 5/Band 7 and Band 3/Band 5*):** Land and water are distinctively separated because soils exhibit strong absorption in the band 7 and high reflectance in band 5. Land appears as lighter tone and water appear darker.
- **Vegetation – (*Band 4/Band 3 and Band 4/Band 5*):** This discriminate between vegetation, water and croplands which is due to the moisture content. Vegetation reflects higher in near IR region and strong absorption in the red region. The lighter the tone, means more vegetation present.
- **Water areas – (*Band 4/Band 3, Band 4/Band 5 and Band 5/Band 7*):** Easily discriminates water bodies from the land. Water absorbs strongly in near IR region and reflects much in band 5. Water body appears darker than vegetation and land which appear lighter.

The mathematical expression of the band ratio function is displayed in *Equation 1*.

$$BandRatio = BR_{i,j,r} = \frac{BN_{i,j,k}}{BN_{i,j,1}} \quad \text{(Eq.1)}$$

where $BR_{i,j,r}$ is the output ratio value for the pixel, at row *i*, column *j*, and $BN_{i,j,k}$ and $BN_{i,j,l}$ is the brightness value at the same location in band *k* and *l*. Both the numerator and the denomerator factors belong to the same image scene.

Classification method

We used Maximum Likelihood (ML) algorithm to classify the images (Rawat and Kumar, 2015; Dewan and Yamaguchi, 2009). Maximum Likelihood was preferred over other classification algorithms due to the robust nature of the Gaussian probability distribution in assigning classes (Mather and Tso, 2010). It has successfully been applied in urban and peri-urban areas to monitor land cover changes (Schneider, 2012). We used training sample features that were extracted (digitised) from GE for each of the defined class. Then the band ratio (as described above) was applied for the respective features. We subjected the single band result to a ML supervised classification using the extracted training sample as ground truth. The classification was done for five classes (bare land, vegetation, water, roads, and buildings), which were later aggregated to three classes of built-up areas (roads and buildings), non-built up areas and water bodies, during the post-classification. A kennel smooth size 3 was used to smoothen the result.

http://www.aloki.hu ● ISSN 1589 1623 (Print) ● ISSN 1785 0037 (Online)
DOI: http://dx.doi.org/10.15666/aeer/1706_1314713168

The advantage of this approach is that it can be applied to various Landsat sensors for this purpose, whereas the established indexes are limited to specific sensors because the bands used are not present in all the array of sensors. This approach is also simple as it involves very little mathematics and does not necessarily need an in-depth understanding for implementation.

Change rate and growth rate calculations

Change and growth rates have been used by (Li et al., 2016; Xu et al., 2011) to examine urban impervious surface distribution and change dynamics where the surface area coverage was determined for various years for Hangzhou and Xiamne cities. Change rate is this paper was calculated using *Equations 2* and *3*.

$$ChangeRate = (CR) = A(x) = \frac{f(x_2) - f(x_1)}{x_2 - x_1} = \frac{y_2 - y_1}{x_2 - x_1} \quad \text{(Eq.2)}$$

where x_2 is the final year, and x_1 is the initial year; the functions are defined as in *Equation 3:*

$$\begin{aligned} f(x_2) &= x_2^{\,2} - (2 \times x_2) \\ f(x_1) &= x_1^{\,2} - (2 \times x_1) \end{aligned} \quad \text{(Eq.3)}$$

Different formulas exist for the calculation of growth rates, however in this study the formula of *Equation 4* (Feeney, 2014) was adopted.

$$GrowthRate = (GR) = T(x) = \left[\frac{present}{past} \right]^{\frac{1}{n}} - 1 \quad \text{(Eq.4)}$$

where *present* and *past* represent the figures for the current and past years respectively. *n* is the interval over which the growth is computed - 10 years for this study (*Fig. 7*).

To assess the spatial distribution of built-up expansion intensity, an annual urban expansion intensity index (AUEII) by (Liu et al., 2000) was adopted and modified to Built-Up Expansion Intensity Index (BUEII) for use as an indicator of the urbanization rate of the study area. BUEII is expressed as in *Equation 5*.

$$BUEII = \frac{A_{n+i} - A_i}{nTA_{n+i}} \times 100\% \quad \text{(Eq.5)}$$

where TA_{n+i} is the total area of the target unit at time $n + i$; A_{n+i} and A_i the built-up area within the target unit at time $n + i$ and i, respectively, and n the interval period (in years).

Accuracy assessment calculation (kappa coefficient)

The *kappa coefficient* measures classification and truth values agreement. With a kappa value of 1 there is a perfect agreement, while a value of 0 means no agreement.

http://www.aloki.hu ● ISSN 1589 1623 (Print) ● ISSN 1785 0037 (Online)
DOI: http://dx.doi.org/10.15666/aeer/1706_1314713168

The kappa coefficient mathematically follows *Equation 6* but can be simply reduced to *Equation 7:*

$$K = \frac{N\sum_{i=1}^{n} m_{i,1} - \sum_{i=1}^{n}(G_i G_i)}{N^2 - \sum_{i=1}^{n}(G_i G_i)} \quad \text{(Eq.6)}$$

where i is the class number; N is the total number of classified values compared to truth values; $m_{i,i}$ is the number of values within class i that have also been classified as class i which values are along the diagonal of the confusion matrix; C_i is the total number of predicted values within class I; G_i is the total number of truth values within class i.

$$Kappa = \frac{(Nb - g)}{N^2 - g} \quad \text{(Eq.7)}$$

where N is the total number of points; b is the sum of correctly mapped points; g is the sum of the products of classes between the ground truth points used and the predicted points digitised.

Results and analysis

Accuracy assessment

We generated the confusion matrix to assess the accuracy of the results. The highest overall accuracy obtained is 87.18% and a lowest of 81.31% with a mean accuracy assessment of 84.25%. The Kappa coefficient was used to evaluate the quality of agreement, either positive or negative. The average kappa coefficient for Accra was 0.7618 using *Equation 6,* which is a simplified rendition for its calculation. The producer accuracy and user accuracy are calculated for each image for each class and are shown in *Table 2*. It was possible to obtain a producer accuracy of 90.91% for built-up area in 1987. The user accuracy for the same year is 84.96%. For built-up areas the producer accuracy ranged between 75.36 and 90.91%, non-built up areas range from 75.00 to 93.27%, and between 81.08 and 92.31% for water bodies. Figures for water bodies seem high because it was easy to identify them within the chosen band combinations, thus reducing the chances of error. Water can even attain a high accuracy of 100% (Elhag, 2017).

Analysis on built-up area coverage

In total, thirteen comparable years were analysed. The entire timeline was divided into five epochs; (i) before 1980, (ii) 1981-1990, (iii) 1991-2000, (iv) 2001-2010 and (v) 2011-2017. These were further grouped into three periods of the *early period (first 3 years)*, *mid period (second 3 years)* and *late period (last 4 years),* of each epoch. This approach made the comparison easier and visually comprehensible. A graph of the gains is shown in *Figure 4*.

http://www.aloki.hu ● ISSN 1589 1623 (Print) ● ISSN 1785 0037 (Online)
DOI: http://dx.doi.org/10.15666/aeer/1706_1314713168

Table 2. *Accuracy assessment table*

Year					Year					CLASS
	PA	UA	OVA	K		PA	UA	OVA	K	
1972	0.8824	0.8824			1999	0.8395	0.8831			BUP
	0.7500	0.7500				0.8667	0.8228			NBUP
	0.8889	0.8889				0.8776	0.8776			WB
			0.8421	0.7548				0.8585	0.7835	
1984	0.7536	0.8254			2004	0.8222	0.9136			BUP
	0.8909	0.7424				0.8831	0.8095			NBUP
	0.8108	0.8696				0.8889	0.8571			WB
			0.8131	0.7195				0.8597	0.7863	
1987	0.9091	0.8929			2006	0.8163	0.8791			BUP
	0.7778	0.7955				0.8667	0.9176			NBUP
	0.8485	0.8485				0.8730	0.7333			WB
			0.8496	0.7695				0.8486	0.7713	
1989	0.8243	0.9385			2009	0.7895	0.8911			BUP
	0.8621	0.7937				0.8889	0.7921			NBUP
	0.8929	0.7813				0.8657	0.8406			WB
			0.8500	0.7635				0.8413	0.7583	
1992	0.7927	0.8904			2011	0.8148	0.9483			BUP
	0.8551	0.7867				0.9327	0.8220			NBUP
	0.8824	0.8333				0.8904	0.8333			WB
			0.8366	0.7521				0.8718	0.8041	
1995	0.8182	0.9231			2014	0.8156	0.8984			BUP
	0.8955	0.7792				0.8673	0.7870			NBUP
	0.8333	0.8333				0.8919	0.8571			WB
			0.8469	0.7673				0.8498	0.7688	
					2017	0.7947	0.9160			BUP
						0.9135	0.7787			NBUP
						0.8676	0.8429			WB
								0.8483	0.7641	

BUP = Built Up Areas; NBUP = Non-Built Up areas; WB = Water Bodies; PA = Producer Accuracy; UA = User Accuracy; OVA = Overall Accuracy; K = Kappa

Non-built up areas generally lost to built-up areas steadily with some anomalies in 2011 and 2008. These anomalies, we think, may be due to the migration from rural-urban into the urban centres which may have contributed to a drastic increase in built-up areas. Constant urban development picked up around these times, and it is fully represented in the graph (*Fig. 4*). Information presented in *Figure 5* compliments that of *Figure 4*. Gaps within the graph indicate years with no data (images). Either images were avoided entirely due to cloud cover or it was missing (sensor failure). The complete mapped area coverages are shown in *Table 3*. It shows the corresponding area coverage of the land covers for respective years.

http://www.aloki.hu ● ISSN 1589 1623 (Print) ● ISSN 1785 0037 (Online)
DOI: http://dx.doi.org/10.15666/aeer/1706_1314713168

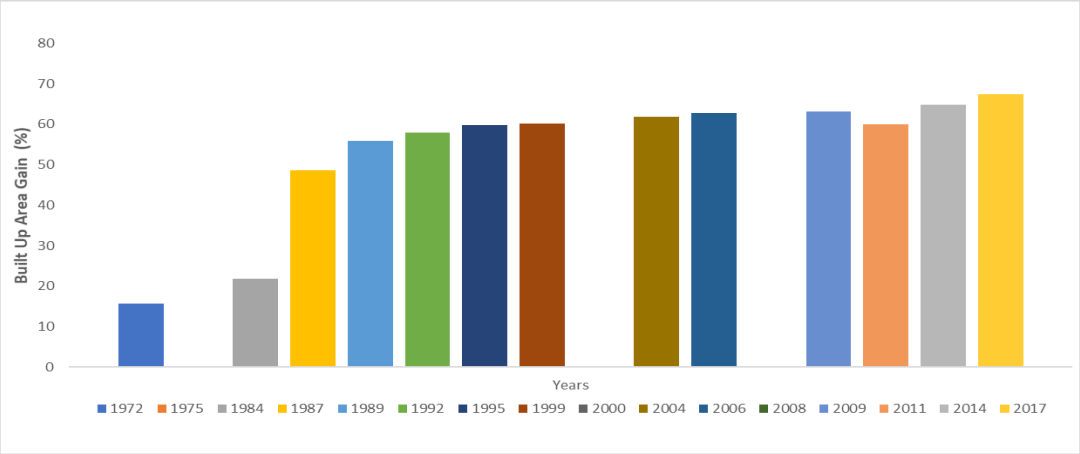

Figure 4. *Graph of built up areas coverage in percentages (%)*

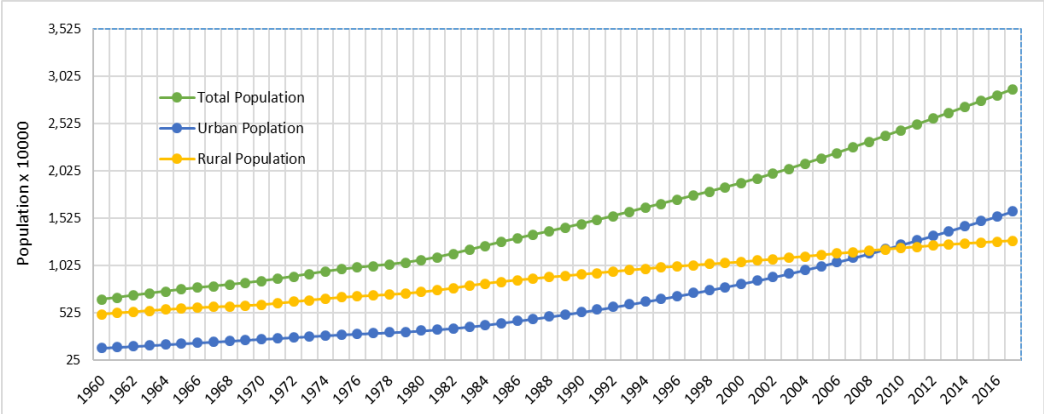

Figure 5. *Population growth in urban and rural areas in Ghana*

Table 3. *Results for area coverage of classification in percentages (%)*

Greater Accra Region							Annual percentage BUP increase based on *Equation 5*
Total land area = 3245 km²							
Year	**BUP%**	**km²**	**NBUP%**	**km²**	**WB%**	**km²**	
1972	15.65	507.84	68.49	2222.50	15.86	514.66	0.52%
1984	21.87	709.68	63.85	2071.93	14.28	463.39	
1987	48.69	1579.99	37.33	1211.36	13.98	453.65	5.68%
1989	55.94	1815.25	30.23	980.96	13.83	448.78	
1992	57.82	1876.26	28.38	920.93	13.80	447.81	
1995	59.84	1941.81	26.40	856.68	13.76	446.51	0.23%
1999	60.12	1950.89	26.25	851.81	13.63	442.29	
2004	61.78	2004.76	24.66	800.22	13.56	440.02	
2006	62.65	2032.99	23.94	776.85	13.41	435.15	0.27%
2009	63.12	2048.24	23.53	763.55	13.35	433.21	
2011	59.89	1943.43	26.85	871.28	13.26	430.29	
2014	64.81	2103.08	22.31	723.96	12.88	417.96	1.24%
2017	67.32	2184.53	19.92	646.40	12.76	414.06	

BUP = Built Up Areas; NBUP = Non-Built Up areas; WB = Water Bodies

http://www.aloki.hu ● ISSN 1589 1623 (Print) ● ISSN 1785 0037 (Online)
DOI: http://dx.doi.org/10.15666/aeer/1706_1314713168

Analysis on built-up change rate

This rate gives an indication of when much built up occurred which can be a measure of the economic status of the region. With an argument, it is assumed that the citizens and not the government do the built-up activities. The change rate is shown in *Figure 6*. It was calculated using *Equations 2* and *3* (Phiri and Nyirenda, 2015). In the second epoch (1991-2000), Accra added 3.83% more to its built-up environment but there was a slight increase of 2.12% during the third epoch (2001-2010). Notwithstanding this small increase it did an increase of 11.04% over the period (2011-2017). By 1980, the built-up areas had increased from 15.65% in 1972 to 21.87% representing a land surface area of 507.84 km^2 and 709.68 km^2, respectively, an increase of only 0.19%. However, by 1989, over 15-17 years, the built-up areas occupied 55.94% of surface area. The highest change occurred between 2001 and 2005 and the lowest occurred between 1996 and 2000 against the previous years, over the last 35 years. The last column of *Table 3* gives annual percentage increase in built-up areas depicting the annual change in size.

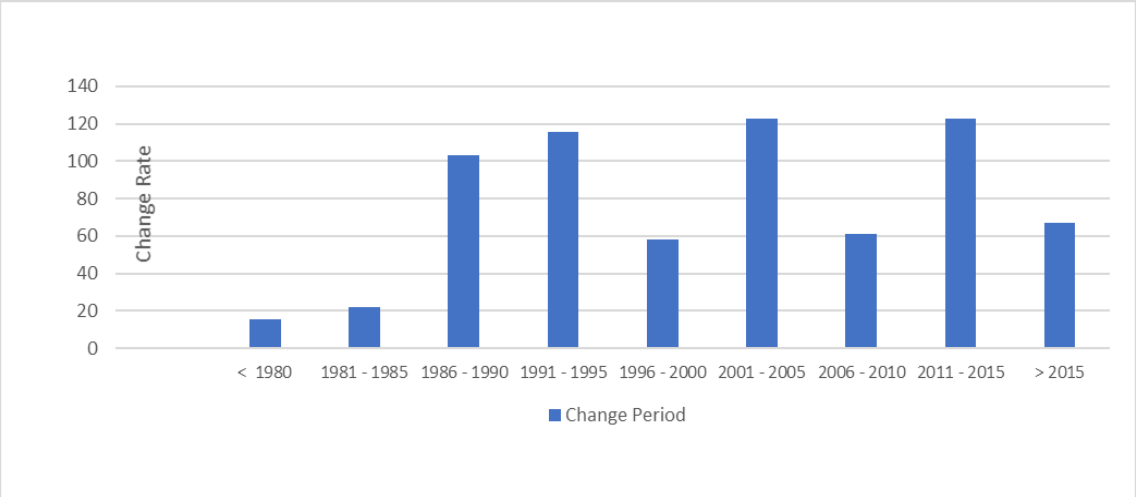

Figure 6. *Graph of annual built-up change rate*

Analysis on built-up growth rate

The GR over the period 1984-1994, 1995-2005 and 2006-2016 were 10.19%, 0.32%, and 0.34% respectively. Over the entire period of 1984-2017, Accra had a built-up growth rate of 11.9%. This figure, a graph of which is in *Figure 7,* does not necessarily mean lack of development (urbanisation) but rather it tells the spatial coverage of development or urbanisation within the region. The high growth rate of Accra in the first decade from 1984 is attributed to stable political environment after various coup d'états from 1966 until 1979. Although it was a military regime for almost the entire period, the country had a stable environment for growth.

There was coup d'état around this time, the economy of the country was very bad and this resulted in a lot of people leaving the country for greener pastures. Built-up areas within the capital were just very low as the economic status of the citizenry was not encouraging. The 1972 urban built-up scenario is depicted in *Figure 8*.

By 1984, the country had a stable government and economic activities had picked up. The country was implementing the Structural Adjustment Programme (SAP) as the

http://www.aloki.hu ● ISSN 1589 1623 (Print) ● ISSN 1785 0037 (Online)
DOI: http://dx.doi.org/10.15666/aeer/1706_1314713168

building foundation of the economy which was destroyed over the 15-year coup d'état period. Physical infrastructure was pursued vigorously by government which resulted in a constant growth by the year 1992 when the country returned to constitutional governance. *Figure 9* shows the change between 1984 and 1992.

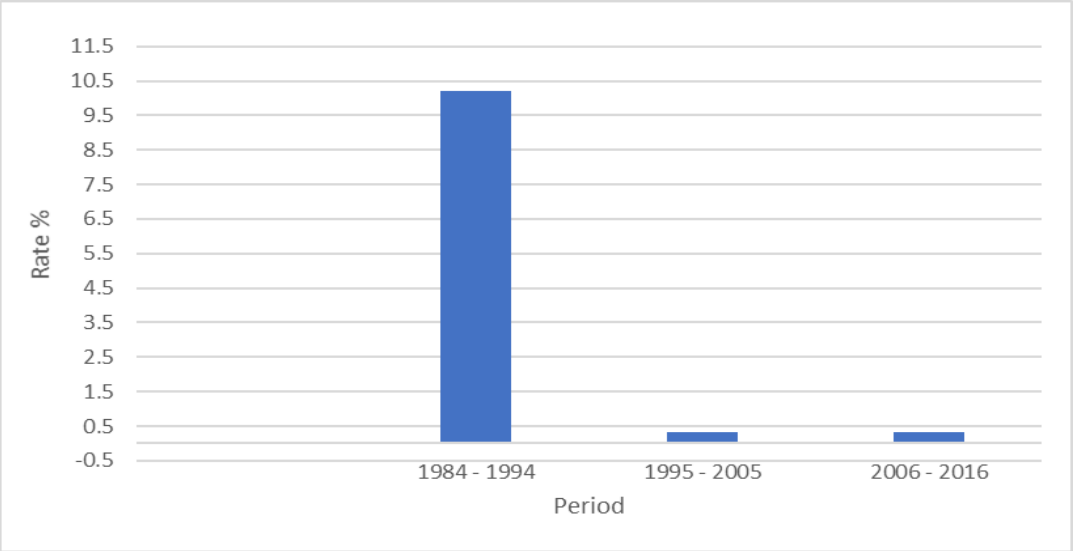

Figure 7. *Decade analysis of built up growth rate*

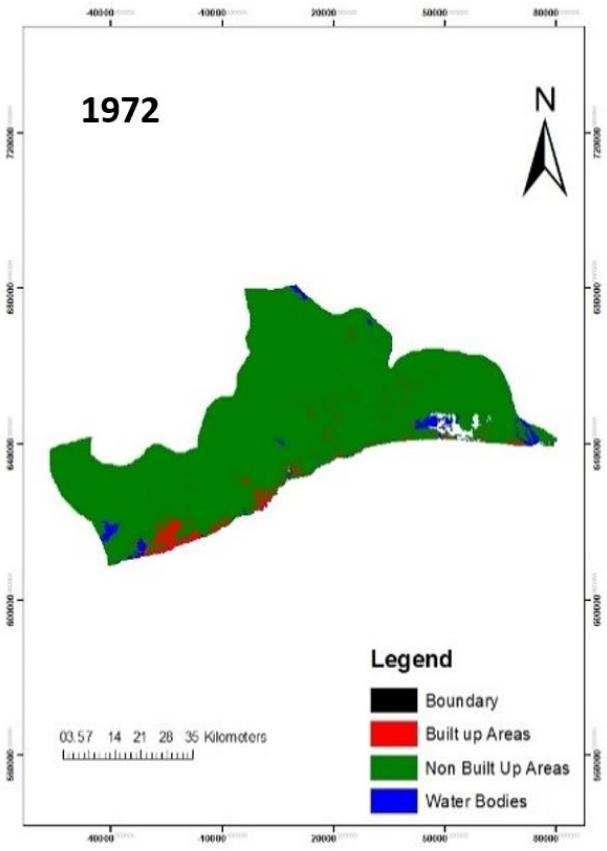

Figure 8. *Map land cover – baseline comparison 1972*

http://www.aloki.hu ● ISSN 1589 1623 (Print) ● ISSN 1785 0037 (Online)
DOI: http://dx.doi.org/10.15666/aeer/1706_1314713168

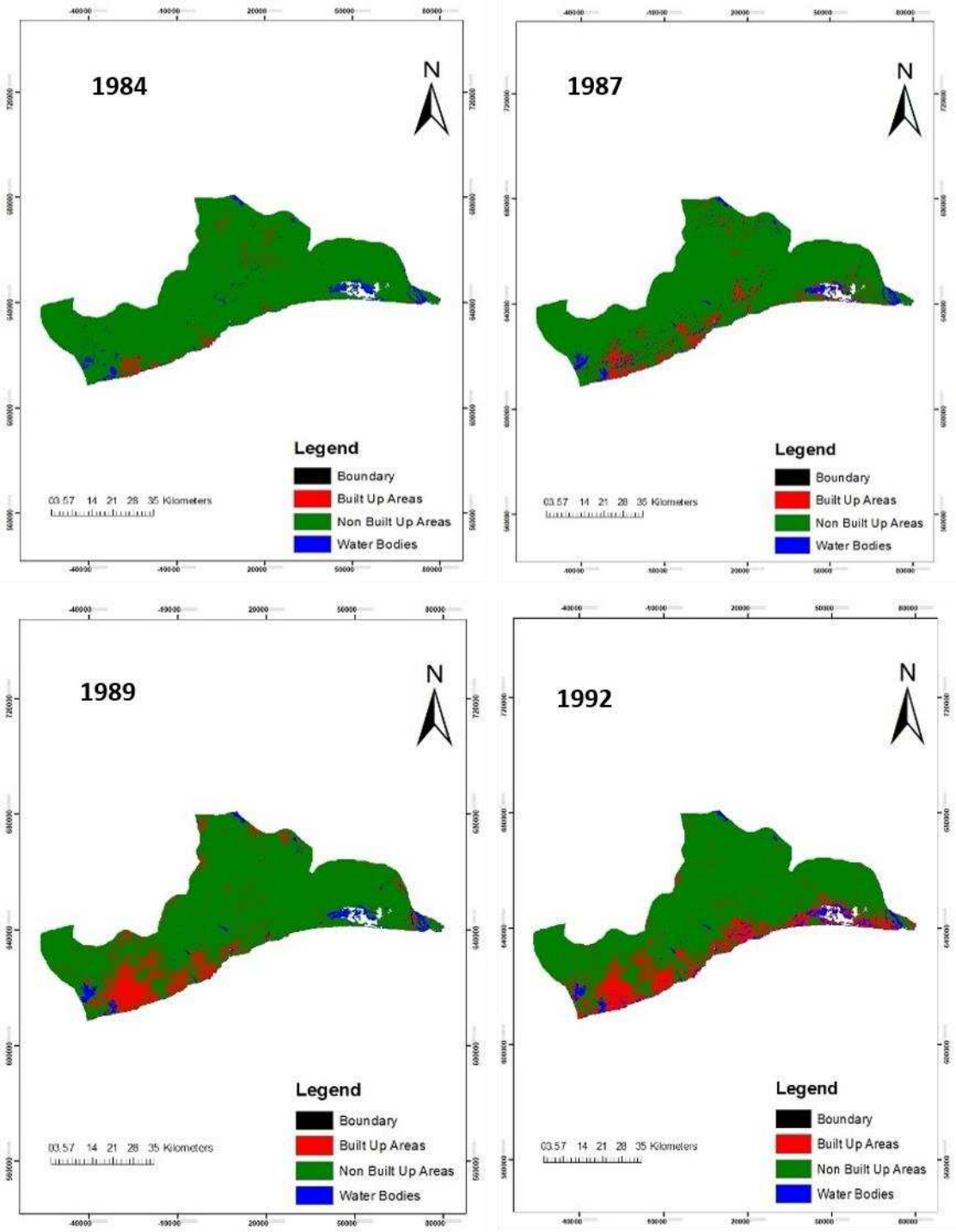

Figure 9. *Map of land cover classification – selected years*

Between 1993 and 1999, there was less development because greater portion of resources was channelled in expanding the country through electrification projects and building of feeder roads. Much of the built up activities was experienced mostly outside the economic capital. After the debt cancellation in 2001, the government had economic space to accelerate infrastructure once more and this increased the built up areas. The gradual increase is adequately shown in *Figure 10*.

http://www.aloki.hu ● ISSN 1589 1623 (Print) ● ISSN 1785 0037 (Online)
DOI: http://dx.doi.org/10.15666/aeer/1706_1314713168

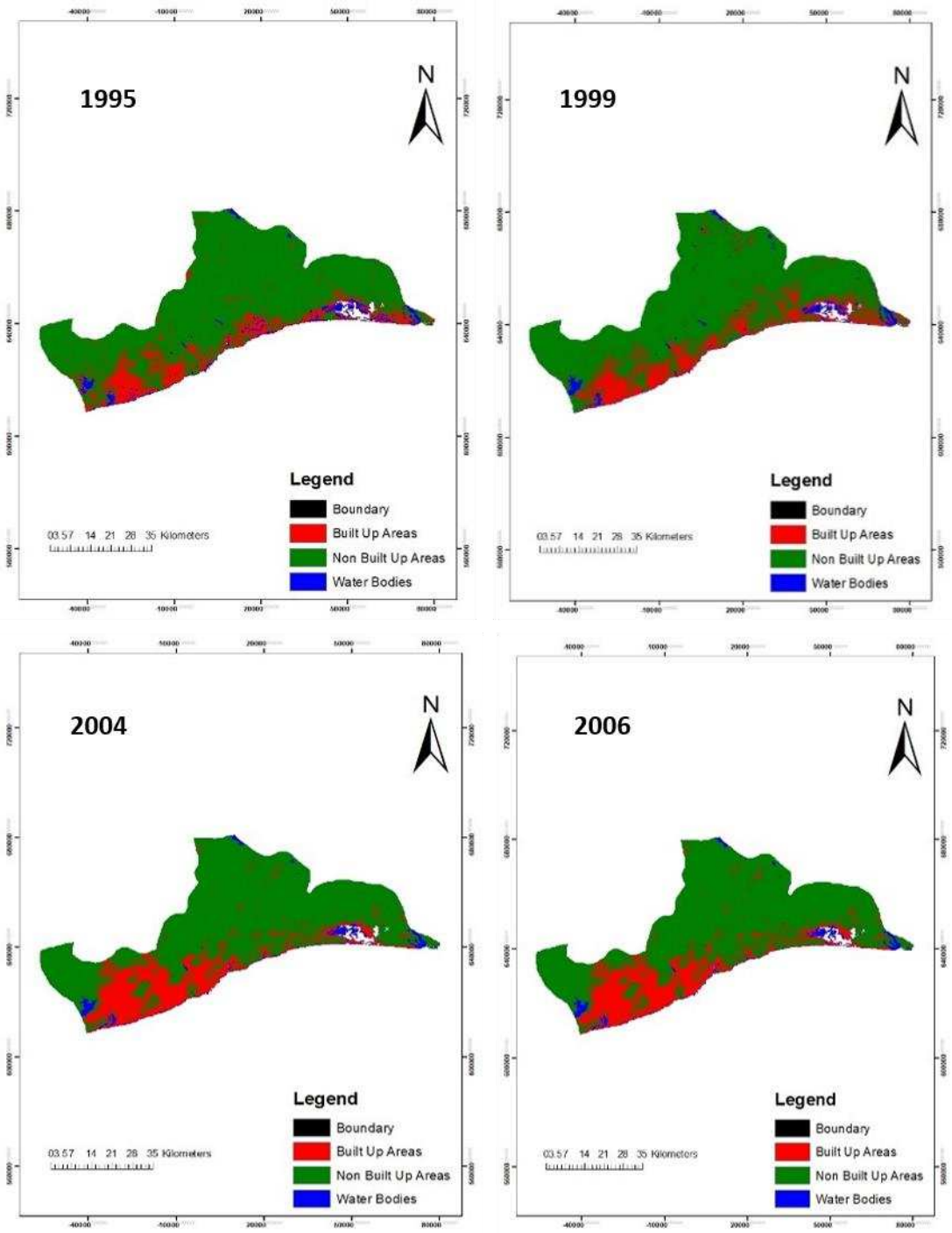

Figure 10. *Map of land cover classification – selected years*

There was a setback in 2007 and 2009 following flooding disaster which resulted in a massive demolishing of structures put up on water ways (dried up streams). The rapid increase in population and massive migration to the economic capital between 2010 and 2014 resulted in rapid housing projects to accommodate the influx. These have their own associated problems as demolishing of houses continues whenever there is flooding. This has seemingly slowed the rapid built up of infrastructure expansion. *Figure 11* shows the apparent scenarios explained above.

http://www.aloki.hu ● ISSN 1589 1623 (Print) ● ISSN 1785 0037 (Online)
DOI: http://dx.doi.org/10.15666/aeer/1706_1314713168

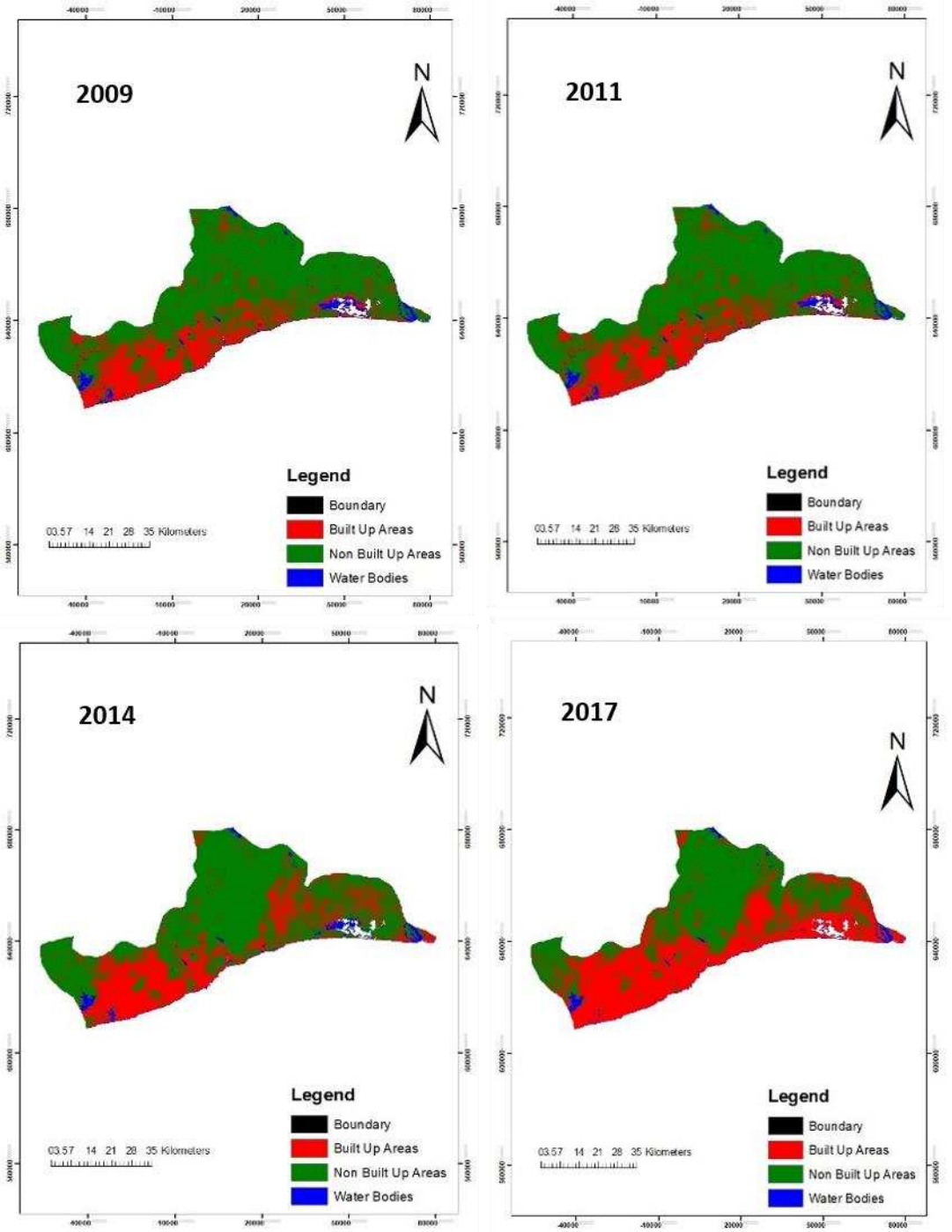

Figure 11. *Map of land cover classification – selected years*

Analysis on non built-up and water bodies performance

Results of the Area coverage percentage indicate a sharp loss of non-built up areas between 1981 and 1987. The 26.52% loss between 1984 and 1987 matches with the 26.82% gain in built up for the same time period. Water bodies lost 3.1% within 37 years translating into an annual loss of 0.08%. The highest loss value for water body

http://www.aloki.hu ● ISSN 1589 1623 (Print) ● ISSN 1785 0037 (Online)
DOI: http://dx.doi.org/10.15666/aeer/1706_1314713168

areas is only 1.58% between 1972 and 1984. In between comparable years, water body areas did not decline by even 1%.

Discussion

Band ratios and band combination

This is a very important image processing technique. The DN value of each pixel of one band is divided by the corresponding pixel value of another band. This yielded new number sets from zero (0/1) to 255 (255/1) which highlight more the specific target feature while suppressing the others. When necessary a rescaling can be done to provide a gray tone image resulting in a truer image because effect of shadows (or topographic) are dealt with (Zhouyu et al., 2006). This is an important advantage because eliminating shadows is still a challenge in a mixed urban environment during classification. Rescaling was not done in this study. Two distinct advantages result from band ratios; the differences in spectral reflectance curves of surface types are highlighted, and then illumination and radiance differ. Band rationing has the effect of removing shadows.

Another important property of two band ratios is that some features can be recognized by simply observing a single ratio. Many band ratios exist but involve the use of more than two bands. A few two band ratios exist but are mostly related to lithological discrimination and mapping and applications in hyperspectral image analysis (Simon et al., 2016; Mohammad et al., 2001).

The spectral reflectance curves, of ground targets provide great insight for information extraction. Usually ratio results of 1 or more is expected since pixels of ratios less than unity is characterized by dark signatures. Hence, ratio bands calculations were chosen to give values more than unity or close to unity. Between any two bands, which will be the numerator and which will be the denominator is carefully adjusted.

Maximum likelihood classification

As a parametric statistical classifier, the analyst training samples are numerically presented to the classifier algorithm by assuming that the distribution of the training sample is normally distributed. All unclassified pixels are assigned classes within the probability density function (Lillesand et al., 2015). The greatest advantage with ML is the quality of training samples. Training samples were collected in a homogeneous cover types as much as possible, since Google Earth provide a high resolution visually for good collection. The classifier develops signatures by taking advantage of the spectra of training set pixels which includes the contributions of all the materials in the training set. It is robust for most topographic and climatic variations which were tested in this study due to the stretch of time period over which topography had been affected due to urbanization. During evaluation in the accuracy assessment, it was manifest that while ML provide higher rates of correct recognition, it also yielded some false alarms. Maximum Likelihood classifier over the years has supported by many remote sensing and geographic information system based software such as ERDAS, with a straight forward in implementation.

Google Earth data

Digitizing training samples for ground truth from this platform gives geometrically-corrected high-resolution image. This serves as a great free source of validating data

http://www.aloki.hu ● ISSN 1589 1623 (Print) ● ISSN 1785 0037 (Online)
DOI: http://dx.doi.org/10.15666/aeer/1706_1314713168

because Google Earth can go back in time to give a real time training data. Google Earth provide high-resolution image that is coupled with other datasets for effective detection and classification (Xu et al., 2016). The class of water bodies like rivers and lakes is featured by their fairly better pixel uniformity and good spectral discrimination. The classification results using a combination of GE imagery and object-based classification techniques can attain an overall accuracy above 70.00% (Hu et al., 2013), which seem to be the situation in this paper.

Statistical analysis on delineated features

As of 2017 the total urban built-up land occupied in Accra was 2184.53 km^2. Total coverage of built up in Accra before 1972 was 507.84 km^2 but gained as much as 597.73 km^2 (34.07%) between 1981 and 1990 to reach 1815.25 km^2. During the second epoch of 1991-2000, the total coverage moved from 1876.26-1950.89 km^2. It increased only from 2004.76 to 2048.24 km^2 within the third epoch of 2001-2010. From 2011-2017 it added up to 241.10 km^2 in coverage. These figures are different from the results obtained by (Osei et al., 2013). According to their findings, urban areas covered 534.2279 km^2 in 2014 but our results indicate 2103.08 km^2 for the same year. We are inclined to say, their analysis might be off since the total land size of Accra as indicated by them is 3693.69 km^2 in 1985 and 3694.70 km^2 in 2014. This is problematic since Greater Accra region was not demarcated again in 2014. The total size since 1960 has remained 3245 km^2 and not what was obtained by them. Again areas covered by water have declined since 1985 due to buildings springing up on waterways which eventually dries the streams. It lost from 15.86% in 1972 to 2.88% by 2014. What is left now are the big rivers and big drains. However, their results showed very little change, 11.80% in 1985 to 11% in 2014. Over the period of 1984-1994, Accra increased its built up areas 7.2%. Over the 37-year study period, non-built up areas lost almost 49% to built-up areas because it gained by almost the same margin by 2017. Water bodies remained fairly stable with only 3.1% decrease over 37 years which means it lost 0.084% annually.

Conclusions

Remote sensing has the exclusive capability to support the extraction of urban features to detect urban growth with associated by-problems as, rise in surface temperatures, high traffic volume or population assessment. Change is very regular with all cities. These changes have both temporal and spatial characteristics which transformations can be temporally measured. Multi-year remote sensing information offers an essential source for monitoring and evaluating these endless changes with sufficient information for spatial urban growth investigation at regional level and at varied spatial and temporal scales. Understanding dynamic interaction between diverse aspects of urban expansion as expansion of built-up area and construction activities is very important as it is a very essential indicator of economic growth of a country. Again, the extraction of urban land-cover and land-use studies help to answer questions associated with these interrelations and its endless changes.

Band ratios have been used for many years in the field of remote sensing to classify terrain cover types. In this paper, we have shown the potential of spectral band ratio features for accurate pixel classification. Two band ratio combinations created in this study exhibit a better discrimination of urban features and patterns of urban growth. It

http://www.aloki.hu ● ISSN 1589 1623 (Print) ● ISSN 1785 0037 (Online)
DOI: http://dx.doi.org/10.15666/aeer/1706_1314713168

looked at the growth rate, growth change and the spatial area coverage of the economic capital of Ghana. This paper utilised the entire archive of Landsat data and does a 10-year varied-year analysis unlike other depiction of only two years, which is inadequate for in-depth analysis. Every algorithm has its own strengths and flaws. To effectively detect built-up areas based on a chosen algorithm, the nature of the input data is important. Depending on the output of this study, we can primarily say that, the quality of the training data required in supervised classification added to the success of the classification stage.

There were some inconsistencies in the built-up rate but this may be attributed to an uncoordinated land tenure system in the city which resulted in settlements springing up at hitherto odd inhabited places. This occurrence add-up positively because they all contribute to the built-up areas. Also, it can negatively impact because during digitising such sparse small areas might not be classified at all, or could be wrongly classified. The study provided here gives information that can be used by decision makers to make informed decisions on spatial planning, economic policy drafting and a real realisation of the translated impact of government economic policies as there is a direct relation between population growth, urbanisation, infrastructure deficits and GDP. Outputs present readers a guide on spectral diversity, band combination and accuracy assessment for urban areas detection.

Finally, the freely obtainable and accessible Google Earth data coupled with the high spatial resolution can serve as a reliable and effective source of data in urban land-use and land-cover mapping and change detection analysis. Another benefit of Google Earth is that it offers images at different time period which is very useful for urban engineers for land-use change detection studies. Although GE has more advantages, few studies have been done on the use of this data source for land-use mapping. Except for its spectral characteristics, it can make full use of the spatial features of objects, which can, to some degrees, strengthen the advantages of GE based data for its high spatial resolution and compensate its limitation of poor spectral information. This paper contributes to the search for simple use of basic classification techniques to classify urban areas over large geographical areas. It was able to adequately classify the targeted features.

Acknowledgements. This research was funded by the National Key R & D plan on Strategic International Scientific and Technological Innovation Cooperation special project (2016YFE0202300), Fundamental Research Funds for the Central Universities (2042016kf0179 and 2042016kf1019), the Wuhan Chen Guang project (2016070204010114), the Guangzhou Science and Technology project (201604020070), the Special Task of Technical Innovation in Hubei Province project (2016AAA018), and the Natural Science Foundation of China (61671332, 41771452 and 41771454).

REFERENCES

[1] Angel, S., Parent, J., Civco, D. L., Blei, A., Potere, D. (2011): The dimensions of global urban expansion: Estimates and projections for all countries, 2000–2050. – Progress in Planning 75(2): 53–107.

[2] Chester, L., Arnold, J., Gibbons, C. J. (1996): Impervious surface coverage: the emergence of a key environmental indicator. – Journal of the American Planning Association 62(2): 243–258.

[3] Cobbinah, P. B., Niminga-Beka, R. (2017): Urbanisation in Ghana: residential land use under siege in Kumasi central. – Cities 60: 388–401.

http://www.aloki.hu ● ISSN 1589 1623 (Print) ● ISSN 1785 0037 (Online)
DOI: http://dx.doi.org/10.15666/aeer/1706_1314713168

[4] Defries, R. S., Rudel, T., Uriarte, M., Hansen, M. (2010): Deforestation driven by urban population growth and agricultural trade in the twenty-first century. – Nature Geoscience 3(3): 178–181.
[5] Dewan, A. M., Yamaguchi, Y. (2009): Using remote sensing and GIS to detect and monitor land use and land cover change in Dhaka Metropolitan of Bangladesh during 1960-2005. – Environmental Monitoring and Assessment 150(1–4): 237–249.
[6] Elhag, M. (2017): Consideration of Landsat-8 spectral band combination in typical Mediterranean forest classification in Halkidiki, Greece. – Open Geosciences 9(1): 468–479.
[7] Estoque, R. C., Murayama, Y. (2015): Intensity and spatial pattern of urban land changes in the megacities of Southeast Asia. – Land Use Policy 48: 213–222.
[8] Feeney, G. (2014): Demography 101 : population growth rates. – The Demography-Statistics-Information Technology Letter #9.
[9] Ghana Statistical Service (2014): 2010 Population & Housing Census. – Accra Metropolitan District Analytical Report.
[10] Ghosh, S., Singh, P., Kumari, M. (2017): Assessment of urban sprawl and land use change dynamics, using remote sensing technique. A study of Kolkata and surrounding periphery, WB, India. – NGCT 2017 : 3rd International Conference on Next Generation Computing Technologies - Springer, Scopus, SCIE, Web of Science, DBLP. 30–31 October, Dehradun, India.
[11] Giles-Corti, B., Kerr, J., Pratt, M. (2017): Contributing to helping to achieve the UN sustainable development goals: truly shifting from niche to norm. – Preventive Medicine 103(September): S1–S2.
[12] Giridharan, R., Ganesan, S., Lau, S. S. Y. (2004): Daytime urban heat island effect in high-rise and high-density residential developments in Hong Kong. – Energy and Buildings 36(6): 525–534.
[13] Guo, W., Lu, D., Wu, Y., Zhang, J. (2015): Mapping impervious surface distribution with integration of SNNP VIIRS-DNB and MODIS NDVI Data. – Remote Sensing 7(9): 12459–12477.
[14] Hettiarachchi, M., Morrison, T. H., Wickramsinghe, D., Mapa, R., De Alwis, A., McAlpine, C. A. (2014): The eco-social transformation of urban wetlands: A case study of Colombo, Sri Lanka. – Landscape and Urban Planning 132: 55–68.
[15] Hu, Q., Wu, W., Xia, T., Yu, Q., Yang, P., Li, Z., Song, Q. (2013): Exploring the use of Google Earth imagery and object-based methods in land use/cover mapping. – Remote Sensing 5(11): 6026–6042.
[16] Inzana, J., Kusky, T., Higgs, G., Tucker, R. (2003): Supervised classifications of Landsat TM band ratio images and Landsat TM band ratio image with radar for geological interpretations of central Madagascar. – Journal of African Earth Sciences 37(1–2): 59–72.
[17] Jokar Arsanjani, J., Helbich, M., de Noronha Vaz, E. (2013): Spatiotemporal simulation of urban growth patterns using agent-based modeling: the case of Tehran. – Cities 32: 33–42.
[18] Kolokotroni, M., Shittu, E., Santos, T., Ramowski, L., Mollard, A., Rowe, K., Wilson, E., Filho, J. P. de B., Novieto, D. (2018): Cool roofs: high tech low cost solution for energy efficiency and thermal comfort in low rise low income houses in high solar radiation countries. – Energy and Buildings 176: 58–70.
[19] Kuang, W., Chi, W., Lu, D., Dou, Y. (2014): A comparative analysis of megacity expansions in China and the U.S.: patterns, rates and driving forces. – Landscape and Urban Planning 132: 121–135.
[20] Li, L., Lu, D., Kuang, W. (2016): Examining urban impervious surface distribution and its dynamic change in Hangzhou metropolis. – Remote Sensing 8(265): 19–24.

http://www.aloki.hu ● ISSN 1589 1623 (Print) ● ISSN 1785 0037 (Online)
DOI: http://dx.doi.org/10.15666/aeer/1706_1314713168

[21] Li, X., Yeh, A. G. O. (2000): Modelling sustainable urban development by the integration of constrained cellular automata and GIS. – International Journal of Geographical Information Science 14(2): 131–152.
[22] Li, X., Liu, X., Gong, P. (2015): Integrating ensemble-urban cellular automata model with an uncertainty map to improve the performance of a single model. – International Journal of Geographical Information Science 29(5): 762–785.
[23] Li, X., Zhou, Y., Zhu, Z., Liang, L., Yu, B., Cao, W. (2018): Mapping annual urban dynamics (1985–2015) using time series of Landsat data. – Remote Sensing of Environment 216: 674–683.
[24] Liu, S., Chuan-jun, W., Hong-quan, S. (2000): A GIS based model of urban land use growth in Beijing. – Acta Geographica Sinica 55(4): 407–416.
[25] Lu, J., Chen, J. H., Tang, Y., Feng, Y., Wang, J. S. (2007): High-rise buildings versus outdoor thermal environment in Chongqing. – Sensors 7(10): 2183–2200.
[26] Mather, P., Tso, B. (2010): Classification Methods for Remotely Sensed Data. 2nd Ed. – CRC, Boca Raton.
[27] Mohammad, M. R., El-Sobky, H., Sedeik, K., Raey, M. El (2001): Application of Band Ratios Identified by HHRR for Recognition of Surface Units using TM Data in SIWA Depression, Western Desert, Egypt. – 22nd Asian Conference on Remote Sensing, 5-9 November 2001, Singapore. Centre for Remote Sensing Imaging, Sensing and Processing (CRISP).
[28] Mohammady, S., Delavar, M. R., Pijanowski, B. C. (2013): Urban growth modelling with artificial neural network and logistic regression. Case study: Sanandaj City, Iran. – Romanian Review of Regional Studies IX (2): 47–60.
[29] Mu, D., Resources, N., Lafayette, W. (2006): Modelling urbanization patterns in two diverse regions of the world. – Journal of Land Use Science 1(2–4): 83–108.
[30] Muniz, R., Garcıa, S., Gonzalez, F., Corrales, J. A. (2003): Use of band rationing for color texture classification. – IbPRIA 606–615.
[31] Osei, F. E., Olutayo Balogun, B., Afrifa, G. (2013): Identifying and quantifying urban sprawl in the Greater Accra Region of Ghana from 1985 to 2014. – International Journal of Science and Research 4(1): 2793–2798.
[32] Phiri, L., Nyirenda, E. (2015): Urban growth analysis for Lusaka City using remote sensing and GIS. – DII-2015 Conference (Development and Investment in Infrastructure Conference). 16–18 September, Livingstone, Zambia.
[33] Potts, D. (2012): Challenging the myths of urban dynamics in Sub-Saharan Africa: the evidence from Nigeria. – World Development 40(7): 1382–1393.
[34] Rahman, M., Ullah, R., Lan, M., Sri Sumantyo, J. T., Kuze, H., Tateishi, R. (2013): Comparison of Landsat image classification methods for detecting mangrove forests in Sundarbans. – International Journal of Remote Sensing 34(4): 1041–1056.
[35] Rawat, J. S., Kumar, M. (2015): Monitoring land use/cover change using remote sensing and GIS techniques: a case study of Hawalbagh block, district Almora, Uttarakhand, India. – Egyptian Journal of Remote Sensing and Space Science 18(1): 77–84.
[36] Roy, D. P., Wulder, M. A., Loveland, T. R., C. E., W., Allen, R., Gerson, M. C., Helder, D., Irons, J. R., Johnson, D. M., Kennedy, R., Scambos, T. A., Schaaf, C. B., Schott, J. R., Sheng, Y., Vermote, E. F., Belward, A. S., Bindschadler, R., Cohen, W. B., Gao, F., Hipple, J. D., Hostert, P., Huntington, J., Justice, C. O., Kilic, A., Kovalskyy, V., Lee, Z. P., Lymburner, L., Masek, J. G., McCorkel, J., Shuai, Y., Trezza, R., Vogelmann, J., Wynne, R. H., Zhu, Z. (2014): Landsat-8: science and product vision for terrestrial global change research. – Remote Sensing of Environment 145: 154–172.
[37] Satterthwaite, D. (2010): The role of cities in sustainable development. – Sustainable Development Insights 4: 1–8.
[38] Schneider, A. (2012): Monitoring land cover change in urban and peri-urban areas using dense time stacks of Landsat satellite data and a data mining approach. – Remote Sensing of Environment 124: 689–704.

http://www.aloki.hu ● ISSN 1589 1623 (Print) ● ISSN 1785 0037 (Online)
DOI: http://dx.doi.org/10.15666/aeer/1706_1314713168

[39] Senanayake, I. P., Welivitiya, W. D. D. P., Nadeeka, P. M. (2013): Urban green spaces analysis for development planning in Colombo, Sri Lanka, utilizing THEOS satellite imagery - a remote sensing and GIS approach. – Urban Forestry and Urban Greening 12(3): 307–314.
[40] Seto, K. C., Kaufmann, R. K., Woodcock, C. E. (2000): Landsat reveals China's farmland reserves, but they're vanishing fast. – Nature 406(6792): 121.
[41] Sharma, R. C., Tateishi, R., Hara, K., Gharechelou, S., Iizuka, K. (2016): Global mapping of urban built-up areas of year 2014 by combining MODIS multispectral data with VIIRS nighttime light data. – International Journal of Digital Earth 9(10): 1004–1020.
[42] Simon, N., Ali, C. A., Mohamed, K. R., Sharir, K. (2016): Best band ratio combinations for the lithological discrimination of the Dayang. – Sains Malayasiana 45(5): 659–667.
[43] Sobrino, J. A., Oltra-Carrió, R., Sòria, G., Bianchi, R., Paganini, M. (2012): Impact of spatial resolution and satellite overpass time on evaluation of the surface urban heat island effects. – Remote Sensing of Environment 117: 50–56.
[44] Songsore, J. (2010): The Urban Transition in Ghana: Urbanization, National Development and Poverty Reduction. – Accra, Ghana.
[45] The World Bank Group (2015): Rising through Cities in Ghana: Ghana Urbanization Review Overview Report. – World Bank, Washington, DC.
[46] Thomas, M., Lillesand, Kiefer, R. W., Chipman, J. W. (2015): Remote Sensing and Image Interpretation. 7th Ed. – John Wiley & Sons Incorporation, New York.
[47] Varshney, A. and Rajesh, E. (2014): A comparative study of built-up index approaches for automated extraction of built-up regions from remote sensing data. – Journal of the Indian Society of Remote Sensing 42(3): 659–663.
[48] Xiang, D. L., Tang, T., Hu, C. B., Fan, Q. H., Su, Y. (2016): Built-up area extraction from PolSAR imagery with model-based decomposition and polarimetric coherence. – Remote Sensing 8(8): 21.
[49] Xu, H., Lin, D., Tang, F., Wei, C. (2011): Remote sensing of impervious surface dynamics of Xiamen City, southeastern China. – Proceedings of the 19th International Conference on Geoinformatics, 24–26 June, Shanghai, China.
[50] Xu, J., Zhao, Y., Zhong, K., Ruan, H., Liu, X. (2016): Coupling modified linear spectral mixture analysis and soil conservation service curve number (SCS-CN) models to simulate surface runoff: Application to the main Urban Area of Guangzhou, China. – Water (Switzerland) 8(12): 550.
[51] Yang, J., Huang, C., Zhang, Z., Wang, L. (2014): The temporal trend of urban green coverage in major Chinese cities between 1990 and 2010. – Urban Forestry and Urban Greening 13(1): 19–27.
[52] Yao, Y., Chen, D., Chen, L., Wang, H., Guan, Q. (2018): A time series of urban extent in China using DSMP/OLS nighttime light data. – PLoS ONE 13(5): 1–24.
[53] Yin, J., Yin, Z., Zhong, H., Xu, S., Hu, X., Wang, J., Wu, J. (2011): Monitoring urban expansion and land use/land cover changes of Shanghai metropolitan area during the transitional economy (1979-2009) in China. – Environmental Monitoring and Assessment 177(1–4): 609–621.
[54] Zhouyu, F., Caelli, T., Nianjun, L., Robles-Kelly, A. (2006): Boosted band ratio feature selection for hyperspectral image classification. – Proceedings of the International Conference on Pattern Recognition. 20–24 August, Hong Kong, pp. 1059–1062.

http://www.aloki.hu ● ISSN 1589 1623 (Print) ● ISSN 1785 0037 (Online)
DOI: http://dx.doi.org/10.15666/aeer/1706_1314713168

THE USE OF ARTIFICIAL NEURAL NETWORKS IN ENERGY USE MODELING IN BROILER FARMS: A CASE STUDY OF MERSİN PROVINCE IN THE MEDITERRANEAN REGION

YELMEN, B.[1*] – ŞAHIN, H. H.[2] – ÇAKIR M. T.[3]

[1]*Adana Metropolitan Municipality, Wastewater Treatment Department, 01120 Adana, Turkey*

[2]*Adana Metropolitan Municipality, 01120 Adana, Turkey*

[3]*Health Institutes of Turkey (TUSEB), 06590 Ankara, Turkey*

**Corresponding author*
e-mail: bekiryelmen@gmail.com

(Received 31st May 2019; accepted 2nd Sep 2019)

Abstract. This study presents the application of Artificial Neural Network (ANN) techniques to estimate the total energy use of broiler farms. Chicken meat is shown as one of the important parameters in the modeling of energy use efficiency of broiler farms. However, the measurement of this extremely important parameter is difficult and takes a long time to obtain the desired results. In order to overcome such difficulties, scientists have tried to develop alternative methods. The farm-scale data used in the study was obtained from 30 broiler farms in Mersin (Turkey) province in 2018. In the application of ANN model, consumed feeds, electricity, fuel, water, broiler farms, chicks, human labor and machinery parameters used in the farm are used as input; broiler poultry meat and fertilizer parameter are used as output. In addition, the total energy equivalent estimates of chicken meat were made using various input combinations to investigate the best results model. The highest coefficient of determination (R^2) (0.936) and the lowest root mean square error (RMSE) and the mean absolute error (MAE) values were found to be 0.232 and 0.019, respectively. The results showed that the ANN model is a very promising approach for the estimation of total energy equivalent of chicken meat in broiler farms.
Keywords: *artificial neural networks, energy efficiency, broiler chicken, sustainable, modeling*

Introduction

The need to provide adequate food for the increasing population of the world has increased energy consumption in agriculture. Increased population and energy demands have forced governments to work on the efficiency of energy use. This issue makes agriculture vulnerable to oil prices (Taki and Yildizhan, 2018). Agriculture, as an efficient part of the economy, plays an important part in national production. With the reduction of energy resources, people will be forced to produce more food with less energy consumption in the future (Rohani et al., 2018). Agriculture is not only an energy consumer but also an important energy supplier (Almasi et al., 2008). Poultry meat offers significant potential to meet human nutritional needs (Folorunsho and Onibi, 2005). 35 g protein of animal origin is recommended for daily intake by FAO (FAO, 2011). In human nutrition, one third of the meat consumed in the world is obtained from broilers (Atilgan and Koknaroglu, 2006). Efficient use of energy in agriculture reduces environmental problems, prevents the destruction of natural resources and develops sustainable agriculture as an economic production system (Hatirli et al., 2005). In animal production systems, energy and feed are the main components of production costs (Rivera-Torres et al., 2010). Energy efficiency relates to the reduction of inputs purchased in agricultural production. The modeling capability

http://www.aloki.hu ● ISSN 1589 1623 (Print) ● ISSN 1785 0037 (Online)
DOI: http://dx.doi.org/10.15666/aeer/1706_1316913183

of ANN has made them the most popular tool for modeling the biological processes of complex systems with nonlinear properties (Kologirou, 1999). Artificial neural networks have a high approach and have a great advantage in a short time such as problem solving (Bechtler et al., 2001). ANN is applied in a wide area such as energy, mathematics, engineering, medicine, economy, environment and agriculture (Safa and Samarasinghe, 2001). ANN is one of the smartest techniques that are flexible and do not require too much physical complex operation (Yazdani et al., 2009). ANN is an optimization algorithm in which the learning process is tried to be modelled mathematically. ANN is a simple approach to a complex process, but uses the basic concepts inherent in the learning processes of people and animals. The ANN imitates the human brain's ability to learn by experimenting to produce solutions to problems that require a person's thinking and observing abilities. Learning in humans occurs by adjusting the synaptic connections between nerve cells (neurons). Since one birth, because of the process of learning by experience, the brain shows a continuous improvement. As the number of experience increases, synaptic connections are adjusted and new connections are created. In this way, learning takes place. This also applies to ANN. Learning is through training, using examples. By processing the input and output data, the training algorithm using this data, it is possible to re-adjust the connection weights until a convergence is achieved (Keskin and Taylan, 2007). ANNs are universal function estimators that work better than traditional function approach methods (Farjam et al., 2014). Classical regression analysis does not give any good results due to the nonlinear complex relations resulting from the nature of the problem. There are other methods that can be used more appropriately in cases of uncertainty. There are various methodologies in the literature, such as artificial neural networks (ANN), fuzzy logic, adaptive neuro-fuzzy systems which can be expressed as flexible methods. ANN models can be used to estimate the performance of the energy efficiency of broiler farms (Yurtoglu, 2005). In efficient energy use in agriculture, mathematical models have been used to find the relationships between the inputs and outputs of a production process (Pahlavan et al., 2012). Mathematical functions are of great importance in finding the relationship between inputs and yield by various methods (Hatirli et al., 2006). In study conducted in Iran using artificial neural networks; total equivalent input and output energy in broiler production was calculated as 153.79 and 27.45 GJ per 1000 birds, respectively (Amid and Gundoshmian, 2016). Rahman and Bala used artificial neural networks to estimate the dry matter of the cannabis plant in Bangladesh using parameters dependent on climatic conditions. They concluded that the best model had two hidden layers, the 6-9-5-1 structure (Rahman and Bala, 2010). Houshyar et al. in the wheat production in Iran, ANN was used. The best model for this study was the GFFN model with a hidden layer and the LM training algorithm with $R^2 = 0.95$ and RMSE = 0.071 (Houshyar et al., 2010). Using artificial neural network, Taki et al. have concluded that the optimal network for the estimated output energy of wheat production has two secret layers, each containing 8 neurons and which can be well predicted (Taki et al., 2012). In another study, Zangeneh et al. have compared the results of the implementation of two different approaches, namely, parametric model (PM) and ANN models, to evaluate the economic indices that benefit economic efficiency, total production costs and the cost ratio of the potato crop (Zangeneh et al., 2011). A study was carried out on the estimation of the energy demand of greenhouses by artificial neural network. In this study R^2, RMSE and MAE were found to be 0.93, 0.187 and 0.058, respectively (Trejo-Perea et al., 2009). Some other non-linear models such as

http://www.aloki.hu ● ISSN 1589 1623 (Print) ● ISSN 1785 0037 (Online)
DOI: http://dx.doi.org/10.15666/aeer/1706_1316913183

artificial neural networks, adaptive neuro-fuzzy inference system and nonlinear similar studies have been used in regression technique (Ekici and Aksoy, 2011; Mellit and Kalogirou, 2011; Talebizadeh and Moridnejad, 2011; Nefeslioglu et al., 2008; Yagiz et al., 2009; Dagdelenler et al., 2011). A multi-layered ANFIS has been used to estimate the yield of agricultural products (Naderloo et al., 2012; Khoshnevisan et al., 2014a, 2014b). In Iran, Heidari et al., in a study done in Yezd province measured energy efficiency of five-input and two-output parameters and broiler units, 16 were found to be fully efficient from 44 poultry farms (Heidari et al., 2011a). Heidari et al. using the Artificial Neural Network models estimated the Benefit Cost Ratio (BCR) of chicken farms in the tropical regions of Iran (Heidari et al., 2011b). The neural network used a multilayered feed network with five neurons (bird cost, labor cost, food cost, fuel cost and electricity cost) in the input layer and a neuron (benefit-cost ratio) in the output layer (Layer structure 5-20-1). Statistical indicators were estimated in R^2, RMSE, MAE and to verify the model. The indicators were calculated at 0.978, 0.002, 0.037 and 2.695 (Heidari et al., 2011b). Sefeedpari et al., in order to estimate the energy consumption of egg production farms in Iran, they used a three-entry ANN model to estimate variables such as fuel energy, electricity and feed energy (Sefeedpari et al., 2012). Atilgan and Koknaroglu according to the results of energy analysis used in broiler production units, showed that larger production units had higher energy efficiency compared to smaller production units (Atilgan and Koknaroglu, 2006). The electricity, fuel and manpower used in the 60,000-capacity brolier farm are reported in the winter 2395.8, 38563.88 and 94.85 MJ, respectively, and in the summer were 3359.5, 66.124, and 94.58 MJ, respectively (Sedaghat Hoseyni et al., 2008). Risse et al., who studied poultry farms as an energy source (Risse et al., 2007). reported that poultry manure saved 283 million gallons of fuel in the United States. In this study, Artificial Neural Network (ANN) models are applied for efficient use of Broiler Farms and estimation of total energy use.

Artificial neural networks (ANN)

ANN is a sub-branch of artificial intelligence. The artificial working principle of the human brain is the artificial systems that have adopted the model. ANN is one of the most popular subjects of modern science with its ability to learn, adapt, ability to work with little information, fast work and identification. ANNs work with the principle of increasing knowledge and experience through learning and producing results by benefiting from the learning (Oztemel, 2003). Environment, agriculture, engineering, medicine, such as employees working in various areas of the sphere of their own areas of expertise, began to develop applications in their own fields. This interest is further strengthened by the theoretical and practical successes. It has been seen that some areas that seem to be unique to human intelligence can be expressed numerically, and thus machines can perform learning and recalling in a surprisingly similar way to human intelligence. Artificial neural networks are a powerful computational system inspired by the structure and learning characteristics of biological neuron cells and are very powerful classifiers in pattern recognition. Artificial neural networks, especially with the development of computer technology, have found a wide range of applications in the field of engineering (Kalogirou, 1999). Artificial neural networks are parallel information processing structures with the following characteristics:

- Inspired by a biological neuron, a mathematical model was introduced.
- It consists of a large number of processing elements connected to each other.
- Connection holds information with weights.

http://www.aloki.hu ● ISSN 1589 1623 (Print) ● ISSN 1785 0037 (Online)
DOI: http://dx.doi.org/10.15666/aeer/1706_1316913183

- A processing element can react dynamically to the input warnings and the response is entirely dependent on local information (the input signal through the connections and link weights that affect the respective processing element).
- It has learning, recalling and generalizing skills thanks to the connection weights set by the training data.

These outstanding features provide the ability to solve complex problems in artificial neural networks. It has found wide application areas in the fields of modeling and control. ANNs are first trained using the available data and then tested with unused data during training. Although training takes quite a long time; they decide very quickly during use. They found a wide range of applications in modeling both linear and nonlinear systems because of their ability to tolerate learning, generalization and errors and to take advantage of faulty samples (Haykin, 1994). ANN is looking at the examples of events and making generalizations about these events, collecting information and using the information they have learned when they have never seen them before and can decide on those examples (Ozcalik and Kucuktufekci, 2003). The concept of artificial neural networks (ANN) emerged with the idea of mimicking the working principles of the human brain on digital computers and the first studies focused on the mathematical modeling of neurons. Studies have shown that neurons exchange information with neighboring neurons. The so-called artificial neural networks are composed of neurons coming together in certain forms. ANN models differ from conventional models with non-algorithmic parallel and distributed information processing capabilities. Thanks to these different features, ANN can easily and quickly perform complex and non-linear accounts. Non-algorithmic and very intense parallel operations can be performed in parallel with the ability to learn and parallel distributed memory has led to new perspectives in the calculation. Input layer neurons transmit values to the next information processing layer elements through links that retrieve input information. This process continues until the output layer is reached. This type of information flow is known as the network feed forward network, which occurs in one direction. A typical ANN model is given in *Figure 1*. ANN models are configured as single or multiple inputs, and single or multiple outputs.

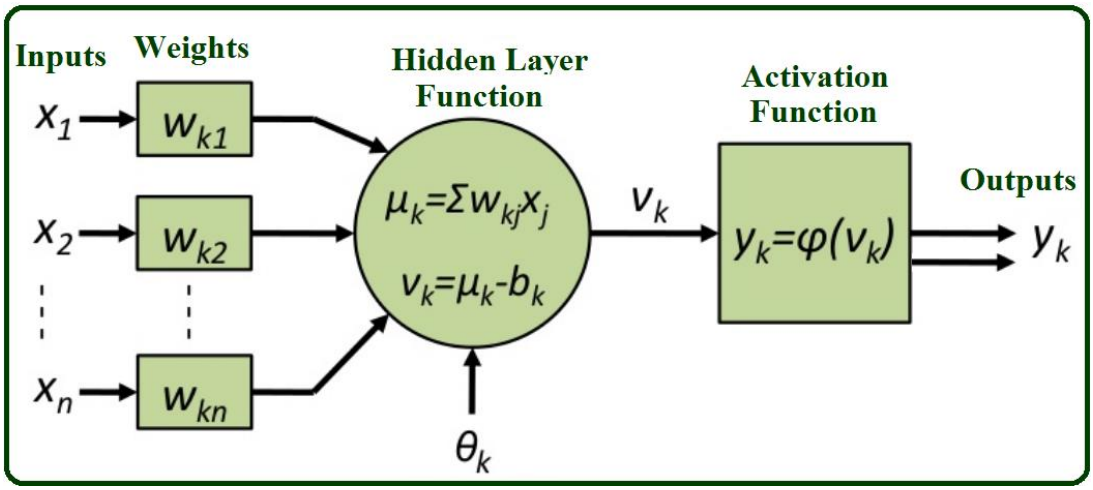

Figure 1. *Artificial neural network model*

http://www.aloki.hu ● ISSN 1589 1623 (Print) ● ISSN 1785 0037 (Online)
DOI: http://dx.doi.org/10.15666/aeer/1706_1316913183

Feed forward back propagation artificial neural network (FFBPANN) model

In this study, ANN (i, j, k) model is created to show input, hidden and output layers of icons i, j and k, respectively. Each layer is composed of many neurons and is bound by weight clusters between layers. The way of attachment and the number of neurons in each part may vary. Communication between neurons in the same section is not allowed. At the beginning of this training process, connection forces are assigned as random values. The learning algorithm changes the force until each iteration is completed with success. When the iteration process reaches a conclusion, the coupling forces obtain and store the available information in the samples used in the training process. When a new input group is presented, an output group is obtained by means of the learned and stored information in the connection forces of the artificial neural network with forward feed. Here, i and k values are 1 and j values are taken as 2, 3, 5, 7, 9, 10, 12 and ANN models are created. In this study, sigmoid function is used as transfer function, and back propagation algorithm based on generalized delta rule is used for ANN training (ASCE, 2000). The article aimed to use Artificial Neural Network (ANN) techniques to assess broiler farm energy consumption as a method that can sufficiently calculate the energy equivalent of chicken meat.

Materials and methods

In this study, data were collected from 30 producers of broiler farms in Mersin. In the Mediterranean region city of Mersin, located south of Turkey. It is located between 36° 48' N and 34° 38' E (*Fig. 2*). The average annual temperature is approximately 19.2 °C and the total annual rainfall is 592.1 mm. Approximately 94% fall from October to May (GDM, 2017).

Figure 2. *The location of the Mersin province involved in the presented study*

Data on the production of broiler farms were collected with face-to-face surveys from the producer in 2018. Samples were selected using randomly selected random sampling method. Using the random sampling method of the producers who are producing in Broyler Farms in Mersin province where the production was made in 2018, the sample size was

http://www.aloki.hu ● ISSN 1589 1623 (Print) ● ISSN 1785 0037 (Online)
DOI: http://dx.doi.org/10.15666/aeer/1706_1316913183

calculated using the following equation (Newbold, 1994): The total number of registered farmers in Mersin in 2018 year was 35039 (GDAE, 2018). The Neyman method was applied to determine of number the farmer(Yamane, 1967).

$$n = \frac{N \times S^2}{(N-1)S^2_x + S^2} \quad \text{(Eq.1)}$$

where n is the required sample size, N population volume, S standard deviation, S_X sample is the standard deviation of the mean (S_X = d / z), z is a reliability coefficient, d is based on the allowable error equation of the sample size (*Eq. 1*) In the Broiler Farms, the number of samples examined for production systems was 414. The permissible error (d) was defined as 5%, and for 95% reliability (z), the sampling size of 414 was calculated. First, the most common production systems for each Broiler Farm were identified, and then all inputs and outputs from the systems were identified and digitized, and then converted to energy units. With the addition of partial energies to the total energies per production unit, the energy inputs of each input were: chicks, human labor, fuel, electricity, feeds, water and machine. In order to estimate the energy in the MJ unit equivalents were used to find the input quantities as presented in *Table 1*.

Table 1. *Energy equivalences for input and outputs*

Particulars	Unit	Energy equivalent (MJ unit^{-1})	Reference
A. Inputs			
1. Chick	kg	10.33	Heidari et al., 2011b
2. Human labour	h	1.96	Karaagac et al., 2011; Mani et al., 2007
3. Diesel fuel	L	47.8	Kitani, 1999
4. Electricity	kWh	11.21	Pisghar et al., 2013
5. Feed	kg	12.98	Anonymous, 2014
6. Water	ton	0.63	Yaldız et al., 1993
7. Machinery (iron)	kg	27.73	Canakci and Akinci, 2006
8. Machinery (plastic)	kg	90	Canakci and Akinci, 2006
B. Outputs			
1. Chicken Meat	kg	10.33	Celik and Ozturkcan, 2003
2. Manure	kg	0.3	Singh, 2002

The data used in this study are the feed consumed in the broiler farms in 2018, the electricity consumed, the fuel consumed, the water consumed; human labor, machine parameters used in farms and chicken meat and fertilizer were obtained from 30 broiler farms in Mersin Province (*Table 1*). Energy equivalences for input and outputs are presented in *Table 2*. Energy input-output analysis in broiler chicken values are given. Poultry Equipment Used On Broiler Farms are given in *Figure 3*.

Statistical analyses of each of these data are given in *Table 3*. In this table, Xort, Sx and Cv represent the mean, standard deviation and variance, values of each data, respectively. The most variable data is water parameter (Cv = 0.564), feed parameter

http://www.aloki.hu ● ISSN 1589 1623 (Print) ● ISSN 1785 0037 (Online)
DOI: http://dx.doi.org/10.15666/aeer/1706_1316913183

has the highest correlation with chicken meat (R = 0.971). *Table 3* shows that the water parameter has the lowest correlation (R = -0.421) with chicken meat.

Table 2. *Energy input-output analysis in broiler chickens*

Particulars	Unit	Quantity per unit area MJ (1000 birds)	Total energy equivalent (MJ/1000 bird)	Percentage of total energy (%)
A. Inputs				
1. Chick	kg	4000	41320	0.848
2. Human labour	h	1005.9	1971.564	0.040
3. Diesel fuel	L	940.8	44970.24	0.923
4. Electricity	kWh	12870.8	144281.668	2.962
5. Feed	kg	357012	4634015.76	95.148
6. Water	ton	41.622	26.22186	0.001
7. Machinery (iron)	kg	5.082	140.92386	0.003
8. Machinery (plastic)	kg	39.711	3573.99	0.073
Total inputs		375837.515	4870300.368	100
B. Outputs				
1. Chicken Meat	kg	245024	2531097.92	99.401
2. Manure	kg	47702.4	15264.768	0.599
Total outputs		292726.4	2546362.688	100
Energy ratio			0.52	

Table 3. *Data used in the study and its statistical analysis*

Data	X_{ort}	S_x	$C_v(S_x/X_{ort})$	Chicken meat and correlation (R)
Chicken meat (kg)	2531097.92	845263.8	0.334	1.000
Manure (kg)	15264.77	7311.824	0.479	0.638
Feed (kg)	4634015.76	1616092	0.349	0.971
Electricity (kWh)	144281.668	57424.1	0.398	0.816
Diesel fuel (L)	44970.24	18527.74	0.412	0.787
Chick (kg)	41320	19255.12	0.466	0.673
Machinery	3714.91	1824.023	0.491	0.619
Human labour	1971.56	1033.1	0.524	0.544
Water	26.22	14.78913	0.564	0.421

Implementation of feed forward back propagation artificial neural network model

Analysis of 414 data from 30 broiler farms consisting of chicken meat and manure from seven input vectors (feeds, electricity, fuel, chicks, machinery, human labor and water) and two output vectors was considered. The data is divided into two groups to form the training and test sets. While constitute 276 data training sets, the remaining 138 data sets, were used as the test set in evaluating the performance of the program to the real values. The estimated network structure in Artificial Neural Networks model for broiler farms is given in *Figure 4*. In this study, for the evaluation of errors, the

http://www.aloki.hu ● ISSN 1589 1623 (Print) ● ISSN 1785 0037 (Online)
DOI: http://dx.doi.org/10.15666/aeer/1706_1316913183

coefficient of determination (R^2), the square root of the mean square error (RMSE) and the mean absolute error (MAE) functions were used.

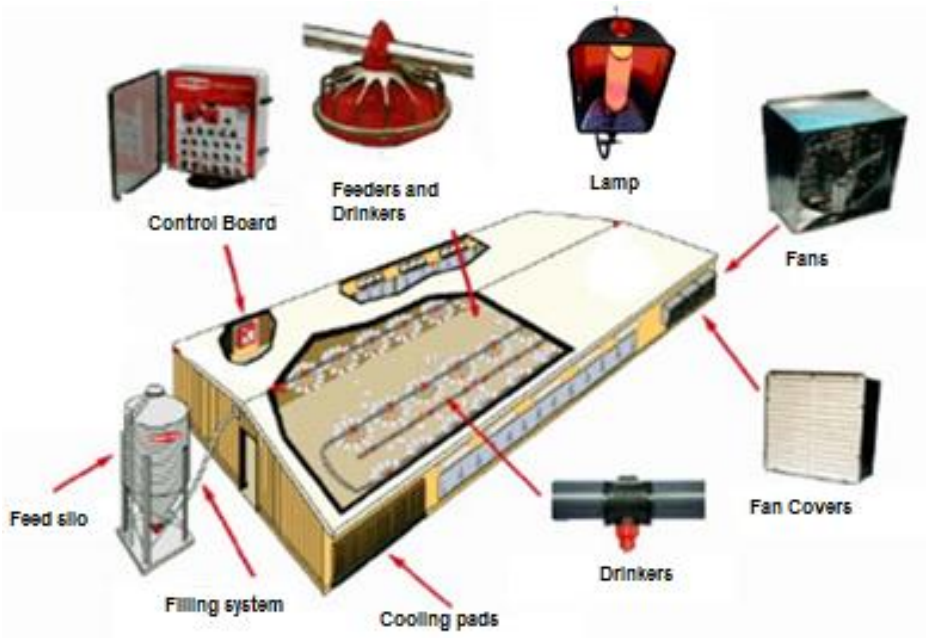

Figure 3. *Poultry equipment used on broiler farms*

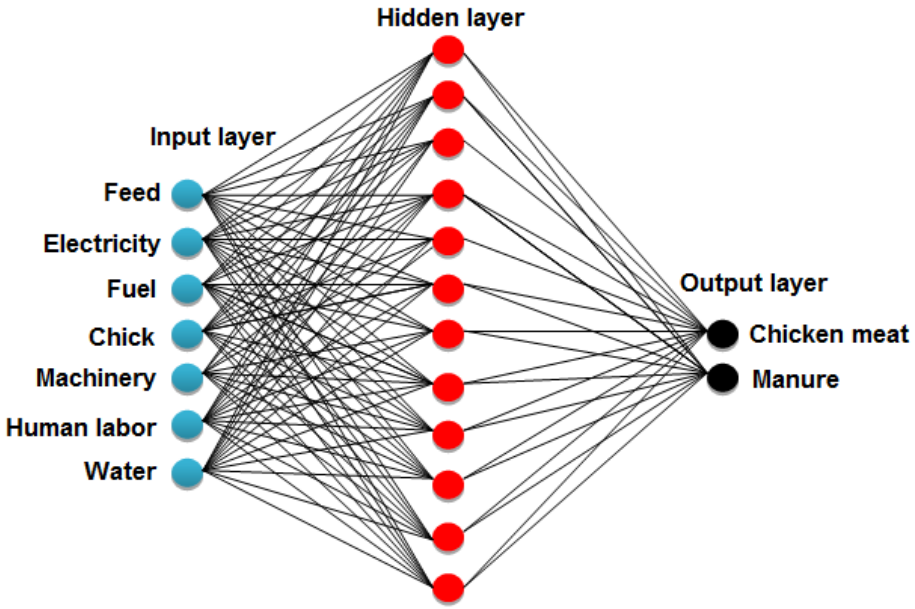

Figure 4. *Network structure estimated in the neural networks model for broiler farms*

In this study, each model was tested with the test data set by training the training data set and the root of the square root mean square (RMSE) was calculated by using *Equation 2* (Landeras et al., 2008). One of the best evaluations used for statistical indices, the root of the mean square error (RMSE), as well as R^2 estimation value were found with *Equation 3*. The related equations are:

http://www.aloki.hu ● ISSN 1589 1623 (Print) ● ISSN 1785 0037 (Online)
DOI: http://dx.doi.org/10.15666/aeer/1706_1316913183

$$RMSE = \sqrt{\frac{\sum_{i=1}^{N}\left(yi - yi^{'}\right)^2}{N}} \quad \text{(Eq.2)}$$

According to the R^2 equation; m is the number of data tested, the estimated data on the Oi neural network, *yi* is the amount of data calculated (Traore et al., 2010).

$$R^2 = \frac{\left[\sum_{i}^{m}(yi - \overline{y})(Oi - \overline{O})\right]}{\sum_{i=1}^{m}(yi - \overline{y})^2 \sum(Oi - \overline{O})^2} \quad \text{(Eq.3)}$$

where $\overline{y}$ is the average of the calculated data amount (yi) and the mean values of the estimated data amounts (Oi) in the $\overline{0}$ artificial neural network. In addition, mean absolute error (MAE) values were calculated (*Eq. 4*) (Trejo-Perea et al., 2009).

$$MAE = \frac{1}{N}\sum_{i=1}^{N}\left|y_i - y_i^{'}\right| \quad \text{(Eq.4)}$$

Sensitivity analysis using feed forward back propagation artificial neural network model

The choice of input parameters to be used in the FFBPANN model is important for the performance of the model (Khoshnevisan et al., 2014b). The effectiveness of the inputs in the model can be determined by sensitivity analysis. For the estimation of chicken meat, each input parameter was used individually and the most sensitive parameter was found with FFBPANN. The results are shown in *Figure 5a-g*. In addition, it was found that which combinations of inputs would give the most effective model by using sensitivity analysis (*Table 4*). As a result of sensitivity analysis, it was observed that all input parameters were important in estimating chicken meat. The feed input parameter is the most effective parameter for poultry meat prediction; Water as the least effective parameter is determined by the sensitivity analysis as shown in *Figure 5a* and *g,* respectively.

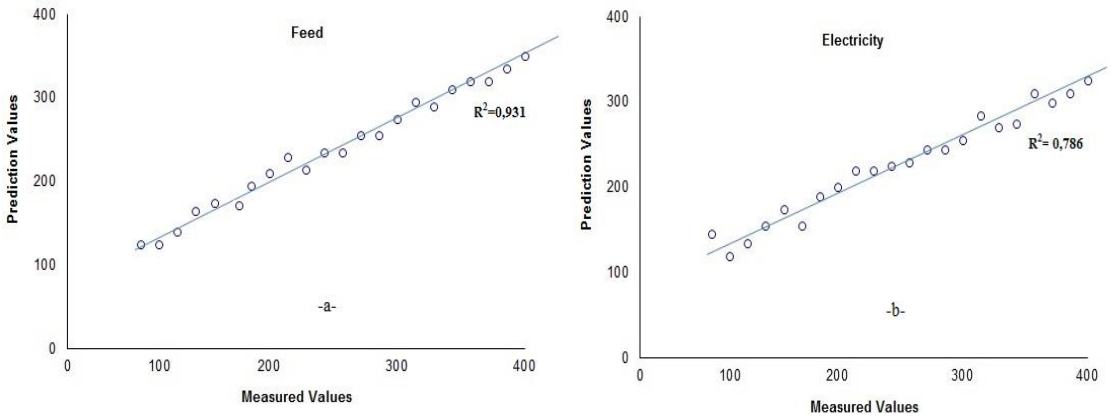

http://www.aloki.hu ● ISSN 1589 1623 (Print) ● ISSN 1785 0037 (Online)
DOI: http://dx.doi.org/10.15666/aeer/1706_1316913183

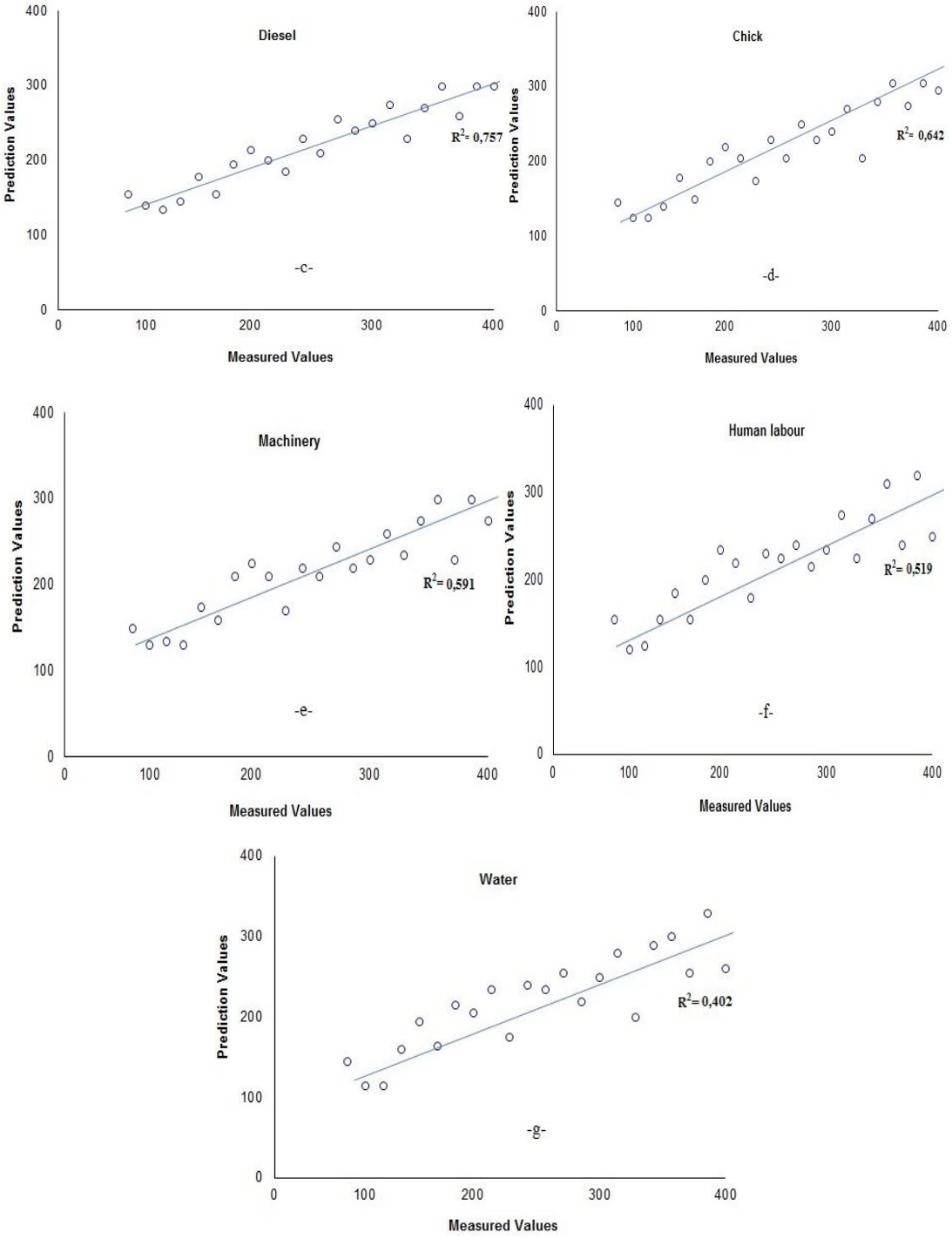

Figure 5. a-g *Determination of performance of each input parameter in poultry meat estimation by FFBPANN*

Table 4. *Determination of the most effective FFBPANN model using sensitivity analysis*

	MAE (%)	**RMSE**	**Determination (R^2)**
Feed + Electricity + Fuel + Chick + Machinery + Human labour + Water	0.019	0.232	0.936

http://www.aloki.hu ● ISSN 1589 1623 (Print) ● ISSN 1785 0037 (Online)
DOI: http://dx.doi.org/10.15666/aeer/1706_1316913183

Determination of the most appropriate FFBPANN model

FFBPANN model, which gives the best result, was obtained after various trial errors. The determination of the FFBPANN model is shown in *Table 5*. RMSE and R^2 performance functions are used to find the most effective FFBPANN model. In this study, the number of secret layer neurons is determined as 12 as seen in *Table 5* after various experiments. The highest performance is the ANN (7.12.2) model. It is also understood from *Table 5* that the maximum number of iterances is 1000 for the training of the model.

Table 5. *Determination of the most effective IBGYYSA model*

ANN (number of neurons in layers)	Number of iterations	Determination factor (R^2)	Root of the mean square error (RMSE)
ANN(7,2,2)	1000	0.885	0.197
ANN(7,3,2)	1000	0.889	0.201
ANN(7,5,2)	1000	0.892	0.207
ANN(7,7,2)	1000	0.896	0.209
ANN(7,9,2	1000	0.852	0.152
ANN(7,10,2)	1000	0.911	0.217
ANN(7,12,2)	1000	0.936	0.232
ANN(7,2,2)	2000	0.861	0.159
ANN(7,3,2)	2000	0.865	0.167
ANN(7,5,2)	2000	0.868	0.171
ANN(7,7,2)	2000	0.872	0.175
ANN(7,9,2	2000	0.843	0.149
ANN(7,10,2)	2000	0.877	0.178
ANN(7,12,2)	2000	0.882	0.186

The model was tested after the training of the FFBPANN model. When the test set chicken meat predictions were compared with the measured chicken meat, it was observed that the estimates of FFBPANN were very close to the observed ones. *Figure 6* shows that the predicted values are very close to the observed values and their tendency is almost equal.

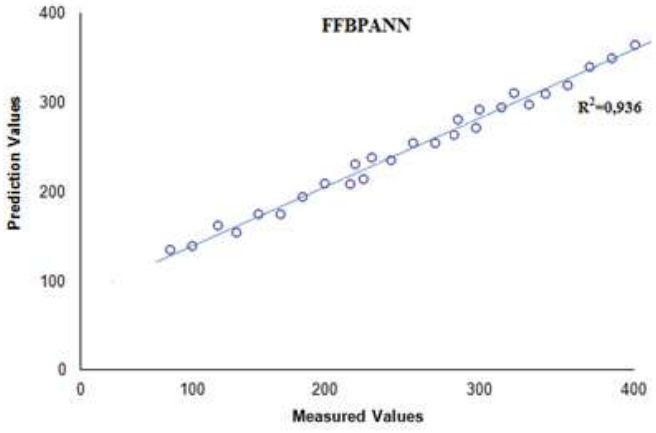

Figure 6. *FFBPANN model chicken meat predictions compared with measured chicken meat*

http://www.aloki.hu ● ISSN 1589 1623 (Print) ● ISSN 1785 0037 (Online)
DOI: http://dx.doi.org/10.15666/aeer/1706_1316913183

Results

In this study, the data obtained from 30 broiler farms in Mersin province by using feed forward, back diffusion artificial neural networks FFBPANN model the energy consumption of poultry was tried to be estimated. In the network structures where the best results for the test and training data are obtained; R^2, MAE and RMSE etc. statistical analyses were performed. Training and test R^2 values showed that the ANN used in this study gave high accuracy results. Each input parameter was used as an input in a separate model and the efficiency levels of each parameter in the estimation of chicken meat were found. As a result of this, the most effective parameter is that feed supply energy. Then the energy of electricity, fuel, chicks, machine and human labor are effective, respectively; water supply energy has been determined as the least effective parameter. Furthermore, sensitivity analysis was performed for the determination of the most effective model due to the fact that an effective Forward Feed Back Artificial Neural Networks FFBPANN model was dependent on the input parameters. As a result of sensitivity analysis, it has been observed that all input supply energy parameters have an influence on the model of Feed, Electricity, Fuel, Chicks, Machines, Human labor and Water, ANN model. As a result, for the broiler farm process, the Advanced Feed Back Flow Artificial Neural Networks model proved that using ANN in the estimation of chicken meat supply energy is a better technique than traditional mathematical modeling. It can be said that Broiler Farms can be used as a very effective model in the evaluation of energy use estimation due to the fact that they provide realistic and reliable estimates thanks to well-trained ANN parameters. The model developed in this study has an acceptable generalization ability. Since it is an effective analysis and identification method to simulate the nonlinear behavior of the Broiler Farms of ANN, it is concluded that it is used as a good performance evaluation method. The highest coefficient of determination (R^2) 0.936 and the lowest root of the mean square error (RMSE) and the mean absolute error (MAE) values were found as 0.232 and 0.019, respectively. Sensitivity analysis showed that all input parameters (Chicken Meat) were important in estimating chicken meat. (Feed) Feed input parameter (Chicken Meat) is the most effective parameter for estimating chicken meat, Water was determined as the least effective parameter by sensitivity analysis.

Based on the findings of this study, ANN topologies are recommended. In the study conducted in the province of Mersin it has been found efficient in the estimation of energy usage of seven inputs, two output parameters and broiler farms by using ANN techniques.

REFERENCES

[1] Almasi, M., Kiani, S., Lavimi, N. (2008): Agricultural Mechanization. 4th Ed. – Jangal, Tehran.

[2] Amid, S., Gundoshmian, M. T. (2016): Modelling energy efficiency in broiler production using multi layer perception artificial neural network approach (case study: Ardabil Province). – Animal Production Research 5(2): 73-85.

[3] Anonymous (2014): CP. Istanbul: layer chicken feed characteristics. – http://www.cpturkiye.com/tr/urunler/yem/kanatli-hayvan-yemleri/yumurta-tavugu-yemleri/.

http://www.aloki.hu ● ISSN 1589 1623 (Print) ● ISSN 1785 0037 (Online)
DOI: http://dx.doi.org/10.15666/aeer/1706_1316913183

[4] ASCE (2000): Task Committee on Application of Artificial Neural Networks in Hydrology (2000): artificial neural networks in hydrology. I: Preliminary concepts. – J. Hydrologic Engrg. ASCE 5(2): 115-123.
[5] Atilgan, A., Koknaroglu, H. (2006): Cultural energy analysis on broilers reared in different capacity poultry houses. – Italian Journal of Animal Science 5: 393-400.
[6] Bechtler, H., Browne, M. W., Bansal, P. K., Kecman, V. (2001): New approach to dynamic modeling of vapour compression liquid chillers: artificial neural networks. – Applied Thermal Engineering 21: 941-953.
[7] Canakci, M., Akinci, I. (2006): Energy use pattern analyses of greenhouse vegetable production. – Energy 31: 1243-56.
[8] Celik, L., Ozturkcan, O. (2003): Effects of dietary supplemental L-carnitine and ascorbic acid on performance, carcass composition and plasma L-carnitine concentration of broiler chicks reared under different temperature. – Archives of Animal Nutrition 57: 27-38.
[9] Dagdelenler, G., Sezer, E. A., Gokceoglu, C. (2011): Some non-linear models to predict the weathering degrees of a granitic rock from physical and mechanical parameters. – Expert Syst. Appl. 38: 7476-7485.
[10] Ekici, B. B., Aksoy, U. T. (2011): Prediction of building energy needs in early stage of design by using ANFIS. – Expert Syst. Appl. 38: 5352-5358.
[11] FAO (2011): Food and Agriculture Organization. – http://www.fao.org/3/i3396e/i3396e.pdf
[12] Farjam, A., Omid, M., Akaram, A., Fazel-Niari, Z. (2014): A neural network based modeling and sensitivity analysis of energy inputs for predicting seed and grain corn yields. – Journal of Agricultural Science and Technology 16: 767-778.
[13] Folorunsho, O. R., Onibi, G. E. (2005): Assessment of the Nutritional Quality of Eviscerated Waste from Selected Chicken Types. – In: Onibi, G. E., Agele, S. O., Adekunle, V. A. J. (eds.) Proceedings of the 1st Annual Conference on Developments in Agriculture and Biological Sciences, 27th April 2005, Akure, Nigeria.
[14] GDAE (2018): Republic of Turkey General Directorate of Agricultural Enterprises. https://www.tarimorman.gov.tr/sgb/Belgeler/SagMenuVeriler/HAYGEM.pdf–
[15] GDM (2017): Republic of Turkey Ministry of Agriculture, Forestry General Directorate of Meteorology. – https://www.mgm.gov.tr/?il=Mersin.
[16] Hatirli, S. A., Ozkan, B., Fert, C. (2005): An econometric analysis of energy input-output in Turkish agriculture. – Renewable and Sustainable Energy Reviews 9: 608-23.
[17] Hatirli, S. A., Ozkan, B., Fert, C. (2006): Energy inputs and crop yield relationship in greenhouse tomato production. – Renew. Energy 31: 427-438.
[18] Haykin, S. (1994): Neural Networks. A Comprehensive Foundation. – Prentice Hall, Upper Saddle River, NJ.
[19] Heidari, M. D., Omid, M., Akram, A. (2011a): Optimization of energy consumption of broiler production farms using Data Envelopment Analysis Approach. – Modern Applied Science 5(3): 69-78.
[20] Heidari, M. D., Omid, M., Akram, A. (2011b): Application of artificial neural network for modeling benefit to cost ratio of broiler farms in tropical regions of Iran. – Research Journal of Applied Science, Engineering and Technology 3(6): 546-52.
[21] Houshyar, E., Sheikh-Davoodi, M., Bahrami, H., Kiani, S., Houshyar, M. (2010): Energy use forecasting for wheat production utilizing artificial neural network. – World Applied Science Journal 10: 958-962.
[22] Karaagac, M. A., Aykanat, S., Cakir, B., Eren, O., Turgut, M. M., Barut, Z. B., Ozturk, H. H. (2011): Energy balance of wheat and maize crops production in Haciali undertaking. – 11th International Congress on Mechanization and Energy in Agriculture Congress, Istanbul, Turkey, pp. 388-391.
[23] Keskin, M. E., Taylan, E. D. (2007): Stochastic modeling of flows in the middle Black Sea basin. – CCE - Chamber of Civil Engineers Technical Magazine 2007: 4271-4291.

http://www.aloki.hu ● ISSN 1589 1623 (Print) ● ISSN 1785 0037 (Online)
DOI: http://dx.doi.org/10.15666/aeer/1706_1316913183

[24] Khoshnevisan, B., Rafiee, S., Mousazadeh, H. (2014a): Application of multi-layer adaptive neuro-fuzzy inference system for estimation of greenhouse strawberry yield. – Measurement 47: 903-910.
[25] Khoshnevisan, B., Rafiee, S., Omid, M., Mousazadeh, H. (2014b): Prediction of potato yield based on energy inputs using multi-layer adaptive neuro-fuzzy inference system. – Measurement 47: 521-530.
[26] Kitani, O. (1999): Energy and Biomass Engineering. CIGR Handbook of Agricultural Engineering. Vol. 5. – ASAE, St. Joseph, MI.
[27] Kologirou, S. (1999): Applications of artificial neural networks in energy systems: a review. – Energy Conversion and Management 40(3): 1073-1087.
[28] Landeras, G., Ortiz-Barredo, A., Lopez, J. J. (2008): Comparison of artificial neural network models and empirical and semi-empirical equations for daily reference evapotranspiration estimation in the Basque Country (Northern Spain). – Agricultural Water Management 95: 553-565.
[29] Mani, I., Kumar, P., Panwar, J. S., Kant, K. (2007): Variation in energy consumption in production of wheat- maize with varying altitudes in hill regions of Himachal Pradesh, India. – Energy 32: 2336-39.
[30] Mellit, A., Kalogirou, S. A. (2011): ANFIS-based modelling for photovoltaic power supply system: a case study. – Renew. Energy 36(1): 250-258.
[31] Naderloo, L., Alimardani, R., Omid, M., Sarmadian, F., Javadikia, P., Torabi, M., Alimardani, F. (2012): Application of ANFIS to predict crop yield based on different energy inputs. – Measurement 45(6): 1406-1413.
[32] Nefeslioglu, H. A., Gokceoglu, C., Sonmez, H. (2008): An assessment on the use of logistic regression and artificial neural networks with different sampling strategies for the preparation of landslide susceptibility maps. – Eng. Geol. 97: 171-191.
[33] Newbold, P. (1994): Statistics for Business and Economics. – Prentice-Hall, Inc. Upper Saddle River, NJ.
[34] Ozcalik, H. R., Kucuktufekci, A. (2003): Linear and inverse modeling of dynamic systems with artificial neural networks. – KSU Journal of Science and Engineering 6(1): 26-35.
[35] Oztemel, E. (2003): Artificial Neural Networks. 3rd Ed. – Papatya Publications, Istanbul.
[36] Pahlavan, R., Omid, M., Rafiee, S., Mousavi-Avval, H. (2012): Optimization of energy consumption for rose production in Iran. – Energy for Sustainable Development 16: 236-241.
[37] Pisghar-Komleh, S. H., Omid, M., Heidari, M. D. (2013): On the study of energy use and GHG (greenhouse gas) emissions in greenhouse cucumber production in Yazd province. – Energy 59: 63-71. DOI: 10.1016/j.energy.2013.07.037.
[38] Rahman, M. M., Bala, B. K. (2010): Modelling of jute production using artificial neural networks. – Biosystems Engineering 105: 350-356.
[39] Risse, M., Das, K. C., Worley, J., Thompson, S. (2007): Poultry Litter as an Energy Source. – Department of Biological and Agricultural Engineering, University of Georgia, Athens. USA.
[40] Rivera-Torres, V., Noblet, J., Dubois, S., van Milgen, J. (2010): Energy partitioning in male growing turkeys. – Poult. Sci. 89(3): 530-538.
[41] Rohani, A., Taki, M., Abdollahpour, M. (2018): A novel soft computing model (Gaussian process regression with K-fold cross validation) for daily and monthly solar radiation forecasting (Part: I). – Renewable Energy 115: 411-422.
[42] Safa, M., Samarasinghe, S. (2001): Determination and modelling of energy consumption in wheat production using neural networks: a case study in Canterbury Province, New Zealand. – Energy 36: 5140-5147.
[43] Sedaghat Hoseyni, S. N., Almasi, M., Minaei, S., Barghaei, A. (2008): Energy Recovery Systems of Industrial Complex for Production of Eggs. – Ferdosi University, Mashhad.

http://www.aloki.hu ● ISSN 1589 1623 (Print) ● ISSN 1785 0037 (Online)
DOI: http://dx.doi.org/10.15666/aeer/1706_1316913183

[44] Sefeedpari, P., Rafiee, S., Akram, A. (2012): Modeling of energy output in poultry for egg production farms using artificial neural networks. – Journal of Animal Production Advances 2(5): 247-253.
[45] Singh, J. M. (2002): On farm energy use pattern in different cropping systems in Haryana, India. – Master of Science Thesis. International Institute of Management University of Flensburg, Sustainable Energy Systems and Management.
[46] Taki, M., Yildizhan, H. (2018): Evaluation the sustainable energy applications for fruit and vegetable productions processes. Case study: greenhouse cucumber production. – Journal of Cleaner Production 199: 164-172.
[47] Taki, M., Ajabshirchi, Y., Mahmoudi, A. (2012): Prediction of output energy for wheat production using artificial neural networks in Esfahan province of Iran. – Journal of Agricultural Technology 8(4): 1229-1242.
[48] Talebizadeh, M., Moridnejad, A. (2011): Uncertainty analysis for the forecast of lake level fluctuations using ensembles of ANN and ANFIS models. – Expert Syst. Appl. 38: 4126-4135.
[49] Traore, S., Wang, Y. M., Kerh, T. (2010): Artificial neural network for modeling reference evapotranspiration complex process in Sudano-Sahelian zone. – Agricultural Water Management 97: 707-714.
[50] Trejo-Perea, M., Herrera-Ruiz, G., Rios-Moreno, J., Castaneda, R., Miranda-Raiza, E. (2009): Greenhouse energy consumption prediction using neural networks models. – International Journal of Agricultural & Biology 11(1): 1-6.
[51] Yagiz, S., Gokceoglu, C., Sezer, E., Iplikci, S. (2009): Application of two nonlinear prediction tools to the estimation of tunnel boring machine performance. – Eng. Appl. Artif. Intell. 22: 818-824.
[52] Yaldiz, O., Ozturk, H. H., Zeren, Y., Bascetincelik, A. (1993): Energy usage in production of field crops in Turkey. – 5th International Congress on Mechanization and Energy in Agriculture, Kusadasi, Turkey, pp. 527-536.
[53] Yamane, T. (1967): Elementary Sampling Theory. – Prentice Hall, Englewood Cliffs, NJ.
[54] Yazdani, M., Saghafian, B., Mahdian, M., Soltani, S. (2009): Monthly runoff estimation using artificial neural networks. – Journal of Agricultural Science and Technology 11: 335-362.
[55] Yurtoglu, H. (2005): Artificial neural network modeling and forecasting methodology: the case of Turkey for some macroeconomic variables. – Thesis. General Directorate of Economic Models and Strategic Research, Ankara.
[56] Zangeneh, M., Omid, M., Akram, A. (2011): A comparative study between parametric and artificial neural networks approaches for economical assessment of potato production in Iran. – Spanish Journal of Agricultural Research 3: 661-671.

http://www.aloki.hu ● ISSN 1589 1623 (Print) ● ISSN 1785 0037 (Online)
DOI: http://dx.doi.org/10.15666/aeer/1706_1316913183

QUERCETIN REDUCES OXIDATIVE STRESS DAMAGE TO REPRODUCTIVE PROFILE INDUCED BY 2,3,7,8-TETRACHLORODIBENZO-*P*-DIOXIN IN MALE ALBINO RATS (*RATTUS NORVEGICUS* L.)

ABDULKAREEM, S. M.* – NANAKALI, N. M.

Department of Biology, College of Education, Salahaddin University-Erbil, Erbil, Iraq (phone: +964-750-478-1809)

**Corresponding author*
e-mail: saman.abdulkareem@su.edu.krd; phone: +964-75-0479-4154

(Received 1st Jun 2019; accepted 2nd Sep 2019)

Abstract. The article aimed to investigate the effect of the antioxidant quercetin (QCT) on male Wistar albino rats under oxidative stress caused by 2,3,7,8-tetrachlorodibenzo-p-dioxin (TCDD), focusing on their reproductive system, in order to find a way to combat declining male productivity. Thirty adult male Wistar rats of body weight ranged from 230 to 250 g were randomly divided into five equal groups (6 per group), designated as normal control (corn oil) and treatments: 10 µg/kg TCDD; 20 mg/kg QCT; 20 mg/kg QCT + 10 µg/kg TCDD (pretreatment of QCT); 10 µg/kg TCDD + 20 mg/kg QCT (post-treatment of QCT), and the treatments were administered intragastrically by gavage for twelve weeks and the study was conducted in Salahaddin University-Erbil, Iraq. In each group, three males were mated with untreated fertile females, and the reproductive and biochemical parameters were evaluated for each group. TCDD significantly reduced the values of sperm quality (motility, viability, and count), serum testosterone, sex ratio, body weight, gonads weight, and testicular antioxidant enzymes (superoxide dismutase, catalase, and glutathione reductase). However, increased sperm abnormality and oxidant biomarker (malondialdehyde) were observed. Concomitant treatment with QCT ameliorated these affected values, especially when QCT treatment was administered 30 min before TCDD dosing.
Keywords: *TCDD, QCT, sperm quality, male fertility, antioxidants*

Introduction

It is believed that biological factors such as contamination of the environment have a considerable impact on male fertility. Various environmental contaminants responsible for the global decline in male reproductive health have been suggested (Erthal et al., 2018). One of these environmental polluters is dioxins, and dioxin-like compounds that are known as endocrine-disrupting and reprotoxic pollutants (Dhanabalan et al., 2011). These substances exerted their cellular and metabolic effects through interactions with the aryl hydrocarbon receptor (AhR) associated with the xenobiotic- (XRE) and antioxidant responsive (ARE) DNA elements (Nguyen et al., 2009). Upstream genes such as the promoter of the cytochrome P450 1A1 (CYP1A1) and another Ah-responsive gene that organizes the expression of the genes participating in the metabolism and detoxification of polycyclic aromatic hydrocarbons such as dioxins and dioxin like-compounds in experimental animals and humans (Mandal, 2005).

Dioxins suchlike 2,3,7,8-tetrachlorodibenzo-*p*-dioxin (TCDD) are leaked as unwanted by-products to the environment from several industrial processes such as the production of certain herbicides, pesticides and plastics, and combustion of plastics and medical waste (Anderson and Fisher, 2002; Hewitt et al., 2006; Lin et al., 2006). Home heating systems, cars exhaust, and cigarette smoke have been found to contain trace

http://www.aloki.hu ● ISSN 1589 1623 (Print) ● ISSN 1785 0037 (Online)
DOI: http://dx.doi.org/10.15666/aeer/1706_1318513197

quantities of dioxin (Fiedler et al., 1990). TCDD is a toxic chemical compound and a widespread potent environmental contaminant, and because of its lipophilicity and long biological half-lives, it bioaccumulates in organisms and biomagnifies in the food web. They enter to human body primarily by eating food rich in animal fat and accumulating in human fatty tissues (Jackson et al., 2017). TCDD can affect male fertility by reducing the number of sperm (Pilsner et al., 2017), changes in motility and in sperm transit time (Sanabria et al., 2016), serum testosterone (Karman et al., 2012), lowering reproductive organs weight (Jin et al., 2010), delayed sexual maturation (Takeda et al., 2012), and can also change the "male/female" sexual ratio of offspring (You et al., 2018).

Quercetin (3,5,7,3',4'-pentahydroxyflavone, QCT), a compound of yellow powder extracted from natural sources and have a potent antioxidant, due to the existence of two pharmacophores, the catechol group in the B-ring and the OH group at situation 3 within the molecule scavenging the free radicals (Nabavi et al., 2015). It is found in several daily foods such as onion, grape, nuts, tea, berries, cabbage, and cauliflower (Azzi et al., 2018). Inal and Kahraman (2000) reported the following biological effects of QCT: anti-cancerous, antiviral, anti-ischemic, anti-inflammatory, and anti-allergenic, in addition to the protective power against atherosclerosis and coronary heart disease.

In animal studies, TCDD exposure has been shown to induce testicular damage and QCT may reduce the male reproductive toxicity of TCDD due to its antagonistic activity against AhR which is activated by TCDD (Ciftci et al., 2012). Melekoglu et al. (2016) reported that TCDD and related substances promote the production of reactive oxygen species (ROS) in the reproductive system. Additionally, several studies have shown that TCDD exposure results in oxidative damage to many tissues, such as the kidney, liver, and testis (Palaniswamy et al., 2014; Slezak et al., 2000).

Though to our knowledge, there are some literary works on the mitigating role of QCT in testicular damage caused by TCDD. Therefore, the purpose of this study was to assess the role of QCT in alleviating the testicular damage caused by TCDD in rats by estimating serum testosterone, sperm qualities, and determining the levels of the oxidant-antioxidant biomarkers activity in the testis.

Materials and methods

Chemicals

2,3,7,8-tetrachlorodibenzo-*p*-dioxin (TCDD; purity > 99%) and quercetin (QCT; purity > 99%) were purchased from Beijing Solarbio Science & Technology Company, Ltd. (Beijing, China), and corn oil (Afia, Saudi Arabia) was obtained from local markets. TCDD was dissolved in corn oil at a dose of 10 μg/kg body weight, and QCT at a dose of 20 mg/kg body weight was also dissolved in corn oil.

Experimental animals

Thirty adult male Wistar rats, *Rattus norvegicus*, used for this study were procured from the Laboratory Animal Center (College of Science, University of Zakho, Duhok Province, Iraq). The rats were acclimated to the animal housing for two weeks before the start of dosing. They were preserved in plastic cages with wire mesh coverings and kept in an air-conditioned and well-ventilated room in a controlled light environment (12-h light/dark cycle) and temperature (22 ± 2 °C). Rats were fed on a balanced rat chow, and water (tap water) provided ad libitum. The local Committees approved the

http://www.aloki.hu ● ISSN 1589 1623 (Print) ● ISSN 1785 0037 (Online)
DOI: http://dx.doi.org/10.15666/aeer/1706_1318513197

experimental protocols for using animals of the Salahaddin University-Erbil, Erbil city, Kurdistan Region of Iraq. The care and handling of the experimental animals were performed according to the precepts of the National Institutes of Health Guide for the Care and Use of Laboratory Animals (NRC, 2011).

Experimental design

The body weight (BW) of the animals ranged between 230 to 250 g. After weighing, the animals randomly divided into five equal groups (n = 6), and the treatment was given intragastrically by gavage for twelve weeks: The 1st group was kept as a normal group and was given corn oil (vehicle). The 2nd group (TCDD group) was orally administered TCDD at a dose of 10 µg/kg BW/day. A dose of 20 mg/kg BW/day of QCT was treated to rats in group 3 (QCT group). In group 4 (QCT-TCDD), rats were treated with TCDD (10 µg/kg BW/day) and QCT (20 mg/kg BW/day) 30 min before TCDD treatment (pre-treatment group), while in group 5 (TCDD-QCT), after 30 min of TCDD administration (10 µg/kg BW/day), animals were treated with 20 mg/kg BW/day of QCT (post-treatment group).

Body weight and gonadosomatic index (GSI)

The rats weighed once per week throughout the experiment and the weight gain determined at the end of the study. The testes and cauda epididymis were removed and weighed to measure the gonado-somatic index (GSI) and epididymal-somatic index (ESI) by the following equation:

$$GSI = \frac{Gonad\ weight\ \times\ 100}{Body\ weight}$$

$$ESI = \frac{Weight\ of\ epididymis\ \times\ 100}{Body\ weight}$$

Serum testosterone concentration

Serum testosterone concentration was measured by the enzyme-linked immunosorbent assay (ELISA) method using DRG ELISA testosterone kit (ELISA EIA-1559, 96 wells; DRG Instruments, GmbH, Marburg, Germany), as directed by the manufacturer's instructions.

Preparation of tissue homogenates

The testis tissue samples were homogenized in extraction solution specialized for each test, using an Ultra-Turrax (Janke and Kunkel IKA, Labortechnik, Germany) homogenizer at 20000 rpm/min. The resulting homogenate was centrifuged at 8000 rpm for 10 min at 4 °C using a cooling centrifuge (Biobase, China). The resulting cell-free supernatant was used for the biochemical analysis. The product was assessed spectrophotometrically according to the manufacturer's protocol.

Lipid peroxidation and anti-oxidant assay

The level of lipid peroxidation of testis tissue was measured spectrophotometrically (EMC^2 GmbH, Germany) by determining the malondialdehyde (MDA) production and

http://www.aloki.hu ● ISSN 1589 1623 (Print) ● ISSN 1785 0037 (Online)
DOI: http://dx.doi.org/10.15666/aeer/1706_1318513197

the antioxidant profiles such as superoxide dismutase (SOD), catalase (CAT), and glutathione reductase (GSH-R) levels were assayed using the kit method supplied by Beijing Solarbio Science & Technology Company, Ltd, (Beijing, China). The results are expressed per unit weight of tissue.

Sperm quality analysis

Spermatozoa were obtained from the right cauda epididymis, which was carefully removed, cleaned, and immediately placed into a pre-warmed container with 1 ml of phosphate-buffered saline (PBS, pH 7.2) at 37 °C and minced with scissors (Narayana et al., 2005). Subsequently, sliced tissue was incubated at 37 °C for 10 min. All epididymal samples were examined for the following parameters:

Sperm motility analysis

Sperm motility was evaluated by counting 200 sperms per rat counted throughout at least 10 fields of view of the sample on a pre-warmed slide (37 °C) under prewarmed coverslip (37 °C) using binocular microscope (Nikon, Japan) with a warmed stage (400× magnification).

Total sperm count

The sperm counting was carried out by diluting the sperm suspension with PBS (1:20) in the pipette with white bead, then mixed gently, after that a drop of the suspension was delivered into the Neubauer hemocytometer in each side of the counting chamber. The hemocytometer was allowed to stand for 5 min for sedimentation, and then sperms were counted under binocular microscope (Nikon, Japan) in large eight squares of 1 mm^2 each area with the exception of the central area for erythrocyte counting of Neubauer's chamber was performed and multiplied by a 5 × 10^4 factor to calculate the total count of spermatozoa in a million/epididymis (Narayana et al., 2005). Counting was only done for those sperms with sperm head located in squared areas.

Sperm viability

In order to determine live-dead spermatozoa, 10 µL of pre-heated eosin-nigrosin stain was placed on a pre-warmed slide (37 °C) then 10 µL of sample suspension was added and mixed gently. A smear of the sample-stain mixture was prepared and dried at room temperature. Samples were analyzed at 1000-fold magnification under a binocular microscope (Nikon, Japan). Two hundred sperms per rat were used for the determination of sperm viability. Unstained (white) sperms are viable, while stained (pink) sperms are dead sperms (Kledmanee et al., 2013).

Sperm abnormality

Sperm morphology was evaluated following smear staining with eosin-nigrosin stain. Slides were viewed with an oil immersion (100× magnification) under a microscope (Nikon, Japan). On each slide, a total of two hundred sperms were examined for each animal, and the total sperm abnormality rates were expressed as percentages (Ciftci et al., 2012).

http://www.aloki.hu ● ISSN 1589 1623 (Print) ● ISSN 1785 0037 (Online)
DOI: http://dx.doi.org/10.15666/aeer/1706_1318513197

Fertility test

At the end of the experiment, fertility and sex ratio was estimated in adult male rats of treated groups and the control of male counterparts. In each group, three males were randomly selected, and each one was mated with three untreated fertile females in separated plastic cages. Detection of sperm in the vaginal smear supposes an early indicator of successful mating. After five days of mixing, every three days, female rats were checked for pregnancy in three days intervals (by checking abdominal size) with calculating the pregnancy percentage for each group. Also, the number and sex ratio (male/female ratio) of newborns in each group was calculated.

Statistical analysis

Data were expressed as mean ± standard deviation (SD) for this experiment. Analyzing of results performed by one-way analysis of variance (ANOVA) followed by Tukey's post hoc test to determine significant differences between the experimental groups using GraphPad Prism 6 version 6.01 for Windows (GraphPad Software 2012). Accepting a conventional 5% level of significance ($P \leq 0.05$), hence, all tests are statistically significant. Significant differences between treatment groups (or comparison of mean values) and appropriate vehicle control were denoted by superscript asterisks symbols *, **, ***; significant differences between TCDD group and the rest treatment groups were denoted by superscript hash symbols #, ##, ###; significant differences between QCT group and the treatment groups were denoted by superscript symbols $, $$, $$$ which represent significance at $p < 0.05$, $p < 0.01$ and $p < 0.001$, respectively.

Results

Metabolic results

Body weight and GSI

Results of mean (±SD) body weight (g), the GSI (%), and the ESI (%) are given in *Table 1*. There was a statistically significant decrease in body weight after twelve weeks of TCDD administration in TCDD group rats in comparison to control and QCT group rats (TCDD: 244.16 ± 13.92 g; Control: 294.83 ± 7.60 g; 286.83 ± 8.18 g, $p < 0.001$). However, co-treatment of QCT with TCDD in both QCT-TCDD and TCDD-QCT group rats reversed this effect of TCDD, but administration of QCT 30 min after TCDD administration was more effective than administration of QCT 30 min before TCDD administration (QCT-TCDD: 303.66 ± 8.71 g; TCDD-QCT: 320.66 ± 10.48 g; TCDD: 244.16 ± 13.92 g, $p < 0.001$).

The GSI and ESI of the TCDD treated rat were significantly lower than that of the control rat (TCDD: 0.387 ± 0.012%, 0.056 ± 0.01%; Control: 0.419 ± 0.021%, 0.075 ± 0.01, $p < 0.05$). The GSI and ESI of the QCT group rats were insignificantly higher than that of the control rats ($p > 0.05$) and significantly greater than that of the TCDD group ($p < 0.001$, $p < 0.01$). Rats received QCT in combination with TCDD (QCT-TCDD) significantly ($p < 0.001$) reduced the adverse effects of TCDD in rats received TCDD alone, which demonstrate increasing of GSIs in comparison to TCDD group. While QCT administration in combination with TCDD (TCDD-QCT) showed a reduction in the adverse effects of TCDD compared to rats received TCDD alone, but the values did not meet any statistical significance ($p > 0.05$).

http://www.aloki.hu ● ISSN 1589 1623 (Print) ● ISSN 1785 0037 (Online)
DOI: http://dx.doi.org/10.15666/aeer/1706_1318513197

Table 1. *Body weight, GSI, and ESI of control and treated groups (n = 6)*

Groups	Body weight (g)	GSI (%)	ESI (%)
Control	294.83 ± 7.60	0.419 ± 0.021	0.075 ± 0.010
TCDD	244.16 ± 13.92***	0.387 ± 0.012*	0.056 ± 0.010*
QCT	286.83 ± 8.18$^{###}$	0.444 ± 0.010$^{###}$	0.076 ± 0.011$^{#}$
QCT-TCDD	303.66 ± 8.71$^{###}$	0.427 ± 0.029$^{###}$	0.065 ± 0.005
TCDD-QCT	320.66 ± 10.48$^{**###\$\$\$}$	0.411 ± 0.033$^{\$}$	0.062 ± 0.009

Testosterone concentration

Relative to the rats of the control group, the plasma testosterone level is significantly reduced in rats administrated with TCDD, whereas the testosterone levels in rats in QCT group were not markedly changed in comparison to control rats (Control: 1.83 ± 0.26; TCDD: 0.31 ± 0.19; QCT: 2.25 ± 0.38, $p < 0.001$, $p > 0.05$).

The results obtained in this study exhibit a significant ($p < 0.001$) decrease of plasma testosterone levels in rats treated with TCDD, but in the QCT-TCDD and TCDD-QCT rats, the value of hormone testosterone is significantly reversed in the blood plasma compared to the TCDD treated group (TCDD: 0.31 ± 0.19; QCT-TCDD: 1.18 ± 0.24; TCDD-QCT: 1.01 ± 0.18, $p < 0.001$, $p > 0.01$). This increase was grown, but it was still lower than the corresponding value in the blood plasma of control group. Plasma testosterone started to increase again after subsiding to approximately 1/6 of the corresponding control value. In rats with QCT administered alone, the testosterone concentration was insignificantly ($p > 0.05$) increased when compared with the corresponding control (*Table 2*).

Table 2. *Testosterone hormone of control and treated groups (n = 6)*

Groups	Testosterone concentration (ng/dl)
Control	1.83 ± 0.26
TCDD	0.31 ± 0.19***
QCT	2.25 ± 0.38$^{###}$
QCT-TCDD	1.18 ± 0.24$^{**###\$\$\$}$
TCDD-QCT	1.01 ± 0.18$^{***##\$\$\$}$

Lipid peroxidation and anti-oxidant assay

Values of the antioxidant enzymes (SOD, CAT, and GSH) and the oxidative biomarker (MDA) in the testis are shown in *Table 3*. A significant elevation in MDA levels was observed in the rats exposed to TCDD, whereas GSH levels, SOD, and CAT activities were meaningfully declined in testis tissues in opposition to the control group rats. Also, there were statistically insignificant changes between the QCT and control groups regarding MDA, SOD, CAT, and GSH levels. Otherwise, the decline in MDA levels and rises in SOD and CAT activities and GSH levels in the group pretreated with QCT (QCT-TCDD) were observed in comparison to the rats exposed to only TCDD. Administration of QCT 30 min after TCDD administration (post-treatment group) improved SOD, CAT, GSH, and MDA levels but these improvements (except MDA level) did not reach the statistical significance when compared with the rats of TCDD group.

http://www.aloki.hu ● ISSN 1589 1623 (Print) ● ISSN 1785 0037 (Online)
DOI: http://dx.doi.org/10.15666/aeer/1706_1318513197

Table 3. *Oxidant and antioxidant assay of control and treated groups (n = 6)*

Groups	MDA (nmol/g)	GSH-R (µg/g)	SOD (U/g)	CAT (U/g)
Control	22.63 ± 7.57	82.09 ± 8.85	83.32 ± 12.39	47.43 ± 8.54
TCDD	54.73 ± 8.66***	39.58 ± 9.45***	45.02 ± 11.94***	22.95 ± 9.18**
QCT	19.88 ± 4.89$^{\#\#\#}$	84.19 ± 9.97$^{\#\#\#}$	89.84 ± 7.02$^{\#\#\#}$	55.85 ± 10.63$^{\#\#\#}$
QCT-TCDD	34.33 ± 10.09$^{\#\#\$}$	56.07 ± 9.13$^{***\#\$\$\$}$	69.64 ± 16.66$^{\#}$	38.25 ± 10.33$^{\#\$}$
TCDD-QCT	39.36 ± 8.83$^{*\#\$\$}$	49.33 ± 8.03$^{***\$\$\$}$	64.38 ± 12.34$^{\$}$	33.66 ± 7.49$^{\$\$}$

Sperm analysis

TCDD-treated rats exhibited a significant reduction in sperm count, motility, and viability percentage, while increased morphologically abnormal sperms in the TCDD group compared with the control and other experimental groups. The sperm numbers, motility, viability, and abnormality were 58.25 × 10^6 ± 5.53, 61.33 ± 8.93%, 51.33 ± 6.47%, and 12.83 ± 1.94%, respectively, in the TCDD group. The corresponding values in the control group were 71.33 × 10^6 ± 6.96, 86.33 ± 7.28%, 84.50 ± 8.33%, and 6.50 ± 1.87%. However, QCT consumption by rats treated with TCDD resulted in significant (QCT-TCDD: $p < 0.001$, TCDD-QCT: $p < 0.01$) ameliorations in all sperm parameters when compared with the TCDD group rats. The corresponding values in the QCT-TCDD group were 67.66 × 10^6 ± 5.90, 78.33 ± 8.16%, 69.83 ± 5.23%, and 7.16 ± 1.47%, and similar amounts in the TCDD-QCT group were 64.25 × 10^6 ± 5.98, 71.67 ± 7.11%, 66.67 ± 4.50%, and 8.66 ± 1.03%, but the results showed that administration of QCT 30 min before TCDD administration was more effective than QCT administration 30 min after TCDD administration. On the other hand, the sperm number, sperm motility, sperm viability, and sperm abnormality were not significantly changed in rats orally received QCT when compared with the rats of the control group, while a considerable change was observed in comparison to TCDD group rats (*Table 4*).

Table 4. *Sperm analysis of control and treated groups (n = 6)*

Groups	Sperm count (million/epididymis)	Sperm motility %	Sperm viability %	Sperm abnormality %
Control	71.33 ± 6.96	86.33 ± 7.28	84.50 ± 8.33	6.50 ± 1.87
TCDD	58.25 ± 5.53*	61.33 ± 8.93***	51.33 ± 6.47***	12.83 ± 1.94***
QCT	71.91 ± 7.76$^{\#\#}$	88.50 ± 7.03$^{\#\#\#}$	86.17 ± 7.19$^{\#\#\#}$	5.16 ± 1.60$^{\#\#\#}$
QCT-TCDD	67.66 ± 5.90	78.33 ± 8.16$^{\#\#}$	69.83 ± 5.23$^{**\#\#\#\$\$}$	7.16 ± 1.47$^{\#\#\#}$
TCDD-QCT	64.25 ± 5.98	71.67 ± 7.11$^{*\$}$	66.67 ± 4.5$^{***\#\#\$\$\$}$	8.66 ± 1.03$^{\#\#\$\$}$

Fertility test

The percentage of pregnant female rats in the group received TCDD was significantly lower than that of the control and QCT group (TCDD: 66.66%; Control: 100%; QCT: 100%, $p < 0.05$). Whereas in the QCT-TCDD and TCDD-QCT group, the pregnancy rate was reversed compared to the TCDD group, but the difference did not attend any statistical significance, and this increase grew but was remain lower than the corresponding value in the control group (QCT-TCDD: 88.88%; TCDD-QCT: 88.88%, $p > 0.05$).

http://www.aloki.hu ● ISSN 1589 1623 (Print) ● ISSN 1785 0037 (Online)
DOI: http://dx.doi.org/10.15666/aeer/1706_1318513197

The sex ratio of the control group's 9 litters (89 embryos), 6 litters of the TCDD group (51 embryos), 9 litters of the QCT group (92 embryos), 8 litters of the QCT-TCDD group (77 embryos) and 8 litters of the TCDD-QCT group (74 embryos) was linked to the visual examination of anogenital distance away and the presence of male genitals (*Table 5*). Our results showed a statistically significant decrease in the sex ratio of embryos in the TCDD group against the control and QCT group rats (TCDD: 27.62 ± 21.14%; Control: 52.01 ± 8.58%; QCT: 53.98 ± 10.26%, $P < 0.05$). In general, QCT treatment significantly increased pregnancy percentage, mean litter size, and sex ratio (male/female ratio) in comparison to TCDD treatment. Additionally, the results exhibited that QCT administration along with TCDD in both QCT-TCDD and TCDD-QCT groups in contrast to TCDD group insignificantly increased pregnancy percentage, mean litter size, and sex ratio percentage. Also, there were no significant changes between QCT-TCDD and TCDD-QCT groups in means of pregnancy percentage, mean litter size, and sex ratio percentage. The QCT substance when given together with TCDD, especially in a group when pre-treated with QCT, brought pregnancy percentage, mean litter size, and sex ratio percentage closer to the control level.

Table 5. *Fertility test of control and treated groups (n = 6)*

Groups	Pregnant female rats (%)	Total No. of male newborns	Total No. of female newborns	Mean litter size	Total sex ratio (%)
Control	100 ± 0.00	46 ± 0.78	43 ± 1.09	9.88 ± 1.05	52.01 ± 8.58
TCDD	66.66 ± 0.50*	21 ± 1.80*	30 ± 2.64	5.66 ± 4.38*	27.62 ± 21.14*
QCT	100 ± 0.00$^{\#}$	50 ± 1.50$^{\#\#}$	42 ± 1.00	10.22 ± 1.64$^{\#}$	53.98 ± 10.26$^{\#}$
QCT-TCDD	88.88 ± 0.33	42 ± 2.12$^{\#}$	35 ± 1.69	8.55 ± 3.46	48.27 ± 19.83
TCDD-QCT	88.88 ± 0.33	38 ± 1.92	36 ± 1.65	8.22 ± 3.30	40.47 ± 24.15

Discussion

Male reproductive disorders, such as a diminution in sperm quality and quantity, have shown an increasing trend in recent years. Several environmental/lifestyle factors (like exposure to dioxins, traffic exhaust fumes, smoking, and obesity) appear to negatively affect both the perinatal and adult testes (Sharpe, 2010; Wang et al., 2017). TCDD was found to increase oxidative stress and inhibit the activity of the antioxidant enzymes in testis and influences the serum level of testosterone hormone. It has also been reported that TCDD decelerates the progressive motility of epididymal sperm (Dhanabalan et al., 2015).

The current data showed the beneficial properties of QCT on TCDD induced reproductive impairment in male rats. We found a reduction in the sperm characteristics of TCDD treated rats compared to control rats. TCDD induced significant oxidative disorders in the testis tissue. Administration of QCT to rats received TCDD markedly decreased the reproductive damage and its oxidative stress induced by TCDD. Similarly, other researchers (Ciftci et al., 2012) found that TCDD produced oxidative stress in rat testes tissue. In addition to significantly decreasing serum testosterone levels, sperm count with its motility as well as increasing abnormal sperm percentage and testicular damages with TCDD dosing. It was thought that spermatological effects of TCDD might be due to its oxidative and histopathological effects.

http://www.aloki.hu ● ISSN 1589 1623 (Print) ● ISSN 1785 0037 (Online)
DOI: http://dx.doi.org/10.15666/aeer/1706_1318513197

The results of the study showed that body weight in TCDD group less gained in comparison to control rats and also GSI and ESI in the rats treated with TCDD decreased. The results of the study are in agreement with previous findings obtained by Seefeld et al. (1984) and Ciftci et al. (2010). They showed that oral TCDD administration decreased body weight compared to control rats. However, Awal et al. (2001) reported that in male rats, exposure to TCDD during adulthood resulted in a reduction in the weights of testes and accessory sex organs, but it still remains unclear which cells of the testis are particularly affected by TCDD. This adverse effects of TCDD, including those related to the endocrine-disrupting activities (Le Magueresse-Battistoni et al., 2017; Decherf and Demeneix, 2011). While, pre and post-treatment with QCT could improve the gonad and body weight in the rats treated with TCDD.

Furthermore, antioxidant defence systems consist of SOD, glutathione peroxidase (GPx), CAT (enzymatic), and GSH (non-enzymatic) protects the cell against oxidative damage in normal physiological conditions. TCDD treatment caused a significant increase in testicular MDA levels in the present study with a decrease in testicular SOD, GSH, and CAT activity compared to the control group. An increased MDA concentration is maybe a consequence of the reduced production of antioxidants in the TCDD treated rats' tissues thereby shifting the accurate balance in favour of ROS, thus leading to an excess of pathologic damage to sperm cells and coincident loss of function (Oyeyipo et al., 2014). The antioxidant superoxide dismutase enzyme dramatically speeds up the dismutation of the superoxide anion to hydrogen peroxide (H_2O_2). Catalase breaks down H_2O_2 to H_2O and O_2, and the glutathione peroxidase/reductase system catalyzes H_2O_2 and lipid hydroperoxide degradation by reduced glutathione. Reducing the activity of SOD, CAT, GSH-R, and GPx could reflect the negative effect of TCDD on antioxidant enzymes in epididymal sperm (Latchoumycandane et al., 2003). Due to the direct damaging effect of TCDD, reduced activity of one or more antioxidant systems leads to increased lipid peroxidation and oxidative stress, resulting in testicular and sperm toxicity.

As pointed out in the introduction that TCDD binds to an AhR in the cytoplasm, the receptor complex (AhR-TCDD) translocates into the nucleus, where AhR heterodimerizes with the Ah receptor nuclear translocator (ARNT), connects to dioxin-responsive enhancer elements and regulates the transcription of target genes (Baba et al., 2005). The mechanisms of TCDD-induced disorders in the reproductive system of mammals have been shown to be multiple, including impairment of spermatogenesis (Foster et al., 2010), steroidogenesis (Adamsson et al., 2009), dropping in the number of testicular cells (Johnson et al., 1994), and induction of cytochrome P450 (CYP) 1 family enzymes, leading to inactivation of steroid hormones (Badawi et al., 2000). The treatment of QCT ameliorated these detrimental effects. These results corroborate the previous findings of Ciftci et al. (2012) and El-Gerbed et al. (2015). Ciftci et al. (2012) reported that QCT could reduce testicular damage caused by TCDD in rats. El-Gerbed et al. (2015) said that exposure to TCDD triggered semen quality to deteriorate, a reduction in fertility indexes, decreased the activity of serum enzymes, and decreased testosterone, in addition to histological changes in the tests. The team also highlighted the effect of QCT in reducing the adverse impact generated by TCDD.

Our results showed decreased male/female ratio in TCDD group rats compared with control group rats. Several studies have shown that exposure to TCDD in humans and animal reduces the male sex ratio of offspring (You et al., 2018; Mocarelli et al., 2000; Rowlands et al., 2006; Ishihara et al., 2007). James (2006) supposes that before

http://www.aloki.hu ● ISSN 1589 1623 (Print) ● ISSN 1785 0037 (Online)
DOI: http://dx.doi.org/10.15666/aeer/1706_1318513197

conception, elevated gonadotropin and low levels of testosterone would have injured and distorted Y- bearing gametes. Song et al. (2018) found that Y chromosome-bearing human spermatozoa were more susceptible to EDCs than spermatozoa with the X chromosome. Ishihara et al. (2010) investigated the effects on sex ratio, sperm concentration, and motility of TCDD exposure. They found that TCDD leads to decreasing Y-bearing/X-bearing sperm ratio. Although it is still unclear why Y spermatozoa are more susceptible to high TCDD levels than X spermatozoa, You et al. (2018) proposed that after exposure to stressful conditions such as endocrine-disrupting chemicals (EDCs), the fertilization capacity according to their chromosome constitution may differ. Interestingly, Y spermatozoa survived at high TCDD concentrations for a shorter time than X spermatozoa. Furthermore, the reduced male sex ratio of births was related to the limited lifespan of Y spermatozoa and they attributed that to the antiandrogenic properties in utero or during lactation in adult rats that might be exposed to dioxin-like compounds and polychlorinated biphenyls (PCBs), leading to permanently changed sperm-transit time through the epididymis and the extra-testicular excurrent duct system (Jongbloet et al., 2002).

Conclusion

In summary, that we really found that rats subjected to TCDD showed reduced sexual activity, low motility with sperm count inhibition, viability, decreased antioxidant enzymes activity, additionally increased sperm abnormality and oxidative biomarker (MDA) in testis tissue. QCT treatment could minimize the effects of TCDD in rats, in part by improving sexual performance and eliminating oxidative damage. Thus, these results suggested that QCT could be used as protective agents against reproductive toxicity induced by TCDD in male rats. Further studies are required to clarify the mechanism of QCT as a therapeutic agent against the toxic effects of TCDD.

Acknowledgements. This study was supported as a PhD plan by Salahaddin University-Erbil, Erbil, Kurdistan Region-Iraq (Administrative order No. 1/1/15738. Signed on December 1, 2015). The authors wish to gratefully thank Rêbwar M. Hama Salih, Sarwar N. Jafar, and Younis M. Saleh for excellent technical support performed for spermatological and biochemical tests.

REFERENCES

[1] Adamsson, A., Simanainen. U., Viluksela, M., Paranko, J., Toppari, J. (2009): The effects of 2,3,7,8-tetrachlorodibenzo-p-dioxin on foetal male rat steroidogenesis. – International Journal of Andrology 32: 575-585.

[2] Anderson, D. R., Fisher, R. (2002): Sources of dioxins in the United Kingdom: the steel industry and other sources. – Chemosphere 46: 371-381.

[3] Awal, M. A., Siddiqi, M. N. H., Kurohmaru, M., Andriana, B. B., Mizukami, T., Kanai, Y., Hayashi, Y. (2001): Biochemical effects of 2, 3, 7, 8-tetrachlorodibenzo-p-dioxin (TCDD) on the sertoli cell culture from prepubertal male Wistar rats. – Journal of Medical Sciences 1: 311-315.

[4] Azzi, J., Jraij, A., Auezova, L., Fourmentin, S., Greige-Gerges, H. (2018): Novel findings for quercetin encapsulation and preservation with cyclodextrins, liposomes, and drug-in-cyclodextrin-in-liposomes. – Food Hydrocolloids 81: 328-340.

http://www.aloki.hu ● ISSN 1589 1623 (Print) ● ISSN 1785 0037 (Online)
DOI: http://dx.doi.org/10.15666/aeer/1706_1318513197

[5] Baba, T., Mimura, J., Nakamura, N., Harada, N., Yamamoto, M., Morohashi, K. I., Fujii-Kuriyama, Y. (2005): Intrinsic function of the aryl hydrocarbon (dioxin) receptor as a key factor in female reproduction. – Molecular and Cellular Biology 25: 10040-10051.

[6] Badawi, A. F., Cavalieri, E. L., Rogan, E. G. (2000): Effect of chlorinated hydrocarbons on expression of cytochrome P450 1A1, 1A2 and 1B1 and 2-and 4-hydroxylation of 17β-estradiol in female Sprague–Dawley rats. – Carcinogenesis 21: 1593-1599.

[7] Ciftci, O., Tanyildizi, S., Godekmerdan, A. (2010): Protective effect of curcumin on immune system and body weight gain on rats intoxicated with 2, 3, 7, 8-Tetrachlorodibenzo-p-dioxin (TCDD). – Immunopharmacology and Immunotoxicology 32: 99-104.

[8] Ciftci, O., Aydin, M., Ozdemir, I., Vardi, N. (2012): Quercetin prevents 2, 3, 7, 8-tetrachlorodibenzo-p-dioxin-induced testicular damage in rats. – Andrologia 44: 164-173.

[9] Decherf, S., Demeneix, B. A. (2011): The obesogen hypothesis: a shift of focus from the periphery to the hypothalamus. – Journal of Toxicology and Environmental Health, Part B 14(5-7): 423-448.

[10] Dhanabalan, S., Jubendradass, R., Latha, P., Mathur, P. P. (2011): Effect of restraint stress on 2, 3, 7, 8 tetrachloro dibenzo-p-dioxin induced testicular and epididymal toxicity in rats. – Human & Experimental Toxicology 30: 567-578.

[11] Dhanabalan, S., Mathur, P. P., Latha, P. (2015): TCDD and corticosterone on testicular steroidogenesis and antioxidant system of epididymal sperm in rats. – Toxicology and Industrial Health 31: 811-822.

[12] El-Gerbed, M. S., El-Saad, A. M. A., Haussein, A. B. (2015): 2, 3, 7, 8-tetrachloro-dibenzo-p-dioxin induced testicular toxicity in rats and the protective effect of quercetin: biochemical, histopathological and immunohistochemical studies. – Journal of Applied Pharmaceutical Science 5: 099-109.

[13] Erthal, R. P., Siervo, G. E., Silveira, L. T., Scarano, W. R., Fernandes, G. S. (2018): Can resveratrol attenuate testicular damage in neonatal and adult rats exposed to 2, 3, 7, 8-tetrachlorodibenzo-p-dioxin during gestation?. – Reproduction, Fertility and Development 30: 442-450.

[14] Fiedler, H., Hutzinger, O., Timms, C. W. (1990): Dioxins: sources of environmental load and human exposure. – Toxicological & Environmental Chemistry 29: 157-234.

[15] Foster, W. G., Maharaj-Briceño, S., Cyr, D. G. (2010): Dioxin-induced changes in epididymal sperm count and spermatogenesis. – Environmental Health Perspectives 118: 458-464.

[16] Inal, M. E., Kahraman, A. (2000): The protective effect of flavonol quercetin against ultraviolet a induced oxidative stress in rats. – Toxicology 154(1-3): 21-29.

[17] Ishihara, K., Warita, K., Tanida, T., Sugawara, T., Kitagawa, H., Hoshi, N. (2007): Does paternal exposure to 2, 3, 7, 8-tetrachlorodibenzo-p-dioxin (TCDD) affect the sex ratio of offspring?. – Journal of Veterinary Medical Science 69: 347-352.

[18] Ishihara, K., Ohsako, S., Tasaka, K., Harayama, H., Miyake, M., Warita, K., Tanida, T., Mitsuhashi, T., Nanmori, T., Tabuchi, Y., Yokoyama, T. (2010): When does the sex ratio of offspring of the paternal 2, 3, 7, 8-tetrachlorodibenzo-p-dioxin (TCDD) exposure decrease: in the spermatozoa stage or at fertilization? – Reproductive Toxicology 29: 68-73.

[19] Jackson, E., Shoemaker, R., Larian, N., Cassis, L. (2017): Adipose tissue as a site of toxin accumulation. – Comprehensive Physiology 7: 1085-1135.

[20] James, W. H. (2006): Offspring sex ratios at birth as markers of paternal endocrine disruption. – Environmental Research 100: 77-85.

[21] Jin, M. H., Hong, C. H., Lee, H. Y., Kang, H. J., Han, S. W. (2010). Toxic effects of lactational exposure to 2, 3, 7, 8-tetrachlorodibenzo-p-dioxin (TCDD) on development of male reproductive system: Involvement of antioxidants, oxidants, and p53 protein. – Environmental Toxicology: An International Journal 25: 1-8.

http://www.aloki.hu ● ISSN 1589 1623 (Print) ● ISSN 1785 0037 (Online)
DOI: http://dx.doi.org/10.15666/aeer/1706_1318513197

[22] Johnson, L., Wilker, C. E., Safe, S. H., Scott, B., Dean, D. D., White, P. H. (1994): 2, 3, 7, 8-Tetrachlorodibenzo-p-dioxin reduces the number, size, and organelle content of Leydig cells in adult rat testes. – Toxicology 89: 49-65.
[23] Jongbloet, P. H., Roeleveld, N., Groenewoud, H. M. (2002): Where the boys aren't: Dioxin and the sex ratio. – Environmental Health Perspectives 110: 1-3.
[24] Karman, B. N., Basavarajappa, M. S., Hannon, P., Flaws, J. A. (2012): Dioxin exposure reduces the steroidogenic capacity of mouse antral follicles mainly at the level of HSD17B1 without altering atresia. – Toxicology and Applied Pharmacology 264: 1-12.
[25] Kledmanee, K., Taweedet, S., Thaijongruk, P., Chanapiwat, P., Kaeoket, K. (2013): Effect of L-cysteine on Chilled carp (Cyprinus carpio) semen qualities. – The Thai Journal of Veterinary Medicine 43: 91-97.
[26] Latchoumycandane, C., Chitra, K. C., Mathur, P. P. (2003): 2, 3, 7, 8-Tetrachlorodibenzo-p-dioxin (TCDD) induces oxidative stress in the epididymis and epididymal sperm of adult rats. – Archives of Toxicology 77: 280-284.
[27] Le Magueresse-Battistoni, B., Labaronne, E., Vidal, H., Naville, D. (2017): Endocrine disrupting chemicals in mixture and obesity, diabetes and related metabolic disorders. – World Journal of Biological Chemistry 8: 108-119.
[28] Lin, L. F., Lee, W. J., Chang-Chien, G. P. (2006): Emissions of polychlorinated dibenzo-p-dioxins and dibenzofurans from various industrial sources. – Journal of the Air & Waste Management Association 56: 1707-1715.
[29] Mandal, P. K. (2005): Dioxin: a review of its environmental effects and its aryl hydrocarbon receptor biology. – Journal of Comparative Physiology B 175: 221-230.
[30] Mark Hewitt, L., Parrott, J. L., McMaster, M. E. (2006): A decade of research on the environmental impacts of pulp and paper mill effluents in Canada: sources and characteristics of bioactive substances. – Journal of Toxicology and Environmental Health, Part B 9: 341-356.
[31] Melekoglu, R., Ciftci, O., Cetin, A., Basak, N., Celik, E. (2016): The beneficial effects of Montelukast against 2, 3, 7, 8-tetrachlorodibenzo-p-dioxin toxicity in female reproductive system in rats. – Acta Cirurgica Brasileira 31: 557-563.
[32] Mocarelli, P., Gerthoux, P. M., Ferrari, E., Patterson Jr, D. G., Kieszak, S. M., Brambilla, P., Vincoli, N., Signorini, S., Tramacere, P., Carreri, V., Sampson, E. J. (2000): Paternal concentrations of dioxin and sex ratio of offspring. – Lancet 355: 1858-1863.
[33] Nabavi, S. F., Russo, G. L., Daglia, M., Nabavi, S. M. (2015): Role of quercetin as an alternative for obesity treatment: You are what you eat! – Food Chemistry 179: 305-310.
[34] Narayana, K., Prashanthi, N., Nayanatara, A., Kumar, H. H. C., Abhilash, K., Bairy, K. L. (2005): Effects of methyl parathion (o, o-dimethyl o-4-nitrophenyl phosphorothioate) on rat sperm morphology and sperm count, but not fertility, are associated with decreased ascorbic acid level in the testis. – Mutation Research/Genetic Toxicology and Environmental Mutagenesis 588: 28-34.
[35] Nguyen, T., Nioi, P., Pickett, C. B. (2009): The Nrf2-antioxidant response element signaling pathway and its activation by oxidative stress. – Journal of Biological Chemistry 284: 13291-13295.
[36] NRC (2011): Guide for the Care and Use of Laboratory Animals. 8th ed. – National Research Council, National Academies Press, Washington, DC. https://www.ncbi.nlm.nih.gov/books/NBK54050/.
[37] Oyeyipo, I. P., Raji, Y., Bolarinwa, A. F. (2014): Antioxidant profile changes in reproductive tissues of rats treated with nicotine. – Journal of Human Reproductive Sciences 7: 41-46.
[38] Palaniswamy, K. S., Vishwanadha, V. P., Singaravelu, S. R. (2014): Fish oil rich in eicosapentaenoic acid protects against oxidative stress-related renal dysfunction induced by TCDD in Wistar rats. – Cell Stress and Chaperones 19: 409-419.

http://www.aloki.hu ● ISSN 1589 1623 (Print) ● ISSN 1785 0037 (Online)
DOI: http://dx.doi.org/10.15666/aeer/1706_1318513197

[39] Pilsner, J. R., Parker, M., Sergeyev, O., Suvorov, A. (2017): Spermatogenesis disruption by dioxins: epigenetic reprograming and windows of susceptibility. – Reproductive Toxicology 69: 221-229.

[40] Rowlands, J. C., Budinsky, R. A., Aylward, L. L., Faqi, A. S., Carney, E. W. (2006): Sex ratio of the offspring of Sprague–Dawley rats exposed to 2, 3, 7, 8-tetrachlorodibenzo-p-dioxin (TCDD) in utero and lactationally in a three-generation study. – Toxicology and applied Pharmacology 216: 29-33.

[41] Sanabria, M., Cucielo, M. S., Guerra, M. T., dos Santos Borges, C., Banzato, T. P., Perobelli, J. E., Leite, G. A. A., Anselmo-Franci, J. A., Kempinas, W. D. G. (2016): Sperm quality and fertility in rats after prenatal exposure to low doses of TCDD: A three-generation study. – Reproductive Toxicology 65: 29-38.

[42] Seefeld, M. D., Keesey, R. E., Peterson, R. E. (1984): Body weight regulation in rats treated with 2, 3, 7, 8-tetrachlorodibenzo-p-dioxin. – Toxicology and Applied Pharmacology 76: 526-536.

[43] Sharpe, R. M. (2010): Environmental/lifestyle effects on spermatogenesis. – Philosophical Transactions of the Royal Society B: Biological Sciences 365: 1697-1712.

[44] Slezak, B. P., Hatch, G. E., DeVito, M. J., Diliberto, J. J., Slade, R., Crissman, K., Hassoun, E., Birnbaum, L. S. (2000): Oxidative stress in female B6C3F1 mice following acute and subchronic exposure to 2, 3, 7, 8-tetrachlorodibenzo-p-dioxin (TCDD). – Toxicological Sciences 54: 390-398.

[45] Song, W. H., Mohamed, E. A., Pang, W. K., Kang, K. H., Ryu, D. Y., Rahman, M. S., Pang, M. G. (2018): Effect of endocrine disruptors on the ratio of X and Y chromosome-bearing live spermatozoa. – Reproductive Toxicology 82: 10-17.

[46] Takeda, T., Fujii, M., Taura, J., Ishii, Y., Yamada, H. (2012): Dioxin silences gonadotropin expression in perinatal pups by inducing histone deacetylases a new insight into the mechanism for the imprinting of sexual immaturity by dioxin. – Journal of Biological Chemistry 287: 18440-18450.

[47] Wang, C. Y., Cui, J. T., Lu, Z. L., Ma, X. L., Wang, J. H., Sun, Y. C. (2017): Effects of aroclor 1254 on the DNA methylation of imprinted genes in the adult mouse sperm. – Applied Ecology and Environmental Research 15: 999-1012.

[48] You, Y. A., Mohamed, E. A., Rahman, M. S., Kwon, W. S., Song, W. H., Ryu, B. Y., Pang, M. G. (2018): 2, 3, 7, 8-Tetrachlorodibenzo-p-dioxin can alter the sex ratio of embryos with decreased viability of Y spermatozoa in mice. – Reproductive Toxicology 77: 130-136.

http://www.aloki.hu ● ISSN 1589 1623 (Print) ● ISSN 1785 0037 (Online)
DOI: http://dx.doi.org/10.15666/aeer/1706_1318513197

EFFECT OF HUMIC ACID AND SULFUR FERTILIZER LEVELS ON SOME PHYSIOLOGICAL TRAITS OF MAIZE (*ZEA MAYS* L.) ON CALCAREOUS SOIL

MARUF, M. T. – MAM-RASUL, G. A.

Department of Natural Resources, College of Agricultural Engineering Sciences, Sulaimani, Iraq
(e-mails/phones: muhamad.maruf@univsul.edu.iq/+964-770-146-8930,
ghafwr.mamrasul@univsul.edu.iq/+964-770-156-3130)

(Received 3rd Jun 2019; accepted 2nd Sep 2019)

Abstract. The field experiment was conducted at two locations, Qlyasan and Kanipanka in Sulaimani governorate, Iraq. The main aim of this research is, to evaluate the impact of adding various levels of Humic Acid and Sulfur rates on maize yield and yield components. Experimental treatments have been organized and a factorial experiment was laid out in a complete randomized block design with three replicates. The treatments included four levels of humic acid, and four levels of sulfur incorporated into the soil. The results showed that the effect was significant at ($P < 0.05$) on the reproductive growth criteria of a maize plant. The number of kernels per ear, the weight of 100 kernels (g), kernel yield (ton ha^{-1}), biological yield (ton ha^{-1}), harvest index and relative yield maize plant from both of locations. While the results showed that the humic acid and sulfur application significantly affected of the number of kernels per raw from Kanipanka and of the ear diameter (cm) from Qlyasan, it did not affect the number of kernels per raw from Qlyasan location and by the ear diameter (cm) from Kanipanka location.
Keywords: *kernels, biological yield, relative yield*

Introduction

Maize (*Zea mays* L.) is the third most important cereal crop in the world after wheat and rice. Maize is a miracle crop called "Queen of Cereals", is grown in more than 130 countries and it belongs to the family of Gramineae (Poaceae), (Shah et al., 2009) and tribe Maydeae, all varieties of the maize belong to a single species which is Zea mays (Sikandar et al., 2007). Iraqi Kurdistan region as a semi-arid region, there is an increasing interest for field crop production and recommended farmers to grow grain crops and vegetables.

An increasing the number of human population continuously increases their demands for food and energy, which require to incorporate the new areas in agricultural as well as increase the crop yield-per unit of area with healthy quality with good nutritional or healthy quality. Generally, the average yield of maize is greater than (4 ton ha^{-1}) (Farnhamet al., 2003). The maize cultivation in Iraq in the last decade increased, because of its importance as previously mentioned, its cultivation focused in the south of Iraq in Wasit, Meesan and AL-Qadeseya governorates, with only (3500 ha) during 1998. In 2014, the cultivated area with maize in Iraq increased to (299500 ha) with average production (4166.5 kg ha^{-1}), Central Statistical Organization of Iraq (2014). The maize cultivation in the Kurdistan region–Iraq has got more attention in last year's. The cultivated area in Kurdistan region roughly is about (1824 ha) with average production about (5138 kg ha^{-1}), (KRG, 2014). In the last decade, the maize production increased about (40%) reaching (840) million tons in the world in 2011 (FAO, 2009).

In terms of nutrient acquisition efficiency by the plant, Maize may have different strategies in response to nutrient deficiency. In addition to that the strategy of Maize cultivation is recently had been introduced to the Kurdistan Iraqi region, and every year

http://www.aloki.hu ● ISSN 1589 1623 (Print) ● ISSN 1785 0037 (Online)
DOI: http://dx.doi.org/10.15666/aeer/1706_1319913217

new high-yielding maize varieties are continually being evolved and introduced by the breeder to be grown by farmers in the area. However, the properties such as economic, quality and grain yield potential of this new Maize not fully aware by the farmers (Hogir, 2016).

Therefore, intensive efforts of the researchers were focused on how to maximize the productivity of this crop through highly nutrient efficient, especially for humic acids and sulfur fertilizers.

Humic acid (HA) is a naturally occurring polymericheterocyclic organic compound with carboxylic ($COOH^-$), phenolic (OH^-), alcoholic and carbonyl fractions extracted from various sources such as lignite, peat, coal, farmyard manure, coirpith besides natural persistence in soil (Sharif et al., 2002). Humic acids is not only found in soil, plants, peat, natural water, rivers, sea sediments, and other chemically and biologically transformed materials but also extracted from lignite, oxidized bituminous coal, leonardite and gyttja (Karaca et al., 2006).

The mechanism of humic acid activity in promoting plant growth is not completely known, but several explanations have been proposed by some researchers such as increasing cell membrane permeability, oxygen uptake, respiration and photosynthesis, phosphate uptake, and root cell elongation (Turkmen et al., 2004). Addition of HA to soil increases the rate of absorption of ions on root surfaces and their penetration into the cells of the plant tissue. Plants show more active metabolism and increased respiratory activity, which are attributed to the intervention of the quinine groups of HA (Atefe and Ali, 2012). The physicochemical and molecular structure and the mechanism of its stimulating effect on various crops and soil conditions have been envisaged by various workers (Singh and Agrawal, 2010; Cordeiro et al., 2011).

The sulfur (S) dynamics and its availability are less studied than other nutrients, even though S is an essential nutrient for crops production (Rheinheimer et al., 2007). Most soil sources of sulfur are in organic matter and are therefore concentrated in the topsoil or plow layer. Elemental sulfur and other forms as found in soil organic matter and some fertilizers are not available to crops. They must be converted to sulfate (SO_4^{2-}) form to become available to crops. This SO_4^{2-} is available to crops when the roots reach this area of the soil. Sulfur is a part of the amino acids cystine, cysteine and methionine and is therefore required for protein formation and hence plant growth. Sulfur is also present in plant oils and is involved in enzyme activation. Many common crop plants contain approximately the same amount of sulfur as they do of phosphorus (Scherer, 2001). Sulfur is a by-product of the oil industries, despite this, it is found in a comparatively large amount in Iraq in the fields of Mashraq, which has a production capacity of one million tons annually, so the addition of sulfur has become a standard method for a number of researchers as a means of managing nutrients in the soil.

This study aims to investigate the influence of humic acids and sulfur individually or mixing on yield characteristics of maize growing under calcareous soil condition.

Review of literature

Humic acid (HA) is a naturally occurring polymericheterocyclic organic compound with carboxylic ($COOH^-$), phenolic (OH^-), alcoholic and carbonyl fractions extracted from various sources such as lignite, peat, coal, farmyard manure, coirpith besides natural persistence in soil (Sharif et al., 2002). Humic acids are not only found in soil, plants, peat, natural water, rivers, sea sediments, and other chemically and biologically

http://www.aloki.hu ● ISSN 1589 1623 (Print) ● ISSN 1785 0037 (Online)
DOI: http://dx.doi.org/10.15666/aeer/1706_1319913217

transformed materials but also extracted from lignite, oxidized bituminous coal, leonardite and gyttja (Karaca et al., 2006). The humic substances are distributed in soil, peat, coal, many upland streams, dystrophic lakes, and ocean water (Stevenson, 1994).

Humic acids are technically not a fertilizer, although in some walks people do consider it. Humic acids are an effective agent to use as a complement to synthetic or organic fertilizers. In many instances, regular humic acids use will reduce the need for fertilization due to the soil and plant ability to make better use of it. In some instances, fertilization can be eliminated entirely if sufficient organic material is present and the soil can become self-sustaining through microbial processes and humus production.

To promote efficient plant absorption of nutrients and reduce environmental pollution, some chemical molecules have been studied (Ertani et al., 2011) these compounds are defined as bio-stimulants such as humic substances.

In many studies, humic and fulvic acids preparations were reported to increase the uptake of mineral elements (Mackowiak et al., 2001), to promote the root length (Canellas et al., 2002), and to increase the fresh and dry weights of crop plants (Chen et al., 2004).

The use of humic acids has been on the increased in last year's. Improvement of soil conditions and establishing equilibrium among plant nutrients are also important for soil productivity and plant production. Humic acids and organically improvement of soil increased the yields of some field crops in several studies (Ulukan, 2008).

The sulfur (S) dynamics and its availability are less studied than other nutrients, even though S is an essential nutrient for crops production (Rheinheimer et al., 2007). In a general overview of the element we can at first, describe sulfur as a solid. It is a pale yellow non-metallic, brittle element and is widely distributed in close proximity to hot springs and volcanoes and is also found in many minerals and ores. Sulfur is one of (16) essential elements for crop growth. Although sulfur is considered as a secondary nutrient, it is often called the fourth major nutrient ranking just below nitrogen, phosphorus, and potassium. It is also an essential nutrient for plant growth and development as it is a part of major metabolic compounds such as amino acids (methionine and cysteine), glutathione, proteins, and sulpho-lipids (Duke and Reisenauer, 1986). Most soil sources of sulfur are in organic matter and are therefore concentrated in the topsoil or plow layer. Elemental sulfur and other forms as found in soil organic matter and some fertilizers are not available to crops. They must be converted to sulfate (SO_4^{2-}) form to become available to crops. This SO_4^{2-} is available to crops when the roots reach this area of the soil. Sulfur is a part of the amino acids cysteine, cysteine and methionine and is therefore required for protein formation and hence plant growth. Sulfur is also present in plant oils and is involved in enzyme activation. Many common crop plants contain approximately the same amount of sulfur as they do of phosphorus (Scherer, 2001).

Maize dry weight increased as elemental sulfur rate increased, after which there was a sharp decrease in dry maize weight. This was mainly due to the significant increase in soil Mn and Zn availability (Karimizarchi and Aminuddin, 2015) and uptake by maize as demonstrated by Karimizarchi et al. (2014). Scherer (2001) provides an overview of soil sulfur transformations describes the diverse forms of organic sulfur in soil and outlines the processes linked to sulfur mineralization that release SO_4^{2-}. Most studies on sulfur mineralization have involved laboratory experimentation. There is limited information on the rates of sulfur mineralization in field soils.

http://www.aloki.hu ● ISSN 1589 1623 (Print) ● ISSN 1785 0037 (Online)
DOI: http://dx.doi.org/10.15666/aeer/1706_1319913217

The maize is the major source of starch in the worldwide. It can be fed to stock as green chop, dry forage, silage or grain. Various fractions of milling processes, also it can be used as animal feed. Furthermore, maize uses in nonfood making products such as drugs, paper goods, paints, textiles (cloths) and ceramics (Jones, 2003).

An increasing the number of human population continuously increases their demands for food and energy, which require to incorporate the new areas in agricultural as well as increase the crop yieldper unit of area with healthy quality with good nutritional or healthy quality. Among all grain crops, the maize has the highest yield per hectare (Du Plessis, 2003). Generally, the average yield of maize is greater than (4 ton ha^{-1}) (Farnham et al., 2003).

The maize cultivation in Iraq in the last decade increased, because of its importance as previously mentioned, its cultivation focused in the south of Iraq in Wasit, Meesan and AL-Qadeseya governorates, with only (3500 ha) during 1998. In 2014, the cultivated area with maize in Iraq increased to (299500 ha) with average production (4166.5 kg ha^{-1}), Central Statistical Organization of Iraq (2014). The maize cultivation in the Kurdistan region–Iraq has got more attention in last year's. The cultivated area in Kurdistan region roughly is about (1824 ha) with average production about (5138 kg ha^{-1}), (Ministry of Agriculture and Irrigation, Kurdistan regional government, Iraq, 2014). In the last decade maize production increased about (40%) reaching (840) million tons in the world in 2011 (FAOSTAT, 2013).

Therefore, intensive efforts of the researchers were focused on how to maximize the productivity of this crop through highly nutrient efficient, especially for humic acids and sulfur fertilizers.

Calcareous soil is a soil that has high levels of both calcium carbonate and magnesium that reduce acidity in the soil and covers more than one-third of the cultivable surface land in the world. Calcareous soil can have differing levels of sand, silt or clay as well as coarse to fine texture. This soil type typically maintains a moderate to high alkalinity (Pasricha et al., 2001).

Calcareous soils are common and widely spreader not only in arid and semiarid regions but also is formed in humid and per humid regions, due to the relatively low leaching and the nature of the weathered parent material such as limestone, shells (Sandstone) or calcareous glacial tills (Brady and Weil, 2002) and relatively young parent material which subjected to slight weathering process (Pal et al., 2000).

Lalljee and Facknath (2001) and Alloway (2008) found that micronutrients solubility in calcareous soils is extremely low because the pH value of these soils is high, which reduces nutrient absorption by plants, finally increases plant requirements to these nutrients. In addition to this, high rate of fertilization with P-fertilizers prompts micronutrients deficiencies in plants. Therefore, micronutrients content in plant dry matter and crops yield will reduce (Salimpour et al., 2010).

Materials and methods

To assess the impact of humic acid and sulfur incorporated into the soil on yield and yield constituents of maize (*Zea mays* L.) cv. Gloria, grown under calcareous soil, the experiment was conducted at two different locations. The first one at Qlyasan Agricultural Research Farm (45.3581 E, 35.5767 N 757 m above sea level) and the second one at Kanipanka Agricultural Research Farm (45.7161 E, 35.3822 N 578 m above sea level) in Sulaimani governorate, Iraq as shown in (*Fig. 1*) during spring

http://www.aloki.hu ● ISSN 1589 1623 (Print) ● ISSN 1785 0037 (Online)
DOI: http://dx.doi.org/10.15666/aeer/1706_1319913217

growing season of (10th and 11th April 2017 to 29th and 27th July 2017) respectively. The experiment includes four levels of humic acid as humate potassium (Humic 85%), obtained from AFICO factory in Jordan, ($H_0 = 0$, $H_1 = 25$, $H_2 = 50$ and $H_3 = 100$ kg HA ha^{-1}) and four levels of sulfur, obtained from LAWA factory in Sulaimani–Iraq, as agricultural sulfur, which contained 99% S ($S_0 = 0$, $S_1 = 500$, $S_2 = 1000$ and $S_3 = 2000$ kg S ha^{-1}) were incorporated into the soil in deep by 5 cm at sowing time. Average of the rainfall and air temperature climatic data of the experiment field locations (Kanipanka and Qlyasan) in 2017 showing in *Tables 1* and *2*.

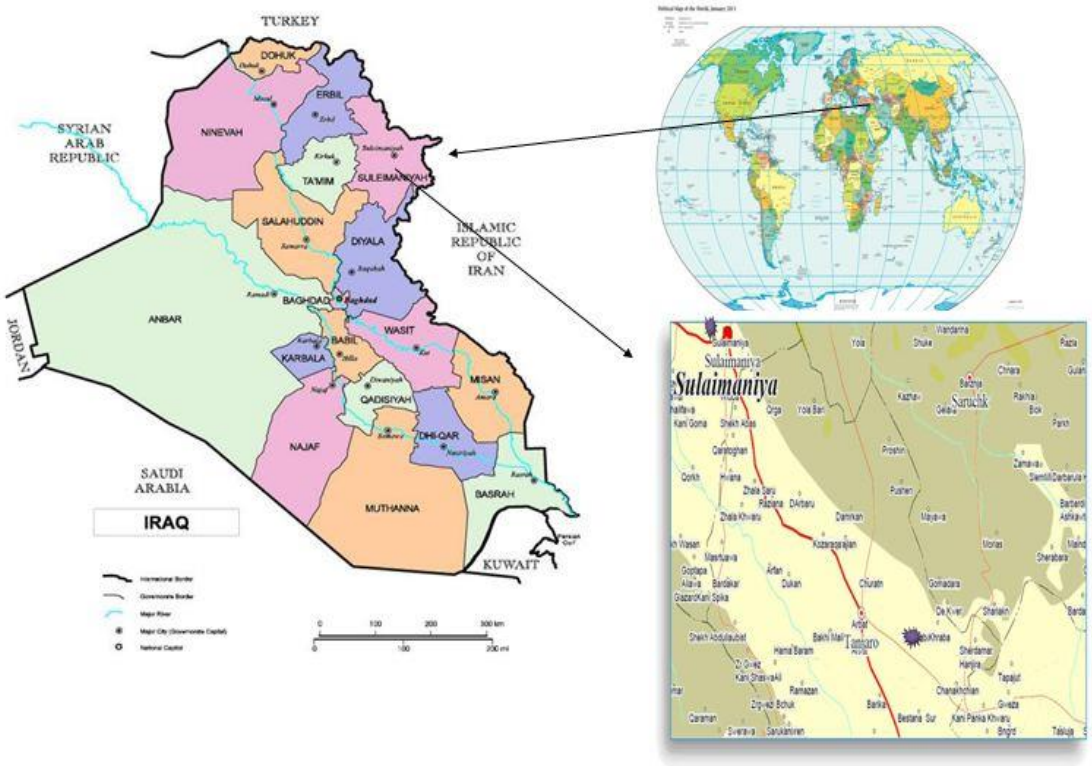

Figure 1. *The location of testing site*

The experiment was conducted on the 622.5 m^2 area (15 m × 41.5 m), in 16 experimental units with three replicates, the area of each experimental unit was 6 m^2 (2 × 3) m, each experimental plot included 3 rows in 3 m length, and the distance between these three was 0.70 m while it was 0.30 m within the rows of the individual plants, to obtain a mean density of 50,000 plants ha^{-1}, and the distance between the experimental units was 0.5 m while the distance between the blocks was 2 m. Experimental treatments have been organized in a factorial experiment by using the complete randomized block design (CRBD) by having three replicates. Treatments were as follows:

T1 = (control)
T2 = 500 kg S ha^{-1}
T3 = 1000 kg S ha^{-1}
T4 = 200 kg S ha^{-1}
T5 = 25 kg HA ha^{-1}
T6 = 25 kg HA ha^{-1} + 500 kg S ha^{-1}
T7 = 25 kg HA ha^{-1} + 1000 kg S ha^{-1}
T8 = 25 kg HA ha^{-1} + 2000 kg S ha^{-1}
T9 = 50 kg HA ha^{-1}
T10 = 50 kg HA ha^{-1} + 500 kg S ha^{-1}
T11 = 50 kg HA ha^{-1} + 1000 kg S ha^{-1}
T12 = 50 kg HA ha^{-1} + 2000 kg S ha^{-1}
T13 = 100 kg HA ha^{-1}
T14 = 100 kg HA ha^{-1} + 500 kg S ha^{-1}
T15 = 100 kg HA ha^{-1} + 1000 kg S ha^{-1}
T16 = 100 kg HA ha^{-1} + 2000 kg S ha^{-1}

http://www.aloki.hu ● ISSN 1589 1623 (Print) ● ISSN 1785 0037 (Online)
DOI: http://dx.doi.org/10.15666/aeer/1706_1319913217

Table 1. *Average of the rainfall and air temperature climatic data of the experiment field location (Kanipanka), in 2017*

Days	April			May			June			July			August		
	Rainfall mm	Temp. °C		Rainfall mm	Temp. °C		Rainfall mm	Temp. °C		Rainfall mm	Temp. °C		Rainfall mm	Temp. °C	
		Max.	Min.		Max.	Min.		Max.	Min.		Max.	Min.		Max.	Min.
1	1.2	20	15	1.2	28	21	0	30	28	0	40	30	0	44	34
2	4.8	21	16	14.5	22	18	0	29	24	0	41	31	0	44	36
3	15.5	16	14	0	27	20	0	33	30	0	42	30	0	43	35
4	11	18	15	0	27	24	0	35	33	0	44	27	0	44	35
5	0	23	19	0	25	22	0	36	28	0	44	27	0	44	36
6	0	24	15	1.2	28	17	0	40	30	0	45	31	0	44	35
7	2.5	21	15	0	28	24	0	40	36	0	42	30	0	44	38
8	0	21	19	0	30	24	0	39	35	0	44	36	0	43	39
9	0	21	16	0	29	26	0	39	36	0	41	34	0	45	37
10	0	19	13	0	32	26	0	41	36	0	43	34	0	44	37
11	3	19	14	0	34	31	0	38	34	0	41	39	0	41	35
12	0	25	22	0	35	27	0	37	34	0	41	35	0	44	36
13	7	28	18	0	32	27	0	39	36	0	39	33	0	45	37
14	8	19	16	0	32	26	0	41	37	0	41	38	0	41	34
15	0	21	18	0	34	30	0	36	32	0	41	38	0	41	35
16	0	22	17	0	33	29	0	35	33	0	42	34	0	41	35
17	0	24	20	0	32	28	0	36	30	0	43	31	0	43	37
18	5	24	19	0	29	20	0	37	32	0	44	35	0	41	36
19	0	22	17	1.3	35	26	0	38	29	0	44	36	0	41	35
20	0	24	21	0	32	27	0	37	31	0	43	35	0	41	36
21	0	24	20	0	27	22	0	34	30	0	44	38	0	42	35
22	0	28	22	0	29	25	0	34	29	0	44	37	0	43	32
23	1	26	22	0	32	27	0	38	35	0	45	35	0	42	34
24	2.5	25	20	0	30	26	0	40	32	0	42	34	0	42	34
25	0	26	20	0	29	27	0	40	31	0	41	37	0	42	34
26	0	26	23	0	34	27	0	40	32	0	40	33	0	42	34
27	0	27	25	0	35	28	0	43	36	0	43	36	0	41	34
28	0	29	25	0	35	27	0	44	35	0	44	38	0	40	32
29	0	31	23	0	36	32	0	41	36	0	44	39	0	42	35
30	0	30	27	0	36	27	0	41	37	0	41	33	0	42	34
31				0	35	29				0	42	31	0	43	32

http://www.aloki.hu ● ISSN 1589 1623 (Print) ● ISSN 1785 0037 (Online)
DOI: http://dx.doi.org/10.15666/aeer/1706_1319913217

Table 2. *Average of the rainfall and air temperature climatic data of the experiment field location (Qlyasan), in 2017*

Days	April			May			June			July			August		
	Rainfall mm	Temp. °C		Rainfall mm	Temp. °C		Rainfall mm	Temp. °C		Rainfall mm	Temp. °C		Rainfall mm	Temp. °C	
		Max.	Min.		Max.	Min.		Max.	Min.		Max.	Min.		Max.	Min.
1	2.6	22	12	0.5	32	22	0	34	24	0	44	36	0	48	40
2	10.2	20	12	15.5	29	24	0	36	22	0	43	36	0	47	36
3	4.9	20	16	0	25	23	0	37	21	0	47	34	0	47	38
4	0	20	18	0	30	19	0	37	31	0	48	35	0	46	38
5	0	24	17	0	31	23	0	41	28	0	47	34	0	48	32
6	0	26	21	0	31	20	0	42	25	0	46	35	0	44	34
7	0	26	21	0	26	19	0	44	29	0	46	35	0	45	36
8	1.7	24	20	0	32	22	0	38	33	0	47	36	0	47	39
9	0	23	20	1.3	34	27	0	38	26	0	39	34	0	46	35
10	0	22	21	0	36	24	0	37	33	0	43	35	0	49	36
11	4	20	16	0	39	24	0	43	31	0	45	28	0	46	35
12	5.5	29	23	0	38	24	0	42	27	0	45	29	0	48	36
13	0	31	29	0	32	22	0	42	36	0	37	33	0	48	37
14	6.2	22	20	0	36	22	0	44	35	0	43	34	0	46	32
15	0	24	17	0	37	24	0	37	35	0	41	28	0	43	31
16	0	23	18	0	36	22	0	38	32	0	44	34	0	44	31
17	0	27	20	0	35	22	0	41	26	0	46	31	0	44	36
18	5.4	29	24	0	34	20	0	42	27	0	46	33	0	37	34
19	0	24	17	2.7	39	33	0	40	29	0	46	33	0	44	34
20	0	24	17	0	33	28	0	40	27	0	45	37	0	43	34
21	0	28	16	0	28	22	0	37	30	0	46	42	0	46	29
22	0	26	20	0	30	22	0	36	24	0	48	37	0	45	32
23	1.5	28	22	0	34	25	0	38	23	0	48	35	0	41	30
24	0.2	26	24	0	31	24	0	41	28	0	44	34	0	41	30
25	0	29	20	0	33	21	0	42	26	0	43	32	0	44	31
26	0	28	20	0	34	20	0	44	32	0	43	33	0	44	30
27	0	29	23	0	35	29	0	47	40	0	45	28	0	44	32
28	0	30	23	0	37	23	0	48	35	0	47	33	0	44	26
29	0	32	26	0	40	24	0	45	31	0	44	32	0	45	30
30	0	34	27	0	40	27	0	45	30	0	44	33	0	44	30
31				0	36	35				0	44	31	0	46	32

http://www.aloki.hu ● ISSN 1589 1623 (Print) ● ISSN 1785 0037 (Online)
DOI: http://dx.doi.org/10.15666/aeer/1706_1319913217

All required management practices were done at proper times, and the standard practices were used for weed control. Soil samples were taken before planting from a depth of 0-40 cm of the soil used in the field experiments. The soil samples were air-dried, filtered by a 2 mm sieve, and kept in plastic bottles until analyzed. (*Table 3*) illustrates the main physical and chemical properties of the soils.

Table 3. *Some physical and chemical properties of soil used in field experiments*

		Location	
		Qlyasan	Kanipanka
Particle size distribution (PSD) g kg^{-1}	Sand	59.68	37.40
	Silt	619.17	500.30
	Clay	321.15	462.30
Textural class		Silty clay loam	Silty clay
Bulk density Mg m^{-3}		1.40	1.50
pH		7.42	7.46
EC dS m^{-1} at 25 °C°		0.38	0.27
Soluble ions mmol L^{-1}	Ca^{2+}	2.0	4.20
	Mg^{2+}	0.81	0.90
	Na^{+}	0.46	0.80
	K^{+}	0.156	2.70
	HCO_3^{-}	2.51	4.20
	SO_4^{2-}	0.789	0.892
Cation exchange capacity (CEC) cmolckg^{-1}		49.82	46.50
Organic matter (OM) g kg^{-1}		19.59	22.50
$CaCO_3$ equivalent g kg^{-1}	Total	215.68	215.50

Physiological parameters were measured as follows: Three plants of each plot were tagged, and all the reproductive growth and vegetative growth parameters were recorded, leaf area per plant, all available leaves of five plants per net plot were collected at 50% milking stage, and leaf length and width were measured. The leaf area was determined by multiplying leaf length and maximum leaf width adjusted by a correction factor of 0.75 (i.e., 0.75 X leaf length X maximum leaf width) as suggested by Francis et al. (1969).

$$\text{Leaf area (LA)} = \text{Length (cm)} \times \text{Maximum width of leaf (cm)} \times 0.75 \quad \text{(Eq.1)}$$

The diameter of the ear of maize was measured at harvest and expressed in centimeter. The randomly selected ears were cleaned, and a number of rows in each ear were counted manually. Then, the average number of rows of selected ears was taken as the number of rows per Ear. The number of Kernel was obtained by manual counting after separation of Kernels from the ear and the row.

At maturity, the crop was harvested on 27/7/2017 for Kanipanka location and 29/7/2017 for Qlyasan location, after reaching the mature physiological stage (when maturity symptoms occur on plants). Six plants were harvested from each treatment which signed previously, the ears were separated from plants, for removing the dust

http://www.aloki.hu ● ISSN 1589 1623 (Print) ● ISSN 1785 0037 (Online)
DOI: http://dx.doi.org/10.15666/aeer/1706_1319913217

from plants, plants washed by tap water, then rinsed three times by distilled water, air dried in dry cabinets chamber at 70 °C till the weight fixed at constant weight, and the plants total dry matter weight were recorded. Then, the plants were chopped into small pieces to enable complete drying and then oven-dried at 70 °C till a constant weight was obtained. The oven-dry weight of dry matter was recorded and expressed in grams per plant. Maize ears were dried, then shelled and the maize grain dried to 15% moisture content. The dry maize grains were weighed from each harvested area. The weight of grain for each experimental unit (6 m^2) was determined, and the yield was expressed in (Mg ha^{-1}). Other yield parameters were also collected.

A small sample of the seeds selected randomly from the grain yield of each experimental unit, and 100 seeds were counted and weighted, to obtain the net weight of 100 seeds (g). Kernel yield (ton ha^{-1}) was obtained in ton per hector according to Wasonga et al. (2008) using the following equation:

$$\text{Kernel yield (ton ha}^{-1}\text{)} = \text{Plant density ha}^{-1} \times \text{Grain yield kg plant}^{-1} \quad \text{(Eq.2)}$$

Higher harvest index indicates a superior conversion of dry matter to grain yield. Many workers currently (Sharma et al., 1987) calculate harvest index for grain crops as a percentage, thus:

$$\text{Harvest index (\%)} = (\text{Kernel yield} / \text{Biological yield}) \times 100 \quad \text{(Eq.3)}$$

The relative yield was calculated by the following equation according to Tisdale et al. (1995):

$$\text{Relative yield} = (\text{yield of the control/ yield of fertilized treatment}) \times 100 \quad \text{(Eq.4)}$$

Data were subjected to analysis of variance (ANOVA) performed by XLSTAT (2016) Package and the differences were compared by Duncan Multiple Range Test (DMRT) at the 5% significance level.

Results

The attained results will be presented as follows:

Vegetative growth criteria

Leaf area (cm^2)

The results in (*Figs. 2* and 3) refer to the significant effect of humic acid and sulfur rate fertilizer on the leaf area (cm^2) of a maize plant. The results showed that the increasing humic acid and sulfur fertilizer application increased the leaf area significantly. The maximum leaf area of maize (78.50 and 77.50 cm^2) was produced by T_{16} from both of locations Qlyasan and Kanipanka, while the minimum leaf area of maize (66.75 cm^2) was produced by T_3 and T_1 from Qlyasan and Kanipanka locations respectively. Similar results were obtained by Erdal et al. (2000) and Abdullah et al. (2016) for humic acid. While the results were obtained by Nader and Nadia (2011) and Habtamu (2015) for sulfur rates, they found that the application of humic acid and sulfur rate fertilizer were affected significantly in the leaf area (cm^2) of maize.

http://www.aloki.hu ● ISSN 1589 1623 (Print) ● ISSN 1785 0037 (Online)
DOI: http://dx.doi.org/10.15666/aeer/1706_1319913217

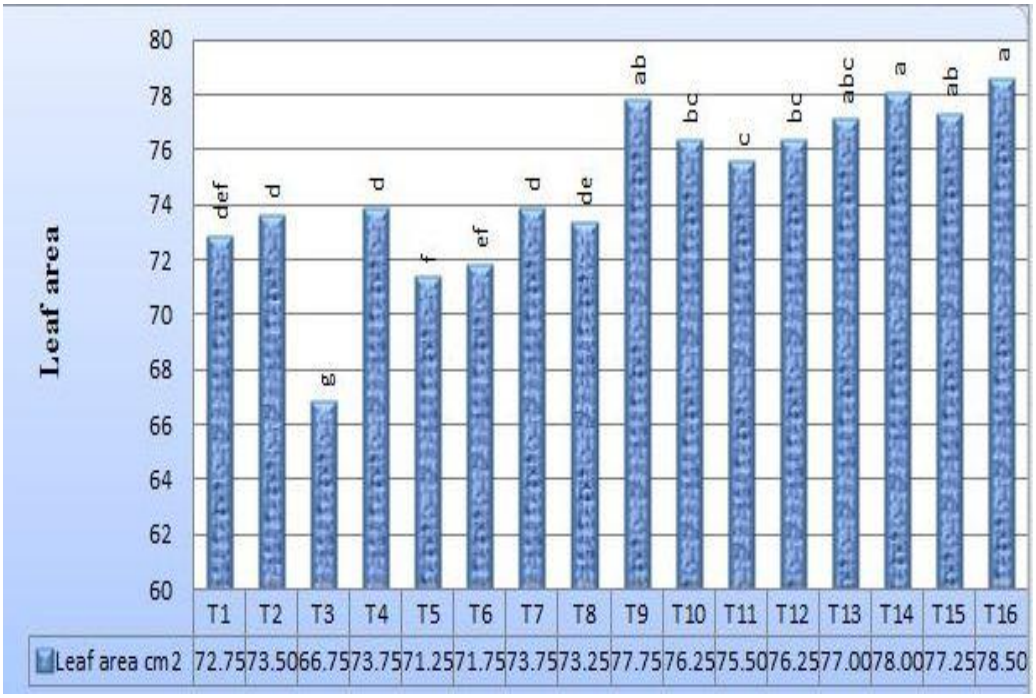

Figure 2. *Influence of humic acid and sulfur on the leaf area of maize from Qlyasan location*

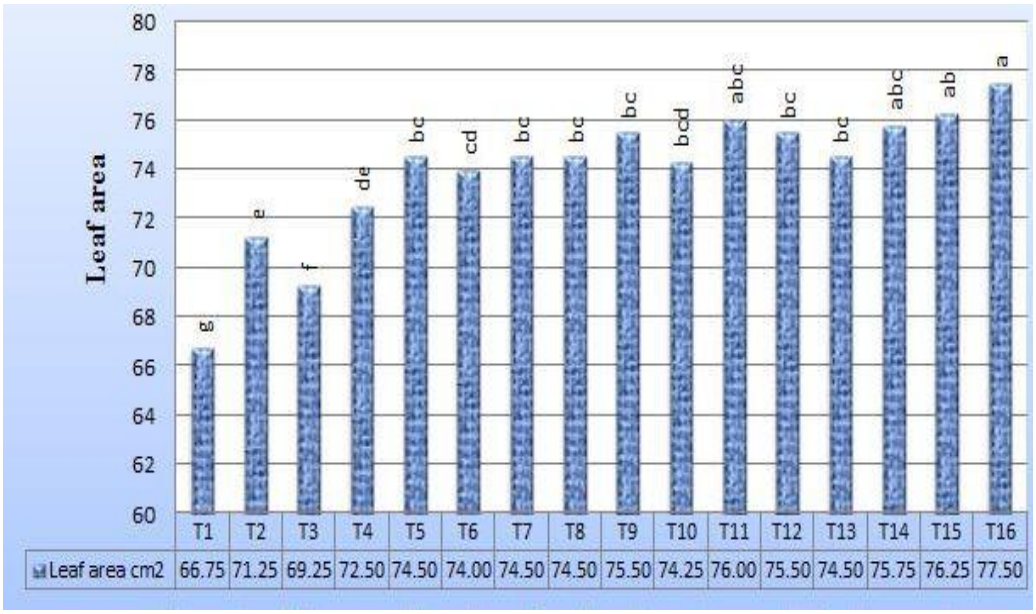

Figure 3. *Influence of humic acid and sulfur on the leaf area of maize from Kanipanka location*

Reproductive growth criteria

Ear diameter (cm)

The data presented in (*Table 4*) shows that the application of humic acid and sulfur rates were affected significantly at ($P < 0.05$ level) on the ear diameter (cm) from the Qlyasan location, the highest value (4.67 cm) was recorded from (T_{16}), while the lowest

http://www.aloki.hu ● ISSN 1589 1623 (Print) ● ISSN 1785 0037 (Online)
DOI: http://dx.doi.org/10.15666/aeer/1706_1319913217

value (4.26 cm) was obtained from (T_{11}). The positive effect of humic acid confirmed with the finding of Ebtisam et al. (2012) and Daur and Ahmed (2013) and similar results obtained by Makary (2002) and Nader and Nadia (2011) for the sulfur rate fertilizer application they referred that the application of humic acid and sulfur are essential to increase the ear characters of the corn plant. While the data present in (*Table 5*) revealed that, the application of different rates of humic acid and sulfur have not significant effects on the ear diameter (cm) from Kanipanka location.

Number of rows per ear

Results from a meaningful comparison of data (*Tables 4* and 5) of study treatments indicate that humic acid and sulfur rate application to the soil were affected significantly on the number of rows per ear of maize. The highest value of the number of rows per ear (16.67) was recorded from (T_{12}), while the lowest value (14.00) was obtained from (T_2) for Qlyasan location, but for Kanipanka location the highest value of the number of rows per ear (17.67) was recorded from (T_{16}), while the lowest value (15.33) was obtained from (T_1). Similar results were obtained by Attia et al. (2013) and Muhammad et al. (2015) for humic acid, and were obtained by Khan et al. (2006) and Habtamu (2015) for sulfur rates application, they found that the application of humic acid and sulfur rate affected significantly on the number of rows per ear of maize.

Table 4. *Influence of humic acid and sulfur rates on reproductive growth criteria of maize from Qlyasan location*

Treat.	Ear diameter (cm)	No. of (row/ear)	No. of (kernel/row)	No. of (kernel/ear)	Weight of 100 kernel (g)	Kernel yield (ton ha^{-1})	Biological yield (ton ha^{-1})	HI %
T_1	4.29 ^{bc}	14.67 ^{bc}	40.81 ^{bc}	598.67 ^{de}	22.65 ^{de}	6.44 ^{hi}	22.79^{f}	28.27^{fgh}
T_2	4.38 ^{c}	14.00 ^{c}	42.31 ^{bc}	598.87 ^{de}	22.26 ^{ef}	6.26 ^{hi}	22.68^{f}	27.59^{gh}
T_3	4.38 ^{c}	14.33 ^{c}	41.79 ^{bc}	598.97 ^{de}	23.28 ^{de}	8.22 ^{d}	23.05^{ef}	35.68^{ab}
T_4	4.29 ^{c}	14.00 ^{c}	42.76 ^{bc}	598.67 ^{de}	21.50 ^{f}	6.83 ^{fgh}	23.21^{def}	29.47^{defg}
T_5	4.45 ^{bc}	14.67 ^{bc}	41.90 ^{bc}	614.67 ^{de}	22.89 ^{de}	5.91 ^{i}	21.34^{cdef}	27.69^{h}
T_6	4.38 ^{c}	14.33 ^{c}	43.07 ^{bc}	616.67 ^{de}	23.14 ^{de}	6.49 ^{ghi}	23.52^{cdef}	27.62^{gh}
T_7	4.29 ^{c}	14.00 ^{c}	42.33 ^{bc}	599.67 ^{e}	22.79 ^{de}	6.77 ^{gh}	23.37^{cdef}	28.99^{efgh}
T_8	4.59 ^{ab}	15.67 ^{ab}	42.00 ^{bc}	658.67 ^{bcd}	23.18 ^{de}	7.47 ^{ef}	23.81^{cde}	31.36^{cdef}
T_9	4.37 ^{c}	14.33 ^{c}	44.33 ^{abc}	635.67 ^{cde}	23.54 ^{cd}	8.00 ^{de}	24.06^{cd}	33.24^{bc}
T_{10}	4.26 ^{c}	14.67 ^{c}	42.33 ^{a}	635.65 ^{bcde}	23.70 ^{cd}	8.93 ^{a}	24.06^{cd}	37.14^{a}
T_{11}	4.45 ^{bc}	14.67 ^{bc}	43.67 ^{c}	640.64 ^{de}	24.61 ^{bc}	9.12 ^{b}	24.13^{bc}	37.79^{a}
T_{12}	4.65 ^{a}	16.67 ^{a}	45.33 ^{ab}	754.67 ^{a}	25.23 ^{b}	7.82 ^{de}	24.14^{bc}	32.38^{bcde}
T_{13}	4.61 ^{ab}	16.00 ^{a}	42.67 ^{bc}	682.67 ^{bc}	26.38 ^{a}	8.20 ^{d}	24.92^{b}	32.94^{bcd}
T_{14}	4.61 ^{ab}	16.33 ^{a}	42.84 ^{bc}	698.67 ^{ab}	26.55 ^{a}	7.12 ^{fg}	26.03^{a}	27.35^{gh}
T_{15}	4.65 ^{a}	16.33 ^{a}	43.81 ^{bc}	695.00 ^{bc}	26.64 ^{a}	9.93 ^{bc}	26.00^{a}	38.20^{a}
T_{16}	4.67 ^{a}	16.33 ^{a}	42.90 ^{bc}	699.67 ^{ab}	27.02 ^{a}	8.44 ^{cd}	26.15^{a}	32.29^{bcde}

Treat. = Treatments, No. = Number, HI = Harvest index

Number of kernels per row and ear

The application of humic acid and sulfur rate fertilizer significantly increased the kernel per row of maize. The highest mean value of kernel per ear (754.67) was

http://www.aloki.hu ● ISSN 1589 1623 (Print) ● ISSN 1785 0037 (Online)
DOI: http://dx.doi.org/10.15666/aeer/1706_1319913217

recorded from (T12), while the lowest mean value of kernel per ear (598.67) was obtained from (T1) for Qlyasan location (*Table 4*), but for Kanipanka location the highest value of kernel per ear (768.00) was recorded from (T16), while the lowest value of kernel per ear (648.33) was obtained from (T2) (*Table 5*). Similar results were obtained by Celiket al. (2010) for humic acid, and the results are in agreement with those obtained by Choudhary et al. (2013) for sulfur rate application, they found that the application of humic acid and sulfur rates affected significantly of the kernel per ear of maize. From the results in (*Tables 4* and *5*) it has been observed that the application of humic acid and sulfur rates have not a significant effect on a number of kernels per row in Qlyasan location but have a significant effect in Kanipanka location.

The weight of 100 kernels (g)

According to the analysis of variance, the mean comparison showed that the application rates of humic acid and sulfur revealed that the weight of 100 kernels (g) of maize was affected significantly at ($P < 0.05$). The results show that significantly increased the weight of 100 kernels (g) of maize from 22.26 g was recorded from (T2) to 27.02 g was recorded from (T16) for Qlyasan location (*Table 4*) and from 27.33 g was recorded from (T1) to 33.92 g was recorded from (T16) for Kanipanka location (*Table 5*). These findings are in coincidence with those recorded by Navigehet al. (2012) and Balbaaet al. (2013) about humic acid, and the results are in agreement with those obtained by Srinivasraoet al. (2010) about the sulfur rate application, they found that the application of humic acid and sulfur rates affected the weight of 100 kernels (g) of maize significantly.

Kernel yield (ton ha^{-1})

The data relating to kernel yield (ton ha^{-1}) are presented in (*Tables 4* and 5), revealed that kernel yield was affected significantly at ($P < 0.05$ level) by the application of humic acid and sulfur rate to the soil. The maximum of kernel yield (9.93 and 9.20 ton ha^{-1}) was produced by T15 and T13, while the minimum kernel yield (6.26 and 7.22 ton ha^{-1}) was produced by T2 and T1 from Qlyasan and Kanipanka locations respectively. Similar results were obtained by Turanet al. (2011), and Awwadet al. (2015) about humic acid and the results are in a harmonic with the finding by Khan et al. (2006) about sulfur rates application, they found that the application of humic acid and sulfur rate affected significantly of the kernel yield (ton ha^{-1}) of maize.

Biological yield (ton ha^{-1})

The result regarding biological yield (ton ha^{-1}) of maize plant showed that the application of humic acid and sulfur rates to the soil was affected significantly at ($P < 0.05$) on biological yield from both locations Qlyasan and Kanipanka. The maximum biological yield (26.15 and 26.54 ton ha^{-1}) was obtained from T16 and T15, while the minimum biological yield (22.68 and 22.6 ton ha^{-1}) was obtained from T2 and T1 for both locations Qlyasan and Kanipanka respectively (*Tables 4* and 5). These results are in a harmonic with those recorded by Gomaa et al. (2014) and Daur and Ahmed (2013) for humic acid, and the results are in agreement with the finding by Khan et al. (2006); Choudhary et al. (2013) and Habtamu (2015) for sulfur rate application, they found that the application of humic acid and sulfur rates affected significantly of the biological yield (ton ha^{-1}) of maize.

http://www.aloki.hu ● ISSN 1589 1623 (Print) ● ISSN 1785 0037 (Online)
DOI: http://dx.doi.org/10.15666/aeer/1706_1319913217

Table 5. *Influence of humic acid and sulfur rates on reproductive growth criteria of maize from Kanipanka location*

Treat.	Ear diameter (cm)	No. of (row/ear)	No. of (kernel/row)	No. of (kernel/ear)	Weight of 100 kernel (g)	Kernel yield (ton ha^{-1})	Biological yield (ton ha^{-1})	HI %
T_1	4.60^{b}	15.33^{de}	42.40^{bcdef}	678.33^{cd}	27.33^{ef}	7.22^{d}	22.6 ^{g}	31.83 ^{cdef}
T_2	4.58^{b}	15.33^{de}	40.52^{f}	648.33^{d}	27.36^{fg}	7.55^{cd}	25.98 ^{abc}	29.06^{h}
T_3	4.58^{b}	15.47^{de}	41.77^{cdef}	654.33^{d}	28.06^{ef}	7.60^{cd}	23.27 ^{fg}	32.69 ^{bcd}
T_4	4.52^{b}	15.33^{de}	44.84^{ab}	686.33^{cd}	26.45^{g}	8.33^{b}	25.44 ^{cd}	32.75 ^{bcd}
T_5	4.61^{b}	16.00^{e}	43.67^{abcde}	698.33^{bcd}	28.87^{e}	7.27^{d}	23.67 ^{f}	30.72 ^{efgh}
T_6	4.61^{b}	16.00^{e}	44.00^{abcde}	704.00^{bcd}	28.86^{e}	7.38^{d}	24.39 ^{e}	30.26 ^{fgh}
T_7	5.64^{a}	16.33^{cde}	41.67^{def}	680.33^{cd}	28.04^{ef}	7.40^{d}	24.58 ^{e}	30.10 ^{fgh}
T_8	4.66^{b}	16.33^{cde}	44.67^{ab}	729.33^{abc}	31.79^{cd}	7.22^{d}	22.95 ^{de}	31.46^{h}
T_9	4.64^{b}	16.33^{cde}	44.67^{abc}	730.00^{abc}	28.43^{ef}	9.04^{a}	25.48 ^{cd}	35.47 ^{a}
T_{10}	4.61^{b}	16.00^{de}	45.67^{a}	730.67^{abc}	28.99^{e}	7.51^{cd}	25.47 ^{cd}	29.50 ^{gh}
T_{11}	4.66^{b}	16.33^{cde}	41.33^{ef}	675.00^{cd}	32.54^{bc}	7.53^{cd}	23.39 ^{fg}	32.30 ^{cde}
T_{12}	4.75^{b}	17.63^{b}	42.68^{ab}	754.16^{a}	31.11^{d}	7.91^{c}	25.38 ^{cd}	31.15 ^{defg}
T_{13}	4.84^{b}	19.00^{a}	39.70^{f}	754.33^{ab}	33.19^{ab}	9.20^{a}	25.62 ^{bcd}	35.93 ^{a}
T_{14}	4.68^{b}	17.00^{bcd}	44.54^{abcd}	757.00^{ab}	33.10^{ab}	8.89^{a}	25.78 ^{bc}	34.51 ^{ab}
T_{15}	4.68^{b}	16.67^{bcde}	45.33^{ab}	755.67^{ab}	32.45^{bc}	8.84^{a}	26.54 ^{a}	33.29 ^{bc}
T_{16}	4.77^{b}	17.67^{bc}	43.49^{abcde}	768.00^{a}	33.92^{a}	9.12^{a}	26.36 ^{ab}	34.61 ^{ab}

Treat. = Treatments, No. = Number, HI = Harvest index

Harvest index %

The statistical analysis of the variance in (*Tables 4* and 5) showed that applying humic acid and sulfur rate for the soil was affected significantly at ($P < 0.05$ level) on harvest index. The highest value of harvest index percentage (38.20% and 35.93%) was recorded from T15 and T13, while the lowest value of harvest index percentage (27.59% and 29.06%) was observed in T2 from Qlyasan and Kanipanka locations respectively. These results for humic acid were in agreement with the results of Celiketal (2010) and Awwadet al. (2015) who found that the harvest index increased owing to the increase of humic acid rates. About the effect of sulfur rates, the results in a harmonic with the results of Szulcet al. (2012), reported that the different levels of a sulfur application significantly affected the grain yield and harvest index of maize plans.

Relative yield percentage

The results regarding the relative yield percentage of maize plant are shown in (*Figs. 4* and *5*) which showed that the humic acid and sulfur rates incorporated into the soil were affected significantly on relative yield from both locations Qlyasan and Kanipanka. The highest value of relative yield percentage (108.96% and 100.05%) was observed in T5 and T8, while the lowest value of relative yield percentage (64.95% and 78.40%) was recorded from T15 and T13 for Qlyasan and Kanipanka locations respectively. These results are in a harmonic with those recorded by Hakanet al. (2011) and Balbaaet al. (2013) for humic acid, and the results are in agreement with the results of Dwivedi et al. (2002) for sulfur rates, they found that applying humic acid and sulfur rates affected significantly and decreased of the relative yield percentage of maize.

http://www.aloki.hu ● ISSN 1589 1623 (Print) ● ISSN 1785 0037 (Online)
DOI: http://dx.doi.org/10.15666/aeer/1706_1319913217

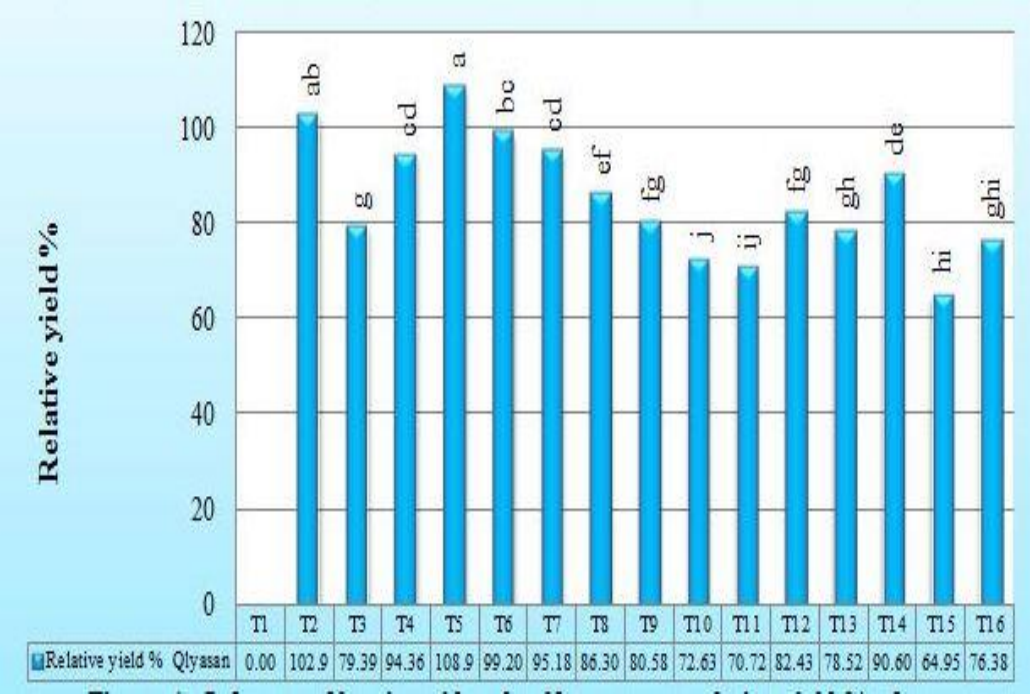

Figure 4. *Influence of humic acid and sulfur on the relative yield % of maize from Qlyasan location*

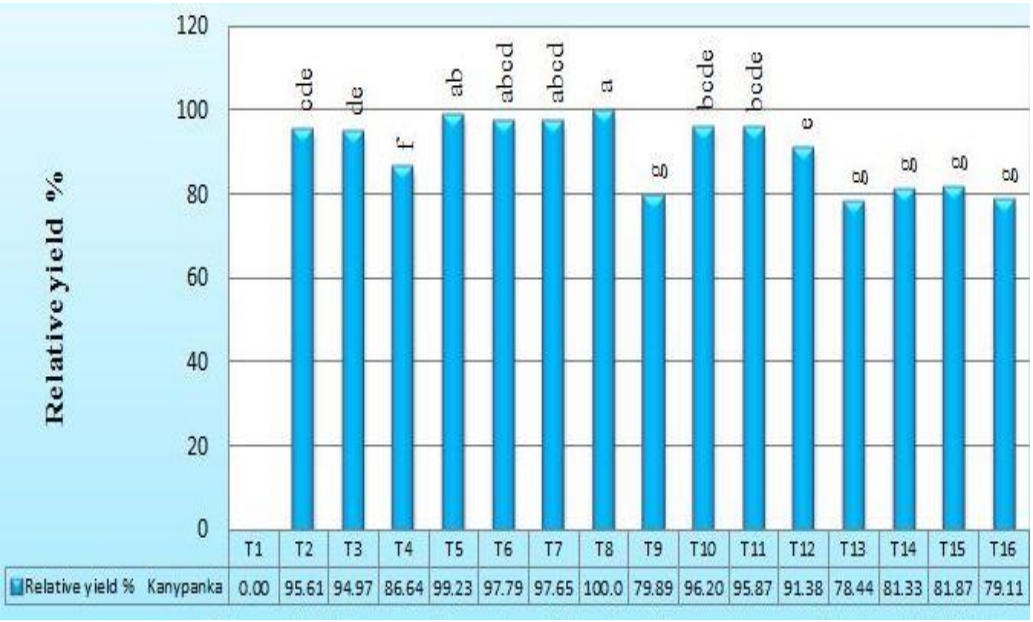

Figure 5. *Influence of humic acid and sulfur on the relative yield % of maize from Kanipanka location*

Discussion

From the above results it has been observed that applying humic acid and sulfur rates in the higher levels (T16 and T15 treatments) have a significant effect on yield and yield constituents of maize in both locations, because the humic acids improve the soil

http://www.aloki.hu ● ISSN 1589 1623 (Print) ● ISSN 1785 0037 (Online)
DOI: http://dx.doi.org/10.15666/aeer/1706_1319913217

structure (Ali et al., 2011) and through various mechanisms which were indicated to plant growth and development, enhance nutrient abundance and absorption (Berbara and Garcia, 2014). Humic acid is crucial for enhancing the abundance of nutrients through the chelation of metallic nutrients, promoting the chelation of various elements and turning them obtainable by the plant and improve the plant growth and nutrient uptake.

This process may be attributed to the distinctive structural properties of humic acid as it has so many oxygen-containing functional groups (CO_2H_2, OH, phenols, and C = O).

Humic acid is vital for modified soil physical properties. Humic acid is essential to increased plant yield through physiological effects such as the impact on the metabolism of plant cells and increasing the leaves area (Nardi et al., 2009). Increased root growth has been attributed to improved soil structure, stimulation of the soil microflora and plant growth regulator effects. For comprehensive reviews of humic acid effects on plants and because sulfur is essential in the structural and enzymatic components in plants, sulfur is a fundamental constituent of some basic amino acids that comprise proteins, and it contributes in chlorophyll synthesis. Moreover, Sulfur optimizes utilization of supplementary nutrients in plants, which are crucial for growth, development of root nodule in legumes in addition to plant protection mechanism since soil pH drops when sulfur is added to the soil.

Many previous studies have indicated that applying humic acid optimizes soil physical configuration, supports preserving soil moisture, raises root absorptivity of water and nutrients, promotes the production of nucleic and amino acids, promotes the action of enzymes and metabolic rate, and subsequently, optimizes yield (Dursunet al., 2002). All these pathway alterations may be attributed to humic acid since it elevates membranes absorbency and enhances the uptake of nutrients Furthermore; humic acid intensifies soil sponginess and enhances root development which in turn contributes to a larger shoot (Garcia et al., 2008). Humic acid optimizes the fresh and dry weight of shoot and root in corn (Cordeiro et al., 2011). Using sulfur fertilizers promotes growth through promoting the absorbency of soil micronutrients which eventually leads to more significant yield quantities (Fayed, 2005). Due to the significance of sulfur in root development, chlorophyll production, and metabolism, heavier fresh and dry weights of plants treated with sulfur-containing humic acid might be attributed to sulfur (Atoosa et al., 2017).

Conclusion

The results of the current work indicate that humic acid has a positive impact on the yield and its components in corn. Using humic acid may decrease the demand for other chemical and biological fertilizers to a reasonable extent. These wanted outcomes might be attributable to its impact on corn growth and physiology. Besides raising yield quantities of corn, humic acid may also contribute to realizing the objectives of agricultural sustainability. Sulfur is a central micronutrient needed for plant growth and development. Because sulfur and humic acid are involved in affecting physiological and biochemical pathways, they have to be studied thoroughly and profoundly In order to grasp better the nutritional mechanisms of sulfur about humic acid and in order to serve as a guideline for developing balanced fertilizer formulas to optimize yield quality and quantity. According to the results obtained from the present research, we guide the

http://www.aloki.hu ● ISSN 1589 1623 (Print) ● ISSN 1785 0037 (Online)
DOI: http://dx.doi.org/10.15666/aeer/1706_1319913217

related directions to farmers in Sulaimani Governorate, Kurdistan Region – Iraq to cultivate the cv. Gloria of maize. It is necessary to implement more studies on other levels of humic substances in maize plant at different dose along with the sulfur and other methods of application for reaping higher yield and quality apart from sustaining the soil health. Evaluation of soil fertility status to other potential maize growing areas should be done to understand the deficiency situation of the nutrients

REFERENCES

[1] Abdullah, N., Muhammad, Y., Muhammad, S., Sultana, S., Ehsan, M., Nazarat, A. (2016): Maize production and nitrogen use efficiency in response to nitrogen application with and without humic acid. – Journal of Animal and Plant Science 6: 1641-1651.

[2] Ali, L. K., Nadia, A. M., El-Maghraby, T. A. (2011): Effect of P and Zn fertilization on wheat yield and nutrient uptake in calcareous soil. – Journal of Soil Science and Agriculture Engineering 2: 555-569.

[3] Alloway, B. J. (2008): Micronutrient Deficiencies in Crop Production in China. – In: Chunqin, Z., Xiaopeng, G., Rongli S., Xiaoyun, F., Fusuo Z. (eds.) Micronutrient Deficiencies in Global Crop Production. Springer, Dordrecht, pp. 127-148.

[4] Atefe, A., Ali, T. (2012): Effect of humic acid on nutrient uptake and physiological characteristic Fragaria ananassa var: Camarosa. – Journal of Biodiversity and Environmental Sciences 6(16): 77-79.

[5] Atoosa, D., Sara, H., Mohammad, A. B., Maryam, D., Mehrdad, B. (2017): The effect of sulfur-containing humic acid on yield and nutrient uptake in olive fruit. – Open Journal of Ecology 7: 279-288.

[6] Attia, A. N., El-Mosury, S. A., Mahgoub, G. M., Darwish, M. M. (2013): Effect of compost rates, humic acid treatments, and nitrogen fertilization rates on growth and yield of maize. – Journal Plant Prods 4: 509-521.

[7] Awwad, M. S., El-Hedek, K. S., Bayoumi, M. A., Eid, T. A. (2015): Effect of potassium humate application and irrigation water levels on maize yield, crop water productivity, and some soil properties. – Journal of Soil Science and Agriculture Engineering 6: 461-482.

[8] Balbaa, M. G., Awad, A. M. (2013): Effect of humic acid and micronutrients foliar fertilization on yield, yield components and nutrients uptake of maize in calcareous soil. – Journal Plant Production 4: 773-785.

[9] Berbara, R. L., Andrés, C. G. (2014): Humic Substances and Plant Defense Metabolism. – In: Ahmad, P., Wani, M. R. (ed.) Physiological Mechanisms and Adaptation Strategies in Plants Under Changing Environment. Springer, New York, pp. 297-319.

[10] Brady, N. C., Weil, R. R. (2002): The Nature and Properties of Soils. 13th Ed. – Prentice Hall, Upper Saddle River, NJ.

[11] Canellas, L. P., Olivares, F. L., Okorokova-Facanha, A. L., Facanha, A. R. (2002): Humic acids isolated from earthworm compost enhance root elongation, lateral root emergence and plasma membrane H-ATPase activity in maize roots. – Plant Physiology l30: 1951-1957.

[12] Celik, H., Ali, V. K., Baris, B. A., Murat, A. T. (2010): Effect of hummus on growth and nutrient uptake of maize under saline and calcareous soil conditions. – Zemdirbyste-Agriculture Journal 97: 15-22.

[13] Chen, Y., Clapp, C. E., Magen, H. (2004b): Mechanisms of plant growth stimulation by humic substances: The role of organic-iron complexes. – Soil Science and Plant Nutrition 50: 1089-1095.

http://www.aloki.hu ● ISSN 1589 1623 (Print) ● ISSN 1785 0037 (Online)
DOI: http://dx.doi.org/10.15666/aeer/1706_1319913217

[14] Choudhary, R., Singh, D., Singh, P., Dadarwal, R. S., Chaudhari, R. (2013): Impact of nitrogen and sulfur fertilization on yield, quality and uptake of nutrient by maize in southern Rajasthan. – Annals of Plant and Soil Research 15: 118-121.
[15] Cordeiro, F. C., Catarina, C. S., Silveira, V., De Souza, S. R. (2011): Humic acid effect on catalase activity and the generation of reactive oxygen species in corn (Zea mays). – Bioscience, Biotechnology, and Biochemistry 75: 70-74.
[16] Daur, I., Ahmed, A. B. (2013): Effect of humic acid on growth and quality of maize fodder production. – Pakistan Journal Botany 45: 21-25.
[17] Dwivedi, S. K., Singh, R. S., Dwivedi, K. N. (2002): Effect of sulfur and zinc nutrition on yield and quality of maize in TypicUstropept soil of Kanpur. – Journal of the Indian Society of Soil Science 50: 70-74.
[18] Du Plessis, J. (2003): Maize Production. – Department of Agriculture, Pretoria, South Africa. www.nda.agric.za/publications.
[19] Duke, S. H., Reisenauer, H. M. (1986): Roles and Requirements of Sulfur in Plant Nutrition. – In: Tabatabai M. A. (ed.) Sulfur in Agriculture. Agronomy Monograph. American Society of Agron., Madison, WI, pp. 123-168.
[20] Dursun, A., Guvenc, I., Turan, M. (2002): Effects of different levels of humic acid on seedling growth and macro and micronutrient contents of tomato and eggplant. – Acta Agrobotanica 56: 81-88.
[21] Ebtisam, I. K., Sabreen, K., Abd El Hady, M. (2012): Improving soil properties, maize yield components grown in sandy soil under irrigation treatments and humic acid application. – Australian Journal of Basic and Applied 6: 587-593.
[22] Erdal, D., Bozkurt, M. A., Cimrin, K. M., Karaca, S., Saglam, M. (2000): Effects of humic acid and phosphorus applications on growth and phosphorus uptake of the corn plant (Zea mays L.) grown in a calcareous soil. – Turkish Journal of Agriculture and Forestry 24: 663-668.
[23] Ertani, A., Francioso, O., Tugnoli, V., Righi, V., Nardi, S. (2011): Effect of commercial lignosulfonate-humate on Zea mays L. metabolism. – Journal of Agricultural and Food Chememistry 59: 11940-11948.
[24] FAOSTAT (2013): Statistical Database of the Food and Agriculture Organization of the United Nations. – FAO, Rome, Italy. http://faostat.fao.org (accessed 4 June 2013).
[25] Farnham, D. E., Benson, G. O., Pearce, R. B. (2003): Corn Perspective and Culture. – In: White, P. J., Johnson, L. A. (eds.) Corn: Chemistry and Technology. American Association of Cerial, Chemicals, Inc., St. Paul, MN, pp. 1-33.
[26] Fayed, T. A. (2005): Effect of some organic manures and biofertilizers on Anna apple trees. Yield and fruit characteristics. – Egypt Journal of Applied Science 20: 176-191.
[27] Food and Agriculture Organization of the United Nations, Statistics Division (FAO) (2009): Maize, Rice and Wheat: Area Harvested, Production Quantity, Yield. FAO, Rome.
[28] Garcia, M. C., Francisca, S. E., Lopez, M. J., Joaquim, M. (2008): Influence of compost amendment on soil biological properties and plants. – Dynamic Soil, Dynamic Plant 1: 1-9.
[29] Gomaa, M. A., Radwan, F. I., Khalil, G. A., Kandil, E. E., El-Saber, M. M. (2014): Impact of humic acid application on productivity of some maize hybrids under water stress conditions. – Middle East Journal of Applied Sciences 4: 668-673.
[30] Hakan, C., VahapKatkat, A., Bulent Asık, B., Turan, M. A. (2011): Effect of foliar-applied humic acid to dry weight and mineral nutrient uptake of maize under calcareous soil conditions. – Communications in Soil Science and Plant Analysis 42: 29-38.
[31] Habtamu, A. D. (2015): Response of maize (Zea mays L.) to different levels of nitrogen and sulfur fertilizers in Chilga District, Amhara National Regional State, Ethiopia. – Basic Research Journal of Soil and Environmental Science 3: 38-49.

http://www.aloki.hu ● ISSN 1589 1623 (Print) ● ISSN 1785 0037 (Online)
DOI: http://dx.doi.org/10.15666/aeer/1706_1319913217

[32] Hogir, S. M. (2016): Interaction effect of maize genotypes and phosphate fertilization on availability of some micronutrients in calcareous soil. – Master of Science Thesis, College of Agriculture, Duhok Univ.
[33] Jones, J. B. (2003): Agronomic Hand Book: Management of Crops, Soils and Their Fertility. – CRC Press, Boca Raton, FL.
[34] Karimizarchi, M., Aminuddin, H. (2015): Effect of elemental sulphur on soil micronutrients mobility. – Journal of Agricultural Science and Food Technology 1: 34-42.
[35] Karimizarchi, M., Aminuddin, H., Khanif, M. Y., Radziah, O. (2014): Elemeantal sulphur application effects on nutrient availability and sweet Maize (Zea mays L.) response in a high pH soil of Malaysia. – Malaysian Journal of Soil Science 18: 75-86.
[36] Karaca, A., Turgay, O. C., Tamer, N. (2006): Effects of a humic deposit (gyttja) on soil chemical and microbiological properties and heavy metal availability. – Biology and Fertility of Soils 42: 585-592.
[37] Khan, M. J., Muhammad, H. K., Riaz, A. K., Muhammad, T. J. (2006): Response of maize to different levels of sulfur. – Communications in Soil Science and Plant Analysis 37: 1-2.
[38] KRG (2014): Ministry of Agriculture and Irrigation, Kurdistan Regional Government, Iraq. – https://krg-moawr.org/ku.
[39] Lalljee, B., Facknath, S. (2001): Effect of Lime on Nutrient Content of Soils, Yield and Nutrient Content of Potato and Infestation by Leaminers. – Food and Agricultural Research Council, Moka, Mauritius, pp. 139-147.
[40] Mackowiak, C. L., Grossl, P. R., Bugbee, B. G. (2001): Beneficial effects of humic acid on micronutrient availability to wheat. – Soil Science Society of America Journal 56: 1744-1750.
[41] Makary, B. S. (2002): Effect of some organic and inorganic fertilizers with sulfur element on the yield of corn and its influence on some soil properties. – Journal of Agricultural Science 27: 1301-1313.
[42] Muhammad, I. K., Mohammad, Q., Muhammad, S., Hamayun, K., Muhammad, A., Muhammad, R. (2015): Response of maize crop to different levels of humic acid. – Life Sciences International Journal 9: 3116-3120.
[43] Nader, R. H., Nadia, M. H. (2011): Effects of elemental sulphur and partial substitution of N-mineral fertilizer by organic amendments on some properties of slight saline soils. – Journal of Applied Sciences Research 7: 2102-2111.
[44] Nardi, S., Carletti, P., Pizzeghello, D., Muscolo, A. (2009): Biological Activities of Humic Substances. – In: Senesi, N., Xing, B., Huang, P. M. (eds.) Biophysico-Chemical Processes Involving Natural Nonliving Organic Matter in Environmental Systems. Wiley, Hoboken, pp. 305-339.
[45] Navigeh, R., Mehrdad, Y., Davood, H. P. (2012): Effect of drought stress and potassium humate application on grain yield-related traits of corn (cv. 604). – Journal of Food, Agriculture and Environment 10: 580-584.
[46] Pal, D. K., Sasog, G. S., Vadivelu, S., Ahiya, R. L., Bhattacharyya, T. (2000): Secondary Calcium Carbonate in Soils in Arid and Semi-Arid Regions of India. – In: Lal, R., Kimble, J. M., Eswaran, H., Stewart, B. A. (eds.) Global Climatic Change and Pedogenic Carbonates. Lewis Publishers, CRS Press, New York, pp. 149-185.
[47] Pasricha, N. S., Bansal, S. K., Golakiya, B. A. (2001): Balanced Nutrition of Groundnut and Other Field Crops Grown in Calcareous Soils of India. – Potash Research Institute of India, Gurugram, pp. 5-19.
[48] Rheinheimer, D. S., Rasche, J. W. A., Osorio, Filho, B. D., Silva, L. S. (2007): Responses to sulphur application and recuperation in greenhouse crops in soils with different clay and organic matter content. – Ciência Rural (CR) 37: 363-371.

http://www.aloki.hu ● ISSN 1589 1623 (Print) ● ISSN 1785 0037 (Online)
DOI: http://dx.doi.org/10.15666/aeer/1706_1319913217

[49] Salimpour, S., Khavazi, K., Nadian, H., Besharati, H., Miransari, M. (2010): Enhancing phosphorous availability to canola (Brassica napus L.) using P solubilizing and sulfur oxidizing bacteria. – Australian Journal of Crop Science 4: 330-334.
[50] Scherer, H. W. (2001): Sulphur in crop production - invited paper. – European Journal of Agronomy14: 81-111.
[51] Shah, S. T., Zamir, S. I., Waseem, M., Ali, A., Tahir, M., Khalid, B. W. (2009): Growth and yield response of maize (Zea mays L.) to organic and inorganic sources of nitrogen. – Pakistan Journal of Life and Social Science 7: 108-111.
[52] Sharif, M., Khattak, R. A., Sarir, M. S. (2002): Effect of different levels of lignitic coal derived humic acid on growth of maize plants. – Communications in Soil Science and Plant Analysis 33: 3567-3580.
[53] Sharma, R. C., Smith, E. L., McNew, R. W. (1987): Stability of harvest index and grain yield in winter wheat. – Crop Science 27: 104-107.
[54] Sikandar, A., Ali, M., Amin, M., Bibi, S., Arif, M. (2007): Effect of plant population on maize hybrids. – Journal of Agricultural and Biological Science 2: 13-20.
[55] Singh, R. P., Agrawal, M. (2010): Effect of different sewage sludge applications on growth and yield of Vigna radiata L. field crop: metal uptake by plant. – Ecological Engineering 36: 969-972.
[56] Srinivasrao, C., Masood, A., Venkateshwaralu, S., Rupa, T. R., Singh, K. K., Sumanta Kundu, S., Prasad, J. V. (2010): Direct and residual effects of integrated sulfur fertilization in maize (Zea mays) - chickpea (Cicer arietinum) cropping system on typic ustochrept. – Indian Journal of Agronomy 55: 259-263.
[57] Stevenson, F. J. (1994): Humus Chemistry: Genesis, Composition, Reactions. – John Wiley & Sons, New York.
[58] Szulc, P., Jan, B., Zajac, M. R. (2012): The effect of soil supplementation with nitrogen and elemental sulfur on chlorophyll content and grain yield of maize (Zea mays L.). – Polish Journal of Environmental Studies 99: 247-254.
[59] Tisdale, S. L., Nelson, W. L., Beaton, J. D., Havlin, J. L. (1995): Soil Fertility and Fertilizer. 5th Ed. – Prentice-Hall of India, New Delhi.
[60] Turan, M. A., Asik, B. B., Katkat, A. V., Celik, H. (2011): The effects of soil-applied humic substances to the dry weight and mineral nutrient uptake of maize plants under soil salinity conditions. – Notulae Botanicae Horti Agrobotanici Cluj-Napoca 39: 171-177.
[61] Turkmen, O., Dursun, A., Turan, M., Erdinc, C. (2004): Calcium and humic acid affect seed germination, growth, and nutrient content of tomato (Lycopersicon esculentum L.) seedlings under saline soil conditions. – Acta Agriculturae Scandinavica, Section B- Soil and Plant Science 54: 168-174.
[62] Ulukan, H. (2008): Humic acid application into field crops cultivation. – KS University Journal Science Engineering 11: 119-128.

http://www.aloki.hu ● ISSN 1589 1623 (Print) ● ISSN 1785 0037 (Online)
DOI: http://dx.doi.org/10.15666/aeer/1706_1319913217

GROWTH AND MARKETABLE POTATO (*SOLANUM TUBEROSUM* L.) TUBER YIELD IN RESPONSE TO FOLIAR APPLICATION OF SEAWEED EXTRACT AND HUMIC ACIDS

WADAS, W.[1*] – DZIUGIEŁ, T.[2]

[1]*Department of Vegetable Crops, Faculty of Natural Sciences, Siedlce University of Natural Sciences and Humanities, B. Prusa 14, 08-110 Siedlce, Poland*

[2]*Voivodeship Plant Health and Seed Inspection Service, Main Inspectorate of Plant Health and Seed Inspection, Żółkiewskiego 17, 05-075 Warszawa-Wesoła, Poland*

**Corresponding author*
e-mail: wanda.wadas@uph.edu.pl; phone: +48-25-643-1296

(Received 3rd Jun 2019; accepted 2nd Sep 2019)

Abstract. The effect of foliar application of seaweed extracts Bio-algeen S90 (*Ascophyllun nodosum*) and Kelpak SL (*Ecklonia maxina*) and humic and fulvic acids from leonardite HumiPlant on plant growth and marketable tuber yield of early potato crop was investigated. The application of seaweed extracts resulted in a faster rate of plant growth. Bio-algeen S90 affected potato growth more than Kelpak SL. The plants grew taller and produced a greater above-ground biomass. With the use of HumiPlant, stems were shorter but had a similar weight to plants in the cultivation without biostimulant. Biostimulants caused enlargement of the assimilation leaf area, but had no effect on the weight of leaves, leaf weight ratio (LWR) or leaf area ratio (LAR). The yield-increasing effect of biostimulants depended on hydrothermal conditions during potato growth. Seaweed extracts produced better results in a warm and a very wet growing season, whereas humic and fulvic acids produced better results in a cool growing season with drought during the tuber growth period.
Keywords: *biostimulant, plant height, above-ground biomass, assimilation leaf area, leaf area ratio (LAR), leaf weight ratio (LWR)*

Introduction

Potato (*Solanum tuberosum* L.) growth and, as a result, tuber yield depends on the site-specific interaction between cultivar and environment, and on the agronomic practices. Potato growth is influenced by many biotic and abiotic stress factors. In sustainable agriculture, biostimulants have been gaining increasing importance. Biostimulants contain a wide range of bioactive compounds that increase plant stress resistance, which allows better use of the cultivar production potential under the environmental conditions of the cultivar area (Calvo et al., 2014; Bulgari et al., 2015). In field crop production, the most commonly used are seaweed extracts and humic acids (Battacharyya et al., 2015; Canellas et al., 2015).

Many plant growth-stimulating compounds such as auxins, cytokinins, gibberellins, betaines, polyamines, abscisic acid, brassinosteroids and minerals were identified from seaweed. These compounds affect cellular metabolism in treated plants, leading to increased tolerance to abiotic stresses, improved plant growth and crop yield (Craige, 2011; Sharma et al., 2014). Most commercial seaweed products are manufactured from red (*Lithothamnium calcareum*) and brown (*Ascophyllum nodosum*, *Ecklonia maxima*, *Sargassum* spp., and *Durvillaea* spp.) microalgae (Craige, 2011). The plant growth-promoting effects of seaweed extracts have been documented in several agricultural and horticultural crops such as tomato, onion, pepper, carrot, potato, wheat, barley and

http://www.aloki.hu ● ISSN 1589 1623 (Print) ● ISSN 1785 0037 (Online)
DOI: http://dx.doi.org/10.15666/aeer/1706_1321913230

maize. Seaweed extract applied via roots or leaves stimulates plant growth in a species-specific manner. The effect of seaweed extract on plant growth depends on the date and dose of application (Haider et al., 2012; Sharma et al., 2014; Begum et al., 2018).

A study carried out in Finland showed that in long-day conditions characterized by a cool and short growing season, the foliar application of the first seaweed extract SM3 (originally called Sea Magic) had a remarkable effect on potato growth and tuber yield (Kuisma, 1989), whereas a later study carried out in Iraq showed that the foliar application of extracts from brown seaweed *Sargassum* Alga 600 and Sea force 2 promoted potato growth and increased tuber yield (Sarhan, 2011). A positive response of potato plant growth and yield to the foliar application of the extracts from *Ascophyllum nodosum* (Primo, Bio-algeen S90) and *Ecklonia maxima* (Keplak SL) was shown in studies carried out in Pakistan and Poland (Haider et al., 2012; Wierzbowska et al., 2015) and the extracts from *Kappaphycus alvarezii* (K sap) and *Gracilaria edulis* (G sap) in a study carried out in India (Prajapati et al., 2016).

Humic substances are able to produce positive effect on the growth, yield and quality of potato (Verlinden et al., 2009). The biostimulant effects of humic substances extracted from naturally humified organic matter, from composts, or from mineral deposition are characterized by both structural and physiological changes in plants. The activity of humic substances is related to their chemical structure (Calvo et al., 2014; Canellas et al., 2015). Humic acids have been reported to stimulate the growth of such crops as wheat, rice, maize, tomato, cucumber, pepper and potato. The effect of humic acids on plant growth depends on their source and concentration and on the date and method (foliar or soil) of application, as well as the plant species (Calvo et al., 2014; Canellas et al., 2015; Alenazi et al., 2016; Zhang et al., 2017). A strong potato response to the application of humic substances originating from leonardite formations in Canada has been reported (Verlinden et al., 2009). Later studies carried out in Poland, Saudi Arabia and China confirmed the positive effect of humic and fulvic acids on potato growth and on tuber yield and quality (Matysiak and Adamczewski, 2010; Alenazi et al., 2016; Zhang et al., 2017). The results of a study carried out in Korea showed that foliar or soil application of fulvic and humic acids had no clear promotional effects on tuber growth or potato yield (Suh et al., 2014).

The application of humic substances (soluble humic and fulvic acids fractions) and seaweed extracts shows inconsistent, yet a generally positive, effect on plant growth. To date, few studies have been focused on the effects of seaweed extracts and humic acids application on early crop potato culture. In our study it was hypothesised that the stimulation of potato plant growth by seaweed extracts and humic acid application would contribute to increase early potato crops. The assumption was also made that the potato response to foliar application of seaweed extracts and humic acids depends on the potato cultivar and environmental conditions. The aim of the study was to determine the effect of seaweed extracts and humic acid application on plant growth and marketable tuber yield of very early potato cultivars.

Materials and methods

Experimental site and season

The field experiment was carried out in central-eastern Poland - 52°03'N, 22°33'E (*Fig. 1*) during three growing season of the 2012-2014 period, on loamy soil (Luvisol) with an acidic-to-slightly-acid reaction (pH in 1 M KCl from 4.7 to 6.3). The content of

http://www.aloki.hu ● ISSN 1589 1623 (Print) ● ISSN 1785 0037 (Online)
DOI: http://dx.doi.org/10.15666/aeer/1706_1321913230

available phosphorus in the soil ranged from 118 to 144 mg P kg^{-1}, potassium from 124 to 208 mg K ha^{-1} and magnesium from 22 to 51 mg Mg kg^{-1} of soil. In each year of the study, spring triticale was grown as a potato forecrop. Farmyard manure was applied in autumn, at rate of 25 t ha^{-1}, and mineral fertilizers were applied in rates 80 kg N (ammonium nitrate), 35 kg P (superphosphate) and 100 kg K (potassium sulphate) per hectare in spring. Potato cultivation was carried out according to common agronomical practice. Colorado potato beetle (*Leptinotarsa decemlineata*) was controlled using Actara 25 WG (thiametoksam) and Apacz 50 WG (chlotianidine).

Figure 1. *Location of experimental site (http://freeworldmaps.net)*

Plant material and experimental design

The field experiment was established in the split-plot design with three replications. The experimental factors were as follows: (i) – type of biostimulant: control treatment without biostimulant, Bio-algeen S90 – 2 L ha^{-1} at the beginning of leaf development stage BBCH 10-11 and 2 L ha^{-1} after two weeks from first treatment, Kelpak SL – 2 L ha^{-1} at the leaf development stage BBCH 14-16 and 2 L ha^{-1} after two weeks from first treatment, HumiPlant – 2 L ha^{-1} at the leaf development stage BBCH 14-16 and 2 L ha^{-1} after one week from first treatment (*Table 1*); (ii) – potato cultivar: 'Denar', 'Lord', 'Miłek' (Polish cultivars registered on the Common Catalogue of Varieties of Agricultural Plant Species CCV).

Table 1. *Characteristics of biostimulants used in the experiment*

Trade name	Source of biologically active compounds	Plant growth-stimulating compounds
Bio-algeen S90	Seaweed extract *Ascophyllum nodosum*	90 groups of chemical compounds including: amino acids, vitamins, alginic acid and other active components of seaweeds, N - 0.02%, P - 0,006%, K - 0,096%, Ca - 0,31%, Mg - 0,021%, B - 16 mg kg^{-1}, Fe - 6,3 mg kg^{-1}, Cu - 0,2 mg kg^{-1}, Mn - 0,6 mg kg^{-1}, Zn - 1,0 mg kg^{-1}, Mo, Se, Co
Kelpak SL	Seaweed extract *Ecklonia maxima*	Auxin - 11 mg L, cytokinin - 0.031 mg L
HumiPlant	Leonardite extract	Humic acid - 12%, fulvic acid - 6%, K_2O - 3%, Fe, Ca, Mn, S, Mg, B, Mo, Zn, Cu

http://www.aloki.hu ● ISSN 1589 1623 (Print) ● ISSN 1785 0037 (Online)
DOI: http://dx.doi.org/10.15666/aeer/1706_1321913230

In successive years, 6-weeks pre-sprouted seed potatoes were planted on the 12th, 18th and 7th and 4 April, with an in-row spacing of 25 cm and 67.5 cm between rows. The average length of sprouts at the time of planting was 15-20 mm. The plots were six rows wide and 4 m long (96 plants per plot). At the tuber formation stage (BBCH 41-43), the length and weight of stems and weight of leaves and assimilation leaf area were determined. The measurements were made on four successive plants per plot. The assimilation leaf area was measured by the weight method based on the weight of pieces with a known diameter and total weight of leaves per plant (Wadas and Kalinowski, 2017). The leaf weight ratio (LWR) and leaf area ratio (LAR) were calculated. LWR and LAR were calculated as the ratio of the weight of leaves/weight of the whole plant and the ratio of assimilation leaf area/weight of the whole plant, respectively (Pietkiewicz, 1985). Potatoes were harvested 75 days after planting (the end of June). The marketable tuber yield (diameter above 30 mm) was determined.

Statistical analysis

The results of a two-way field experiment were analysed statistically by means of analysis of variance (ANOVA) for the split-plot design. The significance of differences was verified using Tukey's test at $p \leq 0.05$ (*Table 2*).

Table 2. *Effect of experimental factors on potato growth and tuber yield*

Experimental factors	Length of stems	Weight of stems	Leaf area	Weight of leaves	Leaf weight ratio (LWR)	Leaf area ratio (LAR)	Tuber yield
Year (Y)	**	**	**	**	**	**	**
Biostimulant (B)	**	**	**	ns	ns	ns	*
Y × B	*	**	**	ns	ns	ns	*
Cultivar (C)	*	**	**	*	**	**	ns
Y × C	ns	**	**	ns	ns	ns	**
B × C	ns	**	**	*	ns	ns	ns
Y × B × C	*	**	*	ns	ns	ns	ns

*Significant at $p \leq 0.05$, **significant at $p \geq 0.01$, ns: non-significant

Weather conditions

The mean air temperatures in the period of potato growth were above or similar to the long-term average (*Table 3*). In 2012 total precipitation in April-June was similar and in 2013 and 2014 above the long-term average and unevenly distributed during potato growth period.

Table 3. *Mean air temperature and precipitation total in potato growing period*

Years	Temperature (°C)			Rainfalls (mm)		
	April	May	June	April	May	June
2012	8.9	14.6	16.3	29.9	53.4	76.2
2013	7.4	15.3	18.0	36.0	105.9	98.8
2014	9.8	13.5	15.4	45.0	92.7	55.4
Many-year mean (1981-2010)	8.3	12.2	16.8	41.2	53.0	63.8

http://www.aloki.hu ● ISSN 1589 1623 (Print) ● ISSN 1785 0037 (Online)
DOI: http://dx.doi.org/10.15666/aeer/1706_1321913230

The most favourable thermal and moisture conditions for early crop potato culture were in the warm and moderately wet growing season of 2012. 2013 was warm and with a heavy rainfall, whereas 2014 was cool with a heavy rainfall after the plant emergence and a drought in the period of tuber growth.

Results

Length and weight of stems

The type of biostimulant had a significant effect on potato growth (*Table 4*). Following the application of Bio-algeen S90, the stems were longer by 2.3 cm, on average, and the average weight of stems was 40 g higher compared with the control object without the growth stimulant. With the application of Kelpak SL the stem lengths were similar and with the application of HumiPlant they were shorter by 3.3 cm, on average, in comparison with the control object, although the stem weights were not significantly different. The effect of tested biostimulants on plant growth depended on weather conditions during the potato growing season. The type of biostimulant had the greatest effect on plant growth in 2014 with a low air temperature and a heavy rainfall after the plant emergence. In that year, after the application of Bio-algeen S90 the weight of stems was higher by 81 g than the plants from the control object without biostimulant, with a comparable length of stems. Following the application of Keplak SL and HumiPlant, stems were shorter by 3.9 cm and 5.0 cm, respectively, compared with the plants from the control object with comparable stem weights.

Table 4. *Length and weight of stems*

Type of biostimulant	Years			Cultivar			Mean
	2012	2013	2014	Denar	Lord	Miłek	
Length of stems (cm)							
Without biostimulant	63.6 b	59.0 ab	82.5 a	72.1	71.8	61.2	68.4 b
Bio-algeen S90	67.6 a	59.7 a	84.8 a	76.5	77.0	58.7	70.7 a
Kelpak SL	67.4 a	56.8 ab	78.6 b	74.3	72.6	55.9	67.6 b
HumiPlant	61.8 b	55.9 b	77.5 b	71.2	70.1	54.1	65.1 c
Mean	65.1 B	57.9 C	80.9 A	73.5 A	72.9 A	57.5 B	
Weight of stems (g)							
Without biostimulant	306 a	208 a	475 b	371 b	311 b	308 a	330 b
Bio-algeen S90	328 a	225 a	556 a	434 a	396 a	280 ab	370 a
Kelpak SL	350 a	189 a	451 b	374 b	369 a	247 b	330 a
HumiPlant	313 a	183 a	451 b	364 b	318 b	264 ab	315 b
Mean	324 B	201 C	483 A	386 A	348 A	348 A	

Means within columns/rows followed by the same lowercase/uppercase letters do not differ significantly at $p \leq 0.05$

The type of biostimulant and cultivar interaction effect on the length of stems was not statistically confirmed. Bio-algeen S90 had a greater effect on the weight of stems of ‘Denar’ and ‘Lord’ than ‘Miłek’ (*Table 4*). The differences were highest in 2014 with a low air temperature and a heavy rainfall after plant emergence.

http://www.aloki.hu ● ISSN 1589 1623 (Print) ● ISSN 1785 0037 (Online)
DOI: http://dx.doi.org/10.15666/aeer/1706_1321913230

The rate of plant growth depended on the cultivar and weather conditions (*Table 4*). Regardless of the treatment (with or without biostimulant), the length and weight of stems were higher for 'Denar' and 'Lord' than for 'Miłek'. The stems were longest and they had the greatest weight in 2014, with the highest air temperature and moderate rainfall in the second half of May.

Weight of leaves and assimilation leaf area

The biostimulants used in the experiment had no significant effect on the weight of leaves, but caused enlargement of the assimilation leaf area, on average, by 366 cm^2 to 664 cm^2 (*Table 5*). The type of biostimulant and year interaction effect on the assimilation leaf area was statistically confirmed. In 2013 with the highest air temperature and a heavy rainfall after plant emergence, the greatest enlargement of assimilation leaf area, on average by 624 cm^2, was caused by Kelpak SL. In 2014 with the lowest air temperature and a heavy rainfall after plant emergence, following the application of Bio-algeen S90, the assimilation leaf area was larger, on average, by 941 cm^2 than the plants from the control object without a biostimulant, with a comparable weight of leaves.

Table 5. *Weight of leaves and assimilation leaf area*

Type of biostimulant	Years			Cultivar			Mean
	2012	2013	2014	Denar	Lord	Miłek	
Weight of leaves (g)							
Without biostimulant	250	171	282	221 a	204 b	279 a	234 a
Bio-algeen S90	246	177	305	243 a	250 a	235 b	243 a
Kelpak SL	262	167	284	238 a	234 ab	241 b	238 a
HumiPlant	256	159	276	238 a	202 b	251 ab	230 a
Mean	254 B	169 C	287 A	235 AB	222 B	251 A	
Assimilation leaf area (cm^2)							
Without biostimulant	7131 b	5411 b	9438 b	7214 a	6425 b	8341 a	7327 b
Bio-algeen S90	7847 a	5746 ab	10379 a	8120 a	8008 a	7845 a	7991 a
Kelpak SL	7964 a	6035 a	9434 b	7871 a	7636 ab	7926 a	7811 a
HumiPlant	7963 a	5947 ab	9170 b	7592 a	6903 b	8584 a	7693 a
Mean	7726 B	5785 C	9605 A	7699 B	7243 C	8174 A	

Means within columns/rows followed by the same lowercase/uppercase letters do not differ significantly at $p \leq 0.05$

The type of biostimulant applied had a greater effect on the weight and assimilation leaf area of 'Lord' than 'Denar' and 'Miłek' (*Table 5*). Following the application of Bio-algeen S90, the weight of 'Lord' leaves was higher by 46 g, on average, and the assimilation leaf area was larger by 1583 cm^2 as compared with the plants from the control object without biostimulant. The differences were highest in 2014 with a low air temperature and a heavy rainfall after the plant emergence.

Regardless of the biostimulant applied, the weight and the assimilation leaf area were higher for 'Miłek' than for 'Denar' and 'Lord'. The plant growth indices were highest in 2014 with the highest air temperature and a moderate rainfall at the end of May (*Table 5*).

http://www.aloki.hu ● ISSN 1589 1623 (Print) ● ISSN 1785 0037 (Online)
DOI: http://dx.doi.org/10.15666/aeer/1706_1321913230

Leaf weight ratio (LWR) and leaf area ratio (LAR)

The biostimulants used in the experiment had no significant effect on the LWR or LAR (*Table 6*). Following the application of biostimulants, the plant growth indices were similar to the control object without biostimulant.

Table 6. *Leaf weight ratio (LWR) and leaf area ratio (LAR)*

Type of biostimulant	Years			Cultivar			Mean
	2012	2013	2014	Denar	Lord	Miłek	
Leaf weight ratio (g g^{-1})							
Without biostimulant	0.446	0.455	0.380	0.388	0.413	0.480	0.427 a
Bio-algeen S90	0.434	0.449	0.366	0.381	0.398	0.471	0.416 a
Kelpak SL	0.435	0.480	0.403	0.409	0.407	0.503	0.440 a
HumiPlant	0.450	0.469	0.387	0.407	0.405	0.494	0.435 a
Mean	0.441 A	0.463 A	0.384 B	0.396 B	0.406 B	0.487 A	
Leaf area ratio (cm^2 g^{-1})							
Without biostimulant	13.50	16.47	12.60	13.10	13.46	16.01	14.19 a
Bio-algeen S90	13.37	15.83	12.50	12.51	13.27	15.93	13.90 a
Kelpak SL	12.72	17.51	13.41	13.63	13.16	16.85	14.55 a
HumiPlant	13.36	16.60	12.89	12.99	12.82	17.04	14.28 a
Mean	13.24 B	16.61 A	12.85 C	13.06 B	13.18 B	16.46 A	

Means within columns/rows followed by the same lowercase/uppercase letters do not differ significantly at $p \leq 0.05$

The LWR and LAR depended on the cultivar and weather conditions during potato growth (*Table* 6). Regardless of the treatment (with or without biostimulant), the LWR and LAR were higher for 'Miłek' than for 'Denar' and 'Lord'. The plant growth indices were lowest in 2014 with the highest air temperature and a moderate rainfall in the second half of May.

Marketable tuber yield

The productive effects of biostimulants used in the experiment were comparable, which was reflected in an increase in the marketable tuber yield in comparison with the cultivation without biostimulant (*Table 7*). In the three years of the study, the marketable tuber yield was higher by 2.15 t ha^{-1}, on average. The yield-increasing effect of biostimulants depended on weather conditions during the potato growing season.

Table 7. *Marketable tuber yield (t ha^{-1})*

Type of biostimulant	Years			Cultivar			Mean
	2012	2013	2014	Denar	Lord	Miłek	
Without biostimulant	39.49 a	29.75 b	29.34 b	31.84	33.10	33.64	32.86 b
Bio-algeen S90	38.96 a	34.64 a	30.62 b	34.49	35.47	34.26	34.74 ab
Kelpak SL	40.22 a	34.12 a	30.62 b	33.50	35.46	36.00	34.99 a
HumiPlant	41.43 a	31.61 ab	32.83 a	34.95	36.21	34.71	35.29 a
Mean	40.02 A	32.53 B	30.86 C	33.69 A	35.06 A	34.65 A	

Means within columns/rows followed by the same lowercase/uppercase letters do not differ significantly at $p \leq 0.05$

http://www.aloki.hu ● ISSN 1589 1623 (Print) ● ISSN 1785 0037 (Online)
DOI: http://dx.doi.org/10.15666/aeer/1706_1321913230

Bio-algeen S90 and Kelpak SL caused the highest increase in marketable tuber yield in the warm and very wet growing season of 2013. With the use of those biostimulants, the marketable tuber yield was higher by 4.63 t ha^{-1}, on average, in comparison with the cultivation without biostimulant. HumiPlant caused the highest increase in marketable tuber yield in 2014 with a low air temperature and, at the same time, insufficient water supply for plants in the period of tuber growth. In that year, following the application of HumiPlant the marketable tuber yield was higher by 3.49 t ha^{-1}. The type of biostimulant and cultivar interaction effect on marketable tuber yield was not statistically confirmed.

The marketable tuber yields of the tested potato cultivars were similar (*Table 7*). The yield of early potato was highest in the warm and moderately wet growing season of 2012.

Discussion

An analysis of plant growth is important to determine the effect of biostimulants on the crop yielding. In the present study, the type of biostimulant applied significantly affected the growth of very early potato cultivars. A faster rate of plant growth was observed with the use of seaweed extracts, than with the use of humic and fulvic acids. Seaweed extracts have more biostimulant potential due to the presence of phytohormones and a number of other compounds promoting plant growth and strengthening stress resistance (Begum et al., 2018). Among the tested seaweed extracts, Bio-algeen S90 (*Ascophyllum nodosum*) had a greater effect on the rate of plant growth than Keplak SL (*Ecklonia maxima*). Bio-algen S90 have more bioactive compounds than Kelpak SL. Following the Bio-algeen S90 application, the plants were higher and produced a greater above-ground biomass. The positive effect of the foliar application of *Ascophyllum nodosum* extract on the growth of medium-early potato cultivar was also shown in a study carried out in Pakistan (Haider et al., 2012). Following the application of HumiPlant, plants were lower but had a similar weight of stems as in the cultivation without biostimulant, which suggests that the stems were thicker. To date studies showed a generally positive effect of humic acids on potato growth. A study carried out in Iraq and Saudi Arabia showed that the application of humic acid promoted the growth of medium-early potato cultivars (Sarhan, 2011; Alenazi et al., 2016), whereas the results of a study carried out in Korea showed that foliar or soil application of humic and fulvic acids had no clear effect on the growth of medium-early potato cultivar (Suh et al., 2014). A study carried out in China showed that foliar application of fulvic acid increased the stem length and diameter of early potato cultivar and prolonged the plant growth period (Zhang et al., 2017), which was no clear confirmed in the present study. Plant response to exogenously applied humic substances depends on the plant species and its ontogeny and environment conditions. Plant growth response to humic substances obtained from leonardite are less than the response to humic substances obtained from peat, composts or vermicomposts (Canellas and Olivares, 2014). Biostimulants had no effect on the weight of leaves, but caused enlargement of the assimilation leaf area under abiotic stress conditions. In the year with the highest air temperature and a heavy rainfall after plant emergence, the assimilation leaf area was the largest after the application of Kelpak SL, whereas in the year with a lowest air temperature and with a heavy rainfall after plant emergence, the assimilation leaf area was the largest after the application of Bio-algeen S90.

http://www.aloki.hu ● ISSN 1589 1623 (Print) ● ISSN 1785 0037 (Online)
DOI: http://dx.doi.org/10.15666/aeer/1706_1321913230

Biostimulants caused enlargement of the assimilation leaf area, but had no significant effect on the share of assimilation organs in the whole plant weight (LWR) or on the weight per unit leaf area (LAR). These indices are determined by the cultivar and plant growth stage, and by the interaction effect between the cultivar and environment (Pietkiewicz, 1985; Lahlou et al., 2003; Wadas and Kalinowski, 2017), which was confirmed in the present study. The LWR and LAR varied with plant growth, due to potato response to weather changes by falling or new growth of leaves (Pietkiewicz, 1985; Camargo et al., 2015).

The yield-increasing effect of biostomulants depended on the hydrothermal conditions during potato growth. The seaweed extracts Bio-algeen S90 and Kelpak SL produced better results in a warm and a very wet growing season. With the use of those biostimulants, the marketable tuber yield (with diameter above 30 mm) was higher by 15.5% in comparison with the cultivation without biostimulant. Seaweed extracts improve the thermal tolerance of plants (Battacharyya et al., 2015), which was confirmed in the present study. Humic and fulvic acids from leonardite produced better results in a cool growing season and with insufficient water supply for plants in a period of tuber growth. With the use of HumiPlant the marketable tuber yield was higher by 12%. Very early potato cultivars showed a differential response to seaweed extracts. Kelpak SL did not have a significant effect on the marketable tuber yield of very early potato cultivar 'Felka', but caused an increase in the yield of very early cultivar 'Volumia'. In a year with a lower air temperature and less rainfall, Bio-algeen S90 caused a higher increase in the total yield of the very early potato cultivar 'Volumia' than Kelpak SL (Erlichowski and Pawińska, 2003; Wierzbowska et al., 2015). Kelpak SL caused an increase in the total tuber yield of medium-early potato cultivars (Matysiak and Adamczewski, 2010). Kelpak SL contains auxins and cytokinins at the level of 350/1. Exogenous auxin plays an important role in tuber formation and plant stress resistance; however, the action of exogenous auxin depends on its concentration and light conditions. The potato growth response to exogenous auxin depends on the plant genotype and carbohydrate status (Kolachevskaya et al., 2019). Cytokinins also have an important effect of plant adaptation to environmental stresses. Under drought conditions, exogenous cytokinins can increase stomatal apertures and transpiration in plant, and have a positive effect on photosynthetic activity (Ha et al., 2012). In the present study, the type of biostimulant and cultivar interaction effect of early crop potato yield was not statistically confirmed. Positive potato response to humic substances originating from leonardite applied to soil or foliar was confirmed in studies carried out by other authors (Verlinden et al., 2009; Matysiak and Adamczewski, 2010). Under water stress, foliar application of humic acids increased leaf water retention and photosynthetic and antioxidant metabolism (Fahramand et al., 2014). Periods of high temperature and drought are becoming more frequent in Central Europe. In east-central Poland, the shortage of rainfall in the growing season of early potato cultivars occurs more often than their excess (Radzka et al., 2015).

A positive correlation was found between the tuber yield and the number of main stems per plant, stem length and diameter (Arslan, 2007; Darabad, 2014). A significant relationship was also found between the tuber yield and LWR and LAR (Zrůst and Čepl, 1991; Wadas and Kalinowski, 2017). In the present study, following the application of Bio-algeen S90, the plants were higher and produced a greater above-ground biomass than in the cultivation without biostimulant, whereas following the application of HumiPlant the stems were shorter at a similar weight as the control

http://www.aloki.hu ● ISSN 1589 1623 (Print) ● ISSN 1785 0037 (Online)
DOI: http://dx.doi.org/10.15666/aeer/1706_1321913230

plants, which suggests that the stems were thicker. Biostimulants caused enlargement of the assimilation leaf area, but had no effect on the weight of leaves. This suggests that the leaves were thinner following the application of biostimulants. As the result, the biostimulants had no significant effect on the LWR or LAR. It often happens that the enlargement of the assimilation leaf area does not result in an increase in the tuber yield, because the rate of photosynthesis per unit of leaf area decreases with an increase in the leaf area (Pietkiewicz, 1985).

Conclusions

This study showed the possibility of improving plant growth in an early crop potato culture with the foliar application of seaweed extracts *Ascophyllum nodosum* (Bio-algeen S90) and *Ecklonia maxima* (Kelpak SL) and humic and fulvic acids from leonardite (HumiPlant). Seaweed extracts caused a faster rate of potato growth. Bio-algeen S90 had a greater effect on plant growth than Kelpak SL. Following the application of Bio-algeen S90, the plants were higher and produced a greater above-ground biomass than in the cultivation without biostimulant. Following the application of HumiPlant, plants were lower but had a similar weight of stems as plants in the cultivation without biostimulant. This suggests that the stems were thicker. Biostimulants caused enlargement of assimilation leaf area, but had no effect on the weight of leaves, which suggests that the leaves were thinner. As a results, the biostimulants had no effect on the leaf weight ratio (LWR) or leaf area ratio (LAR). The biostimulants caused an increase in the marketable tuber yield of early crop potato. The yield-increasing effect of biostimulants depended on the hydrothermal conditions during potato growth. Seaweed extracts produced better results in a warm and a very wet growing season, whereas humic and fulvic acids produced better results in a cool growing season and with a drought in the period of tuber growth. To use humic substances and seaweed extract for promoting plant growth in early crop potato culture, it is necessary to optimize their source and concentration for environmental conditions to achieve the expected outputs.

Acknowledgements. This study was supported by the Polish Ministry of Science and Higher Education under the statutory activities of the Siedlce University of Natural Sciences and Humanities (grant number 218/05/S).

REFERENCES

[1] Alenazi, M., Wahb-Allah, M. A., Abdel-Razzak, H. S., Ibrahim, A. A., Alsadon, A. (2016): Water regimes and humic acid application influences potato growth, yield, tuber quality and water use efficiency. – American Journal of Potato Research 93(5): 463-473. https://doi.org/10.1007/s12230-016-9523-7.

[2] Arslan, B. (2007): Relationships among yield and some yield characters in potato (*S. tuberosum* L.). – Journal of Biological Sciences 7(6): 973-976. https://doi.org/10.3923/jbs.2007.973.976.

[3] Battacharyya, D., Babgohari, M. Z., Rathor, P., Prithiviraj, B. (2015): Seaweed extracts as biostimulants in horticulture. – Scientia Horticulturae 196: 39-48. https://doi.org/10.1016/j.scienta.2015.09.012.

http://www.aloki.hu ● ISSN 1589 1623 (Print) ● ISSN 1785 0037 (Online)
DOI: http://dx.doi.org/10.15666/aeer/1706_1321913230

[4] Begum, M., Bordoloi, B. C., Singha, D. D., Ojha, N. J. (2018): Role of seaweed extract on growth, yield and quality of some agricultural crops: A review. – Agricultural Reviews 39(4): 321-326. https://doi.org/10.18805/ag.r-1838.
[5] Bulgari, R., Cocetta, G., Trivellini, A., Vernieri, P., Ferrante, A. (2015): Biostimulants and crop response: a review. – Biological Agriculture and Horticulture 31(1): 1-17. https://doi.org/10.1080/01448765.2014.964649.
[6] Calvo, P., Nelson, L., Kloepper, J. W. (2014): Agricultural uses of plant biostimulants. – Plant and Soil 383(1-2): 3-41. https://doi.org/10.1007/s11104-014-2131-8.
[7] Camargo, D. C., Montoya, F., Córcoles, J. I., Ortega, J. F. (2015): Modeling the impact of irrigation treatments on potato growth and development. – Agricultural and Water Management 150: 119-128. https://doi.org/10.1016/j.agwat.2014.11.017.
[8] Canellas, L. P., Olivares, F. L. (2014): Physiological responses to humic substances as plant growth promoter. – Chemical and Biological Technologies in Agriculture 1: 1–11. https://doi.org/10.1186/2196-5641-1-3.
[9] Canellas, L. P., Olivares, F. L., Aguiar, N. O., Jones, D. L., Nebbioso, A., Mazzei, P., Piccolo, A. (2015): Humic and fulvic acids as biostimulants in horticulture. – Scientia Horticulturae 196: 15-27. https://doi.org/10.1016/j.scienta.2015.09.013.
[10] Craige, J. S. (2011): Seaweed extract stimuli in plant science and agriculture. – Journal of Applied Phycology 23(3): 37-393. https://doi.org/10.1007/s10811-010-9560-4.
[11] Darabad, G. R. (2014): Study the relationships between yield and yield components of potato varieties using correlation analysis and regression analysis and causality. – International Journal of Plant, Animal and Environmental Sciences 4(2): 584-589.
[12] Erlichowski, T., Pawińska, M. (2003): Biological evaluation of product Kelpak on potato plants. – Progress in Plant Protection 43(2): 606-609 (in Polish).
[13] Fahramand, M., Moradi, H., Noori, M., Sobhkhizi, A., Adibian, M., Abdollahi, S., Rigi, K. (2014): Influence of humic acid on increase yield of plants and soil properties. – International Journal of Farming and Allied Science 3(3): 339-341.
[14] Ha, S., Vankova, R., Yamaguchi-Shinozaki, K., Shinozaki, K., Tran, L-S. P. (2012): Cytokinins: metabolism and function in plant adaptation to environmental stresses. – Trends in Plant Science 17(3): 172-179. https://doi.org/10.1016/j.tplants.2011.12.005.
[15] Haider, M. W., Ayyub, C. M., Pervez, M. A., Asad, H. U., Manan, A., Raza, S. A., Ashraf, I. (2012): Impact of foliar application of seaweed extract on growth, yield and quality of potato (*Solanum tuberosum* L.). – Soil and Environment 31(2): 157-162.
[16] Kolachevskaya, O. O., Lomin, S. N., Arkhipov, D. V., Romanov, G. A. (2019): Auxin in potato: molecular aspects and emerging roles in tuber formation and stress resistance. – Plant Cell Reports 38: 681-698. https://doi.org/10.1007/s00299-019-02395-0.
[17] Kuisma, P. (1989): The effect of foliar application of seaweed extract on potato. – Journal of Agricultural Science in Finland 61(5): 371-377. https://doi.org/10.23986/afsci.72367.
[18] Lahlou, O., Ouattar, S., Ledent, J. F. (2003): The effect of drought and cultivar on growth parameters, yield and yield components of potato. – Agronomie 23(3): 257-268. https://doi.org/10.1051/agro:2002089.
[19] Matysiak, K., Adamczewski, K. (2010): Effect of Moddus 250 EC, Kelpak SL, Algaminoplant, HumiPlant i Yield Plus on the size and structure of potato tuber yield. – Ziemniak Polski 1: 28-32 (in Polish).
[20] Pietkiewicz, S. (1985): An indicator-based analysis of plant growth. – Wiadomości Botaniczne 29(1): 29-42 (in Polish).
[21] Prajapati, A., Patel, C. K., Singh, N., Jain, S. K., Chongtham, S. K., Maheshwari, M. N., Patel, C. R., Patel, R. N. (2016): Evaluation of seaweed extract on growth and yield of potato. – Environment and Ecology 34(2): 605-608.
[22] Radzka, E., Rymuza, K., Lenartowicz, T. (2015): Analysis of hydrothermal conditions and their impact on early potato yields. – Journal of Ecological Engineering 16(2): 120-124. https://doi.org/10.12911/22998993/1866.

http://www.aloki.hu ● ISSN 1589 1623 (Print) ● ISSN 1785 0037 (Online)
DOI: http://dx.doi.org/10.15666/aeer/1706_1321913230

[23] Sarhan, T. Z. (2011): Effect of humic acid and seaweed extracts on growth and yield of potato plant (*Solanum tuberosum* L.) Desiree cv. – Mesopotamia Journal of Agriculture 39(2): 19-27.
[24] Sharma, H. S. S., Fleming, C., Selby, C., Rao, J. R., Martin, T. (2014): Plant biostimulants: a review on the processing of macroalgae and use of extracts for crop management to reduce abiotic and biotic stresses. – Journal of Applied Phycology 26(1): 465-490. https://doi.org/10.1007/s10811-013-0101-9.
[25] Suh, H. Y., Yoo, K. S., Suh, S. G. (2014): Tuber growth and quality of potato (*Solanum tuberosum* L.) as affected by foliar or soil application of fulvic and humic acids. – Horticulture Environment and Biotechnology 55(3): 183-189. https://doi.org/10.1007/s13580-014-0005-x.
[26] Verlinden, G., Pycke, J., Mertens, J., Debersaques, F., Verheyen, K., Baert, G., Bries, J., Haesaert, G. (2009): Application of humic substances results in consistent increases in crop yield and nutrient uptake. – Journal of Plant Nutrition 32(9): 1407-1426. https://doi.org/10.1080/01904160903092630.
[27] Wadas, W., Kalinowski, K. (2017): Effect of titanium on growth of very early-maturing potato cultivars. – Acta Scientiarum Polonorum, Hortorum Cultus 16(6): 125-138. https://doi.org/10.24326/asphc.2017.6.11.
[28] Wierzbowska, J., Cwalina-Ambroziak, B., Głosek-Sobieraj, M., Sienkiewicz, S. (2015): Effect of biostimulators on yield and selected chemical properties of potato tubers. – Journal of Elementology 20(3): 757-768. https://doi.org/10.5601/jelem.2014.19.4.799.
[29] Zhang, Y., Zhou, Q., Li, Y., Xu, C., He, S., Huang, Y., Yang, H., Wang, M., Liu, L., Tang, M. (2017): Effect of fulvic acid on agronomic traits and yield of autumn potato. – Agricultural Science and Technology 18(8): 1448-1451.
[30] Zrůst, J., Čepl, J. (1991): Dependence of early potato yield on some growth characteristics. – Rostlina Výroba 37: 925-933.

http://www.aloki.hu ● ISSN 1589 1623 (Print) ● ISSN 1785 0037 (Online)
DOI: http://dx.doi.org/10.15666/aeer/1706_1321913230

YIELD AND SUGAR CONTENT OF EUROPEAN MAIZE (*ZEA MAYS* L.) CULTIVARS GROWN IN POLAND

GĄSIORowska, B. – PŁAZA, A. – RZĄŻEWSKA, E.* – WARANICA, M.

Agrotechnology Department, Faculty of Natural Sciences, Siedlce University of Natural Sciences and Humanities, Siedlce, Poland
(e-mails: barbara.gasiorowska@uph.edu.pl; anna.plaza@uph.edu.pl; szur@uph.edu.pl)

**Corresponding author*
e-mail: emilia.rzazewska@uph.edu.pl

(Received 4th Jun 2019; accepted 2nd Sep 2019)

Abstract. The work presents results of a research conducted in 2009-2011 to assess the yield and sugar content of selected maize (*Zea mays* L.) cultivars included in the Common Catalogue of Varieties of Agricultural Plant Species (CCA), harvested at various development stages, which affects the quality of animal feed produced, and select cultivars suitable for cultivation under the soil and climatic conditions of Poland. Two factors were examined in the study: A − the harvest date of maize green matter (I − tasseling stage (75% of plants at this stage), II − milk maturity stage (after three weeks), III − wax maturity stage (after another three weeks)); B − cultivars with different earliness of maturity: Pyroxenia – very early, FAO 130, Codimi – early FAO 200, Moschus – early, FAO 220, Alombo – medium early, FAO 230, and Celive – medium early, FAO 245. Total protein yield, dry matter and starch content, soluble sugars and reducing sugars were determined in maize plants. The obtained study results demonstrated that the highest total protein yield was produced by the following maize cultivars: Codimi, Moschus, Alombo and Celive harvested at the wax maturity stage. The highest starch content was determined in the plants of cv. Pyroxenia, Codimi, Alombo and Celive also harvested at the wax maturity stage. Maize plants of all the examined cultivars harvested at the milk maturity stage and cv. Pyroxeni harvested at the tasseling stage had the highest soluble sugars and reducing sugars.
Keywords: *FAO, harvest date, total protein yield, dry matter, starch*

Introduction

As the cultivation area of maize and the crop's economic importance are increasing, there is also an increase in the demand for better cultivars − hybrids. Nowadays, breeding new maize cultivars makes use of heterosis or hybrid vigour which is displayed in the F_1 generation obtained as a result of crossing maternal and paternal inbred lines (Adamczyk, 2001; Sulewska et al., 2011). According to Jha et al. (1998) and Michalski et al. (2002), the role new cultivars play in modern agriculture is of great importance. In the cultivation of maize, breeding of new cultivars is developing dynamically, so it is advisable to study new cultivars recommended for cultivation in Poland, as well as from the CCA Community Catalog with neighboring countries. Thus, it is could prove beneficial to examine new cultivars originating from neighbouring countries and grown under the soil and climatic conditions of Poland. Both yielding and chemical composition of maize green feed are cultivar-related (Korniewicz et al., 2000; Ptaszyńska and Sulewska, 2008; Lynch et al., 2012). In their experiments, Filya (2004) and Komainda et al. (2018) observed that the greatest changes in organic matter chemical composition are associated with maize development stages. The more the harvest date is delayed, the higher increase in soluble sugars and starch content, and the lower the protein content of maize plants. Their contents are the highest when maize plants are at the milk maturity stage. The paucity of Polish literature on the subject

http://www.aloki.hu ● ISSN 1589 1623 (Print) ● ISSN 1785 0037 (Online)
DOI: http://dx.doi.org/10.15666/aeer/1706_1323113238

provided an incentive to conduct this research. Its objective was to assess yielding and sugar content in maize plants of selected cultivars included in the Common Catalogue of Varieties of Agricultural Plant Species (CCA), harvested at various development stages which affect the quality of animal feed produced, and select cultivars suitable for cultivation under the soil and climatic conditions of Poland.

Materials and methods

Field studies were conducted in 2009-2011 on a private holding located in Kowiesy near Siedlce (52° 03' 39" N, 22° 33' 80" E). The field trial was set up on the soil classified as Albic Luvisol (Arenic) characterised by a slight acidity and average available phosphorus, potassium and magnesium contents. The soil's humus content was 1.28%. The experiment was arranged as a split-plot design with three replicates. The area of one plot was 30 m^2. The following two factors were investigated: A − maize green matter harvest date (I − tasseling stage (75% of plants at this stage), II − milk maturity stage (after three weeks), III − wax maturity stage (after another three weeks)); B − cultivars with different earliness of maturity (Pyroxenia – very early FAO 130, Codimi – early FAO 200, Moschus – early FAO 220, Alombo – medium early FAO 230, Celive – medium early FAO 245; *Table 1*). The number of plants per 1 m was 10, and the sowing rate was established based on previous research by Sulewska (2001). Inter-row widths were 0.8 m. Maize was grown in monoculture. In the autumn, cattle manure was applied at the rate of 30 t ha^{-1}.

Table 1. *Characteristics of studied cultivars*

Cultivar	Earliness of maturity	Number FAO
Pyroxenia	Very early	130
Codimi	Early	200
Moschus	Early	220
Alombo	Medium early	230
Celive	Medium early	245

In spring, phosphorus and potassium fertilisers were applied at rates matching soil contents of available elements, that is 60 kg P ha^{-1} and 90 kg K ha^{-1}. Nitrogen fertiliser was applied pre-plant at the rate of 92 kg N ha^{-1} in the spring and followed by maize, the nitrogen rate being increased due to an application of Polifoska 6. Seeds of the examined cultivars were planted in late April. Cv. Pyroxenia (bred by Trnava s.r.o. Slovakia, three-way cross (Tc)) is a hybrid characterised by extreme earliness, a high share of cobs in the yield structure, resistance to increased stand density and rapid increase in cob dry matter. Cv. Codimi (bred by Codimes, France, Tc) is an early maturing variety with a classical stay-green trait, rapid initial growth and a high share of grain dry matter in silage. Its plants are of medium height developing an abundance of wide leaves. Cv. Moschus (bred by Freiherr von Moreau Saatzucht GmbH, Germany, modified three-way cross (MTc)) is an early maturing multiple-use variety displaying the stay-green trait. It produces high yields of grain which easily releases water. Cv. Alombo (bred by Freiherr von Moreau Saatzucht GmbH, Germany, single cross (Sc)) is a multiple-use variety suitable for both grain and silage production even under poorer soil conditions. It has a high yield-production potential and good healthiness. Cv. Celive

http://www.aloki.hu ● ISSN 1589 1623 (Print) ● ISSN 1785 0037 (Online)
DOI: http://dx.doi.org/10.15666/aeer/1706_1323113238

(bred by Cezea a.s., Czech Republic, Sc) is an early maturing hybrid suitable for grain production, cold-tolerant, producing high grain yields, which is indicative of high quality of silage produced from its green matter. The green matter of maize crop was harvested at three dates as set in the methodology. The plant matter was sampled to determine dry matter content, total protein content, starch content, soluble sugars and reducing sugars by means of near infrared spectroscopy (NIRS) using the spectrometer NIR Flex N-500. The analyses were performed at the certified laboratory of the Institute of Technology and Life Sciences in Falenty.

The results of the research were statistically analysed; ANOVA following the linear model for a two factor split-plot design was performed for each characteristic examined, and separation of means was obtained by means of Tukey test at the significance level of 0.05. All the calculations were performed in STATISTICA®, version 12.0 and MS Excel.

The studies were carried out on lessive soil. Maize was grown in monoculture. Nitrogen at a dose of 92 N kg ha $^{-1}$ was applied in spring before sowing maize in the form of urea for the tilling set, the additional nitrogen dose was increased by the use of mineral fertilizer in the form of Polifoska 6. Phosphorus at a dose of 60 P kg ha $^{-1}$ and potassium at a dose of 90 K kg ha $^{-1}$ was applied in the form of multi-component mineral fertilizer-Polifoska 6 in spring.

Weather conditions in the 2009 growing season were moderately favorable for the proper vegetation of corn plants. During the growing season of 2010, weather conditions favored the growth, development and yielding of maize. The vegetation season of 2011 was varied in terms of both rainfall and temperature.

Results

The total protein yield of maize plants

Total protein yield of maize plants varied significantly due to the impact of the experimental factors and their interaction (*Table 2*).

Table 2. *Total protein yield of maize plants (means across 2009-2011), kg ha^{-1}*

Cultivars (B)	**Harvest date (A)**			**Means**
	I	**II**	**III**	
Pyroxenia	656b	1152a	1419b	1076B
Codimi	773a	1068b	1598a	1146A
Moschus	690a	1221a	1624a	1179A
Alombo	878a	1336a	1768a	1327A
Celive	794a	1189a	1755a	1246A
Średnie	758C	1193B	1633A	-
ANOVA	**P-value**		**$LSD_{0.05}$**	
Harvest date (A)	< 0.001		223	
Cultivars (B)	< 0.001		223	
Interaction (AxB)	< 0.001		230	

Values in columns followed by the same small letter and values in rows followed by the same capital letter do not differ significantly at P < 0.05

http://www.aloki.hu ● ISSN 1589 1623 (Print) ● ISSN 1785 0037 (Online)
DOI: http://dx.doi.org/10.15666/aeer/1706_1323113238

The highest total protein yield was produced by maize plants harvested at the wax maturity stage, it being significantly lower at the milk maturity stage and the lowest at the tasseling stage. Cultivars had a significant influence on total protein yield. The yield produced by cv. Codimi, Moschus, Alombo and Celive was the highest and differed insignificantly between the cultivars, it being significantly lower for cv. Pyroxenia only. An interaction between the experimental factors was determined which indicated that the highest total protein content was produced by cv. Codimi, Moschus, Alombo and Celive harvested at the wax maturity stage, it being the lowest for all the examined cultivars harvested at the tasseling stage.

The dry matter content in maize plants

Statistical analysis revealed a significant influence of the experimental factors and their interaction on dry matter content in maize plants (*Table 3*).

Table 3. *Dry matter content in maize plants (means across 2009-2011), g kg^{-1}*

Cultivars (B)	**Harvest date (A)**			**Means**
	I	**II**	**III**	
Pyroxenia	142.1a	243.4a	361.4a	249.0A
Codimi	137.2a	247.4a	356.8a	247.2A
Moschus	131.3a	238.9a	330.3b	233.5A
Alombo	134.1a	216.1b	341.6a	230.6A
Celive	135.8a	218.2b	325.0b	226.3B
Średnie	136.1C	232.8B	343.0A	-
ANOVA	**P-value**		**$LSD_{0.05}$**	
Harvest date (A)	< 0.001		20.1	
Cultivars (B)	< 0.001		20.2	
Interaction (AxB)	< 0.001		23.0	

Values in columns followed by the same small letter and values in rows followed by the same capital letter do not differ significantly at P < 0.05

The highest dry matter content was recorded for maize plants harvested at the wax maturity stage, it being significantly lower at the milk maturity stage and the lowest at the tasseling stage. Cultivars significantly affected dry matter content in maize plants, as well. The highest dry matter content was determined in maize cv. Pyroxenia, Codimi, Moschus and Alombo, it being the lowest in the green matter of maize cv. Celive. An interaction between the experimental factors was confirmed indicating that the highest dry matter content was found in maize plants of cv. Pyroxenia, Codimi, Moschus and Alombo harvested at the wax maturity stage, it being the lowest for all the cultivars harvested at the tasseling stage.

The starch content in maize plants

Starch content in maize plants was significantly affected by harvest date, cultivars and their interaction (*Table 4*).

http://www.aloki.hu ● ISSN 1589 1623 (Print) ● ISSN 1785 0037 (Online)
DOI: http://dx.doi.org/10.15666/aeer/1706_1323113238

Table 4. *Starch content in maize plants (means across 2009-2011), g kg^{-1} d.m.*

Cultivars (B)	Harvest date (A)			Means
	I	II	III	
Pyroxenia	32.0a	280.2a	401.5a	237.8A
Codimi	67.0a	198.8b	394.0a	219.9A
Moschus	50.7a	189.8b	348.7b	196.4B
Alombo	40.6a	159.0c	356.1a	185.2B
Celive	51.7a	176.5b	359.9a	196.0B
Średnie	48.4C	200.8B	372.0A	-
ANOVA	**P-value**		**LSD$_{0.05}$**	
Harvest date (A)	< 0.001		26.2	
Cultivars (B)	< 0.001		32.3	
Interaction (AxB)	< 0.001		48.0	

Values in columns followed by the same small letter and values in rows followed by the same capital letter do not differ significantly at P < 0.05

The highest starch content was recorded in maize plants harvested at the wax maturity stage, it being significantly lower at the milk maturity stage and the lowest at the tasseling stage. Cultivars had a significant influence on starch content in maize plants. The highest starch content was determined in the maize plants of cv. Pyroxenia and Codimi, it being significantly lower in cv. Moschus, Alombo and Celive. An interaction between the experimental factors was confirmed: the highest starch content was recorded in maize plants of cv. Pyroxenia, Codimi, Alombo and Celive harvested at the wax maturity stage, and the lowest for all the examined cultivars harvested at the tasseling stage.

The soluble sugars in maize plants and reducing sugars in maize plants

Statistical analysis demonstrated a significant effect of harvest date and an interaction between harvest dates and cultivars on soluble sugars and reducing sugars in maize plants (*Tables 5* and *6*).

Table 5. *Soluble sugars in maize plants (means across 2009-2011), g kg^{-1} d.m.*

Cultivars (B)	Harvest date (A)			Means
	I	II	III	
Pyroxenia	80.7a	72.1b	33.8b	62.2
Codimi	53.6b	78.5b	39.0b	57.0
Moschus	53.6b	81.3a	50.0a	61.6
Alombo	50.6b	85.6a	55.4a	63.9
Celive	56.3b	82.4a	48.5a	62.4
Średnie	58.9B	80.0A	45.3C	-
ANOVA	**P-value**		**LSD$_{0.05}$**	
Harvest date (A)	< 0.001		9.7	
Cultivars (B)	-		r.n.	
Interaction (AxB)	< 0.001		19.4	

Values in columns followed by the same small letter and values in rows followed by the same capital letter do not differ significantly at P < 0.05

http://www.aloki.hu ● ISSN 1589 1623 (Print) ● ISSN 1785 0037 (Online)
DOI: http://dx.doi.org/10.15666/aeer/1706_1323113238

Table 6. *Reducing sugars in maize plants (means across 2009-2011), g kg^{-1} d.m.*

Cultivars (B)	Harvest date (A)			Means
	I	II	III	
Pyroxenia	51.3a	51.6a	28.7b	43.8
Codimi	43.6a	56.2a	32.1b	44.0
Moschus	42.5b	54.0a	38.6a	45.1
Alombo	42.1b	56.4a	39.1a	45.9
Celive	44.7a	56.7a	41.5a	47.6
Średnie	44.8B	55.0A	36.0C	-
ANOVA	**P-value**		**LSD$_{0.05}$**	
Harvest date (A)	< 0.001		3.0	
Cultivars (B)	-		r.n.	
Interaction (AxB)	< 0.001		7.8	

Values in columns followed by the same small letter and values in rows followed by the same capital letter do not differ significantly at P < 0.05

The largest amounts of soluble sugars and reducing sugars were found in maize plants harvested at the milk maturity stage, them being significantly lower at the tasseling stage and the lowest at the wax maturity stage. An interaction between the experimental factors was confirmed which indicated that the highest amounts of soluble and reducing sugars were characteristic of all the experimental maize cultivars harvested at the milk maturity stage and cv. Pyroxenia plants harvested at the tasseling stage. The lowest soluble sugar contents were determined for maize plants of cv. Pyroxenia, Codimi, Moschus and Celive harvested at the wax maturity stage whereas reducing sugars were the lowest for cv. Pyroxenia and Codimi harvested at the same maturity stage.

Discussion

Maize is a crop plant which provides bulky feed produced in ploughed fields and characterised by many beneficial characteristics, Animal feed produced from the whole plants has a high energy value but a low protein content (Brzóska, 2001; Schittenhelm, 2008). In the present study, the highest total protein yield was obtained from maize plants harvested at the wax maturity stage, which was due to the highest dry matter yield. Similar findings were reported by Stejskalove et al. (2013), Magalhães et al. (2015) and Nowab et al. (2017) who demonstrated that a delay in the harvest of maize plants contributed to an increase in total protein yield. In the study discussed here, cultivars affected the total protein yield, too. Cv. Codimi, Moschus, Alombo and Celive were superlative in terms of total protein yield. Similar relationships were observed by Verbic et al. (1997). In the present work, cv. Pyroxenia produced the lowest total protein yield because it is flint type which has the shortest growing season.

Similarly to Magalhães et al. (2015) and Podkówka et al. (2015), in the experiment presented here a delay in maize harvest was followed by an increase in dry matter. Cultivars had a significant effect on dry matter content in maize plants. The highest concentration of this component was recorded in maize plants of cv. Pyroxenia, Codimi, Moschus and Alombo. Celive was the cultivar with the lowest dry matter content. Also

http://www.aloki.hu ● ISSN 1589 1623 (Print) ● ISSN 1785 0037 (Online)
DOI: http://dx.doi.org/10.15666/aeer/1706_1323113238

Magalhães et al. (2015) found the lowest dry matter content in maize plants of cv. Celive characterised by the longest growing season.

In the present work, the highest starch content was recorded in maize plants harvested at the wax maturity stage. The results are similar to those reported by other authors (Tolera et al., 1998; Yuxiang et al. (2007). When harvest was delayed, there was observed an increase in starch content in the dry matter of green feed, which is closely correlated with maize maturity stage. In the experiment discussed here, significant differences were found between starch content in the dry matter of maize plants representing the experimental cultivars. The concentration of starch was higher in the dry matter of two early maize cultivars, that is Pyroxenia and Codimi. Also Tolera et al. (1999), Strzetelski et al. (2001) and Szempliński et al. (2009) mentioned that starch content was higher in the dry matter of earlier maturing maize cultivars.

In the current work, there was confirmed a significant effect of maize harvest date on soluble sugars and reducing sugars in the plants. The highest concentration of the sugars in the dry matter of maize green matter was recorded when plants had been harvested at the milk maturity stage. A delay in harvest until plants reached the wax maturity stage contributed to a decline in soluble sugars and reducing sugars, and an increase in starch content. The above relationship was also reported by Lynch et al. (2012) and Magalhães et al. (2015). Maize harvest at the wax maturity stage is associated with the highest starch content, which contributes to the production of the best quality silage. Of the examined cultivars, early representatives, that is Pyroxenia adn Codimi, had the most beneficial chemical composition of green matter.

A new approach to the problem to examine cultivars from neighboring international countries in Poland's soil and climate conditions. New cultivars such as Pyroxenia and Codimi are available for cultivation in Poland and provide the best feed.

Conclusions

(1) The highest total protein content was produced by maize cv. Codimi, Moschus, Alombo and Celive harvested at the wax maturity stage. Maize cv. Pyroxenia, Codimi, Moschus and Alombo harvested at the wax maturity stage had the highest dry matter content.

(2) The highest starch content was recorded in maize cv. Pyroxenia, Codimi, Alombo and Celive harvested at the wax maturity stage.

(3) All the examined maize cultivars harvested at the milk maturity stage, and cv. Pyroxenia harvested at the tasseling stage produced the highest amounts of soluble sugars and reducing sugars.

(4) It is necessary to continue research on the cultivation of new cultivars from the CCA community catalogue in Polish soil and climate conditions.

REFERENCES

[1] Adamczyk, J. (2001): The importance of selecting varieties in the cultivation of maize for grain and silage. – Biul. Inf. IŻ - R. XXXIX(1): 29-35 (in Polish).

[2] Brzóska, F. (2001): Nutritional value of fodder from corn. – Biul. Inf. IŻ, R. XXXIX(1): 37-48 (in Polish).

[3] Filya, I. (2004): Nutritive value and aerobic stability of whole crop maize silage harvested at four stages of maturity. – Anim. Feed Sci. Tech. 116: 141-150.

http://www.aloki.hu ● ISSN 1589 1623 (Print) ● ISSN 1785 0037 (Online)
DOI: http://dx.doi.org/10.15666/aeer/1706_1323113238

[4] Jha, P. B., Ghosh, J., Nirala, R. B. P. (1998): Genetic variability and character association in fodder maize. – J. Res. Birsa Agric. Univ. 10(2): 139-143.
[5] Komainda, M., Taube, F., Klub, C., Antje, H. (2018): The effects of maize (Zea Mays L.) hybrid and harvest date on above-and belowground biomass dynamics, forage yield and quality - a trade-off for carbon inputs? – Eur. Jour. Agron. 92: 51-62.
[6] Korniewicz, A., Kosmala, I., Czarnik-Matusewicz, H., Paleczek, B. (2000): The contents of basic nutrients in the grain of different maize hybrids. – Rocz. Nauk Zoot. 27(1): 289-303 (in Polish).
[7] Lynch, J. P., O'Kiely, P., Doyle, E. M. (2012): Yield, quality and ensilage characteristics of whole-crop maize and of the cob and stover components: harvest date and hybrid effect. – Grass Forage Sci. 67(4): 472-487.
[8] Magalhães, A., Rolim, M., Duarte, A., Pedrosa, E., Silva, E. (2015): Chemical attributes of soil and dry mass accumulation of maize fertilized with cassava wastewater. – Engen. Agric. 35(3): 458-469.
[9] Michalski, T., Kruczyńska, H., Kowalik, I. (2002): Yields and quality of ensilaging maize depending on the cultivar and mowing height at harvested. – Acta Sci. Pol. Agric. 1(2): 83-92.
[10] Nawab, A., Anjum, M. M. (2017): Effect of different nitrogen rates on growth, yield and quality of maize. – Mid. East Jour. Agric. Res. 6(1): 107-112.
[11] Podkówka, L., Podkówka, Z., Piwczyński, D., Buko, M. (2015): Effect of cultivar earliness on chemical composition and digestibility of maize grain. – Rocz. Nauk Zoot. 42(2): 155-169 (in Polish).
[12] Ptaszyńska, G., Sulewska, H. (2008): Yield variation of maize hybrids with different growing period in climatic conditions of Central Wielkopolska region. – Acta Sci. Pol. Agric. 7(3): 93-103 (in Polish).
[13] Schittenhelm, S. (2008): Chemical composition and methane field of maize hybrids with contrasting maturity. – Eur. Jour. Agron. 29(2-3): 72-78.
[14] Sulewska, H. (2001): Yielding and nutritive value of maize harvested on green mass depending on some agrotechnical factors. – Rocz. AR Poznań. Rozp. nauk. 315 (in Polish).
[15] Sulewska, H., Adamczyk, J., Rejek, D. (2011): Evaluation of the yield of new hybrids of fodder maize (Zea Mays L.) of Smolice breeding. – Nauka Przy. Tech. 5(1): 1-11.
[16] Stejskalova, M., Hejcmanova, P., Hejcman, M. (2013): Forage value of leaf fodder main European broad-leaved woody species. The role of grassland in a green future. – Grassl. Sci. Europe 18: 85-87.
[17] Strzetelski, A., Jurkiewicz, A., Strzetelski, J. (2001): Maize silage in cattle feed. – Biul. Inf. Inst. Zoot. 39(1): 49-62 (in Polish).
[18] Szempliński, W., Bogucka, B., Wróbel, E. (2009): Suitability of early and mid-early maize hybrids grown in the province of Warmia and Mazury for silage production. – Acta Sci. Pol. Agric. 8(1): 57-68 (in Polish).
[19] Tolera, A., Sundstolb, F., Saidc, A. (1998): The effect of stage of maturity on yield and quality of maize grain and stover. – Anim. Feed Sci. Tech. 75(2): 157-168.
[20] Tolera, A., Berg, T., Sundstolb, F. (1999): The effect of variety on maize grain and crop residue yield and nutritive value of the stover. – Anim. Feed Sci. Technol. 79(3): 165-177.
[21] Verbic, J., Babnik, D., Gregorcic, A., Kmetic, M. (1997): Morphology and chemical composition of two maize hybrids and their influence on silage quality. – Zb. Biotech. Fak. Univ. v Ljubljani Kmetijstvo 70: 175-185.
[22] Yuxiang, Ch., Jing, Ch., Daowei, Z. (2007): Effect of harvest date on shearing force of maize stems. – Liv. Sci. 111(1): 33-44.

http://www.aloki.hu ● ISSN 1589 1623 (Print) ● ISSN 1785 0037 (Online)
DOI: http://dx.doi.org/10.15666/aeer/1706_1323113238

STUDY ON THE NICKEL ADSORPTION CHARACTERISTICS OF LAKE SEDIMENTS AND SOIL

MA, X.[1#] – SUN, J.[1#] – REN, L.[2#] – GUO, M.[1] – WANG, Y.[1*] – HAN, X.[1]

[1]*College of Resources and Environment, Jilin Agricultural University, 130118 Changchun, China*

[2]*Hebei Puni Testing Technology Co., Ltd., 050011 Shijiazhuang, China*

**Corresponding author*
e-mail: 951254609@qq.com; phone: 86-135-0441-9456

[#]*These authors contributed equally to this work*

(Received 5th Jun 2019; accepted 3rd Sep 2019)

Abstract. The test adopted the OECD (Organisation for Economic Co-operation and Development) guideine106 equilibrium adsorption method (Bian et al., 2016), to explore the Ni adsorption behavior of the bottom sediment and black soil of the lake. The isothermal adsorption curve of Ni on sediment and black soil retained an "S" shape, and the Freundlich model and D-R model could sufficiently fit the adsorption of Ni by sediment and soil, and the correlation coefficient r was 0.9859~0.9963; Within 120 min, the adsorption amount of nickel in the sediment and soil reached 99.57% and 99.84% of the total adsorption amount, respectively, and reached equilibrium after 720 min. The final desorption amounts of Ni in sediments and soil accounting for 1.26% and 1.35% of the adsorption amounts, respectively. The amount of Ni adsorbed in the sediment increases with rising temperature, and the adsorption coefficient changes in the following manner: K_f 15 °C < K_f 25 °C < K_f 35 °C, Δ G < 0. The adsorption process of nickel on sediment and soil is spontaneous and high temperature is beneficial to this process. The removal of organic matter from sediment and soil weakened the adsorption of nickel, indicating that organic matter could improve the interception of nickel.
Keywords: *sediment, soil, Ni, adsorption, desorption*

Introduction

The content of nickel (Ni) on the earth ranks the fifth, and it generally exists in the form of ore in nature, and the Ni in the natural water body is basically in the form of sulfide and nitrate (Prithviraj et al., 2014). On October 27, 2017, the World Health Organization's International Agency for Research on Cancer announced that Ni is a class of carcinogen, which can lead to a variety of cancer lesions, such as rectal cancer, oral cancer (De Brouwere et al., 2012). Ni is non-biodegradable and persistent, and is easily enriched in soil and organisms, posing a serious threat to human health. In recent years, with the development of economy and society and the acceleration of industrialization, heavy metal pollution has become a global environmental pollution problem, especially the pollution of heavy metals to the soil environment (Kashulina et al., 2018; Abdelwaheb et al., 2017). A large amount of Ni is released into the environment through mining, atmospheric deposition, fertilizer and pesticide application, and sludge and sewage are irrigated into the soil. The Ni accumulated in the soil may remain in the soil and enter crops through planting and other agricultural activities, or enter water bodies through leaching. Part of the pollutants in the water will enter the sediment of the lake through the action of particle adsorption and sedimentation, which makes the sediment become the important "source" and "sink" of the pollutants, which will produce endogenous pollution. The sediment is an important part of the aquatic ecosystem. Heavy metal pollution can cause great harm to

http://www.aloki.hu ● ISSN 1589 1623 (Print) ● ISSN 1785 0037 (Online)
DOI: http://dx.doi.org/10.15666/aeer/1706_1323913251

aquatic organisms, and thus cause harm to human body and ecosystem (Vukosav et al., 2014). Adsorption of soil and sediment can affect Ni mobility and bioavailability, thus playing a key role in reducing further risks to the environment and humans.

Riparian belt is a transition zone between land and river, and it is an important hub connecting aquatic ecosystem and terrestrial ecosystem. Human agricultural activities are the main source of sediment input to rivers. During rainstorms, a large amount of soil, silt and other materials are transported into rivers through surface runoff, so the sediment and the shore soil have a certain correlation on the components (Zhang et al., 2018). Therefore, it is necessary to study the adsorption characteristics of nickel in sediment and shore soil, and to understand the distribution law of metal nickel between solid and liquid phases. At present, there has been some research on the adsorption of Ni in soil, Sangiumsak (2014) investigates the adsorption of Ni and Zn on different kinds of soils found in the Northeastern Thailand as silty soil and sandy soil. Peng (2017) studied the adsorption and desorption characteristics of heavy metals in soil by soil organic matter and mineral composition, and found that SOM seems to play the most important role in soil adsorption of metal Ni. At present, there are many researches on soil adsorption of heavy metals, but few researches on the comparison between soil and sediment. This paper focuses on the evaluation of the adsorption potential of heavy metal nickel in sediments and soil, and provides theoretical guidance for the prevention of heavy metal contamination of groundwater in soil and sediment.

Materials and methods

Samples for test

Sample collection and basic physical and chemical properties

The tested sediment was taken from Xinlicheng reservoir, Changchun city, Jilin Province, China. The Xinlicheng Reservoir (125°42’57”E, 43°42’57”N) is located in the middle and upper reaches of the Yitong River, 16 km from the center of Changchun. On May 24, 2017, grab dredger was used to collect the surface layer (0-10 cm) sediments of Xinlicheng reservoir. A sampling point was set at the upstream, middle and downstream of the reservoir, and repeated collection was made for three times. After the collected samples were mixed, and after air drying in the room, impurities such as animal and plant residues and stones were removed, and then ground through a 100 mesh sieve and stored for use (Duan et al., 2016). The tested soil was taken from the soil around the entrance of Xinlicheng reservoir. After removing the plants and rocks on the soil surface, five-point sampling method was used to collect the surface soil of 0~20 cm (Wu et al., 2017). The collected samples were naturally dried, removed animal and plant residues, stones and other impurities, and ground through a 100-mesh sieve for preservation. Sampling points are shown in *Figure 1*. The basic physical and chemical properties of samples were shown in *Table 1*.

Table 1. *Physicochemical properties of test samples*

Sample	Unit weight ($g \cdot m^{-3}$)	OM (g/kg)	TN (%)	TP (%)	Ni ($mg \cdot kg^{-1}$)	Mechanical composition (%)			
						Sand	Coarse silt	Fine silt	Clay
Sediment	1.79	41.23	0.15	0.12	29.93	10.48	33.97	24.12	31.43
Black soil	1.65	34.65	0.12	0.09	21.10	4.84	51.43	22.96	20.77

http://www.aloki.hu ● ISSN 1589 1623 (Print) ● ISSN 1785 0037 (Online)
DOI: http://dx.doi.org/10.15666/aeer/1706_1323913251

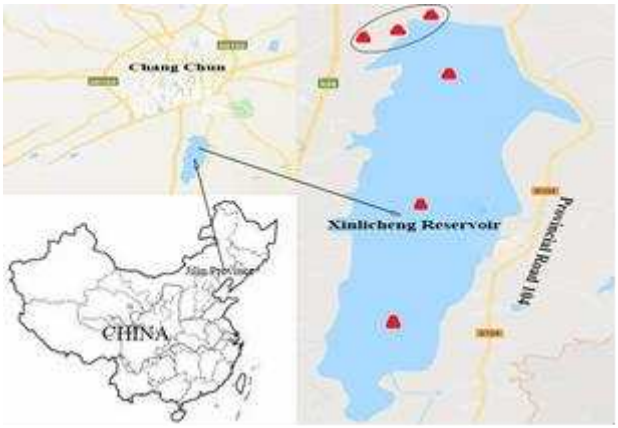

Figure 1. *Schematic diagram of the location of Xinlicheng Reservoir in Changchun City, China*

Test design

Ni isotherm adsorption-desorption

The experiment was conducted with reference to the OECD guideline106 equilibrium adsorption test (OECD). The 1.000 ± 0.0005 g soil samples were taken in 50 ml polyethylene centrifuge tubes, according to the water-soil ratio of 20:1, added 20 ml solution containing different concentrations of Ni background, make the concentration of Ni respectively, 50, 100, 200, 300, 400, 500 $mg \cdot L^{-1}$, after shaking at a constant temperature at 25 °C until adsorption equilibrium, it was centrifuged at 4000 $r \cdot min^{-1}$ for 10 min, filtered, and the concentration of Ni in the supernatant was measured. Immediately after the adsorption, the desorption test was carried out, after removing all the supernatant, added 20 ml deionized water at 25 °C under constant temperature oscillation to desorption balance, and the concentration of Ni in the supernatant was determined.

Adsorption kinetics of Ni

According to the test method in Ni isothermal adsorption-desorption. Added 100 $mg \cdot L^{-1}$ Ni background solution 20 ml for constant temperature oscillation at 25 °C. Samples were taken at the time of 1, 5, 10, 20, 30, 60, 120, 240, 360, 480, 720 and 1440 min, respectively, and centrifuged at 4000 $r \cdot min^{-1}$ for 10 min, then filtered and determined the Ni concentration in the supernatant.

Ni adsorption thermodynamics

According to the test method in Ni isothermal adsorption-desorption. Five Groups of 20 ml solution with Ni concentration of 50, 100, 200, 300, 400 and 500 $mg \cdot L^{-1}$ were prepared, which were placed at 15 °C, 25 °C, 35 °C constant temperature to oscillate to adsorption equilibrium, centrifuged at 4000 $r \cdot min^{-1}$ for 10 min, and filtered to determine the concentration of Ni in the supernatant.

Effects of different organic matter contents on Ni adsorption behavior

The organic matter in the sample was removed by H_2O_2 digestion method, and the experiment was conducted with reference to Ni adsorption thermodynamics.

http://www.aloki.hu ● ISSN 1589 1623 (Print) ● ISSN 1785 0037 (Online)
DOI: http://dx.doi.org/10.15666/aeer/1706_1323913251

All tests were performed in triplicate.

Data processing

Freundlich equation:

$$lg\ q_\varepsilon = lg\ K_f + lg\ C_\varepsilon^{\frac{1}{n}} \quad \text{(Eq.1)}$$

D – R equation:

$$ln\ q_\varepsilon = ln\ q_m - k\varepsilon^2 \quad \text{(Eq.2)}$$

Elovich equation:

$$C = a + b\ ln\ t \quad \text{(Eq.3)}$$

Parabolic diffusion equation:

$$\frac{C}{C_{Ni}} = a + bt^{\frac{1}{2}} \quad \text{(Eq.4)}$$

In *Equation 1,* lgK_f and 1/n respectively represent the adsorption capacity and adsorption strength of the sample to Ni; In *Equation 2,* q_m is the maximum adsorption capacity, K is a constant for the adsorption energy, ε is the adsorption potential of Polanyi. In *Equations 3* and *4:* C_{Ni} and C are the equilibrium adsorption capacity and the adsorption capacity at time t, respectively $mg \cdot kg^{-1}$; a is the adsorption constant related to the maximum adsorption amount, and b is the adsorption rate coefficient, which is a measure of how fast the reaction rate decreases with time. R value represents the correlation coefficient between variables in the sample, and the magnitude of correlation; P value is the test value, which is to test whether the two variables have the same correlation with the samples in the population from which the samples come, and $p < 0.01$ means extremely significant correlation.

Results and discussion

Adsorption-desorption isothermal behavior of Ni in sediment and black soil and its discussion

Adsorption isotherm of Ni in sediment and black soil

Adsorption isotherms of sediment and black soil on Ni are shown in *Figure 2*. It can be seen from *Figure 2* that in the experimental concentration range, when the initial concentration of Ni changes from 50 $mg \cdot L^{-1}$ to 500 $mg \cdot L^{-1}$, the isothermal adsorption line of Ni in sediment and soil showed a tendency of increasing slope, but the adsorption amount did not reach saturation, When the concentration of Ni is 500 $mg \cdot L^{-1}$, the equilibrium adsorption concentration of sediment and soil on Ni were 17.86 and 20.71 $mg \cdot L^{-1}$, respectively, and the equilibrium adsorption amount were 9642.88 and 9585.84 $mg \cdot kg^{-1}$ respectively. According to the classification of isothermal adsorption curves by Giles (1974), it can be seen that the isothermal adsorption curve of the sediment and soil to Ni is “S” type. For this “S” type isothermal adsorption line, the

http://www.aloki.hu ● ISSN 1589 1623 (Print) ● ISSN 1785 0037 (Online)
DOI: http://dx.doi.org/10.15666/aeer/1706_1323913251

data can be analyzed and fitted with Freundlich and D-R models to explain the adsorption mechanism of Ni in sediment and soil, and the fitting parameters are shown in *Table 2*.

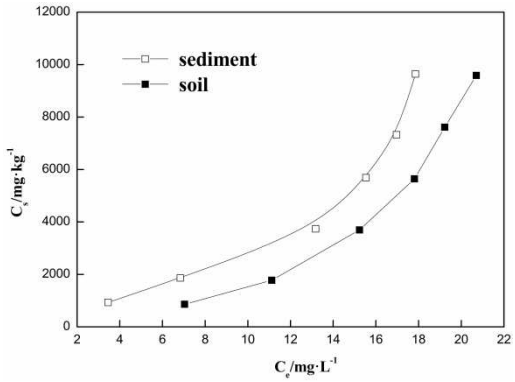

Figure 2. *Adsorption isotherm of Ni in sediment and soil*

Table 2. *The isothermal adsorption fitting parameters of Ni in sediment and soil*

Sample type	Freundlich equation			D-R equation		
	K_f	1/n	r	q_m	k	r
Sediment	3.1906	2.761	0.9891**	31898.2507	68.8476	0.9859**
Soil	1.2562	2.938	0.9963**	26562.0806	78.3844	0.9866**

n = 6, $r_{0.05}$ = 0.811, $r_{0.01}$ = 0.917. **indicate statistical significance at P < 0.01. The same below

It can be seen from *Table 2,* Freundlich equation and D-R equation were used to fit the adsorption isotherms of nickel on sediment and soil, and the correlation coefficients were above 0.98, the fitting results were all significantly correlated ($p < 0.01$). The Freundlich equation has the best fitting effect, the adsorption constant K_f represents the adsorption capacity of Ni on the sediment and the soil. The larger of the K_f, the stronger the adsorption capacity was. The adsorption coefficient K_f of Ni in the sediment was greater than that in the soil, indicating that the adsorption effect of the sediment on nickel was greater than that on the soil. When the concentration of nickel was lower than 500 mg·L^{-1}, the adsorption of Ni on sediments and soil did not reach the saturation state, which may be due to the modification effect of nickel on the bottom sediment and soil surface, forming a new adsorption field, thus promoting the adsorption of nickel in the bottom sediment and soil (Rinklebe et al., 2017). Since the D-R equation describes an ideal adsorption state in which the pores of an adsorbent are completely filled with solutes, the calculated equilibrium adsorption q_m is an ideal state.

The desorption of Ni in sediment and black soil

The desorption amount was often used as an index to indicate the adsorption strength, and can generally be used to illustrate the bonding degree of the colloidal surface active adsorption position with heavy metal ions (Tahervand et al., 2016, 2017). The desorption isotherm and desorption rate of Ni on bottom sediment and soil are shown in *Figure 3*.

http://www.aloki.hu ● ISSN 1589 1623 (Print) ● ISSN 1785 0037 (Online)
DOI: http://dx.doi.org/10.15666/aeer/1706_1323913251

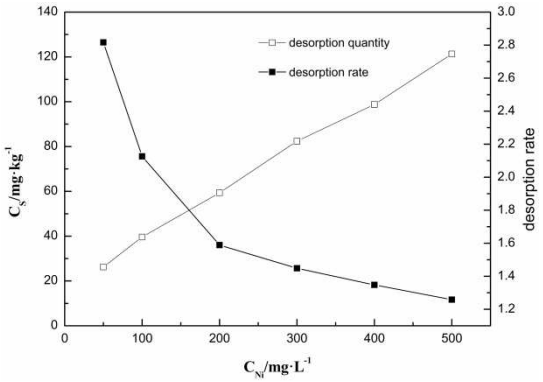

Figure 3. *The desorption amount and desorption rate of Ni in sediment*

As can be seen from *Figure 4*, the desorption of Ni by sediments and soil has a similar trend to that of adsorption, and the desorption of soil and sediment gradually increases with the increase of the initial Ni concentration. The final desorption of Ni by sediments and soil was 121.34 mg·kg^{-1} and 129.78 mg·kg^{-1}, respectively, accounting for 1.26% and 1.35% of the adsorption capacity, respectively.

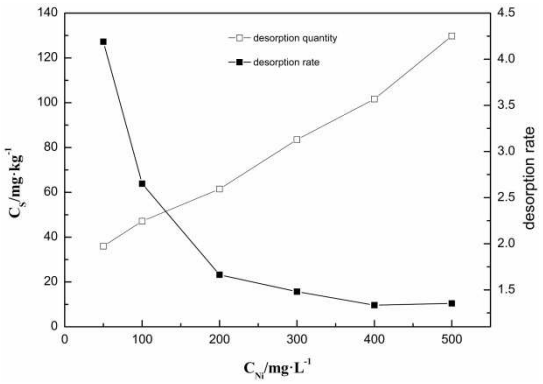

Figure 4. *The desorption amount and desorption rate of Ni in soil*

It can be seen that the adsorption capacity of sediments and soil to Ni was strong, while the desorption capacity was weak. The desorption amount of Ni in sediments was slightly less than that in soil. When the adsorption capacity was low, Ni occupies a high energy adsorption point, and the adsorption was mainly specific adsorption, so the desorption of Ni was difficult. When certain saturation was reached, specific adsorption points gradually decrease, and adsorption of heavy metals in stable sediments and soil was reduced, making it easier to desorption, so desorption also increased (Arancibia et al., 2015). The sediment contains more organic matter than the soil, so it has a stronger adsorption ability to nickel and a stronger fixation ability, leading to less desorption. Low Ni desorption may be the buffer of sediment and soil against heavy metal pollution (Davari et al., 2015). The desorption process can be regarded as the reverse process of soil adsorption process, and all factors affecting adsorption affect the desorption. The desorption data of Ni in sediment and soil are fitted with the Freundlich equation and the D-R equation, and the results are shown in *Table 3*.

http://www.aloki.hu ● ISSN 1589 1623 (Print) ● ISSN 1785 0037 (Online)
DOI: http://dx.doi.org/10.15666/aeer/1706_1323913251

Table 3. *Isothermal desorption fitting parameters of Ni in sediment and soil*

Sample type	Freundlich equation			D-R equation		
	K_f	n	r	q_m	k	r
Sediment	0.7218	0.5727	0.9706**	197.7315	82.1164	0.9338**
Soil	1.1054	0.6496	0.9724**	151.2162	61.7417	0.9052**

n = 6, $r_{0.05}$ = 0.811, $r_{0.01}$ = 0.917

As can be seen from *Table 3,* the correlation coefficient of desorption isotherm of nickel in sediment and soil of Freundlich equation was 0.9937~0.9937, $K_{f\ (sediment)} < K_{f\ (soil)}$. The adsorption capacity of sediment on Ni was strong, but its desorption capacity was weak. Ni adsorbed on sediments and soil is not easy to desorption. Kaur (2018) proposed to use hysteretic coefficient (HI) as a quantitative indicator of the irreversible adsorption degree of the compound in soil.

$$HI = (q^d - q^s)/q^s$$

In the formula, q_d and q_s respectively refer to the adsorption concentration of Ni in the soil during adsorption and desorption at a certain temperature mg·kg^{-1}. When 0.7 < HI < 1.0, the desorption rate was similar to the adsorption rate, and the adsorption isotherm coincides with the desorption isotherm. When HI < 0.7, the desorption rate was lower than the adsorption rate, and the desorption process was positive hysteresis. When HI > 1.0, the desorption process was negative hysteresis (Mosqueravivas et al., 2018). It can be seen from *Table 4* that as the Ni concentration of the background solution increases, the desorption hysteresis coefficient gradually decreases and was much smaller than 0.7, indicating that the desorption rate was much smaller than the adsorption rate. When the initial concentration was the same, $HI_{\ sediment} < HI_{\ soil}$, indicating that the Ni adsorbed on the sediment was more difficult to desorption than the soil.

Table 4. *Ni desorption hysteresis coefficient HI at different concentrations*

Initial concentration (mg/L)	50	100	200	300	400	500
Sediment	0.0290	0.0217	0.0161	0.0147	0.0131	0.0127
Soil	0.0437	0.0273	0.0169	0.015	0.0135	0.0137

Adsorption kinetics of Ni in sediment and black soil

The change of Ni adsorption amount with sediment and black soil with time is shown in *Figure 5*. As can be seen from *Figure 5*, the whole adsorption process can be divided into two stages, namely, rapid adsorption stage and slow equilibrium stage. The concentration of Ni in the solution decreased rapidly in 0-120 min, and the concentration of Ni in the solution was gradually balanced in the 120-1440 min solution. In the 0-120 min, the adsorption amount of Ni to the sediment and soil accounted for 99.57% and 99.84% of the total adsorption, respectively. At the adsorption equilibrium, the maximum adsorption capacity of sediment and soil to Ni was 1881.60 and 1804.58 mg·kg^{-1}. Because there are more adsorption sites on the

http://www.aloki.hu ● ISSN 1589 1623 (Print) ● ISSN 1785 0037 (Online)
DOI: http://dx.doi.org/10.15666/aeer/1706_1323913251

surface of the sediment and soil, Ni can be quickly adsorbed. When more and more adsorption sites are occupied, the reaction rate decreases until the adsorption reaches equilibrium. Ni may form a complex when adsorbed in the sediment and soil, so that the heavy metals adsorbed on its appearance are transferred to the inside of the particles and precipitate on the sediment and soil surface, so that the adsorption of the sediment and soil to the Ni was getting smaller, and finally until it tended to balance (Peng et al., 2018). And the reduction agent in the sediment and soil dissolves from the solid phase to the water phase is a slow dissolution process (Huang et al., 2018).

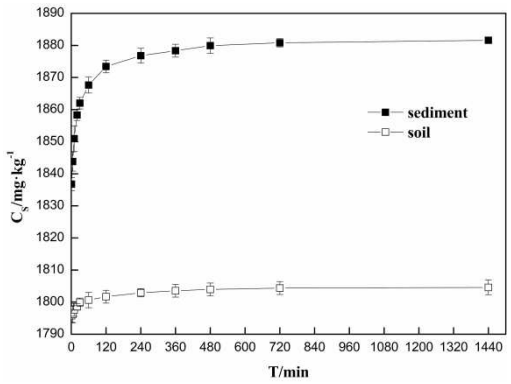

Figure 5. *The adsorption kinetic curve of Ni*

In this experiment, Elovich equation and parabolic diffusion equation were used to fit the adsorption kinetics of Ni in sediment and black soil. The relevant parameters of the fitting are shown in *Table 5*. It can be seen from *Table 5* that Elovich equation has a good fitting effect on the adsorption kinetics of Ni in sediments and black soil, indicating that the adsorption kinetics process is non-uniform diffusion process, and the reaction process is controlled by multiple mechanisms such as diffusion, dissolution and mineralization. The adsorption fitting coefficient r of Ni in lake bottom sediment and soil was 0.9827 and 0.9895, respectively. The greater the constant a value in the Elovich equation, the greater the adsorption rate, so the adsorption amount of the sediment is greater than the adsorption amount of the soil. The fitting of adsorption by parabolic diffusion equation is relatively poor, and the correlation coefficients r were 0.7905 and 0.8813, respectively. In the above model fitting, it can be inferred that the diffusion of particles is not the only mechanism controlling the adsorption process, which is also adsorbed by other adsorbents (Zhu et al., 2015).

Adsorption thermodynamics of Ni in sediment and black soil

The adsorption of Ni by sediment and black soil over time are shown in *Figures 6* and *7*. As can be seen from *Figures 6* and *7*, in the test temperature range, with the increase of temperature, the adsorption amount of sediment and soil to Ni increases gradually, and the adsorption does not reach saturation. The increase of temperature was beneficial to the adsorption of Ni by sediment and soil, and the reaction can be determined to be an endothermic reaction. Heavy metal Ni has good hydration in the test temperature range. When the metal Ni was adsorbed by sediment and soil, it lost its hydrating shell. The process of nickel losing hydrated shell requires some energy, and the process of removing water molecules is endothermic. The higher the temperature is,

http://www.aloki.hu ● ISSN 1589 1623 (Print) ● ISSN 1785 0037 (Online)
DOI: http://dx.doi.org/10.15666/aeer/1706_1323913251

the more favorable it is for the Ni adsorbed on the bottom sediment and soil surface to diffuse into the particles. It is also a benefit for external complexity and internal complexity. It also facilitates the combination of thermodynamic unstable state to stable state transition. Therefore, the adsorption of nickel in sediments and soil increases with temperature.

Table 5. *Parameters of the kinetics adsorption models for Ni in sediment and black soil*

Soil type	Elovich equation			Parabolic diffusion equation			
	a	b	r	a	b	s	r
Sediment	1836.8507	6.8847	0.9827**	293.8471	0.1789	6.3016	0.7905**
Black soil	1795.5288	1.2942	0.9895**	267.2892	0.0346	6.7273	0.8813**

n = 12, $r_{0.05}$ = 0.0.576, $r_{0.01}$ = 0.708

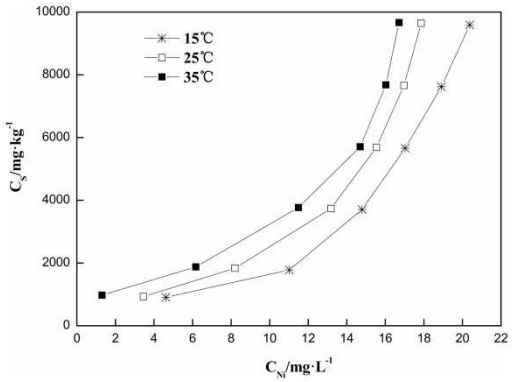

Figure 6. *The effect of different temperature on the adsorption of Ni in the sediment*

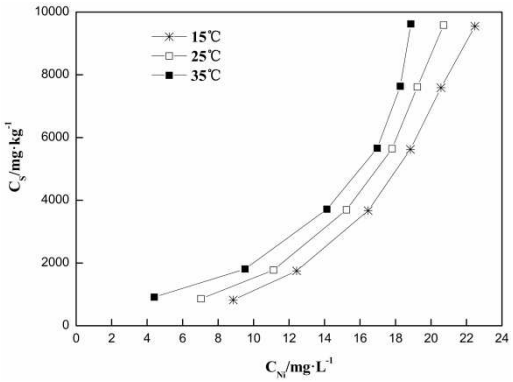

Figure 7. *The effect of different temperature on the adsorption of Ni in the soil*

When the temperature at 15 °C, 25 °C and 35 °C sediment and soil on the adsorption thermodynamics equation of Ni fitting results as shown in *Table 6*. The adsorption thermodynamics of sediment and soil on Ni is well correlated with the thermodynamic fitting of Ni on sediment and soil. The coefficient *R* is between 0.9491 and 0.9975. Sediment and soil on the adsorption of Ni coefficient K_f15°C < K_f25°C < K_f35°C, show

http://www.aloki.hu ● ISSN 1589 1623 (Print) ● ISSN 1785 0037 (Online)
DOI: http://dx.doi.org/10.15666/aeer/1706_1323913251

that the higher the temperature, the stronger the adsorption capacity of sediment and soil nickel. The adsorption reaction can be determined as endothermic reaction.

Table 6. *The isotherm adsorption parameters of Ni at different temperatures*

Sample type	Temperature (°C)	Freundlich equation			D-R equation		
		K_f	n	r	q_m	k	r
Sediment	15	1.9583	0.3554	0.9923**	24814.9828	70.5966	0.9786**
	25	3.1904	0.3621	0.9786**	28899.0866	63.7658	0.9483**
	35	17.0777	0.4513	0.9617**	21947.8305	44.4613	0.9246**
Soil	15	1.0453	0.3419	0.9829**	25954.7285	88.6074	0.9832**
	25	1.2568	0.3406	0.9946**	26562.0767	78.3846	0.9723**
	35	1.4630	0.3384	0.9724**	27134.1593	69.9409	0.9438**

n = 6, $r_{0.05}$ = 0.811, $r_{0.01}$ = 0.917

According to the K_f in the Freundlich equation at different temperatures, the enthalpy change and entropy change are calculated by lnK_f and 1/T, $\Delta G = \Delta H - T\Delta S$. It can be seen from *Table 7* that the ΔG at different temperatures were less than zero, as the rise of environmental temperature, ΔG gradually reduced. It was indicated that the adsorption process of Ni on sediment and soil is spontaneous, and the high temperature is favorable for the spontaneity of adsorption, which is consistent with the fitting results of Langmuir equation and Freundlich equation (Wu et al., 2013; Turp, 2018). It can be seen from the table that $\Delta H > 0$ of Ni in the sediment and soil is indicated as an endothermic reaction. ΔG and ΔH indicated that sediment and soil buffer capacity of Ni, and may have a seasonal migration and activity (Guo et al., 2012).

Table 7. *The thermodynamic parameters of Ni in sediment and soil*

Sample type	Temperature °C	ΔG KJ·mol^{-1}	ΔH KJ·mol^{-1}	ΔS KJ·(mol·K)$^{-1}$
Sediment	15	-1.1707	79.5104	0.2804
	25	-3.9703		
	35	-6.7706		
Soil	15	-0.2308	12.4508	0.0403
	25	-0.6704		
	35	-1.1102		

Effect of organic matter content on adsorption characteristics of Ni

The Ni adsorption by sediment and soil before and after the removal of organic matter are shown in *Figures 8* and *9*. As can be seen from the figure, when organic matter was removed from sediments and soil, and the Ni concentration in the solution was 500 mg·L^{-1}, the adsorption capacity of sediments and soil on Ni decreased by 2.17% and 1.7%, respectively. The above phenomenon indicates that the presence of organic matter can increase the adsorption of Ni by sediment and soil. In the experiment, according to the formula of: contribution rate = ($Q_{original}$-$Q_{removal}$) / $Q_{removal}$. According to this formula, the contribution rate of organic matter in sediment and soil to

http://www.aloki.hu ● ISSN 1589 1623 (Print) ● ISSN 1785 0037 (Online)
DOI: http://dx.doi.org/10.15666/aeer/1706_1323913251

Ni was 2.06% and 1.73% respectively. The higher the content of organic matter is, the greater the contribution rate of organic matter to Ni was, and the adsorption point of sediment to Ni after removing organic matter is greater than that of soil.

There was a significant correlation between the adsorption amount and the content of organic matter. The reason may be that the organic matter entered the sediments and soil to form humus after microbial action. Humus contains carboxyl, phenol hydroxyl and alcohol hydroxyl. These groups can easily complex or chelate with heavy metal elements to form stable compounds, thus improving their adsorption capacity. In addition, polar groups in sediment and soil organic matter, such as hydroxyl group and carboxyl group, can make sediment and soil surface have a large amount of negative charge, thus enhancing the electrostatic adsorption of nickel (Refaey et al., 2014; Yin et al., 2016).

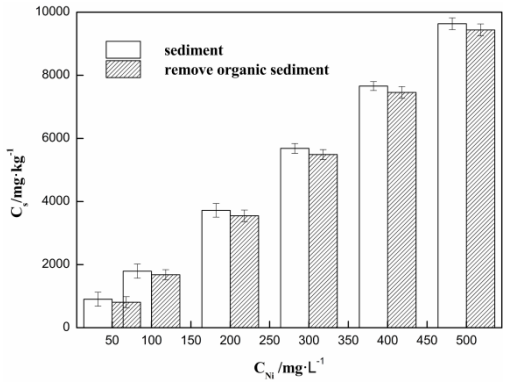

Figure 8. *Adsorption isotherm of Ni under removal of sediment organic before and after*

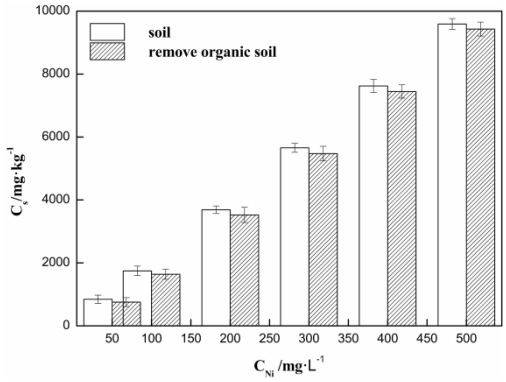

Figure 9. *Adsorption isotherm of Ni under removal of soil organic before and after*

Conclusion

The adsorption characteristics of Ni on the sediment of the lake and the black soil on the shore show that the adsorption of Ni on the sediment was larger than that in the soil, and the adsorption process can be fitted with the Freundlich model and the D-R model. The Freundlich model can better fit the adsorption of Ni by sediment and soil. The correlation coefficient r were 0.9891 and 0.9963, the final desorption amount of sediment and soil to Ni are 121.34 and 129.78 mg·kg^{-1}, which accounts for 1.26% and 1.35% of adsorption, respectively. The initial concentration was the same,

http://www.aloki.hu ● ISSN 1589 1623 (Print) ● ISSN 1785 0037 (Online)
DOI: http://dx.doi.org/10.15666/aeer/1706_1323913251

$HI_{sediment} < HI_{soil}$, indicated that the sediment had a stronger retention capacity to Ni than the soil. The adsorption kinetics of nickel in sediments and black soil can be well fitted by Elovich equation. In the experimental temperature range, the adsorption amount of Ni on the sediment and soil gradually increased with the increase of temperature, and the ΔG value of adsorption thermodynamic parameters is less than 0, which indicates that Ni adsorption process on sediment and shore soil is spontaneous. After removing organic matter, the adsorption capacity of bottom sediment and soil on Ni was weakened, and the adsorption capacity was reduced by 2.02% and 1.70%, respectively, indicating that organic matter could enhance the retention capacity of Ni. These factors may limit or enhance the transport or absorption of metal Ni in soil. This work provides a theoretical framework for the prediction of metal adsorption characteristics and provides a potential help for the prediction of bioavailability, fate and transport of heavy metals in newly contaminated areas. Meanwhile, the interaction between Ni and other heavy metals is expected to be considered in future studies.

REFERENCES

[1] Abdelwaheb, M., Dridi-Dhaouadi, S. (2017): Impact of soil properties on groundwater contamination risks by nickel and lead. – Euro-Mediterranean Conference for Environmental Integration, 22-25 November 2017, Sousse, Tunisia.

[2] Arancibia-Miranda, Nicolás, Silva-Yumi, J., Escudey, M. (2015): Effect of cations in the background electrolyte on the adsorption kinetics of copper and cadmium and the isoelectric point of imogolite. – Journal of Hazardous Materials S0304389415006263.

[3] Bian, W., Ma, X., Wang, F., Zhang, L., Ren, L., Wang, Y. (2016): Study on the adsorption characteristics of ciprofloxacin in saline alkali soil. – Acta Agroenvironmental Sinica 35(10): 1953-1959.

[4] Davari, M., Rahnemaie, R., Homaee, M. (2015): Competitive adsorption-desorption reactions of two hazardous heavy metals in contaminated soils. – Environmental Science & Pollution Research 22(17): 13024-13032.

[5] De Brouwere, K., Buekers, J., Cornelis, C., Schlekat, C. E., Oller, A. R. (2012): Assessment of indirect human exposure to environmental sources of nickel: oral exposure and risk characterization for systemic effects. – Science of the Total Environment 419(0): 25-36.

[6] Duan, Q., Lee, J., Liu, Y., et al. (2016): Distribution of heavy metal pollution in surface soil samples in China: a graphical review. – Bulletin of Environmental Contamination and Toxicology 97(3): 303-309.

[7] Guo, P., Yang, L. I., Zhang, Y. X., Ming, L., Zhang, S., Yue-Ming, L. I. (2012): Effect of freeze-thaw on the adsorption of heavy metals by soil. – Journal of Jilin University 2012(3).

[8] Huang, L., Jin, Q., Tandon, P., Li, A., Du, J. (2018): High-resolution insight into the competitive adsorption of heavy metals on natural sediment by site energy distribution. – Chemosphere 197: 411.

[9] Kashulina, G. M. (2018): Monitoring of soil contamination by heavy metals in the impact zone of copper-nickel smelter on the Kola Peninsula. – Eurasian Soil Science 51(4): 467-478.

[10] Kaur, P., Kaur, P. (2018): Time and temperature dependent adsorption-desorption behaviour of pretilachlor in soil. – Ecotoxicology & Environmental Safety 161: 145.

[11] Mosqueravivas, C. S., Martinez, M. J., GarcíaSantos G., Guerrerodallos, J. A. (2018): Adsorption-desorption and hysteresis phenomenon of tebuconazole in Colombian agricultural soils: experimental assays and mathematical approaches. – Chemosphere 190(2): 393-404.

http://www.aloki.hu ● ISSN 1589 1623 (Print) ● ISSN 1785 0037 (Online)
DOI: http://dx.doi.org/10.15666/aeer/1706_1323913251

[12] Peng, L., Liu, P., Feng, X., Wang, Z., Cheng, T., Liang, Y. (2018): Kinetics of heavy metal adsorption and desorption in soil: developing a unified model based on chemical speciation. – Geochimica et Cosmochimica Acta 224: 282-300.
[13] Prithviraj, D., Deboleena, K., Neelu, N. (2014): Biosorption of nickel by Lysinibacillus sp. BA2 native to bauxite mine. – Exotoxicology and Environmental Safety 107(0): 260-268.
[14] Refaey, Y. B., Jansen, B., Elshater, A. H., Elhaddad, A. A., Kalbitz, K. (2014): The role of dissolved organic matter and its adsorption for the fate of heavy metals in clay-rich soil. – Abstracts of the EGU General Assembly Conference Vienna, Austria, 27 April–02 May, 2014.
[15] Rinklebe, J., Shaheen, S. M. (2017): Redox chemistry of nickel in soils and sediments: a review. – Chemosphere 179: 265-278.
[16] Sangiumsak, N., Punrattanasin, P. (2014): Behaviors of ni and zn adsorption on different soils found in the northeastern Thailand. – Advanced Materials Research 931-932: 681-686.
[17] Tahervand, S., Jalali, M. (2016): Sorption, desorption, and speciation of Cd, Ni, and Fe by four calcareous soils as affected by pH. – Environmental Monitoring & Assessment 188(6): 1-12.
[18] Tahervand, S., Jalali, M. (2017): Sorption and desorption of potentially toxic metals (Cd, Cu, Ni and Zn) by soil amended with bentonite, calcite and zeolite as a function of pH. – Journal of Geochemical Exploration 181. DOI: 10.1016/j.gexplo.2017.07.005.
[19] Turp, S. M. (2018): Mn^{2+} and Cu^{2+} adsorption with a natural adsorbent: expanded perlite. – Applied Ecology and Environmental Research 16(4): 5047-5057.
[20] Vukosav, P., Mlakar, M., Cukrov, N., Željko Kwokal, Pižeta, I., Pavlus, N., et al. (2014): Heavy metal contents in water, sediment and fish in a karst aquatic ecosystem of the Plitvice Lakes National Park (Croatia). – Environmental Science & Pollution Research 21(5): 3826-3839.
[21] Wu, F., Liu, H., Zhang, M., Ma, W., Huang, X., Liu, S., et al. (2017): Adsorption characteristics and the effect of dissolved organic matter on mercury (ii) adsorption of various soils in china. – Journal of Soil Contamination 26(2): 14.
[22] Wu, Y., Yilihan, P., Cao, J., Jin, Y. (2013): Competitive adsorption of Cr (VI) and Ni (II) onto coconut shell activated carbon in single and binary systems. – Water, Air, & Soil Pollution 224(9): 1662.
[23] Yin, B., Zhou, L., Yin, B., Liang, C. (2016): Effects of organic amendments on rice (Oryza sativa L.) growth and uptake of heavy metals in contaminated soil. – Journal of Soils & Sediments 16(2): 537-546.
[24] Zhang, L., Duff, A., Smith, C. J. (2018): Community and functional shifts in ammonia oxidizers across terrestrial and marine (soil/sediment) boundaries in two coastal bay ecosystems. – Environmental Microbiology 20(8).
[25] Zhu, D. N., Zou, S. Z., Zhou, C. S. (2015): Adsorption characteristics of Cd^{2+} in typical soils in karst areas. – China Karst 34(4).

http://www.aloki.hu ● ISSN 1589 1623 (Print) ● ISSN 1785 0037 (Online)
DOI: http://dx.doi.org/10.15666/aeer/1706_1323913251

COMPREHENSIVE ASSESSMENT OF DROUGHT RESISTANCE IN SEEDLINGS OF FIVE ALFALFA (*MEDICAGO SATIVA* L.) CULTIVARS

GUO, H. – GONG, Y. B. – BAO, A. K.*

State Key Laboratory of Grassland Agro-ecosystems; Key Laboratory of Grassland Livestock Industry Innovation, Ministry of Agriculture and Rural Affairs; Engineering Research Center of Grassland Industry, Ministry of Education; College of Pastoral Agriculture Science and Technology, Lanzhou University, Lanzhou, 730020, P. R. China

**Corresponding author*
e-mail: baoaik@lzu.edu.cn; phone: +86-931-891-3447; fax: +86-931-891-3447

(Received 5th Jun 2019; accepted 2nd Sep 2019)

Abstract. Selecting drought-tolerant alfalfa cultivars is conducive to improve the forage yield in arid and semi-arid areas. In this study, drought resistance of five alfalfa (*Medicago sativa* L.) cultivars at the seedling stage was analyzed by using agronomic and physiological indicators. After withholding water for 6 days and then re-watering for 4 days, shoot dry weights of "Longdong" and "Daye" were significantly higher than that of the other cultivars. Under drought stress, "Daye" had healthier plasma membrane with the minimum leaf membrane permeability, while the leaf osmotic potential of "Longdong" and "Gannong No. 3" were significantly lower than that of the other three cultivars. Moreover, "Longdong" showed the highest leaf relative water content. According to the combination of above indicators, the relative drought resistance of the five cultivars decreased in order: "Longdong", "Daye", "Gannong No. 3", "Sandili", and "Rambler". This study suggested that "Longdong" and "Daye" might be more suitable for planting in arid and semi-arid regions.
Keywords: *forages, arid environment, physiological mechanism, agronomic indicators*

Introduction

Drought is one of the most adverse environmental factors causing the reduction of agricultural productivity worldwide (Hassine et al., 2010; Ghaderi et al., 2011). In order to face this challenge, we need to identify suitable crops adapting to drought. Alfalfa (*Medicago sativa* L.) is the most important legume forage, which is rich in vitamins, minerals and phytonutrients (Xiao et al., 2015; Kumar et al., 2018). Establishing alfalfa pastures has played a more and more important role in ecological environment and livestock production of China (Shi et al., 2017). Alfalfa planting areas in China were significantly extended by 74% from 2001 to 2013, and about 70% of them are distributed in northern China, an arid or semi-arid region with water resource shortage (Lu, 2013). Planting alfalfa cultivars with strong drought resistance is one of the fundamental ways for promoting forage productivity and saving the limited water resources in northern China. However, there is a considerable variation of drought tolerance among existing alfalfa cultivars (Guo et al., 2004). Alfalfa is very sensitive to drought during the seedling stage (Kumar, 2011). Therefore, to evaluate the drought tolerance in the seedling stage is necessary for selecting drought-tolerant alfalfa cultivars.

Drought stress can directly disrupt the water balance, decrease the leaf turgor potential, and damage the cell membrane (Ma et al., 2012). On a physiological level, the most important strategy for plants survival in arid environment is osmotic adjustment,

http://www.aloki.hu ● ISSN 1589 1623 (Print) ● ISSN 1785 0037 (Online)
DOI: http://dx.doi.org/10.15666/aeer/1706_1325313261

by which plants can retain the water and maintain the stability of cell membrane (Quan et al., 2016). Therefore, the physiological indicators such as osmotic potential (Ψs), leaf relative water content (RWC) and relative membrane permeability (RMP), were frequently used to evaluate drought resistance of plants (Foster et al., 2012; Cui et al., 2019). However, it is difficult to determine by single physiological indicator and the result tends to unilateralism, since the mechanism of drought resistance in plants is extremely complex (Cattivelli et al., 2008; Wu et al., 2014). On the other hand, the agronomic indicators (such as yield, survival rate, plant height and biomass) are the phenotypes that integrate the various physiological mechanisms in response to stress, but are readily affected by other factors instead of the concerned factor (Noble and Rogers, 1992; Singh et al., 2019). The objective of this study was thus to assess and compare the drought resistance among five alfalfa cultivars at the seedling stage by combining one agronomic indicator (shoot dry weight) and three physiological indicators (leaf RMP, Leaf Ψs and leaf RWC).

Materials and methods

Plant materials, growth conditions and treatments

Seeds of five alfalfa cultivars, "Longdong", "Gannong No.3", "Daye", "Rambler" and "Sandili" collected from the Chinese commercial market were surface sterilized and germinated as described by Bao et al. (2009). The seedlings were transplanted in plastic pots filled with artificial soil with a mixture of perlite, vermiculite and peat moss (v/v, 1:1:1). Each cultivar was transplanted in 60 pots. All the seedlings were grown in the greenhouse in Lanzhou University (36.03°N, 103.40°E; elevation 1520 m) under a 16-h photoperiod (the light flux density was approximately 600 μmol/m^2/s) at 24 ± 2°C and 60 ± 5% of relative humidity, watered with 1/8 Hoagland nutrient solution every 2 days, and seedlings in each pot were thinned to 3 plants after 5 days. The pots were continuously watered with 1/8 Hoagland nutrient solution to maximum field water-holding capacity for 15 days, then nutrient solution was withheld for 6 days and re-watered for 4 days. The seedlings in the control group were watered with 1/8 Hoagland nutrient solution normally. Each treatment was repeated three times, and each repetition contained 10 pots (3 plants/pot). Physiological indicators including leaf relative membrane permeability (RMP), leaf osmotic potential (Ψs) and leaf relative water content (RWC) were measured after water withholding, and shoot dry weight was determined after re-watered.

Measurement of shoot dry weight

After being re-watered for 4 days, the shoots were cut from stem base of seedlings and rinsed with distilled water, then were dried in an oven at 80°C for 48 h and the dry weights of shoots were weighed.

Measurement of leaf RMP, Ψs and RWC

After water withholding for 6 days, the leaves were excised from seedlings. Leaf RMP was determined according to the method reported by Bao et al. (2009) using a conductivity meter (EC215, HANNA, Italy). Leaf Ψs was measured according to the method as described by Wu et al. (2014) using a cryoscopic osmometer (Osmomat-030,

http://www.aloki.hu ● ISSN 1589 1623 (Print) ● ISSN 1785 0037 (Online)
DOI: http://dx.doi.org/10.15666/aeer/1706_1325313261

Gonotec GmbH, Germany). Leaf RWC was calculated through the method mentioned by Ma et al. (2012).

Assessment of drought resistance in five alfalfa cultivars

According to the method as described by Bao et al. (2009), the data of shoot dry weight, leaf RMP, leaf *Ψs* and leaf RWC were converted into relative values (the ratio of value from drought stress to value from control), respectively. Then the relative value of each indicator from each cultivar was standardized by the subordinate function method (Wu et al., 2014). Finally, the relative drought resistance of each cultivars was scored according to standardized values of each indicator by the following formula: [*I* (1) + *I* (2) + *I* (3) + *I* (4)]/4. Where *I* (1-4) refer to the standardized value of shoot dry weight, leaf RMP, leaf *Ψs* and leaf RWC, respectively.

Statistical analysis

All data in this study were analyzed by one-way analysis of variance (ANOVA) using SPSS 13.0 (SPSS inc. USA) and Duncan's Multiple Range test was used to detect significant differences among the means ($P < 0.05$).

Results

Shoot dry weight

After withholding water for 6 days and then re-watering for 4 days, shoot biomass of each cultivar was significantly reduced. The shoot dry weight of "Rambler" showed the largest decline by 35.8% and was significantly lower than that of the other cultivars. Shoot dry weights of "Longdong" and "Xinjiang Daye" only decreased by 9.8% and 12.9%, respectively, and were significantly higher than other three cultivars (*Fig. 1*).

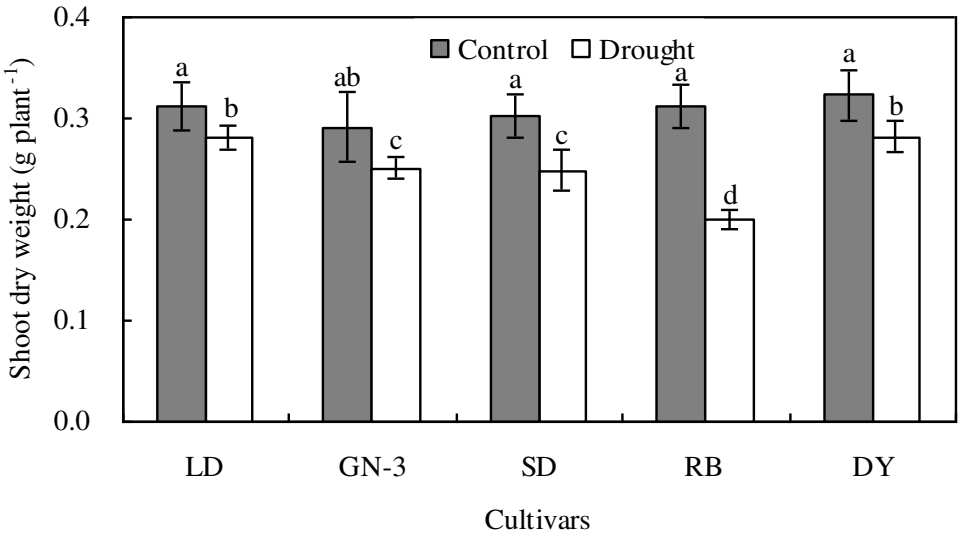

Figure 1. *Shoot dry weights of alfalfa seedlings under control and drought conditions for 6 days, and then re-watering for 4 days. Values are means ± SD (n = 6) and bars indicate SD. Different letters on columns indicate significant difference at P < 0.05 (Duncan's test). LD: "Longdong"; GN-3: "Gannong No. 3"; SD: "Sandili"; RB: "Rambler"; DY: "Xinjiang Daye"*

http://www.aloki.hu ● ISSN 1589 1623 (Print) ● ISSN 1785 0037 (Online)
DOI: http://dx.doi.org/10.15666/aeer/1706_1325313261

Leaf relative membrane permeability (RMP)

After being treated with drought for 6 days, leaf RMP of all cultivars increased sharply. However, the leaf RMP of "Longdong" and "Gannong No. 3" were significantly higher than those of the other cultivars, while "Xinjiang Daye" showed the lowest leaf RMP value, under drought stress (*Fig. 2*).

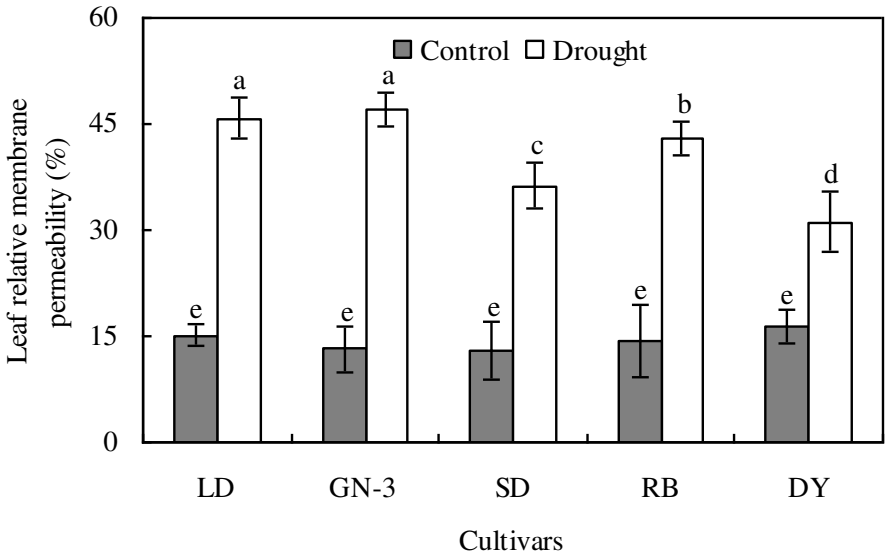

Figure 2. *Leaf relative membrane permeabilities of alfalfa seedlings under control and drought conditions for 6 days. Values are means ± SD (n = 6) and bars indicate SD. Different letters on columns indicate significant difference at P < 0.05 (Duncan's test). LD: "Longdong"; GN-3: "Gannong No. 3"; SD: "Sandili"; RB: "Rambler"; DY: "Xinjiang Daye"*

Leaf osmotic potential (Ψs)

It is observed that leaf *Ψs* of "Longdong" and "Xinjiang Daye" were significantly lower than that of the other three cultivars under the control condition. Under drought stress, leaf *Ψs* of each cultivar significantly decreased, but there were significantly differences among five cultivars, in which "Longdong" and "Gannong No. 3" had the lowest leaf *Ψs* compared to other three cultivars (*Fig. 3*).

Leaf relative water content (RWC)

Under well-watering condition, there was no significant difference in leaf RWC between the five alfalfa cultivars. After withholding water for 6 days, leaf RWC of each cultivar was significantly reduced. Moreover, there were significant differences among five cultivars, of which "Rambler" showed the lowest RWC (decreased by 53.0%), while "Longdong" exhibited the highest RWC (decreased by 35.8%), under drought stress, suggesting that "Longdong" showed stronger water retention ability than other cultivars (*Fig. 4*).

Comprehensive assessment on drought resistance among five cultivars

The relative values of shoot dry weight, leaf RMP, leaf *Ψs* and leaf RWC, were used to evaluate and compare the relative drought resistance of five alfalfa cultivars. From

http://www.aloki.hu ● ISSN 1589 1623 (Print) ● ISSN 1785 0037 (Online)
DOI: http://dx.doi.org/10.15666/aeer/1706_1325313261

the comprehensive assessment, the relative drought resistance of the five cultivars decreased in order: "Longdong", "Xinjiang Daye", "Gannong No. 3", "Sandili" and "Rambler". The result of comprehensive evaluation indicated that "Longdong" and "Xinjiang Daye" had relatively higher drought resistance among five cultivars (*Table 1*).

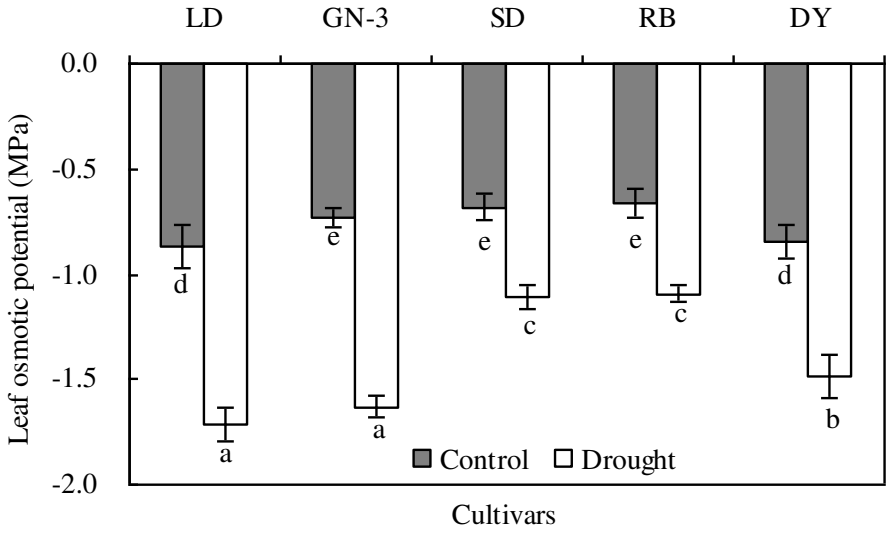

Figure 3. *Leaf osmotic potentials of alfalfa seedlings under control and drought conditions for 6 days. Values are means ± SD (n = 6) and bars indicate SD. Different letters on columns indicate significant difference at P < 0.05 (Duncan's test). LD: "Longdong"; GN-3: "Gannong No. 3"; SD: "Sandili"; RB: "Rambler"; DY: "Xinjiang Daye"*

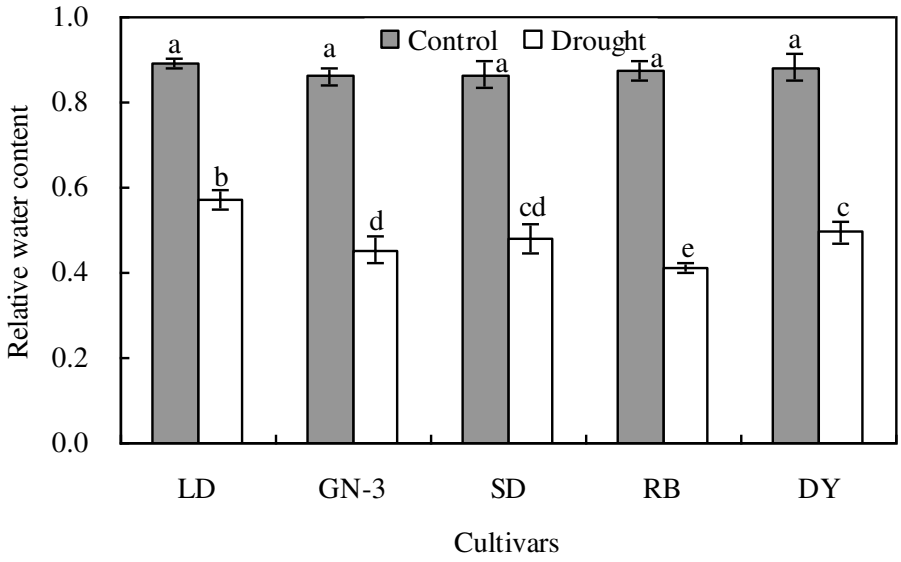

Figure 4. *Leaf relative water contents of alfalfa seedlings under control and drought conditions for 6 days. Values are means ± SD (n = 6) and bars indicate SD. Different letters on columns indicate significant difference at P < 0.05 (Duncan's test). LD: "Longdong"; GN-3: "Gannong No. 3"; SD: "Sandili"; RB: "Rambler"; DY: "Xinjiang Daye"*

http://www.aloki.hu ● ISSN 1589 1623 (Print) ● ISSN 1785 0037 (Online)
DOI: http://dx.doi.org/10.15666/aeer/1706_1325313261

Table 1. *Comprehensive assessment on drought resistance between the five alfalfa cultivars. I (1): shoot dry weight; I (2): leaf relative membrane permeability; I (3): leaf osmotic potential; I (4): leaf relative water content*

Cultivars	*I* (1)	*I* (2)	*I* (3)	*I* (4)	Mean	Order
Longdong	1.00	0.32	0.55	1.00	0.72	1
Xinjiang Daye	0.88	1.00	0.18	0.53	0.65	2
Gannong No.3	0.85	0.00	1.00	0.33	0.54	3
Sandili	0.69	0.47	0.00	0.50	0.41	4
Rambler	0.00	0.30	0.03	0.00	0.08	5

Discussion

As a major abiotic factor, drought can reduce the growth of plants by directly leading to the decrease of shoot yield (Yamaguchi and Sharp, 2010). Therefore, shoot biomass is an important indicator for identifying the stress resistance of higher plants, not only for its ease of measurement, but also due to the fact that it is a direct reaction to the interaction of a variety of physiological mechanisms in plants and external environment (Noble and Rogers, 1992; Wu et al., 2014). Numerous studies have been performed on the effects of drought stress on the seedling growth of alfalfa by focusing on the relationship between water deficit and shoot biomass (Liu et al., 2005; Pang et al., 2011). In the present study, shoot dry weight of five alfalfa cultivars were significantly reduced by water deficit and showed significant difference between cultivars. The similar results were also observed in previous studies on drought response of alfalfa (Kang et al., 2011; Quan et al., 2016). Foliage yield is the primary determinant of plant productivity and economic performance and thus is a momentous criterion for pasture managers to screen cultivars with high-yielding (Liu et al., 2005). Our study demonstrated again that shoot biomass completely can be used as a reliable indicator for evaluating drought resistance in alfalfa cultivars. In addition, this study indicated that other important physiological indicators can also be used as a better basis for assessing the drought resistance of alfalfa cultivars.

Abiotic stresses (including drought) can cause the accumulation of high concentrations of reactive oxygen species (ROS) in plants, which can result in the cell membrane lipid peroxidation, membrane permeability increase and finally inhibit the growth of plants (Wang et al., 2009; Zhang et al., 2018). The ability to maintain stability of membrane structure is closely related to stress resistance of plants, and relative membrane permeability (RMP) is an important indicator reflecting cell membrane stability (Guimarães et al., 2011; Quan et al., 2016). In this study, leaf RMP of five alfalfa cultivars were significantly increased under drought stress, but the increment differed widely among different cultivars. “Xinjiang Daye” showed a significantly lower leaf RMP in comparison to other four cultivars under drought stress, suggesting that it has the relatively higher ability to maintain the stability of membrane structure than other cultivars. This might be resulted from increased antioxidants contents as well as higher antioxidant enzymes activities in drought-tolerant cultivars under drought stress (Kang et al., 2011; Quan et al., 2016).

One of the strategies for plants adapting to arid environment is the accumulation of osmotic adjustment substances, which reduces osmotic potential and thus slows down the water loss of plants (Ma et al., 2012; He et al., 2019). Therefore, the osmotic

http://www.aloki.hu ● ISSN 1589 1623 (Print) ● ISSN 1785 0037 (Online)
DOI: http://dx.doi.org/10.15666/aeer/1706_1325313261

potential (Ψs) is an important physiological indicator for measuring the drought tolerance of plants. In this study, "Longdong" and "Gannong No. 3" showed lowest leaf Ψs under water deficit condition. Interestingly, it was found that leaf Ψs of "Longdong" and "Xinjiang Daye" were significantly lower than that of the other three cultivars under the normal condition, indicating that their adaptability to drought may be stronger than the other cultivars, since the lower initial leaf Ψs means the stronger water retention capacity (Mohamed and Tawfik, 2006; Ma et al., 2012). The data of leaf relative water content (RWC) in this study support this point. Under drought stress, "Longdong" had the highest leaf RWC, followed by "Xinjiang Daye", suggesting that these two cultivars have better water status, which may be due to their lower initial osmotic potential. Previous studies have demonstrated that drought-tolerant alfalfa cultivars showed less water loss and higher water use efficiency in drought conditions (Kang et al., 2011; Quan et al., 2016).

Drought resistance of higher plants is a combination of morphological variations, physiological changes, biochemical metabolisms and gene expression regulation, and there are diverse mechanisms and environmental variables involved in drought responses of plants (Wang et al., 2009), thus it actually hard to be accurately clarified by single indicator (Wu et al., 2014; Yan et al., 2015). In the present study, this point was confirmed again. Generally, there are various results presented by different indicators. Therefore, we developed a comprehensive assessment approach through combining one agronomic indicator and three physiological indicators, which are closely related to drought resistance, and especially, can be easily measured at seedling stage of plants. The results of this assessment clearly showed that the performance of "Longdong" and "Xinjiang Daye" were better than the other three alfalfa cultivars under drought stress, suggesting that these two cultivars may be more suitable for planting in arid and semi-arid regions of northern China.

Conclusion

In this study, we developed a comprehensive assessment procedure for drought resistance of alfalfa seedlings through combining one agronomic indicator and three physiological indicators. The results indicated that there existed great differences in drought resistance among five commercial alfalfa cultivars, in which "Longdong" and "Xinjiang Daye" were more suitable for planting in arid and semi-arid regions of northwestern China, and could be generalized as excellent cultivars with strong resistance. The next step will be to determine the overall adaptability by comprehensively assessing the drought resistance of the different alfalfa cultivars at different growth stages under field conditions, including yield and quality evaluations.

Acknowledgements. This work was supported by the National Key Research and Development Program of China (2017YFC0504804), the National Natural Science Foundation of China (31670405, 31971761) and the Fundamental Research Funds for the Central Universities (lzujbky-2018-k01).

REFERENCES

[1] Bao, A. K., Guo, Z. G., Zhang, H. F., Wang, S. M. (2009): A procedure for assessing the salt tolerance of lucerne (*Medicago sativa* L.) cultivar seedlings by combining agronomic

http://www.aloki.hu ● ISSN 1589 1623 (Print) ● ISSN 1785 0037 (Online)
DOI: http://dx.doi.org/10.15666/aeer/1706_1325313261

and physiological indicators. – New Zealand Journal of Agricultural Research 52: 435-442.

[2] Cattivelli, L., Rizza, F., Badeck, F. W., Mazzucotelli, E., Mastrangelo, A. M., Francia, E., Marè, C., Tondelli, A., Stanca, A. M. (2008): Drought tolerance improvement in crop plants: an integrated view from breeding to genomics. – Field Crops Research 105: 1-14.

[3] Cui, Y. N., Xia, Z. R., Ma, Q., Wang, W. Y., Chai, W. W., Wang, S. M. (2019): The synergistic effects of sodium and potassium on the xerophyte *Apocynum venetum* in response to drought stress. – Plant Physiology and Biochemistry 135: 489-498.

[4] Foster, K., Ryan, M. H., Real, D., Ramankutty, P., Lambers, H. (2012): Drought resistance at the seedling stage in the promising fodder plant tedera (*Bituminaria bituminosa* var. *albomarginata*). – Crop and Pasture Science 63: 1034-1042.

[5] Ghaderi, N., Siosemardeh, A. (2011): Response to drought stress of two strawberry cultivars (cv. *kurdistan* and *selva*). – Horticulture Environment and Biotechnology 52: 6-12.

[6] Guimarães, F. V., Lacerda, C. F., Marques, E. C., Miranda, M. R., Abreu, C. E., Prisco, J. T., Gomes-Filho, E. (2011): Calcium can moderate changes on membrane structure and lipid composition in cowpea plants under salt stress. – Plant Growth Regulation 65: 55-63.

[7] Guo, Z. G., Liu, H. X., Wang, Y. R., Wang, S. M., Cheng, G. D. (2004): Suitability of lucerne cultivars, with respect to root development, to semi-arid conditions in west China. – New Zealand Journal of Agricultural Research 7: 51-59.

[8] Hassine, A. B., Bouzid, S., Lutts, S. (2010): Does habitat of *Atriplex halimus* L. affect plant strategy for osmotic adjustment? – Acta Physiologiae Plantarum 32: 325-331.

[9] He, F. L., Bao, A. K., Wang, S. M., Jin, H. X. (2019): NaCl stimulates growth and alleviates drought stress the salt-secreting xerophyte *Reaumuria soongorica*. – Environmental and Experimental Botany 162: 433-443.

[10] Kang, Y., Han, Y., Torres-Jerez, I., Wang, M., Tang, Y., Monteros, M., Udvardi, M. (2011): System responses to long-term drought and re-watering of two contrasting alfalfa varieties. – The Plant Journal 68: 871-889.

[11] Kumar, S. (2011): Biotechnological advancements in alfalfa improvement. – Journal of Applied Genetics 52: 111-124.

[12] Kumar, T., Bao, A. K., Bao, Z., Wang, F., Gao, L., Wang, S. M. (2018): The progress of genetic improvement in alfalfa (*Medicago sativa* L.). – Czech Journal of Genetics and Plant Breeding 54: 41-51.

[13] Liu, H. X., Guo, Z. G., Wang, S. M., Zhang, Z. H., Wang, Y. R. (2005): A new procedure for evaluating lucerne genotypes for semi-arid land in west China. – New Zealand Journal of Agricultural Research 48: 109-116.

[14] Lu, X. S. (2013): Problems with the development of alfalfa industry in China. – Chinese Journal of Grassland 35: 1-5.

[15] Ma, Q., Yue, L. J., Zhang, J. L., Wu, G. Q., Bao, A. K., Wang, S. M. (2012): Sodium chloride improves photosynthesis and water status in the succulent xerophyte *Zygophyllum xanthoxylum*. – Tree Physiology 32: 4-13.

[16] Mohamed, M. F., Tawfik, A. A. (2006): Dehydration-induced alterations in growth and osmotic potential of callus from six tepary bean lines varying in drought resistance. – Plant Cell, Tissue and Organ Culture 87: 255-262.

[17] Noble, C. L., Rogers, M. E. (1992): Arguments for the use of physiological criteria for improving the salt tolerance in crops. – Plant and Soil 146: 99-107.

[18] Pang, J. Y., Yang, J. Y., Ward, P., Siddique, K. H. M., Lambers, H., Tibbett, M., Ryan, M. (2011): Contrasting responses to drought stress in herbaceous perennial legumes. – Plant and Soil 348: 299-314.

[19] Quan, W., Liu, X., Wang, H., Chan, Z. (2016): Comparative physiological and transcriptional analyses of two contrasting drought tolerant alfalfa varieties. – Frontiers in Plant Science 6: 1256.

http://www.aloki.hu ● ISSN 1589 1623 (Print) ● ISSN 1785 0037 (Online)
DOI: http://dx.doi.org/10.15666/aeer/1706_1325313261

[20] Shi, S. L., Nan, L. L., Smith, K. F. (2017): The current status, problems, and prospects of alfalfa (*Medicago sativa* L.) breeding in China. – Agronomy 7: 1.
[21] Singh, R., Srivastava, P., Singh, P., Sharma, A. K., Singh, H., Raghubanshi, A. S. (2019): Impact of rice-husk ash on the soil biophysical and agronomic parameters of wheat crop under a dry tropical ecosystem. – Ecological Indicators 105: 505-515.
[22] Wang, W. B., Kim, Y. H., Lee, H. S., Kim, K. Y., Deng, X. P., Kwak, S. S. (2009): Analysis of antioxidant enzyme activity during germination of alfalfa under salt and drought stresses. – Plant Physiology and Biochemistry 47: 570-577.
[23] Wu, G. Q., Wang, C. M., Su, Y. Y., Zhang, J. J., Feng, R. J., Liang, N. (2014): Assessment of drought tolerance in seedlings of sugar beet (*Beta vulgaris* L.) cultivars using inorganic and organic solutes accumulation criteria. – Soil Science and Plant Nutrition 60: 565-576.
[24] Xiao, Y., Zhang, J., Jia, T. T., Pang, X. P., Guo, Z. G. (2015): Effects of alternate furrow irrigation on the biomass and quality of alfalfa (*Medicago sativa*). – Agricultural Water Management 161: 147-154.
[25] Yamaguchi, M., Sharp, R. E. (2010): Complexity and coordination of root growth at low water potentials: recent advances from transcriptomic and proteomic analyses. – Plant, Cell and Environment 33: 590-603.
[26] Yan, W., Zhong, Y., Shangguan, Z. (2015): Evaluation of physiological traits of summer maize under drought stress. – Acta Agriculturae Scandinavica, Section B — Soil & Plant Science 66: 1-8.
[27] Zhang, W., Yu, X., Li, M., Lang, D., Zhang, X., Xie, Z. (2018): Silicon promotes growth and root yield of *Glycyrrhiza uralensis* under salt and drought stresses through enhancing osmotic adjustment and regulating antioxidant metabolism. – Crop Protection 107: 1-11.

http://www.aloki.hu ● ISSN 1589 1623 (Print) ● ISSN 1785 0037 (Online)
DOI: http://dx.doi.org/10.15666/aeer/1706_1325313261

EFFECTS OF DIFFERENT MIXTURE RATIOS AND HARVEST PERIODS ON GRASS QUALITY OF TRITICALE (*xTRITICOSECALE* WITTMACK) – FORAGE PEA (*PISUM SATIVUM* L.) INTERCROP

SEYDOSOGLU, S.[1*] – BENGISU, G.[2]

[1]*Field Crops Department, Agricultural Faculty, Siirt University, Siirt, Turkey*

[2]*Field Crops Department, Agricultural Faculty, Harran University, Şanlıurfa, Turkey*

**Corresponding author*
e-mail: seyithanseydosoglu@siirt.edu.tr; phone: + 90-544-645-8100

(Received 6th Jun 2019; accepted 28th Aug 2019)

Abstract. The aim of this study was to determine the effects of different mixture rates and harvest periods on the herbage quality of triticale (*xTriticosecale* Wittmack) and forage pea (*Pisum sativum* L.) intercrops. The research was carried out in Diyarbakir province of Turkey during the winter vegetation period of 2016-2017. The research was carried out in randomized block design in split parcels in which the harvest periods and mixture ratios formed the main parcels and sub-parcels, respectively. In the study, all harvests were conducted at spike and milking period of triticale. The mixing ratios were 100% forage peas (FP), 100% triticale (T), 75% FP + 25% T, 50% FP + 50% T, 25% FP + 75% T. As the harvest periods delayed, crude ash, crude protein, digestible dry matter, dry matter consumption and relative feed value decreased where Acid Detergent Fiber (ADF) and Neutral Detergent Fiber (NDF) rates increased. As the proportion of forage pea in the mixture increased, the ratio of crude protein and ADF increased, while the rate of digestible dry matter decreased. The spiking period of triticale was found to be the suitable harvest period. Sowing mixture at 25% FP + 75% T was superior obtaining good ADF, digestible dry matter and relative feed value. In the case of favorable NDF and crude protein ratios, 75% FP + 25% T proved to be superior to other mixture combinations.
Keywords: *cereal, legume, mixed cropping, feed quality*

Introduction

Intercropping is co-cultivation of two or more plant species in same period in same field. Triticale (× *Triticosecale* Wittmack), as a cereal, is more tolerant to biotic and abiotic stress conditions than wheat. Therefore, it is more suitable for marginal areas (Villegas et al., 2010). Triticale has high adaptability, better nutrient content and higher yield compared to other cereals (Oettler, 2005).

Forage pea is an important and nutritious fodder plant. It is reported that harvesting and weed control is a problem due to the significant lodging when this species is grown sole (Kadziuliene et al., 2011). Intercropping has many advantages. The presence of at least one legume species in the intercrop results with higher quality herbage production. Protein content and feed value increase with this method. In addition, wheat improves resistance to soil erosion where legumes reduce or prevent frost damage. The danger of swelling in animals due to some legumes may be reduced by feeding with these mixtures. Existence of cereals in mixtures also prevents lodging and decay of some legume fodder crops. In mixtures, the herbage gets dry better and more successful results are obtained in case of silage making. In case of existence of legumes in the intercrop; organic matter and nitrogen in the soil also increase. Generally in plants, as the development progressed, the weight increases, but the feed value decreases, which is

http://www.aloki.hu ● ISSN 1589 1623 (Print) ● ISSN 1785 0037 (Online)
DOI: http://dx.doi.org/10.15666/aeer/1706_1326313271

more rapid since cartilage is more rapid in wheat. Therefore, harvest times should be determined based on the development periods of cereals in intercrops (Asik, 2006).

In a study in Spain, Pereira-Crespo et al. (2010), used forage peas and triticale in mixtures where they reported that ADF and NDF content of triticale alone was higher compared to the mixture and sole forage pea. Lithourgidis et al. (2006) reported that they obtained highest crude protein yield from common vetch-triticale mixture containing 65% common vetch and 35% triticale. Karadag and Büyükburç (2004) reported that, with the Hungarian vetch and triticale mixtures, the ratio of crude protein increased when triticale ratio decreased in the mixture.

The ratio of the species in the mixture is very important in terms of yield and quality. In legume and cereal mixtures, with the increase in the ratio of leguminous, dry grass yield generally decreases but in order to obtain the desired quality feeds, the ratio of cereals should not be more than 20% (Yucel and Avci, 2009). In a study conducted in Mediterranean conditions of Turkey, it is reported that with triticale-berseem clover mixtures, 60% berseem clover + 40% triticale rate, and 100% flowering period of berseem clover was best for high yield and good silage quality values (Yucel et al., 2018a). In another study carried out in Mediterranean conditions of Turkey, it is reported that 60% berseem clovers with 40% Italian ryegrass harvested at 100% flowering period of the berseem clover were suitable for high yield and good silage quality values (Yucel et al., 2018b).

The aim of this study was to investigate the effects of mixture ratio and harvest periods on forage quality of triticale and forage pea mixtures cropped in winter season in Diyarbakır condition which is a very important zone for feed and animal production in Turkey.

Materials and methods

Forage pea (*Pisum sativum* L. cv. Gap Pink) and triticale (× *Triticosecale* Wittmack cv. Karma 2000) were used as material in the research. The research was carried out in 2016-2017 winter (November-May) conditions in research fields of "GAP International Agricultural Research and Training Center" in Diyarbakir province of Turkey. Some climate data for the research period from the trial area are presented in *Table 1*.

Table 1. *Some climate data of Diyarbakir province of Turkey*

Month	Average temperature (°C)		Precipitation (mm)	
	2016-2017 season	Long-term	2016-2017 season	Long-term
September	24.2	24.8	5.2	4.1
October	18.8	17.2	13.6	34.7
November	8.2	9.2	52.0	51.8
December	2.4	4.0	135.6	71.4
January	1.5	1.8	20.6	68.0
February	1.5	3.5	3.8	68.8
March	9.4	8.5	90.2	67.3
April	12.8	13.8	98.8	68.7
May	18.8	19.3	30.6	41.3
June	26.9	26.3	2.6	7.9
Total			453.0	484.0

http://www.aloki.hu ● ISSN 1589 1623 (Print) ● ISSN 1785 0037 (Online)
DOI: http://dx.doi.org/10.15666/aeer/1706_1326313271

Climatic data of trial year shows low deviation compared to long-term averages. The study was carried out with 3 replications based on divided parcels in randomized complete blocks design. Harvest times were at main parcels and mixture ratios were at sub-parcels. Harvest times were at two different times; spiking and milking period of triticale in the mixtures. Mixture ratios were 100% forage pea (FP), 100% triticale (T), 75% FP + 25%T, 50%FP + 50%T, and 25%FP + 75%T.

Each parcel was 6 m long containing 10 rows at 20 cm row spacings where both species were mixed before planting. 100 kg/ha forage pea and 220 kg/ha triticale seed applied at planting. Before planting, diammonium phosphate fertilizer (18.46.0) was applied to the parcels in order to provide 40 kg/ha pure nitrogen and 100 kg/ha pure phosphorus (Kir, 2014). Parcel border rows and 0.5 m of row end tails of parcels were eliminated before harvest and 8 m^2 areas of each parcel were harvested. 500 g of harvested green herbage materials were used for the determination of both species in each parcel. These samples were separated into two species (triticale and forage pea) to calculate the ratios of both species in each parcel. Green herbage samples were dried in a drying cabinet for 48 h at 70 °C before determining dry herbage ratios. Then botanical composition rates of dry herbage were determined and each sample was milled for quality analysis. Crude ash, crude protein, ADF and NDF analysis were performed on these milled herbage samples of forage peas and triticale separately and parcel values were calculated according to their ratio in botanical composition in accordance with Yucel et al. (2015). According to this method, during the harvests, 500 grams of green herbage samples taken from the mixture parcels were divided into pea and triticale species and green herbage weights were determined. Then, the proportional weights of the forage pea and triticale plants were calculated and assigned as botanical composition rate. Weende method for raw ash (AOAC, 1990), Kjeldahl method for raw protein (AOAC, 1990) and ANKOM method for ADF and NDF (Van Soest, 1967) were applied for quality analysis. Digestible dry matter (DDM), dry matter consumption (DMC) and relative feed value (RFV) of dry herbage were calculated by using *Equations 1–3* in accordance with Morrison (2003).

$$DDM = 88.9 - (0.779 \times ADF\%) \quad \text{(Eq.1)}$$

$$DMC = \frac{120}{NDF\%} \quad \text{(Eq.2)}$$

$$RFV = \frac{DDM \times DMC}{1.29} \quad \text{(Eq.3)}$$

Variance analysis of the data obtained from the study was conducted by using JUMP statistical package program and the significant averages were grouped into LSD, 5% (Kalayci, 2005).

Results and discussion

Harvest period, mixture rate and harvest period x mixture rate interaction were found statistically significant for crude ash (CA) and crude protein (CP) ratios (*Table 2*). The CA ratio, which was 8.70% at the spike period, decreased to 7.34% at the milking

http://www.aloki.hu ● ISSN 1589 1623 (Print) ● ISSN 1785 0037 (Online)
DOI: http://dx.doi.org/10.15666/aeer/1706_1326313271

period, meaning that the effect of the harvest period was significant on CA ratio. The average lowest CA ratio (7.67%) was obtained from the 75%FP + 25% T mixture and no statistically significant difference was observed between other mixtures. When the CA ratio is examined for the harvest period x mixture interaction; the highest CA ratio was found to be obtained from spiking period at 100% T, 25% FP + 75% T and 50% FP + 50% T mixtures. The lowest CA ratio was obtained from milking period at all applications except 100% FP (*Table 2*).

Table 2. *Rates of crude ash and crude protein examined in the dry herbage (%)*

Mixture rate (MR)		Crude ash ratio (%)			Crude protein ratio (%)		
		Harvest period (HP)			Harvest period (HP)		
		Spiking	Milking	Average	Spiking	Milking	Average
100% FP		8.35c[1]	8.03c	8.19A*	16.42a	15.66a	16.04A
100% T		8.93a	7.30d	8.12A	10.22c	5.50e	7.86E
25% FP + 75% T		8.87ab	7.15d	8.01A	10.27c	8.35d	9.31D
50% FP + 50% T		8.96a	7.28d	8.12A	12.90b	11.21c	12.06C
75% FP + 25% T		8.41bc	6.92d	7.67B	13.51b	12.70b	13.11B
Averages		8.70A+	7.34B	8.02	12.67A	10.69B	11.68
LSD (0.05)	HP	0.20**			0.51**		
	MR	0.32*			0.44**		
	HP × MR	0.47**			1.15**		

*The means with the same capital letter in the same column are not statistically significant different from each other according to the LSD test at $P \leq 0.05$

+The means with the same capital letter in the same row are not statistically significant different from each other according to the LSD test at $P \leq 0.05$

[1]The means of different treatment-harvest stage combinations with the same lower case are not statistically significant different from each other according to the LSD test at $P \leq 0.05$

The effect of harvest period on the CP ratio was found significant. The CP ratio was decreased from 12.67% to 10.69% after the transition from the spike to the milking period. Kim et al. (1990) reported that the CP ratio decreased rapidly due to the reduction in photosynthetic leaf area during the post-spike period. Other investigators also reported decreases in CP ratio following delays in harvest period. For example, Asik (2006) reported a CP ratio decrease from 13.36% to 5.77% at barley-pea mixtures when barley harvest period was delayed from stem elongation stage to yellow dough stage. Kir et al. (2018) also reported CP ratio decrease from 16.3% to 14.0% at Hungarian vetch-cereal mixtures when cereal was progressed transition from booting stage to milk dough stage.

Table 2 shows that the effect of average CP on mixtures is significant. The highest and lowest CP ratio was obtained from sole forage pea with 16.04% and sole triticale with 7.86%, respectively. CP ratio of all mixtures was higher than sole triticale. The high CP ratio of sole pea sources probably from the high ratio of both pods number and leaves/stalk rate. Many investigators was reported an increase in the CP ratio in case of existence of higher proportion of legumes in the mixtures (Kavut et al., 2014; Yildirim and Ozaslan-Parlak, 2016; Kir et al., 2018).

http://www.aloki.hu ● ISSN 1589 1623 (Print) ● ISSN 1785 0037 (Online)
DOI: http://dx.doi.org/10.15666/aeer/1706_1326313271

When *Table 2* is examined; the effect of HP x MR interaction on CP probably was found to be significant. The highest CP ratio was obtained from sole forage pea at milk period while the lowest CP ratio was obtained from sole triticale at milking stage.

The effect of harvest period on ADF and NDF ratios was found significant. There was a statistically significant increase in ADF ratio as the harvest period was delayed (*Table 2*). The mean ADF ratio was increased from 31.29% to 36.20% and the rate of NDF from 44.15% to 48.91% after transition from spiking period to milking period. Many investigators also reported an increase in ADF and NDF ratio with delayed harvest time. For example, Aksoy and Nursoy (2010) reported that, in Hungarian vetch-wheat mixture, the ratio of ADF and NDF ratio varied between 25.94-38.24% and 36.47-57.61%, respectively. Guzelogullari (2012) reported that, in different vetch species at different harvest time, the ADF and NDF ratio was varied between 25.53-34.58% and 33.21-38.68%, respectively. Turgut et al. (2006) observed that, at Hungarian vetch, common vetch and hairy vetch, delays in harvest time was increased NDF ratio. Kir et al. (2018) reported the ADF ratio in Hungarian vetch-cereal mixtures as between 29.5-32.1% and NDF ratio as between 49.7-52.3%. These results are supporting our findings.

When *Table 3* is examined, it can be noticed that averages ADF and NDF values of mixtures were statistically significant. The highest and the lowest ADF ratio was obtained from sole triticale with 37.89% and sole forage pea with 29.95%, respectively. The lowest NDF ratio was also obtained from sole forage pea. Yildirim and Ozaslan-Parlak (2016) found ratio of ADF as 29.59%, NDF as 55.53% for triticale, and ADF as 23.10% and NDF as 46.34% for forage pea. Gocmen and Ozaslan-Parlak (2017), reported the ADF ratio of triticale as 45.16% and NDF ratio as 63.22% and forage pea ADF ratio as 41.23% and NDF ratio as 50.31%. These results are in accordance with our results.

Table 3. *Rates of acid detergent fiber (ADF) and neutral detergent fiber (NDF) examined in the dry herbage (%)*

Mixture rate (MR)		ADF (%)			NDF (%)		
		Harvest period (HP)			Harvest period (HP)		
		Spiking	Milking	Average	Spiking	Milking	Average
100% FP		28.10	31.80	29.95E*	47.60c[1]	39.87g	43.74C
100% T		34.97	40.81	37.89A	51.31a	46.03d	48.67C
25% FP + 75% T		28.67	33.98	31.33D	48.17c	44.25e	46.21B
50% FP + 50% T		31.43	35.68	33.56C	49.61b	48.17c	48.89A
75% FP + 25% T		33.30	38.70	36.00B	47.89c	42.43f	45.16B
Averages		31.29B+	36.20A	33.75	48.91A	44.15B	46.53
LSD (0.05)	HP	1.04**			0.44**		
	MR	0.53**			1.06**		
	HP x MR	n.s.			1.01**		

*The means with the same capital letter in the same column are not statistically significant different from each other according to the LSD test at $P \leq 0.05$

+The means with the same capital letter in the same row are not statistically significant different from each other according to the LSD test at $P \leq 0.05$

[1]The means of different treatment-harvest stage combinations with the same lower case are not statistically significant different from each other according to the LSD test at $P \leq 0.05$

http://www.aloki.hu ● ISSN 1589 1623 (Print) ● ISSN 1785 0037 (Online)
DOI: http://dx.doi.org/10.15666/aeer/1706_1326313271

When *Table 4* is examined, it is noticed that the effect of harvest period on the DDM rate is significant. Significant reductions was realised in the ratio of DDM as the harvest period was delayed. The rate of DDM was 64.52% and 60.70% at the spike period and milking period, respectively. Prolonged vegetation period probably resulted with structural changes in plant tissues with increased ADF ratios and finally these changes decreased DDM rate. One of the most important factors affecting the quality of feed is harvest time. Because the differences in the ADF value due to developmental periods significantly affect the digestibility of the feed (Caddel and Allen, 1997; Cinar, 2012).

The effect of mixtures on DDM ratios was found significant. The highest and lowest DDM ratios were obtained from sole forage pea and sole triticale, respectively (*Table 4*).

In studies conducted by different researchers, the ratio of DDM was between 59.1-68.7% at Hungarian vetch-wheat mixture (Aksoy and Nursoy, 2010), 65.5% at barley, 65.8% at triticale (Canpolat, 2012), 60.7-64.4% at Hungarian vetch-barley (Yilmaz et al. (2014) and average 63.9% at different Hungarian vetch-cereal mixtures (Kir et al., 2018). Our findings were similar to these results.

Table 4. *Rates of digestible dry matter (DDM) and dry matter consumption (DMC) examined in the dry herbage (%)*

Mixture rates (MR)		DDM rate (%)			DMC rate (%)		
		Harvest periods (HP)			Harvest periods (HP)		
		Spiking	Milking	Average	Spiking	Milking	Average
100% FP		67.01	64.13	65.57A*	2.52e[1]	3.01a	2.77A
100% T		61.66	57.11	59.38E	2.34g	2.61d	2.47D
25% FP + 75% T		66.57	62.43	64.50B	2.49e	2.71c	2.60C
50% FP + 50% T		64.42	61.11	62.76C	2.42f	2.49e	2.46D
75% FP + 25% T		62.96	58.75	60.85D	2.51e	2.83b	2.67B
Averages		64.52A+	60.70B	62.61	2.46B	2.73A	2.59
LSD (0.05)	HP	0.42**			0.02**		
	MR	0.81**			0.05**		
	HP x MR	n.s.			0.07**		

*The means with the same capital letter in the same column are not statistically significant different from each other according to the LSD test at $P \leq 0.05$

+The means with the same capital letter in the same row are not statistically significant different from each other according to the LSD test at $P \leq 0.05$

[1]The means of different treatment-harvest stage combinations with the same lower case are not statistically significant different from each other according to the LSD test at $P \leq 0.05$

When the effect of harvest periods on DMC ratio was examined (*Table 4*), statistically significant differences were observed. The rate of DMC was 2.73% at spiking period, and 2.46% at the milking period. DMC rate was significantly decreased when harvest period was delayed. The effect of mixtures on DMC ratios was also found significant (*Table 4*). The highest DMC ratio was obtained from sole forage pea (2.77%), where the lowest was obtained from sole triticale and 50% YB + 50% T mixture.

http://www.aloki.hu ● ISSN 1589 1623 (Print) ● ISSN 1785 0037 (Online)
DOI: http://dx.doi.org/10.15666/aeer/1706_1326313271

The effect of harvest periods on RFV was found significant. A statistically significant decrease was observed in the RFV as the harvest period was delayed (*Table 5*). RFV was 136.69 and 115.64 at the spiking period and milking period, respectively. It was determined that the effect of the different mixtures on the RFV was significant, where the highest and lowest RFV was obtained from sole forage pea and sole triticale, respectively.

Table 5. *Rates of relative feed value (RFV) examined in the dry herbage (%)*

Mixture rates (MR)		RFV		
		Harvest periods (HP)		
		Spiking	**Milking**	**Average**
100% FP		156.42a	125.33c[1]	140.87A*
100% T		124.64c	103.59f	114.11E
25% FP + 75% T		139.94b	120.57d	130.26B
50% FP + 50% T		124.42c	114.60e	119.51D
75% FP + 25% T		138.03b	114.12e	126.08C
Average		136.69A +	115.64B	126.17
LSD (0.05)	HP	1.95**		
	MR	3.27**		
	HP x MR	4.37**		

*The means with the same capital letter in the same column are not statistically significant different from each other according to the LSD test at $P \leq 0.05$

+The means with the same capital letter in the same row are not statistically significant different from each other according to the LSD test at $P \leq 0.05$

[1]The means of different treatment-harvest stage combinations with the same lower case are not statistically significant different from each other according to the LSD test at $P \leq 0.05$

When quality classification of Rohweder et al. (1978) was considered as reference, which is based on the 100% flowering period of clover, where RFV > 151 = premium quality, 151-125 = 1st quality (very good), 124-103 = 2nd quality (good), 102-87 = 3rd quality (medium), 86-75 = 4th quality (bad), < 75 = 5th quality (unacceptable), quality scores ranged between 1st and 2nd quality at different harvest periods and mixture combinations in our study.

In different studies, relative feed value in different harvest periods was between 98-114 for pure triticale (Yucel et al., 2018a), 106-108 for wheat-Hungarian vetch mixture (Aksoy and Nursoy, 2010), 96.2-118.8 for Hungarian vetch-barley (Yilmaz et al., 2014) and 109 for Hungarian vetch-lolium mixture (Kusvuran et al., 2014). Our findings were similar to these results.

Conclusions

Main aim of inclusion of forage pea in triticale is to increase its protein content. Shifting forage pea rate in the mixture from 25% to 50% increases the CP approximately 33% whereas shifting forage pea rate from 50% to 75% increases CP approximately 8%. But in the same time, RFV is 6 points and DMC is 0.2% higher when shifted forage pea rate from 50% to 75%. Milking period of triticale was found the most appropriate harvest period. So, when these important quality parameters

http://www.aloki.hu ● ISSN 1589 1623 (Print) ● ISSN 1785 0037 (Online)
DOI: http://dx.doi.org/10.15666/aeer/1706_1326313271

considered together, it is found appropriate to propose 75% FP + 25%T mixture under arid climate conditions similar to East Anatolia according to this study. Testing morphologically different forage pea and triticale cultivars may produce different information related to the subject which is proposed to future researchers.

Acknowledgements. This study was a part of "TAGEM/17A07/P7/004" coded project which was supported by the General Directorate of Agricultural Research and Policies (TAGEM). Authors thank to TAGEM for their support.

REFERENCES

[1] Aksoy, I., Nursoy, H. (2010): Determination of nutrient composition, rumination properties in rumen, in vitro digestible and relative feed value of Hungarian vetch-wheat mixture in different periods of vegetation. – Kafkas University Journal of Veterinary Medicine 16(6): 925-931 (in Turkish).

[2] AOAC (1990): Official Method of Analysis. 15th. Ed. – Association of Official Analytical Chemists, Washington, DC, pp. 66-88.

[3] Asik, F. F. (2006): Determine the effects of seed rates in mixtures of pea (Pisum sativum L.) + barley (*Hordeum vulgare* L.) and cutting stages on the hay yield and its quality. – Yüksek Lisans Tezi, Uludağ Üniversitesi Fen Bilimleri Enstitüsü, Bursa.

[4] Caddel, J., Allen, E. (1997): Forage Quality Interpretations. – http://virtual,chapingo,mx/dona/paginaCBasicos/f-2117.pdf (access date: 18.02.2019).

[5] Canbolat, O. (2012): Comparison of invitro gas production, digestible organic matter, relative feed value and metabolic energy content of some wheat roughage. – Kafkas University Journal of Veterinary Medicine 18(4): 571-577 (in Turkish).

[6] Cinar, S. (2012): Determination of suitable mixtures of some perennial warm season cereal forage crops with alfalfa (*Medicago sativa* L.) in Cukurova conditions. – PhD Thesis. Çukurova University School of Natural and Applied Sciences, Adana (in Turkish).

[7] Gocmen, N., Ozaslan-Parlak, A. (2017): Determination of mixture rates of barley, oats and triticale with feed pea. – Canakkale Onsekiz Mart University Journal of Agriculture 5(1): 119-124 (in Turkish).

[8] Guzelogulları, E. (2012): The effects of different sowing and harvesting times on the yield and quality of some vetch (*Vicia spp*.) species in Isparta ecological conditions. – Master Thesis. Süleyman Demirel University, School of Natural and Applied Sciences, Isparta (in Turkish).

[9] Kadziuliene, Z., Sarunaite, L., Deveikyte, I. (2011): Ratarstvoi povrtarstvo. – Field and Vegetable Crops Research 48: 183-188.

[10] Kalayci, M. (2005): Models of Variance Analysis for the Use of Jump and Agricultural Research with Examples. – Anadolu Agricultural Research Institute Publications, Anadolu. Publication no: 21 (in Turkish).

[11] Karadag, Y., Buyukburc, U. (2004): Effect of different seed proportion on yield of forage, seed and quality of annual legume and barley (Hordeum vulgare) mixture. – The Indian Journal of Agricultural Sciences 74(5): 265-7.

[12] Kavut, Y. T., Geren, H., Soya, H., Avcioğlu, R., Kir, B. (2014): Effects of rate of mixture and time of harvest on the winter second crop performances of mixtures of some annual legumes and italian ryegrass. – Journal of Ege University, Faculty of Agriculture 51(3): 279-288.

[13] Kim, J. G., Yang, J. S., Han, M. S., Lee, S. B. (1990): Studies on dry matter production and nutritive quality of rye and barley. II. Changes in the chemical components digestibility and net energy value as affected by stage of morphological development. – Herbage Abst. 60(5): 176.

http://www.aloki.hu ● ISSN 1589 1623 (Print) ● ISSN 1785 0037 (Online)
DOI: http://dx.doi.org/10.15666/aeer/1706_1326313271

[14] Kir, H. (2014): Effects of cutting time and mixture ratio on the forage yields and qualities of the mixtures of Hungarian vetch with some cereal species under Kırşehır conditions. – PhD Thesis, Gaziosmanpaşa University, Institute of Science and Technology, Tokat (in Turkish).
[15] Kir, H., Karadag, Y., Yavuz, T. (2018): The factors affecting yield and quality of Hungarian vetch + cereal mixtures in arid environmental conditions. – Fresenius Environmental Bulletin 27(12A): 9049-9059.
[16] Kusvuran, A., Kaplan, M., Nazlı, I., R. (2014): Effects of mixture ratio and row spacing in Hungarıan vetch (Vicia pannonica Crantz.) and annual ryegrass (Lolium multiflorum L.) intercropping system on yield and quality under semi arid climate conditions. – Turkish Journal of Field Crops 19(1): 118-128.
[17] Lithourgidis, A. S., Vasilakoglou, I. B., Dhima, K. V., Dordas, C. A., Yiakoulaki, M. D. (2006): Forage yield and quality of common vetch mixtures with oat and triticale in two seeding ratios. – Field Crops Res. 99: 106-113.
[18] Morrison, J. A. (2003): Hay and Pasture Management. Chap. 8. – Extension Educator, Crop Systems Rock Ford Extension Center. http://iah.aces.uiuc.edu/pdf/ Agronomy_HB/08chapter.pdf (access date: 20.02.2019).
[19] Oettler, G. (2005): The fortune of a botanical curiosity-triticale: past, present and future. – J. Agric. Sci. 143: 329-346.
[20] Pereira-Crespo, S., Fernández-Lorenzo, B., Valladares, J., González-Arráez, A., Flores, G. (2010): Effects of seeding rates and harvest date on forage yield and nutritive value of pea-triticale intercropping. – Options Méditerranéennes A 92: 215-218.
[21] Rohweder, D. A., Barnes, R. F., Jorgensen, N. (1978): Proposed hay grading standards based on laboratory analyses for evaluating quality. – Journal of Animal Science 47(3): 747-759.
[22] Turgut, L., Yanar, M., Kaya, A. (2006): Raw nutrient contents of some vetch species harvested in different maturity stages and their in situ ruminal degradabilities. – Journal of Atatürk University, Faculty of Agriculture 37(2): 181-186.
[23] Van Soest, P. J. (1967): Development of a comprehensive system of feed analyses and its application to forages. – Journal of Animal Science 26: 119-128.
[24] Villegas, D., Casadesus, J., Atienza, S., Martos, V., Maalouf, F., Karam, F., Aranjuelo, I., Nogues, S. (2010): Tritordeum, wheat and triticale yield components under multi-local Mediterranean drought conditions. – Field Crops Res. 116: 68-74.
[25] Yıldırım, S., Parlak-Özaslan, A. (2016): Forage yield, qualty of triticale intercrops with faba bean, pea and vetch at varying seeding ratios. – Journal of Çanakkale University, Faculty of Agriculture 4(1): 77-83.
[26] Yılmaz, Ş., Özel, A., Atak, M., Erayman, M. (2014): Effects of seeding rates on competition indices of barley and vetch intercropping systems in East Mediterranean. – journals.tubitak.gov.tr/openAcceptedDocument. htm? fileID=464949&no=100552 (access date: 18.02.2019).
[27] Yucel, C., Avcı, M. (2009): Effect of different ratios of common vetch (*Vicia sativa* L.) - triticale (*Triticosecale* Whatt) mixtures on forage yields and quality in Cukurova plain in Turkey. – Bulgarian Journal of Agricultural Science 15(4): 323-332.
[28] Yucel, C., Avcı, M., İnal, İ., Yücel, H., Aktaş, A., Hatipoğlu, R. (2015): Effects of different mixing ratios and harvest periods of *Trifolium alexandrinum* triticale and Italian grass on yield and silage quality. – Project Final Report. TAGEM/TA/11/005 (in Turkish).
[29] Yucel, C., Avcı, M., Yucel, H., Sevilmiş, U., Hatipoğlu, R. (2018a): Effects of seed mixture ratio and harvest time on forage yield and silage quality of intercropped berseem clover with triticale. – Fresenius Environmental Bulletin 27(8): 5312-5322.
[30] Yucel, C., İnal, İ., Yucel, D., Hatipoğlu, R. (2018b): Effects of mixture ratio and cutting time on forage yield and silage quality of intercropped Berseem clover and Italian ryegrass. – Legume Research 41(5): 1-8.

http://www.aloki.hu ● ISSN 1589 1623 (Print) ● ISSN 1785 0037 (Online)
DOI: http://dx.doi.org/10.15666/aeer/1706_1326313271

A RADISH (*RAPHANUS SATIVUS* L.) E3 UBIQUITIN LIGASE GENE *RHA2b* ENHANCES SEED DORMANCY AND TOLERANCE TO PREHARVEST SPROUTING IN TRANSGENIC WHEAT (*TRITICUM AESTIVUM* L.)

LI, D. B.[#] – LYU, G. Z.[#] – JIANG, Y. M. – NIU, H. B. – WANG, X. – YIN, J.[*]

National Engineering Research Center for Wheat, State Key Laboratory of Wheat and Maize Crop Science, Collaborative Innovation Center of Henan Grain Crop, Henan Agricultural University, Zhengzhou 450002, China

**Corresponding author*
e-mail: xmzxyj@126.com; phone: +86-371-6355-8203

[#]These authors contributed equally to this work

(Received 9th Jun 2019; accepted 28th Aug 2019)

Abstract. The *RHA2b* gene from radish encodes a transcription factor that is involved in abscisic acid (ABA) signal transduction and is associated with seed dormancy and preharvest sprouting. *RsRHA2b* gene may have the function to improve dormancy and tolerance to PHS in transgenic wheat. The *RsRHA2b* gene was cloned and transferred into Zhengmai 9023 via *Agrobacterium*-mediated stem apex transformation. The results of RT-PCR and southern blot indicated that the *RsRHA2b* gene was integrated into the genomes of the wheat transformants. Seed dormancy and PHS tolerance was significantly enhanced in transgenic plants that stably expressed *RsRHA2b*. In addition, in the presence of 0.5 μmol/L ABA and 5 μmol/L ABA, a significant reduction in weight was found between the transgenic wheat plants and the non-transgenic Zhengmai 9023 plants. Furthermore, the expression of genes involved in *RHA2b*-mediated ABA signal transduction, such as *ABI5, FUS3* and *MAL,* significantly increased at the second leaf stage in ABA-treated transgenic wheat plants. These results show that *RsRHA2b* improves dormancy and preharvest sprouting tolerance in transgenic wheat.
Keywords: *agrobacterium-mediated stem apex transformation, southern blot, abscisic acid, signal transduction, reverse transcription-polymerase chain reaction*

Introduction

Preharvest sprouting (PHS) in wheat (*Triticum aestivum* L.) is the germination of grains in the ears when long-range rainfall or damp conditions occur prior to harvest (Li et al., 2004). PHS is an important issue, which is is not conducive to the stability of wheat production worldwide (Xiao et al., 2002). Seed viability and the hydrolysis of starch and protein in the endosperm are always reduced after PHS (Mohan, 2008). Moreover, PHS creates a favorable environment for serious infections by saprophyte fungi and thus causes heavy losses to grain yield (Castor and Frederiken, 1977). Therefore, there is a need to breed for increased resistance to PHS. Molecular breeding may be an effective method to reduce PHS susceptibility. Wheat is an important cereal crop worldwide, and it is a staple food for many populations. Genetically modified (GM) crops can act as powerful complement to the crops produced by laborious and time consuming conventional breeding methods to meet the worldwide demand for quality foods and help fight malnutrition by enhanced yield, nutritional quality and increased resistance to various biotic and abiotic stresses (Kamthan et al., 2016). PHS and dormancy in wheat have been focuses of numerous researches. *TaRHA2b* and *RsRHA2b* gene may play an important role in seed

http://www.aloki.hu ● ISSN 1589 1623 (Print) ● ISSN 1785 0037 (Online)
DOI: http://dx.doi.org/10.15666/aeer/1706_1327313288

dormancy during germination, which could be used to improve the PHS resistance of wheat. Because of homologous co-suppression in transgenic plants, exogenous genes are usually used for genetic manipulation.

To date, most researchers have agreed that PHS is the result of interactions between genotypes and the environment. Seed dormancy is an adaptive trait that inhibits seed germination and is positively correlated with resistance to PHS (Derera et al., 1977; Gerjets et al., 2010; Gubler et al., 2005; Chen et al., 2008b). The resistance of a seed to PHS is partially influenced by the external environment, but seed dormancy is the most critical determinant (Kucera et al., 2005; Holdsworth et al., 2008). As has been confirmed in many species, seed dormancy is influenced by the internal abscisic acid (ABA) content and the sensitivity to ABA (Groot and Karssen, 1992; Tan et al., 1997). ABA plays a critical role in plant development. Therefore, ABA, including its metabolism and signaling, has long been a focus of research (Grill and Himmelbach, 1998; Raghavendra et al., 2010; Zhu, 2002). ABA is important for plant growth and developmental processes, such as seed maturation, germination and seedling growth. ABA also regulates plant adaptation to various environmental challenges, including drought, salt, cold and other abiotic stresses (Nambara and Marion-Poll, 2003; Yamaguchi Shinozaki and Shinozaki, 2006; Lopez-Molina et al., 2001). During seed maturation, the ABA content in the seed increases significantly, resulting in strong dormancy. After the mature seed absorbs water, it quickly changes from a state of dormancy to a state of germination.

Many regulatory factors and response regulators in ABA signaling act in the signal transduction cascade during seed maturation and in young seedlings. These factors include ABA receptors, regulators and really interesting new gene (RING) finger transcription factors, which regulate the regulatory factors via ubiquitination and via the expression of ABA downstream response regulators (Koornneef et al., 1984). The genes related to ABA include ABI5, FUS3, MAL, and so on (Chiu et al., 2012; Huang et al., 2012; Li et al., 2011). The ubiquitin-proteasome pathway comprises two major components, the ubiquitination machinery, which attaches a ubiquitin or a poly-ubiquitin chain to a substrate, and the 26S proteasome, which degrades poly-ubiquitin-tagged protein substrates (Dreher and Callis, 2007; Moon et al., 2004; Schwechheimer and Schwager, 2004; Smalle and Vierstra, 2004). The ubiquitination of substrate proteins requires three types of enzymes, including E1 enzymes, which are ubiquitin-activating enzymes; E2 enzymes, which are ubiquitin-conjugating enzymes; and E3 enzymes, which are ubiquitin ligases. These three enzyme types act sequentially to catalyze the covalent attachment of the 76-amino-acid ubiquitin to the target protein. The E3 ligases recruit specific substrates and are the key determinants of the specificity of ubiquitination (Smalle and Vierstra, 2004).

RING finger proteins have motifs containing conserved cysteines and histidines. The RING motifs can be classified into three subgroups, including C3HC4 (RING-HC), C3H2C3 (RING-H2) and modified RING domain proteins. RING finger proteins always mediate protein-protein interactions and the formation of multi-protein complexes (Borden, 2000; Stone et al., 2005). At least 477 RING motif-containing proteins that play a critical role in plant developmental processes have been found in *Arabidopsis* (Vierstra, 2009). Some evidence has indicated that RING class E3 enzymes are critical for regulating ABA signaling and are associated with abiotic stress responses in plants (Ko et al., 2006; Zhang et al., 2005, 2007). RHA2a and RHA2b, which are RING finger E3 ligases, can positively regulate the ABA-mediated

http://www.aloki.hu ● ISSN 1589 1623 (Print) ● ISSN 1785 0037 (Online)
DOI: http://dx.doi.org/10.15666/aeer/1706_1327313288

inhibition of germination and act in the early seedling stage. RHA2a can activate positive regulators by mono-ubiquitinating and stabilizing certain key regulators of the ABA signaling pathway (Bu et al., 2009). ANAC019 and ANAC055, two closely related NAC family proteins, were identified as RHA2a-interacting proteins (Bu et al., 2008; Jiang et al., 2009). RHA2b acts additively with RHA2a in regulating ABA signaling. Seeds over-expressing *RHA2a* and *RHA2b* showed increased sensitivity to exogenous ABA, increased dormancy and a significant reduction in germination capacity. RHA2b targets MYB30 degradation to regulate ABA signal transduction (Zheng et al., 2018). Although some progress has been made in understanding the molecular and biological functions of *RHA2b* in *Arabidopsis*, the molecular mechanism of *RHA2b*-mediated ABA signaling is largely unknown. The *AtRHA2b* gene encodes an active E3 ubiquitin ligase that plays a positive regulatory role in ABA signaling and stress responses. The over-expression of *AtRHA2b* leads to ABA-associated phenotypes, such as ABA hyper-sensitivity in seed germination and seedling growth (Li et al., 2011).

In our previous studies, *TaRHA2b* and *RsRHA2b* genes were cloned from wheat and radish (*Raphanus sativus* L.), respectively. The results showed that the proteins encoded by *TaRHA2b* and *RsRHA2b* were consisted of Zinc finger RING-type profiles. Blast and phylogenetic analysis showed that the protein encoded by *TaRHA2b* and *RsRHA2b* shared the identity with *AtRHA2b* from the Arabidopsis. The expression of *TaRHA2b* and *RsRHA2b* genes was significantly tissue-specific. The sensitivity of the *TaRHA2b* and *RsRHA2b* genes to ABA was significantly increased (Li et al., 2019a). The differences in nucleotide polymorphism sites of *RsRHA2b* gene resulted in differences in the three cleavage sites of *BstD102I*, *Cfr10I*, and *HpaII/MspI* (Li et al., 2019b). These results facilitate the exploration of the correlation between the *TaRHA2b* gene and wheat's enhanced resistance to PHS and the development of molecular markers for resistance to PHS.

In the present study, the *RsRHA2b* gene from radish was cloned and then transferred into wheat using *Agrobacterium tumefaciens*. Seed dormancy and ABA sensitivity were significantly enhanced in transgenic wheat lines. These results displayed that *RsRHA2b* gene has the function to improve dormancy and tolerance to PHS in transgenic wheat.

Materials and methods

To clone the *RsRHA2b* gene, mRNA was isolated from the embryos of a local radish variety, "New generation 791". The elite Chinese bread wheat cultivar Zhengmai 9023, a hexaploid wheat cultivar with weak resistance to PHS, which is widely cultivated in Henan Province, was used for transformation.

Construction of a binary vector

The coding sequence and 3'-untranslated region (3'-UTR) of the *RsRHA2b* gene were amplified from radish cDNA via PCR with primers *RsRHA2b*-F2/*RsRHA2b*-R2 (*Table 1*). The PCR-amplified products were cloned into TA vectors (Takara, Dalian, China) and sequenced. A binary vector was constructed based on pCAMBIA3301. The TA vectors including the *RsRHA2b* gene and the pCAMBIA3301 vector were digested with *Bgl*II and *BstE*II. The two digested fragments were ligated together using T4 ligase. The resulting binary vector carried the *phosphinothricin* gene (*bar*) for selection.

http://www.aloki.hu ● ISSN 1589 1623 (Print) ● ISSN 1785 0037 (Online)
DOI: http://dx.doi.org/10.15666/aeer/1706_1327313288

Agrobacterium-mediated stem apex transformation of wheat

Wheat seeds were sterilized with 0.1% $HgCl_2$ for 10 min, then washed five times with sterilized distilled water. The sterilized seeds were germinated at 25 °C in the dark for 2–3 days on filter-containing plates. When the coleoptiles of the seeds reached a certain height (2–4 cm), the shoots were cut using a clean knife. Then, the stem apexes were exposed. Finally, 2–4 μL of resuspended *Agrobacterium* harboring the *RsRHA2b* gene and that had been induced with 100 μmol/L acetosyringone was dropped onto the stem apex for inoculation.

The inoculated seedlings were maintained on medium-containing plates until new leaves grew out, and then the seedlings were transferred into pots. Selection for resistance was performed by spraying the seedlings with a solution containing 160 mg/L basta when the seedlings had 3–4 leaves. The resistant plants were planted in the field.

Propagation of the transgenic lines

The seeds were harvested from the field in 2011. Then, they were grown in a digital biochemical incubator after rigorous screening. When the seedlings had 3–4 leaves, selection for resistance was performed by spraying the seedlings with a solution containing 160 mg/L basta. Genomic DNA and RNA were extracted from young wheat leaves. Then, PCR, reverse transcription-polymerase chain reaction (RT-PCR) and quantitative real-time polymerase chain reaction (qRT-PCR) analyses were conducted on the resistant plants. The seeds of *RsRHA2b* transgenic plants were harvested while the plants were in the digital biochemical incubator. Then, they were grown in the field. They were then grown and screened as in prior years.

DNA and RNA extraction

Genomic DNA was extracted from young wheat leaves. Total RNA was isolated from seeds and leaves using TRIzon reagent (CoWin Biotech Co., China) according to the manufacturer's instructions and treated with RNase-free DNase I (Tiangen, China) before final precipitation with ethanol.

PCR, RT-PCR analysis and southern blot

For the PCR analysis of transgenic plants, a 565 bp *RsRHA2b* product was amplified using PCR with the primers *RsRHA2b*-F1/*RsRHA2b*-R1 (*Table 1*), which were designed based on pCAMBIA3301-*RsRHA2b*. The primers were specific for radish.

For RT-PCR analyses of transgenic plants, approximately 5 μg of total RNA from the shoots of transgenic plants was reverse-transcribed into cDNA using reverse transcriptase (Tiangen, China) and oligo-dT_{18} primers. PCR amplifications were performed using the primers *RsRHA2b*-F2/*RsRHA2b*-R2.

Southern blot analysis was performed using standard procedures. Genomic DNA samples (30 μg) from PCR-positive transgenic wheat plants were digested with *Hind*III overnight at 37 °C. The DNA fragments were separated on 1.0% (w/v) agarose gels and transferred to Hybond N^+ nylon membranes. The PCR-amplified fragment to be used as a probe was further purified and labeled with digoxigenin (DIG)-dUTP using a DIG-High Prime Kit (Roche, Manheim, Germany). Hybridization was conducted at 68 °C. Hybridization and detection were performed using a DIG Nucleic Acid Detection Kit (Roche) according to the manufacturer's instructions.

http://www.aloki.hu ● ISSN 1589 1623 (Print) ● ISSN 1785 0037 (Online)
DOI: http://dx.doi.org/10.15666/aeer/1706_1327313288

qRT-PCR analysis of transgenic wheat plants

For qRT-PCR, the RNA from wheat leaves at 12 h, 24 h, 48 h after treatment with 0 μmol/L, 0.5 μmol/L, or 5 μmol/L ABA was used for reverse transcription (Toyobo, Osaka, Japan). qRT-PCR was performed in a volume of 20 μL containing SYBR Green I PCR Master Mix (Promega, Madison, USA) 10 pmol each of forward and reverse gene-specific primers (*Table 1*), and cDNA (0.2 μmol/L). Gene-specific primers were designed using Primer Premier 5 software. The wheat *ACTIN* gene was co-amplified as an internal control to normalize the total amount of cDNA present in each reaction and to eliminate the differences among the samples. PCR amplification was performed in an iQ5 Cycler (Bio-Rad) under the following conditions: 95 °C for 3 min, followed by 39 cycles of 94 °C for 10 s, 60 °C for 20 s, and 72 °C for 30 s. The plate was read at 72 °C for 30 s. To determine the specificity of each PCR primer pair, a melt curve was generated by incubating the reaction at 95 °C for 10 s, cooling to 65 °C for 10 s and increasing to 95 °C at a rate of 0.5 °C/10 s.

Table 1. *Primer sequences used for PCR, RT-PCR, qRT-PCR and southern blot analysis*

Name	Sequence (5'-3')
RsRHA2b-F1	CCATGGTCCAGCAACAGCAGCAAACA
RsRHA2b-R1	GGTGACCGGAGAAAGCCGCGAGATTAAA
qRT-*RsRHA2b*-F	TGCCCGAGGAGGTCAAGGAG
qRT-*RsRHA2b*-R	CGTGATTGGATGGCTACTATACAAAGTG
RsRHA2b-F2	AGATCTATGGGGTTACAAGGTCAACTCT
RsRHA2b-R2	GGTGACCGGAGAAAGCCGCGAGATTAAA
Trans(gDNA)-F	AGATCTATGGGGTTACAAGGTCAACTCT
Trans(gDNA)-R	GGTGACCGGAGAAAGCCGCGAGATTAAA
Trans(cDNA)-F	AGATCTATGGGGTTACAAGGTCAACTCT
Trans(cDNA)-R	GGTGACCGGAGAAAGCCGCGAGATTAAA
Southernblot(probe)-F	AGATCTATGGGGTTACAAGGTCAACTCT
Southernblot(probe)-R	GGTGACCGGAGAAAGCCGCGAGATTAAA
Ta*ACTIN*-F	GCTGTTCCAGCCATCTCATGT
Ta*ACTI*N-R	CGATCAGCAATTCCAGGAAAC
ABI5-F	GACGGAAGAAGCGGCAGTG
ABI5-R	TCTGAAGCAGCACGAGAAAGG
FUS3-F	GTGGCTGGGTTGCGAGTTAT
FUS3-R	ATCCTGCTCTTGTTGTTTGGC
MAL-F	CTTCCTGTGCTGCCTATTCTG
MAL-R	CCACATGCACTGGACGATAAC

Seed germination test

Intact spikes were harvested at physiological maturity. Grains from the wheat spikes were hand-threshed. The dormant seeds were used for further analysis. Thirty sound grains of each plant were placed crease down on moist filter paper in Petri dishes at 20 °C in the dark for 7 d. The germinated grains were counted every day and

http://www.aloki.hu ● ISSN 1589 1623 (Print) ● ISSN 1785 0037 (Online)
DOI: http://dx.doi.org/10.15666/aeer/1706_1327313288

calculated in terms of the germination index (GI). $GI = (7n1 + 6n2 + \ldots + 1n7)/7N$, where n1, n2, n3, …n7 are the number of grains that had germinated on the 1st day, 2nd day, …7th day, and N is the total number of grains in the assay. The grains from each plant composed a replication, and the experiments were performed in three replicates. Additionally, 30 sound grains of each plant were placed crease down on moist filter paper in Petri dishes at 20 °C in normal conditions (16 h, light:8 h, dark; 20 °C). The germination capacity on the 39th day after sowing was recorded.

Spike sprouting test

Ten spikes of each T5-generation transgenic line harvested from the experimental field were inserted into floral foam (floral foam can retain water to prevent the detached wheat spikes from wilting) at approximately 20-25 °C in a greenhouse. Misting was controlled by a humidifier and checked automatically for 4 d. Under these conditions, a high relative humidity (> 98%) was maintained.

ABA sensitivity assay

Wheat seeds from the transgenic lines and from the non-transgenic Zhengmai 9023 whose dormancy had been broken were tested for ABA sensitivity. Seeds were germinated at 20 °C. At the second leaf stage, they were treated with different concentrations of ABA, including 0 μmol/L, 0.5 μmol/L and 5 μmol/L ABA. Fourteen seedlings from each transgenic line and from non-transgenic Zhengmai 9023 were assayed after being treated for13 d (Saad et al., 2013). The initial fresh weight and final fresh weight of the plants were measured. Then, the difference in weight was calculated. The experiments were performed on three replicates.

Statistical analysis

The GIs, germination capacity and average weight difference of each line were analyzed using Excel software, and Student's *t* test was calculated for relevant data using SPSS software. The figures were created using Origin8 software and Adobe Photoshop CS5 software.

Results

Cloning and analysis of the RsRHA2b gene

The EST database was BLASTed based on the amino acid sequence encoded by the *Arabidopsis* RING finger gene *AtRHA2b* (Gene ID: 814644). Many highly homologous ESTs were found. A cDNA sequence including the entire ORF of the radish RING finger gene *RHA2b* was found using artificial splicing and software analysis based on the radish database. The length of the entire sequence was 697 bp (*Fig. 1*). The ID of the *RsRHA2b* gene was KR349970. The entire coding sequence, plus a 93 bp sequence in the 3'-UTR, was amplified from radish cDNA and was 565 bp in length. The sequence was then used to construct the binary vector pCAMBIA3301-*RsRHA2b* (*Fig. 2*). The constructed vector was further confirmed by sequence analysis (*Fig. 1*) and was then transferred into *Agrobacterium tumefaciens* EHA105. Transgenic wheat plants were obtained to investigate the function of *RsRHA2b*.

http://www.aloki.hu ● ISSN 1589 1623 (Print) ● ISSN 1785 0037 (Online)
DOI: http://dx.doi.org/10.15666/aeer/1706_1327313288

```
1          CCATGGTCCAGCAACAGCAGCAAACACTCTCTCTCTAAAAGAATCTCTCTCTCTCAGGAA
61         GAAGAAGAAGATGGGGTTACAAGGTCAACTATCTGACGTTTCATCAGATTCAATCCCTCT
1                     M  G  L  Q  G  Q  L  S  D  V  S  S  D  S  I  P  L

121        CATGCTCGTTGCTCTCCTCGCTACTTTGTTCAAACACGTCCGCTCTTTCTTCCTCCGCTT
18           M  L  V  A  L  L  A  T  L  F  K  H  V  R  S  F  F  L  R  F

181        CTCCTCCTCCTCCTCTGTCGTCGAAGATGCTTCTCTCTCCATTTCCTCAGGGTTTGCGAA
38           S  S  S  S  S  V  V  E  D  A  S  L  S  I  S  S  G  F  A  N

241        CATCGCCGTACTCGCCGACCAGCTCAAACTCAACCGTCTCTTCTCATACCCCTACGACCA
58           I  A  V  L  A  D  Q  L  K  L  N  R  L  F  S  Y  P  Y  D  H

301        TAAGGCCGCCGCAGCCGCATCCGACTGCATCGTGTGCTTGTCTACACTCAAGACCGGAGA
78           K  A  A  A  A  A  S  D  C  I  V  C  L  S  T  L  K  T  G  E

361        AGAAGTGAGGAAGCTGGGATGCAGACACGTGTTCCACAAACAGTGTTTGGAAGGTTGGCT
98           E  V  R  K  L  G  C  R  H  V  F  H  K  Q  C  L  E  G  W  L

421        TCAACATCTCAATTTTAATTGTCCGCTTTGTAGATCTCCGTTGGTTGGTCGTGGAGGAGG
118          Q  H  L  N  F  N  C  P  L  C  R  S  P  L  V  G  R  G  G  G

481        ATGTGAATCGATCACTTCTTCTTTCTCTCTTCTCTCAGACGCTCAGTGAGTTCTCTTCAT
138          C  E  S  I  T  S  S  F  S  L  L  S  D  A  Q  *

541        TGTCTGATGAACAAAAAAAAAAAAGAAAAGGGAAAGAGAGAAGAAGAGTTTGGGCGTTTT
601        TTTTAATCTCGCGGCTTTCTCCGGTCACC
```

Figure 1. *Nucleotide and deduced amino acid sequences of the RsRHA2b gene*

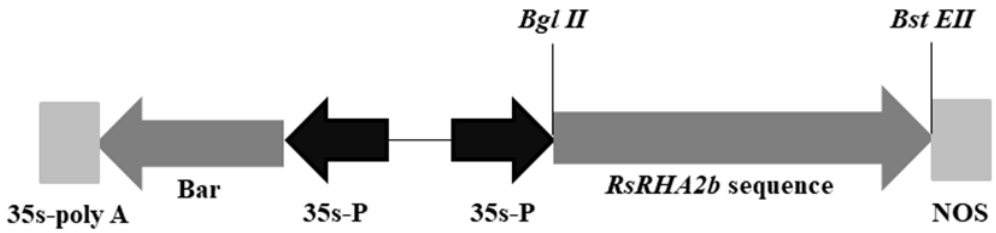

Figure 2. *Structure of the binary vector pCAMBIA3301-RsRHA2b, which was used for transformation. RsRHA2b sequence, RsRHA2b coding sequence plus 93 bp sequence at 3'-UTR; 35S-P, 35S-promoter; Bar, phosphinothricin gene*

Identification of transgenic wheat plants

The transgenic plants were identified using PCR and RT-PCR. As shown in *Figure 3*, the *RsRHA2b* gene fragment was found in the genome of transgenic wheat, and *RsRHA2b* transcripts were also detected. These results showed that the *RsRHA2b* gene was stable in the wheat genome and was stably expressed. Each of the five lines (L1, L2, L3, L4 and L5) showed a single band, indicating independent transformation events (*Fig. 4*). As expected, there was no significant hybridization signal from WT DNA. These results indicated that the *RsRHA2b* gene was integrated into the genomes of the wheat transformants in the selected lines and was inherited by the progeny as a single copy. However, the segregation was not consistent with heredity of a single-copy gene. Ultimately, four transgenic lines, 1471 (100 wheat heads), 1477 (102 wheat heads), 1492 (105 wheat heads) and 1569 (103 wheat heads), were selected for further characterization. Their morphology was similar to that of the non-transgenic Zhengmai 9023.

http://www.aloki.hu ● ISSN 1589 1623 (Print) ● ISSN 1785 0037 (Online)
DOI: http://dx.doi.org/10.15666/aeer/1706_1327313288

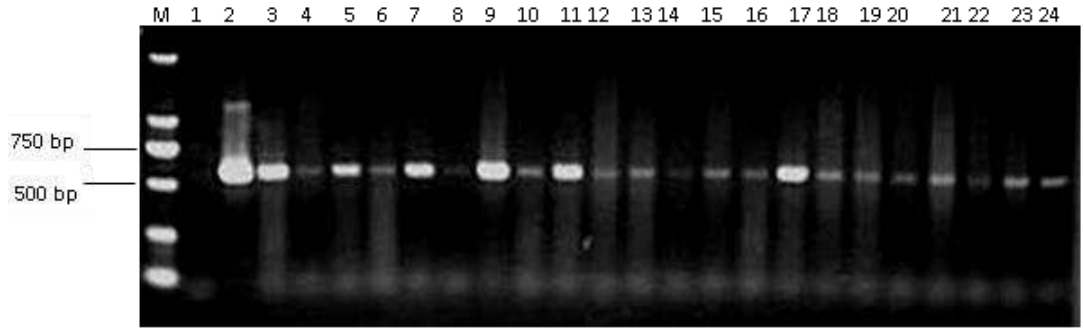

Figure 3. *Identification of transgenic plants by PCR and RT-PCR analyses. DNA was extracted from the leaves of each T5 transgenic line and from non-transgenic Zheng9023. RNA was extracted from the shoots of each T5 transgenic line and non-transgenic Zheng9023. (3-13) DNA fragments between the RsRHA2b coding sequence and the NOS sequence amplified by primers RsRHA2b-F/RsRHA2b-R. (14-24) RT-PCR products of the RsRHA2b sequence amplified from cDNA using primers. RsRHA2b-F/RsRHA2b-R. M, marker 2000; 1, non-transgenic Zheng9023; 2, plasmid pCAMBIA3301-RsRHA2b; 3-13, transgenic lines (DNA); 14-24, transgenic lines (cDNA)*

Figure 4. *Southern blot analysis. L1-7, seven randomly selected T2 PCR-positive lines (L1-7); WT, non-transgenic Zheng9023; P: purified probe product (positive control). Thirty micrograms of HindIII-digested total wheat leaf DNA was fractionated on a 1% agarose gel, blotted onto a nylon membrane, and hybridized with a probe labeled with DIG-11-dUTP*

RsRHA2b has an important role in the regulation of RsRHA2b-mediated seed dormancy

To assay the seed dormancy of transgenic wheat, GIs were investigated using the seeds from the T5 generation. The GIs were significantly lower in the transgenic wheat lines than in the non-transgenic Zhengmai 9023 (*Table 2*). The GIs of the seeds of the transgenic lines ranged from 0.098 to 0.387, a significant reduction, up to 89.9%. In particular, the GI of transgenic line 1477 was 0.098. The germination capacity of the transgenic lines ranged from 0.367 to 0.724, a significant reduction of up to 63.3%. In particular, the germination capacity of the transgenic line 1477 was 0.367. GI value (less than 0.4) was defined as resistance to spike germination. GI value (0.4-0.8) is medium resistance. GI value (more than 0.8) is prone to spike germination (Ma et al., 2014). The GI values of the seeds of the four transgenic lines in this study were all less than 0.4, while the average GI values of the control group were 0.973. Therefore, the retarded seed germination in the transgenic wheat with *RsRHA2b* gene is stably inherited, and *RsRHA2b* can increase seed dormancy.

http://www.aloki.hu ● ISSN 1589 1623 (Print) ● ISSN 1785 0037 (Online)
DOI: http://dx.doi.org/10.15666/aeer/1706_1327313288

Table 2. *Seed germination indexes and germination capacity (on the 39th day after germination) in different T5 transgenic wheat compared with those of non-transgenic Zhengmai 9023*

Transgenic line	Germination index[a] (GI)	Germination capacity[b]
1471	0.217 ± 0.010 b	0.650 ± 0.024 b
1477	0.098 ± 0.003 b	0.367 ± 0.047 b
1492	0.244 ± 0.017 b	0.600 ± 0.024 b
1569	0.387 ± 0.007 b	0.724 ± 0.024 b
CK[c]	0.973 ± 0.012 a	1.000 ± 0.000 a

[a]Germination indexes are the average ± standard error from 10 plants per line
[b]Germination capacity is the average ± standard error from 10 plants per line on the 39th day after germination
[c]CK: non-transgenic Zhengmai 9023
The letters 'a' and 'b': Significant at $P < 0.05$ with Student's *t* test

RsRHA2b effectively regulates RsRHA2b-mediated tolerance to PHS in spikes

To ascertain whether the *RsRHA2b* gene mediates the PHS response, 10 T5-generation plants from each of four transgenic lines, as well as non-transgenic Zhengmai 9023, were assayed for their PHS tolerance. The GI of the transgenic wheat line 1477 was significantly lower than that of the non-transgenic Zhengmai 9023 (*Table 2; Fig. 5*). Seeds from 1477 had just started to germinate while Zhengmai 9023 had a long first leaf. Spikes of 1477 maintained dormancy while Zhengmai 9023 displayed substantial leaves after 4 d of misting. The results showed that the *RsRHA2b* gene can improve PHS tolerance in transgenic wheat plants.

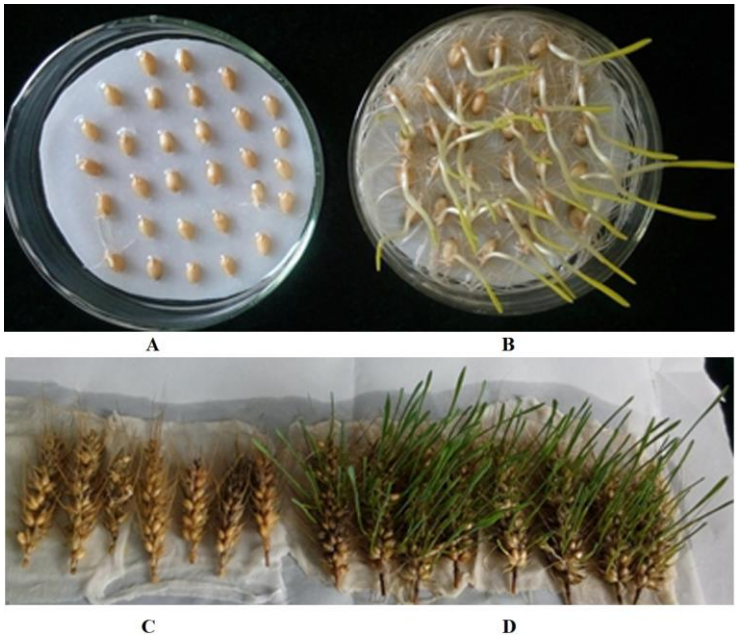

Figure 5. *Seed germination phenotypes of representative seeds and spikes from the T5 transgenic line 1477 and the non-transgenic Zheng9023. (A) Seeds of 1477 and (B) Zheng9023 incubated on a moist filter for 7 d. (C) Spikes of 1477 and (D) Zheng9023 incubated for 4 d under misting conditions*

http://www.aloki.hu ● ISSN 1589 1623 (Print) ● ISSN 1785 0037 (Online)
DOI: http://dx.doi.org/10.15666/aeer/1706_1327313288

Higher sensitivity to exogenous ABA in transgenic plants

The ABA sensitivity of the *RsRHA2b* transgenic wheat plants was assayed. At the second leaf stage, the plants were transferred to Hoagland's liquid medium containing different concentrations of ABA (0 μmol/L, 0.5 μmol/L or 5 μmol/L). In the absence of ABA, the weights of transgenic wheat plants and non-transgenic Zhengmai 9023 were 0.701 g and 0.743 g, respectively (*Table 3*); there was no significant difference between them. However, in the presence of 0.5 μmol/L ABA, the weights of the transgenic wheat plants and non-transgenic Zhengmai 9023 were 0.417 g and 0.597 g, respectively (*Table 3*), and the difference was significant. The inhibitory effect was more apparent when 5 μmol/L ABA was applied. As shown in *Table 3*, with 5 μmol/L ABA, the weights of transgenic wheat plants and of non-transgenic Zhengmai 9023 were 0.274 g and 0.448 g, respectively. Taken together, the ABA sensitivity was significantly improved in transgenic wheat lines containing the *RsRHA2b* gene.

Table 3. *Weight differences in wheat plants with ABA treatment*

Transgenic line		**ABA**	
	0 μmol/L	0.5 μmol/L	5 μmol/L
CK[a]	0.743 ± 0.015 (g)	0.597 ± 0.037 (g) a	0.448 ± 0.006 (g) a
1477	0.701 ± 0.008 (g)	0.417 ± 0.009 (g) b	0.274 ± 0.015 (g) b

[a]CK: non-transgenic Zhengmai 9023
The letters 'a' and 'b': significant at $P < 0.05$ with Student's *t* test

RsRHA2b affects the expression of genes associated with ABA signal transduction

To investigate whether the expression of the *RsRHA2b* gene affected the ABA signal transduction pathways, the expression levels of several genes associated with ABA were analyzed in the T5 transgenic plants and non-transgenic Zhengmai 9023. Three genes, *ABI5* (accession no. AB362818.1), *FUS3* (accession no. AM418838.1, homologous cloning) and *MAL* (accession no. AK334873.1), were found to be closely associated with *RsRHA2b*. As shown in *Figure 6A-C*, the expression of three genes showed an obvious steady increase in transgenic wheat plants after ABA treatment. In the presence of 0.5 μmol/L ABA, the expression levels of *ABI5*, *FUS3*, and *MAL* increased 2.6-fold (48 h, highest level), 25.7-fold (24 h, highest level) and 7.2-fold (48 h, highest level), respectively, in the transgenic wheat plants relative to non-transgenic Zhengmai 9023; in the presence of 5 μmol/L ABA, the expression of the three genes increased 3.8-fold (48 h, highest level), 6.8-fold (24 h, highest level) and 43.5-fold (24 h, highest level), respectively, in the transgenic wheat plants. Taken together, these results indicate that the *RsRHA2b* gene up-regulated the expression of several genes related to seed germination in transgenic wheat.

Discussion

To solve the problem of PHS in wheat, scholars have conducted much research to explore the mechanism of PHS resistance. The conclusions are as follows. First, studies have focused on the apparent physical and physiological characteristics of wheat seeds, such as spike morphology (Zanetti et al., 2000), the color of the seed coat (Torada and Amano, 2002; Bassoi and Flintham, 2005), seed structure and water absorption (King

http://www.aloki.hu ● ISSN 1589 1623 (Print) ● ISSN 1785 0037 (Online)
DOI: http://dx.doi.org/10.15666/aeer/1706_1327313288

and Von Wettstein-Knowles, 2000), seed dormancy (Andreoli et al., 2006; Hughes et al., 2010), ABA content (Gerjets et al., 2010) and α-amylase activity (Major et al., 2001). In the breeding process, grain color, spikelet density, 1000-grain weight and grain width can be used as important reference indexes for wheat varieties resistant to spike germination (Ma et al., 2016). Second, research has focused on the characteristics of genes related to PHS or seed dormancy and the positional cloning of QTLs (Anderson et al., 1993; Chen et al., 2008a; Somers et al., 2007). Third, research has focused on the screening of molecular markers, the mapping of resistance genes and the generation of transgenic lines using genetic engineering methods. PHS resistance in wheat is a quantitative trait, and relevant quantitative trait locuses linked to PHS have been reported on almost all chromosomes (Munkvold et al., 2009; Ogbonnaya et al., 2008). However, PHS-resistant wheat germplasm resources are scarce. Therefore, the use of genetic engineering provides good choices for the improvement of PHS resistance in wheat. The *VP1* and *Trx* genes have been used to improve the PHS resistance of wheat (Li et al., 2009; Huang et al., 2012). Although these attempts have yielded some progress in controlling seed dormancy and PHS, more work is required.

The objective of this study was to determine whether the *RHA2b* gene from radish could improve the PHS tolerance of wheat. The *RsRHA2b* gene was used to improve seed dormancy and PHS tolerance in wheat.

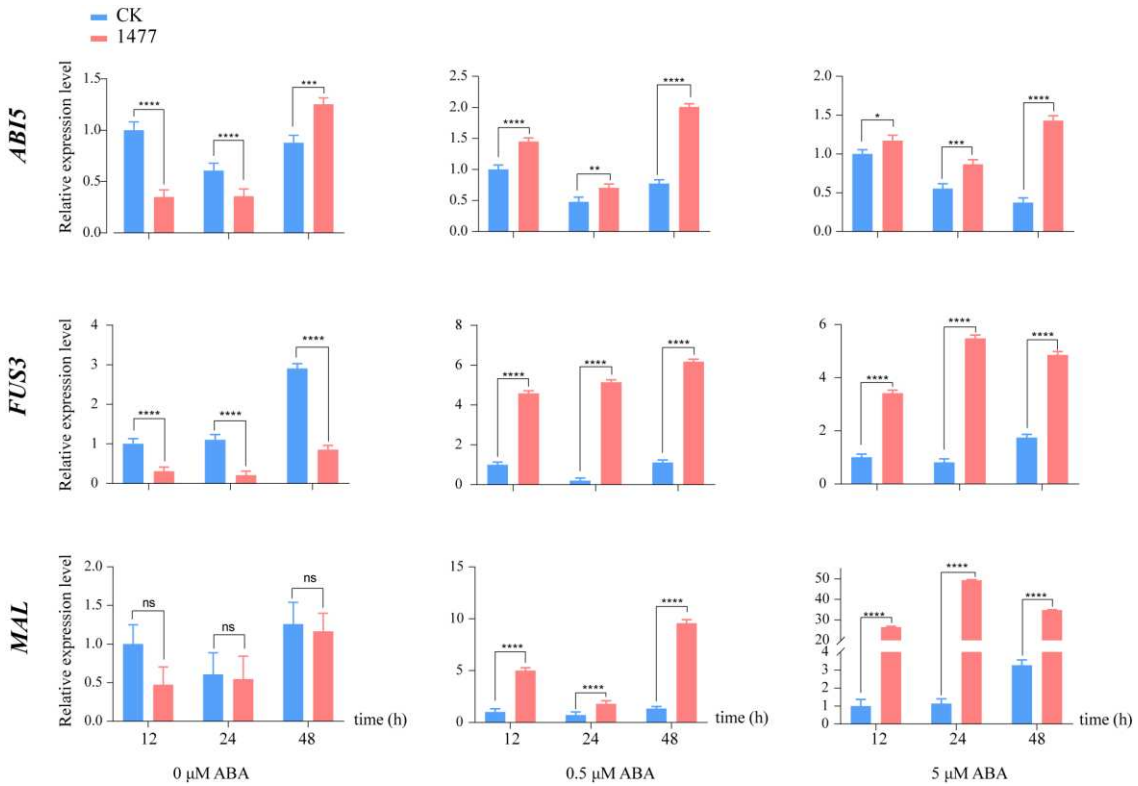

Figure 6. *qRT-PCR analysis of three genes in the T5 generation of transgenic line 1477 and non-transgenic Zheng9023 is presented. RNA was isolated from the leaves at the second leaf stage of the plants. ABI5: a positive regulator of ABA signaling; MAL: involved in the pathways of ABA signaling; FUS3: involved with the regulation of ABA biosynthesis. The symbol '*' indicates statistically differences P < 0.05, the symbol '**' indicates statistically differences P < 0.01; the symbol '***'indicates statistically differences P < 0.001; the symbol '****' indicates statistically differences P < 0.0001 (Two-way ANOVA, Sidak's multiple comparisons test)*

http://www.aloki.hu ● ISSN 1589 1623 (Print) ● ISSN 1785 0037 (Online)
DOI: http://dx.doi.org/10.15666/aeer/1706_1327313288

The success of the *Agrobacterium*-mediated transformation method used here provides a new technique for wheat genetic breeding (Zhao et al., 2006). In this study, the stem apex was used to improve *Agrobacterium*-mediated transformation. Basta was used to select the transgenic lines. The optimum half lethal concentration of basta had not been reported previously. Prior to this study, the concentration was analyzed using concentration gradient experiments. The phenotypes of plants treated with basta solutions of 80 mg/L, 100 mg/L, 120 mg/L, 140 mg/L, 160 mg/L, 180 mg/L, 200 mg/L, 220 mg/L, 240 mg/L, and 260 mg/L were recorded. The results showed that the optimum half lethal concentration of basta was 160 mg/L. This method can provide genetically stable material for further application. As shown in *Figure 3*, the transgenic lines were rigorously screened using basta, PCR and RT-PCR. The seeds from pure transgenic lines, identified based on the segregation ratio of the integrated *RsRHA2b* gene, were used for propagation.

Seed dormancy was stably inherited in transgenic wheat lines carrying the *RHA2b* gene from radish (*Figs. 3* and *4*). GIs and germination capacities were stably reduced in the T5 generation of transgenic wheat lines (*Table 2*). The transgenic lines in the present study had significantly increased tolerance to PHS, indicating that *RsRHA2b* has an important role in regulating seed dormancy and PHS tolerance.

The resistance to dormancy and PHS is regulated by ABA anabolism and ABA signal transduction (Gubler et al., 2005). Additionally, studies on wheat mutants have shown that ABA sensitivity is directly associated with seed dormancy (Kawakami et al., 1997; Noda et al., 2002). Research on the physiological characteristics of wheat has shown that ABA synthesis is important for embryos to remain dormant. However, embryo dormancy is closely associated with the internal ABA content and the sensitivity of embryos to ABA (King, 1993; Morris et al., 1989; Walker-Simmons, 1987). Cultivars with strong dormancy have strong sensitivity to ABA (Morris et al., 1989; Walker-Simmons, 1987; Corbineau et al., 2000). These results demonstrate that both ABA signal transduction and ABA cascade effectors are important for maintaining dormancy and resisting PHS. Increased ABA sensitivity in transgenic wheat may increase survival rates.

In this study, the *RsRHA2b*-regulated ABA sensitivity apparently failed to impair the growth of transgenic wheat plants without exogenous ABA, but with exogenous ABA, smaller weight increases were observed (*Table 3*). Therefore, the exogenous *RsRHA2b* gene may regulate the ABA signaling pathway in transgenic wheat.

Although the *AtRHA2b* gene plays a positive role in regulating ABA signaling and stress responses, the regulatory factors and response regulators associated with *AtRHA2b* are not known. Previous qRT-PCR assays have indicated that ABA treatment increased the expression of several ABA-inducible marker genes, including *RAB18, RD29A, KIN1, AtADH1, RD22* and *RD29B* in wild-type *Arabidopsis* (Li et al., 2011). The regulators associated with ABA and ABA-inducible marker genes were chosen for analysis in transgenic wheat containing the *RsRHA2b* gene. In the present work, three genes, i.e., *ABI5, FUS3* and *MAL,* were found to be significantly associated with *RHA2b*. *ABI5*, a bZIP transcription factor, is a positive regulator of ABA signaling, and its expression can be activated by exogenous ABA treatment (Suzuki et al., 2003; Kobayashi et al., 2008). *FUS3* (FUSCA3) promotes dormancy and prevents the precocious germination of immature seeds by stimulating ABA synthesis (Chiu et al., 2012). MAL is involved in the metabolic pathways of ABA signaling (Huang et al., 2012). The expression of *ABI5, FUS3* and *MAL* significantly increased in the presence

http://www.aloki.hu ● ISSN 1589 1623 (Print) ● ISSN 1785 0037 (Online)
DOI: http://dx.doi.org/10.15666/aeer/1706_1327313288

of 0.5 μmol/L ABA and 5 μmol/L ABA at the second leaf stage in transgenic wheat (*Fig. 6*). Thus, the *RsRHA2b* gene could positively regulate ABA signaling intermediates in transgenic wheat.

The grain germination rate of the over-expressed miR9678 wheat transgenic lines was significantly lower than that of the wild type, and the content of active gibberellin was reduced, leading to significantly increased resistance to spike germination (Guo et al., 2018). The miR9678 can mediate the splicing of long-segment non-coding RNA and produce a series of phasiRNA, which eventually leads to the change of gibberellin metabolism and its regulatory pathway by affecting the expression of gibberellin synthesis gene, thus controlling the germination rate of grain and spike germination (Guo et al., 2018). Based on transgenic wheat containing *RsRHA2b*, the reason for significantly increased tolerance to PHS can be explored by further work.

Conclusion

The *RsRHA2b* gene was integrated into the genomes of the wheat transformants. Transgenic wheat containing the *RsRHA2b* gene showed improved seed dormancy and PHS tolerance. *RsRHA2b* gene plays a significant role in regulating the genes associated with ABA signal transduction. This study provides a promising strategy for breeding wheat cultivars with improved seed dormancy and PHS tolerance using genetic engineering with the *RsRHA2b* gene. However, more work is needed to discover the mechanism of *RsRHA2b*-mediated PHS resistance.

Acknowledgements. This work was supported by the "Twelfth Five-Year" National Science and Technology Projects in Rural Areas (2013BADD04B01-02) and Henan Science and Technology Project (162102110007).

Conflict of interests. Authors state no conflict of interests.

REFERENCES

[1] Anderson, J. A., Sorrells, M. E., Tanksley, S. D. (1993): RFLP analysis of genomic regions associated with resistance to preharvest sprouting in wheat. – Crop Science 33: 453-459.

[2] Andreoli, C., Bassoi, M. C., Brunetta, D. (2006): Genetic control of seed dormancy and pre-harvest sprouting in wheat. – Scientia Agricola 63: 564-566.

[3] Bassoi, M. C., Flintham, J. (2005): Relationship between grain colour and preharvest sprouting-resistance in wheat. – Pesquisa Agropecuária Brasileira 40: 981-988.

[4] Borden, K. L. (2000): RING domains: master builders of molecular scaffolds? – Journal of Molecular Biology 295: 1103-1112.

[5] Bu, Q., Jiang, H., Li, C.-B., Zhai, Q., Zhang, J., Wu, X., Sun, J., Xie, Q., Li, C. (2008): Role of the Arabidopsis thaliana NAC transcription factors ANAC019 and ANAC055 in regulating jasmonic acid-signaled defense responses. – Cell Research 18: 756-767.

[6] Bu, Q., Li, H., Zhao, Q., Jiang, H., Zhai, Q., Zhang, J., Wu, X., Sun, J., Xie, Q., Wang, D., Li, C. (2009): The arabidopsis ring finger E3 ligase RHA2a is a novel positive regulator of abscisic acid signaling during seed germination and early seedling development. – Plant Physiology 150: 463-481.

[7] Castor, L., Frederiken, F. (1977): Seed moulding of grain sorghums caused by Fusarium and Curvularia. – Proc Annu Phytopathol Soc 4: 151.

http://www.aloki.hu ● ISSN 1589 1623 (Print) ● ISSN 1785 0037 (Online)
DOI: http://dx.doi.org/10.15666/aeer/1706_1327313288

[8] Chen, C. X., Cai, S. B., Bai, G. H. (2008a): A major QTL controlling seed dormancy and pre-harvest sprouting resistance on chromosome 4A in a Chinese wheat landrace. – Molecular Breeding 21: 351-358.
[9] Chen, Q. J., Zhang, L. Q., Yang, Y. W., Yuan, Z. W., Xiang, Z. G., Zheng, Y. L., Peng, Z. S., Liu, D. C. (2008b): Dormancy spreads seed germination over a long period with a discontinuous procession in Aegilops tauschii, the D-genome donor species of bread wheat. – International Journal of Agricultural Research 3: 77-82.
[10] Chiu, R. S., Nahal, H., Provart, N. J., Gazzarrini, S. (2012): The role of the Arabidopsis FUSCA3 transcription factor during inhibition of seed germination at high temperature. – BMC Plant Biology 12: 15.
[11] Corbineau, F., Benamar, A., Daniel, C. (2000): Changes in sensitivity to abscisic acid of the developing and maturing embryo of two wheat cultivars with different sprouting susceptibility. – Israel Journal of Plant Sciences 48: 189-197.
[12] Derera, N., Bhatt, G., Mcmaster, G. (1977): On the problem of pre-harvest sprouting of wheat. – Euphytica 26: 299-308.
[13] Dreher, K., Callis, J. (2007): Ubiquitin, hormones and biotic stress in plants. – Annals of Botany 99: 787-822.
[14] Gerjets, T., Scholefield, D., Foulkes, M. J., Lenton, J. R., Holdsworth, M. J. (2010): An analysis of dormancy, ABA responsiveness, after-ripening and pre-harvest sprouting in hexaploid wheat (Triticum aestivum, L.) caryopses. – Journal of Experimental Botany 61: 597-607.
[15] Grill, E., Himmelbach, A. (1998): ABA signal transduction. – Current Opinion in Plant Biology 1: 412-418.
[16] Groot, S. P., Karssen, C. M. (1992): Dormancy and germination of abscisic acid-deficient tomato seeds Studies with the Sitiens mutant. – Plant Physiology 99: 952-958.
[17] Gubler, F., Millar, A. A., Jacobsen, J. V. (2005): Dormancy release, ABA and pre-harvest sprouting. – Current Opinion in Plant Biology 8: 183-187.
[18] Guo, G., Liu, X., Sun, F., Cao, J., Huo, N., Wuda, B., Xin, M., Hu, Z., Du, J., Xia, R. (2018): Wheat miR9678 affects seed germination by generating phased siRNAs and modulating abscisic acid/gibberellin signaling. – The Plant Cell 30: 796-814.
[19] Holdsworth, M. J., Bentsink, L., Soppe, W. J. (2008): Molecular networks regulating Arabidopsis seed maturation, after-ripening, dormancy and germination. – New Phytologist 179: 33-54.
[20] Huang, T., Qu, B., Li, H. P., Zuo, D. Y., Zhao, Z. X., Liao, Y. C. (2012): A maize viviparous 1 gene increases seed dormancy and preharvest sprouting tolerance in transgenic wheat. – Journal of Cereal Science 55: 166-173.
[21] Hughes, K., Griffey, C., Parrish, D., Barbeau, W., Souza, E., Thomason, W. (2010): Preharvest sprouting tolerance in current soft red winter wheat cultivars. – Crop Science 50: 1449-1457.
[22] Jiang, H. L., Li, H. M., Bu, Q. Y., Li, C. Y. (2009): The RHA2a-interacting proteins ANAC019 and ANAC055 may play a dual role in regulating ABA response and jasmonate response. – Plant Signaling & Behavior 4: 464-466.
[23] Kamthan, A., Chaudhuri, A., Kamthan, M., Datta, A. (2016): Genetically modified (GM) crops: milestones and new advances in crop improvement. – Theoretical & Applied Genetics 129: 1639-1655.
[24] Kawakami, N., Miyake, Y., Noda, K. (1997): ABA insensitivity and low ABA levels during seed development of non-dormant wheat mutants. – Journal of Experimental Botany 48: 1415-1421.
[25] King, R., Von Wettstein-Knowles, P. (2000): Epicuticular waxes and regulation of ear wetting and pre-harvest sprouting in barley and wheat. – Euphytica 112: 157-166.
[26] King, R. W. (1993): Manipulation of grain dormancy in wheat. – Journal of Experimental Botany 44: 1059-1066.

http://www.aloki.hu ● ISSN 1589 1623 (Print) ● ISSN 1785 0037 (Online)
DOI: http://dx.doi.org/10.15666/aeer/1706_1327313288

[27] Ko, J. H., Yang, S. H., Han, K. H. (2006): Upregulation of an Arabidopsis RING-H2 gene, XERICO, confers drought tolerance through increased abscisic acid biosynthesis. – The Plant Journal 47: 343-355.
[28] Kobayashi, F., Maeta, E., Terashima, A., Takumi, S. (2008): Positive role of a wheat HvABI5 ortholog in abiotic stress response of seedlings. – Physiologia Plantarum 134: 74-86.
[29] Koornneef, M., Reuling, G., Karssen, C. (1984): The isolation and characterization of abscisic acid-insensitive mutants of Arabidopsis thaliana. – Physiologia Plantarum 61: 377-383.
[30] Kucera, B., Cohn, M. A., Leubner-Metzger, G. (2005): Plant hormone interactions during seed dormancy release and germination. – Seed Science Research 15: 281-307.
[31] Li, C. D., Ni, P. X., Francki, M., Hunter, A., Zhang, Y., Schibeci, D., Li, H., Tarr, A., Wang, J., Cakir, M. (2004): Genes controlling seed dormancy and pre-harvest sprouting in a rice-wheat-barley comparison. – Functional & Integrative Genomics 4: 84-93.
[32] Li, D., Lyu, G., Lyu, J., Niu, H., Wang, X., Yin, J. (2019a): Cloning and characterization of a wheat RING finger gene TaRHA2b whose expression is up-regulated by ABA treatment. – Applied Ecology and Environmental Research 17: 7495-7510.
[33] Li, D. B., Zuo, N., Lyu, G. Z., Du, H. X., Niu, H. B., Yin, J. (2019b): Identification of characteristics of pre-harvest sprouting and differences of TaRHA2b gene sequence among different wheat varieties. – Journal of Henan Agricultural Sciences 48: 6-16.
[34] Li, H., Jiang, H., Bu, Q., Zhao, Q., Sun, J., Xie, Q., Li, C. (2011): The Arabidopsis RING finger E3 ligase RHA2b acts additively with RHA2a in regulating abscisic acid signaling and drought response. – Plant Physiology 156: 550-63.
[35] Li, Y. C., Ren, J. P., Cho, M. J., Zhou, S. M., Kim, Y. B., Guo, H. X., Wong, J. H., Niu, H. B., Kim, H. K., Morigasaki, S. (2009): The level of expression of thioredoxin is linked to fundamental properties and applications of wheat seeds. – Molecular Plant 2: 430-441.
[36] Lopez-Molina, L., Mongrand, S., Chua, N.-H. (2001): A postgermination developmental arrest checkpoint is mediated by abscisic acid and requires the ABI5 transcription factor in Arabidopsis. – Proceedings of the National Academy of Sciences 98: 4782-4787.
[37] Ma, L., Li, Z., Ren, T., Tang, Z., Yan, B., Ren, Z. (2014): Evaluation and validation of molecular marker associated with pre harvest sprouting tolerance in a RIL population. – Journal of Triticeae Crops 34: 435-442.
[38] Ma, W., Zhang, C., Song, X., Feng, J., Cui, Z., Sun, D. (2016): Pre-harvest sprouting resistance in wheat from different wheat regions and its correlation with ear characteristics. – Journal of Triticeae Crops 36: 1269-1274.
[39] Major, B., Kettlewell, P., Scott, R. (2001): Mechanisms leading to excess alpha-amylase activity in wheat (Triticum aestivum, L) grain in the UK. – Journal of Cereal Science 33: 313-329.
[40] Mohan, A. (2008): Pre-harvest sprouting in cereals: a global scenario. – Current Science-Bangalore 94: 704.
[41] Moon, J., Parry, G., Estelle, M. (2004): The ubiquitin-proteasome pathway and plant development. – Plant Cell 16: 3181-3195.
[42] Morris, C., Moffatt, J., Sears, R., Paulsen, G. (1989): Seed dormancy and responses of caryopses, embryos, and calli to abscisic acid in wheat. – Plant physiology 90: 643-647.
[43] Munkvold, J. D., Tanaka, J., Benscher, D., Sorrells, M. E. (2009): Mapping quantitative trait loci for preharvest sprouting resistance in white wheat. – Theoretical and Applied Genetics 119: 1223-1235.
[44] Nambara, E., Marion-Poll, A. (2003): ABA action and interactions in seeds. – Trends in Plant Science 8: 213-217.
[45] Noda, K., Matsuura, T., Maekawa, M., Taketa, S. (2002): Chromosomes responsible for sensitivity of embryo to abscisic acid and dormancy in wheat. – Euphytica 123: 203-209.
[46] Ogbonnaya, F. C., Imtiaz, M., Ye, G., Hearnden, P. R., Hernandez, E., Eastwood, R. F., Van Ginkel, M., Shorter, S., Winchester, J. (2008): Genetic and QTL analyses of seed

http://www.aloki.hu ● ISSN 1589 1623 (Print) ● ISSN 1785 0037 (Online)
DOI: http://dx.doi.org/10.15666/aeer/1706_1327313288

dormancy and preharvest sprouting resistance in the wheat germplasm CN10955. – Theoretical and Applied Genetics 116: 891-902.

[47] Raghavendra, A. S., Gonugunta, V. K., Christmann, A., Grill, E. (2010): ABA perception and signalling. – Trends in Plant Science 15: 395-401.

[48] Saad, A. S., Li, X., Li, H. P., Huang, T., Gao, C. S., Guo, M. W., Cheng, W., Zhao, G. Y., Liao, Y. C. (2013): A rice stress-responsive NAC gene enhances tolerance of transgenic wheat to drought and salt stresses. – Plant Sci 203-204: 33-40.

[49] Schwechheimer, C., Schwager, K. (2004): Regulated proteolysis and plant development. – Plant Cell Reports 23: 353-364.

[50] Smalle, J., Vierstra, R. D. (2004): The ubiquitin 26S proteasome proteolytic pathway. – Annu. Rev. Plant Biol. 55: 555-590.

[51] Somers, D., Ogbonnaya, F. C., Imtiaz, M., Depauw, R. M. (2007): Haplotype diversity of preharvest sprouting QTLs in wheat. – Genome 50: 107-118.

[52] Stone, S. L., Hauksdóttir, H., Troy, A., Herschleb, J., Kraft, E., Callis, J. (2005): Functional analysis of the RING-type ubiquitin ligase family of Arabidopsis. – Plant Physiology 137: 13-30.

[53] Suzuki, M., Ketterling, M. G., Li, Q.-B., Mccarty, D. R. (2003): Viviparous1 alters global gene expression patterns through regulation of abscisic acid signaling. – Plant Physiology 132: 1664-1677.

[54] Tan, B. C., Schwartz, S. H., Zeevaart, J. A., Mccarty, D. R. (1997): Genetic control of abscisic acid biosynthesis in maize. – Proceedings of the National Academy of Sciences 94: 12235-12240.

[55] Torada, A., Amano, Y. (2002): Effect of seed coat color on seed dormancy in different environments. – Euphytica 126: 99-105.

[56] Vierstra, R. D. (2009): The ubiquitin–26S proteasome system at the nexus of plant biology. – Nature Reviews Molecular Cell Biology 10: 385-397.

[57] Walker-Simmons, M. (1987): ABA levels and sensitivity in developing wheat embryos of sprouting resistant and susceptible cultivars. – Plant physiology 84: 61-66.

[58] Xiao, S. H., Zhang, X. Y., Yan, C. S., Lin, H. (2002): Germplasm improvement for preharvest sprouting resistance in Chinese white-grained wheat: an overview of the current strategy. – Euphytica 126: 35-38.

[59] Yamaguchi Shinozaki, K., Shinozaki, K. (2006): Transcriptional regulatory networks in cellular responses and tolerance to dehydration and cold stresses. – Annu. Rev. Plant Biol. 57: 781-803.

[60] Zanetti, S., Winzeler, M., Keller, M., Keller, B., Messmer, M. (2000): Genetic analysis of pre-harvest sprouting resistance in a wheat × spelt cross. – Crop Science 40: 1406-1417.

[61] Zhang, X. R., Garreton, V., Chua, N.-H. (2005): The AIP2 E3 ligase acts as a novel negative regulator of ABA signaling by promoting ABI3 degradation. – Genes & Development 19: 1532-1543.

[62] Zhang, Y., Yang, C., Li, Y., Zheng, N., Chen, H., Zhao, Q., Gao, T., Guo, H., Xie, Q. (2007): SDIR1 is a RING finger E3 ligase that positively regulates stress-responsive abscisic acid signaling in Arabidopsis. – The Plant Cell Online 19: 1912-1929.

[63] Zhao, T. J., Zhao, S. Y., Chen, H. M., Zhao, Q. Z., Hu, Z. M., Hou, B. K., Xia, G. M. (2006): Transgenic wheat progeny resistant to powdery mildew generated by Agrobacterium inoculum to the basal portion of wheat seedling. – Plant Cell Reports 25: 1199-1204.

[64] Zheng, Y., Chen, Z., Ma, L., Liao, C. (2018): The ubiquitin E3 ligase RHA2b promotes degradation of MYB30 in abscisic acid signaling. – Plant Physiology 178: 428-440.

[65] Zhu, J. K. (2002): Salt and drought stress signal transduction in plants. – Annual Review of Plant Biology 53: 247.

http://www.aloki.hu ● ISSN 1589 1623 (Print) ● ISSN 1785 0037 (Online)
DOI: http://dx.doi.org/10.15666/aeer/1706_1327313288

THE EFFECT OF ARTIFICIAL ILLUMINATION ON POSTPONING PLANT PHENOLOGY

YANG, J.[1] – DUAN, R.[2*]

[1]*Faculty of Architecture and Urban Planning, Chongqing University, Chongqing 400030, China (phone: +86-159-0933-4280)*

[2]*School of Arts, Chongqing Technology and Business University, Chongqing 400067, China*

**Corresponding author*
e-mail:dr_optics@163.com ; phone: +86-136-0834-7300

(Received 9th Jun 2019; accepted 28th Aug 2019)

Abstract. The phenology of landscape plural can predict the urban environment and guide the development of the city. The aim of the study is to get the relationship between urban environment and plant phenology. The methods monitored the phenology of the environment and garden plants in the main urban area of Chongqing from 2016 to 2019. And it is concluded that artificial light of garden lighting is between 1000 to 4000 Lx in Chongqing, and the application of LED (Light Emitting Diode) is the highest number. At the same time, the flowering period of trees is more susceptible than that of the shrubs; the flowering period of plants is more susceptible than the evergreen plants; and the fruit period of trees is earlier; the flowering period is prolonged. The flowering stage and flowering period of pruning plants are longer than the plants under natural state. This data should prove useful for future research of the subject.
Keywords: *nightscape lighting, plant phenology, garden plants, environment and phenology*

Introduction

The urban environment has a great impact on plant phenology. Since 1950, the flowering period of urban garden plants has moved 1~3 days ahead in Europe (Menzel, 2002), and from 1902 to 2006, the flowing period for the shrub species in nearly 1/4 of North America also came much earlier (Neil, 2010). In China, the spring phenological period of most plants in urban areas has moved to an earlier date, and the autumn phenological period was delayed (Caruso, 2004). In particular, from 1963 to 2007, the early flowering period of 34 woody plants came 9 days ahead of time, and the full-bloom stage 12 days earlier (Bai et al., 2010). In recent years, nightscape lighting have been widely applied in urban areas above the county level in China, and so far spread to scenic tourist areas and some natural mountains. To celebrate Hangzhou G20 Summit, more than one billion RMB was invested in nightscape, which further triggered the construction of nightscapes in various cities. Now landscape plants have been illuminated at night everywhere in China (Yuan, 2014) The light environment is an important factor affecting plant growth. According to the biological rhythm, plants do not perform photosynthesis at night (Zhang et al, 2012). However, with the artificial lighting, the photosynthesis time of plants is prolonged, affecting their phenology. There is a close relationship between light and plant photosynthesis (Kendrick, 1986). Unlike daylight, the light source intensity, spectral energy distribution and illumination time of artificial light all affect plant phenology (Fukuda et al, 2008).

Chongqing is located in Class V light climate zone in China. It is in the southwestern part of China and the upper reaches of the Yangtze River, falling within the subtropical climate zone, with an average annual temperature of 16~18 °C, an annual rainfall of

http://www.aloki.hu ● ISSN 1589 1623 (Print) ● ISSN 1785 0037 (Online)
DOI: http://dx.doi.org/10.15666/aeer/1706_1328913296

1017.5 mm and a sunshine duration of 1000~1400 h. This city has abundant garden plants, so a large amount of lighting facilities have been built. This paper attempts to study the phenology of garden plants in Chongqing, with a view to finding out the impacts of artificial lighting on the urban forestry ecosystem.

Materials and methods

Selection of materials

25 observation points with landscape lighting in the main urban area of Chongqing were selected for monitoring of landscape lighting and plant phenology. The research location is in *Figure 1*. The parameters recorded included artificial illumination, temperature, humidity and altitude. In each survey area, 20 sampling sites were randomly selected for measurement and each measurement was repeated 3 times. The criteria for material selection were that it had an ornamental value and that it was widely distributed in Chongqing. There were 36 species of woody garden plants, including 16 species of shrubs (8 evergreen and 8 deciduous shrubs) and 20 species of arbors (5 evergreen and 15 deciduous arbors). The selected plants fell within 14 families and 21 genera (see *Table 1*).

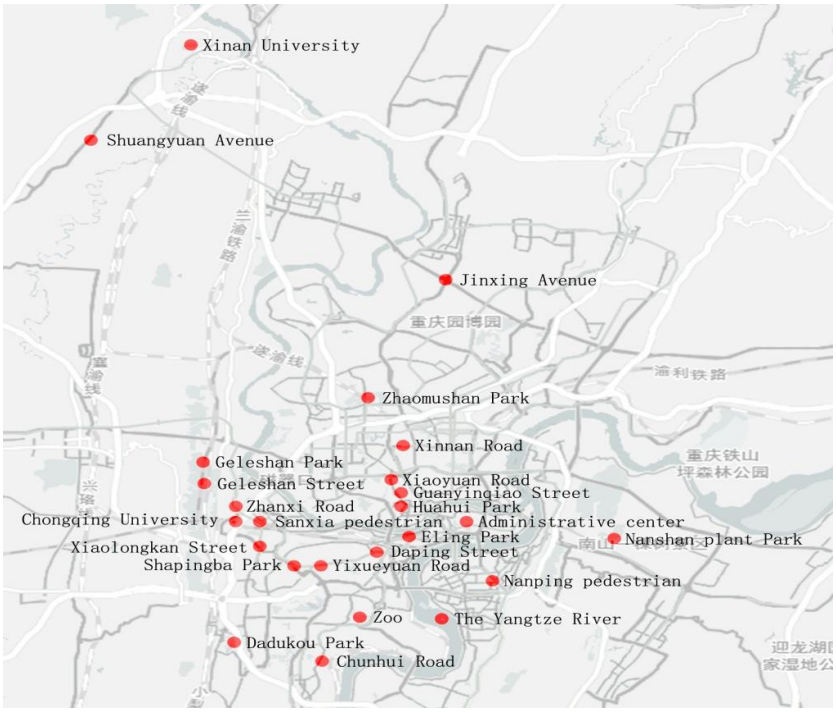

Figure 1. *Research location in Chongqing*

Research method

From January 2017 to December 2018, a total of 36 species of woody plants were monitored. The phenological observations were carried out on specific plants at fixed points in accordance with the Chinese Phenological Observation Method (Wan, 1979) every 4 to 7 days. Each time, the observation on all plants in a survey area must be completed within 3 days. The tree species selected were middle-age plants that were

http://www.aloki.hu ● ISSN 1589 1623 (Print) ● ISSN 1785 0037 (Online)
DOI: http://dx.doi.org/10.15666/aeer/1706_1328913296

robust and had been blossomed and fruited for more than 3 years. In each survey area, 3-5 plants were observed for each species, including at least 15 branches. During the phenological observation, records and pictures were taken. According to the Julian daily conversion method, the length of the corresponding flowering period and the growing season are calculated. In this study, the bud stage, the early flowering stage, the full-bloom stage and the late flowering stage were defined as the flowering phenology; the bud opening stage, the early leaf expansion and the leaf flourishing stage as the leafing phenology; and the bud opening period, the early leaf expansion, the leaf flourishing stage and the leaf fall stage as the leaf phenology. Artificial illumination is measured by professional illuminance meter.

Table 1. *Observation sample land environment factor data table (2016~2019)*

Site	Illumination (lx)	Temperature (°C)	Humidity	Altitude (m)	Architecture proportion (%)	Hard ratio (%)	Plant coverage (%)
1.Guanyinqiao Street	4860	23.21	50.27	265.70	51.18	48.82	13.25
2.Nanping pedestrian	2890	24.90	53.27	290.70	45.93	54.07	16.00
3.Sanxia pedestrian	4050	22.88	48.76	243.90	33.37	66.63	16.85
4.Chunhui Road	1700	25.20	44.54	283.00	23.23	69.02	37.21
5.Daping Street	3980	24.01	56.01	328.80	9.83	38.53	50.30
6.Geleshan Street	1030	20.49	47.97	507.60	33.33	60.01	29.96
7.Jinxing Avenue	2020	23.03	50.80	325.80	40.66	53.41	17.01
8.Shuangyuan Avenue	2510	23.31	47.83	273.80	22.24	69.99	26.37
9.Xiaolong kan Street	2630	22.53	45.34	252.40	18.76	73.12	23.20
10.Xiaoyuan Road	2560	23.10	47.25	275.50	20.26	71.77	33.37
11.Xinnan Road	3020	23.11	57.19	267.20	1.55	40.95	55.12
12.Zhanxi Road	1020	22.51	45.23	252.80	16.14	75.47	25.72
13.The Yangtze River	2200	22.81	59.92	337.33	15.21	76.31	23.76
14.Xinan University	1310	21.35	47.86	265.90	23.14	19.19	55.13
15.Chongqing University	810	22.68	51.61	237.70	27.26	28.41	41.14
16.Yixueyuan Road	2320	21.26	49.08	327.09	27.01	32.97	40.73
17.Dadukou Park	1010	22.45	56.74	279.10	13.25	12.47	63.37
18.Zoo	2020	22.93	42.07	255.70	7.35	16.81	62.77
19.Eling Park	2910	22.27	59.62	347.67	6.37	12.82	64.19
20.Administrative center	3210	22.01	47.88	276.78	2.96	9.68	66.36
21.Huahui Park	2820	21.24	54.01	283.80	4.02	18.43	47.13
22.Shapingba Park	1810	21.80	46.79	250.80	2.38	8.26	82.43
23.Geleshan Park	510	19.38	54.00	573.80	0.82	5.18	59.78
24.Nanshan plant Park	1100	21.05	49.60	525.50	6.80	15.14	74.36
25.Zhaomushan Park	5530	20.95	52.22	460.80	0.83	2.59	94.10

Results

Artificial light source types in garden lighting

The types of artificial light sources in garden nightscape were analyzed with the survey data, through which, the utilization of these light sources were obtained, as shown in *Figure 1*. According to statistics, the garden nightscape sources mainly include metal halide lamps, high pressure sodium lamps and LEDs. Traditional light sources accounted for 20% of the total surveyed ones, followed by white LEDs (39%),

http://www.aloki.hu ● ISSN 1589 1623 (Print) ● ISSN 1785 0037 (Online)
DOI: http://dx.doi.org/10.15666/aeer/1706_1328913296

yellow LEDs (6.8%), red LEDs (5.4%), violet LED (2.7%) and green LED (2.5%). Due to the transient nature, long service life and high luminous efficiency, LED light is gradually replacing the traditional light source as the dominant light source in landscape lighting (Pousset et al, 2010).

Illumination of artificial light sources in garden lighting

At present, the illumination intensity of garden nightscape lighting is generally high, resulting in extremely serious light pollution. Statistics of the illumination intensity applied in garden lighting are shown in *Figure 2*. As can be seen, the illumination intensity of garden nightscape lighting ranges mainly between 1000~4000 lx, accounting for 74% of the quantity surveyed; the illumination intensity for key plants ranges between 5000~6000 lx, accounting for 14% of the total surveyed quantity; most fluorescent lighting has an intensity of 1000 lx or below, accounting for 12% of the total quantity. In the garden lighting practice, an illumination intensity of 1000~4000 lx can meet people's usage and aesthetic needs, and such intensity is also the most widely applied (Duan, 2015).

Phenological characteristics of plants in the urban environment

36 plants radiated by artificial light sources were observed, and the averages of the flowering period (early flowering, full blossom and late flowering) and the mature fruiting period were compared with those recorded in Flora of China, Flora of Chongqing Jinyun Mountain and Flora of Sichuan. According to *Table 2*, among the 36 observed plants, 18 showed obviously earlier flowering periods, and 5 experienced earlier fruiting periods. All other plants showed consistent phonological periods with those recorded (see *Table 2*).

Phenological sensitivity of plants in the urban environment

The plants experiencing earlier flowering periods included 2 species of evergreen shrubs, accounting for 25% of all evergreen shrubs; 5 species of deciduous shrubs, accounting for 63% of all deciduous shrubs; 3 species of evergreen arbors, accounting for 60% of all evergreen arbors; and 8 species of deciduous arbors, accounting for 53% of all deciduous arbors. In terms of the fruiting period, the evergreen shrubs, deciduous shrubs and evergreen arbors had consistent phenological periods with the historical records, and only 5 of the deciduous arbors experienced earlier fruiting, which accounted for 45% of all deciduous arbors (see *Fig. 2*).

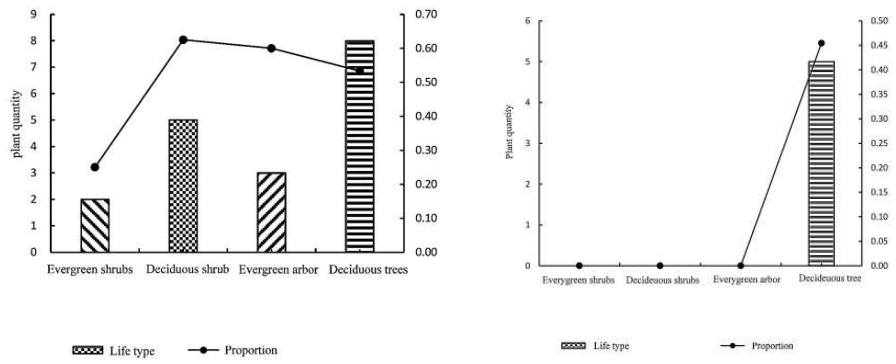

Figure 2. *Life type and advance proportion*

http://www.aloki.hu ● ISSN 1589 1623 (Print) ● ISSN 1785 0037 (Online)
DOI: http://dx.doi.org/10.15666/aeer/1706_1328913296

Table 2. *Historical comparison of plant phenology*

Plant name	Florescence			Fruit period		
	Observation (month)	Record	Change	Observation	Record	Change
Pittosporum tobira (Thunb.) Ait.	Late April	Mar to May	-	Mid-Sep	Sep to Oct	-
Loropetalum chinense Oliv. Var. Rubrum Yieh	Late Feb to Mid-April	Apr to May	Advanced	*	*	*
Michelia figo (Lour.) Spreng.	Late March to early May	Mar to May	-	*	Jul to Aug	-
Jasminum mesnyi Hance	Late March to Early April	Dec to Aug	Advanced	*	Mar to May	-
Gardenia jasminoides Ellis var. grandiflora Nakai.	Late May	Mar to July	-	*	May to Dec	-
Gardenia jasminoides Ellis	Mid-May to Early Jun	Mar to July	-	*	May to Dec	-
Camellia japonica L.	Late Jan to Late Mar	Jan to Apr	-	*	*	*
Nandina domestica	Mid-May to Early Jun	Mar to Jun	-	Early Sep	May to Nov	-
Cercis chinensis	Early Mar to Early Apr	Mar to Apr	-	Mid-Aug	Aug to Nov	-
Rhododendronsimsii&R. spp.	Early Mar to Late Apr	Apr to May	Advanced	Mid-Aug	Aug to Nov	-
Rhododendron simsii Planch.	Late Apr to Late May	Jun to Aug	Advanced	Early Nov	Nov to Dec	-
Chimonanthus praecox (Linn.) Link	Early Jun to Mid-Mar	Mar to Apr	Advanced	Early Jun	Apr to Dec	-
Magnolia liliiflora Desr.	March	to Mar	-	Early Sep	Aug to Sep	-
Ligustrum × vicaryi Hort	Late Apr to Late Apr	May to Jun	Advanced	Mid-Jul	Jul to Aug	-
Ligustrum sinense Lour.	Late Mar to Late Apr	Mar to Jun	Advanced	Mid-Oct	Sep to Dec	-
Chaenomeles speciosa (Sweet) Nakai	Mid-Feb to Mid-Mar	Feb to Apr	-	Early Sep	Sep to Oct	-
Michelia alba DC.	March	Apr to Sep	Advanced	*	*	*
Michelia chapensis Dandy	Early Mar to Late Apr	Mar to Apr	-	*	Aug to Sep	-
Michelia maudiae Dunn	Early Feb to Early Mar	Feb to Mar	-	*	Sep to Oct	-
Cinnamomum japonicum Sieb.	Late Mar to Late Apr	Apr to May	Advanced	Late Aug	Jul to Sep	-
Cinnamomum porrectum	April	May to Jun	Advanced	Late Aug	Jul to Sep	-
Michelia alba DC.	Early Feb to Early Mar	Feb to Mar		Late Aug	Aug to Sep	-
Magnolia soulangeana Soul.-Bod.	Late Feb to Late Mar	Feb to Mar		Late Aug	Aug to Sep	-
Acer palmatum ‘Atropurpureum’	Apr	May	Advanced	Late Jun	Sep	Advanced
Lagerstroemia indica L.	Mid-Jun to Mid-Sep	Apr to Sep	-	Late Oct	Sep to Dec	-
Prunus Cerasifera Ehrhar f. atropurpurea (Jacq.) Rehd.	Late Feb to Late Mar	Mar to Apr	Advanced	Late May	Aug to Sep	Advanced
Prunus × blireana cv. Meiren	Early Feb to Early Mar	Mar to Apr	Advanced	*	*	-
Malus halliana Koehne	Late Feb to Late Apr	Mar to Apr	Advanced	Mid-Aug	Sep to Oct	Advanced
Malus halliana Koehne	Mid-Mar to Early Apr	Mar to Apr	-	Early Aug	Aug to Sep	-
Amygdalus persica L.	Late Feb to Late Mar	Mar to Apr	Advanced	Early Aug	Aug to Sep	-
Prunus persica ‘Atropurpurea’	Late Mar to Mid-Apr	Mar to Apr	-	Late Aug	Aug to Sep	-
Prunus mume	Feb	Dec to Mar	-	Mid-Jun	-	*
Prunus x yedoensis	Mar	Apr	Advanced	Mid-Apr	May	Advanced
Cerasus serrulata	Late Mar to Mid-Apr	Mar to Apr	-	*	*	*
Cerasus subhirtella (Miq.) Sok.	Mid-Feb to Early Mar	Apr	Advanced	Early Apr	May	Advanced
Cerasus serrulata (Lindl.) G. Don ex London	Early Mar to Early Apr	Apr to May	Advanced	Late Apr	*	*

Through comparative analysis, as shown in *Figure 2,* the flowering period of the arbors under artificial lighting changed more obviously than that of the shrubs, and that of the deciduous plants experienced more obvious changes than the evergreen ones. Of the species in life forms experiencing earlier flowing periods, most are deciduous shrubs and deciduous arbors, and their proportions were also high in terms of quantity. However, in terms of the fruiting period, only deciduous arbors experienced earlier fruiting, which was consistent with the results regarding the flowering period.

http://www.aloki.hu ● ISSN 1589 1623 (Print) ● ISSN 1785 0037 (Online)
DOI: http://dx.doi.org/10.15666/aeer/1706_1328913296

Plant phenology under the urban management mode

An independent sample T test was performed on the selected woody plants to analyze the phonological differences between different landscape management modes. The survey areas of Chinese Loropetalum herb included the Three Gorges Square, Xinnan Road, Southwest University, Chongqing University, Zoo, Eling Park, Shaping Park, Flower Garden, and Nanshan Botanical Garden; those of michelia figo included Eling Park and Nanshan Botanical Garden; and those of the sample plots of ligustrum sinense included Daping, Star Avenue and Flower Garden. The analysis results are shown in *Figure 3*.

Under landscape lighting, after being pruned, the bud stage, the early flowering stage and the full blossom stage of woody plants came significantly later than those in the natural state, but the difference between the two states was not significant in the late flowering stage, nor are those in the bud opening stage, the early leafing stage and the leaf flourishing stage. Data show that, under the natural state, woody plants would blossom earlier and longer, but that there is no difference in leafing, probably because woody plants in the natural state are older and have larger ground diameters, making the flowering period earlier; and also because pruned woody plants will preferentially undergo vegetative growth, which is a response to the environmental change.

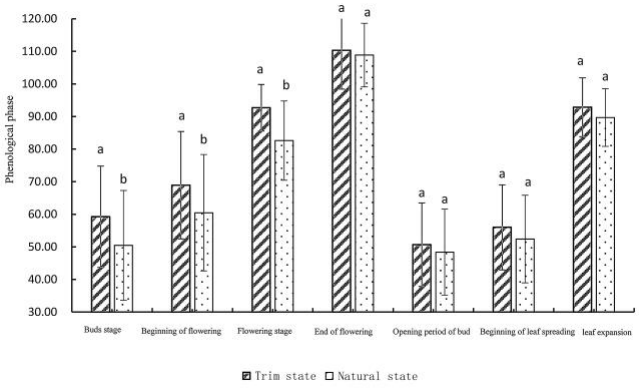

Figure 3. *Difference phenological period under different garden management modes*

Discussion

Artificial illumination has significant impacts on the phenology of woody landscape plants (Wang et al., 2012; Kulchin et al., 2018). The high-pressure sodium lamp has a discontinuous spectrum, with a peak value ranging between 570 and 600 mm; the metal halide lamp has a spectral peak ranging between 500 and 600 nm; the white and yellow LEDs contain much blue and red light; and the chromatic spectrum of LEDs has a narrow range. According to the absorption behaviour of the plant with respect to the light source spectrum, the spectra of low-light-intensity high-pressure sodium lamps and LED colour light sources have little effect on plant growth, while those of white and yellow LEDs and metal halide lamp have obvious impacts thereon. The results of the research verified this conclusion.

Artificial illumination is a direct factor affecting plant phenology and the paper-making plants. The flowering period is more sensitive to artificial light than the fruiting period, so it is more suitable as an indicator of the impact of artificial light on plant

http://www.aloki.hu ● ISSN 1589 1623 (Print) ● ISSN 1785 0037 (Online)
DOI: http://dx.doi.org/10.15666/aeer/1706_1328913296

phenology. Through analysis of the differences between the phenological periods of 5 arbors in urban and rural areas, it is found that the phenological period in urban areas is 4 days ahead of that in the rural one (Hu, 2013). This study also finds that artificial light, temperature, floor area ratio and proportion of rigid pavement can promote and extend the flowering and leafing of the plants and delay their defoliation; and that the increase of altitude and vegetation coverage has the opposite effect. For pruned woody plants, the bud, early flowering and full-blossom stages are all significantly later than those for plants in the natural state, but the difference between the two states is not so significant in the bud opening, early leafing and leaf flourishing stages (Jia et al., 2019). There is a certain relationship between the stem diameter of the plant and the flowering period, and after being pruned, woody plants would preferentially undergo vegetative growth under the artificial light (Chen, 2007), resulting in much earlier and longer flowering period of woody plants in the natural state.

Conclusion

The wide application of artificial nightscape lighting in the urban areas affects the phenology of garden plants and does harm to the forest growth, which is not conducive to the urban ecological environment. Through the monitoring on the phenology of garden plants in the artificial light environment in Chongqing, this study preliminarily obtains the current range of landscape illumination, applications of spectra and the phenological changes of garden plants, such as the flowering period and fruiting period, which provide information and data for the research on the phenology of landscape plants in Chongqing and also allow people to see the harm of artificial light environment to the landscape plants and the paper-making plants. Future research will focus on the effects of the illumination intensity, spectral energy distribution and illumination time of artificial light sources on plant phenology so as to provide basis for rational use of artificial lighting.

Acknowledgements. My paper is supported by the Technical Project of Chongqing Education Commission (KJQN201900818) and the Scientific research project of high-level talents in Chongqing Technology and Business University (950318046).

REFERENCES

[1] Bai J., Ge, Q., et al. (2010): The relationship between the phenology of woody plants in Xi'an and the climatic factors. – Acta Phytoecologica Sinica 34(11): 1274-1282.
[2] Caruso, C. M. (2004): The quantitative genetics of floral trait variation in Lobelia: potential constraints on adaptive evolution. – Evolution 58(4): 732-740.
[3] Chen, F., Yang, Y., et al. (2007): Flowering phenology and its influencing factors of Lagerstroemia indica in urban gardens of southern Sichuan. – The Journal of Ecology 7: 1841-1846.
[4] Duan, R., Yang, C., et al. (2015): Elements and methods of planning and design of garden nightscape lighting. – Lights and Lighting 4: 49-52.

http://www.aloki.hu ● ISSN 1589 1623 (Print) ● ISSN 1785 0037 (Online)
DOI: http://dx.doi.org/10.15666/aeer/1706_1328913296

[5] Fukuda, N., Fujitan, M., et al. (2008): Directional blue light irradiation triggers epidermal cell elongation of abaxial side resulting in inhibition of leaf epinasty in geranium under red light condition. – Sci. Hort.115: 176-182.
[6] Hertzog, M., Wang, M., Mony, J., Börjesson, K. (2019): Strong light–matter interactions: a new direction within chemistry. – Chemical Society Reviews 48(3): 937-961.
[7] Hu, H. (2013): Effects of Urban Landscape Pattern on Plant Phenology in Urban and Rural Gradients. – East China Normal University, Shanghai.
[8] Jia, X., Wang, M. (2019): The Impact of Green Supply Chain Management Practices on Competitive Advantages and Firm Performance. – In: Liu, X. (ed.) Environmental Sustainability in Asian Logistics and Supply Chains. Springer, Singapore.
[9] Kendrick, R. E., Kronenborg, G. H. M. (eds.) (1986): Photomorphogenesis in Plants. 2nd Ed. – Kluwer Academic Publishers, Dordrecht.
[10] Kulchin, Y. N., Nakonechnaya, O. V., et al. (2018): Plant morphogenesis under different light intensity. – Defect and Diffusion Forum 386: 201-206.
[11] Menzel, A. (2002): Phenology: its importance to the global change community. – Climatic Change 54(4): 379-385.
[12] Neil, K. L., Landrum, L., Wu, J. G. (2010): Effects of urbanization on flowering Phenology in the metropolitan Phoenix region of USA. Findings from herbarium records. – Journal of Arid Environments 74(4): 440-444.
[13] Pousset, N., Rougié, B., Razet, A. (2010): Impact of current supply on LED color. – Lighting - Research and Technology 42: 371-383.
[14] Wan, M., Liu, X. (1979): Chinese Phenological Observation Method. – Science Press, Beijing.
[15] Wang, Y., Tao, J., et al. (2012): Leaf functional traits of 6 evergreen broad-leaved tree species at seedling stage under different light conditions. – Forestry Science 48(11): 23-29.
[16] Yuan, H. (2014): Urban nightscape and nightscape lighting analysis and evaluations on typical nightscape cases in Nanjing. – Master Thesis, Blekinge Institute of Technology, Karlskrona, Sweden.
[17] Zhang, X., Chen, Z., et al. (2012): Effects of urbanization on flowering phenology of plants. – Safety and Environmental Engineering 19(6): 1-7.

http://www.aloki.hu ● ISSN 1589 1623 (Print) ● ISSN 1785 0037 (Online)
DOI: http://dx.doi.org/10.15666/aeer/1706_1328913296

PRELIMINARY STUDY ON THE ROCK WEATHERING EFFECT OF *BACILLUS MUCILAGINOSUS*

WU, Q.[1] – HU, H.[2,3*] – HE, L.[1]

[1]*School of Biological and Food Engineering, Anyang Institute of Technology, Anyang, Henan 455000, China*

[2]*Collaborative Innovation Center of Sustainable Forestry in Southern China of Jiangsu Province, Nanjing Forestry University, 159 Longpan Road, Nanjing, Jiangsu 210037, China*

[3]*Key Laboratory of Soil and Water Conservation and Ecological Restoration in Jiangsu Province, Nanjing Forestry University, 159 Longpan Road, Nanjing, Jiangsu 210037, China*

**Corresponding author*
e-mail: 531208831@qq.com

(Received 9th Jun 2019; accepted 28th Aug 2019)

Abstract. In order to explore the mechanism of the microbial weathering of rock, study the covering green process on rocks and improve the ecological environment, the soil forming effect of weathering granite, gneiss and sandstone was studied. Using ICP–OES and SEM method, the species and capacity of metabolites produced by *Bacillus mucilaginosus* in the fermentation process, concentrations of various elements released from the granite, gneiss, and sandstone and rock surface morphology were assessed. Results showed that metabolites such as organic acids, amino acids and polysaccharides formed by the *B. mucilaginosus* had significant differences among three types of rocks, concerning their quantities, granite > gneiss > sandstone; metabolites mentioned above could destroy the structure of the rock, which released many oxides. According to the amount of oxides leached from the three kinds of rock fermentation liquid, more oxides such as SiO_2, Na_2O, P_2O_5, Fe_2O_3, Al_2O_3, CaO, K_2O, MgO, TiO_2 were dissolved from the fermentation liquid of the granite. MnO was dissolved in the highest quantities in the fermentation broth of gneiss, more than that of granite and sandstone. The result indicated that the *B. mucilaginosus* had an obvious weathering effect on three kinds of rocks, especially on the weathering ability of granite.
Keywords: *Bacillus mucilaginosus, weathering, granite, gneiss, sandstone*

Introduction

Silicate minerals are widely distributed in nature, about one-third of all the known minerals (Du, 1984). Because of the excessive exploitation of ore in the last century, bare rock was everywhere, which had led to land degradation and a sharp decline in biodiversity (Fang et al., 2016), and ecological environment needs to be repair. However, under the natural condition, relying on the physical and chemical weathering, changing bare rock to soil usually takes 20000 years to form 1 m thick soil (Yang, 2013). Therefore, in order to promote the restoration of degraded ecological environment, it is urgent to have good bacterial species resources of ecological restoration and effective vegetation restoration methods. The evolution of hard rock into a bioactive and porous soil requires an extremely complex process of weathering and soil formation. All kinds of organisms living in soil fundamentally change the physical, chemical and biochemical properties of soil parent material, and promote the formation and evolution of soil (Li, 2006). Hall believes that in the environment with biological existence, biological weathering rocks can play a leading role under certain conditions (Hall et al., 2005). Microorganisms are widely attached to the rock surface, which can

http://www.aloki.hu ● ISSN 1589 1623 (Print) ● ISSN 1785 0037 (Online)
DOI: http://dx.doi.org/10.15666/aeer/1706_1329713309

affect the weathering of rocks and minerals and promote the formation of soil through growth and reproduction and the formation of biofilms (Ehrlich, 1999). Researches showed that the main microorganisms weathering the rock minerals were *B. mucilaginosus* (Zeng, 2016), *Burkolderia solanacearum* (Barker, 1998), *Pseudomonas protegens* (Wu et al., 2017a; Wu, 2016), *Bacillus megatherium* (Wu et al., 2017b), *Aspergillus niger* (Wu, 2018, 2019), *Rhizobium tropici* (Wang et al., 2015), *Penicillium oxalicum* (Song et al., 2015) and so on. The weathering effects of these microorganisms on mineral rocks include direct dissolution and mechanical damage, and indirect chemical corrosion. By reducing pH value and producing organic acids or inorganic acids, these microorganisms dissolve rock components and accelerate the release of Si, Al, Ca, Mg, K and other elements from rocks (Welchm, 1993; Vandevivere et al., 1994; Sun et al., 2018; Zhang et al., 2018; Zhou et al., 2015; Li et al., 2017), which are directly supplied to plant growth and utilization (Ge and Li, 2017; Li et al., 2016).

B. mucilaginosus is an important functional bacterium widely used in microbial fertilizers. It decomposes rock minerals through mechanical damage, mineral complex, acidolysis, enzymatic hydrolysis, reduction and complexation (Zeng, 2018; Man, 2015). Štyriaková et al. studied the infection of *B. mucilaginosus* on basalt, granite and gneiss at different temperatures and leaching tests on potassium, calcium, magnesium, silicon, iron and aluminum, and found that the influence of temperature on microbial weathering of rocks and the change of element extraction was obvious (Štyriaková, 2012). Xiao Guoguang et al. studied the release of metabolites (organic acids, amino acids and polysaccharides) of *B. mucilaginosus* under laboratory conditions, and believed that all metabolites had a certain weathering effect on plagioclase (Xiao, 2013). To date, however, no one has discussed the effect of *B. mucilaginosus* on weathered soils of granite, gneiss, and sandstone.

In this experiment, the metabolites released by weathering of granite, gneiss and sandstone, and the ability of dissolution of Si, K and other elements were compared and studied by using the *B. mucilaginosus* under laboratory conditions, which aimed at a deeper understanding of the effects and mechanism of the *B. mucilaginosus* weathering mineral rocks, cleared the role of the microbial weathering of rock, and screened good strains of weathering rock minerals, thus to provide important clues for clarifying the soil generating process, the ecological restoration, the development of sustainable agriculture and a series of scientific problems.

Materials and method

Materials

Bacteria

A *B. mucilaginosus* was isolated, purified and screened from the soil in Key Laboratory of Soil and Water Conservation and Ecological Restoration in Jiangsu Province, Nanjing Forestry University, China. It was identified as a *B. mucilaginosus* by biochemical analysis and 16s rDNA. The strain formed a raised colorless transparent colony on the nitrogen-free silicate medium, and the colony was smooth in surface, neat in its edge, with viscous and elastic, and could be drawn into silk. Its form was rod, gram reaction was negative, the optimum growth temperature was 28 C, and it was cultured for 3 d on the N-containing medium.

http://www.aloki.hu ● ISSN 1589 1623 (Print) ● ISSN 1785 0037 (Online)
DOI: http://dx.doi.org/10.15666/aeer/1706_1329713309

Rock sample

The tested granite samplings were taken from the closed mine in Jinding mountain, Wuzhong district, Suzhou; the sandstone samplings from the Yuyang mountain in Suzhou, and the gneiss samplings from the Lingzhou mine in Lianyungang. According to the XRD analysis of the collected rock samples, the mineral composition of the granite: quartz 30-35%, plagioclase 20-25% and potassium feldspar 25-30%, mica 10-15%, chlorite or vermiculite < 5%, the collected rock was porphyritic granite; Main mineral composition of gneiss: quartz 30-35%, Plagioclase 45-50%, Mica 15-20%; Main mineral composition of sandstone: quartz > 95%; A small amount of feldspar; small amounts of iron, etc. The chemical compositions (%) by X-ray fluorescence analysis were shown in *Table 1*. The rock powder was sieved with a 100 mesh sieve for experiment.

Table 1. *Chemical compositions (%) of the tested rocks*

Rock type	Chemical composition (%)										
	SiO_2	TiO_2	Al_3O_2	Fe_2O_3	MnO	MgO	CaO	Na_2O	K_2O	P_2O_5	Other
Granite	74.29	0.20	13.54	1.88	0.37	0.28	0.78	3.49	4.78	0.04	0.35
Gneiss	78.12	0.22	11.67	1.18	0.47	0.27	0.66	5.72	0.98	0.01	0.70
Sandstone	97.45	0.06	0.99	0.53	0.09	0.04	0.08	0.17	0.16	0.01	0.51

N-containing medium

Sucrose 10 g, KCl 0.1 g, (NH_4) SO_4 1.0 g, $CaCO_3$1.0 g, $Na_2HPO_4 \cdot 12H_2O$ 2.0 g, $MgSO_4 \cdot 7H_2O$ 1.0 g, distilled water 1.0 L.

The *B. mucilaginosus* were cultured on N-containing medium for 3 d to activate the bacteria. The pH value was adjusted by 0.1 mol• L^{-1} HCl and NaOH in the preparation of N-containing medium.

Experimental methods

The test of weathering rock by B. mucilaginosus

The *B. mucilaginosus* was inoculated in 250 mL culture solution for 56 h, centrifuged at 5000 rpm for 10 min, and then washed with sterile water for 3 times, and 600 mL of sterile water was added as the inoculation solution. 150 mL liquid medium was first added into a 500 mL triangular flask, and then 5 g granite powder or 5 g gneiss powder or 5 g sandstone powder was added. Sterile filter membrane was used for sealing. 121 C high pressure sterilization for 20 min, to add 5% *B. mucilaginosus* spore suspension (10^7/mL) at 28℃ (plus or minus 0.5 C) for static culture after cooling, and the contents of organic acids, polysaccharides, pH value, Si, Fe, Al, Ca, K and Mg in the fermentation broth were determined at 2 d, 5 d, 10 d, 15 d, 22 d and 30 d respectively. Compare with no bacteria, repeat three times. The experimental period was 30 d (Wu, 2018).

Observation of the surface morphology of weathering rock by B. mucilaginosus

The powders of granite, gneiss, and sand rock were collected respectively after experiment processing, and dried at 50 C. Then the samples were fixed, sprayed gold.

http://www.aloki.hu ● ISSN 1589 1623 (Print) ● ISSN 1785 0037 (Online)
DOI: http://dx.doi.org/10.15666/aeer/1706_1329713309

The surface characteristics of rocks were observed using a Scanning Electron Microscopy (SEM) (Neo Scope JCM - 5000) after 30 d.

Method of measurement

Determination of organic acids

1 mL of filtered fermented liquid after cultured 10 d was sucked up and put into the centrifuge tube with 10 mL from the test samples treated by the spore suspension liquid of *B. mucilaginosus*, 200 μL of 50% H_2SO_4 were add into it, which was centrifuged with 10000 r/min for 5 min, 500 μL of supernatant were taken, and filtered with the 0.45 μm filter membrane, the contents of 6 kinds of organic acids (oxalic acid, tartaric acid, citric acid, acetic acid, malic acid and succinic acid) were determined by means of High Performance Liquid Chromatography (HPLC, 1260 Infinity, Agilent Technologies, USA) method (Wu, 2018).

Determination of amino acids

2 mL of filtered fermented liquid after cultured 10 d were sucked up and put into the centrifuge tube with 10 mL from the test samples treated by the spore suspension liquid of *B. mucilaginosus*, 2 mL of sulfosalicylic acid solution were accurately added into it, blended and vibrated overnight at 4 C; then 1 mL of EDTA-Na solution with 50 g/L and 1 mL of HCl solution with 0.06 mol/L were added into it, mixed, and centrifuged with 10,000 r/min for 5 min, their supernatant liquids were sucked up, and freeze-dried; then 1 mL of sodium citrate buffer solution was added to make the concentration of amino acid be in the best detection range, and the contents of different amino acids in the fermentation liquid were determined by the amino acid tester (Germany, sykam S-433D) (Wu, 2018).

Determination of polysaccharides

2 mL of filtered fermented liquid after cultured 10 d were sucked up and put into the centrifuge tube with 10 mL from the test samples treated by the spore suspension liquid of *B. mucilaginosus*, which was centrifuged with 8 000 r/min for 20 min, their supernatant liquids were taken, 60 mL of anhydrous ethanol were added, and put into refrigerator at 4 C for 1 h; then centrifuged with 6 000 r/min for 20 min, washed and precipitated with 95% of ethanol, anhydrous ethanol and ether precipitation respectively, the polysaccharide crude products were obtained after centrifugation, the removing protein processing were conducted by the Sevag reagent (chloroform: isoamyl alcohol = 4 : 1), and then dialyzed using deionized water, frozen at - 80 C after about 24 h, freeze-dried, a pure polysaccharide was gained and weighted, thus contents of polysaccharide in the fermented liquid of *B. mucilaginosus* were determined and compared in different rocks (Wu, 2018).

Determination of the elements in the fermentation fluid

5 mL fermented liquid of cultured 2 d, 5 d, 10 d, 15 d, 30 d were respectively taken to centrifuge with 5000 r/min for 10 min from the test samples treated by the spore suspension liquid of *B. mucilaginosus*, then their supernatants were fetched and put into the volumetric flask to be constant volume with 50 mL, 5 mL of measured liquids were taken, and added 1 drop of concentrated nitric acid into it, the contents of various

http://www.aloki.hu ● ISSN 1589 1623 (Print) ● ISSN 1785 0037 (Online)
DOI: http://dx.doi.org/10.15666/aeer/1706_1329713309

element of the processed samples were determined by inductively coupled plasma emission spectrometer Inductively Coupled Plasma Optical Emission Spectr (ICP-OES) (the Vista MXP type, USA).

Results

Changes of the metabolites formed by B. mucilaginosus in different rocks

Change trend of pH value of fermented liquids for B. mucilaginosus in different rock conditions

Figure 1 presented the change trend of pH value of fermented liquids for *B. mucilaginosus* with cultured time. It can be found that, with the extension of cultured time, pH value of the fermented liquids decreased first and then increased; within the cultivation of 1-10 d time, pH value declined rapidly, when cultivated 10 d, the pH value achieved minimum, subsequently, with the extension of cultured time, pH value had a rising trend gradually; Under different rock conditions, the variation trend of pH value was similar, the rangeability of pH value varied differently, with the highest pH value (4.59) in sandstone, secondly pH value (4.48) in gneiss, and lowest pH value (4.34) in granite, but three all were significantly lower than the control pH value (5.88, $p < 0.05$). In the experimental system containing *B. mucilaginosus*, the pH value first decreased and then increased, which may be because of *B. mucilaginosus* producing metabolites such as organic acids, polysaccharides and amino acids, which were gradually ionized as H+, resulting in a lower pH value of fermentation broth. The increase of pH value in the later stage of the experiment may be related to the autolysis of bacterial cells.

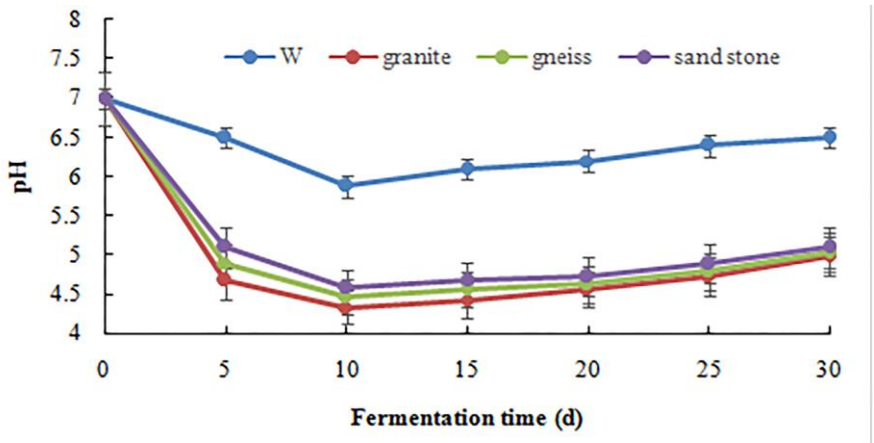

Figure 1. *Change of contents of pH values of the fermented liquids for B. mucilaginosus in different rocks*

Changes of types and contents of organic acids in the fermented liquids of B. mucilaginosus in different rocks

Organic acid is one of metabolites of *B. mucilaginosus*, reflects the ability of mineral leaching and silicon dissolving of *B. mucilaginosus* to a certain extent. The contents of 6 organic acids (oxalic acid, citric acid, malic acid, tartaric acid, acetic acid and succinic acid) in the fermentation broth of *B. mucilaginosus* at the 10th d were measured (at this

http://www.aloki.hu ● ISSN 1589 1623 (Print) ● ISSN 1785 0037 (Online)
DOI: http://dx.doi.org/10.15666/aeer/1706_1329713309

time, the pH value of the fermentation liquids was the smallest, as shown in *Fig. 1*). The contents of organic acids in the fermentation fluids in different rocks were found to be significantly different (*Fig. 2*). Among them, the contents of various organic acids in the fermentation fluids for granite were highest, followed by gneiss, and the lowest the sandstone, and three all were significantly higher than the control (without rock) ($p < 0.05$, *Table 2*). From the perspective of the types of organic acids, the three types of rocks all produced six organic acids, while the control produced only five organic acids, without citric acid; From the perspective of the contents of organic acid, among 6 kinds of organic acid, of tartaric acid were the most (1225.51), followed by glucose acid (1077.29), succinic acid (198.55), malic acid (116.61), and oxalic acid (76.11) and citric acid (55.78) the lower.

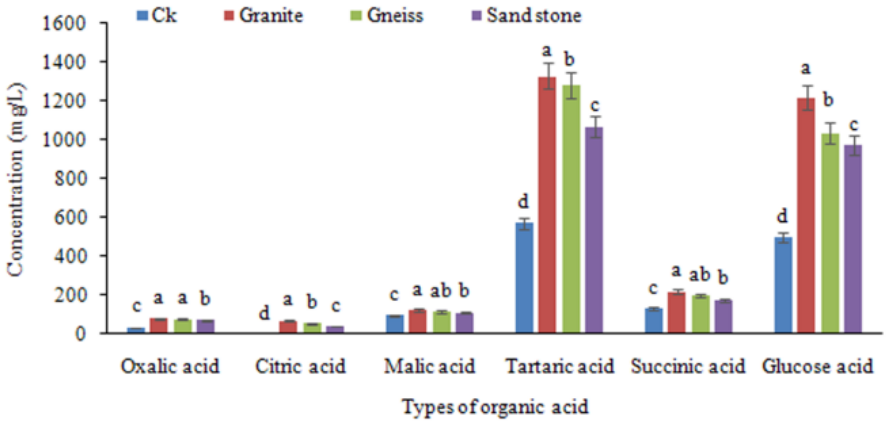

Figure 2. *Types and contents of organic acids in the fermented liquids of B. mucilaginosus for different rocks*

Changes of amino acid contents in the fermentation liquids of B. mucilaginosus for different rocks

Table 2 showed the types and contents of amino acids in the fermentation liquids at the cultured 10th d. It was obvious that the types and content of amino acids in the fermentation fluids between different rocks were different. 19 kinds of amino acids were detected out in fermented liquids for granite and gneiss, 18 kinds of amino acids for sandstone (methionine was not detected out), and just 8 kinds of amino acids for the control (without rock), which suggested that the types of amino acid produced in fermented liquids in added rock powder were more than in control (without rock powder). In other words, the rock powder to add in the fermented liquid stimulated *B. mucilaginosus* to produce more amino acids.

It can be seen from *Table 2* that the contents of amino acids in fermented liquids of *B. mucilaginosus* in different rocks were significant different, and its size sequence was granite > gneiss > sandstone > control, and the composition of amino acids was different obviously in different rock except control. Among them, the contents of alanine were the most, followed by cysteine, glutamic acid, glycine, leucine, isoleucine, methionine content in the least. This result further indicates that different rocks stimulate the fermentation broth of silicate bacteria to produce different metabolites, that is to say, microorganisms have certain selectivity to destroy the mineral rocks with different structures.

http://www.aloki.hu ● ISSN 1589 1623 (Print) ● ISSN 1785 0037 (Online)
DOI: http://dx.doi.org/10.15666/aeer/1706_1329713309

Table 2. *Types and contents of amino acids in the fermented liquids of B. mucilaginosus for different rocks*

Types of amino acids (μg/L)		Culture environment			
		Without rock (Ck)	**Granite**	**Gneiss**	**Sandstone**
Nonpolar amino acid	Glycine	0.619 ± 0.040c	1.633 ± 0.045a	1.450 ± 0.025a	1.006 ± 0.002b
	Alanine	—	2.112 ± 0.063a	1.366 ± 0.042b	1.016 ± 0.02c
	Valine	—	0.788 ± 0.002a	0.568 ± 0.002b	0.478 ± 0.002c
	Leucine	0.412 ± 0.004d	1.483 ± 0.021a	1.096 ± 0.036b	0.636 ± 0.004c
	Isoleucine	—	1.432 ± 0.033a	0.738 ± 0.005b	0.776 ± 0.003b
	Proline	—	0.509 ± 0.001a	0.326 ± 0.004c	0.423 ± 0.005b
	Methionine	0.086 ± 0.001c	0.185 ± 0.009b	0.332 ± 0.003a	—
	Tryptophan	—	0.175 ± 0.002b	0.123 ± 0.002c	0.223 ± 0.001a
	Phenylalanine	—	0.359 ± 0.001b	0.450 ± 0.003a	0.432 ± 0.003ab
Polar amino acid	Tyrosine	0.239 ± 0.033c	0.462 ± 0.003a	0.455 ± 0.005a	0.316 ± 0.003b
	Threonine	0.083 ± 0.001c	0.222 ± 0.004a	0.178 ± 0.002b	0.218 ± 0.001a
	Serine	—	0.246 ± 0.002a	0.218 ± 0.002b	0.076 ± 0.001c
	Cysteine	—	1.976 ± 0.058a	0.968 ± 0.003b	0.561 ± 0.004c
	Asparaginate	—	0.122 ± 0.003a	0.114 ± 0.001b	0.105 ± 0.001c
Alkaline amino acid	Histidine	0.126 ± 0.037c	0.654 ± 0.042a	0.582 ± 0.005a	0.402 ± 0.003b
	Arginine	—	0.964 ± 0.065a	0.866 ± 0.004b	0.749 ± 0.005c
	Lysine	—	1.043 ± 0.068a	0.916 ± 0.003b	0.815 ± 0.002c
Acidic amino acid	Aspartic acid	1.134 ± 0.081c	1.546 ± 0.032a	1.324 ± 0.035b	1.101 ± 0.021c
	Glutamic acid	0.215 ± 0.051b	1.685 ± 0.422a	1.555 ± 0.046a	1.360 ± 0.036a

"—" indicates that data is not detected

Changes of polysaccharide contents in the fermentation fluids of B. mucilaginosus for different rocks

The contents of polysaccharides in the fermentation liquid at cultured 10th d were shown in *Figure 3*. It can be seen that there were obvious differences in the contents of polysaccharides in the fermentation liquid of *B. mucilaginosus* for different rocks. The contents of polysaccharide in the fermentation liquids of *B. mucilaginosus* in the addition of rock powders were significantly higher than that of the control (without rock powder), indicating that the rock powder added in the medium stimulates the *B. mucilaginosus* to produce more polysaccharides. At the same time, we can see from *Figure 3* that the *B. mucilaginosus* have different effect of yielding sugars in different rocks. Among them, the contents of polysaccharide in the fermentation liquids in granite were the highest, which had no significant difference with gneiss, but was significantly higher than that of sandstone and control.

The weathering effect of the B. mucilaginosus on different rocks

The dissolution effect of the B. mucilaginosus on the elements in different rocks

Figure 4 showed the dissolution effect of *B. mucilaginosus* on different oxides in granite, gneiss and sandstone. The data in the figure were obtained from the content of oxide in the fermentation broth minus that of the control (without *B. mucilaginosus*). It was observed from the figure that with the increase of culture time, concentration of

http://www.aloki.hu ● ISSN 1589 1623 (Print) ● ISSN 1785 0037 (Online)
DOI: http://dx.doi.org/10.15666/aeer/1706_1329713309

each oxide was significantly increased, a good growth effect of the *B. mucilaginosus* in the culture liquids added rock was showed, which indicated that the three kinds of rocks could promote the growth and reproduction of *B. mucilaginosus*, and further showed that *B. mucilaginosus* had a certain weathering effect on the three kinds of rocks. According to the amount of oxides leached from the three kinds of rock fermentation liquid, more oxides such as SiO_2, Na_2O, P_2O_5, Fe_2O_3, Al_2O_3, CaO, K_2O, MgO, TiO_2 were dissolved from fermentation liquid in the granite. Compared with sandstone, they increased by 17.28, 5.71, 2.27, 22.96, 5.99, 17.15. 16.80, 1.93 and 0.65 mg/L respectively; compared with gneiss, they increased by 14.24, 3.51, 1.48, 6.80, 1.55, 5.39, 1.93, 0.70 and 2.43 mg/L, respectively. MnO was dissolved in the highest quantities in the fermentation broth of gneiss, more than that of granite and sandstone, which was increased by 0.41 mg/L and .50 mg/L, respectively.

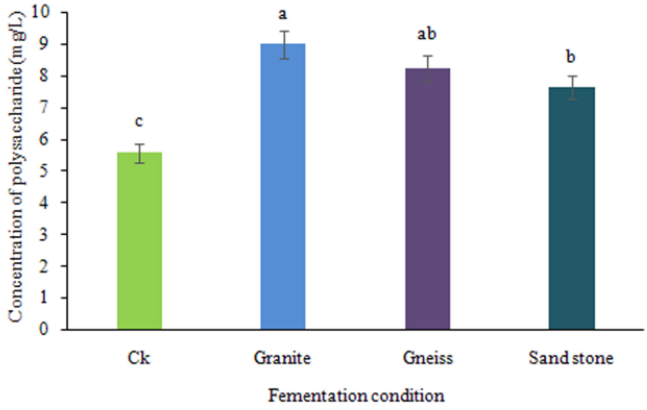

Figure 3. *Change of contents (mg/L) of polysaccharide in the fermentation liquids of B. Mucilaginosus for different rocks*

It can also be seen from *Figure 4* and *Table 1* that the weathering effect of *B. mucilaginosus* on rocks is closely related to the structural components of rocks. In addition to SiO_2, TiO_2 and Na_2O, in general, the higher the content of a certain chemical component in rocks, the more the chemical component dissolved by *B. mucilaginosus*. For example, granite and gneiss have similar structural components, mainly composed of quartz and feldspar, so the weathering effect of the two kinds of rock fermentation liquid is also similar. The main reason why the element dissolution of gneiss is lower than that of granite is that the content of this element in the rock component is slightly lower than that of granite. The main component of sandstone is quartz, the content of SiO_2 is greater than 95%, and the content of other element oxides is less, so the dissolution concentration of oxides of other nine elements in the three types of rocks is low. It should be pointed out that the content of SiO_2 in sandstone is extremely high, ranking the first among the three types of rocks, but its dissolution concentration is the lowest, and the reason remains to be further discussed.

Morphological changes and analysis of rock samples before and after dissolution

The observation results of fore-and-aft of granite, gneiss and sandstone weathered by B. mucilaginosus with the scanning electron microscope were shown in *Figure 5*.

http://www.aloki.hu ● ISSN 1589 1623 (Print) ● ISSN 1785 0037 (Online)
DOI: http://dx.doi.org/10.15666/aeer/1706_1329713309

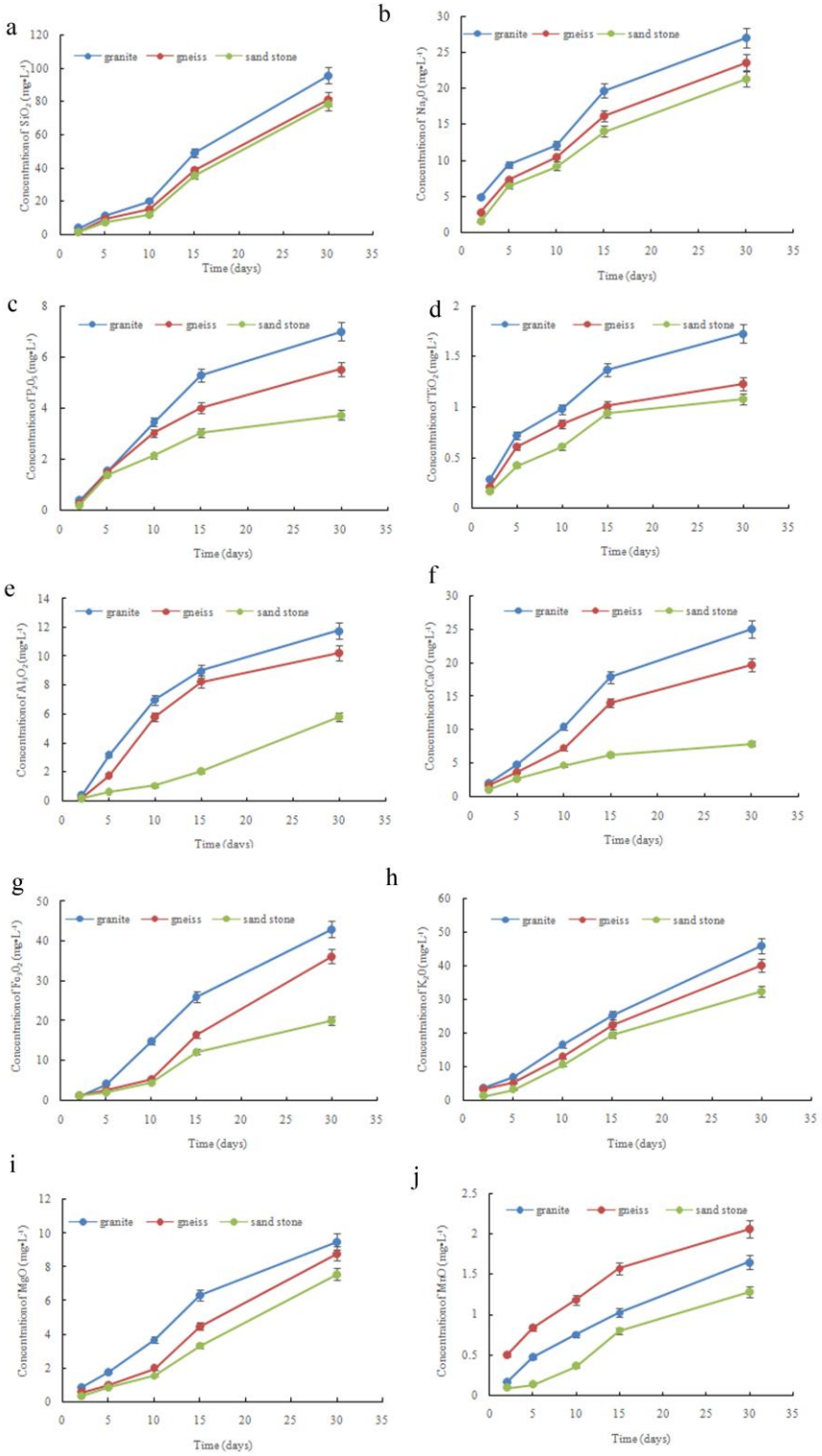

Figure 4. *The concentration of various oxides in the fermentation broth of B. mucilaginosus for different rocks*

Figure 5a, b, c were surface appearance of granite, gneiss, and sandstone rock that were not contacted with *B. mucilaginosus* respectively, it can be seen that the surface of rock particles was smooth, angular, obvious uneven shape, complete crystal structure;

http://www.aloki.hu ● ISSN 1589 1623 (Print) ● ISSN 1785 0037 (Online)
DOI: http://dx.doi.org/10.15666/aeer/1706_1329713309

Figure 5f was the surface topography of sandstone corroded by *B. mucilaginosus* at cultured 30 d, its surface structure was basically destroyed, blurred edges and corners, with some small caves and fractures; *Figure 5e* was the surface appearance of gneiss rock corroded by *B. mucilaginosus* at cultured 30 d, and its angular surface became smooth, the large corner angle and the bulge were broken up into smaller angular and smaller particles, with more corrosion holes and cracks. *Figure 5d* was the surface appearance of granite corroded by *B. mucilaginosus* at cultured 30 d. It can be seen from the *Figure 5d* that the surface structure of granite was completely destroyed, its raised edges and corners was completely blurred, and its surface became rough and uneven. These fully demonstrated that the *B. mucilaginosus* had obvious weathering effect on the surface of three kinds of rocks, and the weathering effect of granite was most distinct.

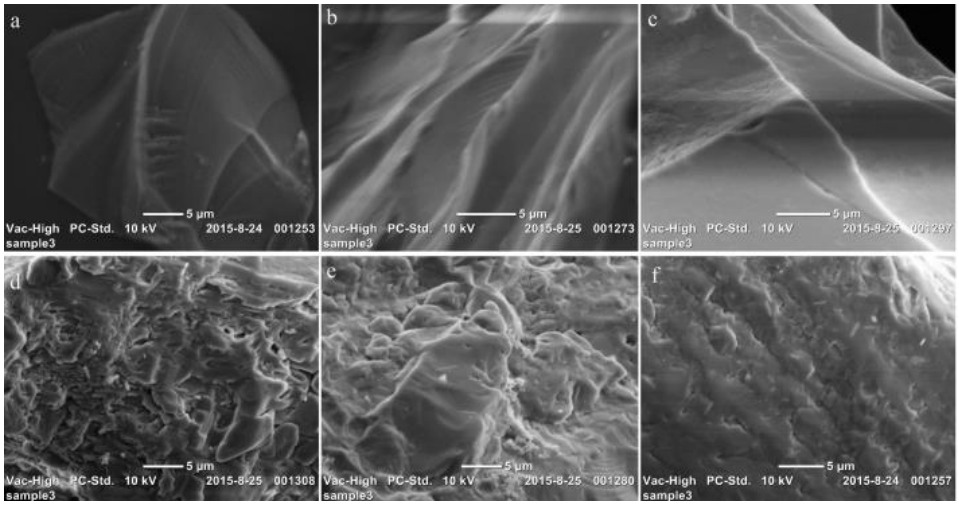

Figure 5. *Electron micrograph of B. mucilaginosus before and after weathering rocks. a - control for weathered granite; b - control for weathered gneiss; c - control for weathered sandstone; d - photograph for weathered granite; photograph for weathered gneiss; f - photograph for weathered sandstone*

Discussion

Most researchers believe that acid hydrolysis is an important way for microorganisms to promote rock and mineral weathering. In this experiment, organic acids such as oxalic acid, citric acid and succinic acid produced in the fermentation broth had good dissolution effects on granite, gneiss and sandstone. It has been proved by studies that under the condition of mineral properties and the same pH value, organic acid solution is more likely to dissolve silicate minerals than inorganic acid solution (Bennett, 1996), because organic acid has both acid dissolution and complexation in the dissolution of silicate minerals, and complexation plays an important role in the dissolution of silicate minerals by organic acid.

Previous studies have shown that *B. mucilaginosus* can promote the weathering of potassium feldspar, illite, quartz, plagioclase and kaolin (Sun, 2006; Ren, 2015). The results showed that *B. mucilaginosus* also had obvious weathering effect on granite, gneiss and sandstone. This was basically consistent with the results of previous studies. However, compared with Sun Side's experiment of promoting silica, plagioclase and

http://www.aloki.hu ● ISSN 1589 1623 (Print) ● ISSN 1785 0037 (Online)
DOI: http://dx.doi.org/10.15666/aeer/1706_1329713309

kaolinite to dissolve silicon and aluminum by using the JXF strain of *B. mucilaginosus* (Sun, 2008), two kinds of organic acids (acetic acid and succinic acid) and three kinds of amino acids (tryptophan, threonine and histidine) were detected in the fermentation broth. These metabolites undoubtedly play an important role in the weathering of rocks by *B. mucilaginosus*.

The fermentation broth of *B. mucilaginosus* could dissolve the elements contained in granite, gneiss and sandstone, such as phosphorus, potassium, silicon, sodium, magnesium, iron and calcium. With the extension of fermentation time, the content of released elements increased. Among them, the weathering effect of the granite was best, followed by gneiss, that of the sandstone was weak. The results of this study fully confirmed that *B. mucilaginosus* could promote weathering of granite, gneiss and sandstone, and elucidate its dissolution effect on phosphorus, potassium, silicon, sodium, magnesium, iron and calcium and other elements, but its dissolution effect had certain selectivity to rock types. Phosphorus and potassium are essential macroelements for plants. Sodium, magnesium, iron and calcium are essential microelements for plants. Although silicon is not a necessary element for plants, it is also a beneficial element. Once applied to the restoration of abandoned rock mining areas, *B. mucilaginosus* will promote the dissolution of available nitrogen, phosphorus, potassium, silicon, sodium, magnesium, iron and calcium in the soil, increase the contents in the soil, improve the status of soil nutrient poverty, so as to enable plants to obtain sufficient nutrients to promote the growth of plants (Zhang et al., 2016).

Granite, gneiss and sandstone are widely distributed in China, which are the three rock types in Jiangsu province. Their bare rock needs repairing. The experiment results showed that the *B. mucilaginosus* could effectively weather the three rocks. Its application in the restoration of bare rock will undoubtedly help to solve the problems of soil erosion and vegetation growth in Jiangsu province and even the whole country, and it is of great significance and value to accelerate the rock slope greenization project and realize the sustainable development of ecological environment. As for how *B. mucilaginosus* mixes with other microbial species, plant seeds, soil, etc. remains to be further studied.

Conclusion

In the fermentation broth of *B. mucilaginosus* added with granite, gneiss and sandstone respectively, their pH values showed a tendency of first decreasing and then increasing with the extension of culture time.

B. mucilaginosus can promote the dissolution effect of granite, gneisses and sandstone by secreting organic acids, amino acids, polysaccharides and other metabolites. Different rocks stimulate *B. mucilaginosus* to produce different metabolites. The contents of various organic acids, amino acids and polysaccharides in the fermentation liquid of granite were the highest, followed by gneiss, and sandstone was the lowest. More 9 kinds of oxides such as SiO_2, Na_2O, P_2O_5, Fe_2O_3, Al_2O_3, CaO, K_2O, MgO and TiO_2 were dissolved in fermentation broth added with granite.

B. mucilaginosus can significantly promote the weathering of granite, gneiss and sandstone, especially granite. SEM observation showed that after 30 days of dissolution by *B. mucilaginosus*, the edges and corners of sandstone rock became blurred, the edges and corners of gneiss rock smooth, and the convex edges and corners of granite surface rough, and obvious corrosion pits appeared in all three kinds of rocks.

http://www.aloki.hu ● ISSN 1589 1623 (Print) ● ISSN 1785 0037 (Online)
DOI: http://dx.doi.org/10.15666/aeer/1706_1329713309

This paper provided a good seed resources for solving the problem of rapid soil formation of exposed rocks in abandoned mining areas and a new idea and solution for ecological restoration of degraded habitats. However, the effective combination of *B. mucilaginosus* with other microbial species, plant seeds and soil still needs to be further studied.

Acknowledgements. This research was supported by the positioning research project of Forest Ecosystem of Changjiang River Delta in Jiangsu Province, the Engineering Project 'Three New' for Forestry in Jiangsu Province (lysx [2013] 10), a project funded by the Priority Academic Program Development of Jiangsu Higher Education Institutions, the open project of the Key Laboratory of Soil and Water Conservation and Ecological Restoration in Jiangsu Province, and a Fund Project of the Anyang Institute of Technology (YJJ2015011).

REFERENCES

[1] Barker, W. W., Banfield, J. F. (1998): Zones of chemical and physical interaction at interfaces between microbial communities and minerals: a model. – Geomicrobiology Journal 15(3): 223-244.
[2] Bennett, P. C., Hiebert, F. K., Wan, J. C. (1996): Microbial colonization and weathering of silicates in a petroleum-contaminated groundwater. – Chemical Geology 132(1-4): 45-53.
[3] Du, L. T., Huang, Z. Z. (1984): Valence dipolarization in silicate rocks. – Geochimica 13(3): 273-281 (in Chinese).
[4] Ehrlich, H. L. (1998): Geomicrobiology: its significance for geology. – Earth-Science Reviews 45(1-2): 45-60.
[5] Fang, Y., Ma, R. T., An, S. S. et al. (2016): Heidaigou opencast coal mine: soil enzyme activities and soil physical and chemical properties under different vegetation restoration. – Environmental Science 37(3): 1121-1127 (in Chinese).
[6] Ge, H. L., Ji, X. E. (2017): Screening, Identification and promoting effects of potassium-solubilizing bacteria in rhizosphere of cucumber. – Northern Horticulture 41(13): 21-25 (in Chinese).
[7] Hall, K., Arocena, J. M., Boelhouwers, J. et al. (2005): The influence of aspect on the biological weathering of granites: observations from the Kunlun Mountains, China. – Geomorphology 67(1-2): 171-188.
[8] Li, J., Yuan, H. S., Wang, W. et al. (2016): Isolation of silicate bacteria from paddy field and determination of activity of the strain. – Ecological Science 35(1): 103−108 (in Chinese).
[9] Li, S., Li, F. C., Cheng, L. J. (2006): Recent development in bio-weathering research. – Mineral Resources and Geology 20(6): 577-582 (in Chinese).
[10] Li, Y., Li, F. C., Yang, G. et al. (2017): Comparing elements dissolution from biotite bio-weathering by bacteria and fungi. – Chinese Journal of Soil Science 48(1): 86-93 (in Chinese).
[11] Man, L. Y., Xiao, G. G., Zhang, X. Z. (2015): Bioleaching of bauxite by silicate bacteria and change of bacterial community structure during leaching process. – Journal of Central South University (Science and Technology) 46(2): 394-403 (in Chinese).
[12] Ren, L. L., Li, Y. X., Chen, Y. (2015): Research progress on silicate bacteria potassium releasing. – Experiment Science and Technology 13(2): 209-211 (in Chinese).
[13] Song, M., Peng, Y. X., Pedruzzi, I. et al. (2015): Bioweathering and K release of K-bearing minerals by Penicillium oxalicum. – Microbiology China 42(7): 1410-1417 (in Chinese).

http://www.aloki.hu ● ISSN 1589 1623 (Print) ● ISSN 1785 0037 (Online)
DOI: http://dx.doi.org/10.15666/aeer/1706_1329713309

[14] Štyriaková, I., Štyriak, I., Oberhansli, H. (2012): Rock weathering by indigenous heterotrophic bacteria of Bacillus spp. at different temperature: a laboratory experiment. – Mineralogy and Petrology 105(3-4): 135-144.
[15] Sun, D. S., Zhang, X. Z., Zhang, Q. (2006): Leaching effects of metabolites of silicate bacterium on silicate minerals. – Mining and Metallurgical Engineering 26(3): 39-42 (in Chinese).
[16] Sun, D. S., Wan, Q., Zhao, X. P. (2008): Metabolites of Bacillus mucilaginous JXF and their desiliconization effect. – Mining and Metallurgical Engineering. 28(3): 52-56 (in Chinese).
[17] Sun, H. Z., Song, P., Du, J. et al. (2018): Identification of silicate bacterium and its breeding by UV mutation. – Genomics and Applied Biology 37(3): 1225-1230 (in Chinese).
[18] Vandevivere, P., Welch, S. A., Ullman, W. J. et al. (1994): Enhanced dissolution of silicate minerals by bacteria at near-neutral pH. – Microbial Ecology 27(3): 241-251.
[19] Wang, R. R., Wang, Q., He, L. Y. et al. (2015): Isolation and the interaction between a mineral-weathering Rhizobium tropici Q34 and silicate minerals. – World Journal of Microbiology and Biotechnology 31(5): 747-753.
[20] Welch, S. A., Ullman, W. J. (1993): The effect of organic acids on plagioclase dissolution rates and stoichiometry. – Geochimica et Cosmochimica Acta 57(12): 2725-2736.
[21] Wu, Q. F., Hu, H. B. (2019): The influence of environmental factors on Aspergillus niger granite weathering. – Applied Ecology and Environmental Research 17(1): 395-408.
[22] Wu, Q. F., Fu, L., Lu, Z. F. (2016): Purification and molecular identification experiments of microbe in soil. – Journal of Anyang Institute of Technology 15(4): 27-29 (in Chinese).
[23] Wu, Q. F., Hu, H. B., Zhang, X. (2018): Effect of *Aspergillus niger* and its metabolites on weathering of granite. – Journal of Nanjing Forestry University (Natural Sciences Edition) 42(1): 81-88 (in Chinese).
[24] Wu, Y. W., Zhang, J. C., Guo, X. P. et al. (2017a): Identification of efficient strain applied to mining rehabilitation and its rock corrosion mechanism: based on boosted regression tree analysis. – Environmental Science 38(1): 283-293 (in Chinese).
[25] Wu, Y. W., Zhang, J. C., Wang, L. J. et al. (2017b): A rock-weathering bacterium isolated from rock surface and its role in ecological restoration on exposed carbonate rocks. – Ecological Engineering 101(1): 162-169.
[26] Xiao, G. G., Sun, D. S., Cao, F. (2013): Weathering of silicate minerals by metabolites produced by silicate bacteria in culture experiments. – Mineral Petrol. 33(3): 8-15 (in Chinese).
[27] Yang, J. L., Zhang, G. L., Huang, L. M. (2013): Rock weathering and soil formation rates of a forested watershed in the typical subtropical granite area. – Acta Pedolocica Sinica 50(2): 253-259 (in Chinese).
[28] Zeng, Q. (2016): Research progress on the mechanism of silicate bacteria on mineral weathering. – Science and Wealth 8(5): 931 (in Chinese).
[29] Zhang, H. F., He, G., Wu, L. Y. et al. (2018): Screening, identification and cultivated condition optimization of high efficiency potassium solubilization and desilication fungus strain. – Soils 50(5): 85-92 (in Chinese).
[30] Zhang, Y. X., Lei, P., Xu, Z. Q. et al. (2016): Screening of a high-efficiency phosphate solubilizing bacterium Bacillus subtilis JT-1 and its effects on soil micropecology and wheat growth. – Jiangsu Agricultural Science 32(5): 1037-1080 (in Chinese).
[31] Zhou, D. Z., Chen, Y., Cao, F. et al. (2015): Effects of chemical mutation on bacterial extracting potassium from potassium-rich sandshale. – The Chinese Journal of Nonferrous Metals 25(3): 824-833 (in Chinese).

http://www.aloki.hu ● ISSN 1589 1623 (Print) ● ISSN 1785 0037 (Online)
DOI: http://dx.doi.org/10.15666/aeer/1706_1329713309

TOXIC EFFECTS OF CHLORPYRIFOS AND Cr^{6+} ON RED CALIFORNIAN EARTHWORM (*EISENIA FETIDA*)

TU, B. H. – GUI, S. – SUN, C. P. – ZHAO, Y.* – XIAO, X. – ZHANG, S.*

School of Environmental and Safety Engineering, Changzhou University, Changzhou, Jiangsu 213164, China

**Corresponding authors*
e-mail/phone: zhaoyuan@cczu.edu.cn/+86-159-6123-8081 (Y. Zhao); zhangsheng@cczu.edu.cn/+86-139-5122-6900 (S. Zhang)

(Received 9th Jun 2019; accepted 28th Aug 2019)

Abstract. Eisenia fetida are commonly used for water and soil ecotoxicology tests. Here, we use Eisenia fetida as a model organism to investigate the effect of cartap and Cr^{6+} on the physiological and biochemical indicators, such as mortality, protein content, superoxide dismutase (SOD), catalase (CAT) and malondialdehyde (MDA). The results showed that with an increasing content of cartap, protein contents in Eisenia fetida increased in the beginning, then decreased, and finally stabilized after prolonged exposure. In the case of increasing Cr^{6+}, protein contents in Eisenia fetida decreased in the beginning, then increased, and finally decreased after prolonged exposure. The SOD activity in Eisenia fetida was simulated under low concentration and short durations of contaminations, while the SOD activity decreased after prolonged exposure. Meanwhile, under low contaminations, CAT contents were stimulated. The MDA contents in Eisenia fetida were significantly negatively correlated with SOD activity. This indicated that when the organisms are subjected to pollutant stress, the activity of SOD will be rapidly induced for removing excess oxygen free radicals and producing H_2O_2, accompanied by enhanced activity of CAT converting H_2O_2 to H_2O. With the prolonged exposure time, the SOD activity decreased, and the organisms were harmed by oxidative damage with enhanced MDA contents.
Keywords: *chlorpyrifos, ecotoxicity, superoxide dismutase, catalase, malondialdehyde*

Introduction

With the rapid development of China's industrialization, heavy metal content in farmland soils and water bodies severely exceeds the standard, seriously affecting the quality of agricultural products and endangering human health (Yu and Liu, 2011). This issue gained the attention of all countries. Heavy metal pollution does great harm to aquatic and soil ecosystems, affecting the physiological activities of aquatic plants such as respiration and photosynthesis, and inhibiting their growth (He et al., 2008). Affect the metabolism and growth of aquatic animals, such as cadmium affecting fish growth, interfering with fish endocrine (Wang et al., 2015). Heavy metals cause loss of activity in proteins and enzymes in the human body, accumulating in certain organs of the human body, causing chronic poisoning (Zhao et al., 2007). Among them, Cr^{6+} and Pb are more toxic, and they are more easily absorbed in the human body and are carcinogenic to the human body (Teng et al., 2014). When pesticides are applied, they are easy to remain on the surface of soil and agricultural products. Under the action of enzymes, metabolic processes such as hydrolysis, dechlorination and oxidation occur, and are transmitted to the human body through the food chain. In particular, some of the larger molecular weights are more soluble and easily absorbed by crops (Chen, 2014; Xia, 2008; Huang, 2002). When pesticides are applied, they are easy to remain on the surface of soil and agricultural products. Under the action of enzymes, metabolic processes such as hydrolysis, dechlorination and oxidation occur, and are transmitted to the human body

http://www.aloki.hu ● ISSN 1589 1623 (Print) ● ISSN 1785 0037 (Online)
DOI: http://dx.doi.org/10.15666/aeer/1706_1331113327

through the food chain. In particular, some of the larger molecular weights are more soluble and easily absorbed by crops (Xiao and Zhao, 2005). In addition, crops also absorb some residual pesticides from the soil and enter the crops through enrichment, which affects crop safety (Liu et al, 2002).

Traditional chemical analysis methods can accurately quantify the content of major components in pollutants, but can not directly reflect the environmental and biological toxicity of various toxic substances (Su et al, 2011). The biotoxicity method is a rapid monitoring method that reflects the overall toxicity of various toxic pollutants to the environment (Liao and Chen, 2007). Is a oligochaete terrestrial animal, one of the most biomass soil organisms, and a source of food for many birds and other organisms. It is located in the terrestrial ecosystem at the lowest level of the bio-chain and is easier in the food chain. The transfer of pollutants plays an important role in maintaining the stability of farmland ecosystems and the entire soil ecosystem, but it is likely to have more enrichment of heavy metals and pesticides in the body. In addition, alfalfa can improve the soil structure through feeding, excavation, etc., help the degradation of organic decay substances in the soil, maintain soil fertility, and affect soil physical and chemical properties. Because the soil moisture content, pH value and other changes can affect the cockroaches, cockroaches are highly sensitive to pollutants, and are highly susceptible to pollutants leading to changes in survival, genetics, etc. Therefore, cockroaches as ecotoxicology indicator organism for facilitating related research (Wang et al, 2012). Thus, our study aimed at (i) studying the toxic effects of Cr^{6+} on Eisenia fetida, and (ii) determining whether Eisenia fetida is suitable as an indicator of soil ecotoxicity.

Materials and methods

Acute toxicity test

Chlorpyrifos, with a purity of 98.8%, from Shanghai Institute of Pesticide; potassium dichromate（$K_2Cr_2O_7$, Purchased from Sinopharm Chemical Reagent Co., Ltd. Before the experiment, the chlordane and potassium dichromate were prepared and formulated into a 1000 $mg \cdot L^{-1}$ stock solution, which was sealed and stored at 4 °C for use. Eisenia fetida, Purchased from a professional carp farm in Jiangsu (*Fig. 1a*). Before the test, it was pre-cultured for a period of time in the laboratory. During the test, adult mature ticks with a body weight of about 0.3 g were selected.

Experiment method

Clean up the gut of the earthworm

Pick up the sexually mature adult cockroaches in the pre-cultivated red scorpion, wash them with ultrapure water and put them into a beaker. The bottom of the beaker is covered with filter paper and moistened with appropriate amount of water. Seal with plastic wrap and use the anatomical needle. Make holes in the cling film. Place the beaker in a constant temperature incubator at 20 ± 1 °C, humidity 80 to 85%, and clear the intestines for 1 day and night in the dark.

Contamination

The median expected toxicity was determined according to the literature. Pre-experiment was performed before the formal test to find the maximum lethal

http://www.aloki.hu ● ISSN 1589 1623 (Print) ● ISSN 1785 0037 (Online)
DOI: http://dx.doi.org/10.15666/aeer/1706_1331113327

concentration LD_{100} and the minimum lethal concentration of the pollutants, and the formal test concentration was set according to the preliminary experiment. The double-layer double-circle qualitative filter paper was placed in a glass culture dish, and 4 mL of the test concentration reagent was accurately absorbed on the filter paper, and 10 replicates with one test organism were set for each treatment, and a blank control group was set at the same time. Rinse the sputum after the intestines and blot the excess water on the surface and place one in each glass dish for the test. Seal with plastic wrap, place the glass culture dish in a constant temperature incubator at 20 ± 1 °C, adjust the humidity to 80% to 85%, culture in the dark for 72 h, and at 24 h, 48 h and 72 h recorded the survival of sputum.

Figure 1. *(a) The test organism Eisenia fetida; (b) sexually mature adult worms; and (c) toxicity test*

Data processing

The dose-effect model (DRC) of the toxicity of mixed pollutants was nonlinearly fitted by origin 8.5 software, and the LC_{50} values of the earthworms 24 h, 48 h and 72 h were calculated by nonlinear regression equation and passed SPSS software. Calculate a 95% confidence interval. The significance of different treatment was tested using Duncan's multiple-range test at $p < 0.05$ after one-way analysis of variance (ANOVA) in SPSS 20.2.

Experiment on earthworm physiological and biochemical indexes

Pollutant addition method

1. Blank control of experimental methods

In the blank test, 4 mL of deionized water was accurately absorbed and uniformly poured onto the glass culture dish with double layer and double coil qualitative filter paper.

2. Method of adding pyrrolidin

Accurately weigh the standard product of pyrrolide 1.02 g, dissolve with deionized water at a constant volume of 100 mL volumetric flask, configured into 10,000 $mg \cdot L^{-1}$ pyrrolide standard product mother liquid, is now used. Deionized water was used to dilute the mother solution of pyroridin with the concentration gradient of 0.5, 1.0, 1.5, 2.0 and 2.5 $mg \cdot L^{-1}$, respectively. Double layer and double coil qualitative filter paper was placed in a 9 cm diameter glass culture dish, and the diluted solution 4 mL was uniformly poured on the filter paper.

http://www.aloki.hu ● ISSN 1589 1623 (Print) ● ISSN 1785 0037 (Online)
DOI: http://dx.doi.org/10.15666/aeer/1706_1331113327

3. Add methods of Cr^{6+}

Accurately weigh the dried potassium dichromate standard 0.565 g, dissolve it in water, use deionized water to fix the volume of 100 mL volumetric flask, and configure it into 1000 mg· L^{-1} potassium dichromate standard storage liquid. The mother solution of potassium dichromate was extracted and diluted with deionized water into 5 experimental solutions with concentration gradient of 1.0, 2.0, 3.0, 4.0 and 5.0 mg· L^{-1}. Double layer and double coil qualitative filter paper was placed in a 9 cm diameter glass culture dish, and the diluted solution 4 mL was uniformly poured on the filter paper.

Earthworm in vivo biochemical index test experiment

1. Test for determination of protein content

Earthworm samples from each treatment group at 24 h, 48 h and 72 h of exposure were collected, and the weight of the tissue to be measured was accurately weighed. 0.86% normal saline was added according to the proportion of weight (g): volume (mL) = 1:9. Mechanical homogenation was performed in ice water bath. The supernatant was diluted into 2% tissue homogenate with normal saline at 1:4, and was to be tested.

Blank tube, standard tube and measuring tube were set up in the experiment, in which double steaming water was added into the blank tube, protein standard substance 0.563 g/L was added into the standard tube, and homogenized earthworm tissues were placed in the measuring tube. In the test, the sample was first added with coomath bright blue color developing liquid, mixed and set for 10 min, then the absorbance value of each tube was measured at 595 nm by a colorimetric cup with a light diameter of 1 cm with ultraviolet spectrophotometer and double steaming water for zero adjustment. According to the measured absorbance, the protein content of the tissue homogenate with 2% concentration of earthworm sample was determined by the calculation formula shown below:

$$\text{Protein Concentration in the Sample(gprotj/L)} = \frac{\text{Measured value (OD)} - \text{Blank value (OD)}}{\text{standard value (OD)} - \text{Blank value (OD)}} \times \text{Standard concentration} \times \text{Dilution multiple before sample determination} \quad \text{(Eq.1)}$$

2. Determination of total superoxide dismutase activity

Respectively collected 24 h, 48 h and 72 h exposure when the earthworm samples of each treatment group accurately according to weight of the organization, by weight (g): the ratio of volume (mL) = 1:9 add 0.86% saline, ice water bath conditions, mechanical preparation of 10% homogenate and serum, use refrigerated centrifuge (Thermo Multifuge X1R) homogenate good earthworm tissue fluid under the condition of 2500 r/min centrifuge for 10 min. Remove the supernatant and test.

Test tube and set up the determination of the tube and the care, determination of the tube with samples, the care of the same volume of double steaming water, room temperature static 10 min, the use of ultraviolet spectrophotometer (Multiskan™ GO, Thermo Scientific), double steaming water zero, light diameter 1 cm colorimetric cup at the wavelength of 550 nm, determine the absorbance value of each tube. Because SOD has a specific inhibitory effect on superoxide anion radicals, resulting in the formation

http://www.aloki.hu ● ISSN 1589 1623 (Print) ● ISSN 1785 0037 (Online)
DOI: http://dx.doi.org/10.15666/aeer/1706_1331113327

of nitrite reduction, colorimetric determination of the tube absorbance value is lower than the care of the absorbance value, substituted into the formula to calculate SOD activity. The calculation formula is as follows:

$$\text{Total vitality (U/mgprot)} = \frac{\text{Control value (OD)} - \text{Measured value (OD)}}{\text{Control value (OD)}} \div 50\% \times \frac{\text{Total volume of reaction liquid}}{\text{Sampling quantity}} \div \text{Protein Concentration in the Sample to be Measured (mgprot/ml)} \quad \text{(Eq.2)}$$

3. Determination of catalase (CAT) activity

Respectively collected 24 h, 48 h and 72 h exposure when the earthworm samples of each treatment group accurately according to weight of the organization, by weight (g): the ratio of volume (mL) = 1:9 add 0.86% saline, ice water bath conditions, mechanical preparation of 10% homogenate and serum, use refrigerated centrifuge homogenate good earthworm tissue fluid under the condition of 2500 r/min centrifuge for 10 min. Take supernatant and normal saline (0.86%) and prepare 5% tissue homogenate according to 1:1 volume ratio.

The care and measurement tubes were operated according to the kit purchased by Nanjing Jiancheng Institute of Biological Engineering.

Ultraviolet spectrophotometer, double evaporation water zero, light diameter 0.5 cm colorimetric cup at the wavelength of 240 nm colorimetric, determine the absorbance value of each tube. The calculation formula is as follows:

$$\text{CAT vitality (U/mgprot)} = \frac{(\text{Control value (OD)} - \text{Measured value}) \times 271}{60 \times \text{Sampling quantity}} \times \text{Protein Concentration in the Sample to be Measured} \quad \text{(Eq.3)}$$

4. Determination of malondialdehyde (MDA)

Earthworm samples from each treatment group at 24 h, 48 h and 72 h of exposure were collected, and the weight of the tissue to be measured was accurately weighed. 0.86% normal saline was added according to the proportion of weight (g): volume (mL) = 1:9. Mechanical homogenation was performed in ice water bath. Take the supernatant and dilute it with normal saline at 1:4 to 2% tissue homogenate for testing.

The test set blank tube, standard tube, measuring tube and pair of care, according to the operation of the kit, the use of ultraviolet spectrophotometer, double steaming water zero, light diameter 0.5 cm colorimetric cup at the wavelength of 405 nm colorimetric, determine the absorbance value of each tube. The calculation company is as follows:

$$\text{MDA content (nmol/mgprot)} = \frac{\text{Measured value (OD)} - \text{Blank value (OD)}}{\text{standard value (OD)} - \text{Blank value (OD)}} \times \text{Standard concentration} \div \text{Protein Concentration in the Sample to be Measured} \quad \text{(Eq.4)}$$

http://www.aloki.hu ● ISSN 1589 1623 (Print) ● ISSN 1785 0037 (Online)
DOI: http://dx.doi.org/10.15666/aeer/1706_1331113327

Results

Toxicity test of chlorpyrifos and Cr^{6+} on earthworms

The toxicity test results of chlorpyrifos and Cr^{6+} on earthworms are shown in *Table 1*. The results show that both drugs have a certain degree of toxicity on earthworms, and the toxicity increases with the extension of exposure time. The experimental results showed that the survival rate of earthworms was 100%. When the poisoning time was 24 h, the single toxicity value of chlorpyrifos and Cr^{6+} on earthworms was significantly different, and the order of toxicity was > Cr^{6+} of chlorpyrifos. Among them, the most toxic was pyroridin, with a 24-h LC_{50} value of 14.30 (13.57-15.02) $mg \cdot L^{-1}$, followed by Cr^{6+}, and a 24-h LC_{50} value of 104.42 (99.20-109.64) $mg \cdot L^{-1}$. Two drugs are longer duration of canister and toxic, canister for 48 h, chlorpyrifos, Cr^{6+} 48 h-LC_{50} were 12.36 (11.74 12.98), 71.53 (67.95 75.11) $mg \cdot L^{-1}$, toxicity increased 1.16 and 1.46 times respectively, chlorpyrifos toxicity is still the strongest, is 5.79 times that of Cr^{6+} infected time for 72 h., chlorpyrifos, Cr^{6+} toxicity continue to strengthen, the strongest toxicity is still chlorpyrifos, 72-h LC_{50} value was 10.43 (9.91-10.95) mg· l-1, and the toxicity of cyanilon and Cr^{6+} was 1.19 times and 1.78 times stronger than that of cyanilon 48 h after exposure, respectively.

Table 1. *Single toxicity of cartap, Cr^{6} on earthworm*

	24 h LC_{50} $mg \cdot L^{-1}$	**95% confidence interval $mg \cdot L^{-1}$**	**48 h LC_{50} $mg \cdot L^{-1}$**	**95% confidence interval $mg \cdot L^{-1}$**	**72 h LC_{50} $mg \cdot L^{-1}$**	**95% confidence interval $mg \cdot L^{-1}$**
Methyl ethyl chloride	14.30	13.57-15.02	12.36	11.74-12.98	10.43	9.91-10.95
Cr^{6+}	104.42	99.20-109.64	71.53	67.95-75.11	40.21	38.20-42.22

Effects of pyroridin, Cr^{6+} and the biochemical indexes on earthworms

Effects of pyroridin and Cr^{6+} on the protein content of earthworms

Protein is composed of 20 kinds of amino acid, is an important part of the cell is the foundation of many life processes, is responsible for performing the life activities of the main functional molecules, easily happened due to the impact of certain factors in degeneration or other changes, thus could be obtained by using the studies of the changes of protein material toxicity mechanism of relevant information. Studies have shown that soil contaminated with pesticides and heavy metals can cause changes in the protein content of earthworms.

The experiment set up five treatment groups of 0.5, 1.0, 1.5, 2.0 and 2.5 $mg \cdot L^{-1}$. Earthworm samples were collected for pretreatment at 24 h, 48 h and 72 h respectively, and the protein content was determined. The results were shown in *Figure 2*.

As can be seen from *Figure 2,* the protein content of earthworms changed to different degrees after the exposure of pyroridin at different concentrations. The protein content of the infected earthworms was higher than that of the blank control group, which may be caused by the stimulation of pollutants and the stress proteins produced by the earthworm body, such as c-reactive protein (CRF) and fibrin connective protein (Fn), etc., which may lead to the increase of the protein content of earthworms (Ling, 2004). When the exposure time of 24 h, the earthworm body protein content increased with the

http://www.aloki.hu ● ISSN 1589 1623 (Print) ● ISSN 1785 0037 (Online)
DOI: http://dx.doi.org/10.15666/aeer/1706_1331113327

increase of concentration of test presents a trend of reducing the rise, were relatively blank control group increased by 12.9%, 12.9%, 43.57%, 29.59% and 23.8%, the concentration of 1.5 $mg \cdot L^{-1}$ when the maximum, the protein content of 144% times as blank group, then gradually reduce the protein content, may be due to chlorpyrifos has strong tag and stomach poison, start acting on earthworm skin table, send the earthworm appear after stress reaction or worms infected body metabolic disorders cause the protein content is higher, With the increase of the concentration, the toxin ACTS on the stomach of earthworms and destroys the protein synthesis, resulting in the decrease of protein content (Xue and Pei, 2000).

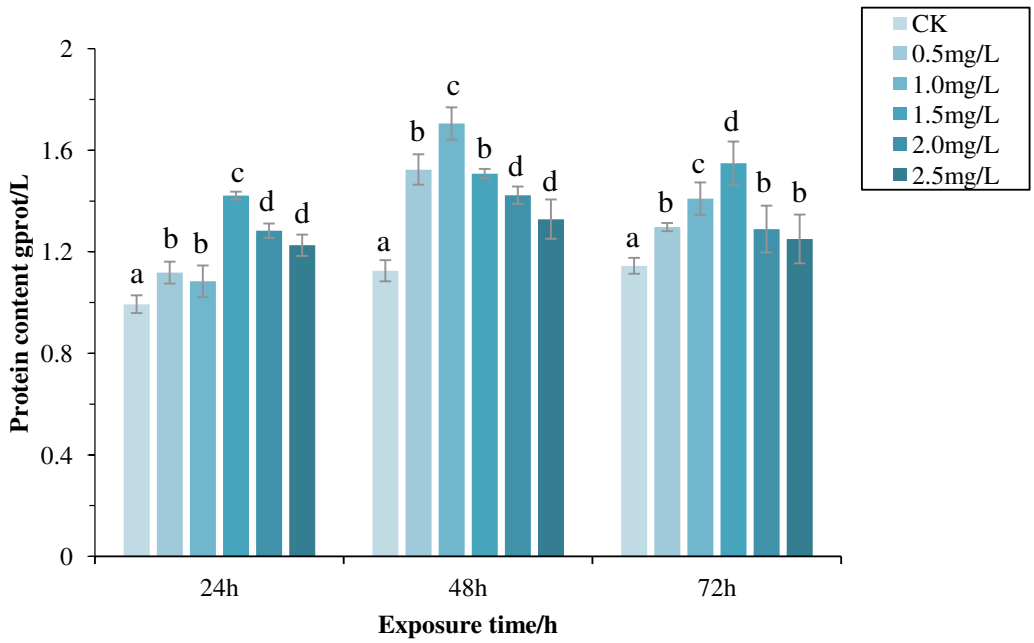

Figure 2. *Effect of cartap with different concentrations on protein contents of earthworm after single exposure 24, 48 and 72 h. Different lowercase letters indicate significant differences between treatments, as revealed by one-way ANOVA with Duncan's multiple-range test at* $p < 0.05$

Earthworms were treated with Cr^{6+} solution of 1, 2, 3, 4 and 5 $mg \cdot L^{-1}$, and earthworms were collected at 24, 48 and 72 h for protein content determination. The results are shown in *Figure 2*.

As can be seen from *Figure 3,* the protein content of blank treated earthworms decreased slightly with the exposure time and was lower than that of Cr^{6+} infected earthworms, which may be related to the stress protein produced by the body stress response of earthworms after being poisoned. When the exposure time was 24 h, with the increase of Cr^{6+} concentration, the protein content of earthworms presented an increasing trend, indicating that earthworms produced more stress proteins in the short term, which led to the increase of protein content in the body. When the exposure time was 48 h, the content of earthworm in vivo was first decreased, then increased and then decreased. When the Cr^{6+} concentration was 4 $mg \cdot L^{-1}$, the maximum value was 1.52 gprot/L, which was 1.30 times higher than that of the blank group. At 72 h of exposure, the change trend of protein content first decreased and then increased to a stable level, and it was lower than the blank value when the Cr^{6+} concentration was

http://www.aloki.hu ● ISSN 1589 1623 (Print) ● ISSN 1785 0037 (Online)
DOI: http://dx.doi.org/10.15666/aeer/1706_1331113327

3 $mg \cdot L^{-1}$, which may be due to the fact that with the extension of exposure time, earthworms were stressed and the absorption of digestive tract cells was destroyed (Sun et al, 2011). This leads to decreased protein content.

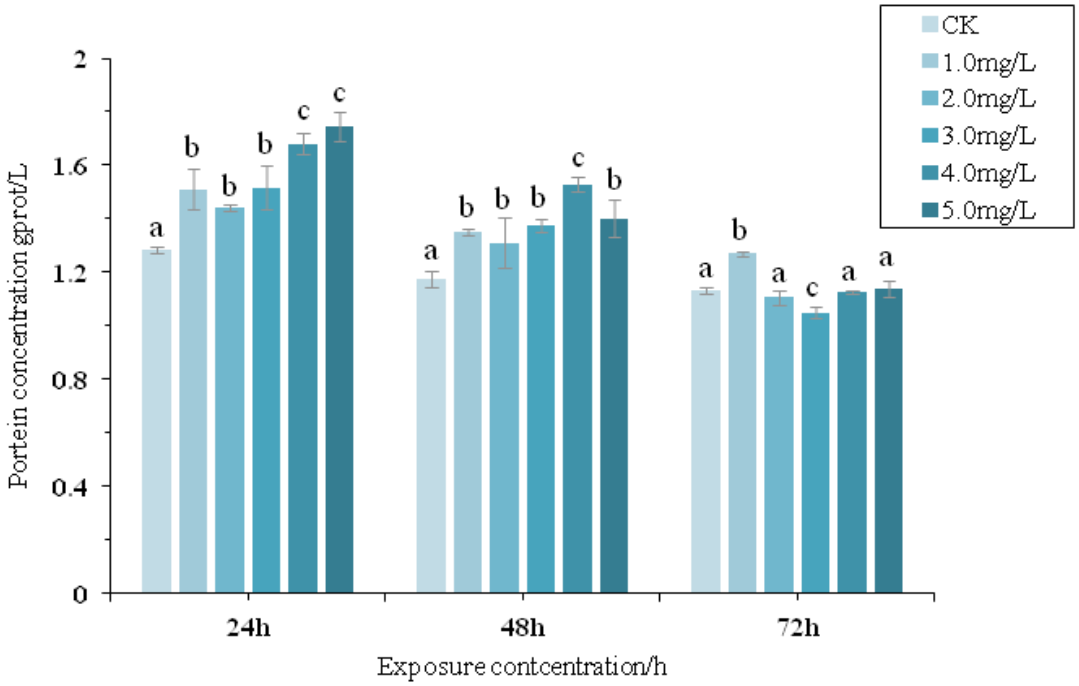

Figure 3. *Effect of Cr^{6+} with different concentrations on protein contents of earthworm. Different lowercase letters indicate significant differences between treatments, as revealed by one-way ANOVA with Duncan's multiple-range test at $p < 0.05$*

Effect of pyroridin and Cr^{6+} on SOD content in earthworms

The experiment set up five treatment groups of 0.5, 1.0, 1.5, 2.0 and 2.5 $mg \cdot L^{-1}$. Earthworm samples were collected for pretreatment at 24 h, 48 h and 72 h, respectively, to determine the content of SOD in vivo.

It can be seen from *Figure 4* that the SOD activity of earthworms infected with chlorpyrifos at different concentrations showed different trends in different poisoning time. SOD activity first decreased and then increased at 24 h after poisoning, then increased at 48 h and then decreased at 72 h after poisoning. Exposure time of 24 h, the low concentration of chlorpyrifos examination in the SOD activity of SOD vitality is higher than the blank group, were higher than that of blank control group 10.93%, 3.02%, 2.06%, 5.51% and 19.04%, obviously when the concentration of 1.5 $mg \cdot L^{-1}$ basic comparative with the SOD vitality of blank control group, with the increase of concentration, the higher SOD vigor, chlorpyrifos is mainly applied to earthworms in the stomach, in the early infected by epidermal cells after absorption, the body's antioxidant defense response, SOD activity was induced. Infected time 48 h, chlorpyrifos role in earthworms in the stomach, earthworms affects the body metabolism, inhibit SOD activity, lower overall than 24 h, and SOD activity in vivo in contrast to the 24 h trends, the concentration of 2.0 $mg \cdot L^{-1}$, reach the maximum, then the SOD activity decreased, but speculation is that as the extension of exposure time, SOD is consumed, and enzyme activity reduced. Exposure time of 72 h, the earthworm

http://www.aloki.hu ● ISSN 1589 1623 (Print) ● ISSN 1785 0037 (Online)
DOI: http://dx.doi.org/10.15666/aeer/1706_1331113327

body total SOD vigor decreasing trends, and much lower than the blank control group, who is probably the most prolonged and the increase of concentration, SOD activity significantly reduced, because the earthworm when suffer less stress, increased the amount of oxygen free radical, in order to remove excess oxygen free radicals and reduce the membrane lipid peroxidation, induction of SOD content increases, the stress levels increase, the body is not enough to resist oxidation, severely damage, enzyme activity is also reduced (Xue and Pei, 2000).

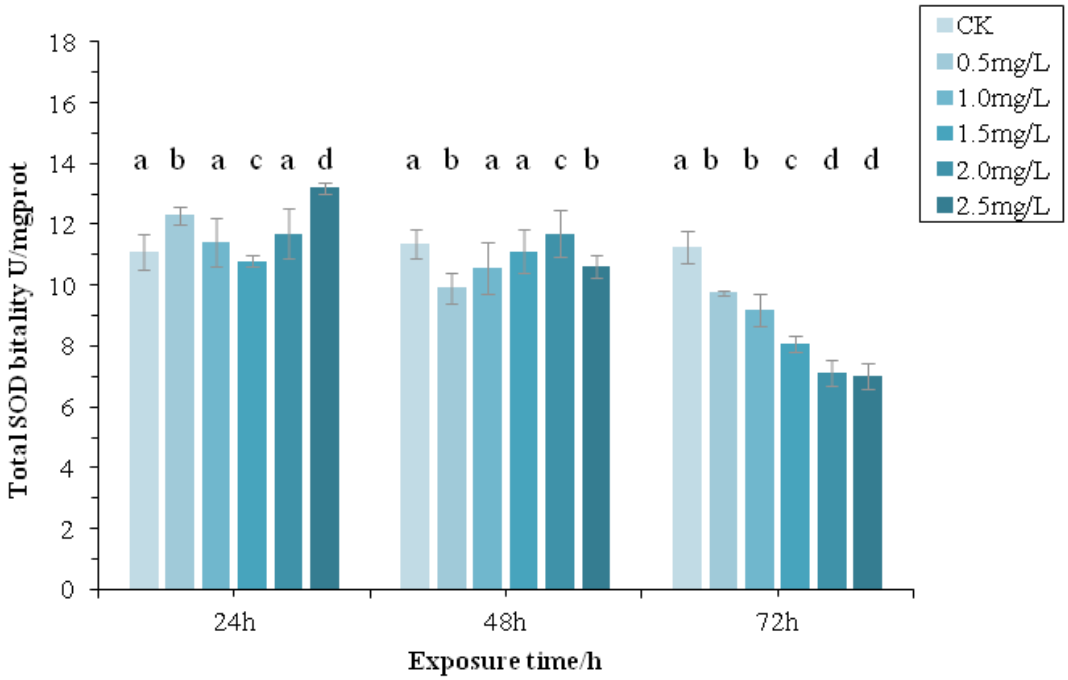

Figure 4. *Effect of cartap with different concentrations on SOD activity of earthworm after single exposure 24, 48 and 72 h. Different lowercase letters indicate significant differences between treatments, as revealed by one-way ANOVA with Duncan's multiple-range test at* $p < 0.05$

In the experiment, Cr^{6+} was set as the concentration of 1.0, 2.0, 3.0, 4.0 and 5.0 mg·L^{-1}. Earthworm samples were collected for pretreatment at 24 h, 48 h and 72 h, respectively, to determine the content of superoxide dismutase (SOD) in vivo.

By *Figure 5,* exposed to the Cr^{6+}, earthworms + pollution, the SOD activity in the body as the canister to the extension of time is reduced, the highest SOD activity in 24 h, may be due to the superoxide dismutase (SOD) is the first line of organism to resist oxidation, so under pollution stress the body to make quick oxidation reaction, induction of enhanced SOD activity, remove excess oxygen free radicals, avoid lipid oxidation reaction. Infected when the time for 24 h, according to the processing of SOD activity were blank control group 145%, 156%, 174%, 148% and 133%, with the increase of concentration of Cr^{6+} processing in earthworm body SOD activity showed a trend of lower after the first rise, the maximum SOD activity was in Cr^{6+} concentration of 3.0 mg·L^{-1}, compared with the blank control group, SOD activity increased by 74.12%. SOD activity decreased at 72 h after exposure compared with that at 24 h and 48 h after exposure, which may be because earthworms were severely affected by Cr^{6+}

http://www.aloki.hu ● ISSN 1589 1623 (Print) ● ISSN 1785 0037 (Online)
DOI: http://dx.doi.org/10.15666/aeer/1706_1331113327

stress, the body was seriously damaged, and SOD activity decreased. The above results showed that Cr^{6+} pollution could significantly induce SOD activity in earthworms at the early stage of infection. When the exposure time was more than 48 h, the SOD activity in earthworms decreased significantly. Under the stress of heavy metal pollution, earthworms produce a large number of oxygen free radicals in the body. In order to reduce the damage caused by oxygen free radicals to themselves, antioxidant enzyme activity increases. However, with the extension of the exposure time, the body is seriously damaged, and various internal balances are broken, and enzymes are gradually consumed to maintain the steady state, thereby reducing the SOD activity.

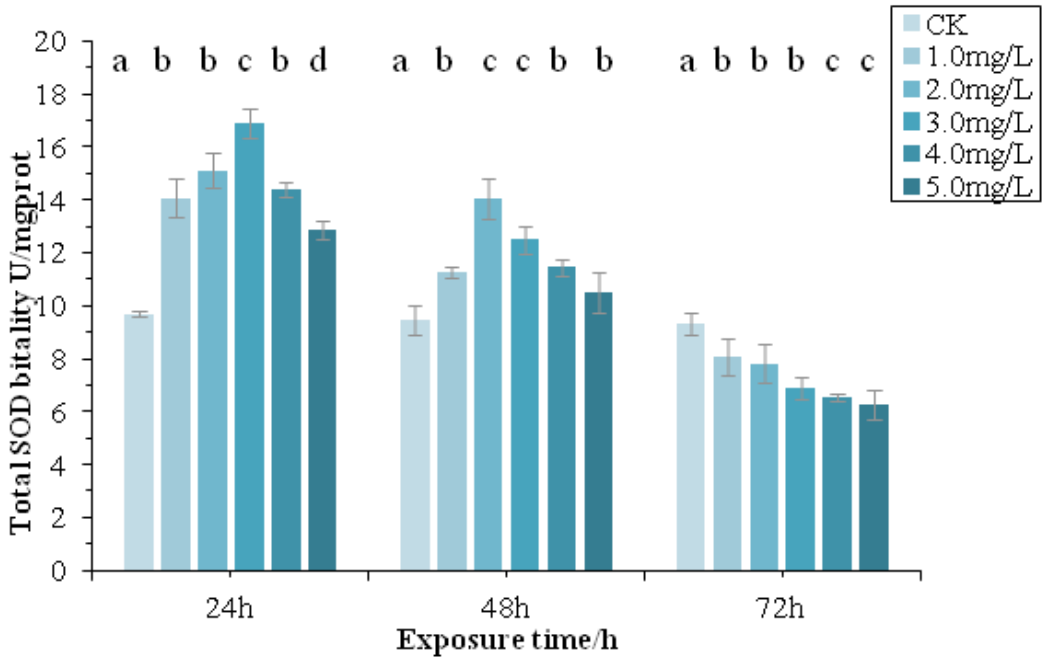

Figure 5. *Effect of Cr^{6+} with different concentrations on SOD activity of earthworm after single exposure 24, 48 and 72 h. Different lowercase letters indicate significant differences between treatments, as revealed by one-way ANOVA with Duncan's multiple-range test at $p < 0.05$*

Effect of pyroridin, Cr^{6+} and Pb on the content of CAT in earthworms

CAT as a biological enzyme systems is an important antioxidant defensive function, existence of red blood cells in most organisms, and some cells of oxygen in the body, usually with the GSH-Px synergy, the product of the free radicals SOD disproportionation H_2O_2 into harmless H_2O and O_2, eliminate free radical and lipid peroxide formation, pollutants stress can lead to the active content changes, so the test in earthworm body of CAT as a biomarker research.

The experiment set up five treatment groups of 0.5, 1.0, 1.5, 2.0 and 2.5 $mg \cdot L^{-1}$. Earthworm samples were collected for pretreatment at 24 h, 48 h and 72 h, respectively, to determine the catalase (CAT) content in vivo.

From *Figure 6,* you can see that when infected 24 h, the earthworm treated by chlorpyrifos induced rapidly rising, the CAT activity was obviously in the kill moth when chlorpyrifos is 0.5 $mg \cdot L^{-1}$ peak, with the increase of chlorpyrifos concentration, the CAT inside its body content is on the decline, probably because with the increased

http://www.aloki.hu ● ISSN 1589 1623 (Print) ● ISSN 1785 0037 (Online)
DOI: http://dx.doi.org/10.15666/aeer/1706_1331113327

concentration of cells in the body chlorpyrifos, nature is the CAT activity. When infected time for 48 h, earthworm body CAT activity increased with the increase of concentration of chlorpyrifos was reduced after the first rise trend, when chlorpyrifos is 2.0 mg · L $^{-1}$ peak, compared with 24 h, slash, CAT content decrease respectively 52.18%, 46.51%, 41.24%, 46.51% and 41.24%, may be due to the early infected cells absorb less chlorpyrifos, vicarious induced the CAT activity increased, with the extension of time, the activity of CAT back to normal levels. CAT activity increased first and then decreased with the increase of pyrrolidan concentration at 72 h, and reached the maximum when pyrrolidan concentration was 1 mg·L^{-1}. Compared with 48 h, CAT activity was more stable, which may be due to the adaptive reaction of earthworms to pyrrolidan, and the enzyme activity reached a stable state.

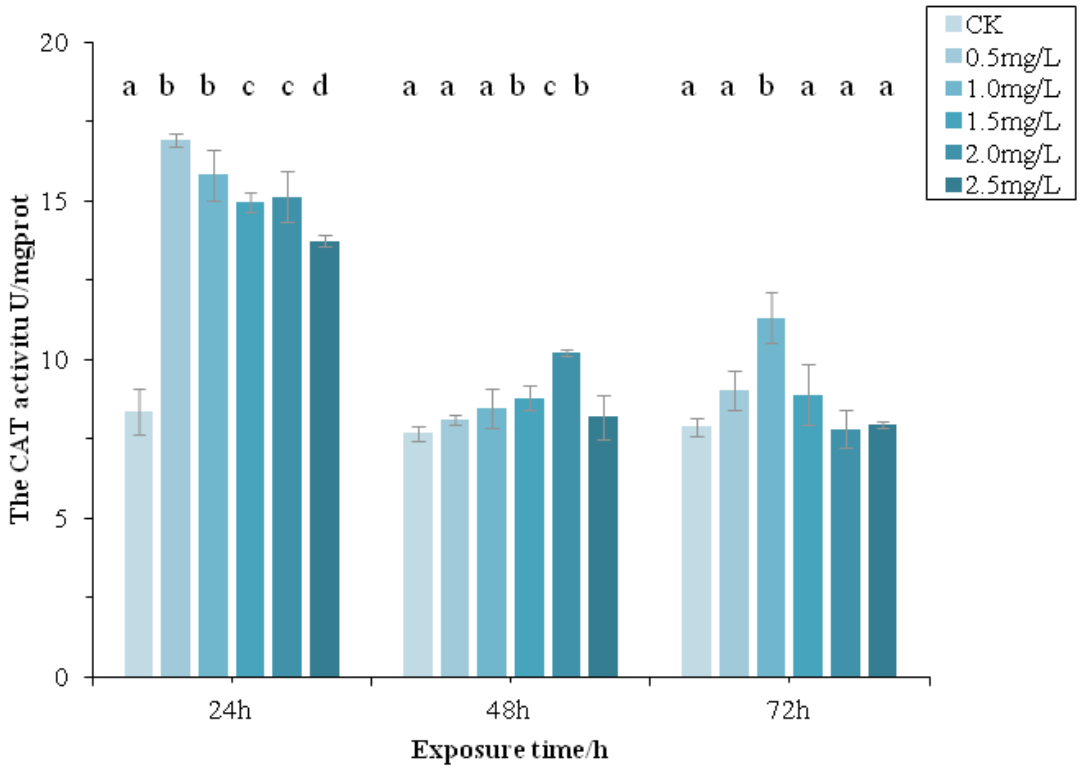

Figure 6. *Effect of cartap with different concentrations on CAT activity of earthworm after single exposure 24, 48 and 72 h. Different lowercase letters indicate significant differences between treatments, as revealed by one-way ANOVA with Duncan's multiple-range test at* $p < 0.05$

In the experiment, Cr^{6+} was set as the concentration of 1.0, 2.0, 3.0, 4.0 and 5.0 mg· l-^{1}. Earthworm samples were collected for pretreatment at 24 h, 48 h and 72 h, respectively, and the CAT content in vivo was determined, as shown in *Figure 7.*

By *Figure 7* you can see that when infected time for 24 h, the earthworm body CAT activity of Cr^{6+} treatment was obviously higher than that of blank control group, obviously with the increase of concentration of Cr^{6+} CAT activity is "S" shape change, Cr^{6+} concentration of 2 mg·L^{-1} peak, is at the beginning of the canister, the earthworm intimidation, induction of SOD and CAT activity, CAT is mainly used to produce the H_2O_2, consumption of SOD with elevated Cr^{6+} concentration, the cell absorption Cr^{6+}

http://www.aloki.hu ● ISSN 1589 1623 (Print) ● ISSN 1785 0037 (Online)
DOI: http://dx.doi.org/10.15666/aeer/1706_1331113327

increase, SOD activity continues to strengthen, to produce a large amount of H_2O_2, The activity of CAT was inhibited. With the increase of concentration, SOD activity decreased and CAT activity recovered. When the time of exposure was 48 h, the time of exposure was prolonged and the stress of the body was enhanced. The CAT activity of earthworms in each group was increased to reduce the oxidative damage of the body, and the change trend was first increased and then decreased. The maximum CAT activity also appeared when the Cr^{6+} concentration was $2mg \cdot L^{-1}$. When the time of exposure was 72 h, the change trend was similar to that of 48 h, and the overall decrease was relatively small compared with that of 48 h. With the extension of exposure time, the CAT activity of earthworm in the blank control group was relatively stable without obvious fluctuation. The exposure time of the group treated with Cr^{6+} at different concentrations was basically inverted u-shaped at 24 h, 48 h and 72 h.

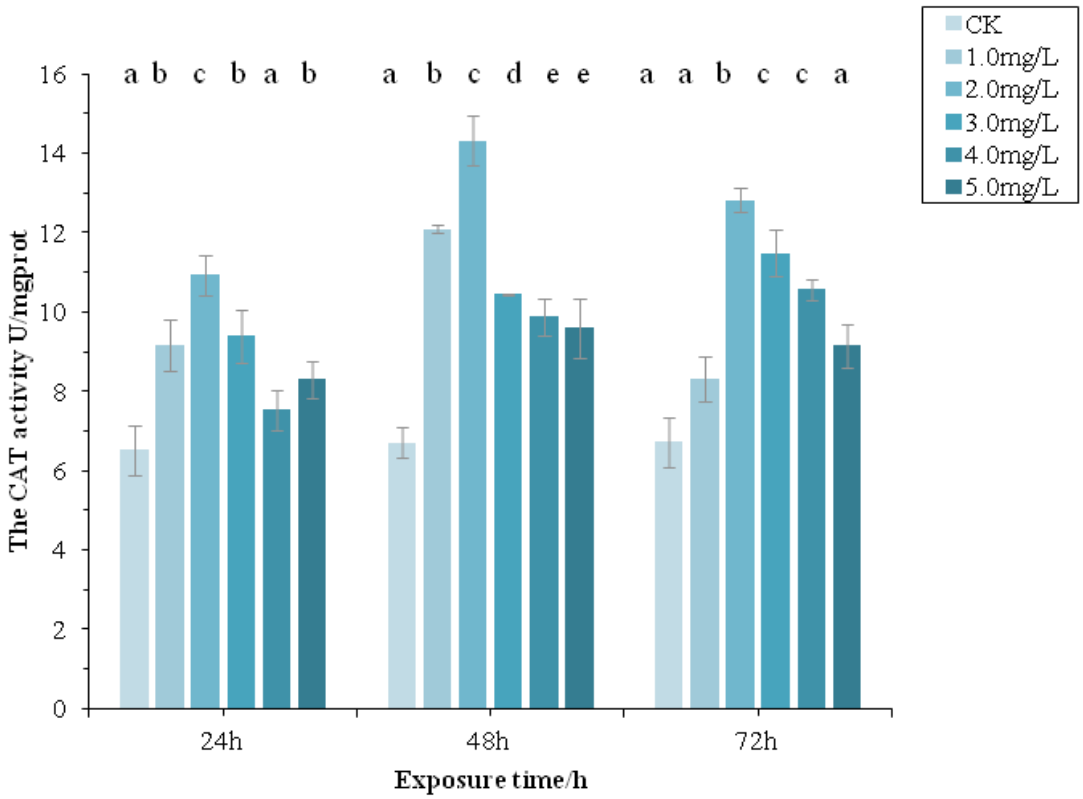

Figure 7. *Effect of Cr^{6+} with different concentrations on CAT activity of earthworm after single exposure 24, 48 and 72 h. Different lowercase letters indicate significant differences between treatments, as revealed by one-way ANOVA with Duncan's multiple-range test at $p < 0.05$*

Effects of chlorpyrifos and Cr^{6+} on MDA content in earthworms

Earthworm under environmental stresses can produce ROS metabolism, the body through a series of antioxidant way to eliminate, when the degree of oxidation than compensatory ability to eliminate the oxidation and anti-oxidation system will lose the original balance appear oxidative stress response, at this point, the antioxidant enzyme system (SOD, CAT, POD, GSH-Px) such as enzyme activity, enhance antioxidant capacity. Malondialdehyde (MDA) is an excess ROS oxidative lipid product that

http://www.aloki.hu ● ISSN 1589 1623 (Print) ● ISSN 1785 0037 (Online)
DOI: http://dx.doi.org/10.15666/aeer/1706_1331113327

directly reflects the degree of peroxidative injury. Therefore, malondialdehyde (MDA) in earthworm was used as an important indicator of peroxidation level in organism.

1. Effect of pyrrolidan on MDA content in earthworms

In the experiment, pyroridin was set as 0.5, 1.0, 1.5, 2.0 and 2.5 $mg \cdot L^{-1}$ concentrations. Earthworm samples were collected for pretreatment at 24 h, 48 h and 72 h respectively, and malondialdehyde (MDA) content in vivo was determined. The results were shown in *Figure 8*.

By *Figure 8* can be concluded that chlorpyrifos infected by different concentration of earthworms in infected time after 24 h, 48 h, 72 h, the overall trend of decrease the MDA content in the body, speculated that this phenomenon is because at the beginning of the virus, worm surface stress by chlorpyrifos, antioxidant defense system is not fully, the body by oxidative damage, leading to lipid oxidation product MDA content rise rapidly, as the antioxidant defense system open, all kinds of antioxidant enzyme activity, eliminates the excessive oxygen free radicals, reduce MDA content.

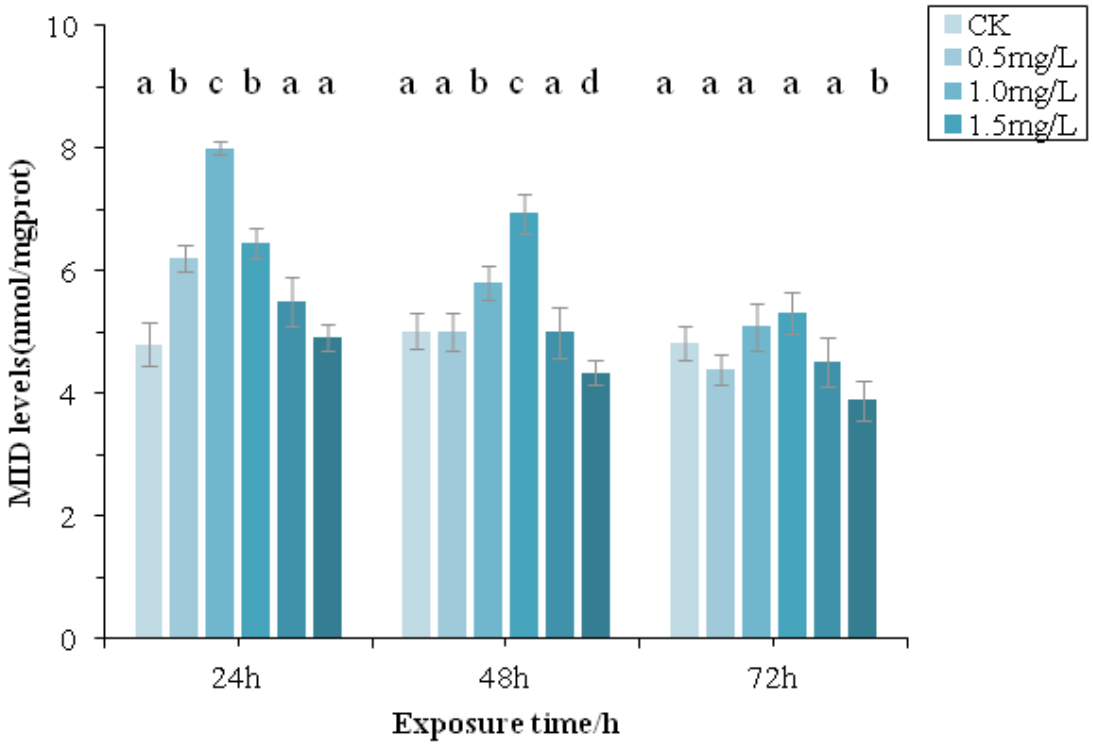

Figure 8. *Effect of cartap with different concentrations on MDA content of earthworm after single exposure 24, 48 and 72 h. Different lowercase letters indicate significant differences between treatments, as revealed by one-way ANOVA with Duncan's multiple-range test at* $p < 0.05$

2. Effects of Cr^{6+} on MDA content in earthworms

In the experiment, Cr^{6+} was set as the concentration of 1.0, 2.0, 3.0, 4.0 and 5.0 $mg \cdot L^{-1}$. Earthworm samples were collected for pretreatment at 24 h, 48 h and 72 h respectively, and malondialdehyde (MDA) content in vivo was determined, as shown in *Figure 9*.

http://www.aloki.hu ● ISSN 1589 1623 (Print) ● ISSN 1785 0037 (Online)
DOI: http://dx.doi.org/10.15666/aeer/1706_1331113327

It can be concluded from *Figure 8* that the content of malondialdehyde (MDA) in earthworms with different concentrations of Cr^{6+} varied in different poisoning time ranges after single exposure. Chlorpyrifos infected by different concentration of earthworms in infected time after 24 h, the MDA content in the body as a whole was reduced after the first rise trend, but with the blank control group, MDA content was not significantly change, is due to the earthworm itself is Cr^{6+} stress and oxidative stress response, antioxidant system effectively resist Cr^{6+} oxidative damage to the body. Infected time 72 h, with the canister to the extension of time, the earthworm body by oxidative damage degree aggravating, increased MDA content accumulation in the body, a trend of reducing the rise on the whole, were higher than the blank control group 48.23%, 69.88%, 77.12%, 47.23% and 43.21%, in Cr^{6+} concentration of 3.0 $mg \cdot L^{-1}$ MDA content is the highest, while the concentration of earthworms body oxidative damage is the most serious.

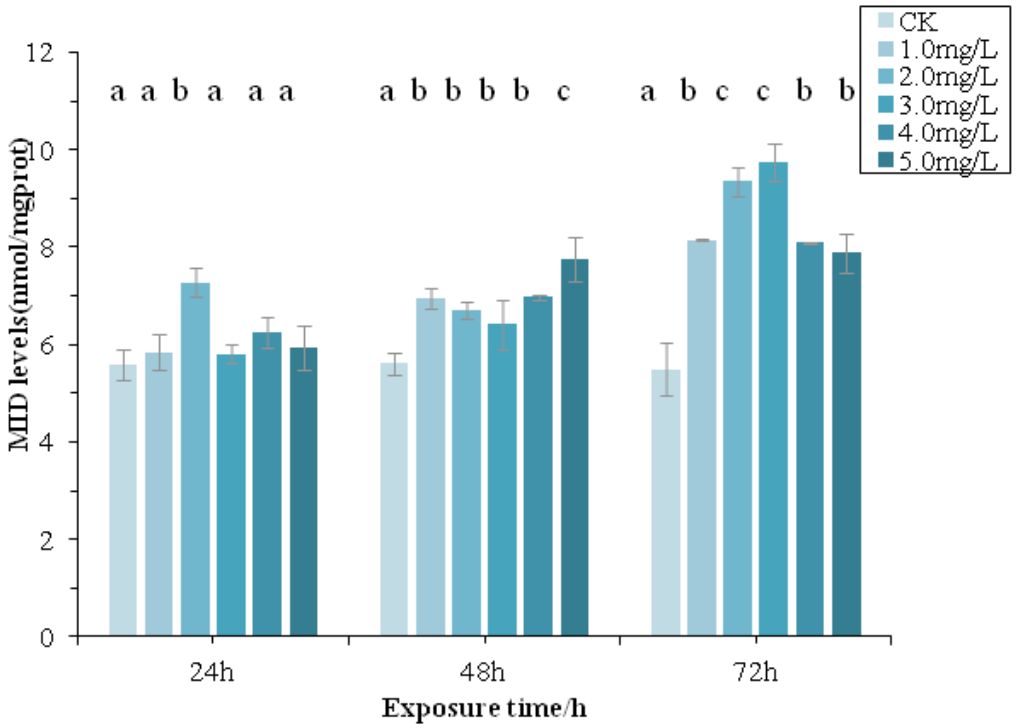

Figure 9. *Effect of Cr^{6+} with different concentrations on MDA content of earthworm after single exposure 24, 48 and 72 h. Different lowercase letters indicate significant differences between treatments, as revealed by one-way ANOVA with Duncan's multiple-range test at $p < 0.05$*

Discussion

Test to select chlorpyrifos, Cr^{6+} to the single toxicity test of earthworm, record the different influence on earthworm mortality after a single drug, and calculate the chlorpyrifos, Cr^{6+} in 24 h, 48 h and 72 h exposure when single LC_{50} value of earthworms, after two or three kinds of drug toxicity of earthworms size order: chlorpyrifos > Cr^{6+}, and with the extension of exposure time and enhance the toxic. Select chlorpyrifos, Cr^{6+} to the single toxicity test of earthworm, record the different influence on earthworm mortality after a single drug, and calculate the chlorpyrifos, Cr^{6+} in 24 h, 48 h and 72 h exposure when single LC_{50} value of earthworms, after two or

http://www.aloki.hu ● ISSN 1589 1623 (Print) ● ISSN 1785 0037 (Online)
DOI: http://dx.doi.org/10.15666/aeer/1706_1331113327

three kinds of drug toxicity of earthworms size order: chlorpyrifos > Cr^{6+}, and with the extension of exposure time

Total protein content reflects the sum of all types of enzymatic and non-enzymatic cellular proteins. When the chlorpyrifos single action, the earthworm body protein changes have the regularity, as the chlorpyrifos concentration increases the protein content first increases then decreases, as the time of infection extends the protein content first increases after tends to be stable. SOD in earthworms is sometimes induced and a dynamic balance is maintained to meet the needs of organisms to eliminate O^{2-} but the balance can be easily disrupted by the stress of pollutants (Ma et al., 2017). SOD activity in vivo was induced in a short period of time with low concentration, and decreased with the extension of the exposure time. The CAT activity of earthworm decreased with the increase of pyrrolidine concentration and decreased with the extension of time. MDA is the product of lipid peroxidation and has been used to assess oxidative stress in earthworms (Xue et al., 2009). The content of MDA in earthworms is regular. With the increase of the concentration of pyroridin, the content of MDA increases first and then decreases. With the extension of the poisoning time, the content of MDA decreases, possibly because the body is less damaged by oxidation. When Cr^{6+} acted alone, the protein content of earthworm decreased first and then increased with the increase of Cr^{6+} concentration, and the protein content of earthworm showed a trend of decrease with the extension of the duration of infection.

After single action of Cr^{6+}, the activity of SOD in earthworms first increased and then decreased, and the activity decreased with the extension of the poisoning time. CAT activity in vivo increased first and then decreased with the increase of Cr^{6+} concentration, and increased with the extension of exposure time. There was no obvious rule between the change of MDA content and the concentration of Cr^{6+} in vivo. As a whole, MDA content increased with the extension of the exposure time, indicating that the body was aggravated by oxidative damage.

Generally, single toxicity test of chlorpyrifos and Cr^{6+} on earthworms was carried out, and the effect of different drugs on the mortality of earthworms was recorded. Similar result was also reported before (Oliveira et al., 2018). The order of toxicity of two drugs on earthworms was obtained: chlorpyrifos > Cr^{6+}, and the toxicity increased with the extension of exposure time.

Potential synergistic effects of chemicals interactions were highlighted recently because of existence of complicated synergistic and antagonistic responses, which might cause serious ecological problems (Yang et al., 2017). Here, joint effects of chlorpyrifos and Cr^{6+} on earthworms were studied. The changes of SOD activity, CAT activity and MDA content in earthworms infected with chlorpyrifos and Cr^{6+} at sublethal dose were significant ($p < 0.05$). The results showed that when the body was under the stress of pollutants, the first antioxidant defense was activated, and the activity of SOD in the body was rapidly induced to remove excessive oxygen radicals in the body and generate H_2O_2 (Ma et al., 2017). Subsequently, the activity of CAT was enhanced and H_2O_2 was converted into H_2O. With the extension of poisoning time, SOD activity decreased and MDA content increased, indicating that the degree of oxidative damage to the body increased. Therefore, both SOD activity and MDA content can be used as indicators for earthworms to cope with oxidative stress and the degree of oxidative damage to the body.

http://www.aloki.hu ● ISSN 1589 1623 (Print) ● ISSN 1785 0037 (Online)
DOI: http://dx.doi.org/10.15666/aeer/1706_1331113327

Conclusion

In conclusion, distinctive toxicity effects on Eisenia fetida under different chlorpyrifos and Cr^{6+} stress levels were generally indicated by levels of enzyme activity/content impact, in terms of protein content, SOD, CAT and MDA activities. Generally, enzyme activity of Eisenia fetida may be sensitive indicators of chemical stress. However, in order to appropriately assess the ecological risk, more studies should be focused on long-term effects of chemical mixtures at different concentrations on earthworms.

Acknowledgements. This research was funded by Changzhou Science and Technology Support Program (Social Development) (CE20175060); Natural Science Research Project of Universities in Jiangsu Province (16KJB610001)

Conflict of interests. The authors declare no conflict of interests.

REFERENCES

[1] Chen, C. (2014): Study on Combined Toxic Effects of Pesticide Residues Mixed Pollution. – Chinese Academy of Agricultural Sciences, Beijing.
[2] He, G., Geng, C. G., Luo, R. (2008): Treatment of heavy metal pollution and its influence on aquatic plants. – Guizhou Agricultural Science 36(3): 147-150.
[3] Huang, Q. H. (2002): Current situation of pesticide residues in vegetables and countermeasures. – Fujian Agricultural Science and Technology 5: 43-44.
[4] Liao, Y. Y., Chen, R. F. (2007): Effects of sublethal concentrations of Cu, Pb, Cd and Hg on the larva of swimming crab triwarts. – Journal of Environmental Science 27(8): 1347-1358.
[5] Ling, S. F. (2004): Effects of dichlorvos on water-soluble protein in loach muscle and its analysis. – Fisheries Science 23(2): 20-21.
[6] Liu, C. C., Men, W. J., Liu, Y. J. (2002): Soil pollution by pesticides and bioremediation of contaminated soil. – Soil and Crops 18(4): 291-292.
[7] Ma, T., Zhou, W., Chen, L., et al. (2017): Toxicity effects of di-(2-ethylhexyl) phthalate to Eisenia fetida at enzyme, cellular and genetic levels. – PLoS One 12(3): e0173957.
[8] Oliveira Resende, A. P., Santos, V. S. V., Campos, C. F., et al. (2018): Ecotoxicological risk assessment of contaminated soil from a complex of ceramic industries using earthworm Eisenia fetida. – Journal of Toxicology and Environmental Health, Part A 81(20): 1058-1065.
[9] Su, L. M., Liu, H. Q., Li, Z. Q. (2011): Combined toxic effects of three pesticides and three heavy metals on luminescent bacteria. – Journal of Northeast Normal University (Natural Science) 43(4): 137-140.
[10] Sun, S. X., Tao, R., Zhang, Q. J. (2012): Effects of disulfonate and disulfonate on the protein content of earthworms. – Journal of Jiangxi Agricultural University 2: 298-303.
[11] Teng, Y. G., Wu, J., Lu, S. (2014): Soil and soil environmental quality monitoring in China: a review. – Environment International 69: 177-199.
[12] Wang, J., Ren, T. J., Wang, F. Q. (2015): Toxic effect of heavy metal cadmium on aquatic animals and its mechanism. – China Feed 17: 25-27.
[13] Wang, Y., Cang, T., Zhao, X. (2012): Comparative acute toxicity of twenty-four insecticides to earthworm, Eisenia fetida. – Ecotoxicology & Environmental Safety 79(6): 122-128.
[14] Xia, S. J. (2008): Pesticide Toxicology. – Chemical Industry Press, Beijing.
[15] Xiao, J., Zhao, J. B. (2005): Effects of pesticide pollution on ecological environment and countermeasures. – Anhui Agricultural Science 33(12): 2376-2377.

http://www.aloki.hu ● ISSN 1589 1623 (Print) ● ISSN 1785 0037 (Online)
DOI: http://dx.doi.org/10.15666/aeer/1706_1331113327

[16] Xue, X. T., Pei, Y. Z. (2000): Anthracene to black Jun effects of superoxide dismutase (SOD). – Journal of Fisheries 24(3): 217-220.
[17] Xue, Y. G., Gu, X. Y., Wang, X. R., et al. (2009): The hydroxyl radical generation and oxidative stress for the earthworm Eisenia fetida exposed to tetrabromobisphenol A. – Ecotoxicol 18(6): 693-699.
[18] Yang, G., Chen, C., Wang, Y., et al. (2017): Mixture toxicity of four commonly used pesticides at different effect levels to the epigeic earthworm, Eisenia fetida. – Ecotoxicology and Environmental Safety 142: 29-39.
[19] Yu, X. L., Liu, Q. (2011): Heavy metal pollution in water and its impact on human health. – Green Technology 10: 123-126.
[20] Zhao, Q. G., Huang, G. Q., Qian, H. Y. (2007): Ecological agriculture and food safety. – Acta Pedologica Sinica 44(6): 1127-1134 (in Chinese).

http://www.aloki.hu ● ISSN 1589 1623 (Print) ● ISSN 1785 0037 (Online)
DOI: http://dx.doi.org/10.15666/aeer/1706_1331113327

ARSENIC POLLUTION CHARACTERISTICS AND VARIATION TRENDS IN YANGZONGHAI LAKE, CHINA

ZHANG, Y. X.[1,2] – SHI, J. S.[1*] – LIU, J. T.[1] – ZHOU, B.[1]

[1]The Institute of Hydrogeology and Environmental Geology, C.A.G.S.
No. 268, Zhonghuabei Street, Shijiazhuang 050061, People's Republic of China
(phone: + 86-311-6759-8512; fax: +86-311-6759-8661)

[2]China University of Geosciences
No. 29, College Road, Haidian District, Beijing 100083, People's Republic of China
(phone/fax: +86-10-8232-2005)

**Corresponding author*
e-mail: 124582556@qq.com; phone: +86-311-6759-8559

(Received 9th Jun 2019; accepted 28th Aug 2019)

Abstract. In order to ascertain the status quo and variation trend of arsenic pollution in Yangzonghai Lake, China, the water samples of Yangzonghai Lake, sediment and interstitial water were collected and the total amount and morphological composition of arsenic were determined. The spatial distribution of arsenic was analyzed and the variation trends of arsenic pollution was evaluated. The results showed that the arsenic content of lake water in December 2016 was between 0.029-0.036 mg/L. The arsenic content in interstitial water is generally lower than 0.005 mg/L. The average content of arsenic in 0-2, 2-4, 4-6, 6-8 cm sediments are 50.5 mg/kg, 40.1 mg/kg, 33.6 mg/kg and 32.5 mg/kg, respectively. The high arsenic area is mainly distributed in the north and south shores, and gradually decreases from the coastal areas to the lake center. As the depth increases, arsenic content in the sediment gradually decreases. The arsenic in the sediment is still mainly in residual fraction, followed by organic fraction and oxide fraction. With the passage of time, the arsenic in the sediment gradually transforms from oxide fraction and organic fraction to residual fraction. The release of arsenic in the sediment is limited and the ecological risk is minimal.
Keywords: *arsenic, morphology, interstitial water, sediment, variation trend*

Introduction

Arsenic is a serious pollutant with potentially harmful effects (Huang et al., 2018; Zhang et al., 2015). Due to its recalcitrance, strong biotoxicity, bioaccumulation and biomagnification effect, arsenic contamination has been attracting much attention (Barrett et al., 2019; Jakobsen et al., 2018; Romero-Freire et al., 2014). In 2008, a serious arsenic pollution incident occurred in Yangzonghai Lake, one of the nine highland lakes in Yunnan Province. From April to October 2008, the arsenic content of Yangzonghai Lake rose sharply from 5 $\mu g \cdot L^{-1}$ to 134 $\mu g \cdot L^{-1}$ (Bi et al., 2014), and the water quality decreased from class II to inferior class V. According to the investigation, the source of arsenic pollution derived from a chemical plant on the hill in the southwest corner of the lake. The area belongs to karst landform area. The underground of the chemical plant area is carbonate rock and caves, and the karst is strongly developed. The high-arsenic wastewater discharged by the chemical plant in violation of regulations enters the karst zone through the soil, and then enters the lake from the spring formed by the fracture of the karst zone. The pollution incident has brought a huge impact on the production and life of the surrounding residents, directly threatening drinking water safety of more than 20,000 people around, causing inconvenience to irrigation of crops around the lake. The livelihood of hundreds of fishermen on both

http://www.aloki.hu ● ISSN 1589 1623 (Print) ● ISSN 1785 0037 (Online)
DOI: http://dx.doi.org/10.15666/aeer/1706_1332913340

sides of the river is worrying, and the surrounding tourism and holiday industry is also suffering from heavy losses, so it has aroused widespread concern in society (Wang et al., 2011). The team of Academician Chen Jing of Yunnan University has carried out arsenic pollution control in Yangzonghai Lake since 2009 (Chen et al., 2015) by adopting the process of atomization spray of $FeCl_3$ solution to remove arsenic from lake water. According to reports, the water quality of Yangzonghai Lake has been restored to Class III in November 2016. However, up to now, there is yet no detailed report on the status and variation trends of arsenic content in lakes and sediments after the treatment, and the stability of arsenic in sediments needs further investigation. Based on this, the author conducted systematic sampling and analysis of Yangzonghai Lake water and sediments in December 2016, found out the total amount and morphological composition of arsenic in lake water and sediment, and analyzed spatial distribution of arsenic in water bodies, sediments and sediment interstitial waters. Combining the sample analysis of 2008-2010 (Zhang et al., 2012), the variation trend and risk of arsenic were evaluated. This means important guiding significance for the further management of Yang Zonghai and the restoration of water environment.

Materials and methods

Study area

Yangzonghai lake (E102°59'-103°02', N24°51'-24°58') belongs to the Nanpanjiang water system of the Pearl River Basin. The lake surface is spindle-shaped, 2.5 km wide from east to west, 12.7 km long from north to south, and 32.3 km long on the lakeshore. The drainage area is 286 km^2, the lake area is 31.9 km^2 (at water level 1770 m), the deepest point is 29.1 m, the water storage capacity is 604 million m^3, and the water exchange period is 13 years (Chen, 2008). The nourishment source mainly comes from natural rainfall, Yangzong Great River and Qixing River catchment, artificial water of Baiyi River and underground water. The lake water flows into Nanpan River through the only outlet, Tangchi River.

Sampling and analysis

In December 2016, systematic sampling of lake water and sediment was carried out, as shown in *Figure 1* and *Table 1*. A total of 19 water samples were taken and 120 groups of sediment samples were collected. In order to analyze the arsenic content in the lake water, 7 sampling points were arranged along the north-south axis of the lake center, and the sampling numbers were S01-S07. Using the "MEGA-MONSOON sampling pump" produced in the United States, water samples of 0.5, 10 m depth were collected at S01 and S07, water samples of 0.5, 10, and 20 m depth were collected at S02-S06. The samples were stored in a 250 ml plastic bottle and a total of 19 samples were taken. To analyze the content and morphological characteristics of arsenic in the sediment, an average of 30 sampling points were arranged in the lake. Sample collection and stratification were performed using the "LENZ type sediment sampler" produced by HYDRO-BIOS, Germany. For each sampling point, 1-layer sample was taken from the top to the bottom at 2 cm intervals and 4 layers were taken. The samples were placed in a plastic ziplock bag and sealed for preservation, and 120 groups of samples were taken.

After the water samples were collected, the "Hash multi-parameter field test box" was used to quickly measure the indicators like pH value, conductivity, dissolved

http://www.aloki.hu ● ISSN 1589 1623 (Print) ● ISSN 1785 0037 (Online)
DOI: http://dx.doi.org/10.15666/aeer/1706_1332913340

oxygen on the site; the collected water sample was filtered by a 0.45 μm disposable pinhole filter, added with 1% volume of HNO_3 with a concentration of 1:1 for total arsenic analysis. The samples were sent to the Guangdong Province Material Testing Center for testing. After the sediment samples were collected, they were divided into 2 parts, one of which was dried in shade in the laboratory, removed with animal and plant residues and stones, ground, screened through a 200 mesh nylon sieve, and analyzed for arsenic and its seven binding fraction (including water soluble fraction, ion exchange fraction, carbonate fraction, oxide fraction, humic acids fraction, strong organic fraction, residual fraction) (Liu et al., 2018); for the other one, interstitial water was prepared using "centrifugation method", and the sample was placed in a plastic centrifuge cup, centrifuged at 5000 r/min for 20 min, with upper layer interstitial water taken for analysis of indicators like total arsenic. The test of sediment and interstitial water was completed by Guangdong Province Material Testing Center.

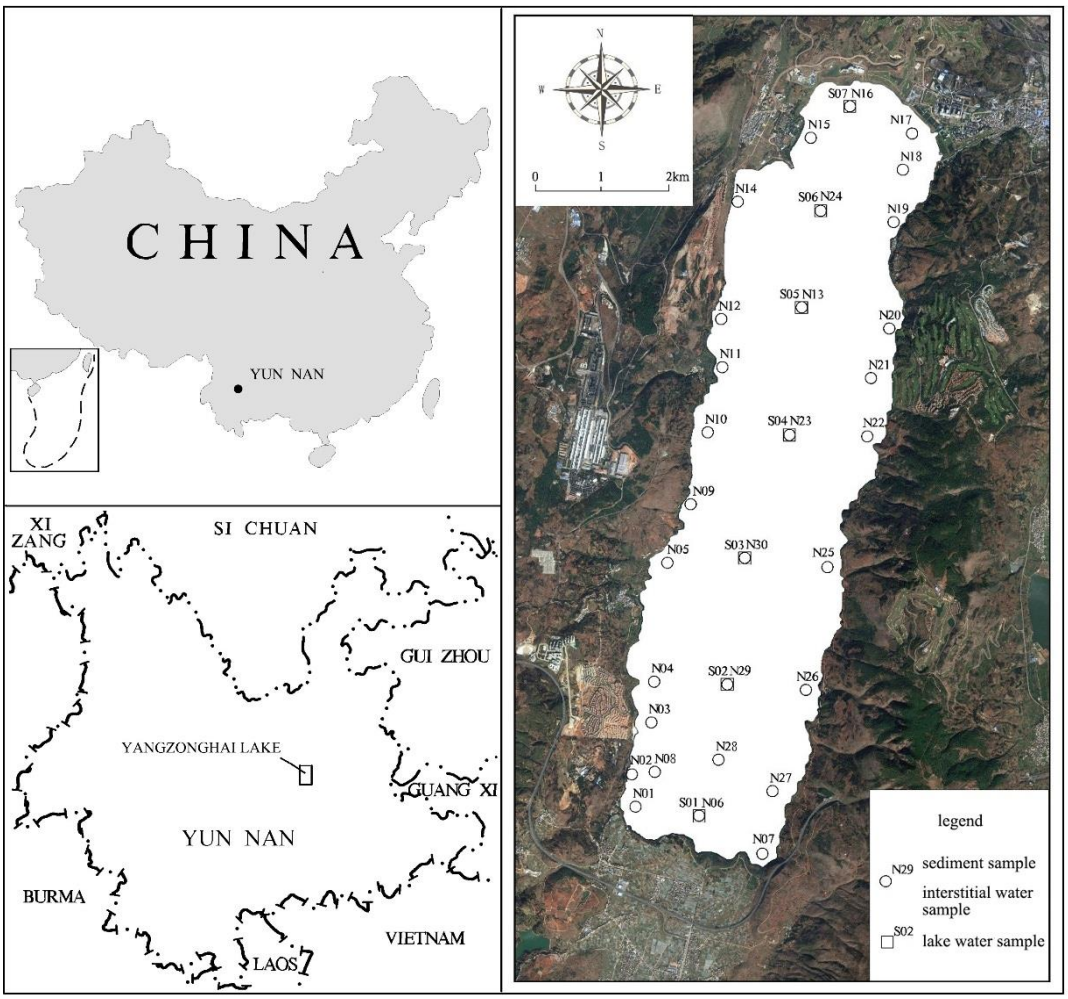

Figure 1. *Sampling points*

The descriptive statistical parameters were calculated with Microsoft Office Excel 2016. The positions of sample locations were recorded as a coordinate system using a GPS receiver. The kriging interpolations of the contaminant concentrations were computed with the MapGIS 6.7.

http://www.aloki.hu ● ISSN 1589 1623 (Print) ● ISSN 1785 0037 (Online)
DOI: http://dx.doi.org/10.15666/aeer/1706_1332913340

Table 1. *GPS coordinates of the sampling points*

Sampling points	GPS coordinates		Sampling points	GPS coordinates	
N01	102°58’57”	24°52’01”	N16 (S07)	103°00’46”	24°57’45”
N02	102°58’54 “	24°52’17”	N17	103°01’19”	24°57’32”
N03	102°59’04 “	24°52’42”	N18	103°01’15”	24°57’14”
N04	102°59’05”	24°53’02”	N19	103°01’10”	24°56’49”
N05	102°59’12”	24°54’00”	N20	103°01’08”	24°55’57”
N06 (S01)	102°59’31”	24°51’57”	N21	103°00’59”	24°55’32”
N07	103°00’05”	24°51’39”	N22	103°00’58”	24°55’04”
N08	102°59’07”	24°52’18”	N23 (S04)	103°00’16”	24°55’04”
N09	102°59’24”	24°54’29”	N24 (S06)	103°00’31”	24°56’54”
N10	102°59’32”	24°55’04”	N25	103°00’37”	24°53’59”
N11	102°59’39”	24°55’36”	N26	103°00’27”	24°52’59”
N12	102°59’39”	24°56’00”	N27	103°00’10”	24°52’09”
N13 (S05)	103°00’21”	24°56’06”	N28	102°59’41”	24°52’24”
N14	102°59’46”	24°56’58”	N29 (S02)	102°59’45”	24°53’01”
N15	103°00’25”	24°57’29”	N30 (S03)	102°59’53”	24°54’03”

Results and analysis

Arsenic in lake water

The pH value of the lake water is between 7.95-9.01, with an average of 8.69, which is alkaline. There is no obvious regularity in the horizontal distribution. In the vertical distribution, the pH value decreases slightly as the water depth increases. The conductivity is between 442-524 μS/cm, the average value is 463 μS/cm, with relatively uniform distribution vertically. The dissolved oxygen is between 5.91-6.12 mg/L, with an average value of 6.07 mg/L, which decreases slightly as water depth increases. The results of the 2010 survey showed that the average pH value of the lake water was 8.66, which also decreased slightly with the increase of water depth; the average conductivity was 456 μS/cm, and the distribution was relatively uniform. It can be seen that in recent years, regardless of content or distribution characteristics, field indicator characteristics of the lake water show no significant changes and the overall characteristics of the lake water environment is relatively stable.

According to the results of this survey, the dissolved arsenic content in Yangzonghai Lake water ranges from 0.029 to 0.036 mg/L, with an average of 0.033 mg/L. According to the Surface Water Environmental Quality Standard (GB 3838-2002), it belongs to Class III water. In the vertical distribution, the arsenic content does not change much, but the arsenic content at the depth of 10 m is slightly higher than that of 0.5 m in the surface layer and 20 m in the bottom layer. The arsenic content at the depth of 10 m is more concentrated than that of 0.5 m and 20 m, and the distribution difference is relatively small. In the horizontal distribution, from south to north, the arsenic content in each lake depth is basically reduced gradually. Among them, the maximum difference of arsenic content in the depth of 0.5 m is 0.007 mg/L, the maximum difference of arsenic content in the depth of 10 m is 0.003 mg/L, and the maximum difference of arsenic content in the depth of 20 m is 0.005 mg/L, which also reflects that in the horizontal distribution, surface lake water and bottom lake water

http://www.aloki.hu ● ISSN 1589 1623 (Print) ● ISSN 1785 0037 (Online)
DOI: http://dx.doi.org/10.15666/aeer/1706_1332913340

have relatively obvious distribution differences, and the arsenic content of lake water is stable at 10 m depth.

Previous studies have shown that the As content in the lake water in October 2008 ranged from 0.130 to 0.190 mg/L (Qi et al., 2010). By September 2009, the average content of As in lake water and sediment was 0.161 mg/L (Wang et al., 2011). By April 2010, the total As content in Yangzonghai water was 0.083 mg/L (Zhang et al., 2012). It can be seen that the arsenic content of Yangzonghai Lake reached a peak value in 2009 and gradually decreased thereafter. As of 2016, the arsenic content of lake water decreased to an average of 0.033 mg/L, a decrease of about 78%. In 2010, there was a significant difference in the vertical distribution of arsenic in the lake. The arsenic content in the lower layer was significantly higher than that in the upper layer. However, there was no significant difference in the arsenic content of the lake in the vertical direction. This is due to the fact that the sampling in 2010 was during the control of spraying agents. In the flocculation and sedimentation process, the sedimentation of the lower layer of water is later than that of the upper layer of water, or the sedimentation effect is reduced as the action progresses. In this investigation, after the sedimentation process ended, the lake water was evenly mixed, which caused the phenomenon.

Arsenic in interstitial water

The arsenic content in 0-2 cm sediment interstitial water is between 0.0004-0.0629 mg/L and the average value is 0.0082 mg/L. The arsenic content in the 2-4 cm sediment interstitial water is between 0.0006-0.0227 mg/L and the average value is 0.0042 mg/L. The arsenic content in 4-6 cm sediment interstitial water is between 0.0004-0.0222 mg/L and the average value is 0.0038 mg/L. The arsenic content in 6-8 cm sediment interstitial water is between 0.0002 and 0.0170 mg/L, and the average value is 0.0031 mg/L.

The arsenic content in interstitial water is generally low. Except for the surface interstitial water of the N18 point, the arsenic content is less than 0.05 mg/L in all the samples, and the arsenic content of most samples is less than 0.005 mg/L. As the depth increases, the average arsenic content decreases sharply. The arsenic content in the 0-2 cm layer is nearly twice that of the 2-4 cm layer, while the average arsenic content in the three layers below 2 cm decreases, but the variation is small. In terms of the distribution ratio, the proportion of samples with arsenic content less than 0.005 mg/L gradually increases, and the proportion of other ranges gradually decreases. By 4-6 cm and 6-8 cm, the proportion of arsenic content in different ranges has become stable. Comparison of the interstitial water arsenic content in each sampling point reveals that the vertical distribution of arsenic generally decreases with the increase of sediment depth, but the local area is also more complicated. The arsenic content of 17 points increases linearly with depth, and that of 6 points shows fluctuation state of increasing first and then decreasing. The two accounts for 3/4 of the total number of samples. There are 6 points with wavelike rises, only arsenic at one point rises linearly, and the two accounts for about 1/4 of the number of samples, as shown in *Figure 2*.

In the 0-2 cm interstitial water, the relatively high arsenic area is concentrated in two areas. One is Tangchi Town and Shijiazui area on the north shore. The arsenic content of the four sampling points in this area, N15, N16, N17 and N18, is above 0.01 mg/L, and the number is the highest in point N18 (0.0629 mg/L). The other is located near the N30 point in the south of the lake center, where the relatively high arsenic distribution

http://www.aloki.hu ● ISSN 1589 1623 (Print) ● ISSN 1785 0037 (Online)
DOI: http://dx.doi.org/10.15666/aeer/1706_1332913340

is only caused by N30 (0.0219 mg/L), and the distribution range is small. Arsenic content in other areas is generally low, basically within 0.005 mg/L. In 2-4 cm pore water, the arsenic content is obviously lower than that of the upper layer, and the relatively high value points are concentrated in the north shore area. Here, the arsenic content of the four sampling points is still above 0.01 mg/L, and the highest value point is changed from N18 to N15 (0.0227 mg/L). However, high value area of the lake center has disappeared, the arsenic content in the whole lake area is basically less than 0.004 mg/L, and arsenic content in some areas is below 0.002 mg/L. In the 4-6 cm interstitial water, the relatively high value points are concentrated in two areas. One is still near the north shore, but the area with figure larger than 0.01 mg/L has been reduced. It is mainly concentrated around N15 and N18, and the highest value still appears in N15 (0.0222 mg/L). The other area appears in the 30-mu area of the West Bank, with a small distribution range concentrated around N11 point carrying arsenic content of 0.0154 mg/L. Except the two areas, the arsenic content in other areas is basically within 0.004 mg/L, and the area with a figure below 0.002 mg/L is further expanded. In the 6-8 cm interstitial water, the relatively high value points are concentrated only in the north shore area. The arsenic content of the three sampling points of N15, N16 and N18 is above 0.01 mg/L, and the highest value point is still N15 (0.0170 mg/L). The arsenic content of other areas drops to within 0.002 mg/L, as shown in *Figure 3*.

Arsenic in sediment

The determination of arsenic in the sediment shows that the arsenic content of the 0-2 cm sediment is between 16.2-230.0 mg/kg, with an average of 50.5 mg/kg and a coefficient of variation of 94%. The arsenic content in 2-4 cm sediment interstitial water is between 15.1-136.0 mg/kg, with an average of 40.1 mg/kg and a coefficient of variation of 76%. The arsenic content in 4-6 cm sediment interstitial water is between 11.7-96.4 mg/kg, with an average of 33.6 mg/kg and a coefficient of variation of 62%. The arsenic content in 6-8 cm sediment interstitial water is between 11.8-148.0 mg/kg, with an average of 32.5 mg/kg and a coefficient of variation of 79%. Samples with an arsenic content of less than 25 mg/kg are substantially uncontaminated, and the proportion of samples in each layer ranges from 37% to 60%, with the ratio from top to bottom significantly increased, as shown in *Figure 4*. The sample with arsenic content between 25-50 mg/kg is slightly polluted, and the proportion of samples in each layer is between 27% and 37%, with the proportion of 0-6 cm basically unchanged and that at 6-8 cm decreased to some extent. The samples with arsenic content between 50-100 mg/kg are moderately polluted, and the proportion of samples in each layer is between 10%-17%, showing wavelike decrease from top to bottom. The samples with arsenic content higher than 100 mg/kg is heavily polluted, and the proportion of samples in each layer is between 0%-10%, showing wavelike decrease of first decrease and then increase from top to bottom and the amplitude is big. It can be seen that as the sampling depth increases, arsenic content in the sediment gradually decreases on the whole, and the heavily polluted sediment is still mainly distributed in the surface layer.

Arsenic in the sediment has very obvious difference in horizontal distribution. The high arsenic area is mainly distributed in Tangeying, Xinjie of south shore and Sanying and Tangchi town of north shore. The arsenic content is generally above 50 mg/kg, and the arsenic content in the central area of the lake is relatively low. Generally, it is lower than 25 mg/kg, and characteristics of gradually spreading to the lake center along the

http://www.aloki.hu ● ISSN 1589 1623 (Print) ● ISSN 1785 0037 (Online)
DOI: http://dx.doi.org/10.15666/aeer/1706_1332913340

pollution source on the shore are demonstrated in overall, and there is obvious pollution halo characteristic, as shown in *Figure 5*.

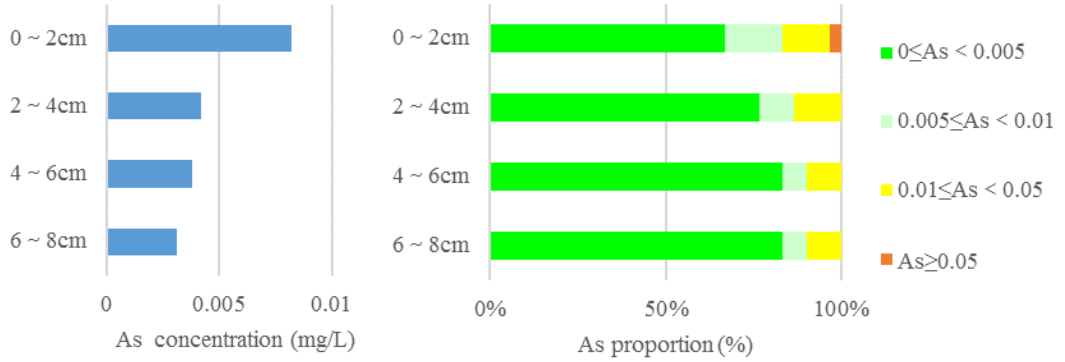

Figure 2. *Average content and proportion of arsenic in interstitial water*

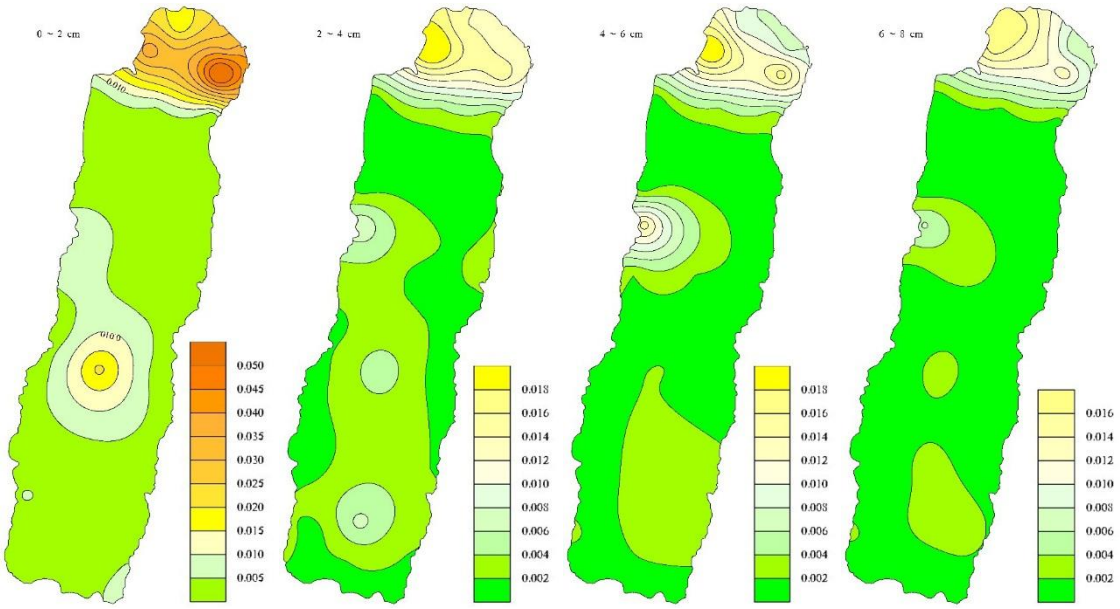

Figure 3. *Distribution of arsenic content in interstitial water (mg/L)*

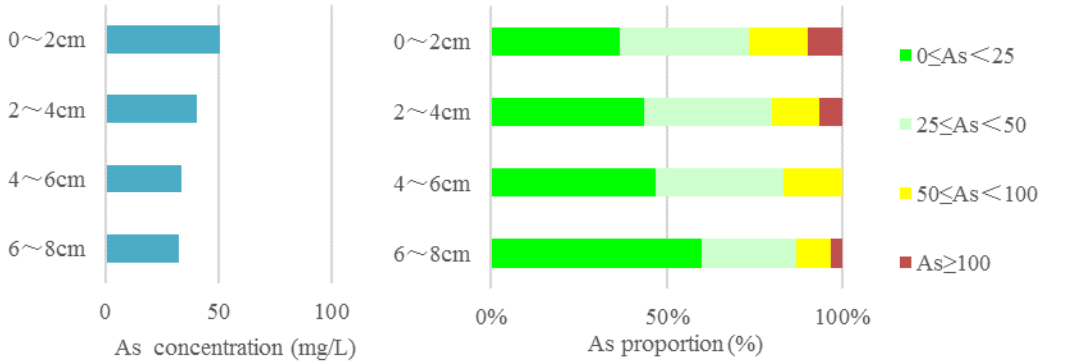

Figure 4. *Average content and proportion of arsenic in sediment (mg/L)*

http://www.aloki.hu ● ISSN 1589 1623 (Print) ● ISSN 1785 0037 (Online)
DOI: http://dx.doi.org/10.15666/aeer/1706_1332913340

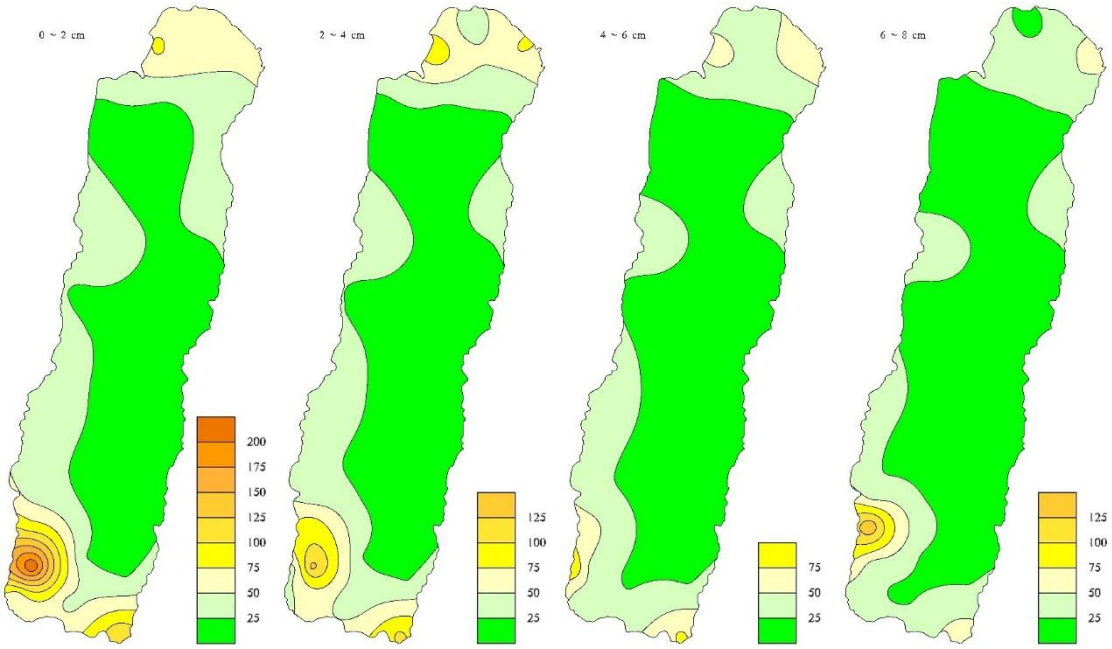

Figure 5. *Spatial distribution of arsenic content in sediments (mg/kg)*

Specifically, in the 0-2 cm sediment, the area with the highest arsenic content is located at N08, N02, N03 points near Tangeying and N07 point near Xinjie, and the arsenic content is 230 mg/kg and 164 mg/kg, 85.4 mg/kg and 121 mg/kg, respectively, followed by Tangchi Town of north shore where the arsenic content of N15, N16 and N17 points in the coastal areas is 77.9 mg/kg, 66.8 mg/kg and 74.3 mg/kg, respectively. In the 2-4 cm sediment, the high arsenic distribution area on both the north and south shores decreases to different extents. The arsenic content of N08 point in Tangeying is still the highest, being 136 mg/kg, followed by that of N07 point of Xinjie and the content is 104 mg/kg. The high arsenic area in north shore is reduced to the vicinity of Sanying N15 point and Tangchi N17 point, and the arsenic content is 92.9 mg/kg and 77.9 mg/kg, respectively. In the 4-6 cm sediment, the high arsenic zone is once again reduced and concentrated around Tangeying N02, Xinjie N07, Sanying N15 and Tangchi N17 points, with arsenic content being 96.4 mg/kg, 77.8 mg/kg, 62.9 mg/kg and 70.9 mg/kg, respectively. In the 6-8 cm sediment, the arsenic content in the vicinity of Tangeying increases, increasing to 148 mg/kg at N03 point, while area of other high arsenic zones continues to shrink, and the arsenic content in most of the lake area is maintained within 25 mg/kg.

Previous studies have shown that the arsenic content in the sediment at the end of October 2008 ranged from 54.86 to 193.29 mg/kg (Qi et al., 2010). By September 2009, the average content of arsenic in the sediment was 46.96 $mg \cdot kg^{-1}$ (Wang et al., 2011). The data in 2010 showed that the arsenic content in the sediment increased to 6.05-396.49 mg/kg, and the average content of As in the 0-2, 2-4, 4-6 and 6-8 cm sediments was 155.66. 52.01, 29.78, 19.22 mg/kg, respectively (Zhang et al., 2012). On the one hand, the arsenic content in the sediments of each layer in this sampling has dropped significantly, and the surface arsenic content has the largest decline, which is about 1/4 of the 2010 test data. Due to the implementation of arsenic treatment by sedimentation, the sedimentation process resulted in a higher arsenic content in the sediment at the end

http://www.aloki.hu ● ISSN 1589 1623 (Print) ● ISSN 1785 0037 (Online)
DOI: http://dx.doi.org/10.15666/aeer/1706_1332913340

of 2010. After 2014, the arsenic content of the sediment decreases quite obviously, and the arsenic content in the lake water does not rise, indicating that the arsenic in the sediment is less likely to be reversely dissolved into the lake water. On the other hand, the vertical distribution characteristics of the sediment are gradually complicated. At the end of 2010, the vertical distribution of sediment arsenic content decreased significantly with depth. The maximum value of arsenic appears in the surface sediment. Only the maximum arsenic content at 2 points appears in the lower sediment. The arsenic content of these two points is generally low, both lower than 20 mg/kg, and the difference in arsenic content between the layers is extremely small, which basically reflects the natural deposition state. In this sampling result, the maximum arsenic content of 11 points appears in the lower sediment, and the maximum arsenic content of 5 points appears in the 6-8 cm sediment.

The decrease in the total arsenic amount in the sediment and the abnormal distribution of arsenic in each layer found in this investigation may be caused by the following reasons: Affected by the arsenic removal and sedimentation process, as the arsenic content in the lake water decreases, the arsenic content in sedimentation particles is also reduced, then the low arsenic sediment covers the previous high arsenic sediment; The migration of sediment arsenic to the lower layer or surrounding sediment under the disturbance of lake water; Under the disturbance of the lake water, the sediment agitation phenomenon appears.

Arsenic exists in different binding states in the sediment and shows different mobility, bioavailability and ecotoxicity (Desbarats et al., 2017; Hossain et al., 2016). The mass fractions of water soluble fraction, ion exchange fraction and carbonate fraction are relatively low, and the sum of the three accounts for 0.55% of the total amount on average, and there is almost no change in the vertical distribution. Arsenic in water soluble fraction, ion exchange fraction and carbonate fraction is sensitive to environmental changes, which can be released under neutral conditions. Easy to migrate and transform, it can be absorbed by plants and carries high potential ecological risks (Zhou, 2017). The arsenic in oxide fraction accounts for 6.82% of the total amount on average, up to 27.20% at the highest, and the proportion decreases with increase of depth in the vertical distribution. This form is a wrapped or precipitated part of arsenic linked to iron-manganese oxide, which belongs to a strong ion bonding chemical form. It is not easily released under stable external conditions, but when the water body has a reduced redox potential or is in hypoxia, this bound arsenic may be reduced to a bioavailable state (Wang et al., 2015). The humic acid fraction and strong organic fraction are mainly chelated by organic matter such as animal and plant residues, humus and arsenic in the sediment. When the external conditions change little, the arsenic in this state is relatively stable, which has small environmental hazard. The sum of the two accounts for 8.97% on average, up to 23.25% at the highest, and the proportion also decreases with the increase of depth in the vertical distribution. The residual state is mainly present in the crystal lattice of primary minerals and secondary silicate minerals. It is very stable and does not participate in the rebalanced distribution of water-sediment systems (Huang et al., 2010, 2016a), which contributes little to migration and bioavailability of arsenic in sediments, so it is generally considered safe to the environment. The arsenic in the Yangzonghai sediment mainly exists in the form of residual fraction, with the average content accounting for 83.66% of the total, up to 93.79% at the highest, and the proportion increases with the increase of depth in the vertical distribution, as shown in *Figure 6*.

http://www.aloki.hu ● ISSN 1589 1623 (Print) ● ISSN 1785 0037 (Online)
DOI: http://dx.doi.org/10.15666/aeer/1706_1332913340

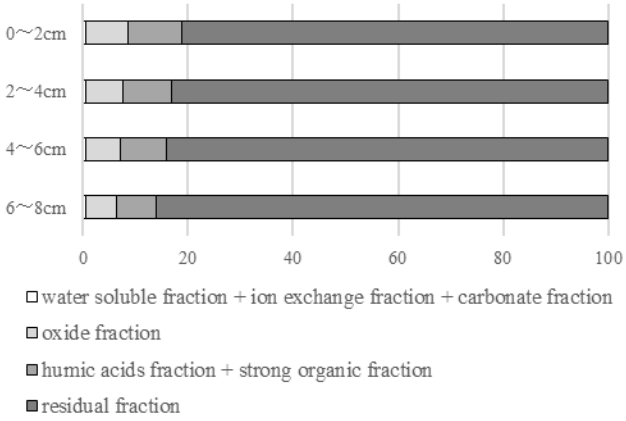

Figure 6. *Ratio of different fraction of arsenic in sediments (%)*

According to the study in 2010, the proportion of residual arsenic in the 0-2, 2-4, 4-6 and 6-8 cm sediments was 58%, 65%, 69% and 78%, respectively, which was increased to 81%, 83%, 84% and 86% respectively in this investigation. Meanwhile, content of arsenic in other forms decreased. It reflects that the form of arsenic in the sediment gradually changes to a more stable residual fraction over time. On the one hand, it is affected by the aging mechanism of arsenic in the soil (Huang et al., 2016b). On the other hand, flocculant used in the treatment work may also be one of the reasons for increased proportion of residual state arsenic in the sediment (Li et al., 2015).

In summary, the form of arsenic in the sediment is mainly in residual fraction, followed by the organic fraction and the oxide fraction, and the sum of the three accounts for more than 99% of the total amount. The content of water soluble fraction, ion exchange fraction and carbonate fraction is extremely low, and environmental influence is limited. The vertical distribution of various binding states of arsenic shows that with the continuous sedimentation process, the arsenic in the sediment gradually transforms from oxide fraction and organic fraction to the residual fraction. Therefore, in a more stable lake environment, the release of arsenic in the sediment is limited and the ecological risk is minimal.

Comparing the test results of interstitial water and sediment, it was found that there was no significant correlation between the two. The generation and direction of interstitial water are restricted and affected by various conditions, such as sediment pollution level, sedimentation physiochemical properties, redox conditions and hydrodynamic influence. The environment in Yangzonghai area is complex, and the total arsenic content in the sediment and arsenic content in various binding states do not determine the arsenic content in the interstitial water.

The vertical distribution characteristics of sediment interstitial water are often used to determine whether there is release of substance from the sediment to the lake (Wang et al., 2016). Generally speaking, if there is a phenomenon that substance in the sediment is released to the lake water, there is often a curve tendency that substance content increases first and then decreases as the depth increases. In this investigation, the arsenic content in the sediment interstitial water in most areas of Yangzonghai decreased significantly with the increase of sediment depth. Therefore, it can be inferred that there is no release of sediment arsenic into the lake water.

http://www.aloki.hu ● ISSN 1589 1623 (Print) ● ISSN 1785 0037 (Online)
DOI: http://dx.doi.org/10.15666/aeer/1706_1332913340

Conclusions

In December 2016, the arsenic content of Yangzonghai Lake was between 0.029-0.036 mg/L, with an average of 0.033 mg/L. It has reached the Class III water standard, and the arsenic content is evenly distributed in different depths of the lake. The sediment interstitial water is weakly alkaline. The arsenic content in the interstitial water in Tangchi of north shore is relatively high, up to 0.0629 mg/L at the highest, while arsenic content in other areas is generally lower than 0.005 mg/L, and the content is very small. Vertically, as the depth increases, the arsenic content mainly declines rapidly. The average content of arsenic in 0-2, 2-4, 4-6, 6-8 cm sediments was 50.5 mg/kg, 40.1 mg/kg, 33.6 mg/kg and 32.5 mg/kg, respectively. Horizontally, the high arsenic area is mainly distributed on both sides of the north and south shore, which gradually decreases from the coastal side toward the lake center. Vertically, as the depth increases, arsenic content in the sediment gradually decreases on the whole, and heavily polluted sediment is still mainly distributed in the surface layer. Morphological analysis shows that arsenic in the sediment is mainly in residual state, followed by organic matter binding state and iron-manganese oxide binding state, and the sum of the three accounts for more than 99% of the total amount. The water soluble fraction, ion exchange fraction and carbonate fraction are extremely low in content and has limited environmental impact. With the passage of time, the arsenic in the sediment gradually transforms from oxide fraction and organic fraction to residual fraction, tending to be more stable. That is to say, the lake treatment has achieved remarkable results, the release of arsenic in the sediment is limited, the possibility of reverse dissolution is small, and the ecological risk is minimal.

Acknowledgements. The study was financially supported by projects of China Geological Survey (No. DD20160308 and No. DD20190331).

REFERENCES

[1] Barrett, P. M., Hull, E. A., Burkart, K., Hargrave, O., McLean, J., Taylor, V. F., Jackson, B. P., Gawel, J. E., Neumann, R. B. (2019): Contrasting arsenic cycling in strongly and weakly stratified contaminated lakes: evidence for temperature control on sediment–water arsenic fluxes. – Limnology and Oceanography 64(3) 1333-1346.

[2] Bi, J. P., Liu, C., Li, S. Z. (2014): Variation of water quality of Yangzonghai Lake affected by arsenic pollution (in Chinese). – Water Resources Protection 30(1): 84-89.

[3] Chen, J., Zhang, S., Yang, X. J., Huang, Z. J., Wang, S. X., Wang, C., Wei, Q. Y., Zhang, G. L., Xiao, J. (2015): Arsenic Removal by Coagulation Process and the Field Expanding Experiments for Yangzonghai Lake (in Chinese). – Environmental Science 36(1): 202-208.

[4] Chen, Y. J. (2008): Research on precaution and control of water pollution in Yangzong Lake (in Chinese). – Environmental Science Survey 27(3): 28-31.

[5] Desbarats, A. J., Pal, T., Mukherjee, P. K., Beckie, R. D. (2017): Geochemical evolution of groundwater flowing through arsenic source sediments in an aquifer system of West Bengal, India. – Water Resources Research 53(11): 8715-8735.

[6] Hossain, I., Anjum, N., Tasnim, T. (2016): Removal of arsenic from contaminated water utilizing tea waste. – International Journal of Environmental Science & Technology 13(3): 843-848.

[7] Huang, G. X., Sun, J. C., Jing, J. H., Zhang, Y. X., Liu, J. T., Wang, J. C., Xiang, X. P., Chen, X., Cui, H. W. (2010): Distribution of arsenic in water and soil in the

http://www.aloki.hu ● ISSN 1589 1623 (Print) ● ISSN 1785 0037 (Online)
DOI: http://dx.doi.org/10.15666/aeer/1706_1332913340

representative area of the Pearl River Delta (in Chinese). – Zhongshan Daxue Xuebao/Acta Scientiarum Natralium Universitatis Sunyatseni 49(1): 131-137.

[8] Huang, G. X., Chen, Z. Y., Wang, J., Hou, Q. X., Zhang, Y. (2016a): Impact of temperature on the aging mechanisms of arsenic in soils: fractionation and bioaccessibility. – Environmental Science and Pollution Research 23(5): 4594-4601.

[9] Huang, G. X., Chen, Z. Y., Zhang, Y., Liu, F., Wang, J., Hou, Q. (2016b): Changes of arsenic fractionation and bioaccessibility in wastewater-irrigated soils as a function of aging: Influence of redox condition and arsenic load. – Geoderma 280: 1-7.

[10] Huang, K., Liu, Y., Yang, C., Duan, Y., Yang, X., Liu, C. (2018): Identification of Hydrobiogeochemical processes controlling seasonal variations in arsenic concentrations within a riverbank aquifer at Jianghan Plain, China. – Water Resources Research 54(7): 4294-4308.

[11] Jakobsen, R., Kazmierczak, J., Sø, H. U., Postma, D. (2018): Spatial variability of groundwater arsenic concentration as controlled by hydrogeology: conceptual analysis using 2-D reactive transport modeling. – Water Resources Research 54(12): 10254-10269.

[12] Li, Z. Y., Yang, C. L., Li, S. Y., Zhang, Y., Liu, R. B., Liu, K., Shen, S. L. (2015): Speciation and distribution of arsenic and its stability assessment in Lake Yangzonghai sediments after arsenic pollution remediation (in Chinese). – Environmental Science & Technology 38(2): 41-47.

[13] Liu, G. N., Chen, M., Li, W. Q., Gong, W. W. (2018): A critical review on the speciation and development of sequential extraction procedures for arsenic in soils (in Chinese). – Journal of Agro-Environment Science 37(12): 2629-2638.

[14] Qi, J. Y., Xu, Z. Y., Li, X. P., Fang, J. D., Huang, J. H. (2010): Study on source and speciation distribution characteristics of arsenic in Yangzonghai Lake waters (in Chinese). – Journal of Anhui Agricultural Sciences 38(20): 10789-10792.

[15] Romero-Freire, A., Sierra-Aragón, M., Ortiz-Bernad, I., Martín-Peinado, F. J. (2014): Toxicity of arsenic in relation to soil properties: implications to regulatory purposes. – Journal of Soils & Sediments 14(5): 968-979.

[16] Wang, J., Liu, F., Chen, Z. Y., Sun, J. C., Zhang, Y., Huang, G. X. (2015): Effect of sample pretreatment on the fractionation of arsenic in anoxic soils. – Environmental Science and Pollution Research 22(11): 8367-8374.

[17] Wang, W., Liu, X., Wang, Y., Guo, X., Lu, S. (2016): Analysis of point source pollution and water environmental quality variation trends in the Nansi Lake basin from 2002 to 2012. – Environmental Science and Pollution Research 23(5): 4886-4897.

[18] Wang, Z. H., He, B., Pan, X. J., Zhang, K. G., Wang, C., Sun, J., Yun, Z. J., Jiang, G. B. (2011): The levels, trends and risk assessment of arsenic pollution in Yangzonghai Lake, Yunnan (in Chinese). – Scientia Sinica Chimica 41(3): 556-564.

[19] Zhang, J., Li, T., Yang, Y. L., Liu, H. G., Wang, Y. Z. (2015): Erratum to: arsenic concentrations and associated health risks in Laccaria mushrooms from Yunnan (SW China). – Biological Trace Element Research 165(2)233-234.

[20] Zhang, Y. X., Xiang, X. P., Zhang, Y., Chen, X., Liu, J. T., Wang, J. C., Zhang, Y. J., Sun, J. C. (2012): Distribution and sources of arsenic in Yangzonghai Lake, China (in Chinese). – Environmental Science 33(11): 3768-3777.

[21] Zhou, X. (2017): Arsenic distribution and source in groundwater of Yangtze River Delta economic region, China. – Journal of Groundwater Science and Engineering 5(4): 343-353.

http://www.aloki.hu ● ISSN 1589 1623 (Print) ● ISSN 1785 0037 (Online)
DOI: http://dx.doi.org/10.15666/aeer/1706_1332913340

STUDY ON ECOLOGICAL RISK ASSESSMENT OF DIFFERENT LAND USE TYPES BASED ON HMER MODEL – TAKING THE DAXIA RIVER IN GANSU, CHINA AS AN EXAMPLE

WANG, S. – ZHANG, C.* – JI, H. – ZHANG, Y. – LOU, T.

College of Computer Science & Engineering, Northwest Normal University, Lanzhou 730070, China

**Corresponding author*
e-mail: dearzhangchang@qq.com

(Received 10th Jun 2019; accepted 28th Aug 2019)

Abstract. The effective heavy metal content of soil indicates ecological environmental risks. The study takes the typical watershed area in northwestern China as a research area. The real-time and rapid risk assessment of ecological environment can be achieved through the monitoring value of normalized difference vegetation index (NDVI) of remote sensing information and environmental factors, and a heavy metal ecological risk assessment model (HMER) for the evaluation of the watershed is built. The research results show that the change of the effective heavy metal content in different areas of the watershed is affected to some extent by the influence of geographical location and human activities. Among them NDVI and the content of heavy metals, precipitation and temperature, and a nonlinear relationship between the average heavy metal content and the ecological risk index HRI. The establishment of HMER research model is applied to different land use types to evaluate the ecological risk level of the watershed, explore the ecological risk level of different land use types in the same region, and in different regions. The results of the study emphasize that the risk assessment of the watershed can be carried out through remote sensing information and environmental factors.
Keywords: *soil, heavy metals, HMER, land use type, NDVI*

Introduction

Soil safety is closely related to agricultural production, food safety, human health and ecological health (Shi et al., 2019). At present, about 20% of China's land ecological environment is under high risk, with a total area of about 0.11 billion km^2 (Liu and Zhang, 2010). Among them, the effective pollution status of heavy metals in soil environment has received increasing attention (Yang et al., 2018). Studies have shown that heavy metals pose a high risk of environmental exposure by spreading and accumulating between plants (the main pathways includes crops and vegetables) and animals (Sawut et al., 2018). The heavy metal environmental hazard released by the ecological chain link process has a negative impact on the viability of urban trees (Yu et al., 2018). Frequent human activities accelerate the release of heavy metal activity, causing heavy metals in the soil to pose a public health threat (Doabi et al., 2018).

In different land use types, soil moisture content will change (Tang et al., 2018). Physical properties such as soil texture, porosity, structure, and chemical properties such as absorption and cushioning are also different (Liang et al., 2018). As the content of heavy metals in soil is related to these properties of soil, there are differences in the distribution and quantity accumulation of heavy metals in soil of different land use types (Su et al., 2013), which leads to the phenomenon that the content of heavy metals in soil of different land types is different (Wang et al., 2016). Some scholars have carried out ecological assessment studies on the production of heavy metals in different

http://www.aloki.hu ● ISSN 1589 1623 (Print) ● ISSN 1785 0037 (Online)
DOI: http://dx.doi.org/10.15666/aeer/1706_1334113354

land use types in the same area (Zhou et al., 2017). Some scholars have used different evaluation methods to study the status of heavy metal pollution (Liu et al., 2013). The reasons for these differences and the relationship between soil physical and chemical properties and heavy metals under different land use types need further verification (Wu et al., 2018). Traditional evaluation methods all require field sampling, but due to the weather, geographical location and other factors, the difficulty of sampling is increased, and the sample processing time is also relatively long. These factors cause great obstacles to further study and understanding of regional heavy metal ecological risk.

This paper studies the impact of human activities on environmental and ecological risks from the perspective of land use types and the correlation between climatic and environmental factors and heavy metals. The precipitation, temperature and NDVI of the study area are analyzed. The extraction and comparison of different land use types were carried out, and then the remote sensing data and environmental data and the ecological assessment model of the average content of heavy metals were established in the soil over a long period of time. The relationship between different land use types and ecological risk index was explored, and then the remote sensing data was used to estimate the distribution of heavy metals in the basin and construct an ecological risk assessment model. The research methods are applied to different land use types in the same area and the same land use types in different areas to determine their ecological risk levels. Because of the difficulty of sampling different land use types in the basin area, it is more accurate to carry out ecological risk assessment for the study basin area. The research results provide a theoretical reference for the assessment of soil heavy metal ecological risk in small and medium watersheds, the prevention and treatment of heavy metals in farmland and the methods of restoration.

Materials and methods

Research area overview

The research area is the Daxia River which flows through the southwestern part of Gansu Province in China. The study area is located between 102°02'~103°23' East longitudes and 34°51'~35°48' North latitude. There are two river sources in the Daxia River, namely Xiahe and Luohe (Yang, 2013). The Daxia River originates in the southern part of Tongren County and the west of Xiahe County in Qinghai Province, and flows through Qingshui Gorge in Xiahe County, passes through Tumen Gate and enters Maji Town of Linxia County, and passes through Yinji and Xinji Towns into Linxia City. From the estuary, the river enters the Liujiaxia Reservoir and merges into the Yellow River. It is called "the first-level tributary of the upper reaches of the Yellow River" (Wang, 2016). According to the water conservancy department in Linxia Prefecture, 45.5% of the river water resources in the area are affected by different levels of anthropogenic pollution, and 11.6% has water quality that is lower than the drinking standard. More than 90% of municipal water resources are threatened by water security (Chen, 2015). In terms of the geographical distribution of water pollution, the water quality of the main stream is higher than in the tributaries, and the upstream water quality is better than the downstream. A major source of water pollution is the mines (Luo, 2017). Water conservation in the Daxia River Basin is regarded as an important foundation for the sustainable social and economic development in the ethnic minority areas (Lin, 2015).

http://www.aloki.hu ● ISSN 1589 1623 (Print) ● ISSN 1785 0037 (Online)
DOI: http://dx.doi.org/10.15666/aeer/1706_1334113354

Source and processing of remote sensing data

Remote-sensing data are mainly provided by the Geospatial Data Cloud (http://www.gscloud.cn/) and the Landsat 8 OLI_Thermal Infrared Sensor (TIRS) remote sensing satellite data from the LANDSAT series of data provided by the United States Geological Survey (USGS) (https://earthexplorer.usgs.gov/). The applied remote sensing image is in the period from 2015 (January to December) to 2017 (January to December), and its spatial resolution is 30 m × 30 m. The ENVI software was used to calculate the corresponding NDVI values for radiometric calibration, image mosaic, image cropping, and atmospheric correction on the smoke image of the study area, and to remove the outliers and center standardization. The NDVI is defined as the ratio of the difference between near-infrared (NIR) and visible-red-red (R) bands and the sum of the two bands, NDVI = (NIR-R) / (NIR + R). In vegetation remote sensing, NDVI is the most widely used, as (1) NDVI can be applied to detect vegetation growth status, vegetation coverage, and to eliminate some radiation errors; (2) negative values indicate that the ground cover is cloud, water, snow, etc., with a high reflection for visible light; 0 means rock or bare soil, where NIR and R is approximately equal; positive values indicate vegetation coverage, and the positive value increases with increasing coverage (Yuan and Gu, 2018). The average monthly NDVI of the study area from 2015 (January to December) to 2017 (January to December) is shown in *Figure 1*.

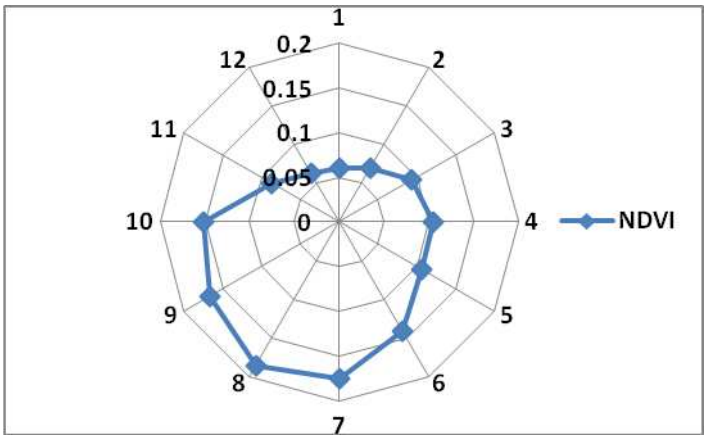

Figure 1. *NDVI monthly average*

Source and treatment of heavy metal data

In order to determine the number of samples more reasonably, this paper uses the Cochran method to estimate the optimal number of samples and sampling points for the construction constructed with pure random sampling of the study area. And there are 114 sampling points, including 24 fixed sampling points and 90 random sampling points. Among them, the fixed sampling point refers to the point to be collected every time, and the random sampling point is the point that is not necessarily collected every month, which can make the sample closer to the real situation. The main sampling time for this study is 2015 (January to December) to 2017 (January to December). Among them, the sample collection is performed once a month. The distribution of sampling points is shown in *Figure 2*. When collecting samples, a hand-held GPS device was used, and a plastic spoon was used to take 0-20 cm of the upper layer of the bottom

http://www.aloki.hu ● ISSN 1589 1623 (Print) ● ISSN 1785 0037 (Online)
DOI: http://dx.doi.org/10.15666/aeer/1706_1334113354

mud. The soil sample was dried and ground, after passing through a 200-mesh nylon sieve. In addition, the sample was processed by microwave digestion. Finally, the content of heavy metals was determined by inductively coupled plasma optical emission spectrometer (ICP-OES). By combining remote sensing images and combining field visits to study areas, we learn about the main sources of heavy metals in the study area, such as plant emissions, and the use of pesticides.

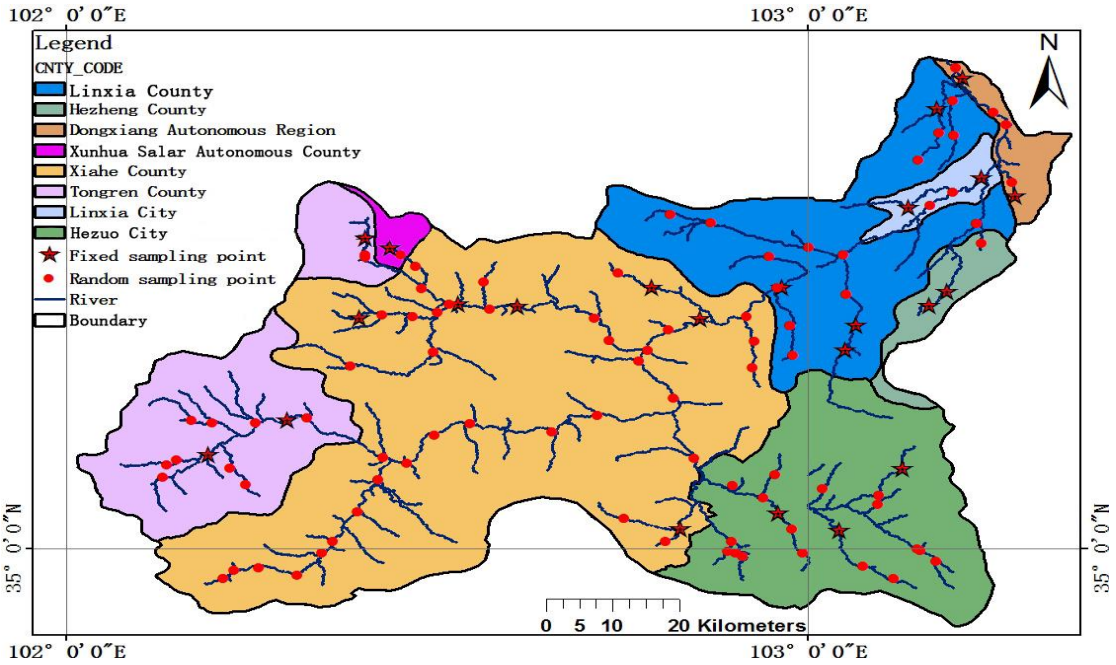

Figure 2. *Study area sampling point map*

Source and treatment of precipitation and temperature

Surface meteorological data from the China Meteorological Data Network (http://data.cma.cn/site/index.html) is typically used as the main source of precipitation and temperature data. Monthly average temperature and monthly average precipitation data from January 2015 to December 2017 was obtained for the study.

Results and discussion

Relationship between regional factors

Impact of climatic factors on NDVI

As the seasons change, the value of NDVI will change due to variations in moisture and temperature (Wang et al., 2018) Changes in vegetation cover are also affected by the combined or synergistic effects of hydrological conditions (such as temperature, precipitation, and humidity) (Liu et al., 2018). Due to little variation in pH and land use type in the study area, this paper focuses on the differences in precipitation and temperature. The amount of precipitation, temperature, and NDVI is affected to some extent by human activities. The monthly average NDVI values from January 2015 to December 2017, the monthly average precipitation and the monthly average temperature were used for correlation analysis.

http://www.aloki.hu ● ISSN 1589 1623 (Print) ● ISSN 1785 0037 (Online)
DOI: http://dx.doi.org/10.15666/aeer/1706_1334113354

It can be observed that the correlation between monthly average NDVI value and monthly average precipitation is 0.807, and the correlation between monthly average NDVI value and monthly mean temperature is 0.808. The relationship between temperature and NDVI ($P = 0.01 < 0.05$), and precipitation and NDVI ($P = 0.02 < 0.05$) are statistically significant. Details are shown in *Figure 3a, b*.

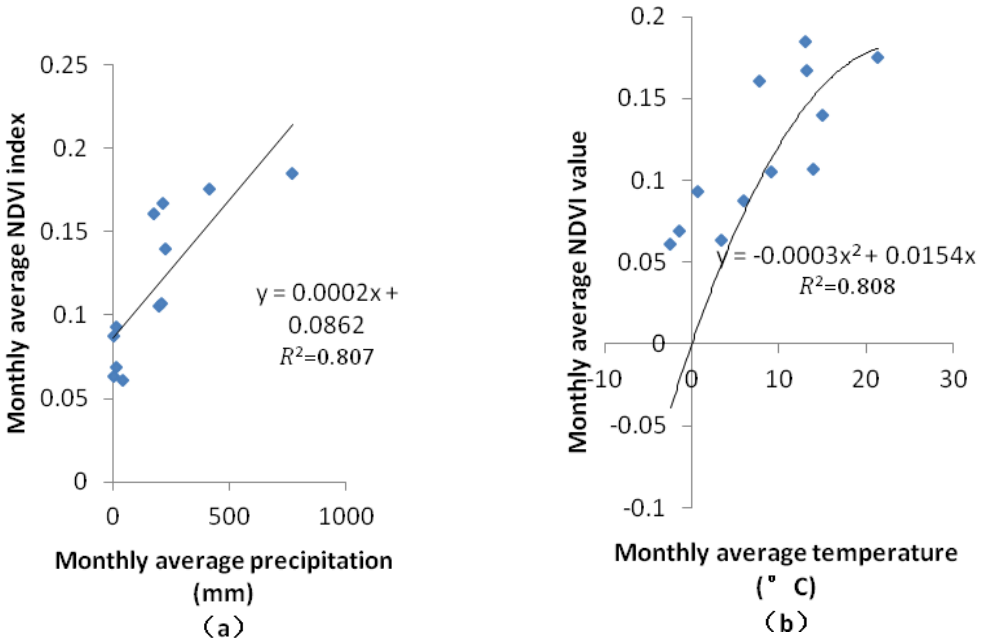

Figure 3. *Relationship between NDVI and precipitation temperature*

Influence of climatic factors on heavy metal content

Field measurements showed evidence of the presence of Cd, Cr, Cu, Pb, and as in the research area. The content of heavy metals is related to the migration of heavy metals. The speed of migration is linked to precipitation and temperature, and the cumulative effect of heavy metals in organisms is related to climatic factors (Ahonen et al., 2018). The soil heavy metal content is significantly correlated with the annual average precipitation and temperature at the sampling point (Zhou et al., 2018). Human activities indirectly affect the content of heavy metals by affecting climate change. The monthly average heavy metal content of the five elements was calculated, and a correlation analysis was undertaken for monthly precipitation and monthly average temperature. The correlation between monthly heavy metal content and precipitation was -0.79, and the correlation between monthly heavy metal content and temperature was -0.784, and the significance was sig. = 0.03, sig. = 0.02, respectively. The average heavy metal content in soil is negatively correlated with precipitation and temperature. Erosion and rainfall runoff will reduce the content of heavy metals (Li et al., 2011). An increase in temperature causes increased acidity and an increase in the activity of heavy metal ions, which means that the heavy metal content increases. However, the increase of heavy metal active ions means that the water solubility of heavy metal ions increases. Thus, heavy metal content can be seasonal, increasing with an increase in temperatures. The scouring effect is notable, and will reduce the heavy metal content of the soil. Details are shown in *Figure 4a, b*.

http://www.aloki.hu ● ISSN 1589 1623 (Print) ● ISSN 1785 0037 (Online)
DOI: http://dx.doi.org/10.15666/aeer/1706_1334113354

Ecological risk assessment model

Remote sensing data prediction of heavy metal average content model

The heavy metal content, the average monthly NDVI, the monthly average precipitation, and the monthly average temperature data from 2015 (January to December) to 2017 (January to December) in the Daxia River Basin were modeled using SPSS20 statistical software. The modeling result was $R^2 = 0.866$.

$$H = -0.002P - 54.2876N - 0.042T + 34.443 \quad \text{(Eq.1)}$$

where H is the average heavy metal content, P and T are the precipitation amount and temperature, respectively; N is the NDVI value.

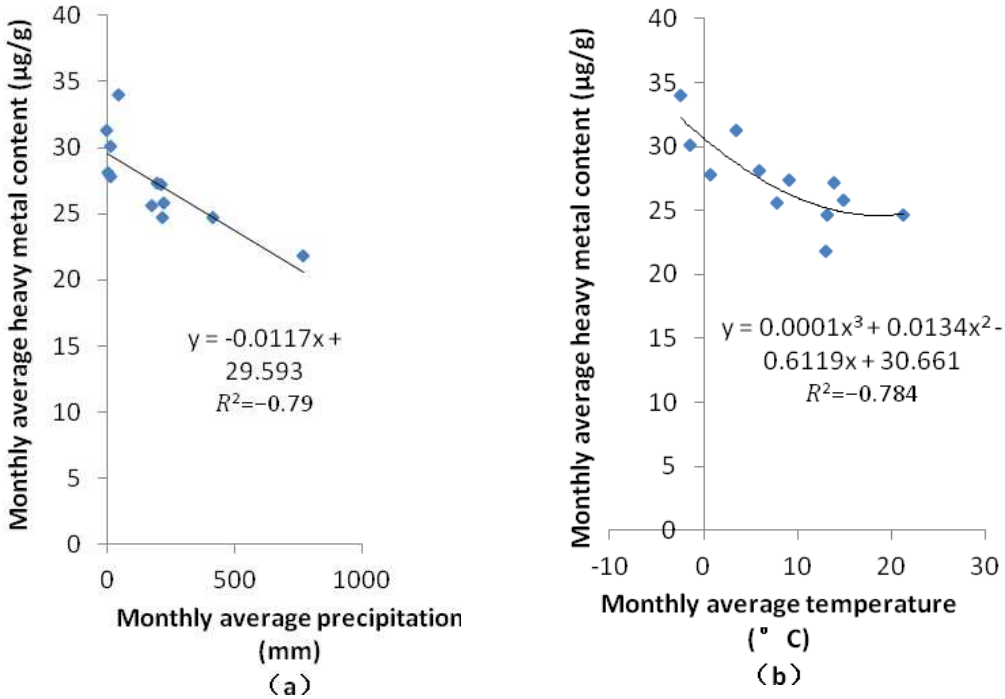

Figure 4. *Relationship between monthly heavy metal content and water purification temperature*

From 2015 (January to December) to 2017 (January to December), the fixed sampling points of the study area and the values of the random sampling points are measured. After treatment, the content of heavy metals was determined by inductively coupled plasma optical emission spectrometer (ICP-OES), and then the values were averaged. The comparison with the average heavy metal content of the soil predicted by *Equation 1* is as follows. *Equation 1* can be used to predict the average heavy metal content of the study area. From *Figure 5*, the average heavy metal content in August is the lowest. The vegetation in August is the lushest, and the vegetation has an inhibitory effect on the dissolution of heavy metal content in the soil.

http://www.aloki.hu ● ISSN 1589 1623 (Print) ● ISSN 1785 0037 (Online)
DOI: http://dx.doi.org/10.15666/aeer/1706_1334113354

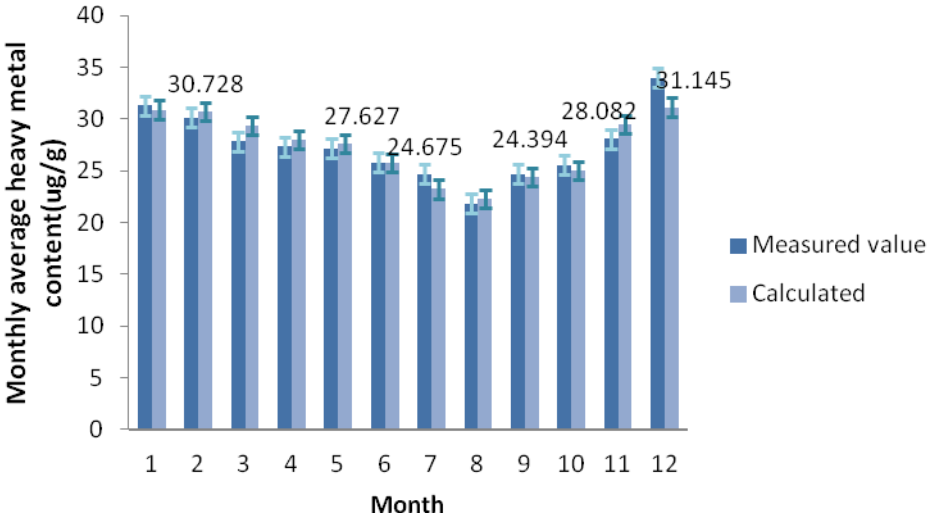

Figure 5. *Comparison of measured and calculated values of monthly heavy metal content*

Establishment of ecological risk assessment model

The Hakanson Ecological Risk Index is a commonly used potential ecological risk assessment index for heavy metals (Hakanson, 1980) which predicts the slow release processes and potential effects of heavy metals in the soil. In response to this potential hazard, the Swedish environmentalist Lars Hakanson introduced the potential ecological risk index (HRI) in 1980.

$$HRI = \sum_{i=1}^{n} E_r^i = \sum_{i=1}^{n} T_r^i \cdot C_r^i = \sum_{i=1}^{n} T_r^i \cdot \frac{C_f^i}{C_z^i} \quad \text{(Eq.2)}$$

where: HRI is the potential ecological risk index of n kinds of heavy metals in the sample. E_r^i is the single potential ecological risk index of the sample heavy metal I; T_r^i is the toxicity response coefficient of the T heavy metal I; C_r^i is the pollution coefficient of the heavy metal I; C_f^i is the measured value of the heavy metal i in the sample, and C_z^i is the specific gravity metal value of the uncontaminated sediment before industrialization. (This can also be replaced by the local sediment background value.) The geochemical background values of the heavy metals in the study area (Wang and Lian, 1993) are shown in *Table 1*, and the classification criteria for the potential ecological hazard index of heavy metals (Li et al., 2015) are shown in *Table 2*.

The size of HRI value is related to the content of heavy metal. Therefore, the average heavy metal content H calculated in *Equation 1* is the independent variable, and the HRI calculated by *Equation 2* is the dependent variable, and the linear fitting is performed. The fitting result is shown in *Table 3*.

Table 1. *Geochemical background values of soil heavy metals in the study area (Wang and Lian, 1993)*

Project	Copper	Lead	Arsenic	Cadmium	Chromium
Background values	28. 91	20.83	14.03	0.130	75.35

http://www.aloki.hu ● ISSN 1589 1623 (Print) ● ISSN 1785 0037 (Online)
DOI: http://dx.doi.org/10.15666/aeer/1706_1334113354

Table 2. *Classification criteria for potential ecological hazard index of heavy metals (Li et al., 2015)*

Risk level	E_r^i	*HRI*	Potential ecological risk
A	< = 40	< = 150	Low
B	40~80	150~300	Medium
C	80~160	300~600	Slightly serious
D	160~320	600~1200	Serious
E	> 320	> 1200	Extremely serious

E_r^i is the potential ecological hazard index of heavy metals I; HRI is the potential ecological risk index

Table 3. *Fitting results of HRI and average heavy metal content*

Model type	Linear function	Logarithmic function	Countdown function	Quadratic function	Cubic function	Composite function	Power function
Correlation	0.731	0.682	0.629	0.88	0.893	0.825	0.785

By comparing the fitting results, the cubic function fitting is ideal, the cubic formula is selected, and the specific fitting *Equation 3* is the remote heavy metal ecological risk assessment model (HMER) follows:

$$HMER = 0.02H^3 - 0.718H^2 + 228.034 \quad \text{(Eq.3)}$$

where H represents the average heavy metal content calculated in *Equation 1;* HMER represents the ecological risk assessment value, and its classification is referred to *Table 2*.

Using the data from 2018 (January to June) for verification, a comparison between the verification result and the sampling result in shown in *Figure 6* (Numbers 1-12 and Numbers 13 to 19 are the data of the sample area and verification area, respectively). The relationship between the watershed heavy metal ecological risk index, RRI, and the meteorological remote sensing information can be expressed by *Equation 3*.

Model application

Application of different land use type models in the same area

Due to the relatively large difficulty of different land use types in the whole study area, this method is used to evaluate the ecological risks of different land use types.

By using ENVI software to read, inlay, trim, and atmospheric correction of remote sensing images with less cloud cover, the unsupervised classification K-Means and the combination of on-site surveys are used to classify the land as shown in *Figure 7*. The map is processed by Majority/Minority analysis, and the clustering process is carried out to ensure the continuity of the space. The filtering problem is also used to solve the island problem in the picture, so the image is close to the real situation. In this study, land types are mainly divided into water area, grassland, town, cultivated land and woodland, as shown in *Figure 7*. Among them, the NDVI value is usually in the range

http://www.aloki.hu ● ISSN 1589 1623 (Print) ● ISSN 1785 0037 (Online)
DOI: http://dx.doi.org/10.15666/aeer/1706_1334113354

of [-1, 1]. The negative value of the waters is normal. When the waters are extracted, the water bodies may have positive values because some vegetation grows in the water and floats on the water surface. Similarly, when extracting land use types such as grassland, woodland, cultivated land, and towns, it may be affected by the background of the plant canopy, such as soil, wet ground, snow, dead leaves, roughness, etc., and will get negative values. NDVI values of each land use type were calculated by using mask and other operations, as shown in *Table 4.*

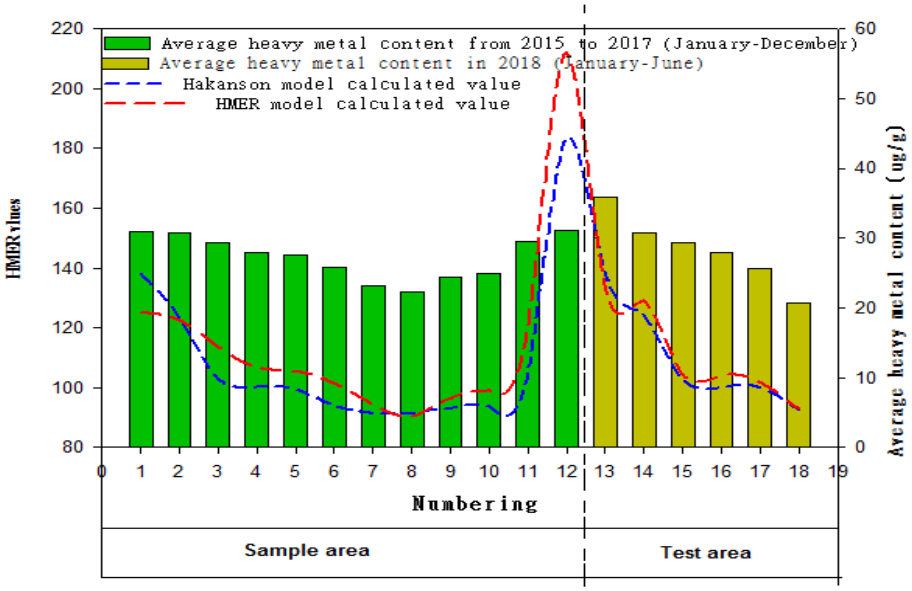

Figure 6. *Comparison of the HMER model and the Hakanson model*

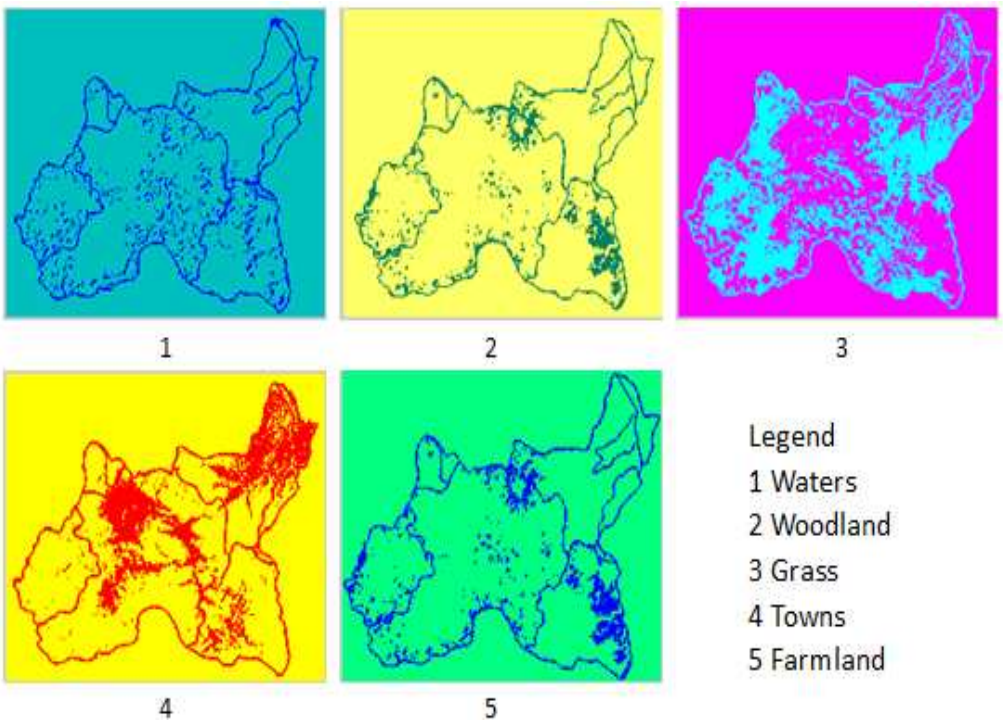

Figure 7. *Daxiahe land use type classification map*

http://www.aloki.hu ● ISSN 1589 1623 (Print) ● ISSN 1785 0037 (Online)
DOI: http://dx.doi.org/10.15666/aeer/1706_1334113354

Table 4. *NDVI values for different land use types*

Types	Min	Max	Stdev	Total
Waters	-0.76625	0.59237	0.104546	7014712
Grassland	-0.4982	0.62051	0.198214	10064524
Town	-0.74373	0.600615	0.126054	8560026
farmland	-0.72819	0.624793	0.130765	542308
woodland	-0.70428	0.606539	0.362047	729353

According to *Equation 1,* the different land use types of average NDVI value of the heavy metal content in the research area, precipitation, temperature factors, in order to compare the influence of different land use types on heavy metal content, the average rainfall and temperature in different areas of the process, to get the precipitation and temperature in the whole area. The corresponding NDVI value, precipitation and temperature, etc. were substituted into the corresponding formula. The results are shown in *Table 5*.

Table 5. *Ecological risk levels of different land use types in the Daxia River Basin*

Types	HMER	Risk level	Potential ecological risk index
Waters	-21.5568	A	Low
Grassland	113.5366	A	Low
Town	168.7537	B	Medium
Farmland	144.7092	A	Low
Woodland	69.37197	A	Low

It can be seen from *Table 5* that the waters are negative and do not participate in the discussion. The potential risk index of grassland, farmland and forest land is low pollution, and the HMER index of woodland is the lowest. It can be inferred that the planting of woodland in this study area can help inhibit the heavy metals and reduce the ecological risk. The ecological risk level of the town is medium. Due to the large urban population, human activities are frequent. It can be seen that the impact of human activities on soil heavy metal content is positive, so the ecological risk level of towns is high.

Application of different land use types in different regions

Read, mosaic, crop, and atmospheric correction of remote sensing images with less cloud content by using ENVI software. The land is classified using unsupervised classification K-Means and combined with on-site surveys. Then, using mask technology, according to the administrative boundaries of each small area, it is divided and the NDVI value is calculated, as shown in *Figure 8* and use the average of the precipitation in each area from 2015 to 2017 and the temperature average to be substituted into *Equations 1* and *3,* as shown in *Table 6*.

It can be seen from *Table 6* that the ecological risk pollution levels of different land use types in small areas are low or medium, among which the ecological risk levels of grassland, farmland and forest land in Dongxiang County, Linxia City, Llinxia County,

http://www.aloki.hu ● ISSN 1589 1623 (Print) ● ISSN 1785 0037 (Online)
DOI: http://dx.doi.org/10.15666/aeer/1706_1334113354

Hezuo City, Xiahe county, Hezheng county, Xunhua Salar Autonomous County and Tongren County are all low. The ecological risk levels of Dongxiang County, Linxia City, Linxia County, Hezuo city, Xiahe County, Hezheng County and Xunhua Salar Autonomous County were all medium, while the ecological risk levels of Tongren County were low.

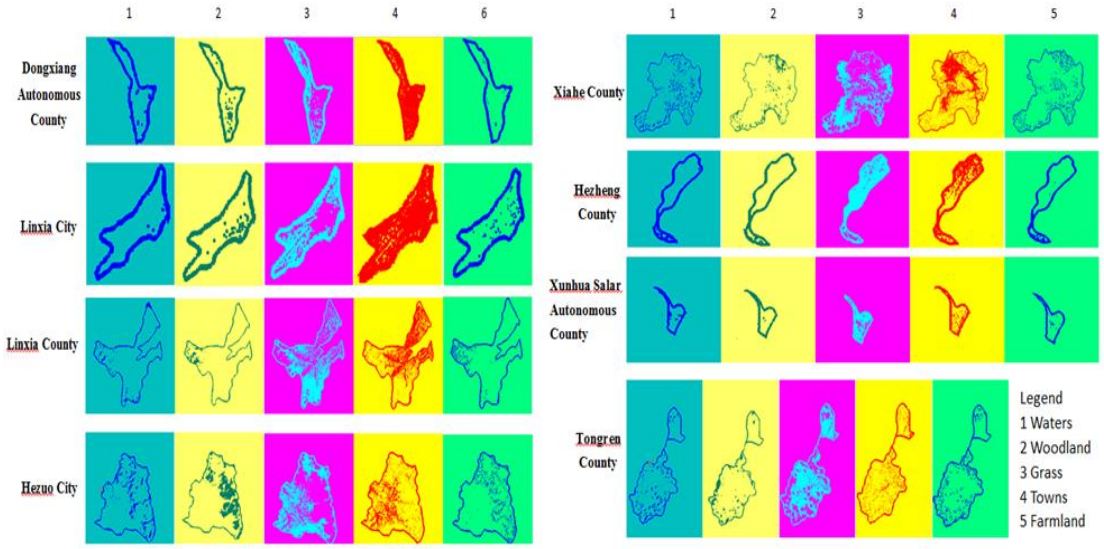

Figure 8. *Small area land use type*

Table 6. *Ecological risk levels of different land use types in small areas*

Region	Grass		Towns		Farmland		Woodland		Waters
	P-I	P-L	P-I	P-L	P-I	P-L	P-I	P-L	
Dongxiang County	85.365	A-L	243.455	B-M	143.4	A-L	70.365	A-L	No
Linxia City	83.215	A-L	270.532	B-M	148.653	A-L	68.447	A-L	No
Linxia County	97.117	A-L	184.663	B-M	146.637	A-L	72.256	A-L	No
Hezuo City	132.419	A-L	168.321	B-M	84.571	A-L	40.752	A-L	No
Xiahe County	140.327	A-L	179.988	B-M	79.634	A-L	56.766	A-L	No
Hezheng County	63.021	A-L	193.365	B-M	139.521	A-L	86.329	A-L	No
Xunhua Salar Autonomous County	86.130	A-L	153.654	B-M	136.774	A-L	12.114	A-L	No
Tongren County	74.557	A-L	68.776	A-L	66.521	A-L	38.123	A-L	No

A-L: A-low; B-M: B-medium; P-I: pollution index; P-L: pollution level

Combined with the remote sensing image map (*Fig. 5*) and the local interview survey, we can see that there are many towns in Dongxiang county, Linxia city and Linxia county. Human activities (factory emissions, transportation, etc.) cause high ecological risk assessment, and the ecological risk pollution index is close to 150 (close to c-heavy). Therefore, Dongxiang County, Linxia City and Linxia County can increase the planting of forest land to alleviate the ecological risk of this area.

http://www.aloki.hu ● ISSN 1589 1623 (Print) ● ISSN 1785 0037 (Online)
DOI: http://dx.doi.org/10.15666/aeer/1706_1334113354

Conclusion

From Jan 2015 to Dec 2017, the NDVI of the study area increased, in areas where humans live in more areas, the NDVI value is lower. The NDVI is significantly affected by precipitation and temperature. The correlation coefficient between precipitation and NDVI is 0.807, and the correlation coefficient between temperature and NDVI is 0.808. It can be seen that the temperature has a greater influence on the NDVI. The heavy metal content was negatively correlated with temperature and precipitation, and the correlation coefficients were -0.79 and -0.784, respectively.

The ecological risk level of land use types in grassland, cultivated land and forest land in the Daxia River Basin is low. The town is medium. The overall ecological risk is better. The ecological risk pollution levels of different land use types in small areas are also low or medium, including the grasslands of Dongxiang County, Linxia City, Linxia County, HeZuo City, Xiahe County, Hezheng County, Xunhua Salar Autonomous County and Tongren County. The ecological risk grades of cultivated land and forest land are all low. The land use types are Dongxiang County, Linxia City, Linxia County, Hezuo City, Xiahe County, Hezheng County, Xunhua Salar Autonomous County, and the ecological risk level of Tongren County is low. The towns of Dongxiang County, Linxia City and Linxia County are more distributed, and their ecological risk pollution index is close to heavy pollution. Therefore, Dongxiang County, Linxia City and Linxia County can increase the planting of forest land to alleviate the ecological risk of the area. This paper establishes remote sensing data and average heavy metal content model in the Daxia River Basin. The ecological risk assessment HMER model and method, through data verification shows that the model has potential application value and certain degree of implementation. It laid the foundation for the subsequent heavy metal pollution of the soil in the study area.

The model under study has an intentional significance for the risk assessment of the Daxia River Basin. Whether the HMER model has a more accurate assessment effect on the basin area of other vegetation and industrial types remains to be studied by the researchers. The follow-up work of this paper is mainly to study the data monitoring through data sensors and establish intelligent data detection and analysis in order to increase the efficiency of the relevant staff.

Acknowledgments. This work was supported by the National Natural Science Foundation of China under Grant No.61563047.

REFERENCES

[1] Ahonen, S. A., Hayden, B., Leppänen, J. J., Kahilainen, K. K. (2018): Climate and productivity affect total mercury concentration and bioaccumulation rate of fish along a spatial gradient of subarctic lakes. – Science of the Total Environment 637: 1586-1596.

[2] Chen, N. H. (2015): Discussion on the causes and countermeasures of water environment problems in Linxia Prefecture. – Agricultural Science & Technology and Information, (12): 91-92.

[3] Doabi, S. A., Karami, M., Afyuni, M., Yeganeh, M. (2018): Pollution and health risk assessment of heavy metals in agricultural soil, atmospheric dust and major food crops in Kermanshah province, Iran. – Ecotoxicology and Environmental Safety 163: 153-164.

[4] Hakanson, L. (1980): An ecological risk index for aquatic pollution control. A sedimentological approach. – Water Research 14(8): 975-1001.

http://www.aloki.hu ● ISSN 1589 1623 (Print) ● ISSN 1785 0037 (Online)
DOI: http://dx.doi.org/10.15666/aeer/1706_1334113354

[5] Li, Q., Li, T. L., Liu, D. X., Jin, Z. H. (2011): Characteristics of rainwater runoff pollution in different land use types in Tianjin. – Environmental Pollution & Control 33(7): 22-26.
[6] Li, Y. W., Cao, C., Ju, T. Z., Zhao, X. T., Mu, R. Q., Liu, S. Q., Du, M. Z (2015): Soil heavy metal pollution characteristics and ecological risk assessment of vegetable soils in different areas of Baiyin City. – Journal of Ecology 34(11): 3205-3213.
[7] Liang, B., Nie, X. G., Yang, D. S., Wan, D., Fang, J. P., Zhao, W.(2018): Analysis of soil physical properties of five typical land use patterns in the lower reaches of the Niyang River Basin in Tibet. – Journal of Northwest A&F University (Natural Science Edition) 46(1): 119-128.
[8] Lin, Y. H. (2015): Investigation and analysis of water environment status and pollution causes in the Daxia River Basin. – People's Yellow River 37(1): 74-78.
[9] Liu, J. L., Zhang, J. T. (2019): Current status and treatment of heavy metal pollution in soil. – Shandong Industrial Technology 7: 209.
[10] Liu, W., Zheng, B. H., Fu, Q., Luo, Y. P., Wang, M. (2013): Application of water pollution index method in river water quality evaluation. – Environmental Monitoring in China 29(3): 49-55.
[11] Liu, Y., Li, L., Chen, X., Zhang, R., Yang, J. (2018): Temporal-spatial variations and influencing factors of vegetation cover in Xinjiang from 1982 to 2013 based on GIMMS-NDVI3g. – Global and Planetary Change 169: 145-155.
[12] Luo, R. Q. (2017): Discussion on the causes and countermeasures of water environment problems in Linxia Prefecture. – Agricultural Science & Technology 2: 36-37.
[13] Sawut, R., Kasim, N., Maihemuti, B., Hu, L., Abliz, A., Abdujappar, A., Kurban, M. (2018): Pollution characteristics and health risk assessment of heavy metals in the vegetable bases of northwest China. – Science of the Total Environment 642: 864-878.
[14] Shi, R. G., Zhang, Y. W., Xu, M. M., Zheng, X. Q., Zhao, Z. S. (2019): Evaluation and source analysis of heavy metal pollution in soils in Tianjin Suburbs. – Journal of Agro-Environment Science 38(5): 1069-1078.
[15] Su, W., Chen, M. H., Shen, G. S. (2013): Distribution characteristics and ecological risk of heavy metal Pb in soils of different land use types in suburbs of Changchun City. – Journal of Anhui Agricultural Sciences 41(31): 12303-12305.
[16] Tang, M., Zhao, X. N., Gao, X. D., Zhang, C., Wu, P. (2018): Characteristics of soil moisture in different land use types in loess hilly region. – Chinese Journal of Applied Ecology 29(3): 765-774.
[17] Wang, S. P., Lian, B. (1993): Characteristics and distribution of soil environmental background value in Gansu Province. – Journal of Gansu Environmental Research and Monitoring 23(3): 1-7.
[18] Wang, S. Z. (2016): Discussion on planning and design of Daxiahe flood control project in Xiahe County, Gannan Prefecture. – Journal of Gansu Agriculture (20): 39-41.
[19] Wang, X., Ciais, P., Wang, Y., Zhu, D. (2018): Divergent response of seasonally dry vegetation to climatic variations in dry and wet seasons. – Glob Change Biol 24: 4709-4717.
[20] Wang, Z. X., Guo, Q. W., Yang, Z. H., Sun, G. Q., Ye, W. S., Hu, X. B. (2016): A land use-based spatial analysis method for human health risk assessment of heavy metals in soil and its application in Zhuzhou City, Hunan Province, China. – Journal of Central South University 23(8): 1915-1923.
[21] Wu, J. N., Long, J., Liu, L. F., Wu, Q. S., Huang, B. C., Zhang, J. M. (2018): Characteristics and evaluation of heavy metal pollution in soils of different land use types in typical lead-zinc mineralization areas. – Earth and Environment 46(6): 561-570.
[22] Yang, Q., Li, Z., Lu, X., Duan, Q., Huang, L., Bi, J. (2018): A review of soil heavy metal pollution from industrial and agricultural regions in China: pollution and risk assessment. – Science of the Total Environment 642: 690-700.

http://www.aloki.hu ● ISSN 1589 1623 (Print) ● ISSN 1785 0037 (Online)
DOI: http://dx.doi.org/10.15666/aeer/1706_1334113354

[23] Yang, Z. H. (2013): Discussion on water quality status assessment and protection measures in Daxia River Basin. – Gansu Science and Technology 31(6): 38-40.
[24] Yu, K., Van Geel, M., Ceulemans, T., Geerts, W., Ramos, M. M., Serafim, C., ... Ameglio, T. (2018): Vegetation reflectance spectroscopy for biomonitoring of heavy metal pollution in urban soils. – Environmental Pollution 243: 1912-1922.
[25] Yuan, S. C., Gu, F. G. (2018): Study on vegetation coverage classification based on normalized index (NDVI) taking Guizhou Province as an example. – Environmental Technology 24(3): 38-42.
[26] Zhou, P., Wen, A. B., Shi, Z. L., Yan, D. C., Long, Y. (2017): Distribution characteristics and pollution evaluation of heavy metals in different land use soils in the Three Gorges Reservoir Area. – Transactions of the Chinese Society of Agricultural Machinery 48(7): 207-213.
[27] Zhou, Y., Aamir, M., Liu, K., Yang, F., Liu, W. (2018): Status of mercury accumulation in agricultural soil across China: spatial distribution, temporal trend, influencing factor and risk assessment. – Environmental Pollution 240: 116-124.

http://www.aloki.hu ● ISSN 1589 1623 (Print) ● ISSN 1785 0037 (Online)
DOI: http://dx.doi.org/10.15666/aeer/1706_1334113354

A REVIEW OF CHRYSANTHEMUM, THE EASTERN QUEEN IN TRADITIONAL CHINESE MEDICINE WITH HEALING POWER IN MODERN PHARMACEUTICAL SCIENCES

SHAHRAJABIAN, M. H.[1,2#] – SUN, W.[1,2#] – ZANDI, P.[3] – CHENG, Q.[1,2*]

[1]*Biotechnology Research Institute, Chinese Academy of Agricultural Sciences, Beijing 100081, China*

[2]*Nitrogen Fixation Laboratory, Qi Institute, Building C4, No. 555 Chuangye, Jiaxing 314000, Zhejiang, China*

[3]*Institute of Environment and Sustainability, Development in Agriculture, Chinese Academy of Agricultural Sciences, Beijing 100081, China*

[#]*These authors equally contributed to this paper.*

**Corresponding author*
e-mail: chengqi@caas.cn

(Received 12th Jun 2019; accepted 28th Aug 2019)

Abstract. Chrysanthemum is famous as the Queen of the East grown mainly in China and Japan. Chrysanthemum is the second most important plant in both the ornamental industry and traditional Chinese medicine. The most important chemical extracts of Chrysanthemum include flavonoids, betaine, choline and vitamin B1. Thirteen important compounds of chrysanthemum flowers are acacetin-7-0-beta-D-glucopyranoside, luteolin, luteolin-7-O-beta-D-glucopyranoside, acaciin, acacetin 7-0-(6$^{//}$-0-alpha-L-rhamnopyranosyl)-beta-sophoroside, 3-0-caffeoylquinic acid, syringaresinol 0-beta-D-glucopyranoside, 5,7-dihydroxychromone, uracil, p-gydroxybenzoic acid, 4-0-beta-D-glucopyranosyloxybenzoic acid, boscialin and blumenol A. The most outstanding health benefits of chrysanthemum tea are easing stress and anxiety, improving cardiovascular health, protect against oxidative damage, inhibit inflammation, support healthy immune function, improve eye health and lower risk for osteoporosis. In traditional Chinese medicine, chrysanthemum is a cold herb which helps dispel pathogenic heat, helps the liver, improves eyesight and aids detoxification. To conclude, treatment with natural Chinese herbal medicine especially chrysanthemum, non-synthetic drug is recommended for an organic life.
Keywords: *health benefits, Asian medicinal science, western pharmaceutical science, herbal medicine, silk road*

Introduction

Traditional Chinese medicine is a system of medicine based on acupuncture, acupressure, Chinese herbs, cupping, diet and moxibustion (Soleymani and Shahrajabian, 2012, 2018; Ogbaji et al., 2018; Shahrajabian et al., 2018, 2019a, b, c). Traditional medicine refers to health practices, knowledge, approaches and beliefs incorporating plants and herbs based on both ancient and modern pharmaceutical science (Sharajabian et al., 2019d, e, f, 2020). Chrysanthemum with high ornamental value is a one of the ten most popular traditional flowers in China and one of the most popular cut flowers in the world (Sun et al., 2011; Wang et al., 2014; Chung et al., 2018). Wang et al. (2014) stated that there are more than 20,000 chrysanthemum cultivars in the world and about 7,000 cultivars in China. The objective of this review is survey on some important modern and ancient pharmaceutical sciences of chrysanthemum.

http://www.aloki.hu ● ISSN 1589 1623 (Print) ● ISSN 1785 0037 (Online)
DOI: http://dx.doi.org/10.15666/aeer/1706_1335513369

Materials and methods

All relevant papers in the English language of researchers from different countries were collected. The keywords of chrysanthemum, traditional Chinese medicine, traditional Asian medicine, modern pharmaceutical science, health benefits and western medicine were searched in Google Scholar, Scopus, Research Gate and PubMed.

Results and discussion

Chrysanthemum occurrence and cultivation

In Chinese culture, ancient Chinese scholars consider chrysanthemum as a symbol of nobility and integrity and long prized by ordinary people for its medicinal properties. Teixeria (2003) mentioned that, chrysanthemum is the world's second most economically important floricultural crop, following rose. In China, it is found most often in Zhejiang, Anhui, Henan and Sichuan provinces. Imtiaz et al. (2019) also noted that chrysanthemum is native to China and was first cultivated as a flowering herb back in the 15th century BC, and it was believed that this plant had the power of life. Chrysanthemum is famous as Queen of the East, and also known as autumn flower (Saicharan et al., 2017). In traditional Chinese medicine, chrysanthemum provides mildly cold energy, and it has special affinity to the energy channels that lead to the lungs, liver, spleen and kidneys. Chrysanthemum tea is an herbal infusion made from the dried flowers of the chrysanthemum plant in ancient China, and it was used as an herbal remedy in traditional Chinese medicine (TCM) as early as 1500 B.C. Its petals consumed in the form of a salad has the perception of causing longevity. *Chrysanthemum* commonly called as gul-e-daudi or golden flower autumn queen has been cultivated for more than 2000 years ago in Iran. It belongs to the family of Asteraceae, and it behaves both as an annual as well as perennial flowering crop (Kalia, 2015). It is the world's second most important floricultural crop only after Rose (Kalia, 2015). The National Chrysanthemum Society of Britain lists over 600 cultivars of this plant (Datta, 2013). Klie et al. (2014) has shown that chrysanthemum is a segmental allohexaploid with an ambiguous pattern of inheritance. Chrysanthemums require well-drained soil and full sunlight to grow and successfully bloom. Plants grown with less light will become weak, spindly and produce few flowers. Chrysanthemums are shallow rooted and do best if planted high, which means that frequent watering may be necessary during times of high heat and little rainfall. The best defense against adverse weather conditions is to provide good drainage so that water does not accumulate around the plants and promote ice formation. Cicek Atikmen et al. (2014) found that 12.5% fresh mushroom compost and 25% exhausted mushroom compost were the best ratios for cultivation of chrysanthemum. Chrysanthemum white rust (CWR) is one of the primary diseases on chrysanthemum which has been considered as a quarantine disease in many countries (Dong et al., 2018). List of some chrysanthemum varieties is presented in *Table 1*. Qualitative characters of 20 genotypes of chrysanthemum is shown in *Table 2*. Genotypes of *C. morifolium* is shown in *Table 3*. Performance of chrysanthemum genotypes for vegetative characters is presented in *Table 4*. Length of flowering, diameter of flowering stem, diameter of flower bud, diameter of most open inflorescence, plant height, and number of inflorescences per pot of chrysanthemum is presented in *Table 5*. Phytochemical characteristics evaluated in chrysanthemum plants (average of three cultivars) with and without application Si is shown in *Table 6*. Chukki

http://www.aloki.hu ● ISSN 1589 1623 (Print) ● ISSN 1785 0037 (Online)
DOI: http://dx.doi.org/10.15666/aeer/1706_1335513369

et al. (2018) indicated that *Chrysanthemum indicum* flower has the potential for Congo red dye reduction from aqueous solution. A number of disease plague chrysanthemus, are Septoria Leaf Spot, Powdery Mildew and virus diseases such as mosaic and stunt or virus-like diseases such as aster yellows. A number of insects such as Aphids, Caterpillars, Leafhoppers, Leaminers, Plant Bugs and Spider Mites may hurt the crops. Chrysanthemums cultivars reveal amazing colours, shapes types of inflorescence and a varied growth (Carvalho-Zanao et al., 2012). Plants are generally raised through suckers and terminal cuttings. It has been said that micro propagation to be very efficient technique for the fast and disease free raising of *Chrysanthemum* plants (Kalia, 2015). Cojocariu et al. (2018) noted that knowing the particular architecture can improve the correct application of chrysanthemum culture technologies as properly positioning of the crops into the appropriate fertility plots, adequate application of fertilizers, and mechanical maintenance of chrysanthemum crops in order to protect the root system of the plants. Yasemin et al. (2017) reported that flower diameters, disc florets, number of flowers, shoot height, root collar thickness, root and shoot fresh weights were negatively affected in 150 and 200 mM NaCl treatments. Liu and Xiao (2018) reported that fourteen compounds were isolated and identified as stigmata-4-ene-3-one (1), calenduladiol-3β-O- palmitate (2), 16β,22α-dihydroxypseudotaraxasterol-3β-O-palmitate (3), α-amyrin (4), urs-12-ene-3β,16β-diol (5), 3β-hydroxyurs- 12-ene-11-one (6), arnidiol (7), maniladiol (8), 3β-hydroxyolean-12-ene-11-one (9), luteolin (10), apigenin (11), apigenin-7,4'- dimethyl ether (12), genkwanin (13), and 1-linoleic acid glycerate (14). Carvalho-Zanao et al. (2012) reported that silicon has promoted improvements both in quantitative and qualitative aspects when supplied to some ornamental species produced in these conditions. Lee and Van Iersel (2008) found that saline water may be more readily available and can have the added benefit of reduced plant height, which is an important quality characteristic for floriculture crops such as chrysanthemum. The effect of growth substrates over the nutrients of *chrysanthemum* plant is shown in *Table 7*. The effect of growth substrates over the nutrients of chrysanthemum plant is presented in *Table 8*. Germination rate of seeds is shown in *Table 9*. Kalia (2015) indicated that *Chrysanthemum* can be multiplied in large scale through micro propagation using right concentration of the auxins. She clearly indicates that the above problems can be minimized by micro propagation of *Chrysanthemum*.

Table 1. *List of some chrysanthemum varieties (Kumar et al., 2014)*

Cultivars	Cultivars
Kanchil	Pusa Anmol
Glumohr	Yellow Bangla
Shayamal	Sharad Mala
Sadwin Yellow	Star White
White Andaman	TERI
Aparjita	Poornima White
Sadbhawna	Waters May
Flirt	Beauty
Neelima	Jubilee
White Prolific	Maghi Orange
Ravikiran	Maghi White
Birbal Sahni	Maghi Yellow
Shukla	Kalvin Orange

http://www.aloki.hu ● ISSN 1589 1623 (Print) ● ISSN 1785 0037 (Online)
DOI: http://dx.doi.org/10.15666/aeer/1706_1335513369

Yellow Charm	Diana
Pink Cloud	Pankaj
Kajole	Kalvin Pink
Gaity	Sonali Tara
Geetanjali	Mother Teressa
Star Pink	Pinked White
Korean Small	Gajra
Yellow Star	Santa Dine
Ajay	Red Shringar
Meghavi	Shwet Shringar
Yellow Gold	White Anemone
Lalpari	Mahatma Gandhi
Red Gold	Raja Orange
Vasantika	Tokyo Soldier
Kundan	Korean Small
Kargil	Kalvin Yellow
Shanti	Greenish White
Taichen Queen	Ajay
Star Yellow	Texas Gold
Snowball	Yellow Reflex
President Viger	Golden Yellow
Jayanti	Red D spoon
Dolly Orange	Annual Chrysanthemum
Liliput	Annual Chrysanthemum
FDL	

Table 2. *Qualitative characters of 20 genotypes of chrysanthemum (Prakash et al., 2018)*

Genotypes	Flower colour	Disc colour	Type of flower
Thai Chin Queen	Orange	*	Double
Pusa arunoday	Pink	Yellow	Double
Yellow charm	Yellow	Yellow	Semi-double
Pusa sona	Yellow	Yellow	Semi-double
Pusa centenary	Yellow	*	Double
Pusa aditya	Yellow with orange center	Orange	Semi-double
Sunny	Blood red	*	Double
Pusa kesari	Saffron	*	Double
Sadbhavana	Dark orange	Yellow	Semi-double
Lalith	White	*	Double
Ajay	Pink	*	Double
Pusa Chitraksha	Deep magenta	Yellow	Semi-double
Basanthi	Yellow	Yellow	Semi-double
Ramlal dada	Yellow	*	Single
Haldighati	Dark yellow	*	Double
Star white	White	*	Double
Lal pari	Red	Yellow	Semi-double
Jaya	White	*	Double
Ajay orange	Orange	*	Double
Lilyput	Yellow	*	Double

http://www.aloki.hu ● ISSN 1589 1623 (Print) ● ISSN 1785 0037 (Online)
DOI: http://dx.doi.org/10.15666/aeer/1706_1335513369

Table 3. *Genotypes of C. morifolium (Kaur et al., 2018)*

Plant tag no.	Genotypes name	Color	Plant tag no.	Genotypes name	Color
V1	Aparajita	Yellow	V9	Celtic	Green
V2	Fortune	White	V10	Paiwer-W	White
V3	Anastasia	White	V11	HF-164	Yellow Purple
V4	Charlia	Purple Yellow	V12	Paladov Dark	Orange
V5	Vanilla Sorbet	Cream	V13	Tocovar-6	Red
V6	Paladov Sunny	Yellow	V14	Papaya	Orange
V7	White Double	White	V15	Cologne	White
V8	Braca Splendid	Magenta			

Table 4. *Performance of chrysanthemum genotypes for vegetative characters (Kaur et al., 2018)*

Population No.	Genotypes	Plant spread (cm)	No. of branches per plant	No. of leaves per plant	No. of flowers per stem	No. of flowers per cut flower	Flower size (cm)
V1	Aparajita	26.06	13.66	156.33	4.73	55.44	3.73
V2	Fortune	31.86	15.06	140.93	5.46	60.34	5.73
V3	Anastasia	17.86	7.53	51.00	4.33	27.33	5.43
V4	Charlia	22.40	18.46	252.73	4.46	52.38	3.28
V5	Vanilla Sorbet	12.13	10.06	73.93	2.60	23.80	3.92
V6	Paladov Sunny	16.26	11.26	82.13	2.86	31.74	2.59
V7	White Double	23.80	13.26	156.00	4.26	46.16	5.71
V8	Braca Splendid	21.26	9.46	75.40	3.53	34.13	5.15
V9	Celtic	21.00	6.20	57.46	4.26	26.11	3.04
V10	Paiwer-W	23.66	9.33	98.33	4.60	43.93	5.11
V11	HF-164	20.93	8.06	72.00	2.93	21.74	5.13
V12	Paladov Dark	13.66	6.00	34.66	2.20	20.53	4.58
V13	Tocovar-6	23.00	12.00	145.40	3.13	38.87	5.05
V14	Papaya	19.40	10.13	99.46	3.06	38.88	5.21
V15	Cologne	18.73	9.40	77.86	2.13	19.78	4.93
C.D. at 5% level of significance		3.63	3.29	5.58	1.56	1.99	0.17

Table 5. *Length of flowering (LFS), diameter of flowering stem (DFS), diameter of flower bud (DFB), diameter of most open inflorescence (DI), plant height (PH), and number of inflorescences per pot (NI) of chrysanthemum cultivar (Carvalho-Zanao et al., 2012)*

Cultivar	PH (cm)	DI (cm)	LFS (cm)	DFS (cm)	DFB (cm)	NI (unit/pot)
Coral Charm	55.35a	5.15c	44.94a	44.94a	0.99a	22.50c
White Reagan	56.31a	6.87b	45.09a	45.09a	1.01a	29.17a
Indianapolis	48.67b	7.81a	41.10a	41.10a	1.16a	24.50b
CV (%)	6.42	3.85	6.51	6.51	6.34	15.15

http://www.aloki.hu ● ISSN 1589 1623 (Print) ● ISSN 1785 0037 (Online)
DOI: http://dx.doi.org/10.15666/aeer/1706_1335513369

Table 6. *Phytochemical characteristics evaluated in chrysanthemum plants as a function of the application of Si (average of three cultivars) (Carvalho-Zanao et al., 2012)*

Variables	Without Si	With Si	CV (%)
Length of flowering stem (cm)	39.99a	39.22a	7.42
Diameter of flowering stem (cm)	0.38a	0.37a	6.51
Diameter of flower bud (cm)	1.00a	1.03a	6.34
Diameter of the most open inflorescence (cm)	6.65a	6.58a	3.85
Height of plant (cm)	48.73a	49.45a	6.42
Number of inflorescences per pot	25.11a	25.67a	15.15
Production of root dry matter (g)	2.88a	2.87a	20.60
Production of leaf dry matter (g)	7.36a	6.86a	14.49
Production of stems dry matter (g)	11.36a	11.50a	15.57
Production of inflorescence dry matter (g)	7.62a	7.49a	19.58
Production of dry matter of the shoots (g)	26.34a	25.84a	11.16
Cycle (days)	88.54a	88.50a	7.55
Shelf life (days)	26.89a	27.00a	6.21

Averages followed by distinct letters different significantly among each other by Turkey's test, $p < 0.05$

Table 7. *The effect of growth substrates over the nutrients of chrysanthemum plant (Cicek Atikmen et al., 2014)*

Growth substrates	Total N (%)	Total P (%)	Total K (%)	Total Na (ppm)	Total Ca (%)
100% P	4.04^{ns}	1.07A	6.36^{ns}	695^{ns}	1.81E
12.5% FMC + 87.5% P	3.90	0.79CD	7.14	513	2.01CDE
25% FMC + 75% P	3.84	0.87BC	6.81	581	1.86DE
50% FMC + 50% P	3.62	0.66D	6.55	739	2.48AB
12.5% FMC + 25% Perlite + 62.5% P	3.98	0.80CD	6.68	705	2.07BCD
25% FMC + 25% Perlite + 50% P	3.83	0.79CD	7.27	607	2.31ABC
50% FMC + 25% Perlite + 25% P	3.75	0.84BCD	7.20	597	2.44AB
12.5% EMC + 87.5% P	3.71	0.93ABC	6.82	784	2.25ABCD
25%EMC + 75% P	3.91	0.95ABC	6.70	619	2.19ABCDE
50% EMC + 50% P	3.81	0.93ABC	6.83	526	2.57A
12.5% EMC + 25% Perlite + 62.5% P	3.80	1.07A	7.05	614	2.57A
25% EMC + 25% Perlite + 50% P	3.91	1.09A	6.75	599	2.26ABCD
50% EMC + 25% Perlite + 25% P	3.84	1.00A	7.20	579	2.34ABC

ns: non-significant, $p < 0.01$. P = Peat, FMC = Fresh MC, EMC = Exhausted MC

Table 8. *The effect of growth substrates over the nutrients of chrysanthemum plant (Cicek Atikmen et al., 2014)*

Growth substrates	Total Mg (%)	Total Fe (ppm)	Total Mn (ppm)	Total Zn (ppm)	Total Cu (ppm)
100% P	1.00A	701A	96BC	144BC	17A
12.5% FMC + 87.5% P	0.86CD	405CD	88BC	166B	14BC
25% FMC + 75% P	0.84D	354D	103BC	100C	15ABC
50% FMC + 50% P	0.94ABC	306D	136A	49D	14C
12.5% FMC + 25% Perlite + 62.5% P	0.90BCD	463BCD	90BC	48D	15ABC
25% FMC + 25% Perlite + 50% P	0.92ABCD	505BCD	86.29C	156B	14C
50% FMC + 25% Perlite + 25% P	0.95ABC	464BCD	118AB	224A	16ABC
12.5% EMC + 87.5%P	0.95ABC	566ABC	101BC	175B	16ABC
25%EMC + 75%P	0.92ABCD	659AB	92BC	156B	16ABC
50% EMC + 50% P	0.95ABC	702A	81C	161B	14C
12.5% EMC + 25% Perlite + 62.5%P	0.98AB	495BCD	99BC	160B	15ABC
25% EMC + 25% Perlite + 50% P	0.97AB	466BCD	81C	155B	16ABC
50% EMC + 25% Perlite + 25%P	1.01A	474BCD	93BC	170B	17AB

ns: non-significant, $p < 0.01$. P = Peat, FMC = Fresh MC, EMC = Exhausted MC

http://www.aloki.hu ● ISSN 1589 1623 (Print) ● ISSN 1785 0037 (Online)
DOI: http://dx.doi.org/10.15666/aeer/1706_1335513369

Table 9. *Germination rate of seeds (Wang et al., 2014)*

Cultivars	Seed germination rate (%)
QX-081	0
QX-006	0
QX-003	0
Q10-33-2	66.7 ± 8.3
Nannongxiangbin	0
Nannonghongcheng	57.1 ± 6.5
QX-001	66.7 ± 4.7
Nannongjinhe	27.5 ± 4.5
Q10-33-1	23.9 ± 4.3

Values given are mean ± standard deviation

Medicinal uses and potential health benefits in traditional and modern medicine industry

In traditional Chinese medicine (TCM), chrysanthemum flowers are plants that belong to the Cool/Acrid herbs that release the exterior category. Herbs which release the exterior aim to treat the early stages of diseases that affect the upper respiratory tract, the eyes, the ears, the nose, the throat or the skin. In some Eastern cultures, chrysanthemums are also a symbol of good luck, wealth, happiness, and longevity. In Chinese medicine, chrysanthemums are a versatile herb called Ju Hua. In Chinese traditional medicine, Ju Hua is considered to be a fragrant, cool, and light herb. Also, it is used for cooling heat in the liver channel, especially when it manifests as dry, red or painful eyes. Yang et al. (2019) discovered that the *Chrysanthemum morifolium* flower is widely used in China and Japan as a food, beverage, and medicine for many diseases. Chrysanthemum tea is naturally caffeine-free which makes it a great alternative to drinks containing caffeine like black tea and coffee. It has been reported that *Chrysanthemum morifolium* has many antioxidant activities including resisting fatigue, improving the function of cardiovascular system, and lowering the levels of serum lipid (Wang and Xiao, 2013; Yu et al., 2013). The healing benefits of *Chrysanthemum morifolium* are closely related to the composition and content of phenolic compounds (Liu et al., 2013), and apigenin-7-O-glucoside is one of the most active phenolic compounds in chrysanthemum flowers (Wang et al., 2018). Sassi et al. (2008) found that chrysanthemum acts as an antibiotic against a variety of pathogens. Marongiu et al. (2009) reported that the extract of a fresh plant can be applied to skin infections. Liang Yu et al. (2010) and Michalowska and Lema-Ruminska (2018) reported that chrysanthemums have many health-promoting properties used in medicine. Bose et al. (2003) found that chrysanthemum s boiled roots were used as a headache remedy, young sprouts and petals were eaten as salad and leaves were brewed for a festive drink. Chrysanthemum has aesthetic values, antigenotoxic, antioxidative and antimutagenic properties. 13 different types of Chrysanthemums are: Single blooms, Quilled blooms, Spider blooms, Anemone, Pompons, Decorative blooms, Reflex and Incurve blooms, Reflex mums, Brush or Thistle Chrysanthemums, Unclassified, Spoon mums, Cushion mums and Miscellaneous mums. Terpenes concentrations used for sensory analyses is shown in *Table 10*. Compounds identified from Chrysanthemum morifolium Huangju by UHPLC-Q-TOF-MS is presented in *Table 11*. Antioxidant activities of apigenin-7-

http://www.aloki.hu ● ISSN 1589 1623 (Print) ● ISSN 1785 0037 (Online)
DOI: http://dx.doi.org/10.15666/aeer/1706_1335513369

O-glucoside, apihenon and glucose is shown in *Table 12*. The chemical compositions of Chrysanthemum essential oil (CHEO) is presented in *Table 13*. Essential oil composition of *Chrysanthemum cinerariifolium* is shown in *Table 14*. Some health benefits of chrysanthemums are for allergies, hypertension (high blood pressure0, tightening of the chest, anxiety, skin conditions such as boils, vertigo, eyes that are inflamed, headaches, sore throats, colds and tinnitus. The health benefits of chrysanthemum is shown in *Table 15*. The most important health benefits of chrysanthemum tea is presented in *Table 16*. Samples and origins of the studies *Chrysanthemum morifolium* tea from China is shown in *Table 17*. Common traditional Chinese medicine formulas in which chrysanthemum flowers are used is shown in *Table 18*.

Table 10. *Terpenes concentrations used for sensory analyses (Niu et al., 2018)*

Terpenes	Concentration (mg/L)
α-pinene	3083
Camphene	2780
β-pinene	355
β-myrcene	787
α-phellandrene	523
dl-limonene	8192
Cis-ocimene	53
α-terpinolen	7566
Caryophyllene	775
β-farnesene	243
Germacrene B	985
Alcohols	
Linalool	2974
D-fenchyl alcohol	1178
Eudesmol	1177
Borneol	183
Isoborneol	3065
4-terpineol	866

Table 11. *Compounds identified from Chrysanthemum morifolium Huangju by UHPLC-Q-TOF-MS (Wang et al., 2018)*

No.	RT	Formula	$[M-H]^-$	Score	MS/MS	Identification
1	4.833	C16H18O9	353.08785	97.69	191.05644, 248.97382, 112.98560	Chlorogenic acid
2	11.442	C21H20O11	447.09376	87.93	285.03972	Luteolin-7-O-glucoside
3	17.242	C25H24O11	515.12035	95.93	353.08736, 179.03450, 173.04544, 135.04501, 191.05577	3,5-dicafeoylquinic acid
4	19.575	C25H24O12	431.09920	95.44	268.03810, 269.04341	Apigenin-7-O-Glucoide
5	21.275	C21H18O11	445.07743	79.28	269.04514, 113.02422	Apigenin-7-O-glucuronide
6	22.208	C24H22O14	533.09396	94.85	489.10472, 285.04009	Luteolin-7-O-6″-malonylglucoside
7	32.767	C15H10O5	269.04627	94.96	117.03469, 151.00383, 149.02439	Apigenin

http://www.aloki.hu ● ISSN 1589 1623 (Print) ● ISSN 1785 0037 (Online)
DOI: http://dx.doi.org/10.15666/aeer/1706_1335513369

Table 12. *Antioxidant activities of apigenin-7-O-glucoside, apihenon and glucose (Wang et al., 2018)*

±	ABTS (EC_{50})	DPPH (EC_{50})	FI (EC_{50})
Apigenin-7-O-glucoside	5.49 ± 0.74^{a}	/	/
Apigenin	0.68 ± 0.01^{b}	/	/
Glucose	/	/	/
BHT	0.17 ± 0.00^{b}	0.41 ± 0.01^{a}	/
Ascorbic acid	0.12 ± 0.00^{b}	0.11 ± 0.00^{b}	/
Rutin	0.52 ± 0.10^{b}	0.52 ± 0.07^{a}	/
EDTA	/	/	0.32 ± 0.03

Each value is expressed as the mean ± standard deviation (n = 3). Means with different letters with in a column are significantly different ($p < 0.01$). ABTS and DPPH, effective concentration at which 50% of radicals are scavenged (mg/mL); FI, ferrous ion chelating power; effective concentration at which 50% of ferrous ions are chelated (mg/mL). Positive controls were: BHT, ascorbic acid, rutin and EDTA. / , no data obtained from the EC_{50} model Y = 100 / (1 + 10^((LogEC50-C)*HillSlope))

Table 13. *The chemical compositions of chrysanthemum essential oil (CHEO) (Lin et al., 2019)*

Composition	Proportion (%)	Composition	Proportion (%)
Borneol	19.55 ± 0.031	α-Curcumene	1.25 ± 0.021
B-Slinene	16.25 ± 0.052	Eucalyptol	1.11 ± 0.013
Camphor	13.48 ± 0.021	Pentanoic acid	1.05 ± 0.018
Guaia-3,9-diene	5.26 ± 0.019	Butanoic acid, 3-methyl-,1,7,7-trimethylbicyclo[2.2.1]hept-2-yl ester	1.0 ± 0.007
Hexaoxa-cycloocatdecane	4.16 ± 0.012	1,4,7,10,13,16-Hexaoxacyclooctadecane	0.92 ± 0.011
Cyclopropa-naphthalene	2.69 ± 0.015	3-Cyclohexene-1-methanol, alpha., alpha., 4-trimethyl	0.92 ± 0.003
1,4,7,10,13,16-Hexaoxacycloocladecane	2.33 ± 0.004	1-Phenyl-2-propanol	0.63 ± 0.011
3-ethylidence-1-methylcyclopentene	1.88 ± 0.008	Octaethylene glycol	0.56 ± 0.042
Tetramethyl-undeca-2,6,9-trien-8-one	1.42 ± 0.014	3,6,9,12,15-Pentaoxanonadecan-1-ol	0.27 ± 0.026

Table 14. *Essential oil composition of Chrysanthemum cinerariifolium (Shrestha et al., 2014)*

RI	Compound	%	RI	Compound	%
809	2-Hexanol	0.8	1217	Trans-Carveol	0.4
854	(2E)-Hexenal	0.4	1225	Neoiso-Dihydrocarveol	0.3
856	(3Z)-Hexenol	2.3	1261	Cis-Chrysanthenyl acetate	0.5
890	2-Hexen-1-ol	0.3	1270	Unidentified	1.4
891	n-Hexanol	1.0	1311	(Z)-Patchenol	0.9
941	α-Pinene	0.2	1315	Unidentified	1.9
981	1-Octen-3-ol	1.5	1356	Eugenol	0.5
992	Dehydro-1,8-cineole	0.4	1419	(E)-Caryophyllene	0.9
994	6-Methyl-5-hepten-2-ol	0.2	1458	(E)-β-Farnesene	0.4
996	3-Octanol	0.2	1477	Trans-Cadina-1(6),4-diene	0.2

http://www.aloki.hu ● ISSN 1589 1623 (Print) ● ISSN 1785 0037 (Online)
DOI: http://dx.doi.org/10.15666/aeer/1706_1335513369

1016	α-Terpinene	0.3	1481	ϒ-Muurolene	4.6
1024	p-Cymene	0.2	1484	ar-Curcumene	0.3
1028	Limonene	0.2	1497	α-Zingiberene	1.0
1030	1,8-Cineole	2.4	1516	cis-Dihydroagarofuran	0.7
1032	Benzyl alcohol	0.2	1525	δ-Cadinene	1.7
1043	Phenylacetaldehyde	0.4	1534	Italicene Ether	0.3
1066	Cis-Sabinene hydrate	0.4	1550	Unidentified	1.0
1097	Trans-Sabinene hydrate	0.7	1552	Unidentified	0.9
1100	Linalool	0.2	1559	Unidentified	1.2
1103	Filifolone	2.3	1565	(E)-Nerolidol	0.3
1105	Hotrienol	1.1	1576	Germacrene D-4-ol	1.4
1112	2-Phenylethyl alcohol	1.2	1581	ar-Turmerol	0.5
1120	Isophorone	1.0	1583	Caryophyllene oxide	2.1
1125	Chrysanthenone	7.6	1601	Viridiflorol	2.2
1138	trans-Pinocarveol	3.3	1609	Humulene epoxide II	0.2
1144	Camphor	11.0	1628	1-epi-Cubenol	1.1
1162	Cis-Chrysanthenol	4.4	1631	Caryophylla-4(12),8(13)-dien-5α-ol	0.8
1165	Borneol	3.5	1633	Caryophylla-4(12),8(13)-dien-5β-ol	1.9
1166	δ-Terpineol	0.4	1642	τ-Muurolol	2.7
1173	Cis-Pinocamphone	0.2	1646	α-Muurolol (= Torreyol)	0.5
1176	Terpinen-4-ol	3.6	1651	β-Eudesmol	0.4
1190	α-Terpineol	1.2	1655	α-Cadinol	4.8
1193	Methyl salicylate	1.3	1686	Caryophylla-4(15)5,10(14)-trien-1α-ol	0.8
1195	Myrtenol	1.0	1691	Shyobunol	3.4
1202	Nopol	0.4	1737	Oplopalone	1.2
1207	Verbenone	0.5	1954	Hexadecanoic acid	0.3
1208	Trans-3(10)-Caren-2-ol	0.2	2108	(E)-Phytol	0.2
				Total identified	93.7

Table 15. *The health benefits of chrysanthemum*

1-	Increase the metabolism in the body, which can help people to lose weight, improve circulation, regulate hormone levels, and even improve neurotransmitter activity
2-	Prevent certain chronic illnesses, in part because it helps fight free radicals, prevents cellular mutations, and protects body against numerous illnesses which cause by free radicals
3-	Improve vision. Chrysanthemum tea can also improve eyesight, and also can protect against diseases such as cataracts, macular, degeneration, neuropathy and even blurry vision
4-	It may help to improve bone density and even prevent osteoporosis. This is due to its many naturally occurring minerals, including calcium and magnesium
5-	It may boost immune system because of its high levels of Vitamin C and A
6-	It may help unclog arteries and improve overall heart health
7-	It may help alleviate varicose veins
8-	Help ease digestive issues, eliminating a lot of digestive problems and keeping body in less pain with fewer stomach problems
9-	It may help alleviate dryness and itchiness in the eyes
10-	Rejuvenate the brain and alert the senses
11-	Detoxify the liver, making body healthier overall, as well as make the cholesterol numbers lower
12-	It may help alleviate pimples, acne, and other skin problems
13-	It may lower body temperature, and can help relieve the pain
14-	It may help feeling better without the nasty side effects that chemical medicines may have, particularly prescription

http://www.aloki.hu ● ISSN 1589 1623 (Print) ● ISSN 1785 0037 (Online)
DOI: http://dx.doi.org/10.15666/aeer/1706_1335513369

Table 16. *The most important health benefits of chrysanthemum tea*

1-	Anti-inflammatory
2-	Increase immune system
3-	Strengthens bones
4-	Prevents chronic diseases
5-	Improve eyesight
6-	Increase metabolic rate
7-	Maintains cardiovascular health
8-	Relaxes nerves
9-	Treats cough and cold
10-	Detoxifies body

Table 17. *Samples and origins of the studies Chrysanthemum morifolium tea from China (Wang et al., 2019)*

Samples	Company	Origins
C. morigolium Gongju	Beijing Tongrentang Health Pharmaceutical Industry Co., Ltd	Huangshan city, Anhui province
C. morifolium Hangbaiju	Beijing Tongrentang Health Pharmaceutical Industry Co., Ltd	Tongxiang city, Zhejiang Province
C. morifolium Taiju	Beijing Zhang Yiyuan Jinqiao Tea Co., Ltd.	Zhongwei city, Ningxia Hui Autonomous Region
C. morifolium Boju	Bozhou Zhongyitang Chinese Medicinal Materials Sales Co., Ltd.	Bozhou city, Anhui Province
C. morifolium Chuju	Anhui Jutai Chuju Herb Science and Technology Co., Ltd.	Chuzhou city, Anhui Province
C. morifolium Huangju	Huangshan Dingxiangwu Ecological Agriculture Development Co., Ltd.	Shangrao city, Jiangxi Province

Table 18. *Common TCM formulas in which chrysanthemum flowers are used*

1-	For hypertension combine chrysanthemum flowers with dangelions and honeysuckle flowers
2-	For improving vision, relieving tinnitus and headaches combine chrysanthemum flowers with goji berries
3-	For exterior wind-heat with symptoms of headache, colds, sore throat combine chrysanthemum flowers with wild mint, platycodon roots, and greater burdock fruits
4-	For high blood pressure combine chrysanthemum flowers with gambir stems and thorns, cassia seeds and white peony roots
5-	For liver and kidney Yin deficiency combine chrysanthemum flowers with glossy privet fruits and goji berries
6-	For external wind heat with fever, sore throat, chills and red eyes combine chrysanthemum flowers with mulberry leaves, forsythia fruits, wild mint and platycodon roots
7-	For deficient kidney and liver Yin patterns with symptoms such as dizziness, vertigo, blurred vision, headache and hypertension combine chrysanthemum flowers with heal-all spikes, gambir stems and thorns and Baikal skullcap roots
8-	For wind-heat headache combine chrysanthemum flowers with angelica roots and Szechuan lovage roots
9-	For liver or wind-heat with red and painful eyes combine chrysanthemum flowers with cassia seeds and mulberry leaves

http://www.aloki.hu ● ISSN 1589 1623 (Print) ● ISSN 1785 0037 (Online)
DOI: http://dx.doi.org/10.15666/aeer/1706_1335513369

Conclusions

Chrysanthemum is the second most important plants in both ornamental industry and traditional Chinese medicine. Chrysanthemums, often called mums or chrysanths (family *Asteraceae*, genus *Chrysanthemum*), are one of the most important crops in the flower industry. Chrysanthemum is both a source of beautification and high medicinal characteristics. In some Eastern cultures, chrysanthemums are also a symbol of good luck, wealth, happiness, and longevity. In Chinese medicine, chrysanthemums are a versatile herb called Ju Hua. In Chinese traditional medicine, Ju Hua is considered to be a fragrant, cool, and light herb. Also, it is used for cooling heat in the liver channel, especially when it manifests as dry, red or painful eyes. It has tremendously diverse in morphologies including flower shapes, sizes, colors and plant architecture. Thirteen important compounds of chrysanthemum flowers are acacetin-7-0-beta-D-glucopyranoside, luteolin, luteolin-7-O-beta-D-glucopyranoside, acaciin, acacetin 7-0-($6^{//}$-0-alpha-L-rhamnopyranosyl)-beta-sophoroside, 3-0-caffeoylquinic acid, syringaresinol 0-beta-D-glucopyranoside, 5,7-dihydroxychromone, uracil, p-gydroxybenzoic acid, 4-0-beta-D-glucopyranosyloxybenzoic acid, boscialin and blumenol A. Some health benefits of chrysanthemums are for allergies, hypertension (high blood pressure0, tightening of the chest, anxiety, skin conditions such as boils, vertigo, eyes that are inflamed, headaches, sore throats, colds and tinnitus. In traditional Chinese medicine, chrysanthemum is a cold herb which helps dispel pathogenic heat, helps the liver, improves eyesight and aids detoxification. In TCM, chrysanthemum tea has been used for varicose veins, atherosclerosis, acne, influenza, sore throat, fever, angina (Chest pain), common cold symptoms, high blood pressure, inflammation, HIV/AIDS, dizziness and type 2 diabetes. Integrative use of modern agriculture and science of traditional Chinese herbs with new technologies will play an important role in sustainable agriculture and food systems. More clinical researches are necessary to uncover the numerous substances and their impacts on chrysanthemum that contribute to public health.

Conflict of interests. No potential conflict of interests was reported by the authors.

REFERENCES

[1] Bose, T. K., Yadav, L. P., Pal, V. A., Parthasarathy, Das, P. (2003): Commercial Flowers. Vol. II. – Naya Udyog, Kolkata, India.

[2] Carvalho-Zanao, M. P., Zanao Junior, L. A., Barbosa, J. G., Grossi, J. A. S., De A Vila, V. T. (2012): Yield and shelf life of chrysanthemum in response to the silicon application. – Hort. Bras 30(3): 403-408.

[3] Chukki, J., Abinandan, S., Shanthakumar, S. (2018): *Chrysanthemum indicum* microparticles on removal of hazardous Congo red dye using response surface methodology. – Int. J. Ind. Chem https://doi.org/10.1007/s40090-018-0160-5.

[4] Chung, Y. S., Jun, T., Lee, Y. G., Jung, J. A., Won, S. Y., Hwang, Y. J., Silva, R. R., Choi, S. C., Kim, C. (2018): A genetic linkage map of wild *Chrysanthemum* species indigenous to Korea and its challenges. – Int. J. Agric. Biol 20: 2708-2716.

[5] Cicek Atikmen, N., Kutuk, C., Karahan, G. (2014): Response of chrysanthemum (*Chrysanthemum morifolium*) to fresh and exhausted mushroom compost substrates in greenhouse conditions. – Bulletin UASVM Horticulture 71(2): 233-239.

http://www.aloki.hu ● ISSN 1589 1623 (Print) ● ISSN 1785 0037 (Online)
DOI: http://dx.doi.org/10.15666/aeer/1706_1335513369

[6] Cojocariu, A., Chelariu, E. L., Tanase, C. (2018): Adventitious roots development and root system architecture of chrysanthemum cuttings. – J. Plant Develop 25: 91-98.
[7] Datta, S. K. (2013): *Chrysanthemum morifolium* Ramar. A unique genetic material for breeding. – Sci Cult 7-8: 307-313.
[8] Dong, L., Huang, Z., Liu, D., Zhu, P., Lv, S., Li, N., Mao, H. (2018): Transcriptome analysis of chrysanthemum in responses to white rust. – Sci Hort 233: 421-430.
[9] Imtiaz, M., Khattak, A. M., Ali Khan, M., Jalal, F., Hussain, S., Said, F., Bo, H. (2019): Rapid in-vitro propagation of *chrysanthemum morifolium* through shoot bud explants. – Pak. J. Bot 51(3).
[10] Kalia, R. (2015): Effect of different concentrations of auxins on the regeneration of *Chrysanthemum Morif Olium* plantlets. – Int. J. Tech. Res. Applic 3(6): 106-107.
[11] Kaur, M., Dahiya, D. S., Kumar, S., Yadav, G., Malik, A. (2018): Appraisal for flower yield and genetic correlation of *Chrysanthemum morifolium* genotypes in semi-arid Haryana. – J. Pharmacogn Phytochem 7(4): 1267-1272.
[12] Kumar, G., Singh, K. P., Prasad, K. V., Rana, M. K., Namita, Panwark, S. (2014): Genetic diversity analysis of chrysanthemum (*Chrysanthemum grandiflorum*) cultivars using RAPD markers. – Indian J. Agr. Sci 84(11): 1323-8.
[13] Klie, M., Schie, S., Linde, M., Debener, T. (2014): The type of ploidy of *Chrysanthemum*is not black or white: a comparison of a molecular approach to published cytological methods. – Front Plant Sci 479: 1-8.
[14] Lee, M. K., van Iersel, M. W. (2008): Sodium chloride effects on growth, morphology, and physiology of chrysanthemum (*Chrysanthemum* × *morifolium*). – HortScience 43(6): 1888-1891.
[15] Liang-Yu, W., Hong-Zhou, G., Xun-Lei, W., Jian-Hui, Y., Jian-Liang, L., Yue-Rong, L. (2010): Analysis of chemical composition of *Chrysanthemum indicum* flowers by GC/MS and HPLC. – J. Med. Plants Res 4(5): 421-426.
[16] Lin, L., Mao, X., Sun, Y., Rajivgandhi, G., Cui, H. (2019): Antibacterial properties of nanofibers containing chrysanthemum essential oil and their application as beef packaging. – Int. J. Food Microbiol 292: 21-30.
[17] Liu, F., Ong, E. S., Li, S. F. (2013): A green and effective approach for characterization and quality control of *chrysanthemum* by pressurized hot water extraction in combination with HPLC with UV absorbance detection. – Food Chem 141: 1807-1813.
[18] Liu, L. L., Xiao, Z. B. (2018): Chemical constituents from flowers of *Chrysanthemumindicum*. – Chinese Traditional and Herbal Drugs 49(22): 5254-5258.
[19] Marongiu, B., Piras, A., Porcedda, S., Porcedda, S., Tuveri, E., Laconi, S., Deidda, D., Maxia, A. (2009): Chemical and biological comparisons on supercritical extracts of *Tanacetum cinerariifolium* (Trevir) Sch. Bip., with three related species of *Chrysanthemums of Sardinia* (Italy). – Nat. Prod. Res 23: 190-199.
[20] Michalowska, E., Lema-Ruminska, J. (2018): ISSR markers in the genetic diversity of Chrysanthemum plants derived via somatic embryogenesis. – Zeszyty Problemowe Postepow Nauk Rolniczych 594: 17-25.
[21] Niu, Y., Sun, X., Xiao, Z., Wang, P., Wang, R. (2018): Olfactory impact of terpene alcohol on terpenes aroma expression in *Chrysanthemum* essential oils. – Molecules 23: 2803.
[22] Ogbaji, P. O., Li, J., Xue, X., Shahrajabian, M. H., Egrinya, E. A. (2018): Impact of bio-fertilizer or nutrient solution on Spinach (*Spinacea Oleracea*) growth and yield in some province soils of P. R. China. – Cercetari Agronomice in Moldova 2(174): 43-52.
[23] Prakash, A., Kumar, M., Kumar, A., Kumar, M., Gupta, A., Badal, S. (2018): Performance and flower characterization of chrysanthemum (*Dendranthema grandiflora Tzvelev*) genotypes under agro-climatic region of western Uttar Pradesh. – Int. J. Chem. Stud 6(5): 1439-1442.

http://www.aloki.hu ● ISSN 1589 1623 (Print) ● ISSN 1785 0037 (Online)
DOI: http://dx.doi.org/10.15666/aeer/1706_1335513369

[24] Saicharan, M., Anitha, V., Kameshwari, L., Srilatha, D. (2017): Seasonal incidence of insect pests of chrysanthemum in Maddur and Palgutta villages of Ranga Reddy district, Telangana. – Int. J. Farm Sci 7(4): 141-143.
[25] Sassi, A. B., Harzallah-Skhiri, N., Bourgougnon, N., Aouni, M. (2008): Antimicrobial activities of four Tunisian *Chrysanthemum* species. – Indian J. Med. Res. 127: 183-192.
[26] Shahrajabian, M. H., Sun, A., Cheng, Q. (2018): A review of goji berry (*Lycium barbarum*) in traditional Chinese medicine as a promising organic superfood and superfruit in modern industry. – Academia Journal of Medicinal Plants 6(12): 437-445.
[27] Shahrajabian, M. H., Sun, W., Cheng, Q. (2019a): The power of natural Chinese medicine, ginger and ginseng root in an organic life. – Middle-East J. Sci. Res 27(1): 64-71.
[28] Shahrajabian, M. H., Sun, W., Cheng, Q. (2019b): Traditional Chinese medicine and agriculture; organic life and sustainability for future. – GSC Biological and Pharmaceutical Sciences 7(01): 091-095.
[29] Shahrajabian, M. H., Sun, W., Cheng, Q. (2019c): Clinical aspects and health benefits of ginger (*Zingiber officinale*) in both Traditional Chinese and modern industry. – Acta Agriculturae Scandinavica, Section B-Soil & Plant Science. DOI: 10.1080/09064710.2019.1606930.
[30] Shahrajabian, M. H., Khoshkharam, M., Sun, W., Cheng, Q. (2019d): The effect of pretreatment factors on seed germination and seedling growth of (*Pimpinella anisum* L.). – Middle East J. Sci. Res 5(1): 86-93.
[31] Shahrajabian, M. H., Sun, W., Cheng, Q. (2019e): A review of ginseng species in different regions as a multipurpose herb in traditional Chinese medicine, modern herbology and pharmacological science. – J. Med. Plants. Stud 13(10): 213-226.
[32] Shahrajabian, M. H., Sun, W., Cheng, Q. (2019f): Modern pharmacological actions of Longan fruits and their usages in traditional herbal remedies. – J. Med. Plants. Stud 7(4): 179-185.
[33] Shahrajabian, M. H., Khoshkharam, M., Zandi, P., Sun, W., Cheng, Q. (2020): The influence of temperatures on germination and seedling growth of pyrethrum (*Tanacetum Cineraiifolium*) under drought stress. – International Journal of Advanced Biological and Biomedical Research 8(1): 9-39 (in press).
[34] Shrestha, S., Satyal, P., Pandit, G., Setzer, W. N. (2014): Chemical composition of the essential oil from the aerial parts of *Chrysanthemum cinerariifolium* growing in Nepal. – Am. J. Essent. Oi. Nat 2(2): 01-03.
[35] Soleymani, A., Shahrajabian, M. H. (2012): Response of different cultivars of fennel (*Foeniculum vulgare*) to irrigation and planting dates in Isfahan, Iran. – Res Crops 13(2): 656-660.
[36] Soleymani, A., Shahrajabian, M. H. (2018): Changes in germination and seedling growth different cultivars of cumin to drought stress. – Cercetari Agronomice in Moldova 1(173): 91-100.
[37] Sukmawani, R., Haerumank, M., Sulistyowati, L., Perdana, T. (2015): Sustainable development model of *Chrysanthemum* agribusiness. – Int. J. Agric. Sci. Res 5(1): 11-18.
[38] Sun, C. Q., Huang, Z. Z., Wang, Y. L. et al. (2011): Overcoming prefertilization barriers in the wide cross between *Chrysanthemum grandiflorum* (Ramat.) Kitmaura and *C. nankingense* (Nakai) Tzvel. By using special pollination techniques. – Euphytica 178(2): 195-202.
[39] Teixeria da Silva. (2003): Chrysanthemum organogenesis through think cell layer technology and plant growth regulator control. – Asian J. Plant Sci 2(6): 505-514.
[40] Wang, J., Xiao, H. (2013): Discrimination of different white *chrysanthemum* by electronic tongue. – J. Food. Sci. Technol 50: 986-992.
[41] Wang, F., Zhang, F. J., Chen, F. D., Fang, W. M., Teng, N. J. (2014): Identification of Chrysanthemum (*Chrysanthemum morifolium*) self-incompatibility. – Hindawi Article ID 625658.

http://www.aloki.hu ● ISSN 1589 1623 (Print) ● ISSN 1785 0037 (Online)
DOI: http://dx.doi.org/10.15666/aeer/1706_1335513369

[42] Wang, Y., Xu, Z., Huang, Y., Wen, X., Wu, Y., Zhao, Y., Ni, Y. (2018): Extraction, purification and hydrolysis behavior of apigenin-7-O-glucoside from *Chrysanthemum morridolium* tea. – Molecules 23: 2933.
[43] Wang, Y., Xu, Z., Wu, Y., Li, M., Pang, S., Liang, Z., Ni, Y. (2019): Effect of weakly basic conditions on the separation and purification of flavonoids and glycosides from *Chrysanthemum morifolium* tea. – Molecules 24: 297.
[44] Yang, P. F., Yang, Y. N., He, C. Y., Chen, Z. F., Yuan, Q. S., Zhao, S. C., Fu, Y. F., Zhang, P. C., Mao. D. B. (2019): New caffeoylquinic acid derivatives and flavanone glycoside from the flowers of *Chrysanthemum morifolium* and their bioactivities. – Molecules 24: 850.
[45] Yasemin, S., Koksal, N., Ozkaya, A., Yener, M. (2017): Growth and physiological responses of *Chrysanthemum paludosum* under salinity stress. – J. Biol. Environ. Sci 11(32): 59-66.
[46] Yu, Y., Zhu, C., Wang, S., Song, W., Yang, Y., Shi, J. (2013): Homosecoiridoid alkaloids with amino acid units from the flower buds of *Lonicera japonica*. – J. Nat. Prod 76(12): 2226-2233.

http://www.aloki.hu ● ISSN 1589 1623 (Print) ● ISSN 1785 0037 (Online)
DOI: http://dx.doi.org/10.15666/aeer/1706_1335513369

A REVIEW OF ASTRAGALUS SPECIES AS FOODSTUFFS, DIETARY SUPPLEMENTS, A TRADITIONAL CHINESE MEDICINE AND A PART OF MODERN PHARMACEUTICAL SCIENCE

SHAHRAJABIAN, M. H.[1,2#] – SUN, W.[1,2#] – CHENG, Q.[1,2*]

[1]*Biotechnology Research Institute, Chinese Academy of Agricultural Sciences, Beijing 100081, China*

[2]*Nitrogen Fixation Laboratory, Qi Institute, Building C4, No. 555, Chuangye County, Jiaxing 314000, Zhejiang, China*

[#]*These authors equally contributed to this paper.*

**Corresponding author*
e-mail: chengqi@caas.cn

(Received 12th Jun 2019; accepted 28th Aug 2019)

Abstract. Astragalus is a common Traditional Chinese Medicinal plant and is a widely used herbal product in China and other countries. Saponins, polysaccharides, amino acids, flavonoids, organic acid, glycosides, alkaloid, and trace elements, are the major classes of chemical compounds occurring in the species of Astragalus genus. In Traditional Chinese Medicine, Astragalus is considered to be effective in the treatment of diabetes, mellitus, nephritis, leukemia, uterine cancer, besides its tonic agent and diuretic effects. Some uses of Astragalus are in the treatment of kidney and urinary problems, digestion, liver problems, female reproductive system problems, muscular, skin problems, cardiovascular and blood related issues, immune and lymphatic system, nervous system, respiratory system, and for some specific diseases. It helps protect the body against various types of stress such as physical and emotional stress. Astragalus root has anti-aging properties, and also help in the prevention of bone loss. *Astragali radix*, the root of *Astragalus membranaceus* Bunge, has been reported to exert hepatoprotective effects, anti-oxidative effects, antiviral activity, anti-oxidative effects, anti-hypertensive effects, and immunostimulant properties; it has also been reported to strengthen superficial resistance, drainage action and new tissue growth. More clinical studies are necessary to discover the effects of Astraglaus.
Keywords: *health benefits, traditional Asian medicine, Yin-Yang balance, Silk Road, herbal medicine*

Introduction

Chinese herbs have been used as traditional medicine immune booster for human being for thousands of years in China (Yin et al., 2009; Shahrajabian et al., 2018). More than 3 million tons of herb medicines were produced in China, and their medicinal parts were consumed in traditional Chinese medicine (TCM) clinic (Soleymani and Shahrajabian, 2012, 2018; Zhang et al., 2016; Ogbaji et al., 2018). In traditional Chinese medicine, some herbals have been used for anti-aging since ancient times (Liu et al., 2017). *Astragalus membranaceus* as one of the most important Qi tonifying adaptogenic herbs in traditional Chinese medicine has a long history of medicinal use (Yang et al., 2010; Zhong et al., 2012; Liu et al., 2017). In traditional Chinese medicine, which laid a lot of emphasis on Qi (vital energy) and Yin-Yang balance (negative and positive equilibrium). Chinese herbs have used as traditional medicine immune booster for human being for thousands of years in China and many parts of Asia (Shahrajabian

http://www.aloki.hu ● ISSN 1589 1623 (Print) ● ISSN 1785 0037 (Online)
DOI: http://dx.doi.org/10.15666/aeer/1706_1337113382

et al., 2019a, b, c, 2020; Sun et al., 2020). The goal of this review is survey on some important ancient and modern pharmaceutical sciences of astragalus.

Materials and methods

All relevant papers in the English language of researchers from different countries were collected. The keywords of astragalus, traditional Chinese medicine, traditional Asian medicine, modern pharmaceutical science, health benefits and western medicine were searched in Google Scholar, Scopus, Research Gate and PubMed.

Results and discussion

Astragalus in traditional Chinese medicine and other parts of the world

Astragalus is considered as benefiting Qi and helping to pass water (Li et al., 2011). It has been used as therapy for Wei Zheng, a term for skeletal muscle fatigue and wasting (Zhou and Mei, 2014). The dried root of *A. membranaceus*, first documented in Shennong Bencao Jing (Shennong's Classic of Materia Medica, 200-300 AD), is one of the most popular health promoting herbal medicines commonly used in China for more than 2000 years. In modern Chinese medicine, it is used in Fu zheng therapy as an immune stimulant (Ionkova et al., 1997). Also known as Huang Qi (Chinese), Milk-Vetch (English), Hwanggi (Korean), and Ogi (Japanese) (Chou et al., 2007; Li et al., 2019). It is sold in dietary supplements in tea or capsule form in the USA, and in the tea, beverages, soup, and trail mix (gorp) in Asia (Song et al., 2008; Zhang et al., 2011). Chinese milk vetch (*Astragalus sinicus* L.) is also a traditional leguminous green manure which plays an important role in maintaining paddy soil fertility and in the popularizing of the double-rice farming system in southern China; it is ploughed into soil at full blooming stage and serves as an alternative to chemical nitrogen fertilizer in the region (Zhu et al., 2012). *Astragalus membranaceus* was originally described in the Shennong's Classic of Meteria medica, the earliest complete Pharmacopoeia of China written from Warring States Period to Han Dynasty (Hei et al., 2005; Auyeung et al., 2016). It is valued for its ability to strengthen the primary energy of the body which we know as the immune system, as well as the metabolic, respiratory and eliminative functions (Liu et al., 2017). This fact is being increasingly substantiated by pharmacological studies showing that it can increase telomerase activity, and has antioxidant, anti-inflammatory, immuneregulatory, anticancer, antitumor, antioxidant, hypolipidemic, antihyperglycemic, hepatoprotective, expectorant, immunomodulatory activity, and diuretic effects (Anon, 2003; Ma et al., 2011; Zhao et al., 2011). *Astragalus membranaceus* (Fisch.) Bunge. has been widely used an anti-osteoporosis herb is traditional Chinese medicine for many years (Du et al., 2004; Wong et al., 2007; Xi et al., 2008; Jiao et al., 2014). In Traditional Chinese Medicine, *Astragalus membranaceus* is a major component in a prescription to treat chronic phlegmatic disorders and general gastrointestinal disturbances including stomach ulcer, chronic diarrhea and intestinal inflammation (Kim et al., 2008; Yang et al., 2014). Other researchers have reported the values of Astraglaus s roots in traditional Chinese medicine with the function of strengthening exterior and promoting health for thousands of years (Ma et al., 2017; Zhao et al., 2011). Traditional Chinese herbs are generally applied in the form of multi-herb formulas in medical treatments and as dietary supplements (Takagi and Ishii, 1967; Li et al., 2011). Lu et al. (2013) reported that *Radix Astragali* is the root

http://www.aloki.hu ● ISSN 1589 1623 (Print) ● ISSN 1785 0037 (Online)
DOI: http://dx.doi.org/10.15666/aeer/1706_1337113382

of *Astragalus membranaceus* Bunge, and as a famous traditional Chinese medicine (TCM), it has been used to improve muscle wasting-related disorders for a long history. They have also introduced Astragalus polysaccharide (APS) as an important bioactive and a therapeutic agent in the management of muscle wasting. *Astragalus trojanus* Stev. is an endemic plant mostly found in eastern and central Anatolia (1300-3500 m), central Aegean region and slopes of Toros mountain (1300-2300 m) in Turkey (Nartop et al., 2015). This genus is widely distributed throughout the temperate and arid regions of the world, and is principally located in Asia (1500 species), North American (500 species) and South American (150 species), and Europe (120 species), but also on mountains in Africa, However, the centre of origin and biodiversity of Astragalus plants is Eurasia, especially the mountainous parts of South-Western and South-Central Asia (Lysiuk and Darmohray, 2016). Iran alone, being the richest centre of Astragalus habitation, shelters more than 850 species, 527 of which are endemic in the flora of Iran (Ranjbar and Karamian, 2002; Aslanipour et al., 2017; Ghasemian-Yadegari et al., 2017). Aslanipour et al. (2017) stated that the crude drugs prepared from Astragalus roots are used for treating some illnesses such as leukemia, respiratory infections and diabetes in Iranian folk medicine. In South Eastern Turkey (Anatolia district), the aqueous extract of the roots of different *Astragalus spp*. are traditionally used against leukemia and for its wound-healing properties (Yesilada et al., 2005; Nalbantosy et al., 2012; Napolitano et al., 2013). In the district of Anatolia, located in South Eastern Turkey, an aqueous extract of the roots of Astragalus is traditionally used against leukemia and for its wound healing properties (Bedir et al., 2001). *Astragalus corniculatus* Bieb. (Fabaceae) is distributed in Southeastern Romania, South Ukraine and Moldova (Tutin et al., 1972). *Astragalus Tragacantha L.* (Fabaceae) is a western Mediterranean perennial cushion-like plant species well-adapted to drought that grows even in the trace metal and metalloid polluted soils (Salducci et al., 2019). It has been reported that Astragalus is an adaptogen and is usually used in combination with other herbs, such as, ginseng, Echinacea, and glossy privet. Astragalus is primarily used in American medicine to potentiate the function of the immune system and in cardiovascular disease. In traditional Chinese medicine, it is used for influenza and the common cold (McKenna et al., 2002). Nishiyama et al. (1995) reported that in traditional oriental medicine, it is conventional to combine different herbs in order to achieve a variety of treatment purposes simultaneously, or to enhance a single effect without causing severe side effects. Erect milkvetch (*Astragalus adsurgens* Pall.), also as a palatable forage, are also widely used in returning farmland to grassland, it has an important role in restoring the degraded ecosystems and could be an effective and applicable to improve soil nutrients and prevent further soil degradation and erosion, because it grows rapidly, and was characterized by barren-tolerance, wide adaptability and strong resistance (Wang and Wang, 2013).

Bioactive phytochemicals, medicinal uses and potential health benefits of Astragalus in traditional and modern medicine industry

Constituents of the dried roots of *Astragalus spp*. *Radix Astragali* provide significant protection against heart, brain, kidney, intestine, liver and lung injury in various models of oxidative stress-related disease (Hong et al., 1992; Shahzad et al., 2016). Zhang et al. (2007) stated that Astragalus is an important traditional Chinese medicine (TCM), and now widely used an immune modulator, especially to support immune health for various chronic degenerative diseases. Recently, *Astragalus radix* was proved efficacious to be an adjunctive therapy medicine for cancers (Wang et al., 2003). In the

http://www.aloki.hu ● ISSN 1589 1623 (Print) ● ISSN 1785 0037 (Online)
DOI: http://dx.doi.org/10.15666/aeer/1706_1337113382

Bulgarian traditional medicine, *Astragalus glycyphyllos* is used an antihypertensive, diuretic and anti-inflammatory remedy (Nikolov, 2006). Major classes of compounds of Astragalus species (*Table 1*) are polysaccharides, saponins and isoflavonoids, alkaloid, choline, betaine, folic acid, organic acid, various amino acids, mucoitin, gum, cellulose and fourteen trace elements, including selenium, zinc, and iron, which are essential micronutrients for man and animals (Bedir et al., 2000; Block and Mead, 2003; Yin et al., 2006; Lu et al., 2016). Astragalus genera are the richest source of cycloartanes, the unique triterpenoids with a characteristics 9,19-cyclopropane (Nartop et al., 2015). According to the systematic review by a Chinese scientists on the chemical constituents of the plants (*genus Astragalus* L.) more than 140 cycloartane-type triterpene glycosides, 60 flavonoids and 18 different polysaccharides have been identified so far (Li et al., 2014). Under high soil moisture and wet conditions, Astragalus is susceptible to root rot caused by fungi, which is the main constraint to cultivation. Land must be well drained for Astragalus. Loose soil and raised beds can be used to control soil moisture (Shannon et al., 2014). The chemical structures and chain conformations of polysaccharides play a vital role in their biological activities; however, polysaccharides belong to a structurally diverse class of macromolecules (Jin et al., 2014). Cycloastragenol (CA) is the main aglycon of many cycloartane-type glycosides which only found in Astragalus genus, extends T cell proliferation by increasing telomerase activity which helps the delay the onset of cellular aging (Valenzuela et al., 2009). Astragalus root also contains a series of cycloartane triterpene glycosides, including astragalosides I-VIII, acetylastragaloside, isoastragaloside I and III, astramembrannin II, cycloastragenol, cyclosieversigenis, soyasaponin I, soyasapogenol B, and lupeol (Ko and Chik, 2009). Among these, *Astragalus membranaceus* has a high content of astragaloside IV, which is commonly used as a qualitative marker.

Table 1. *Astragalus membranaceus main compounds*

Compound	Effect
Flavonoids	Plant metabolites with antioxidant effects; give plants yellow color
Isoflavones	Polyphenolic compounds that are classified as phytoestrogens; formononetin is one of the prominent ones
Lectin	Carbohydrate-binding proteins
Polysaccharides	Carbohydrates whose molecules contain linked monosaccharides; starch, inulin, cellulose
Saponins	Amorphous glycosides of terpenes and steroids that can form emulsions and can foam (soap-like); Astragaloside IV is one the most-studied saponins in Huang Qi

On the basis of traditional Chinese medicine view of cancer, causes are endogenous causes and exogenous causes. Endogenous causes are the seven emotional states (anger, grief, fear, worry, over joy, shock and melancholy) can be seen as the way that stress, worry, over work, and emotional grief can suppress the immune system and allow predispositions for cancer growth to take hold. So, while it can seem simplistic to attribute cancer to normal emotions such as sadness, worry, fear, etc., the TCM view is that when these emotions are excessive, prolonged or unresolved, they can cause disease. The concept of Jing in TCM can be likened to the role of genetics in cancer, which is an important factor indeed. Exogenous causes consists of six exogenous causes for all illness, including cancer, are climatic factors of wind, cold, dampness, dryness,

http://www.aloki.hu ● ISSN 1589 1623 (Print) ● ISSN 1785 0037 (Online)
DOI: http://dx.doi.org/10.15666/aeer/1706_1337113382

summer heat and fire. And, other miscellaneous causes are environmental causes, dietary causes, and drugs. The TCM concepts of yin/yang balance, the need for calmness of mind, absence of strife, the practice of health promotion through movement, all support modern ideas on the role of psychological, neurological and immunological health in cancer prevention (Shahrajabian et al., 2019d, e, f, g, h). Liu et al. (2011) reported that in many parts of the world, especially in China and Germany, the combined use of herbal treatment and conventional cancer treatment is far more widespread than in America. They have also mentioned that 66.44% of cancer patients in China combined the use of herbal medicine with Western treatment. A prospective, controlled study conducted in Israel (Yaal-Hahoshen et al., 2011) found significant improvement in anemia and neutropenia in breast cancer patients who were given an herbal mixture containing Huang Qi and other Chinese herbs. Rios and Waterman (1997) reported that cycloastragenol (CAG) is a secondary metabolite isolated from Radix Astragali, present in all known *Astragalus spp*., CAG (9,19-cycloanostane-3,6,16,25-tetrol,20,24-epoxy-(3β, 6α,16β,20R,24S); is both a triterpene aglycone and the most common genuine aglycone in the bioactive triterpenoid saponins called astragalosides. *Astragalus polysaccharides* (APS) are one of the main efficacious principles of Radix Astragali (*Astragalus membranaceus*), which is reported to have anti-oxidant, anti-diabetic, anti-hypertensive, and immunomodulatory activities (Wu and Chen, 2004; Wu et al., 2005). It has been noted that the crude polysaccharide extract of A. membranaceus was mainly composed of carbohydrates with small amount of proteins (Cho and Leung, 2007). It has been demonstrated that the main components of the ethylacetate extract of Astragalus were isoflavonids such as calycosin-7-O-β-D-glycoside, formononetin-7-O-β-D-glycodie and (6R, 10R)-9,10-dimethoxypterocarpan-3-O-βD-glycoside, and these glycosides and other their aglycones were proved to exhibit strong antioxidant activity (Zhang et al., 2007). Li et al. (2010) also mentioned that the dried root of Astragalus contains 2'4'-dihydroxy-5,6-dimethoxyisoflavone, kumatakenin, choline, betaine, polysaccharides, saponins, glucuronic acid, sucrose, amino acids, traces of folic acid and astraisoflavanin. So many other scientists also revealed that *Astragalus membranaceus* has a notable functional role in various pharmacopoeias as a herbal immunomodulator and an anti-diabetic drug (Wei et al., 2011; Agyeman et al., 2013). Its roots have been used in many state-approved Chinese Herbal formulas for the treatment of diabetes (Jai et al., 2003; Wei et al., 2011). Some experiments have showed that Astragalus exhibits immunomodulating and immunorestorative effects both in vitro and in vivo (Guo et al., 2005), and have shown preliminary promise against the experimental coccidial infection when used in conjunction with vaccine (Cho and Leung, 2007). Song et al. (2017) reported that Astragalus extract mixture HT042 is a combination of three standardized herbal extracts from *Astragalus membranaceus* root, *Elutherococcus senticosus* stem, and *Phlomis umbrosa* root, and it has been developed to promote height growth in children with short stature. Sun et al. (2012) revealed that *Astragalus membranaceus* is a popular traditional Chinese medicine, commonly used in Chinese herb prescription to treat liver disease, and the extract prepared from the roots of *Astragalus membranaceus* and *Paeonia lactiflora* demonstrated better hepatoprotective activity than the herbs used individually. Ko and Chik (2009) demonstrated that root extract of *Astragalus membranaceus* administrated orally and locally can protect rats against hapten-induced colitis through attenuation of TNF-αand IL-1βand up-regulating of Il-10. Shen et al. (2008) indicated that *Astragalus membranaceus* has a potential role in treating allergic

http://www.aloki.hu ● ISSN 1589 1623 (Print) ● ISSN 1785 0037 (Online)
DOI: http://dx.doi.org/10.15666/aeer/1706_1337113382

asthma. Zhang et al. (2009) *Astragalus membranaceus* and its effective components are effective in reducing fasting blood glucose and albuminuria levels, in reversing the glomerular hyperfiltration state, and in ameliorating the pathological changes of early diabetic nephropathy in rat models. Ko and Chik (2009) demonstrates that both oral and locally administered *Astragalus membranaceus* possess protective effects against experimental colitis through differential modulation of colonic cytokines. Yang et al. (2013) found that *Astragalus membranaceus* polysaccharide (AMP) has antitumor activity in vivo at least partly via improving immune responses of host organism, and seems to be safe and effective for the use of anti-tumor therapy. Lv et al. (2017) suggest that *Astragalus polysaccharide* (APS) which is a bioactive extract of *Astragalus membranaceus* may represent a natural therapeutic approach for treating inflammatory bowel disease, such as ulcerative colitis. Yan et al. (2010) found that administration of *Astragalus mongholicus* polysaccharides could significantly increase serum and liver antioxidant enzyme activities in mice and decrease peroxidative lipid levels. Jalsrai et al. (2010) found that doses of *Astragalus mongholicus* extract which did not interfere with locomotor activity and situational anxiety appear to be useful in the treatment of convulsive disorders. Kim et al. (2016) highlighted the ability of *Astragalus membranaceus* to facilitate sperm development and semen quality. Tian et al. (2016) reported that Astragalus may be beneficial as an adjuvant therapy in the treatment of type 2 diabetes. Zhou et al. (2018) demonstrated that the extract from *Astragalus membranaceus* with water extraction-ethanol supernatant method inhibit cell growth and induce apoptosis in cultured breast cancer cells. This effect astragalus extract to suppress breast cancer cells growth was associated with its ability to inhibit PI3K/Akt/mTOR activity. Maresca et al. (2017) concluded that the 50% hydroalcoholic extract of Astragali radix is a valuable candidate for the adjuvant treatment of articular disease. Liu et al. (2017) concluded that the appropriate dose of Astragalus depends on several factors, such as the user's age, health status, and several other conditions. They have also found that natural products are not always necessarily safe, and dosages can be important. Sheng et al. (2005) found that one of the most important biological role of saponins is modulating the cellular oxidant antioxidant balance.

Conclusions

Traditional Chinese medicinal materials have been used for thousands of years and are believed to be abundant, safe, and inexpensive. Astragalus has been used in Chinese traditional medicine as an immunity booster for almost 2000 years. The genus Astragalus is a member of the Fabaceae of Legume family and it is native to northern China and Mongolia. It is widely distributed in China, Siberia, and northern Korea. Some actions of *Astragalus membranaceus* are anti-viral, anti-bacterial, immune system enhancing, immune stimulant, anti-infective some viruses, adaptogen, cardio-tonic, diuretic, hypotensive, anti-oxidant, immunomodulator, hypoglycaemic, circulatory stimulant, vasodilator, anti-fatigue, anti-cancer and hepatoprotective. Chemical constituents are polysaccharides, triterpenoid saponins (Astragalosides), flavonoids, choline, phytosterols, volatile oils, amino acids (Asparagine, Gamma-aminobutyric acid, Canavanine), aglycones, coumarins, astrapterocarpan, betaine, calcium, copper, isoflavonoids, rich in potassium and magnesium. Astragalus membranaceus classically prescribed in TCM in combination with other Chinese medicinal herbs as a dried root, powdered or as a decoction, with the combination depending on the desired therapeutic

http://www.aloki.hu ● ISSN 1589 1623 (Print) ● ISSN 1785 0037 (Online)
DOI: http://dx.doi.org/10.15666/aeer/1706_1337113382

effect and the specific TCM diagnosis. Polysaccharides in Astragalus intensify phagocytosis in reticuloendothelial systems, stimulate pituitary-adrenal cortical activity, and restore depleted red blood cell formations in bone marrow. Astragalus uses are in kidneys problems, strengthens the kidneys, incontinence and frequent urination, urinary tract infection, gastric ulcers, decreased appetite, chronic diarrhea, strengthens the spleen, poor digestion, liver problems, viral hepatitis, strengthen the liver, postpartum fever, uterine bleeding, topical adjuvant therapy for chronic viral cervicitis, vaginitis, edema, lupus, rheumatoid arthritis, myasthenia gravis, strengthens and builds bone marrow, excessive sweating, night sweats, slow healing wounds, increasing white blood cell count, leukopenia, ischemic heart disease, angina pectoris, recovery from severe loss of blood, diabetes, anemia, high blood pressure, heart palpitations, congestive heart failure, strengthens the blood, increases interferon production, impaired immunity, chronic viral infections, general debility, increases energy, HIV/AIDS, cancer, myalic encephalomyelitis (chronic fatigue syndrome), improves sleep quality, upper respiratory infection, common cold, chemotherapy, radiation therapy, flu, combats coxsackie B myocarditis, amerlirate side effects of drugs, appropriate herb for weak and elderly. Isoflavonoids, such as calycosin-7-O-β-D-glucoside, ononin, astraisoflavan-7-O-β-D-glucoside, calycosin and formononetin, are principle bioactive compounds found in Radix astragali-based drugs or foods. In summary, Astragalus is an ancient herb for modern medicine which can promote good health and as drugs to treat diseases. Further clinical researches are necessary to uncover various substances and their effects on astragalus which contribute to public health.

REFERENCES

[1] Agyemang, K., Han, L., Liu, E., Zhang, Y., Wang, T., Gao, X. (2013): Recent advances in *Astragalus membranaceus* anti-diabetic research: pharmacological effects of its phytochemical constituents. – Evid-Based Compl Alt Med Article ID 654643.

[2] Anon (2003): *Astragalus membranaceus*. Monograph. – Altern Med Rev 8: 72-77.

[3] Aslanipour, B., Gulcemal, D., Nalbantsoy, A., Yusufoglu, H., Bedir, E. (2017): Cycloartane-type glycosides from *Astragalus brachycalyx* FISCHER and their effects on cytokine release and hemolysis. – Phytochem Lett 21: 66-73.

[4] Auyeung, K. K., Han, Q. B., Ko, J. K. (2016): *Astragalus membranaceus*: a review of its protection against inflammation and gastrointestinal cancers. – Am J Chin Med. 44: 1-22.

[5] Bedir, E., Calis, I., Piacente, S., Pizza, C., Khan, I. A. (2000): New flavonol glycoside from the aerial parts of *Astragalus vulneraria*. – Chem. Pharm. Bull. 48(12): 1994-1995.

[6] Bedir, E., Calis, I., Dunbar, C., Sharan, R., Buolamwini, J. K., Khan, I. A. (2001): Two novel cycloartane-type triterpene glycosides from the roots of *Astragalus prusianus.* – Tetrahedron 57: 5961-5966.

[7] Block, K. I., Mead, M. N. (2003): Immune system effects of Echinacea, ginseng, and astragalus: a review. – Integr Cancer Ther. 2(3): 247-267.

[8] Cho, W. C., Leung, K. N. (2007): In vitro and in vivo immunomodulating and immunorestorative effects of *Astragalus membranaceus*. – J Ethnopharmacol 113: 132-141.

[9] Chou, M.-X., Wei, X.-Y., Chen, D.-S., Zhou, J.-C. (2007): A novel nodule-enhanced gene encoding a putative universal stress protein from *Astragalus sinicus*. – J. Plant Physiol 164: 764-772.

[10] Du, S. H., Meng, Z. (2004): The treatment of *Astragalus membranaceus* (Fisch.) Bunge. for nephrasthenia syndrome and headache. – J Trad. Chi. Med. 45: 250.

http://www.aloki.hu ● ISSN 1589 1623 (Print) ● ISSN 1785 0037 (Online)
DOI: http://dx.doi.org/10.15666/aeer/1706_1337113382

[11] Ghasemian-Yadegari, J., Nazemiyeh, H., Hamedeyazadan, S., Fathiazad, F. (2017): Secondary metabolites from the roots of *Astragalus maximus*. – Res J Pharmacog 4(2): 31-38.
[12] Guo, F. C., Kwakkel, R. P., Williams, C. B., Suo, X., Li, W. K., Verstegen, M. W. (2005): Coccidiosis immunization: effects of mushroom and herb polysaccharides on immune responses of chickens infected with Eimeria tenella. – Avian Dis 49: 70-73.
[13] Hei, Z. Q., Huang, H. Q., Zhang, J. J., Chen, B. X., Li, X. Y. (2005): Protective effect of *Astragalus membranaceus* on intestinal mucosa reperfusion injury after hemorrhagic shock in rats. – World J Gastroenterol 11: 4986-4991.
[14] Hong, C. Y., Ku, J., Wu, P. (1992): *Astragalus membranaceus* stimulates human sperm motility in vitro. Am J Chin Med. 20: 289-294. – Trop J Pharm Res 15(9): 1897-1901.
[15] Ionkova, I., Kartnig, T., Alfermann, W. (1997): Cycloartane saponin production in hairy root cultures *Astragalus Mongholicus*. – Phytochemistry 45(8): 1597-1600.
[16] Jalsrai, A., Grecksch, G., Becker, A. (2010): Evaluation of the effects of *Astragalus mongholicus Bunge* saponin extract on central nervous system functions. – J Ethnopharmacol 131: 544-549.
[17] Jiao, J., Wei, F.-Y., Gai, Q.-Y., Wang, W., Luo, M., Fu, Y.-J., Ma, W. (2003): A pilot-scale homogenization-assisted negative pressure cavitation extraction of Astragalus polysaccharides. – Int J Biol Macromol 67: 189-194.
[18] Jin, M., Zhao, K., Huang, Q., Shang, P. (2014): Structural features and biological activities of the polysaccharides from *Astragalus membranaceus*. – Int J Biol Macromol 64: 257-266.
[19] Kim, S. W., Fan, M. Z., Applegate, T. J. (2008): Nonruminant nutrition symposium on natural phytobiotics for health of young animals and poultry: mechanisms and application. – J. Anim. Sci 86: E138-E139.
[20] Kim, W., Kim, D. R., Chang, M. S., Park, S. K. (2016): *Astragalus membranaceus* augment sperm parameters in male mice associated with cAMP-responsive element modulator and activator of CREM in testis. – J Tradit Complement Med 6: 294-298.
[21] Ko, J. K., Chik, C. W. (2009): The protective action of *radix Astragalus membranaceus* against hapten-induced colitis through modulation of cytokines. – Cytokine 47: 85-90.
[22] Li, C.-Y., Chen, H.-Y., Liu, W.-P., Rui, W. (2019): Multi-fingerprint profiling combined with chemometric methods for investigating the quality of Astragalus polysaccharides. – Int. J. Biol. Macromol. 123: 766-774.
[23] Li, H., Nie, D., Wang, C., Fang, J., Li, D. (2016): Anti-osteoporosis activity of *Astragalus membranaceusBunge* extract in experimental rats. – Trop J Pharm Res 15(9): 1897-1901.
[24] Li, M., Xu, Y., Yang, W., Li, J., Xu, X., Zhang, X., Chen, F., Li, D. (2011): In vitro synergistic anti-oxidant activities of solvent-extracted fractions from *Astragalus membranaceus* and *Glycyrrhiza uralensis*. – LWT-Food Sci Technol 44: 1745-1751.
[25] Li, R., Chen, W.-C., Wang, W.-P., Tian, W.-Y., Zhang, X.-G. (2010): Antioxidant activity of Astragalus polysaccharides and antitumour activity of the polysaccharides and siRNA. – Carbohyd Polym 82: 240-244.
[26] Li, X., Qu, L., Dong, Y., Han, L., Liu, E., Fang, S., Zhang, Y., Wang, T. A. (2014): A review of recent research progress on the Astragalus genus. – Molecules 19(11): 18850-18880.
[27] Liu, J., Li, X., Liu, J., Ma, L., Li, X., Fonnebo, V. (2011): Traditional Chinese medicine in cancer care: a review of case reports published in Chinese literature. – Forsch Komplementmed 18(5): 257-263.
[28] Liu, P., Zhao, H., Luo, Y. (2017): Anti-aging implications of *Astragalus membranaceus* (Huangqi): A well-known Chinese tonic. – Aging Dis 8(6): 868-886.
[29] Lu, L., Wang, D.-T., Shi, Y., Yin, Y., Wei, L.-B., Zou, Y.-C., Huang, B., Zhao, Y., Wang, M., Wan, H., Li, C. J., Diao, J.-X. (2013): Atsragalus polysaccharide improves muscle atrophy from dexamethasone-and peroxide-induced injury in vitro. – Int. J. Biol. Macromol 61: 7-16.

http://www.aloki.hu ● ISSN 1589 1623 (Print) ● ISSN 1785 0037 (Online)
DOI: http://dx.doi.org/10.15666/aeer/1706_1337113382

[30] Lu, L., Huang, Y.-F., Chen, D.-X., Wang, M., Zou, Y.-C., Wan, H., Wei, L.-B. (2016): Astragalus polysaccharides decrease muscle wasting through Akt/mTOR, ubiquitin proteasome and autophagy signalling in 5/6 nephrectomised rats. – J Ethnopharmacol 186: 125-135.
[31] Lv, J., Zhang, Y., Tian, Z., Liu, F., Shi, Y., Liu, Y., Xia, P. (2017): Astragalus polysaccharides protect against dextran sulphate sodium-induced colitis by inhibiting NF-κß activation. – Int J Biol Macromol 98: 723-729.
[32] Lysiuk, R., Darmohray, R. (2016): Pharmacology and ethnomedicine of the genus Astragalus. – Int. J. Pharmacol. Phytochem 3: 46-53.
[33] Ma, J., Qiao, Z., Xiang, X. (2011): Aqueous extract of *Astragalus mongholicus* ameliorates high cholesterol diet induced oxidative injury in experimental rat models. – J. Med Plant Res 5: 855-858.
[34] Ma, Y., Liu, C., Qu, D., Chen, Y., Huang, M., Liu, Y. (2017): Antibacterial evaluation of silver nanoparticles synthesized polysaccharides from *Astragalus membranaceus* roots. – Biomed Pharmacother 89: 351-357.
[35] Maresca, M., Micheli, L., Cinci, L., Bilia, A. R., Ghelardin, C., Di, L., Mannelli, C. (2017): Pain relieving and protective effects of *Astragalus hydroalcoholic* extract in rat arthritis models. – J Pharm Pharmacol 1858-1870.
[36] McKenna, D. J., Hughes, K., Jones, K. (2002): Astragalus. – Altern Ther Health Med. 8(6): 34-40.
[37] Nalbantsoy, A., Nesil, T., Yilmaz-Dilsiz, O., Aksu, G., Khan, S., Bedir, E. (2012): Evaluation of the immunomodulatory properties in mice and in vitro anti-inflammatory activity of cycloartane type saponins from *Astragalus species*. – J. Ethnopharmacol 139: 574-581.
[38] Napolitano, A., Akay, S., Mari, A., Bedir, E., Pizza, C., Piacente, S. (2013): An analytical approach based on ESI-MS, LC-MS and PCA for the quali-quantitative analysis of cycloartane derivatives in *Astragalus spp*. – J Pharmaceut Biomed 85: 46-54.
[39] Nartop, P., Gurel, A., Akgun, I. H., Bedir, E. (2015): Astragaloside IV and cycloastragenol production capacity of *Astragalus trojanus Calli*. – Rec. Nat. Prod. 9(1): 49-61.
[40] Nikolov, S. (2006): Astragalus glycyphyllos. – In: Nikolov, S. (ed.), Specializirana enciklopedia na lechebnite rastenia. BAS, Sofia, pp. 317-318.
[41] Nishiyama, N., Wang, Y. L., Saito, H. (1995): Beneficial effects of S-113m, a novel herbal prescription, on learning impairment model in mice. – Biol Pharm Bull 18: 1498-1503.
[42] Ogbaji, P. O., Li, J., Xue, X., Shahrajabian, M. H., Egrinya, E. A. (2018): Impact of bio-fertilizer or nutrient solution on Spinach (*Spinacea Oleracea*) growth and yield in some province soils of P. R. China. – Cercetari Agronomice in Moldova 2(174): 43-52.
[43] Ranjbar, M., Karamian, R. (2002): Astragalus sect. Astragalus (Fabaceae) in Iran: complementary notes with a key to the species. – Nordic. J. Bot. 2: 177-181.
[44] Rios, J. L., Waterman, P. G. (1997): A review of the pharmacology and toxicology of Astragalus. – Phytother. Res. 11: 411-418.
[45] Salducci, M.-D., Folzer, H., Issartel, J., Rabier, J., Masotti, V., Prudent, P., Affre, L., Hardion, L., Tatoni, T., Laffont-Schwob, I. (2019): How can a rare protected plant cope with the metal and metalloid soil pollution resulting from part industrial activities? Phytometabolites, antioxidant activities and root symbiosis involved in the metal tolerance of *Astragalus tragacantha*. – Chemosphere 217: 887-896.
[46] Shahrajabian, M. H., Sun, W., Cheng, Q. (2018): A review of Goji berry (*Lycium barbarum*) in traditional Chinese medicine as a promising organic superfood and superfruit in modern industry. – Academia Journal of Medicinal Plants 6(12): 437-445.
[47] Shahrajabian, M. H., Sun, W., Cheng, Q. (2019a): The influence of traditional Iranian and Chinese medicine on western and Islamic countries. – Asian J. Med. Bio. Res 5(2): 94-99.

http://www.aloki.hu ● ISSN 1589 1623 (Print) ● ISSN 1785 0037 (Online)
DOI: http://dx.doi.org/10.15666/aeer/1706_1337113382

[48] Shahrajabian, M. H., Sun, W., Cheng, Q. (2019b): Modern pharmacological actions of Longan fruits and their usages in traditional herbals remedies. – J. Med. Plants. Stud 7(4): 179-185.
[49] Shahrajabian, M. H., Khoshkharam, M., Zandi, P., Sun, W., Cheng, Q. (2019c): Jujube, a super-fruit in traditional Chinese medicine, heading for modern pharmacological science. – J. Med. Plants. Stud 7(4): 173-178.
[50] Shahrajabian, M. H., Sun, W., Cheng, Q. (2019d): The power of natural Chinese medicine, ginger and ginseng root in an organic life. – Middle East J. Sci. Res 27(1): 64-71.
[51] Shahrajabian, M. H., Sun, W., Cheng, Q. (2019e): Clinical aspects and health benefits of ginger (*Zingiber officianle*) in both traditional Chinese medicine and modern industry. – Acta Agriculturae Scandinavica, Section B-Soil & Plant Science 1-11.
[52] Shahrajabian, M. H., Sun, W., Cheng, Q. (2019f): Traditional Chinese medicine and agriculture; organic life and sustainability for future. – GSC Biol. Pharm. Sci 7(1): 091-095.
[53] Shahrajabian, M. H., Sun, W., Cheng, Q. (2019g): A review of ginseng species in different regions as a multipurpose herb in traditional Chinese medicine, modern herbology and pharmacological science. – J Med. Plants Res 13(10): 213-226.
[54] Shahrajabian, M. H., Khoshkharam, M., Sun, W., Cheng, Q. (2019h): The effect of pretreatment factors on seed germination and seedling growth of anise (*Pimpinella anisum* L.). – Middle East J. Sci 5(1): 86-93.
[55] Shahrajabian, M. H., Khoshkharam, M., Zandi, P., Sun, W., Cheng, Q. (2020): The influence of temperatures on germination and seedling growth of pyrethreum (*Tanacetum cineraiifolium*) under drought stress. – International Journal of Advanced Biological and Biomedical Research 8(1): 29-39 (in press).
[56] Shahzad, M., Shabbir, A., Wojcikowski, K., Wohlmuth, H., Gobe, G. C. (2016): The Antioxidant Effects of Radix Astragali (*Astragalus membranaceus* and Related Species) in Protecting Tissues from Injury and Disease. – Curr Drug Targets 17: 1331-1340.
[57] Shannon, D. A., Wang, M., Kemppainen, B., Mitchell, C. C., Salmasi, S. Z. (2014): Adaptation of *Astragalus membranaceus* varieties to Southeastern United States: growth, root development and Astragaloside IV content. – J. Med. Plants. Stud 2(3): 80-91.
[58] Shen, H.-H., Wang, K., Li, W., Ying, Y.-H., Gao, G. X., Li, X.-B., Huang, H.-Q. (2008): *Astragalus membranaceus* prevents airway hyperreactivity in mice related to Th2 response inhibition. – J Ethnopahrmacol 116: 363-369.
[59] Sheng, B. W., Cheng, H. F., Zhao, J., He, D. L., Nan, X. Y. (2005): *Astragalus membranaceus* reduces free radical-mediated injury to renal tubules in rabbits receiving high-energy shock waves. – Chinese Medic J (England) 118: 43-49.
[60] Soleymani, A., Shahrajabian, M. H. (2012): Response of different cultivars of fennel (*Foeniculum vulgare*) to irrigation and planting dates in Isfahan, Iran. – Res Crops 13(2): 656-660.
[61] Soleymani, A., Shahrajabian, M. H. (2018): Changes in germination and seeding growth of different cultivars of cumin to drought stress. – Cercetari Agronomice in Moldova 1(173): 91-100.
[62] Song, J., Lee, D., Min, B., Bae, J.-S., Chang, G. Y., Kim, H. (2017): Safety evaluation of Astragalus extract mixture HT042 and its constituent herbs in Sprague-Dawley rats. – Phytomedicine 32: 59-67.
[63] Song, J. Z., Yiu, H., Qiao, C. F., Han, Q. B., Xu, H. X. (2008): Chemical comparison and classification of Radix Astragali by determination of isoflavonoids and astragalosides. – J. Pharm. Biomed. Anal. 47: 399-406.
[64] Sun, W.-Y., Wang, L., Liu, H., Li, X., Wei, W. (2012): A standardized extract from Paeonia lactiflora and *Astragalus membranaceus* attenuates liver fibrosis induced by porcine serum in rats. – Int J Mol Med 29: 491-498.

http://www.aloki.hu ● ISSN 1589 1623 (Print) ● ISSN 1785 0037 (Online)
DOI: http://dx.doi.org/10.15666/aeer/1706_1337113382

[65] Sun, W., Shahrajabian, M. H., Qiman, H. (2020): Soybean seeds treated with single walled carbon naotubes (SwCNTs) showed enhanced drought tolerance during germination. – International Journal of Advanced Biological and Biomedical Research 8(1): 9-16 (in press).
[66] Takagi, K., Ishii, Y. (1967): Peptic ulcer inhibiting properties of a new fraction from licorice root (FM100). 1. Experimental peptic ulcer and general pharmacology. – Arzneimittel-Forschung 17(12): 1544-1547.
[67] Tian, H., Lu, J., He, H., Zhang, L., Dong, Y., Yao, H., Feng, W., Wang, S. (2016): The effect of Astragalus as an adjuvant treatment in type 2 diabetes mellitus: A (preliminary) meta-analysis. – J Ethnopahrmacol 191: 206-215.
[68] Toshkova, R. A., Krasteva, I. N., Wesselinova, D. W., Nikolov, S. D. (2007): Influence of purified saponin mixture from *Astragalus corniculatus Bieb*. On phagocytic cells in Graffi-tumor bearing hamsters. – J Ethnopharmacol 109: 394-399.
[69] Tutin, T. G., Heywood, V. H., Burges, N. A., Mooze, D. M., Valeutine, D. H., Walters, S. M., Webb, D. A. (1972): Flora Europea. Vol. 2. – Cambridge University Press, Cambridge, pp. 108-124.
[70] Valenzuela, H. F., Fuller, T., Edwards, J., Finger, D., Molgora, B. (2009): Cycloastragenol extends T cell proliferation by increasing telomerase activity. – J. Immunol 182: 90-30.
[71] Wang, Y. P., Li, X. Y., Song, C. Q., Hu, Z. B. (2002): Effect of astragaloside IV on T, B lymphocyte proliferation and peritoneal macrophage function in mice. – Acta Pharmacol. Sin. 23: 263.
[72] Wang, Z.-B., Wang, Q.-Y. (2013): Cultivating erect milkvetch (*Astragalus adsurgens Pall*.) (Leguminosae) improved soil properties in loess hilly and gullies in China. – J. Integr. Agric 12(9): 1652-1658.
[73] Wei, D. X., Yu, N. Z., Ya, O. Z. (2011): Traditional Chinese medicines in treatment of patients with type 2 diabetes mellitus. – Evidence-Based Complementary and Alternative Medicine Article ID 726723.
[74] Wong, R. W., Rabie, B., Benedus, M., Hagg, U. (2007): The effects of *Rhizoma Curculiginis* and *Astragalus membranaceus (Fisch.)* Bunge. extracts on bones. – J Chi. Med. 2: 13-14.
[75] Wu, F., Chen, X. (2004): A review of pharmacological study on *Astragalus membranaceus (Fisch) Bge*. – Zhong Yao Cai 27: 232-234.
[76] Wu, Y., Ou-Yang, J.-P., Wu, K., Wang, Y., Zhou, Y.-F., Wen, C.-Y. (2005): Hypoglycemic effect of Astragalus polysaccharide and its effect on PTP1B[1]. – Acta Pharm Sin 26(3): 345-352.
[77] Xi, M., Hai, C., Tang, H., Fang, K., Liang, X. (2008): Antioxidant and antiglycation properties of total saponins extracted from traditional Chinese medicine used to treat diabetes mellitus. – Phytother. Res. 22(2): 228-237.
[78] Yaal-Hahoshen, N., Maimon, Y., Siegelmann-Danieli, N., Lev-Ari, S., Ron, I. G., Sperber, F., Samuels, N., Shoham, J., Merimsky, O. (2011): A prospective, controlled study of the botanical compound mixture LCS101 for chemotherapy-induced haematological complications in breast cancer. – Oncologist 16(9): 1197-1201.
[79] Yan, H., Xie, Y., Sun, S., Sun, X., Ren, F., Shi, Wang, S., Zhang, W., Li, X., Zhang, J. (2010): Chemical analysis of *Astragalus mongholicus* polysaccharides and antioxidant activity of the polysaccharides. – Carbohydrate Polymers 82: 636-640.
[80] Yang, B., Xiao, B., Sun, T. (2013): Antitumor and immunomodulatory activity of *Astragalus membranaceus* polysaccharides in H22 tumor-bearing mice. – Int J. Biol Macromol 62: 287-290.
[81] Yang, M., Lin, H.-B., Gong, S., Chen, P.-Y., Geng, L.-L., Zeng, Y.-M., Li, D.-Y. (2014): Effect of Astragalus polysaccharides on expression of TNF-α, IL-1βand NFATc4 in a rat model of experimental colitis. – Cytokine 70: 81-86.

http://www.aloki.hu ● ISSN 1589 1623 (Print) ● ISSN 1785 0037 (Online)
DOI: http://dx.doi.org/10.15666/aeer/1706_1337113382

[82] Yang, X., Huang, S., Chen, J., Song, N., Wang, L., Zhang, Z., Deng, G., Zheng, H., Zhu, X.-Q., Lu, F. (2010): Evaluation of the adjuvant properties of *Astragalus membranaceus* and *Scutellaria baicalensis GEORGI* in the immune protection induced by UV-attenuated Toxoplasma gondii in mouse models. – Vaccine 28: 737-743.

[83] Yesilada, E., Bedir, E., Calis, I., Takaishi, Y., Ohmoto, Y. (2005): Effects of triterpene saponins from Astragalus species on in vitro cytokine release. – J. Ethnopharmacol 96: 71-77.

[84] Yin, G., Jeney, G., Racz, T., Xu, P., Jun, X., Jeney, Z. (2006): Effect of two Chinese herbs (*Astragalus radix* and *Scutellaria radix*) on non-specific immune response of tilapia Orechromis niloticus. – Aquaculture 253: 39-47.

[85] Yin, G., Ardo, L., Thompson, K. D., Adams, A., Jeney, Z., Jeney, G. (2009): Chinese herbs (*Astragalus radix* and *Ganoderma lucidum*) enhance immune response of carp, Cyprinus carpio, and protection against *Aeromonas hydrophila*. – Fish Shellfish Immunol 26: 140-145.

[86] Zhang, J., Xie, X., Li, C., Fun, P. (2009): Systematic review of the renal protective effect of *Astragalus membranaceus* (root) on diabetic nephropathy in animal models. – J. Ethnopharmacol 126: 189-196.

[87] Zhang, L. J., Liu, H. K., Hsiao, P. C., Kuo, L. M., Lee, I. J., Wu, T. S., Chiou, W. F., Kuo, Y. H. (2011): New isoflavonoid glycosides and related constituents from Astragali Radix (*Astragalus memberanaceus*) and their inhibitory activity on nitric oxide production. – J. Agric. Food Chem. 59: 1131-1137.

[88] Zhang, X., Sun, Y. G., Cheng, M. C., Wang, Y. Q., Xiao, H. B., Liang, X. M. (2007): Simultaneous quantification of three isoflavonoid glyconsides in rabbit plasma after oral administration of *Astragalus mongholicus* extract by high-performance liquid chromatography coupled with electrospray. – Anal Chim Acta 602: 252-258.

[89] Zhang, Y., Li, X., Ruan, J., Wang, T., Dong, Y., Hao, J., Liu, E., Han, L., Gao, X., Wang, T. (2016): Oleanane type saponins from the stems of *Astragalus membranaceus (Fisch.) Bge*. Var. mongholicus (Bge.) Hsiao. – Fitoterapia 109: 99-105.

[90] Zhao, L. H., Ma, Z. X., Zhu, J., Yu, X. H., Weng, D. P. (2011): Characterization of polysaccharide from *Astragalu radix* as the macrophage stimulator. – Cell Immunol 271(2): 329-334.

[91] Zhong, R. Z., Yu, M., Liu, H. W., Sun, H. X., Cao, Y., Zhou, D. W. (2012): Effects of dietary Astragalus polysaccharide and *Astragalus membranaceus* root supplementation on growth performance, rumen fermentation, immune responses, and antioxidant status of lambs. – Anim Feed Sci Tech 174: 60-67.

[92] Zhou, K., Mei, X. Y. (2014): Study on preventive and therapeutic effects of *Astagali radix* on denervated tibial muscle atrophy in rats. – Zhongguo Zhong Yao Za Zhi 39: 1083-1087.

[93] Zhou, R., Chen, H., Chen, J., Chen, X., Wen, Y., Xu, L. (2018): Extract from *Astragalus membranaceus* inhibit breast cancer cells proliferation via PI3K/AKT/mTOR signalling pathway. – Complement Altern Med 18: 83.

[94] Zhu, B., Yi, L.-X., Hu, Y.-G., Zeng, Z.-H., Tang, H.-M., Yang, G.-L., Xiao, X.-P. (2012): Effects of Chinese Milk Vetch (*Astragalus sinicus L.*) residue incorporation on CH_4 and N_2O emission from a double-rice paddy soil. – J. Integr. Agric 11(9): 1537-1544.

http://www.aloki.hu ● ISSN 1589 1623 (Print) ● ISSN 1785 0037 (Online)
DOI: http://dx.doi.org/10.15666/aeer/1706_1337113382

PARASITIC ACTIVITY OF POWDERY MILDEW (PATHOGEN STRAIN HMLAC226) ON PROSTRATE KNOTWEED (*POLYGONUM AVICULARE* L.) AT VARIOUS LOCATIONS OF SHENYANG, NORTHEAST CHINA

IQBAL, M. F.[1,2] – FENG, Y. L.[1*] – LIU, M. C.[1] – LU, X. R.[1] – NASIR, M.[3] – SIKANDAR, A.[4]

[1]*College of Bioscience and Biotechnology, Shenyang Agricultural University No. 120 Dongling Road, Shenyang, Liaoning Province 110866, China*

[2]*Department of Agriculture, Adaptive Research Farm, Gujranwala, Punjab, Pakistan*

[3]*Plant Protection Department, Institute of Cotton Research, CAAS, Anyang, Henan, China*

[4]*Nematology Institute of Northern China, No. 120 Dongling Road, Shenyang, Liaoning Province 110866, China*

**Corresponding author*
e-mail: yl_feng@tom.com; phone: +86-24-8848-7163; fax: +86-24-8849-2799

(Received 13th Jun 2019; accepted 28th Aug 2019)

Abstract. Prostrate knotweed (*Polygonum aviculare* L.) is a persistent native weed of China. This weed is characterized by high genetic and biological plasticity having a capacity to spread on a landscape scale. The present study planned to investigate the infection of a plant parasitic powdery mildew on *P. aviculare* on a landscape scale in three different locations of Shenyang during 2018. These locations were selected with a control treatment for proper comparison. Different growth parameters were observed and calculated by coefficient of determination (R^2). Maximum temperature (Maxt) ranged 25-30 °C and Minimum temperature (Mint) between 17-20 °C with relative humidity 64-78% played a vital role for the emergence and flourishing of pathogen pressure on the plant. The elevated value of $R^2 = 0.97$ for Mint with *RMSE* (Root Mean Square Error) < 5 recorded excellent prediction followed by $R^2 = 0.82$ with RMSE < 5-10 for Maxt recorded very good model prediction. Highly significant ($P < 0.001$) height of *Polygonum aviculare* was recorded (23.125 ± 0.59) in parasite free plants compared to (20.99 ± 0.96) location-I having Mean ± SD. Both temperature ranges has a significant effect ($P < 0.0001$) with ($F = 5.917$; $P < 0.0001$; $F = 25.721$; $P < 0.0001$) three locations; however, the effect of the locations on plants height (*P. aviculare*) did not differ statistically ($F = 2.102$; $P > 0.05$) between two temperature ranges from 25-30 °C and 17-20 °C. According to our findings, plant parasitic powdery mildew (pathogen strain HMLAC226) affected significantly with growth characteristics of prostrate knotweed.
Keywords: *ecology, landscape, native plant, transect method, Liaoning-Province*

Introduction

Prostrate knotweed (*Polygonum aviculare* L.) is an annual native weed to Europe, introduced in China during 2004 (Coquillat, 1951; Flora, 2004; Ma et al., 2013), initially collected in Canada in 1821 and widespread in the globe (Costea and François, 2005). Its extensive distribution is credited to elevated genetic polymorphism and phenotypic agility (Meerts, 1995) and spread in soyabean, rice, maize, sweet potato, cotton, sugarcane, orchards and other agricultural crops (Tottman and Wilson, 1990). This weed grows in poorly aerated heavy compacted soil with 3.5 pH (You et al., 2005). *P. aviculare* L. belongs to Polygonaceae family grow up to 30.50-91 cm long with tiny elliptic lanceolate

http://www.aloki.hu ● ISSN 1589 1623 (Print) ● ISSN 1785 0037 (Online)
DOI: http://dx.doi.org/10.15666/aeer/1706_1338313394

foliage. Its foliage is opposite, lance form to rectangle and 12.50-63.50 mm elongated, silver, papery casing at every nodule, flowers are present in the groups in clusters (Severoglu et al., 2012). Due to its taproot system, the roots of full-grown plants reached up to 70 cm in alluvial soils. However, thick parallel inferior roots were dispersed in the upper segment (15-25 cm) of soil (Costea and François, 2005).

Prostrate knotweed seeds require moist-cold stratification for germination (Batlla et al., 2009). The seeds of this weed lose dormancy in March and April and germinate in a single flush between March and May. Its flowers are hermaphroditic and self pollinated (Meerts et al., 1990). In California, more than 36 insect taxa were documented to feed on the nectar of this weed; however, both above ground and terrestrial insects were attracted on the flowers (Bugg et al., 1987).

Recently many studies that endeavour to work out the fiscal worth of the ecosystem services provided by plant life have paid their attention on both native and deliberately cultured landscapes floral communities (Bolund et al., 1999; Chen et al., 2008; Tyrväinen et al., 2005). Now the ecologists approach to understand that an assessable level of ecological functionality can be accomplished by a sophisticated collection of species (Hobbs et al., 2009; Pickett et al., 2008). At the functional level, natural urban flora can be measured and prolonged in the logic that it is performing an extensive assortment of experimental ecosystem services on subsidiary terra firma with a negligible contribution of continuation possessions (Rink, 2009; Del and Peter, 2010).

Powdery mildews (*Erysiphe polygoni*; Erysiphales family Erysiphaceae) are significant cluster of fungi, capable for causing diseases in natural flora. This pathogen has 873 species with 17 genera (Braun, 2012) attack on 10,000 species of angiosperms in the world (Braun, 2012). The most imperative, key pervasive and easily predictable invasive pathogen of prostrate knotweed (*P. Aviculare*) is powdery mildew (*Erysiphe polygoni*), strain HMLAC226, gene JN621872 through DQ490766 ITS sequence present in Mengyin, Shandong, China (Pintye et al., 2012). The attack symptoms are grayish-white, powdery mat visible on the upper surface of leaves (Abkhoo, 2009). The pathogen reduce photosynthesis, increase respiration, transpiration, and or caused the growth retarded (Severoglu et al., 2012).

The fungal spores shifted through air to the newly introduced host plant and its growth started on epidermal cells of the leaf by means of haustoria (Carlile et al., 2001) and put the haustoria into mesophyll cells of prostrate knotweed (Takamatsu et al., 1998). However, moderate temperature and humidity (%) played a significant role for flourishing and spreading pathogen infection (Koike et al., 2007) that becomes the base of significant loss to the landscape of China.

The article aimed to determine parasitic powdery mildew (pathogen strain HMLAC226) on certain physiological characteristics of prostrate knotweed. These characteristics studied at different temperatures ranges and in various locations of Shenyang using determination coefficient (R^2) and Root Mean Square Error (*RMSE*) under Liaoning Key Laboratory for Biological Invasions and Global Changes, College of Bioscience and Biotechnology, Shenyang Agricultural University, Shenyang China.

Materials and methods

Experimental site

The studied areas northern part in China having the hilly area that edges into South Korea. During survey we selected three locations randomly (location I having latitude

http://www.aloki.hu ● ISSN 1589 1623 (Print) ● ISSN 1785 0037 (Online)
DOI: http://dx.doi.org/10.15666/aeer/1706_1338313394

41°49.490 N and longitude = 123° 35.397 E; location II having latitude 41°48.851N and longitude = 123° 33.464 E; location III having latitude 41°49.760 N and longitude = 123° 34.141 E) respectively (*Fig. 1B*). Maximum annual temperature (Maxt) ranges between (8.30 to 36.10 °C) and minimum (Mint) -32.90 to 12.40 °C but the annual rainfall was 698.5 mm with relative humidity 62-78% (*Fig. 1A*).

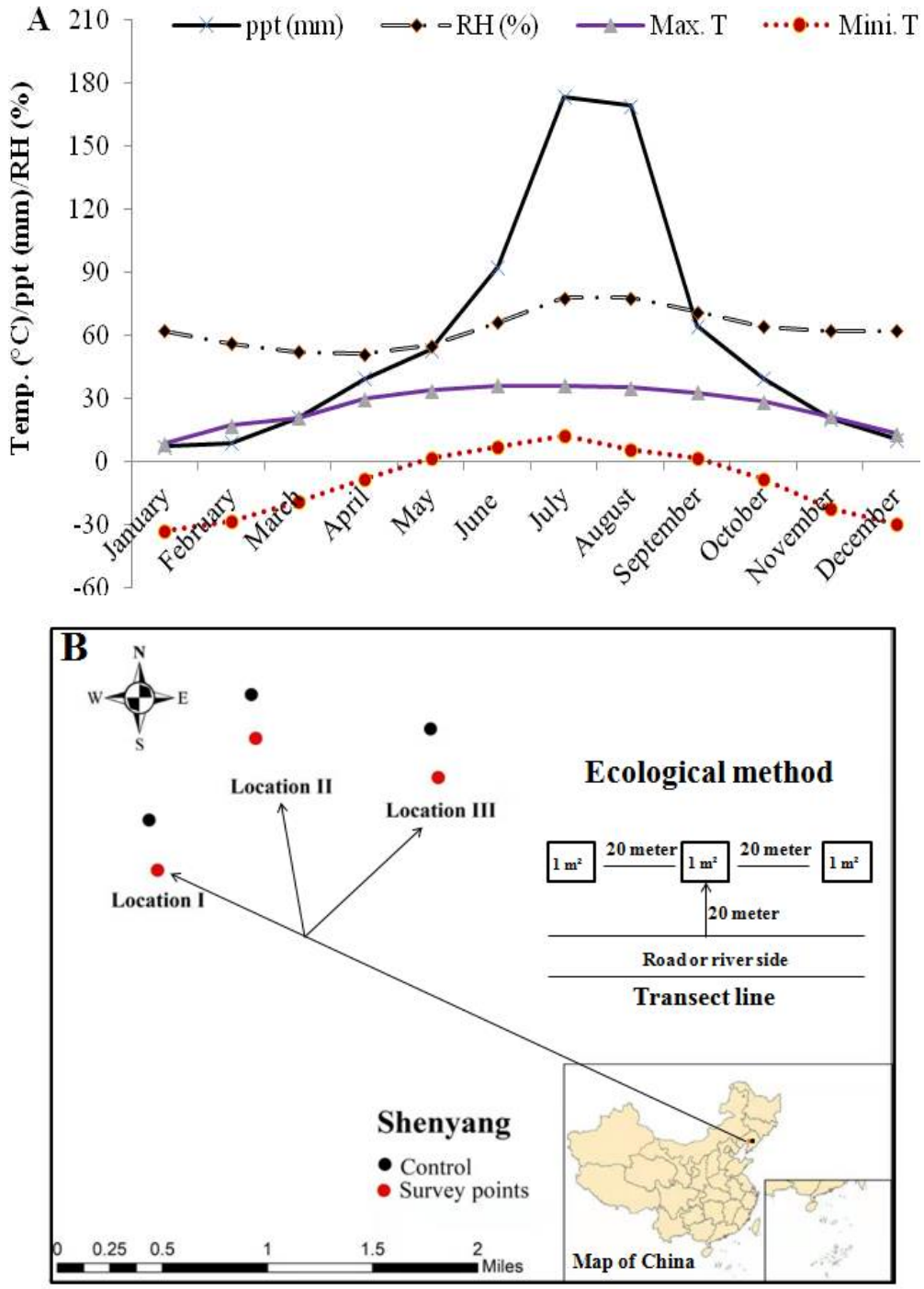

Figure 1. *(**A**) Monthly climatic data of Shenyang for the year 2018 (data sourced from Chinese meteorological data base). (**B**) Three studied locations and control was the average of these three locations using mapping software ESRI (ArcGis, 2013) and 1 m^2= one square meter*

http://www.aloki.hu ● ISSN 1589 1623 (Print) ● ISSN 1785 0037 (Online)
DOI: http://dx.doi.org/10.15666/aeer/1706_1338313394

Experimental design

Ecological survey was conducted in three locations of Shenyang by line transect ecological method of sampling in field conditions during 2018. During ecological survey in July, prostrate knotweed leaves infected with powdery mildew (*Erysiphe polygoni*) and its pathogen strain HMLAC226 was selected. The transect line was sixty meter long parallel to the roadside and collected three points twenty meters in one side of the transect (*Fig. 1B*) and data were recorded using quadratic methods (100 × 100 cm). Control point was also selected in these three locations having three replications at each location in same environmental cues. The selected surveyed points were observed during peak season for three weeks and temperature data were recorded on the spot and calculated. However, after collection of the temperature data from three locations, maximum and minimum temperature was calculated. Three whole knotweed plants in each quadratic ring were selected randomly and uprooted keeping in view no any part of the plant was damaged by external or physical injury. A sum total of nine plants collected from three quadratic rings from each sampling point, uprooted along with control plants or pathogen free plants (selected from close observations), taken in the laboratory for measuring its growth parameters and other characteristics. Control plants were the average of disease free plants collected within three locations. The initial pathogen symptoms were present on the leaves just like dusted flour. Powdery mildew usually starts off as circular, powdery white spots, which can appear on leaves, stems of the plant. However, control plants or pathogen free plants were selected from the same environmental conditions near to the infected community of knotweed populations.

Pathogen identification

Powdery mildew-infected leaves of *P. aviculare* from these three locations and examined under microscope under microscope (Olympus DP 80 model) with the magnification of 20 µm and 200 µm. The spore slides were prepared using cedar wood oil (artificial, Shanghai specimen model factory, China) which was pale-yellow to yellow in color. The drops solution of this oil was xylene based with acid value < 60 mg KOH g^{-1} was used and identified the pathogen with the help of available literature (Braun, 1987; Braun and Takamatsu, 2000; Braun et al., 2003) on morphometric characteristics of the pathogen (*Fig. 2*).

Growth parameter measurement

Plant height (cm), root length (cm), number of lateral and main branches was measured; however, all leaves were removed separately from randomly selected nine plants from each sampling point. The leaf area was measured by destructive method (Ahmad et al., 2015; Aldesuquy et al., 2014).

Re-modification of the evolving model

The regression-type relationship carried out for developing the model for treatments and comparison of RMSE with R^2. The regression model was set out to determine the effect of different growth parameters ultimately gave the information about model fitness of how far away the fitted line is from the reference line. The researchers previously exposed that how condensed or scattered the observed points are around the fitted line, which alternatively revealed about the validity and good-fit of the model

http://www.aloki.hu ● ISSN 1589 1623 (Print) ● ISSN 1785 0037 (Online)
DOI: http://dx.doi.org/10.15666/aeer/1706_1338313394

(Hossain et al., 2017). For the evaluation of different growth parameters in an experiment with n observations and agreement between predicted and actual values was purposed with root mean square error (RMSE) that was defined by *Equation 1* (Debaeke et al., 1997; Ahmed et al., 2019).

$$RMSE = \sqrt{1/n \times \sum_{j=1}^{n} ((Yield_{mes} - Yield_{sim})^2} \quad \text{(Eq.1)}$$

Where n is the number of observations, $yield_{mes}$ represents actual cumulative percent, $yield_{sim}$ is predicted cumulative percentage (Mayer and Butler, 1993). RMSE gave a magnitude of the characteristic variation between predicted and actual values. The RMSE categorized to assess the precision of the model (Royo et al., 2010) reported that RMSE < 5 means awesome prediction; 5-10, very good prediction; 10-15, good prediction; > 15, inadequate prediction. The lowest RMSE designated the appearance of the model fitness had optimized.

Statistical analyses

The above ecological indices were focused on analysis of variance through invasion condition at different locations with analysis of variance (ANOVA) test. The mean differences between locations growth characters were calculated using Tukey's HSD (Honest Significance Test), post hoc on Fishers's LSD test, these tests were performed using SPSS statistical software (version 13.0; Inc., Chicago, IL, USA) and R (version 3.3.1) package (Nigussie et al., 2017; Rcore, 2016). The geographic coordinates were recorded using GPS navigator and map of the studied locations was designed by ArcGIS version 10.2 software (ArcGis, 2013).

Results

The data recorded highly significant ($P < 0.001$) plant height of *P. aviculare* in uninfected powdery mildew control ($23.125 + 0.59$) compared to (20.99 ± 0.96) location-I, location-II (19.42 ± 0.53) having Mean ± SD. Statistically highly significant ($P < 0.0001$) root length (cm) was recorded in control treatment (21.08 ± 0.40) comparable with location-I (18.87 ± 0.80) recording significant result ($P < 0.01$). Leaf area (cm^2), number of main branches and number of lateral branches differed significantly ($P < 0.01$) in control compared to other but illustrated non-significant ($P > 0.05$) result with rest of locations at Shenyang (*Table 1*). The experiment deliberated that the effectiveness of powdery mildew (*Erysiphe polygoni*) significantly reduced the plant height, root length, leaf area and lateral branches significantly; but do not differ statistically with main branches of the selected prostrate knotweed (*P. aviculare*).

Different growth parameters calculated by co-efficient of determination (R^2). The studied maximum temperature (Maxt) ranged 25-30 °C, minimum temperature (Mint) between 17-20 °C with relative humidity 64-78% was played a significant role for the emergence and flourishing of pathogen pressure on the plant; however, elevated value of $R^2 = 0.97$ for Mint with RMSE < 5 recording awesome model prediction followed by $R^2 = 0.82$ with RMSE < 5-10 for Maxt recording very good model prediction (*Table 2*).

http://www.aloki.hu ● ISSN 1589 1623 (Print) ● ISSN 1785 0037 (Online)
DOI: http://dx.doi.org/10.15666/aeer/1706_1338313394

Table 1. *Effect of different growth parameters of Polygonum aviculare L. at different locations*

Weed	Plant height (cm)	Root length (cm)	Leaf area (cm^2)	Main branches	Lateral branches
Control	23.125 ± 0.59^a	21.08 ± 0.40^a	2.71 ± 0.31^a	7.63 ± 0.74^a	3.38 ± 0.52^a
Location-I	20.99 ± 0.96^b	18.87 ± 0.80^b	2.42 ± 0.14^b	7.00 ± 0.76^a	2.50 ± 0.53^b
Location-II	19.42 ± 0.53^c	16.18 ± 1.00^c	2.32 ± 0.14^b	6.88 ± 0.64^a	2.50 ± 0.53^b
Location-III	19.84 ± 1.00^c	16.26 ± 1.04^c	2.30 ± 0.15^b	7.38 ± 0.52^a	2.63 ± 0.52^b
C. V.	0.57	2.24	0.003	0.016	-0.03
S.E.	0.217	0.336	0.050	0.133	0.104
LSD	$P < 0.001$	$P < 0.001$	$P < 0.01$	$P > 0.05$	$P < 0.05$

C.V. = component variance; the same letter do not differ statistically from each other at 5% significance level ($P > 0.05$); however, means having different letters indicated statistically significant result ($P < 0.05$) or ($P < 0.01$) or ($P < 0.001$), LSD = least significant Difference; (mean ± SD), S. D. = standard deviation, S.E. = standard error

Table 2. *Regression model for growth parameter of Polygonum aviculare L. showing comparison of co-efficient determination (R^2) with RMSE during 2018*

Weed	Regression model	R^2	RMSE
Prostrate knotweed (*P. aviculare L.*)	PH = -0.5769 x H + 21.24	0.50	20.17
	Rl = -1.5488 x R + 22.482	0.42	51.16
	LA = 7.4975 x A + 0.5067	0.35	26.94
	Mb = 0.1875 x M + 6.7083	0.52	1.75
	Lb = 0.0625 x L + 2.4167	0.75	0.11
	Maxt. (°C) = 0.93 x Ma + 26.069	0.82	8.55
	Mint. (°C) = 1.4375 x Mi + 15.547	0.97	4.28

PH = plant height; Rl = root length; LA = leaf area; Mb = number of main branches; Lb = number of lateral branches; Maxt = maximum temperature; Mint = minimum temperature; R^2 = coefficient of determination; RMSE = root mean square error

However, the value of $R^2 = 0.75$ with RMSE = 0.11 described strong model fitting in the experiment. The polynomial relationship for number of main branches also displayed a linear arc pattern which strung with an initial linear stage followed by moderate asymptotic trend at the growth stage by R^2 (0.52) with RMSE (1.75) indicated the good model prediction. The values more than 15 indicated insufficient prediction of the model fitness. Maximum, minimum temperature was effecting significantly ($F = 5.917$; $P < 0.0001$; $F = 25.721$; $P < 0.0001$); however, the interaction between location with height of the *P. aviculare* did not differ statistically ($F = 2.102$; $P > 0.05$) between two temperature ranges from 25-30 °C and 17-20 °C (*Table 3*). The root length of the *P. aviculare* was affected highly significant ($F = 54.41$; $P < 0.0001$) with height and locations showed its plasticity but there interaction (PH x L) to total variance was strongly trait specific recording non-significant result ($F = 3.796$; $P > 0.05$).

The plant height was recorded significant result ($F = 3.796$; $P < 0.05$) with leaf length; however, plant height showed high significant ($F = 7.900$; $P < 0.001$) result with location. The interaction between leaf length and location (Ll × L) with height ($F = 0.579$; $P > 0.05$) did not correlated statistically; however, it was also a trait specific.

http://www.aloki.hu ● ISSN 1589 1623 (Print) ● ISSN 1785 0037 (Online)
DOI: http://dx.doi.org/10.15666/aeer/1706_1338313394

Table 3. *Analysis of variance of the interaction of maximum, minimum temperature, with location, plant height, leaf length of P. aviculare on four locations during 2018*

Parameter	Source	d.f.	MS	*F*
Maxt	Location (L)	2	10.778	5.917***
	Plant height (PH)	1	3.828	2.102NS
	L x PH	2	1.514	0.831NS
Mint	L	2	18.111	25.721***
	PH	1	0.193	0.274NS
	L x PH	2	0.399	0.567NS
Rl	PH	1	66.82	54.141***
	L	2	20.18	16.353***
	PH x L	2	1.13	0.912NS
PH	Ll	1	2.483	3.796*
	L	2	5.167	7.900**
	Ll x L	2	0.379	0.579NS

The range of maximum temperature = Maxt. was 25-30 °C and minimum temperature = Mint. was 17-20 °C; location = L; plant height = H; Leaf length = Ll in northeast regions. For each effect, we show the mean square (MS); degree of freedom (DF); F and P value. Significance level is P > 0.05

The fresh leaves infected with powdery mildew scrapped off gently into small pieces. These infected leaves were examined under microscope. In our study, the first symptoms visible as powdery white scraps on the upper portion of foliage further developed to plentiful hyphal development on the upper and lower sides of the leaves (*Fig. 2a*). Infected leaves become chlorotic with warped periphery resulted in early defoliation. Hyphal appressoria were well developed, lobed (*Fig. 2d*) and present in opposed pairs (*Fig. 2*).

Cleistothecium was emerged and conidiophores appeared cylindrical and appressorium was observed and identified on 200 µm (*Fig. 2c, 2d*). The cells of conidiophores formed in a round straightway in shape. The conidia produced in the single oval-shaped round to oblong. Germ tubes recorded in the perihilar portion of conidia and identified with 20 µm magnification under microscope (*Fig. 2b*).

Discussion

The study regarding parasitic activity of powdery mildew (*Erysiphe polygoni* L.) having its pathogen strain HMLAC226 recorded on native prostrate knotweed (*Polygonum aviculare* L.) investigated best prediction model of coefficient of determination (R^2). These results correlated with previously explicated investigations that leaf area measured in grassland exposed good performance $R^2 = 0.88$ with RMSE = 0.96 (Francone et al., 2014).

Our results were in accordance to the researchers who reported that stable temperature models were accustomed to predict the evolution under changing temperatures. However, the pathogen development pressure reduced quickly at elevated temperatures than at lower temperatures comparable to optimum temperature (Xu, 1999).

http://www.aloki.hu ● ISSN 1589 1623 (Print) ● ISSN 1785 0037 (Online)
DOI: http://dx.doi.org/10.15666/aeer/1706_1338313394

The temperature effect in this experiment are in line with the researchers who reported in their experiments that the prevalence of powdery mildew propelled by moderate temperatures (21-30 °C). Elevated temperatures can delay or stop the growth and spore formation of *Erysiphe*. Vulnerability of times depleted increases with elevated temperature, maximum temperature ranged between 22-27 °C played a vital role for the germination of conidia (Peduto et al., 2013).

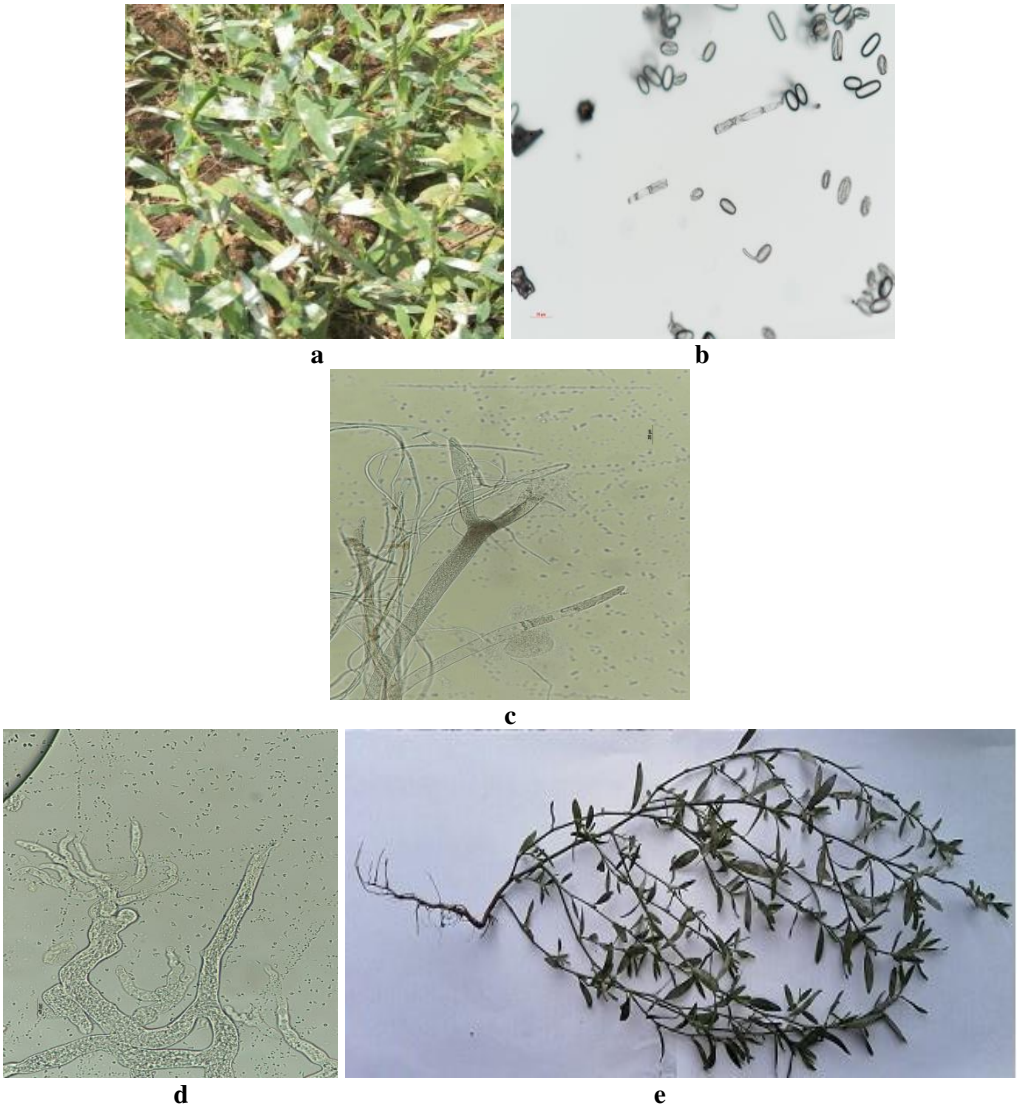

Figure 2. *Different stages of powdery mildew infection on Polygonum aviculare a. Infection; b. germ tube; c. Cleistothecium, Conidiophore; d. Appressorium; e. Healthy plant*

Exclusive growth models were fit to the expansion rate data with high significance value (Miller et al., 2003). As well as lower rate of development, supra-optimal temperatures resulted in higher spores mortality and faster rate at which leaves become resistant due to faster host growth than lower temperatures. This was the most likely explanation of the results obtained from inoculated plants exchanged between 20-30 °C (Xu, 1999).

http://www.aloki.hu ● ISSN 1589 1623 (Print) ● ISSN 1785 0037 (Online)
DOI: http://dx.doi.org/10.15666/aeer/1706_1338313394

Our morphological results were in accordance with the researchers who reported that the spores of fungi present on the inoculated plants were similar in morphology compared to examine by diseased plants, fulfilling the Koch's postulates (Han et al., 2016). Prostrate knotweed (*E. polygoni*) is well known fungi distributed in the United States, Europe (United Kingdom, Czech Republic, Romania, Finland, and the former the Soviet Union), and China, Taiwan, Nepal, India (Lebeda et al., 2007) and Korea (Han et al., 2016). This study is in accordance with the investigations that powdery mildew was cosmopolitan and showed plant parasitic properties for angiosperm plants. Some species of *E. polygoni* are harmful specifically in agriculture and caused economic damage (Severoglu and Ozyigit, 2012); however, some may use as biological control agents (BCA's) on native and invasive weeds.

The Chinese climates vary from region to region with different ecological conditions and temperature fluctuates haphazardly resulted pathogen pressure can be increased. Our study was focused on prostrate knotweed (*Polygonum aviculare* L.), a plant parasitic powdery mildew (*E. polygoni*) investigated at roadsides, gardens and landscape range. This is a preliminary systematic study was conducted to identify powdery mildew in its conidial morphological states on prostrate knotweed and study its growth parameters compared to control. During field survey the infection of *E. polygoni* was observed on *Rumex acetosa*, *Plantago asiatica*, *Syringa oblata* and *Taraxacum mongolicum* which may become promising candidate for biological control agent (BCA's) in future.

Conclusion

Powdery mildew pathogen strain HMLAC226 is an important emerging parasitic agent of prostrate knotweed (*P. aviculare*) widespread as serious disease throughout the world. The symptom of this disease appeared with favorable environmental conditions demonstrated significant damage to the leave tissues. Maximum 25-30 °C and minimum temperature 17-20 °C along with 64-78% relative humidity are most conducive for pathogen establishment. According to the above analysis and findings, we encouraged researchers and ecologists to explore plant-pathogen interaction mechanism, resistance mechanism, host specificity test and genetic diversity in future.

Acknowledgements. This study was supported by the National Key R&D Program of China (2017YFC1200101), the National Natural Science Foundation of China (31470575, 31670545 and 31971557).

Author's contributions. All authors have contributed equally to this paper.

Conflict of interests. All authors declare no conflict of interests.

REFERENCES

[1] Abkhoo, J. (2009): Powdery mildews causing fungi in Iran. – Mycopath 13: 51-55.
[2] Ahmad, S., Ali, H., Ur Rehman, A., Khan, R. J. Z., Ahmad, W., Fatima, Z., Abbas, G., Irfan, M., Ali, H., Khan, M. A. (2015): Measuring leaf area of winter cereals by different techniques: A comparison. – Pak. J. Life Soc. Sci 13: 117-125.
[3] Ahmed, M., Ji, M., Qin, P., Gu, Z., Liu, Y., Sikandar, A., Iqbal, M. F., Javeed, A. (2019): Phytochemical screening, total phenolic and flavonoids contents and antioxidant activities

http://www.aloki.hu ● ISSN 1589 1623 (Print) ● ISSN 1785 0037 (Online)
DOI: http://dx.doi.org/10.15666/aeer/1706_1338313394

of *Citrullus colocynthis* L. and *Cannabis sativa* L. – Applied Ecology and Environmental Research 17: 6961-6979.

[4] Aldesuquy, H., Baka, Z., Mickky, B. (2014): Kinetin and spermine mediated induction of salt tolerance in wheat plants: Leaf area, photosynthesis and chloroplast ultrastructure of flag leaf at ear emergence. – Egyptian Journal of Basic and Applied Sciences 1: 77-87.

[5] ArcGis, E. (2013): Version 10.2. 0. – Environmental Systems Research Institute, Redlands.

[6] Batlla, D., Grundy, A., Dent, K. C., Clay, H. A., Finch-Savage, W. E. (2009): A quantitative analysis of temperature-dependent dormancy changes in *Polygonum aviculare* seeds. – Weed Research 49: 428-438.

[7] Bolund, P., Hunhammar, S. (1999): Ecosystem services in urban areas. – Ecological Economics 29: 293-301.

[8] Braun, U. (1987): A monograph of the Erysiphales (powdery mildews). – Beihefte zur Nova Hedwigia 89: 1-700.

[9] Braun, U. (2012): Taxonomic Manual of Erysiphales (Powdery Mildews). – CBS Biodiversity Series 11. CBS-KNAW Fungal Biodiversity Centre, Utrect.

[10] Braun, U., Takamatsu, S. (2000): Phylogeny of *Erysiphe*, *Microsphaera*, *Uncinula* (Erysipheae) and *Cystotheca*, *Podosphaera*, *Sphaerotheca* (Cystotheceae) inferred from rDNA ITS sequences - some taxonomic consequences. – Schlechtendalia 4: 1-33.

[11] Braun, U., Takamatsu, S. (2013): Phylogeny of Erysiphe, *Microsphaera, Uncinula* (Erysipheae) and *Cystotheca, Podosphaera, Sphaerotheca* (Cystotheceae) inferred from rDNA ITS sequences–some taxonomic consequences. – Schlechtendalia 4: 1-33.

[12] Braun, U., Cunnington, J. H., Brielmaier-Liebetanz, U., Ale-Agha, N., Heluta, V. (2003): Miscellaneous notes on some powdery mildew fungi. – Schlechtendalia 10: 91-95.

[13] Bugg, R., Ehler, L., Wilson, L. (1987): Effect of common knotweed (*Polygonum aviculare*) on abundance and efficiency of insect predators of crop pests. – Hilgardia 55: 1-52.

[14] Carlile, M. J., Watkinson, S. C., Gooday, G. W. (2001): The Fungi. – Gulf Professional Publishing, Houston, TX.

[15] Chen, Wendy, Y., Jim, C. Y. (2008): Assessment and valuation of the ecosystem services provided by urban forests. – Ecology, Planning, and Management of Urban Forests, Springer.

[16] Cook, R. T. A., Inman, A. J., Billings, C. (1997): Identification and classification of powdery mildew anamorphs using light and scanning electron microscopy and host range data. – Mycological Research 101: 975-1002.

[17] Coquillat, M. (1951): Sur les plantes les plus communes a la surface du globe. – Publications de la Société Linnéenne de Lyon 20: 165-170.

[18] Costea, M. T., François, J. (2005): The biology of Canadian weeds. 131. *Polygonum aviculare* L. – Canadian Journal of Plant Science 85: 481-506.

[19] Debaeke, P., Caussanel, J. P., Kiniry, J. R., Kafiz, B., Mondragon, G. (1997): Modelling crop: weed interactions in wheat with ALMANAC. – Weed Research 37: 325-341.

[20] Del, T., Peter (2010): Spontaneous urban vegetation: reflections of change in a globalized world. – Nature and Culture 5: 299-315.

[21] Flora of China. (2004): *Polygonum aviculare* (Linnaeus). – Species Plantarum. 1(5):362-363 (1753).

[22] Francone, C., Pagani, V., Foi, M., Cappelli, G., Confalonieri, R. (2014): Comparison of leaf area index estimates by ceptometer and Pocket LAI smart app in canopies with different structures. – Field Crop Research 155: 38-41.

[23] Han, G. S., Kim, B. S., Choi, I. Y., Cho, S. E., Shin, H. D. (2016): First report of powdery mildew caused by *Erysiphe polygoni* on *Homalocladium platycladum* in Korea. – Plant Disease 100: 2170-2170.

[24] Hobbs, R. J., Higgs, E., Harris, J. A. (2009): Novel ecosystems: implications for conservation and restoration. – Trends in Ecology & Evolution 24: 599-605.

http://www.aloki.hu ● ISSN 1589 1623 (Print) ● ISSN 1785 0037 (Online)
DOI: http://dx.doi.org/10.15666/aeer/1706_1338313394

[25] Hossain, S. A. A. M., Wang, L., Chen, T., Li, Z. (2017): Leaf area index assessment for tomato and cucumber growing period under different water treatments. – Plant, Soil and Environment 63: 461-467.
[26] Koike, S., Gladders, P., Paulus, A. 2007. Vegetable Diseases: A Color Handbook. – Academic Press. San Diego, California, USA.
[27] Lebeda, A., Mieslerová, B., Rybka, V., Sedlářová, M., Petrželová, I. (2007): First record of powdery mildew on *Homalocladium platycladum* in the Czech Republic. – Plant Pathology 56: 722-722.
[28] Ma, J. S., Yan, X. L., Shou, H. Y. (2013): The Checklist of the Chinese Invasive Plants. – China Higher Education Press, Beijing.
[29] Mayer, D. G., Butler, D. G. (1993): Statistical validation. – Ecological Modelling 68: 21-32.
[30] Meerts, P. (1995): Phenotypic plasticity in the annual weed *Polygonum aviculare*. – Botanica Acta 108: 414-424.
[31] Meerts, P., Briane, J. P., Lefèbvre, C. (1990): A numerical taxonomic study of the *Polygonum aviculare* complex (Polygonaceae) in Belgium. – Plant Systematics and Evolution 173: 71-89.
[32] Miller, T. C., Gubler, W. D., Geng, S., Rizzo, D. M. (2003): Effects of temperature and water vapor pressure on conidial germination and lesion expansion of *Sphaerotheca macularis* f. sp. fragariae. – Plant Disease 87: 484-492.
[33] Nigussie, S. T., Amare, S. A., Manaye, M. M., Edget, M. B., Ashenafi, A. H., Girum, F. B., Tesfaye, B. H. (2017): Invasion and impacts of *Xanthium strumarium* in Borena Zone of Oromia Region, Ethiopia. – Journal of Coastal Life Medicine 5: 350-355.
[34] Peduto, F., Backup, P., Hand, E. K., Janousek, C. N., Gubler, W. D. (2013): Effect of high temperature and exposure time on *Erysiphe necator* growth and reproduction: revisions to the UC Davis Powdery Mildew Risk Index. – Plant Disease 97: 1438-1447.
[35] Pickett, S. T. A., Cadenasso, M. L., Grove, J. M., Groffman, P. M., Band, L. E., Boone, C. G., Burch, W. R., Grimmond, C. S. B., Hom, J., Jenkins, J. C. (2008): Beyond urban legends: an emerging framework of urban ecology, as illustrated by the Baltimore Ecosystem Study. – BioScience 58: 139-150.
[36] Pintye, A., Bereczky, Z., Kovács, G. M., Nagy, L. G., Xu, X., Legler, S. E., Váczy, Z., Váczy, K. Z., Caffi, T., Rossi, V. (2012): No indication of strict host associations in a widespread mycoparasite: grapevine powdery mildew (Erysiphe necator) is attacked by phylogenetically distant Ampelomyces strains in the field. – Phytopathology 102: 707-716.
[37] Rcore, T. (2016): R: A Language and Environment for Statistical Computing. – R Foundation for Statistical Computing, Vienna, Austria. http://www.R-project.org.
[38] Rink, D. (2009): Wilderness: The nature of urban shrinkage? The debate on urban restructuring and restoration in Eastern Germany. – Nature and Culture 4: 275-292.
[39] Royo, E. A., Torra, J., Conesa, J. A., Forcella, F., Recasens, J. (2010): Modeling the emergence of three arable bedstraw (Galium) species. – Weed Science 58: 10-15.
[40] Severoglu, Z., Ozyigit, Ibrahim, I. (2012): Powdery mildew disease in some natural and exotic plants of Istanbul, Turkey. – Pak. J. Bot 44: 387-393.
[41] Takamatsu, S., Hirata, T., Sato, Y. (1998): Phylogenetic analysis and predicted secondary structures of the rDNA internal transcribed spacers of the powdery mildew fungi (Erysiphaceae). – Mycoscience 39: 441-453.
[42] Tottman, D. R., Wilson, B. J. (1990): Weed control in small grain cereals. In: Hance, R. J., Holly, K., eds. – Weed Control Handbook: Principles. Oxford, UK: Blackwell, 30-328.
[43] Tyrväinen, L., Pauleit, S., Seeland, K., de Vries, S. (2005): Benefits and Uses of Urban Forests and Trees. – In: Konijnendijk, C., Nilsson, K., Randrup, T., Schipperijn, J. (eds.) Urban Forests and Trees. Springer, Berlin.

http://www.aloki.hu ● ISSN 1589 1623 (Print) ● ISSN 1785 0037 (Online)
DOI: http://dx.doi.org/10.15666/aeer/1706_1338313394

[44] Xu, X.-M. (1999): Effects of temperature on the length of the incubation period of rose powdery mildew (*Sphaerotheca pannosa* var. rosae). – European Journal of Plant Pathology 105: 13-21.
[45] You, J. F., He, Y. F., Yang, J. L., Zheng, S. J. (2005): A comparison of aluminum resistance among Polygonum species originating on strongly acidic and neutral soils. – Plant and Soil 276: 143-151.

http://www.aloki.hu ● ISSN 1589 1623 (Print) ● ISSN 1785 0037 (Online)
DOI: http://dx.doi.org/10.15666/aeer/1706_1338313394

MINERAL ADDITIVES AND CACTUS ADDED TO ENRICHED ANIMAL MANURE AS COMPOST FOR ENHANCING CHICKPEA AGRICULTURAL EFFICIENCY

ELFADIL, S.* – JAOUAD, A. – MAHROUZ, M. – BOUCHDOUG, M.

Team of Search, Innovation, Sustainable Development, Green Chemistry and Expertises, Semlalia Faculty of Science, Cadi Ayyad University, 24000 Marrakech, Morocco (phone: +212-5-2443-4649; fax: +212-5-2443-6769)

**Corresponding author*
e-mail: elfadilsaida@gmail.com; phone: +212-6-3887-5242; fax: +212-5-2443-6769

(Received 17th Jun 2019; accepted 28th Aug 2019)

Abstract. In this research we studied the effect of compost including phosphate flotation waste, phosphogypsum and cactus on chickpea (*Cicer arietinum* L.*)* plant growth and yield for 4 months under greenhouse systems in morocco. Chickpea development presented elevated variability. Phosphate flotation waste, contrary to the phosphogypsum, had positive effects on chickpea productivity; significant increase in biomass yield was demonstrated under phosphate flotation waste treatment (38.16%) and combination of phosphate flotation waste and cactus (48.87%). Phosphate flotation waste improved chickpea yield parameters and its effect was even more significant while adding cactus. Cactus might be a good material for enhancing the absorbance of nutrients by plants. When the phosphate flotation waste-cactus combination was optimal, supplementary parameters productivity was registered in certain situations. Furthermore, this research was the first to establish that the mixture including phosphate flotation waste, manure and cactus could not only enhance plant yield and growth but further assume for long-term agricultural productivity and right soil fertility.
Keywords: *phosphate flotation waste, phosphogypsum, cactus, physicochemical characterization of treatments, soil physicochemical properties, chickpea yield*

Introduction

Intensive cultivation and the failure to implement effective soil conservation practices for chickpea (*Cicer arietinum* L.*)* to meet the global demand has damaged the natural supply, and soil fertility and nutrients. Looking forward to obtaining a good fertility of soil and optimal yield, cultivated lands require proper management and recycling of organic wastes on land to protect agricultural soils.

In the last years, ammonium nitrate has been the best-known origin of nitrogen (N) on behalf of soil amendment in crop fertilization. Though, relative to else Nitrogen origin, ammonium nitrate is fairly luxurious and its production is probably to decrease during the decades to come (Wang et al., 2016). Under such scene, animal manure is getting more increasingly employed as an N origin nutriment for crop agriculture. To the same effect, in various countries, phosphorous (P) is the major growth restricting soil fertility; phosphate amendments have a critical role in pacing agricultural activity to shift human food productivity to the levels observed today. Though Yi et al. (2017) emphasize the utilizable deposits of phosphate are very restricted.

Further, evidencing the rooted dependency of food production on soil nutrients such P, in an alarming way (Cordel et al., 2009) prognostic a worldwide revolution in P production to arise by 2030. Yet the amendment production acknowledges the turn down in quantity and quality of international reserves along with the increasing costs of mining, meeting out and caring of P (Childers et al., 2011). Besides to these problems,

http://www.aloki.hu ● ISSN 1589 1623 (Print) ● ISSN 1785 0037 (Online)
DOI: http://dx.doi.org/10.15666/aeer/1706_1339513405

there is a rising appreciation of the environmental expenses of the present system of food production. Unfortunate nutrient running of soils and sustained use of synthetic amendments have had harmful effects on soil fertility (Ke et al., 2017). To maintain food industry in excess of time and to provide effective utilization of accessible resources with maximum competence, it is crucial that enhanced methods and techniques for completing crop productivities are considered and agreed (Ganesapillai et al., 2015).

To this fact, Phosphate Flotation Waste (PFW) generated from beneficiation of Moroccan phosphate rocks is of great concern in composting as a low-grade phosphate rock (Elfadil et al, 2016). Phosphate rock, and for consequence PFW have been acknowledged as an alternating source for P nutrient. In Morocco, it is estimated that there are approximately 260 million tons of phosphate rock deposits and that material will present a shameful source of phosphate fertilizer for crop production (Tanner, 1961). Unfortunately, phosphor is not readily available to the plants in soils with a pH > 5.5– 6.0. Because of this, extension services are reluctant to recommend it and farmers are hesitant to utilize phosphate rock directly. furthermore, It was reported by Luo et al. (2013) and Hu et al. (2007) that phosphogypsum, the main by-product of phosphoric acid production, might be effective in composting in the sense where he can reducing NH_4 emissions during by increasing SO_4^{2-} content of the compost, and Luo et al. (2013) indicated that the addition of phosphogypsum at a rate of 10% of total compost mixture (dry weight) decreased NH_3 emissions significantly during pig manure composting.

Besides, cactus has been recommended as a bio-adsorbent because of it high retention (Sakr et al., 2015); so can it considered as a good quality–low charge substituted fertilizer that can offer a well-off source of amendment to improve agricultural productivity?

This research presents an original approach to increase soil fertility by the combined application including Phosphate flotation waste PFW, phosphogypsum (Pg), cactus and animal manure. While the use of Phosphate rock enriched composts has been the question of current studies (Moharana and Biswas, 2016), there have been awfully no information on the application of PFW, Pg and cactus in soils. Therefore, in the present study, the application of Phosphate flotation waste, phosphogypsum and cactus enriched animal manure on the plant development reply parameters of Chickpea (*Cicer arietinum L.*) was inquired.

Materials and methods

Sampling and sample pretreatment

Animal manure was obtained from forty farms in Chichaoua city with good-balanced regimes. Fresh manure samples were composed in air-tight comprising and refrigerated less than 20 °C to keep away from ammonia volatilization (Ke et al., 2017). The results of this study are summarized in *Table 1*.

Phosphate flotation waste and phosphogypsum tailings with 43.8% Ca_3PO_4 (20.05% P_2O_5) were obtained from industrial mines of Khouribga. Commercial grade Triple Super-Phosphate (TSP) with 45% P_2O_5 was obtained from Moroccan Institute for Agronomic Research in Settat city (INRA Settat). Composts are prepared with various mixtures of these raw materials;

Prior to the study, TSP was crushed and screened to size less than 2.5 mm.

http://www.aloki.hu ● ISSN 1589 1623 (Print) ● ISSN 1785 0037 (Online)
DOI: http://dx.doi.org/10.15666/aeer/1706_1339513405

the details of the treatments is: T1: the control (soil without addition); T2: soil and manure compost; T3: soil and compost of manure and PFW (6:4); T4: soil and compost of manure and phosphogypsum (6:4); T5: soil and compost of manure, PFW and cactus age under 6 mouth) (6:3:1); T6: soil and compost of manure, PFW and cactus (age above 6 mouth) (6:3:1); T7: soil and TSP. Three doses were applied of each treatment: 0.06 t/ha, 0.6 t/ha and 6 t/ha.

The experiments were carried out in the laboratory with an average room temperature of 25 ± 3 °C and relative humidity as 60%.

Table 1. *Nutritional statues of soil, compost, and soil compost mixes at the begining of the trial*

Treatments	Total N (mg.g^{-1} of dry matter)	Avail. N (µg.g^{-1} of dry matter)	P_2O_5 (%)	Avail. P (µg.g^{-1} of dry matter)	K_2O (%)	Avail. K (µg.g^{-1} of dry matter)
T1	3.33	832.62	1.23	729	8.03	856
T21	4.26	951.00	5.84	5843.23	9.12	1525.00
T22	5.32	1112.23	6.23	6421.21	10.42	1952.00
T23	6.53	1541.22	6.69	7011.55	11.23	2214.00
T31	6.26	953.00	7.84	5845.23	11.12	1527.00
T32	6.65	1113.56	7.56	6422.54	11.75	1953.33
T33	8.68	1542.55	8.02	7012.88	12.56	2215.33
T41	6.88	953.62	8.46	5845.85	11.74	1527.62
T42	7.20	1114.11	8.11	6423.09	12.30	1953.88
T43	9.57	1544.26	9.73	7014.59	14.27	2217.04
T51	5.04	951.78	6.62	5844.01	9.90	1525.78
T52	5.73	1112.64	6.64	6421.62	10.83	1952.41
T53	7.27	1541.96	7.43	7012.29	11.97	2214.74
T61	2.98	949.72	4.56	5841.95	7.84	1523.72
T62	3.85	1110.76	4.76	6419.74	8.95	1950.53
T63	6.12	1540.81	6.28	7011.14	10.82	2213.59
T71	8.59	955.33	10.17	5847.56	13.45	1529.33
T72	11.32	1118.23	12.23	6427.21	16.42	1958.00
T73	13.35	1548.04	13.51	7018.37	18.05	2216.48

T1: the control; T21: soil and 0.06 t/ha of manure compost; T22: soil and 0.6 t/ha of manure compost; T23: soil and 6 t/ha of manure compost; T3: soil and compost of manure and PFW; T4: soil and compost of manure and phosphogypsum; T5: soil and compost of manure, PFW and cactus (age under 6 mouth); T6: soil and compost of manure, PFW and cactus (age above 6 mouth); T7: soil and TSP

Experimental mode

A greenhouse experiment with chickpea plants was conducted from the beginning of September to the beginning of January 2015 (140 days) at the National institute of agronomic research (INRA) site located in Settat (Morocco), located at an altitude of about 400 m, Lambert coordinates X: 292.413 and Y: 263.664.

The site is located in the semi-arid bioclimatic stage with an average rainfall of between 300 and 350 mm concentrated between the months of October and May and a very temperate average temperature varying between 5 °C during the months December and January to 38 °C during the summer. Compound soil samples were obtained from a profundity of 0.2 m from the surface and screened throughout a 6 mm hole. The soil

http://www.aloki.hu ● ISSN 1589 1623 (Print) ● ISSN 1785 0037 (Online)
DOI: http://dx.doi.org/10.15666/aeer/1706_1339513405

used was red loam with 4.33% gravel, 92.84% sand and 2.83% fine; this soil was used for its proper properties and its impermeability. Trays (0.44 × 0.32 × 0.14 m) were packed with 4 kg of air-dried soil and studied with 3 replications. Trays were approved as plant divide arrays. Every array included plant replicates of the soil treatments, on a network including 3 rows by 18 columns of trays. Inside every array, the soil treatments were owed depending on a randomized complete block (RCB) plan, consequently this group of plant pots inside every line incorporated one repeat. 6 composts, prepared from phosphate flotation waste, phosphogypsum, animal manure and cactus, were additional to the respective trays 2 days previous to kernel planting and sprayed to ensure proper dissolution of composts in the soil. Trays were divided into plant slots and 3 seeds were planted in both pots at a profundity of 30 mm in greenhouse (*Fig. 1*). After germination, plants were watered down to 3 per slot for all the plates. All plants were periodically watered with de-ionized water through the research period. Upon maturity (about 4 months following planting the seeds) all plants were reaped and the plants phisico-morphological characteristics and biomass yield were identified. Preliminary pot experiment was set up with a set of 7 treatments.

For the seven treatments except the control, 3 doses are adopted with 3 replications:

- A dose of 0.06 t/ha of compost was selected for fertilization so 2 g of each compost. This dose was applied to the individual plots at the level of each treatment.
- A dose of 0.6 t/ha so 20 g of each compost.
- A maximum dose of 6 t/ha so 200 g of each compost.

During the experimental period, homogeneous irrigation (50 l for each plot) without chemical fertilizing was carried out regularly every five days with tap water using a drip system.

a **b** **c**

Figure 1. *(a, b) Layout of pot and greenhouse experiment. (c) Nodules on treated chickpea plants from pot experiment*

Plant physicochemical analysis

The unamended soil was included for its primary characteristics (*Table 2*). Post-harvesting, oven dried at 40 °C, plants was grinded at 2 mm screen. All the samples were characterize for total phosphorus, total nitrogen, total potassium and transferable cations (P, K, and N); pH was measured in 0.01 M $CaCl_2$ (1: 5) (Simpson, 1988). Total phosphorus and nitrogen were determined by means of the Dumas incineration method

http://www.aloki.hu ● ISSN 1589 1623 (Print) ● ISSN 1785 0037 (Online)
DOI: http://dx.doi.org/10.15666/aeer/1706_1339513405

at 900 °C with an oxygen run rate of 125 ml min^{-1}. P, N and K transferable were measured using absorption method. Exchangeable cations P (Olsenet al., 1960), K and N were measured using absorption method.

The contents of the air party of chickpea in fertilizing elements, in trace elements and in heavy metals, are determined by the Inductively Coupled Plasma Atomic Emission Spectroscopy (*ICP*-AES) to the laboratory Reminex of the company Managem of Marrakesh Morocco.

Table 2. *Effect of manure and different rates of compost amendments alone and in combination on growth promotion of chickpea plants compared to mineral fertilizer TSP after 140 d*

Treatment	Number of pods	Weight of pods (g)	Number of seeds	Weight of seeds (g)	Yield plant biomass (g)	Root length (cm)
T3	15.00a(2.70)	2.70abc(0.40)	6.67a(4.27)	1.97ab(0.11)	8.58b (0.44)	16a(1.17)
T5	8.14abc(0.89)	3.61a(0.04)	6.86a(3.18)	2.73a(0.03)	8.17b(0.76)	13.86b(0.67)
T6	8.20abc(0.64)	2.10abc(0.08)	4.80abc(1.10)	1.48ab(0.02)	11.24ab(1.00)	17.70ab(1.64)
T4	5.00bc(1.00)	0.96c(0.03)	2.33c(1.80)	0.64b(0.07)	5.20b(0.39)	16.78ab(1.32)
T6	7.40bc(0.51)	3.05ab(0.08)	6.00ab(2.00)	2.21ab(0.08)	16.68a(1.90)	17.80ab(2.38)
T2	11.00ab(1.54)	2.79abc(0.17)	5.67abc(3.04)	1.98ab(0.08)	10.46ab(1.01)	20.33a(1.67)
T1	3.00c(0.11)	1.09c(0.02)	2.00c(0.23)	0.53b(0.01)	8.24b(0.67)	17.17ab(1.75)

T1: the control (soil without addition); T2: soil and manure compost; T3: soil and compost of manure and PFW; T4: soil and compost of manure and phosphogypsum; T5: soil and compost of manure, PFW and cactus (age under 6 mouth); T6: soil and compost of manure, PFW and cactus (age above 6 mouth); T7: soil and TSP. Data are given as mean of three replicates (standard deviation)

Physiological analysis

The harvest of pods and plants was started on 140-day-old plants and the following characteristics were recorded for each collected plant: number and weight of pods, number and weight of seeds.

The roots of each plant were washed carefully and their lengths were determined.

Statistical analysis

The plant development data was originated to track normal distribution screening homogeneity of variances with correlation analysis. The data was statistically analyzed throughout SAS at a level of significance set at $P < 0.05$ using Anova followed by Dancun as a post-hoc test.

Results and discussion

Soil, compost, and potting mixture analysis

Nutrient condition of the soil, Composts and potting mixtures of soil and compost is exposed in *Table 1*. Among the macrofertilizers, availability of P was the uppermost, tracking by K and then N in the Composts, while soil presented upper concentrations of available N, tracking by K, and afterward P. Comparison of the results showed that the compost contained higher amounts of all macronutrients analyzed compared with the control. Upon substitution of soil with Composts, availability of macronutrients like N,

http://www.aloki.hu ● ISSN 1589 1623 (Print) ● ISSN 1785 0037 (Online)
DOI: http://dx.doi.org/10.15666/aeer/1706_1339513405

P, and K in potting mixtures increased significantly with increasing proportions of compost substitutions (*Table 1*).

Chickpea biomass production

The treatments studied and the responsiveness of plant growth characteristics have been presented (*Tables 2* and *3)*. Intended for all treatments, the efficiency of PFW enriched animal manure was originated to be improved than that of the control (*Table 2*; $p < 0.05$). Relative to seeds weight, following tendency was showed for the control and 6 different treatments with all the three doses: T5 > T7 > T2 > T3 > T6 > T4 > T1 (*Fig. 2d*). A parallel tendency was showed for pods weight with the control, cactus 2 and phosphogypsum providing the lowly value. Relative to total plant biomass a different pattern was apparent: T7 > T6 > T2 > T3 > T1 > T5 > T4 (*Fig. 2c*); significant augment in biomass yield was confirmed in treatments T3 (38.16%) and T5 (28.87%) (*Fig. 2a*). However, enhancement of plant root length was most pronounced under T62 (0.06 t ha^{-1} of T2) (*Fig. 2b*).

Table 3. *Correlation matrix between quality parameters of PFW enriched composts*

Temperature	pH	K_2O	K_{ech}	Nitrate	P_2O_5	P_{assi}
pH	1.00000	0.19944* 0.5343	0.78039 0.0027	0.58550 0.0455	0.86056 0.0003	0.78785 0.0023
K_2O		1.00000	0.97254* 0.8227	0.31061* 0.6258	-0.28143* 0.8755	-0.05033* 0.8766
K_{ech}			1.00000	-0.94788 < .0001	-0.31589* 0.3172	-0.49368* 0.1029
Nitrate				1.00000	0.57492* 0.0505	0.59263 0.0423
P_2O_5					1.00000	0.95821 < .0001
P_{assi}						1.00000

*Correlation is significant at the 0.05 level

With compost input of 0.6 t P_2O_5 ha^{-1} to the soil, a different tendency was presented with rising compost dose adding. The majority of plant growth responsiveness parameters responded positively as P addition was augmented to 0.6 t ha^{-1}. Additional supplementation with P had resulting to decrease growth characteristics relatively to previous treatments while the results were still improved than that of the control. Hosseinpur et al. (2011) indicated comparable results for chickpea where they recommended that, rising application of inorganic P fertilizer further than 40 kg P ha^{-1} reduce leguminous P-fixation. They also recommend that for the benefits of starter P to be performed and the yield of chickpea to be improved, levels as significant as 0.6 kg N ha^{-1} could be necessary for optimizing the yields. While PFW input of 0.6 t P_2O_5 ha^{-1} yields positive results relatively to the control for all treatments, supplementary resource-use performance might be ensured throughout the optimal P additive identify. This study reports 0.6 t ha^{-1} as a positive level of chickpea agriculture. For instance, allowing for pod number as the responsiveness parameter; treatment T5 (6 t P ha^{-1})

http://www.aloki.hu ● ISSN 1589 1623 (Print) ● ISSN 1785 0037 (Online)
DOI: http://dx.doi.org/10.15666/aeer/1706_1339513405

relative to T5 (0.6 t P ha^{-1}) showed that supplementary P addition results in reduced number of pods (T5 is 86% of T4) nevertheless still considerably higher than the control T1 ($p < 0.05$) (*Table 2*). Parallel result and watching of tendency for P addition to soils cultivating chickpeas was indicated by many authors (Saini et al., 2004; Wei et al., 2015; Iyer et al., 2017).

On the other hand, mineral amendments have larger agronomic competence for the reason that their elements are available and effortlessly captivated by plants. This would be due to the rapid release of nutrients to soils and plants, as demonstrated by Abdelhamid et al. (2004) in a study comparing the economic profitability of inorganic and organic fertilizers in faba bean (*Vicia faba L.*). On the other hand, the dose of 0.6 t ha^{-1} of manure compost is much more efficient than 0.06 or 6 t ha^{-1}. These results (*Table 2; Fig. 2*) show the value and necessity of using low doses in case of low availability of organic materials. This confirms the studies of Ukem (2010) who advocate the use of small quantities of compost in vegetable and soybean crops.

Effect of cactus addition on chickpea biomass production

Cactus with PFW resulting in enhanced chickpea growth as well as dry matter increase could be awarded to mechanisms as the creation of indoleacetic acid along with dissolving of unsolvable phosphate alongside with uncharacterized characteristics making fertilizers more willingly available for plant uptake. Cactus facilitates enhanced mineral nutrient absorption as a result of varying the physiological rank along with morphological characteristic of inoculated roots, and therefore promotion of root growth is considered as one of the major markers by which the beneficial effect of plant growth promotion by cactus is measured. Increased root length in the seed treatments may thus be influenced by cactus (*Table 2; Figs. 2* and *3*).

Increase in growth as well as dry matter build-up in chickpea plants in the combined a of high compost use substitution as well as cactus and manure was better than the amount of their individual applications, possibly as an effect of the synergistic input of both parameters in the enhancement of the physico-chemical characteristics and nutritional factors. The benefits of this combination are more likely to synchronize nutrient release from the compost and soil with plant nutrition demand as well as involvement of cactus and manure modulation of the plant root architecture for more efficient acquisition of soil nutrients. In this study, cactus with manure improved the tested parameters of growth due to their synergistic effect. This supposed that manure substitution separately was powerless to provide the plants with enough quantities of willingly available fertilizers as well as enhancement of plant growth unlike the combinations.

Effect of toxicity of the novel composts on chickpea plant

Heavy metals are regarded as trace elements due to their existence in low contents (in ppm) in different eco-systems (Meharg, 2011). Their bio-assimilates is affected by various physical parameters (temperature, adsorption...), chemical parameters (thermodynamic equilibrium, complexation kinetics, lipid solubility…) (Hamelink, 1994) and biological parameters (species characteristics, biochemical/physiological adaptation…) (Martin, 1995).

The contents in cadmium and lead were low for all the treatments (< 2 ppm and < 26 ppm respectively); also the concentrations of nickel and chromium were weak

http://www.aloki.hu ● ISSN 1589 1623 (Print) ● ISSN 1785 0037 (Online)
DOI: http://dx.doi.org/10.15666/aeer/1706_1339513405

and stay below the international standards: AFNOR norme. The copper and zinc concentrations of the various plants were superior with regard to the no amended treatment especially for the treatment which contains of the small cactus, what can be to explain by the strong adsorption of the cactus of the zinc and the copper.

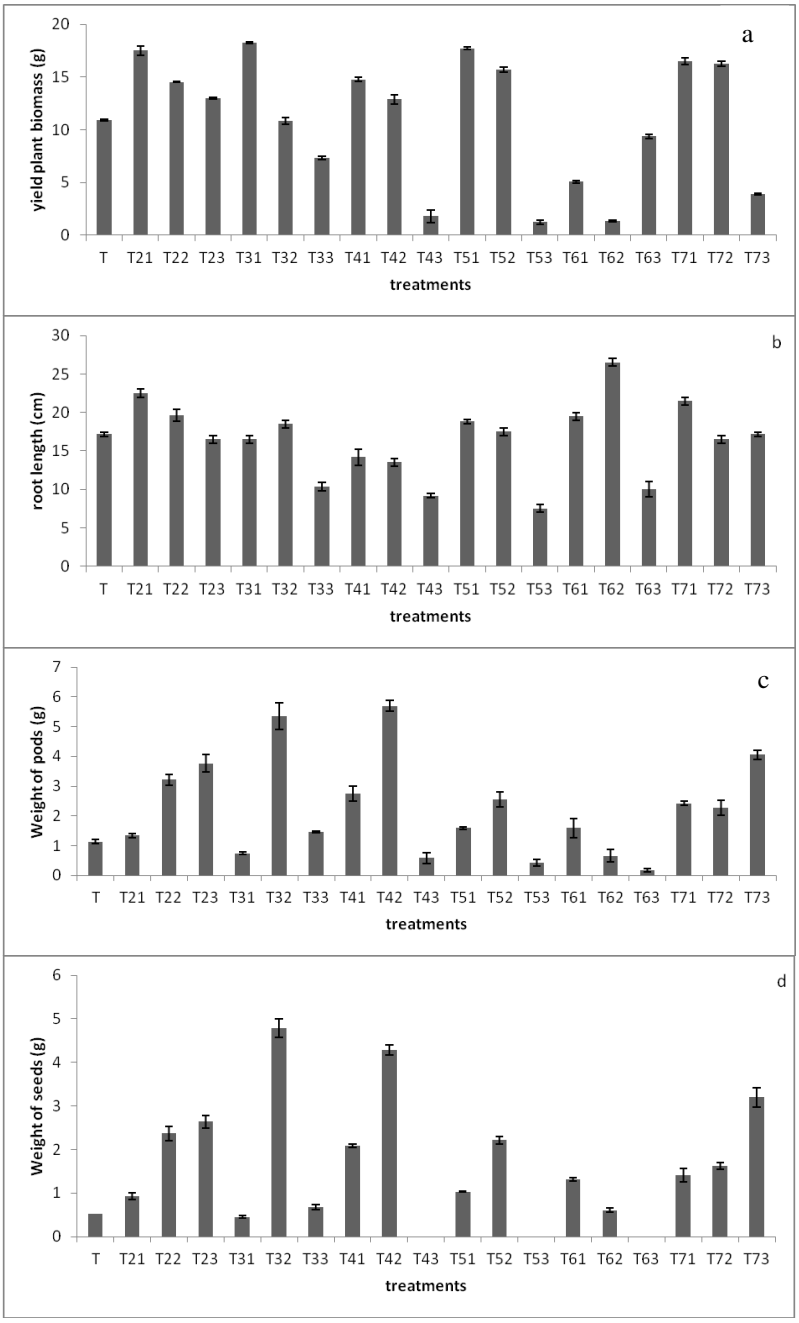

Figure 2. *Influence of enriched composts on (a) yield plant biomass; (b) root length; (c) Weight of pods; (d) Weight of seeds per plant in the various treatments. T1: the control; T21: soil and 0.06 t/ha of manure compost; T22: soil and 0.6 t/ha of manure compost; T23: soil and 6 t/ha of manure compost; T3: soil and compost of manure and PFW; T4: soil and compost of manure and phosphogypsum; T5: soil and compost of manure, PFW and cactus (age under 6 mouth); T6: soil and compost of manure, PFW and cactus (age above 6 mouth); T7: soil and TSP. Modulation values are back transformed from loge means. LSD5% value is therefore the least significant ratio (LSR5%)*

http://www.aloki.hu ● ISSN 1589 1623 (Print) ● ISSN 1785 0037 (Online)
DOI: http://dx.doi.org/10.15666/aeer/1706_1339513405

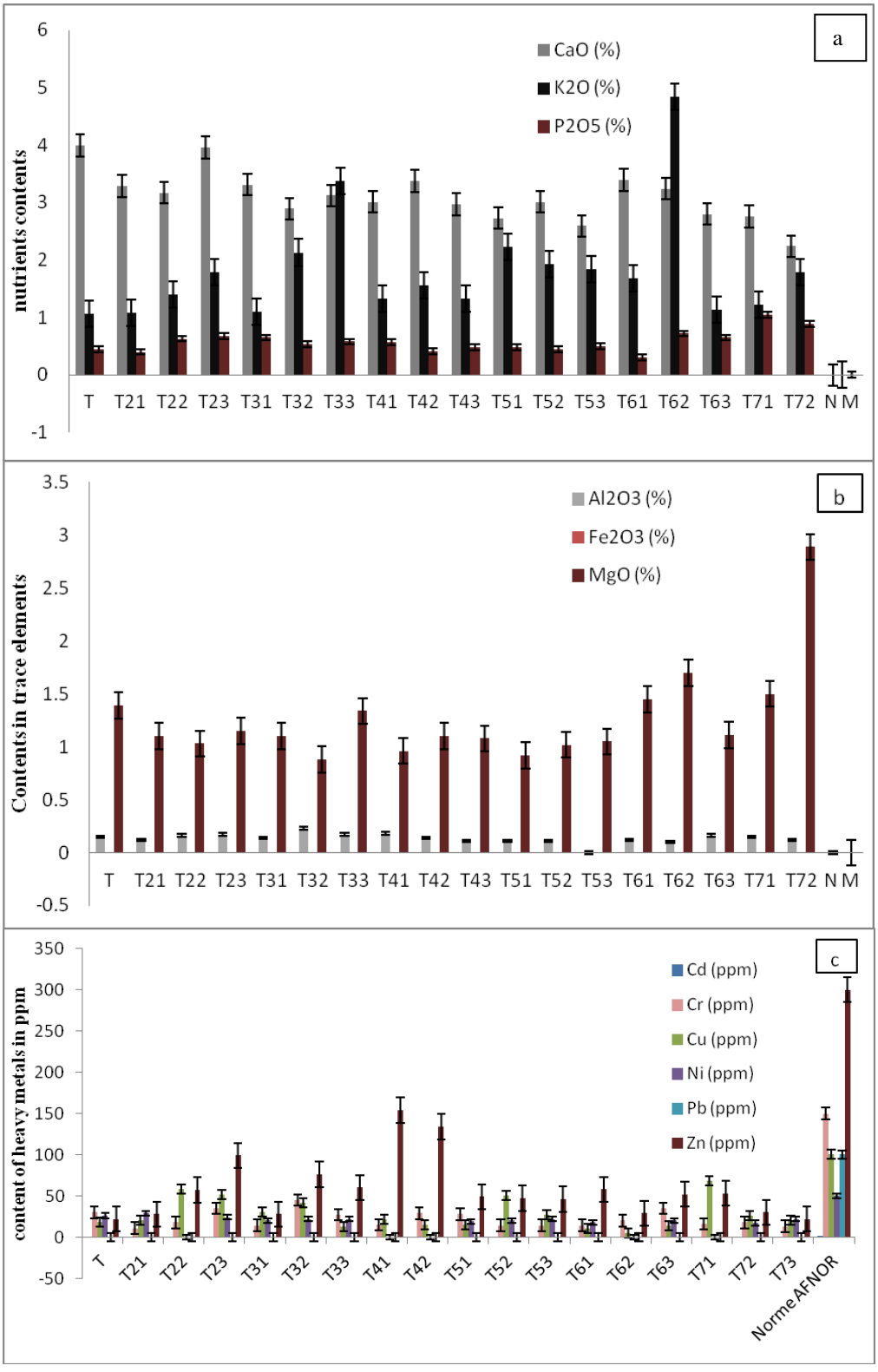

Figure 3. *Contents in nutrients (a), traces elements (b) and elements metallic tracks (c) in chickpea plant in the various treatments. T1: the control; T21: soil and 0.06 t/ha of manure compost; T22: soil and 0.6 t/ha of manure compost; T23: soil and 6 t/ha of manure compost; T3: soil and compost of manure and PFW; T4: soil and compost of manure and phosphogypsum; T5: soil and compost of manure, PFW and cactus (age under 6 mouth); T6: soil and compost of manure, PFW and cactus (age above 6 mouth); T7: soil and TSP*

http://www.aloki.hu ● ISSN 1589 1623 (Print) ● ISSN 1785 0037 (Online)
DOI: http://dx.doi.org/10.15666/aeer/1706_1339513405

Conclusion

This research confirmed an approach to fertilize plants via the combined application of wastes resources; PFW, phosphogypsum, animal manure and cactus. That confirmed the elevated performance observed in reactivates parameters of Cicer arietinum as the product of treatment T4 (PFW at 0.6 t P_2O_5 ha^{-1} and cactus at 0.6 kg P ha^{-1}). The addition of PFW and phosphogypsum fitting nature of Cicer arietinum, chemical analyses of soil subsequent the harvest presented an augmentation in total soil phosphorus; cactus have clear beneficial effect to increased supply of Phosphorus, changes in the growth rate of chickpea and absorption of heavy metals by plants.

Unfortunately, some of the studied treatments exacerbate certain problems with mineral additives, especially regarding heavy metals accumulations. For this reason, research is in progress to ameliorate the physicochemical conditions for using these additives improvers and also to investigate the links between heavy metals accumulation in cultivated soils, the physical and hydraulic properties, and soil productivity.

Acknowledgments. The authors would like to thank anonymous reviewer for his useful comments and the high ministry of education of morocco. Mr A. Bousetta (Reminex Unit – Managem Morocco), is thanked for the help concerning ICP analysis. The authors would like Mr E. El Mzouri the Director of INRA Settat Morocco.

REFERENCES

[1] Abdelhamid, M., Horiuchi, T., Oba, S. (2004): Composting of rice straw with oilseed rape cake and poultry manure and its effects on faba bean (Vicia faba L.) growth and soil properties. – Bioresource Technology 93: 183-189. http://dx.doi:10.1016/j.biortech.2003.10.012.

[2] Childers, D., Corman, J., Edwards, M., Elser, J. (2011): Sustainability challenges of phosphorus and food: solutions from closing the human phosphorus cycle. – BioScience 61: 117-124. http://dx.doi:10.1525/bio.2011.61.2.6.

[3] Cordell, D., Drangert, J., White, S. (2009): The story of phosphorus: global food security and food for thought. – Global Environmental Change 19: 292-305. http://dx.doi:10.1016/j.gloenvcha.2008.10.009.

[4] Elfadil, S., Bouchdoug, M., Jaouad, A. (2016): Physico-chemical characterization of phospahtes flotation waste and its potential us as a composting amendment. – IJIR 2(5): 71-77.

[5] Ganesapillai, M., Simha, P., Zabaniotou, A. (2015): Closed-loop fertility cycle: realizing sustainability in sanitation and agricultural production through the design and implementation of nutrient recovery systems for human urine. – Sustainable Production and Consumption 4: 36-46. http://dx.doi:10.1016/j.spc.2015.08.004.

[6] Hamelink, J. (1994): Bioavailability. – Lewis Publishers, Boca Raton.

[7] Hosseinpur, A., Kiani, S., Halvaei, M. (2011): Impact of municipal compost on soil phosphorus availability and mineral phosphorus fractions in some calcareous soils. – Environmental Earth Sciences 67: 91-96. http://dx.doi:10.1007/s12665-011-1482-1.

[8] Hu, T., Zeng, G., Huang, D., Yu, H., Jiang, X., Ai, I. F., Huang, G. (2007): Use of potassium dihydrogen phosphate and sawdust as adsorbents of ammoniacal nitrogen in aerobic composting process. – Journal of Hazardous Materials 141: 736-744. http://dx.doi:10.1016/j.jhazmat.2006.07.027.

http://www.aloki.hu ● ISSN 1589 1623 (Print) ● ISSN 1785 0037 (Online)
DOI: http://dx.doi.org/10.15666/aeer/1706_1339513405

[9] Iyer, B., Rajput, M., Rajkumar, S. (2017): Effect of succinate on phosphate solubilization in nitrogen fixing bacteria harbouring chick pea and their effect on plant growth. – Microbiological Research 202: 43-50. http://dx.doi:10.1016/j.micres.2017.05.005.

[10] Ke, J., Xing, X., Li, G., Ding, Y., Dou, F., Wang, S., Liu, Z., Tang, S., Ding, C., Chen, L. (2017): Effects of different controlled-release nitrogen fertilisers on ammonia volatilisation, nitrogen use efficiency and yield of blanket-seedling machine-transplanted rice. – Field Crops Research 205: 147-156. http://dx.doi:10.1016/j.fcr.2016.12.027.

[11] Luo, Y., Li, G., Luo, W., Schuchardt, F., Jiang, T., Xu, D. (2013): Effect of phosphogypsum and dicyandiamide as additives on NH3, N2O and CH4 emissions during composting. – Journal of Environmental Sciences 25: 1338-1345. http://dx.doi:10.1016/s1001-0742(12)60126-0.

[12] Martin, M. (1995): Plants as biomonitors: indicators for heavy metals in the terrestrial environment VCH. – Phytochemical Analysis 6: 112-112. http://dx.doi:10.1002/pca.2800060209.

[13] Meharg, A. (2011): Trace elements in soils and plants. 4th edition. By A. Kabata-Pendias. – Experimental Agriculture 47: 739-739. http://dx.doi:10.1017/s0014479711000743.

[14] Moharana, P., Biswas, D. (2016): Assessment of maturity indices of rock phosphate enriched composts using variable crop residues. – Bioresource Technology 222: 1-13. http://dx.doi:10.1016/j.biortech.2016.09.097.

[15] Olsen, S., Watanabe, F., Cole, C. (1960): Effect of sodium bicarbonate on the solubility of phosphorus in calcareous soils. – Soil Science 89: 288-291. http://dx.doi:10.1097/00010694-196005000-00010.

[16] Sakr, F., Sennaoui, A., Elouardi, M., Tamimi, M., Assabbane, A. (2015): Étude de l'adsorption du Bleu de Méthylène sur un biomatériau à base de Cactus (Adsorption study of Methylene Blue on biomaterial using cactus). – J. Mater. Environ. Sci. 6(2): 397-406. https://www.jmaterenvironsci.com/Document/vol6/.../48-JMES-1115-2014-Sakr.pdf.

[17] Saini, V., Bhandari, S., Tarafdar, J. (2004): Comparison of crop yield, soil microbial C, N and P, N-fixation, nodulation and mycorrhizal infection in inoculated and non-inoculated sorghum and chickpea crops. – Field Crops Research 89: 39-47. http://dx.doi:10.1016/j.fcr.2004.01.013.

[18] Simpson, K. (1988): Plant analysis. Edited by D. J. Reuter and J. B. Robinson. Melbourne: Inkata Press. – Experimental Agriculture 24: 129-129. http://dx.doi:10.1017/s0014479700015775.

[19] Tanner, C. (1961): Book review: fertiliser report and statistics, 1959. – Outlook on Agriculture 3: 98-98. http://dx.doi:10.1177/003072706100300211.

[20] Ukem, B. (2010): Effect of a complementary application of Algifol nutrient solution and npk on growth, flowering and yield of tomato in a northern guinea savanna soil of Nigeria. – Global Journal of Agricultural Sciences 8. http://dx.doi:10.4314/gjass.v8i2.51892.

[21] Wang, Y., Dong, H., Zhu, Z., Li, L., Zhou, T., Jiang, B., Xin, H. (2016): CH4, NH3, N2O and NO emissions from stored biogas digester effluent of pig manure at different temperatures. – Agriculture, Ecosystems & Environment 217: 1-12. http://dx.doi:10.1016/j.agee.2015.10.020.

[22] Wei, Y., Zhao, Y., Xi, B., Wei, Z., Li, X., Cao, Z. (2015): Changes in phosphorus fractions during organic wastes composting from different sources. – Bioresource Technology 189: 349-356. http://dx.doi:10.1016/j.biortech.2015.04.031.

[23] Yi, K., Wang, D., QiYang, Li, X., Chen, H., Sun, J., An, H., Wang, L., Deng, Y., Liu, J., Zeng, G. (2017): Effect of ciprofloxacin on biological nitrogen and phosphorus removal from wastewater. – Science of the Total Environment 605-606: 368-375. http://dx.doi:10.1016/j.scitotenv.2017.06.215.

http://www.aloki.hu ● ISSN 1589 1623 (Print) ● ISSN 1785 0037 (Online)
DOI: http://dx.doi.org/10.15666/aeer/1706_1339513405

DESIGN AND APPLICATION OF BARCODE DIAMETER-AT-BREAST-HEIGHT TAPE IN FOREST INVENTORIES

ZHOU, D. Q. – HE, X. J.* – CHEN, G. W.

The Third Surveying and Mapping Institute of Guizhou Province, Guiyang 550004, China
(e-mail: 214955874@qq.com (Zhou, D. Q.), 521010515@qq.com (Chen, G. W.);
phone/ fax: +86-1-307-8590-698)

**Corresponding author*
e-mail: 623094714@qq.com; phone/ fax: +86-1-307-8590-698

(Received 17th Jun 2019; accepted 2nd Sep 2019)

Abstract. Diameter at breast height (DBH) is one of the most important factors in forest inventories. A diameter tape is a traditional tool for measuring DBHs and is often used to obtain references when testing other DBH tools. However, reading measurements with this tool is subjective and may result in low-accuracy values. In this paper, two types of diameter tapes with barcoding (black & white tape and multicolour tape) were designed based the traditional diameter tape. A new algorithm was designed and developed as an application that can be installed on a smartphone with a wide-angle camera to decode and store readings of these new tapes. This system was tested in typical forest plots. The results showed that when comparing the mean values measured multiple times with reference values obtained with a traditional tape, the bias was not particularly significant (1.3 mm). The RMSE of measurements using these new tools (5.6 mm) was smaller than that obtained using a traditional tool (9.2 mm). Furthermore, this new approach reduced the subjectivity of different observers reading the data. Therefore, these new tapes may be better alternatives to a traditional tape.
Keywords: *forest inventory, standing tree, diameter at breast height, smartphone, automatic measurement*

Introduction

Field survey is an important means of gathering information from forests. The information collected usually includes diameter at breast height (DBH), tree height and crown width, which can be used to estimate stock volume and biomass models (Maia et al., 1999; Drexhage and Colin, 2001; Popescu et al., 2003; Ouimet et al., 2008) and to establish remote sensing inversion models (Riaño et al., 2003; Wieser et al., 2017). The accuracy of the collected information directly determines the accuracy of such models. DBH is easier to measure and more important than other variables. DBH has strong correlations with tree height, stock volume and biomass (Gering and May, 1995; Popescu et al., 2003; Ouimet et al., 2008; Sumida et al., 2013). Therefore, the accuracy, efficiency, and objectivity of DBH measurements are of great interest.

Caliper and diameter tape are traditional measurement tools. These tools are inefficient and yield subjective results because they require contact with the trees and the manual reading of measurements. Some new, non-contact tools, such as relascopes and dendrometers, have been developed and used for DBH measurements. Kalliovirta et al. (2005) tested a laser-relascope, which is a combination of a relascope and a dendrometer, under typical forest conditions. They compared the measurements with the values gathered by a steel caliper and obtained a standard error of 8.2 mm. The accuracy of the laser-relascope measurements depends on distance, tree measurement time, DBH and observer experience.

http://www.aloki.hu ● ISSN 1589 1623 (Print) ● ISSN 1785 0037 (Online)
DOI: http://dx.doi.org/10.15666/aeer/1706_1340713421

Terrestrial laser scanning (TLS) and mobile laser scanning (MLS) are considered alternatives to traditional measurement tools. These devices can be used to scan a sample plot and generate three-dimensional (3-D) point cloud data with high position accuracy. Through filtering, reconstruction and some additional steps, sample plot information including DBH measurements can be obtained from the data (Watt, 2005; Maas et al., 2008; Liang et al., 2012; Yu et al., 2013; Saarinen et al., 2013; Liang et al., 2014a; Srinivasan et al., 2015; Vastaranta et al., 2015; Olofsson and Olsson, 2017). Maas et al. (2008) used single-station and multi-station observations to measure the DBH of trees and compared the results with traditional caliper measurements. They found that the multiple-scan data was superior to the single-scan data, with a root mean squared error (RMSE) of 1.5 cm vs. an RMSE of 3.2 cm. Liang et al. (2014a) tested an MLS system composed of a high-performance laser scanner, a navigation unit, and a six-wheeled all-terrain vehicle in forest inventories, and the RMSE of the estimations of DBH was 2.36 cm. However, the high expense of the devices and the limited availability of cloud-processing software for the obtained cloud data of sample plots may limit the applications of TLS and MLS for forestry measurements.

A camera is another effective measuring tool that has been widely used in forest inventory (Juujarvi et al., 1998; Melkas et al., 2008; Liang et al., 2014b; Miller et al., 2015; Varjo et al., 2019). The device is typically used in one of two ways (to analyze a single photo attached to some conditions or a point cloud generated from multiple photos). Melkas et al. (2008) tested a laser-camera that combined a digital reflex camera with an integrated laser line generator. Tree diameters measured with the device were compared with measurements conducted with a steel caliper. The standard error of the diameter observations was 6 mm (5.3%), and the proportion of bias was 2.5 mm. However, this method may not be as efficient as the direct use of a diameter tape. Liang et al. (2014b) evaluated a point cloud generated from an uncalibrated hand-held camera and compared with measurements obtained with a steel tape. The RMSE of the DBH estimates of individual trees was 2.39 cm, which means that the results may not be very accurate. The color point cloud generated by this approach can be processed in the same way as a point cloud obtained by TLS or MLS, but the automated image matching procedure is very difficult and introduces more redundant error than does a TLS method.

A smartphone is a device that integrates sensors such as a wide-angle camera, gyro system, and GPS. As a low-cost, portable and developable device, the smartphone has been widely used in various industries including forest inventory (Villasante and Fernandez, 2014; Bijak and Sarzyński, 2015; Vastaranta et al., 2015; Molinier et al., 2016; Qu et al., 2017). Vastaranta et al. (2015) evaluated a related app (TRESTIMATM) in conducting sample plot measurements and included a function to measure stem diameter automatically. The app was used to measure basal area median tree diameter (DgM) in the test. The measurements were compared with values obtained by a caliper. Biases for the DgM measurements varied from -1.4% to 3.1%, and the RMSE ranged from 5.2% to 11.6% among different tree species. Clearly, these errors are larger than desired.

Although many advanced devices have been used for DBH measurements, a caliper and diameter tape are still considered the most accurate measurement tools, and measurements obtained with these devices have been widely used as true values for comparison tests. However, the observations made with these two instruments and the recording of results are subjective, which will affect the validity of comparative tests.

http://www.aloki.hu ● ISSN 1589 1623 (Print) ● ISSN 1785 0037 (Online)
DOI: http://dx.doi.org/10.15666/aeer/1706_1340713421

To the present authors' knowledge, no tool has yet been developed that measures diameter as accurately as these two traditional tools and that does not yield subjective measurements.

In this study, a new diameter tape (barcode diameter tape) was developed. The scale on this tape was coded with special barcodes to allow measurements to be decoded and recorded using a smartphone with a wide-angle camera. A new algorithm to read and parse images with the barcodes was designed and developed into a smartphone application. This system seeks to obtain measurements of the same level of accuracy as traditional measurement tools and to overcome the subjectivity of observations and records. The new system was tested in typical forest conditions, and the accuracy of the DBH measurements was examined.

Barcode diameter tape

Structure of the barcode diameter tape

Diameter tape is a tool for measuring the diameter (D) of a tree at breast height. The measurement principle of conventional diameter tape is to measure the circumference (C) of the tree at breast height. D is obtained by the formula D=C/π. Thus, a linear relationship can be found between DBH and circumference, wherein each π cm on the diameter tape is equal to 1 cm DBH (*Fig. 1*). The unit interval on the diameter tape is designed for the π cm, sub-scale value for π/10, and the readout values from the tape are the DBH values.

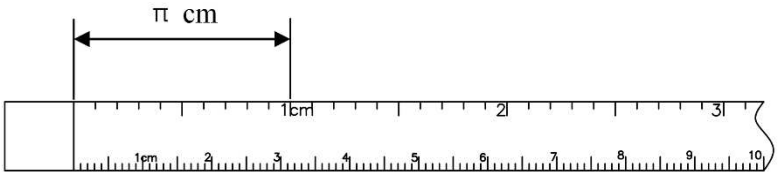

Figure 1. *Scale sample of traditional diameter tape*

The new barcode diameter tape designed in this paper separates the fractional area from the integer area without a dual scale (*Fig. 2*).

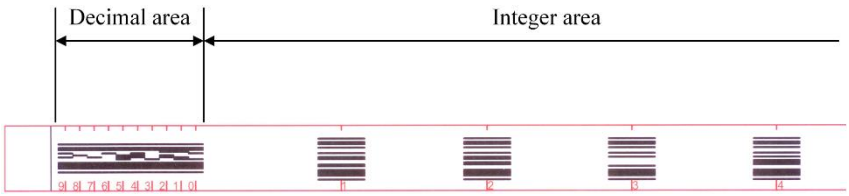

Figure 2. *Scale sample of barcode diameter tape*

The integer area of the scale interval is π cm; the fractional area of the overall length is π cm, with ten scales from 0-9; and the length of the scale interval is π/10 cm. The measurement principle of conventional diameter tape is shown in *Figure 3a*; the DBH of the tree is read along the bottom edge of the tape where the left and right ends of the tape cross at the 0-line. The measurement principle of the designed diameter tape is

http://www.aloki.hu ● ISSN 1589 1623 (Print) ● ISSN 1785 0037 (Online)
DOI: http://dx.doi.org/10.15666/aeer/1706_1340713421

shown in *Figure 3b*. The user reads the integer value before zero on the scale and the minimum scale value from the integer value to zero on the scale, which is the sum of the integer value within the fractional area and the fractional value corresponding to the integer scale (*Fig. 3*).

Principle of barcode encoding

A barcode can accurately represent numeric and alphabetic data using patterns (black lines and white lines) that can be read rapidly. The diameter tape is a tool used to obtain numeric diameter data, and 1D barcode can represent its corresponding value. However, there is an excessive number of standard patterns of existing barcodes. For example, the classic European Article Number (EAN-13) encoding standard contains 113 patterns. Each pattern is 0.33 mm in width according to conventional standards. The total width of the barcode is approximately 38 mm, which requires a tape greater than 38 mm in width. However, the width of conventional diameter tape is approximately 10 mm and thus does not meet the requirements of existing encoding standards. Therefore, two sets of simple barcodes were designed in this study: a set of black & white barcodes, and a set of multicolor barcodes.

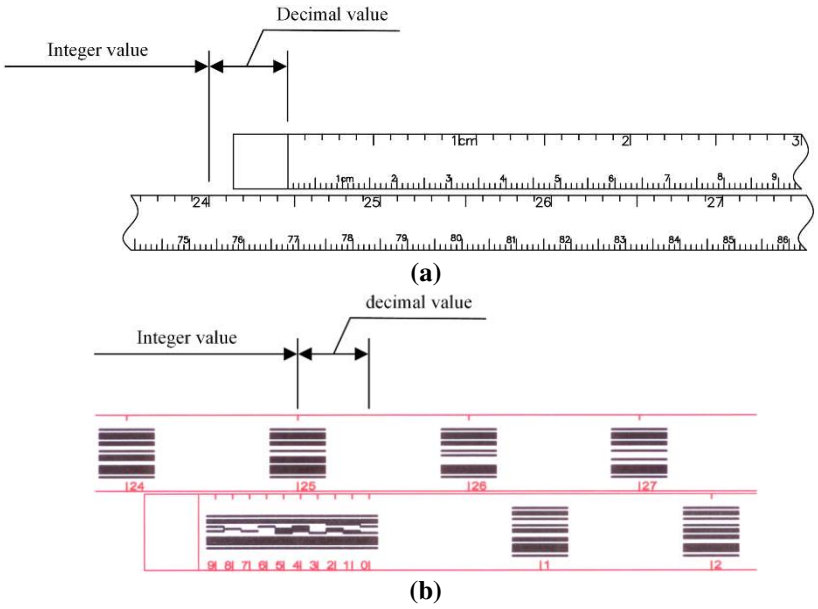

Figure 3. *Comparison of readout principle of diameter tapes*

The redesigned barcode consists of Left Quiet Zone, Start Character, Data Character, Stop Character and Right Quiet Zone. The pattern values of each zone except Data Character are shown in *Table 1*. In the set of black & white barcodes, the Data Character field refers to the EAN code and uses 7 patterns to represent a digit; the numbers corresponding to the code are shown in *Table 2*. The integer area requires two digits with 14 patterns, whereas the fractional area requires only one digit with 7 patterns. Different width-encoding modes are used for integer area and fractional area to allow the two parts to be distinguished accurately. The pattern width design is 0.4 mm, so the total tape width is 14 mm. Due to the limited space (3.14 mm) between scale lines in the fractional area, we made the pattern length 3.14 mm. The results are shown in *Figure 2*.

http://www.aloki.hu ● ISSN 1589 1623 (Print) ● ISSN 1785 0037 (Online)
DOI: http://dx.doi.org/10.15666/aeer/1706_1340713421

The structure of the multicolor barcodes is identical to that of black & white barcodes, except that two new colors (red and green) are added, which transforms the binary barcode to a quaternary barcode such that each zone can be represented with fewer patterns. The pattern values are shown in *Table 1* and *Table 2*. The pattern width design is 0.6 mm; thus, the total width is 9.6 mm. The results are shown in *Figure 4*.

Table 1. *Corresponding zone patterns of black & white and multicolor barcode*

Barcode type	Zone Pattern			
	Left Quiet Zone	Start Character	Stop Character	Right Quiet Zone
Black & White	000000	101	111101	000000
Multicolor	000	10	21	0000

"0": white; "1": black; "2": red; "3": green

Table 2. *Corresponding pattern of data characters*

Digit	Pattern of data character	
	Black &White	Multicolor
0	1010010	120
1	1100110	130
2	1101100	110
3	1000010	200
4	1011100	210
5	1001110	230
6	1010000	220
7	1000100	300
8	1001000	330
9	1010100	310

Figure 4. *Design of color barcode DBH tape*

Principle of barcode decoding

The redesigned barcode has two parts: an integer area and a fractional area. Neither part follows existing standard code, and there is no ready-made open source library or decoding methods to choose from. In this paper, a new set of decoding schemes was designed to meet the use of barcode diameter tape. The scheme can be used for decoding both black & white barcode and multicolor barcode. The decoding flowchart is shown in *Figure 5*.

Typically, a barcode-containing image (*Fig. 6*) can be captured through a camera-equipped device using the barcode diameter to measure DBH. The color of each pattern in the image can be determined by the values of the three channels of R, G and B. For example, the three-channel values for red are 255, 0, and 0 theoretically. However, the channel values are usually affected by the reflectivity and uniformity of light under natural conditions. In this paper, 3-channel values of the pixels on the mid-perpendicular of the image are counted, and the upper and lower quartiles are obtained. As shown in the

http://www.aloki.hu ● ISSN 1589 1623 (Print) ● ISSN 1785 0037 (Online)
DOI: http://dx.doi.org/10.15666/aeer/1706_1340713421

Table 3, if the pixel's R-channel value is greater than the upper quartile (UQ) of this channel and the G- and B-channel values are less than their respective lower quartiles (LQs), then the pixel color is considered red.

To read the value represented by the barcode, the integer and fractional areas should be found in the image; in *Figure 7*, this means finding Points ①-④. If searching down from right above the image, the pixel color goes through the sequence of "(non-white)-(white)-(non-white & non-black)-(black)", and the last black pixel is on the topmost module. The width of this pattern can be obtained by continuing to search down, and the midpoint of the module is Point ①. Similarly, Point ④ can be obtained through bottom-up search. However, if the midpoint of Point ① and Point ④ is adjusted as the starting point for searching Point ② and Point ③, the product may not conform to this sequence.

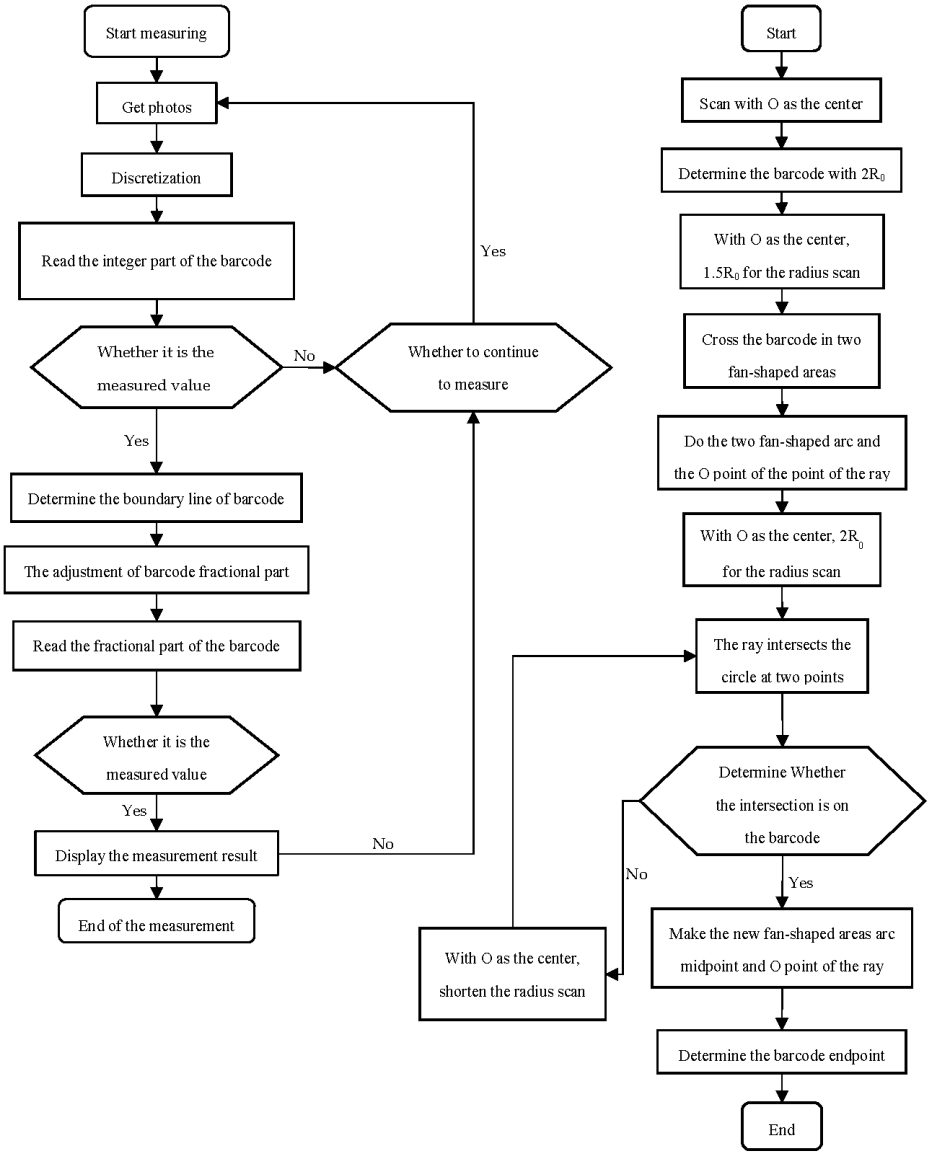

Figure 5. *Flowchart of the decoding method*

http://www.aloki.hu ● ISSN 1589 1623 (Print) ● ISSN 1785 0037 (Online)
DOI: http://dx.doi.org/10.15666/aeer/1706_1340713421

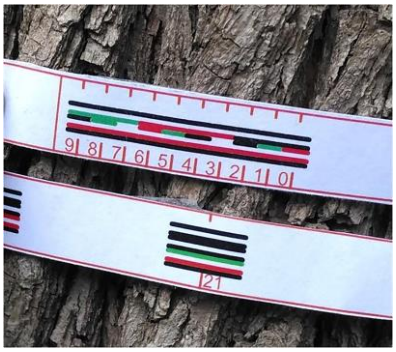

Figure 6. *Typical captured barcode-containing image*

Table 3. *Pixel channel characteristics of different colors*

color	R-channel value		G-channel value		B-channel value	
	<LQ	>UQ	<LQ	>UQ	<LQ	>UQ
white	-	Y	-	Y	-	Y
black	Y	-	Y	-	Y	-
red	-	Y	Y	-	Y	-
green	Y	-	-	Y	Y	-

"LQ": lower quartile; "UQ": upper quartile; "Y": yes

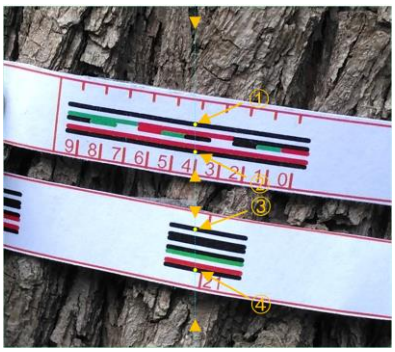

Figure 7. *Procedure of edge detection*

In this paper, the search starting points are adjusted to the pixel points at the corresponding distance above and below the midpoint. These starting points must be in the gap of tape or in the white area of the tape corresponding to the search direction. The distance is determined by the pattern structures of the barcode diameter tapes, which are shown in *Figure 8*. For black & white barcode diameter tape (*Fig. 8a*), the number of patterns between Point ① and Point ④ is calculated by *Equation 1*:

$$T = (23 - 0.5 + 6) + 2g + (9.5 + 16 - 0.5) = 53.5 + 2g \quad \text{(Eq.1)}$$

and the distance D should meet the following condition (*Equation 2*):

$$\frac{[(23 - 0.5 + 6) - T/2]N}{T} < D < \frac{[T/2 - (23 - 0.5)]N}{T} \quad \text{(Eq.2)}$$

http://www.aloki.hu ● ISSN 1589 1623 (Print) ● ISSN 1785 0037 (Online)
DOI: http://dx.doi.org/10.15666/aeer/1706_1340713421

where N is the number of pixels between Point ① and Point ④. This interval will be the smallest when g=0, and the range of D will be as follows (*Equation 3*):

$$0.0327N < D < 0.0421N \quad \text{(Eq.3)}$$

Similarly, the smallest interval of multicolor barcode diameter tape is as follows (*Equation 4*):

$$0.0319N < D < 0.0532N \quad \text{(Eq.4)}$$

This allows the algorithm to be adapted to both types of tapes, with values in the range of the following (*Equation 2*):

$$0.0327N < D < 0.0421N \quad \text{(Eq.5)}$$

After determining the inner patterns and outmost patterns (or Points ①-④), the distance (D12) between Point ① and Point ② and the distance (D34) between Point ③ and Point ④ can be calculated, and the wider distance can be considered the integer area. In *Figure 7*, the area between Point ③ and Point ④ will be seen as the integer area. If the number of patterns in the integer area is M, the space between Point ③ and Point ④ is equally divided into M-1 parts, with each equidistant point being the midpoint of each pattern. In this way, the color type of the equidistant points can be read and compared with the code library to obtain the corresponding value.

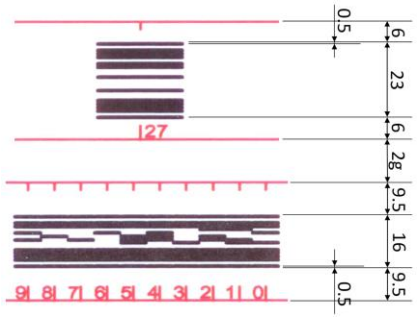

(a)

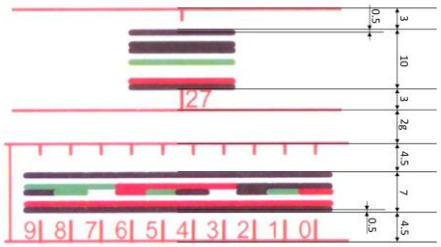

(b)

Figure 8. *Pattern distribution of barcodes. The unit is "Patterns", and "2 g" represents the gap width (number of patterns) between the integer area and fractional area of the tape*

http://www.aloki.hu ● ISSN 1589 1623 (Print) ● ISSN 1785 0037 (Online)
DOI: http://dx.doi.org/10.15666/aeer/1706_1340713421

The reading of the fractional area is primarily based on the corresponding integer area scale. However, it is difficult to ensure that there is no gap between the integer part and fractional part of tape and that the two parts are parallel during typical measurement. A new algorithm was developed to eliminate these difficulties, and the algorithm diagram is shown in *Figure 9*. From the figure, we can see that each mid-perpendicular of the pattern in the integer area crosses the corresponding scale line of the integral area, which can determine the scale position of the integer. In this context, the special pattern in the integer area that is closest to the fractional area is chosen as the target for obtaining a mid-perpendicular, and the endpoints of this pattern can be used to calculate the mid-perpendicular. The new algorithm needs to find the endpoints of this pattern; the new algorithm diagram is shown in *Figure 9*.

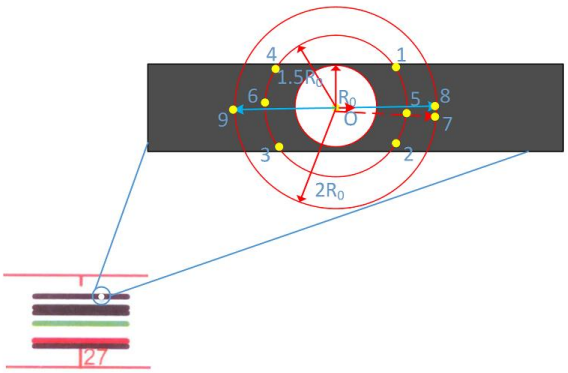

Figure 9. *Principle of the decoding algorithm*

In this algorithm, a circle, which has its center at Point O (Point ③ in *Figure 7*) and a radius of 2 pixels, is determined. If all the pixels in the circle have the same color type as Point O, the radius of the circle is gradually increased until a pixel of a color type different from the color type of Point O appears in the circle. At the end of this process, the pattern width is $2R_0$ assuming a radius of R_0. With Point O as the center and $1.5R_0$ as the radius of a circle, the circle will intersect with the pattern at arc (12)ˆ and arc (34)ˆ. Point 5 and Point 6 are the midpoints of arc (12)ˆ and arc (34)ˆ, respectively. With the midpoint as the center and $2R_0$ as the radius of a circle, the ray passing through Point O and Point 5 intersects with the circle at Point 7. If Point 7 is in the pattern, it will be corrected to the midpoint 8 of the arc where Point 7 is located. Then, the radius of circle continues to be increased until the intersection of the circle with the corresponding ray is not included in the pattern. The target endpoint should be close to this intersection point and can be obtained by adjusting the intersection point. Similarly, another endpoint can be obtained using this method. These two endpoints are similar to Point A, B in *Figure 10*, and Point C, D, E, F can be obtained by the same method. As shown in *Figure 10*, the mid-perpendicular of Point A, B intersects Line AB at Point P0 and Line CD at Point P1. To amend the error caused by the non-parallel and gap between the integer and fractional parts of the tape, the target fractional code is the code that is intersected by the line passing through Point P (midpoint of Point P0 and P1) and perpendicular to Line CD or the code between Point S1 and S2. The value can be read in a way similar to that of the integer area.

http://www.aloki.hu ● ISSN 1589 1623 (Print) ● ISSN 1785 0037 (Online)
DOI: http://dx.doi.org/10.15666/aeer/1706_1340713421

Materials and Methods

The profile of the study sites

Two plots in Xiangshan (40.00°N, 116.19°E), located in Beijing, China, were selected for study. A total of 94 standing trees in the plots (each 25*25 m) were investigated; descriptive statistics of the plots are summarized in *Table 4*. The tree species in Plot 1 are mainly conifer species, and those in Plot 2 are broad-leaved species. The data in the table were obtained using a caliper. The DBH of each tree was measured by six different observers, and the average values were taken as the true values of the trees.

Since the principles of the black & white barcode tape and the multicolor barcode tape are the same, the test data were obtained by a multicolor barcode tape. To study the subjectivity of different researchers in measuring DBH and the effect of observer experience on DBH measurement, the data were measured by six different observers. Numbered patches were attached to the breast height of trees as reference points to ensure that each measurement was collected at the same height.

The reference values were measured using a traditional diameter tape. For comparison with the measurement results obtained by barcode tape, each diameter was measured by the same six different observers.

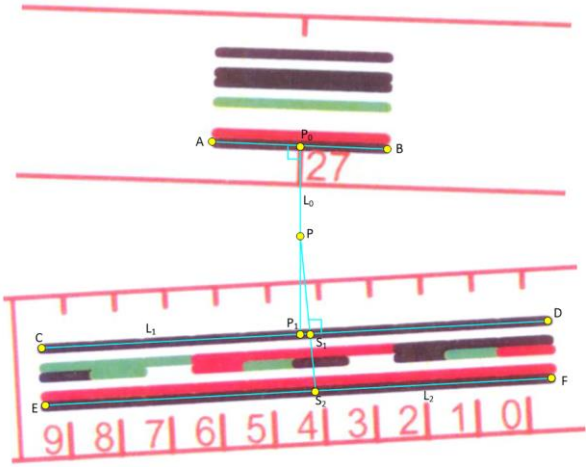

Figure 10. *Adjustment and reading of fractional area*

Table 4. *Summary statistics of DBH in the plots*

Plot	Species	N	Mean(cm)	S.D.(cm)	Minimum(cm)	Maximum(cm)
1	Platycladus orientalis	50	18.2	9.6	6.2	50.7
	Acer truncatum	4	8.0	2.0	6.2	10.4
2	Catalpa ovata	37	20.6	5.6	9.5	30.0
	Sophora japonicum	3	43.3	6.9	36.6	50.5

Methods

Error observation

To estimate the central trend and variability of measurements obtained by different observers using the barcode tape, bias, relative BIAS, root mean squared error (RMSE)

http://www.aloki.hu ● ISSN 1589 1623 (Print) ● ISSN 1785 0037 (Online)
DOI: http://dx.doi.org/10.15666/aeer/1706_1340713421

and relative RMSE were used as evaluation indicators, as defined in (*Equation 6*) - (*Equation 9*).

$$Bias = \frac{1}{n}\sum_{i=1}^{n}(d_i - d_{ri}) \quad \text{(Eq.6)}$$

$$Bias\% = \frac{Bias}{\overline{d_r}} \times 100\% \quad \text{(Eq.7)}$$

$$RMSE = \sqrt{\frac{\sum_{i=0}^{n}(d_i - d_{ri})^2}{n}} \quad \text{(Eq.8)}$$

$$RMSE\% = \frac{RMSE}{\overline{d_r}} \times 100\% \quad \text{(Eq.9)}$$

where d_i is the ith measurement, d_{ri} is the ith reference value, $\overline{d_r}$ is the mean of references, and n is the number of measurements.

Generally, the measurements obtained by the traditional diameter tape are widely used as the reference values. Because these values also contain errors and because the purpose of this paper is to compare the accuracy of measurements between a traditional diameter tape and a barcode tape, the measurements obtained by a traditional diameter tape cannot be used as reference values. In this paper, when estimating the bias of the barcode tape measurements, the mean values of observations using the traditional diameter tape by six different observers were taken as the reference values. Furthermore, when comparing the variability of the measurements obtained by the diameter tape and the barcode tape, the means of measurements obtained using the barcode tape by the six different observers were considered as reference values.

Dependence of measurement error

The purpose of using a barcode tape is to reduce the subjectivity of human-read measurements or the differences in measurements between observers. A linear mixed model can detect differences between groups and is suitable for identifying the error associated with different observers. The model is defined as *Equation 10*:

$$y = X\beta + U\xi + \varepsilon \quad \text{(Eq.10)}$$

where y is an $n \times 1$ observation vector, β is the p×1 fixed parameters vector, X is the $n \times p$ matrix of the independent variables associated with the fixed parameters, ξ is the $q \times 1$ intragroup effect parameters vector, U is the $n \times q$ matrix of the explanatory variables associated with the intragroup effect parameters, and ε is a $n \times 1$ random error vector.

In this paper, measurement errors were treated as dependent variables, the intercept was the only fixed effect, and observer was considered a random variable. The proportion of errors in the total errors caused by different observers was used as a basis for comparison.

http://www.aloki.hu ● ISSN 1589 1623 (Print) ● ISSN 1785 0037 (Online)
DOI: http://dx.doi.org/10.15666/aeer/1706_1340713421

Results and Discussion

The measurements of DBH obtained by different observers are shown in *Table 5*. When the mean measurements observed by the traditional tool were used as the reference values, diameter was on average underestimated by 1.3 mm. However, this bias was not significant (0.67%). When the within-group means were used as the reference values, the bias variability (-1.8~1.4 mm) of the traditional tool was larger than that of the barcode tape (-0.7~0.7 mm). RMSE is an indicator used to assess variability. When the observer used the new measurement tool, regardless of whether the within-group or between-group means were selected as the reference values, the measurement values had less variability (2.71%, 3.92%) than those obtained with the traditional tool (4.46%).

Table 5. *Accuracies of the DBH measurements by observers M1-M6 (n = 94 trees measured by each observer)*

	Observer	Bias (W)	Bias% (W)	Bias (B)	Bias% (B)	RMSE (W)	RMSE% (W)	RMSE (B)
traditional diameter tape	M1	-1.8	-0.88%	-	-	13.5	6.55%	-
	M2	-0.1	-0.07%	-	-	9.8	4.74%	-
	M3	1.4	0.68%	-	-	4.4	2.14%	-
	M4	-0.1	-0.05%	-	-	14.3	6.96%	-
	M5	0.2	0.12%	-	-	8.5	4.14%	-
	M6	0.5	0.23%	-	-	4.6	2.23%	-
	Mean	0.0	0.00%	-	-	9.2	4.46%	-
barcode tape	M1	-0.7	-0.32%	-1.0	-0.50%	4.2	2.03%	5.6
	M2	0.1	0.07%	-0.2	-0.11%	5.6	2.73%	7.7
	M3	-0.1	-0.07%	-0.5	-0.25%	4.1	2.01%	3.9
	M4	0.7	0.34%	0.3	0.16%	7.2	3.50%	10.9
	M5	-0.5	-0.24%	9.5	4.86%	9.0	4.37%	13.3
	M6	0.1	0.04%	-0.3	-0.14%	3.3	1.63%	6.3
	Mean	-0.1	-0.03%	1.3	0.67%	5.6	2.71%	7.9

"W" means the within-group evaluations; "B" means the between-group evaluations; M1-M6 means different observers

Regarding the variability of measurements obtained with the diameter tape, 13.7% was due to differences among observers. When using the barcode tape, the corresponding value was 0%. However, if the means of measurements obtained with the traditional tape were selected as the reference values, the corresponding value was 21.0%. This larger variability was due to the differences between the mean values of different measurement tools; thus, the barcode tape was unable to eliminate the differences between observers. However, this new tool can reduce this difference. To determine the reduction in this difference, many comparative tests should be conducted over the long term.

The measurement results are expected to be better than the results from the remote sensing, such as relascope, TLS, MLS and camera. Kalliovirta et al. (2005) evaluated the availability of laser-relascope in forest inventory and reported an 8.2 mm standard error of DBH estimations, i.e. 4.7% from the mean diameter; obviously, the results have greater variability compared to our results due to our new tool using a contact measurement method. Vastaranta et al. (2009) evaluated the accuracy of the laser-camera in estimating the DBH of the tree; their results showed the standard errors

http://www.aloki.hu ● ISSN 1589 1623 (Print) ● ISSN 1785 0037 (Online)
DOI: http://dx.doi.org/10.15666/aeer/1706_1340713421

of DBH measurements were 8.3 mm and 8.5 mm. Although the device used a method of automatically estimating the DBHs to avoid subjective interference, it is less accurate than our tool because it is also a remote sensing measurement tool. Miller et al. (2015) used the digital photogrammetry to obtain point clouds to estimate the DBHs of the trees; the RMSE of the DBH estimation of individual trees was 2.39 cm. This approach avoided subjective interference and improved work efficiency, but its accuracy is still lower than our tool due to limited camera resolution and processing methods. Obviously, the accuracy of the barcode DBH tape data shows that it has the potential to measure DBH accurately. The results in this study indicated that the barcode DBH tape is an attractive and accurate technology for DBH measurements, which may be applied as the references to former remote sensing methods.

Conclusions

In this study, two barcode diameter tapes (black & white and multicolor barcode tapes) were designed. A new decoding algorithm was designed and developed as an application that was installed on a mobile phone with a wide-angle camera for parsing and recording the measurements of these new diameter tapes. The system was tested under typical forest conditions. When the mean values obtained with a traditional diameter tape were selected as reference values, the bias of the measurements was not significant (1.3 mm). The RMSE of the DBH was 5.6 mm. In addition, the DBM measurements obtained with a traditional tape were biased; specifically, they tended to be overestimates. The results also showed that the new tool could reduce the subjectivity of observers when reading observations and potentially replace traditional diameter tapes.

In the future, many comparative trials should be conducted to determine the precise amount of subjective improvement attained with the barcode tape. These tests should be conducted under different forest conditions, such as different canopy closures, ages, and forest types. In addition, there are some problems with the algorithm that cannot be completely solved. For example, when the angle between the integer tape and decimal tape is too large, the decimal value may not be accurately determined. This problem should be assessed quantitatively and appropriately resolved.

REFERENCES

[1] Bijak, S., Sarzyński, J. (2015): Accuracy of smartphone applications in the field measurements of tree height. – Folia Forestalia Polonica 57.

[2] Drexhage, M., Colin, F. (2001): Estimating root system biomass from breast-height diameters. – Forestry 74: 491-497.

[3] Gering, L. R., May, D. M. (1995): The Relationship of Diameter at Breast Height and Crown Diameter for Four Species Groups in Hardin County, Tennessee. – Southern Journal of Applied Forestry 19: 177-181.

[4] Juujarvi, J., Heikkonen, J., Brandt, S. S., Lampinen, J. (1998): In Digital-image-based tree measurement for forest inventory, Intelligent Robots and Computer Vision XVII: Algorithms, Techniques, and Active Vision. – International Society for Optics and Photonics: 114-124.

[5] Kalliovirta, J., Laasasenaho, J., Kangas, A. (2005): Evaluation of the Laser-relascope. – Forest Ecology and Management 204: 181-194.

http://www.aloki.hu ● ISSN 1589 1623 (Print) ● ISSN 1785 0037 (Online)
DOI: http://dx.doi.org/10.15666/aeer/1706_1340713421

[6] Liang, X., Hyyppä, J., Kaartinen, H., Holopainen, M., Melkas, T. (2012): Detecting Changes in Forest Structure over Time with Bi-Temporal Terrestrial Laser Scanning Data. – ISPRS International Journal of Geo-Information 1: 242-255.
[7] Liang, X., Hyyppä, J., Kukko, A., Kaartinen, H., Jaakkola, A., Yu, X. (2014a): The Use of a Mobile Laser Scanning System for Mapping Large Forest Plots. – Geoscience and Remote Sensing Letters, IEEE 11: 1504-1508.
[8] Liang, X., Jaakkola, A., Wang, Y., Hyyppä, J., Honkavaara, E., Liu, J., Kaartinen, H. (2014b): The Use of a Hand-Held Camera for Individual Tree 3D Mapping in Forest Sample Plots. – Remote Sensing 6: 6587-6603.
[9] Maas, H. G., Bienert, A., Scheller, S., Keane, E. (2008): Automatic forest inventory parameter determination from terrestrial laser scanner data. – International Journal of Remote Sensing 29: 1579-1593.
[10] Maia Araujo, T., Higuchi, N., Carvalho, J. (1999): Comparison of formulae for biomass content determination in a tropical rain forest site in the state of Para Â, Brazil. – Forest Ecology and Management 117: 43-52.
[11] Melkas, T., Vastaranta, M., Holopainen, M. (2008): Accuracy and efficiency of the Laser-camera. – SilviLaser: 17-19.
[12] Miller, J., Morgenroth, J., Gomez, C. (2015): 3D modelling of individual trees using a handheld camera: Accuracy of height, diameter and volume estimates. – Urban Forestry & Urban Greening 14: 932-940.
[13] Molinier, M., Lopez-Sanchez, C., Toivanen, T., Korpela, I., Corral-Rivas, J. J., Tergujeff, R., Häme, T. (2016): Relasphone—Mobile and Participative In Situ Forest Biomass Measurements Supporting Satellite Image Mapping. – Remote Sensing 8: 869-891.
[14] Olofsson, K., Olsson, H. (2017): Estimating tree stem density and diameter distribution in single scan terrestrial laser measurements of field plots: a simulation study. – Scandinavian Journal of Forest Research 33: 1-20.
[15] Ouimet, R., Camiré, C., Brazeau, M., Moore, J.-D. (2008): Estimation of coarse root biomass and nutrient content for sugar maple, jack pine, and black spruce using stem diameter at breast height. – Canadian Journal of Forest Research 38: 92-100.
[16] Popescu, S., Wynne, R., Nelson, R. (2003): Measuring individual tree crown diameter with lidar and assessing its influence on estimating forest volume and biomass. – Canadian Journal of Remote Sensing 29: 564-577.
[17] Qu, Y., Wang, J., Song, J., Wang, J. (2017): Potential and Limits of Retrieving Conifer Leaf Area Index Using Smartphone-Based Method. – Forests 8: 217.
[18] Riaño, D., Meier, E., Allgöwer, B., Chuvieco, E., Ustin, S. (2003): Modeling airborne laser scanning data for the spatial generation of critical forest parameters in fire behavior modeling. – Remote Sensing of Environment 86: 177-186.
[19] Saarinen, N., Vastaranta, M., Vaaja, M., Lotsari, E., Jaakkola, A., Kukko, A., Kaartinen, H., Holopainen, M., Hyyppä, H., Alho, P. (2013): Area-Based Approach for Mapping and Monitoring Riverine Vegetation Using Mobile Laser Scanning. – Remote Sensing 5: 5285-5303.
[20] Srinivasan, S., Popescu, S., Eriksson, M., Sheridan, R., Ku, N.-W. (2015): Terrestrial Laser Scanning as an Effective Tool to Retrieve Tree Level Height, Crown Width, and Stem Diameter. – Remote Sensing Letters 7: 1877-1896.
[21] Sumida, A., Miyaura, T., Torii, H. (2013): Relationships of tree height and diameter at breast height revisited: Analyses of stem growth using 20-year data of an even-aged Chamaecyparis obtusa stand. – Tree physiology 33.
[22] Varjo, J., Henttonen, H., Lappi, J., Heikkonen, J., Juujärvi, J. (2019): Digital horizontal tree measurements for forest inventory.
[23] Vastaranta, M., Latorre, E. G., Luoma, V., Saarinen, N., Holopainen, M., Hyyppä, J. (2015): Evaluation of a Smartphone App for Forest Sample Plot Measurements. – Forests 6: 1179-1194.

http://www.aloki.hu ● ISSN 1589 1623 (Print) ● ISSN 1785 0037 (Online)
DOI: http://dx.doi.org/10.15666/aeer/1706_1340713421

[24] Villasante, A., Fernandez, C. (2014): Measurement errors in the use of smartphones as low- cost forestry hypsometers. – Silva Fennica 48: 11.
[25] Watt, P., Donoghue, D. (2005): Measuring forest structure with terrestrial laser scanning. – International Journal of Remote Sensing 26.
[26] Wieser, M., Mandlburger, G., Hollaus, M., Otepka, J., Glira, P., Pfeifer, N. (2017): A Case Study of UAS Borne Laser Scanning for Measurement of Tree Stem Diameter. – Remote Sensing 9: 1154.
[27] Yu, X., Liang, X., Hyyppä, J., Kankare, V., Vastaranta, M., Holopainen, M. (2013): Stem biomass estimation based on stem reconstruction from terrestrial laser scanning point clouds. – Remote Sensing Letters 4: 344-353.

http://www.aloki.hu ● ISSN 1589 1623 (Print) ● ISSN 1785 0037 (Online)
DOI: http://dx.doi.org/10.15666/aeer/1706_1340713421

APPLICATION OF BRYOPHYTE RHIZOID-ASSOCIATED BACTERIA INCREASES SILICON ACCUMULATION AND GROWTH IN MAIZE (*ZEA MAYS* L.) SEEDLINGS

HU, L.[1,2] – XU, C. C.[3] – WANG, J.[1] – CHEN, D. Q.[1] – ZENG, R. S.[1] – SONG, Y. Y.[1] – CHEN, D. M.[1*]

[1]*Key Laboratory of Ministry of Education for Genetics, Breeding and Multiple Utilization of Crops, College of Crop Science, Fujian Agriculture and Forestry University, Fuzhou, China*

[2]*Key Laboratory of Beibu Gulf Environment Change and Resources Utilization of Ministry of Education, Nanning Normal University, Nanning, China*

[3]*College of Life Sciences, Fujian Agriculture and Forestry University, Fuzhou, China*

**Corresponding author*
e-mail: dongmeijj@163.com; phone: +86-130-1572-5866; fax: +86-591-8378-9483

(Received 19th Jun 2019; accepted 2nd Sep 2019)

Abstract. Silicon (Si) enhances plant resistance to various forms of stress. However, the availability of Si as a plant nutrient is frequently limited. Bryophytes are able to grow on the surface of rocks and buildings with high Si accumulation. Therefore, bryophyte rhizoids might harbor microorganisms capable of solubilizing Si. In this study, silicate solubilizing bacteria (SSB) were isolated from the rhizoids of the bryophyte *Hypnum plumaeforme* L. to examine their effects on Si weathering and growth of maize (*Zea mays* L.). Molecular phylogeny and 16S rRNA gene sequence analysis demonstrated that the dominant bacterial strain B1-5 was a member of the *Kosakonia* genus. The concentrations of soluble Si released from the feldspar and quartz powder in liquid media with strain B1-5 inoculation were higher than those of the control. B1-5 inoculation in pot soil significantly increased the water-extractable Si content in soil, improved Si uptake and accumulation in maize plants, and promoted seedling growth. These results not only prove the existence of SSB in bryophyte rhizoids, but also demonstrate a new approach to searching for effective biological Si fertilizers.
Keywords: *silicate solubilizing bacteria, microbial weathering, molecular phylogeny, Kosakonia, biological fertilizer*

Introduction

Silicon (Si) is the second most abundant element after oxygen in soil. It occurs mostly in the form of dioxide and silicates (Myshlyaeva and Krasnoshchekov, 1974), which cannot be directly used by plants. Only water-soluble monosilicic acid [$Si(OH)_4$], a product of the weathering of rocks and soil minerals, is available to plants (Epstein, 1994; Raven, 1983). Si has not yet been recognized as an essential nutrient element for plants, but its beneficial effects on resistance have been extensively reported in numerous crops (Epstein, 1999). In 2015 Si was listed as a "beneficial substance" by the International Plant Nutrition Institute, USA (Reynolds et al., 2016). Increasing evidences indicate that Si can alleviate both biotic and abiotic stresses including pathogens, herbivores, extreme temperature, water deficiency, high salinity and nutrient stresses (Debona et al., 2017; Ma, 2004; Wu et al., 2017). Nitrogen (N), phosphorus (P) and potassium (K) fertilizers are widely applied in agricultural production, but Si fertilizer is usually neglected. Si deficiency frequently occurs as a result of Si removal by continuous crop harvest (Liang et al., 2015). Thus, it is of significance to effectively convert unavailable Si in the soils into a form plants can utilize.

http://www.aloki.hu ● ISSN 1589 1623 (Print) ● ISSN 1785 0037 (Online)
DOI: http://dx.doi.org/10.15666/aeer/1706_1342313433

Soil microbes play a crucial role in nutrient availability and mineral weathering from primary minerals (Vessey, 2003). Most related studies focused on the P and K solubilizing abilities of some microorganisms as seen in *Table 1*.

Table 1. *Studies of phosphate and potassium solubilizing bacteria in crops*

Crop name	Solubilizing capacity	Citation
Barely (*Hordeum vulgare* L.)	P	Mehrvarz and Chaichi, 2008
Wheat (*Triticum aestivum* L.)	P	Afzal et al., 2005
Wheat (*Triticum aestivum* L.)	K	Sheng and He, 2006
Pepper (*Capsicum annuum* L.)	P and K	Han and Lee, 2006
Cucumber (*Cucumis sativus* L.)	P and K	Han and Lee, 2006
Tobacco (*Nicotiana tabacum* L.)	K	Zhang and Kong, 2014
Cotton (*Gossypium barbadense* L.)	K	Sheng, 2005
Rape (*Brassica campestris* L.)	K	Sheng, 2005
Peanut (*Arachis hypogaea* L.)	K	Youssef et al., 2010
Sesame (*Sesamum indicum* L.)	K	Youssef et al., 2010
Ryegrass (*Lolium rigidum* L.)	K	Xiao et al., 2017
Maize (*Zea mays* L.)	K	Singh et al., 2010

The role of silicate solubilizing bacteria (SSB), which can solubilize silicon from silicate bearing mineral and rocks (Bosecker, 1997), is largely ignored. Use of highly-efficient SSB is a promising approach for enhancing crop yield and defense in Si deficient soil.

An analysis of the Si contents in 175 plant species collected from a botanical garden shows that Bryophyta (3.46%) contains the highest Si, following by Pteridophyta (1.4%), Gymnospermae (0.5%), Angiospermae (0.13%) (Takahashi and Miyake, 1976a, b, c), suggesting that bryophytes are Si accumulators with high Si content. Therefore, we speculated that bryophyte rhizoids harbor certain SSB capable of solubilizing Si from poor nutrient habitats.

In the present study, our aims were to: (1) isolate and characterize bryophyte rhizoids-associated silicate bacteria, (2) determine the Si-solubilizing ability of selected bacteria, and (3) examine the effect of soil inoculation with selected bacteria on Si availability in the soil, Si uptake and plant growth in maize.

Materials and methods

Plants, soil and mineral

Bryophyte *Hypnum plumaeforme* was collected from rock walls in the back hill on Jinshan Campus of Fujian Agriculture and Forestry University, Fuzhou, China (119°54' E, 26°05' N) in July, 2018. Bryophytes from eight random sampling locations were kept in sterilized plastic Petri-dishes until the isolation experiment began in the same day.

The soils for maize potting were collected from a hillside near the university campus. The soil was a red soil (Typic Hapludults) (Soil Survey Staff, 2010). The properties of the soil were: pH (1:2.5 w/v water) 5.5; organic C 10.03 $g \cdot kg^{-1}$; total N 1.28 $g \cdot kg^{-1}$; available N 19.3 $mg \cdot kg^{-1}$; total P 0.13 $g \cdot kg^{-1}$; available P 12.6 $mg \cdot kg^{-1}$; total K 2.05 $g \cdot kg^{-1}$; available K 154.6 $mg \cdot kg^{-1}$, water-extractable Si 34.3 $mg \cdot kg^{-1}$. Seeds of

http://www.aloki.hu ● ISSN 1589 1623 (Print) ● ISSN 1785 0037 (Online)
DOI: http://dx.doi.org/10.15666/aeer/1706_1342313433

maize (*Zea mays*, cultivar Yuecai) were obtained from the Crop Research Institute, Guangdong Academy of Agricultural Sciences, Guangzhou, China.

Mineral powders, feldspar ($KAlSi_3O_8$, SiO_2 68.09%) and quartz (SiO_2 98.81%), were manufactured by Foshan Hongda Ceramics Co., Ltd and passed through 0.075 mm mesh sieve. The powders were rinsed three times in pure water to eliminate soluble Si.

Isolation of silicate bacteria from bryophyte rhizoids

All collected bryophytes were slightly shaken to remove sands loosely adhering to the rhizoids. The rhizoids with the remaining adherd soil were swayed in 25 mL sterile water with tweezers, and the water was transferred to a 50 mL plastic tubes. The tubes were shaken with a vortex mixer for 15 s. The mixture was kept at room temperature for 30 min. The serially diluted suspension was plated on the surface of Aleksandrov's medium for silicate bacterial culture containing 0.5% sucrose, 0.05% $MgSO_4 \cdot 7H_2O$, 0.5% $FeCl_3$, 0.2% Na_2HPO_4, 0.01% $CaCO_3$, 0.1% $KAlSi_3O_8$, and 2% Agar, pH 7.2 (Hu et al., 2018). The Petri-dishes were placed in an incubator at 28 °C for 5 d. The growth of bacteria was checked every day. Fast-growing isolates with different morphology were further purified. The pure colonies were inoculated into liquid medium and preserved in 25% glycerol solution at -80 °C for future use.

Mineral dissolution experiment

The dominant strain was selected to test the ability to solubilize the mineral. The liquid medium consisted of 1% sucrose, 0.05% yeast extract, 0.1% NH_4SO_4, 0.2% Na_2HPO_4, 0.05% $MgSO_4 \cdot 7H_2O$, 0.01% NaCl, 0.01% $CaCO_3$, 5 g mineral powder, pH 7.2. Each conical flask (250 mL) contained 100 mL autoclaved liquid medium and 5 mL bacterial inocula (10^6 cfu mL^{-1}) as inoculation treatment. Five mL of sterilized inoculum were also added to the liquid medium to serve as control.

Feldspar and quartz were used as Si mineral respectively in two separate experiments. The inoculation and corresponding control were replicated three times. Each flask was maintained at 180 rpm for 7 d at 28 °C. The fermented broth was centrifuged at 8000 *g* for 20 min. The solubilized Si concentration in the supernatant was determined using the colorimetric molybdenum blue method described by Pettersson and Karlberg (1999).

Molecular identification

Genomic DNA was extracted using the DNA extraction Kit (Qiagen, USA) according to the manufacture's protocol. The universal primers for 16S rRNA sequence amplification were 27F (5′-GTTTGATCCTGGCTCAG-3′) and 1492R (5′-GGTTACCTTGTTACGACTT-3′) (Lin et al., 2012). The PCR reaction system had a volume of 25 μl, including Taq PCR Master Mix 12.5 μl, primer 2 μl, ddH_2O 9.5 μl, and DNA template 1 μl. The PCR was performed as follows: hot start at 94 °C for 5 min, followed by 30 cycles of denaturation at 94 °C for 30 s, annealing at 55 °C for 30 s, and extension at 72 °C for 60 s. A final extension step lasted 8 min at 72 °C. The PCR products were purified and sequenced by Shanghai Biosune Biological Technology Co., Ltd. The sequencing results were analyzed using NCBI database to find the closely related homologous sequences.

The sequence and the reference sequences with the highest similarities were aligned using Clustalx 1.83 and phylogenetic analyses was done using MEGA version 4 with

http://www.aloki.hu ● ISSN 1589 1623 (Print) ● ISSN 1785 0037 (Online)
DOI: http://dx.doi.org/10.15666/aeer/1706_1342313433

the neighbor-joining method, p-distance and 1000 bootstrap replicates (Tamura et al., 2007; Thompson et al., 1997).

Pot experiment

Maize seeds were surface-sterilized with 10% H_2O_2 for 10 min, and then rinsed 5 times with distilled water. The seeds were soaked in distilled water for 24 h, and then pre-germinated for 48 h at 28 °C. One seedling was transplanted to a 1 L plastic pot with 750 g dry sterilized soil. The soil were autoclaved thrice in three consecutive days. Meanwhile, the cells in cultured bacterial broth were collected by centrifugation at 8000 *g* for 20 min at 4 °C and washed with sterilized tap water. The pelleted cells were resuspended with sterilized water and then the cells were adjusted to around 10^6 cfu mL^{-1} as determined by a standard growth curve based on optical density reading at 600 nm using a spectrophotometer (Ling et al., 2009). The experiment was established with two groups: one group was inoculated with 10 mL bacterial suspension as inoculation treatment, and the other group was added with 10 mL distilled water as control. A total of 20 pots with maize plants were divided into two groups. After 7 d, all plants were fertilized with 50 mL Hoagland nutrient solution (Hoagland and Arnon, 1950).

All plants were harvested 5 weeks after transplanting. The roots were washed and cleaned, and stem diameters were measured. All plants samples were dried at 70 °C for 3 d, then weighed. The Si contents of dry samples were then analyzed by molybdenum blue colorimetric method described by Dannon and Wydra (2004). The water-extractable Si content of air-dry soil samples (1:10 w/v water) was determined by colorimetric molybdenum blue method described by Wang et al. (2004).

Statistical analysis

Si concentrations in culture solution, growth indexes and Si content of plants and soils were analyzed using t-test ($P < 0.05$) to determine difference between bacterial inoculation and control. All analyses were performed with the SPSS 13.0 software package (SPSS Inc.).

Results and discussion

Isolation silicate bacteria from the bryophyte rhizoids

Si-solubilizing bacterial isolates were obtained from the bryophyte *Hypnum plumaeforme* rhizoids on rock walls (*Fig. 1A*), and one of them showed the dominant colony which was named as B1-5, and kept for further study. On the Aleksandrov plates, the strain B1-5 formed round, smooth, convex, slimy, elastic, translucent and colorless colonies (*Fig. 1B*). Silicate solubilizing bacteria (SSB) can solubilize silicon from silicate mineral (Bosecker, 1997). Bryophyte with high Si-accumulation mostly can grow on the surface of rocks and buildings. So it raises the possibility that some SSB may adhere to the bryophyte rhizoids.

Molecular identification based on 16S rRNA analysis

About 1500 bp band was obtained from the amplification of 16S rRNA gene sequence from the strain B1-5. The 16S rRNA gene sequence of B1-5 clones was submitted to GenBank with accession number MH051262. Phylogenetic analysis

http://www.aloki.hu ● ISSN 1589 1623 (Print) ● ISSN 1785 0037 (Online)
DOI: http://dx.doi.org/10.15666/aeer/1706_1342313433

showed that B1-5 and all 6 *Kosakonia* species formed a branch, and that other outgroup species formed different branches (*Fig. 2*). Thus, the B1-5 strain belongs to the *Kosakonia* genus. *Figure 2* also showed that strain B1-5 shared the highest sequence similarities with *Kosakonia cowanii*. Thus, strain B1-5 was identified as a member of *Kosakonia*.

Several *Kosakonia* species isolated from soils and trees promote plant growth (Brady et al., 2013). Diazotrophic bacteria, *K. pneumoniae* and *K. radicincitans* were found to be associated sugarcane at Northeast Region of Brazil (Antonio et al., 2016). *K. radicincitans* improves fruit yield and quality of *Solanum lycopersicum* (Berger et al., 2017). *K. radicincitans* alters *Arabidopsis thaliana* root and root exudate metabolism (Witzel et al., 2017). *K. pseudosacchari* sp. nov., an endophyte of *Zea mays* was isolated (Kaempfer et al., 2016).

Si solubilizing activity of the bacteria

The ability of strain B1-5 to solubilize Si was assessed in liquid media containing mineral powders of $KAlSi_3O_8$ and SiO_2 (*Fig. 3*). After 7 days of incubation, a significant increase in soluble Si concentration of the medium with $KAlSi_3O_8$ ($t = -5.344$, $df = 4$, $P = 0.006$) or SiO_2 ($t = -43.466$, $df = 4$, $P < 0.001$) supplement was observed in inoculated versus control seedlings.

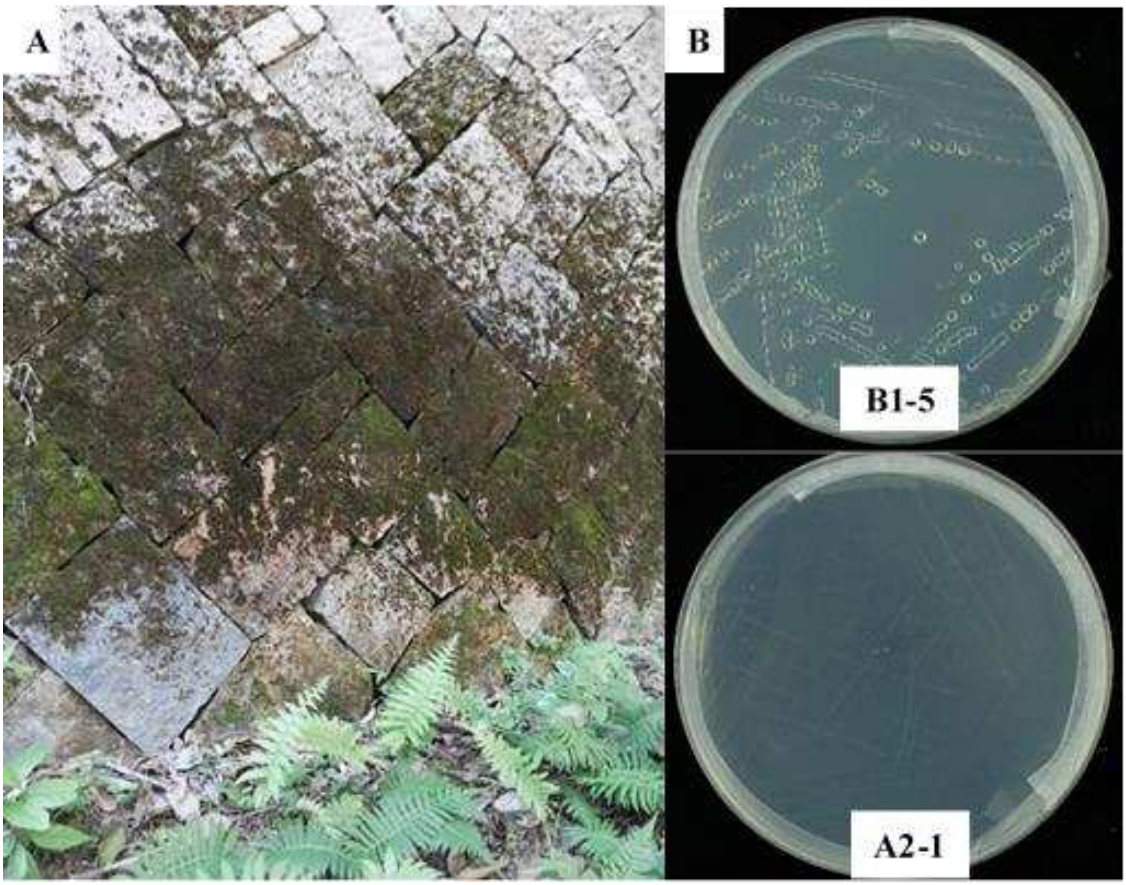

Figure 1. *Habitat of bryophyte Hypnum plumaeforme on rock walls (A). Characteristics of strains B1-5 and A2-1 colonies after grown on Aleksandrov medium for 48 h (B)*

http://www.aloki.hu ● ISSN 1589 1623 (Print) ● ISSN 1785 0037 (Online)
DOI: http://dx.doi.org/10.15666/aeer/1706_1342313433

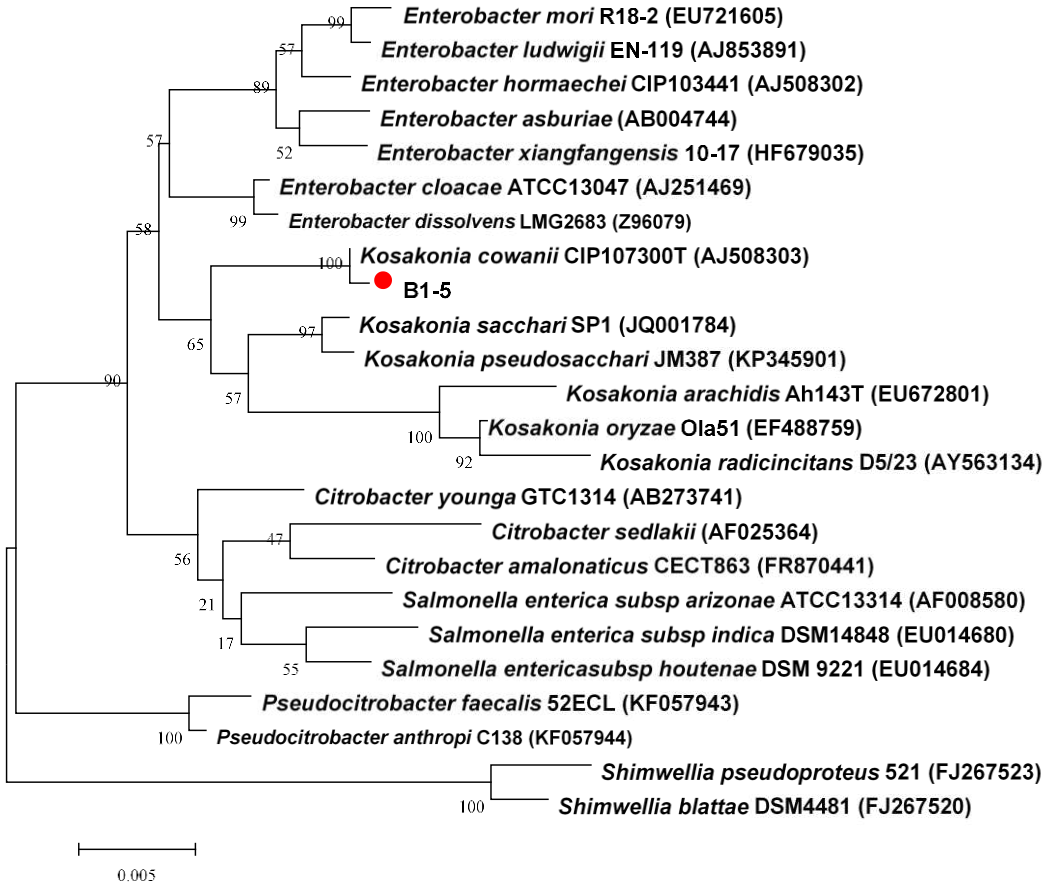

Figure 2. *Phylogenetic dendrogram based on comparative analysis of the 16S rRNA gene sequence, showing the relationship among strain B1-5 and other related species and genera. The GenBank sequence accession numbers were indicated in brackets after the strain names. The dendrogram was generated using the neighbour-joining method in the bootstrap test (1000 replicates)*

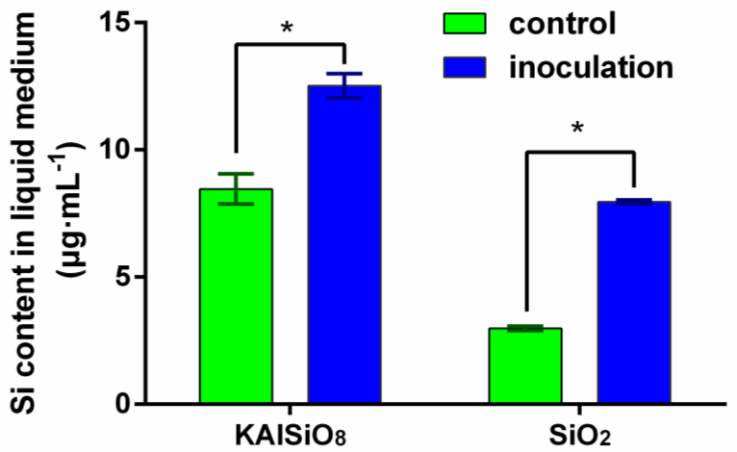

Figure 3. *Si content in $KAlSi_3O_8$ - (A) and SiO2 -containing (B) liquid medium with and without inoculation with the isolated silicate bacterium strain B1-5. Si content was determined 7 d after inoculation with strain B1-5. Significant differences ($P < 0.05$) between inoculation and non-inoculated control are indicated by asterisk above bars. Values are mean ± standard error from three replicates*

http://www.aloki.hu ● ISSN 1589 1623 (Print) ● ISSN 1785 0037 (Online)
DOI: http://dx.doi.org/10.15666/aeer/1706_1342313433

Here we found the B1-5 bacterial strain was able to solubilize silicate from Si-bearing mineral in fermentation liquid. Indeed, microbial leaching is a simple and effective technology for metal extraction from low-grade ores and mineral concentrates, and this method is being increasingly applied in mining industry (Bosecker, 1997). Mineral weathering mechanism has been increasingly clarified in terms of chemical weathering processes. These microbes have been indicated to accelerate the dissolution of silicates by perturbing mineral–water equilibria and reaction dynamics, the production of chelating agents, proton, organic ligands, hydroxyl anion, extracellular polysaccharides and enzymes, and silicate precipitation by metal sorption at the cell membrane (Bennett et al., 2001). However, the influence of bacteria in this process and its molecular mechanisms are still unclear (Uroz et al., 2009).

Effect of strain B1-5 on maize growth and Si content in soil and plants

Maize seedlings grown in soils inoculated with B1-5 showed greater shoot diameter ($t = -4.745$, $df = 18$, $P < 0.001$) and dry biomass ($t = -2.634$, $df = 18$, $P = 0.017$) than un-inoculated plants (*Fig. 4*). Soil inoculation with B1-5 strain significantly increased the growth of maize plants.

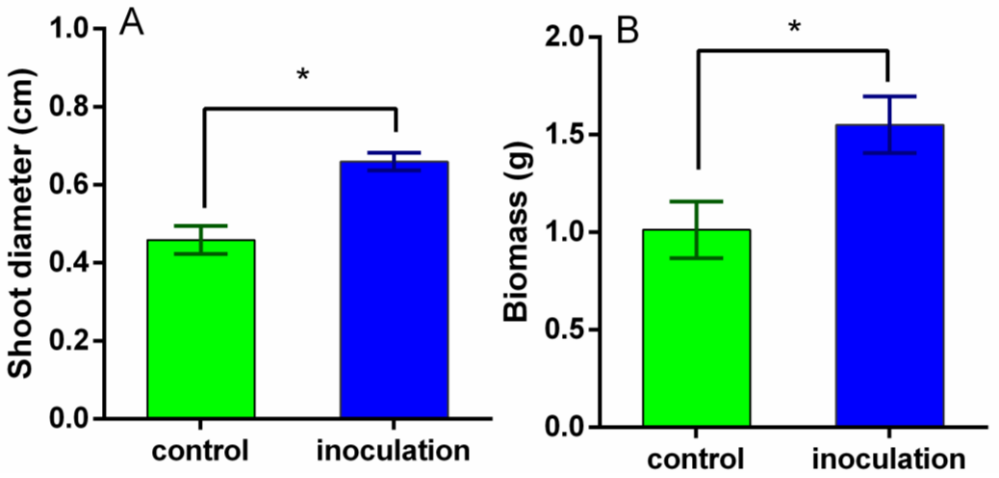

Figure 4. *Shoot diameter (A) and biomass (B) of maze seedlings grown in the soil with and without inoculation of strain B1-5. Significant differences ($P < 0.05$) between inoculation and non-inoculated control are indicated by asterisk above bars. Values are mean ± standard error from ten replicates*

The soluble Si content in the soil inoculated with B1-5 strain was higher than that in un-inoculated control ($t = -3.67$, $df = 18$, $P = 0.001$) (*Fig. 5A*). Maize plants grown in inoculated soil showed significantly higher Si level in shoots ($t = -2.55$, $df = 18$, $P = 0.020$) and roots ($t = -2.228$, $df = 18$, $P = 0.039$) than those in un-inoculated plants (*Fig. 5B*). Inoculation with B1-5 strain significantly increased soluble Si release from the soil and Si uptake by maize plants.

Our study clearly illustrated that the growth and Si content of maize plants were improved by inoculation with B1-5 strain via enhancement of soil Si availability and plant Si uptake. This is consistent with the findings that SSB, *Bacillus circulans Burkholderia eburnean* and *Enterobacter ludwigii*, increased the release of Si in soil and Si acquisition by plants (Kang et al., 2017; Lee et al., 2019; Zahra et al., 1984). Many studies have

http://www.aloki.hu ● ISSN 1589 1623 (Print) ● ISSN 1785 0037 (Online)
DOI: http://dx.doi.org/10.15666/aeer/1706_1342313433

showed that Si application improves the growth of monocot crops including rice, sugarcane (*Saccharum officinarum*) and turf (*Lolium perenne*) (Nanayakkara et al., 2008; Savant et al., 1999; Snyder, 2001). Moreover, two field experiments in India have also reported that silicon solubilizing bacteria improve silicon uptake and crop yield in rice and sugarcane (Brindavathy et al., 2012; Pedda et al., 2016).

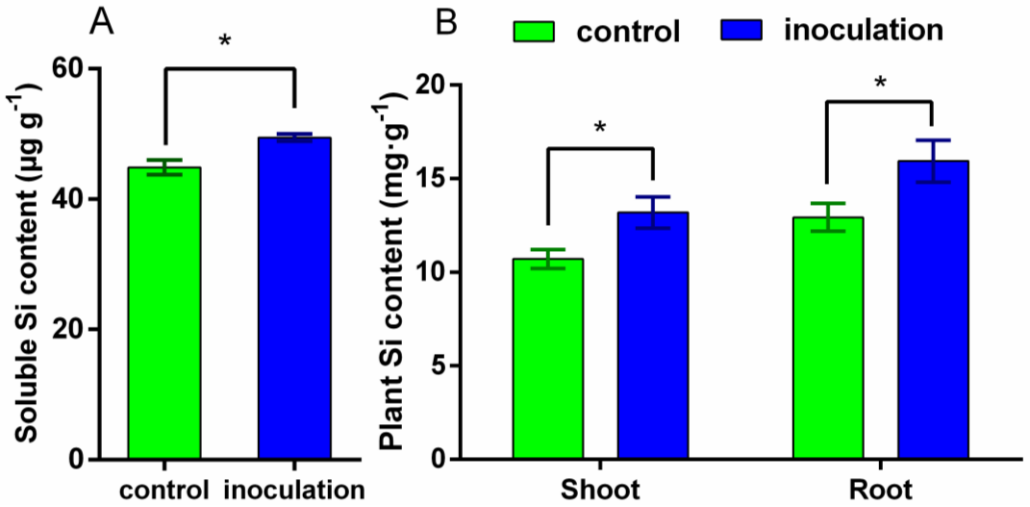

Figure 5. *(A) Soluble Si content in strain B1-5-inoculated and un-inoculated soils. (B) Si content in the shoots (left) and roots (right) of maize seedlings grown in strain B1-5-inoculated and un-inoculated soils. Significant differences ($P < 0.05$) between inoculation and control are indicated by asterisk by different letters above bars. Values are mean ± standard error from ten replicates*

Conclusion

In conclusion, this study not only highlights the existence of bryophyte rhizoids-associated silicate solubilizing bacteria, but also opens up a new approach searching for Si-solubilizing bacteria to increase Si availability in soil. Use of silicate solubilizing bacteria biofertilizer may serve as an important approach to increase Si availability and crop production. More detailed mechanisms of microbiological molecular biology and metabonomics about mineral weathering await further research.

Acknowledgements. This work was supported by the National Natural Science Foundation of China (31670414, 31770474), Fujian Provincial Excellent Youth Science Foundation (2017J06010), and Fujian-Taiwan Joint Innovative Center for Germplasm Resources and Cultivation of Crop (FJ 2011 Program, NO.2015-75).

REFERENCES

[1] Afzal, A., Ashraf, M., Asad, S. A., Farooq, M. (2005): Effect of phosphate solubilizing microorganisms on phosphorus uptake, yield and yield traits of wheat (*Triticum aestivum* L.) in rainfed area. – Int J Agric Biol 7: 207-209.

[2] Antonio, C. D. S., Rouws, L. F. M., Teixeira, K. R. S., Reis, V. M. (2016): Diazotrophic bacteria associated to sugarcane varieties cropped at northeast region of Brazil. – Revista Brasileirade Ciencias Agrarias 11: 272-280.

http://www.aloki.hu ● ISSN 1589 1623 (Print) ● ISSN 1785 0037 (Online)
DOI: http://dx.doi.org/10.15666/aeer/1706_1342313433

[3] Bennett, P. C., Rogers, J. R., Choi, W. J., Hiebert, F. K. (2001): Silicates, silicate weathering, and microbial ecology. – Geomicrobiol J 18: 3-19.
[4] Berger, B., Baldermann, S., Ruppel, S. (2017): The plant growth-promoting bacterium *Kosakonia radicincitans* improves fruit yield and quality of *Solanum lycopersicum*. – J Sci Food Agric 97: 4865-4871.
[5] Bosecker, K. (1997): Bioleaching: metal solubilization by microorganisms. – FEMS Microbiol Rev 20: 591-604.
[6] Brady, C., Cleenwerck, I., Venter, S., Coutinho, T., De Vos, P. (2013): Taxonomic evaluation of the genus *Enterobacter* based on multilocus sequence analysis (MLSA). – Syst Appl Microbiol 36: 309-319.
[7] Brindavathy, R., Dhara, N., Rajasundari, K. (2012): Biodissolution of Silica by Silicon Bacteria in Sugarcane Rhizosphere. – Res J Agri Sci 3: 1042-1044.
[8] Dannon, E. A., Wydra, K. (2004): Interaction between silicon amendment, bacterial wilt development and phenotype of *Ralstonia solanacearum* in tomato genotypes. – Physiol Mol Plant Pathol 64: 233-243.
[9] Debona, D., Rodrigues, F. A., Datnoff, L. E. (2017): Silicon's role in abiotic and biotic plant stresses. – Annu Rev Phytopathol 55: 85-107.
[10] Epstein, E. (1994): The anomaly of silicon in plant biology. – P Natl Acad Sci USA 91: 11-17.
[11] Epstein, E. (1999): Silicon. – Annu Rev Plant Biol 50: 641-664.
[12] Han, H. S., Lee, K. D. (2006): Effect of co-inoculation with phosphate and potassium solubilizing bacteria on mineral uptake and growth of pepper and cucumber. – Plant Soil Environ 52: 130-136.
[13] Hoagland, D. R., Arnon, D. I. (1950): The water-culture method for growing plants without soil. – Calif Agric Exp Stn Circ 347: 357-359.
[14] Hu, L., Xia, M., Lin, X., Xu, C., Zeng, R., Song, Y. (2018): Earthworm gut bacteria increase silicon bioavailability and acquisition by maize. – Soil Biol Biochem 125: 215-221.
[15] Kaempfer, P., McInroy, J. A., Doijad, S., Chakraborty, T., Glaeser, S. P. (2016): *Kosakonia pseudosacchari* sp nov., an endophyte of Zea mays. – Syst Appl Microbiol 39: 1-7.
[16] Kang, S. M., Waqas, M., Shahzad, R., You, Y. H., Asaf, S., Khan, M. A., Lee, K. E., Joo, G. J., Kim, S. J., Lee, I. J. (2017): Isolation and characterization of a novel silicate-solubilizing bacterial strain *Burkholderia eburnea* CS4-2 that promotes growth of japonica rice (*Oryza sativa* L. cv. Dongjin). – Soil Sci Plant Nutr 63: 233-241.
[17] Lee, K. E., Adhikari, A., Kang, S. M., You, Y. H., Joo, G. J., Kim, J. H., Kim, S. J., Lee, I. J. (2019): Isolation and characterization of the high silicate and phosphate solubilizing novel strain *Enterobacter ludwigii* GAK2 that promotes growth in rice plants. – Agronomy 9: 144.
[18] Liang, Y., Nikolic, M., Belanger, R., Haijun, G., Song, A. (2015): Silicon in Agriculture. From Theory to Practice. – Springer, Dordrecht.
[19] Lin, W., Wang, Y., Li, B., Pan, Y. (2012): A biogeographic distribution of magnetotactic bacteria influenced by salinity. – ISME J 6: 475-479.
[20] Ling, T. Y., Jong, H. J., Apun, K., Sulaiman, W. H. W. (2009): Quantifying Escherichia coli release from soil under high-intensity rainfall. – T ASABE 52: 785-792.
[21] Ma, J. F. (2004): Role of silicon in enhancing the resistance of plants to biotic and abiotic stresses. – J Plant Nutr Soil Sci 50: 11-18.
[22] Mehrvarz, S., Chaichi, M. R. (2008): Effect of phosphate solubilizing microorganisms and phosphorus chemical fertilizer on forage and grain quality of barely (*Hordeum vulgare* L.). – Agri Environ Sci 3: 822-828.
[23] Myshlyaeva, L. V., Krasnoshchekov, V. V. (1974): Analytical Chemistry of Silicon. – Wiley, New York.

http://www.aloki.hu ● ISSN 1589 1623 (Print) ● ISSN 1785 0037 (Online)
DOI: http://dx.doi.org/10.15666/aeer/1706_1342313433

[24] Nanayakkara, U. N., Uddin, W., Datnoff, L. E. (2008): Application of silicon sources increases silicon accumulation in perennial ryegrass turf on two soil types. – Plant Soil 303: 83-94.
[25] Pedda, K. S., Mohiuddin, G., Balasubramaniam, P., Mahendran, P. P. (2016): Performance of silicate solubilizing bacteria on silicon uptake and yield of rice under lowland ecosystem. – J Appl Nat Sci 8: 55-59.
[26] Pettersson, Å. K., Karlberg, B. (1999): Simultaneous determination of orthophosphate and silicate in brackish water. – Anal Chim Acta 378: 183-189.
[27] Raven, J. A. (1983): The transport and function of silicon in plants. – Biological Reviews 58: 179-207.
[28] Reynolds, O. L., Padula, M. P., Zeng, R., Gurr, G. M. (2016): Silicon: potential to promote direct and indirect effects on plant defense against arthropod pests in agriculture. – Front Plant Sci 7. DOI: 10.3389/fpls.2016.00744.
[29] Savant, N., Korndörfer, G., Datnoff, L., Snyder, G. (1999): Silicon nutrition and sugarcane production: a review. – J Plant Nutr 22: 1853-1903.
[30] Sheng, X. F. (2005): Growth promotion and increased potassium uptake of cotton and rape by a potassium releasing strain of Bacillus edaphicus. – Soil Biol Biochem 37: 1918-1922.
[31] Sheng, X. F., He, L. Y. (2006): Solubilization of potassium-bearing minerals by a wild-type strain of Bacillus edaphicus and its mutants and increased potassium uptake by wheat. – Can J Microbiol 52: 66-72.
[32] Singh, G., Biswas, D. R., Marwaha, T. S. (2010): Mobilization of potassium from waste mica by plant growth promoting rhizobacteria and its assimilation by maize (*zea mays*) and wheat (*triticum aestivum*): a hydroponics study under phytotron growth chamber. – J Plant Nutr 33: 1236-1251.
[33] Snyder, G. H. (2001): Calibration of soil and plant silicon analysis for rice production. – J Plant Nutr 24: 1071-1084.
[34] Soil Survey Staff. (2010): Keys to Soil Taxonomy. 11th Ed. – USDA Natural Resources Conservation Service, Washington, DC.
[35] Takahashi, E., Miyake, Y. (1976a): Distribution of silica accumulator plants in the plant kingdom (1) Monocotyledons. – J Sci Soil Manu Jpn 47: 296-300.
[36] Takahashi, E., Miyake, Y. (1976b): Distribution of silica accumulator plants in the plant kingdom (2) Dicotyledons. – J Sci Soil Manu Jpn 47: 301-306.
[37] Takahashi, E., Miyake, Y. (1976c): Distribution of silica accumulator plants in the plant kingdom (3) Gymnospermae, Pteridophyta, Bryophyta. – J Sci Soil Manu Jpn 47: 333-337.
[38] Tamura, K., Dudley, J., Nei, M., Kumar, S. (2007): MEGA4: Molecular evolutionary genetics analysis (MEGA) software version 4.0. – Mol Biol Evol 24: 1596-1599.
[39] Thompson, J. D., Gibson, T. J., Plewniak, F., Jeanmougin, F., Higgins, D. G. (1997): The CLUSTAL_X windows interface: flexible strategies for multiple sequence alignment aided by quality analysis tools. – Nucleic Acids Res 25: 4876-4882.
[40] Uroz, S., Calvaruso, C., Turpault, M. P., Freyklett, P. (2009): Mineral weathering by bacteria: ecology, actors and mechanisms. – Trends Microbiol 17: 378-387.
[41] Vessey, J. K. (2003): Plant growth promoting rhizobacteria as biofertilizers. – Plant Soil 255: 571-586.
[42] Wang, Jim, J., Dodla, Syam, K., Henderson, Rodney, E. (2004): Soil silicon extractability with seven selected extractants in relation to colorimetric and ICP determination. – Soil Science 169: 861-870.
[43] Witzel, K., Strehmel, N., Baldermann, S., Neugart, S., Becker, Y., Becker, M., Berger, B., Scheel, D., Grosch, R., Schreiner, M., Ruppel, S. (2017): Arabidopsis thaliana root and root exudate metabolism is altered by the growth-promoting bacterium *Kosakonia radicincitans* DSM 16656(T). – Plant Soil 419: 557-573.

http://www.aloki.hu ● ISSN 1589 1623 (Print) ● ISSN 1785 0037 (Online)
DOI: http://dx.doi.org/10.15666/aeer/1706_1342313433

[44] Wu, G. Q., Liu, H. L., Feng, R. J., Wang, C. M., Du, Y. Y. (2017): Silicon ameliorates the adverse effects of salt stress on sainfoin (*Onobrychis viciaefolia*) seedlings. – Plant Soil Environ 63: 545-551.
[45] Xiao, Y., Wang, X., Chen, W., Huang, Q. (2017): Isolation and identification of three potassium-solubilizing bacteria from rape rhizospheric soil and their effects on ryegrass. – Geomicrobiol J 34. DOI: 10.1080/01490451.01492017.01286416.
[46] Youssef, G. H., Seddik, W. M. A., Osman, M. A. (2010): Efficiency of natural minerals in presence of different nitrogen forms and potassium dissolving bacteria on peanut and sesame yields. – J Am Sci 6: 647-660.
[47] Zahra, M. K., Monib, M., Abdel-Al, S. I., Heggo, A. (1984): Significance of soil inoculation with silicate bacteria. – Zentralblatt für Mikrobiologie 139: 349-357.
[48] Zhang, C., Kong, F. (2014): Isolation and identification of potassium-solubilizing bacteria from tobacco rhizospheric soil and their effect on tobacco plants. – Appl Soil Ecol 82: 18-25.

http://www.aloki.hu ● ISSN 1589 1623 (Print) ● ISSN 1785 0037 (Online)
DOI: http://dx.doi.org/10.15666/aeer/1706_1342313433

DIET INFLUENCES THE ACCUMULATION OF SHORT-CHAIN FATTY ACIDS ASSOCIATED WITH THE GUT MICROBIOTA IN THE GRASS CARP (*CTENOPHARYNGODON IDELLUS*) HINDGUT

LI, Z. F.[1,2] – XIE, J.[1,2*] – YU, E. M.[1,2] – WANG, G. J.[1,2] – ZHANG, X. K.[3] – YU, D. G.[1,2] – ZHANG, K.[1,2] – GONG, W. B.[1,2]

[1]*Key Laboratory of Tropical and Subtropical Fishery Resource Application and Cultivation, Pearl River Fisheries Research Institute, Chinese Academy of Fishery Sciences, No.1, Xingyu Road, Liwan, Guangzhou, Guangdong 510380, China*

[2]*Guangdong Ecological Remediation of Aquaculture Pollution Research Center, Guangzhou, Guangdong 510380, China*

[3]*Research Center of Aquatic Organism Conservation and Water Ecosystem Restoration in Anhui Province, Anqing Normal University, Anqing, Anhui 246011, China*

**Corresponding author*
e-mail: xiejunhy01@126.com; phone: +86-20-8161-6178

(Received 19th Jun 2019; accepted 28th Aug 2019)

Abstract. Diet changes the composition and function of the gut microbiota (GM). Short-chain fatty acids (SCFAs) are mainly produced through carbohydrate fermentation by the GM. It remains unclear whether changing the diet influences the accumulation of SCFAs in the grass carp (*Ctenopharyngodon idellus*) gut. To address this question, we compared SCFA accumulation with GM changes in the hindgut contents of grass carp in groups fed hybrid giant napier (*Pennisetum sinese* Roxb, HG), formula feed (FG), and broad bean (*Vicia faba*, BG). Our results showed that diet significantly influenced the SCFA concentrations in the hindgut of grass carp. By eliminating the influences of dietary SCFA, acetate and total SCFA accumulation in the hindgut of grass carp turned out to be positively associated with dietary cellulose contents. Most of the enriched bacterial biomarkers in the HG group that consumed the most dietary cellulose were SCFA-producing bacteria. These results implied that diet could regulate the relative abundances of potential SCFA-producing bacteria and SCFA accumulation in the grass carp hindgut. These findings shed light onto GM functions related to SCFA production and associative functions between SCFAs and the GM of grass carp.
Keywords: *aquaculture, carbohydrate fermentation, cellulose, high-throughput sequencing, microbial metabolism*

Introduction

In mammals, short-chain fatty acids (SCFAs) such as acetate, butyrate, and propionate are essential host energy sources (Stevens and Hume, 1998; Spiljar et al., 2017; Leblanc et al., 2017), which act as signal-transduction molecules via G protein-coupled receptors and as epigenetic regulators of gene expression by inhibiting histone deacetylase (Kasubuchi et al., 2015; Cohen et al., 2017). SCFAs are involved in regulating glucose and lipid metabolism, stimulating the proliferation and differentiation of intestinal enterocytes, and reducing the intestinal pH (thereby promoting the absorption of minerals by increasing their solubility) (Barczynska et al., 2016; Postler and Ghosh, 2017). SCFAs are also key regulators of virtually every aspect of the intestinal immune system, and they play key roles in the prevention and treatment of metabolic syndromes, bowel disorders, and cancer (Kasubuchi et al., 2015; Postler and Ghosh, 2017; Fukuda et al., 2012; Flint et al., 2015; Safari et al., 2016). Although

http://www.aloki.hu ● ISSN 1589 1623 (Print) ● ISSN 1785 0037 (Online)
DOI: http://dx.doi.org/10.15666/aeer/1706_1343513453

comparatively less research has been conducted with fish than with mammals, high intestinal SCFA concentrations occur in some marine herbivorous fishes and SCFAs produced by the hindgut microbiota are used as a blood fuel for energy purposes or for lipid synthesis by the host fish (Clements et al., 1994; Clements and Choat, 1995, 1997; Seeto et al., 1996; Mountfort et al., 2002).

Naturally, SCFAs are mainly produced through carbohydrate fermentation by gut microbiota in the host's intestines (Flint et al., 2015; Clements and Choat, 1995; Mountfort et al., 2002; Hao et al., 2017b). However, with the collapse of wild fishery resources, aquaculture has become the main way to produce fish protein. In addition, formula feed has replaced natural food to become the primary, or even sole food for cultured fish.

Diet is believed to be the major factor that changes the composition and functions of fish gut microbiota (Ni et al., 2014a; Faith and Gordon, 2011; Claesson et al., 2012; Bolnick et al., 2015; Miyake et al., 2015; Hao et al., 2017a). In addition, the quantities and number of SCFA species are markedly influenced by carbohydrate substrates (Hao et al., 2017a; Mountfort et al., 1993; Kihara and Sakata, 1997, 2002). Kihara and Sakata (2002) reported that alpha starch is the best substrate for producing SCFAs in the tilapia (*Oreochromis niloticus*) gut by microbial fermentation. Mountfort et al. (1993) isolated a bacterium, *Eubacterium* sp. P-1 (DSM 6788), from the mullet gut contents, which anaerobically ferments pectin to produce 163 mol acetate, 30 mol ethanol, 88 mol methanol, and 48 mol formate per 100 mol pectin monomer, whereas it anaerobically ferments hexose in cellobiose or starch to produce 39 mol acetate, 128 mol ethanol, and 41 mol formate per 100 mol hexose. However, it remains unclear whether changing the diet from natural food to artificial feed reduces SCFA accumulation in the fish gut. Since acetate absorption is driven by an SCFA concentration gradient between the blood and intestines, and the rates of absorption increase with intestinal concentrations (Titus and Ahearn, 1991), the answer to the question will show which feed formula promotes SCFA accumulation in hindgut and enhances the growth and health of fish, considering there are many studies have shown that using SCFAs and their salts as feed supplements enhance fish production (Goosen et al., 2011; Ringø, 1992; Da et al., 2013).

Grass carp (*Ctenopharyngodon idella*) is one of the most important native Chinese freshwater herbivorous fish, representing the largest freshwater aquaculture product worldwide (Ni et al., 2014a; FAO, 2014; Wang et al., 2015). Recently, a high-density culture formulation of grass carp feed with broad bean (*Vicia faba*) or formula feed in ponds has started spreading in China. The changes of the gut microbiota in grass carp caused by diet were described previously (Ni et al., 2014a). However, given that broad bean and formula feeds contain high protein and low cellulose concentrations, it is unclear whether those changes alter SCFA accumulation in the hindgut of grass carp. Considering the usability of carbohydrate substrates in fermentation by the gut microbiota, the nutritional contents of feeds, and the co-evolution between the gut microbiota and host's feeding habits, we hypothesized that whereas feeding formula feeds would increase grass carp growth and SCFA fermentation in the hindgut, feeding natural grass would enrich the cellulose- degrading bacteria in the hindgut of grass carp. To test this hypothesis, we compared the compositions of gut microbiota with cellulose levels and SCFA accumulation in hindgut of grass carp fed hybrid giant napier (*Pennisetum sinese* Roxb), formula feed, and broad beans.

http://www.aloki.hu ● ISSN 1589 1623 (Print) ● ISSN 1785 0037 (Online)
DOI: http://dx.doi.org/10.15666/aeer/1706_1343513453

Materials and methods

Experimental design and sample collection

The experiment was conducted in the precise aquaculture base of the Pearl River Fisheries Research Institute of China (113°13′02″ E, 23°04′07″ N) over a period of 60 days from May 23, 2015 to July 24, 2015. Grass carps weighing approximately 500 g individually from the same parents was collected from an artificial pond at Foshan Tongwei Fisheries Co. (Guangdong, China). The experiment was divided into three groups. Each group, including 30 individuals, was fed with hybrid giant napier (H), formula feed (F), or broad bean (B), respectively. The daily feed amount was 3% of the total weight of grass carps in formula feed group and broad bean group, and 10% of the total weight of grass carps in hybrid giant napier group. The uneaten feed was removed after 1 h of feeding. Broad beans were marinated in fresh water 24 h before they were fed to grass carp. After 2 months of being fed hybrid giant napier, formula feed, or marinated broad bean at 09:00 and 16:00 each day in the artifificial pond, three carps in each diet group were collected and euthanized by submersion in 60 mg/L tricaine methane sulfonate solution.

After two months, the grass carp were dissected under sterile conditions to obtain their hindgut contents for total microbial DNA extraction and SCFA concentration measurements, according to a previously described method (Ni et al., 2014a; Li et al., 2018). The groups were named based on the feed type. For example, FG indicates that the microbiota was collected from the hindgut of grass carp fed with formula feed.

Determination of nutritional contents in feeds

The crude fiber contents, crude ash contents, crude protein contents, and crude fat contents in fresh hybrid giant napier, marinated broad beans, and formula feed were determined according to standard methods (ISO 6541:1981, ISO 5984:2002, ISO 5983:1979, and ISO 6492:1999).

Determination of SCFA concentrations

SCFAs (acetate, propionate, butyrate, iso-butyrate, valerate, and iso-valerate) in feeds and the hindgut contents of grass carp fed with different feeds were analyzed by gas chromatography using the method proposed by Schwiertz et al. (2012), with some modifications. Briefly, each sample of 300 mg (wet weight) was weighed (10^{-4} g precision) and placed in a 2-ml EP tube with 1.2 ml ddH_2O. The mixture was vortexed for 30 s, homogenized in a ball mill for 4 min at 45 Hz, and sonicated for 5 min in ice water. The mixture was centrifuged at 5,000 rpm for 20 min at 4 °C, and the supernatant (0.6 ml) was collected for metabolite extraction. Next, 0.15 ml H_2SO_4 (50%) and 50 μg SCFA/ml ether were added to each supernatant, after which the supernatant was vortexed for 30 s and centrifuged (10 min, 12000 rpm, 4 °C). The supernatant was passed through a nylon filter (0.45 μm) into a gas chromatography vial. SCFAs were analyzed using a GC2025 gas chromatograph (Shimazdu; Kyoto, Japan) with an automatic injector (AOC20i) at 240 °C, using a flame-ionization detector (Shimadzu Deutschland GmbH, Duisburg, Germany) at 240 °C, equipped with an HP-Innowax capillary column (Agilent, Santa Clara, USA; 30 m × 0.25 mm i.d. × 0.25 μm f.d.). The injection volume was 1 μl, the carrier gas was helium (flow rate, 1 ml/min), and the mode of injection was splitless. The oven temperature program was 50 °C for 3 min,

http://www.aloki.hu ● ISSN 1589 1623 (Print) ● ISSN 1785 0037 (Online)
DOI: http://dx.doi.org/10.15666/aeer/1706_1343513453

followed by an increase to 180 °C (held for 0 min) at 8 °C /min, and a further increase to 200 °C (held for 5 min) at 50 °C/min. Other parameters used were: gas helium flow, 30 ml/min; hydrogen flow, 40 ml/min; and airflow, 400 ml/min.

DNA extraction and sequencing

Total genomic DNA was extracted from the gut samples using a Gut Microbial DNA Extraction Kit (Omega, USA). DNA concentrations and purities were evaluated using 1% agarose gels. DNA samples were diluted to 1 ng/μl using sterile water before amplification was performed (Li et al., 2017).

The V4 region of the 16S rRNA gene was amplified using primers 515F and 806R, which contain sample-specific barcodes (Yan et al., 2016). PCR was performed in 30-μl reaction volumes with 15 μl of the Phusion® High-Fidelity PCR Master Mix (New England BioLabs, USA), 0.2 μM of the forward and reverse primers, and approximately 10 ng of template DNA. The thermal cycling conditions used were as follows: initial denaturation at 98 °C for 1 min; followed by 30 cycles of denaturation at 98 °C for 10 s, annealing at 50 °C for 30 s, and elongation at 72 °C for 60 s; and a final elongation step at 72 °C for 5 min (Li et al., 2018).

The PCR products were mixed with the same volume of 1× loading buffer (containing SYBR Green) and electrophoresed on 2% agarose gels for detection. Samples between 400 and 450 bp in size were chosen for further experiments. The PCR products were mixed at an equidensity ratio; then, the mixed PCR products were purified using the GeneJET Gel Extraction Kit (Thermo Scientific, USA).

Sequencing libraries were constructed using the NEB Next® Ultra™ DNA Library Prep Kit (NEB, USA), according to the manufacturer's recommendations, and index codes were added. The library quality was assessed using a Qubit@ 2.0 Fluorometer (Thermo Scientific, USA) and an Agilent Bioanalyzer 2100 system (Agilent Technologies, USA). Finally, the libraries were sequenced using the Illumina MiSeq platform, and 250-bp paired-end reads were generated.

Sequence data analysis

Paired-end reads from the original DNA fragments were merged using FLASH software. Paired-end reads were assigned to each sample based on the sample-specific barcodes. Sequences analysis was performed using the UPARSE software package with the UPARSE-OTU and UPARSE-OTUref algorithms (Edgar, 2013). QIIME 1.9.0 software (Caporaso et al., 2010) and the vegan package (Dixon, 2003) in the R platform (R Core Team, 2014) were used to analyze alpha (within samples) and beta (among samples) diversity. Sequences with $\geq 97\%$ similarity were assigned to the same operational taxonomic units (OTUs). We selected representative sequences for each OTU and used the RDP classifier to annotate the taxonomic information for each representative sequence (Wang et al., 2007). To compute alpha diversities, we rarified the OTU table and calculated three metrics: Chao1 estimated species abundance, observed species estimated as the number of unique OTUs found in each sample, and the Shannon index. Rarefaction curves were generated based on these three metrics.

Correspondence analysis (CA), non-parametric multivariate analysis of variance (MANOVA) (Anderson, 2001), and non-parametric significance testing of differences were conducted using the vegan package in the R platform. A heatmap profile was drawn using HemI 1.0 (Deng et al., 2014).

http://www.aloki.hu ● ISSN 1589 1623 (Print) ● ISSN 1785 0037 (Online)
DOI: http://dx.doi.org/10.15666/aeer/1706_1343513453

All sequencing data were deposited in the NCBI Sequence Read Archive (SRA) under accession number SRP080980. The SRA records can be accessed at http://www.ncbi.nlm.nih.gov/sra/SRP080980.

SCFA data analysis

Statistical analysis was performed using R software, version 3.0.1. Data are displayed as the mean ± standard error (S.E.). The Kruskal–Wallis test was applied to analyze global differences among three groups. Tukey's method was used as a post-hoc test for multiple comparisons of means.

Results

Nutrient content in the three feeds and growth of grass carp

As expected, fresh hybrid giant napier contained the highest content of crude fiber (23.96 ± 1.68%, dry matter), followed by formula feed (9.70 ± 0.46%, dry matter) and marinated broad beans (1.98 ± 0.89%, dry matter). Fresh hybrid giant napier contained the lowest content of crude protein (12.36 ± 1.92%, dry matter), followed by formula feed (28.78 ± 0.00%, dry matter) and marinated broad beans (31.78 ± 1.86%, dry matter) (*Table 1*).

Table 1. *Nutrient contents in three feeds used to feed grass carp (% dry matter). The superscripted lowercase letters indicate significant differences observed between different feeds. The same superscripted letters reflect cases where no significant difference was found, whereas different superscripted letters represent cases where significant differences were found ($p < 0.05$)*

Nutrient component	Hybrid giant napier (%)		Broad bean (%)		Formula feed (%)	
	Mean	S. E.	Mean	S. E.	Mean	S. E.
Crude fiber content	23.96^{a}	1.68	1.98^{c}	0.89	9.70^{b}	0.46
Crude ash content	13.33^{a}	1.20	3.76^{c}	0.00	7.53^{b}	0.07
Crude protein content	12.36^{a}	1.92	31.78^{c}	1.86	28.78^{b}	0.00
Crude fat content	3.23^{b}	0.13	$< 1.11^{*a}$	NA	5.42^{c}	0.26

*The content of crude fat in the marinated broad beans was below the limit of detection

At the start of the experiment, the average weights of grass carp in groups fed hybrid giant napier, formula feed, and marinated broad bean were 501.5 ± 20.17 g, 501.33 ± 15.00 g, and 498.83 ± 21.44 g, respectively. No significant differences were observed. However, at the end of the two-month experiment, the average weights were 680.17 ± 15.17 g, 918.00 ± 46.67 g, and 602.50 ± 10.50 g, respectively. The weight increases were 178.67 ± 13.67 g, 416.67 ± 53.33 g, and 103.67 ± 15.11 g, which represented significant differences, in each case (*Appendix 1*).

Concentrations of SCFAs in feeds and gut contents of grass carp fed different feeds

The concentrations of acetate, propionate, and i-valerate in broad beans were the highest among the three feeds, whereas the absolute concentrations of all SCFAs in the

http://www.aloki.hu ● ISSN 1589 1623 (Print) ● ISSN 1785 0037 (Online)
DOI: http://dx.doi.org/10.15666/aeer/1706_1343513453

hindguts of grass carp fed with formula feed were the highest (1.95 ± 1.06 mmol/kg, 0.54 ± 0.16 mmol/kg, and 0.13 ± 0.01 mmol/kg for acetate, propionate, and butyrate, respectively), followed by those from grass carp fed marinated broad beans and fresh hybrid giant napier (*Table 2*). Although the absolute concentrations were different, the three most dominant SCFAs in the guts of all of grass carp fed with different feeds were acetate, propionate, and butyrate. The ratios of their concentrations (approximately 14.3: 2.5: 1) were similar in all grass carp contents (*Table 2*). These results showed that the SCFA concentrations in the feeds and the metabolic activity of the hindgut microbiota markedly influenced SCFA concentrations in the hindgut of grass carp.

Table 2. *Absolute concentrations of short-chain fatty acids (SCFAs) in the three feeds and in the hindguts of grass carp fed with the three feeds. HG, hindgut contents of grass carp fed with fresh hybrid giant napier (Pennisetum sinese Roxb); BG, hindgut contents of grass carp fed with marinated broad beans (Vicia faba); FG, hindgut contents of grass carp fed with formula feed; H, fresh hybrid giant napier; B, marinated broad beans; F, formula feed. The superscripted lowercase letters indicate significant differences observed between different feeds. The same superscripted letter shows instances where no significant difference was found, and different superscripted letters indicate cases where significant differences ($p < 0.05$) were found. Data are displayed as the mean ± standard error (S.E.)*

	Sample size	Acetate (mmol/kg)	Propionate (mmol/kg)	Butyrate (mmol/kg)	Iso-butyrate (mmol/kg)	Valerate (mmol/kg)	Iso-valerate (mmol/kg)
HG	3	0.31 ± 0.03	0.02 ± 0.00^a	0.01 ± 0.00^a	0.01 ± 0.00^a	0.00 ± 0.00^a	0.00 ± 0.00^a
BG	3	1.07 ± 0.51	0.14 ± 0.03^a	0.04 ± 0.02^a	0.01 ± 0.00^a	0.00 ± 0.00^a	0.01 ± 0.00^a
FG	3	1.95 ± 1.06	0.54 ± 0.16^b	0.13 ± 0.01^b	0.03 ± 0.00^b	0.02 ± 0.00^b	0.03 ± 0.00^b
H	3	0.14 ± 0.01	0.01 ± 0.00	0.01 ± 0.00	0.01 ± 0.00	0.00 ± 0.00	0.00 ± 0.00
B	3	1.82 ± 1.15	0.26 ± 0.34	0.05 ± 0.06	0.02 ± 0.01	0.01 ± 0.00	0.04 ± 0.01
F	3	1.05 ± 0.04	0.20 ± 0.01	0.08 ± 0.00	0.02 ± 0.00	0.01 ± 0.00	0.02 ± 0.00

To measure the SCFA increment in the hindgut region of grass carp fed with different feeds, the ratios of SCFA concentrations in the hindgut of each group to those in the feed were calculated. In terms of the total SCFA concentration (i.e., the sum of the concentrations of acetate, propionate, butyrate, iso-butyrate, valerate, and iso-valerate), the ratio for HG was the highest (1.98), followed by those for FG (1.95) and BG (0.58). The crude fiber contents in different feeds positively associated with SCFA ($R^2 = 0.890$) and acetate ($R^2 = 0.989$) increments in grass carp, but negatively associated with propionate ($R^2 = 0.895$) and butyrate ($R^2 = 0.837$) increases (*Fig. 1*). These findings implied that incremental changes of SCFAs, especially acetate in the hindguts of grass carp, were associated with the fiber contents of feeds.

Gut microbiota composition of grass carp fed different feeds

In this study, 451,160 high-quality spliced sequences from 9 samples were obtained. To eliminate the impediment of sequencing depths for each sample in determining the reliability, each sample was re-sampled at 29,918 sequences to assess their microbiotas. After re-sampling, 628 OTUs from 284 genera were detected using the criterion of 97% sequence similarity. An average of 190 OTUs (ranging from 93

http://www.aloki.hu ● ISSN 1589 1623 (Print) ● ISSN 1785 0037 (Online)
DOI: http://dx.doi.org/10.15666/aeer/1706_1343513453

to 310) were detected in each sample (*Appendix 2*). The alpha diversity (Chao1 and Shannon indexes) of the gut microbiota was highest in the BG group, followed by the HG group, and lowest in the FG group (*Appendix 2*). The rarefaction curves of the OTUs showed that the sequence datasets could be used to represent the diversities and structures of each microbiota (*Appendix 3*).

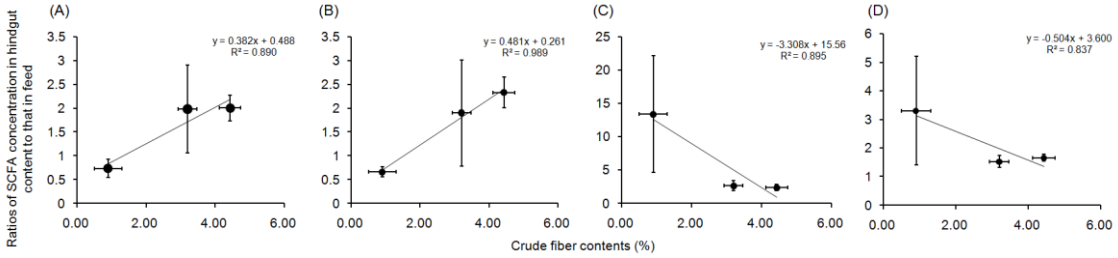

Figure 1. *Ratios of SCFA concentrations in the hindguts of grass carp to those in different feeds. (A) Ratios of all SCFA concentrations (i.e. total concentrations of acetate, propionate, butyrate, iso-butyrate, valerate, and iso-valerate). (B) Ratios for acetate. (C) Ratios for propionate. (D) Ratios for butyrate*

Except for a minority of sequences (ranging from 0.03% to 0.17%) that could not be classified into any phylum, 19 phyla consisting of 1 Archaea phylum and 18 Bacteria phyla were found. Fusobacteria (40.92%), Proteobacteria (26.40%), Firmicutes (25.04%), Bacteroidetes (5.61%), and Cyanobacteria (1.46%) were the dominant phyla in the gut microbiota of the grass carp (*Fig. 2A*). In this study, differences in the phylum compositions of the gut microbiota among the grass carp fed different diets were observed. The relative abundance of Bacteroidetes in the hindgut microbiota of the BG group was significantly higher than that found with the other diets, whereas the relative abundance of Fusobacteria was significantly lower (*Fig. 2B*). The relative abundance of Firmicutes in the hindgut microbiota of the FG group was significantly lower than that in the other groups (*Fig. 2B*). Moreover, the relative abundance of Proteobacteria in the BG group was significantly higher than that of the HG group (*Fig. 2B*). These results indicated that diet could fundamentally change the gut microbiota composition at the phylum level.

CA based on the OTUs and genus compositions of the samples showed a clear separation of the community composition among three treatment groups and revealed that diet significantly changed the hindgut microbiota of grass carp (*Fig. 3A* and *B*). MANOVA also revealed distinct differences among the gut microbiota of grass carp fed with different feeds ($P < 0.05$).

Fifty-three dominant genera (relative abundances > 0.1% in at least one sample) was detected. They clustered into three different groups according to diet (*Fig. 4A*). The relative abundances of *Cetobacterium* in the FG and HG were obviously higher than those in the BG group. The relative abundances of *Lactobacillus*, *Pediococcus*, *Bacillus*, an unidentified Streptophyta genus, and an unidentified Staphylococcaceae genus in the HG group were obviously higher than those in the FG and BG groups. The relative abundances of *u114* of Fusobacteriaceae and an unidentified Betaproteobacteria genus in the FG group were obviously higher than those in the BG and HG groups, whereas the relative abundances of *Bacteroides*, *Tolumonas*, an unidentified Lachnospiraceae genus, and an unidentified Enterobacteriaceae genus

http://www.aloki.hu ● ISSN 1589 1623 (Print) ● ISSN 1785 0037 (Online)
DOI: http://dx.doi.org/10.15666/aeer/1706_1343513453

were obviously higher in the BG group than those in the HG and FG groups (*Fig. 4A*). LEfSe results showed that the increased genus biomarkers in the HG group mostly concentrated in *Lactobacillus*, *Pediococcus*, *Streptococcus*, *Enterococcus*, and *Leptotrichia*; the increased genus biomarkers in the BG group mostly concentrated in *Rhodobacter* and *Uliginosibacterium*; and the increased genus biomarker in the FG group was mostly represented by *Fusobacteria* (*Fig. 4B*).

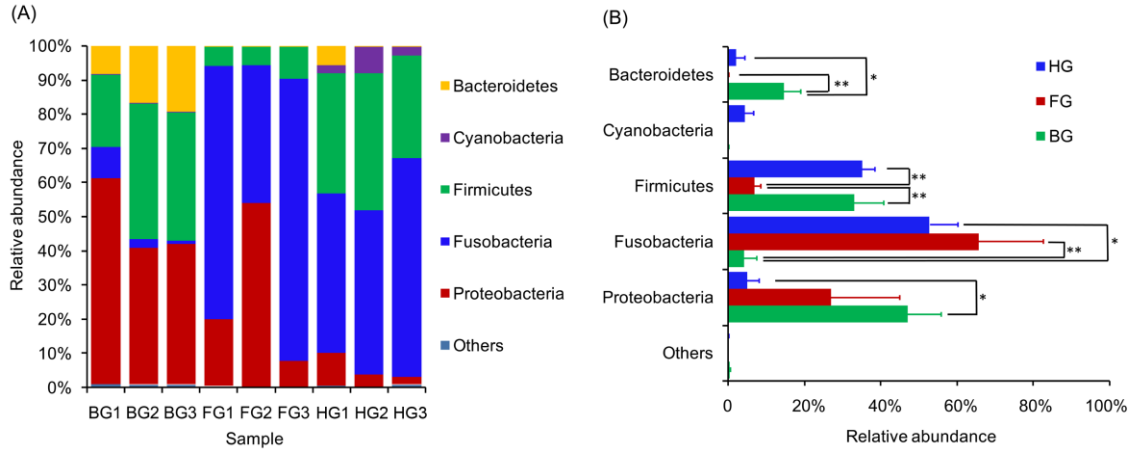

Figure 2. *Phylum compositions of the gut microbiota in grass carp fed with different feeds. (A) The relative abundance of each bacterial phylum in each hindgut microbiota of grass carp fed with different feeds. (B) Significant differences in phylum abundances were found between the gut microbiota of grass carp fed with different feeds. FG, HG, and BG indicate the hindgut microbiota of grass carp fed with formula feed, fresh hybrid giant napier, and marinated broad beans, respectively. *p < 0.05, **p < 0.01*

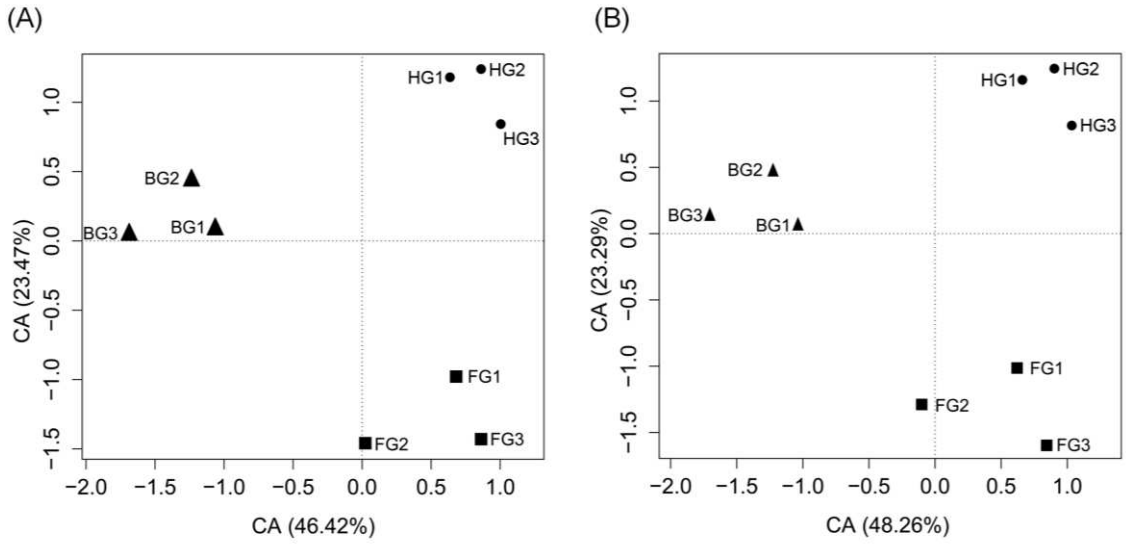

Figure 3. *Correspondence analysis (CA) profiles of the gut microbiota genotypes in grass carp fed with different feeds. (A) and (B) show the CA profiles after analysis, based on the OTU and genus compositions, respectively. FG, HG, and BG indicate the hindgut microbiota of grass carp fed with formula feed, fresh hybrid giant napier, and marinated broad beans, respectively*

http://www.aloki.hu ● ISSN 1589 1623 (Print) ● ISSN 1785 0037 (Online)
DOI: http://dx.doi.org/10.15666/aeer/1706_1343513453

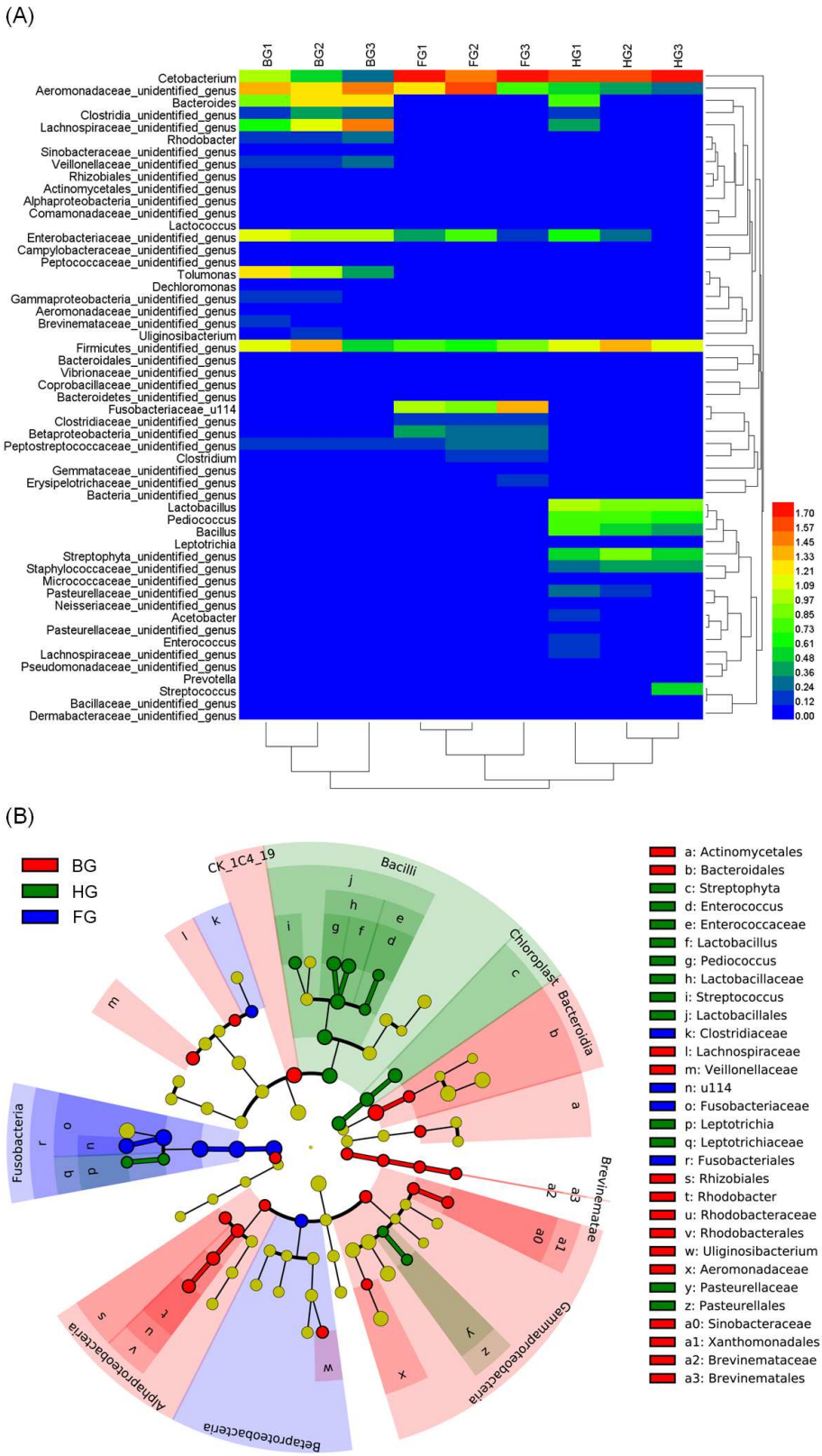

Figure 4. *Heatmap (A) and LEfSe (B) profiles showing the relative abundances of significantly different gut microbiota OTUs in grass carp fed with different feeds. FG, HG, and BG indicate the hindgut microbiota of grass carp fed with formula feed, fresh hybrid giant napier, and marinated broad beans, respectively*

http://www.aloki.hu ● ISSN 1589 1623 (Print) ● ISSN 1785 0037 (Online)
DOI: http://dx.doi.org/10.15666/aeer/1706_1343513453

Discussion

Effects of diet on hindgut SCFA accumulation and the growth of grass carp

Our results showed that changing the diet from natural food to formula feed significantly influenced the accumulation of SCFAs in the hindgut of grass carp (*Table 2*). Two dietary factors influenced SCFA accumulation in the hindgut of grass carp. Firstly, the diet directly supplied SCFAs to the hindgut of grass carp. Although SCFAs are thought to be mainly produced through carbohydrate fermentation by microorganisms, all three feeds had detectable SCFAs in this study (*Table 2*). Secondly, the amounts and species of SCFAs are significantly influenced by carbohydrate substrates (Hao et al., 2017a; Mountfort et al., 1993; Kihara and Sakata, 1997; Probert et al., 2004; Geraylou et al., 2014). Starch is seemingly more easily utilized to produce SCFAs through fermentation by gut microbiota in many fish (Kihara and Sakata, 1997; Van, 1994; Leenhouwers et al., 2007). This could explain the increased growth in grass carp fed formula feed compared with those fed with hybrid giant napier or broad beans, as formula feed contains more starch and higher luminal concentrations of SCFAs (*Table 2*).

Proportional model and concentrations of SCFA metabolites in the grass carp hindgut

In mammals and fishes, the SCFA metabolites produced during gut fermentation were mostly acetate, propionate, and butyrate (Clements et al., 1994; Hao et al., 2017b; Bergman, 1990; Smith et al., 1996; Cook and Sellin, 1998), and these metabolites were produced at different ratios. Acetate accumulation was most abundant (~60%), followed by propionate (~25%) and then, to a much lesser degree, by butyrate (~15%) in human intestines (Fukuda et al., 2012). Although the ratios of acetate, propionate, and butyrate fluctuate among different species, the trends of these ratios (acetate > propionate ≥ butyrate) were identical between mammals and fishes (Clements et al., 1994; Hao et al., 2017b; Bergman, 1990; Smith et al., 1996), with few exceptions in marine fishes (Kandel et al., 1994). Mountfort et al. (2002) reported the ratio of their concentrations in three species of marine fish as ranging from approximately 6.4: 3.2: 1 to 28.8: 9.8: 1, on average. In this study, the ratio of these concentrations was approximately 14.3: 2.5: 1 (*Table 2*). Therefore, changes in the acetate concentration primarily influenced the concentration of total SCFAs.

We found that the SCFA concentration in the grass carp hindgut ranged from 0.35 to 2.70 mmol/kg, which is similar to findings reported by Hao et al. (2017a), but were lower than those reported by Paris et al. (Paris et al., 1977). Clements et al. (2014) compared the SCFA concentrations in the hindgut contents of 18 fishes. The SCFA concentrations ranged from 1.70 to 38.00 mM. In addition, the SCFA concentrations in hindgut contents of freshwater herbivore fish were commonly lower than in other fishes (Clements et al., 2014).

Effect of dietary crude fiber contents on the SCFA increment of the grass carp hindgut microbiota

Gut microbiota ferment dietary cellulose to SCFAs as energy sources and signal-transduction molecules in humans and mammals (Spiljar et al., 2017; Postler and Ghosh, 2017; Bindels et al., 2012; Hullar and Fu, 2014). Data from previous studies

http://www.aloki.hu ● ISSN 1589 1623 (Print) ● ISSN 1785 0037 (Online)
DOI: http://dx.doi.org/10.15666/aeer/1706_1343513453

also indicated that the gut microbiota in herbivorous fish are capable of cellulose fermentation (Hao et al., 2017a, b; Ni et al., 2014a). Hao et al. (2017a) studied the influence of diets on the SCFA concentrations in the grass carp hindgut. Although they found that diets influenced SCFA concentrations in the hindgut, the influence of dietary SCFA concentrations was not demonstrated. The association between SCFA concentrations and the dietary cellulose contents was also not analyzed. However, the intestinal SCFA concentrations were clearly influenced by the dietary contents, as also shown in this study. Here, we used the ratios of intestinal SCFA concentrations to dietary SCFA concentrations to (i) exclude the influence of dietary SCFA concentrations on intestinal SCFA concentrations and to (ii) determine the SCFA increment. We found that the SCFA increment associated positively with the dietary cellulose contents in the three diets. The acetate increment, which represented the largest proportion of SCFAs, was highly positively associated with the dietary cellulose contents, but the increments of propionate and butyrate associated negatively with the dietary cellulose contents (*Fig. 1*). These results implied that acetate was probably produced in the hindgut of grass carp through cellulose fermentation, and the produced rates were faster than hindgut-absorption rates in the HG and FG, as the ratios were more than 1. However, most propionate and butyrate were probably not produced through cellulose fermentation, and their production and absorption in the hindgut were probably influenced by other undetected factors.

Effect of dietary cellulose contents on the structure of grass carp hindgut microbiota

In our study, we verified that the diet significantly changed the hindgut microbiota of grass carp, as reported previously (Ni et al., 2014b; Hao et al., 2017a). Changes in the hindgut microbiota of grass carp fed different diets also emerged at the phylum, genus, and OTU levels (*Figs. 2–4*). Similar to previous reports in grass carp and other fish (Hao et al., 2017b; Ni et al., 2014b; Miyake et al., 2015; Zhang et al., 2017), we found that Fusobacteria, Proteobacteria, Firmicutes, Bacteroidetes, and Cyanobacteria were the dominant phyla in the gut microbiota of the grass carp. However, their relative abundances acutely fluctuated between individuals fed different feeds or living in different habitats. Proteobacteria species dominate the intestines of many fish species, with differences found in the resident microbes (Zhang et al., 2017; Xia et al., 2014; Piazzon et al., 2017). Overgrowth of Proteobacteria was commonly associated with gut microbial dysbiosis and over-accumulation of energy in mammals. For instance, in Western-style diets, which are low in fiber, decreased beneficial Bacteroidetes and increased Proteobacteria levels are found, compared with those in a high-fiber diet (Geraylou et al., 2013). Dulski et al. (2018) speculated that Proteobacteria inhabiting the gut microbiota at an early stage of life are a necessary component of the pikeperch (*Sander lucioperca*) microbiome that may support proper nutrition of the fish. Fusobacteria species also dominated the intestines of grass carp in this study, as observed in other studies (Xia et al., 2014). However, the relative abundance of Fusobacteria species showed large fluctuations among different individuals under different conditions (Xia et al., 2014; Piazzon et al., 2017). Fusobacteria has been found to produce butyric acid as a major product of fermentation (Anand et al., 2016), and some species have been associated with diseases in mammals (Bennett and Eley, 1993).

CA of the 16S rRNA gene-sequencing results also revealed that gut bacterial communities from grass carp fed different diets formed different clusters (*Fig. 3A* and *B*). The *Pediococcus*, *Lactobacillus*, *Streptococcus*, *Enterococcus*, and *Leptotrichia*

http://www.aloki.hu ● ISSN 1589 1623 (Print) ● ISSN 1785 0037 (Online)
DOI: http://dx.doi.org/10.15666/aeer/1706_1343513453

genus biomarkers increased in the HG group (*Fig. 4B*). They were mostly represented by the Bacilli class, which contains many SCFA-producing bacteria, such as *Pediococcus* and *Lactobacillus* (Leblanc et al., 2017; Johansson et al., 1998; Li et al., 2016b, 2009; Dar et al., 2015).

Fermentation of cellulose by the gut microbiota is a major source of SCFA production (Leblanc et al., 2017; Kasubuchi et al., 2015; Flint et al., 2015). The grass carp is basically herbivorous (Ni et al., 2014a; Wu et al., 2012), and its cellulose-degrading capability is important for improving the utilization rate of plant polysaccharides and the production of SCFAs (Li et al., 2016a). In this study, most bacteria showing changes in abundance were related to SCFA production. For instance, the relative abundances of *Cetobacterium* in the HG and FG groups were obviously higher than that in the BG group. Tsuchiya et al. (2008) reported that the *Cetobacterium* abundance positively associated with acetic and propionic acid production through fermentation. The ratios of the SCFA concentrations in the HG and FG hindgut contents of grass carp to those in the feed were also obviously higher.

The ability of both lactobacilli and *Pediococcus* to produce SCFAs is well documented (Leblanc et al., 2017; Zhang et al., 2017). For instance, Geraylou et al. (2013) found that arabinoxylan-derived oligosaccharides could stimulate the growth of lactic acid bacteria and *Clostridium* sp. in the sturgeon gut and enhance the SCFA levels in the hindgut of sturgeon. Within 24 h, supplementation of *Lactobacillus salivarius* JCM 1230 and *Lactobacillus agilis* JCM 1048 in a simulated chicken cecum significantly increased propionate and butyrate formation (Meimandipour et al., 2010). Moreover, *L. acidophilus* CRL 1014 was also reported to increase the SCFA concentrations in a simulated human microbial ecosystem (Sivieri et al., 2013). Recently, *Lactobacillus rhamnosus* GG was included in a study with a mix of probiotic strains and prebiotics, where it could metabolize these prebiotics, leading to SCFA production (Leblanc et al., 2017). In our study, the relative abundances of *Lactobacillus* in the HG group were obviously higher compared to the other groups (*Fig. 4A*), as was the SCFA-production capability (*Fig. 1A*). Bacterial strains of *Pediococcus* have been widely reported as SCFA-producing bacteria (Dineshkumar, and Renu, 2008; Taheri et al., 2015). For instance, Iehata et al. (2010) reported *Pediococcus* sp. Ab1 treatment could improve the gut environment of the abalone, *Haliotis gigantea*. In our study, the relative abundances of *Pediococcus* in the HG group were obviously higher those in the other groups (*Fig. 4A*). Bacterial strains of *Bacillus* and *Bacteroides* were also reported to cause cell lysis and to be capable of SCFA and branched-chain short fatty acid biosynthesis (Kaneda, 1963; Mayhew et al., 1975; Dreher et al., 1976; Tsuchido et al., 1985; Pogribna et al., 2010; Ray et al., 2012; Hong et al., 2017). For instance, Li et al. (2016a) isolated some cellulolytic *Bacillus* strains from the gut contents of grass carp. Ray et al. (2012) reported that many *Bacillus* sp. could produce cellulase. Bacilli is the primary producers of butyrate (Flint et al., 2015; Kaoutari et al., 2013; Levy et al., 2016). Our results showed that the elevated genera in the HG group were mostly represented by Bacilli (*Fig. 4B*). These results implied that cellulolytic bacteria would be enriched with high-cellulose substrates in the hindgut of grass carp. In addition, SCFAs were also indirectly produced from other intermediates that were produced by polysaccharide fermentation. For instance, lactate, which is produced by many members of the human gut microbiome, can serve as a substrate for the bacterial production of propionate (e.g., *Coprococcus catus*) and butyrate (e.g., *Eubacterium hallii* and *Anaerostipes caccae*) (Duncan et al., 2004; Reichardt et al., 2014). These findings imply

http://www.aloki.hu ● ISSN 1589 1623 (Print) ● ISSN 1785 0037 (Online)
DOI: http://dx.doi.org/10.15666/aeer/1706_1343513453

that bacteria related to the SCFA concentration may not directly produce SCFAs, although they can increase the SCFA concentrations in the gut.

Conclusions

We conducted the first quantitative analysis of the association between SCFA accumulation and the dietary cellulose contents in this study. We found that the HG, which contained the highest dietary cellulose, exhibited the highest SCFA increase, even though the absolute concentration of SCFAs was higher in the FG, which contained more easily fermentable polysaccharides. Moreover, SCFA-producing bacteria, such as *Lactobacillus*, *Pediococcus*, and *Bacillus*, were significantly enhanced in the hindgut microbiota of the HG group. These results implied that the dietary cellulose content influenced the production of SCFAs in the grass carp hindgut by regulating the relative abundances of gut bacteria related to SCFA production. In addition, our results implied that adding appropriate proportion of cellulose or grass meal to grass carp feed could help to regulate the intestinal microbiota, and thereby increasing the content of SCFAs and increasing the growth and health of grass carp. However, the regulating mechanism of intestinal microbiota of grass carp to the productions of SCFAs needed to further study. These results would provide important reference for the design of grass carp feed formulation, and expand our understanding of the relationship between intestinal microbiota and grass carp metabolism.

Acknowledgements. We sincerely appreciate Yifei Wang and Wen Lou for their help in catching the experimental fish. We wish to thank Guangdong Meilikang BioScience, Ltd., for his help in analyzing the sequencing data and generating the pictures. This work was supported by the Central Public-interest Scientific Institution Basal Research Fund CAFS [2019XT0405, 2017HY-ZC0503] and the Modern Agro-industry Technology Research System [CARS-45-21].

REFERENCES

[1] Anand, S., Kaur, H., Mande, S. S. (2016): Comparative in silico analysis of butyrate production pathways in gut commensals and pathogens. – Frontiers in Microbiology 7: 1945.

[2] Anderson, M. J. (2001): A new method for non-parametric multivariate analysis of variance. – Austral Ecology 26: 32-46.

[3] Barczynska, R., Slizewska, K., Litwin, M., Szalecki, M., Kapusniak, J. (2016): Effects of dietary fiber preparations made from maize starch on the growth and activity of selected bacteria from the *Firmicutes*, *Bacteroidetes*, and *Actinobacteria* phyla in fecal samples from obese children. – Acta Biochimica Polonica 63: 261-266.

[4] Bennett, K. W., Eley, A. (1993): Fusobacteria: new taxonomy and related disease. – Journal of Medical Microbiology 39: 246-254.

[5] Bergman, E. N. (1990): Energy contributions of volatile fatty acids from the gastrointestinal tract in various species. – Physiological Reviews 70: 567-590.

[6] Bindels, L. B., Porporato, P., Dewulf, E. M., Verrax, J., Neyrinck, A. M., Martin, J. C., et al. (2012): Gut microbiota-derived propionate reduces cancer cell proliferation in the liver. – British Journal of Cancer 107(8): 1337-1344.

[7] Bolnick, D. I., Snowberg, L. K., Hirsch, P. E., Lauber, C. L., Org, E., Parks, B., et al. (2015): Individual diet has sex-dependent effects on vertebrate gut microbiota. – Nature Communications 5: 4500.

http://www.aloki.hu ● ISSN 1589 1623 (Print) ● ISSN 1785 0037 (Online)
DOI: http://dx.doi.org/10.15666/aeer/1706_1343513453

[8] Caporaso, J. G., Kuczynski, J., Stombaugh, J., Bittinger, K., Bushman, F. D., Costello, E. K., et al. (2010): QIIME allows analysis of high-throughput community sequencing data. – Nature Methods 7: 335-336.
[9] Claesson, M. J., Jeffery, I. B., Conde, S., Power, S. E., O'Connor, E. M., Cusack, S., et al. (2012): Gut microbiota composition correlates with diet and health in the elderly. – Nature 488(7410): 178-184.
[10] Clements, K. D., Choat, J. H. (1995): Fermentation in tropical marine herbivorous fishes. – Physiological Zoology 68(3): 355-378.
[11] Clements, K. D., Choat, J. H. (1997): Comparison of herbivory in the closely-related marine fish genera *Girella* and *Kyphosus*. – Marine Biology 127: 579-586.
[12] Clements, K. D., Angert, E. R., Montgomery, W. L., Choat, J. H. (2014): Intestinal microbiota in fishes: what's known and what's not. – Molecular Ecology 23(8): 1891-1898.
[13] Clements, K. D., Gleeson, V. P., Slaytor, M. (1994): Short-chain fatty acid metabolism in temperate marine herbivorous fish. – Journal of Comparative Physiology - Part B 164: 372-377.
[14] Cohen, L. J., Esterhazy, D., Kim, S. H., Lemetre, C., Aguilar, R. R., Gordon, E. A., et al. (2017): Commensal bacteria make GPCR ligands that mimic human signalling molecules. – Nature 549(7670): 48-53.
[15] Cook, S. I., Sellin, J. H. (1998): Review article: short chain fatty acids in health and disease. – Alimentary Pharmacology and Therapeutics 12: 499-507.
[16] Da, S. B., Fdn, V., Jlp, M., Ferreira, G. S., Seiffert, W. Q. (2013): Salts of organic acids selection by multiple characteristics for marine shrimp nutrition. – Aquaculture 384(6): 104-110.
[17] Dar, M. A., Pawar, K. D., Jadhav, J. P., Pandit, R. S. (2015): Isolation of cellulolytic bacteria from the gastro-intestinal tract of *Achatina fulica*, (Gastropoda: Pulmonata) and their evaluation for cellulose biodegradation. – International Biodeterioration and Biodegradation 98: 73-80.
[18] Deng, W., Wang, Y., Liu, Z., Cheng, H., Xue, Y. (2014): HemI: a toolkit for illustrating heatmaps. – Plos One 9(11): e111988.
[19] Dineshkumar, N., Renu, A. (2008): Preparation of a probiotic fermented milk using a native isolate of *Pediococcus pentosaceus* MTCC 5151. – Research Journal of Biotechnology 3(3): 28-31.
[20] Dixon, P. (2003): VEGAN, a package of R functions for community ecology. – Journal of Vegetation Science 14(6): 927-930.
[21] Dreher, R., Poralla, K., König, W. A. (1976): Synthesis of omega-alicyclic fatty acids from cyclic precursors in *Bacillus subtilis*. – Journal of Bacteriology 127(3): 1136-1140.
[22] Dulski, T., Zakęś, Z., Ciesielski, S. (2018): Characterization of the gut microbiota in early life stages of pikeperch *Sander lucioperca*. – Journal of Fish Biology 92(1): 94-104.
[23] Duncan, S. H., Louis, P., Flint, H. J. (2004): Lactate-utilizing bacteria, isolated from human feces, that produce butyrate as a major fermentation product. – Applied and Environmental Microbiology 70(10): 5810-5817.
[24] Edgar, R. C. (2013): UPASE: highly accurate OUT sequences from microbial amplicon reads. – Nature Methods 10(10): 996-998.
[25] Faith, J. J., Gordon, J. I. (2011): Predicting a human gut microbiota's response to diet in gnotobiotic mice. – Science 333(6038): 101-104.
[26] FAO (2014): The state of world fisheries and aquaculture 2014. Opportunities and challenges. – Food and Agriculture Organization of the United Nations, Rome.
[27] Flint, H. J., Duncan, S. H., Scott, K. P., Louis, P. (2015): Links between diet, gut microbiota composition and gut metabolism. – The Proceedings of the Nutrition Society 74(1): 13-22.

http://www.aloki.hu ● ISSN 1589 1623 (Print) ● ISSN 1785 0037 (Online)
DOI: http://dx.doi.org/10.15666/aeer/1706_1343513453

[28] Fukuda, S., Toh, H., Hase, K., Oshima, K., Nakanishi, Y., Yoshimura, K., et al. (2012): Bifidobacteria can protect from enteropathogenic infection through production of acetate. – Nature 469(5): 543-547.
[29] Geraylou, Z., Rurangwa, E., Wiele, T. V. D., Courtin, C. M., Delcour, J. A., Buyse, J., Ollevie, F. (2014): Fermentation of Arabinoxylan-oligosaccharides, oligofructose and their monomeric sugars by hindgut bacteira from Siberian sturgeon and African catfish in batch culture *in vitro*. – Journal of Aquaculture Research and Development 5(3): 230.
[30] Geraylou, Z., Souffreau, C., Rurangwa, E., Maes, G. E., Spanier, K. I., Courtin, C. M., et al. (2013): Prebiotic effects of arabinoxylan oligosaccharides on juvenile Siberian sturgeon (*Acipenser baerii*) with emphasis on the modulation of the gut microbiota using 454 pyrosequencing. – FEMS Microbiology Ecology 86(2): 357-371.
[31] Goosen, N. J., Görgens, J. F., Wet, L. F. D., Chenia, H. (2011): Organic acids as potential growth promoters in the South African abalone Haliotis midae. – Aquaculture 321(3): 245-251.
[32] Hao, Y. T., Wu, S. G., Jakovlić, I., Zou, H., Li, W. X., Wang, G. T. (2017a): Impacts of diet on hindgut microbiota and short-chain fatty acids in grass carp (*Ctenopharyngodon idellus*). – Aquaculture Research 48(11): 5595-5605.
[33] Hao, Y. T., Wu, S. G., Xiong, F., Tran, N. T., Jakovlić, I., Zou, H., et al. (2017b): Succession and Fermentation Products of Grass Carp (*Ctenopharyngodon idellus*) Hindgut Microbiota in Response to an Extreme Dietary Shift. – Frontiers in Microbiology 8: 1585.
[34] Hong, C., Chen, Y., Li, L., Chen, S., Wei, X. (2017): Identification of a key gene involved in branched-chain short fatty acids formation in Natto by transcriptional analysis and enzymatic characterization in *Bacillus subtilis*. – Journal of Agricultural and Food Chemistry 65(8): 1592-1597.
[35] Hullar, M. A. J., Fu, B. C. (2014): Diet, the gut microbiome, and epigenetics. – Cancer Journal 20(3): 170-175.
[36] Iehata, S., Inagaki, T., Okunishi, S., Nakano, M., Tanaka, R., Maeda, H. (2010): Improved gut environment of abalone *Haliotis gigantea* through *Pediococcus* sp. Ab1 treatment. – Aquaculture 305(1): 59-65.
[37] Johansson, M. L., Nobaek, S., Berggren, A., Nyman, M., Björck, I., Ahrné, S., et al. (1998): Survival of *Lactobacillus plantarum* DSM 9843 (299v), and effect on the short-fatty acid content of faeces after ingestion of a rose-hip drink with fermented oats. – International Journal of Food Microbiology 42(1-2): 29-38.
[38] Kandel, J. S., Horn, M. H., Van, A. W. (1994): Volatile fatty acids in the hindguts of herbivorous fishes from temperate and tropical marine waters. – Journal of Fish Biology 45: 527-529.
[39] Kaneda, T. (1963): Biosynthesis of branched chain fatty acids. – Journal of Biological Chemistry 238(4): 1222-1228.
[40] Kaoutari, A. E., Armougom, F., Gordon, J. I., Raoult, D., Henrissat, B. (2013): The abundance and variety of carbohydrate-active enzymes in the human gut microbiota. – Nature Reviews Microbiology 11(7): 497-504.
[41] Kasubuchi, M., Hasegawa, S., Hiramatsu, T., Ichimura, A., Kimura, I. (2015): Dietary gut microbial metabolites, short-chain fatty acids, and host metabolic regulation. – Nutrients 7(4): 2839-2849.
[42] Kihara, M., Sakata, T. (2002): Production of short-chain fatty acids and gas from various oligosaccharides by gut microbes of carp (*Cyprinus carpio* L.) in micro-scale batch culture. – Comparative Biochemistry and Physiology - Part A 132: 333-340.
[43] Kihara, M., Sakata, T. (1997): Fermentation of dietary carbohydrates to short-chain fatty acids by gut microbes and its influence on intestinal morphology of a detritivorous teleost tilapia (*Oreochromis niloticus*). – Comparative Biochemistry and Physiology – Part A 118(4): 1201-1207.

http://www.aloki.hu ● ISSN 1589 1623 (Print) ● ISSN 1785 0037 (Online)
DOI: http://dx.doi.org/10.15666/aeer/1706_1343513453

[44] Leblanc, J. G., Chain, F., Martín, R., Bermúdez-Humarán, L. G., Courau, S., Langella, P. (2017): Beneficial effects on host energy metabolism of short-chain fatty acids and vitamins produced by commensal and probiotic bacteria. – Microbial Cell Factories 16(1): 79.

[45] Leenhouwers, J. I., Ortega, R. C., Jaj, V., Schrama, J. W. (2007): Digesta characteristics in relation to nutrient digestibility and mineral absorption in Nile tilapia (*Oreochromis niloticus* L.) fed cereal grains of increasing viscosity. – Aquaculture 273(4): 556-565.

[46] Levy, M., Thaiss, C. A., Elinav, E. (2016): Metabolites: messengers between the microbiota and the immune system. – Genes and Development 30(14): 1589-1597.

[47] Li, H., Wu, S., Wirth, S., Hao, Y., Wang, W., Zou, H., et al. (2016a): Diversity and activity of cellulolytic bacteria, isolated from the gut contents of grass carp (*Ctenopharyngodon idellus*) (Valenciennes) fed on Sudan grass (*Sorghum sudanense*) or artificial feedstuffs. – Aquaculture Research 47(1): 153-164.

[48] Li, J., Hou, J., Zhang, P., Liu, Y., Xia, R., Ma, X. (2016b): Comparative study of intestinal microbial community structure in different species of carp in aquaponics system. – South China Fisheries Science 12(6): 42-50 (in Chinese).

[49] Li, W., Huan, X., Zhou, Y., Ma, Q., Chen, Y. (2009): Simultaneous cloning and expression of two cellulase genes from bacillus subtilis newly isolated from golden takin (*budorcas taxicolor bedfordi*). – Biochemical and Biophysical Research Communications 383(4): 397-400.

[50] Li, Z., Che, J., Xie, J., Wang, G., Yu, E., Xia, Y., et al. (2017): Microbial succession in biofilms growing on artificial substratum in subtropical freshwater aquaculture ponds. – FEMS Microbiology Letters 364(4): fnx017.

[51] Li, Z., Yu, E., Wang, G., Yu, D., Zhang, K., Gong, W., Xie, J. (2018): Broad Bean (*Vicia faba* L.) Induces intestinal inflammation in grass Carp (*Ctenopharyngodon idellus* C. et V) by increasing relative abundances of intestinal gram-negative and flagellated bacteria. – Frontiers in Microbiology 9: 1913.

[52] Mayhew, J. W., Onderdonk, A. B., Gorbach, S. L. (1975): Effects of time and growth media on short-chain fatty acid production by *Bacteroides fragilis*. – Applied Microbiology 29(4): 472-475.

[53] Meimandipour, A., HairBejo, M., Shuhaimi, M., Azhar, K., Soleimani, A. F., Rasti, B., Yazid, A. M. (2010): Gastrointestinal tract morphological alteration by unpleasant physical treatment and modulating role of *Lactobacillus* in broilers. – British Poultry Science 51(1): 52-59.

[54] Miyake, S., Ngugi, D. K., Stingl, U. (2015): Diet strongly influences the gut microbiota of surgeonfishes. – Molecular Ecology 24(3): 656-672.

[55] Mountfort, D. O., Grant, W. D., Morgan, H., Rainey, F. A., Stackebrandt, E. (1993): Isolation and characterization of an obligately anaerobic, pectinolytic, member of the genus *Eubacterium* from mullet gut. – Archives of Microbiology 159(3): 289-295.

[56] Mountfort, D. O., Campbell, J., Clements, K. D. (2002): Hindgut fermentation in three species of marine herbivorous fish. – Applied and Environmental Microbiology 68(3): 1374-1380.

[57] Ni, J., Yan, Q., Yu, Y., Zhang, T. (2014a): Factors influencing the grass carp gut microbiome and its effect on metabolism. – FEMS Microbiology Ecology 87(3): 704-714.

[58] Ni, J., Yan, Q., Yu, Y., Zhang, T. (2014b): Fish gut microecosystem: a model for detecting spatial pattern of microorganisms. – Chinese Journal of Oceanology and Limnology 32(1): 54-57.

[59] Paris, H., Murat, J. C., Castilla, C. (1977): Etude des acides grasvolatilsdans l'intestintroise speces de Poissons Teleosteens. – Comptes Rendus des Seances de la Societe de Biologieet de ses Filiales 171: 1297-1301.

http://www.aloki.hu ● ISSN 1589 1623 (Print) ● ISSN 1785 0037 (Online)
DOI: http://dx.doi.org/10.15666/aeer/1706_1343513453

[60] Piazzon, M. C., Calduchginer, J. A., Fouz, B., Estensoro, I., Simómirabet, P., Puyalto, M., et al. (2017): Under control: how a dietary additive can restore the gut microbiome and proteomic profile, and improve disease resilience in a marine teleostean fish fed vegetable diets. – Microbiome 5(1): 164.

[61] Pogribna, M., Freeman, J. P., Paine, D., Boudreau, M. D. (2010): Effect of *Aloe vera* whole leaf extract on short chain fatty acids production by *Bacteroides fragilis*, *Bifidobacterium infantis* and *Eubacterium limosum*. – Letters in Applied Microbiology 46(5): 575-580.

[62] Postler, T. S., Ghosh, S. (2017): Understanding the holobiont: How microbial metabolites affect human health and shape the immune system. – Cell Metabolism 26(1): 110-130.

[63] Probert, H. M., Apajalahti, J. H. A., Rautonen, N., Stowell, J., Gibson, G. R. (2004): Polydextrose, lactitol, and fructo-oligosaccharide fermentation by colonic bacteria in a three-stage continuous culture system. – Applied and Environmental Microbiology 70(8): 4505-4511.

[64] R Core Team. (2014): R: A language and environment for statistical computing. – R Foundation for Statistical Computing, Vienna, Austria. http://www.r-project.org/.

[65] Ray, A. K., Ghosh, K., Ringø, E. (2012): Enzyme-producing bacteria isolated from fish gut: a review. – Aquaculture Nutrition 18(5): 465-492.

[66] Reichardt, N., Duncan, S. H., Young, P., Belenguer, A., Mcwilliam, L. C., Scott, K. P., et al. (2014): Phylogenetic distribution of three pathways for propionate production within the human gut microbiota. – The ISME Journal 8(6): 1323-1335.

[67] Ringø, E. (1992): Effects of dietary formate and acetate on growth and lipid digestibility in Arctic charr, *Salvelinus alpinus* (L.). – Fiskeridirektoratets Skrifter Serie Ernaering 5: 17-24.

[68] Safari, R., Hoseinifar, S. H., Kavandi, M. (2016): Modulation of antioxidant defense and immune response in zebra fish (*Danio rerio*) using dietary sodium propionate. – Fish Physiology and Biochemistry 42(6): 1733-1739.

[69] Schwiertz, A., Taras, D., Schäfer, K., Beijer, S., Bos, N. A., Donus, C., Hardt, P. D. (2012): Microbiota and SCFA in lean and overweight healthy subjects. – Obesity 18(1): 190-195.

[70] Seeto, G. S., Veivers, P. C., Clements, K. D., Slaytor, M. (1996): Carbohydrate utilisation by microbial symbionts in the marine herbivorous fishes *Odax cyanomelas* and *Crinodus lophodon*. – Journal of Comparative Physiology - Part B 165: 571-579.

[71] Sivieri, K., Morales, M. L. V., Adorno, M. A. T., Sakamoto, I. K., Saad, S. M. I., Rossi, E. A. (2013): *Lactobacillus acidophilus* CRL 1014 improved "gut health" in the SHIME reactor. – BMC Gastroenterology 13(1): 100.

[72] Smith, T. B., Wahl, D. H., Mackie, R. I. (1996): Volatile fatty acids and anaerobic fermentation in temperate piscivorous and omnivorous freshwater fish. – Journal of Fish Biology 48(5): 829-841.

[73] Spiljar, M., Merkler, D., Trajkovski, M. (2017): The immune system bridges the gut microbiota with systemic energy homeostasis: focus on TLRs, mucosal barrier, and SCFAs. – Frontiers in Immunology 8: 1353.

[74] Stevens, C. E., Hume, I. D. (1998): Contributions of microbes in vertebrate gastrointestinal tract to production and conservation of nutrients. – Physiological Reviews 78(2): 393-427.

[75] Taheri, H. R., Moravej, H., Malakzadegan, A., Tabandeh, F., Zaghari, M., Shivazad, M., Adibmoradi, M. (2015): Efficacy of *Pediococcusacidl actici*-based probiotic on intestinal coliforms and villus height, serum cholesterol level and performance of broiler chickens. – African Journal of Biotechnology 9(44): 7564-7567.

[76] Titus, E., Ahearn, G. A. (1991): Transintestinal acetate transport in a herbivorous teleost: Anion exchange at the basolateral membrane. – Journal of Experimental Biology 156: 41-61.

http://www.aloki.hu ● ISSN 1589 1623 (Print) ● ISSN 1785 0037 (Online)
DOI: http://dx.doi.org/10.15666/aeer/1706_1343513453

[77] Tsuchido, T., Hiraoka, T., Takano, M., Shibasaki, I. (1985): Involvement of autolysin in cellular lysis of *Bacillus subtilis* induced by short- and medium-chain fatty acids. – Journal of Bacteriology 162(1): 42-46.
[78] Tsuchiya, C., Sakata, T., Sugita, H. (2008): Novel ecological niche of *Cetobacterium somerae*, an anaerobic bacterium in the intestinal tracts of freshwater fish. – Letters in Applied Microbiology 46(1): 43-48.
[79] Van, S. P. J. (1994): Nutritional Ecology of the Ruminant. 2nd Ed. – Cornell University Press, Ithaca.
[80] Wang, Q., Garrity, G. M., Tiedje, J. M., Cole, J. R. (2007): Naïve Bayesian classifier for rapid assignment of rRNA sequences into the new bacterial taxonomy. – Applied and Environmental Microbiology 73(16): 5261.
[81] Wang, Y., Lu, Y., Zhang, Y., Ning, Z., Li, Y., Zhao, Q., et al. (2015): Erratum: the draft genome of the grass carp (*Ctenopharyngodono idellus*) provides insights into its evolution and vegetarian adaptation. – Nature Genetics 47(8): 625-631.
[82] Wu, S., Wang, G., Angert, E. R., Wang, W., Li, W., Zou, H. (2012): Composition, diversity, and origin of the bacterial community in grass carp intestine. – Plos One 7(2): e30440.
[83] Xia, J. H., Lin, G., Fu, G. H., Wan, Z. Y., Lee, M., Wang, L., et al. (2014): The intestinal microbiome of fish under starvation. – BMC Genomics 15(1): 266.
[84] Yan, Q., Li, J., Yu, Y., Wang, J., He, Z., Van Nostrand, J. D., et al. (2016): Environmental filtering decreases with fish development for the assembly of gut microbiota. – Environmental Microbiology 18(12): 4739-4754.
[85] Zhang, Z., Li, D., Refaey, M. M., Xu, W. (2017): High spatial and temporal variations of microbial community along the Southern catfish gastrointestinal tract: insights into dynamic food digestion. – Frontiers in Microbiology 8: 1531.

APPENDIX

Appendix 1. *Weight increments of grass carp feed two months of hybrid giant napier (HG), formula feed (FF), or marinated broad beans (BB), respectively*

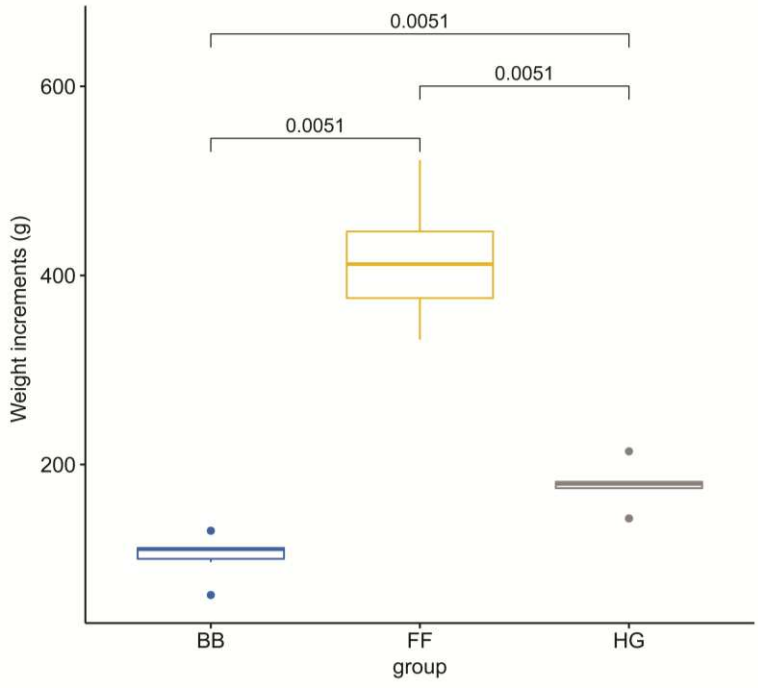

http://www.aloki.hu ● ISSN 1589 1623 (Print) ● ISSN 1785 0037 (Online)
DOI: http://dx.doi.org/10.15666/aeer/1706_1343513453

Appendix 2. *Sequencing information of samples for microbiota analysis. FG, HG, and BG indicate the hindgut microbiota of the grass carp fed formula feed, hybrid giant napier, and marinated broad beans, respectively*

Sample ID	Raw sequence	Clean sequence	Effective sequence	Average length (nt)	Q30	OUT number	Chao1 index	Shannon index
BG1	55,159	55,115	52,782	253	97.13	277	418.973	3.533
BG2	54,108	54,075	50,859	253	97.13	291	350.381	3.57
BG3	63,421	63,375	60,402	253	97	310	415	3.208
HG1	62,086	60,662	57,635	253	96.98	209	246.561	3.366
HG2	60,888	58,019	55,007	253	96.71	126	165	2.704
HG3	59,094	57,268	55,248	252	96.88	198	265.097	2.408
FG1	34,651	34,636	32,466	252	97.01	99	118.333	1.873
FG2	43,641	43,617	39,371	253	97.04	93	118.87	2.071
FG3	51,364	51,322	47,390	252	97.12	103	146.938	2.025

Appendix 3. *OTU rarefaction curves of the samples. FG, HG, and BG indicate the hindgut microbiota of the grass carp fed formula feed, hybrid giant napier, and marinated broad beans, respectively*

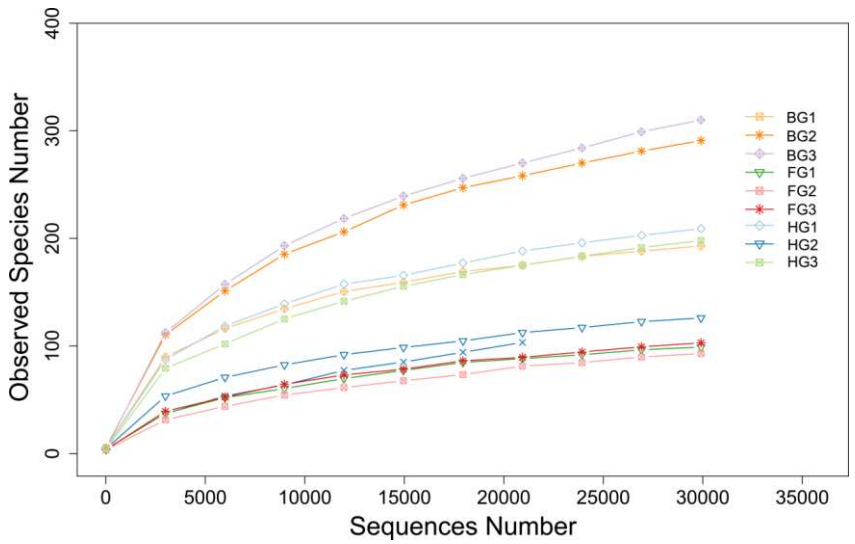

http://www.aloki.hu ● ISSN 1589 1623 (Print) ● ISSN 1785 0037 (Online)
DOI: http://dx.doi.org/10.15666/aeer/1706_1343513453

CHARACTERISTICS OF DECOMPOSITION AND NUTRIENT RELEASE OF CORN STRAW UNDER DIFFERENT ORGANIC FERTILIZER REPLACEMENT RATES

HE, H. – ZHANG, Y. T – WEI, C. Z. – LI, J. H.*

Key Laboratory of Oasis Eco-Agriculture, Xinjiang Production and Construction Corps, College of Agronomy, Shihezi University, Road of North 4th, Shihezi City, Xinjiang 832003, China

**Corresponding author*
e-mail: ljh630703@163.com

(Received 2nd Jul 2019; accepted 2nd Sep 2019)

Abstract. In this study, the nylon net bag method was used to explore the characteristics of straw decomposition and nutrient release under different organic fertilizer replacement rates, which provided a scientific basis for rational straw returning in corn (*Zea mays* L.) planting. The results showed that the characteristics of straw decomposition and nutrient release in different treatments were fast in the early stage (0-20 d) and slow in the late stage (20-100 d). At the end of decomposition (100 d), the decomposition rate and nutrient release rate were 47.69%-56.07%, 47.55%-61.73%, 47.40%-62.67%, 48.04%-66.35% and 82.20%-100.00%, respectively, decomposition rate and nutrient release rate were 8%OF (organic fertilizer replaces 8% N fertilizer) > 16%OF (organic fertilizer replaces 16% N fertilizer) > 24%OF (organic fertilizer replaces 24% N fertilizer) > CF (only chemical fertilizer) > CK (no fertilizer control). Through the model ($y = a \cdot x^b$) analysis of nutrient release rate, the time until complete release of C, N, P, and K was predicted to be 206-275 d, 167-271 d, 153-248 d, and 85-150 d, respectively, and it was verified that the nutrient release characteristics of fertilization treatment (CF, 8%OF, 16%OF, 24%OF) in this experiment were potassium (K) > phosphorus (P) > nitrogen (N) > carbon (C), and CK was K > P > N ≈ C. Based on the model and correlation analysis, the recommended organic fertilizer replacement rate is 12%, and according to the characteristics of straw decomposition and nutrient release, a strategy of rational straw returning and fertilization management was proposed.

Keywords: *corn straw returning, corn planting, nutrient, fertilizer reduction, fertilization strategy, model, prediction*

Introduction

Corn is China's main food and feed crop, and it plays an important strategic role in achieving food security. Excessive application of chemical fertilizers in agricultural production to ensure the increase of crop yields has caused problems such as increased planting costs, low nutrient use efficiency, reduced soil fertility, and agricultural non-point source pollution, and threatened the sustainable development of agro-ecology in China (Fischer, 2010; Jin and Zhou, 2018). In the past decade, corn has contributed 31.8% of the total increase in chemical fertilizer use in China. In 2015, the Ministry of Agriculture of China put forward the *2020 Fertilizer Use Zero Growth Action Plan* to reduce the use of chemical fertilizers (Jin et al., 2015). Therefore, reducing the consumption of chemical fertilizer in corn production is bound to be conducive to the realization of "Fertilizer Use Zero Growth". The increase in corn yield also produces many straw resources. Crop straw is a kind of biomass resource, but it has not been used reasonably. There are high amounts of straws being burned and discarded, which not only causes waste of resources but also brings a series of environmental issues, among them, straw burning has discharged many CO_2, CO, particulate matter, etc.,

http://www.aloki.hu ● ISSN 1589 1623 (Print) ● ISSN 1785 0037 (Online)
DOI: http://dx.doi.org/10.15666/aeer/1706_1345513472

which wastes biomass energy and causes losses for the agricultural carbon pool, serious air pollution and soil health hazards (Feng et al., 2011; Sun et al., 2016; Li and Wang, 2013; Zhang et al., 2016). Therefore, reducing the use of chemical fertilizers and the effective use of straw resources has become a major challenge for sustainable development of green and traditional agriculture.

At present, straw returning and organic fertilizer replacing part of chemical fertilizer has become the main measures to realize the effective utilization of straw resources and reduce the use of chemical fertilizer. After organic fertilizer replaces part of chemical fertilizer, it can reduce the amount of chemical fertilizer, improve the physical and chemical properties and buffering properties of soil, improve soil fertility and microbial activity, and coordinate the balanced supply of nutrients in soil (Liu et al., 2013; Fu et al., 2017; Wen et al., 2018). Crop straw is an important renewable resource in the agricultural ecosystem. It contains abundant C, N, P, K and trace elements (Wang et al., 2010). After returning to the field, soil microorganisms and enzymes act together to decompose, release C, N, P, K and other nutrients to the soil, and provide crop absorption and utilization (Becker et al., 2014), which can improve soil fertility and soil physical and chemical properties, it can reduce the negative impact of burning straw on the ecological environment. Straw returning is the most economical and sustainable way to use straw resources (Yin et al., 2017).

In recent years, to solve the problems of waste of agricultural resources and alleviate the excessive application of chemical fertilizer, soil degradation and agricultural non-point source pollution, the nutrients released during the decomposition of crop straw are used to reduce the amount of chemical fertilizer application. Therefore, the research on crop straw decomposition has become a hot topic of many scholars' attention (Abdou et al., 2016; Wang et al., 2018; Gong et al., 2018). Some studies have found that with the increase of decomposition days, the decomposition rate and nutrient release rate of straw gradually increase and the decomposition speed gradually decreases. The decomposition rate of different straws is fast in the early stage and slow in the later stage (Li et al., 2009; Dai et al., 2010; Dai et al., 2017). The application of chemical fertilizer or decomposition agent in the soil can promote the decomposition of straw (Chen et al., 2016; Ngatia et al., 2014). For the different crop straw or the different forms and contents of nutrients in the straw, the release rates of nutrients are different. Some studies found that K > P > N > C (Dai et al., 2010; Wu et al., 2011), and others found that K > P > C > N (Li et al., 2017). Therefore, the study of the characteristics of straw decomposition and nutrient release is the theoretical basis for guiding straw returning in agricultural production.

There are many studies on straw decomposition, but there are few studies on straw decomposition under different organic fertilizer replaces chemical fertilizer rate. Xinjiang Province is one of the major corn planting regions in China. The resources of corn straw are abundant but not effectively utilized, and it has great potential to straw returning. At the same time, the phenomenon of excessive fertilization in production is more common. Therefore, this study is based on the phenomenon that straw resources are not effectively utilized and excessive fertilization. The nylon net bag method was used to carry out decomposition experiments because this method has little impact on soil water transport and is closer to the actual situation in the field; this method is suitable for studying the decomposition of crop straw in arid and semi-arid regions (Lin et al., 1992; Bocock and Gilbert, 1957). To explore the

http://www.aloki.hu ● ISSN 1589 1623 (Print) ● ISSN 1785 0037 (Online)
DOI: http://dx.doi.org/10.15666/aeer/1706_1345513472

characteristics of decomposition and nutrient release of corn straw under different organic fertilizer replacement rate under equal nutrient conditions, establish and analyse decomposition and nutrient models, dynamically monitor and predict them, and recommend suitable organic fertilizer replacement rate, To provide a scientific basis for straw returning and rational fertilization in corn cultivation is of great significance for the effective utilization of straw resources and to reduce chemical fertilizer application and sustainable development of agriculture.

Materials and methods

Site description

The experimental site is located in the Demonstration Park of Agricultural Technology (DPAT) in Yining, Xinjiang, Northwest China (43°55'30"N, 81°33'29''E), the site has an elevation of 683 m and is moderate temperate arid inland mountain climate, four seasons are clear and sunshine is sufficient. The annual precipitation is 250-551.7 mm, the annual average temperature and maximum temperature are 10.6 °C and 35.8 °C, respectively, the effective accumulated temperature ≥ 10 °C is 3621.2 °C, the annual duration of sunshine is 2792.7 h, and the frostless season is 154-184 d. The soil type is irrigated lime-calcareous soil, and the physicochemical properties of the soil tillage layer (0-20 cm) are as follows: pH, 7.71; alkali N, 85.95 mg kg^{-1}; available K, available P, 23.94 mg kg^{-1}; 229.24 mg kg^{-1}; soil organic C, 7.38 g kg^{-1}; total N, 0.96 g kg^{-1}.

Materials

The experimental straw is corn straw (comprised the stems, leaves, and sheaths) preserved after harvesting and drying in the experimental site in 2017, and its initial nutrient contents were as follows: C, 413.50 g kg^{-1}; N, 19.47 g kg^{-1}; P, 3.09 g kg^{-1}; and K, 17.53 g kg^{-1}, C/N ratio, 21.24, C/P ratio, 133.82, C/K ratio, 23.59. The local conventional fertilizers (NPK fertilizer) mainly uses urea (contains 46.0% N), diammonium phosphate (contains 18.0% N, 48.0% P_2O_5), potassium sulfate (contains 51.0% K_2O); the commercial organic fertilizer (contains 1.77% N, 1.95% P_2O_5, 0.53% K_2O).

Experimental design

The experiment was conducted from 8 May to 16 August 2018. On the basis of equal nutrient conditions, straw decomposition experiments under different organic fertilizer replacement rates were carried out, and five treatments were set up: (1) CK: no fertilizer control; (2) CF: only chemical fertilizer; (3) 8%OF: organic fertilizer replaces 8% N fertilizer; (4) 16%OF: organic fertilizer replaces 16% N fertilizer; (5) 24%OF: organic fertilizer replaces 24% N fertilizer. Before spring tillage, commercial organic fertilizer, 40% N fertilizer and P and K fertilizer were applied as base fertilizer, and the remaining 60% N fertilizer was artificially applied urea (ditch application) at jointing stage. The fertilization scheme is shown in *Table 1*. Random block arrangement was adopted, with three replicates per treatment, and the area of the plot was 32.4 m^2 (4 m × 8.1 m), and the corn (*Zea mays* L., *cv.* Xinyu 50) is planted in the plot, the row spacing is 50.0 cm (8 rows in total), plant spacing is 21.5 cm, the planting density is 9.3×10^4 plants hm^{-2}.

http://www.aloki.hu ● ISSN 1589 1623 (Print) ● ISSN 1785 0037 (Online)
DOI: http://dx.doi.org/10.15666/aeer/1706_1345513472

Table 1. *Fertilization schemes for different treatments*

Treatment	*k* (%)	Base fertilizer						Topdressing chemical-N	Total nutrient contents		
		Chemical fertilizer			Organic fertilizer						
		N	P_2O_5	K_2O	N	P_2O_5	K_2O	N	N	P_2O_5	K_2O
CK	-	0	0	0	0	0	0	0	0	0	0
CF	0	120.0	180.0	60.0	0	0	0	180.0	300.0	180.0	60.0
8%OF	8	96.0	153.0	52.5	24.0	27.0	7.5	180.0	300.0	180.0	60.0
16%OF	16	72.0	127.5	45.0	48.0	52.5	15.0	180.0	300.0	180.0	60.0
24%OF	24	48.0	100.5	37.5	72.0	79.5	22.5	180.0	300.0	180.0	60.0

According to the organic fertilizer replacement rate (*k*), the replacement N content is calculated, and the organic fertilizer dosage and PK replacement amount are calculated according to the nutrient content of organic fertilizer

The decomposition experiment adopts the nylon net bag method, and the corn straw is dried and pulverized into 3 to 5 cm, mixed, weighed 30.0 g (equivalent to 5000 kg ha^{-1}, half amount of returning to the field) and then placed in a nylon net bag (whose length × width was 30 cm × 20 cm, with a pore diameter of 0.125 mm), after which the opening of each bag was tightly closed, and the bags were laid flat about 2 cm high, and each treatment was 15 bags, and the experiment was a total of 75 bags (5 treatments × 3 replicates × 5 samples). After corn emerged 2-3 cm, the bag was buried. The specific operational steps of the buried bag: at the centre of each plot, nylon net bags were buried 10 cm below the 2-6 inter-row tillage layers. When landfilling, the soil 10 cm depth between rows of corn is taken out, the soil deep in the 2 cm is dug out (no landfill), then the nylon net bag is laid horizontally, and then the soil is filled back and compacted to the level with the ground (*Fig. 1*). The experimental period was 100 days, and 15 nylon net bags were taken every 20 days for 5 times, and recorded the precipitation and temperature conditions during the decomposition period (*Fig. 2*). To avoid the interference of topdressing on the determination of nutrient content of corn straw residues, no topdressing was carried out in the area where straw was buried.

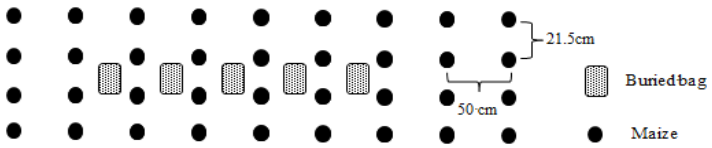

Figure 1. *Schematic diagram of buried bag of corn straw*

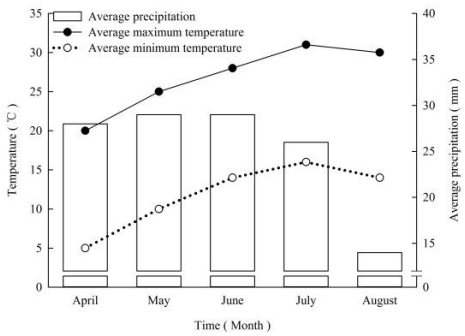

Figure 2. *Temperature during decomposition experimental period*

http://www.aloki.hu ● ISSN 1589 1623 (Print) ● ISSN 1785 0037 (Online)
DOI: http://dx.doi.org/10.15666/aeer/1706_1345513472

Sampling and chemical analysis

Sampling began on May 28, 2018, sampling was performed at 20, 40, 60, 80, and 100 days (decomposition day is 20, 40, 60, 80 and 100 days) after the bag was buried (sampling a total of 5 times), and August 16th, 2018 was the last sample. After sampling, the surface of the nylon net bag and the root debris were removed, and the nylon net bag was rinsed clean, then the straw in the net bag was taken out and placed in an oven (KJ-DY02, Kejie Company, China) at 65 °C to dry to constant weight. The dry weight of the straw was measured, and the sieve was passed through a 1 mm sieve to determine the C, N, P, and K of the straw.

The dry matter weight of the straw was determined by a drying-weighing method. The carbon (C) of straw was determined by potassium dichromate (133 mmol L^{-1} $K_2Cr_2O_7$) external heating (at 170-180 °C) method. After the corn straw sample (0.25 g) was digested by the sulfuric acid-hydrogen peroxide (H_2SO_4-H_2O_2) at 380 °C, the nitrogen (N) of straw was determined by Nessler's colorimetry method (722N, JKI Company, China), the phosphorus (P) of straw was determined by vanadium molybdate yellow colorimetric method (722N, JKI Company, China), the potassium (K) of straw was determined by flame photometer method (FP640N, OEM Company, China). The above indicators are determined by reference to Bao (2000).

Statistical analysis and calculation

Data processing, analysis and plotting were performed using Microsoft Excel 2010 and SPSS 17.0 software. Correlation analyses were performed using the Pearson method.

Organic fertilizer replacement rates in different treatments were calculated as follows:

$$k = \frac{\text{Organic fertilizer N contact}}{\text{Total N contact}} \quad \text{(Eq.1)}$$

Calculate the decomposition rate, decomposition speed, nutrient release rate, and C/N ratio methods (Liu et al., 2016; Huang et al., 2017) (*Eqs. 2-5*):

$$\text{Decomposition rate (\%)} = \frac{M_0 - M_t}{M_0} \times 100\% \quad \text{(Eq.2)}$$

$$\text{Decomposition speed (g day}^{-1}\text{)} = \frac{M_0 - M_t}{t} \quad \text{(Eq.3)}$$

$$\text{Nutrient release rate (\%)} = \frac{M_0 \cdot C_0 - M_t \cdot C_t}{M_0 \cdot C_0} \times 100\% \quad \text{(Eq.4)}$$

$$\text{Ratio of C to nutrients in straw residue} = \frac{C_t\ (C)}{C_t\ (N,\ P \text{ or } K)} \quad \text{(Eq.5)}$$

where *t* (d) *is the decomposition day;* M_0 (g) is the initial straw dry weight; M_t (g) is the straw dry weight at t; C_0 (g kg^{-1}) is the initial straw nutrient content; C_t (g kg^{-1}) is the straw nutrient content at t.

Models of straw decomposition rate and nutrient release rate under different decomposition days (Chapman, 1997; Stanford, et al., 1972; Chen et al., 2009):

http://www.aloki.hu ● ISSN 1589 1623 (Print) ● ISSN 1785 0037 (Online)
DOI: http://dx.doi.org/10.15666/aeer/1706_1345513472

$$y = a \cdot x^b \quad \text{(Eq.6)}$$

where y is the decomposition rate or nutrient release rate; x is the decomposition day; a is the release rate of some nutrients in straw which can be achieved quickly; b is the release rate growth parameter, indicating that the release rate increases faster.

Results

Straw decomposition characteristics

As the decomposition progresses, the decomposition rate increased, and the decomposition speed decreased. The whole decomposition process showed the characteristic of fast in the early stage and slows in the later stage (*Fig. 3*). In the first 20 days, the decomposition speed was faster, reaching 254.83-308.83 mg d^{-1} and the decomposition rate increased rapidly, reaching 16.99%-20.59%, accounting for 33.43%-36.72% of the total decomposition rate, both decomposition rate and decomposition speed were 8%OF > 16%OF > 24%OF > CF > CK. After 20 days, the decomposition speed began to decrease, and then it was relatively stable, and the decomposition rate was slowed down. At the end of decomposition (100 d), decomposition speed was 143.33-170.00 mg d^{-1}, and the decomposition rate reached 47.69%-56.07%. The order of decomposition rate and decomposition speed was 8%OF > 16%OF > 24%OF > CF > CK.

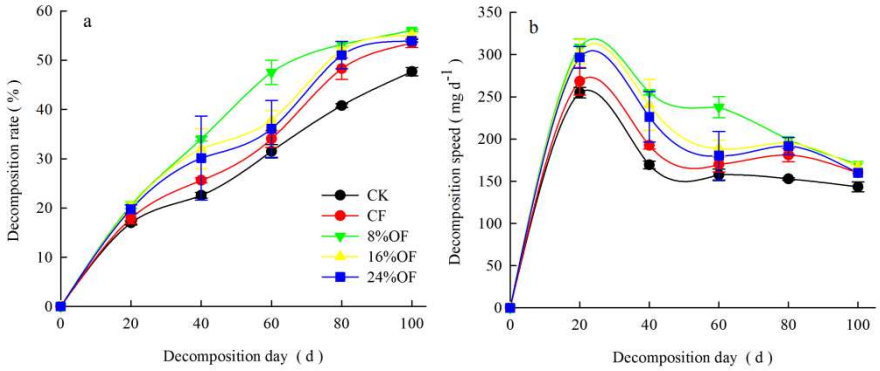

Figure 3. *Decomposition characteristics of corn straw under different amounts of returned straw. In the figure, a and b represent the decomposition rate and decomposition speed, respectively*

Nutrient release characteristics

The nutrient release characteristics are similar to the decomposition characteristics, showing that nutrient release was faster in the early stage (0-20 d) and slower in the late stage (20-100 d) (*Fig. 4*). The release rates of C, N, P and K in each treatment were 14.72%-25.91%, 14.99%-20.46%, 16.90%-23.68%, and 42.10%-61.36%, respectively, accounting for 30.96%-46.83%, 29.91%-34.79%, 34.15%-35.88% and 47.62%-61.36% of the total release rate, respectively, and the order of each nutrient release rate is K > P > C > N. After 20 days, the release rate of each nutrient increased slowly, and at 80 days, the K treated with 8%OF had been completely released. At the end of decomposition (100 d), the release rates of C, N, P and K in each treatment were

http://www.aloki.hu ● ISSN 1589 1623 (Print) ● ISSN 1785 0037 (Online)
DOI: http://dx.doi.org/10.15666/aeer/1706_1345513472

47.55%-61.73%, 47.40%-62.67%, 48.04%-66.35% and 82.20%-100.00% respectively. Among them, the order of release of nutrients in fertilization treatments (CF, 8%OF, 16%OF and 24%OF) were K > P > N > C, and the order of release of nutrients in CK treatment was K > P > N ≈ C.

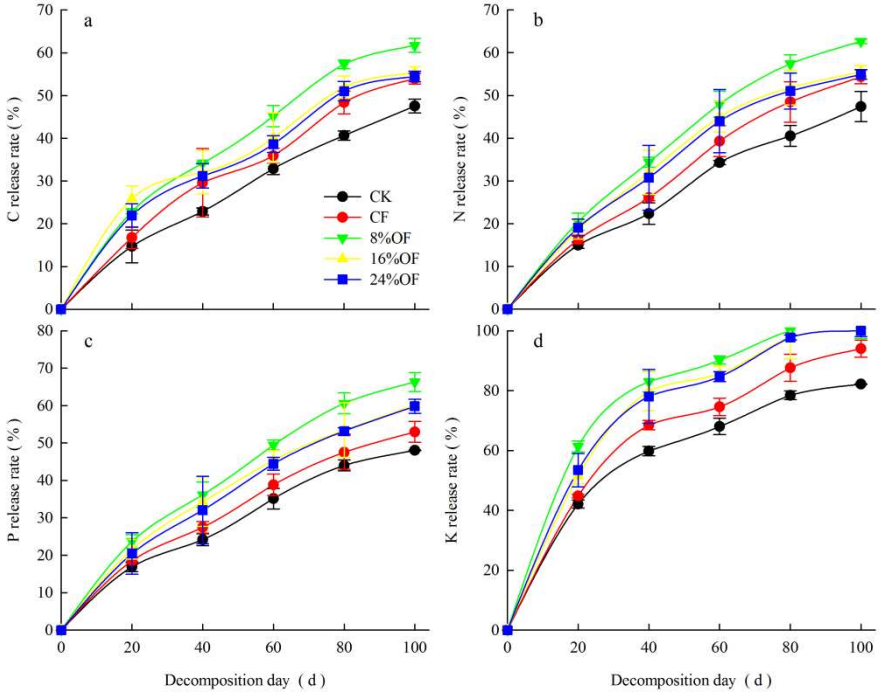

Figure 4. *Dynamic changes in C, N, P and K release rates of corn straw. In the figure, a, b, c, and d represent the nutrient release rates of C, N, P, and K, respectively*

The rate of nutrient release from corn straw increased faster in the early stage (0-20 d) and decreased in the late stage (20-100 d) (*Fig. 5*). In the first 20 days, the release rates of C, N, P, and K in straw reached 91.33-160.72 mg d^{-1}, 4.38-5.97 mg d^{-1}, 0.78-1.10 mg d^{-1}, and 11.07-16.14 mg d^{-1}, respectively. After 100 days of decomposition, the release rates of C, N, P, and K decreased to 58.98-76.58 mg d^{-1}, 2.60-3.55 mg d^{-1}, 0.45-0.62 mg d^{-1}, and 4.32-5.26 mg d^{-1}, respectively. After 100 days of decomposition, the release rates of C, N, P and K decreased to 58.98-76.58 mg d^{-1}, 2.60-3.55 mg d^{-1}, 0.45-0.62 mg d^{-1} and 4.32-5.26 mg d^{-1}, respectively, which were 35.42%-57.99%, 36.80%-44.09%, 41.45%-43.97%, 58.01%-67.40%, compared with the pre-decomposition period (0-20 d). During the whole decomposition process, the release rate of each nutrient in different treatments was 8%OF > 16%OF > 24%OF > CF > CK.

Changes of C and nutrients (N, P, and K) ratio of straw residue

As seen from *Figure 6,* the C/N ratio, the C/P ratio and the C/K ratio of the different treatments are substantially similar. Therefore, the different organic fertilizers replacement rate does not change the overall release characteristics of the nutrients. During the whole decomposition process, the C/N ratio fluctuated around 21, and there was a significant downward trend in the first 20 days. After 40 days, the C/N ratio of each treatment ranged from 20.8 to 20.98 (*Fig. 6a*). In the first 20 days, the C/P ratio increased rapidly, and P released the fastest. The order of the C/P ratio was

http://www.aloki.hu ● ISSN 1589 1623 (Print) ● ISSN 1785 0037 (Online)
DOI: http://dx.doi.org/10.15666/aeer/1706_1345513472

8%OF > 16%OF > 24%OF > CF > CK, which was consistent with the P release characteristics. The C/P ratio decreased rapidly from 20 to 40 days, and stabilized after 40 days, ranging from 115.40 to 130.94 (*Fig. 6b*). The C/K ratio continued to increase with decompression days. In the first 60 days, the order of C/K ratio was 8%OF > 16%OF > 24%OF > CF > CK. At 80 days, K of 8%OF was completely released. At 100 days, K of 16%OF and 24%OF was completely released, and CF (185.08) was higher than CK (69.54), which was consistent with the characteristics of K release (*Fig. 6c*).

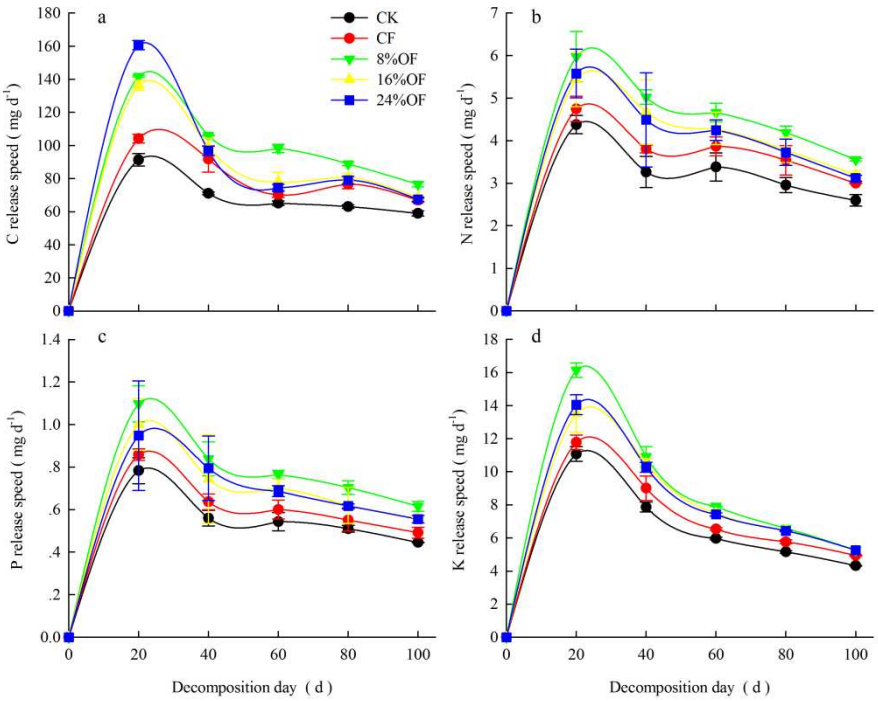

Figure 5. *Dynamic changes in C, N, P and K release speeds of corn straw. In the figure, a, b, c, and d represent the nutrient release speeds of C, N, P, and K, respectively*

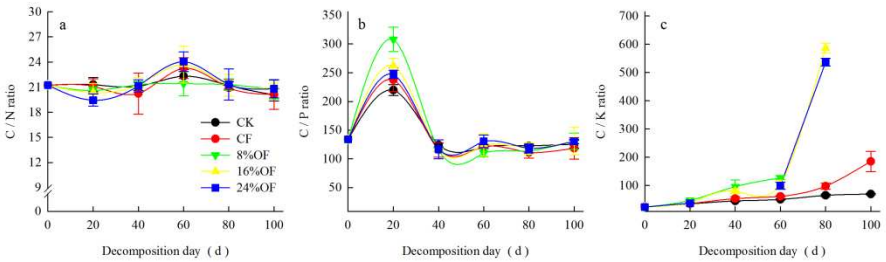

Figure 6. *Changes of C and nutrients (N, P, and K) ratio of straw residue during decomposition of corn straw. In the figure, a, b and c represent the C/N ratio, C/P ratio and C/K ratio, respectively*

Model analysis and prediction of decomposition rate and nutrient release rate

The decomposition rate, nutrient release rate (y) and decomposition days (x) were fitted to the regression equation, in accordance with the power function model $y = a \cdot x^b$

http://www.aloki.hu ● ISSN 1589 1623 (Print) ● ISSN 1785 0037 (Online)
DOI: http://dx.doi.org/10.15666/aeer/1706_1345513472

(*Table 2*). It can be seen that the parameter a of the decomposition rate and the nutrient release rate of the fertilization treatments (CF, 8%OF, 16%OF and 24%OF) were both 8%OF > 16%OF > 24%OF > CF, and the parameter b has no obvious change, therefore, fertilization can promote the decomposition and nutrient release of straw, and the treatment effect of organic fertilizer replaces chemical fertilizer is more obvious. At the same time, the model can also predict that the days of complete decomposition and C N, P, and K complete release in different treatments are 217-330 d, 206-275 d, 167-271 d, 153-248 d and 85-150 d, respectively, The days required for complete decomposition is 8%OF < 16%OF < CF < 24%OF < CK and the days required for the complete release of C N, P, and K is 8%OF < 16%OF < 24%OF < CF < CK. The nutrient release rate of fertilization treatments (CF, 8%OF, 16%OF and 24%OF) were K > P > N > C, and the nutrient release rate of CK was K > P > N ≈ C, which was consistent with the test results.

Table 2. *Model analysis of decomposition time (x) and decomposition rate and nutrient release rate (y) of corn straw under different treatments*

Item (%)	Treatments	Equation	R^2	*P* value	Prediction days (d)
Decomposition rate	CK	$y = 2.2231x^{0.6566}$	0.9728	0.002	330
	CF	$y = 2.0603x^{0.7031}$	0.9759	0.002	251
	8%OF	$y = 3.0781x^{0.6472}$	0.9774	< 0.001	217
	16%OF	$y = 3.0109x^{0.6353}$	0.9846	0.001	248
	24%OF	$y = 2.8552x^{0.640}$	0.9796	0.001	259
C release rate	CK	$y = 1.5653x^{0.7407}$	0.9964	< 0.001	275
	CF	$y = 1.9414x^{0.7255}$	0.9919	< 0.001	229
	8%OF	$y = 3.3395x^{0.6383}$	0.9946	< 0.001	206
	16%OF	$y = 2.6449x^{0.6781}$	0.9992	0.003	213
	24%OF	$y = 2.5403x^{0.6801}$	0.9997	0.001	222
N release rate	CK	$y = 1.5659x^{0.7421}$	0.9999	< 0.001	271
	CF	$y = 1.7486x^{0.7491}$	0.9934	< 0.001	222
	8%OF	$y = 2.0592x^{0.7589}$	0.9931	< 0.001	167
	16%OF	$y = 1.9148x^{0.7543}$	0.9842	0.001	190
	24%OF	$y = 1.8954x^{0.7536}$	0.9883	0.001	193
P release rate	CK	$y = 1.6477x^{0.7449}$	0.9863	0.001	248
	CF	$y = 1.7839x^{0.7498}$	0.9938	< 0.001	215
	8%OF	$y = 2.1747x^{0.762}$	0.9961	< 0.001	153
	16%OF	$y = 2.0211x^{0.7574}$	0.9981	< 0.001	173
	24%OF	$y = 1.9719x^{0.756}$	0.9974	< 0.001	181
K release rate	CK	$y = 12.248x^{0.4197}$	0.9893	< 0.001	150
	CF	$y = 11.969x^{0.4526}$	0.9763	0.002	111
	8%OF	$y = 25.049x^{0.3109}$	0.9586	0.004	85
	16%OF	$y = 15.846x^{0.4121}$	0.9452	0.006	88
	24%OF	$y = 17.214x^{0.3913}$	0.9661	0.003	90

http://www.aloki.hu ● ISSN 1589 1623 (Print) ● ISSN 1785 0037 (Online)
DOI: http://dx.doi.org/10.15666/aeer/1706_1345513472

Correlation analysis of decomposition rate and nutrient release rate under different organic fertilizer replacement rates, and recommending organic fertilizer replacement rate

During the whole decomposition process, there was no significant correlation ($P > 0.05$) between organic fertilizer replacement rate and decomposition rate or nutrient release rate, but there was a significant positive correlation between decomposition rate and nutrient release rate ($P < 0.05$) (*Table 3*), therefore, the nutrient release rate of the treatment with the high decomposition rate is also higher. The regression equation fitting of the relationship between organic fertilizer replacement rate (k is 0, 8%, 16%, and 24%, respectively) and decomposition rate (y) conforms to the one-variable quadratic function (*Schedule 1*).

Table 3. *Correlation analysis of decomposition rate and nutrient release rate (y) under different organic fertilizer replacement rate (k)*

Decomposition day	Item	Decomposition rate	Nutrient release rate			
			C	N	P	K
20 d	*k*	0.570	0.633	0.495	0.219	0.303
	Decomposition rate	1	0.947*	0.974**	0.961**	0.920*
40 d	*k*	0.416	0.176	0.431	0.410	0.528
	Decomposition rate	1	0.936*	0.998**	1.000**	0.989**
60 d	*k*	-0.077	0.100	0.397	0.378	0.503
	Decomposition rate	1	0.970**	0.863	0.899*	0.847
80 d	*k*	0.439	0.089	0.071	0.240	0.658
	Decomposition rate	1	0.963**	0.961**	0.885*	0.977**
100 d	*k*	0.034	-0.177	-0.182	0.340	0.775
	Decomposition rate	1	0.916*	0.914*	0.894*	0.965**

* and **: Correlation coefficients significant at $P < 0.05$ and $P < 0.01$, respectively

Schedule 1. *Regression analysis of organic fertilizer replacement rate (k) and decomposition rate (y)*

Item (%)	Time (d)	Equation	R^2	*P* value	Best *k* (%)	Prediction y (*k* = 12%) (%)
Decomposition rate	20	$y = -0.0123k^2 + 0.3606k + 18.040$	0.8958	0.131	15	20.60
	40	$y = -0.0402k^2 + 1.1083k + 26.147$	0.8565	0.158	14	33.66
	60	$y = -0.0598k^2 + 1.3913k + 35.579$	0.5506	0.081	12	43.66
	80	$y = -0.0598k^2 + 1.3913k + 35.579$	0.8543	0.410	14	53.04
	100	$y = -0.0144k^2 + 0.3501k + 53.681$	0.8664	0.032	12	55.81

At the end of decomposition, the best organic fertilizer replacement rate was 12%, which is determined that the recommended organic fertilizer replacement rate was 12%, and bring it into the (*Schedule 2*) equation, predicting the decomposition rates and C, N, P and K release rates for different days (20 d, 40 d, 60 d, 80 d and 100 d) ranged from 20.60% to 55.81%, 25.02% to 59.08%, 19.77% to 59.69%, 23.03% to 64.11% and 57.31% to 100.00%, respectively. The predicted value satisfies the experiment result of

http://www.aloki.hu ● ISSN 1589 1623 (Print) ● ISSN 1785 0037 (Online)
DOI: http://dx.doi.org/10.15666/aeer/1706_1345513472

K > P > N > C. Finally, the regression equation was fitted to the decomposition rate and nutrient release rate under the recommended organic fertilizer replacement rate (k = 12%), which is consistent with the power function $y = a \cdot x^b$ model (*Table 4*). Through the model, it can be predicted that the days for complete decomposition and the days for complete release of C, N, P and K under the organic fertilizer replacement rate of 12% are 176 d, 163 d, 159 d, 153 d, and 65 d, respectively (*Table 4*), and compared with the best treatment of 8%OF (k = 8%) in the experiment, it was advanced by 41 d, 43 d, 8 d, 0 d, and 20 d, respectively.

Schedule 2. *Regression analysis of organic fertilizer replacement rate (k) and nutrient release rate (y)*

Item (%)	Time (d)	Equation	R^2	*P* value	Prediction y (k = 12%) (%)
C release rate	20	$y = -0.0391k^2 + 1.1716k + 16.593$	0.9820	0.014	25.02
	40	$y = -0.0212k^2 + 0.5417k + 30.023$	0.7031	0.617	33.47
	60	$y = -0.0422k^2 + 1.0498k + 36.835$	0.6478	0.081	43.36
	80	$y = -0.0386k^2 + 0.9591k + 49.32$	0.5871	0.024	55.27
	100	$y = -0.0339k^2 + 0.7523k + 54.93$	0.5083	0.011	59.08
N release rate	20	$y = -0.0145k^2 + 0.4312k + 16.681$	0.6193	0.190	19.77
	40	$y = -0.0373k^2 + 1.0413k + 26.67$	0.8077	0.183	33.79
	60	$y = -0.0379k^2 + 1.0481k + 39.985$	0.7598	0.102	47.10
	80	$y = -0.038k^2 + 0.9371k + 49.445$	0.5630	0.218	55.22
	100	$y = -0.0349k^2 + 0.7702k + 55.47$	0.4748	0.025	59.69
P release rate	20	$y = -0.0247k^2 + 0.638k + 18.927$	0.7596	0.264	23.03
	40	$y = -0.0427k^2 + 1.1723k + 27.978$	0.8744	0.415	35.9
	60	$y = -0.0453k^2 + 1.2474k + 39.711$	0.7263	0.018	48.16
	80	$y = -0.0522k^2 + 1.3782k + 48.861$	0.5717	0.143	57.88
	100	$y = -0.0535k^2 + 1.4628k + 54.256$	0.6384	0.024	64.11
K release rate	20	$y = -0.0569k^2 + 1.5666k + 46.706$	0.4714	0.091	57.31
	40	$y = -0.0634k^2 + 1.8421k + 69.468$	0.8403	0.013	82.44
	60	$y = -0.0652k^2 + 1.886k + 75.804$	0.7854	0.001	89.05
	80	$y = -0.0492k^2 + 1.5342k + 88.435$	0.8581	< 0.001	99.76
	100	$y = -0.0233k^2 + 0.7823k + 94.338$	0.9333	< 0.001	100.00

Table 4. *Model of corn straw decomposition and nutrient release under recommended organic fertilizer replacement rate (k = 12%)*

Item (%)	Equation	R^2	*P* value	Time prediction (d)
Decomposition rate	$y = 0.7872x^{0.9856}$	0.9995	< 0.001	176
C release rate	$y = 1.8596x^{0.7828}$	0.9996	< 0.001	163
N release rate	$y = 1.8764x^{0.7844}$	0.9999	< 0.001	159
P release rate	$y = 1.928x^{0.7851}$	0.9999	< 0.001	153
K release rate	$y = 3.3484x^{0.8138}$	0.9987	< 0.001	65

As shown in *Figure 7*, it is recommended that the straw returned per hectare under the replacement rate of organic fertilizer, after 100 days of decomposition, the release

http://www.aloki.hu ● ISSN 1589 1623 (Print) ● ISSN 1785 0037 (Online)
DOI: http://dx.doi.org/10.15666/aeer/1706_1345513472

amounts of C, N, P, and K are 1209.26 kg, 57.53 kg, 9.81 kg, and 86.77 kg, respectively. Among them, most of the nutrients released in the first 20 days were 512.12 kg, 19.05 kg, 3.52 kg, and 49.73 kg, accounting for 42.35%, 33.12%, 35.92%, 57.31% of the total release of C, N, P and K, which accorded with the characteristics of decomposition and nutrient release in this experiment.

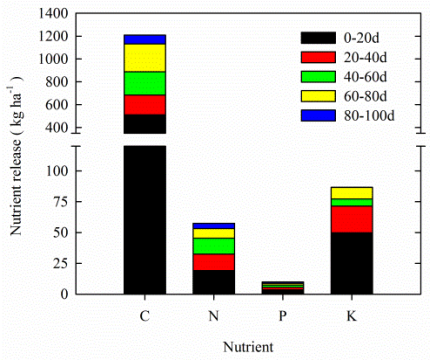

Figure 7. *Nutrient release under recommended organic fertilizer replacement rate (k = 12%) during corn growth period*

Discussion

Decomposition and nutrient release characteristics of straw

(1) Decomposition characteristics

This study found that the characteristics of decomposition and nutrient release during the whole decomposition process are fast in the early stage (0-20 d) and slow in the later stage (20-100 d), which is similar to previous studies (Wu et al., 2011; Zhao et al., 2011; Yang et al., 2015). It may be because: in the early stage of decomposition, corn straw contains a large amount of easily decomposable organic substances, which are easily used by microorganisms, resulting in faster decomposition; As the decomposition progresses, the easily decomposable organic matter in the straw is gradually reduced, and the remaining mainly coarse fibers and lignin which are difficult to decompose are difficult to be easily utilized by microorganisms, resulting in slow decomposition in the later stage (Li et al., 2009; Summerell and Burgess, 1989). In addition, temperature and precipitation in climatic conditions can also affect straw decomposition (Gupta and Singh, 1981). This experiment began in May, when the temperature rises and precipitation increases (*Fig. 1*), which improves microbial activity and promotes straw decomposition. At the later stage, excessive temperature inhibited microbial activity, which inhibited straw decomposition (Zhou et al., 2015; Nakajima et al., 2016).

(2) Nutrient release characteristics

There was a significant positive correlation ($P < 0.05$) between the decomposition rate and nutrient release rate (*Table 3*). Therefore, the nutrient release rate of high decomposition rate treatment was also higher. At the end of the experiment (100 d), the order of nutrient release rate was K > P > N > C, which was consistent with most studies (Dai et al., 2010; Gong et al., 2018; Liu et al., 2016). The nutrient release rate depends mainly on the morphology of each nutrient (C, N, P, and K) in the straw. Among them, the K content in the straw is high and mainly exists in the ionic state,

http://www.aloki.hu ● ISSN 1589 1623 (Print) ● ISSN 1785 0037 (Online)
DOI: http://dx.doi.org/10.15666/aeer/1706_1345513472

which is easy to release; The P content in the straw is low, over 60% is in the ionic state, the release is faster, and the rest is more difficult to decompose, resulting in slower release in the later stage, so the K release is faster than P (Wang et al., 2013; Dai et al., 2017). C and N are the main components of straw, mainly insoluble organic matter, which is easier to release in the early stage. The remaining part is mainly organic matter with high cementation and difficult to decompose, resulting in a slower release of C and N (Murayama, 2010; Chen et al., 2016; Tang et al., 2016).

(3) Changes of C and nutrients (N, P, and K) ratio of straw residue

Changes of C and nutrients (N, P, and K) ratio of straw residue during the decomposition process can not only reflect the characteristics of the overall release of nutrients after the crop straw is returned to the field, but also reveal its relationship with the decomposition and nutrient release (*Fig. 6*). C/N ratio of straw is a major factor affecting straw decomposition and microbial activity (Ahlam, 2004). In the first 20 days, decomposition and nutrient release was the fastest, because the reduction of C/N ratio promoted decomposition (Dai et al., 2010), and the late C/N ratio was close to the appropriate range of microbial growth 25-30:1 (Devêvre and Horwath, 2000), but the C in the straw is mainly in the form of lignin, which is difficult to be used by microorganisms, leading to the slowing down of decomposition and nutrient release (Summerell and Burgess, 1989; Li et al., 2009), and the change in C/N ratio also reflects that the characteristics of decomposition and nutrient release is fast in the early stage (0-20 d) and slow in the later stage (20-100 d) (*Figs. 3–5*). The change of C/P ratio and C/K ratio of straw reflects that the release degree of nutrients of C, P and K is K > P > C (*Fig. 4*), and reflected the characteristics of nutrient release from different treatments are 8%OF > 16%OF > 24%OF > CF > CK.

(4) Models of decomposition and nutrient release

Through the establishment of decomposition and nutrient release models (*Table 2*), dynamic monitoring of straw decomposition and nutrient release from different treatments can be performed, and the days for complete decomposition and complete release of nutrients can be predicted, and verified the characteristics of decomposition and nutrient release in this experiment (*Figs. 3–5*). Therefore, the establishment of the model helps to establish a reasonable return time, which is of great significance for guiding reasonable straw returning.

Effects of different organic fertilizer replacement rates on straw decomposition and nutrient release and prediction of organic fertilizer replacement rate

The decomposition rate and nutrient release rate were 8%OF > 16%OF > 24%OF > CF > CK (*Figs. 3–4*). It can be seen that with the increase of the replacement rate of organic fertilizer, the decomposition rate, and nutrient release rate first increased and then decreased, and the fertilization treatments (CF, 8%OF, 16%OF and 24%OF) were higher than that without fertilizer application (CK), and the effect of organic fertilizer replacement treatment was obvious. It is because, on the one hand, chemical fertilizers are fast, but the utilization rate is low. Organic fertilizers improve soil physical and chemical properties and promote microbial activities and reproduction, but organic fertilizers release nutrients at a slower rate. The replacement of some chemical fertilizers by organic fertilizers can coordinate inorganic and organic

http://www.aloki.hu ● ISSN 1589 1623 (Print) ● ISSN 1785 0037 (Online)
DOI: http://dx.doi.org/10.15666/aeer/1706_1345513472

nutrients, meet the nutrient requirements of crops, and improve soil fertility, thereby promoting microbial activities and straw decomposition (Hao et al., 2012). Some studies have also found that the application of chemical fertilizers in the soil can also promote the decomposition of straw, and the corn straw is decomposed faster under high fertility conditions (Zheng et al., 2004; Wang et al., 2009). According to the characteristics of fertilizer efficiency of chemical fertilizer and organic fertilizer, with the increase of organic fertilizer replacement rate, the available nutrients in the soil are reduced. The crop growth in the plot absorbs available nutrients from the soil, and there exists nutrient competition between crop growth and decomposition, thus inhibiting straw decomposition (Azam et al., 1991).

The correlation analysis (*Table 3*) shows the whole decomposition process. The organic replacement rate will not change the characteristics of the whole decomposition and nutrient release of corn straw, but the appropriate organic replacement rate can effectively coordinate the nutrient balance, promote the decomposition and nutrient release. Therefore, it is very important to determine the organic replacement rate for straw decomposition. In this study, model analysis of decomposition rates and nutrient release rates under different organic fertilizer replacement rates (*Schedule 1*) was performed to determine a recommended organic fertilizer replacement rate of 12% and a decomposition and nutrient release model was established (*Table 4*). Predicting the complete time required for decomposition and releasing is better than the optimal treatment (8%OF). Therefore, the recommendation of the replacement rate of organic fertilizer has important guiding significance for the comprehensive management of straw returning and rational fertilization.

The strategy of straw returning and rational fertilization in corn planting

Corn is one of the three major food crops in the world. It needs a lot of nutrients; excessive application of chemical fertilizer not only increases the cost of agricultural production but also causes soil acidification and agricultural pollution. This study found that suitable organic fertilizer replacement efficiency is conducive to the efficient use of straw resources and reduce the use of chemical fertilizer. Taking this experimental area as an example, the recommended fertilization amount is 300.0 kg N ha^{-1}, 180.0 kg P_2O_5 ha^{-1}, 60.0 kg K_2O ha^{-1}, On the basis of recommending the replacement rate of organic fertilizer 12%, the return of straw is carried out, and the fertilization scheme: the application of N, P_2O_5, K_2O in the form of chemical fertilizer is 264.0 kg ha^{-1}, 140.3 kg ha^{-1} and 49.2 kg ha^{-1}, respectively; the organic fertilizer is 2033.9 kg ha^{-1} kg ha^{-1}, of which the N, P_2O_5, K_2O contents are 36.0 kg ha^{-1}, 39.7 kg ha^{-1}, 10.8 kg ha^{-1}, respectively. During the growth period of corn (100 d), the release of N, P and K was equivalent to 19.18%, 5.45% and 144.61% of the fertilization amount of NPK fertilizer, and the K release amount exceeded the fertilization amount of K fertilizer, at the same time, a many C is released (*Fig. 7*), which effectively increases soil organic matter content (Wang et al., 2017). According to the characteristics of nutrient release from straw, it is fast in the early stage (0-20 d), slow in the late stage (20-100 d) and K > P > N > C. This study proposes that organic fertilizer and straw are applied as base fertilizers, while reducing the application amount of chemical fertilizers in base fertilizers. According to the general nutrient absorption characteristics of corn, the absorption of N, P and K was less in the seedling stage, the jointing stage was significantly increased, and the peak was reached from the booting stage to the heading stage (Denbaly and Vroomen, 1993), and reasonable fertilization measures were

http://www.aloki.hu ● ISSN 1589 1623 (Print) ● ISSN 1785 0037 (Online)
DOI: http://dx.doi.org/10.15666/aeer/1706_1345513472

formulated: reduce or delay the application of K fertilizer, increase N and P fertilizer after jointing stage, increase N fertilizer in the late stage of decomposition, avoid nutrient competition of corn and straw decomposition, promote corn growth and straw decomposition, and ensure crop yield, to achieve efficient utilization of straw resources and reduce the application of chemical fertilizer.

Conclusion

This study found that the straw decomposition and nutrient release characteristics of the whole decomposition process under different organic fertilizer replacement rates are fast in the early stage (0-20 d) and slow in the late stage (0-100 d). At the end of decomposition (100 d), the decomposition rate and nutrient release rate were 8%OF > 16%OF > 24%OF > CF > CK, and the nutrient release characteristics of fertilization treatment were K > P > N > C, while CK was K > P > N ≈ C. Through the establishment and analysis of decomposition and nutrient release models ($y = a \cdot x^b$), dynamic monitoring and prediction of decomposition and nutrient release during corn growth period can be carried out, and the characteristics of decomposition and nutrient release in this experiment can be verified. Through the establishment of different organic fertilizer replacement rate and nutrient release model and correlation analysis, the recommended organic fertilizer replacement rate was determined to be 12%, and according to the characteristics of nutrient release in this study, the strategy of comprehensive management of reasonable straw returning and fertilization in corn planting was proposed: On the basis of recommending the organic fertilizer replacement rate (k = 12%), the return of straw is carried out, Organic fertilizer and straw are applied as base fertilizer, and the amount of chemical fertilizer applied in the base fertilizer is reduced. This study is limited to the nutrient release of straw, and the nutrient absorption characteristics of corn needs further research, combined with the release characteristics of straw nutrients, which is conducive to the development of more scientific straw returning and fertilization management measures.

Acknowledgements. This research was supported by the National Key Research and Development Program of China (2017YFD0201808, 2018YFD0200406) and the National Natural Science Foundation of China (31660598, 31360501).

REFERENCES

[1] Abdou, G., Ewusi-Mensah, N., Nouri, M., Tetteh, F. M., Safo, E. Y., Abaidoo, R. C. (2016): Nutrient release patterns of compost and its implication on crop yield under Sahelian conditions of Niger. – Nutrient Cycling in Agroecosystems 105(2): 117-128.

[2] Ahlam, E. B. (2004): Assessment of rate of decomposition and nutrient release from leaf residue of some tree species. – MSc. Thesis Desertification and Desert Cultivation Studies Institute, University of Khartoum, Khartoum.

[3] Azam, F., Lodhi, A., Ashraf, M. (1991): Availability of soil and fertilizer nitrogen to wetland rice following wheat straw amendment. – Biology and Fertility of Soils 11(2): 97-100.

[4] Bao, S. D. (2000): Analysis of Soil Agrochemistry. – China Agriculture Press, Beijing, pp. 30-107.

http://www.aloki.hu ● ISSN 1589 1623 (Print) ● ISSN 1785 0037 (Online)
DOI: http://dx.doi.org/10.15666/aeer/1706_1345513472

[5] Becker, R., Bubner, B., Remus, R., Wirth, S., Ulrich, A. (2014): Impact of multi-resistant transgenic Bt maize on straw decomposition and the involved microbial communities. – Applied Soil Ecology 73(1): 9-18.
[6] Bocock, K. L., Gilbert, O. J. W. (1957): The disappearance of leaf litter under different woodland conditions. – Plant and Soil 9(2): 179-185.
[7] Chapman, S. J. (1997): Barley straw decomposition and s immobilization. – Soil Biology and Biochemistry 29(2): 109-114.
[8] Chen, J., Zhao, B. Z., Zhang, J. B., Shen, L. L., Zhang, H., Qin, S. W. (2009): Research on process of fluvo-aquic soil organic carbon mineralization in initial stage of maize growth under long-term different fertilization. – Soils 41(5): 719-725.
[9] Chen, S., Liu, Z. R., Zeng, K. (2016): Effect of straw-decomposing inoculant on decomposition of rice straw. – Chinese Journal of Environmental Engineering 10(2): 839-844.
[10] Dai, W. C., Gao, M., Lan, M. L., Huang, R., Wang, J. Z., Wang, Z. F., Han, X. F. (2017): Nutrient release patterns and decomposition characteristics of different crop straws in drylands and paddy fields. – Chinese Journal of Eco-Agriculture 25(2): 188-199.
[11] Dai, Z. G., Lu, J. W., Li, X. K., Lu, M. X., Yang, W. B., Gao, X. Z. (2010): Nutrient release characteristic of different crop straws manure. – Transactions of the Chinese Society of Agricultural Engineering 26(6): 272-276(5).
[12] Denbaly, M., Vroomen, H. (1993): Dynamic fertilizer nutrient demands for corn: a cointegrated and error-correcting system. – American Journal of Agricultural Economics 75(1): 203-209.
[13] Devêvre, O. C., Horwath, W. R. (2000): Decomposition of rice straw and microbial carbon use efficiency under different soil temperatures and moistures. – Soil Biology and Biochemistry 32(11): 1773-1785.
[14] Feng, W., Zhang, L. Q., Pang, Z. W., Guo, S. Z. (2011): The economic and environmental analysis of crop residues burning and reutilization in China. – Chinese Agricultural Science Bulletin 27(6): 350-354.
[15] Fischer, G., Winiwarter, W., Cao, G. Y., Ermolieva, T., Hizsnyik, E., Klimont, Z., et al. (2010): Implications of population growth and urbanization on agricultural risks in China. – Population and Environment 33(2-3): 243-258.
[16] Fu, W., Liu, K. P., Chen, H. S., Chen, X. B., Lin, H. F., Zhang, W., Wang, K. L. (2017): Effect of partial replacement of inorganic N with organic manure on crop yield and soil nutrient balance in arable ecosystem in karst peak-cluster depression. – Chinese Journal of Eco-Agriculture 25(6): 812-820.
[17] Gong, Z. P., Deng, N. Z., Song, Q. L., Li, Z. T. (2018): Decomposing characteristics of maize straw returning in Songnen Plain in long-time located experiment. – Transactions of the Chinese Society of Agricultural Engineering 34(8): 139-145.
[18] Gupta, S. R., Singh, J. S. (1981): The effect of plant species, weather variables and chemical composition of plant material on decomposition in a tropical grassland. – Plant and Soil 59(1): 99-117.
[19] Hao, X. Y., Gao, W., Wang, Y. J., Huang, S. W., Tang, J. W., Jin, J. Y. (2012): Effects of combined application of organic manure and chemical fertilizers on yield and quality of tomato and soil nitrate leaching loss under greenhouse condition. – Journal of Agro-Environment Science 31(3): 538-547.
[20] Huang, T. M., Wang, Z. H., Hou, Y. Y., Gu, C. M., Li, X., Zheng, X. F. (2017): Effects of nitrogen application on decomposition and nutrient release of returned maize straw in Guanzhong Plain, Northwest China. – Chinese Journal of Applied Ecology 28(7): 2261-2268.
[21] Jin, S., Zhou, F. (2018): Zero growth of chemical fertilizer and pesticide use: China's objectives, progress and challenges. – Journal of Resources and Ecology 9(1): 50-58.

http://www.aloki.hu ● ISSN 1589 1623 (Print) ● ISSN 1785 0037 (Online)
DOI: http://dx.doi.org/10.15666/aeer/1706_1345513472

[22] Jin, S. Q., Zhou, F., Shen, G. Y. (2015): Feasible routes for reducing chemical fertilizer use with dual goals of agricultural development and non-point source pollution prevention. – Environmental Protection 43(8): 50-53.
[23] Li, F. Y., Wang, J. F. (2013): Estimation of carbon emission from burning and carbon sequestration from biochar producing using crop straw in China. – Transactions of the Chinese Society of Agricultural Engineering 29(14): 1-7.
[24] Li, F. Y., Sun, X. F., Feng, W. Q., Qin, Y. S., Wang, C. Q., Tu, S. H. (2009): Nutrient release patterns and decomposing rates of wheat and rapeseed straw. – Journal of Plant Nutrition and Fertilizers 15(2): 374-380.
[25] Li, Z. Y., Tang, H. Q., Meng, Y. C., He, T. G., Wang, J., Hu, J. M., Li, T. T., Zhang, Y. (2017): Characteristics of decomposition and nutrients release of *Dolichos lablab,* L.'straw under different incorporation methods. – Soil and Fertilizer Sciences in China 2: 130-135.
[26] Lin, X. X., Wu, S. L., Che, Y. P. (1992): Nylon bag method for determination of decomposition rate of organic matter in arid and semi-dry regions. – Soils 24(6): 315-318.
[27] Liu, J., Zhang, J., Qin, W. J., Yang, C. C., Xie, J., Xiang, X. J., Cao, W. D., Xu, C. X. (2016): Decomposition and nutrient release characteristics of different *Vicia villosa* green manure applications in red soil uplands of South China. – Acta Prataculturae Sinica 25(10): 66-76.
[28] Liu, Y. R., Xiang, L. I., Shen, Q. R., Xu, Y. C. (2013): Enzyme activity in water-stable soil aggregates as affected by long-term application of organic manure and chemical fertiliser. – Pedosphere 23(1): 111-119.
[29] Murayama, S. (2010): Decomposition kinetics of straw saccharides and synthesis of microbial saccharides under field conditions. – European Journal of Soil Science 35(2): 231-242.
[30] Nakajima, M., Cheng, W., Tang, S., Hori, Y., Yaginuma, E., Hattori, S., Tawaraya, K., Xu, X. K. (2015): Modeling aerobic decomposition of rice straw during the off-rice season in an andisol paddy soil in a cold temperate region of Japan: effects of soil temperature and moisture. – Soil Sci Plant Nutr 7: 1-9.
[31] Nakajima, M., Cheng, W., Tang, S., Hori, Y., Yaginuma, E., Hattori, S., Tawaraya, K., Xu, X. K. (2016): Modeling aerobic decomposition of rice straw during the off-rice season in an andisol paddy soil in a cold temperate region of Japan: effects of soil temperature and moisture. – Soil Science and Plant Nutrition 62(1): 90-98.
[32] Ngatia, L. W., Reddy, K. R., Nair, P. K. R., Pringle, R. M., Palmer, T. M., Turner, B. L. (2014): Seasonal patterns in decomposition and nutrient release from East African savanna grasses grown under contrasting nutrient conditions. – Agriculture Ecosystems and Environment 188(15): 12-19.
[33] Stanford, G., Smith, S. J. (1972): Nitrogen mineralization potentials of soils. – Soil Science Society of America Journal 36(3): 465-472.
[34] Summerell, B. A., Burgess, L. W. (1989): Decomposition and chemical composition of cereal straw. – Soil Biology and Biochemistry 21(4): 551-559.
[35] Sun, J. F., Peng, H. Y., Chen, J. M., Wang, X. M., Wei, M., Li, W. J., et al. (2016): An estimation of CO_2 emission via agricultural crop residue open field burning in China from 1996 to 2013. – Journal of Cleaner Production 112(12): 2625-2631.
[36] Tang, S. R., Cheng, W. G., Hu, R. G., Guigue, J., Kimani, S. M., Tawaraya, K., Xu, X. K. (2016): Simulating the effects of soil temperature and moisture in the off-rice season on rice straw decomposition and subsequent CH_4, production during the growth season in a paddy soil. – Biology and Fertility of Soils 52(5): 739-748.
[37] Wang, J., Zhang, L., Pang, H. C., Zhang, J. (2017): Returning granulated straw for accelerating decomposition rate and improving soil fertility. – Transactions of the Chinese Society of Agricultural Engineering 33(6): 177-183.

http://www.aloki.hu ● ISSN 1589 1623 (Print) ● ISSN 1785 0037 (Online)
DOI: http://dx.doi.org/10.15666/aeer/1706_1345513472

[38] Wang, W., Chen, C. L., Wu, X. H., Xie, K. J., Yin, C. M., Hou, H. J., Xie, X. L. (2018): Effects of reduced chemical fertilizer combined with straw retention on greenhouse gas budget and crop production in double rice fields. – Biology and Fertility of Soils 55: 89-96.
[39] Wang, X. D., Chen, X. N., Wang, C. X., Tian, X. H., Wu, F. (2009): Decomposition of corn stalk in cropland with different fertility. – Transactions of the Chinese Society of Agricultural Engineering 25(10): 252-257.
[40] Wang, Y. J., Bi, Y. Y., Gao, C. Y. (2010): The assessment and utilization of straw resources in China. – Agricultural Sciences in China 9(12): 1807-1815.
[41] Wang, Y. Z., Chen, X., Shi, Y. (2013): Phosphorus availability in cropland soils of China and related affecting factors. – Chinese Journal of Applied Ecology 24(1): 260-268.
[42] Wen, Y. C., Zhang, Y. D., Yuan, L., Li, W., Li, Y. Q., Lin, Z., Zhao, B. Q. (2018): Crop yield and soil fertility response to commercial organic fertilizer substituting chemical fertilizer. – Scientia Agricultura Sinica 51(11): 2136-2142.
[43] Wu, J., Guo, X. S., Wang, Y. Q., Xu, Z. Y., Lu, J. W. (2011): Decomposition characteristics of rapeseed and wheat straw sunder different rice cultivations and straw mulching models. – Agricultural Sciences in China 44(16): 3351-3360.
[44] Yang, H. X., Zhou, M. H., Li, J. L., Liang, B., Sui, F. G. (2015): Decay and nutrient release in *Vulpia myuros* grasses, a species suitable for soil conservation in temperate zone orchards. – Acta Prataculturae Sinica 24(4): 208-213.
[45] Yin, H., Zhao, W., Li, T., Cheng, X., Liu, Q. (2017): Balancing straw returning and chemical fertilizers in China: role of straw nutrient resources. – Renewable and Sustainable Energy Reviews 81: 2695-2702.
[46] Zhang, L., Liu, Y., Hao, L. (2016): Contributions of open crop straw burning emissions to PM2.5 concentrations in China. – Environmental Research Letters 11(1): 014014.
[47] Zhao, N., Zhao, H. B., Yu, C. W., Cao, Q. H., Li, M., Cao, W. D., Gao, Y. J. (2011): Nutrient releases of leguminous green manures in rainfed lands. – Plant Nutrition and Fertilizer Science 17(5): 1179-1187.
[48] Zheng, D. M., Jiang, Y. J., Lu, S. Q., Zhu, C. Y. (2004): Study on decomposition and humification coefficient of organic fertilizer in arid region. – Soils and Fertilizers Sciences in China (2): 15-19.
[49] Zhou, G. X., Chen, L., Zhang, C. Z., Zhang, J. B. (2015): Effects of temperature and moisture on microbial community function responsible for straw decomposition. – Soils 47(5): 911-918.

http://www.aloki.hu ● ISSN 1589 1623 (Print) ● ISSN 1785 0037 (Online)
DOI: http://dx.doi.org/10.15666/aeer/1706_1345513472

INHIBITORY EFFECTS OF SOME PESTICIDES AND METALS ON CARBONIC ANHYDRASE PURIFIED FROM SHABUT FISH (*BARBUS GRYPUS*) GILL TISSUE

YERLIKAYA, E.

School of Health, Siirt University, 56100 Siirt, Turkey
(e-mail: emrahyerlikaya@siirt.edu.tr; phone: +90-484-223-1224/4054; fax: +90-484-223-5156)

(Received 7th Jul 2019; accepted 2nd Sep 2019)

Abstract. Carbonic anhydrase enzyme catalyzes the reversible inter-conversion of CO_2 and HCO_3. The enzyme is crucial for the osmotic balance and acid–base regulation in the fish. It is well-known that gills of fish play the most important role in acid–base relevant ion transfer, the transfer of H^+ and/or HCO_3, for the maintenance of systemic pH. Many researches have shown that fish are the species that is the most susceptible to environmental toxins. In addition, these toxins firstly encounter the gill tissue in fish. In this study, the carbonic anhydrase enzyme was purified 198.6-folds with 58.8% yield from Shabut Fish (*Barbus grypus*) gill tissue by Sepharose-4B-L-tyrosine-sulfanilamide affinity column. The specific activity was determined as 2.92 EU/mg protein. The molecular weight determined by sodium dodecyl sulfate–polyacrylamide gel electrophoresis was found to be about 29.9 kDa. Inhibitory effects of some pesticides (Spinosad and Dimethoate) and metal ions (Al^{3+}, Cu^{2+}, Ba^{2+}, Fe^{2+}, Mn^{2+}, Se^{2+}) were examined on the purified carbonic anhydrase enzyme. Inhibition graphics were drawn in order to find the IC_{50} values of metals and pesticides showing inhibition. The kinetic parameters of this enzyme were determined for its esterase activity, with 4-nitrophenyl acetate as substrate.
Keywords: *pollution, inhibition, enzyme, chromatography, catalysis*

Introduction

According to the records of the Food and Agriculture Organization, Shabut, also known as *Barbus grypus*, is one of the most significant fish species listed in the fresh waters of Iraq and in the rivers along South and Southwest Iran, the Karoon river, and also in The Euphrates River and Tigris Rivers in Turkey (Olgunoglu et al., 2011). Shabut is one of the leading fish species of Siirt/Botan Stream which contributes to the city's economy.

In nature it is known that carbonic anhydrases (CAs, EC 4.2.1.1) are some of the most efficient enzymes probably due to the fact that uncatalyzed CO_2 hydration is a very slow process at neutral pH, and the physiologic demands for its conversion to ionic, soluble species (i.e., bicarbonate and protons) are very high. Actually, CO_2 is generated in most metabolic oxidative processes, and being a gas, it must be converted to soluble products quickly and efficiently. Otherwise, it could accumulate and damage cells and other organelles in the gaseous state without such an efficient hydration catalyst as the CAs (Supuran, 2018). At least 16 different CA isozymes have important roles in diverse processes, such as physiological pH control and gas balance, calcification, and photosynthesis, have been described in higher vertebrates up to this point. The role of CA in fish gills is considered to be related to gas exchange, acid-base balance, osmoregulation, ion regulation, and clearance of the waste products from nitrogenous metabolism. The shape of distribution of CA activity among gills pairs shows variety depending on habitat and osmoregulatory behavior of the animal. Gill epithelium is the first tissue of the organism exposed to the aquatic environment, and because of this, it is the primary frontier for the harmful effects of environmental pollutant in the case of fish (Lopez Mananes et al., 2000; Randall and Daxbaeck, 1984; Dincer et al., 2016; Hisar et al., 2004).

http://www.aloki.hu ● ISSN 1589 1623 (Print) ● ISSN 1785 0037 (Online)
DOI: http://dx.doi.org/10.15666/aeer/1706_1347313483

The gill tissue is the primary tissue contacting with the contaminants in the water. Because of its small diffusion distance and large surface area between the blood and water, the gills are initially affected by contaminants such as pesticides and metals (Demir et al., 2016). In general, the gill cells react rapidly to several chemicals to handle tissue damage or physiological impairment. Chemicals may have a negative impact on the overall gill function, improving fish sensitivity to toxic compounds and potentially causing fish mortality (Cerqueira and Fernandes, 2002). Lately, the contamination of aquatic environment by pollutants has become a big problem. They are a threat to public water supplies and can damage aquatic life (Koca et al., 2005). Pesticides are substances that are used to kill or control the organisms considered to be destructive. The most broadly used ones are insecticides, herbicides, fungicides and rodenticides. They are the most common contaminants of the environment and cause water, soil and air pollution. They can also pile up in the living organisms like humans, animals, and so on (Anwar, 1997). They are attracted attention owing to the fact that they stay in the environment for a long time, can accumulate in food, and have a constant presence in food and drinking water (Tiemann, 2008). Generally, pesticides can interfere into rain water, irrigation water or river, plants and may be harmful for specific enzymes. It is known that many compounds, metal ions and pesticides can be hazardous for the living organisms in water. Scientific studies on pesticides make clear that these compounds show their destructive effects by inhibiting the enzymes even at low concentrations (Ceyhun et al., 2010).

Heavy metals have a toxic impact that is proportional to their concentration in fish. Heavy metals bring about toxicity in aquatic environments and this heavy metal damage is a crucial factor in many toxicological and pathological processes (Ekinci and Beydemir, 2010; Soyut and Beydemir, 2008). At the same time, heavy metals may lead to oxidative damage by decreasing the cellular antioxidant capacity and by directly rising the cellular concentration of reactive oxygen species (Topal et al., 2014; Ekinci et al., 2008). It has been reported that heavy metals and pesticides principally enter into the human/animal body through ingestion, such as food materials, inhalation and dermal contact, such as emissions of waste material in the form of smoke, dust particle, fume of chemicals from several industrial activities, such as mining, and manufacturing of batteries (Singh et al., 2017).

The aim of the study is to purificate and examine the inhibition effects of the some pesticides and metals on the activity of CA enzyme from Shabut Fish (*Barbus grypus*) gill tissue in the Tigris basin. Since it is frequently consumed by the people of the region and has high economic value, Shabut Fish was chosen as the source in the study. In addition, since CA enzyme has never been purified from this fish species before, this fish species was preferred in the study. The other aim of the study is the determination of some biochemical parameters of purified enzyme. For this purpose, the enzyme was isolated from gill of this fish. It was determined the inhibitory effects of these chemicals using 4-nitrophenyl acetate (4-NPA) as a substrate.

Methods and materials

Chemicals and devices

All chemicals used in this study were the highest grade purity available and were obtained from Sigma and E. Merck (Darmstadt, Germany). Sepharose 4B activated by CNBr, protein assay reagents, and chemicals for electrophoresis were obtained from Sigma-Aldrich Chemie (Taufkirchen, Germany). A UV–Visible spectrophotometer

http://www.aloki.hu ● ISSN 1589 1623 (Print) ● ISSN 1785 0037 (Online)
DOI: http://dx.doi.org/10.15666/aeer/1706_1347313483

(VWR UV-6300PC Double Beam Spectrophotometer) was used for the determination of enzyme activity. The peristaltic pump used for enzyme purification was (Masterflex L/S Digital Pump System 77921-60), the centrifuge machine was purchased from Thermo Scientific/Megafuge 16R and the electrophoresis system was a Bio-Rad Mini-PROTEAN®System.

Preparation of homogenate

Shabut Fish (*Barbus grypus*) gill tissues were obtained commercially from fishermen in Siirt/Botan Stream, Turkey. Gill tissues were brought to Siirt University Science and Technology Application and Research Center Laboratory in accordance with the cold chain rule. They (about 50 g) were cut off carefully with aid of scalpel for avoiding damage and were washed three times with 0.9% NaCl to eliminate blood and other contaminants. After the tissues were lysed by liquid nitrogen, were taken in 50 mM Tris-SO_4 buffer (pH 7.4). The homogenate was centrifuged for 60 min (15.000 rpm at + 4 °C). The pH of the resulting supernatant was adjusted to 8.7 with solid Tris and loaded onto the affinity column.

Purification of CA from Shabut Fish (Barbus grypus) gill by affinity chromatography

The solution was applied to a Sepharose 4B-L-tyrosine sulfanilamide affinity column equilibrated with 25 mM Tris–HCl/0.1 M Na_2SO_4 (pH 8.7). The affinity gel was washed with 25 mMTris–HCl/22 mM Na_2SO_4 (pH 8.7). CA was eluted with 0.1 M $NaCH_3COO$/0.5 M $NaClO_4$ (pH 5.6). The 280 nm absorbance of the protein in the column effluents was determined spectrophotometrically. All of the purification steps were performed at 4 °C.

Esterase activity assay

The CA activity was assayed by the esterase method by following the change in absorbance at 348 nm of 4-NPA hydrolyzed to 4-nitrophenolate ion in the presence of the enzyme, over a period of 3 min at 25 °C, using a UV–Vis spectrophotometer according to the Verpoorte procedure (Verpoorte et al., 1967). The enzymatic reaction, in a total volume of 1.0 mL, contained 0.59 mL Tris–SO4 buffer solution (50 mM, pH 7.4), 0.36 mL 4-NPA (3.0 mM), and 0.05 mL enzyme. The control cuvette did not contain enzyme solution. One enzyme unit of CA esterase activity is defined as hydrolysis of 1 μmol 4-NPA to p-nitrophenol and acetate in 1 min. Briefly, 4-NPA is hydrolyzed into p-nitrophenol and acetate by CA, and p-nitrophenol absorbance is determined spectrophotometrically at 348 nm for CA esterase activity. The absorbance of the non-catalyzed 4-NPA in this buffer was always subtracted from the enzymatic measurements reported in this article (Senturk et al., 2011). K_M and V_{max} values were calculated for NPA by Lineweaver–Burk graph (Lineweaver–Burk, 1934).

Protein determination

During each purification steps, protein determination was performed spectrophotometrically at 595 nm according to the Bradford method, using bovine serum albumin as the standard (Bradford, 1976).

http://www.aloki.hu ● ISSN 1589 1623 (Print) ● ISSN 1785 0037 (Online)
DOI: http://dx.doi.org/10.15666/aeer/1706_1347313483

SDS polyacrylamide gel electrophoresis

Sodium dodecyl sulfate–polyacrylamide gel electrophoresis (SDS-PAGE) was carried out according to the method of Laemmli for the determination of purity and molecular weight of the Shabut Fish (*Barbus grypus*) gill CA using a 5% (w/v) stacking gel and 12% (w/v) separating gel (Laemmli, 1970). The molecular weight of the enzyme was determined using different protein markers from 8.5 kDa to 70 kDa. R_f values were also calculated for the enzyme and standard proteins, and R_f–LogMW graph was obtained (*Fig. 1*).

Optimum pH determination

In order to determine the optimum pH, K-phosphate and Tris–SO_4 buffers were used in the pH range of 5.0–7.5 and 7.0–9.0, respectively.

Optimum temperature determination

For determination of the optimum temperature, enzyme activity was assayed at different temperatures in the range from 5 to 70 °C. The desired temperature was provided by using a Grant bath.

Optimum ionic strength determination

For determination of optimum ionic strength, enzyme activity was determined using different concentrations of Tris–SO_4 buffer, pH: 7.5, in the range from 10 mM to 1000 mM.

Inhibition effect of some pesticides and metals on CA enzyme activity

The inhibitory effects of some pesticides (Spinosad and Dimethoate) and metal ions (Al^{3+}, Cu^{2+}, Ba^{2+}, Fe^{2+}, Mn^{2+}, Se^{2+}) were determined on Shabut Fish (*Barbus grypus*) gill CA enzyme activity. The effects of inhibitors were examined in the five diverse 4-NPA concentrations for each inhibitor. The CA activities were measured for different concentrations of inhibitors in spectrophotometer cuvette (1.0 mL). Control activity was assumed to be 100% in the absence of inhibitor. Reduced 50% activity of enzyme by used inhibitor concentration (IC_{50}) was calculated from the graphs using conventional polynominal regression software (Microsoft Office 2010, Excel).

Results

In present study, CA enzyme was purified from the Shabut Fish (*Barbus grypus*) gill tissue for the first time. The purification of the gill CA was carried out in one stage by chromatography column on L-tyrosine sulfonamide coupled to Sepharose 4B. The Shabut Fish (*Barbus grypus*) gill CA was purified with a specific activity of 2.92 EU/mg protein (198.6-folds) with a yield of 58.8% (*Table 1*).

To establishment of molecular weight of the enzyme, R_f values were also calculated for the enzyme and standard proteins, and R_f–LogMW graph was obtained according to Laemmli' method (*Fig. 1*). It was obtained a single protein band, evidence of purified enzyme having a molecular weight of the subunit was approximately 29.9 kDa, based on SDS-PAGE (*Fig. 2*). SDS-PAGE is one of the most greatly used laboratory methods to separate biological macromolecules including proteins and nucleic acids. In this

http://www.aloki.hu ● ISSN 1589 1623 (Print) ● ISSN 1785 0037 (Online)
DOI: http://dx.doi.org/10.15666/aeer/1706_1347313483

separation method, macromolecules are differentiated according to their electrophoresis mobility, which is a function of the length, conformation, and charge of the molecule. Ordinarily, macromolecules as proteins may be run in their native state or in denatured forms. To separate molecules based on their lengths, samples are run in denaturing conditions (Atasever et al., 2013).

Some biochemical parameters of enzyme were investigated such as optimum pH, optimum temperature and optimum ionic strength. The optimum pH, optimum temperature and optimum ionic strength were determined to be 7.5 Tris–SO_4 buffer, 40 °C and 50 mM Tris–SO_4 buffer for the CA enzyme, respectively. K_M and V_{max} values were calculated for NPA by Lineweaver–Burk graph. K_M constants were calculated as 0.32 mM, V_{max} values as 0.0025 mol × min^{-1} for NPA.

The inhibitory effects of some pesticides (Spinosad and Dimethoate) and metal ions (Al^{3+}, Cu^{2+}, Ba^{2+}, Fe^{2+}, Mn^{2+}, Se^{2+}) on CA purified from the Shabut Fish (*Barbus grypus*) gill tissue were determined. For the compounds showing inhibitory effects, the IC_{50} value was determined by activity% vs inhibitor concentration graphs for each compound. *Table 2* shows the *in vitro* effect of metal ions (Al^{3+}, Cu^{2+}, Ba^{2+}, Fe^{2+}, Mn^{2+} and Se^{2+}) on CA purified from the Shabut Fish (*Barbus grypus*) gill tissue. IC_{50} values of Al^{3+}, Cu^{2+}, Ba^{2+}, Fe^{2+} and Se^{2+} ions were determined to be 0.355, 3.46, 0.77, 0.303 and 1.57 mM, respectively.

Inhibition data for some pesticides (Spinosad and Dimethoate) on this enzyme are exhibited in *Table 3*. Very low IC_{50} values were obtained such as 0.41 and 0.52 mM in the presence of the Spinosad and Dimethoate as inhibitors (*Fig. 3a, b*).

Table 1. *Summary of purification procedure of CA enzyme from Shabut Fish (Barbus grypus) gill tissue*

Purification Steps	Activity (EU/ml)	Total volume (ml)	Protein (mg/ml)	Total protein (mg)	Total activity	Specific activity (EU/mg)	Yield %	Purification fold
Homogenate	45.33	30	2050	92250	1360	0.0147	100.0	1.0
Sepharose-4B-L tyrosine-sulfanilamide affinity chromatography	80	10	27.44	274.4	800	2.92	58.8	198.6

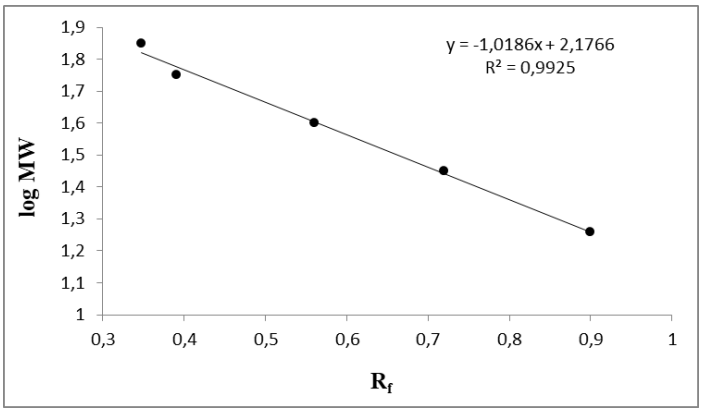

Figure 1. *Standard R_f–LogMW graph molecular weight of CA from Shabut Fish (Barbus grypus) gill tissue using the SDS-PAGE results*

http://www.aloki.hu ● ISSN 1589 1623 (Print) ● ISSN 1785 0037 (Online)
DOI: http://dx.doi.org/10.15666/aeer/1706_1347313483

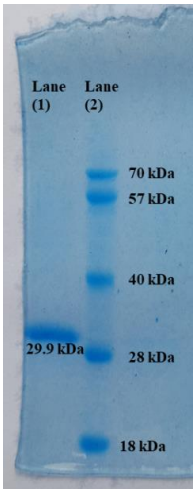

Figure 2. *SDS-PAGE analysis of purified Shabut Fish (Barbus grypus) gill tissue CA enzyme. Lane (1) CA enzyme purified from the gill tissue of Shabut Fish (Barbus grypus), (29.9 kDa). Lane (2) standard proteins (70 kDa), (57 kDa), (40 kDa), (28 kDa), (18 kDa)*

Table 2. *IC_{50} values for metal ions on CA enzyme from Shabut Fish (Barbus grypus) gill tissue*

Inhibitors	IC_{50}	Inhibitors	IC_{50}
Al^{3+}	0.355 mM	Se^{2+}	1.57 mM
Fe^{2+}	0.303 mM	Ba^{2+}	0.77 mM
Cu^{2+}	3.46 mM	Mn^{2+}	No inhibition (1-15 mM)

Table 3. *IC_{50} values for some pesticides on CA enzyme from Shabut Fish (Barbus grypus) gill tissue*

Inhibitors	IC_{50}	Inhibitors	IC_{50}
Spinosad	0.41 mM	Dimethoate	0.52 mM

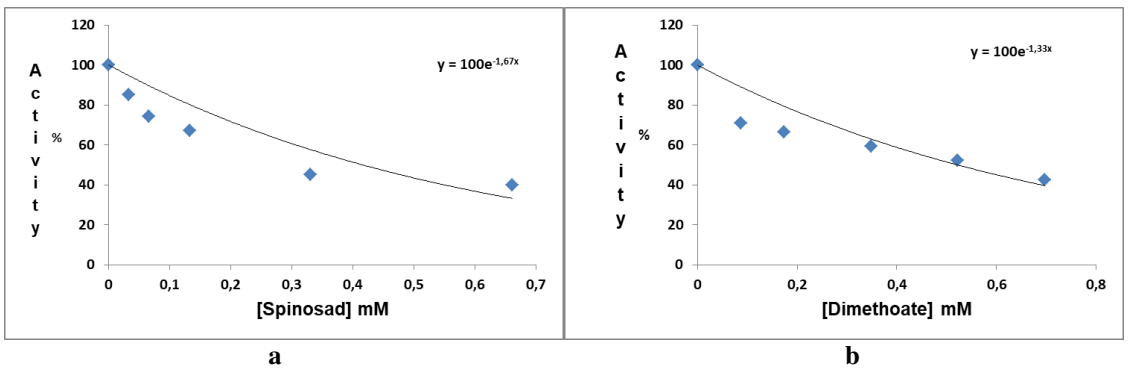

a **b**

Figure 3. *IC_{50} graph of **a** Spinosad and **b** Dimethoate*

These findings may be helpful for comparing CAs from different vertebrate species, their susceptibility to inhibition of various compound classes and also for understanding

http://www.aloki.hu ● ISSN 1589 1623 (Print) ● ISSN 1785 0037 (Online)
DOI: http://dx.doi.org/10.15666/aeer/1706_1347313483

the toxic effect of some pesticides and metal ions in endangered fish species. Some physiological aspects of CA-mediated processes in this type of less investigated vertebrate are in fact poorly understood, since most of the CA pharmacological/environmental researches have been done with the human and rodent enzymes. This research made from fish gill is important in this aspect.

Discussion and conclusion

Metals and pesticides generally have a negative effect on metabolism. Pesticides commonly used in agricultural fields and metals with industrial waste are particularly important determinants of the health of land and aquatic organisms. In recent years, issues such as the rapid increase in the use of pesticides in agriculture and the disposal of industrial wastes to the environment are need attention. When the distribution of heavy metals in the ecological system is examined, it is observed that the human hand is more effective in spreading to the environment than natural cycles. Kacar et al. studied to determine the concentrations of heavy metals (Cr, Mn, Fe, Co, Ni, Cu, Zn, Cd and Pb) in liver, gill and muscle of *Barbus grypus* in Batman Dam, Turkey. Their results indicated that heavy metal concentrations were higher in the liver and gill, while it was lower in the muscle (Kacar et al., 2017a). In another study, Kacar et al. studied the heavy metal concentrations in the tissues of fish taken seasonally from the Batman Dam. Their results indicated that in the winter; Cr, Fe, Ni, Co, Zn and Pb accumulations in the gills were more than in all seasons (Kacar et al., 2017b).

CO_2, produced in fish tissues, is hydrated quickly by the CA enzyme, converted into bicarbonate, and transported in the blood. Approximately, 98% of the transported and stored CO_2 is in the bicarbonate form (Demirdag et al., 2013). CA is a crucial enzyme in several other important physiological processes. For instance, the gills of aquatic organisms function in respiratory gas exchange, salt transport, and acid–base balance and CA can function in all three processes. The multiple functions of CA are a result of multiple isoforms that are localized to specific subcellular compartments/fractions within the gill (Cudennec et al., 2006; Sender et al., 1999). It has been understood that nearly all chemical reactions in the metabolism of the living organisms are catalyzed by enzymes, and the enzyme activities are influenced (decreased or increased) by many chemical substances including pesticides, fungicides, drugs and metal ions even at low concentrations (Soydan et al., 2017; Ozaslan et al., 2017). There are numerous studies about inhibition of CA enzyme activity with different pesticide and metals reported in the literature. For instance, Demirdag et al. investigated the inhibitory effects of some metals on the enzymatic activity of sheep liver CA. They found *in vitro* inhibition of the metals in the order of $Cu^{2+} > Zn^{2+} > Cd^{2+} > Co^{2+} > Ni^{2+}$ (Demirdag et al., 2012a). In another study, Ceyhun et al. studied the inhibitory effects of some metals on the enzymatic activity of the teleost fish *Dicentrarchus labrax* liver CA. Their results indicated that metal ions (Al^{3+}, Cu^{2+}, Pb^{2+}, Co^{3+}, Ag^{1+}, Zn^{2+} and Hg^{2+}) inhibited the enzyme activity at low concentrations (0.0692, 0.0715, 0.1128, 0.3165, 0.3790, 0.39 and 0.4484 mM), respectively (Ceyhun et al., 2011). Furthermore, Demirdag et al. investigated inhibitor effects of pesticides such as cyhalothrin, cypermethrin, dichlorvos, methamidophos, chlorpyrifos and methylparathion on purified enzyme from the European Seabass liver (Demirdag et al., 2012b). They showed that pesticides inhibit the enzyme even at very small concentrations. Soydan et al. studied the inhibitory effects of some pesticides on the enzymatic activity of Apis mellifera CA.

http://www.aloki.hu ● ISSN 1589 1623 (Print) ● ISSN 1785 0037 (Online)
DOI: http://dx.doi.org/10.15666/aeer/1706_1347313483

Their results indicated that IC_{50} values for the tebuconazole, propoxur, carbaryl, carbofuran, simazine and atrazine pesticides were 0.0030, 0.0321, 0.0031, 0.0087, 0.0273 and 0.0165 mM, respectively (Soydan et al., 2017). In another study, Kılınc et al. studied the inhibitory effects of chlorpyrifos, cypermethrin, dichlorvos, glyphosate isopropylamine and lambda cyhalomethrin pesticides on the enzymatic activity of the sheep stomach CA-II. Their results indicated that glyphosate isopropylamine and dichlorvos were found to have the highest inhibitory effects on the purified enzyme (Kılınc et al., 2015). From the studies mentioned above, it can be distinctly understood that many pesticides and metals have inhibitory effects on CA enzyme activity. Hence, in this study; the inhibitory effects of some widely used pesticides and metals on the activity of purified Shabut Fish (*Barbus grypus*) gill CA enzyme are investigated (*Tables 2* and *3*). As gill carbonic anhydrases contact primary with habitat of fish, investigation of these functions' performance is necessary how affected by environmental factors. In this study, the carbonic anhydrase enzyme was purified for the first time from Shabut Fish (*Barbus grypus*) gill tissue, in a single step, by using affinity chromatography. Furthermore, this enzyme has been inhibited by the some pesticides inhibitors (Spinosad and Dimethoate), with the IC_{50} values of 0.41 mM and 0.52 mM, respectively.

Hisar et al. (2006) reported that the CA was purified 104.8-folds with a specific activity of 55.6 EUx (mg protein)$^{-1}$ from the rainbow trout gills by using Sepharose 4B-L-tyrosine-sulfanilamide affinity column. (Demirdag et al., 2015) purified a fish enzyme from Agrı Balık Lake trout gill (*Salmo trutta labrax*) and achieved a purification of 303.9-folds with a specific activity of 4130.4 EUx (mg protein)$^{-1}$ and recovery of 79.3% using the identical technique. It is indicated that the carbonic anhydrases derived from various organisms have molecular mass of from 18.9 to 29.3 kDa (Smith and Ferry, 2000). The subunit molecular weight of the Shabut Fish (*Barbus grypus*) gill CA enzyme was found to be about 29.9 kDa by SDS-PAGE. The values obtained are in harmony with the literature as seen. Dincer et al. (2016) reported that the molecular weight of the gill CA from Russian Sturgeon Fish (*Acipenser gueldenstaedtii*) is about 29 kDa while Hisar et al. (2006) reported that it to be 27 kDa from the rainbow trout gills and 29 kDa from Russian Sturgeon Fish erythrocyte (Kolayli et al., 2011).

Data of *Table 2* show that the gill CA was inhibited by metal ions, with IC_{50} values in the range of 0.303–3.46 mM. The most inhibitory ion was Fe (II) and the least inhibitory was Cu (II). Heavy metals possess different toxicological impacts on living organisms, especially in fish. It is that enter the food chain are not discharged from fish and are so accumulated in their bodies. Then, they can be ingested by humans via the consumption of fish. Thus, heavy metal ions probably do constitute a great danger for this fish, or at least they do inhibit significantly the CA found in the gill. Pesticides have been found to be a more potent inhibitor of gill CA when it is compared to heavy metals. It was observed that some pesticides such as (Spinosad and Dimethoate) inhibited the enzyme at very small concentrations such as 0.41 and 0.52 mM. Most of the enzyme studies in the literature are on humans and animals. Researches on the effects of environmental pollutants such as pesticides and metals on fish are limited. As the number of such studies demonstrating the metabolic effects of environmental pollutants on fish increases, we can become a more conscious society. It would be beneficial for researchers to give direction to their research by taking this into consideration.

http://www.aloki.hu ● ISSN 1589 1623 (Print) ● ISSN 1785 0037 (Online)
DOI: http://dx.doi.org/10.15666/aeer/1706_1347313483

Consequently, Shabut Fish (*Barbus grypus*) gill CA enzyme was purified in a one step affinity chromatography procedure for the first time, and analyzed characteristic features. In addition, inhibitory effects of some pesticides and metals on enzyme activity were reported. In the light of these results, the Shabut Fish (*Barbus grypus*) gill CA enzyme is inhibited by some environmental pollutants such as pesticides (Spinosad and Dimethoate) and metal ions (Al^{3+}, Cu^{2+}, Ba^{2+}, Fe^{2+} and Se^{2+}). Owing to their toxicity, pesticides and metal ions affect not only the target organisms but also animals and humans which are being exposed to these compounds. Therefore, some measures have to be taken to prevent excessive diffusion to the environment when using these compounds. As a precaution, farmers should be informed about the use of pesticides and trained on this subject at short intervals. Besides, harmful effects on health of these chemical substances must be considered carefully and the usage of them must be kept under control. The industries near the water supplies must be more conscious about the factory waste and metal residues. The fish in fresh water and sea have been consumed as an important food source until now and will be consumed in the future. Thus, due to the mixing of the pesticides through the rain and irrigation waters into the Siirt/Botan Stream, aquatic organisms in this area are at great risk of chemical toxicity.

REFERENCES

[1] Anwar, W. A. (1997): Biomarkers of human exposure to pesticides. – Environment Health Perspectives 105: 801-806.

[2] Atasever, A., Ozdemir, H., Gulcin, I., Kufrevioglu, O. I. (2013): One-step purification of lactoperoxidase from bovine milk by affinity chromatography. – Food Chem. 136(2): 864-870.

[3] Bradford, M. M. (1976): A rapid and sensitive method for the quantitation of microgram quantities of protein utilizing the principle of protein-dye binding. – Anal Biochem 72: 248-254.

[4] Cerqueira, C. C., Fernandes, M. N. (2002): Gill tissue recovery after copper exposure and blood parameter responses in the tropical fish Prochilodus scrofa. – Ecotoxicol. Environ. Saf. 52: 83-91.

[5] Ceyhun, S. B., Senturk, M., Erdogan, O., Kufrevioglu, O. I. (2010): *In vitro* and *in vivo* effects of some pesticides on carbonic anhydrase enzyme from rainbow trout (oncorhynchus mykiss) gills. – Pestic Biochem Physiol 97: 177-181.

[6] Ceyhun, S. B., Senturk, M., Yerlikaya, E., Erdogan, O., Kufrevioglu, O. I., Ekinci, D. (2011): Purification and characterization of carbonic anhydrase from the teleost fish *Dicentrarchus labrax* (European seabass) liver and toxicological effects of metals on enzyme activity. – Environ Toxicol Pharm. 32: 69-74.

[7] Cudennec, B., Rousseau, M., Lopez, E., Fouchereau-Peron, M. (2006): CGRP stimulates gill carbonic anhydrase activity in molluscs via a common CT/CGRP receptor. – Peptides 27: 2678-2682.

[8] Demir, Y., Oruc, E., Topal, A. (2016): Carbonic anhydrase activity responses and histopathological changes in gill and liver tissues after acute exposure to chromium in brown trout juvenile. – Hacettepe J. Biol. Chem. 44(4): 515-523.

[9] Demirdag, R., Comakli, V., Kuzu, M., Yerlikaya, E., Senturk, M. (2015): Purification and characterization of carbonic anhydrase from Agrı Balık Lake trout gill (*Salmo trutta labrax*) and effects of sulfonamides on enzyme activity. – J Biochem Molecular Toxicology 29(3): 123-128.

http://www.aloki.hu ● ISSN 1589 1623 (Print) ● ISSN 1785 0037 (Online)
DOI: http://dx.doi.org/10.15666/aeer/1706_1347313483

[10] Demirdag, R., Comakli, V., Senturk, M., Ekinci, D., Kufrevioglu, O. I., Supuran, C. T. (2013): Purification and characterization of carbonic anhydrase from sheep kidney and effects of sulfonamides on enzyme activity. – Bioorg Med Chem 21: 1522-1525.
[11] Demirdag, R., Yerlikaya, E., Aksakal, E., Kufrevioglu, O. I., Ekinci, D. (2012b): Influence of pesticides on the pH regulatory enzyme, carbonic anhydrase, from European Seabass liver and bovine erythrocytes. – Environ Toxicol Pharm. 34: 218-222.
[12] Demirdag, R., Yerlikaya, E., Kufrevioglu, O. I. (2012a): Purification of carbonic anhydrase-II from sheep liver and inhibitory effects of some heavy metals on enzyme activity. – J Enzyme Inhib Med Chem. 27(6): 795-799.
[13] Dincer, B., Ekinci, A. P., Akyuz, G., Kurtoglu, I. Z. (2016): Characterization and inhibition studies of carbonic anhydrase from gill of Russian Sturgeon Fish (*Acipenser gueldenstaedtii*). – J Enzyme Inhib Med Chem. 31(6): 1662-1665.
[14] Ekinci, D., Beydemir, S. (2010): Purification of PON1 from human serum and assessment of enzyme kinetics against metal toxicity. – Biol Trace Elem Res. 135: 112-120.
[15] Ekinci, D., Beydemir, S., Kufrevioglu, O. I. (2008): *In vitro* inhibitory effects of some heavy metals on human erythrocyte carbonic anhydrases. – J Enzyme Inhib Med Chem. 22(6): 745-750.
[16] Hisar Aras, S., Hisar, O., Yanık, T., Aras, S. M. (2004): Inhibitory effects of ammonia and urea on gill carbonic anhydrase enzyme activity of rainbow trout (*Oncorhynchus mykiss*). – Environ Toxicol Pharm 17: 125-128.
[17] Hisar, O., Beydemir, S., Bulbul, M., Yanık, T. (2006): Kinetic properties of carbonic anhydrase purified from gills of rainbow trout (Oncorhynchus mykiss). – J Appl Anim Res 30: 185-188.
[18] Kacar, E., Karadede Akın, H., Cicek, T., Unlu, E. (2017b): Seasonal variations of heavy metals in water, sediment and tissues of two freshwater fish species (*Cyprinion macrostomum* and *Capoeta trutta*) from the Batman Dam (Tigris Basin), Turkey. – Fresenius Environmental Bullet 26(6): 4187-4193.
[19] Kacar, E., Karadede Akın, H., Ugurlu, P. (2017a): Determination of heavy metals in tissues of *Barbus grypus* (Heckel, 1843) from Batman Dam, Turkey. – Turkish Journal of Fisheries and Aquatic Sciences 17: 787-792.
[20] Kılınc, N., Isgor, M. M., Sengül, B., Beydemir, S. (2015): Influence of pesticide exposure on carbonic anhydrase II from sheep stomach. – Toxicology and Industrial Health 31(9): 823-830.
[21] Koca, Y. B., Koca, S., Yildiz, S., Gurcu, B., Osanc, E., Tuncbas, O., et al. (2005): Investigation of histopathological and cytogenetic effects on Lepomis gibbosus (*Pisces: Perciformes*) in the Cine stream (Aydin/Turkey) with determination of water pollution. – Environ. Toxicol. 20: 560-571.
[22] Kolayli, S., Karahalil, F., Sahin, H., et al. (2011): Characterization and inhibition studies of an a-carbonicanhydrase from the endangered sturgeon species Acipenser gueldenstaedti. – J Enzyme Inhib Med Chem.26: 895-900.
[23] Laemmli, U. K. (1970): Cleavage of structural proteins during the assembly of the head of bacteriophage T4. – Nature 227: 680-5.
[24] Lineweaver, H., Burk, D. (1934): The determination of enzyme dissocation constants, J. Am. Chem. Soc., 56(3): 658-666.
[25] Lopez Mananes, A. A., Magnoni, L. J., Goldemberg, A. L. (2000): Brancial carbonic anhydrase (CA) of gills of Chasmagnathus granulata (*Crustacea decapoda*). – Comp Biochem Physiol 127B: 85-95.
[26] Olgunoglu, A. I., Olgunoglu, M. P., Artar, E. (2011): Seasonal changes in biochemical composition and meat yield of Shabut (*Barbus grypus*, Heckel 1843). – Iranian Journal of Fisheries Sciences Short Communication 10(1): 181-187.

http://www.aloki.hu ● ISSN 1589 1623 (Print) ● ISSN 1785 0037 (Online)
DOI: http://dx.doi.org/10.15666/aeer/1706_1347313483

[27] Ozaslan, M. S., Demir, Y., Kufrevioglu, O. I., Ciftci, M. (2017): Some metals inhibit the Glutathione S-transferase from Van Lake fish gills. – J Biochem Mol Toxicol. 31: e21967. https://doi.org/10.1002/jbt.21967.
[28] Randall, D. J., Daxbaeck, C. (1984): Oxygen and Carbon Dioxide Transfer across Fish Gills. – In: Hoar, W. S., Randall, D. J. (eds.) Fish Histology. Vol. 10A. Academic Press, New York.
[29] Sender, S., Bottcher, K., Cetin, Y., Gros, G. (1999): Carbonic anhydrase in the gills of seawaterand freshwater-acclimated flounders Platichthys flesus: purification, characterization, and immunohistochemical localization. – J Histochem Cytochem 47: 43-50.
[30] Senturk, M., Gulcin, I., Beydemir, S., Kufrevioglu, O. I., Supuran, C. T. (2011): *In Vitro* inhibition of human carbonic anhydrase I and II isozymes with natural phenolic compounds. – Chem. Biol. Drug Des. 77(6): 494-499.
[31] Singh, N., Gupta, K. V., Kumar, A., Sharma, B. (2017): Synergistic effects of heavy metals and pesticides in living systems. – Frontiers in Chemistry 5: 70.
[32] Smith, K. S., Ferry, J. G. (2000): Prokaryotic carbonic anhydrases, reviews. – FEMS Microbiol 24: 335-366.
[33] Soydan, E., Guler, A., Bıyık, S., Senturk, M., Supuran, C. T., Ekinci, D. (2017): Carbonic anhydrase from Apis mellifera: purification and inhibition by pesticides. – J Enzyme Inhib Med Chem. 32(1): 47-50.
[34] Soyut, H., Beydemir, S. (2008): Purification and some kinetic properties of carbonic anhydrase from rainbow trout (*Oncorhynchus mykiss*) liver and metal inhibition. – Protein Pept. Lett. 15(5): 528-535.
[35] Supuran, C. T. (2018): Carbonic Anhydrases and Metabolism. – Metabolites 8(2): 25.
[36] Tiemann, U. (2008): *In vivo* and *in vitro* effects of the organochlorine pesticides DDT, TCPM, methoxychlor, and lindane on the female reproductive tract of mammals: a review. – Reprod Toxicol. 25(3): 316-326.
[37] Topal, A., Atamanalp, M., Oruc, E., Demir, Y., Beydemir, S., Isik, A. (2014): *In vivo* changes in carbonic anhydrase activity and histopathology of gill and liver tissues after acute exposure to chlorpyrifos in rainbow trout. – Arh. Hig. Rada Toksikol. 65: 377-385.
[38] Verpoorte, J. A., Mehta, S., Edsall, J. T. (1967): Esterase activities of human carbonic anhydrases B and C. – J Biol Chem 242: 4221-9.

http://www.aloki.hu ● ISSN 1589 1623 (Print) ● ISSN 1785 0037 (Online)
DOI: http://dx.doi.org/10.15666/aeer/1706_1347313483

EFFECTS OF SALINE STRESS ON *IN VITRO* SEED GERMINATION AND SEEDLING GROWTH OF SOME TURKISH FIG CULTIVARS (*FICUS CARICA* L.)

PAKYÜREK, M.[1*] – DUMANOĞLU, H.[2]

[1]*Department of Horticulture, Faculty of Agriculture, Siirt University, 56100 Siirt, Turkey*

[2]*Department of Horticulture, Faculty of Agriculture, Ankara University, 06110 Ankara, Turkey*

**Corresponding author*
e-mail: mine.pakyurek@siirt.edu.tr

(Received 3rd Jul 2019; accepted 2nd Sep 2019)

Abstract. In this study, saline stress tolerance/sensitivity levels, germination rate of the seeds, and seedling growth of eight fig cultivars (Morgüz, Sarılop, Yeşilgüz, Sultan Selim, Halebi, Bursa Siyahı, Göklop and Izmir Bardacık) of Turkey were examined by *in vitro* screening. In fig, this is the first and guiding study reporting *in vitro* germination performance of the seeds in saline conditions for fig researchers. Salt stress *in vitro* condition was established by adding 0, 85.5, 171.1 and 342.5 mM NaCl to the MS basal medium in current experiment. In the examinations carried out 45 days after seedling, none of the cultivars could be obtained at a dose of 342.5 NaCl. Highest seed germination rates were determined in Sultan Selim (79.5%) and Bursa Black (75.0%) cultivars at 171.1 mM NaCl concentration. In other cultivars, this ratio has changed between 0.0-40.0%. High germination rate (90% <) and plant growth under the observed 85.5 mM NaCl dose was determined for Sultan Selim and Bursa Siyahı cultivars. The seeds and seedlings of Sarılop cultivar, one of the major cultivars for dried fig production, have been found sensitive to salt stress.
Keywords: *fruit, fig (Ficus carica L.), salinity tolerance, stress physiology, germination criteria*

Introduction

The fig, a subtropical fruit (*Ficus carica* L.) is grown in many parts of the world with mild climate. Turkey is one of the countries in the world with the largest share of producing and exporting figs. According to the latest reports, 305.7 thousand tons of fig are produced over 50.3 thousand hectares in Turkey. This value (1152.8 thousand tons) reaches 26.5% of the global fig production (FAO, 2017). Turkey is a very rich country in terms of the genetic resources of figs (Ercişli, 2004). Fig genetic diversity in Turkey is very valuable for classical and modern fig breeding programs. As indicated in previous studies, the genetic diversity found in cultivated plants and wild relatives provides rich resources for targeted cultivation characteristics and gene discovery that have not been used sufficiently yet (Ismail and Horie, 2017). It is important to reveal the genetic potential of the cultivars in terms of targeted character development. To evaluate genotypes in a short time, *in vitro* screening method can grant great convenience and time-saving. This technique has many advantages over *ex vitro* conditions to investigate the complex response of plants to stress factors as under aseptic and controlled environmental conditions (Jain, 2001; Lokhande et al., 2011; Rai et al., 2011). There are many studies in the literature that use these techniques for drought, salinity and other stress factors (Tal, 1994; Shibli et al., 2007; Shatnawi et al., 2009).

http://www.aloki.hu ● ISSN 1589 1623 (Print) ● ISSN 1785 0037 (Online)
DOI: http://dx.doi.org/10.15666/aeer/1706_1348513492

Figs are moderately tolerant (EC 3-5 dS m^{-1}) plants to the soil salinity (Mass and Hoffman, 1977; Golombek and Lüdders, 1994). The land where figs grow in the world usually contains above average saline levels. Therefore, salinity is a major problem for figs today and in the future (Golombek and Lüdders, 1994; Zarei et al., 2016; Soliman and Alhady, 2017). The result of dry and hot climatic conditions of the country, low precipitation and especially the improper irrigation practices implemented in the agricultural and landscaping applications, salinity problems arise in such areas where there are drainage problems. Salinity, one of the abiotic stress factors, negatively affects both the agricultural soil and the plants grown in the soil that is under the threat of salinity (Yılmaz et al., 2011). Against these stress factors, high yield producing and stress resistant species should be designated and cultivated in areas with salinity problem (Shannon, 1978; Epstein, 1985; Ashraf et al., 1986; Singh et al., 2018). Due to the expensive and difficult methods to eliminate the salinity problem in the cultivated land, salt-resistant plant species and the more tolerant genotypes of these species have been studied in recent years (Singh et al., 2018). Concordantly, seed reproduction has crucial value in the fig hybridization as well as in the seed reproduction mediated seedling production (Hartmann et al., 2011; Zarei et al., 2016; Nimbolkar et al., 2016).

In this study, seed germination and seedling growth performances of eight Turkish fig cultivars under salt pressure were resolved to effectively utilize *in vitro* screening technique. Likewise, the capability of germination of fig seeds under saline conditions has been demonstrated for the first time with this study by the wide application doses of NaCl and the susceptible/tolerance fig cultivars.

Materials and methods

Herein, mature seeds formed as a result of free pollination were used as vegetable material as Morgüz, Sarılop, Yeşilgüz, Sultan Selim, Halebi, Bursa Siyahı, Göklop, and İzmir Bardacık fig cultivars. For this purpose, the ripen fruits were obtained in season from Aydın Erbeyli Fig Research Institute located at 37° 51' 56.0" – 27° 39' 53.3" coordinates. First of all, the seeds are washed in the laboratory environment after being washed out and cleaned in a solution with sodium hypochlorite (5% active chlorine) with 0.1% (v/v). 20 g/L sucrose and 6 g/L agar containing hormone-free MS (Murashige and Skoog, 1962) medium were used as the main nutrient medium and the pH of the medium was set to 5.8. 0, 85.5, 171.1 and 342.5 mM NaCl were added to the basic nutrient medium. In the experiments, 25 ml medium in 100×15 mm petri dishes were used. 25 seeds were planted in each petri dish. While working with four replicas, the seeds were allowed to germinate for 45 days under saline stress. The cultures were incubated at 25 ± 1 °C under 16-h photoperiod with 35 $\mu mol \cdot m^{-2} \cdot s^{-1}$ supplied by cool-white fluorescent lamps. The number of seeds germinated during the trial period was recorded daily. At the end of the experiment, germination rate (%), seedling height (mm), number of leaves (pieces/seedling rootstock) and root length (mm) were recorded.

Data were analysed according to Minitab Package Program (MINITAB Inc.). Analysis of variance (ANOVA) was applied with the F test ($P < 0.05$). Significant differences were determined based on a 5% error limit with Duncan test and differences were determined with the help of letters. Angle values of percentages were used in the analysis.

http://www.aloki.hu ● ISSN 1589 1623 (Print) ● ISSN 1785 0037 (Online)
DOI: http://dx.doi.org/10.15666/aeer/1706_1348513492

Results and discussion

In this study, the interaction between the germination rates, seedling height, number of leaves and root length in terms of various doses of NaCl was found to be statistically significant (*Table 1*). In terms of germination rate, the seeds of Sultan Selim, Bursa Siyahı, Göklop, and İzmir Bardacık were found to have statistically similar high germination rates at 0 mM and 85.5 mM NaCl concentrations. However, germination rates in Morgüz, Sarılop, Yeşilgüz and Halebi seeds decreased significantly compared to control in 85.5 mM application. Significant decrease in germination rates was recorded in 171.1 mM NaCl concentration. In this saline concentration, no germination occurred in Sarılop and Yeşilgüz seeds. However, germination rates of 79.5% and 75.0% were determined in the seeds of Sultan Selim and Bursa Siyahı respectively which are the highest values of 171.1 mM NaCl administration. No germination was noted at a concentration of 342.5 mM saline in any of the fig cultivars (*Table 1*).

Seedling height values decreased in all genotypes with increasing salt concentration. Moreover, the seedling height of Sultan Selim and Bursa Siyahı has the highest values compared to other cultivars in increasing saline concentrations (*Table 1*). The number of leaves in seedlings decreased significantly with elevated NaCl concentration in all cultivars. At 85.5 mM NaCl concentration, Sultan Selim, Bursa Siyahı and Halebi had a higher number of leaves than the others. There was no significant difference in the number of leaves between cultivars in 171.1 mM NaCl concentration (*Table 1*). The longest roots in 85.5 NaCl concentrations were recorded in Bursa Siyahı (52.4 mm), İzmir Bardacık (50.9 mm) and Sultan Selim (46.7 mm). The root length was significantly reduced in all cultivars at the 171.1 mM NaCl concentration. There was no significant difference among cultivars at this concentration (*Table 1*).

This is the first scientific study to reveal germination performances of fig seeds under saline stress. However, there are studies conducted on this subject in other woody plant species, albeit limited. Although all of these studies vary according to genotypes, germination rates and plant growth in seeds have been reported to be significantly decreased with an increasing salt concentration in the environment (Vijayan et al., 2003; Rahneshana et al., 2018). Similar findings were obtained in our study as well. Experiments showed that germination rates of fig seeds under saline stress manifested a great change depending on the type of cultivars and NaCl concentrations. *In vitro* conditions, the germination rate in fig cultivars on nutrient media (control- no NaCl) was 83-98%. At 85.5 mM (0.5%) NaCl concentration, the germination rate in fig cultivars was 10.3-99%, and at the highest NaCl concentration 171.1 mM (1%) the germination rate in fig cultivars was 0-79.5% (*Table 1*). NaCl causes an increase in osmotic pressure in the environment and prevents the seed from receiving water (Ardakani, 2015). NaCl leads to ionic stress as well as osmotic effect. It can also affect the activity of many enzymes that play a key role in lipid degradation (Zaghdoudi et al., 2015). In our study, one of the striking findings was that there was no germination in Yeşilgüz and Sarılop in the nutrient medium containing 171.1 mM NaCl. On the contrary, the same saline stress onto Sultan Selim and Bursa Siyahı has the highest germination rates 79.5% and 75.0% respectively. These results are vital for salinity resistant fig breeding since the elimination of the salinity originate problems depends on improvements of the cultivated genotypes salinity resistance (Athar and Ashraf, 2009).

http://www.aloki.hu ● ISSN 1589 1623 (Print) ● ISSN 1785 0037 (Online)
DOI: http://dx.doi.org/10.15666/aeer/1706_1348513492

Table 1. *Effects of NaCl concentrations on in vitro seed germination and seedling growth of Turkish fig cultivars*

Cultivar	0 mM NaCl			85.5 mM NaCl			171.1 mM NaCl			342.5 mM NaCl		
	(1) Germination ratio (%)											
Morgüz	97.3	AB[x]	A	64.0	D	b	10.7	C	c	-	A	d
Sarılop	83.0	D	A	44.0	E	b	-	D	c	-	A	c
Yeşilgüz	84.0	D	A	10.3	F	b	-	D	c	-	A	c
Sultan Selim	98.0	A	A	99.0	A	a	79.5	A	b	-	A	c
Halebi	93.0	BCD	A	80.0	C	b	40.0	B	c	-	A	d
Bursa Siyahı	90.0	CD	A	91.2	B	a	75.0	A	b	-	A	c
Göklop	96.0	ABC	A	92.0	B	a	36.0	B	b	-	A	c
İzmir Bardacık	96.0	ABC	A	89.3	BC	a	9.3	C	b	-	A	c
	(2) Seedling height (mm)											
Morgüz	21.3 ± 0.7[y]	D	A	7.2 ± 0.4	BC	b	4.0 ± 1.2	A	c	-		
Sarılop	24.8 ± 1.1	BC	A	7.4 ± 0.3	BC	b	-			-		
Yeşilgüz	18.4 ± 1.1	E	A	5.9 ± 0.7	C	b	-			-		
Sultan Selim	28.2 ± 2.0	A	A	15.5 ± 1.0	A	b	5.4 ± 0.3	A	c	-		
Halebi	26.0 ± 1.0	AB	A	9.4 ± 0.6	B	b	5.3 ± 0.4	A	c	-		
Bursa Siyahı	25.7 ± 2.3	ABC	A	13.7 ± 0.3	A	b	6.2 ± 0.8	A	c	-		
Göklop	22.7 ± 1.4	CD	A	9.5 ± 0.2	B	b	4.8 ± 0.3	A	c	-		
İzmir Bardacık	23.4 ± 2.0	BCD	A	7.6 ± 1.0	BC	b	4.4 ± 0.6	A	c	-		
	(3) Leaf number											
Morgüz	6.5 ± 0.4	CD	A	3.7 ± 0.1	CDE	b	1.8 ± 0.3	A	c	-		
Sarılop	5.7 ± 0.5	D	A	3.5 ± 0.2	DE	b	-			-		
Yeşilgüz	6.1 ± 0.5	D	A	3.1 ± 0.2	E	b	-			-		
Sultan Selim	8.6 ± 0.3	A	A	5.0 ± 0.2	A	b	1.7 ± 0.2	A	c	-		
Halebi	7.1 ± 0.4	BC	A	4.4 ± 0.5	ABC	b	2.1 ± 0.1	A	c	-		
Bursa Siyahı	7.8 ± 0.4	B	A	4.9 ± 0.1	AB	b	2.1 ± 0.1	A	c	-		
Göklop	6.2 ± 0.1	D	A	4.1 ± 0.2	BCD	b	2.0 ± 0.1	A	c	-		
İzmir Bardacık	6.4 ± 0.4	CD	A	3.8 ± 0.1	CDE	b	2.0 ± 0.1	A	c	-		
	(4) Root length (mm)											
Morgüz	48.1 ± 5.3	AB	A	34.4 ± 7.7	B	b	3.8 ± 0.6	A	c	-		
Sarılop	43.0 ± 5.0	BC	A	18.5 ± 5.6	C	b	-			-		
Yeşilgüz	58.4 ± 4.8	A	A	23.3 ± 5.7	C	b	-			-		
Sultan Selim	46.0 ± 1.3	BC	A	46.7 ± 0.7	A	a	4.7 ± 0.4	A	b	-		
Halebi	35.0 ± 2.2	C	A	21.5 ± 3.2	C	b	3.4 ± 0.5	A	c	-		
Bursa Siyahı	44.0 ± 1.7	BC	A	52.4 ± 5.1	A	a	3.7 ± 0.3	A	b	-		
Göklop	39.1 ± 4.1	BC	A	34.6 ± 5.7	B	a	2.6 ± 0.4	A	b	-		
İzmir Bardacık	39.7 ± 0.6	BC	B	50.9 ± 3.1	A	a	5.6 ± 0.8	A	c	-		

Source	P-values			
	(1)	(2)	(3)	(4)
Cultivar (C)	0.000	0.000	0.000	0.000
Treatment (T)	0.000	0.000	0.000	0.000
C × T	0.000[*]	0.016[***]	0.004[**]	0.000[*]

[x]For each parameter, different capital letters within a column indicate significant differences among cultivars in each treatment, and different small letters within a row show significant differences among treatments in each cultivar

[y]Data presented as mean ± standard error of mean

[*], [**], [***]Significant at $P < 0.001$, $P < 0.01$ and $P < 0.05$, respectively

http://www.aloki.hu ● ISSN 1589 1623 (Print) ● ISSN 1785 0037 (Online)
DOI: http://dx.doi.org/10.15666/aeer/1706_1348513492

The lack of germination of the seeds in the high saline conditions is the biggest factor limiting the obtaining of plants (Zaghdoudi et al., 2015). Procurement of water, retaining chloroplast function and ion homeostasis dictates the plant competence in enduring saline stress. In addition to those, osmotically controlling metabolites, some proteins, enzymes that confine free radicals play an important role in the plant homeostasis during germination (Parvaiz and Satyawati, 2008).

Tolerance of the plants to saline stress generally varies according to their development stages (Zaghdoudi et al., 2015). It has been reported by different researchers that salinity reduces water intake in seeds, inhibits germination by suppressing genes encoding GA biosynthetic enzymes, and also reduces germination rate due to stimulating ABA accumulated in tissues (Doğan and Budaklı Çarpıcı, 2016; Kim and Park, 2008; Li et al., 2016). In our study, increasing salt rates significantly decreased germination rates of fig genotypes. However, germinated seeds continued to grow on the same saline media for approximately 30 days. The response of seedlings to saline stress varies according to the saline levels and in general, high saline levels have decreased plant growth significantly. Halted or impaired plant growth in high saline stress stems form, in particular: ion toxicity, nutrient constraints, osmotic and oxidative stress. These mechanisms lead to disruption in the membrane lipids, proteins, and nucleic acids via the inflated levels of reactive oxygen species. Sodium toxicity is the main stress factor in the high saline lands by causing an increased rate of accumulation of reactive oxygen species (Mudgal et al., 2010). In our study, we found that the size of the seedlings in six cultivars was reduced by approximately 80% at 171.1 nM NaCl concentration compared to no saline control. Bursa Siyahı was the least susceptible to saline stress in the size of the seedlings reduction (75.9%). In all cultivars, germination can take place at 85.5 mM NaCl dose, while the Bursa Siyahı and Sultan Selim cultivars are less affected by saline stress than other fig cultivars with respect to the size of the seedlings. Saline stress leads to a 45% decline in the size of the seedlings in Bursa Siyahı and Sultan Selim compared to no saline control. In other cultivars, this reduction ratio reached up to 70%. Another crucial finding in our study is that the root length in the Bursa Siyahı and Sultan Selim cultivars did not curtail compared to the control at the 85.5 mM NaCl concentration. In terms of root development, the 85.5 mM NaCl dose did not pose any threat in these cultivars. Therefore, Bursa Siyahı and Sultan Selim are defined as saline stress-tolerant fig cultivars. However, in the Sarılop and Yeşilgüz cultivars we have reported as sensitive to salt, root growth at the dose of 85 mM NaCl decreased by 60% compared to the no saline control. Saline stress tolerant plant species underwent certain adaptation to manage this stressful condition. A boost in the root/canopy ratio, changes in chlorophyll content, adjustments in the leaf anatomy contributes to hinder leaf ion toxicity. Hence, water homeostasis is maintained by these adaptations and photosynthesis can be sustained without any hindrance (Acosta-Motos et al., 2017). Our findings are partially compatible with the findings of Emek (2018), who investigated the response of Bursa Siyahı to saline stress *in vitro*. Emek (2018), in his study, evaluated the effects of 0, 40, 80, 120, 240, 320 and 480 mM NaCl concentrations on the plant growth in Bursa Siyahı after 6-week incubation. According to this research, plants were healthy at 0-80 mM NaCl concentrations, browning at 120-240 mM NaCl concentrations and chlorosis and deaths were detected at 320-480 mM concentrations. The researcher stated that the observations in Bursa Siyahı were done up to 120 mM NaCl. In our study, observations were made in 6 fig cultivars up to 171.1 mM NaCl concentration. However, in this study, we recommend the use of the

http://www.aloki.hu ● ISSN 1589 1623 (Print) ● ISSN 1785 0037 (Online)
DOI: http://dx.doi.org/10.15666/aeer/1706_1348513492

dose of 85.5 mM NaCl, which is more reliable in evaluating the response of many fig genotypes to saline stress as a result of plant growth, because some plants do not survive after exceeding this concentration. Abdolinejad and Shekafandeh (2014) investigated the effects of different saline concentrations (0, 80, 120 and 160 mM) in *in vitro* conditions on two Persian fig cultivars: Anjir Sabz and Shah Anjir. At 160 mM NaCl concentration, Anjir Sabz reported having more chloride ion accumulation. Soliman and Alhady (2017) revealed that in their *in vitro* replication study with five local fig cultivars, a five-week salt application resulted in a significant reduction in plant growth and rooting. In another study conducted with Brown Turkey and Royal cultivars of fig, salt was applied to irrigation water (Alswalmeh et al., 2015). This study announced that the Brown Turkey variant was less affected by saline stress than the Royal variant. In another *in vitro* replication study on Black Mission, Brown Turkey and Brunswick fig cultivars, different concentrations of NaCl were applied to replicating media containing different plant growth regulators. In the study, Black Mission, Brunswick, and Brown Turkey are listed as the most resistant cultivars to saline stress in Saudi Arabia respectively (Metwali et al., 2014). The effects of seven NaCl doses ranging from 1000-7000 mg L^{-1} (17.1-119.7 mM) on plant growth in four fig cultivars were tested *in vitro* (Yehia et al., 2018). Researchers suggested that 7000 mg L^{-1} (119.7 mM) NaCl is lethal. However, six fig genotypes showed development at 171.1 mM NaCl concentration in our study. The number of leaves of fig genotypes was recorded between 3.1 and 5.0 in 85.5 mM NaCl concentration. Yehia et al. (2018), reported that the number of leaves ranges between 2.4-4.0 at 5000 mg L^{-1} (85.5 mM) NaCl in the six-week-old plants. These values are consistent with our findings. In another study, saline stress resistance of four fig genotypes was tested by addition of 0.6, 4, 6, 8 dS m^{-1} saline containing water (6, 40, 60, 80 mM). Researchers found a negative correlation between increasing saline concentration and plant development. Of note, SxK genotype was determined as the most tolerant variant in their study (Zarei et al., 2016).

Conclusion

In this study, the growth performance of eight Turkish figs cultivars against saline stress was compared successfully *in vitro*. At 0 nM, 85.5 nM, 171.1 nM and 342.5 mM NaCl concentrations and 45 days after seed germination rate (%), seedling height (mm), number of leaves (pieces/seedling rootstock) and root length (mm) were assessed. The tolerance against saline stress differences between fig genotypes could be determined at highest 171.1 mM NaCl concentration regarding germination of seeds occur *in vitro*. In the study, the highest NaCl dose in which fig genotypes can be evaluated according to seedling development criteria was determined as 85.5 mM. A higher NaCl dose (171.1 mM), there were no germination in Sarılop and Yeşilgüz genotypes. When the germination rates and seedling growth were evaluated, it was revealed that Sultan Selim and Bursa Siyahı fig genotypes were more tolerant to saline stress than others. Sarılop, which is an important fig genotype in a dried fig market, was assigned as the most susceptible fig genotype to saline stress.

Most effective solution against prevailing salinity problem in agricultural areas is the development of tolerant cultivars and rootstocks to saline stress. Ratio of seed germination, which is important for hybridization and seedling production in fruit species, must be determined to the select genotypes under stress conditions in breeding

http://www.aloki.hu ● ISSN 1589 1623 (Print) ● ISSN 1785 0037 (Online)
DOI: http://dx.doi.org/10.15666/aeer/1706_1348513492

programs. Turkey is one of the important gene centers of the fig so it has large genetic variability for producing new fig cultivars tolerance to saline conditions by plant breeders of this country. In fig, this is the first study reporting *in vitro* germination performance of the seeds in salt conditions although some studies exist on the development of seedlings under salinity stress. It can be mentioned that a guiding and useful study has been presented for future fig breeding programmes.

REFERENCES

[1] Abdolinejad, R., Shekafandeh, A. (2014): Responses of two figs (*Ficus carica* L.) cultivars under salt stress via *in vitro* condition. – Agriculture Science Developments 3: 194-199.
[2] Acosta-Motos, J. R., Ortuno, M. F., Bernal-Vicente, A., Diaz-Vivancos, P., Sanchez-Blanco, M. J., Hernandez, J. A. (2017): Plant responses to salt stress: adaptive mechanisms. – Agronomy 7: 18.
[3] Alswalmeh, H. A., Al-Obeed, R. S., Omar, A. E. K. (2015): Effect of water salinity on seedlings growth of Brown Turkey and Royal fig cultivars. – The Journal of Agriculture and Natural Resources Sciences 2: 510-516.
[4] Ardakani, M. J. (2015): Effect of salinity on germination and deployment of *Pistachio vera* var. Badami. – European Journal of Experimental Biology 5: 57-59.
[5] Ashraf, M., McNaily, T., Bradshaw, A. D. (1986): The potential for evaluation of salt (NaCl) tolerance of seven grass species. – New Phytologist 103: 299-309.
[6] Athar, H. R., Ashraf, M. (2009): Strategies for Crop Improvement against Salinity and Drought Stress: An Overview. – In: Ashraf, M., Ozturk, M., Athar, H. R. (eds.) Salinity and Water Stress. Springer, Dordrecht, pp. 1-16.
[7] Doğan, R., Budaklı Çarpıcı, E. (2016): Effects of different salt concentrations on germination of some triticale lines. – KSU Journal of Natural Science 19: 130-135 (In Turkish).
[8] Emek, Y. (2018): Effects of salinity on the morphology of the 'Bursa Siyahı', fig (*Ficus carica* L.) cultivar *in vitro* conditions. – KSU Journal of Natural Sciences 21: 292-296.
[9] Epstein, E. (1985): Salt-tolerant crops: origins, development, and prospects of the concept. – Plant and Soil 89: 187-198.
[10] Ercişli, S. (2004): A short review of the fruit germplasm resources of Turkey. – Genetic Resources and Crop Evolution 51: 419-435.
[11] FAO (2017): Fig Production. – Food and Agriculture Organization of the United Nations, Rome. http://www.fao.org.
[12] Golombek, S. D., Lüdders, P. (1994): Effects of short-term salinity on leaf gas exchange of the fig (*Ficus carica* L.). – Plant and Soil 148: 21-27.
[13] Hartmann, H. T., Kester, D. E., Davies, F. T., Geneve, R. L. (2011): Plant Propagation: Principle and Practices. – Prentice-Hall, London.
[14] Ismail, A. M., Horie, T. (2017): Genomics, physiology, and molecular breeding approaches for improving salt tolerance. – Annual Review of Plant Biology 68: 405-434.
[15] Jain, S. M. (2001): Tissue culture-derived variation in crop improvement. – Euphytica 118: 153-166.
[16] Kim, S. G., Park, C. M. (2008): Gibberellic acid-mediated salt signaling in seed germination. – Plant Signaling & Behavior 3: 877-879.
[17] Li, W., Yamaguchi, S., Khan, M. A., An, P., Liu, X., Tran, L. S. P. (2016): Roles of gibberellins and abscisic acid in regulating germination of *Suaeda salsa* dimorphic seeds under salt stress. – Frontiers in Plant Science 6: 1-10.
[18] Lokhande, V. H., Nikam, T. D., Patade, V. Y., Ahire, M. L., Suprasanna, P. (2011): Effects of optimal and supra-optimal salinity stress on antioxidative defence, osmolytes

http://www.aloki.hu ● ISSN 1589 1623 (Print) ● ISSN 1785 0037 (Online)
DOI: http://dx.doi.org/10.15666/aeer/1706_1348513492

and *in vitro* growth responses in *Sesuvium portulacastrum* L. – Plant Cell, Tissue and Organ Culture 104: 41-49.

[19] Metwali, E. M. R., Hemaid, I. A. S., Al-Zahrani, H. S., Howlader, S. M., Fuller, M. P. (2014): Influence of different concentrations of salt stress on *in vitro* multiplication of some fig (*Ficus carica* L.) cultivars. – Life Science Journal 11: 386-397.

[20] Mudgal, V., Madaan, N., Mudgal, A. (2010): Biochemical mechanism of salt tolerance in plants: a review. – International Journal of Botany 6: 136-143.

[21] Murashige, T. and Skoog, F. (1962): A revised medium for rapid growth and bio assays with tobacco tissue cultures. – Physiologia Plantarum 15: 473-497.

[22] Nimbolkar, P. K., Shiva, B., Rai, A. K. (2016): Rootstock breeding for abiotic stress tolerance in fruit crops. – International Journal of Agriculture, Environment and Biotechnology (IJAEB) 9: 375-380.

[23] Parvaiz, A., Satyawati, S. (2008): Salt stress and phyto-biochemical responses of plants - a review. – Plant Soil and Environment 54: 89-99.

[24] Rahneshana, Z., Nasibi, F., Moghadam, A. A. (2018): Effects of salinity stress on some growth, physiological, biochemical parameters and nutrients in two pistachio (*Pistacia vera* L.) rootstocks. – Journal of Plant Interactions 13: 73-82.

[25] Rai, M. K., Kalia, R. K., Singh, R., Gangola, M. P., Dhawan, A. K. (2011): Developing stress tolerant plants through *in vitro* selection-an overview of the recent progress. – Environmental and Experimental Botany 71: 89-98.

[26] Shannon, M. C. (1978): Testing salt tolerance variability among tall wheat grass lines. – Agronomy Journal 70: 719-722.

[27] Shatnawi, M., Faouri, A., Al-Mazraawi, M., Shibli, R., Makhadmeh, I. (2009): Tissue culture and salt stress in *Chrysanthemum morifolium*. – Acta Horticulture 829: 189-196.

[28] Shibli, R. A., Kushad, M., Yousef, G. G., Lila, M. A. (2007): Physiological and biochemical responses of tomato microshoots to induced salinity stress with associated ethylene accumulation. – Plant Growth Regulation 51: 159-169.

[29] Singh, A., Sharma, D. K., Kumar, R., Kumar, A., Yadav, R. K., Gupta, S. K. (2018): Soil Salinity Management in Fruit Crops: A Review of Options and Challenges. – In: Gupta, S. K., Goyal, M. R., Singh, A. (eds.) Engineering Practices for Management of Soil Salinity: Agricultural, Physiological, and Adaptive Approaches. CRC Press, Apple Academic Press Inc. Waretown NJ.

[30] Soliman, H. I. A., Alhady, M. R. A. A. (2017): Evaluation of salt tolerance ability in some fig (*Ficus carica* L.) cultivars using tissue culture technique. – Journal of Applied Biology & Biotechnology 5: 29-39.

[31] Tal, M. (1994): *In vitro* selection for salt tolerance in crop plants: theoretical and practical considerations. – *In Vitro* Cellular & Developmental Biology-Plant 30: 175-180.

[32] Vijayan, K., Chakraborti, S. P., Ghosh, P. D. (2003): *In vitro* screening of mulberry (*Morus* spp.) for salinity tolerance. – Plant Cell Reports 22: 350-357.

[33] Yehia, T. A., AbdAllatif, A. M., Saleh, M. A. E. F., Elazab, R. M. (2018): *In vitro* evaluation of four fig cultivars grown under salinity stress. – Bioscience Research 15: 117-123.

[34] Yılmaz, E., Tuna, A. L., Bürün, B. (2011): Tolerance strategies developed by plants to the effects of salt stress. – C. B. U. Journal of Science 7: 47-66.

[35] Zaghdoudi, M., Baatour, O., Bensalem, N., Ouerghi Abidi, Z. (2015): Effect of saline conditions on germination and enzymatic activity in two varieties of *Linum usitatissimum* seeds. – Journal of New Sciences, Agriculture and Biotechnology 17: 629-638.

[36] Zarei, M., Azizi, M., Rahemi, M., Tehranifar, A. (2016): Evaluation of NaCl salinity tolerance of four fig genotypes based on vegetative growth and ion content in leaves, shoots, and roots. – HortScience 51: 1427-1434.

http://www.aloki.hu ● ISSN 1589 1623 (Print) ● ISSN 1785 0037 (Online)
DOI: http://dx.doi.org/10.15666/aeer/1706_1348513492

FATE OF IMPORTANT MEDICINAL PLANTS IN THE EASTERN HIMALAYA IN CHANGING CLIMATE SCENARIOS: A CASE OF *PANAX PSEUDOGINSENG* WALL.

KUMAR, D.[1*] – SINGH, M.[2] – SHARMA, S.[2]

[1]*G. B. Pant National Institute of Himalayan Environment & Sustainable Development, Sikkim Regional Centre, Pangthang, Gangtok 737101, Sikkim, India (phone: +91-359-223-7328)*

[2]*G. B. Pant National Institute of Himalayan Environment & Sustainable Development, Head Quarters, Kosi-Katarmal, Almora 263643, Uttarakhand, India*

**Corresponding author*
e-mail: devendrawii@gmail.com; phone: +91-800-137-3435

(Received 28th Aug 2017; accepted 25th Oct 2019)

Abstract. Monitoring the impact of climate change on forest ecosystems, particularly at the species level, can be currently observed in many parts of the world. In this study, Maxent species distribution modelling algorithm was used to predict the suitable habitat for the medicinally important species; *Panax pseudoginseng* in Sikkim Himalaya. The nineteen bioclimatic variables from Worldclim database were used to predict the current potential distribution. Representative Concentration Pathway (RCP) 4.5 and RCP 8.5 scenarios of IPCC 5th assessment was used for predicting the future distribution of species in 2050 and 2070. The Maxent model performed better than random with an average test AUC (Area under Curve) value 0.927 under the predicted current distribution. The projected distribution in future under the both RCPs scenarios showed upward shift of species (i.e., gain in suitable habitat area) in high elevation area over the years of 2050 and 2070. Areas with suitable climatic conditions predicted to decline by the 2050s and the 2070s under both RCP scenarios. The application of predictive Maxent modelling approach presented here may provide policymakers and conservationists, with a useful tool for prediction of species in future climate with only presence distribution records and therefore, can be an effective approach for species restoration and conservation actions.
Keywords: *Himalaya, climate change, conservation, Panax pseudoginseng, medicinal plants*

Introduction

Various components of a landscape (physical, biological and socio economic) are being affected by climate change, mostly along regional temperature changes where impacts due to changes in snow, ice and permafrost regions have influenced ground instability, enhanced glacial melt, enlargement and increase of glacial lakes in mountain regions, hence early and increased spring peak discharges in rivers (IPCC, 2014). Responses of species to impacts of climate change have been manifested in changes in phenology (Corlett et al., 1998; Settele et al., 2016), earlier onset of spring (Mohandass et al., 2015), migration process (Saltré et al., 2015), and lengthening of growing season (IPCC, 2014; Singh and Kushwaha, 2016). Changes in the abundance and distribution range of some species, changes in community composition, and local extinctions of species have been attributed to climate change (Davis and Shaw, 2001; Thomas et al., 2004; Moritz and Agudo, 2013; Maclean et al., 2015). The response of climate change on species distribution could be more rapid and expected to be faster in higher altitude areas, where species occur close to their physiological tolerance (Innes, 1991; Diaz and Bradely, 1997; Gratani, 2014). At regional scale these changes affects the natural

http://www.aloki.hu ● ISSN 1589 1623 (Print) ● ISSN 1785 0037 (Online)
DOI: http://dx.doi.org/10.15666/aeer/1706_1349313511

distribution of species, causing temporal reproductive isolation or even towards the extinction (Araujo et al., 2005; Schröter et al., 2005; Priti et al., 2016; Yi et al., 2016). To reduce the species extinction rates and conservation of its natural habitats in human dominated landscape, delineating protected areas are often the strategy by which conservation can be ensured. Species distribution models (SDMs) is useful in taking important decisions in developing conservation strategies particularly for poorly known or other species (Guisan and Thiller, 2005; Guisan et al., 2013; Cuyckens et al., 2016; de Siqueira et al., 2009; Kumar, 2012; Perez-Garcia et al., 2013; Khanum et al., 2013; Shrestha and Bawa, 2014; Sohel et al., 2016) by providing a strong predictive framework for identifying additional natural populations of species (Menon et al., 2010), and relocating the threatened population of species to natural suitable habitats (Adhikari et al., 2012).

The Himalayan region is experiencing warming at higher rate than the global average (three times high, 0.06 °C/year; Shrestha et al., 2012). Being a biodiversity hotspot region, Himalaya, and sensitivity towards climate change, information in this region is not adequate and limited to few studies on the aspects of response of species towards climate change (Saran et al., 2010; Kumar, 2012; Forrest et al., 2012; Telwala et al., 2013; Shrestha and Bawa, 2014; Manish et al., 2016). Therefore, this globally important region warrants more understanding on species response towards the climate changes and ecosystem functioning also due to its distinctive evolutionary history and rich species diversity (Pandit and Babu, 1998; Pandit et al., 2007).

Eastern Himalayan region has unique assemblage of endemic plant species and many of them are known for their medicinal values, and among them is *Panax pseudoginseng* Wall., also known as *Himalayan Ginseing* is a well known high value medicinal plant. The species is also one of the threatened plant species describes in Red Data Book of India (Nayar and Sastry, 1990). State of Sikkim in the Eastern part of Indian Himalayan region has 31% of the total geographical area under legal protection of protected area network through one National Park and seven Wildlife Sanctuaries which is much higher than the average of country (~4% of total geographical area). Whether the current situation of protected area network in Sikkim Himalaya would encompass the distribution of *P. pseudoginseng*, and what level of research and conservation strategies are required for protection and conservation to manage the natural habitats of *P. pseudoginseng* are key questions on the face of rapid climate changing scenario. In this rationale objectives of this study are: (1) to determine the important climatic variables that enhance prediction for *P. pseudoginseng* in current climatic situations, (2) to model the present predictive distribution range of *P. pseudoginseng* and potential future distribution under two climate change emission scenarios i.e., Representative Concentration Pathways (RCP 4.5 and RCP 8.5) for 2050 and 2070 year, and (3) to propose conservation strategies and management options under different scenarios.

Materials and methods

Study area

Sikkim State in Indian Himalayan Region (IHR) is located between 27°00'46" to 28°07'48" N latitudes and 88°00'58" to 88°55'25" E longitudes (*Fig. 1*). The State encompasses four districts (i.e., North Sikkim, East Sikkim, South Sikkim and West Sikkim) covering 7,096 km^2 geographical area. This mountainous state has - natural gradient of altitude ranging from 300 m to 8,586 m amsl. Biogeographically, Sikkim is

http://www.aloki.hu ● ISSN 1589 1623 (Print) ● ISSN 1785 0037 (Online)
DOI: http://dx.doi.org/10.15666/aeer/1706_1349313511

part of Eastern Himalayan region and has been categorized in two biogeographic zones (Trans Himalaya and Himalaya) of India (Rodgers et al., 2002) - Trans-Himalaya - Sikkim (1C) and Eastern Himalaya (2D). Broad representative vegetation types (Champion and Seth, 1968) of the Eastern Himalayan region of India are tropical moist deciduous, subtropical broad leaved forests, Broad leafed and conifer mixed forests, wet temperate forests, sub alpine forests, and alpine meadows (moist and dry alpine scrubs). Protected Area Network in the Sikkim includes seven Wildlife Sanctuaries (Shingba Rhododendron Sanctuary, Kyongnosla Alpine Sanctuary, Pangolakha Wildlife Sanctuary, Fambonglho Wildlife Sanctuary, Maenam Wildlife Sanctuary, Barsey Rhododendron Sanctuary and Kitam Bird Sanctuary), and one National Park (Khangchendzonga NP), covering a total area of 2183.1 km^2, which is 30.8% of the total geographical area of the State.

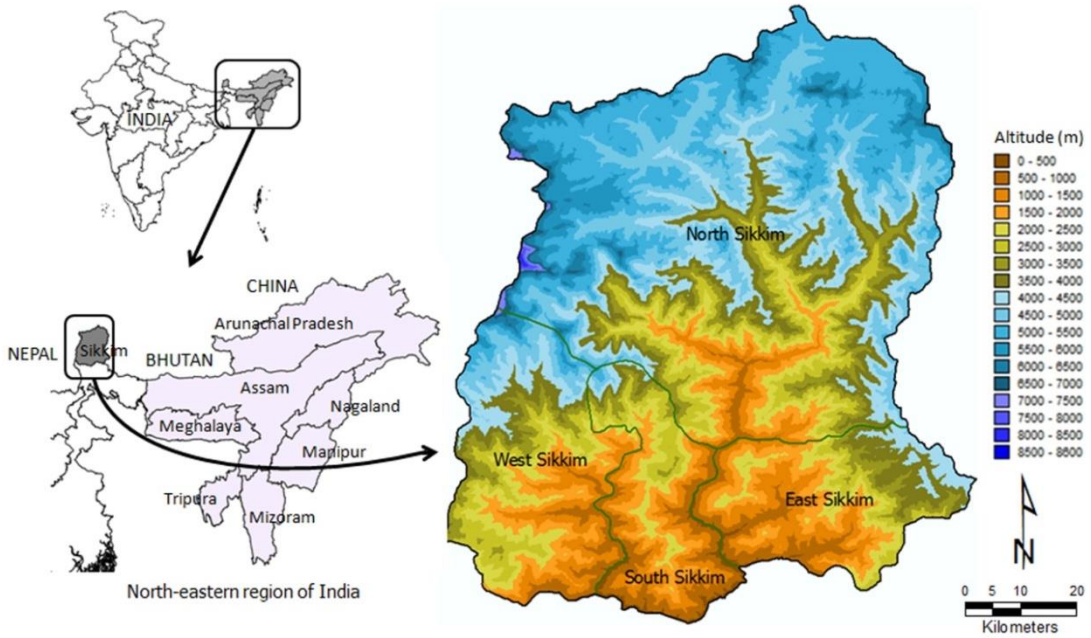

Figure 1. *Map of study area showing the districts and elevation gradients of Sikkim Himalaya*

Study species

Panax pseudoginseng Wall. (Araliaceae) [syn. *Aralia pseudoginseng* (Wall.) Benth. ex C.B. Clarke; *Aralia quinquefolia* Decne. & Planch. var. pseudoginseng (Wall.) Burkill; *Panax schinseng* var. *nepalensis* Nees; *Panax sikkimensis* R.N. Banerjee] is commonly known as *Himalayan Ginseng*, *Indian Ginseng* and *False Ginseng*. It is a perennial herb that grows up to 50 cm in height (Clarke, 1879). It is distributed in temperate zone of thick conifer-oak mixed and Himalayan birch forests where the soils has deep humus content. The species starts flowering during the months of May-June and fruiting during July-October. The flowers are terminal, unequal, umbellate and pale green or orange-yellow in colour. Its bear's dull green to black fruits measuring 3-5 mm with a black spot at the top part. Medicinally the Himalayan Ginseng is well-liked to known as elixir of life and its rhizomes uses for preparation of rejuvenating and revitalizing tonic. It is used to increase longevity, mental agility and to check hypertension. Locally it is used as a haemostatic for treating conditions such as

http://www.aloki.hu ● ISSN 1589 1623 (Print) ● ISSN 1785 0037 (Online)
DOI: http://dx.doi.org/10.15666/aeer/1706_1349313511

vomiting and coughing up of blood, blood in the urine or stool, bleeding nose and hemorrhagic disease.

Known habitats of *P. pseudoginseng* in this study are under sub-alpine zone between 3000 and 4000 m amsl, which comprises locations those remain moist for 8-9 months, and dry season for 3-4 months. A cold climate is normal for all the locations and dew, frosts or days under snow occur as regular events at some locations. The plant normally grows under shade and most abundantly under canopy of *Abies densa*, *Betula* spp., *Lithocarpus pachyphyllus* and *Rhododendron* spp., however, occasionally it can be found in open forests also.

Species presence data

Herbarium records of the species were analyzed from the collection of Botanical Survey of India, Sikkim Office. All the herbarium sheets (12 in number) were geo-referenced through location of collections on the maps, this was followed by field surveys and ten new locations were also recorded, thus leading to a total of 22 locations for current presence data. These locations were transferred to GIS platform using Arc GIS software.

Environmental predictors

Nineteen bioclimatic variables are available from WorldClim database (http://www.worldclim.org) at a resolution of approximately 1 km (Hijmans et al., 2005) was used for distribution modeling of *P. pseudoginseng*. These variables, derived principally from monthly temperature and precipitation data (*Table 1*), have proven relevance in modeling species distribution (Pearson and Dawson, 2003; Irfan-Ullah et al., 2007; Loiselle et al., 2008; Khanum et al., 2013). Intergovernmental Panel on Climate Change (IPCC) 5 data for future climate projection conditions for the years 2050s and 2070s were obtained from the Consultative Group on International Agricultural Research (CGIAR)'s Research Program on Climate Change, Agriculture and Food Security (CCAFS) climate data archive (http://www.ccafs-climate.org/) to project the potential distribution in future.

The future climatic projection datasets are based on of IPCC 5th assessment and were calibrated and downscaled using the current climatic data. Instead of using single global circulation model (GCM), we used data from three different global climate models for reducing the uncertainty. MRI-CGCM3, CSIRO-MK3.6 and HadGEM2-CC global climate models were selected for modeling the future prediction (Khanum et al., 2013; Barber, 2015; Dotchamou et al., 2016). Each GCM was tested under two future greenhouse gas concentration trajectories, called Representative Concentration Pathways (RCP) i.e., RCP 4.5 and RCP 8.5 for the periods 2050 and 2070. The RCP 4.5 ("intermediate stabilization pathways") was developed by Pacific Northwest National Laboratory's in the United States. It is relatively stable scenario in which total radiative forcing reaches 4.5 W/m^2 and stabilized shortly after 2100, without overshooting the long-run radiative forcing target level (Clarke et al., 2007; Smith and Wigley, 2006; Wise et al., 2009). The RCP 8.5 was developed by the International Institute for Applied System Analysis in Austria. It is characterized by increasing greenhouse gas emissions throughout the 21st century and radioactive forcing is predicted to reach up to 8.5 W/m^2 by 2100 (Riahi et al., 2007; Riahi et al., 2011). These two scenarios are being used by various workers to analyze impacts of climate change on predictive species

http://www.aloki.hu ● ISSN 1589 1623 (Print) ● ISSN 1785 0037 (Online)
DOI: http://dx.doi.org/10.15666/aeer/1706_1349313511

distribution modeling (Monahan et al., 2013; Shrestha and Bawa, 2014; Li et al., 2015; Kang et al., 2016; Sohel et al., 2016; York et al., 2016). For future potential distribution predictions of *P. pseudoginseng*, we ran separate models (*Appendix*) and also by averaging the results (ensemble approach) from the CGCM3, CSIRO-MK3 and HadGEM2-CC future climate models (Araujo and New, 2007).

Table 1. *Percentage contribution (average of over twenty replicate runs) and permutation importance of the climatic variables in the Maxent models for Panax pseudoginseng*

Climatic variable	Code	Unit	Percentage contribution	Permutation importance
Annual mean temperature [AMT]	Bio1	°C	-	-
Mean diurnal range temperature {Mean of monthly (max temp - min temp)}[MDRT]	Bio2	°C	-	-
Isothermality (Bio2/Bio7) (* 100) [ISO]	**Bio3**		0.1	0.3
Temperature seasonality (Standard deviation *100) [TS]	Bio4		-	-
Maximum temperature of warmest month [MTWM]	Bio5	°C	-	-
Minimum temperature of coldest month [MTCM]	Bio6	°C	-	-
Temperature annual range (Bio5-Bio6) [TAR]	**Bio7**	°C	0.8	0.0
Mean temperature of wettest quarter [MTWQ]	Bio8	°C	-	-
Mean temperature of driest quarter [MTDQ]	Bio9	°C	-	-
Mean temperature of warmest quarter [MTWAQ]	**Bio10**	°C	8.5	21.9
Mean temperature of coldest quarter [MTCQ]	**Bio11**	°C	25.6	76.6
Annual precipitation [AP]	Bio12	mm	-	-
Precipitation of wettest month [PWM]	Bio13	mm	-	-
Precipitation of driest month [PDM]	Bio14	mm	-	-
Precipitation seasonality (Coefficient of variation) [PS]	**Bio15**		60.2	0.7
Precipitation of wettest quarter [PWQ]	Bio16	mm	-	-
Precipitation of driest quarter [PDQ]	Bio17	mm	-	-
Precipitation of warmest quarter [PWAQ]	**Bio18**	mm	4.8	0.6
Precipitation of coldest quarter [PCQ]	Bio19	mm	-	-

Predictive Maxent modeling

For the prediction modelling, maximum entropy based technique i.e., Maxent ver. 3.3.3k (http://www.cs.princeton.edu/~schapire/Maxent/) was chosen due to its better performance with small sample sizes relative to other modelling algorithms (Elith et al., 2006). This programme attempts to estimate a species distribution by finding the probability distribution of species occurrence i.e., closest to uniform subject to the constraint that the mean environmental conditions by the model should be close to the empirical average of the conditions at the presence localities (Phillips et al., 2006; Phillips and Dudik, 2008; Elith et al., 2011).

A total of twenty replicate runs were set for model building and averaged the result. In the replicated runs the cross validation technique was used, where samples divided into replicate folds and each fold was used for test data. Jackknife test and percent variable contributions were used to estimates the relative influence of different predictor variables, which estimate the training gain of every variable and recommend the best interpreter for the prediction of distribution of species. The AUC (area under curve), area under the ROC (Receiver Operating Characteristics) curve, was used to evaluate model performance. However, ROC AUC provides a threshold-independent measure of model performance compared to that of null expectations, such should provides an overall picture of the predictive nature of models (Stockwell and Peterson, 2002;

http://www.aloki.hu ● ISSN 1589 1623 (Print) ● ISSN 1785 0037 (Online)
DOI: http://dx.doi.org/10.15666/aeer/1706_1349313511

Fawcett, 2006). An AUC statistic closer to 0.5, indicates that model did not perform better than random whereas closer to 1.0, indicates perfect discrimination (Swets, 1988). Araujo et al. (2005) recommended the following interpretation of AUC for the models generated, viz., excellent if AUC > 0.90; Good if 0.80 > AUC < 0.90; Acceptable if 0.70 > AUC < 0.80; Bad if 0.60 > AUC < 0.70; Invalid if 0.50 > AUC < 0.60.

The multi-collinearity test was conducted using pairwise Pearson's correlation coefficient (r) to examine the cross-correlation among the climatic variables using the ENM tool (Warren et al., 2010). The variables with cross-correlation coefficient value of $\geq +0.90$ were excluded from the analysis (see *Table A1* in the *Appendix*). Based on such criterion, 13 bioclimatic variables were excluded and only 6 bioclimatic variables were used in the final model to predict the effect of climate change on the future distribution of *P. pseudoginseng*. For validating the model robustness a 10 percentile training presence threshold rule was executed over a twenty replicated model runs (Pearson et al., 2004). Other parameters were set to default as the program is already calibrated on a wide range of species datasets as suggested by Phillips and Dudik (2008). To avoid erroneous predictions of suitable habitat under future climate scenarios for 2050 and 2070 'fade by clamping' option was used in Maxent, which removes heavily clamped pixels from the final predictions (Fielding and Bell, 1997; Phillips et al., 2006). For each of the three habitat models, including the current *P. pseudoginseng* potential distribution and the two future predictions under the RCP scenarios (2050 and 2070), we calculated the total area of habitats, and amounts of stable/no change (areas of the current potential range predicted to remain suitable), unsuitable, lost (areas not predicted to remain suitable in future), and gained habitats (areas that are predicted to be suitable future that are not currently suitable) areas for each of the two future models under 2050 and 2070 years.

Results

The selected climatic variables, 6 in number, provided a satisfactory prediction of the potential current distribution of species (*P. pseudoginseng*) evident by mean test AUC value of 0.927 ± 0.043, and considered excellent (Araujo et al., 2005). Amongst these climatic variables, precipitation seasonality (PS) and mean temperature of coldest quarter (MTCQ) appeared significant for the occurrence of the species (collectively contributed to 85.8% of the model's variance; *Table 1*) indicating role of moisture and cold environment as apparent by contribution of Mean temperature of warmest quarter (MTWAQ) and precipitation of warmest quarter (PWAQ). Temperature annual range (TAR) and isothermality (ISO) made the lowest contribution to the predictive model. Considering the permutation importance, MTCQ had the maximum influence on model and contributed to 76.6%, followed by mean temperature of warmest quarter (MTWAQ), i.e., 21.9% (*Table 1*). Climatic profiles (based on the occurrence records; minimum, maximum and mean value of nineteen current climatic variables) for the species under investigation are presented in *Table 2*.

The current suitable habitats for *P. pseudoginseng,* covering 14.4% of the total geographical area, are confined to mainly in central part of North Sikkim district, north-eastern part of East Sikkim district, north-western part of West Sikkim district, with some patches in northern part of South Sikkim district (*Fig. 2a*). The Jackknife test estimated the training gains of each predictor variable, when a variable is used in separation, when it is excluded, and when all variables are utilized. The graph of

http://www.aloki.hu ● ISSN 1589 1623 (Print) ● ISSN 1785 0037 (Online)
DOI: http://dx.doi.org/10.15666/aeer/1706_1349313511

Jackknife predictor test indicates that the MTCQ and PS as main factors influencing the distribution pattern and has highest training gain (*Fig. 3a*). The response curve of *P. pseudoginseng* showed that the predicted habitat suitability area was initially increased sharply with increasing PS and was bell shaped with MTCQ (*Fig. 3b, c*). Areas with suitable climatic conditions for *P. pseudoginseng* are predicted to decline by the 2050s and the 2070s under both RCP scenarios. Averaged future predictions from three climatic models under an intermediate scenario (RCP 4.5) of 2050 showed loss of suitable area (190.88 km^2; 2.69%); while further loosing the suitable habitat area over the year 2070 (266.1 km^2; 3.75%) (*Fig. 2b, c; Table 3*). The loss of suitable habitat area in average model of RCP 4.5 scenario was predicted mainly in patches form of northern part of West Sikkim and central parts of North Sikkim districts for year 2050, whereas in 2070 the loss predicted continuously over the north-western part of West Sikkim, northern part of South Sikkim, north-eastern part of East Sikkim and, central and north-eastern part of North Sikkim districts (*Fig. 2b, c*). Conversely, in higher scenario (RCP 8.5) the loss of suitable habitat areas was predicted continuously in northern part of West and South Sikkim districts, and in patches form of north-eastern parts of North and East Sikkim districts for year 2050, whereas in 2070 the loss predicted continuously over the entire four districts of Sikkim (*Fig. 2d, e*). However, the loss of suitable area predicted under a RCP 8.5 was more than RCP 4.5 for 2050 (307.26 km^2; 4.3%), which further continuously lost predicted suitable habitat over the year of 2070 (63,509 km^2; 8.95%) (*Fig. 2d, e; Table 3*). Those scenarios also decreased the number of suitable patches (i.e. no change/stable) in RCPs 4.5 by 8.21% to 7.51% and RCP 8.5 by 6.57% to 1.95%, over the years 2050 to 2070 respectively. Another common feature for projected distribution in future climate models under the both RCPs scenarios (4.5 and 8.5), was the upward shift of species (i.e., gain in suitable habitat area) in high elevation area over the years of 2050 and 2070.

Table 2. *Climatic profile of Panax pseudogensing based on herbarium and presence records*

Climatic variable	Code	Unit	Min.	Max.	Mean	SD
Annual mean temperature [AMT]	Bio1	°C	3.1	8.2	4.9	1.6
Mean diurnal range temperature {Mean of monthly (max temp - min temp)}[MDRT]	Bio2	°C	9.6	13.0	12.1	1.0
Isothermality (Bio2/Bio7) (* 100) [ISO]	Bio3		45.0	47.0	45.8	0.6
Temperature seasonality (Standard deviation *100) [TS]	Bio4		4271.0	5561.0	5167.5	380.2
Maximum temperature of warmest month [MTWM]	Bio5	°C	14.3	18.3	15.8	1.3
Minimum temperature of coldest month [MTCM]	Bio6	°C	-13.1	-4.0	-10.3	2.5
Temperature annual range (Bio5-Bio6) [TAR]	Bio7	°C	21.1	28.2	26.2	2.1
Mean temperature of wettest quarter [MTWQ]	Bio8	°C	9.4	13.3	11.0	1.3
Mean temperature of driest quarter [MTDQ]	Bio9	°C	-3.2	3.2	-1.1	1.8
Mean temperature of warmest quarter [MTWAQ]	Bio10	°C	9.4	13.3	11.0	1.3
Mean temperature of coldest quarter [MTCQ]	Bio11	°C	-4.2	2.2	-2.1	1.9
Annual precipitation [AP]	Bio12	mm	626.0	1400.0	806.0	211.7
Precipitation of wettest month [PWM]	Bio13	mm	126.0	319.0	168.6	51.9
Precipitation of driest month [PDM]	Bio14	mm	3.0	9.0	5.3	1.7
Precipitation seasonality (Coefficient of variation) [PS]	Bio15		73.0	90.0	81.4	5.8
Precipitation of wettest quarter [PWQ]	Bio16	mm	340.0	818.0	449.8	132.0
Precipitation of driest quarter [PDQ]	Bio17	mm	20.0	49.0	28.1	8.7
Precipitation of warmest quarter [PWAQ]	Bio18	mm	340.0	818.0	449.8	132.0
Precipitation of coldest quarter [PCQ]	Bio19	mm	30.0	62.0	40.1	9.7

http://www.aloki.hu ● ISSN 1589 1623 (Print) ● ISSN 1785 0037 (Online)
DOI: http://dx.doi.org/10.15666/aeer/1706_1349313511

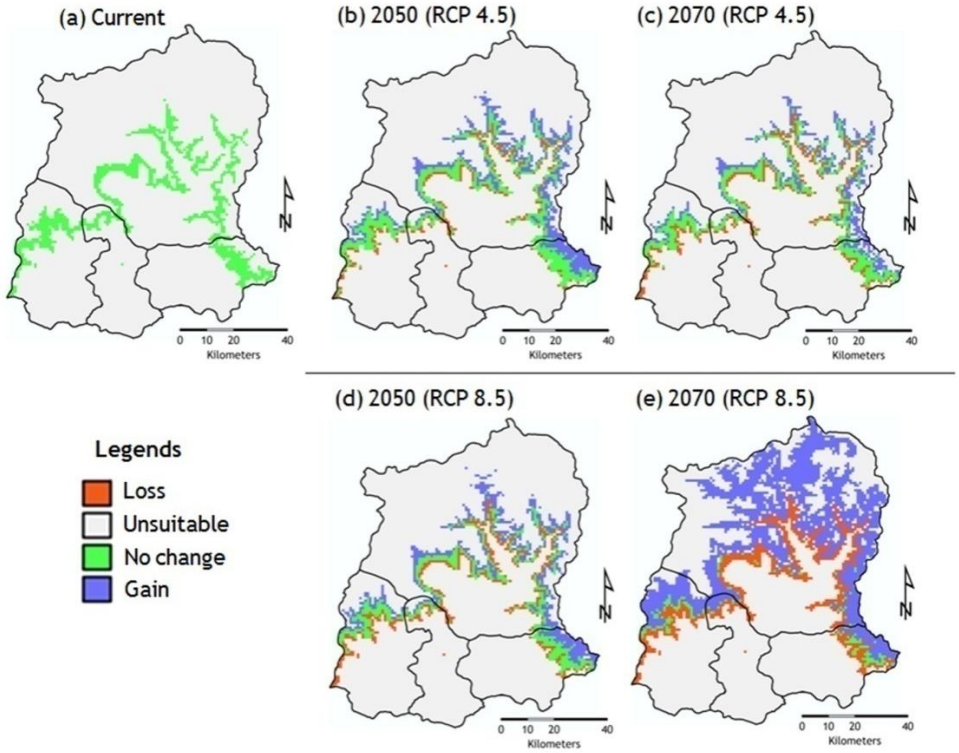

Figure 2. *Predicted (a) current and (b-e) future (Suitable/no change, loss, gain and unsuitable) habitats of P. pseudoginseng for the years 2050 and 2070, under RCP 4.5 and RCP 8.5 climate change scenarios*

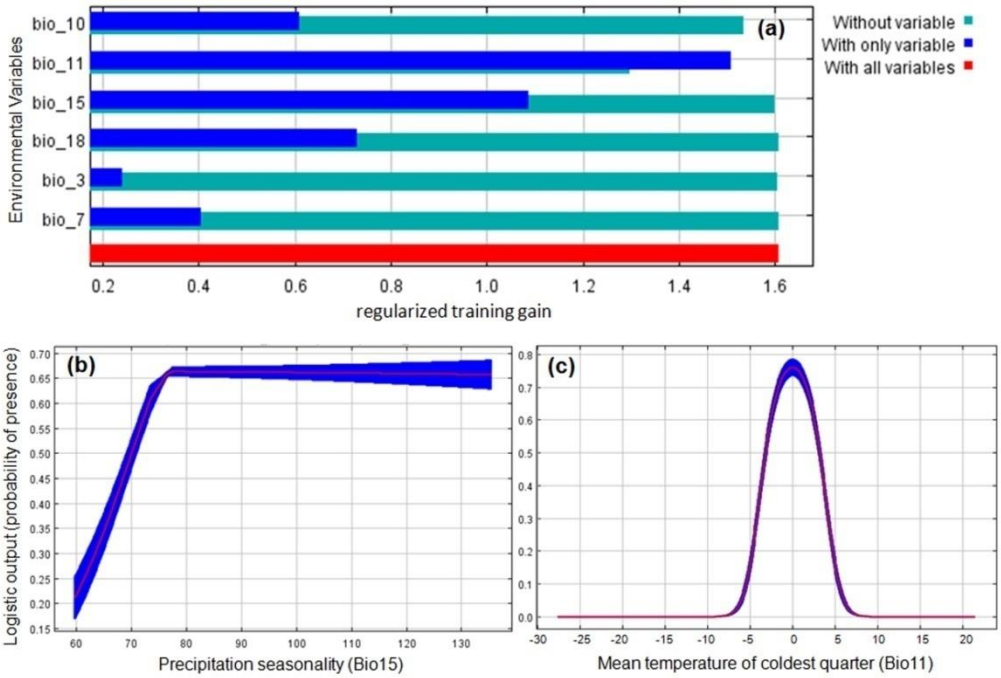

Figure 3. *(a) Jackknife regularized training gain, showing the relative predictive power of bioclimatic variable; and (b) response curves showing the relationships between probability of presence of a species and climatic variables. (Values shown are average of twenty replicate run)*

http://www.aloki.hu ● ISSN 1589 1623 (Print) ● ISSN 1785 0037 (Online)
DOI: http://dx.doi.org/10.15666/aeer/1706_1349313511

Table 3. *Predicted suitable habitat areas for P. pseudogensing under each climate change scenarios*

Classes	Area (km^2)					Area (%)				
	Current	RCP 4.5		RCP 8.5		Current	RCP 4.5		RCP 8.5	
		2050	2070	2050	2070		2050	2080	2050	2070
Suitable/No change	1,025	582.58	507.36	466.21	138.37	14.44	8.21	7.15	6.57	1.95
Loss		190.88	266.10	307.26	635.09		2.69	3.75	4.33	8.95
Gain		491.04	374.67	510.91	1871.92		6.92	5.28	7.20	26.38
Unsuitable		5,831.49	5,947.87	5,811.62	4,450.61		82.18	83.82	81.90	62.72

Discussion

The modelling result suggests that the suitable habitat area for *Panax pseudoginseng* (*Himalayan Ginseng*) would shrink under the predicted levels of climate change in future. The Maxent model performed better than random, with satisfactory mean test AUC value. Maxent predicted the upward shifts of (i.e., more than 4000 m high elevated zones) *P. pseudoginseng* suitable area under the both intermediate and high scenarios, with greater risk of habitat loss from current suitable predicted areas in Sikkim Himalaya. Field observation suggest the *Himalayan Ginseng* is highly dependent on local climates, the plant thrives only when there is moist soil humus content at places ranging between 3000-4000 m elevations, due to this the species has confined distribution in eastern Himalayan region of India. Maxent model result shows, predicted suitable habitat area under the current climatic condition would become unsuitable in predicted future climate change scenarios, resulting in local extinction of the species.

Considering climate sensitive plants, the seasonality (such as temperature, rainfall, humidity, soil temperature, soil moisture content and day length) expose them to regular periodic changes in the quality and abundance of resources (Franklin et al., 1992). All of these factors are known to play a role, only or in combination with, in triggering the phenological or physiological changes. Some species may be capable of adapting to future climatic condition through phenological changes (such as early or late flowering/fruiting) or through adaptation towards microclimate conditions responsible for survival of its natural population. In this investigation, *Himalayan Ginseng* showed the range expansions of suitable habitat towards higher elevated zones in future climate change scenarios, which may be to make possible through adaptation towards the changes in local climatic condition. Khanum et al. (2013) showed similar results of adaptation and range expansion of species for predicting the impact of climate change of three important medicinal asclepiads in Pakistan. Midgley et al. (2006) suggested that, in predicting the impact of climate changes on plant species the dispersal of seed is also a regulating factor for adaptation of species. A study across twenty-six mountains in Switzerland demonstrated that, the alpine flora expanded their ranges upward towards the peaks (Grabherr et al., 1994; Pauli et al., 1996) and a similar study by Moiseev and Shiyatov (2003) showed the upward movement of treelines in Siberia.

While generalizing the ecosystem responses towards the rapid warming in the Himalayan region, Singh et al. (2010) have reported that the woody species of higher elevated zones have began to invade the alpine meadows, and result in a complex series of changes in ecosystem functioning process with involvement of the soil subsystems. Another hypothesis is the future exploitations pressure on this plant species will make coping difficult against the climate changes and this could cause the extinction of this species despite good showing in the current and future climate suitable habitats (Svenning et al.,

http://www.aloki.hu ● ISSN 1589 1623 (Print) ● ISSN 1785 0037 (Online)
DOI: http://dx.doi.org/10.15666/aeer/1706_1349313511

2009). The present study shows that *Himalayan Ginseng* is threatened under the predicting climate change scenarios in Sikkim, Himalaya; a similar kind of results have been reported from another studies for economically important species, viz., studies on Baobab trees by Sanchez et al. (2011); on medicinal Asclepiads in Pakistan by Khanum et al. (2013); on Caterpiller fungus in Nepal by Shrestha and Bawa (2014) and on *Dysoxylum binectariferum* by Sohel et al. (2016) in northeastern part of Bangladesh. Another parameter such as soil and land transformations would also become the contributing factor for predicting the species response in climate change (Pearson and Dawson, 2005), but the present study did not incorporate these parameters, due to unavailability of datasets.

Species with known economic importance value experiences pressures, (i.e., loss of natural habitats from climate change events, changes in landuse and land cover patterns, and overexploitation) because of their known utility (Pandit et al., 2007). These threats adversely affect natural plant resources in Himalayan region of India. The high medicinal important is responsible for their extraction from the wild which has already reduced the population sizes of *Himalayan Ginseng* in the natural population (Pandit and Babu, 1998). Loss of natural habitats due to deforestation, developmental works and expansion of agricultural practices have driven many of the endemic and medicinally important plant species to the brink of extinction in Himalaya region (Pandit et al., 2007). The *Himalayan Ginseng* is already listed as threatened taxa in the Red Data Book of India (Nayar and Sastry, 1990). On regional scale the climate change is one of the greatest challenges for conserving the biodiversity and forests ecosystems. Changes have already reported in different region, including impact of change on plant biodiversity in Europe (Thuiller et al., 2005), plant species vulnerability to climate change in Peninsular Thailand (Trisurat et al., 2011), declines of woody plant species ranges under climate change in Yunnan, China (Zhang et al., 2014) and extinction of freshwater swamp forest trees (*Pongamia pinnata* and *Barringtonia acutangula*) of Bangladesh in climate change scenarios (Deb et al., 2016).

Conservation of natural plant resources at species level has often failed owing to lack of proper knowledge of the target species in term of habitat suitability. The application of Ecological Niche Models (ENMs) to extract simple inventory data (such as presence records of species) may provide predictions of species under changing climates at both regional and local scale, and the models may be used to make recommendations for policymakers and conservationists in dealing with potential climate change (Sanchez et al., 2011). Here, we used the maximum entropy based modelling techniques, as implemented in the ENM software Maxent (Phillips et al., 2006; Elith et al., 2006, 2011), to summarize the climatic niche of the *Himalayan Ginseng* to predict changes in climate change emission scenarios. Maxent accounts for some consequences, for example, it does not estimate the probability of occurrence directly, but rather the environmental suitability for the species that can be mapped in a geographic space (Royle et al., 2012). Considerably, it is the most widely used and has good predictive power capabilities (Elith et al., 2006). Maxent have been used extensively for investigating plant and animal responses to climate change (Trisurat et al., 2011; Chitale and Behera, 2012; Khanum et al., 2013; Kumar, 2013; Shrestha and Bawa, 2014; Alamgir et al., 2015; Cuyckens et al., 2016; Sohel et al., 2016).

Conservation strategies

Considering the results in this study by predictive Maxent modelling on distribution of *Himalayan Ginseng* in Sikkim Himalaya, there will be moderate to high impacts under the future climate change scenarios. The most of suitable habitat area predicted for this plant

http://www.aloki.hu ● ISSN 1589 1623 (Print) ● ISSN 1785 0037 (Online)
DOI: http://dx.doi.org/10.15666/aeer/1706_1349313511

species might already be devoid of populations due to transformation of landuse, and overexploitations by local people for economic gain. A recent investigation on predicting the impact of climate change on a tree species (*Dysoxylum binectariferum*) in north-eastern part of Bangladesh by Sohel et al. (2016) suggested that the combined effect of human induced anthropogenic factors and change in climate condition in future will increase the extent of unsuitable habitat for the plant. Therefore, successful management plan for conserving the natural population in human dominated landscape is needed which can be used to address the issues and generate connectivity across protected areas (Urbina-Cardona and Flores-Villela, 2010). Besides designating a new protected area, the existing protected areas should have successful management plan for conservation and restoration of key species. These management plans should consider ecotourism, restriction of grazing, firewood collection and forest fire, involving the field researchers, NGOs and local communities. The subtropical to temperate and alpine areas of Sikkim is of special conservation interest as it is also suitable area for the conservation of key species such as the Snow Leopard (Sathyakumar et al., 2011b; Forrest et al., 2012), Red Panda (Ghose et al., 2011), Rhododendrons (Kumar, 2012) and for Galliformes (Sathyakumar et al., 2011a) in different protected area of Sikkim. This is also the area where *Himalayan Ginseng* exhibits the highest generic diversity (Sharma and Pandit, 2011).

Another possible conservation strategy for *Himalayan Ginseng*, especially for areas at high risk of habitat loss, e.g., in Pangolakha Wildlife Sanctuary and Barsey Rhododendron Sanctuary (*Fig. 2*), could be compensated by ex situ germplasm collection and micropropagation techniques, as suggested by Sanchez et al. (2011) for Baobab trees in Africa. Moreover, results of habitat loss do not necessarily suggest extinction but certainly increase the local extinction risk (Alarcón and Cavieres, 2015). The Convention on Biodiversity (CBD) suggested that a minimum representation of species habitat at ecosystem level should be under protection between 10-12% (Burgess et al., 2005; Tear et al., 2005), or 17% for terrestrial ecosystems (Moilanen et al., 2013). In this study, the current network of PAs accomplishes and even surpasses this suggestion area (at 30.8%) where, most of the natural population of *Himalayan Ginseng* are growing (*Fig. 4*). *Table 4* showed the area statistics of predicted potential habitats for *Himalayan Ginseng* in current climatic condition under different PAs network of Sikkim. The most effective strategy for protecting the *Himalayan Ginseng* viable populations in the areas of suitable future habitat is through conservation or sustainable utilization (Sanchez et al., 2011). For example, if local peoples are made aware that they may reap higher economic benefits from this plant left in their natural habitat than if grown as a crop this change in priority of action would yield better conservation outcome for the *Himalayan Ginseng*.

Table 4. *Present projection of suitable habitat area of P. pseudogensing in different PAs of Sikkim*

Protected area		**Predicted potential area habitat for *P. pseudogensing***	
Name	**Area (km^2)**	**km^2**	**%**
Khangchendzonga National Park	1784.00	290.46	16.28
Shingba Rhododendron Sanctuary	43.00	18.77	43.65
Kyangnosla Alpine Sanctuary	31.00	18.71	60.35
Pangolakha Wildlife Sanctuary	128.00	36.55	28.55
Maenam Wildlife Sanctuary	35.34	0.56	1.58
Barsey Rhododendron Sanctuary	104.00	8.60	8.27
Total	**2125.34**	**373.65**	**17.58**

http://www.aloki.hu ● ISSN 1589 1623 (Print) ● ISSN 1785 0037 (Online)
DOI: http://dx.doi.org/10.15666/aeer/1706_1349313511

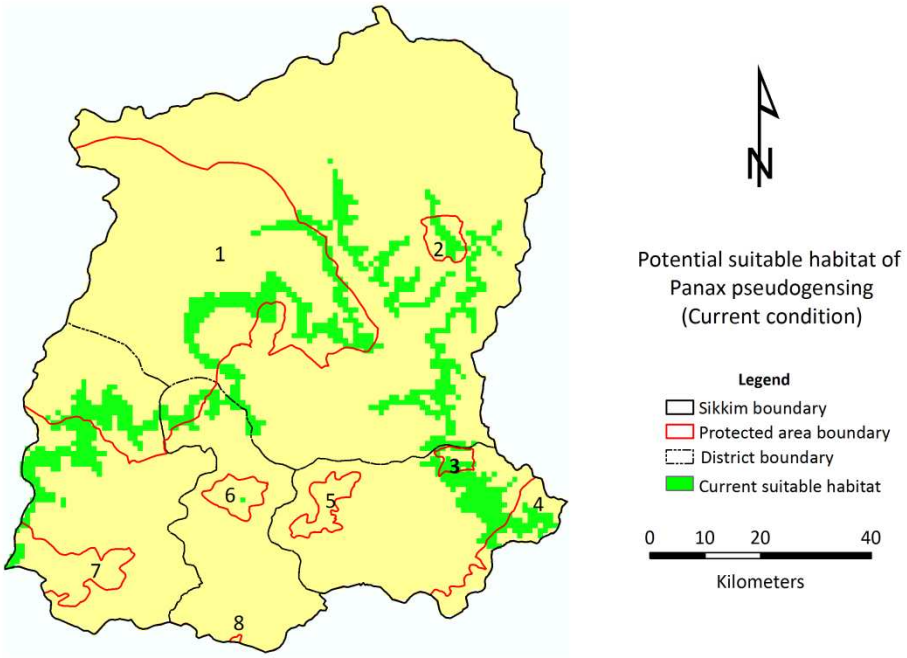

Figure 4. *Predicted current potential habitat of P. pseudogensing overlaid on existed protected areas (red color lines) networks of Sikkim Himalaya. (1: Khangchendzonga National Park; 2: Shingba Rhododendron Sanctuary; 3: Kyangnosla Alpine Sanctuary; 4: Pangolakha Wildlife Sanctuary; 5: Fambunglho Wildlife Sanctuary; 6: Maenam Wildlife Sanctuary; 7: Barsey Rhododendron Sanctuary; 8: Kitam Bird Sanctuary)*

Acknowledgments. The facilities provided by the Director, G.B. Pant National Institute of Himalayan Environment and Sustainable Development, Uttarakhand are gratefully acknowledged. This research did not receive any specific grant from funding agencies in the public, commercial, or not-for-profit sectors. The authors are also thankful to the Scientist In-charge, Botanical Survey of India, Sikkim Himalayan Circle, for providing information and providing access to the herbarium specimens.

REFERENCES

[1] Adhikari, D., Barik, S. K., Upadhaya, K. (2012): Habitat distribution modelling for reintroduction of *Ilex khasiana* Purk., a critically endangered tree species of northeastern India. – Ecological Engineering 40: 37-43.

[2] Alamgir, M., Mukul, S. A., Turton, S. M. (2015): Modelling spatial distribution of critically endangered Asian elephant and Hoolock gibbon in Bangladesh forest ecosystems under a changing climate. – Applied Geography 60: 10-19.

[3] Alarcón, D., Cavieres, L. A. (2015): In the right place at the right time: habitat representation in protected areas of South American Nothofagus-dominated plants after a dispersal constrained climate change scenario. – PLoS One 10: e0119952.

[4] Al-Qaddi, N., Vessella, F., Stephan, J., Al-Eisawi, D., Schirone, B. (2016): Current and future suitability areas of kermes oak (*Quercus coccifera* L.) in the Levant under climate change. – Regional Environmental Change 17: 143-156.

[5] Araujo, M. B., New, M. (2007): Ensemble forecasting of species distribution. – Trends in Ecology and Evolution 22: 42-47.

[6] Araujo, M. B., Pearson, R. G., Thuiller, W., Erhard, M. (2005): Validation of species-climate impact models under climate change. – Global Change Biology 11: 1504-1513.

http://www.aloki.hu ● ISSN 1589 1623 (Print) ● ISSN 1785 0037 (Online)
DOI: http://dx.doi.org/10.15666/aeer/1706_1349313511

[7] Barber, Q. E. C. (2015): Assessing the vulnerability of rare plants using climate change velocity, habitat connectivity and dispersal ability. – Ph.D Thesis, University of Alberta.
[8] Buisson, L., Thuiller, W., Casajus, N., Lek, S., Grenouillet, G. (2010): Uncertainty in ensemble forecasting of species distribution. – Global Change Biology 16: 1145-1157.
[9] Burgess, N., Küper, W., Mutke, J., Brown, J., Westaway, S., Turpie, S., Meshack, C., Taplin, J., McClean, C., Lovett, J. C. (2005): Major gaps in the distribution of protected areas for threatened and narrow range Afrotropical plants. – Biodiversity and Conservation 14: 1877-1894.
[10] Champion, H. G., Seth, S. K. (1968): A Revised Survey of the Forest Types of India. – Government of India, New Delhi.
[11] Chitale, V. S., Behera, M. D. (2012): Can the distribution of sal (*Shorea robusta* Gaertn. f.) shift in the northeastern direction in India due to changing climate? – Current Science 102: 1126-1135.
[12] Clarke, C. B. (1879): Aralia L. – In: Hooker, J. D. (ed.) Flora of British India. Vol II. Reeve and Co., London, pp 721-722.
[13] Clarke, L. E., Edmonds, J. A., Jacoby, H. D., Pitcher, H., Reilly, J. M., Richels, R. (2007): Scenarios of Greenhouse Gas Emissions and Atmospheric Concentrations. Sub-report 2.1a of Synthesis and Assessment Product 2.1. – Climate Change Science Program and the Subcommittee on Global Change Research, Washington, DC.
[14] Corlett, R. T., Lafrankie, Jr. J. V. (1998): Potential impacts of climate change on tropical Asian forests through an influence on phenology. – Climate Change 39(2): 439-453.
[15] Cuyckens, G. A. E., Christie, D. A., Domic, A. I., Malizia, L. R., Renison, D. (2016): Climate change and the distribution and conservation of the world's highest elevation woodland in the South American Altiplano. – Global and Planetary Change 137: 79-87.
[16] Davis, M. B., Shaw, R. G. (2001): Range shifts and adaptive responses to Quaternary climate change. – Science 292(5517): 673-679.
[17] de Siqueira, M. F., Durigan, G., de Marco Júnior, P., Peterson, A. T. (2009): Something from nothing: using landscape similarity and ecological niche modeling to find rare plant species. – Journal for Nature Conservation 17(1): 25-32.
[18] Deb, J. C., Rahman, H. T., Roy, A. (2016): Freshwater swamp forest trees of Bangladesh face extinction risk from climate change. – Wetlands 36(2): 323-334.
[19] Diaz, H. F., Bradley, R. S. (1997): Temperature variations during the last centaury at high altitude elevation sites. – Climate Change 36: 253-279.
[20] Dotchamou, F. T., Atindogbe, G., Sode, A. I., Fonton, H. N. (2016): Density and spatial distribution of *Parkia biglobosa* pattern in Benin under climate change. – Journal of Agriculture and Environment for International Development 110(1): 173-194.
[21] Dowling, C. R. (2015): Using Maxent modeling to predict habitat of mountain Pine Beetle in response to climate change. – Ph.D. Thesis, University of Southern California.
[22] Elith, J., Graham, C. H., Anderson, R. P., Dudik, M., Ferrier, S., Guisan, A., Hijmans, R. J., Huettmann, F., Leathwick, J. R., Lehmann, A., Li, J., Lohmann, L. G., Loiselle, B. A., Manion, G., Moritz, C., Nakamura, M., Nakazawa, Y., Overton, J. M., Peterson, A. T., Phillips, S. J., Richardson, K., Scachetti-Pereira, R., Schapire, R. E., Soberon, J., Williams, S., Wisz, M. S., Zimmermann, N. E. (2006): Novel methods improve prediction of species distribution from occurrence data. – Ecography 29: 129-151.
[23] Elith, J., Phillips, S., Hastie, T., Dudik, M., Chee, Y. E., Yates, C. J. (2011): A statistical explanation of Maxent for ecologists. – Diversity and Distributions 17: 43-47.
[24] Fawcett, T. (2006): An introduction to ROC analysis. – Pattern Recognition Letters 27: 861-874.
[25] Fielding, A. H., Bell, J. F. L. (1997): A review of methods for the assessment of prediction errors in conservation presence/absence models. – Environmental Conservation 24(1): 38-49.
[26] Forrest, J. L., Wikramanayake, E., Shrestha, R., Areendran, G., Gyeltshen, K., Maheshwari, A., Mazumdar, S., Naidoo, R., Thapa, G. J., Thapa, K. (2012): Conservation

http://www.aloki.hu ● ISSN 1589 1623 (Print) ● ISSN 1785 0037 (Online)
DOI: http://dx.doi.org/10.15666/aeer/1706_1349313511

and climate change: assessing the vulnerability of snow leopard habitat to treeline shift in the Himalaya. – Biological Conservation 150: 129-135.

[27] Franklin, J., Swanson, F., Harmon, M., Perry, D., Spies, T., Dale, V., McKee, A., Ferrell, W., Means, J., Gregory, S., Lattin, J., Schowalter, T., Walter, D. (1992): Effects of Global Climatic Change on Forests in Northwestern North America. – In: Peters, R. L., Lovejoy, T. E. (eds.) Global Warming and Biological Diversity. Yale University Press, New Haven, CT, pp. 244-257.

[28] Ghose, P. S., Sharma, B., Chakraborty, R., Legshey, K. (2011): Status of Red Panda in Sikkim: A Case Study in East Sikkim. – In: Arrawatia, M. L., Tambe, S. (eds.) Biodiversity of Sikkim - Exploring and Conserving a Global Hotspot. Information and Public Relations Department, Government of Sikkim, Gangtok, India, pp. 363-378.

[29] Grabherr, G., Gottfried, M., Pauli, H. (1994): Climate effects on mountain plants. – Nature 369: 448.

[30] Gratani, L. (2014): Plant phenotypic plasticity in response to environmental factors. – Advances in Botany. http://dx.doi.org/10.1155/2014/208747.

[31] Guisan A., Thuiller, W. (2005): Predicting species distribution: offering more than simple habitat models. – Ecology Letters 8: 993-1009.

[32] Guisan, A., Tingley, R., Baumgartner, J. B., Naujokaitis-Lewis, I., Sutcliffe, P. R., Tulloch, A. I. T., Regan, T. J., Brotons, L., McDonald-Madden, E., Mantyka-Pringle, C., Martin, T. G., Rhodes, J. R., Maggini, R., Setterfield, S. A., Elith, J., Schwartz, M. W., Wintle, B. A., Broennimann, O., Austin, M., Ferrier, S., Kearney, M. R., Possingham, H. P., Buckley, Y. M. (2013): Predicting species distributions for conservation decisions. – Ecology Letters 16: 1424-1435.

[33] Hansen, A. J., Phillips, L. B. (2015): Which tree species and biome types are most vulnerable to climate change in the US Northern Rocky Mountains? – Forest Ecology and Management 338: 68-83.

[34] Hijmans, R. J., Cameron, S. E., Parra, J. L., Jones, P. G., Jarvis, A. (2005): Very high resolution interpolated climate surfaces for global land areas. – International Journal of Climatology 25: 1965-1978.

[35] Innes, J. L. (1991): High-altitude and high latitude tree growth in relation to past, present and future global climate change. – The Holocene 1: 168-173.

[36] IPCC (2014): Summary for Policymakers. In: Field, C. B., Barros, V. R., Dokken, D. J., Mach, K. J., Mastrandrea, M. D., Bilir, T. E., Chatterjee, M., Ebi, K. L., Estrada, Y. O., Genova, R. C., Girma, B., Kissel, E. S., Levy, A. N., MacCracken, S., Mastrandrea, P. R., White, L. L. (eds.) Climate Change 2014: Impacts, Adaptation, and Vulnerability. Part A: Global and Sectoral Aspects. Contribution of Working Group II to the Fifth Assessment Report of the Intergovernmental Panel on Climate Change. – Cambridge University Press, Cambridge, UK and New York, NY, pp. 1-32.

[37] Irfan-Ullah, M., Amartnath, G., Murthy, M. S. R. and Peterson, A. T. (2007): Mapping the geographic distribution of *Agalia bourdillonii* Gamble (Meliaceae), an endemic and threatened plant, using ecological niche modeling. – Biodiversity and Conservation 16: 1917-1925.

[38] Kang, W., Minor, E. S., Lee, D., Park, C. R. (2016): Predicting impacts of climate change on habitat connectivity of *Kalopanax septemlobus* in South Korea. – Acta Oecologica 71: 31-38.

[39] Khanum, R., Mumtaz, A. S., Kumar, S. (2013): Predicting impacts of climate change on medicinal asclepiads of Pakistan using Maxent modeling. – Acta Oecologica 49: 23-31.

[40] Koo, K. A., Kong, W. S., Nibbelink, N. P., Hopkinson, C. S., Lee, J. H. (2015): Potential effects of climate change on the distribution of cold-tolerant evergreen broadleaved woody plants in the Korean peninsula. – PLoS One 10(8): p.e0134043.

[41] Kumar, D. (2013): Distribution and mapping of selected tree species in different forest types of lower Assam region of India. – Ph.D. Thesis, North-Eastern Hill University, Shillong, India.

http://www.aloki.hu ● ISSN 1589 1623 (Print) ● ISSN 1785 0037 (Online)
DOI: http://dx.doi.org/10.15666/aeer/1706_1349313511

[42] Kumar, P. (2012): Assessment of impact of climate change on Rhododendrons in Sikkim Himalayas using Maxent modelling: limitations and challenges. – Biodiversity and Conservation 21: 1251-1266.
[43] Li, R., Xu, M., Wong, M. H. G., Qiu, S., Li, X., Ehrenfeld, D., Li, D. (2015): Climate change threatens giant panda protection in the 21st century. – Biological Conservation 182: 93-101.
[44] Loiselle, B. A., Jorgensen, P. M., Consiglio, T., Jimenez, I., Blake, J. G., Lohmann, L. G., Montiel, O. M. (2008): Predicting species distributions from herbarium collections: does climate bias in collection sampling influence model outcomes? – Journal of Biogeography 35: 105-116.
[45] Maclean, I., Hopkins, J. J., Bennie, J., Lawson, C. R., Wilson, R. J. (2015): Microclimates buffer the responses of plant communities to climate change. – Global Ecology and Biogeography 24(11): 1340-1350.
[46] Manish, K., Telwala, Y., Nautiyal, D. C., Pandit, M. K. (2016): Modelling the impacts of future climate change on plant communities in the Himalaya: a case study from Eastern Himalaya, India. – Modeling Earth Systems and Environment 2: 92. DOI: 10.1007/s40808-016-0163-1.
[47] Marini, M. A., Barbet-Massin, M., Martinez, J., Prestesc, N. P., Jiguet, F. (2010): Applying ecological niche modelling to plan conservation actions for the Red-spectacled Amazon (*Amazona pretrei*). – Biological Conservation 143(1): 102-112.
[48] Menon, S., Soberon, J., Li, X. G., Peterson, A. T. (2010): Preliminary global assessment of terrestrial biodiversity consequences of sea-level rise mediated by climate change. – Biodiversity and Conservation 19: 1599-1609.
[49] Midgley, G. F., Hughes, G. O., Thuiller, W., Rebelo, A. G. (2006): Migration rate limitations on climate change induced range shifts in Cape Proteaceae. – Diversity and Distributions 12: 555-562.
[50] Mohandass, D., Zhao, J. L., Xia, Y. M., Campbell, M. J., Li, Q. J. (2015): Increasing temperature causes flowering onset time changes of alpine ginger Roscoea in the Central Himalayas. – Journal of Asia-Pacific Biodiversity 8(3): 191-198.
[51] Moilanen, A., Anderson, B. J., Arponen, A., Pouzols, F. M., Thomas, C. D. (2013): Edge artefacts and lost performance in national versus continental conservation priority areas. – Diversity and Distributions 19: 171-183.
[52] Moiseev, P. A., Shiyatov, S. G. (2003): The Use of Old Landscape Photographs for Studying Vegetation Dynamics at the Tree Line Ecotone in the Ural Highlands, Russia. – In: Nagy, L. (ed.) Alpine Biodiversity in Europe. Springer-Verlag, Berlin, pp. 423-436.
[53] Monahan, W. B., Cook, T., Melton, F., Connor, J., Bobowski, B. (2013): Forecasting distributional responses of limber pine to climate change at management-relevant scales in Rocky Mountain National Park. – PLoS One 8(12): p.e83163.
[54] Moritz, C., Agudo, R. (2013): The future of species under climate change: resilience or decline? – Science 341(6145): 504-508.
[55] Nayar, M. P., Sastry, A. R. K. (1990): Red Data Book of Indian Plants. Vol. 3. – Botanical Survey of India, Kolkatta.
[56] Pandit, M. K., Babu, C. R. (1998): Biology and conservation of *Coptis teeta* Wall: an endemic and endangered medicinal herb of Eastern Himalaya. – Environmental Conservation 25(3): 262-272.
[57] Pandit, M. K., Sodhi, N. S., Koh, L. P., Bhaskar, A., Brook, B. W. (2007): Unreported yet massive deforestation driving loss of endemic biodiversity in Indian Himalaya. – Biodiversity and Conservation 16: 153-163.
[58] Pauli, H., Gottfried, M., Grabherr, G. (1996): Effects of climate change on mountain ecosystems: upward shifting of mountain plants. – World Research Review 8: 382-390.
[59] Pearson, R. G., Dawson, T. P. (2003): Predicting the impacts of climate change on the distribution of species: Are bioclimate envelope models useful? – Global Ecology and Biogeography 12: 361-371.

http://www.aloki.hu ● ISSN 1589 1623 (Print) ● ISSN 1785 0037 (Online)
DOI: http://dx.doi.org/10.15666/aeer/1706_1349313511

[60] Pearson, R. G., Dawson, T. P. (2005): Long-distance plant dispersal and habitat fragmentation: identifying conservation targets for spatial landscape planning under climate change. – Biological Conservation 123: 389-401.
[61] Pearson, R. G., Dawson, T. P., Liu, C. (2004): Modelling species distributions in Britain: a hierarchical integration of climate and land-cover data. – Ecography 27: 285-298.
[62] Perez-Garcia, N., Font, X., Ferre, A., Carreras, J. (2013): Drastic reduction in the potential habitats for alpine and subalpine vegetation in the Pyrenees due to twenty-first-century climate change. – Regional Environmental Change 13(6): 1157-1169.
[63] Phillips, S. J., Dudik, M. (2008): Modeling of species distributions with Maxent: new extensions and a comprehensive evaluation. – Ecography 31: 161-175.
[64] Phillips, S. J., Anderson, R. P., Schapire, R. E. (2006): Maximum entropy modeling of species geographic distributions. – Ecological Modelling 190: 231-259.
[65] Priti, H., Aravind, N. A., Shaanker, R. U., Ravikanth, G. (2016): Modeling impacts of future climate on the distribution of Myristicaceae species in the Western Ghats, India. – Ecological Engineering 89: 14-23.
[66] Riahi, K., Grübler, A., Nakicenovic, N. (2007): Scenarios of long-term socio-economic and environmental development under climate stabilization. – Technological Forecasting and Social Change 74(7): 887-935.
[67] Riahi, K., Krey, V., Rao, S., Chirkov, V., Fischer, G., Kolp, P., Kindermann, G., Nakicenovic, N., Rafai, P. (2011): RCP-8.5: exploring the consequence of high emission trajectories. – Climatic Change 109: 33. DOI: 10.1007/s10584-011-0149-y.
[68] Rodgers, W. A., Panwar, H. S., Mathur, V. B. (2000): Wildlife Protected Area Network in India: A Review, Executive Summary. – Wildlife Institute of India, Dehradun.
[69] Royle, J. A., Chandler, R. B., Yackulic, C., Nichols, J. D. (2012): Likelihood analysis of species occurrence probability from presence-only data for modelling species distributions: Likelihood analysis of presence-only data. – Methods in Ecology and Evolution 3(3): 545-554.
[70] Saltré, F., Duputié, A., Gaucherel, C., Chuine, I. (2015): How climate, migration ability and habitat fragmentation affect the projected future distribution of European beech. – Global Change Biology 21(2): 897-910.
[71] Sanchez, A. C., Osborne, P. E., Haq, N. (2011): Climate change and the African baobab (*Adansonia digitata* L.): the need for better conservation strategies. – African Journal of Ecology 49: 234-245.
[72] Saran, S., Joshi, R., Sharma, S., Padalia, H., Dadhwal, V. K. (2010): Geospatial modeling of Brown oak (Quercus semecarpifolia) habitats in the Kumaun Himalaya under climate change scenario. – Journal of the Indian Society of Remote Sensing 38: 535-547.
[73] Sathyakumar, S., Poudyal, K., Bhattacharya, T., Bashir, T. (2011a): Galliformes of Khangchendzonga Biosphere Reserve, Sikkim, Inidia. – In: Arrawatia, M. L., Tambe, S. (eds.) Biodiversity of Sikkim-Exploring and Conserving a Global Hotspot. Information and Public Relations Department, Government of Sikkim, Gangtok, India.
[74] Sathyakumar, S., Bashir, T., Bhattacharya, T., Poudyal, K. (2011b): Assessing mammal distribution and abundance in intricate eastern Himalayan habitats of Khangchendzonga, Sikkim, India. – Mammalia 75: 257-268.
[75] Schröter, D., Cramer, W., Leemans, R., Prentice, I. C., Araújo, M. B., Arnell, N. W., Bondeau, A., Bugmann, H., Carter, T. R., Gracia, C. A., de la Vega-Leinert, A. C., Erhard, M., Ewert, F., Glendining, M., House, J. I., Kankaanpää, S., Klein, R. J., Lavorel, S., Lindner, M., Metzger, M. J., Meyer, J., Mitchell, T. D., Reginster, I., Rounsevell, M., Sabaté, S., Sitch, S., Smith, B., Smith, J., Smith, P., Sykes, M. T., Thonicke, K., Thuiller, W., Tuck, G., Zaehle, S., Zierl, B. (2005): Ecosystem service supply and vulnerability to global change in Europe. – Science 310(5752): 1333-1337.
[76] Settele, J., Bishop, J., Potts, S. G. (2016): Climate change impacts on pollination. – Nature Plants 2: 16092. DOI: 10.1038/nplants.2016.92.

http://www.aloki.hu ● ISSN 1589 1623 (Print) ● ISSN 1785 0037 (Online)
DOI: http://dx.doi.org/10.15666/aeer/1706_1349313511

[77] Sharma, S. K., Pandit, M. K. 2011. A morphometric analysis and taxonomic study of *Panax bipinnatifidus* Seem. (Araliaceae) species complex from Sikkim Himalaya, India. – Plant Systematics and Evolution 297: 87-98.
[78] Shrestha, U. B., Bawa, K. S. (2014): Impact of climate change on potential distribution of Chinese caterpillar fungus (*Ophiocordyceps sinensis*) in Nepal Himalaya. – PLoS One 9(9): e106405. DOI: 10.1371/journal.pone.0106405.
[79] Shrestha, U. B., Gautam, S., Bawa, K. S. (2012): Widespread climate change in the Himalayas and associated changes in local ecosystems. – PLoS One 7(5): e36741. DOI: 10.1371/journal.pone.0036741.
[80] Singh, K. P., Kushwaha, C. P. (2016): Deciduousness in tropical trees and its potential as indicator of climate change: A review. – Ecological Indicators 69: 699-706.
[81] Singh, S. P., Singh, V., Skutsch, M. (2010): Rapid warming in the Himalayas: ecosystem responses and development options. – Climate and Development 2: 1-13.
[82] Smith, S. J., Wigley, T. M. L. (2006): Multi-gas forcing stabilization with minicam. – The Energy Journal 3: 373-392.
[83] Sohel, S. I., Akhter, S., Ullah, H., Haque, E., Rana, P. (2016): Predicting impacts of climate change on forest tree species of Bangladesh: evidence from threatened *Dysoxylum binectariferum* (Roxb.) Hook. f. ex Bedd. (Meliaceae). – iForest 10: 154. DOI: 10.3832/ifor1608-009.
[84] Stockwell, D. R. B., Peterson, A. T. (2002): Effects of sample size on accuracy of species distribution models. – Ecological Modelling 148: 1-13.
[85] Svenning, J. C., Harlev, D., Sørensen, M. M., Balslev, H. (2009): Topographic and spatial controls of palm species distributions in a montane rain forest, southern Ecuador. – Biodiversity and Conservation 18: 219-228.
[86] Swets, J. (1988): Measuring the accuracy of diagnostic systems. – Science 240: 1285-1293.
[87] Tear, T. H., Kareiva, P., Angermeier, P. L., Comer, P., Czech, B., Kautz, R., Landon, L., Mehlman, D., Murphy, K., Ruckelshaus, M., Scott, J. M., Wilhere, G. (2005): How much is enough? The recurrent problem of setting measurable objectives in conservation. – BioScience 55: 835.
[88] Telwala, Y., Brook, B. W., Manish, K., Pandit, M. K. (2013): Climate-induced elevational range shifts and increase in plant species richness in a Himalayan biodiversity epicentre. – PLoS One 8(2): e57103.
[89] Thomas, C. D., Cameron, A., Green, R. E., Bakkenes, M., Beaumont, L. J., Collingham, Y. C., Erasmus, B. F., De Siqueira, M. F., Grainger, A., Hannah, L., Hughes, L. (2004): Extinction risk from climate change. – Nature 427(6970): 145-148.
[90] Thuiller, W., Lavorel, S., Araújo, M. B., Sykes, M., Prentice, I. C. (2005): Climate change threats to plant diversity in Europe. – Proceedings of National Academy of Sciences 102: 8245-8250.
[91] Thuiller, W., Broennimann, O., Hughes, G. O., Alkemade, J. R. M., Midgley, G. F., Corsi, F. (2006): Vulnerability of African mammals to anthropogenic climate change under conservative land transformation assumptions. – Global Change Biology 12: 424-440.
[92] Trisurat, Y., Rajendra, P., Shrestha, B., Kjelgren, R. 2011. Plant species vulnerability to climate change in peninsular Thailand. – Applied Geography 31: 1106-1114.
[93] Urbina-Cardona, J. N., Flores-Villela, O. (2010): Ecological niche modeling and prioritization of conservation area networks for Mexican herpetofauna. – Conservation Biology 24(4): 1031-1041.
[94] Warren, D. L., Glor, R. E., Turelli, M. (2010): ENMTools: a toolbox for comparative studies of environmental niche models. – Ecography 33: 607-611.
[95] Wise, M., Calvin, K., Thomson, A., Clarke, L., Bond-Lamberty, B., Sands, R., Smith, S. J., Janetos, A., Edmonds, J. (2009): Implications of limiting CO_2 concentrations for land use and energy. – Science 324: 1183-1186.

http://www.aloki.hu ● ISSN 1589 1623 (Print) ● ISSN 1785 0037 (Online)
DOI: http://dx.doi.org/10.15666/aeer/1706_1349313511

[96] Yi, Y. J., Cheng, X., Yang, Z. F., Zhang, S. H. (2016): Maxent modeling for predicting the potential distribution of endangered medicinal plant (*H. riparia* Lour) in Yunnan, China. – Ecological Engineering 92: 260-269.
[97] York, E. M., Butler, C. J., Lord, W. D. (2016): Global decline in suitable habitat for *Angiostrongylus* (=Parastrongylus) *cantonensis*: the role of climate change. – PLoS One 9(8): e103831. DOI: 10.1371/journal.pone.0103831.
[98] Zhang, Y., Wang, Y., Zhang, M., Ma, K. (2014): Climate change threats to protected plants of China: an evaluation based on species distribution modeling. – Chinese Science Bulletin 59(34): 4652-4659.

APPENDIX

Uncertainty among model predictions

It should be noted that only three global circulation models (GCMs; MRI-CGCM3, CSIRO-MK3.6 and HadGEM2-CC) under two future climate scenarios (RCP 4.5 and 8.5) were used in this study (*Fig. A1*).

Figure A1. *Differences in future potential predictions, among three different Global Circulation Models (GCMS) viz.; CGCM3, CSIRO-MK3 and HadGEM2-CC for Panax pseudoginseng. Where cyan color shows unsuitable prediction, yellow color shows predicted suitable habitat area by at least one of the GCMs, green color shows predicted suitable habitat area by two GCMs, and red shows predicted suitable habitat area by all three GCMs*

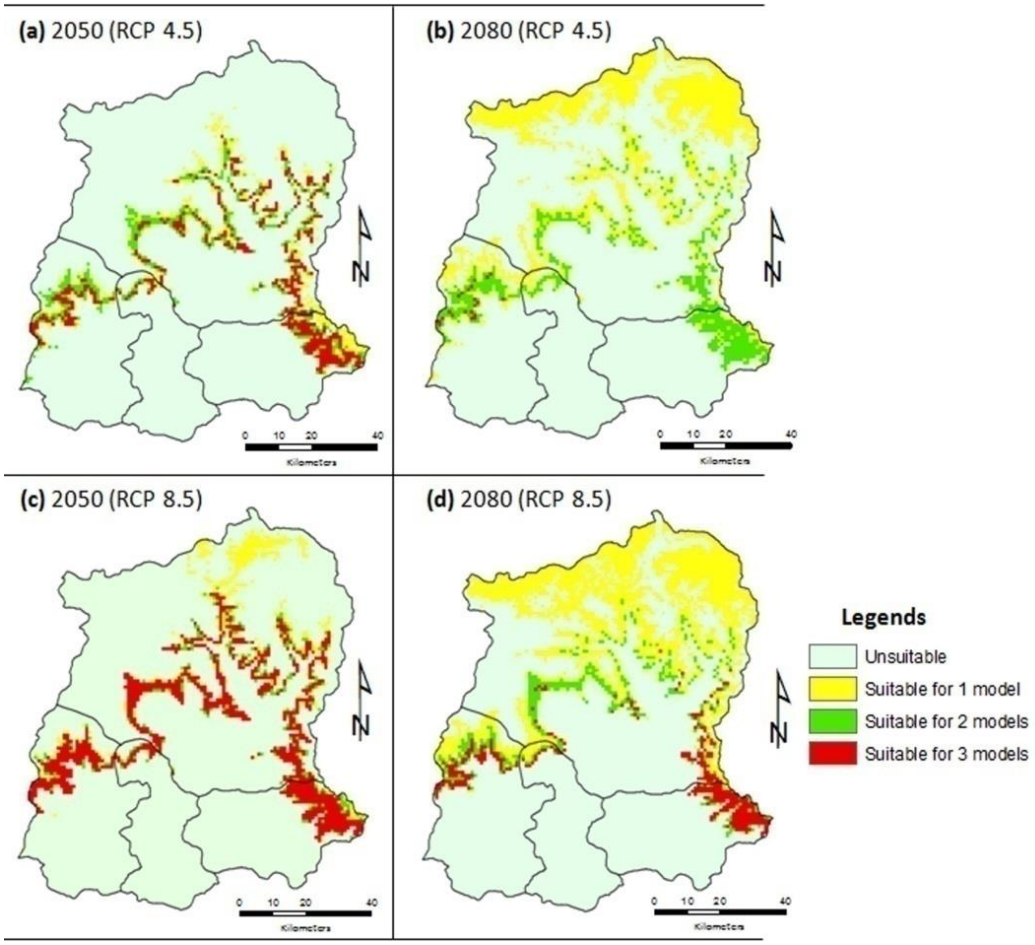

http://www.aloki.hu ● ISSN 1589 1623 (Print) ● ISSN 1785 0037 (Online)
DOI: http://dx.doi.org/10.15666/aeer/1706_1349313511

Other scenarios and GCMs could give different results. Buisson et al. (2010) accounted that the Maxent or other modeling algorithms used could yield large variation in projections, followed by GCM, whose contribution increased over time. In order to report for certain future uncertainty Buisson et al. (2010) recommended using several GCMs and scenarios. Model projections also depend on the year. The years 2050 and 2070 are commonly used in studies dealing with the impacts of climate change on biodiversity (Thuiller et al., 2006; Khanum et al., 2013; Dowling, 2015; Hansen and Phillips, 2015; Koo et al., 2015; Al-Qaddi et al., 2016; Deb et al., 2016; Sohel et al., 2016). As expected, projections for 2070 displayed more negative impacts than projections for 2050(described by Thuiller et al., 2006; York et al. 2014) in RCP 8.5 scenario of climate change. However, in RCP 4.5 scenario projections for 2050 and 2070 displayed less likely to negative impacts.

A pertinent question which arises while studying the potential future distribution of a species is the validity and/or accuracy of the GCM and scenarios commonly used for this purpose, as different GCM from different climatic research centers show different results. However, to date, this is the best data available, and it is still commonly used to study the potential effect of climate change on species' distributions (Buisson et al., 2010; Marini et al., 2010; Khanum et al., 2013; Dowling, 2015; Hansen and Phillips 2015; Koo et al., 2015; Al-Qaddi et al., 2016; Deb et al., 2016; Sohel et al., 2016; Kang et al., 2016). The precautionary principle suggests that the uncertainty about predicted changes in climate does not justify lack of action. It is better to use the data which is available and carry out the studies required to make recommendations for conservation.

Table A1. *Pairwise correlation matrix (Pearson's correlation coefficients, r) between bioclimatic variables. Variables showing (r) ≥ 0.9 were excluded from the analysis, and only six variables included in this study (i.e., Bio3, Bio7, Bio10, Bio11, Bio15 and Bio18)*

Variables	Bio1	Bio2	*Bio3*	Bio4	Bio5	Bio6	*Bio7*	Bio8	Bio9	*Bio10*	*Bio11*	Bio12	Bio13	Bio14	*Bio15*	Bio16	Bio17	*Bio18*
Bio2	-0.518																	
Bio3	0.319	0.208																
Bio4	-0.592	0.975	0.008															
Bio5	0.850	0.008	0.476	-0.088														
Bio6	0.925	-0.794	0.201	-0.853	0.591													
Bio7	-0.586	0.987	0.063	0.997	-0.075	-0.849												
Bio8	0.957	-0.249	0.401	-0.334	0.966	0.776	-0.326											
Bio9	0.977	-0.678	0.269	-0.748	0.724	0.984	-0.742	0.875										
Bio10	0.957	-0.249	0.401	-0.334	0.966	0.776	-0.326	1.000	0.875									
Bio11	0.980	-0.670	0.269	-0.740	0.732	0.982	-0.734	0.881	1.000	0.881								
Bio12	0.742	-0.955	-0.022	-0.968	0.280	0.936	-0.974	0.515	0.862	0.515	0.856							
Bio13	0.646	-0.970	-0.060	-0.977	0.160	0.879	-0.982	0.401	0.785	0.401	0.778	0.986						
Bio14	0.741	-0.887	0.200	-0.954	0.313	0.928	-0.942	0.528	0.860	0.528	0.852	0.952	0.934					
Bio15	-0.200	-0.573	-0.104	-0.575	-0.588	0.147	-0.567	-0.434	-0.013	-0.434	-0.026	0.413	0.551	0.424				
Bio16	0.657	-0.974	-0.046	-0.984	0.169	0.890	-0.989	0.412	0.796	0.412	0.789	0.990	0.998	0.946	0.532			
Bio17	0.814	-0.897	0.127	-0.946	0.395	0.971	-0.941	0.613	0.917	0.613	0.890	0.979	0.943	0.976	0.316	0.955		
Bio18	0.657	-0.974	-0.046	-0.984	0.169	0.890	-0.989	0.412	0.796	0.412	0.789	0.990	0.998	0.946	0.532	1.000	0.955	
Bio19	0.870	-0.840	0.181	-0.900	0.494	0.984	-0.893	0.696	0.951	0.696	0.856	0.951	0.894	0.953	0.194	0.909	0.990	0.864

http://www.aloki.hu ● ISSN 1589 1623 (Print) ● ISSN 1785 0037 (Online)
DOI: http://dx.doi.org/10.15666/aeer/1706_1349313511

A SURVEY ON WEED MANAGEMENT IN DRY LENTIL FIELDS

PALA, F.

Department of Plant Protection, Faculty of Agriculture, Siirt University, Siirt, Turkey
(e-mail: firatpala@siirt.edu.tr; phone: +90-484-212-1111)

(Received 23rd Oct 2018; accepted 7th Jan 2019)

Abstract. A questionnaire consisting of 20 questions about weed, herbicide, tillage and crop rotation was applied to 100 lentil farmers to determine the current state of a weed problem in lentil fields in 2016. Common weeds were determined charlock mustard (*Sinapis arvensis* L., 36%), devil-on-all-sides (*Ranunculus arvensis* L., 16%), cleavers (*Galium aparine* L., 11%), makhobeli (*Cephalaria syriaca* L., 8%), and knapweed (*Centaurea depressa* L., 8%), respectively. The majority of participants used aclonifen (89%) as a post-emergence to control broadleaf, besides, clethodim (26%), haloxyfop-methyl-ester (17%), tepraloxydim (16%), quizalofop p-ethyl (15%), and fluazifop p-butyl (6%) for grass, respectively, and as a total herbicide glyphosate (4%) as well. But, respondents (66%) stated that lentils had crop injury from aclonifen. Growers took into account the price (43%), herbicides (38%), weeds (10%) and crop rotation (9%) to choose herbicides. Managing weeds with hand-picked (76%) were common in areas that did not use herbicides. Preventive measures were used such as crop rotation (61%), late sowing (10%), and deep tillage (4%), furthermore, farmers planted wheat (91%) and barley (9%) as a preceding crop. In this study, dissatisfaction was determined by the efficacy and selectivity of aclonifen which is registered herbicide on lentils in Turkey. Lentils have a short stature, slow early-season growth rate, and open-canopy growth habit, which make them poor competitors with broadleaf weeds. So weed management in the early period such as pre-planting, pre-emergence or early post-emergence herbicides, and IMI herbicide-tolerant lentil varieties (Clearfield) have been investigated.
Keywords: *lentils*, *mustard, aclonifen, crop rotation, late sowing, plow tillage*

Introduction

Lentils (*Lens culinaris* Medik.), which is well-known as nutritious food, is one of the important crops cultivated in the cool season. It grows as an annual bushy leguminous plant typically 20-45 cm tall, which produces many small purse- shaped pods containing one to two lens-shaped seeds each (SPG, 2017). It is not only a rich source of improved nutrition for people but also provides nutritious straw for animals. Lentil contains about 11 per cent water, 25 percent protein and 60 percent carbohydrate. The important lentil growing countries of the world are India (18.00 million ha), Canada (12.17 million ha), Turkey (2.43 million ha), Iran (1.68 million ha), Australia (1.62 million ha), Bangladesh 1.24 (million ha), Syria (1.11 million ha), USA (1.04 million ha) respectively. Turkey ranks third in the world in respect of production as well as area followed by India and Canada (FAOSTAT, 2014). One-third of the country's production of lentil is provided by Diyarbakir province (TUIK, 2016).

Lentil production provides several agronomic advantages and opportunities to increase profit margins. Besides tolerating drought conditions, cool temperatures, and a wide variety of soil types, leguminous pulse crops can also help fix nitrogen in the soil. However, growers should be aware of the challenges and opportunities of managing weeds in these crops (Pala et al., 2018). The common problem is weeds in lentils widely cultivated such as Native red, Firat-87, Seyran-96, Cagil, Altintoprak and Sakar. Weed management in varieties is generally considered to be a poor competitor due to its slow establishment and limited vegetative growth. Their productivity is adversely affected by the presence of weeds (Swanton et al., 2015). Lentil yield loss from the competition

http://www.aloki.hu ● ISSN 1589 1623 (Print) ● ISSN 1785 0037 (Online)
DOI: http://dx.doi.org/10.15666/aeer/1706_1351313521

with weeds can range as high as 80% (Beniwal and Dalkiran, 1995; Yenish et al., 2009). On the other hand, it is known that weeds host the sloe bug (*Dolycoris baccarum* L.) and gorse shieldbug (*Piezodorus lituratus* F.) that causing chalking problem on lentil (Akkaya, 2004; Ozberk et al., 2014). The prominent weed species infesting lentil crop are charlock mustard (*Sinapis arvensis* L.), field bindweed (*Convolvulus arvensis* L.), volunteer wheat (*Triticum* spp.), wild oat (*Avena* spp.), knapweed (*Centaurea depressa* M. Bieb), cow cockle (*Vaccaria pyramidata*), vetch (*Vicia* sp.), cleavers (*Galium aparine*), volunteer barley (*Hordeum vulgare*), pheasant's (*Adonis aestivalis*), fumitory (*Fumaria officinalis* L.) etc. (Guncan, 2014; Tepe, 2014; Kraehmer, 2016; Pala et al., 2018). The concept that high input provided for higher yield, also pose high risk, if weeds are not controlled.

Climate change and applied agricultural practices cause changes in the populations of harmful organisms (pests, pathogens, and weeds) that cause significant losses in crop plants (Flood, 2010; Ucak et al., 2017). Cultural practices to decrease weed pressure in lentil crops include prevention, seedbed preparation, variety selection, proper sowing and, crop establishment, insect and disease management. For example, Baird et al. (2009) observed that increasing the seeding density of lentil translated into increased yield and decreased weed biomass. However, while cultural practices such as allelopathy, cover crops, and crop rotations are at the backbone of integrated weed management (IWM) plan, they alone may not be enough to secure adequate weed control in lentil fields (Pala et al., 2018). In addition, cultivation of soil with smart sensitive cultivator, monitoring of plants and pests with a drone and local intervention, and the application of steam and soil disinfection on field crops, vegetables and fruits and the control of diseases, pests, and weeds should be investigated (Pala et al., 2017).

Mechanical weed control practices in lentil, such as harrowing or rotary hoeing fields in fall, after the emergence of weeds but before lentil planting. Also to control weeds generally hand weeding is in practice but it is now costly as well as difficult because of the non-availability of labor in peak periods (Bhan and Kukula, 1987). Crop rotation is one of the other powerful tools to manage weed problems. To high persistence herbicides commonly used in small grain crops such as iodosulfuron, metsulfuron, chlorsulfuron sulfosulfuron etc. can damage subsequent annual legumes, including lentil (Kraehmer, 2012; SPG, 2017). There are a number of herbicides registered to control grassy weeds in lentil, but few options exist for control of broadleaf weeds (Brand et al., 2007). To applicability and success of herbicides in lentil fields depend on the cropping system, land preparation methods, soil conditions, and weed problems. For example, challenge (aclonifen) is a selective herbicide that is in the diphenyl ether group, it is used for postemerge against broadleaf weed in lentils. When it applies at recommended rates provides effective control on some broadleaf weeds, but it is not effective enough some broad-leaved weeds or ineffective, in addition, it can cause crop damage in stressful conditions of cold weather, low fertility, disease, or insect damage. Also, although pursuit (imazethapyr) can be used to manage broadleaf weeds in no-till or minimum tillage systems, it has many application restrictions due to crop safety concerns, including leaf chlorosis, stand reduction, and decreased yields, especially cold and wet conditions occurring within a week of application can severely damage the crop (Friesen and Wall, 1986; Muehlbauer et al., 1995; Ghosheh and El-Shatnawi, 2003). These methods can be supported by other mechanical and cultural processes such as tillage, late sowing, and rotation (Kayan and Adak, 2006; Dogan, 2014). However, lentil is sensitive to weed competition. Weed growth reduces lentil yields by competing

http://www.aloki.hu ● ISSN 1589 1623 (Print) ● ISSN 1785 0037 (Online)
DOI: http://dx.doi.org/10.15666/aeer/1706_1351313521

for light, moisture, and nutrients. It is known that available practices in the control of weeds in lentil fields are inadequate (Harper, 1977; Swanton et al., 2015). The USA and Canada developed lentil varieties tolerant to the imidazolinone (an acetolactate synthase [ALS]-inhibitor) herbicides through mutation breeding in order to deal with the shortcomings in broadleaf weed control in lentil (Chant, 2004; Slinkard et al., 2007). Weed control in these ALS inhibitor herbicide-tolerant lentil varieties was initially excellent and, as a consequence, they have had very high adoption rates. Hence lentil is a suitable model crop to study on weeds and weed management due to the limitations of weed control for this crop.

In order to develop economic, effective and environmentally friendly IWM tactics in lentil, where weed competition is weak, it is necessary to monitor the distribution and the prevalence of weed species which are primarily a problem. There have been a limited number of studies on weed species in our country and in our province, but no detailed and up-to-date studies have been found. With this view, the study has undertaken the determination of existing weed control techniques in lentil fields.

Material and methods

The survey was conducted in Diyarbakir where it is located in the Southeastern Anatolia Region (SAR) of Turkey in spring 2016 (*Fig. 1*). Lentil is mainly grown in the non-irrigated areas.

Figure 1. *Location of surveys, Diyarbakir Turkey*

The most lentil growing districts, cultivated fields and sample number are given in *Table 1*.

The surveys were carried out in the Bismil, Cermik, Cinar, Dicle, Egil, Ergani, Hani, Hazro, Kayapinar, Silvan, and Sur. Sampling size and the settlements of the interviews were determined purposively according to the Turkish Statistical Institute (TUIK) database. In this regard, 100 farm enterprises were determined and interviewed to represent the study area. A questionnaire containing questions regarding a) common weeds agronomic practices including tillage, irrigation, crop rotation, fertilization,

http://www.aloki.hu ● ISSN 1589 1623 (Print) ● ISSN 1785 0037 (Online)
DOI: http://dx.doi.org/10.15666/aeer/1706_1351313521

harvesting b) weed management practices, c) problematic weed rankings, d) knowledge of weed management and e) efficiency of extension services; was prepared and each grower was interviewed for answering the questionnaire. Using the proportional sample volume formula (*Eq. 1*) (Newbold, 1995).

$$n = \frac{N.p(1-p)}{(N-1)\sigma^2_{px} + p(1-p)} \quad \text{(Eq.1)}$$

The formula; σ^2_{px} = Variance of rate (90% confidence interval and 5% 5% tolerance), n: Sample volume, N: The main mass represents. p: rate (p: 0.5). The data collected during the survey were analyzed by using frequencies and simple percentages.

Table 1. *Districts surveyed in Diyarbakir province and number of samples taken (TUIK, 2016)*

Districts	Lentils field (ha)*	The number of participants
Bismil	24.580	48
Cermik	1.700	16
Cinar	3.350	12
Dicle	600	10
Egil	411	6
Ergani	5.500	3
Hani	521	1
Hazro	450	1
Kayapinar	800	1
Silvan	9.000	1
Sur	6.500	1
Total	**53.412**	**100**

Results and discussion

The outcome of the survey two out of three of the participants in the survey was between 30-50 years of age. Approximate half of them had education up to primary school and one-third of them had a secondary school. This shows the education level was low and a very small portion of respondents had higher graduate degrees. The farmers were asked; since how long you have been grown lentil. Response was 1-10, 10-20, 20-30 and > 30 years which ranged 19, 28, 45, and 8 respectively. The area of lentil production was < 5, 5-10, 10-20, 20-50, > 50 ha with percentages of 9, 38, 35, 12, and 6% respectively. This value showed that tw- thirds of the farmers produce lentil in the fields between 10 and 50 ha.

The preceding crops of lentil are wheat 91% and barley 9% (*Table 2*). The results of the survey showed that all of the farmers planted cereal before lentil production. Crop rotation strongly affects the density and composition of weed flora because the different crops in rotation require different agricultural practices and herbicide. Due to continuously changing agricultural practices as a result of crop rotation; the adaptation's success of certain species to a specific area under sole or mono-cropping could be prevented (Kayan and Adak, 2006; Erman et al., 2008; Dogan, 2014). Tepe et al. (2004)

http://www.aloki.hu ● ISSN 1589 1623 (Print) ● ISSN 1785 0037 (Online)
DOI: http://dx.doi.org/10.15666/aeer/1706_1351313521

reported that crop rotation is an important part of a good weed control program in lentil agriculture. Certain weeds, especially broadleaf weeds in lentil, may be less difficult to control in a farming system having preceding crops such as cereal. Other benefits of crop rotation may include a reduction in insects, diseases and nematode problems in lentil.

Table 2. *The preceding crops of lentil grown by farmers in survey*

Preceding crop	Percentage (%)
Wheat	91
Barley	9
Total	**100**

When the respondents were asked for the tillage practices being used by them in lentil agriculture, 12% of respondents stated that the tillage practices included the plow in autumn, and 88% cultivator and harrow tillage before planting. Planting with the seeders/planters system is opted by the growers in the region. The 87% of respondents stated that they planted seeds after the rain due to moisture, and the rest before the rain in dry soil. When asked the effect of tillage systems on weed density, 76% of respondents stated that deep plowing reduces weed density. When asked for previous crop residue, the majority of respondents answered that they burned them usually. Previous crop residue and tillage practices can affect weed population dynamics, including weed seed distribution and abundance in the soil seed bank (Mulugeta and Stoltenberg, 1997). There are reports that weed control was improved by using plow for tillage (Durutan et al., 1989; Pala et al., 2000; Camara et al., 2003). When asked for irrigation and fertilization, 100% of respondents answered that they did not use both of them in lentil production. This crop produces a dry climate and does not need to use fertilizer in Diyarbakir. The most problematic weed species in the lentil field are represented in *Table 3*. *Sinapis arvensis* L. as a broadleaf, and *Avena fatua* L. as a grass were the first most problematic weeds, respectively. In the study carried out, important weed species found in the lentil fields were adapted to the agricultural products in winter and spread especially in these fields. For this reason, these species, which are found in the field of surveillance, are among the important weeds, which are problematic both in countries such as Canada and India, and in beans and pulses in our country (Holm et al., 1977; Guncan, 2014; Tepe, 2014; Kraehmer, 2016; SPG, 2017). So, this shows that the problematic weed species stated by farmers are similar to the majority of species reported in the lentil fields.

Weeds emerging in lentil fields and trouble for farmers are mostly broadleaves such as *S. arvensis, R. Arvensis,* and *G. aparine.* Majority of participants stated they combined tillage, hand-picking, and herbicides commonly. 89% of them used to control broadleaf weeds by using aclonifen as a chemical broadleaf weeds control method (*Table 4*). Hand-picking (76%) was common in areas that do not use herbicides. Guncan (2014) stated that fewer herbicides are available for use in lentil. It is known just there is just one registered herbicide for broadleaf weeds in the lentil fields of Turkey.

Participants used clethodim, haloxyfop-methyl-ester tepraloxydim, quizalofop p-ethyl, fluazifop p-butyl for grass ratios 26, 17, 16, 15, 6%, respectively (*Table 5*). But, 66% of aclonifen reported phytotoxicity, also few farmers (4%) applied glyphosate, pre-emergence.

http://www.aloki.hu ● ISSN 1589 1623 (Print) ● ISSN 1785 0037 (Online)
DOI: http://dx.doi.org/10.15666/aeer/1706_1351313521

Table 3. *According to participants noxious weeds in lentil fields*

Weed species	Percentage (%)
Sinapis arvensis L.	36
Ranunculus arvensis L.	16
Galium aparine L.	11
Cephalaria syriaca L.	8
Centaurea depressa L.	8
Avena fatua L.	7
Vicia sativa L	6
Adonis aestivalis L.	3
Vaccaria pyramidata Medik.	3
Fumaria officinalis L.	1
Triticum aestivum L	1
Total	**100**

Table 4. *Herbicides used to control broadleaf weeds in lentil fields*

Herbicides for broadleaf	Percentage (%)
Aclonifen*	89
No chemical**	11
Total	**100**

*Post-emergence for broadleaf. **Hand-picking

Table 5. *Herbicides used to control grass weeds in lentil fields*

Herbicides for grass	Percentage (%)
Clethodim*	26
Haloxyfop*	17
Tepraloxydim*	16
Quizalofop*	15
Fluazifop*	6
No chemical**	20
Total	**100**

*Post-emergence for grass. **Hand-picking

The preventive measures were used in lentil fields by farmers such as crop rotation, late planting, deep tillage in order of 61, 10, 4% (*Table 6*).

Participants took into account the price (43%), herbicides (38%), weeds (10%) and crop rotation (9%) to choice weed management in the survey, respectively (*Table 7*).

Lentil has an early-season slow growth and open-canopy growth habit, which makes them poor competitors with weeds, so the control of weeds in the early period is too important. But we do not have much of a pre-plant, pre-emergence or post-emergence herbicide choice, especially to control of the broadleaf weeds emerging in lentil fields. Also, there is dissatisfaction with the efficacy and selectivity of aclonifen, the only registered herbicide in Turkey. This survey emphasizes the need to define the effects of

http://www.aloki.hu ● ISSN 1589 1623 (Print) ● ISSN 1785 0037 (Online)
DOI: http://dx.doi.org/10.15666/aeer/1706_1351313521

weeds in lentil fields and to understand the effects of management on weed populations. It is essential to control weeds as tillage pre-plant, and herbicides post-plant are used in lentil production areas. Weed management systems significantly affect weed control and yield crops. Therefore, weed management in lentil has been a major challenge for crop producers from the start of agriculture.

Table 6. *Preventive measures and mechanical applications against weeds in lentil*

Cultural measures and tillage	Percentage (%)
Crop rotation	61
Late sowing	10
Plow tillage	4
Others*	25
Total	**100**

*Varieties, roller, more seeds, intra-row etc.

Weeds compete for factors such, nutrients, water and light, also some weeds host many plant pathogens and insects harmful to lentil, preventing certain agricultural practices in a fit and rapid manner. It was important that cultural measures (crop rotation with 61% and late sowing with 10%) were the first choice for preventing weeds from damaging lentil yield and quality.

Table 7. *Considerations when choosing methods for controlling weeds*

The matters considerations	Percentage (%)
Price	43
Herbicide diversity	38
Weeds	10
Crop rotation	9
Total	**100**

The fluctuations in labor, fuel and herbicide prices from year to year caused the input cost (price 43%) to be the main concern of farmers when deciding on weed control. In order to carry out economic analyzes in an appropriate way, it was understood that current studies on critical period and economic threshold were needed.

Conclusions

The available major agricultural issues are to feed the world without contaminating the environment. Weeds are the most important constraints in lentil production. Despite the fact that cereals are planted as previous crops, the fact that grains are not mentioned by farmers as a major weed problem is related to the destruction of grains by tillage and late sowing of lentils. The fact that weeds are problematic in the lentil production areas of the weeds expressed as a problem indicates that the farmers recognize weeds. Farmers complained that the market is not enough herbicides for broadleaf weeds control unlike the herbicides used in the control for grasses. It is good but insufficient to make crop rotation by little more than half of the farmers. It is also observed that the late tillage and plow deep tillage are not aware of the importance of weed control by

http://www.aloki.hu ● ISSN 1589 1623 (Print) ● ISSN 1785 0037 (Online)
DOI: http://dx.doi.org/10.15666/aeer/1706_1351313521

participants. While the method of weed control is chosen in lentil fields, firstly, the low cost and the availability of herbicides determine the behavior of farmers. As a result, the survey showed weeds, which are expressed as a problem in lentil fields by participants, have been the common weeds that cause significant yield losses in lentils and showed that the cultural measures, mechanical and chemical weed control are insufficient. To this end, herbicides are used to control weeds; however, overconfidence on herbicides is not sustainable in the long run. Therefore, there is a need to develop integrated weed management strategies in the lentil production systems, which aim to reduce the weed seed bank before lentil sowing and reduce weed emergence and weed growth in lentils. It was shown that weed management practices are inadequate in lentil fields. So new tactics should be improved such as imidazolinone (IMI) tolerant non-transgenic crops called Clearfield lentil varieties by ethyl methanesulfonate (EMS) which is a mutagenic, teratogenic, and possibly carcinogenic organic compound.

REFERENCES

[1] Akkaya, A., 2004. The studies of chalky spot factors causing yield and quality loss on red lentil and their control possibilities in Southeastern Anatolia Region. Plant Protection Research Institute, Diyarbakir, Turkey.
[2] Baird, J., Shirtliffe, S., Walley, F. (2009): Optimal seeding rate for organic production of lentil in the northern Great Plains. – Can J Plant Sci 89: 455-464.
[3] Beniwal, S. P. S., Kaiser, W. J., Dalkiran, H. (1995): Biotic Constraints to the Production of Lentils and Their Management in the Highlands of West Asia and North Africa. – Ed. J. D. H. Keating and I Kusmenoglu, Ankara.
[4] Bhan, V. M., Kukula, S. (1987): Weed and their control in chickpea (*Cicer arietinum* L.). – CAB International, Wallingford, Oxon, pp. 319-328.
[5] Brand, J., Yaduraju, N. T., Shivakumar, B. G., McMurray, L. (2007): Weed Management. – In: Yadav, S. S., McNeil, D. L., Stevenson, P. C. (eds.) Lentil—An Ancient Crop for Modern Times. Springer, Dordrecht, pp. 159-172.
[6] Camara, K. M., Payne, W. A., Rasmussen, P. E. (2003): Long-term effect of tillage, nitrogen and rainfall on winter wheat yields in the Pacific Northwest. – Agron J. 95: 828-835.
[7] Chant, S. R. (2004): Imidazolinone tolerance in lentil (*Lens culinaris* Medik.). – M.Sc. Thesis. University of Saskatchewan, Saskatoon, SK, Canada.
[8] Dogan, Y., Togay, T., Togay, A. (2014): Effect of different sowing time on yield and yield components of lentil (*Lens culinaris* Medic.) varieties in Mardin Kiziltepe conditions. – Journal of Tekirdag Agricultural Faculty 11(2): 51-58.
[9] Durutan, N., Guler, M., Karaca, M., Meyveci, K., Avcin, A., Eyuboglu, H. (1989): Effect of various components of the management package on weed control in dryland agriculture. – In: Soil and Crop Management of Improved Water Use Efficiency in Rainfed Areas. Proceedings of an International Workshop, Ankara, Turkey.
[10] Erman, M., Tepe, I., Bukun, B., Yergin, R., Taskesen, M. (2008): Critical period of weed control in winter lentil under non-irrigated conditions in Turkey. – African Journal of Agricultural Research 3(8): 523-530.
[11] FAOSTAT (2014): Food and Agriculture Organization of the United Nations. – http://www.fao.org/faostat/en/#home.
[12] Flood J: The importance of plant health to food security. Food Secur., 2(3): 215–231.
[13] Friesen, G. H., Wall, D. A. (1986): Tolerance of lentil (*Lens culinaris* Medik.) to herbicides. – Can J Plant Sci 66: 131-139.

http://www.aloki.hu ● ISSN 1589 1623 (Print) ● ISSN 1785 0037 (Online)
DOI: http://dx.doi.org/10.15666/aeer/1706_1351313521

[14] Ghosheh, H. Z., El-Shatnawi, M. K. (2003): Broadleaf weed control in chickpeas (*Cicer arietinum*), faba beans (Vicia faba) and lentils (*Lens culinaris*). – Acta Agron Hungarica 51: 427-444.
[15] Guncan, A. (2014): Weed Management. – Selcuk University Publisher, Konya.
[16] Harper, J. L. (1977): The Population Biology of Plants. – Academic Press, London.
[17] Holm, L. G., Plucknett, D. L., Pancho, J. V., Herberger, J. P. (1977): The World's Worst Weeds, Distribution and Biology. – East-West Center University Press of Hawaii, Honolulu.
[18] Kayan, N., Adak, M. S. (2006): Effect of soil tillage and weed control methods on weed biomass and yield of lentil (*Lens culinaris* Medic.). – Agronomy and Soil Science 52(6): 697-704.
[19] Kraehmer, H. (2012): Innovation: changing trends in herbicide discovery. – Outlooks Pest Manag. 23: 115-118.
[20] Kraehmer, H. (2016): Atlas of Weed Mapping. – Wiley and Sons. Ltd., Chichester, pp. 87-104.
[21] Muehlbauer, F. J., Kaiser, W. J., Clement, S. L., Summerfield, R. J. (1995): Production and breeding of lentil. – Advances in Agronomy 54: 283-332.
[22] Mulugeta, D., Stoltenberg, D. E. (1997): Weed and seedbank management with integrated methods as influenced by tillage. – Weed Sci. 45: 706-715.
[23] Newbold, P. (1995): Statistics for Business and Economics. – Prentice Hall Inc., Upper Saddle River, NJ.
[24] Ozberk, İ., Tanrikulu, O. M. (2014): A study on some grading factors affecting marketing price of red lentil (*L. culinaris* Medik.) in South-East Anatolia. – Journal of Field Crops Central Research Institute 23(1): 1-6.
[25] Pala, F., Mennan, H., Demir, A. (2017): Investigation of problems and considerations on weed control methods in field crops of Diyarbakir. – International Conference on Multidisciplinary, Science, Engineering and Technology, Bitlis, Turkey.
[26] Pala, F., Mennan, H., Demir, A., Ocal, A., Karipcin, M. Z., Pakyurek, M., Aydin, M. H. (2017): Effect on weed control of soil disinfection with steam in strawberry farms. – 4th International Regional Development Conference, Malatya, Turkey.
[27] Pala, F., Mennan, H., Demir, A. (2018): Determination of the weed species, frequency and density in lentil fields in Diyarbakir province. – Turkish Journal of Weed Science 21(1): 33-42.
[28] Slinkard, A., Vandenberg, A., Holm, F. (2007): Lentil plants having increased resistance to imidazolinone herbicides. – US Patent 7,232,942 B2.
[29] SPG (2017): Saskatchewan pulse growers. – http://saskpulse.com/growing/lentils/.
[30] Swanton, C. J., Nkoa, R., Blackshaw, R. E. (2015): Experimental methods for crop weed competition studies. – Weed Sci. 63(1): 2-11.
[31] Tepe, I. (2014): Weed Management. – Sidas Medya Agriculture Publisher No: 31, Izmir, Turkey.
[32] Tepe, I., Erman, M., Yazlik, A., Levent, R., Ipek, K. (2004): Effect of different control methods on weeds, yield components and nodulation in the spring lentil. – Turk J. Agric. For. 28: 49-56.
[33] TUIK (2016): Turkish Statictical Institute. – http://www.turkstat.gov.tr/Start.do.
[34] Ucak, A. B., Kaplan, C., Inal, B., Gencoglan, S. (2017): Effects of different irrigation levels on mediterranean corn borer (*Sesamia nonagrioides* Lefebvre) populations and effects of fatty acids in corn borer preferences. Fresenius Environmental Bulletin, 26(12A): 8211-8220.
[35] Yenish, J. P., Larsen, R., Pala, M., Haddad, A. (2009): Weed Management. – In: Erskin, W., Meuhlbauer, F. J., Sarker, A., Sharma, B. (eds.) The Lentil Botany, Production and Uses. CABI, Oxfordshire, UK.

http://www.aloki.hu ● ISSN 1589 1623 (Print) ● ISSN 1785 0037 (Online)
DOI: http://dx.doi.org/10.15666/aeer/1706_1351313521

PHYSICOCHEMICAL, CYTOTOXICITY AND GENOTOXICITY ASSESSMENT OF PALM OIL MILL EFFLUENT ON V79 CELLS

AWANG, N.* – MUSTAFFA, S. N. – MENG, C. K.

Environmental Health and Industrial Safety Programme, Faculty of Health Sciences, Universiti Kebangsaan Malaysia, Jalan Raja Muda Abdul Aziz, 50300 Kuala Lumpur, Malaysia

**Corresponding author*
e-mail: norm@ukm.edu.my

(Received 1st Dec 2018; accepted 15th Feb 2019)

Abstract. Palm oil mill effluent (POME) is the wastewater produced from palm oil refining activities like oil extraction, washing and cleaning processes in the mill that require an effective treatment before being discharged into waterways due to the effects it may have on the environment. The study was conducted in one of the mills that are located in Jerangau, Terengganu. This study was conducted to determine the physicochemical characteristics of POME on four different ponds which was mixing pond, facultative pond, algae pond and discharged pond. Discharged pond was the last pond for the POME treatment before it is discharged into the nearby river. The physicochemical parameters that have been determined to evaluate POME were pH, temperature, BOD, COD and TSS. The physicochemical characterization was carried out to determine the profile of POME at that time and the results showed that all parameters exceed the standards set by the Regulations of the Environmental Quality (Industrial Effluent) Regulations 2009 Standard B of the Environmental Quality Act 1974 except the temperature. In addition, this study also aimed to determine and compare the effects of cytotoxicity and genotoxicity of POME between the four ponds towards V79 cells. The cytotoxicity can be determined using MTT assay to evaluate the cytotoxic effect of POME on V79 cells. Meanwhile the genotoxicity was determined by using the alkaline comet assay to evaluate the genotoxic effect of POME on V79 cells. The study found that the POME in all ponds showed the cytotoxic effects on V79 cells and the POME in discharged pond showed the highest IC_{50} value compared to the other ponds which was 75% v/v. By using the IC_{25}, the treatment towards V79 cells showed the value of the moments tail in the discharged pond was the lowest compared to the others which was 0.898 ± 0.561. The values of the tail moment are much lower when compared to the positive control which was 6.58 ± 1.383. Therefore, it can be concluded that the POME in a discharged pond had a lowest cytotoxic and genotoxic effects on V79 cells compared to other ponds.
Keywords: *genotoxicity, palm oil mill effluent, physicochemical characterizations, V79 cells*

Introduction

Malaysia is the largest producer and exporter of palm oil. By 2010, Malaysia has contributed 41% of the world production for palm oil. While the palm oil industry has been recognized for its contribution towards economic growth and rapid development, it has also led to environmental pollution due to the production of large quantities of by-product from the oil extraction process (Rupani et al., 2010). The waste products from palm oil processing consist of oil palm trunks (OPT), oil palm fronds (OPF), empty fruit bunches (EFB), palm pressed fibres (PPF) and palm kernel shells, less fibrous material such as palm kernel cake and liquid discharge palm oil mill effluent (POME) (Rupani et al., 2010; Sulaiman, 2010). Among the waste generated, POME is considered the most harmful waste for the environment if discharged untreated (Rupani et al., 2010). POME is a thick brownish liquid that contains high amounts of total solids (40,500 mg/L), oil and grease (4000 mg/L), COD (50,000 mg/L) and BOD (25,000 mg/L). The disposal of this highly polluting effluent is becoming a major problem if it is not being treated

http://www.aloki.hu ● ISSN 1589 1623 (Print) ● ISSN 1785 0037 (Online)
DOI: http://dx.doi.org/10.15666/aeer/1706_1352313532

properly besides a stringent standard limit imposed by The Malaysian Department of Environment for effluent discharged (Latif Ahmad et al., 2003).

The discharge of effluents without proper treatment to the environment will lead to the severe pollution and will affect to the people. POME contains fatty acids, protein, carbohydrates and other plant materials in a high volumes which is capable to change the parameters of the environment, especially BOD, DO and COD levels (Verla et al., 2014). In addition, the effluent also contains a colloidal suspension that affects the water such as a brown solid color, colloidal and oily (Latif Ahmad et al., 2003). It was identified as the major source of water pollution in Malaysia. If it is not treated before being discharge, this effluent would be a major problem to the environment (Lai et al., 2011).

This study discovers the cytotoxic and genotoxic effect of POME towards V79 cells that can be beneficial as safety alert to industries and community. Besides that, this study also comparing the cytotoxicity and genotoxicity effects between four ponds of POME at the mills. This research study has proven that there were cytotoxic effects and genotoxic effects that can be seen in the POME for four ponds. The in vitro cytotoxicity and genotoxicity study in this work will help the researchers to uncover the critical issue regarding the health risk associated with wastewater produced from palm oil refining activities and increase awareness among industrial practisers, thus leading towards more efficient and safe wastewater management.

Materials and methods

Materials

Chemicals used in this study were trypan blue solution, ethidium bromide (TBR), sodium hydrogen carbonate ($NaHCO_3$), hydrochloric acid (HCl), sodium hydroxide (NaOH), sodium chloride (NaCl), disodium hydrogen phosphate (Na_2HPO_4), triton X-100, distilled water, low melting agar (LMA) and normal melting agar (NMA). In addition, COD digestion reagent low range and high range for measuring COD from Hach Company (USA), powdered DMEM medium (supplemented with L-Glutamine and without sodium bicarbonate hydrogen) obtained from Gibco, US also used. Other chemicals were fetal bovine serum (FBS) obtained from JR Scientific USA, and penicillin/streptomycin from PAA (Germany). MTT tetrazolium salt from Sigma-Aldrich, USA and a dimethylsulfoxide (DMSO) solution from Fiesher Scientific, UK is also used in this study. Finally, the materials used are ethyl diamine disodium tetraacetate (Na2-EDTA), potassium chloride (KCl) and potassium dihydrogen phosphate (KH_2PO_4) from Ajax Chemical Laboratories, Unilab (NSW, Australia).

Sampling location and time

The study was conducted at one of the mills that are located at Terengganu. The mill produced the products such as crude palm oil (CPO) and kernel palm oil. The sampling was conducted on November, 2016. The samples were taken in the morning which was at 10 am until 1 pm and the samples taken was three times (triplicate) from each ponds which the effluents was collected. There are four ponds of effluent at the palm oil mill where all the product of filtration and purification will be stored in those ponds before being discharged into a nearby river. The four ponds were mixing pond, facultative pond, algae pond and discharged pond.

http://www.aloki.hu ● ISSN 1589 1623 (Print) ● ISSN 1785 0037 (Online)
DOI: http://dx.doi.org/10.15666/aeer/1706_1352313532

Physicochemical analysis

The physicochemical properties that are being determined in this study were pH and temperature. The readings of these parameters were determined during the sampling because the readings are direct reading (in-situ). In addition, the reading of biochemical oxygen demand (BOD), chemical oxygen demand (COD) and total suspended solids (TSS) were also be determined. All the three readings of these parameters are analyzed *ex-situ* where the reading of this parameter evaluated in the laboratory using appropriate equipment.

Cell line

The cytotoxicity study was performed on V79 cell line, which is a type of lung fibroblast cells derived from Chinese hamster male, Cricetulus griseus. The cells were cultured in complete growth media Dulbecco's Modified Eagle's Medium (DMEM) enriched with 10% fetal bovine serum (FBS) and 1% penicillin/streptomysin.

Cell viability assay

The viability of V79 cells were determine using 3-(4, 5-dimethylthiazol-2-yl)-2, 5-diphenyltetrazolium bromide (MTT) assay (Mossman, 1983). Cells were seeded in a sterile 96-well microplate at density of 5 × 104 cells/mL and incubated for 24 h. Later, the medium in each well was discarded and replaced with a fresh medium containing tested samples at concentrations 100, 50, 25, 12.5 and 6.25% v/v. After 24 h treatment, 20 µL of 5 mg/mL MTT solution was added to each well and incubated for 4 h. An approximate of 180 µL of media was removed and added with 180 µL DMSO in each well. After 15 min incubated, the plate was agitated using orbital shaker to ensure the complete dissolve of the crystal formazan. The Optical Density (OD) of each well was measured at 570 nm wavelength using iMark Microplate Reader (BioRad, USA). The inhibitory concentration that induced cytotoxicity in 50% cell population (IC_{50}) was calculated and compared with the positive control. Menadione was used as positive control and untreated cells as a negative control.

Alkaline comet assay

The genotoxic effect of POME on V79 cells was assessed using comet assay, carried out under alkaline condition (Singh et al., 1988). The cells were seeded in 6-well plate at density of 5 × 104 cells/mL and incubated for 24 h. After 24 h, the media was discarded from each well and replaced with a fresh media containing water sample treatment and incubated for next 24 h. The procedure was performed in dark condition to avoid any interfering factors that can contribute to DNA damage such as direct radiation from the light. After that, the cells were harvest and pellet was collected. Then, the pellet was suspended in 3 mL PBS and then was aliquot 1 mL each into eppendorf tube. The tubes were then centrifuged at 2500 rpm for 5 min at 4 °C. The pellet was then washed with PBS and centrifuged again. Later, the pellet was collected and stored in cold condition.

Fully frosted slides were covered with 0.6% normal melting point (NMP) agarose. When this slide was solidified, a second layer containing the cells mixed with 0.6% low melting point (LMP) agarose was placed on the slide. After 5 min of solidification on ice, the slides were covered with 0.6% LMP agarose. They were then immersed for 1 to

http://www.aloki.hu ● ISSN 1589 1623 (Print) ● ISSN 1785 0037 (Online)
DOI: http://dx.doi.org/10.15666/aeer/1706_1352313532

24 h in 4 °C lysis solution. The slides were then placed on a horizontal gel-electrophoresis tank, facing the anode. The fresh electrophoretic buffer was filled into the tank in which the slides were put for 20 min to allow DNA unwinding and the expression of alkali-labile sites. Denaturation and electrophoresis were performed at 4 °C under dim light. Electrophoresis was carried out for 20 min at 25 V (300 mA). Subsequently, the slides were rinsed gently three times with a neutralization buffer in order to remove excess alkali and detergents. Then, each slide was stained with 30 µL ethidium bromide covered with a cover-slip. Fifty randomly selected cells were analyzed per sample. The slides were examined at 250× magnifications with a fluorescence microscope equipped with a 515-560 nm excitation filter and a 590 nm barrier filter, and images of cells were analyzed with the computerized image analysis system Comet Score III. The tail length was evaluated to quantify DNA damage.

Statistical analysis

All the investigated data were statistically analyzed using (SPSS). The comparisons between groups were done by one way analysis of variance (ANOVA). The level of statistical significance was set at P value of < 0.05.

Results and discussion

Physicochemical analysis

Table 1 showed the mean values ± SEM (standard error mean) for each parameter (pH, temperature, BOD, COD and TSS) in different types of ponds. The Environmental Quality (Industrial Effluent) Regulations 2009 Standard B, Environmental Quality Act 1974 was used as a standard for comparison. The pH value obtained for effluent sample in mixing, facultative, algae and discharge ponds was 4.51 ± 0.20, 7.62 ± 0.16, 8.58 ± 0.29 and 8.91 ± 0.12 respectively. All the values were below the standard limit allowed by the Environmental Quality (Industrial Effluent) Regulations 2009 Standard B, the Environmental Quality Act 1974 (pH 5.5- 9.0) except for effluent sample from mixing pond which has the acidic pH. This might be due to the accumulation of raw POME in mixing pond as the effluent collected in mixing pond was directly from the mill. As the POME underwent biodegradation process along the way to the next ponds which were facultative, algae and discharge ponds, the effluent turned out to be basic and increase the pH in the respective ponds. Biodegradation occurred whereas the active microorganisms used up organic materials in POME as their nutrients and decomposed them into methane, carbon dioxide, hydrogen sulphide and water. According to Okwute and Nnennaya (2007), the pH of the raw POME released is acidic but after the biodegradation occurs, it gradually turns into alkali. This is because long-term POME retention in each pond causes biodegradation to occur where it depends on active microorganisms, which use organic ingredients in POME as nutrients and ultimately elaborate these organic substances in the form of simple products such as methane, carbon dioxide, Hydrogen sulfide and water (Okwute and Nnennaya, 2007; Jameel et al., 2011).

For the temperature, the average value obtained from the mixing pond, facultative pond, algae pond and the discharged pond were 32.80 ± 0.61 °C, 30.00 ± 0.20 °C, 27.60 ± 0.20 °C and 27.47 ± 1.88 °C, respectively. Based on the standards, the temperature obtained did not exceed the temperature permitted (40 °C). However, the

http://www.aloki.hu ● ISSN 1589 1623 (Print) ● ISSN 1785 0037 (Online)
DOI: http://dx.doi.org/10.15666/aeer/1706_1352313532

temperature in mixing pond was slightly higher (32.8 °C) compared to another ponds. This is because mixing pond was the first pond introduced with effluent discharged from the mill which was normally in high temperature (80-90 °C) (Khalid et al., 1992). Nevertheless, the temperature of the effluent decreased by time as heat released. In our study, the sampling was conducted after a certain period the effluent was released (the effluent released in the morning), and thus gave the lower monitored temperature compared to the temperature when effluent was first released. Besides, the temperature also dropped as the effluent flew to the next ponds and that was why we could observe the temperature in the each pond was lower compared to the pond before.

Table 1. *Average value of pH, temperature, BOD, COD and TSS for POME obtained in mixing ponds, facultative ponds, algae ponds and discharged ponds*

Ponds	Parameters				
	pH	Temperature (°C)	BOD (mg/L)	COD (mg/L)	TSS (mg/L)
Mixing	4.51 ± 0.20	32.80 ± 0.61	25600.00 ± 300.00	2241.33 ± 18.95	22524.00 ± 2340.00
Facultative	7.62 ± 0.16	30.00 ± 0.20	71.00 ± 2.00	338.67 ± 7.02	151.67 ± 14.04
Algae	8.58 ± 0.29	27.60 ± 0.20	35.00 ± 2.65	161.33 ± 4.04	45.67 ± 4.16
Discharged	8.91 ± 0.12	27.47 ± 1.88	25.00 ± 3.61	136.00 ± 3.61	34.33 ± 4.16

In the other hand, the BOD and COD in mixing and facultative ponds were higher than standard limit. The value allowed for both BOD and COD were 50 and 200 mg/L. The value for BOD and COD in mixing pond were 25600.00 ± 300.00 and 2241.33 ± 18.95 mg/L, while in the facultative pond the value for both were 71.00 ± 2.00 and 338.67 ± 7.02 mg/L. Meanwhile, BOD and COD content in algae and discharge ponds were still in allowed level.

Meanwhile, the TSS value for mixing and facultative ponds exceeded the standard limit (100 mg/L) compared to the other two ponds. The value for each pond was 22524.00 ± 2340.00 mg/L, 151.67 ± 14.04 mg/L, 45.67 ± 4.16 mg/L and 34.33 ± 4.16mg/L respectively for each pond.

The results obtained for parameters of biochemical oxygen demand (BOD), chemical oxygen demand (COD) and total suspended solids (TSS) showed that the average value for those parameters of POME in the mixing pond was the highest than the others. The mixing pond normally contained the raw POME which was first released from the mill. Raw POME was a high pollution wastewater with high BOD and COD which can cause severe pollution to the environment that eventually polluted the water sources (Lam et al., 2011). Therefore, the values of BOD, COD and TSS in the mixing pond were higher compared to the other ponds. The BOD and COD values are important indicator to define the composition of wastewater and its effects towards the environment (Jameel et al., 2011). However, the content of BOD, COD and TSS decreased as the effluent distributed to the next ponds which were facultative, algae and discharged ponds, the value decreased. This was due to some processes that took place along the way the POME was released, such as a pre-treatment in the mixing pond, and biological treatments in the facultative and algae ponds. The pre-treatment was performed to reduce the suspended solids and oils by using flocculation, solvent extraction, adsorption and membrane separation processes (Latif et al., 2003).

http://www.aloki.hu ● ISSN 1589 1623 (Print) ● ISSN 1785 0037 (Online)
DOI: http://dx.doi.org/10.15666/aeer/1706_1352313532

According to Wong (1980), the treatment system of POME usually consists of anaerobic and aerobic treatments. Aerobic treatment was required to reduce the concentration of BOD to produce effluents that comply with national effluent discharge standards (Salihu and Alam, 2012).

Based on the results of the study, all parameters such as pH, COD, BOD and TSS of POME in mixing pond were exceed the specified limits except for the temperature where the values are still in the range. Whereas the result obtained in the facultative pond for all parameters were above the prescribed standard except for pH and temperature. Meanwhile, for algae ponds and discharged pond, all parameters such as pH, temperature, BOD, COD and TSS do not exceed the prescribed standards.

Cytotoxicity of palm oil mill effluent sample on V79 cells

Figures 1–4 showed a graph of cell viability against sample concentration from each tested pond. The viability of V79 cells exhibited a decrease in concentration-dependent manner for sample from each pond. Based on *Figure 1,* the percentage of cell viability was 106.73 ± 0.025, 103.20 ± 0.026, 82.58 ± 0.05%, 57.88 ± 0.067% and 6.46 ± 0.03% at concentrations 6.25, 12.5, 25, 50 and 100% v/v. The IC50 was obtained at concentration 58% v/v. Meanwhile, for facultative pond (*Fig. 2*), IC50 value was 61% v/v. The cell viability reduced from 79.8 ± 0.018, 76.06 ± 0.028, 64.21 ± 0.029 59.32 ± 0.032% and 8.84 ± 0.01% for concentrations 6.25, 12.5, 25, 50 and 100% v/v. Next, IC50 concentration for sample from algae pond (*Fig. 3*) was determined at 62% v/v with cell viability decreased from 99.4 ± 0.043, 101.77 ± 0.022, 80.52 ± 0.014, 60.84 ± 0.024 and 13.85 ± 0.012% for concentrations as previous. For the discharged pond (*Fig. 4*), the graph also showed a slight increase in cell viability for concentrations 6.25, 12 and 5.25% v/v in which the viability was 94.8 ± 0.011, 107.33 ± 0.063, and 109.19 ± 0.051 respectively. However, the viability started to decrease to 83.02 ± 0.018 and 15.48 ± 0.015% when treated with 50 and 100% v/v sample. The IC50 value obtained was 72% v/v. Based on all the graphs displayed, we can observed that there were some points in the graphs where the cell viability at certain concentration was higher from the previous concentration and this might be due to adaptive response of the cells towards the certain concentration (Klassen and Eaton, 2001).

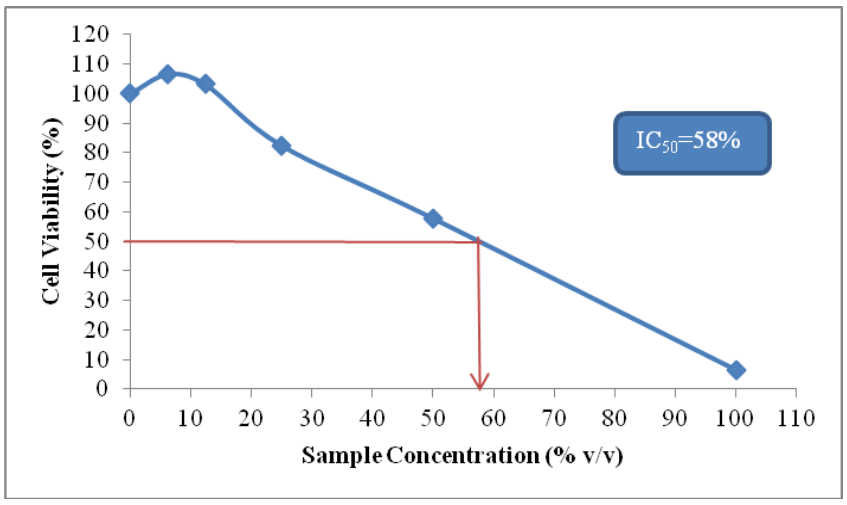

Figure 1. *The viability of the V79 cell against the effluent sample concentration of the mixing pond after being treated for 24 h*

http://www.aloki.hu ● ISSN 1589 1623 (Print) ● ISSN 1785 0037 (Online)
DOI: http://dx.doi.org/10.15666/aeer/1706_1352313532

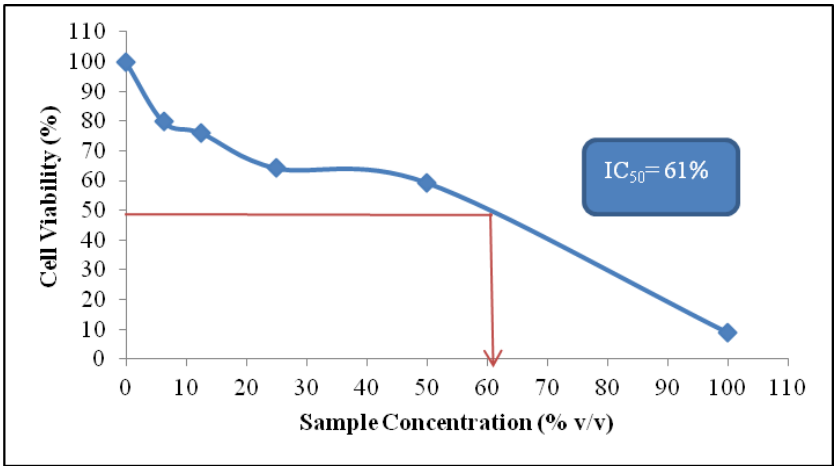

Figure 2. *The viability of V79 cell against the concentration of effluent samples from the facultative pond after being treated for 24 h*

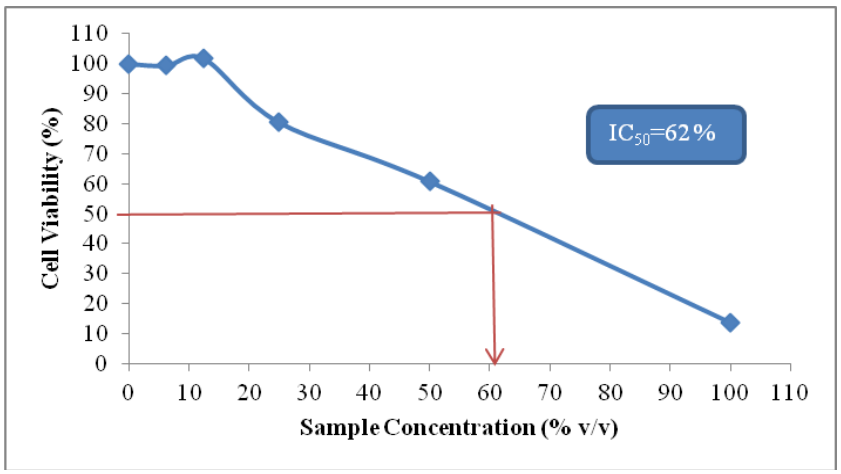

Figure 3. *The viability of the V79 cell against the effluent sample concentration of the algae pond after being treated for 24 h*

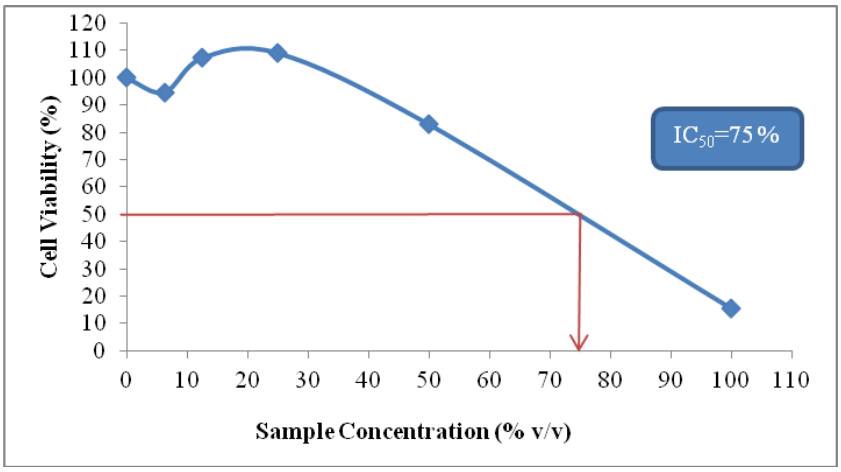

Figure 4. *The viability of the V79 cell against the concentration of the effluent sample from the discharged pond after being treated for 24 h*

http://www.aloki.hu ● ISSN 1589 1623 (Print) ● ISSN 1785 0037 (Online)
DOI: http://dx.doi.org/10.15666/aeer/1706_1352313532

Based on the result obtained, the cytotoxicity of POME in the mixing pond was the highest than the others. The highly cytotoxicity of POME in mixing pond was caused by the content of oil and grease compounds present in the mixing pond where those compound can cause cytotoxic effects to POME. The highly oil and grease content is due to the production of POME directly from the mill without any treatment. The high content of oil and grease was proven by Latif Ahmad et al. (2003) where he stated that the raw sample consists of high oil and grease (191 mg/L). Furthermore, the production of raw POME is from the oil extraction, washing and cleaning process in the mill and it contained cellulose, fat, oil and grease (Rupani et al., 2010). In addition, oils and greases are considered dangerous pollutants especially in aquatic environments, since these compounds are highly toxic to aquatic organisms (Agamuthu, 1995).

On the other hand, the cytotoxicity of POME in discharged pond was the lowest compared to other ponds. The decrease of cytotoxicity in the discharged pond was due to the presence of biological treatments in the facultative pond and algae pond. POME in the discharged pond was the result from the treatment on those ponds. This biological treatment depends largely on active microorganisms, which use organic ingredients in POME as nutrients and ultimately degradation of these organic matter into simple products such as methane, carbon dioxide, hydrogen sulfide and water (Jameel et al., 2011). In addition, according to Azbar and Yonar (2004), wastewater treatment of palm oil refinery industry based on coagulation and biological methods caused in the overall removal of 92-96% COD, 83-98% TSS and 93-95% oil.

Genotoxicity

Comparison of DNA damages between mixing pond, facultative ponds, algae ponds and discharged pond

Figure 5 showed the tail moment of V79 cell treated with concentration IC25 of effluent sample from each pond together with menadione and untreated cells as positive and negative controls. The IC25 values was choose as the treatment concentration in order to avoid the highly damaged cells have gone into apoptosis and that the fragmented DNA disappeared from the gel, leaving only relatively undamaged cells.

Based on the bar graph, cells treated with POME from mixing pond gave tail moment 1.948 ± 0.187 while for the facultative pond the tail moment was 1.560 ± 0.220. Meanwhile, the tail moment value 1.234 ± 0.204 and 0.898 ± 0.561. was attributed for both algae and discharged ponds. On the other side, the tail moment values for positive and negative controls were 6.58 ± 1.383 and 0.328 ± 0.200, respectively. However, the genotoxic effecs of POME from all the four ponds was not significant when compared to negative control at $p < 0.05$.

Nevertheless, the genotoxic effect still could be detected in each pond as the tail moment was formed based on alkaline comet assay conducted. For example, POME sample from mixing pond induced the highest tail moment formation compared to other ponds. This might due to the presence of phenolic compounds in raw POME accumulated in mixing pond and suggested with finding by Jameel et al. (2011) that reported palm oil refineries contained some phenolic compounds such as Gallic, protocatechuic, 4-hydroxybenzoic, 4-hydroxylphenylacetic, caffeic, syringic acid, p-coumaric and ferulic acid. Based on Li et al. (2005), they found that phenol is a genotoxin evidence that can cause DNA damage. However, the biological treatments carried out as the effluent move to the next ponds eliminated those phenolic compounds

http://www.aloki.hu ● ISSN 1589 1623 (Print) ● ISSN 1785 0037 (Online)
DOI: http://dx.doi.org/10.15666/aeer/1706_1352313532

(Hussain et al., 2015) and thus, decreased the toxicity of POME by ponds. That was why the tail moment observed in this study reduced by ponds.

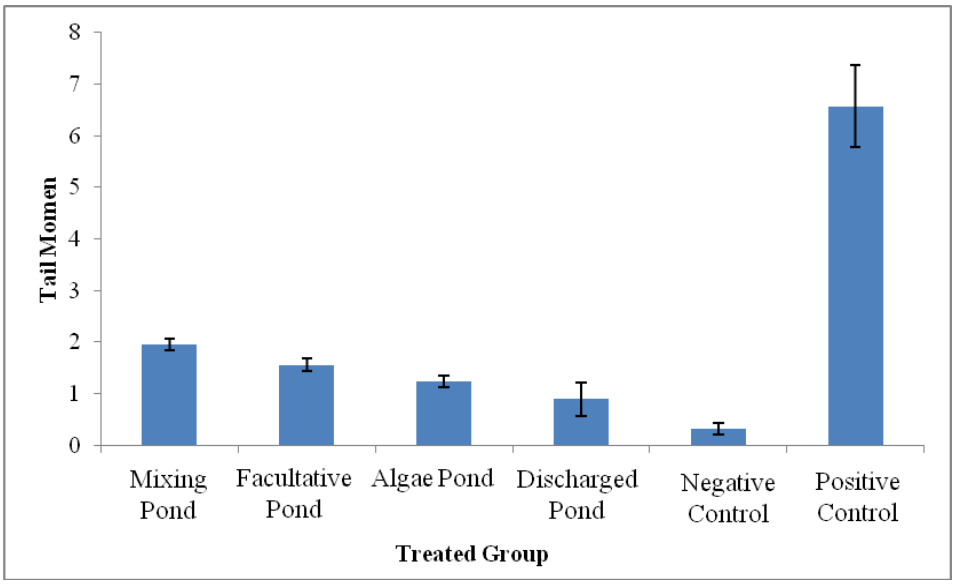

Figure 5. *Comparison of the tail moment of V79 cell for negative control, positive control and effluent samples for each pond which were mixing pond, facultative pond, algae pond and discharged pond according to their respective concentration of* IC_{25}

Conclusion

From this study, the physicochemical assessment of POME from the mixing and facultative ponds at the sampling location in Terengganu has exceeded the standard limit allowed by the Environmental Quality (Industrial Effluent) Regulations 2009 Standard B, Environmental Quality Act 1974. The other two ponds which were algae and discharged ponds were still under control. However, the MTT and alkaline comet assays conducted showed that POME sample from all ponds have cytotoxic and DNA damage effects towards V79 cells based on IC50 values and tail moments values obtained. Even though the treatment processes in each pond might be able to reduce the effects of POME before it was discarded into the nearby river, the long term effect of exposure of this wastewater is still under concern. Thus, a more efficient and proper management and treatment of wastewater in the sampling location are still required. For example is by performing a pre-treatment of POME wastewater using ultrafiltration membrane technique which coupled with absorption treatment (Azmi and Yunos, 2014). The ultrafiltration treatment coupled with adsorption treatment as pre-treatment is and advantageous method for the POME treatment. This treatment offer the easier operating conditions, more ability to combine with two technique and easier control of the system.

Acknowledgements. We would like to thank Palm oil mill at Jerangau, Terengganu for the cooperation given. Technical support from the laboratory assistants of Faculty of Health Sciences Universiti Kebangsaan Malaysia is gratefully acknowledged.

http://www.aloki.hu ● ISSN 1589 1623 (Print) ● ISSN 1785 0037 (Online)
DOI: http://dx.doi.org/10.15666/aeer/1706_1352313532

REFERENCES

[1] Agamuthu, P. (1995): Palm Oil Mill Effluent Treatment and Utilization. – In: Sastry, C. A., Hashim, M. A., Agamuthu, P. (eds.) Waste Treatment Plant. Narosa Publishing House, New Delhi pp: 338-360.

[2] Azbar, N., Yonar, T. (2004): Comparative evaluation of a laboratory and full-scale treatment alternatives for the vegetable oil refining industry wastewater. – Process Biochemistry 39(7): 869-875.

[3] Azmi, N. S., Yunos, K. F. M. (2014): Wastewater treatment of palm oil mill effluent (POME) by ultrafiltration membrane separation technique coupled with adsorption treatment as pre-treatment. – Agriculture and Agricultural Science Procedia 2: 257-264.

[4] Hussain, A.,. Dubey, S. K., Kumar, V. (2015): Kinetic study for aerobic treatment of phenolic wastewater. – Water Resources and Industry 11: 81-90.

[5] Jameel, P.,. Idris, Z. M., Alam, M. Z. (2011): Effects of physicochemical parameters on the production of phenolic acids from palm oil mill effluent under liquid-state fermentation by Aspergillus niger. – Food Chemistry Journal 124: 1595-1602.

[6] Khalid, A. R., Mustafa, W. A. W. (1992): External benefits of environmental regulation: resource recovery and the utilisation of effluents. – The Environmentalist 12: 277-285.

[7] Klassen, C. D., Eaton, D. L. (2001): Casarett's and Doull's Toxicology: Principle of Toxicology. – McGraw Hill, New York.

[8] Lai, M. E., Lheang, L. S., Salimon, J. (2011): Effectiveness Of Palm Oil Sewage Treatment Using Zero Sewage Technology. – UKM Coolocium, Bangi.

[9] Lam, M. K., Lee, K. T. (2011): Renewable and sustainable bioenergies production from palm oil mill effluent (POME): Win-win strategies toward better environmental protection. – Biotechnology Advances 29: 124-141.

[10] Latif, A., Suzylawati, I., Norliza, I., Subhash, B. (2003): Removal of suspended solids and residual oil from palm oil mill effluent. – Journal of Chemical Technology and Biotechnology 78(9): 971-978.

[11] Latif Ahmad, A., Ismail, S., Bhatia, S. (2003): Water recycling from palm oil mill effluent (POME) using membrane technology. – Desalination 157(1): 87-95.

[12] Li, Y., Qu, M., Sun, L., Wu, Y., Chen, Y., Chen, H., Kong, Z and Liu, Z. (2005): Genotoxicity study of phenol and ocresol using the micronucleus test and the comet assay. – Toxicological & Environmental Chemistry 87: 3365-372.

[13] Okwute, L. O., Nnennaya, I. R. (2007): The environmental impact of palm oil mill effluent (POME) on some physicochemical parameters and total aerobic bioload of soil at a dump site in Anyigba, Kogi State, Nigeria. – African Journal of Agricultural Research 2(12): 656-662.

[14] Rupani, P. F., Singh, R. P., Ibrahim, M. H., Esa, N. (2010): Review of current palm oil mill effluent (POME) treatment methods: vermicomposting as a sustainable practice. – World Applied Sciences Journal 10(10): 1190-1201.

[15] Salihu, A., Alam, M. Z. (2012): Palm oil mill effluent: a waste or a raw material? – Journal of Applied Sciences Research 8(1): 466-473.

[16] Singh, N. P., Mc Coy, M. T., Tice, R. R., Schneider, E. L. (1988): A simple technique for quantitation of low levels of DNA damage in individual cells. – Exp Cell Res 175: 184-191.

[17] Sulaiman, A. (2010): Accelerated start-up of a semi-commercial digester tank treating palm oil mill effluent with sludge seeding for methane production. – World Appl. Sci. J 8(2): 247-258.

[18] Verla, A. W., Adowei, P., Verla, E. N. 2014): Physicochemical and microbiological characteristic of palm oil mill effluent (POME) in Nguru: Aboh Mbaise, Eastern Nigeria. – Acta Chimica & Pharmaceutica Indica 4(3): 119-125.

[19] Wong, K. K. (1980): Application of ponding systems in the treatment of palm oil mill and rubber mill effluents. – Pertanika Journal 3(2): 133-141.

http://www.aloki.hu ● ISSN 1589 1623 (Print) ● ISSN 1785 0037 (Online)
DOI: http://dx.doi.org/10.15666/aeer/1706_1352313532

INVESTIGATING CONTRIBUTIONS OF GASES, METEOROLOGICAL PARAMETERS, AND AEROSOLS TOWARDS TROPOSPHERIC OZONE VARIABILITIES OVER MEGACITY LAHORE (PAKISTAN)

PARVEZ, S. – RANA, A. D. – UL-HAQ, Z.* – BATOOL, S. A. – ALI, M. – TARIQ, S. – MAHMOOD, K. – BANO, S.

GIS and Remote Sensing Group, Department of Space Science, University of the Punjab Lahore, Pakistan

**Corresponding author*
e-mail: zia.spsc@yahoo.com

(Received 19th Mar 2019; accepted 4th Jul 2019)

Abstract. We investigated contributions of some tropospheric gases, meteorological parameters, and aerosol burden measured as aerosol optical depth (AOD) towards Tropospheric Ozone ($TropoO_3$) variabilities over Lahore by developing a stepwise multiple linear regression model. The tropospheric gases include; Methane (CH_4), Carbon Monoxide (CO), Carbon Dioxide (CO_2), and Sulphur Dioxide (SO_2), whereas the meteorological parameters include; cloud fraction (CLF), outgoing long-wave radiation (OLR), relative humidity (RH), temperature (Temp), and surface wind-speed (WS). Data products of these parameters have been retrieved from various satellite sensors during October 2004 – September 2015. Time series distributions of both observed and modeled $TropoO_3$ concentrations show similar increasing trends except for few months. Moreover, monthly-means of these observed and modeled $TropoO_3$ concentrations indicate similar decreasing trends with maximum during spring and summer (monsoon) seasons. Based upon weighted contributions of standardized regression coefficients, modeled $TropoO_3$ concentration was found dependent upon OLR[0.458], WS[0.262], CLF[0.256] $TropoSO_2$[–0.097], TropoCO[–0.231], and RH[–0.320] out of all parameters used in this study. Modeled $TropoO_3$ concentrations were validated against an independent source of $TropoO_3$ concentrations retrieved from original subtracted product of OMI-MLS over Lahore and the results were found in good agreement. The study is unique and would be helpful for further research investigations.
Keywords: *regression modeling, atmospheric outlook of Lahore, ozone contributors, ecology, atmospheric remote sensing*

Introduction

$TropoO_3$ is one of the short-lived but major atmospheric pollutants that plays a key role towards climate change (UNEP and WMO, 2011) by modifying the chemical composition of the troposphere and its oxidation capacity (Gauss et al., 2003). It is considered as a primary precursor for the production of hydroxyl radical (OH), that acts as an oxidizing agent severely disturbing the occurrence of tropospheric trace gases (Seinfeld and Pandis, 2016). $TropoO_3$ absorbs short-wave solar radiations and after attenuation re-radiates it in the form of long-wave radiations (Shan et al., 2008; Pal, 2010; Tan et al., 2014). $TropoO_3$ has harmful effects on human health, vegetation health & yield, and sensitive ecosystems (EPA, 2003; The Royal Society, 2008; Avnery et al., 2011; Burney and Ramanathan, 2014). Also, $TropoO_3$ is one of the major anthropogenic greenhouse gases, which is responsible for global warming (IPCC, 2013). Ozone in troposphere is either produced from chemical reactions of NO_x, CH_4, CO, and volatile organic compounds (VOCs) through non-linear, complex, and feedback-regulated processes in the presence of solar radiations (El-Fadel et al., 2002; Pulikesi et al., 2006;

http://www.aloki.hu ● ISSN 1589 1623 (Print) ● ISSN 1785 0037 (Online)
DOI: http://dx.doi.org/10.15666/aeer/1706_1353313553

Stevenson et al., 2006; Young, 2013; Seinfeld and Pandis, 2016) or transported directly from the stratosphere (Hsu and Prather, 2009). From an ecological point of view, both increased emission and destruction of VOCs by $TropoO_3$ may affect several of their multiple functions (Lerdau and Slobodkin, 2002; Holopainen, 2004; Van, 2009; Yuan et al., 2009). There are a number of anthropogenic and natural sources of these $TropoO_3$ precursors e.g.; crop-residue burning, biomass burning, fossil fuel combustion, enhancement of volatile organic compounds through convections of CO and aerosols, vehicular emissions, industrial processing, energy production activities, waste management, lightning NO_x, and soil emissions (Jaeglé et al., 2004; Satheesh and Moorthy, 2005; Stevenson et al., 2006; Aghedo et al., 2007; Wang et al., 2012; Ganesan et al., 2013; Ul-Haq et al., 2014). Anthropogenic activities pose numerous threats to the functioning, structural growth and diversity of natural and semi-natural ecosystems (Bobbink, 1989). Globally, an increase of 36% in $TropoO_3$ burden has been reported since 1850 (Cooper et al., 2014). $TropoO_3$ has strong effects on ecological interactions based on VOC signaling (Pinto et al., 2010).

Various natural, meteorological and anthropogenic factors are responsible for $TropoO_3$ concentration variability. Natural factors include; seasons, Earth-Sun distance, and location (altitude, latitude, and longitude), meteorological factors include; temperature, precipitation, humidity, soar flux, and wind speed, while anthropogenic factors include; emissions from precursor pollutants, biomass burning, vehicular emissions, and industrial processing (Ahmad and Aziz, 2013; Iqbal et al., 2014). Aerosols decrease $TropoO_3$ formation in polluted areas (Satheesh and Moorthy, 2005; Xing et al., 2017) and also decline its concentration after reacting with tropospheric gases (Sahoo et al., 2005). The primary objective of this study is to investigate the potential contributions of major tropospheric gases, meteorological parameters, and aerosol burden towards $TropoO_3$ variability over Lahore. $TropoO_3$ monitoring is being carried out either by onboard satellite sensors (Cooper et al., 2014; Ziemke et al., 2014) or via ground-based stations (Fioletov et al., 2008). Remote sensing techniques provide cost-effective, synoptic and repetitive coverages for spatio-temporal monitoring of tropospheric gases, meteorological parameters, and aerosol burden either at large or small scales. Whereas, data acquisition via ground-based stations is expensive, time-consuming, and almost impossible for inaccessible areas. The present study is carried out by retrieving datasets from onboard satellite sensors including; AIRS, AMSU-A, MODIS, MOPITT, OMI, and TRMM, as well as GLDAS model. To the best of our knowledge, no detailed study has so far been published for assessing $TropoO_3$ variability as functions of remotely sensed major tropospheric gases, meteorological parameters, and aerosol burden over Lahore.

Material and Methods

Location and description of the study area

Metropolitan corporation Lahore (31.5204°N, 74.3587°E) is the capital city of the Punjab province in Pakistan. As per 6th Population Census 2017 results, Lahore is the second-most populous city and financial hub of Pakistan after Karachi having population over 11 million and an area of 1,172 km^2 (*Figure 1*). Lahore is bounded by Sheikhupura District on the north and west bifurcated by Ravi River, Kasur District on its south, and Wagah Border along Indian province Punjab on the east. Lahore is the 16th largest and rapidly growing city in the world (CMF, 2018). Being financial hub, Lahore contains all types of Industrial, manufacturing, construction, business, and IT related activities

http://www.aloki.hu ● ISSN 1589 1623 (Print) ● ISSN 1785 0037 (Online)
DOI: http://dx.doi.org/10.15666/aeer/1706_1353313553

including but not limited to; pharmaceutical and chemical factories, steel mills, construction materials, power generation, manufacturing of motor vehicles, home appliance, electronics, leather goods, and paper products (Alam et al., 2012; Ali et al., 2014). Major air pollution sources in Lahore include automobile emissions, road dust, and biomass burning along with air pollutants transported from nearby regions (Alam et al., 2010, 2014). The Indian states of Punjab, Haryana, and Uttar Pradesh (shown in *Figure 1*) are reported to be the well-known air-pollutant emission sources from large scale rice and wheat crops generated residue burning and periodically transported to Lahore (Sidhu and Beri, 2008; Badarinath et al., 2009; Mishra and Shibata, 2012). Lahore falls under hot semi-arid and wet category based on the Köppen climate classification system with highly hot and wet summers (heavy monsoon rainfalls with frequent dust storms during June to September), while dry and cold winters (from December to February). Spring (March to May) and autumn (September to November with extensive crop residue burning in the surrounding regions) seasons are also observed in Lahore (Ali et al., 2014).

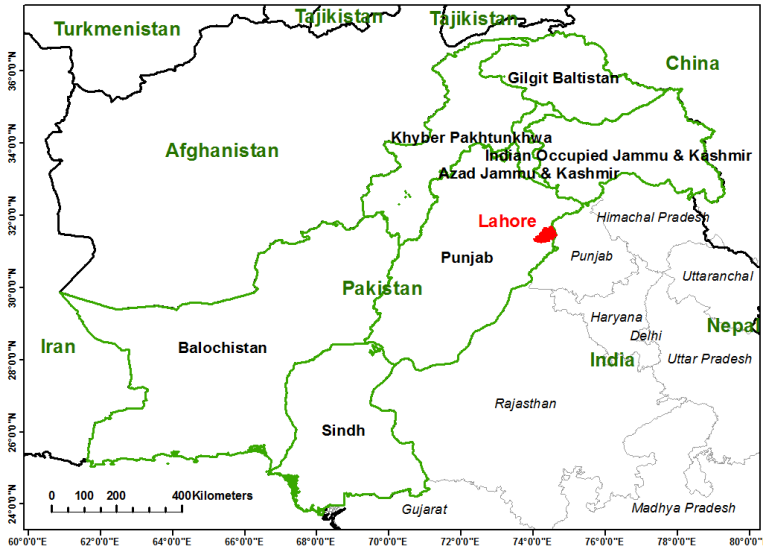

Figure 1. *Map showing the geographical location of Lahore (31.5204°N, 74.3587°E). (Source: https://www.statsilk.com/maps/download-free-shapefile-maps)*

Datasets

Host of satellite borne sensors have been providing online data products for monitoring and analyzing atmospheric gases, meteorological parameters, and aerosol burden measured as aerosol optical depth (AOD). For current study, we retrieved monthly-mean data products of TropoCH_4, TropoCO_2, CLF, and OLR, while daily datasets of RH, and surface temperature over Lahore from Atmospheric Infrared Sounder (AIRS, Pagano et al., 2003; Abed, 2017) and the Advanced Microwave Sounding Unit-A (AMSU-A, Aumann et al., 2003) onboard AURA satellite operational since 2002. The combined use of AIRS and AMSU-A data products basically offers new as well as improved measurements (Susskind et al., 2003). Data products of TropoNO_2 (daily), TropoO_3 (monthly-mean), and planetary boundary layer SO_2 (monthly-mean) were acquired from NASA's EOS Ozone Monitoring Instrument (OMI) onboard Aura satellite launched in a sun-synchronous polar orbit on July 15, 2004 at an altitude of 705 km and inclination of

http://www.aloki.hu ● ISSN 1589 1623 (Print) ● ISSN 1785 0037 (Online)
DOI: http://dx.doi.org/10.15666/aeer/1706_1353313553

98.2° (Levelt et al., 2006a; Ziemke et al., 2011). OMI provides almost global coverage daily with a resolution of 13×24 km^2 at nadir while 13×100 km^2 at off-nadir (Boersma et al., 2006). It consists of hyperspectral imaging sensors to record radiances in the range of 270–500 nm (Levelt et al., 2006a,b). Additionally, monthly-mean data of TropoCO was retrieved from MOPITT onboard Terra, whereas, AOD from MODIS onboard Aqua deep blue. The datasets of surface level precipitation rate and near surface wind speed over Lahore were obtained from Tropical Rainfall Measuring Mission (TRMM, Liu et al., 2012) and Global Land Data Assimilation System (GLDAS, Fang et al., 2009), respectively. For validation of our resultant modeled, the original TropoO_3 data product of subtracted monthly-means of Total Column Ozone retrievable from OMI and Stratospheric Column Ozone retrievable from MSL onboard Aura satellite was utilized (Ziemke et al., 2006). Details about all the data products of major tropospheric gases, meteorological parameters, and aerosols used for this study are given in *Table 1*.

Methodology

We developed a bivariate correlation matrix representing tropospheric gases (CH_4, CO, CO_2, NO_2, O_3, and SO_2), meteorological parameters (CLF, OLR, PR, RH, Temp, and WS), and aerosol burden over Lahore using monthly-mean remotely sensed data during October 2004 – September 2015 (shown in *Table 2*). Each parameter mentioned in *Table 2* has either positive value (shown in blue colored bar) or negative value (shown in red colored bar), which indicates the type of correlation between the respective parameters. Longer the length of colored bars (either blue or red), stronger would be the correlation (either positive or inverse, respectively) between the corresponding parameters. Whereas, colored bars having smaller lengths (smaller values either positive or negative) indicate weaker correlations. In *Table 2*, correlation values written in bold text are significant at the 0.01 level (2-tailed), whereas, in italic text are significant at the 0.05 level (2-tailed). Respective statistical significance values, against each correlations of *Table 2*, are mentioned in *Table 3*. The highest statistical significance values at the 0.01 level (2-tailed) are highlighted in bold text, whereas, the statistical significance values at the 0.05 level (2-tailed) are mentioned in italic text in *Table 3*. The values written in regular text indicate least significance values. The highest correlation value [0.73] with 99% significance at 0.00 level (2-tailed) indicates that PR & CLF (meteorological parameters) are found to be positively highly correlated with each other in the study area during the observation period. Other higher positive correlations significant at 0.00 level (2-tailed) are; RH & CLF [0.70], RH & PR [0.69], Temp & AOD [0.69], and Temp & OLR [0.66]. Next equally higher but opposite correlations significant at 0.00 level (2-tailed) are; OLR & TropoO_3 [0.61], and TropoO_3 & TropoCO [–0.61]. Remaining relatively higher correlations significant at 0.00 level (2-tailed) are; WS & TropoO_3 [0.57], TropoCO_2 & TropoCH_4 [0.54], RH & TropoCH_4 [0.54], WS & TropoCO [–0.54], and RH & OLR [–0.52]. The parameters used in this study having weaker correlations with each other significant at 0.00 level (2-tailed) are (in descending order); OLR & CLF [–0.48], RH & TropoO_3 [–0.46], PR & AOD [0.45], PR & TropoCH_4 [0.45], RH & AOD [0.41], WS & TropoCO_2 [0.40], Temp & TropoCH_4 [0.39], AOD & TropoCH_4 [0.34], Temp & PR [0.33], OLR & TropoCO [–0.31], Temp & TropoO_3 [0.28], TropoNO_2 & TropoCO_2 [0.28], CLF & TropoCH_4 [0.27], WS & CLF [0.25], TropoCO_2 & TropoCO [–0.23], WS & TropoNO_2 [0.23], and TropoSO_2 & TropoO_3 [–0.23]. Out of all the tropospheric gases used in this study, TropoO_3 and TropoCO are found to be highly but inversely correlated with each other, whereas, TropoCO_2 and TropoCH_4 are next highly

http://www.aloki.hu ● ISSN 1589 1623 (Print) ● ISSN 1785 0037 (Online)
DOI: http://dx.doi.org/10.15666/aeer/1706_1353313553

and positively correlated gases significant at 0.01 level (2-tailed). Other tropospheric gases with weaker correlations including positive as well as inverse significant at 0.00 level (2-tailed) are; TropoNO_2 & TropoCO_2 [0.28], TropoCO_2 & TropoCO [–0.23], and TropoSO_2 & TropoO_3 [–0.23]. Only one correlation (least and positive) significant at 0.05 level (2-tailed) was found between TropoSO_2 & TropoNO_2 [0.18]. Positive as well as inverse correlations with 95% significance at 0.05 level (2-tailed) observed from this study are; OLR & AOD [0.22], CLF & TropoSO_2 [–0.22], AOD & TropoCO [–0.21], CLF & AOD [0.19], WS & RH [–0.19], and TropoSO_2 & TropoNO_2 [0.18]. All these correlations are also comparatively weaker ones.

Table 1. *Metadata of data retrieved from different satellite sensors (level-3 products) and models used in this study*

Product Name/Version	Sensor/ Model	Units	Spatial Resolution	Temporal Resolution	Observation Period	Description
a) Tropospheric Gases						
TropoCH_4 – Tropospheric Methane (AIR3STM_VMR_A.700hPa v006)	AIRS/ AMSU-A	ppbv	0.25°x0.25°	Daily	2002 – current	Tropospheric
TropoCO – Tropospheric Carbon Monoxide (MOP03JM v007)	MOPITT	ppbv	1° x 1°	Daily	2000 – current	Tropospheric
TropoCO_2 – Tropospheric Carbon Dioxide (AIR3C2M mole fraction v005)	AIRS/ AMSU-A	ppm	1° x 1°	Daily	2002 – current	Tropospheric
TropoNO_2 – Tropospheric Nitrogen Dioxide (OMNO2d v003)	OMI	x10^{15} molecules cm^{-2}	0.25°x0.25°	Daily	2004 – current	Tropospheric
TropoO_3 – Tropospheric Ozone (AIR3STM_VMR_A.700hPa v006)	AIRS/ AMSU-A	ppbv	0.25°x0.25°	Daily	2002 – current	Tropospheric
TropoSO_2 – Tropospheric Sulphur Dioxide (OMSO2e_PBL v003)	OMI	DU	0.25°x0.25°	Daily	2004 – current	Planetary boundary layer
b) Meteorological Parameters						
CLF – Cloud Fraction (AIRX3STM v006)	AIRS/ AMSU-A	Unit less	1° x 1°	Daily	2002 – current	Total column
OLR – Outgoing Long-wave Radiation (AIRX3STM v006)	AIRS/ AMSU-A	W m^{-2}	1° x 1°	Daily	2002 – current	Top of the atmosphere
PR – Precipitation Rate (TMPA/3B43 v007)	TRMM	mm $month^{-1}$	0.25°x0.25°	Monthly	1998 – current	Surface level
RH – Relative Humidity (AIRX3STD v006)	AIRS/ AMSU-A	%	1° x 1°	Daily	2002 – current	925 hPa
Temp – Air Temperature (AIRX3STD v006)	AIRS/ AMSU-A	Kelvin	1° x 1°	Daily	2002 – current	925 hPa
WS – Wind Speed (GLDAS_NOAH025_M v2.1)	GLDAS Model	m s^{-1}	0.25°x0.25°	Monthly	2000 – current	Near surface level
c) Aerosols						
AOD – Aerosol burden measured as Aerosol Optical Depth (MOD08_M3_550 v006)	MODIS	Unit less	1° x 1°	1–2 days	2002 – current	Total column
d) Independent data product of TropoO_3 for Model Validation						
TropoO_3 – Tropospheric Ozone OMI/MLS tropospheric ozone (original product)	OMI-MLS	ppbv	1° x 1.25°	Monthly-mean	2004 – current	Tropospheric

http://www.aloki.hu ● ISSN 1589 1623 (Print) ● ISSN 1785 0037 (Online)
DOI: http://dx.doi.org/10.15666/aeer/1706_1353313553

Table 2. *Bivariate correlation matrix representing monthly-mean data of tropospheric gases including TropoCH₄ (ppbv), TropoCO (ppbv), TropoCO₂ (ppm), TropoNO₂ (x10¹⁵ molecules cm⁻²) and TropoSO₂ (DU); major meteorological parameters including cloud fraction (CLF, unit less), outgoing long-wave radiation (OLR, W m⁻²), precipitation rate (PR, mm month⁻¹), relative humidity (RH, %), temperature at 925 hPa (Temp, K) and surface wind speed (WS, m s⁻¹); and aerosol burden measured as aerosol optical depth (AOD, unit less) over Lahore during October 2004 – September 2015*

Parameters	$TropoCH_4$	TropoCO	$TropoCO_2$	$TropoNO_2$	$TropoO_3$	$TropoSO_2$	AOD	CLF	OLR	PR	RH	Temp
TropoCO	-0.14											
$TropoCO_2$	**0.54**	**-0.23**										
$TropoNO_2$	-0.15	0.01	**0.28**									
$TropoO_3$	-0.07	**-0.61**	0.14	-0.06								
$TropoSO_2$	-0.02	0.13	0.08	*0.18*	**-0.23**							
AOD	**0.34**	*-0.21*	-0.01	0.07	0.09	0.01						
CLF	**0.27**	-0.17	0.01	-0.09	-0.07	*-0.22*	*0.19*					
OLR	0.07	**-0.31**	-0.06	-0.15	**0.61**	-0.05	*0.22*	**-0.48**				
PR	**0.45**	-0.16	0.02	-0.15	0.00	-0.12	**0.45**	**0.73**	-0.10			
RH	**0.54**	0.12	0.03	-0.15	**-0.46**	-0.03	**0.41**	**0.70**	**-0.52**	**0.69**		
Temp	**0.39**	-0.16	-0.11	-0.14	**0.28**	0.01	**0.69**	-0.09	**0.66**	**0.33**	0.11	
WS	-0.12	**-0.54**	**0.40**	**0.23**	**0.57**	-0.13	0.04	**0.25**	0.10	0.14	*-0.19*	-0.11

Correlations in bold text are significant at the 0.01 level (2-tailed). Correlations in Italic are significant at the 0.05 level (2-tailed). Blue color indicates positive correlations, and red color indicates negative/inverse correlations. Longer the length of colored bars (either blue or red), stronger would be the correlation (either positive or inverse, respectively) between the corresponding parameters

Table 3. *Based upon correlation matrix discussed in Table 2 above, matrix showing statistical significance values of tropospheric gases including TropoCH₄ (ppbv), TropoCO (ppbv), TropoCO₂ (ppm), TropoNO₂ (×10¹⁵ molecules cm⁻²) and TropoSO₂ (DU); major meteorological parameters including cloud fraction (CLF, unit less), outgoing long-wave radiation (OLR, W m⁻²), precipitation rate (PR, mm month⁻¹), relative humidity (RH, %), temperature at 925 hPa (Temp, K) and surface wind speed (WS, m s⁻¹); and aerosol burden measured as aerosol optical depth (AOD, unit less) over Lahore during October 2004 – September 2015*

Parameter	$Tropo\ CH_4$	Tropo CO	$Tropo\ CO_2$	$Tropo\ NO_2$	$Tropo\ O_3$	$Tropo\ SO_2$	AOD	CLF	OLR	PR	RH	Temp
TropoCO	0.11											
$TropoCO_2$	**0.00**	**0.01**										
$TropoNO_2$	0.08	0.94	**0.00**									
$TropoO_3$	0.39	**0.00**	0.12	0.50								
$TropoSO_2$	0.77	0.13	0.36	*0.03*	**0.01**							
AOD	**0.00**	*0.02*	0.95	0.41	0.31	0.89						
CLF	**0.00**	0.06	0.91	0.30	0.44	*0.01*	*0.03*					
OLR	0.41	**0.00**	0.51	0.09	**0.00**	0.58	*0.01*	**0.00**				
PR	**0.00**	0.06	0.83	0.09	0.97	0.17	**0.00**	**0.00**	0.26			
RH	**0.00**	0.18	0.76	0.08	**0.00**	0.68	**0.00**	**0.00**	**0.00**	**0.00**		
Temp	**0.00**	0.07	0.22	0.11	**0.00**	0.97	**0.00**	0.29	**0.00**	**0.00**	0.22	
WS	0.15	**0.00**	**0.00**	**0.01**	**0.00**	0.13	0.63	**0.00**	0.27	0.12	*0.03*	0.22

The numbers written in bold text are statistical significance values for significant correlations at the 0.01 level (2-tailed). The numbers written in italic text are statistical significance values for significant correlations at the 0.05 level (2-tailed)

Annual trends (slopes and y-intercepts), overall changes (%), and R^2 of tropospheric gases, meteorological parameters, and aerosol optical depth over Lahore using their annual-means from October 2004 to September 2015 are tabulated in *Table 4*. All tropospheric gases except TropoCO indicate an increasing trend. Maximum positive

http://www.aloki.hu ● ISSN 1589 1623 (Print) ● ISSN 1785 0037 (Online)
DOI: http://dx.doi.org/10.15666/aeer/1706_1353313553

slope of 4.93±0.18 with R^2=0.99 observed for TropoCH_4 (having high correlations [0.54] significant at 0.01 level with TropoCO_2 and RH) indicates a maximum increasing trend than other gases used for this study. Similarly, slopes of PR (3.21±1.08) with maximum change of 49.61% (having strong correlation with CLF), and TropoCO_2 (1.97±0.04, having high correlation with TropoCH_4) show relatively increasing trends during the study period. However, a relatively large negative slope of TropoCO (–3.48±0.54) shows a decreasing trend over Lahore, which may be due to an overall decrease in TropoCO (-23.8%) during the entire study period. Moreover, TropoCO has inverse but high correlations significant at 0.01 level with TropoO_3 and WS. Relatively higher positive slopes (~21%) have been noticed for TropoNO_2, CLF, and WS, whereas little negative slopes have been observed for OLR (–0.05±0.21) and temperature (–0.10±0.04). It is worth mentioning here that the monthly-mean temperature values over Lahore during October 2004 – September 2015 show a little increasing trend (*Figure 3* refers).

Table 4. *Annual trends (linear equation showing slopes and y-intercepts), overall change (%), and R^2 based on annual-means of tropospheric gases including TropoCH_4, TropoCO, TropoCO_2, TropoNO_2 and TropoSO_2; major meteorological parameters including cloud fraction (CLF), outgoing long-wave radiation (OLR), precipitation rate (PR), relative humidity (RH), temperature (Temp) and surface wind speed (WS); and aerosol burden measured as aerosol optical depth (AOD) over Lahore during October 2004 – September 2015*

Parameter	Annual Trend Line	Overall Change (%)	R^2
TropoCH_4 (ppbv)	$y = (4.93\pm0.18)x + (1799.10\pm1.35)$	2.92	0.99
TropoCO (ppbv)	$y = -(3.48\pm0.54)x + (202.36\pm3.94)$	–23.80	0.81
TropoCO_2 (ppm)	$y = (1.97\pm0.04)x + (377.07\pm0.27)$	5.40	1.00
TropoNO_2 ($\times10^{15}$ molecules cm^{-2})	$y = (0.06\pm0.02)x + (2.23\pm0.17)$	21.62	0.40
TropoO_3 (ppbv)	$y = (0.29\pm0.08)x + (47.91\pm0.62)$	6.18	0.54
TropoSO_2 (DU)	$y = (0.00\pm0.00)x + (0.06\pm0.02)$	13.27	0.01
CLF (unit less)	$y = (0.00\pm0.00)x + (0.19\pm0.02)$	21.47	0.29
OLR (W m^{-2})	$y = -(0.05\pm0.21)x + (302.66\pm1.52)$	–0.18	0.01
PR (mm $month^{-1}$)	$y = (3.21\pm1.08)x + (32.62\pm7.97)$	49.61	0.47
RH (%)	$y = (0.41\pm0.15)x + (40.71\pm1.13)$	9.94	0.42
Temp (K at 925 hPa)	$y = -(0.10\pm0.04)x + (300.50\pm0.30)$	–0.37	0.38
WS (m s^{-1})	$y = (0.05\pm0.01)x + (1.86\pm0.08)$	21.43	0.66
AOD (unit less)	$y = (0.01\pm0.00)x + 0.62\pm0.02$	10.69	0.39

Results and Discussion

Parametric out-look of Lahore

Tropospheric gases

Concentrations of major tropospheric gases have been compared with those of TropoO_3 over Lahore during October 2004 – September 2015 and are shown in *Figure 2*. Large variations have been observed in TropoCH_4, TropoCO, and TropoNO_2, whereas, TropoCO_2 and TropoSO_2 show comparatively little variations. We also noticed that all tropospheric gases indicate increasing trends except TropoCO. Gradual increasing trend in TropoCH_4 indicates gradual increasing activities responsible for Methane production (Paddy crops, animals, industrial activities, and vehicular emissions etc.) in the study area

http://www.aloki.hu ● ISSN 1589 1623 (Print) ● ISSN 1785 0037 (Online)
DOI: http://dx.doi.org/10.15666/aeer/1706_1353313553

during the study period. Similarly, gradual increasing trend in $TropoCO_2$ is an indication of increased activities causing carbon dioxide to increase (Agricultural activities, population, animals, industrial activities, and vehicular emissions etc.) in Lahore. Whereas, slopes of $TropoNO_2$ and $TropoSO_2$ are quite gentle showing little increase similar to that of $TropoO_3$.

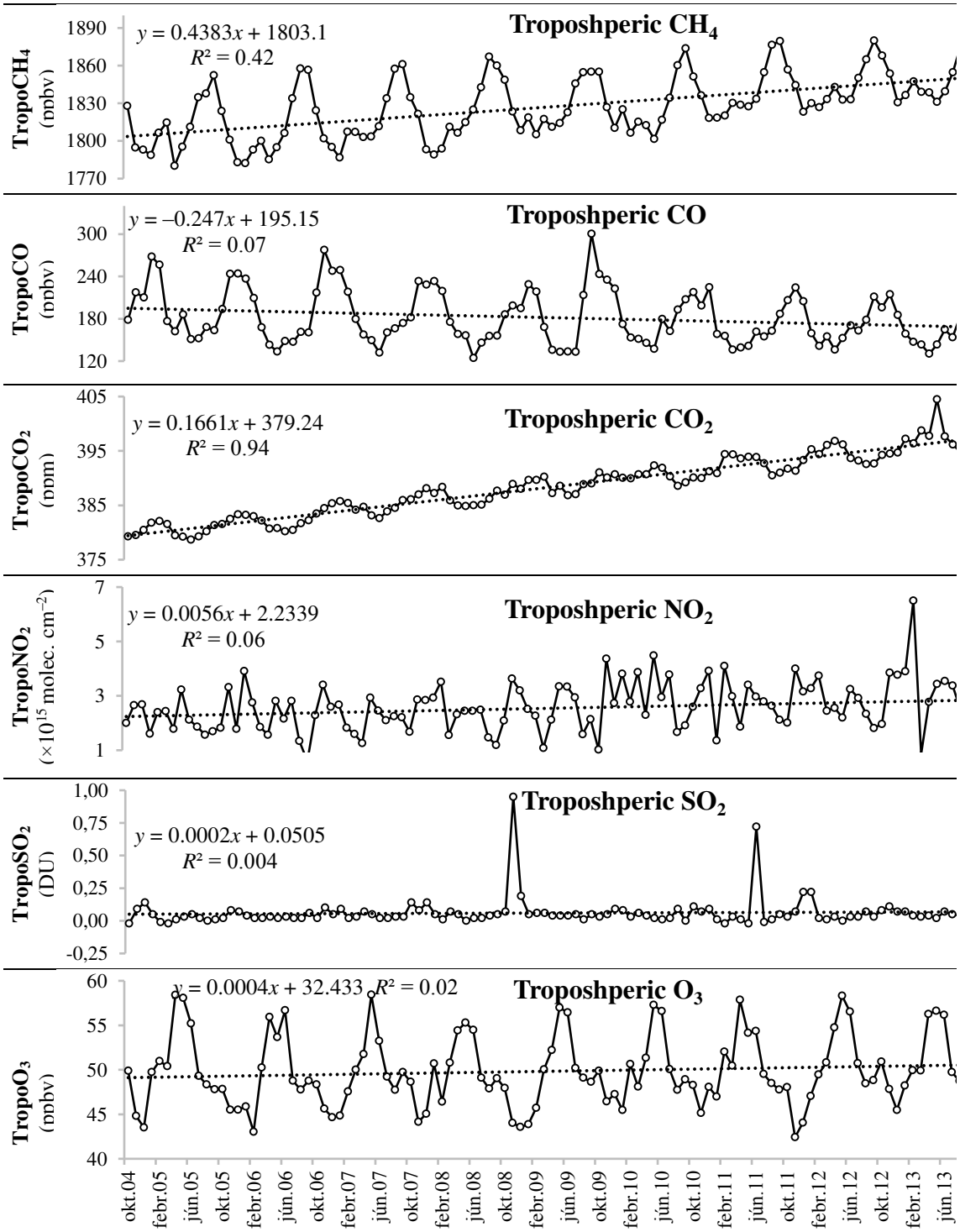

Figure 2. *Time series monthly-mean variations of major tropospheric gases over Lahore during October 2004 – September 2015. Dotted lines correspond to respective trend lines*

http://www.aloki.hu ● ISSN 1589 1623 (Print) ● ISSN 1785 0037 (Online)
DOI: http://dx.doi.org/10.15666/aeer/1706_1353313553

Meteorological parameters

Monthly-mean data products of major meteorological parameters as well as aerosol burden measured as Aerosol Optical Depth (AOD) have been compared with $TropoO_3$ concentrations over Lahore during October 2004 – September 2015 and are shown in *Figure 3*. Large variations have been observed in all parameters similar to that of $TropoO_3$ during the entire study period. Positive slopes of all parameters including $TropoO_3$, except OLR, indicate increasing trends during the study period. Comparatively larger slope value of PR indicates a gradual increase in precipitation in the study area.

$TropoO_3$

Maximum concentration of $TropoO_3$ has been reported during spring and summer seasons across the globe (e.g., Cooper et al., 2014). Accordingly, maximum concentrations have been observed in $TropoO_3$ over Lahore during spring and summer (monsoon) seasons (March to July) in Pakistan shown in *Figure 4*. Major causes of this increased $TropoO_3$ concentration over Lahore are mainly due to increased ozone precursor gas emissions, enhanced biomass burning activities, biogenic emissions, polluted air-masses migrated from nearby regions, removal of NO_2 concentration due to increased OH radicalization (Yienger and Levy, 1995), photolysis of water vapors which reduces NO_2 concentration during high rainfall in monsoon (Jacob, 2003; Ghude et al., 2009; Seinfeld and Pandis, 2016), and enhanced intrusion of O_3 from stratosphere (Noreen et al., 2018). An overall decreasing trend has been observed in the monthly-mean values of observed $TropoO_3$ concentration over Lahore (slope=–0.4303, y-intercept=52.786, and R^2=0.1614) during the study period.

Modeling $TropoO_3$ concentration over Lahore

In order to investigate $TropoO_3$ dependencies, monthly-mean values of major tropospheric gases, meteorological parameters, and aerosol burden over Lahore during October 2004 – September 2015 have been incorporated in multiple linear regression model (e.g., Engel-Cox et al., 2004; Lin et al., 2012), mentioned in *Equation (1)*;

$$\text{Objective or Dependent Variable} = a_o + \sum(b_n \times w_n) + \varepsilon \qquad \text{(Eq.1)}$$

where a_o is an intercept, b=1,2,3,..…n are regular (unstandardized) regression coefficients, w=1,2,3,…...n are regressors or independent variables, and ε is an error term associated with the regression analysis. The resultant multiple linear regression model used in this study to model $TropoO_3$ (Objective/Dependent Variable) as functions of tropospheric gases, meteorological parameters, and aerosol burden (regressors or independent variables) is mentioned in *Equation (2)* below;

$$\begin{aligned} \text{TropoO}_3\text{(monthly mean)} &= a_0 + b_1 \times \text{TropoCH}_4 \\ &+ b_2 \times \text{TropoCO} \\ &+ b_3 \times \text{TropoCO}_2 + \\ b_4 \times \text{TropoNO}_2 &+ b_5 \times \text{TropoSO}_2 + b_6 \times \text{CLF} \\ &+ b_7 \times \text{OLR} + \\ b_8 \times \text{PR} + b_9 \times \text{RH} &+ b_{10} \times \text{Temp} + b_{11} \times \text{WS} \\ &+ b_{12} \times \text{AOD} + \varepsilon \end{aligned} \qquad \text{(Eq.2)}$$

http://www.aloki.hu ● ISSN 1589 1623 (Print) ● ISSN 1785 0037 (Online)
DOI: http://dx.doi.org/10.15666/aeer/1706_1353313553

where a_o is an intercept, b_1, b_2, b_3,……b_{12} are regular (unstandardized) regression coefficients; TropoCH_4, TropoCO, TropoCO_2, TropoNO_2, TropoSO_2, CLF, OLR, PR, RH, Temp, WS, and AOD are the monthly-mean regressors or independent variables; and ε is an error term associated with the regression analysis. The multiple linear regression model mentioned in *Equation (2)* closely measures the intrinsic relationships of TropoO_3 with all regressors, separately. Therefore, this model offers better predictability of TropoO_3 based on relative impacts with all regressors than by simple linear model which is based only upon single regressor.

To improve the results of *Equation (2)*, stepwise multiple linear regression procedure (Lin et al., 2012) was adopted. Resultant stepwise multiple linear regression model shown in *Table 5* was generated. The model provides statistical information for modeling TropoO_3 concentrations based upon weighted contributions from its regressors. This procedure simultaneously regresses multiple variables (gases, meteorological parameters, and aerosol burden) and removes un-important parameter(s) from the model. *Table 5* shows that the modeled TropoO_3 is mainly dependent upon OLR, WS, CLF, TropoSO_2, TropoCO, and RH out of all regressors mentioned in *Equation (2)*. The standardized regression coefficients (β) obtained from the stepwise multiple linear regression model show weight-wise dependence of TropoO_3 upon OLR [β=0.458] with the highest contribution, followed by nearly equivalent contributions from WS [β=0.262] and CLF [β=0.256], whereas, the least contribution has been observed from RH [β=–0.320]. This model also reveals that TropoSO_2 [β=–0.097] and TropoCO [β=–0.231] are negatively contributing against TropoO_3 concentration over Lahore during the study period. The values of multiple error (r=0.85) and standard error (2.14) for this TropoO_3 model appear to be reasonable.

A subsequent bivariate correlation matrix representing observed TropoO_3, modeled TropoO_3, and the parameters which contributed in the modeled TropoO_3 concentration (OLR, WS, CLF, TropoSO_2, TropoCO, and RH) as mentioned in *Table 5* above was generated and is shown in *Table 6* below. Blue color indicates positive correlations, while red color indicates negative/inverse correlations. Longer the length of colored bars (either blue or red), stronger would be the correlation (either positive or inverse, respectively) between the corresponding parameters. In *Table 6*, correlation values written in bold text are significant at the 0.01 level (2-tailed), whereas, in italic text are significant at the 0.05 level (2-tailed). Respective statistical significance values, against each correlations of *Table 6*, are written in *Table 7*. The highest statistical significance values at the 0.01 level (2-tailed) are highlighted in bold text, whereas, the statistical significance values at the 0.05 level (2-tailed) are mentioned in italic text in *Table 7*. The values written in regular text indicate least significance values. All correlations shown in *Table 6* exhibit the same corresponding values as mentioned in *Table 2* above along with additive correlation values against modeled TropoO_3. All bivariate correlations with the modeled TropoO_3 concentration are significant at 0.01 level (2-tailed) except for CLF. The highest correlation value [0.85] with 99% significance at 0.00 level (2-tailed) between modeled and observed TropoO_3 concentrations over Lahore during the study period reveals the high suitability of the modeled developed in this study mentioned in *Table 5* above. Out of two tropospheric gases used in this model, modeled TropoO_3 is found to be highly but inversely correlated with TropoCO [–0.72], whereas, OLR [0.71] and WS [0.68] are the next highly and positively correlated meteorological parameters significant at 0.01 level (2-tailed).

http://www.aloki.hu ● ISSN 1589 1623 (Print) ● ISSN 1785 0037 (Online)
DOI: http://dx.doi.org/10.15666/aeer/1706_1353313553

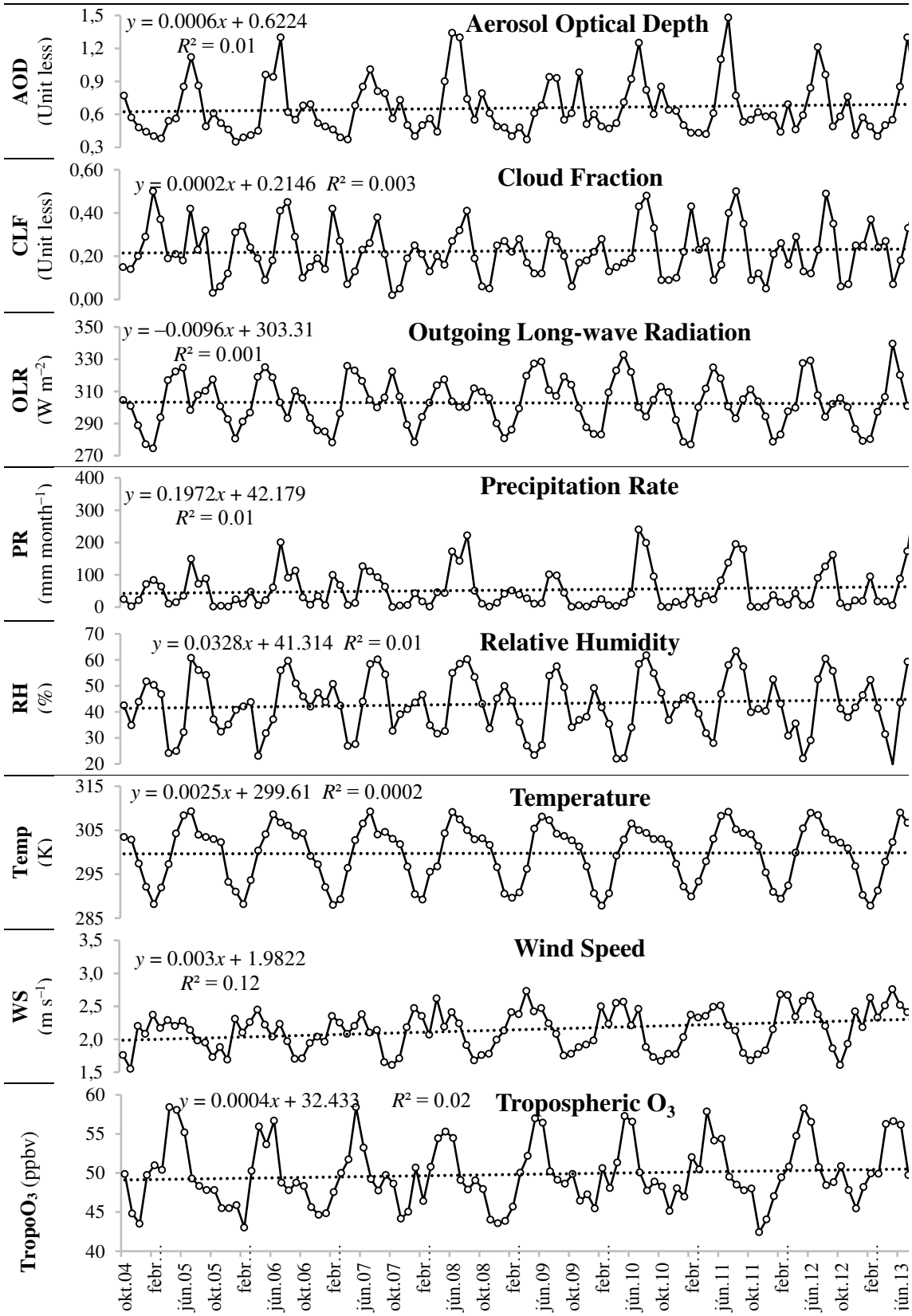

Figure 3. *Time series monthly-mean variations of $TropoO_3$ and major meteorological parameters over Lahore during October 2004 – September 2015. Dotted lines correspond to respective trend lines*

http://www.aloki.hu ● ISSN 1589 1623 (Print) ● ISSN 1785 0037 (Online)
DOI: http://dx.doi.org/10.15666/aeer/1706_1353313553

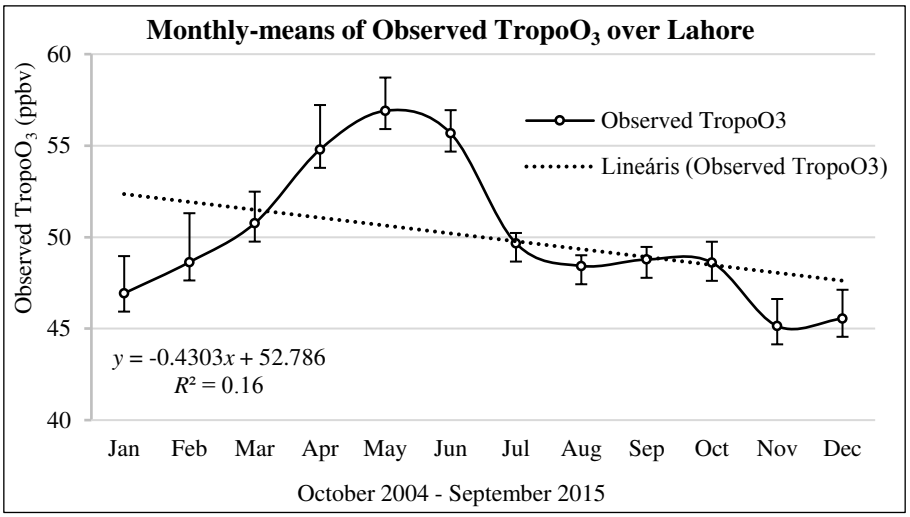

Figure 4. *Monthly-means of Observed $TropoO_3$ concentration (ppbv) over Lahore during October 2004 – September 2015. Dotted line corresponds to the trend line*

Table 5. *Stepwise multiple linear regression model developed to model $TropoO_3$ (ppbv) variations based upon weighted contributions of monthly-mean data of OLR (W m^{-2}), WS (m s^{-1}), CLF (unit less), $TropoSO_2$ (DU), TropoCO (ppbv), and RH (%) over Lahore during October 2004 – September 2015*

Stepwise multiple linear regression model equation	Multiple *r*	Standard Error
$TropoO_3$ (monthly-mean) = 12.706 + 0.127*OLR*[0.458] + 3.213*WS*[0.262] + 9.078*CLF*[0.256] – 3.648*TropoSO*$_2$[–0.097] – 0.026*TropoCO*[–0.231] – 0.121*RH*[–0.320]	0.85	2.14

The values in parentheses are Standardized Regression Coefficients (Beta, β) representing regressor's relative weightage on modeled $TropoO_3$ concentrations in descending order, although these coefficients do not take part in calculations

Table 6. *Bivariate correlation matrix representing monthly-mean data of observed $TropoO_3$, OLR (W m^{-2}), WS (m s^{-1}), CLF (unit less), $TropoSO_2$ (DU), TropoCO (ppbv), and RH (%) as well as modeled $TropoO_3$ concentrations over Lahore during October 2004 – September 2015*

Parameters	Observed $TropoO_3$	OLR	WS	CLF	$TropoSO_2$	TropoCO	RH
OLR	**0.61**						
WS	**0.57**	0.10					
CLF	-0.07	**-0.48**	**0.25**				
$TropoSO_2$	**-0.23**	-0.05	-0.13	*-0.22*			
TropoCO	**-0.61**	**-0.31**	**-0.54**	-0.17	0.13		
RH	**-0.46**	**-0.52**	*-0.19*	**0.70**	-0.03	0.12	
Modeled $TropoO_3$	**0.85**	**0.71**	**0.68**	-0.07	**-0.27**	**-0.72**	**-0.53**

Correlations in bold text are significant at the 0.01 level (2-tailed). Correlations in Italic are significant at the 0.05 level (2-tailed). Blue color indicates positive correlations, and red color indicates negative/inverse correlations. Longer the length of colored bars (either blue or red), stronger would be the correlation (either positive or inverse, respectively) between the corresponding parameters

http://www.aloki.hu ● ISSN 1589 1623 (Print) ● ISSN 1785 0037 (Online)
DOI: http://dx.doi.org/10.15666/aeer/1706_1353313553

Table 7. *Based upon correlation matrix discussed in Table 6 above, matrix showing statistical significance values of observed TropoO_3, OLR (W m^{-2}), WS (m s^{-1}), CLF (unit less), TropoSO_2 (DU), TropoCO (ppbv), and RH (%) as well as modeled TropoO_3 concentrations over Lahore during October 2004 – September 2015*

Parameters	Observed TropoO_3	OLR	WS	CLF	TropoSO_2	TropoCO	RH
OLR	**0.00**						
WS	**0.00**	0.27					
CLF	0.44	**0.00**	**0.00**				
TropoSO_2	**0.01**	0.58	0.13	*0.01*			
TropoCO	**0.00**	**0.00**	**0.00**	0.06	0.13		
RH	**0.00**	**0.00**	*0.03*	**0.00**	0.68	0.18	
Modeled TropoO_3	**0.00**	**0.00**	**0.00**	0.42	**0.00**	**0.00**	**0.00**

The numbers written in bold text are statistical significance values for significant correlations at the 0.01 level (2-tailed). The numbers written in italic text are statistical significance values for significant correlations at the 0.05 level (2-tailed)

Other inverse correlations of the modeled TropoO_3 significant at 0.00 level (2-tailed) are noticed against RH [–0.53] and TropoSO_2 [–0.27]. The least and inverse correlation having 95% significance at 0.05 level (2-tailed) is against CLF [–0.07].

The observed TropoO_3 datasets retrieved directly from the AIRS/AMSU-A sensor over Lahore during October 2004 – September 2015 and the modeled TropoO_3 concentration values obtained from of the resultant step-wise multiple linear regression model (discussed in *Table 5* above) have been plotted in *Figure 5*.

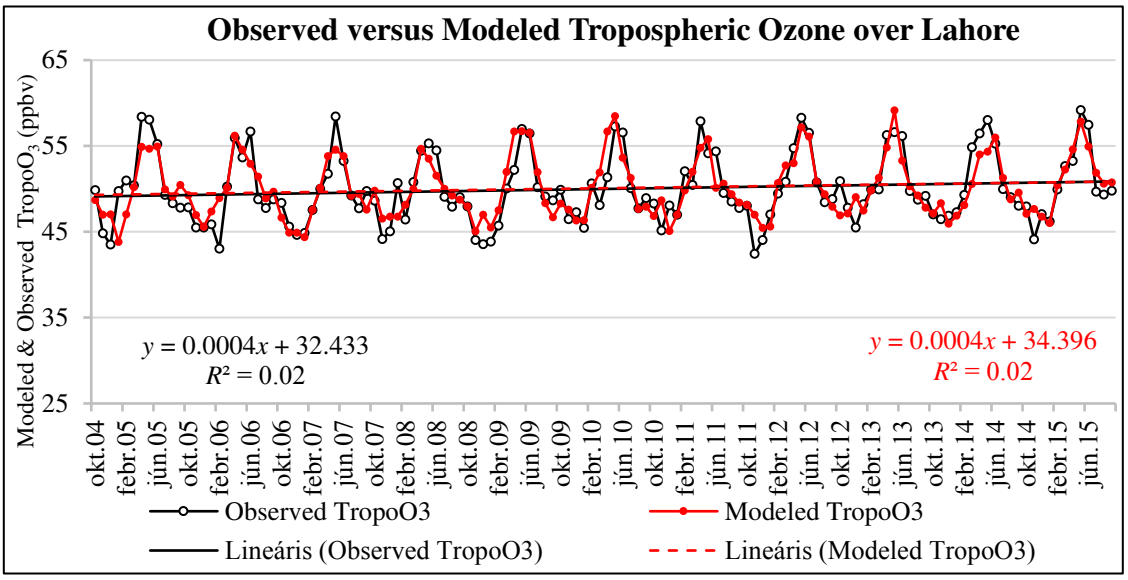

Figure 5. *Comparison of observed versus modeled time-series TropoO_3 (ppbv) concentrations over Lahore during October 2004 – September 2015. Dotted lines correspond to respective trend lines*

Time series distributions of these observed and modeled TropoO_3 concentrations show similar increasing and consistent trends except during the months of May 2005, Feb 2006, May 2007, Dec 2008, Nov 2011, Dec 2012, May 2014, and Nov 2014. The highest value in the modeled TropoO_3 concentration has been notice for the month of May 2013.

http://www.aloki.hu ● ISSN 1589 1623 (Print) ● ISSN 1785 0037 (Online)
DOI: http://dx.doi.org/10.15666/aeer/1706_1353313553

Monthly-mean data analysis of modeled $TropoO_3$ concentration indicate a similar pattern as that of the observed $TropoO_3$ concentration over Lahore during the study period as shown in *Figure 6(a)*. We find higher concentrations of both modeled and observed $TropoO_3$ during spring and summer (monsoon) seasons, whereas, minima during the winter season. A similar observation about $TropoO_3$ variation was reported by Ahmad and Aziz, 2013. Our modeled $TropoO_3$ variation attributes a similar decreasing trend (slope=–0.3254, y-intercept=52.192, and R^2=0.12) over Lahore during the study period. Scatter plot drawn between observed and modeled $TropoO_3$ indicates a linear positive trend having a slope 0.732 and y-intercept 13.469 with R^2=0.73 as shown in *Figure 6(b)*.

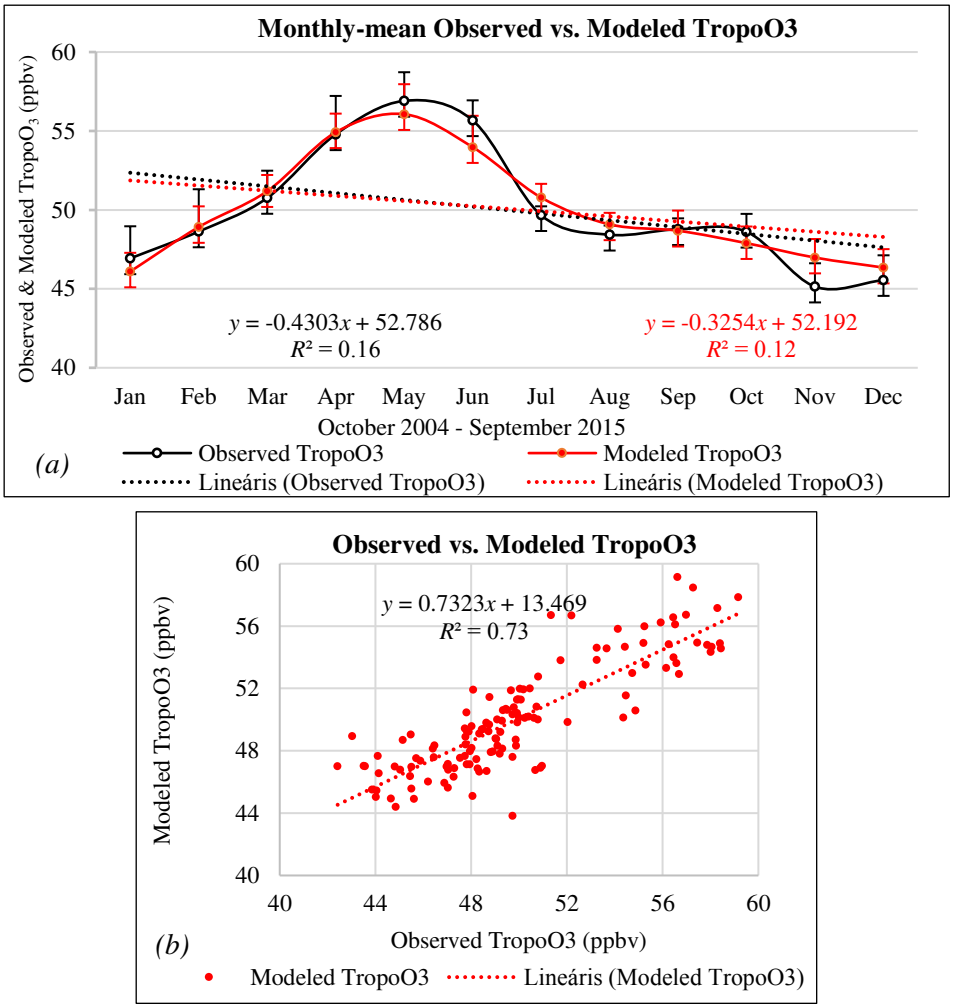

Figure 6. *(a) Monthly-means of observed $TropoO_3$ (used as dependent variable) and modeled $TropoO_3$ concentrations (all data in ppbv) over Lahore during October 2004 – September 2015. (b) Scatter plot of observed versus modeled $TropoO_3$ concentrations (ppbv). Dotted lines correspond to respective trend lines*

Annual trends, overall change (%), and R^2 based on annual-means of observed and modeled $TropoO_3$ concentrations over Lahore during October 2004 – September 2015 were calculated and are mentioned in *Table 8*.

http://www.aloki.hu ● ISSN 1589 1623 (Print) ● ISSN 1785 0037 (Online)
DOI: http://dx.doi.org/10.15666/aeer/1706_1353313553

Table 8. *Annual trends (slopes and y-intercepts), overall change (%), and R^2 based on annual-means of observed and modeled $TropoO_3$ concentrations over Lahore during October 2004 – September 2015*

Parameter	Annual Trend Line	Overall Change (%)	R^2
Observed $TropoO_3$ (ppbv)	$y = (0.29\pm0.08)x + (47.91\pm0.62)$	6.18	0.54
Modeled $TropoO_3$ (ppbv)	$y = (0.23\pm0.06)x + (48.48\pm0.42)$	4.89	0.62

Overall similar increasing concentrations of both observed (6.18%, R^2 = 0.54), and modeled (4.89%, R^2 = 0.62) $TropoO_3$ indicate good agreement of resultant model devised in this study. The slope of observed $TropoO_3$ [0.29±0.08] is little larger than that of the observed $TropoO_3$ [0.23±0.06], however, the values of y-intercepts of both concentrations are nearly similar. The increase in $TropoO_3$ concentration observed in Lahore and adjoining areas during the study period is possibly due to increased anthropogenic activities including; population and traffic densities, industrial activities, infrastructure development activities, and biomass burning etc. These results are almost in agreement with those obtained by Noreen et al 2018 for ozone column over Lahore. Some other studies had also discussed about the $TropoO_3$ concentrations, and production of its precursors through different anthropogenic activities (e.g., Kulkarni et al., 2010; Lal et al., 2012; Ahmad and Aziz, 2013).

Model validation

Modeled $TropoO_3$ concentrations were crossed checked against an independent source of $TropoO_3$ concentrations. For this purpose, original $TropoO_3$ data product of subtracted monthly-means of Total Column Ozone retrievable from OMI and Stratospheric Column Ozone retrievable from MSL onboard Aura satellite was utilized (available at https://acd-ext.gsfc.nasa.gov/Data_services/cloud_slice/new_data.html). $TropoO_3$ product calculated by mean volume mixing ratio (in ppbv) formatted in 1-degree (latitude) by 1.25-degree (longitude) resolution was extracted for Lahore during October 2004 – September 2015. Our modeled as well as the observed $TropoO_3$ (used as dependent variable) concentrations have been plotted in *Figure 7* against these independently available product of OMI-MLS $TropoO_3$ concentrations (ppbv) over Lahore during the study period.

The results show similar seasonality patterns as well as trends in all three datasets with good agreements in their slopes and error values mentioned in *Figure 7*. These promising results validate our resultant model. OMI-MLS $TropoO_3$ concentrations have been plotted against secondary axis due to its wider data range. OMI/MLS data measurements have some anomalies especially during 2007 and 2009 (Ziemke et al., 2006).

To further investigate this validation process, monthly-mean data of OMI-MLS $TropoO_3$ (independent data) was compared with modeled as well as observed $TropoO_3$ concentrations over Lahore during October 2004 – September 2015 (shown in *Figure 8*). Monthly-mean graphical patterns, slopes, and trends in all three datasets are similar with higher concentrations during the spring and summer (monsoon) seasons, whereas, minima during the winter season shown in *Figure 8(a)*. Comparison of scatter plots drawn between OMI-MLS $TropoO_3$ (independent data), and observed $TropoO_3$ (used as

http://www.aloki.hu ● ISSN 1589 1623 (Print) ● ISSN 1785 0037 (Online)
DOI: http://dx.doi.org/10.15666/aeer/1706_1353313553

dependent variable) against modeled $TropoO_3$ concentrations shown in *Figure 8(b)* indicates similar linear positive trends.

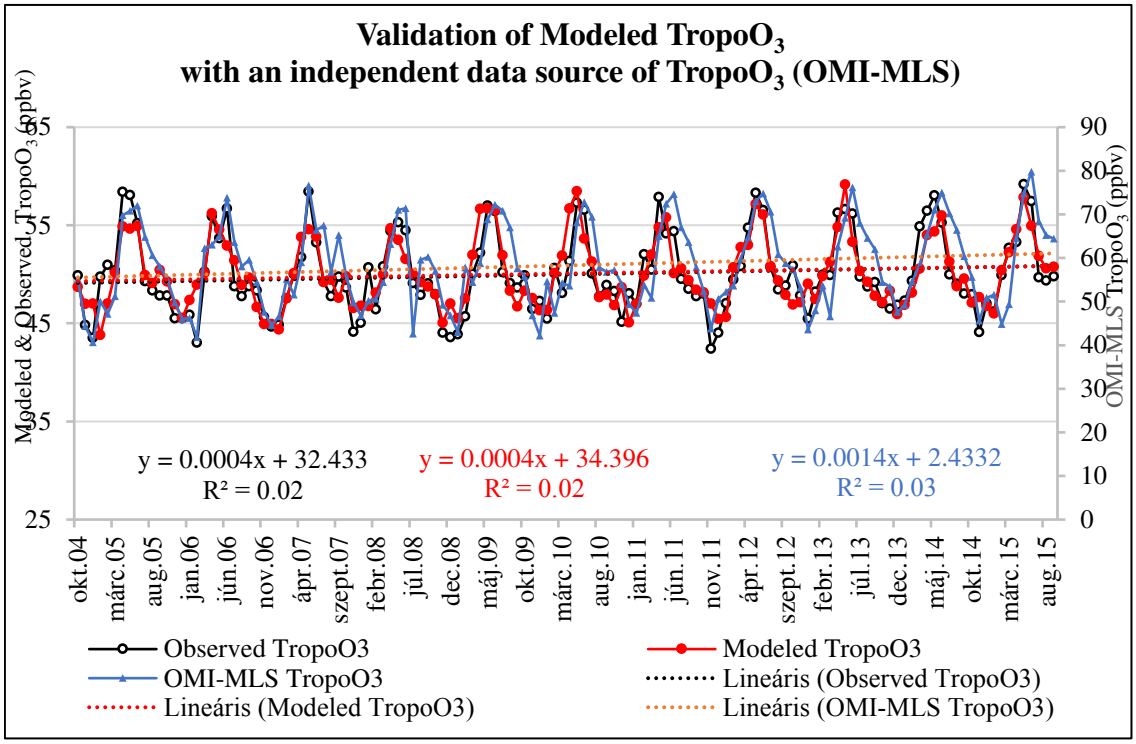

Figure 7. *Validation of modeled and observed (used as dependent variable) $TropoO_3$ (ppbv) against an independent source of $TropoO_3$ concentrations (ppbv) retrieved from OMI-MLS data product over Lahore during October 2004 – September 2015. Dotted lines correspond to respective trend lines*

Conclusions

The proposed step-wise multiple linear regression model reveals weighted contributions of major factors OLR, WS, and CLF, $TropoSO_2$, TropoCO, and RH (based on standardized regression coefficient, β) against $TropoO_3$ variability over Lahore during September 2004 – October 2015. Stepwise multiple linear regression modelling technique opted to model $TropoO_3$ concentrations over Lahore has shown highly consistent results as compared with the $TropoO_3$ observations retrieved directly from OMI satellite sensor. The trend-line of scatter plot drawn between observed and modeled $TropoO_3$ provides a steady linear increase analogous correlation with an overall increase of 6.18% in observed $TropoO_3$, while 4.89% in modeled $TropoO_3$ over Lahore during the study period. Based on the resultant value of multiple correlation coefficient (r=0.854) it can confidently be asserted that the stepwise multiple linear regression model opted to predict $TropoO_3$ over Lahore is quite reasonable. The modeled $TropoO_3$ concentrations were validated against an independent source of $TropoO_3$ concentrations retrieved from original subtracted product of OMI-MLS over Lahore for the study period and the results were found in good agreement. This study of modeling $TropoO_3$ variation as functions of satellite observations of major tropospheric gases, meteorological parameters, and aerosol burden over Lahore acquired during October 2004 – September 2015 using stepwise multiple

http://www.aloki.hu ● ISSN 1589 1623 (Print) ● ISSN 1785 0037 (Online)
DOI: http://dx.doi.org/10.15666/aeer/1706_1353313553

linear regression modelling technique is quite unique. The study would be helpful for further research investigations in this domain as well as provide useful information for policy/decision makers in Lahore, Pakistan.

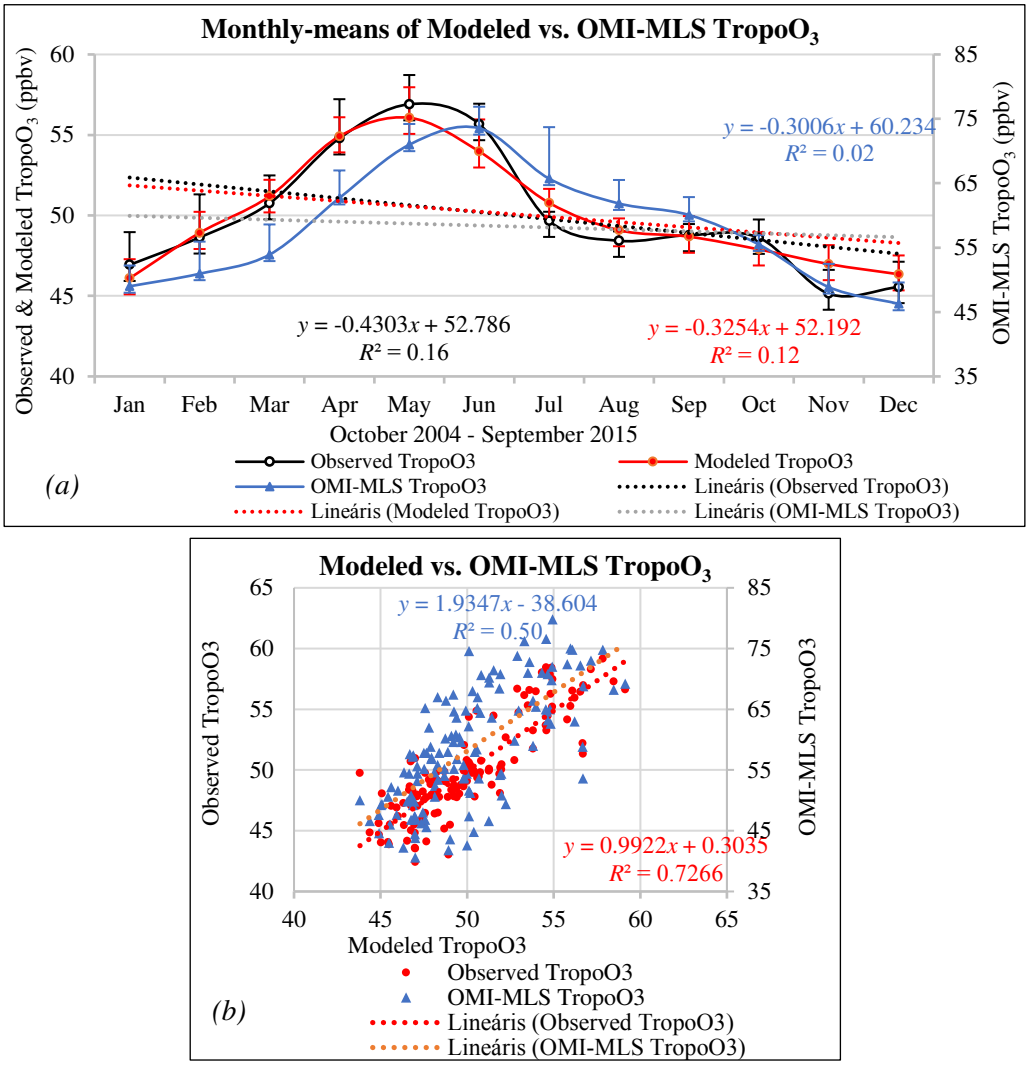

Figure 8. *(a) Monthly-means of OMI-MLS TropoO₃ (independent data), observed TropoO₃ (used as dependent variable) and modeled TropoO₃ concentrations (all data in ppbv) over Lahore during October 2004 – September 2015. (b) Scatter plot of OMI-MLS TropoO₃ (independent data), and observed TropoO₃ (used as dependent variable) against modeled TropoO₃ concentrations (all data in ppbv). Dotted lines correspond to respective trend lines*

Acknowledgements. Authors gratefully acknowledge the project teams of AIRS/AMSU-A, GLDAS_NOAH, MODIS, OMI, and TRMM for online provision of related datasets and necessary information about error analyses.

REFERENCES

[1] Abed, F. G., Al-Salihi, A., Jasim, M. R. (2017): Space-borne observation of methane from atmospheric infrared sounder: data analysis and distribution over Iraq. – Journal of Applied and Advanced Research 2(4): 256-264. Doi:10.21839/jaar.2017.v2i4.100.

http://www.aloki.hu ● ISSN 1589 1623 (Print) ● ISSN 1785 0037 (Online)
DOI: http://dx.doi.org/10.15666/aeer/1706_1353313553

[2] Aghedo, A. M., Schultz, M. G., Rast, S. (2007): The influence of African air pollution on regional and global tropospheric ozone. – Atmos. Chem. Phys. 7(5): 1193-1212. Doi:10.5194/acp-7-1193-2007.

[3] Ahmad, S. S., Aziz, N. (2013): Spatial and Temporal Analysis of Ground Level Ozone and Nitrogen Dioxide Concentration across the Twin Cities of Pakistan. – Environmental Monitoring and Assessment 185: 3133-3147. Doi:10.1007/s10661-012-2778-7.

[4] Alam, K., Iqbal, M. J., Blaschke, T., Qureshi, S., Khan, G. (2010): Monitoring spatiotemporal variations in aerosols and aerosol-cloud interactions over Pakistan using MODIS data. – Adv. Space Res. 46: 1162-1176. Doi:10.1016/j.asr.2010.06.025.

[5] Alam, K., Trautmann, T., Blaschke, T., Majid, H. (2012): Aerosol optical and radiative properties during summer and winter season over Lahore and Karachi. – Atmos. Environ. 50: 234-245. Doi:10.1016/j.atmosenv.2011.12.027.

[6] Alam, K., Trautmann, T., Blaschke, T., Subhan, F. (2014): Changes in aerosol optical properties due to dust storms in the Middle East and Southwest Asia. – Remote Sens. Environ. 143: 216-227. Doi:10.1016/j.rse.2013.12.021.

[7] Ali, M., Tariq, S., Mahmood, K., Daud, A., Batool, A., ul-Haq, Z. (2014): A study of aerosol properties over Lahore Pakistan) by using AERONET data. – Asia-Pacific J Atmos Sci. 50(2): 153-162. Doi: 10.1007/s13143-014-0004-y.

[8] Aumann, H. H., Chahine, M. T., Gautier, C., Goldberg, M. D., Kalnay, E., McMillin, L. M., Revercomb, H., Rosenkranz, P. W., Smith, W. L., Staelin, D. H., Strow, L. L., Susskind, J. (2003): AIRS/AMSU/HSB on the aqua mission: design, science objectives, data products, and processing systems. – IEEE Trans. Geosci. Rem. Sens. 41: 253-264. Doi: 10.1109/TGRS.2002.808356.

[9] Avnery, S., Mauzerall, D. L., Liu, J., Horowitz, L. W. (2011): Global crop yield reductions due to surface ozone exposure: 2. Year 2030 potential crop production losses and economic damage under two scenarios of O_3 pollution. – Atmos. Environ. 45(13): 2297-2309. Doi:10.1016/j.atmosenv.2011.01.002.

[10] Badarinath, K. V. S., Shailesh, K. K., Anu, R. S., Krishna, V. P. (2009): Analysis of aerosol and carbon monoxide characteristics over Arabian Sea during crop residue burning period in the Indo-Gangetic plains using multi-satellite remote sensing datasets. – J. Atmos. Sol. Terr. Phys. 71: 1267-1276. Doi:10.1016/j.jastp.2009.04.004.

[11] Bobbink, R. (1989): Impacts of tropospheric ozone and airborne nitrogenous pollutants on natural and semi-natural ecosystems: A commentary. – New Phytologist 139(1): 161-168. Doi:10.1046/j.1469-8137.1998.00175.x.

[12] Boersma, K., Eskes, H., Veefkind, J., Brinksma, E., Sneep, M., van der Oord, G., Levelt, P., Stammes, P., Gleason, J., Bucsela, E. (2006): Near-real time retrieval of tropospheric NO_2 from OMI. – Atmos. Chem. Phys. Dis. 6(6): 12301-12345. Doi:10.5194/acpd-6-12301-2006.

[13] Burney, J., Ramanathan, V. (2014): Recent climate and air pollution impacts on Indian agriculture. – Proc. Natl. Acad. Sci. 111(46): 16319-16324.

[14] CMF (2018): City Mayors Foundation, UK. – www.citymayors.com (accessed on 11 July 2018).

[15] Cooper, O. R., Parrish, D. D., Ziemke, J., Balashov, N. V., Cupeiro, M., Galbally, I. E., Gilge, S., Horowitz, L., Jensen, N. R., Lamarque, J.-F., Naik, V., Oltmans, S. J., Schwab, J., Shindell, D. T., Thompson, A. M., Thouret, V., Wang, Y., Zbinden, R. M. (2014): Global distribution and trends of tropospheric ozone: An observation-based review. – Elem Sci Anth 2: 29. Doi:10.12952/journal.elementa.000029.

[16] El-Fadel, M., Zein, M., Nuwayhid, I., Jamali, D., Sadek, S. (2002): Environmental Management of Ozone in Beirut Urban Areas. – Environmental Management and Health 13: 471-494. Doi:10.1108/09566160210441780.

[17] Engel-Cox, J. A., Holloman, C. H., Coutant, B. W., Hoff, R. M. (2004): Qualitative and quantitative evaluation of MODIS satellite sensor data for regional and urban scale air quality. – Atmos. Environ. 38(16): 2495-2509. Doi:10.1016/j.atmosenv.2004.01.039.

http://www.aloki.hu ● ISSN 1589 1623 (Print) ● ISSN 1785 0037 (Online)
DOI: http://dx.doi.org/10.15666/aeer/1706_1353313553

[18] EPA (2003): National air quality and emissions trends report, Special Studies Edition. – Environmental Protection Agency, US EPA. EPA/454/R-03-005, North Carolina.
[19] Fang, H., Beaudoing, H. K., Rodell, M., Teng, W. L., Vollmer, B. E. (2009): Global Land Data Assimilation System (GLDAS) Products, Services and Application from NASA Hydrology Data and Information Services Center (HDISC). – ASPRS 2009 Annual Conference; 8-31 March 2009; Baltimore, MD US.
[20] Fioletov, V., Labow, G., Evans, R., Hare, E., Köhler, U., McElroy, C., Miyagawa, K., Redondas, A., Savastiouk, V., Shalamyansky, A. (2008): Performance of the ground-based total ozone network assessed using satellite data. – J. Geophys. Res. Atmos. 113(D14): 313. Doi:10.1029/2008JD009809.
[21] Ganesan, A. L., Chatterjee, A., Prinn, R. G., Harth, C. M., Salameh, P. K., Manning, A. J., Hall, B. D., Mühle, J., Meredith, L. K., Weiss, R. F., O'Doherty, S., Young, D. (2013): The variability of methane, nitrous oxide and sulfur hexafluoride in Northeast India. – Atmospheric Chemistry and Physics 13: 10633-10644. Doi:10.5194/acp-13-10633-2013.
[22] Gauss, M., Myhre, G., Pitari, G., Prather, M. J., Isaksen, I. S. A., Berntsen, T. K., Brasseur, G. P., Dentener, F. J., Derwent, R. G., Hauglustaine, D. A., Horowitz, L. W., Jacob, D. J., Johnson, M., Law, K. S., Mickley, L. J., Müller, J. -F., Plantevin, P. -H., Pyle, J. A., Rogers, H. L., Stevenson, D. S., Sundet, J. K., van Weele, M., Wild, O. (2003): Radiative forcing in the 21st century due to ozone changes in the troposphere and the lower stratosphere. – J. Geophys. Res. 108(D9): 4292. Doi:10.1029/2002JD002624.
[23] Ghude, S. D., der Arj, V., Beig, G., Fadnavis, S., Polade, S. D. (2009): Satellite derived trends in NO2 over the major global hotspot regions during the past decade and their inter-comparison. – Environ. Pollut. 157(6): 1873-1878. Doi:10.1016/j.envpol.2009.01.013.
[24] Holopainen, J. K. (2004): Multiple functions of inducible plant volatiles. – Trends Plant Sci. 9: 529-533.
[25] Hsu, J., Prather, M. J. (2009): Stratospheric variability and tropospheric ozone. – J. Geophys. Res. Atmos. 114:D6. http://dx.doi.org/10.1029/2008JD010942 retrieved from https://escholarship.org/uc/item/09q010cs.
[26] IPCC (2013): Climate Change 2013: The Physical Science Basis. – In: Stocker, T. F., Qin, D., Plattner, G. K., Tignor, M., Allen, S. K., Boschung, J., Nauels, A., Xia, Y., Bex, V., Midgley, P. M. (eds.). Contribution of Working Group I to the Fifth Assessment Report of the Intergovernmental Panel on Climate Change. Cambridge University Press, Cambridge, United Kingdom and New York, NY, USA, 1535 pp.
[27] Iqbal, M. A., Kim, K. -H., Shon, Z. -H., Sohn, J. -R., Jeon, E. -C., Kim, Y. -S., Oh, J. -M. (2014): Comparison of Ozone Pollution Levels at Various Sites in Seoul, a Megacity in Northeast Asia. – Atmospheric Research 138: 330-345. Doi:10.1016/j.atmosres.2013.12.003.
[28] Jacob, D. J. (2003): The oxidizing power of the atmosphere. – In: Potter, T. D., Colman, B. (eds.). Handbook of weather, climate and water. John Wiley & Sons. pp 1-1020. ISBN: 978-0-471-21489-2.
[29] Jaeglé, L., Martin, R., Chance, K., Steinberger, L., Kurosu, T., Jacob, D. J., Modi, A., Yoboué, V., Sigha-Nkamdjou, L., Galy-Lacaux, C. (2004): Satellite mapping of rain-induced nitric oxide emissions from soils. – J. Geophys. Res. Atmos. 109:D21. Doi:10.1016/j.atmosres.2013.12.003.
[30] Kulkarni, P. S., Ghude, S. D., Bortoli, D. (2010): Tropospheric ozone trend over three major inland Indian cities: Delhi, Hyderabad and Bangalore. – Anna. Geophys. 28(10): 1879-1885. Doi:10.5194/angeo-28-1879-2010.
[31] Lal, D., Ghude, S. D., Patil, S., Kulkarni, S. H., Jena, C., Tiwari, S., Srivastava, M. K. (2012): Tropospheric ozone and aerosol long-term trends over the Indo-Gangetic plain (IGP), India. – Atmos. Res. 116: 82-92. Doi:10.1016/j.atmosres.2012.02.014.
[32] Lerdau, M., Slobodkin, L. (2002): Trace gas emissions and species-dependent ecosystem services. – Trends Ecol. Evol. 17: 309-312. Doi:10.1016/S0169-5347(02)02535-1.

http://www.aloki.hu ● ISSN 1589 1623 (Print) ● ISSN 1785 0037 (Online)
DOI: http://dx.doi.org/10.15666/aeer/1706_1353313553

[33] Levelt, P. F., van den Oord, G. H. J., Dobber, M. R., Malkki, A., Visser, H., de Vries, J., Stammes, P., Lundell, J. O. V., Saari, H. (2006a): The Ozone Monitoring Instrument. – IEEE Transactions on Geoscience and Remote Sensing 44: 1093-1101. Doi:10.1109/TGRS.2006.872333.

[34] Levelt, P. F., Hilsenrath, E., Leppelmeier, G. W., van den Oord, G. B. J., Bhartia, P. K., Tamminen, J., de Haan, J. F., Veefkind, J. P. (2006b): Science objectives of the Ozone Monitoring Instrument. – IEEE Transactions on Geoscience and Remote Sensing 44(5): 1199-1208. Doi:10.1109/TGRS.2006.872336.

[35] Lin, M., Tao, J., Chan, C. -Y., Cao, J. -J., Zhang, Z. -S., Zhu, L. -H., Zhang, R. -J. (2012): Regression analyses between recent air quality and visibility changes in megacities at four haze regions in China. – Aerosol Air Qual. Res. 12: 1049-1061. Doi:10.4209/aaqr.2011.11.0220.

[36] Liu, S. N., Zhou, T., Wei, L. Y., Shu, Y. (2012): The spatial distribution of forest carbon sinks and sources in China. – Chin. Sci. Bull. 57: 1699-1707. Doi:10.1007/s11434-012-4998-1.

[37] Mishra, A. K., Shibata, T. (2012): Synergistic analyses of optical and microphysical properties of agricultural crop residue burning aerosols over the Indo-Gangetic Basin (IGB). – Atmos. Environ. 57: 205-218. Doi:10.1016/j.atmosenv.2012.04.025.

[38] Noreen, A., Khokhar, M. F., Zeb, N., Yasmin, N., Hakeem, K. R. (2018): Spatio-temporal assessment and seasonal variation of tropospheric ozone in Pakistan during the last decade. – Environ. Sci. Pollut. Res. 25(9): 8441-8454. Doi:10.1007/s11356-017-1010-2.

[39] Pagano, T. S., Aumann, H. H., Hagan, D. E., Overoye, K. (2003): Prelaunch and in-flight radiometric calibration of the atmospheric infrared sounder (AIRS). – IEEE Trans. Geosci. Rem. Sens. 41(2): 265-273. Doi:10.1109/TGRS.2002.808324.

[40] Pal, C. (2010): Variability of Total Ozone over India and Its Adjoining Regions during 1997-2008. – Atmospheric Environment 44: 1927-1936. Doi:10.1016/j.atmosenv.2010.01.028.

[41] Pinto, D. M., Blande, J. D., Souza, S. R., Nerg, A. M., Holopainen, J. K. (2010): Plant Volatile Organic Compounds (VOCs) in Ozone (O3) Polluted Atmospheres: The Ecological Effects. – J Chem Ecol 36(1): 22-34. Doi:10.1007/s10886-009-9732-3.

[42] Pulikesi, M., Baskaralingam, P., Rayudu, V. N., Elango, D., Ramamurthi, V., Sivanesan, S. (2006): Surface ozone measurements at urban coastal site Chennai, in India. – Journal of Hazardous Materials 137: 1554-1559. Doi:10.1016/j.jhazmat.2006.04.040.

[43] Sahoo, A., Sarkar, S., Singh, R. P., Kafatos, M., Summers, M. E. (2005): Declining Trend of Total Ozone Column over the Northern Parts of India. – International Journal of Remote Sensing 26: 3433-3440. Doi:10.1080/01431160500076467.

[44] Satheesh, S. K., Moorthy, K. K. (2005): Radiative effects of natural aerosols: A review. – Atmos. Environ. 39(11): 2089-2110. Doi:10.1016/j.atmosenv.2004.12.029.

[45] Seinfeld, J. H., Pandis, S. N. (2016): Atmospheric Chemistry and Physics: from air pollution to climate change. 3rd Edt. – John Wiley & Sons. ISBN-13: 978-1-118-94740-1.

[46] Shan, W. P., Yin, Y. Q., Zhang, J. D., Ding, Y. P. (2008): Observational Study of Surface Ozone at an Urban Site in East China. – Atmospheric Research 89: 252-261. Doi:10.1016/j.atmosres.2008.02.014.

[47] Sidhu, B. S., Beri, V. (2008): Rice residue management: farmer's perspective. – Indian Journal of Air Pollution Control VIII(I): 61-67.

[48] Stevenson, D., Dentener, F., Schultz, M., Ellingsen, K., Van Noije, T., Wild, O., Zeng, G., Amann, M., Atherton, C., Bell, N. (2006): Multimodel ensemble simulations of present-day and near-future tropospheric ozone. – J. Geophys. Res. Atmos. 111(D8): D08301. Doi:10.1029/2005JD006338.

[49] Streets, D. G., Canty, T., Carmichael, G. R., Defoy, B., Dickerson, R. R., Duncan, B. N., Edwards, D. P., Haynes, J. A., Henze, D. K., Houyoux, M. R., Jacob, D. J., Krotkov, N. A., Lamsal, L. N., Liu, Y., Lu, Z., Martin, R. V., Pfister, G. G., Pinderm, R. W., Salawitch, R. J., Wecht, K. J. (2013): Emissions Estimation from Satellite Retrievals: A Review of

http://www.aloki.hu ● ISSN 1589 1623 (Print) ● ISSN 1785 0037 (Online)
DOI: http://dx.doi.org/10.15666/aeer/1706_1353313553

Current Capability. – Atmospheric Environment 77: 1011-1042. Doi:10.1016/j.atmosenv.2013.05.051.

[50] Susskind, J., Barnet, C. D., Blaisdell, J. M. (2003): Retrieval of atmospheric and surface parameters from AIRS/AMSU/HSB data in the presence of clouds. – IEEE Trans. Geosci. Rem. Sens. 41: 390-409. Doi: 10.1109/TGRS.2002.808236.

[51] Tan, K. C., Lim, H. S., MatJafri, M. Z. (2014): Analysis of Total Column Ozone in Peninsular Malaysia Retrieved from SCIAMACHY. – Atmospheric Pollution Research 5: 42-51. Doi:10.5094/APR.2014.006.

[52] The Royal Society (2008): Ground-level Ozone in the 21st Century: Future Trends, Impacts and Policy Implications. – The Royal Society, London. Science policy report 15/08. ISBN: 978-0-85403-713-1.

[53] Ul-Haq, Z., Tariq, S., Ali, M., Mahmood, K., Batool, S. A., Rana, A. D. (2014): A Study of Tropospheric NO_2 Variability over Pakistan Using OMI Data. – Atmospheric Pollution Research 5: 709-720. Doi:10.5094/APR.2014.080.

[54] UNEP and WMO (2011): Integrated assessment of black carbon and tropospheric ozone. – United Nations Environment Programme, Nairobi.

[55] Van Dingenen, R., Dentener, F. J., Raes, F., Krol, M. C., Emberson, L., Cofala, J. (2009): The global impact of ozone on agricultural crop yields under current and future air quality legislation. – Atmos. Environ. 43(3): 604-618. Doi:10.1016/j.atmosenv.2008.10.033.

[56] Wang, L., Emmerich, J. S., Persily, A. K., Lina, C. C. (2012): Carbon Monoxide Generation, Dispersion and Exposure from Indoor Operation of Gasoline-Powered Electric Generators under Actual Weather Conditions. – Building and Environment 56: 283-290. Doi:10.1016/j.buildenv.2012.03.016.

[57] Xing, J., Wang, J., Mathur, R., Wang, S., Sarwar, G., Pleim, J., Hogrefe, C., Zhang, Y., Jiang, J., Wong, D.-C., Hao, J. (2017): Impacts of aerosol direct effects on tropospheric ozone through changes in atmospheric dynamics and photolysis rates. – Atmospheric Chemistry and Physics. Copernicus Publications, Katlenburg-Lindau, Germany 17: 9869-9883. Doi:10.5194/acp-17-9869-2017.

[58] Yienger, J. J., Levy, H. (1995): Empirical Model of Global Soil-Biogenic Noχ Emissions. – Journal of Geophysical Research 100 (D6): 11447-11464. Doi:10.1029/95JD00370.

[59] Young, P., Archibald, A., Bowman, K., Lamarque, J. -F., Naik, V., Stevenson, D., Tilmes, S., Voulgarakis, A., Wild, O., Bergmann, D. (2013): Pre-industrial to end 21st century projections of tropospheric ozone from the Atmospheric Chemistry and Climate Model Intercomparison Project (ACCMIP). – Atmos. Chem. Phys. 13(4): 2063-2090. Doi:10.5194/acp-13-2063-2013.

[60] Yuan, J. S., Himanen, S., Holopainen, J. K., Chen, F., Stewart, C. N. Jr. (2009): Smelling global climate change: mitigation of function for plant volatile organic compounds. – Trends Ecol. Evol. 24: 323-331. Doi: 10.1016/j.tree.2009.01.012.

[61] Ziemke, J., Chandra, S., Labow, G., Bhartia, P., Froidevaux, L., Witte, J. (2011): A global climatology of tropospheric and stratospheric ozone derived from Aura OMI and MLS measurements. – Atmos Chem Phys 11(17): 9237-9251. Doi:10.5194/acp-11-9237-2011.

[62] Ziemke, J., Olsen, M., Witte, J., Douglass, A., Strahan, S., Wargan, K., Liu, X., Schoeberl, M., Yang, K., Kaplan, T. (2014): Assessment and applications of NASA ozone data products derived from Aura OMI/MLS satellite measurements in context of the GMI chemical transport model. – J. Geophys. Res. Atmos. 119(9): 5671-5699. Doi:10.1002/2013JD020914.

http://www.aloki.hu ● ISSN 1589 1623 (Print) ● ISSN 1785 0037 (Online)
DOI: http://dx.doi.org/10.15666/aeer/1706_1353313553

STUDY OF SEED DORMANCY ORIGINS IN THREE ATLAS PISTACHIO ECOTYPES (*PISTACIA ATLANTICA* DESF.)

LABDELLI, A.[1,2] – ADDA, A.[1] – BOUCHENAFA, N.[1] – REBIAI, A.[3] – ZEBIB, B.[4] – MERAH, O.[5,6*]

[1]*Laboratory of Agro-Biotechnology and Nutrition in Semi-Arides Zones, Ibn Khaldoun University of Tiaret, Tiaret, Algeria*

[2]*Scientific and Technical Research Centre for Arid Areas (CRSTRA), BP 1682 RP, Biskra, Algeria*

[3]*University of El Oued, VTRS Laboratory, P. O. Box 789, El-Oued, Algeria*

[4]*Agronutition SAS Laboratories, Parc Activestre, 3 allée de l'Orchidée, F-31390 Carbonne, France*

[5]*Laboratoire de Chimie Agro-industrielle, LCA, Université de Toulouse, INRA, Toulouse, France*

[6]*Département Génie Biologique, IUT A, Université Paul Sabatier, Auch, France*

**Corresponding author*
e-mail: othmane.merah@ensiacet.fr

(Received 4th Apr 2019; accepted 2nd Sep 2019)

Abstract. The Atlas pistachio (*Pistacia atlantica* Desf.), a rustic tree distributed in different bioclimatic areas, is rapidly declining, particularly in Algeria. Among the actions to be undertaken is the launch of a restocking program. Nevertheless, Atlas pistachio seed dormancy is an obstacle limiting its germination and obtaining seedlings. The aims of the present study are to define the nature of seed germination inhibitors and to propose pretreatments that would limit their effects. Seeds were collected from three locations in Algeria. Quantitative and qualitative traits of phenolic compounds and total antioxidant activity were determined at three levels, namely, seed, epicarp and kernel. Germination was investigated in seeds with epicarp, epicarp removed, and with or without H_2O_2 treatment. Results showed that whole seed germination is not effective. Scarification by removing epicarp did not improve the germination rate. Chemical analyses indicated that seeds, kernel and epicarp were rich in total phenolic compounds. These compounds are known to limit seed germination in several species. Application of hydrogen peroxide induced a significant increase in seed germination rate in the three ecotypes. H_2O_2 caused inhibition of polyphenol compounds effects on germination. The results indicated that the inhibitory effect of phenolic compounds can be found at the kernel level instead of the epicarp. However, studied genotypes indicated that only one ecotype was distinguished by seed dormancy that originated in the epicarp and kernel.
Keywords: *pistachio, seeds, germination, inhibition, polyphenols*

Introduction

Wild pistachio (*Pistacia atlantica* Desf.) is a rustic and xerophytic tree, adapted to dry climates. In Algeria, it even inhabits pre-Saharan areas where it plays important roles on the ecological and socio-economic levels. It is a tree species of the genus *Pistacia* L. which is endangered in Algeria. This species has been declining from year to year in response to anthropogenic factors and, in addition, due to the problems related to its regeneration. Similarly, plants that beyond the emergence stage by escaping pastures are confronted with arid climate problems that cause even more damage (Ait Said et al., 2011). Atlas pistachio produces oilseeds rich in polyunsaturated fatty acids,

http://www.aloki.hu ● ISSN 1589 1623 (Print) ● ISSN 1785 0037 (Online)
DOI: http://dx.doi.org/10.15666/aeer/1706_1355513565

mainly oleic and linoleic acid (Yousfi et al., 2002; Farhoosh et al., 2009; Yazdanpanah and Baghereyanmanesh, 2015) and exhibit orthodox storage characteristics (Joley, 1960; Ayfer and Serr, 1961).

Seed germination is one of the most important stages of the plant life cycle. Germination in the narrow sense is an exceptionally complex process that begins with water uptake and is associated with many metabolic, cellular, and molecular events, which enable the radicle to emerge from the seed (Barba-Espín et al., 2012). The efficient progression of germination determines the nature of seedling formation and the proper development of mature plants. However, *Pistacia atlantica* seeds present a dormancy phenomenon which greatly limits their germination.

Seed dormancy is separated into two types, the first imposed by the epicarp and the second by the embryo (Joley, 1960; Bewley and Black, 1994). The endocarp can reduce the imbibition rate (Crane and Forde, 1974). Embryonic dormancy is related to the environmental conditions which occur at the time of harvest and when maturation of seeds takes place (Vallèe et al., 1999). Seeds of this tree are encompassed by a hard epicarp, which makes germination difficult (Isfendiyaroglu and Özeker, 2001; Abu-Qaoud, 2007).

Phenolic compounds are the products of secondary metabolism in plants, providing essential functions in their reproduction and growth, acting as defense mechanisms against pathogens, parasites, and predators, as well as contributing to the color of plants (Liu, 2007). The inhibitory effects of phenolic compound on seed germination are closely related to the regulation of endogenous auxins, epicarp permeability and oxygen supply to the embryo (Bewley and Black, 1994). Polyphenols and flavonoids produced in the fruit or seed can inhibit germination (Baskin and Baskin, 1998). The reactivation of metabolism following seed imbibition may supply an important source of reactive oxygen species (ROS) (Bailly, 2004). Hydrogen peroxide (H_2O_2) is a reactive molecule that plays a dual role in plant physiological and developmental processes, and in resistance to stress. The accumulation of H_2O_2 and of other ROS has been identified in seed physiology during imbibition and during early stages of germination (Schopfer, 2001; Bailly, 2004).

Preservation of the Atlas pistachio requires protection of the existing population, as well as planting of new trees. Realization of this last operation is based on the mastery seed germination and seedling production. Nevertheless under different conditions, the germination of pistachio seeds, though slow, requires the removal of factors which reduce its rate.

The poor germination of Atlas pistachio seeds seriously limits its regeneration. Different treatments have been used to increase the germination rate, without characterizing the factors that are responsible for seed dormancy. Abu Qaoud (2007) showed that germination rate was improved by seed scarification, which explains that seed dormancy is due to the mechanical resistance of the epicarp.

This study attempts to define the biochemical factors imposing the seed dormancy and their variation through the genetic variability thus the limitation of their effects by pretreatments application.

Materials and methods

Plant materials

Seeds of *Pistacia atlantica* accessions were collected from 10 trees in each of three locations in Algeria from the beginning of October to November 2015 (*Table 1; Figs. 1* and *2*).

http://www.aloki.hu ● ISSN 1589 1623 (Print) ● ISSN 1785 0037 (Online)
DOI: http://dx.doi.org/10.15666/aeer/1706_1355513565

Table 1. *Geographical data of Algerian studied zones where seeds sampling are collected*

Designation	Bioclimatic stage	Altitude (m)	Latitude (N)	Longitude (E)
Djelfa	Arid	630	34°02'11"	03°40'22"
Bechar	Hyper-arid	979	32°04'6"	02°18'5"W
Batna	Semi-arid	1027	35°37'10"	6°22'13"

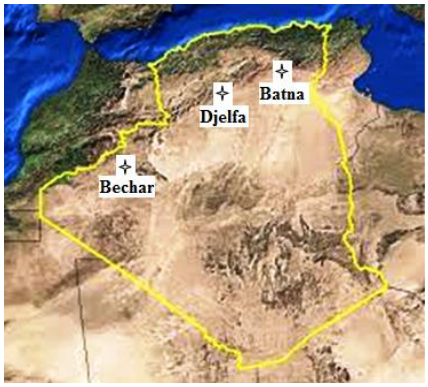

Figure 1. *Repartition map of the different sites of Pistacia atlantica ecotypes*

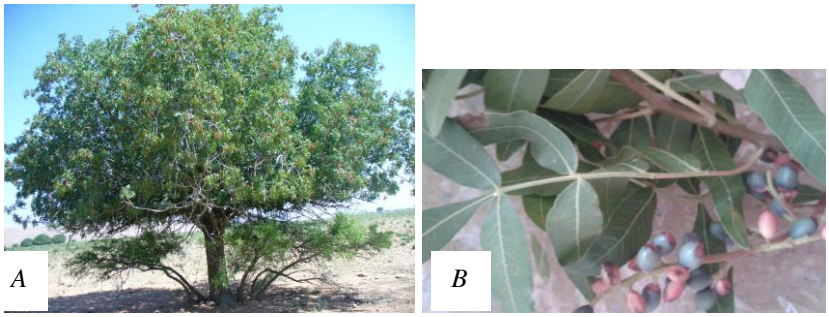

Figure 2*. Atlas Pistachio tree (A) and twigs with fruits (B)*

Biochemical analysis

Plant sampling and preparation of extracts

One gram of each sample of seed, kernel and epicarp were crushed into powder using a mortar grinder (RM 200-Retsch) mixed with 20 ml of methanol and stirred for 48 h in the dark at room temperature. The mixture was filtered through a GHP filter with 0.45 µm pores. The solvent was then removed under reduced pressure in a rotary evaporator at 60 °C. The residue (crude extract) was dissolved in 3 ml of methanol for analysis.

Determination of total phenolic compounds

The total polyphenol content (TPC) was quantified using the Folin-Ciocalteau phenol reagent, according to the protocol of Singleton et al. (1999). The method is based on the colored reaction of phenolic compounds with the reagent. Folin-Ciocalteau reagent is reduced to a blue colored oxide at pH 9.0 upon reaction with phenols. In a typical

http://www.aloki.hu ● ISSN 1589 1623 (Print) ● ISSN 1785 0037 (Online)
DOI: http://dx.doi.org/10.15666/aeer/1706_1355513565

experiment, 200 µl of the final methanolic solution was mixed with 1 ml of Folin-Ciocalteu reagent (10%) and 0.8 ml of Na_2CO_3 (7.5%). After incubation for 30 min at room temperature in dark, the absorbance was determined at 765 nm using a UV-1800 spectrophotometer (Shimadzu UV–VIS). Results were expressed as mg of gallic acid equivalent per g of fresh weight (mg GAE/g FW). For each sample three replicates were analyzed. The choice of methanol as solvent was based on the results of Belyagoubi et al. (2016), who showed that crude methanolic extracts were more effective than petroleum ether, chloroform, acetone and water extracts for determining total phenolic content and antioxidant activity of *P. atlantica* seeds.

Evaluation of total antioxidant activity (TAA)

The total antioxidant activity (TAA) of methanolic extract samples was estimated using the phosphomolybdenum method of Prieto et al. (1999), based on the reduction of Mo (VI) to Mo (V) by the extractedion and subsequent formation of a specific green phosphate/Mo (V) complex at acidic pH. Aliquots (1 ml) of reagent solution (0.6 M sulfuric acid, 28 mM sodium phosphate and 4 mM ammonium molybdate) were added to 100 µL of each sample (three replicates) and incubated at 95 °C for 90 min. The mixture was then cooled at room temperature. The absorbance of all samples was measured at 695 nm. Total antioxidant activity was expressed as mg gallic acid equivalent per g of fresh weight (mg GAE/g FW).

Qualitative analysis of phenolic compounds

The chromatographic system for the separation, analysis of phenolic acids and flavonoids were carried out with Shimadzu model prominence liquid chromatography, thermostatic column compartment, online degasser and an UV-visible detector model SPD-20A (operating at 268 nm). An analytical column used was a Shim-pack VP-ODS C18 (4.6 mm×250 mm, 5 µm), (Shimadzu Co., Japan). A binary gradient linear system consisting of acetonitrile (A) and 0.2% acetic acid in water (B) was used. Gradient method was generated by starting with 90% B; then decreasing to 86% B in 6 min, to 83% B in 16 min, to 81% B in 23 min, to 77% B in 28 min, held at 77% B in 28-35 min, to 60% B in 38 min, to 90% B in 50 min; at a flow rate of 1 mL/min. Quantification of separated peaks was performed by calibration with standard gallic acid (GA), chlorogenic acid (CGA), vanillic acid (VA), caffeic acid (CA), p-coumaric acid (p-CA), vanillin (V), rutin (RU), naringin (NAR), and quercetin (QE). The volume injected is 20 µl. The phenolic compositions were quantified by plotting a standard curve with the respective standards (*Fig. 1*).

Seed germination rate

Seeds of *Pistacia atlantica* (*Fig. 2*) were divided into two groups, with and without epicarp (achieved by mechanical scarification). They were imbibed in distilled water (control) or 4% H_2O_2 as pretreatment for 48 h. A total of 216 seeds were used for each ecotype (with and without epicarp) and were placed in Petri dishes (9 cm diameter) with filter paper moistened with distilled water. The experimental design was completely randomized with three replications per treatment. Seeds were incubated at 25 °C in the dark. The rate germination (G %) was calculated according to the following equation: G% = (NGG / NTG) × 100, where NGG was the number of germinated seeds and NTG was the total number of tested seeds.

http://www.aloki.hu ● ISSN 1589 1623 (Print) ● ISSN 1785 0037 (Online)
DOI: http://dx.doi.org/10.15666/aeer/1706_1355513565

Statistical analysis

All data were subjected to a one- and two-way analysis of variance (ANOVA) using the STATISTICA software package (StatSoft, Tulsa, USA). Mean comparison was performed by Duncan test at 5% probability level.

Results

Polyphenols and antioxidant activity

The results (*Table 2*) showed that there was a significant ecotype effect on the TPC content at the seed, epicarp and kernel level. Regarding the TAA, there was a significant effect only in relation to seed content.

Our results indicated that the phenolic compound content of the epicarp was significantly higher than seed or kernel, irrespective of the geographic origins (*Table 2*). The highest TPC content of the epicarp was observed in seeds from Djelfa and the lowest in seeds fromn Bechar. In the kernel, the total phenolic content increased by 20% from values in Bechar seeds to those from Djelfa (*Table 2*). The TAA at the seed level depended significantly on the nature of the ecotypes studied. However, seed origin had only a small influence on this activity in epicarp and kernel (*Table 2*). Total antioxidant activity was extremely different in seeds from different locations and values varied by nearly two-fold between ecotypes from Bechar and those from Batna (*Table 2*). The total antioxidant activity was highest at the epicarp level and the lowest values at the kernel level (*Table 2*). Indeed, TAA in the epicarp was nearly 1.7 and 4.5 times that in the whole seed and kernel, respectively (*Table 2*). Moreover, the higher the TPC value, the higher the antioxidant activity, irrespective of seed origin or the specific seed part investigated.

Table 2. *Means values of total phenolic contents (TPC) and total antioxidant activity (TAA) founded in seed, kernel and epicarp of Pistacia atlantica harvested from three geographic zones in Algeria*

Ecotype	TPC (mg GAE/g FW)			TAA (mg GAE/g FW)		
	Seed	Kernel	Epicarp	Seed	Kernel	Epicarp
Djelfa	257.7 ± 2.7^{a}	93.6 ± 5.8^{a}	450.4 ± 17.9^{a}	71.8 ± 14.2^{a}	42.34 ± 1.57^{a}	115.5 ± 3.8^{a}
Bechar	237.8 ± 2.4^{b}	77.7 ± 0.2^{b}	367.4 ± 32.5^{b}	82.0 ± 6.9^{a}	44.84 ± 8.55^{a}	87.2 ± 20.1^{a}
Batna	192.7 ± 3.6^{c}	81.7 ± 6.1^{b}	324.8 ± 1.8^{b}	49.4 ± 10.1^{b}	36.37 ± 5.60^{a}	126.7 ± 30.3^{a}
Mean	229.4	84.3	380.9	67.74	41.18	109.8
F values	57.1^{***}	8.76^{*}	26.6^{**}	7.1^{*}	1.6^{ns}	2.8^{ns}

*, **, ***: Significant at $P \leq 0.05$; $P \leq 0.01$; $P \leq 0.001$, respectively. ns: not significant. F values Means indicated by different letters are significantly different using the Duncan test at 0.05 probability and the significance of ecotype Factor it also displayed

Phenolic identification by HPLC

The phenolic compounds including gallic acid, chlorogenic Acid, vanillic acid, caffeic acid, Vanillin, p-coumaric acid, rutin, naringin and quercetin were identified and quantified in epicarp, kernel and seed (*Table 3a, b*).

http://www.aloki.hu ● ISSN 1589 1623 (Print) ● ISSN 1785 0037 (Online)
DOI: http://dx.doi.org/10.15666/aeer/1706_1355513565

The phenolic acid contents, which consist mainly of gallic and chlorogenic acids, are variable according to the ecotypes, at the three measurement sites (*Table 3a, b*). The highest phenolic acids content was recorded at the epicarp of Djelfa (D) seeds with 94.15 mg/gFW and the lowest value was measured at the Batna seeds epicarp (B) with 0.206 mg/gFW.

The results indicated that the quercetin is the major flavonoids constituent, identified in epicarp as well as in seed and kernel extracts. The total flavonoids highest levels were found in the epicarp of Djelfa and Batna seeds with respective values of 459.86 mg/gFW and 104.48 mg/gFW. The lowest levels of total flavonoids were found in the three ecotypes kernels, where the lowest grade has reached 2.26 mg/gFW (Bechar).

Finally, the results show that the different constituents of the Atlas pistachio seeds are poor in tannins. The condensed tannins are present at a low level, only in the epicarp of Djelfa and Batna ecotypes.

Table 3a. *Quantitative and qualitative analysis by HPLC of phenolic acids (mg/g FW) of seed, kernel and epicarp in different ecotypes*

	Ecotypes	**Gallic acid**	**Chlorogenic acid**	**Vanilic acid**	**Caffeic acid**	**p-Coumaric acid**	**Total phenolic acids**
Seed	Djelfa	6.277	9.83	0.094	ND	0.156	16.357
	Bechar	6.437	9.705	0.073	0.034	0.146	16.246
	Batna	1.462	3.482	ND	0.012	0.031	4.988
Kernel	Djelfa	1.649	1.515	0.059	0.080	ND	3.303
	Bechar	1.700	3.833	0.018	ND	ND	5.550
	Batna	0.468	1.497	ND	ND	ND	1.965
Epicarp	Djelfa	48.8	43.858	0.824	0.39	0.279	94.15
	Bechar	1.622	0.917	ND	ND	ND	2.54
	Batna	0.041	0.126	0.019	0.021	ND	0.206

ND: not determined

Table 3b. *Quantitative and qualitative analysis by HPLC of flavonoids and tanins (mg/g FW) of seed, kernel and epicarp in different ecotypes*

		Flavonoids				**Tannins**
	Ecotypes	**Rutin**	**Naringin**	**Quercetin**	**Total flavonoids**	**Vanillin**
Seed	Djelfa	1.025	0.07	43.985	45.08	0.111
	Bechar	1.133	0.297	41.798	43.228	ND
	Batna	0.128	0.211	42.845	43.183	ND
Kernel	Djelfa	0.144	ND	2.937	3.081	ND
	Bechar	0.133	ND	2.126	2.259	ND
	Batna	0.258	ND	7.154	7.413	ND
Epicarp	Djelfa	5.459	1.51	452.894	459.863	0.07
	Bechar	0.21	ND	23.391	23.602	ND
	Batna	0.254	0.091	104.134	104.479	0.091

ND: not determined

http://www.aloki.hu ● ISSN 1589 1623 (Print) ● ISSN 1785 0037 (Online)
DOI: http://dx.doi.org/10.15666/aeer/1706_1355513565

Seed germination rate

Seed germination was tested with or without an epicarp. The results showed that in both situations, seed germination was significantly influenced by ecotype origin, H_2O_2 treatment and their interaction (*Table 4*). No germination was observed, whatever the geographical origin, for whole seeds or for seeds without an epicarp. Pretreatment with H_2O_2 significantly increased the germination rate in all of the ecotypes studied (*Table 4*). However, the interaction between H_2O_2 treatment and seed origin had a significant effect on seed germination rate (*Table 3*). This relationship mirrored distinct reactions based on the seed origin with respect to the H_2O_2 pretreatment. In fact, H_2O_2treatment induced germination of seeds with or without an epicarp. Nevertheless, results of pretreatment with H_2O_2 were different depending on the presence of an epicarp or not (*Table 5*). Indeed germination rate of seeds without an epicarp with H_2O_2 application was 50% was higher than in whole seeds similarly treated with H_2O_2. Moreover, the ecotypes reacted differently to H_2O_2 pretreatment. The Batna ecotype had a 50% germination rate, while the lowest germination rate was observed in the Djelfa ecotype (*Table 5*). This difference in germination rate between Djelfa and Batna ecotype was reported for whole seeds and for seeds without an epicarp.

Table 4. *F-Test values and the significance of ecotype, H_2O_2 treatment and their interaction effects on seed germination on four ecotypes of Pistacia atlantica, with and without epicarp*

	Ecotype	**H_2O_2 Treatment**	**Ecotype*Treatment**
Seeds (with epicarp)	3.58^{ns}	45.74^{***}	3.5^{ns}
Seeds (without epicarp)	22.39^{***}	143.97^{***}	22.3^{***}

***Significant at $P \leq 0.001$; ns: not significant

Table 5. *Germination rate of seeds with or without epicarp, treated or not with H_2O_2 from three ecotypes of Pistacia atlantica*

Ecotype	**Treatment**	**Germination rate (%)**	
		With epicarp	**Without epicarp**
Djelfa	Control	0.00	0.00
Djelfa	H_2O_2	11.11 ± 11	14.7 ± 2.94
Bechar	Control	0.00	0.00
Bechar	H_2O_2	19.44 ± 8.3	25 ± 13.8
Batna	Control	0.00	0.00
Batna	H_2O_2	33.33 ± 0	50 ± 8.3

Discussion

Our results showed that removal of the epicarp did not improve seed germination whatever the ecotype (*Table 4*). This discrepancy may be a result of several environmental and genetic factors. Moreover, our results suggest that seed dormancy is chemical in nature and concerned, not only with the epicarp, but also the kernel (*Tables 4* and *5*). Among the chemical components that are involved in seed dormancy, phenols and their antioxidant activities are often cited (Panngom et al., 2018). Several methods have been used to overcome seed dormancy and to improve the seed

http://www.aloki.hu ● ISSN 1589 1623 (Print) ● ISSN 1785 0037 (Online)
DOI: http://dx.doi.org/10.15666/aeer/1706_1355513565

germination rate. Among these methods, the use of chemicals has been reported to be more effective (Wada et al., 2011; Barba-Espin et al., 2012; Panuccio et al., 2014; Panngom et al., 2018). In our study, we demonstrated that pretreatment with H_2O_2 greatly increased seed germination rates (*Table 5*). Similar findings have been reported using chemical components to break seed dormancy and increase seed germination in several species, including pea, coriander, carrot, zinnia and quinoa (Wada et al., 2011; Barba-Espin et al., 2012; Panuccio et al., 2014; Szopińska, 2014; Panngom et al., 2018). Many studies report that the progression of seed germination by hydrogen peroxide treatment may be the result of the oxidation of germination inhibitors present in the epicarp and pericarp (Duval and NeSmith, 2000; Ogawa and Iwabuchi, 2001; Conner, 2008; Klein et al., 2008; Huarte and Garcia, 2009; Panngom et al., 2018). The positive effect of H_2O_2 on seed germination has been explained by production of O_2 resulting by scavenging of H_2O_2 for the mitochondrial respiration and metabolic activities (Katzman et al., 2001). Chen et al. (1993) reported that H_2O_2 is useful in cracking hard seeds, allowing them to interact with water. The results obtained here showed that the origin of seed dormancy is related to both the kernel and the epicarp. Indeed, total phenol content and their antioxidant activities were higher in both compartments of the seed (*Table 2*). However, this result was dependent on the origin of the seeds used. Seeds from Batna locality showed similar inhibitory effects in the epicarp and kernel. Moreover, even though total phenol content was four times higher in the epicarp than in the kernel, antioxidant activity of the epicarp was only 2.5 times higher than the kernel. These results could be explained by the presence of chemical components other than phenols acting as antioxidants.

Total polyphenol compounds are mainly involved in the inhibition of seed germination in this plant species which limits water or oxygen absorption or both. Phenolic compounds and alkaloids that can be found in the epicarp and pericarp may inhibit seed germination (Tao and Buta, 1986; Gross and Parthier, 1994; Bhattacharyya et al., 1999). Isfendiyaroglu and Özeker (2001) reported that flavonoids and phenylpropanes played important roles in seed dormancy. Under natural conditions, the presence of total polyphenol compounds in seeds is effective in plant resistance to environmental conditions (Khoyerdi et al., 2016). The pretreatment with H_2O_2 that induced the germination (*Tables 3* and *4*) demonstrated that dormancy in Atlas pistachio seeds has a chemical basis. Among the functions of H_2O_2 is the oxidation of total phenolic compounds, contributing to the decomposition of the germination inhibitors (Ogawa and Iwabuchi, 2001). Klein et al. (2008) reported that faster germination of eastern gamagrass seeds exposed to H_2O_2 may result from breaking down the inhibitors present in the pericarp, although there may also be a direct physical scarifying effect of this compound. Some studies have reported that H_2O_2 is involved abscisic acid catabolism and gibberellin synthesis that, in turn, activates germination (Barba-Espin et al., 2012 and Panngom et al., 2018). The results also showed that the antioxidant activity increases with the increase of the polyphenol content of seeds. The antioxidant activity of phenolic compounds is mainly due to their redox properties, which allow them to act as reducing agents, hydrogen donors and singlet oxygen quenchers. Therefore reduces the endogenous concentration of ROS would improve seed germination (Sangmin et al., 2010).

The results of the present study showed that Atlas pistachio seeds (*Pistacia atlantica* Desf.) were characterized by a dormancy that inhibits their germination under optimal conditions. Seed scarification (removal of the epicarp) did not modify the germination

http://www.aloki.hu ● ISSN 1589 1623 (Print) ● ISSN 1785 0037 (Online)
DOI: http://dx.doi.org/10.15666/aeer/1706_1355513565

rate whatever the ecotype. Biochemical analysis showed seeds were rich in total phenolic compounds that were probably at the origin of their dormancy. This hypothesis was partly confirmed by the increase in germination rate after treatment of seeds with hydrogen peroxide. In fact, the total phenolic compounds were not only present in the epicarp but also the kernel, which may explain the absence of germination after scarification. Moreover, the distribution (content) of phenols between the kernel and the epicarp was different depending on ecotype studied. It seems that for ecotypes from Djelfa and Bechar, inhibition of germination was essentially localized at the level of the kernel, whereas for the ecotype from Batna this inhibition involved both the epicarp and the kernel. Further investigations are needed to confirm these results and to study the effect of different durations of pretreatment with H_2O_2 or other chemicals.

Conclusion

The low germination rates of Atlas pistachio seeds are due to their dormancy. This dormancy is of chemical nature and is localized at the level of the pericarp and kernel. It is explained by their high content of phenolic compounds that limit their metabolic reactivation during the emergence of latent life during their germination. In fact, there had been an absence of germination of whole or scarified seeds. Germination improved significantly after pretreatment with hydrogen peroxide (H_2O_2). The application of H_2O_2, which is one of the ROS, would inhibit the effects of phenolic compounds, accelerate the dormancy emergence and consequently improve the germination rate of *Pistacia atlantica*.

REFERENCES

[1] Abu-Qaoud, H. (2007): Effect of scarification, gibberellic acid and stratification on seed germination of three *Pistacia* species. – An Najah Univ J. Res (N. Sc.) 2(1): 1-11.

[2] Ait Said, S., Fernandez, C., Greff, S., Derridj, A., Gauquelin, T., Mevy, J. P. (2011): Inter-population variability of leaf morpho-anatomical and terpenoid patterns of *Pistacia atlantica* Desf. ssp. *atlantica* growing along an aridity gradient in Algeria. – Flora 206: 397-405.

[3] Ayfer, M., Serr, E. F. (1961): Effects of gibberellin and other factors on seed germination and early growth in *Pistacia* species. – Proceedings of the American Society for Horticultural Science 77: 308-315.

[4] Bailly, C. (2004): Active oxygen species and antioxidants in seed biology. – Seed Science Research 14: 93-107.

[5] Barba-Espín, G., Hernández, J. A., Diaz-Vivancos, P. (2012): Role of H_2O_2 in pea seed germination. – Plant Signaling & Behavior 7(2): 193-195.

[6] Baskin, C. C., Baskin, J. M. (1998): Seeds. – Academic Press San Diego, CA.

[7] Belyagoubi, L., Belyagoubi-Benhammou, N., Atik-Bekkara, F., Coustard, J. M. (2016): Effects of extraction solvents on phenolic content and antioxidant properties of *Pistacia atlantica* Desf. fruits from Algeria. – International Food Research Journal 23: 948-953.

[8] Bewley, J. D., Black, M. (1994): Seeds. Physiology of Development and Germination. – Plenum Press, New York.

[9] Bhattacharyya, S., Das. B., Ghose, T. K., Bhattacharya, S. (1999): Investigation on seed germination of *Nyctanthesarbour-tristis* (*Oleraceae*) in relation to the phenol content. – Seed Science and Technology 27: 321-327.

[10] Chen, Z., Silva, H., Klessing, D. F. (1993): Active oxygen species in the induction of plant systemic acquired resistance by salicylic acid. – Science 262: 1883-1886.

http://www.aloki.hu ● ISSN 1589 1623 (Print) ● ISSN 1785 0037 (Online)
DOI: http://dx.doi.org/10.15666/aeer/1706_1355513565

[11] Crane, J. C., Forde, H. I. (1974): Improved *Pistacia* seed germination. – California Agriculture 28: 8-9.
[12] Conner, P. J. (2008): Effects of stratification, germination temperature and pre-treatment with gibberellic acid and hydrogen peroxide on germination of 'Fry' muscadine (*Vitis rotundifolia*) seed. – Hort. Sci. 43: 853-856.
[13] Duval, J. R., Ne Smith, D. S. (2000): Treatment with hydrogen peroxide and seed coat removal or clipping improve germination of 'Genesis' triploid watermelon. – HortiScience 35: 85-86.
[14] Farhoosh, R., Haddad Khodaparast, M. H., Sharif, A. (2009): Bene hull oil as a highly stable and antioxidative vegetable oil. – European Journal of Lipid Science and Technology 111: 1259-65.
[15] Gross, D., Parthier, B. (1994): Novel natural substances acting in plant growth regulation. – Journal of Plant Growth Regulation 13: 93-114. http://dx.doi.org/10.1007/BF00210953.
[16] Huarte, R., Garcia, M. D. (2009): *Tripsacum dactyloides* (L.) L. (*Poaceae*) caryopsis dormancy and germination responses to scarification, hydrogen peroxide and phytohromes. – Seed Sci. Technol. 37: 544-553.
[17] Isfendiyaroglu, M., Özeker, E. (2001): The relation between phenolic compounds and seed dormancy in *Pistacia* spp. – Options Méditerranéennes 56: 227-232.
[18] Joley, L. E. (1960): Experiences with propagation of the genus *Pistacia*. – Proceedings of the Plant Propagators' Society 10: 287-292.
[19] Katzman, L. S., Taylor, A. G., Langhans, R. W. (2001): Seed enhancements to improve spinach germination. – HortiScience 36: 979-981.
[20] Khoyerdi. F. F., Shamshiri, M. H., Estaji, A. (2016): Changes in some physiological and osmotic parameters of several pistachio genotypes under drought stress. – Scientia Horticulturae 198: 44-51. http://dx.doi.org/10.1016/j.scienta.2015.11.028.
[21] Klein, J. D., Wood, L. A., Geneve, R. L. (2008): Hydrogen peroxide and color sorting improves germination and vigor of eastern gamagrass (*Tripsacum dactyloides*) seeds. – Acta Horticulturae 782: 93-97.
[22] Liu, R. H. (2007): Whole grain phytochemicals and health. – Journal of Cereal Science 46: 207-219.
[23] Ogawa, K., Iwabuchi, M. (2001): A mechanism for promoting the germination of *Zinnia elegans* seeds by hydrogen peroxide. – Plant Cell Physiology 42: 286-291.
[24] Panngom, K., Chuesaard, T., Tamchan, N., Jiwchan, T., Srikongsritong, K., Park, G. (2018): Comparative assessment for the effects of reactive species on seed germination, growth and metabolisms of vegetables. – Scientia Horticulturae 227: 85-91.
[25] Panuccio, M. R., Jacobsen, S. E., Akhtar, S. S., Muscolo, A. (2014): Effect of saline water on seed germination and early seedling growth of the halophyte quinoa. – AoB Plants 6(plu047): 1-18.
[26] Prieto, P., Pineda, M., Aguilar, M. (1999): Spectrophotometric quantitation of antioxidant capacity through the formation of a phosphomolybdenum complex: Specific application to the determination of vitamin E. – Analytical Biochemistry 269: 337-341.
[27] Sangmin, L., Sang-Gyu, K., Chung-Mo, P. (2010): Salicylic acid promotes seed germination under high salinity by modulating antioxidant activity in Arabidopsis. – New Phytologist 188: 626-637.
[28] Schopfer, P. (2001): Hydroxyl radical-induced cell-wall loosening in vitro and in vivo: implications for the control of elongation growth. – The Plant Journal 28: 679-678.
[29] Singleton, V. L., Orthofer, R., Lamuela-Raventos, R. M. (1999): Analysis of total phenols and other oxidation substrates and antioxidants by means of Folin-Ciocalteu reagent. – Methods in Enzymology 299: 152-178.
[30] Szopińska, D. (2014): Effects of hydrogen peroxide treatment on the germination, vigour and health of *Zinnia elegans* seeds. – Folia Hort. 26(1): 19-29.

http://www.aloki.hu ● ISSN 1589 1623 (Print) ● ISSN 1785 0037 (Online)
DOI: http://dx.doi.org/10.15666/aeer/1706_1355513565

[31] Tao, K. L. J., Buta, J. G. (1986): Differential effects of camptothecin and interaction with plant hormones on seed germination and seedling growth. – Plant and Growth Regulation 4: 219-226.
[32] Vallèe, C., Bilodeau, G., De Lanaudière, C. J. (1999): Les techniques de culture en multicellules. – Quebecois Institute of the Decorative Development of Horticulture, Saint-Nicolas, Québec, Canada.
[33] Wada, S., Kennedy, J. A., Reed, B. M. (2011): Seed-coat anatomy and proanthocyanidins contribute to the dormancy of Rubus seed. – Scientia Horticulturae 130: 762-768.
[34] Yazdanpanah, E., Baghereyanmanesh, R. (2015): Quantitative analysis of the seed oil from *Pistacia atlantica* var. *mutica* in boyer ahmad. – Indian Journal of Fundamental and Applied Life Sciences 5(4): 84-87.
[35] Yousfi, M., Nedjmi, B., Bellal, R., Ben Bertal, D., Pallad, G. (2002): Fatty acids and sterols of *Pistacia atlantica* fruit oil. – Journal of the American Oil Chemists' Society 79: 1049-1050.

http://www.aloki.hu ● ISSN 1589 1623 (Print) ● ISSN 1785 0037 (Online)
DOI: http://dx.doi.org/10.15666/aeer/1706_1355513565

EVALUATION OF REGION AND SUBREGION-BASED HEIGHT-DIAMETER MODELS FOR DAHURIAN LARCH (*LARIX GMELINII*) IN DAXING'AN MOUNTAINS IN CHINA

ENZINGA, G. Y.[1] – JIANG, L.-C.[2*]

[1]*Forest Management Department, College of Forestry, Hexing Road, Xiangfang District, 150040 Harbin, China*

[2]*Northeast Forestry University, Harbin, Heilongjiang Province, China*

*****Corresponding author*
e-mail: jlichun@nefu.edu.cn

(Received 4th Apr 2019; accepted 31st Oct 2019)

Abstract. Using the felled tree data, subregions-based height-diameter models were developed for Dahurian larch (*Larix gmelinii* Rupr) in Daxing'an Mountains in China. Thirty frequently used nonlinear growth functions were fitted to individual tree height-diameter data. A total of 2411 for Dahurian larch trees were collected and measured. Parameter estimates and evaluation statistics were calculated using SAS PROC NLIN procedure for overall model, three regional models, and ten subregional models. The non-linear extra sum of squares method was used to assimilate the difference of the height-diameter relationships among different subregions. The results indicate that the Chapman-Richards growth function show the best for fitting tree height-diameter relationships at regional and subregional levels with a root mean square error RMSE = 2.193 and coefficient determination $R^2 = 0.8221$. It was revealed that, Dahurian larch height-diameter relationships showed the several differences among these regions and subregions ($P < 0.0001$) when overall, regional and subregional model was applied to predict tree height separately in each region and subregion. Among the 45 pairs of subregions, only four subregion pairs (e.g., XL versus SBZ, XL versus HJY, SBZ versus HJY, and XL versus JGDQ) showed the non-significant difference F-value ($P > 0.05$) and the data from those subregions were combined and applied to others subregions; all comparisons show the difference. The tree height-diameter relationships of Dahurian larch are significantly different among the geographic regions in Daxing'an Mountains, depending on local climatic, soil, and ecological conditions.

Keywords: *Chapman-Richards model, non-linear extra sum of square method, full model, reduced model, forest management*

Introduction

Individual tree diameter at breast height (D) and total height are the most fluently measured variables in study of forest inventory and growth and yield modeling. In practice, tree diameters can be readily measured inexpensively. However, collect tree height data are fairly more difficult and expensively. Often total tree heights are obtained by estimations from observed tree diameter at breast height outside bark. To estimate individual tree volume and site index, and describe stand growth dynamics and succession over time, necessitates accurate height–diameter models (Botkin et al., 1972; Curtis, 1967). Particularly in the northern and northeastern provinces of China, the genus Dahurian larch (*Larix gmelinii* Rupr.) is economically and ecologically important for tree species in China (Leng et al., 2008). Dahurian forests cover an area and volume in the forests of these provinces of 92.9 and 87.6 percent, respectively, of the total Dahurian in the country (Zang et al., 2016). It is a deciduous needle leaf conifer that is adapted to growing in very harsh climates and is widely distributed over a range from 72° 31' N 105° 03' E. In the Daxing'an Mountains forest ecosystem in northern China, it is the

http://www.aloki.hu ● ISSN 1589 1623 (Print) ● ISSN 1785 0037 (Online)
DOI: http://dx.doi.org/10.15666/aeer/1706_1356713591

dominant tree species (Jiang et al., 2016). Recently, Dai and Jiang (2015) developed and evaluated 12 non-linear height-diameter models for Dahurian larch from three regions in Daxing'an Mountain of northeast China. They found that the Chapman-Richards function was one of the best models for this species across the study region. In this study, we will develop and evaluate 30 nonlinear diameter models for Dahurian larch in three regions subdivided into 10 subregions and we will select the best model according to the goodness-of-fit statistics. With a large number of models, we could expect that the best model for Dahurian larch could be other that of Chapman-Richards as found to the study quoted above. However, if another model is found better than for Chapman Richard; then this will lead us to understand that the Chapman-Richards is not the best suitable model for the Dahurian larch in the Daxing'an mountain, so there is another model better than this one. However, the height-diameter relationship of a given species is highly dependent on climatic patterns (e.g., temperature and precipitation). Application of regional models to local ecological sites may lead to biased predictions for tree heights knowing that these subregions are specified by climatic regimes (e.g. temperature and precipitation), soil moisture and nutrient regimes, and vegetation types. The variations are expected during their comparisons. Examples of models that represent such variation are found (Zhang et al., 2002; Özçelik et al., 2014; Huang, 1999; Huang et al., 1999, 2000; Huang and Titus, 1994; Peng et al., 2001 Pillsbury et al., 1995).

In recent years, the principles of multifunction, multipurpose and ecologically based forest management were approved in China. Therefore, in order to help forest managers and practitioners more realize the differences in these relationships among different subregions, the subregion-based height-diameter models are necessary. to: (1) evaluate tree height-diameter models for Dahurian larch at regional and subregional scales in Daxing'an Mountains at Northeast China; (2) establish the comparison of differences of the height-diameter relationships among the ten subregions; (3) evaluate the consequences and biases of incorrectly applying regional and subregional height-diameters models in different subregions.

Materials and methods

Study area and data

The study area is the cold temperate forest regions in Daxing'an Mountain in Heilongjiang Province and eastern part of Inner Mongolia, from 121° 12′ E to 127° 00′ E and from 50° 10′ N to 53° 33′ N in Northeastern China. The climate is continental monsoon climate. The average annual precipitation ranges from 500 to 750 mm. The mean annual temperature is between -1 and -2.8 °C, and the average January and July air temperatures are about -28 °C and +20 °C, respectively (*Table 1*). The study area was assigned to three distinct regions (Zhang et al., 1992): the eastern slope of Northern part of Daxing'an Mountains (NDXAM), the northwest of the northern slope of Yilehuli Mountains (NWYLHLM), and the southeast of the northern slope of Yilehuli Mountains (SAYLHLM). Sample trees were assigned to ten subregions in NWYLHLM, SAYLHLM, and NDXAM regions (*Fig. 1*). The NWYLHLM region covers four subregions, including Xilinji (XLJ), Tuqiang (TQ), Amuer (AME), Huzhong (HZ); The SAYLHLM region covers four subregions, including Xinlin (XL), Tahe (TH), Shibazhan (SBZ), Hanjiayuan (HJY); the NDXAM region covers two subregions, including Songling (SL), Jiagedaqi (JGDQ). These subregions are specified by climatic schemes (e.g., temperature and precipitation), soil moisture and nutrient regimes, and vegetation types.

http://www.aloki.hu ● ISSN 1589 1623 (Print) ● ISSN 1785 0037 (Online)
DOI: http://dx.doi.org/10.15666/aeer/1706_1356713591

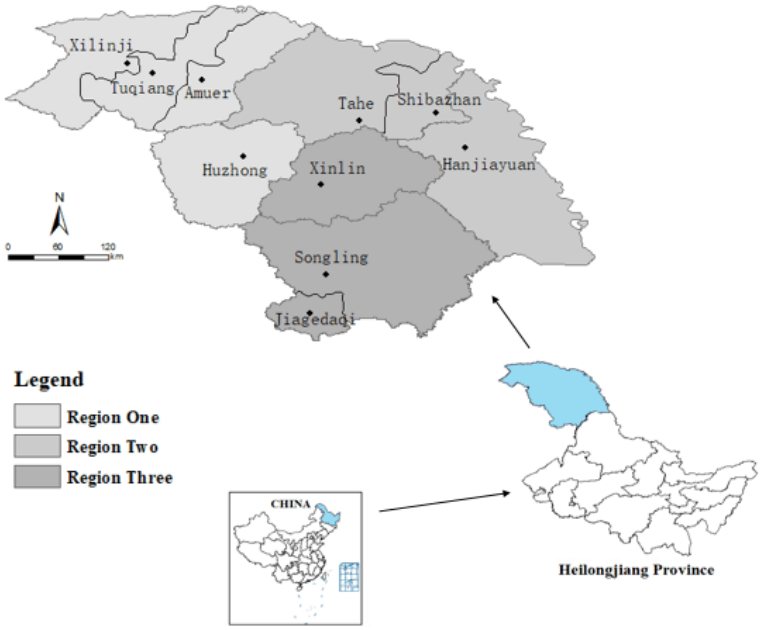

Figure 1. *Simple map of ecoregion classification of study area in the Northeast, China*

Table 1. *Summary of climatic variables*

Subregions	AMT (C)	AMP (mm)
SL	-3	600
JGDQ	-1.2	450
XL	-2.6	514
TH	-2.4	463
HZ	-4.3	498
SBZ	-2.5	471
HJY	-2	510
XLJ	-7.5	500
TQ	-5.5	460
AME	-5	455

AMT – annual mean temperature; AMP – annual mean precipitation

A total of 2411 destructively sampled Dahurian larch trees were used in this study. These trees were felled throughout the forest inventory areas of northeast China and all sampled trees were selected to ensure a representative distribution across a range of height and diameter classes within stands varying in density, height, site condition, age and stand structure. The data is from an existing database, and was collected from December 2004 and February 2005. For developing taper and individual tree volume equations the data set was initially used. Diameters at breast height were measured for all sampled trees (D, defined as 1.3 m above the ground) outside bark, and total height (H). Trees possessing broken tops, obvious cankers or crooked boles were excluded from the analysis. Summary statistics for tree diameter and total height are provided for each subregion, the NDXAM, YLHLM-NW and YLHLM-SA regions, and all data combined (Overall) in *Table 2*.

http://www.aloki.hu ● ISSN 1589 1623 (Print) ● ISSN 1785 0037 (Online)
DOI: http://dx.doi.org/10.15666/aeer/1706_1356713591

Table 2. *Summary of tree diameter at breast height (D) and total height (H) for subregional and regional data sets*

Subregion	N	D (cm)				H (m)			
		Mean	STD	Min	Max	Mean	STD	Min	Max
SL	214	29.15	14.07	5.5	55.1	19.59	5.41	7.1	29.2
JGDQ	524	27.27	13.24	5.4	61.0	18.3	4.83	6.4	30.8
XL	190	30.94	12.57	6.0	63.4	19.34	3.99	8.4	29.5
TH	203	21.98	12.32	5.2	50.6	15.34	5.37	5.1	26.5
HZ	215	23.53	11.61	5.1	48.8	16.13	4.69	4.5	25.9
SBZ	237	27.46	13.33	5.4	56.6	17.93	4.72	6.1	26.1
HJY	128	26.79	12.38	5.2	50.8	17.72	4.60	6.6	26.5
XLJ	224	16.00	9.00	5.1	62.0	15.76	4.21	7.2	24.6
TQ	191	23.98	14.59	5.2	56.0	17.45	5.25	6.5	28.5
AME	285	33.68	13.00	5.1	72.2	22.37	4.87	7.3	33.9
NWYLHLM	915	24.94	13.86	5.1	72.2	18.26	5.53	4.5	34.0
SAYLHLM	758	26.75	13.10	5.2	63.4	17.56	4.93	5.1	29.5
NDXAM	738	27.82	13.50	5.4	61.0	18.67	5.03	6.4	30.8
Overall	2411	26.39	13.57	5.1	72.2	18.16	5.21	4.5	34.0

N – sample size (number of trees), STD – standard deviation, Min. – minimum, Max. – maximum

Data analysis

The 30 height–diameter equations listed in Fang and Bailey (1998), Huang et al. (2000, 1992) and Peng et al. (2001) were examined and evaluated to select the best model for further analyses. The equations chosen for the comparison were concentrated on the verification of the height-diameter relationship, as shown by plotting tree height against D on a provincial basis (Huang, 1999). All selected functions are shown in *Table 3*. The validity of a homogeneous variance was investigated. In several studies, we observed the significant evidence of unequal error variances (Huang et al., 1992), while here there were not. Under this circumstance, weighted least-squares may not significantly improve model performance but may increase model fit slightly (Zhang, 1997). Therefore, ordinary nonlinear least-squares were used for parameter estimation instead than weighted least-squares. Every model was assessed using a coefficient of determination (R^2) and root mean square error (RMSE).

Table 3. *Height-diameter functions selected for evaluation*

Function number and form	References
(1) $H = 1.3 + \frac{D^2}{(a+bD)^2}$	Loetsch et al. (1973)
(2) $H = 1.3 + \frac{a}{(1+D^{-1})^b}$	Curtis (1967)
(3) $H = 1.3 + ae^{-b/(D+c)}$	Ratkowsky (1990)
(4) $H = 1.3 + a(1-e^{-bD^c})$	Yang et al. (1978)
(5) $H = 1.3 + a(1-e^{-bD})^c$	Richards (1959)

http://www.aloki.hu ● ISSN 1589 1623 (Print) ● ISSN 1785 0037 (Online)
DOI: http://dx.doi.org/10.15666/aeer/1706_1356713591

(6) $H = 1.3 + e^{(a+\frac{b}{D+1})}$	Wykoff et al.(1982)
(7) $H = 1.3 + aD^{bD^{-c}}$	Sibbesen (1981)
(8) $H = 1.3 + ae^{-bD^{-c}}$	Zeide (1989)
(9) $H = 1.3 + ae^{-b\,e^{-cD}}$	Winsor (1932)
(10) $H = ae^{-\exp(-b(D-c))}$	Seber and Wild (1989)
(11) $H = a(1 - exp\{-bD^c\})$	Bailey (1979)
(12) $H = 1.3 + ae^{b/D}$	Loetsch et al. (1973)
(13) $H = 1.3 + 10^a D^b$	Burkhart and Strub (1974); Buford (1986); Larson (1986); Watts (1983)
(14) $H = 1.3 + aD/(b + D)$	Bates and Watts (1980); Ratkowsky (1990)
(15) $H = 1.3 + a(1 - e^{-bD})$	Bates and Watts (1980); Ratkowsky (1990)
(16) $H = 1.3 + \frac{aD}{(D+1)} + bD$	Watts (1983)
(17) $H = 1.3 + a/(1 + be^{-cD}$	Paerl and Reed (1920)
(18) $H = a(1 - b\ \ exp\{-cD^d\})$	Bailey (1979), Seber and Wild (1989)
(19) $H = 1.3 + D^2/(a + bD + cD^2)$	Curtis (1967); Prodan (1968)
(20) $H = 1.3 + ae^{b/(D+c)}$	Ratkowsky (1990)
(21) $H = 1.3 + a/(1 + b^{-1}D^{-c}$	Ratkowsky and Reedy (1986)
(22) $H = e^{a+b/(D+1)}$	Wykoff et al. (1982), Huang and Titus (1992)
(23) $H = aD/(b + D)$	Tang (1994), Bates and Watts (1980), Ratkowsky and Reedy (1986)
(24) $H = a\ \ exp\{-bexp[-cD^d]\}$	Zeide (1993)
(25) $H = a + bD + cD^2$	Henricksen (1950), Curtis (1967)
(26) $H = 1.3 + aD^b$	Stoffels and van Soest (1953); Stage, 1975
(27) $H = a/(1 + e^{-b(D-c)}$	Seber and Wild (1989)
(28) $H = a + b/(D + c)$	Tang (1994)
(29) $H = ae^{b/(D+c)}$	Ratkowsky (1990), Huang and Titus (1992)
(30) $H = a(1 - e^{-bD})$	Meyer (1940), Farr et al. (1989), Moffat et al. (1991)

H = total height (m); D = diameter at breast height outside bark (cm); a, b, c, d = parameters to be estimated; e = base of the natural logarithm (≈2.71828); 1.3 = a constant commonly used to avoid the prediction of a height less than 1.3 meters when D is small

Through comparisons, the Chapman-Richards function was considered one of the best nonlinear functions for describing the relationship between height and diameter of the Dahurian larch and selected as the base model. The function on Chapman-Richards as represented by the following equation:

http://www.aloki.hu ● ISSN 1589 1623 (Print) ● ISSN 1785 0037 (Online)
DOI: http://dx.doi.org/10.15666/aeer/1706_1356713591

$$H = 1.3 + a\left[1 - e^{-b.D}\right]^{c} \quad \text{(Eq.1)}$$

where: H: total tree height (m); D: tree diameter at breast height (cm); a: the asymptotic parameter; b: the rate parameter; c: the shape parameter.

The Chapman-Richards function was fit to: (1) the overall data (N = 2411); (2) the NWYLHLM region data (915); (3) the SAYLHLM region data (758); (4) the NDXAM region data (738); (5) each of ten subregions separately. Parameter estimates and evaluation statistics were calculated using SAS PROC NLIN procedure (SAS Institute, Inc., 1999) for overall model, three regional models, and ten subregional models. The non-linear extra sum of squares method was used (Bates and Watts, 1988) to assimilate the difference of the height-diameter relationships among different subregions. The non-linear extra sum of squares method demands the fitting of full and reduced models and has commonly been applied to evaluate if separate models needed for different species or different geographic regions (Huang, 2000; Peng, 2001; Zhang, 2002; Corral-Rivas et al., 2004, 2007; Castedo-Dorado et al., 2005). The full model varieties to different sets of parameters for each subregion and is gotten by enlarging each parameter by including an associated parameter and a dummy variable to distinguish among subregions. The reduced model corresponds to the same set of global parameters for all subregions. Using Indicator (dummy) variable approach, the full model of the Chapman-Richards function can be written as:

$$H = 1.3 + \left(a + \sum_{i=1}^{k} a_i z_i\right)\left[1 - e^{-\left(b + \sum_{i=1}^{k} b_i z_i\right).DBH}\right]^{\left(c + \sum_{i=1}^{k} c_i z_i\right)} \quad \text{(Eq.2)}$$

(1) To evaluate the overall differences among regions. Two indicator variables (k = 2) are needed in *Equation 2* for three regions. They are set as follows:
If region = NWYLHLM, $z_1 = 1$, $z_2 = 0$;
If region = SAYLHLM, $z_1 = 0$, $z_2 = 1$;
If region = NDXAM, $z_1 = 0$, $z_2 = 0$.

(2) To evaluate the differences between the three regions. A total of 3 region pairs can be formulated to test the pairwise differences between the three regions. The 3 testing pairs require 3 full models that take the form of *Equation 2*, and 3 reduced models that take the form of *Equation 1*. For example, to test the difference between region NWYLHLM vs. SAYLHLM, one indicator variable (k = 1) can be defined: if region = NWYLHLM, $Z_1 = 1$; and if region = SAYLHLM $Z_1 = 0$. Similarly, the full model (*Eq. 2*) has 6 estimable parameters.

(3) To evaluate the overall differences among subregions. Nine indicator variables (k = 9) are needed in *Equation 2* for ten subregions. They are defined as follows:
If subregion = SL, $z_1 = 1$, all other $z_i = 0$;
If subregion = JGDQ, $z_2 = 1$, all other $z_i = 0$;
If subregion = XL, $z_3 = 1$, all other $z_i = 0$;
If subregion = TH, $z_4 = 1$, all other $z_i = 0$;
If subregion = HZ, $z_5 = 1$, all other $z_i = 0$;
If subregion = SBZ, $z_6 = 1$, all other $z_i = 0$;
If subregion = HJY, $z_7 = 1$, all other $z_i = 0$;
If subregion = XLJ, $z_8 = 1$, all other $z_i = 0$;
If subregion = TQ, $z_9 = 1$, all other $z_i = 0$;

http://www.aloki.hu ● ISSN 1589 1623 (Print) ● ISSN 1785 0037 (Online)
DOI: http://dx.doi.org/10.15666/aeer/1706_1356713591

If subregion = AME, all other $z_i = 0$.

(4) To evaluate the differences between the ten subregions: A total of 45 subregion pairs can be formulated to test the pairwise differences between the ten subregions. The 45 testing pairs require 45 full models that take the form of *Equation 2*, and 45 reduced models that take the form of *Equation 1*. For example, to test the difference between subregion SL vs XL, one indicator variable (k = 1) can be defined: if subregion = SL, $Z_1 = 1$; and if subregion = XL, $Z_1 = 0$. Similarly, the full model (*Eq. 2*) has 6 estimable parameters. All the reduced models for these tests take the form of *Equation 1* with 3 parameters. The nonlinear extra sum of squares for comparing the full and reduced models follows an F-distribution and uses the following expression:

$$F = \frac{(SSE_R - SSE_F)/(df_R - df_F)}{(SSE_F)/(df_F)} \quad \text{(Eq.3)}$$

where SSE_R and df_R are the error sum of squares and degrees of freedom related with the reduced model and SSE_F and df_F are error sum of squares and degrees of freedom related with a full model. Generally, the F-test is meaningful if the p-value for the test is least than 0.05.

To evaluate the performances of applying a height-diameter model to different subregion; each of the fourteen models (overall model, three regional models, and ten subregional models) was used to predict total tree heights for each subregion. Using the observed and predicted total tree heights, the following criteria were used to assess the predictive capability and significant test (Zhang et al., 2002; Cutini et al., 2013; Peng et al., 2004):

$$\bar{e} = \frac{\sum_{i=1}^{m}(H_i - \hat{H}_i)}{m} \quad \text{(Eq.4)}$$

$$S_e = \sqrt{\frac{\sum_{i=1}^{m}\left(e_i - \bar{e}_i\right)^2}{m-1}} \quad \text{(Eq.5)}$$

$$\bar{e}\% = \frac{\bar{e}}{\bar{H}} X\ 100 \quad \text{(Eq.6)}$$

$$t = \frac{\bar{e}}{S_{e/\sqrt{m}}} \quad \text{(Eq.7)}$$

where e_i is the unlike between the observed (Hi) and predicted ($\hat{H}i$) height for the i the observation (i = 1, 2,…, m) with m being the number of observations in the concerned subregion, $\bar{e}$ is mean prediction error; Se is the standard deviation of the prediction error; $\bar{e}\%$ is percent prediction error, $\bar{H}$ is the mean of observed heights; t is a t-test used to test the null hypothesis that the mean prediction error equals zero. Although overall evaluation ($\bar{e}$, $\bar{e}\%$ and t-test) are good indicators of the consequences of inappropriately applying a height-diameter model in different subregions, they may not be indicated the quality of prediction for different diameter classes in each of the ten subregions. Therefore, the height-diameter models (Overall model, three regional models, and ten subregional models) were further assessed by use of plots of prediction errors against diameter classes (5-cm diameter intervals) in each of the ten subregions.

http://www.aloki.hu ● ISSN 1589 1623 (Print) ● ISSN 1785 0037 (Online)
DOI: http://dx.doi.org/10.15666/aeer/1706_1356713591

Results and discussion

Selection of the height-diameter model

Parameter estimates and fitting statistics for the candidate models are listed in *Table 4*.

The t-statistics for the parameters of these functions were all significant at the significant level of 0.0001. The coefficient of determination (R^2) of all functions was within the range from 0.7607 to 0.8221, and the RMSE was within the range from 2.193 to 2.5347 m. The Chapman-Richards function (model 5) had the smallest RMSE value and highest R^2 value.

Table 4. *Comparison of height-diameter on the Dahurian larch model fitting data set*

Function	Estimated coefficients				n	RMSE	R^2
	a	b	c	d			
(1)	0.6543	0.0304	-	-	2411	2.2024	0.8194
(2)	27.2134	10.2849	-	-	2411	2.2642	0.8091
(3)	32.5708	16.7877	6.3255	-	2411	2.2044	0.8191
(4)	25.9089	0.049	0.0593	-	2411	2.206	0.8205
(5)	25.9018	0.0392	0.8114	-	2411	2.193	0.8221
(6)	2.3244	-8.7643	-	-	2411	2.3006	0.8029
(7)	3.5664	1.5361	1.05	-	2411	2.287	0.8052
(8)	43.2886	4.5309	0.5037	-	2411	2.198	0.8217
(9)	23.7396	1.7099	0.0712	-	2411	2.2414	0.813
(10)	2.887	0.3362	19	-	2411	2.5347	0.7607
(11)	117.0832	0.0345	0.4507	-	2411	2.2738	0.8074
(12)	26.8223	-9.6581	-	-	2411	2.2814	0.8061
(13)	0.5519	0.4863	-	-	2411	2.287	0.8052
(14)	32.8961	21.5312	-	-	2411	2.2024	0.8194
(15)	24.1895	0.0541	-	-	2411	2.2223	0.8161
(16)	9.025	0.3143	-	-	2411	2.4634	0.7739
(17)	23.0775	3.2223	0.0955	-	2411	2.2715	0.8079
(18)	77.0078	0.1805	-1.8397	-0.0792	2411	2.2205	0.7749
(19)	-0.216	-0.9696	0.8704	-	2411	2.2024	0.8194
(20)	31.1265	-17.1302	5.5443	-	2411	2.2049	0.8189
(21)	32.8964	0.0464	-	-	2411	2.2024	0.8194
(22)	2.32433	-8.7608	-	-	2411	2.3006	0.8029
(23)	25.0865	0.9393	0.0467	-	2411	2.2141	0.8175
(24)	97.2516	0.428	-2.4736	-0.1904	2411	2.2091	0.8203
(25)	32.1933	0.0451	1.0246	-	2411	2.2027	0.8194
(26)	3.56433	0.4863	-	-	2411	2.2872	0.8052
(27)	24.4738	0.0916	-1.0217	-	2411	2.2647	0.8091
(28)	34.8772	17.1059	0.9376	-	2411	2.2009	0.8197
(29)	32.563	-16.7739	6.3157	-	2411	2.2044	0.8191
(30)	24.9065	0.0603	-	-	2411	2.2416	0.8129

Functions are shown in *Table 2*. The higher R^2 values are found in functions 5, 8 and 4, respectively

http://www.aloki.hu ● ISSN 1589 1623 (Print) ● ISSN 1785 0037 (Online)
DOI: http://dx.doi.org/10.15666/aeer/1706_1356713591

Fitting the Chapman-Richards model to regional and subregional data

Based on the Chapman-Richards function, *Table 5* shows the sample sizes, parameter estimates, and mean square errors (MSE) for all the fourteen fitted models (overall model, three regional models, and ten subregional models). The four regional models (Overall, NWYLHLM, SAYLHLM, and NDXAM) have different model MSEs and parameter estimates. Among the ten subregional models, the lowest MSE value was found in the XLJ subregion (MSE = 2.1909), while the highest MSE value was found in the JGDQ subregion (MSE = 4.5703). The asymptote parameter (a in *Table 5*) ranged from 19.9264 to 32.8497, rate parameter (b in *Table 5*) ranged from 0.0197 to 0.1225, and shape parameter (c in *Table 5*) ranged from 0.6323 to 1.559. The parameter estimates varied among the ten subregions, indicating that each subregion may have a different height-diameter relationship with others.

Table 5. *Parameter estimations and model MSE of Chapman-Richards function for the regional and subregional models*

Subregion	N	a	b	c	MSE
SL	214	32.8497	0.0197	0.6323	2.9089
JGDQ	524	23.7489	0.052	0.9244	4.5703
XL	190	22.8785	0.0591	1.0135	3.2597
TH	203	23.2172	0.0583	1.2253	3.5829
HZ	215	19.9264	0.093	1.559	3.7469
SBZ	237	21.9893	0.0662	1.0635	3.3236
HJY	128	21.6856	0.0761	1.3459	3.5877
XLJ	224	20.3106	0.1225	1.4833	2.1909
TQ	191	23.8895	0.0539	0.8703	2.9696
AME	285	29.5955	0.0358	0.8211	3.5748
NWYLHLM	915	23.1747	0.0561	0.8434	5.0139
SAYLHLM	758	20.6695	0.0942	1.3421	4.9493
NDXAM	738	26.6823	0.0318	0.6735	3.9431
Overall	2411	25.4937	0.0421	0.8381	4.7716

N: sample size (number of trees); a, b, c: three parameters of Chapman-Richards function; MSE: model mean squared error

Comparison of height-diameter models among subregions and between regions

The fitting results of the reduced and full height-diameter models on combination data are provided in *Table 6* (first row). The F-test result reveals that there are overall significant differences ($P < 0.05$) among subregions. Since the divergences may be caused by as few as two or as many as all of the subregions implicated, indicator variable approach was also carried out for every eventual pair of subregions then, the source of the differences could be identified and data from similar subregion can be combined. Same analyses were realized for others subregions pairs and F-values were calculated (*Table 6*).

http://www.aloki.hu ● ISSN 1589 1623 (Print) ● ISSN 1785 0037 (Online)
DOI: http://dx.doi.org/10.15666/aeer/1706_1356713591

Table 6. *F-test for testing the differences between subregions*

Subregion pairs	n	Full model			Reduced model			Extra sum of squares		
		SSE_F	*P*F	d*f*F	SSE_R	*P*R	d*f*R	d*f*R-d*f*F	F-value	Prob > *F*
Combined	2411	8384.62	30	2381	11489.91	3	2408	27	32.6599	< 0.0001
SL-JGDQ	738	2987.39	6	732	3197.37	3	735	3	17.1503	< 0.0001
SL-XL	404	1215.82	6	398	1432.11	3	401	3	23.5886	< 0.0001
SL-TH	417	1322.84	6	411	1644.46	3	414	3	33.3093	< 0.0001
SL-HZ	429	1400.62	6	423	1897.39	3	426	3	50.0105	< 0.0001
SL-SBZ	451	1383.98	6	445	1688.71	3	448	3	32.6613	< 0.0001
SL-HJY	342	1054.72	6	336	1273.91	3	339	3	23.2741	< 0.0001
SL-XLJ	438	1090.46	6	432	1344.92	3	435	3	33.6032	< 0.0001
SL-TQ	405	1164.55	6	399	1259.24	3	402	3	10.8145	< 0.0001
SLAME	499	1614.37	6	493	1767.71	3	496	3	15.6082	< 0.0001
JGDQ-XL	714	2990.69	6	708	2998.95	3	711	3	0.65198	0.5818
JGDQ-TH	727	3097.71	6	721	3309.85	3	724	3	16.4596	< 0.0001
JGDQ-HZ	739	3175.48	6	733	3412.48	3	736	3	18.2358	< 0.0001
JGDQ-SBZ	761	3158.84	6	755	3194.41	3	758	3	2.8332	0.0374
JGDQ-HJY	652	2829.59	6	646	2876.78	3	649	3	3.5915	0.0135
JGDQ-XLJ	748	2865.32	6	742	3211.65	3	745	3	29.8955	< 0.0001
JGDQ-TQ	715	2939.41	6	709	3001.53	3	712	3	4.9941	0.001
JGDQ-AME	809	3389.23	6	803	4268.31	3	806	3	69.4259	< 0.0001
XL-TH	393	1326.13	6	387	1403.78	3	390	3	7.5532	< 0.0001
XL-HZ	405	1403.91	6	399	1518.73	3	402	3	10.8774	< 0.0001
XL-SBZ	427	1387.27	6	421	1394.93	3	424	3	0.7754	0.5081
XL-HJY	318	1058.01	6	312	1073.08	3	315	3	1.4806	0.2197
XL-XLJ	414	1093.75	6	408	1295.78	3	411	3	25.1214	< 0.0001
XL-TQ	381	1167.84	6	375	1228.81	3	378	3	6.5251	< 0.0001
XL-AME	475	1617.66	6	469	2329.86	3	472	3	68.8285	< 0.0001
TH-HZ	418	1513.73	6	412	1575.63	3	415	3	5.6159	0.0008
TH-SBZ	440	1494.29	6	434	1614.13	3	437	3	11.6025	< 0.0001
TH-HJY	331	1165.03	6	325	1197.56	3	328	3	3.0253	0.0297
TH-XLJ	427	1200.76	6	421	2044.52	3	424	3	98.6095	< 0.0001
TH-TQ	394	1274.86	6	388	1645.46	3	391	3	37.5979	< 0.0001
TH-AME	488	1724.67	6	482	2476.83	3	485	3	70.0693	< 0.0001
HZ-SBZ	452	1572.06	6	446	1669.39	3	449	3	9.2041	< 0.0001
HZ-HJY	343	1242.81	6	337	1281.43	3	340	3	3.4912	0.016
HZ-XLJ	439	1278.54	6	433	1855.69	3	436	3	65.1539	< 0.0001
HZ-TQ	406	1352.63	6	400	1717.23	3	403	3	35.9388	< 0.0001
HZ-AME	500	1802.45	6	494	2905.22	3	497	3	100.746	< 0.0001
SBZ-HJY	365	1226.17	6	359	1241.61	3	362	3	1.5059	0.2126
SBZ-XLJ	461	1261.91	6	455	1511.42	3	458	3	29.9889	< 0.0001
SBZ-TQ	428	1336.11	6	422	1441.02	3	425	3	11.0583	< 0.0001
SBZ-AME	522	1785.81	6	516	2670.94	3	519	3	85.2504	< 0.0001
HJY-XLJ	352	932.648	6	346	1217.74	3	349	3	35.2549	< 0.0001
HJY-TQ	319	1006.74	6	313	1138.21	3	316	3	13.6241	< 0.0001
HJY-AME	413	1456.56	6	407	2042.31	3	410	3	54.5582	< 0.0001
XLJ-TQ	415	1042.47	6	409	1135.14	3	412	3	12.1191	< 0.0001
XLJ-AME	509	1492.29	6	503	1691.66	3	506	3	22.3999	< 0.0001
TQ-AME	476	1566.39	6	470	1858.71	3	473	3	29.2372	< 0.0001

The F-values were calculated according to *Equation 3*. The number of observations is represented by *n*; *p* is the number of parameters; SSE_F, d*f*F, SSE_R and d*f*R are the sum of squared errors and the degrees of freedom associated with the full and reduced models, respectively

http://www.aloki.hu ● ISSN 1589 1623 (Print) ● ISSN 1785 0037 (Online)
DOI: http://dx.doi.org/10.15666/aeer/1706_1356713591

Among the 45 pairs of subregions, only four subregion pairs (e.g., XL versus SBZ, XL versus HJY, SBZ versus HJY, and XL versus JGDQ) showed the non-significant difference F-value ($P > 0.05$). Therefore, the data from these three subregions (XL, SBZ, and HJY) were then combined, and seven new subregion pairs were formed as follows:
Subregion (XL + SBZ + HJY) and SL;
Subregion (XL + SBZ + HJY) and JGDQ;
Subregion (XL + SBZ + HJY) and TH;
Subregion (XL + SBZ + HJY) and HZ;
Subregion (XL + SBZ + HJY) and XLJ;
Subregion (XL + SBZ + HJY) and TQ;
Subregion (XL + SBZ + HJY) and AME

Subsequent F-tests show that the height-diameter relationship for the combined subregions (XL + SBZ + HJY) is different from those for SL, JGDQ, TH, HZ, XLJ, TQ and AME ($P < 0.05$, *Table 7*).

Table 7. *F-test for testing the differences between combined subregions (XL + SBZ + HJY) with each subregion*

Subregion pairs	n	Full model			Reduced model			Extra sum of squares		
		SSE_F	*P*F	d*f*F	SSE_R	*P*R	d*f*R	d*f*R-d*f*F	F-value	Prob > *F*
(XL + SBZ + HJY) - SL	766	2467.85	6	763	2870.74	3	766	3	41.5217	< 0.0001
(XL + SBZ + HJY) - JGDQ	1076	4242.71	6	1073	4288.13	3	1076	3	3.8286	0.0096
(XL + SBZ + HJY) - TH	755	2578.16	6	752	2708.07	3	755	3	12.6308	< 0.0001
(XL + SBZ + HJY) - HZ	767	2655.93	6	764	2778.32	3	767	3	11.7353	< 0.0001
(XL + SBZ + HJY) - XLJ	776	2345.77	6	773	2780.56	3	776	3	47.7581	< 0.0001
(XL + SBZ + HJY) - TQ	743	2419.87	6	740	2567.41	3	743	3	15.0381	< 0.0001
(XL + SBZ + HJY) - AME	837	2869.69	6	834	4205.94	3	837	3	129.4491	< 0.0001

The F-values were calculated according to *Equation 3*. The number of observations is represented by *n*; *p* is the number of parameters; SSE_F, d*f*F, SSE_R and d*f*R are the sum of squared errors and the degrees of freedom associated with the full and reduced models, respectively

Based on regional classification in *Table 2*, Dahurian larch has three regions with three pairs (NWYLHLM, SAYLHLM, and NDXAM), the three pairs require the fittings of the 6 nonlinear regression models to give error sums of squares, so that the F-test can be carried out for each pair. The F-test also indicates that there are over significant differences ($P < 0.05$) among regions (*Table 8*, first row). All of the three regional paired comparisons produced significant F values, suggesting that significant different height-diameter equations are required.

Table 8. *F-test for testing the differences between regions*

Region pairs	n	Full model			Reduced model			Extra sum of squares		
		SSE_F	*P*F	d*f*F	SSE_R	*P*R	d*f*R	d*f*R-d*f*F	F-value	Prob > *F*
Combined	2411	10425.81	9	2402	11489.91	3	2408	6	40.8582	< 0.0001
NWYLHLM-SAYLHLM	1673	7228.47	6	1667	8286.89	3	1670	3	81.3629	< 0.0001
NWYLHLM-NDXAM	1653	7717.78	6	1647	7925.83	3	1650	3	14.7998	< 0.0001
SAYLHLM-NDXAM	1496	5905.44	6	1490	6218.61	3	1493	3	26.3381	< 0.0001

The F-values were calculated according to *Equation 3*. The number of observations is represented by *n*; *p* is the number of parameters; SSE_F, d*f*F, SSE_R and d*f*R are the sum of squared errors and the degrees of freedom associated with the full and reduced models, respectively

http://www.aloki.hu ● ISSN 1589 1623 (Print) ● ISSN 1785 0037 (Online)
DOI: http://dx.doi.org/10.15666/aeer/1706_1356713591

Prediction errors of applying regional and overall models to each subregion

According to the above F-tests, there were significant differences for most subregion pairs in the height-diameter relationships. It has been shown that there are statistically significant differences between the tested subregions, but that does not imply that these differences have practical importance. In practice, incorrectly applying a height-diameter model in these subregions may result in prediction biases. To understand the consequences, all 14 models (overall model, NWYLHLM model, SAYLHLM model, NDXAM model, and ten subregional models) were used to predict total tree heights for a given subregion individually. The mean prediction error ($\bar{e}$), the percent prediction error ($\bar{e}$%), and the t-test for testing the null hypothesis that means prediction error equals zero were shown in *Tables 9* and *10.*

Table 9. *Prediction error of applying the overall model to each subregion*

Subregion	N	$\bar{H}$ (m)	$\hat{H}$ (m)	$\bar{e}$	$\bar{e}$%	Se	t	p-value
SL	214	19.58	18.99	0.58	2.99	1.79	4.79	< 0.0001
JGDQ	524	18.29	18.55	-0.26	-1.42	2.14	-2.77	0.005
XL	240	18.7	19.54	-0.83	-4.48	2.08	-6.24	< 0.0001
TH	203	15.34	16.69	-1.35	-8.83	1.92	-10.01	< 0.0001
HZ	215	16.12	17.44	-1.31	-8.18	2.02	-9.56	< 0.0001
SBZ	237	17.93	18.56	-0.63	-3.51	1.88	-5.13	< 0.0001
HJY	128	17.7	18.55	-0.83	-4.69	1.93	-4.87	< 0.0001
XLJ	224	15.75	14.42	1.33	8.45	1.66	11.98	< 0.0001
TQ	191	17.44	17.02	0.41	2.41	1.75	3.29	0.001
AME	285	22.36	20.52	1.84	8.24	1.99	15.64	< 0.0001

N – sample size, $\bar{H}$ – average of observed tree height, $\hat{H}$ – average of predicted tree height from the overall model, $\bar{e}$ – average of prediction error, $\bar{e}$ % – percent prediction error, Se – standard deviation of prediction error

The overall model was used to predict trees heights in each subregion, over or under predictions occurred for different subregions. The p-value of the t-test was less than 0.05 for each of the ten subregions. On average, the overall model under-estimate (i.e., positive prediction error %) trees heights from 2.4% to 8.45% for subregions SL, XLJ, TQ and AME, and over-estimate (i.e., negative prediction error %) tree heights from -1.42% to -8.83% for subregions JGDQ, XL, TH, HZ, SBZ and HJY (*Table 9*). *Table 10* shows that when applying NWYLHLM model in each subregion, there is no difference between NWYLHLM–SL; NWYLHLM–TQ, while there is a difference in the others regions and subregions.

The same applies to SAYLHLM model, when the model is applied in each subregion, there is no difference between SAYLHLM–(subregions SBZ and HJY); there is a difference between others regions and subregions. When NDXAM model is applied in each subregion, there is no difference between NDXAM–(subregions JGDQ, XL, and TQ), although there is a difference between others regions and subregion. The prediction biases ranged from -11.97 to 8.46% in NWYLHLM model; from -3.52 to 13.82% in SAYLHLM model; from -8.69 to 8.58% in NDXAM model. Then, applying

http://www.aloki.hu ● ISSN 1589 1623 (Print) ● ISSN 1785 0037 (Online)
DOI: http://dx.doi.org/10.15666/aeer/1706_1356713591

regional height-diameters models in different subregions displays the variations bias in the predictions of heights that cannot help forest managers to predict the height of the model from other regions and make good decisions.

Table 10. *Prediction errors of applying regional models to each subregion*

Region	N	$\bar{H}$ (m)	$\hat{H}$ (m)	ē	ē%	Se	t	p-value
NWYLHLM model								
NWYLHLM-SL	214	19.58	19.74	-0.16	-0.75	1.70	-1.4043	0.1616
NWYLHLM-JGDQ	524	18.29	18.81	-0.51	-2.8	2.17	-5.4094	< 0.0001
NWYLHLM-XL	190	19.33	19.95	-0.62	-3.32	1.82	-4.7005	< 0.0001
NWYLHLM-TH	203	15.34	17.17	-1.83	-11.97	2.06	-12.6611	< 0.0001
NWYLHLM-HZ	215	16.12	17.87	-1.74	-10.83	1.96	-13.0251	< 0.0001
NWYLHLM-SBZ	237	17.93	18.79	-0.85	-4.79	1.82	-7.2495	< 0.0001
NWYLHLM-HJY	128	17.72	18.84	-1.12	-6.32	1.94	-6.5253	< 0.0001
NWYLHLM-XLJ	224	15.75	15.14	0.60	3.84	1.57	5.7623	< 0.0001
NWYLHLM-TQ	191	17.44	17.38	0.06	0.36	1.73	0.511	0.6099
NWYLHLM-AME	285	22.36	20.47	1.89	8.46	2.26	14.0901	< 0.0001
SAYLHLM model								
SAYLHLM-SL	214	19.58	18.10	1.48	7.55	1.91	11.3093	< 0.0001
SAYLHLM-JGDQ	524	18.29	17.72	0.57	3.13	2.14	6.1232	< 0.0001
SAYLHLM-XL	190	19.33	19.02	0.31	1.62	1.8	2.4013	0.0173
SAYLHLM-TH	203	15.34	15.88	-0.54	-3.52	1.91	-4.0206	< 0.0001
SAYLHLM-HZ	215	16.12	16.67	-0.54	-3.38	1.97	-4.0435	< 0.0001
SAYLHLM-SBZ	237	17.93	17.71	0.21	1.22	1.85	1.8183	0.0702
SAYLHLM-HJY	128	17.72	17.76	-0.03	-0.22	1.88	-0.2369	0.8131
SAYLHLM-XLJ	224	15.75	13.57	2.17	13.82	1.65	19.644	< 0.0001
SAYLHLM-TQ	191	17.44	16.1	1.34	7.68	1.75	10.5944	< 0.0001
SAYLHLM-AME	285	22.36	19.6	2.75	12.34	2.08	22.2962	< 0.0001
NDXAM model								
NDXAM-SL	214	19.58	18.99	0.58	2.99	1.77	4.8474	< 0.0001
NDXAM-JGDQ	524	18.29	18.54	-0.24	-1.34	2.15	-2.6219	0.0089
NDXAM-XL	190	19.33	19.85	-0.51	-2.66	1.84	-3.8427	< 0.0001
NDXAM-TH	203	15.34	16.67	-1.33	-8.69	1.93	-9.8154	< 0.0001
NDXAM-HZ	215	16.12	17.41	-1.29	-8	2.03	-9.2785	< 0.0001
NDXAM-SBZ	237	17.93	18.55	-0.62	-3.45	1.9	-5.0114	< 0.0001
NDXAM-HJY	128	17.72	18.53	-0.8	-4.56	1.94	-4.7005	< 0.0001
NDXAM-XLJ	224	15.75	14.40	1.35	8.58	1.67	12.0851	< 0.0001
NDXAM-TQ	191	17.44	17.03	0.41	2.38	1.76	3.2542	0.001
NDXAM-AME	285	22.36	20.53	1.83	8.2	1.97	15.6945	< 0.0001

N – sample size, $\bar{H}$ – average of observed tree height, $\hat{H}$ – average of predicted tree height from the model, **ē** – average of prediction error, ē % – percent prediction error, S_e – standard deviation of prediction error

http://www.aloki.hu ● ISSN 1589 1623 (Print) ● ISSN 1785 0037 (Online)
DOI: http://dx.doi.org/10.15666/aeer/1706_1356713591

Figure 2 illustrates the average prediction errors across 5-cm D classes when NDXAM, NWYLHLM, SAYLHLM, Overall, and subregion models are applied to predict tree height in each of the ten subregions separately. Clearly, large negative values of the Overall model are observed in the TH and HZ subregions due an overestimation of large-sized trees. We also noticed negative values in the subregions JGDQ, XL, SBZ, and HJY. Large positive values of the Overall model are observed in the AME and XLJ subregions; it was also revealed that underestimations with positive values are observed in the SL and TQ subregions.

Prediction errors of applying subregional model to each subregion

Table A1 (*Appendix*) shows that when the ten subregional models were applied to each subregion, they generally performed well only in the subregions in which the models were developed (p-value for t-test > 0.05 for testing that the mean prediction error equals zero). Otherwise, the models produced significant prediction errors. The prediction biases ranged from -10.84% to 7.32% in SL; from -7.64% to 9.87% in JGDQ; from -5.89% to 11% in XL; from -0.17% to 18.3% TH; from -0.18% to 16.69% HZ; from -5.97% to 12.09% in SBZ; from -3.32% to 12.85% HJY; from -14.2% to 10.28% in XLJ; from -12.22% to 7.35% in TQ; from -17.02% to 2.44% in AME. The p-values of the mean prediction biases were calculated using the paired t-test procedure explained. When a model developed from one subregion was applied to other subregions, we found over- or underestimations significant. Sometimes, in order to know how well a model from one subregion will perform when it is used in a different subregion, the calculated percent prediction error can be used as a criterion for estimating as an approximation. The percent prediction error can serve as an accurate indicator to determine the applicability of a fitted model. It is possible to create an acceptable ē% according to the prediction intervals or select voluntarily without taking into account any statistical test, but it will have to depend on the required accuracy and available resources. The height-diameter models from several subregions may be used interchangeably for the height-diameter models, if a ± 5% average bias for height predictions is enabling.

Figure 3 shows the height-diameter performance when each subregional model is applied to predict tree height separately in each of the ten subregions. Compared to the overall and region models, the subregional model more closely followed the actual values for all subregions and indicated that subregional height-diameter model should be needed.

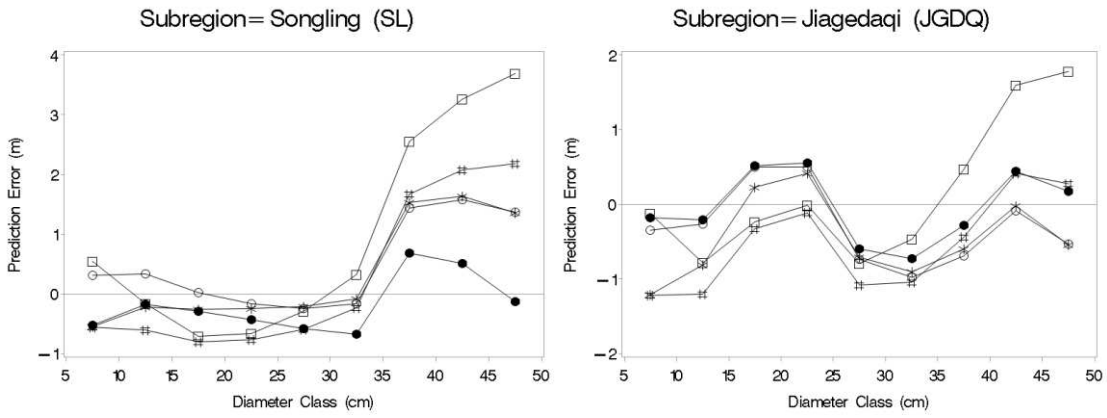

http://www.aloki.hu ● ISSN 1589 1623 (Print) ● ISSN 1785 0037 (Online)
DOI: http://dx.doi.org/10.15666/aeer/1706_1356713591

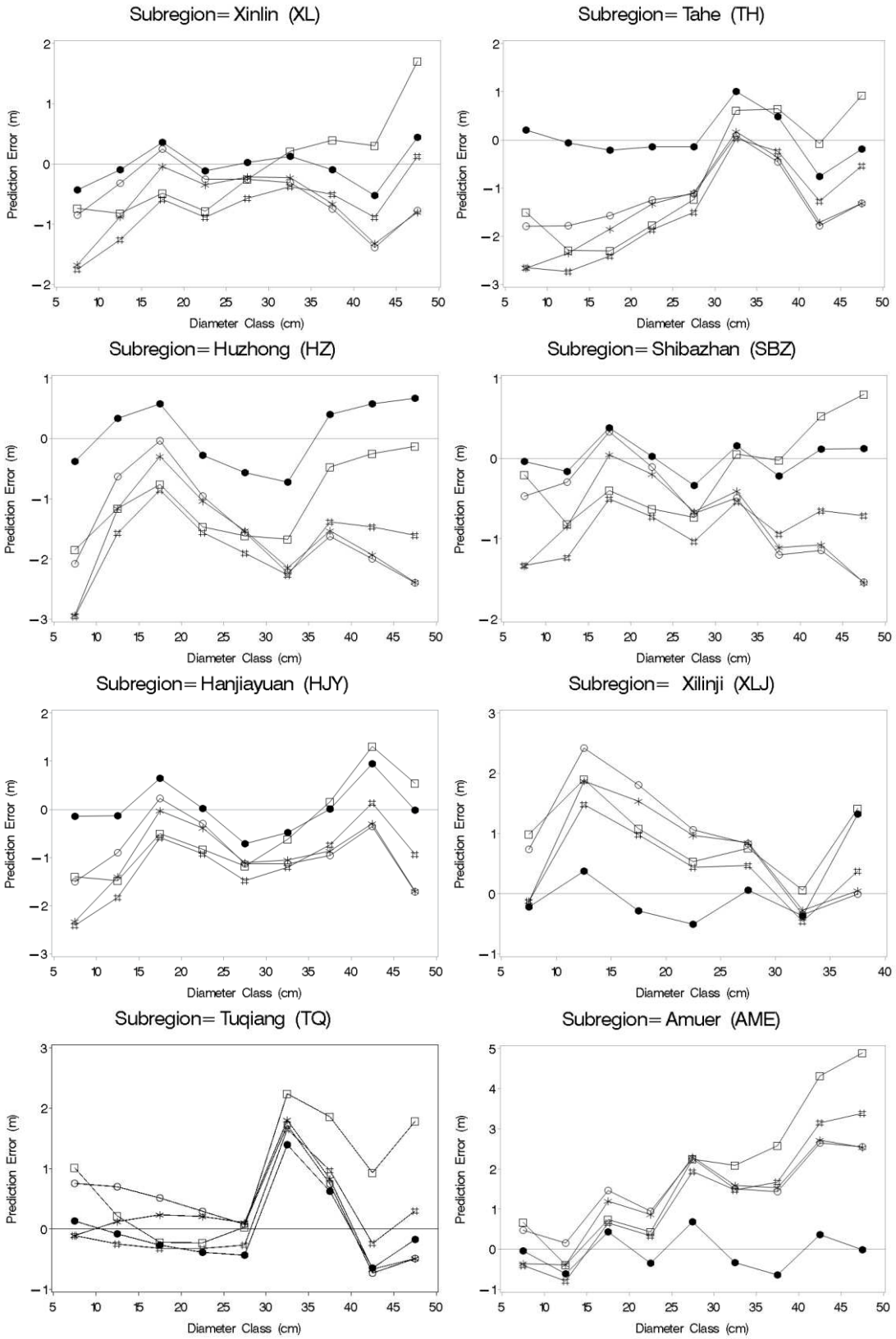

Figure 2. *Average prediction errors (m) across 5-cm diameter classes when the NDXAM, NWYLHLM, SAYLHLM regional models and the Overall model are applied to predict tree heights in each of the ten subregions. The overall and the subregion model with symbols NDXAM (hash), NWYLHLM (square), SAYLHLM (star), Overall (circle) and Subregion (dot)*

http://www.aloki.hu ● ISSN 1589 1623 (Print) ● ISSN 1785 0037 (Online)
DOI: http://dx.doi.org/10.15666/aeer/1706_1356713591

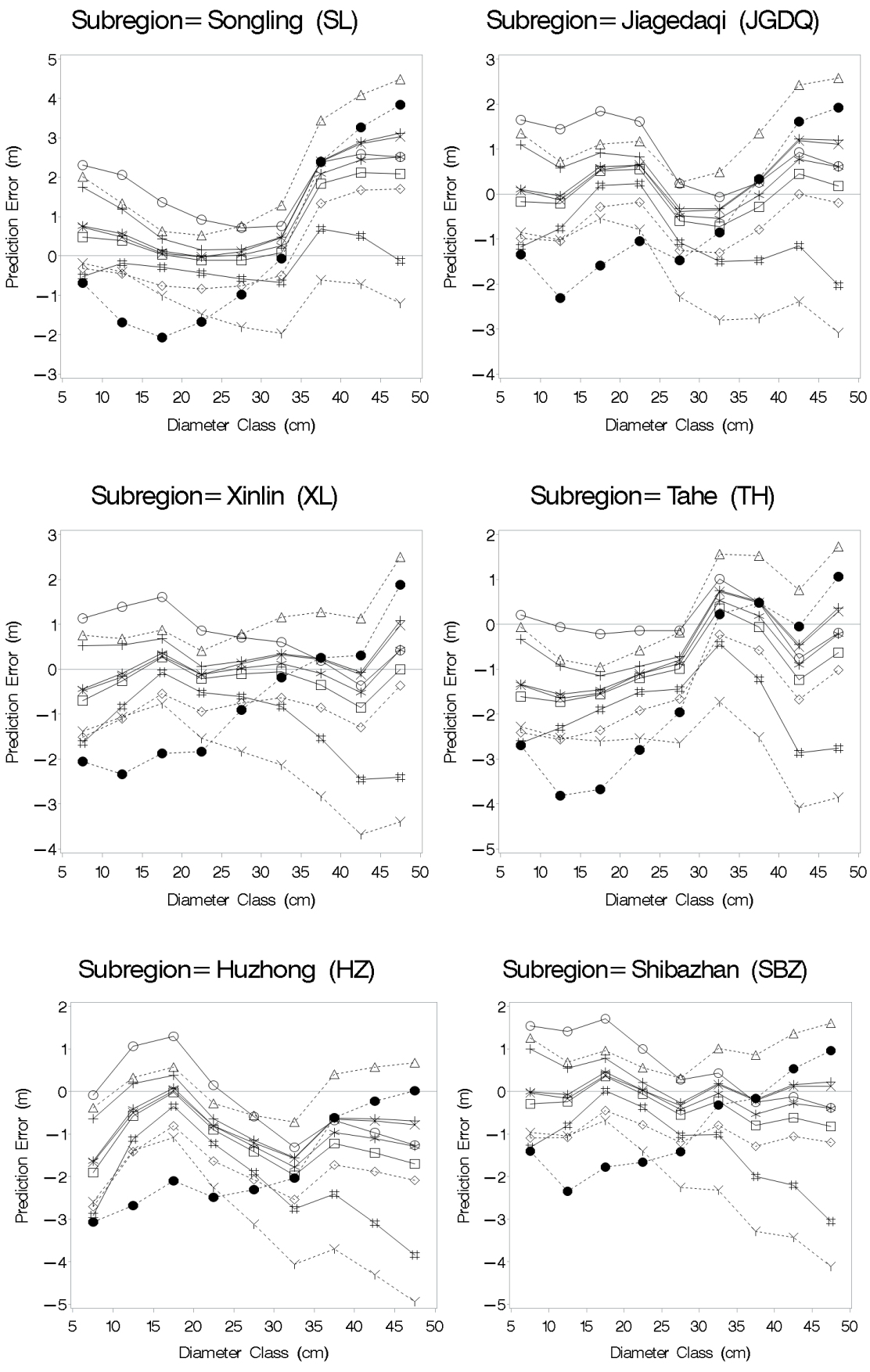

http://www.aloki.hu ● ISSN 1589 1623 (Print) ● ISSN 1785 0037 (Online)
DOI: http://dx.doi.org/10.15666/aeer/1706_1356713591

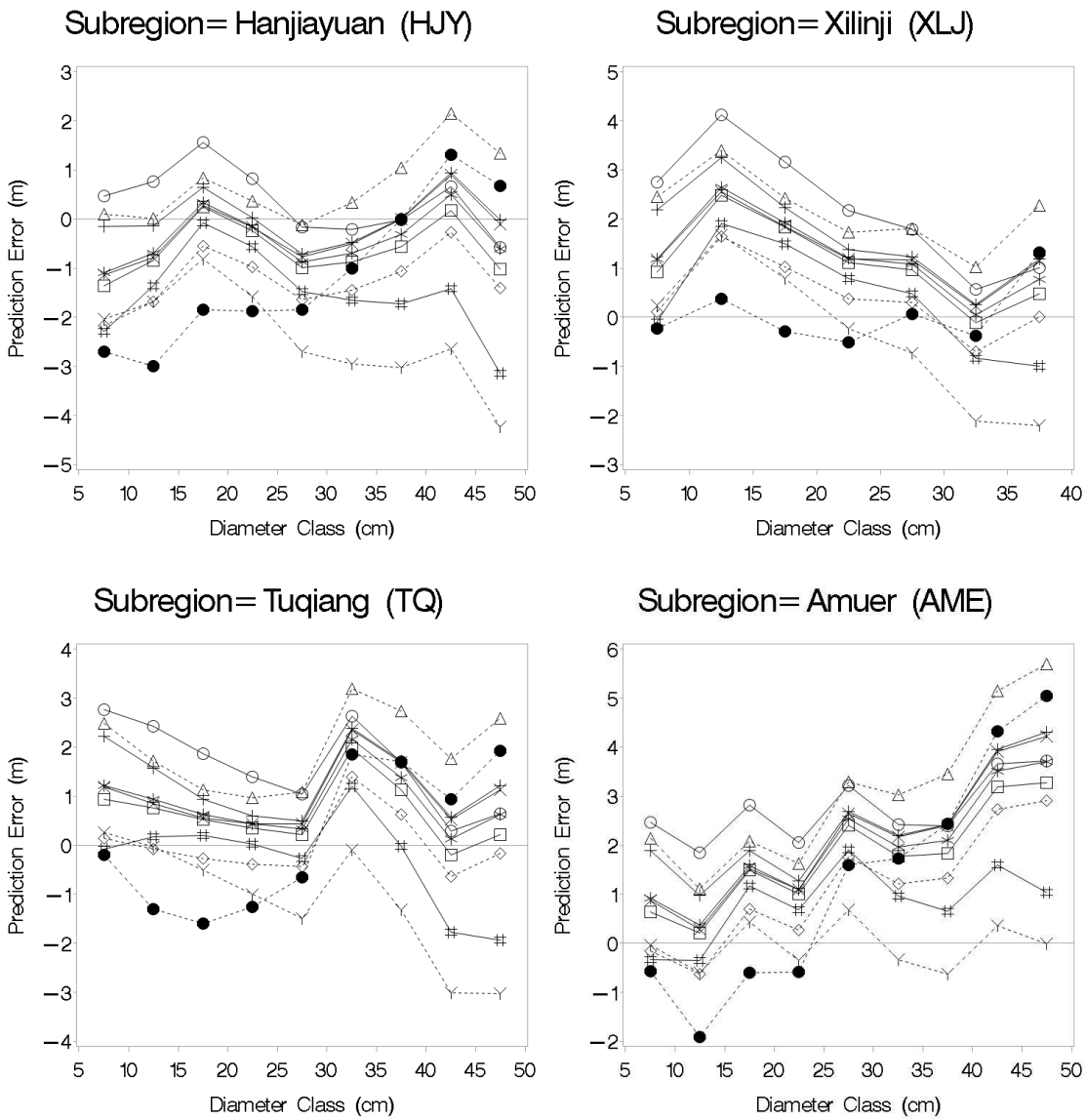

Figure 3. *Average prediction errors (m) across 5-cm diameter classes when each subregional model is applied to predict tree heights in each of the ten subregions with symbols: SL (hash), JGDQ (square), XL (star), TH (circle), SBZ (X), HJY (plus), HZ (triangle), XLJ (dot), TQ (diamond) and AME (Y)*

In the forest literature, there is a high number of local and generalized height-diameter equations available (Gadow et al., 2001; Soares and Tomé, 2002; Lopéz et al., 2003; Temesgen and Gadow, 2004; Brooks and Wiant, 2007; Stankova et al., 2013; Xu et al., 2014; Zhao et al., 2013; Adamec et al., 2015; Hassanzad et al., 2016; Yan-qiong et al., 2015). 30 nonlinear growth functions were fitted to a species of trees and 10 subregions in the Daxing'an Mountain at northeast China, based on their appropriate mathematical features and possible biological interpretation of parameters. The results from model statistics suggested that all thirty models fitted equally well to the tree height-diameter data of the species and the best is Chapman-Richards model. The analysis reveals that the height-diameter relationship is statistically different between the subregions identified in the current study. This was waited because biogeoclimatic

http://www.aloki.hu ● ISSN 1589 1623 (Print) ● ISSN 1785 0037 (Online)
DOI: http://dx.doi.org/10.15666/aeer/1706_1356713591

conditions are not identical among different subregions. A climatic division is formed between the mountains, they differ from the arid region to the west as a result of the precipitation they take from the southeast winds and create a relatively humid climate (precipitation is more than 20 inches [500 mm] annually). The coldest part of eastern China is the northern mountain region with very rigorous winters (mean temperature -18 °F [-28 °C]) and large areas under permafrost. With January temperatures approximately -21 °C, annual rainfall of 10-12 inches (250-300 mm) and light relative snowfall, the southern region of the range is much warmer and drier than in the north. To the south, forests cover the higher ground above 5,000 feet (1500 m), while the highest meadows cover most of the area (https://www.britannica.com/editor/the-editors-of encyclopedia-Britannica/4419: Mountains China). But the rapidity and the characteristics of its growth are affected by the unique features of the subregions. It was revealed that, Dahurian larch height-diameter relationships showed the differences among these subregions. The using of separate height-diameter models for NWYLHLM, SAYLHLM and NDXAM regions; likewise, because of the singular characteristics of the subregions in landforms, geology, vegetation, and climate separate height-diameter relationships for the Xilinji (XLJ), Tuqiang (TQ), Amuer (AME), Huzhong (HZ), Xinlin (XL), Tahe (TH), Shibazhan (SBZ), Hanjiayuan (HJY), Songling (SL), Jiagedaqi (JGDQ), all are provable, as this is shown from the F-test results in *Tables 6, 7* and *8*. Therefore, the combination of all climatic, environmental and vegetation factors plays an important role in determining the different height-diameter relationships among ten subregions. Subsequent F- tests suggest that the height-diameter equation for the combined subregions (XL + SBZ + HJY) is different from those for SL, JGDQ, TH, HZ, XLJ, TQ and AME subregions (*Table 7*). Therefore, according to the F-tests, eight height-diameter equations relating to eight distinctly different subregion groups were separated. Analyzing of the subregion-based height-diameter models for Dahurian larch in Daxing'an Mountain suggested that the height-diameter relationships for XL, SBZ, and HJY subregions are statistically the same. The sameness of height-diameter patterns between XL, SBZ and HJY subregions is probably due to the similarity in habitats that stands of Dahurian larch.

It is apparent from *Table A1* (*Appendix*) outcome of the calculated $\bar{e}$, Se, and $\bar{e}$%. It is demonstrated by examples values over and underestimated when the height-diameter equation from XLJ was served to predict the tree height in subregion AME 10.28% underestimate appeared. Relatively, the value of $\bar{e}$ was 2.29 and for Se was equal to 2.95. When the height-diameter equation from subregion XLJ was served to predict the tree height in subregion TH, -14.2% an overestimate was observed. Carefully, the prediction errors values of $\bar{e}$ and Se were -2.17% and 2.48%. Globally, the percent prediction error varies from 16.69% an underestimate to -16.5% overestimate. The mean prediction errors vary from an underestimate of 3.73 (HZ applied to AME) to overestimate of 2.66 (AME applied to HZ). The paired t-test procedure outlined in Snedecor and Cochran (1989) was used to calculate the t-values of the mean prediction biases. It was revealed that significant over- or underestimations appeared when a model developed from one subregion was used to other subregions.

Founded on development data, we observed that the best-fitting model was the Chapman Richards model, which gives the most precise estimates with MSE values from 2.1909 to 4.5703 for all subregions (*Table 5*). When we fitted the Korf equation in each subregion, we found that this equation produced a largest parameter asymptotic, which is means the Korf equation doesn't have stability. This characteristic of the Korf

http://www.aloki.hu ● ISSN 1589 1623 (Print) ● ISSN 1785 0037 (Online)
DOI: http://dx.doi.org/10.15666/aeer/1706_1356713591

function was also observed in Cross-validation of Non-linear Growth Functions (Zhang, 1997). The Chapman-Richards function was used to describe the height-diameter in several previous studies. Huang et al. (1992) declared that, when there is a weak relationship between the dependent and independent variables, this function approaches the asymptote too quickly. In this study, we found that the Chapman Richards model as the best for Dahurian larch produced some of the most satisfactory fits among many alternative model forms, considering the model mathematical features, biological interpretation of parameters, and accurate prediction. However, the performance of models, such as the Weibull, Schnute, Exponential and others was also very good. Comparing the model root mean squared errors (RMSE), the Richards, Korf and Weibull functions had relatively smaller RMSEs than the other twenty seven equations (*Table 4*).

Conclusion

Our study results suggest that there are distinct variations in height-diameter relationships for Dahurian larch among different subregions in the three forest regions (NDXAM, YLHLM-NW, and YLHLM-SA) in Daxing'an Mountain at northeast China. Usually, ecoregion-based height-diameter models report predictions with more reliability on a regional basis and avoid the likely expected errors that may arise while models are enforced in others areas. However, at any location where the data is favorable, it is advisable to develop different models by different ecoregions.

Acknowledgements. This research was financially supported by the National Natural Science Foundation of China (31570624), Applied Technology Research and Development Plan Project of Heilongjiang Province (GA19C006), and Fundamental Research Funds for Central Universities.

Conflict of interests. The authors declare that they have no conflict of interests.

REFERENCES

[1] Adamec, Z., Drápela, K. (2015): Generalized additive models as an alternative approach to the modelling of the tree height-diameter relationship. – J. For. Sci. 61: 235-243.
[2] Bates, D. M., Watts, D. G. (1980): Relative curvature measures of nonlinearity. – J. Roy. Stat. Soc. B, 42: 1-16.
[3] Bates D. M., Watts, D. G. (1988): Nonlinear Regression Analysis and Its Applications. – Wiley, New York.
[4] Botkin, D. B., Janak, J. F., Wallis, J. R. (1972): Some ecological consequences of a computer model of forest growth. – The Journal of Ecology 849-872.
[5] Brooks, J. R., Wiant, H. V. (2007): Evaluating Ecoregion-Based Height-Diameter Relationship of Five Economically Important Appalachian Hardwood Species in West Virginia. – In: Mc Roberts, R. E., Reams, G. A., Van Deusen, P. C., McWilliams, W. H. (eds.) Proceedings of the Seventh Annual Forest Inventory and Analysis Symposium, 3-6 October, Portland, OR.
[6] Buford, M. A. (1986): Height-diameter relationship at age 15 in loblolly pine seed sources. – For. Sci. 32: 812-818.
[7] Burkhart, H. E., Strub, M. R. (1974): A Model for Simulation of Planted Loblolly Pine Stands. – In: Fries, J. (ed.) Growth Models for Tree and Stand Simulation. Royal College of Forestry, Stockholm, pp. 128-135.

http://www.aloki.hu ● ISSN 1589 1623 (Print) ● ISSN 1785 0037 (Online)
DOI: http://dx.doi.org/10.15666/aeer/1706_1356713591

[8] Castedo-Dorado, F., Anta, M. B., Parresol, B. R., Gonzalez, J. G. A. (2005): A stochastic height-diameter model for maritime pine ecoregions in Galicia (Northwestern Spain). – Ann Forest Science 62: 455-465.
[9] Corral-Rivas, J. J., Álvarez González, J. G., Ruiz, A. D., Gadow, K. V. (2004): Compatible height and site index models for five pine species in El Salto, Durango (Mexico). – Forestry Ecology Management 201: 145-160.
[10] Corral-Rivas, J. J., Diéguez-Aranda, U., Castedo, F., Corral, S. A. (2007): Merchantable volume system for major pine species in El Salto, Durango (Mexico). – Forestry Ecology Management 238: 118-129.
[11] Curtis, R. O. (1967): Height-diameter and height-diameter-age equations for second-growth Douglas-fir. – Forest Science 13: 365-375.
[12] Cutini, A., Chianucci, F., Manetti, M. C. (2013): Allometric relationships for volume and biomass for stone pine (Pinus pinea L.) in Italian coastal stands. – iForest 6: 331-337.
[13] Dai, Z. D., Jiang, L. C. (2015): Ecoregion based height-diameter models for Larix gmelinii Rupr in Daxing'an' Mountains. – Bulletin of Botanical Research 35(4): 583-589 (in Chinese).
[14] Fang, Z., Bailey, R. (1998): Height–diameter models for tropical forests on Hainan Island in southern China. – Forest Ecology and Management 110: 315-327.
[15] Farr, W. A., DeMars, D. J., Dealy, J. E. (1989): Height and crown width related to diameter for open-grown western hemlock and Sitka spruce. – Can. J. For. Res. 19: 1203-1207.
[16] Gadow, K. Real, P., Álvarez Gonzáles, J. G. (2001): Modelización del Crecimiento y la Evolución de los Bosques. – IUFRO World Series, Vol. 12, Vienna.
[17] Hassanzad, I., Navroodi, Alavi, S. J., Ahmadi, M. K., Radkarimi, M. (2015): Comparison of different non-linear models for prediction of the relationship between diameter and height of velvet maple trees in natural forests (case study: Asalem Forests, Iran). – Journal of Forest Science 62(2): 65-71.
[18] Huang, S. (1999): Ecoregion-based individual tree height-diameter models for lodgepole pine in Alberta. – Western Journal of Applied Forestry 14: 186-193.
[19] Huang, S., Titus, S. J. (1992): Comparison of nonlinear height-diameter functions for major Alberta tree species. – Canada Forestry Resources 22(9): 1297-1304.
[20] Huang, S., Titus, S. J. (1994): An age-independent individual tree height prediction model for boreal spruce–aspen stands in Alberta. – Canadian Journal of Forest Research 24: 1295-1301.
[21] Huang, S., Price, D., Morgan, D., Titus, S. (1999): Validation of ecoregion-based taper equations for white spruce in Alberta. – The Forestry Chronicle 75: 281-292.
[22] Huang, S., Price, D., Titus, S. J. (2000): Development of ecoregion-based height–diameter models for white spruce in boreal forests. – Forest Ecology and Management 129: 125-141.
[23] Henricksen, H. A. (1950): Height-diameter curve with logarithmic diameter. – Dansk Skovforen. Tidsskr. 35: 193-202.
[24] Institute SAS (1999): SAS/STAT user's Guide, Version 8. – SAS Institute, Cary, NC.
[25] Jiang, Y., Zhang, J., Han, S., Chen, Z., Setälä, H., Yu, J., Zheng, X., Guo, Y., Gu, Y.(2016): Radial growth response of Larix gmelinii to climate along a latitudinal gradient in the greater Khingan Mountains. – Northeastern China Forests 7: 295.
[26] Larson, B. C. (1986): Development and growth of even-aged stands of Douglas-fir and grand fir. – Can. J. For. Res. 16: 367-372.
[27] Leng, W., He, H. S., Bu, R., Dai, L., Hu, Y., Wang, X. (2008): Predicting the distributions of suitable habitat for three larch species under climate warming in Northeastern China. – Forest Ecology and Management 254: 420-428.
[28] Loetsch, F., ZoÈhrer, F., Haller, K. E. (1973): Forest Inventory. Vol. 2. – BLV Verlagsgesellschaft mbH, München.

http://www.aloki.hu ● ISSN 1589 1623 (Print) ● ISSN 1785 0037 (Online)
DOI: http://dx.doi.org/10.15666/aeer/1706_1356713591

[29] Lopéz, Sánchez, C. A., Gorgoso, J. J., Castedo, F., Rojo, A., Rodríguez, R., Álvarez González, J. G., Sánchez Lynch, T. B., Murphy, P. A. (2003): A compatible height prediction and projection system for individual trees in natural, even-aged shortleaf pine stands. – For Sci 41: 194-209.
[30] Meyer, H. A. (1940): A mathematical expression for height curves. – J. For. 38: 415-420.
[31] Moffat, A. J., Matthews, R. W., Hall, J. E. (1991): The effects of sewage sludge on growth and foliar and soil chemistry in pole-stage Corsican pine at Ringwood Forest, Dorset, UK. – Can. J. For. Res. 21: 902-909.
[32] Özçelik, R., Yavuz, H., Karatepe, Y., Gürlevik, N., Kiri, Ş. R. (2014): Development of ecoregion-based height-diameter models for 3 economically important tree species of southern Turkey. – Turkish Journal of Agriculture and Forestry 38: 399-412.
[33] Pearl, R., Reed, L. J. (1920): On the rate of growth of the population of the United States since 1970 and its mathematical representation. – Proc. Natl. Acad. Sci. U.S.A. 6: 275-288.
[34] Peng, C., Zhang, L., Liu, J. (2001): Developing and validating nonlinear height–diameter models for major tree species of Ontario's boreal forests. – Northern Journal of Applied Forestry 18: 87-94.
[35] Peng, C., Zhang, L., Zhou, X., Dang, Q., Huang, S. (2004): Developing and evaluating tree height-diameter models at three geographic scales for black spruce in Ontario. – Northern Journal of Applied Forestry 21: 83-92.
[36] Peng, C. H. (1999): Nonlinear height-diameter models for nine boreal forest tree species in Ontario. – Forest Research Report. Ontario Forest Research Institute, Marie, ON, Canada.
[37] Pillsbury, N. H., McDonald, P. M., Simon, V. (1995): Reliability of Tanoak volume equations when applied to different areas. – Western Journal of Applied Forestry 10: 72-78.
[38] Prodan M (1968): Forest Biometrics (English Ed.). – Pergamon Press, Oxford (German ed. 1961).
[39] Ratkowsky, D. A. (1990): Handbook of Nonlinear Regression. – Marcel Dekker, Inc., New York.
[40] Ratkowsky, D. A., Reedy, T. J. (1986): Choosing near-linear parameters in the four-parameter logistic model for radio ligand and related assays. – Biometrics 42: 575-582.
[41] Richards F (1959): A flexible growth function for empirical use. – Journal of Experimental Botany 10: 290-301.
[42] Seber, G. A. F., Wild, C. J. (1989): Nonlinear Regression. – John Wiley and Sons, New York.
[43] Sibbesen E (1981): Some new equations to describe phosphate sorption by soils. – European Journal of Soil Science 32: 67-74.
[44] Snedecor, G. W., Cochran, W. G. (1989): Statistical Methods. Eighth Ed. – Iowa State University, Ames, IA.
[45] Soares, P., Tomé, M. (2002): Height-diameter equation for first rotation eucalypt plantations in Portugal. – Forest Ecology Management 166: 99-109.
[46] Stage, A. R. (1975): Prediction of height increment for models of forest growth. – USDA For. Serv. Res. Pap. INT-164.
[47] Stankova, T. V., Diéguez-Aranda, U. (2013): Height-diameter relationships for Scots pine plantation in Bulgaria: optimal combination of model type and application. – Ann For Res 56: 149-163.
[48] Stoffels, A., van Soest, J. (1953): The main problems in sample plots. 3. height regression. – Ned Bosbouwtijdschr. 25: 190-199 (English summary in For. Abstr. 15: 77).
[49] Tang, S. (1994): Self-adjusted height-diameter curves and one entry volume model. – Forest Research 7(5): 512-518 (in Chinese).

http://www.aloki.hu ● ISSN 1589 1623 (Print) ● ISSN 1785 0037 (Online)
DOI: http://dx.doi.org/10.15666/aeer/1706_1356713591

[50] Temesgen, H., Gadow, K. V. (2004): Generalized height-diameter models an application for major tree species in complex stands of interior British Columbia. Europe. – Journal Forests Resources 123: 45-51.
[51] Watts, S. B. (1983): Forestry Handbook for British Columbia. 4th Ed. – Forestry Undergraduate Society, Vancouver, B.C.
[52] Winsor, C. P. (1932): The Gompertz curve as a growth curve. – Proc. Natl. Acad. Sci. U.S.A. 18: 1-7.
[53] Wykoff, W. R., Crookston, N. L., Stage, A. R. (1982): User's Guide to the Stand Prognosis Model. – Intermountain Forest and Range Experiment Station, Ogden, UT.
[54] Xu, H., Sun, Y., Wang, X., Fu, Y., Dong, Y., Li Y (2014): Nonlinear mixed-effects (NLME) diameter growth models for individual China-fir (*Cunninghamia lanceolata*) trees in southeast China. – PLoS One 9: e104012. DOI: 10.1371/journal.pone.0104012 PMID: 25084538.
[55] Yan-qiong, L., et al. (2015): Development and evaluation of models for the relationship between tree height and diameter at breast height for Chinese-fir plantations in subtropical China. – PLoS One 10(4): e0125118. DOI: 10.1371/journal.pone.0125118.
[56] Yang, R. C., Kozak, A., Smith, J. H. G. (1978): The potential of Weibull-type functions as flexible growth curves. – Canadian Journal of Forest Research 8: 424-431.
[57] Zhang, H., Lei, X., Zeng, W. (2016): Height–diameter equations for larch plantations in northern and northeastern China: a comparison of the mixed-effects, quantile regression and generalized additive models. – Forestry 89: 434-445.
[58] Zhang, L. (1997): Cross-validation of non-linear growth functions for modelling tree height– diameter relationships. – Annals of Botany 79: 251-257.
[59] Zhang, L., Peng, C., Huang, S., Zhou, X. (2002): Development and evaluation of ecoregion-based jack pine height-diameter models for Ontario. – The forestry Chronicle 78: 530-538.
[60] Zhang, W. R., Sheng, W. T., Jiang, Y. X., Zhou, Z. X., Wang, X. S. (1992): Classification of forest site system in China. – Forest Research 5(3): 251-262 (in Chinese).
[61] Zhao, M. F., Xiang, W. H., Tian, D. L., Deng, X. W., Huang, Z. H., Zhou, X. L., et al. (2013): Effects of increased nitrogen deposition and rotation length on long-term productivity of Cunninghamia lanceolata plantation in southern China. – PLoS One 8(2): e55376. doi: 10.1371/journal.pone.0055376 PMID: 23390533.
[62] Zeide, B. (1989): Accuracy of equations describing diameter growth. – Can. J. For. Res. 19:1283-1286.
[63] Zeide, B. (1993): Analysis of growth equations. – For. Sci. 39(3): 594-616.

APPENDIX

Table A1. *Prediction errors of applying a specific subregion model to each subregion*

Subregion	N	$\bar{H}$ (m)	$\hat{H}$ (m)	ē	ē%	Se	t	p-value
Songling model								
SL-SL	214	19.58	19.57	0.01	0.06	1.68	0.1149	0.9085
SL-JGDQ	524	18.29	19.02	-0.72	-3.95	2.26	-7.3121	< 0.0001
SL-XL	190	19.33	20.42	-1.09	-5.64	2.03	-7.3741	< 0.0001
SL-TH	203	15.34	17	-1.66	-10.84	1.97	-12.1121	< 0.0001
SL-HZ	215	16.12	17.74	-1.62	-10.06	2.17	-10.9611	< 0.0001
SL-SBZ	237	17.93	19.04	-1.11	-6.21	2.09	-8.1781	< 0.0001

http://www.aloki.hu ● ISSN 1589 1623 (Print) ● ISSN 1785 0037 (Online)
DOI: http://dx.doi.org/10.15666/aeer/1706_1356713591

SL-HJY	128	17.72	18.96	-1.24	-7.004	2.09	-6.7131	< 0.0001
SL-XLJ	224	15.75	14.61	1.15	7.32	1.76	9.7611	< 0.0001
SL-TQ	191	17.44	17.49	-0.3	-1.72	1.86	-2.2211	0.0273
SL-AME	285	22.36	21.24	1.12	5.02	1.91	9.9303	< 0.0001
Jiagedaqi model								
JGDQ-SL	214	19.58	18.69	0.88	4.53	1.89	6.8569	< 0.0001
JGDQ-JGDQ	524	18.29	18.32	-0.06	-0.03	2.13	-0.0691	0.9446
JGDQ-XL	190	19.33	19.56	-0.22	-1.15	1.79	-1.7174	0.0875
JGDQ-TH	203	15.34	16.51	-1.17	-7.64	1.94	-8.5851	< 0.0001
JGDQ-HZ	215	16.12	17.25	-1.13	-7.02	1.97	-8.3971	< 0.0001
JGDQ-SBZ	237	17.93	18.33	-0.36	-2.04	1.83	-3.0661	0.0024
JGDQ-HJY	128	17.72	18.32	-0.6	-3.38	1.9	-3.5661	0.0005
JGDQ-XLJ	224	15.75	14.31	1.45	9.21	1.62	13.3751	< 0.0001
JGDQ-TQ	191	17.44	16.78	0.66	3.82	1.72	5.3497	< 0.0001
JGDQ-AME	285	22.36	20.15	2.2	9.87	2.08	17.8962	< 0.0001
Xinlin model								
XL-SL	214	19.58	18.46	1.12	5.72	1.94	8.4179	< 0.0001
XL-JGDQ	524	18.29	18.09	0.2	1.11	2.13	2.1867	0.0292
XL-XL	190	19.33	19.33	-0.01	-0.07	1.79	-0.0113	0.913
XL-TH	203	15.34	16.32	-0.98	-6.4	1.95	-7.1721	< 0.0001
XL-HZ	215	16.12	17.07	-0.95	-5.89	1.96	-7.1032	< 0.0001
XL-SBZ	237	17.93	18.08	-0.14	-0.83	1.82	-1.2612	0.209
XL-HJY	128	17.72	18.12	-0.4	-2.27	1.89	-2.4052	0.0176
XL-XLJ	224	15.75	14.12	1.63	10.36	1.61	15.1591	< 0.0001
XL-TQ	191	17.44	16.55	0.89	5.12	1.71	7.1867	< 0.0001
XL-AME	285	22.36	19.91	2.46	11	2.13	19.4831	< 0.0001
Tahe model								
TH-SL	214	19.58	17.75	1.82	9.32	1.8	14.8481	< 0.0001
TH-JGDQ	524	18.29	17.31	0.98	5.38	2.19	10.2822	< 0.0001
TH-XL	190	19.33	18.71	0.62	3.24	1.86	4.6291	< 0.0001
TH-TH	203	15.34	15.32	0.01	0.07	1.88	0.0922	0.9265
TH-HZ	215	16.12	16.15	-0.02	-0.17	2.07	-0.2123	0.8413
TH-SBZ	237	17.93	17.32	0.61	3.41	1.96	4.8031	< 0.0001
TH-HJY	128	17.72	17.32	0.39	2.21	1.94	2.2817	< 0.0241
TH-XLJ	224	15.75	12.87	2.88	18.3	1.76	24.5241	< 0.0001
TH-TQ	191	17.44	15.63	1.81	10.41	1.85	13.5143	< 0.0001
TH-AME	285	22.36	19.38	2.98	13.34	1.95	25.7151	< 0.0001
Huzhong model								
HZ-SL	214	19.58	17.29	2.29	11.71	2.25	14.8871	< 0.0001
HZ-JGDQ	524	18.29	17.02	1.27	6.96	2.21	13.1672	< 0.0001
HZ-XL	190	19.33	18.19	1.13	5.89	1.86	8.4074	< 0.0001
HZ-TH	203	15.34	15.37	-0.02	-0.18	2.06	-0.1951	0.8454
HZ-HZ	215	16.12	16.13	-0.06	-0.04	1.92	0.0495	0.9605
HZ-SBZ	237	17.93	16.97	0.95	5.31	1.84	7.9651	< 0.0001
HZ-HJY	128	17.72	17.12	0.61	3.46	1.92	3.6063	0.0004
HZ-XLJ	224	15.75	13.23	2.52	16	1.57	23.9041	< 0.0001

http://www.aloki.hu ● ISSN 1589 1623 (Print) ● ISSN 1785 0037 (Online)
DOI: http://dx.doi.org/10.15666/aeer/1706_1356713591

HZ-TQ	191	17.44	15.43	2.01	11.54	1.77	15.6723	< 0.0001
HZ-AME	285	22.36	18.63	3.73	16.69	2.41	26.0481	< 0.0001
Shibazhan model								
SBZ-SL	214	19.58	18.28	1.3	6.63	2.06	9.2178	< 0.0001
SBZ-JGDQ	524	18.29	18.32	0.29	1.58	2.2	3.0113	0.0027
SBZ-XL	190	19.33	19.14	0.19	0.98	1.8	1.4579	0.1465
SBZ-TH	203	15.34	16.25	-0.91	-5.97	2	-6.5171	< 0.0001
SBZ-HZ	215	16.12	16.99	-0.86	-5.38	1.94	-6.5532	< 0.0001
SBZ-SBZ	237	17.93	17.93	0.01	0.08	1.81	0.0136	0.9891
SBZ-HJY	128	17.72	17.99	-0.27	-1.55	1.9	-1.6311	0.1053
SBZ-XLJ	224	15.75	14.13	1.62	10.29	1.57	15.3814	< 0.0001
SBZ-TQ	191	17.44	16.44	1	5.77	1.72	8.0997	< 0.0001
SBZ-AME	285	22.36	19.66	2.7	12.09	2.24	20.3611	< 0.0001
Hanjiayuan model								
HJY-SL	214	19.58	18.01	1.57	8.02	2	11.4452	< 0.0001
HJY-JGDQ	524	18.29	17.66	0.62	3.43	2.15	6.6657	< 0.0001
HJY-XL	190	19.33	18.95	0.38	1.97	1.8	2.9166	0.003
HJY-TH	203	15.34	15.85	-0.51	-3.32	1.93	-3.7491	0.0002
HJY-HZ	215	16.12	16.65	-0.52	-3.28	1.95	-3.9623	0.0001
HJY-SBZ	237	17.93	17.64	0.28	1.59	1.84	2.3845	0.0178
HJY-HJY	128	17.72	17.72	-0.06	-0.03	1.87	-0.0362	0.9709
HJY-XLJ	224	15.75	13.54	2.2	14	1.66	19.8661	< 0.0001
HJY-TQ	191	17.44	16.01	1.43	8.21	1.76	11.2541	< 0.0001
HJY-AME	285	22.36	19.49	2.87	12.85	2.17	22.3332	< 0.0001
Xilinji model								
XJL-SL	214	19.58	19.23	0.58	2.99	2.82	3.0329	0.002
XJL-JGDQ	524	18.29	18.86	-0.56	-3.08	2.52	-5.1112	0.0006
XJL-XL	190	19.33	19.81	-0.47	-2.44	2.2	-2.956	0.003
XJL-TH	203	15.34	17.52	-2.17	-14.2	2.48	-12.5232	< 0.0001
XJL-HZ	215	16.12	18.18	-2.05	-12.75	2.06	-14.5824	< 0.0001
XJL-SBZ	237	17.93	18.76	-0.83	-4.63	2.08	-6.1391	< 0.0001
XJL-HJY	128	17.72	18.97	-1.25	-7.07	2.25	-6.3312	< 0.0001
XJL-XLJ	224	15.75	15.75	-0.001	-0.006	1.47	-0.0113	0.991
XJL-TQ	191	17.44	17.45	-0.02	-0.01	2.11	-0.0142	0.989
XJL-AME	285	22.36	20.06	2.29	10.28	2.95	13.1434	< 0.0001
Tuqiang model								
TQ-SL	214	19.58	19.31	0.27	1.39	1.96	2.0221	0.0443
TQ-JGDQ	524	18.29	18.94	-0.64	-3.54	2.13	-6.9321	< 0.0001
TQ-XL	190	19.33	20.16	-0.82	-4.26	1.79	-6.3132	< 0.0001
TQ-TH	203	15.34	17.21	-1.87	-12.22	1.98	-13.4612	< 0.0001
TQ-HZ	215	16.12	17.94	-1.81	-11.28	1.96	-13.6241	< 0.0001
TQ-SBZ	237	17.93	18.93	-1	-5.57	1.82	-8.4541	< 0.0001
TQ-HJY	128	17.72	18.97	-1.24	-7.05	1.9	-7.4122	< 0.0001
TQ-XLJ	224	15.75	15.07	0.68	4.33	1.59	6.4182	< 0.0001
TQ-TQ	191	17.44	17.45	-0.04	-0.02	1.71	-0.0351	0.9717
TQ-AME	285	22.36	20.72	1.64	7.35	2.15	12.8821	< 0.0001

http://www.aloki.hu ● ISSN 1589 1623 (Print) ● ISSN 1785 0037 (Online)
DOI: http://dx.doi.org/10.15666/aeer/1706_1356713591

Amuer model								
AME-SL	214	19.58	20.61	-1.03	-5.26	1.73	-8.7121	< 0.0001
AME-JGDQ	524	18.29	20.08	-1.78	-9.76	2.31	-17.7735	< 0.0001
AME-XL	190	19.33	21.57	-2.23	-11.57	2.03	-15.1721	< 0.0001
AME-TH	203	15.34	17.95	-2.61	-17.02	1.92	-19.2912	< 0.0001
AME-HZ	215	16.12	18.78	-2.66	-16.5	2.19	-17.7521	< 0.0001
AME-SBZ	237	17.93	20.1	-2.16	-12.09	2.14	-15.5414	< 0.0001
AME-HJY	128	17.72	20.05	-2.33	-13.19	2.08	-12.7122	< 0.0001
AME-XLJ	224	15.75	15.37	0.38	2.44	1.82	3.1623	0.001
AME-TQ	191	17.44	18.38	-0.93	-5.353	2.04	-6.3121	< 0.0001
AME-AME	285	22.36	22.368	-0.02	-0.01	1.88	-0.0282	0.983

N – sample size, $\overline{H}$ – average of observed tree height, $\hat{H}$ – average of predicted tree height from the model, $\bar{e}$ – average of prediction error, $\bar{e}$ % – percent prediction error, S_e – standard deviation of prediction error

http://www.aloki.hu ● ISSN 1589 1623 (Print) ● ISSN 1785 0037 (Online)
DOI: http://dx.doi.org/10.15666/aeer/1706_1356713591

MICROMORPHOLOGICAL ASSESSMENT OF LEAVES OF *AMARANTHUS CAUDATUS* L. CULTIVATED ON FORMULATED SOIL TYPES

JIMOH, M. O.[1] – AFOLAYAN, A. J.[1*] – LEWU, F. B.[2]

[1]*Medicinal Plants and Economic Development (MPED) Research Centre, Department of Botany, University of Fort Hare, Alice 5700, South Africa*
(e-mail: moajay006@gmail.com)

[2]*Department of Agriculture, Cape Peninsula University of Technology, Wellington Campus, Wellington 7654, Cape Town, South Africa*
(e-mail: LewuF@cput.ac.za)

**Corresponding author*
e-mail: aafolayan@ufh.ac.za; phone: +27-82-202-2167

(Received 6th Apr 2019; accepted 13th Jun 2019)

Abstract. This study examined the modification of foliar characters in the leaf of *Amaranthus caudatus* cultivated on formulated soils. The soil types namely; sandy clay loam, silty clay loam, clayey loam and loam were experimentally derived from sieved soil particles of sand, silt and clay that were re-mixed in relative proportions proposed by the United States Department of Agriculture (USDA, 1951) while unfractionated soil served as the control. The Energy Dispersive X-Ray Spectroscopy (SEM-EDX) showed variation in percentage elemental composition of the epidermal layers. Harvests from clayey loam soil (with relative equal compositions of sand, silt and clay) had the highest composition of the following elements; nitrogen, oxygen, sodium, phosphorus, calcium and zinc whereas other elements were present in various proportions on epidermal surfaces of harvests from other soils. The Scanning Electron Microscope revealed non-glandular dish-like peltate trichomes with membranous lids attached in some cases. On the abaxial layer, stomata densities of the harvests from various soils were in this order: clayey loam > loam > sandy clay loam > control soil > silty clay loam. This research, therefore, provided supportive data on the effect of formulated soil on stomatal development and distribution in *Amaranthus caudatus.*
Keywords: *Amaranthus caudatus, foliar characters, spectroscopy, stomata, dish-like peltate trichomes*

Introduction

Grain amaranths were important crops to the people of Mayan, Aztec and Incas of the pre-Columbian era. They belong to the family Amaranthaceae (now including former family Chenopodiaceae), comprising of grain crops, vegetables, ornamental herbs, shrubs and dye plants numbering about 2500 species globally (The Angiosperm Phylogeny Group, 2009; Christenhusz and Byng, 2016; Kadereit et al., 2003). The existence of wide taxonomic and morphology characters between and within *Amaranthus* species (Juan et al., 2007) makes it important to study possible cause due to environmental factors. *Amaranthus caudatus* is one of the few ancient dicotyledonous pseudo cereals of Amaranthaceae. Its origin has been traced to the Andean countries and it is well known to survive in marginal climates where other crops cannot be easily cultivated (Jimoh et al., 2018).

The technique of micromorphology has proven to be more reliable in provision of data for germplasm identification and in unravelling structures of taxonomic importance that are embedded in plant cell or tissue for adequate knowledge of genetic diversity

http://www.aloki.hu ● ISSN 1589 1623 (Print) ● ISSN 1785 0037 (Online)
DOI: http://dx.doi.org/10.15666/aeer/1706_1359313605

(Costea et al., 2006; Shah et al., 2018). Also, for the enhancement of cultivars for better yield, it is important to understand the magnitude of environmental influence on these factors (Rastogi and Shukla, 2013).

Many environmental conditions such as moisture, light, temperature and a host of other geographic factors have been reported to affect genetic make-up of species naturally or artificially. The soil environment plays a key role in plant gene expression (Viger et al., 2015). Also, it has been well established that soil texture determines the moisture retention capacity and water infiltration rate which in turn influences the amount of nutrients available to plant although for different soil structures, the two factors are inversely related (Olesen et al., 1999; Rabot et al., 2018). The photosynthetic biochemistry of plant coupled with soil factor and other environmental conditions drive the mechanism for stomatal acclimation to atmospheric carbon IV oxide (Maherali et al., 2002; Pillitteri and Torii, 2012). Since environmental condition is capable of altering the entire plant structures such as leaf size, stem girth and root length; its overall effect on stomatal size, density, distribution and conductivity cannot be underestimated (Casson and Gray, 2008; Maherali et al., 2002; Jimoh et al., 2019a).

Apart from being a depot for bioactive compounds, plant leaf houses important organs responsible for physiological functions and stomata, useful in taxonomic characterization. For example, epidermal features have been recently recognized as supportive tool for systematic delimitation within and between species implying that foliar micromorphology is a true reflection of interaction between plant and its environment (Fank-De-Carvalho et al., 2010; Sharaibi and Afolayan, 2017; Stuessy, 2009). The core objective of this research therefore, was to investigate induced morphological adjustments to foliar characteristics of *Amaranthus caudatus* cultivated plants on different soil types and incorporate newly acquired information into existing taxonomic database for the species.

Materials and methods

Experimental soil formulation

Top soil collected from the University of Fort Hare's Research Farm in May 2017 was air dried under shade for 4 weeks. The dried soil was later filtered with iron sieves of the designated mesh into parent particle sizes of clay (<2 μm), silt (<50–2 μm) and sand (<2000–50 μm). Experimental soil was then formulated by mixing sieved soil particles in relative proportions proposed by the United States Department of Agriculture (United States Department of Agriculture & Natural Resources Conservation Service, 1983) soil texture triangle as shown in *Table 1*.

Table 1. *Experimental soil formulation in proportions recommended by soil texture triangle technique (USDA, 1951)*

S/N	Soil types	% Sand	% Silt	% Clay
1	Control soil (SF_1)	Unfractionated	Unfractionated	Unfractionated
2	Sandy clay loam (SF_2)	66	13	21
3	Silty clay loam (SF_3)	10	60	30
4	Clayey loam (SF_4)	36	30	34
5	Loam (SF_5)	40	40	20

http://www.aloki.hu ● ISSN 1589 1623 (Print) ● ISSN 1785 0037 (Online)
DOI: http://dx.doi.org/10.15666/aeer/1706_1359313605

Plant material and experimental design

Seeds of *A. caudatus* collected from seedbank of the Medicinal Plants and Economic Development (MPED) Research Centre, Department of Botany, University of Fort Hare were broadcast in seedling trays and transplanted after three weeks into pots filled with the control and formulated soils types (*Table 1*) arranged in the green house in a Completely Randomised Design (CRD) in three replicates (*Fig. 1*). The experiment was conducted in the greenhouse (set at an average temperature of 25 °C; 64% relative humidity), sited on the roof of the Department of Botany building. At flowering stage, fresh and mature leaves were collected at five nodes to the shoot apices, from three different pots representing each of the soil types. Portions of 2-3 cm^2 were cut off from the standard median part of the leaf blade close to the mid-rib in preparation for micromorphological examination.

Figure 1. *Potted experiment of Amaranthus caudatus in a green house*

Scanning electron microscopy and energy dispersive X-ray spectroscopy (SEM-EDX)

Cut sections of the leaf were fixed in 6% glutaraldehyde solution buffered with 0.05 M sodium cacodylate (pH 7.5) for 24 h. The samples were soaked in distilled water and dehydrated in graded ethanol (10-100% concentration series) for 20 min per rinse (Munien et al., 2015). Samples were then soaked in 100% ethanol and dried in a Hitachi HCP-2 critical point drier. Dried specimens were fixed with two sided adhesive carbon tape on aluminium stubs and coated with a thin layer of gold using an Elko IB-3 Ion Coater. The abaxial and adaxial surfaces were examined in a JEOL (JSM-6390LV) Scanning Electron Microscope (SEM) operating at an accelerated voltage of 10-15 kV at different magnifications. The Energy Dispersive X-Ray Spectroscopy (produced by Thermo Electron Corporation, 6733B-IUUSN, USA) and the Noran System Six Imaging Software both connected to SEM were respectively used to analyse the elemental composition of the treated samples and capture electron images (Sharaibi and Afolayan, 2017). Both qualitative and quantitative features on the abaxial and adaxial layers of the leaf epidermis were assessed. Quantitative features examined were number

http://www.aloki.hu ● ISSN 1589 1623 (Print) ● ISSN 1785 0037 (Online)
DOI: http://dx.doi.org/10.15666/aeer/1706_1359313605

of trichomes; stomata density and distance between two stomata. The qualitative characters considered were stomata distribution; trichome types, size, shape and distribution; presence or absence of peltate scale; and oil sac frequency on both layers.

Statistical analysis

Data obtained from all treatments were analysed and expressed as mean ± standard deviation (SD) of 3 replicates. A MINITAB 17 statistical package was used to separate means of various replicate data for EDX percentage elemental compositions, stomata densities and distances between stomata.

Results

Foliar micromorphological characters

Stomata

Stomata types and distribution: Leaves are amphistomatic with both layers characterized by sunken, anomocytic stomata lacking subsidiary cells. Stomata were found to be prevalent on the abaxial surface than the adaxial in all soil types (*Fig. 2*).

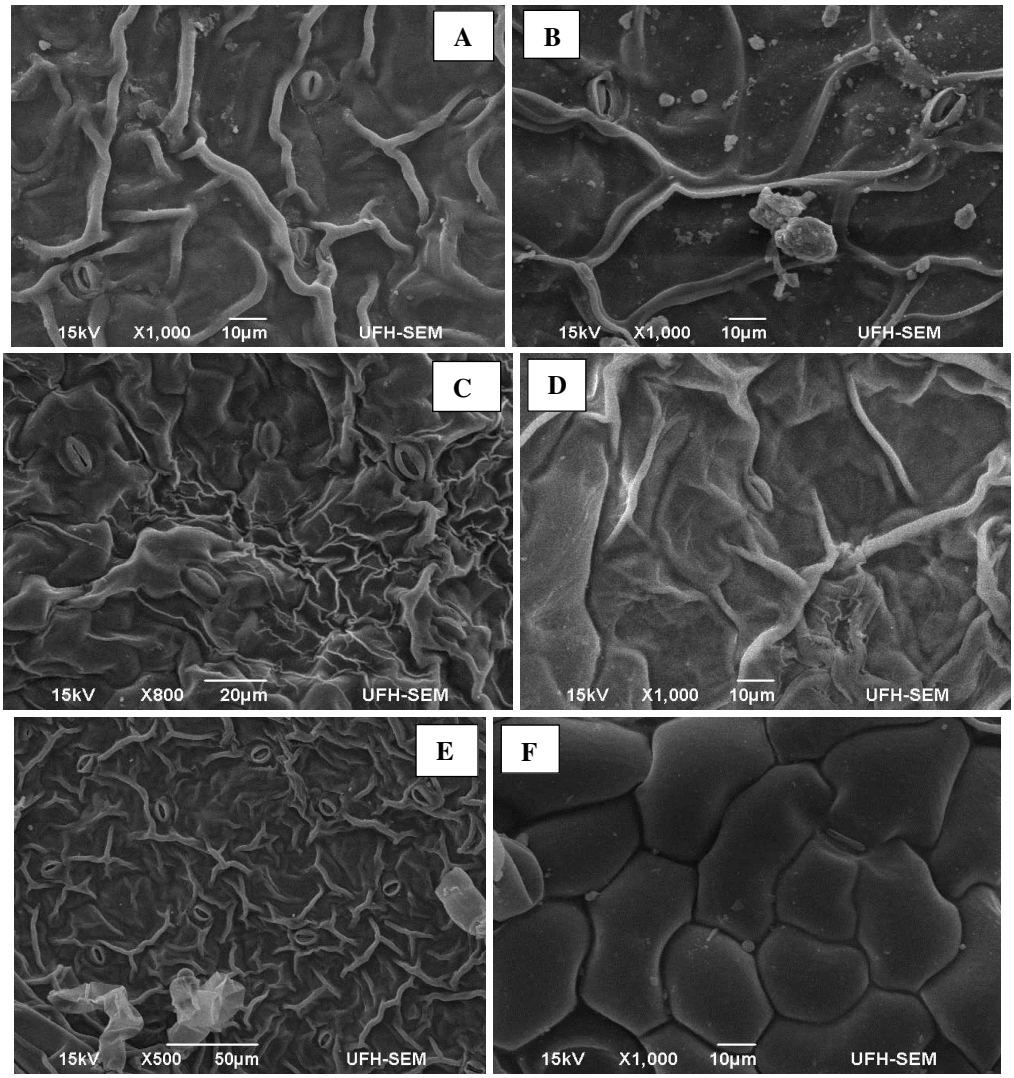

http://www.aloki.hu ● ISSN 1589 1623 (Print) ● ISSN 1785 0037 (Online)
DOI: http://dx.doi.org/10.15666/aeer/1706_1359313605

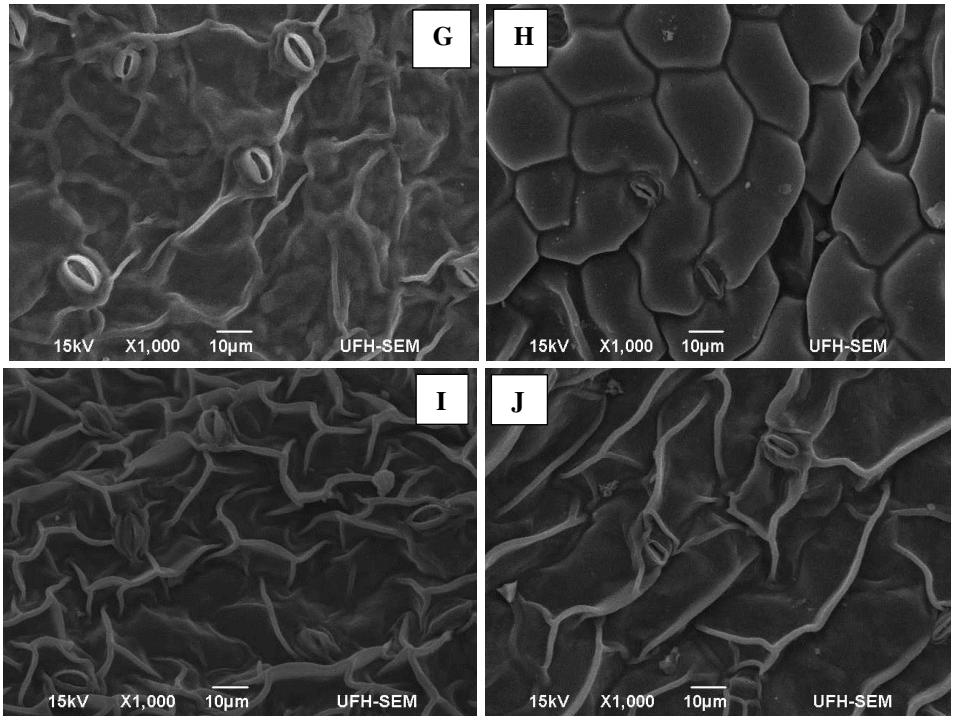

Figure 2. *Plates A, C, E, G & I showing stomata number and distributions on abaxial layers; Plates B, D, F, H & J indicating stomata number and distributions on adaxial layers of A. caudatus cultivated on control soil, sandy clay loam, silty clay loam, clayey loam and loam respectively*

Stomata density: This is defined as number of stomata per unit area. From SEM micrographs, stomata densities were higher on abaxial layers. In all soil types, the highest density (abaxial: 521.7 ± 0.5 stomata/mm^2; adaxial: 248.4 ± 0.3 stomata/mm^2) was observed in the clayey loam, followed by loam (abaxial: 397.5 ± 0.7 stomata/mm^2; adaxial: 198.8 ± 0.5 stomata/mm^2), sandy clay loam (abaxial: 372.7 ± 0.5 stomata/mm^2; adaxial: 99.4.4 ± 0.3 stomata/mm^2), control soil (abaxial: 223.6 ± 0.5 stomata/mm^2; adaxial: 99.4 ± 0.3 stomata/mm^2) and silty clay loam (abaxial: 198.8 ± 0.5 stomata/mm^2; adaxial: 99.4.4 ± 0.3 stomata/mm^2) with the least stomatal density (*Table 2*). The same stomata densities were evaluated for the adaxial layers of control (SF_1), sandy clay loam (SF_2) and silty clay loam (SF_3) soils. This was due to the fact that the same numbers of stomata were observed in their respective SEM micrographs.

Table 2. *Effect of soil types on stomata characteristics*

Leaf indices	**Adaxial surface**				
Soil types	SF1	SF2	SF3	SF4	SF5
Stomatal density (mm^{-2})	99.38 ± 0.47^b	99.38 ± 0.47^b	99.38 ± 0.47^b	248.44 ± 0.47^a	198.75 ± 0.94^{ab}
Distance between stomata (mm^2)	128.07 ± 6.92^a	153.53 ± 43.01^a	75.53 ± 13.3^b	41.13 ± 5.73^b	52.6 ± 9.22^b
	Abaxial surface				
Soil types	SF1	SF2	SF3	SF4	SF5
Stomatal density (mm^{-2})	223.60 ± 0.82^a	372.66 ± 0.82^b	198.75 ± 2.67^c	521.73 ± 0.82^a	397.51 ± 1.25^{ab}
Distance between stomata (mm^2)	51.93 ± 6.82^b	53.67 ± 5.73^b	60.43 ± 7.01^b	34.43 ± 4.91^c	50.03 ± 4.43^b

*Letters a, ab, b and c are different values of mean separations obtained from MINITAB 17

http://www.aloki.hu ● ISSN 1589 1623 (Print) ● ISSN 1785 0037 (Online)
DOI: http://dx.doi.org/10.15666/aeer/1706_1359313605

Trichomes

Different kinds of trichomes namely; capitate, multicellular glandular, acicular and non-glandular dish-shaped peltate trichomes were seen on both layers of the epidermis of the plant samples examined. In some soils, the dish-shaped peltate trichomes had attached lids while in other cases, lids were absent. Both acicular and capitate trichomes were abundant on the upper surface than the lower surface (*Fig. 3*).

Distance between stomata

The distance between stomata and stomata density followed a characteristic trend. As stomata density increases, the distance decreases. Stomata were farthest away from one another on sandy clay loam (adaxial: 153.5 ± 14.3μm) and closest on clayey loam (abaxial: 34.4 ± 1.6μm) with each soil type following the trend earlier mentioned (*Table 2*).

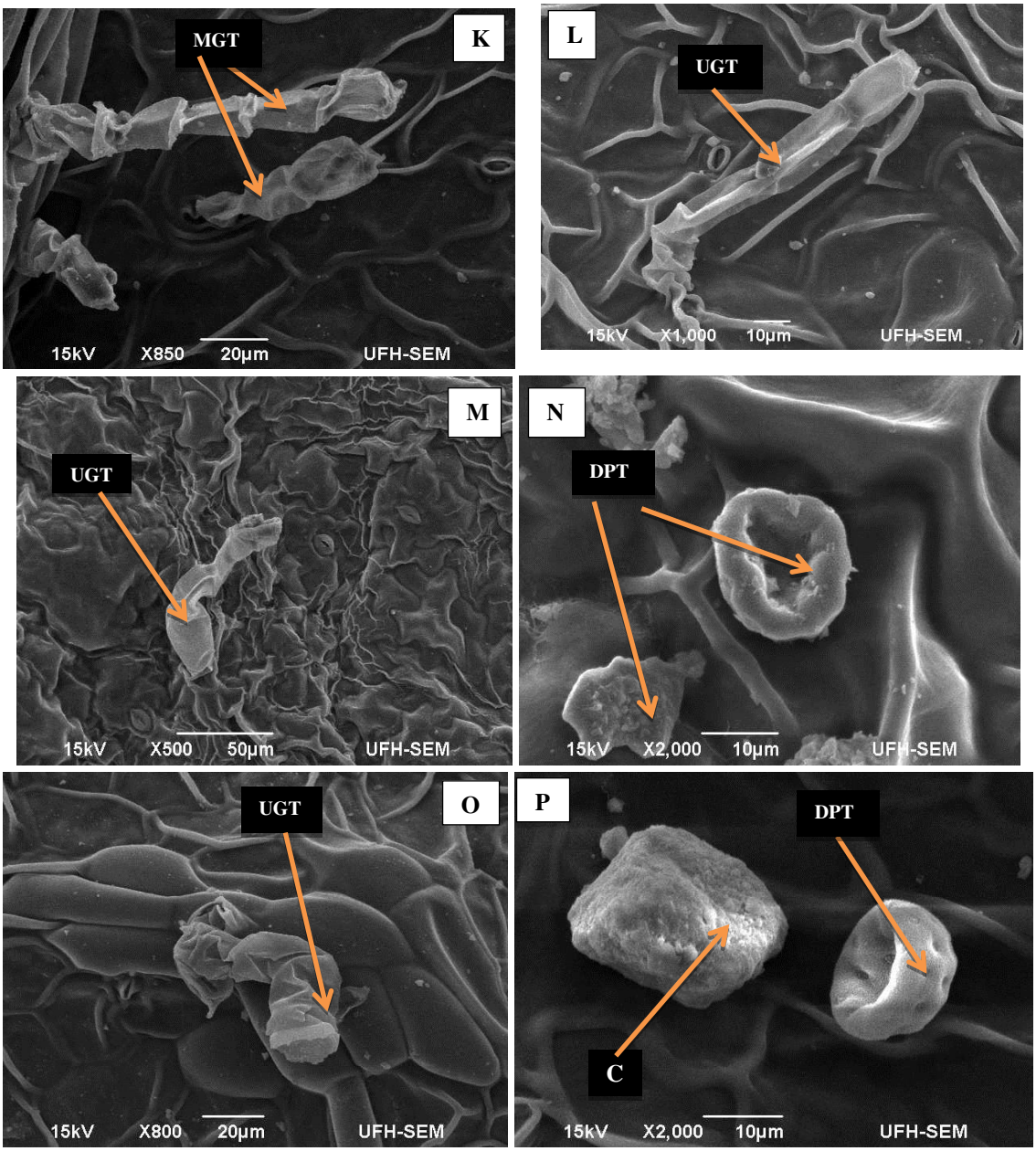

http://www.aloki.hu ● ISSN 1589 1623 (Print) ● ISSN 1785 0037 (Online)
DOI: http://dx.doi.org/10.15666/aeer/1706_1359313605

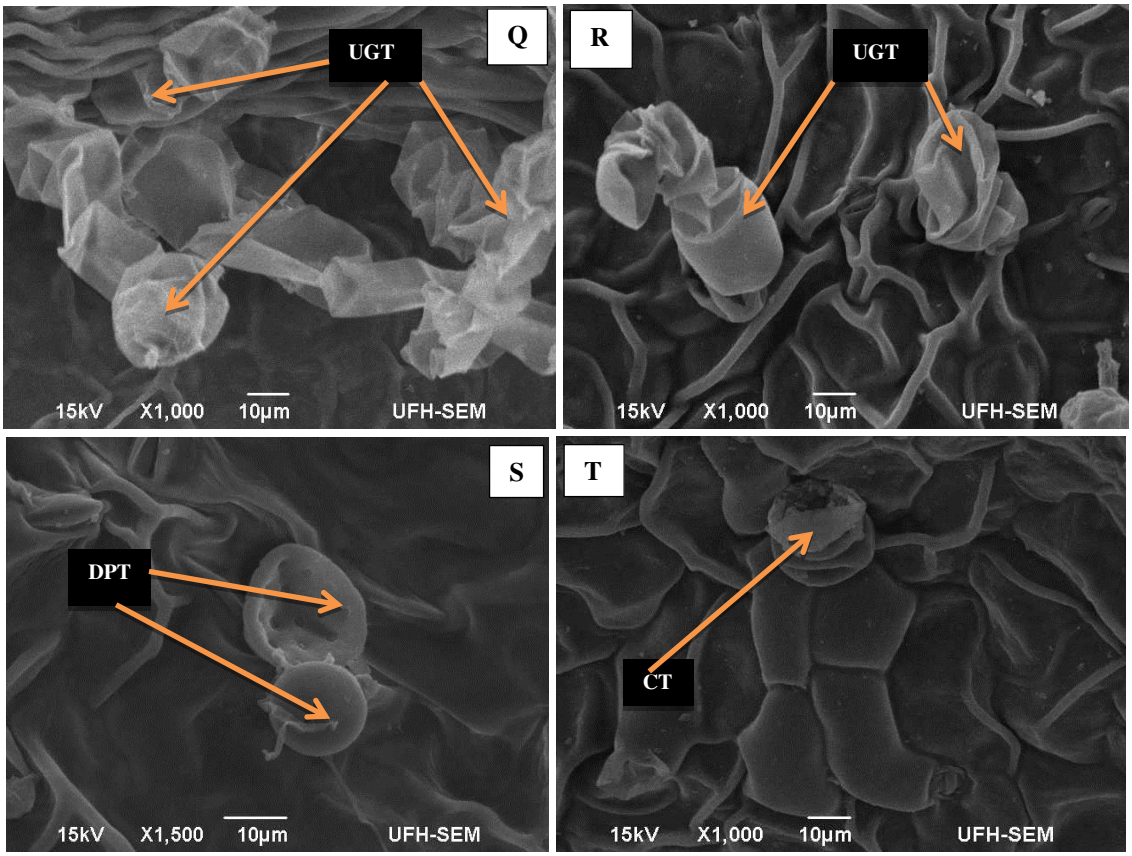

Figure 3. *Plates K, L, M, N & O showing different trichomes on abaxial layers; Plates P, Q, R, S & T indicating trichomes on adaxial layers of A. caudatus cultivated on control soil, sandy clay loam, silty clay loam, clayey loam and loam respectively. MGT = multicellular glandular trichome; UGT = unicellular glandular trichome; DPT = dish-like peltate trichome; CT = capitate trichome; C = crystal*

Epidermal cells

The epidermal cell walls in all soil types were irregular in shape, with curved anticlinal walls but later assumed polygonal shape when swollen. The anticlinal walls became straight when turgid, conferring the polygonal shape on the epidermal cell (*Fig. 4W & X*). The epidermal cells on the adaxial layer developed into distinct polygonal sacs that may serve as storage facilities for essential oil, water or phytochemicals. Also, crystal deposits were found on the epidermal layers which may indicate the presence of chemicals that offer mechanical support to the leaf (*Fig. 4*).

Energy dispersive X-ray (EDX) spectroscopy

The EDX analysis of the epidermal layers revealed percentage atomic composition of various elements as presented in *Table 3*. Presumably, high presence of gold was due to the gold coating. Beryllium was found in high quantity only in the control soil whereas it is absent in the plant grown on formulated soils. Elements such as carbon, nitrogen, oxygen, sodium, magnesium, silicon, phosphorus, sulphur, potassium and calcium were found in quantifiable amount from all harvested plants. Plants harvested from the control soil (SF_1) and sandy clay loam (SF_2) lack aluminium which is present in low

http://www.aloki.hu ● ISSN 1589 1623 (Print) ● ISSN 1785 0037 (Online)
DOI: http://dx.doi.org/10.15666/aeer/1706_1359313605

quantity in the harvest from other soil types. Chlorine, iron, manganese and zinc were found in extremely low amount although still lacking in some harvested samples of *A. caudatus* (*Table 3*; *Fig. 5*).

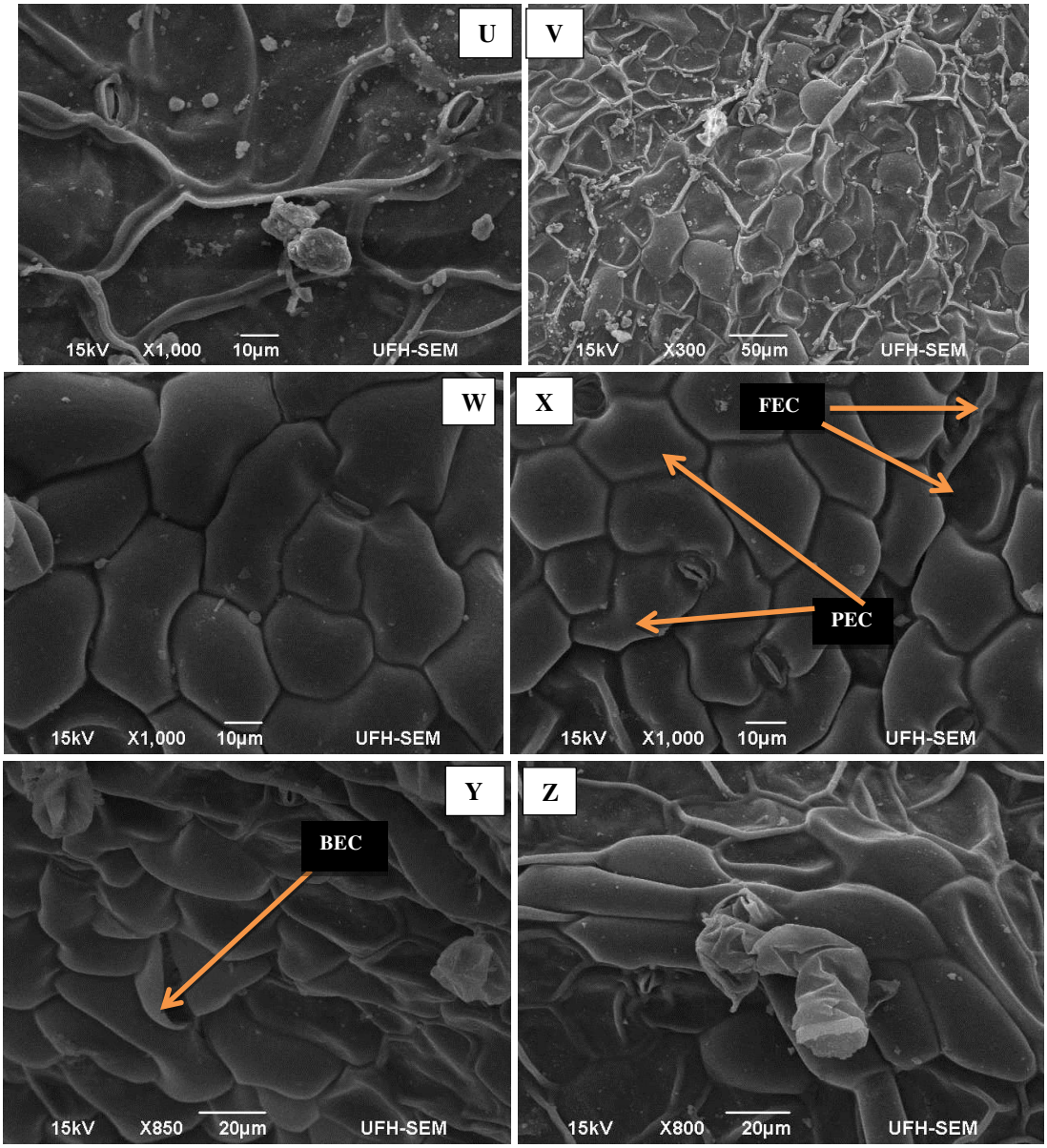

Figure 4. *Plates U & V showing flaccid epidermal cells on abaxial and adaxial layers of harvest from the control soil respectively; Plate W & X indicating turgid epidermal cells on adaxial layers of A. caudatus cultivated on sandy clay loam and clayey loam respectively.; Plate Y showing burst epidermal sac on adaxial layer of harvest from loam soil; Plate Z indicating swollen epidermal cell on adaxial layer of harvest from silty clayey loam*

Discussion

The taxonomic significance of micro-characters in delimiting *Amaranthus* species has been explored deeply; however, there is dearth of information on modifications induced by soil types to distribution, types and frequency of these characters. Recent investigations by Costea et al. (2006) and Ogundipe and Kadiri (2012) revealed some

http://www.aloki.hu ● ISSN 1589 1623 (Print) ● ISSN 1785 0037 (Online)
DOI: http://dx.doi.org/10.15666/aeer/1706_1359313605

diagnostic micro-molecular characters in Amaranthaceae. Among these ultra-structures of interest are stomata and trichomes. This study established how soil type modulates stomata densities, trichome types, sizes, frequency and protrusion of epidermal cells due to storage of water, accumulation of essential oils and phytochemicals.

The amphistomatic nature of the epidermal layers of *A. caudatus* remained intact in all soil types although with varying stomatal densities, distribution and, development of solitary, dish-like stellate trichomes that play major roles in secretion and storage of bioactive compounds (Ogundipe and Kadiri, 2012; Wagner et al., 2004). From the figures presented in this study, stomata densities increased in the order $SF_3 < SF_1 < SF_2 < SF_5 < SF_4$ (abaxial) and $SF_1 = SF_2 = SF_3 < SF_5 < SF_4$ (adaxial). This implies that SF_4 (clayey loam) with the highest clay content provided the most suitable environment for stomata development and proliferation than other soil types. This may not be unconnected with increased clay content (compared to other soil formulations) that must have conferred high water retention capacity on the soil since water retention capacity depends on soil physical characteristics (Rawls et al., 1991; Rabot et al., 2018). Thus, the plant may have been compelled to evolve an adaptive mechanism for a more efficient evapotranspiration, leading to increased number of stomata on both epidermal layers. Also, all harvested samples from different soils followed the common trend of higher stomata index on the abaxial layers compared to the adaxial (Babber and Dhingra, 1985; De Micco et al., 2011; Jimoh and Olowokudejo, 2017).

The non-glandular dish-shaped peltate trichomes are being reported for *Amaranthus caudatus* for the first time. This kind of trichome was not observed in the plant harvested from the control and clayey loam. In addition, no lid was found in the abaxial layer of plant harvested from silty clay loam. Also, membranous lid was seen attached to the trichomes on the adaxial surfaces of harvest from loam and sandy clay loam. This observation is a key contribution to the taxonomy of *Amaranthus caudatus* in particular, and Amaranthaceae at large.

Table 3. *Percentage compositions of the elements in A. caudatus leaf epidermis by EDX spectroscopy*

Elements	SF_1	SF_2	SF_3	SF_4	SF_5
Beryllium	8.83 ± 0.33	0	0	0	0
Carbon	31.20 ± 0.60	29.15 ± 0.67	26.60 ± 0.73	27.88 ± 1.16	30.00 ± 0.69
Nitrogen	5.03 ± 1.24	5.38 ± 1.67	2.98 ± 1.60	6.86 ± 2.10	4.48 ± 1.58
Oxygen	20.77 ± 0.42	23.91 ± 0.55	19.95 ± 0.54	26.83 ± 0.74	24.43 ± 0.54
Sodium	0.73 ± 0.07	2.03 ± 0.17	1.26 ± 0.10	3.00 ± 0.11	0.83 ± 0.09
Magnesium	1.10 ± 0.08	1.26 ± 0.11	1.74 ± 0.12	0.62 ± 0.07	1.24 ± 0.11
Aluminium	0	0	0.15 ± 0.06	0.04 ± 0.04	0.05 ± 0.05
Silicon	0.84 ± 0.08	0.03 ± 0.03	0.07 ± 0.06	0.08 ± 0.07	0.22 ± 0.05
Phosphorus	0.43 ± 0.11	0.53 ± 0.13	0.75 ± 0.15	0.81 ± 0.18	0.41 ± 0.13
Sulphur	0.53 ± 0.11	0.47 ± 0.14	1.28 ± 0.18	1.18 ± 0.19	0.29 ± 0.15
Chlorine	0.32 ± 0.05	0.09 ± 0.07	0.12 ± 0.08	0	0
Potassium	3.53 ± 016	4.68 ± 0.22	3.34 ± 0.22	3.96 ± 0.29	1.54 ± 0.18
Calcium	0.14 ± 0.07	0.72 ± 0.10	0.51 ± 0.11	1.68 ± 0.15	0.27 ± 0.09
Iron	0	0.20 ± 0.20	0	0	0
*Gold	26.56 ± 4.09	31.28 ± 5.19	40.92 ± 5.70	26.42 ± 6.57	35.24 ± 5.18
Manganese	0	0.26 ± 0.18	0.22 ± 0.20	0	0
Zinc	0	0	0.11 ± 0.11	0.65 ± 0.65	0

*High percentage of gold was presumably due to the gold plating

http://www.aloki.hu ● ISSN 1589 1623 (Print) ● ISSN 1785 0037 (Online)
DOI: http://dx.doi.org/10.15666/aeer/1706_1359313605

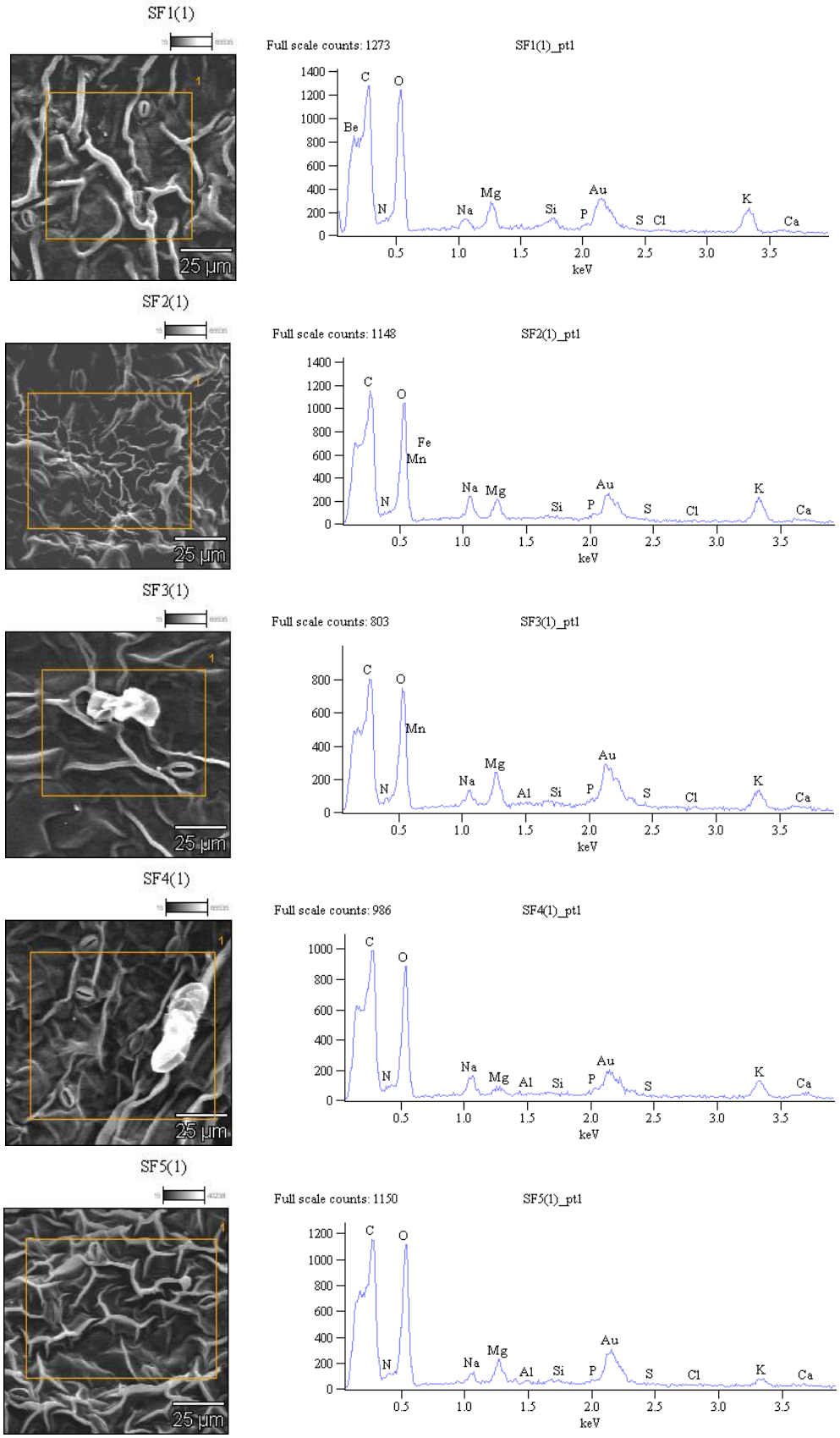

Figure 5. *Percentage compositions of elements in A. caudatus leaf epidermis by EDX spectroscopy. SF1 = control soil; SF2 = sandy clay loam; SF3 = silty clay loam; SF4 = clayey loam; SF5 = loam*

http://www.aloki.hu ● ISSN 1589 1623 (Print) ● ISSN 1785 0037 (Online)
DOI: http://dx.doi.org/10.15666/aeer/1706_1359313605

The analysis of percentage compositions of the elements in *A. caudatus* by EDX spectroscopy of the leaf epidermis revealed variations in elemental composition of the plant with regard to nutrient derived from the respective soil types used for cultivation. For example, harvests from clayey loam soil (with relative equal compositions of sand, silt and clay) had the highest composition of the following elements; nitrogen, oxygen, sodium, phosphorus, calcium and zinc whereas other elements were present in different proportions on epidermal surfaces of harvests from other soils. This finding might be a precursor to the highest biological activities recorded in harvests from clayey loam as reported in Jimoh et al., (2019b). This further corroborates earlier reports that nutrient uptake from the soil affects percentage composition of elements in plants (Ogundola et al., 2017; Ahmed et al., 2013).

Conclusion

Findings from this research revealed that formulated soil types modified the foliar epidermal characteristics in *Amaranthus caudatus*. Also, variabilities in stomatal densities and percentage elemental composition of the harvests further indicated that the relative proportion of primary soil particles (sand, silt and clay) in the formulated soils affects both nutrient uptake and the capacity for evapotranspiration via the stomata. The presence of special trichome; the dish-like non-glandular peltate trichome and other types may not be unconnected with secretion of essential phytochemicals responsible for high therapeutic effect of the plant. Undoubtedly, these soil types-induced modifications could be useful in achieving a robust taxonomic delimitation in *Amaranthus caudatus* as results obtained explained further, the impact of environment on foliar development.

Acknowledgements. Authors wish to acknowledge Dr Elizabeth Famewo Aladejana of MPED Research Centre and the Govan Mbeki Research and Development Centre respectively for their technical and financial support.

Conflict of interests. We declare no conflict on this manuscript.

REFERENCES

[1] Ahmed, A. H. H., Darwish, E., Alobaidy, M. G. (2013): Effect of putrescine and humic acid on growth, yield and chemical composition of cotton plants grown under saline soil conditions. – American-Eurasian Journal of Agricultural and Environmental Sciences 13(4): 479-497.

[2] Babber, S., Dhingra, H. R. (1985): Foliar epidermal studies in Amaranthaceae. – Current Science Association 54(14): 707-709.

[3] Casson, S., Gray, J. E. (2008): Influence of environmental factors on stomatal development. – New Phytologist 178(1): 9-23.

[4] Christenhusz, M. M. J., Byng, J. W. (2016): The number of known plants species in the world and its annual increase. – Phytotaxa 261(3): 201-217.

[5] Costea, M., Brenner, D. M., Tardif, F. J., Tan, Y. F., Sun, M. (2006): Delimitation of *Amaranthus cruentus* L. and *Amaranthus caudatus* L. using micromorphology and AFLP analysis: an application in germplasm identification. – Genetic Resources and Crop Evolution 53: 1625-1633.

http://www.aloki.hu ● ISSN 1589 1623 (Print) ● ISSN 1785 0037 (Online)
DOI: http://dx.doi.org/10.15666/aeer/1706_1359313605

[6] De Micco, V., Arena, C., Vitale, L., Aronne, G. (2011): Anatomy and photochemical behaviour of Mediterranean *Cistus incanus* winter leaves under natural outdoor and warmer indoor conditions. – Botany 89: 677-688.
[7] Fank-De-Carvalho, S. M., Gomes, M. R. de A., Silva, P. Í. T., Báo, S. N. (2010): Leaf surfaces of *Gomphrena* spp. (Amaranthaceae) from Cerrado biome. – Biocell 34(1): 23-35.
[8] Jimoh, M. O., Olowokudejo, J. D. (2017): Leaf epidermal morphology and petiole anatomy of the genus *Anthocleista* Afzel. ex R. Br . (Gentianaceae). – Journal of Tropical Agriculture 55(2): 121-133.
[9] Jimoh, M. O., Afolayan, A. J., Lewu, F. B. (2018): Suitability of *Amaranthus* species for alleviating human dietary deficiencies. – South African Journal of Botany 115: 65-73. https://doi.org/10.1016/j.sajb.2018.01.004.
[10] Jimoh, M. O., Afolayan, A. J., Lewu, F. B. (2019a): Germination response of *Amaranthus caudatus* L. to soil types and environmental conditions. – Thaiszia Journal of Botany 29(1): 85-100.
[11] Jimoh, M. O., Afolayan, A. J., Lewu, F. B. (2019b): Antioxidant and phytochemical activities of *Amaranthus caudatus* L. harvested from different soils at various growth stages. – Scientific Reports 9: 12965
[12] Juan, R., Pastor, J., Alaiz, M., Vioque, J. (2007): Electrophoretic characterization of *Amaranthus* L. seed proteins and its systematic implications. – Botanical Journal of the Linnean Society 155(1): 57-63.
[13] Kadereit, G., Borsch, T., Weising, K., Freitag, H. (2003): Phylogeny of Amaranthaceae and Chenopodiaceae and the evolution of C4 photosynthesis. – International Journal of Plant Sciences 164(6): 959-986.
[14] Maherali, H., Reid, C. D., Polley, H. W., Johnson, H. B., Jackson, R. B. (2002): Stomatal acclimation over a sub ambient to elevated CO2 gradient in a C3/C4 grassland. – Plant, Cell and Environment 25(4): 557-566. http://doi.wiley.com/10.1046/j.1365-3040.2002.00832.x 23 December 2018.
[15] Munien, P., Naidoo, Y., Naidoo, G. (2015): Micromorphology, histochemistry and ultrastructure of the foliar trichomes of *Withania somnifera* (L.) Dunal (Solanaceae). – Planta 242(5): 1107-1122.
[16] Ogundipe, O. T., Kadiri, A. B. (2012): Comparative foliar epidermal morphology of the West African species of Amaranthaceae Juss. – Feddes Repertorium 123(2): 97-116.
[17] Ogundola, A. F., Bvenura, C., Afolayan, A. J. (2017): Morphological assessment of the roots, stems and leaves of *Solanum nigrum* L. Cultivated on different soil types. – Applied Ecology and Environmental Research 15(1): 787-798.
[18] Olesen, T., Moldrup, P., Gamst, J. (1999): Solute Diffusion and Adsorption in Six Soils along a Soil Texture Gradient. – Soil Science Society of America Journal 63(3): 519-524. https://www.soils.org/publications/sssaj/abstracts/63/3/SS0630030519 4 April 2019.
[19] Pillitteri, L. J., Torii, K. U. (2012): Mechanisms of Stomatal Development. – The Annual Review of Plant Biology 63: 591-614. www.annualreviews.org (accessed on 4 April 2019).
[20] Rabot, E., Wiesmeier, M., Schlüter, S., Vogel, H. J. (2018): Soil structure as an indicator of soil functions: a review. – Geoderma 314: 122-137. https://doi.org/10.1016/j.geoderma.2017.11.009.
[21] Rastogi, A., Shukla, S. (2013): Amaranth: a new millennium crop of nutraceutical values. – Critical Reviews in Food Science and Nutrition 53(2): 109-125.
[22] Rawls, W. J., Gish, T. J., Brakensiek, D. L. (1991): Estimating Soil Water Retention from Soil Physical Properties and Characteristics. – In: Stewart, B. A. (ed.) Advances in Soil Science. Springer-Verlag, New York, pp. 213-234. http://link.springer.com/10.1007/978-1-4612-3144-8_5 (accessed on 4 April 2019).
[23] Shah, S. N., Ahmad, M., Zafar, M., Razzaq, A., Malik, K., Rashid, N., Ullah, F., Iqbal, M., Zaman, W. (2018): Foliar epidermal micromorphology and its taxonomic

http://www.aloki.hu ● ISSN 1589 1623 (Print) ● ISSN 1785 0037 (Online)
DOI: http://dx.doi.org/10.15666/aeer/1706_1359313605

implications in some selected species of Athyriaceae. – Microscopy Research and Technique. https://doi.org/10.1002/jemt.23055.

[24] Sharaibi, O. J., Afolayan, A. J. (2017): Micromorphological characterization of the leaf and rhizome of *Agapanthus praecox* subsp. praecox Willd. (Amaryllidaceae). – Journal of Botany. https://doi.org/10.1155/2017/3075638.

[25] Stuessy, T. F. (2009): Plant Taxonomy : The Systematic Evaluation of Comparative Data. – Columbia University Press, New York.

[26] The Angiosperm Phylogeny Group (2009): An update of the Angiosperm phylogeny group classification for the orders and families of flowering plants: APG III. – Botanical Journal of the Linnean Society 161(2): 105-121.

[27] United States Department of Agriculture & Natural Resources Conservation Service (1983): National Soil Survey Handbook (NSSH). NRCS Soils. – https://www.nrcs.usda.gov/wps/portal/nrcs/detail/soils/ref/?cid=nrcs142p2_054242 (accessed on 5 April 2019).

[28] Viger, M., Hancock, R. D., Miglietta, F., Taylor, G. (2015): More plant growth but less plant defence? First global gene expression data for plants grown in soil amended with biochar. – GCB Bioenergy 7(4): 658-672.

[29] Wagner, G. J., Wang, E., Shepherd, R. W. (2004): New approaches for studying and exploiting an old protuberance, the plant trichome. – Annals of Botany 93(1): 3-11.

http://www.aloki.hu ● ISSN 1589 1623 (Print) ● ISSN 1785 0037 (Online)
DOI: http://dx.doi.org/10.15666/aeer/1706_1359313605

RAINFALL FREQUENCY ANALYSIS USING FRECHET AND LOG-LOGISTIC DISTRIBUTIONS OF SITES OF AZAD JAMMU AND KASHMIR, PAKISTAN

HUSSAIN, Z.[1*] – ABBAS, K.[2]

[1]*Research Center for Modelling and Simulation (RCMS), National University of Sciences and Technology (NUST), H-12, Islamabad, Pakistan*

[2]*Department of Statistics, University of Azad Jammu and Kashmir, Muzaffarabad, Pakistan (phone: +92-51-9085-5739)*

**Corresponding author*
e-mail: zami_cr@yahoo.com, zamir@rcms.nust.edu.pk

(Received 10th Apr 2019; accepted 4th Jul 2019)

Abstract. The paper illustrates the application of at-site frequency analysis using relatively non-traditional probability distributions adopting four methods of parameter estimation using annual maximum rainfall series (AMRS) (from 1980 to 2015) of three sites; Muzaffarabad, Garhi Dupatta and Kotli of Azad Jammu and Kashmir, Pakistan. Critical assumptions related to AMRS for frequency analysis have been validated through run test (to check the randomness of AMRS at each site) and Mann Whitney test (to check the distribution of AMRS at given sites as identical or not). Two probability distributions; Frechet and Log-logistic have been used as candidate distributions to model AMRS at given sites. The parameters of these distributions have been estimated using four methods; Probability Weighted Moments Estimation (PWME), Maximum Likelihood Estimation (MLE), Bayesian Estimation (BE) and Moments Estimation (ME) methods. The Kolmogorov Smirnov test has been used as goodness-of-fit criteria. The results show suitability of the selected probability distributions for the observed AMRS series at given sites with BE and MLE methods as adequate for estimation. Moreover, the results indicate that ME method is not a preferred choice for the estimation of parameters and quantiles for various return periods.
Keywords: *at-site frequency analysis, Bayesian estimation, maximum likelihood estimation, method of moments, probability weighted moments*

Introduction

Frequency analysis is a technique for estimation of a specific event that occurs frequently. Estimation of a return period of geophysical events, for instance, extreme rainfall or floods of a site or many sites (together, assuming a homogeneous region) which occurs rarely is a familiar problem in environmental engineering. For rainfall frequency analysis (RFA), usually, at site and regional approaches with various typical probability distributions are in practice for the estimation of quantiles. Success depends on the availability and span of the observed data along with nature of the associated variables (site characteristics) having strong correlations with the observed data series at given sites. With the introduction of several new class of probability distributions in the literature, it is very important to examine the suitability of these distributions with optimum method of estimation for analysing the extremes of geophysical, hydrological and meteorological events like earthquakes, floods, rainfall, etc. It will bring variability in the choice of selecting best-fit distribution for the estimation of extreme events. The current study has used two atypical probability distributions in the family of extreme value distributions namely Frechet distribution (FD) and Log-logistic distribution

http://www.aloki.hu ● ISSN 1589 1623 (Print) ● ISSN 1785 0037 (Online)
DOI: http://dx.doi.org/10.15666/aeer/1706_1360713623

(LLD), with four methods of estimation of parameters to estimate rainfall quantiles for T-years return period.

Climate is a composition of temperature, sunshine, pressure, wind speed, humidity, rainfall and clouds, etc. Rainfall is an important characteristic as it can cause disasters like land slide or floods if extremely befallen. Scarcity of rainfall also affects the water management systems hence impacts agricultural productions. Pakistan is a populated country, economy based on agriculture and high vulnerable index to ecological disasters, like rainfall and floods. Therefore, it is also important to have estimates of rainfall using suitable methods in numerous climate zones of the country. This study illustrates the results of at-site frequency analysis using two relatively new probability distributions with four methods of estimation using rainfall data of three sites of Azad Jammu and Kashmir, Pakistan. The results of this study will be useful in terms of introducing new probability distributions, to bring variety and flexibility in the choice of probability distributions, for modelling of extreme events with various methods of estimation. The estimated quantiles with best suitable estimation method(s) would also be useful for officials dealing with water resources management and disasters management of the study area.

Based on the aforementioned details, the major objectives of the study are:

- Assessing the suitability of FD and LLLD for modelling extremes of rainfall using four methods of estimation namely Maximum Likelihood Estimation (MLE), Bayesian Estimation (BE), Moments Estimation (ME) and Probability Weighted Moments Estimation (PWME)
- Estimating rainfall quantiles for various return periods of the most suitable method(s) of estimation

Moreover, to establish the usefulness of the adopted methodology, in general, the quantile estimates obtained through this study has been compared with the results of the previously published study. The comparison reveals that the results are comparable in terms of forecasting the magnitude of extreme events at given sites for shorter as well as longer return periods.

Literature review

Various probability distributions with different methods of estimations using regional as well as at-site approach have been applied in the literature for modelling rainfall data all over the world including Pakistan. Some of the published international and indigenous studies are summarized below.

International studies

Zalina et al. (2002) performed rainfall frequency analysis using eight probability distributions including Gamma, Generalized Normal, Generalized Pareto, Generalized Extreme Value, Gumbel, Log Pearson Type III, Pearson Type III and Wakeby distribution to estimate extreme rainfall in Malaysia. The variable of analysis was annual maximum rainfall series of seventeen stations located in Peninsular Malaysia. The study concluded that the Generalized Extreme Value distribution is the most appropriate distribution for the study area.

Mohamed and Ibrahim (2016) analyzed annual rainfall data for fourteen rainfall stations in Sudan. Five distributions namely Normal, Log Normal, Gamma, Weibull and

http://www.aloki.hu ● ISSN 1589 1623 (Print) ● ISSN 1785 0037 (Online)
DOI: http://dx.doi.org/10.15666/aeer/1706_1360713623

Exponential have been used and the study concluded that Normal and Gamma distributions are suitable probability distributions to model rainfall data.

Bahrawi (2018) investigates annual rainfall data of more than 20 stations in Makkah Al-Mukarramah, Saudi Arabia using Lognnormal, Normal, Extreme Value Type I, Pearson Type III and Log-Pearson Type III distributions. Different distributions have been identified as best-fitted distribution for different regions with suitability of Log-normal for 36% of the rainfall stations.

Few other studies include the work of Mo et al. (2019) in South China using Generalized Extreme Value and Generalized Pareto distributions with MLE method for analyzing rainfall data of eight gauging stations and concluded that Generalized Pareto distribution performed better relative to Generalized Extreme Value distribution. Liang et al. (2017) performed L-moments based regional frequency analysis and compared the results with at-site analysis using Generalized Extreme Value distribution analyzing rainfall data in the Taihu basin China; Wang et al. (2017) applied regional approach using fuzzy c-means and L-moments to analyze precipitation extremes in Mainland China; and Alam et al. (2018) performed at-site rainfall frequency analysis using Generalized Extreme Value, Pearson Type III and Log Pearson Type III probability distributions for various sites of Bangladesh and concluded that different probability distributions are suitable for different sites with Generalized Extreme Value distribution suitable for 36% of the stations.

Case studies of Pakistan

There are few published studies performing rainfall frequency analysis of different sites/areas of Pakistan using at-site or regional approach with various probability distributions using different methods of estimation of parameters and quantiles. Some of them are briefly summarized below:

Amin et al. (2016) performed at-site frequency analysis using four probability distributions; Log Pearson Type-III, Normal, Gumbel Maximum and Log-Normal distributions to model annual maximum rainfall for sites in the northern areas of Pakistan. The study concluded that the Normal and Log Pearson Type-III distributions are best-fit distributions for the study area. Iqbal and Ali (2013) performed at-site frequency analysis using extreme annual rainfall of four cities of Punjab and concluded that the General Extreme Value distribution is the best-fitted distribution for the study area. Shahzadi (2013) and Shahzadi et al. (2013) performed L-moments based regional frequency analysis using annual maximum rainfall series of 23 stations of Pakistan. The study area was divided into three homogenous regions. The study concluded that Generalized Normal, Generalized Extreme Value and Generalized Logistic distributions are suitable to model the observed data series for the regions under study. The study area of Shahzadi et al. (2013) includes the sites used in this study with similar variable of analysis, i.e. annual maximum rainfall series. Therefore, a comparison of the estimates provided by Shahzadi et al. (2013) with the results of current study has been provided in the later section of the paper, to establish the usefulness of the current methodology. In another study, Hussain et al. (2017) illustrated the application of regional rainfall frequency analysis using rainfall data of seven sites of Sindh, Pakistan with annual maximum monthly rainfall totals as variable of analysis. The study concluded that three distributions namely: Generalized Normal, Pearson Type III and Generalized Pareto are suitable for the observed data series of the study region. Ahmad et al. (2017) performed L-moments based regional frequency analysis using annual total

http://www.aloki.hu ● ISSN 1589 1623 (Print) ● ISSN 1785 0037 (Online)
DOI: http://dx.doi.org/10.15666/aeer/1706_1360713623

rainfall of 30 met sites of Pakistan. The study area (includes sites from Sindh, Punjab, Balochistan and Northern Areas) was divided into four homogeneous regions with different three-parameters probability distributions identified as best-fitted probability distributions. Ahmad et al. (2016) performed at site frequency analysis using annual daily maximum rainfall series. Different probability distributions have been used with methods of estimations as L-moments, TL moments and LH moments. The study area includes 9 sites from Sindh, 7 sites from Balochistan, 6 sites from Punjab, 3 sites from Khyber Pakhtunkhwa and 3 sites from Northern Areas of Pakistan. Hussain et al. (2010) applied Box-cox transformed hierarchical Bayesian multivariate spatio-temporal interpolation method to estimate space time monthly precipitation in the monsoon periods during 1974 to 2000, using 27 years monthly average rainfall data of 51 stations in Pakistan. Khan et al. (2017) performed regional frequency analysis using monthly precipitation data from 1999 to 2012 at 17 stations of Northern areas and Khyber Pakhtunkhwa. L-moments and partial L-moments have been used as estimation methods with four three-parameter probability distributions. The study concluded the suitability of Generalized Pareto distribution using L-moments and Generalized Normal distribution using partial L-moments for the study region.

The aforementioned details show that both at-site and regional approaches have been adopted to analyse rainfall frequency analysis in Pakistan using some typical probability distributions with various methods of estimation of parameters but non of the studies have used FD and LLD to model the extremes of rainfall in Pakistan.

Materials and methods

Study area and data utilized

The study area consists of three sites of Azad Jammu and Kashmir (AJ&K) namely Muzaffarabad, Kotli and Garhi Dupatta. AJ&K commonly known as Pakistan administered Kashmir borders Pakistan's Punjab province to the south and Khyber Pakhtunkhwa province to the west. It has a total area of 13,297 km^2 with a total population of 4,045,366 as per the 2017 census of Pakistan. The northern part of AJ&K encompasses the lower area of the Hamalayas. The region receives rainfall in both the winter and the summer. However, in the summer season, monsoon floods of the rivers Jhelum and Leepa are common due to extreme rainfall and snow melting. The southern parts of AJ&K including Kotli usually have extremely hot weather in summers and moderate cold weather in winters. This area receives rainfall mostly in monsoon (from June to September). The central and the northern parts of AJ&K including Muzaffarabad have moderate hot weather in summers and very cold (chilly) in winter with snowfall occurs in December and January.

Annual maximum rainfall series (AMRS) in millimeters, i.e. maximum value from the daily rainfall record of each year has been selected for the analysis, which usually considered as an important variable for rainfall frequency analysis as used in a number of case studies mentioned in the literature review section. Data for the years 1980 to 2015 have been used, provided by Pakistan Meteorological Department, head office Karachi, Pakistan. The site characteristics along with few summary statistics and geographical locations of the three sites are presented in *Table 1* and *Figure 1*, respectively. The descriptive statistics provided in *Table 1* are useful to understand the general trends and tendencies of AMRS at given sites.

http://www.aloki.hu ● ISSN 1589 1623 (Print) ● ISSN 1785 0037 (Online)
DOI: http://dx.doi.org/10.15666/aeer/1706_1360713623

Among the three sites, Garhi Dupatta has the highest average value of observed AMRS as 75.72 mm whereas the average of observed AMRS at Kotli and Muzaffarabad is 59.91 mm and 74.46 mm, respectively. To observe the dispersion around mean of the given data series, standard deviation has been calculated which shows that there exist variations in the observed data series at different sites. The highest variation has been observed in AMRS of site Muzaffarabad.

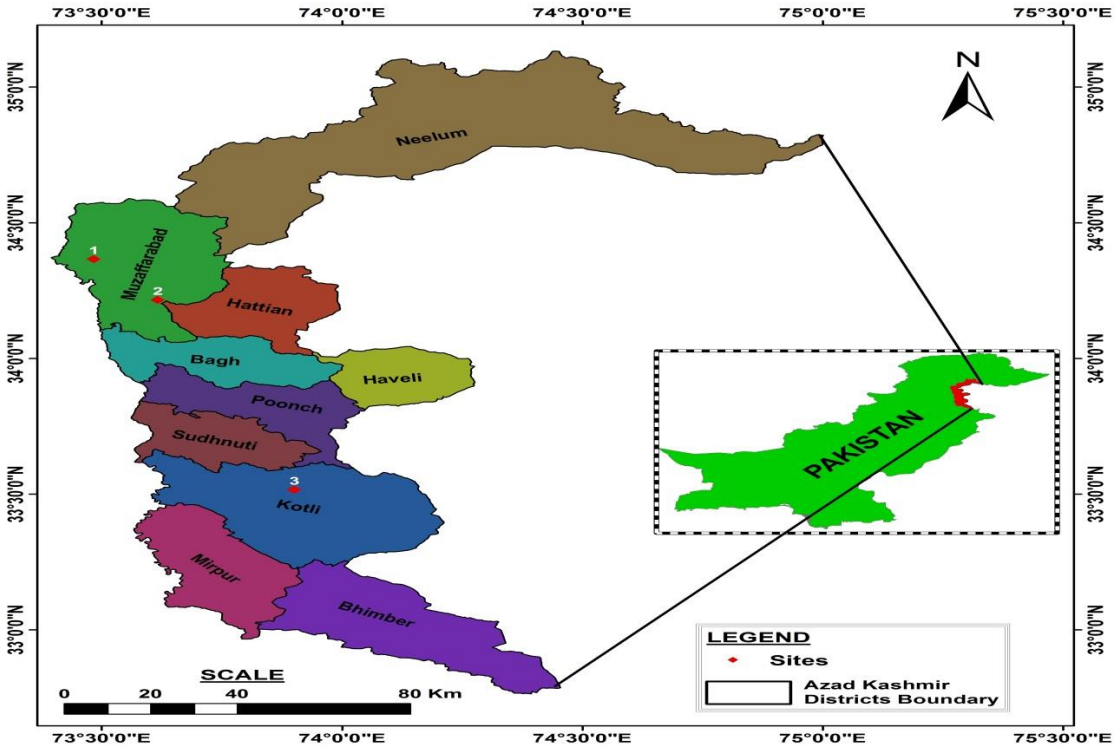

Figure 1. *Study area and geographical locations of the three sites of AJ&K, Pakistan*

Table 1. *Site characteristics and descriptive statistics of the data series at three sites*

Site name	Lat	Lon	Ele (m)	n	Mean (mm)	SD (mm)	CV	Min (mm)	Max (mm)	Skew
Garhi Dupatta	34°13’	73°37’	813.50	36	75.72	11.32	14.95	32.15	184.27	1.12
Kotli	33°31’	73°54’	614.00	36	59.91	24.55	40.98	28.72	129.28	1.29
Muzaffarabad	34°22’	73°29’	702.04	36	74.46	31.43	42.21	30.55	153.98	1.09

Lat, Lon, and Ele are the Latitude, Longitude and Elevation of the sites, mm denotes millimeters while n, SD, CV, Min, Max and Skew are the number of observations, standard deviation, coefficient of variation, minimum value, maximum value and moments measure of skewness of the observed data series at each site, respectively

Coefficient of variation (CV) has been calculated as a relative measure of dispersion. The values of CV show that the least consistency exists in AMRS of Muzaffarabad, followed by Kotli and Garhi Dupatta. The coefficient of skewness ranges from 1.09 to 1.29 indicates that the distribution associated to the observed data series at these sites is positively skewed (non-normal). Therefore, it would be appropriate to select positively skewed distribution(s) as candidate(s) for the observed data series at given sites. The

http://www.aloki.hu ● ISSN 1589 1623 (Print) ● ISSN 1785 0037 (Online)
DOI: http://dx.doi.org/10.15666/aeer/1706_1360713623

maximum of the observed AMRS at respective sites so far is 184.27 mm at Garhi Dupatta, 129.28 mm at Kotli and 153.98 mm at Muzaffarabad.

For rainfall frequency analysis, there exists certain commonly used probability distributions with variations in the methods of estimation as discussed in the literature review. However, this study has introduced FD and LLD to model the rainfall data at given sites using different methods of estimation. The illustration of the results of this application provides flexibility to the researchers performing inferential statistics of extreme events using probability distribution(s).

Basic assumptions of the observed data series

The procedure of rainfall frequency analysis is usually based on few assumptions related to the observed data series at given sites. For instance, the observed data series at given sites is random and identically distributed. Therefore, to check these assumptions Run test for randomness (Bradley, 1968) and Maan-Whitney test (Mann and Whitney, 1947) for identical distribution of the data series at given site have been utilized. Furthermore, Kolmogorov Smirnov (KS) test has been used as goodness-of-fit measure.

Estimation methods

For the two selected probability distributions, i.e. FD and LLD, four estimation methods, i.e. MLE, PWME, ME and BE methods have been used for the estimation of parameters and quantiles. Few details related to the procedures are:

FD was introduced by Maurice Frechet in 1927 for largest extremes (Frechet, 1927). It is a special case of Extreme value distribution (EVDs) and used to model the extreme events like floods, maximum rainfall, river discharge in hydrology, etc. The reason for selecting this probability distribution for the analysis is that various published studies related to rainfall frequency analysis found Generalized Extreme Value distribution as appropriate to model extremes of rainfall in Pakistan. Therefore, the idea is to provide a suitable alternative to bring flexibility in the choice of available probability distributions for modeling rainfall data. The probability density function (PDF) of FD is

$$f(x,\alpha,\beta) = \frac{\alpha}{\beta}\left(\frac{\beta}{x}\right)^{\alpha+1} exp\left[-\left(\frac{\beta}{x}\right)^{\alpha}\right], x > 0, \alpha, \beta > 0, \quad \text{(Eq.1)}$$

where α is the shape parameter and β is the scale parameter.

The LLD is also a type of extreme value distribution. It can be used for model the extreme values like maximum daily one day rainfall, river discharge per day or per month, etc. The PDF of LLD is:

$$f(x,\alpha,\beta) = \frac{\left(\frac{\beta}{\alpha}\right)\left(\frac{x}{\alpha}\right)^{\beta-1}}{\left[1+\left(\frac{x}{\alpha}\right)^{\beta}\right]^2}, x > 0, \alpha, \beta > 0, \quad \text{(Eq.2)}$$

where α is scale and β is shape parameter.

Estimates of parameters for FD using MLE

Let $x_1, x_2, , x_3, , \ldots, x_n$ be a random sample of size 'n' from two parameters FD, then the likelihood of function of *Equation 1* is:

http://www.aloki.hu ● ISSN 1589 1623 (Print) ● ISSN 1785 0037 (Online)
DOI: http://dx.doi.org/10.15666/aeer/1706_1360713623

$$L(x,\alpha,\beta) = \alpha^n \beta^{n\alpha} \pi_{i=1}^n x_i^{-(\alpha+1)} \exp\left[-\sum_{i=1}^n \left(\frac{\beta}{x_i}\right)^\alpha\right], \quad \text{(Eq.3)}$$

The log-likelihood function is:

$$logL(x,\alpha,\beta) = nlog\alpha + n\alpha log\beta - (\alpha+1)\sum_{i=1}^n logx_i - \sum_{i=1}^n \left(\frac{\beta}{x_i}\right)^\alpha, \quad \text{(Eq.4)}$$

The score equations are

$$\frac{\partial logL}{\partial \alpha} = \frac{n}{\alpha} + nlog\beta - \sum_{i=1}^n logx_i - \sum_{i=1}^n \left(\frac{\beta}{x_i}\right)^\alpha \log\left(\frac{\beta}{x_i}\right) = 0, \quad \text{(Eq.5)}$$

$$\frac{\partial logL}{\partial \beta} = \frac{n\alpha}{\beta} - \alpha\beta^{(\alpha-1)} \sum_{i=1}^n \left(\frac{1}{x_i}\right)^\alpha = 0. \quad \text{(Eq.6)}$$

The above equations cannot be written in closed form, therefore, the BFGS (Broyden Fletcher GoldFarb Shanno), available in the R software, have been used to estimate α and β with MLE.

Estimates of parameters for FD using PWME

The Probability weighted Moments proposed by Greenwood et al. (1979) has the following form

$$M_{p,r,s} = \int X^p \{F(x)^r\}\{1-F(x)\}^s dF(x), \quad \text{(Eq.7)}$$

Hosking et al. (1985) presented the special case

$$B_r = E[X\{F(X)\}^r], r = 0,1,2,3,\ldots \quad \text{(Eq.8)}$$

For any population, the r^{th} non-central moments can be expressed as

$$\alpha_r = M_{1,0,r} = E[X\{1-F(X)\}^r], \quad \text{(Eq.9)}$$

by putting r = 1, 0 in *Equation 9*,

$$\alpha_0 = \beta\tau\left(1-\frac{1}{\alpha}\right), \alpha > 1, \quad \text{(Eq.10)}$$

$$\alpha_1 = \frac{\beta\tau(1-\frac{1}{\alpha})(2-2^{\frac{1}{\alpha}})}{2}, \quad \text{(Eq.11)}$$

from observed sample, the corresponding r^{th} moments are

$$a_r = n^{-1} \frac{\sum_{i=1}^n \binom{n-i}{r} X_i}{\binom{n-1}{r}}, \quad \text{(Eq.12)}$$

by substituting r = 1, 0 in *Equation 12*,

http://www.aloki.hu ● ISSN 1589 1623 (Print) ● ISSN 1785 0037 (Online)
DOI: http://dx.doi.org/10.15666/aeer/1706_1360713623

$$a_0 = \bar{X}, \quad \text{(Eq.13)}$$

$$a_1 = \frac{\sum_{i=1}^{n}(n-1)x_i}{n(n-1)}, \quad \text{(Eq.14)}$$

Then equating *Equations 10* and *11* to *Equation 13* and *14*, estimates of α and β for FD using PWME are:

$$\hat{\alpha}_{PWM} = \frac{log2}{log2+loga_0-loga_1}, \quad \text{(Eq.15)}$$

$$\hat{\beta}_{PWM} = \frac{\bar{X}}{\tau(1-\frac{1}{\alpha})}, \alpha > 1 \quad \text{(Eq.16)}$$

Estimates of parameters for FD using ME

The r^{th} moment for FD is

$$E(X^r) = \beta^r \tau\left(1-\frac{r}{\alpha}\right), \quad \text{(Eq.17)}$$

by substituting r = 1, 2 respectively in *Equation 17*, the first and second moments for FD, i.e.

$$m_1^* = \bar{X}, \quad \text{(Eq.18)}$$

$$m_2^* = E(X^2) = \beta^2 \tau\left(1-\frac{2}{\alpha}\right), \quad \text{(Eq.19)}$$

By solving *Equations 18* and *19* using iterative method, the estimates of α and β for FD using ME can be obtained.

Estimates of parameters for FD using BE

The estimates of α and β using BE can be obtained by considering the reference prior, developed by Abbas and Tang (2015), i.e.

$$\pi_R(\alpha,\beta) = \frac{1}{\alpha\beta}, \quad \text{(Eq.20)}$$

Then the joint posterior distribution for α and β is

$$\pi_{(\alpha,\beta|x)} = \frac{\alpha^{n-1}\beta^{n\alpha-1}\pi_{i=1}^{n}x_i^{-(\alpha+1)}\exp[-\sum_{i=1}^{n}(\frac{\beta}{x_i})^{\alpha}]}{\int_0^{\infty}\int_0^{\infty}\alpha^{n-1}\beta^{n\alpha-1}\pi_{i=1}^{n}x_i^{-(\alpha+1)}\exp[-\sum_{i=1}^{n}(\frac{\beta}{x_i})^{\alpha}]d\alpha d\beta}, \quad \text{(Eq.21)}$$

Laplace approximation can be used to obtain the estimates of α and β using BE.

Estimates of parameters for LLD using MLE

Let $x_1, x_2, , x_3, , \ldots, x_n$ be a random sample of size 'n' from LLD, then the likelihood of function of *Equation 2* is:

http://www.aloki.hu ● ISSN 1589 1623 (Print) ● ISSN 1785 0037 (Online)
DOI: http://dx.doi.org/10.15666/aeer/1706_1360713623

$$L(x_i;\alpha,\beta) = \beta^n \alpha^{-n\beta} \pi_{i=1}^n x_i^{\beta-1} \pi_{i=1}^n [1 + \left(\frac{x_i}{\alpha}\right)^{\alpha}]^{-2}, \quad \text{(Eq.22)}$$

Then the log-likelihood function can be written as:

$$logL(x_i;\alpha,\beta) = nlog\beta - n\beta log\alpha + (\beta-1)\sum_{i=1}^{n} logx_i - 2\sum_{i=1}^{n} \log\left[1 + \left[\frac{x_i}{\alpha}\right]^{\beta}\right], \quad \text{(Eq.23)}$$

Derivatives of *Equation 23* with respect to α and β are:

$$\frac{\partial logL}{\partial \alpha} = -\frac{n\beta}{\alpha} + \frac{2\beta}{\alpha}\sum_{i=1}^{n} \frac{(\frac{x_i}{\alpha})^{\beta}}{(1+(\frac{x_i}{\alpha})^{\beta})} = 0, \quad \text{(Eq.24)}$$

$$\frac{\partial logL}{\partial \beta} = \frac{n}{\beta} - nlog\alpha + \sum_{i=1}^{n} logx_i - 2\sum_{i=1}^{n} \frac{(\frac{x_i}{\alpha})^{\beta} \log(\frac{x_i}{\alpha})}{\left[1+(\frac{x_i}{\alpha})^{\beta}\right]} = 0. \quad \text{(Eq.25)}$$

Equations 24 and *25* do not have a closed form solution. Therefore, these may be solved to obtain the estimates of parameters of LLD using BFGS method which is available in R software.

Estimates of parameters for LLD using PWME

The estimates of α and β can be obtained as:

$$\beta_r = \frac{\alpha\Gamma(\frac{1}{\beta}+r+1)\Gamma(1-\frac{1}{\beta})}{\Gamma(r+2)}, \quad \text{(Eq.26)}$$

by putting $r = 0, 1$ respectively, in *Equation26*, we get

$$\beta_0 = \alpha\Gamma\left(\frac{1}{\beta}+1\right)\Gamma\left(1-\frac{1}{\beta}\right), \quad \text{(Eq.27)}$$

$$\beta_1 = \frac{\alpha}{2}\Gamma(\frac{1}{\beta}+2)\Gamma\left(1-\frac{1}{\beta}\right), \quad \text{(Eq.28)}$$

Their corresponding sample moments are

$$\widehat{\beta_r} = \frac{\sum_{i=1}^{n} \binom{i-1}{r} x_i}{n\binom{n-1}{r}}, \quad \text{(Eq.29)}$$

put $r = 0, 1$ respectively, in *Equation29*, we have

$$\hat{\beta}_0 = \bar{X}, \quad \text{(Eq.30)}$$

$$\widehat{\beta_1} = \sum_{i=1}^{n} \frac{x_i(i-1)}{n(n-1)}. \quad \text{(Eq.31)}$$

By comparing *Equantion27* and *Equation28* to *Equantion30* and *Equation31*, estimates of α and β through PWME can be obtained.

http://www.aloki.hu ● ISSN 1589 1623 (Print) ● ISSN 1785 0037 (Online)
DOI: http://dx.doi.org/10.15666/aeer/1706_1360713623

Estimates of parameters for LLD using ME method

The r^{th} moment for LLD is:

$$E(X^r) = \int_0^\infty x^r f(x;\alpha,\beta)dx, \quad \text{(Eq.32)}$$

$$E(X^r) = \alpha^r \Gamma\left(\frac{r}{\beta}+1\right)\Gamma\left(1-\frac{r}{\beta}\right), \quad \text{(Eq. 33)}$$

By putting r = 1, 2 respectively in *Equation33*, the first and second moments for LLD are:

$$m_1^* = E(X) = \alpha\Gamma\left(\frac{1}{\beta}+1\right)\Gamma\left(1-\frac{1}{\beta}\right) = \bar{X}, \quad \text{(Eq.34)}$$

$$m_2^* = E(X^2) = \alpha^2\Gamma\left(\frac{2}{\beta}+1\right)\Gamma\left(1-\frac{2}{\beta}\right). \quad \text{(Eq.35)}$$

By solving *Equation34* and *Equantion35* by iterative method, the estimates of α and β through ME can been obtained.

Estimates for LLD using BE

Estimates of parameters for LLD using BE are obtained by considering the reference prior developed by Abbas and Tang (2016). The joint posterior distribution of α and β is:

$$\pi_{(\alpha,\beta|x)} = \frac{\alpha^{-n\beta-1}\beta^{n-1}\pi_{i=1}^n x_i^{\beta-1}\pi_{i=1}^n[1+\left(\frac{x_i}{\alpha}\right)^\beta]^{-2}}{\int_0^\infty\int_0^\infty \alpha^{-n\beta-1}\beta^{n-1}\pi_{i=1}^n x_i^{\beta-1}\pi_{i=1}^n[1+(\frac{x_i}{\alpha})^\beta]^{-2}d\alpha d\beta}. \quad \text{(Eq.36)}$$

Here Metropolis within Gibbs sampling algorithm has been used to obtain the Bayesian estimates.

Results and discussion

Initial data screening

To check for the randomness and identical distribution of the observed data series at given sites, *Table 2* illustrates the results of Run test and Maan-Whitney statistics (W). The corresponding p-values of observed number of runs indicates that the AMRS at given sites is random. For the calculation of W, the data series at each site has been divided into two groups. The corresponding p-values of W provide sufficient evidence that the observed data series at each site is identically distributed. Both the tests (Run test and Maan-Whitney) have been performed using 5% level of significance.

Estimation of probability distributions

The estimates of parameters of the two selected probability distributions along with p-values of Kolmogorov Smirnov (KS) test (used as a goodness of fit measure) are illustrated in *Table 3*. Based on the corresponding p-values, in general, all the methods of estimation have passed the goodness of fit criteria for the three sites considering both

http://www.aloki.hu ● ISSN 1589 1623 (Print) ● ISSN 1785 0037 (Online)
DOI: http://dx.doi.org/10.15666/aeer/1706_1360713623

the selected probability distributions at 5 percent level of significance. However, observing closely, the values of ME have the highest value of KS statistic so as the lowest p-values for both the probability distributions for the three sites. It indicates that the method of moments may not be a preferable choice for the estimation of parameters for the given data series at three sites. These results are consistent with the general practice of the application of extreme value probability distributions that the methods of moments is not an optimal choice for the data series having skewed distribution.

In particular, for FD the corresponding p-values of KS test are approximately similar with MLE and BE methods for Garhi Dupatta and Muzaffarabad, while PWME method have near similar tendency to MLE and BE as the skewness in the observed data series increases for the site Kotli. Similar tendencies hold for LLD (with PWME having similar tendency comparable to MLE and BE for Garhi Dupatta and Muzaffarabad); while MLE method outperforms for the site Kotli. Therefore, the results suggest that both the distributions (FD and LLD) using MLE and BE methods are suitable (with PWME method as a good alternative, if the observed data series exhibit large skewness) for modeling extremes of rainfall.

To graphically visualize the performance of both the probability distributions with four methods of estimation, the plots of probability density functions of FD and LLD have been constructed and presented in *Figure 2*. These graphs also suggest that, in general; the selected distributions are suitable for the observed data series at given sites. Particularly, for LLD, the behavior of pdf with BE method is relatively different for the sites Kotli and Muzaffarabad; while for the site Garhi Dupatta with PWME the curve seems to fit the observed data adequately and the performance of MLE, BE and ME methods is approximately similar. On the other hand, for FD, the graph using BE and MLE are comparable for all the three sites. These results are consistent with the findings of KS test.

Based on the aforementioned details both the distributions are suitable to model the extremes of rainfall with MLE or BE as preferred methods of estimation.

The quantile estimates for various return periods for each site can be obtained using the quantile function of the selected probability distribution(s). These quantiles have been calculated using MLE, BE and PWME methods (as ME is not a preferred choice of estimation). The results are illustrated in *Table 4*. The results of *Table 4* show that the estimated quantiles for F = 0.90 (10 year return period) and so on are greater than the average values of AMRS at given site. Moreover, the magnitude of 100 year return period is greater the maximum value of the observed AMRS (see *Table 1*) for the three sites (for both the probability distributions). These results are useful for the officials and researchers dealing with disasters and water resources management of the study for proper planning and effective management.

Table 2. *Results of run test and Maan-Whitney (W) statistics*

Site name	n	Runs	P-values	Groups	W	P-values
Garhi Dupatta	36	17	0.6920	18, 18	339	0.8619
Kotli	36	19	0.7510	18, 18	340	0.8371
Muzaffarabad	36	20	0.6750	18, 18	346	0.6927

n is the number of observations at each site, Runs are the observed number of runs, W is the calculated test statistic for Maan-Whitney test. These tests are performed at 5% level of significance

http://www.aloki.hu ● ISSN 1589 1623 (Print) ● ISSN 1785 0037 (Online)
DOI: http://dx.doi.org/10.15666/aeer/1706_1360713623

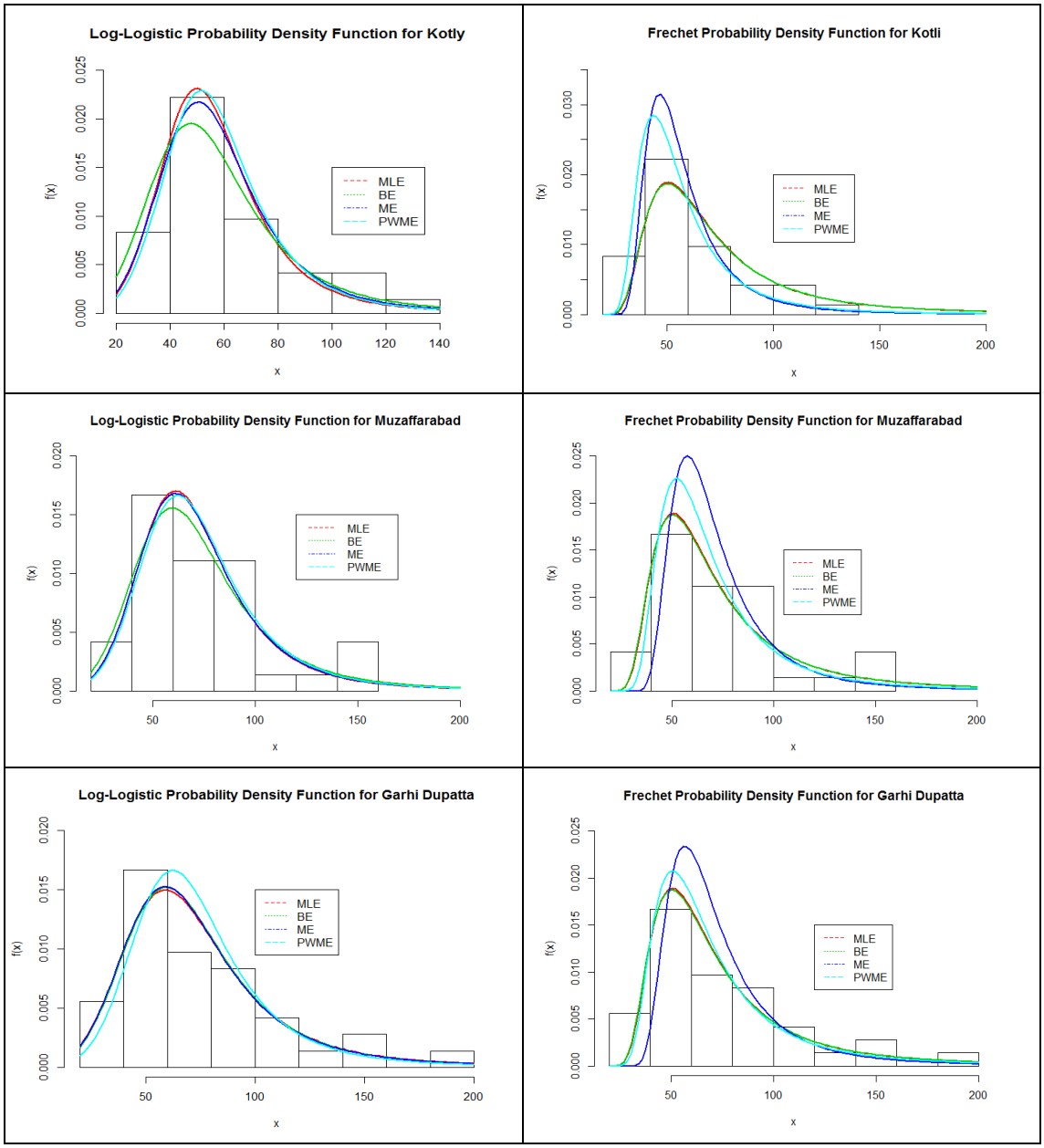

Figure 2. *Plots of probability density function of Log-Logistic and Frechet distribution for three sites using four estimation methods*

Table 3. *Estimates of parameters and goodness of fit measure for FD and LLD*

For FD

Muzaffarabad				
Methods	**A**	**B**	**KS**	**P-values**
MLE	2.7462	56.6804	0.0971	0.8539
BE	2.7103	56.5792	0.0995	0.8336
ME	4.0172	60.8367	0.1344	0.4912
PWME	3.3454	57.4418	0.1269	0.5645

http://www.aloki.hu ● ISSN 1589 1623 (Print) ● ISSN 1785 0037 (Online)
DOI: http://dx.doi.org/10.15666/aeer/1706_1360713623

Garhi Dupatta				
MLE	2.5047	55.0170	0.1026	0.8056
BE	2.4705	54.8953	0.1014	0.8162
ME	3.7203	60.5172	0.1778	0.1817
PWME	3.0015	55.9328	0.1281	0.5523
Kotli				
MLE	3.2386	46.9789	0.0924	0.8899
BE	3.1941	46.9301	0.0929	0.8868
ME	4.1011	49.2182	0.1258	0.5749
PWME	3.5121	47.0087	0.0965	0.8587
For LLD				
Muzaffarabad				
Methods	**A**	**B**	**KS**	**P-values**
MLE	68.0016	4.3984	0.0855	0.9346
BE	67.9053	3.9635	0.0687	0.9913
ME	69.2406	4.7908	0.1183	0.6507
PWME	68.1396	4.3437	0.0852	0.9363
Garhi Dupatta				
MLE	67.9686	3.7960	0.0795	0.9631
BE	68.0521	3.8644	0.0825	0.9502
ME	69.3718	4.3719	0.11589	0.6761
PWME	67.5925	3.8496	0.0758	0.9757
Kotli				
MLE	54.3723	4.8122	0.0906	0.9036
BE	54.0521	3.9565	0.1097	0.7381
ME	55.9075	4.9094	0.1243	0.5908
PWME	55.3301	4.5832	0.1115	0.7200

MLE, BE, ME and PWME are estimates using Maximum Likelihood Estimation, Bayesian Estimation, Moments Estimation and Probability Weighted Moments Estimation methods. KS are the calculated values of Kolmogorov Smirnov test

Table 4. *Quantiles estimates for various return periods for each site using selected probability distributions and three methods of estimation*

For Muzaffarabad						
Distributions	**Estimation methods**	**Quantile estimates (in millimeters) with non-exceedance probability F/return period (years)**				
		0.10/(1)	**0.50/(2)**	**0.90/(10)**	**0.99/(100)**	**0.999/(1000)**
Frechet	MLE	41.83	64.77	128.62	302.63	701.09
	BE	41.59	64.77	129.79	308.87	723.54
	PWME	49.43	66.65	106.52	191.20	339.55
Log-Logistic	MLE	41.26	68.00	112.07	193.30	326.96
	BE	39.01	67.91	118.21	216.47	387.88
	PWME	41.75	69.24	109.43	114.83	339.56

http://www.aloki.hu ● ISSN 1589 1623 (Print) ● ISSN 1785 0037 (Online)
DOI: http://dx.doi.org/10.15666/aeer/1706_1360713623

For Garhi Dupatta

Distributions	Estimation methods	Quantile estimates (in millimeters) with non-exceedance probability F/return period (years)				
		0.10/(1)	**0.50/(2)**	**0.90/(10)**	**0.99/(100)**	**0.999/(1000)**
Frechet	MLE	39.44	63.69	135.11	345.24	867.28
	BE	39.17	63.67	136.50	353.35	899.03
	PWME	42.36	63.20	118.38	258.98	558.59
Log-Logistic	MLE	38.10	67.97	121.25	228.05	419.27
	BE	38.54	68.05	120.16	223.49	406.49
	PWME	38.20	67.59	119.61	223.00	406.53

For Kotli

Distributions	Estimation methods	Quantile estimates (in millimeters) with non-exceedance probability F/return period (years)				
		0.10/(1)	**0.50/(2)**	**0.90/(10)**	**0.99/(100)**	**0.999/(1000)**
Frechet	MLE	36.31	52.61	94.11	194.43	396.43
	BE	36.15	52.64	94.93	198.11	407.96
	PWME	37.07	52.18	89.22	174.19	335.99
Log-Logistic	MLE	34.44	54.37	85.83	141.28	228.40
	BE	31.01	54.05	94.19	172.67	309.71
	PWME	34.26	55.33	89.37	150.80	249.71

Comparison with previously published study

Though the illustrated results of this study indicates that the selected probability distributions are suitable to model the rainfall data at given sites so as the estimated quantiles are useful but the precedence through practical comparison of the adopted methodology (as an acceptable alternative to the conventional methods) is still requisite. To do so, the quantile estimates for 1, 10 and 100 year return period of this study have been compared with the quantiles provided by Shahzadi et al. (2013). Few details of the comparison are: the study of Shahzadi et al. (2013) has been selected as it is the only study with similar variable for analysis, i.e. annual maximum rainfall series and the same set of sites. The sites Muzaffarabad, Garhi Dupatta and Kotli were included in Region 2 by Shahzadi et al. (2013) and Generalized Extreme Value, Generalized Normal and Generalized Logistic distributions identified as regional distributions (for more details and regional quantiles see *Table 5* of Shahzadi et al., 2013). Those estimated regional quantiles are utilized to estimate the quantiles for the specific sites (for comparison) using index flood method, i.e. those estimates of regional quantiles (for 1, 10 and 100 year return period) are multiplied by the mean of the respective sites provided in *Table 1* of this study. The results are illustrated in *Table 5*. The comparison (of *Tables 4* and *5*) reveals that, for all the three sites, the estimates of FD and LLD distributions with BE, MLE and PWME are quite close to the results of L-moments based regional frequency analysis with Generalized Extreme Value, Generalized Normal and Generalized Logistic distributions for shorter return period, i.e. 1 and 10 year. Moreover, for longer return period, i.e. 100 year, LD distribution with BE method and FD with PWME method provides comparative results to the results of Shahzadi et al. (2013), hence can be a preferred choice to model the extremes of rainfall.

http://www.aloki.hu ● ISSN 1589 1623 (Print) ● ISSN 1785 0037 (Online)
DOI: http://dx.doi.org/10.15666/aeer/1706_1360713623

Table 5. *Quantiles for 1, 10 and 100 year return period of Shahzadi et al. (2013)*

For Muzaffarabad				
Distributions	**Estimation methods**	**Return period (years)**		
		1	**10**	**100**
Generalized extreme value	L-moments based regional frequency analysis	40.66	117.05	206.55
Generalized normal	L-moments based regional frequency analysis	40.51	118.47	201.94
Generalized logistic	L-moments based regional frequency analysis	40.51	201.94	213.40
For Garhi Dupatta				
Distributions	**Estimation methods**	**Return period (years)**		
		1	**10**	**100**
Generalized extreme value	L-moments based regional frequency analysis	41.34	119.03	210.05
Generalized normal	L-moments based regional frequency analysis	41.19	120.47	205.35
Generalized logistic	L-moments based regional frequency analysis	41.19	116.38	217.01
For Kotli				
Distributions	**Estimation methods**	**Return period (years)**		
		1	**10**	**100**
Generalized extreme value	L-moments based regional frequency analysis	32.71	94.18	166.19
Generalized normal	L-moments based regional frequency analysis	32.59	95.32	162.48
Generalized logistic	L-moments based regional frequency analysis	32.59	92.08	171.70

Conclusions

The study illustrates application of two atypical probability distributions with four methods of estimation of parameters to model the behavior of AMRS at three sites of AJ&K, Pakistan. Some of the major conclusions are:

i. The observed data series at given sites is random and identically distributed as validated by Run test and Man Whitney test.
ii. Summary statistics have shown that there exists variations in the observed data series and the distribution related to the observed data series at given sites is positively skewed.
iii. In general, both the distributions with suggested methods for the estimation of parameters have passed the goodness of fit criteria of KS test. However, the tendency of the KS values along with corresponding p-values have suggested that ME method is no a preferred choice for estimation.
iv. The graphs of probability density functions for FD and LLD have also illustrated that both the probability distributions are suitable for the observed data series at given sites. Moreover, the trends and tendencies of probability density functions are dissimilar using various methods of estimation. However, the results are in agreement with the results of KS test.
v. The study suggest that both the probability distributions using MLE and BE methods are preferred choice for modeling the extremes of rainfall of the study area. These results are encouraging to adopt relatively atypical probability distributions for the estimation of extreme events, like floods, rainfall, etc. This will bring diversity and flexibility in the choice of selection of a probability distribution for the modeling of extremes of geophysical events.
vi. The quantiles for various return periods have been calculated using the quantiles functions of the selected probability distributions. The estimated

http://www.aloki.hu ● ISSN 1589 1623 (Print) ● ISSN 1785 0037 (Online)
DOI: http://dx.doi.org/10.15666/aeer/1706_1360713623

quantiles for 10 year return period and above are greater than the average values of the observed data series at given sites. Moreover, the estimates of 100 year return period are greater than the maximum values of the observed data series for all the three sites. Therefore, the concerned officials have to adopt preemptive measures in advance to deal with these extreme events of such magnitude.

vii. To establish the usefulness of the selected distributions along with the adopted methods of estimation, the quantiles for 1, 10 and 100 year return period are compared with the previously published studies related to this area of study and variable of analysis. The comparison reveals that LD distribution with BE method and FD distribution with PWME method provides comparative results relative to L-moments based rainfall frequency analysis using popular three-parameter distributions, especially for longer return period, i.e. 100 year.

The study provides useful guidelines for the concerned officials of study area, home-grown farmers, meteorologists studying precipitation and rainwater management planning. Moreover, the study provides illustration of some new probability distributions with different methods of parameter estimation for at site frequency analysis of extreme events. The procedure can be adopted in general to bring diversity and flexibility in the choice of probability distributions for modeling of extremes of events like floods, rainfall, etc.

Acknowledgements. We are thankful to the editorial office of the journal and anonymous reviewer(s) for their constructive comments and suggestions to improve the quality of the paper. We are also grateful to Pakistan Meteorological Department (CDPC, Head Office Karachi) for providing the rainfall data for the study.

REFERENCES

[1] Abbas, K., Tang, Y. (2015): Analysis of Frechet distribution using reference priors. – Communications in Statistics - Theory and Methods 44: 14: 2945-2956.

[2] Abbas, K., Tang, Y. (2016): Objective Bayesian analysis for log-logistic distribution. – Communications in Statistics-Simulation and Computation 45(8): 2782-2791.

[3] Ahmad, I., Abbas, A., Saghir, A., Fawad, M. (2016): Finding probability distributions for annual daily maximum rainfall in Pakistan using linear moments and variants. – Polish Journal of Environmental Studies 25(3): 925-937.

[4] Ahmad, I., Abbas, A., Fawad, M. (2017): A study on regional frequency analysis of annual total rainfall in Pakistan using method of linear moments. – NUST Journal of Engineering Sciences 10(1). http://journals.nust.edu.pk/index.php/njes/article/view/157.

[5] Alam, M. A., Emura, K., Farnham, C., Yuan, J. (2018): Best-fit probability distributions and return periods for maximum monthly rainfall in Bangladesh. – Climate 6(9). DOI: 10.3390/cli6010009.

[6] Amin, M. T., Rizwan, M., Alazba, A. A. (2016): A best-fit probability distribution for the estimation of rainfall in northern regions of Pakistan. – Open Life Sciences 11(1): 432-440.

[7] Bahrawi, J. A. (2018): Rainfall distribution and its characteristics in Makkah Al-Mukarrahmah Region, Saudi Arabia. – Applied Ecology and Environmental Research 16(4): 4129-4144.

http://www.aloki.hu ● ISSN 1589 1623 (Print) ● ISSN 1785 0037 (Online)
DOI: http://dx.doi.org/10.15666/aeer/1706_1360713623

[8] Bradley, J. V. (1968): Distribution-Free Statistical Tests. – Prentice Hall, Upper Saddle River, NJ.
[9] Frechet, M. (1927): Sur la loi de probabilite de l'ecart maximum. – Annales de la Societe Polonaise de Mathematique 6: 93-116.
[10] Greenwood, J. A., Landwehr, J. M., Matalas, N. C., Wallis, J. R. (1979): Probability weighted moments: definition and relation to parameters of several distributions expressible in inverse form. – Water Resour Res 15: 1049-1054.
[11] Hosking, J. R., Wallis, J. R., Wood, E. F. (1985): Estimation of the generalized extreme-value distribution by the method of probability-weighted moments. – Technometrics 27(3): 251-261.
[12] Hussain, I., Spöck, G., Pilz, J., Yu, H.-L. (2010): Spatio-temporal interpolation of precipitation during monsoon periods in Pakistan. – Advances in Water Resources 33(8): 880-886.
[13] Hussain, Z., Shahzad, M. N., Abbas, K. (2017): Application of regional rainfall frequency analysis on seven sites of Sindh, Pakistan. – KSCE Journal of Civil Engineering 21(5): 1812-1819.
[14] Iqbal, M. J., Ali, M. (2013): A probabilistic approach for estimating return period of extreme annual rainfall in different cities of Punjab. – Arabian Journal of Geosciences 6(7): 2599-2606.
[15] Khan, S. A., Hussain, I., Hussain, T., Faisal, M., Muhammad, Y. S., Mohamd Shoukry, A. (2017): Regional frequency analysis of extremes precipitation using L-moments and partial L-moments. – Advances in Meteorology. DOI: 10.1155/2017/6954902.
[16] Liang, Y., Liu, S., Guo, Y., Hua, H. (2017): L-moment-based regional frequency analysis of annual extreme precipitation and its uncertainty analysis. – Water Resources Management 31(12): 3899-3919.
[17] Mann, H. B., Whitney, D. R. (1947): On a test of whether one of two random variables is stochastically larger than the other. – Annals of Mathematical Statistics 18(1): 50-60.
[18] Mo, C., Ruan, Y., He, J., Jin, J., Liu, P. Sun, G. (2019): Frequency analysis of precipitation extremes under climate change. – International Journal of Climatology 39(3): 1373-1387.
[19] Mohamed, M. T., Ibrahim, A. A. (2016): Fitting probability distributions of annual rainfall in Sudan. – SUST J. Eng. Comput. Sci. 17(2): 34-39.
[20] Shahzadi, A. (2013): A review: regional frequency analysis of annual maximum rainfall in monsoon region of Pakistan using L-moments. – International Journal of Advanced Statistics and Probability 1(3): 97-101.
[21] Shahzadi, A., Akhter, A. S., Saf, B. (2013): Regional frequency analysis of annual maximum rainfall in monsoon region of Pakistan using L-moments. – Pakistan Journal of Statistics and Operation Research 9(1): 111-136.
[22] Wang, Z., Zeng, Z., Lai, C., Lin, W., Wu, X., Chen, X. (2017): A regional frequency analysis of precipitation extremes in Mainland China with fuzzy c-means and L-moments approaches. – International Journal of Climatology DOI: 10.1002/joc.5013.
[23] Zalina, M. D., Desa, M. N. M., Nguyen, V. T. A., Kassim, A. H. M. (2002): Selecting a probability distribution for extreme rainfall series in Malaysia. – Water Science and Technology 45(2): 63-68.

http://www.aloki.hu ● ISSN 1589 1623 (Print) ● ISSN 1785 0037 (Online)
DOI: http://dx.doi.org/10.15666/aeer/1706_1360713623

PROGRESSIVE ALTERATIONS IN MINERAL PROFILING OF CITRUS INFECTED WITH CANKER CAUSED BY *XANTHOMONAS AXONOPODIS* PV. *CITRI* (HASSE)

HAMEED, A.[1,4] – ATIQ, M.[1*] – JAVED, N.[1] – AHMAD, A.[2,4] – AHMED, Z.[3,4]

[1]*Department of Plant Pathology, University of Agriculture, Faisalabad, Pakistan*

[2]*Department of Agronomy, University of Agriculture, Faisalabad, Pakistan*

[3]*Department of Plant Breeding & Genetics, University of Agriculture, Faisalabad, Pakistan*

[4]*Center for advanced studies in Agriculture and Food Security (CAS), University of Agriculture Faisalabad, Pakistan*

**Corresponding author*
e-mail: dratiq1@yahoo.com; phone: +92-333-4396-981

(Received 10th Apr 2019; accepted 12th Jul 2019)

Abstract. Mineral nutrients are important factors in plant-disease interactions. Experiments were conducted under Completely Randomized Block Design (CRD) with three replications to find out the alterations in mineral status of citrus leaves infected with the canker. Leaves of susceptible (Grapefruit, Succari, Kinnow) and resistant (Kumquat, Jaffa, China lemon) varieties of inoculated and un-inoculated citrus plant leaves from 6 varieties were collected and analyzed by using Nested Structured Design to check the ionic status of nutrients and minerals. Variations ($p \leq 5$) were observed in the mineral status among the treatment groups (Un-inoculated and inoculated), types (susceptible and resistant) and in the citrus varieties in response of citrus canker infection. Resistant type of plants expressed 6.88, 1.39, 8.33, 2.19, 1.84, 1.46, 1.56, 2.82 and 1.89 while susceptible type expressed 5.39, 1.13, 5.90, 1.89, 1.44, 1.11, 1.03, 1.81 and 0.92 variations in concentration of N and P (%) while K, Ca, Mg, Na, Zn, Fe and Cu in (ppm) respectively. Susceptible varieties accumulated lower concentrations as compared to resistant varieties which have an increased level of minerals. Plants become more prone to pathogen infection due to the deficiency of these nutrients which help the plants in restricting the pathogens.
Keywords: *citrus canker, mineral nutrients, plant-disease interaction, CRD, nested structured design*

Introduction

Citrus is the most important cash and fruit crop grown all over the world. It grows best under tropical and subtropical ecological conditions (Jagtap et al., 2012; Wali et al., 2013). Worldwide, its total production estimated at 115 Million Metric Tons (MMT) while in case of Pakistan, it was 3.6 MMT (Memon, 2017). Citrus has much supplementary usage in various kinds of food and beverages having traditionally medicinal values (Gurib, 2006). Citrus is valuable due to its rich nutritional grade and is more precious because of its highly dietary status. It has large amount of sugars, amino acids, organic acids, vitamins, antioxidants like flavonoides, terpenes, macro and micronutrients minerals (calcium, magnesium) along with rich source of vitamin C (Ladaniya et al., 2010). In Pakistan, citrus area is 20.7 million hectares with 36 million tons production (Memon, 2017). Pakistan earned 17.78 billion Pakistani rupees (PKR) by exporting 3.8 million tonns kinnow during the year of 2017 (Memon, 2017). Citrus is spoiled by nearly one hundred and fifty pathogens and disorders caused by fungal, viral and bacterial diseases like canker, greening (HLB), scab, gummosis, whithertip, greecy spot, black spot, decline and citrus tristeza virus

http://www.aloki.hu ● ISSN 1589 1623 (Print) ● ISSN 1785 0037 (Online)
DOI: http://dx.doi.org/10.15666/aeer/1706_1362513642

which results in severe losses but canker caused by *Xanthomonas axonopodis* pv. *citri (Xac)* is one of the major threat among all the constraints faced by the citrus crop in Pakistan (Ware, 2015). Pakistan which is one of the major exporters of citrus in the world, facing a huge economic losses due to this disease. During 2015-16, 144 consignments of citrus were rejected by the European Union due to the infection of *Xac* (Pervaiz, 2015). Overall, the yield losses due to canker is increasing day by day (Sahi et al., 2007).

Bacteria gain entry in to the leaves through stomata, wounds/injuries and penetrate into the intercellular spaces of leaves and attaches to the mesophyll cells using type III secretary system and releases effecter proteins (toxins) which causes hypertrophy, hyperplasia and and causes multiple infection and produces water soaked lesion with yellow hollow. Epidermis gets raised and began to rupture. After two weeks of infection, the watery lesions began to dry and form necrotic lesions. Copper-based chemicals are used in conventional management of canker. No doubt, these chemicals expressed quick response against canker but are not eco-friendly and have ill effects on human health. So, there is dire need to develop an alternate strategy which should be cost effective with least residual effects and is eco-friendly (Kumar et al., 2011). *Xac* forms a bio film on leaf surface and gains entry in to leaves via natural leaf openings or the wounds. Upon bacterial invasion the defense mechanism of plant which is composed of a series of well coordinated molecular networks is triggered, various transcriptomic reprogramming events, ultra-structural reinforcements and physiological changes takes place in a series of defense related events. The first line of plant's defence involves production of reactive oxygen species (ROS) as a part of PAMP-Triggered immunity (PTI). The second line of defense is triggered when certain pathogen effecter molecules are recognized by the R gene products which results in multiple responses including HR response and programmed cell death for pathogen confinement and preventing disease spread (Roeschlin et al., 2017).

Mineral nutrients are essential not only for plant growth and development but also play an important role in plant-disease interaction as well as in reducing disease to a tolerable level (Bradbury, 2016). Nutrients are not responsible for disease severity and resistance but they also take part in the disease development by fluctuating the functioning of the plants or the expansion of disease (Arshadi et al., 2013). Sometime, these nutrients may increase the plant growth which ultimately effects the pathogenic infection and their deficiency also takes the plant towards susceptibility against the pathogen (Bruning and Gabriel, 2003). In the same way these nutrients influence the disease susceptibility by inducing the chemical alterations in the host plant (Mubeen et al., 2015). When a pathogen attacks, it affects the physiology of plant and reduced nutrient uptake, assimilation, absorption, mobility and their consumption. In diseased tissues, translocation or consumption of nutrients are influenced by pathogens, result in nutrient deficiencies. These nutrients have a sound effect on all the key components which play role in the disease severity. Besides, plants have more chances of damage by pathogens that suffer with low level of nutrients which are necessary for building cell walls and other structural tissues (Ryan et al., 2011). In most of the bacterial diseases of plants, pathogen enter and multiply in to the host through the xylum vessels which is the main system for transportation of water and nutrients from the roots to the leaves (Honger et al., 2016). The presence of these pathogenic bacteria produce ooze and slime within the vessels which causing blockage of nutrients, produce rough water soaked lesions on the leaves and after on surface of fruits. Some plant nutrients play a vital role in reducing the capability of bacteria to produce vessels blocking slime (Spann and Schumann, 2010). In sustainable agriculture, management of nutrients has received little attention for control of disease. The physiological functions of plant nutrients are generally well

http://www.aloki.hu ● ISSN 1589 1623 (Print) ● ISSN 1785 0037 (Online)
DOI: http://dx.doi.org/10.15666/aeer/1706_1362513642

understood but still there is a little knowledge regarding the relationship between plant-pathogens and nutrients. It is reported that fundamental essential macro and micro nutrients for healthy citrus plants are N, P, K, Mg, Fe, Ca, S, Zn, Cu and B (Zekri and Obreza, 2015). Pathogen uses these nutrients in their growth and development, reduced their accessibility to the host plants and enhancing susceptibility of plant towards various infections (Sahi et al., 2010). Enhancement of plant health is an effective way of combating citrus canker. When bacteria attack on citrus plant, it induces different changes in its metabolism. It interferes with its defense mechanism by disturbing its ionic content which ultimately leads to disease development. A method for the enrichment of plant health and strengthening its defense mechanism against the pathogen attack is to analyze the mineral profile of healthy and diseased plants. The present study was designed to find out the biochemical alterations happened after the disease attack in citrus plants to pave the way towards successful management of citrus canker. For this purpose, mineral profiling of inoculated and un-inoculated plants of susceptible and resistant citrus varieties was conducted.

Materials and methods

One year old seedlings of six varieties (Grape fruit, Succari, Kinnow, Kumquat, Jaffa and China lemon) were collected from the research area Institute of Horticultural Science, University of Agriculture Faisalabad (UAF). All varieties were sown in three replications in pots (30 × 15 cm) containing field soil (sandy clay) previously sterilized by drenching 1% solution of formaline using a Completely Randomized Block Design (CRD) in the green house, research area of Department of Plant Pathology UAF. All the recommended horticultural practices were exercised including the doses of fertilizers and number of irrigations to keep the plants in healthy condition. Soil health analysis was also done to fulfill all requirements of minerals. A standard soil mix (2:1 clay and sand) was used in all experiments. The soil mixture tested 73 lb./acre phosphorus, 242 lb./acre exchangeable potassium. It was partially sterilized by (i) autoclaving for 2 h at 121 °C and 15 psi (ii) fumigating in a sealed plastic container in which 1% formalin solution injected. The soil mixtures were aerated for seven days after treatment. Leaves showed characteristics symptoms of canker were collected in brown paper bags (10" × 12") from research area of Institute of Horticultural Sciences and brought to the citrus pathology lab to isolate *Xac* by using streaking method. Nutrient Agar (NA) media (Beef extract 3 g, Peptone 5 g, Glucose 2.5 g and Agar 15 g, 1000 ml distilled water for 1 L media) was used to isolate *Xac*. For the preparation of inoculums for pathogencity, bacterial culture was grown overnight in 10 ml nutrient broth at 25 °C and put on shaker (RTSK-0300, Robus United Kingdom) at 200 rpm. Inoculum was measured equivalent to 10^8 colony-forming units (*cfu*) per ml with the help of spectrophotometer (Hitachi U-2001, model 121-003) (Francis et al., 2010). Inoculation was done at morning in the green house by using syringe method (using a 1 cm^3 needleless tuberculin syringe). Bacterial suspension (approximately 2 µl) was infiltrated into the leaf until the water-soaked area reached about 6 mm in diameter. Three areas on each side of the leaf mid-vein were infiltrated. Disease incidence was confirmed via Koch's postulates (Juhasz et al., 2013). For mineral analysis, total 300 samples (150 inoculated & 150 un-inoculated), 50 (25 healthy & 25 diseased) from each variety one time after inoculation were collected. Disease symptoms were appeared on the susceptible and resistant type of varieties after the inoculation (*Fig. 1*).

http://www.aloki.hu ● ISSN 1589 1623 (Print) ● ISSN 1785 0037 (Online)
DOI: http://dx.doi.org/10.15666/aeer/1706_1362513642

Figure 1. *Disease symptoms after the inoculation of Xac on susceptible (left) and resistant (right) varieties*

Estimation of mineral gradient in citrus cultivar

The leaves samples comprising of inoculated and un-inoculated groups both from resistant and susceptible reaction types were taken, stored in the refrigerator (Dawlance DW 550) and standard analytical method were employed for the determination of different biochemical compound via 'Nested Structured Design (Gomez and Gomez, 1984). Leaves were surface sterilized by using 0.2% NaOCl solution to eliminate all debris, followed by washing with 0.8% HCL solution (to remove metallic contamination from them) and then with de-ionized water (to get rid of previous two solutions). After this, leaves were first air dried, later placed inside brown paper bags (23 × 15 cm) and then subjected to oven (BST/HAO-1122) drying at 70 °C for 3 days (72 h approx.) to attain a constant weight. After drying the leaf samples were grind in to a fine powder by using sterilized mortar and pestle. After thoroughly grinding, samples (100 mg) were boiled in 10 ml of 1.4 M nitric acid on a hotplate (TH-550; Advantec, Tokyo, Japan) at 100 °C for 25-30 min. The solution was left for cooling, afterwards the sample suspension was diluted up to 250 time using distilled water and analysis for determining concentrations of key elements including; N, P, K, Zn, Mg, Ca, Fe and Na were done by following Bhargava and Raghupathi (1995) method. Potassium, Zinc, Magnesium, Calcium, Iron and Sodium contents were measured on ppm (parts per million) while Nitrogen and Phosphorus were recorded on percent basis.

Estimation of phosphorus from citrus leaves

Sample solution of 0.1 ml was prepared by wet digestion method. Solution was taken in a volumetric flask (ASTM-E288) and 1 ml of ammonium molybdate reagent [$(NH_4)_6Mo_7O_{24}.4H_20$] along with 8.6 ml of distilled water was added. Amino nephtholsulphonic acid ($C_{10}H_9NO_4S$) was added after swirling the flask to mix solution. Sample solution placed at 720 nm on a spectrophotometer (Hitachi U-2001, model 121-003) and absorbency was measured by using distilled water as a reagent blank. Absorbency was compared to previously prepared standard curve (Bolts and Mellon, 1948; Fiske and Subbarow, 1925) by atomic absorption spectrometer (Hitachi polarized Zeeman) for determination of phosphorous concentration.

http://www.aloki.hu ● ISSN 1589 1623 (Print) ● ISSN 1785 0037 (Online)
DOI: http://dx.doi.org/10.15666/aeer/1706_1362513642

Determination of potassium and sodium from leaves of diseased and healthy citrus plants

Determination of sodium and potassium contents was done by using Flame phorometer (PFP-7, Janway). Potassium chloride and sodium chloride were used as standards for the measurement of K and Na respectively. Four concentrations 10, 20, 30 and 40 ppm for both potassium and sodium were used for preparing the standard curves. Fresh working standards were prepared immediately before use.

Estimation of copper, magnesium, iron, calcium and zinc from citrus leaves

Determination of Calcium (Ca), Magnesium (Mg), iron (Fe), Copper (Cu) and zinc (Zn) was done using a spectrophotometer (Hitachi U-2001, model 121-003). Standards that used for the estimation of these ions were Iron sulphate ($FeSO_4$), Magnesium sulphate ($MgSO_4$), Zinc oxide (ZnO), Calcium chloride ($CaCl_2$) and Copper sulphate ($CuSO_4$). For obtaining standard curves, concentrations 10, 20, 40, 80 and 100 ppm for Ca; 2, 2.5, 3, and 3.5 ppm for Cu; 5, 10, 15 and 20 ppm for Mg; 0.2, 0.3, 0.5 and 2 ppm for zinc and 1, 2 and 3 ppm for iron were used. Standard solutions were prepared just before this activity. Atomic absorption spectrophotometer (GA 3202 HGA) was used for the analysis of these minerals both from resistant and healthy cultivars of citrus.

Estimation of total nitrogen from diseased and healthy citrus leaves

Determination of total nitrogen from the sample was done by using Micro Kjeldahl method (46MC; Quickfit, England) (Kjeldahl, 1983). Proper amount of sample was oven-dried (D6450 Hanus; Heraeus) and taken in long neck Kjeldahl flask. Concentrated sulphuric acid of 25 ml and five grams of digestion mixture containing K_2SO_4 and $CuSO_4$ was added. For boiling of the sample, Digestion hood (KB8S Kjeldatherm) was used. Contents of flask were distilled by using distilled water in 250 ml volumetric flask (ASTM-E288). 10 ml of this solution was distilled in micro Kjeldhal distillation apparatus (VAP20, Garhardt) in the presence of 10 ml of 40% sodium hydroxide (NaOH) solution. Ammonia produce in this reaction which was collected in a beaker containing 10 ml of 2% boric acid (H_3BO_3) solution. Boric acid with two drops of methyl red was used as an indicator. The solution was titrated against standard 0.1N sulphuric acid to light pink point. *Equation 1* was used to calculate the percentage of nitrogen.

$$\text{Nitrogen } \% = \frac{0.1 \text{ N } H_2SO_4 \times 0.0014 \times 250}{\text{WI} \times 100} \times 100 \qquad \text{(Eq.1)}$$

Total percentage of crude protein present in sample was estimated using *Equation 2.*

$$\text{Crude protein} = \text{Nitrogen } \% \times 6.25 \qquad \text{(Eq.2)}$$

Statistical analysis

The plant samples (all varieties) were divided in 2 groups i.e. un-inoculated and inoculated. Further each group contained of 2 reaction types: i) resistant, ii) susceptible, three susceptible citrus varieties were used: Grapefruit, Succari and Kinnow and three resistant varieties Kumquat, Jaffa and China lemon. Leaves sample of un-inoculated and

http://www.aloki.hu ● ISSN 1589 1623 (Print) ● ISSN 1785 0037 (Online)
DOI: http://dx.doi.org/10.15666/aeer/1706_1362513642

inoculated plants from resistant varieties with a disease incidence ranging from 0-5% and susceptible plants showing above 25% incidence were acquired from the research area Department of Plant pathology near Center of Advanced Studies (CAS) University of Agriculture Faisalabad during 2018. For estimation of mineral contents, standard analytical methods via Nested Structured Design (Gomez and Gomez, 1984) were used and data were statistically analyzed by using PROC MiXED procedure of the Statistical Analysis System (SAS, 2009).

Results

Determination of minerals contents of N, P, K, Na, Zn, Ca, Mg, Fe and Cu from inoculated and un-inoculated citrus plant

Samples of un-inoculated and inoculated with *Xac* both from susceptible and resistant plants were addressed for the determination of N, P, K, Ca, Mg, Na, Zn, Fe and Cu. Inoculated and un-inoculated citrus varieties expressed significant variations (on an average 3.31% across inoculated plants) and (on an average 8.91% across un-inoculated plants) which point out that nitrogen contents were clearly affected by the attack of *Xac.* Resistant and susceptible type showed 6.88% and 5.39% variation at $p \leq 0.05$ and "Type" Component expressed 92.41% total variance. Total nitrogen variability which variety exhibited was 0.83% (*Table 1*). Resistant cultivar "Kumquat" displayed maximum nitrogen amount at 7.23% and susceptible cultivar "Grape fruit" minimum at 5.20% (*Table 2*). In case of phosphorus, there was seen a significant variation between inoculated (0.68%) and un-inoculated (1.81%) cultivars during the infection. Resistant and susceptible varieties showed total variance of 93.00% with 1.39% and 1.13% on individual basis respectively at $p \leq 0.05$ while the variance between the varieties that observed was 1.40%. Maximum and minimum concentrations of phosphorus were accounted by Jaffa (1.46%) and China lemon (1.00%) respectively (*Tables 3* and *4*). Total variability of potassium contents exhibited by the group was 11.09 and in case of type were 88.61% on canker infection (*Table 5*). Resistant and susceptible varieties showed significant variation averaging 8.33 and 5.90 ppm respectively. Inoculated (3.58 ppm) and un-inoculated (10.65 ppm) citrus cultivars also expressed significant variation under *Xac* infection. Resistant cultivar named as kumquat displayed maximum potassium concentration (8.60 ppm) while minimum concentration of potassium was expressed by Grape fruit (5.66 ppm) at $p \leq 0.05$ (*Table 6*).

Regarding the calcium concentration, statistically significant difference was attained by the group having total variance of 4.08% (on an average 1.36 ppm in case of inoculated citrus plants and 2.11 ppm for un-inoculated plants) as shown in *Table 7*. In the same way, resistant cultivars expressed 2.19 ppm while susceptible cultivars showed 1.89 ppm variation as compared to the types which had 91.84% variability in the result of canker infection at $p \leq 0.05$. Significant variation was also expressed by the varieties with the amount of 1.46% of the total variance. Calcium concentrations of 2.26, 2.11, and 2.19 ppm were showed by Kumquat, Jaffa, and China lemon (resistant types), while 1.75, 1.86, and 2.06 ppm concentrations were shown by susceptible varieties Grape fruit, Succari, and Kinnow, respectively as given in *Table 8*. Magnesium articulated a total variability of 4.93% with a significant variation between the inoculated (0.63 ppm) and un-inoculated (2.65 ppm) under the disease conditions. On an average, 1.84 ppm and 1.44 ppm were observed in case resistant and susceptible citrus varieties respectively with a total variation of 93.27%. Varieties showed a total variance of

http://www.aloki.hu ● ISSN 1589 1623 (Print) ● ISSN 1785 0037 (Online)
DOI: http://dx.doi.org/10.15666/aeer/1706_1362513642

0.72 ppm for magnesium. Resistant variety Kumquat expressed maximum concentration of magnesium with 1.90 ppm and susceptible variety Grape fruit showed minimum magnesium contents with amount of 1.19 ppm (*Tables 9* and *10*).

In group, sodium concentration had significant variation in inoculated and un-inoculated citrus varieties expressed (on average 0.62% across inoculated plants) and (on average 1.95% across uninoculated plant) as given in *Table 11* and significant variations (92.19%) were attained by resistant and susceptible cultivar averaging 1.46 ppm and 1.11 ppm respectively. Kumquat with 1.60 ppm and Grape fruit with 1.03 ppm expressed maximum and minimum sodium concentration (*Table 12*).

Table 1. *Nested ANOVA of mineral concentrations of nitrogen in inoculated and un-inoculated citrus plant leaves*

Nitrogen (%)							
SOV	**DF**	**SS**	**MS**	**F value**	**Pr > F**	**Variance component**	**% of total**
Type (A)	1	845.712	845.712	27.457	0.035*	15.091	92.41
Group (B)	2	61.603	30.801	25.163	0.000*	1.095	6.71
Variety (C)	8	9.792	1.224	135.849	0.000*	0.135	0.83
Error	96	0.865	0.009	-	-	0.009	0.06
Total	107	917.973	-	-	-	16.330	-

*Significant

Table 2. *Amount of nitrogen in reaction groups (inoculated and un-inoculated), types (resistant and susceptible) and in varieties of citrus plant leaves*

Nitrogen (%)												
Varieties (C)	**Kumquat**		**Jaffa**		**China Lemon**		**Grape fruit**		**Succari**		**Kinnow**	
Type (A)	**Resistant**						**Susceptible**					
Group (B)	**Inoc.**	**Uninoc.**	**Inoc.**	**Uninoc.**	**Inoc.**	**Uninoc.**	**Inoc.**	**Uninoc.**	**Inoc.**	**Uninoc.**	**Inoc.**	**Uninoc.**
Amount of N in (C)	4.12	10.3	3.63	9.36	3.96	9.85	2.46	7.96	2.80	8.15	3.16	7.80
Av. amount of N in (C)	7.23		6.49		6.91		5.20		5.47		5.48	
Av. amount of N in (A)	Resistant = 6.88 Susceptible = 5.39											
Av. amount of N in (B)	Un-inoculated = 8.91 Inoculated = 3.31											

Table 3. *Nested ANOVA of mineral concentrations of phosphorus in inoculated and un-inoculated citrus plant leaves*

Phosphorus (%)							
SOV	**DF**	**SS**	**MS**	**F value**	**Pr > F**	**Variance component**	**% of total**
Type (A)	1	34.566	34.566	32.205	0.030*	0.620	93.00
Group (B)	2	2.146	1.073	12.668	0.003*	0.037	5.49
Variety (C)	8	0.677	0.084	111.594	0.000*	0.009	1.40
Error	96	0.072	0.000	-	-	0.001	0.11
Total	107	37.464		-	-	0.667	-

*Significant

http://www.aloki.hu ● ISSN 1589 1623 (Print) ● ISSN 1785 0037 (Online)
DOI: http://dx.doi.org/10.15666/aeer/1706_1362513642

Table 4. *Amount of phosphorus in reaction groups (inoculated and un-inoculated), types (resistant and susceptible) and in varieties of citrus plant leaves*

Phosphorus (%)												
Varieties (C)	**Kumquat**		**Jaffa**		**China Lemon**		**Grape fruit**		**Succari**		**Kinnow**	
Type (A)	**Resistant**						**Susceptible**					
Group (B)	**Inoc.**	**Uninoc.**	**Inoc.**	**Uninoc.**	**Inoc.**	**Uninoc.**	**Inoc.**	**Uninoc.**	**Inoc.**	**Uninoc.**	**Inoc.**	**Uninoc.**
Amount of N in (C)	0.82	1.98	0.76	1.85	0.84	2.07	0.45	1.55	0.55	1.67	0.78	1.76
Av. amount of N in (C)	1.40		1.30		1.46		1.00		1.11		1.27	
Av. amount of N in (A)	Resistant = 1.39 Susceptible = 1.13											
Av. amount of N in (B)	Un-inoculated = 1.81 Inoculated = 0.68											

Table 5. *Nested ANOVA of mineral concentrations of potassium in inoculated and un-inoculated citrus plant leaves*

Potassium (ppm)							
SOV	**DF**	**SS**	**MS**	**F value**	**Pr > F**	**Variance component**	**% of total**
Type (A)	1	1351.077	1351.077	16.834	0.055	23.534	88.61
Group (B)	2	160.513	80.256	113.793	0.000*	2.946	11.09
Variety (C)	8	5.642	0.705	600.956	0.000*	0.078	0.29
Error	96	0.1127	0.001	-	-	0.001	0.00
Total	107	1517.346	-	-	-	26.559	-

*Significant

Table 6. *Amount of potassium in reaction groups (inoculated and uninoculated), types (resistant and susceptible) and in varieties of citrus plant leaves*

Potassium (ppm)												
Varieties (C)	**Kumquat**		**Jaffa**		**China Lemon**		**Grape fruit**		**Succari**		**Kinnow**	
Type (A)	**Resistant**						**Susceptible**					
Group (B)	**Inoc.**	**Uninoc.**	**Inoc.**	**Uninoc.**	**Inoc.**	**Uninoc.**	**Inoc.**	**Uninoc.**	**Inoc.**	**Uninoc.**	**Inoc.**	**Uninoc.**
Amount of N in (C)	5.08	12.12	4.34	11.71	4.77	11.97	2.25	9.07	2.68	9.11	2.36	9.40
Av. amount of N in (C)	8.60		8.02		8.37		5.66		6.16		5.88	
Av. amount of N in (A)	Resistant = 8.33 Susceptible = 5.90											
Av. amount of N in (B)	Un-inoculated = 10.65 Inoculated = 3.58											

http://www.aloki.hu ● ISSN 1589 1623 (Print) ● ISSN 1785 0037 (Online)
DOI: http://dx.doi.org/10.15666/aeer/1706_1362513642

Table 7. *Nested ANOVA of mineral concentrations of calcium in inoculated and un-inoculated citrus plant leaves*

Calcium (ppm)							
SOV	**DF**	**SS**	**MS**	**F value**	**Pr > F**	**Variance component**	**% of total**
Type (A)	1	49.410	49.410	40.390	0.024*	0.892	91.84
Group (B)	2	2.446	1.223	8.002	0.012*	0.040	4.08
Variety (C)	8	1.223	0.152	6.011	0.000*	0.014	1.46
Error	96	2.441	0.025	-	-	0.025	2.62
Total	107	55.521	-	-	-	0.972	-

*Significant

Table 8. *Amount of calcium in reaction groups (inoculated and un-inoculated), types (resistant and susceptible) and in varieties of citrus plant leaves*

Calcium (ppm)												
Varieties (C)	**Kumquat**		**Jaffa**		**China Lemon**		**Grape fruit**		**Succari**		**Kinnow**	
Type (A)	**Resistant**						**Susceptible**					
Group (B)	**Inoc.**	**Uninoc.**	**Inoc.**	**Uninoc.**	**Inoc.**	**Uninoc.**	**Inoc.**	**Uninoc.**	**Inoc.**	**Uninoc.**	**Inoc.**	**Uninoc.**
Amount of N in (C)	1.59	2.94	1.39	2.83	1.49	2.88	1.05	2.44	1.17	2.55	1.47	2.65
Av. amount of N in (C)	2.26		2.11		2.19		1.75		1.86		2.06	
Av. amount of N in (A)	Resistant = 2.19 Susceptible = 1.89											
Av. amount of N in (B)	Un-inoculated = 2.11 Inoculated = 1.36											

Table 9. *Nested ANOVA of mineral concentrations of magnesium in inoculated and un-inoculated citrus plant leaves*

Magnesium (ppm)							
SOV	**DF**	**SS**	**MS**	**F value**	**Pr > F**	**Variance component**	**% of total**
Type (A)	1	104.725	104.725	36.827	0.026*	1.887	93.27
Group (B)	2	5.687	2.843	18.499	0.001*	0.100	4.93
Variety (C)	8	1.229	0.153	7.065	0.000*	0.015	0.72
Error	96	2.088	0.021	-	-	0.022	1.08
Total	107	113.731	-	-	-	2.023	-

* = Significant

http://www.aloki.hu ● ISSN 1589 1623 (Print) ● ISSN 1785 0037 (Online)
DOI: http://dx.doi.org/10.15666/aeer/1706_1362513642

Table 10. *Amount of magnesium in reaction groups (inoculated and un-inoculated), types (resistant and susceptible) and in varieties of citrus plant leaves*

Magnesium (ppm)												
Varieties (C)	**Kumquat**		**Jaffa**		**China Lemon**		**Grape fruit**		**Succari**		**Kinnow**	
Type (A)	**Resistant**						**Susceptible**					
Group (B)	**Inoc.**	**Uninoc.**	**Inoc.**	**Uninoc.**	**Inoc.**	**Uninoc.**	**Inoc.**	**Uninoc.**	**Inoc.**	**Uninoc.**	**Inoc.**	**Uninoc.**
Amount of N in (C)	0.74	3.06	0.65	2.93	0.83	2.82	0.45	2.13	0.56	2.33	0.70	2.47
Av. amount of N in (C)	1.90		1.78		1.82		1.29		1.45		1.59	
Av. amount of N in (A)	Resistant = 1.84 Susceptible = 1.44											
Av. amount of N in (B)	Un-inoculated = 2.62 Inoculated = 0.65											

Table 11. *Nested ANOVA of mineral concentrations of sodium in inoculated and un-inoculated citrus plant leaves*

Sodium (ppm)							
SOV	**DF**	**SS**	**MS**	**F value**	**Pr > F**	**Variance component**	**% of total**
Type (A)	1	47.733	47.733	28.194	0.034*	0.853	92.19
Group (B)	2	3.386	1.693	13.945	0.002*	0.058	6.29
Variety (C)	8	0.971	0.121	193.395	0.000*	0.013	1.45
Error	96	0.060	0.000	-	-	0.001	0.07
Total	107	52.151	-	-	-	0.925	-

*Significant

Table 12. *Amount of sodium in reaction groups (inoculated and un-inoculated), types (resistant and susceptible) and in varieties of citrus plant leaves*

Sodium (ppm)												
Varieties (C)	**Kumquat**		**Jaffa**		**China Lemon**		**Grape fruit**		**Succari**		**Kinnow**	
Type (A)	**Resistant**						**Susceptible**					
Group (B)	**Inoc.**	**Uninoc.**	**Inoc.**	**Uninoc.**	**Inoc.**	**Uninoc.**	**Inoc.**	**Uninoc.**	**Inoc.**	**Uninoc.**	**Inoc.**	**Uninoc.**
Amount of N in (C)	0.95	2.25	0.63	2.05	0.72	2.16	0.44	1.64	0.55	1.85	0.44	1.75
Av. amount of N in (C)	1.60		1.34		1.44		1.03		1.20		1.09	
Av. amount of N in (A)	Resistant = 1.46 Susceptible = 1.11											
Av. amount of N in (B)	Un-inoculated = 1.95 Inoculated = 0.62											

http://www.aloki.hu ● ISSN 1589 1623 (Print) ● ISSN 1785 0037 (Online)
DOI: http://dx.doi.org/10.15666/aeer/1706_1362513642

In case of zinc, significant variation was displayed by the inoculated and un-inoculated citrus plants with the amount of 0.41 ppm and 2.19 ppm respectively (*Table 13*). Likewise, significant variation was also observed in resistant (1.56 ppm) and susceptible (1.03 ppm) citrus plants with total variability of about 86.06 of zinc. Kumquat (1.68 ppm) showed maximum concentration of zinc while Grape fruit (0.92 ppm) expressed minimum zinc concentration (*Table 14*). 15.82, 83.24 and 0.91% total variability was observed in groups, type and varieties respectively in case of iron contents under the disease stress conditions (*Table 15)*. Minimum and maximum iron concentration was showed by Grape fruit (1.60 ppm) and Jaffa (2.65 ppm) respectively (*Table 16*). Both inoculated (1.67 ppm) and un-inoculated (2.14 ppm) citrus plant leaves showed significant variation in cupper contents on pathogen infection. Resistant and susceptible plant also expressed significant variations of 1.89 and 0.92 ppm respectively with 59.87% of the total variance. Varieties showed a total variance of 1.89 ppm for copper. Kumquat (2.05 ppm) and Grape fruit (0.79 ppm) displayed their maximum and minimum concentration of copper contents after the attack of *Xac.* (*Tables 17* and 18).

Table 13. *Nested ANOVA of mineral concentrations of zinc in inoculated and un-inoculated citrus plant leaves*

Zinc (ppm)							
SOV	**DF**	**SS**	**MS**	**F value**	**Pr > F**	**Variance component**	**% of total**
Type (A)	1	84.388	84.388	14.277	0.043*	1.453	86.06
Group (B)	2	11.821	5.910	27.234	0.000*	0.211	12.49
Variety (C)	8	1.736	0.217	477.795	0.000*	0.024	1.43
Error	96	0.043	0.000	-	-	0.000	0.03
Total	107	97.989	-	-	-	1.689	-

*Significant

Table 14. *Amount of zinc in reaction groups (inoculated and un-inoculated), types (resistant and susceptible) and in varieties of citrus plant leaves*

Zinc (ppm)												
Varieties (C)	**Kumquat**		**Jaffa**		**China Lemon**		**Grape fruit**		**Succari**		**Kinnow**	
Type (A)	**Resistant**						**Susceptible**					
Group (B)	**Inoc.**	**Uninoc.**	**Inoc.**	**Uninoc.**	**Inoc.**	**Uninoc.**	**Inoc.**	**Uninoc.**	**Inoc.**	**Uninoc.**	**Inoc.**	**Uninoc.**
Amount of N in (C)	0.50	2.87	0.46	2.43	0.49	2.63	0.31	1.54	0.34	1.65	0.35	1.96
Av. amount of N in (C)	1.68		1.44		1.56		0.92		0.99		1.15	
Av. amount of N in (A)	Resistant = 1.56 Susceptible = 1.03											
Av. amount of N in (B)	Un-inoculated = 2.19 Inoculated = 0.41											

http://www.aloki.hu ● ISSN 1589 1623 (Print) ● ISSN 1785 0037 (Online)
DOI: http://dx.doi.org/10.15666/aeer/1706_1362513642

Table 15. *Nested ANOVA of mineral concentrations of iron in inoculated and un-inoculated citrus plant leaves*

Iron (ppm)							
SOV	**DF**	**SS**	**MS**	**F value**	**Pr > F**	**Variance component**	**% of total**
Type (A)	1	171.032	171.032	11.324	0.048*	2.888	83.24
Group (B)	2	30.208	15.104	52.905	0.000*	0.549	15.82
Variety (C)	8	2.284	0.285	325.848	0.000*	0.032	0.91
Error	96	0.084	0.000	-	-	0.001	0.03
Total	107	203.608	-	-	-	3.469	-

*Significant

Table 16. *Amount of Iron in reaction groups (inoculated and un-inoculated), types (resistant and susceptible) and in varieties of citrus plant leaves*

Iron (ppm)												
Varieties (C)	**Kumquat**		**Jaffa**		**China Lemon**		**Grape fruit**		**Succari**		**Kinnow**	
Type (A)	**Resistant**						**Susceptible**					
Group (B)	**Inoc.**	**Uninoc.**	**Inoc.**	**Uninoc.**	**Inoc.**	**Uninoc.**	**Inoc.**	**Uninoc.**	**Inoc.**	**Uninoc.**	**Inoc.**	**Uninoc.**
Amount of N in (C)	1.55	4.39	1.24	4.06	1.42	4.25	0.55	2.97	0.71	2.94	0.85	3.13
Av. amount of N in (C)	2.97		2.65		2.84		1.60		1.83		1.99	
Av. amount of N in (A)	Resistant = 2.82 Susceptible = 1.81											
Av. amount of N in (B)	Un-inoculated = 3.57 Inoculated = 1.05											

Table 17. *Nested ANOVA of mineral concentrations of cupper in inoculated and un-inoculated citrus plant leaves*

Cupper (ppm)							
SOV	**DF**	**SS**	**MS**	**F value**	**Pr > F**	**Variance component**	**% of total**
Type (A)	1	58.904	58.904	4.085	0.041*	0.824	59.87
Group (B)	2	28.840	14.420	61.560	0.000*	0.525	38.19
Variety (C)	8	1.874	0.234	292.980	0.000*	0.026	1.89
Error	96	0.076	0.000	-	-	0.001	0.06
Total	107	89.695	-	-	-	1.376	-

*Significant

http://www.aloki.hu ● ISSN 1589 1623 (Print) ● ISSN 1785 0037 (Online)
DOI: http://dx.doi.org/10.15666/aeer/1706_1362513642

Table 18. *Amount of copper in reaction groups (inoculated and un-inoculated), types (resistant and susceptible) and in varieties of citrus plant leaves*

Copper (ppm)												
Varieties (C)	**Kumquat**		**Jaffa**		**China Lemon**		**Grape fruit**		**Succari**		**Kinnow**	
Type (A)	**Resistant**						**Susceptible**					
Group (B)	**Inoc.**	**Uninoc.**	**Inoc.**	**Uninoc.**	**Inoc.**	**Uninoc.**	**Inoc.**	**Uninoc.**	**Inoc.**	**Uninoc.**	**Inoc.**	**Uninoc.**
Amount of N in (C)	1.09	3.01	0.86	2.54	1.01	2.85	0.25	1.34	0.36	1.46	0.42	1.66
Av. amount of N in (C)	2.05		1.70		1.93		0.79		0.91		1.04	
Av. amount of N in (A)	Resistant = 1.89 Susceptible = 0.92											
Av. amount of N in (B)	Un-inoculated = 2.14 Inoculated = 0.67											

Discussion

Mineral nutrients have a crucial role to play in plant- disease interaction. Determination of the effects of nutrients on disease development is based upon some major factors like concentration and forms of elements, disease type and weather conditions. Disease severity can be reduced by the accurate provision of nutrients and by understanding the dynamics between the nutritional status of plants and pathogens (Vandermeer et al., 2010). Establishment of pathogen on host surface, rate of penetration and development of disease are depending upon histological or morphological attributes of plant which are influenced by nutritional status of plant. Different types of nutrients have a distinct impact on resistance/susceptibility of host and virulence of pathogens which lead towards various kinds of alterations and consequences in the form of stresses (Bhaduri et al., 2014). Plants need balanced and in time availability of all required nutrients for their growth and development. This plant are more resistant against the various types of biotic and abiotic stresses, protected from new pathogenic infections and also enables to restrict existing infection better than the plants received deficient from proper nutrients supply. In the present study, nutritional requirements like N, P, K, Ca, Mg, Zn, Fe, Cu and B of citrus plant leaves for their growth and development was observed.

In plants, nitrogen is a major element for many compounds of great significance such as protein, coenzymes, amino acid, amides, nucleic acids, nucleotides, chlorophyll, cytosine and auxins (Lakitan, 2007). Nitrogen deficiency in plant happens due to the excessive run-off and leaching. Plants responded abruptly to the application of nitrogen because it required for normal growth and development (Spann and Schumann, 2010). Its deficiency produces many other symptoms while excess availability of nitrogen also favors some diseases in plants (Dordas, 2008). In present study, it was observed that inoculated citrus varieties contained less amount of nitrogen while un-inoculated and resistant cultivars have high nitrogen contents that were also witnessed by Zekri and Obreza (2015).

Plants get high energy compounds like phospholipids, nucleic acids, coenzymes NAD, NADP, ATP and several others by the utilization of phosphorus (Huber and Graham, 1999; Spann and Schumann, 2010). Better root development due to the phosphorus nutrition may survive plants from the attack of various pathogens (Huber, 2007). In the current study, there was a clear difference of phosphorus accumulation in inoculated and

http://www.aloki.hu ● ISSN 1589 1623 (Print) ● ISSN 1785 0037 (Online)
DOI: http://dx.doi.org/10.15666/aeer/1706_1362513642

uninoculated plants of both resistant and susceptible varieties. Findings of this study associated with the conclusions of Amusa et al. (2005), who experienced variations in phosphorus concentration between inoculated and un-inoculated plant.

Potassium is essential in enzyme activation; many of these enzymes are involved in carbohydrate metabolism. It is also helpful in controlling different plant diseases and pests. In the cellular functions, potassium acts as a mobile regulator for several activities of enzymes which ultimately reduces overall severity of disease. Nitrogen balances with the potassium particularly affect plants susceptibility against the disease (Dordas, 2008). Further, potassium has a great influence on plant physiological functions like hardening of tissues, opening of stomata, rate of photosynthesis and infestation degree of intensity (Huber and Graham, 1999; Rice, 2007; Spann and Schumann, 2010). Disease susceptibility is also linked with the deficiency of potassium because it has major role in plant metabolism. Under its deficiency, the synthesis of starch, protein and cellulose is impaired. In current study, we found that un-inoculated and resistant citrus varieties contained more potassium concentration as compare to the inoculated and diseased varieties which is also confirmed by Olanya et al. (2000). Sodium is taken up by the plants in the form of Na^+ and great variations were observed in inoculated and un-inoculated citrus varieties during this study. Susceptible and infected citrus varieties accumulated less sodium concentration than resistant and un-infected varieties. Closely related findings were reported by Jadon and Shah (2012) which verify the findings of ongoing study.

Calcium is absorbed by the plant in the form of Ca^+ cation and specifically used in growth of roots and leaves, microbial activities and in the uptake of other essential nutrients. It also helps in defense of plants against the penetration of pathogen and disease resistance. Calcium being a structural and functional component of plant cell wall and membrane acts as a secondary messenger within the symplast in signaling pathways (Rice, 2007). It also plays a key role in maintaining cell integrity and permeability because it is a main part of middle lamella in the form of calcium pectate (Spann and Schumann, 2010). Reduction in the concentration of calcium in plants leads towards the susceptibility against the disease. Calcium also act as a barrier in the regulation of sugars and amino acid molecules in between the cells (from the cytoplasm to the apoplast), which stimulate in the case of calcium reduction and increase the chance of pathogen infection (Marschner, 1995). In current studies, a reduction in calcium concentrations inside infected leaves of citrus plant were observed which was further confirmed and supported by the findings of Amusa et al. (2005).

Magnesium takes part in chlorophyll synthesis, in photosynthesis as central atom for chlorophyll and in carbohydrates metabolism (Devlin and Witham, 1983; Spann and Schumann, 2010). Since Mg is a vital element of structural tissues and take part in different physiological and biochemical processes. It is necessary for integrity and safeguarding of ribosomes and is associated with growth factors, mitosis, protein level, carbohydrates metabolism and oxidative phosphorylation. It also takes part in respiration, DNA and RNA synthesis, energy transfer reactions and also acts as a co-factor for many enzymes (Marschner, 2011). In current study an increase in magnesium contents was observed in resistant and un-inoculated citrus plants as compare to the susceptible and inoculated varieties which showed a significant reduction in Mg contents due to the attack of pathogen and these results are in accordance with the conclusions of Jadon and Shah (2012).

Zinc is important for plants due to its role in resistance to various plant diseases. It acts as a co-factor for various enzymes but the actual role in disease resistance is unclear (Rice, 2007). Application of zinc to the soils reduced the attack of root pathogens

http://www.aloki.hu ● ISSN 1589 1623 (Print) ● ISSN 1785 0037 (Online)
DOI: http://dx.doi.org/10.15666/aeer/1706_1362513642

especially in vegetable crops (Kalim et al., 2003). It plays a significant role in starch and protein formation. A considerable variation in zinc concentration was observed in citrus varieties where there was a less concentration of zinc in inoculated and susceptible varieties as compare to un-inoculated and resistant varieties. Results of present study is supported by the work of Marschner (1995) and Dordas (2008) who also reported decrease in concentration of Zn due to disease.

Fe has a significant and lethal effect on the plant pathogens and its deficiency reduced the xylem lignifications (Evans et al., 2007). A clear variation was observed in the case of iron contents where leaves of un-inoculated and resistant citrus cultivars expressed high amount of Fe contents as compare to inoculated and susceptible one on the infection as witnessed by Zekri and Obreza (2003). It may due to the effect that plant pathogens generally have higher requirement of Fe and act as a virulence factor during the course of disease. The only justification may be the association of iron as a component of various flavoproteins (Metalloflavoproteins) which take part in biological oxidation and increase as a result of inoculation with the pathogen. Iron is found in iron-prophyrn proteins, which include cytochromes, peroxidases and catalases (these proteins may be responsible for increased catabolic activities in susceptible plants) and also act as a co-factor in reduction-oxidation reactions (Devlin and Witham, 1983). Copper is an important component of lignin and have a key role in protein and carbohydrate metabolism and acts as catalyst in different metabolic activities of the plant (Imran and Gurmani, 2011). In current study, reduction in copper contents was observed on the attack of *Xac.* It was confirmed from this study that there is a relationship between nutrients and disease occurrence because pathogen wants nutrients for their growth. Same results of relationship between nutrients and disease severity were reported by Zekri and Obreza (2015).

Conclusion

Reduction in concentrations of minerals like nitrogen, phosphorus, potassium, calcium, magnesium, zinc, sodium, and copper in the diseased host plants were due to the utilization of minerals by the pathogen for its growth and survival. Timely provision of these macro and micro nutrients to plants is helpful in fortification of physical and biochemical processes of citrus plants and also in enhancing the resistance of plants against the canker.

Acknowledgements. Authors are highly thankful to the Higher Education Commission of Pakistan (NRPU-6373) for funding this study.

REFERENCES

[1] Amusa, N., Ashaye, O., Oladapo, M., Oni, M. (2005): Guava fruit anthracnose and the effects on its nutritional and market values in Ibadan, Nigeria. – World Journal Agricultural Sciences 1: 169-172.

[2] Arshadi, F., Sijam, K., Awang, Y. B. (2013): Genetic diversity of *Xanthomonas axonopodis* subsp. *citri*, causal agent of citrus canker. – Journal of Plant Protection Research 53: 312-316.

[3] Bhaduri, D., Rakshit, R., Chakraborty, K. (2014): Primary and secondary nutrients-a boon to defense system against plant diseases. – International Journal of Bio-resource and Stress Management 5: 461-466.

http://www.aloki.hu ● ISSN 1589 1623 (Print) ● ISSN 1785 0037 (Online)
DOI: http://dx.doi.org/10.15666/aeer/1706_1362513642

[4] Bhargava, B. S., Raghupathi, H. B. (1995): Analysis of Plant Materials for Macro and Micro Nutrients. – In: Tandon, H. L. S. (eds.) Methods of Analysis of Soils, Plants, Waters and Fertilizers. Fertilizer Development and Consultation Organisation, New Delhi, pp. 61-62.
[5] Bolts, D. F., Mellon, M. G. (1948): Spectrophotometric determination of phosphorus as molybdi-phosphoric acid. – Analytical Chemistry 27: 749.
[6] Bradbury, K. (2016): An introduction to citrus fruit. – Pakistan journal of Plant Pathology 5(1): 52-60.
[7] Brunings, A. M., Gabriel, D. W. (2003): *Xanthomonas citri*: breaking the surface. – Molecular Plant Pathology 4: 141-157.
[8] Devlin, R. M., Witham, F. H. (1983): Plant Physiology. – Wardsworth Pub. Co., Belmont, CA.
[9] Dordas, C. (2008): Role of nutrients in controlling plant diseases in sustainable agriculture. A review. – Agronomy for Sustainable Development 28: 33-46.
[10] Evans, I., Solberg, E., Huber. D. M. (2007): Copper and Plant Disease. – In: Datnoff, L. E. et al. (eds.) Mineral Nutrition and Plant Disease. American Phytopathological Society, St. Paul, MN, pp. 177-188.
[11] Fiske, C. A., Subbarow. I. (1925): The colorimetric determination of phosphorus. – Journal of Biological Chemistry 66: 375.
[12] Francis, M. I., Peña, A., Graham, J. H. (2010): Detached leaf inoculation of germplasm for rapid screening of resistance to citrus canker and citrus bacterial spot. – European Journal of Plant Pathology 127: 571-578.
[13] Gomez, A. A., Gomez, K. A. (1984): Statistical Procedures for Agricultural Research. – John Wiley and Sons, New York.
[14] Gurib-Fakim, A. (2006): Medicinal plants: traditions of yesterday and drugs of tomorrow. – Molecular Aspects of Medicine 27: 1-93.
[15] Honger, J., Essuman, E., Cornelius, E. (2016): The incidence, severity and aetiology of a bacterial canker disease of citrus in Ghana. – West African Journal of Applied Ecology 24: 31-44.
[16] Huber, D. M. (2007): Nitrogen and Plant Disease. – In: Datnoff, L. E. et al. (eds.) Mineral Nutrition and Plant Disease. American Phytopathological Society, St. Paul, MN, pp. 31-44.
[17] Huber, D. M., Graham, R. D. (1999): The role of nutrition in crop resistance. Mineral nutrition of crops. – Fundamental Mechanisms and Implications 18: 169.
[18] Imran, M., Gurmani, Z. A. (2011): Role of macro and micro nutrients in the plant growth and development. – Science, Technology and Development 30(3): 36-40.
[19] Jadon, K., Shah, R (2012): Effect of Drechslera bicolor infection on physiology of bell pepper. – Journal of Plant Pathology & Microbiology 3: 126.
[20] Jagtap, G. P., Thosar, R. U., Dey, U. (2012): Evaluation of plant extracts and bioagents for the control of gummosis of mandarin orange (*Citrus reticulata* blanko) caused by *Phytophthora* species. – African Journal of Agricultural Research 7(32). DOI: 10.5897/AJAR12.214.
[21] Juhasz, C. C., leduc, A., Boyer, C., Guérin, F., Vernière, C., Pruvost, O., Wonni, I., Ouedraogo, L. (2013): First report of *Xanthomonas citri* pv. *citri* causing asiatic citrus canker in burkina faso. – Plant Disease 97: 1653-1653.
[22] Kalim, S., Luthra, Y. P., Gandhi, S. K. (2003): Cowpea root rot severity and metabolic changes in relation to manganese application. – Journal of Phytopathology 151: 92-97.
[23] Kjeldahl, J. (1983): Determination of protein nitrogen in food products. – Encyclopedia of Food and Agricultural Ethics 28: 757-759.
[24] Kumar, N., Ebel, R. C., Roberts, P. D. (2011): Antioxidant metabolism of grapefruit infected with *Xanthomonas axonopodis* pv. *citri*. – Environmental and Experimental Botany 71: 41-49.

http://www.aloki.hu ● ISSN 1589 1623 (Print) ● ISSN 1785 0037 (Online)
DOI: http://dx.doi.org/10.15666/aeer/1706_1362513642

[25] Ladanyia, M., Ladaniya, M. (2010): Citrus Fruit: Biology, Technology and Evaluation. – Academic Press, Amsterdam.
[26] Lakitan, B. (2007): Fundamentals of Plant Physiology. – Raja Grafindo Persada, Jakarta.
[27] Lee, H. A. (1918): Further data on the susceptibility of rutaceous plants to citrus-canker. – Journal of Agricultural Research 15: 661-665.
[28] Marschner, H. (1995): Mineral Nutrition of Higher Plants. 2nd Ed. – Academic Press, Amsterdam.
[29] Memon, N. A. (2017): Citrus Fruit (Kino). Punjab Produced 98% of Production. – Pakistan Bureau of Statistics 2016-2017, Islamabad.
[30] Mubeen, M., Arshad, M. I. H., Iftikhar, H. M., Irfan, U. M., Bilqees, I. (2015): Biochemical charecterization of *Xanthomon asaxonopodis* pv. *citri*: a gram negative bacterium causing citrus canker. – International Journal of Science and Nature 6(2): 151-154.
[31] Olanya, O., El-Bedewy, R., Ojiambo, P., Ewell, P., Hakiza, J. (2001): Relationships of Fungicide Application to Late Blight Development and Potato Growth Parameters in the Tropical Highlands of Uganda and Kenya. – International Potato Center 1990-2000, Lima, Peru.
[32] Pervaiz, S. (2015): Fruit, vegetable fail to enter European Union. A report. – http://the dailystar.net/business.
[33] Rice, R. W. (2007): The Physiological Role of Minerals in the Plant. – In: Datnoff, L. E. et al. (eds.) Mineral Nutrition and Plant Disease. American Phytopathological Society Press, St. Paul, MI, pp. 9-29.
[34] Roeschlin, R. A., Favaro, M. A., Chiesa, M. A., Alemano, S., Vojnov, A. A., Castagnaro, A. P., Filippone, M. P., Gmitter, F. G., Gadea, J., Marano, M. R. (2017): Resistance to citrus canker induced by a variant of *Xanthomonas citri* ssp. *citri* is associated with a hypersensitive cell death response involving autophagy-associated vacuolar processes. – Molecular Plant Pathology18: 1267-1281.
[35] Ryan, R. P., Vorhölter, F.-J., Potnis, N., Jones, J. B., Van Sluys, M.-A., Bogdanove, A. J., Dow, J. M (2011): Pathogenomics of *Xanthomonas*: understanding bacterium–plant interactions. – Nature Reviews Microbiology 9: 344-355.
[36] Sahi, S. T., Ghazanfar, M. U., Afzal, M., Rashed, A., Habib, A. (2007): Incidence of citrus canker disease caused by *Xanthomonas axonopodis* pv. *citri* (Hasse) dows on Kinnow (*Citrus reticulata*) and its chemotherapy. – Pakistan Journal of Botany 39: 13-19.
[37] Sahi, S. T., Ghazanfar, M. U., Afzal, M., Wakil, W., Habib, A. (2010): Influence of inoculation with ascochyta lentis mineral contents (Na, Ca, Mg, Zn, Cu and Fe) of susceptible and resistant lines of lentil (*Lens culinaris medik*.). – Pakistan Journal of Botany 42: 375-382.
[38] SAS Institute Inc. (2009): SAS Procedures Guide. Version 9.3. Third Edition. SAS Programming Tips: www.ats.ucla.edu/STAT/SAS/library/nesug00/bt3005. – SAS Institute Inc., Cary, NC.
[39] Schubert, T. S., Rizvi, S. A., Sun, X., Gottwald, T. R., Graham, J. H., Dixon, W. N. (2001): Meeting the challenge of eradicating citrus canker in Florida—again. – Plant Disease 85: 340-356.
[40] Spann, T. M., Schumann, A. W. (2010): Mineral Nutrition Contributes to Plant Disease and Pest Resistance. – University of Florida, IFAS Extension, Gainesville, FL.
[41] Spann, T., Schumann, A. (2012): Using good horticultural practices to maintain yield of HLB-affected groves. – Cell 772: 473-4142.
[42] Vandermeer, J., Perfecto, I., Philpott, S. (2010): Ecological complexity and pest control in organic coffee production: uncovering an autonomous ecosystem service. – BioScience 60: 527-537.
[43] Wali, S., Munir, F., Mahmood, T. (2013): Phylogenetic studies of selected citrus species based on chloroplast gene, rps14. – International Journal of Agricultural Biology 15: 357-361.

http://www.aloki.hu ● ISSN 1589 1623 (Print) ● ISSN 1785 0037 (Online)
DOI: http://dx.doi.org/10.15666/aeer/1706_1362513642

[44] Ware, M. (2015): Oranges: health benefits, nutritional information. – https://www.medicalnewstoday.com/articles/272782.php.
[45] Zekri, M., Obreza, T. (2015): Macronutrient Deficiencies in Citrus: Nitrogen. Phosphorus, and Potassium. – University of Florida. IFAS Extension, Gainesville, FL. http://edis. ifas.ufl.edu/ss420.

http://www.aloki.hu ● ISSN 1589 1623 (Print) ● ISSN 1785 0037 (Online)
DOI: http://dx.doi.org/10.15666/aeer/1706_1362513642

EVOLUTION AND IDENTIFICATION OF SOME DATE PALM (*PHOENIX DACTYLIFERA* L.) CULTIVARS GROWN IN THE EL-DAKHLA OASIS, EGYPT

SALAMA, M. I.[1] – OMAR, A. K.[1] – EL-MORSY, A. A.[1] – OMAR, A. A.[1,2*] – ALAMELDEIN, S. M.[3] – ALY, K. M.[4]

[1]*Kafresheikh University, Faculty of Agriculture, Horticulture Dept., Kafr El-Sheikh 33516, Egypt*

[2]*Institute of Research and Consulting, King Faisal University, Hofuf, Kingdom of Saudi Arabia*

[3]*Horticulture Department, Faculty of Agriculture, Tanta University, Tanta 31527, Egypt*

[4]*Date Palm Research and Development, Agricultural Research Center, Giza, Egypt*

**Corresponding author*
e-mail: alaa.omr@agr.kfs.edu.eg, akomar@kfu.edu.sa; phone: +20-109-740-8240

(Received 13th Apr 2019; accepted 19th Jun 2019)

Abstract. This study was carried out during two consecutive seasons on five date palm cultivars grown under the "environmental conditions". of El- Dakhla oasis, New Valley governorate, Egypt. Five date palm cultivars (Bartamoda, Sakoty, Soltany, Sewy and Barhy) were evaluated using morphological characteristics as well as inter- simple sequence repeats (ISSR) as DNA fingerprinting. Results revealed that, Barhy had the highest values through most of the study, it obtained the highest values in leaflet area (161.59 and 176.70 cm^2), fruit weight (15.23 and 16.33 g), flesh weight (13.89 and 14.99 g), flesh percentage (91.11 and 91.76%), number of bunches (18.8 and 18.66) and yield/palm (195.4 and 197.21 kg). In this study, the total number of ISSR bands were 52 bands, 31 bands were polymorphic "59.61%" and 21 bands were monomorphic "40.38%". The polymorphic bands contained 20 unique bands, these unique bands could be used to "discriminate" between the studied five date palm cultivars.
Keywords: *RAPD, morphological characteristics, DNA, ISSR*

Introduction

Dates are dioecious perennial monocotyledon fruit trees that belong to the Arecaceae family. Date palm (*Phoenix dactylifera* L.) is one of the most important and oldest fruit trees cultivated by man, it is considered to be the oldest tree with great genetic diversity (Popenoe, 1973). Date palm is an important fruit crop in Egypt where the total annual production of date fruits is about 1,730,000 tonnes (FAO Statistics, 2018). It is the most common fruit tree grown in semiarid and arid regions it plays an important role in the protection of interplant cropping system and the stabilization of the ecological system (Hasnaou et al., 2011). For this reason date palm is considered one of the suitable trees which could be cultivated in the new reclaimed desert regions. In Egypt, date palm is one of the most important fruits and widely distributed in different districts, where they are harvested and market at three stages of their development. The Arabic names for the various stages of development of dates are the terms used universally. After pollination, date fruits initially have a slow growth period essentially due to cell division up to the end of the six weeks from pollination. Thereafter fruits enter into the rapid phase of growth which is termed the "Kimiri" stage when fruits are young and green in color (16 weeks from pollination). Fruits then begin to change color and reach maximum weight and size at the "Khalal" (also called "Bisr") stage (20 weeks from pollination); this is considered as the

http://www.aloki.hu ● ISSN 1589 1623 (Print) ● ISSN 1785 0037 (Online)
DOI: http://dx.doi.org/10.15666/aeer/1706_1364313655

maturi- ty stage. Fruits enter the ripening or "Rutab" stage (22 weeks from pollination) when the fruit begins to soften, lose moisture content and astringency, and starts acquiring a dark and less attractive color (Kassem, 2012). Finally, fruits con- tinue to lose their fresh weight and reach the lowest value at the "Tamr" stage (23 weeks from pollination) which may be considered as the senescence stage (Hobani et al., 2003; Taain, 2013). Soft cultivars are harvested and used at the "Khalal" and "Rutab" stages, but semi-dry and dry cultivars are harvested and used at the "Tamr" stage (Riad, 1993). Among all Egyptian governorates, New Valley ranked the fourth position after Sharkia, Behaira and Aswan according to acreage and the number of female palms. It is well known fact that morphological plasticity is a major weak point in assessment of phenotypic diversity. However, the study on inheritance of agronomic traits of fruit trees (citrus) is known to be controlled by multiple genes, which can be authenticated only through morphological characterization (Liu and Deng, 2007). The correct identification palms based on physiological and morphological markers is usually not possible until fruits are produced. Moreover, the characterization and evaluation of genetic diversity based on large set of phenotypic data is often difficult to assess due to environmental influences (Sedra et al., 1998). Molecular markers based on DNA sequence proved to be an ideal means for the identification and estimation of relatedness among genotypes of different origin. Different markers based on DNA sequences have been developed in the previous years for DNA fingerprinting and genome mapping (Naz et al., 2014). DNA-based molecular markers have been employed to provide reliable useful information on the genetic diversity, relationship between cultivars, DNA fingerprinting, and pedigree analysis (Ayesh, 2017; Haider, 2017; Purayil et al., 2018). Recently, inter simple sequence repeats (ISSR) markers have been emerged as an alternative system with reliability and advantages of microsatellites (SSRs) (Cregan, 1992). The ISSR strategy was therefore performed to access the DNA diversity among crop genotypes (Zehdi et al., 2004). ISSR markers are also believed to be simple, rapid, inexpensive and highly reproducible due to their primer length and to the high stringency achieved to be one of the most efficient techniques that can rapidly reveal high polymorphism and determine genetic diversity in date palm (Zehdi et al., 2004). Determination of genetic relationships among date palm cultivars is of major importance for characterization of date palm germplasm, breeding programs, and conservation purposes. The present study signifies the applicability of ISSR marker system in detecting genetic diversity of date palm cultivars. This may facilitate the conservation and improvement of date palm cultivars in the future. The aim of the study is the analysis of the genetic diversity among a set of Egyptian date palm varieties.

The aim of this work was elucidating the differences on growth, fruiting aspects and identify the genetic diversity between five date palm cultivars namely "Bartamoda", "Sakoty", "Soltany", "Sewy" and "Barhy".

Materials and methods

The present study was carried out during the two successive seasons of 2016 and 2017 on evaluated vegetative growth, physical and chemical fruit properties as well as genetic diversity analysis of some date palm cultivars grown at private orchards of El-Dakhla Oasis, New Valley governorate, Egypt (which lies between 22° and 31° North latitudes and between 25° and 35° East longitudes. Its climate (comprising a mild and wet winter from November to April and a hot and dry summer from May to October) is suitable for the production of many field and horticultural crops (Directorate of

http://www.aloki.hu ● ISSN 1589 1623 (Print) ● ISSN 1785 0037 (Online)
DOI: http://dx.doi.org/10.15666/aeer/1706_1364313655

Intelligence, 2011).). These cultivars are classified and nominated according to their moisture content in to three groups as follows: a) dry date palm cultivars (Bartamoda, Sakoty and Soltany) b) semidry date palm cultivars (Sewy) c) soft date palm cultivars (Barhy). Three trees were chosen for each cultivar of about 23-25 years old, grown in sandy loam soil. The palms were similar in vigor and received the same orchard management. The inflorescences of the trees under this study were manually pollinated by one source of pollen. At first week of October vegetative characteristics of chosen trees were measured in both seasons. Leave length (m), umber of leaflet, number of spines, leaflet area (cm^2), leave zone (m), spine length (cm), leaflet length (cm) and leaflet width (cm) were measured. Total yield was determined at harvest, each spathe was weighed separately using weighing balance and was expressed in kilogram (kg). For fruit properties fifty fruits were randomly taken from each palm. Physical properties of fruits included fruit and seed weight as well as flesh weight, percentage of flesh, fruit length, seed length and fruit dimensions. The chemical constituents included: Moisture content was determined in about 50 g of chopped flesh sample which was taken and dried in draft oven at 70 °C until a constant weight was obtained, soluble solids content (SSC) was determined by using a hand refractometer according to Chen and Mellenthin (1981). Titratable acidity percentage in the flesh expressed as percentage by titration against NaOH (0.1 N) using phenolphethaline as an indicator as described by A. O.A.C. (1985). Total and reducing sugars concentration were determined according to Lan and Eynon method as described by the A.O.A.C. (1985).

Molecular analysis

DNA extraction

Fresh leaves of date palm were collected separately from different strains and cultivar. Then DNA extraction was performed as described by Dellaporta et al. (1983). About 0.1 g (fresh weight) of plant tissues was ground to fine powder in liquid N_2 using mortar and pestle. Before the tissue thawed, 1 ml extraction buffer (100 mM Tris-HCl pH 8.0, 50 mM EDTA and 0.5 M NaCl) and 0.2 ml 20% SDS were added. The mixture was incubated at 65°C in water bath for 20 minutes. Then 1 ml of phenol, chloroform and isoamyl alcohol (25: 24: 1) was added. Centrifugation was performed at 10,000 rpm for 10 min. The supernatants of each sample were transferred separately to new tubes, and then 1 ml of chloroform and isoamyl alcohol (24:1) was added. Centrifugation was performed at 10,000 rpm for 10 minutes. The supernatants of each sample were transferred separately to a new tube, then 1 ml of isopropanol was added and then kept overnight in a freezer. Centrifugation was performed at 10,000 rpm for 10 min. The resulted pellets containing DNA were re-suspended in 1 ml ethanol. Centrifugation was performed at 10,000 rpm for 2 min. The DNA pellets were re-suspended in 200 TE buffer (10 mM Tris-HCl pH 8.0 and 1 mM EDTA). DNA purity and quantity was determined by UV -spectrophotometer and gel electrophoresis.

ISSR-PCR analysis

ISSR-PCR reactions were conducted using five primers. Amplification was conducted in 25 µl reaction volume containing the following reagents: 2.5 µl of dNTPs (2.5 mM), 2.5 µl Mgcl2 (2.5 mM), and 2.5 µl of 10 × buffer, 3.0 µl of primer (10 pmol), 3.0 µl of template DNA (25 ng/µl), 1 µl of Taq polymerase (1U/µl) and 12.5 µl of sterile dd H_2O. the PCRs were programmed for one cycle at 94 °C for 4 min followed

http://www.aloki.hu ● ISSN 1589 1623 (Print) ● ISSN 1785 0037 (Online)
DOI: http://dx.doi.org/10.15666/aeer/1706_1364313655

by 45 cycles of 1 min at 94 °C, 1 min at 40-48 °C (according to the primer), 2 min at 72 °C, then the reaction was finally stored at 72 °C for 10 min. The PCR products were separated on a 1.5% agarose gels and fragments sizes were estimated with the 100 bp ladder DNA marker (Fermentas.com).

Inter simple sequence repeat (ISSR-PCR) procedure

PCR reactions were conducted using 5 arbitrary 10-mer primers. Their names and sequences are shown in *Table 1*.

Table 1. *List of the primer names and their nucleotide sequences used in the study for ISSR procedure.*

No.	Name	Sequence	Annealing temp.
1	14A	5' CTC TCT CTC TCT CTC TTG 3'	40
2	44B	5' CTC TCT CTC TCT CTC TGC 3'	40
3	HB-09	5' ACC CGC AAGG 3'	48
4	HB-12	5' CACCACCACGC 3'	45
5	HB-15	5' GTG GTG GTG GC 3'	48

Statistical analysis

The experiment was set as randomized complete block design with three replicates (each palm as a replicate) per treatment (cultivar) according to Little and Hills (1972) and analyzed by the standard methods according to Snedecor and Cochran (1980). The new L.S.D. test was used for comparison between means. The DNA bands generated by each primer were counted and their molecular sizes were compared with those of the DNA markers. The bands scored from DNA profiles generated by each primer were pooled together. Then the presence or absence of each DNA band was treated as calculate genetic similarity and to construct dendrogram tree among the studied date palm seedling strains and Bartamoda cultivars. Calculation was achieved using Dice Similarity Coefficients (Dice, 1945) as implemented in the computer program SPSS-10.

Results and discussion

Vegetative measurements

Data presented in *Table 2* showed the vegetative measurements of five date palm cultivars. Results showed that Soltany cv. gave the highest values of leaf length (5.39 and 5.53 m) and number of spins (54.2 and 53.66).

While Barhy cv., had the highest value of leaflet area (161.59 and 176.70 cm^2). Also, results indicated that Sewy cv. recorded the highest of leaflet zone/leave (3.37 and .366 m). Sakoty cv., gave the highest value of number of leaflet (212 and 214). On other hand, Bartamoda cv., gave the lowest value of leaf length (3.57 m), number of leaflet (173.2) and number of spines (25.2) in the first season and the number of leaflet (179.66) and leaflet zone/leave (2.81 m) in the second season. These results are in agreement with Abdalla (1979) found that with Iraq and Egyptian date palm cultivars, i.e., Brahee, Hallawy, Sayer and Samany the number of spines per leaf and spine length were in the average of 15-29 and 4-13 cm, respectively.

http://www.aloki.hu ● ISSN 1589 1623 (Print) ● ISSN 1785 0037 (Online)
DOI: http://dx.doi.org/10.15666/aeer/1706_1364313655

Table 2. *Some morphological measurements of five date palm cultivars grown under New Valley condition during 2016 and 2017 seasons*

Strains	Leaf length (m)		No-of leaflet		No-of spines		Leaflet area (cm^2)		Leaflet zone/leave (m)	
	2016	2017	2016	2017	2016	2017	2016	2017	2016	2017
Bartamoda cv	3.57d	4.65c	173.2d	179.66d	25.2c	27.33c	130.06b	126.52bc	2.8b	2.81b
Sakoty	3.67d	3.68c	212a	214a	25.6c	25.33c	98.31c	96.85c	2.92b	2.86b
Soltany	5.39a	5.53a	198.2b	200.66b	54.2a	53.66a	134.06ab	124.06bc	3.52a	3.43ab
Sewy	3.37a	5.2a	187c	197.33b	27.2c	28.66c	132.30ab	149.53ab	3.37a	3.66a
Barhy	4.37c	4.38b	186.8c	190c	33.8b	34.33b	161.59a	176.70a	3.02b	3.17ab

Values with the same letter in the same column are not significant at ($P \geq 0.05$)

Yield parameters, number of bunches and fruit physical characteristics

It is clear from obtained data in *Tables 3* and *4* and *Fig. 1* showed that Barhy cv., had the highest values in most studied fruit physical characteristics as compared to other studied cultivars. It, was gave the highest fruit weight (15.23 and 16.33 g), flesh weight (13.89 and 14.99 g) and flesh percentage (91.11 and 91.76%). While, Sewy cv. gave the highest seed weight (1.71 and 1.80 g).

Table 3. *Yield parameters, number of bunches and fruit physical characteristics of five date palm cultivars grown under New Valley condition during first season (2016)*

Strains	Fruit weight (g)	Flesh weight (g)	Seed weight (g)	Seed length (cm)	Fruit length (cm)	Fruit diameter (cm)	Flesh %	No-bunch/ palm	Yield/ palm
Bartamoda cv	6.17d	5.16d	1.00c	2.3b	4.38b	2.04c	83.77c	10cd	89cd
Sakoty	8.34c	7.42c	0.91c	2.74a	5.00a	1.98c	88.98ab	8.8d	80.5d
Soltany	11.16b	9.52b	1.64a	2.46ab	3.36e	2.00c	85.16c	12.2bc	98.16c
Sewy	14.70a	12.98a	1.71a	2.4b	4.18c	2.58b	88.28b	13.8b	132.2b
Barhy	15.23a	13.89a	1.34b	1.8c	3.62d	3.12a	91.11a	18.8a	195.4a

Values with the same letter in the same column are not significant at ($P \geq 0.05$)

On other hand, Sakoty cv. gave the lowest value of fruit diameter (1.98 and 1.96 cm) and seed weight (0.91 and 0.91g). Also, Bartamoda cv., recorded the lowest value of flesh percentage (83.77 and 82.63%).

Table 4. *Yield parameters, number of bunches and fruit physical characteristics of five date palm cultivars grown under New Valley condition during second season (2016)*

Strains	Fruit weight (g)	Flesh weight (g)	Seed weight (g)	Seed length (cm)	Fruit length (cm)	Fruit diameter (cm)	Flesh %	No-bunch/ palm	Yield/ palm
Bartamoda cv	6.19d	5.11d	1.07cd	3.69a	4.43b	2.1c	82.63c	9.66c	91.0cd
Sakoty	8.45c	7.54c	0.91d	2.83a	5.06a	1.96d	89.17ab	9.0c	81.0d
Soltany	11.76b	10.16b	1.6ab	2.4a	3.46e	2.03cd	86.29b	12.33b	94.61e
Sewy	16.03a	14.23a	1.80a	2.5a	4.2c	3.63b	88.72ab	13.66b	124.06b
Barhy	16.33a	14.99a	1.34bc	1.8a	3.66d	3.2a	91.76a	18.66a	197.21a

Values with the same letter in the same column are not significant at ($P \geq 0.05$)

http://www.aloki.hu ● ISSN 1589 1623 (Print) ● ISSN 1785 0037 (Online)
DOI: http://dx.doi.org/10.15666/aeer/1706_1364313655

Figure 1. *The fruit of five date palm cultivars.* ***1*** *Bartamoda,* ***2*** *Sakoty,* ***3*** *Soltany,* ***4*** *Sewy, and* ***5*** *Barhy*

Regarding number of bunches and yield/palm, Barhy cv., had the highest number of bunches (18.8 and 18.66) and yield/palm (195.4 and 197.21 kg) followed by Sewy cv. in both seasons. On other hand, Sakoty cv. gave the lowest number of bunches (9 and 8.8) and yield/ palm (80.5 and 81 kg). These results are in harmony with present results those obtained by Abo-Rekab et al. (2014), Idris et al. (2014), Mortazavi et al. (2015), Nasir et al. (2015), Omaima, et al. (2015), Qadri et al. (2016), Abd-El Hamed, et al. (2017). Who found that Sakoti gave the lowest seed weight in both seasons (0.961 and 0.985 g, respectively) (Abo Rekab et al., 2010). These data are in agreement with El-Merghany et al. (2013) they found that Barhy cv. gave the highest yield/palm in the second season.

Chemical properties

Data presented in *Table 5* showed the chemical properties of five date palm cultivars. Results showed that Sewy cv. gave the highest value of reducing and total sugar (65.41 and 64.88) and (74.64 and 74.46) respectively, while Barhy cv. recorded the highest moisture % (31.56 and 31.23%) as compared to other date palm cultivars.

http://www.aloki.hu ● ISSN 1589 1623 (Print) ● ISSN 1785 0037 (Online)
DOI: http://dx.doi.org/10.15666/aeer/1706_1364313655

Table 5. *Fruit chemical properties of five date palm cultivars grown under New Valley condition during 2015 and season (2016)*

Cultivars	Moisture %		T.S.S		Acidity %		Reducing sugars		Non-reducing sugar %		Total sugar %	
Seasons	**2016**	**2017**	**2016**	**2017**	**2016**	**2017**	**2016**	**2017**	**2016**	**2017**	**2016**	**2017**
Bartamoda	14.26d	14.61d	78.76ab	79.87a	0.136d	0.137c	7.33d	7.48e	63.22a	63.23a	70.56bc	71.04b
Sakoty	12.93e	12.96e	78.42b	78.31b	0.199b	0.200b	10.20c	10.06d	60.12b	61b	71.06b	71.06b
Soltany	17.4c	17.36c	79.58a	78.48b	0.223a	0.223a	11.4c	11.7c	58.46c	58.4c	69.86c	70.00b
Sewy	23.96b	23.87b	78.2b	77.85b	0.037e	0.046d	65.41a	64.88a	9.23e	9.58e	74.64a	74.46a
Barhy	31.56a	31.23a	57.83c	58.16c	0.187c	0.188b	37.66b	38.00b	14.00d	13.66d	51.66d	51.66c

Values with the same letter in the same colum are not significant at ($P \geq 0.05$)

Also, Soltany cv. had the highest of acidity (0.223 and 0.223%). On other hand, Bartamoda cv. gave the lowest value of reducing sugar (7.33 and 7.48%). While, Sakoty cv. had the lowest of moisture % (12.93 and 12.96%). Also, Barhy cv. recorded the lowest of total sugars (51.66 and 51.66). These results are in agreement with many researchers such as Gadalla et al. (2013), Idris et al. (2014), Mortazavi et al. (2015), Nasir et al. (2015), El-Salhy et al. (2016), Qadri et al. (2016), Abd-El Hamed et al. (2017), who found that Barhy at khalal stage gave the lowest total sugars percentage (51 and 50%) in both season. Youssef et al. (1998) found that total sugars concentration in fruits of eight date palm cultivars (from different areas of Upper Egypt) were ranged from 73.65 to 81.77% for dry cultivars.

Identification of ISSR-PCR markers

To determine the genetic relationships among the 5 date palm cultivars, ISSR profile resulting from using 5 tested primers, i.e. 14A, 44B, HB- 09, HB-12 and HB-15 were illustrated in *Table 6* and *Figure 2*.

Table 6. *The ISSR analysis products produced by the five primers investigated of ten date palm seedlings strains as well as Bartamoda cultivar. (1 means presence and 0 means absence)*

Band no.	M.W bp	Sewy	Soltany	Bartamoda	Sakoty	Barhy
		14A				
1	565	1	1	1	1	1
2	435	0	0	0	0	1
3	370	1	1	0	1	1
4	315	1	1	0	0	0
5	265	0	0	1	0	0
Total		3	3	2	2	3
Band no.	**M.W bp**	**44B**				
1	825	0	0	0	0	1
2	690	0	1	0	0	0
3	510	0	0	0	1	0
4	425	0	0	0	0	0
5	355	1	1	0	1	1
6	280	1	1	1	1	1
7	225	1	1	1	1	1
8	190	1	1	1	1	1
Total		4	5	3	5	5

http://www.aloki.hu ● ISSN 1589 1623 (Print) ● ISSN 1785 0037 (Online)
DOI: http://dx.doi.org/10.15666/aeer/1706_1364313655

Band no.	M.W bp	HB-09				
1	985	1	0	1	0	0
2	880	0	1	0	1	1
3	860	0	0	0	0	0
4	735	1	0	1	0	0
5	615	0	1	0	1	1
6	520	0	0	0	0	0
7	450	1	1	0	0	0
8	415	1	1	1	1	1
9	355	1	1	1	1	1
10	315	1	1	1	0	1
11	250	1	1	1	1	1
12	215	1	1	1	1	1
13	180	1	1	1	1	1
Total		9	9	8	7	8
Band no.	**M.W bp**	**HB-12**				
1	985	1	0	1	1	1
2	880	0	0	1	1	1
3	860	1	0	0	0	0
4	735	1	0	1	1	1
5	615	1	0	1	1	1
6	520	1	0	1	1	1
7	450	1	1	1	1	1
8	415	1	0	1	1	1
9	355	1	0	1	1	1
10	315	0	1	1	0	0
Total		8	2	9	8	8
Band no.	**M.W bp**	**HB-15**				
1	2075	0	0	0	0	0
2	1600	1	1	0	1	1
3	1370	1	1	0	1	1
4	1355	1	1	0	0	0
5	1150	1	1	1	1	1
6	1115	1	1	0	1	1
7	910	0	0	0	0	0
8	825	1	1	0	0	0
9	800	1	1	0	1	1
10	575	1	1	1	1	1
11	510	1	1	1	1	1
12	415	1	1	1	1	1
13	310	1	1	0	1	1
14	275	1	1	1	1	1
15	220	1	1	1	0	0
16	150	1	1	1	1	1
Total		14	14	7	9	9

A total number of 52 ISSR bands were obtained of these 31 bands were polymorphic (59.61%) and 21 were monomorphic (40.38%) both primer HB-12 and 14A exhibited high polymorphism percentage (90 and 80%), respectively. On the other hand, primer HB-09 exhibited low polymorphism (46.15%). Primer 14A showed three specific fragments two of them was positive markers with molecular size 435 bp and 265 bp for

http://www.aloki.hu ● ISSN 1589 1623 (Print) ● ISSN 1785 0037 (Online)
DOI: http://dx.doi.org/10.15666/aeer/1706_1364313655

Barhy and Bartamoda cultivars and the other specific fragments was negative marker with molecular size 370 p for Bartamoda cultivar. Primer 44B showed four specific fragments, three of them was positive markers with molecular size 825, 690 and 510 bp for Barhy, Soltany and Sakoty, respectively, and the other specific fragment was negative markers for Bartamoda cultivar. Primer HB-09 showed specific fragment (315 bp) as negative marker for Sakoty cultivar. Primer HB-12 Showed specific fragment, one of them was positive marker with molecular size 860 bp for Sewy cultivar and the other specific fragments (six markers) was negative marker for Soltany cultivar. Primer HB-15 showed specific fragment, each these fragments were negative markers for Bartamoda cultivar (*Table 7* and *Fig. 2*).

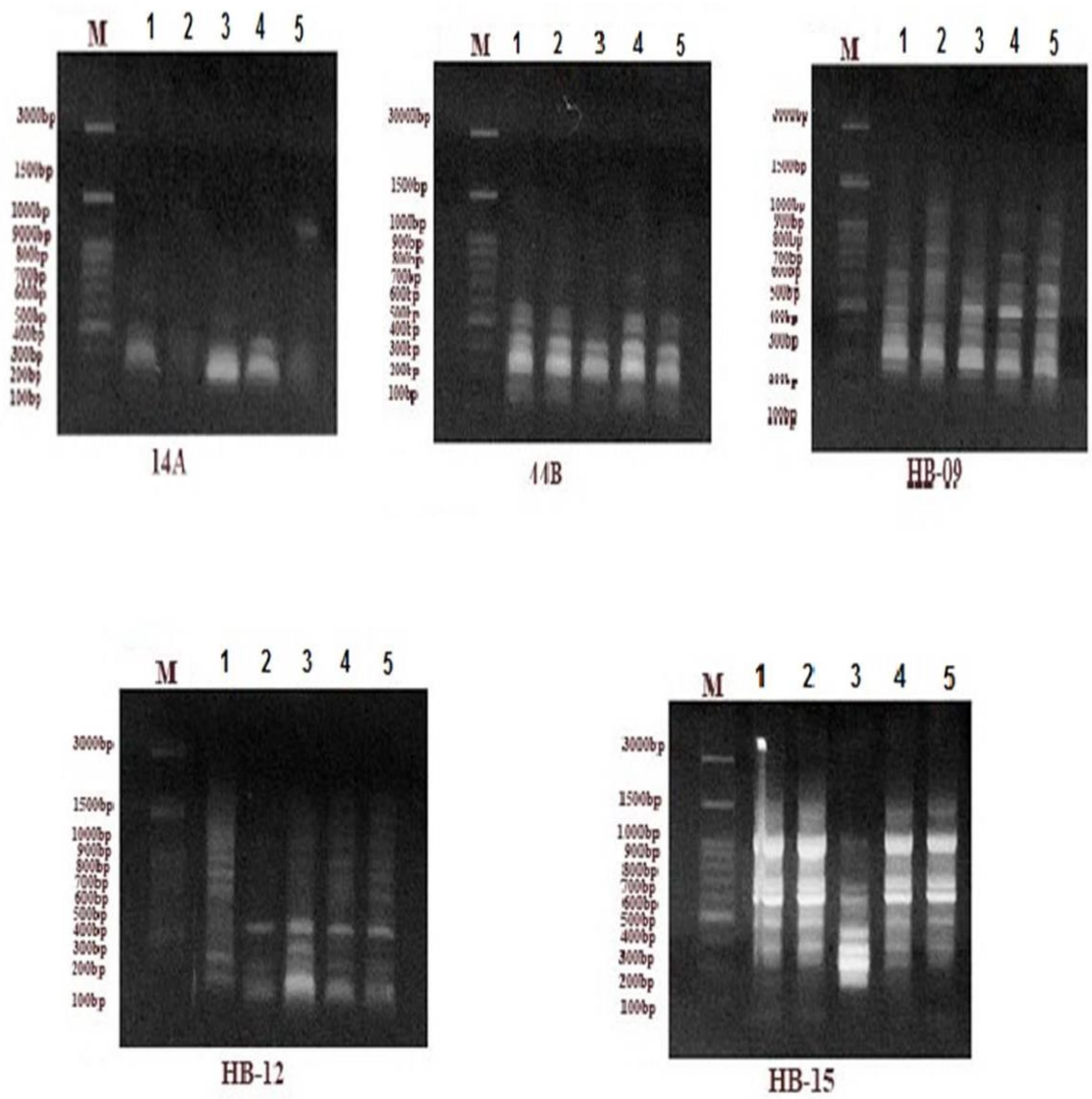

Figure 2. *ISSR products generated with primers 14A, 44B, HB-09, HB-12 and HB-15 in five date palm cultivars cultivar. (1: Sewy, 2: Soltany, 3: Bartamoda, 4: Sakoty, 5: Barhy)*

A total number of 52 ISSR bands were obtained of these 31 bands were polymorphic (59.61%) and 21 were monomorphic (40.38%) both primer HB-12 and 14A exhibited high polymorphism percentage (90 and 80%), respectively. On the other hand, primer

http://www.aloki.hu ● ISSN 1589 1623 (Print) ● ISSN 1785 0037 (Online)
DOI: http://dx.doi.org/10.15666/aeer/1706_1364313655

HB-09 exhibited low polymorphism (46.15%). Primer 14A showed three specific fragments two of them was positive markers with molecular size 435 bp and 265 bp for Barhy and Bartamoda cultivars and the other specific fragments was negative marker with molecular size 370 p for Bartamoda cultivar. Primer 44B showed four specific fragments, three of them was positive markers with molecular size 825, 690 and 510 bp for Barhy, Soltany and Sakoty, respectively, and the other specific fragment was negative markers for Bartamoda cultivar. Primer HB-09 showed specific fragment (315 bp) as negative marker for Sakoty cultivar. Primer HB-12 Showed specific fragment, one of them was positive marker with molecular size 860 bp for Sewy cultivar and the other specific fragments (six markers) was negative marker for Soltany cultivar. Primer HB-15 showed specific fragment, each these fragments were negative markers for Bartamoda cultivar (*Table 6* and *Fig. 2*).

Table 7. *Total number of bands, polymorphic band, monomorphic band, unique band and polymorphic %*

Primer name	Total band	Polymorphic band	Monomorphic band	Unique band	Polymorphic %
14A	5	4	1	3	80
44B	8	4	4	4	50
HB-09	13	6	7	1	46
HB-12	10	9	1	7	90
HB-15	16	8	8	5	50
Total	52	31	21	19	-

Genetic similarity and cluster analysis based on ISSR-markers

The ISSR data were used to estimate the genetic similarity among five date palm cultivars by using UPGMA computer analysis as presented in *Table 8*.

Table 8. *Genetic similarity matrices among the ten dry seedlings strains as well as Bartamoda cultivar accessions as compute according to Dice coefficient from ISSR*

Similarity	Sewy	Soltany	Bartamoda	Sakoty
Soltany	0.81	1.00		
Bartamoda	0.77	0.61	1.00	
Sakoty	0.84	0.78	0.76	1.00
Barhy	0.84	0.78	0.77	1.00

The highest similarity index (1.00) was recorded between Barhy and Sakoty date palm cultivar, while the lowest similarity index (0.61) was detected between Bartamoda and Soltany.

A dendrogram for the genetic relationship among the five date palm cultivars was drawn in *Figure 3* which separated cultivars into two major cluster.

The first cluster contained the Bartamoda cultivar while the second cluster was divided into two subcluster where the first sub cluster included Soltany cultivar, while the second sub cluster consisted of two group, the first group included Sakoty and Bartamoda cultivars, whereas the second group included Sewy cultivar. The results of

http://www.aloki.hu ● ISSN 1589 1623 (Print) ● ISSN 1785 0037 (Online)
DOI: http://dx.doi.org/10.15666/aeer/1706_1364313655

ISSR are in harmony with Sami et al. (2004). They concluded that the cultivar Siwi characterized by a unique positive marker (OPB05 $_{1700}$ bp). Zeinab et al. (2014) reported that using ISSR analysis which gave two specific DNA band with molecular size 640 and 160 bp were absent (negative marker) for Shamia and Sakoty cultivar, respectively.

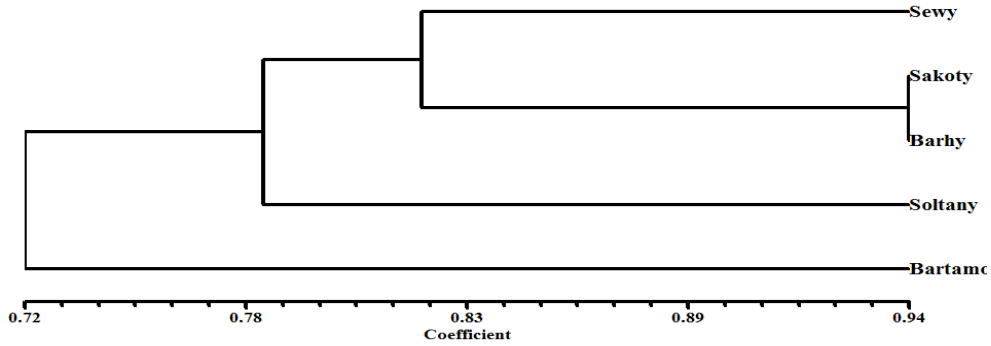

Figure 3. *Dendrogram for the five date palm cultivars as accessions constructed from the ISSR data using unweighed pair-group arithmetic (UPGMA) and similarity matrices computed according to Dice coefficient*

Conclusion

This morphological variation showed that the date palm varieties accessions under study were phenotypically different individuals. The results indicated the existence of diverse accessions in date palm germplasm in spite of similar morphological characters present in genotypes.

Thus, the SSR markers are effective to identify diversity or closeness in genotypes which may contribute to fasten the breeding programs and help in date palm crop improvement.

REFERENCES

[1] A.O.A.C. (1985): Methods of Analysis 14th Ed. – Association of Official Agriculture Chemists, Washington. DC.

[2] Abdalla, M. Y. (1979): Studies on some soft date cultivar. – MSc Thesis, Fac. Agric., Zagazig Univ., Egypt.

[3] Abd-El Hamed, K., Darwesh Rasmia, S. S., Zayed, E. M. M. (2017): Evaluation physical and chemical characteristics of some seedlings date palm fruits (Maghal) in the North Delta Egypt. – International Journal of Advances in Agricultural Science and Technology 4(7): 13-32.

[4] Abo-Rekab, Z. A., Gadalla, E. G., Mohamed, S. Y. (2010): Morphological, physiological and molecular genetic evaluation of the most important Egyptian dry date palm. – J. Biol. Chem. Environ. Sci. 5(3): 23-47.

[5] Abo-Rekab, Z. A., Ghada, A., El-Kafrawy, T. M., Madboly, E. A. (2014): Physico-chemical characters and molecular genetic evaluation of selected dry date palm seedling trees. – Middle East Journal of Applied Sciences 4(4): 931-941.

[6] Ayesh, B. M. (2017): Genotyping and Molecular Identification of Date Palm Cultivars Using Inter-Simple Sequence Repeat (ISSR) Markers. – In: Al-Khayri, J., Jain, S., Johnson, D. (eds.) Date Palm Biotechnology Protocols. Vol. II. Methods in Molecular Biology. Vol. 1638. Humana Press, New York.

http://www.aloki.hu ● ISSN 1589 1623 (Print) ● ISSN 1785 0037 (Online)
DOI: http://dx.doi.org/10.15666/aeer/1706_1364313655

[7] Chen, P. M., Mellenthin, W. M. (1981): Effect of harvest date on ripening capacity and post-harvest life of d' Anjoupears'. – J. Amer. Soc. Hort. Sci. 106(1): 38-42.
[8] Cregan, B. (1992): Simple sequence repeats DNA length polymorphism. – Prole. 2: 18-22.
[9] Dellaporta, S. L., Wood, J., Hicks, J. B. (1983): A plant DNA mini preparation. Version III. – Plant Mol. Biol. 1: 19-21.
[10] Dice, L. R. (1945): Measures of the amount of ecologic association between species. – Ecology 26: 297-302.
[11] Directorate of Intelligence (2011): "CIA - World Fact-book". Information on the history, people, government, economy, geography, communications, transportation, military, and transnational issues for 267 world entities. – January 17 2013<https://www.cia. gov/library/publications/the-world-factbook/index. Html.
[12] El-Merghany, S., Zan El-Daen, E. M. A. (2013): Evaluation of some date palm cultivars grown under Toshky conditions'. – Plant Production, Mnsoura Univ. 4(8): 1207-1218.
[13] El-Salhy, A. M., Ibrahim, R. A., Gadalla, E. G., Khalil, H. K. H. (2016): Evaluation of some seeded dry date palm grown under Aswan climatic condition. – Assiut J. Agric. Sci. 47(4): 136-155.
[14] FAO Statistics (2018): http://www.fao.org/statistics/en. – Accessed on 23 July 2018.
[15] Gadalla, E. G., Abeer, H. I., Ahmed, E. F. S. (2013): Behavior of some Egyption dry cultivars and Barhee cv. Date palm produced from tissue culture under Shark Al- Oinat condition El –Wadi El –Gadid governorate. – J of Appl. Sci. 32(12).
[16] Haider, N. (2017): Determining Phylogenetic Relationships Among Date Palm Cultivars Using Random Amplified Polymorphic DNA (RAPD) and Inter-Simple Sequence Repeat (ISSR) Markers. – In: Al-Khayri, J., Jain, S., Johnson, D. (eds.) Date Palm Biotechnology Protocols Volume II. Methods in Molecular Biology, Vol. 1638. Humana Press, New York.
[17] Hasnaoui, A. M., Elhoumaizi, A., Hakkou, A., Wathelet, B., Sindic, M. (2011): Physicochemical characterization, classification and quality evaluation of date palm fruits of some Moroccan cultivars. – J. Sci. Res. 3(1): 139-149.
[18] Hobani, A. I., Thottam, A. N. M., Ahmed, K. A. M. (2003): Development of a neural network classifier for date fruit varieties using some physical attributes. – Agric. Res. Cent. King Saud Univ. Res. Bul. 126: 5-18.
[19] Idris, T. I. M., Hussein, F. A., Said, A. E., Elsadig, E. H. (2014): Evaluation of some dry seedling date selections from the Northern State, Sudan. – Sudanese Journal of Agricultural Sciences 1: 30-35.
[20] Kassem, H. A. (2012): The response of date palm to calcarous soil fertilization. – Journal of Soil Science and Plant Nutrition 12(1): 45-58.
[21] Little, T. M., Hills, F. J. (1972): Statistical methods in Agricultural Research. – University of California, Davis.
[22] Liu, Y. Z., Deng, X. X. (2007): Citrus breeding and genetics in China. – The Asian Australian J Pl Sci Biotech 1: 23-28.
[23] Mortazavi, S. M. H., Azizollahi, F., Moalemi, N. (2015): Some quality attributes and biochemical properties of nine Iranian date (Phoenix dactylifera L.) cultivars at different stages of fruit development. – International Journal of Horticultural Science and Technology 2(2): 161-171.
[24] Nasir, M. U., Hussain, S., Jabbar, S., Rashid, F., Khalid, N., Mehmood, A. (2015): A review on the nutritional content, functional properties and medicinal potential of dates. – Science Letters 3(1): 17-22.
[25] Naz, S., Shahzadi, K., Rashid, S., Saleem, F., Zafarullah, A., Ahmad, S. (2014): Molecular characterization and phylogenetic relationship of different citrus varieties of Pakistan. – J Animal Pl Sci 24: 315-20.

http://www.aloki.hu ● ISSN 1589 1623 (Print) ● ISSN 1785 0037 (Online)
DOI: http://dx.doi.org/10.15666/aeer/1706_1364313655

[26] Omaima, M., Hafez, Malaka Saleh, A., Ashour, N. E., Mostafa, E. A. M., Naguib, M. M. (2015): Evaluation of some pollen grain sources on yield and fruit quality of samany date palm cv. (Phoenix dactylifera L.). – Middle East Journal of Agriculture 4(1): 27-30.
[27] Popenoe, P. (1973): The Date Palm. – Field Research Projects Coconut Grove, Miami, Florida.
[28] Purayil, F. T., Robert, G. A., Gothandam, K. M., et al. (2018): Genetic variability in selected date palm (Phoenix dactylifera L.) cultivars of United Arab Emirates using ISSR and DAMD markers. – 3 Biotech 8: 109.
[29] Qadri, R. W. K., Waheed, S., Haider, M. S., Khan, I., Naqvi, S. A., Bashir, M., Khan, M. M. (2016): Physiochemical characterization of fruits of different date palm (Phoenix dactylifera L.) varieties grown in Pakistan. – The Journal of Animal & Plant Sciences 26(5): 1268-1277.
[30] Riad, M. (1993): The Date Palm Sector in Egypt. – In: Ferry, M., Greiner, D. (eds.) Le palmier dattier dans l'agriculture d'oasis des pays méditerranéens. Options Méditerranéennes: Série A. Sémin aires Méditerranéens; n. 28. CIHEAM, Zaragoza, pp. 45-53.
[31] Sami, S. A, Ebtissam, H. H., Samer, E. M., Hanaiya, A. E. (2004): Genomic diversity in date palm (*phoenix dactylifera* L.) as revealed by AFLPs in comparison to RAPDs and ISSRs. – Arab J. Biotch. 8(1).
[32] Sedra, H., Lashermers, P., Trouslot, P., Combes, C., Hamon, P. (1998): Identification and genetic analysis of date palm (Phoenix dactylifera L.) varieties from Morocco using RAPD markers. – Euphytica 103: 75-82.
[33] Snedecor, G. W., Cochran, W. G. (1980): Statistical Methods. 6th Ed. – J. B. H. Publishing Comm., Oxford.
[34] Taain, D. A. (2013): Study on physico-chemical and physiological characteristics of date palm fruits (Phoenix dactylifera L.) cv. Um-aldehin. – Pakist. J. Agri. Sci. 50(1): 1-5.
[35] Youssef, M. K. E., Abou-El-Hawa, S. T., Seleim, M. A., Ramadan, B. R. (1998): Evaluation of chemical composition of various types of Upper Egypt dates. – Assiut Journal of Agricultural Sciences 29(3): 33-52.
[36] Zehdi, S. L., Sakka, H. L., Rhouma, A., Ould Mohamed Salemy, A., Marrakchi, M. L., Trifi, M. L. (2004): Analysis of Tunisian date palm germplasm using simple sequence repeat primers. – African J. of Biotech. 3(4): 215-219.
[37] Zeinab, A. A, Gada, A. A, El- Kafrawy, T. M., Essam, A. M. (2014): Physicochemical and molecular genetic evaluation of selected dry date palm seedling trees. – Middle East J. Appl. Sci. 4(4): 931-941.

http://www.aloki.hu ● ISSN 1589 1623 (Print) ● ISSN 1785 0037 (Online)
DOI: http://dx.doi.org/10.15666/aeer/1706_1364313655

RESPONSE OF LABILE ORGANIC MATTER FRACTIONS TO PLASTIC FILM REMOVAL DURING MAIZE (*ZEA MAYS* L.) GROWTH IN SEMIARID FARMLAND SOIL

WANG, S. J.[1] – LUO, S. S.[2*] – LI, S. Q.[3*]

[1]*College of Resource and Environment, Key Laboratory of Soil Resource Sustainable Utilization for Jilin Province Commodity Grain Bases, Jilin Agricultural University, Changchun 130118, China*

[2]*Key Laboratory of Mollisols Agroecology, Northeast Institute of Geography and Agroecology, Chinese Academy of Sciences, Changchun 130102, China*

[3]*State Key Laboratory of Soil Erosion and Dryland Farming on the Loess Plateau, Chinese Academy of Sciences and Ministry of Water Resource, Yangling 712100, China*

**Corresponding authors*
e-mail: shasha0705@hotmail.com; sqli@ms.iswc.ac.cn

(Received 17th Apr 2019; accepted 15th Nov 2019)

Abstract. Understanding the differences of labile soil organic matter between plastic film mulching at all growing stages (FM) and plastic film removal after the silking stage (RM) is essential to identify changes in soil quality and N availability. Compared to the FM treatment, the RM treatment significantly decreased the microbial biomass C (MBC) content, water soluble organic C content in the 0-20 cm layer and extractable organic C content in 2011 at milk stage (R3); however, it significantly increased the MBC content at planting time (PT) or the 6th leaf stage (V6) of the next growing season. Moreover, compared with the FM treatment, the RM treatment significantly increased the microbial biomass N content from silking stage to physiological maturity (R6) in the 0-20 cm layer and extractable organic N (EON) content at R6 in 2012; however, it significantly decreased the water soluble organic N (WSON) content at R3 and the WSON and EON contents at PT or V6 of the next growing season. Thus, plastic film mulching with film removal during the maize reproductive stages could be an excellent option for maintaining soil quality and improving soil N availability in the temperature- and rainfall-limited regions of northwest China.
Keywords: *plastic film mulching, microbial biomass carbon, microbial biomass nitrogen, dissolved organic carbon, dissolved organic nitrogen*

Introduction

Plastic film mulching is a worldwide agricultural technology with direct economic and environmental benefits, such as improving crop productivity, increasing water-use efficiency, improving soil quality, reducing greenhouse gas emissions, and reducing nitrate leaching (Wang et al., 2017; Liu et al., 2014b, 2015, 2016). The Loess Plateau has a typical semi-arid monsoon climate, in which maize (*Zea mays* L.) is one of the most common grain crops; however, low temperature and drought in the early growth stage of spring crops often lead to low crop yield (Liu et al., 2009). Up to this day, plastic film mulching has been widely used on the Loess Plateau (Zhou et al., 2012; Liu et al., 2014c; Li et al., 2018), which can significantly improve crop yield by increasing soil moisture and topsoil temperature (Liu et al., 2010; 2014a; Bu et al., 2013b). The rainy season on the Loess Plateau ranges from July to September and coincides with the spring maize reproductive stages (RS) (Liu et al., 2010). During this period, plastic film mulching is detrimental to crop yield, in some conditions (e.g., high air temperatures),

http://www.aloki.hu ● ISSN 1589 1623 (Print) ● ISSN 1785 0037 (Online)
DOI: http://dx.doi.org/10.15666/aeer/1706_1365713672

most likely because it increases soil temperature and accelerates leaf and root senescence during the spring maize RS (Liu et al., 2010, 2014a). Compared with plastic film mulching for the entire maize growing season, plastic film removal during the spring maize RS decreased the leaf and root senescence rate and increased the final crop yield (Liu et al., 2014a; Luo et al., 2016). Although there are some reports about the effects of different mulching periods during crop growing season on crop yield and soil properties (Wang et al., 2009; Luo et al., 2016), there is limited information about the effects of plastic film removal during the spring maize RS on labile soil organic matter (SOM) pools, relative to retaining them throughout the whole maize growing season. Our previous studies have shown that plastic film removal during the spring maize RS significantly increased soil organic carbon (SOC), total nitrogen (TN), extractable organic C (EOC), $KMnO_4$-oxidizable C ($KMnO_4$-C) and C management index (CMI) in the 0-20 cm layer, as well as light fraction organic C (LFOC), light fraction organic N (LFON), microbial biomass C (MBC), EOC, extractable organic N (EON), $KMnO_4$-C and CMI in the 20-40 cm layer after the 5-yr cultivation (Luo et al., 2016).

As labile SOM pools, soil microbial biomass and dissolved organic matter are strongly affected by soil management and therefore sensitive and important parameters of soil fertility and quality (Haynes, 2005). Soil microorganisms are responsible for transforming organic matter into inorganic nutrients (Ryan et al., 2009). Dissolved organic matter (DOM) represents a mobile source of energy and food for soil microorganisms (Kalbitz et al., 2000) and a primary source of mineralizable N, P and S, thus making a significant contribution to nutrient availability and cycling (Haynes, 2005). Accordingly, measuring labile SOM fractions such as MBC, microbial biomass N (MBN), water soluble organic C (WSOC), water soluble organic N (WSON), EOC and EON are essential to identifying changes in soil quality and fertility. A few studies have investigated the effects of fertilization and plastic film mulching on the changes of soil microbial biomass during maize growth (Liang et al., 2011; Liu et al., 2014c). Until now, little has been known about the effects of plastic film removal during the spring maize RS on the changes of soil microbial biomass and other labile SOM fractions in semiarid farmland. This study was designed to: (1) reveal the impacts of plastic film removal during the spring maize RS on the labile SOM pools during the whole maize growth; and (2) evaluate the effects on soil fertility and environmental sustainability. We hypothesized that the changes in labile organic C and N pools with the plant growth vary largely between retaining and removing plastic film during the spring maize RS, thereby generate the cumulative effect of early season residue inputs for the next growing season. This information will be useful for understanding the SOM dynamics and developing the integrated management practices to improve SOM quantity and quality in a spring maize cropping system on the semiarid Loess Plateau.

Materials and methods

Site description

The study was conducted in 2011 and 2012 at Changwu Agricultural and Ecological Experimental Station (35.28°N, 107.88°E, 1200 m altitude), which is located in semiarid area on the Loess Plateau of China (*Fig. 1*). The environmental information and soil properties of study site were described in Luo et al. (2016). The annual mean air temperature is 9.7 °C, and the average annual precipitation from 1957 to 2010 is 582 mm with 73% of this falls during the maize growth season. The soil at the study site

http://www.aloki.hu ● ISSN 1589 1623 (Print) ● ISSN 1785 0037 (Online)
DOI: http://dx.doi.org/10.15666/aeer/1706_1365713672

is developed from loess and had a silt loam texture according to the USDA texture classification system. The soil properties at the top 20 cm were: bulk density 1.3 g cm^{-3}, pH 8.4, SOC 8.2 g kg^{-1}, TN 1.05 g kg^{-1}, mineral N 28.8 mg kg^{-1}, available phosphorus (Olsen-P) 20.7 mg kg^{-1}, and available potassium (NH_4OAc-K) 133.1 mg kg^{-1} in April 2009, prior to the start of the experiment (Luo et al., 2016).

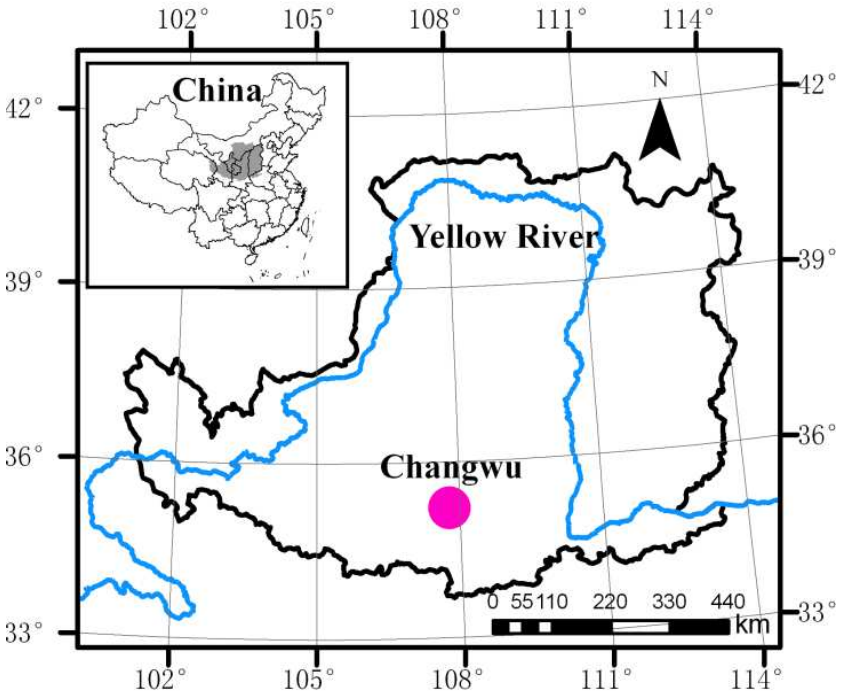

Figure 1. *The location of Changwu Agricultural and Ecological Experimental Station (35.28°N, 107.88°E, 1200 m altitude) on the Loess Plateau of China. (Luo et al., 2019)*

Experimental design and field management

The detail information of experimental design and field management were described in Luo et al. (2016). We applied two treatments, including plastic film mulching during all growing stages (FM) and plastic film removal at the silking stage (RM), to maize plots with a density of 85,000 plants ha^{-1}. A high-yielding maize hybrid (Pioneer 335) was used in this study. The treatments were applied to 56 m^2 (8 m × 7 m) plots arranged in a randomly block design with three replicates. After ridging the treatment plots, chemical fertilizers were broadcast over the soil at a rate of 90 kg N ha^{-1} in the form of urea (containing 46% N), 40 kg P ha^{-1} in the form of calcium super phosphate (12% P_2O_5), 80 kg K ha^{-1} in the form of potassium sulfate (45% K_2O), and 30 t ha^{-1} organic manure was broadcast over the soil; the soil was then plowed to mixed the fertilizer into the subsurface. Plastic film (0.005 mm thick, 1.2 m wide and transparent) was used to cover the soil. The maize was planted at 5 cm deep using a hole-sowing machine on 21 and 28 April in 2011 and 2012, respectively, and maize plants were harvested on 5 and 19 September in 2011 and 2012, respectively.

All of the plots were top-dressed twice with 67.5 kg N ha^{-1} (urea, 46% N) during the 10th leaf stage (V10) and silking stage (R1) recorded according to the standardized maize development stage system (Ritchie et al., 1992), using the same handheld device as used for sowing.

http://www.aloki.hu ● ISSN 1589 1623 (Print) ● ISSN 1785 0037 (Online)
DOI: http://dx.doi.org/10.15666/aeer/1706_1365713672

Sampling and measurements

The standardised maize development stage system was used to identify the vegetative (VS, from seedling emergence to silking) and reproductive (RS, from silking to physiological maturity) stages of the entire growing season (Ritchie et al., 1992). During the growing season, three adjacent plants were sampled at the 6th leaf stage (V6), V10, R1, milk stage (R3) and physiological maturity (R6) to measure the aboveground biomass. At maturity, the grain yield was measured for all plants selected from a 10 m^2 area in each plot. The aboveground biomass and grain yield were determined based on the average of three plot replicates, and all samples were dried to a constant weight in a fan oven at 75 °C.

Soil samples were collected at planting time (PT, before fertilization and sowing), V6, V10, R1, R3 and R6. At each plot, soil cores were drilled randomly using a 4-cm diameter auger with five replications and then mixed together to form one composite sample for every soil depth (0-20 cm and 20-40 cm). Soil moisture of each sample was measured after removing visible plant residues and sands, and then soil sample passed through a 2-mm sieve. The samples were refrigerated (0-4 °C) until MBC, MBN, WSOC, WSON, EOC and EON were determined.

MBC and MBN were measured using a modified chloroform fumigation-extraction method (Brookes et al., 1985; Vance et al., 1987). Briefly, 12.5 g fresh soil samples were fumigated with alcohol-free chloroform at 25 °C for 24 h. Excess chloroform was removed by repeated evacuation, the fumigated and non-fumigated samples promptly were extracted with 50 mL 0.5 mol L^{-1} K_2SO_4 (soil/solution ratio of 1:4 w/v) on a rotary shaker at 220 r min^{-1} for 0.5 h. After shaking, the supernatant was filtered using a membrane filter, and then filtrate was immediately frozen at -20 °C. Total organic C concentration in the filtrate was measured using an automated total organic C analyzer (TOC-Vcph, Shimadzu, Japan). Total soluble N in the filtrate was followed by alkaline persulfate oxidation and measured by dual-wavelength ultraviolet spectrophotometry (Norman et al., 1985; Cabrera and Beare, 1993). MBC and MBN were calculated by taking the difference between total organic C and soluble N of the fumigated and non-fumigated soils, respectively. A K_C value of 0.45 (Vance et al., 1987) and a K_N value of 0.54 (Brookes et al., 1985) were used to calculate the C and N content of the microbial biomass.

WSOC and WSON were extracted from 20 g fresh soil with 40 mL deionized water (soil/solution ratio of 1:2 w/v) at 25 °C. After shaking at 250 r min^{-1} for 0.5 h, and then centrifuging for 10 min at 8000 r min^{-1}, the supernatant was filtered using a 0.45-μm membrane filter, and then filtrate was immediately frozen at -20 °C (Liang et al., 1998). EOC and EON were extracted from 10 g of fresh soil with 50 mL 0.5 mol L^{-1} K_2SO_4 (soil/solution ratio of 1:5 w/v) at 25 °C. After shaking for 1 h at a speed of 220 r min^{-1}, the supernatant was filtered using a 0.45-μm membrane filter, and then filtrate was immediately frozen at -20 °C (Jones and Willett, 2006). Total organic C concentration in the filtrate was measured using an automated total organic C analyzer (TOC-Vcph, Shimadzu, Japan). The filtrate was later defrosted at room temperature and analyzed for mineralization N (NH_4^+-N and NO_3^--N) with a continuous flow analyzer (FLOWSYS, Italy), and total soluble N by dual-wavelength ultraviolet spectrophotometry after alkaline persulfate oxidation (Cabrera and Beare, 1993; Norman et al., 1985). Total organic N concentration in the filtrate was calculated by taking the difference between total soluble N and mineralization N.

http://www.aloki.hu ● ISSN 1589 1623 (Print) ● ISSN 1785 0037 (Online)
DOI: http://dx.doi.org/10.15666/aeer/1706_1365713672

Statistical analysis

The effects of plastic film removal on the measured parameters were evaluated using Independent-Samples T-Test. In all cases, differences were deemed to be significant if $p < 0.05$ using SPSS version 20.0.

Results

Air temperature and precipitation

The monthly precipitation and mean air temperature at the study site during the two experimental years were measured at the Changwu meteorological monitoring station, which is situated within 50 m of the experimental site (*Fig. 2*). One wet year occurred in 2011 and one dry year occurred in 2012 compared with the average for the preceding 54 yr (1957–2010). In this study site, the annual mean air temperatures were both 9.4 °C in two years, and the precipitation was 644 mm in 2011 and 481 mm in 2012. During the maize growth season (May to September), the mean air temperature was 18.2°C in 2011 and 18.7 °C in 2012, which is lower than the 54-yr mean (19.0 °C), and the precipitation was 14% greater than the 54-yr mean (426 mm) in 2011 and 15% less than the 54-yr mean in 2012. The precipitation during the rainy season (July to September) was 25% greater than the 54-yr mean (310 mm) in 2011 and close to the 54-yr mean in 2012. Compared with the 54-yr mean, the precipitation was greater in spring maize reproductive stages of 2011, and lower in spring maize vegetative stages of 2012. The mean air temperature during the rainy season was 18.4 °C in 2011 and 19.1 °C in 2012, which is lower than the 54-yr mean (19.8 °C).

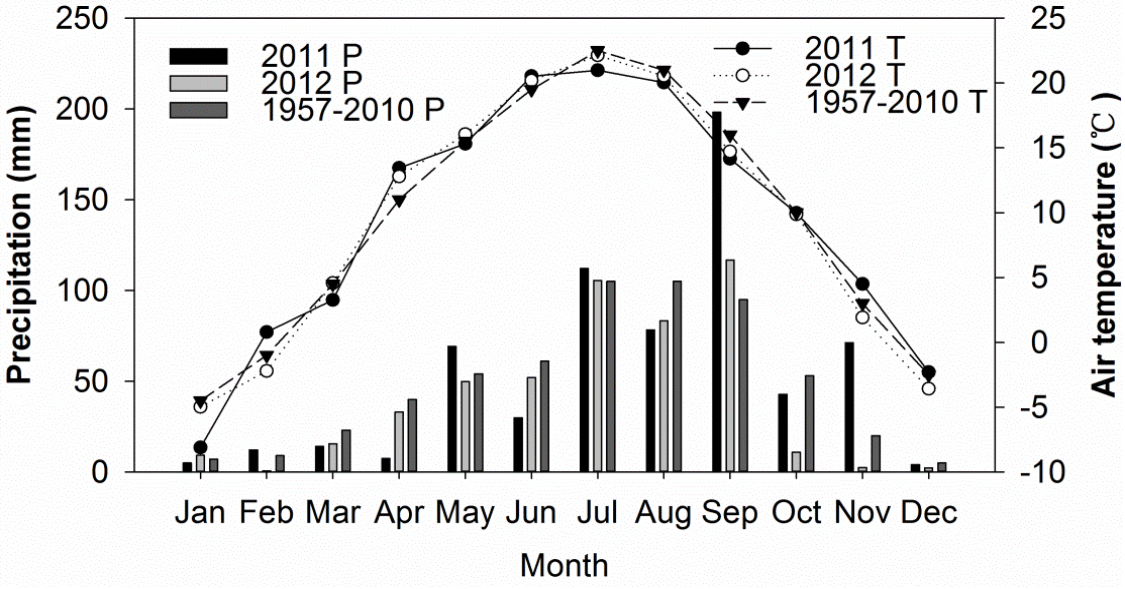

Figure 2. *The monthly precipitation (P) and mean air temperature (T) at the study site*

Total aboveground biomass and grain yield

Compared with the FM treatment, the RM treatment significantly increased the total aboveground biomass at V6 and V10 in 2011 and at V10 in 2012 (*Table 1*). However,

http://www.aloki.hu ● ISSN 1589 1623 (Print) ● ISSN 1785 0037 (Online)
DOI: http://dx.doi.org/10.15666/aeer/1706_1365713672

there was no significant difference in the total aboveground biomass between the two treatments from R1 to R6 (*Table 1*). *Table 1* shows that plastic film removal had no significant effect on the aboveground biomass during the RS (from R1 to R6) of the current growing season, but it may promote the aboveground biomass during the VS (V6 or V10) of the next growing season. Compared with the FM treatment, the RM treatments lightly increased the grain yield by 8.7% in 2011 and 4.1% in 2012, while the differences were not significant (*Table 1*).

Table 1. *Effects of plastic film mulching (FM) and removal (RM) on the total aboveground biomass and grain yield in 2011 and 2012*

Sampling time		Total aboveground biomass (t ha^{-1})		Grain yield (t ha^{-1})	
		FM	RM	FM	RM
2011	V6	0.58b	0.71a		
	V10	4.92b	5.71a		
	R1	12.76a	11.78a		
	R3	19.69a	19.67a		
	R6	23.56a	24.43a	14.42a	15.67a
2012	V6	0.75a	0.76a		
	V10	5.25b	5.83a		
	R1	11.63a	11.79a		
	R3	17.10a	16.85a		
	R6	23.65a	24.17a	14.57a	15.17a

Means (n = 3) followed by different lowercase letters within a row are significantly ($p < 0.05$) different between mulching practices. V6, V10, R1, R3, R6 denote the 6th leaf stage, the 10th leaf stage, silking stage, milk stage and physiological maturity, respectively

Microbial biomass C and N

Microbial biomass C content ranged from 175.9 to 454.0 mg kg^{-1} in the 0-20 cm layer (*Fig. 3a, b*), compared to a range of 107.9 to 227.8 mg kg^{-1} in the 20-40 cm layer (*Fig. 3c, d*). The MBC content was higher in the 0-20 cm layer than that in the 20-40 cm layer ($p < 0.001$). Meanwhile, the MBC content was higher during the wet year (2011) than that during the dry year (2012) at sampling times from V6 to R1 ($p < 0.001$). For most of sampling times, the two layers had a similar trend in the MBC content. Compared with the FM treatment, the MBC content under RM significantly increased at V6 in 2011 and at PT in 2012 in the 0-20 cm layer (*Fig. 3a, b*), as well as at PT in 2011 and 2012 in the 20-40 cm layer (*Fig. 3c, d*); the MBC content under RM significantly decreased at R3 in 2011 and 2012 in the 0-20 cm layer (*Fig. 3a, b*). *Figure 2* shows that plastic film removal had a significant negative effect on the MBC content at R1 of the current growing season in the 0-20 cm layer, but it may promote the MBC content at PT or V6 of the next growing season in the two layers.

Microbial biomass N content ranged from 17.5 to 76.9 mg kg^{-1} in the 0-20 cm layer (*Fig. 3e, f*), compared to a range of 14.2 to 37.3 mg kg^{-1} in the 20-40 cm layer (*Fig. 3g, h*). The MBN content was higher in the 0-20 cm layer than that in the 20-40 cm layer

http://www.aloki.hu ● ISSN 1589 1623 (Print) ● ISSN 1785 0037 (Online)
DOI: http://dx.doi.org/10.15666/aeer/1706_1365713672

($p < 0.001$). The MBN content was lower during the wet year (2011) than that during the dry year (2012) at sampling times from V10 to R6 ($p < 0.001$). For most of sampling times, the two layers had a similar trend in the MBN content.

Water soluble organic C and N

Water soluble organic C content ranged from 51.2 to 122.7 mg kg^{-1} in the 0-20 cm layer (*Fig. 4a, b*), compared to a range of 29.3 to 76.5 mg kg^{-1} in the 20-40 cm layer (*Fig. 4c, d*). The WSOC content was higher in the 0-20 cm layer than that in the 20-40 cm layer ($p < 0.001$). For most of sampling times, the two layers had a similar change trend in the WSOC content. In 2011, compared with the FM treatment, the RM treatment generally decreased the WSOC content in the 0-20 cm layer, whereas increased that in the 20-40 cm layer (*Fig. 4a, c*). Compared with the FM treatment, the RM treatment significantly decreased the WSOC content in the 0-20 cm layer at PT in 2011 and at R3 and R6 in 2012 (*Fig. 4a, b*), whereas significantly increased that in the 20-40 cm layer from R1 to R6 in 2011 and from V10 to R3 in 2012 (*Fig. 4c, d*). *Figure 3* shows that plastic film removal had a significant active effect on the WSOC content in the 20-40 cm layer during the rainy season (from R1 to R3) in two years.

Water soluble organic N content ranged from 2.6 to 20.0 mg kg^{-1} in the 0-20 cm layer (*Fig. 4e, f*), compared to a range of 1.5 to 15.5 mg kg^{-1} in the 20-40 cm layer (*Fig. 4g, h*). For most of sampling times, the two layers had a similar change trend in the WSON content. Compared with the FM treatment, the RM treatment significantly decreased the WSON content in the 0-20 and 20-40 cm layers at R3 in two years (*Fig. 4e-h*); meanwhile, the RM treatment significantly decreased the WSON content in the 20-40 cm layer at PT in two years and at V6 and R6 in 2012 (*Fig. 4g, h*). *Figure 3* shows that plastic film removal had a significantly negative effect on the WSON content in the whole 0-40 cm layer at R3 and this negative effect may persist into the early stage of the next growing season in the 20-40 cm layer.

Extractable organic C and N

Extractable organic C content ranged from 58.7 to 144.3 mg kg^{-1} in the 0-20 cm layer (*Fig. 5a, b*), compared to a range of 27.9 to 68.1 mg kg^{-1} in the 20-40 cm layer (*Fig. 5c, d*). The EOC content was higher in the 0-20 cm layer than that in the 20-40 cm layer ($p < 0.001$). For most of sampling times, the two layers had a similar change trend in the EOC content. Compared with the FM treatment, the RM treatment significantly decreased the EOC content in the 0-20 and 20-40 cm layers at R3 in 2011 (*Fig. 5a, c*); meanwhile, the RM treatment significantly decreased the EOC content at R3 in the 0-20 cm layer in 2012 (*Fig. 5b*). *Fig. 4* shows that plastic film removal had a significantly negative effect on the EOC content in the 0-20 cm layer at R3 in two years and this negative effect may extend into the 20-40 cm layer at R3 in the wet year (2011).

Extractable organic N content ranged from 8.2 to 26.0 mg kg^{-1} in the 0-20 cm layer (*Fig. 5e, f*), compared to a range of 5.6 to 16.2 mg kg^{-1} in the 20-40 cm layer (*Fig. 5g, h*). The EON content was higher in the 0-20 cm layer than that in the 20-40 cm layer ($p < 0.001$). For most of sampling times, the two layers had a similar change trend in the EON content. Compared with the FM treatment, the RM treatment significantly decreased the EON content in the 0-20 cm layer from PT to V10 in 2012 (*Fig. 5f*) and in the 20-40 cm layer at PT in two years (*Fig. 5g, h*), but the RM treatment significantly increased the EON content in the 0-20 and 20-40 cm layers at R6 in 2012 (*Fig. 5f, h*).

http://www.aloki.hu ● ISSN 1589 1623 (Print) ● ISSN 1785 0037 (Online)
DOI: http://dx.doi.org/10.15666/aeer/1706_1365713672

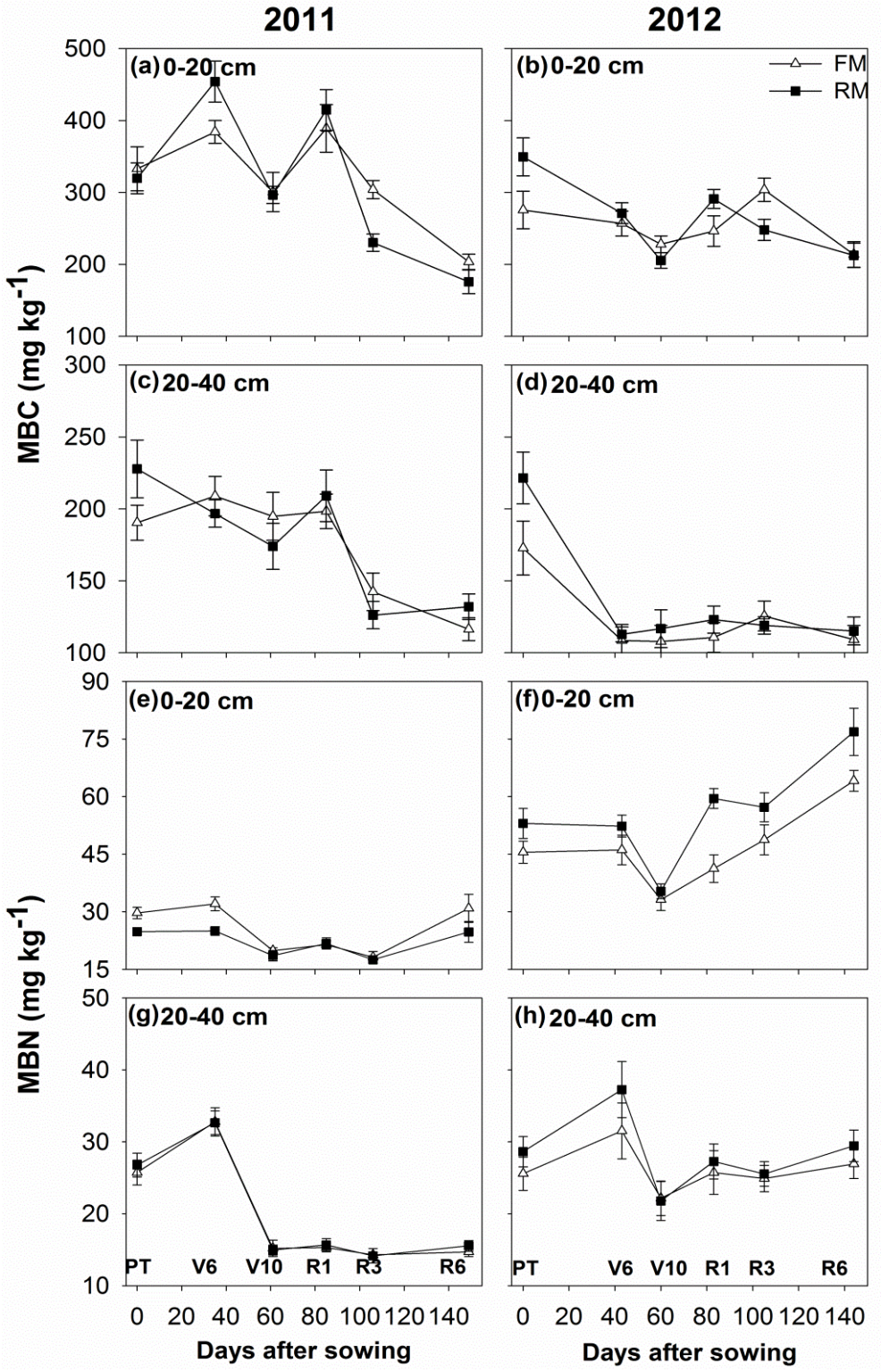

Figure 3. *Microbial biomass C and N under different mulching practices in the 0-20 and 20-40 cm layers during the maize growing season in 2011 and 2012. Error bars represent standard errors of the means (n = 3). FM denote the treatment with plastic film mulching during all growing stages, RM denote the treatment with plastic film removal at the silking stage. PT, V6, V10, R1, R3, R6 denote the planting time before fertilization and sowing, the 6th leaf stage, the 10th leaf stage, silking stage, milk stage and physiological maturity, respectively*

http://www.aloki.hu ● ISSN 1589 1623 (Print) ● ISSN 1785 0037 (Online)
DOI: http://dx.doi.org/10.15666/aeer/1706_1365713672

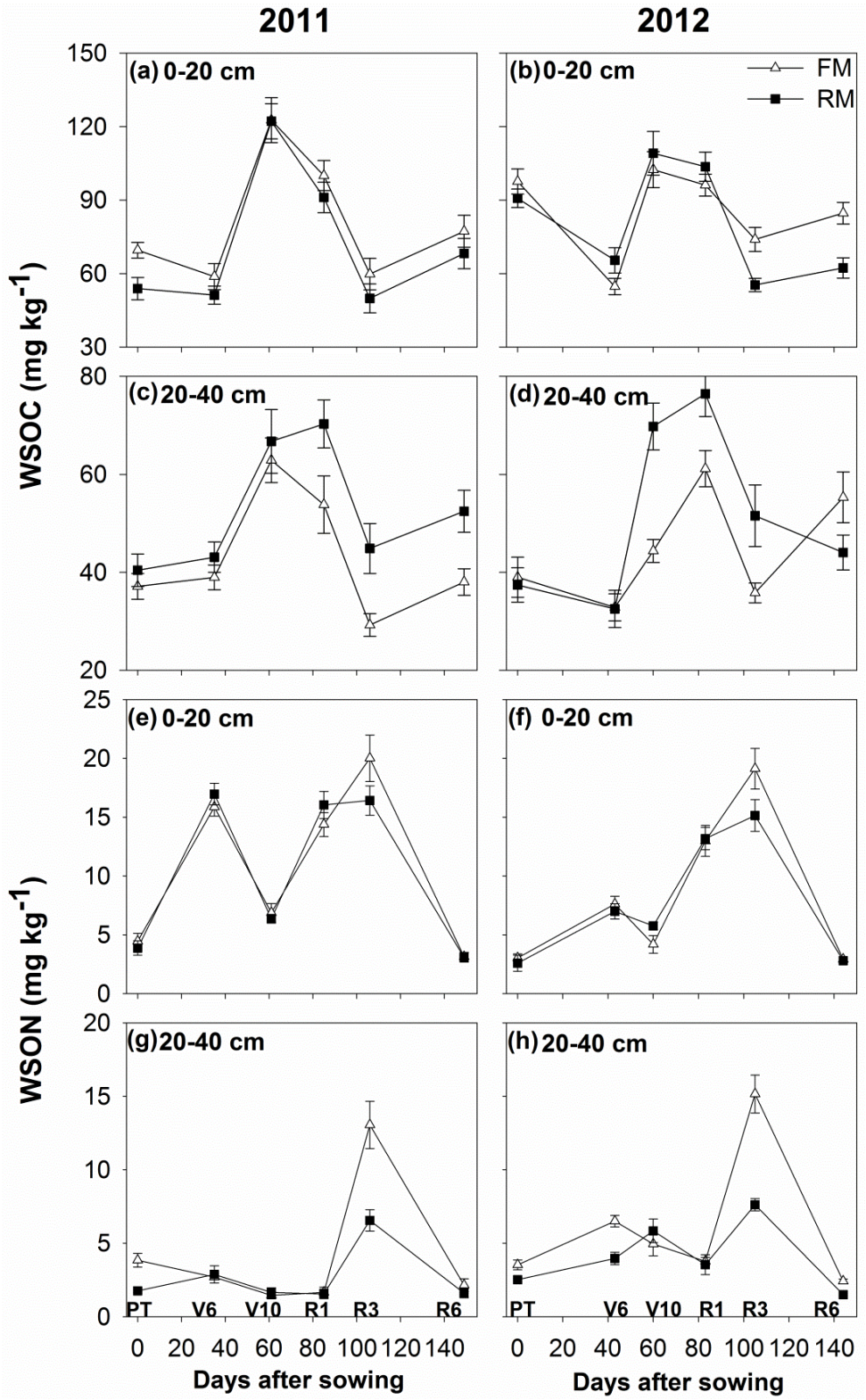

Figure 4. *Water soluble organic C and N under different mulching practices in the 0-20 and 20-40 cm layers during the maize growing season in 2011 and 2012. Error bars represent standard errors of the means (n = 3). FM denote the treatment with plastic film mulching during all growing stages, RM denote the treatment with plastic film removal at the silking stage. PT, V6, V10, R1, R3, R6 denote the planting time before fertilization and sowing, the 6th leaf stage, the 10th leaf stage, silking stage, milk stage and physiological maturity, respectively*

http://www.aloki.hu ● ISSN 1589 1623 (Print) ● ISSN 1785 0037 (Online)
DOI: http://dx.doi.org/10.15666/aeer/1706_1365713672

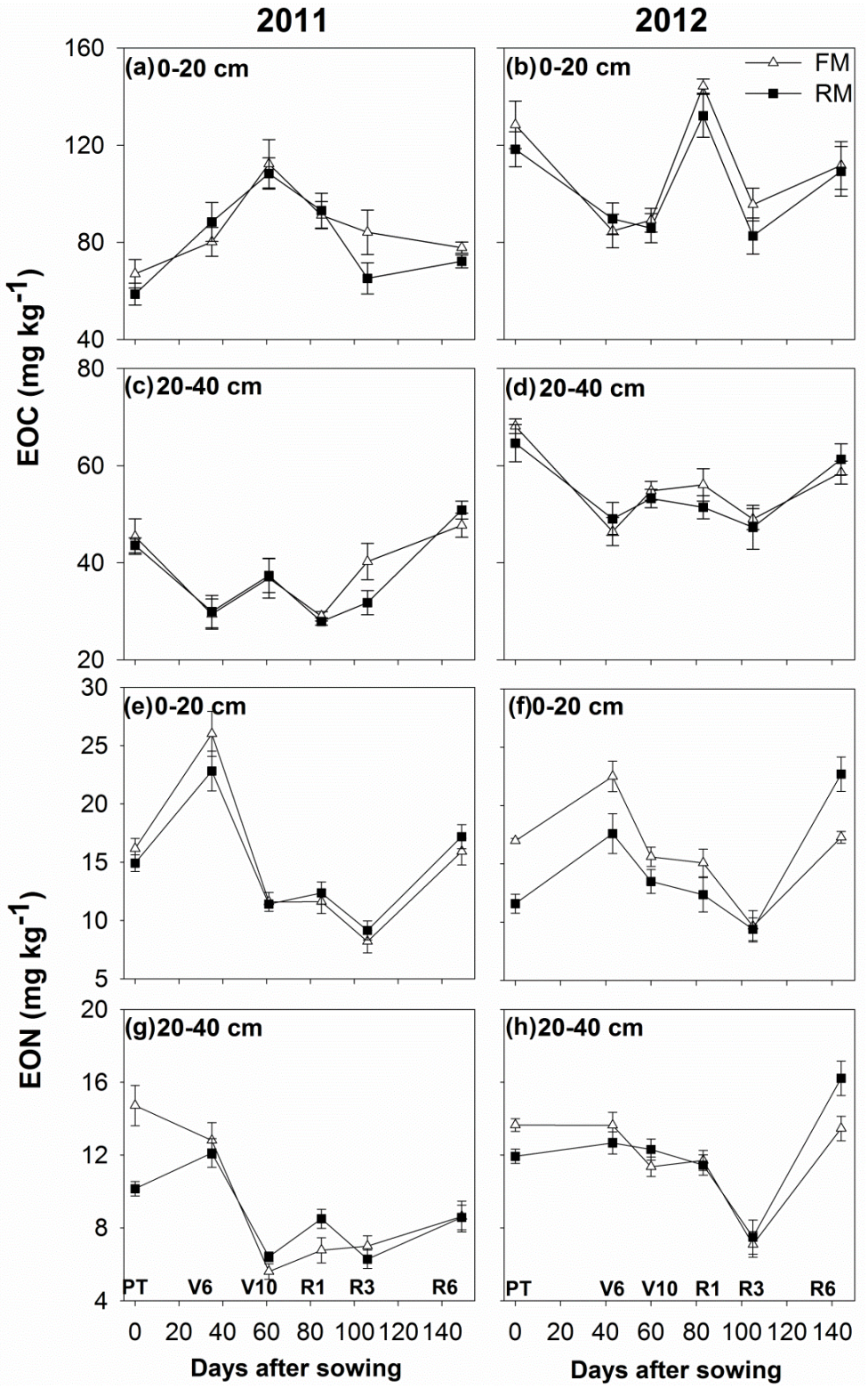

Figure 5. *Extractable organic C and N under different mulching practices in the 0-20 and 20-40 cm layers during the maize growing season in 2011 and 2012. Error bars represent standard errors of the means (n = 3). FM denote the treatment with plastic film mulching during all growing stages, RM denote the treatment with plastic film removal at the silking stage. PT, V6, V10, R1, R3, R6 denote the planting time before fertilization and sowing, the 6th leaf stage, the 10th leaf stage, silking stage, milk stage and physiological maturity, respectively*

http://www.aloki.hu ● ISSN 1589 1623 (Print) ● ISSN 1785 0037 (Online)
DOI: http://dx.doi.org/10.15666/aeer/1706_1365713672

Discussion

Effects of plastic film removal on soil microbial biomass C and N

Maintenance of satisfactory level of SOC and TN are necessary for crop productivity and sustainable agro-ecosystems (Dong et al., 2018), because they play crucial roles in the soil quality and fertility (Zhao et al., 2015). Soil nitrogen (N) is one of the necessary nutrients for plant growth and development, as well as a major nutrient limiting factor for crop yield (Karra et al., 2018; Huang et al., 2018). Soil organic N content of approximately 70%-90% in surface soil could not only maintain soil N fertility (Xu et al., 2003), but also has an important function for soil N supply capacity (Ju et al., 2004). However, it is difficult to detect the significant changes of SOC and TN in response to management practices in the short-term (Haynes, 2005; Gong et al., 2009). It is known that soil C and N cycling in agro-ecosystems is mediated by soil microorganisms. Due to the rapid generation time of soil microbial biomass, MBC and MBN are thought to be the most labile SOM fractions (Brookes, 2001; Chen et al., 2009). MBC regulates soil organic matter decomposition, and MBN represents both a source and sink of mineral N; thus, they play key roles in maintaining agricultural ecosystems sustainability. Our previous studies have shown that the RM treatment could decrease soil water and temperature during the maize RS compared with the FM treatment (Bu et al., 2013a; Liu et al., 2014a). The lower topsoil moisture and temperature might decrease the decay of plant roots (Liu et al., 2014a), which could lead to increased input of root biomass and rhizodeposits under the RM treatment. In this study, plastic film removal had a significant negtive effect on the MBC contentat R1 of the current growing season in the 0-20 cm layer, but it may promote the MBC content at PT or V6 of the next growing season in the two layers (*Fig. 3*). Meanwhile, the higher topsoil moisture and temperature provide more substrates for promoting microbial biomass activity, which could lead to higher microbial biomass (Li et al., 2004; Zhou et al., 2012). Taken together, these observations suggest that plastic film removal significantly increased soil microbial biomass at PT or V6 (the maize VS), which was affected by the cumulative effect of early season residue inputs; however, it significantly decreased soil microbial biomass at R3 (the maize RS), which was affected by the lower topsoil moisture and temperature during the current growing season. Moreover, the uptake capacities of inorganic and organic N by plants varied with development stages and seasonal changes (Simon et al., 2011). In this study, plastic film removal generally increased the MBN content in the dry year (2012), especially in the upper layer of the maize RS (*Fig. 3*). Considering soil microbes generally compete effectively against plant roots for mineral N in soils (Dunnet al., 2006), plant roots may shift towards enhancing the utilization of organic N to avoid the intense competition between plants and microbes during the active growing stages (e.g., the maize RS with high N demands), when plant N demands are highest in the fields with low N availability (Rennenberg et al., 2009). These results probably reflect that the plastic film removal decreases the decay of plant roots, therefore increases the plant N demands; therefore, the increasing plant N demand enhances the utilization of organic N by plants and increases the microbial N immobilization.

Effects of plastic film removal on soil dissolved organic C and N

Dissolved organic matter (DOM) is the main source of available C and nutrients (e.g., N and P) for soil microorganisms and plants, therefore, largely governs nutrient

http://www.aloki.hu ● ISSN 1589 1623 (Print) ● ISSN 1785 0037 (Online)
DOI: http://dx.doi.org/10.15666/aeer/1706_1365713672

cycling in soil ecosystems (Marschner and Kalbitz, 2003). Although DOM fractions (e.g., dissolved Organic C (DOC) and dissolved Organic N (DON)) constitute only a very small proportion of the total SOM pool, they respond rapidly to the changes in soil moisture and temperature resulting from management practices (Luo et al., 2015a, b; 2016). Among the DOM fractions, DOC is retained in mineral soil horizons mostly by sorption onto mineral surfaces (Kaiser and Guggenberger, 2000), and is a readily available substrate for microorganisms and contains a mineralizable proportion of up to 95% (Don and Kalbitz, 2005); meanwhile, DON is composed of amino acids and other light organic molecules, and may represent a labile N source for soil microorganisms (Jones and Kielland, 2002). Dissolved organic C and N pools have been measured in various extracts, e.g., hot water (hot water extractable), cold water (simply water soluble, refer to WSOC and WSON used in this study), 0.5 M K_2SO_4 (refer to EOC and EON used in this study), and 2 M KCl etc (Ghani et al., 2003; Jones and Willett, 2006).

WSOC is composed of an array of molecules generally reflecting the composition of total SOC because the soluble phase tends to be in equilibrium with the solid phase of SOC (Chantigny, 2003), and is regarded as an indicator of soil quality and functioning (Saviozzi et al., 2001). In this study, compared with the FM treatment, the RM treatment significantly decreased the WSOC content in the 0-20 cm layer, whereas significantly increased that in the 20-40 cm layer at R3 in two years (*Fig. 4*). This most likely reflects that the plastic film removal helps the upper WSOC infiltrate into the lower layer with soil water migration during the rainy season. EOC is the primary energy source for soil microorganisms and is an indicator of the carbon availability to soil microorganisms; moreover, microbial metabolites also constitute a significant proportion of EOC (Kalbitz et al., 2000). In this study, compared with the FM treatment, the RM treatment significantly decreased the EOC content in the 0-20 cm layer at R3 in two years; however, in the 20-40 cm layer, this negative effect was significant in the wet year (2011) and insignificant in the dry year (2012) (*Fig. 5*). These results probably reflect that plastic film removal leads to a lower microbial reproduction rate and is more significant in the case of wet year and upper layer (high soil water content condition). DON is derived from microbial degradation of fresh and partially decomposed organic residues, including autochthonous soil organic N (Murphy et al., 2000). In general, the salt solution (e.g., 0.5 M K_2SO_4) extracted more soil organic N than coldwater. A salt extraction may disturb the adsorption equilibrium on soil surfaces, and organic N measured in these extracts may include N originally adsorbed on the surface of soil mineral and organic clays (Murphy et al., 2000). WSON is widely used as a surrogate for DON in soil solutions and includes the DON present in macropores and some smaller pores (Chantigny et al., 2008). In this study, compared with the FM treatment, the RM treatment significantly decreased the WSON content at R3, which may persist into the early stage of the next growing season in the 20-40 cm layer (*Fig. 4*). Taken together, these observations suggest that plastic film removal leads to the less release of soluble N that occurs after microbial degradation of the crop residues and/or the more utilization of soluble N by plants. Meanwhile, compared with the FM treatment, the RM treatment generally decreased the EON content during the maize VS period, but significantly increased the EON content at R6 in 2012 (*Fig. 5*). Taken together, these observations suggest that plastic film removal reduces the release of EON, which may be due to the less amounts of extracted N that are originally adsorbed on the surface of soil mineral and organic clays and/or the greater amounts of extracted N that are reused by soil microbes.

http://www.aloki.hu ● ISSN 1589 1623 (Print) ● ISSN 1785 0037 (Online)
DOI: http://dx.doi.org/10.15666/aeer/1706_1365713672

Conclusions

Removing plastic film during the maize RS may promote the aboveground biomass during the VS (V6 or V10) of the next growing season. Meanwhile, compared with the FM treatment, the RM treatment significantly decreased soil microbial biomass and SOM mineralization, whereas significantly increased soil microbial N immobilization at R3 of the current growing season; however, it significantly increased soil microbial biomass, whereas significantly decreased the DON pools at PT or V6 of the next growing season. Thus, plastic film mulching with film removal during the maize RS could be an excellent option for enhancing crop productivity, improving soil N availability and maintaining soil quality in the temperature- and rainfall-limited region of northwest China. The response of net soil organic nitrogen mineralization to RM should be further investigated in the future.

Acknowledgements. This research was financially supported by the National Key Research and Development Plan (2017YFD0201807, 2017YFD0200100), National Natural Science Foundation of China (41701332), and Jilin Provincial Science and Technology Development Project of China (20180520048JH).

REFERENCES

[1] Brookes, P. C. (2001): The soil microbial biomass: concept, measurement and applications in soil ecosystem research. – Microbes and Environments 16: 131-140.

[2] Brookes, P. C., Landman, A., Pruden, G., Jenkinson, D. S. (1985): Chloroform fumigation and the release of soil-nitrogen—a rapid direct extraction method to measure microbial biomass nitrogen in soil. – Soil Biology & Biochemistry 17: 837-842.

[3] Bu, L. D., Zhu, L., Liu, J. L., Luo, S. S., Chen, X. P., Li, S. Q. (2013a): Source–sink capacity responsible for higher maize yield with removal of plastic film. – Agronomy Journal 105(3): 591-598.

[4] Bu, L. D., Liu, J. L., Zhu, L., Luo, S. S., Chen, X. P., Li, S. Q., Hill, R. L., Zhao, Y. (2013b): The effects of mulching on maize growth, yield and water use in a semi-arid region. – Agricultural Water Management 123: 71-78.

[5] Cabrera, M. L., Beare, M. H. (1993): Alkaline persulfate oxidation for determining total nitrogen in microbial biomass extracts. – Soil Science Society of America Journal 57: 1007-1012.

[6] Chantigny, M. H. (2003): Dissolved and water-extractable organic matter in soils: a review on the influence of land use and management practices. – Geoderma 113: 357-380.

[7] Chantigny, M. H., Angers, D. A., Kaiser, K., Kalbitz, K. (2008): Extraction and Characterization of Dissolved Organic Matter. – In: Carter, M. R., Gregorich, E. G. (eds.) Soil Sampling and Methods of Analysis. 2nd Ed. Canadian Society of Soil Science. CRC Press, Boca Raton, FL, pp 617-635.

[8] Chen, H., Hou, R., Gong, Y., Li, H., Fan, M., Kuzyakov, Y. (2009): Effects of 11 years of conservation tillage on soil organic matter fractions in wheat monoculture in Loess Plateau of China. – Soil & Tillage Research 106: 85-94.

[9] Don, A., Kalbitz, K. (2005): Amounts and degradability of dissolved organic carbon from foliar litter at different decomposition stages. – Soil Biology & Biochemistry 37: 2171-2179.

[10] Dong, Q., Yang, Y., Yu, K., Feng, H. (2018): Effects of straw mulching and plastic film mulching on improving soil organic carbon and nitrogen fractions, crop yield and water

http://www.aloki.hu ● ISSN 1589 1623 (Print) ● ISSN 1785 0037 (Online)
DOI: http://dx.doi.org/10.15666/aeer/1706_1365713672

use efficiency in the Loess Plateau, China. – Agricultural Water Management 201: 133-143.
[11] Dunn, R. M., Mikola, J., Bol, R., Bardgett, R. D. (2006): Influence of microbial activity on plant-microbial competition for organic and inorganic nitrogen. – Plant and Soil 289: 321-334.
[12] Ghani, A., Dexter, M., Perrott, K. W. (2003): Hot-water extractable carbon in soils: a sensitive measurement for determining impacts of fertilisation, grazing and cultivation. – Soil Biology & Biochemistry 35: 1231-1243.
[13] Gong, W., Yan, X. Y., Wang, J. Y., Hu, T. X., Gong, Y. B. (2009): Long-term manuring and fertilization effects on soil organic carbon pools under a wheat–maize cropping system in North China Plain. – Plant and Soil 314: 67-76.
[14] Haynes, R. J. (2005): Labile organic matter fractions as central components of the quality of agricultural soils: an overview. – Advances in Agronomy 85: 221-268.
[15] Huang, D. D., Chen, X. W., Cao, G. J., Liang, A. Z., Jia, S. X., Liu, S. X. (2018): Effects of long-term conservation tillage on soil nitrogen content and organic nitrogen components in a Chinese mollisol. – Applied Ecology and Environmental Research 16(5): 5517-5528.
[16] Jones, D. L., Kielland, K. (2002): Soil amino acid turnover dominates the nitrogen flux in permafrost-dominated taiga forest soils. – Soil Biology & Biochemistry 34: 209-219.
[17] Jones, D. L., Willett, V. B. (2006): Experimental evaluation of methods to quantify dissolved organic nitrogen (DON) and dissolved organic carbon (DOC) in soil. – Soil Biology & Biochemistry 38: 991-999.
[18] Ju, X. T., Liu, X. J., Zhang, F. S. (2004): Effects of long-term fertilization on soil organic nitrogen fractions. – Scientia Agricultura Sinica 37(1): 87-91.
[19] Kaiser, K., Guggenberger, G. (2000): The role of DOM sorption to mineral surfaces in the preservation of organic matter in soils. – Organic Geochemistry 31: 711-725.
[20] Kalbitz, K., Solinger, S., Park, J. H., Michalzik, B., Matzner, E. (2000): Controls on the dynamics of dissolved organic matter in soils: a review. – Soil Science 165: 277-304.
[21] Karra, R., Maslouhi, A., Bamba, Y. O. (2018): Modeling of nitrogen transport in variably saturated soils. – Applied Ecology and Environmental Research 2(6): 1427-1444.
[22] Li, F. M., Song, Q. H., Jjemba, P. K., Shi, Y. C. (2004): Dynamics of soil microbial biomass C and soil fertility in cropland mulched with plastic film in a semiarid agro-ecosystem. – Soil Biology & Biochemistry 36: 1893-1902.
[23] Liang, B., Yang, X. Y., He, X. H., Zhou, J. B. (2011): Effects of 17-year fertilization on soil microbial biomass C and N and soluble organic C and N in loessial soil during maize growth. – Biology and Fertility of Soils 47: 121-128.
[24] Liang, B. C., Mackenzie, A. F., Schnitzer, M. (1998): Management-induced change in labile soil organic matter under continuous corn in eastern Canadian soils. – Biology and Fertility of Soils 26: 88-94.
[25] Liu, C. A., Jin, S. L., Zhou, L. M., Jia, Y., Li, F. M., Xiong, Y. C., Li, X. G. (2009): Effects of plastic film mulch and tillage on maize productivity and soil parameters. – European Journal of Agronomy 31: 241-249.
[26] Liu, J. L., Bu, L. D., Zhu, L., Luo, S. S., Chen, X. P., Li, S. Q. (2014a): Optimizing plant density and plastic film mulch to increase maize productivity and water-use efficiency in semiarid areas. – Agronomy Journal 106: 1138-1146.
[27] Liu, J. L., Zhu, L., Luo, S. S., Bu, L. D., Chen, X. P., Yue, S. C., Li, S. Q. (2014b): Response of nitrous oxide emission to soil mulching and nitrogen fertilization in semi-arid farmland. – Agriculture Ecosystems & Environment 188: 20-28.
[28] Liu, J. L., Zhan, A., Chen, H., Luo, S. S., Bu, L. D., Chen, X. P., Li, S. Q. (2015): Response of nitrogen use efficiency and soil nitrate dynamics to soil mulching in dryland maize (*Zea mays* L.) fields. – Nutrient Cyclingin Agroecosystems 101: 271-283.

http://www.aloki.hu ● ISSN 1589 1623 (Print) ● ISSN 1785 0037 (Online)
DOI: http://dx.doi.org/10.15666/aeer/1706_1365713672

[29] Liu, J. L., Chen, X. P., Zhan, A., Luo, S. S., Chen, H., Jiang, H. B., Huang, X. Y., Li, S. Q. (2016): Methane uptake in semiarid farmland subjected to different mulching and nitrogen fertilization regimes. – Biology and Fertility of Soils 52: 941-950.
[30] Liu, X. E., Li, X. G., Hai, L., Wang, Y. P., Fu, T. T., Turner, N. C., Li, F. M. (2014c): Film-Mulched Ridge–Furrow Management Increases Maize Productivity and Sustains Soil Organic Carbon in a Dryland Cropping System. – Soil Science Society of America Journal 49: 1182-1185.
[31] Liu, Y., Yang, S. J., Li, S. Q., Chen, X. P., Chen, F. (2010): Growth and development of maize (*Zea mays* L.) in response to different field water management practices: Resource capture and use efficiency. – Agricultural and Forest Meteorology 150: 606-613.
[32] Luo, S. S., Zhu, L., Liu, J. L., Bu, L. D., Yue, S. C., Shen, Y. F., Li, S. Q. (2015a): Sensitivity of soil organic carbon stocks and fractions to soil surface mulching in semiarid farmland. – European Journal of Soil Biology 67: 35-42.
[33] Luo, S. S., Zhu, L., Liu, J. L., Bu, L. D., Yue, S. C., Shen, Y. F., Li, S. Q. (2015b): Mulching effects on labile soil organic nitrogen pools under a spring maize cropping system in semiarid farmland. – Agronomy Journal 107: 1465-1472.
[34] Luo, S. S., Zhu, L., Liu, J. L., Bu, L. D., Yue, S. C., Shen, Y. F., Li, S. Q. (2016): Response of labile organic C and N pools to plastic film removal from semiarid farmland soil. – Soil Use and Management 32(4): 535-542.
[35] Luo, S. S., Wang, S. J., Yao, P. Y., Guo, D., Li, X. J., Li, S. Q., Tian, C. J. (2019): Soil microbial communities under film mulching and N fertilization in semiarid farmland. – Nutrient Cycling in Agroecosystems 114: 157-170.
[36] Marschner, B., Kalbitz, K. (2003): Controls of bioavailability and biodegradability of dissolved organic matter in soils. – Geoderma 113: 211-235.
[37] Murphy, D. V., Macdonald, A. J., Stockdale, E. A., Goulding, K. W. T., Fortune, S., Gaunt, J. L., Poulton, P. R., Wakefield, J. A., Webster, C. P., Wilmer, W. S. (2000): Soluble organic nitrogen in agricultural soil. – Biology and Fertility of Soils 30: 374-387.
[38] Norman, R. J., Edberg, J. C., Stucki, J. W. (1985): Determination of nitrate in soil extracts by dual-wavelength ultraviolet spectrophotometry. – Soil Science Society of America Journal 49: 1182-1185.
[39] Rennenberg, H., Dannenmann, M., Gessler, A., Kreuzwieser, J., Simon, J., Papen, H. (2009): Nitrogen balance in forest soils: nutritional limitation of plants under climate change stresses. – Plant Biology 11: 4-23.
[40] Ritchie, S. W., Hanway, J. J., Benson, G. O. (1992): How a Corn Plant Develops. – Special Report No. 48. Iowa State University, Cooperative Extension Service, Ames, IA, http://maize.agron.iastate.edu/corngrows.html.
[41] Ryan, J., Masri, S., Singh, M. (2009): Seasonal changes in soil organic matter and biomass and labile forms of carbon as influenced by crop rotations. – Communications in Soil Science and Plant Analysis 40: 188-199.
[42] Saviozzi, A., Levi-Minzi, R., Cardelli, R., Riffaldi, R. (2001): A comparison of soil quality in adjacent cultivated, forest and native grassland soils. – Plant and Soil 233: 251-259.
[43] Simon, J., Dannenmann, M., Gasche, R., Holst, J., Mayer, H., Papen, H., Rennenberg, H. (2011): Competition for nitrogen between adult European beech and its offspring is reduced by avoidance strategy. – Forest Ecology and Management 262: 105-114.
[44] Vance, E. D., Brookes, P. C., Jenkinson, D. S. (1987): An extraction method for measuring soil microbial biomass-C. – Soil Biology & Biochemistry 19: 703-707.
[45] Wang, F. X., Feng, S. Y., Hou, X. Y., Kang, S. Z., Han, J. J. (2009): Potato growth with and without plastic mulch in two typical regions of Northern China. – Field Crops Research 110: 123-129.
[46] Wang, L., Li, X. G., Lv, J., Fu, T., Ma, Q., Song, W., Wang, Y. P., Li, F. M. (2017): Continuous plastic-film mulching increases soil aggregation but decreases soil pH in semiarid areas of China. – Soil & Tillage Research 167: 46-53.

http://www.aloki.hu ● ISSN 1589 1623 (Print) ● ISSN 1785 0037 (Online)
DOI: http://dx.doi.org/10.15666/aeer/1706_1365713672

[47] Xu, Y. C., Shen, Q. R., Ran, W. (2003): Content and distribution of forms of organic N in soil and particle size fractions after long-term fertilization. – Chemosphere 50(6): 739-745.
[48] Zhao, X., Wu, P., Gao, X., Persaud, N. (2015): Soil quality indicators in relation to land use and topography in a small catchment on the Loess Plateau of China. – Land Degradation & Development 26(1): 54-61.
[49] Zhou, L. M., Jin, S. L., Liu, C. A., Xiong, Y. C., Si, J. T., Li, X. G., Gan, Y. T., Li, F. M. (2012): Ridge-furrow and plastic-mulching tillage enhances maize–soil interactions: Opportunities and challenges in a semiarid agroecosystem. – Field Crops Research 126: 181-188.

http://www.aloki.hu ● ISSN 1589 1623 (Print) ● ISSN 1785 0037 (Online)
DOI: http://dx.doi.org/10.15666/aeer/1706_1365713672

CARBON EMISSION ASSESSMENT OF AN URBAN COMMUNITY

ZHAO, R. – HUANG, Y. – YAO, M. X. – ZHAN, L. P. – PENG, D. P.*

Faculty of Geosciences and Environmental Engineering, Southwest Jiaotong University, Chengdu 611756, China

**Corresponding author*
e-mail: pdp0330@swjtu.cn

(Received 22nd Apr 2019; accepted 12th Jul 2019)

Abstract. This study constructs a community carbon emission assessment system based on the greenhouse gas emissions inventory of the Intergovernmental Panel on Climate Change (IPCC). The system contains three activities, namely, building service, transport, and waste treatment and disposal. A street community in Ya'an, Sichuan, China is taken as a typical case for the study, and its carbon emissions during 2015–2017 are measured to demonstrate the practical application of the proposed assessment system. The results indicate that electricity consumption, transport, and natural gas consumption contribute the most carbon emissions in the community, accounting for 40.3%, 25.6%, and 25.1% of the total emissions on average over the 3 years. The study has policy implications for low carbon consumption, and thus, can promote sustainable community development. Limitations regarding the measurement are given to lay the foundations for future research.
Keywords: *IPCC inventory, building service, transport, waste disposal, sustainable development*

Introduction

Residential living is a notable source of carbon emissions, accounting for about 30% of global emissions (Natarajan et al., 2011; Xu et al., 2015). In urban communities, which act as spaces for daily residential life, carbon emission assessment is an effective way to identify the most carbon-intensive sector and to provide insight into emissions reduction and energy savings, thereby promoting low-carbon development (Kennedy et al., 2009).

Carbon emission assessment for households has been discussed by a number of studies. Kenny and Gray (2009) established a metabolism model for urban households to measure their carbon emissions from the perspectives of energy consumption and waste disposal. Using this model, Christen et al. (2011) further incorporated transport, building usage, and food into the assessment of carbon emission. The results were compared with actual emissions monitoring results to validate the model. Kellett et al. (2013) improved the emission model based on the theory of carbon balance. However, the indirect carbon emissions associated with residential activities were omitted. Life cycle assessment (LCA), an emerging environmental assessment tool, can effectively measure the environmental impact of a product or service at all stages of its life cycle (Hellweg and Canals, 2014). The application of LCA is effective in revealing the embodied carbon emissions from household activities, thereby allowing holistic carbon accounting (Jones and Kammen, 2011). For example, Cuéllar-Franca and Azapagic (2012) used LCA to measure the carbon emissions from three types of common residences in the United Kingdom. Heinonen et al. (2013) applied LCA to dividing the boundaries of household activities into 12 categories to measure their carbon emissions. Wang et al. (2015) coupled LCA with input–output analysis to measure the indirect carbon emissions from household consumption. A similar approach was implemented by Miehe et al. (2016), who assessed the carbon emissions of households to determine their spatial heterogeneity.

http://www.aloki.hu ● ISSN 1589 1623 (Print) ● ISSN 1785 0037 (Online)
DOI: http://dx.doi.org/10.15666/aeer/1706_1367313684

Ding et al. (2019) employed process life cycle assessment (PLCA) to measure direct and indirect carbon emissions by China's households.

However, carbon emission assessment of urban communities is scarcely considered in relevant literature. Although LCA is an insightful method for carbon emission assessment, it is difficult for unpractised engineers or designers to use owing to its complexity in the division of the system's boundary, and the acquisition of available data (Chen and Corson, 2014; Zhao et al., 2018a). In such a context, there have been requests for a simplified method to facilitate implementation of assessment in managerial practice, thus to help decision-makers better understand the assessment results and their associated decomposition (Zhang et al., 2018).

The present study aims to fill this gap by applying an assessment to community carbon emissions of various sectors based on the greenhouse gas (GHG) emissions inventory of the Intergovernmental Panel on Climate Change (IPCC), including direct and indirect emissions. Yucheng District in Ya'an City, Sichuan Province, China is taken as the case region for the assessment, owing to its progress in the development of a low-carbon community. The sector with the largest carbon emission in the area is identified, in order to develop policy implications for the creation of low-carbon lifestyles, thereby promoting sustainable regional development.

Methods and data

The Kyoto Protocol classifies carbon emissions into three categories, namely: (1) direct emissions from fossil fuel combustion; (2) indirect emissions from energy consumption, such as power use, cooling, and heating; and (3) emissions from a product or service (Andrew and Cortese, 2011). As households consume various categories of products or services, it is difficult to determine their emissions levels (Fan et al., 2012). Hence, this study mainly focuses on the carbon emissions from use of buildings, transport, and waste disposal within a community. These activities define the emissions boundary for the community, as shown in *Figure 1*.

Carbon emissions measurement

Carbon emissions are GHG emissions measured by carbon dioxide equivalent (Lin et al., 2013a; Zhao et al., 2017). The carbon emission of an urban community is measured as follows (IPCC, 2006):

$$E_i = L_i \times EF_i \times PV_p \quad \text{(Eq.1)}$$

where E_i is the carbon emissions from the i-th activity, L_i represents the i-th activity level, EF_i denotes the emissions factor corresponding to the i-th activity, and PV_p is the global warming potential of the p-th GHGs, where CO_2 (PV_1), CH_4 (PV_2), and N_2O (PV_3) are 1, 28, and 265, respectively.

The direct carbon emissions (E_1) produced by fossil fuels consumptions are calculated as follows (Ou et al., 2010):

$$E_1 = \sum_j (A_{1j} \times LC_j \times CC_j \times OC_j) \times \frac{44}{12} \times PV_1 \quad \text{(Eq.2)}$$

http://www.aloki.hu ● ISSN 1589 1623 (Print) ● ISSN 1785 0037 (Online)
DOI: http://dx.doi.org/10.15666/aeer/1706_1367313684

where A_{1j} refers to the consumption of the j-th fuel (kg), LC_j is the lower heating value of the j-th fuel (kJ/kg), CC_j is the carbon content per unit of heating value of the fuel (kg/kJ), and OC_j refers to the oxidation rate (%).

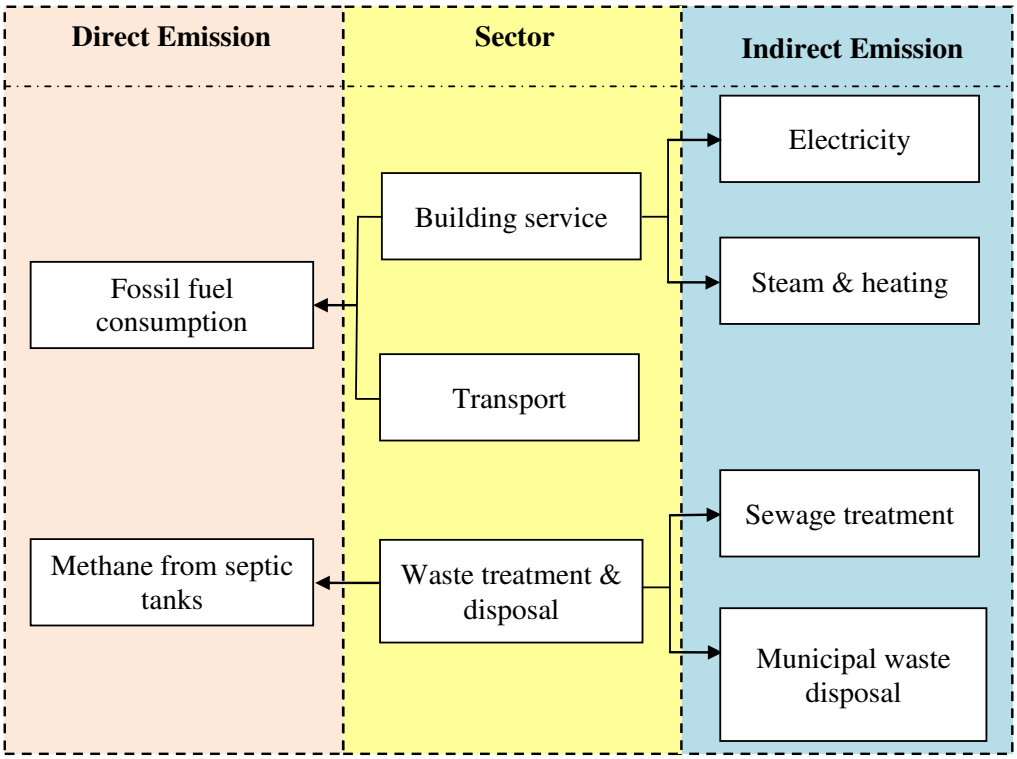

Figure 1. *Boundary of an urban community carbon emission assessment system*

The direct carbon emissions E_2 from septic tanks, which can be calculated based on the amount of escaped CH_4, are (Diaz-Valbuena et al., 2011):

$$E_2 = \left(A_{2j} \times \mathrm{DOC}_j \times \alpha_j - R_{2j}\right) \times \frac{16}{12} \times PV_2 \quad \text{(Eq.3)}$$

where A_{2j} is the amount of the waste disposed by the j-th septic tank (kg), DOC_j represents the degradable organic carbon content of the j-th septic tank (kg/kg), α_j refers to the disposal rate for the degradable organic carbon in the j-th septic tank (%), and R_{2j} is the amount of recovered CH_4 of the j-th septic tank (kg).

Indirect carbon emissions include emissions from electricity consumption, heating, and waste treatment and disposal. In particular, the indirect emissions from electricity consumption (E_3) are calculated as follows (Bi et al., 2011):

$$E_3 = A_3 \times F_3 \times PV_1 \quad \text{(Eq.4)}$$

where A_3 is power consumption (kWh), and F_3 is the average emission factor of the regional power grid (kg/kWh).

Indirect carbon emissions from heating (E_4) are calculated as follows (Bi et al., 2011):

http://www.aloki.hu ● ISSN 1589 1623 (Print) ● ISSN 1785 0037 (Online)
DOI: http://dx.doi.org/10.15666/aeer/1706_1367313684

$$E_4 = PV_1 \times \sum_j \left(S_j \times t_j \times F_{4j} \right) \quad \text{(Eq.5)}$$

where S_j is the residential area by using the j-th type of heating system (m^2), t_j is the time spent using the j-th heating system (h), and F_{4j} is the carbon emission intensity of using the j-th heating system (kg/(m^2·h)).

The carbon emissions from waste treatment and disposal are mainly composed of emissions from sewage treatment and municipal waste disposal. Among them, the carbon emissions from sewage treatment (E_5) are primarily converted from CH_4 and N_2O, and are calculated as follows (Listowski et al., 2011):

$$E_5 = [(TOW \times B_0 \times MCF_5) - R_5] \times PV_2 + C_N \times F_{N2O} \times 44/28 \times PV_3 \quad \text{(Eq.6)}$$

where TOW refers to the total amount of organic matters in the sewage (kg/kg), B_0 is the maximum production capacity of methane (kg/kg), MCF_5 is the methane correction factor, R_5 is the amount of recovered methane (kg), C_N refers to the nitrogen content in the sewage (kg/kg), and F_{N2O} refers to the N_2O emissions factor of the sewage (kg/kg).

The nitrogen content C_N in the sewage is calculated as follows (Listowski et al., 2011):

$$C_N = (P \times P_r \times C_{NPR} \times F_{NON\text{-}CON} \times F_{IND\text{-}COM}) - C_S \quad \text{(Eq.7)}$$

where P is the population (person), P_r is the per capita protein consumption (kg/person), C_{NPR} refers to the nitrogen content of proteins (kg/kg), $F_{NON\text{-}CON}$ refers to the non-consumption protein factor in the wastewater, $F_{IDN\text{-}COM}$ refers to the industrial and commercial protein factor, with a default value of 1.25, and C_S refers to the nitrogen removed from the sludge (kg).

The carbon emissions (E_6) generated from the disposal of municipal waste are measured as follows (Huang et al., 2018):

$$E_6 = (MSW_F \times L_0 - R_6) \times (1 - OX) \times PV_2 + PV_1 \times IW \times CCW \times FCF \times EF \times 44/12 \quad \text{(Eq.8)}$$

where MSW_F refers to the amount of municipal waste disposed in landfills (kg), L_0 refers to the methane production potential of the landfills (kg/kg), R_6 refers to the amount of recovered methane (kg), OX is the oxidation factor, IW refers to the total amount of municipal waste treated by incineration (kg), CCW refers to the carbon content of the municipal waste (%), FCF refers to the proportion of mineral carbon to the total carbon of the municipal waste (%), and EF is the combustion efficiency of incinerators (%).

The methane production potential (L_0) of landfills is measured as follows (Huang et al., 2018):

$$L_0 = MCF_6 \times DOC \times DOC_F \times F \times 16/12 \quad \text{(Eq.9)}$$

where MSF_6 refers to the methane correction factor of landfills (%), DOC is the content of degradable organic carbon in the municipal waste (kg/kg), DOC_F is the fraction of degradable organic carbon, and F refers to the proportion of methane in landfill gases.

http://www.aloki.hu ● ISSN 1589 1623 (Print) ● ISSN 1785 0037 (Online)
DOI: http://dx.doi.org/10.15666/aeer/1706_1367313684

Data sources

This study takes a community in Ya'an city as a case example to assess its carbon emissions from 2015 to 2017. The community was established in March 2002. It covers a total area of 1.8 square kilometers. It consists of administrative departments, vocational and technical colleges, primary schools, shops, and residential quarters. There are a total of 14,311 residents and 835 shops. Through a community survey, the major sources of carbon emissions have been identified, as shown in *Table 1*. Since the community has not established a central heating system, the carbon emissions are measured by electricity and natural gas consumption from household heating.

Table 1. *Identification of sources of carbon emission*

Activity	Emission source	Emission category
Building service	Natural gas consumption	Direct
	Electricity consumption	Indirect
Transport	Gasoline consumption	Direct
Waste treatment and disposal	Waste landfill disposal	Indirect
	Sewage treatment	Indirect

The data corresponding to different activity levels are shown in *Table 2*. The electricity and natural gas consumption of administrative departments, colleges, and primary schools, as well as their gasoline consumption from transport are obtained directly through questionnaire survey. Owing to a large number of households and shops in the community, a sample survey was conducted to obtain the corresponding activity levels.

Table 3 shows the emission coefficients, which are given priority over local emission coefficients, including the lower heating value of natural gas, the ratio of landfill disposal, and the degradable organic carbon content. The remaining emission factors are the default values provided by the Guide of Provincial Greenhouse Gases Inventory.

Results

The assessment results of the community from 2015 to 2017 are shown in *Table 4*. The carbon emissions for these 3 consecutive years are 14,446.69 t, 20,651.10 t, and 26,137.19 t, respectively. It is apparent that the carbon emissions of the community increase gradually, but their contributions differ by source.

From the perspective of carbon emission decomposition, *Figure 2a–c* illustrates that electricity consumptions contribute most of the total emissions during the period 2015–2017, accounting for 40.3% on average. The survey revealed that residents used a large variety of household appliances in their daily lives. In particular, because Ya'an has not implemented a central heating system, residents mainly rely on air conditioners for heating in winter, resulting in excessive power consumption and associated carbon emissions. The emissions caused by transport are the second largest, accounting for 25.6% of the total on average over the 3 years, followed by emissions from gas consumptions (25.1%). The findings are similar to those of Kellett et al. (2013) and Li et al. (2015), indicating that energy consumption and transport are major sources for household carbon emissions.

http://www.aloki.hu ● ISSN 1589 1623 (Print) ● ISSN 1785 0037 (Online)
DOI: http://dx.doi.org/10.15666/aeer/1706_1367313684

Table 2. *Activity levels of different emission sources in the case community*

Emission source	Data acquisition	Activity level			Unit
		2015	2016	2017	
Community population	Capita	9263	12982	14311	person
Natural gas consumption	Consumption	1,603,604	2,808,096	3,604,023	m^3
Electricity consumption	Consumption	10,305,642	15,852,530	20,760,705	kWh
Gasoline consumption	Consumption	1,944,096	2,303,386	2,922,453	L
CH_4 release from sewage treatment	Total organic matter	33.57	33.30	23.59	t
Waste disposal	Yield	3007.8	3363.7	3458	kg
N_2O release from sewage treatment	Per capita protein consumption	25.185			kg/person
	Non-consumption protein factor	1.5			%
	Protein factor in the sewage	1.25			%
	Nitrogen content in proteins	0.16			kg/kg
	Nitrogen removal by sludge	0			kg

Table 3. *Data of emission coefficient*

Emission source		Emission coefficient	Unit	Value	Source
Electricity consumption		Average emissions factor of the regional power grid	kg/kWh	0.5257	NDRC (2014)
Natural gas consumption		Lower heating value	kJ/m^3	34541	Field survey
		Carbon content per unit of heating	kg/kg	15.32	NDRC (2011)
		Carbon oxidation rate	%	99	NDRC (2011)
Gasoline consumption		Lower heating value	kJ/kg	43,070	SAC (2008)
		Carbon content per unit of heating	kg/kg	18.90	NDRC (2011)
		Carbon oxidation rate	%	98	NDRC (2011)
Sewage treatment	CH_4 emission	Maximum production capacity of CH_4	kg/kg	0.6	NDRC (2011)
		Methane correction factor	%	0.165	NDRC (2011)
		Amount of recovered CH_4	kg	0	NDRC (2011)
	N_2O emission	N_2O emissions factor	kg/kg	0.005	NDRC (2011)
Landfill disposal		Ratio of landfill disposal	%	100	Field survey
		Degradable organic carbon	kg/kg	0.1588	Local environmental protection agency
		Methane correction factor	%	40	NDRC (2011)
		Proportion of DOC	%	50	NDRC (2011)
		Proportion of CH_4 to landfill gases	%	50	NDRC (2011)
		Amount of recovered CH_4	kg	0	NDRC (2011)
		Oxidation factor	%	10	NDRC (2011)

http://www.aloki.hu ● ISSN 1589 1623 (Print) ● ISSN 1785 0037 (Online)
DOI: http://dx.doi.org/10.15666/aeer/1706_1367313684

Table 4. *Carbon emissions of the case community*

Emission source	Carbon emissions (t)		
	2015	2016	2017
Natural gas consumption	3,080.34	5,394.03	6,922.92
Transport	4,250.73	5,036.31	6,389.88
Electricity consumption	5,417.68	8,333.68	10,913.90
Municipal waste disposal	1,604.87	1,794.77	1,845.08
Sewage treatment	93.08	92.32	65.41
Total emissions	14,446.69	20,651.10	26,137.19

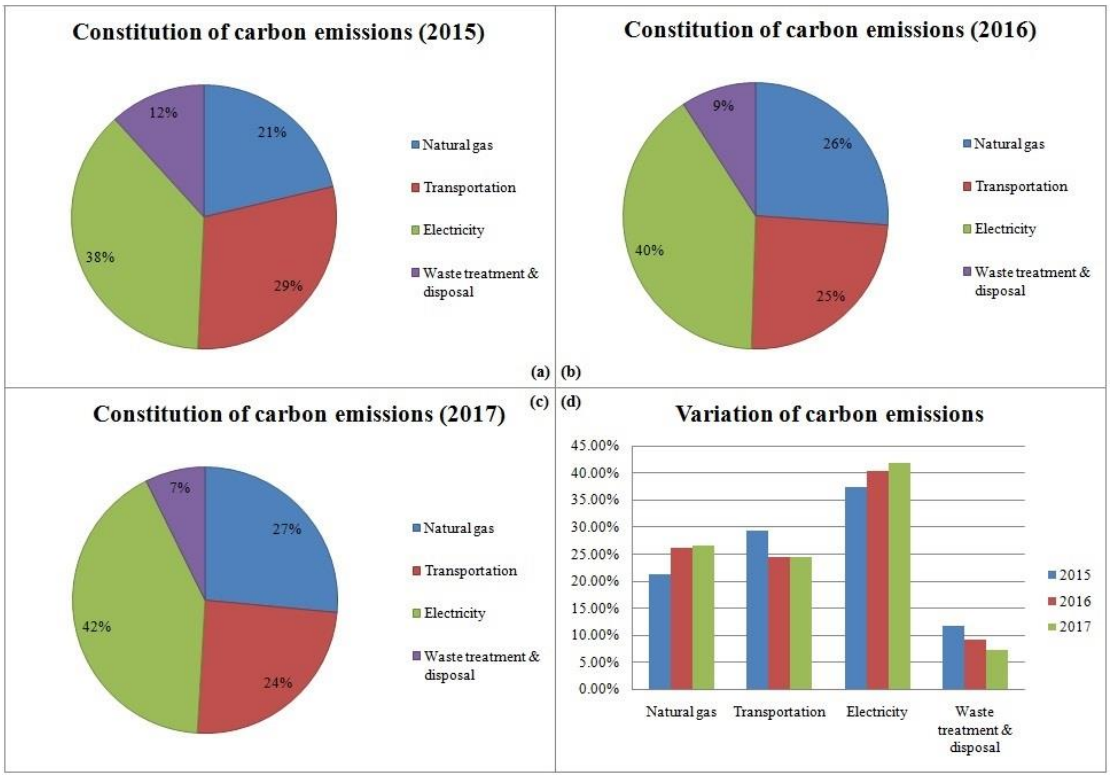

Figure 2. *The constitution of carbon emissions regarding the community*

Figure 2d shows that the proportions of carbon emissions contributed by electricity and natural gas consumptions increase gradually during the period 2015–2017. This may correspond to the population growth in the community. The carbon emissions contributed by transport increase slowly. On the contrary, the proportion of carbon emissions from waste treatment and disposal decreases during the 3 years. This may be the result of the promotion of waste sorting and recycling in the community, thereby reducing the volumes of landfill disposal.

Decomposition of the carbon emissions from building service

The carbon emissions of the community building usage in 2015, 2016, and 2017 are 8,498 t, 13,738 t, and 17,836 t, respectively. *Figure 3* shows that there are primarily three types of community building services that produce carbon emissions, namely,

http://www.aloki.hu ● ISSN 1589 1623 (Print) ● ISSN 1785 0037 (Online)
DOI: http://dx.doi.org/10.15666/aeer/1706_1367313684

residential buildings, retail shops, and administrative departments. The emissions of the first two categories increase significantly during these 3 years.

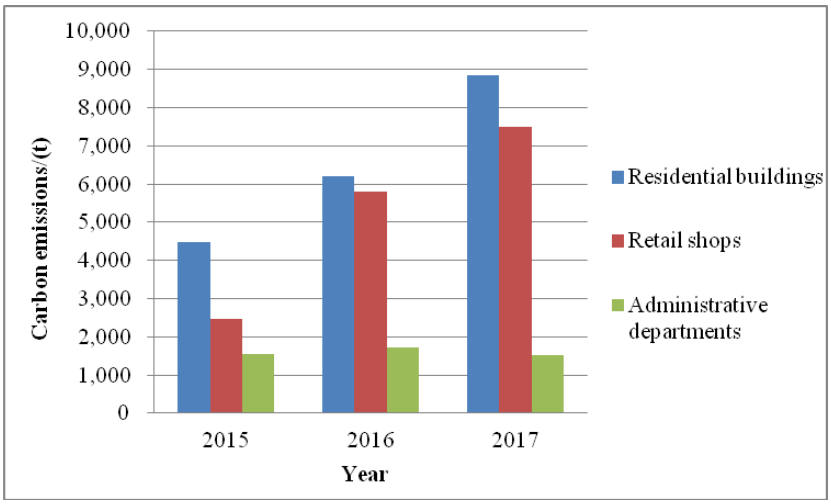

Figure 3. *Carbon emissions from usage of various buildings*

Decomposition of the carbon emissions from transport

The carbon emissions from transport in 2015, 2016, and 2017 are 4,250 t, 5,036 t, and 6,389 t, respectively, a significant increase, as shown in *Figure 4*. According to the survey, the transportation vehicles in the community are mainly comprised of private cars and business cars, of which the former contribute most of the carbon emissions.

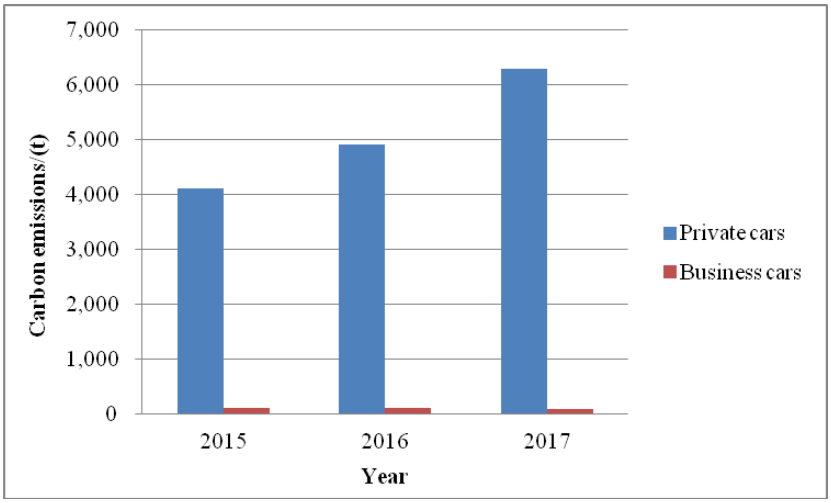

Figure 4. *Carbon emissions from transport*

Decomposition of the carbon emissions from waste treatment and disposal

Figure 5 shows that the carbon emissions from waste treatment and disposal in 2015, 2016, and 2017 are 1,698 t, 1,887 t, and 1,910 t, respectively. These account for approximately 4.7% of the total carbon emissions from the community. Sewage treatment contributes to less carbon emissions than waste disposal does.

http://www.aloki.hu ● ISSN 1589 1623 (Print) ● ISSN 1785 0037 (Online)
DOI: http://dx.doi.org/10.15666/aeer/1706_1367313684

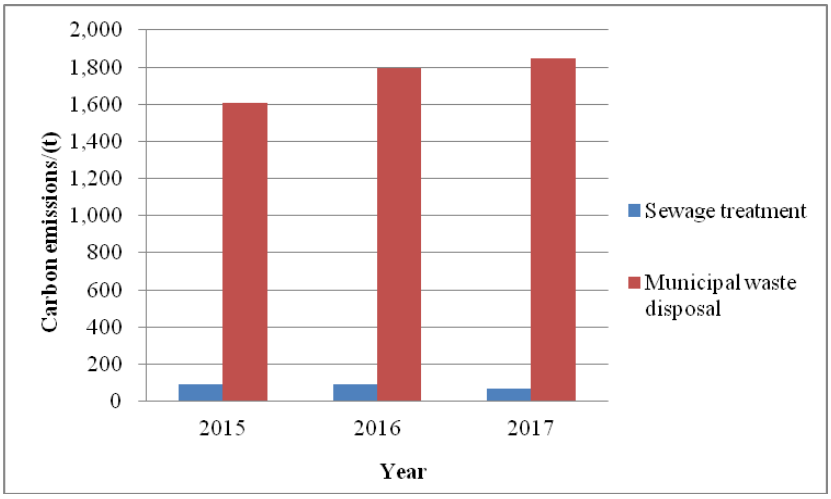

Figure 5. *Carbon emissions from waste treatment and disposal*

Discussion

According to the assessment results, this study finds that electricity consumptions contribute most of the community's carbon emissions. This is similar to the findings of Lin et al. (2013b), indicating that more attention needs to be paid to emissions reduction of power supply. Transport and natural gas consumption account for 25.6% and 25.1%, respectively, of the total carbon emissions in the community, which is in line with the result of Ahmad et al. (2015). However, Büchs and Schnepf (2013) as well as Lee and Lee (2014) concluded that transport produces the most household carbon emissions. This difference may be due to variations in the boundary division, as the latter two studies incorporated long-distance travel of residents into the carbon emissions assessment by transport. Waste treatment and disposal produce a certain amount of carbon emissions, but the contribution is relatively small, indicating that it is not the key emissions source of the community (Kenny and Gray, 2009; Shirley et al., 2012).

Although electricity and natural gas consumptions are important sources of carbon emissions, our field survey reveals that there are huge variations among households. For example, the maximum average electricity consumption is 181 kWh per month while the minimum is only 74 kWh per month, indicating a polarization of carbon emission in the daily lives of households. In addition, there is large potential for emission reduction regarding transport in the community, since the residents mainly choose to use private cars. Thus, public transport can be encouraged through, for example, community buses and shared bicycles to reduce transport carbon emissions.

The research results have policy implications for low-carbon living. This study may provide impetus for the design of a community "carbon credit" incentive program (Zhao et al., 2018b). Through such a policy, the public can obtain credits to offset their carbon footprints through a number of environmentally friendly activities, such as green consumption, low carbon transport, waste sorting, and recycling (Starkey, 2012).

Conclusion

This study applies the IPCC GHG emissions inventory to assess the carbon emissions of a community located in Ya'an City during 2015–2017. The sector that

http://www.aloki.hu ● ISSN 1589 1623 (Print) ● ISSN 1785 0037 (Online)
DOI: http://dx.doi.org/10.15666/aeer/1706_1367313684

contributes to the largest emission is identified to propose appropriate policies on implementation of low carbon development. The results show that electricity, transport, and natural gas consumptions are the three largest emission sources, accounting for 40.3%, 25.6%, and 25.1% of the total, respectively. The energy consumption behavior significantly influences the community carbon emissions. Private cars leave large room for transport emission reduction of the community. The carbon emissions of waste treatment and disposal are lower than those of community building service and transport.

This study has certain limitations, mainly reflected in the uncertainties of the assessment results. First, the energy consumptions of shops and households are based upon the sampling estimation. Second, a number of default emission factors are used instead of actual measured values, which may have an impact on the results. Future study should focus on establishing a holistic inventory of emission related activities, and a corresponding emission factor database, to enable dynamic updates on urban community carbon emissions.

Acknowledgements. This study is sponsored by National Natural Science Foundation of China (No. 41571520), Sichuan Science and Technology Program (No. 2019JDJQ0020; 2019YJ0244; 2017SZ0169), Sichuan Province Circular Economy Research Center Fund (No. XHJJ-1802).

REFERENCES

[1] Ahmad, S., Baiocchi, G., Creutzig, F. (2015): CO2 emissions from direct energy use of urban households in India. – Environmental Science & Technology 49(19): 11312-11320.

[2] Andrew, J., Cortese, C. L. (2011): Carbon disclosures: comparability, the carbon disclosure project and the greenhouse gas protocol. – Australasian Accounting, Business and Finance Journal 5(4): 5-18.

[3] Bi, J., Zhang, R., Wang, H., Liu, M., and Wu, Y. (2011): The benchmarks of carbon emissions and policy implications for China's cities: case of Nanjing. – Energy Policy 39(9): 4785-4794.

[4] Büchs, M., Schnepf, S. V. (2013): Who emits most? Associations between socio-economic factors and UK households' home energy, transport, indirect and total CO2 emissions. – Ecological Economics 90: 114-123.

[5] Chen, X., Corson, M. S. (2014): Influence of emission-factor uncertainty and farm-characteristic variability in LCA estimates of environmental impacts of French dairy farms. – Journal of Cleaner Production 81: 150-157.

[6] Christen, A., Coops, N. C., Crawford, B. R., Kellett, R., Liss, K. N., Olchovski, I., Tooke, T. R., van der Laan, M., Voogt, J. A. (2011): Validation of modeled carbon-dioxide emissions from an urban neighborhood with direct eddy-covariance measurements. – Atmospheric Environment 45(33): 6057-6069.

[7] Cuéllar-Franca, R. M., Azapagic, A. (2012): Environmental impacts of the UK residential sector: life cycle assessment of houses. – Building and Environment 54: 86-99.

[8] Diaz-Valbuena, L. R., Leverenz, H. L., Cappa, C. D., Tchobanoglous, G., Horwath, W. R., Darby, J. L. (2011): Methane, carbon dioxide, and nitrous oxide emissions from septic tank systems. – Environmental Science & Technology 45(7): 2741-2747.

[9] Ding, N., Liu, J., Kong, Z., Yan, L., Yang, J. (2019): Life cycle greenhouse gas emissions of Chinese urban household consumption based on process life cycle assessment: Exploring the critical influencing factors. – Journal of Cleaner Production 210: 898-906.

http://www.aloki.hu ● ISSN 1589 1623 (Print) ● ISSN 1785 0037 (Online)
DOI: http://dx.doi.org/10.15666/aeer/1706_1367313684

[10] Fan, J., Guo, X., Marinova, D., Wu, Y., Zhao, D. (2012): Embedded carbon footprint of Chinese urban households: structure and changes. – Journal of Cleaner Production 33: 50-59.
[11] Heinonen, J., Jalas, M., Juntunen, J. K., Ala-Mantila, S., Junnila, S. (2013): Situated lifestyles: I. How lifestyles change along with the level of urbanization and what the greenhouse gas implications are—a study of Finland. – Environmental Research Letters 8(2): 025003.
[12] Hellweg, S., i Canals, L. M. (2014): Emerging approaches, challenges and opportunities in life cycle assessment. – Science 344(6188): 1109-1113.
[13] Huang, J., Zhao, R., Huang, T., Wang, X., Tseng, M. L. (2018): Sustainable municipal solid waste disposal in the belt and road initiative: a preliminary proposal for Chengdu city. – Sustainability 10(4): 1147.
[14] Intergovernmental Panel on Climate Change (IPCC) (2006): IPCC guidelines for national greenhouse gas inventories. – http://www.ipcc-nggip.iges.or.jp./public/2006gl/index.html. Accessed on 19.03.2019.
[15] Jones, C. M., Kammen, D. M. (2011): Quantifying carbon footprint reduction opportunities for US households and communities. – Environmental Science & Technology 45(9): 4088-4095.
[16] Kellett, R., Christen, A., Coops, N. C., van der Laan, M., Crawford, B., Tooke, T. R., Olchovski, I. (2013): A systems approach to carbon cycling and emissions modeling at an urban neighborhood scale. – Landscape and Urban Planning 110: 48-58.
[17] Kennedy, C., Steinberger, J., Gasson, B., Hansen, Y., Hillman, T., Havranek, M., Pataki, D., Phdungsilp, A., Ramaswami, A., Mendez, G. V. (2009): Greenhouse gas emissions from global cities. – Environmental Science & Technology 43(19): 7297-7302.
[18] Kenny, T., Gray, N. F. (2009): A preliminary survey of household and personal carbon dioxide emissions in Ireland. – Environment International 35(2): 259-272.
[19] Lee, S., Lee, B. (2014): The influence of urban form on GHG emissions in the US household sector. – Energy Policy 68: 534-549.
[20] Li, Y., Zhao, R., Liu, T., Zhao, J. (2015): Does urbanization lead to more direct and indirect household carbon dioxide emissions? Evidence from China during 1996–2012. – Journal of Cleaner Production 102: 103-114.
[21] Lin, J., Liu, Y., Meng, F., Cui, S., Xu, L. (2013a): Using hybrid method to evaluate carbon footprint of Xiamen City, China. – Energy Policy 58: 220-227.
[22] Lin, T., Yu, Y., Bai, X., Feng, L., Wang, J. (2013b): Greenhouse gas emissions accounting of urban residential consumption: a household survey based approach. – PloS One 8(2): e55642.
[23] Listowski, A., Ngo, H. H., Guo, W. S., Vigneswaran, S., Shin, H. S., Moon, H. (2011): Greenhouse gas (GHG) emissions from urban wastewater system: future assessment framework and methodology. – Journal of Water Sustainability 1(1): 113-125.
[24] Miehe, R., Scheumann, R., Jones, C. M., Kammen, D. M., Finkbeiner, M. (2016): Regional carbon footprints of households: a German case study. – Environment, Development and Sustainability 18(2): 577-591.
[25] Natarajan, S., Padget, J., Elliott, L. (2011): Modelling UK domestic energy and carbon emissions: an agent-based approach. – Energy & Buildings 43(10): 2602-2612.
[26] National Development and Reform Commission (NDRC) (2011): Guide of Provincial Greenhouse Gases Inventory. – http://www.cbcsd.org.cn/sjk/nengyuan/standard/home/20140113/download/shengjiwenshiqiti.pdf. Accessed on 19.03.2019 (in Chinese).
[27] National Development and Reform Commission (NDRC) (2014): Average Carbon Dioxide Emission Factors of China Regional Power Grid in 2011 and 2012. – http://www.cec.org.cn/d/file/huanbao/xingyexinxi/qihoubianhua/2014-10-10/5fbcb57bcd163a1059cf224b03b751d8.pdf. Accessed on 19.03.2019 (in Chinese).

http://www.aloki.hu ● ISSN 1589 1623 (Print) ● ISSN 1785 0037 (Online)
DOI: http://dx.doi.org/10.15666/aeer/1706_1367313684

[28] Ou, X., Zhang, X., and Chang, S. (2010): Alternative fuel buses currently in use in China: life-cycle fossil energy use, GHG emissions and policy recommendations. – Energy Policy 38(1): 406-418.
[29] Pandey, D., Agrawal, M., Pandey, J. S. (2011): Carbon footprint: current methods of estimation. – Environmental Monitoring and Assessment 178(1-4): 135-160.
[30] Shirley, R., Jones, C., Kammen, D. (2012): A household carbon footprint calculator for islands: case study of the United States Virgin Islands. – Ecological Economics 80: 8-14.
[31] Standardization Administration of China (SAC) (2008): General principles for calculation of comprehensive energy consumption. – http://c.gb688.cn/bzgk/gb/showGb?type=online&hcno=F2113A2857611297ECF9A1683BE77F15. Accessed on 10.03.2019 (in Chinese).
[32] Starkey, R. (2012): Personal carbon trading: a critical survey Part 2: Efficiency and effectiveness. – Ecological Economics 73: 19-28.
[33] Wang, Z., Liu, W., Yin, J. (2015): Driving forces of indirect carbon emissions from household consumption in China: an input–output decomposition analysis. – Natural Hazards 75(2): 257-272.
[34] Xu, X., Tan, Y., Chen, S., Yang, G., Su, W. (2015): Urban household carbon emission and contributing factors in the Yangtze River Delta, China. – PloS One 10(4): e0121604.
[35] Zhang, G., Ge, R., Lin, T., Ye, H., Li, X., Huang, N. (2018): Spatial apportionment of urban greenhouse gas emission inventory and its implications for urban planning: a case study of Xiamen, China. – Ecological Indicators 85: 644-656.
[36] Zhao, R., Min, N., Geng, Y., He, Y. (2017): Allocation of carbon emissions among industries/sectors: an emissions intensity reduction constrained approach. – Journal of Cleaner Production 142: 3083-3094.
[37] Zhao, R., Geng, Y., Liu, Y., Tao, X., and Xue, B. (2018a): Consumers' perception, purchase intention, and willingness to pay for carbon-labeled products: a case study of Chengdu in China. – Journal of Cleaner Production 171: 1664-1671.
[38] Zhao, R., Xu, Y., Wen, X., Zhang, N., Cai, J. (2018b): Carbon footprint assessment for a local branded pure milk product: a lifecycle based approach. – Food Science and Technology 38(1): 98-105.

http://www.aloki.hu ● ISSN 1589 1623 (Print) ● ISSN 1785 0037 (Online)
DOI: http://dx.doi.org/10.15666/aeer/1706_1367313684

COMBINED EFFECT OF TILLAGE AND SOWING METHODS ON RICE-WHEAT PRODUCTIVITY

KAHLON, M. S.* – DHINGRA, M.

Department of Soil Science, Punjab Agricultural University, Ludhiana 141004, Punjab, India

**Corresponding author*
e-mail: dr.mskahlon@rediffmail.com

(Received 23rd Apr 2019; accepted 16th Jul 2019)

Abstract. Crop establishment methods and tillage practices significantly influence crop productivity by altering soil physical environment, root distribution and plant growth. The present study includes a combination of tillage practices for both rice and wheat i.e. deep tillage before rice (DTR) as well as wheat (DTW) along with conventional tillage before rice and wheat (CTRW) in main plots. The crop establishment methods i.e. no-tillage with residue (NTR) in wheat and direct seeded rice (DSR) were practiced in sub plots. These treatments were compared with traditional practices i.e. conventional tillage in wheat (CTW) and puddled transplanting in rice (PTR). It was reported that DTR and DTW results in 8% and 12% higher grain yields of rice and wheat, respectively over CTRW. Irrespective of crop establishment methods followed in rice, the NTR in wheat results in 7% higher wheat grain yield than CTW. The reduced soil mechanical resistance under deep tillage resulted in 18% and 22% more root length densities of rice and wheat than CT. Thus, among tillage practices, DTR and DTW and among crop establishment methods PTR and NTR are appropriate practices for sustaining crop productivity of rice-wheat systems in northwest India.
Keywords: *penetration resistance, deep tillage, direct seeding, puddled transplanting, water productivity*

Introduction

Rice-wheat is a prominent cropping system of Northwest India. The commonly followed practice in rice cultivation is puddled transplanting and for wheat it is conventional tillage (CT). These conventional practices are leading to soil degradation, poor productivity and environmental risks. For sustaining crop and water productivity of rice–wheat system, new tillage practices along with crop establishment methods need to be studied. No doubt puddling controls weed, reducing deep percolation losses of nutrients and water, but it also causes soil structural breakdown and create hard pan at shallow soil depth, which hinders root and water penetration and also cause poor aeration for succeeding wheat crop. Since, wheat is a deep rooted crop and requires favorable soil conditions without compaction for proper root proliferation. Many researchers have reported adverse effect of puddling on the yield of a subsequent wheat crop (Arora et al., 2006; Farooq et al., 2008; Gangwar et al., 2004). Sharma et al. (2003) noted that the negative effect of puddling on wheat is more pronounced in medium- to fine-textured soils than in light-textured soils. Ishaq et al. (2001) observed that subsoil compaction resulted in a reduction of both water and nutrient use efficiency in wheat by 38% owing to decreased root length. Unproductive losses of water in traditional rice cultivation resulted in alarming fall in water table that threatens sustainability of rice production. This fall has resulted in increased energy requirement and cost of pumping groundwater, increased tube well installation cost and deteriorated the ground water quality (AICRP, 2009; Kamra et al., 2002). Thus, there is a need to explore alternate techniques that can sustain rice production and are resource conservative. The underground water is being over exploited by excessive pumping to meet the water

http://www.aloki.hu ● ISSN 1589 1623 (Print) ● ISSN 1785 0037 (Online)
DOI: http://dx.doi.org/10.15666/aeer/1706_1368513699

requirement of transplanted rice. As a consequence, it has been causing a sharp decline in ground water table. Therefore, need has been felt to develop technically viable and economically feasible alternate techniques for growing rice in this region. The preliminary research conducted at Punjab Agricultural University indicated that DSR could be a viable alternative to PTR. The DSR offers many advantages such as more efficient water use, high tolerance to water deficit, less methane gas emission, reduced cultivation cost, prevents the formation of hard pan in sub-soil and minimizes labour input (Balasubramanian and Hill, 2002). It is more conducive to mechanization and also eliminates transplanting shock. However, the rice yield in most cases was higher (8-80%) under puddled transplanted rice (PTR) than under direct seeder rice (DSR). Other studies reported no difference in yield of rice under both crop establishment methods (Bajpai and Tripathi, 2000; Hobbs et al., 2002; Sharma et al., 1995, 2005). In India, yields were significantly lower (9-28%) in DSR than in PTR. However, DSR has several advantageous in poorly drained areas, it can be established earlier than PTR and does not incur growth delays from transplant injury; hence, it may hasten physiological maturity, reducing vulnerability to late-season drought (Tuong et al., 2000). Naklang et al. (1996) note that DSR had more root biomass than PTR. Some findings suggest that DSR achieves higher tiller density, leaf area, and vegetative biomass (Dingkuhn et al., 1990; Schnier et al., 1990), and that yields match or exceed PTR (Naklang et al., 1996; Saleh and Bhuiyan, 1995). Cultural practices like deep tillage in advance of soil puddling attempt to preserve the advantages of PTR while expanding the rooting zone above the plough sole. Akhtar and Quereshi (1999) found a depth-wise increase in root distribution from 12 to 20 cm and a yield benefit of 30% with adoption of deep tillage prior to PTR. By contrast, deep tillage preceding DSR may breech pre-existing plough soles, potentially exacerbating hazards posed by drought, weeds, and nutrient deficiencies from changes to the field water balance. As soil water dynamics in DSR is different from that of PTR, this is likely to affect water and nutrient uptake, and ensuing growth and crop yields. In semi-arid subtropical climatic conditions, DSR is expected to respond to changes in soil physical environment caused by deep tillage resulting in improved crop productivity. Deep tillage has emerged as a better option to improve deep root growth (advantageous for water extraction during drought in upland rice) of rice cultivars. Tillage under intensive cropping system has the additional challenges of ensuring high water use, nutrient use and energy use efficiencies through deeper and denser crop rooting (Gajri et al., 2002). The deep tillage before wheat also helps in enhancing root proliferation and enabling the plant to explore water and nutrient from deeper layers. Since, management of huge quantity of paddy straw produced every year is a serious problem in the region. Its management through no-tillage and surface residue retention (NTR) is another viable option for sustaining productivity. Keeping these points in view, a field study was conducted on sandy loam soil with the objective to evaluate impact of deep tillage on rice-wheat productivity under two crop establishment methods as DSR and PTR in rice and NTR and CT in wheat, respectively.

Materials and methods

Study area

This field experiment was conducted at the Research farm of Department of Soil Science, Punjab Agricultural University, Ludhiana. The site represent the Indo-gangetic alluvial plains situated at 30° 56’ N latitude and 75° 52’ E longitudes with an altitude of

http://www.aloki.hu ● ISSN 1589 1623 (Print) ● ISSN 1785 0037 (Online)
DOI: http://dx.doi.org/10.15666/aeer/1706_1368513699

247 m above the mean sea level. The area is characterized by sub-tropical and semi-arid type of climate with hot and dry summer from April to June followed by hot and humid period during July to September and cold winters from November to January. The summer temperature touches 45 °C with dry summer spells. Winter experiences frequent frosty spells especially in December and January and minimum temperature dips up to 0.5 °C. The climatic data of study period is presented in *Figure 1*. The experiment comprised of three main tillage practices namely deep tillage before rice (DTR), deep tillage before wheat (DTW) and conventional tillage in both rice and wheat (CTRW). While, two methods of crop establishment for rice i.e. puddled transplanted rice (PTR) and direct seeded rice (DSR) and two methods of sowing for wheat i.e. no-tillage with residue (NTR) and conventional tillage (CT) kept in sub plots. The experiment was replicated thrice with plot dimensions of 4.0 m width and 10.0 m length. In CT plots the field was disked twice followed by two cultivators and one planking operation while in DT the field was deep ploughed up to 45 cm depth with 50 cm apart and then CT operations were performed for conventional till plots and only deep till operation was performed where, wheat has to be sown by no till practice. In NTR the sowing of wheat was made directly under no-till conditions with retention of loose crop residue and standing rice stubbles in the field. In PTR the rice seedlings of 30 day old nursery were transplanted in field, while in DSR the wet rice seed was sown directly with drill. The sole DT operation was performed even in no-tillage plots excluding all other CT practices i.e. disking, cultivator and planking operations. The soil was neutral, non calcareous in nature and sandy loam in texture (*Typic Ustochrept).* The data pertaining to physico-chemical characteristics of the studied soil is presented in *Table 1*. The sowing of DSR was performed following all recommended packages of practices in the first week of June, while PTR was transplanted in second week of June and wheat was sown in the first week of November. The row to row spacing was maintained as 20 cm in both rice and wheat. The harvesting of wheat and rice were performed in the month of April and October, respectively. The in-situ and laboratory determination were made for various soil physico-chemical characteristics at the end of the experiment.

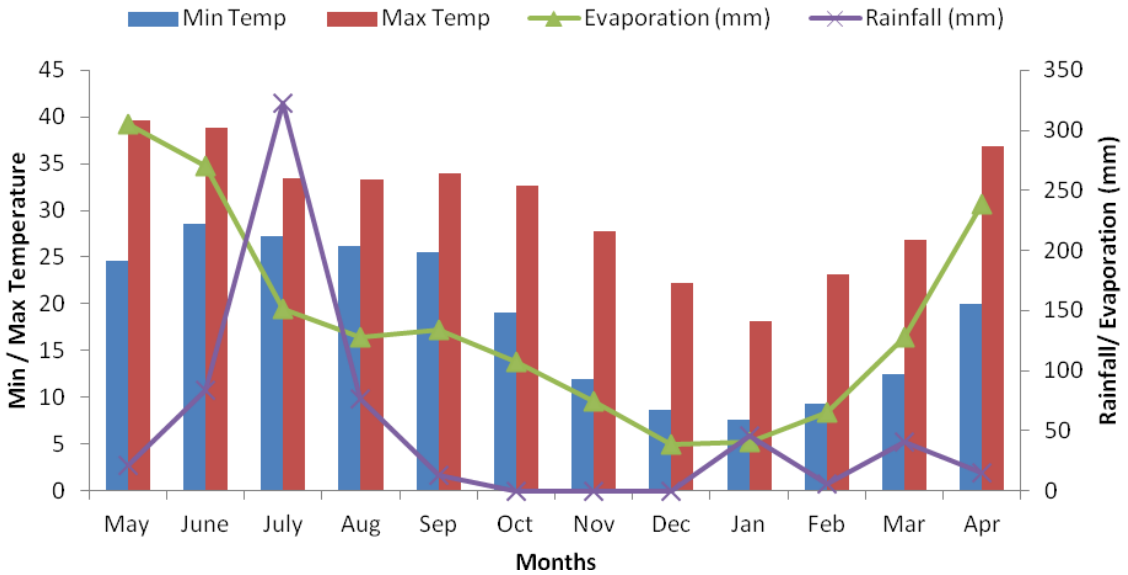

Figure 1. *Climatic data for the study year*

http://www.aloki.hu ● ISSN 1589 1623 (Print) ● ISSN 1785 0037 (Online)
DOI: http://dx.doi.org/10.15666/aeer/1706_1368513699

Table 1. *Soil parameters of experimental site*

Depth (cm)	pH	EC (dS m^{-1})	OC (%)	BD (Mg m^{-3})	Soil water content (%)		Sand (%)	Clay (%)
					FC	PWP		
0-10	8.46	0.38	0.42	1.44	20.9	9.8	68.5	19.7
10-20	8.33	0.29	0.31	1.53	22.1	10.3	63.2	22.8
20-30	8.30	0.23	0.24	1.62	24.4	11.8	60.6	24.6
30-40	8.24	0.19	0.21	1.57	26.7	12.6	58.3	25.7
40-50	8.21	0.16	0.21	1.53	27.3	13.7	54.7	27.8

EC = electrical conductivity; OC = organic carbon; BD = bulk density, FC = field capacity; PWP = permanent wilting point

Soil properties measurement

The in-situ determination of soil bulk density (ρ_b) was made with the help of cylindrical core having 7.5 cm height and 8.0 cm diameter at 0-15 and 15-30 cm depth. The cores were dried in an oven at 105 °C till the weight of the soil becomes constant. As given in *Equation 1,* the ratio of dry soil mass (M_s) and internal volume (V_t) of the cylindrical ring is expressed as ρ_b of soil (Mg m^{-3}) (Blake and Hartge, 1986).

$$BD = Ms / Vt \quad \text{(Eq.1)}$$

The penetration resistance (PR) of soil was measured with hand-held digital cone penetrometer (CP40II; Rimik electronics, RFM Australia) at five randomly selected locations within a plot. The soil PR was recorded up to 60 cm depth.

Soil infiltration rate was determined using double ring infiltrometer method while the saturated hydraulic conductivity (K_s) was determined using constant head method (Reynolds et al., 2002). For K_s determination undisturbed soil cores (8 cm diameter and 7.5 cm length) were collected from 0-7.5 and 7.5-15 cm depth. Samples were saturated in the laboratory. Saturated soil sample along with core was connected with another core and to avoid the water leakage grease was applied in the jointing place on the top of previous core. A thin layer of water was slowly poured on top of the sample by using siphons connected to a constant head device (Mariotte apparatus). The volume of water that percolates through the sample was measured at definite intervals of time. The K_s was calculated using *Equation 2.*

$$Ks = Q \times L / A \times t\,(H + L) \quad \text{(Eq.2)}$$

where: Ks = saturated hydraulic conductivity (cm hr^{-1}); Q = volume of percolate collected (cm^3); L = length of soil column (cm); A = cross sectional area of soil column (cm^2); t = time (hr); H = depth of water above soil (cm).

Determination of plant parameters, crop and water productivity

During the crop growing period of both the crops the agronomic data on plant height, straw and grain yield was recorded. The grain yield of both the crops were recorded in kg from 24 m^2 area in each plot and finally expressed in t ha^{-1}. The root distribution was measured at 120 days after sowing (DAS) in both rice and wheat, respectively. The root

http://www.aloki.hu ● ISSN 1589 1623 (Print) ● ISSN 1785 0037 (Online)
DOI: http://dx.doi.org/10.15666/aeer/1706_1368513699

samples were collected up to 40 cm depth in rice and 70 cm depth in wheat. For root sampling, the soil cores were taken with the help of core sampler of 5 cm diameter. Samples were taken in between the plant rows. The root-soil cores were then collected and washed in plastic nets. Roots were carefully separated from the soil by washing the nets under water. The washed roots were further cleaned to remove any leftover weed roots, seed and other organic debris. The root length density (RLD) (cm cm^{-3}) was calculated from the total length of roots measured by scanner to the volume of the core.

The water productivity (WP) was calculated by dividing the grain yield of corresponding treatment with the total water use (IW + RF + PWU) in particular treatment.

IW = amount of irrigation water applied (cm)
RF = rainfall during crop growth period (cm)
PWU = profile water use (cm)

The data collected on various aspects of the investigations were statistically analysed as prescribed by Cochran and Cox (1967) and adapted by Cheema and Singh (1991) in statistical package CPCS-I. The treatment comparisons were made at 5% level of significance.

Results

Land management impacts on soil mechanical and water transmission characteristics

Result revealed that soil bulk density (BD) was significantly influenced by tillage and crop establishment methods at both 0-15 and 15-30 cm soil depth (*Table 2*). Minimum soil BD (Mg m^{-3}) was recorded in DTW (1.53) followed by DTR (1.55) and maximum in CTRW (1.58) at 0-15 cm depth. Similar trend was observed for 15-30 cm depth. Among crop establish methods, lesser mean BD was recorded under DSR as compared to PTR for both the depth. Among combination of treatments the PTR-CT results in maximum BD (1.58 Mg m^{-3}), while DSR-NTR records minimum BD (1.53 Mg m^{-3}). However, these effects were found to be non significant (*Table 2*). The data pertaining to effect of tillage on mean penetration resistance (PR) is presented in *Figure 2*.

Table 2. *Effect of tillage practices and crop established methods on soil bulk density (Mg m^{-3}) at 0-15 and 15-30 cm soil depth*

Tillage practices	Crop establishment methods				Mean	Crop establishment methods				Mean
	DSR		PTR			DSR		PTR		
	NTR	CT	NTR	CT		NTR	CT	NTR	CT	
	(0-15 cm)					(15-30 cm)				
DTR	1.53	1.54	1.56	1.57	1.55	1.64	1.66	1.68	1.71	1.67
DTW	1.51	1.52	1.54	1.55	1.53	1.62	1.62	1.65	1.67	1.64
CTRW	1.55	1.56	1.60	1.61	1.58	1.67	1.68	1.71	1.73	1.70
Mean	1.53	1.54	1.57	1.58		1.64	1.65	1.68	1.70	
LSD (<0.05)	Tillage = 0.03 Crop establishment methods = 0.02					Tillage = 0.04 Crop establishment methods = 0.03				

DTR = Deep tillage before rice; DTW = Deep tillage before wheat; CTRW = Conventional tillage before rice and wheat; DSR = direct seeded rice; PTR = puddled transplanted rice; NTR = no-tillage with residue; CT = conventional tillage

http://www.aloki.hu ● ISSN 1589 1623 (Print) ● ISSN 1785 0037 (Online)
DOI: http://dx.doi.org/10.15666/aeer/1706_1368513699

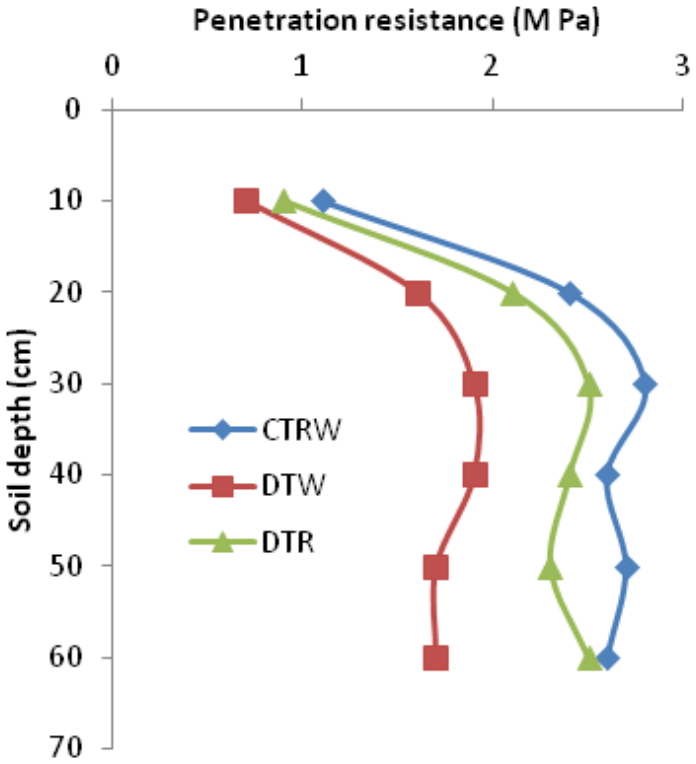

Figure 2. *Soil penetration resistance under different tillage practices (DTR = deep tillage before rice; DTW = deep tillage before wheat; CTRW = conventional tillage before rice and wheat)*

The PR is a measure of soil strength and the force required by the plant root to penetrate into the soil pores. The penetration resistance of soil increased with increase in soil depth. Likewise soil BD, the PR was also found to be significantly affected by tillage practices i.e. lowest PR was recorded under DTW (1.7 M Pa) and maximum under CTRW (2.9 M pa) at 30 cm soil depth. The data pertaining to steady state infiltration rate (IR) under different tillage practices has been presented in *Table 3*.

Table 3. *Effect of tillage practices and crop establishment methods on soil infiltration rate and saturated hydraulic conductivity (cm hr^{-1})*

Main tillage practices	Crop establishment methods				Mean	Crop establishment methods				Mean
	DSR		PTR			DSR		PTR		
	NTR	CT	NTR	CT		NTR	CT	NTR	CT	
	Infiltration rate (cm hr^{-1})					Saturated hydraulic conductivity (cm hr^{-1})				
DTR	1.4	1.1	1.1	0.8	1.1	1.8	1.5	1.6	1.4	1.6
DTW	1.7	1.5	1.4	1.1	1.4	2.1	1.7	1.6	1.5	1.7
CTRW	1.1	0.8	0.9	0.7	0.9	1.6	1.2	1.4	1.2	1.4
Mean	1.4	1.1	1.1	0.9		1.8	1.5	1.5	1.4	
LSD (<0.05)	Tillage = 0.4 Crop establishment methods = 0.3					Tillage = 0.3 Crop establishment methods = 0.3				

DTR = Deep tillage before rice; DTW = Deep tillage before wheat; CTRW = Conventional tillage before rice and wheat; DSR = direct seeded rice; PTR = puddled transplanted rice; NTR = no-tillage with residue; CT = conventional tillage

http://www.aloki.hu ● ISSN 1589 1623 (Print) ● ISSN 1785 0037 (Online)
DOI: http://dx.doi.org/10.15666/aeer/1706_1368513699

The steady state IR was higher under DTW (1.4 cm hr^{-1}) followed by DTR (1.1 cm hr^{-1}) and least in CTRW (0.9 cm hr^{-1}). However, among crop establishment methods higher mean IR was recorded in DSR than PTR. Likewise infiltration rate, maximum saturated hydraulic conductivity was recorded in DTW (1.7 cm hr^{-1}) followed by DTR (1.6 cm hr^{-1}) and least in CTRW (1.4 cm hr^{-1}). Among crop establishment methods maximum saturated hydraulic conductivity was recorded in DSR-NTR (1.8 cm hr^{-1}) and minimum in PTR-CT (1.4 cm hr^{-1}).

Plant height and root distribution

Data pertaining to plant height under different land management practices is presented in *Table 4*. The data revealed that, plant height significantly affected both by tillage and crop establishment methods. Maximum rice plant height was recorded in PTR-CT (102.8 cm) and least in DSR-HS (100.1 cm). Among main tillage practices, significantly higher rice mean plant height was recorded in DTR (103.0 cm) followed by DTW (101.3 cm) and lowest in CTRW (99.8 cm). In wheat also, the DTW recorded significantly higher plant height (104.0 cm) followed by DTR (102.3 cm) and least in CTRW (100.1 cm). However, among crop establishment methods maximum wheat mean plant height was observed in NTR-PTR (103.2 cm) and least in CT-DSR (100.7 cm). The mean root length density (RLD) of rice differed significantly under various tillage and crop establishment methods at different soil depths. The mean rice RLD in surface soil layer (10 cm) was 16 percent higher under DTR-PTR than DTR-CTRW (*Fig. 3*). However, at lower soil depths i.e. 20, 30 40 and 50 cm the RLD was observed to be 33%, 43%, 23% and 17% higher under DTR-DSR than CTRW, respectively.

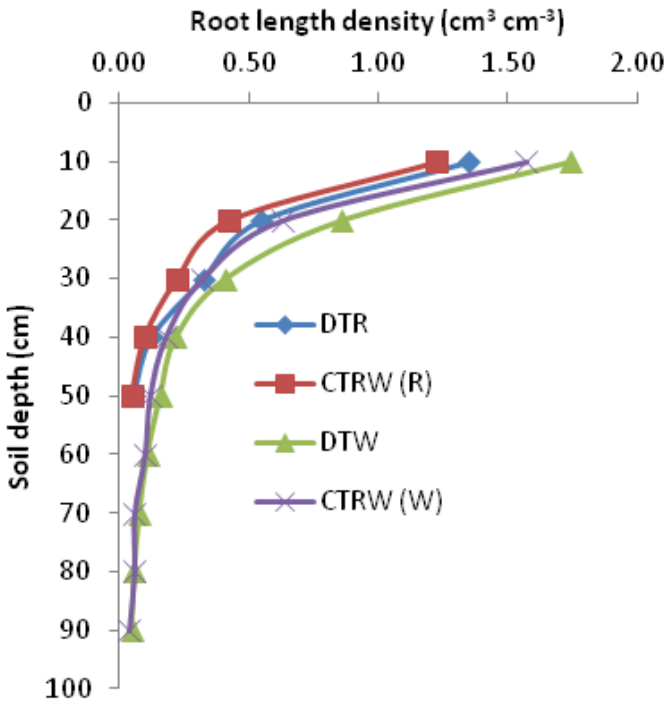

Figure 3. *Rice root length densities of rice and wheat under different tillage practices (DTR = deep tillage before rice; DTW = deep tillage before wheat; CTRW (R) = conventional tillage before rice and wheat for rice root; CTRW (W) = conventional tillage before rice and wheat for wheat*

http://www.aloki.hu ● ISSN 1589 1623 (Print) ● ISSN 1785 0037 (Online)
DOI: http://dx.doi.org/10.15666/aeer/1706_1368513699

Table 4. *Effect of tillage practices and crop establishment methods on plant height of rice and wheat*

Tillage practices	Crop establishment methods				Mean	Crop establishment methods				Mean
	DSR		PTR			DSR		PTR		
	NTR	CT	NTR	CT		NTR	CT	NTR	CT	
	Rice plant height (cm)					Wheat plant height (cm)				
DTR	101.2	102.6	103.3	104.8	103.0	102.8	101.5	102.7	102.2	102.3
DTW	100.3	100.7	101.7	102.6	101.3	103.6	102.1	105.8	104.7	104.0
CTRW	98.9	99.3	100.4	100.9	99.8	100.3	98.4	101.2	100.5	100.1
Mean	100.1	100.9	101.8	102.8		102.2	100.7	103.2	102.5	
LSD (<0.05)	Tillage = 1.3 Crop establishment methods = 0.9					Tillage = 1.6 Crop establishment methods = 1.1				

DTR = Deep tillage before rice; DTW = Deep tillage before wheat; CTRW = Conventional tillage before rice and wheat; DSR = direct seeded rice; PTR = puddled transplanted rice; NTR = no-tillage with residue; CT = conventional tillage

Crop and water productivity of rice and wheat

The rice straw as well as grain yield was found to be significantly more under DTR (7.0 t ha^{-1}) followed by DTW (6.7 t ha^{-1}) and least in CTRW (6.4 t ha^{-1}). Among crop establishment methods maximum rice straw yield was recorded in PTR-CT (7.5 t ha^{-1}) and minimum in DSR-HS (5.9 t ha^{-1}). Similarly maximum rice grain yield was recorded in DTR (6.1 t ha^{-1}) and minimum in CTRW (5.6 t $ha^{-1)}$ (*Table 5*).

Table 5. *Effect of tillage practices and crop establishment methods on rice straw and grain yield (t/ha)*

Tillage practices	Crop establishment methods				Mean	Crop establishment methods				Mean
	DSR		PTR			DSR		PTR		
	NTR	CT	NTR	CT		NTR	CT	NTR	CT	
	Rice straw yield (t/ha)					Rice grain yield (t/ha)				
DTR	6.1	6.7	7.2	7.8	7.0	5.4	5.9	6.3	6.7	6.1
DTW	5.9	6.5	6.9	7.5	6.7	5.4	5.7	6.1	6.4	5.9
CTRW	5.7	6.0	6.5	7.2	6.4	5.1	5.4	5.6	6.1	5.6
Mean	5.9	6.4	6.9	7.5		5.3	5.7	6.0	6.4	
LSD (<0.05)	Tillage = 0.3 Crop establishment methods = 0.6					Tillage = 0.4 Crop establishment methods = 0.5				

DTR = Deep tillage before rice; DTW = Deep tillage before wheat; CTRW = Conventional tillage before rice and wheat; DSR = direct seeded rice; PTR = puddled transplanted rice; NTR = no-tillage with residue; CT = conventional tillage

Among crop establishment methods maximum rice grain yield was recorded in PTR-CT (6.4 t ha^{-1}) and minimum in DSR-HS (5.3 t ha^{-1}). In wheat, maximum straw yield was recorded in DTW (5.9 t ha^{-1}) and minimum in CTRW (5.3 t ha^{-1}). Among crop establishment methods maximum wheat straw yield was recorded in PTR-NTR (6.1 t ha^{-1}) and minimum in DSR-CT (5.1 t ha^{-1}). Grain yield of wheat was also observed to be highest in DTW (5.2 t ha^{-1}) and least in CTRW (4.6 t ha^{-1}) (*Table 6*). The

http://www.aloki.hu ● ISSN 1589 1623 (Print) ● ISSN 1785 0037 (Online)
DOI: http://dx.doi.org/10.15666/aeer/1706_1368513699

DTR-NTR out yielded wheat productivity by 14% than DSR-CT. The water productivity of rice and wheat was found to be significantly affected by tillage practices and crop establishment methods. Maximum WP in rice was recorded in DTR (5.35 kg ha^{-1} mm^{-1}) and least in CTRW (3.92 kg ha^{-1} mm^{-1}) (*Fig. 4*). However, among crop establishment methods the maximum WP was recorded in PTR-CT followed by PTR-NTR, DSR-CT and least in DSR-NTR. Similarly, in wheat, maximum WP was observed in DTW (15.14 kg ha^{-1} mm^{-1}) and least in DSR-CT (13.24 kg ha^{-1} mm^{-1}) (*Fig. 5*). Under crop establishment methods the maximum WP was recorded under NTR-PTR followed by CT-PTR, NTR-DSR and least in CT-DSR.

Table 6. *Effect of tillage practices and crop establishment methods on wheat straw and grain yield (t/ha)*

Tillage practices	Crop establishment methods				Mean	Crop establishment methods				Mean
	DSR		PTR			DSR		PTR		
	NTR	CT	NTR	CT		NTR	CT	NTR	CT	
	Wheat straw yield (t/ha)					Wheat grain yield (t/ha)				
DTR	5.3	5.1	6.0	5.8	5.6	4.6	4.4	5.1	4.8	4.7
DTW	5.6	5.3	6.4	6.1	5.9	5.1	4.9	5.6	5.3	5.2
CTRW	5.2	4.8	5.8	5.4	5.3	4.5	4.2	4.9	4.7	4.6
Mean	5.4	5.1	6.1	5.8		4.7	4.5	5.2	4.9	
LSD (<0.05)	Tillage = 0.2 Crop establishment methods = 0.5					Tillage = 0.3 Crop establishment methods = 0.4				

DTR = Deep tillage before rice; DTW = Deep tillage before wheat; CTRW = Conventional tillage before rice and wheat; DSR = direct seeded rice; PTR = puddled transplanted rice; NTR = no-tillage with residue; CT = conventional tillage

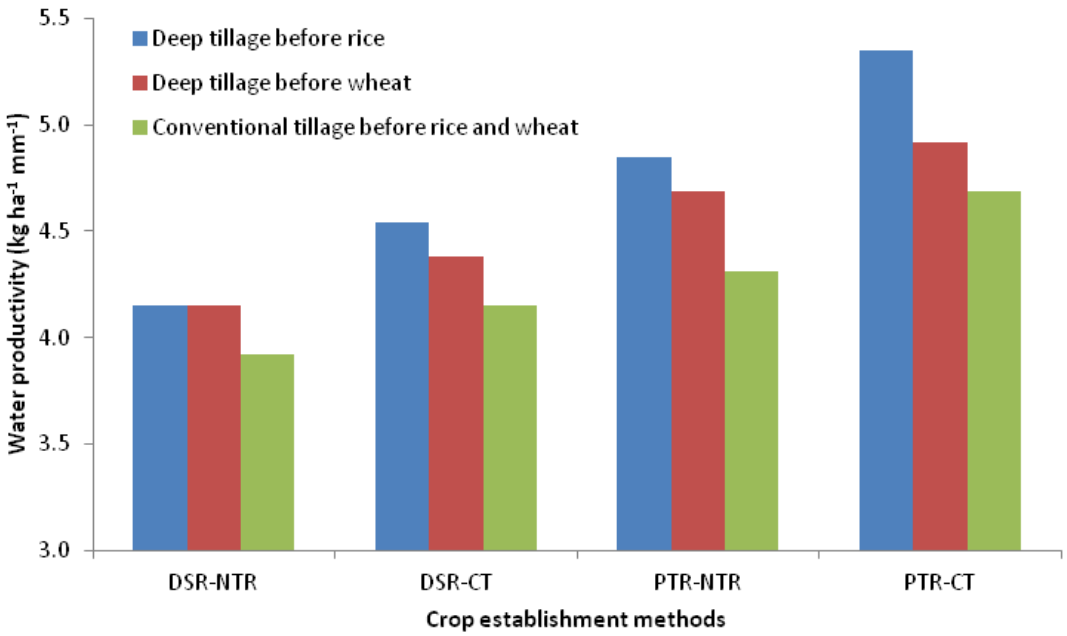

Figure 4. *Water productivity of rice under different tillage practices and crop establishment method (DSR = direct seeded rice; PTR = puddled transplanted rice; NTR = no-tillage with residue; CT = conventional tillage)*

http://www.aloki.hu ● ISSN 1589 1623 (Print) ● ISSN 1785 0037 (Online)
DOI: http://dx.doi.org/10.15666/aeer/1706_1368513699

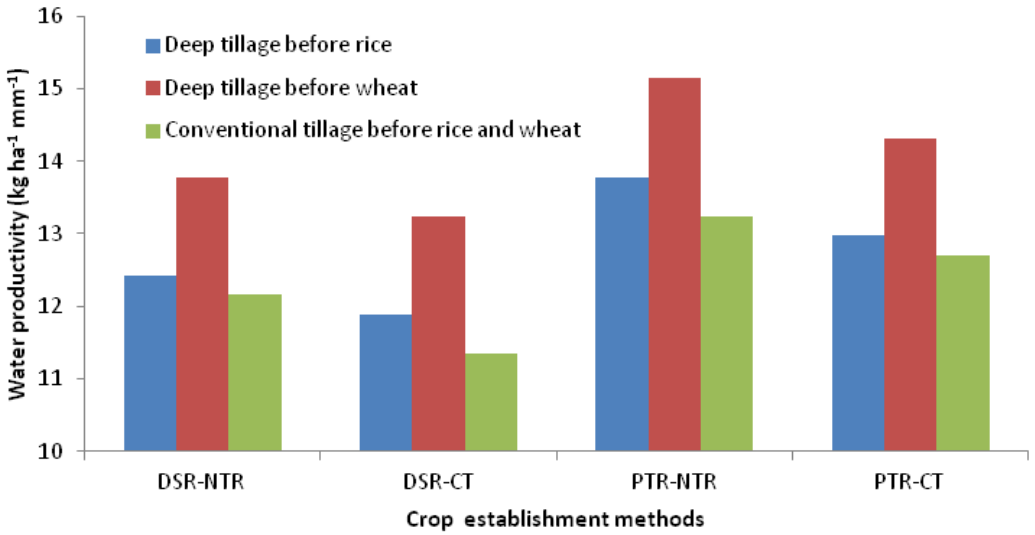

Figure 5. *Water productivity of wheat under different tillage practices and crop establishment method (DSR = direct seeded rice; PTR = puddled transplanted rice; NTR = no-tillage with residue; CT = conventional tillage)*

Discussion

Effect of tillage and crop establishment methods on soil compaction and water transmission

Conventional tillage practices including puddling in rice and performing five field operations for seed bed preparation in wheat have lead to destruction of soil structure by breaking macro aggregates into micro aggregates. Also due to physical compression there is formation of hard pan and increased bulk density at sub surface layer, which hinders growth of wheat roots to deeper depths. The bulk density of soil increases with the number of traffic passes and intensity whereas infiltration rate decreases with number of passes. However, with deep tillage practice due to shattering of soil up to 45 cm depth and 50 cm apart, the hard pan lying at 15-25 cm depth broken down leading to loosening of soil which further helps in increasing soil; water infiltration and saturated hydraulic conductivity of the soil. Among crop establishment the DSR showed lesser bulk density than PTR. This might be due to lesser number of field operations in DSR than PTR and also due to puddling and transplanting the chances of soil compaction increases as observed through higher bulk density and penetration resistance values. Prasad and Balanagoudar (2017) also reported lower soil bulk density in DSR than PTR as puddling resulted in destruction of soil aggregates and dispersion of soil particles to form compact layer having low porosity. Commonly all tillage practices accounts to reduced bulk density to the depth of tillage operation (Erbach et al., 1992; Osunbitan et al., 2005) and water infiltration rate was greater in tilled than no-tilled soil (Ferreras et al., 2000).

The water transmission characteristics of soil are also observed to be significantly affected by tillage and crop establishment methods. The various physical properties of soil such as bulk density, porosity and water holding capacity are fundamental indicators that show the effect of tillage on soils hydraulic properties (Strudley et al., 2008). The deep tillage improves soil properties by reducing soil bulk density and penetration resistance in the tilled layer (Varsa et al., 1997) and by altering soil porosity,

http://www.aloki.hu ● ISSN 1589 1623 (Print) ● ISSN 1785 0037 (Online)
DOI: http://dx.doi.org/10.15666/aeer/1706_1368513699

increasing hydraulic conductivity and infiltration rate (Laddha and Totawat, 1997). Sojka et al. (1997) also found that deep tillage increases soil porosity, saturated and unsaturated hydraulic conductivity, improves the aeration status which leads to increased soil moisture storage (Velykis, 2004) in the loosened soil layer. Chan and Mead (1989) noticed that tilled soils exhibited greater hydraulic conductivities than untilled soils and attributed the difference to decreased soil bulk density and improved porosity than in soils under no tillage conditions. Higher infiltration rate recorded in DT than CT may be due to ample amount of macro pores which led to fast entry of water into the soil profile. Almouti et al. (2007) reported increase in infiltration rate with increase in tillage depth; the probable cause might be the decrease in bulk density.

Effect of tillage and crop establishment on crop growth and productivity

The deep tillage reduces the soil compaction, thereby increasing the water availability to the crops by facilitating well developed root system. Many reports over the world have shown that tillage practices influence root growth and crop yield by altering soil properties such as soil structure, water, aeration, fertility and other factors having strong influence on crop yield, water and fertilizer use efficiency of crops (Acharya and Sharma, 1994; Holanda et al., 1998; Lampurlanes and Cantero-Martinez, 2003). Cai et al. (2014) observed that DT to a soil depth of 50 cm have significantly improved root morphology and thereby increases the resistance to environmental stress. The various studies have reported that DT can increase the crop yield and resource use efficiency, largely due to the improved physical, biological, and hydraulic properties of the soil (Jabro et al., 2009). Further, soil manipulation and loosening by DT permits greater water movement and aeration in the soil, facilitates better root proliferation to deeper layers and allows the deeper chemical movement as compared to untilled soil (Diaz-Zorita, 2000; Strudley et al., 2008). High soil strength often limits the root proliferation to deeper layers and thus hinders the usage of water and nutrient resources (Bengough et al., 2011). The higher RLD under deep tilled conditions could be due to improved physical conditions of the soil which facilitates better root proliferation due to reduced mechanical resistance. The DSR do not perform well from productivity point of view. This may be due to higher weed infestation and iron deficiency. As above ground biomass is the function of the below ground biomass, i.e. root system. Better the root system more will be the exploration of soil volume by plant roots for water and nutrients, more will be the translocation of water and nutrients and hence the above ground biomass. Thus, higher grain yield was recorded under deep tillage than conventional tillage in both rice and wheat crops. However, among crop establishment methods, the PTR performed significantly better than DSR. The shallow and compacted topsoil in conventional tilled plots not only restricts the root development of plants, but hinders their absorption of nutrients and water (Wang et al., 2008). This could be due to the negative effect of residue retained on the following DSR crop. There was a consistent trend for poorer growth of DSR following wheat mulched with rice straw, suggesting the need to examine the possibility of allelopathic effects of surface rice straw retention in direct seeded rice-wheat systems (Gupta et al., 2016). The deep tillage reduces soil strength and soil bulk density (Laddha and Totawat, 1997), improves water storage in the soil, enhances the root growth (Holloway and Dexter, 1991) thereby increases crop production (Ghosh et al., 2006) as compared to conventional tillage. The crop productivity was higher under tillage depth of 35 cm as compared to tillage depth of 15 cm (Zhang and Li, 2010). Sub-soil compaction reduced both the water and

http://www.aloki.hu ● ISSN 1589 1623 (Print) ● ISSN 1785 0037 (Online)
DOI: http://dx.doi.org/10.15666/aeer/1706_1368513699

nutrient use efficiencies of wheat by about 38% in a fine loamy soil (Ishaq et al., 2001). Deep tillage (chiseling), decreases soil bulk density and penetration resistance of this compact layer, increases depth of rooting, profile water use and yield of following wheat crop. Mosaddeghi et al. (2009) found that soil conditions under a zero-tillage conservation system were better than those under conventional system in arid and semi-arid environments. Residues accumulation in the soil acts as mulch which protects the soil from soil aggregate destruction enhances infiltration of water. It is an important organic source for retaining and improving soil fertility (Wang et al., 2002).

Conclusion

The deep tillage before wheat and rice improves crop and water productivity. Among crop establish methods puddled transplanted rice significantly improved rice yield and in wheat no-tillage with residue out yielded conventional tillage. The deep tillage provides healthy soil environment by reducing soil compaction and allowing water and roots to move to deeper soil layers. The greater root proliferation under deep tillage helps in extracting water and nutrient from lower soil depths. Thus, deep tillage helps in reducing mechanical strength and enhancing water transmission. Thus, in northwest Indian conditions in rice deep tillage along with puddled rice transplanting and in wheat, deep tillage along with no-tillage and residue are appropriate tillage and crop establishment techniques for enhancing crop and water productivity. However, further research needs to be carried out on impact of different tillage practices under variable irrigation and nitrogen regimes on cereals and pulse based cropping systems.

REFERENCES

[1] Acharya, C., Sharma, P. (1994): Tillage and mulch effects on soil physical environment, root growth, nutrient uptake and yield of maize and wheat on an Alfisol in north-west India. – Soil Till. Res. 32: 291-302.

[2] AICRP (2009): All India Coordinated Project on Management of salt Affected Soils and Use of Saline Water in Agriculture Biennial Report (2006-08). – Central Soil Salinity Research Institute, Karnal, Haryana, India.

[3] Akhtar, M. S., Quereshi, S. Q. (1999): Soil hydraulic properties and rice root development as influenced by tillage. – Pakistan J. Biol. Sci. 2(4): 1245-1251.

[4] Alamouti, M. Y., Navabzadeh, M. (2007): Investigation of plowing depth effect on some soil physical properties. – Pak J Biol Sci.10: 4540-14.

[5] Arora, V. K., Gajri, P. R., Uppal, H. S. (2006): Puddling, irrigation, and transplanting time effects on productivity of rice–wheat system on a sandy loam soil of Punjab, India. – Soil Till. Res. 85: 212-220.

[6] Bajpai, R. K., Tripathi, R. P. (2000): Evaluation of non-puddling under shallow water tables and alternative tillage methods on soil and crop parameters in a rice–wheat system in Uttar Pradesh. – Soil Till. Res. 55: 99-106.

[7] Balasubramanian, V., Hill, J. E. (2002): Direct Seeding of Rice in Asia: Emerging Issues and Strategic Research Needs for the 21st Century. – In: Pandey, S., Mortimer, M., Wade, L., Tuong, T. P., Lopez, K., Hardy, B. (eds.) Direct Seeding: Research Strategies and Opportunities. International Rice Research Institute, Los Banos, Philippines, pp.15-39.

[8] Bengough, A. G., McKenzie, B. M., Hallett, P. D., Valentine, T. A. (2011): Root elongation, water stress, and mechanical impedance: a review of limiting stresses and beneficial root tip traits. – J Exp Bot 62: 59-68.

http://www.aloki.hu ● ISSN 1589 1623 (Print) ● ISSN 1785 0037 (Online)
DOI: http://dx.doi.org/10.15666/aeer/1706_1368513699

[9] Blake, G. R., Hartge, K. H. (1986): Bulk Density. – In: Klute, A. (ed.) Methods of Soil Analysis. ASA, Madison, WI, pp 363-75.
[10] Cai, H. G., Ma, W., Zhang, X. Z., Ping, J. Q., Yan, X. G., Liu, J. Z., Yuan, J. C., Wang, L. C., Ren, J. (2014): Effect of subsoil tillage depth on nutrient accumulation, root distribution, and grain yield in spring maize. – Crop J 2: 297-307.
[11] Chan, K. Y., Mead, J. A. (1989): Water movement and macroporosity of an Australian Alfisol under different tillage and pasture conditions. – Soil Till Res14: 301-10.
[12] Cheema, H. S., Singh, B. (1991): Software Statistical Package CPCS-1. – Department of Statistics, PAU, Ludhiana.
[13] Cochran, W. G., Cox, G. M. (1967): Experimental Designs. – John Wiley, New York.
[14] Diaz-Zorita, M. (2000): Effects of deep-tillage and nitrogen fertilization interactions on dryland corn (Zea mays L.) productivity. – Soil Till Res 54: 11-19.
[15] Dingkuhn, M., Schnier, H. F., DeDatta, S. K., Dorffling, K., Javellana, C., Pamplona, R. (1990): Nitrogen fertilization of direct seeded flooded vs. transplanted rice. II. Interactions among canopy properties. – Crop Sci. 30(6): 1284-1292.
[16] Erbach, D. C., Benjamin, J. G., Cruse, R. M., Elamin, M. A., Mukhtar, S., Choi, C. H. (1992): Soil and corn response to tillage with paraplow. – Transactions of the ASAE 35: 1347-1354.
[17] Farooq, M., Basra, S. M. A., Asad, S. A. (2008): Comparison of conventional puddling and dry tillage in rice–wheat system. – Paddy Water Environ. 6: 397-404.
[18] Ferreras, L. A., Costa, J. L., Garcia, F. O., Pecorari, C. (2000): Effect of no-tillage on some physical properties of structural degraded Petrocalcic Paleudoll of southern Pampa of Argentina. – Soil Till Res 54: 31-39.
[19] Gajri, P. R., Arora, V. K., Parihar, S. S. (2002): Tillage for Sustainable Cropping. – Food Products Press, New York.
[20] Gangwar, K. S., Singh, K. K., Sharma, S. K. (2004): Effects of tillage on growth, yield and nutrient uptake in wheat after rice in Indo-Gangetic Plains of India. – J. Agric. Sci. 142: 453-459.
[21] Ghosh, P. K., Mohanty, M., Bandyopadhyay, K. K., Painuli, D. K., Misra, A. K. (2006): Growth, competition, yield advantage and economics in soybean/pigeonpea intercropping system in semi-arid tropics of India: I. Effect of subsoiling. – Field Crops Res 96: 80-89.
[22] Gupta, N., Yadav, S., Humphreys, E., Kukal, S. S., Balwinder-Singh., Eberbach, P. L. (2016): Effects of tillage and mulch on the growth, yield and irrigation water productivity of a dry seeded rice-wheat cropping system in north-west India. – Field Crops Res 196: 219-36.
[23] Hobbs, P. R., Singh, Y., Giri, G. S., Lauren, J. G., Duxbury, J. M. (2002): Direct Seeding and Reduced Tillage Options in the Rice-Wheat Systems of the Indo-Gangetic Plains of South Asia. – In: Pandey, S., Mortimer, M., Wade, L., Tuong, T. P., Hardy, B. (eds.) Direct Seeding in Asian Rice Systems: Strategic Research Issues and Opportunities. International Rice Research Institute, Los Banos, Philippines, pp. 201-205.
[24] Holanda, F., Mengel, D., Paula, M., Carvaho, J., Bertoni, J. (1998): Influence of crop rotations and tillage systems on phosphorus and potassium stratification and root distribution in the soil profile. – Comm Soil Sci Plant Anal 29: 2383-94.
[25] Holloway, R. E., Dexter, A. R. (1991): Tillage and compaction effect on soil properties, root growth and yield of wheat during drought in a semi-arid environment. – Soil Tech 4: 233-53.
[26] Ishaq, M., Hassan, A., Saeed, M., Ibrahim, M., Lal, R. (2001): Sub soil compaction effects on crops in Punjab, Pakistan. I. Soil physical properties and crop yield. – Soil Till. Res. 59: 57-65.
[27] Jabro, J. D., Stevens, W. B., Evans, R. G., Iversen, W. M. (2009): Tillage effects on physical properties in two soils of the Northern Great Plains. – Appl Eng Agric 25: 377-82.

http://www.aloki.hu ● ISSN 1589 1623 (Print) ● ISSN 1785 0037 (Online)
DOI: http://dx.doi.org/10.15666/aeer/1706_1368513699

[28] Kamra, S. K., Khajanchi, L., Singh, O. P., Boonstra, J. (2002): Effects of pumping on temporal changes in groundwater quality. – Agric Water Manage 56: 169-78.
[29] Laddha, K. C., Totawat, K. L. (1997): Effects of deep tillage under rainfed agriculture on production of sorghum (Sorghum biocolor L. Moench) intercropped with green gram (Vigna radiate L. Wilczek) in western India. – Soil Till Res 43: 241-50.
[30] Lampurlanes, J., Cantero-Martinez, C. (2003): Soil bulk density and penetration resistance under different tillage and crop management systems and their relationship with barley root growth. – Agron J 95: 526-36.
[31] Mosaddeghi, M. R., Mahboubi, A. A., Safadoust, A. (2009): Short-term effects of tillage and manure on some soil physical properties and maize root growth in a sandy loam soil in western Iran. – Soil Till Res 104: 173-179.
[32] Naklang, A. K., Fukai, B. S., Nathabut, A. K. (1996): Growth of rice cultivars by direct seeding and transplanting under upland and lowland conditions. – Field Crops Res. 48: 115-123.
[33] Osunbitan, J. A., Oyedele, D. J., Adekalu, K. O. (2005): Tillage effects on bulk density, hydraulic conductivity and strength of a loamy sand soil in southwestern Nigeria. – Soil Till Res 82(1): 57-64.
[34] Prasad, S. L., Balanagoudar, S. R. (2017): Soil quality assessment in selected dry direct seeded rice and puddled paddy field in agro climatic zone 2 of Northern Karnataka. – Int J Pure Appl Biosci. 5(3): 362-368.
[35] Reynolds, W. D., Elrick, D. E., Youngs, E. G. (2002): Single-Ring and Double or Concentric-Ring Infiltrometers. – In: Dane, J. H., Topp, G. C. (eds.) Methods of Soil Analysis. Soil Sci Soc Am, Madison, WI, pp. 821-26.
[36] Saleh, A. F. M., Bhuiyan, S. I. (1995): Crop and rainwater management strategies for increasing productivity of rainfed lowland rice systems. – Agric. Syst. 49: 259-276/
[37] Schnier, H. F., Dingkuhn, M., DeDatta, S. K., Mengel, K., Faronilo, J. E. (1990): Nitrogen fertilization of direct seeded flooded vs. transplanted rice. I. Nitrogen uptake, photosynthesis, growth, and yield. – Crop Sci. 30: 1276-1284.
[38] Sharma, P. K., Ladha, J. K., Bhushan, L. (2003): Soil Physical Effects of Puddling in Rice-Wheat Cropping Systems. – In: J. K. Ladha, J. E. Hill, J. M. Duxbury, R. K. Gupta, and, R. J. Buresh (eds.) Improving the Productivity and Sustainability of Rice-Wheat Systems: Issues and Impacts. ASA, CSSA, SSSA, Madison, WI. ASA Special Publication 65: 97-113.
[39] Sharma, S. K., Tomar, R. K., Gangwar, K. S. (1995): Effects of crop establishment and tillage practices on yield and economics of irrigated rice (Oryzasativa)–wheat (Triticum aestivum) system. – Ind. J. Agric. Sci. 65: 636-638.
[40] Sharma, S. K., Pandey, D. K., Gangwar, K. S., Tomar, O. K. (2005): Effect of crop establishment methods on performance of rice (Oryzasativa) cultivars and their effects on succeeding wheat (Triticum aestivum). – Ind J. Agron. 50: 253-255.
[41] Sojka, R. E., Home, D. J., Ross, C. W., Baker, C. J. (1997): Subsoiling and surface tillage effects on soil physical properties and forage oat stand and yield. – Soil Till Res 40: 125-44.
[42] Srinivasa Prasad, L., Balanagoudar, S. R. (2017): Soil quality assessment in selected dry-direct seeded rice (dry-dsr) and puddled paddy fields in agro climatic zone 2 of northern Karnataka. – Int. J. Pure App. Biosci. 5(3): 362-368.
[43] Strudley, M. W., Green, T. R., Ascough, J. C. (2008): Tillage effects on soil hydraulic properties in space and time. – Soil Till Res 99: 4-48.
[44] Tuong, T. P., Singh, A. K., Siopongco, J. D. L. C., Wade, L. J. (2000): Constraints to high yield of dry-seeded rice in the rainy season of a humid tropic environment. – Plant Prod. Sci. 3: 164-172.
[45] Varsa, E. C., Chong, S. K., Abolaji, J. O., Farquhar, D. A., Olsen, F. J. (1997): Effect of deep tillage on soil physical characteristics and corn (Zea mays L.) root growth and production. – Soil Till Res 43: 219-28.

http://www.aloki.hu ● ISSN 1589 1623 (Print) ● ISSN 1785 0037 (Online)
DOI: http://dx.doi.org/10.15666/aeer/1706_1368513699

[46] Velykis, A. (2004): Effect of subsoiling on agrophysical properties of compacted clay loam soil. Subsoil compaction-distribution, processes and consequences. – Adv Geoecol 32: 325-30.
[47] Wang, H. Q., Bouman, B. A. M., Zhao, D. L., Wang, C., Moya, P. F. (2002): Aerobic Rice in Northern China: Opportunities and Challenges. – In: Bouman, B. A. M., Heengsdijk, H., Hardy, B., Bindraban, P. S., Tuong, T. P. and Ladha, J. K. (Eds.). Proc of the International Workshop on Water Wise Rice Production, 8-11 April 2002, IRRI, Los Banos, Phillipines, pp. 143-54.
[48] Wang, J. D., Gong, S. H., Sui, J., Xu, H., Yu, Y. D. (2008): Effects of drip irrigation frequency on the farmland soil water-heat distribution and spring maize growth in North China. – Trans Chinese Soc Agric. Engg. 24: 39-45.
[49] Zhang, S. H., Li., S. K. (2010): Domestic and Foreign Corn Industrial Technology Development Report. – China Agricultural Science and Technology Press, Beijing.

http://www.aloki.hu ● ISSN 1589 1623 (Print) ● ISSN 1785 0037 (Online)
DOI: http://dx.doi.org/10.15666/aeer/1706_1368513699

CHARACTERISTICS OF POPULATION INDICATORS OF BROWN HARE (*LEPUS EUROPAEUS* PALL.) OBTAINED DURING GROUP HUNTING IN THE REGION WITH THE HIGHEST DENSITY IN WESTERN PART OF THE LUBLIN REGION IN POLAND

FLIS, M.[1] – RATAJ, B.[2*]

[1]*Department of Ethology of Animals and Hunting, Faculty of Animal Sciences and Bioeconomy, University of Life Sciences in Lublin, 20-950 Lublin, Poland (ORCID 0000-0001-7429-3158)*

[2]*Polish Hunting Association, District Board Nowy Sącz, 33-300 Nowy Sącz, Poland*

**Corresponding author*
e-mail: brataj66@gmail.com

(Received 23rd Apr 2019; accepted 11th Jul 2019)

Abstract. The research was conducted in the hunting season 2017/18, during three group hunts. In total, 129 shot hares were covered. During the tests, body weight, age, and sex were determined. The achieved results indicate that the size of hunting harvest at the level of about 3 individuals/100 ha should be accepted as the highest in Poland, which is also a confirmation of the highest density of this species. They are also a confirmation of high individual condition expressed by body weight of both young (4.10 kg) and adults (4.65 kg). The structure of sex and age, as well as calculated reproduction rates (1.63) and reproductive success (2.42) indicate that the assessed population has developing features. The conducted research on the parameters characterizing the hare population in the area covered by the studies indicate high individual condition as well as reproductive potential, which allows to deduce about the potentially high potential for reconstruction of the number of hares.
Keywords: *brown hare, body mass, age structure, sex structure, Lublin Upland*

Introduction

In the last decades, a decreasing trend of the hare population has been observed in most European countries. Also in our country, the number and local density ratios, in many regions, have remained at a low and very low level for many years (Pielowski, 1976; Burel and Baudry, 1990; Dziedzic et al., 2002; Flis, 2009, 2016; Jezierski, 2004; Nasiadka and Dziedzic, 2014).

Although it is quite difficult to identify the unambiguous cause of this unfavorable trend, the most frequent changes are the changes in agrocenoses that are the main habitat for this species. Intensification of agriculture affecting quite significantly the heterogeneity of hare living environments, combined with the increase in the mechanization of all agrotechnical operations and the frequent use of plant protection products contributes to a significant simplification of agrocenosis structures (Lewandowski and Nowakowski, 1993; Panek and Kamieniarz, 1999; Dziedzic et al., 2000; Schmidt et al., 2004; Kryński et al., 2007; Kamieniarz et al., 2013; Schai-Braun et al., 2015; Panek, 2018). Another not less important factor influencing the hare population dynamics is predation, mainly free-living foxes (Pielowski, 1979; Goszczyński and Wasilewski, 1992; Panek et al., 2006; Panek, 2007; Wasilewski, 2007). The number of these predators in recent years has increased quite dramatically,

http://www.aloki.hu ● ISSN 1589 1623 (Print) ● ISSN 1785 0037 (Online)
DOI: http://dx.doi.org/10.15666/aeer/1706_1370113711

which in turn was caused by the elimination of the basic mortality factor which was rabies. It is conditioned by the fact of conducting nationwide action of immunization of free-living foxes against rabies, starting from 2002 (Flis et al., 2017, 2018). Nevertheless, nowadays, in the conditions of low densities of hares populations occurring in many regions of the country, predation of foxes in hares in agrocenoses plays less and less influence on the dynamics of their numbers. The composition of the fox diet is more and more often sources of anthropogenic origin and small mammals (Gołdyn et al., 2003; Hušek et al., 2015; Panek, 2018). In addition, the negative impact of synanthropic predation on the population and thus the functioning of the population is also not without significance (Flis, 2013; Nasiadka and Dziedzic, 2014).

Quite significant factors affecting the dynamics of hares are also numerous disease entities. Coccidiosis and parasitic diseases are most often mentioned. However, bacterial and viral diseases such as brucellosis and hemorrhagic hare disease - EBHS and many other slightly less common (Pikula et al., 2004; Dubinský et al., 2010; Decors et al., 2011; Chroust et al., 2012; Kornaś et al., 2014; Nasiadka and Dziedzic, 2014; Flis et al., 2016). All described elements have a negative effect, and at the same time have a comprehensive impact on the functioning of the population of this species and they have led to a drastic reduction in densities. In the 70s of the last century, the average population density in our country remained at the level of about 50 individuals per 100 areas of field hunting grounds (Pielowski, 1976, 1979). At the beginning of the 21st century, the average level of hares density in the country was varied in individual regions and was in the range of 5-9 individuals/100 ha (Dziedzic et al., 2002; Wasilewski, 2007; Flis, 2009, 2016).

The most frequently used measure of the individual quality and health status as well as the survival rates of wild animals is the individual condition resulting directly from the body weight. This indicator, combined with climatic factors and intra-population parameters such as sex structure and age structure, determines the reproductive potential of the population. As a rule, individuals in a lower individual condition are more susceptible to natural selection factors (Frylestam, 1980; Hackländer, 2011; Flis, 2015).

The aim of the study was to assess the individual condition expressed by the body weight of males and females of young and adult hares in conditions of hunting areas with high acquisition of this species. The assessment also included sex structure and age indicators that directly affect the reproductive potential of this species.

Material and methods

Characteristics of the research area

The research was conducted in two hunting districts with a total area of 13.600 ha, the forest cover of which is 25.2%. They are located in the western part of the Lublin region, in the mesoregion of Kotlina Chodelska and the northern part of Wzniesienia Urzędowskie, in Poland, near the town of Opole Lubelskie (according to the WGS 84 reference system, the geographical coordinates are; width: 51°08′51″N, length: 21°58′08″E) (*Fig. 1*). This region is characterized by the presence of fertile soils of the chernozem type on the loess ground (Kondracki, 2000). Despite fairly fertile soils, it is distinguished by significant fragmentation of agricultural crops, and thus large heterogeneity of field environments. Field crops are dominated by plants with high soil requirements, with particular reference to orchards and plantations of perennial soft fruits, mainly raspberries and currants. In the agricultural landscape, there are numerous

http://www.aloki.hu ● ISSN 1589 1623 (Print) ● ISSN 1785 0037 (Online)
DOI: http://dx.doi.org/10.15666/aeer/1706_1370113711

wastelands as well as small wooded enclaves and forest complexes (Witek, 1991). Heterogeneity evaluation of the natural environment of agrocenoses in the area of research, performed according to the method proposed by Schrödel (1991) showed an average size of individual fields at the level of 0.95 ha, while the average distance between landscape elements ranged from 0.5 to 0.7 km. In turn, the relative length of contour lines in agrocenoses having significant impact on the functioning of small game population, despite the variation in individual regions of the study area, was on average at 0.1-0.2 km/km^2. All described elements determine quite significant mosaicism of field environments, creating almost optimal conditions for living and functioning of the hare population (Pielowski, 1979).

Figure 1. *Location of the research area*

Material for research

The research material were hares fired during collective hunts in November and December 2017. The hares were shot in the area with the highest density in the Lublin region. The annual number of assessments carried out by hunters indicate that the region has an average annual population size over the last 5 years, estimated at 1,100 individuals. With reference to the field surface of the area where the research was carried out, there is a density of 10 individuals per 1 km^2. In total, the analyzes were

http://www.aloki.hu ● ISSN 1589 1623 (Print) ● ISSN 1785 0037 (Online)
DOI: http://dx.doi.org/10.15666/aeer/1706_1370113711

carried out on 129 hares, of which 51 were male and another 78 females. Among the shots were 80 young hares and 49 adults. Additionally, in order to determine the level of compaction, a hunting analysis of this species was made during the last five hunting seasons.

Methods and measurements

All hares were weighed directly after the shot. Weighing was carried out with an accuracy of 0.1 kg. Gender assessments were made based on the appearance of secondary sexual characteristics. The hog age was also determined directly in the field on the basis of the palpation assessment of the occurrence or disappearance of the Stroh mark (cartilaginous elbow base cap). Such an assessment allows the division of hares into young (up to 1 year old) and adult (over 1 year old) (Stroh, 1931; Pielowski, 1979) (*Fig. 2*).

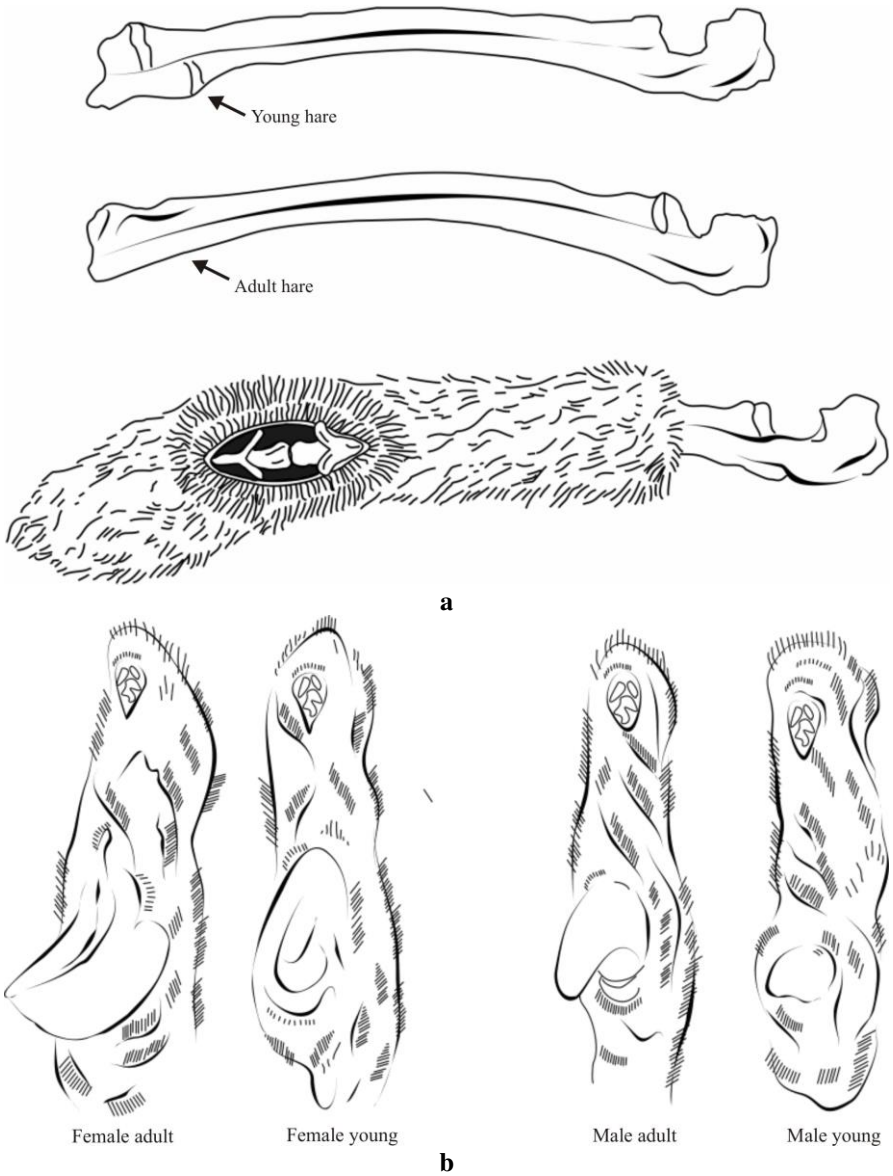

Figure 2. *Recognition of the age of shot hares based on the Stroh sign (a) and gender based on the appearance of the external reproductive organs (b)*

http://www.aloki.hu ● ISSN 1589 1623 (Print) ● ISSN 1785 0037 (Online)
DOI: http://dx.doi.org/10.15666/aeer/1706_1370113711

Analysis

The whole material was divided into age-gender groups, which allowed to determine the sex structure index and the age of the animals obtained. In order to determine the differences between average body weight values depending on the sex in separate age groups, hares were made a one-way analysis of variance. In order to verify the possible occurrence of differences between the averages, calculations were made using the Tukey test, in the Statistica program. The reproductive index and reproductive success rate were used to describe the dynamics of the population size (Pintur et al., 2006).

The reproduction rate was calculated as the ratio of the number of young hares that survived to the hunting season per 1 adult animal:

$$Wr = \frac{Njuv}{Nad} \quad \text{(Eq.1)}$$

The reproductive success rate was defined as the ratio of the number of young hares that survived to the hunting period per 1 adult female:

$$Wsr = \frac{Njuv}{Nadf} \quad \text{(Eq.2)}$$

Results

In the last five hunting seasons, hiring the hares in the areas constituting the research area showed a clear upward trend (*Fig. 3*). In this period, on average, over 300 hares were acquired in the circumferences constituting the research area on an annual basis (data from hunts conducted in this area by the hunting club). The acquisition rate from 100 ha of field area increased by over 100%, and on average in the hunting season more than 3 hares were obtained from every 100 ha of field area. This result in recent years is certainly the highest in Poland.

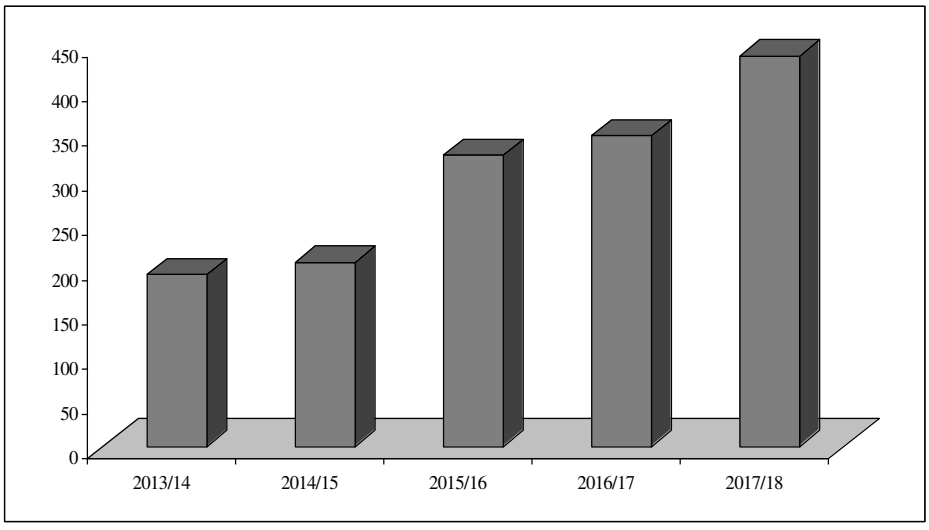

Figure 3. *The number and acquisition of a hare with 100 ha of area by shooting in the last 5 hunting seasons in the areas constituting the research area*

http://www.aloki.hu ● ISSN 1589 1623 (Print) ● ISSN 1785 0037 (Online)
DOI: http://dx.doi.org/10.15666/aeer/1706_1370113711

The analyzes of hog body mass development carried out show a significant variation of this characteristic between young and adult individuals and the relative stabilization of young and adult hares in the sexual groups (*Table 1*). The average body weight of 35 young males was 4.18 kg and young females were lower by 0.14 kg. This difference was not statistically significant ($p > 0.05$). The average body weights of adult females and males varied only 0.02 kg. On the other hand, predictably, adult hares were much heavier than the young ones. The least stable was the weight value of young females, which is confirmed by the calculated values of standard deviation.

Table 1. *Mean and standard deviation of body weight (kg) of acquired hares*

Item	Male		Female		Totality	
	Young	Adult	Young	Adult	Young	Adult
n	35	16	45	33	80	49
$\overline{x}$	4.18_x	4.63_y	4.04_x	4.65_y	4.10	4.65
SD	0.22	0.23	0.43	0.23	0.36	0.23

The structure of the sex of hares obtained showed significant variation in the age groups (*Fig. 4*). Both females prevailed in both young and adult animals. In young hares, the sex structure index was 1:1.29 and in adults it was 1:2.06. The age structure of shot hares was differentiated by gender (*Fig. 5*), however, in both sexual groups, young animals predominated. In males, the age structure index was 1:0.46 in favor of young animals. In females, the prevalence of juveniles was slightly lower, and the age structure index was at the level of 1:0.73, also in favor of individuals up to one year old. The calculated population reproduction (*Eq. 1*) rate was 1.63, and the reproductive success (*Eq. 2*) rate was 2.42.

Discussion

Hunting hares in the last hunting seasons in the area covered by the research should be assessed as very high. The average index obtained from 100 ha of area, at the level of about 3 individuals, is not much lower than the size of this species given by Flis (2015), in the area of Wyżyna Lubelska in the hunting season 2004/05-2013/14. It is also close to the lowest indicators of this parameter in the 10-year monitoring period in the experimental circuit located also in the Lublin Upland (Flis, 2016), which data reflect the average national level from the beginning of the twenty-first century (Dziedzic et al., 2002). Densities in central and western Poland given by Kamieniarz and others (2013) in 2006, depending on the season, were within the range of 4.1-9.5 individuals, while the results of the same studies in Germany showed density at the level of 18.8-48.4 individuals/100 ha. Research conducted in Turkey also indicates the diversified density of this species, depending on the type of environment and the season, at the level within the range of 1.6-7.6/100 ha (Demirbas, 2015). The compaction index in Hungary in the 2014/15 season was in the range of 13-17 individuals/100 ha (Farkas et al., 2016). Nevertheless, in some European countries there are areas in which the population density is much higher and often exceeds 20 individuals per 100 ha area (Pikula et al., 2004; Pintur et al., 2006). The obtained results indicate, that in the area of research, the population density of this species is undoubtedly one of the highest in Poland, which is confirmed by the distributions of collective hunting and calculated index of acquisition from 100 ha.

http://www.aloki.hu ● ISSN 1589 1623 (Print) ● ISSN 1785 0037 (Online)
DOI: http://dx.doi.org/10.15666/aeer/1706_1370113711

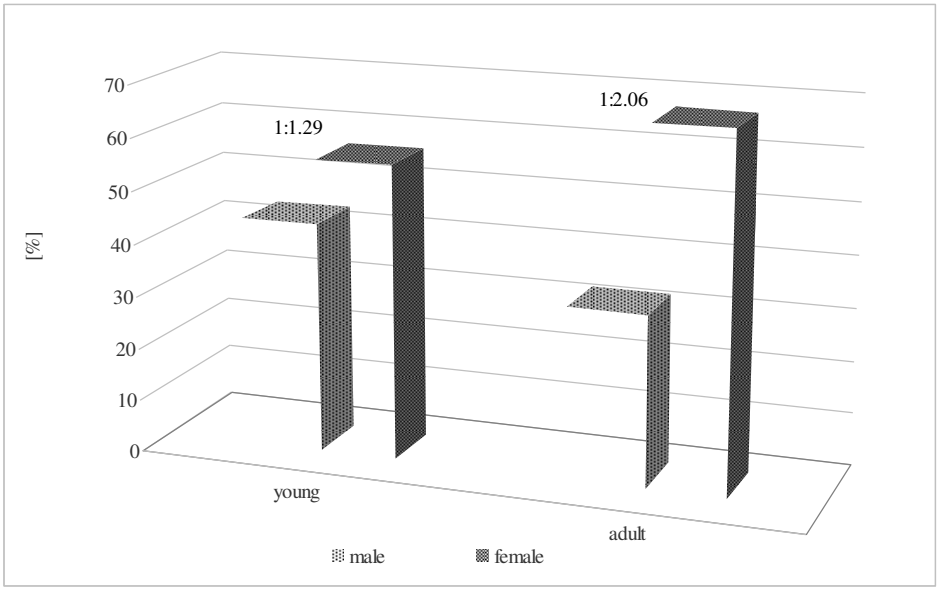

Figure 4. *Gender structure of acquired hares*

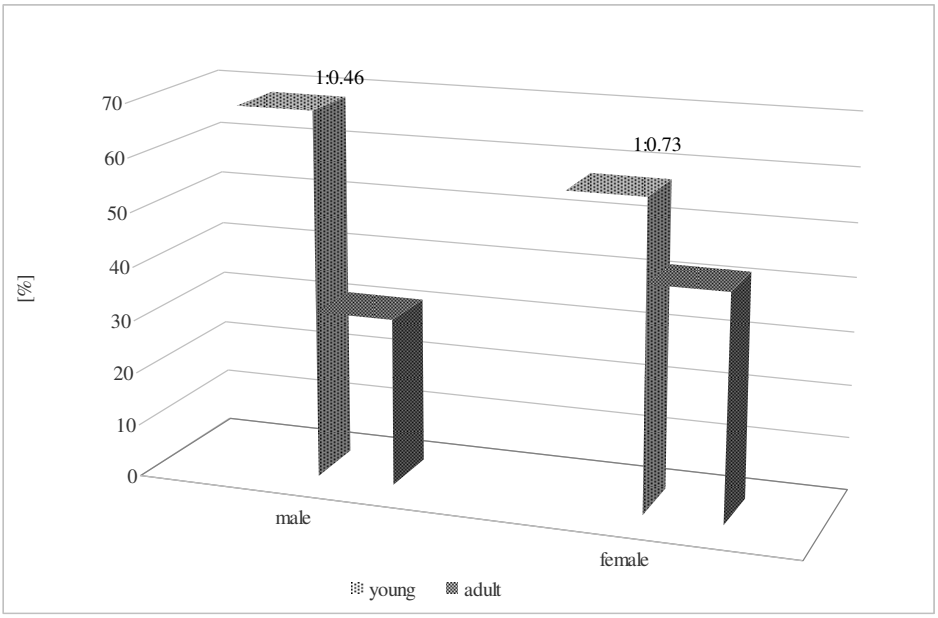

Figure 5. *Age structure of acquired hares*

The presented body weight results of both male and female hares are higher than those of Flis (2015) conducted in the hunting grounds of the Lublin Upland in the 2014/15 season. Currently, body mass is also slightly higher compared to the average values of this feature in the area of the Lublin Upland and Podlasie obtained in studies conducted in the mid-90s of the last century (Dziedzic et al., 1998). In turn, in Misiorowska and other studies (2014) conducted in areas of the highest population size of this species in our country, average hare body weight varied (3.42-4.32 kg), and a statistically significant difference between the averages was recorded only in age

http://www.aloki.hu ● ISSN 1589 1623 (Print) ● ISSN 1785 0037 (Online)
DOI: http://dx.doi.org/10.15666/aeer/1706_1370113711

groups. Also in the region of Central Pomerania in the years 1998-2001, significant differences between the hare body mass were found only in age groups, and the average value of this feature was 4.13 kg (Mysłek et al., 2004). The obtained data is also higher than in Croatia in the hunting season 2004/2005, given by Pintura and others (2006), as well as in Hungary in both age and gender groups (Farkas et al., 2016). Therefore, high density indicators in the area of research do not adversely affect the body weight of animals, because it is higher compared to the results presented by other authors from recent years, both from Poland and other European countries.

The obtained sex structure and age structure indicators showing a clear advantage of females and young individuals, regardless of gender, in the study population, are very optimistic, as they indicate that in the research area, the population exhibits developing features, which should directly affect its further development. The values of the reproduction rate and reproductive success indicate a high reproductive potential of the analyzed population, and thus suggest that there should be further dynamic growth. In the presented results, the reproduction rate was definitely higher than that from Misiorowska and other results (2014) carried out in the areas with the highest number of hares in Poland in the hunting season 2009/10, which ranged from 0.36 to 1.26. In turn, the reproductive success rate is only slightly lower than the upper value described by the same authors who fell within the range of 0.7-2.7. Pintur et al. (2006), conducting research in the diverse environments of Croatia in the 2004/05 hunting season, showed that the reproduction rate was environment-dependent and ranged from 0.61 to 1.50. In the same studies, the reproductive success rate was set at 1.33 to 3.40. In turn, in research conducted near Nitra in Slovakia, the value of the reproduction rate depending on the season was within the range of 0.76-0.92, and the reproductive success rate from 1.61 to 2.10 (Méres et al., 2016). Thus, the described indicators are within the upper range of this species obtained in some European countries.

Conclusions

1. The amount of hares obtained in recent hunting seasons on an average level of about 3 individuals from 100 hectares, confirms the high population density index, which can certainly be described as the highest in Poland and one of the highest in Europe.
2. The body weight of the hares obtained, both young (4.10 kg) and adults (4.65 kg) indicates that the individual condition of the animals is high, and the values of this feature definitely outweigh those from other regions of the country, as well as in some European countries.
3. The structure of sex with a clear predominance of females and the structure of the age where young specimens dominated, indicates a high reproductive potential of the population in the research area, and thus also shows the features of the developing population. This is also confirmed by the high values of the reproduction rate - 1.63 and the reproductive success rate, which value was 2.42.
4. Analysis of the basic parameters characterizing the population of the hares in the area covered by the study indicates that despite the decline in numbers in many countries, there are areas characterized by the existence of populations with high individual quality and reproductive potential. Thus, it allows to deduce about the potential possibilities of rebuilding the number of hares.

http://www.aloki.hu ● ISSN 1589 1623 (Print) ● ISSN 1785 0037 (Online)
DOI: http://dx.doi.org/10.15666/aeer/1706_1370113711

REFERENCES

[1] Burel, F., Baudry, J. (1990): Structural dynamic of hedgerow network landscape in Brittany, France. – Landscape Ecology 4(4): 197-210.
[2] Chroust, K., Vodnansky, M., Pikula, J. (2012): Parasite load of European brown hares in Austria and Czech Republic. – Veterinarni Medicina 57(10): 551-558.
[3] Dubinský, P., Vasilková, Z., Hurníková, Z., Miterpáková, M., Slamečka, J., Jurčík, R. (2010): Parasitic infections of the European brown hare (*Lepus europaeus* Pallas, 1778) in south−western Slovakia. – Helmintologia 47(4): 219-225.
[4] Decors, A., Lesage, C., Jourdain, E., Giraud, P., Houbron, P., Vanhem, P., Madani, N. (2011): Outbreak of tularemia in brown hares (Lepus europaeus) in France, January to March 2011. – Euro Surveillance 16(28): pii: 19913.
[5] Demirbas, Y. (2015): Density of European hare and red fox in different habitats of Kirikkale Province (Central Anatolia), with a low level in hare number and an expected correlation in spring. – Acta Zoologica Bulgarica 67(4): 515-520.
[6] Dziedzic, R., Flis, M., Olszak, K., Wójcik, M., Beeger, S. (1998): Masa ciała zajęcy na Wyżynie Lubelskiej i Podlasiu. – Annales UMCS XVI (35, EE): 261-267.
[7] Dziedzic, R., Dzięciołowski, R., Bresiński, W., Wasilewski, M., Flis, M., Wójcik, M., Beeger, S., Olszak, K., Czyżowski, P., Przypaśniak, J., Wawrzyniak, P. (2000): Wpływ czynników środowiskowych na dynamikę i pozyskanie zajęcy w latach 1989−1999. – Materiały konferencji „Zwierzyna drobna jako elementy bioróżnorodności środowiska przyrodniczego", Włocławek.
[8] Dziedzic, R., Kamieniarz, R., Majer-Dziedzic, B., Wójcik, M., Beeger, S., Flis, M., Olszak, K., Żontała, M. (2002): Przyczyny spadku populacji zająca szaraka w Polsce. – Wyd. Ministerstwo Środowiska. Fundacja Ekonomistów Środowiska i Zasobów Naturalnych.
[9] Farkas, P., Kusza, S., Majzinger, I. (2016): Analysis of some population parameters of the brown hare (*Lepus europaeus* Pallas, 1758) in two hunting areas on the Hungarian great plain. – Lucrări Ştiinţifice 18(1): 71-74.
[10] Flis, M. (2009): Zmienność zagęszczeń i preferencji siedliskowych zajęcy w warunkach obwodu łowieckiego w latach 1998−2008. – Roczniki Naukowe Polskiego Towarzystwa Zootechnicznego 5(1): 139-147.
[11] Flis, M. (2013): Synanthropic predators as an environmental threat. – Annales UMSC Sectio EE XXXI: 1: 1-9.
[12] Flis, M. (2015): Zróżnicowanie wieku, płci oraz masy ciała zajęcy w warunkach niskiego zagęszczenia na Wyżynie Lubelskiej. – Sylwan 159(7): 579-585.
[13] Flis, M. (2016): Zróżnicowanie zagęszczenia oraz preferencji siedliskowych zajęcy w warunkach obwodu łowieckiego położonego na Wyżynie Lubelskiej. – Sylwan 16(10): 829-836.
[14] Flis, M., Nozdryn-Płotnicki Z, Wrona, Z., Piórkowski, J. (2016): Zapalenie ziarniniakowe układu rozrodczego u zająca szaraka (*Lepus europaeus* Pall. 1778) - opis przypadku. – Życie Weterynaryjne 91(8): 579-581.
[15] Flis, M., Grela, E. R., Gugała, D. (2017): Occurrence of rabies in Poland in 2011-2015 in relation to the free-living fox population. – Medycyna Weterynaryjna 73(1): 43-47.
[16] Flis, M., Grela, E. R., Gugała, D. (2018): Efektywność doustnej immunizacji lisów wolno żyjących w ograniczaniu wścieklizny w latach 2011-2015. – Medycyna Weterynaryjna 74(3): 203-208.
[17] Frylestam, B. (1980): Reproduction in the European hare in southern Sweden. – Ecography 3(1): 74-80.
[18] Gołdyn, B., Hromada, M., Surmacki, A., Tryjanowski, P. (2003): Habitat use and diet of the red fox *Vulpes vulpes* in an agricultural landscape in Poland. – Zeitschrift für Jagdwissenschaft 49: 191-200.

http://www.aloki.hu ● ISSN 1589 1623 (Print) ● ISSN 1785 0037 (Online)
DOI: http://dx.doi.org/10.15666/aeer/1706_1370113711

[19] Goszczyński, J., Wasilewski, M. (1992): Predation of foxes on a hare population in central Poland. – Acta Theriologica 37(4): 329-338.
[20] Hackländer, K., Zeitlhofer, C., Ceulemans, T., Suchentrunk, F. (2011): Continentality affects body condition and size but not yearly reproductive output in female European hares (*Lepus europaeus*). – Mammalians Biology - Zeitschrift für Säugetierkunde 76: 662-664.
[21] Hušek, J., Panek, M., Tryjanowski, P. (2015): Predation risk drives habitat-specific sex ratio in a monomorphic species, the brown hare (Lepus europaeus). – Ethology 121(6): 593-600.
[22] Jezierski, W. (2004): Zając - ginący gatunek. – Łowiec Polski 6: 12-15.
[23] Kamieniarz, P., Voigt, U., Panek, M., Strauss, E., Niewęgłowski, H. (2013): The effect of landscape structure on the distribution of brown hare *Lepus europaeus* in farmlands of Germany and Poland. – Acta Therriologica 58(1): 39-46.
[24] Kondracki, J. (2000): Geografia Regionalna Polski. – PWN, Warszawa.
[25] Kryński, A., Chudzińska−Popek, M., Majdecka, T. (2007): Środowisko współczesnych agrocenoz a sytuacja zająca szaraka. – Nauka łowiectwu. Cz. 2. Zającowi na ratunek. Wyd. Samorząd Województwa Mazowieckiego, Warszawa, pp. 110-113.
[26] Kornaś, S., Wierzbowska, I., Wajdzik, M., Kowal, J., Basiaga, M., Nosal, P. (2014): Endoparasites of European brown hare (*Lepus europaeus*) from Southern Poland based on necropsy. – Annals of Animal Science 14(2): 297-306.
[27] Lewandowski, K., Nowakowski, J. (1993): Spatial distribution of brown hare *Lepus europaeus* in habitats of various types of agriculture. – Acta Theriologica 38(4): 435-442.
[28] Méres, J., Ostrihoň, M., Slamečka, M., Kaštier, J. (2016): Population structure of brown hare (Lepus europaeus): a case study in selected areas of Nitra region [2013]. – Acta Facultatis Forestalis Zvolen 55(suppl. 1).
[29] Misiorowska, M., Ludwisiak, Ł., Nasiadka, P. (2014): Wybrane parametry populacyjne zająca szaraka (*Lepus europaeus* L.) w rejonach największej liczebności gatunku w Polsce. – Sylwan 158(12): 901-910.
[30] Mysłek, P., Kalasińska, E., Bartyzel, B. (2004): Size of the brown hare (*Lepus europaeus* Pallas 1778) living in Central Pomerania in Poland. – Zoologia Poloniae 49(1-4): 237-244.
[31] Nasiadka, P., Dziedzic, R. (2014): Podręcznik najlepszych praktyk ochrony kuropatwy i zająca. Dla różnorodności biologicznej. – Centrum Koordynacji Projektów Środowiskowych, Warszawa, pp. 66-118.
[32] Panek, M. (2007): Drapieżnictwo lisów na zającach. – Nauka łowiectwu. Cz. 2. Zającowi na ratunek. Wyd. Samorząd Województwa Mazowieckiego, Warszawa, pp. 96-105.
[33] Panek, M. (2018): Habitat factors associated with the decline in brown hare abundance in Poland in the beginning of the 21st century. – Ecological Indicators 85: 915-920.
[34] Panek, M., Kamieniarz, R. (1999): Relationships between density of brown hare *Lepus europaeus* and landscape structure in Poland in the years 1981−1995. – Acta Theriologica 44: 67-75.
[35] Panek, M., Kamieniarz, R., Bresiński, W. (2006): The effect of experimental removal of red foxes *Vulpes vulpes* on spring density of brown hares *Lepus europaeus* in western Poland. – Acta Theriologica 51: 187-193.
[36] Pielowski, Z. (1976): On the Present State and Perspectives of the European Hare Breeding in Poland. – In: Pucek, Z., Pielowski, Z. (eds.) Ecology and Management of European Hare Populations. PWRiL, Warszawa, pp. 25-27.
[37] Pielowski, Z. (1979): Zając. Monografia przyrodniczo−łowiecka. – PWRiL, Warszawa.
[38] Pikula, J., Beklova, M., Holesovska, Z., Treml, F. (2004): Ecology of european brown hare and distribution of natural foci of tularemia in the Czech Republik. – Acta Veterinaria Brno 73(2): 267-273.

http://www.aloki.hu ● ISSN 1589 1623 (Print) ● ISSN 1785 0037 (Online)
DOI: http://dx.doi.org/10.15666/aeer/1706_1370113711

[39] Pintur, K., Popović, N., Alegro, A., Severin, K., Slavica, A., Kolić, E. (2006): Selected indicators of brown hare (Lepus europaeus Pallas, 1778) population dynamics in northwestern Croatia. – Veterinarski Arhiv 76: 199-209.
[40] Schai-Braun, S. C., Reichlin, T. S., Ruf, T., Klansek, E., Tataruch, F., Arnold, W., Hackländer, K. (2015): The European hare (*Lepus europaeus*): A picky herbivore searching for plant parts rich in fat. – PloS One 10(7): e0134278.
[41] Schmidt, N. M., Asferg, T., Forchhammer, M. C. (2004): Long-term patterns in European brown hare population dynamics in Denmark: effects of agriculture, predation and climate. – BMC Ecology 4: 1-7.
[42] Schrödl, G. (1991): Ein Stichprobenverfahren zur Biotopcharakterisierung Niederwildgebieten. – Beitrage zur Jagd und Wildforschung XVII: 93-98.
[43] Stroh, G. (1931): Zwei sichere Altersmerkmale beim Hasen. – Berliner Tierärztl. Wschr. 47: 180-181.
[44] Wasilewski, M. (2007): Drapieżnictwo a zwierzyna drobna. – Nauka łowiectwu. Cz. 1. Kryzys zwierzyny drobnej i sposoby przeciwdziałania. Wyd. Samorząd Województwa Mazowieckiego, Warszawa, pp. 34-38.
[45] Witek, T. (1991): Warunki przyrodnicze produkcji rolnej: woj. lubelskie. – IUNiG, Puławy.

http://www.aloki.hu ● ISSN 1589 1623 (Print) ● ISSN 1785 0037 (Online)
DOI: http://dx.doi.org/10.15666/aeer/1706_1370113711

ARBUSCULAR MYCORRHIZAL SYMBIOSIS ALLEVIATES DROUGHT STRESS IMPOSED ON WHEAT PLANTS (*TRITICUM AESTIVUM* L.)

METWALLY, A.[1,2*] – AZOOZ, M.[3] – NAFADY, N.[2] – EL-ENANY, A.[2,4]

[1]*Biological Sciences Department, Faculty of Science, King Faisal University Hofuf 31982, Saudi Arabia*

[2]*Botany and Microbiology Department, Faculty of Science, Assiut University Assiut 71516, Egypt*

[3]*Botany Department, Faculty of Science, South Valley University, Qena 83523, Egypt*

[4]*Biological Sciences Department, Sajer Faculty of Science and Arts, Shaqra University, Saudi Arabia*

[*]*Corresponding author*
e-mail: ametwally@kfu.edu.sa

(Received 25th Apr 2019; accepted 15th Nov 2019)

Absract. The aim of this study was to determine the contribution of native arbuscular mycorrhizal fungi (AMF) inoculation to growth, pigmentation and grain yield of wheat plants (*Triticum aestivum* L.) grown under different levels of water deficiency [D0, 100% Field Capacity (FC); D1, 75% FC; D2, 50% FC and D3, 25% FC]. The results suggested that AMF inoculation has a beneficial effect on plant drought tolerance and effectively improved biomass and crop productivity of wheat plants grown under drought. Mycorrhizal symbiosis alleviates the inhibitory effect of drought stress via improving water status and chlorophyll biosynthesis of wheat plants. Mycorrhizal colonization increased gradually and was higher at the maturity stage under a low level of drought (D1). The mycorrhizal wheat plants had higher shoot phosphorous than non-mycorrhizal plants at all samplings regardless of levels of drought stress. In general, with all treatments, the content of photosynthetic pigment fractions was inhibited as the level of drought increased in the soil pot experiment. However, the photosynthetic pigment contents of mycorrhizal wheat plant leaves were significantly ($p<0.05$) greater than those of non-mycorrhizal ones. The study/ concluded that the native mycorrhizae alleviate the drought stress by enhancement of the process of phosphorus uptake, pigment biosynthesis and accumulation of plant metabolites and may be used as a biofertilizer.
Keywords: *arbuscular mycorrhizal, drought stress, biofertilizer, phosphorus, wheat*

Introduction

Water shortage is considered one of the most significant environmental factors that affect plant growth and limit plant development and productivity in many arid and semiarid regions of the world. Also, seasonal water deficiency sometimes occurs in non-arid regions. Drought has a sharp decline in crop productivity, although many of these crops have many improved characteristics to withstand water shortage conditions (Bohnert et al., 1995; Zhu et al., 2012). Water deficit negatively influences the growth and metabolism of many plants, the response of plants differs depending on plant genotype, developmental stage, severity and duration of the stress (El-Enany et al., 2013, 2014).

Soil microorganisms are a very important component in the plant/soil system (Abd-Alla et al., 2014a,b; Kannenberg and Phillips, 2017). Symbionts can improve plant resistant to abiotic stresses by enhancing both plant nutrition and protection against the oxidative damage produced by the water deficiency (Ruíz-Lozano, 2003) and heavy metals (Rivera-

http://www.aloki.hu ● ISSN 1589 1623 (Print) ●ISSN1785 0037 (Online)
DOI: http://dx.doi.org/10.15666/aeer/1706_1371313727

Becerril et al., 2005). The symbiotic relation between arbuscular mycorrhizal fungi (AMF) and most plants provides nutrients, stimulates plant growth and increases the tolerance of plants against the stress (Barea et al., 2005; Abdel Latif and Chaoxing, 2014; Kyriazopouls et al., 2014; Shinde and Thakur, 2015). Arbuscular mycorrhizal fungi (AMF) can form mutualistic symbiotic associations with the roots of 80% of all terrestrial plant species (Smith and Read, 2008; Patale and Shinde, 2014). The AM symbiosis induced a higher improvement of physiological parameters in drought-sensitive plants than in drought-tolerant plants and drought-sensitive plants obtained higher physiological benefit from the AM symbiosis (Quiroga et al., 2017). Plants grown under water deficiency have a lower stomatal conductance in order to conserve water. Previous studies have indicated that drought stress severely affects plant growth through various mechanisms, such as reduced leaf water potential, reduced rate of cell division, and altered plant water and nutrient relationships. Consequently, CO_2 fixation is inhibited and photosynthetic rate reduced, resulting in less assimilate production for growth and yield of plants (Celebi et al., 2010; Farooq et al., 2012; Shinde and Singh, 2017).

There is considerable evidence suggesting that AMF has the potential to increase the tolerance of their host plants to water deficit stress (Asrar et al., 2012; Lazcano et al., 2014; Xiao-Qing et al., 2017). Studies have shown that the extraradical mycelia of AM fungi transfer water to their host plants under low soil moisture conditions and the AM fungi improve plant growth, development and yield (Augé et al., 2007), enhanced nutrient uptake (Michalis et al., 2013), an increase in the root hydraulic conductance (Bárzana et al., 2012), alterations in the soil's water retention properties (Augé, 2001), or improved osmotic adjustment (Aroca et al., 2007) and antioxidant activity (Bompadre et al., 2014). The beneficial functions of AMF may be of great importance to climate change, particularly with respect to water shortage and to the revegetation of degraded ecosystems; including coal mine spoil banks (Khalvati et al., 2010).

Wheat (*Triticum aestivum* L.) is the major food crop plants, are known to be commonly associated with AM fungi, which inhabit in agricultural soils contributing physiologically and ecologically to the health of both plants and soils (Li et al., 2012). Colonization of roots by AM fungi has been shown to increase the drought resistance of wheat (Al-Karaki and Clark, 1998). Therefore, our aim in the present study was to evaluate the potential of native species of AMF to mitigate the adverse effects of drought stress on wheat growth and for improved grain yield.

Material and Methods

Production of mycorrhizal inoculum

Native adapted AM fungi were isolated from the arid environment [Al-Uqair coast, Al-Ahsa, Saudi Arabia, (25°39'35.8"N 50°11'25.6"E)] and propagated for inoculums production. The most abundant mycorrhizal species selected and morphologically identified according to Schüessler and Walker (2010). Native AM fungi were propagated on maize (*Zea mays.* L) as host plant on the sterilized clay-sand mixture (50% soil and 50% sand). Plants were cultured in the greenhouse for 3 months. The roots colonized by AM fungi were checked during the culture, and the presence of spores was confirmed by sieving. One hundred grams of soil containing a mixture of mycorrhizal spores, extra-radical hyphae, and roots fragments applied as mixture culture inoculum. Non-mycorrhizal maize roots and sterilized soil used for the control treatment.

http://www.aloki.hu ● ISSN 1589 1623 (Print) ●ISSN1785 0037 (Online)
DOI: http://dx.doi.org/10.15666/aeer/1706_1371313727

Experimental design and growth conditions

Wheat grains (*Triticum aestivum* L.) were surface sterilized and grown in plastic pots filled with 4 kg sterilized soil at different levels of drought (D0, 100% FC-D1, 75% FC-D2, 50% FC and D3, 25% FC). The seedlings were thinned to 10 plants one week after germination. All pots were fertilized with 50 mg N-KNO_3 g^{-1} soil. Solutions of K_2HPO_4 were prepared and P was added at 30 or 60 mg^{-1} g soil. A control treatment was also included. The experiment in a completely randomized design was performed by fifty- gram inoculum of AMF mixture and placed in pots below the grain of the tested plant (approximately contain 90–100 spores/10 g soil). Pots of the control treatments received the same volume of autoclaved inoculums. All pots contain 10 seedlings were kept in the greenhouse with day and night temperatures of 27 and 15˚C, respectively, day and night relative humidity of 70 and 80%, respectively, and a photoperiod of 14 h. Each treatment was replicated three times.

Growth parameters and grain yield

After 42 days of planting, some wheat plants were removed gently from the pots, washed with water. Then, plants were separated into shoots and roots and part of fresh roots and shoots were immediately frozen for analysis. The dry weights of the plants were recorded by placed the samples in an oven at 80°C until the dry weight was constant. At maturity, yield components [spike length, the number of grains per spike, grain yield per plant and 100- grain weight (seed index)] were determined on 3 plants for each treatment. Also, days to flowering and days to maturity were recorded for all treatments.

Estimation of mycorrhizal colonization

Root segments were separated from the plant, washed and then cut into one centimeter long pieces. The segments were cleared with 10% (w/v) KOH at 70^{o}C for 20 min and stained with 0.5% (w/v) Trypan blue. The stain was prepared by mixing water, glycerin and lactic acid in proportions 1:1:1 (v/v/v). Mycorrhizal colonization was assessed by the method of Brundrett et al. (1984). Frequency of mycorrhizas (F%), the intensity of mycorrhizal colonization in the root (M%), and arbuscule frequency in roots (A%) was calculated according to Trouvelot et al. (1986) using the MYCOCALC (http://www.dijon. inra.fr/mychintec/Mycocalc-prg/download.html) program.

Quantification of phosphoros mycorrhizal dependency

According to Plenchette et al. (1983), the dependency of mycorrhizal plants growth and Phosphorous (P) uptake were calculated as:

$$\frac{[\text{P content (M)} - \text{P content (NM)}]}{\text{P content (M)}} \times 100 \qquad \text{(Eq.1)}$$

where M, mycorrhizal plants and NM, non-mycorrhizal plants.

The concentration of P in the shoot was determined after digestion in a mixture of concentrated nitric and perchloric acids (4:1). Each sample was placed in 50 mL measuring flasks and 10 mL of the acid mixture was added. The mixture was first heated on fry pans to 90°C for 30 min, and then temperature increased to 140°C to remove excess nitric acid. De-ionized water was added to make up to definite volume of

http://www.aloki.hu ● ISSN 1589 1623 (Print) ●ISSN1785 0037 (Online)
DOI: http://dx.doi.org/10.15666/aeer/1706_1371313727

the primary extract. An aliquot of this primary extract was diluted for determining phosphorus shoot concentration spectrophotometrically (Olsen and Sommers, 1982).

Determination of photosynthetic pigments

The fractions of pigments (chlorophyll a, chlorophyll b and carotenoids) were estimated using the spectrophotometric method recommended by Lichtenthaler (1987). The photosynthetic pigments were extracted from a definite weight of fresh leaf samples in 5 ml of 95% ethyl alcohol at 60˚C, until colorless. Then the total volume was completed to 10 ml with 95% ethyl alcohol and absorbance readings were followed with a spectrophotometer (Unico UV-2100 spectrophotometer. The extinction was measured against a blank of pure 95% ethyl alcohol at three wavelengths of 452, 644 and 663 nm. The concentration of chlorophylls and carotenoids were calculated as mg/g FW using the following equations:

$$\text{Chlorophyll a} = (13.36 \times A_{663}) - (0.918 \times A_{644}) \quad \text{(Eq.2)}$$

$$\text{Chlorophyll b} = (27.49 \times A_{664}) - (3.87 \times A_{663}) \quad \text{(Eq.3)}$$

$$\text{Carotenoids} = (4.2 \times A_{452}) - [(0.0264 \times \text{Chl.a}) + (0.46 \times \text{Chl.b})] \quad \text{(Eq.4)}$$

Statistical analysis

The data were subjected to one-way ANOVA using the SPSS 10.0 software program. Means and standard errors were calculated for 3 replicate values. Means were compared by Duncan's multiple range test and statistical significance was determined at a 5% level.

Results

A total number of 7 morphotypes of native species of AMF were recovered from rhizosphere plants grown in a harsh environment. Based on the number of spores the seven species in stressed soils were *Acaulospora* sp., *A. bireticulata* (Rothwell & Trappe), *A. capsicula* Blaszk., *Glomusaggregatum* Schenck and Smith, *G. clarum* Nicolson & Schenck, *G. geosporum* (Nicol. & Gerd.) Walkerand *G. mosseae* (Nicol. & Gerd.) Gerd. & Trappe. The most common native species (*Acaulospora capsicula*,*Glomus aggregatum* ,and *Glomus geosporum*) were propagated and used as mixture inoculum for further experiments.

The experiment was conducted on *Triticum aesativum* L. under different levels of drought (D0, D1, D2, and D3) and inoculated with or without a mixture of native AM fungi to grow for 3 months. Under well-watered conditions, mycorrhizal inoculation significantly increased all the growth parameters. The fresh and dry weights of mycorrhizal plants increased significantly than non-mycorrhizal plants. The drought treatments significantly reduced the growth criteria of both the mycorrhizal and nonmycorrhizal plants (*Table 1*). The data indicated that drought treatments were significantly ($p > 0.05$) reduced fresh or dry weights of wheat plant roots especially at the highest levels of drought (D2 and D3) as compared by reference control (D0). Inoculation of wheat plants with AM fungi stimulated the growth, especially the plants under drought. The data presented in *Table 1* shows that all water deficit levels exerted an inhibitory effect on the root and shoot dry yield of non-mycorrhizal wheat plants. On

http://www.aloki.hu ● ISSN 1589 1623 (Print) ●ISSN1785 0037 (Online)
DOI: http://dx.doi.org/10.15666/aeer/1706_1371313727

the other side, the fresh and dry shoot weights of mycorrhizal plants showed an increase at all drought levels as compared with control plants.

Analysis of the data revealed that drought significantly affected days to flowering of wheat plants of which delayed as compared with control. Days to the flowering of mycorrhizal wheat plants grown under drought stress were significantly early flowering than those of their respective non-mycorrhizal counterparts. The period of maturity of wheat spike plants showed the effectiveness of mycorrhizal inoculation as shown in *Table 2*.

Table 1. *Growth parameters of wheat plants in response to mycorrhizal inoculation grown under different levels (D0, D1, D2, and D3) of drought stress*

Parameters		Treatments							
		D0		D1		D2		D3	
		NM	M	NM	M	NM	M	NM	M
Shoot	Fresh Weight (g)	7.08 ± 0.27 **e**	8.38 ± 0.39 **f**	6.28 ± 0.34 **d**	7.12 ± 0.44 **e**	5.12 ± 0.31 **ab**	5.95 ± 0.52 **cd**	4.59 ± 0.28 **a**	5.54 ± 0.24 **bc**
	Dry Weight (g)	1.87 ± 0.18 **cd**	2.24 ± 0.14 **e**	1.58 ± 0.15 **bc**	1.90 ± 0.13 **d**	1.43 ± 0.11 **ab**	1.72 ± 0.16 **cd**	1.23 ± 0.08 **a**	1.69 ± 0.14 **cd**
	Length (cm)	81.67 ± 3.51 **cd**	89.33 ± 6.03 **d**	76.67 ± 6.03 **bc**	81.33 ± 3.05 **cd**	64.33 ± 3.50 **b**	72.67 ± 4.50 **bc**	56.33 ± 4.10 **a**	75.33 ± 6.02 **bc**
Root	Fresh Weight (g)	0.70 ± 0.07 **cd**	0.90 ± 0.13 **e**	0.64 ± 0.11 **bc**	0.79 ± 0.06 **de**	0.51 ± 0.04 **ab**	0.63 ± 0.03 **bc**	0.45 ± 0.04 **a**	0.59 ± 0.05 **bc**
	Dry Weight (g)	0.17 ± 0.03 **bcd**	0.20 ± 0.02 **d**	0.16 ± 0.01 **abc**	0.18 ± 0.01 **cd**	0.14 ± 0.01 **ab**	0.17 ± 0.01 **bc**	0.13 ± 0.02 **a**	0.16 ± 0.01 **abc**
	Length (cm)	51.33 ± 5.51 **bcd**	56.33 ± 7.37 **d**	44.00 ± 6.56 **abc**	63.00 ± 4.58 **d**	42.00 ± 7.93 **ab**	54.67 ± 7.76 **cd**	34.67 ± 4.50 **a**	52.67 ± 4.50 **bcd**

*NM nonmycorrhizal wheat plants; M, mycorrhizal wheat plants. Means in each column followed by the same letter are not significantly different ($P < 0.05$) as determined by Duncan's test. Values are the means of three replications

Table 2. *Yield components of wheat plants in response to mycorrhizal inoculation grown under different levels (D0, D1, D2, and D3) of drought stress*

Parameters	Treatments							
	D0		D1		D2		D3	
	NM	M	NM	M	NM	M	NM	M
Days to Flowering	96.67 ± 1.52 **b**	86.33 ± 3.06 **a**	95.67 ± 3.06 **b**	88.00 ± 2.00 **a**	101.67 ± 1.53 **ab**	89.00 ± 2.65 **a**	104.33 ± 1.15 **c**	94.33 ± 3.15 **b**
Days to Maturity	130.33 ± 2.52 **c**	121.67 ± 1.53 **a**	131.00 ± 3.61 **c**	124.67 ± 1.53 **ab**	135.67 ± 1.32 **d**	127.33 ± 2.08 **bc**	138.00 ± 2.65 **da**	128.33 ± 1.45 **bc**
Spike Length (cm)	8.67 ± 0.32 **cd**	9.70 ± 0.56 **e**	7.93 ± 0.51 **bc**	9.37 ± 0.15 **de**	7.43 ± 0.71 **ab**	8.93 ± 0.25 **de**	6.77 ± 0.40 **a**	8.10 ± 0.20 **bc**
Number of Grains/Spike	42.67 ± 4.51 **de**	48.6 ± 4.21 **e**	35.00 ± 3.71 **bc**	38.00 ± 3.78 **cd**	29.00 ± 2.52 **ab**	36.00 ± 4.04 **cd**	24.67 ± 2.00 **a**	33.33 ± 1.53 **bc**
Grain Yield /Plant (g)	14.27 ± 2.25 **e**	16.99 ± 0.29 **f**	13.88 ± 0.30 **de**	14.47 ± 0.49 **e**	12.12 ± 0.47 **b**	13.19 ± 0.69 **cd**	11.12 ± 0.33 **a**	12.38 ± 0.24 **bc**
Seed Index (100 grain weight in g)	31.75 ± 0.27 **cd**	37.18 ± 1.15 **bc**	30.15 ± 1.22 **d**	32.02 ± 2.13 **cd**	26.87 ± 2.90 **b**	30.42 ± 1.37 **bcd**	21.72 ± 1.82 **a**	27.31 ± 2.01 **b**

*NM nonmycorrhizal wheat plants; M, mycorrhizal wheat plants. Means in each column followed by the same letter are not significantly different ($P < 0.05$) as determined by Duncan's test. Values are the means of three replications

http://www.aloki.hu ● ISSN 1589 1623 (Print) ●ISSN1785 0037 (Online)
DOI: http://dx.doi.org/10.15666/aeer/1706_1371313727

The data showed that amongst all the treatments, days to maturity significantly ($P<0.05$) delayed under drought stress. Yield and its component consider the main target for the activity of plants. So the data recorded in *Table 2* show that wheat plants inoculated with AMF caused a marked effect on the seed yield per plant and its components (spike length, grains of a spike, grains per plants and grains index, the weight of 100 seeds) in comparison to the treated plants. The data in *Table 2* demonstrated that/ spike length of water deficit at all levels was significantly decreased with increased water deficit level in soil, especially at high water stress levels. The highest values of spike length obtained from wheat plants inoculated with AMF, while the minimum spike length recorded from non-mycorrhizal plants grown at high water deficit treatment soil. These results showed a general trend of an increase in grain per spike with inoculation of treated plants (*Table 2*). Seed index weight of 100 grains (g) was recorded and the data revealed that grain index was significantly increased in mycorrhizal wheat inoculated plant than those uninoculated wheat plants. The root colonization rate was affected by substrate, inoculation, and the interaction of the substrate with drought stress or inoculation. In general, different levels of drought stimulated development the frequencies of root colonization (F%), the intensity of root cortex colonization (M%), and arbuscular development (A%) by *Acaulospora capsicula*, *Glomus aggregatum*, and *Glomus geosporum* at different growth stages in wheat plants as shown in *Table 3*.

Table 3. *Mycorrhizal colonization of wheat plants under different levels (D0, D1, D2, and D3) of drought stress*

Growth stages	Mycorrhizal colonization (%)	Drought levels			
		D0	D1	D2	D3
Vegetative	F %	48.0	52.0	43.0	36.0
	M %	21.3	20.0	17.0	15.3
	A %	16.7	13.0	8.0	5.3
Flowering	F %	63.0	69.0	60.0	49.0
	M %	54.0	58.0	49.0	43.3
	A %	36.3	42.3	35.6	29.0
Maturity	F %	83.3	85.0	75.0	62.0
	M %	57.2	62.0	53.0	55.0
	A %	53.3	58.0	44.3	48.0

*F%: Frequency of mycorrhizal root segments, M%: the intensity of mycorrhizal colonization in the root, A%: Arbuscule frequency in roots

The microscopic assessment confirmed that plants of non-inoculation treatment were not colonized by AMF. As is evident from *Table 3*, at the vegetative stage, the highest value of frequency of mycorrhizal root segments recorded under a low level of drought. At the flowering stage, mycorrhizal colonization increased as compared with those of vegetative stage, and F%, M %, and A% recorded a maximum value under a low level of drought.

It was observed that the highest mycorrhizal colonization was recorded at the maturity stage (as compared with those of vegetative and flowering stage). Frequency percentage of mycorrhizae in roots reduced at the vegetative stage by about 4%, whereas increased by about 8% and 5% in flowering stage and maturity, respectively at low drought level (D1). The moderate (D2) and high (D3) drought levels obviously reduced the percentage of arbuscular mycorrhizae frequency in roots at the different

http://www.aloki.hu ● ISSN 1589 1623 (Print) ●ISSN1785 0037 (Online)
DOI: http://dx.doi.org/10.15666/aeer/1706_1371313727

stages of plant growth. The mycorrhizae in roots of wheat plants consisted of arbuscules, vesicles, as well as intra-and extraradical hyphae. The arbuscules and vesicles were patchily distributed along the roots examined. The intraradical hyphae were evenly distributed and frequently formed coils.

The phosphorus content of wheat plant shoots inoculated with AMF grown at different levels of the drought was represented in *Fig. 1A*. The data revealed that P uptake was significantly reduced by drought treatments. The P contents of wheat shoots were used as indicators of mycorrhizal activity in the soil. Mycorrhizal inoculation of the wheat plant significantly raised the P uptake especially at low drought level (D1) and shoots of mycorrhizal wheat plants had significantly higher concentrations of P than those of nonmycorrhizal wheat plants.

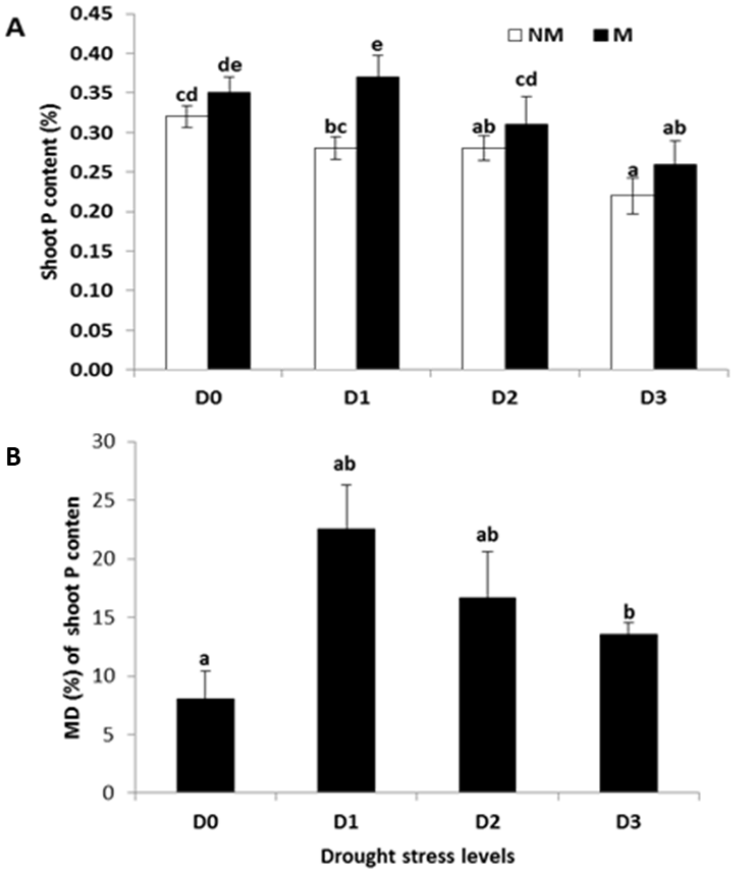

Figure 1. *Effect of different levels (D0, D1, D2, and D3) of drought on/ (A) wheat shoot phosphorus content (%); (B) Mycorrhizal dependency of P wheat shoot content (%). Means in each column followed by the same letter are not significantly different (P < 0.05) as determined by Duncan's test. Values are the means of three replications*

Photosynthetic pigments

The content of the photosynthetic pigments (chlorophyll a, chlorophyll b and carotenoids) of mycorrhizal and non-mycorrhizal in wheat plant leaves are presented as mg g^{-1} leaf fresh weight in *Figure 2*. The current study shows that photosynthetic pigment fractions are significantly affected water deficit and mycorrhizal inoculation as indicated by significant two-way interaction based on ANOVA. In general, with all

http://www.aloki.hu ● ISSN 1589 1623 (Print) ●ISSN1785 0037 (Online)
DOI: http://dx.doi.org/10.15666/aeer/1706_1371313727

treatments, the content of photosynthetic pigment fractions was decreased as the level of drought increased in the soil pot experiment.

However, the contents of photosynthetic pigments of mycorrhizal wheat plant leaves were significantly ($p<0.05$) greater than those of non-mycorrhizal ones. In non-mycorrhizal plants a significant reduction in total pigments was recorded at high water deficit (D3).

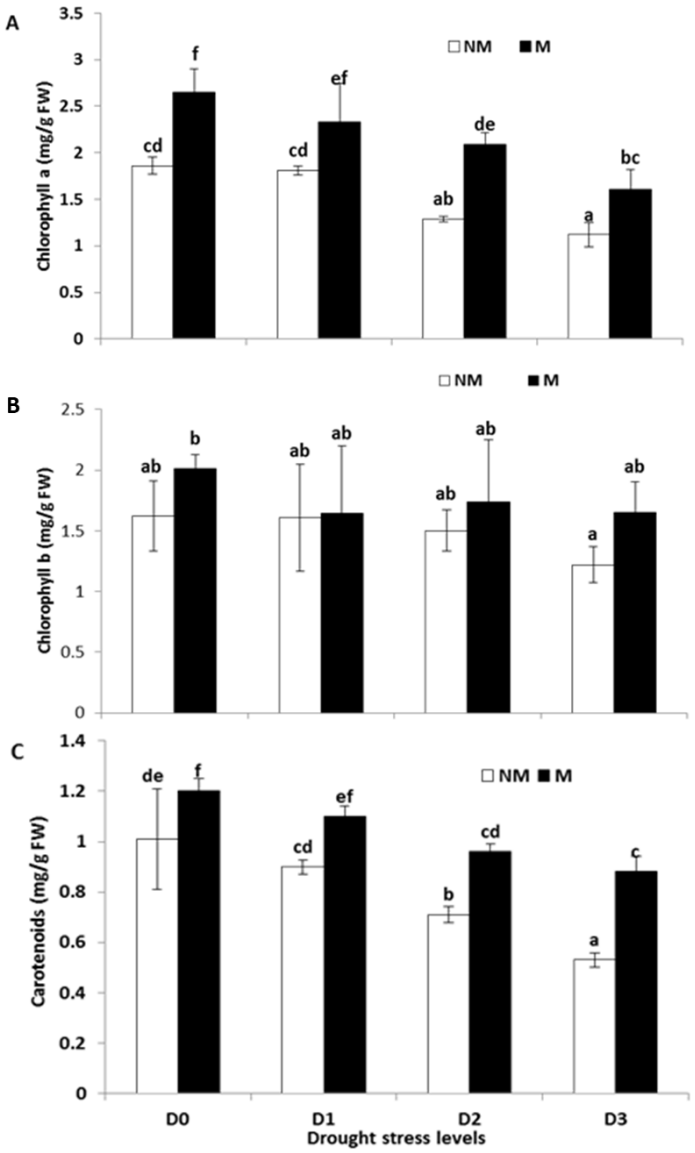

Figure 2. *Chlorophyll a (A); chlorophyll b (B); and carotenoids (C) contents in leaves of wheat plants inoculated with mycorrhizal fungi grown under different levels (D0, D1, D2 ,and D3) of drought stress. Means in each column followed by the same letter are not significantly different ($P < 0.05$) as determined by Duncan's test. Values are the means of three replications*

Analysis of variance of chlorophyll contents showed that mycorrhizal colonization significantly improved chlorophyll concentrations. Also, the interaction of drought and mycorrhizal inoculation exhibited a stimulatory effect on the different types of photosynthetic pigments (*Fig. 2*).

http://www.aloki.hu ● ISSN 1589 1623 (Print) ●ISSN1785 0037 (Online)
DOI: http://dx.doi.org/10.15666/aeer/1706_1371313727

Discussion

In the present study, drought decreased the fresh and dry weights of wheat plants which are recorded by many studies (Auge, 2001; Celebi et al., 2010; Kyriazopouls et al., 2014). Previous reports have indicated that drought stress severely affects plant growth through various mechanisms, such as reduced leaf water potential, reduced rate of cell division, and altered plant water and nutrient relationships (Boomsma and Vyn, 2008; Kilic and Yagbasanlar, 2010; Farooq et al., 2012). The positive effect of AMF on wheat growth under different levels of drought suggested that the application of AMF technology may be a sustainable method for improving plant performance under the adverse conditions (Kyriazopouls et al., 2014; Malik et al., 2017). AM symbiosis drives an increase in the leaf area and coarse root mass and improves the plant-soil water relationship under drought stress, which can affect various physiological processes. The improvement of biomass in mycorrhizal plants may also be due to the enhanced water uptake (Subramanian et al., 2006; Habibzadeh et al., 2013). Our results in *Table 2* are in accordance with the current tendency for reduced use of agrochemicals, research is currently aimed at crop yield improvement and at yield sustainability; thus, microbial-based approaches have been proposed to improve crop yield (Covacevich et al., 2007). In this respect, numerous researchers have reported improvement in biomass production and grain yield in the grain of cereals after inoculation with AMF (Tarafdar and Marschner, 1994). The fungal filaments outside the root system can spread and explore soil areas not reachable by plant roots. One centimeter of colonized roots might produce 50 to 150 cm of extraradical hyphae (Harley, 1989). Through this mechanism, AMF associations may improve crop yield by increasing the capacity of plants to obtain nutrients that are relatively immobile in the soil such as phosphorus (P).

Our results in accordance with most studies which indicated that drought stress decreased the colonization rates (Kohler et al., 2009; El-Mesbahi et al., 2012) and may be due to the adaptation of AMF isolates to different substrates and different behaviors of plants under drought stress (Gholamhoseini et al., 2013). The decrease of root colonization by drought stress is due to reducing spore germination and plant photosynthetic capacity (Wu et al., 2013; Xiao-Qing et al., 2017). Michalis et al. (2013) concluded that soil moisture can have various effects on AMF spore germination and thus root colonization. Moreover, drought modifies various features of the root system which, in turn, may influence the degree of colonization and the frequency of different AM fungal structures (Fusconi and Berta, 2012). Some results opposite to our studies and showed that mycorrhizal colonization increased with increasing intensity of drought stress (Zhao et al., 2015). They concluded that under drought stress, watering caused lighter compaction, better pore structure and soil aeration, which benefits the development of mycorrhizae.

Drought stress may reduce nutrient mineralization by lowering nutrient availability (Heidari and Karami, 2014). Mycorrhizal symbiosis may improve plant nutrition, which is generally regarded as an important drought tolerance mechanism (Smith and Read, 2008; Li et al., 2012). Hijikata et al. (2010) noticed that the activity of high-affinity P transporters on the plasma membrane of extraradical hyphae is most likely directly involved in enhanced drought tolerance in plants. In the present study, the P contents in mycorrhizal plants were consistently higher than those in non-mycorrhizal plants, regardless of the intensity of drought stress. The increase in P concentrations of mycorrhizal plants may provide more RNA to meet the protein synthesis needs, resulting in a higher plant growth rate (Matzek and Vitousek, 2009). Under drought conditions, the RNA-directed synthesis of some protein or enzymes may be of physiological importance in helping the plants withstand drought stress (Fan and Liu, 2011).

http://www.aloki.hu ● ISSN 1589 1623 (Print) ●ISSN1785 0037 (Online)
DOI: http://dx.doi.org/10.15666/aeer/1706_1371313727

The results obtained showed that wheat plants under drought stress were strongly mycorrhizal dependent (*Fig. 1B*). The lowest mycorrhizal dependency recorded at the control drought level. SchiiBler et al. (2001) stated that arbuscular mycorrhiza is formed in about 80% of land plants with soil fungi belonging to *Glomeromycota*. Arbuscular mycorrhizal plants can take up more soil nutrients especially phosphate (P), micronutrients such as copper and zinc, than non-mycorrhizal plants (Smith and Read, 1997). They concluded that the growth of a host plant can be improved by mycorrhizal colonization provided that soil available P is a limiting factor for plant growth. The degree of growth improvement is affected by factors such as host plant species, fungal species, and soil conditions.

Analysis of variance of chlorophyll contents (*Fig. 2*) revealed that mycorrhizal colonization significantly improved chlorophyll concentrations and the interaction of drought and mycorrhizal inoculation exhibited a stimulatory effect on the different types of photosynthetic pigments. Chlorophyll status is a key index for evaluating plant photosynthetic efficiency and environmental stress. Augé (2001), Gemma et al. (1997) and Azooz and Youssef (2010) are in agreement with the results of other proved the differences of chlorophyll *a*, chlorophyll *b* and chlorophyll *a* + *b* concentrations were significant between AM and non-AM maize plants under drought stress conditions (Zafari et al., 2017). They suggest that drought stress interferes less with chlorophyll synthesis and/or more with chlorophyll breakdown (Evelin et al., 2009) or protects pigments against (Kyriazopouls et al., 2014) oxidative damage generated by drought (Shinde and Thakur, 2015). Drought stress caused a great decline in the chlorophyll *a*, chlorophyll *b* and the total chlorophylls content in many plant varieties investigated by some authors in non-mycorrhizal than mycorrhizal in plants (Ommen et al., 1999; Manivannan et al., 2007; Evelin et al., 2009). Also, unchanged chlorophyll level during drought stress has been reported in other species, depending on the duration and severity of drought (Kpyoarissis et al., 1995). The decrease in chlorophyll under drought stress may result in chloroplast damage caused by active oxygen species (Herbinger et al., 2002). Consequently, the rate of photosynthesis decreased (Kawamitsu et al., 2000) due to lower stomatal conductance in order to conserve water and the resistance of the stomata to CO_2 entry probably is the main factor limiting photosynthesis under drought, resulting in less assimilate production for growth and yield of plants.

Conclusion

The mycorrhizal root colonization rate was significantly affected by drought stress levels or the stages of plant growth of wheat plants. Also, it can be concluded that the AMF enhances the absorption of phosphorus and other nutritional elements and then improves the nutritional status of wheat plants during drought stress which resulted in an increase in chlorophyll contents than control plants. In spite of better performance of inoculation with mycorrhizae, there are still certain aspects that need critical consideration. One important aspect is the evaluation of this approach under natural field conditions. Most of the previous studies were conducted under controlled conditions, and the response of these organisms observed under such conditions may vary significantly in view of the variable ecology of these microorganisms in the natural environment. Additionally, the researches also have to face other harsh conditions like the toxicity of heavy metals and pathogen attacks. Therefore, the role of these microorganisms for providing relief from other stresses.

http://www.aloki.hu ● ISSN 1589 1623 (Print) ●ISSN1785 0037 (Online)
DOI: http://dx.doi.org/10.15666/aeer/1706_1371313727

Acknowledgment. The authors extend their gratitude to the Deanship of Scientific Research (DSR), King Faisal University, Saudi Arabia, for providing a fund of the current work (DSR, project No. 150161).

REFERENCES

[1] Abd-Alla, M. H., El-Enany, A. E., Bagy, M. K., Bashandy, S. R. (2014a): Alleviating the inhibitory effect of salinity stress on nod gene expression in *Rhizobium tibeticum* - fenugreek (*Trigonella foenum graecum*) symbiosis by isoflavonoids treatment. – Journal of Plant Interaction 9: 275-284.

[2] Abd-Alla, M. H., El-Enany, A. E., Nafady, N. A., Khalaf, D. M., Morsy, F. M. (2014b): Synergistic interaction of *Rhizobium leguminosarum* bv. *viciae* and arbuscular mycorrhizal fungi as a plant growth-promoting biofertilizers for faba bean (*Vicia faba* L.) in alkaline soil. – Microbiological Research 169: 49-58.

[3] Abdel Latef, A. A. H., Chaoxing, H. (2014): Does Inoculation with Glomus mosseae Improve Salt Tolerance in Pepper Plants? – Journal of Plant Growth Regulation 33: 644-653.

[4] Al-Karaki, G. N., Clark, R. B. (1998): Growth, mineral acquisition, and water use by mycorrhizal wheat grown under water stress. – Journal of Plant Nutrition 21: 263-276.

[5] Aroca, R., Porcel, R., Ruiz-Lozano, J. M. (2007): How does arbuscular mycorrhizal symbiosis regulate root hydraulic properties and plasma membrane aquaporins in *Phaseolus vulgaris* under drought, cold and salinity stresses? – New Phytologist 173: 808-816.

[6] Asrar, A. A., Abdel-Fattah, G. M., Elhindi, K. M. (2012): Improving growth, flower yield, and water relations of snapdragon (*Antirhinum majus* L.) plants grown under well-watered and water stress conditions using arbuscular mycorrhizal fungi. – Photosynthetica 50: 305-316.

[7] Augé, R. M. (2001): Water relations, drought ,and vesicular-arbuscular mycorrhizal symbiosis. – Mycorrhiza 11: 3-42.

[8] Augé, R. M., Toler, H. D., Moore, J. L., Cho, K., Saxton, A. M. (2007): Comparing contributions of soil versus root colonization to variations in stomatal behavior and soil drying in mycorrhizal *Sorghum bicolor* and Cucurbita. – Journal of Plant Physiology 164: 1289-1299.

[9] Azooz, M. M., Youssef, M. M. (2010): Evaluation of heat shock and salicylic acid treatments as inducers of drought stress tolerance in hassawi wheat. – American Journal of Plant Physiology 5: 56-70.

[10] Barea, J. M., Werner, D., Azcón-Guilar, C., Azcón, R. (2005): Interactions of arbuscular mycorrhiza and nitrogen-fixing symbiosis in sustainable agriculture. – In: Werner, D., Newton, W. E. (eds.) Nitrogen Fixation in Agriculture, Forestry, Ecology, and the Environment. Springer Netherlands pp: 199-222.

[11] Bárzana, G., Aroca, R., Paz, J. A., Chaumont, F., Martinez-Ballest, M. C., Carvajal, M. I. (2012): Arbuscular mycorhhizal symbiosis increases relative apoplastic water flow in roots of the host plant under both well-watered and drought stress conditions. – Annals of Botany 109: 1009-1017.

[12] Bohnert, H. J., Nelson, D. E., Jensen, R. G. (1995): Adaptations to environmental stresses. – The Plant Cell 7: 1099-1111.

[13] Bompadre, M. J., Silvani, V. A., Bidondo, L. F., Ríos de Molina, M. D. C., Roxana, P. C., Pardo, A., Galicia, M. G. (2014): Arbuscular mycorrhizal fungi alleviate oxidative stress in pomegranate plants growing under different irrigation conditions. – Botany 92: 187-193.

[14] Boomsma, C. R., Vyn, T. J. (2008): Maize drought tolerance: potential improvements through arbuscular mycorrhizal symbiosis? – Field Crops Research 108: 14-31.

http://www.aloki.hu ● ISSN 1589 1623 (Print) ●ISSN1785 0037 (Online)
DOI: http://dx.doi.org/10.15666/aeer/1706_1371313727

[15] Brundrett, M. C., Piche, Y., Peterson, R. L. (1984): A new method for observing the morphology of vesicular-arbuscular mycorrhizae. – Canadian Journal of Botany 62: 2128-2134.
[16] Celebi, S. Z., Demir, S., Celebi, R., Durak, E. D., Yilmaz, I. H. (2010): The effect of arbuscular mycorrhizal fungi (AMF) applications on the silage maize (*Zea mays* L.) yield in different irrigation regimes. – European Journal of Soil Biology 46: 302-305.
[17] Covacevich, F., Echeverria, H. E., Aguirrezabal, L. (2007): Soil available phosphorus status determines indigenous mycorrhizal colonization into a field and glasshouse-grown spring wheat in Argentina. – Applied Soil Ecology 35: 1-9.
[18] El-Enany, A. E., Al-Anazi, A. D., Nahla, D., Al-Taisan, W. A. (2013): Role of antioxidant enzymes in amelioration of water deficit and waterlogging stresses on *Vigna Sinensis* plants. – Journal of Biology and Earth Sciences 1: 144-153.
[19] El-Enany, A. E., Morsy, F., Nahla, D. (2014): Impact of water stress on growth criteria and alcohol dehydrogenase activity of three legume plants. – Minia Science Bulletin 25: 29-51.
[20] El-Mesbahi, M. N., Azcón, R., Ruiz-Lozano, J. M., Aroca, R. (2012): Plant potassium content modifies the effects of arbuscular mycorrhizal symbiosis on root hydraulic properties in maize plants. – Mycorrhiza 22: 555-564.
[21] Evelin, H., Kapoor, R., Giri, B. (2009): Arbuscular mycorrhizal fungi in alleviation of salt stress: a review. – Annals of Botany 104: 1263-1280.
[22] Fan, Q. J., Liu, J. H. (2011): Colonization with arbuscular mycorrhizal fungus affects growth: drought tolerance and expression of stress-responsive genes in *Poncirus trifoliate*. – Acta Physiologae Plantarum 33: 1533-1542.
[23] Farooq, M., Hussain, M., Wahid, A., Siddique, K. H. M. (2012): Drought stress in plants - an overview. – In: Aroca, R. (ed.) Plant Responses to drought Stress: from morphological to molecular features. Springer, Berlin Heidelberg, pp. 1-33.
[24] Fusconi, A., Berta, G. (2012): Environmental stress and role of arbuscular mycorrhizal symbiosis. – In: Ahmad, P., Prasad, M. N. V. (eds.) Abiotic Stress Responses in Plants: Metabolism, Productivity and Sustainability. Springer, New York, pp. 197-214.
[25] Gemma, J. N., Koske, R. E., Roberts, E. M., Jackson, N., De Antonis, K. (1997): Mycorrhizal fungi improve drought resistance in creeping bentgrass. – Journal of Turfgrass Science 73: 15-29.
[26] Gholamhoseini, M., Ghalavand, A., Dolatabadian, A., Jamshidi, E., Khodaei-Joghan, A. (2013): Effects of arbuscular mycorrhizal inoculation on growth yield, nutrient uptake and irrigation water productivity of sunflowers grown under drought stress. – Agricultural Water Management 117: 106-114.
[27] Habibzadeh, Y., Pirzad, A., Zardashti, M. R., Jalilian, J., Eini, O. (2013): Effects of Arbuscular Mycorrhizal Fungi on Seed and Protein Yield under Water-Deficit Stress in Mung Bean. – Agronomy Journal 105: 79-84.
[28] Harley, J. L. (1989): The significance of mycorrhizal. – Mycological Research 92: 129-139.
[29] Heidari, M., Karami, V. (2014): Effects of different mycorrhiza species on grain yield, nutrient uptake and oil content of sunflower under water stress. – Journal of the Saudi society of agricultural sciences 13: 9-13.
[30] Herbinger, K., Tausz, M., Wonisch, A., Soja, G., Sorger, A., Grill, D. (2002): Complex interactive effects of drought and ozone stress on the antioxidant defense systems of two wheat cultivars. – Plant Physiology and Biochemistry 40: 691-696.
[31] Hijikata, N., Murase, M., Tani, C., Ohtomo, R., Osaki, M., Ezawa, T. (2010): Polyphosphate has a central role in the rapid and massive accumulation of phosphorus in extraradical mycelium of an arbuscular mycorrhizal fungus. – New Phytologist 186: 285-289.

http://www.aloki.hu ● ISSN 1589 1623 (Print) ●ISSN1785 0037 (Online)
DOI: http://dx.doi.org/10.15666/aeer/1706_1371313727

[32] Kannenberg, S. A., Phillips, R. P. (2017): Soil microbial communities buffer physiological responses to drought stress in three hardwood species. – Oecologia 183: 631-641.
[33] Kawamitsu, Y., Driscoll, T., Boyer, J. S. (2000): Photosynthesis during desiccation in an Intertidal Alga and a Land Plant. – Plant and Cell Physiology 41(3): 344-353.
[34] Khalvati, M., Bartha, B., Dupigny, A., Schröder, P. (2010): Arbuscular mycorrhizal association is beneficial for growth and detoxification of xenobiotics of barley under drought stress. – Journal of Soils and Sediments 10: 54-64.
[35] Kilic, H., Yagbasanlar, T. (2010): The Effect of Drought Stress on Grain Yield, Yield Components and some Quality Traits of Durum Wheat (*Triticum turgidum* ssp. durum) Cultivars. – Notulae Botanicae Horti Agrobotanici Cluj-Napoca 38: 164-170.
[36] Kohler, J., Caravaca, F., del Mar, A. M., Roldán, A. (2009): Elevated CO_2 increases the effect of an arbuscular mycorrhizal fungus and a plant-growth-promoting rhizobacterium on structural stability of a semiarid agricultural soil under drought conditions. – Soil Biology and Biochemistry 41: 1710-1716.
[37] Kpyoarissis, A., Petropoulou, Y., Manetas, Y. (1995): Summer survival of leaves in a soft-leaved shrub (*Phlomis fruticosa* L., Labiatae) under Mediterranean field conditions:avoidance of photoinhibitory damage through decreased chlorophyll contents. – Journal of Experimental Botany 46: 1825-1831.
[38] Kyriazopouls, A. P., Orfanoudakis, M., Abraham, E. M., Parissi, Z. M., Serafidou, N. (2014): Effects of Arbuscular Mycorrhiza Fungi on Growth Characteristics of *Dactylis glomerata* L. under Drought Stress Conditions. – Notulae Botanicae Horti Agrobotanici Cluj-Napoca 42: 132-137.
[39] Lazcano, C. F. B., Barrios-Masias, F. H., Jackson, L. E. (2014): Arbuscular mycorrhizal effects on plant water relations and soil greenhouse gas emissions under changing moisture regimes. – Soil Biology and Biochemistry 74: 184-192.
[40] Li, Y., Cheng, Y. L., Li, M., Lin, X. G., Liu, R. J. (2012): Effects of arbuscular mycorrhizal fungal communities on soil quality and the growth of cucumber seedlings in a greenhouse soil continuously planting cucumber. – Pedosphere 22: 79-87.
[41] Lichtenthaler, H. K. (1987): Chlorophylls and carotenoids: Pigments of photosynthetic biomembranes. – Methods in Enzymology 148: 350-382.
[42] Malik, N. S. A., Alberto, N., McKeever, L. C. (2017): Mycorrhizal Inoculation Increases Growth and Induces Changes in Specific Polyphenol Levels in Olive Saplings. – Journal of Agricultural Science 9(2): doi:10.5539/jas.v9n2p1.
[43] Manivannan, P., Abdul Jaleel, C., Sankar, B., Kishorekumar, A., Somasundaram, R., Lakshmanan, G. M. A., Panneerselvam, R. (2007): Growth, biochemical modifications and proline metabolism in *Helianthus annuus* L. as induced by drought stress. – Colloids and Surfaces B: Biointerfaces 59: 141-149.
[44] Matzek, V., Vitousek, P. M. (2009): N:P stoichiometry and protein:RNA ratios in vascular plants:an evaluation of the growth-rate hypothesis. – Ecology Letters 12: 765-771.
[45] Michalis, O., Ioannides, I. M., Ehaliotis, C. (2013): Mycorrhizal inoculation affects arbuscular mycorrhizal diversity in watermelon roots but leads to improved colonization and plant response under water stress only. – App Soil Ecol 63: 112-119.
[46] Olsen, S. R., Sommers, L. E. (1982): Phosphorus. – In: Page, A. L., Miller, R. H., Keeney, D. R. (eds.) Methods of soil analysis, part 2. Chemical and Microbiological Properties. ASA, SSSA, Madison, Wis, pp 403-430.
[47] Ommen, O. E., Donnelly, A., Vanhoutvin, S., van Oijen, M., Manderscheid, R. (1999): Chlorophyll content of spring wheat flag leaves grown under elevated CO_2 concentrations and other environmental stresses within the ESPACE-wheat project. – European Journal of Agronomy 10: 197-203.

http://www.aloki.hu ● ISSN 1589 1623 (Print) ●ISSN1785 0037 (Online)
DOI: http://dx.doi.org/10.15666/aeer/1706_1371313727

[48] Patale, S. W., Shinde, B. P. (2014): Effect of water and salt stress on Bt-Cotton inoculated with AM fungi. – Indian Journal of Research Studies in Pure and Applied Science 2: 50-56.
[49] Plenchette, C., Fortin, J. A., Furlan, V. (1983): Growth response of several plant species to mycorrhiza in soil of moderate P fertility. I. mycorrhizal dependency under field conditions. – Plant and Soil 70: 199-209.
[50] Quiroga, G., Erice, G., Aroca, R., Chaumont, F., Ruiz-Lozano, J. M. (2017): Enhanced Drought Stress Tolerance by the Arbuscular Mycorrhizal Symbiosis in a Drought-Sensitive Maize Cultivar Is Related to a Broader and Differential Regulation of Host Plant Aquaporins than in a Drought-Tolerant Cultivar. – Frontiers in Plant Science 8: doi.org/10.3389/fpls.2017.01056.
[51] Rivera-Becerril, F., van Tuinen, D., Martin-Laurent, F., Metwally, A., Dietz, K-J., Gianinazzi, S., Gianinazzi-Pearson, V. (2005): Molecular changes in *Pisum sativum* L. roots during arbuscular mycorrhiza buffering of cadmium stress. – Mycorrhiza 16: 51-60.
[52] Ruíz-Lozano, J. M. (2003): Arbuscular mycorrhhizal symbiosis and alleviation of osmotic stress. New perspectives for molecular studies. – Mycorrhiza 13: 309-317.
[53] Schueßler, A., Schwarzott, D., Walker, C. (2001): A new fungal phylum, the Glomeromycota: phylogeny and evolution. – Mycological Research 105: 1413-1421.
[54] Schueßler, A., Walker, C. (2010): The Glomeromycota: a species list with new families and genera. – Edinburgh & Kew, UK: The Royal Botanic Garden; Munich, Germany: Botanische Staatssammlung Munich; Oregon, USA: Oregon State University. URL:http://www.amf-phylogeny.com. ISBN-13:978- 1466388048; ISBN-10:1466388048.
[55] Shinde, B. P., Thakur, J. (2015): Influence of Arbuscular mycorrhizal fungi on chlorophyll, proteins, proline and total carbohydrates content of the pea plant under water stress condition. – International Journal of Current Microbiology and Applied Sciences 4: 809-821.
[56] Shinde, B. P., Singh, N. (2017): Effect of Arbuscular Mycorrhizal Fungi on Growth Parameters of Sweet Corn under NaCl Salinity. – International Journal of Current Microbiology and Applied Sciences 6: 1317-1325.
[57] Smith, S. E., Read, D. J. (1997): Mycorrhizal symbiosis. – 2nd ed. Academic Press, London.
[58] Smith, S. E., Read, D. J. (2008): Mineral nutrition, toxic element accumulation and water relations of arbuscular mycorrhizal plants. – In: Smith, S. E., Read, D. J. (eds.) Mycorrhizal Symbiosis. 3rd ed. pp. 145-18. Academic Press, London.
[59] Subramanian, K. S., Santhanakrishnan, P., Balasubramanian, P. (2006): Responses of field grown tomato plants to arbuscular mycorrhizal fungal colonization under varying intensities of drought stress. – Scientia Horticulturae 107: 245-253.
[60] Tarafdar, J. C., Marschner, H. (1994): Efficiency of VAM hyphae in utilization of organic phosphorus by wheat plants. – Soil Science and Plant Nutrition 40: 593-600.
[61] Trouvelot, A., Kough, J., Gianinazzi-Pearson, V. (1986): Evaluation of VA infection levels in root systems. – In: Gianinazzi-Pearson, V., Gianinazzi, S. (eds.) Research for estimation methods having a functional significance, Physiological and Genetical Aspects of Mycorrhizae. INRA Press, Paris, France, pp. 217-221.
[62] Wu, Q. S., Srivastava, A. K., Zou, Y. N. (2013): AMF-induced tolerance to drought stress in citrus: A review. – Scientia Horticulturae 164: 77-87.
[63] Xiao-Qing, T., Li, H. E., Ying-Ning, Z. (2017): Alleviation of Drought Stress in White Clover after Inoculation with Arbuscular Mycorrhizal Fungi. – Notulae Botanicae Horti Agrobotanici Cluj-Napoca 45: 220-224.
[64] Zafari, M., Ebadi, A., Godehkahriz, S. J. (2017): Effect of seed Inoculation on *Alfalfa* Tolerance to water deficit stress. – Notulae Botanicae Horti Agrobotanici Cluj-Napoca 45: 82-88.

http://www.aloki.hu ● ISSN 1589 1623 (Print) ●ISSN1785 0037 (Online)
DOI: http://dx.doi.org/10.15666/aeer/1706_1371313727

[65] Zhao, R., Guo, W., Bi, N., Guo, J., Wang, L. J., Zhao, J., Zhang, J. (2015): Arbuscular mycorrhizal fungi affect the growth, nutrient uptake and water status of maize (*Zea mays* L.) grown in two types of coal mine spoils under drought stress. – Applied Soil Ecology 88: 41-49.

[66] Zhu, X. C., Song, F. B., Liu, S. Q., Liu, T. D., Zhou, X. (2012): Arbuscular mycorrhizae improve photosynthesis and water status of *Zea mays* L. under drought stress. – Plant, Soil and Environment 58: 186-191.

http://www.aloki.hu ● ISSN 1589 1623 (Print) ●ISSN1785 0037 (Online)
DOI: http://dx.doi.org/10.15666/aeer/1706_1371313727

MODELLING OF EXTREME RAINFALL IN PUNJAB: PAKISTAN USING BAYESIAN AND FREQUENTIST APPROACH

AHMAD, I.[1, 2, 4*] – AHMAD, T.[3] – ALMANJAHIE, IBRAHIM M.[1,2]

[1]*Department of Mathematics, College of Science, King Khalid University, Abha 62529, Kingdom of Saudi Arabia*

[2]*Statistical Research and Studies Support Unit, King Khalid University, Abha 62529, Kingdom of Saudi Arabia*

[3]*Department of Statistical Sciences, University of Padova, Padova 35121, Italy*

[4]*Department of Mathematics and Statistics, Faculty of Basic and Applied Sciences, International Islamic University, 44000 Islamabad, Pakistan*

**Corresponding author*
e-mail: ishfaq.ahmad@iiu.edu.pk

(Received 25th Apr 2019; accepted 25th Oct 2019)

Abstract. In this study we compared the efficiency of frequentist approach with Bayesian approach by carrying out extreme value analysis of Annual Maximum Daily Rainfall (AMDR). For frequentist frequency analysis of AMDR, we used the data of one station i.e. Lahore in Punjab province, Pakistan while for Bayesian analysis we used the data of three other neighboring stations as prior information. During frequentist approach, Generalized Extreme Value (GEV) was found to be a best-fit distribution on the data. In frequentist method, the parameters of GEV distribution were estimated using Maximum Likelihood Estimation (MLE), while in the Bayesian framework the Markov Chain Monte Carlo (MCMC) simulation technique along with Metropolis-Hasting algorithm and Gibbs sampler were implemented. Findings of this study indicate that despite the asymptotic requirements of the MLE, its performance can be enhanced by adopting the Bayesian MCMC paradigm. In order to acquire the posterior densities of GEV parameters, non-informative and informative priors based on the historical data of surrounding weather stations were employed. The result of Bayesian MCMC might be affected by the choice of priors. In addition, the performance of the parameters estimation methods was verified by employing several robustness measures. Robustness measures results proved that the Bayesian MCMC method performed better than MLE in estimating GEV parameters and future return levels. Therefore, the findings of these analyses could be helpful in adopting proper flood protection measures and designing infrastructures of culverts, buildings, bridges and dams in the region.
Keywords: *annual maximum daily rainfall, generalized extreme value, the Markov Chain Monte Carlo, maximum likelihood estimation, Bayesian paradigm, priors specification*

Abbreviations: AMDR: Annual Maximum Daily Rainfall; GEV: Generalized Extreme Value; MLE: Maximum Likelihood Estimation; MCMC: Markov Chain Monte Carlo; UNFCC: United Nations Framework on Climate Change; FFC: Federal Flood Commission; POT: Peak over a Threshold; GP: Generalized Pareto; GLO: Generalized Logistic; L-moment: Linear moment; mm: millimeters; SE: Standard Error; RRMSE: Relative Root Mean Square Error; RASE; Relative Absolute Square Error; PPCC: Probability Plot Correlation Coefficient; CV: Coefficient of Variation; SD: Standard Deviation; FA: Frequency Analysis; CI: Confidence Intervals; GB: Gibbs Sampler; M-H: Metropolis-Hasting; MLEs: Maximum Likelihood Estimates

Introduction

Extreme rainfall events are frequently connected with climatic fluctuations which may cause a series of natural disasters such as heavy floods and landslides. According to the United Nations Framework on Climate Change (UNFCC) the human lives, animal lives, and water resources, agricultural lands, food security, and coastal zones will be heavily affected

http://www.aloki.hu ● ISSN 1589 1623 (Print) ● ISSN 1785 0037 (Online)
DOI: http://dx.doi.org/10.15666/aeer/1706_1372913748

due to climatic changes in Asia. Pakistan is situated in the western part of the Indian subcontinent, with Afghanistan and Iran on the western borders, India on the eastern borders, and the Arabian Sea to the south. It is an agricultural country. The country with 70% of its population depends on agriculture and its products (Faisal and Sadiq, 2009). Most of the agricultural lands and other living organisms depend on rain-water. Rainfall occurs in Pakistan, not only in summer but also in winter. In summer, rainfall happens frequently during the monsoon period (from early July to September). The top-months of the monsoon rainfall in Pakistan are July and August (Ahmad et al., 2014, 2016). Rainfall is a major source of water for agriculture and energy production. According to Adnan and Khan (2009), the 60% of the total annual rainfall in Pakistan is due in summer. All Kharif crops are more dependent on monsoon rainfalls. These crops are also known as summer or monsoon crops. The major Kharif crops are rice, maize, cotton, jowar, bajra etc. Furthermore, winter rains are very beneficial for Rabi crops in the country (Shamshad, 1988; Ahmad et al., 2016). Rabi crops are sown at the beginning of winter season. The major Rabi crops are wheat, gram, peas and barley etc. Rabi crops are also known as winter or spring crops. In Pakistan, rainwater plays an important role in hydroelectricity and agricultural production. Agriculture is considered as the backbone of Pakistan's economy, but unfortunately, heavy rainfalls cause loss of lives, crops and infrastructures. This fact is undeniable that the society and the economy of any country can be affected due to extreme environmental events (Shabri et al., 2011). Therefore, the suitable modelling of extreme events can be done through statistical analysis.

The main purpose of the statistical analysis of extreme values is to enumerate the stochastic behavior of extreme environmental events (Smith, 1989; Coles et al., 2001). The most meteorological variables, such as rainfall, wind speed, temperature, floods and precipitation, are of under consideration because they have a terrific influence on humans and thus it is crucial to portray their behavior statistically due to their extreme positions.

Due to monsoon season in Pakistan; as heavy rainfalls are anticipated to take place frequently every year. According to the Federal Flood Commission (FFC) Pakistan, it is estimated that about cumulative financial loss US$ 38.171 million during the past 70 years. Around 616,598 km^2 of the total land area of Pakistan is prone to flood, some 197,275 villages were damaged and 12,330 people have lost their lives due to 24 major floods. Being a developing country like Pakistan, natural disasters unquestionably cripples the country's output. It is evident that any extreme environmental event is unpredictable. Nevertheless, the influence of heavy rainfall events may be abridged by precautionary measures based on the results from statistical analysis of Annual Maximum Daily Rainfall (AMDR) series, as suggested by Zin et al. (2010), Khamkong (2012) and Diriba et al. (2014). The major objective of statistical modelling of extreme rainfall was to estimate the quantiles that might occur for the next years to come.

There are two main statistical approaches to model AMDR series, namely the block maxima and peak over a threshold (POT). The block maxima approach models the highest value of each year collected from the large sample, whereas (POT) approach requires the observations that exceed a certain level of threshold in the collected data (Pickands, 1975; Davison and Smith, 1990). However, according to Madsen et al. (1997) and Eastoe and Tawn (2012) the block maxima is preferred since the method in selecting the appropriate threshold in (POT) procedure sometimes can be complex.

The AMDR series needs to be modelled by appropriate probability distributions that provide the better inferences of the future behaviour of extreme rainfalls. Various kinds of statistical distributions often are able to be used in AMDR. They are Generalized Extreme

http://www.aloki.hu ● ISSN 1589 1623 (Print) ● ISSN 1785 0037 (Online)
DOI: http://dx.doi.org/10.15666/aeer/1706_1372913748

Value (GEV), Gumbel, Generalized Pareto (GP), Generalized Logistic (GLO) and the lognormal distribution. Because of their suitability to modelling of extreme value, these probability distributions have numerous applications for environmental data (e.g., An and Pandey, 2005; Furrer and Katz, 2008; Chikobvu and Sigauke, 2013; Jonathan and Ewans, 2013; Diriba et al., 2015; Ahmad et al., 2016). Several studies based on frequentist approaches have been conducted for finding the best fit distribution and modelling the AMDR data in Pakistan by Rasul et al. (2004), Haroon and Rasul (2009), Rasul et al. (2009) and Ahmad et al. (2014, 2016). Ahmad et al. (2016) suggested that the (GEV) and (GP) are the most suitable distribution for the AMDR series in the different regions of Pakistan.

In this study, the five extreme value statistical distributions (such as GP, GEV, GLO, Pearson Type-III and Log-Normal three parameter) are applied to the extreme rainfall data of Lahore station of the Punjab province by using the frequentist procedure via linear moment (L-moment) estimation method. However, the results demonstrate the tendency that the GEV distribution among all others fits the data in a more appropriate way, attention is therefore limited to the GEV distribution.

Meanwhile, extreme data are sporadic by their nature, the statistical inference on extremes may be improved by the addition of other sources of information through a prior distribution. Unlike frequentist approaches (maximum likelihood and L-moments), a Bayesian analysis of extreme values is also not dependent on the fundamental assumptions that are required by the asymptotic theory of frequentist approaches (Smith, 1985; Coles et al., 2001; Smith, 2002). In addition, according to Hamed and Rao (2000) the MLE method that was unable to get an appropriate estimate with a small sample. The Bayesian method can be employed in estimating the parameter of GEV distribution. The basic theory of the Bayesian paradigm about extreme values has been discussed by many authors in a number of outstanding articles and books (Coles and Tawn, 1996, 2005; Beirlant et al., 2006; Naghettini, 2017, p. 505). In this study, the researcher has focused on its applications by using the GEV distribution. Additionally, the primary purpose of this article is the comparison of both estimation methods by using the robustness measures. The first one is the MLE method and the second one is the Bayesian method. In Bayesian analysis, the non-informative priors and informative priors based on the historical data of neighboring stations in term of extreme quantiles are formulated. In the previous study, Ahmad et al. (2014) discussed the behaviour of monsoon rainfalls in Pakistan through kappa distribution by employing L-moments estimation method. In another study Ahmad et al. (2016) used the data of extreme rainfall of 28 stations in Pakistan and found the best fit distribution among five extreme value distributions. After finding the best fit distribution the researcher carried out at-site frequency analysis on the same data by using L-moments and Trimmed L-moment estimation methods. However, they did not use the Bayesian paradigm for the modelling of extreme rainfall in Pakistan. The main purpose of this paper, therefore, is to study the extremes of rainfall by applying the GEV distribution to the Lahore station data, the province of Punjab, Pakistan. The frequentist approach, i.e. MLE and the Bayesian method were applied (Coles and Tawn, 1996; Diriba et al., 2017). The effects of non-informative and informative priors on the estimate of GEV parameters and return level are investigated and compared with MLE results. Despite the application of the Bayesian approach is progressively prevalent in many areas, a challenge when using this method is the computational problems. This can be solved by the application of Markov Chain Monte Carlo (MCMC) simulations (Coles et al., 2001). Moreover, the previous studies conducted on Bayesian Paradigm by using MCMC were Coles and Tawn (1996), Coles et al. (2003), Smith (2005) and Eli et al. (2012). The rest paper is organized as follows. We commence with description of data used in this study. Next, the probability

http://www.aloki.hu ● ISSN 1589 1623 (Print) ● ISSN 1785 0037 (Online)
DOI: http://dx.doi.org/10.15666/aeer/1706_1372913748

distribution and parameters estimation methods used in this study will be described. After that, the results and discussion section of our analysis will be presented. Later on, the conclusion, recommendations concerning the plan for future studies will be discussed in final section.

Materials and methods

Data description

The modeling of extreme rainfalls in the province Punjab, Pakistan, the data of daily rainfall of Lahore station had been acquired from Pakistan Metrological Center Karachi for the period of 1985 to 2014, which is recorded in millimeters (mm). Data have been selected on the following standard criteria like as length of the data, variability, quality, urbanization and climate change. After that, the Annual Maximum Daily Rainfall (AMDR) series were extracted from the daily rainfall series. AMDR series is a single maximum value for any specific year and station among the all values of recorded daily rainfall. The AMDR series for 30 years of the same length were considered. For construction of informative priors for the Bayesian analysis, extreme rainfall characteristics of three sites at various distances from Lahore station were selected, namely Faisalabad, Sialkot and Jhelum.

The selected stations for informative priors were located to the south-west, north-east and north-west of Lahore station. Additionally, they are 118 km, 105 km, 164 km from Lahore station, respectively. The plots under spatial network comprise of selected weather stations studied in present research are shown in *Figure 1*. This study have 25 years of data at the same time points from 1990-2014 for each station considered for construction of informative priors.

Figure 1. *Spatial plots of network weather stations used in study for the period of 1985-2014*

Summary statistics of the selected stations

The statistical parameters for the amount of AMDR data of four selected stations are briefed in *Table 1*. Where the minimum, maximum, mean, standard deviation (SD), coefficient of variation (CV), skewness and kurtosis of AMDR series of the all included stations in this study are given. The AMDR data designates that the annual daily rainfall

http://www.aloki.hu ● ISSN 1589 1623 (Print) ● ISSN 1785 0037 (Online)
DOI: http://dx.doi.org/10.15666/aeer/1706_1372913748

was strongly positively skewed and highly leptokurtic for Jhelum station. It is also noted that AMDR data for Sialkot station is positively skewed and platykurtic. The CV of AMDR around 42-45% in the province Punjab, Pakistan.

Table 1. *Summary statistics of the annual maximum daily rainfall (AMDR) data for the selected stations*

Study locations	Stations			
	Lahore	**Faisalabad**	**Jhelum**	**Sialkot**
Minimum (mm)	29.40	25.00	54.90	45.00
Maximum (mm)	189.70	136.00	242.20	207.50
Mean	90.45	63.43	99.40	110.10
Standard deviation	38.32	27.66	44.56	47.44
Coefficient of variation	42.35	43.61	44.83	47.44
Coefficient of skewness	0.91	1.05	1.52	0.71
Kurtosis	3.35	4.02	5.29	2.34

The fundamental assumptions

Primarily, it is compulsory to check the basic assumptions of data before conducting the further analysis of an annual maximum series in the field of statistical hydrology; because the final results may be ambiguous without fulfilling the assumptions. The fundamental assumption of hydrological data are randomness, independence, homogeneity and stationarity. We tested these assumptions using different tests such as NERC test for randomness, Wald-Wolfowitz for independence, Mann-Whitney test for homogeneity with respect to location parameters and Spearman rank correlation test for stationarity. The results of these tests given in *Table 2* are calculated by using (ALEA 2.0) software.

Table 2. *Results of different tests for basic assumptions at 5% level of significance*

Study locations	NERC (P-value)	Wald-Wolfowitz (P-value)	Mann-Whitney (P-value)	Spearman Rank (P-value)
Lahore	-0.7445 (0.2283)	1.3505 (0.0884)	-0.3940 (0.3468)	0.7895 (0.2149)
Faisalabad	1.9358 (0.1264)	0.5230 (0.3005)	-2.0117 (0.1021)	2.4021 (0.0820)
Jhelum	1.0423 (0.1486)	1.5812 (0.0569)	-1.8043 (0.0556)	-1.3981 (0.0810)
Sialkot	-0.7445 (0.2283)	0.5039 (0.3072)	-0.4770 (0.3167)	0.2767 (0.3910)

The probability value of these tests for each stations is more than 5% level of significance showed that the relevant assumptions of the data are fulfilled, and the available data can be used for further frequency analysis (FA).

http://www.aloki.hu ● ISSN 1589 1623 (Print) ● ISSN 1785 0037 (Online)
DOI: http://dx.doi.org/10.15666/aeer/1706_1372913748

Generalized extreme value distribution

Jenkinson (1955) introduced the GEV distribution for the three limiting cases for maxima. Furthermore, the GEV distribution is very extensively used for the design structure of extreme events. Engineers, hydrologist and business analyst are most commonly used GEV distribution in the recent decade. Because, the risk always linked with the extreme type events such as risk in business, the stock market, and also risk is related to extreme floods, heavy rainfall, high wind speed and extreme temperature etc. The GEV probability density function and distribution function of a random variable w is given by:

$$f(w_i,\xi,\mu,\sigma)=\frac{1}{\sigma}\left[1+\xi\frac{(w_i-\mu)}{\sigma}\right]^{-\left(1+\frac{1}{\xi}\right)}\exp\left[-\left\{1+\xi\frac{(w_i-\mu)}{\sigma}\right\}^{-\frac{1}{\xi}}\right] \quad \text{(Eq.1)}$$

The range of w is: $-\infty < w \le \mu+\frac{\sigma}{\xi}$ if $\xi>0$; $-\infty < w \le \infty$ if $\xi=0$; $\mu+\frac{\sigma}{\xi} < w \le \infty$ if $\xi<0$.

$$F(w,\xi,\mu,\sigma)=\exp\left[-\left\{1+\xi\frac{(w-\mu)}{\sigma}\right\}^{-\frac{1}{\xi}}\right] \quad \text{(Eq.2)}$$

where $\{w:1+\xi(w-\mu)/\sigma\}$ and μ,σ and ξ are location, scale and shape parameters of GEV distribution (Beirlant et al., 2006). The shape parameter affects the nature of upper tail of the GEV distribution. Additionally, GEV distribution is the mixture of three limiting extreme value distributions i.e., Gumbel distribution, Freshet distribution and Weibull distribution. If $\xi\to 0$ the GEV distribution in *Equation 2* relates to the Gumbel distribution.

$$F(w,\xi,\mu,\sigma)=\exp\left[-\exp\left(-\frac{(w-\mu)}{\sigma}\right)\right];-\infty<w<\infty \quad \text{(Eq.3)}$$

It means that the probability of obtaining the maximum high observation come to be very small exponentially. For $\xi>0$ the GEV distribution in *Equation 2* converts to Frechet distribution, which is considered by a heavy tail that declines polynomially. Hence, obtaining higher values of maximum are larger probability in comparison with a Gumbel distribution. For $\xi<0$ the distribution in *Equation 2* becomes negative Weibull distribution and this is bounded above (Coles et al., 2003; Karim, 1995; Gingras and Adamowski, 1992). Consequently, there is a finite value that the maximum cannot exceed.

Parameter estimation of GEV distribution

Maximum Likelihood Estimation (MLE) method was primarily articulated by a German mathematician Johann Carl Friedrich Gauss. But later as a general method of

http://www.aloki.hu ● ISSN 1589 1623 (Print) ● ISSN 1785 0037 (Online)
DOI: http://dx.doi.org/10.15666/aeer/1706_1372913748

estimation was initially developed by a British statistician Sir Ronald Aylmer Fisher in his series of papers discussed by Gupta (1982). MLE method involved a function that maximizes the parameters of the distribution, the function is known as the likelihood function. Likelihood function reaches to the maximum value when equating it to the conditions of unknowns and an identical number of equations in the system, whose solution produce the MLE estimators for unknown distribution parameters. The author was used MLE method to estimate the GEV distribution parameters. The density function of GEV distribution is given in *Equation 1*. Therefore the joint likelihood function associated with $w_1, w_2, ..., w_m$ follows from *Equation 1*.

$$L(\mu,\sigma,\xi;w_1,w_2,...,w_m)=\frac{1}{\sigma^m}\prod_{i=1}^{m}\left[1+\xi\frac{(w_i-\mu)}{\sigma}\right]^{-\left(1+\frac{1}{\xi}\right)}\times\exp\left[-\sum_{i=1}^{m}\left\{1+\xi\frac{(w_i-\mu)}{\sigma}\right\}^{-\frac{1}{\xi}}\right] \quad \text{(Eq.4)}$$

The maximum likelihood estimates of the parameters μ,σ and ξ, say $\hat{\mu},\hat{\sigma}$ and $\hat{\xi}$, are calculated by maximizing the logarithm of *Equation 4,* that is, maximizing

$$l(\mu,\sigma,\xi;w_1,w_2,..,w_m)=m\log\sigma-\left(1+\frac{1}{\xi}\right)\sum_{i=1}^{m}\log\left[1+\xi\frac{(w_i-\mu)}{\sigma}\right]-\sum_{i=1}^{m}\left\{1+\xi\frac{(w_i-\mu)}{\sigma}\right\}^{-\frac{1}{\xi}} \quad \text{(Eq.5)}$$

With respect to unknown parameters, say μ,σ and ξ. In other words, the log-likelihood function i.e., $\ln[L(\mu,\sigma,\xi;w_1,w_2,...,w_m)]=l(\mu,\sigma,\xi;w_1,w_2,..,w_m)$ is maximized instead of $L(\mu,\sigma,\xi;w_1,w_2,...,w_m)$, which simplifies the complication and gives the easy solution to the system. In a continuous parameter space the shape parameter of Gumbel distribution, $\xi=0$ is a single point, it will not be estimated by maximizing this log likelihood with probability 1. In practice the maximization of log likelihood functions is done by numerically iterations e.g., with a quasi-Newton procedure (Diriba et al., 2014, 2015).

Return level estimation for GEV distribution

The attention of extreme climatic events analysis does not sometimes lie on the estimates of GEV parameters, however the application of the fitted model to estimate the other measures. For illustration, it is very important the forecast of future extreme rainfall and heavy floods to make a proper plan to reduce its negative impact (for example landslides, human lives, animals and destruction of infrastructures such as power stations, buildings and roads) and return level or quantiles are used for such forecast. In other word, return level estimates play a dynamic role in rainfall frequency analysis to finding the future risk connected with a return period corresponding to a fitted model. The return level for GEV model corresponding the return period $T=\frac{1}{p}$ is acquired through quantile function, which is the inverse of *Equation 2* given by Coles (2001), denoted by w_p where $\mathrm{F}(w_p)=1-p$ and $0<p<1$.

http://www.aloki.hu ● ISSN 1589 1623 (Print) ● ISSN 1785 0037 (Online)
DOI: http://dx.doi.org/10.15666/aeer/1706_1372913748

$$w_p = \begin{cases} \mu - \frac{\sigma}{\xi}\left[1 - \{-\log(1-p)\}^{-\xi}\right], \xi \neq 0 \\ \mu - \sigma \log\{-\log(1-p)\}, \xi = 0 \end{cases} \quad \text{(Eq.6)}$$

The return level w_p is a quantile of considered GEV distribution corresponding to the upper tail probability p. The ML estimate of the return level w_p, denoted by $\hat{w}_p$ is found by substituting the ML estimates $\hat{\mu}, \hat{\sigma}$ and $\hat{\xi}$. The standard error (SE) of $\hat{w}_p$ are acquired via delta method (Rao, 1973).

Bayesian paradigm

The Bayesian approach has been extensively used in extreme rainfall frequency analysis. Bayesian statistical analysis depends on Bayes Theorem, which describes us how to update prior information about parameters and hypotheses using the additional information of data, to produce posterior beliefs suggested (Jackman, 2009). According to Naghettini (2017) and Tang and Ang (2007) difference between Bayesian and frequentist approaches are based on the parameters of given probability distribution.

In a classical approach, the parameters have fixed, but unknown, they are estimated from given sample by maximizing the likelihood function. But in Bayesian approach the parameters are treated as random, they have their own probability distribution. The parameters are updated on the basis of prior knowledge and sample information, the updated information is called the posterior information of the parameters.

As in MLE method, suppose AMDR $w = (w_1, w_2, ..., w_m)$ are independently and identically distributed and their distribution belongs to a parametric family i.e. GEV. However, the parameters of GEV distribution (μ, σ and ξ) are treated as random variables for which the author describes the prior distributions. Let $\theta = (\mu, \sigma, \xi)$ and suppose the prior information about parameter θ can be articulated by a probability density function $g_\theta(\theta)$ with no reference to the actual data. After multiplication of likelihood and prior information using Bayes theorem to get the posterior density of θ has the form:

$$\pi(\theta / w) = \frac{L(\theta / w) g_\theta(\theta)}{\int_\Theta L(\theta / w) g_\theta(\theta) d\theta} \propto L(\theta / w) g_\theta(\theta) \quad \text{(Eq.7)}$$

where $L(\theta / w)$ is the likelihood function of GEV distribution given in *Equation 4* and $\pi(\theta / w)$ is the posterior distribution for θ. Furthermore, the integral is taken over the parameter space Θ. In this paper, both the non-informative and informative priors were used. The description about construction of these prior are given in previous sections.

Priors specification

Non-informative priors

The main demur in the use of Bayesian frame work is the requirement for postulating a prior knowledge $g_\theta(\theta)$. When the minimal or no information is available, the

http://www.aloki.hu ● ISSN 1589 1623 (Print) ● ISSN 1785 0037 (Online)
DOI: http://dx.doi.org/10.15666/aeer/1706_1372913748

Bayesian analysis is performed by using objective or non-informative and Jeffery's priors. The non-informative priors (also known as diffuse, flat or vague priors) used to indicate a set of principles about the concerned parameters of GEV distribution, because to betoken that the meaningful information of extreme rainfall is quite inaccessible at the moment. The AMDR series have a GEV distribution i.e., $W_i \sim GEV(\mu,\sigma,\zeta)$, the likelihood function is given in *Equation 4*. The parametrization $\varphi = \log\sigma$ is used in the place of σ, for the purpose of easier work to the specification of prior, σ is inhibited to be positive. The tri-variate normal distribution based on $\theta' = (\mu,\varphi,\xi)$ is used with prior density as follows:

$$g_\theta(\theta) \propto \frac{1}{\sigma}\exp\left\{-\frac{1}{2}(\theta' - u)^T \sum^{-1}(\theta' - u)\right\} \quad \text{(Eq.8)}$$

where the mean vector u is symmetric positive definite (3×3) covariance matrix and $\sum$ must be quantified. The prior density is preferred to be

$$g(\mu,\varphi,\xi) = g(\mu)g(\varphi)g(\xi) \quad \text{(Eq.9)}$$

The marginal priors of $g_\mu(.), g_\varphi(.)$ and $g_\xi(.)$ are:

$$\mu \sim N(0,10000)$$
$$\varphi \sim LN(0,10000)$$
$$\xi \sim N(0,100)$$

These are known as independent normal priors with large variances. The larger variances are preferred enough to create the distribution nearly flat, comparable to prior obliviousness (Eli et al., 2012; Fawcett and Walshaw, 2008).

Informative priors

Since the nonexistence of expert knowledge on extreme rainfalls in Lahore station, we have articulated the prior knowledge for the Bayesian analysis from rainfall characteristics of nearby weather stations in the same province. Hence, the informative priors were constructed by employing the approach given by (Coles and Tawn, 1996). Prior information were elicited in term of extreme quantiles. The brief description of the technique given in the following paragraph.

Remember that return level w_p [= q_p Coles and Tawn (1996) notation] for GEV distribution corresponding with the return period of $\frac{1}{p}$ is given in *Equation 6,* therefore $F(q_p) = 1-p$, and where $F(.)$ is the cumulative distribution function of GEV in *Equation 2*. Let q_{p_i}, $i = 1,2,3$ with $p_1 > p_2 > p_3$, be the quantiles calculated from the past extreme rainfall data of the nearby weather stations in the province Punjab other than Lahore. So, the independent quantiles q_{p_i} are calculated for each nearby station by means of ML estimates of GEV parameters in *Eq. 2*. A joint prior distribution for given

http://www.aloki.hu ● ISSN 1589 1623 (Print) ● ISSN 1785 0037 (Online)
DOI: http://dx.doi.org/10.15666/aeer/1706_1372913748

probabilities $p_1 > p_2 > p_3$ could be elicited from the quantiles ($q_{p_1}, q_{p_2}, q_{p_3}$) discuss by Coles and Tawn (1996). One slight compilation with this approach is that parameters must be ordered q_{p_i}, $i = 1,2,3$, i.e. $q_{p_1} < q_{p_2} < q_{p_3}$. Hence, the suggest quantile differences, because of the assumption of independent priors on q_{p_i}, $i = 1,2,3$ would not be valid.

$$\left.\begin{aligned} \tilde{q}_1 &= q_{p_1} - e_1 \\ \tilde{q}_2 &= q_{p_2} - q_{p_1} \\ \tilde{q}_3 &= q_{p_3} - q_{p_2} \end{aligned}\right\} \quad \text{(Eq.10)}$$

where e_1 is a physical lower end point for the process variable (rainfall) or naturally considered to be $e_1 = 0$. Perceive that the quantile differences confirm the ordering of quantiles. The marginal priors on the quantile differences are now supposed to independent Gamma distribution with parameters $(\alpha_i^*, \beta_i^*), i = 1,2,3,$ we can take in the form

$$\tilde{q}_{p_i} \sim gamma(\alpha_i^*, \beta_i^*),\ \alpha_i^* > 0, \beta_i^* > 0;\ i = 1,2,3. \quad \text{(Eq.11)}$$

From *Equations 10* and *11* we can get the joint prior for the (α_i^*, β_i^*), $i = 1,2,3$ in following form:

$$g(q_{p_1}, q_{p_2,} q_{p_3}) \propto \tilde{q}_{p_1}^{\alpha_1^*-1} \exp(-\beta_1^* \tilde{q}_{p_1}) \times \prod_{i=2}^{3} \tilde{q}_{p_i}^{\alpha_i^*-1} \exp(-\beta_i^* \tilde{q}_{p_i}) \quad \text{(Eq.12)}$$

provided that $q_{p_1} < q_{p_2} < q_{p_3}$. Then utilize *Equation 6* in *Equation 12* and multiplying by the Jacobean (J) of the transformation from ($q_{p_1} < q_{p_2} < q_{p_3}$) to $\theta = (\mu, \sigma, \xi)$, it gives to an expression for the prior in term of the GEV distribution parameters θ. Further, this can be written as

$$g_\theta(\theta) \propto \prod_{i=1}^{3} \tilde{q}_{p_i}^{\alpha_i^*-1} \exp\left(-\frac{\tilde{q}_{p_i}}{\beta_i^*}\right) \times J \quad \text{(Eq.13)}$$

provided that $q_{p_1} < q_{p_2} < q_{p_3}$. The Jacobean used in *Equation 13* is given by

$$J = \begin{cases} \dfrac{\sigma}{\xi^2} \left| \sum_{i<j} (-1)^{i+j} (y_i \times y_j) \log\left(\dfrac{y_j}{y_i}\right) \right|, [i, j \in \{1,2,3\}; \xi \neq 0 \\ \dfrac{\sigma}{2} \left| \sum_{i<j} (-1)^{i+j} \log y_i \times \log y_j \times \log\left(\dfrac{y_j}{y_i}\right) \right|, [i, j \in \{1,2,3\}; \xi = 0 \end{cases} \quad \text{(Eq.14)}$$

http://www.aloki.hu ● ISSN 1589 1623 (Print) ● ISSN 1785 0037 (Online)
DOI: http://dx.doi.org/10.15666/aeer/1706_1372913748

where $y_i = -\log(1-p_i), i = 1,2,3.$ The posterior density $\pi(\theta / w)$ is found by replacing the likelihood and prior density given in *Equations 5* and *12,* respectively, in *Equation 7*. However, the analytical calculation for *Equation 7* is completely intractable, because of the involvement of integrals in denominator. Therefore, the features of posterior distribution $\pi(\theta / w)$ of θ is to be estimated by using Markov Chain Monte Carlo (MCMC) method with the combination of Gibbs Sampler and Metropolis-Hastings algorithm.

In Bayesian analysis, to estimate the return levels, usually, the vectors of simulated values are found by employing the marginal posterior distributions of GEV parameters. Return level q_p is obtained for a specified return period $\frac{1}{p}$ by substituting the simulated samples of GEV parameters from posterior distribution. Furthermore, the summary statistics can easily be acquired.

Robustness measures

On the basis of robustness measures, the authors will also compare the performance between the classical (MLE) and Bayesian MCMC methods (both for non-informative and for informative priors) in estimating GEV parameters and return levels for AMDR data of Lahore weather station in the province Punjab, Pakistan.. The selected robustness measures are relative root mean square error (RRMSE), relative absolute square error (RASE) and probability plot correlation coefficient (PPCC). The first two measure comprises the assessment on the difference between the observed and the estimated values under the presumed distribution, while the third one is measure the relationship between the ordered values and associated estimated values (Zawiah et al., 2009). The formulae are given as:

$$RRMSE = \sqrt{\frac{1}{n}\sum_{i=1}^{n}\left(\left|\frac{w_{i:n} - \hat{q}(F_i)}{w_{i:n}}\right|\right)^2} \quad \text{(Eq.15)}$$

$$RASE = \frac{1}{n}\sum_{i=1}^{n}\left|\frac{w_{i:n} - \hat{q}(F_i)}{w_{i:n}}\right| \quad \text{(Eq.16)}$$

$$PPCC = \frac{\sum_{i=1}^{n}(w_{i:n} - \bar{x})(\hat{q}(F_i) - \bar{q}(F_i))}{\sqrt{\sum_{i=1}^{n}(w_{i:n} - \bar{x})^2 \sum_{i=1}^{n}(\hat{q}(F_i) - \bar{q}(F_i))^2}} \quad \text{(Eq.17)}$$

where $w_{i:n}$ represents the observed sample values of *ith* order statistics of a random sample of size n, and $\hat{q}(F_i)$ are estimated quantiles linked with the *ith* Weibull plotting position, F. The Weibull plotting is defined as follows:

$$F = \frac{i}{n+1}$$

http://www.aloki.hu ● ISSN 1589 1623 (Print) ● ISSN 1785 0037 (Online)
DOI: http://dx.doi.org/10.15666/aeer/1706_1372913748

where i denote the ranks of the observations arranged in ascending order. The minimum values of RRMSE and RASE will show the best method. In contrast, the value of PPCC that is closest to -1 or 1 will be reflected as the best method for elucidation the behavior of extreme rainfalls in Punjab, Pakistan.

Results and discussion

GEV distribution using MLE

To analyze the AMDR data, GEV distribution is fitted to the extreme rainfall values. The parameters of the fitted model are estimated by MLE method. Maximum likelihood estimates with their SE in (parentheses) and the 95% confidence interval (CI) in [square brackets] for fitted model at Lahore Station are given in *Table 3*. It can be seen that the entire results of the fitted model (i.e. GEV) supports the AMDR data.

Table 3. *Parameter estimates of location, scale and shape of GEV distributions, their standard errors and confidence interval*

Study locations	**Location ($\hat{\mu}$)** **(SE)** **[CI]**	**Scale ($\hat{\sigma}$)** **(SE)** **[CI]**	**Shape ($\hat{\xi}$)** **(SE)** **[CI]**
Lahore	72.8995 (5.9325) [61.2686, 84.5208]	28.6298 (4.3780) [20.0469, 37.2029]	0.0317 (0.1461) [-0.2544, 0.3180]

Furthermore, before calculating the return levels, we should have to check the goodness of fit of our model. The adequacy of the chosen model can be checked using the quantiles, probability and return level plot. The plots for GEV distributions fitted to the data of Lahore station are given in *Figure 2*. The quantiles and probability plots shows that the assumptions required for the GEV distributions have been fulfilled.

The return levels for best fitting model (i.e. GEV) could be estimated for next '*T'* year after base year using *Equation 6*. Therefore, the return levels estimates will be time varying. An estimate of the rainfall that the authors might assume to see at Lahore station in the next '*T*' years by employing the MLEs of the parameters in GEV distribution. Before estimating $\hat{w}_p$, the number of years should be converted to the probability (i.e. $p = \frac{1}{T}$). The predicted amount of maximum rainfall, that is, in context of return level, corresponding to return periods in *Figure 2* suggests that the return level falls below the 20-year return periods. Furthermore, it can be noted that the 95% confidence bounds are becoming very distant from the straight line for the return periods beyond the 20 years. Return levels for different return periods with corresponding the 95% CIs were estimated using the profile likelihood methods are given in *Table 4*.

Therefore, the return levels for AMDR increased slowly for the higher return periods. It can be seen that from *Table 4,* the profile likelihood intervals were gradually wider as return period increased.

This supports with the results showed in the return level plots given in *Figure 2*. However, since the profile likelihood method takes into account the skewness of the parameter distributions, it gives more accurate results for longer return periods.

http://www.aloki.hu ● ISSN 1589 1623 (Print) ● ISSN 1785 0037 (Online)
DOI: http://dx.doi.org/10.15666/aeer/1706_1372913748

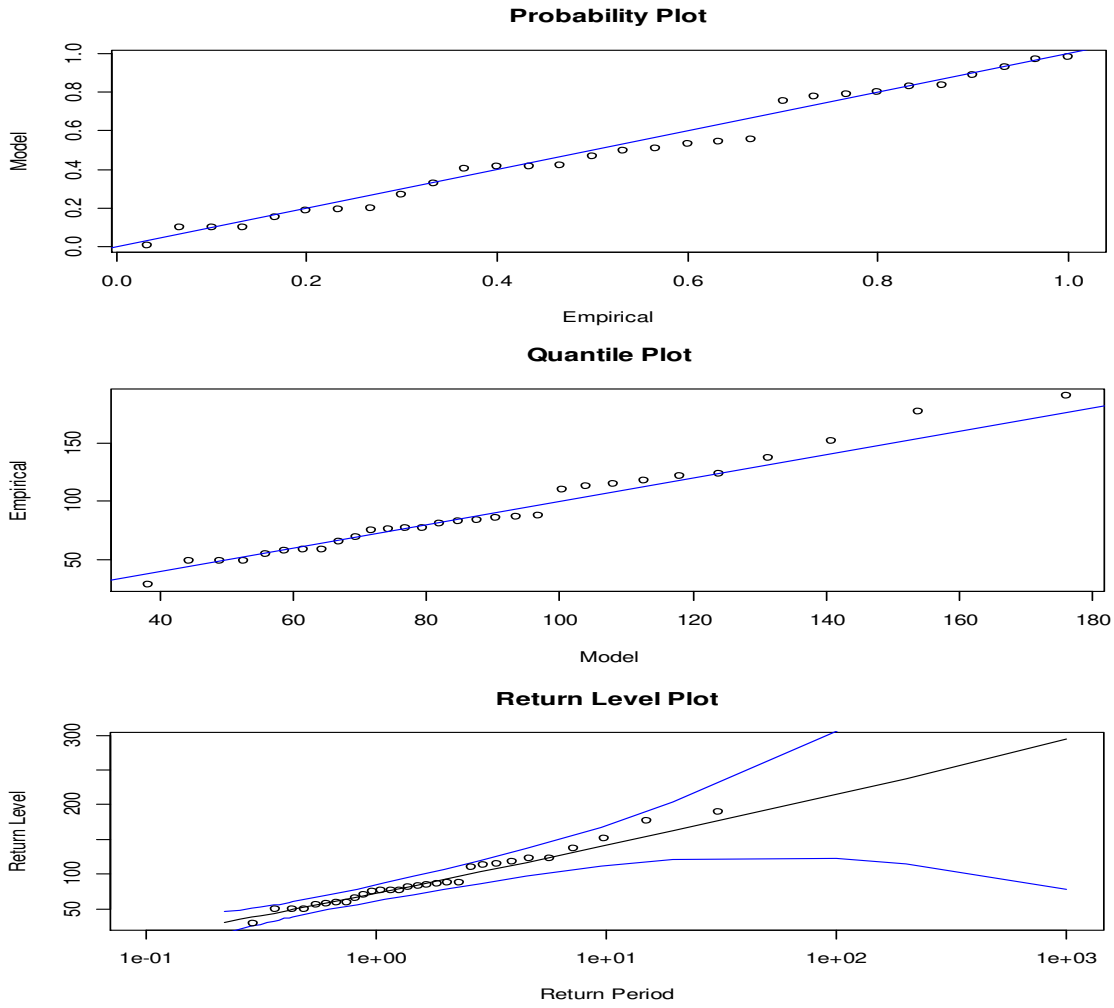

Figure 2. *Diagnostic plots based on profile likelihood method to assess goodness-of-fit of the GEV distribution fitted to AMDR data. From top to bottom: probability, quintile and return level*

Table 4. *Return level and 95% profile likelihood confidence intervals for 10, 25, 50, 75 and 100-year return levels of AMDR based on MLE*

Return periods	Return levels	Profile likelihood confidence intervals
10	139.6837	(118.3549, 187.0867)
25	169.2826	(138.9474, 263.5811)
50	191.8235	(153.1579, 340.1084)
75	205.1583	(160.5263, 393.9222)
100	214.7013	(166.8421, 437.5112)

Bayesian analysis

In Bayesian analysis, we were employed the non-informative and informative priors to the extreme rainfall data of Lahore weather station. The non-informative priors used (Coles and Tawn, 2005) were constructed for GEV parameters by assuming there is no reliable prior information available about the parameters given in priors specification

http://www.aloki.hu ● ISSN 1589 1623 (Print) ● ISSN 1785 0037 (Online)
DOI: http://dx.doi.org/10.15666/aeer/1706_1372913748

subheading (*non-informative priors*). Non-informative independent priors for GEV parameters were assumed $g(\mu) \sim N(0,10000)$; $g(\varphi) \sim LN(0,10000)$ and $g(\xi) \sim N(0,100)$.

The scale parameter of GEV (i.e. σ) was reparametrized as $\varphi = \log(\sigma)$ to hold the positivity of this parameter. The Gaussian distribution having zero mean and higher variance impose the flat marginal priors (also known as diffuse or vague priors), which show the absence of external information. The MCMC technique with combination of Gibbs Sampler (GB) and Metropolis-Hasting (M-H) algorithm was applied to AMDR series. Different starting points were used in simulations to check that the chains had converged to the original series and all the chains mixed well. The posterior means, standard deviation (SD) and 95% CIs of the parameters are given in *Table 4*. Furthermore, the posterior means, standard deviations (SD) are close to ML parameter of GEV distribution (see *Table 3*). The CIs of posterior parameters are little bit wider as compared to MLEs. It is expected that for flat-priors that posteriors means of GEV parameters with their CIs would be close to MLEs because they incorporate little information to the likelihood.

The informative priors were articulated by using historical records of rainfall data from three nearby weather stations to Lahore station. Moreover, the prior distributions were elicited using the method given by Coles and Tawn (1996) and discussed in subheading (*informative priors*) with quantiles $p_i = 10^{-i}$; for $i = 1,2,3$. By using this procedure, we have found $\tilde{q}_{p_1} \sim gamma(25.9065,4.015)$, $\tilde{q}_{p_2} \sim gamma(0.5702,117.4019)$ and $\tilde{q}_{p_3} \sim gamma(0.0999,804.3856)$ from Faisalabad weather station data. Similarly, the informative prior priors for Sialkot and Jhelum weather station were elicited by applying the same procedure. The posterior means and SD of GEV parameters with CIs are also given in *Table 5*. It can be seen the posterior means and CIs for GEV parameters based informative prior are close posterior means and CIs of non-informative priors.

Table 5. *Posterior means, standard deviations and confidence intervals for GEV parameters to AMDR data of Lahore weather station*

Study locations	**Parameters estimate of GEV distribution**		
	Location ($\hat{\mu}$) **(SE)** **[CI]**	**Scale ($\hat{\sigma}$)** **(SE)** **[CI]**	**Shape ($\hat{\xi}$)** **(SE)** **[CI]**
Non-informative priors	72.5232 (6.3956) [60.362, 85.5687]	31.0642 (5.1108) [22.7240, 42.6316]	0.0527 (0.1501) [-0.2130, 0.3696]
Informative priors			
Faisalabad	70.4847 (5.8650) [59.2650, 82.3369]	28.3486 (4.4383) [21.1682, 38.4110]	-0.0006 (0.1108) [-0.2169, 0.2179]
Sialkot	73.40324 (6.2712) [61.3944, 86.1910]	31.76948 (4.9098) [23.7582, 42.9742]	0.07116 (0.1429) [-0.2006, 0.3549]
Jhelum	72.76406 (6.3700) [60.6154, 85.6824]	31.00531 (4.9640) [22.8808, 42.2235]	0.05265 (0.1430) [-0.2077, 0.3497]

http://www.aloki.hu ● ISSN 1589 1623 (Print) ● ISSN 1785 0037 (Online)
DOI: http://dx.doi.org/10.15666/aeer/1706_1372913748

The informative priors constructed from the surrounding weather stations reduced the posterior SD for all GEV parameters as compared to non-informative priors and MLEs. This abatement in the SD would possibly overcome in uncertainty due to using extra information from the surrounding weather stations. This impact became most important for the SD of location, scale and shape parameters.

The estimated posterior densities plots of GEV parameters are given in *Figure 3*. It can be noticed that the distributions of location and shape parameters are symmetrical for non-informative and informative priors, while the shape parameter is negatively skewed for the prior elicited from the Faisalabad weather station that is situated at 118 km distance from Lahore. But the densities of location, scale and shape parameters have high peaks at center for the informative priors which were constructed using the Faisalabad and Sialkot data.

The densities for scale parameter were slightly positively skewed for non-informative and for all informative priors. It can be observed from densities plots, the densities of location, scale and shape parameters are shifted lift for the priors elicited from Sialkot and Jhelum data. These variations indicate that the posterior results might be changed due to the choice of priors. Furthermore, the distance between a weather station was used to articulate priors and Lahore weather station.

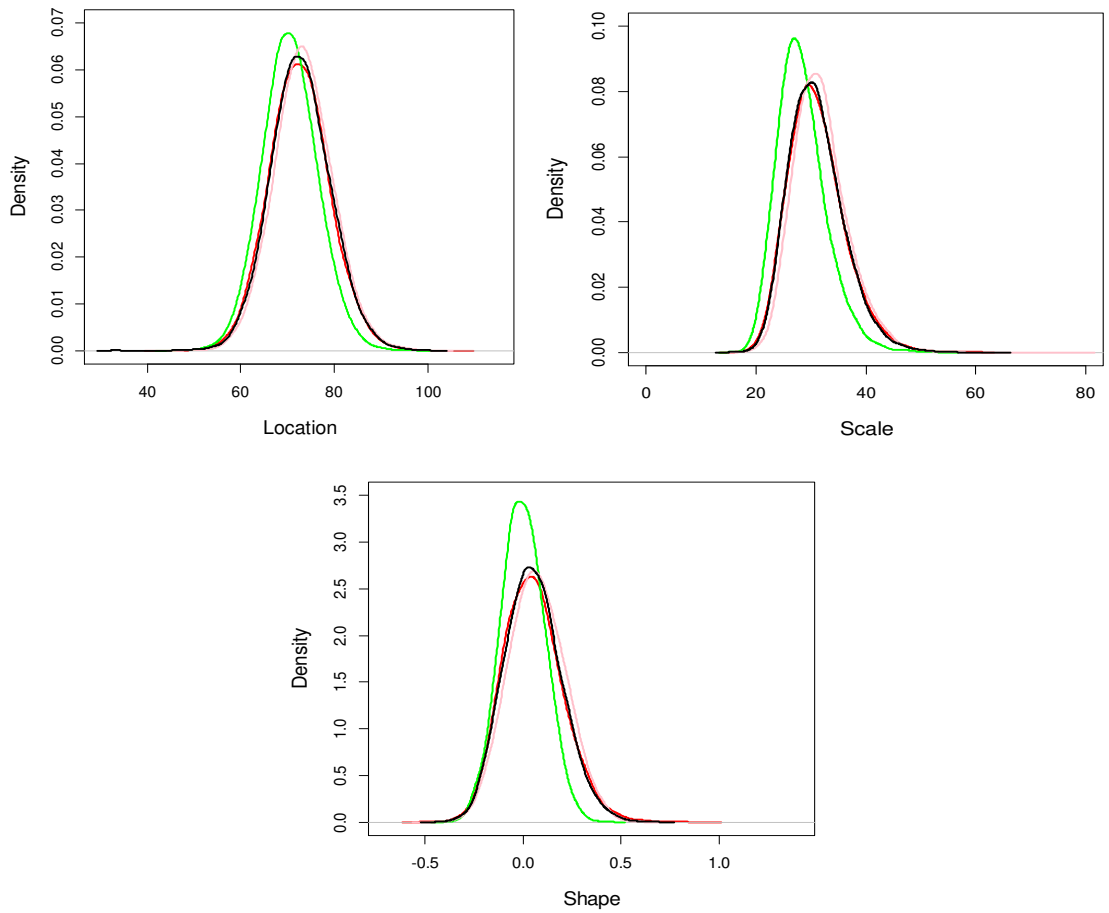

Figure 3. *Posterior densities plots of the GEV parameters to AMDR data using non-informative (red line) and informative priors (green line for Faisalabad, pink line for Sialkot and black line for Jhelum)*

http://www.aloki.hu ● ISSN 1589 1623 (Print) ● ISSN 1785 0037 (Online)
DOI: http://dx.doi.org/10.15666/aeer/1706_1372913748

Priors effect on return level

To look at how the non-informative and informative priors have affected the return levels, the authors obtained the posterior densities of the return levels. Additionally, the posterior density plots were constructed by employing the observations vectors obtained from the marginal posterior distributions of GEV parameters in *Equation 3,* for $0 < p < 1$. This process was carried out to attain the posterior densities of return levels for 10, 25, 50, 75, and 100 years return periods. Therefore, the posterior densities of these return levels for both non-informative and informative priors are given in *Figure 4*. The return level densities were symmetric and peaks high for the prior formulated from the Faisalabad weather station data, while the all other densities of the return levels were positively skewed and mesokurtic for both non-informative and the informative priors obtained from the Sialkot and Jhelum data. From this skewness, it can be cleared that the uncertainty might reproduce in the model for founding upper limits of the return levels as compare to lower limits for higher return periods (Coles and Tawn, 2005; Diriba et al., 2015). Furthermore, the posterior median of AMDR data for Lahore weather station was calculated. The results for different return periods are given in *Table 6*. The posterior medians of return levels for both non-informative and informative prior are not much different to their parallel MLEs. Moreover the results of *Tables 6* and *4* showed that the posterior medians of return levels for non-informative priors and informative priors constructed from nearby stations except Faisalabad are higher than MLEs across all considered return periods. The variations in higher medians of return levels (i.e. 75, 100) are smaller as compared to lower return levels. Hence the medians of returns levels vary due to distance of these stations (Faisalabad, Sialkot and Jhelum) and Lahore weather station, which was used to informative priors construction. However, the results of return level against different return periods are higher as compared to previous study which was conduct by Ahmad at el. (2016). Therefore, it is undeniable that these results are significant for policy implications in the region. They are also beneficial for meteorologists and hydrologists in water resource management.

Table 6. *Posterior medians for 10, 25, 50, 75 and 100-year return levels of AMDR using both non-informative and informative priors*

Priors	**Return levels**				
	10	**25**	**50**	**75**	**100**
Non-informative	146.7440	180.7501	207.0989	222.8688	234.2373
Informative					
Faisalabad	134.2359	161.0712	180.9693	192.5310	200.712
Sialkot	150.9387	187.5129	216.2855	233.6831	246.3059
Jhelum	146.8390	180.7752	207.0684	222.8045	234.1485

Robustness measures

On the basis of result given in *Table 7,* it can be decided the Bayesian MCMC paradigm for both non-informative and informative priors is slightly performed better than MLE. Because, the smaller values of RRMSE and RASE show little difference between the observed and estimated values. Furthermore, the smaller value of RRMSE and RASE corresponding to informative priors also indicate that Bayesian MCMC

http://www.aloki.hu ● ISSN 1589 1623 (Print) ● ISSN 1785 0037 (Online)
DOI: http://dx.doi.org/10.15666/aeer/1706_1372913748

method provide more precise results, when the expert prior were used in estimation. With the support of the results of PPCC test, it can be declared that Bayesian MCMC method was superior in modeling of extreme rainfall in the Punjab, Pakistan.

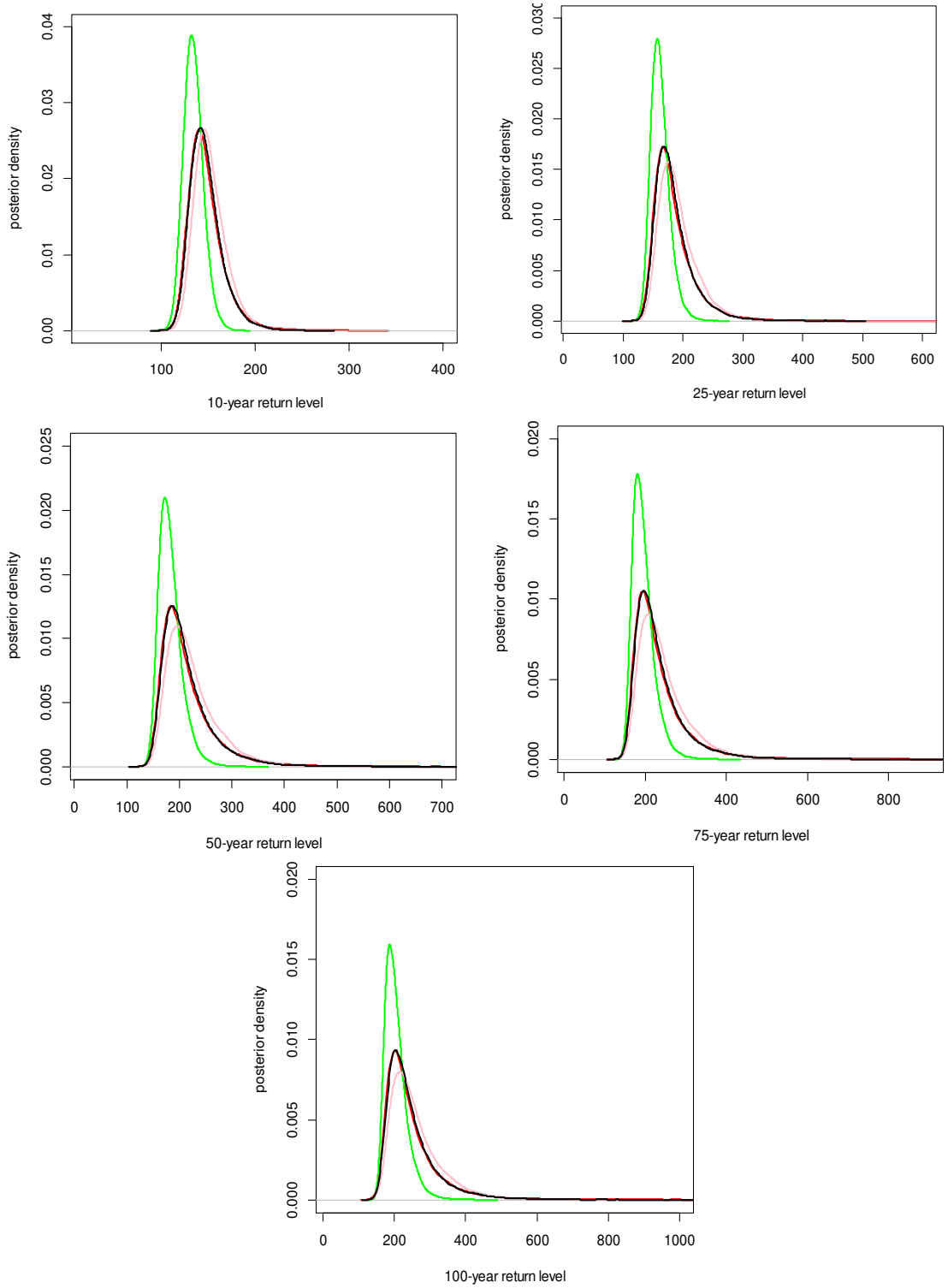

Figure 4. *Posterior median densities plots for the 10, 25, 50, 75 and 100 year return levels using AMDR data using non-informative (red line) and informative priors (green line for Faisalabad, pink line for Sialkot and black line for Jhelum)*

http://www.aloki.hu ● ISSN 1589 1623 (Print) ● ISSN 1785 0037 (Online)
DOI: http://dx.doi.org/10.15666/aeer/1706_1372913748

Table 7. *Comparison of performance between MLE and Bayesian method (both for non-informative and informative priors)*

Method of estimation	Test of robustness		
	RRMSE	**RASE**	**PPCC**
MLE	0.68443	0.66774	0.8858
Bayesian			
Non-informative priors	0.67973	0.66050	0.9123
Informative priors			
Faisalabad	0.64670	0.63706	0.97211
Sialkot	0.65682	0.63957	0.96455
Jhelum	0.66143	0.63781	0.96054

Conclusion

Our objective was to conduct the extreme value analysis for the modelling of AMDR data of Lahore weather station, Punjab, Pakistan through frequentist and Bayesian approaches. The AMDR data was shown to follow GEV distribution which has a positive shape parameter, frequently appealing as it has a finite upper limit. In frequentist method, the return levels for (10, 25, 50, 75 and 100 years) were estimated by using parameter estimates obtained via MLE. These results indicated that there would be an extreme rain event occurring in future. In addition, the authors used Bayesian MCMC approach, which provide a more efficient analysis and predictions. Therefore, the results found for both non-informative and informative priors using MCMC techniques and were compared with MLEs and each other. As the posterior means of best fit distribution parameter estimates attained using non-informative priors were close to MLEs of parameters. In addition, the influence of the informative priors used in the statistical analysis on posterior mean and SE depend on the distance among the weather stations used for construction of informative priors and the weather station where GEV model was best fitted. Furthermore, the SE of posterior means of the parameters were smaller due to shorter distance. The smaller values of robustness measures were directed precision of Bayesian MCMC method (both for non-informative and informative priors). Although, the Bayesian analysis offers a more suitable and straight way to handling and expressing uncertainties suggested (Coles et al., 2003).

The Bayesian paradigm presented in this study to model the behavior extreme event at Lahore weather station is suitable when climatological information is scare. The limitation of the method is that it considers the behavior of extreme rainfall is same over the weather stations in the province from which the data were acquired. However, the extreme rainfall behavior at different parts of the province Punjab can be affected by the topography of the area and other information. To construct the prior distributions for weather stations in addition to historical records, the authors suggest that the Bayesian analysis should utilize this kind of information. Moreover, this study shows that the effects of informative priors on posterior means and accuracy of parameter estimates of GEV depend on distance. In general, the results of this work are very helpful to future plan in the designing of dam, bridges, culverts, and flood control devices in the province Punjab, Pakistan. These findings could be enhanced further with the practice of spatial modelling and this is the theme of future research.

http://www.aloki.hu ● ISSN 1589 1623 (Print) ● ISSN 1785 0037 (Online)
DOI: http://dx.doi.org/10.15666/aeer/1706_1372913748

Acknowledgements. The Deanship of Scientific Research at King Khalid University. Kingdom of Saudi Arabia funded this work through research groups program under the project number RGP-1/102/40.

REFERENCES

[1] Adnan, S., Khan, A. H. (2009): Effective rainfall for irrigated agriculture plains of Pakistan. – Pakistan Journal of Meteorology 6(11): 61-72.
[2] Ahmad, I., Mahmood, I., Malik, I. R., Arshad, I. A., Iqbal, Z. (2014): Probability analysis of monthly rainfall on seasonal monsoon in Pakistan. – International Journal of Climatology 34(3): 827-834.
[3] Ahmad, I., Abbas, A., Saghir, A., Fawad, M. (2016): Finding probability distributions for annual daily maximum rainfall in Pakistan using linear moments and variants. – Polish Journal of Environmental Studies 25(3).
[4] An, Y., Pandey, M. D. (2005): A comparison of methods of extreme wind speed estimation. – Journal of Wind Engineering and Industrial Aerodynamics 93(7): 535-545.
[5] Beirlant, J., Goegebeur, Y., Segers, J., Teugels, J. L. (2006): Statistics of Extremes: Theory and Applications. – John Wiley & Sons, New York.
[6] Chikobvu, D., Sigauke, C. (2013): Modelling influence of temperature on daily peak electricity demand in South Africa. – Journal of Energy in Southern Africa 24(4): 63-70.
[7] Coles, S., Tawn, J. A. (1996): A Bayesian analysis of extreme rainfall data. – Applied Statistics 6(10): 463-478.
[8] Coles, S., Tawn, J. (2005): Bayesian modelling of extreme surges on the UK east coast. – Philosophical Transactions of the Royal Society of London A: Mathematical, Physical and Engineering Sciences 363(1831): 1387-1406.
[9] Coles, S., Bawa, J., Trenner, L., Dorazio, P. (2001): An Introduction to Statistical Modeling of Extreme Values. Vol. 208. – Springer, London.
[10] Coles, S., Pericchi, L. R., Sisson, S. (2003): A fully probabilistic approach to extreme rainfall modeling. – Journal of Hydrology 273(1-4): 35-50.
[11] Davison, A. C., Smith, R. L. (1990): Models for exceedances over high thresholds. – Journal of the Royal Statistical Society. Series B (Methodological): 393-442.
[12] Diriba, T. A., Debusho, L. K., Botai, J., Hassen, A. (2014): Analysis of extreme rainfall at East London, South Africa. – Annual Proceedings of the South African Statistical Association Conference 2014(1): 25-32.
[13] Diriba, T. A., Debusho, L. K., Botai, J. (2015): Modeling extreme daily temperature using generalized Pareto distribution at Port Elizabeth, South Africa. – Annual Proceedings of the South African Statistical Association Conference 2015(1): 41-48).
[14] Diriba, T. A., Debusho, L. K., Botai, J., Hassen, A. (2017): Bayesian modelling of extreme wind speed at Cape Town, South Africa. – Environmental and Ecological Statistics 24(2): 243-267.
[15] Eastoe, E. F., Tawn, J. A. (2012): Modelling the distribution of the cluster maxima of exceedances of subasymptotic thresholds. – Biometrika 99(1): 43-55.
[16] Eli, A., Shaffie, M., Zin, W. Z. W. (2012): Preliminary study on Bayesian extreme rainfall analysis: a case study of Alor Setar, Kedah, Malaysia. – Sains Malaysiana 41(11): 1403-1410.
[17] Faisal, N., Sadiq, N. (2009): Climatic zonation of Pakistan through precipitation effectiveness index. – Pak. J. Meteorol 6(16): 51-60.
[18] Fawcett, L., Walshaw, D. (2008, June). Modelling environmental extremes. – Short Course for the 19th Annual Conference of the International Environmentrics Society, June 8, Kelowna, Canada.
[19] Furrer, E. M., Katz, R. W. (2008): Improving the simulation of extreme precipitation events by stochastic weather generators. – Water Resources Research 44(12).

http://www.aloki.hu ● ISSN 1589 1623 (Print) ● ISSN 1785 0037 (Online)
DOI: http://dx.doi.org/10.15666/aeer/1706_1372913748

[20] Gingras, D., Adamowski, K. (1992): Coupling of nonparametric frequency and l-moment analyses for mixed distribution identification 1. – JAWRA Journal of the American Water Resources Association 28(2): 263-272.
[21] Gupta, S. C. (1982): Fundamentals of Mathematical Statistics: A Modern Approach. – Sultan Chand and Sons, New Delhi.
[22] Hamed, K., Rao, A. R. (2000): Flood Frequency Analysis. – CRC Press, Boca Raton, FL.
[23] Haroon, M. A., Rasul, G. (2009): Principal component analysis of summer rainfall and outgoing long-wave radiation over Pakistan. – Pakistan Journal of Meteorology 5(10).
[24] Jackman, S. (2009): Bayesian Analysis for the Social Sciences. Vol. 846. – John Wiley & Sons, Chicherster.
[25] Jenkinson, A. F. (1955): The frequency distribution of the annual maximum (or minimum) values of meteorological elements. – Quarterly Journal of the Royal Meteorological Society 81(348): 158-171.
[26] Jonathan, P., Ewans, K. (2013): Statistical modelling of extreme ocean environments for marine design: a review. – Ocean Engineering 62: 91-109.
[27] Karim, M. A., Chowdhury, J. U. (1995): A comparison of four distributions used in flood frequency analysis in Bangladesh. – Hydrological Sciences Journal 40(1): 55-66.
[28] Khamkong, M. (2012): Statistical modeling of annual monthly maximum rainfall in upper northern region of Thailand. – The 6th International Days of Statistics and Economics, 13-15 September, Prague.
[29] Madsen, H., Pearson, C. P., Rosbjerg, D. (1997): Comparison of annual maximum series and partial duration series methods for modeling extreme hydrologic events: 2. Regional modeling. – Water Resources Research 33(4): 759-769.
[30] Naghettini, M. (ed.) (2017): Fundamentals of Statistical Hydrology. – Springer, Cham.
[31] Pickands III, J. (1975): Statistical inference using extreme order statistics. – The Annals of Statistics 3(1): 119-131.
[32] Rao, C. R. (1973): Linear Statistical Inference and Its Applications. Vol. 2. – Wiley, New York, pp. 263-270.
[33] Rasul, G., Sixiong, Z., Qingcun, Z. (2004): A diagnostic study of record heavy rain in twin cities Islāmābad-Rāwalpindi. – Advances in Atmospheric Sciences 21(6): 976-988.
[34] Rasul, G., Chaudhry, Q. Z., Mahmood, A. (2009): Numerical simulation of heavy rainfall case in South Asia. – Pakistan Journal of Meteorology 6(11).
[35] Shabri, A. B., Daud, Z. M., Ariff, N. M. (2011): Regional analysis of annual maximum rainfall using TL-moments method. – Theoretical and Applied Climatology 104(3-4): 561-570.
[36] Shamshad, K. M. (1988): The Meteorology of Pakistan. First Ed. – Royal Book Company Publishers, Karachi.
[37] Smith, E. (2005): Bayesian modelling of extreme rainfall data. – Doctoral Dissertation, University of Newcastle upon Tyne (unpublished).
[38] Smith, E. P. (2002): An Introduction to Statistical Modeling of Extreme Values. – Springer, London.
[39] Smith, R. L. (1985): Maximum likelihood estimation in a class of non-regular cases. – Biometrika 72(1): 67-90.
[40] Smith, R. L. (1989): Extreme value analysis of environmental time series: an application to trend detection in ground-level ozone. – Statistical Science 4(4): 367-377.
[41] Tang, W. H., Ang, A. (2007): Probability Concepts in Engineering: Emphasis on Applications to Civil & Environmental Engineering. – Wiley, New York.
[42] Zawiah, W. Z. W., Jemain, A. A., Ibrahim, K., Suhaila, J., Sayang, M. D. (2009): A comparative study of extreme rainfall in Peninsular Malaysia: with reference to partial duration and annual extreme series. – Sains Malaysiana 38(5): 751-760.
[43] Zin, W. Z. W., Jamaludin, S., Deni, S. M., Jemain, A. A. (2010): Recent changes in extreme rainfall events in Peninsular Malaysia: 1971-2005. – Theoretical and Applied Climatology 99(3-4): 303.

http://www.aloki.hu ● ISSN 1589 1623 (Print) ● ISSN 1785 0037 (Online)
DOI: http://dx.doi.org/10.15666/aeer/1706_1372913748

SENSITIVITY OF ARBUSCULAR MYCORRHIZAL FUNGI IN OLD-GROWTH FORESTS: DIRECT EFFECT ON GROWTH AND SOIL CARBON STORAGE

ULLAH, S.[1*] – MUHAMMAD, B.[1] – AMIN, R.[1] – ABBAS, H.[1] – MUNEER, M. A.[2]

[1]*College of Forestry, Beijing Forestry University, Beijing 100083, China*

[2]*College of Grassland Science, Beijing Forestry University, Beijing 100083, China*

**Corresponding author*
e-mail: Saifkhan@bjfu.edu.cn, saif.haryankot@outlook.com; phone: +86-188-1079-7267

(Received 1st May 2019; accepted 11th Jul 2019)

Abstract. Arbuscular mycorrhizal association is ubiquitous and can be found in majority of natural habitats. Arbuscular mycorrhizal fungi (AMF) play a key role in the absorption of plant nutrients, soil aggregation and fertility. The basic role of AMF in the plant growth is to increase the absorption and translocation of relatively immobile ions and elements. In the past, studies have focused primarily on the mycorrhiza development and their general role in the growth of plants. Here, in this review manuscript, we highlight the role of AMF in the growth of old forests. In many studies, it has been found that concentration of phosphorous (P) decreases with the stand age which as a result leads to phosphorous (P) deficiency. This phosphorous (P) deficiency is considered as a cause of slow growth of old forests. In this review article, we argued that apart from the low concentration of phosphorous (P), weak arbuscular mycorrhizal associations are also a cause of slow growth of old forests. Furthermore, we also highlight the ecological role of AMF in the soil carbon storage. AMF provide physical (hyphae frame) and chemical support (Glomalin) to the dispersed soil particles to create stable aggregated soil structure. The Glomalin compound which is released by AMF acts like a glue and consequently increases soil aggregation. The soil organic matters stored in soil aggregates are less exposed to decomposition. Hence, soil can be used as a large sink where a huge amount of carbon can be stored in the form of soil organic matters which as a result can contribute to the mitigation of global climate change.
Keywords: *spore germination, Glomalin, phosphorous (P), heavy metals, soil aggregation*

Introduction

The permanency and functioning of a terrestrial ecosystem are determined by plant biodiversity and species composition (Bond et al., 1993; Tilman and Downing, 1994; Naeem et al., 1994; Tilman et al., 1996; Hooper and Vitousek, 1997; Wang et al., 2006, 2008). The collaboration between aboveground and belowground mechanisms in all terrestrial ecosystems impacts community and ecosystem-level processes (Wardle et al., 2004). Typically, in a terrestrial ecosystem, different mycorrhizal symbiotic links develop between plants and fungi in an extensive range (Finlay, 2008). These symbiotic associations are abundant and occur in 75 to 80% plants (Clasen et al., 2018). Mycorrhizal association plays very important role in ecosystem which improves plants growth and existence through a mutualistic relationship (Kernaghan, 2005) as can be seen in *Figure 1*. There is a give-and-take influence or "feedback" between plants and mycorrhizal fungi. For instance, the diversity of mycorrhiza promotes several plants community traits which in turn can promote mycorrhizal diversity (Castelli and Casper, 2003; Reynolds et al., 2003).

The term 'Mycorrhiza' was first used in 1885 by Frank to define the modified root structures of forest trees (Frank, 2005). In the mycorrhizal associations, arbuscular

http://www.aloki.hu ● ISSN 1589 1623 (Print) ● ISSN 1785 0037 (Online)
DOI: http://dx.doi.org/10.15666/aeer/1706_1374913758

mycorrhizal fungi (AMF) is the result of the mutual adaptation of plants and fungi (Smith and Smith, 1990). AMF symbiosis is one of the oldest association on ground and hired in to the phylum Glomeromycota and order Glomales (Smith and Read, 1997; Schüßler, 2002).

In terrestrial ecosystem, AMF is the essential component (Smith and Read, 2008) and can be found in many herbaceous plant communities in abundance (Allen et al., 1995; Kennedy et al., 2005). Generally, the distribution of AMF species is dependent on many factors, for instance, environmental conditions and host plant species (Koske, 1981; Hetrick and Bloom, 1986). Hence, richness and diversity of AMF vary across different community types (Gai et al., 2009).

Previous studies have focused primarily on the mycorrhiza development and their general role in the growth of plants. Here, in this review manuscript, we highlight the role of AMF in the growth of old forests. In many studies, it has been found that concentration of phosphorous (P) decreases with stand age which as a result leads to phosphorous (P) deficiency (Jiao et al., 2013; Li et al., 2013). This phosphorous (P) deficiency is considered as a cause of slow growth of old forests. In this review article, we argue that apart from the low concentration of phosphorus, weak Arbuscular mycorrhizal associations are also a cause of the slow growth. We suggest that the growth of old forests can be made better if suitable environment for the germination and development of arbuscular mycorrhizal fungi (AMF) associations is provided which as a result can increase above ground biomass. Furthermore, we considered a portion on the ecological role of AMF in the soil carbon storage. The Glomalin compound which is released by AMF plays a very important role in the soil aggregation. The soil organic matters stored in soil aggregates are less exposed to decomposition. In this study, we highlight the importance of soil as a large sink where a huge amount of carbon can be stored in the form of soil organic matters which as a result can mitigate the problem of global climate change.

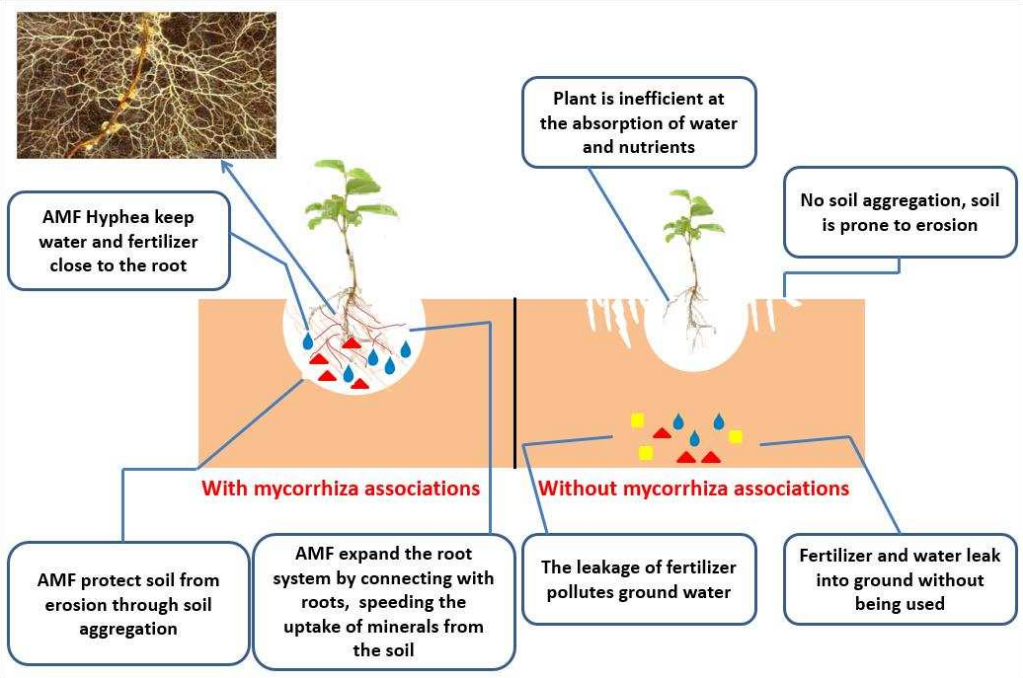

Figure 1. *Mycorrhiza associations play a key role in the growth of a plant*

http://www.aloki.hu ● ISSN 1589 1623 (Print) ● ISSN 1785 0037 (Online)
DOI: http://dx.doi.org/10.15666/aeer/1706_1374913758

Role of AMF in forest growth

The main role of AMF is to increase the absorption and translocation of relatively immobile ions and elements (Cooper and Tinker, 1981; Liu et al., 2000). These immobile ions (phosphate, ammonium and nitrate) and elements (such as P, Zn, Ca, S and N) are translocated through hyphae of AMF. In return, AMF receive carbon from the plant in the form of photosynthates (*Fig. 2*). About 5 to 10% of plants taken carbon during photosynthesis is usually released to the soil via roots (Farrar et al., 2003; Zhang et al., 2016).

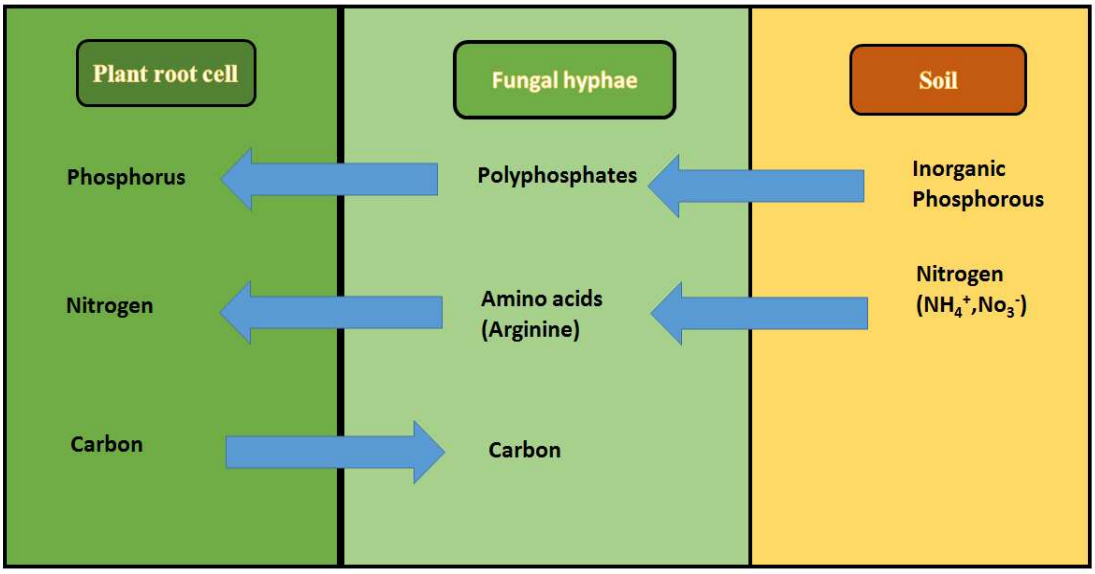

Figure 2. *Mutual nutrient supply between plant and AMF hyphae (Selosse and Rousset, 2011)*

Among AMF translocated immobile elements, phosphorous (P) is considered one of the primary nutrients for plant growth (Hinsinger, 2001). In soil, phosphorous (P) usually present in both organic and inorganic forms. Majority of it is in insoluble form as in acid soil, phosphate ions are mostly adsorbed in the form of Fe and Al phosphates, while in alkaline and calcareous soils, it is adsorbed in the form of Ca and Mg phosphates (Mehrotra, 2005). As already mentioned, AMF plays a very important role in the up-taking of these phosphorous (P) immobile ions (Cooper and Tinker, 1981; Liu et al., 2000). It is found that AMF is more efficient than plant roots at up-taking of phosphorous (P). The rate of up-taking can be six times faster than root hairs (Bolan, 1991). The up-taking phosphorous (P) is needed to maintain optimum plant quality, cell division, plant metabolisms, reproduction and energy storage (Zapata and Zaharah, 2002; Epstein, 1972). Moreover, phosphorous (P) plays an important role in the availability of nutrients, root development, root morphology and its branching (López-Bucio et al., 2003; Jin et al., 2005). The deficiency of phosphorous (P) usually leads to undersized, necrotic and erect leaves, lateral buds and subnormal root development. Hence, the availability of phosphorous (P) is very important for the growth of forest and it has been found that the growth of some regions is more effected by Phosphorous (P) than Nitrogen (N) (Jiao et al., 2013). The reason behind it is that AMF do not directly increase the up-taking of nitrogen but actually help plant in absorbing phosphorus which as a result also affects the absorption of other nutrients such as nitrogen (Mehrotra, 2005).

http://www.aloki.hu ● ISSN 1589 1623 (Print) ● ISSN 1785 0037 (Online)
DOI: http://dx.doi.org/10.15666/aeer/1706_1374913758

As stated earlier, the concentration of phosphorous (P) does not remain the same with the stand age and it decreases with the passage of time from early successional stage to late successional stage (Li et al., 2013; Jiao et al., 2013). As a result, many old forests with phosphorous (P) deficiency, have less growth, productivity and less carbon biomass. Here we propose that phosphorous (P) deficiency is not the only reason behind the slow growth of old forests. There are other factors which are accounted for the slow growth such as AMF spore germination and spore density. In a forest, AMF spore germination and AMF spore density are directly connected to the up-taking of phosphorous (P) which means that less spore germination and less spore density result in the decrease of phosphorous (P) absorption which is the case for an old forest. There are many factors which affect spore germination and spore density such as plant cover, soil sampling depth, soil fertility, seasonal variations, altitudinal gradient, soil moister, PH, and heavy metals concentration (Hepper and Smith, 1976; Jansa et al., 2005; Weissenhorn et al., 1993; He et al., 2002; Pawlowska and Charvat, 2004a). But here we discuss only three factors, e.g. heavy metals concentrations, soil fertility and plant cover which can be important in the context of old growth forests. The first factor, heavy metal concentration affects the initial stage of spore germination of AMF. It has been found that from early successional stage to late successional stage, the concentrations of heavy metals (Zn, Fe, Cu) increases which has negative impact on the initial stage of AMF spore germination (Li et al., 2013; Jiao et al., 2013; Pawlowska and Charvat, 2004b). The other two factors are related to spore density. Generally, increase in the concentration of different elements (e.g. N. Ca, K, and Mn) with stand age indicates increase in the fertility. It is well known that AMF possess higher spores density in low fertile soil due to slower decomposition rates and longer lived roots which is not the case for old forests (Eissenstat and Yanai, 1997; Zak and Pregitzer, 1998; Lovelock et al., 2003; Nadelhoffer, 2000). On other hand, plant cover which increases with the stand age of a forest negatively affects the spore density (He et al., 2002). Spore density and spore germination are crucial stages for AMF occurrence, distribution and colonization which play important role to provide phosphorous (P) for growth. Hence, apart from the phosphorous (P) deficiency, increase in the heavy metals concentration, fertility and plant cover also affect the growth of old forests through weak arbuscular mycorrhizal associations. Hence, we claim that the growth of old forests can be made better if suitable environment for the germination and development of arbuscular mycorrhizal fungi (AMF) associations is provided.

Here, we suggest that the development of rich food sites (like grasslands) around the boundaries of old forests can improve the distribution and density of AMF spores inside the old forests. The food sites will attract mammals, rodents, ungulates, migratory and local birds (endozochoorous co-dispersers, transfer usable propagules of both mutual associates-plants and AM fungi) (Bueno and Moora, 2019) that can spread spores of arbuscular mycorrhiza through bird droppings and faeces in old forests. In addition, the use of information and communication technology (ICT) for the management of old forests can improve plant community structure, ecosystem health, biodiversity and above ground biomass.

Role of AMF in soil carbon storage

Globally, forest soil contains approximately half of the earth terrestrial carbon (1146 × 1015 g) and about two-thirds of this amount is retained in soil pools (Dixon et al., 1994; Goodale et al., 2002). Understanding of the mechanisms through which we

http://www.aloki.hu ● ISSN 1589 1623 (Print) ● ISSN 1785 0037 (Online)
DOI: http://dx.doi.org/10.15666/aeer/1706_1374913758

can control soil carbon storage is crucial for the climate change (Averill et al., 2014). The soil organic carbon pool is an important regulator of the carbon exchange between biosphere and atmosphere. In order to achieve carbon loss-gain balance and mitigate global climate change, the soil carbon storage should be increased (Díaz et al., 2009). Soil carbon storage is directly related to the microbial community contribution, dynamics, biomass, balance between formation and degradation of microbial by-products and indirectly related with carbon cycling and soil aggregation (Six et al., 2006). To increase the storage capacity of the soil for carbon, the role of AMF cannot be ignored. As can be seen from *Figure 2,* the transfer of carbon from the host plant to AMF hyphae occurs in the form of photosynthates. This transfer usually takes place within few hours (Johnson et al., 2002). It has been found that the presence of mycorrhizal associations increases significantly plant carbon assimilation during photosynthesis (Miller et al., 2002; Grimoldi et al., 2006; Calderón et al., 2012) and as a result can increase carbon induction into soil (Grimoldi et al., 2006). AMF take carbon from the host plant in exchange for phosphorous (P) to expand the hyphae network. Generally a large fraction of soil carbon is labile and can readily undergo changes and decomposition if exposed to high moisture and temperature (Davidson and Janssens, 2006). Any significant increase in the decomposition of soil organic matter (SOM) can make the problem of global climate change severe. So we need to protect this soil organic matter from decomposition and as result we can dump more and more carbon inside soil in the form of SOM. This can be done if we store SOM in soil aggregates. In soil aggregation, insoluble Glomalin glycoprotein produced by AMF hyphae and spore plays very important role (Driver et al., 2005; Gonzalez-Chavez et al., 2004). The hyphae which behave like wall boards and soil particles which behave like insulation fills spaces between these boards (hyphae). The Glomalin covers it like a protective layer of paint on a wall (*Fig. 3*). Glomalin is very important for the stability of these soil aggregates. In the case of weak aggregation, aggregates can easily eroded by rainfall and all the organic matter and nutrients stored in these aggregates will be lost.

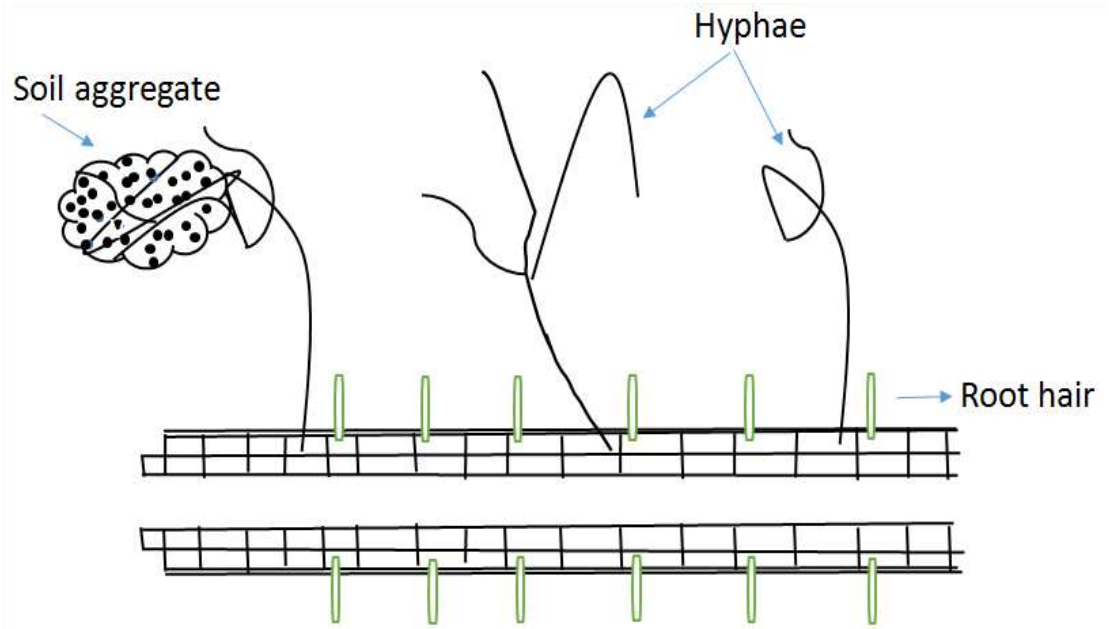

Figure 3. *Hyphae collect soil particles and then coat it with Glomalin to form soil aggregates (Rillig, 2004)*

http://www.aloki.hu ● ISSN 1589 1623 (Print) ● ISSN 1785 0037 (Online)
DOI: http://dx.doi.org/10.15666/aeer/1706_1374913758

Glomalin for the first time was discovered by soil scientist Sara F. Wright of the United States Department of Agriculture (USDA) and Agricultural Research Service (ARS) in 1996 (Wright and Upadhyaya, 1996). Glomalin is a compound which is not soluble in water and also resistant to heat degradation. Glomalin is still not defined biochemically. It consists of 4 to 6% Hydrogen, 33 to 49% Oxygen, 36 to 59% Carbon, 3-5% Nitrogen and 0.03 to 0.1% Phosphorus. Glomalin has reddish color and it is because of the 0.8 to 8.8% of Iron. This range of Iron concentration makes Glomalin resistive to degradation, increases thermal stability and strengthens Glomalin antimicrobial properties (Fokom et al., 2012).

As already explained, AMF especially Vesicular Arbuscular Mycorrhizal (VAM) is very important for the growth of a plant because of the hyphae hair like projections which can explore soil better than plant roots for different nutrients. Fungus supply different nutrients especially Phosphorus to the plant and in return plant provides carbon to the fungus for the growth. The excreted Glomalin covers the hyphae with hydrophobic sheet to stop any leakage of nutrients. When the roots grow and hyphae stop supply of nutrients, the Glomalin is generally released to the soil where it sticks to the organic materials and minerals. In soil, its presence increases soil aggregation and because of its ability to protect organic matters inside aggregates, it is also associated with carbon sequestration (Rillig et al., 1999). Functions of Glomalin can be summarized as:

- Acts like glue and helps in soil aggregation (Wright and Upadhyaya, 1998)
- Mitigates water and soil erosion (Andrade et al., 1998)
- Increases percolation of water (Prasad et al., 2018)
- Increases retention of water close to the roots (Bitterlich et al., 2018)
- Makes improvements to the recycling of nutrients (Singh, 2012)
- Improves carbon and nitrogen storage (Ariza et al., 2008)

Summary and future perspectives

To summarize, we have reviewed the role of AMF in the growth of old forests. Previously, researchers have found that low concentration of phosphorous (P) is the main cause of the slow growth of old forests. In this review article, we argued that apart from the low concentration of phosphorus, weak Arbuscular mycorrhizal association is also a cause of the slow growth. In old growth forests, the concentration of heavy metals has increased with the stand age which negatively affects the initial germination stage of AMF spores. Furthermore, an increase in fertility and plants cover with stand-age also decreased AMF spore density. These all factors over all affected the AMF associations in the old forests. Thus we claim that the growth of old forests can be improved provided that spore germination and spore density are increased which as a result can increase above ground biomass. In this study, we suggested that the development of rich food sites (like grasslands) around the boundaries of old forests can improve the distribution and density of AMF spores inside the old forests. The food sites will attract mammals, rodents, ungulates, migratory and local birds (endozochoorous co-dispersers, transfer usable propagules of both mutual associates-plants and AM fungi) that can spread spores of arbuscular mycorrhiza through bird droppings and faeces in the old forests. In addition, the use of information and communication technology (ICT) for the management of old forests can improve plant community structure, ecosystem health, biodiversity and above ground biomass. Apart from the role of AMF in the old forests,

http://www.aloki.hu ● ISSN 1589 1623 (Print) ● ISSN 1785 0037 (Online)
DOI: http://dx.doi.org/10.15666/aeer/1706_1374913758

we also highlighted the importance of AMF in soil aggregation. The Glomalin compound which is released by AMF (spores and hyphae) acts like glue and consequently increase soil aggregation. The soil organic matters stored in soil aggregates are less exposed to decomposition. Hence, soil can be used as a large sink where a huge amount of carbon can be stored in the form of soil organic matters which as result can mitigate the problem of global climate change.

Acknowledgements. We are grateful to all referees for their comments and suggestions which have improved our article a lot. We would also like to thank Prof. XiangPing Wang and Dr. Arif Ullah for their valuable discussion and suggestions. This study was supported by the National Key Research and Development Program of China (#2017YFC0503901) and National Natural Science Foundation of China (31870430).

REFERENCES

[1] Allen, E. B., Allen, M. F., Helm, D. J., Trappe, J. M., Molina, R., Rincon, E. (1995): Patterns and regulation of mycorrhizal plant and fungal diversity. – Plant and Soil 170(1): 47-62.

[2] Ariza, M., Boutton, T., Gonzalez Chavez, M. d. C., Filley, T. (2008): Carbon and nitrogen storage in glomalin-related soil protein during grassland-to-woodland succession. – American Geophysical Union Abstract B23B-0412.

[3] Averill, C., Turner, B. L., Finzi, A. C. (2014): Mycorrhiza-mediated competition between plants and decomposers drives soil carbon storage. – Nature 505(7484): 543.

[4] Bitterlich, M., Franken, P., Graefe, J. (2018): Arbuscular mycorrhiza improves substrate hydraulic conductivity in the plant available moisture range under root growth exclusion. – Frontiers in Plant Science 9(301). DOI: 10.3389/fpls.2018.00301.

[5] Bolan, N. (1991): A critical review on the role of mycorrhizal fungi in the uptake of phosphorus by plants. – Plant and Soil 134(2): 189-207.

[6] Bond, W., Schulze, E., Mooney, H. (1993): Biodiversity and Ecosystem Function. – Springer-Verlag, Berlin.

[7] Bueno, G., Moora, M. (2019): Commentary. How do arbuscular mycorrhizal fungi travel? – New Phytologist 222(2): 645-647. DOI: 10.1111/nph.15722.

[8] Calderón, F. J., Schultz, D. J., Paul, E. A. (2012): Carbon allocation, belowground transfers, and lipid turnover in a plant–microbial association. – Soil Science Society of America Journal 76(5): 1614-1623.

[9] Castelli, J. P., Casper, B. B. (2003): Intraspecific AM fungal variation contributes to plant–fungal feedback in a serpentine grassland. – Ecology 84(2): 323-336.

[10] Clasen, B. E., Silveira, A. d. O., Baldoni, D. B., Montagner, D. F., Jacques, R. J. S., Antoniolli, Z. I. (2018): Characterization of ectomycorrhizal species through molecular biology tools and morphotyping. – Scientia Agricola 75(3): 246-254.

[11] Cooper, K. M., Tinker, P. (1981): Translocation and transfer of nutrients in vesicular-arbuscular mycorrhizas: IV. Effect of environmental variables on movement of phosphorus. – New Phytologist 88(2): 327-339.

[12] Davidson, E. A., Janssens, I. A. (2006): Temperature sensitivity of soil carbon decomposition and feedbacks to climate change. – Nature 440(7081): 165.

[13] Díaz, S., Hector, A., Wardle, D. A. (2009): Biodiversity in forest carbon sequestration initiatives: not just a side benefit. – Current Opinion in Environmental Sustainability 1(1): 55-60.

[14] Dixon, R. K., Solomon, A., Brown, S., Houghton, R., Trexier, M., Wisniewski, J. (1994): Carbon pools and flux of global forest ecosystems. – Science 263(5144): 185-190.

http://www.aloki.hu ● ISSN 1589 1623 (Print) ● ISSN 1785 0037 (Online)
DOI: http://dx.doi.org/10.15666/aeer/1706_1374913758

[15] Driver, J. D., Holben, W. E., Rillig, M. C. (2005): Characterization of glomalin as a hyphal wall component of arbuscular mycorrhizal fungi. – Soil Biology and Biochemistry 37(1): 101-106.
[16] Eissenstat, D., Yanai, R. (1997): The ecology of root lifespan. – Advances in Ecological Research 27: 1-60.
[17] Epstein, E. (1972): Mineral Nutrition of Plants: Principles and Perspectives. – John Wiley and Sons New York.
[18] Farrar, J., Hawes, M., Jones, D., Lindow, S. (2003): How roots control the flux of carbon to the rhizosphere. – Ecology 84(4): 827-837.
[19] Finlay, R. D. (2008): Ecological aspects of mycorrhizal symbiosis: with special emphasis on the functional diversity of interactions involving the extraradical mycelium. – Journal of Experimental Botany 59(5): 1115-1126.
[20] Fokom, R., Adamou, S., Teugwa, M., Boyogueno, A. B., Nana, W., Ngonkeu, M., Tchameni, N., Nwaga, D., Ndzomo, G. T., Zollo, P. A. (2012): Glomalin related soil protein, carbon, nitrogen and soil aggregate stability as affected by land use variation in the humid forest zone of south Cameroon. – Soil and Tillage Research 120: 69-75.
[21] Frank, B. (2005): On the nutritional dependence of certain trees on root symbiosis with belowground fungi (an English translation of AB Frank's classic paper of 1885). – Mycorrhiza 15(4): 267-275.
[22] Gai, J., Christie, P., Cai, X., Fan, J., Zhang, J., Feng, G., Li, X. (2009): Occurrence and distribution of arbuscular mycorrhizal fungal species in three types of grassland community of the Tibetan Plateau. – Ecological Research 24(6): 1345.
[23] Gonzalez-Chavez, M., Carrillo-Gonzalez, R., Wright, S., Nichols, K. (2004): The role of glomalin, a protein produced by arbuscular mycorrhizal fungi, in sequestering potentially toxic elements. – Environmental Pollution 130(3): 317-323.
[24] Goodale, C. L., Apps, M. J., Birdsey, R. A., Field, C. B., Heath, L. S., Houghton, R. A., Jenkins, J. C., Kohlmaier, G. H., Kurz, W., Liu, S. (2002): Forest carbon sinks in the Northern Hemisphere. – Ecological Applications 12(3): 891-899.
[25] Grimoldi, A. A., Kavanová, M., Lattanzi, F. A., Schäufele, R., Schnyder, H. (2006): Arbuscular mycorrhizal colonization on carbon economy in perennial ryegrass: quantification by 13CO2/12CO2 steady-state labelling and gas exchange. – New Phytologist 172(3): 544-553.
[26] He, X., Mouratov, S., Steinberger, Y. (2002): Spatial distribution and colonization of arbuscular mycorrhizal fungi under the canopies of desert halophytes. – Arid Land Research and Management 16(2): 149-160.
[27] Hepper, C., Smith, G. (1976): Observation's on the germination of Endogone spores. – Transactions of the British Mycological Society 66(2): 189-194.
[28] Hetrick, B. A. D., Bloom, J. (1986): The influence of host plant on production and colonization ability of vesicular-arbuscular mycorrhizal spores. – Mycologia 78(1): 32-36.
[29] Hinsinger, P. (2001): Bioavailability of soil inorganic P in the rhizosphere as affected by root-induced chemical changes: a review. – Plant and Soil 237(2): 173-195.
[30] Hooper, D. U., Vitousek, P. M. (1997): The effects of plant composition and diversity on ecosystem processes. – Science 277(5330): 1302-1305.
[31] Jansa, J., Mozafar, A., Frossard, E. (2005): Phosphorus acquisition strategies within arbuscular mycorrhizal fungal community of a single field site. – Plant and Soil 276(1-2): 163-176.
[32] Jiao, F., Wen, Z.-M., An, S.-S., Yuan, Z. (2013): Successional changes in soil stoichiometry after land abandonment in Loess Plateau, China. – Ecological Engineering 58: 249-254.
[33] Jin, J., Wang, G., Liu, X., Pan, X., Herbert, S. J. (2005): Phosphorus application affects the soybean root response to water deficit at the initial flowering and full pod stages. – Soil Science & Plant Nutrition 51(7): 953-960.

http://www.aloki.hu ● ISSN 1589 1623 (Print) ● ISSN 1785 0037 (Online)
DOI: http://dx.doi.org/10.15666/aeer/1706_1374913758

[34] Johnson, D., Leake, J., Read, D. (2002): Transfer of recent photosynthate into mycorrhizal mycelium of an upland grassland: short-term respiratory losses and accumulation of 14C. – Soil Biology and Biochemistry 34(10): 1521-1524.
[35] Kennedy, N., Edwards, S., Clipson, N. (2005): Soil bacterial and fungal community structure across a range of unimproved and semi-improved upland grasslands. – Microbial Ecology 50(3): 463-473.
[36] Kernaghan, G. (2005): Mycorrhizal diversity: cause and effect. – Pedobiologia 49(6): 511-520.
[37] Koske, R. (1981): A preliminary study of interactions between species of vesicular-arbuscular fungi in a sand dune. – Transactions of the British Mycological Society 76(3): 411-416.
[38] Li, Y., Yang, F., Ou, Y., Zhang, D., Liu, J., Chu, G., Zhang, Y., Otieno, D., Zhou, G. (2013): Changes in forest soil properties in different successional stages in lower tropical China. – PloS One 8(11): e81359.
[39] Liu, A., Hamel, C., Hamilton, R., Ma, B., Smith, D. (2000): Acquisition of Cu, Zn, Mn and Fe by mycorrhizal maize (Zea mays L.) grown in soil at different P and micronutrient levels. – Mycorrhiza 9(6): 331-336.
[40] López-Bucio, J., Cruz-Ramirez, A., Herrera-Estrella, L. (2003): The role of nutrient availability in regulating root architecture. – Current Opinion in Plant Biology 6(3): 280-287.
[41] Lovelock, C. E., Andersen, K., Morton, J. B. (2003): Arbuscular mycorrhizal communities in tropical forests are affected by host tree species and environment. – Oecologia 135(2): 268-279.
[42] Mehrotra, V. (2005): Mycorrhiza: Role and Applications. – Allied Publishers, New Delhi.
[43] Miller, R., Miller, S., Jastrow, J., Rivetta, C. (2002): Mycorrhizal mediated feedbacks influence net carbon gain and nutrient uptake in Andropogon gerardii. – New Phytologist 155(1): 149-162.
[44] Nadelhoffer, K. J. (2000): The potential effects of nitrogen deposition on fine-root production in forest ecosystems. – New Phytologist 147(1): 131-139.
[45] Naeem, S., Thompson, L. J., Lawler, S. P., Lawton, J. H., Woodfin, R. M. (1994): Declining biodiversity can alter the performance of ecosystems. – Nature 368(6473): 734-737.
[46] Pawlowska, T. E., Charvat, I. (2004a): Heavy-metal stress and developmental patterns of arbuscular mycorrhizal fungi. – Applied and Environmental Microbiology 70(11): 6643-6649.
[47] Pawlowska, T. E., Charvat, I. (2004b): Heavy-metal stress and developmental patterns of arbuscular mycorrhizal fungi. – Appl. Environ. Microbiol 70(11): 6643-6649.
[48] Prasad, M., Chaudhary, M., Ramakrishnan, S. (2018): Glomalin: a miracle protein for soil sustainability. – Indian Farmer 5(09): 1092-1100.
[49] Reynolds, H. L., Packer, A., Bever, J. D., Clay, K. (2003): Grassroots ecology: plant–microbe–soil interactions as drivers of plant community structure and dynamics. – Ecology 84(9): 2281-2291.
[50] Rillig, M. C. (2004): Arbuscular mycorrhizae, glomalin, and soil aggregation. – Canadian Journal of Soil Science 84(4): 355-363.
[51] Rillig, M. C., Wright, S. F., Allen, M. F., Field, C. B. (1999): Rise in carbon dioxide changes soil structure. – Nature 400(6745): 628.
[52] Schüßler, A. (2002): Molecular Phylogeny, Taxonomy, and Evolution of Geosiphon Pyriformis and Arbuscular Mycorrhizal Fungi. – In: S. E. Smith, F. A. Smith (eds.) Diversity and Integration in Mycorrhizas. Springer, Dordrecht, pp. 75-83.
[53] Selosse, M.-A., Rousset, F. (2011): The plant-fungal marketplace. – Science 333(6044): 828-829.
[54] Singh, P. K. (2012): Role of glomalin related soil protein produced by arbuscular mycorrhizal fungi - a review. – Agric Sci Res J 2(3): 119-125.

http://www.aloki.hu ● ISSN 1589 1623 (Print) ● ISSN 1785 0037 (Online)
DOI: http://dx.doi.org/10.15666/aeer/1706_1374913758

[55] Six, J., Frey, S., Thiet, R., Batten, K. (2006): Bacterial and fungal contributions to carbon sequestration in agroecosystems. – Soil Science Society of America Journal 70(2): 555-569.
[56] Smith, S., Smith, F. (1990): Structure and function of the interfaces in biotrophic symbioses as they relate to nutrient transport. – New Phytologist 114(1): 1-38.
[57] Smith, S., Read, S. (1997): Mycorrhizal Symbiosis. 2nd Ed. – Academic Press, San Diego, CA.
[58] Smith, S., Read, D. (2008): Mycorrhizal Symbiosis. 3rd Ed. – Academic Press, San Diego, CA.
[59] Tilman, D., Downing, J. A. (1994): Biodiversity and stability in grasslands. – Nature 367(6461): 363.
[60] Tilman, D., Wedin, D., Knops, J. (1996): Productivity and sustainability influenced by biodiversity in grassland ecosystems. – Nature 379(6567): 718.
[61] Wang, X., Fang, J., Zhu, B. (2008): Forest biomass and root–shoot allocation in northeast China. – Forest Ecology and Management 255(12): 4007-4020.
[62] Wang, X. P., Tang, Z. Y., Fang, J. Y. (2006): Climatic control on forests and tree species distribution in the forest region of northeast China. – Journal of Integrative Plant Biology 48(7): 778-789.
[63] Wardle, D. A., Bardgett, R. D., Klironomos, J. N., Setälä, H., Van Der Putten, W. H., Wall, D. H. (2004): Ecological linkages between aboveground and belowground biota. – Science 304(5677): 1629-1633.
[64] Weissenhorn, I., Leyval, C., Berthelin, J. (1993): Cd-tolerant arbuscular mycorrhizal (AM) fungi from heavy-metal polluted soils. – Plant and Soil 157(2): 247-256.
[65] Wright, S. F., Upadhyaya, A. (1996): Extraction of an abundant and unusual protein from soil and comparison with hyphal protein of arbuscular mycorrhizal fungi. – Soil Science 161(9): 575-586.
[66] Zak, D. R., Pregitzer, K. S. (1998): Integration of Ecophysiological and Biogeochemical Approaches to Ecosystem Dynamics. – In: Pace, M. L., Groffman, P. M. (eds.) Successes, Limitations, and Frontiers in Ecosystem Science. – Springer, New York, pp. 372-403.
[67] Zapata, F., Zaharah, A. (2002): Phosphorus availability from phosphate rock and sewage sludge as influenced by the addition of water soluble phosphate fertilizer. – Nutrient Cycling in Agroecosystems 63(1): 43-48.
[68] Zhang, L., Xu, M., Liu, Y., Zhang, F., Hodge, A., Feng, G. (2016): Carbon and phosphorus exchange may enable cooperation between an arbuscular mycorrhizal fungus and a phosphate-solubilizing bacterium. – New Phytologist 210(3): 1022-1032.

http://www.aloki.hu ● ISSN 1589 1623 (Print) ● ISSN 1785 0037 (Online)
DOI: http://dx.doi.org/10.15666/aeer/1706_1374913758

ESTIMATION OF EVAPOTRANSPIRATION FOR IRRIGATED ARTIFICIAL GRASSLANDS IN TYPICAL STEPPE AREAS USING THE METRIC MODEL

WANG, J.[1,2] – LI, H. P.[1,2] – LU, H. Y.[1,2*] – ZHANG, R. Q.[1,2] – CAO, X. S[2] – TONG, C. F.[2] – ZHENG, H. X.[2]

[1]*State Key Laboratory of Simulation and Regulation of Water Cycle in River Basin, China Institute of Water Resources and Hydropower Research, Beijing, China*

[2]*Institute of Water Resources for Pastoral Area, China Institute of Water Resources and Hydropower Research, Hohhot, China*

**Corresponding author*
e-mail: haiyuan_lu@126.com

(Received 5th May 2019; accepted 16th Jul 2019)

Abstract. Irrigated artificial grasslands can help in achieving a large amount of forage in the Inner Mongolia typical steppe areas of China. However, developing irrigated artificial grasslands requires the consumption of water resources, and also affects the hydrological cycle. In this study, mapping evapotranspiration at high resolution with internalized calibration (METRIC) model has been used to estimate regional evapotranspiration during the crop growth season (from May to September) in irrigated artificial grasslands in 2011. The results were verified based on the data obtained from eight monitoring points of irrigated silage maize farms using water balance method, with a mean relative error value of 13.8%. The average evapotranspiration for irrigated artificial grasslands during the crop growth season is 611.42 mm. To further analyze the consumption of local water resources, concept of groundwater consumption (GW) is proposed. The GW value for irrigated artificial grasslands during the crop growth season was estimated to be 457.96 mm; the GW values at each of these farms, including Woyuan cow, Maodeng, Baiyinxile, Hezhongmumin, exceeded 400 mm. The results show that these areas, which exhibit high water consumption face difficulties in water resource management, particularly when there is no external water supply.
Keywords: *remote sensing, precipitation, Landsat images, underlying surface, water balance*

Introduction

Irrigated artificial grasslands are arable lands planted with artificial herbage in pastoral areas. It is supplemented by modern irrigation facilities to achieve a high forage yield. Irrigated artificial grasslands can produce a large amount of forage in the Inner Mongolia typical steppe areas of China (Niu and Jiang, 2004). The development and construction of irrigated artificial grasslands on a significant scale in the areas with better water resources can improve the yield of high-quality forage and resolve the problem of livestock forage shortage. This can also play an important role in improving the carrying capacity of pastures, thereby reducing the pressure on natural steppes and promoting water-forage-livestock system balance (Lu et al., 2016, 2018). However, irrigated artificial grasslands in the Inner Mongolia typical steppe areas are restricted by arid climate. In most cases, irrigation can only be obtained via pumping groundwater, because these areas are mainly distributed in the semi-arid region of Eurasia (Tong et al., 2004), in which the vast majority of the rivers are seasonal inland rivers (Batnasan, 2003), among which hydrological and geographical features are characterized by precipitation rarely flowing into rivers or groundwater. Evapotranspiration (ET) is the main mode of water vapor exchange between the underlying surface and atmosphere (Yamanaka et al., 2007). This hydrographic feature has led to a lack of local surface

http://www.aloki.hu ● ISSN 1589 1623 (Print) ● ISSN 1785 0037 (Online)
DOI: http://dx.doi.org/10.15666/aeer/1706_1375913776

water resources, which in turn makes it difficult for agricultural development. The Xilin River is the only seasonal inland river in the basin, and supplies water for various purposes, except irrigation. Therefore, the water required for irrigating artificial grasslands is sourced from local groundwater, in addition to precipitation. Owing to limited precipitation, crops grown on artificial grasslands must be irrigated. Pumping groundwater to satisfy the crop growth needs of irrigated artificial grasslands bring benefits to the regional economy, but consumes a large amount of groundwater, affecting the hydrological cycle in the steppe areas. The advantages and disadvantages of this water consumption need to be determined. Therefore, accurate monitoring of the water consumption for irrigated artificial grasslands, especially local groundwater consumption, can help determine regional irrigation water consumption and water resource management decisions (Liou and Kar, 2014; Pedro-Monzonís et al., 2015; Numata et al., 2017; Talsma et al., 2018).

Many ET monitoring and estimation methods have emerged with related theoretical research. These include the water balance method, aerodynamics methods, and scintilla meter measurements (Bowen, 1926; Thornthwaite, 1948; Howell et al., 1991; Rana and Katerji, 2000). These methods have displayed the ability to describe the characteristic rules of the ET processes at micro and farmland scales in detail (Liou and Kar, 2014). In addition, they have also provided important references and basic information for water vapor exchanges on underlying surfaces, decision-making with respect to farmland irrigation, comprehensive water resource management, and so forth (Long and Singh, 2013; French et al., 2015; Xu et al., 2015). However, in terms of regional ET estimation, owing to fluctuations in weather conditions and the dynamic nature of water-heat transfer processes (Gao et al., 2008), it has been determined that these traditional point-scale monitoring methods and approaches cannot fully reflect the actual characteristics of spatial changes in ET (Su et al., 2003; Cai et al., 2009; Monteith and Unsworth, 2013; Taherparvar and Pirmoradian, 2018). It has been determined that remote sensing technology can offer a new approach for regional ET estimation. Because of the spatial continuity and large span characteristics of remote sensing, the water that is consumed during ET can be derived directly, without the need to quantify other complex hydrological processes (Trezza et al., 2013).

ET models using remote sensing technology have been developed in recent years, including empirical methods and mechanism methods. Many achievements in theory innovation and method techniques have been presented (Khand et al., 2017). Among these proposed methods, two-source energy balance (TSEB), surface energy balance index (SEBI), simplified surface energy balance index (S-SEBI), surface energy balance algorithm for land (SEBAL), mapping evapotranspiration at high resolution with internalised calibration (METRIC) model have been widely used to calculate regional ET based on the theory of energy balance (Menenti, 1993; Norman et al., 1995; Bastiaanssen et al., 1998; Roerink et al., 2000; Su, 2002; Allen et al., 2007; Yang et al., 2010). As a typical representative of estimating regional ET by using remote sensing, the METRIC model is a variant of the SEBAL model that implements the residual method to calculate regional ET (Spiliotopoulos et al., 2017; Zamani Losgedaragh and Rahimzadegan, 2018). The METRIC model has been successfully used in many areas, as a physical model for high-precision estimation of regional ET (Allen et al., 2007, 2013; Morton et al., 2013; Paço et al., 2014; Reyes-González et al., 2017; Spiliotopoulos et al., 2017).

http://www.aloki.hu ● ISSN 1589 1623 (Print) ● ISSN 1785 0037 (Online)
DOI: http://dx.doi.org/10.15666/aeer/1706_1375913776

The objective of this paper is to use high-resolution Landsat images as an example to estimate the regional ET for irrigated artificial grasslands in the Inner Mongolia typical steppe areas by the METRIC model. Based on the development model of current groundwater by irrigated artificial grasslands, groundwater consumption (GW) and its law in the crop growth season are analyzed to accurately simulate and monitor the hydrological cycle in the Inner Mongolia typical steppe areas.

Materials and methods

Study area

The Xilin River Basin is a typical inland river basin in the Inner Mongolia typical steppe areas of China (Chen, 2002). The basin, with an area of approximately 11,172 km^2 (115.53°−117.25°E, 43.41°−44.63°N), has a typical continental temperate semi-arid climate. In accordance with the statistical data of the Xilinhot Station detailed on the National Meteorological Data website, the multi-year (period 1971-2011) average precipitation, ET from the water surface, air temperature, and wind speed are 263.5 mm, 1,904 mm, 3 °C, and 3.4 m s^{-1}, respectively. The average precipitation gradually decreases from the southeast to northwest (Sheng, 2017) (*Fig. 1*).

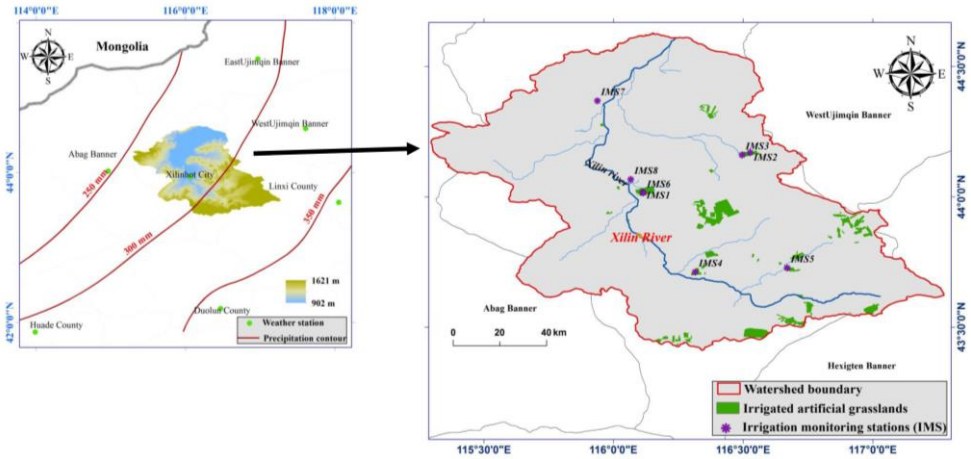

Figure 1. *Distribution for irrigated artificial grasslands in Xilin River Basin*

The planted area of the irrigated artificial grasslands in 2011 was approximately 257.3 km^2 (*Fig. 1*). The crops were silage maize (128.6 km^2), potato (96.5 km^2), alfalfa (25.8 km^2), and green millet (6.4 km^2). The management departments included co-ops (such as Hezhongmumin farm) and companies (Woyuan cow farm, Maodeng farm, Baiyinxile farm). Because of the effective accumulated temperature restriction, the crop growth season is from May to September every year with an irrigation quota of 400-700 mm. These crops bring benefits to the regional economy while consumes a large amount of water. In addition, amid limited precipitation, the crops grown on artificial grasslands must be irrigated. However, there is only one seasonal inland river in the basin, the Xilin River that supplies water for various purposes except irrigation. Therefore, the water required for irrigating artificial grasslands is sourced from local groundwater, apart from precipitation. Irrigation has a great impact on local water resource management.

http://www.aloki.hu ● ISSN 1589 1623 (Print) ● ISSN 1785 0037 (Online)
DOI: http://dx.doi.org/10.15666/aeer/1706_1375913776

Data

Landsat images

In this study, Landsat-5 and Landsat-7 images were chosen to estimate ET. In the data bands of these images, visible light and near-infrared bands have a high spatial resolution of 30 m, which satisfies the validation requirements for the spatial accuracy of ET estimation results in this study. In combination with the cloud cover of the study area, the effective 8-day sunshine data during the crop growth season (from May to September) of 2011 (day of the year from 121 to 273) were used to calculate the long-time scale of ET (*Table 1*). All the data were obtained from the United States Geological Survey (http://glovis.usgs.gov/).

Table 1. *Landsat-5/7 TM data information (PATH 124, ROW 29/30)*

Date	Day of the year (DOY)	Cloud coverage (%)	Sensor
2011/04/12	102	1	Landsat-5
2011/05/14	134	8	Landsat-5
2011/05/22	142	23	Landsat-7
2011/08/02	214	0	Landsat-5
2011/08/10	222	0	Landsat-7
2011/09/11	254	0	Landsat-7
2011/09/19	262	2	Landsat-5
2011/10/05	278	6	Landsat-5

Meteorological data

Meteorological data included air temperature, wind velocity, water vapor pressure, solar radiation, humidity, and precipitation in the seven weather stations of East Ujimqin Banner, Abag Banner, Huade County, West Ujimqin Banner, Xilinhot City, Linxi County, and Duolun County (*Fig. 1*). Among these, the air temperature data were used to calculate the surface temperature and net radiation by the METRIC model; the wind velocity data to calculate the aerodynamic resistance by the METRIC model; and the water vapor pressure data to calculate atmospheric transmittance and surface albedo by the METRIC model (Bastiaanssen et al., 1998; Allen et al., 2007). Other parameters such as solar radiation and humidity were used to calculate reference crop evapotranspiration (ET_0) by FAO Penman-Monteith equation (Allen et al., 1998). The meteorological data were obtained from the National Meteorological Data Information Center (http://data.cma.cn/).

Evapotranspiration measurement data

The ET measurement data were obtained from the eight irrigation monitoring stations (IMS) (*Fig. 1*). The crop cultivated in the monitoring station was silage maize. The average volumetric weight of soil was 1.54 - 1.82 g cm^{-3} for a thickness varying from 0 to 100 cm. The field water holding capacity (θ_f) was 14.3% - 19.0% (accounting for the dry soil weight), and the buried depth of the groundwater level was over 3 m. Based on water balance method, the water consumption data of the silage maize growth period were calculated to evaluate the results of the METRIC model.

http://www.aloki.hu ● ISSN 1589 1623 (Print) ● ISSN 1785 0037 (Online)
DOI: http://dx.doi.org/10.15666/aeer/1706_1375913776

Methods

METRIC model

The SEBAL model is the theoretical basis of the METRIC model (Bastiaanssen et al., 1998a, b; Allen et al., 2007). In the model, by considering the interference of the underlying surface elevation, slope gradient, slope direction, and other factors, the surface information obtained through remote sensing are converted to surface albedo, surface emissivity, vegetation index, roughness length, surface temperature, and other characteristic parameters. This model is combined with the meteorological observational data of the underlying surfaces to calculate the regional ET (Allen et al., 2007; González-Dugo et al., 2012). The theoretical equation is given as follows:

$$LE = R_n - G - H \quad \text{(Eq.1)}$$

where LE is the latent energy consumed by ET; R_n is the net radiation; G is the soil heat flux; and H is the sensible heat flux. Each energy component is generally expressed in W m^{-2}.

(1) Net radiation

R_n denotes the difference in the whole-band radiation quantity between the downward projection from the sky (including the sun and the atmosphere) and the upward projection from the Earth's surface (including soil, plants, and water). This parameter represents the main power source for the energy and water transmission of the underlying surfaces (Allen et al., 2007):

$$R_n = (1-\alpha)K_{in} + (L_{in} - L_{out}) - (1-\varepsilon)L_{in} \quad \text{(Eq.2)}$$

where α is the surface albedo (dimensionless); K_{in} is the incoming short-wave radiation (W m^{-2}); L_{in} is the incoming long-wave radiation (W m^{-2}); L_{out} is the outgoing long-wave radiation (W m^{-2}); and ε is the broad-band surface emissivity (dimensionless).

(2) Soil heat flux

G refers to the part of energy stored in vegetation and soil due to conduction, and its changes are mainly affected by net radiation, surface temperature and the vegetation cover on underlying surfaces. For the comprehensive analysis in this study, the achievements of Wright and Bastiaanssen are referred as follows (Wright, 1982; Bastiaanssen et al., 1998):

$$G = \frac{T_s - 273.15}{\alpha}(0.0038\alpha + 0.0074\alpha^2) \times (1 - 0.978NDVI^4)\ R_n \quad \text{(Eq.3)}$$

where T_s is the surface temperature (K); and NDVI is the normalized difference vegetation index (dimensionless).

(3) Sensible heat flux

H is a parameter, describing the exchange of energy between land surfaces and atmosphere, in which energy is transferred from the Earth's surface to the atmosphere

http://www.aloki.hu ● ISSN 1589 1623 (Print) ● ISSN 1785 0037 (Online)
DOI: http://dx.doi.org/10.15666/aeer/1706_1375913776

through convection or conduction. The calculation of H in the METRIC model is based on the following assumptions: dry and wet pixels exist in the study area; and there is a linear relationship between the temperature difference dT ($dT = T_1$-T_2) at z_1 and z_2 above the height of the zero-plane displacement and T_s. The space interpolation of the meteorological data on the underlying surfaces can then be avoided. Furthermore, the errors due to T_s are corrected to calibrate the calculation results of each pixel in remote sensing imaging through the elevation, slope gradient, and slope direction:

$$H = \rho_{air} c_p \frac{dT}{r_a} \quad \text{(Eq.4)}$$

where ρ_{air} is the air density (kg m^{-3}); c_p is the air specific heat capacity at a constant pressure (1,004 J kg^{-1} K^{-1}); and r_a is the aerodynamic resistance between two near surface heights, which has been calculated by the Monin–Obukhov theory (Allen et al., 2007); The calculation equations is given as follows:

$$dT = aT_{s,adtum} + b \quad \text{(Eq.5)}$$

$$T_{s,adtum} = T_s + 0.0065\Delta Z \quad \text{(Eq.6)}$$

where a and b are empirical constants; $T_{s,adtum}$ is the surface temperature adjusted to a common elevation data for each image pixel by using a digital elevation model and customized lapse rate (K); For non-planar areas, it is necessary to use the numerical elevation difference ΔZ for the corrections; and ΔZ is the difference between the elevation of each pixel and the reference elevation (m).

Dry and wet pixels are the two extreme pixels required for calculation using the METRIC model. Dry pixels refer to the dry idle wasteland or bare land areas without vegetation cover; these pixels are characterized by high temperature and almost zero ET (Bastiaanssen et al., 1998; Allen et al., 2007). In this study, dry pixels approximately satisfied LE≈0. The dry end of the dT function is estimated by rearranging *Equation 4* for a selected dry pixel in the image:

$$dT_{dry} = \frac{(R_n - G)_{dry} r_{a\,dry}}{\rho_{air\,dry} c_p} \quad \text{(Eq.7)}$$

where $r_{a\,dry}$ is r_a computed for the roughness and stability conditions of the dry pixel; and $\rho_{air\,dry}$ is ρ_{air} calculated at the dry pixel.

Wet pixels refer to areas with adequate water supply, dense vegetation growth, low temperatures and potential ET levels in the remote sensing images (Bastiaanssen et al., 1998; Allen et al., 2007). These could include completely covered areas or open water masses with good plant growth. For the wet pixels, H≈0 is usually set in the SEBAL model, and such H values are considered in the METRIC model (Allen et al., 2007).

$$dT_{wet} = \frac{(R_n - G - H)_{wet} r_{a\,wet}}{\rho_{air\,wet} c_p} \quad \text{(Eq.8)}$$

http://www.aloki.hu ● ISSN 1589 1623 (Print) ● ISSN 1785 0037 (Online)
DOI: http://dx.doi.org/10.15666/aeer/1706_1375913776

where $r_{a\ wet}$ is ra computed for the roughness and stability conditions of the wet pixel; $\rho_{air\ wet}$ is ρ_{air} calculated at the wet pixel.

The distribution of dT is obtained by extracting the information regarding the dry and wet pixels (de la Fuente-Sáiz et al., 2017). The values for a and b in *Equation 5* are estimated from these two pairs of dT and associated $T_{s,adtum}$.

$$a = \frac{dT_{dry} - dT_{wet}}{T_{s,adtum,dry} - T_{s,adtum,wet}} \quad \text{(Eq.9)}$$

$$b = dT_{dry} - aT_{s,adtum,dry} \quad \text{(Eq.10)}$$

(4) Surface parameters

Surface parameters contain α, ε, NDVI, T_s and Momentum roughness length (Z_{om}) which are crucial in the atmospheric-surface interaction and consequently affect the ET estimation. Among them, α is computed by integrating band reflectance within the short-wave spectrum using a weighting function (Allen et al., 2007); ε is computed using an empirical equation (Tasumi, 2003); NDVI is the ratio of the differences in reflectivity for the near-infrared band and red band to their sum (Allen et al., 2007); T_s is computed the single window algorithm proposed by Qin (Qin et al., 2010); Z_{om} for each image is specified by the corresponding NDVI (Allen et al., 2007).

(5) Long-time scale of the daily evapotranspiration

In addition, it is assumed that the instantaneous ET ratio (EF_{inst}, $EF_{inst} = \mathrm{LE_{inst}}/(R_n\text{-}G)_{\mathrm{inst}}$) is equal to the daily ET ratio (EF_d, $EF_d = \mathrm{LE_d}/(R_n\text{-}G)_{\mathrm{d}}$), when the instantaneous ET is used to calculate the daily ET ($\mathrm{ET_d}$) (Bastiaanssen et al., 1998a, b). In this study, in order to estimate long-time scale of the daily ET, the daily reference ET ratio ($\mathrm{ET_rF}$ is the ratio between $\mathrm{ET_d}$ and daily $\mathrm{ET_0}$, $\mathrm{ET_rF} = \mathrm{ET_d}/\mathrm{ET_0}$) of the eight DOYs were calculated, and the crop growth season was divided into seven intervals (*Table 1*). Each interval consisted of two DOYs of effective sunshine satellite images. Thereafter, by assuming that the $\mathrm{ET_rF}$ change between two adjacent effective sunshine days is linearly correlated with the DOY, interpolation was used to calculate the daily ET during the period:

$$ET_{d,DOY} = (c \times DOY + d) \times ET_{0,DOY} \quad \text{(Eq.11)}$$

$$c = \frac{ET_r F_n - ET_r F_m}{DOY_n - DOY_m} \quad \text{(Eq.12)}$$

$$d = ET_r F_n - c \times DOY_n \quad \text{(Eq.13)}$$

where c and d are constants; $\mathrm{ET_{d,DOY}}$ and $\mathrm{ET_{0,DOY}}$ are the daily ET and $\mathrm{ET_0}$ between two adjacent effective sunshine days respectively; and $\mathrm{ET_rF_n}$ and $\mathrm{ET_rF_m}$ are the $\mathrm{ET_rF}$ when the DOY is n and DOY is m, respectively (DOY_n: 278,262,254,222,214,142,134; DOY_m: 262,254,222,214,142,134,102).

http://www.aloki.hu ● ISSN 1589 1623 (Print) ● ISSN 1785 0037 (Online)
DOI: http://dx.doi.org/10.15666/aeer/1706_1375913776

Evapotranspiration of silage maize at irrigation monitoring stations by the METRIC model

The evapotranspiration of silage maize consumed by the crops were calculated using the water balance method as follows (Kang, 2007):

$$ET_{IMS} = P_a + I - L + K - \Delta W \quad \text{(Eq.14)}$$

where ET_{IMS} is the ET value of IMS; P_a is the effective precipitation; I denotes irrigation; L is the amount of deep leakage; and K is the groundwater recharge amount. Because of the fact that the buried depth of the groundwater was greater than 3 m, as per the observations of a buried negative pressure meter, groundwater recharge was observed to be minimal; therefore, $K \approx 0$. ΔW represents the variation in planned soil moisture layer during the growth cycle of silage maize. All the above parameters are in units of mm (*Fig. 2a*).

Groundwater consumption for irrigated artificial grasslands

Each irrigated artificial grassland is regarded as an independent land unit. According to the "one piece of sky corresponding to one piece of land," a land unit is divided into three spatial structure components: atmosphere, irrigated artificial grasslands, and groundwater. The inflow of water to irrigated artificial grasslands during the crop growth season includes P_a from the atmosphere, and K and I from groundwater. Water consumed by irrigated artificial grasslands includes ET from irrigated artificial grasslands to the atmosphere, and L from the irrigated artificial grasslands to groundwater. It is considered that the local groundwater supplements the unsaturated zone of the irrigated artificial grasslands. This water is still stored in the irrigated artificial grasslands; thus, it is classified as internal consumption of local water resources. The rest of the water separates from the irrigated artificial grasslands by ET, which is the net consumption and defined as the local groundwater consumption. From another perspective, for the amount of water consumed by the irrigated artificial grasslands on the underlying surface, and aside from the P_a supply of the atmosphere, the remainder of the water is sourced from groundwater. Therefore, GW is estimated using the difference between ET and P_a (*Fig. 2b*).

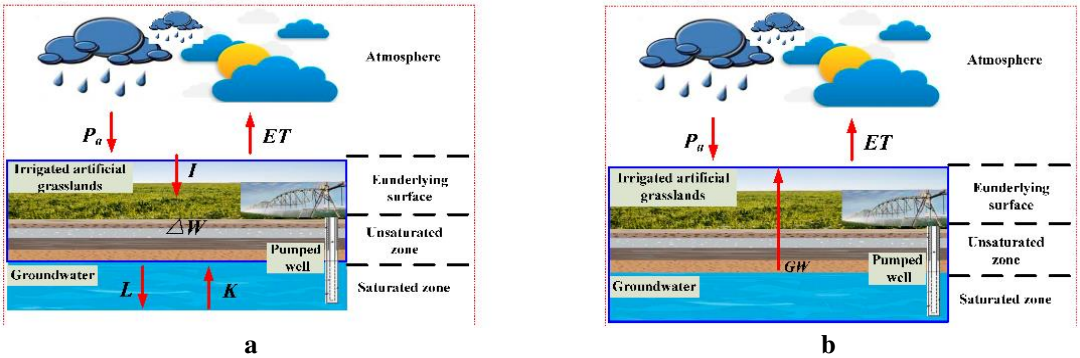

Figure 2. *Water balance for irrigated artificial grasslands: (a) evapotranspiration of silage maize based on water balance; (b) groundwater consumption for irrigated artificial grasslands based on water balance*

http://www.aloki.hu ● ISSN 1589 1623 (Print) ● ISSN 1785 0037 (Online)
DOI: http://dx.doi.org/10.15666/aeer/1706_1375913776

The GW was calculated using the water balance for irrigated artificial grasslands as follows:

$$GW = ET - P_a \quad \text{(Eq.15)}$$

$$P_a = \sum P_s \times \sigma \quad \text{(Eq.16)}$$

where P_s denotes a single rainfall; and σ is the effective precipitation coefficient, which is determined from the measured data. For areas without measured data, the following values can be referred to as: $\sigma = 0$ when $P_s < 5$ mm; $\sigma = 1.0$ when $5 < P_s \leq 50$ mm; $\sigma = 0.7$ - 0.8 when $P_s > 50$ mm (Kang, 2007).

The value of GW is the net groundwater consumption of the irrigated artificial grasslands in the Inner Mongolia typical steppe areas (*Fig. 2b*). By calculating the value of GW during the crop growth season, it is possible to visually reflect the amount of local water consumed by the irrigated artificial grasslands.

Comparison of ET_{METRIC} and ET_{IMS}

ET_{METRIC} was accurately estimated by computing the mean absolute error (MAE) and mean relative error (MRE). The values of MAE and MRE were computed as follows (Mayer and Butler, 1993):

$$MAE = \frac{\sum_{i=1}^{n} \left| ET_{METRIC} - ET_{IMS} \right|}{n} \quad \text{(Eq.17)}$$

$$MRE = \frac{1}{n} \sum_{i=1}^{n} \left| \frac{ET_{METRIC} - ET_{IMS}}{ET_{IMS}} \right| \times 100\% \quad \text{(Eq.18)}$$

where ET_{METRIC} is the estimated ET by the METRIC model; and n is the number of observations.

Results and discussion

Estimated accuracy of evapotranspiration by METRIC model

All the crops grown at the eight monitoring stations were silage maize, with an average growth period of 97 days. The irrigation methods included central pivot sprinkler irrigation (CPSI), drip irrigation (DI), low-pressure pipeline irrigation (LPPI), and semi-fixed irrigation (SFI). The average actual water consumption of silage maize during the growth period was determined to be 445.10 mm using *Equation 14*. The average value of ET_{METRIC} of silage maize in the eight stations during the growth period was determined to be 428.73 mm, in which MAE = 16.37 mm and MRE = 13.8%. By summarizing the previous research results, Kalma reviewed the various estimation methods of different remote sensing ET, and observed that when compared with the ground-based ET measurement value, the majority of the relative errors ranged from 15.0% to 30.0% (Kalma et al., 2008). Therefore, in this study it was believed that the accuracy of long-term scale ET estimation was reasonable and consistent with the

http://www.aloki.hu ● ISSN 1589 1623 (Print) ● ISSN 1785 0037 (Online)
DOI: http://dx.doi.org/10.15666/aeer/1706_1375913776

previous research related conclusions (Allen et al., 2011; Lian and Huang, 2015) (*Table 2*).

The estimation results summarized in *Table 2* show that the MRE of CPSI and DI is lower than that of SFI and LPPI by approximately 32.1% and the cause of this phenomenon was analyzed in this study. The ET_{METRIC} is the regional comprehensive water consumption of the underlying surface. Within the corresponding time period, the researchers randomly sampled the field water consumption data, and CPSI and DI was employed to reflect the actual situation of field water consumption more objectively than SFI and LPPI, because historical measured data are applied to confirm that the uniformity of CPSI and DI is better than that of SFI and LPPI. Therefore, ET_{IMS} by SFI and LPPI may not accurately reflect the regional comprehensive water consumption as CPSI and DI do.

Table 2. *Comparison of ET_{METRIC} and ET_{IMS} during the growth period of silage maize*

No.	Irrigation type	Growth cycle (DOY-DOY)	P_a (mm)	I (mm)	L (mm)	ΔW (mm)	ET_{IMS} (mm)	ET_{METRIC} (mm)	Absolute error (mm)	Relative error (%)
IMS1	CPSI	140-243	133.40	450.00	/	36.38	547.03	511.26	35.77	6.5
IMS2	CPSI	145-243	127.30	337.50	/	5.28	459.52	470.32	10.80	2.3
IMS3	CPSI	145-243	127.30	375.00	/	35.48	466.83	490.83	24.00	5.1
IMS4	CPSI	152-243	127.30	405.00	/	33.62	498.69	469.55	29.14	5.8
IMS5	CPSI	152-243	127.30	375.00	/	41.00	461.31	479.02	17.72	3.8
IMS6	DI	156-250	127.30	142.00	1.73	-10.54	278.11	308.53	30.42	10.9
IMS7	LPPI	145-243	127.30	90.00	/	-8.46	225.76	311.47	85.71	38.0
IMS8	SFI	145-243	127.30	495.00	/	-1.26	623.56	388.86	234.70	37.6

Evapotranspiration for irrigated artificial grasslands in the crop growth season

The value of ET for the irrigated artificial grasslands in the Xilin River Basin during the crop growth season varied from 241.99-741.55 mm, with an average of 611.42 mm, standard deviation of 80.73 mm, and daily average ET intensity of 4.0 mm d^{-1} (*Fig. 3a*). Because of the combined effects of climatic conditions, irrigation water volume, soil texture, vegetation cover, and other factors, the estimation of ET shows obvious spatial differentiation characteristics. For example, the water consumption in the CPSI areas were significantly higher than that in the surrounding areas that are not effectively irrigated (*Fig. 3b-e*).

Groundwater consumption for irrigated artificial grasslands and its law for different periods

Precipitation and effective precipitation for irrigated artificial grasslands

The values of P and P_a for the irrigated artificial grasslands, which were determined to be 207.18 mm and 153.46 mm in 2011, respectively (*Table 3*) were obtained from precipitation statistics of the seven weather stations. The Linxi County and Duolun County stations in the southeast part of the basin presented the greatest precipitation, while the Abag Banner station in the northwest part of the basin showed the least. P values during the crop growth season show a parabolic change of first increasing, and then decreasing, with the maximum appearing in July.

http://www.aloki.hu ● ISSN 1589 1623 (Print) ● ISSN 1785 0037 (Online)
DOI: http://dx.doi.org/10.15666/aeer/1706_1375913776

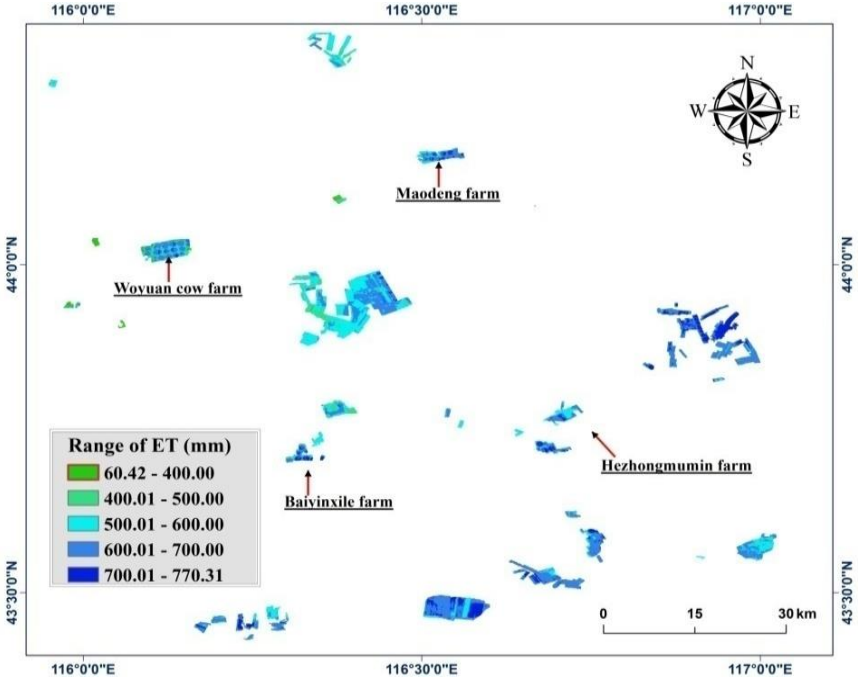

(a) ET_{METRIC} values for irrigated artificial grasslands

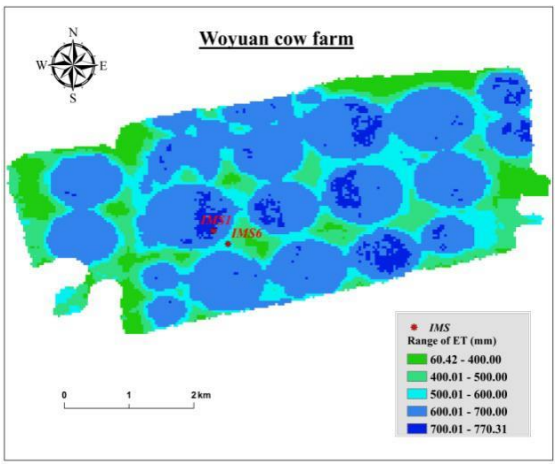

(b) ET_{METRIC} values of Woyuan cow farm

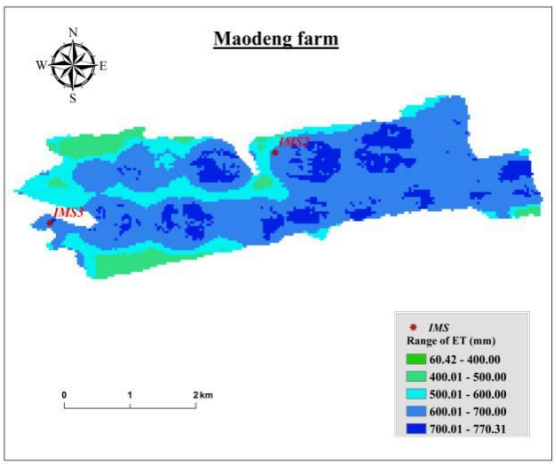

(c) ET_{METRIC} values of Maodeng farm

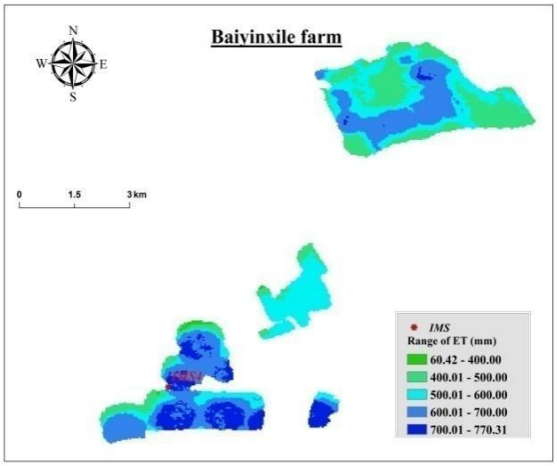

(d) ET_{METRIC} values of Baiyinxile farm

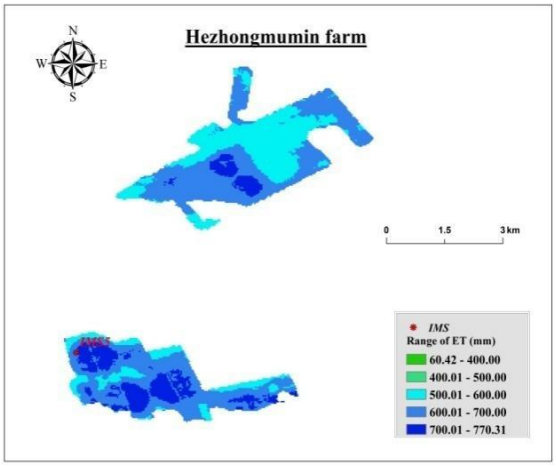

(e) ET_{METRIC} values of Hezhongmumin farm

Figure 3. *ET_{METRIC} values for irrigated artificial grasslands in the crop growth season*

http://www.aloki.hu ● ISSN 1589 1623 (Print) ● ISSN 1785 0037 (Online)
DOI: http://dx.doi.org/10.15666/aeer/1706_1375913776

Table 3. *Accumulation of precipitation and effective precipitation in the crop growth season in 2011*

Weather station (location)	P P_a	May (mm)	Jun. (mm)	Jul. (mm)	Aug. (mm)	Sep. (mm)	Accumulation (mm)
EastUjimqin Banner (116.97°E,45.52°N)	P	19.2	21.9	68.7	34.0	21.9	165.7
	P_a	6.1	16.0	51.0	22.5	13.2	108.8
Abag Banner (114.95°E,44.02°N)	P	23.0	30.2	50.5	4.9	10.2	118.8
	P_a	9.4	12.9	39.7	0.0	5.9	67.9
Huade County (114.00°E,1.90°N)	P	36.1	45.0	45.7	42.7	9.8	179.3
	P_a	32.6	26.1	21.8	37.6	0.0	118.1
WestUjimqin Banner (117.60°E,44.58°N)	P	29.2	27.7	230.2	4.3	7.9	299.3
	P_a	15.0	20.9	202.1	0.0	0.0	238.0
Xilinhot City (116.07°E,43.95°N)	P	23.9	57.1	77.2	18.1	3.6	179.9
	P_a	6.1	51.0	64.3	12.0	0.0	133.4
Linxi County (118.07°E,43.60°N)	P	10.5	58.4	263.8	31.9	12.6	377.2
	P_a	0.0	50.1	187.6	29.5	5.4	272.6
Duolun County (116.47°E,42.18°N)	P	25.9	75.7	83.8	19.4	16.4	221.2
	P_a	8.5	73.4	64.2	18.4	10.7	175.2

P and P_a of the irrigated artificial grasslands were calculated on the basis of the inverse distance weighted interpolation method (*Fig. 4*). The results indicate that the corresponding spatial distribution trend of precipitation decreases from southeast to northwest (*Fig. 4a*), which is consistent with the trend of precipitation statistics in China for many years (Huang et al., 2011; Sheng, 2017). Thus, it can be concluded that the interpolation results are valid.

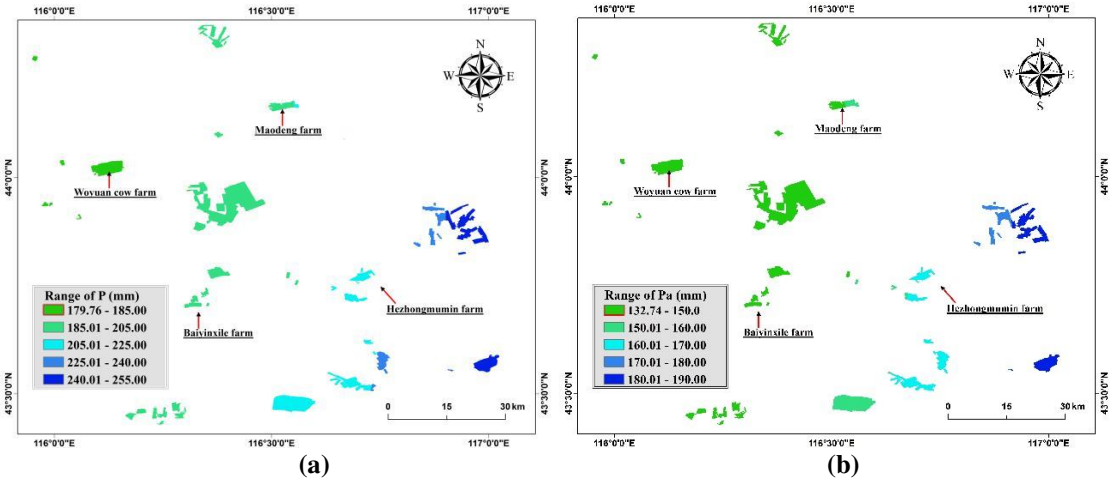

(a) **(b)**

Figure 4. *Precipitation and effective precipitation values of irrigated artificial grasslands in the crop growth season: (a) precipitation of irrigated artificial grasslands; (b) effective precipitation of irrigated artificial grasslands*

Groundwater consumption for irrigated artificial grasslands

The value of GW of the irrigated artificial grasslands during the crop growth season in 2011 was calculated to be 457.86 mm by using *Equation 15*. According to statistics,

http://www.aloki.hu ● ISSN 1589 1623 (Print) ● ISSN 1785 0037 (Online)
DOI: http://dx.doi.org/10.15666/aeer/1706_1375913776

the planted area of the irrigated artificial grasslands in 2011 was approximately 257.3 km^2, and the equivalent water volume was approximately 118 million m^3. In addition, it can be observed that at Woyuan cow farm, Maodeng farm, Baiyinxile farm, and Hezhongmumin farm, the value of GW of groundwater exceeded 400 mm (*Fig. 5b-e*). The local water consumption in these areas was significantly higher than other areas, making high water consumption areas.

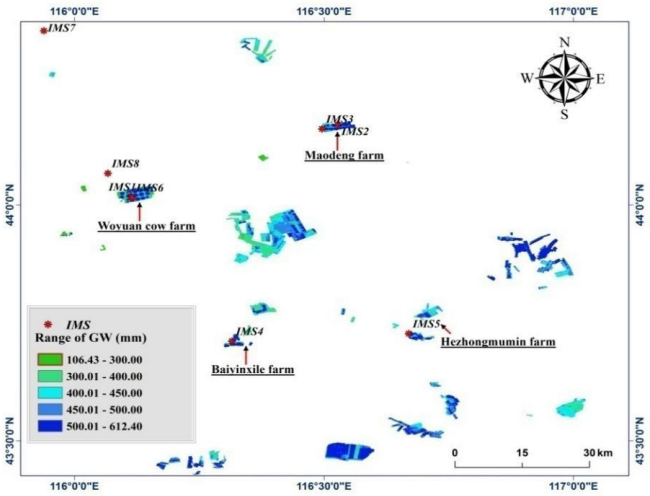

(a) GW values of Xilin River Basin

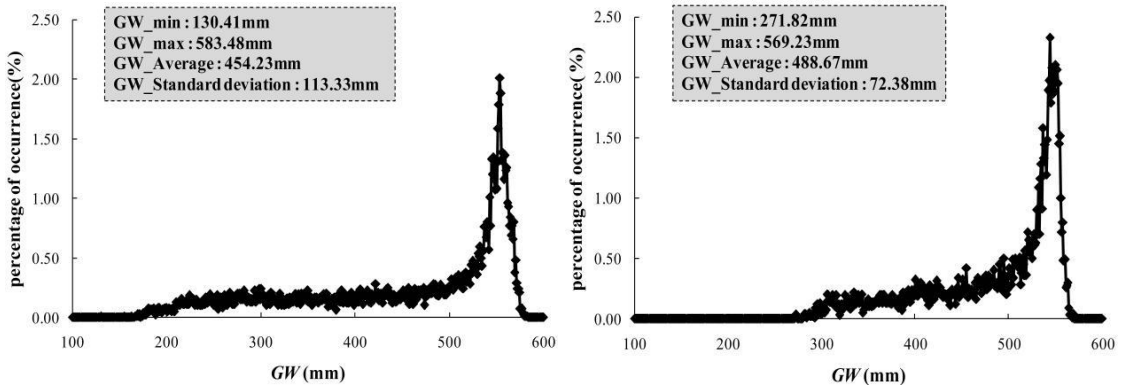

(b) GW values of Woyuan cow farm

(c) GW values of Maodeng farm

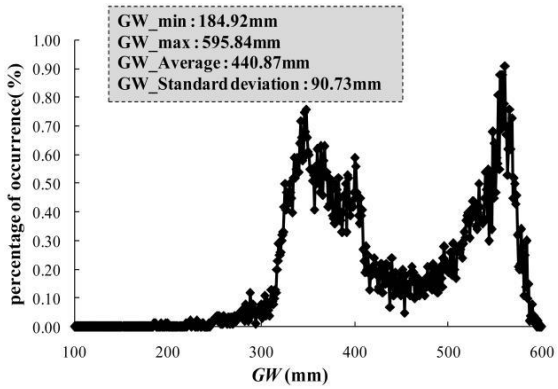

(d) GW values of Baiyinxile farm

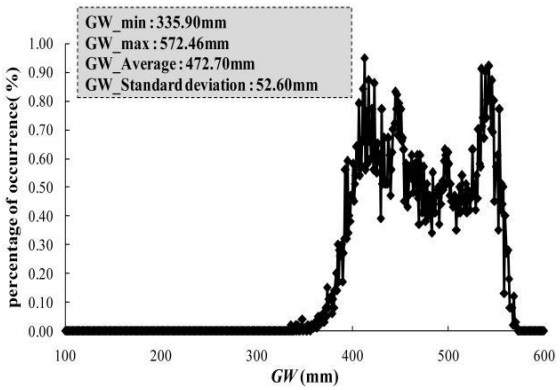

(e) GW values of Hezhongmumin farm

Figure 5. *Groundwater consumption values for irrigated artificial grasslands during the crop growth season*

http://www.aloki.hu ● ISSN 1589 1623 (Print) ● ISSN 1785 0037 (Online)
DOI: http://dx.doi.org/10.15666/aeer/1706_1375913776

Laws of groundwater consumption in different periods

The crop growth season of the irrigated artificial grasslands is divided into five periods by month, with an accumulated 153 days (*Table 4*). In accordance with the Landsat images and meteorological data, the values of ET, P_a, and GW in different periods were obtained (*Table 4; Fig. 6*).

Table 4. *Groundwater consumption of the irrigated artificial grasslands in different periods (all parameters are in units of mm)*

	May	**Jun.**	**Jul.**	**Aug.**	**Sep.**	**Accumulation**
DOY_m - DOY_n	121 - 151	152 - 181	182 - 212	213 - 243	244 - 273	153
*Avg.*ET	71.22	136.72	141.63	160.45	101.40	611.42
Avg.P_a	7.28	44.80	86.25	12.86	2.27	153.46
*Avg.*GW	63.94	91.92	55.38	147.59	99.13	457.96

*Avg.*ET, *Avg.*P_a, *Avg.*GW are calculated by average of ET_{METRIC} values, P_a values, GW values in the Xilin River Basin, respectively

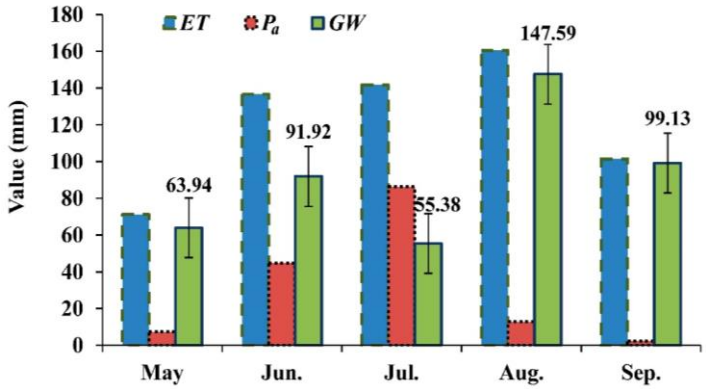

Figure 6. *Laws of groundwater consumption in different periods (all parameters are in units of mm)*

The values of ET_{METRIC} of the irrigated artificial grasslands during the crop growth season show a parabolic change of "first increasing, and then decreasing". With the increase in temperature, the value of ET is the maximum in July and August. The change in values of ET are highly consistent with the water consumption laws of crop growth (Tong et al., 2014). However, because of the influence of precipitation, the variation in the values of GW and ET change during different periods are significantly different, with details as follows: During the high-water consumption period of the crop growth season (July), precipitation is higher, while the values of GW of the irrigated artificial grasslands are relatively low. In addition, the value of precipitation in the study area is significantly lower in August, which results in the water consumption of the underlying surface being chiefly provided by regional groundwater resources, and the value of GW for the irrigated artificial grasslands is maximum. The above results show that the change in the values of GW are affected by not only the crop growth period on the underlying surface but also by weather factors such as precipitation, which cannot be ignored.

http://www.aloki.hu ● ISSN 1589 1623 (Print) ● ISSN 1785 0037 (Online)
DOI: http://dx.doi.org/10.15666/aeer/1706_1375913776

Conclusions

In this study, the METRIC model was used for estimating the regional ET of the irrigated artificial grasslands in the Inner Mongolia typical steppe areas. The results were verified through the water balance method of eight irrigation monitoring points, with an MRE = 13.8%. Combined with the previous remote sensing estimation of regional ET, the results show that the use of the METRIC model to estimate the ET of the Xilin River Basin, which is located in a typical steppe area, is reliable.

To analyze the consumption of local water resources, the spatial structure of the irrigated artificial grasslands are reclassified. The value of GW is introduced as the net consumption of local groundwater resources. Furthermore, the value of GW during the crop growth season in the Xilin River Basin is calculated. The crops planted over an area of 257.3 km^2 of the irrigated artificial grasslands consumed a total of 118 million m^3 of groundwater during the crop growth season. The net groundwater consumption of each of the farms, including that of Woyuan cow farm, Maodeng farm, Baiyinxile farm and Hezhongmumin farm, exceeded 400 mm. These areas with high water consumption face difficulties in water resource management, particularly when there is no external water supply**.**

The water consumption of the underlying surface of a typical steppe is complex, and has several influencing factors such as climate and anthropogenic influence. In addition, its characteristic laws are variable at different time scales. In order to determine the impact of irrigation artificial grasslands on local groundwater resources, future studies performed on GW should be conducted based on monitoring data of groundwater level.

Acknowledgements. This work was supported by the special fund of State Key Laboratory of Simulation and Regulation of Water Cycle in River Basin (Grant NO. SKL2018TS01), and China Institute of Water Resources and Hydropower Research (Grant NO. MK2016J09).

REFERENCES

[1] Allen, R. G., Pereira, L. S., Raes, D., Smith, M. (1998): Crop Evapotranspiration: Guidelines for Computing Crop Water Requirements. – FAO Irrigation and Drainage Paper No. 56. FAO, Rome.

[2] Allen, R. G., Tasumi, M., Morse, A., Trezza, R., Wright, J. L., Bastiaanssen, W., Kramber, W., Lorite, I., Robison, C. W. (2007a): Satellite-based energy balance for mapping evapotranspiration with internalized calibration (METRIC)—applications. – Journal of Irrigation and Drainage Engineering 133: 395-406.

[3] Allen, R. G., Tasumi, M., Trezza, R. (2007b): Satellite-based energy balance for mapping evapotranspiration with internalized calibration (METRIC)—model. – Journal of Irrigation and Drainage Engineering 133: 380-394.

[4] Allen, R. G., Pereira, L. S., Howell, T. A., Jensen, M. E. (2011): Evapotranspiration information reporting: I. Factors governing measurement accuracy. – Agricultural Water Management 98: 899-920.

[5] Allen, R. G., Burnett, B., Kramber, W., Huntington, J., Kjaersgaard, J., Kilic, A., Kelly, C., Trezza, R. (2013): Automated calibration of the METRIC-Landsat evapotranspiration process. – JAWRA Journal of the American Water Resources Association 49: 563-576.

[6] Bastiaanssen, W. G. M., Menenti, M., Feddes, R. A., Holtslag, A. A. M. (1998a): The surface energy balance algorithm for land (SEBAL). Part 1: Formulation. – Journal of Hydrology 212: 801-811.

http://www.aloki.hu ● ISSN 1589 1623 (Print) ● ISSN 1785 0037 (Online)
DOI: http://dx.doi.org/10.15666/aeer/1706_1375913776

[7] Bastiaanssen, W. G. M., Pelgrum, H., Wang, J., Ma, Y., Moreno, J. F., Roerink, G. J., Wal, D. T. V. (1998b): A remote sensing surface energy balance algorithm for land (SEBAL). Part 2: Validation. – Journal of Hydrology 212: 213-229.
[8] Batnasan, N. (2003): Freshwater issues in Mongolia. – Proceeding of the National Seminar on IRBM in Mongolia, Ulaanbaatar.
[9] Bowen, I. S. (1926): The ratio of heat losses by conduction and by evaporation from any water surface. – Physical Review 27: 779-787.
[10] Cai, X., Xu, Z., Su, B., Yu, W. (2009): Distributed simulation for regional evapotranspiration and verification by using remote sensing (in Chinese with English abstract). – Transactions of the Chinese Society of Agricultural Engineering 25: 154-160.
[11] Chen, S. (2002): Study the land use/land cover change and cycle of Xilin River Basin by remote sensing and GIS (in Chinese). – University of Chinese Academy of Sciences (the Institute of Remote Sensing Applications), Beijing.
[12] de la Fuente-Sáiz, D., Ortega-Farías, S., Fonseca, D., Ortega-Salazar, S., Kilic, A., Allen, R. (2017): Calibration of METRIC model to estimate energy balance over a drip-irrigated apple orchard. – Remote Sensing 9. https://doi.org/10.3390/rs9070670.
[13] French, A. N., Hunsaker, D. J., Thorp, K. R. (2015): Remote sensing of evapotranspiration over cotton using the TSEB and METRIC energy balance models. – Remote Sensing of Environment 158: 281-294.
[14] Gao, Y. C., Long, D., Li, Z. L. (2008): Estimation of daily actual evapotranspiration from remotely sensed data under complex terrain over the upper Chao River basin in North China. – International Journal of Remote Sensing 29: 3295-3315.
[15] González-Dugo, M., Gonzalez-Piqueras, J., Campos, I., Balbontín, C., Calera, A. (2012): Estimation of surface energy fluxes in vineyard using field measurements of canopy and soil temperature. – Remote Sensing and Hydrology (Proceedings of a symposium held at Jackson Hole, Wyoming, USA, September 2010) IAHS 352: 59-62.
[16] Howell, T. A., Schneider, A. D., Jensen, M. E. (1991): History of Lysimeter Design and Use for Evapotranspiration Measurements. – Lysimeters for Evapotranspiration and Environmental Measurements, ASCE, Honolulu, Hawaii, 23-25 July, pp. 1-9.
[17] Huang, Y., Feng, G. L., Dong, W. J. (2011): Temporal changes in the patterns of extreme air temperature and precipitation in the various regions of China in recent 50 years (in Chinese). – Acta Meteorologica Sinica 69: 125-136.
[18] Kalma, J. D., Mcvicar, T. R., Mccabe, M. F. (2008): Estimating land surface evaporation: a review of methods using remotely sensed surface temperature data. – Surveys in Geophysics 29: 421-469.
[19] Kang, S. Z. (2007): Conspectus of Agricultural Soil and Water Engineering (in Chinese). – Chinese Agricultural Press, Beijing.
[20] Khand, K., Kjaersgaard, J., Hay, C., Jia, X. (2017): Estimating impacts of agricultural subsurface drainage on evapotranspiration using the Landsat imagery-based METRIC model. – Hydrology 4. DOI: 10.3390/hydrology4040049.
[21] Lian, J., Huang, M. (2015): Evapotranspiration estimation for an oasis area in the Heihe River basin using Landsat-8 images and the METRIC model. – Water Resources Management 29: 5157-5170.
[22] Liou, Y.-A., Kar, S. (2014): Evapotranspiration estimation with remote sensing and various surface energy balance algorithms—a review. – Energies 7: 2821-2849.
[23] Long, D., Singh, V. P. (2013): Assessing the impact of end-member selection on the accuracy of satellite-based spatial variability models for actual evapotranspiration estimation. – Water Resources Research 49: 2601-2618.
[24] Lu, H. Y., Li, H. P., Gao, Z. Y., Wang, D. X., Wang, J. (2016): Water and land resources allocation model of pastoral area based on grassland ecological conservation (in Chinese with English abstract). – Transactions of the Chinese Society of Agricultural Engineering 32: 123-130.

http://www.aloki.hu ● ISSN 1589 1623 (Print) ● ISSN 1785 0037 (Online)
DOI: http://dx.doi.org/10.15666/aeer/1706_1375913776

[25] Lu, H. Y., Li, H. P., Wang, J., Gao, Z. Y. (2018): Regulation model and application for water-land-forage-livestock balance in pastoral areas (in Chinese with English abstract). – Transactions of the Chinese Society of Agricultural Engineering 34: 87-95.
[26] Mayer, D. G., Butler, D. G. (1993): Statistical validation. – Ecological Modelling 68: 21-32.
[27] Menenti M (1993): Parameteraization of Land Surface Evaporation by Means of Location Dependent Potential Evaporation and Surface Temperature Range. – In: Bolle, H.-J., Feddes, R. A., Kalma, J. D. (eds.) Exchange Processes at the Land Surface for a Range of Space and Time Scales. Proceedings of an International Symposium Held at Yokohama, Japan, 13-16 July. IAHS Press, Wallingford, UK.
[28] Monteith, J. L., Unsworth, M. H. (2013): Microclimatology of Radiation: (iii) Interception by Plant Canopies and Animal Coats. – In: Monteith, J. L., Unsworth, M. H. (eds.) Principles of Environmental Physics (4th Ed.). Academic Press, Boston, pp. 111-133.
[29] Morton, C. G., Huntington, J. L., Pohll, G. M., Allen, R. G., McGwire, K. C., Bassett, S. D. (2013): Assessing calibration uncertainty and automation for estimating evapotranspiration from agricultural areas using METRIC. – JAWRA Journal of the American Water Resources Association 49: 549-562.
[30] Niu, S. L., Jiang, G. M. (2004): Function of artificial grassland in restoration of degraded natural grassland and its research advance (in Chinese). – Chin. J. Appl. Ecol. 15: 1662-1666.
[31] Norman, J. M., Kustas, W. P., Humes, K. S. (1995): Source approach for estimating soil and vegetation energy fluxes in observations of directional radiometric surface temperature. – Agricultural and Forest Meteorology 77: 263-293.
[32] Numata, I., Khand, K., Kjaersgaard, J., Cochrane, M., Silva, S. (2017): Evaluation of Landsat-based METRIC modeling to provide high-spatial resolution evapotranspiration estimates for Amazonian forests. – Remote Sensing 9: 46.
[33] Paço, T. A., Pôças, I., Cunha, M., Silvestre, J. C., Santos, F. L., Paredes, P., Pereira, L. S. (2014): Evapotranspiration and crop coefficients for a super intensive olive orchard. An application of SIMDualKc and METRIC models using ground and satellite observations. – Journal of Hydrology 519: 2067-2080.
[34] Pedro-Monzonís, M., Solera, A., Ferrer, J., Estrela, T., Paredes-Arquiola, J. (2015): A Review of water scarcity and drought indexes in water resources planning and management. – Journal of Hydrology 527: 482-493.
[35] Qin, Z., Karnieli, A., Berliner, P. (2010): A mono-window algorithm for retrieving land surface temperature from Landsat TM data and its application to the Israel-Egypt border region. – International Journal of Remote Sensing 22: 3719-3746.
[36] Rana, G., Katerji, N. (2000): Measurement and estimation of actual evapotranspiration in the field under Mediterranean climate: a review. – European Journal of Agronomy 13: 125-153.
[37] Reyes-González, A., Kjaersgaard, J., Trooien, T., Hay, C., Ahiablame, L. (2017): Comparative analysis of METRIC model and atmometer methods for estimating actual evapotranspiration. – International Journal of Agronomy 2017: 1-16.
[38] Roerink, G. J., Su, Z., Menenti, M. (2000): S-SEBI: A simple remote sensing algorithm to estimate the surface energy balance. – Physics and Chemistry of the Earth, Part B: Hydrology, Oceans and Atmosphere 25: 147-157.
[39] Sheng, X. (2017): Handbook of Characteristic Values of Rivers and Lakes in Inner Mongolia Autonomous Region (in Chinese). – Inner Mongolia University Press, Inner Mongolia, China.
[40] Spiliotopoulos, M., Holden, N. M., Loukas, A. (2017): Mapping evapotranspiration coefficients in a temperate maritime climate using the METRIC model and Landsat TM. – Water 9: 23.

http://www.aloki.hu ● ISSN 1589 1623 (Print) ● ISSN 1785 0037 (Online)
DOI: http://dx.doi.org/10.15666/aeer/1706_1375913776

[41] Su, Z. (2002): The surface energy balance system (SEBS) for estimation of turbulent heat fluxes. – Hydrology & Earth System Sciences 6: 85-99.
[42] Su, Z., Yacob, A., Wen, J., Roerink, G., He, Y., Gao, B., Boogaard, H., van Diepen, C. (2003): Assessing relative soil moisture with remote sensing data: theory, experimental validation, and application to drought monitoring over the North China Plain. – Physics and Chemistry of the Earth, Parts A/B/C 28: 89-101.
[43] Taherparvar, M., Pirmoradian, N. (2018): Estimation of rice evapotranspiration using reflective images of Landsat satellite in Sefidrood irrigation and drainage network. – Rice Science 25: 111-116.
[44] Talsma, C. J., Good, S. P., Jimenez, C., Martens, B., Fisher, J. B., Miralles, D. G., McCabe, M. F., Purdy, A. J. (2018): Partitioning of evapotranspiration in remote sensing-based models. – Agricultural and Forest Meteorology 260-261: 131-143.
[45] Tasumi, M. (2003): Progress in operational estimation of regional evapotranspiration using satellite imagery. – Thesis (Ph.D.), University of Idaho, USA.
[46] Thornthwaite, C. W. (1948): An approach toward a rational classification of climate. – Geographical Review 38: 55-94.
[47] Tong, C., Wu, J., Yong, S., Yang, J., Yong, W. (2004): A landscape-scale assessment of steppe degradation in the Xilin River basin, Inner Mongolia, China. – Journal of Arid Environments 59: 133-149.
[48] Tong, C. F., Li, H. P., Bai, B., Zheng, H. X., Wang, J., Yang, Y. S., Miao, H. L. (2014): Study on water requirement rule and optimization irrigation quota of alfalfa in Xilin River basin (in Chinese). – Chinese Agricultural Science Bulletin 2014(29): 188-191.
[49] Trezza, R., Allen, R. G., Tasumi, M. (2013): Estimation of Actual evapotranspiration along the middle Rio Grande of New Mexico using MODIS and Landsat imagery with the METRIC model. – Remote Sensing 5: 5397-5423.
[50] Wright, J. L. (1982): New evapotranspiration crop coefficients. – Journal of the Irrigation & Drainage Division 108: 57-74.
[51] Xu, D., Liu, Y., Yang, D., Zhang, B. Z. (2015): Evapotranspiration scale effect and temporal-spatial scale expansion (in Chinese). – Science China Press, Beijing.
[52] Yamanaka, T., Kaihotsu, I., Oyunbaatar, D., Ganbold, T. (2007): Summertime soil hydrological cycle and surface energy balance on the Mongolian steppe. – Journal of Arid Environments 69: 65-79.
[53] Yang, D., Chen, H., Lei, H. (2010): Estimation of evapotranspiration using a remote sensing model over agricultural land in the North China Plain. – International Journal of Remote Sensing 31: 3783-3798.
[54] Zamani Losgedaragh, S., Rahimzadegan, M. (2018): Evaluation of SEBS, SEBAL, and METRIC models in estimation of the evaporation from the freshwater lakes (case study: Amirkabir dam, Iran). – Journal of Hydrology 561: 523-531.

http://www.aloki.hu ● ISSN 1589 1623 (Print) ● ISSN 1785 0037 (Online)
DOI: http://dx.doi.org/10.15666/aeer/1706_1375913776

NITROUS OXIDE EMISSION AND PRODUCTION PATHWAYS UNDER ALTERNATE WETTING-DRYING CONDITIONS IN RICE PADDY SOILS

ABID, A. A.[1] – ZHANG, Q.[1,2*] – AFZAL, M.[1] – DI, H.[1]

[1]*Zhejiang Provincial Key Laboratory of Agricultural Resources and Environment, Key Laboratory of Environment Remediation and Ecological Health, Ministry of Education, Zhejiang University, Hangzhou 310058, P. R. China*

[2]*College of Environmental and Resource Sciences, Zhejiang University, Hangzhou, 310058, P. R. China*

**Corresponding author*
e-mail: qczhang@zju.edu.cn; phone: +86-571-8898-2413

(Received 5th May 2019; accepted 28th Aug 2019)

Abstract. The aim of this study was to evaluate the relative contributions of nitrification and denitrification in rice paddy soils under various water events. A laboratory incubation study was conducted in China to quantify N_2O production during alternate wetting and drying cycle (AWD) versus permanent flooding (PF). The soils were treated with long-term chemical fertilizer (CF); chemical fertilizer plus pig manure (PMCF); and chemical fertilizer plus rice straw (SRCF) for 5 years. The results showed that N_2O flux during AWD was consistently higher than PF. The highest N_2O flux during AWD was 1.94 mg m^{-2} h^{-1}. The PMCF and SRCF soils had higher N_2O emissions compared to CF and CK soils. Ammonia oxidizer community peaks were found at 60% field capacity (FC) ($p < 0.0001$), while, for denitrifier, this increase was maintained for a certain period of time (10d) and then started to decrease. Autotrophic nitrification appeared to be an important and dominant process of N_2O emissions during AWD and PF, contributed 79.03% of N_2O emissions during AWD, while 36.53% during PF. Thus, the results concluded that under AWD event the addition of pig manure and rice straw plus chemical fertilizer significantly increased the N_2O flux, by stimulating the growth of microbial communities.
Keywords: *N_2O, flux, water events, pig manure, rice straw, ^{15}N stable isotopes*

Introduction

Ecosystems are adversely affected by the global warming if actions to mitigate it are not taken. Besides industrial emissions, biological processes can also contribute to the greenhouse gas emissions (GHG), especially nitrous oxide (N_2O). N_2O is an important greenhouse gas and its concentration in the atmosphere is comparatively lower than CO_2 concentration but its global warming potentials (GWP) is relatively 265 times higher over 100 years than that of CO_2 (IPCC, 2013). Agricultural soils contribute about 60% to anthropogenic N_2O emissions which is mainly due to fertilizer application (Charles et al., 2017; Liu et al., 2017). Fertilization of agricultural soils is considered to be an important source of N_2O emissions, which contributes about 13-24% of annual emissions (IPCC, 2007). Among these agricultural soils, rice paddy soils are considered to be a main source of N_2O emissions. Rice is a staple food for half of the world's population and approximately 155 million ha. is grown annually, around the globe (Abid et al., 2018).

Alternating wetting and drying (AWD) practice is a common practice which is being used to save water in rice fields. AWD reduce water use by 23-33% in rice paddy soils (Carrijo et al., 2017). It has been used in many countries such as Philippines (Belder et

http://www.aloki.hu ● ISSN 1589 1623 (Print) ● ISSN 1785 0037 (Online)
DOI: http://dx.doi.org/10.15666/aeer/1706_1377713792

al., 2004), China (Cabangon et al., 2004) and Japan (Chapagain and Yamaji, 2010). The AWD practice has been found to give higher or equal rice yield (Zhang et al., 2009) compared to conventional practice, i.e. continuous flooding practice, where surplus of N_2O is produced during this process (Peng et al., 2011). However, the underlying causes, e.g. microbial mechanisms of N_2O emissions are generally unknown.

Nitrous oxide is mainly emitted by nitrification and denitrification processes (Wrage et al., 2001), and both processes may occur in soil simultaneously (Abbasi and Adams, 2000; Garrido et al., 2002; Webster and Hopkins, 1996). To what extent each of these processes contributes to the N_2O emissions in the rice during AWD and permanent flooding (PF) are not fully understood. This is mainly attributed to oxygen content of the soil, and further estimation of water filled pore space (WFPS) has been considered as a major influencing factor. Nitrogen stable isotopes with acetylene (C_2H_2) can offer a precise information about nitrogen cycle in ecosystems (Ostrom et al., 2002). It is of interest to use ^{15}N as a tracer because a negligible isotope fractionation is being used as a tracer during biological processes. Acetylene (C_2H_2) inhibits NH_3^+ oxidation at low concentration (10 Pa) and start to inhibit N_2O reductase at high concentration (10 kPa) during denitrification (Berg et al., 1982). Also, C_2H_2 may inhibit NH_4^+ oxidation by autotrophs but inhibition by heterotrophic nitrifiers is not documented (Moir et al., 1996; Hynes and Knowles, 1982; Daum et al., 1998). Recently, stable isotope signatures coupled with C_2H_2 (10 Pa; 0.01% v/v) are being used to estimate N_2O source and relative contributions of denitrification, heterotrophic nitrification and autotrophic nitrification processes in soil (Baggs et al., 2003; Stevens et al., 1997).

The obvious benefits of implementing AWD strategy are to save irrigation water and reduce CH_4 emissions. On the other hand, the combined effect of long term fertilization and AWD on N_2O is still inconclusive. Also, the N_2O production source during AWD and PF events is still poorly understood. Therefore, the objectives of the present study were: (1) to determine the potential of AWD to produce N_2O from rice paddies as compared to the normal practice of rice (PF); (2) to determine the effect of long term organic (PMCF, SRCF) and inorganic (CF) fertilizers along with different water events (AWD, PF) on N_2O gas emissions; and (3) to quantify the contribution of different processes (nitrification, denitrification) to N_2O emissions under AWD and PF related to long term fertilization, using ^{15}N stable isotopes in combination with C_2H_2.

Materials and methods

Soil sampling site

A long-term fertilized experiment (LTFE) was conducted from 2010 to 2014 and soil samples were collected. This site was located in Jintan county, Jiangsu province, China (120° 0' 41" East, 29° 57' 9" North). The annual mean precipitation and temperature of study area are 1452.5 mm and 16.27 °C, respectively. A rice paddy field was selected with 5-yr canola-rice rotation history. The soil samples were grouped into four treatment groups, including no fertilization (CK), 100% chemical fertilization (CF: N 314 kg ha^{-1}, P_2O_5 31.5 kg ha^{-1}, K_2O 153 kg ha^{-1}), pig manure compost plus 50% chemical fertilization (PMCF: Pig manure 6000 kg ha^{-1} + N 157 kg hm^{-2}, P_2O_5 31.5 kg ha^{-1}, K_2O 153 kg ha^{-1}) and rice straw plus 50% chemical fertilization (SRCF: rice straw 6000 kg ha^{-1} + N 157 kg ha^{-1}, P_2O_5 31.5 kg ha^{-1}, K_2O 153 kg ha^{-1}). Just after the rice harvested in 2014, five soil cores were collected at a depth of 15 cm from three replicates of each treatment and five hundred grams of soils were packed. The soil cores

http://www.aloki.hu ● ISSN 1589 1623 (Print) ● ISSN 1785 0037 (Online)
DOI: http://dx.doi.org/10.15666/aeer/1706_1377713792

were put in sterile plastic bags, zipped and transported to the laboratory and stored at 4 °C. Each replicated sample was divided and one sub sample was air-dried and sieved through a 2.0 mm for subsequent chemical analysis and another sub sample was incubated under different dry and wet conditions.

Incubation design

The incubation was carried out at 25 °C with two water events including: (a) alternating with 7 days continuous flooding followed by 7 days of air-drying (AWD); (b) permanent flooding for 14 days (PF). The detailed methodology of the incubation experiment was as follows (*Fig. 1*). Two hundred g of soil collected from CK, CF, PMCF and SRCF treatments were put in 1000 mL glass pots and to make flooding conditions additional water was added. For AWD, soils were incubated as flooded for 7 days, with gas and soil samples were collected after 1 and 7 days of flooding incubation (100%FC, 1 d; 100%FC, 7 d). Then the water was removed to reach 80% field capacity (80%FC, 10 d) and 60% field capacity (60%FC, 14 d), samples were also collected at 80%FC, 10 d and 60%FC, 14 d). For PF, the same treatments were incubated with flooded conditions for 14 d and gas and soil samples were collected after 1, 7, 10 and 14 d. Headspace gas samples were collected after 1, 7, 10 and 14 d immediately after closing the jars and 30 min later using a hypodermic needle and a polypropylene syringe. These gas samples were used to analyze the isotopic ^{15}N-N_2O. N_2O was calculated using GC 2010 plus (Shimadzu).

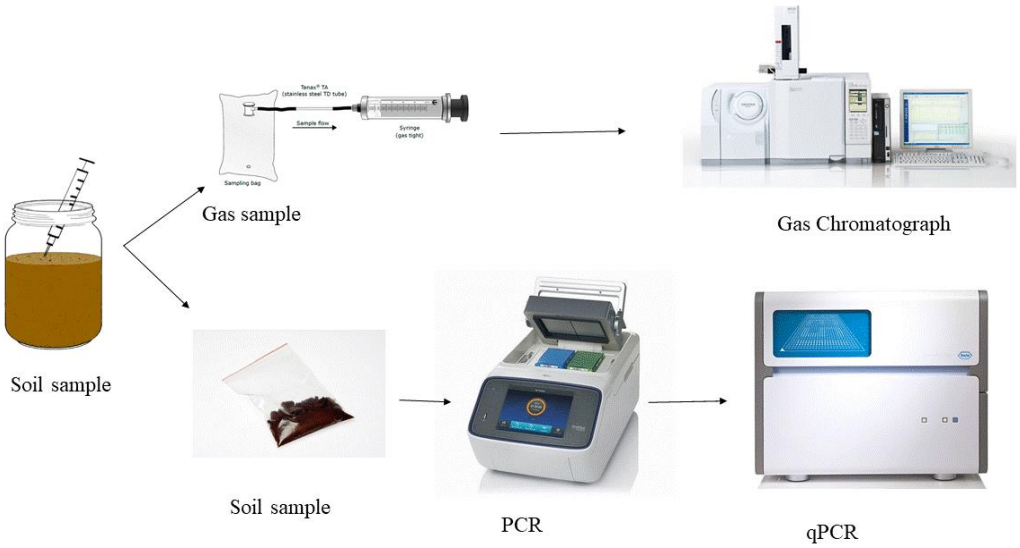

Figure 1. *Schematic diagram of whole study plan*

After 14 days of incubation, all soils were treated with (a) $^{14}NH_4{}^{15}NO_3$, (b) $^{15}NH_4{}^{15}NO_3$, (c) $^{15}NH_4{}^{15}NO_3 + C_2H_2$ (0.01% v/v), and (d) no N addition. $^{14+15}N$ was applied at 200 mg total N m^{-2} (20% atom % excess ^{15}N) combined with C_2H_2 (10 Pa) (*Table 1*). Additional water was added to achieve the desired moisture contents (flooding). Also, three replicates of each treatment was created for gas analyses. To create gas-tight incubations, the lids of the jars were then closed. Five ml (1% v/v in air) of C_2H_2 gas was injected to the headspace of a further three replicates of the $^{15}NH_4{}^{15}NO_3$ fertilizer treatments (treatment c) (*Table 1*) to make a final concentration of

http://www.aloki.hu ● ISSN 1589 1623 (Print) ● ISSN 1785 0037 (Online)
DOI: http://dx.doi.org/10.15666/aeer/1706_1377713792

0.01% (v/v) which was considered sufficient to inhibit oxidation of NH_3^+ (Bateman and Baggs, 2005). Five days after fertilizer additions, the jars were opened because inhibition continued for about 3 days after 0.01% (v/v) C_2H_2 addition, and there was no effect of jars opening on trace gas production (Bateman and Baggs, 2005). Seven days after fertilizer addition, 20 ml gas samples were collected at 0 and 30 min after closing the glass jars from each treatment using poly-pyrine syringe. The ^{15}N was analyzed using isotope ratio mass spectrometer (Europa PDZ 20:20).

Table 1. *Outline of the ^{15}N fertilizer and C_2H_2 inhibition treatments used to estimate the contribution of denitrification and autotrophic and heterotrophic nitrification to ^{15}N-N_2O emissions*

Treatment	Source of ^{15}N-N_2O
(a) $^{14}NH_4{}^{15}NO_3$	Denitrification
(b) $^{15}NH_4{}^{15}NO_3$	Denitrification and nitrification (autotrophic and heterotrophic)
(c) $^{15}NH_4{}^{15}NO_3$ + C_2H_2(0.01% v/v)	Denitrification and heterotrophic nitrification
(d) (c) minus (a)	Heterotrophic nitrification

q-PCR to determine the abundance of nitrifiers and denitrifiers

After 1, 7, 10 and 14 d of different water application, soil samples were collected and 0.5 g sampled soil was used to extract DNA using TAKARA DNA standard protocol. Nano drop technology was also used to quantify DNA (Nano Drop Technologies, Wilmington, DE, USA). Real time quantitative PCR was used to quantify the abundance of denitrifier (*nirS, nir*K) and nitrifier (AOA *amo*A, AOB *amo*A) communities. Serial dilutions of linearized plasmids were used to produce standard curves by using cloned AOA, AOB, *nirS* and *nir*K genes amplified from denitrifying and nitrifying strains. The cloning kit (V007 TsingKe China) was used to prepare standard (www.tsingke.net). The qPCR primers sets used to target desired genes are indicated in *Table 2*. A reaction mixture of 20 μL containing 1 μL target gene primer, SYBR Premix 10 μL, total DNA template 1 μL, and deionized distilled water to make final volume 20 μL. The copy number of these plasmids was directly calculated based on the concentrations and lengths (base pairs) of them. The copy number of the target genes in unknown soil DNA were analyzed by comparing with their reactive standard curves.

Table 2. *Real-time PCR primer sets, conditions of the assay*

Target gene base pairs		Primer	Nucleotide sequence (5'-3')	Annealing temperature and time	Reference
Bacterial *amo*A	491 bp	amoA-1F amoA-2R	GGGGTTTCTACTGGTGGT CCCCTCKGSAAAGCCTTCTTC	55 °C for 45 s	Rotthauwe et al., 1997
Archaeal *amo*A	635 bp	amoAF amoAR	STAATGGTCTGGCTTAGACG GCGGCCATCCATCTGTATGT	53 °C for 45 s	Francis et al., 2005
nirK	472 bp	F1aCu R3Cu	ATCATGGTSCTGCCGCG GCCTCGATCAGRTTGTGGTT	63 °C for 30 s	Hallin and Lindgren, 1999
nirS	425 bp	Cd3aF R3 Cd	GTSAACGTSAAGGARACSGG GASTTCGGRTGSGTCTCTTGA	57 °C for 30 s	Throbäck et al., 2004

http://www.aloki.hu ● ISSN 1589 1623 (Print) ● ISSN 1785 0037 (Online)
DOI: http://dx.doi.org/10.15666/aeer/1706_1377713792

Statistical analysis

SPSS 16.0 package was used to perform all statistical (SPSS, Chicago, IL, USA). One way analysis of variance (ANOVA) test was used to analyze significant differences among different treatments. ANOVA, followed by the least significant difference (LSD) test, in which $P < 0.05$ was considered statistically significant. Also, Duncan's Multiple Range Test was used to determine significant mean differences. Correlation analysis was performed to analyze the correlation between variables. All results were accepted at significant probability 0.05.

Results

N_2O gas emission

Nitrous oxide (N_2O) fluxes of the incubated soils showed different trends during AWD and PF events (*Fig. 2*). N_2O flux increased with reducing moisture contents over time during AWD. N_2O emitted over 14 days (60% FC) was significantly higher ($P < 0.001$) throughout the experiment during AWD than PF. While comparing fertilizer treatments, the highest emissions were recorded from SRCF (1.88 mg m^{-2} h^{-1}) and PMCF (1.34 mg m^{-2} h^{-1}) over 14 days, which were 12 and 20 times greater than those over 10 days and 7 days of AWD, respectively. N_2O emissions from fertilized soils decreased after one day throughout trial period but were greater than unfertilized controls. The highest fluxes were measured at 60% FC over 14 days. In the CK and CF treatments, N_2O fluxes were minimal over 1 day which was 0.02 and 0.01 mg m^{-2} h^{-1}, while the treatments of PMCF and SRCF showed slightly higher N_2O emissions, ranging from 0.12 to 0.28 mg m^{-2} h^{-1} with same moisture contents. No significant differences were observed in total N_2O produced over 1 day and 7 days of flooded conditions. During AWD, the emissions of N_2O increased when exposed to air-drying conditions after continuous flooding over one week. While During PF, the fluxes significantly decreased with time and the lowest fluxes were measured over 14 days of continuous flooding ($P < 0.0001$).

Sources of N_2O

Labelling of ^{15}N is the only way to differentiate N pool, as a possible substrate for N_2O production. N_2O emitted from C_2H_2 treatments could be produced either by heterotrophic nitrification or denitrification (treatment c), and ^{15}N-N_2O production from $^{14}NH_4{}^{15}NO_3$ (treatment a) could be produced by denitrification (*Table 1*). The difference in the emissions of ^{15}N-N_2O between the $^{14}NH_4{}^{15}NO_3$ (treatment a) and $^{15}NH_4{}^{15}NO_3$ (treatment b) was attributed to nitrification, and the difference in the emissions of ^{15}N-N_2O between $^{14}NH_4{}^{15}NO_3$ (treatment a) and $^{15}NH_4{}^{15}NO_3 + C_2H_2$ (treatment c) was used to quantify heterotrophic nitrification. Results of the present study showed relatively higher ^{15}N-N_2O emissions were measured during AWD than PF (*Fig. 3*) but this relation was not significant. The total ^{15}N-N_2O emissions were recorded during AWD condition in PMCF and SRCF treatments (0.23, 0.24 mg m^{-2} h^{-1}), which were significantly higher than CK and CF treatments. ^{15}N-N_2O emissions during 60% FC in the presence of C_2H_2 were significantly lower than the other treatments, indicating autotrophic nitrification as main contributor to N_2O emissions (*Table 2*). In the presence of C_2H_2, N_2O produced was accredited to denitrification and/or heterotrophic nitrification. A strong significant positive correlation was found between autotrophic nitrification nitrous oxide production,

http://www.aloki.hu ● ISSN 1589 1623 (Print) ● ISSN 1785 0037 (Online)
DOI: http://dx.doi.org/10.15666/aeer/1706_1377713792

indicating autotrophic nitrification as a predominant ^{15}N-N_2O source during both AWD and PF ($P < 0.01$, $R^2 = 0.77$) (*Table 3; Fig. 4*). The maximum N_2O production from autotrophic nitrification was 0.19 mg N m^{-2} h^{-1} during AWD. Between 57 and 72% of N_2O production during both AWD and PF emitted from autotrophic nitrification in all fertilized treatments and significantly higher compared to CK. The mean ^{15}N-N_2O emissions during AWD were 0.89 mg N m^{-2} h^{-1}, contributing 79% by autotrophic nitrification, while during PF, the N_2O emissions were 0.13 mg N m^{-2} h^{-1}, and 52% was contributed by denitrification and 36% by autotrophic nitrification (*Table 4*).

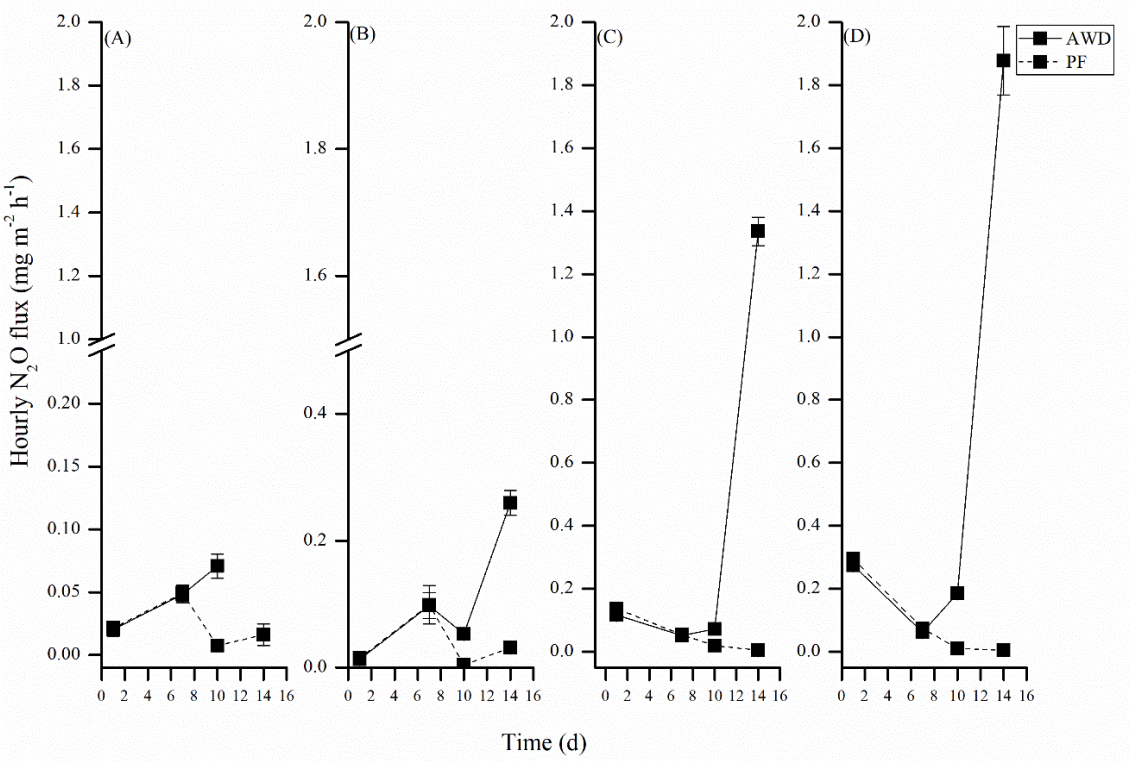

Figure 2. *Hourly N_2O emission (mg m^{-2} h^{-1}) from (A) CK, (B) CF, (C) PMCF and (D) SRCF treatments after 1, 7, 10 and 14 days of different water treatment incubation. AWD represents alternate drying and flooding conditions while PF represents permanent flooding conditions. Arrow bar represents standard deviation. CK: control, CF: Chemical fertilization, PMCF: Pig manure plus chemical fertilizer, SRCF: Rice straw plus chemical fertilizer*

Table 3. *Correlation of total isotopic $^{15}N_2O$ with denitrification, heterotrophic nitrification and autotrophic nitrification (n = 8)*

	Total $^{15}N_2O$ flux	**Denitrification**	**Heterotrophic nitrification**	**Autotrophic nitrification**
Total $^{15}N_2O$ flux	1.00	0.03	0.36	0.88**
Denitrification	0.03	1.00	0.50*	-0.44
Heterotrophic nitrification	0.36	0.50*	1.00	0.05
Autotrophic nitrification	0.88**	-0.44	0.05	1.00

*Correlation is significant at level 0.05
**Correlation is significant at level 0.01

http://www.aloki.hu ● ISSN 1589 1623 (Print) ● ISSN 1785 0037 (Online)
DOI: http://dx.doi.org/10.15666/aeer/1706_1377713792

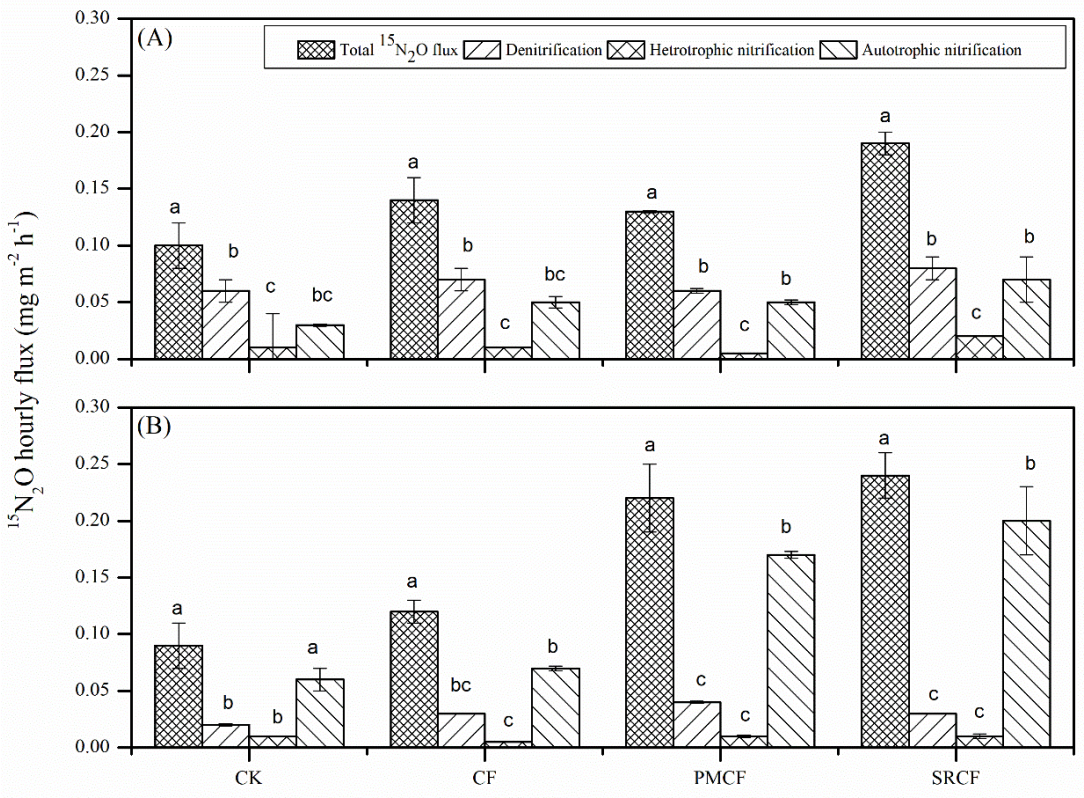

Figure 3. *Hourly isotopic N_2O emission (mg m^{-2} h^{-1}) and the emission come from denitrification, heterotrophic and autotrophic nitrification from (A) PF and (B) AWD conditions. Arrow bar represents standard deviation (n = 3). Different letters show significant differences among treatments (P < 0.05). CK: control, CF: Chemical fertilization, PMCF: Pig manure plus chemical fertilizer, SRCF: Rice straw plus chemical fertilizer*

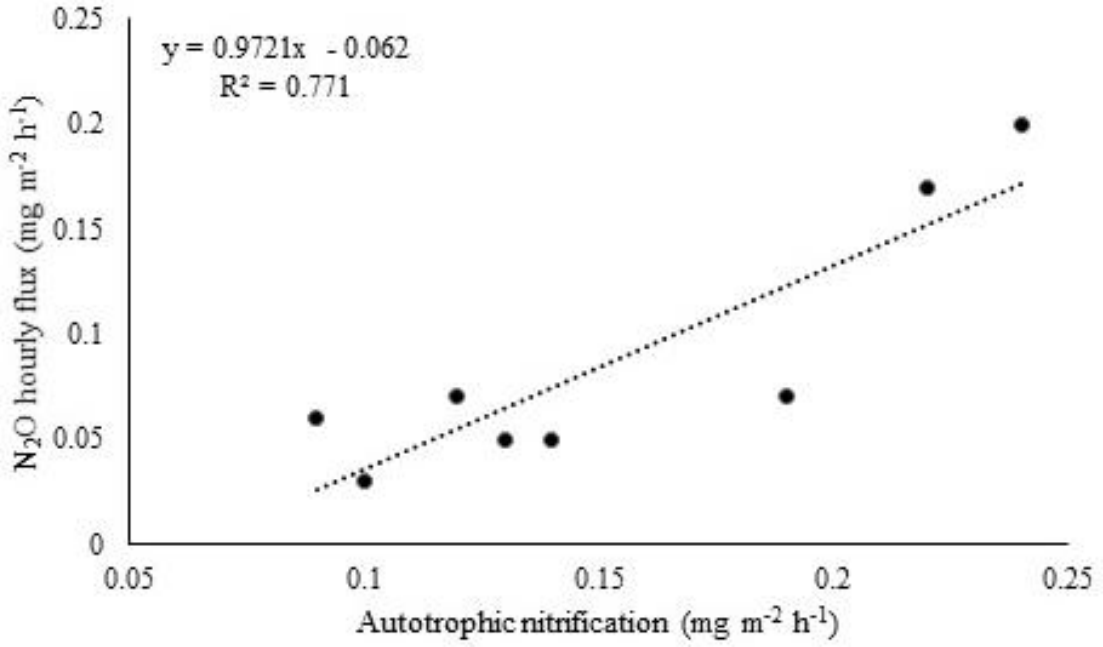

Figure 4. *Correlation between total $^{15}N_2O$ emission and autotrophic nitrification*

http://www.aloki.hu ● ISSN 1589 1623 (Print) ● ISSN 1785 0037 (Online)
DOI: http://dx.doi.org/10.15666/aeer/1706_1377713792

Table 4. *Mean hourly emission of $^{14+15}N_2O$ emission (mean ± S.D), total and percentage (%) contribution of denitrification, heterotrophic and autotrophic nitrification during AWD and PF events (n = 4)*

	AWD	**PF**
	60% FC, 14 d	**Flooding, 14 d**
Total $^{14+15}N_2O$ emission (mg m^{-2} h^{-1})		
$^{14}N_2O$ hourly flux	0.89 ± 0.22	0.15 ± 0.01
$^{15}N_2O$ hourly flux	0.16 ± 0.06	0.13 ± 0.03
Contributing processes (mg m^{-2} h^{-1})		
Denitrification	0.03 ± 0.01 (16.12%)	0.07 ± 0.01 (52.88%)
Heterotrophic nitrification	0.01 ± 0.00 (5.16%)	0.01 ± 0.01 (10.57%)
Autotrophic nitrification	0.12 ± 0.06 (79.03%)	0.05 ± 0.01 (36.53%)

AWD: alternate wetting and drying, PF: permanent flooding

Abundance of nitrifier and denitrifier

The AOA *amo*A gene abundance was found in the range of 2.16E + 06 - 1.61E + 08 copies g^{-1} of the soil (*Fig. 5*). The copy numbers increased with time during both AWD and PF events. The AOA *amo*A gene abundance was found significantly higher at 60% FC (14 days) in the CK, PMCF and SRCF ($P < 0.0001$). While, during PF, PMCF only increased AOA *amo*A gene abundance, especially after 10 days and 14 days.

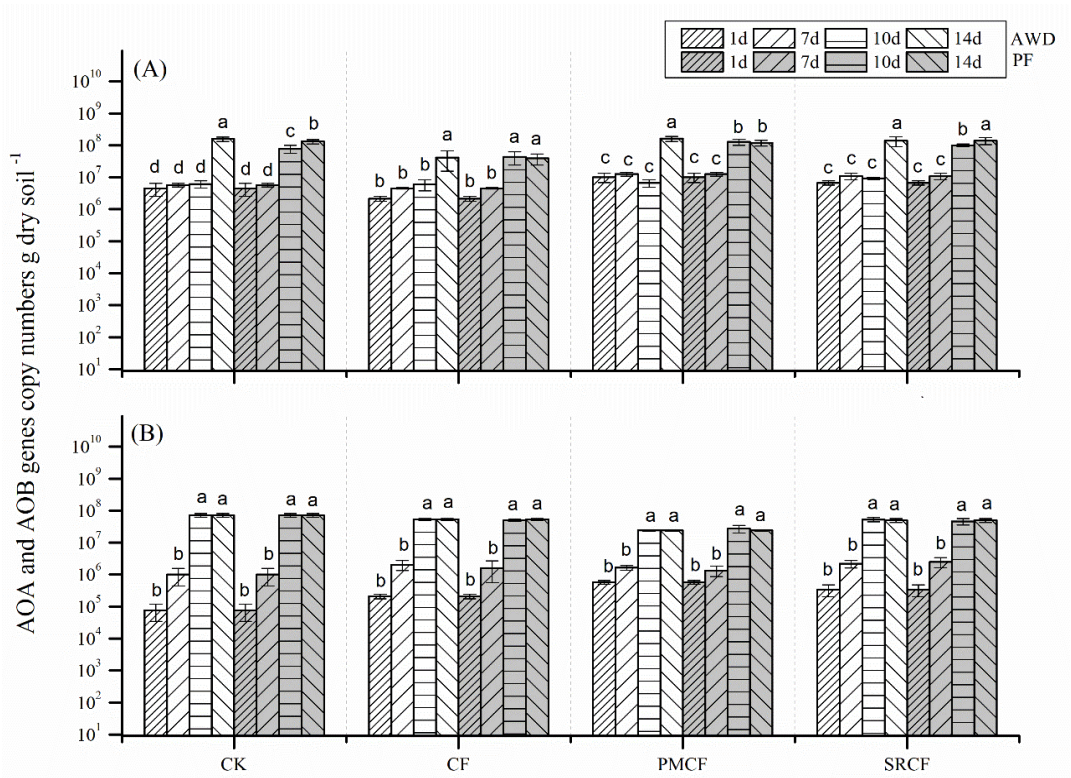

Figure 5. *Abundance of (A) AOA and (B) AOB gene (copy numbers g dry $soil^{-1}$) after 1, 7, 10 and 14 days of incubation during AWD and PF events. AWD represents alternate drying and flooding conditions while PF represents permanent flooding conditions. Arrow bar above the line shows standard deviation (n = 3, P < 0.0001). CK: control, CF: Chemical fertilization, PMCF: Pig manure plus chemical fertilizer, SRCF: Rice straw plus chemical fertilizer*

http://www.aloki.hu ● ISSN 1589 1623 (Print) ● ISSN 1785 0037 (Online)
DOI: http://dx.doi.org/10.15666/aeer/1706_1377713792

The AOB *amo*A gene abundance was found in the range of 7.68E + 04 - 7.13E + 07 copy numbers g^{-1} of dry soil, with the highest value at 60% FC (14 days) in CK and CF treatments (*Fig. 5*). While, during AWD, a gradual increase in copy numbers were noted with time and relatively high at 80% FC and 60% FC. Also, during PF, this increase in copy numbers were recorded with time in all treatments. It was interesting that significant increases in copy numbers were found in CK and CF treatments during early stages ($P < 0.0001$). After 14 d, significant differences were noted between treatments.

The abundance of the *nir*S gene significantly increased with time during both water events. Significant differences were found among treatments during the later stage of experiment ($P < 0.0001$). During PF event, this increase in copy numbers were in certain limit and after that it started to decrease or remain constant. Moreover, relatively higher gene abundances were found in PMCF and SRCF during the whole trial period during both water events.

Although the abundance of *nir*K gene varied with time under all moisture conditions i.e. 60% FC and 100% FC. The high genes abundance was found during flooded condition in all treatments but relatively higher abundance was in PMCF treatment (*Fig. 6*). The highest value (6.94E + 06) of *nir*K was observed in the PMCF treatment after 14 days of PF.

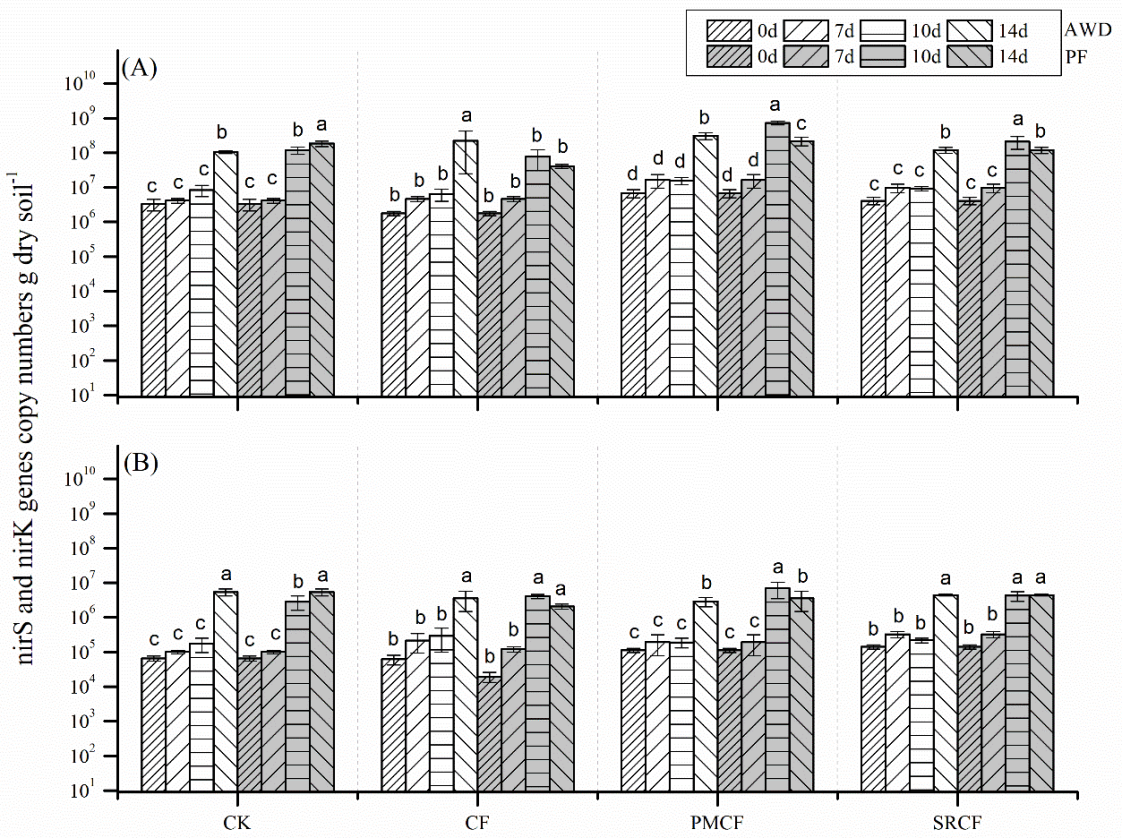

Figure 6. *Abundance of (A) nirS and (B) nirK genes (copy numbers g dry soil^{-1}) after 1, 7, 10 and 14 days of incubation during AWD and PF events. AWD represents alternate drying and flooding conditions while PF represents permanent flooding conditions. Arrow bar above the line shows standard deviation (n = 3, P < 0.0001). CK: control, CF: Chemical fertilization, PMCF: Pig manure plus chemical fertilizer, SRCF: Rice straw plus chemical fertilizer*

http://www.aloki.hu ● ISSN 1589 1623 (Print) ● ISSN 1785 0037 (Online)
DOI: http://dx.doi.org/10.15666/aeer/1706_1377713792

Proportion of greenhouse gases emission associated with microbial biomass and water condition

The relationship of nitrifiers and denitrifiers with N_2O emissions under AWD and PF conditions are given in *Table 5*. A significant correlation was observed between AOB and N_2O emissions during both AWD and PF, suggesting that AOB is responsible for N_2O emissions whatever the water events are (AWD or PF). The correlation between N_2O and nitrifiers and denitrifiers suggested that N_2O emissions is mainly affected by AOB.

Table 5. *Correlation between N_2O, AOA, AOB and nirK genes (n = 24)*

	N_2O	**AOA**	**AOB**	***nir*S**	***nir*K**
N_2O	1.00	-0.96**	0.54*	0.11	0.92**
AOA	-0.96**	1.00	-0.36	-0.29	-0.81**
AOB	0.54*	-0.36	1.00	0.01	0.81**
*nir*S	0.11	-0.29	0.01	1.00	0.01
*nir*K	0.92*	-0.81**	0.81**	0.01	1.00

*Correlation is significant at level 0.05 (two tail test)
**Correlation is significant at level 0.01 (two tail test)

Discussion

Effect of moisture contents on N_2O emissions

A plethora of previous literature have described the significant changes in N_2O emissions during alternate flooding and air drying events in paddy fields (Toyoda et al., 2011; Nishimura et al., 2011). AWD generally promotes N_2O emissions compared to PF in most of studies (Prieme and Christensen, 2001; Wu et al., 2017; Zou et al., 2005; Hou et al., 2012). Although, significant higher N_2O fluxes were observed when the water was removed from the all treatments (10d, 14d), confirmed by earlier findings (Toyoda et al., 2011; Nishimura et al., 2004, 2011). Jorgensen et al. (1998) and Scholes et al. (1997) have reported a rise in N_2O flux during AWD after submerged conditions, and these results were due to the combined effect of high microbial activity and escape of entrapped N_2O (Rice and Smith, 1982). Moreover, the N_2O emissions in PMCF, SRCF and CF treatments were greater than control (CK) suggesting that the application of long-term inorganic or organic fertilizers increase N_2O productions during soil drying-rewetting events (*Fig. 2*). This high N_2O emission in the PMCF and SRCF might be due to the high concentration of organic N fertilizer in the PMCF and SRCF. In this study, N_2O fluxes were positively affected by fertilization (CF, PMCF, and SRCF). Similar results were reported in previous studies conducted in rice paddies (Hou et al., 2012; Zou et al., 2005) presenting that fertilization had a noticeable effect on N_2O emissions because majority of inorganic N is supplied by fertilization in the form of NH_4^+-N and NO_3^--N, which promotes N_2O production (Liu et al., 2015). Harrison-Kirk et al. (2013) revealed N_2O fluxes increased exponentially by increasing C up to 50 mg g^{-1} soil by organic fertilizer application. It is interesting that N_2O fluxes always showed the following order: CK < CF < PMCF < SRCF during whole trial period.

http://www.aloki.hu ● ISSN 1589 1623 (Print) ● ISSN 1785 0037 (Online)
DOI: http://dx.doi.org/10.15666/aeer/1706_1377713792

Effect of water conditions on nitrifier and denitrifier abundance based on long term fertilization

AOA abundance in our results was more dominant compared to AOB, which was consistent with previous studies (He et al., 2007; Alam et al., 2013). This increase in AOA compared to the abundance of AOB might be due to high AOA affinity for oxygen (Szukics et al., 2009). However, Soil pH is another sole factor which may increase AOA abundance, producing favorable conditions for AOA in the paddy fields. Meanwhile, AOB abundance was mainly increased by pH (Nicol et al., 2008). In addition, some previous studies revealed that fertilization rate is the main driver of AOB and AOA abundances to decrease or remain unaffected (Zhong et al., 2016; Di et al., 2014). Also, the influence of fertilizer application on AOA and AOB were reported in some other filed studies (Dai et al., 2013; Alam et al., 2013) and laboratory incubation (Di et al., 2009). NH_4^+ availability produced by organic nitrogen mineralization or either by added inorganic NH_4^+ is the sole factor responsible for the abundance of AOA and AOB (Tourna et al., 2008). However, the pH might influence NH_4^+availability because under low pH it would be ionized to NH_4^+ (Nicol et al., 2008; He et al., 2007). Therefore, in the rice paddies, the drop of soil pH by fertilization, was a more significant factor to increase the availability of substrate for AOA.

The abundances of *nirK* and *nirS* genes had dramatically increased with time after 7 days in AWD and in PF until 10 days and then maintained or decreased (after 14 days). These results were in agreement with previous study of Uchida et al. (2014), indicated that under the absolute anaerobic conditions, the denitrifier abundance was reduced. In addition, the denitrifier abundance was influenced by flooding-drying pattern because denitrifier growth usually stimulate near anaerobic conditions (Uchida et al., 2014; Di et al., 2014). Alternatively, Cui et al. (2016) recognized a notable increase in denitrifiers abundance (*nirK*, *nirS*) after long-term fertilization which is similar to our results in which the abundance of denitrifiers were found high in PMCF and SRCF treatments. Hamonts et al. (2013) reported that dissolved organic carbon (DOC), NO_3^- and NO_2^- might increase denitrifiers copy numbers in fertilized soils. Moreover, low pH is recognized to reduce the assembly and turnover of N_2O reductase (Bergaust et al., 2010). In a recent study, DOC and NO_3^- contents increased by fertilization could decrease soil pH (data not shown). Together, these factors might have led to a neutral effect on the denitrifiers abundances.

Contribution of nitrification and denitrification on N_2O emissions with respect to water conditions

Nitrous oxide in soil are produced by various N transformation processes, i.e. nitrification (heterotrophic or autotrophic) and denitrification (Ruser et al., 2006; Beare et al., 2009; Hayakawa et al., 2009). However, in rice paddy soil, the water contents and fertilization rate are the main drivers for particular N transformation process. According to our results, the main contributor to N_2O production was autotrophic nitrification at 60% FC while denitrification was the predominant source during PF, consistent with Bateman and Baggs (2005). It is interesting that denitrification and autotrophic nitrification produce equally in PMCF and SRCF treatments during PF events and this relation is not significant however in CK and CF this relation was significant. The predominant contribution of autotrophic nitrification might be due to favorable conditions for substrate and O_2 diffusion. Similarly, autotrophic nitrification contributed

http://www.aloki.hu ● ISSN 1589 1623 (Print) ● ISSN 1785 0037 (Online)
DOI: http://dx.doi.org/10.15666/aeer/1706_1377713792

equally during PF because it proceeds under limited short-term O_2 during process of nitrifier denitrification (Poth and Focht, 1985; Goreau et al., 1980; Wrage et al., 2001 Bollmann and Conrad, 1998). In addition, nitrifier denitrification at higher water level might be another reason of high autotrophic nitrification contribution (Bollmann and Conrad, 1998). Alternatively, at high concentration of 200 kg N ha^{-1} NH_4NO_3 (>10 μg g^{-1}) inhibited the conversion of N_2O to N_2 for a limited time because NO_3^- is more suitable electron acceptor over N_2O (Blackmer and Bremner, 1978). Although, a very low heterotrophic nitrification contribution was observed during both water events, and this might be due to a limited C and O_2 availability for heterotrophic nitrification or that N_2O emission during heterotrophic nitrification process was unable to be detected (Bateman and Baggs, 2005). I has been assumed that both denitrification and nitrification processes had contribution to N_2O emission at 60% FC. In addition, the contribution of nitrification in fertilization treatments was higher than denitrification because fertilization always promotes nitrification in the soil.

Conclusions

Rewetting and drying conditions had an important impact on N_2O emissions, growth of denitrifier and nitrifier communities along the experiment. However, denitrifier and ammonia oxidizer growth (AOA, AOB, *nir*S, *nir*K) were significantly affected by soil moisture contents. Meanwhile, AWD event promoted N_2O fluxes compared to PF. PMCF and SRCF increased N_2O emissions during both water events (AWD, PF). After finding out the dominant contributor it had been evaluated that autotrophic nitrification had a dominant role in both AWD and PF conditions. Moreover, a significant correlation between the N_2O emission and AOB copy numbers were found in different wetting-drying conditions, showing that AOB has dominant role in N_2O emission by the process of nitrification. Thus present study emphasizes that the PF water conditions are the better option to mitigate nitrous oxide form terrestrial environment to atmospheric environment. However, further study needed to emphasize the underlying process of nitrous oxide emissions.

Acknowledgments. The authors gratefully acknowledge the financial support of The National Natural Science Foundation of China (41877044), The National Key Basic Research Program of China (2015CB150502), The National Key Research and Development Program of China (2016YFD0801103) and Hangzhou Science and Technology Bureau Project (179464).

REFERENCES

[1] Abbasi, M. K., Adams, W. A. (2000): Gaseous N emission during simultaneous nitrification–denitrification associated with mineral N fertilisation to a grassland soil under field conditions. – Soil Biol. Biochem. 32: 1251-1259.

[2] Abid, A. A., Zhang, Q. C., Wang, J. W., Di, H. J. (2018): Nitrous Oxide fluxes and nitrifier and denitrifier communities as affected by dry-wet cycles in long term fertilized paddy soils. – Appl. Soil Eco. 125: 81-87.

[3] Alam, M. S., Ren, G. D., Lu, L., Zheng, Y., Peng, X. H., Jia, Z. J. (2013): Conversion of upland to paddy field specifically alters the community structure of archaeal ammonia oxidizers in an acid soil. – Biogeosciences 10: 5739-5753.

http://www.aloki.hu ● ISSN 1589 1623 (Print) ● ISSN 1785 0037 (Online)
DOI: http://dx.doi.org/10.15666/aeer/1706_1377713792

[4] Baggs, E. M., Richter, M., Cadisch, G., Hartwig, U. A. (2003): Denitrification in grass swards is increased under elevated atmospheric CO_2. – Soil Biol. Biochem. 35: 729-732.
[5] Bateman, E. J., Baggs, E. M. (2005): Contributions of nitrification and denitrification to N_2O emissions from soils at different water-filled pore space. – Biol. Fert. Soils. 41(6): 379-388.
[6] Beare, M. H., Gregorich, E. G., Georges, P. S. (2009): Compaction effects on CO_2 and N_2O production during drying and rewetting of soil. – Soil Biol. Biochem. 41(3): 611-621.
[7] Belder, P., Bouman, B. A. M., Cabangon, R., Guoan, L., Quilang, E. J. P., Yuanhua, L., Spiertz, J. H. J., Tuong, T. P. (2004): Effect of water-saving irrigation on rice yield and water use in typical lowland conditions in Asia. – Agricultural Water Management 65: 193-210.
[8] Berg, P., Klemedtsson, L., Rosswall, T. (1982): Inhibitory effect of low partial pressures of acetylene on nitrification. – Soil Biol. Biochem. 14: 301-303.
[9] Bergaust, L., Mao, Y., Bakken, L. R., Frostegard, A. (2010): Denitrification response patterns during the transition to anoxic respiration and posttranscriptional effects of suboptimal pH on nitrogen oxide reductase in Paracoccus denitrificans. – Appl. Environ. Microb. 76: 6387-6396.
[10] Blackmer, A. M., Bremner, J. M. (1978): Inhibitory effect of nitrate on reduction of N_2O to N_2 by soil microorganisms. – Soil Biol. Biochem. 10: 187-191.
[11] Bollmann, A., Conrad, R. (1998): Influence of O_2 availability on NO and N_2O release by nitrification and denitrification in soils. – Global Change Bio. 4: 387-396.
[12] Cabangon, R. J., Tuong, T. P., Castillo, E. G., Bao, L. X., Lu, G., Wang, G., Cui, Y., Bouman, B. A. M., Li, Y., Chen, C., Wang, J. (2004): Effect of irrigation method and N-fertilizer management on rice yield, water productivity and nutrient-use efficiencies in typical lowland rice conditions in China. – Paddy and Water Environment 2: 195-206.
[13] Carrijo, D. R., Lundy, M. E., Linquist, B. A. (2017): Rice yields and water use under alternate wetting and drying irrigation: a meta-analysis. – Field Crops Res. 203: 173-180.
[14] Chapagain, T., Yamaji, E. (2010): The effects of irrigation method, age of seedling and spacing on crop performance, productivity and water-wise rice production in Japan. – Paddy Water Environ. 8: 81-90.
[15] Charles, A., Rochette, P., Whalen, J. K., Angers, D. A., Chantigny, M. H., Bertrand, N. (2017): Global nitrous oxide emission factors from agricultural soils after addition of organic amendments: a meta-analysis. – Agric. Ecosyst. Environ. 236: 88-98. https://doi.org/10.1016/j.agee.2016.11.021.
[16] Cui, P., Fan, F., Yin, C., Song, A., Huang, P., Tang, Y., Zhu, P., Peng, C., Li, T., Wakelin, S. A., Liang, Y. (2016): Long-term organic and inorganic fertilization alters temperature sensitivity of potential N_2O emissions and associated microbes. – Soil Biol. Biochem. 93: 131-141.
[17] Dai, Y., Di, H. J., Cameron, K. C., He, J. Z. (2013): Effects of nitrogen application rate and a nitrification inhibitor dicyandiamide on ammonia oxidizers and N_2O emissions in a grazed pasture soil. – Sci. Total Environ. 465: 125-135.
[18] Daum, M., Zimmer, W., Papen, H., Kloos, K., Nawrath, K., Bothe, H. (1998): Physiological and molecular biological characterization of ammonia oxidation of the heterotrophic nitrifier Pseudomonas putida. – Curr. Microbiol. 37: 281-288.
[19] Di, H. J., Cameron, K. C., Shen, J. P., Winefield, C. S., O'Callaghan, M., Bowatte, S., He, J. Z. (2009): Nitrification driven by bacteria and not archaea in nitrogen-rich grassland soils. – Nature Geoscience 2: 621-624.
[20] Di, H. J., Cameron, K. C., Podolyan, A., Robinson, A. (2014): Effect of soil moisture status and a nitrification inhibitor, dicyandiamide, on ammonia oxidizer and denitrifier growth and nitrous oxide emissions in a grassland soil. – Soil Biol. Biochem. 73: 59-68.

http://www.aloki.hu ● ISSN 1589 1623 (Print) ● ISSN 1785 0037 (Online)
DOI: http://dx.doi.org/10.15666/aeer/1706_1377713792

[21] Garrido, F., Hénault, C., Gaillard, H., Pérez, S., Germon, J. C. (2002): N_2O and NO emissions by agricultural soils with low hydraulic potentials. – Soil Biol. Biochem. 34: 559-575.
[22] Goreau, T. J., Kaplan, W. A., Wofsy, S. C., McElroy, M. B., Valois, F. W., Watson, S. W. (1980): Production of NO_2^- and N_2O by nitrifying bacteria at reduced concentrations of oxygen. – Appl. Environ. Microbiol. 40: 526-532.
[23] Hamonts, K., Balaine, N., Moltchanova, E., Beare, M., Thomas, S., Wakelin, S. A., O'Callaghan, M., Condron, L. M., Clough, T. J. (2013): Influence of soil bulk density and matric potential on microbial dynamics inorganic N transformations, N_2O and N_2 fluxes following urea deposition. – Soil Biol. Biochem. 65: 1-11.
[24] Harrison-Kirk, T., Beare, M. H., Meenken, E. D., Condron, L. M. (2013): Soil organic matter and texture affect responses to dry/wet cycles: effects on carbon dioxide and nitrous oxide emissions. – Soil Biol. Biochem. 57: 43-55.
[25] Hayakawa, A., Akiyama, H., Sudo, S., Yagi, K. (2009): N_2O and NO emissions from Andisol field as influenced by pelleted poultry manure. – Soil Biol. Biochem. 41(3): 521-529.
[26] He, J., Shen, J., Zhang, L., Zhu, Y., Zheng, Y., Xu, M., Di, H. (2007): Quantitative analyses of the abundance and composition of ammonia-oxidizing bacteria and ammonia oxidizing archaea of a Chinese upland red soil under long-term fertilization practices. – Environ. Microbiol. 9: 2364-2374.
[27] Hou, H., Peng, S., Xu, J., Yang, S., Mao, Z. (2012): Seasonal variations of CH_4 and N_2O emissions in response to water management of paddy fields located in Southeast China. – Chemosphere 89: 884-892.
[28] Hynes, R. K., Knowles, R. (1982): Effect of acetylene on autotrophic and heterotrophic nitrification. – Can. J. Microbiol. 28: 334-340.
[29] IPCC (2007): Climate Change: The Physical Science Basis. – In: Solomo, S., Qin, D., Manning, M., et al. (eds.) Contribution of Working Group I to the Fourth Assessment Report of the Intergovernmental Panel on Climate Change (IPCC). Cambridge University Press, Cambridge.
[30] IPCC (2013): Summary for Policymakers. – In: Stocker, T. F., Qin, D., Plattner, G. K., Tignor, M., Allen, S. K., Boschung, J., Nauels, A., Xia, Y., Bex, V., Midgley, P. M. (eds.) Climate Change 2013: The Physical Science Basis. Contribution of Working Group I to the Fifth Assessment Report of the Intergovernmental Panel on Climate Change. Cambridge University Press, Cambridge, UK, New York. https://www.ipcc.ch/pdf/assessment-report/ar5/wg1/WGIAR5_SPM_brochure_en.pdf.
[31] Jorgensen, R. N., Jorgensen, B. J., Nielsen, N. E. (1998): N_2O emission immediately after rainfall in a dry stubble field. – Soil Biol. Biochem. 30: 545-546.
[32] Liu, C., Yao, Z., Wang, K., Zheng, X. (2015): Effects of increasing fertilization rates on nitric oxide emission and nitrogen use efficiency in low carbon calcareous soil. – Agr. Ecosys. Environ. 203: 83-92.
[33] Liu, R., Hayden, H. L., Suter, H., Hu, H., Lam, S. K., He, J. (2017): The effect of temperature and moisture on the source of N2O and contributions from ammonia oxidizers in an agricultural soil. – Biol Fertil. Soils. 53: 141-152. https://doi.org/10.1007/s00374-016-1167-8.
[34] Moir, J. W. B., Crossman, L. C., Spiro, S., Richardson, D. J. (1996): The purification of ammonia monooxygenase from Paracoccus denitrificans. – FEMS Lett. 387: 71-74.
[35] Nicol, G. W., Leininger, S., Schleper, C., Prosser, J. I. (2008): The influence of soil pH on the diversity, abundance and transcriptional activity of ammonia oxidizing archaea and bacteria. – Environ. Microbiol. 10: 2966-2978.
[36] Nishimura, S., Sawamoto, T., Akiyama, H., Sudo, S., Yagi, K. (2004): Methane and nitrous oxide emissions from a paddy field with Japanese conventional water management and fertilizer application. – Global Biogeochem. Cycles 18: GB2017.

http://www.aloki.hu ● ISSN 1589 1623 (Print) ● ISSN 1785 0037 (Online)
DOI: http://dx.doi.org/10.15666/aeer/1706_1377713792

[37] Nishimura, S., Akiyama, H., Sudo, S., Fumoto, T., Cheng, W. G., Yagi, K. (2011): Combined emission of CH_4 and N_2O from a paddy field was reduced by preceding upland crop cultivation. – Soil Sci. Plant Nutr. 57: 167-178.
[38] Ostrom, N. E., Hedin, L. O., von Fischer, J. C., Robertson. G. P. (2002): Nitrogen transformations and nitrate removal at a soil-stream interface: a stable isotope approach. – Ecological Applications 12: 1027-43.
[39] Peng, S. Z., Hou, H. J., Xu, J. Z., Mao, Z., Abudu, S., Luo, Y. F. (2011): Nitrous oxide emissions from paddy fields under different water managements in southeast China. – Paddy Water Environ. 9: 403-411.
[40] Poth, M., Focht, D. D. (1985): ^{15}N kinetic analysis of N_2O production by Nitrosomonas europaea an examination of nitrifier denitrification. – Appl. Environ. Microbiol. 49: 1134-1141.
[41] Prieme, A., Christensen, S. (2001): Natural perturbations, drying-wetting and freezing-thawing cycles, and the emission of nitrous oxide, carbon dioxide and methane from farmed organic soils. – Soil Biol. Biochem. 33: 2083-2091.
[42] Rice, C. W., Smith, M. S. (1982): Denitrification in no-till and plowed soils. – Soil Sci. Sot. Am. J. 46: 1168-l 173.
[43] Ruser, R., Flessa, H., Russow, R., Schmidt, G., Buegger, F., Munch, J. C. (2006): Emission of N_2O, N_2 and CO_2 from soil fertilized with nitrate: Effect of compaction, soil moisture and rewetting. – Soil Biol. Biochem. 38(2): 263-274.
[44] Scholes, M. C., Martin, R., Scholes, R. J., Parsons, D., Winstead, E. (1997): NO and N_2O emissions from savanna soils following the first simulated rains of the season. – Nutrient Cycling in Agro. Eco. Systems 48: 115-122.
[45] Stevens, R. J., Laughlin, R. J., Burns, L. C., Arah, J. R. M., Hood, R. C. (1997): Measuring the contributions of nitrification and denitrification to the flux of nitrous oxide from soil. – Soil Biol. Biochem. 29: 139-151.
[46] Szukics, U., Hackl, E., Zechmeister-Boltenstern, S., Sessitsch, A. (2009): Contrasting response of two forest soils to nitrogen input: rapidly altered NO and N_2O emissions and nirK abundance. – Biol. Fert. Soils 45: 855-863.
[47] Tourna, M., Freitag, T. E., Nicol, G. W., Prosser, J. I. (2008): Growth, activity and temperature responses of ammonia-oxidizing archaea and bacteria in soil microcosms. – Environ. Microbiol. 10: 1357-1364.
[48] Toyoda, S., Yano, M., Nishimura, S., Akiyama, H., Hayakawa, A., Koba, K., Sudo, S., Yagi, K., Makabe, A., Tobari, Y., Ogawa, N. O., Ohkouchi, N., Yamada, K., Yoshida, N. (2011): Characterization and production and consumption processes of N_2O emitted from temperate agricultural soils determined via isotopomer ratio analysis. – Global Biogeochem Cycles 25: GB2008.
[49] Uchida, Y., Wang, Y., Akiyama, H., Nakajima, Y., Hayatsu, M. (2014): Expression of denitrification genes in response to a waterlogging event in a Fluvisol and its relationship with large nitrous oxide pulses. – FEMS Microbiol. Ecol. 88: 407-423.
[50] Webster, E. A., Hopkins, D. W. (1996): Contributions from different microbial processes to N_2O emissions from soil under different moisture regimes. – Biol. Fertil. Soils 22: 331-335.
[51] Wrage, N., Velthof, G. L., van Beusichem, M. L., Oenema, O. (2001): Role of nitrifier denitrification in the production of nitrous oxide. – Soil Biol. Biochem. 33: 1723-1732.
[52] Wu, K., Chen, Z., Li, X., Xu, J., Li, J., Wang, K., Wang, H., Wang, S., Dong, X. (2017): Flow behavior of gas confined in nanoporous shale at high pressure: real gas effect. – Fuel 205: 173-183.
[53] Zhang, X., Wong, M., Feng, X., Wang, K. (2009): Identification of soil heavy metal sources from anthropogenic activities and pollution assessment off fuyang County, China. – Environ. Monit. Assess. 154(1): 439-449.
[54] Zhong, W., Bian, B., Gao, N., Min, J., Shi, W., Lin, X., Shen, W. (2016): Nitrogen fertilization induced changes in ammonia oxidation are attributable mostly to bacteria

http://www.aloki.hu ● ISSN 1589 1623 (Print) ● ISSN 1785 0037 (Online)
DOI: http://dx.doi.org/10.15666/aeer/1706_1377713792

rather than archaea in greenhouse-based high N input vegetable soil. – Soil Biol. Biochem. 93: 150-159.

[55] Zou, J. W., Huang, Y., Jiang, J. Y. (2005): A 3-year field measurement of methane and nitrous oxide emissions from rice paddies in China: effects of water regime, crop residue, and fertilizer application. – Glob Biogeochem. Cycles. DOI: 10.1029/2004 gb002401.

http://www.aloki.hu ● ISSN 1589 1623 (Print) ● ISSN 1785 0037 (Online)
DOI: http://dx.doi.org/10.15666/aeer/1706_1377713792

BIOSYNTHESIS AND CHARACTERIZATION OF SILVER NANOPARTICLES USING FIG (*FICUS CARICA)* LEAVES: A POTENTIAL ANTIMICROBIAL ACTIVITY

ACAY, H.

Department of Nutrition and Dietetic, School of Health, Mardin Artuklu University
Mardin, Turkey
(e-mail: hilalacay@gmail.com)

(Received 10th May 2019; accepted 16th Jul 2019)

Abstract. Environmentally friendly methods for obtaining nanomaterials see a great interest. In addition to being inexpensive, the easy implementation process and the advantages of synthesis without toxic chemicals are the main reasons of interest. In this study, silver nanoparticles (AgNPs) were successfully synthesized using fig (*Ficus carica*) leaf extract. The formation and the presence of AgNPs were observed using ultraviolet-visible spectrophotometry (UV-Vis). Peaks with a maximum wavelength of 419 nm are identified in the measurements. Phytochemicals in the extract responsible for functional groups providing reduction and stability were evaluated using Fourier transform infrared spectroscopy (FT-IR) data. The Scanning electron microscopy-Energy Dispersive X-Ray Spectrum (SEM-EDX) analysis showed that the AgNPs were spherical and the elemental composition contained mostly silver. X-ray diffractometer (XRD) results revealed that the peaks 111°, 200°, 220° and 311° belong to the characteristic structure of silver and have a crystal dimension of 17.30 Nm using Debye-Scherrer equation. In thermogravimetric - differential thermal analysis (TGA-DTA) analysis, the degradation temperatures of AgNPs were evaluated. AgNPs showed antimicrobial activity on various microorganisms even at very high concentrations. As a solution to the antimicrobial search, it can be developed in medical industry.
Keywords: *XRD, SEM, TGA-DTA, AgNPs, Ficus carica*

Introduction

Nanomaterials are used in medical, electronic, food and cosmetic industries, textile industry, agricultural applications and many other areas (Alqahtani et al., 2017; El-Batal et al., 2018; Silva-Ichante et al., 2018; Rolim et al., 2019). Among nanomaterials, AgNPs have a large facial area, good thermal and electrical conductivity (Elemike et al., 2016). AgNP are obtained using different methods (*Fig. 1*) (Mittal et al., 2013). Since physical and chemical methods are being synthesized by using high amounts of energy and toxic chemicals, they are a disadvantage compared to biological methods. Biological source synthesis methods are cheaper and the process is simpler and easier. It also makes these methods more advantageous because they do not contain toxic chemicals during the synthesis phase (Pantidos and Horsfall, 2014; Tippayawat et al., 2016; Kanchi et al., 2018). Phytochemicals such as polyphenols, flavonoids, proteins, alcohols and sugars found in plants, rather than harmful chemicals, are responsible for both reduction and stability (Kumar et al., 2015). Phytochemicals are responsible for the synthesis of AgNPs by reducing the Ag+ form to AgO (Prakash et al., 2013). Obtaining nanoparticles from plant sources provides advantages such as easy processing and no culture (Pallela et al., 2018). Furthermore, AgNPs have been shown to exhibit anti-microbial activity in some studies (Veerasamy et al., 2011; Ghosh et al., 2012; Ashajyothi et al., 2016).

http://www.aloki.hu ● ISSN 1589 1623 (Print) ● ISSN 1785 0037 (Online)
DOI: http://dx.doi.org/10.15666/aeer/1706_1379313802

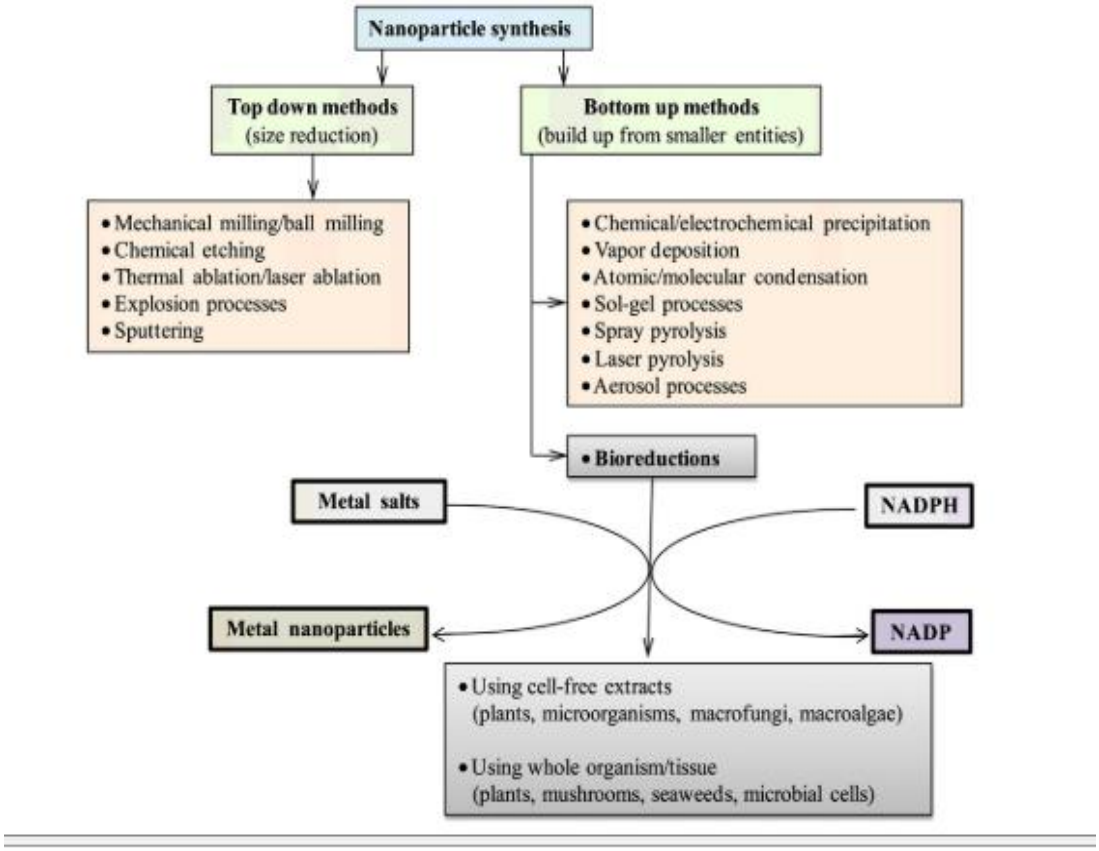

Figure 1. *Nanoparticle forming methods (Mittal et al., 2013)*

The aim of this study is to synthesize AgNPs with fig (Ficus carica) leaf extract in an inexpensive and simple way and to investigate the anti-microbial effects of these NPs characterized by different analysis data.

Materials and methods

Plant leaf

Fig *(Ficus carica)* leaf used in the study was obtained from Mardin, Sultan Village/Turkey in May-June 2018. 500 g samples stored in the Microbiology-Biochemistry Research Laboratory of Mardin Artuklu University

Microorganisms

For testing antimicrobial activity; *Escherichia coli* ATCC 25922, Staphylococcus *aureus* ATCC 25923, *Streptococcus pyogenes* ATCC 19615 *Pseudomonas* aeruginosa ATCC 27853, standard bacterial strains with *Candida albicans* ATCC 10231 strains are available in the Microbiology-Biochemistry Research Laboratory of Mardin Artuklu University.

http://www.aloki.hu ● ISSN 1589 1623 (Print) ● ISSN 1785 0037 (Online)
DOI: http://dx.doi.org/10.15666/aeer/1706_1379313802

Preparation of fig (Ficus carica) leaf extract and silver nitrate ($AgNO_3$) solution

The green leaves of fig fruit were collected in the center of Mardin, Sultan Village/Turkey. After washing with tap water, washing was done several times with distilled water. Dried leaves were minimized prior to preparation of the extract. 100 g was taken and mixed with 500 ml distilled water and left to boil. After boiling, the room was cooled and filtered several times by using the rough filter paper first and then the Whattman No.1 filter paper. After being filtered for several times, it was kept at +4 °C for synthesis. 1 mM aqueous solution was prepared with silver nitrate (AgNO3) of 99.8% purity was purchased from Alfa Aesar.

Synthesis and characterization

500 ml extract and 2000 ml $AgNO_3$ solution were mixed and kept constant in room conditions. The color change was observed for 50 min depending on the time. The presence of AgNPs was checked by examining absorbance values for the color change using Perkin Elmer one UV Visible Spectrophotometer. The characterization of silver nanoparticles was carried out as follows according to the methods described earlier (Baran, 2018). FTIR analysis was performed to evaluate phytochemicals responsible for reduction by using Perkin Elmer Spectrum One. The post-synthesized content in liquid form was centrifuged with OHAUS FC 5706 model device at 6,000 rpm for 25 min and the particles used for further characterization steps were precipitated. The particles were dried at 65 °C. RadB-DMAX II computer-controlled Energy Dispersive X-Ray diffractometer (EDX) was used to evaluate the elemental composition of the particles. Morphological images were examined with scanning electron microscope EVO 40 LEQ (SEM) data. The crystal structure of the particles was evaluated by RadB-DMAX II computer-controlled X-ray diffractometer (XRD) analysis. Crystalline particle size was determined by using the debye-Scherrer equation, using the Shimadzu TGA-50 device to control the decomposition temperature of the particles with TGA-DTA.

Determination of antimicrobial effects of silver nanoparticles

The antimicrobial effects of the particles on gram negative *Escherichia coli* ATCC 25922, *P. aeruginosa* ATCC 27853, gram positive *Staphylococcus aureus* ATCC 29213, *S. pyogenes* ATTC 19615 bacteria and *Candida albicans* yeast were determined by using micro dilution method to determine the minimum inhibition concentration (MIC). In practice, the muller Hilton medium was added to the microplate wells and incubated overnight at 37 °C by addition of an appropriate amount of the microorganism mixture and the AgNP solution adjusted to 0.5 in turbidity according to the Mc Farland standard. The lowest concentration in the absence of reproduction after incubation was determined as the MIC value (El-Batal et al., 2018; Vishwasrao et al., 2018). Commercial antibiotics were used as control for Gram (+) (vancomycin), Gram (-) (colistin) bacteria and fungus (fluconazole). In addition, the effect of $AgNO^3$ solution was investigated. The study was performed with 3 repetitions and the mean values were determined as MIC value.

Results and discussion

After mixing 1 mM $AgNO_3$ solution with leaf extract, the color rapidly changed from light to dark brown was observed after 30 min. Maximum absorbance data at 419 nm is given in *Figure 2*.

http://www.aloki.hu ● ISSN 1589 1623 (Print) ● ISSN 1785 0037 (Online)
DOI: http://dx.doi.org/10.15666/aeer/1706_1379313802

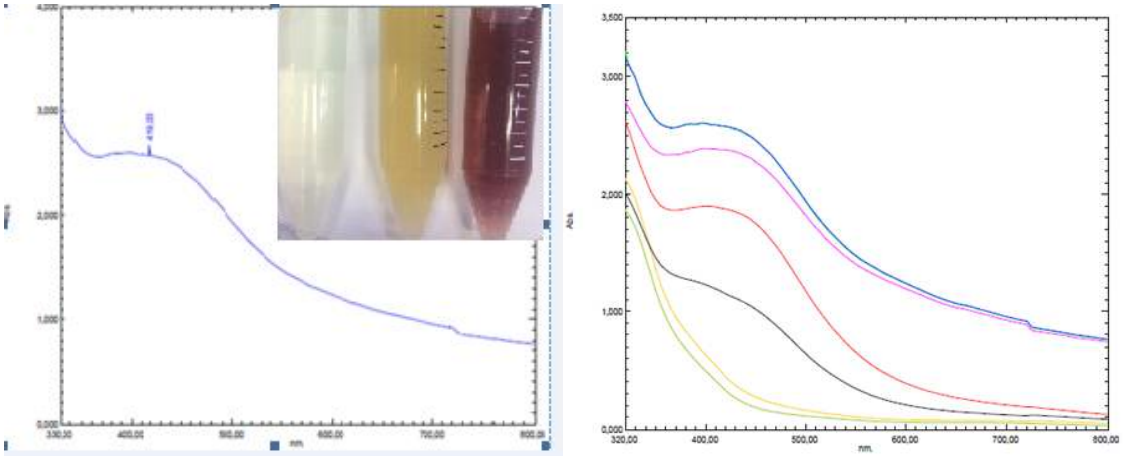

Figure 2. *UV-Vis. analysis result data*

Functional groups involved in the reduction of AgNPs were investigated by FTIR analysis (*Fig. 3*).

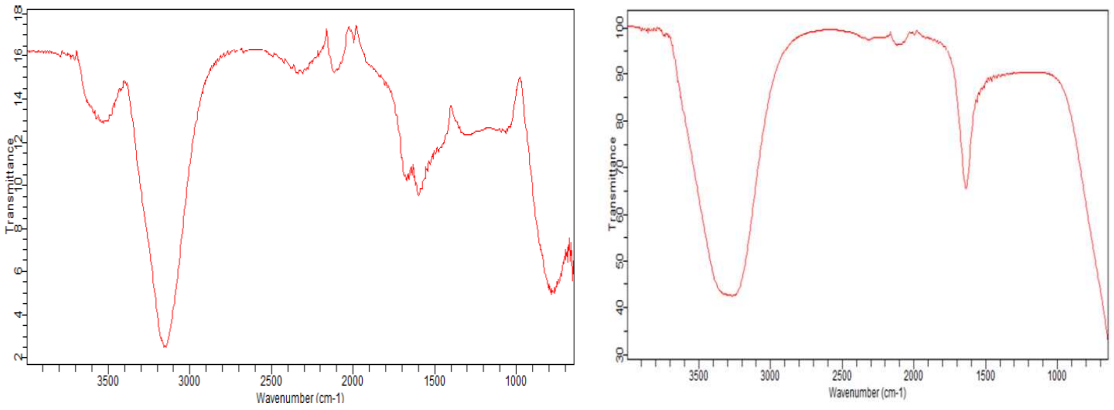

Figure 3. *With FTIR analysis result data.* ***A*** *Extract,* ***B*** *evaluation of functional groups after synthesis*

In the XRD results, the peaks 111°, 200°, 220° and 311° are the peaks that correspond to 2 θ, which represent the cubic crystal structure of silver (*Fig. 4*). The numerical values corresponding to these peaks were found to be 38.10, 44.24, 64.54 and 77.50. The crystal size of AgNPs were calculated 17.30 nm by using the Debye-Scherrer formula (*Eq. 1*) (Baran, 2019).

$$D = K\lambda / (\beta \cos\theta) \qquad \text{(Eq.1)}$$

In *Equation 1:* D = particle size (nm), K = fixed (0.90), λ = wavelength X-ray (1.5406°A), β = half of the highest peak value is specified in radians (FWHM), θ = fracture angle.

When the SEM analysis data were examined, it was found that AgNPs were in spherical appearance (*Fig. 5*).

http://www.aloki.hu ● ISSN 1589 1623 (Print) ● ISSN 1785 0037 (Online)
DOI: http://dx.doi.org/10.15666/aeer/1706_1379313802

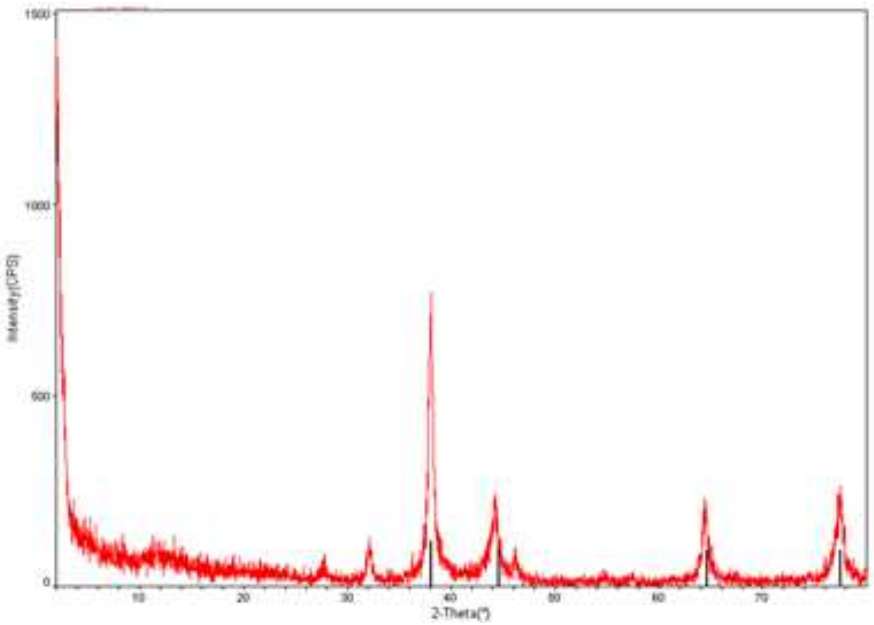

Figure 4. *Investigation of crystal structure and silver phases of AgNPs by XRD analysis*

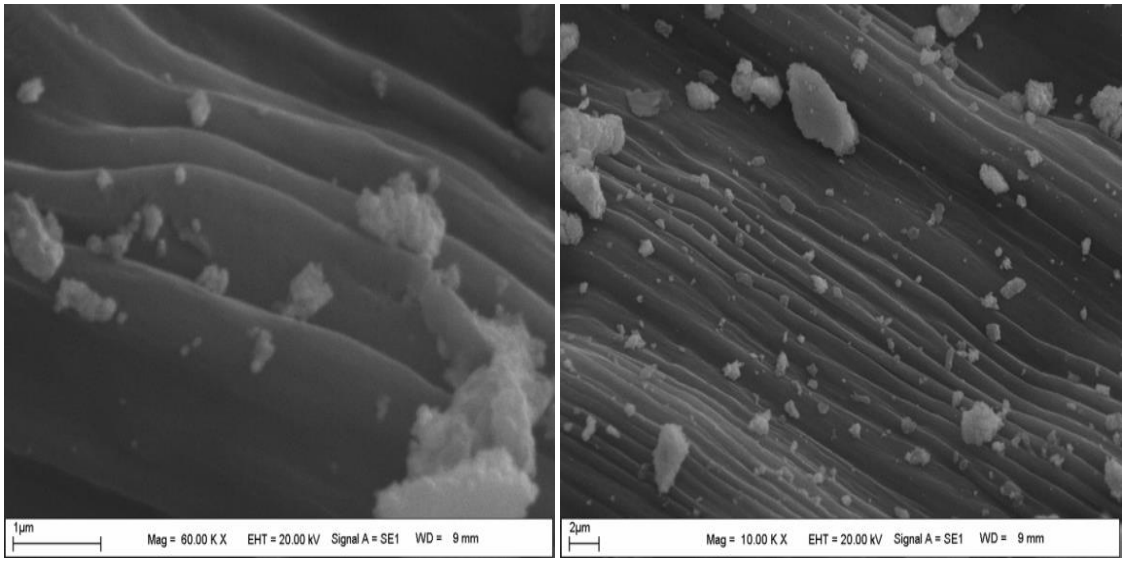

Figure 5. *Evaluation of morphology of AgNPs in SEM results*

The results of EDX showed a large percentage of the element content (*Fig. 6*). The TGA-DTA findings of the synthesized AgNPs were analyzed at a flow rate of 20 mL/min in the N_2 (g) atmosphere with a heating rate of 10 °C/min between 12 and 1000 °C (*Fig. 7*) (Eren and Baran, 2019).

In the study, AgNPs were found to be effective at lower concentrations than antibiotic and 5 mM silver nitrate solution. The MIC values of *S. aureus, S. pyogenes E. coli P. aeruginosa* and *C. albicans* respectively *0.225, 0.056, 0.112, 0.112* and *0.450 mg* L^{-1} results were obtained (*Table 1*). Compared with silver nitrates and antibiotics, AgNPs synthesized using plant extract can be used as an alternative to existing antibiotics as a result.

http://www.aloki.hu ● ISSN 1589 1623 (Print) ● ISSN 1785 0037 (Online)
DOI: http://dx.doi.org/10.15666/aeer/1706_1379313802

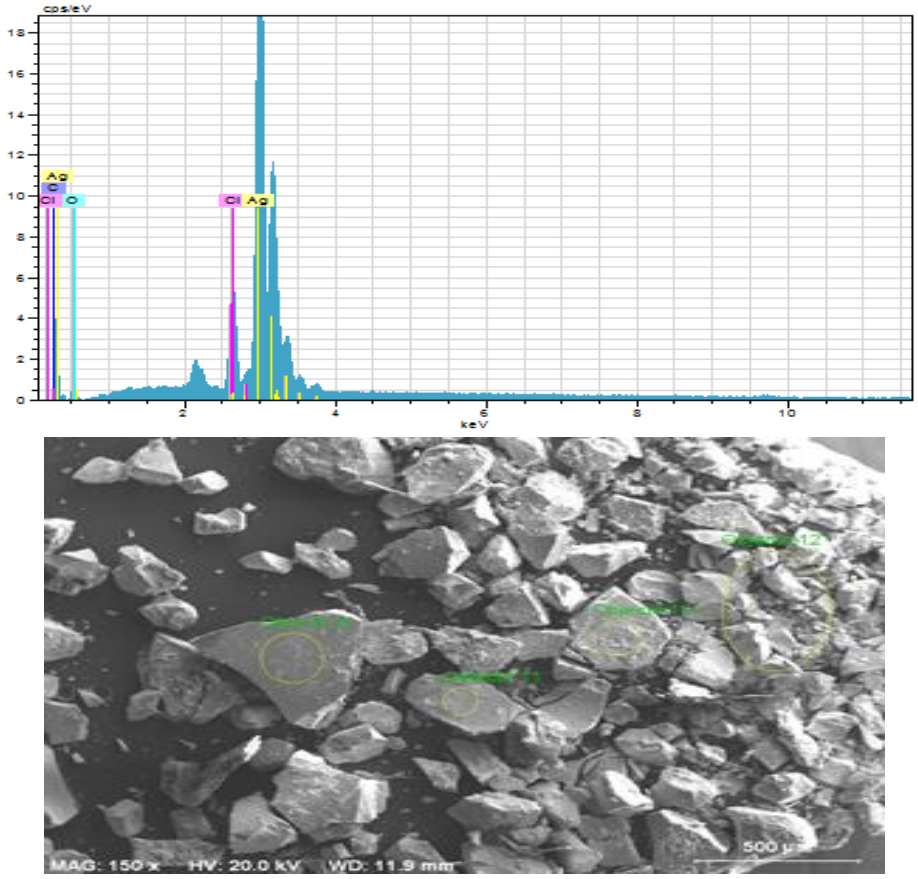

Figure 6. *Analysis of the elemental composition by the EDX analysis of AgNPs*

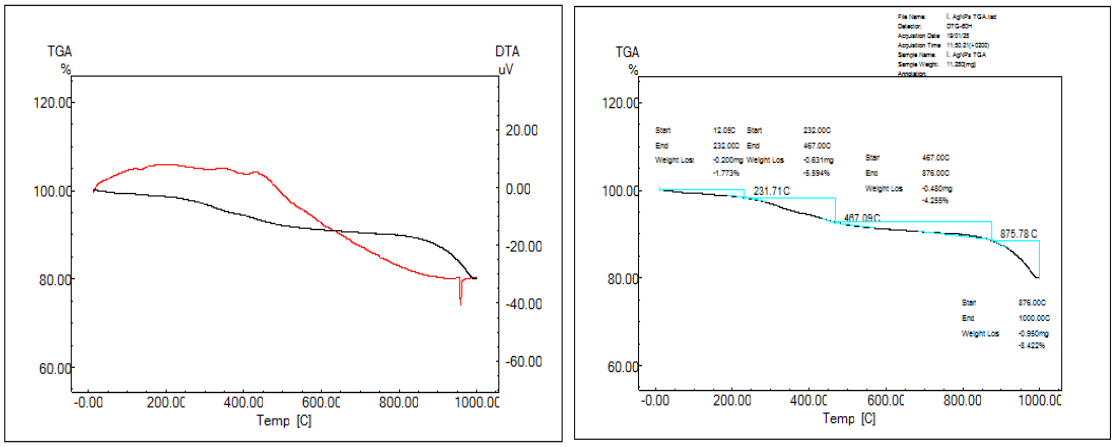

Figure 7. *TGA-DTA data of the synthesized nanoparticle*

In the synthesis of AgNPs using the fig leaf extract, the dark brown color change vibrations on the plasma surface and the UV-Vis. The data on the maximum absorbance of 419 nm in spectrophotometer measurements gives us characteristic data showing the formation and presence of AgNPs (Link and Wang, 1999; Hemmati et al., 2019). In similar synthesis studies of plant origin there are values of absorbance supporting this data (Shahverdi et al., 2007; Kumar et al., 2017; Selvakumar et al., 2018). The peak at

http://www.aloki.hu ● ISSN 1589 1623 (Print) ● ISSN 1785 0037 (Online)
DOI: http://dx.doi.org/10.15666/aeer/1706_1379313802

3529 cm^{-1} is – NH stretching, the peak at 1599 cm^{-1} may belong to – C = O or I amide band, and the peak in cm^{-1} 3180 is considered to be phenol or alcohol-induced-OH. During the formation of nanoparticles, role of -OH, -NN and C = O groups shift in the reduction is shown. In the synthesis studies to obtained AgNPs, almost identical functional groups were said to be responsible for reduction (Baran, 2019). In the XRD results, the peaks 111°, 200°, 220° and 311° are the peaks that correspond to 2 θ, which represent the cubic crystal structure of silver. Some studies have characterized these data with AgNPs (Narayanan and Sakthivel, 2010; Hemmati et al., 2019). The crystal size of AgNPs was calculated 17.30 nm by using the Debye-Scherrer formula. After the synthesis of nanoparticles, there are studies that calculate crystal size using this equation (Senapati et al., 2014; Palanisamy et al., 2017). The SEM results indicate that AgNPs have spherical morphology. In other studies, it has been reported that AgNPs have a spherical appearance (Pugazhendhi et al., 2018; Vishwasrao et al., 2018; Rolim et al., 2019).

Table 1. *MIC values of Synthesized silver nanoparticles (AgNP) (mg mL^{-1}) on Silver nitrate solution and vancomycin, fluconazole, colistin antibiotics, S. Aureus, S. pyogenes, S. albicans and E. Coli, P. aeruginosa microorganisms*

	Organism	**AgNPs**	**Silver nitrat**	**Antibiotic**
Gram positive	*S. aureus ATCC 29213*	0.225	2.65	1
	S. pyogenes ATTC 19615	0.056	1.32	1
Gram negative	*E. coli* ATCC25922	0.112	0.66	2
	P. aeruginosa ATCC 27853	0.112	0.66	2
Fungi	*C. albicans*	0.450	0.66	2

In the EDX analysis, it was observed that the content of the element belonged largely to silver. In similar studies, the element composition was evaluated (Owaid et al., 2015; Khan et al., 2018; Acay et al., 2019). In TGA-DTA data, it is understood that the mass loss of the nanoparticles at 12-232 °C is due to moisture and the mass loss at 232-467 °C is due to the structure of the extract and that the material is now gradually degraded at 467-876 °C in *Figure 5* (Baran et al., 2018; Baran, 2019). We have investigated the effective antimicrobial activity of AgNPs. This activity was effective even at lower concentrations than commercial antibiotic and 5 mM silver nitrate solution. Studies have shown that AgNPs have a negative effect on the reproduction of microorganisms and that they have put pressure on them (Pugazhendhi et al., 2018). These NPs produce ROS (Reactive Oxygen Species), suppressing the membrane structure, proteins, DNA and other vital functions of microorganisms and suppressing their function (Acay et al., 2019). Environmentally friendly synthesis methods for the production of nanomaterials are in the focus of interest due to their lack of toxic chemicals, economical and easier synthesis process. At the same time, the fields of use are becoming widespread every day.

http://www.aloki.hu ● ISSN 1589 1623 (Print) ● ISSN 1785 0037 (Online)
DOI: http://dx.doi.org/10.15666/aeer/1706_1379313802

Conclusions

The advantages of nanoparticles synthesized by biological methods are hygienic working environment, health and environmental protection, less waste and providing the most stable products. Green-synthesized Ag-NPs can be evaluated in a variety of applications including cardiovascular implants, dentistry, medicine, therapeutics, biosensors, agriculture and more, both now and in the future. In this context, It was synthesized AgNPs from the leaves of the *Ficus carica* plant with an easy, inexpensive, environmentally friendly method and without creating any special conditions (temperature, rinse, light, etc.). It was revealed that these particles are in a spherical view with a maximum absorption of 419 nm and that the crystal particle size is 17.30 nm. The degradation temperatures of these AgNPs were found to be 876 °C, and this is an indication of the durability of the product. It was found that these particles showed strong anti-microbial activity. NPs increasingly used for medical applications are of great interest as an approach to killing or reducing the activity of a large number of microorganisms. As a result, the AgNPs obtained is an alternative that can be developed and used in biotechnological and medical applications

REFERENCES

[1] Acay, H., Baran, M. F., Eren, A. (2019): Investigating antimicrobial activity of silver nanoparticles produced through green synthesis using leaf extract of common grape (Vitis vinifera). – Applied Ecology and Environmental Research 17(2): 4539-4546.

[2] Alqahtani, F. S., Alshebly, M. M., Govindarajan, M., Senthilmurugan, S., Vijayan, P., Benelli, G. (2017): Green and facile biosynthesis of silver nanocomposites using the aqueous extract of Rubus ellipticus leaves: toxicity and oviposition deterrent activity against Zika virus, malaria and filariasis mosquito vectors. – J Asia Pac Entomol 20(1): 157-164.

[3] Ashajyothi, C., Prabhurajeshwar, C., Handral, H. K., Kelmani, C. R. (2016): Investigation of antifungal and anti-mycelium activities using biogenic nanoparticles: an eco-friendly approach. – Environ Nanotechnology Monit Manag 5: 81-87.

[4] Baran, M. F. (2018): Green synthesis of silver nanoparticles (AgNPs) using Pistacia terebinthus leaf extract: antimicrobial effect and characterization EJONS. – International Journal on Mathematic, Engineering and Natural Sciences (5)67-75.

[5] Baran, M. F. (2019): Synthesis, characterization and investigation of antimicrobial activity of silver nanoparticles from Cydonia oblonga leaf. – Applied Ecology and Environmental Research 17(2): 2583-2592.

[6] Baran, M. F., Koç, A., Uzan, S. (2018): Synthesis, characterization and antimicrobial applications of silver nanoparticles (AgNPs) with kenger (Gundelia tournefortii) leaf. – EJONS International J on Math, Eng and Natural Sci 5(2): 44-52.

[7] El-Batal, A. I., Al-Hazmi, N. E., Mosallam, F. M., El-Sayyad, G. S. (2018): Biogenic synthesis of copper nanoparticles by natural polysaccharides and Pleurotus ostreatus fermented fenugreek using gamma rays with antioxidant and antimicrobial potential towards some wound pathogens, Microb Pathog 118(March): 159-169.

[8] Elemike, E. E., Onwudiwe, D. C., Mkhize, Z. (2016): Eco-friendly synthesis of AgNPs using Verbascum thapsus extract and its photocatalytic activity. – Mater Lett 185: 452-455.

[9] Eren, A., Baran, M. F. (2019): Green synthesis, characterization and antimicrobial activity of silver nanoparticles (AgNPs) from maize (Zea mays). – Applied Ecology and Envıronmental Research 17(2): 4097-4105.

http://www.aloki.hu ● ISSN 1589 1623 (Print) ● ISSN 1785 0037 (Online)
DOI: http://dx.doi.org/10.15666/aeer/1706_1379313802

[10] Ghosh, S., Patil, Ahire, Kitture, R., Kale, S., Pardesi, Cameotra, Bellare, J., Dhavale, Jabgunde, Chopade, B. (2012): Synthesis of silver nanoparticles using Dioscorea bulbifera tuber extract and evaluation of its synergistic potential in combination with antimicrobial agents. – Int J Nanomedicine 7: 483-496.

[11] Hemmati, S., Rashtiani, A., Zangeneh, M. M., Mohammadi, P., Zangeneh, A., Veisi, H. (2019): Green synthesis and characterization of silver nanoparticles using Fritillaria flower extract and their antibacterial activity against some human pathogens. – Polyhedron 158(May): 8-14.

[12] Kanchi, S., Kumar G., Lo, A. Y., Tseng, C. M., Chen, S. K., Lin, C. Y. et al. (2018): Exploitation of de-oiled jatropha waste for gold nanoparticles synthesis: a green approach. – Arab J Chem 11(2) 247-255.

[13] Khan, A. U., Yuan, Q., Zia Ul Haqkhan, Ahmad, A., Khan, F. U., Tahir, K., Shakeel, M., Ullah, S. (2018): An eco-benign synthesis of AgNPs using aqueous extract of Longan fruit peel: antiproliferative response against human breast cancer cell line MCF-7, antioxidant and photocatalytic deprivation of methylene blue. – J Photochem Photobiol B Biol. 183: 367-373.

[14] Kumar, B., Smita, K., Cumbal, L., Debut, A. (2015): Green synthesis of silver nanoparticles using Andean blackberry fruit extract. – Saudi J Biol Sci 24(1) 45-50.

[15] Kumar, V., Singh, D. K., Mohan, S., Gundampati, R. K., Hasan, S. H. (2017): Photoinduced green synthesis of silver nanoparticles using aqueous extract of Physalis angulata and its antibacterial and antioxidant activity. – J Environ Chem Eng 5(1) 744-756.

[16] Link, S., Wang, Z. L. (1999): Alloy formation of gold - silver nanoparticles and the dependence of the plasmon absorption on their composition. – J. Phys. Chem. B 103(18): 3529-3533.

[17] Mittal, A. K., Chisti, Y., Banerjee, U. C. (2013): Synthesis of metallic nanoparticles using plant extracts. – Biotechno Adv 31(2): 346-356.

[18] Narayanan, K. B., Sakthivel, N. (2010): Phytosynthesis of gold nanoparticles using leaf extract of Coleus amboinicus Lour. – Mater Charact 61(11): 232-1238.

[19] Owaid, M. N., Raman, J., Lakshmanan, H., Al-Saeedi, S. S. S., Sabaratnam, V., Ali Abed, I. (2015): Mycosynthesis of silver nanoparticles by Pleurotus cornucopiae var. citrinopileatus and its inhibitory effects against Candida sp. – Mater Lett 153: 186-190.

[20] Palanisamy, S., Rajasekar, P., Vijayaprasath, G., Ravi, G., Manikandan, R., Marimuthu, P. N. (2017): A green route to synthesis silver nanoparticles using Sargassum polycystum and its antioxidant and cytotoxic effects: an in vitro analysis. – Mater Lett 189: 196-200.

[21] Pallela, P. N. V. K., Ummey, S., Ruddaraju, L., Pammi, S. V. N., Yoon, S. G. (2018): Ultra Small, mono dispersed green synthesized silver nanoparticles using aqueous extract of Sida cordifolia plant and investigation of antibacterial activity. – Microb Pathog 124: 63-69.

[22] Pantidos, N., Horsfall, L. E. (2014): Biological synthesis of metallic nanoparticles by bacteria, fungi and plant. – J Nanomed Nanotechnol 5(5): 10.

[23] Prakash, P., Gnanaprakasam, P., Emmanuel, R., Arokiyaraj, S., Saravanan, M. (2013): Green synthesis of silver nanoparticles from leaf extract of Mimusops elengi, Linn. for enhanced antibacterial activity against multi drug resistant clinical isolates. – Colloids Surfaces B Biointerfaces 108: 255-259.

[24] Pugazhendhi, S., Palanisamy, P. K., Jayavel, R. (2018): Synthesis of highly stable silver nanoparticles through a novel green method using Mirabillis jalapa for antibacterial, nonlinear optical applications. – Opt Mater (Amst) 79: 457-463.

[25] Rolim, W. R., Pelegrino, M. T., De Araújo, L. B., Ferraz, L. S., Costa, F. N., Bernardes, J. S., Rodigues, T., Brocchi, M., Seabra, A. B. (2019): Green tea extract mediated biogenic synthesis of silver nanoparticles: Characterization, cytotoxicity evaluation and antibacterial activity. – Appl Surf Sci 463(August): 66-74.

http://www.aloki.hu ● ISSN 1589 1623 (Print) ● ISSN 1785 0037 (Online)
DOI: http://dx.doi.org/10.15666/aeer/1706_1379313802

[26] Selvakumar, P., Sithara, R., Viveka, K., Sivashanmugam, P. (2018): Green synthesis of silver nanoparticles using leaf extract of Acalypha hispida and its application in blood compatibility. – J Photochem Photobiol B Biol 182(December): 52-61.
[27] Senapati, S., Syed, A., Khan, S., Pasricha, R., Khan, M. I., Kumar, R., Ahmad, A. (2014): Extracellular biosynthesis of metal sulfide nanoparticles using the fungus Fusarium oxysporum. – Curr Nanosci 10(4): 588-595.
[28] Shahverdi, A. R., Minaeian, S., Shahverdi, H. R., Jamalifar, H., Nohi, A. A. (2007): Rapid synthesis of silver nanoparticles using culture supernatants of Enterobacteria: a novel biological approach. – Process Biochem 42(5) 919-923.
[29] Silva-Ichante, M., Reyes-Vidal, Y., Bácame-Valenzuela, F. J., Ballesteros, J. C., Arciga, E., Ţălu, S., Méndez-Albores, S., Trejo, G. (2018): Electrodeposition of antibacterial Zn-Cu/silver nanoparticle (AgNP) composite coatings from an alkaline solution containing glycine and AgNPs. – J Electroanal Chem 823(June): 328-334.
[30] Tippayawat, P., Phromviyo, N., Boueroy, P., Chompoosor, A. (2016): Green synthesis of silver nanoparticles in aloe vera plant extract prepared by a hydrothermal method and their synergistic antibacterial activity. – J Peer 4: 1-15.
[31] Veerasamy, R., Xin, T. Z., Gunasagaran, S., Xiang, T. F. W., Yang, E. F. C., Jeyakumar, N., Dhanaraj, S. A. (2011): Biosynthesis of silver nanoparticles using mangosteen leaf extract and evaluation of their antimicrobial activities. – J Saudi Chem Soc 15: 113-120.
[32] Vishwasrao, C., Momin, B., Ananthanarayan, L. (2018): Green synthesis of silver nanoparticles using sapota fruit waste and evaluation of their antimicrobial activity. – Waste and Biomass Valorization 4(3). DOI: 10.1007/s12649-018-0230-0.

http://www.aloki.hu ● ISSN 1589 1623 (Print) ● ISSN 1785 0037 (Online)
DOI: http://dx.doi.org/10.15666/aeer/1706_1379313802

FARMERS' WILLINGNESS TO PAY FOR THE ECOSYSTEM SERVICES OF ORGANIC FARMING: A LOCALITY STUDY IN VALIKAMAM AREA OF SRI LANKA

SOORIYAKUMAR, K.* – SIVASHANKAR, S. – SIREERANHAN, A.

Department of Agricultural Economics, Faculty of Agriculture, University of Jaffna, Sri Lanka (phone: +94-21-206-0173; fax: +94-21-206-0175)

**Corresponding author*
e-mail: kzs0008@tigermail.auburn.edu; phone: +94-76-320-3126; fax: +94-21-206-0175

(Received 12th May 2019; accepted 28th Aug 2019)

Abstract. This study investigates the farmers' willingness to pay for ecosystem services of organic farming in Valikamam area of Sri Lanka. Choice modeling employed indicates that farmers are willing to pay more for big reduction in nitrate leaching and soil quality improvement than biodiversity improvement. It indicates that farmers give more weight to the short term benefit than the long term sustainable benefit. Income and education level of farmers positively influence farmer's willingness to pay for soil quality improvement and Biodiversity. Young farmers are willing to pay more for soil quality improvement than old farmers. It shows that young farmers are willing to invest more to develop the farms than old farmers as young farmer value economic objective more than old farmers do. Middle aged farmers are willing to pay more for biodiversity. As middle aged farmers value social actions, environment responsibility more than young farmers do and are willing to invest more than old farmers do, middle aged farmers are willing to pay more for biodiversity than other farmers. Increasing farmer's income, organizing awareness programs on sustainable agriculture and providing subsidies could be the most effective ways to adopt organic farming in Valikamam.
Keywords: *biodiversity, choice modeling, conditional logit model, nitrate leaching, soil quality*

Introduction

Ecosystems provide a range of services which are very important to human well-being, livelihoods, health and survival. Ecosystem functions provide goods and services that satisfy human needs, directly or indirectly. Therefore, a growing human population and associated increasing food demands make the challenge to maintain and enhance ecosystem services in agriculture greater than in other ecosystems. Jaffna district in Sri Lanka is facing many problems such as high nitrate level in ground water, declining soil fertility, loss of biodiversity and declining crop productivity due to the overuse of agrochemical in agricultural production. Intensive agriculture that utilizes large quantities of inputs in the form of fertilizers, pesticide, labour and capital made it possible to grow enough food to meet the current global needs. However, these practices lead to environmental damage and degradation of several ecosystem services. Agro ecosystems not only provide ecosystem services but also consume them. Agro ecosystem is a highly managed ecosystem and provides food, forage, fiber, energy and pharmaceuticals. This agro ecosystem strongly depends on ecosystem services provided by natural ecosystem. Supporting ecosystem services comprise of genetic biodiversity for the use of breeding, soil formation, soil fertility, nutrient cycling and water purification (Sandhu et al., 2010). Regulating services include the services of pollinators and natural enemies (Power, 2010).

http://www.aloki.hu ● ISSN 1589 1623 (Print) ● ISSN 1785 0037 (Online)
DOI: http://dx.doi.org/10.15666/aeer/1706_1380313815

As the economic value of ecosystem services is substantial, the utilization of these services for the long-term sustainability of agro-ecosystems and their ability to provide increased production while maintaining ecosystem services becomes very imperative (Sandhu et al., 2005). Sustainable agriculture seeks to make the best use of nature's goods and services while maintaining them for future generations. Organic agriculture is considered to be one of the production systems that aim to achieve sustainability by utilizing and maintaining ecosystem services. The estimated value of several ecosystem services is very high in organic agriculture than that of intensive agriculture. It is well known that organic agriculture delivers more environmental benefits than does intensive farming. Organic farming reduces the use of labour, fuel and agrochemicals and lowers external costs to human health and the environment (Sandhu et al., 2005). Scientists have been involved in enhancing the knowledge about how ecosystem services are produced for over a decade. Most studies had focused on estimating the value of one or two well understood ecosystem services. Better understanding of the processes of ecosystem could help to predict the range of ecosystem services from that ecosystem (Polasky, 2008). The valuation of ecosystem services generally includes both market and non-market valuation. Since agricultural commodities are traded in markets, valuing the provisioning services of agriculture is relatively simple.

Value of supporting services of ecosystems such as pollination services and biological control services can be estimated from in the quantity or quality of agricultural production when the services are removed or degraded (e.g. Losey and Vaughan, 2006; Gallai et al., 2009). Replacement cost method can be used to estimate the values of biological control as pesticides replace natural pest control and values of pollination services as hand-pollination replaces pollination by bees. Non-market valuation methods are used to estimate both the use value and the non-use value of various environmental amenities (Mendelsohn and Olmstead, 2009). Non-market valuation can be based on revealed preference or stated preference. In contingent valuation method, consumers are asked what they would be willing to pay for the ecosystem service. The goal of valuing ecosystem services is to use that information to form policies and incentives for sustainable management of ecosystems. There are difficulties in managing ecosystem services since many ecosystem services are public goods. Farmers' agronomic practices may strongly influence the ecosystem services available to others. Policy makers are facing challenges on how to use emerging information about ecological production functions and valuation to develop policies and incentives to achieve sustainable ecosystem management. In US and many European countries, incentives are provided to the farmers through government program to support for environmentally sound farming practices that support ecosystem services. The impacts of these programs are inconsistent, however, and their success is debated (e.g. Baulcombe et al., 2009).

Market imperfections of environmental goods and services distort their real prices or values and also consumers' willingness to pay on them cannot be readily observed. Market imperfections exist when public goods, externalities, and incomplete markets or property rights are involved (Baumol and Oates, 1975). Market imperfections have been categorized into public goods, externalities, and incomplete markets or property rights (Baumol and Oates, 1975). Since environmental resources produce benefits or costs for which markets do not provide an appropriate price, Market for these benefits and costs can be imperfect. Economic valuation methods generally can be divided into two broad categories: revealed preference methods and stated preference methods (Freeman,

http://www.aloki.hu ● ISSN 1589 1623 (Print) ● ISSN 1785 0037 (Online)
DOI: http://dx.doi.org/10.15666/aeer/1706_1380313815

1993). Revealed preference methods depend on actual consumer behavior in the market. Stated preference method is used to estimate the value of non-market goods and services. In the stated preference method respondents were asked to state their preferences in one or more hypothetical scenarios (Mitchell and Carson, 1989). Stated preference methods could estimate both use and nonuse values. Use values are the monetary value of the utility derived from the direct or indirect consumption of a good or service. Nonuse values are less tangible and are naturally motivated by the wish to leave some existing assets to future generations.

Contingent valuation approach estimates respondent's maximum willingness to pay for a hypothetical change in an environmental good or service (Mitchell and Carson, 1989; Hanley et al., 2001). Conjoint analysis and choice modeling both value the multiple attributes of a product. Conjoint valuation analyzes one combination of attributes at a time. Choice modeling analyzes the values for multiple attributes of a product and their tradeoffs simultaneously (Merino-Castello, 2003). Multi-attribute techniques can be grouped into two categories: preference-based approaches, choice-based approaches. Preference-based approaches ask individuals to rate alternative scenarios on a cardinal scale, whereas choice-based approaches ask consumers to choose among alternative products on ordinal scale. Conjoint analysis is a technique that applied in marketing for many years, but it has recently been employed in economics (Louviere, 1991). The application of conjoint analysis to environmental economics is limited. Choice experiments have some advantages over contingent valuation methods.

In contingent valuation method, Respondents are asked to state their maximum willingness to pay for the improved good or service. The improvements in goods or services are needed to describe precisely. A problem arises in this approach is that if any errors in the information discovered after the fact cannot be changed. However, the choice experiment approach depends on the representation of a choice situation using a range of attributes. Therefore, it relies less on precise description of the good or service, but more on description of the situation. In choice experiment approach, respondents are asked about a sample of events drawn from the universe of possible events of that type (Louviere, 1994). Using attributes and levels of specific choice situations, choice modeling approach are used to make choice sets of attributes that reflect different states of the environment. Individuals are asked to choose their preferred alternative choice set from different choice sets. Thus, the choice modeling approach makes each individual tradeoff between the attributes of the situation. When a cost factor is included as one of attributes in a choice set, it becomes possible to estimate economic values of the other attributes. Choice modeling is attractive for environmental valuation because this type of analysis is based on random utility theory (McFadden, 1974; Ben-Akiva and Lerman, 1989).

The objectives of this study are to estimate the values of ecosystem services of organic farming such as reduction of nitrate leaching, improvement of soil quality improvement and biodiversity and make suggestions or recommendation to policy makers in local and central government to encourage organic farming in Valikamam area in Jaffna district. Intensive agriculture in Valikamam area created many environmental problems such as high nitrate level in ground water, declining of soil fertility, loss of biodiversity and declining crop productivity. Jaffna district is one of the districts in Sri Lanka that is endowed with significant natural and human resources that can be exploited for the agricultural purposes. The total land area including inland water

http://www.aloki.hu ● ISSN 1589 1623 (Print) ● ISSN 1785 0037 (Online)
DOI: http://dx.doi.org/10.15666/aeer/1706_1380313815

is 1025.2 km^2 (Jaffna District Secretariat, 2014). Jaffna district is divided into four sub divisions. They are Islands, Thenmarachi, Vadamarachi, and Valikamam. Total population of the district is around 600,000. Agriculture and fisheries have been the principle economic activities of the district. Agriculture sector is the leading sector and 1/3 of the population mainly depends on agriculture. About 86,000 families are engaged in agriculture while 15,000 families engage in fishing. Agriculture in the district contributes substantially to the GDP of the country. Agriculture is the dominant productive sector in the Jaffna district. *Figure 1* shows five divisional secretariats of Valikamam area: Valikamam East, Valikamam North, Valikamam South, Valikamam South west and Valikamam West. Total populations of those areas are 73087, 37579, 51099, 52423, and 48703, respectively. The climatic condition and the soil type of this area are conducive for the agricultural activities (Jaffna District Secretariat, 2014).

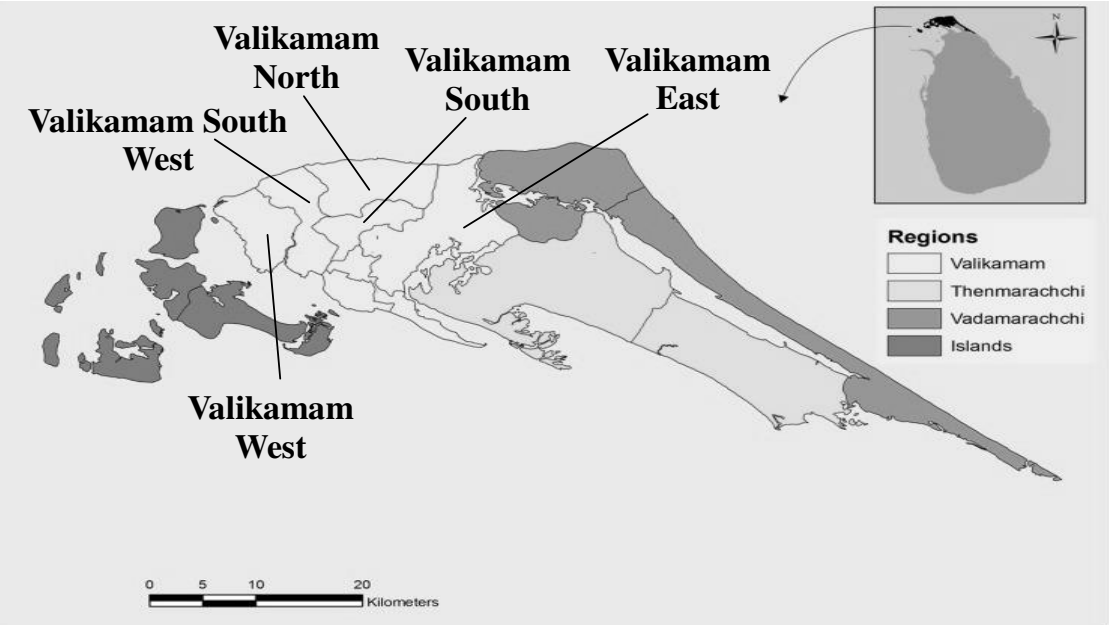

Figure 1. *Map of Jaffna District*

Methodology

Our primary aim is to assess marginal economic values of ecosystem services and benefits to the society; hence we employ choice modeling that is one of stated preference techniques. Discrete Choice Experiment (DCE) initially developed by Louviere and Hensher (1982) and Louviere and Woodworth (1983). The first application of a DCE in valuing environmental goods was reported by Adamowicz et al. (1994). In the recent years, the number of applications of choice modeling has significantly increased and become a popular stated preference method for environmental valuation. A complete summary of this valuation method can be found in Ben-Akiva and Lerman (1985), Louviere et al. (2000), Train (2003), Hensher et al. (2005) and Kanninen (2007). Choice modeling aims to assess the utility that individuals derive from the attributes of non-market environmental good or service under valuation. Choice modeling can also provide the opportunity to understand the trade-offs between different attributes (Adamowicz et al., 1998; Jin et al., 2006).

http://www.aloki.hu ● ISSN 1589 1623 (Print) ● ISSN 1785 0037 (Online)
DOI: http://dx.doi.org/10.15666/aeer/1706_1380313815

Choice modeling was formulated in a random utility framework that permits measurement of the values of non-market goods and services. The Utility function (U) is a function of an observable component (indirect utility function) and an unobservable error component,

$$U = V + \varepsilon \quad \text{(Eq.1)}$$

where V is the indirect utility function and ε is the stochastic error term. We assume that the indirect utility is a linear form,

$$V_i = \beta_i X_{ki} + \alpha m = \beta_1 + \beta_2 x_{2i} + \beta_3 x_{3i} + \ldots + \beta_k x_{ki} + \alpha_i m_i \quad \text{(Eq.2)}$$

where ($X_{ki} = \{x_{1,2}, \ldots, x_k\}$) is a vector of k attributes associated with alternative i, β is a coefficient vector, m_i is income for a respondent choosing the alternative i bundle, and α is the coefficient vector of income. If the stochastic error term is logistically Gumbel distributed (Type I extreme value distributed), the choice probability for alternative i is given by

$$\Pr(i) = \frac{\exp(\rho V_i)}{\sum_{j \in C}^{J} \exp(\rho V_i)} \quad \text{(Eq.3)}$$

where ρa positive scale parameter and C is is the choice set for an individual. For convenience we generally make the assumption$\rho = 1$. To estimate willingness to pay for a change from the status quo state to the chosen state, the following formula is used:

$$V_i(X_i, y) + \varepsilon_i = V_j(X_j, m - CV) + \varepsilon_j \quad \text{(Eq.4)}$$

where V_i and V_j represent utility before and after the change and CV is compensating variation, the amount of money that makes the respondent indifferent between the status quo and the proposed scenario. Conditional logit model can be applied to estimate the welfare measure in *Equation 4*. *Equation 4* can be restated as:

$$\beta_i X_{ki} + \alpha_i m + \varepsilon_i = \beta_j X_{kj} + \alpha_j (m - CV) + \varepsilon_j \quad \text{(Eq.5)}$$

α_i and α_j are assumed to be equal if marginal utility of income for a respondent is constant. The welfare change is estimated by:

$$CV = -\frac{1}{\alpha}\left[(\beta_i (X_{ki} - X_{kj}) + (\varepsilon_i - \varepsilon_j)\right] \quad \text{(Eq.6)}$$

In conditional logit model, coefficient of k attributes across the all alternatives are the same, and $\beta_i = \beta_j$; only the attribute levels differ across the alternatives. Under this condition, welfare change is estimated by the following:

$$CV = -\frac{1}{\alpha}\left[(\beta (X_{ki} - X_{kj}) + (\varepsilon_i - \varepsilon_j)\right] \quad \text{(Eq.7)}$$

http://www.aloki.hu ● ISSN 1589 1623 (Print) ● ISSN 1785 0037 (Online)
DOI: http://dx.doi.org/10.15666/aeer/1706_1380313815

Equation 7 is used to estimate welfare changes in ecosystem services, assuming the impact of the attributes across the all alternatives same.

The attributes of selected ES provided by organic farming in this study were nitrate leaching, soil quality improvement, and biodiversity enhancement of organic farming. Each attribute has several discrete levels of delivery. For the nitrate leaching from organic farming, there were three levels present to respondents: big reduction (50% reduction in nitrate leaching to ground water; small reduction (20% reduction in nitrate leaching to ground water); and no change from current level of nitrate leaching to ground water. The attribute of soil quality of organic farming is limit to two level: soil quality improving and no change. The third attribute, biodiversity enhancement of organic farming is limit to two levels; more variety and no change.

The choice modeling surveys contain multiple choice sets about alternative policies for improving three ecosystem services. In the surveys, before the choice set questions, respondents were briefed about the three attributes of ecosystem services and associated cost to the household. The cost to the household, the payment vehicle, was defined as an additional annual payment to the regional office of environmental authority responsible for management of the environment. The discrete range of cost alternatives given to respondents was LKR 10, LKR 30, LKR 60, and LKR 100. In the choice questions, respondents were asked to select an option they favoured the most out of the three alternatives provided. Each option contains the three attributes and the cost to the household with various levels of attribute combinations. The cost to the household in option A was designed higher than in option B, and option C was set as the status quo across all choice sets. Respondents were asked to answer similar types of choice questions sets multiple times. As there are three levels for nitrate leaching attributes, two levels in the soil and biodiversity attributes, and four levels in the cost to household, there are 2^2 x3 x4 factorial designs. For statistically efficient choice designs, a D-efficient design excluding unrealistic cases was adapted to each of the choice questions. Definitions of selected Ecosystem Service Attributes on cropping farms are presented in *Table 1*. So 48 orthogonal choice combinations are possible but it is impossible to include the all the choices into to the questionnaire and impossible to ask the respondent to select the choice among the choice sets, so we reduce the number of choices in to half. We select 24 choice combinations among the 48 orthogonal combinations. Here we assume, interaction effects between attributes are insignificant. Among 24 choices, 3 unrealistic options were excluded, so 21 choices were selected. "No change" in the current attributes levels (Option C) was included in the each choice set. Levels of the attributes change from one alternative to the other except option C. Attributes, levels, payment of cost, organic farming benefits, and different levels of intensive organic farming are briefly introduced to the farmers during the survey. Each option in the choice set has different level of intensive organic farming. A sample of choices from 21 choices was given in the *Appendix*. In this study only four attributes with few levels were selected to reduce the number of choices and allows farmers to make a clear choice. After giving brief knowledge to the farmers individuals are asked to select the most preferred alternative among the choice sets. Conditional logit model was estimated for the selection of choices.

For this study, 107 farmers from Valikamam east and 104 farmers from rest of the Valikam area, a total of 211 farmers were randomly selected. Data were gathered from personal interviews with Farmers using structured questionnaire. Questionnaire include farmer's demographic and social characteristics such as age education, income, residents

http://www.aloki.hu ● ISSN 1589 1623 (Print) ● ISSN 1785 0037 (Online)
DOI: http://dx.doi.org/10.15666/aeer/1706_1380313815

in rural or urban area and occupation, number of people in household, number of children, agricultural farming practices, environmental problems in their area and the 21 intensive organic farming management scenarios. Discrete choice modeling was used to estimate the economic value of three non-marketed ecosystem services: water quality improvement, soil quality improvement and Biodiversity enhancement associated with organic farming. Definitions of the effect codes for attributes and variable description are presented in *Tables 2* and *3,* respectively. Farmers' age and education level were categorized into 4 groups and income was classified into two groups.

Table 1. *Definitions of selected ecosystem service attributes on cropping farms*

Attributes	Levels	Definitions
Nitrate leaching	Big reduction (NLB) Small reduction (NLS) No change	50% reduction in nitrate leaching to ground water 20% reduction in nitrate leaching to ground water Maintain current nitrate leaching to ground water
Soil quality	Improved (SQ) No change	Soil organic matter and structure are improved Maintain current slow rate of soil degradation
Bio diversity	More variety (BD) No change	More variety of species on crop farms Maintain current variety of species on crop Farms
Cost to household	10:30:60:100	Annual payment to a regional office (LKR) Next five years

Table 2. *Effect codes: choice modeling*

Attributes	Variables	
Nitrate leaching	NLB	1 if big reduction; 0 if small reduction; -1 if no change
	NLS	1 if small reduction; 0 if big reduction; -1 if no change
Soil quality	SQ	1 if improved; -1 if no change
Biodiversity	BD	1 if more variety; -1 if no change

Table 3. *Variable description*

Variable	Description	Unit
East	Valikamam East	1 if Valikamam East; 0 if other areas
Income1	Income	1 if monthly income is less than 135 USD (20,000 LKR) 0 if monthly income is 135 USD (20,000 LKR) and more
Edu1	Education level	1 if farmer's education is $\leq 5^{th}$ grade Otherwise 0
Edu2	Education level	1 if 5^{th} grade < farmer's education $\leq$ 8th grade Otherwise 0
Edu3	Education level	1 if 8^{th} grade < farmer's education $\leq$ 11th grade Otherwise 0
Age 1	Age	1 if farmer's age is $\leq$ 40 years Otherwise 0
Age 2	Age	1 if 40 years < farmer's age $\leq$ 55 years Otherwise 0
Age 3	Age	1 if 55 < farmer's age $\leq$ 65 years Otherwise 0

http://www.aloki.hu ● ISSN 1589 1623 (Print) ● ISSN 1785 0037 (Online)
DOI: http://dx.doi.org/10.15666/aeer/1706_1380313815

Results and discussion

The descriptive statistics of Valikamam east and rest of the Valikamam are given in *Table 4*. The descriptive statistics show that farmers from both places have almost similar statistics regarding income level and farmers age, but on average farmers from rest of the Valikamam have higher education level than the farmers from Valikamam East.

Table 4. *Descriptive statistics*

Variable	East of Valikamam					Rest of Valikamam				
	Obs	**Mean**	**Std. dev.**	**Min**	**Max**	**Obs**	**Mean**	**Std. dev.**	**Min**	**Max**
Income	3,204	10981	7663	3000	45000	3,120	10782	7463	3000	50000
Age	3,204	53	11	30	82	3,120	53	11	27	80
Education	3,204	8.8	3.2	2	13	3,120	10	2.7	2	13

Five conditional logit models were developed using effective codes for three ecosystem service attributes. Results of five conditional logit model were presented in *Table 5*. As a simple model, model 1 includes no social characteristics and no dummy values for divisional area of Valikamam and estimated as a simple pooled model. All variables except small reduction in nitrate leaching are significant at 5% level. The negative coefficient of cost indicates that farmers are likely to accept the policy option with lower cost to them. Dummy values for Valikamam East and rest of the Valikamam are included in the Model 2 as interaction terms with each ecosystem service attribute. The interaction term of Valikamam East and biodiversity is negative and significant at 5% level. It indicates that farmers from Valikamam east are willing to pay less for biodiversity than farmers from rest of Valikamam. Social characteristics such as income, education level and age are included in model 3, 4 and 5, respectively.

Mean welfare values from the improvement of each ecosystem service were estimated by using *Equation 7* and the Estimated mean willingness to pay for each attribute were presented in *Table 6*. Mean welfare values of big reduction in nitrate leaching and soil quality improvement are almost similar between Valikamam east and rest of the Valikamam, which are around 0.53 USD (80 LKR) and 0.52 USD (79 LKR) per annum respectively. Farmers in Valikamam east give less weight for the improvement of biodiversity when compared to the farmers in rest of the Valikamam area. Farmers in Valikamam East and rest of the Valikamam are willing to pay for biodiversity improvement 0.1 USD (10 LKR) and 0.2 USD (30 LKR) per annum respectively. Mean welfare values of all three ecosystem services in Valikamam East and rest of the Valikamam are 1.25 USD (188 LKR) and 1.05 USD (158 LKR) per farm household per year respectively. Farmers from both areas are willing to pay more for large reduction in nitrate leaching and soil quality improvement policies than the policy for biodiversity improvement. This result indicates that, for the farmers from both areas, the big reduction in nitrate leaching and soil quality improvement are more important than the improvement in biodiversity. This indicates that farmers give more weight to the short term benefit than the long term sustainable benefit.

http://www.aloki.hu ● ISSN 1589 1623 (Print) ● ISSN 1785 0037 (Online)
DOI: http://dx.doi.org/10.15666/aeer/1706_1380313815

Table 5. *Conditional logit model*

	Model 1	Model 2	Model 3	Model 4	Model 5
NLB	0.565**	0.562**	0.644**	0.711**	0.639**
NLS	-0.047	-0.038	0.204	0.177	0.265
SQ	0.435**	0.433**	0.636**	0.789**	0.628**
BD	0.228**	0.258**	0.254**	0.369**	0.236*
COST	-0.016**	-0.016**	-0.016**	-0.016**	-0.016**
East × NLB		0.013	0.012	-0.045	-0.043
East × NLS		-0.033	-0.036	0.003	0.007
East × SQ		-0.028	-0.027	-0.046	-0.038
East × BD		-0.152**	-0.153**	-0.167**	-0.161**
Income1 × NLB			-0.09	-0.061	-0.002
Income1 × NLS			-0.274**	-0.298**	-0.320**
Income1 × SQ			-0.227**	-0.177**	-0.163**
Income1 × BD			0.009	0.042	0.025
Educa1 × NLB				0.005	0.011
Educa1 × NLS				-0.054	-0.057
Educa1 × SQ				-0.218**	-0.206**
Educa1 × BD				-0.209**	-0.192**
Educa2 × NLB				-0.303**	-0.290*
Educa2 × NLS				0.300**	0.296*
Educa2 × SQ				-0.231**	-0.214**
Educa2 × BD				-0.088	-0.075
Educa3 × NLB				-0.051	-0.074
Educa3 × NLS				-0.011	0.009
Educa3 × SQ				-0.236**	-0.252**
Educa3 × BD				-0.186**	-0.189**
Age1 × NLB					0.193
Age1 × NLS					-0.131
Age1 × SQ					0.186**
Age1 × BD					0.108
Age2 × NLB					0.064
Age2 × NLS					-0.119
Age2 × SQ					0.215**
Age2 × BD					0.176**
Age3 × NLB					-0.093
Age3 × NLS					-0.033
Age3 × SQ					0.122
Age3 × BD					0.197**

**Significant at 1% level, *significant at 5% level

Table 6. *Mean WTP per farming family per year USD (LKR)*

Area	NLB	SQ	BD
Rest of Valikamam	0.53 (79.88)	0.52 (78.5)	0.2 (29.5)
Valikamam East	0.5 (74.50)	0.49 (73.8)	0.06 (9.38)

http://www.aloki.hu ● ISSN 1589 1623 (Print) ● ISSN 1785 0037 (Online)
DOI: http://dx.doi.org/10.15666/aeer/1706_1380313815

Total willingness to pay for these ecosystem services attributes can be calculated from the mean values. According to the Jaffna District statistics, there are about 12353 farming families from Valikamam East and 19450 families from rest of the Valikamam. Based on these numbers and estimated mean willingness to pay, the total WTP for each ecosystem services are estimated and presented in *Table 7*. Results of these models show that farmers who get monthly income less than 135 USD (20,000 LKR) are willing to pay less for soil quality of improvement than farmers who get monthly income more than 135 USD (20,000 LKR).

Table 7. *Total WTP per farming family per year USD (million LKR)*

Area	NLB	SQ	BD
Rest of Valikamam	10400 (1.56)	10200 (1.53)	4000 (0.6)
Valikamam East	6133 (0.92)	6066 (0.91)	800 (0.12)
Total	16533 (2.48)	16266 (2.44)	4800 (0.72)

The interaction term of education levels with Soil Quality and Biodiversity attributes are negative and significant at 5% level. It indicates that farmers who have education level of 11^{th} grade or below are willing to pay less for soil quality improvement and Biodiversity than farmers who have education level above 11^{th} grade. The interaction terms of age with soil quality attributes is positive and significant at 5% level. It indicates that farmers who are 55 years old or below are willing to pay more for soil quality improvement than who are above 55 years old. The interaction terms of age and biodiversity attributes indicates that farmers whose age is between 40 years and 65 years are willing to pay more for biodiversity than farmers whose age are below 40 years and above 65 years. These findings are consistent with the previous study which found that young farmers were the most active at developing their farms and old farmers were the least active. Young farmers value economic objective slightly more than old farmers, whereas they valued social actions, environment responsibility objectives less than did others (Rantamäki-Lahtinen and Väre, 2012).

Conclusion

Welfare values for changes in levels of three ecosystem services associated with organic farming were estimated using choice modeling method. Estimated mean willingness to pay for each attribute indicates that farmers from both areas are willing to pay more for large reduction in nitrate leaching and soil quality improvement policies than the policy for biodiversity improvement. Soil quality is directly linked to the agricultural productivity and farmers waste their economic resources due to strong nitrate leaching. Nitrate leaching increase the nitrate level in the ground water which is used as drinking water and causes health problem. Therefore, for farmers, the both big reduction in nitrate leaching and soil quality improvement became more important than the improvement in biodiversity. It also indicates that farmers give more weight to the short term benefit than the long term sustainable benefit.

Farmers from both places have almost similar statistics regarding income level and farmers age, but on average farmers from rest of the Valikamam have higher education level than the farmers from Valikamam East. Therefore, Farmers' unawareness about

http://www.aloki.hu ● ISSN 1589 1623 (Print) ● ISSN 1785 0037 (Online)
DOI: http://dx.doi.org/10.15666/aeer/1706_1380313815

the benefits of biodiversity in Valikamam east might be one of the reasons for low willingness to pay for biodiversity improvement. Total willingness to pay for all three ecosystem services in rest of the Valikamam and Valikamam East are 24600 USD (3.69 million LKR) and 13000 USD (1.95 million LKR) per year respectively. It shows that there is a potential to impose minimal tax on farmers and provide this tax revenue as a subsidy to the farmers who practice organic farming. This will encourage more farmers to practice organic farming. Farmers with lower monthly income are willing to pay less for soil quality of improvement than farmers with higher monthly income. Farmers with lower education level are willing to pay less for soil quality improvement and Biodiversity than farmers with higher education level. Young farmers are willing to pay more for soil quality improvement than old farmers. Middle aged farmers are willing to pay more for biodiversity than young and old farmers. It indicates that young farmers are willing to invest more to develop the farm than middle aged and old farmers. As middle aged farmers value social actions, environment responsibility more than young farmers do and are willing to invest more than old farmers do, middle aged farmers are willing to pay more for biodiversity. This study concludes that creating opportunities to earn extra money from off-farm and on-farm economic activities and organizing awareness program on the benefits of reducing nitrate leaching and improving soil quality and biodiversity for farmers, especially young and middle aged farmers and providing subsidy to the farmers who practice organic farming from the tax revenue collected by Central Environmental Authority could be an effective way to adopt organic farming in Valikamam area.

REFERENCES

[1] Adamowicz, W., Louviere, J., Williams, M. (1994): Combining revealed and stated preference methods for valuing environmental amenities. – Journal of Environmental Economics and Management 26: 271-292.
[2] Adamowicz, W., Boxall, P., Williams, M., Louviere, J. (1998): Stated preference approaches for measuring passive use values: choice experiment and contingent valuation. – American Journal of Agricultural Economics 80: 64-75.
[3] Baulcombe, D., Crute, I., Davies, B., Dunwell, J., Gale, M., Jones, J., Ptetty, J., Sutherland, W., Toulmin, C. (2009): Reaping the Benefits: Science and the Sustainable Intensification of Global Agriculture. – The Royal Society, Policy Document 11/09, London.
[4] Baumol, W. J., Oates, W. E. (1975): The Theory of Environmental Policy. – Prentice Hall, Englewood Cliffs, NJ
[5] Ben-Akiva, M., Lerman, S. (1985): Discrete Choice Analysis. – MIT, Cambridge, MA.
[6] Freeman, A. M. (1993): The measurement of environmental and resource values: theory and methods. – Resources for the Future, Washington, DC.
[7] Gallai, N., Salles, J. M., Settele, J., Vaissière, B. E. (2009): Economic valuation of the vulnerability of world agriculture confronted with pollinator decline. – Ecological Economics 68: 810-821.
[8] Hanley, N., Mourato, A., Wright, R. (2001): Choice modeling approaches: a superior alternative for environmental evaluation? – J. Econ. Survey 15(3): 435-462.
[9] Hensher, D. A., Rose, J. M., Greene, W. H. (2005): Applied Choice Analysis. A Primer. – Cambridge University Press, New York.
[10] Jaffna District Secretariat (2014): Jaffna District Statistical Handbook. – Jaffna District Secretariat, Sri Lanka.
[11] Kanninen, B. J. (ed.) (2007): Valuing Environmental Amenities Using Stated Choice Studies. – Springer, Dordrecht.

http://www.aloki.hu ● ISSN 1589 1623 (Print) ● ISSN 1785 0037 (Online)
DOI: http://dx.doi.org/10.15666/aeer/1706_1380313815

[12] Losey, J. E., Vaughan, M. (2006): The Economic Value of Ecological Services Provided by Insects. – Bioscience 56: 311-323.
[13] Louviere, J. (1991): Best-Worst Scaling: A Model for the Largest Difference Judgments. – Working Paper, University of Alberta.
[14] Louviere, J., Hensher, D. A. (1982): On the design and analysis of simulated choice or allocation experiments in travel choice modelling. – Transportation Research Record 890: 11-17.
[15] Louviere, J., Woodworth, G. (1983): Design and analysis of simulated consumer choice or allocation experiments: an approach based on aggregate data. – Journal of Marketing Research 20: 350-367.
[16] Louviere, J., Hensher, D. A., Swait, J. (2000): Stated Choice Methods: Analysis and Applications. – Cambridge University Press, Cambridge.
[17] McFadden, D. (1973): Conditional Logit Analysis of Qualitative Choice Behavior. – In: Zarembka, P. (ed.) Frontiers in Econometrics. Academic Press, New York.
[18] Mendelsohn, R., Olmstead, S. (2009): The economic valuation of environmental amenities and disamenities: Methods and applications. – Annual Review of Environment and Resources 34: 325-347.
[19] Merino-Castello, A. (2003): Eliciting Consumer Preferences Using Stated Preference Discrete Choice Models: Contingent Ranking versus Choice Experiments. – Department of Economics and Business, Pompeu Fabra University, Barcelona, Spain. http://www.econ.upf.edu/docs/papers/downloads/705.pdf. – Accessed in May 2011.
[20] Mitchell, R., Cameron, R., Carson, T. (1986): The Use of Contingent Valuation Data for Benefit-Cost Analysis in Water Pollution Control. Final Report to the U.S. Environmental Protection Agency, September. – U.S. Environmental Protection Agency, Washington, DC.
[21] Polasky, S. (2008): What's nature done for you lately: measuring the value of ecosystem services. – Choices 23(2): 42-46.
[22] Rantamäki-Lahtinen, L. M., Väre, M. (2012): Strategic objectives and development plans of beginning farmers. – Agricultural and Food Science 21(4): 430-439.
[23] Sandhu, H. S., Wratten, S. D., Cullen, R., Hale, R. (2005): Evaluating nature's services on Canterbury arable farmland. Technical Report. – National Centre for Advanced Bio-Protection Technologies, Lincoln University, Lincoln.
[24] Sandhu, H. S., Wratten, S. D., Cullen, R. (2010): Organic agriculture and ecosystem services. – Environmental Science & Policy 13: 1-7.
[25] Power, A. G. (2010): Ecosystem services and agriculture: tradeoffs and synergies. – Philos. Trans. Roy. Soc. B 365: 2959-2971.
[26] Train, K. (2003): Discrete Choice Methods with Simulation. – Cambridge University Press, New York.

APPENDIX

1. Please tick the option that you most prefer

	Option A	**Option B**	**Option C**
Nitrate leaching	Big reduction	Small reduction	No change
Soil quality	Improvement	No change	No change
Biodiversity	More variety	More variety	No change
Payment for the option (Rs. per year for next 5 years)	Rs. 100	Rs. 10	Rs. 0

Option A ☐ Option B ☐ Option C ☐

http://www.aloki.hu ● ISSN 1589 1623 (Print) ● ISSN 1785 0037 (Online)
DOI: http://dx.doi.org/10.15666/aeer/1706_1380313815

2. Please tick the option that you most prefer

	Option A	**Option B**	**Option C**
Nitrate leaching	Big reduction	No change	No change
Soil quality	No change	Improvement	No change
Biodiversity	More variety	No change	No change
Payment for the option (Rs. per year for next 5 years)	Rs. 100	Rs. 10	Rs. 0

Option A ☐ Option B ☐ Option C ☐

3. Please tick the option that you most prefer

	Option A	**Option B**	**Option C**
Nitrate leaching	Small reduction	Big reduction	No change
Soil quality	Improvement	No change	No change
Biodiversity	No change	More variety	No change
Payment for the option (Rs. per year for next 5 years)	Rs. 100	Rs. 60	Rs. 0

Option A ☐ Option B ☐ Option C ☐

http://www.aloki.hu ● ISSN 1589 1623 (Print) ● ISSN 1785 0037 (Online)
DOI: http://dx.doi.org/10.15666/aeer/1706_1380313815

TRANSCRIPTIONAL DYNAMICS OF EARLY DEVELOPING TOMATO (*SOLANUM LYCOPERSICUM* L.) FRUIT BASED ON RNA-SEQ ANALYSIS

EDRIS, S.[1,2,3*] – ABO-ABA, S.[1,4] – ALGANDABY, M. M.[1] – ALSHAMRANI, E. M. M.[1] – ATEF, A.[1] – RAMADAN, A. M.[1,5] – GADALLA, N. O.[1,6] – SABIR, M. J. S.[7] – EL-DOMYATI, F. M.[1,3] – MAKKI, R. M.[1] – HAJRAH, N. H.[1] – SABIR, M. J.[1] – ABDEL-HAMID, A. M. E.[8] – QARI, S. H.[9] – JANSEN, R. K.[1,10] – AL-QUWAIE, D. A. H.[11] – BAHIELDIN, A.[1,3]

[1]*Department of Biological Sciences, Faculty of Science, King Abdulaziz University (KAU), Jeddah, Saudi Arabia*

[2]*Princess Al-Jawhara Al-Brahim Centre of Excellence in Research of Hereditary Disorders (PACER-HD), Faculty of Medicine, King Abdulaziz University (KAU), Jeddah, Saudi Arabia*

[3]*Department of Genetics, Faculty of Agriculture, Ain Shams University, Cairo, Egypt*

[4]*Department of Microbial Genetics, Genetic Engineering and Biotechnology Division, National Research Centre, Giza, Egypt*

[5]*Agricultural Genetic Engineering Research Institute (AGERI), Agriculture Research Center (ARC), Giza, Egypt*

[6]*Department of Genetics and Cytology, Genetic Engineering and Biotechnology Division, National Research Center, Dokki, Egypt*

[7]*Department of Computer Science, Faculty of Computer and Information Technology, King Abdulaziz University (KAU), Jeddah 21589, Saudi Arabia*

[8]*Department of Biological and Geological Sciences, Faculty of Education, Ain Shams University, Cairo, Egypt*

[9]*Department of Biology, Aljumum University, College, Umm Al-Qura University, Makkah, Saudi Arabia*

[10]*Department of Integrative Biology, University of Texas at Austin, Austin, TX, USA*

[11]*Department of Biological Sciences, Rabigh College of Science and Arts, King Abdulaziz University (KAU), Rabigh, Saudi Arabia*

**Corresponding author*
e-mail: seedris@kau.edu.sa; phone: +966-59-366-2384; ORCID ID: 0000-0002-2810-3736

(Received 13th May 2019; accepted 20th Aug 2019)

Abstract. Tomato (*Solanum lycopersicum* L.) is one of the most popular vegetable species grown worldwide. Functional genomic analysis of genes in the early flower and fruit stages are the key factors for genetic enhancement of tomato fruits for increased yield and quality. In the current study, RNA-Seq datasets were generated for the Chico cultivar at six growth stages, 0, 3, 5, 7, 9 and 12 days after pollination (DAP). The computational analysis of transcriptomes and heat map showed close relationships among transcripts regulated at 3 and 5 DAP and at 7 and 9 DAP, whereas transcripts regulated at 12 DAP were more distant. Annotated transcripts and KEGG analysis showed that starch and sucrose pathway experienced the most dynamic changes resulting in the synthesis of several soluble sugars, e.g., sucrose, β-D-fructose, α-D-glucose, trehalose, maltose and 1,4-β-D-xylan. Enzymes

http://www.aloki.hu ● ISSN 1589 1623 (Print) ● ISSN 1785 0037 (Online)
DOI: http://dx.doi.org/10.15666/aeer/1706_1381713831

activated in this pathway included levansucrase, phosphotransferse, invertase, pectin methyl esterase (PME), glucan synthase and cellulase. In general, the results provided improved insights into the mechanisms underlying early fruit development in tomatoes.
Keywords: *Chico III, analysis, pPCR, KEGG, starch and sucrose pathway, PME2.1, WIV-1(sacA), PTS (scrA), LS (sacB), cellulose (phd) and sph1(cre or glucan synthase)*

Introduction

Tomato (*Solanum lycopersicum* L.) is one of the most important vegetable crops worldwide due to its economic and agronomic importance (Zhang et al., 2016). Cultivated tomatoes are diploid with 12 chromosomes and a genome size of approximately 950 Mb with 35,000 genes (Guigó Serra et al., 2012) and wild forms range from diploids to hexaploids (Bonierbale et al., 1988; Gupta et al., 2013). Tomato fruit development begins with fertilization and ends at the red ripe stages (Gillaspy et al., 1993; Picken, 1984). Wild tomatoes are important for tomato breeding and also cultivating plants belonging to family Solanaceae because information gained from studies in tomato genome sequencing can be applied to these plants (Kimura and Sinha, 2008).

Functional genomic analysis at the fruit ripening stage with mature, full-sized green fruit has been studied intensively (Gapper et al., 2014), while studies at earlier stages of fruit development are limited. The early developmental stage is very important for tomato fruit formation because the fruit weight and size are widely dependent on the pericarp cell number which is genetically controlled during cell division (Xiao et al., 2008), which leads to cell expansion and increases in average cell size. Transcription factors organizing early steps of the development also appear to have roles in tomato flower and fruit development (Silva et al., 2014). DNA replication is essential during both phases, although it is followed by mitosis in the earlier phase and endomitosis (replication progresses several times without mitosis) in the later phase. The resulting cells can possess multiple genome copies (polyploidy); an important process during cell expansion (Bergervoet et al., 1996).

Parallel with these processes, differentiation of the tissues into pericarp (fruit wall), peel, placenta and locular tissue ("jelly") is completed (Bertin, 2005; Mintz-Oron et al., 2008). Many of the final fruit quality parameters, such as size, shape, taste (soluble solids), texture (wateriness, mealiness), firmness, proneness to cracking, peelability, and properties during processing (viscosity), are co-determined during early stages by signals of some hormones that are stimulated in pericarp developmental stages. Carbohydrates are the main component in early developed tomato fruits. Metabolism of carbohydrates is regulated by many genes that contribute to cell wall synthesis (Zhang et al., 2016).

Web-based resources for genetic control and development of tomato are available at Tomato Genetics Resource Center (TGRC) (http://tgrc.ucdavis.edu) which contains a collection of wild relatives and miscellaneous genetic stocks of tomato (Kimura and Sinha, 2008). Expressed sequence tags (ESTs) library largely replaced microarray technologies in most plant systems because it provides a large-scale picture of gene expression during ripening in tomato (Gapper et al., 2014) and responses to treatment or environmental stresses (Bahieldin et al., 2015a). However, RNA-Seq provides an accurate statistical assessment of gene expression and clusters of genes based on their expression patterns (Bahieldin et al., 2015b). Therefore, RNA-Seq datasets of gene expression in tomato were generated in the present study and verification of gene

http://www.aloki.hu ● ISSN 1589 1623 (Print) ● ISSN 1785 0037 (Online)
DOI: http://dx.doi.org/10.15666/aeer/1706_1381713831

expression profiles involved in several metabolic pathways shed the light on genetic mechanisms that might regulate early developmental stage and the formation of fruit during ripening stage in tomato.

Materials and methods

Plant material

Tomato cv. Chico III seeds were germinated in pots filled with Peat moss soil and grown in the glasshouse under controlled conditions (16-h-light/8-h-dark cycle at 21 ± 2 °C (day/night), light intensity of ~200 uE m^{-2} s^{-1} for the 16-h photoperiod and 80% humidity) (Zhan et al., 2018). Recovered plantlets were watered every other day for 60 days until buds started to develop. Then, flower and bud samples were taken at six growth stages, i.e., 0 day after pollination (DAP), 3 DAP, 5 DAP, 7 DAP, 9 DAP and 12 DAP. Each sample was collected from two pots with four plants each in order to recover enough RNA for further analysis.

RNA extraction, library construction and sequencing

Total RNAs were extracted using SV Total RNA Isolation System (Promega) and the Truseq™ RNA Sample Prep Kit (Illumina) was utilized for library construction following the manufacturer's instructions. Then, the library was shipped to Beijing Genomics Institute (BGI) in China for sequencing on Illumina HiSeq™ 2000. For every sequencing read, the indexes were trimmed using SeqPrep program (https://github.com/jstjohn/SeqPrep) and the paired ends were merged . The remaining optimized reads were mapped to the tomato reference genome (ftp://ftp.solgenomics.net/tomato_genome/annotation/ITAG2.3_release/) using Tophat (Trapnell et al., 2009) and SOAPaligner/soap2 software (http://soap.genomics.org.cn) (Robinson et al., 2010). The mapped reads were then assembled with Cufflink (Trapnell et al., 2010). The experiment was submitted to National Center for Biotechnology Information (NCBI) as BioProject accession number PRJNA298353 and as BioSample accession numbers SAMN04214820 to SAMN04214831. RNA-Seq reads were placed in Sequence Read Archive (SRA) database (http://www.ncbi.nlm.nih.gov/Traces/sra/) under the accession number SUB1151548. The differential expression profiling and further annotation analysis utilized the merged and assembled sequences, as well as the original genome annotations.

The Bowtie aligner software of trinity package (http://trinityrnaseq.sourceforge.net/analysis/extract_proteins_from_trinity_transcripts.html) was used to predict the mapping of the assembled transcripts reads to the reference genome and annotated genes or open reading frames (ORFs). Sequence-similarity Blast searches of transcripts were conducted against the tomato reference genome, the NCBI genome database (http://www.ncbi.nlm.nih.gov/), the gene ontology (GO) database (http://www.geneontology. org/) and the Kyoto encyclopedia of genes and genomes (KEGG) database (http://www.genome.jp/kegg/) (Kanehisa and Goto, 2000).

GO terms for tomato transcripts were obtained using Blast2GO (v.2.3.5) (http://www.blast2go.org/) with default parameters (Kanehisa and Goto, 2000). Differential expression analysis was performed via Tophat (http://tophat.cbcb.umd.edu/) and Cufflinks (http://cufflinks.cbcb.umd.edu/) programs and RPKM (Reads per kilobase of exon model per million mapped fragments) values were detected within 95%

http://www.aloki.hu ● ISSN 1589 1623 (Print) ● ISSN 1785 0037 (Online)
DOI: http://dx.doi.org/10.15666/aeer/1706_1381713831

confidence limit. Differential expression was calculated according to the count values of each transcript in the library using edge R software (Robinson et al., 2010). False discovery rate (FDR) of < 0.05 and $\log^2$ fold-change ($\log^2$ FC) of ≥ 1 were used as the thresholds for judging significant differences in transcript expression. Transcripts with $\log^2$ FC of < 0.25 were assumed to have no change in expression levels.

Data verification via qRT-PCR

Quantitative real-time reverse transcriptase (qRT-PCR) consideration was performed to verify the expression patterns of randomly selected transcripts of RNA-Seq datasets. Aliquots of the originally purified RNA samples were reverse-transcribed using the PrimeScript RT Reagent kit with gDNA Eraser (Takara, Dalian, China) following the manufacturer's protocol. Eight gene-specific qRT-PCR primer pairs (18-20 bp) (*Table 1*) were designed using primer Premier 5.0 software (Premier Biosoft International, Palo Alto, CA). These genes are *sacB(LS)*, *scrA(PTS)*, *sacA(WIV-1), PME, xyl1, cre (Glucan synthase)* and *phd (Cellulase)* encode enzymes at the starch and sucrose metabolic pathway. RNA-Seq data indicated that these eight genes were regulated during fruit development. Of which, the first four genes were downregulated, while the other three genes were upregulated. qRT-PCR was performed using SybrGreenqRT-PCR master mix (Ruian Biotechnologies, Shanghai, China) in an ABI 7500 FAST Real-Time PCR system (Applied Biosystems, Foster City, CA, USA). PCR conditions were 2 min at 95 °C, followed by 40 cycles of heating at 95 °C for 10 s and annealing/extension at 60 °C for 40 s and 72 °C for 2 min. Three replicates were performed, and the amplicons were used for melting curve analysis to check the amplification specificity. The relative expression level of each gene was calculated as $2^{-(\Delta\Delta Ct)}$ and the housekeeping gene glyceraldehyde-3-phosphate dehydrogenase or GAPDH (accession no. U93208) from *S. lycopersicum* was used to normalize the amount of template cDNA added in each reaction.

Table 1. *Primer sequences for selected genes used for validating RNA-Seq datasets*

Gene symbol	Accession number	Sequence (5'- > 3')	Amplicon (bp)
GAPDH	NM_001247874	AATTGGCCGATTGGTTGCTC GAAGGGATCGTTCACTGCGA	73
sacB (LS)	NM_001247250	ATCGCGGAGAAGGAAGCAAA ACTACCCGGTGGCAATGTAG	117
scrA (PTS)	NM_001247449	TGGCTAGATTGCCACAACTCG CCAGCTGTTGGGATTCCTCAT	86
sacA (WIV-1)	NM_001246913	TCGCGAGTTTAGACAAGGCA CCAAGACCACCTTGAACCGT	103
PME	NM_001247019	TGGCGATAAAGCTGAAACTGA ATAACCACCACCCCACAACC	111
XYL1	NM_001246981	GTGGAAGGCTCCCAATGACA GGGTAGTTTGTGGCAGGGTT	97
cre (*glucan synthase)*	NM_001247033	TCGCTAGCGGAAAATTGCTT TTCGTCATCCTTTGACGTGC	111
Phd (cellulase)	NM_001247953	CCCAGACGAGCGTTCAGATT	98

http://www.aloki.hu ● ISSN 1589 1623 (Print) ● ISSN 1785 0037 (Online)
DOI: http://dx.doi.org/10.15666/aeer/1706_1381713831

Results

Transcriptomic analysis

RNA-Seq analysis of flowers and buds harvested from tomato cultivar Chico III was done at early fruit development stages ranging from 0, 3, 5, 7, 9 and 12 DAP. Over 24 Gb of data were generated from six datasets comprising 274,981,532 paired-end reads of 90 bp in length after trimming. The dataset of each sample had > 44 million reads, which represented a sufficient read density for the subsequent quantitative analysis of gene expression (*Table 2*).

The clean sequence reads were aligned to the tomato reference genome database allowing two base mismatches. Alignment and assembly resulted in 27,527 transcripts in the transcriptome. This number represents over 65% of the genes available in the tomato Unigene database (42,257), and 29.2-43.1% were differentially expressed with ≥ 2 fold at different time points compared to the control (0 DAP) (*Table 2*). The percentage of transcripts of different sizes with 150-200, 200-600, 600-1000, 1000-1600, 1600-2200, 2200-3000 and > 3000 bp were 8.14, 32.53, 20.28, 20.72, 9.44, 5.41 and 3.48%, respectively (*Fig. 1*). The latter four size categories more likely recover fragments long enough to likely detect function domains of the transcripts. The total number of transcripts expressed at different time points was 4335 in the control group (0 DAP), while 2588 at 3 DAP, 3529 at 5 DAP, 3549 at 7 DAP, 4054 at 9 DAP and 5,968 at 12 DAP.

The heat map indicated that the differential response at 0 DAP was distinct from the later stages (*Fig. 2*). Transcripts regulated at 3 and 5 DAP and 7 and 9 DAP clustered together, and transcripts regulated at 12 DAP were more distant compared to these four stages. A Venn diagram was constructed to compare the yield of transcripts shared between the following pairs of developmental stages, e.g., 0/3 DAP, 0/7 DAP and 0/12 DAP (*Fig. 3*). The number of shared transcripts were 8,054 (A + AB + AC + ABC), 8,750 (B + AB + BC + ABC) and 11,875 (C + AC + BC + ABC), respectively out of the total of 14,182 different transcripts. The highest number of shared transcripts was across the three stages (5307) followed by 0 and 7 DAP (1,871). The highest number of unique transcripts (3,276) in the developmental stage pairs was 0/12 DAP followed by 0/7 DAP (981). These unique transcripts across the three developmental stages indicate the occurrence of differential expression during the flowering stages.

Table 2. *Number of reads sequenced and mapped to the tomato reference genome*

Time point	0 DAP	3 DAP	5 DAP	7 DAP	9 DAP	12 DAP
Clean bases (bp)	4,149,898,380	4,046,486,040	4,033,137,780	4,079,245,860	4,220,982,000	4,218,587,820
Clean no. reads	46,109,982	44,960,956	44,812,642	45,324,954	46,899,800	46,873,198
% Aligned reads	82.02	81.92%	85.21%	82.86%	85.23%	83.75%
% Unique matches	36.58	49%	38.33	35.12	34.32	33.42
% Multi-position matches	45.44	45.43%	46.88	47.74	50.91	50.33
% Unaligned reads	17.98	18.08%	14.79	17.14	14.77	16.25
No. differentially expression genes (≥2 fold)	-	8.045	9.465	8.750	9.678	11875
% Differentially expression genes (≥2 fold)	-	29.23	34.38	31.79	35.16	43.1

http://www.aloki.hu ● ISSN 1589 1623 (Print) ● ISSN 1785 0037 (Online)
DOI: http://dx.doi.org/10.15666/aeer/1706_1381713831

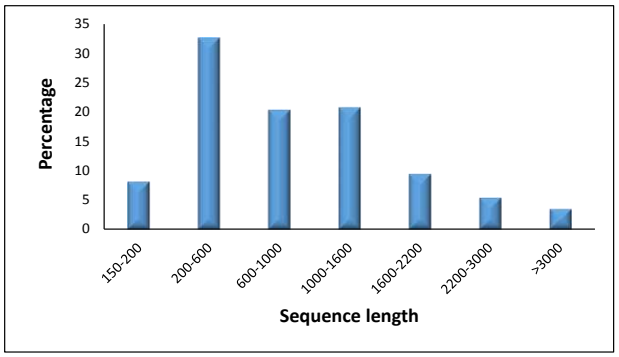

Figure 1. *Length distribution of the transcript sequences detected in early fruit development transcriptomes*

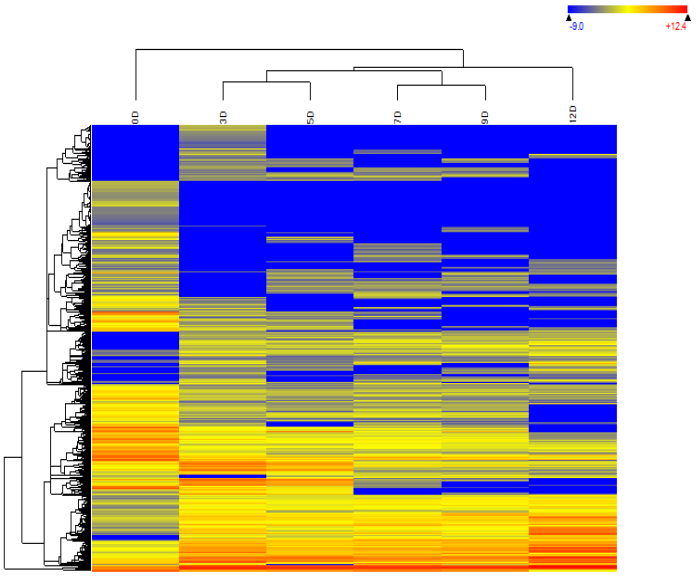

Figure 2. *Heat map analysis of all transcripts at the different time courses*

Figure 3. *Venn diagram of expressed transcripts at 3 (A), 7(B) and 12 (C) DAP compared with those at 0 DAP*

http://www.aloki.hu ● ISSN 1589 1623 (Print) ● ISSN 1785 0037 (Online)
DOI: http://dx.doi.org/10.15666/aeer/1706_1381713831

Annotated transcripts with known function were classified into 52 functional groups, including 13 in cellular component (*Fig. 4*), 12 in molecular function (*Fig. 5*) and 19 in biological process (*Fig. 6*) categories comprising 1,364 regulated transcripts. In the cellular component category, 337 transcripts were regulated. Of which, 96, 75, 56 and 37 transcripts were regulated in the "cell", "organelle", "membrane" and "extracellular region", respectively (*Fig. 4*). In the molecular function category, 251 transcripts were regulated. Of which, 90, 88, 22 and 13 transcripts were regulated in the "catalytic activity", "binding", transporter activity" and "nucleic and binding transcription factor activity", respectively (*Fig. 5*). In the biological process category, 778 transcripts were regulated and most of these belong to "metabolic process" (118), followed by "cellular process" (105), "single organism process" (101), "response to stimulus" (68), "biological regulation" (58), cellular component organization or biogenesis (54) and "developmental process" (49) (*Fig. 6*). Results of the functional groups indicate that the highest activities were at the cell, organelle and membrane levels as well as at the extracellular region level. These activities induced catalysis, binding, transportation and those required for transcription factors binding in the nucleus and cytoplasm. Major processes include metabolism and responses to stimulation and development. The latter two processes are essential for the flower in early developmental stages.

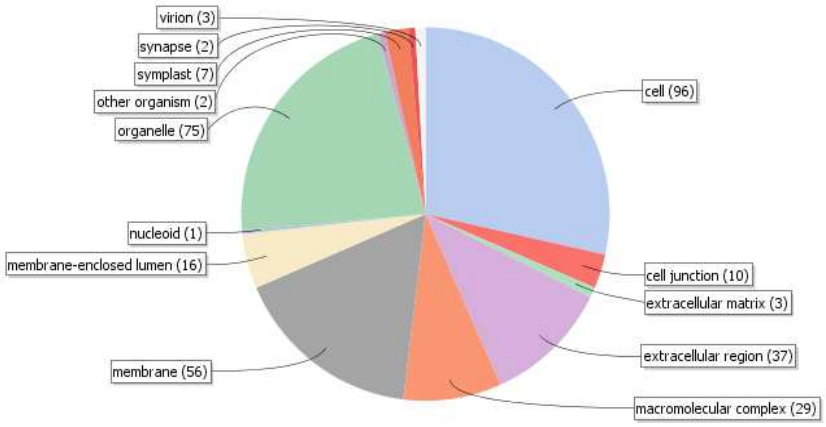

Figure 4. *Gene ontology (GO) terms of transcripts by the level 2. All transcripts were assigned to at least one GO term and were grouped under the cellular component category*

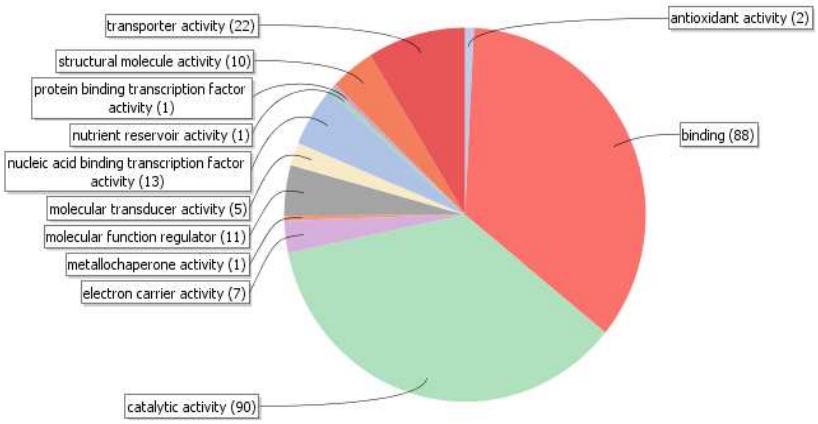

Figure 5. *Gene ontology (GO) terms of transcripts by the level 2. All transcripts were assigned to at least one GO term and were grouped under the molecular function category*

http://www.aloki.hu ● ISSN 1589 1623 (Print) ● ISSN 1785 0037 (Online)
DOI: http://dx.doi.org/10.15666/aeer/1706_1381713831

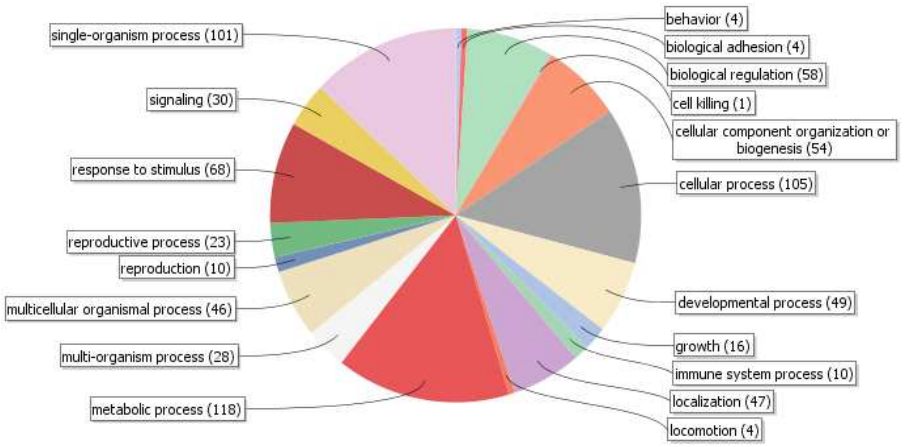

Figure 6. *Gene ontology (GO) terms of transcripts by the level 2. All transcripts were assigned to at least one GO term and were grouped under the biological process category and filtered by cutoff = 5*

Verification of RNA-Seq data

In order to verify the gene expression profiles of enzymes involved in starch and sucrose metabolism obtained from the RNA-Seq datasets, quantitative real-time PCR was utilized. Eight genes were selected for the analysis based on their regulation during starch and sucrose metabolic pathway. They are *scrA*, *sacB*, *phd*, *cre*, *sacA*, *pg2*, *pme* and *xyl1* (*Fig. 7*). These genes encode phosphotransferse (EC:2.7.1.69), levansucrase (EC:2.4.1.10), cellulase (EC:3.2.1.4), glucan synthase (EC:2.4.1.34), invertase (EC:3.2.1.26), exopolygalacturonase (EC:3.2.1.67), pectin methylesterase (EC:3.1.1.11) and beta-xylosidase (EC:3.2.1.37).

Figure 8 shows that eight genes were divided into three groups depending on its expression profile, first group were down regulated containing *PME2.1, PTS (scrA), Cellulose (phd) and sph1(cre or Glucan synthase)*, the second pattern was up-regulated *WIV-1(sacA) and the third* pattern was partially down regulated *LS (sacB).*

Discussion

The results are concomitant with those of Silva et al. (2014) who found that miR156-targeted *S. lycopersicum* SBP genes were dynamically expressed in developing flowers and ovaries as the cell is active in metabolism and likely to be sensitive to external stimuli. Hydrolase, transferase and oxidoreductase enzymes are predominant across the different stages of fruit development (*Fig. 9*). Recent reports indicate that one family of the hydrolases, e.g., xyloglucan endotransglycosylase/hydrolase (XTH), plays an important role in the remodeling of cell wall hemicelluloses during ripening (Han et al., 2015). One of the transferase families, e.g., quercetin-3-O-glucosyl transferases (3-GT), has a role in forming the flavonoid quercetin-3-rutinoside or rutin during tomato fruit ripening (Capanoglu et al., 2012). One important enzyme family of oxidoreductase, or quinone oxidoreductase, is ripening-induced and catalyzes the formation of 4-hydroxy-2,5-dimethyl-3(2H)-furanone (HDMF), the key flavor compound in strawberry (Klein et al., 2007). Family of this enzyme has previously been isolated from kiwi, raspberry and tomato as natural products (Schwab, 2013).

http://www.aloki.hu ● ISSN 1589 1623 (Print) ● ISSN 1785 0037 (Online)
DOI: http://dx.doi.org/10.15666/aeer/1706_1381713831

Kyoto Encyclopedia of Genes and Genomes (KEGG) has recently moved the exopolygalacturonase enzyme to the "pentose and glucuronate interconversions" pathway, while the latter two enzymes were moved to "amino sugar and nucleotide sugar metabolism" pathway. The correlation coefficients (R2) ranged in value between 0.9900 and 1.0000, and PCR amplification efficiencies over 94% were obtained from the standard curves generated using a 10-fold serial dilution of cDNA.

KEGG annotation assigned 846 transcripts to 89 KEGG pathways. The pathway most strongly represented was "starch and sucrose metabolism" (seven activated enzymes). Tomato fruit is very powerful sink for carbohydrate especially in early stages of development. Sucrose is the major photoassimilate transported from photosynthetic leaves to developing fruit. Carbohydrates comprise the most abundant and widely distributed food components derived from plants. Their contents vary greatly in tomato fruit during development and ripening. Selection in this fruit was oriented towards sweetness as sugar, mainly sucrose, glucose and fructose, level (~60% of the total fruit dry weight) is the indicator of ketchup's quality (O'donoghue et al., 1994). Invertase enzyme cleaves sucrose, which may regulate the rate of carbon import to developing tomato fruit (Fei Wang, 1993). It was demonstrated that changes in sugar composition contribute to alterations in fruit size. Mach (Fridman et al., 2004) discussed the role of apoplastic invertase, which contributes to starch accumulation in pericarp and columella tissues, in determining the soluble solids content of mature fruit (Dinar and Stevens, 1981; Schaffer and Petreikov, 1997).

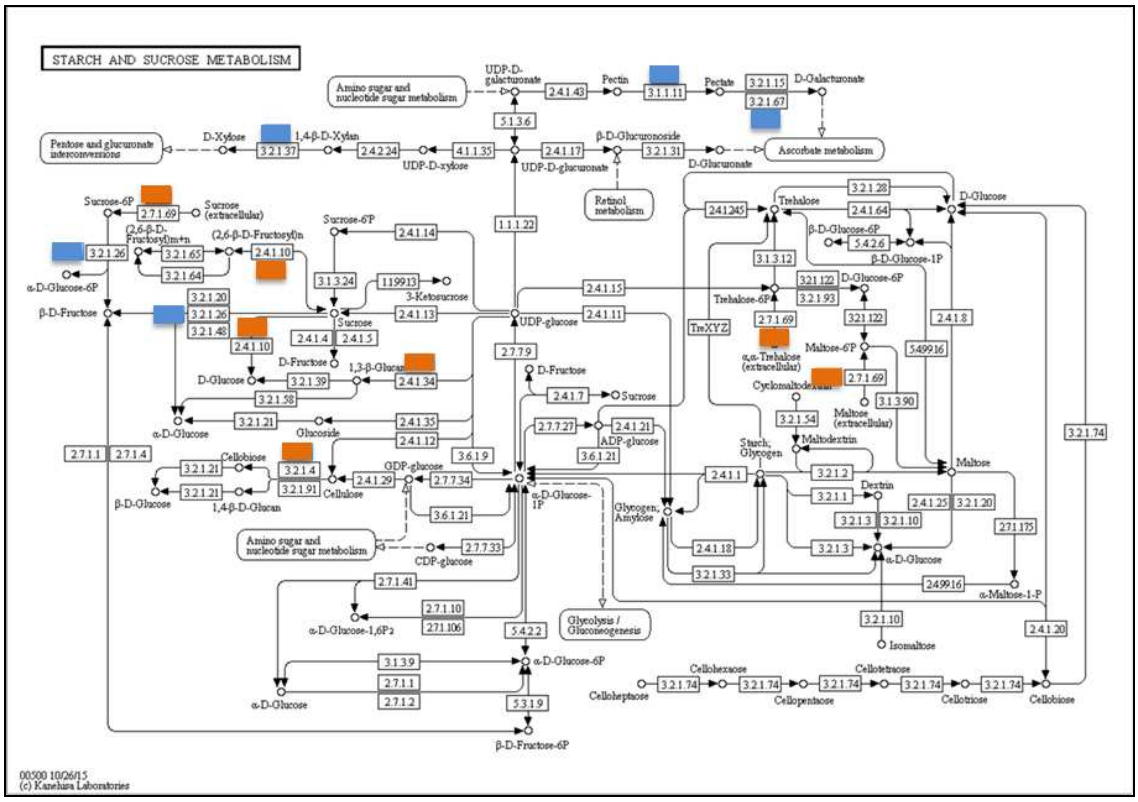

Figure 7. *Enzymes in the starch and sucrose metabolic pathway during early stages of tomato fruit development at 12 versus 0 DAP. Upregulated (or activated) (blue box), downregulated (or repressed) (orange box). (Source: https://www.genome.jp/kegg-bin/show_pathway?ko00500)*

http://www.aloki.hu ● ISSN 1589 1623 (Print) ● ISSN 1785 0037 (Online)
DOI: http://dx.doi.org/10.15666/aeer/1706_1381713831

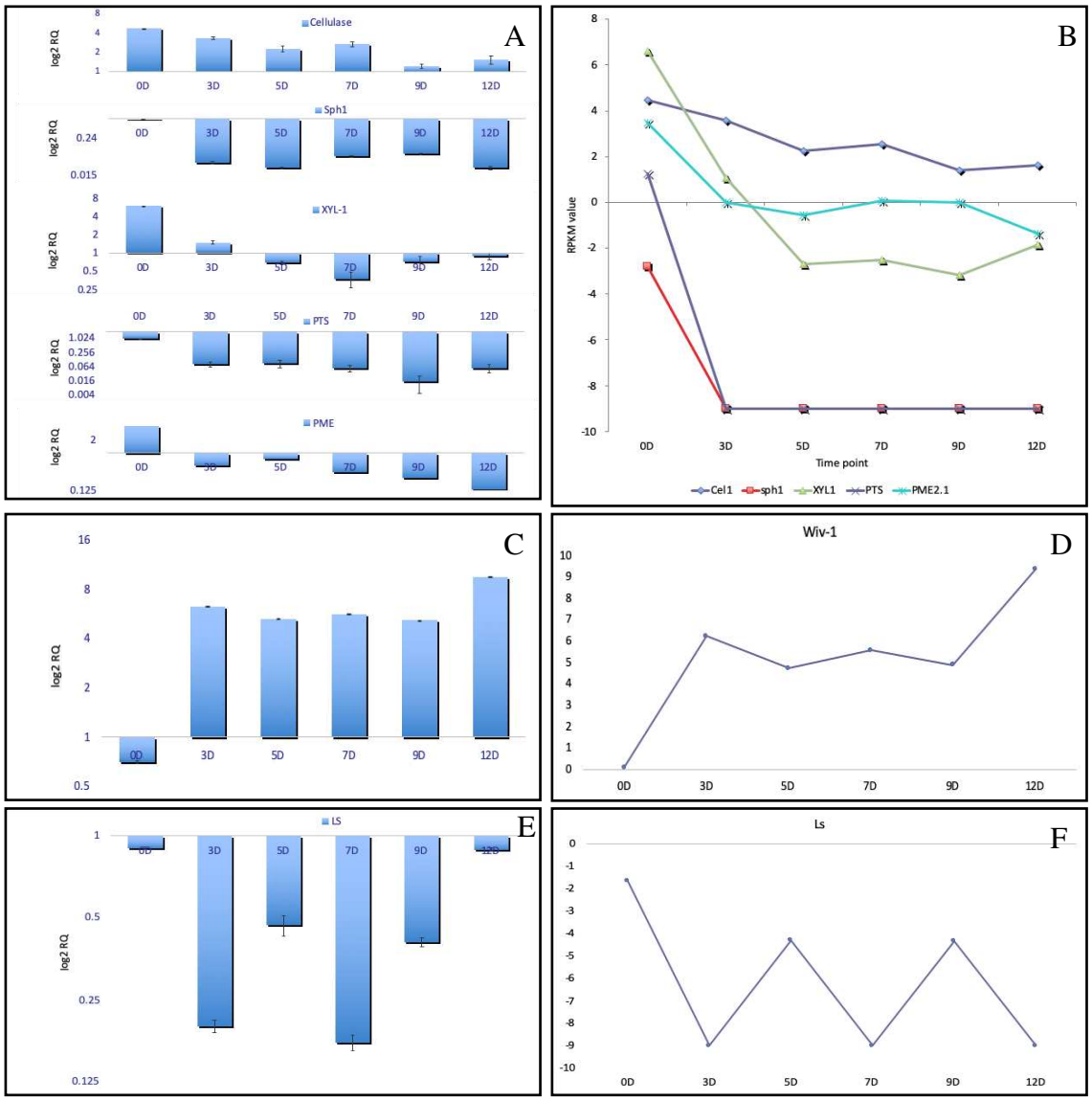

Figure 8. *Gene expression verification of PME2.1, WIV-1(sacA), PTS (scrA), LS (sacB), Cellulose (phd) and sph1(cre or Glucan synthase) genes using qPCR. A and B representing the down regulation pattern on both real time PCR results and RNAseq data respectively, C and D representing the up-regulation pattern of WIV-1(sacA), E and F representing fluctuated down regulation of LS (sacB) gene expression*

Invertase and sucrose synthase, along with the other regulated enzymes of the starch and sucrose metabolism in the present study seem to play a major role during early development of tomato fruits. It is well-known that sucrose, fructose and glucose are stored in the cell vacuole (Mach, 2014).

Figure 8 indicates the overproduction of several soluble sugars, e.g., sucrose, β-D-fructose, α-D-glucose, trehalose, maltose and D-xylose. This conclusion was reached as enzymes upstream these sugars were activated, enzymes downstream them were suppressed or both. Sucrose accumulated due to the suppression of levansucrase (encoded by *sacB*) and phosphotransferase (encoded by *scrA*), while β-D-fructose and α-D-glucose accumulated due to activation of invertase (encoded by *sacA*). High

http://www.aloki.hu ● ISSN 1589 1623 (Print) ● ISSN 1785 0037 (Online)
DOI: http://dx.doi.org/10.15666/aeer/1706_1381713831

activity of the enzyme also results in the synthesis of D-glucose and D-galactose in the "galactose metabolism" pathway (data provided upon request). Trehalose and maltose also accumulated due to suppression of phosphotransferase. In addition, the high activity of the enzyme pectin methyl esterase (PME) can result in approaching "Ascorbate metabolism". Two other enzymes, glucan synthase and cellulase (or endo-1,4 β-D-glucanase), were suppressed. This action results in the accumulation of UDP-glucose and cellulose, respectively (*Fig. 1*).

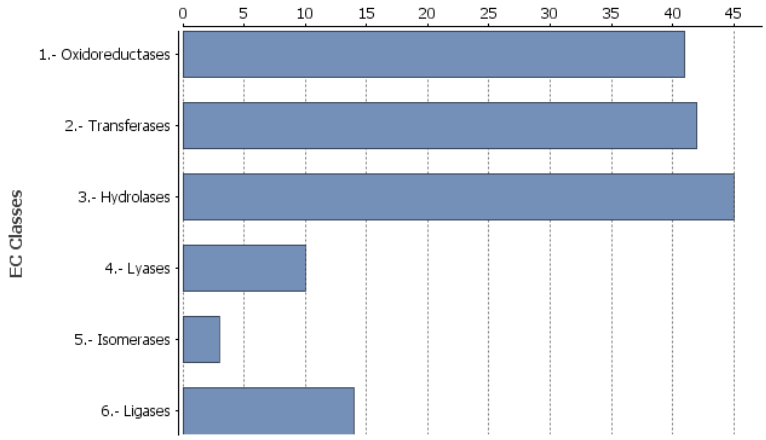

Figure 9. *Enzyme code distributions. All transcripts were aligned to the GO database to predict possible enzymatic functions. the total putative proteins were functionally classified into 6 groups*

Invertase is encoded by the *invertase 5* (or *lin5*) gene, accumulates in the cell wall and is known to act exclusively in flowers and young fruit (Fridman and Zamir, 2003). The enzyme is important in controlling total soluble solid content in these two organs. Overexpression of the enzyme resulted in increased partitioning of photosynthates to the fruit, hence, enhanced fruit yield (Baxter et al., 2005; Fridman et al., 2004; Schauer et al., 2006).

Zanor et al. (Zanor et al., 2009) reported that knockdown of the gene resulted in decreased levels of glucose and fructose in the fruit. The knockdowns were also characterized by the reduction in fruit size, seed number per plant and levels of phytohormones (LeClere et al., 2008).

Cellulase activity has previously been identified to contribute to cell wall disassembly and fruit softening (Brummell and Harpster, 2001). In avocado, cellulose was also found to contribute to the fruit ripening process (O'donoghue et al., 1994; Pesis et al., 1978). It is likely that this enzyme is suppressed at early stages of fruit development to allow complete maturity before the fruit commits to softening, while high cellulase activity in the abscission zone results in organ abscission in tomato (Brummell et al., 1999; Lashbrook et al., 1994, 1998; Sexton et al., 1980).

β-d-xylosidase was previously reported to have a role in the hydrolysis of arabinoxylans, xylans, and xyloglucans (Takizawa et al., 2014). The gene was shown to be involved in pear and tomato fruit development and ripening (Itai et al., 1999; Sozzi et al., 2002). The enzyme was also potentially involved in the softening process in strawberry (*Fragaria ananassa*) fruit (Bustamante et al., 2006). Frenkel et al. (1998) indicated that the production of methanol as well as ethanol in mature tomato fruit is

http://www.aloki.hu ● ISSN 1589 1623 (Print) ● ISSN 1785 0037 (Online)
DOI: http://dx.doi.org/10.15666/aeer/1706_1381713831

positively regulated by activation of pectin methylesterase (PME). The explanation of these results is based on the fact that suppression of the ethanol ADH-catalyzed production is due to methanol accumulation during tomato fruit ripening (Brummell and Harpster, 2001). Earlier reports indicated that mRNA/protein stability and delayed protein synthesis influence the level of PME activity during the development of tomato fruit (Harriman et al., 1991).

Conclusion

The computational analysis of transcriptomes and heat map showed close relationships among transcripts regulated at 3 and 5 DAP and at 7 and 9 DAP. Transcripts regulated at 12 DAP were more distant compared to the latter four stages. Annotated transcripts and KEGG analysis showed that starch and sucrose pathway experienced the most dynamic change resulting in the synthesis of several soluble sugars and activation of some enzymes. In general, the results provide better insights on the mechanisms underlying early flower and fruit development in tomatoes, which will be valuable for genetic enhancement of tomato fruits in the future.

The authors recommended for further studies to complete all stages involved on fruit repining and development to get complete picture about tomato fruit development.

Acknowledgements. This project was funded by the Deanship of Scientific Research (DSR), King Abdulaziz University, Jeddah, under Grant no. (19-3-1432/HiCi). The authors, therefore, acknowledge with thanks DSR technical and financial support.

REFERENCES

[1] Bahieldin, A., Atef, A., Sabir, J. S., Gadalla, N. O., Edris, S., Alzohairy, A. M., Radhwan, N. A., Baeshen, M. N., Ramadan, A. M., Eissa, H. F. (2015a): RNA-Seq analysis of the wild barley (H. spontaneum) leaf transcriptome under salt stress. – Comptes Rendus Biologies 338(5): 285-297.

[2] Bahieldin, A., Atef, A., Shokry, A. M., Al-Karim, S., Al Attas, S. G., Gadallah, N. O., Edris, S., Al-Kordy, M. A., Omer, A. M. S., Sabir, J. S. (2015b): Structural identification of putative USPs in Catharanthus roseus. – Comptes Rendus Biologies 338(10): 643-649.

[3] Baxter, C. J., Carrari, F., Bauke, A., Overy, S., Hill, S. A., Quick, P. W., Fernie, A. R., Sweetlove, L. J. (2005): Fruit carbohydrate metabolism in an introgression line of tomato with increased fruit soluble solids. – Plant and Cell Physiology 46(3): 425-437.

[4] Bergervoet, J. H., Berhoeven, H. A., Gilissen, L. J., Bino, R. J. (1996): High amounts of nuclear DNA in tomato (Lycopersicon esculentum Mill.) pericarp. – Plant Science 116(2): 141-145.

[5] Bertin, N. (2005): Analysis of the tomato fruit growth response to temperature and plant fruit load in relation to cell division, cell expansion and DNA endoreduplication. – Annals of Botany 95(3): 439-447.

[6] Bonierbale, M. W., Plaisted, R. L., Tanksley, S. D. (1988): RFLP maps based on a common set of clones reveal modes of chromosomal evolution in potato and tomato. – Genetics 120(4): 1095-1103.

[7] Brummell, D. A., Harpster, M. H. (2001): Cell wall metabolism in fruit softening and quality and its manipulation in transgenic plants. – Plant Molecular Biology 47(1-2): 311-340.

http://www.aloki.hu ● ISSN 1589 1623 (Print) ● ISSN 1785 0037 (Online)
DOI: http://dx.doi.org/10.15666/aeer/1706_1381713831

[8] Brummell, D. A., Hall, B. D., Bennett, A. B. (1999): Antisense suppression of tomato endo-1, 4-β-glucanase Cel2 mRNA accumulation increases the force required to break fruit abscission zones but does not affect fruit softening. – Plant Molecular Biology 40(4): 615-622.
[9] Bustamante, C. A., Rosli, H. G., Añón, M. C., Civello, P. M., Martínez, G. A. (2006): β-Xylosidase in strawberry fruit: isolation of a full-length gene and analysis of its expression and enzymatic activity in cultivars with contrasting firmness. – Plant Science 171(4): 497-504.
[10] Capanoglu, E., Beekwilder, J., Matros, A., Boyacioglu, D., Hall, R. D., Mock, H. P. (2012): Correlation of rutin accumulation with 3-o-glucosyl transferase and phenylalanine ammonia-lyase activities during the ripening of tomato fruit. – Plant Foods for Human Nutrition 67(4): 371-376.
[11] Dinar, M., Stevens, M. (1981): The relationship between starch accumulation and soluble solids content of tomato fruits. – Journal American Society for Horticultural Science 106: 415-418.
[12] Fei Wang, A. S., Brenner, M., Smith, A. (1993): Sucrose synthase, starch accumulation, and tomato fruit sink strength. – Plant Physiol. 101: 321-327.
[13] Frenkel, C., Peters, J. S., Tieman, D. M., Tiznado, M. E., Handa, A. K. (1998): Pectin methylesterase regulates methanol and ethanol accumulation in ripening tomato (Lycopersicon esculentum) fruit. – Journal of Biological Chemistry 273(8): 4293-4295.
[14] Fridman, E., Zamir, D. (2003): Functional divergence of a syntenic invertase gene family in tomato, potato, and Arabidopsis. – Plant Physiology 131(2): 603-609.
[15] Fridman, E., Carrari, F., Liu, Y.-S., Fernie, A. R., Zamir, D. (2004): Zooming in on a quantitative trait for tomato yield using interspecific introgressions. – Science 305(5691): 1786-1789.
[16] Gapper, N. E., Giovannoni, J. J., Watkins, C. B. (2014): Understanding development and ripening of fruit crops in an 'omics' era. – Horticulture Research 1: 14034.
[17] Gillaspy, G., Ben-David, H., Gruissem, W. (1993): Fruits: a developmental perspective. – The Plant Cell 5(10): 1439.
[18] Guigó Serra, R., Câmara Ferreira, F., Consortium, T. G. (2012): The tomato genome sequence provides insights into fleshy fruit evolution. – Nature 485(7400): 635-641.
[19] Gupta, S., Shi, X., Lindquist, I. E., Devitt, N., Mudge, J., Rashotte, A. M. (2013): Transcriptome profiling of cytokinin and auxin regulation in tomato root. – Journal of Experimental Botany 64(2): 695-704.
[20] Han, Y., Zhu, Q., Zhang, Z., Meng, K., Hou, Y., Ban, Q., Suo, J., Rao, J. (2015): Analysis of xyloglucan endotransglycosylase/hydrolase (XTH) genes and diverse roles of isoenzymes during persimmon fruit development and postharvest softening. – PloS One 10(4): e0123668.
[21] Harriman, R. W., Tieman, D. M., Handa, A. K. (1991): Molecular cloning of tomato pectin methylesterase gene and its expression in Rutgers, ripening inhibitor, nonripening, and never ripe tomato fruits. – Plant Physiology 97(1): 80-87.
[22] Itai, A., Kawata, T., Tanabe, K., Tamura, F., Uchiyama, M., Tomomitsu, M., Shiraiwa, N. (1999): Identification of 1-aminocyclopropane-1-carboxylic acid synthase genes controlling the ethylene level of ripening fruit in Japanese pear (Pyrus pyrifolia Nakai). – Molecular and General Genetics MGG 261(1): 42-49.
[23] Kanehisa, M., Goto, S. (2000): KEGG: kyoto encyclopedia of genes and genomes. – Nucleic Acids Research 28(1): 27-30.
[24] Kimura, S., Sinha, N. (2008): Tomato (Solanum lycopersicum): A Model Fruit-Bearing Crop. – CSH Protoc. DOI: 10.1101/pdb.emo105.
[25] Klein, D., Fink, B., Arold, B., Eisenreich, W., Schwab, W. (2007): Functional characterization of enone oxidoreductases from strawberry and tomato fruit. – Journal of Agricultural and Food Chemistry 55(16): 6705-6711.

http://www.aloki.hu ● ISSN 1589 1623 (Print) ● ISSN 1785 0037 (Online)
DOI: http://dx.doi.org/10.15666/aeer/1706_1381713831

[26] Lashbrook, C. C., Gonzalez-Bosch, C., Bennett, A. B. (1994): Two divergent endo-beta-1, 4-glucanase genes exhibit overlapping expression in ripening fruit and abscising flowers. – The Plant Cell 6(10): 1485-1493.
[27] Lashbrook, C. C., Giovannoni, J. J., Hall, B. D., Fischer, R. L., Bennett, A. B. (1998): Transgenic analysis of tomato endo-β-1, 4-glucanase gene function. Role of cell in floral abscission. – The Plant Journal 13(3): 303-310.
[28] LeClere, S., Schmelz, E. A., Chourey, P. S. (2008): Cell wall invertase-deficient miniature1 kernels have altered phytohormone levels. – Phytochemistry 69(3): 692-699.
[29] Mach, J. (2014): Modeling sugar metabolism in tomato fruit. – The Plant Cell 26(8): 3222-3223.
[30] Mintz-Oron, S., Mandel, T., Rogachev, I., Feldberg, L., Lotan, O., Yativ, M., Wang, Z., Jetter, R., Venger, I., Adato, A. (2008): Gene expression and metabolism in tomato fruit surface tissues. – Plant Physiology 147(2): 823-851.
[31] O'donoghue, E., Huber, D. J., Timpa, J., Erdos, G., Brecht, J. (1994): Influence of avocado (Persea americana) Cx-cellulase on the structural features of avocado cellulose. – Planta 194(4): 573-584.
[32] Pesis, E., Fuchs, Y., Zauberman, G. (1978): Cellulase activity and fruit softening in avocado. – Plant Physiology 61(3): 416-419.
[33] Picken, A. (1984): A review of pollination and fruit set in the tomato (Lycopersicon esculentum Mill.). – Journal of Horticultural Science 59(1): 1-13.
[34] Robinson, M. D., McCarthy, D. J., Smyth, G. K. (2010): edgeR: a Bioconductor package for differential expression analysis of digital gene expression data. – Bioinformatics 26(1): 139-140.
[35] Schaffer, A. A., Petreikov, M. (1997): Sucrose-to-starch metabolism in tomato fruit undergoing transient starch accumulation. – Plant Physiology 113(3): 739-746.
[36] Schauer, N., Semel, Y., Roessner, U., Gur, A., Balbo, I., Carrari, F., Pleban, T., Perez-Melis, A., Bruedigam, C., Kopka, J. (2006): Comprehensive metabolic profiling and phenotyping of interspecific introgression lines for tomato improvement. – Nature Biotechnology 24(4): 447-454.
[37] Schwab, W. (2013): Natural 4-hydroxy-2,5-dimethyl-3(2H)-furanone (Furaneol(R)). – Molecules 18(6): 6936-51.
[38] Sexton, R., Durbin, M. L., Lewis, L. N., Thomson, W. W. (1980): Use of cellulase antibodies to study leaf abscission. – Nature 283: 873-874.
[39] Silva, G. F. F. e., Silva, E. M., da Silva Azevedo, M., Guivin, M. A. C., Ramiro, D. A., Figueiredo, C. R., Carrer, H., Peres, L. E. P., Nogueira, F. T. S. (2014): microRNA156-targeted SPL/SBP box transcription factors regulate tomato ovary and fruit development. – The Plant Journal 78(4): 604-618.
[40] Sozzi, G. O., Fraschina, A. A., Navarro, A. A., Cascone, O., Greve, L. C., Labavitch, J. M. (2002): α-L-Arabinofuranosidase activity during development and ripening of normal and ACC synthase antisense tomato fruit. – HortScience 37(3): 564-566.
[41] Takizawa, A., Hyodo, H., Wada, K., Ishii, T., Satoh, S., Iwai, H. (2014): Regulatory specialization of xyloglucan (XG) and glucuronoarabinoxylan (GAX) in pericarp cell walls during fruit ripening in tomato (Solanum lycopersicum). – PloS One 9(2): e89871.
[42] Trapnell, C., Pachter, L., Salzberg, S. L. (2009): TopHat: discovering splice junctions with RNA-Seq. – Bioinformatics 25(9): 1105-1111.
[43] Trapnell, C., Williams, B. A., Pertea, G., Mortazavi, A., Kwan, G., Van Baren, M. J., Salzberg, S. L., Wold, B. J., Pachter, L. (2010): Transcript assembly and quantification by RNA-Seq reveals unannotated transcripts and isoform switching during cell differentiation. – Nature biotechnology 28(5): 511-515.
[44] Xiao, H., Jiang, N., Schaffner, E., Stockinger, E. J., van der Knaap, E. (2008): A retrotransposon-mediated gene duplication underlies morphological variation of tomato fruit. – Science 319(5869): 1527-1530.

http://www.aloki.hu ● ISSN 1589 1623 (Print) ● ISSN 1785 0037 (Online)
DOI: http://dx.doi.org/10.15666/aeer/1706_1381713831

[45] Zanor, M. I., Osorio, S., Nunes-Nesi, A., Carrari, F., Lohse, M., Usadel, B., Kühn, C., Bleiss, W., Giavalisco, P., Willmitzer, L. (2009): RNA interference of LIN5 in tomato confirms its role in controlling Brix content, uncovers the influence of sugars on the levels of fruit hormones, and demonstrates the importance of sucrose cleavage for normal fruit development and fertility. – Plant Physiology 150(3): 1204-1218.

[46] Zhan, Y., Qu, Y., Zhu, L., Shen, C., Feng, X., Yu, C. (2018): Correction: transcriptome analysis of tomato (Solanum lycopersicum L.) shoots reveals a crosstalk between auxin and strigolactone. – PloS One 13(9): e0204873.

[47] Zhang, S., Xu, M., Qiu, Z., Wang, K., Du, Y., Gu, L., Cui, X. (2016): Spatiotemporal transcriptome provides insights into early fruit development of tomato (Solanum lycopersicum). – Sci Rep 6: 23173.

http://www.aloki.hu ● ISSN 1589 1623 (Print) ● ISSN 1785 0037 (Online)
DOI: http://dx.doi.org/10.15666/aeer/1706_1381713831

EXPERIMENTAL STUDY OF SINGLE-ROTOR UAV ON DROPLET DEPOSITION DISTRIBUTION IN SOYBEAN FIELD

ZHANG, K. F. – ZHANG, Z. – ZHANG, Y. H. – LI, H.*

College of Mechanical and Electrical Engineering, Henan Agricultural University, Zhengzhou 450002, China

**Corresponding author*
e-mail: chungbuk@163.com

(Received 20th May 2019; accepted 28th Aug 2019)

Abstract. It is particularly important to improve soybean yield and its management in the middle and late stage. Therefore, in view of the difficult problems of traditional field management machines, such as difficult operation, seedling pressing and so on. In this paper, the following two aspects of experimental research are carried out: the wind field distribution characteristics of single-rotor Unmanned Aerial Vehicle (UAV); the contrast test of the deposition distribution of different types of UAV. The spray test of single-rotor UAV in the middle and late stage of soybean was carried out to optimize the operation parameters of UAV. The experimental data is provided to improving the application of field management and UAV application technology in the middle and late stages of soybean production. The results show that the droplets of single rotor UAV can reach the lower part of soybean canopy, and the density of droplets can be more than 15/cm2. The data also provides technical support for experimental study.
Keywords: *plant protection, unmanned aerial vehicle, Huang-Huai-Hai area, wind field, droplet density*

Introduction

Agriculture is the foundation of China's economic construction and development, and the guarantee of the country's prosperity and strength. For a long time, soybean has been loved by people all over the world because of its high quality edible oil, excellent plant protein and many kinds of active substances which are beneficial to the human body (Yang, 2010; Chen et al., 2017[a]; Zhang et al., 2015). Soybean, as a feed crop, food crop, oil crop, cash crop and vegetable crop, has a large cultivation area and yield in the United States, Brazil and other countries. With a long planting history, China is one of the major producers of soybean (Zhang, 2007).

In recent years, the domestic demand for soybean has increased year by year, but the soybean output in our country is far from satisfying the domestic demand, which leads to a situation where we have to rely on a large number of imported foreign soybeans. This situation directly threatens the food security of China (Yang et al., 2008; Chen et al., 2017[b]).

Figure 1 shows the statistics of Chinese soybean imports from 2012 to 2017. According to the statistics of the General Administration of Customs from January to December 2017, the total amount of imported soybeans has reached 9.55×10^7 t, an increase of 1.16×10^7 t compared to 8.391×10^7 t in 2016.The data of the National Bureau of Statistics shows that the total output of legumes (soybeans and other miscellaneous beans) in China is about 1.9×10^7 t, which is the direct result of the 6.52×105 hm^2 increase in soybean planting area (Lou et al., 2017).

At present, the largest soybean production area in China includes three provinces in northeast China, followed by the summer soybean production area in Huang-Huai-Hai region, where the annual soybean production accounts for about 30% of the total

http://www.aloki.hu ● ISSN 1589 1623 (Print) ● ISSN 1785 0037 (Online)
DOI: http://dx.doi.org/10.15666/aeer/1706_1383313844

soybean production in China. Compared with the large-scale self-propelled spraying machinery and the operation mode of agricultural plant protection aircraft in the three provinces of northeast China, soybean plant protection in Huang-Huai-Hai area is mainly carried out by manual sprayer and backpack motor sprayer. This limits the operation of large-scale plant protection machinery because of the characteristics of land management mode and small plot in Huang-Huai-Hai area. At the same time, the development of pesticide application technology in our country, especially the development of pesticide application machinery, is lagging behind in the worsening of diseases and insect pests (Liu et al., 2015; Chen et al.,2017[c]; Qin et al., 2014). There are still many problems in the prevention and control of disease and pests, and the demand for soybean in China has been high all the time, but the soybean output cannot meet the change of this situation, which results in the need to import a large number of foreign soybeans, posing a direct threat to food security in our country. 86% soybean demand depends on imports and the imports in 2017 set a high record again, which is a further increase trend.

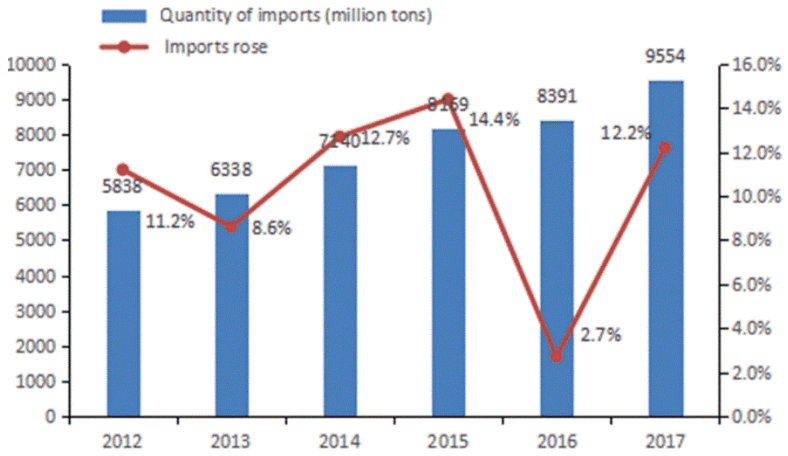

Figure 1. *Soybean import quantity statistics*

The development of UAV for plant protection in recent years has offered a new idea for soybean field plant protection (Jin et al., 2016). Single-rotor UAV has been widely used in agricultural plant protection because of its single wind field, uniform spraying, strong penetration, etc. (Gong and Fu, 2008; Guo et al., 2014; Xu et al., 2017). In order to solve the problems existing in soybean field management at the present stage, single rotor plant protection UAV was used in the field experiment in the middle and late stage of soybean, in order to solve the difficulty of traditional field management machine, which enter the soybean field in the middle and late stage of soybean, whose ridge was sealed. It solves pressing seedlings and other difficult problems, too. The field operation parameters of UAV were optimized, and the experimental data and technical support were provided for the application of field management and UAV application technology in the middle and late stages of soybean production. So wind field tests for a single-rotor UAV were carried out in this paper.

The influence of operation speed, flight height and the addition of flight control auxiliary equipment on droplets deposition was analyzed, and the optimal operation parameters in different periods were obtained. Providing field operation and the

http://www.aloki.hu ● ISSN 1589 1623 (Print) ● ISSN 1785 0037 (Online)
DOI: http://dx.doi.org/10.15666/aeer/1706_1383313844

optimization of key operation parameters for the applicability of plant protection unmanned aerial vehicle in soybean, are to solve the problem of landing for traditional spraying way during the middle and late stage.

Wind field tests for single-rotor UAV

Material

The test model is the electric single-rotor UAV (Mercury one), which is powered by a high-performance polymer lithium battery and is equipped with a remote control and a matching spray system, as is shown in *Figure 2*.The spray rod is adjustable which is installed with two fan-shaped spray nozzles with spray width of generally 7 m, different types of sprayers can be changed according to the use of different pesticides. Meanwhile, in order to measure wind speed, wind direction and temperature and humidity, we need to prepare multichannel anemometer, computer, temperature and humidity tester (CEM DT-615), portable anemometer (LB-SD2) and timer.

Figure 2. *Anelectric single-rotor UAV (Mercury one)*

Test method

The experiment was carried out in an experiment plot of Henan Agricultural University. During the test, the wind direction and wind speed were measured with a multichannel anemometer and a handheld anemometer (LB-SD2) at the test site. A temperature and humidity tester (CEM DT-615) is used to record the temperature of the test site and the time required for the test is recorded by a timer. The schematic diagram of the working principle is shown in *Figure 3*.

The wind field test of single-rotor plant UAV needs to determine the boundary of wind field. The multichannel anemometer and the handheld anemometer were used to find the boundary of the wind field (wind speed less than 0.2 m/s), and the boundary of the wind field was recorded.

Before the wind field test was carried out, it was necessary to determine the measurement point of the test, which started from the vertical bottom of the rotor of the UAV (as shown in the *Fig. 3*). Below the rotor of the plant protection UAV was the "O" point of the center. The wind field was measured all the way to the boundary, which was measured with a tape ruler every 0.5 meters. And eight directions were measured in one torus. In the direction of height Z, the height of soybean at branching stage and pod-setting stage were recorded at 0.5 m, 1 m, 1.5 m and 2 m respectively. The median

http://www.aloki.hu ● ISSN 1589 1623 (Print) ● ISSN 1785 0037 (Online)
DOI: http://dx.doi.org/10.15666/aeer/1706_1383313844

volume diameter (D_{50}) of agriculture flat-fan nozzle were used (Zhao et al., 2009).The spraying dose was 450 L/ha. The speed of the UAV was 5 m/s. The experiments had been replicated for three times.

Through the wind field test, the best flying altitude range of the single-rotor UAV was obtained. Within the same scope, the single-rotor plant UAV can achieve better spray drop deposition distribution compared to the multi-rotor UAVs.

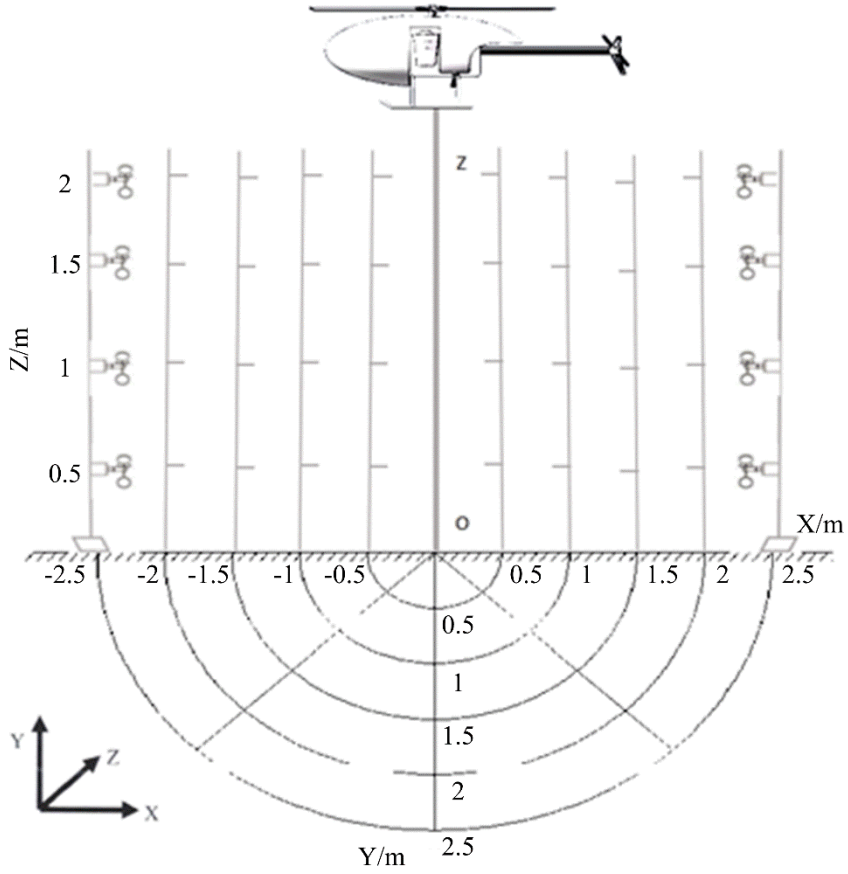

Figure 3. *Wind farm test layout*

Results and discussion

In the wind field test, the temperature is 17.5 °C, the wind speed is 0.2 ~ 1.5 m/s and the wind direction are southwest. During the experiment, the head of the drone was placed westward, and the fixed height of the drone was adjusted to 2.88 m. The measured data of each measurement point in the test are shown in *Table 1*.

As shown in *Figure 4*, the wind speed distribution of 0.5 m, 1 m, 1.5 m and 2 m from the plant canopy below the rotor shows that the distribution of wind field at different altitudes is basically similar. With the decrease of distance from the plant canopy, the wind speed is smaller. The decrease of the velocity below the center of the rotor is the fastest. From the wind field test data of *Table 1* and *Figure 4* and the simulation diagram of actual wind field test, it can be seen that the wind speed increases gradually with the increase of the center distance of the rotor axis in the range of rotor span of the single-rotor UAV. Outside the wingspan of the rotor, the wind speed decreases

http://www.aloki.hu ● ISSN 1589 1623 (Print) ● ISSN 1785 0037 (Online)
DOI: http://dx.doi.org/10.15666/aeer/1706_1383313844

gradually. In the rotor height direction, the wind speed increases first and then declines with the rise of the distance from the rotor. The trend is that the maximum wind speed is in the range of 1.5 m below the rotor, and the wind speed reaches about 12 m/s.

Table 1. *Wind field test data*

X/m	Y/m	Z/m	Wind (m/s)	X/m	Y/m	Z/m	Wind (m/s)	X/m	Y/m	Z/m	Wind (m/s)	X/m	Y/m	Z/m	Wind (m/s)
0.0	-2.5	1.0	0.3	0.0	-2.5	1.5	1.5	0.0	-2.5	2.0	1.9	0.0	-2.5	2.5	2.1
-0.5	-0.5	1.0	5.7	-0.5	-0.5	1.5	7.8	-0.5	-0.5	2.0	9.8	-0.5	-0.5	2.5	11.0
-1.0	-1.0	1.0	7.1	-1.0	-1.0	1.5	10.5	-1.0	-1.0	2.0	9.9	-1.0	-1.0	2.5	9.4
-1.5	-1.5	1.0	7.0	-1.5	-1.5	1.5	4.0	-1.5	-1.5	2.0	2.1	-1.5	-1.5	2.5	2.8
-2.0	-2.0	1.0	3.5	-2.0	-2.0	1.5	1.0	-2.0	-2.0	2.0	0.8	-2.0	-2.0	2.5	0.5
-2.5	-2.5	1.0	1.9	-2.5	-2.5	1.5	0.0	-2.5	-2.5	2.0	0.0	-2.5	-2.5	2.5	0.3
-0.5	0.0	1.0	6.4	-0.5	0.0	1.5	7.1	-0.5	0.0	2.0	9.4	-0.5	0.0	2.5	11.0
-1.0	0.0	1.0	6.8	-1.0	0.0	1.5	8.2	-1.0	0.0	2.0	9.4	-1.0	0.0	2.5	11.3
-1.5	0.0	1.0	7.7	-1.5	0.0	1.5	4.9	-1.5	0.0	2.0	3.1	-1.5	0.0	2.5	1.9
-2.0	0.0	1.0	7.3	-2.0	0.0	1.5	5.2	-2.0	0.0	2.0	4.3	-2.0	0.0	2.5	2.9
2.5	0.0	1.0	2.2	2.5	0.0	1.5	0.5	2.5	0.0	2.0	0.8	2.5	0.0	2.5	1.7
-0.5	0.5	1.0	5.7	-0.5	0.5	1.5	7.8	-0.5	0.5	2.0	9.8	-0.5	0.5	2.5	11.0
-1.0	1.0	1.0	7.1	-1.0	1.0	1.5	10.5	-1.0	1.0	2.0	9.9	-1.0	1.0	2.5	9.4
-1.5	1.5	1.0	7.0	-1.5	1.5	1.5	4.0	-1.5	1.5	2.0	2.1	-1.5	1.5	2.5	2.8
-2.0	2.0	1.0	3.5	-2.0	2.0	1.5	1.0	-2.0	2.0	2.0	0.8	-2.0	2.0	2.5	0.5
-2.5	2.5	1.0	1.9	-2.5	3.5	1.5	0.0	-2.5	2.5	2.0	0.0	-2.5	2.5	2.5	0.3
0.0	0.5	1.0	4.0	0.0	0.5	1.5	4.5	0.0	0.5	2.0	7.1	0.0	0.5	2.5	6.1
0.0	1.0	1.0	7.5	0.0	1.0	1.5	7.1	0.0	1.0	2.0	5.2	0.0	1.0	2.5	5.6
0.0	1.5	1.0	3.3	0.0	1.5	1.5	0.3	0.0	1.5	2.0	0.0	0.0	1.5	2.5	0.8
0.0	2.0	1.0	2.8	0.0	2.0	1.5	1.9	0.0	2.0	2.0	1.5	0.0	2.0	2.5	2.4
0.0	2.5	1.0	2.1	0.0	2.5	1.5	0.3	0.0	2.5	2.0	0.0	0.0	2.5	2.5	0.3
0.5	0.5	1.0	5.7	0.5	0.5	1.5	7.8	0.5	0.5	2.0	9.8	0.5	0.5	2.5	11.0
1.0	1.0	1.0	7.1	1.0	1.0	1.5	10.5	1.0	1.0	2.0	9.9	1.0	1.0	2.5	9.4
1.5	1.5	1.0	7.0	1.5	1.5	1.5	4.0	1.5	1.5	2.0	2.1	1.5	1.5	2.5	2.8
2.0	2.0	1.0	3.5	2.0	2.0	1.5	1.0	2.0	2.0	2.0	0.8	2.0	2.0	2.5	0.5
2.5	2.5	1.0	1.9	2.5	2.5	1.5	0.0	2.5	2.5	2.0	0.0	2.5	2.5	2.5	0.3
0.5	0.0	1.0	6.4	0.5	0.0	1.5	7.1	0.5	0.0	2.0	9.4	0.5	0.0	2.5	11.0
1.0	0.0	1.0	6.8	1.0	0.0	1.5	8.2	1.0	0.0	2.0	9.4	1.0	0.0	2.5	11.3
1.5	0.0	1.0	7.7	1.5	0.0	1.5	4.9	1.5	0.0	2.0	3.1	1.5	0.0	2.5	1.9
2.0	0.0	1.0	7.3	2.0	0.0	1.5	5.2	2.0	0.0	2.0	4.3	2.0	0.0	2.5	2.9
2.5	0.0	1.0	2.2	2.5	0.0	1.5	0.5	2.5	0.0	2.0	0.8	2.5	0.0	2.5	1.7
0.5	-0.5	1.0	5.7	0.5	-0.5	1.5	7.8	0.5	-0.5	2.0	9.8	0.5	-0.5	2.5	11.0
1.0	-1.0	1.0	7.1	1.0	-1.0	1.5	10.5	1.0	-1.0	2.0	9.9	1.0	-1.0	2.5	9.4
1.5	-1.5	1.0	7.0	1.5	-1.5	1.5	4.0	1.5	-1.5	2.0	2.1	1.5	-1.5	2.5	2.8
2.0	-2.0	1.0	3.5	2.0	-2.0	1.5	1.0	2.0	-2.0	2.0	0.8	2.0	-2.0	2.5	0.5
2.5	-2.5	1.0	1.9	2.5	-2.5	1.5	0.0	2.5	-2.5	2.0	0.0	2.5	-2.5	2.5	0.3

It can be seen from *Figure 5* that the wind speed gradually decreases with the decrease of the rotor height within the span of the rotor, and the wind speed is affected by the plant canopy effect about 0.5 m away from the plant canopy, and the wind speed decreases gradually from the center of the rotor to the outside. Outside the wingspan, the wind velocity in the direction of height is not obviously weakened.

http://www.aloki.hu ● ISSN 1589 1623 (Print) ● ISSN 1785 0037 (Online)
DOI: http://dx.doi.org/10.15666/aeer/1706_1383313844

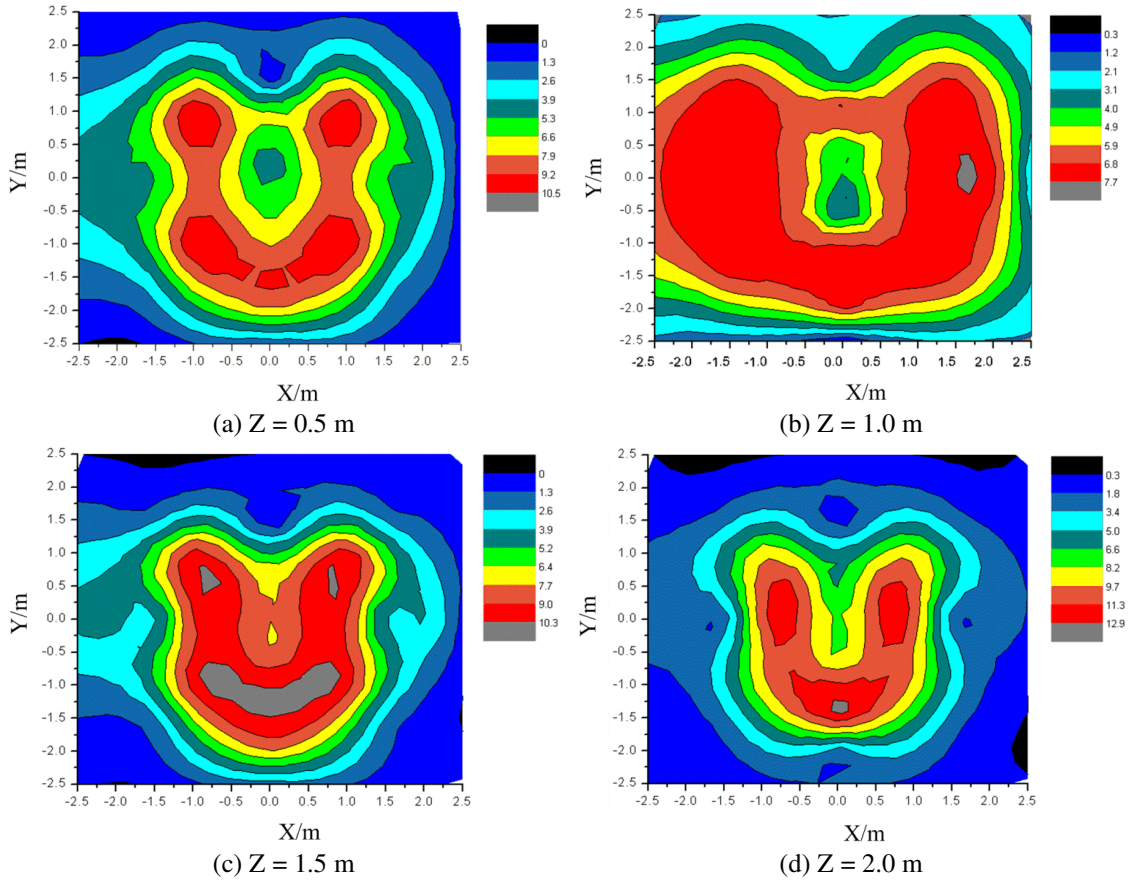

(a) Z = 0.5 m (b) Z = 1.0 m

(c) Z = 1.5 m (d) Z = 2.0 m

Figure 4. *Different heights wind farm test plan. (Note: Z is the height from the plant canopy)*

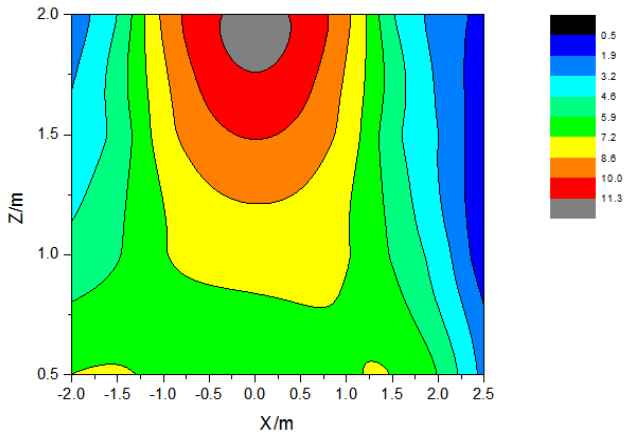

Figure 5. *Wind farm distribution map in the vertical direction of the rotor*

Taking the plant canopy as the reference and the rotor axis of the single-rotor UAV as the center, the vertical wind field were measured vertically up the plant canopy, and the vertical wind field data were obtained. The following conclusions are drawn from the analysis:

1. At the same height from the plant canopy, the wind velocity value is positively correlated with the axis distance within the wingspan range, and the wind

http://www.aloki.hu ● ISSN 1589 1623 (Print) ● ISSN 1785 0037 (Online)
DOI: http://dx.doi.org/10.15666/aeer/1706_1383313844

speed increases gradually with the increase of the distance, and decreases gradually beyond the wingspan range until the boundary of the wind field.
2. In the direction of altitude, the value of wind velocity is positively correlated with the height off the plant canopy.
3. The maximum wind speed is 1-2.5 m above the plant canopy, and the maximum wind speed is 12.9 m/s. Therefore, in the field operation, the flying altitude of the single-rotor UAV is best within this range, which is favorable for the airflow and droplets to reach the bottom of the canopy.
4. Under the influence of plant canopy effect, turbulence will appear in the wind field below 1 m, and there is no definite rule.

Spray deposition contrast test

In order to test the difference between single-rotor plant UAV and multi-rotor plant protection drone, different models were selected to carry out. The spray tests of S40 single rotor, M23 electric four rotors and M8A electric eight rotor plant protection UAV were carried out in soybean field, and the spray drop deposition distribution of different types of UAV was compared and analyzed.

Materials and methods

Experimental laboratory materials and equipment

In order to compare the effects of droplet deposition with Mercury 1 electric single-rotor UAV, three different UAV were prepared for soybean field experiments, as shown in *Figure 6*. The parameters of the three UAV are shown in *Table 2*.

(a) S40

(b) M23

(c) M8A

Figure 6. *Three kinds of UAV*

http://www.aloki.hu ● ISSN 1589 1623 (Print) ● ISSN 1785 0037 (Online)
DOI: http://dx.doi.org/10.15666/aeer/1706_1383313844

Table 2. *Main parameters*

Type	S40	M23	M8A
Size (mm × mm × mm)	2165 × 2400 × 720	1318 × 1318 × 685	1360 × 1360 × 650
Maximum (load/L)	20	10	10
Flight speed(m/s)	5	5	5
Flight height(m)	1-3	1-3	1-3
Spraying width(m)	4-7	4-6	4-5
Number of sprinklers	5	4	6

Reagent preparation

The analytical instrument is micro-spectrophotometer with a maximum absorption wavelength of 508 nm. First, prepare labeling group, use500 ml volumetric flask to prepare 1 g/L liquid containing carmine, extract 50 ul, 150 ul, 250 ul, 350 ul, 450 ul, 550 ul, 650 ul, 750 ul, 850 ul, 950 ul solution with pipette to be placed in 10 ml volumetric flask, balance, measure the absorbance, repeat each test three times to obtain average standard curve. In order to indicate deposition quantity with ratio of carmine, curve model of absorbance versus carmine solution concentration was established. Determination coefficient was calculated by linear regression curve fitting as $R^2 = 0.997$. As measurement of deposition quantity needs test of dilution concentration, relationship between carmine solution concentration and absorbance was obtained via variable conversion:

$$C = 0.0363A - 0.0016 \quad \text{(Eq.1)}$$

where C is mass concentration (g/L) of the carmine solution and A is absorbance of the carmine solution.

Test method

The experiment was carried out in Liangshan county demonstration base of "Research on high-yield and high-efficiency mechanization production technology and supporting equipment of soybean". The experiment was carried out in the middle and late stages of soybean growth. The row spacing and plant height of soybean in the experimental field were 40 cm and 90 cm respectively. The spray liquid used in this experiment is 4 g/L rouge aqueous solution, and the droplet collection card is used to collect the droplet. In the field experiment of soybean, three groups of spray tests were compared in the range of spraying in the same plant protection unmanned aerial vehicle (UAV) operation, and 8 points were continuously arranged at 1.2 m interval in the transverse direction, and 8 points were arranged continuously in the same plant protection unmanned aerial vehicle (UAV) operation. Longitudinally: corresponding transverse, control test every 5 meters, continuous arrangement of 3 each collecting point, the upper, middle and lower layers are arranged to collect droplets acquisition card (*Fig. 7*). Every time the plant protection drone flies along the set axis, in order to stabilize the test operation, the aircraft hovers and takes off at 10 m in the acquisition point, and stops operation after 10 min away from the acquisition point. The temperature and humidity meter and wind speed and wind direction meter were used to measure and record the environmental parameters during the plant protection unmanned aerial vehicle operation.

http://www.aloki.hu ● ISSN 1589 1623 (Print) ● ISSN 1785 0037 (Online)
DOI: http://dx.doi.org/10.15666/aeer/1706_1383313844

Figure 7. *Collection point layout*

Results and discussion

Test results of droplet deposition distribution

The data of droplet deposition and density of droplet deposition are shown in *Table 3*.

Table 3. *Mean value of droplet deposition*

Number	S40 Electric single rotor		M23 Electric four rotor		M8A Electric eight rotor	
	Deposits ($cm^{2)}$	Deposition ($\mu L/cm^2$)	Deposits ($cm^{2)}$	Deposition ($\mu L/cm^2$)	Deposits ($cm^{2)}$	Deposition ($\mu L/cm^2$)
A0-1	39.2	0.210	23.0	0.047	18.5	0.036
A0-2	62.0	0.122	21.4	0.018	18.0	0.016
A0-3	11.8	0.027	5.2	0.003	5.8	0.004
A1-1	27.1	0.125	15.7	0.012	41.1	0.067
A1-2	29.7	0.526	21.8	0.022	45.9	0.072
A1-3	20.4	0.049	11.9	0.010	15.4	0.026
A2-1	44.5	0.330	41.1	0.115	61.7	0.977
A2-2	45.3	0.149	43.4	0.097	58.6	0.264
A2-3	9.5	0.030	13.8	0.012	21.6	0.047
A3-1	35.1	0.302	21.3	0.035	40.2	0.104
A3-2	17.2	0.207	42.6	0.066	78.7	0.236
A3-3	6.9	0.014	8.7	0.006	29.5	0.084
A4-1	37.2	0.281	35.1	0.055	16.2	0.027
A4-2	28.4	0.068	13.6	0.017	26.8	0.033
A4-3	8.8	0.049	7.3	0.011	10.5	0.022
A5-1	55.1	0.595	51.7	0.105	63.1	0.211
A5-2	41.4	0.278	64.4	0.143	55.0	0.217
A5-3	8.7	0.043	29.7	0.053	12.5	0.028
A6-1	53.2	0.406	26.8	0.040	50.4	0.109
A6-2	23.8	0.086	36.8	0.035	35.2	0.101
A6-3	4.3	0.016	10.8	0.014	10.8	0.026
A7-1	29.9	0.194	24.4	0.068	22.9	0.044
A7-2	24.6	0.105	67.9	0.179	32.1	0.125
A7-3	6.0	0.014	34.6	0.046	10.3	0.017

http://www.aloki.hu ● ISSN 1589 1623 (Print) ● ISSN 1785 0037 (Online)
DOI: http://dx.doi.org/10.15666/aeer/1706_1383313844

Analysis of droplet distribution uniformity

As shown in *Figure 8*, the three UAV were all carried out under the best operating parameters. It can be seen from *Figure 8*, the deposition distribution of droplets in each collecting point is different under different operating parameters. The deposition amount and uniformity of each collecting point are relatively good on the whole, and the droplets of each collecting point are relatively good. The coefficient of variation is 37.37%, the coefficient of variation is 69.34%, and the coefficient of variation is 110.88%. The coefficient of variation reflects the droplet deposition uniformity of the UAV, and the results show that the droplet distribution uniformity of the single rotor UAV is better than that of the multi-rotor UAV as a whole.

It also can be concluded that the drift on the right side is larger than that on the left side, and the drift is smaller when the operating speed is 5 m/s. It can be seen from that there is little difference in droplets deposition data collected from at different operating parameters. Under different operating parameters, it can be concluded that the single-rotor UAV has a single and stable downwind field and less ground loss and drift.

The wind field of S40 single-rotor plant UAV is relatively stable. It has a strong penetrating and a better droplet deposition and uniformity. The six nozzles of M8A eight-rotor UAV are arranged under the fuselage, and there is disturbance between the wind field, so the distribution of turbulence is not uniform. The M23 four-rotor drone with one nozzle under each rotor, has enough atomization and less deposition.

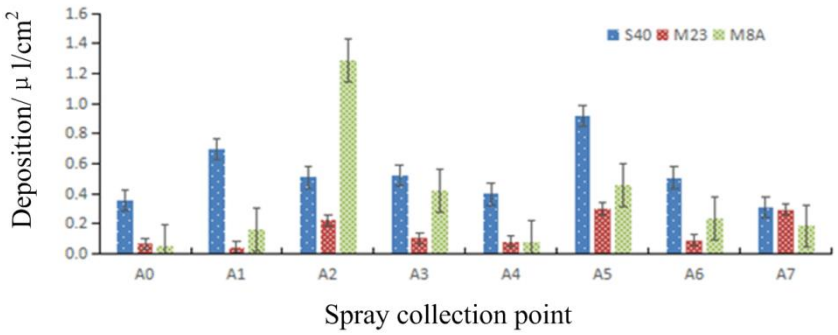

Figure 8. *Plant protection UAV deposition layout*

Comparative analysis of penetration of fog droplets

As can be seen from *Figure 8*, the density of droplets in each sampling point of soybean canopy can reach 15/cm^2. As shown in *Figure 9*, the distribution of droplets in the upper, middle and lower canopy of three UAV can be visualized to show the penetration of droplets in different UAVs.

Figure 9 shows when the S40, M23, and M8A UAVs are operated, droplets can reach the lower layer of the soybean blade. The density of droplets deposited in the lower layers decreased gradually. The density of droplets in the middle layer of soybean decreased by 14.75% compared with that in the upper layer, and that in the lower layer decreased by 71.85% compared with that in the middle layer. During the spraying operation with M23 electric four-rotor UAV, the droplet density of the middle blade is higher than that of the upper layer and the lower layer, and the deposition density of the middle layer is higher than that of the lower layer. The density of droplets in the lower

http://www.aloki.hu ● ISSN 1589 1623 (Print) ● ISSN 1785 0037 (Online)
DOI: http://dx.doi.org/10.15666/aeer/1706_1383313844

layer was 60.77% less than that in the middle layer. During the spraying operation with the M8A electric eight-rotor UAV, the droplet deposition density of the middle layer blade was 10.27% higher than that of the upper layer blade, and the lower layer was 66.67% lower than that of the middle layer.

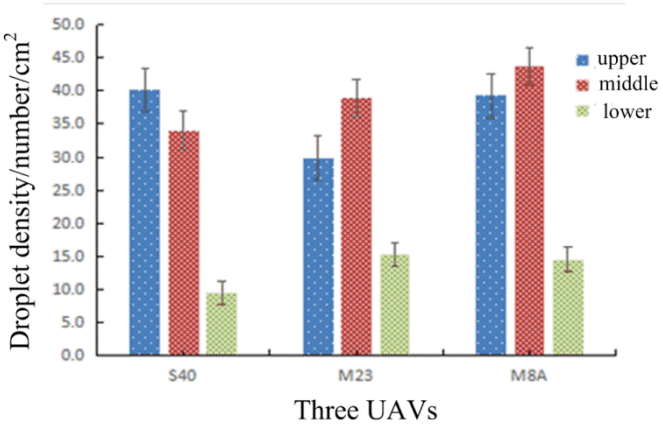

Figure 9. *Droplet distribution in soybean canopy*

Conclusions

The main parameters of S40 electric single rotor, M23 electric four rotor and M8A electric eight rotor UAV are briefly introduced. The spray experiments in the soybean pod period are carried out with these models.

Under different operating parameters, height and velocity have significant influence on the deposition and distribution of droplets. As the wind field of the single-rotor plant protection unmanned aerial vehicle is single, droplets can reach the bottom of the soybean canopy under different working parameters. At different speeds and heights, the deposition amount and distribution uniformity of droplets are different. The deposition density of upper, middle and lower canopy droplets of soybean has certain regularity. The results of droplet deposition show that the droplets of single rotor and multi-rotor UAV can reach the lower part of soybean canopy, and the density of droplets can be more than 15/cm^2. The single rotor UAV has a single wind field, uniform distribution and strong penetration.

Acknowledgements. The authors would like to thank the National Soybean Industry Technical System Foundation of China (Contract No. CARS-04), the Natural Science Foundation of Henan Province (Contract No. 162300410155) and the Natural Science Foundation of China (Contract No. 31501213) for their supports of this work. Furthermore, the authors would sincerely thank the reviewers for their very professional suggestions on this study.

REFERENCES

[1] Chen, S. D., Lan, Y. B., Li, J. Y., Xu, X. J., Wang, Z. G., Peng, B. (2017a): Evaluation and test of effective spraying amplitude of plant protection UAV during aerial spraying. – Journal of Agricultural Engineering 33(7): 82-90.

http://www.aloki.hu ● ISSN 1589 1623 (Print) ● ISSN 1785 0037 (Online)
DOI: http://dx.doi.org/10.15666/aeer/1706_1383313844

[2] Chen, S. D., Lan, Y. B., Li, J. Y., Zhou, Z. Y., Liu, A. M., Xu, X. J. (2017b): Comparison of effects of aerial spraying and artificial spraying on rice application. – Journal of South China Agricultural University 38(4): 103-109.
[3] Chen, S. D., Lan, Y. B., Zhou, Z.Y., Liao, J., Zhu, Q.Y. (2017c): Effects of spray parameters of small plant protection UAV on droplet deposition in orange canopy. – Journal of South China Agricultural University 38(5): 97-102.
[4] Gong, Y., Fu, X. M. (2008): Aeronautical application technology in modern agriculture. – Agricultural Equipment Technology 34(6): 26-29.
[5] Guo, Y. W., Yuan, H. Z., He, X. K., Shao, Z. R. (2014): General situation and prospect analysis of agricultural aviation plant protection development in China. – China Journal of Plant Protection 34(10): 78-82.
[6] Jin, X., Dong, X., Yan, X. J., Yan, H. R. (2016): Design and test of target spray system for 3WGZ-500 sprayer. – Journal of Agricultural Machinery 47(7): 21-27.
[7] Liu, K. X. (2015): Development status of agricultural aviation industry in Russia, Japan and South Korea. – Age Agricultural Machinery 42(7): 169.
[8] Lou, S. Y., Xue, X. Y., Gu, W., Cui, L. F., Zhou, Q. Q., Wang, X. (2017): Research status and trend of Agricultural Plant Protection Unmanned aerial vehicle. – Agricultural Mechanization Research 39(12): 1-6, 31.
[9] Qin, W. C., Xue, X. Y., Zhou, L. X., Zhang, S. C., Sun, Z., Kong, W., Wang, B. K. (2014): Effect of spray parameters of unmanned helicopter on droplet deposition distribution in maize canopy. – Journal of Agricultural Engineering 30(5): 50-56.
[10] Xu, Y., Xiao, Y. J., Liu, J. H., Zhou, J. S., Song, X. Q., Dai, X. H. (2017): Impact of drones on agricultural modernization. – Agricultural Services 34(16): 43.
[11] Yang, H. Q. (2010): Analysis and discussion on the current situation of soybean industry in China. – China Seed Industry 4: 18-20.
[12] Yang, W. Y., Yong, T. W., Ren, W. J. (2008): Develop industry soybean, revitalize soybean industry. – Soybean Science 27(1): 1-7.
[13] Zhang, F. S. (2007): Study on the Effect of Plant Protection on Grain Production Safety in China. – Fujian Agricultural and Forestry University, Fujian.
[14] Zhang, S. C., Xue, X. Y., Qin, W. C., Xun, Z., Ding, S. M., Zhou, L. X. (2015): Simulation and experiment of N-3 type agricultural unmanned helicopter's airborne application drift. – Journal of Agricultural Engineering 31(3): 87-93.
[15] Zhao, H., Song, J. L., Zeng, A. J., He, X. K. (2009): Correlations between dynamic surface tension and droplet diameter. – Transactions of the Chinese Society for Agricultural Machinery 40(8): 74-79.

http://www.aloki.hu ● ISSN 1589 1623 (Print) ● ISSN 1785 0037 (Online)
DOI: http://dx.doi.org/10.15666/aeer/1706_1383313844

HIGHSTAND SEA-LEVEL IN THE HOLOCENE INFERRED FROM BURIED PEAT AND DIATOM ASSEMBLAGES FROM NORTH COAST OF THE YELLOW SEA, CHINA

FANG, J.[1] – LI, Y.[2] – GUAN, X.[2*] – HU, K.[2*]

[1]*School College of Geography and Environmental Science, Tianjin Normal University, Tianjin 300387, China*

[2]*School of Ocean Sciences, China University of Geosciences, Beijing 100083, China*

**Corresponding authors*
e-mail: guanxy@cugb.edu.cn (Guan, X.); huke@cugb.edu.cn (Hu, K.)

(Received 20th May 2019; accepted 10th Sep 2019)

Abstract. Understanding the sea-level change in the geological past is helpful for the future coastal protection. Information of sea-level changes has been documented in various archives in the coasts. In this study, the well-preserved peat in three representative Holocene ditches in Dayanghe Plain in the Yellow Sea China were investigated using radiocarbon dating and diatom analysis. The widely distributed buried peats at elevation of ca. 2-10 m above sea-level (a.s.l.) in Dayanghe Plain are classified as marsh and limnological peats, which were formed after seawater receding from the drowned ditches. The peat layers lower than 4 m a.s.l., overlain the marine sediments conformably, correspond to the late-Holocene regression. Timing of the highstand sea-level in North Coast of North Yellow Sea is limited to 6182-5466 cal. a BP by radiocarbon dating. Shell banks at west of the Dagu Mountain which was at a 7-10 m height were thought not to be indicative of the Holocene highstand sea-level.
Keywords: *diatom assemblages, sea-level rise, radiocarbon dating, peatland, Yellow Sea*

Introduction

The Yellow Sea is one of margin seas in East China, located at the low-gradient shelf between the Chinese mainland and the Korean Peninsula. Thick sediments have been deposited in the Yellow Sea since the Late Pleistocene (Zheng, 1991), containing rich palaeo-environmental information under the sea-level changes in the geological past (Chappell et al., 1996; Kim and Kennett, 1998; Yokoyama et al., 2001; Chappell, 2002; IPCC, 2007; Liu et al., 2004). A multitude of investigations and research on relative sea-level change and environmental evolution in east China have been carried out during the last half century (e.g. Zhao, 1996). Multiple transgressions since late Pleistocene were defined widely in the Bohai Sea, Yellow Sea and East China Sea. Corresponding to the global sea-level change (Shi et al., 2016), three transgression-regression cycles are identified in the coast stratigraphy (Zhao, 1986; Wang et al., 1986; IOCAS, 1985). The transgression-regression sequences have been studied in the chronology (e.g. Liu et al., 2016; Li et al., 2019; Yi et al., 2013), sedimentary processes (e.g. Yi et al., 2012; Liu et al., 2016; Wang et al., 2015), sea-level change (Yi et al., 2012; Liu et al., 2004; Xue, 2014) and driven factors, e.g. palaeo-climate and environment during the geological past (e.g. IOCAS, 1985; Yi et al., 2012).

The uppermost transgressive succession overlying the widely distributed peat or organic-rich sandy interlayer over the coastal areas in the east marginal seas results from the Holocene sea-level rise. The pattern of the Holocene sea-level has been well studied using benthic foraminiferal and stable isotopic approaches with well-established

http://www.aloki.hu ● ISSN 1589 1623 (Print) ● ISSN 1785 0037 (Online)
DOI: http://dx.doi.org/10.15666/aeer/1706_1384513857

radiocarbon chronology (Kim and Kennett, 1998; Liu et al., 2004). Several approaches have been employed for a well understanding of environmental evolution and sea-level change during the Holocene in North Yellow Sea. Peats and shell bars in the Liaodong coastal stratigraphy are likely to deposit during the Holocene sea-level highstand and then dated using radiocarbon (GIGCAS, 1977; Wang et al., 1991; Gao, 1986, 1992). Environmental evolution was interpreted by pollen (GIGCAS, 1977; Liu, 1992), foraminiferal (Yang, 1985) and archeological record (Shi, 2006). Static tectonic movement or slow subsidence in coast of the North Yellow Sea was proposed in former research, e.g. Xiao (1981), Ding (1958) and Zhao (2000), while some researchers assumed a relatively slow uplifting occurring identified by abrasion terrace which is 250 a.s.l. in Dalian, coastal bars and terraces in Liaodong Peninsula (Liu, 1986; Xia et al, 1986). Although the timing of the Holocene transgression in the North Yellow Sea is well restricted, the transgressive process and height of sea-level highstand are still not precisely confirmed mainly due to lack of stratigraphic correlation and reliable sea-level indicators on the background of tectonic uplifting in the North Coast of the Yellow Sea (Fu et al., 1989, 1995; Wei et al., 1984; Zhong and Chang, 1988; Lu, 1985).

Widely distributed marsh peat in the coastal plain is treated as the marker for sea-level highstand (Shennan and Horton, 2002; Engelhart and Horton, 2012). However, the peat formation could be misunderstood due to lack of identification of the contacting layer. As sensitive to salinity, pH and temperature, diatom is a well indicator to the water-lain sedimentary environments, such as the coast and lacustrine (Kosugi, 1988; Horton, 1997; Horton et al, 2006, 2007). In this paper, we investigated the well-preserved peat in the three representative ditches in the Dayanghe Plain, the North Coast of the North Yellow Sea. Diatom analysis was applied to identify the types of peat in the different depths. The timing of the marsh peat, indicating the Holocene sea-level highstand, was determined using radiocarbon dating.

Materials and methods

Study area

The Yellow Sea is a margin sea of China with average water depth of 60-80 m. It is covered by seawater due to the subsidence of the Zhe-Min Uplift in the early Quaternary (Jin and Yu, 1978; Qin et al., 1989; Yi et al., 2014), Yellow sea is geographically divided into two parts, the North Yellow sea and the South Yellow sea, by Dabie-Linjin fault zone (Qin et al., 1989). The North Yellow Sea is a semi-enclosed sea surrounded by Shandong peninsula, Liaodong peninsula and Korea peninsula. It is a fault basin during Cenozoic on the base of Jiaoliao palaeo-Uplift. Since the Late Tertiary, regional subsidence and stable sedimentation have occurred in the whole Yellow sea, remarked by process of depression sedimentation (IOCAS, 1985; Qin et al., 1989). Current system in the North Yellow sea contains the Yellow Sea Warm Current (YSWC), which is known as a branch of Tsushima Current, and the coastal currents along Chinese and Korean coasts (*Fig. 1a*). The tide in the North Coast of the Yellow sea is irregularly semidiurnal in range of 4.08 m (Qin et al., 1989). Due to the strong tide and the flat terrain, 6-10 km wide tidal flat develops in the coastal area. The sedimentary process is dominated mainly by fluvial and tide currents from alluvial plain, estuary to tidal flat.

The study area is the Dayanghe alluvial plain located in southern Liaodong Peninsula. The plain is divided into several small drowned ditches. Sediments in the

http://www.aloki.hu ● ISSN 1589 1623 (Print) ● ISSN 1785 0037 (Online)
DOI: http://dx.doi.org/10.15666/aeer/1706_1384513857

Dayanghe alluvial plain were mainly transported by two local rivers, the Dayanghe River and the Xiaoyanghe River, both originating in the region of Xiuyan in the North Liaoning Province. The Dayanghe River, with length of 201 km, flows from the northeast direction into study area. While the Xiaoyanghe River, 57.40 km long, flows from the northwest direction into study area. These two rivers meet in the north of alluvial plain, and turn to the direction of south, pouring into the Yellow Sea. The average slopes of Dayanghe alluvial plain are 0.6 and 0.2‰, respectively (*Fig. 1b*).

The Holocene stratigraphy in southern Liaodong Peninsula was studied in sedimentology, pollen analysis and radiocarbon dating. Southern Liaodong Peninsula was influenced by transgression in early and mid-Holocene, as a result of the regional sea-level rise to the highstand sea-level, then declining with fluctuation to a stable sea-level as present (GIGCAS, 1977). Timing of high-stand sea level between 8000 and 6000 a BP is mainly determined by dating the widely distributed peat layer and shell bar (GIGCAS, 1977; Wang et al., 1991; Gao, 1986, 1992; Fu et al., 1995). Archeological records in southern Liaodong Peninsula provide the evidence of the Holocene transgression using the shells excavated in archeological sites (Shi, 2006).

The Bohai Sea, Yellow Sea and East China Sea are the three marginal seas of China. Current system in Yellow Sea is shown in *Figure 1a* (1. Yellow Sea Warm Current (YSWC), 2. Yellow Sea Coastal Current (YSCC), 3. Taiwan Warm Current (TWC), 4. North Yellow Sea Coastal Current (NYSCC), 5. Zhe-Min Coastal Current (ZMCC), 6. Tsushima Strait Warm Current (TSWC)). Sites of the studied boreholes in the North Coast of the Yellow Sea are shown in *Figure 1b* (Source of the Digital Elevation Model: http://srtm.csi.cgiar.org/).

Studied boreholes

To investigate the stratigraphic characteristics in the Early and Middle Holocene in the Dayanghe alluvial plain, three boreholes (referred to as LD-1, LD-2 and LD-3, *Fig. 1b*) from Dayanghe plain were drilled with the manual sampling device in the three representative ditches. Elevation of each borehole was measured by using level points on topographical map in scale 1:10 000 (1956 Yellow Sea elevation system) and leveling instrument.

The length of core LD-1 (39°55’32”N, 123°13’35”E, elevation 4.9 m a.s.l.; *Fig. 2*) was 550 cm. The top 113 cm of the core consists of silt, with the upper part in yellow-brown and the lower part in grey-brown. A 37 cm-thick layer contains brown-black peat, which can be recognized widely in this area. The depth of brown-grey clayey silt is from 150-165 cm, while the lower blue-grey layer, containing vegetation debris, is from 165 cm to 505 cm. The lowest part contains brown silt with breccias (505-550 cm).

Core LD-2 (39°55’42”N, 123°39’48”E, elevation 6.5m a.s.l.; *Fig. 1*), 560 cm long, can be described as follows: 0-205 cm, silt with the upper part (0-150 cm) in yellow-brown and the lower part (150-205 cm) in grey-brown; 205-238 cm, brown-grey clay with two thin organic-rich layers; 238-266 cm, brown-black peat layer; 266-505 cm, blue-grey organic-rich silt layer; 505-560 cm, blue-grey medium sand with gravels.

Core LD-3 (40°01’21”N, 123°38’35”E, elevation 4.8 m a.s.l.; *Fig. 1*), with the length of 400 cm, is described as follows: 0-35 cm, brown-grey silt; 35-86 cm, dark grey clay; 86-123 cm, coarse sand in light grey with gravels; 123-150 cm, peat layer; 150-170 cm, brown-black clay with organic-rich materials; 170-352 cm, silty clay in light blue; 352-400 cm, coarse sand in dark grey with gravels.

http://www.aloki.hu ● ISSN 1589 1623 (Print) ● ISSN 1785 0037 (Online)
DOI: http://dx.doi.org/10.15666/aeer/1706_1384513857

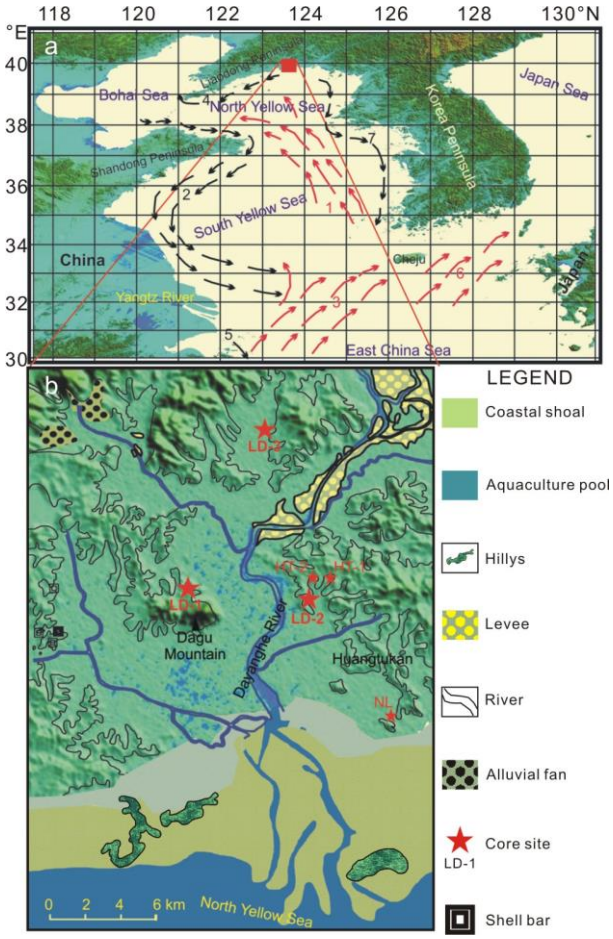

Figure 1. *Location of study area.* ***a*** *shows the marginal seas in the East China and the location of the Dayanghe alluvial plain.* ***b*** *shows the geomorphological characteristics of the Dayanghe alluvial plain and the drilling sites.*

Several additional boreholes were drilled to investigate the stratigraphy in both three ditches. Peat or black organic-rich clay layers distribute widely in these three ditches, with brownish clay/silt layer overlying and blue clay layer underlying. Peat or black organic-rich layer between 2 m and 4 m a.s.l. can be recognized as a mark layer, while peat in 9 m in ditch LD-1, in 7 m and 10 m in ditch LD-2 were distinguished from the mark peat layer not only the appearance of height, but also the contacting layers as the peat layer develops between gravely coarse sand, gravely coarse sand and brownish clay/silt layer in ditch LD-1 and LD-2, respectively.

To compare with the previous research, two boreholes were drilled in region of the Huangtukan (labeled as HT-1 and HT-2, *Fig. 1b*), which were sampled for investigation of peat layer and diatom analysis and comparison. The elevations of HT-1 and HT-2 are 11.0 m and 10.8 m, respectively. Peat layer appears in 8.80 m a.s.l. in core HT-1, with underlying grey peat-clay layer, while in 8.35 m a.s.l. in core HT-2, with underlying blue-grey medium and coarse sand. Borehole NL was drilled in the modern coast area, at east of the Dayanghe River estuary, for diatom analysis and radiocarbon dating (*Fig. 1b*). Top elevation of this borehole is 4.7 m a.s.l., described as: -0.55 - -1 m a.s.l., yellowish medium sand; 1.7 - -0.55 m a.s.l., light-grey fine sandy silt and clay interlayers with shell; 4.7-1.7 m a.s.l., brown-grey silt/light-grey silt.

http://www.aloki.hu ● ISSN 1589 1623 (Print) ● ISSN 1785 0037 (Online)
DOI: http://dx.doi.org/10.15666/aeer/1706_1384513857

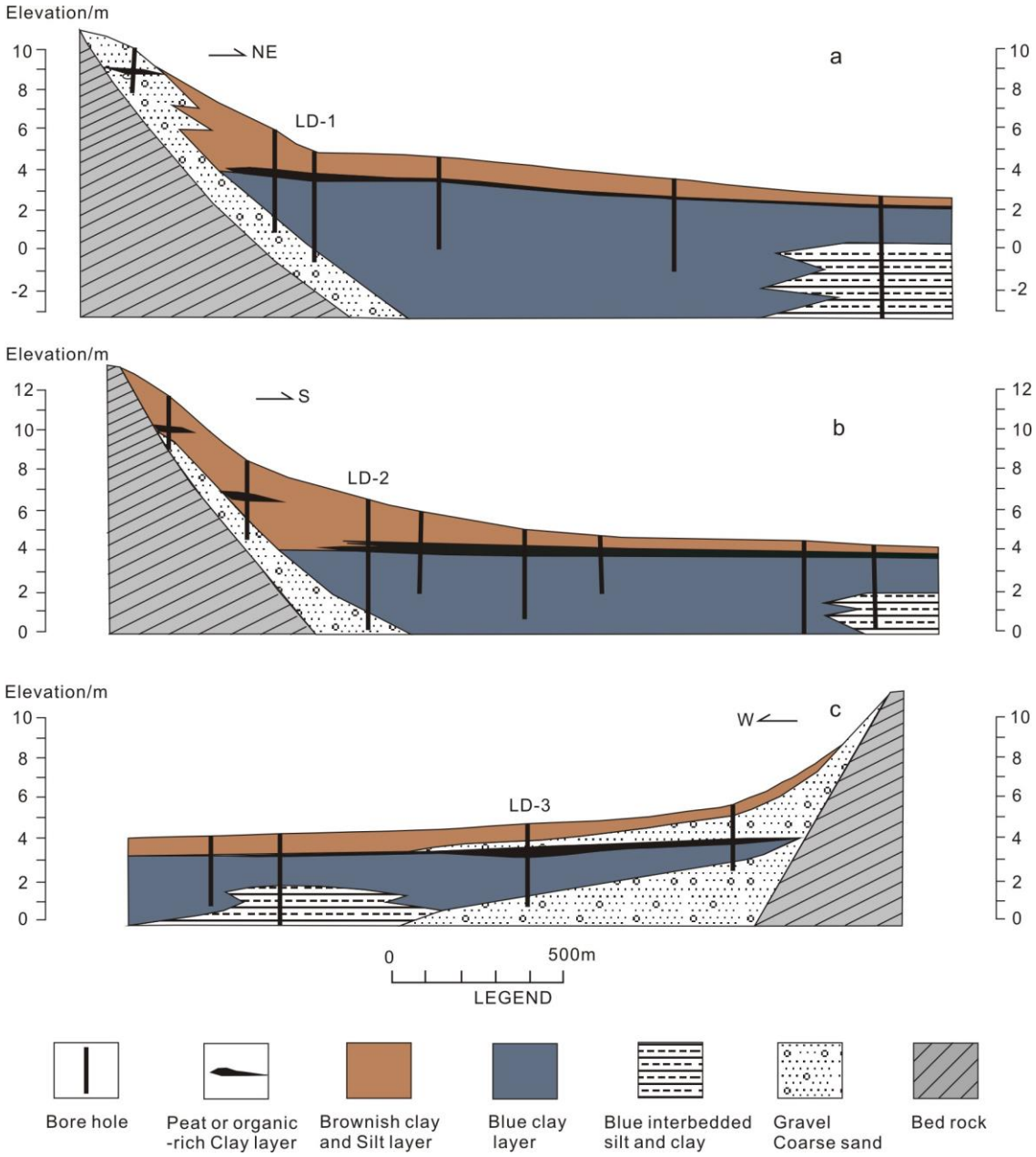

Figure 2. *Stratigraphic distribution in three ditches*

Radiocarbon dates

Three samples from the bottom of peat layers were extracted for radiocarbon dating. All radiocarbon dating experiments were conducted at Center for Chronological Research, Nagoya University, using the Accelerator Mass Spectrometry (AMS) method. Radiocarbon dates were calibrated using Calib 5.0.1 (Stuiver et al., 2005). All ages (*Table 1*) are reported as calibrated calendar ^{14}C ages before AD 1950 (cal BP).

Diatom analysis

4-6 g sediments were collected at -20 cm intervals for diatom analysis. Samples were pre-treated with 30% H_2O_2 to remove organic matter, rinsed with deionized water for

http://www.aloki.hu ● ISSN 1589 1623 (Print) ● ISSN 1785 0037 (Online)
DOI: http://dx.doi.org/10.15666/aeer/1706_1384513857

several times. The coarse sand and gravel fraction were removed by sedimentation method. After abundant precipitation, 1 mL of liquid was removed to cover slip by transfer pipet, then dried and agglutinated with ground slide by resin. 4-6 slices were made for one sample. Diatom assemblages were identified at 400× magnification on microscope (smaller individuals at 1000× magnification). At least 200 diatom valves were counted and identified from each slice. Diatom identification and nomenclature were based on KASHINA (1986), KOSUGI (1988) and ANDO and FUJIMOTO (1990). Based on the living environment, three kinds of diatom were classified, as 1) marine-brackish species (M-B), living in marine and inner bay environment under seawater; 2) brackish-fresh species (B-F), living in environment influenced by mixture of fresh water and brackish water, but not existing in marine environment; 3) fresh species (F), living in the fresh water environments, such as wetland, marsh and river, etc.

Table 1. *Radiocarbon date on materials from core LD-1, LD-2, LD-3 AND NL*

Core	Samples elevation a.s.l. (m)	Materials	$\delta^{13}C$	Conventional ^{14}C age/a BP	Calibrated age/a cal BP	
					Intercept	Range
LD-1	3.40	Peat	-28.8	4721 ± 160	5466	5286-5645
LD-2	3.84	Peat	-27.9	5242 ± 140	6052	5895-6208
LD-3	3.3	Peat	-26.4	4707 ± 140	5466	5288-5603
NL	-0.5	Shell	-1.2	5784 ± 180	6182	5985-6378

Results and discussion

Diatom analysis for core LD-1

Core LD-1 was divided into four diatom assemblage zones (*Fig. 3a*).

Zone I (505-330 cm)

Marine-brackish species, including marine species *Thalassionema nitzschioides*, indicate the open marine environment. *Cyclotella stylorum, Paralia sulcata, Actinocyclus* spp.*, Cosinodiscus* spp. are indicative of the inner bay environment. Brackish species *Diploneis smithii* are found in the lower part of blue-grey layer in Zone I. The component of species above reaching 75-95% is related to a process of transgression that this area was covered by seawater.

Zone II (505-330 cm)

In Zone II, the marine-brackish species decrease from 94 to 61%, while an increase of brackish-fresh and fresh species from 6 to 40% indicate a process of regression with a w seawater influence and a stronger influence by freshwater.

Zone III (163-150 cm)

Various species appear in Zone III. 20% are marine-brackish, while the fresh and brackish-fresh species reach 80%, including *Pinnularia* spp. (29%), which inhabited in marsh environment, and the fresh-brackish species *Rhopalodia gibberula*, 14% of total species. The dominating assemblages with mixture of fresh and brackish-fresh taxa are commonly observed in the wetland environment influenced by seawater.

http://www.aloki.hu ● ISSN 1589 1623 (Print) ● ISSN 1785 0037 (Online)
DOI: http://dx.doi.org/10.15666/aeer/1706_1384513857

Zone IV (150-133 cm)

In Zone IV, constrained to the peat layer, nearly all taxa were fresh species, with wetland species *Pinnularia* spp. (34-47%), *Eunotia* spp. (3-8%) and *Cymbella* spp. (5-11%), and fresh benthonic species *Hantzschia amphioxys* (6-11%). The diatom assemblages in the peat layer showed a wetland environment influenced rarely by seawater.

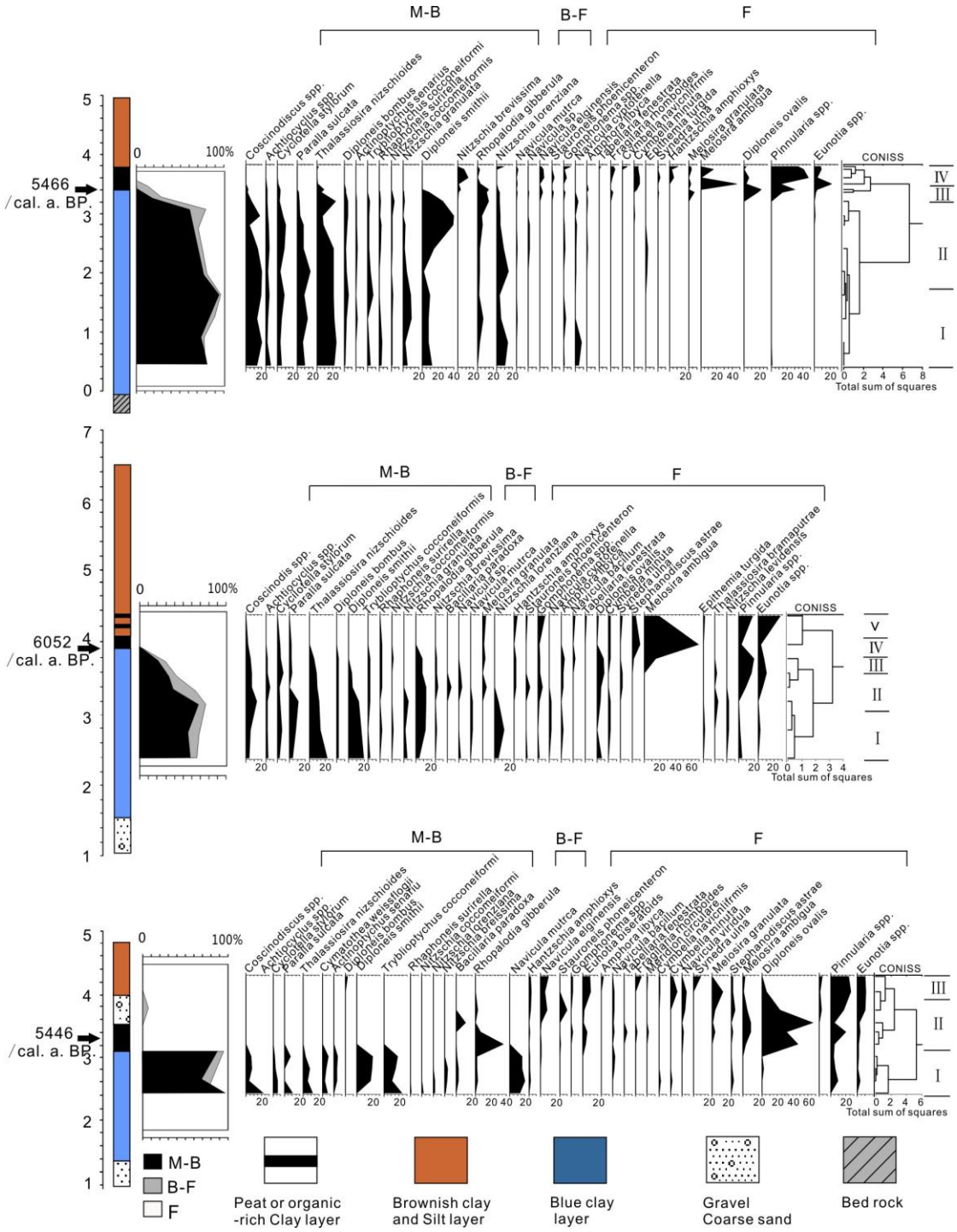

Figure 3. *Result of diatom analysis for three cores,* ***a, b*** *and* ***c*** *are correspondence of LD-1, LD-2 and LD-3, respectively.*

http://www.aloki.hu ● ISSN 1589 1623 (Print) ● ISSN 1785 0037 (Online)
DOI: http://dx.doi.org/10.15666/aeer/1706_1384513857

Diatom analysis for core LD-2

Core LD-1 was divided into five diatom assemblage zones (*Fig. 3b*).

Zone I (430-350 cm)

The main taxa are marine-brackish species (57-66%), accompanied by fresh species (22-32%) and fresh-brackish species (5-12%). Among the taxa, Percentage of the marine indicator taxa, *Thalassionema nitzschioides*, was 12-14%, while marine-brackish species such as *Diploneis smithii* were reaching 12-18%, indicating a drowned ditch environment.

Zone II (350-290 cm)

With the same lithological characteristics as Zone I, Zone II contained nearly the same diatom assemblages, with a notably declining trend of marine-brackish species from 66% to 34% and increase of fresh and fresh-brackish species. The indicators of the marsh and wetland such as *Pinnularia* spp. and *Eunotia* spp. with a percentage of 15-20%, show there was a declining trend of sea-level, accompanied by environment changing from drowned ditches to salty marsh.

Zone III (290-266 cm)

In Zone III, constrained to upper part of blue-grey peaty clay layer, the marine-brackish species declined to 21%, with an increase of fresh species to 69%. The marsh and wetland indicators such as *Pinnularia* spp. and *Eunotia* spp. were with a percentage of 29%. The limnological environment indicator *Melosira ambigua*, known as a plankton species, appeared within this interval with a percentage of 16%, indicating a salty marsh environment covered by water.

Zone IV (266-230 cm)

Zone IV is the peat layer, containing only 4% marine species and nearly 95% were fresh species. The marsh and wetland indicators such as *Pinnularia* spp. and *Eunotia* spp. declined to 6%, accompanied by limnological environment taxa such as plankton *Melosira ambigua* and *Stephanodiscus astrae* with a drastic increase to 87%. It suggests that the environment changed from a marsh wetland to limnological environment.

Zone V (230-205 cm)

The brown-black peat and brown-grey silt occur in Zone V. *Pinnularia* spp. and *Eunotia* spp. increased rapidly, with the percentage of 18% and 28%, respectively. *Melosira ambigua* and *Stephanodiscus astrae* decline to 19% and 5%, respectively. We infer that the environment changed from fresh lake to marsh and wetland covered by shallow water.

Diatom analysis for core LD-3

Three diatom assemblage zones were found in core LD-3 (*Fig. 3c)*.

Zone I (290-170 cm)

In Zone I, marine-brackish species dominated with a percentage of 68-98%. There was an increase trend of *Diploneis smithii* from 16% to 35%, indicating a period of inner bay environment covered by shallow seawater.

http://www.aloki.hu ● ISSN 1589 1623 (Print) ● ISSN 1785 0037 (Online)
DOI: http://dx.doi.org/10.15666/aeer/1706_1384513857

Zone II (170-80 cm)

Zone II was characterized by conspicuous increase of fresh species without marine-brackish species, although constrained to a combination of peaty clay, peat and coarse sand with gravels layers. A fresh lake environment appeared in this period, characterized by a significant increase of fresh limnological taxa such as *Melosira ambigua* and *Stephanodiscus astrae* with percentage of 24-67%.

Zone III (80-35 cm)

In Zone III, *Melosira ambigua* and *Stephanodiscus astrae* met a clear declining trend to 3-5%, with *Pinnularia* spp. and *Eunotia* spp. increasing rapidly reaching 35%. A stream environment indicator *Gamphonena* spp. appeared in this zone (6-11%), indicating a wetland environment influenced by stream.

Diatom analysis for core HT-1 and HT-2

Peat, grey peat in core HT-1 and blue-grey medium and coarse sand in core HT-2 were employed for diatom analysis. Results from both the cores show that few diatom species exist in underlying layers with small amount of fresh species such as *Pinnularia* spp., *Eunotia* spp. and *Hantzschia amphioxys*.

Diatom analysis for core NL

Overlying the yellowish medium sand to 4.2 m a.s.l., M-B species play a dominate role, containing *Coscinodiscus excentricus,* indicator of coastal environment and inner bay, and *Thaiassionema nitzschioides*, indicator of coastal environment, with significant percentages of 33-25% and 10-28%, respectively. A declining trend of the number of diatoms above 4.2 m a.s.l. is observed, with the dominant species indicative of freshwater environment, such as *Pinnularia* spp. and *Eunotia* spp. (18-37% and 18-25%, respectively).

Diatom species and covered water change

The diversity of diatom assemblage in Core LD-1 shows that the environment changed gradually from the bottom to the top, as marine-brackish species dominated in the lower part, while fresh-brackish and fresh species dominated in the upper part, suggesting that the environment varied from drowned ditch covered to salty marsh, and then to fresh wetland and marsh. The gradual change shows that the sediments provide continuous environment records, documenting the waning of seawater influence. Diatom species in the peat layer were mostly fresh indicators, especially inhabited in marsh and wetland environment, while the underlying part contained brackish-fresh species with gradual increase of brackish-marine diatoms, which indicated that these organic-rich materials were formed in a marsh environment with sea level regressed in the semi-enclosed drowned ditch. Hence, the base of peat layer which contacted with underlying layer can be used as the turning point from sea-level highstand to regression, with 3.40 m a.s.l. The calibrated radiocarbon age of 5466 cal. a B.P., indicating that the shoreline retreated from 5466 a B.P. from the position of core LD-1 with elevation of *ca.* 3.40 m a.s.l.

Sedimentary environment change can be identified from the vertical change of diatom assemblages in Core LD-2. From the bottom of LD-2, five diatom assemblage

http://www.aloki.hu ● ISSN 1589 1623 (Print) ● ISSN 1785 0037 (Online)
DOI: http://dx.doi.org/10.15666/aeer/1706_1384513857

zones were constrained to drowned ditch covered by seawater, drowned ditch with shallow seawater, salty marsh, lacustrine bog and wetland, respectively. Similar with LD-1, the peat layer contacted conformably with underlying part, which contained gradual increase of fresh-brackish species from the base to the top, showing a gradual declining of sea level. The radiocarbon date showed that the seawater had regressed from the small drowned ditch since 6052 cal. a B.P., in height of 3.84 m a.s.l.

Without gradual change of the diatom assemblages, the fresh-species dominant peat directly contacted with underlying by marine-brackish sedimentary layer in core LD-3, in disagreement with the cores LD-1 and LD-2. It is likely related to erosion or drastic increase of fresh water level. The elevation of 3.10 m a.s.l. for the peat layer in core LD-3 is thus not applicable to indicate the sea-level in this site. The radiocarbon date is 5446 cal. a BP for this peat layer.

Peatlands and its implication of the mid-Holocene sea level change

The Dayanghe Plain is geomorphologically separated into several drowned ditches with a static sedimentary environment. The distribution of the buried peat layers in these three drowned ditches could be recognized from the boreholes. The elevation of the peat layer declines from head to mouth, corresponding to the sea-level regression. Determined by diatom assemblages, this layer is classified as the marsh or limnological peat, rarely influenced by seawater. The distribution of peat in LD-3 ditch indicates that seawater reached to the LD-3 ditch, which is 20 km to the present estuary, occupying the whole Dayanghe Plain. The lower blue-grey clay layer likely resulted from shallow marine environment during the Early-Middle Holocene. The boundary of peat and the lower blue-grey layer corresponds to seawater regression in the Dayanghe Plain. In the LD-3 ditch, peat and black clay appeared at elevations of 6.4 m and 9.0 m a.s.l., whereas the underlain sediment succession contains no marine-brackish species. Therefore, the noncontinuous peat and organic-rich clay in the LD-3 ditch are not result of the Holocene sea-level change.

It demonstrates that the boundary between the peat layer and the blue-grey marine strata is approximately 4 m a.s.l. in the head of ditches. It is consistent with the mean high tide line at that time. The tidal range in this area is 4.08 m at present, with mean regional sea-level in 0.36 m a.s.l. We assume that the situation in mid-Holocene was consistent with present, and the mean sea level could be calculated as: high tide level minus half of the tidal range (4 – 4.08 / 2 m = 1.96 m), which implies that the sea-level was approximately 1.60 m higher than present. Although one radiocarbon date for the LD-3 peat is doubtful to indicate the seawater regression due to the unconformable contact between the peat and the underlain silt layer, the age results from cores LD-1 and LD-2 suggested the Holocene regression started during 6052-5466 cal. a BP. It challenges the outcomes from the previous studies. The buried peat at the height of 8 m a.s.l. in Huangtukan area has been thought to be related to the high sea-level since 7840 cal. a BP. Similarly, the shell banks in the west Dagu Mountain at height of 7-10 m a.s.l. have been considered as the result of sea-level rise and tectonic uplifts, which was 3-6 m higher than result from buried peat and diatom analysis. Moreover, the upper grey silt layer in core NL, deposited in the coastal environment, was dated back to 6182 cal. a BP using the shell collected from the bottom of this layer. It suggests that seawater reached to the Dayanghe Plain not before ca. 6000 cal. a BP. More evidence was provided by diatom analysis from cores drilled in Huangtukan area. Buried peat was found in core HT-1 and HT-2, in height of 8.80 and 8.50 m a.s.l., respectively.

http://www.aloki.hu ● ISSN 1589 1623 (Print) ● ISSN 1785 0037 (Online)
DOI: http://dx.doi.org/10.15666/aeer/1706_1384513857

Only several diatom species inhabiting in fresh water were found in lower parts of both two cores. Therefore, the peat in the Huangtukan area is not indicative of sea-level change during the Holocene.

The sea-level of 1.60 m higher than the present during the Holocene sea-level highstand is also supported by the results of the previous research in Japanese coastal areas, e.g. Hokkaido, Tsugaru Plain, Osaka Bay and Tamagawa. They suggested that the sea-level highstand occurred during 6000-5500 cal. a B.P. The sea-level was 0-5 m higher than the present (UMITSU, 1994). Therefore, the height of highstand sea-level in the North Coast of the Yellow Sea in the Middle Holocene (6052-5466 cal. a BP) is constrained to ca. 1.60 m a.s.l. by radiocarbon dating and diatom analysis approaches.

Conclusions

Using diatom assemblage analysis and radiocarbon dating approaches, the sea-level highstand and the timing of the sea-level highstand termination in the North Coast of the Yellow Sea were investigated. We draw our conclusions as follows.

(1) The widely distributed buried peat, at elevation of 2-10 m a.s.l. in the Dayanghe Plain was classified as marsh and limnological peat, which formed after seawater regressing from the drowned ditches. Only the peat layer below 4 m a.s.l., contacting the lower marine section conformably, were related to regression.

(2) The peatland at < 4 m a.s.l. formed during the period of 6182-5466 cal. a BP, indicating the Holocene highstand sea-level was 1.60 m higher than the present.

(3) According to the diatom assemblages in the studies cores, the shell banks at west of Dagu Mountain at height of 7-10 m is not indicative of sea-level change. The shell banks are also excluded as sea-level indicator as they are much higher than the results of the regional sea-level investigations.

(4) It is necessary to investigate the notches, terraces and buried peat in the adjacent areas for comparison to better understand the Holocene sea-level change.

REFERENCES

[1] Ando, K., Fujimoto, K. (1990): Paleo-environmental history and sea-level records based on the diatom assemblages in the middle part of the Arakawa lowland, Central Japan. – The Quaternary Research 29: 427-437.

[2] Chappell, J. (2002): Sea level changes forced ice breakouts in the Last Glacial cycle: new results from coral terraces. – Quaternary Science Reviews 21: 1229-1240.

[3] Chappell, J., Omura, A., Esat, T., McCulloch, M., Pandolfi, J., Ota, Y., Pillans, B. (1996): Reconciliaion of late Quaternary sea levels derived from coral terraces at Huon Peninsula with deep sea oxygen isotope records. – Earth and Planetary Science Letters 141: 227-236.

[4] Ding, X. (1958): Problem uplifting or subsidence in coastal zone, Liaoning. – China Quaternary Research 1: 160-165.

[5] Engelhart, S. E., Horton, B. P. (2012): Holocene sea level database for the Atlantic coast of the United States. – Quaternary Science Reviews 54: 12-25.

[6] Fu, W., Li, G., Wei, C. (1989): Late Quaternary shoreline migration along the eastern coast of Liaodong Peninsula. – Oceanologia et Limnologia Sinica 20: 252-262.

[7] Fu, W., Wang, G., Liu, G. (1995): Peat deposition and sea level change in Holocene, Liaoning. – Journal of Oceanography of Huanghai & Bohai Seas 13: 23-32.

http://www.aloki.hu ● ISSN 1589 1623 (Print) ● ISSN 1785 0037 (Online)
DOI: http://dx.doi.org/10.15666/aeer/1706_1384513857

[8] Gao, F. (1986): The relation between formation of peat in seaside area of Bohai Sea and North Yellow Sea and sea level fluctuation since the Late Wuerm-glaciation. – Scientia Geographica Sinica 6: 56-63.
[9] Gao, S., Li, Y., Liu, G. (1992): Sedimentary characters and sea level change recorded by sand and gravel bank-lagoon system in coastal zone, Liaoning. – Acta Geographica Sinica 47: 129-137.
[10] GIGCAS (1977): The natural environment changes last10000 years in South Liaoning Province. – Science in China (Series A) 6: 603-614.
[11] Horton, B. P. (1997): Quantification of the indicative meaning of a range of Holocene sea-level index points from the western North Sea. – Doctoral dissertation, Durham University.
[12] Horton, B. P., Corbett, R., Culver, S. J., Edwards, R. J., Hillier, C. (2006): Modern saltmarsh diatom distributions of the Outer Banks, North Carolina, and the development of a transfer function for high resolution reconstructions of sea level. – Estuarine, Coastal and Shelf Science 69: 381-394.
[13] Horton, B. P., Zong, Y., Hillier, C., Engelhart, S. (2007): Diatoms from Indonesian mangroves and their suitability as sea-level indicators for tropical environments. – Marine Micropaleontology 63: 155-168.
[14] IOCAS (1985): Bohai Sea Geology. – Science Press, Beijing.
[15] IPCC (2014): Climate Change 2014: Impacts, Adaptation, and Vulnerability (edited by Field, C. B., Barros, V. R. et al.) – Cambridge University Press, New York.
[16] Jin, X., Yu, P. (1978) Preliminary study on geomagnetic field and tectonics of continental shelf of the East China Sea. – Marine Sciences 3: 94-96.
[17] Kashina, K. (1986): Holocene successions of diatom fossil assemblages in alluvium, and those relations to paleo-geographical changes. – Geographical Review of Japan 59: 383-403.
[18] Kim, J. M., Kennett, J. P. (1998): Paleoenvironmental changes associated with the Holocene marine transgression, Yellow Sea (Hwanghae). – Marine Micropaleontology 34: 71-89.
[19] Kosugi, M. (1988): Class ification of living diatom assemblages as the indicator of environments, and its application to reconstruction of paleoenvironments. – The Quaternary Research 27: 1-20.
[20] Li, G., Li, P., Liu, Y., Qiao, L., Ma, Y., Xu, J., Yang, Z. (2014): Sedimentary system response to the global sea level change in the East China Seas since the last glacial maximum. – Earth-Science Reviews 139: 390-405.
[21] Li, Y., Tsukamoto, S., Shang, Z., Tamura, T., Wang, H., Frechen, M. (2019): Constraining the transgression history in the Bohai Coast China since the Middle Pleistocene by luminescence dating. – Marine Geology: 416.
[22] Liu, G., Han, M. (1986): New discovery of residual coastal sediments in Dalian. – Acta Oceanologica Sinica 6: 793-796.
[23] Liu, G., Gao, S., Li, Y. (1992): Sedimentary environment and sea level fluctuation in Holocene, Dalian area. – Geographical Research 11: 38-45.
[24] Liu, J., Wang, H., Wang, F., Qiu, J., Saito, Y., Lu, J., Zhou, L., Xu, G., Du, X., Chen, Q. (2016): Sedimentary evolution during the last ~1.9Ma near the western margin of the modern Bohai Sea. – Palaeogeography, Palaeoclimatology, Palaeoecology 451: 84-96.
[25] Liu, J. P., Milliman, J. D., Gao, S., Cheng, P. (2004): Holocene development of the Yellow River's subaqueous delta, North Yellow Sea. – Marine Geology 209: 45-67.
[26] Lu, Y. (1985): Displacement of shoreline and neotectonic movement in the eastern China during the Holocene. – Proceedings of Collection of Quaternary Coastline Symposium, China, pp. 76-87.
[27] Qin, Y. S., Zhao, Y. Y., Chen, L. R., Zhao, S. L. (1989): Geology of the Yellow Sea. – China Ocean Press, Beijing.

http://www.aloki.hu ● ISSN 1589 1623 (Print) ● ISSN 1785 0037 (Online)
DOI: http://dx.doi.org/10.15666/aeer/1706_1384513857

[28] Shennan, I., Horton, B. (2002): Holocene land-and sea-level changes in Great Britain. – Journal of Quaternary Sciences 17: 511-526.
[29] Shi, B. (2006): Archeological record for high stand sea level in Holocene, Liaodong Peninsula. – Sichuan Cultural Relics: 37-41.
[30] Stuiver, M., Reimer, P. J., Reimer, R. W. (2005): CALIB 5.0.1. WWW Program and Documentation. – www.calib.org.
[31] Umitsu, M. (1994): Late Quaternary Environment and Landform Evolution of Riverine Coastal Lowlands. – Kokon-Shoin, Tokyo.
[32] Wang, F., Li, J., Chen, Y., Fang, J., Zong, Y., Shang, Z., Wang, H. (2015): The record of mid-Holocene maximum landward marine transgression in the west coast of Bohai Bay, China. – Marine Geology 359: 9-95.
[33] Wang, Q., Li, F., Li, Y., Gao, X. (1986): Shoreline Changes in West-Southern Coastal Plain of the Bohai Sea Since 150 ka. – In: Qin, Y. S., Zhao, S. (eds.) Late Quaternary Sea-Level Changes. China Ocean Press, Beijing, pp. 62-71.
[34] Wang, S., Zhang, W. (1991): Preliminary discussion on coastal change in Liaodong Peninsula during Holocene. – Progress of Geomorphology and Quaternary 1986: 199-201.
[35] Wei, C., Li, G., Fu, W. (1984): A preliminary study on the development of the mud-flat coast of the north Yellow Sea. – Marine Geology & Quaternary Geology 4: 35-42.
[36] Xia, H., Zhang, X. (1986): Coastal topography and the reflection of neotectonic movement in coastal zone in Liaodong Peninsula. – Seismology and Geology 3: 40-49.
[37] Xiao, R., Tang, C. (1981): Differentiation of marine geomorphology in Liaodong Peninsula. – Journal of Northeast Normal University 1981: 83-90.
[38] Xue, C. (2014): Missing evidence for stepwise postglacial sea level rise and an approach to more precise determination of former sea levels on East China Sea Shelf. – Marine Geology 348: 2-62.
[39] Yang, W., Lin, J. (1985): Preliminary Notes on Holocene Transgression in the Southeast Coast of Liaodong Peninsula. – Chinese Journal of Geology 2: 196-201.
[40] Yi, L., Yu, H., Ortiz, J. D., Xu, X., Qiang, X., Huang, H., Shi, X., Deng, C. (2012): A reconstruction of late Pleistocene relative sea level in the south Bohai Sea, China, based on sediment grain-size analysis. – Sedimentary Geology 281: 88-100.
[41] Yi, L., Lai, Z., Yu, H., Xu, X., Su, Q., Yao, J., Wang, X., Shi, X. (2013): Chronologies of sedimentary changes in the south Bohai Sea, China: constraints from luminescence and radiocarbon dating. – Boreas 42: 267-284.
[42] Yi, L., Ye, X., Chen, J., Li, Y., Long, H., Wang, X., Du, J., Zhao, S., Deng, C. (2014): Magnetostratigraphy and luminescence dating on a sedimentary sequence from northern East China Sea: Constraints on evolutionary history of eastern marginal seas of China since the Early Pleistocene. – Quaternary International 349: 16-326.
[43] Yokoyama, Y., Esat, T. M., Lambeck, K. (2001): Coupled climate and sea-level changes deduced from Huon Peninsula coral terraces of the last ice age. – Earth and Planetary Science Letters 193: 579-587.
[44] Zhao, G., Liu, X., Ma, S., Tian, S., He, S. (2000): Crustal deformation of coastal zone based on tidal record in China. – Seismology and Geology 22(4): 371-378.
[45] Zhao, S. (1986): Transgression and Coastal Changes in Bohai Sea and Its Vicinities since the Late Pleistocene. – In: Yunshan Qin, S. Z. (ed.) Late Quaternary Sea-Level Changes. China Ocean Press, Beijing.
[46] Zhao, X. (1996): China Climate and Sea-Level Change: Trend and Influence. – Shandong Science and Technology Press, Shandong.
[47] Zheng, G. (1991): Quaternary Geology in the Yellow Sea. – Science Press, Beijing.
[48] Zhong, Y., Gao, C. B. (1988): Sea level changes in the Holocene and crustal movement in the past 5000 years in the Liaodong Peninsula. – Marine Sciences 1: 4-8.

http://www.aloki.hu ● ISSN 1589 1623 (Print) ● ISSN 1785 0037 (Online)
DOI: http://dx.doi.org/10.15666/aeer/1706_1384513857

STUDY ON SEAWATER INTRUSION AND INFLUENCING FACTORS BASED ON THE ADVECTION-DISPERSION EQUATION

ZHANG, L.[1] – JIANG, Z.[2*] – WANG, H.[3] – QI, Q.[1] – ZHU, Y.[4]

[1]*School of Civil Engineering, Shijiazhuang Tiedao University, 050043 Shijiazhuang, China*

[2] *China Railway Guangzhou Group Hainan Railway Co., Ltd., 570100 Haikou, China*

[3]*Shijiazhuang City Water Conservancy and Hydropower Engineering Department, 050000 Shijiazhuang, China*

[4]*Hebei Institute of Water Science, 050000 Shijiazhuang, China*

**Corresponding author*
e-mail: 599787051@qq.com

(Received 21st May 2019; accepted 16th Oct 2019)

Abstract. The purpose of this study was to explain the phenomenon of seawater intrusion (SWI) by numerical simulation and analysis. In this paper, a numerical method was introduced for solving the one-dimensional advection-dispersion equation by the explicit finite difference method, and the corresponding convergence conditions and the boundary attenuation factor, β, were given, which can be convenient in studying the impact of different influencing factors on seawater intrusion. Additionally, the effects of six hydraulic factors on seawater intrusion were explored under steady state, namely, hydraulic conductivity, longitudinal dispersivity, hydraulic gradient, flux, evaporation and rainfall. Moreover, two different seawater intrusion types were also studied, namely active seawater intrusion and passive seawater intrusion. Meanwhile, the control variates method was adopted to explore the influence of a single factor on seawater invasion. According to the calculated results, with the increase of hydraulic conductivity, longitudinal dispersion, flux and evaporation, the degree of it will be aggravated, but the rainfall can play a role in mitigating seawater intrusion. Besides, under active seawater intrusion conditions, the growth of the numerical value of hydraulic gradient will aggravate seawater intrusion, while under passive seawater intrusion conditions, it will slow down the degree of invasion. All in all, the results and achievements are consistent with the actual situation, which can explain the phenomenon of seawater intrusion.
Keywords: *seawater intrusion, numerical simulation, explicit finite difference method, active and passive seawater intrusion, seepage tank*

Introduction

In coastal and island areas, seawater intrusion (SWI) has become one of the major geological hazards due to the over-exploitation of groundwater (Li et al., 1996). Seawater intrusion arising from aquifer depletion is often classified as active or passive, depending on whether seawater moves in the same direction as groundwater flow or not (Werner, 2017). Generally, hydrodynamic and hydrogeological conditions are essential for the formation of seawater intrusion (Xue et al., 1992). There are a variety of factors affecting seawater intrusion, which can also be divided into hydrodynamic factors and hydrogeological factors under natural conditions excluding human factors. Hydrodynamic factors include hydraulic gradient, flux, evaporation, rainfall, recharge and tidal action, while hydrogeological factors include hydraulic conductivity, longitudinal dispersivity, adsorption and porosity (Chen et al., 2013). According to the *Technical regulations for monitoring and evaluating sea water intrusion* issued by the

http://www.aloki.hu ● ISSN 1589 1623 (Print) ● ISSN 1785 0037 (Online)
DOI: http://dx.doi.org/10.15666/aeer/1706_1385913874

State Oceanic Administration (Mao, 2014), the concentration of chloride ion at 250 mg/L can evaluate the degree of seawater intrusion.

Zhao et al. (2018) investigated the effects of some influencing factors on seawater-freshwater mixing zones, namely, saturated hydraulic conductivity, porosity, molecular diffusivity, longitudinal and transverse dispersivity, by analyzing their uncertainty and sensitivity for the predicted seawater-freshwater mixing zones in simulation experiments. Moreover, based on the measured data of groundwater level and content in the transition zone, Zhang et al. (2015) and Zhen et al. (2015) found that there was a significant negative correlation between the seasonal variation of groundwater level and the seasonal variation of groundwater content. Then, Zhang (2015) determined that the correlation coefficient was above 0.92. Adel et al. (2014) found that salinization of fresh groundwater is highly associated with groundwater withdrawal based on historical hydraulic heads data. Qing et al. (2013) determined that rainfall and tidal effects have an important impact on seawater intrusion, and that rainfall can lower the degree of seawater intrusion. Liu et al. (2007) obtained that the increase of elevation difference between seawater and freshwater level will increase the speed of SWI. Zhang and Chen et al. (2015) proposed that local groundwater is subjected to anthropogenic activities and geochemical processes, such as evaporation, water-rock interaction, and ion exchange, thus affecting the degree of seawater intrusion. Emna et al. (2018) found local shallow groundwater is threatened by seawater intrusion because of the reduced rainfall and recharge capacity.

Based on the above research contents, six hydraulic factors were considered including hydraulic conductivity, longitudinal dispersivity, hydraulic gradient, flux, evaporation and rainfall in this paper. In order to study the influence of these six hydraulic factors on seawater intrusion and its final steady state, the control variates method was adopted in this paper. With other conditions unchanged, the influence of the change of one factor on the final steady state was considered separately. In this paper, the explicit finite difference method was adopted to solve the one-dimensional advection-dispersion equation. The purpose of this method was to simulate the real salt migration phenomenon from the viewpoint of numerical calculation, analyze the mechanism of seawater intrusion, and explain the influence of various factors on the seawater intrusion under both steady state and two kinds of SWI types, active SWI and passive SWI (active seawater intrusion and passive seawater intrusion).

The one-dimensional advection-dispersion equation has been widely applied to describe the transportation process, which is utilized for the study of seawater intrusion (Yu, 2018). Compared with two-dimensional and three-dimensional models, it requires fewer parameters and remains as a simple and feasible method, and it is convenient to study the impact of the above six hydraulic factors on seawater intrusion. Nie et al. (2002) explained the problem of seawater intrusion through the advection-dispersion model of miscible fluid. Purnaditya et al. (2018) developed the mathematical model of groundwater flow and solute transport which is applicable to seawater intrusion mechanism.

With respect to solve one-dimensional advection-dispersion equation by finite difference method, Yu et al. (2018), from China, implemented Homotopy Analysis Method (HAM) to solve the one-dimensional advection-dispersion equation. Savovic et al. (2012), from Russia, solved one-dimensional advection– dispersion equation with variable coefficients by using explicit finite difference method and shown that explicit

http://www.aloki.hu ● ISSN 1589 1623 (Print) ● ISSN 1785 0037 (Online)
DOI: http://dx.doi.org/10.15666/aeer/1706_1385913874

finite difference method is effective and accurate for solving the equation. Yang et al. (2016), from China, proposed a boundary value method for solving fractional order advection-dispersion equation. In the traditional numerical solution of the advection-dispersion equation, the longitudinal dispersivity coefficient is often regarded as a constant, but it is directly proportional to the size of the flow velocity. When the distribution of the flow velocity in space is not equal, neither the velocity nor the longitudinal dispersivity coefficient can be regarded as a constant. Comparing the methods described above, the methods presented in this paper combined the characteristics of seawater intrusion, considering active SWI and passive SWI, introducing the boundary attenuation factor, and giving the convergence conditions, which can simulate the real situation of seawater intrusion.

Therefore, the article aimed to study seawater intrusion through the introduction of a numerical method to solve the one-dimensional advection-dispersion equation using the finite difference method, and additionally investigated influencing factors, the effect strength of a single such factor, and seawater intrusion types.

Research methods

One-dimensional advection-dispersion equation

In the steady seepage field, if the change of water density caused by the change of solute concentration can be ignored by solving the advection-dispersion equation, the flow equation and the solute transport equation can be solved independently. The velocity components in the seepage field are obtained from the solution of the flow equation, and then the velocity is substituted into the advection-dispersion equation as input. This method called decoupling method has high computational efficiency (Zheng et al., 2016). In this paper, the decoupling method was adopted to solve the problem of the flow velocity term in the advection-dispersion equation. According to the different influencing factors, different formulas for calculating the velocity term were given. The velocity term was substituted for the difference formula of the concentration, and the calculation results were expressed as the spatial distribution of chloride ion concentration in the seepage interval under this single influencing factor.

In the paper, the one-dimensional advection-dispersion equation was taken as the research object. It was considered that seawater and freshwater were miscible, regardless of source and sink terms, and the porosity n is constant (Khakimov et al., 2017).

$$\frac{\partial c}{\partial t} = \frac{\partial}{\partial x}(D_l \frac{\partial c}{\partial x}) - \frac{\partial}{\partial x}(V_x c) \quad \text{(Eq.1)}$$

$$V_x = -k \frac{\partial h}{\partial x} \quad \text{(Eq.2)}$$

$$D_l = \alpha_L |V_x| \quad \text{(Eq.3)}$$

In the above equations, k is the hydraulic conductivity, unit m/s; D_l represents the longitudinal dispersivity coefficient, which is the physical quantity reflecting the dispersivity of soluble substances through the permeable media, unit m^2/s; a_L represents the longitudinal dispersivity, unit m.

http://www.aloki.hu ● ISSN 1589 1623 (Print) ● ISSN 1785 0037 (Online)
DOI: http://dx.doi.org/10.15666/aeer/1706_1385913874

Explicit differentiation of differential equations

In terms of one-dimensional advection-dispersion seawater intrusion model, there are two kinds of cases. Namely, the one case that seawater head is higher than freshwater head is defined as active SWI, and the other case that freshwater head is higher than seawater head is defined as passive SWI (Badaruddin et al., 2017). Under active SWI conditions, $h_0 > h_N$, as shown in *Figure 1,* the direction of flow velocity is the same as the direction of salt migration as well as the direction of X-axis. Furthermore, under passive SWI conditions, $h_0 < h_N$, as shown in *Figure 2,* the direction of velocity is opposite to the direction of salt migration as well as the direction of the X-axis. The diffusion of salinity under constant flux, head and steady-state conditions was studied in this paper. Therefore it is assumed that the water head and flow velocity have reached a steady state before salinity diffusion.

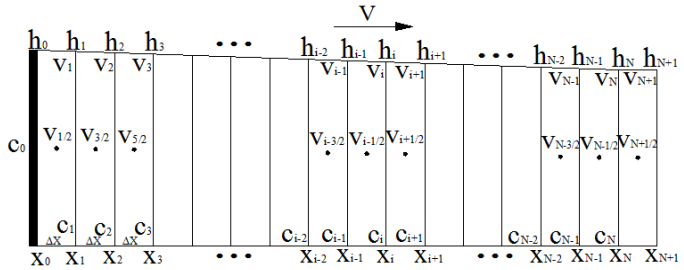

Figure 1. *The seepage interval node division under active SWI conditions*

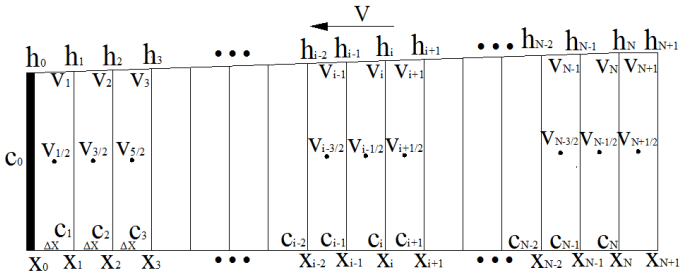

Figure 2. *The seepage interval node division under passive SWI conditions*

Under active SWI conditions, *Equation 1* can be transformed into differential iterative formula as follows:

$$\frac{c_i^{n+1}-c_i^n}{\Delta t}=\frac{\alpha_L[V_{i+\frac{1}{2}}(c_{i+1}^n-c_i^n)-V_{i-\frac{1}{2}}(c_i^n-c_{i-1}^n)]}{(\Delta x)^2}-\frac{V_i c_i^n-V_{i-1}c_{i-1}^n}{\Delta x}\quad(1\le i<N)\qquad\text{(Eq.4)}$$

When $i=N$, then $c_{N+1}^n=\beta c_N^n$, $V_{N+1/2}=V_N$, β is the boundary attenuation factor, and its value is between [0,1], reflecting the degree of attenuation of the concentration at the boundary. Therefore, *Equation 1* can be transformed into *Equation 5* as follows:

$$\frac{c_N^{n+1}-c_N^n}{\Delta t}=\frac{\alpha_L[V_N(\beta-1)c_N^n-V_{N-\frac{1}{2}}(c_N^n-c_{N-1}^n)]}{(\Delta x)^2}-\frac{V_N c_N^n-V_{N-1}c_{N-1}^n}{\Delta x}\quad(i=N)\qquad\text{(Eq.5)}$$

http://www.aloki.hu ● ISSN 1589 1623 (Print) ● ISSN 1785 0037 (Online)
DOI: http://dx.doi.org/10.15666/aeer/1706_1385913874

Equations 4 and *5* can be transformed into standard difference formulas as follows:

$$\begin{cases} \Delta t/(\Delta x)^2 = \lambda \\ c_i^{n+1} = \lambda\alpha_L V_{i+\frac{1}{2}} c_{i+1}^n + [1-\lambda(\alpha_L V_{i+\frac{1}{2}} + \alpha_L V_{i-\frac{1}{2}} + \Delta x V_i)]c_i^n + \lambda(\alpha_L V_{i-\frac{1}{2}} + \Delta x V_{i-1})c_{i-1}^n (1 \le i < N) \\ c_N^{n+1} = \left\{[1-\lambda[\alpha_L(1-\beta)V_N + \alpha_L V_{N-\frac{1}{2}} + \Delta x V_N]\right\} c_N^n + \lambda(\alpha_L V_{N-\frac{1}{2}} + \Delta x V_{N-1})c_{N-1}^n \quad (i = N) \end{cases} \quad \text{(Eq.6)}$$

The value of Δx and Δt should satisfy the corresponding convergence conditions. Under active SWI conditions, when the value of Δx and Δt should satisfy *Equation 7,* the one-dimensional explicit difference schemes are absolutely convergent.

$$1 - \frac{\Delta t}{(\Delta x)^2}(\alpha_L V_{i+\frac{1}{2}} + \alpha_L V_{i-\frac{1}{2}} + \Delta x V_i) \ge 0 \quad \text{(Eq.7)}$$

q stands for flux per unit width, whose calculation equation is shown in *Equation 8,* and its unit is m^2/s (Qi, 2016).

$$q = \frac{k\left(h_0^2 - h_N^2\right)}{2L} \quad \text{(Eq.8)}$$

Equation 9 is for calculating node water head height under active SWI conditions.

$$h_i = \sqrt{h_0^2 - i\frac{(h_0^2 - h_N^2)\Delta x}{L}} \quad \text{(Eq.9)}$$

Equations 10 and *11* are for calculating flow velocity under active SWI conditions.

$$V_i = \frac{q}{h_i} = \frac{k(h_0^2 - h_N^2)}{2L\sqrt{h_0^2 - i\frac{(h_0^2 - h_N^2)\Delta x}{L}}} \quad \text{(Eq.10)}$$

$$V_{i+\frac{1}{2}} = \frac{k(h_i - h_{i+1})}{\Delta x} = \frac{k(\sqrt{h_0^2 - i\frac{(h_0^2 - h_N^2)\Delta x}{L}} - \sqrt{h_0^2 - (i+1)\frac{(h_0^2 - h_N^2)\Delta x}{L}})}{\Delta x} \quad \text{(Eq.11)}$$

Under passive SWI conditions, the calculated value of the velocity substituted is negative. Considering that D_l, the longitudinal dispersivity coefficient, is not affected by the forward or negative effect of the velocity, but only related to its size, *Equation 1* can be transformed into *Equation 12* as shown below to ensure that the coefficients of the velocity term in the explicit difference equation are forward.

$$\frac{c_i^{n+1} - c_i^n}{\Delta t} = \frac{\alpha_L[V'_{i+\frac{1}{2}}(c_{i+1}^n - c_i^n) - V'_{i-\frac{1}{2}}(c_i^n - c_{i-1}^n)]}{(\Delta x)^2} + \frac{V'_i c_i^n - V'_{i-1} c_{i-1}^n}{\Delta x} \quad (1 \le i < N) \quad \text{(Eq.12)}$$

Similarly, *Equation 12* can be transformed into standard difference formulas as follows:

http://www.aloki.hu ● ISSN 1589 1623 (Print) ● ISSN 1785 0037 (Online)
DOI: http://dx.doi.org/10.15666/aeer/1706_1385913874

$$\begin{cases} \Delta t/(\Delta x)^2 = \lambda \\ c_i^{n+1} = \lambda\alpha_L V'_{i+\frac{1}{2}} c_{i+1}^n + [1-\lambda(\alpha_L V'_{i+\frac{1}{2}} + \alpha_L V'_{i-\frac{1}{2}} - \Delta x V'_i)]c_i^n + \lambda(\alpha_L V'_{i-\frac{1}{2}} - \Delta x V'_{i-1})c_{i-1}^n (1 \le i < N) \\ c_N^{n+1} = \left\{[1-\lambda[\alpha_L(1-\beta)V'_N + \alpha_L V'_{N-\frac{1}{2}} - \Delta x V'_N]\right\} c_N^n + \lambda(\alpha_L V'_{N-\frac{1}{2}} - \Delta x V'_{N-1})c_{N-1}^n \qquad (i = N) \end{cases} \quad \text{(Eq.13)}$$

Under passive SWI conditions, its convergence conditions are shown as below:

$$\begin{cases} 1 - \dfrac{\Delta t}{(\Delta x)^2}(\alpha_L V'_{i+\frac{1}{2}} + \alpha_L V'_{i-\frac{1}{2}} - \Delta x V'_i) \ge 0 \\ \alpha_L V'_{i-\frac{1}{2}} - \Delta x V'_{i-1} \ge 0 \end{cases} \quad \text{(Eq.14)}$$

Equation 15 is for calculating node water head height under passive SWI conditions.

$$h'_i = \sqrt{h_N^2 - (N-i)\frac{(h_N^2 - h_0^2)\Delta x}{L}} \quad \text{(Eq.15)}$$

Equations 16 and *17* are for calculating flow velocity under passive SWI conditions.

$$V'_i = \frac{q}{h'_i} = \frac{k(h_N^2 - h_0^2)}{2L\sqrt{h_N^2 - (N-i)\frac{(h_N^2 - h_0^2)\Delta x}{L}}} \quad \text{(Eq.16)}$$

$$V'_{i+\frac{1}{2}} = \frac{k(h'_i - h'_{i+1})}{\Delta x} = \frac{k(\sqrt{h_N^2 - (N-i)\frac{(h_N^2 - h_0^2)\Delta x}{L}} - \sqrt{h_0^2 - (N-i+1)\frac{(h_N^2 - h_0^2)\Delta x}{L}})}{\Delta x} \quad \text{(Eq.17)}$$

In order to study the effects of discharge variation, precipitation and evaporation on seawater intrusion, the flux is changed by keeping the hydraulic gradient constant and controlling the water head on both sides to increase at the same time.

The effects of rainfall and evaporation are considered to be uniform in the seepage field, and water exchange exists in each subzone. The position diagram of the influencing factors such as flow change, precipitation and evaporation was drawn, as shown in *Figure 3*.

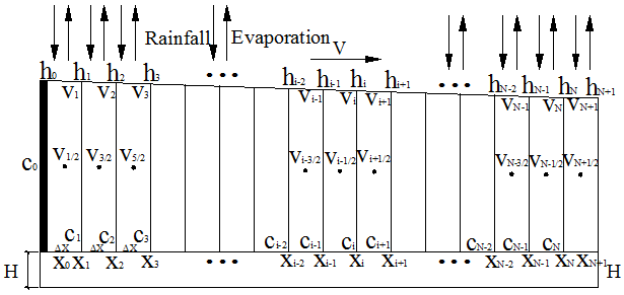

Figure 3. *Influencing relationship of flux, rainfall and evaporation*

As shown in *Figure 3, H* represents the numerical value of simultaneous rise of water head on both sides. If *H* is positive, it means water head would increase H meters

http://www.aloki.hu ● ISSN 1589 1623 (Print) ● ISSN 1785 0037 (Online)
DOI: http://dx.doi.org/10.15666/aeer/1706_1385913874

simultaneously on both sides. Conversely, negative H means decreasing. That is to say, the seawater head rises *H* meters, at the same time, the fresh water level also rises *H* meters. Meanwhile, the hydraulic gradient does not change. However, the flux changes with the change of *H*, which is a special flow quantity change, thus affecting the seepage velocity and the final concentration distribution. The formulas for calculating discharge, head and velocity can be seen in *Equation 18.*

$$\begin{cases} q_H = \dfrac{k[(h_0+H)^2-(h_N+H)^2]}{2L} \\ h_{H_i} = \sqrt{h_0^2 - i\dfrac{(h_0^2-h_N^2)\Delta x}{L}} + H \\ V_{H_i} = \dfrac{q_H}{h_H}, V_{H_{i+\frac{1}{2}}} = \dfrac{k(h_{H_i}-h_{H_{i+1}})}{\Delta x} \end{cases} \quad \text{(Eq.18)}$$

As to rainfall and evaporation, the influencing factors on seawater intrusion, the annual average rainfall is represented by *R*, and the annual average evaporation is represented by *E*. The unit is mm/yr, and 1 mm/yr = 3.171 $\times 10^{-11}$ m/s. Rainfall and evaporation are directly affected on the unit seepage length, and water exchange occurs in each spatial grid. Rainfall and evaporation will affect the flux in the seepage region. Thus, the flow velocity and salt diffusion are affected.

Under active SWI conditions, the equations of flux and flow velocity under the influence of the evaporation factor were shown below.

$$\begin{cases} q_{E_i} = \dfrac{k\left(h_0^2-h_N^2\right)}{2L} - iE \\ V_{E_i} = \dfrac{q_{E_i}}{h_i}, V_{E_{i+\frac{1}{2}}} = \dfrac{k(h_i-h_{i+1})}{\Delta x} \end{cases} \quad \text{(Eq.19)}$$

Under active SWI conditions, the equations of flux and flow velocity under the influence of the rainfall factor were shown below.

$$\begin{cases} q_{R_i} = \dfrac{k\left(h_0^2-h_N^2\right)}{2L} + iR \\ V_{R_i} = \dfrac{q_{R_i}}{h_i}, V_{R_{i+\frac{1}{2}}} = \dfrac{k(h_i-h_{i+1})}{\Delta x} \end{cases} \quad \text{(Eq.20)}$$

Under passive SWI conditions, the equations of flux and flow velocity are similar to those under active SWI conditions.

Numerical examples

It is assumed that there is a seepage tank, which is used to simulate seawater invasion. The length of the tank is 1.5 m, the width is 0.1 m, and $k = 0.0001$ m/s, $\alpha_L = 0.2$ m. The left side is the boundary of constant head and concentration, the left side of seawater head is 0.5 m, and the initial chloride ion

http://www.aloki.hu ● ISSN 1589 1623 (Print) ● ISSN 1785 0037 (Online)
DOI: http://dx.doi.org/10.15666/aeer/1706_1385913874

concentration of the left side seawater is 18.000 mg/L, which can be prepared by seawater salinometer measuring. The right side is the fixed head boundary, the fresh water head on the right side is 0.35 m, and the chloride ion concentration is 0. Under this condition, it is considered that there is no concentration decay at the right side boundary ($c_{N+1}^n = c_N^n$), which is a case of active SWI, as shown in *Figure 4.* As to passive SWI, in the left side, the seawater head is 0.35 m and the initial chloride ion concentration is 0; and in the right side, the fresh water head is 0.5 m and the initial chloride ion concentration is 18.000 mg/L, as shown in *Figure 5.* Besides, the physical photograph of the applied seepage tank is shown in *Figure 6.* Taking $\Delta x = 0.03$ m, $\Delta t = 100$ s and $\beta = 1$, the relationship will be calculated between the steady concentration and the diffusion distance of seawater salt in the seepage field after 6,000 iterations. The initial and boundary conditions are as shown below.

$$\begin{cases} \dfrac{\partial C}{\partial t} = \dfrac{\partial}{\partial x}(a_L|V_x|\dfrac{\partial C}{\partial x}) - \dfrac{\partial}{\partial x}(V_x C) \qquad (0 < x < 1.5, t > 0) \\ C|_{t=0} = 0 \\ C|_{x=0} = 18000 \\ \dfrac{\partial V}{\partial x}|_{x=1.5} = 0 \end{cases} \tag{Eq.21}$$

While the finite difference method to calculate the above examples are used, under the condition of convergence, after 6000 iterations, the concentration of the node position basically does not change with the increase of iterations. Meanwhile, the calculation results represent the chloride ion concentration under steady state, then the degree of seawater intrusion in the region will be judged.

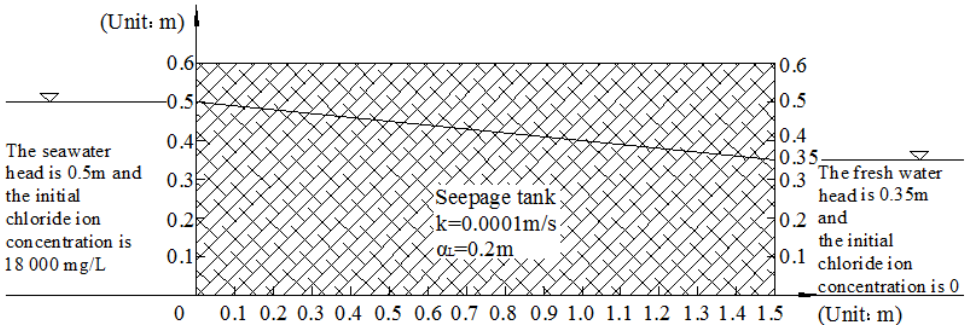

Figure 4. *The seepage tank size and boundary conditions under active SWI conditions*

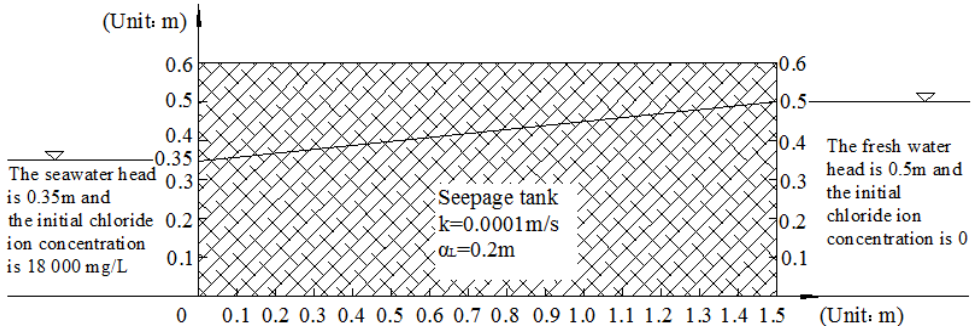

Figure 5. *The seepage tank size and boundary conditions under passive SWI conditions*

http://www.aloki.hu ● ISSN 1589 1623 (Print) ● ISSN 1785 0037 (Online)
DOI: http://dx.doi.org/10.15666/aeer/1706_1385913874

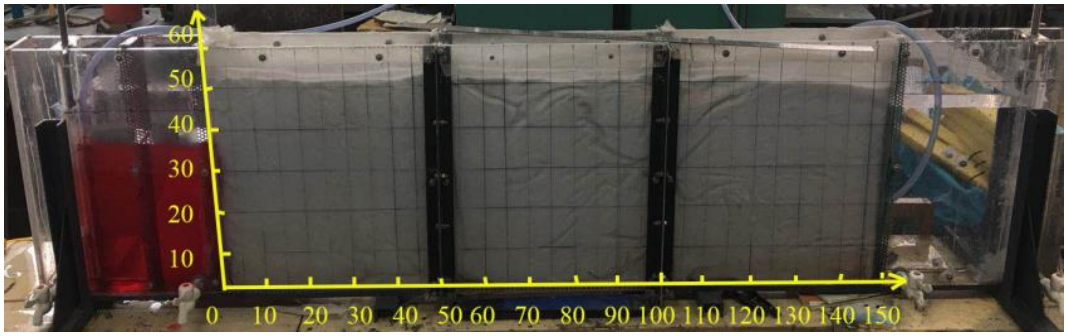

Figure 6. *The physical photograph of the applied seepage tank (unit, cm)*

Result discussion

The effects of six hydraulic factors on seawater intrusion were explored in this paper, namely, hydraulic conductivity, longitudinal dispersivity, hydraulic gradient, flux, evaporation and rainfall. Besides, the initial and boundary conditions utilized for calculation and simulation were based on the contents described in the numerical examples above. In this paper, the finite difference method was utilized to solve one-dimensional advection-dispersion equation. Meanwhile, the control variates method was adopted to explore the influence of a single factor on seawater invasion. After iteration calculation, the distribution of chloride ion concentration in the seepage field was compared under steady state.

Hydraulic conductivity

Hydraulic conductivity k, which is defined as the unit flux under the unit hydraulic gradient, represents the difficulty of fluid passing through the pore framework. The hydraulic conductivity can affect the flow velocity of seepage flow and the salt migration. In order to study the influence of hydraulic conductivity on salt migration, five different numerical values of hydraulic conductivity were formulated in this paper, namely, $k = 0.00005$ m/s, 0.0001 m/s, 0.00015 m/s, 0.0002 m/s and 0.00025 m/s. Hydraulic conductivity of sandy soil is related to many factors, such as material composition, particle size, shape, gradation and compactness of soils (Liu et al., 2017), and it can be monitored nondestructively and rapidly in real time by the resistivity measurement (Yuan et al., 2019).

Keeping other conditions unchanged, considering the forward and reverse seepage type conditions, the influence of hydraulic conductivity on seawater intrusion and its final state was analyzed, as shown in *Figure 7*.

According to the calculated results, the concentration of the final steady state rises with the increase of the hydraulic conductivity, but its growth rate is small. In the steady seepage field, the hydraulic conductivity is the time that affects the salinity to reach the final steady state. The larger the hydraulic conductivity is, the smaller the time to reach the steady state will be. Moreover, the hydraulic conductivity is forwardly correlated with the degree of seawater invasion.

Longitudinal dispersivity

Longitudinal dispersivity is related to the properties of porous media, unit m, describing the degree of the dispersion in the migrating direction of flow, which is one

http://www.aloki.hu ● ISSN 1589 1623 (Print) ● ISSN 1785 0037 (Online)
DOI: http://dx.doi.org/10.15666/aeer/1706_1385913874

of the most important parameters representing the dispersion feature of aquifer (Cheng, 2002), and it can be compute by the dispersive-area (DA) method and the linear graphic (LG) method (Zhang et al., 2010). Therefore, five different numerical values of longitudinal dispersivity were formulated in this paper, namely, $\alpha_L = 0.1$ m, 0.2 m, 0.3 m, 0.4 m and 0.5 m. Keeping other conditions unchanged, considering the forward and reverse seepage type conditions, the influence of longitudinal dispersivity on seawater intrusion and its final state was analyzed, as shown in *Figure 8.*

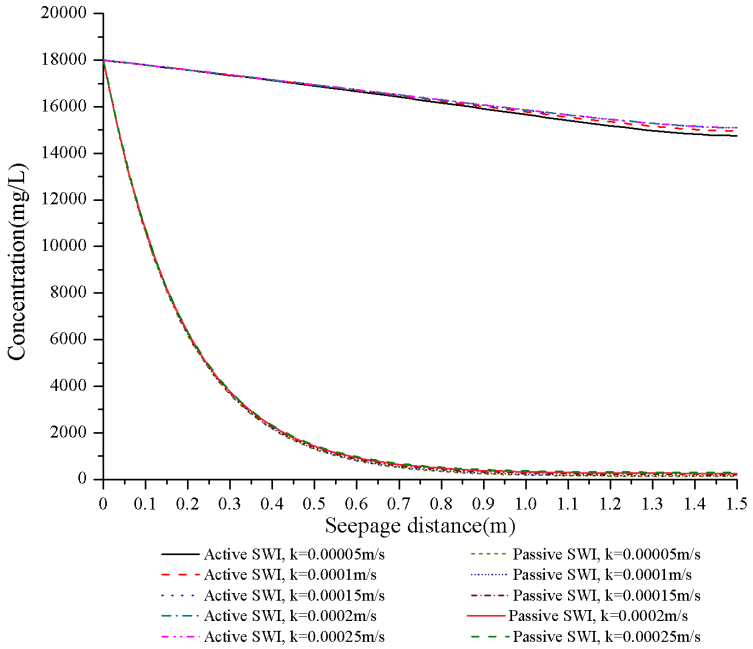

Figure 7. *The concentration distribution map under the changing hydraulic conductivity*

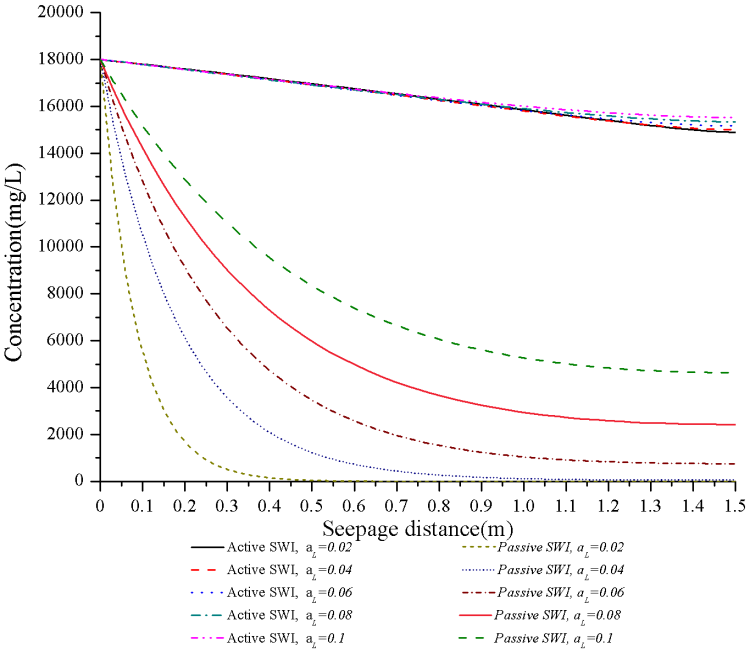

Figure 8. *The concentration distribution map under the changing longitudinal dispersivity*

http://www.aloki.hu ● ISSN 1589 1623 (Print) ● ISSN 1785 0037 (Online)
DOI: http://dx.doi.org/10.15666/aeer/1706_1385913874

According to the calculated results, when the longitudinal dispersivity increases in the test condition, the concentration under steady state also grows, indicating that the longitudinal dispersivity is forwardly correlated with seawater intrusion. From *Figure 8* it is found that the longitudinal dispersivity has a great influence on the degree of seawater intrusion under both steady state and passive SWI conditions, and this phenomenon is particularly evident under passive SWI conditions but inapparent under active SWI conditions. The greater the longitudinal dispersivity is, the severer the seawater invasion will be under both active and passive SWI conditions.

Hydraulic gradient

Hydraulic gradient, *J*, refers to the loss of head per unit distance of flow, $J = |h_0 - h_N| / L$. Five different numerical values of hydraulic gradient were formulated in this paper, namely, J = 0.1 m, 0.2 m, 0.3 m, 0.4 m and 0.5 m. Keeping other conditions unchanged, considering the forward and reverse seepage type conditions, the influence of hydraulic gradient on seawater intrusion and its final state was analyzed, as shown in *Figure 9*.

According to the calculation results, under the condition of active SWI, with the increase of the numerical value of hydraulic gradient, the concentration of chloride ion shows an increasing trend in the seepage field. However, under passive SWI conditions, with the increase of the numerical value of hydraulic gradient, the concentration of chloride ion decreases in the seepage field. That is to say, when the groundwater head increases, it will slow down the degree of seawater intrusion. On the contrary, when the head is reduced, the degree of seawater intrusion will be aggravated. In addition, this phenomenon is particularly evident under active and passive SWI conditions. Finally, the results of numerical simulation are the same as the achievements by the field measurements of Zhang et al. (2015) and also accord with the numerical experiments of Werner (2017).

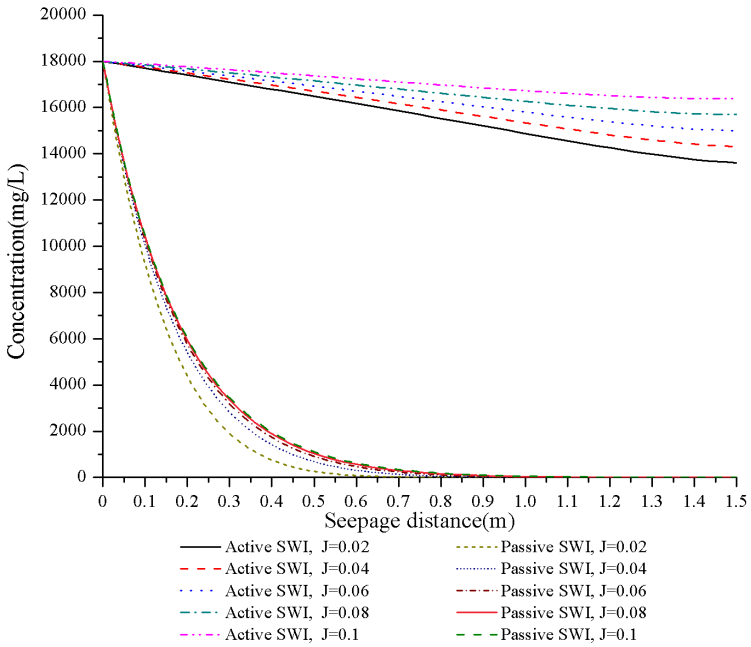

Figure 9. *The concentration distribution map under the changing hydraulic gradient*

http://www.aloki.hu ● ISSN 1589 1623 (Print) ● ISSN 1785 0037 (Online)
DOI: http://dx.doi.org/10.15666/aeer/1706_1385913874

Flux

With the influence of flux, it was proposed that under the condition of constant hydraulic gradient, the water heads on the left and right sides should be raised or lowered at the same time, so as to make the flux increase or decrease while the hydraulic gradient remains unchanged. In order to explore the distribution of salt migration and chloride ion concentration under steady-state in different flow states, five working conditions were proposed. They were water head on both sides dropping by 0.1 m and by 0.05 m, respectively, water head remaining unchanged and water head on both sides rising by 0.05 m and by 0.1 m. Keeping other conditions unchanged, considering under the forward and reverse seepage types, the influence of flux on seawater intrusion under steady state was analyzed, as shown in *Figure 10*.

According to the calculation results, under active SWI conditions, the concentration of the final steady state increases with the increase of the flux. Although the final concentration also rises under passive SWI conditions, it was also slightly in terms of the extent of growth. Therefore, the flux was forwardly correlated with the degree of seawater intrusion.

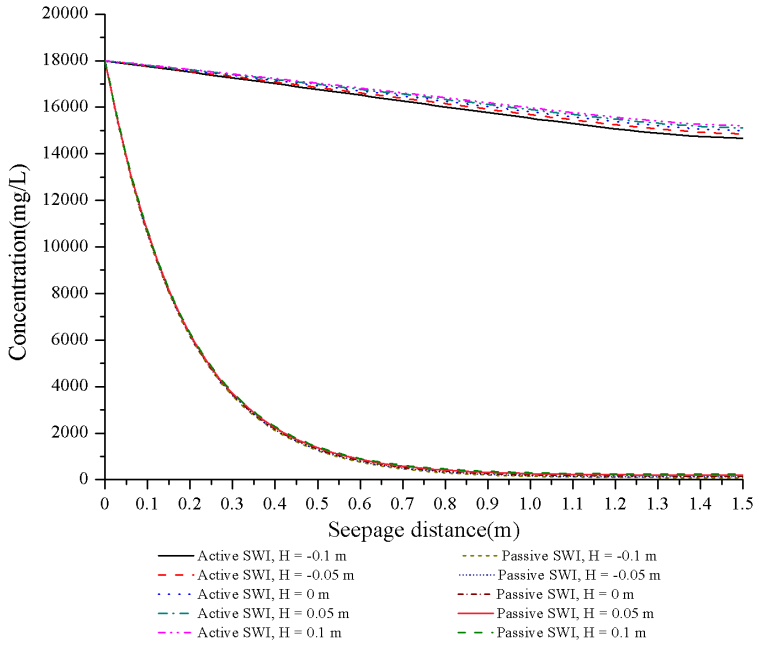

Figure 10. *The concentration distribution map under the changing flux*

Annual average evaporation

Evaporation refers to the amount of water that evaporates into the air over a certain period of time, which is usually expressed in millimeters of the thickness of the evaporated water layer, and it can be measured by the evaporimeter. In extremely arid areas, the average annual evaporation can reach more than 3000 mm/yr, for example, in western Ordos Plateau, China (Sun et al., 2017). Therefore, five different numerical values of annual average evaporation were formulated in this paper, namely, 1000 mm/yr, 2000 mm/yr, 3000 mm/yr and 4000 mm/yr, 5000 mm/yr. Keeping other conditions unchanged, considering the forward and reverse seepage type conditions, the

http://www.aloki.hu ● ISSN 1589 1623 (Print) ● ISSN 1785 0037 (Online)
DOI: http://dx.doi.org/10.15666/aeer/1706_1385913874

influence of annual average evaporation on seawater intrusion and its final state was analyzed, as shown in *Figure 11*.

According to the calculated results, under active SWI conditions, with the increase of the average annual evaporation, the concentration of the final steady state increases with a small range. Although the final concentration also grows under passive SWI conditions, it was also insignificantly in terms of the extent of growth. Therefore, the annual average evaporation was forwardly correlated with the degree of seawater intrusion. That is to say, the greater the degree of evaporation is, the severer the seawater invasion will be.

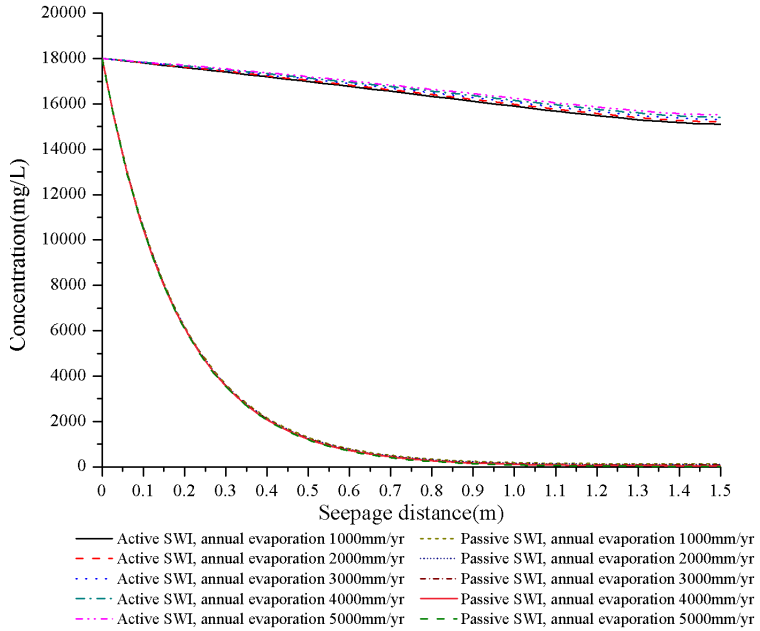

Figure 11. *The concentration distribution map under the changing annual average evaporation*

Annual average rainfall

Rainfall refers to the depth of the water layer falling to the ground in a certain period of time, which is generally measured by the rainfall measuring cylinder. The average annual rainfall in China is about 630 mm/yr, but in some extremely humid areas, the average annual rainfall can reach more than 10.000 mm/yr. Therefore, five different numerical values of annual average rainfall were formulated in this paper, namely, 0 mm/yr, 1000 mm/yr, 2000 mm/yr, 3000 mm/yr and 4000 mm/yr. Keeping other conditions unchanged, considering the forward and reverse seepage type conditions, the influence of annual average rainfall on seawater intrusion and its final state was analyzed, as shown in *Figure 12*.

According to the calculated results, under active SWI conditions, with the increase of average annual rainfall, the concentration in the final steady state decreases with a small extent. Under passive SWI conditions, the concentration also reduces slightly. Therefore, the rainfall is negatively correlated with the seawater invasion degree, and rainfall can slow down the degree of seawater invasion. Finally, the results of numerical simulation accord with the achievements of Qing et al. (2013).

http://www.aloki.hu ● ISSN 1589 1623 (Print) ● ISSN 1785 0037 (Online)
DOI: http://dx.doi.org/10.15666/aeer/1706_1385913874

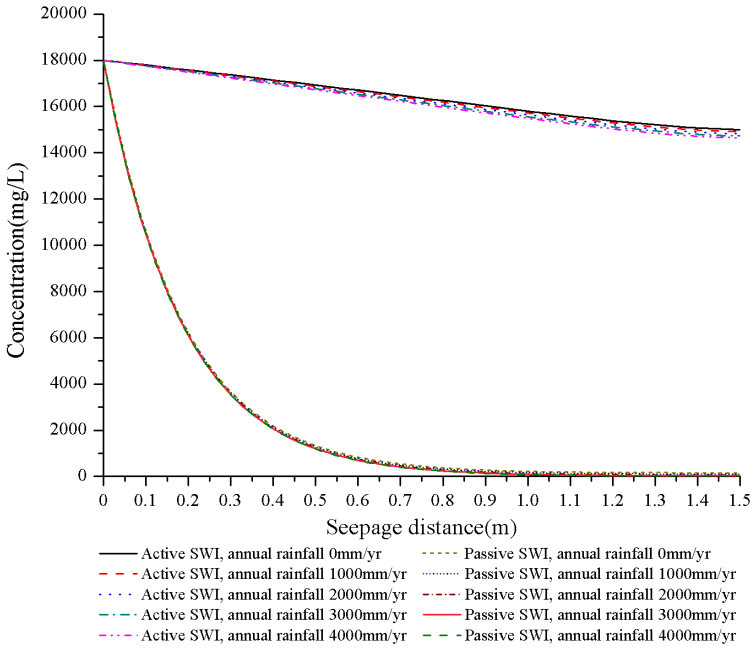

Figure 12. *The concentration distribution map under the changing annual average rainfall*

Conclusion

(1) In this paper, this numerical simulation method of solving one-dimensional advection-dispersion equation by explicit finite difference method can obtain distribution of chloride ion concentration at spatial nodes under steady state. Moreover, this method can be utilized to explore the influence of different factors on the degree of seawater intrusion, and the results and achievements are efficient, robust, reliable and consistent with the actual situation, which can explain the phenomenon of seawater intrusion. In addition, the numerical method for solving the one-dimensional advection-dispersion equation by the explicit finite difference method is correct and worthy of being used for reference. Compared with the one-dimensional advection-dispersion equation, the two-dimensional equation can more accurately explain the salt transport process under different SWI conditions. Therefore, it should be worth studying with the two-dimensional Taylor's theorem and finite difference method.

(2) It can be seen from the results of numerical simulation that, with the increase of the numerical value of hydraulic conductivity, longitudinal dispersivity, flux and evaporation capacity, the degree of seawater invasion will be aggravated, but the rainfall can play a role in mitigating seawater intrusion. Besides, under active SWI conditions, the growth of the numerical value of hydraulic gradient will aggravate seawater intrusion, while under passive SWI conditions, it will slow down the degree of invasion. As for the reason, the six factors can affect the distribution of groundwater velocity field (the size and direction of groundwater velocity), thus affecting seawater intrusion. In addition, some other factors should be worth studying, for example, pumping positions and pumping quantity.

(3) It can be seen from the results of numerical simulation that under both active and passive SWI conditions, the above six hydraulic factors have a significant influence, to a certain extent, on the seawater intrusion under steady state. Furthermore, the effect of hydraulic gradient on seawater intrusion is greatly obvious under both active and

http://www.aloki.hu ● ISSN 1589 1623 (Print) ● ISSN 1785 0037 (Online)
DOI: http://dx.doi.org/10.15666/aeer/1706_1385913874

passive SWI conditions. Additionally, it is found that the longitudinal dispersivity has a great influence on the degree of seawater intrusion under both steady state and passive SWI conditions, and this phenomenon is particularly evident under passive SWI conditions but inapparent under active SWI conditions.

Acknowledgements. This paper can be completed thanks to the help of Professor Shaoxiong Zhang, who gave this paper some professional guidance. At the same time, I am also grateful for the help of Professor Gaoyue Rong on the writing of this paper. This paper was supported by the Natural Science Fund of Hebei Province (Grant No. E2017210094).

REFERENCES

[1] Adel, Z., Amira, M., Lahcen, Z., Jamila, T. (2014): Understanding groundwater chemistry using multivariate statistics techniques to the study of contamination in the Korba unconfined aquifer system of Cap-Bon (North-east of Tunisia). – Journal of African Earth Sciences 3: 1-15.

[2] Badaruddin, S., Werner, A. D., Morgan, L. K. (2017): Characteristics of active seawater intrusion. – Journal of Hydrology 551: 632-647.

[3] Chen, G. Q. (2013): Mechanisms Underlying of Seawater Intrusion and Evaluation of Early Warning Systems in the Laizhou Bay Area. – East China Normal University, Shanghai.

[4] Cheng, J. M. (2002): Analysis on field scale effect of dispersivity in consideration of relative reliability level of data. – Hydraulic Journal 2: 90-94.

[5] Cui, Z., Chen, G. Q., Xu, X. Y. (2015): Mechanism and assessment of seawater intrusion in the Northern Changshan Island. – Marine Environmental Science 34: 930-936.

[6] Emna, B., Moez, B., Ikram, J., Nabila, A., Jalila, M., Hafedh, K., Salem, B. (2018): Hydrochemical and statistical studies of the groundwater salinization combined with MODPATH numerical model: case of the Sfax coastal aquifer, Southeast Tunisia. – Arabian Journal of Geosciences 11(4).

[7] Khakimov, E., Chung, S. Y., Senapathi, V., Elzain, H. E., Son, J. (2017): The characteristics of hydrogeological parameters of unconsolidated sediments in the Nakdong River delta of Busan City, Korea. – Journal of Soil and Groundwater Environment 22(3): 27-41.

[8] Li, G., Chen, C. X. (1996): The development and trend in researches of saltwater intrusion. – Earth Science Frontiers 3: 161-169.

[9] Liu, X. H. (2007): Experimental Analysis of Seawater Intrusion Speed in Sands. – Dalian Maritime University, Dalian.

[10] Liu, Y., Zhao, Y. R. (2017): Experimental study on influence factors of permeability coefficients of sand soil. – Journal of Jiangsu Construction 185: 88-91.

[11] Mao, Y. T. (2014): Technical Regulations for Sea Water Invasion Monitoring (Trial Implementation). – Department of Environmental Protection, State Oceanic Administration, Qingdao.

[12] Miao, Q. (2013): Effects of Precipitation and Tide on Seawater Intrusion in the Laizhou Bay. – First Institute of Oceanography, State Oceanic Administration, Qingdao.

[13] Nie, J., Zhao, Q. S. (2002): Research status and development trend on the seawater intrusion mathematical model. – Journal of Anshan Normal University 4: 16-18.

[14] Purnaditya, N. P., Soeryantono, H., Marthanty, D. R. (2018): Proposing mathematical model for seawater intrusion phenomena in the coastal aquifer. – MATEC Web of Conferences 197: 10003.

[15] Qi, Q. L. (2016): Hydraulics. – China Railway Press, Beijing.

http://www.aloki.hu ● ISSN 1589 1623 (Print) ● ISSN 1785 0037 (Online)
DOI: http://dx.doi.org/10.15666/aeer/1706_1385913874

[16] Savovic, S., Djordjevich, A. (2012): Finite difference solution of the one-dimensional advection- diffusion equation with variable coefficients in semi-infinite media. – International Journal of Heat and Mass Transfer 55(15-16): 4291-4294.
[17] Sun, J., Wang, Q. M., Liu, J. (2018): Change of the potential evapotranspiration in western Ordos Plateau: taking Etoke County as an example. – Journal of Irrigation and Drainage 11: 84-90.
[18] Werner, A. D. (2017): On the classification of seawater intrusion. – Journal of Hydrology 11: 619-631.
[19] Xue, Y. Q., Xie, C. H., Wu, J. C. (1992): Seawater invasion. – Hydrogeology and Engineering Geology 19: 29-34.
[20] Yang, S. L. (2016): Boundary value methods for solving the fractional advection-dispersion equation. – Journal of Computational Mathematics of Colleges and Universities 38: 350-356.
[21] Yu, C., Wang, H., Fang, D. F. (2018): Semi-analytical solution to one-dimensional advective-dispersive- reactive transport equation using homotopy analysis method. – Journal of Hydrology 565: 422-428.
[22] Yuan, Z. H., Wang, Y. R., Peng, C., Mei, L., Wang, L. Y. (2019): Measurement of sands permeability coefficient based on electrical resistivity. – Journal of Yangzhou University (Natural Science Edition) 3: 60-65.
[23] Zhang, J., Wang, M. Y., Zhang, L. (2010): Suitability of numerical simulation for two computations of longitudinal dispersivity in heterogeneous media. – Journal of East China University of Science and Technology (Natural Science Edition) 6: 796-800.
[24] Zhang, W. J., Chen, X., Tan, H. B., Zhang, Y. F., Cao, J. F. (2015): Geochemical and isotopic data for restricting seawater intrusion and groundwater circulation in a series of typical volcanic islands in the South China Sea. – Marine Pollution Bulletin 93(1-2): 153-162.
[25] Zhang, Y. H. (2015): Application of the change groundwater level in analysing seawater intrusion. – Marine Environmental Science 34: 788-791.
[26] Zhao, Z. W., Zhao, J., Xin, P., Hua, G. F., Jin, G. Q. (2018): Uncertainty and sensitivity analyses of the simulated seawater-freshwater mixing zones in steady-state coastal aquifers. – China Ocean Engineering 4: 489-502.
[27] Zheng, C. M., Bennett, G. D. (2016): Applied Contaminant Transport Modelling. 2nd Ed. – Higher Education Press, Beijing.

http://www.aloki.hu ● ISSN 1589 1623 (Print) ● ISSN 1785 0037 (Online)
DOI: http://dx.doi.org/10.15666/aeer/1706_1385913874

VARIATION CHARACTERISTICS, INFLUENCING FACTORS AND HYDROLOGICAL CONDITIONS OF THE REVERSE FLOW FROM MEKONG RIVER TO TONLE SAP LAKE

LI, C. W.* – YOU, Z. Q. – LI, A. Q. – XU, Z. M. – YAO, W. – HUANG, L. Y.

Changjiang Institute of Survey, Planning, Design and Research, Wuhan 430010, China

**Corresponding author: Li Changwen*
e-mail: lichangwen@cjwsjy.com.cn

(Received 21st May 2019; accepted 2nd Sep 2019)

Abstract. In order to understand the interactive mechanism between Mekong River and Tonle Sap Lake, long-series hydrological statistics were studied to analyze the variation characteristics, influencing factors and hydrological conditions of the reverse flow from Mekong River to Tonle Sap Lake. It was found that the reversal in the flood season lasts 122 days, with the flow volume reaching 37.7 billion m^3 and flood peak flow reaching 8402 m^3/s on average. The reversal reaches the maximum in August, accounting for 43% of the total yearly volume and 17.7% of the flow in Mekong River. Main factors influencing reversal flow include the difference in the runoff and water level between Mekong River and Tonle Sap Lake, and the water level of Tonle Sap River. The hydrological conditions presupposed that the reversal flow is linearly correlated to the product of water-level of Tonle Sap River to the power of 1.36 multiplied by that water-level difference to the power of 0.46. The result is expected to provide a scientific basis for the management of Mekong Delta and Tonle Sap Lake.
Keywords: *river-lake relationship, reverse flow, backflow intensity, water level difference*

Introduction

Lancang-Mekong River is the most important transboundary river in Asia that runs through six countries including China, Myanmar, Laos, Thailand, Cambodia and Vietnam. It stretches over a total of 4880 km and drains an area of 812400 km^3 (Royal et al., 2010; Mekong River Commission, 2011). The main stream of Mekong River is connected to the Tonle Sap Lake – the largest freshwater lake in Southeast Asia (with an annual average level of water at 4.64 m, covering an area of 6177 km^2 and a volume of 15.1 billion m^3) via the Tonle Sap River in Phnom Penh. The Lancang-Mekong River basin is shown in *Figure 1*.

Tonle Sap Lake closely resembles the Poyang Lake, China's largest freshwater lake, because they are both seasonal freshwater lakes with water flowing in and flowing out. Besides, Yangtze River connects with Poyang Lake at Hukou, and Mekong River connects with Tonle Sap Lake at Phnom Penh, giving rise to a complicated and world-famous river-lake relationship where the water of the lake drains into the river or the water in the river flows back to the lake (Cochrane et al., 2014; Luo et al., 2008; Hu et al., 2011; Fang et al., 2012). So far, there have been many systematic studies on the correlation between Yangtze River and Poyang Lake (Huo, 2011; Zhong et al., 2008; Yin et al., 2007; Hu et al., 2007; Dai et al., 2015; Zhang et al., 2014, 2015; Guo et al., 2012), and the conclusions show that the river-lake relationship has complicated internal mechanisms which are demonstrated in several ways including the main stream's drainage capacity, the river-connected-lake channel's capacity to diverge flows and discharge sediments, as well as the lake's flood control capacity. Among the few studies on the relationship between Mekong River and Tonle Sap Lake (Mekong River

http://www.aloki.hu ● ISSN 1589 1623 (Print) ● ISSN 1785 0037 (Online)
DOI: http://dx.doi.org/10.15666/aeer/1706_1387513895

Commission, 2005; Republic of Korea et al., 2008), most of them focus on the time and volume of the reverse flow from Mekong River to Tonle Sap Lake or analyze the balance between the inflow and outflow of water in Tonle Sap Lake. However, there are no in-depth studies on the variation characteristics of duration and volume of the reversal flow, and research on factors influencing the reversal flow and related hydrological conditions is also absent. Therefore, it is advisable to make full use of the latest research achievements on the correlation between Yangtze River and Poyang Lake to probe into the correlation between Mekong River and Tonle Sap Lake while giving due attention to the differences between Poyang Lake and Tonle Sap Lake.

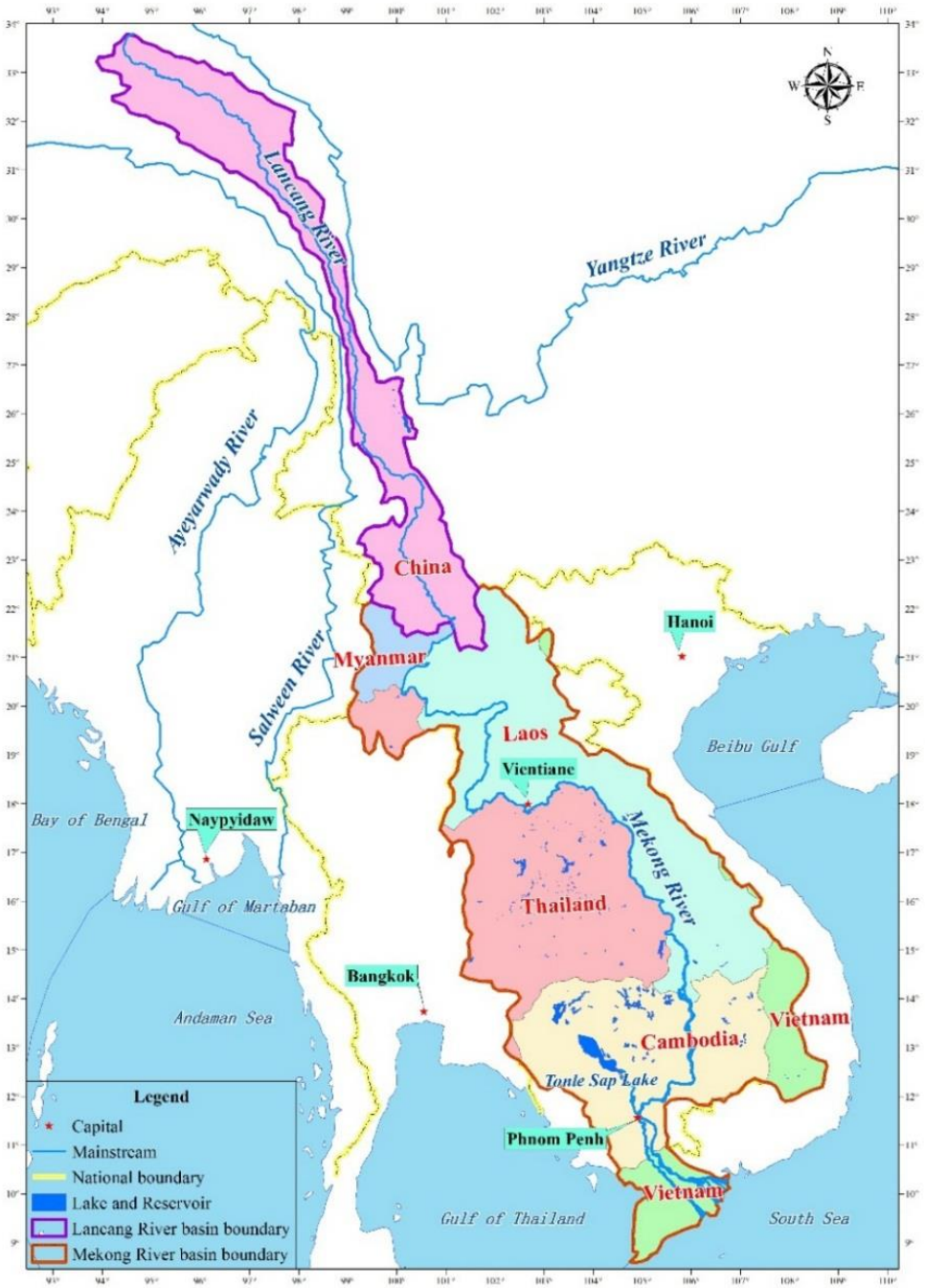

Figure 1. *Watershed map of Lancang-Mekong River*

http://www.aloki.hu ● ISSN 1589 1623 (Print) ● ISSN 1785 0037 (Online)
DOI: http://dx.doi.org/10.15666/aeer/1706_1387513895

Salient geomorphic differences

Poyang Lake is a lake when the water level is high, but it resembles a river when the water level is low, creating a unique landscape of a wide stretch of lake in the flood season while a narrow watercourse in the dry season. The maximum surface area of the lake (3708 km^2) accounts for 2.29% of the area of the whole basin (162200 km^2) (Mak et al., 2012; Changjiang Institute of Survey, Planning, Design and Research, 2015; You et al., 2013; Li et al., 2018a). In contrast, the terrain of Tonle Sap Lake is plain; the average gradients for the outlet watercourse of Tonle Sap Lake, the lake area and the watercourse of Tonle Sap River are 0.0988‰, 0.0024‰ and 0.0354‰, respectively. The water surface gradient is mild, which averages at 0.0062‰ and reaches its maximum at 0.0189‰. The maximum surface area of the lake equals approximately 17.75% of the total area of the basin (86000 km^2), thus Tonle Sap Lake retains the appearance of a lake both in the flood and the dry seasons. As Tonle Sap Lake is situated in a plain, its difference of water level, surface area and volume in flood and dry seasons fall below those of Poyang Lake. In the case of Poyang Lake, when it reaches the highest water level at 20.7 m, its surface area reaches 3708 km^2 and its volume 30.363 billion m^3; when it falls to its lowest water level at 4.01 m, its surface area shrinks to 28.7 km^2 and its volume to 63 million m^3; the ratio of these two extreme surface areas is 129, and that of the extreme volumes is 482. In the case of Tonle Sap Lake, when it reaches the highest water level at 10.54 m, its surface area is 15261 km^2 and its volume is 78.7 billion m^3; when it reaches the lowest water level at 1.11 m, its surface area shrinks to 2053 km^2 and its volume to 780 million m^3; the ratio of the extreme surface areas is 7 and that of the extreme volumes is 101. The largest surface of Tonle Sap Lake is 4.12 times as large as that of Poyang Lake, and its maximum volume 2.59 times as much as that of Poyang Lake; while its minimum surface area and minimum volume are 71.53 times and 12.38 times the size of Poyang Lake, respectively (Li et al., 2018a). The map of Tonle Sap Lake in different hydrological conditions is shown in *Figure 2*.

Geomorphic differences in the watercourse

The mainstream of Yangtze River in Hukou section is located between the upper reaches and the lower reaches of the river. Embankments are built to defend tremendous flood that may occur every two decades, and optimal coordination of the upper stream and the local flood detention-retention basin will meet the requirement to defend a flood resembling that happened in 1954. The mainstream of Mekong River that runs through Phnom Penh is located at the Mekong Delta in Cambodia where a low plain prevails, and the flow discharge capacity of the river in this section is far from enough to handle the enormous flow volume from the upper stream. When the water level of Kompong Cham reaches above 13 m, vast flooding plain of left and right banks in Mekong River are easily inundated through the branch watercourses or irrigation channels, resulting in inundation that lasts an annual average of 19 to 48 days, with an annual average overland flood volume in the floodplain of approximate 42.3 billion m^3 (Changjiang Water Resources Commission of the Ministry of Water Resources, 2019).

Different inflow from the mainstream

The mainstream of Yangtze River in Hukou station has a surface area of 1.68 million km^2, accounting for 93% of the area of the whole basin, and is about

http://www.aloki.hu ● ISSN 1589 1623 (Print) ● ISSN 1785 0037 (Online)
DOI: http://dx.doi.org/10.15666/aeer/1706_1387513895

338 km away from the boundary with the lower-stream tidal areas at Datong station. The surface area of the entrance where Tonle Sap River drains into Mekong River is about 749000 km^2, accounting for 92% of the total area of the basin. Aside from the inflow from the upper stream, the mainstream of Mekong at Phnom Penh is also subject to tidal movements in the downstream area. As a result, the flood lasts long in this region and subsides slowly, with an average rate of flood flow at 1.5 to 2.0 km/h.

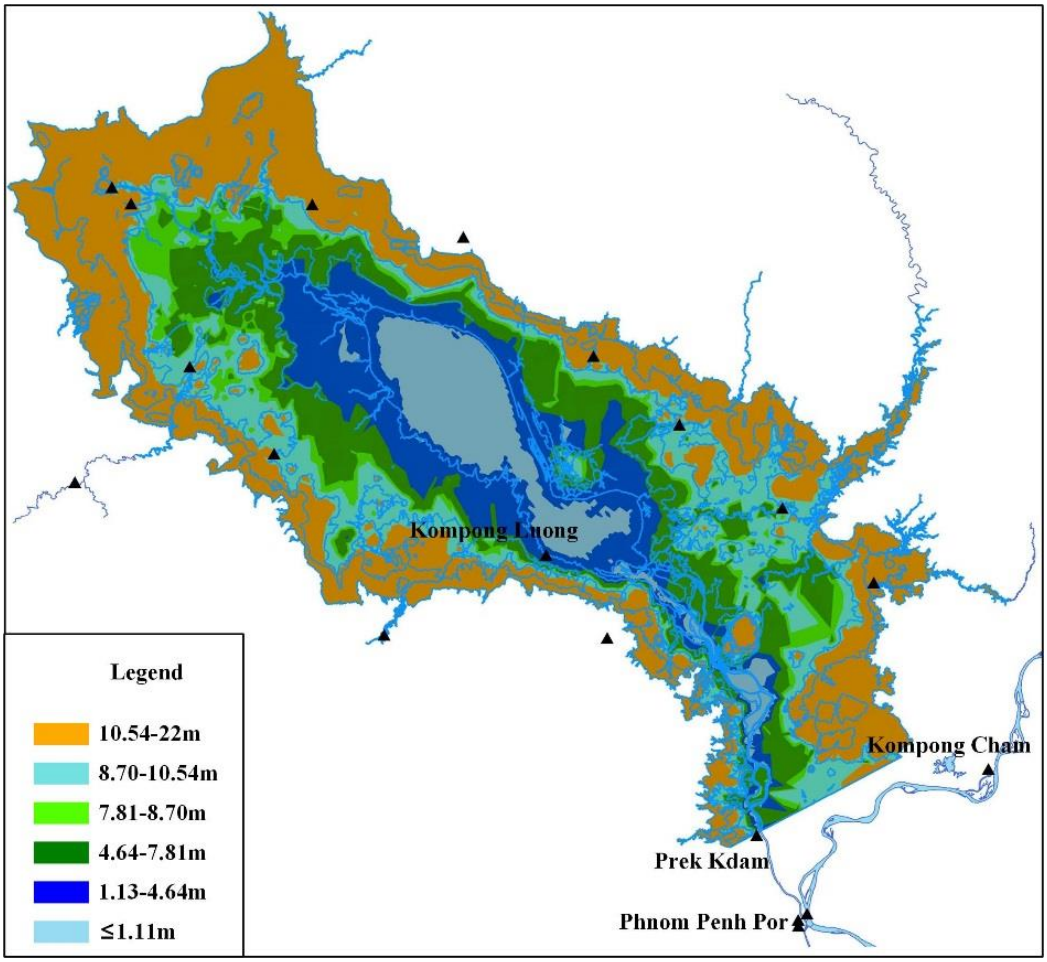

Figure 2. *Area distribution of Tonle Sap Lake under different characteristic stage*

Different water exchange intensity between Mekong River and Tonle Sap Lake

Due to conditions of the watercourses, geomorphic features and inflow of water, Tonle Sap Lake is much more capable than Poyang Lake in terms of flood control and water storage (Li et al., 2018a, b). The water exchange between Mekong River and Tonle Sap Lake is more frequent and active than that between Yangtze River and Poyang Lake. Every year on average, the reversal flow from Mekong River to Tonle Sap Lake lasts 122 days and the volume of the reverse flow reaches 37.7 billion m^3. In contrast, the reversal flow from Yangtze River to Poyang Lake lasts an average of 15 days every year, merely 12% of that from Mekong River to Tonle Sap Lake, and the annual average volume of the reverse flow is 2.843 billion m^3, only 7.5% of that from Mekong River to Tonle Sap Lake (Li et al., 2018c; Changjiang Water Resources Commission of the Ministry of Water Resources, 2013).

http://www.aloki.hu ● ISSN 1589 1623 (Print) ● ISSN 1785 0037 (Online)
DOI: http://dx.doi.org/10.15666/aeer/1706_1387513895

Poyang Lake accounts for a crucial part in the watershed of Yangtze River and the overall ecological system; likewise, Tonle Sap Lake plays an important part in the watershed of Mekong River and the ecological system. Therefore, it is the key to ensure the ecological health of the river and the lake by fully understanding the correlation between Mekong River and Tonle Sap Lake and providing a scientific basis for river and lake regulation. By referring to the research achievements on the relationship between Yangtze River and Poyang Lake, this study made use of long-series hydrological data of several hydrological monitoring stations on the mainstream of Mekong River (*Fig. 2*), including the Kompong Cham station, Phnom Penh Port station on Tonle Sap Lake, Prek Kdam Station and Kompong Luong Station, to analyze the characteristics of changes in water volume, influencing factors and hydrological conditions of the reverse flow from Mekong River to Tonle Sap Lake. Here, the Kompong Cham station is similar to Jiujiang Station on Yangtze River, the Phnom Penh Port station is a stream gauging station, which is similar to Hukou station on Poyang Lake, the Prek Kdam Station is a hydrological station, which is similar to Xingzi Station on Poyang Lake in terms of the water-level monitoring location, but similar to Hukou Station on Poyang Lake in terms of the flow monitoring location, the Kompong Luong Station is also a stream gauging station, which is similar to Duchang Station on Poyang Lake.

The objectives of this study were as follows: 1) characterize the variation of duration and volume of reversal flow from Mekong River to Tonle Sap Lake; 2) identify the major factors of reversal flow; 3) analyze the hydrological conditions of reversal flow.

It is expected to facilitate an in-depth understanding of the interactive mechanism between Mekong River and Tonle Sap Lake, and provide a scientific basis for the integrated treatment of Tonle Sap Lake, thereby better understand the interactive mechanism between Yangtze River and Poyang Lake.

Materials and methods

Study area

Tonle Sap Lake basin is situated on the Cambodia Mekong Delta, and covers a total area of 81,763 km^2. It is the important sub-area within the Lower Mekong Basin due to its complex hydrological and ecological system, rich biodiversities and critical basin development issues (Mak et al., 2012). The Tonle Sap Lake, located at the center of the sub-area as shown on *Figure 3,* is the largest permanent freshwater lake in Southeast Asia. The Lake is connected to the Mekong through the Tonle Sap River at Chaktomuk conjunction in Phnom Penh, about 120 km to the southwest outlet of the Lake. The lake is 371 km long, with an area of around 2,744 km^2 in the dry season and during the wet season it can swell to four or seven times this area. The most prominent feature of the sub-area is the Tonle Sap Lake with its interesting hydrological and ecological functions for the whole Mekong River basin. The water flow of the Tonle Sap River and lake is closely related to the hydrological performance of the Mekong River. The lake discharges water (out-flow), through the Tonle Sap River, into the Mekong River during the dry season. During the wet season, however, the Mekong River becomes bloated by run-off, thus forces the Tonle Sap River to reverse its flow direction (from out-flow to in-flow), filling the lake instead of draining it. The inflow inundates the surrounding forested floodplains, and supports the rich biodiversity of the lake eco-system.

http://www.aloki.hu ● ISSN 1589 1623 (Print) ● ISSN 1785 0037 (Online)
DOI: http://dx.doi.org/10.15666/aeer/1706_1387513895

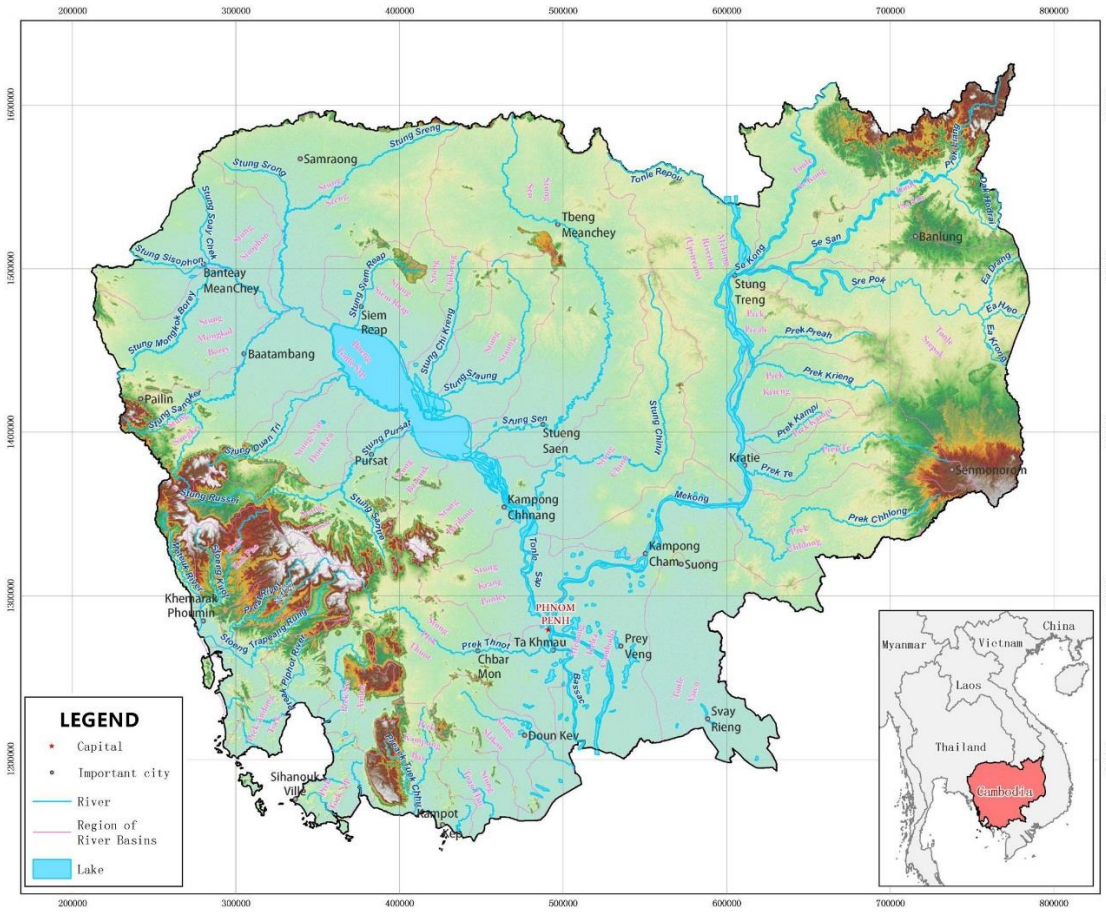

Figure 3. *Map of River Basin in Cambodia*

Hydrological stations and data collection

There are are four controlling hydrological stations installed on the Tonle Sap Lake Area and Cambodia Mekong Delta, namely, Kompong Cham Station, Phnom Penh Port Station, Prek Kdam Station and Kompong Luong Station, as shown in *Figure 2*. Among them, Kampong Cham Station is located at the mainstream of Mekong River, with a distance of around 103 km from the exit of Tonle Sap River and a catchment area of 660,000 km^2 which accounts for 81% of the total area of the whole basin; Phnom Penh Port Station is located at the end of the Tonle Sap River, with a distance of about 1 km from the exit of Tonle Sap River, so it can be used as the water level representative station at the intersection of the Mekong River and the Tonle Sap River; Prek Kdam Station is the inflow-outflow controlling station of Tonle Sap Lake, about 32 km from the exit of Tonle Sap River; Kampong Luong Station is the water-level representative station of Tonle Sap Lake, which is about 172 km far from the exit of Tonle Sap River.

The hydrological data for the above four river-lake controlling stations collected from Ministry of Water Resources and Meteorology in Cambodia and Mekong River Commission are not homogenous, because not all records started in the same time and/or not all stations have the same number of records. 52 years of daily discharge data from 1960 to 2011 is available for Kompong Cham Station, 58 years of daily water level data from 1960 to 2017 is available for Phnom Penh Port Station, 17 years

http://www.aloki.hu ● ISSN 1589 1623 (Print) ● ISSN 1785 0037 (Online)
DOI: http://dx.doi.org/10.15666/aeer/1706_1387513895

of daily water level data from 1995 to 2011 and 58 years of daily water level data from 1960 to 2017 are available for Prek Kdam Station, and 19 years of daily water level data from 1999 to 2017 is available for Kampong Luong Station.

To ensure the consistency of hydrological analysis, the discharge data with the same period from 1995 to 2011 of Kompong Cham Station and Prek Kdam Station, and the water level data with the same period from 1999 to 2011 of Phnom Penh Port Station, Prek Kdam Station and Kampong Luong Station were used. The water level data uses the Cambodian National Elevation Datum (M.S.L. Hatein datum).

Data analysis

The inflow from the Mekong River via the Tonle Sap River can be computed from the observed discharge data at Prek Kdam Station. Therefore, the timing of when flow reversal occurs, the variation characteristics of duration and volume of reversal flow, and the ratio of the reverse volume accounts for the total volume of Mekong River at the Kompong Cham Station, which are of importance for the ecological functioning of the Tonle Sap system and wider Lower Mekong River Basin, have been statistically analysed at the Prek Kdam monitoring site. The water level at Phnom Penh Port Station, Prek Kdam Station and Kampong Luong Station and a correction for backwater based on the water level difference between Phnom Penh Port and Kampong Luong were used to identify the major factors and hydrological conditions of reversal flow from Mekong River to Tonle Sap Lake.

Results

Time series variation characteristics of reversal volume

According to measured flow records from 1995 to 2011 at the Prek Kdam station, this study concluded the duration and volume of reverse flow from Mekong River to Tonle Sap Lake during flood seasons, as shown in *Figures 4* and *5*. It can be seen that the flow reversal from Mekong River to Tonle Sap Lake occurs every year, and the reverse flow duration is long and reversal volume is large. On average, it lasts 122 days and reaches 37.7 billion m^3 in volume every year. The reversal occurs from May to October, especially from July to September – these three months account for 71% of the whole time and 88.6% of the total amount of reversal in a year. The reversal usually reaches its maximum in August during which flow reversal happens every day and reaches an annual average volume of 16.2 billion m^3, making up 43% of the yearly total.

According to *Figure 4,* the longest duration of backflow lasted 149 days in 1999, and the shortest lasted 73 days in 1995, with a variation amplitude of 76 days and a variation coefficient of 0.14. The maximum annual reversal volume is 49.6 billion m^3 in 2005 and the minimum is 21.3 billion m^3 in 1998, with a variation amplitude of 28.3 billion m^3 and a variation coefficient of 0.24. The annual average of flood peak flow from Mekong River was 8402 m^3/s, with the maximum at 10679 m^3/s in 1997 and the minimum at 4584 m^3/s. Thus, the maximum/minimum ratio of flood peak flow and annual volume were both 2.33. In general, the reversal duration and volume increased slightly year by year, with the average reversal duration increased by one day per year, and the average reversal volume increased by 365 million m^3 per year.

http://www.aloki.hu ● ISSN 1589 1623 (Print) ● ISSN 1785 0037 (Online)
DOI: http://dx.doi.org/10.15666/aeer/1706_1387513895

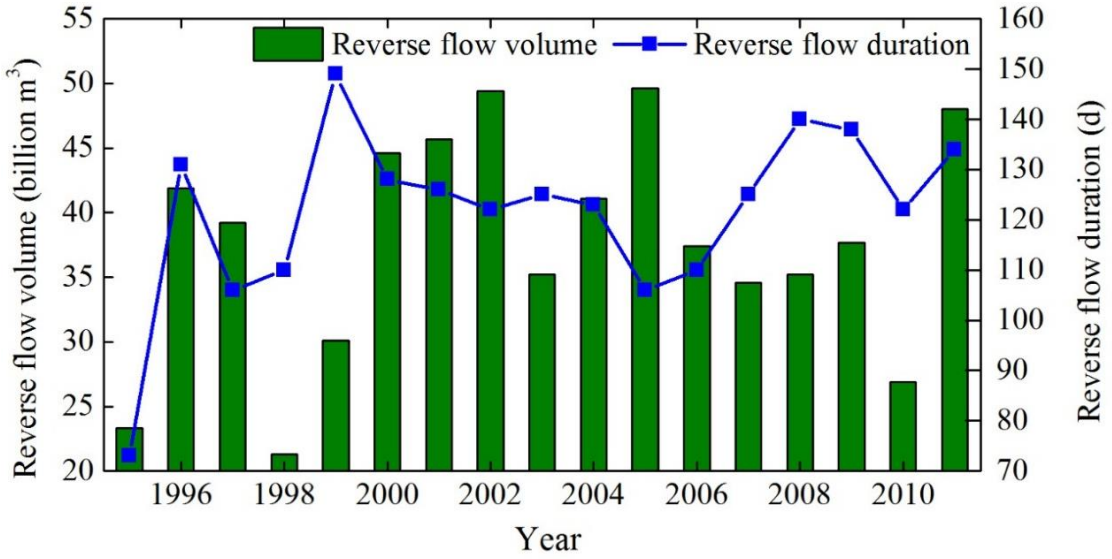

Figure 4. *Inter-annual variation of reverse flow duration and volume from Mekong River to Tonle Sap Lake*

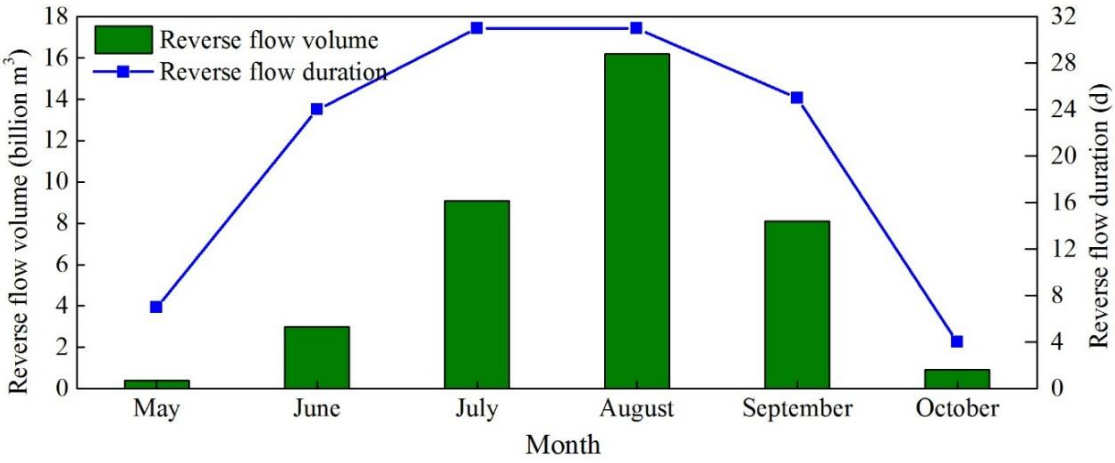

Figure 5. *Annual distribution of reverse flow duration and volume from Mekong River to Tonle Sap Lake*

Proportion of reverse volume to total volume from Mekong river in the same period

According to flood statistics from 1995 to 2011, this study achieved the ratio of the reverse volume against the total volume from Mekong River at the Kompong Cham station, as shown in *Figure 6*. By means of reversal flow, Tonle Sap Lake regulates and stores 10% to 18% (averaged at 14%) of the total flood volume of Mekong River in the flood season. The diversion percentage reaches the peak in August at 17.7%, followed by July (16.6%), June (13.2%), September (10.5%), May (8.9%) and October (8.5%). When the backward flow reaches the peak, the Tonle Sap Lake reduces the flood peak discharge of Mekong River by 15% to 24%, averaged at 20% over the from 1995 to 2011. Overall, the annual variation of the proportion of reverse volume to total volume from Mekong River in the same period is not obvious, and it is slightly increasing.

http://www.aloki.hu ● ISSN 1589 1623 (Print) ● ISSN 1785 0037 (Online)
DOI: http://dx.doi.org/10.15666/aeer/1706_1387513895

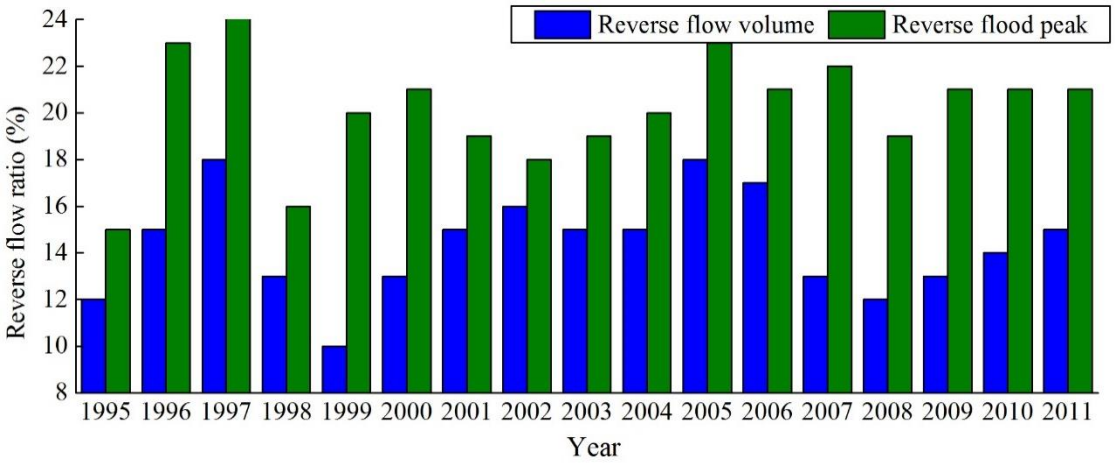

Figure 6. *The ratio of reverse flow volume in flood season accounting for Mekong River runoff in the same period*

Discussion

Influencing factors of reversal flow

The factors that affect the reversal flow from Mekong River to Tonle Sap Lake include the inflow of Mekong River, incoming water from the tributaries of Tonle Sap Lake, runoff difference (or water level difference) between Mekong River and Tonle Sap Lake, tidal water level difference at the beginning of flood season, etc.

(1) Runoff of Kompong Cham Station in Mekong River

According to the observation data in the flood season (May - October) from 1995 to 2011, the correlation between the flood runoff of Kompong Cham Station in mainstream of Mekong River and reversal flow volume is shown in *Figure 7*. It can be seen that the correlation is scattered, indicating that the flood runoff of the Mekong River is not a decisive factor of reversal flow.

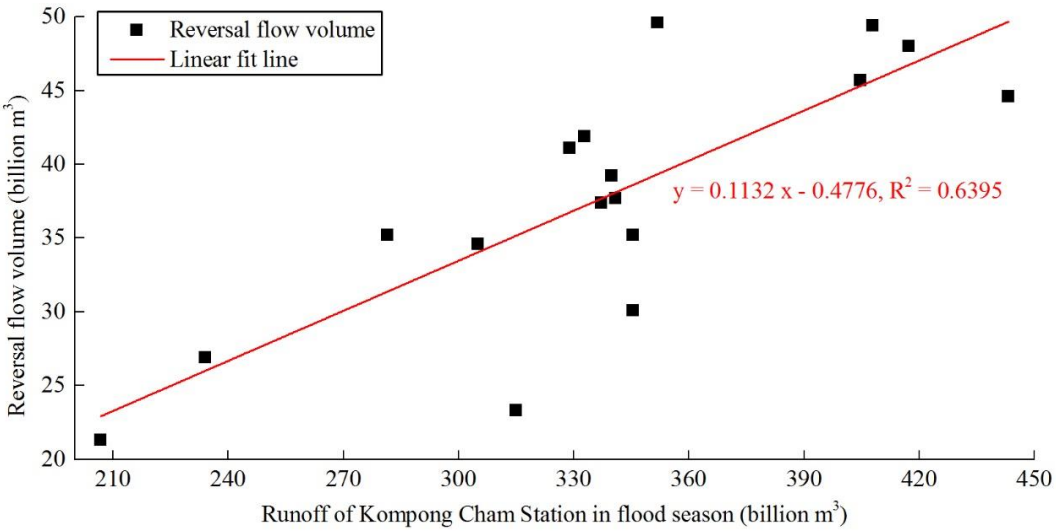

Figure 7. *Correlation between the flood runoff of Kompong Cham Station in mainstream of Mekong River and reversal flow volume*

http://www.aloki.hu ● ISSN 1589 1623 (Print) ● ISSN 1785 0037 (Online)
DOI: http://dx.doi.org/10.15666/aeer/1706_1387513895

The flow of Kampong Cham Station at the main stream of Mekong River when the flow reversal of Tonle Sap River occurs is shown in *Figure 8*. It can be seen that when the flow of Kampong Cham Station is above 3000 m^3/s, the phenomenon of backflow may occur. Among them, the probability of backflow is the largest when the flow of Kampong Cham Station is from 10000 to 40,000 m^3/s, which accounts for 67.31% of the total days of backflow. The reversal flow increases with the rise of the flow of Kampong Cham Station, but the correlation between them is scattered. In May when the runoff of Mekong River is small, the probability and flow of backflow are the minimum, with average annual reverse duration of only 7 days and reverse flow of 471 m^3/s. From June to July, the runoff of Mekong River has increased significantly, and the probability and flow of backflow increased accordingly, with average annual backflow duration of 24 days and 31 days respectively, and average reverse flow of 1286 m^3/s and 3407 m^3/s respectively. In August, the runoff of Mekong River above Phnom Penh reaches the peak, which accounts for 21.0%~23.1% of the annual runoff, makes the reversal probability and backflow reach the maximum, the backflow has occurred in the whole month, and the average reversal flow is 6049 m^3/s. From September to October, with the increase of inflow from the tributaries of Tonle Sap Lake (reaches its peak) and the decrease of runoff from Mekong River, the probability of backflow and the reversal flow began to decline, with average backflow time of 25 days and 4 days, and average reverse flow of 3775 m^3/s and 2392 m^3/s, respectively.

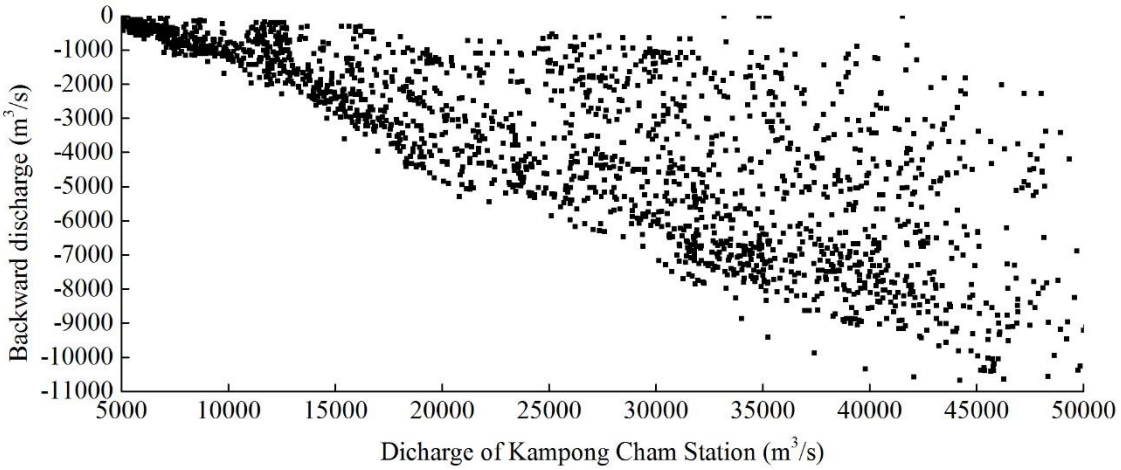

Figure 8. *The flow of Kampong Cham Station when the flow reversal of Tonle Sap River occurs*

Figure 9 compares the average daily runoffs between the Kompong Cham station on Mekong River and the Prek Kdam station on Tonle Sap River during the flood season from June to September in multiple years from 1995 to 2011. It shows that the volume of reversal flow increases with the increase of discharge from the Mekong River (expressed by the rate of increase) and has little connection with the rate of flow of Mekong River.

(2) River-lake runoff difference

Figure 10 compares the discharge from Mekong River and that from Tonle Sap Lake for multiple years from 1995 to 2011. It shows that the ratio of discharge of Mekong River against that of Tonle Sap Lake reaches the peak in August (15:1), followed by

http://www.aloki.hu ● ISSN 1589 1623 (Print) ● ISSN 1785 0037 (Online)
DOI: http://dx.doi.org/10.15666/aeer/1706_1387513895

July (11:1), September (10:1) and June (8:1), October (7:1) and May (5:1). The volume of reverse flow follows the same order in time (i.e. August marks the maximum and May the minimum), which implies the influence of the difference in the runoff between Mekong River and Tonle Sap Lake on the volume of the reverse flow.

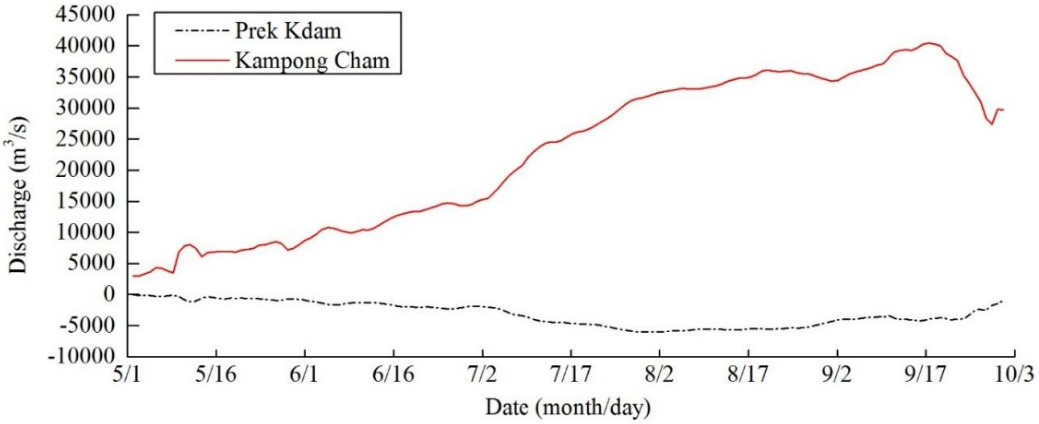

Figure 9. *Multi-year average daily discharge of Prek Kdam station and Kompong Cham station in reversal flow season*

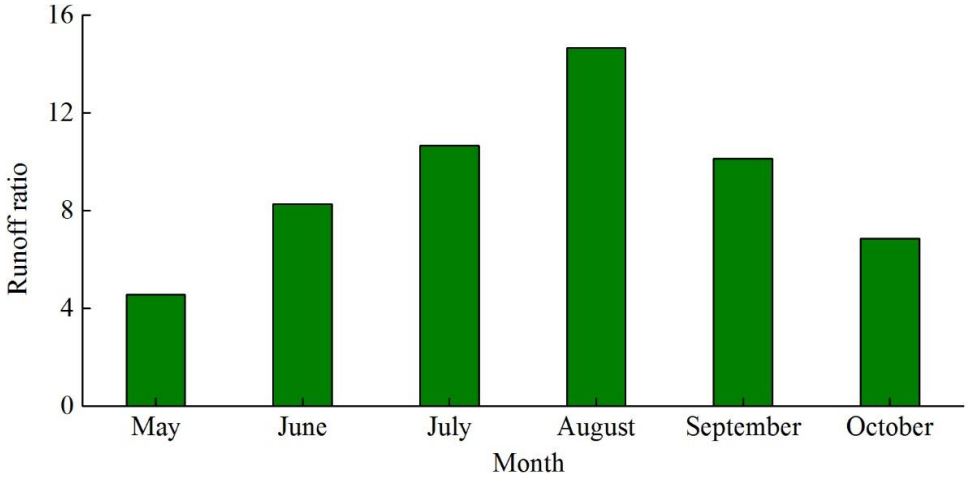

Figure 10. *Monthly runoff ratio between Mekong River and Tonle Sap Lake*

The deviation (the annual value - the average value of the years from 1995 to 2011) of the runoff difference between Kampong Cham Station in Mekong River and Tonle Sap Lake area during the flood season and the deviation of backwater volume were compared and shown in *Figure 11*. It can be seen that in 2001, 2002, 2005 and 2011, the runoff of Mekong River in flood season is abundance, and that of Tonle Sap Lake area is dry, so the backwater volume in each year is more than the average annual value; the runoff of Mekong River in 2006 and 2007 is dry, and that of Tonle Sap Lake area is abundance, so the backwater volume is less than the average annual value. In general, the amount of backwater is basically corresponding to the river-lake runoff difference, except for the partial years, which indicates that the reverse flow is not only related to the inflow from Mekong River and Tonle Sap Lake, but also affected by other factors.

http://www.aloki.hu ● ISSN 1589 1623 (Print) ● ISSN 1785 0037 (Online)
DOI: http://dx.doi.org/10.15666/aeer/1706_1387513895

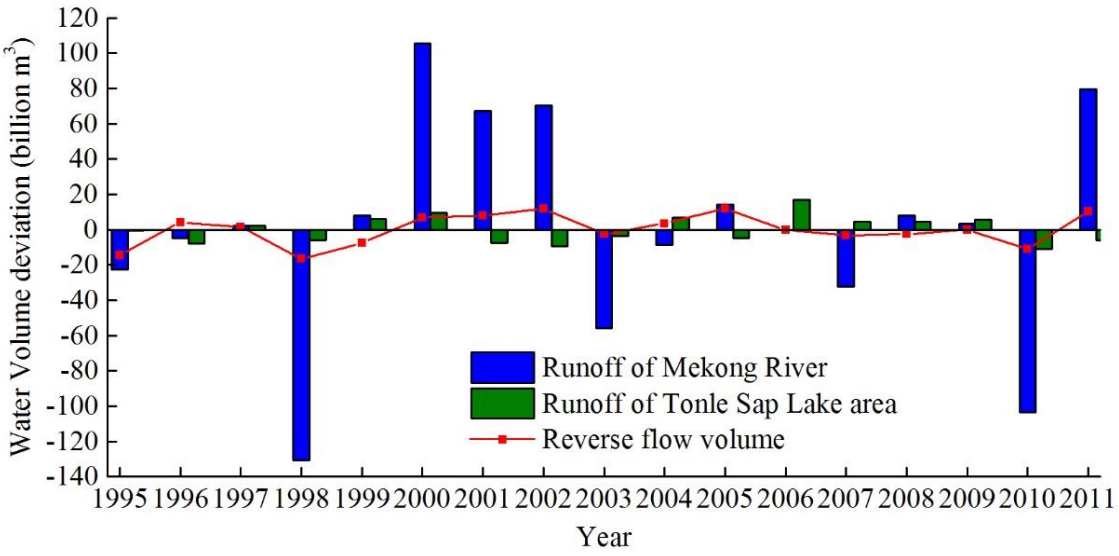

Figure 11. *The deviation comparison between river-lake runoff difference and backwater volume during the flood season*

(3) River-lake water level difference

The water level of Phnom Penh Port, Prek Kdam and Kampong Luong stations in the Tonle Sap Lake area in 2001 is shown in *Figure 12*. It can be seen that when the flood of Mekong River backward flows into the Tonle Sap Lake, the water levels of the above three stations are successively lowered from the bottom to the upper, indicating that the water level difference between Mekong River and Tonle Sap Lake is one of the conditions for the reversal flow of Mekong River.

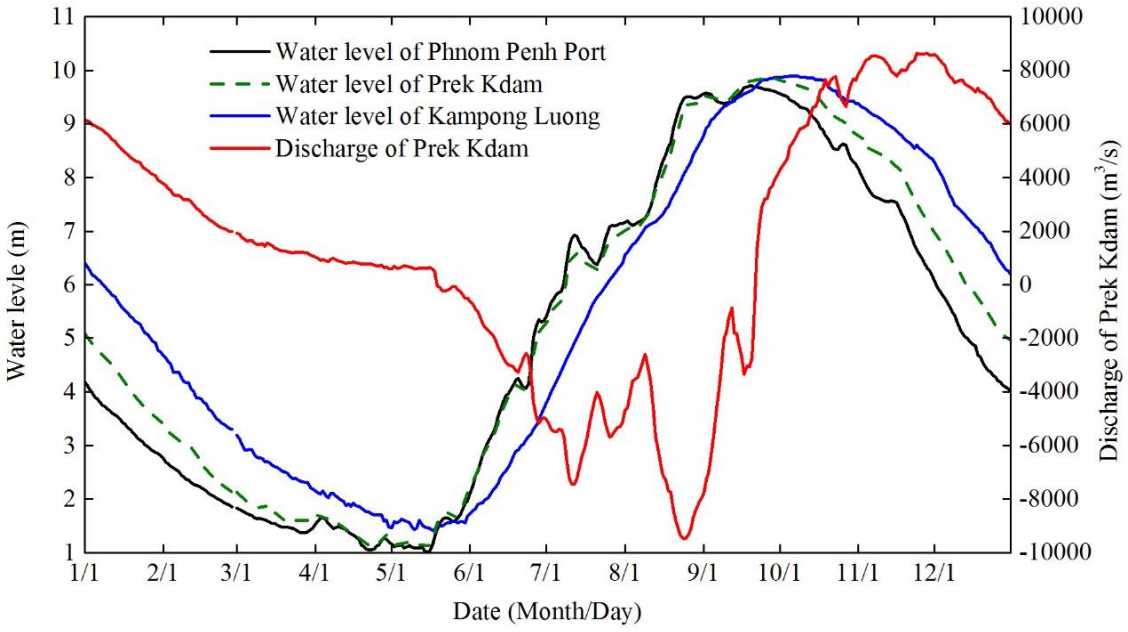

Figure 12. *Water level process in 2001 of hydrological stations in Tonle Sap Lake area*

http://www.aloki.hu ● ISSN 1589 1623 (Print) ● ISSN 1785 0037 (Online)
DOI: http://dx.doi.org/10.15666/aeer/1706_1387513895

According to long-series statistics of the daily water level obtained from major monitoring stations, the water level during the flood season in Mekong River changes more frequently than that in Tonle Sap Lake. The annual average increase rate of water-level declines from 0.16 m/d at the Kampong Cham station on Mekong River, to 0.09 m/d at the Phnom Penh Port station at the Tonle Sap River entrance, 0.08 m/d at the Prek Kdam station on Tonle Sap River and 0.06 m/d at the Kampong Luong station on the Tonle Sap Lake. It indicates that difference in the level of water between Mekong River and Tonle Sap Lake, when the former is higher than the latter, is the major hydrodynamic force that drives the reversal flow, as shown in *Figure 13*.

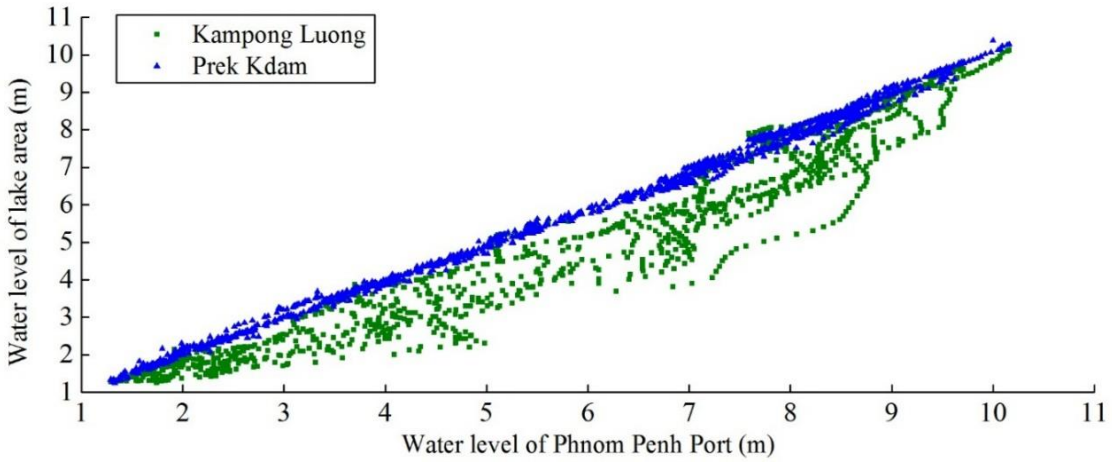

Figure 13. *Water level correlation among Prek Kdam station, Kompong Luong station and Phnom Penh Port station*

Figure 14 shows the correlation between the reverse flow and the difference in the water level between the river and the lake at the Prek Kdam station. It can be seen that the water level difference between the water level at the Kompong Luong station and the water level at the Phnom Penh station is negative most of the time (92%), which indicates that difference in the water level is a major contributor to the reversal flow.

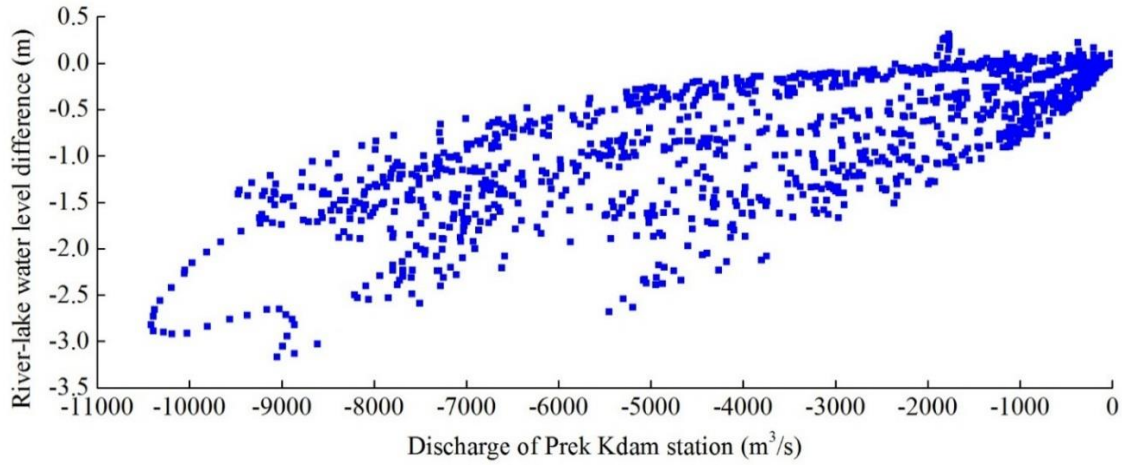

Figure 14. *Correlation between discharge and water level difference in Prek Kdam station*

http://www.aloki.hu ● ISSN 1589 1623 (Print) ● ISSN 1785 0037 (Online)
DOI: http://dx.doi.org/10.15666/aeer/1706_1387513895

According to statistics, the reverse flow from Mekong River to Tonle Sap Lake increases with the increase of difference in their water levels when the water level at the Prek Kdam remains the same, as shown in *Figure 15*.

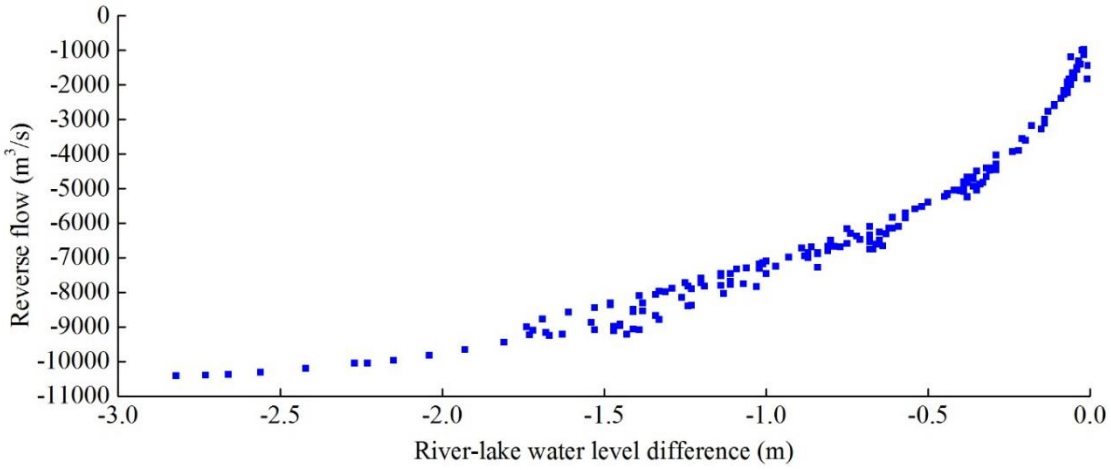

Figure 15. *Correlation between backward discharge and water level difference when the water level of Prek Kdam station reaches 8~9 m*

With the difference in the water level between Mekong River and Tonle Sap Lake as the parameter, this study plots a chart of the average daily flow of Tonle Sap River at the Prek Kdam station, the average daily water level of Tonle Sap Lake at the Kompong Luong station and the average daily flow of Mekong River at the Kompong Cham station. The cluster of correlation between the amount of reverse flow and the flow of Mekong River, as well as the correlation between the water level of Tonle Sap Lake and the discharge of Mekong Lake are established according to the center of point groups, as shown in *Figure 16*. It can be seen that when the difference in the levels of water between Mekong River and Tonle Sap Lake remains constant, the amount of reverse flow increases with the increase of the flow of Mekong River; when the flow of Mekong River remains constant, the volume of reverse flow increases with the increase of difference in the water levels. Therefore, the discharge from Mekong River and the difference in the levels of water are both factors of the reverse flow, and the difference in runoffs directly determines the difference in the levels of water.

(4) Water level of Tonle Sap River

According to statistics from 1999 to 2011, the reverse flow increases linearly with the rise of water level at the Prek Kdam station when the river-lake water level difference remains constant, as shown in *Figure 17*. Therefore, the water level of Tonle Sap River accounts for another factor that influences the reversal flow.

(5) Tidal water level difference at the beginning of flood season

According to the analysis, only the reversal flow at the beginning of the flood period from May to June may be affected by the tides in the South China Sea. The average tidal range is less than 0.2 m, which may result in backflow phenomenon when the daily average water level of Kampong Luong Station in Tonle Sap Lake is higher than that of

http://www.aloki.hu ● ISSN 1589 1623 (Print) ● ISSN 1785 0037 (Online)
DOI: http://dx.doi.org/10.15666/aeer/1706_1387513895

Phnom Penh Port Station in Tonle Sap River. According to the statistics from 1999 to 2011, the phenomenon occurred for 34 days in total for 10 years. Except for the water level difference between Mekong River and Tonle Sap Lake reached 0.29 m on May 15, 1999, the river-lake water level difference on other dates was less than 0.12 m. The average river-lake water level difference is 0.05 m, and daily average backflow is 147 m^3/s.

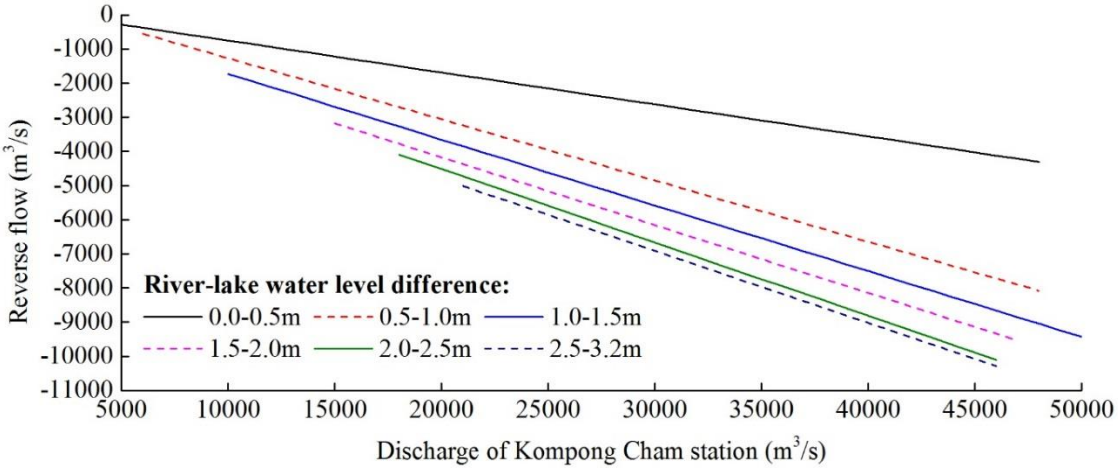

Figure 16. *Correlation between the discharge of Prek Kdam station and Kompong Cham station*

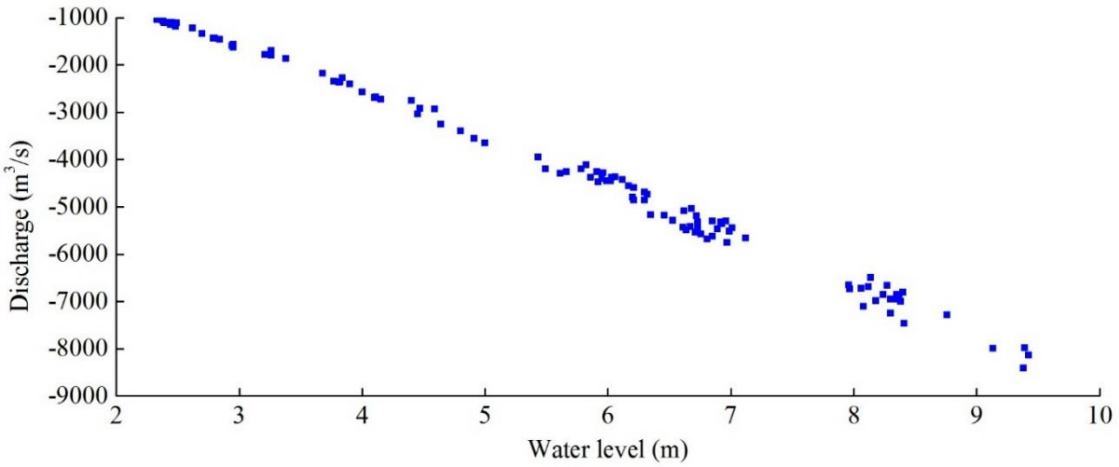

Figure 17. *Correlation between water level and discharge of Prek Kdam station when the water level difference between Mekong River and Tonle Sap Lake reaches 0.8~1.0 m*

Hydrological conditions of the reversal flow

The time, duration and volume of reversal flow are closely linked to the hydrological conditions of Mekong River and Tonle Sap Lake. In light of the geomorphic and hydrological features of Cambodia Mekong Delta and Tonle Sap Lake area, this study selects the water level difference between Mekong River and Tonle Sap Lake (representing the flow resistance) and the water level at the Prek Kdam Station (representing the wetted cross-section area of Tonle Sap River) as the control indices to

http://www.aloki.hu ● ISSN 1589 1623 (Print) ● ISSN 1785 0037 (Online)
DOI: http://dx.doi.org/10.15666/aeer/1706_1387513895

study the hydrological conditions of reversal flow. The water level difference between the Kompong Luong Station and Phnom Penh Station is the precondition for the reverse flow as it leads to a difference in the potential energy between the Mekong River and the Tonle Sap Lake. The water level at the Prek Kdam Station is the driving condition of the reversal. When the flow rate remains constant, the higher the water level is, the larger the wetted cross-section area of Tonle Sap River and the larger the discharge will be.

According to statistics from 1999 to 2011, the correlation between the reverse flow and the river-lake water level difference under different water levels at the Prek Kdam station is shown in *Figure 18* and *Table 1*. It can be found that when the water level at the Prek Kdam station remains the same, the reverse flow increases with the increase of the water-level difference between Mekong River and Tonle Sap Lake; when the reverse flow remains the same, the river-lake water level difference declines with the increase of the water level at the Prek Kdam station; when the river-lake water-level difference remains the same, the reverse flow rises as the water level at the Prek Kdams station rises. The correlation coefficient between the reverse flow and the water-level difference between Mekong River and Tonle Sap Lake varies from 0.85 to 0.98 when the water level at the Prek Kdam station varies from 1.0 to 10.5 m, and the correlation is stronger when the water level is higher.

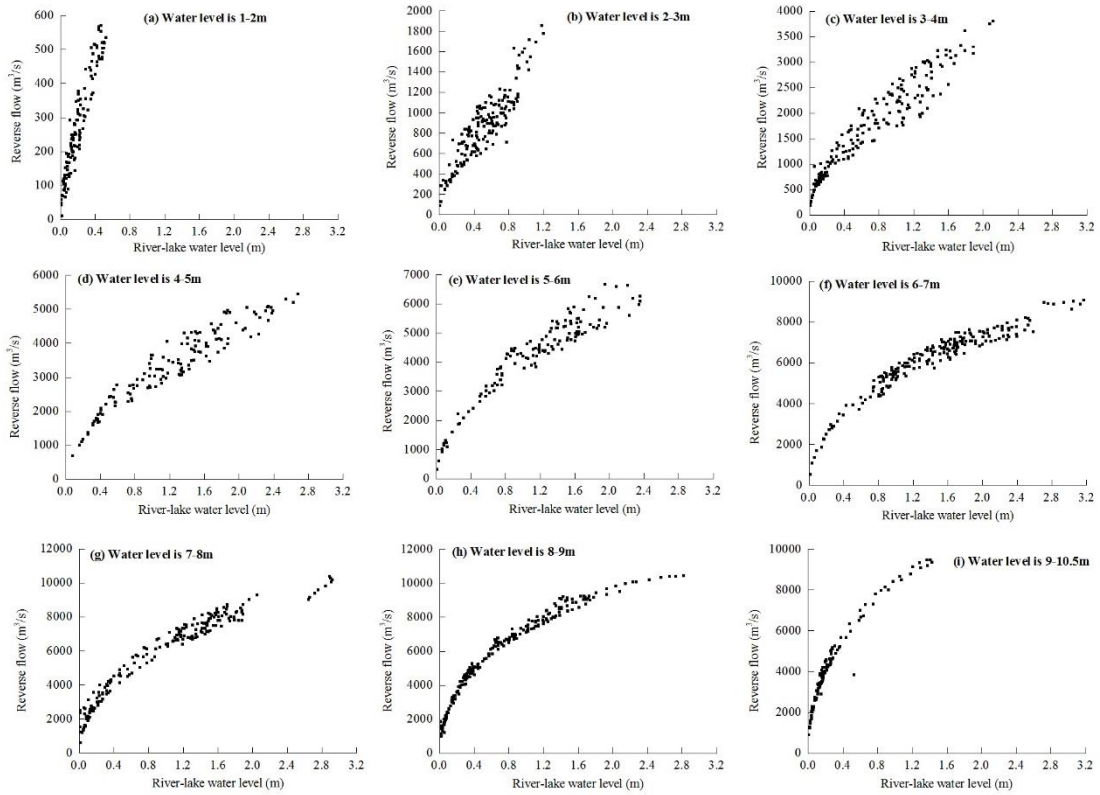

Figure 18. *Correlation between reverse flow and river-lake water level difference*

As the reverse flow and the water-level difference are positively correlated to the water level at the Prek Kdam station, the product of the water-level difference and the water level of the Prek Kdam station are set as the independent variable to identify its correlation to the reverse flow. On the basis of sufficient simulation and analyses, two

http://www.aloki.hu ● ISSN 1589 1623 (Print) ● ISSN 1785 0037 (Online)
DOI: http://dx.doi.org/10.15666/aeer/1706_1387513895

respective power function coefficients are assigned to the water-level difference and the water level at the Prek Kdam station to reduce the error of simulation. On that basis, this study builds an optimization model for the correlation among the reverse flow, the water-level difference, and the water level at the Prek Kdam station, as shown in *Equation 1* and *Figure 19*. It shows that the reverse flow is linearly correlated to the water-level difference and the water level at the Prek Kdam station, and the correlation coefficient reaches 0.9966, which proves the rationality of the model.

$$Q_{PK} = -413.73H + 80.54 = -413.73h_{PK}^{1.36}\left|h_{KL} - h_{JBG}\right|^{0.46} + 80.54 \quad \text{(Eq.1)}$$

where Q_{PK} refers to the discharge (m^3/s) at the Prek Kdam station; h_{JBG}, h_{PK} and h_{KL} are the respective water level (m) at the Phnom Penh station, the Prek Kdam station and the Kompong Luong station.

Table 1. *Correlation coefficient between reverse flow and river-lake water level difference*

Water level of Prek Kdam station (m)	a	b	Correlation coefficient R^2
1.0~2.0	852.49	0.7029	0.8751
2.0~3.0	1264.3	0.5542	0.8489
3.0~4.0	2203	0.5306	0.9554
4.0~5.0	3059.3	0.5599	0.9472
5.0~6.0	4072.1	0.5419	0.9753
6.0~7.0	5318.6	0.4838	0.9757
7.0~8.0	6321.5	0.4258	0.9247
8.0~9.0	7304.9	0.4526	0.9690
9.0~10.5	8549.5	0.4741	0.9779

The correlation between the reverse flow and the water-level difference is presented as $Q_{PK} = a \cdot (h_{JBG} - h_{KL})^b$, where Q_{PK} denotes the reverse flow at the Prek Kdam station (m^3/s), h_{KL} and h_{JBG} denote the respective level of water (m) at the Kompong Luong station and the Phnom Penh station; a and b are the fitting parameters

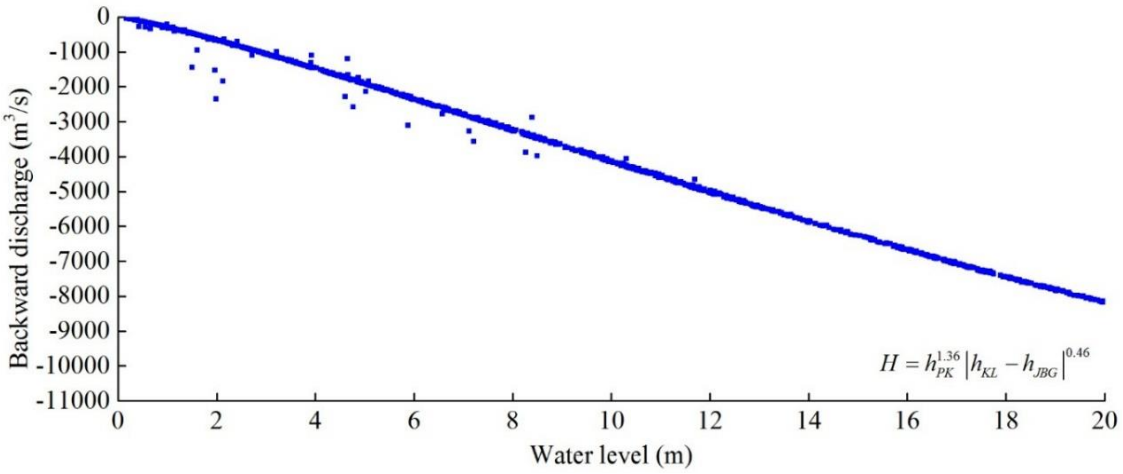

Figure 19. *Correlation among reverse flow, water level difference and water level of Prek Kdam station*

http://www.aloki.hu ● ISSN 1589 1623 (Print) ● ISSN 1785 0037 (Online)
DOI: http://dx.doi.org/10.15666/aeer/1706_1387513895

According to quantitative analysis by *Equation 1,* the relationship among the reverse flow from Mekong River to Tonle Sap Lake, the water level at the Prek Kdam station and the difference in the water level between Mekong River and Tonle Sap Lake are achieved, as shown in *Table 2.* It shows that the reverse flow is small when the water level of Tonle Sap Lake is low or when the water level difference is small, and the reverse flow rises when the water level of Tonle Sap Lake or the hydraulic head difference increases. That is to say, the volume of reverse flow is positively correlated to the water level difference between Mekong River and Tonle Sap Lake. When the reverse flow reaches 3000 m^3/s, the required hydraulic head difference between Mekong River and Tonle Sap Lake declines from 1.31 m, 0.68 m, 0.40 m, 0.26 m, 0.17 m to 0.12 m as the water level at the Prek Kdam station rises from 4 m, 5 m, 6 m, 7 m, 8 m and 9 m. When the water level at the Prek Kdam station remains at 8m, the respective reverse flow from Mekong River to Tonle Sap Lake are 3000 m^3/s, 4000 m^3/s, 5000 m^3/s, 6000 m^3/s, 7000 m^3/s, 8000 m^3/s and 9000 m^3/s when the hydraulic head difference between Mekong River and Tonle Sap Lake reaches 0.17 m, 0.30 m, 0.48 m, 0.71 m, 0.99 m, 1.36 m and 1.84 m. When the difference in the water level between Mekong River and Tonle Sap Lake is 1 m, the respective water level of the Prek Kdam station needs to reach 2.11 m, 3.33 m, 4.38 m, 5.33 m, 6.23 m, 7.11 m, 7.98 m, 8.88 m and 9.86 m so that the reverse flow can reach 1000 m^3/s, 2000 m^3/s, 3000 m^3/s, 4000 m^3/s, 5000 m^3/s, 6000 m^3/s, 7000 m^3/s, 8000 m^3/s and 9000 m^3/s.

Table 2. *Correlation among reverse flow from Mekong River to Tonle Sap Lake, river-lake water level difference and water level of Prek Kdam station*

Water level of Prek Kdam station (m)	**Water level difference between Mekong River and Tonle Sap Lake (m), reverse flow (m^3/s)**				
	0.1	**0.5**	**1**	**1.5**	**2**
2	245	634	920	1138	1322
3	502	1194	1707	2099	2429
4	798	1844	2622	3215	3711
5	1127	2572	3642	4448	5113
6	1487	3366	4737	5749	6564
7	1875	4212	5877	7064	7981
8	2289	5096	7022	8322	9259
9	2727	6000	8126	9442	10275
10	3185	6905	9137	10329	10885

Conclusion

According to the statistical analysis, some conclusions are included as follows:

(1) The flood reversal flow from Mekong River lasts long and is large in volume during the flood season. For long series of years on average, the reversal lasts 122 days and the volume of reverse flow is 37.7 billion m^3, with the flood peak remaining at 8402 m^3/s. The reversal volume accounts for 14% of the volume of Mekong River in the same time period and cuts 20% of the flood peak on average for years. The reversal occurs mainly from July to September and the maximum volume of reverse flow occurs in August, accounting for 43% of the volume in a whole year and 17.7% of the total volume from Mekong River in the same time period. The volume of reverse flow shows

http://www.aloki.hu ● ISSN 1589 1623 (Print) ● ISSN 1785 0037 (Online)
DOI: http://dx.doi.org/10.15666/aeer/1706_1387513895

little change over the years and the extreme ratio of the volume and flood peak of reverse flow remain at 2.33.

(2) The reverse flow is mainly subject to factors including the difference in runoff between Mekong River and Tonle Sap Lake, the difference in the water level between Mekong River and Tonle Sap Lake, and the water level of Tonle Sap River. Among these factors, the difference in runoff determines the difference in the water level. When the water level at Tonle Sap River remains constant, the volume of reverse flow increases as the difference in the water level between the river and the lake (flow resistance) increases. When the difference in the water level remains constant, the volume of reverse flow increases as the water level (the wetted cross-section area) of Tonle Sap River increases.

(3) The hydrological conditions of the reverse flow include the difference in the water level between the river and the lake and the water level at Tonle Sap River. When the water level of Mekong River exceeds that of Tonle Sap Lake, the reverse flow is linearly correlated to the product of the water level of Tonle Sap River to the power of 1.36 multiplied by that water-level difference between Mekong and Tonle Sap Lake to the power of 0.46. When the level of water at the Prek Kdam station on Tonle Sap Lake is 8 m, the hydraulic head difference between the river and the lake needs to reach 0.17 m, 0.30 m, 0.48 m, 0.71 m, 0.99 m, 1.36 m and 1.84 m so that the reverse flow can reach 3000 m^3/s, 4000 m^3/s, 5000 m^3/s, 6000 m^3/s, 7000 m^3/s, 8000 m^3/s, 9000 m^3/s respectively. When the difference in the water level between the river and the lake is 1 m, the water level at the Prek Kdam station has to reach 2.11 m, 3.33 m, 4.38 m, 5.33 m, 6.23 m, 7.11 m, 7.98 m, 8.88 m and 9.86 m, hence the reverse flow can reach 1000 m^3/s, 2000 m^3/s, 3000 m^3/s, 4000 m^3/s, 5000 m^3/s, 6000 m^3/s, 7000 m^3/s, 8000 m^3/s, 9000 m^3/s, respectively.

Objective understanding the variation characteristics, influencing factors and hydrological conditions of the reverse flow from Mekong River to Tonle Sap Lake is conducive to the comprehensive management of Cambodia Mekong Delta and Tonle Sap Lake area. Limited to data conditions, this study is mainly based on the flow records from 1995 to 2011 and the water level records from 1999 to 2011, so further collection and analysis based longer series of hydrological data are needed in the future. The regulation and storage effect of Tonle Sap Lake on the flood of Mekong River, and the positioning of Tonle Sap Lake from the perspective of overall flood control of Mekong River should be further studied. In addition, in order to further study the internal mechanisms of the relationship between Mekong River and Tonle Sap Lake, the discharge capacity of Mekong River, the diversion flow and discharge sediments capacity of Tonle Sap River, the flood control capacity of Tonle Sap Lake should be considered, so it is recommended to strengthen the prototype observation of the river topography.

Acknowledgments. This research was financially supported by the National Key Research and Development Program of China (2017YFC0405301) and China-Asean Maritime Cooperation Fund "Langcang-Mekong Water Resources Cooperation Project".

REFERENCES

[1] Changjiang Institute of Survey, Planning, Design and Research (2015): Study on Variation and Influence of Relationship between Yangtze River and Poyang Lake. – Changjiang Institute of Survey, Planning, Design and Research, Wuhan.

http://www.aloki.hu ● ISSN 1589 1623 (Print) ● ISSN 1785 0037 (Online)
DOI: http://dx.doi.org/10.15666/aeer/1706_1387513895

[2] Changjiang Water Resources Commission of the Ministry of Water Resources (2013): Study on the Changes of Hydrological Regime in Poyang Lake and Related Influence on Water Control Project. – Changjiang Water Resources Commission of the Ministry of Water Resources, Wuhan.
[3] Changjiang Water Resources Commission of the Ministry of Water Resources (2019): Outline of Master Plan on Water Resources of Cambodian. – Changjiang Water Resources Commission of the Ministry of Water Resources, Wuhan.
[4] Cochrane, T. A., Arias, M. E., Piman, T. (2014): Historical impact of water infrastructure on water levels of the Mekong River and the Tonle Sap system. – Hydrology and Earth System Sciences 18(11): 4529-4541.
[5] Dai, X., Wan, R. R., Yang, G. S. (2015): Non-stationary water level fluctuation in China's Poyang Lake and its interactions with Yangtze River. – Journal of Geographical Sciences 25(3): 274-288.
[6] Fang, C. M., Cao, W. H., Mao, J. X., et al. (2012): Relationship between Poyang Lake and Yangtze River and influence of Three Georges Reservoir. – Journal of Hydraulic Engineering 43(2): 175-181.
[7] Guo, H., Hu, Q., Zhang, Q., et al. (2012): Effects of the Three Gorges Dam on Yangtze River flow and river interaction with Poyang Lake, China: 2003-2008. – Journal of Hydrology 416/417: 19-27.
[8] Hu, C. H., Ruan, B. Q. (2011): Study on key technologies of Poyang Lake water control project. – Journal of China Institute of Water Resources and Hydropower Research 9(4): 243-248.
[9] Hu, Q., Song, F., Guo, H., et al. (2007): Interactions of the Yangtze river flow and hydrologic processes of the Poyang Lake, China. – Journal of Hydrology 347(1/2): 90-100.
[10] Huo, Y. (2011): Poyang Lake Morphological Characteristics and Its Response to Runoff and Sediment of Poyang Lake Basin. – Nanjing University, Nanjing.
[11] Li, C. W., You, Z. Q., Yao, W. (2018a): Study on the Flood Storage Function of Tonle Sap Lake. – Proceedings of 2018 Annual Conference of Chinese Hydraulic Engineering Society. Third Volume. China Water Power Press, Beijing.
[12] Li, C. W., Huang, L. Y., Wang, C. P., et al. (2018b): Study on Flood Control Planning of Mekong Delta in Cambodia. – Proceedings of 2018 Annual Conference of Chinese Hydraulic Engineering Society. Fifth Volume. China Water Power Press, Beijing.
[13] Li, C. W., You, Z. Q., Yao, W., et al. (2018c): Study on Hydrologic Condition of Water Exchange between Mekong River and Tonle Sap Lake. – Proceedings of 2018 Annual Conference of Chinese Hydraulic Engineering Society One Belt One Road·Go Out. Changjiang Press, Wuhan.
[14] Luo, X. P., Zheng, L., Qi, S. H., et al. (2008): Analysis on flow and sediment transportation variation of the Poyang Lake into the Yangtze River. – Yangtze River 39(6): 12-14.
[15] Mak, S., Pheng, S., Khuon, K., et al. (2012): Profile of the Sub-Area Stung Treng (SA-9C). – Cambodia National Mekong Committee, Phnom Penh.
[16] Mekong River Commission (2005): Overview of the Hydrology of the Mekong Basin. – Mekong River Commission, Vientiane, Laos.
[17] Mekong River Commission (2011): Atlas Planning of the Lower Mekong River Basin. – Mekong River Commission, Phnom Penh.
[18] Republic of Korea, Korea International Cooperation Agency, Korea Water Resources Corporation (2008): Master Plan of Water Resources Development in Cambodia. – Ministry of Water Resources and Meteorology, the Kingdom of Cambodia, Phnom Penh.
[19] Royal Haskoning, Deltares, UNESCO-IHE (2010): Structural Measures and Flood Proofing in the Lower Mekong Basin. – Mekong River Commission, Vientiane.
[20] Yin, H. F., Liu, G. R., Pi, J. G., et al. (2007): On the river-lake relationship of the middle Yangtze reaches. – Geomorphology 85(3/4): 197-207.

http://www.aloki.hu ● ISSN 1589 1623 (Print) ● ISSN 1785 0037 (Online)
DOI: http://dx.doi.org/10.15666/aeer/1706_1387513895

[21] You, Z. Q., Yu, Q. H., Xu, Z. M. (2013): Master Plan on Poyang Lake Area. – Proceedings of 2013 Annual Conference of Chinese Hydraulic Engineering Society. Chinese Hydraulic Engineering Society, Guangzhou.
[22] Zhang, Q., Ye, X. C., Werner, A. D., et al. (2014): An investigation of enhanced recessions in Poyang Lake: comparison of Yangtze River and local catchment. – Journal of Hydrology 517: 425-434.
[23] Zhang, Z. X., Chen, X., Xu, C. Y., et al. (2015): Examining the influence of river-lake interaction on the drought and water resources in the Poyang Lake basin. – Journal of Hydrology 522: 510-521.
[24] Zhong, Z. Y., Hu, W. Z. (2008): On relation of river and lake. – Yangtze River 39(1): 20-22.

http://www.aloki.hu ● ISSN 1589 1623 (Print) ● ISSN 1785 0037 (Online)
DOI: http://dx.doi.org/10.15666/aeer/1706_1387513895

IMPACT OF SOIL MANAGEMENT ON BIODIVERSITY OF EPIGEIC GROUPS

IVANIČ PORHAJAŠOVÁ, J.[1*] – PETROVIČOVÁ, K.[1] – MLYNEKOVÁ, E.[2] – ERNST, D.[3] – BABOŠOVÁ, M.[1] – NOSKOVIČ, J.[1] – KRUMPÁLOVÁ, Z.[4]

[1]Department of Environment and Zoology, Faculty of Agrobiology and Food Resources Slovak University of Agriculture in Nitra, Tr. A. Hlinku 2, 949 76 Nitra, Slovak Republic (phone: +421-37-641-4470)

[2]Department of Animal Husbandry, Faculty of Agrobiology and Food Resources Slovak University of Agriculture in Nitra, Tr. A. Hlinku 2, 949 76 Nitra, Slovak Republic

[3]Department of Crop Production, Faculty of Agrobiology and Food Resources Slovak University of Agriculture in Nitra, Tr. A. Hlinku 2, 949 76 Nitra, Slovak Republic

[4]Department of Ecology and Environmental Science, Faculty of Natural Sciences Constantine the Philosopher University in Nitra, Tr. A. Hlinku 1, 949 01 Nitra, Slovak Republic

[*]Corresponding author
e-mail: Jana.Porhajasova@uniag.sk; phone: +421-37-641-4470

(Received 22nd May 2019; accepted 25th Oct 2019)

Abstract. The aim of this study was to assess the effect of ecological and integrated farming on the occurrence of epigeic animal groups. The earth trap method was used, were exposed in *Pisum sativum* and *Hordeum vulgare*. The experiment was performed from 2015 to 2017 at the research fields of the Plant Biology and Ecology Centre in Nitra. During the three-year period, 11,866 exemplars were collected from 21 taxonomic groups. Under integrated farming of 5,456 exemplars belonging to 20 groups were collected, in the ecological farming of 6,410 exemplars belonging to 19 groups were collected. The decreasing tendency of abundance in most groups was recorded. Both types of farming showed the Coleoptera, Acarina, Araneida, Collembola as the highly dominant groups. The Opilionida occurred subdominantly. The occurrence of others was recedent or subrecedent. The presence of these animal groups in the agroecosystem increases its biodiversity. The impact of cultivated crops, temperature and type of farming on occurrence of animal epigeic groups was significant. The impact of precipitation was non-significant. The faunistic similarity was of 85.71%, the identity of dominancy was of 95.57%. The highest value of diversity was recorded in the integrated farming with *Pisum sativum*, in ecological farming with *Hordeum vulgare*.
Keywords: *Coleoptera, ecological farming, ground traps, integreted farming*

Introduction

The soil is an important natural resource, and few phenomena on our planet match the complexities of the processes in it. Farming is the most widely used environ technology with its positive and negative impacts on the land. The agricultural land is a type of modified land with a significant human influence and with a disturbed course of natural processes. Biodiversity loss, an important consequence of agricultural intensification, can lead to reductions in agroecosystem functions and services. Increasing crop diversity through rotation may alleviate these negative consequences by restoring positive aboveground–belowground interactions. Compared to the natural ecosystems, in agroecosystems the biodiversity is more reduced (Tieman et al., 2015),

http://www.aloki.hu ● ISSN 1589 1623 (Print) ● ISSN 1785 0037 (Online)
DOI: http://dx.doi.org/10.15666/aeer/1706_1389713908

but according to Baranová et al. (2015) the artificial habitats often provides the shelter of biodiversity in anthropogenic land, because of its valuable natural biotope analogs.

One of the indicators reflecting the biotope burden is soil edaphone, which is an important component of biocoenosis and an important bioindicator of environmental quality. Fazekašová and Bobuľovská (2012) reported that communities of soil organism play an irreplaceable role in decomposition of organic matter, in cycle of biogenic elements of carbon, nitrogen, sulfur, phosphorus, in transformation and degradation of waste and toxic substances, etc. and its presence is irreplaceable. Afterwards, the impact of soil organisms becomes a key component of the strategy leading to the sustainability of the soil ecosystem. The biodiversity of epigeic groups, including its abundance in soil, directly depends on the abiotic and biotic factors that are typical of the biotope. In the agroecosystems, in addition to the natural factors, there is also a strong human impact, such as soil cultivation, crop rotation, cultivated crop, organic and artificial fertilizer inputs, and more. These interventions affect the level of agroecosystems biodiversity and contributes mainly to the reduction of the edaphic groups abundance (Baranová et al., 2013; Porhajašová et al., 2013).

In general, floristic and faunistic biodiversity in ecological farming systems is higher than in integrated systems. However, if integrated systems are well managed, it can also improve the biodiversity in agricultural areas (Bavec and Bavec, 2014; Dobrovodská et al., 2019).

The aim of this study was to asses the epigeic groups biodiversity in stands of *Pisum sativum* and *Hordeum vulgare* cultivated under the conditions of ecological and integrated farming.

Materials and methods (Experimental)

The collection of epigeic material was carried out by the earth traps method in 2015 to 2017 during the growing season (April to October) in stands of *Pisum sativum* and *Hordeum vulgare* cultivated under the conditions of ecological and integrated farming. Both types of management are governed by the following principles. Integrated management is based on ensuring sustainable management, achieving higher quality yields without burdening the environment, maintaining or improving soil fertility, a consistent system approach to all cultivation technology to optimize the economic and environmental aspects of production. Organic farming is based on the assumption that crops use natural resources, for example to combat pests, maintain or increase soil fertility, etc. Without resorting to synthetic chemicals such as fertilizers, pesticides, antibiotics, and without the use of any organisms that have been genetically modified. In this way, more natural, healthier and nutritious foods are obtained. In addition, it helps to achieve greater environmental sustainability, with minimal impact on the environment. One earth trap was located in the center of the plot is exposed in the crops under investigation. A solution of 4% formaldehyde was used as a fixing liquid. Traps were collected at monthly intervals (once a month), the collected biological material was determined in the department's conditions according to keys (Hůrka, 1996; Pokorný, 2002, 2004).

Epigeic groups of monitored agroecosystems were evaluated on the basis of abundance, dominance and species identity according to Jaccard (IA), dominance identity according to Renkonnen and on the basis of diversity degree according to

http://www.aloki.hu ● ISSN 1589 1623 (Print) ● ISSN 1785 0037 (Online)
DOI: http://dx.doi.org/10.15666/aeer/1706_1389713908

Shannon-Weaver (H´) (Losos et al., 1994). Prediction of the richness of edaphic animal species was performed and the homeostasis of agroecosystems was evaluated.

Study area

The monitored area is located in the western part of the Žitava upland on the site of Nitra – Dolná Malanta (research fields of the Plant Biology and Ecology Centre, the Faculty of Agrobiology and Food Resources of the Slovak University of Agriculture, GPS 48°31´ N, 18°14´E) in the lower part of the Selenec stream and its tributaries (Hrnčiarová, 2001), (*Fig. 1*). The altitude of monitored area is of 175 to 180 m above sea level.

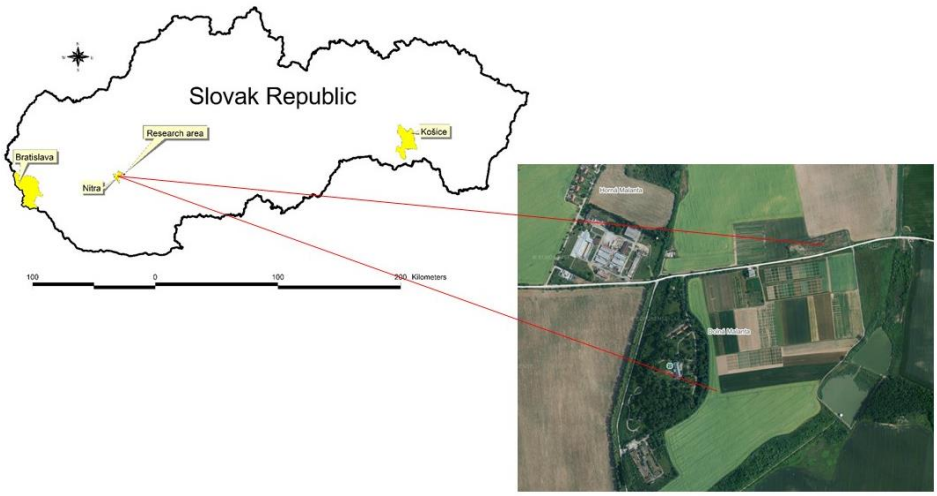

Figure 1. *Map of study area – Dolná Malanta*

The research was performed in stands of *Pisum sativum* and *Hordeum vulgare* cultivated under the conditions of ecological and integrated farming. Legumes have a lower autoregulatory and compensatory ability than cereals. Therefore, good soil preparation, soil types and agroecological conditions play an important role in pea cultivation technology (Candráková, 2014; Černý et al., 2017).

Data analyses

Diversity and equitability were calculated using the Shannon Diversity Index – H' by PAST software (Hammer, 2015).

The prediction – rarefaction of the richness of edaphic animal groups was performed by the PAST software using a confidence interval of 95% based on the amount of caught dragonfly material in the *Pisum sativum* and *Hordeum vulgare* stands cultivated under the conditions of ecological and integrated farming.

The data distribution normality of the individuals of animal epigeic groups from monitored areas was tested by the Shapiro-Wilks W test. Due to the violation of the data distribution normality, non-parametric tests – Friedman (ANOVA) and Kruskal-Wallis test (ANOVA) were used to H_0 hypotheses testing. We observed the influence of factors (temperature, total rainfall, management (integrated, ecological), type of cultivated crop (*Pisum sativum, Hordeum vulgare*)) on the number of individuals of individual epigeic

http://www.aloki.hu ● ISSN 1589 1623 (Print) ● ISSN 1785 0037 (Online)
DOI: http://dx.doi.org/10.15666/aeer/1706_1389713908

groups. Post hot test (LSD test) we added statistical significance of pairs in combination year, farming, plant in Friedman´s test. H_0 hypotheses were tested at the significance level of $p\alpha = 0.05$ (if $p > p\alpha$, we cannot reject H_0 at the level of selected statistical significance of $p\alpha = 0.05$) (i) random selection comes from a normal distribution file, (ii) the number of individuals of the animal epigeic groups does not differ due to the type of farming and the type of crop cultivated, (iii) the average monthly temperature had not an effect on the number of individuals in the animal epigeic groups, (iiii) the average monthly precipitation had not an effect on the number of individuals in the animal epigeic groups. The data matrix with the number of individuals of the all animal epigeic groups was used.

To the data analysis the statistical program Statistics Cz, version 7.0 was used (StatSoft, Inc.).

Results and Discussion

The exemplars of 11,866 pieces of the animal epigeic groups belonging to 21 taxonomic groups, which are part of the zoological taxonomic unit Arthropoda, during the three-year period were collected. Of the number of individuals obtained, 5,456 individuals belonging to 20 groups were collected within under the integrated farming conditions. Exemplars of 6,410 pieces belonging to 19 taxonomic groups were collected in the ecological farming (*Tables 1, 2*). Muridae and Larvae were not further determined, it represented the developmental stages of the epigeic groups present.

Table 1. *Integrated farming – abundance and dominance of animal epigeic groups in Pisum sativum and Hordeum vulgare stands*

Epigeic group	***Pisum sativum***					***Hordeum vulgare***						
	2015	***2016***	***2017***	***∑*****	***D*(%)***	***2015***	***2016***	***2017***	***∑*****	***D*(%)***	***∑*****	***D*(%)***
Anura	2	-	-	2	0.08	4	-	-	4	0.13	6	0.11
Acarina	565	222	144	931	37.16	524	372	54	950	32.19	1881	34.47
Araneida	112	46	86	244	9.74	128	43	56	227	7.69	471	8.63
Auchenorrhyncha	8	5	4	17	0.67	7	4	6	17	0.58	34	0.65
Coleoptera	279	337	327	943	37.66	521	407	191	1119	37.94	2062	37.79
Collembola	53	35	14	102	4.07	116	150	23	289	9.79	391	7.16
Dermaptera	14	-	15	29	1.17	13	11	11	35	1.18	64	1.17
Diplopoda	18	13	14	45	1.78	20	26	8	54	1.84	99	1.83
Diptera	2	1	4	7	0.29	8	3	3	14	0.47	21	0.38
Formicoidea	33	7	2	42	1.67	40	15	-	55	1.86	97	1.78
Hymenoptera	2	7	6	15	0.58	12	6	6	24	0.81	39	0.73
Chilopoda	4	-	3	7	0.28	2	3	3	8	0.27	15	0.27
Isopoda	8	7	3	18	0.75	2	7	4	13	0.44	31	0.57
Lacertidae	-	1	-	1	0.04	-	-	-	-	-	1	0.01
Larvae	3	2	5	10	0.39	8	3	6	17	0.57	27	0.49
Lumbricidae	2	5	1	8	0.32	6	2	-	8	0.28	16	0.28
Opilionida	17	22	45	84	3.35	31	26	60	117	3.96	201	3.68
∑**	**1122**	**710**	**673**	**2505**	**100**	**1442**	**1078**	**431**	**2951**	**100**	**5456**	**100**

(D* – dominance; ∑** - total)

http://www.aloki.hu ● ISSN 1589 1623 (Print) ● ISSN 1785 0037 (Online)
DOI: http://dx.doi.org/10.15666/aeer/1706_1389713908

Table 2. *Ecological farming – abundance and dominance of animal epigeic groups in Pisum sativum and Hordeum vulgare stands*

Epigeic group	*Pisum sativum*					*Hordeum vulgare*						
	2015	*2016*	*2017*	∑**	*D*(%)*	*2015*	*2016*	*2017*	∑**	*D*(%)*	∑**	*D*(%)*
Acarina	763	321	116	1200	32.19	569	372	119	1060	39.51	2260	35.26
Araneida	159	32	47	238	6.38	123	29	44	196	7.31	434	6.77
Auchenorrhyncha	2	-	3	5	0.13	3	6	6	15	0.57	20	0.31
Coleoptera	955	416	359	1730	46.42	252	412	189	853	31.79	2583	40.29
Collembola	91	110	11	212	5.68	81	99	28	208	7.75	420	6.55
Dermaptera	11	8	41	60	1.61	8		43	51	1.9	111	1.73
Diplopoda	18	11	10	39	1.07	22	21	6	49	1.83	88	1.37
Diptera	4	5	1	10	0.27	9	6	5	20	0.75	30	0.47
Formicoidea	41	4	10	55	1.47	18	21	16	55	2.05	110	1.72
Heteroptera	-	-	-	-	-	-	3	-	3	0.11	3	0.05
Hymenoptera	4	5	4	13	0.35	7	6	13	26	0.98	39	0.61
Chilopoda	2	-	-	2	0.05	-	-	5	5	0.18	7	0.11
Isopoda	4	5	2	11	0.29	9	3	2	14	0.52	25	0.39
Larvae	8	1	4	13	0.35	6	3	4	13	0.48	26	0.41
Lumbricidae	9	4	1	14	0.38	3	4	-	7	0.25	21	0.32
Opilionida	38	38	34	110	2.95	25	33	40	98	3.65	208	3.24
Orthoptera	4	-	3	7	0.18	-	4	-	4	0.15	11	0.17
Siphonaptera	-	8	-	8	0.23	-	6	-	6	0.22	14	0.23
∑**	**2113**	**968**	**646**	**3727**	**100**	**1135**	**1028**	**520**	**2683**	**100**	**6410**	**100**

(D* – dominance; ∑** - total)

Acarina and Coleoptera were assessed as an eudominant groups in both types of farming and in both crops cultivated. Araneida and Collembola were dominant (*Tables 1, 2*). With integrated farming in stands of *Pisum sativum*, the dominant group was Araneida. In the *Hordeum vulgare* stands the Araneida and Collembola were dominant. With ecological farming, the Araneida and Collembola groups were dominant in both crops cultivated. The occurrence of Acarina is limited by many factors, especially by its dependence on the substrate type. Gormsen et al. (2006) states that the ending of agricultural measures, i.e. soil management is associated with an increase of the Acarina population. Fox et al. (2017) confirmed the increase of Acarina abundance in soil with application of organic fertilizers. Authors also confirmed higher number of Acarina in soil with shallow ploughing than in soil with deep ploughing applied. According to Boháč et al. (2015), the Coleoptera represents a large and functionally dominant group of soil macrofauna, which sensitively reacts to anthropogenic activity in forest but also in non-forest habitats. Coleoptera, especially Carabidae, represent an important bioindicating organisms in both artificial and natural ecosystems. Authors Tieman et al. (2015) and Vician et al. (2011, 2018) state that the main factors affecting the diversity of its communities are elements of environment such as vegetation, humidity, temperature and shadow. Migration of Coleoptera is significantly affected by microclimatic conditions of the habitat. According to Baranová et al. (2013), the species variability of Carabidae (Coleoptera) is mainly influenced by soil moisture, herbal stratum of 0-200 mm, intensity of agrotechnical interventions and

http://www.aloki.hu ● ISSN 1589 1623 (Print) ● ISSN 1785 0037 (Online)
DOI: http://dx.doi.org/10.15666/aeer/1706_1389713908

humus content. Carabidae (Coleoptera) react sensitively to the toxic substances (herbicides, insecticides), pH change and soil moisture and to the excessive use of artificial fertilizers (Vician et al., 2011; Tieman et al., 2015; Nietupski et al., 2015). In agroecosystems, macropterous species of Carabidae (Coleoptera) with a smaller body size are predominate. It is an indicator of lower ecological stability of the agroecosystems (Langraf et al., 2017, 2018, 2019). The abundance of Araneida and Collembola was almost equal in both monitored types of farming. According to Vician et al. (2015), the arachnocenosis are most sensitive to insecticide application and soil cultivation. During the monitored years, the abundance of Araneida and Collembola in both cultivated crops decreased. The most frequent occurrence of these groups was recorded in 2015, which is probably related to the appropriate climatic conditions of the environment (temperature and precipitation). In the integrated farming system, reducing the number of agrotechnical interventions affects the increase of Araneida and Coleoptera abundance. The population of Collembola varies in abundance and species representation, depending on the type of vegetation and soil conditions. The impact of agricultural management, such as crop harvesting, insecticide and herbicide application and conventional ploughing, has a significant negative effect on the occurrence of Collembola, but the application of organic fertilizers has a positive effect on the increase of its populations (Querner et al., 2008; Jasinski et al., 2016). The subdominant representation in both types of crops and in both types of farming was recorded with Opilionida. Recedent representation was recorded with groups of Dermaptera, Diplopoda and Formicoidea. The others groups were subrecedent. Even though its low presence, its importance in ecosystems is irreplaceable (e.g. Heteroptera are involved in the elimination of acarinocenoses and Thysanoptera, Orthoptera regulates insect pests, Diplopoda are an important saprophytophages, Dermaptera performs the function as a saprophages to polyphagous nocturnal insects). Presence of this epigeic groups contributes to the biodiversity of agroecosystems and also to its ecological stability. It showed that also intensively exploited agroecosystems allow the existence of a relatively wide range of zoofauna. Recorded epigeic groups represents a diversified component of soil fauna. These groups are characterized by different adaptations to the soil environment and different sensitivity to the stress (Porhajašová et al., 2012). The abundance and biodiversity of these epigeic groups supports the natural conditions of ecosystems (Kalivoda et al., 2010; Swaminathan, 2014). According to Lenoir and Lennartsson (2010) believe that the high abundance and dominance of Coleoptera, Araneida and Formicoidae in agroecosystems is mainly related to its trophic preference and tolerance to the soil environment.

In addition to the quantitative evaluation of the obtained epigeic material, qualitative indicators were identified. The qualitative composition of populations influences mainly the vegetation cover, abiotic and biotic environmental factors in the form of intra-species and inter-species relationships which depends on environmental conditions.

Based on the calculated values of faunistic similarity (85.71%), when two types of farming were compared, it can be stated that the ecological and integrated farming are the similar types of ecosystems.

Based on the dominance of populations mutual in both cultivation systems, the dominance identity value was of 95.57%.

The diversity value in the *Pisum sativum* stands cultivated under the conditions of integrated farming was of H´ = 2.61 (H´min = 2.56, H´max = 2.65), in the ecological farming it was of H´ = 2.40 (H´min = 2.36, H 'max = 2.44). In the stands of

http://www.aloki.hu ● ISSN 1589 1623 (Print) ● ISSN 1785 0037 (Online)
DOI: http://dx.doi.org/10.15666/aeer/1706_1389713908

Hordeum vulgare, the value of diversity in integrated farming reached of H´ = 2.62 (H´min = 2.57, H´max = 2.66), in ecological farming it was of H´ = 2.67 (H´min = 2.61, H 'max = 2.71).

The equitability value is in the range of e = 0 – 1, more balanced communities has an equitability value reaching of 1. The value of equitability in the *Pisum sativum* integrated cultivation system was of e = 0.68, in the *Hordeum vulgare* e = 0.69; in ecological cultivation system of *Pisum sativum* e = 0.63, in *Hordeum vulgare* e = 0.70. The equitability values are relatively low, reflecting imbalances number of specimens represented by individual taxa.

On the basis of the total species richness of the taxa of all the areas studied (the number of individuals), the prediction of the richness of animal epigeic groups of the monitored areas was predicted by the individual rarefraction with confidence interval of 95% (*Fig. 2*).

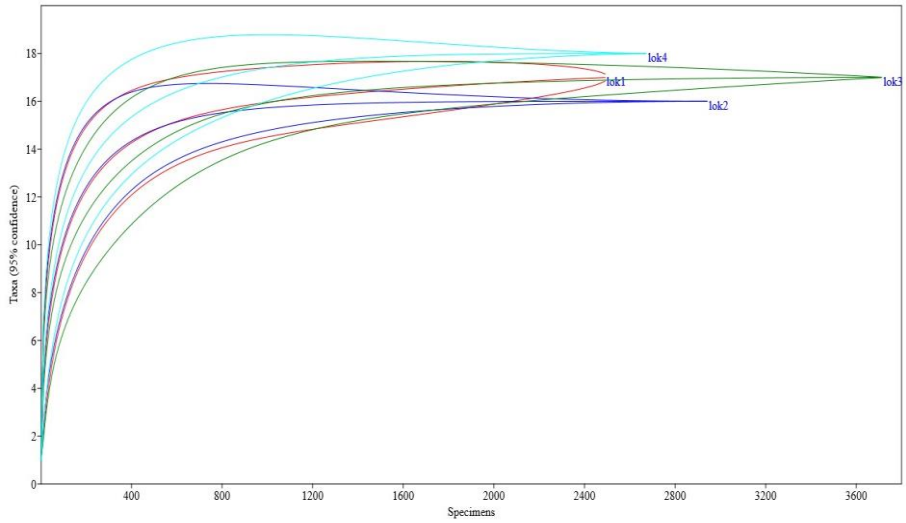

Figure 2. *Rarefaction curves of prediction of animal epigeic groups in integrated Pisum sativum (lok 1), Hordeum vulgare (lok 2) and ecological farming Pisum sativum (lok 3) a Hordeum vulgare (lok 4)*

The length of the rarefaction curve is a reflection of row saturation and prediction confidence. The cultivated area of *Pisum sativum* under the ecological farming (N = 3,727 individuals, 17 animal groups, predicted 18) had the longest rarefaction curve, indicating a greater predictive value for the prediction. According to experimental results, this site had the most complete spectrum of animal epigeic groups. Locations in stands of *Pisum sativum* (N = 2,505 individuals, confirmed 17, predicted 17 animal groups) and *Hordeum vulgare* (N = 2,951 individuals, confirmed 16, predicted 17 animal groups) with integrated farming and locality in stands of *Hordeum vulgare* (N = 2,683 individuals, confirmed 18, predicted 19 animal epigeic groups) with ecological farming were characterized by a short rarefaction curves, reflecting a reserve in animal epigeic saturation and a higher degree of prediction uncertainty. According to Litavský et al. (2018), Vician et al. (2015) and Filho et al. (2016) reported that the presence of epigeic groups in the soil in different types of ecosystems is mainly related to its trophic preference, but also to its tolerance to particular habitat conditions.

http://www.aloki.hu ● ISSN 1589 1623 (Print) ● ISSN 1785 0037 (Online)
DOI: http://dx.doi.org/10.15666/aeer/1706_1389713908

Using the non-parametric Friedman test, the effect of the farming method and the type of cultivated crop on the number of individuals of the animal epigeic groups was tested (H0: the number of individuals of animal epigeic groups was not differ due to the type of farming and type of cultivated crop, pα = 0.05). The result of the test is of p = 0.00, H0 is rejected at a significance level of 95%. Our experimental data showed that the farming and crop cultivated type had an impact on the number of individuals of animal epigeic groups (*Fig. 3*).

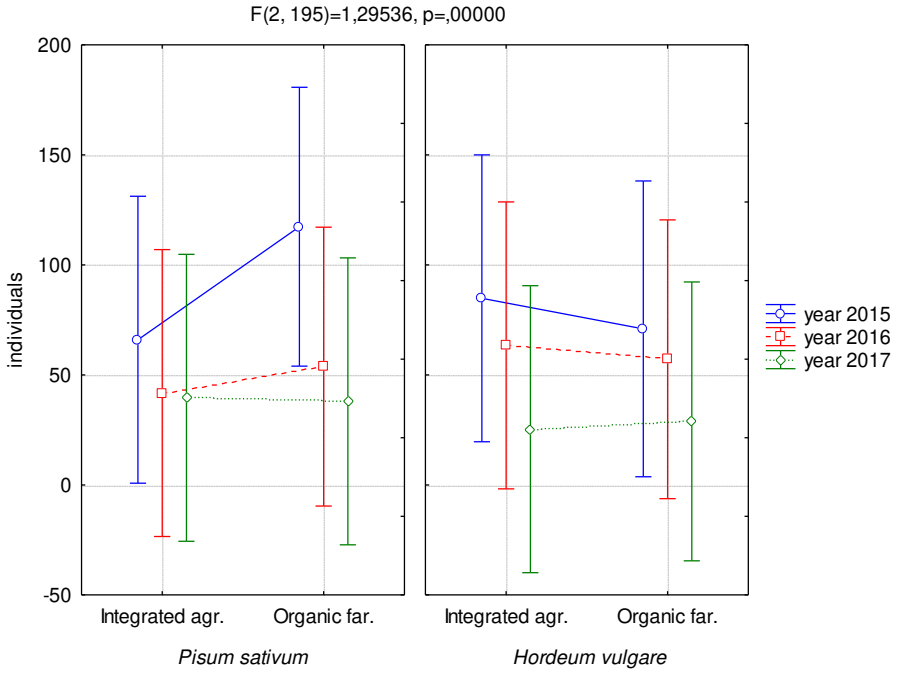

Figure 3. *Impact of farming and crop cultivated type on the number of individuals of animal epigeic groups*

By the Post hot test we have identified which management pairs differ at the level of statistical significance (pα = 0.05) during the years 2015 - 2017 (p < 0.05). The results are shown in *Table 3*.

In the stands of *Pisum sativum* cultivated under the conditions of ecological farming, an average number of individuals was higher than in the same crop cultivated under the conditions of integrated farming. However, in the stands of *Hordeum vulgare* cultivated under the conditions of integrated farming, an average number of individuals was higher.

In view of the impact of the cultivated crop (*Pisum sativum, Hordeum vulgare*) on the occurrence of animal epigeic groups, it is mainly the creation of suitable conditions, shading, moisture, realized agrotechnical interventions during crop cultivation, etc.

Using the non-parametric Kruskal-Wallis test, the effect of the average monthly temperature on the number of individuals of animal epigeic groups was tested (H0: the average monthly temperature had not an effect on the number of individuals of animal epigeic groups, pα = 0.05). The result of the test is of p = 0.01, H0 is rejected at a significance level of 95%. Our experimental data showed that the average monthly temperature had an impact on the number of individuals of animal epigeic groups during the research period (*Fig. 4*).

http://www.aloki.hu ● ISSN 1589 1623 (Print) ● ISSN 1785 0037 (Online)
DOI: http://dx.doi.org/10.15666/aeer/1706_1389713908

Table 3. *Results of Post hot test*

	1	***2***	***3***	***4***	***5***	***6***	***7***	***8***	***9***	***10***	***11***	***12***
1	-	0.69	0.03	0.92	0.05	0.96	0.79	0.85	0.05	0.39	0.05	0.42
2	0.69	-	0.48	0.77	0.36	0.65	0.50	0.55	0.33	0.02	0.32	0.02
3	0.03	0.48	-	0.32	0.10	0.24	0.16	0.19	0.09	0.05	0.09	0.05
4	0.92	0.77	0.32	-	0.54	0.87	0.71	0.77	0.51	0.03	0.49	0.04
5	0.05	0.36	0.10	0.54	-	0.64	0.79	0.74	0.96	0.71	0.94	0.78
6	0.96	0.65	0.24	0.87	0.64	-	0.83	0.89	0.61	0.04	0.59	0.05
7	0.05	0.50	0.16	0.71	0.79	0.83	-	0.94	0.76	0.54	0.73	0.58
8	0.85	0.55	0.19	0.77	0.74	0.89	0.94	-	0.70	0.04	0.68	0.05
9	0.05	0.33	0.09	0.51	0.96	0.61	0.76	0.70	-	0.76	0.97	0.82
10	0.39	0.02	0.05	0.03	0.73	0.04	0.54	0.04	0.76	-	0.79	0.94
11	0.05	0.32	0.09	0.49	0.94	0.59	0.73	0.68	0.97	0.79	-	0.84
12	0.42	0.02	0.05	0.04	0.78	0.05	0.58	0.05	0.82	0.94	0.84	-

Comments: 1 = the year 2015, integrated farming, *Pisum sativum*; 2 = the year 2015, integrated farming, *Hordeum vulgare*; 3 = the year 2015, ecological farming, *Pisum sativum*; 4 = the year 2015, ecological farming, *Hordeum vulgare*; 5 = the year 2016, integrated farming, *Pisum sativum*; 6 = the year 2015, integrated farming, *Hordeum vulgare*; 7 = the year 2016, ecological farming, *Pisum sativum*; 8 = the year 2016, ecological farming, *Hordeum vulgare*; 9 = the year 2017, integrated farming, *Pisum sativum*; 10 = the year 2017, integrated farming, *Hordeum vulgare*; 11 = the year 2017, ecological farming, *Pisum sativum*; 12 = the year 2017, ecological farming, *Hordeum vulgare*

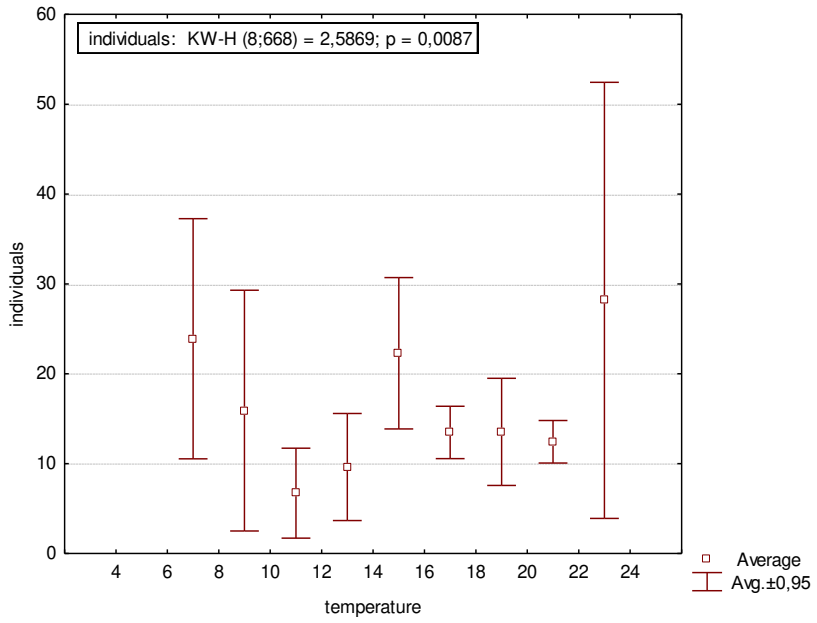

Figure 4. *Impact of average monthly temperature on the number of individuals of animal epigeic groups*

The impact of the average monthly precipitation on the number of individuals of animal epigeic groups (H0: average monthly precipitation had not an effect on the number of individuals of animal epigeic groups, pα = 0.05) was also tested by the Kruskal-Wallis test. The result of the test is of p = 0.34, H0 is not rejected at a significance level of 95%. Our experimental data showed that the average monthly precipitation had not an impact on the number of individuals of animal epigeic groups during the research period (*Fig. 5*).

http://www.aloki.hu ● ISSN 1589 1623 (Print) ● ISSN 1785 0037 (Online)
DOI: http://dx.doi.org/10.15666/aeer/1706_1389713908

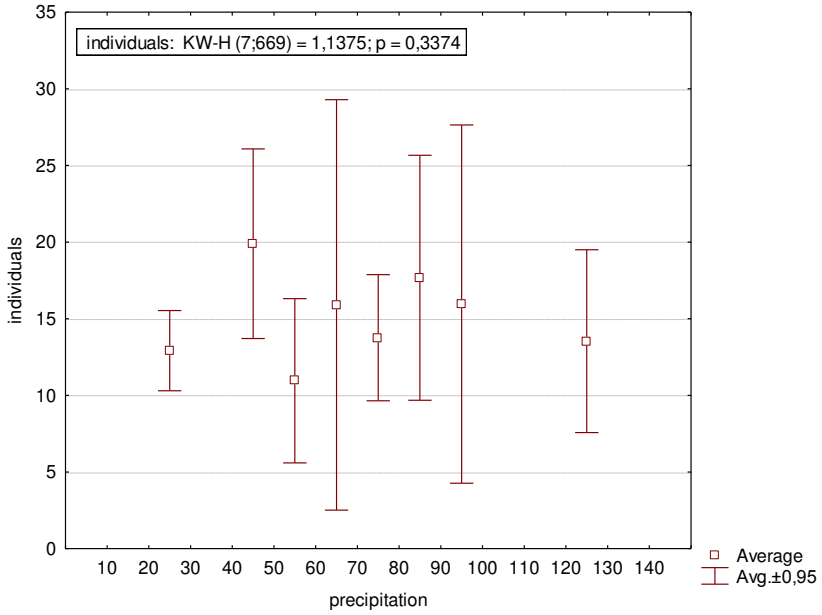

Figure 5. *Impact of average monthly precipitation on the number of individuals of animal epigeic groups*

Conclusions

The impact of two types of farming, integrated and ecological, on the occurence of animal epigeic groups was monitored during the three-year period. The individuals of 11,866 pieces belonging to 21 taxonomic groups were collected. Within the integrated farming of 5,456 individuals, with the determination of 20 groups, within the ecological farming of 6,410 individuals belonging to 19 groups. Coleoptera, Acarina, Araneida and Collembola were dominant in the both types of farming. The occurrence of Opilionida was subdominant. The occurrence of Dermaptera, Diplopoda, Formicoidea, Isopoda, Lumbricidae and others was evaluated as recedent and subrecedent. The impact of cultivated crop, temperature and the type of farming on animal epigeic groups was significant. The impact of precipitation was non-significant. According to different types of farming comparison, the faunistic similarity was of 85.71%, the dominance identity of 95.57%. The higher value of diversity was recorded in integrated farming with *Pisum sativum*, in ecological farming with *Hordeum vulgare*. In conclusion, the abiotic and biotic environmental factors had an effect on the qualitative composition of present animal populations.

Acknowledgements. This research is supports by the project KEGA 021SPU-4/2017.

REFERENCES

[1] Baranová, B., Fazekašová, D., Jászay, T., Manko, P. (2013): Ground beetle (Coleoptera: Carabidae) community of arable land with different crops. – Folia Faunistica Slovaca 18(1): 21-29.

http://www.aloki.hu ● ISSN 1589 1623 (Print) ● ISSN 1785 0037 (Online)
DOI: http://dx.doi.org/10.15666/aeer/1706_1389713908

[2] Baranová, B., Manko, P., Jászay, T. (2015): Waste dumps as local biodiversity hotspots for soil macrofauna and ground beetles (Coleoptera:Carabidae) in the agricultural landscape. – Ecological Engineering 81: 1-13.
[3] Bavec, M., Bavec, F. (2014): Impact of Organic Farming on Biodiversity. – In: Lo, Y. H., Blanco, J. A., Shovonlal, R. (eds.) Biodiversity in Ecosystems. Linking Structure and Function. https://doi.org/10.5772/58974.
[4] Boháč, J., Jahnová, Z. (2015): Land Use Changes and Lanscape Degradation in Central and Eastern Europe in the Last Decades: Epigeic Ivertebrates as Bioindicators of Landscape Changes. – In: Arman, R. H., Hanninen, O. (eds.) Environmental Indicators 395-419.
[5] Candráková, E. (2014): Preparing of the soil under *Pisum sativum*. – http://www.agroporadenstvo.sk/rastlinna-vyroba-strukoviny?article=384. Accessed on 23 January 2019.
[6] Černý, I., Pačuta, V., Ernst, D., Gažo, J. (2017): Dependence of yield formation and sugar content on sugar beet varieties and annual agroecological conditionns. – Listy cukrovarnické a řepařské 133(12): 379-384.
[7] Dobrovodská, M., Kanka, R., David, S., Kolár, J., Špulerová, J., Štefunková, D., Mojses, M., Petrovič, F., Krištín, A., Stašiov, S., Halada, Ľ., Gajdoš, P. (2019): Assessment of the biocultural value of traditional agricultural landscape on a plot-by-plot level: case studies from Slovakia. – Biodiversity and Conservation 28(10): 2615-2645.
[8] Fazekašová, D., Bobuľovská, L. (2012): Soil organisms as an Indicator of Quality and Environmental Stress in the Soil Ecosystem. – Environment 46(2): 103-106.
[9] Filho, L. C., Filho, O. K., Baretta, D., Tanaka, C. A., Sonsa, J. P. (2013): Collembola Community Structure as a Tool to Assess Land Use Effects on Soil Quality. – Rev. Bras. Cienc. Solo 40: 1-17.
[10] Fox, C. A., Miller, J. J., Joschko, M., Drury, C. F., Reynolds, W. D. (2017): Earthworm population dynamics as a consequence of long-term and recently imposed tillage in a clay loam soil. – Can. J. Soil. Sci 97(4): 561-579.
[11] Gormsen, D., Hedlung, K., Wang, H. F. (2006): Diversity of soil mite communities when managing plant communities on set-aside arable land. – Aplied Soil Ecology 31(1-2): 147-158.
[12] Hammer, Q. (2015): Past Paleontological Statistics Version 3.05. – Reference manual [CD]. University of Oslo: Natural History Museum.
[13] Hrnčiarová, T. (2001): Ecological optimization of agricultural landscape (model area Dolná Malanta). – The Bratislava.
[14] Hůrka, K. (1996): Carabidae of the Czech and Slovak Republics. – Kabourek Zlín.
[15] Jasinski, M., Twardowski, J., Tendziagolska, E. (2016): The occurrence of soil mesofauna in organic crops. – Jour. of Research and Applications in Agricultural Engineering 61(3): 193-199.
[16] Kalivoda, H., Petrovič, F., Kalivodová, E., Kürthy, A. (2010): Influence of the landscape structure on the butterfly (Lepidoptera, Hesperioidae and Papilionidae) and bird (Aves) taxocenoses in Veľké Leváre (SW) Slovakia). – Ekologia Bratislava 29(4): 337-359.
[17] Langraf, V., Petrovičová, K., David, S., Ábelová, M., Schlarmannová, J. (2017): Body volume in ground beetles (Carabidae) reflects biotope disturbance. – Folia Oecologica 44(2): 114-120.
[18] Langraf, V., Petrovičová, K., David, S., Kanská, M., Nozdrovická, J., Schlarmannová, J. (2018): Change Phenotypic Traits in Ground Beetles (Carabidae) Reflects Biotope Disturbance in Central Europe. – J. Entomol. Res. Soc. 20(2): 119-129.
[19] Langraf, V., Petrovičová, K., David, S., Nozdrovická, J., Petrovič, F., Schlarmannová, J. (2019): The Bioindication Evaluation of Ground Beetles (Coleoptera: Carabidae) in Three Forest Biotopes in the Southern Part of Central Slovakia. – Ekologia Bratislava 38(1): 25-36.

http://www.aloki.hu ● ISSN 1589 1623 (Print) ● ISSN 1785 0037 (Online)
DOI: http://dx.doi.org/10.15666/aeer/1706_1389713908

[20] Lenoir, L., Lennartsson, T. (2010): Effects of timing of grazing on arthropod communities in semi-natural grasslands. – Journal of Insect Science 10: 33-42.
[21] Litavský, J., Stašiov, S., Svitok, M., Michalková, E., Majzlan, O., Žarnovičan, H., Fedor, P. (2018): Epigeon communities of harvestmen (Opiliones) in Panonian Basin floodplain forests: an interaction with environmental parameters. – Biologia 73(8): 753-763.
[22] Losos, B., Gulička, J., Lellák, J., Pelikán, J. (1984): Ecology of animals. – SPN Publishing, The Prague.
[23] Nietupski, M., Kosewska, A., Lemkowska, B. (2015): Grassland with calcareous gyttja soil in the Olstan Lake District as specific habitats for ground beetles (Coleoptera: Carabidae). – Baltic Journal of Coleopterology 15(1): 57-70.
[24] Pokorný, V. (2002): Book of Coleoptera. – Paseka Publishing, The Prague.
[25] Pokorný, V., Šifner, F. (2004): Book of Insecta. – Paseka Publishing, The Prague.
[26] Porhajašová, J., Noskovič, J., Babošová, M., Rakovská, A. (2012): Biodiversity of epigeic groups in conditions of growing *Salix viminalis L.* – Acta Universitatis Prešoviensis LIV(7): 5-13.
[27] Porhajašová, J., Šustek, Z., Noskovič, J., Babošová, M. (2013): The effect of application of organic fertilizers on the Dynamics of occurence of carabid species (Carabidae, Coleoptera). – Journal Central European Agriculture 14(2): 251-272.
[28] Querner, P., Erhard, Ch., Gusenleitner, J. (2008): Collembolla (Insecta). – Checklisten der Fauna Österreichischen Akademie der Wissenschaften, Wien 24: 1-26.
[29] Swaminathan, R. (2014): Ground Beetles (Coleoptera: Carabidae): Their Potential as Bio-agents in Agroecosystems. – Basic and Applied Aspects of Biopesticides 12: 225-233.
[30] Tieman, L. K., Grandy, A. S., Atkinson, E. E., Marin-Spiotta, E., McDaniel, M. D. (2015): Crop rotational diversity enhances belowground communities and functions in a agroecosystem. – Ecology Letters 18(8): 761-771.
[31] Vician, V., Stašiov, S., Kočík, K., Hazuchová, L. (2011): The structure of community Coeloptera: Carabidae on various farmed areas in the Podpoľanie region and their indication. – Acta Facultatis Ecologiae 24-25: 123-131.
[32] Vician, V., Svitok, M., Kočík, K., Stašiov, S. (2015): The influence of agricultural management on the structure of ground beetle (Coleoptera: Carabidae) assemblages. – Biologia 70(2): 240-252.
[33] Vician, V., Svitok, M., Michalková, E., Lukáčik, I., Stašiov, S. (2018): Influence of tree species and soil properties on ground beetle (Coleoptera: Carabidae) communities. – Acta Oecologica 91: 120-126.

http://www.aloki.hu ● ISSN 1589 1623 (Print) ● ISSN 1785 0037 (Online)
DOI: http://dx.doi.org/10.15666/aeer/1706_1389713908

ANALYZING THE IMPACTS OF SOCIOECONOMIC FACTORS ON NUTRITIONAL DIET IN PAKISTAN USING COMPOSITIONAL DATA ANALYSIS (CODA)

AMJAD, M.* – AKBAR, M. – KHAN, M. S. R. – NOOR, F. – ULLAH, H.

Department of Mathematics and Statistics, Faculty of Basic and Applied Sciences, International Islamic University, 44000 Islamabad, Pakistan

**Corresponding author*
e-mail: amjaduaar.bkk@gmail.com; phone: +92-333-890-4769

(Received 22nd May 2019; accepted 9th Sep 2019)

Abstract. This study is conducted to analyze the effect of socioeconomic factors on households' diet pattern w.r.t shares of calorie intakes from protein, fat and carbohydrate in Pakistan. Cross sectional data are taken from a national level survey i.e. Household Integrated Income and Consumption survey (HIICS) 2015-2016. Compositional Data analysis (CODA) regression approach is followed to compare the effects of explanatory variables on share of calorie intakes from protein versus share of calorie intakes from fat and share of calories intake from carbohydrate versus shares of calories intake from protein and fat. Moreover, elasticities of macronutrient shares from household income, household size, dependency ratio and wealth index are also computed. The model's results explore that rising households' income causes an increase in fat consumption and a decrease in protein and carbohydrate consumption. The household size and rural areas are important factors increasing fat consumption to a higher degree than protein and carbohydrate consumption. Our findings matched with existing literature and they have the benefit to help the substitution effects between macronutrients in the setting of nutrition change. This study is very helpful to know the importance of healthy dietary balance and to avoid the non-communicable diseases as obesity and heart diseases at household level of Pakistan.
Keywords: *calories, macronutrient shares, elasticity, ternary diagram, regression model*

Introduction

Macronutrients are required in diet, as each makes energetic functions in the body by providing energy (calories). Each of the macronutrients, i.e. carbohydrate, protein, and fat, has different properties that affect health but all are considered source of energy. The optimum stability of their dietary contribution has been a topic of discussion for many years (Carreiro et al., 2016) and unbalance in the proportion of these macronutrients may increase the risk of chronic diseases and obesity. For a given calorie intakes, if one macronutrient share increases, then one or more other macronutrient shares decrease definitely. For instance, a diet containing high fat would be low in carbohydrate or protein. Hence, unbalance shares of macronutrients consumption may adversely affect Body mass index (BMI) (Miller et al., 1990; Ahluwalia et al., 2009; Austin et al., 2011 and Satia et al., 2002). Furthermore, the acceptable macronutrient distribution ranges (AMDR) for healthy adults are given as 20–35%, 45–65%, 10–35% shares of energy from fat, carbohydrate and protein respectively to minimize the risk of coronary heart diseases, diabetes, and obesity recommended by the Food and Nutrition Board of the Institute of Medicine (Institute of Medicine, 2005). The risk of non-communicable diseases (NCD) may increase when the shares of these macronutrients are out of these acceptable rages. Overall, the NCD contributed 63% of the total 57 million deaths in 2008 and nearly 80% of these NCD related deaths occurred in developing countries (WHO, 2010). Previous studies show

http://www.aloki.hu ● ISSN 1589 1623 (Print) ● ISSN 1785 0037 (Online)
DOI: http://dx.doi.org/10.15666/aeer/1706_1390913929

that obesity is an important cause of NCD and can lead to severe cardiovascular morbidity and early deaths. The prevalence of obesity has increased globally during the past 30 years due to macronutrients malnutrition (Swinburn et al., 2011 and WHO, 2018). As a result of imbalance diet in term of macronutrients shares, overweight and obesity are increasing in developing countries. Protein-energy malnutrition is the most significant risk factor for diseases and deaths which particularly affects hundreds of millions of pregnant women and young children (Olaf and Michael, 2005). Low-carbohydrate, high-protein diets can be a better choice for weight loss, increased satiety, and improved metabolic parameters (Kushner and Doerfler, 2008).

Pakistan is among the countries with high prevalence of obesity (Tanzil and Jamali, 2016). Findings of Satti and Khalid (2019) show that overweight and obesity prevalence is 21% and 9% respectively in Pakistani adults. According to WHO, 46% of all deaths in 2008 with estimated deaths in males and females of around 380,000 and 300,000 respectively are due to NCD in Pakistan (WHO, 2013). According to estimates of global disease burden research, Pakistan ranks 9th among 188 countries in obese population (Ng, et al., 2014) and 40% of reproductive age Pakistani women are either overweight or obese (NIPS and ICF, 2013). Hence, health situation is alarming in Pakistan due to rising obesity and all other Non-communicable diseases. To overcome this alarming situation, public health policy may be helpful for balancing of diet and of macronutrient shares. It requires to understand the factors affecting diet pattern in term of macronutrient shares at household level in Pakistan.

In order to estimate the association between nutrient intakes and socioeconomic factors, various regression models are frequently used with the different regressors and the different nutrients and calories intakes as response variables (Liaskos and Lazaridis, 2003; You et al., 2016; Akerele et al., 2014; Iyangbe and Orewa, 2009; Zhou, et al., 2018 and Trinh, et al., 2018). All the previous studies in Pakistan explain the importance of macronutrients consumption or volumes from food items. For example (Shabnam et al., 2016) show that the calorie and macronutrient consumption at household level depend upon food prices in Pakistan. Khattak and Khan (2009) explore imbalance energy intakes w.r.t macronutrients in female students of Pakistan. Shakoor et al., (2017) show that the majority of Pakistani female students had low consumption of macronutrients than recommended levels except fat.

To the best of authors' knowledge, no study has been conducted to analyze the factors affecting unbalance diet pattern in term of macronutrients shares at household level in Pakistan. Hence, major objective of this study is to fill this gap in literature by analyzing the impact of some important factors on macronutrient shares in energy intake at household level in Pakistan. This study is conducted to fill this research gap in the literature of food security in Pakistan. Moreover, Compositional data analysis (CODA) is considered instead of conventional regression inference to analyze macronutrients shares as the response variable and to avoid the problem of unbalance diet. CODA is known as a well traditional area of statistics with various areas of application, such as geology or economics (Egozcue et al., 2011; Pawlowsky-Glahn et al., 2015). This CODA technique has been applied recently in the field of nutritional and medical epidemiology (Dumuid et al., 2018; Leite, 2016; Mert et al., 2018). Hence, CODA technique is considered to analyze the phenomenon under consideration. Rest of the article contains material and methods, results, discussion and concluding remarks in the following sections.

http://www.aloki.hu ● ISSN 1589 1623 (Print) ● ISSN 1785 0037 (Online)
DOI: http://dx.doi.org/10.15666/aeer/1706_1390913929

Materials and methods

Materials and methods consists of three sub-sections, i.e. theoretical framework and specification of model, data and description of variables, and methodology of analysis.

Theoretical framework and model's specification

To investigate the impact of socio-economic factors and households characteristics on the Nutrition status or macronutrients intake follows the conceptual frame work (world food program, 2012) of food and nutrition security at household level which is the extension of UNICEF (1991) and Smith and Haddad (2000). This conceptual frame work is the composition of three main layers of causes, i.e. immediate causes, underlying causes and basic causes and each comprises of different factors. The factors at basic causes affect the factors at underlying causes which in turn influence the factors at immediate causes. Our response variable is macronutrient intakes which belongs to immediate level causes whereas the explanatory variables are taken from other two layers of causes in the conceptual frame work. Thus, the theoretical model of macronutrients shares is specified as follows:

$$M_i = \beta_0 + \beta' X' + \varepsilon_i \quad \text{(Eq.1)}$$

where M_i shows the shares of macronutrients from total energy intakes of ith households, β_0 represents constant term, β' is the vector of slopes and X' is vector of explanatory variables while ε_i is the error term.

Data and description of variables

This study uses data taken from Household integrated income and consumption survey (HIICS) 2015-2016 published by Pakistan Bureau of Statistics. This survey was collected in 2015-2016 by applying two stage stratified random sampling technique. Its sample comprises of 24238 households from all the four provinces of Pakistan. However, our sample size for this study is 14948 households due to non-availability of data regarding some variables. In this survey quantities of 72 food items are given from different food groups like meat, fish, milk, cheese, eggs, fresh fruits, dry fruits, vegetables (fresh/chilled/frozen/dried), sugar, jam, honey, chocolate & confectionery, condiments and spices (whole and powder), non-alcoholic beverages, readymade food eaten out of home, public places, offices, bread & cereals, and edible oils.

We calculate total calorie intake (in Kcal), protein and fat intakes (in grams) per day from all consumed food items for each household using Food Consumption table for Pakistan (Khan et al., 2001). The amount of protein and fat in grams are converted into calories for each household by multiplying 4 and 9 respectively (Trinh et al., 2018). Then we compute per capita calorie consumption (namely Cal_p), per capita volume of calories calculated from protein V_P, and per capita volume of calories calculated from fat V_F as follows. An per capita calorie consumption (Cal_p) is calculated by dividing the total consumption of calories per day by an adult equivalence conversion factor (AE) computed for each household. An adult equivalence conversion factor is the ratio between calorie requirement of individual according to age and the estimated adult reference value (Claro, et al., 2010). Similarly, per capita calories from fat and protein are computed for each household using the above procedure. Three types of macronutrients (Fat, protein and carbohydrate) are the source of total calorie intakes per capita, so the following

http://www.aloki.hu ● ISSN 1589 1623 (Print) ● ISSN 1785 0037 (Online)
DOI: http://dx.doi.org/10.15666/aeer/1706_1390913929

relation exist between total per capita calorie intakes and macronutrients which help to calculate the per capita volume of calorie intake calculated from carbohydrate V_C

$$1 \text{ gram protein} = 4 \text{ kcal}$$

$$1 \text{ gram Fat} = 9 \text{ kcal}$$

$$V_p = 4 \times \text{Protein in grams}$$

$$V_F = 9 \times \text{Fat in grams}$$

$$Cal_p = V_F + V_p + V_C$$

$$V_C = Cal_p - V_p - V_F$$

$$Cal_p = \frac{\text{Total calorie intakes of household per day}}{AE}$$

$$AE = \frac{\text{Requirement of individual according to age}}{Adult\ reference\ value}$$

The shares of macronutrient S_F, S_P and S_C are defined as proportion of calorie from fat, protein and carbohydrate respectively as follows.

$$S_F = \frac{V_F}{Cal_F}, S_P = \frac{V_P}{Cal_F}, S_C = 1 - S_F - S_P$$

Some socioeconomic and demographic factors are taken as explanatory variables on the basis of the theoretical framework while considering availability of data. These explanatory variables include residential status, marital status of household head, paid employment dummies of father, mother and couple, Provinces dummies of Punjab, Sindh, Khyber Pakhtunkhwa (KPK) and Baluchistan, household head age, family size, dependency Ratios, dummies of livestock, own cultivation and Benazir income support programme (BISP), per capita income and education dummies of father and mother like no education, primary education, middle education and high education. The description of all the variables used by the study is given in *Table 1* whereas *Table 2* presents descriptive statistics of the variables.

Table 2 shows that the total number of calories per capita is 2451.5 calories which mean that, while households of Pakistan fulfil their calories requirement according to FAO (2013) is 2440 calories per person. Descriptive results show that 626.7, 283.66 and 1541.2 calories come from the Fat, protein and carbohydrate respectively. The sum of the volumes of calories from these three macronutrients equal to 2451.5 calories. The shares of calories from Fat, protein and carbohydrate are 25.9%, 11.4%, and 62.7% respectively and *Table 2* also represents the percentages of all categories of Categorical variables which included for the analysis.

Methodology of analysis

Methodology of analysis consists of two sub sections i.e. introduction to CODA, and compositional regression model to explain macronutrient shares.

http://www.aloki.hu ● ISSN 1589 1623 (Print) ● ISSN 1785 0037 (Online)
DOI: http://dx.doi.org/10.15666/aeer/1706_1390913929

Table 1. *Description of the variables*

Notations	Variables label	Description	Notations	Variables label	Description
Cal_p	Calories volume	Calories per capita	EM_i^c	Couple paid employment	Couple paid employment = 1 & zero otherwise
V_F	Fat volume	Number of calories from fat	V_P	Protein volume	Number of calories from protein
S_F	Fat shares	Shares of calories from fat	V_C	Carbohydrate volume	Number of calories from carbohydrate
S_C	Carbohydrate shares	Shares of calories from carbohydrate	S_P	Protein shares	Shares of calories from protein
$Size_i$	Household size	Number of family members in the household	EM_i^m	Maternal paid employment	Mother paid employment = 1 & zero otherwise
I_i	Monthly income of household	Total monthly income in rupees	EM_i^p	Paternal paid employment	Father paid employment = 1 & zero otherwise
Res_i	Residential status	Rural = 1 & zero otherwise	E_i^{mp}	Maternal primary education	Mother primary education = 1 & zero otherwise
Age_i^h	Age of household head	HH age in years	E_i^{mm}	Maternal middle education	Mother middle education = 1 & zero otherwise
Mar_i^H	HH marital status	HH married = 1 & zero otherwise	E_i^{mh}	Maternal high education	Mother high education = 1 & zero otherwise
L_i	Ownership of livestock	Household's ownership of livestock = 1& zero otherwise	E_i^{pp}	Paternal primary education	Paternal primary education = 1 & zero otherwise
P_i^{kp}	KPK origin	Household's origin of KPK = 1 & zero otherwise	E_i^{pm}	Paternal middle education	Paternal middle education = 1 & zero otherwise
P_i^p	Punjab origin	Punjab origin = 1 & zero otherwise	E_i^{ph}	Paternal high education	Paternal high education = 1 & zero otherwise
P_i^s	Sindh origin	Sindh origin = 1 & zero otherwise	W_i	Wealth index	Wealth index of households
C_i	Households' cultivation of agricultural land	Household involve in cultivation = 1 & zero otherwise	DR_i	Dependency ratio	Dependency ratio of households

http://www.aloki.hu ● ISSN 1589 1623 (Print) ● ISSN 1785 0037 (Online)
DOI: http://dx.doi.org/10.15666/aeer/1706_1390913929

Table 2. *Descriptive statistics of variables*

Variables	Description	Mean/(SD)/Percentage
Cal	Number of calories per capita	2451.5 (900.43)
V_F	Number of calories from fat	626.7(281.8)
V_P	Number of calories from protein	283.6(121.6)
V_C	Number of calories from carbohydrate	1541.1(630.5)
S_F	Shares of calories from fat	25.9% (8.1%)
S_P	Shares of calories from protein	11.4% (1.8%)
S_C	Shares of calories from carbohydrate	62.7% (8.7%)
Res_i	Residential status 0 = Urban 1 = Rural	 74.8% 25.2%
Mar_i^H	Marital status of household head 0 = Unmarried 1 = Married	 10.1% 89.9%
L_i	Livestock 0 = No 1 = Yes	 99% 1%
C_i	Own cultivation 0 = No 1 = Yes	 92.47% 7.53%
EM_i^p	Paternal paid employment 0 = No 1 = Yes	 40.23% 59.77%
EM_i^M	Maternal paid employment 0 = No 1 = Yes	 91.13% 8.87%
EM_i^C	Couple paid employment 0 = No 1 = Yes	 95.54% 5.46%
P_i	Province 0 = Baluchistan 1 = Punjab 2 = Sindh 3 = KPK	 8.7% 45.24% 27.05% 19.01%
E_i^P	Paternal education 0 = No education 1 = Primary education 2 = Middle education 3 = High education	 7.59% 37.42% 51.73% 3.26%
E_i^M	Maternal education 0 = No education 1 = Primary education 2 = Middle education 3 = High education	 46.89% 24.19% 27.34% 1.58%

http://www.aloki.hu ● ISSN 1589 1623 (Print) ● ISSN 1785 0037 (Online)
DOI: http://dx.doi.org/10.15666/aeer/1706_1390913929

Introduction to CODA

We can not apply traditional methods of regression when the dependent or independent variable consists of a vector of shares (Aitchison, 1982; Pawlowsky-Glahn, et al., 2015) because these shares are positive real numbers and carry relative information with constant sum (Chen et al., 2017). In the previous studies, many types of models are used to apply regression with shares (Morais et al., 2018). When a vector of shares (e.g. the shares of macronutrients) is the response variable and other regressors are traditional quantitative or qualitative variables, a proposed model known as CODA (compositional data analysis) is considered as the valid modelling technique (Trinh et al., 2018, Egozcue et al., 2011, Pawlowsky-Glahn et al., 2015, Aitchison, 1986). This model depends on a log-ratio transformation of shares. In the simplex space S^D, a composition S of D shares can be denoted as

$$S^D = \{S = (S_1, S_2, \ldots\ldots\ldots\ldots, S_D)' = S_j > 0, j = 1, \ldots. D; \sum_{j=1}^{D} S_j = 1\}$$

It is interesting to know that if the total sum of these fitted shares equal to one, then we cannot apply classical regression models directly. These shares are therefore converted using the transformation of an isometric log-ratio (ILR) (Egozcue et al., 2003) (for example) in D-1 coordinates which can be denoted in the classical Euclidean space so that the linear regression models can be applied separately to the D-1 coordinates. These coordinates of ILR are explained as follows (Trinh et al., 2018):

$$ilr\,(S) = W'\,log\,(S) = S^* = (S^*_1\ ,\ldots\ldots,\ S^*_{D-1})'$$

where W defined as the $D \times (D-1)$ contrast matrix (Chen et al., 2017) which helps the forecasting of shares on the orthogonal basis of S^D. For instance, we have D = 3, it is possible to use the following contrast matrix (this matrix used by the function "ilr" in R package "Composition"):

$$W = \begin{bmatrix} -\frac{1}{\sqrt{6}} & -\frac{1}{\sqrt{2}} \\ -\frac{1}{\sqrt{6}} & \frac{1}{\sqrt{2}} \\ \sqrt{\frac{2}{3}} & 0 \end{bmatrix}$$

Guiding to the following two ILR coordinates of $S = (S_1, S_2, S_3)$:

$$S^*_1 = \frac{1}{\sqrt{2}}\, log \frac{S_2}{S_1}$$

$$S^*_2 = \frac{2}{\sqrt{6}}\, log \frac{S_3}{\sqrt{S_2 S_1}}$$

In this shape, the first ILR coordinate S^*_1 protein shares have all the relative data of S_2 compared to the fat shares. Similarly, the second ILR coordinate S^*_2 carbohydrate shares have all the data of S_3 compared to the geometric mean respectively of the remaining protein and fat shares (Muller et al., 2016). At the end, with the help of the inverse

http://www.aloki.hu ● ISSN 1589 1623 (Print) ● ISSN 1785 0037 (Online)
DOI: http://dx.doi.org/10.15666/aeer/1706_1390913929

transformation to go back to the simplex to interpret the shares model. This inverse transformation is defined as

$$ilr^{-1}(S^*) = C(exp(WS^*))'.$$

Here, C(.) denote the closure operation which permitting to go from a vector of volumes V to a vector of shares S

$$C(V_1, \ldots, V_D)' = \left(\frac{V_1}{\sum_{j=1}^{D} v_j}, \ldots\ldots, \frac{V_D}{\sum_{j=1}^{D} v_j}\right)' = (S_1, \ldots, S_D)'.$$

Compositional regression model for macronutrient shares

We want to check the impact of socioeconomic factors and household characteristics of Pakistani households on macronutrient composition. *Equation 1* can be written as an adapted compositional regression model as follows (Trinh et al., 2018):

$$\begin{gathered} S_i = a_0 \bigoplus_{k=1}^{K} (Z_{ki}) \odot b_k \oplus \epsilon_i \\ S_i = a_0 \oplus Age_i^h \odot b_1 \oplus Size_i \odot b_2 \oplus Res_i \odot b_3 \oplus Mar_i^H \odot b_4 \\ \oplus P_i^{kp} \odot b_5 \oplus P_i^p \odot b_6 \oplus P_i^s \odot b_7 \oplus I_i \odot b_8 \oplus EM_i^c \odot b_9 \oplus EM_i^m \odot b_{10} \oplus EM_i^p \odot b_{11} \\ \oplus E_i^{mp} \odot b_{12} \oplus E_i^{mm} \odot b_{13} \oplus E_i^{mh} \odot b_{14} \oplus E_i^{pp} \odot b_{15} \oplus E_i^{pm} \odot b_{16} \oplus E_i^{ph} \odot b_{17} \oplus \\ L_i \odot b_{18} \oplus DR_i \odot b_{19} \oplus W_i \odot b_{20} \oplus C_i \odot b_{21} \epsilon_i \end{gathered} \quad \text{(Eq.2)}$$

In *Equation 2,* $S = (S_F, S_P, S_C)'$ i represents the ith households and $\boldsymbol{Z_k}$ are classical regressors as $Res_i, Mar_i^H, P_i^{kp}, P_i^p, P_i^s, EM_i^c, EM_i^m, EM_i^p, E_i^{mp}, E_i^{mm}, E_i^{mh}, E_i^{pp}, E_i^{pm}, E_i^{ph}, L_i,$ *and* C_i are the dummy variables representing residential status, household head marital status, Khyber Pakhtunkhwa origin, Punjab origin, Sindh origin, couple paid employment, maternal paid employment, paternal paid employment, maternal primary, middle, and high education, paternal primary, middle, and high education, livestock and own cultivation respectively. $Age_i^h, Age_i^{sh}, Size_i, Size_i^2 I_i, DR_i,$ *and* W_i are the variables representing household head age, household head age square, household size, household size square, household total income, dependency ratio and wealth index respectively. Detailed explanation of the variables is provided in *Table 1*.

As in Dumuid et al. (2018), Muller et al. (2016) and Nguyen et al. (2018) for the fitting and interpretation of the model in *Equation 2,* we required to run $D - 1 = 2$ ordinary linear regression model, i.e. one for every ILR coordinates of S: S^*_1 and S^*_2 for each period j = 1,2 (Egozcue et al., 2012).

$$\begin{gathered} S^*_{j,i} = a_{0j}{}^* + \sum_{k=1}^{K} b^*_{j,k} X_{ki} \check{n}^*_{j,i} \\ S^*_{j,i} = a_{0j}{}^* + b^*_{j,1} Age_i^h + b^*_{j,2} Size_i + b^*_{j,3} Res_i + b^*_{j,4} Mar_i^H + \\ b^*_{j,5} P_i^{kp} + b^*_{j,6} P_i^P + b^*_{j,7} P_i^S + b^*_{j,8} I_i + b^*_{j,9} EM_i^c + b^*_{j,10} EM_i^m + \\ b^*_{j,11} EM_i^p + b^*_{j,12} E_i^{mp} + b^*_{j,13} E_i^{mm} + b^*_{j,14} E_i^{mh} + b^*_{j,15} E_i^{pp} + b^*_{j,16} E_i^{pm} + \\ b^*_{j,17} E_i^{ph} + b^*_{j,18} L_i + b^*_{j,19} DR_i + b^*_{j,20} W_i + b^*_{j,21} C_i + \check{n}^*_{j,i} \end{gathered} \quad \text{(Eq.3)}$$

http://www.aloki.hu ● ISSN 1589 1623 (Print) ● ISSN 1785 0037 (Online)
DOI: http://dx.doi.org/10.15666/aeer/1706_1390913929

where $a_{0j}{}^{*}$, $b^{*}{}_{j,k}$, $\epsilon^{*}{}_{j}$ are the j^{th} ILR coordinates of a_0, b_k, ϵ.

Since we fit the two transformed models in *Equation 3* using the method of ordinary least square (OLS) and ϵ^{*} is assumed to follow normal distribution. The model's parameters calculation in the simplex and *Equation 2* can be obtained by using inverse transformation from the transformed model in *Equation 3* computed parameters. For example:

$$\hat{b}_2 = C(exp(W\,\hat{b}^{*}_2))', where\ \hat{b}_2 = (\hat{b}^{*}_{1,2}, \hat{b}^{*}_{2,2})'$$

All parameters are estimated in compositional regression model using the method of OLS. The value of compositional models can be assessed to the share data, called adjusted "R^{2}" (Van den Boogaart and Tolosana-Delgado, 2013). The adjusted R-squared value shows that our compositional models explain about 11.87% and 12.54% of the total compositional data variability, respectively. To estimate the parameters of compositional regression model, the package " Compositions" in R language has been used. The R package " Plotly" used to make ternary diagrams.

Results

Results consist of three sub sections i.e. comparison of urban and rural households, results of compositional regression model and Elasticities of macronutrients shares.

Comparison of urban and rural households

Figure 1 displays that the overall households in our sample have on the average 2283 calories per capita per day which looks nearly equal to the requirement of (FAO). But the rural households consume on the average 2657.56 calories which is higher than urban households as well as overall average of households which is 2196.15. We can see the clearly difference between the macronutrients shares in calories for both regions.

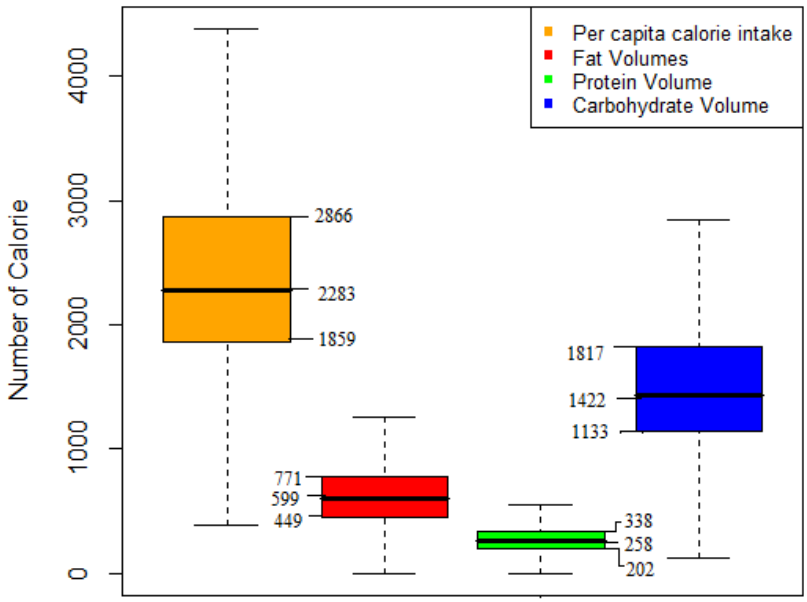

Figure 1. *Per capita calorie intake and volume of macronutrients using overall households*

http://www.aloki.hu ● ISSN 1589 1623 (Print) ● ISSN 1785 0037 (Online)
DOI: http://dx.doi.org/10.15666/aeer/1706_1390913929

Figures 2 and *3* show the comparison of urban and rural site of per capita calorie intake and volume of macronutrient shares using box plot which bases on lower quartile, median and upper quartile. The rural region has the high median i.e. 2627.56 per capita calorie than urban region i.e. 2196.15 calories. Lower and upper quartiles of the rural households of calories are 2082.71 and 3370.31 respectively which are more than urban households i.e. 1807.82 and 2697.25 respectively. Similarly, all three macronutrient shares of rural site having greater values of lower, median and upper quartile compared to the urban households. According to *Table 3,* it is clear to see that there is significant difference between all variables of urban and rural areas.

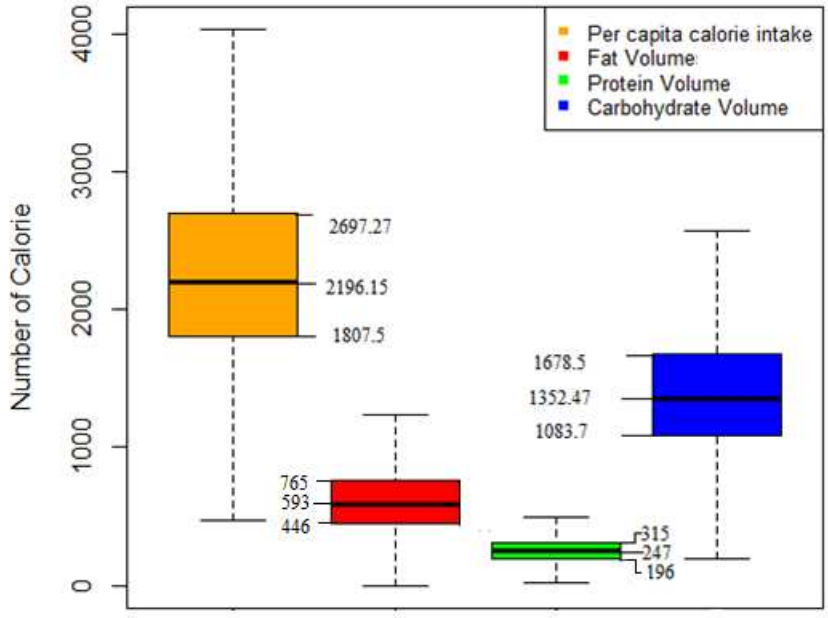

Figure 2. *Per capita calorie intake and volume of macronutrients using urban site*

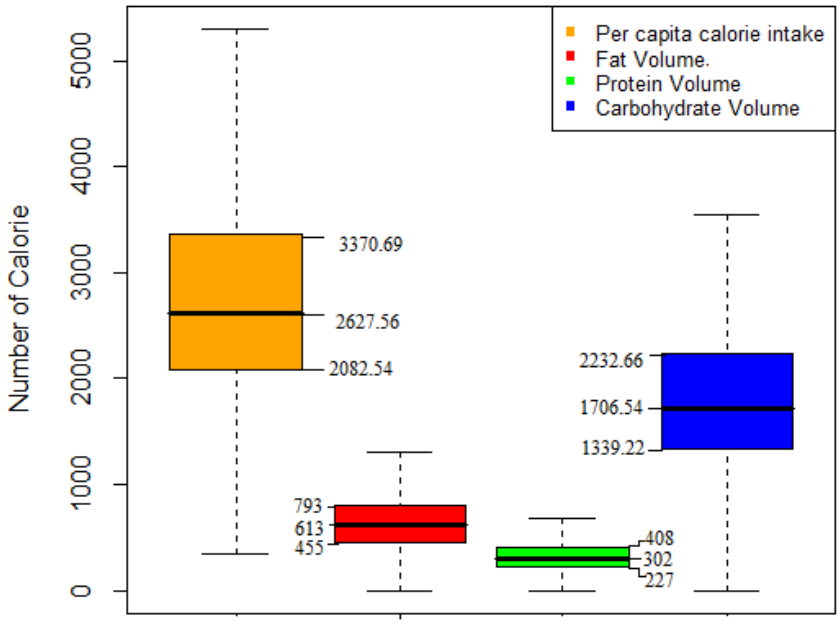

Figure 3. *Per capita calorie intake and volume of macronutrients using rural site*

http://www.aloki.hu ● ISSN 1589 1623 (Print) ● ISSN 1785 0037 (Online)
DOI: http://dx.doi.org/10.15666/aeer/1706_1390913929

Table 3. *Comparison of means using unpaired t test*

Variables	Region	Mean	Standard deviation	95% confidence interval	t-value	P-value
Per capita calorie intake	Urban	2836.93	1079.13	2802.4-2871.4	26.94	0.0000
	Rural	2321.813	790.68	2307.1-2336.4		
Calories from fat	Urban	639.31	288.74	630.1-648.5	3.12	0.0018
	Rural	622.42	279.30	617.2-627.6		
Calories from protein	Urban	331.41	144.65	326.7-336.0	24.84	0.0000
	Rural	267.52	108.19	265.5-269.5		
Calories from carbohydrate	Urban	1866.1	764.9	1841.7-1890.6	32.26	0.0000
	Rural	1431.8	535.9	1421.9-1441.7		

H_0 = there is no difference between means, versus H_A = there is difference between means

Figure 4 represents the tri plot of three macronutrients shares in calories for urban households. This figure shows that most of the urban households have more than 30% shares of carbohydrate, but a few have 40% or below. According to this ternary diagram most of the urban households have less than 20% shares of protein in calories. It can be seen that most urban families have less than 60% shares of fat in calories. *Figure 5* shows the ternary plot of macronutrient shares for rural households and this represents that all rural households have more than 40% shares of carbohydrate and less than 20% shares of protein. All households in the rural region have less than 60% shares of fat in calories. Moreover, t test is employed to test the difference between means of calories intake, shares of calories intake from fat, protein and carbohydrate assuming that there are two independent samples consisting of rural and urban households. The results are reported in *Table 3*. All the t statistics are significant which shows that there is significant difference between rural and urban households w.r.t energy intake from the three macronutrients.

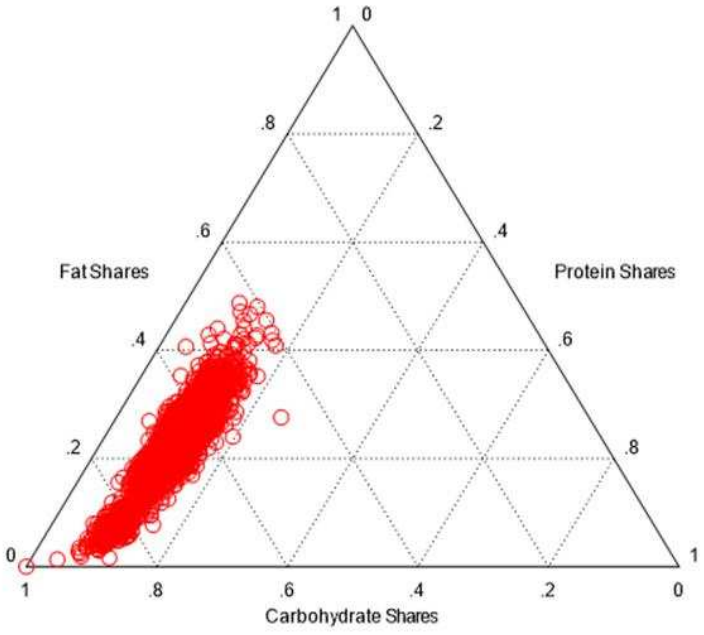

Figure 4. *Ternary diagram of urban site*

http://www.aloki.hu ● ISSN 1589 1623 (Print) ● ISSN 1785 0037 (Online)
DOI: http://dx.doi.org/10.15666/aeer/1706_1390913929

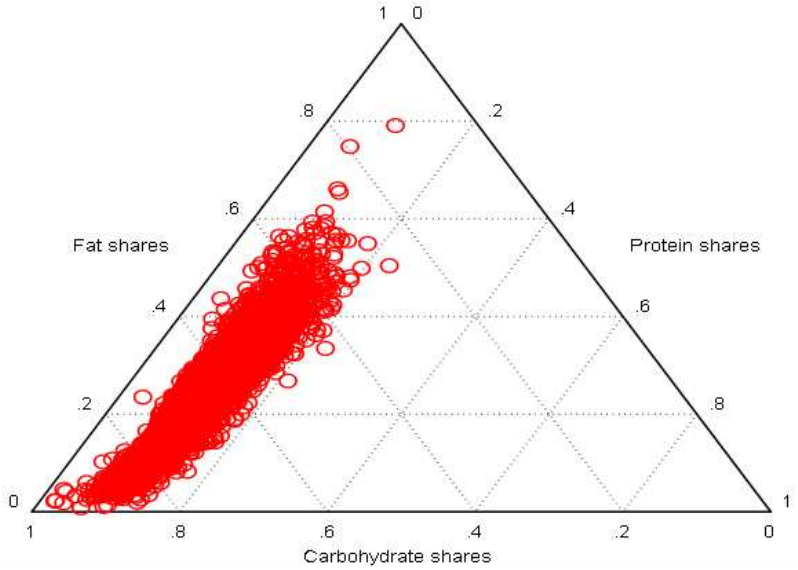

Figure 5. *Ternary diagram of rural site*

Compositional regression model results

We now fit a CODA regression model describing the impacts of socioeconomic factors on macronutrients shares using estimation method of OLS. The First isometric log ratio (ILR) coordinate compares protein against fat shares, while second ILR coordinate compares carbohydrate versus geometric mean of fat and protein shares. *Tables 4* and 5 describe the parameters of the compositional model in ILR coordinates. The two ILR coordinates treated as response variables and associated with explanatory variables.

Estimation results given in *Tables 4* and *5* are interpreted as (Trinh et al., 2018 and Dumuid et al., 2018). *Table 4* shows the coefficients of first coordinate consisting of protein versus fat shares. Estimate of income shows that 1% rise of income for a given household causes decline of the relative dominance of protein versus fat share ($e^{0.0798} = 1.083$) approximately by 0.083%. This analysis shows that rising household's income is not helpful to improve protein shares in calories than fat shares. Similarly, an increase of one more year of household head age, the relative dominance of protein share ($e^{0.00158} = 1.0058$) decreases approximate by 0.0058%. The impact of household size and dependency ratio on the protein share as 1 more person increase of family member and dependency ratio then relative dominance of this first ILR coordinate ($e^{0.0105} = 1.0105$ *and* $e^{0.1148} = 1.13$) increase approximately 0.0105% and 0.13% respectively to fat share. These results are in line with Trinh et al., (2018).

The first ILR coordinate is explained by residential status, hence $Z^{\wedge(\text{protein})^*}{}_1 = 1.56$ is the fitted value of the coordinate $Z^{(\text{protein})^*}{}_1$ for rural while $Z^{\wedge(\text{protein})^*}{}_1 = 1.7696$ for urban. It means that the relative dominance of protein in the composition response is ($e^{1.56} = 4.75$) for rural and ($e^{1.7696} = 5.8685$) for urban. Further, it can be conclude that the relative dominance of protein for rural households is $e^{0.0628} = 1.0648$ times greater than for urban households. Coefficient estimate of marital status of household head shows that a household with married head compared to a household with unmarried head would likely to have more share of protein versus fat. The relative dominance of protein shares for province Sindh is less than other provinces and dominance of protein shares for

http://www.aloki.hu ● ISSN 1589 1623 (Print) ● ISSN 1785 0037 (Online)
DOI: http://dx.doi.org/10.15666/aeer/1706_1390913929

Khyber Pakhtunkhwa is 1.064 times greater than for other provinces compared to fat shares. Hence, the households of KPK compared to other households are likely to have more shares of calories obtained from protein than fat. Similarly, the relative domination of protein shares versus fat share for the households operating agricultural land and the households having livestock are 1.07 and 1.06 times greater than the households who are not operating agricultural land and the households who have not livestock. All educational dummies of maternal and paternal may not be helpful to improve protein shares compared to fat shares in the balanced diet. The households with education of maternal and paternal may increase their fat shares in the diet.

Table 4. *Results of compositional regression model in ILR coordinate for protein versus fat shares*

$S^*_1 = \frac{1}{\sqrt{2}} log \frac{S_P}{S_F}$ (protein versus fat shares) is response variable				
Variables	**Description**	**Coefficients**	**S. E.**	**P-value**
Intercept		-0.22260	0.04268	0.0000 ***
Age_i^h	Age of household head	-0.00158	0.00019	0.0000 ***
$Size_i$	Household size	0.01058	0.00087	0.0000 ***
Res_i	Residential status	0.06282	0.00563	0.0000 ***
Mar_i^H	HH marital status	0.02804	0.00773	0.0002 ***
P_i^{kp}	KPK province	0.04640	0.00887	0.0000 ***
P_i^P	Punjab province	0.01065	0.00816	0.19193
P_i^S	Sindh province	-0.02352	0.00850	0.00574 ***
I_i	Monthly income of household	-0.07980	0.00847	0.0000 ***
EM_i^c	Couple paid employment	0.01760	0.01486	0.23630
EM_i^m	Maternal paid employment	-0.01120	0.01199	0.34668
EM_i^p	Paternal paid employment	-0.00410	0.00500	0.40955
E_i^{mp}	Maternal primary education	-0.05890	0.00578	0.0000 ***
E_i^{mm}	Maternal middle education	-0.02404	0.00641	0.00018 ***
E_i^{mh}	Maternal high education	0.03182	0.02007	0.11296
E_i^{pp}	Paternal primary education	-0.00448	0.00855	0.71178
E_i^{pm}	Paternal middle education	-0.02044	0.00868	0.0185 **
E_i^{ph}	Paternal high education	-0.04422	0.01496	0.00312***
L_i	Own livestock	0.06330	0.00930	0.01578**
DR_i	Dependency ratio	0.12230	0.01107	0.0000 ***
W_i	Wealth index	0.00033	0.00160	0.83564
C_i	Own cultivation	0.12236	0.00932	0.0000 ***

Significance codes: 1% '***' 5% '**' 10%'*'

Table 5 shows the coefficients of second coordinate i.e. carbohydrate shares vs geometric mean of fat and protein shares. 1% increase of income for a given household results into decline of carbohydrate share ($e^{0.2101} = 1.2289$) approximately by 0.233 with respect to geometric mean of other fat and protein shares. The second ILR coordinate

http://www.aloki.hu ● ISSN 1589 1623 (Print) ● ISSN 1785 0037 (Online)
DOI: http://dx.doi.org/10.15666/aeer/1706_1390913929

shows that the households with high income have low proportion of carbohydrate share in calories than other shares. Household size shows positive impact while dependency ratio shows inverse impact on the relative dominance of carbohydrate share versus fat and protein share in energy intake.

Table 5. *Results of compositional regression model in ILR coordinate for carbohydrate versus other shares*

$S^*_2 = \frac{2}{\sqrt{6}} log \frac{S_C}{\sqrt{S_P S_F}}$ **(carbohydrate versus geometric mean of protein and fat shares) is response variable**				
Variables	**Description**	**Coefficients**	**S. E.**	**P-value**
Intercept		2.112	0.4588	0.0000 ***
Age_i^h	Age of household head	0.00004	0.00021	0.81611
$Size_i$	Household size	0.00779	0.00094	0.0000 ***
Res_i	Residential status	0.05770	0.00605	0.0000 ***
Mar_i^H	HH marital status	-0.00866	0.00831	0.29747
P_i^{kp}	KPK province	-0.01009	0.00952	0.28891
P_i^P	Punjab province	-0.11390	0.00878	0.0000 ***
P_i^S	Sindh province	-0.06990	0.00914	0.0000 ***
I_i	Monthly income of household	-0.21010	0.00910	0.0000 ***
EM_i^c	Couple paid employment	0.04965	0.01598	0.001887***
EM_i^m	Maternal paid employment	-0.01281	0.01290	0.32031
EM_i^p	Paternal paid employment	0.01922	0.00583	0.000354***
E_i^{mp}	Maternal primary education	0.01062	0.00622	0.18785
E_i^{mm}	Maternal middle education	0.00791	0.00689	0.25144
E_i^{mh}	Maternal high education	0.00363	0.01935	0.060564 *
E_i^{pp}	Paternal primary education	-0.01280	0.00921	0.16414
E_i^{pm}	Paternal middle education	-0.04318	0.00933	0.0000 ***
E_i^{ph}	Paternal high education	-0.06311	0.01608	0.00087***
L_i	Own livestock	0.02518	0.02958	0.39450
DR_i	Dependency ratio	-0.03912	0.01190	0.00101***
W_i	Wealth index	-0.00197	0.00172	0.25016
C_i	Own cultivation	-0.00198	0.00990	0.84250

Significance codes: 1% '***' 5% '**' 10%'*'

Coefficient estimate of residential status shows that the rural households compared to urban households have more dominance of carbohydrate share than fat and protein shares. Results show positive impact of couple paid employment and Household head paid employment on carbohydrate shares versus fat and protein shares. The relative dominance of carbohydrate share for households having couple and Household head paid employment ($e^{0.0496} = 1.05$ *and* $e^{0.0192} = 1.02$) 1.05 and 1.02 times larger than other households respectively.

http://www.aloki.hu ● ISSN 1589 1623 (Print) ● ISSN 1785 0037 (Online)
DOI: http://dx.doi.org/10.15666/aeer/1706_1390913929

In second ILR coordinates, the negative coefficients show that the dominance of carbohydrate share for Province Punjab and Sindh 1.12 and 1.07 times less than base category Baluchistan province respectively. The households which lie in the province Punjab and Sindh have less carbohydrate shares proportion in calories than base category Baluchistan. Hence these two provinces have more proportion of protein and fat shares than carbohydrate shares. The effect of educational dummy variables like middle and high education of household head on carbohydrate shares is not useful. The dominance of carbohydrate shares compares to other shares for these variables is less than households which do not have an education.

Elasticities of macronutrients shares

Elasticity is very popular tool to overcome the difficult interpretation of coefficients in ILR regression. For regressors X, the elasticity of response variable Y calculates the change rate between two values of response variable Y.

To link these findings with the existing previous studies, we also use standard classical linear regression model to explain the shares of macronutrients by same household characteristics than in the model (1) as estimated separately for each share of macronutrients using ordinary least square (OLS).

$$S_{j,i} = a_{0_j} + \sum_{k=1}^{K} \beta_{0_{j,k}} X_{ki} + \varepsilon_{j,i} \qquad for\ j = 1,2,3$$

Now elasticities of macronutrient shares define with respect to different regressors as

$$Elast\,(S_{j,i}, X_i) = \frac{\frac{\partial S_{j,i}}{S_{j,i}}}{\frac{\partial X_i}{X_i}} = \frac{\partial (S_{j,i})}{\partial (X_i)} = \beta_{j,k}$$

The elasticity is the fix term which is independent of considered households. For these households, the elasticity of the macronutrient share S_j depends on all intakes of macronutrient shares, that is households diet balance.

Elasticities of macronutrient shares relative to income, household size, dependency Ratio and wealth index are presented in *Table 6*. It is clear that fat share is the most elastic income based macronutrient. The positive change rate of 1% of household's income is linked on the average to a positive change rate of 1.15% in the shares of fat, 0.47% increase in protein share, and 0.50% decrease in carbohydrate share in the total calories consumption. Similar is the case of dependency ratio which shows that as dependency ratio increases, it causes to increase the share of fat and protein with a decline in carbohydrate share. However, wealth index shows opposite effects as these are negative for fat and protein but positive for carbohydrate. Moreover, The positive change rate of 1% of family members in the household links on average to a positive change rate of 0.0028% in the share of fat whereas it agrees to a negative rate of change of 0.000466% and 0.0008877% for protein and Carbohydrate respectively. *Figure 6* represents the box plot of income elasticities with respect to macronutrient shares. The lower quartiles of fat, protein and carbohydrate shares are 0.8086, 0.4101 and -0.5298 respectively. The median of fat, protein and carbohydrate shares are 0.9411, 0.4572, -0.4749 and upper quartiles are 1.1163, 0.5095 and -0.4295 respectively.

http://www.aloki.hu ● ISSN 1589 1623 (Print) ● ISSN 1785 0037 (Online)
DOI: http://dx.doi.org/10.15666/aeer/1706_1390913929

Table 6. *Elasticities of shares*

Shares	Income	Household size	Dependency ratio	Wealth index
Fat	1.1559	0.002804	0.00108	-0.00027
Protein	0.4692	-0.000463	0.04167	-0.000183
Carbohydrate	-0.5043	-0.00087	-0.00797	0.000101

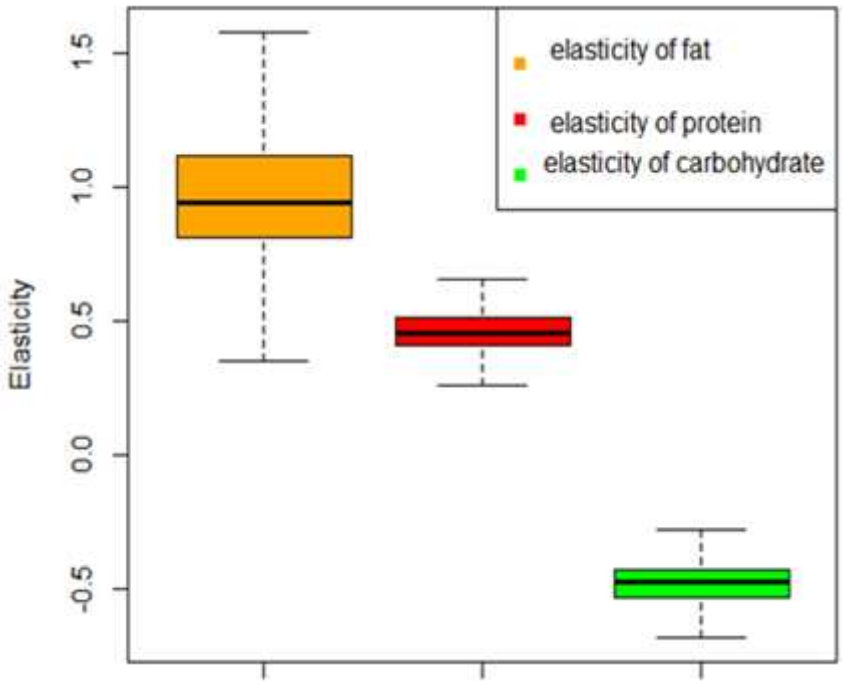

Figure 6. *Box plot of income elasticities of macronutrients consumption shares*

Discussion

Comparison of urban and rural households shows that there is significant difference in calorie intakes as well as in the volume of all macronutrients. The people residing in rural areas consume more calories than urban people because they are involved in heavy physical work in field, which need more energy. The results of income are consistent with the fact that the households with high income use more fatty foods than protein foods. These results are in line with the findings of Trinh et al., (2018) which shows that the fat shares in calories increase when food expenditure increase. This implies that rising household's income is not helpful to improve protein and carbohydrate shares in calories than fat shares. The results show that household size is directly related to more consumption of protein and carbohydrate compared to fat in diet. Most of the households live in rural areas which have more share of calories obtained from protein and carbohydrate than fat because they consume large amount of vegetables and dairy products like as milk, yogurt and cheese than urban.

The study explores that maternal and paternal education is not helpful in improving protein and carbohydrate shares of energy intake in Pakistan. It implies that education is playing an effective role to increase the shares of fat in calories at household level in Pakistan. In the case of Pakistan, knowledge related to nutrition and health practices is

http://www.aloki.hu ● ISSN 1589 1623 (Print) ● ISSN 1785 0037 (Online)
DOI: http://dx.doi.org/10.15666/aeer/1706_1390913929

not part of syllabus at school or college level and therefore, most of the educated people are not aware about the concepts related to balanced food and nutrition, the food items containing macronutrients shares in calories. It implies that education without awareness of nutrition does not affect eating pattern. Moreover, estimates of all other education dummies also support the view that education is not performing well in healthy diet in term of protein and carbohydrate shares in Pakistan. The results of household head paid employment and couple paid employment dummies are not consistent with all shares of macronutrients. It implies that the healthy diet in term of macronutrient shares do not depend on paid employment of couple and household head.

Conclusion and policy implementation

CODA model is employed to evaluate the role of some important socioeconomic and demographic factors on balancing of macronutrient shares in energy consumption at household level as a case study of Pakistan. Cross sectional data of households are taken from a national level survey data, i.e. HIICS-2015-16. Household per capita income, residential status, household size, Dependency Ratio, household head and couple paid employment, Sindh dummy, middle and high educational dummies of household head also play significant role for carbohydrate shares than other shares. We may conclude that the rising income of households increases fat consumption and decreases protein and carbohydrate consumption. It implies that significant increase of households' income level will make economic access easy which may improve fat consumption in Pakistan. It induces that policy steps to raise overall households' income level on the basis of higher economic growth rate may be the most effective tool to fulfil fat requirement in healthy diet. Household size and rural residence are key factors for increasing fat shares than other shares. Hence, effective family planning strategies and birth control programs must be implemented in order to improve fat shares. Paternal education is another important factor for increasing fat shares and the low educational level leads to a reduction in protein and carbohydrate consumption. It implies that education is not playing an important role for protein and carbohydrate shares in balance diet. It is because diet related topics are not part of syllabus in education system of Pakistan and even educated people are not aware of the importance of healthy diet. Hence, it is strongly recommended that the topics of nutrition and balance diet along with its all health related impacts must be included as part of syllabus at primary and secondary education levels in order to make awareness of educated parents as well as children. The livestock and own cultivation cause to improve protein shares. Hence, development of agricultural sector and live stock is imperative to tackle the problem of protein shares in balanced diet in Pakistan

We calculated and compared the elasticities of macronutrient shares using income, household size, dependency ratio and wealth index. Our findings support to the existing literature, the most elastic macronutrient is fat share with respect to the income, household size and dependency ratio compared to other shares. But the carbohydrate share is negatively elastic to income, household size and dependency ratio. Moreover, for example the positive elasticity of macronutrient shares with respect to income represent that the positive impact of income on macronutrient shares.

In this study the important results are very helpful to support the previous studies about the development of nutritional diets at the national level. There is strong correlation between nutritional change and the non-communicable diseases risk factor

http://www.aloki.hu ● ISSN 1589 1623 (Print) ● ISSN 1785 0037 (Online)
DOI: http://dx.doi.org/10.15666/aeer/1706_1390913929

such as heart diseases an obesity (Bloom et al., 2012), country level strategies are required to help Pakistani people to recover their pattern of diet with respect to macronutrients.

In additional research, same kind of studies which based on dietary shares of macronutrients can be done for other countries to see the entire food consumption pattern. Moreover, focusing on the association between macronutrient shares in calories and non-communicable diseases as obesity and heart diseases at the country level will be very interesting.

REFERENCES

[1] Ahluwalia, N., Ferrières, J., Dallongeville, J., Simon, C., Ducimetière, P., Amouyel, P., Arveiler, D., Ruidavets, J. B. (2009): Association of macronutrient intake patterns with being overweight in a population-based random sample of men in France. – Diabetes & Metabolism 35(2): 129-136.

[2] Aitchison, J. (1982): The statistical analysis of compositional data. – Journal of the Royal Statistical Society: Series B (Methodological) 44(2): 139-60.

[3] Aitchison, J. (1986): CODA: A Microcomputer Package for the Statistical Analysis of Compositional Data. – Chapman and Hall, London.

[4] Akerele, D., Kebiru Ibrahim, M., Adewuyi, S. (2014): Socioeconomic determinants of protein and calorie consumption and potential risk of protein-energy malnutrition among households in South-West Nigeria. – International Journal of Social Economics 41(1): 75-88.

[5] Austin, G. L., Ogden, L. G., Hill, J. O. (2011): Trends in carbohydrate, fat, and protein intakes and association with energy intake in normal-weight, overweight, and obese individuals: 1971–2006. – The American Journal of Clinical Nutrition 93(4): 836-843.

[6] Bloom, D. E., Cafiero, E., Jané-Llopis, E., Abrahams-Gessel, S., Bloom, L. R., Fathima, S., O'Farrell, D. (2012): The Global Economic Burden of Noncommunicable Diseases. Program on the Global Demography of Aging (No. 8712). – World Economic Forum, Geneva.

[7] Carreiro, A. L., Dhillon, J., Gordon, S., Higgins, K. A., Jacobs, A. G., McArthur, B. M., Redan, B. W., Rivera, R. L., Schmidt, L. R., Mattes, R. D. (2016): The macronutrients, appetite, and energy intake. – Annual Review of Nutrition 36: 73-103.

[8] Chen, J., Zhang, X., Li, S. (2017): Multiple linear regression with compositional response and covariates. – Journal of Applied Statistics 44(12): 2270-2285.

[9] Claro, R. M., Levy, R. B., Bandoni, D. H., Mondini, L. (2010): Per capita versus adult-equivalent estimates of calorie availability in household budget surveys. – Cadernos de Saude Publica (26): 2188-2195.

[10] Dumuid, D., Stanford, T. E., Martin-Fernández, J. A., Pedišić, Ž., Maher, C. A., Lewis, L. K., Hron, K., Katzmarzyk, P. T., Chaput, J. P., Fogelholm, M., Hu, G. (2018): Compositional data analysis for physical activity, sedentary time and sleep research. – Statistical Methods in Medical Research 27(12): 3726-3738.

[11] Egozcue, J. J., Pawlowsky-Glahn, V., Mateu-Figueras, G., Barcelo-Vidal, C. (2003): Isometric logratio transformations for compositional data analysis. – Mathematical Geology 35(3): 279-300.

[12] Egozcue, J. J., Daunis-I-Estadella, J., Pawlowsky-Glahn, V., Hron, K., Filzmoser, P. (2011): Simplicial regression. The normal model. – Journal of Applied Probability and Statistics 6(1): 87-108.

[13] Institute of Medicine (2005): Dietary Reference Intakes for Energy, Carbohydrate, Fiber, Fat, Fatty Acids, Cholesterol, Protein, and Amino Acids (Macronutrients). – National Academy Press, Washington, DC.

http://www.aloki.hu ● ISSN 1589 1623 (Print) ● ISSN 1785 0037 (Online)
DOI: http://dx.doi.org/10.15666/aeer/1706_1390913929

[14] Iyangbe, C. O., Orewa, S. I. (2009): Determinants of daily protein intake among rural and low-income urban households in Nigeria. American-Eurasian. – Journal of Scientific Research 4(4): 290-301.
[15] Khan, M. A., Khan, M. A., Planning Commission (2001): Food Composition Table for Pakistan. Peshawar. – University of Agriculture, Peshawar.
[16] Khattak, M. M. A. K., Khan, M. N. (2009): Deficient intakes of energy and macronutrients in Pakistani female students assessed by composite. – Asian. J. Clin. Nutr 1: 97-101.
[17] Kushner, R. F., Doerfler, B. (2008): Low-carbohydrate, high-protein diets revisited. – Current Opinion in Gastroenterology 24(2): 198-203.
[18] Leite, M. L. C. (2016): Applying compositional data methodology to nutritional epidemiology. – Statistical Methods in Medical Research 25(6): 3057-3065.
[19] Liaskos, G., Lazaridis, P. (2003): The demand for selected food nutrients in Greece: the role of socioeconomic factors. – Agricultural Economics Review 4(389-2016-23385): 93-106.
[20] Mert, M. C., Filzmoser, P., Endel, G., Wilbacher, I. (2018): Compositional data analysis in epidemiology. – Statistical Methods in Medical Research 27(6): 1878-1891.
[21] Miller, W. C., Lindeman, A. K., Wallace, J., Niederpruem, M. (1990): Diet composition, energy intake, and exercise in relation to body fat in men and women. – The American Journal of Clinical Nutrition 52(3): 426-430.
[22] Morais, J., Thomas-Agnan, C., Simioni, M. (2018): Using compositional and Dirichlet models for market share regression. – Journal of Applied Statistics 45(9): 1670-1689.
[23] Muller, I., Hron, K., Fiserova, E., Smahaj, J., Cakirpaloglu, P., Vancáková, J. (2016): Interpretation of compositional regression with application to time budget analysis. – arXiv 1609.07887.
[24] National Institute of Population Studies (NIPS) [Pakistan] ICF International (2013): Pakistan Demographic and Health Survey 2012–13. – NIPS, Pakistan.
[25] Ng, M., Fleming, T., Robinson, M., Thomson, B., Graetz, N., Margono, C., Mullany, E. C., Biryukov, S., Abbafati, C., Abera, S. F., Abraham, J. P. (2014): Global, regional, and national prevalence of overweight and obesity in children and adults during 1980–2013: a systematic analysis for the Global Burden of Disease Study 2013. – The Lancet 384(9945): 766-781.
[26] Nguyen, T. H. A., Laurent, T., Thomas-Agnan, C., Ruiz-Gazen, A. (2018): Analyzing the impacts of socio-economic factors on French departmental elections with CODA methods. – TSE Working Paper n. 18-961, October 2018.
[27] Olaf, M., Michael, K. (2005): Malnutrition and health in developing countries. – Canadian Medical Association Journal 173(3): 279-286.
[28] Pawlowsky-Glahn, V., Buccianti, A. (2011): Compositional Data Analysis. – Wiley, London.
[29] Pawlowsky-Glahn, V., Egozcue, J. J., Tolosana-Delgado, R. (2015): Modeling and Analysis of Compositional Data. – John Wiley & Sons, New York.
[30] Satia-Abouta, J., Patterson, R. E., Schiller, R. N., Kristal, A. R. (2002): Energy from fat is associated with obesity in US men: results from the Prostate Cancer Prevention Trial. – Preventive Medicine 34(5): 493-501.
[31] Satti, M. N., Khalid, M. (2019): Prevalence and Determinants of Overweight and Obesity Among Adults in Pakistan. – Population & Health Working Paper Series PIDE-CPHSP-2. Pakistan Institute of Development Economics Islamabad.
[32] Shabnam, N., Santeramo, F. G., Asghar, Z. Seccia, A. (2016): The impact of food price crises on the demand for nutrients in Pakistan. – Journal of South Asian Development 11(3): 305-327.
[33] Shakoor, H., Khan, S., Samiullah, M., Zeb, F., Iqbal, U., Khattak, F. H. (2017): nutritional status and dietary intake of boarder female students of the University of Agriculture, Peshawar, Pakistan. – Khyber Medical University Journal 9(2).

http://www.aloki.hu ● ISSN 1589 1623 (Print) ● ISSN 1785 0037 (Online)
DOI: http://dx.doi.org/10.15666/aeer/1706_1390913929

[34] Sheet, P. (2012): Nutrition at the World Food Programme. – World Food Programme, Rome.
[35] Smith, L. C., Haddad, L. J. (2000): Explaining Child Malnutrition in Developing Countries: A Cross-Country Analysis (Vol. 111). – Intl Food Policy Res Inst, Washington, DC.
[36] Swinburn, B. A., Sacks, G., Hall, K. D., McPherson, K., Finegood, D. T., Moodie, M. L., Gortmaker, S. L. (2011): The global obesity pandemic: shaped by global drivers and local environments. – The Lancet 378(9793): 804-814.
[37] Tanzil, S., Jamali, T. (2016): Obesity, an emerging epidemic in Pakistan-a review of evidence. – J Ayub Med Coll Abbottabad 28(3): 597.
[38] Trinh, H. T., Morais, J., Thomas-Agnan, C., Simioni, M. (2018): Relations between socio-economic factors and nutritional diet in Vietnam from 2004 to 2014: new insights using compositional data analysis. – Statistical Methods in Medical Research 28(8): 2305-2325.
[39] UNICEF (1991): Conceptual Framework of the Causes of Malnutrition. – UNICEF, New York.
[40] Van den Boogaart, K. G., Tolosana-Delgado, R. (2013): Analyzing Compositional Data with R. – Springer, Heidelberg.
[41] World Health Organization (2010): Global Status Report on Noncommunicable Diseases 2010: Description of the Global Burden of NCDs, Their Risk Factors and Determinants. – World Health Organization, Geneva. http://www.who.int/entity/nmh/.
[42] World Health Organization (2018): World Health Statistics 2018: Monitoring Health for the SDGs, Sustainable Development Goals. – WHO, Geneva.
[43] World Health Organization Editor (2013): Global Tuberculosis Report 2013. – http://www.who.int/nmh/countries/pak_en.pdf?ua=1.
[44] You, J., Imai, K. S., Gaiha, R. (2016): Declining nutrient intake in a growing China: Does household heterogeneity matter? – World Development 77: 171-191.
[45] Zhou, L., Chen, X., Lei, L. (2018): Intra-household allocation of nutrients in an opening China. – International Journal of Environmental Research and Public Health 15(4): 700.

http://www.aloki.hu ● ISSN 1589 1623 (Print) ● ISSN 1785 0037 (Online)
DOI: http://dx.doi.org/10.15666/aeer/1706_1390913929

COMBINED PENETROMETER AND STANDING WAVE RATIO PROBE TO MEASURE COMPACTNESS AND MOISTURE CONTENT OF SOILS

TIAN, H.[1,3,4] – GAO, C.[2] – ZHAO, Y.[1,3,4*]

[1]*School of Technology, Beijing Forestry University, Beijing 100083, China*

[2]*School of Computer and Information Engineering, Beijing Technology and Business University, Beijing 100048, China*

[3]*Beijing Laboratory of Urban and Rural Ecological Environment, Beijing Municipal Education Commission, Beijing 100083, China*

[4]*Key Lab of State Forestry Administration for Forestry Equipment and Automation, Beijing 100083, China*

**Corresponding author*
e-mail: yandongzh@bjfu.edu.cn; phone: +86-158-1021-0957

(Received 23rd May 2019; accepted 28th Aug 2019)

Abstract. Compactness and moisture content are important and mutually influential soil parameters that affect plant growth, nutrient absorption, and nutrient transportation. To simultaneously measure these two parameters, we developed a combined penetrometer standing wave ratio (PSWR) probe; acceleration measurement was facilitated to eliminate the error caused by varying penetration speeds. The performance of the instrument was analyzed and verified through laboratory and field measurements. The cone-index measurements from an SC-900 sensor and the moisture content calculated by the drying method and a TDR sensor were used to evaluate the performance. The results prove that acceleration compensations can improve the accuracy of cone-index measurements. Further, the sensitive range of the PSWR probe was the area a 10 cm diameter. The linear-fitting coefficient of output voltage and volumetric moisture content exceeded 0.96, and the output was stable; therefore, the moisture content measurements using the PSWR probe were validated. Furthermore, the accuracy and stability of measurements using the PSWR probe and a TDR sensor were similar. The field-measurement results agreed with the results from the drying method, and satisfied the practical implementation requirements. Conclusively, the validated efficiency and the cost-effective stainless-steel structure of the probe render it suitable for practical applications.
Keywords: *cone index, soil volumetric moisture content, penetrating acceleration, measuring radius, performance analysis*

Introduction

Soil is a loose, porous, dielectric material composed of water, air, and soil particles (Schaap, et al., 1997). The compactness and moisture content are important soil parameters that affect the plant growth, water movement, seedling emergence, and root penetration (Cui et al., 2015; Goutal et al., 2013; Ogée and Brunet, 2002). In early days, soil compactness was measured primarily by destructive sampling (Ronai and Shmulevich, 1995); later, instruments based on pressure-based soil cone-index measurement (ASABE Standards, 2009; Erbach et al., 1991; Pillinger et al., 2018; Perumpral, 1987), microwave reflection measurement (Luo and Perumpral, 1995; Zoughi et al.,1994), and volume and porosity measurement were used (Ronai and Shmulevich, 1995). In the recent years, CT technology has been used to scan the soil to

http://www.aloki.hu ● ISSN 1589 1623 (Print) ● ISSN 1785 0037 (Online)
DOI: http://dx.doi.org/10.15666/aeer/1706_1393113944

analyze its compactness (Mossadeghi-Björklund et al., 2016). The measurement techniques for soil moisture are primarily classified into sampling and in-situ techniques. Drying method is typically used to analyze the moisture content in the sampling techniques, and electrical measurements are conducted in localization techniques. In 1980, Topp et al. proposed the use of time-domain reflectometry in the field of soil moisture measurement (Topp et al., 1980). The Topp equation brought a new dimension to the soil moisture evaluation. In addition, many scholars have developed moisture measurement devices using electrical measurement methods (Jin-Hong et al., 2008; Tranter et al., 2008; Zegelin et al., 1989).

Topp et al. initiated the research on the simultaneous measurement of compactness and moisture of the soil. For this purpose, they attempted to combine a cone penetrometer with a TDR moisture sensor. They installed a waveguide coil and mounted it on a static cone for simultaneous measurement (Topp, 2003; Yanuka et al., 1988). Vaz et al. installed the waveguide coil on the conical head of a dynamic cone (Vaz et al., 2001; Vaz and Hopmans, 2001). However, this device takes 10 min to complete a measurement, and its practical application is difficult; therefore, it is still in the laboratory research stage. Subsequently, Hummel proposed a composite sensor combining the cone-index and near-infrared methods (Hummel et al., 2004). Although this sensor could quickly synchronize the measurement, it had a complicated structure and was expensive. In 1997, Singh et al. proposed to embed an FD-type soil-moisture sensor on the head of the cone to ensure that the measurement structure of the cone is not damaged (Singh et al., 1997). Sun et al. further embedded FD-type moisture sensors into cones in 2003 and developed composite sensors in 2004 (Sun et al., 2004). Lin et al. designed a composite cone-index and moisture measurement device in 2014 (Lin et al., 2014). In order to avoid the influence of uneven insertion speed on the measurement results of compactness, ASABE stipulates that penetration speed should be uniform with a maximum penetration speed of 30 $mm \bullet s^{-1}$ (ASABE Standards, 2009).

The concept of combined measurement of compactness and moisture content was previously presented and designed, but there are two disadvantages in the existing systems. First, during the practical application, the operator faces difficulties in maintaining a uniform speed of penetration, which leads to errors in the cone-index measurement; second, such instruments are very expensive. Therefore, this study aimed to design and evaluate a low-cost standing wave ratio probe to be used in combination with a cone penetrometer to determine the moisture content and compactness of the soil, and to reduce the error caused by the non-uniform penetration speed by facilitating acceleration measurement. The combined PSWR probe was first tested in the laboratory, and the results were analyzed. Further, field measurements were conducted, and the results are presented.

Materials and methods

PSWR probe design

As shown in *Figure 1a,* the structure of the penetrometer consists of a cone head, a connecting rod, and a fixed base. The cone head and the connecting rod are marked with scales to measure the insertion depth of the probe with an accuracy of 1 mm. The connecting rod is a hollow steel tube of outer diameter 10 mm, inner diameter 4 mm, and length 700 mm. It is connected to a pressure sensor through the thread; the pressure sensor and acceleration sensor are installed on the base. The cone head is fabricated

http://www.aloki.hu ● ISSN 1589 1623 (Print) ● ISSN 1785 0037 (Online)
DOI: http://dx.doi.org/10.15666/aeer/1706_1393113944

according to American Society of Agriculture and Biological Engineers (ASABE) requirements; the conical diameter is 20 mm and conical angle is 30°. The double-metal-ring SWR probe is mounted on the cone head to form the PSWR probe.

The double-metal-ring SWR probe is shown in *Figure 1b*. Two metal rings are mounted on a solid nylon column with grooves, and three PVC rings are installed between them for insulation, the probe spacing is 10 cm. The metal rings are connected using wires as electrodes to the circuit, which measures the SWR. The wires and metal rings are welded together and installed in the grooves. The circuit, which measures the SWR, is located on the upper part of the probe to reduce the error caused by a change in the impedance around the wires, and is filled with waterproof glue to render it waterproof. The probe has an overall length of 150 mm. The fabricated physical model is shown in *Figure 1c*.

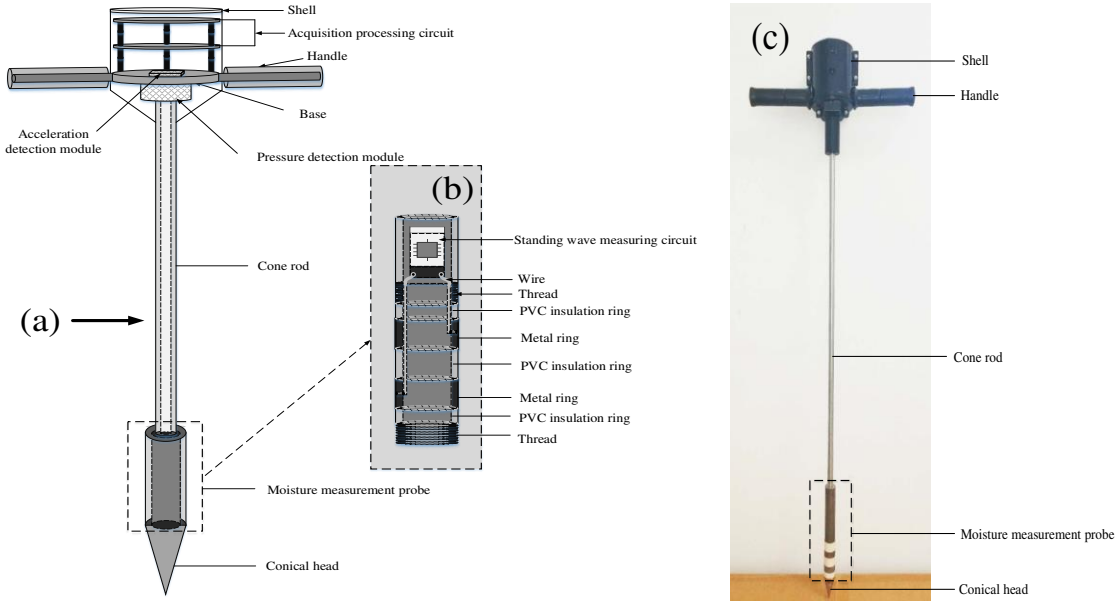

Figure 1. *The assembly of a combined PSWR probe is illustrated: (a) Detailed schematic diagram showing the parts of the instrument; (b) Components of the double-metal-ring SWR probe are detailed; (c) Photograph of the actual physical model fabricated during the study is shown*

Soil compactness measurement based on cone index

The ASABE (formerly the American Society of Agricultural Engineers) stipulates that when the standard cone is penetrated into the soil at a constant speed, the average pressure per unit area is the cone index (*CI*), which can be used to characterize the soil compactness (ASAE S313.3 FEB04., 1998; ASABE Standards, 2009). The formula to calculate *CI* is as follows *Equation 1:*

$$CI = N / S = (F + G) / S \quad \text{(Eq.1)}$$

where N is the pressure at the bottom of the cone head, S is the bottom area of the cone head, F is the external force exerted by a person on the penetrometer, and G is the force due to gravity on the instrument.

http://www.aloki.hu ● ISSN 1589 1623 (Print) ● ISSN 1785 0037 (Online)
DOI: http://dx.doi.org/10.15666/aeer/1706_1393113944

However, during the actual measurement, it is difficult to maintain a uniform insertion speed; therefore, errors persist in the measurement results because of the complexity in the soil composition and non-standard manual operation. Hence, this study suggests a synchronous measurement of the external force (F) and acceleration (a) during the insertion of the cone. The pressure at the bottom of the cone can be calculated as follows *Equation 2:*

$$N = F + G - m * a \quad \text{(Eq.2)}$$

where m is the cone instrument quality. With this pressure, the corrected cone index can be calculated according to *Equation 1,* and the error caused by the variation in the velocity during the insertion can be eliminated.

Measuring volumetric moisture content of soil based on SWR

Moisture sensors based on SWR measure the dielectric constant of the soil. When high-frequency electromagnetic waves propagate along a transmission line, some of the incident waves are reflected by the probe placed in soil of different dielectric constant, because the impedance of the probe does not match with the impedance of the transmission line. Due to the interference of the reflected wave and the incident wave, a standing wave is formed on the transmission line, which causes a change in the voltage difference across the transmission line (Gaskin et al., 1996; Paltineanu et al., 1997). The moisture sensor designed in this study consists of a 100 MHz crystal oscillator, coaxial transmission line, and double-metal-ring probe (*Fig. 2*). The voltage difference across the transmission line can be expressed as follows *Equation 3:*

$$\Delta U = 2A \frac{Z_P - Z_L}{Z_P + Z_L} \quad \text{(Eq.3)}$$

where A is the electromagnetic wave amplitude (V), Z_P is the probe impedance (Ω), and Z_L is the transmission-line impedance (Ω). Z_L is dependent on the physical dimensions and the dielectric constant of the insulating material (50 Ω in this research). Z_P is determined by the probe size, soil permittivity, and operating frequency. The probe size and operating frequency are fixed values, which implies that a difference in the soil dielectric constant at the measurement site will change the impedance of the measuring probe, which results in a change in the voltage difference (ΔU) across the transmission line. The volumetric moisture content of soil has a relatively unique mathematical relationship with its dielectric constant (Topp, 2003; Yanuka et al., 1988); therefore, the moisture content can be measured by measuring the probe impedance.

Filed sampling and instrument

The soil samples were collected from Beijing Gongqing Forest Farm (116.73° E, 40.11° N) and Beijing Forestry University Sanqingyuan Experimental Base (116.34° E, 40.00° N), which are primarily used for teaching and research in the Beijing Forestry University. These sites experience a typical continental climate, with an average annual temperature of 11.6 °C and an average annual precipitation of 600 mm. Areas of uniform soil were identified at the collection sites, and 30 kg of soil samples were extracted. These samples were dried (48 h, 105 °C) in an oven shown in *Figure 3d*.

http://www.aloki.hu ● ISSN 1589 1623 (Print) ● ISSN 1785 0037 (Online)
DOI: http://dx.doi.org/10.15666/aeer/1706_1393113944

After drying, the samples were screened through a 40-mesh sieve shown in *Figure 3c* to remove impurities, such as stones, dead branches, fallen leaves, and roots. Thus, the soil samples for the experiment were obtained, which were identified as sand soil (sand mass fraction 85%, powder mass fraction 10%, clay mass fraction 5%) shown in *Figure 3a* and clay loam soil (sand mass fraction 11%, powder mass fraction 71%, clay mass fraction 18%) shown in *Figure 3b*.

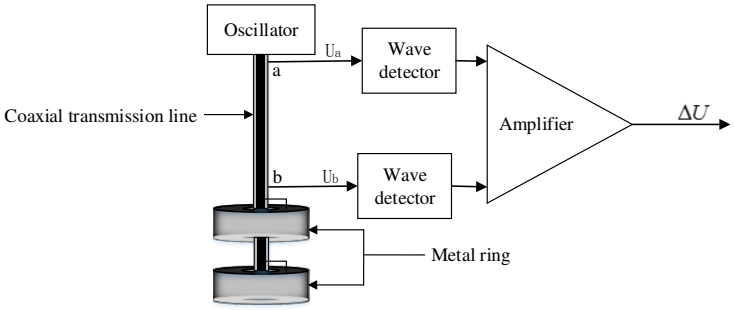

Figure 2. *Diagram of the moisture sensor based on the standing wave ratio, and the measurement circuit. U_a and U_b are output voltages at Point a and Point b on the coaxial transmission line, respectively. ΔU is the differential output voltage between Point a and Point b*

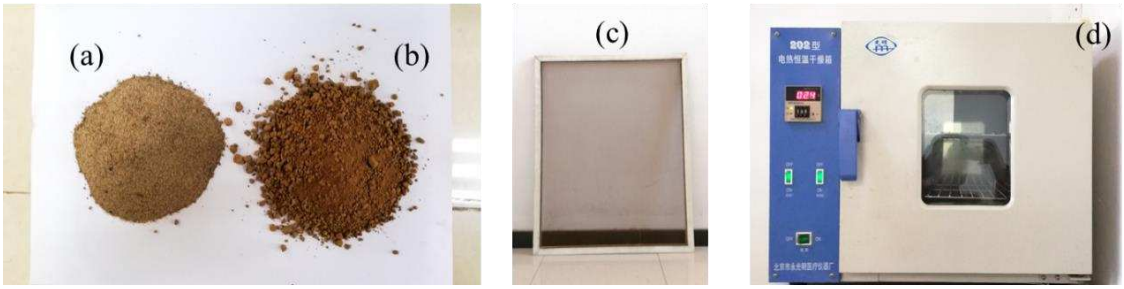

Figure 3. *The details of soil sampling are presented: (a) Picture of the sampled sand soil; (b) Picture of the sampled clay loam soil; (c) 40-mesh sieve used for screening the impurities; (d) Drying oven used for drying the samples*

The contrast instrument is SC-900 sensor (American Spectrum production, measuring unit KPa, resolution is 35 KPa, measurement accuracy is 103 KPa, the range is 0-45 cm and 0-7000 KPa, maximum insertion speed is 25 mm•s-1, maximum load is 95.25 kg) and TDR sensor (German IMKO production, model TRIME-PICO32, measurement range 0-100% volume moisture content, measurement accuracy ± 2%, probe diameter 3.5 mm and probe length 110 mm).

The field experiments were conducted at Beijing Forestry University Forest Farm (altitude 642 m, 116°4’36”E, 40°3’42”N) and Beijing Forestry University Sanqingyuan Experimental Field (altitude 52 m, 116°20’15”E, 40°0’44”N).

Experimental procedure

Two different soil samples of 10 kg each were weighed by a precision electronic weighing machine. A certain quantity of water was added to the samples and mixed thoroughly. The samples were detained for 48 h until the water movement attained

http://www.aloki.hu ● ISSN 1589 1623 (Print) ● ISSN 1785 0037 (Online)
DOI: http://dx.doi.org/10.15666/aeer/1706_1393113944

equilibrium, and were subsequently placed in PVC buckets (20 cm high, 30 cm diameter) and compacted uniformly using a nylon rod (50 cm length, 5 cm diameter). Different trials were conducted by varying the water quantity and compaction of the soil samples; the combined probe was inserted into the soil samples to a penetration depth of 20 cm, and the pressure and acceleration of the penetrations were recorded. The compactness of the samples was also measured using an SC-900 soil compactness meter, the SC-900 sensor is mounted on permanent magnet direct current motor (BXTL150, made in China, working voltage 12 V, power 30 W), the rotation of the motor drives the gear to rotate, which makes the SC-900 sensor move vertically downward uniformly (12 $mm \bullet s^{-1}$) along the guide rail to ensure that the SC-900 sensor measurement can obtain accurate soil compactness and be used as the true value of sample. The relation between the pressure and acceleration during the penetration were analyzed, and the effect of variation in the acceleration on the measurement results was investigated. The sensitive range of the double-metal-ring probe was analyzed by HFSS (High Frequency Structure Simulator) modeling and experimental analyses. Lumped port excitation method was assigned, and the value of frequency was set as 100 MHz and fill dielectric constant as 21 (corresponding to a volumetric moisture content of 36%). The metal ring was the ideal electric field boundary; a cylindrical body of diameter 20 cm and height 20 cm was assumed as the radiation boundary. Meanwhile, the soil column used for the experiment was thinned in steps of 1 cm thickness, the volumetric water content, compactness and height of soil columns remain unchanged, and the combined probe was inserted into the center of the sample; the output voltage of the probe corresponding to the diameter of the soil column was recorded for each step. After the calibration of the combined probe by the drying method, the accuracy and stability of the moisture measurement were analyzed by comparing the results with that from a TDR soil moisture sensor. Field experiments were finally carried out to verify the performance in practical conditions.

Results and discussion

Relationship between penetration acceleration and pressure

The acceleration (a) and force (F) data observed during the penetration were normalized, and the variations in pressure and acceleration are shown in *Figure 4*. Initially, the penetration force (F) remains constant before the cone makes contact with the soil; it increases gradually as the cone touches the soil and continues the penetration, and then decreases rapidly to zero when penetration is stopped after reaching a certain depth (20 cm in this case). Meanwhile, because it is difficult to main a uniform cone penetration manually, there is a fluctuation in the acceleration along the vertical direction. The initial penetration acceleration (a) varies drastically when the cone reaches the soil, and the variation decreases as the cone continues to penetrate into the soil. The influence on the force at the bottom surface of the cone was calculated using *Equation 2,* and the measurement results after the acceleration correction were calculated. *Table 1* is the measurement results of soil samples with different compactness and the depth of measurement is 10 cm. It can be observed that the measurement error is reduced by measuring the penetration acceleration of the cone.

http://www.aloki.hu ● ISSN 1589 1623 (Print) ● ISSN 1785 0037 (Online)
DOI: http://dx.doi.org/10.15666/aeer/1706_1393113944

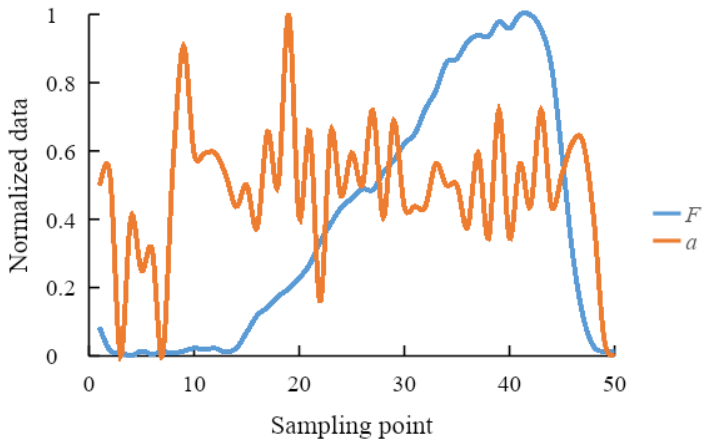

Figure 4. *Variation in penetration pressure (F) and acceleration (a) during the cone penetration are plotted after normalization*

Table 1. *The results obtained from the two sensors are tabulated for comparison. For the composite sensor, the results before and after the acceleration correction are presented along with the corresponding error values*

Sample number	SC-900 measurement results (KPa)	Combined PSWR probe			
		Cone index (not counting acceleration)		Cone index (calculation acceleration)	
		Measurement results (KPa)	Relative error ($cm^3 \cdot cm^{-3}$)	Measurement results (KPa)	Relative error ($cm^3 \cdot cm^{-3}$)
1	344	379.47	10.31%	363.55	5.68%
2	380	392.90	3.40%	379.33	0.18%
3	421	442.79	5.18%	428.70	1.83%
4	526	541.28	2.90%	532.68	1.27%
5	632	658.95	4.26%	651.75	3.12%

PSWR probe detection sensitive area

The HFSS software was used to establish the simulation model of the probe. The electric field distribution of the annular probe is shown in *Figure 5*. It can be seen that the electric field strength gradually decreases as the diameter increases; at the boundary of 10 cm diameter, the electric field strength attenuates to 8 V/m (1% of the center electric field strength). The variation of soil column diameter is shown in *Figure 6*. The variation of the voltage with the diameter of the soil column is shown in *Figure 7;* the output voltage begins to decrease rapidly when the diameter is 10 cm, indicating that the sensitive range of the probe is within 10 cm diameter from the cone. Hence, to ensure accuracy in the measurement, it should be guaranteed that the soil within 10 cm diameter around the cone is uniform and does not contain debris and other impurities.

Laboratory experiment for calibration

For different values of volumetric moisture content of the soil samples, the corresponding voltage of the combined probe was measured and recorded; the relationship between the voltage and the volumetric moisture content is shown in

http://www.aloki.hu ● ISSN 1589 1623 (Print) ● ISSN 1785 0037 (Online)
DOI: http://dx.doi.org/10.15666/aeer/1706_1393113944

Figure 8. For the clay loam and sand samples, the linear-fitting coefficient of output voltage and volumetric moisture content were 0.9694 and 0.9824, respectively, and the fitting determination coefficients were higher than 0.96. This indicates that the output voltage has a good linear relationship with the volumetric moisture content, and the volumetric moisture content can be calculated by fitting the curve.

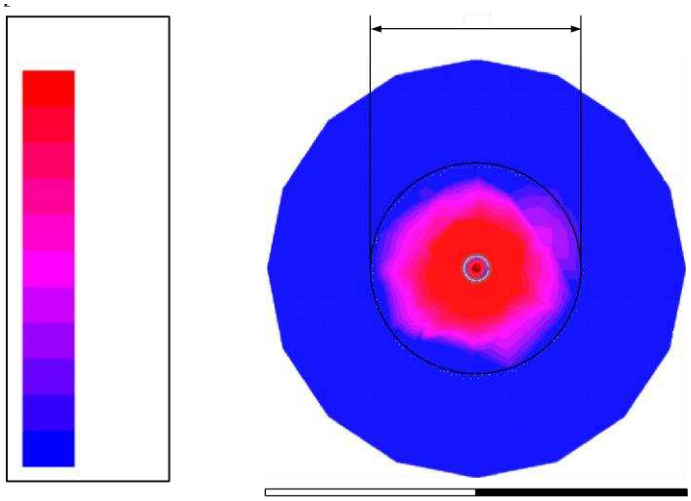

Figure 5. *Electrical field distribution of double-metal-ring probe obtained by simulation is shown: top view of the model, which shows the distribution along the plan*

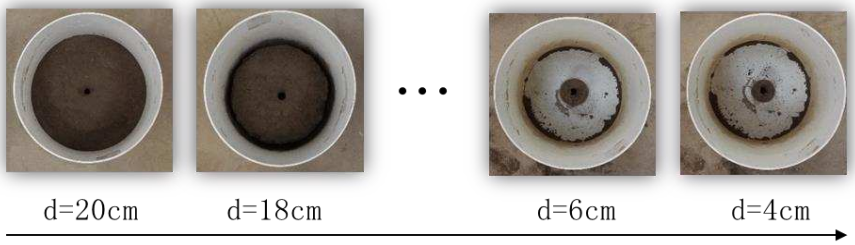

Figure 6. *The gradual reduction of the soil column thickness of the sample during the metal-ring lateral-diameter test process is shown*

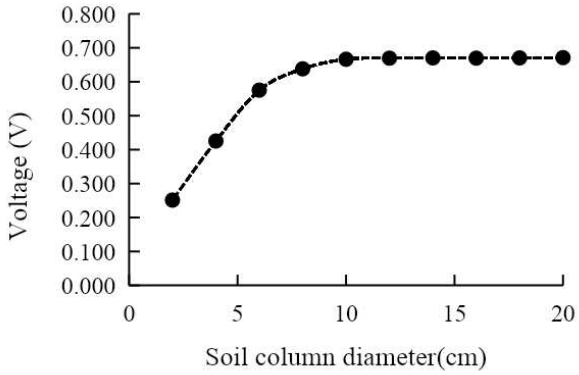

Figure 7. *The variation in the output voltage with the diameter of the soil column is illustrated*

http://www.aloki.hu ● ISSN 1589 1623 (Print) ● ISSN 1785 0037 (Online)
DOI: http://dx.doi.org/10.15666/aeer/1706_1393113944

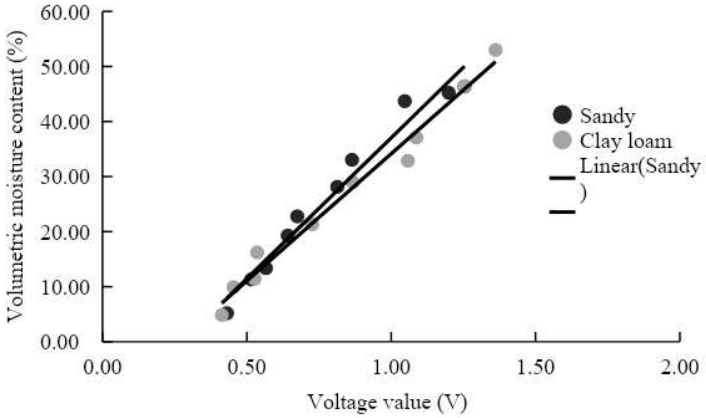

Figure 8. *Relationship between the volumetric moisture content and the voltage value is depicted*

Laboratory measurement

Figure 9 shows the variation in the volumetric moisture content of the soil measured by the probe in 100 repeated measurements in a sand sample of diameter 100 cm and height 20 cm. It can be observed that the measurement results fluctuate very less; the maximum and minimum values of volumetric moisture content were 10.68% and 8.74%, respectively, and the standard deviation was 0.49%. Therefore, it is verified that the PSWR probe can be used for repeated measurements.

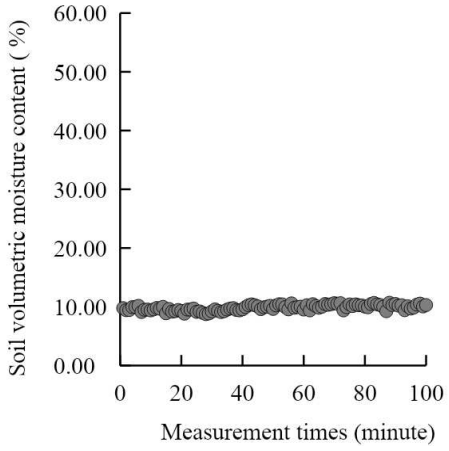

Figure 9. *Results obtained from the repetitive measurements of moisture content are plotted*

Figure 10 is a comparison of the results obtained from the proposed PSWR probe and TDR sensor in two soil types; twelve samples of different volumetric moisture content were prepared for each soil type. Measurement soil volumetric moisture content of the same sample with PSWR probe and TDR sensor respectively. It can be observed from *Figure 10* that the results from the proposed probe are consistent with those from the TDR sensor. The results from the proposed PSWR probe and the TDR sensor were linearly fitted, as shown in *Table 2*. The fitting determination coefficients prove that the measurement accuracies of the two devices are comparable, which satisfies the requirements of practical application.

http://www.aloki.hu ● ISSN 1589 1623 (Print) ● ISSN 1785 0037 (Online)
DOI: http://dx.doi.org/10.15666/aeer/1706_1393113944

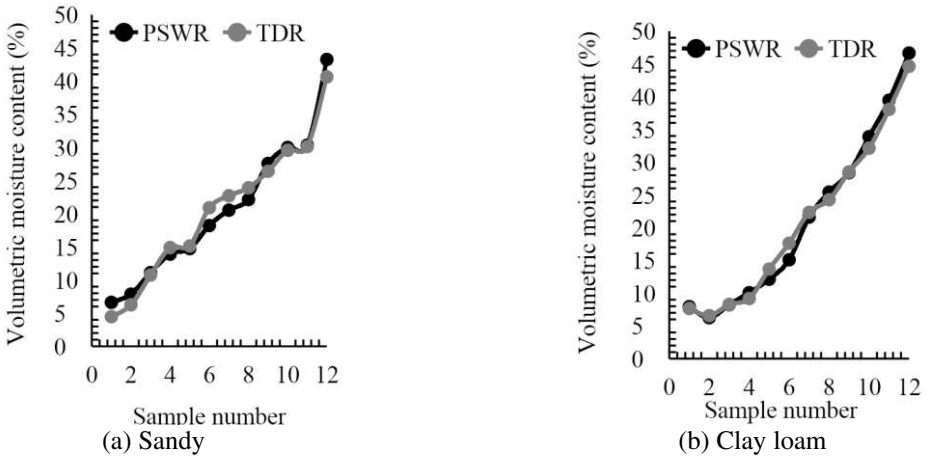

Figure 10. *The measurement results of the two devices are plotted together for comparison: Comparison of results obtained in (a) sandy soil, (b) clay loam soil*

Table 2. *The linear fitting expression and fitting determination coefficient (R^2) of the results from the two devices are tabulated*

Soil type	Linear fit expression	R^2
Sandy	y = 0.9745x + 0.4743	0.975
Clay loam	y = 0.9555x + 1.2446	0.9881

Six samples of different volumetric moisture contents prepared using clay loam were subjected to three measurements per sample, simultaneously with the TDR sensor and the proposed PSWR probe, and the samples were dried to obtain the actual values of the volumetric moisture content. The data was recorded and the standard deviation of the measurements was calculated. As shown in *Figure 11,* the error fluctuation in the measurements of the six samples are approximately equivalent; the standard deviation of the results from the PSWR probe and TDR sensor were obtained as 2.32 and 1.63, respectively. This indicates that the measurement stability of the PSWR probe is equivalent to that of the TDR sensor.

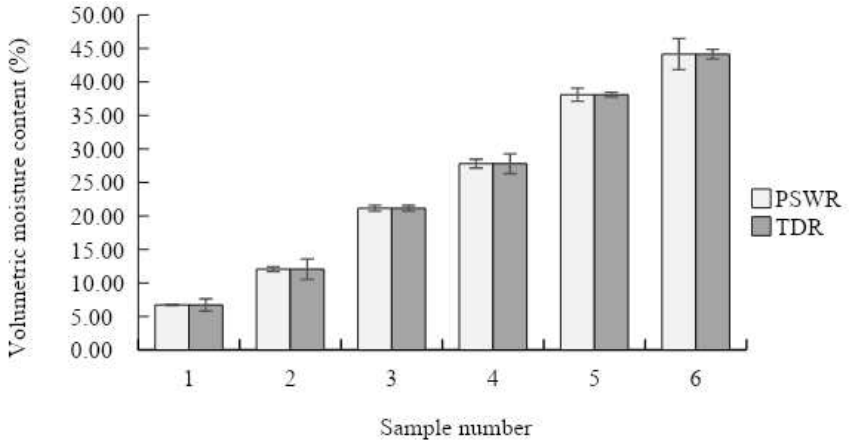

Figure 11. *The moisture content obtained using the two devices are plotted to compare the measurement stability*

http://www.aloki.hu ● ISSN 1589 1623 (Print) ● ISSN 1785 0037 (Online)
DOI: http://dx.doi.org/10.15666/aeer/1706_1393113944

Field measurement

A square, flat land of area 9 m^2 was selected at the sites, and the volumetric moisture content at five points were measured by the combined probe and by the drying method, as shown in *Figure 12*. The measurement depth was 20 cm, and the comparison of measurement results is shown in *Table 3.* It can be observed that the measurement results are comparable; the maximum error was obtained as 2.10%, which is less than 3%; therefore, the proposed probe meets the accuracy requirements for practical use.

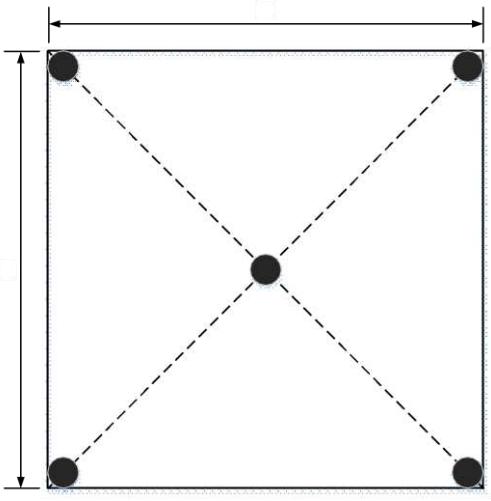

Figure 12*. This diagram illustrates the points selected for the field measurements at the site*

Table 3. *The field measurement results obtained using the proposed probe and the drying method are tabulated for both the sites, θ_V is drying method and θ_S is PSWR method*

Measuring point	Sanqingyuan experimental field		Forest farm	
	θ_V ($cm^3\ cm^{-3}$)	θ_S ($cm^3\ cm^{-3}$)	θ_V ($cm^3\ cm^{-3}$)	θ_S ($cm^3\ cm^{-3}$)
1	18.86%	19.90%	16.89%	17.21%
2	21.44%	21.85%	15.67%	17.35%
3	23.45%	21.35%	15.18%	16.39%
4	21.11%	19.61%	14.80%	16.57%
5	21.22%	20.05%	16.96%	15.16%

Three sites were randomly selected in the field experimental site, The comparison of measurement results is shown in *Figure 13,* the soil compactness was measured by SC-900 sensor and PSWR, the measured depth was 2.5 cm, 5.0 cm, 7.5 cm and 10.0 cm. The results showed that the accuracy of PSWR measurement was the same as that of SC-900 sensor, and met the practical application requirements.

Advantages of combined PSWR probe

The existing compactness sensors based on cone index method are difficult to ensure uniform penetration due to manual operation, resulting in measurement errors due to different vertical velocities (Alaoui and Diserens, 2018; Pillinger et al., 2018; Lin et al., 2014). Moreover, the internationally recognized TDR sensor for moisture measurement has the disadvantage of high price and easy damage of probe (Rudnick et al., 2018; Sun

http://www.aloki.hu ● ISSN 1589 1623 (Print) ● ISSN 1785 0037 (Online)
DOI: http://dx.doi.org/10.15666/aeer/1706_1393113944

et al., 2004; Yan et al., 2018). In view of the above shortcoming, the PSWR probe can simultaneously measure soil compactness and moisture content, the measurement error can be effectively reduced, and the accuracy of cone-index measurement can be improved by synchronously measuring the acceleration during the penetration. In addition, the PSWR probe has a lesser manufacturing cost and a more stable ring structure, and the soil compactness and volumetric moisture content can be measured synchronously by PSWR probe.

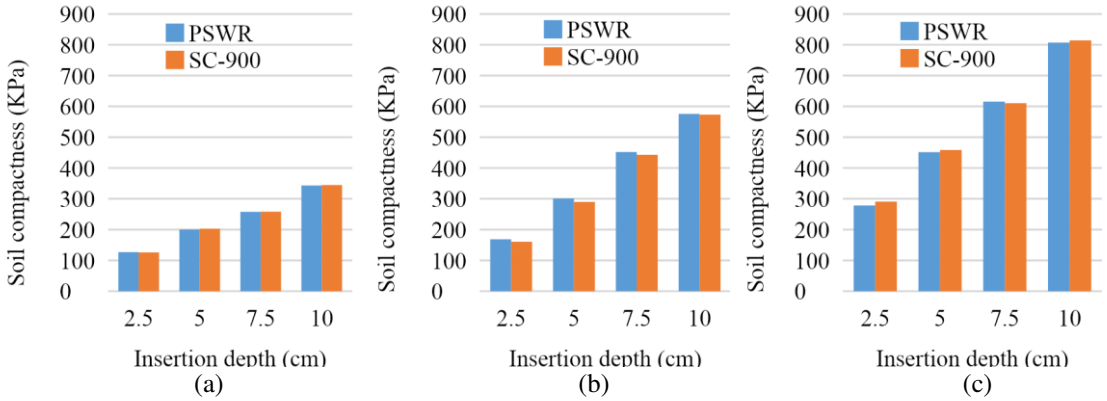

Figure 13. *Comparison of field soil compactness measurement. (a) First, (b) second, (c) third measurement site*

Conclusions

In this study, a combined penetrometer-SWR probe was designed and its performance was evaluated. Considering the errors caused by a varying penetration speed due to manual insertion during the cone-index measurement, we proposed to include synchronized acceleration measurement during the penetration process, and studied the acceleration and external force during the penetration process. The measurements errors were computed by comparing the results with that obtained from an SC-900 sensor, and the variation in the error after the acceleration compensation was observed. In addition, the measurement range of the double-metal-ring probe was analyzed and tested, and its performance was compared with that of a TDR sensor after calibration. Based on the experimental results, the following conclusions can be drawn:

First, there is a fluctuation in the penetration acceleration in the vertical direction, which causes a measurement error because of the complexity in the soil composition and non-standard manual operation during the penetration. The PSWR probe reduces the measurement error and improves the measurement accuracy by simultaneously measuring penetration acceleration.

Second, the HFSS simulation analysis and experiments show that the sensitive range of the PSWR probe designed in this study is within 10 cm diameter around the cone. To ensure accuracy in the results, the point of measurement should be selected such that the soil within a diameter of 10 cm is uniform and does not contain other impurities, such as gravel.

Third, calibration of the PSWR probe in the laboratory indicates that the output voltage has a significant linear relationship with the volumetric moisture content of the soil. The indoor tests prove that the moisture measurement probe can maintain a stable

http://www.aloki.hu ● ISSN 1589 1623 (Print) ● ISSN 1785 0037 (Online)
DOI: http://dx.doi.org/10.15666/aeer/1706_1393113944

output across multiple measurements; the results are comparable to that of a TDR sensor in terms of accuracy and stability.

Finally, the field measurement results obtained using the combined probe was compared to the drying-measurement results, and the maximum error in the volumetric moisture content measurement was obtained as 2.10%, which is less than 3%. This implies that the measurements by the combined probe are consistent with the results from the drying method, which satisfies the requirements for the practical implementation of the proposed probe.

Soil volumetric water content is closely related to soil compactness, soil porosity and soil bulk density, exploring the coupling relationship between them and establishing the coupling model will be the focus of future research.

Acknowledgements. This work is supported by the Fundamental Research Funds for the Central Universities (Grant No.2019YC15), the National Key Research and Development Program of China (Grant No.2017YFD0600901) and Special Fund for Beijing Common Construction Project.

REFERENCES

[1] Alaoui, A., Diserens, E. (2018): Mapping soil compaction. A review. – Current Opinion in Environmental Science & Health 5: 60-66.
[2] ASABE Standards (2009): EP542: Procedures for Using and Reporting Data Obtained With the Soil Cone Penetrometer. – ASABE, St. Joseph, MI.
[3] ASAE S313.3 FEB04. (1998): Soil Cone Penetrometer. – ASAE, S. America.
[4] Cui, F., Wu, Z. Y., Wang, L., et al. (2015): Application of the ground penetrating radar ARMA power spectrum estimation method to detect moisture content and compactness values in sandy loam. – Journal of Applied Geophysics 120: 26-35.
[5] Erbach, D. C., Kinney, G. R., Wilcox, A. P., et al. (1991): Strain gage to measure soil compaction. – Transactions of the ASAE 34(6): 2345-2348.
[6] Gaskin, G. J., Miller, J. D. (1996): Measurement of soil water content using a simplified impedance measuring technique. – Agric. Eng. Res. 63: 153-159.
[7] Goutal, N., Keller, T., Défossez, P., et al. (2013): Soil compaction due to heavy forest traffic: measurements and simulations using an analytical soil compaction model. – Annals of Forest Science 70(5): 545-556.
[8] Hummel, J. W., Ahmad, I. S., Sudduth, K. A., et al. (2004): Simultaneous soil moisture and cone index measurement. – Transactions of the ASAE 47(3): 607-618.
[9] Jin-Hong, X. U., Rui-Song, X. U., Miao, L. (2008): Quantitative analysis of moisture content and fieldspectrum of red soil. – Science of Surveying & Mapping 33(5): 43-45.
[10] Lin, J., Sun, Y., Lammers, P. S. (2014): Evaluating model-based relationship of cone index, soil water content and bulk density using dual-sensor penetrometer data. – Soil & Tillage Research 138: 9-16.
[11] Luo, X., Perumpral, J. V. (1995): Study on soil strength with microwave reflection loss. – Transactions of the Chinese Society of Agricultural Engineering 11(1): 46-51.
[12] Mossadeghi-Björklund, M., Arvidsson, J., Keller, T., et al. (2016): Effects of subsoil compaction on hydraulic properties and preferential flow in a Swedish clay soil. – Soil & Tillage Research 156: 91-98.
[13] Ogée, J., Brunet, Y. (2002): A forest floor model for heat and moisture including a litter layer. – Hydrol. 255: 212-233.
[14] Paltineanu, I. C., Starr, J. L. (1997): Real-time soil water dynamics using multisensor capacitance probes: laboratory calibration. – Soil Sci. Soc. Am. J. 61: 1576-1585.

http://www.aloki.hu ● ISSN 1589 1623 (Print) ● ISSN 1785 0037 (Online)
DOI: http://dx.doi.org/10.15666/aeer/1706_1393113944

[15] Perumpral J. V. (1987): Cone penetrometer applications - a review. – Trans. ASAE 30(4): 0939-0944.
[16] Pillinger, P., Géczy, A., Hudoba, Z., et al. (2018): Determination of soil density by cone index data. – Journal of Terramechanics 77: 69-74.
[17] Ronai, D., Shmulevich, I. (1995): Comparative analysis of some soil compaction measurement techniques. – International Agrophysics 9(3): 165-182.
[18] Rudnick, D. R., Lo, T., Singh, J., et al. (2018): Reply to comments on "Performance assessment of factory and field calibrations for electromagnetic sensors in a loam soil." – Agricultural Water Management 203: 272-276.
[19] Schaap, M. G., Bouten, W., Verstraten, J. M. (1997): Forest floor water content dynamics in a Douglas fir stand. – Hydrol. 201: 367-383.
[20] Singh, G., Das, B. M., Chong, M. K. (1997): Measurement of moisture content with a penetrometer. – Geotechnical Testing Journal 20(3): 317-323.
[21] Sun, Y., Schulze Lammers, P., Ma, D. (2004): Evaluation of a combined Penetrometer for simultaneous measurement of penetration resistance and soil water content. – Journal of Plant Nutrition and Soil Science 167: 745-751.
[22] Topp, G. C. (2003): Laboratory calibration, in-field validation and use of a soil penetrometer measuring cone resistance and water content. – Vadose Zone Journal 2(4): 633-641.
[23] Topp, G. C., Davis, J. L., Annan, A. P. (1980): Electromagnetic determination of soil water content: Measurements in coaxial transmission lines. – Water Resources Research 16(3): 574-582.
[24] Tranter, G., Minasny, B., Mcbratney, A. B., et al. (2008): Comparing spectral soil inference systems and mid-infrared spectroscopic predictions of soil moisture retention. – Soil Science Society of America Journal 72(5): 1394-1400.
[25] Vaz, C. M. P., Hopmans, J. W. (2001): Simultaneous measurement of soil penetration resistance and water content with a combined penetrometer–TDR moisture probe. – Soil Sci. Soc. Am. 65(1): 4-12.
[26] Vaz, C. M. P., Bassoi, L. H., Hopmans, J. W. (2001): Contribution of water content and bulk density to field soil penetration resistance as measured by a combined cone penetrometer–TDR probe. – J. Soil & Tillage Research 60(1): 35-42.
[27] Yan, X., Zhao, Y., Cheng, Q., et al. (2018): Determining forest duff water content using a low-cost standing wave ratio sensor. – Sensors 18(647): 1-11.
[28] Yanuka, M., Topp, G. C., Zegelin, S., et al. (1988): Multiple reflection and attenuation of time domain reflectometry pulses: theoretical considerations for applications to soil and water. – J. Water Resources Research 24(7): 939-944.
[29] Zegelin, S. J., White, I., Jenkins, D. R. (1989): Improved field probes for soil water content and electrical conductivity measurement using time domain reflectometry. – Water Resources Research 25(11): 2367-2376.
[30] Zoughi, R., Gray, S., Nowak, P. S. (1994): Cement paste compressive strength estimation using nondestructive microwave reflectometry. – Proceedings of SPIE - The International Society for Optical Engineering 2275: 89-93.

http://www.aloki.hu ● ISSN 1589 1623 (Print) ● ISSN 1785 0037 (Online)
DOI: http://dx.doi.org/10.15666/aeer/1706_1393113944

EFFECT OF TEMPERATURE AND PRECIPITATION ON STEM BIOMASS AND COMPOSITION OF WHITE BIRCH (*BETULA PLATYPHYLLA*) IN DAXING'ANLING MOUNTAINS INNER MONGOLIA, CHINA

KHAN, D.[1*] – DIN, E. U.[7] – MUNEER, M. A.[2] – HAYAT, M.[3] –KHAN, T. U.[4] – ASIF, M.[1] – SHAH, S.[1] – UDDIN, S.[5] – MUNIR, M. Z.[5] – ZAIB-UN-NISA[5,6] – YIHONG, Z.[1]– HUANG, H.[1*] – GAO, L.[1*]

[1]College of Forestry, Beijing Forestry University
No 35 Qinghua East Road, Haidian District, 100083 Beijing, China

[2]College of Grassland Science, Beijing Forestry University
No 35 Qinghua East Road, Haidian District, 100083 Beijing, China

[3]College of Soil and Water Conservation, Beijing Forestry University
No 35 Qinghua East Road, Haidian District, 100083 Beijing, China

[4]College of Nature Conservation, Beijing Forestry University
No 35 Qinghua East Road, Haidian District, 100083 Beijing, China

[5]School of Biological Sciences and Technology, Beijing Forestry University
No 35 Qinghua East Road, Haidian District, 100083 Beijing, China

[6]Sorghum Research Sub-Station, Dera Ghazi Khan, Punjab, Pakistan

[7]College of Environmental Sciences and Engineering, Beijing Forestry University, Beijing 100083, China

[*]Corresponding authors
e-mail: dilawarafridi333@hotmail.com, gaolushuag@bjfu.edu.cn, huago_huang@bjfu.edu.cn

(Received 23rd May 2019; accepted 16th Oct 2019)

Abstract. Forests play a major role in the regional and global carbon cycle. Climate change events have become serious issue, forests from various geographical regions have different sensitivities to climate variation. Therefore, we examine the effect of annual precipitation and annual temperature from 1950-2016 of white birch (Be*tula platyphylla)* stem biomass and composition in Daxing'anling Mountain Inner Mongolia China. We conduct a field survey, a total of 27 plots were established as the research area. In this study, we used allometric equation including the following components: diameter at breast height (DBH) and tree height (H). Our result showed that the response of *Betula platyphylla* stem biomass has a strong correlation with annual precipitation (R^2 = 0.80), and with temperature (R^2 = 0.75). A positive correlation was found for height with annual precipitation (R^2 = 0.76) and annual temperature (R^2 = 0.51). Additionally, a slightly positive correlation was observed for density with annual precipitation (R^2 = 0.26) and annual temperature (R^2 = 0.20). Our results also predicted that competition for survival played a significant role in tree growth. To achieve fast tree growth and high stem biomass response, systematically based forest management strategies, including thinning operation and selective cuttings could be established even under harsh Mongolian weather conditions. Our finding could suggest forest management guidelines for the normal growth of *Betula platyphylla* forest.
Keywords: *Betula platyphylla, stem biomass, forest ecosystem, global warming, carbon stock*

http://www.aloki.hu ● ISSN 1589 1623 (Print) ●ISSN1785 0037 (Online)
DOI: http://dx.doi.org/10.15666/aeer/1706_1394513959

Introduction

Understanding the prediction and response of forest ecosystem to climate change is a crucial challenge for scientists worldwide (Pan et al., 2013). During the last decade, most studied forest ecosystem characters are the tree biomass and carbon storage. The knowledge of the forest distribution is an essential feature for the conservation strategies, including the reduction of global warming by carbon store in forest ecosystem (Saatchi et al., 2011; Baccini et al., 2012). To study boreal forest is particularly important because they store 460 billion tons of carbon in their biomass and soil, which is equal to the total atmospheric carbon stock (Pan et al., 2011), and process 40 billion tons of carbon annually (Beer et al., 2010). Because they cover a large area of land and play an important role in global climate, regulating energy balance and evaporation at the earth. Inverse modeling of biomass and carbon sink sources from the latitudinal distribution of atmospheric carbon dioxide concentration indicates that a major terrestrial carbon sink is located in ecosystem of the northern hemisphere (Tans et al., 1990; Menon et al., 2007) and also believed that significant fraction of this carbon sink occurs in the northern boreal forest (Hyvönen et al., 2007). Boreal forests also contribute to the diversity, richness, productivity in Daxing'anling Mountain in Inner Mongolia China, which exists under a wide range of harsh environmental conditions (Fang et al., 2012). Recently, boreal forest to sequester a substantial amount of atmospheric carbon dioxide and store carbon in its biomass has focus attention from worldwide (Kasischke, 2000; Donato et al., 2011; Alongi, 2014). A recently conducted study on *Larix gmelinii* and *Betula platyphylla* suggested that stem biomass have a strong correlation with annual precipitation and maximum temperature (Khan et al., 2019).

Northern Mongolia Daxing'anling Mountains is the transaction zone between Siberian taiga and Asian steppes. This line of transaction takes place over several hundred kilometers from north to south (Walter, 1974). The climate of this region is strongly seasonal, characterized by short mild summers and long very cold winter with annual precipitation and temperature variation (Korpela et al., 2013). More than 90% annual precipitation fall as rain during the growing season and another hand annual temperature in Mongolia increased by 2014 ◦C from last 70 years, which is higher than the rise of global average temperature. Precipitation almost decreases in every region at least 0.1 mm/year (Oyuntuya et al., 2015). Further decreasing of precipitation is expected in inner mountains (Sato et al., 2007). Current climate change, is considered the main driver of the vegetation change and observation showed that regional climatic variation has resulted in change in the natural and biological system, such as snow melting and the extension of growing season in the mid-high latitude areas (Douville, 2006; Shea et al., 2015; Rangecroft et al., 2016). Forest degradation significantly impact carbon stock (Baccini et al., 2012), and the recent climatic trend is already impacting forest biomass worldwide (Phillips et al., 2009). Recent studied describe that precipitation and temperature influence the forest ecosystem. Such as a change in temperature and precipitation is directly associated with global warming (Hidalgo-Muñoz et al., 2011; Coumou and Rahmstorf, 2012; Coumou et al., 2013; Omondi et al., 2014). During the last decades, due to the change of precipitation and temperature, many forest sites are replaced by steppe vegetation, while the composition of remaining species changes in the favor of pioneer tree species. Therefore, regeneration of different species increase their interest, while the effect the growth of the native tree species such as white birch (*Betula platyphylla)* (Dulamsuren et al., 2011; Khishigjargal et al., 2014; Gradel et al., 2017). *Betula platyphylla* growth pattern relationship with climate change is also useful for the forecast of species distribution and forest productivity (James, 2011; De Grandpré et al., 2011).

http://www.aloki.hu ● ISSN 1589 1623 (Print) ●ISSN1785 0037 (Online)
DOI: http://dx.doi.org/10.15666/aeer/1706_1394513959

Betula platyphylla was also known as, Manchurian birch or Asian white birch. *Betula platyphylla* is one of the common tree species in Daxing'anling Mountains Inner Mongolia. This species is drought sensitive, have good resistance against frost and able to grow under different climatic condition (Gradel et al., 2017). *Betula platyphylla* had good economic value and its height can reach up to 27 m along with the life duration of 140 years (Zyryanova et al., 2010). It is also one of the pioneer tree species from the south forest outposts in Inner Mongolia. Still, it is the most dominant tree species in the forest instead of human disturbance, cutting and use is a fire due to its fast sprouting capability (Otoda et al., 2013). It is important to protect this species to maintain their forest cover because of its play a significant role in biomass storage as we as in carbon sequestration potential (Hansen et al., 2013). Numerous approaches examine to understand forest biomass. Some are based on a comparison of remote sensing data with standing variables, such as diameter, height, and density to estimate above-ground biomass of trees (Baraloto et al., 2011). This type of correlative studies provide spatially explicit and to verified the estimate the above-ground biomass for an extensive assessment of carbon stock (Saatchi et al., 2011). This method has great importance for mapping carbon stock and evaluating risk from land-use change, which is beneficial for policy involvements (Asner and Mascaro, 2014).

Therefore, allowed the author to investigate the effect of climatic factors and stand characteristics of stem biomass allocation pattern of *Betula platyphylla* species. Although the dataset of China has used to evaluate the temperature effect on biomass allocation in the forest (Lie and Xue, 2016). While data about the effect of climatic factors on stem biomass and composition of *Betula platyphylla* forest is still lacking. Therefore, we want to find out the relationship between climatic factors such as precipitation and temperature from 1950-2016 with *Betula platyphylla* stem biomass. We also want to examine the influence of climatic factors on the height and density of Betula platyphylla.

Material and methods

Study area

Daxing'anling mountains are located at (E'7118.19.10-W'126.41.52, N'47.48.35-S53.33.12) in the Heilongjiang province of China which cover the area of 83000 km^2 with an altitude of 3556 m (*Figure 1*). This area has cold continental monsoon weather with an annual temperature of 2.8°C. Annual precipitation mostly received in July to August from 350-500 mm. snow covers the land for five months in the winter season, which have depth up to 30-50 cm in the forest area with wind flow of 1106 miles per hours. *Betula platyphylla* is the dominant tree species along Dahurian larch (Larix gmelini), Scots pine (Pinus sylvestris var), Mongolian oak (mongolica) among others are common tree species. During the months of summer from April to July of each year usually occur thunderstorms, lightning fires which become a cause burning to this area.

Field data collection

To take forest data a field survey was conducted in 2017 in Daxing'anling mountain of Inner Mongolia Autonomous Region of China. We used a random sampling method and a total of 27 circular plots was taken in the study area. Each selected sampling plot have a radius of 17.84 m. To find out stem biomass and carbon stock of *Betula platyphylla* stand forest, tree diameter at breast height (DBH), tree height (H) and Density (D) were measured in the study area.

http://www.aloki.hu ● ISSN 1589 1623 (Print) ●ISSN1785 0037 (Online)
DOI: http://dx.doi.org/10.15666/aeer/1706_1394513959

Climatic data collection

Climatic factors, such as annual precipitation and annual temperature from 1950 to 2016 were chosen as the parameters in the study area of Daxing'anling Mountain Inner Mongolia, China (*Figure 2*). Data of annual precipitation and annual temperature were download from the (0.50) grid data with help of KNMI climate Explorer [https://climexp.knmi.nl]. The climate station was uniformly distributed in northeastern Inner Mongolia China. Climatic data of each sample plot was download from its coordinate using a global positioning system (GPS) with an accuracy of 1-meter distance. It is used to extract the geographical data of each sample plot. Climate record has been assessed by China metrological administration (CMA) to assure consistency with continuity and to maintain the quality of instrument location and relocation of the stations.

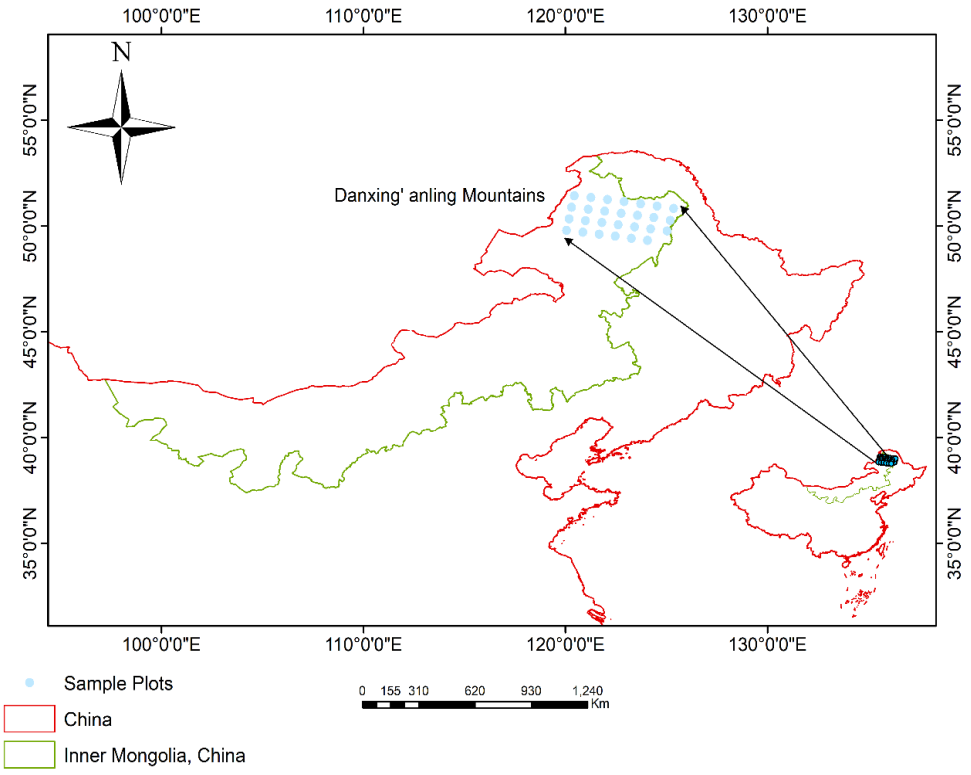

Figure 1. *Geographical Mapping of the study area. Map showing the geographic location of Betula platyphylla plots in Daxing'anling Mountains Inner Mongolia, China*

Stem biomass estimation

Several allometric equations have been developed by researchers to estimate biomass of different tree species using several variables as predictors or independent variables. DBH, total height, volume, basal area, density, and crown radius are the common variables used for estimation of tree biomass (Chave et al., 2005; Mandal et al., 2013; Goodman et al., 2014). The allometric equation gives us a result of the linear and nonlinear correlation between variables in two dimensions (Picard et al., 2012). The quality of the allometric equation is necessary for ensuring the accuracy of forest biomass estimation. It is not only the matter of error but also a statistical toll during the

http://www.aloki.hu ● ISSN 1589 1623 (Print) ●ISSN1785 0037 (Online)
DOI: http://dx.doi.org/10.15666/aeer/1706_1394513959

process should be considered (Picard et al., 2012). Stem biomass should be measured from the recommended component such as diameter at the breast height and height of the tree (H) (Chave et al., 2006). A model is considered reasonable if it yields estimates with minimum standard error (SEE), the minimum sum of the square of the residual error (SSE) throughout the range of data, does not give negative estimates and does not show a decrease in biomass with an increase in diameter or height (Ali et al., 2016).

The following allometric equation was used for *Betula platyphylla* to find out stem biomass and carbon stock which is developed by (Cheng and Li, 1989).

$$Ws = 0.1193 (D2\ H)\ 0.8372 \quad \text{(Eq.1)}$$

To estimate the stem biomass having a coefficient of determination of (R^2) of 0.1193. Where (Ws), is the stem biomass, tree diameter at breast height (D) and tree height (H). To find out total stem biomass per plot was summed for all plots and average to get the mean stem biomass, which was then converted to tons per hectare. Biomass fraction analysis was used to convert the value to its carbon equivalent. Carbon stock was determined as the product of the carbon sink and corresponding biomass of the individual tree.

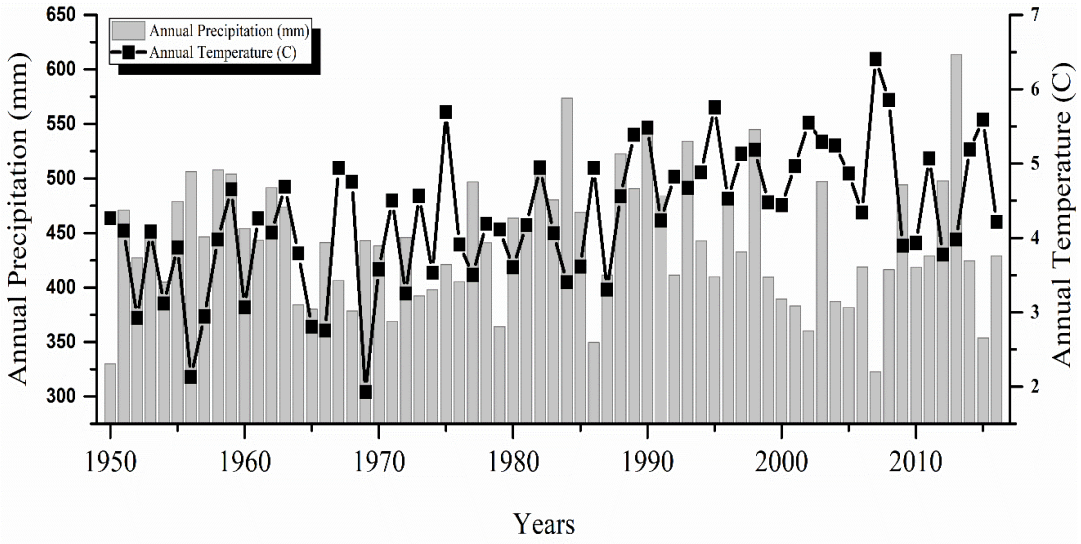

Figure 2. *Yearly climate diagram. Yearly climate diagram of annual precipitation and annual temperature from 1950-2016 in Daxing'anling Mountain Inner Mongolia, China*

Statistical analysis

Regression analysis was performed between dependent variables like stem biomass and carbon stock with explanatory variables like diameter, density, height and climatic variables Such as annual precipitation and annual temperature. The coefficient of determination (R^2) and probability level ($p \leq 0.05$) was used to determine the quality of curves. To check the variables relationship accuracy, we used linear regression analysis to check the variables relationship accuracy. All statistical analysis Analyses were performed using Origin-2016.

http://www.aloki.hu ● ISSN 1589 1623 (Print) ●ISSN1785 0037 (Online)
DOI: http://dx.doi.org/10.15666/aeer/1706_1394513959

Results

The growing stock of Betula platyphylla

Betula platyphylla is the second most dominant species of Daxing'anling Mountains Inner Mongolia China, instead of human's disturbance, cutting and fires, due to its sprouting capability. The result revealed that average stem density ranged from 71.7 ± 21.6 (trees ha^{-1}) while, the total range between low to high stem density was 34.0 ± 111.0 (trees ha^{-1}). The mean diameter of the tree was in the range of 16.3 ± 3.3 (cm) to 11.4 ± 23.8 (cm). The value of average height ranges from 20.8 ± 4.49 (m) to 14.0 ± 29.0 (m), (*Table 1*).

Table 1. *Growing stock characteristics of Betula platyphylla*

No	*Betula platyphylla*	Average density	Average diameter	Average height
1	Mean & Standard deviation	71.7±21.6	16.3±3.3	20.8±4.4
2	Minimum & Maximum	34.0±111.0	11.4±23.8	14.0±29.0

In order to study the relationship between stem biomass (ton/ha), height (m), density (ha^{-1}) with annual precipitation (mm) and annual temperature (^{0}C) regression models were developed in detail which is given below in (*Table 2*).

Table 2. *Relationship type, equation and R^2 value of the Betula platyphylla stand*

Climatic factor	Parameters	Relationship type	Equation	R^2 Value
Precipitation	Stem biomass	Polynomial, Linear	y = -115.9592+ 0.6129*x	0.8014
	Height	Polynomial, Linear	y = -21.9297 + 0.1015*x	0.7674
	Density	Polynomial, Linear	y = 81.8608+ 12.4413*x	0.0696
Temperature	Stem biomass	Polynomial, Linear	y = 81.8608+ 12.4413*x	0.7562
	Height	Polynomial, Linear	y = 12.4017 + 1.7366*x	0.5144
	Density	Polynomial, Linear	y = 54.3686 + 3.5805*x	0.0921

Relationship of precipitation (mm) and temperature (^{0}C) with stem biomass (ton/ha), height (m) and density (ha^{-1}) of *Betula platyphylla*

Biomass and carbon stock of Betula platyphylla with climatic factors

Total tree biomass distribution of *Betula platyphylla* forest was recorded at a range of 142.2±26.2 (ton/ha) with, variation from minimum to maximum 26.2±188.3 (ton/ha) was absorbed. While the total average stem biomass 142 (ton/ha) were found. Carbon stock recorded at the range of 68.7 ± 23.0 to 23.0 ± 134.4 (ton/ha) with, total average carbon stock of 71 (ton/ha) in the study area. The total average precipitation 421 (mm) recorded with the range of 421.2±38.3 along, variation from minimum to maximum 38.3±490.0 mm. The temperature range was 4.9±1.8 to 1.8±134.4 (^{0}C) with a total average temperature of 5 (^{0}C), which are given in the following (*Table 3*).

Effect of climatic factors on stem biomass, height, and density of Betula platyphylla

To study the influence of climatic variables such as annual precipitation and annual temperature from 1950-2016 on stem biomass, height and density of *Betula platyphylla* in Daxing'anling Mountains Inner Mongolia. Annual precipitation and annual temperature have a positive correlation with *Betula platyphylla* stem biomass and height. While a negative correlation was absorbed with a density of *Betula platyphylla*.

http://www.aloki.hu ● ISSN 1589 1623 (Print) ●ISSN1785 0037 (Online)
DOI: http://dx.doi.org/10.15666/aeer/1706_1394513959

According to coefficient correlation ($P \leq 0.05$), the result showed that annual precipitation ($R^2 = 0.80$) and annual temperature ($R^2 = 0.75$) have the strongest correlation with stem biomass (*Figure 3*).

While, height have strong correlation with annual precipitation ($R^2 = 0.76$) and annual temperature ($R^2 = 0.51$), respectively (*Figure 4*).

Table 3. *Biomass and carbon parameters with climatic variables of Betula platyphylla*

Betula platyphylla	**Mean & Standard deviation**	**Minimum± Maximum**
Stem Biomass	142.2±26.2	26.2±188.3
Carbon Stock	68.7±23.0	23.0±134.4
Precipitation	421.2±38.3	38.3±490.0
Temperature	4.9±1.8	1.8±134.4

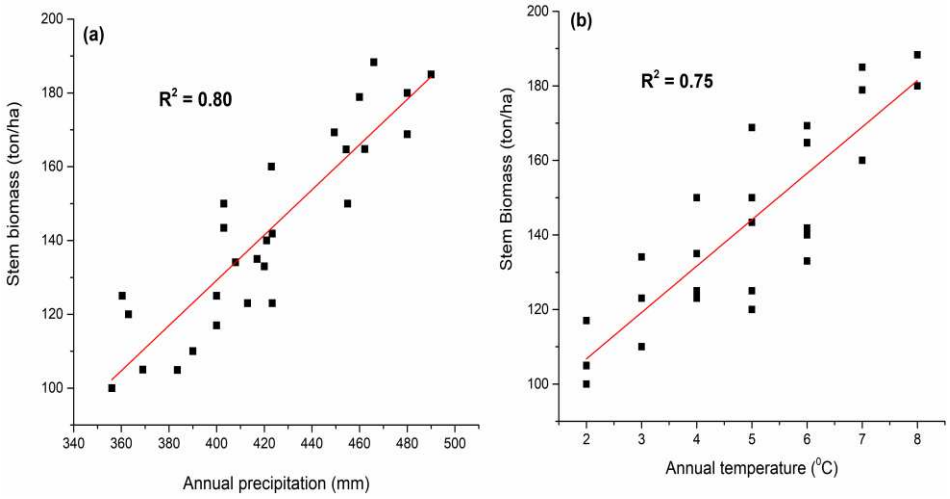

Figure 3. *Stem biomass correlation with annual precipitation and temperature. Betula platyphylla stem biomass correlation with Annual precipitation (a) and Annual temperature (b) from 1950 – 2016*

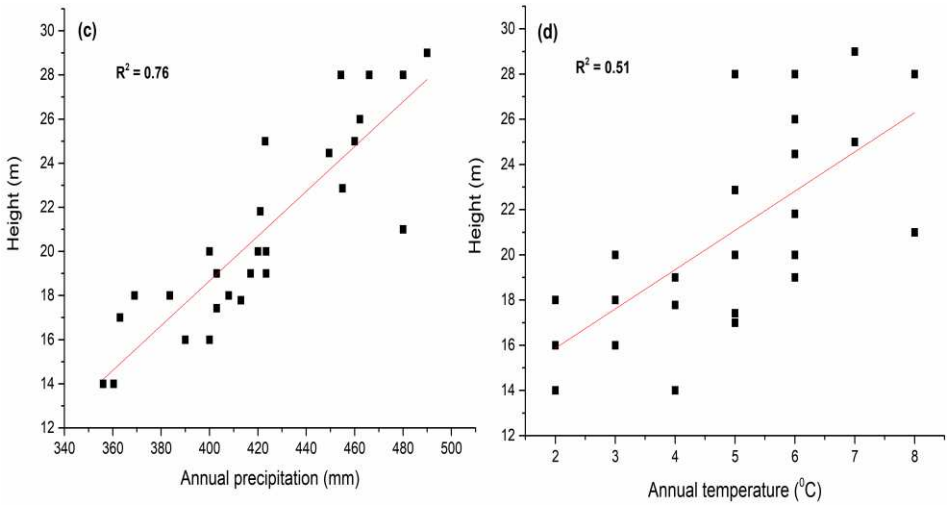

Figure 4. *Height correlation with annual precipitation and temperature. Betula platyphylla height correlation with Annual precipitation (c) and Annual temperature (d) from 1950 – 2016*

http://www.aloki.hu ● ISSN 1589 1623 (Print) ●ISSN1785 0037 (Online)
DOI: http://dx.doi.org/10.15666/aeer/1706_1394513959

In addition, slightly positive correlation was found between *Betula platyphylla* density with annual precipitation (R^2 = 0.26) and annual temperature (R^2 = 0.20) (*Figure 5*).

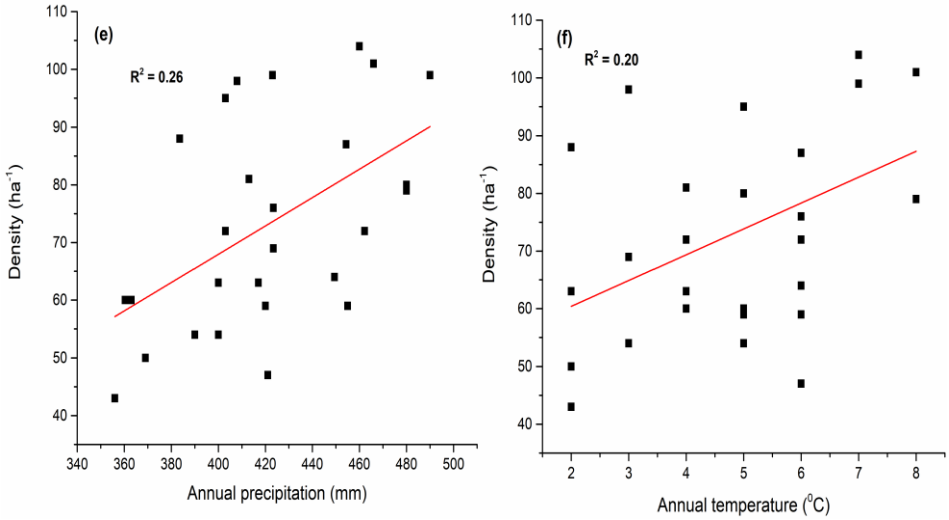

Figure 5. *Density correlation with annual precipitation and temperature. Betula platyphylla density correlation with Annual precipitation (e) and Annual temperature (f) from 1950 – 2016*

Discussion

Daxing'anling Mountains of Inner Mongolia is the important region of northern China. It is located at the high latitude of the northern hemisphere. Which is considered the most sensitive zone to global climate change (Dai et al., 2002; Wang et al., 2012). *Betula platyphylla* forest of this region plays a key role in the contribution of global carbon flux (Wang et al., 2006; Cai et al., 2015), as well as, in the establishment of forest lands consequent harvest and wildfires (Wang et al., 2015). It holds 8.39 million hectare of forest land and 0.76 billion m^3 of timber stock, respectively (Fang et al., 2001; Wang et al., 2006). Wide distribution with transaction character from boreal to the temperate zone, make it important in its prime production and carbon sequestration potential (Wang et al., 2006, 2008). Boreal forests in Inner Mongolia also have tremendous carbon storage mainly due to their vast forest area and living wood stock volume, though their coverage and carbon density lag behind many other provinces in China. Thus, as a whole, they play a significant role in the Chinese terrestrial ecosystem carbon cycle and in turn play an important role in the global carbon cycle (Sun et al., 2008). Meanwhile, there are many challenges as well as opportunities for a long-time forest in the area is lack of management with the extensive degradation of existent stands and poor stand quality and low productivity. The aggravation of desertification accompanying warming and drying trend under climate change is a huge threat to the forests.

Forest vegetation under different climate conditions reacts with a different way to their climatic factors. Climatic variables assessment of the last 66 year annual precipitation and annual temperature predict positive correlation with *Betula platyphylla*. *Betula platyphylla* stem biomass has a strong correlation with annual precipitation (R^2 = 0.80), and annual temperature (R^2 =0.75). While, positive correlation was found

http://www.aloki.hu ● ISSN 1589 1623 (Print) ●ISSN1785 0037 (Online)
DOI: http://dx.doi.org/10.15666/aeer/1706_1394513959

for height with annual precipitation (R^2 = 0.76) and annual temperature (R^2 = 0.51). Forests response positively to the impact of rising precipitation and temperature (Fang et al., 2003; Piao et al., 2005), and they have a positive effect on forest biomass (Lindner et al., 2010). Increase in precipitation and temperature will increase the absorption of carbon dioxide in the forest vegetation (Grant et al., 2004). In term of, stand age had an influence on forest carbon storage. Increasing of stand age also increase carbon storage capacity (Yu et al., 2017). At last, at last, the carbon storage in the forest decreases to a relatively stable level, due to the limiting of hydraulic resistance (Zaehle et al., 2006), and the growth of wood become very slow, which is almost not change (Liu et al., 2012). Some studies also predicted that precipitation and temperature are the main climatic factors that affect forest vegetation in the mid-western United States and China (Peckham et al., 2012), Russia (Alexeyev et al., 1995), Canada, and the Netherlands (Nabuurs and Mohren, 1993) among other places. While the response of vegetation types to precipitation and temperature has differed among places. The rising of precipitation and temperature have been found to increase the forest biomass in colder and wetter ecoregions (Dymond et al., 2015), but reduce the net rate of stem biomass in the Amazon rainforest (Brienen et al., 2015), and the growth rates of mature rainforests (Hopkin, 2007).

Additionally, the results showed that precipitation and temperature were significantly affected by plant density. Due to which the response of density of *Betula platyphylla* has a slightly positive correlation with the annual precipitation (R^2 = 0.035) and annual temperature (R^2 = 0.09), Similarly to the previous studies on tropical elevation transect forest (Leuschner et al., 2007; Girardin et al., 2010). Increase in plant density creates the interplant competition over light and precipitation which cause the disturbance in the balance of growth regulators. Under these conditions, plant density increases while, decrease in light and precipitation penetration into middle and lower layers of canopy and auxin decomposition (Imam and Ranjbar, 2000). Increase in plant density had a significant effect on *Betula platyphylla* plant height. Which tends to decrease because the plants compete over other growth affecting parameters than light (Mukhopadhyay and Sen, 1997).

Generally, denser *Betula platyphylla* stands forest results in higher total production, but the growth of the individual trees will be small (Ohtsuka et al., 2005). The increased volume production can though easily be lost through damages caused by wind or snow (Nykänen et al., 1997). With an increased number of stems density, the dimension decreases, while the volume concentrates in weaker dimensions (Coomes and Allen, 2007). The utility of wood products will be increased with lower stem densities (King et al., 2006). When pre-commercial thinning is performed competition for light and nutrition will decrease and the single stem will have the possibility to increase its diameter growth (Pothier, 2002; Karp and Shield, 2008). The main role of *Betula platyphylla* Silviculture is to have dense stands initially and then successively widening the spacing between the stems (Almgren, 1990). The green crown should never be smaller than half the stem length (Lapidge et al., 2000; Hörnfeldt, 2014). Since shad intolerant species like *Betula platyphylla* has a strong relationship between tree crown diameter and growth (Dolezal et al., 2004). *Betula platyphylla* stands with less than 50% of the living crown will have a small possibility to respond positively to future thinning (Dolezal et al., 2004). Thus, other stand variables such as height, diameter, and stem biomass could be important parameters to driving this observation,

http://www.aloki.hu ● ISSN 1589 1623 (Print) ●ISSN1785 0037 (Online)
DOI: http://dx.doi.org/10.15666/aeer/1706_1394513959

however, the data of wood density in mountain forests is infrequent and requires more sampling effort (Chave et al., 2009).

Demonstrating to find out stem biomass quantification in the *Betula platyphylla* forest in Daxing'anling Mountain. The destructive sampling method was not possible in our study site. That's why we attempt to minimize the uncertainty, we used the allometric equation developed in a similar climate condition with similar tree composition (Cheng and Li, 1989). In general tree diameter at the breast height and height of the tree is commonly used is a parameter to find out tree biomass in most equations (Wang, 2006; Dong et al., 2014; Wang et al., 2017). Furthermore, its depend on research goals and three components to investigate tree biomass with the help of equation (Zou et al., 2015; Kralicek et al., 2017).

Thus, during 1950–2016, the response of stem biomass and height of *Betula platyphylla* forest have a strong correlation with annual precipitation and annual temperature. While density has a negative correlation. That's mean, it also needs further research on forest management and the relative contribution of human activities to forest vegetation in Inner Mongolia.

Conclusion

In this study, we examined the effect climate factors, such as precipitation and temperature from 1950-2016 on *Betula platyphylla* forest ecosystem in Daxing'anling Mountains Northeast China. The response of *Betula platyphylla* to precipitation and temperature was positively correlated with stem biomass and tree height but negatively correlated with the density. Which predict that forest ecosystem also needs a proper management practice for normal growth. As we know, forests are an important component of the global carbon cycle. *Betula platyphylla* forest management can contribute towards emissions reductions and to carbon sequestration. To increase *Betula platyphylla* forest capacity regarding biomass and carbon sequestration providing incentives for the maintenance of future and existing forest resource, enhancing regeneration to increase species composition and stocks, increase people participation in forest management, decelerating hot spot for carbon sequestration and protected area.

Acknowledgements. This study was supported by grant from Key Project of National Key Research and Development Plan（2017YFC0504003-1). We are thankful to the funding agency and all people how helped us during this study.

REFERENCES

[1] Alexeyev, V., Birdsey, R., Stakanov, V., Korotkov, I. (1995): Carbon in vegetation of Russian forests: methods to estimate storage and geographical distribution. – Water, Air, and Soil Pollution 82: 271-282.

[2] Ali, A., Iftikhar, M., Ahmad, S. N., Muhammad, S., Khan, A. A. (2016): Development of allometric equation for biomass estimation of Cedrus deodara in dry temperate forests of Northern Pakistan. – Journal of Biodiversity and Environmental Sciences 9: 43-50.

[3] Almgren, G. (1990): Lövskog: björk, asp och al i skogsbruk och naturvård: Skogsstyr.

[4] Alongi, D. M. (2014): Carbon cycling and storage in mangrove forests. – Annual review of marine science 6: 195-219.

http://www.aloki.hu ● ISSN 1589 1623 (Print) ●ISSN1785 0037 (Online)
DOI: http://dx.doi.org/10.15666/aeer/1706_1394513959

[5] Asner, G. P., Mascaro, J. (2014): Mapping tropical forest carbon: Calibrating plot estimates to a simple LiDAR metric. – Remote Sensing of Environment 140: 614-624.
[6] Baccini, A., Goetz, S. J., Walker, W. S., Laporte, N. T., Sun, M., Sulla-Menashe, D., Hackler, J., Beck, P. S. A., Dubayah, R., Friedl, M. A., Samanta, S., Houghton, R. A. (2012): Estimated carbon dioxide emissions from tropical deforestation improved by carbon-density maps. – Nature climate change 2: 182-185.
[7] Baraloto, C., Rabaud, S., Molto, Q., Blanc, L., Fortunel, C., Hérault, B., Dávila, N., Mesones, I., Rios, M., Valderrama, E. Fine, P. V. A. (2011): Disentangling stand and environmental correlates of aboveground biomass in Amazonian forests. – Global change biology 17: 2677-2688.
[8] Beer, C., Reichstein, M., Tomelleri, E., Ciais, P., Jung, M., Carvalhais, N., Rödenbeck, C. (2010): Terrestrial gross carbon dioxide uptake: global distribution and covariation with climate. – Science: 1184984.
[9] Brienen, R. J. W., Phillips, O. L., Feldpausch, T. R., Gloor, E., Baker, T. R. (2015): Long-term decline of the Amazon carbon sink. – Nature 519: 344-348.
[10] Cai, H., Di, X., Chang, S. X., Wang, C. K., Shi, B., Geng, P. F., Jin, G. Z. (2015): Carbon storage, net primary production, and net ecosystem production in four major temperate forest types in northeastern China. – Canadian Journal of Forest Research 46: 143-151.
[11] Chave, Jr., Andalo, C., Brown, S., Cairns, M. A., Chambers, J. Q., Eamus, D., Fölster, H., Fromard, F., Higuchi, N., Kira, T., Lescure, J.-P., Nelson, B. W., Ogawa, H., Puig, H., Riéra, B., Yamakura, T. (2005): Tree allometry and improved estimation of carbon stocks and balance in tropical forests. – Oecologia 145: 87-99.
[12] Chave, J., Muller-Landau, H. C., Baker, T. R., Easdale, T. A., Steege, H., Webb, C. O. (2006): Regional and phylogenetic variation of wood density across 2456 neotropical tree species. – Ecological applications 16: 2356-2367.
[13] Chave, J., Coomes, D., Jansen, S., Lewis, S. L., Swenson, N. G., Zanne, A. E. (2009): Towards a worldwide wood economics spectrum. – Ecology letters 12: 351-366.
[14] Cheng, Y. X., Li, Z. X. (1989): A study on biomass of three main forest types in Larix gmelinii forest. – Inner Mongolia Forestry Investigation and Design 4: 89-100.
[15] Coomes, D. A., Allen, R. B. (2007): Mortality and tree-size distributions in natural mixed-age forests. – Journal of Ecology 95: 27-40.
[16] Coumou, D., Rahmstorf, S. (2012): A decade of weather extremes. – Nature Climate Change 2: 491-496. Nature Publishing Group. doi.
[17] Coumou, D., Robinson, A., Rahmstorf, S. (2013): Global increase in record-breaking monthly-mean temperatures. – Climatic Change 118: 771-782.
[18] Dai, L., Wu, G., Zhao, J., Kong, H. M., Shao, G. F., Deng, H. B. (2002): Carbon cycling of alpine tundra ecosystems on Changbai Mountain and its comparison with arctic tundra. – Science in China Series D: Earth Sciences 45: 903.
[19] De Grandpré, L., Tardif, J. C., Hessl, A., Pederson, N., Conciatori, F., Green, T. R., Oyunsanaa, B., Baatarbileg, N. (2011): Seasonal shift in the climate responses of Pinus sibirica, Pinus sylvestris, and Larix sibirica trees from semi-arid, north-central Mongolia. – Canadian Journal of Forest Research 41: 1242-1255.
[20] Dolezal, J., Ishii, H., Vetrova, V. P., Sumida, A., Hara, T. (2004): Tree growth and competition in a Betula platyphylla–Larix cajanderi post-fire forest in central Kamchatka. – Annals of Botany 94: 333-343.
[21] Donato, D. C., Kauffman, J. B., Murdiyarso, D., Kurnianto, S., Stidham, M., Kanninen, M. (2011): Mangroves among the most carbon-rich forests in the tropics. – Nature geoscience 4: 293.
[22] Dong, L., Zhang, L., Li, F. (2014): A compatible system of biomass equations for three conifer species in Northeast, China. – Forest Ecology and Management 329: 306-317.
[23] Douville, H. (2006): Impact of regional SST anomalies on the Indian monsoon response to global warming in the CNRM climate model. – Journal of climate 19: 2008-2024.

http://www.aloki.hu ● ISSN 1589 1623 (Print) ●ISSN1785 0037 (Online)
DOI: http://dx.doi.org/10.15666/aeer/1706_1394513959

[24] Dulamsuren, C., Hauck, M., Leuschner, H. H., Leuschner, C. (2011): Climate response of tree-ring width in Larix sibirica growing in the drought-stressed forest-steppe ecotone of northern Mongolia. – Annals of Forest Science 68: 275-282.
[25] Dymond, C. C., Beukema, S., Nitschke, C. R., Coates, K. D., Scheller, R. M. (2015): Carbon sequestration in managed temperate coniferous forests under climate change. – Biogeosciences Discussions 12.
[26] Fang, J., Chen, A., Peng, C., Zhao, S., Ci, L. (2001): Changes in forest biomass carbon storage in China between 1949 and 1998. – Science 292: 2320-2322.
[27] Fang, J., Piao, S., Field, C. B., Pan, Y., Guo, Q., Zhou, L., Peng, C., Tao, S. (2003): Increasing net primary production in China from 1982 to 1999. – Frontiers in Ecology and the Environment 1: 293-297.
[28] Fang, J., Shen, Z., Tang, Z., Wang, X., Wang, Z., Feng, J., Liu, Y., Qiao, X., Wu, X., Zheng, C. (2012): Forest community survey and the structural characteristics of forests in China. – Ecography 35: 1059-1071.
[29] Girardin, C. A. J., Malhi, Y., Aragao, L., Mamani, M., Huaraca Huasco, W., Durand, L., Feeley, K. J., Rapp, J., Silva-Espejo, J. E., Silman, M., Salinas, N., Whittaker, R. J. (2010): Net primary productivity allocation and cycling of carbon along a tropical forest elevational transect in the Peruvian Andes. – Global change biology 16: 3176-3192.
[30] Goodman, R. C., Phillips, O. L., Baker, T. R. (2014): The importance of crown dimensions to improve tropical tree biomass estimates. – Ecological applications 24: 680-698.
[31] Gradel, A., Haensch, C., Ganbaatar, B., Dovdondemberei, B., Nadaldorj, O., Günther, B. (2017): Response of white birch (Betula platyphylla Sukaczev) to temperature and precipitation in the mountain forest steppe and taiga of northern Mongolia. – Dendrochronologia 41: 24-33.
[32] Grant, R. F., Arain, A., Arora, V., Barr, A., Black, T. A., Chen, J., Wang, S., Yuan, F., Zhang, Y. (2004): Modelling temperature effects on CO2 and energy exchange in temperate and boreal coniferous forests. – AGU Spring Meeting Abstracts.
[33] Hansen, M. C., Potapov, P. V., Moore, R., Hancher, M., Turubanova, S. A., Tyukavina, A., Thau, D., Stehman, S. V., Goetz, S. J., Loveland, T. R., Kommareddy, A., Egorov, A., Chini, L., Justice, C. O., Townshend, J. R. G. (2013): High-resolution global maps of 21st-century forest cover change. – Science 342: 850-853.
[34] Hidalgo-Muñoz, J., Argüeso, D., Gámiz-Fortis, S., Esteban-Parra, M. J., Castro-Díez, Y. (2011): Trends of extreme precipitation and associated synoptic patterns over the southern Iberian Peninsula. – Journal of Hydrology 409: 497-511.
[35] Hopkin, M. (2007): Rising temperatures "will stunt rainforest growth". – Nature 659.
[36] Hörnfeldt, R. (2014): Silviculture adapted to multiple goals in Swedish small scale forestry. – Acta Universitatis Agriculturae Sueciae: 1652-6880; 2014:42.
[37] Hyvönen, R., Ågren, G. I., Linder, S., Persson, T., Cotrufo, M. F., Ekblad, A., Freeman, M., Grelle, A., Janssens, I. A., Jarvis, P. G., Kellomäki, S., Lindroth, A., Loustau, D., Lundmark, T., Norby, R. J., Oren, R., Pilegaard, K., Ryan, M. G., Sigurdsson, B. D., Strömgren, M., van Oijen, M., Wallin, G. (2007): The likely impact of elevated [CO2], nitrogen deposition, increased temperature and management on carbon sequestration in temperate and boreal forest ecosystems: a literature review. – New Phytologist 173: 463-480.
[38] Imam, Y., Ranjbar, G. (2000): Effect of plant density and drought stress at vegetative growth stage on yield, yield components and water use efficiency in grain corn. – Iranian Journal of Agricultural Researches 2: 118-129.
[39] James, T. M. (2011): Temperature sensitivity and recruitment dynamics of Siberian larch (Larix sibirica) and Siberian spruce (Picea obovata) in northern Mongolia's boreal forest. – Forest Ecology and Management 262: 629-636.
[40] Karp, A., Shield, I. (2008): Bioenergy from plants and the sustainable yield challenge. – New Phytologist 179: 15-32.

http://www.aloki.hu ● ISSN 1589 1623 (Print) ●ISSN1785 0037 (Online)
DOI: http://dx.doi.org/10.15666/aeer/1706_1394513959

[41] Khan, D., Muneer, M. A., Nisa, Z. U., Shah, S., Amir, M., Saeed, S., Uddin, S., Munir, M. Z., Gao, L., Huang, H. (2019): Effect of Climatic Factors on Stem Biomass and Carbon Stock of Larix gmelinii and Betula platyphylla in Daxing'anling Mountain of Inner Mongolia, China. – Advances in Meteorology, 2019.
[42] Kasischke, E. S. (2000): Boreal ecosystems in the global carbon cycle. – Fire, climate change, and carbon cycling in the boreal forest (Springer): 19-30.
[43] Khishigjargal, M., Dulamsuren, C., Leuschner, H. H., Leuschner, C., Hauck, M. (2014): Climate effects on inter-and intra-annual larch stemwood anomalies in the Mongolian forest-steppe. – Acta oecologica 55: 113-121.
[44] King, D. A., Davies, S. J., Tan, S., Md. Noor, N. S. (2006): The role of wood density and stem support costs in the growth and mortality of tropical trees. – Journal of Ecology 94: 670-680.
[45] Korpela, K., Delgado, M., Henttonen, H., Korpimäki, E., Koskela, E., Ovaskainen, O., Pietiäinen, H., Sundell, J., Yoccoz, N. G., Huitu, O. (2013): Nonlinear effects of climate on boreal rodent dynamics: mild winters do not negate high-amplitude cycles. – Global Change Biology 19: 697-710.
[46] Kralicek, K., Huy, B., Poudel, K. P., Temesgen, H., Salas, C. (2017): Simultaneous estimation of above-and below-ground biomass in tropical forests of Viet Nam. – Forest Ecology and Management 390: 147-156.
[47] Lapidge, M., Godden, M., Keynes, S. (2000): Anglo-Saxon England. – Cambridge University Press.
[48] Leuschner, C., Moser, G., Bertsch, C., Röderstein, M., Hertel, D. (2007): Large altitudinal increase in tree root/shoot ratio in tropical mountain forests of Ecuador. – Basic and Applied Ecology 8: 219-230.
[49] Lie, G., Xue, L. (2016): Biomass allocation patterns in forests growing different climatic zones of China. – Trees 30: 639-646.
[50] Lindner, M., Maroschek, M., Netherer, S., Netherer, S., Kremer, A., Barbati, A., Garcia-Gonzalo, J., Seidl, R., Delzon, S., Corona, P., Kolström, M., Lexer, M. J., Marchetti, M. (2010): Climate change impacts, adaptive capacity, and vulnerability of European forest ecosystems. – Forest Ecology and Management 259: 698-709.
[51] Liu, Y. C., Yu, G. R., Wang, Q. F., Zhang, Y. J. (2012): Huge carbon sequestration potential in global forests. – Journal of Resources and Ecology 3: 193-201.
[52] Mandal, R. A., Yadav, B. K. V., Yadav, K. K., Dutta, I. C., Haque, S. M. (2013): Development of allometric equation for biomass estimation of eucalyptus camaldulensis: a study from Sagarnath Forest, Nepal. – Int J Biodiv Ecosyst 1: 1-7.
[53] Menon, S., Denman, K. L., Brasseur, G. (2007): Couplings between changes in the climate system and biogeochemistry. – Lawrence Berkeley National Lab. (LBNL), Berkeley, CA (United States).
[54] Mukhopadhyay, D., Sen, S. (1997): Augmentation of growth variables and yield components of plants yielding spices by foliar application of diazotrophic bacteria. – Indian Journal of Agricultural Research 31: 1-9.
[55] Nabuurs, G., Mohren, G. (1993): Carbon in Dutch forest ecosystems. – NJAS wageningen journal of life sciences 41: 309-326.
[56] Nykänen, M.-L., Peltola, H., Quine, C. P., Kellomäki, S., Broadgate, M. (1997): Factors affecting snow damage of trees with particular reference to European conditions. – Silva Fennica 31(2): 193-213.
[57] Ohtsuka, T., Akiyama, T., Hashimoto, Y., Inatomi, M., Sakai, T., Jia, S., Mo, W., Tsuda, S., Koizumi, H. (2005): Biometric based estimates of net primary production (NPP) in a cool-temperate deciduous forest stand beneath a flux tower. – Agricultural and Forest Meteorology 134: 27-38.
[58] Omondi, P. A., Awange, J. L., Forootan, E., Ogallo, L., Barakiza, R., Girmaw, G. B., Fesseha, I., Kululetera, V., Kilembe, C., Mbati, M. M., Kilavi, M., King'uyu, S. M., Omeny, P., Njogu, A. K., Badr, E. M., Musa, T. A., Muchiri, P., Bamanya, D.,

http://www.aloki.hu ● ISSN 1589 1623 (Print) ●ISSN1785 0037 (Online)
DOI: http://dx.doi.org/10.15666/aeer/1706_1394513959

Komutungaet, E. (2014): Changes in temperature and precipitation extremes over the Greater Horn of Africa region from 1961 to 2010. – International Journal of Climatology 34: 1262-1277.

[59] Otoda, T., Sakamoto, K., Hirobe, M., Undarmaa, J., Yoshikawa, K. (2013): Influences of anthropogenic disturbances on the dynamics of white birch (Betula platyphylla) forests at the southern boundary of the Mongolian forest-steppe. – Journal of forest research 18: 82-92.

[60] Oyuntuya, S., Dorj, B., Shurentsetseg, B. (2015): Agrometeorological information for the adaptation to climate change. Почвы степных и лесостепных экосистем Внутренней Азии и проблемы их рационального использования: 135-140.

[61] Pan, Y., Birdsey, R. A., Fang, J., Houghton, R., Kauppi, P. E., Kurz, W. A., Phillips, O. L., Shvidenko, A., Lewis, S. L., Canadell, J. G., Ciais, P., Jackson, R. B., Pacala, S. W., McGuire, A. D., Piao, S., Rautiainen, A., Sitch, S., Hayes, D. (2011): A large and persistent carbon sink in the world's forests. – Science: 1201609.

[62] Pan, Y., Birdsey, R. A., Phillips, O. L., et al. (2013): The structure, distribution, and biomass of the world's forests. – Annual Review of Ecology, Evolution, and Systematics 44: 593-622.

[63] Peckham, S. D., Gower, S. T., Buongiorno, J. (2012): Estimating the carbon budget and maximizing future carbon uptake for a temperate forest region in the US. – Carbon balance and management 7: 6.

[64] Phillips, O. L., Aragão, L. E., Lewis, S. L., et al. (2009): Drought sensitivity of the Amazon rainforest. – Science 323: 1344-1347.

[65] Piao, S., Fang, J., Zhou, L., Zhu, B., Tan, K., Tao, S. (2005): Changes in vegetation net primary productivity from 1982 to 1999 in China. – Global Biogeochemical Cycles 19.

[66] Picard, N., Saint André, L., Henry, M. (2012): Manual for building tree allometric equations: from the field to the prediction. – Food and Agriculture Organization of the United Nations, Centre de Coopération Internationale en Recherche Agronomique, Rome.

[67] Pothier, D. (2002): Twenty-year results of precommercial thinning in a balsam fir stand. – Forest Ecology and Management 168: 177-186.

[68] Rangecroft, S., Suggitt, A. J., Anderson, K., Harrison, S. (2016): Future climate warming and changes to mountain permafrost in the Bolivian Andes. – Climatic Change 137: 231-243.

[69] Saatchi, S. S., Harris, N. L., Brown, S., Lefsky, M., Mitchard, E. T. A., Salas, W., Zutta, B. R., Buermann, W., Lewis, S. L., Hagen, S., Petrova, S., White, L., Silman, M., Morel, A. (2011): Benchmark map of forest carbon stocks in tropical regions across three continents. – Proceedings of the National Academy of Sciences 108: 9899-9904.

[70] Sato, T., Kimura, F., Kitoh, A. (2007): Projection of global warming onto regional precipitation over Mongolia using a regional climate model. – Journal of Hydrology 333: 144-154.

[71] Shea, J. M., Immerzeel, W., Wagnon, P., Vincent, C., Bajracharya, S. (2015): Modelling glacier change in the Everest region, Nepal Himalaya. – The Cryosphere 9: 1105-1128.

[72] Sun, C., Chen, L., Chen, L., Han, L., Bass, S. (2008): Global Forest Product Chains. – www.iisd.org.

[73] Tans, P. P., Fung, I. Y., Takahashi, T. (1990): Observational contrains on the global atmospheric CO2 budget. – Science 247: 1431-1438.

[74] Walter, H. (1974): The vegetation of Eastern Europe, Northern Asia and Central Asia. – Regional vegetation monographs, Vol. VII. The vegetation of Eastern Europe, Northern Asia and Central Asia. Regional vegetation monographs, Vol. VII.

[75] Wang, C. (2006): Biomass allometric equations for 10 co-occurring tree species in Chinese temperate forests. – Forest Ecology and Management 222: 9-16.

[76] Wang, X., Fang, J., Tang, Z., Zhu, B. (2006): Climatic control of primary forest structure and DBH–height allometry in Northeast China. – Forest Ecology and Management 234: 264-274.

http://www.aloki.hu ● ISSN 1589 1623 (Print) ●ISSN1785 0037 (Online)
DOI: http://dx.doi.org/10.15666/aeer/1706_1394513959

[77] Wang, H.-m., Saigusa, N., Zu, Y.-g., Wang, W.-j., Yamamoto, S., Kondo, H. (2008): Carbon fluxes and their response to environmental variables in a Dahurian larch forest ecosystem in northeast China. – Journal of forestry research 19: 1-10.
[78] Wang, H., Wang, W., Qiu, L., Su, D. X. (2012): Differences in biomass, litter layer mass and SOC storage changing with tree growth in Larix gmelinii plantations in Northeast China. – Acta Ecol. Sin 32: 833-843.
[79] Wang, X., Weng, Y., Liu, G., Krasowski, M. J., Yang, C. P. (2015): Variations in carbon concentration, sequestration and partitioning among Betula platyphylla provenances. – Forest Ecology and Management 358: 344-352.
[80] Wang, X., Bi, H., Ximenes, F., Ramos, J., Li, Y. (2017): Product and residue biomass equations for individual trees in rotation age Pinus radiata stands under three thinning regimes in New South Wales, Australia. – Forests 8: 439.
[81] Yu, Y., Chen, J. M., Yang, X., Fan, W., Li, M., He, L. (2017): Influence of site index on the relationship between forest net primary productivity and stand age. – PloS one 12: e0177084.
[82] Zaehle, S., Sitch, S., Prentice, I. C., Liski, J., Cramer, W., Erhard, M., Hickler, T., Smith, B. (2006): The importance of age-related decline in forest NPP for modeling regional carbon balances. – Ecological applications 16: 1555-1574.
[83] Zou, W.-T., Zeng, W.-S., Zhang, L.-J., Zeng, M. (2015): Modeling crown biomass for four pine species in China. – Forests 6: 433-449.
[84] Zyryanova, O. A., Terazawa, M., Koike, T., Zyryanov, V. I. (2010): White birch trees as resource species of Russia: their distribution, ecophysiological features, multiple utilizations. – Eurasian Journal of Forest Research 13: 25-40.

http://www.aloki.hu ● ISSN 1589 1623 (Print) ●ISSN1785 0037 (Online)
DOI: http://dx.doi.org/10.15666/aeer/1706_1394513959

BIOLOGICAL ENHANCEMENT BASED ON CAST PROCESS AND DENITRIFICATION PERFORMANCE OF SOLID CARBON SOURCE FOR LOW C/N DOMESTIC SEWAGE

XIAO, J.

School of Civil and Architectural Engineering, Liaoning University of Technology
Jinzhou 121001, P. R. China
(e-mail:xiaojing@lnut.edu.cn)

(Received 24th May 2019; accepted 25th Oct 2019)

Abstract. In winter, low sludge activity, low microbial abundance and low C/N directly affect the quality of wastewater and the removal of total nitrogen in wastewater treatment plants. In this paper, the CAST process for treating low C/N domestic sewage is selected as the experimental reactor, and the method of a combining solid carbon source with biological reinforcement is used to raise the discharge of effluent up to the standard. The target bacteria were immobilized with artificial filler, and different bacterial components were placed in different positions of CAST reactor. The ammonia nitrogen, total nitrogen and COD in the effluent of the system were measured, and the changes of microbial community structure in the treatment process were analyzed by PCR-DGGE technology, so as to determine the effect of solid carbon source and biological reinforcement on the denitrification performance of CAST process.
Keywords: *domestic sewage, activated sludge, high efficiency denitrification, aerobic denitrifying bacteria, community structure*

Introduction

Nitrogen discharged into it will have a great impact on the water body. Therefore, denitrification is an important part of sewage treatment. At present, sewage treatment plants around the world need to be upgraded, and efficient denitrification is a key issue in sewage treatment (Adouani et al., 2015). For domestic sewage, the main influent nitrogen is ammonia nitrogen. At present, the denitrification process in activated sludge system is mainly composed of nitrification process and denitrification process. Any link of the process is limited, which will affect the final denitrification effect of the system and directly affect the quality of the effluent (Magrí et al., 2012). For the traditional denitrification principle of activated sludge system, the main factors that restrict the nitrification process include insufficient aeration and low abundance of nitrifying bacteria; the main factors that restrict the denitrification process include excessive aeration leading to the restriction of denitrifying bacteria and insufficient carbon source restricting the denitrification process (Bellucci et al., 2013).

In this paper, Cyclic Activated Sludge Technology (CAST) process for treating low C/N domestic sewage was selected as the experimental reactor. Biological enhancement and solid carbon source were used to enhance the denitrification performance of the reactor. Nitrification and denitrification can improve the denitrification performance simultaneously. Nitrifying bacteria, anoxic denitrifying bacteria, aerobic denitrifying bacteria and corn cob solid carbon source were used to enhance the denitrification performance of CAST process for treating low C/N domestic sewage (Chen et al., 2016). The changes of COD, NH_4^+-N and TN in the control group and the experimental group with biological agents and corncob were investigated during the experiment. The changes of activated sludge community structure in the two reactors were analyzed by

http://www.aloki.hu ● ISSN 1589 1623 (Print) ●ISSN1785 0037 (Online)
DOI: http://dx.doi.org/10.15666/aeer/1706_1396113974

PCR-DGGE technology, and the adaptability and stability of artificial enhanced biological agents in the system were determined.

Materials and Methods

Experimental materials

Strains and activated sludge

Nitrobacteria were gathered from the compound nitrifying agent M preserved in the laboratory. Anoxic denitrifying bacteria come from the compound anoxic denitrifying bacteria agent Q preserved in the laboratory. Aerobic denitrifying bacteria were compounded by *P.sp., P.stutzeri, P.aeruginosa* according to 1:1:1. Activated sludge is taken from the surplus sludge of Sewage Treatment Plant close to river in a county.

Corncob

Corn cob for experiment comes from Shapingba District of Chongqing City and is cut after recycling, screened by 1 mesh screen, and then screened by 2 meshes screen. Corncobs on the screen were used as experimental materials. Corncobs were about 1-2 cm in diameter. Two days after drying in an oven at 30℃, it was stored in a dryer.

Inlet

The background monitoring of the influent quality of domestic sewage treatment plant close to river in a county was carried out. The actual influent COD was 100-150 mg/L, TN was 20-40 mg/L, and NH_4^+-N was 15-30 mg/L. In order to better simulate the water quality of the sewage treatment plant, the water used in this experiment was diluted and $(NH_4)_2SO_4$ and $NaNO_3$ were prepared for school domestic sewage. The control of COD was about 150 mg/L, TN was about 40 mg/L, and NH_4^+-N was about 30 mg/L. It is generally considered that the wastewater with COD less than 200 mg/L and wastewater COD/TN is 5.6.

Table 1. *Model of experimental instrument*

Instrument	Manufacturer	Model
Bed temperature incubator	Shanghai Fuma Experimental Equipment Co., Ltd.	QYC200
Digital display electrothermal incubator	Shanghai Boxun Industrial Co., Ltd. Medical Equipment Factory	HPX-9297MBE
Super Clean Workbench	Shanghai Boxun Industrial Co., Ltd. Medical Equipment Factory	SW-CJ-ICU
One-thousandth balance	Metler Toledo	AL104-IC
optical microscope	Motic	BA200

Design and operation of CAST reactor

Two groups of parallel reactors were set up, the control group and the experimental group respectively, the reactor schematic diagram is shown in *Figure 1*. Volumes of anaerobic selective zone, pre-reaction zone and main reaction zone in CAST reactor are 10.5L, 12L and 126L, respectively. The anaerobic selective zone L×B×H = (300×100×350) mm; the pre-reaction zone is L-type, 300 mm long, 100 mm wide on the top and 200 mm wide on the bottom, 350 mm high on the front and 600 mm high on

http://www.aloki.hu ● ISSN 1589 1623 (Print) ●ISSN1785 0037 (Online)
DOI: http://dx.doi.org/10.15666/aeer/1706_1396113974

the back; the main reaction zone L×B×H = (700×300×600) mm. The operation period is set up to be 4 hours, water intake 1 hour, aeration 2 hours, standing 1 hour, drainage 1 hour, and aeration begins during water intake. MLSS is set at 3500 mg/L, water filling ratio is 1/3, reflux ratio of mixed liquid is 30%, bottom microporous explosion is used, DO is controlled at aeration stage to be 4.0-5.0 mg/L. During the experiment, no sludge was discharged and reactor operated at room temperature, and the temperature was about 20℃.

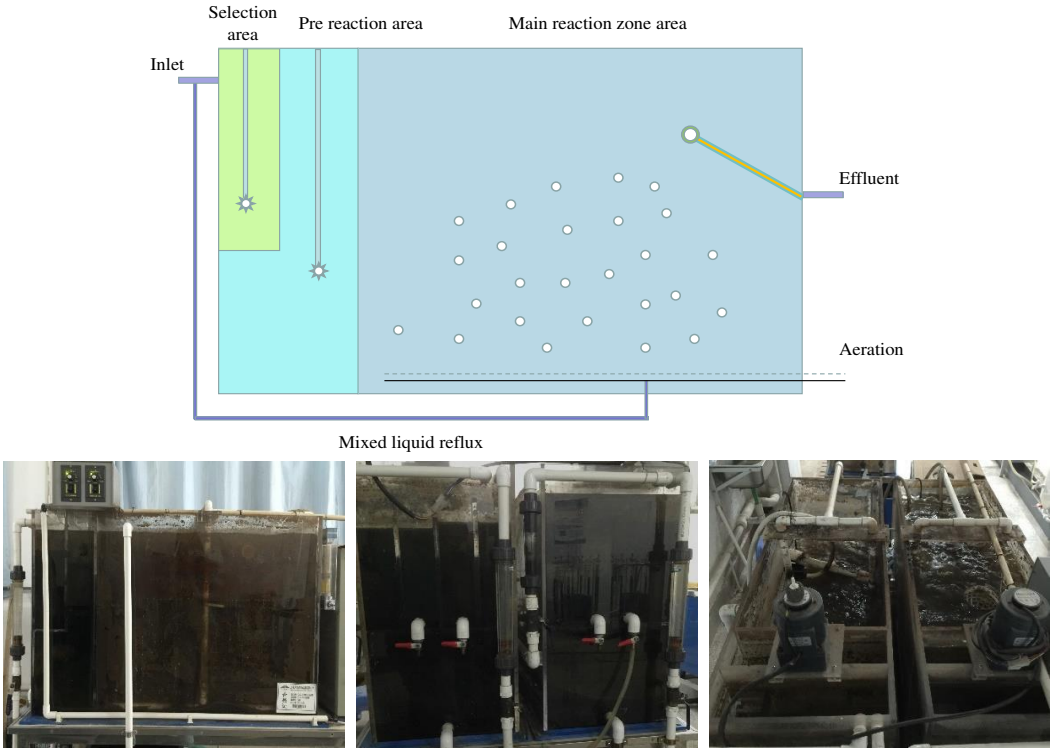

Figure 1. *Diagram and physical diagram of CAST reactor*

PCR-DGGE method of sewage sludge

Principle of PCR-DGGE

By using polyacrylamide gel with chemical denaturant gradient, DGGE can dissolve PCR products differently. The same length of different DNA was amplified in the process of PCR, so all DNA fragments in the product of PCR had the same length, but the nucleotide sequence was different. Through the DGGE experiment, different DNA fragments will stop migration at different positions of the gel due to the different chain breaking behavior along the chemical gradient. Therefore, PCR-DGGE technology can distinguish sequence differences with the same size fragments.

DNA extraction and PCR amplification from sludge

DNA extraction method was carried out according to the instructions of OMEGA soil DNA extraction kit. The 16SrDNA V3 region was selected as the amplification region, and the common primers 338F-GC and 518R were used as the primers. Marker

http://www.aloki.hu ● ISSN 1589 1623 (Print) ●ISSN1785 0037 (Online)
DOI: http://dx.doi.org/10.15666/aeer/1706_1396113974

uses DL2000 and the corresponding fragment size from top to bottom is 2000, 1000, 750, 500, 250, 100.

Primer sequence is:

338-GC: 5`-CGCCCGCCGCGCGCGGCGGGCGGGGCGGGG
GCACGGGGGGACTCCT ACGGGAGGCAGCAG -3`
518R: 5`- ATTACCGCG GCT GCTGG-3`

PCR reaction system was as follows: Total reaction volume was 50 μL, including 10×Taq buffer 5 μL, dNTPmix 4 μL, upstream and downstream primers (10 μM) 2 μL, DNA template 4 μL, Taq enzyme 0.5 μL, sterilized ultra-pure water 32.5 μL. Reaction conditions were as follows: pre-reaction at 95℃ for 5 minutes; denaturation at 95℃ for 1 minute; annealing at 58℃ for 45 s; elongation at 72℃ for 1 minute; reaction cycle 35 times and elongation at 72℃ for 5 minutes.

DGGE experimental steps

Preparation of gel for DGGE: Firstly, after 24 g urea was completely dissolved in water bath at 50℃, 10 ml deionized formamide, 3.896 g acrylamide, 0.1038 g methylene bisacrylamide, 1 ml 50×TAE and 50 μL glycerol were added to the volume of 50 mL. Finally, 80 μL 10% persulfate amine and 110 μL TEMED were added rapidly. After mixing, gel was poured immediately and placed for more than 3 hours to be gelled.

Silver staining: 1) Fixation: fixed with 10% glacial acetic acid of 300 mL for 30 minutes; 2) Cleaning: rinsed with deionized water for 3 times, 2 minutes each time; 3) Silver staining: added 37% formaldehyde 400 mL in 0.1% $AgNO_3$ solution, dyed with this silver staining solution for 25 minutes; 4) Washing: washed with pre-cooled deionized water for three times, the time was 30S, 15S, 30S, respectively. 5) Development: weigh 15 g NaOH, 0.19 g sodium tetraborate, dissolve in sterile deionized water, constant volume to 1000 mL, add 1.5 mL 37% formaldehyde (before use). The developer was used to develop for 12-15 minutes. The development time should not be too long, when the development is less than what you need, it will be terminated in advance, and color rendering time can be prolonged in winter. 6) Termination: When the strip appears, terminate for 3 minutes with fixative. Wash twice, 2 minutes each time (note: if the termination time is too long, the strip will fade). After developing, the UVP gel imaging system was photographed and stored under white light and analyzed by Quantity One-4.6.2 software.

Result and Discussion

Design of experimental group

CAST process for treating low C/N domestic sewage was selected as the experimental reactor in this paper. CAST process is completely mixed in space, anaerobic, anoxic and aerobic in time (Dvorák et al., 2013). If the aeration process and static precipitation process are not properly controlled, it will easily lead to the short anoxic section in the system due to excessive aeration, which directly affects the denitrification process. The main removal site of organic matter is the main reaction area, heterotrophic bacteria carry out nutrient metabolism under aerobic condition to achieve carbon removal; the main reaction area is also the main place for nitrogen removal. By controlling DO in the reactor, nitrification and denitrification can be realized in the same reactor, and then nitrogen removal can be realized.

http://www.aloki.hu ● ISSN 1589 1623 (Print) ●ISSN1785 0037 (Online)
DOI: http://dx.doi.org/10.15666/aeer/1706_1396113974

Phosphorus-accumulating bacteria can absorb excessive phosphorus by PHB in the main reaction zone under aerobic conditions, forming phosphorus-rich sludge, and then complete phosphorus removal through sludge discharge (Duan et al., 2012). In addition, sludge-water separation is realized at the end of one cycle in the main reactor. During the settling stage, the reactor does not receive water, which ensures a good static settling effect. In this stage, denitrifying bacteria can denitrify by using carbon sources in sludge.

CAST process usually has better carbon removal effect, but nitrogen and phosphorus removal is limited (Fang et al., 2015). (1) Nitrification is incomplete. Nitrification is mainly realized in the main reaction zone of CAST process. In the aeration stage, NH_4^+-N is oxidized to NO_3^--N and NO_2^--N by nitrifying bacteria and nitrosobacteria. In this process, nitrifying bacteria compete with heterotrophic bacteria DO, which makes nitrification need longer aeration time, which directly leads to lower water filling in CAST process, the ratio of influent volume to total volume is difficult to improve in each cycle, and the volume utilization rate is low. (2) Denitrification is not complete. CAST process consists of two parts of denitrification, 20% of which is refluxed to realize denitrification using front-end carbon sources; 80% of denitrification is achieved in the main reaction zone, mainly in the period of static precipitation and drainage, but after sludge precipitation, sludge and water are insufficiently mixed, nitrate can not effectively contact with activated sludge, which limits denitrification. The main reaction zone of CAST process can achieve anaerobic, deficient and good plugging flow in time, and realize simultaneous nitrification and denitrification. However, the changing environment also leads to the failure of dominant bacteria to play their role to the greatest extent at all stages. At the same time, the abundance of dominant microorganisms will also be affected by environmental changes, resulting in a decline in abundance.

Denitrification performance of CAST process for treating low C/N domestic sewage is affected by many factors. Considering from the point of view of microorganisms and carbon sources, it mainly includes low types and abundance of denitrifying microorganisms and insufficient organic matter content in low C/N water body. In view of the above problems, biological enhancement and solid carbon source were used to enhance the denitrification performance of the reactor (Huang et al., 2013).

(1) Selection of biofortifier and solid carbon source. The selection of biofortifier mainly starts with the species and abundance of denitrifying bacteria. As far as the CAST process is concerned, it mainly includes nitrifying bacteria to strengthen the nitrification process and denitrifying bacteria to strengthen the denitrification process. In order to remedy the shortage of denitrification caused by the short anoxic section in the same reactor, anoxic denitrifying bacteria and aerobic denitrifying bacteria were selected as denitrifying bacteria. Corn cob was selected as the additional carbon source of CAST process. By adding corn cob, the system C/N was improved, which provided conditions for efficient denitrification of the system.

(2) Dosage mode of biofortifier. In order to immobilize microorganisms to the greatest extent, the method of combining polyethylene biological filler with biofortifier with rough surface and loose fibers was adopted. The fillers with diameter of 80 mm were selected, and the biofortifier was first expanded, then the fillers were connected in series and immersed in the bacterial solution for film hanging. Five days later, the filler was added to the reactor.

http://www.aloki.hu ● ISSN 1589 1623 (Print) ●ISSN1785 0037 (Online)
DOI: http://dx.doi.org/10.15666/aeer/1706_1396113974

(3) The way of adding solid carbon source of corn cob. In order to ensure that the solid carbon source of corn cob does not cause secondary pollution to the reactor, polyethylene biological filler was used to wrap and fix the reactor. The combination of corn cob and filler not only can provide carbon source for the system, but also can be used as biological carrier to increase the microbial abundance of the system. In order to improve the space utilization rate of solid carbon source of corncob and avoid unnecessary waste of carbon source of corncob, the biofortifier was fixed on the solid carbon source of Corncob by spraying microbial agent, and then added to the reactor. Carbon release experiments show that 80% of the carbon source will be released in the first two days of corn cob immersion. When the system needs additional carbon source for a long time, in order to avoid secondary pollution caused by high COD in the initial stage of solid carbon source immersion, the corn cob should be immersed for two days before drying and then using. When the system needs to add carbon source for short-term emergency treatment, corn cob soaking solution can be used instead of methanol which is currently used more (Huang et al., 2013; Islas-García et al., 2015).

(4) Reactor was operated initially. In order to investigate the carbon and nitrogen removal performance of the system and determine the solid carbon source dosage of corn cob in the experimental group, COD, NH_4^+-N and TN were measured in a stable CAST reactor for 5 consecutive days.

(5) Solid carbon source of corn cob and the dosage of biofortifier in the experimental group were preliminarily determined. The results of background monitoring for 5 days showed that the quality of artificial controlled influent water was basically stable, COD was about 150 mg/L, TN was about 35 mg/L and NH_4^+-N was about 25 mg/L. The effluent COD is about 50 mg/L, NH_4^+-N is about 10 mg/L, the removal rate is about 60%, TN is about 25 mg/L, the removal rate is about 30%. The denitrification performance of corn cob combined with biofortifier in activated sludge system showed that when corn cob existed in activated sludge system for 20 days, the removal rate of NO_3^--N of 30 mg/L was maintained at 35%-40%. In order to achieve the initial TN standard of CAST process, the rough calculation group needs to add 500 g solid carbon source of corncob. Corn cob solid carbon source is hung in series at the back end of CAST main reaction zone. The number of nitrifying bacteria film-forming fillers is 16 in a series, which are vertically attached to the front end of the main reaction zone of CAST in series, and 12 in a series of denitrifying bacteria film-forming fillers, which are vertically attached to the front and back end of the main reaction zone of CAST respectively. In order to enhance the mixing degree of microorganisms and water and avoid sludge loss, all packings in series are fixed at the bottom, and the top packings are guaranteed below the water surface at the end of the reactor drainage (Krustok et al., 2015).

Packing observation of CAST reactor experimental group

Solid carbon source of filler and corncob after 20 days operation of CAST reactor is observed in *Fig. 2*. Microscopic observation showed that there were a large number of microorganisms on the surface of film-forming filler and corncob., which could be fixed by bio-strengthening bacteria agent to reduce bacterial loss, increase the microbial abundance on the filler, and then increase the contact area of sludge during the static settling period, which was conducive to the improvement of the nitrogen removal performance of the reactor (Joo et al., 2005).

http://www.aloki.hu ● ISSN 1589 1623 (Print) ●ISSN1785 0037 (Online)
DOI: http://dx.doi.org/10.15666/aeer/1706_1396113974

Effect of bioaugmentation and solid carbon source on denitrification performance of CAST process

In order to investigate the ability of corn cob and biofortifier to improve the denitrification performance in low C/N domestic sewage treatment, a pilot study was carried out by using CAST process to treat low C/N domestic sewage (Jianhua et al., 2016). The experimental results are shown in *Figure 3*.

Figure 2. *Physical drawings of stuffing and corncob after film hanging*

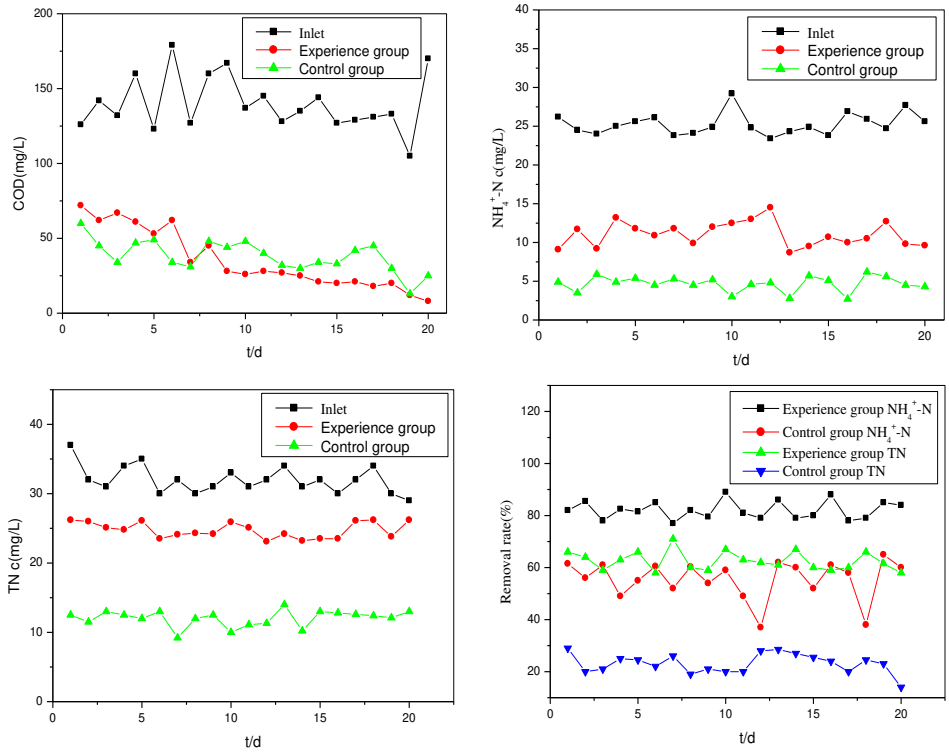

Figure 3. *Changes of water quality index of reactor before and after intensification treatment*

The change of COD in the effluent of the experimental group and the control group showed that the effluent COD of the control group was basically stable and the average COD in the effluent was 41.8 mg/L, reaching the first grade A standard (50 mg/L). The effluent COD of the experimental group did not increase significantly. Before 9 days,

http://www.aloki.hu ● ISSN 1589 1623 (Print) ●ISSN1785 0037 (Online)
DOI: http://dx.doi.org/10.15666/aeer/1706_1396113974

the effluent COD was similar to that of the control group and maintained at about 45 mg/L (Lu et al., 2014). After that, COD decreased slightly, and the average COD of effluent was 30.1 mg/L, and remained below 50 mg/L all the time. It is speculated that the nitrogen removal performance of the system and the utilization rate of microbial carbon source may be improved by adding biofortifier, which may lead to the decrease of COD in the effluent of the experimental group. The results showed that the COD of effluent from the experimental tissues did not increase significantly. When corn cob was used as carbon source of external reinforcement in activated sludge system, it would not cause secondary pollution to the raw water. The change of NH_4^+-N concentration in the effluent of the experimental group and the control group showed that the removal rate of NH_4^+-N in the control group was limited. The average removal rate of NH_4^+-N in the effluent was 11.35 mg/L, which was about 55%. The effluent NH_4^+-N concentration in the experimental group was significantly lower than that in the control group, with an average NH_4^+-N concentration of 4.58 mg/L. The addition of nitrifying bacteria increases the abundance of nitrifying bacteria in the system (Liu et al., 2015). When the aeration condition is the same, increasing the abundance of nitrifying bacteria can enhance the nitrification and reduce the concentration of NH_4^+-N in the system.

The change of TN concentration in the effluent of the experimental group and the control group showed that the removal rate of TN in the control group was low, and the average TN concentration in the effluent was 25.03 mg/L. The TN concentration in effluent of the experimental group was significantly lower than that of the control group, with an average concentration of 12.11 mg/L, reaching the first a standard (15 mg/L). Bioaugmentation has an obvious effect on the removal rate of TN in the system (Quan et al., 2011). It is speculated that bioaugmentation improves the denitrification performance of the system. Anoxic denitrifying bacteria increase the abundance of conventional denitrifying bacteria in the system, and then improve the denitrification performance of the system under anoxic conditions (Szogi et al., 2015). Anaerobic, anoxic and aerobic alternation occurs in the same vessel in CAST process, which makes it difficult to strictly control dissolved oxygen. After the main reaction zone stops aeration, there is no anoxic stirring in the system, resulting in short anoxic period in the main reaction zone of CAST and insufficient slurry mixing in the anoxic period, which directly restricts denitrification and denitrification of the system (Shoda and Ishikawa, 2014). Adding aerobic denitrifying bacteria can realize the nitrification and denitrification process at the same time under the aeration condition in the main reaction zone of CAST, and improve the denitrification performance of the system (Urakawa et al., 2006).

The removal rates of NH_4^+-N and TN in the experimental group and the control group showed that the experimental group had obvious effect on the denitrification of the system. Denitrification performance of CAST process for treating low C/N domestic sewage can be improved by the combination of bio-intensifying bacteria and solid carbon source of corncob.

Electron microscopic analysis of CAST reactor sludge

The initial sludge of the experimental group and the control group and the sludge after 20 days of operation were observed by scanning electron microscopy. The results are shown in *Fig. 4*. A and B represent the sludge at the initial stage of the experiment and the sludge after 20 days of reactor operation. The results showed that at the beginning of the experiment, the sludge structure of the experimental group and the

http://www.aloki.hu ● ISSN 1589 1623 (Print) ●ISSN1785 0037 (Online)
DOI: http://dx.doi.org/10.15666/aeer/1706_1396113974

control group was basically the same, crisp and porous, and filamentous bacteria and bacilli could be clearly seen (Skouteris et al., 2012; Pan et al., 2015). After 20 days of operation of the reactor, the sludge structure of the experimental group basically did not change much, a large number of rod-shaped bacteria could be clearly seen, and the sludge performance was good. The structure of the control group was slightly loose. It was speculated that the starvation of some microorganisms in the activated sludge might be due to insufficient carbon sources in the water, and the sludge structure began to loosen.

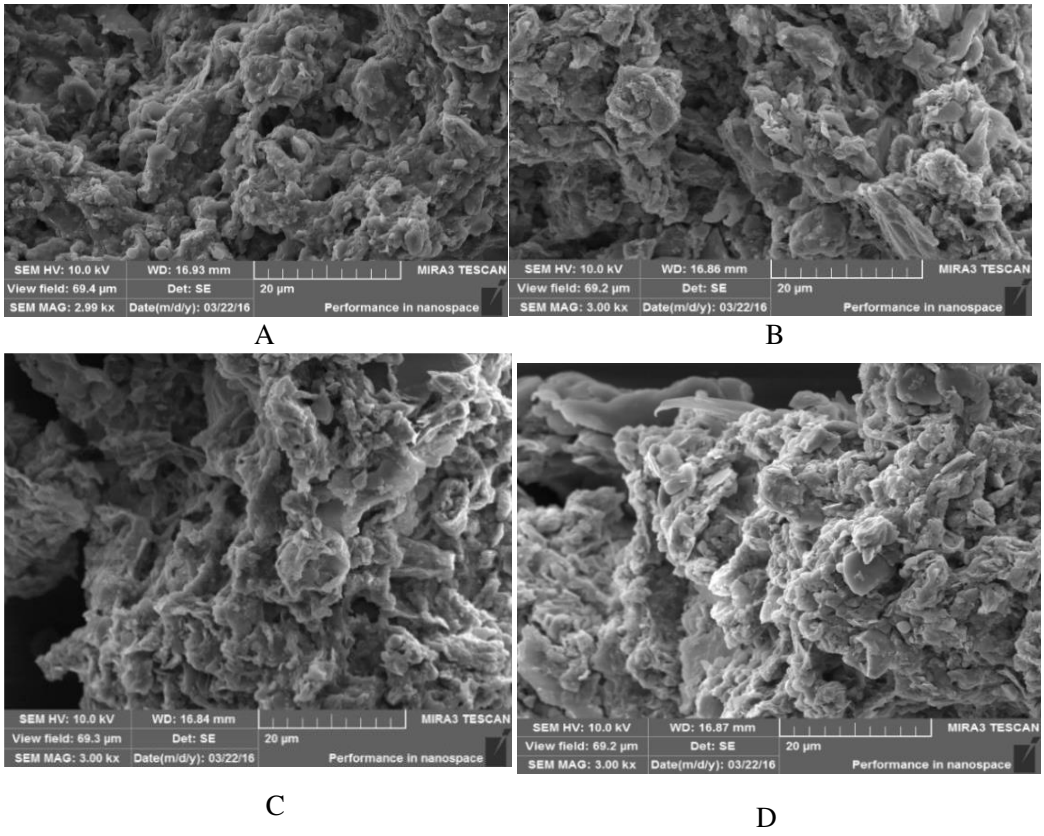

Figure 4. *A-D: Electron Microscopic Scanning of Sludge from Two Reactors at Different Stages*

Analysis of sludge community structure in CAST reactor

Results of sludge PCR in DNA16SrDNAV3 region

The results of 16SrDNAV3 region PCR amplification of total DNA of the samples are shown in *Fig. 5*. From the figure, we can see that all the DNA of the five samples was amplified. The size of the fragments is about 250 bp. The band brightness is suitable and there is no non-specific amplification, which meets the requirements of the follow-up DGGE experiments.

Analysis of sludge community structure

The sludge DGGE and swimming lane recognition maps of the experimental group and the control group after 20 days of operation are shown in *Fig. 6*, respectively. A is the band corresponding to the added anoxic denitrifying agent, B is the band

http://www.aloki.hu ● ISSN 1589 1623 (Print) ●ISSN1785 0037 (Online)
DOI: http://dx.doi.org/10.15666/aeer/1706_1396113974

corresponding to the added nitrifying agent, C is the band corresponding to the added aerobic denitrifying agent, D is the band of sludge after 20 day operation of the experimental group reactor and E is the band of sludge after 20 days operation of the control group reactor.

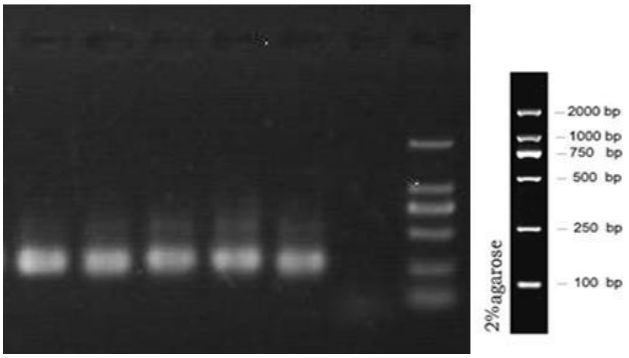

Figure 5. *Gel electrophoresis of PCR product in total DNA16SrDNAV3 region of sample*

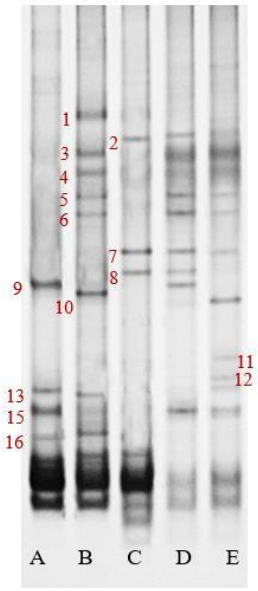

Figure 6. *Sludge DGGE Map. A: anoxic denitrifying bacteria agent; B: nitrifying bacteria agent; C: good nutrient denitrifying bacteria agent; D: Sludge in the experimental group after 20 days; E: Sludge in control group after 20 days*

DGGE map showed that the bands below No. 17 were not separated and no analysis was done. As far as the obvious characteristic bands are concerned, the added anoxic denitrifying bacteria agent includes three characteristic bands, 9, 13 and 15 respectively; the added nitrifying bacteria include six characteristic bands, 1, 3, 4, 5, 6 and 10 respectively; and the added aerobic denitrifying bacteria include three characteristic bands, 2, 7 and 8, respectively. In the control group, 2, 3, 4, 5, 6, 7, 10, 13 and 15 bacterial agents were detected, which indicated that the above eight bacterial species existed in the original activated sludge system and were not exotic and had good adaptability. The dominant denitrifying bacteria in the control group were 3, 4, 10, 2, 7,

http://www.aloki.hu ● ISSN 1589 1623 (Print) ●ISSN1785 0037 (Online)
DOI: http://dx.doi.org/10.15666/aeer/1706_1396113974

13 and 15, and the characteristic strips in the experimental group were 2, 3, 4, 5, 6, 7, 8, 9 and 15. Analysis of the sludge bands of the experimental group and the control group after 20 days of operation showed that compared with the control group, the abundances of the experimental group 2, 3, 5, 6, 7 and 15 increased, the abundances of 4 decreased, and the abundances of 10 and 13 completely disappeared. The change of dominant nitrifying bacteria in the control group showed that the addition of biofortifier gradually replaced the dominant nitrifying bacteria corresponding to 4 in the original activated sludge system, completely replaced the corresponding nitrifying bacteria of 10, and increased the abundance of nitrifying bacteria corresponding to 3, 5 and 6, and gradually became the dominant nitrifying bacteria in the system. The change of dominant denitrifying bacteria in the control group showed that the dominant denitrifying bacteria corresponding to 13 in the original activated sludge system were completely replaced and the corresponding denitrifying bacteria of 2, 7, 13 and 15 were strengthened by adding biofortifier. In addition to the above characteristic bands, 11 and 12 bands of sludge in the control group disappeared. It was speculated that the corresponding strains of 11 and 12 bands were heterotrophic bacteria. While the species and abundance of denitrifying bacteria increased, the species of heterotrophic bacteria decreased. In addition to the above characteristic bands, 8 and 9 in the sludge Atlas of the experimental group are new bands, representing an aerobic denitrifying bacteria and anoxic denitrifying bacteria, which belong to exotic microorganisms. The appearance of 8 and 9 bands indicates that 8 and 9 corresponding strains can exist stably in the sludge system, and 9 bands corresponding denitrifying bacteria gradually become the dominant denitrifying bacteria of the experimental group.

In summary, 2, 3, 4, 5, 6, 7, 10, 13 and 15 of the added biofortifiers exist in the original sludge system, indicating that the above eight bacteria are not alien species and have high stability. The enrichment of 4 decreased and 10 and 13 completely disappeared, indicating that the corresponding strains of 4 were gradually replaced, and the corresponding strains of 10 and 13 were completely replaced within 20 days. The abundance of 2, 3, 5, 6, 7 and 15 strains increased, which indicated that the six strains could grow steadily in the system. The corresponding strains of 1 in the added biofortifier were not detected in the sludge of the experimental group, which indicated that the two strains could not exist stably in the system. The corresponding strains of 8 and 9 could exist stably in the sludge of the experimental group, and the denitrifying bacteria corresponding to 9 bands gradually became the dominant denitrifying bacteria in the experimental group.

Among the six kinds of nitrifying bacteria added, there are three kinds which can exist stably in the system; among the three kinds of anoxic denitrifying bacteria added, there are two kinds which can exist stably in the system length; and among the three kinds of aerobic denitrifying bacteria added, there are three kinds which can exist stably in the system length. The results showed that the structure of denitrification bacteria and the denitrification performance of the sludge system could be effectively improved by adding biofortifier.

Conclusion

In view of the low denitrification performance of CAST process in treating low C/N domestic sewage, biological strengthening and solid carbon source were used to enhance the denitrification performance of CAST process. By increasing the abundance

http://www.aloki.hu ● ISSN 1589 1623 (Print) ●ISSN1785 0037 (Online)
DOI: http://dx.doi.org/10.15666/aeer/1706_1396113974

of nitrifying bacteria and anoxic denitrifying bacteria, the abundance and species of denitrifying microorganisms in the system can be improved; by adding aerobic denitrifying bacteria, the problem of inadequate denitrification caused by too short anoxic section in the same reactor in CAST process can be remedied; by adding corn cob solid carbon source, the carbon source in the treatment of low C/N wastewater system can be increased. This experiment can overcome the limitation of denitrification process caused by excessive aeration and insufficient carbon source.

(1) The COD of the effluent of the reactor with corn cob solid carbon source and nitrifying bacteria, anoxic denitrifying bacteria and aerobic denitrifying bacteria was maintained at about 30 mg/L, the average effluent concentration of NH_4^+-N decreased from 11.35 mg/L to 4.58 mg/L in the control group, and the average effluent TN concentration decreased from 25.03 mg/L to 12.11 mg/L in the control group. The average removal rate of NH_4^+-N in the bio-enhanced reactor increased from 55.8% to 82.1% in the control group, and the average removal rate of TN increased from 23.2% to 62.3% in the control group. The addition of biological agents improves the abundance of denitrifying microorganisms in sludge, increases the types of denitrifying microorganisms, and then improves the denitrification performance of the system, so that the effluent reaches the first A standard. When corn cob is used as carbon source of external reinforcement in activated sludge system, the COD of effluent is stable and low, which will not cause secondary pollution to raw water.

(2) The sludge of the experimental group strengthened by bio-agent and solid carbon source of corncob did not change significantly after 20 days of operation of the reactor. The structure of the sludge was compact and filamentous bacteria and bacilli could be observed obviously. Under the condition of insufficient carbon source in the water environment, the sludge structure of the control group becomes loose and has a certain solution.

(3) Among the six kinds of nitrifying bacteria added, there are three kinds which can exist stably in the system, two of the three kinds of anoxic denitrifying bacteria added can exist stably in the system length, and three kinds of the three kinds of aerobic denitrifying bacteria added can exist stably in the system length. The results showed that the addition of biofortifier could effectively increase the species and abundance of denitrifying microorganisms, change the structure of denitrifying bacteria in sludge system, and improve the denitrification performance of the system.

When corn cob is added to the activated sludge system as a solid carbon source, the amount of corn cob can not be controlled accurately, which may cause secondary pollution. It is suggested that in the future practical application, when external carbon sources need to be added urgently, the leaching solution soaked in corn cob for 2 days should be used instead of the liquid carbon sources commonly used at present; when carbon sources need to be provided slowly for a long time, the corn cob after 2 days should be added to avoid the secondary pollution of water caused by the large amount of COD leached in the initial stage.

Acknowledgements. This work was supported by Liaoning Provincial Natural Science Foundation of China (201602377).

http://www.aloki.hu ● ISSN 1589 1623 (Print) ●ISSN1785 0037 (Online)
DOI: http://dx.doi.org/10.15666/aeer/1706_1396113974

REFERENCES

[1] Adouani, N., Limousy, L., Lendormi, T., Sire, O. (2015): N2O and NO emissions during wastewater denitrification step: Influence of temperature on the biological process. – Comptes Rendus Chimie 18(1): 15-22.
[2] Bellucci, M., Ofiţeru, I. D., Head, I. M., Curtis, T. P., Graham, D. W. (2013): Nitrification in hybrid bioreactors treating simulated domestic wastewater. – Journal of Applied Microbiology 115(2): 621-630.
[3] Chen, J., Gu, S., Hao, H., Chen, J. (2016): Characteristics and metabolic pathway ofAlcaligenessp. TB for simultaneous heterotrophic nitrification-aerobic denitrification. – Applied Microbiology and Biotechnology 100(22): 9787-9794.
[4] Duan, X., Zhou, J., Qiao, S., Yin, X., Tian, T., Xu, F. (2012): Start-up of the anammox process from the conventional activated sludge in a hybrid bioreactor. – Journal of Environmental Sciences 24(6): 1083-1090.
[5] Dvorák, L., Svojitka, J., Wanner, J., Wintgens, T. (2013): Nitrification performance in a membrane bioreactor treating industrial wastewater. – Water Research 47(13): 4412-4421.
[6] Fang, H., Wang, Z., Li, J., Wang, Y. (2015): Denitriding characteristics of a heterotrophic nitrification-aerobic denitrification strain Alcaligenes faecalis No. 4. – Chinese Journal of Environmental Engineering 9(2): 983-988.
[7] Huang, X., Li, W., Zhang, D., Qin, W. (2013): Ammonium removal by a novel oligotrophic Acinetobacter sp. Y16 capable of heterotrophic nitrification–aerobic denitrification at low temperature. – Bioresource Technology 146: 44-50.
[8] Islas-García, A., Vega-Loyo, L., Aguilar-López, R., Xoconostle-Cázares, B., Rodríguez-Vázquez, R. (2015): Evaluation of hydrocarbons and organochlorine pesticides and their tolerant microorganisms from an agricultural soil to define its bioremediation feasibility. – Journal of Environmental Science and Health, Part B 50(2): 99-108.
[9] Jianhua, L., Wenjing, L., Takahashi, J. (2016): High strength ammonium removal in sludge digestate by Alcaligenes faecalis strain No. 4 with heterotrophic nitrification and aerobic denitrification. – Chinese Journal of Environmental Engineering 10(4): 1621-1626.
[10] Joo, H. S., Hirai, M., Shoda, M. (2005): Nitrification and Denitrification in High-Strength Ammonium byAlcaligenes faecalis. – Biotechnology Letters 27(11): 773-778.
[11] Krustok, I., Odlare, M., Truu, J., Nehrenheim, E. (2015): Inhibition of nitrification in municipal wastewater-treating photobioreactors: Effect on algal growth and nutrient uptake. – Bioresource Technology 202: 238-243.
[12] Liu, Y., Wang, Y., Li, Y., An, H., Lv, Y. (2015): Nitrogen removal characteristics of heterotrophic nitrification-aerobic denitrification by Alcaligenes faecalis C16. – Chinese Journal of Chemical Engineering 23(5): 827-834.
[13] Lu, J., Jin, Q., He, Y., He, X., Zhao, J. (2014): Simultaneous Removal of Phenol and Ammonium Using Serratia sp. LJ-1 Capable of Heterotrophic Nitrification-Aerobic Denitrification. – Water, Air & Soil Pollution 225: 2125.
[14] Magrí, A., Vanotti, M. B., Szogi, A. A. (2012): Anammox sludge immobilized in polyvinyl alcohol (PVA) cryogel carriers. – Bioresource Technology 114: 231-240.
[15] Pan, Y. T., Ni, B.-J., Lu, H. J., Chandran, K., Richardson, D., Yuan, Z. G. (2015): Evaluating two concepts for the modelling of intermediates accumulation during biological denitrification in wastewater treatment. – Water Research 71: 21-31.
[16] Quan, L. M., Khanh, D. P., Hira, D., Fujii, T., Furukawa, K. (2011): Reject water treatment by improvement of whole cell anammox entrapment using polyvinyl alcohol/alginate gel. – Biodegradation 22(6): 1155-1167.
[17] Shoda, M., Ishikawa, Y. (2014): Heterotrophic nitrification and aerobic denitrification of high-strength ammonium in anaerobically digested sludge by Alcaligenes faecalis strain No. 4. – Journal of Bioscience and Bioengineering 117(6): 737-741.

http://www.aloki.hu ● ISSN 1589 1623 (Print) ●ISSN1785 0037 (Online)
DOI: http://dx.doi.org/10.15666/aeer/1706_1396113974

[18] Skouteris, G., Hermosilla, D., López, P., Negro, C., Blanco, Á. (2012): Anaerobic membrane bioreactors for wastewater treatment: A review. – Chemical Engineering Journal 198-199: 138-148.

[19] Szogi, A. A., Vanotti, M. B., Ro, K. S. (2015): Methods for Treatment of Animal Manures to Reduce Nutrient Pollution Prior to Soil Application. – Current Pollution Reports 1(1): 47-56.

[20] Urakawa, H., Kurata, S., Fujiwara, T., Kuroiwa, D., Maki, H., Kawabata, S., Hiwatari, T., Ando, H., Kawai, T., Watanabe, M., Kohata, K. (2006): Characterization and quantification of ammonia-oxidizing bacteria in eutrophic coastal marine sediments using polyphasic molecular approaches and immunofluorescence staining. – Environmental microbiology 8(5): 787-803.

http://www.aloki.hu ● ISSN 1589 1623 (Print) ●ISSN1785 0037 (Online)
DOI: http://dx.doi.org/10.15666/aeer/1706_1396113974

GENETIC INHERITANCE OF GRAIN YIELD AND ITS RELATED TRAITS IN MAIZE (*ZEA MAYS* L.) UNDER WATER DEFICIT

RAMZAN, M.[1*] – AHSAN, M.[1] – SADAQAT, H. A.[1] – AWAN, F. S.[2]

[1]*Department of Plant Breeding and Genetics, University of Agriculture, Faisalabad, Pakistan*

[2]*Centre of Agricultural Biochemistry and Biotechnology, University of Agriculture, Faisalabad, Pakistan*

**Corresponding author*
e-mail: madiharamzan2301@gmail.com

(Received 24th May 2019; accepted 11th Oct 2019)

Abstract. Drought stress is one of the major yield limiting factors and causes significant yield losses in different crops. This study was conducted to screen the 50 maize accessions of diverse origin of Pakistan against moisture deficit on the basis of their performance *vis.*, plant height, cob length, kernel rows per ear, kernels per ear, leaf area, days to 50% anthesis, grain yield, 100-seed weight, chlorophyll contents, stomata size, harvest index and drought index. Drought stress was imposed through alternate irrigation (10 recommended irrigations) and normal irrigation (no drought stress) (15 recommended irrigations). The germplasm consisting of 8 parents and 15 crosses was evaluated in field under normal and water deficit conditions in spring season. Out of these 50 accessions five drought and three drought sensitive lines were selected. The selected drought resistant lines were crossed with drought sensitive lines (testers) in line × tester mating design and were evaluated on the basis of yield and yield contributing traits. The inbred lines W64TMS and W82-3 expressed higher general combining ability (GCA) for grain yield, and other yield related traits (cobs per plant, grains per cob, 100-seed weight) under normal and water deficit conditions. The F1 hybrids W64TMS × USSR150 and W82-3 × 150P-1 showed higher specific combining ability (SCA) for grain yield and other related traits under normal and drought stress. Positive correlation was observed between grain yield and cob length, cob diameter, kernel rows per ear, kernels per ear, plant height, number of leaves per plant, leaf area, chlorophyll content, 100-seed weight, stomata size and stomata frequency. It was suggested that the present breeding material may be used for the improvement of grain yield and water deficit tolerance in maize.
Keywords: *moisture deficit, germplasm, accessions, general combining ability*

Introduction

Maize (*Zea mays* L.) is an important food and feed crop due to its high demand as compared to wheat and rice. In 2020 in developing countries maize demand would increase as compared to wheat and rice owing to high consumption as fresh and treated forms like sweeteners, maize bread, corn flakes, maize chips, corn flour, and corn porridge. Moreover maize is used as raw material in industries like textile, refineries, foundry, fermentation, and food industries for production of ethanol as biofuel for vehicles, corn oil, dextrose, corn syrup and alcohol for beverages. In developed countries 40-80% maize used as fodder for livestock (Farnham et al., 2003).

Water deficit is a major factor of abiotic stress which diminishes the grain yield of many crops (Aslam et al., 2015). Maize plants are sensitive to water shortage due to extraordinary evaporation and weak root structure (Abayomi et al., 2012). Globally 20-25% of total planting area of maize is affected by drought stress (Golbashy et al., 2007). Water shortage at flowering stage in maize causes 40-85% yield loss (Bänziger et al., 2002) and at anthesis to grain filling 40-80% yield losses are caused. The deficiency of water reduces photosynthesis, turgor in phloem cells and flow of sucrose from

http://www.aloki.hu ● ISSN 1589 1623 (Print) ● ISSN 1785 0037 (Online)
DOI: http://dx.doi.org/10.15666/aeer/1706_1397513988

conducting cells to sink (seeds) (Sevanto et al., 2014). Moisture deficit limits vegetative growth by decreasing the leaf water contents (Valentovic et al., 2006) and stomatal transpiration/conductance (Anjum et al., 2011). Drought stress damages the membranes (Awasthi et al., 2014), chlorophyll (Rahbarian et al., 2011), photosynthesis (Anjum et al., 2011) due to stomatal or non-stomatal link (Sehgal et al., 2018). Drought stress cause severe losses at reproductive growth stage compared to vegetative growth stage owing to flower abortion, poor kernel set and reduced numbers of seeds (Pushpavalli et al., 2014; Seghatoleslami et al., 2008). Moreover, moisture deficit at grain filling stage reduced the seed size owing to slow down of grain filling rate and duration (Moradi et al., 2013; Sehgal et al.,. 2018).

Drought stress is single most important factor which adversely affects the maize production (Nelson et al., 2007; Nuccio et al., 2015). Water deficiency reduced the survival rate of seedling and cause increase of post-pollination embryo abortion ultimately leading to reduction of yield (Chohan et al., 2012; Kakumanu et al., 2012; Mao et al., 2015). Limited supply of water negatively affects plant development and photosynthesis (Yordanov et al., 200). Water deficit results stunted plant growth, tassel blast, top firing, wilting, low plant density, silk delay and poor seed set which ultimately decreases of grain yield (Chen et al., 2015). To improve tolerance against water deficit, the use of genetics is a main factor. Agronomic interventions also have their significance however; genetic solutions are more cost effective and sustainable (Edmeades et al., 2004) as agronomic practices depend on input availability, skill in soil preparation and crop management but genetics can crammed in kernel and easily amended (Campos et al., 2004). Under drought stress, development of drought-resistant germplasm is an effective and feasible approach (Athar and Ashraf, 2009). For breeding it is indispensable to find the superior genotypes to develop the high yielding hybrids (Ganagappa et al., 1997). The general combining ability (GCA) and specific combining ability (SCA) are essential breeding approaches. General combining ability has main character in yield parameters (Ali et al., 2013; Kanwal et al., 2019; Sindagi et al., 1997) and specific combining ability is more effective as compare the general combining ability for kernel yield. The current study was conducted to i) screen inbred lines for various physio-genetic traits under limited water conditions, ii) development of water deficit tolerant F1 crosses in maize and iii) to estimate gene action, general and specific combining ability effects.

Material and methods

Experimental site, collection and screening of genetic material

This study was conducted in the field of the Department of Plant Breeding & Genetics, University of Agriculture, Faisalabad (latitude 31° N, longitude 73° E, altitude 184.4 m above sea level), Pakistan during 2014 to 2016.

The seed of 50 maize genotypes were taken from maize research group of the Department of Plant Breeding & Genetics, University of Agriculture Faisalabad. The germplasm particularly accomplished for water deficit tolerance and the studied parameters have direct and indirect correlation with water deficit tolerance. Seeds of collected genotypes were multiplied by self-pollination during 2014. Genetic purity within each genotype was maintained by controlled pollination. The collected maize germplasm was evaluated against water deficit stress during spring season under normal and stress condition. Seeds of 50 genotypes were sown in triplicate in the field of the Department of Plant Breeding and Genetics, University of Agriculture Faisalabad. Line

http://www.aloki.hu ● ISSN 1589 1623 (Print) ● ISSN 1785 0037 (Online)
DOI: http://dx.doi.org/10.15666/aeer/1706_1397513988

to line and plant to plant space were kept 0.75 m and 0.25 m, respectively with total crop area of 40 × 50 m. Suggested agronomic and plant safety measures were practiced to nourish crop. Two irrigation treatments were:
T_0: Normal irrigations (15 recommended irrigation)
T_1: Alternate irrigation was skipped (10 irrigations)

Drought stress was imposed by skipping the alternate irrigation (10 irrigations) compared to normal (15 recommended irrigations). Data were recorded on ten random plants per replication from each experiment for the physiological and agronomic parameters. The 5 water deficit tolerant lines were selected.

Recording of data

Number of days to 50% tasselling, 50% silking, anthesis-silking interval and leaf area

Plants with in replication were measured to have started anthesis, if one anther becomes visible. Number of days taken to tasselling was counted from the date of sowing to the time when 50% plants completed tasselling. Plants with in replication were measured to be at silking if at least one silk on a plant emerges. Number of days to 50% silking was recorded by counting the number of days from date of sowing to the date when 50% plants complete emergence of silks. Anthesis-silking interval (ASI) is the period between the maturity tasseling and silking. It was calculated by subtraction of days to 50% silking from days to 50% tasseling. For leaf area measurement length and width of three leaves was measured from top, mid and bottom on each selected and guarded plant with measuring tape in cm. Leaf area was calculated with the following equation after taking average (Montgomery and Cheo, 1971):

$$\text{Leaf area (cm}^2\text{)} = \text{length (cm)} \times \text{width (cm)} \times 0.75$$

Yield and yield contributing traits

Plant height and numbers of leaves was measured from ten plants per replication with the help of meter rod from tassel to ground surface in centimeters and was averaged. Length of ear was measured after harvesting in (cm) with the help of measuring tape from selected plants of replication. Cob diameter of each plant was calculated with measuring tape in centimeters from 10 selected plants of each entry. Leaf angle was measured from fifth leaf of each plant with the help of protractor from 10 plants of each entry. Leaf rolling was measured of each plant by scaling from 1 to 5 from 10 selected plants of each entry.

Numbers of grain rows per ear were counted from each cob of the selected 10 plants and was averaged. The total number of kernels threshed from the ears was counted manually. It was recorded in grams with an electronic balance from three samples obtained each from the bulk grain produce obtained from the ear-marked plants and was averaged. The kernels of each ear were threshed separately and weighed with electric balance. Harvest index was calculated from each plant per replication with the help of following formula. The biological yield was recorded by drying complete plants under shade which was used for the calculations of total harvesting index.

$$\text{HI} = (\text{Grain yield} / \text{Biological yield}) \times 100$$

Drought index was calculated for selected plants with the help of following formula:

http://www.aloki.hu ● ISSN 1589 1623 (Print) ● ISSN 1785 0037 (Online)
DOI: http://dx.doi.org/10.15666/aeer/1706_1397513988

$$DI=\frac{\text{Yield under drought condition}}{\text{Yield under normal condition}}+\frac{\text{Mean performance under drought condition}}{\text{Mean performance under normal condition}}$$

Biometrical approaches

Analysis of variance

The recorded data on maize germplasm for assessment of variability were analyzed using analysis of variance following Steel et al. (1997). A computer software Statistical was used for the analysis.

Line × Tester analysis was conducted as proposed by Kempthorne (1957) to estimate the GCA and SCA effects. Heterosis over mid parent and better parent was determined following the method of Falconer and Mackay (1996). To find the strength of relationship among traits correlation analysis was used as proposed by Kwon and Torrie (1964).

Combining ability effects were calculated according to following formulae:

Estimation of general combining ability (GCA) effects

$$\textbf{Lines}: gi = \{(xj.. / tr) - (x\ldots / ltr)\}$$

$$\textbf{Testers}: gt = \{(x.j. / lr) - (x\ldots / ltr)\}$$

where: l = number of lines; t = number of testers; r = number of replications; xi.. = Total number of F_1 resulting from crossing ith lines with all the testers; x... = Total of all the crosses.

Estimation of specific combining ability (SCA) effects

$$si = \{(xij.) / r) - (xi.. / tr) - (x.j. / lr) + x\ldots / ltr$$

where: xij = total of F_1 resulting from crossing ith lines with jth tester; xi = total of all the crosses of ith line with all testers; xj = Total of all the crosses of jth tester with all lines.

Data analysis

The means were computed and data for all the traits of genotypes were subjected to ordinary analysis of variance (Steel et al., 1997) in order to determine genotypic differences. Biplot analysis based on Principal Component Analysis (PCA) was made using statistical package (XLSTAT) for the selection of tolerant and susceptible genotypes on the basis of all traits along with yield.

Results

Genetic variability

Significant differences were observed among the genotypes for all studied traits. Treatments were significantly different for all the traits except leaf rolling. Genotypes × treatments interaction was also significant for all the traits (*Table A1* in the *Appendix*).

Principle component analysis

Genotype away from origin is good performer relative to the genotypes nearer to the origin. Principal component analysis (PCA 3) showed that accessions 4, 19, 12, 37, 26

http://www.aloki.hu ● ISSN 1589 1623 (Print) ● ISSN 1785 0037 (Online)
DOI: http://dx.doi.org/10.15666/aeer/1706_1397513988

and 28 were fall in quadrate I and accessions 30, 33, 50, 39, 22 and 13 were fall in quadrate IV. The PCA 4 showed that accessions 4, 19, 26, 37 and 9 were fall in quadrate I and accessions 1, 30 and 50 were fall in quadrate IV. The genotypes in quadrate I was selected as lines and in quadrate IV was selected as testers (*Figs. 1* and *2*).

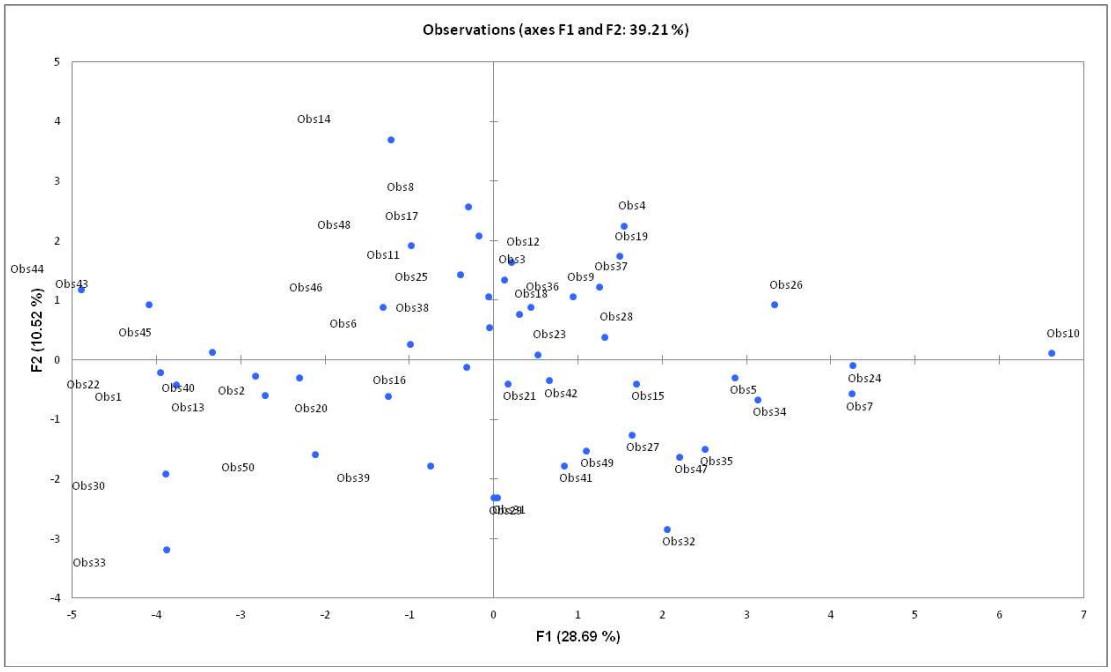

Figure 1. *Biplot analysis based on principal components analysis (PCA) for maize genotypes under normal conditions*

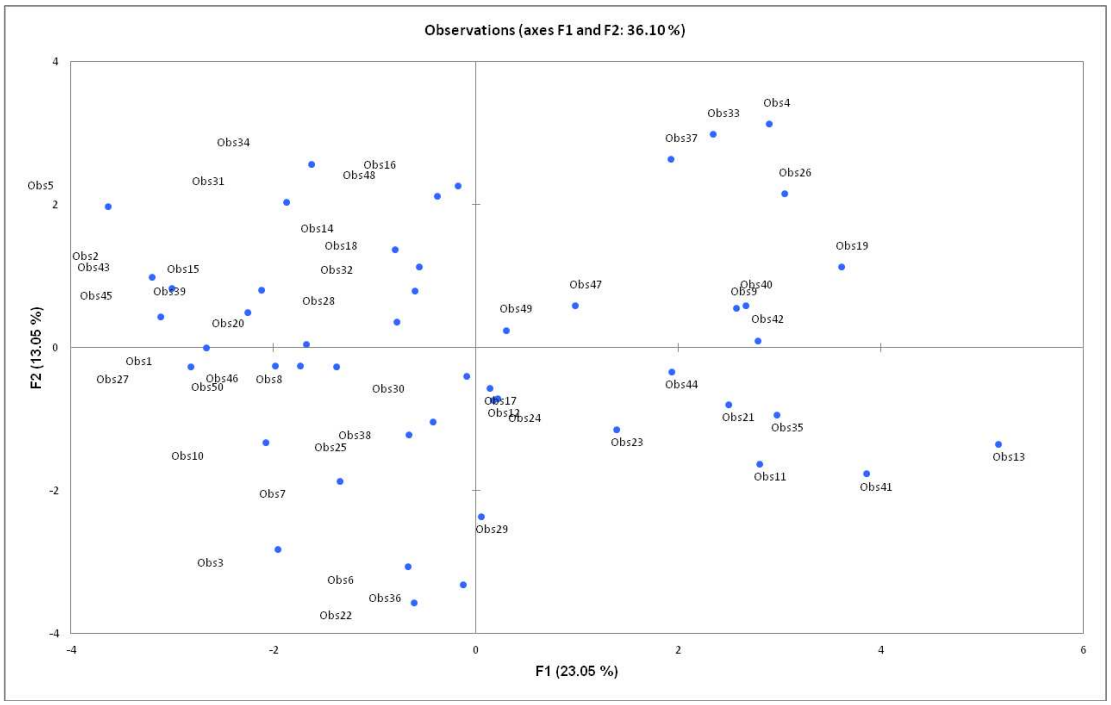

Figure 2. *Biplot analysis based on principal components analysis (PCA) for maize genotypes under water deficit conditions*

http://www.aloki.hu ● ISSN 1589 1623 (Print) ● ISSN 1785 0037 (Online)
DOI: http://dx.doi.org/10.15666/aeer/1706_1397513988

General combining ability effects

Under normal condition (no drought stress) the general combining ability (GCA) test indicated that lines A427-2 showed maximum GCA effects for leaf area and leaf temperature. Line W64TMS revealed maximum values of GCA for seed per cob, rows of kernel per cob, 100 seed weight, and harvest index. For grain yield, chlorophyll content, stomata size and harvest index significant effects were observed in line W82-3 (*Table 1*). Maximum GCA was observed in line A556 for days to 50% anthesis, leaf area, leaf angle and leaf temperature. Line W64TMS expressed positive significant GCA effects for grain yield.

Table 1. *General combining ability effects of lines and testers for various traits of maize under normal conditions*

Traits	Lines					Testers		
	A427-2	**W64TMS**	**W82-3**	**N-18**	**A556**	**M14**	**USSR150**	**150P-1**
Plant height	7.911	-8.422*	-0.311	-5.311	6.133	9.711*	-0.755	-8.955*
Days to 50% silking	0.00	-0.22	-1.111	-0.22	-1.55	-0.244	-0.44	0.688*
Days to 50% anthesis	-0.155	-0.266	-1.37*	0.288	1.511**	0.111	-0.355	0.244
Interval	-0.177	-0.178	-0.511	0.489*	0.377	0.333*	0.066	-0.400*
Number of leaves	0.311	0.644	-0.688*	-0.577	0.311	-0.466	0.200	0.266
Leaf area	25.911*	-29.97*	-38.53*	-19.97	62.57**	10.044	24.177*	-34.22*
Leaf angle	-0.866	-1.422	0.577	-1.088	2.800*	0.911	0.311	-1.22*
Leaf rolling	-0.09*	0.004	0.111*	-0.043	0.02	-0.115*	0.04*	0.074*
Grain per Cob	0.488	38.266**	-11.06*	-21.844**	-5.84	-17.17**	-21.77**	38.95**
kernel rows per ear	0.003	0.466*	-0.111	0.333	-0.66*	0.133	0.00	-0.133
Cob diameter	-0.844*	0.488	-0.622*	0.822*	0.155	0.022	0.088	-0.11
Cob length	0.311	0.311	-0.022	-0.244	-0.355	0.733*	-0.66*	-0.066
Plant yield	4.334	9.788*	8.897*	-5.825*	-17.19**	0.248	-0.161	-0.086
100-SW	-0.41	1.24*	0.379	0.052	-1.23	0.652	-0.794	0.142
Chlorophyll content	-5.321*	-0.421	3.411*	2.067	0.264	-2.128	0.284	1.843
Leaf temperature	0.897*	0.641	-2.15*	-0.38	1.008*	-0.593	1.04*	-0.453
Stomata size	-33.70*	-1.179	14.36*	20.19**	0.32	13.70*	-7.22	-6.47
Stomata frequency	0.111	0.555	-0.787*	0.889*	-0.777*	0.22	0.15	-0.37
Epidermal cells	-0.466*	0.533*	-0.24	0.200	-0.022	-0.66*	0.002	0.66*
Harvest index	-0.45	1.162*	0.979*	-0.487	-1.204*	-1.152**	-0.259	1.412**
Drought index	-0.034*	0.020*	0.008	0.003	0.002	-0.005	0.006	-0.004

*Significant at 0.05 probability level. **Significant at 0.01 probability level

Under normal condition (no drought stress) testers M14 expressed good GCA effects for plant height, anthesis-silking interval, and stomata size. Positive GCA effects were observed in USSR150 for leaf area, leaf rolling and leaf temperature. Tester 150p-1 considered s good general combiner leaf rolling, grains per cob, epidermal cells and harvest index. The tester M14 had positive significant GCA effect for cob length, it is good general combiner because cob length is directly proportional to kernels per ear.

Under water deficit conditions genotypes showed different response for GCA in all parameters (*Table 2*). Line A427-2 considered as good combiner for plant height, days taken to 50% anthesis, anthesis-silking interval, chlorophyll content, stomata size and stomata frequency due to good GCA. Line W64TMS had greater effects for anthesis-silking interval, grain per cob, grain yield, and harvest index. The W82-3 line revealed good GCA effects for days to 50% silking, days to 50% anthesis, leaves per plant, cob

http://www.aloki.hu ● ISSN 1589 1623 (Print) ● ISSN 1785 0037 (Online)
DOI: http://dx.doi.org/10.15666/aeer/1706_1397513988

length grain yield, leaf temperature and harvest index. The line A556 exhibited significant GCA effects for cob diameter and cob length. In testers M14 showed favorable GCA effects for leaves per plant, cob diameter, chlorophyll content and leaf temperature. Tester USSR150 had good GCA effects for days taken to 50% silking, days taken to 50% anthesis, grain yield,100 seed weight and stomata frequency (*Table 2*).

Table 2. *General combining ability effects of lines and testers for various traits of maize under water deficit conditions*

Traits	Lines					Testers		
	A427-2	**W64TMS**	**W82-3**	**N-18**	**A556**	**M14**	**USSR150**	**150P-1**
Plant height	7.78*	2.77	-0.66	3.00	-12.88**	1.48	-2.77	1.288
Days to 50% silking	0.155	-1.73**	1.488**	-0.844*	0.933*	-1.977**	1.488**	0.488*
Days to 50% anthesis	0.600*	-1.400**	1.266**	-1.288**	0.822*	-2.466**	1.600**	0.866*
Interval	0.444*	0.333*	-0.222	-0.444*	-0.111	-0.488*	0.111	0.377*
Number of leaves	1.33	-0.22	0.555*	-0.676*	-1.00	0.511*	-0.622*	0.111
Leaf area	-1.866	5.244	-3.53	2.355	-2.200	9.800	-2.466	-7.33
Leaf angle	1.22	1.22	-5.44*	2.89*	0.11	1.55	-2.77*	1.22
Leaf rolling	-0.02	-0.05	-0.04	0.02	0.097*	-0.284*	0.125*	0.159*
Grain per Cob	-0.86	27.46*	5.133	-18.311	-13.42	-23.00	-23.8	46.8*
kernel rows per ear	-0.178	0.044	-0.400	0.266	0.27	0.266	-0.66*	0.400*
Cob diameter	-0.511*	-0.066	-0.067	-0.288	0.933*	0.755*	-0.177	-0.577*
Cob length	-0.955*	0.044	0.600*	-0.177	0.488*	0.089	-0.244	0.155
Plant yield	1.606	6.504**	6.751**	-8.129**	-6.733**	-1.982	4.366*	-2.383*
100-SW	-0.861	0.517	0.169	-0.215	0.389	0.237	0.835*	-1.07
Chlorophyll content	3.073**	1.362	1.151	-2.404*	-3.182*	2.437*	1.677*	-4.115*
Leaf temperature	0.144	-0.522	1.033*	-1.388*	0.733*	1.431*	-0.58*	-0.842*
Stomata size	18.65**	-12.92*	-12.96*	-0.97	8.21	4.48	-4.34	-0.140
Stomata frequency	0.489*	-0.066	-0.400	-0.288	0.266	-0.377*	0.422*	-0.044
Epidermal cells	-0.044	0.511*	-0.155	-0.266	-0.044	-0.266	-0.066	0.33
Harvest index	-0.782*	1.004*	1.208*	-0.525	-0.904*	-1.086**	-0.494	1.580**

*Significant at 0.05 probability level. **Significant at 0.01 probability level

Specific combining ability effects

Under normal conditions (no drought stress) specific combining ability (SCA) effects of crosses indicated that cross A427 × M14 showed positive SCA effects for kernel rows per ear and leaf temperature. Cross W64TMS × USSR150 had positive and significant SCA effects for cob length, anthesis-silking interval, plant yield, and harvest index (*Table 3*). Cross W64TMS × 150P-1 showed positive and significant SCA effects for cob diameter, kernel rows per ear, grins per cob, plant yield, chlorophyll content, stomata size, and harvest index. Cross W82-3 × 150P-1 exhibited positive and significant SCA effects for cob length, grains per cob, plant yield, and harvest index. Cross N-18 × M14 showed positive and significant SCA effects for cob length, cob diameter, kernel rows per cob, anthesis-silking interval, plant yield and stomata size (*Table 3*). Under drought stress significant SCA effects were observed in cross A427 × M14 for days to 50% silking, days to 50% anthesis and anthesis-silking interval, and stomata size. Cross A427 × 150P-1 exhibited significant SCA effects for number of leaves per plant, kernel rows per cob, leaf angle, anthesis-silking interval, stomata size, and harvest index. Cross W64TMS × USSR150 revealed positive and significant SCA effects for plant height, leaf area, anthesis-silking interval, plant yield, stomata

http://www.aloki.hu ● ISSN 1589 1623 (Print) ● ISSN 1785 0037 (Online)
DOI: http://dx.doi.org/10.15666/aeer/1706_1397513988

frequency, and harvest index (*Table 4*). Cross W82-3 × 150P-1 showed positive and significant SCA effects for number of leaves per plant, cob length, number of grains per cob, plant yield, and harvest index. Cross N-18 × M14 had positive SCA effects for plant height, number of leaves per plant, leaf area, kernel rows per cob, leaf angle and leaf temperature. Cross N-18 × USSR150 revealed positive and significant SCA effects for cob diameter, anthesis-silking interval and 100 seed weight. Cross N-18 × 150P-1 showed positive and significant SCA values for cob diameter, anthesis-silking interval and 100 seed weight (*Table 4*).

Discussion

Drought stress negatively affected the grain yield and yield contributing traits in maize (*Tables 2* and *3*). Different management approaches are used to avoid yield losses in maize such as water management and agronomic practices as sowing on beds etc. However, developments of drought tolerant germplasm are the main tools which are explored across the world to improve the production of maize under moisture deficit conditions (Ali et al., 2017; Aslam et al., 2015). The different genotypes of maize had genetic variability against drought stress (*Tables 1–3*) which could be explored by the screening of different germplasms (Aslam et al., 2015). To develop tolerant genotypes creation of genetic variability and gene combination through intercrossing of targeted parents is the main practices most widely used owing to intercrossing followed by suitable selection which develop an ideotype plant which is suitable for environment specific cultivation (Bänziger et al., 2000; Kanwal et al., 2019; Mahmood et al., 2019). Maximum GCA was recorded in line A556 for days to 50% anthesis, leaf area and line W64TMS had significant GCA for grain yield (*Tables 1–3*) as assessment of yield limiting traits with morphological approaches help conventional breeding for yield improvements (Cattivelli et al., 2008; Ali et al., 2013). The selection of superior traits is a good general combiner for evolving high yield hybrids through transgressive segregation, the similar findings were reported by (Ivy and Howlader, 2000; Paul and Duara, 1991).

The cross W82-3 × 150P-1 had positive SCA effects for number of leaves per plant, cob length, number of grains per cob, plant yield, and harvest index (*Tables 1–4*). Cross W64TMS × USSR150 had significant SCA effects for cob length, anthesis-silking interval, plant yield, and harvest index (*Table 3*), the longer is ear length the higher will be grain yield and similar findings were found by different scientist across the world (Konak et al., 2001; Mendoza et al., 2001; Rahman et al., 2010). Against drought stress, yield and yield contributing traits are primary target for yield improvement. Moreover, secondary traits are also important for yield improvements as they had strong positive correlation with grain yield and are easy to measure (Edmeades et al., 2001). The association of near isogenic lines helped the breeder to find association of targeted secondary traits with economic yield (Bänziger et al., 2000; Ali et al., 2014) as economic yield is the ultimate goal. Under drought stress, testers M14 had positive GCA effects for leaves per plant, cob diameter, chlorophyll content and leaf temperature. While, tester USSR150 had good GCA for days taken to 50% silking, days taken to 50% anthesis, grain yield, 100 seed weight and stomata frequency (*Table 2*) and the intrapopulation improvement for drought stress can be done through plant selection, pre-performance, test crosses using individual plants and parental testers (Bänziger et al., 2000; Ali et al., 2016).

http://www.aloki.hu ● ISSN 1589 1623 (Print) ● ISSN 1785 0037 (Online)
DOI: http://dx.doi.org/10.15666/aeer/1706_1397513988

Table 3. *Specific combining ability affects under normal conditions*

Crosses	PH	NOL	LA	CL	CD	KR	K/E	L ang	DS	DA	Int	PY	100 SW	LR	LT	Chl.	SS	SF	EC	HI
A427 × M14	5.95	0.35	-6.71	0.155	-1.35*	1.20*	14.178	0.53	-1.20*	-0.77	0.44	-4.05	1.42	-0.10*	1.78*	4.16	-27.6*	0.55	0.66	-1.322*
A427 × USSR150	6.28	0.35	38.84	-1.84**	-0.68	-0.57	4.067	2.75	2.35**	1.66*	-0.55	8.97	-4.88*	0.16**	1.40*	-3.63	-39.5**	-0.55	-0.66	0.223
A427 × 150P-1	-16.82*	1.35*	58.06*	-0.17	0.42	-1.35*	7.067	-6.91*	0.91	0.11	-0.55	-15.6*	-0.92	-0.02	1.90*	-7.77*	-54.4**	-0.22	0.77*	1.513*
W64TMS × M14	14.84*	1.57*	-17.1	-0.62	-0.02	-1.13*	38.178**	0.75	0.35	-1.55*	-1.88**	3.79	1.400	0.155*	2.06*	-3.46	-14.2	0.44	1.00*	-0.546
W64TMS × USSR150	-48.6**	1.02	-111**	0.82*	-0.02	0.53	3.178	-9.46**	-1.42*	-0.44	0.88*	32.00**	1.50	0.028	1.27	-7.62*	-26.9*	1.44*	0.55	2.784**
W64TMS × 150P-1	-18.91*	0.02	-74.51*	0.22	1.24*	2.00**	156.77**	1.466	0.00	-0.31	-0.95*	11.91*	1.82	0.134*	-2.79**	16.78**	30.6*	-1.04*	1.66*	5.957**
W82-3 × M14	9.755	-1.64*	27.04	0.55	-1.42*	-1.77**	-46.66**	1.688	1.22*	0.46	-0.62	1.43	-1.91	0.054	-7.03**	7.51*	50.5**	-1.48*	-1.33*	1.177*
W82-3 × USSR150	17.31*	-0.97	5.6	0.22	0.022	0.77	9.00	1.355	-1.88*	-1.42*	0.044	2.45	2.73*	-0.04	0.96	-0.81	-15.5	-0.48	0.11	-0.649
W82-3 × 150P-1	-11.68	0.57	-132**	1.11*	-1.42*	0.00	64.44**	-0.311	0.22	-0.75	-0.95*	10.43*	1.05	0.135*	-1.63*	-2.37	-3.54	-1.48*	0.00	1.533*
N-18 × M14	-8.13	-2.31*	-71.8*	2.22*	1.57*	2.00**	5.778	-0.866	-2.55**	0.02	2.15**	10.04*	1.66	-0.32*	-2.86**	-7.70*	59.88**	0.84	-1.44**	0.698
N-18 × USSR150	-5.04	0.62	-13.11	-1.711**	1.778	0.133	-99.28**	1.00	-0.80	-0.91	-0.15	-8.15	-1.99	0.027	0.31	11.82**	42.61**	2.15**	1.33*	-2.76**
N-18 × 150P-1	10.28	-2.04*	10.77	-0.71	-0.55	-0.64	-61.06**	-1.77	0.42	0.53	0.17	-15.96*	1.42	0.044	-1.30	3.58	12.80	0.377	-0.66	-1.464*
A556 × M14	17.17*	-0.04	84.66**	1.28*	1.22*	0.24	-58.4*	1.22	1.64*	2.64*	1.17*	-10.06*	0.82	-0.28**	2.63*	-9.31*	-6.48	0.377	-1.55**	-4.35**
A556 × USSR150	25.51*	0.17	224.77**	-1.48*	-0.55	-0.86*	-47.62*	6.22*	-0.91	-1.02*	0.17	-36.2**	-2.13	0.07	2.32*	1.96	-3.90	-1.62**	-1.33*	-1.147*
A556 × 150P-1	2.06	0.95	-23.11	-0.04	-0.22	-0.53	10.37	2.33	1.64*	1.75	0.62	9.10*	-2.02	-0.02	0.96	-3.13	-4.08	0.711	0.88*	-1.633*

PH = plant height, NOL = number of leaves, LA = Leaf area, CL = Cob length, CD = Cob diameter, KR = Kernel rows per ear, K/C = Kernel per ear, L ang = Leaf angle, DS = days to silking, DA = Days to anthesis, Int = Interval, PY = plant yield, 100SW = 100 Seed weight, LR = Leaf rolling, LT = Leaf temperature, Chl = Chlorophyll content, SS = Stomata size, SF = Stomata frequency, EC = Epidermal cells, HI = Harvest index

http://www.aloki.hu ● ISSN 1589 1623 (Print) ● ISSN 1785 0037 (Online)
DOI: http://dx.doi.org/10.15666/aeer/1706_1397513988

Table 4. *Specific combining ability affects under water deficit conditions*

Crosses	PH	NOL	LA	CL	CD	KR	K/E	L ang	DS	DA	Int	PY	100 SW	LR	LT	Chl	SS	SF	EC	HI
A427 × M14	-6.37	0.26	-3.13	0.022	0.24	0.177	13.33	-4.88*	3.97**	5.133**	1.155**	-2.70	0.96	0.024	-1.09*	0.073	28.77*	-0.28	1.37*	-0.938
A427 × USSR150	9.28	-0.51	-15.9	-1.31*	2.20**	-2.04**	23.00*	0.11	7.53**	7.133**	-0.400	12.23**	-2.00*	0.404**	-0.76	-0.64	0.026	1.26*	-0.51	-0.938
A427 × 150P-1	6.06	1.04*	-15.8	-1.53**	-1.20**	1.066*	-1.66	6.77*	-5.02**	-3.533**	1.488**	-13.6**	-2.07*	0.482**	-2.65**	-3.10*	20.9*	1.60**	-0.51	1.357*
W64TMS × M14	0.400	1.93**	6.64	0.24	0.355	-1.60**	37.44**	0.11	0.311	0.355	0.044	1.59	0.72	-0.07	0.43	2.11	-18.5	0.155	0.60	-0.464
W64TMS × USSR150	14.95*	-0.73*	37.86*	-0.42	-1.53**	-0.26	-11.77	-3.77	-5.13**	-4.422	0.711*	23.46**	1.68	0.173*	-3.35**	3.52*	-29.7*	1.26*	1.04*	2.500**
W64TMS × 150P-1	-5.11	-1.93**	-44.2*	1.022*	-0.48	1.77**	159.13**	2.77	1.84**	3.066**	1.22**	7.30*	-1.48	0.094	-0.41	-5.60**	-20.9*	-1.75**	0.84	5.856**
W82-3 × M14	2.55	1.28**	18.02	0.68	1.06*	0.88*	-24.53*	-0.55	-2.26**	-3.60**	-1.33**	-1.95	-1.52	-0.33**	3.58**	-0.55	10.77	-0.20	-1.04*	2.863**
W82-3 × USSR150	-2.00	0.17	-27.2	-0.53	0.40	1.33*	12.13	-7.22*	2.84**	3.400**	0.55*	-2.63	0.57	-0.10	-0.30	0.322	-17.17*	-0.53	0.28	-1.134*
W82-3 × 150P-1	0.66	2.40**	1.911	1.91**	-0.71*	-1.33*	84.91**	1.11	0.511	0.622	0.111	6.61*	-1.51	0.000	2.45**	-1.45	7.40	-0.97*	0.40	1.693*
N-18 × M14	36.22**	1.06*	36.13*	-0.42	-0.26	2.00**	0.689	8.88**	-6.93**	-8.488**	-1.55**	-4.94	-1.33	-0.51**	1.33*	0.322	-7.09	-1.86*	-1.15*	-0.414
N-18 × USSR150	-18.17*	-1.3**	-9.66	0.622	0.57*	-1.95**	-95.4**	0.44	-1.155*	-0.533	0.622*	-6.66*	2.33*	0.124	-1.49*	2.52	-12.2	-0.28	0.11	-3.02**
N-18 × 150P-1	-6.51	-1.44**	-3.44	-0.377	-0.20	0.48	-43.13**	-2.88	3.73**	1.800**	-1.93**	-13.74**	-0.37	-0.019	-2.09**	-4.76*	7.08	0.266	-0.77	-0.121
A556 × M14	-24.06**	-1.88**	-16.0	0.066	1.80**	0.26	-95.13**	5.44*	-4.48**	-4.86**	-0.377	-4.28	1.29*	-0.36**	2.05*	6.11**	8.40	0.27	-0.77	-4.89**
A556 × USSR150	-20.73*	-1.33**	0.11	0.177	1.68**	-1.06*	-70.68**	-6.22*	4.84**	4.022**	-0.822*	-0.19	2.42*	0.153*	2.37**	4.33*	33.06**	0.82*	-1.33*	-0.368
A556 × 150P-1	12.82*	1.00*	34.66*	-0.155	0.46	0.26	11.75	-0.11	-0.600	-0.088	0.511*	-0.45	0.32	-0.04	-0.08	-3.21*	-10.6	0.26	1.44*	-1.96*

PH = plant height, NOL = number of leaves, LA = Leaf area, CL = Cob length, CD = Cob diameter, KR = Kernel rows per ear, K/C = Kernel per ear, L ang = Leaf angle, DS = days to silking, DA = Days to anthesis, Int = Interval, PY = plant yield, 100SW = 100 Seed weight, LR = Leaf rolling, LT = Leaf temperature, Chl = Chlorophyll content, SS = Stomata size, SF = Stomata frequency, EC = Epidermal cells, HI = Harvest index

http://www.aloki.hu ● ISSN 1589 1623 (Print) ● ISSN 1785 0037 (Online)
DOI: http://dx.doi.org/10.15666/aeer/1706_1397513988

Conclusions

The inbred lines W64TMS and W82-3 expressed higher general combining ability (GCA) for grain yield, and other yield related traits (cobs per plant, grains per cob, 100-seed weight) under normal and water deficit conditions. The F1 hybrids W64TMS × USSR150 and W82-3 × 150P-1 showed higher SCA for grain yield and other related traits under normal and drought stress. It was suggested form our findings that the present breeding material may be used for the improvement of grain yield and water deficit tolerance in maize.

REFERENCES

[1] Abayomi, Y. A., Awokola, C. D., Lawal, Z. O. (2012): Comparative evaluation of water deficit tolerance capacity of extra-early and early maize genotypes under controlled conditions. – J. Agric. Sci. 4: 54.

[2] Ali, F., Ahsan, M., Ali, Q., Kanwal, N. (2017): Phenotypic stability of Zea mays grain yield and its attributing traits under drought stress. – Frontiers in Plant Science 8: 1397.

[3] Ali, Q., Ahsan, M., Ali, F., Aslam, M., Khan, N. H., Munzoor, M., Mustafa, H. S. B., Muhammad, S. (2013): Heritability, heterosis and heterobeltiosis studies for morphological traits of maize (Zea mays L.) seedlings. – Advancements in Life Sciences 1(1): 52-63.

[4] Ali, Q., Ali, A., Ahsan, M., Ali, S., Khan, N. H., Muhammad, S., Abbas, H. G., Nasir, I. A., Husnain, T. (2014): Line × Tester analysis for morpho-physiological traits of *Zea mays* L. seedlings. – Advancements in Life Sciences 1(4): 242-253.

[5] Ali, Q., Ahsan, M., Malook, S., Kanwal, N., Ali, F., Ali, A., Ahmed, W., Ishfaq, M., Saleem, M. (2016): Screening for drought tolerance: comparison of maize hybrids under water deficit condition. – Advancements in Life Sciences 3(2): 51-58.

[6] Anjum, S., Xie, A., Wang, X. Y., Saleem, L. C., Man, M. F., Lei, W. (2011): Morphological, physiological and biochemical responses of plants to drought stress. – Afr. J. Agric. Res. 6: 2026-2032.

[7] Araus, J. L., Slafer, G. I.; Reynolds, M. P.; Royo. C. (2002): Plant breeding and water deficit in C_3 cereals: what should we breed for? – Ann. Bot. 89: 925-940.

[8] Aslam, M., Maqbool, M. A., Cengiz, R. (2015): Drought Stress in Maize (*Zea mays* L.) Effects, Resistance Mechanisms, Global Achievements and Biological Strategies for Improvement. – Springer, Cham. DOI: 10.1007/978-3-319-25442-5.

[9] Athar, H. R., Ashraf, M. (2009): Strategies for Crop Improvement against Salinity and Drought Stress: An Overview. – In: Ashraf, M., Ozturk, M., Athar, H. R. (eds.) Salinity and Water Stress. Springer Science, Heidelberg.

[10] Awasthi, R., Kaushal, N., Vadez, V., Turner, N. C., Berger, J., Siddique, K. H. (2014): Individual and combined effects of transient drought and heat stress on carbon assimilation and seed filling in chickpea. – Funct. Plant Biol. 41: 1148-1167.

[11] Bänziger, M., Edmeades, G. O., Beck, D., Bellon, M. (2000): Breeding for Drought and Nitrogen Stress Tolerance in Maize: from Theory to Practice. – CIMMYT, Mexico.

[12] Bänziger, M., Edmeades, G. O., Lafitte, H. R. (2002): Physiological mechanisms contributing to the increased N stress tolerance of tropical maize selected for drought tolerance. – Field Crop Res. 75: 223-233.

[13] Campos, H., Cooper, M., Habben, J. E., Edmeades, G. O., Schussler. J. R. (2004): Improving drought tolerance in maize a view from industry. – Field Crops Res. 90: 19-34.

[14] Cattivelli, L., Rizza, F., Badeck, F. W.; Mazzucotelli, E., Mastrangelo, A. M., Francia, E., Mare, C., Tondelli, A., Stanca, A. M. (2008): Drought tolerance improvement in crop plants: an integrative view from breeding to genomics. – Field Crop Res 105: 1-14.

http://www.aloki.hu ● ISSN 1589 1623 (Print) ● ISSN 1785 0037 (Online)
DOI: http://dx.doi.org/10.15666/aeer/1706_1397513988

[15] Chen, D., Wang, S., Cao, B., Cao, D., Leng, G., Li, H., Yin, L., Shan, L., Deng, X. (2015): Genotypic variation in growth and physiological response to drought stress and re-watering reveals the critical role of recovery in drought adaptation in maize seedlings. – Front Plant Sci. 6: 1241.
[16] Chohan, M. S. M., Saleem, M., Ahsan, M., Asghar, M. (2012): Genetic analysis of water stress tolerance and various morpho-physiological traits in *Zea mays,* L. using graphical approach. – Pak. J. Nutr. 11: 489-500.
[17] Edmeades, G. O., Cooper, M., Lafitte, R., Zinselmeier, C., Ribaut, J. M., Habben, J. E., Löffler, C., Bänziger, M. (2001): Abiotic Stresses and Staple Crops. – In: Proceedings of the third International Crop Science Congress. CABI, Hamburg.
[18] Edmeades, G. O., McMaster, G. S., White, J. W., Campos, H. (2004): Genomics and the physiologist: bridging the gap between genes and crop response. – Field Crop. Res. 90: 5-18.
[19] Falconer, D. S., Mackay, T. F. C. (1996): Introduction to Quantitative Genetics. 4th Ed. – Benjamin Cummings, England.
[20] Farnham, I. M., Johannesson, K. H., Singh, A. K., Hodge, V. F., Stetzenbach, K. J. (2003): Factior analytical approaches for evaluating groundwater trace element chemistry data. – Anal. Chim. Acta 490: 123-138.
[21] Golbashy, M., Ebrahim, M., Khorasani, S. K., Chaukan, R. (2010): Evaluation of drought tolerance of some corn (*Zea mays* L.) hybrids in Iran. – Afr. J. Agric. Res. 5: 2714-2719.
[22] Ivy, N. A., Howlader, M. S. (2000): Combining ability in maize. – Bangladesh J. Agril. Res. 25: 385-392.
[23] Kakumanu, A., Ambavaram, M. M., Klumas, C., Krishnan, A., Batlang, U., Myers, E., Grene, R., Pereira, A. (2012): Effects of drought on gene expression in maize reproductive and leaf meristem tissue revealed by RNA-Seq. – Plant Physiol. 160: 846-867.
[24] Kanwal, N., Ali, F., Ali, Q., Sadaqat, H. A. (2019): Phenotypic tendency of achene yield and oil contents in sunflower hybrids. – Acta Agriculturae Scandinavica, Section B - Soil & Plant Science 13: 1-6.
[25] Kempthorne, O. (1957): An Introduction to Genetic Statistics. – John Wiley and Sons, New York, pp. 468-472.
[26] Konak, C., Unay, A., Serter, E., Basal, H. (2001): Estimation of combining ability effects, heterosis and heterobeltiosis using line × tester method in maize. – Turkish J. Field Crops. 4: 19.
[27] Kwon, S. H., Torrie, J. H. (1964): Heritability and interrelationship of trait of two soybean populations. – Crop Sci. 4: 196-198.
[28] Mahmood, T., Mustafa, H. S., Aftab, M., Ali, Q., Malik, A. (2019): Super canola: newly developed high yielding, lodging and drought tolerant double zero cultivar of rapeseed (Brassica napus L.). – Genetics and Molecular Research 18(2).
[29] Mao, H., Wang, H., Liu, S., Li, Z., Yang, X., Yan, J., Li, J., Tran, L. S., Qin, F. A. (2015): Transposable element in a NAC gene is associated with drought tolerance in maize seedlings. – Nat Commun. 6: 8326.
[30] Mendoza, M., Oyervides, A., Lopez. A. (2000): New maize cultivars with agronomic potential for the humid tropics. – Agronomia Mesoamericana 11: 83-88.
[31] Montgomery, K. R., Cheo, P. C. (1971): Effect of leaf thickness on ignitibility. – Forest Science 17(4):475-8.
[32] Moradi, R., Alizadeh, Y., Nezami, A., Eshghizadeh, H. R. (2013): Study of Lentil (*Lens culinaris* Medik.) seed size on germination and seedling properties in drought stress condition. – Iran. J. Field Crops Res. 11: 39-40.
[33] Nelson, D. E., Repetti, P. P., Adams, T. R., Creelman, R. A., Wu, J., Warner, D. C., Anstrom, D. C., Bensen, R. J., Castiglioni, P. P., Donnarummo, M. G., Hinchey, B. S. (2007): Plant nuclear factor Y (NF-Y) B subunits confer drought tolerance and lead to

http://www.aloki.hu ● ISSN 1589 1623 (Print) ● ISSN 1785 0037 (Online)
DOI: http://dx.doi.org/10.15666/aeer/1706_1397513988

improved corn yields on water-limited acres. – Proc. Natl. Acad. Sci. USA 104: 16450-16455.

[34] Nuccio, M. L., Wu, J., Mowers, R., Zhou, H., Meghji, M., Primavesi, L. F., Paul, M. J., Chen, X., Gao, Y., Haque, E., Basu, S. S. (2015): Expression of trehalose-6-phosphate phosphatase in maize ears improves yield in well-watered and drought conditions. – Nat. Biotechnol. 33: 862-869.

[35] Paul, S. K., Duara, R. K. (1991): Combining ability studies in maize (*Zea mays* L.). – Intl. J. Tropics. Agric. 9: 250-254.

[36] Pushpavalli, R., Zaman-Allah, M., Turner, N. C., Baddam, R., Rao, M. V., Vadez, V. (2014): Higher flower and seed number leads to higher yield under water stress conditions imposed during reproduction in chickpea. – Funct. Plant Biol. 42: 162-174.

[37] Rahbarian, R., Khavari-Nejad, R., Ganjeali, A., Bagheri, A., Najafi, F. (2011): Drought stress effects on photosynthesis, chlorophyll fluorescence and water relations in tolerant and susceptible chickpea genotypes. – Acta Biol. Crac. Ser. Bot. 53: 47-56.

[38] Rahman, H., Arifuddin, Shah, Z., Shah, S. M. A., Iqbal, M., Khalil, I. H. (2010): Evaluation of maize S2 lines in testcross combinations I: flowering and morphological traits. – Pak. J. Bot. 42: 1619-1627.

[39] Seghatoleslami, M. J., Kafi, M., Majidi, E. (2008): Effect of drought stress at different growth stages on yield and water use efficiency of five proso millet (*Panicum miliaceum* L.) genotypes. – Pak. J. Bot. 40: 1427-1432.

[40] Sehgal, A., Sita, K., Kumar, J., Kumar, S., Singh, S., Siddique, K. H. M., Nayyar, H. (2017): Effects of drought, heat and their interaction on the growth, yield and photosynthetic function of lentil (*Lens culinaris* Medikus) genotypes varying in heat and drought sensitivity. – Front. Plant Sci. 8: 1776.

[41] Sehgal, A., Sita, K., Siddique, K. H. M., Kumar, R., Bhogireddy, S., Varshney, R. K., HanumanthaRao, B., Nair, R. M., Prasad, P. V., Nayyar, H. (2018): Drought or/and heat-stress effects on seed filling in food crops: impacts on functional biochemistry, seed yields, and nutritional quality. – Front. Plant Sci. DOI: 10.3389/fpls.2018.01705.

[42] Sevanto, S. (2014): Phloem transport and drought. – J. Exp. Bot. 65: 1751-1759.

[43] Sindagi, S. S., Kulkarni, R. S., Seetharam, A. (1997): Line × tester analysis of the combining ability in sunflower (*Helianthus annuus* L.). – The Sunflower Newslet. 3: 11-12.

[44] Steel, R. G. D., Torrie, J. H., Dicky, D. A. (1997): Principles and Procedures of Statistics. A Biometrical Approach. 3rd Ed. – McGraw Hill Book Co. Inc., New York, pp. 400-428.

[45] Valentovic, P., Luxova, M., Kolarovic, L., Gasparıkova, O. (2006): Effect of osmotic stress on compatible solutes content, membrane stability and water relations in two maize cultivars. – Plant Soil Environ. 52: 186-191.

[46] Yordanov, I., Velikova, V., Tsonev, T. (2000): Plant responses to drought, acclimation and stress tolerance: review. – Photosynthetica 38: 171-186.

http://www.aloki.hu ● ISSN 1589 1623 (Print) ● ISSN 1785 0037 (Online)
DOI: http://dx.doi.org/10.15666/aeer/1706_1397513988

APPENDIX

Table A1. *Mean squares values from analysis of variance for yield related traits in maize accessions*

Source of variation	Genotypes (G)	Treatments (T)	G*T	Error
Degree of freedom	49	1	49	198
Plant height	2228.9**	43176.0**	1852.6**	1.0
Number of leaves	6.758**	322.403**	11.526**	0.354
Cob length	9.765**	340.204**	8.627**	0.158
Leaf area	54289**	1602498**	25165**	2
Cob diameter	5.084**	377.149**	5.690**	0.264
Kernel rows	8.713**	979.213**	8.193**	1.302
Kernels per cob	18887**	119920**	17080**	6
Grain yield	893.8**	41564.6**	1047.9**	3.2
100 seed weight	35.81**	2856.53**	56.78**	1.20
Leaf angle	218.856**	110.413**	249.475**	0.515
Leaf rolling	412.97	1565.68	412.76	409.36
Days to 50% silking	32.32**	1391.05**	46.50**	5.58
Days to 50% anthesis	39.60**	2809.08**	58.07**	5.69
Anthesis-silking interval	4.510**	246.613**	4.491**	0.101
Leaf temperature	57.69**	4396.84**	51.84**	0.73
Chlorophyll content	289.5**	64102.9**	343.6**	0.5
Stomata size	15318**	1423663**	16476**	49
Stomata frequency	9.882**	257.613**	12.770**	1.329
Epidermal cells	20.885**	657.120**	20.467**	1.600
Harvest index	37.2**	11325.3**	31.2**	0.3

**Highly significant differences ($P < 0.01$); Df = degree of freedom; SOV = source of variation

http://www.aloki.hu ● ISSN 1589 1623 (Print) ● ISSN 1785 0037 (Online)
DOI: http://dx.doi.org/10.15666/aeer/1706_1397513988

A COMPARISON OF BIOACTIVE CONSTITUENTS AND IN VITRO ANTIOXIDANT POTENTIAL OF ASTHMA WEED (*EUPHORBIA HIRTA*), WITH THOSE OF OTHER ANTI-ASTHMATIC PLANTS GROWING IN TABUK REGION, SAUDI ARABIA

AL-MUTAIRI, K. A. – MOBIN, M. – KHAN, M. N.*

Department of Biology, Faculty of Science, University of Tabuk, Tabuk 71491, Saudi Arabia

**Corresponding author*
e-mail: nasirmn4@gmail.com

(Received 24th May 2019; accepted 25th Oct 2019)

Abstract. *Euphorbia hirta* (asthma weed) has been documented as an effective herb for the treatment of asthma and associated symptoms. This study was aimed at comparing the bioactive constituents and *in vitro* antiradical activity of asthma weed with other commonly growing anti-asthmatic plants such as *Pergularia tomentosa*, *Dipterygium glaucum* and *Acalypha indica* in Tabuk region of Saudi Arabia. The results showed that the total phenol and flavonoid content of methanolic leaf extract of *E. hirta* was highest compared to the other anti-asthmatic plants. *E. hirta* was also recorded to have the maximum total antioxidant capacity, 1, 1-diphenyl-2-picryl-hydrazyl (DPPH) antiradical activity and nitric oxide (NOX) scavenging activity. However, hydrogen peroxide scavenging activities and metal chelating activities were as the highest for the methanolic extracts of *D. glaucum* and *P. tomentosa*, respectively compared to the other anti-asthmatic plants. It may be concluded that the abundance of phenol and flavonoids along with maximum antioxidant capacity, DPPH antiradical activity and NOX scavenging activity of *E. hirta* makes it worthy of using as an effective anti-asthmatic plant.
Keywords: *flavonoids, oxidative stress, antioxidant capacity, antiradical scavenging activity, phenols*

Introduction

Asthma is a chronic lung disease, inducing narrowing of airways and changes in the levels of eosinophils, mast cells, lymphocytes, cytokines and other inflammatory cell products (Rivera et al., 2011). Asthma is a common chronic disease that is estimated to affect as many as 339 million people worldwide (WHO, 2018). However, Bousquet et al. (2005) predicted that 100 million more will be affected by asthma by 2025. It causes a high global burden of death and disability, with around 1000 people dying each day from asthma, and is in the top 20 causes of years of life lived with disability (WHO, 2018). Nearly 2 million people are affected by asthma in the Kingdom of Saudi Arabia. There are no complete cures of asthma and currently available modern therapies have been associated with many side effects. So, to find an effective low risk, a non-drug strategy that may furnish a valuable adjunctive or alternative therapy in asthma management is both alluring and timely.

Of late, medicinal plants have attracted a huge interest due to the inherent antioxidant potential of the phytochemicals that reduce the free-radical induced oxidative damage. It is estimated that 80% of the world population rely on drugs obtained from plants, for their primary health care needs (WHO, 2019). It has been established that climate change may affect the chemical composition and, ultimately the survival of some medicinal plants. Climate change has a remarkable effect on secondary metabolites and other compounds that plants produce, which are usually the basis for their medicinal

http://www.aloki.hu ● ISSN 1589 1623 (Print) ● ISSN 1785 0037 (Online)
DOI: http://dx.doi.org/10.15666/aeer/1706_1398914000

activity (Khan et al., 2016; Yang et al., 2018). Phytochemical screening by several workers has unveiled the presence of various bioactive constituents such as phenols, flavonoids, alkaloids, terpenoids and saponins (Altemimi et al., 2017; Verma et al., 2018; Sai et al., 2019; Batool et al., 2019). Medicinal plants that may be employed for the treatment of asthma should have anti-allergic, anti-inflammatory, antihistaminic and immunomodulatory properties. It has been observed that the supplements with antioxidant properties are potentially effective in decreasing the degree of bronchoconstriction as they suppress the pro-inflammatory episodes by counteracting reactive oxygen species and reactive nitrogen species (Kurutas, 2016; Bagatini et al., 2018).

Tabuk, the northern province of Saudi Arabia (*Fig. 1*) is a region largely characterized by asymmetrical topography ranging from plains to low and high mountains that create a highly distinct environmental variable of extreme cold to extreme hot (Khan et al., 2016). Diversified topography coupled with varied environmental conditions supports the growth of several medicinally important plants in this region. Of these, *Euphorbia hirta (Euphorbiaceae)*, *Pergularia tomentosa* (Asclepiadaceae), *Dipterygium glaucum* (Capparidaceae) and *Acalypha indica* (*Euphorbiaceae*) have long been used in traditional medicine to treat asthma (Kumar et al., 2010; Youssouf et al., 2007; Zahidin et al., 2017; Alamgeer et al., 2018; Rayyan et al., 2018). *Euphorbia hirta* is known as asthma weed, spurge or milkweed and used to treat respiratory complications. Although, various studies have been performed on the phytochemical constituents of these plants, but meagre research was carried out on the comparative study of antioxidant potential of these plants. Therefore, the objective of the current study was to compare the antioxidant potential and secondary metabolites of asthma weed with other anti-asthmatic plants found in Tabuk region.

Figure 1. *Map showing sampling site (Tabuk, Saudi Arabia). (Source: Google images)*

Materials and methods

Plant collection

The plants were collected from Tabuk, the Northern Province of Saudi Arabia (latitude 28°22'59" N; 36°34'59" E, altitude 773 m). The region is characterized by its

http://www.aloki.hu ● ISSN 1589 1623 (Print) ● ISSN 1785 0037 (Online)
DOI: http://dx.doi.org/10.15666/aeer/1706_1398914000

hyper-arid climate, high evaporation rate and low precipitations during December to February. The region is bounded by Red sea on the west to the Hufa depressions in the east. Four plant species (*E. hirta, P. tomentosa, D. glaucum and A. indica*) were collected at flowering stage. At collection site five 10 m × 10 m plots, at the distance of 20 m each, were established randomly during the study. Four plants of each species from each plot were collected randomly. Finally, five healthy plants of each species were selected and were used for assessing various characteristics. The plant materials were authenticated by Dr. M. Nasir Khan. Collected plants were dried in shade under dark. Air-dried leaf samples were ground to a fine powder (80 mesh) using an electric blender and stored in a clean labeled air-tight container as replicates for assessing various characteristics.

Plant extracts

Powdered leaf sample (100 g) of each plant was extracted with methanol for 24 h using Soxhlet apparatus (Borosil, BRL_3840020). The extracts were separated from the solids by filtration with Whatman No. 1 filter paper. The remaining solids were extracted twice with the same methanol and extracts combined. The extracts were concentrated under reduced pressure at 45 °C in a rotary evaporator (EYELA, Tokyo, Japan) and kept in a refrigerator at 4 °C until analyzed.

Estimation of total phenol

The content of total phenols was estimated by the Folin-Ciocalteu method with little modification of Cevallos-Casals and Cisneros-Zevallos et al. (2005). From each sample, 0.5 ml of methanolic extract was added to 2.5 ml of Folin-Ciocalteu reagent and 2 ml of sodium carbonate 1 M. The tubes were incubated at 45 °C for 30 min. The absorbance of total phenolics was measured at 765 nm using Hewlett Packard, UV/visible light. Total phenolics content was expressed as mg gallic acid equivalents per g dry weight.

Estimation of total flavonoids

Total flavonoid content in the methanolic extracts was measured spectrophotometrically (CE 2021, Cecil, Cambridge, England), following the method of Marinova et al. (2005). 4 ml of water was added to 1 ml (500 mg/ml) extract or standard catechin solution and 0.3 ml of 5% $NaNO_2$. After keeping it for 5 min, 0.3 ml 10% $AlCl_3$ was added. To this mixture, after 6 min 2 ml 1 M NaOH was added and the total volume was made up to 10 ml with water. The solution was thoroughly mixed, and the absorbance was recorded against a prepared reagent blank at 510 nm. Total flavonoid content of was expressed as catechin equivalents in mg per g dry weight.

Assay of total antioxidant capacity

Total antioxidant capacity was determined by the method described by Prieto et al. (1999). 0.1 ml of methanolic plant extract was added to 1 ml of reagent solution (0.6 mol/l sulfuric acid, 28 mmol/l sodium phosphate and 4 mmol/l ammonium molybdate). The tubes were heated at 95 °C for 90 min. The absorbance of each solution was recorded at 695 nm against a blank. The antioxidant capacity was expressed as mg gallic acid equivalent per gram dry weight (mg GAE/g DW).

http://www.aloki.hu ● ISSN 1589 1623 (Print) ● ISSN 1785 0037 (Online)
DOI: http://dx.doi.org/10.15666/aeer/1706_1398914000

Anti-radical capacity

Determination of 1, 1-diphenyl-2-picryl-hydrazyl (DPPH) free radical scavenging

The free radical scavenging capacity of methanolic extracts of different plants was recorded using DPPH method as described by Thaipong et al. (2006). 5 ml of 0.004% freshly prepared methanolic solution of DPPH (2, 2-diphenyl-1-picrylhydrazyl) were added to 50 µl of different concentrations of sample. After 30 min in the dark at room temperature, the absorbance was recorded spectrophotometrically against a blank at 517 nm. DPPH free radical scavenging activity was expressed as the percentage inhibition.

Nitric oxide (NOX) scavenging activity

To estimate NOX radical inhibition activity, method described by Marcocci et al. (1994) was followed with little modifications. Briefly, sodium nitropruside (5 mM, pH 7.4) in phosphate buffer saline was mixed with 3 ml of different concentrations of methanolic plant extracts and incubated at 25 °C for 150 min. From this incubated solution, 0.5 ml was taken and mixed with 0.5ml Griess reagent [(1.0 ml sulfanilic acid reagent (0.33% in 20% glacial acetic acid at room temperature for 5 min with 1 ml of naphthylethylenediamine dichloride (0.1% w/v)]. After 30 min of incubation, absorbance was recorded at 540 nm. A standard solution of ascorbic acid was treated in the same way with the Griess reagent as a positive control. NOX scavenging activity was expressed as the percentage inhibition.

Hydrogen peroxide (H_2O_2) scavenging activity

The ability of the extracts to scavenge H_2O_2 was estimated based on the method of Ruch et al. (1989). A solution of H_2O_2 (40 mM) was prepared in phosphate buffer (pH 7.4). The concentration of H_2O_2 was determined by absorption at 230 nm using a spectrophotometer. Plant extracts in methanol were added to a H_2O_2 solution (0.6 ml, 40 mM). The absorbance of H_2O_2 at 230 nm was noted after 10 min against a blank solution containing phosphate buffer without H_2O_2. Ascorbic acid was used as positive control. H_2O_2 scavenging activity was expressed as the percentage inhibition.

Metal chelating activity

The formation of ferrous ion-ferrozine complex was recorded to estimate the ferrous level according to Decker and Welch (1990). The reaction mixture consisted of different concentration of plant extracts and 0.1 ml of 2 mM ferrous chloride. 0.2 ml of 5 mM ferrozine was added to this mixture to initiate the reaction and left to stand at room temperature for 10 min. The absorbance of the solution was measured at 562 nm. Ascorbic acid was used as positive control. The chelating activity was expressed as percentage of inhibition.

Statistical analyses

The data were analyzed statistically using analysis of variance (ANOVA), data were presented as average of five determinations with LSD at 5% ± SE. Differences between the means were compared by Duncan's multiple-range test at the level of $p < 0.05$ using SPSS Ver. 11 statistical software (SPSS Inc., Chicago, IL, USA). IC_{50} values were calculated by employing linear regression analysis.

http://www.aloki.hu ● ISSN 1589 1623 (Print) ● ISSN 1785 0037 (Online)
DOI: http://dx.doi.org/10.15666/aeer/1706_1398914000

Results and discussion

Asthma is an inflammatory disease of the lungs and the present endevour is to control the inflammation. As in *Table 1,* methanolic leaf extracts of *E. hirta, P. tomentosa, D. glaucum and A. indica* showed significant amount of phenolic compounds. The total phenol content of the investigated plants differed significantly. *E. hirta*, the asthma weed has 13.9%, 21.1% and 7.3% more phenol than the *P. tomentosa*, *D. glaucum* and *A. indica*, respectively. We have recorded a higher amount of total phenol in these anti-asthmatic plants than that of other anti-asthmatic plants such as *Matricaria recutita* (Al-Dabbagh et al., 2019) but lower than the *Helichrysum* species (Albayrak et al., 2010).

Table 1. *Total phenols, flavonoids and antioxidant capacity of methanolic extracts of leaves of anti-asthmatic plants Euphorbia hirta, Pergularia tomentosa, Dipterygium glaucum and Acalypha indica*

Anti-asthmatic plants	Total phenols (mg GAE/g DW)	Total flavonoids (mg CE/g DW)	Antioxidant capacity (mg GAE/g DW)
Euphorbia hirta	87.7 ± 4.2	74.3 ± 3.1	67.4 ± 3.2
Pergularia tomentosa	75.5 ± 3.1	51.7 ± 2.1	61.2 ± 2.9
Dipterygium glaucum	69.2 ± 2.9	45.7 ± 2.0	54.9 ± 2.3
Acalypha indica	81.3 ± 3.7	58.7 ± 2.7	63.7 ± 3.5
LSD at 5%	3.09	2.41	1.86

Average of five determinations is presented with LSD at 5% ± SE

Flavonoids, low-molecular weight polyphenolic plant secondary metabolites are known to play a role in prevention and management of asthma. Recent *in vitro and in vivo* studies on anti-allergic and anti-asthmatic properties of flavonoids have strongly indicated that a suitable intake of flavonoids may complement the dietary treatment and/or preventive strategy for asthma or other allergic diseases in humans (Tanaka, 2014; Tanaka et al., 2019). Perusal of the data shows a significant difference among the species in the level of flavonoids (*Table 1*). Higher level of flavonoids were noted in the asthma weed *E. hirta* (74.3 ± 3.1 mg CE/g DW) which was 30.4%, 38.5% and 21% higher than *P. tomentosa* (51.7 ± 2.1 mg CE/g DW), *D. glaucum* (45.7 ± 1.98 mg CE/g DW) and *A. indica* (58.7 ± 2.7 mg CE/g DW), respectively. Garcia-Larsen et al. (2018) have found a direct association between flavonoid intake and asthma prevalence and severity.

We carried out the phosphomolybdenum assay to determine the antioxidant capacity of methanolic leaf extracts of *E. hirta*, *P. tomentosa*, *D. glaucum* and *A. indica*. This method is based on the reduction of Mo (VI) to Mo (V) by the antioxidant compounds and the formation of green Mo (V) complexes with a maximal absorption at 695 nm (Prieto et al., 1999). Analysis of variance showed that there was a significant difference among the studies plant species for antioxidant capacity. The methanolic extract of *E. hirta* had the maximum antioxidant activity with a value of 67.4 mg GAE/g DW. The minimum antioxidant capacity was recorded in the methanolic extract of *D. glaucum* with a value of 54.9 mg GAE/g DW (*Table 1*). Anti-asthmatic plant s such as *Eriobotrya japonica* and *Tussilago farfara* showed a much higher antioxidant capacity than the plants which we studied (Song et al., 2010; Norani et al., 2019). Phytochemical

http://www.aloki.hu ● ISSN 1589 1623 (Print) ● ISSN 1785 0037 (Online)
DOI: http://dx.doi.org/10.15666/aeer/1706_1398914000

attributes such as flavonoids, carotenoids and cinnamic acid derivatives have been ascribed to contribute to the total antioxidant capacity (Tyśkiewicz et al., 2019). As, we know that oxidative stress is strongly linked with most of the features of asthma. The phytochemical preparations that are being able to scavenge these free radicals may help to relieve the symptoms of asthma. The free radical scavenging activities of methanolic leaf extracts of *E. hirta*, *P. tomentosa*, *D. glaucum* and *A. indica* were assessed by DPPH method. DPPH, stable free radicals that accept an electron or hydrogen radical and get converted in to yellow-coloured diphenylpicylhydrazine, a diamagnetic molecule. The reduction capacity of DPPH is estimated by decrease in the absorbance at 517 nm induced by antioxidants. As shown in *Figure 2,* the DPPH radical scavenging activities of methanolic leaf extracts of different plants shown to occur in a dose-dependent manner. The concentration required to inhibit 50% radical-scavenging activity (IC_{50}) was established from the results of a series of concentrations evaluated. A lower IC_{50} value corresponds to a larger scavenging activity. The rank order of potency showed that the methanolic leaf extracts of *E. hirta* was 2.7-, 2.5- and 1.9 -fold more powerful than the

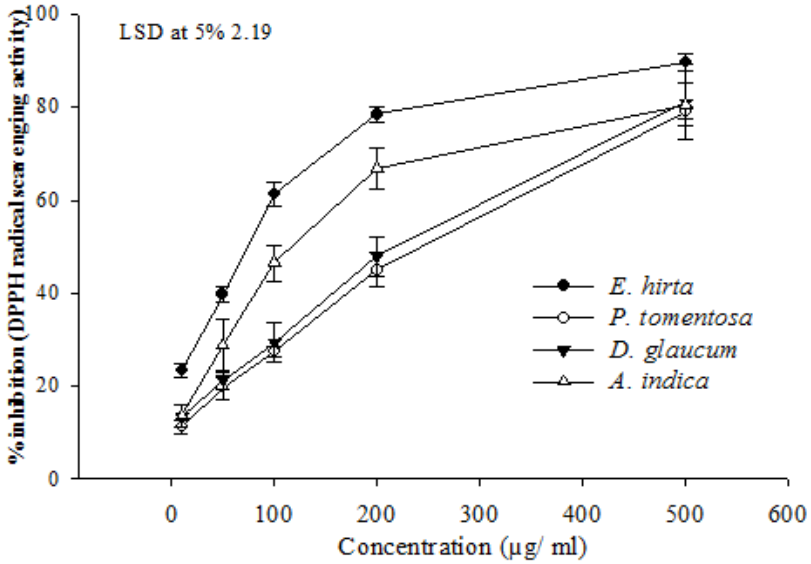

Figure 2. *DPPH radical scavenging activities of the methanolic extracts of anti-asthmatic plants Euphorbia hirta, Pergularia tomentosa, Dipterygium glaucum and Acalypha indica. Average of five determinations is presented with LSD at 5% ± SE*

P. tomentosa, *D. glaucum* and *A. indica*, respectively. The scavenging effect of methanolic extracts on the DPPH radical expressed as IC_{50} values was in the following order: *E. hirta* > *A. indica* > *D. glaucum* > *P. tomentosa* (*Fig. 3*). The substantial antioxidant activity of *E. hirta* could be due to the presence of sesquiterpene lactones and quercetin in flavonoids in the methanolic extracts (Williams et al., 2004; Gupta et al., 2017).

H_2O_2 is very lethal as being able to cross the biological membrane and serve as a precursor for potentially toxic hydroxyl radical (Das and Roychoudhury, 2014). The hydroxyl radical is an extremely reactive free radical capable of damaging almost every molecule found in living cells (Das and Roychoudhury, 2014). As in *Figure 3,* the methanolic leaf extracts of all the plants investigated, have shown a concentration

http://www.aloki.hu ● ISSN 1589 1623 (Print) ● ISSN 1785 0037 (Online)
DOI: http://dx.doi.org/10.15666/aeer/1706_1398914000

dependent H_2O_2 scavenging activity. Statistical analysis of the data shows a significant difference ($p < 0.05$) among the plants in relation to H_2O_2 scavenging activity. Lowest H_2O_2 scavenging activity was recorded for *E. hirta* which was 1.6-, 1.9- and 1.1-fold lower than *P. tomentosa*, *D. glaucum* and *A. indica*, respectively (*Fig. 3*). The H_2O_2 scavenging activity of methanolic extracts expressed as IC_{50} values was in the following order: *D. glaucum* > *P. tomentosa* > *A. indica* > *E. hirta* (*Fig. 3*). According to Mobin et al. (2014), H_2O_2 scavenging activity of these methanolic extracts could be assigned to the presence of active constituents that that may donate electrons to H_2O_2 and thereby neutralizing it to water.

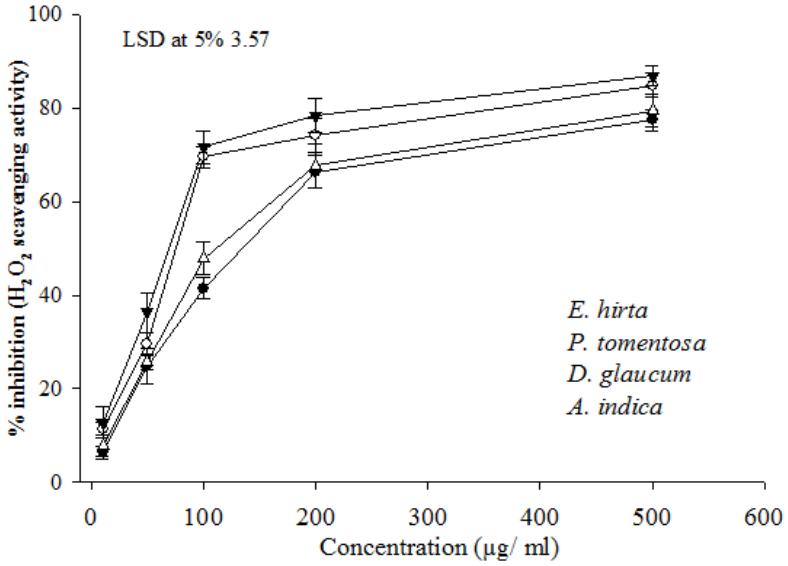

Figure 3. *H_2O_2 scavenging activities of the methanolic extracts of anti-asthmatic plants Euphorbia hirta, Pergularia tomentosa, Dipterygium glaucum and Acalypha indica. Average of five determinations is presented with LSD at 5% ± SE*

According to Terao (2009), NOX regulates many pathological conditions, especially acute inflammatory condition. Nitrite and peroxynitrite anions are generated when oxygen reacts with the excess NOX that may acts as free radicals (Radi, 2018). In this study, methanolic leaf extracts of all the investigated plants compete with oxygen to react with NOX and thus inhibits the generation of the anions in a dose dependent manner. As in *Figure 4* the highest NOX scavenging activity among the analyzed plant extracts were displayed by *E. hirta* ($IC_{50} = 135$ µg/ml). We noted that the NOX scavenging activity of *E. hirta* was 1.2-, 1.4- and 1.1-fold more than *P. tomentosa*, *D. glaucum* and *A. indica*, respectively (*Fig. 4*). The bioactive constituents of *E. hirta* include flavonoids (quercetin and myrcetin), sterols, tannins, and triterpenoids (Attah et al., 2013; Onyeka et al., 2018; Salehi et al., 2019). The abundance of these bioactive substances makes them powerful scavengers.

As in *Figure 5,* the metal chelating ability of the methanolic leaf extracts of *E. hirta, P. tomentosa*, *D. glaucum* and *A. indica* were quantified by the formation of ferrous ion-ferrozine complex of red colour which absorbs at 562 nm (Yamaguchi et al., 2000). The ability of a chelating agent to form σ bond with a metal, may act as effective scavenger as they lower the redox potential and stabilize the oxidised metal ion (Duh et al., 1999). In the present study the plants show a significant difference response in metal chelating

http://www.aloki.hu ● ISSN 1589 1623 (Print) ● ISSN 1785 0037 (Online)
DOI: http://dx.doi.org/10.15666/aeer/1706_1398914000

activity. Highest and lowest metal chelating activity was noted in *P. tomentosa* and *D. glaucum*, respectively. Based on IC_{50} value, the rank order of potency for metal chelating activity of methanolic leaf extracts of all the samples were; *P. tomentosa* > *E, hirta* > *A. indica* > *D. glaucum* (*Fig. 6*). Fe^{2+}, a transition metal can transfer a single electron and can trigger a series of radical reactions even with non-transition metals. Fe^{2+}- chelating activity depends on flavonoid structures, however, the position of the hydroxyl ion in the molecule determines the proton donating and radical scavenging activity as suggested by Mira et al. (2002), Hou et al. (2003) and de Castilho et al. (2018).

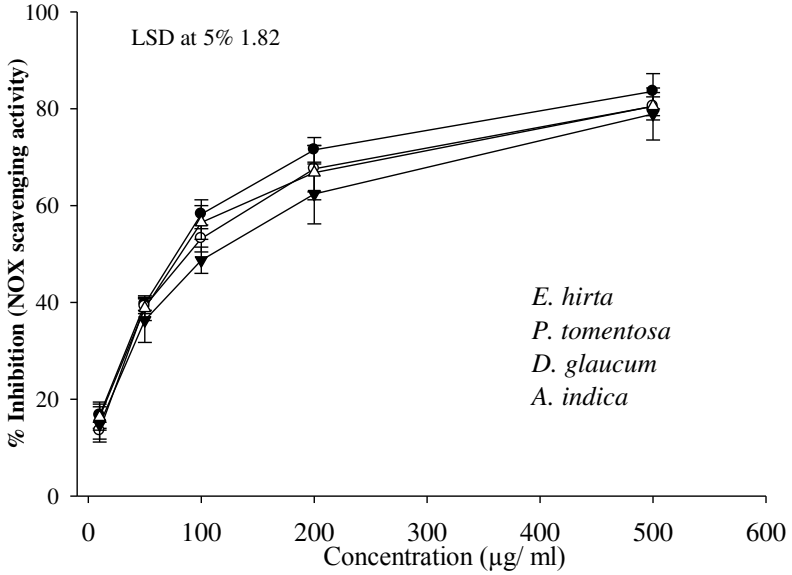

Figure 4. *Nitric oxide (NOX) scavenging activities of the methanolic extracts of anti-asthmatic plants Euphorbia hirta, Pergularia tomentosa, Dipterygium glaucum and Acalypha indica. Average of five determinations is presented with LSD at 5% ± SE*

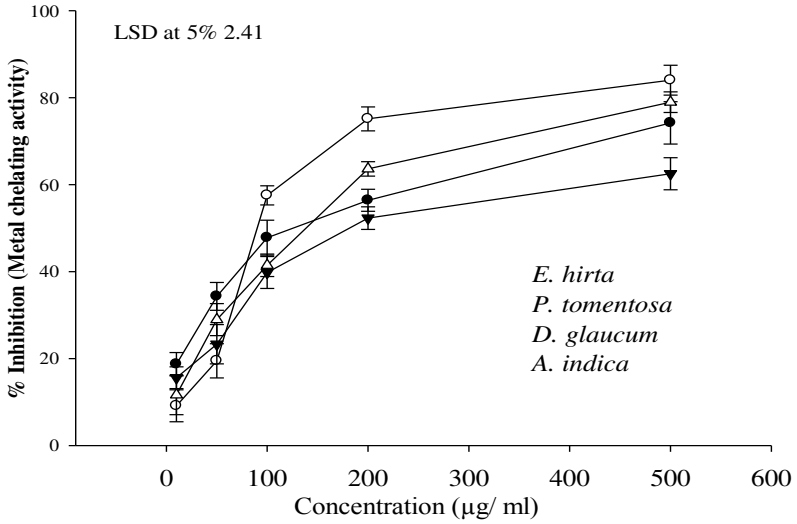

Figure 5. *Metal chelating activities of the methanolic extracts of anti-asthmatic plants Euphorbia hirta, Pergularia tomentosa, Dipterygium glaucum and Acalypha indica. Average of five determinations is presented with LSD at 5% ± SE*

http://www.aloki.hu ● ISSN 1589 1623 (Print) ● ISSN 1785 0037 (Online)
DOI: http://dx.doi.org/10.15666/aeer/1706_1398914000

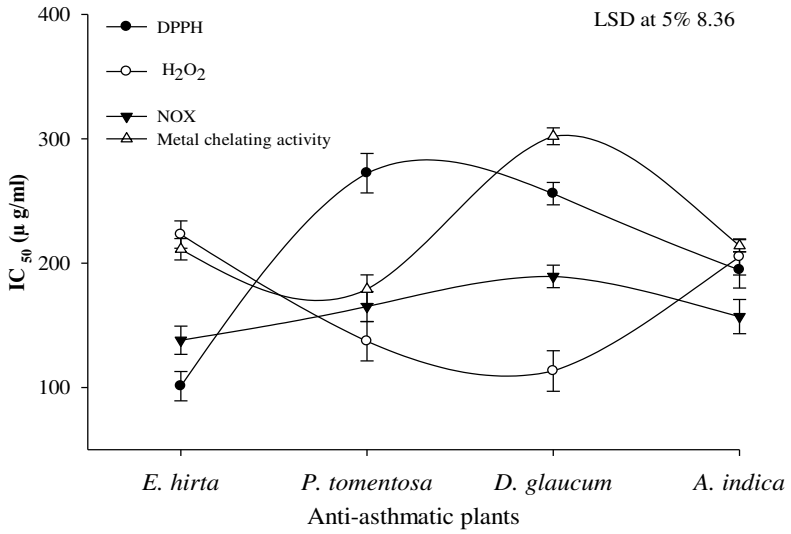

Figure 6. *IC_{50} value (µg/ml) of DPPH radical scavenging, hydrogen peroxide (H_2O_2) scavenging, nitric oxide (NOX) scavenging and metal chelating activities of the methanolic extracts of anti-asthmatic plants Euphorbia hirta, Pergularia tomentosa, Dipterygium glaucum and Acalypha indica. Average of five determinations is presented with LSD at 5% ± SE*

Conclusions

The findings of the present study have provided the biochemical evidences for the ethno-pharmacological applications of these anti-asthmatic plants. Based on statistical analysis of the data, it can be postulated that affluence of phenol and flavonoids along with maximum antioxidant capacity, DPPH antiradical activity and NOX scavenging activity in *E. hirta* makes it worthy of using as an effective anti-asthmatic plant. However, future work should be directed towards the isolation, identification and mode of action of bioactive constituents responsible for strong anti-asthmatic action of these plants.

Acknowledgements. Financial support (Project no. S-0243-1439) by Deanship of Scientific Research (DSR), University of Tabuk is gratefully acknowledged. Authors are also thankful to the Dean, Faculty of Science and head of the Biology Department, University of Tabuk.

REFERENCES

[1] Alamgeer., Younis, W., Asif, H., Sharif, A., Riaz, H., Bukhari, I. A., Assiri, A. M. (2018): Traditional medicinal plants used for respiratory disorders in Pakistan: a review of the ethno-medicinal and pharmacological evidence. – Chinese Medicine 13: 48. https://doi.org/10.1186/s13020-018-0204-y.

[2] Albayrak, S., Aksoy, A., Sagdic, O., Hamzaoglu, E. (2010): Compositions, antioxidant and antimicrobial activities of *Helichrysum* (Asteraceae) species collected from Turkey. – Food Chemistry 119: 114-122.

[3] Al-Dabbagh, B., Elhaty, I. A., Elhaw, M., Murali, C., Al Mansoori, A., Awad, B., Amin, A. (2019): Antioxidant and anticancer activities of chamomile (*Matricaria recutita* L.). – BMC Research Notes 12: 3. DOI: 10.1186/s13104-018-3960-y.

http://www.aloki.hu ● ISSN 1589 1623 (Print) ● ISSN 1785 0037 (Online)
DOI: http://dx.doi.org/10.15666/aeer/1706_1398914000

[4] Altemimi, A., Lakhssassi, N., Baharlouei, A., Watson, D. G., Lightfoot, D. A. (2017): Phytochemicals: extraction, isolation, and identification of bioactive compounds from plant extracts. – Plants 6: 42. DOI: 10.3390/plants6040042.

[5] Attah, S. K., Ayeh-Kumi, P. F., Sittie, A. A., Oppong, I. V., Nyarko, A. K. (2013): Extracts of *Euphorbia hirta* Linn. (Euphorbiaceae) and *Rauvolfia vomitoria* Afzel (Apocynaceae) demonstrate activities against *Onchocerca volvulus Microfilariae in vitro.* – BMC Complementary and Alternative Medicine 13: 66. DOI: 10.1186/1472-6882-13-66.

[6] Bagatini, M. D., Jeandre Jaques. J. A. S., de Oliveira, C. S., de Oliveira, G. A., Pillat, M. M., Mânica, A., Moser, C. S., dos Santos, L. D., Ulrich, H. (2018): Oxidative Stress: Noxious but Also Vital. – In: Atukeren, P. (ed.) Novel Prospects in Oxidative and Nitrosative Stress. InTech Open Publishers, London. DOI: 10.5772/intechopen.73394.

[7] Batool, R., Khan, M. R., Sajid, M., Ali, S., Zahra, Z. (2019): Estimation of phytochemical constituents and in vitro antioxidant potencies of Brachychiton populneus (Schott & Endl.) R. Br. – BMC Chemistry13: 10.1186/s13065-019-0549-z.

[8] Bousquet, J., Annesi-Maesano, I., Carat, F., Leger, D., Rugina, M., Pribil, C., El Hasnaoui, A., Chanal, I. (2005): Characteristics of intermittent and persistent allergic rhinitis: DREAMS study group. – Clinical & Experimental Allergy 35: 728-732.

[9] Cevallos-Casals, B., Byrne, D., Okie, W. R., Cisneros-Zevallos, L. (2005): Selecting new peach and plum genotypes rich in phenolic compounds and enhanced functional properties. – Food Chemistry 96: 273-280.

[10] Das, K., Roychoudhury, A. (2014): Reactive oxygen species (ROS) and response of antioxidants as ROS-scavengers during environmental stress in plants. – Frontiers in Environmental Science https://doi.org/10.3389/fenvs.2014.00053.

[11] de Castilho, T. S., Matias, T. B., Nicolini, K. P., Nicolin, J. (2018): Study of interaction between metal ions and quercetin. – Food Science and Human Wellness 7: 215-219.

[12] Decker, E. A., Welch, B. (1990): Role of ferritin as a lipid oxidation catalyst in muscle food. – Journal of Agricultural and Food Chemistry 38: 674-677.

[13] Duh, P. D., Tu, Y. Y., Yen, G. C. (1999): Antioxidant activity of water extract of harng Jyur (*Chrysanthemum morifolium* Ramat). – LWT - Food Science and Technology 32: 269-277.

[14] Garcia-Larsen, V., Thawer, N., Charles, D., Cassidy, A., van Zele, T., Thilsing, T., Ahlström, M., Haahtela, T., Keil, T., Matricardi, P. M., Brożek, G., Kowalski, M. L., Makowska, J., Niżankowska-Mogilnicka, E, Rymarczyk, B., Loureiro, C., Bom, A. T., Bachert, C., Forsberg, B., Janson, C., Torén, K., Potts, J. F., Burney, P. G. J. (2018): Dietary intake of flavonoids and ventilatory function in European adults: a GA^2 LEN study. – Nutrients 10: 95. 10.3390/nu10010095.

[15] Gupta, S. S., Azmi, L., Mohapatra, P. K., Rao, C. V. (2017): Flavonoids from whole plant of *Euphorbia hirta* and their evaluation against experimentally induced gastroesophageal reflux disease in rats. – Pharmacognosy Magazine 13(Suppl 1): S127-S134. DOI: 10.4103/0973-1296.203987.

[16] Hou, W. C., Lin, R. D., Cheng, K. T., Hung, Y. T., Cho, C. H., Hwang, S. Y., Lee, M. H. (2003): Free radical scavenging activity of Taiwanese native plants. – Phytomedicine 10: 170-175.

[17] Khan, M. N., Mobin, M., Abbas, Z. K., ALMutairi, K. A. (2016): Impact of varying elevations on growth and activities of antioxidant enzymes of some medicinal plants of Saudi Arabia. – Acta Ecologica Sinica 36: 141-148.

[18] Kumar, S., Malhotra, R., Kumar, D. (2010): *Euphorbia hirta*: Its chemistry, traditional and medicinal uses, and pharmacological activities. – Pharmacognosy Reviews 4: 58-61. DOI: 10.4103/0973-7847.65327.

[19] Kurutas, E. B. (2016): The importance of antioxidants which play the role in cellular response against oxidative/nitrosative stress: current state. – Nutrition Journal 15: 71. DOI: 10.1186/s12937-016-0186-5.

http://www.aloki.hu ● ISSN 1589 1623 (Print) ● ISSN 1785 0037 (Online)
DOI: http://dx.doi.org/10.15666/aeer/1706_1398914000

[20] Marcocci, L., Maguire, J. J., Droy, M. T. (1994): The nitric oxide scavenging properties of Gingo biloba extract EGb 761. – Biochemical and Biophysical Research Communications 15: 748-755.
[21] Marinova, D., Ribarova, F., Atanasova, M. (2005): Total phenolics and flavonoids in Bulgarian fruits and vegetables. – Journal of Chemical Technology and Metallurgy 40: 255-260.
[22] Mira, L., Fernandez, M. T., Santos, M., Rocha, R., Florencio, M. H., Jennings, K. R. (2002): Interactions of flavonoids with iron and copper ions: a mechanism for their antioxidant activity. – Free Radical Research 36: 1199-1208.
[23] Mobin, M., Khan, M. N., Zahid, K. A. A. (2014): Studies on the *in vitro* antiradical activity, phenol and flavonoid contents of Saudi medicinal plants of the family Asteraceae having xanthine-inhibitor activities. – World Journal of Pharmacy and Pharmaceutical Sciences 4: 41-52.
[24] Norani, M., Ebadi, M-T., Ayyari, M. (2019): Volatile constituents and antioxidant capacity of seven *Tussilago farfara* L. populations in Iran. – Scientia Horticulturae 57: 108635. https://doi.org/10.1016/j.scienta.2019.108635.
[25] Onyeka, I. P., Suleiman, M. M., Bako, S. P. (2018): Toxicity effects of methanolic extract of *Euphorbia hirta* - honey mixture in albino rats. – Journal of Pharmacognosy & Natural Products 4: 1. DOI: 10.4172/2472-0992.1000147.
[26] Prieto, P., Pineda, M., Aguilar, M. (1999): Spectrophotometric quantification of antioxidant capacity through the formation of a phosphomolybdenum complex: specific application of vitamin E. – Analytical Biochemistry 269: 337-341.
[27] Radi, R. (2018): Oxygen radicals, nitric oxide, and peroxynitrite: Redox pathways in molecular medicine. – Proceedings of the National Academy of Sciences 115: 5839-5848. https://doi.org/10.1073/pnas.1804932115.
[28] Rayyan, W. A., Alshammari, S. A. G., AL-Sammary, A. M. F., AL-Shammari, M. S. S., Seder, N., Qatoosh, L. F. A., Bostami, M., Mansoor, K., Hamad, M. F., Al-Majali, I. S., Daiyyah, W. A. (2018): The phytochemical analysis and antimicrobial activity of *Pergularia tomentosa* in north east Kingdom of Saudi Arabia KSA. – Biomedical and Pharmacology Journal 11: 4. http://biomedpharmajournal.org/?p=23959.
[29] Rivera, D. G., Hernández, I., Merino, N., Luque, Y., Álvarez, A., Martín, Y., Amador, A., Nuevas, L., Delgado, R. (2011): *Mangifera indica* L. extract (Vimang) and mangiferin reduce the airway inflammation and Th2 cytokines in murine model of allergic asthma. – Journal of Pharmacy and Pharmacology 63: 1336-1345. 10.1111/j.2042-7158.2011.01328.x.
[30] Ruch, R. J., Cheng, S. J., Klaunig, J. E. (1989): Prevention of cytotoxicity and inhibition of intercellular communication by antioxidant catechins isolated from Chinese green tea. – Carcinogenesis 10: 1003-1008.
[31] Sai, K., Thapa, R., Devkota, H. P., Joshi, K. R. (2019): Phytochemical screening, free radical scavenging and α-amylase inhibitory activities of selected medicinal plants from Western Nepal. – Medicines 6: 70. https://doi.org/10.3390/medicines6020070.
[32] Salehi, B., Iriti, M., Vitalini, S., Antolak, H., Pawlikowska, E., Kręgiel, D., Sharifi-Rad, J., Oyeleye, S. I., Ademiluyi, A. O., Czopek, K., Staniak, M., Custódio, L., Coy-Barrera, E., Segura-Carretero, A., de la Luz Cádiz-Gurrea, M., Capasso, R., Cho, W. C., Seca, A. M. L. (2019): Euphorbia-derived natural products with potential for use in health maintenance. – Biomolecules 9: 337. https://doi.org/10.3390/biom9080337.
[33] Song, F-L., Gan, R-Y., Zhang, Y., Xiao, Q., Kuang, L., Li, H-B. (2010): Total phenolic contents and antioxidant capacities of selected Chinese medicinal plants. – International Journal of Molecular Sciences 11: 2362-2372.
[34] Tanaka, T. (2014): Flavonoids for allergic diseases: present evidence and future perspective. – Current Pharmaceutical Design 20: 879-85.

http://www.aloki.hu ● ISSN 1589 1623 (Print) ● ISSN 1785 0037 (Online)
DOI: http://dx.doi.org/10.15666/aeer/1706_1398914000

[35] Tanaka, T., Iuchi, A., Harada, H., Hashimoto, S. (2019): Potential beneficial effects of wine flavonoids on allergic diseases. – Diseases 7: 8. https://doi.org/10.3390/diseases7010008.
[36] Terao, J. (2009): Dietary flavonoids as antioxidants. – Forum of Nutrition 61: 87-94.
[37] Thaipong, K., Boonprakob, U., Crosby, K., Cisneros-Zevallosc, L. (2006): Comparison of ABTS, DPPH, FRAP, and ORAC assays for estimating antioxidant activity from guava fruit extracts. – Journal of Food Composition and Analysis 19: 669-675.
[38] Tyśkiewicz, K., Konkol, M., Kowalski, R., Rój, E., Warmiński, K., Krzyżaniak, M., Gil, L., Stolarski, M. J. (2019): Characterization of bioactive compounds in the biomass of black locust, poplar and willow. – Trees. https://doi.org/10.1007/s00468-019-01837-2.
[39] Verma, R., Balaji, B. S., Dixit, A. (2018): Phytochemical analysis and broad spectrum antimicrobial activity of ethanolic extract of *Jasminum mesnyi* Hance leaves and its solvent partitioned fractions. – Bioinformation 14: 430-439. DOI: 10.6026/97320630014430.
[40] WHO (2018): The Global Asthma Report. – Global Asthma Network, Auckland, New Zealand.
[41] WHO (2019): Global Report on Traditional and Complementary Medicine 2019. – World Health Organization, Geneva.
[42] Williams, R. J., Spencer, J. P. E., Rice-Evans, C. (2004): Flavonoids: antioxidants or signaling molecules? – Free Radical Biology & Medicine 36: 838-849.
[43] Yamaguchi, F., Ariga, T., Yoshimara, Y., Nakazawa, H. (2000): Antioxidant and antiglycation of carcinol from *Garcina indica* fruit rind. – Journal of Agricultural and Food Chemistry 48: 180-185.
[44] Yang, L., Wen, K-S., Ruan, X., Zhao, Y-X., Wei, F., Wang, Q. (2018): Response of plant secondary metabolites to environmental factors. – Molecules 23: 762. DOI: 10.3390/molecules23040762.
[45] Youssouf, M. S., Kaiser, P., Tahir, M., Singh, G. D., Singh, S., Sharma, V. K., Satti, N. K., Haque, S. E., Johri, R. K. (2007): Anti-anaphylactic effect of *Euphorbia hirta*. – Fitoterapia 78: 535-9.
[46] Zahidin, N. S., Saidin, S., Zulkifli, R. M., Muhamad, I., Ya'akob, H., Nur, H. (2017): A review of *Acalypha indica* L. (Euphorbiaceae) as traditional medicinal plant and its therapeutic potential. – Journal of Ethnopharmacology http://dx.doi.org/10.1016/j.jep.2017.06.019.

http://www.aloki.hu ● ISSN 1589 1623 (Print) ● ISSN 1785 0037 (Online)
DOI: http://dx.doi.org/10.15666/aeer/1706_1398914000

ANALYSIS OF THE FACTORS AFFECTING THE ADOPTION OF ORGANIC FARMING IN TURKEY: THE CASE OF SAMSUN PROVINCE

CUKUR, T.[1*] – KIZILASLAN, N.[2] – KIZILASLAN, H.[2]

[1]*Department of Marketing and Advertising, Milas Vocational School, Muğla Sıtkı Koçman University, Milas, Muğla, Turkey*

[2]*Department of Agricultural Economics, Agricultural Faculty, Tokat Gaziosmanpaşa University, Tokat, Turkey*

**Corresponding author*
e-mail: tayfun.cukur@hotmail.com; phone: +90-252-211-3263; fax: +90-252-211-1879

(Received 24th May 2019; accepted 3rd Sep 2019)

Abstract. Organic farming is an environmentally friendly agricultural system which is very important in terms of the environment, human and plant and animal health. Thanks to organic farming, soil and water resources and air are protected from excessive contamination. In this respect, organic farming also contributes to the sustainable use of natural resources. Seen from this perspective, the adoption and application of organic farming by farmers is very important. This research was conducted to determine the factors affecting the adoption of organic farming by farmers. The study was executed in the Bafra district of Samsun province in Turkey. Within the context of the study, face-to-face administration of a questionnaire to a total of 54 farmers from nine different villages was performed. The proportional sampling method was used to determine the number of producers to be surveyed. It was determined that the most important factors are the health factors for farmers to adopt organic farming. They are followed by environmental protection factors, economic factors, social factors and innovativeness factors. All the farmers participating in the current study were determined to want to go on with organic farming in the future.
Keywords: *farmers' preference, organic agriculture, conversion, adoption, environment*

Introduction

The history of organic farming dates back to the 1940s, first each country started its development in itself and then its structure and trade developed worldwide. The first worldwide organization was founded in 1972 with the establishment of International Federation of Organic Agriculture Movements (IFOAM). World trade began to develop in the late 1970s and reached the market size in the 1980s (Altındişli and Aksoy, 2010). Organic farming is an alternative production method that aims to improve not only the quantity but also the quality of production and includes human and environmentally friendly production systems for reestablishing the natural equilibrium which is lost as a result of faulty practices in the ecological system, and prohibits the use of synthetic chemical pesticides, hormones and mineral fertilizers while recommending the use of organic and green fertilization and alternation (Aksoy and Altındişli, 1999).

Organic farming started in Turkey in 1984-85 with the demand of European companies for the production of traditional products such as dried fruits and nuts organically (Aksoy, 2002). The organic farming model generally implemented in Turkey is carried out in the form of contract farming between companies and organic producers. According to these contracts, the producers stipulate not to use synthetic fertilizers and pesticides in line with the direction of the project managers of the organic

http://www.aloki.hu ● ISSN 1589 1623 (Print) ● ISSN 1785 0037 (Online)
DOI: http://dx.doi.org/10.15666/aeer/1706_1400114008

companies and carry out other necessary agricultural practices (use of organic inputs and agricultural methods) (Demiryürek, 2011).

In 2018, the number of farmers engaged in organic plant production was 54666. The total area of organic farming was 365889.54 hectare. When organic animal production data for the year 2018 was analyzed, it was found that a total of 148 farmers raise organic animals. When the data for the organic beekeeping were examined, it was found that 334 farmers were in the business of organic beekeeping and the number of hives under such conditions was 51742 (Anonymous, 2019a).

Organic farming started in Samsun province in 1994 with the production of organic hazelnuts. The use of pesticides and chemical fertilizers in areas other than Bafra and Çarşamba plains is quite low. In this respect, Samsun has an important potential for organic farming. In 2018, the number of farmers engaged in organic crop farming in Samsun province was 1013. The total area of organic farming was 3343.65 hectare (Anonymous, 2019a). In the current study, it was aimed to reveal the process of adoption of organic farming and the factor affecting this process in the Bafra district of the Samsun province.

Materials and methods

The main material of the current study is made up of the data collected by means of face-to-face administration of a questionnaire to a total of 54 producers engaged in organic farming in the villages of Çalköy, Darboğaz, Dikencik, Elifli, İkizpınar, Köseli, Ozan, Sürmeli and Uluağaç in the Bafra district of the Samsun province in Turkey (*Fig. 1*). Moreover, previous research on organic farming has also been capitalized on.

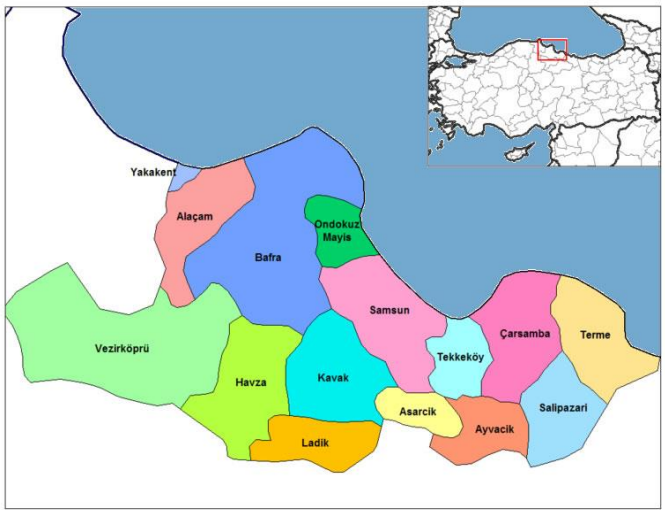

Figure 1. *Map of Samsun Province. (Source: Anonymous, 2019b)*

The questionnaire consists of four parts. These parts are; socio-economic features of the producers, general features of the agricultural enterprises, the farmers' state of plant production and the farmers' state of organic production. The questionnaires were administered in February and March, 2017.

http://www.aloki.hu ● ISSN 1589 1623 (Print) ● ISSN 1785 0037 (Online)
DOI: http://dx.doi.org/10.15666/aeer/1706_1400114008

After the research data had been collected, the analysis process was initiated. In the analysis of the collected data, means and frequencies were calculated. Moreover, in order to determine the farmers' attitudes towards organic farming, a five-point Likert scale was used. The obtained results are summarized in tables and then interpreted and evaluated.

Results

Socio-economic features of the farmers

Within the context of the socio-economic features, the farmers' age, gender, education level, the number of people in the family, income sources, income level and their membership to any agricultural association were investigated in the current study. Of the participating farmers, 92.59% are males and 7.41% are females. The mean age of the participating farmers was found to be 59.54. When the education levels of the farmers were examined, it was found that 53.70% are elementary school graduates, 16.67% are middle school graduates, 12.96% are high school graduates, 11.11% are university graduates, 3.70% are literate and 1.86% are illiterate. The mean number of members in the family was found to be 5.15.

It was determined that 87.04% of the farmers do not keep their business records regularly. All the farmers participating in the current study were found to be a member to an agricultural association. When the agricultural associations subscribed were examined, it was found that all of them are members to the Chamber of Agriculture.

It was also found that the participating farmers are engaged in the production of many organic products. These products include nuts, walnuts, wheat, corn, eggplant, peppers, apples, strawberries, tomatoes, cucumbers and beans. The production areas of these products are as follows: Nut 20.67 decares, walnut 13.30 decares, wheat 3 decares, corn 10 decares, eggplant 2 decares, pepper 2 decares, apple 5.50 decares, strawberry 3 decares, tomato 2 decares, cucumber 3.67 decares, bean 1.37 decares.

Some characteristics of the farms investigated

The farms investigated were found to have 45.06 decares arable land on average and the number of average parcels was calculated to be 6.56. In the current research, it was determined that all of the farmers perform their agricultural activities on the property land. Besides, it was determined that 11.11% of the farmers conduct their agricultural activities on the rented land and that only one producer conducts his/her agricultural activities in the jointly operated land. In the current research, it was also found that 11.11% of the farmers are also engaged in animal breeding.

In the current research, 79.63% of the farmers were found to have non-agricultural income sources. The farmers were asked the question "How is your income level compared to other farmers in your village?" Majority of the farmers (77.78%) were found to be in the middle income group, 14.81% were found to be in the low income group and 7.41% were found to be in the high income group.

Findings related to organic farming

When how the farmers were first introduced to the concept of organic farming was examined, it was found that 57.41% of them first heard of the concept of organic farming from agricultural associations, 12.96% from universities, 11.11% from

http://www.aloki.hu ● ISSN 1589 1623 (Print) ● ISSN 1785 0037 (Online)
DOI: http://dx.doi.org/10.15666/aeer/1706_1400114008

television and radio, 9.26% from books/journals/newspapers, 5.56% from friends and relatives and 3.70% from pioneering farmers. When the farmers were asked the question "How long time passed between your first introduction to the concept of organic farming and your starting organic farming?", 66.67% stated that they immediately started, 24.07% stated that they started 1 to 5 years later and 9.26% stated that they started after 5 years had passed. When how long the farmers had been in the business of organic farming was investigated, it was found that 92.59% had been in the business of organic farming for 0-5 years, 5.56% had been in the business of organic farming for 6-10 years and 1.85% for 11-20 years.

In the current study, it was determined that the most effective factors on the adoption of organic farming by the farmers are health factors. They are followed by environmental protection factors, economic factors, social factors and innovativeness factors (*Table 1*).

Table 1. *Factors affecting the adoption of organic farming*

	Not effective at all		**Little effective**		**Effective**		**Very effective**		**Extremely effective**		**Scale mean**
	n	**%**	**n**	**%**	**n**	**%**	**n**	**%**	**n**	**%**	
Environmental protection factors	0	0.00	0	0.00	1	1.85	38	70.37	15	27.78	4.26
Innovativeness factors	0	0.00	53	98.15	1	1.85	0	0.00	0	0.00	2.02
Economic factors	0	0.00	27	50.00	26	48.15	1	1.85	0	0.00	2.52
Social factors	0	0.00	28	51.85	25	46.30	1	1.85	0	0.00	2.50
Health factors	0	0.00	0	0.00	1	1.85	14	25.93	39	72.22	4.70

The percentage of the farmers thinking that organic farming does not any effect on the income level was found to be 77.78. While 11.11% of the farmers stated that organic farming has an income increasing effect, 11.11% stated that it has an income decreasing effect.

The primary purpose why the farmers are engaged in organic production is to produce healthy products (*Table 2*).

Table 2. *The purpose why the farmers are engaged in organic production*

	Not effective at all		**Little effective**		**Effective**		**Very effective**		**Extremely effective**		**Scale mean**
	n	**%**	**n**	**%**	**n**	**%**	**n**	**%**	**n**	**%**	
Producing healthy products	0	0.00	0	0.00	0	0.00	5	9.26	49	90.74	4.91
Environmentally sensitive production	0	0.00	1	1.85	0	0.00	4	7.41	49	90.74	4.87
Getting subsidies	0	0.00	3	5.56	22	40.74	19	35.19	10	18.52	3.67
Existence of control at every stage	0	0.00	0	0.00	5	9.26	20	37.04	29	53.70	4.44
Greater marketing opportunities	1	1.85	6	11.11	25	46.30	15	27.78	7	12.96	3.39
Higher product prices	1	1.85	21	38.89	24	44.44	7	12.96	1	1.85	2.74
Innovativeness	1	1.85	43	79.63	9	16.67	1	1.85	0	0.00	2.19

http://www.aloki.hu ● ISSN 1589 1623 (Print) ● ISSN 1785 0037 (Online)
DOI: http://dx.doi.org/10.15666/aeer/1706_1400114008

When the ways through which the farmers engaged in organic production market their products were examined, it was found that 77.78% of the farmers market their products through wholesalers while 22.22% market their products in local markets.

Among the problems encountered by the farmers while performing organic production, first place is taken by lack of consciousness on the part of consumers with 35.19%. On the other hand, 7.40% of the farmers were found to have no problem in organic production (*Table 3*).

Table 3. *Problems encountered while performing organic production*

	n	**%**
Low yield	15	27.78
High costs	15	27.78
Lack of consciousness on the part of consumers	19	35.19
All	1	1.85
No problem	4	7.40
Total	54	100.00

It was found that according to the producers, the most important characteristics differentiating organic farming from conventional farming are producing quality food (44.44%) and protecting nature (44.44%) (*Table 4*).

Table 4. *Characteristics differentiating organic farming from conventional farming*

	n	**%**
Guarantee for purchasing due to contracted production	4	7.42
Quality food production	24	44.44
Protecting nature	24	44.44
Having high profits	2	3.70
Total	54	100.00

It was found that all the farmers participate in meetings, trainings and seminars organized in their villages and find these training activities useful.

All of the participating farmers were found to be willing for going on with organic farming in the future. A high majority of the farmers (77.78%) were found to want to go on with organic farming as healthy products are created through organic farming. The percentage of the farmers wanting to go on with organic farming as it does not harm nature was found to be 9.25 (*Table 5*).

Table 5. *The reasons for the farmers' going on with organic farming*

	n	**%**
More subsidies	1	1.85
No harm to nature	5	9.25
No pesticides	3	5.56
Quality food	3	5.56
Healthy products	42	77.78
Total	54	100.00

http://www.aloki.hu ● ISSN 1589 1623 (Print) ● ISSN 1785 0037 (Online)
DOI: http://dx.doi.org/10.15666/aeer/1706_1400114008

It was found that the information most needed by the farmers about organic farming is technical information. Other subjects for which the farmers need information are subsides, legal regulations and prices (*Table 6*).

Table 6. *Subjects for which the farmers need information in relation to organic production*

	None		Little		Some		Much		Very much		Scale mean
	n	%	n	%	n	%	n	%	n	%	
Technical information	0	0.0	10	18.52	12	22.22	11	20.37	21	38.89	3.80
Legal regulations	5	9.26	22	40.74	25	46.30	2	3.70	0	0.00	2.44
Price	4	7.41	33	61.11	14	25.93	3	5.56	0	0.0	2.30
Subsidies	1	1.85	17	31.48	26	48.15	5	9.26	5	9.26	2.93

Discussion

In the current study conducted to determine the factors affecting the adoption of organic farming in Samsun province, it was found that the most effective factors are health factors. That is, the farmers stated that due to the negative effects of chemical inputs used in conventional production on human health, they turned to organic farming. Similarly, Karki et al. (2011) found that health awareness and environmental awareness affected the decision of farmers to switch to organic farming. In a study conducted by Çukur and Işın (2008), it was found that the economic aspect of agriculture is very important for farmers, the ecological aspect of agriculture is important and the social aspect of agriculture is relatively less important. Rezvanfar et al. (2011) determined that there were many factors affecting the adoption of organic farming by farmers, including the socio-economic characteristics of farmers, the characteristics of enterprises, the information sources of farmers, the membership of farmers to farmer associations and the attitudes of farmers. Ceylan et al. (2010) found that economic and environmental factors were effective in farmers' adoption of organic farming. In a study conducted by Meda et al. (2018) in Burkina Faso, it was found that fertilizer support and the use of credit for grain production facilitated farmers' adoption of organic cotton production. Crawford et al. (2015) found that the communication network between farmers is very useful for the farmers engaged in organic farming. In the study conducted by Azam and Shaheen (2019), it was determined that there are 5 important factors in the adoption of organic farming. These factors were identified as economic, social, marketing, tillage and government policy.

It was determined that the majority of the farmers started organic production immediately after hearing of the concept of organic farming and had been in the business of organic farming at least for five years. Burton et al. (2003) also found in the first 5 years, the rate of adoption of organic farming is high. In a study conducted by Kallas et al. (2009), it was found that farmers who like to take risks, who care about the environment and who create employment in their businesses adopt organic farming in a shorter time. In a study conducted by Issa and Hamm (2017) with fresh vegetable and fruit producers, it was determined that farmers have positive views on organic farming and intend to switch to organic farming within 5 years.

A significant proportion of farmers think that their starting organic farming has no notable effect on their income. Artukoglu et al. (2009) determined that the income level of the farmers did not have an effect on their decisions to adopt organic farming.

http://www.aloki.hu ● ISSN 1589 1623 (Print) ● ISSN 1785 0037 (Online)
DOI: http://dx.doi.org/10.15666/aeer/1706_1400114008

In the current study, it was found that according to the producers, the most important characteristics differentiating organic farming from conventional farming are producing quality food and protecting nature. In the current study, it was found that the meetings, trainings and seminars organized in villages about organic farming were found to be beneficial by the producers. Sodjinou et al. (2015) found that communication with agricultural extension services facilitated the adoption of organic farming by farmers. The research conducted by Adebayo and Oladele (2013) has revealed a positive relationship between the frequency of communication with extentionists and the adoption of organic farming by farmers.

In the current research, it was determined that all of the farmers wanted to continue their organic production in the future. In a study conducted by Çukur (2015) however it was determined that farmers do not want to continue organic production in the future as they do not have sufficient knowledge about organic farming.

Conclusion

It was determined that all of the farmers interviewed in the study wanted to continue their organic production in the future and their aim was to cultivate healthy products. This is important for the sustainability of organic farming. Agricultural extension and training programs should be implemented for the adoption of organic farming by more farmers in the district. For this purpose, it is necessary to identify the regions that are suitable for organic farming in the district and where the use of chemical inputs is very low and works should be conducted for farmers to adopt organic farming.

In the current research, it was determined that farmers need technical knowledge about organic farming and they also need information about subsidies, legal regulations and prices. Therefore, a comprehensive extension program should be prepared and put into practice to provide farmers with extension and consultancy services.

In the current study, it was determined that most of the farmers did not keep their business records. Business records are an important source of data for farmers to make the right decision. Therefore, farmers should be informed about the importance of keeping business records.

Consumers should be informed about the importance of the products of organic farming for health and their awareness about organic farming should be increased. The number of organic markets should be increased to make it easier for consumers to access organic products.

Organic farming is very important for sustainable agriculture. The increase in organic farming subsidies is thought to be effective in the adoption of organic farming by more farmers.

Determination of the factors that affect farmers' adoption of organic agriculture seems to be important in terms of using it as data for the development of policies related to organic farming.

REFERENCES

[1] Adebayo, S. A., Oladele, O. I. (2013): Vegetable farmers' attitude towards organic agriculture practices in South Western Nigeria. – Journal of Food, Agriculture & Environment 11(2): 548-552.

http://www.aloki.hu ● ISSN 1589 1623 (Print) ● ISSN 1785 0037 (Online)
DOI: http://dx.doi.org/10.15666/aeer/1706_1400114008

[2] Aksoy, U. (2002): Turkey. – In: Al Bitar, L. (ed.) Report on Organic Agriculture in the Mediterranean Area. CIHEAM, Bari, pp.147-159.
[3] Aksoy, U., Altındişli, A. (1999): Ecological Agricultural Products in the World and Turkey Production, Export and Development Facilities. – İstanbul Chamber of Commerce Publication No 1999-70, İstanbul (in Turkish).
[4] Altındişli, A., Aksoy, U. (2010): Status of organic agriculture in the world and Turkey. – Turkey Agricultural Engineering VII. Technical Congress, Ankara, pp. 213-227 (in Turkish).
[5] Anonymous (2019a): Statistics. – https://www.tarimorman.gov.tr/Konular/Bitkisel-Uretim/Organik-Tarim/Istatistikler.
[6] Anonymous (2019b): Map of Samsun's districts. – http://www.istanbul-rehber.com/harita/il/samsun-haritasi.asp.
[7] Artukoglu, M. M., Tarkan, E., Gencler, F., Miran, B. (2009): Evaluating the factors of transition in organic cotton production for farmers: case of Salihli, Turkey. – Bulg. J. Agric. Sci. 15: 77-83.
[8] Azam, M. S., Shaheen, M. (2019): Decisional factors driving farmers to adopt organic farming in India: a cross-sectional study. – International Journal of Social Economics 46(4): 562-580.
[9] Burton, M., Rigby, D., Young, T. (2003): Modelling the adoption of organic horticultural technology in the UK using Duration Analysis. – The Australian Journal of Agricultural and Resource Economics 47(1): 29-54.
[10] Ceylan, İ. C., Olhan, E., Köksal, Ö. (2010): Determination of the effective factors on organic olive cultivation decision. – African Journal of Agricultural Research 5(23): 3164-3168.
[11] Crawford, C., Grossman, J., Warren, S. T., Cubbage, F.(2015): Grower communication networks: Information sources for organic farmers. – Journal of Extension 53(3).
[12] Çukur, T., Işın, F. (2008): Industrial tomato farmers view of multifunctionality of agriculture concept in Torbalı district of İzmir. – Ege Journal of Agricultural Research 45(3): 185-193 (in Turkish).
[13] Çukur, T. (2015): Conventional dairy farmers converting to organic dairy production in Turkey. – Polish Journal of Environmental Studies 24(4): 1543-1551.
[14] Demiryürek, K. (2011): The concept of organic agriculture and current status of in the world and Turkey. – Journal of Agricultural Faculty of Gaziosmanpasa University 28(1): 27-36 (in Turkish).
[15] Issa, I., Hamm, U. (2017): Adoption of organic farming as an opportunity for Syrian farmers of fresh fruit and vegetables: an application of the theory of planned behaviour and structural equation modelling. – Sustainability 9: 1-22.
[16] Kallas, Z., Serra, T., Gil, J. M. (2009): Farmer's objectives as determinant factors of organic farming adoption. – 113th EAAE Seminar "A resilient European Food Industry and Food Chain in a Challenging World", Chania, Crete, Greece.
[17] Karki, L., Schleenbecker, R., Hamm, U. (2011): Factors influencing a conversion to organic farming in Nepalese tea farms. – Journal of Agriculture and Rural Development in the Tropics and Subtropics 112(2): 113-123.
[18] Meda, Y. J. M., Egyir, I. S., Zahonogo, P., Donsaananang, J., Atewamba, C. (2018): Institutional factors and farmers' adoption of conventional, organic and genetically modified cotton in Burkina Faso. – International Journal of Agricultural Sustainability 16(1): 40-53.
[19] Rezvanfar, A., Eraktan, G., Olhan, E. (2011): Determine of factors associated with the adoption of organic agriculture among small farmers in Iran. – African Journal of Agricultural Research 6(13): 2950-2956.
[20] Sodjinou, E., Glin, L. C., Nicolay, G., Tovignan, S., Hinvi, J. (2015): Socio economic determinants of organic cotton adoption in Benin, West Africa. – Agricultural and Food Economics 3(12): 1-22.

http://www.aloki.hu ● ISSN 1589 1623 (Print) ● ISSN 1785 0037 (Online)
DOI: http://dx.doi.org/10.15666/aeer/1706_1400114008

TRANSFERRING *NOD*D2, *NOD*D3 GENES FROM *RHIZOBIUM LEGUMINOSARUM, NIF*H2 AND *NIF*H3 GENES FROM *AZOTOBACTER CHROOCOCCUM* TO *BACILLUS MEGATERIUM*

TALABANI, SH. K.[1*] – KHIDER, A. K.[2] – FATTAH, O. A.[1]

[1]*Soil and Water Sciences Department, College of Agricultural Sciences, University of Sulaimani, Sulaimani, Kurdistan Region of Iraq*
(e-mail: omar.fattah@univsul.edu.iq; phone: +964-770-153-6011)

[2]*Biology Department, College of Education Scientific, University of Salahaddin, Erbil, Kurdistan Region of Iraq*
(e-mail: dradelkamal51@yahoo.com phone: +964-750-447-2908)

**Corresponding author*
e-mail: shahen.fazil@univsul.edu.iq; phone: +964-770-158-6531

(Received 25th May 2019; accepted 10th Sep 2019)

Abstract. The present study aimed to transfer *nod* and *nif* genes from *Rhizobium* and *Azotobacter* to *Bacillus* by: the transformation technique which used to transfer *nod*D2 and *nod*D3 from *Rhizobium leguminosarum* to *Bacillus megaterium*; and the conjugation mechanism which performed the transfer of *nif*H2 and *nif*H3 from *Azotobacter chroococcum* to transformant *Bacillus megaterium*. The results showed that: 12 colonies were obtained after transformation on Sperber's agar plates which contained tetracycline and ampicillin. While after conjugation; 166 colonies were obtained on Sperber's agar plates which contained ampicillin and erthymycinem, indicating that the transformation and conjugation were successful. To confirm this, a molecular study was performed based on the followings: the extraction of the plasmid DNA from *Rhizobium leguminosarium* and transformant *Bacillus megaterium* to detect *nod*D genes; and the extraction of the genomic DNA from *Azotobacter chroococcum* and transformant-conjugant *Bacillus megaterium* to detect *nif*H genes by PCR and gel electrophoresis. The PCR products on gel electrophoresis showed that *Rhizobium leguminosarium* and transformant *Bacillus megaterium* contained *nod*D2 and *nod*D3; and *Azotobacter chroococcum* and transformant-conjugant *Bacillus megaterium* contained *nif*H2 and *nif*H3. Furthermore, the new *Bacillus megaterium* which obtained these genes successfully, can be used as biofertilizer for nitrogen fixation and phosphorus solubilization at the same time.
Keywords: *nod gene, nif gene, DNA transferring, PCR, Gel electrophoresis*

Introduction

Rhizobium and *Azotobacter* interact with a wide range of other soil microorganisms in the rhizosphere of plants. These interactions are sometimes stimulatory where they increase the growth response of the host in the presence of other microorganisms (Kennedy and Islam, 2001; Nosheen et al., 2011). *Azotobacter* and *Rhizobium* are known to be good non-symbiotic and symbiotic nitrogen fixers, respectively (Siddiqui et al., 2014). This biological nitrogen fixation process in *Azotobacter*, and between *Rhizobium* strains and their legume partners can happen under low levels of available nitrogen with the help of many different genes such as *nod, nif, fix*, production of polysaccharides, competition, infection process, and host specificity (Shamseldin, 2013). *Rhizobium nod* genes, and their product, *Nod* Factor (NF), have been recognized as essential for the development of nitrogen-fixing nodules on legume roots (Lerouge et al., 1990). *Nod*D is present in all *rhizobia* (Shamseldin, 2013). *Nod*D is the core signaling protein, reacting to

http://www.aloki.hu ● ISSN 1589 1623 (Print) ● ISSN 1785 0037 (Online)
DOI: http://dx.doi.org/10.15666/aeer/1706_1400914024

plant flavonoids then binding to nod boxes, binding sites upstream of nod genes, typically *nod*A and/or *nod*B, trigger the expression of a *nod* gene cascade and thus the construction of the *Nod* Factor (Jones et al., 2007). The *nif* genes are able to fix nitrogen in both the free-living and symbiotic states, and the *nif* genes can transcript in both free-living and symbiotic diazotrophs (Dixon and Kahn, 2004). The expression and regulation of *nif* genes, while sharing common features in all or most of the nitrogen-fixing organisms in nature, have distinct characteristics and qualities that differ from one diazotroph to another (Spaink et al., 1998). The structural gene *nif*H, as an important *nif* gene, is involved in the formation of the Fe-protein complex (Cocking, 2003), and *nif*H is the gene that encodes the iron protein subunit of nitrogenase, which is highly conserved among all nitrogen-fixing groups and serves as an ideal molecular marker for these microorganisms (Deslippe and Egger, 2006). *Bacillus megaterium* has the ability to solubilize phosphorus, which is good for the plant (Velineni and Brahmaprakash, 2011). *Bacillus megaterium* produces organic compounds such as lactic acid, gluconic acid, citric acid, succinic acid, propionic acid and enzymes that help solubilize the fixed phosphorus into exchangeable form (Agrilife, 2008).

In the bacterial population, DNA can be transferred from one organism to another by the horizontal transfer mechanism. The DNA thus transferred by the lateral/horizontal method can be stably incorporated in the recipient, and changes the genetic composition of the recipient permanently. Three broad mechanisms mediate efficient movement of DNA between cells: transformation, conjugation, and transduction (Acharya, 2013). Bacterial plasmid transformation is a process by which genetic material, often a plasmid, is inserted into a bacterial cell. Though transformation does occur naturally, scientists have developed many techniques to ensure DNA uptake by bacterial cells (Yoo, 2010). Genetic transformation occurs when a cell takes up (takes inside) and expresses a new piece of genetic material—DNA, and it literally means change caused by genes and involves the insertion of one or more gene(s) into an organism in order to change the organism's traits, this new genetic information often provides the organism with a new trait which is identifiable after transformation (www.explorer.bio-rad.com). Transformation takes place to a limited extent in many bacteria. But laboratory techniques have been developed that increase the rate of DNA uptake. (www.kullabs.com). Bacterial transformation is a process which involves genetic alteration of bacteria by the incorporation and stable expression of foreign genetic material from the environment or surrounding medium. Since DNA is a very hydrophobic molecule, it will not normally pass through a bacterial cell membrane. In order to uptake foreign DNA, the bacterial cells must first be made competent. Competence is the ability of a cell to take up extracellular DNA from its environment (www.himedialabs.com. a). In bacteria, the haploid genome is a single circular chromosome. This differs from eukaryotic genomes like those of plants and animals, where the genetic material is diploid and arranged into linear chromosomes. Bacteria can also possess additional nonessential pieces of circular DNA called plasmids (www.towson.edu/cse). Plasmids are small circles of DNA that contain an origin of replication (ori) and a small number of genes, some of which may confer a survival advantage on a host. Some plasmids can transfer between different species; even between different kingdoms (Slonczewski, 2006). Plasmid transformation into bacterial competent cells is a key technique in molecular cloning (Tu et al., 2005).

Many bacteria from different species frequently exchange their genetic materials by a process called conjugation, which occurs by cell-to-cell contact (Fernandez-Lopez et al.,

http://www.aloki.hu ● ISSN 1589 1623 (Print) ● ISSN 1785 0037 (Online)
DOI: http://dx.doi.org/10.15666/aeer/1706_1400914024

2005). Conjugation is a recombination process where two live bacteria come together, and the donor cell transfers genetic material to the recipient cell. Conjugating bacteria are of two mating types. Certain "male" types (designated as F+) donate their DNA, and other "female types" (designated as F-) receive the DNA, F- cells become F + when they acquire a small amount of DNA. Hence the F factor is called as the Fertility factor. In contemporary microbiology, the donor's F factors are known to be plasmids which are extra-chromosomal elements. The factors (plasmids) contain about 20-30 genes, most of which are associated with conjugation. These genes encode enzymes that replicate DNA during conjugation and structural proteins needed to synthesize special pili at the cell surface which known as F pili or sex pili, these hair-like fibers contact the recipient bacteria, and then retract so that the surfaces of donor and recipient are very close or touching one another. At the area of contact, a channel or conjugation bridge is formed. Once contact via sex pili has been made, the F factor (plasmid) begins replicating by the rolling circle mechanism. A single strand of the factor then passes over or through the channel to the recipient. When it arrives, enzymes synthesize a complementary strand, and a double helix is formed. The double helix bends to a loop and reforms an F factor (plasmid), thereby completing the conversion of the recipient from F- cell to F + cell. Meanwhile, back in the donor cell a new strand of DNA forms, to complement the leftover strand of the F plasmid. The transfer of F factors involves no activity of the bacterial chromosome; therefore the recipient does not acquire new genes other than those on the F factor (www.himedialabs.com).

Transformation process holds key step in molecular biology (Das et al., 2017), and it has been a handy tool in several areas of bacterial research because the genotype of a strain can be deliberately changed in a very specific way by transforming with an appropriate DNA fragment. For example, transformation is used widely in genetic engineering (Pimda and Bunnag, 2010). The goals of gene transfer experiments with other organisms are to study gene regulation and to obtain stable inheritance and expression of new characteristics (Moses, 1987).

Conjugation gene transfer is considered to be an important mechanism for the establishment of new genetic traits in diverse environments (Hausner and Wuertz, 1999). Conjugation is used in nature to share beneficial genetic material between bacteria, such as antibiotic resistance. However, manually inserting genes into the F-plasmid would allow for scientists to have bacteria transfer almost any gene to other cells (Griffiths et al., 2000).

Materials and methods

The country and location of the study

The present study was performed in Sulaimani city/Iraq. All bacteria were isolated from the organic farm of Bakrajow, and the molecular studies were done at the laboratories. The farm and the laboratories are located inside the College of Agricultural Sciences, University of Sulaimani.

Isolation of bacteria

Rhizobium leguminosarium spp. were isolated from healthy, unbroken, firm and pink nodules of Broad bean from the organic farm of Bakrajow using YMA medium in accordance with Agrawal et al., 2012, while *Azotobacter chroococcum spp.* were

http://www.aloki.hu ● ISSN 1589 1623 (Print) ● ISSN 1785 0037 (Online)
DOI: http://dx.doi.org/10.15666/aeer/1706_1400914024

isolated from Bakrajow soil on modified Ashby's medium according to Marwa et al., 2010, and *Bacillus megaterium* was isolated from same soil using Sperber's medium based on Shiva et al., 2010.

Purification of isolated bacteria

A loop of actively growing of each bacterial species (48 h old surface film) was streaked on their selective media, the growth was observed depending on the type of bacteria, *R. leguminosarium* and *B. megaterium* after 24-48 h and *A. chroococcum* after 3-7 days at 28 °C of incubation. The well separated and apparently un-contaminated colonies appearing on the plates were streaked on agar medium, plating and picking were repeated at least 4-5 times.

Maintenance and storage of bacterial culture

The cultures were maintained for a short time at slant medium, and for a long time in 20% glycerol and stored at -70 °C (Ausabel et al., 2003) without losing their activity.

Identification of bacteria by molecular protocol

Depending on the molecular protocol, *B. megaterium* was identified by the extraction of genome DNA using PrestoTM Mini gDNA Bacteria Kit Protocol to detect and check the presence of *B. megaterium* in the region by two random primers, *R. leguminosarium* was identified by the extraction of plasmid DNA using Genetbio, PrmePrep Plasmid DNA isolation kit to detect the *nod*D2 and *nod*D3 genes which we wanted to transfer to the *B. megaterium* by the transformation process, and *A. chroococcum* was identified by extraction of genomic DNA using PrestoTM Mini gDNA Bacteria Kit Protocol to detect the *nif*H2 and *nif*H3 genes which we wanted to transfer to the transformant *B. megaterium* by the conjugation process using specific primers for each gene in order to obtain a new model of the *B. megaterium* which would contain both of the *nod* and *nif* genes and then could be used as bio-fertilizers to provide available nitrogen and phosphorus to plants.

PCR amplification conditions

The conditions of PCR amplification: for *nod*D2 and *nod*D3 were performed according to the modified method of Del Cerro et al., 2015a at cycling conditions consisted of a single cycle of 95 °C for 10 min, followed by 45 cycles of 95 °C for 2 min, 60 °C for 30 s and 72 °C for 30 s, and a final extension cycle at 72 °C for 6 min, while PCR reactions for *nif*H2 and *nif*H3 were done in accordance with Setubal et al., 2009), and for random primers 1 and 2 of *B. megaterium* was carried out in accordance with Patil et al., 2013). The forward, reverse and random primers are shown in *Table 1*.

Gel electrophoresis (Helmut et al., 2004)

Gel electrophoresis was used to identify the extraction of each of genome DNA, chromosomal DNA, and plasmid DNA, and it was also used to check the DNA amplification of each product by dissolving 0.5, 1, 1.5 and 2% (w/v) of agarose gel depending on the size of amplified DNA in 100 ml (IX) TBE buffer by heating it in a micro-wave oven for 3 min, then cooling the solvent to 45 °C at room temperature. The gel was stained with 5 µl of 5 $mg.ml^{-1}$ ethidium bromide, and the gel was soaked in a

http://www.aloki.hu ● ISSN 1589 1623 (Print) ● ISSN 1785 0037 (Online)
DOI: http://dx.doi.org/10.15666/aeer/1706_1400914024

gel tank containing TBE. The gel tank was covered by a lid, and electrophoresis was run at (80 to 100 V) for 2-3 h depending on the product. DNA fragments were visualized at 312 nm with a UV- transilluminator image.

Table 1. *The forward, reverse and random primers used*

Primer	Sequence (5'-3')	Nucleotide	Reference
*nod*D2- F-	(GTA GGC CAT AAT GTC CAG A)	19	Del Cerro et al., 2015a
*nod*D2- R-	(GCG GCT TTA TAC TCA CCA)	18	
*nod*D3- F-	(GAG CTA CCT CGA CTG CTA)	18	Del Cerro et al., 2015b
*nod*D3- R-	(CTA CCG CCA TGA TCA CCA)	18	
*nif*H2- F-	(CGCCGGCGCAGTGTTTGCGG)	20	Setubal et al., 2009
*nif*H2 -R-	(CACTCGTTGCAGCTGTCGGC)	20	
*nif*H3- F-	(CGATGACTGAAGACTGAACGAG)	22	Setubal et al., 2009
*nif*H3 -R-	(AAGGTGCGGTCAGGAGAGAA)	20	
Random primer1	(GGT GCG GGA A)	10	Patil et al., 2013
Random primer2	(GTA GTC ATA T)	10	

Antibiotics resistance test

Table 2 shows the 8 common antibiotics including Chloramphenicol, Gentamycin, Tetracycline, Ampicillin, Cefotaxim, Erthymycine, Streptomycin and Rifampicin which were used for testing the sensitivity of: *R. leguminosarium* and *B. megaterium* for transformation technique, and transformant *B. megaterium* and *A. chroococcum* for conjugation process.

Table 2. *The antibiotics used in accordance with Shoukry et al., 2013; American Type Culture Collection, 2013; Giacopello et al., 2016*

Antibiotic	Recommended stock concentration	Recommended working concentration
Chloramphenicol	10 mg/ml in ethanol	25 µg/mL
Gentamycin	10 mg/ml	10 µg/mL
Tetracycline	10 mg/ml in (50% D.W + 50% ethanol)	10 µg/mL
Ampicillin	10 mg/ml in water	20 µg/ml
Cefotaxime	10 mg/ml in water	30 µg/ml
Erthymycine	10 mg/ml in water	15 µg/ml
Streptomycin	10 mg/ml in water	10 µg/ml
Rifampicin	10 mg/ml in methanol	5 µg/ml

Preparation of competent cells from B. megaterium

A modified method of Sambrook et al., 1989 was used for the preparation of competent cells of *B. megaterium* for transformation. An overnight culture of *B. megaterium* was prepared by suspending a colony from a fresh Sperber's plate in 100 ml of Sperber's broth medium. The culture was incubated in a shaking incubator at 100 rpm for 24 h at 28 °C, then 10 ml of this culture was suspended in 90 ml of

http://www.aloki.hu ● ISSN 1589 1623 (Print) ● ISSN 1785 0037 (Online)
DOI: http://dx.doi.org/10.15666/aeer/1706_1400914024

fresh Sperber's broth and grown at 28 °C for 90 min in a shaking incubator until an OD $_{600}$ nm of approximately 0.3-0.6 was attained, then 10 ml aliquots was centrifuged at 4000 Xg for 10 min at 4 °C to pellet the cells. After that, the supernatant was discarded and cells were re-suspended in 10 ml of 0.1 M $CaCl_2$ over 1 h on ice, and re-centrifuged twice, following the third washing with 5 ml 0.1 M $CaCl_2$. Finally the cells were re-centrifuged and gently re-suspended in 2 ml of ice-cold 0.1 M $CaCl_2$ containing 20% glycerol. The cells could be used immediately for transformation or stored at -20 °C.

Bacterial transformation (Ausabel et al., 2003)

A total of 200 µl of competent cells (*B. megaterium*) were mixed with 2 µl of the extracted plasmid from *R. leguminosarium* in a tube, and the tube was left on ice for 30 min. After that the tube was incubated for 30 s at 42 °C in a water bath and then placed on ice for 5 min, then 800 µl of Sperber's broth was added and the tube was incubated at 28 °C for 1 h. Then the cells were centrifuged at 6000 Xg for 1 min. Next, the pellet was re-suspended in 200 µl of Sperber's broth. A total of 100 µl of the cells were plated out on Sperber's agar medium containing two antibiotics which were used as genetic markers. After post-incubation at 28 °C for 28 h the colonies were screened, then the molecular study was performed using PCR and gel electrophoresis techniques for detection of transferred *nod*D2 and *nod*D3 genes in transformant *B. megaterium* that transferred by transformation process.

Bacterial conjugation (Olsen et al., 1992)

A 10 ml of modified Ashby's broth medium was inoculated with a single colony of *A. chroococcum* (donor cell), and 10 ml of Sperber's broth medium was inoculated with a single colony of transformant *B. megaterium* (recipient cell), then they were incubated at 28 °C for 48 h. with shaking at 100 rpm. After incubation, 0.8 ml of the *A. chroococcum* (donor cells) were mixed with 0.2 ml of transformant *B. megaterium* (recipient cells) and 1 ml of Sperber's broth, the mixture was incubated at 28 °C for 3 h under aerobic condition. Then 0.1 ml of the conjugated mixture was spread on Sperber's agar medium plates containing two antibiotics that were used as genetic markers, and control plates were prepared by spreading 0.1 ml for each donor and recipient suspensions separately on agar plates containing the same markers, then all plates were incubated at 28 °C till the colonies appeared. To verify the transfer of nitrogen fixation genes (*nif* genes) from *A. chroococcum* to transformant *B. megaterium*, the transformant-conjugant colonies were screened, then the molecular study was performed using PCR and gel electrophoresis techniques for the detection of transferred *nif*H2 and *nif*H3 genes, that were transferred by conjugation process, in transformant-conjugant *B. megaterium*.

Results

DNA isolation from bacteria

The DNA was isolated from bacterial cultures, and the molecular method based on the extraction of the genomic DNA from *A. chroococcum* and *B. megaterium* and plasmid DNA from *R. leguminosarium,* which were detected by agarose gel electrophoresis, the results are shown in *Figure 1* lane 2, 4, 6 respectively.

http://www.aloki.hu ● ISSN 1589 1623 (Print) ● ISSN 1785 0037 (Online)
DOI: http://dx.doi.org/10.15666/aeer/1706_1400914024

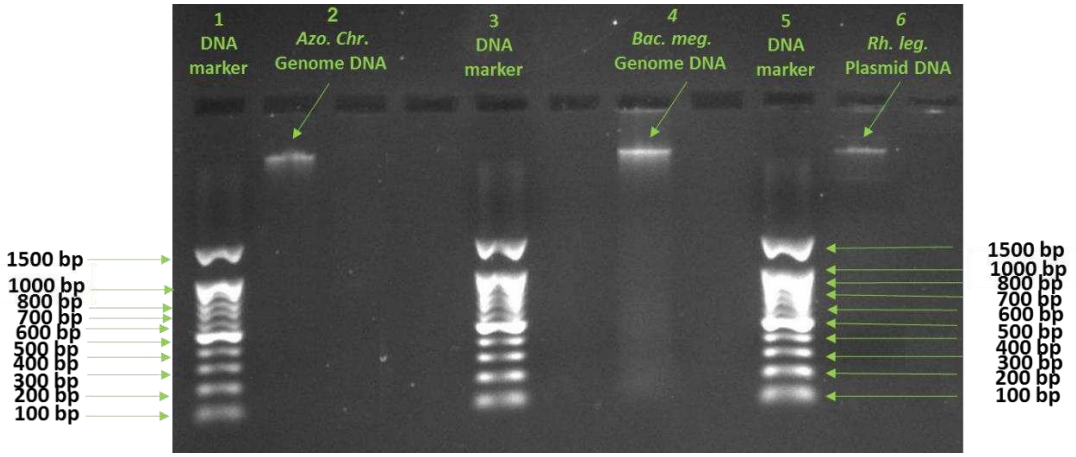

Figure 1. *Agarose gel electrophoresis shows DNA marker lanes 1, 3, and 5, extracted chromosomal DNA from A. chroococcum, genome DNA from B. megaterium and plasmid DNA from R. leguminosarium lanes 2, 4 and 6, respectively*

Molecular based identification of Bacillus megaterium

The PCR amplification was performed to check the presence of *B. megaterium* in the region using two random primers. The PCR products showed high amplification rate and reproducible banding pattern which confirmed the existence of *B. megaterium* (*Fig. 2,* lanes 2 and 3).

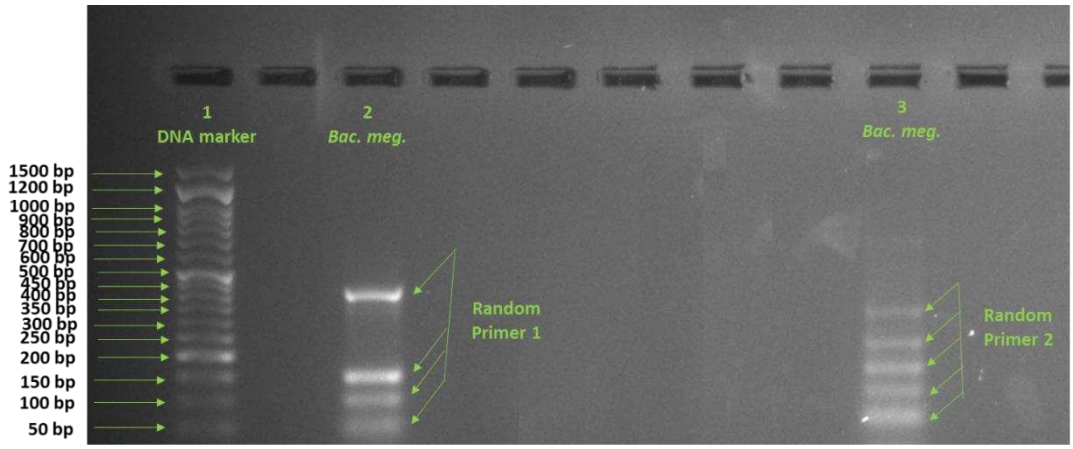

Figure 2. *Agarose gel electrophoresis shows the PCR amplified products of the B. megaterium generated using 10-mer random primers: Lane 1: DNA marker, lanes 2 and 3: random primers 1 and 2 respectively (+ve PCR products)*

Antibiotics resistance of R. leguminosarium, B. megaterium, transformant B. megaterium and A. chroococcum

The resistance screening of *R. leguminosarium, B. megaterium*, Transformant *B. megaterium,* and *A. chroococcum* was evaluated for eight antibiotics that are widely used. Depending on the results in a *Table 3,* tetracycline and ampicillin were used as genetic markers for transformation experiment, while ampicillin and erthymycine were used as genetic markers for the conjugation experiment.

http://www.aloki.hu ● ISSN 1589 1623 (Print) ● ISSN 1785 0037 (Online)
DOI: http://dx.doi.org/10.15666/aeer/1706_1400914024

Table 3. *Antibiotics Resistance of R. leguminosarium, B. megaterium, Transformant B. megaterium and A. chroococcum*

Antibiotic	*R. leguminosarium*	*B. megaterium*	Transformant *B. megaterium*	*A. chroococcum*
Chloramphenicol	R	S	R	R
Gentamycin	R	S	R	S
Tetracycline	S	R	R	R
Ampicillin	R	S	S	R
Cefotaxim	R	S	R	S
Erthymycine	R	R	R	S
Streptomycin	R	S	R	S
Rifampicin	R	S	R	R

S = Sensitive R = Resistance

Transformation of plasmid genes (nodD2 and nodD3) from R. leguminosarium to B. megaterium by transformation process

Transformation experiment was carried out to transfer the genes responsible for the nodulation (*nod*D genes) which were *nod*D2 and *nod*D3 from *R. leguminosarium* to *B. megaterium.* After the transformation, 12 colonies were gained on Sperber's medium supplied with tetracycline and ampicillin as genetic markers and the colonies were resistant to both antibiotics. These results confirmed that the resulting colonies were transformant colonies and the transformation technique was successful between *R. leguminosarium* and *B. megaterium*. To confirm if *nod*D2 and *nod*D3 genes transferred from *R. leguminosarium* to *B. megaterium* by transformation technique, the molecular study was performed using specific primers to detect the *nod*D2 and *nod*D3 genes in transformant cells and compared to the *nod*D2 and *nod*D3 genes in *R. leguminosarium* by PCR technique and gel electrophoresis.

PCR amplification of nodD2 and nodD3

After extraction and purification of plasmid DNA from *R. leguminosarium*, *B. megaterium* and transformant *B. megaterium* using the Genetbio, PrmePrep Plasmid DNA isolation kit according to the manufacturer's protocol, PCR and gel electrophoresis were carried out in order to amplify and check the existenc of *nod*D2 and *nod*D3 in the plasmid DNA of *R. leguminosarium, B. megaterium* and transformant *B. megaterium* using specific oligonucleotide primers that flank the DNA sequence to be amplified.

Figure 3 shown positive PCR products on gel electrophoresis in *R. leguminosarium* and transformant *B. megaterium* which contained *nod*D2-F- and *nod*D2-R- primers with 100 bp in lanes 2 and 4, respectively, while in *Figure 4*, the results show the positive amplification on gel electrophoresis of *nod*D3 in *R. leguminosarium* and transformant *B. megaterium* with 150 bp in lanes 2 and 4, respectively using *nod*D3-F- and *nod*D3-R- primers, but the negative control and *B. megaterium* were negative PCR products and they did not produce bands, which can be seen in lanes 3 and 5, respectively in *Figures 3* and *4*.

http://www.aloki.hu ● ISSN 1589 1623 (Print) ● ISSN 1785 0037 (Online)
DOI: http://dx.doi.org/10.15666/aeer/1706_1400914024

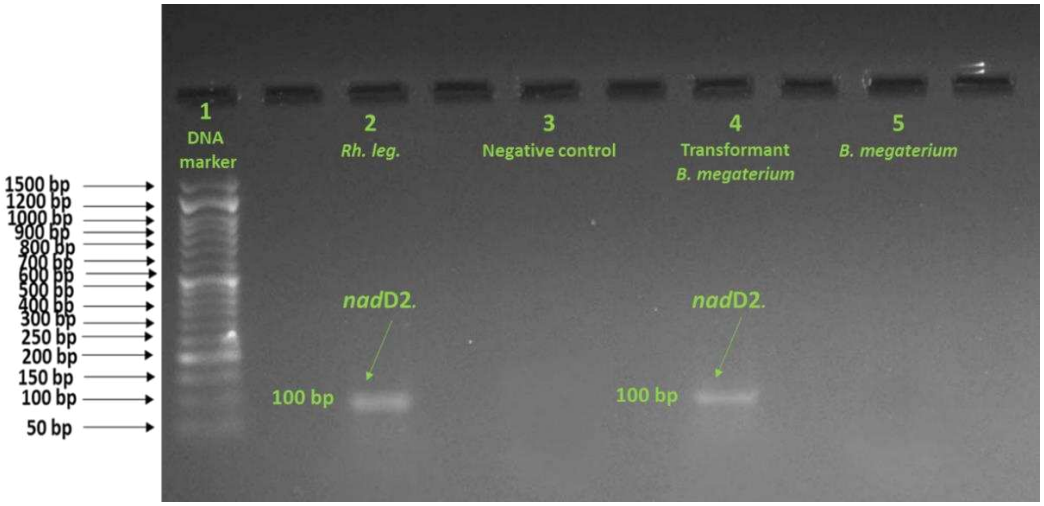

Figure 3. *Agarose gel electrophoresis shows the PCR amplified products of the nodD2 gene (100 bp). Lane 1: DNA marker, lane 2: R. leguminosarium (+ve PCR product), lane 3: negative control (-ve PCR product), lane 4: transformant B. megaterium (+ve PCR product) and lane5: B. megaterium (-ve PCR product)*

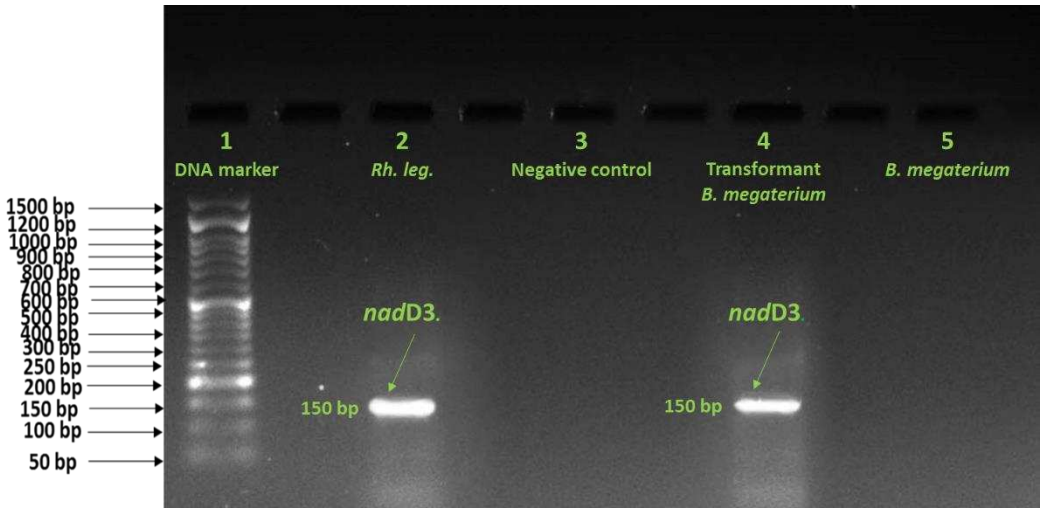

Figure 4. *Agarose gel electrophoresis shows the PCR amplified products of the nodD3 gene (150 bp). Lane 1: DNA marker, lane 2: R. leguminosarium (+ve PCR product), lane 3: negative control (-ve PCR product), lane 4: transformant B. megaterium (+ve PCR product) and lane5: B. megaterium (-ve PCR product)*

Transferring of chromosomal genes (nifH2 and nifH3) from A. chroococcum to transformant B. megaterium by conjugation process

Conjugation experiment was done between *A. chroococcum* as donor cells and transformant *B. megaterium* as recipient cells to investigate the transference ability of nitrogen fixation genes (*nif*H genes) which were *nif*H2 and *nif*H3 from isolated *A. chroococcum* to transformant *B. megaterium*. *A. chroococcum* was successful in conjugation technique with transformant *B. megaterium*, and (166) transformant-conjugant colonies were obtained on Sperber's agar plates containing ampicillin and

http://www.aloki.hu ● ISSN 1589 1623 (Print) ● ISSN 1785 0037 (Online)
DOI: http://dx.doi.org/10.15666/aeer/1706_1400914024

erthymycine. In order to confirm the mobilization of nitrogen fixation genes (*nif*H2 and *nif*H3) from donor to recipient, a molecular study using PCR technique and gel electrophoresis was done for detecting these genes in each of *A. chroococcum, B. megaterium,* and transformant-*conjugant B. megaterium.*

PCR amplification of nifH2 and nifH3

After extraction and purification of genomic DNA from *A. chroococcum*, *B. megaterium* and transformant-conjugant *B. megaterium* using the PrestoTM Mini gDNA Bacteria Kit according to the manufacturer's protocol, PCR was performed for amplification of *nif*H2 and *nif*H3 via the use of specified oligonucleotide primers that flanked the DNA sequence to be amplified, and gel electrophoresis was carried out in order to check the presence of *nif*H2 and *nif*H3 in the chromosomal DNA of *A. chroococcum*, *B. megaterium,* and transformant-conjugant *B. megaterium*.

Results in *Figure 5* indicated that *A. chroococcum* and transformant-conjugant *B. megaterium* samples which contained *nif*H2-F and *nif*H2-R primers exhibit positive PCR products of *nif*H2 on the gel in lanes 2 and 4 respectively with (250 bp). Also the results in *Figure 6* indicated that the gel electrophoresis shows positive amplification of *nif*H3 (130 bp) in *A. chroococcum* and transformant-conjugant *B. megaterium* samples using *nif*H3 -F- and *nif*H3 -R- primers and they produced clear bands in lanes 2 and 4, respectively, while *B. megaterium* and negative control were shown negative PCR products in lanes 3 and 5, respectively and they did not produce bands in *Figures 5* and *6*.

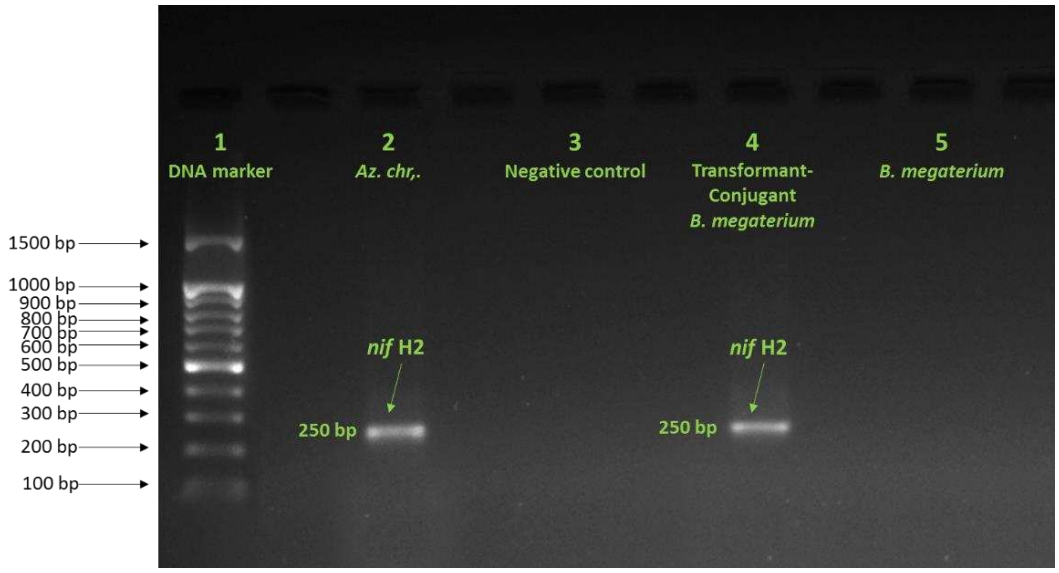

Figure 5. *Agarose gel electrophoresis shows the PCR amplified products of the nifH2 gene (250 bp). Lane 1: DNA marker, lane 2: A. chroococcum (+ve PCR product), lane 3: negative control (-ve PCR product), lane 4: transformant-conjugant B. megaterium (+ve PCR product) and lane5: B. megaterium (-ve PCR product)*

Discussion

This research work was carried out to find out the transference ability of *nod*D2 and *nod*D3 genes from *R. leguminosarium* by transformation technique, and *nif*H2 and

http://www.aloki.hu ● ISSN 1589 1623 (Print) ● ISSN 1785 0037 (Online)
DOI: http://dx.doi.org/10.15666/aeer/1706_1400914024

*nif*H3 genes from *A. chroococcum* by conjugation process, to the *B. megaterium* in order to obtain a new model of *B. megaterium* which can then be used as a biofertilizer that provides available nitrogen and phosphorus for plants. *Nod*D genes act as a family of regulatory genes (Kidaj and Wielbo, 2010). The *nod* genes are controlled by *nod*D genes, *nod*D proteins act as transcriptional activators of inducible nod genes (Kumari and Sinha, 2011). *Nif*H acts as dinitrogenase reductase, obligate electron donor to dinitrogenase during dinitrogenase turn over and are required for FeMo-Co biosynthesis and apodinitrogenase maturation (Shamseldin, 2013). The region of chromosome which contain *nifK, nifD, nifM, nifA, nifN, nifB, nifQ, nifZ, nifP, nifF, nifW, nifB, nifL* and *nifY* genes are located between the fragment of chromosome which contains *nif*H1, *nif*H2, *nif*H3 and the fragment containing *nif*V, *nif*S and *nif*U (Hamilton et al., 2011). So the importance of the *nod*D genes which are located on the plasmid, and *nif*H genes which are located between fragments of chromosomal DNA, and their role in nitrogen fixation process gave importance to our choice of these genes for this study.

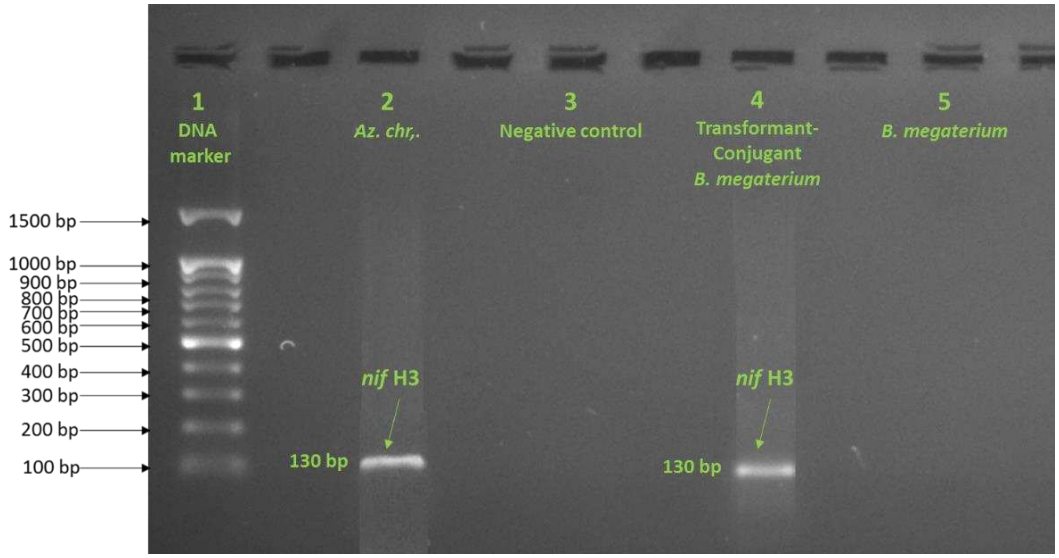

Figure 6. *Agarose gel electrophoresis shows the PCR amplified products of the nifH3 gene (130 bp). Lane 1: DNA marker, lane 2: A. chroococcum (+ve PCR product), lane 3: negative control (-ve PCR product), lane 4: transformant-conjugant B. megaterium (+ve PCR product) and lane5: B. megaterium (-ve PCR product)*

Firstly, *R. leguminosarium, A. chroococcum* and *B. megaterium* were isolated and identified by classical and molecular approach, classical approach included cultural, morphological and biochemical tests (the results did not show), while molecular characterizations of isolated bacteria based on the detection of genomic DNA of *B. megaterium* and *A. chroococcum* and the plasmid DNA of *R. leguminosarium*, have been successfully applied (*Fig. 1* lanes 2, 4, 6 respectively), and PCR technique and gel electrophoresis were carried out to detect and check the presence of *B. megaterium* by using two random primers 1 and 2. The banding patterns were intense, clear and reproducible which confirmed the existence of *B. megaterium* in the region (*Fig. 2*) lanes 2 and 3. Previous studies by Shiva et al. (2010) and Patil et al. (2013) indicated the presence of *B. megaterium* in a different area by these primers. Also the molecular study to identify *R. leguminosarium* was depended on the detection of the *nod*D2

http://www.aloki.hu ● ISSN 1589 1623 (Print) ● ISSN 1785 0037 (Online)
DOI: http://dx.doi.org/10.15666/aeer/1706_1400914024

*nod*D3 on the plasmid using specific complementary primers by PCR technique and gel electrophoresis, because nodulation genes (nod genes) are located on the plasmid which is also called mega plasmid. Kumari and Sinha, 2011; Giraud et al., 2007 indicated that the common nodulation genes (*nod* ABCD) are found in all bacteria that nodulate legumes, and Black et al. (2012) reported that all fourteen species of *Rhizobium* contained *nodD,* as well Rossen et al. (1985) showed and confirmed the presence of *nod*D in *R. leguminosarium*, and for the detection of the *nif*H2 and *nif*H3 in the *A. chroococcum* using specific complementary primers to amplify them, PCR and gel electrophoresis were carried out after extracting the genomic DNA of the *A. chroococcum*. Previous studies by Dashti (2011), Khider (2012), Abid (2013) and Mohamed (2017) proved the existence of different *nif* H genes in *A. chroococcum* in some regions of Kurdistan. Iraq.

The transformation technique was based on the extraction of the plasmid from *R. leguminosarium* and preparation of the competent cells from *B. megaterium* in order to transfer *nod*D2 and *nod*D3 genes from *R. leguminosarium* to *B. megaterium*, The process succeeded when 12 colonies were gotten on Sperber's agar plates containing tetracycline and ampicillin which were used as genetic markers, these transformant colonies may be due to transferring the plasmid DNA from *R. leguminosarium* to *B. megaterium*, to confirm that, PCR technique and gel electrophoresis were carried out to amplify and detect the presence of the *nod*D2 and *nod*D3 genes in each of *R. leguminosarium, B. megaterium* and transformant *B. megaterium* using specific complementary primers after extracting the plasmid DNA from them. The results presented in *Figures 3* and *4* showed positive PCR products of *nod*D2 with 100 bp and *nod*D3 with 150 bp for *R. leguminosarium* in lane 2 and transformant *B. megaterium* in lane 4, and negative PCR products for negative control in lane 3 and *B. megaterium* in lane 5 and they did not produce any bands, these results indicated that the plasmid transferred to transformant bacteria by transformation process. Mohamed (2017) also transferred *nod*C from *R. leguminosarium* to *B. megaterium* by the transformation technique and proved the success of the process between these two bacteria.

Based on these results, the conclusion is that the plasmid with all the *nod* genes (*nod*A, *nod*B, *nod*C *nod*D, *nod*E, nodF, *nod*G, *nod*I, *nod*M, *nod*P, and other *nod* genes) were transferred to the *B. megaterium* and all of them expressed and encoded for nitrogen fixation process in transformant cells, because all of them were located on the plasmid DNA. Plasmid transformation into bacterial competent cells is a key in molecular cloning technique (Tu et al., 2005). Plasmids are replicating circular pieces of DNA, they are smaller than the bacterial genome which encoded their transfer by replication into another bacterial strain or species. They can carry and transfer multiple resistance genes, which may be located on a section of DNA capable of transfer from one plasmid to another or to the genome-transposon or jumping gene (Snyder and Champness, 1997). Chemical transformation includes the usage of calcium chloride, this mode of transformation is easy to perform and requires a minimum number of equipment (www.himedialabs.com a). Because bacteria hosts are not readily convertible to transgenic cells, they need to be treated chemically with calcium chloride and physically with heat shock (Jones & Bartlett Learning, LLC., 2016). Cohen and his colleges in 1973 successfully transformed R-factor and recombinant plasmids into *E. coli* cells using a calcium chloride method, since that time this method has been widely used due to its convenience (Tu et al., 2005).

http://www.aloki.hu ● ISSN 1589 1623 (Print) ● ISSN 1785 0037 (Online)
DOI: http://dx.doi.org/10.15666/aeer/1706_1400914024

The conjugation technique was based on the transfer of *nif*H2 and *nif*H3 genes from *A. chroococcum* which acted as donor cells to *B. megaterium* which acted as recipient cells. The process succeeded when 166 colonies were obtained on Sperber's agar plates containing ampicillin and erthymycine that were used as genetic markers. The growth of the transformant-conjugant colonies may be due to the formation of the conjugation bridge between the donor and recipient bacteria and transmission of ori T genes across this bridge (Snyder and Champness, 1997). To prove the completion of the conjugation process, PCR technique and gel electrophoresis were carried out to amplify and detect the presence of the *nif*H2 and *nif*H3 genes in each of *A. chroococcum, B. megaterium* and transformant-conjugant *B. megaterium* using specific complementary primers. The results in *Figures 5* and *6* showed positive PCR products of *nif*H2 with (250 bp) and *nif*H3 with (130 bp) for *A. chroococcum* in lane 2 and transformant-conjugant *B. megaterium* in lane 4, and negative PCR products for negative control in lane 3 and *B. megaterium* in lane 5 and they did not produce any bands. The conjugation technique of *nif* genes have been proved and reported previously by Davis et al. (2000) when they transferred many *nif* genes from *A. chroococcum* to *Klebsiella pneumonia* and they observed the expression of these genes in transconjugant bacteria, while Khider (2011) and Dashti (2011) transferred some chromosomal *nif* genes by conjugation from *A. chroococcum* to *Lactobacillus planetarium*, also Mohamed (2017) proved this process by transferring some chromosomal *nif* genes from *A. chroococcum* to *B. megaterium.* Many bacteria from different species frequently exchange their genetic materials by a conjugation process which occurs by cell-to-cell contact. This process has been extensively studied because of its significance in genetic manipulation studies (Fernandez-Lopez et al., 2005) as well as in horizontal gene transfer and the resulting spread of multiple antibiotic resistance and virulence.

Conclusion

As a result, the two techniques: transformation to transfer *nod*D2 and *nod*D3, and conjugation to transfer *nif*H2 and *nif*H3 to *Bacillus megaterium* cells were succeeded perfectly. The aim of the presented manuscript is to obtain a new bacteria containing beneficial genes besides its advantageous genes that can be used as an important biofertilizer to plants. Our recommendation is using a new *Bacillus megaterium* bacteria that received *nod* and *nif* genes as a biofertilizer for providing nitrogen by two methods and solubilized phosphorus for plant nutrition, and improving the quality and quantity of plants.

Acknowledgment. We wish to thank Assistant Professor Dr. Zaid Khalaf Khidhir and Professor Dr. Nawroz Abdul-razzak Tahir from the Faculty of the Agricultural Sciences University of Sulaimani for their cooperation.

REFERENCES

[1] Abid, S. A. (2013): Microbiological and molecular biology study of *Azotobacter* species from Bakrajow soil in Sulaimani. – M.Sc. Thesis. Faculty of Agricultural Sciences, University of Sulaimani, Kurdistan.

[2] Acharya, T. (2013): Gene transfer mechanism in bacteria and its types. – Microbe Online. Xinqipolymer.com.

http://www.aloki.hu ● ISSN 1589 1623 (Print) ● ISSN 1785 0037 (Online)
DOI: http://dx.doi.org/10.15666/aeer/1706_1400914024

[3] Agrawal, P. K., Agrawal, S., Singh, U., Katiyar, N., Verma, S. K. (2012): Phenotypic characterization of *rhizobia* from legumes and its application as a bioinoculant. – Journal of Agricultural Technology 8(2): 681-692.
[4] Agrilife. Biosolutions for Soils & Crops (2008*): Bacillus megaterium* BioFertilizer, approved for use in organic agriculture. – www.agrilife.in.
[5] American Type Culture Collection (2013): Antibiotic and selection reagent usage for resistant *E. coli* cells. – www.atcc.org.
[6] Ausabel, F. M., Brent, R., Kingfton, R. E., Moore, D. D., Feidman, J. G., Smith, J. A, Ftruhl, K. (2003): Current Protocol Molecular Biology. 1st Ed. – John Wiley and Sons, Inc, New York.
[7] Black, M., Moolhuijzen, P., Chapman, B., Barrero, R., Howieson, J., Hungria, M., Bellgard, M. (2012): The Genetics of Symbiotic Nitrogen Fixation: Comparative Genomics of 14 *Rhizobia* Strains by Resolution of Protein Clusters. – Genes 3: 138-166. DOI: 10.3390. www.mdpi.com/journal/genes.
[8] Cocking, E. C. (2003): Endophytic colonization of plant roots by nitrogen-fixing bacteria. – Plant and Soil 252(1): 169-175.
[9] Cohen, S. N., Chang, A. C., Boyer, H. W., Helling, R. B. (1973): Construction of biologically functional bacterial plasmid in vitro. – National Academy of Sciences of the Unites States of America 70(11): 3240-3244.
[10] Das, M., Raythata, H., Chatterjee, S. (2017): Bacterial transformation: What? Why? How? and When? – Annual Research & Review in Biology 16(6): 1-11.
[11] Dashti, A. M. K. (2011): Isolation and Characterization of *Azotobacter spp*. – Ph.D. thesis: Erbil Soils, and Study the Effect of Biofertilzer (*Azotobacter chroococcum* and transconjugant *Lactobacillus plantarum*) on Nutrient Uptake by Wheat. Ministry of High Education and Scientific Research, University of Salahaddin/Erbil, Kurdistan.
[12] Davis, N., Cannon, L., Wilson, A., Williams, T. (2000): Expression of *Azotobacter* nitrogen fixation genes (*nif*) in *Klebsiella*. – J. Gen. Microbiol. 105(4): 321-330.
[13] Del Cerro, P., Rolla-Santos, A. A. P., Gomes, D. F. Marks, B. B., et al. (2015a). Regulatory *nod*D1 and *nod*D2 genes of *Rhizobium tropici* strain CIAT 899 and their roles in the early stages of molecular signaling and host-legume nodulation. – BMC Genomics 16(1): 251. DOI: 10.1186/s12864-015-1458-8.
[14] Del Cerro, P., Rolla-Santos, A. A. P., Gomes, D. F. Marks, B. B, et al. (2015b). Opening the "black box" of *nod*D3, *nod*D4 and *nod*D5 genes of *Rhizobium tropici* strain CIAT 899. – BMC Genomics 16: 864. DOI: 10.1186/s12864-015-2033-z.
[15] Deslippe, J., Egger, K. (2006): Molecular diversity of *nif*H genes from bacteria associated with high arctic dwarf shrubs. – Microb. Ecol. 51: 516-525.
[16] Dixon, R., Kahn, D. (2004): Genetic regulation of biological nitrogen fixation. – Nature Reviews Microbiology 2(8): 621-631.
[17] Fernandez-Lopez, R., Machon C., Longshaw C. M., Martin S., Molin S., Zechner E. L., Espinosa M., Lanka E., de la Cruz, F. (2005): Unsaturated fatty acids are inhibitors of bacterial conjugation. – Microbiol 151: 3517-3526.
[18] Giacopello, C., Foti, M., Mascetti, A., Grosso, F., Ricciardi, D., Fisichella, V., Lo Piccolo, M. F. (2016): Antimicrobial resistance patterns of *Enterobacteriaceae* in European wild bird species admitted in a wildlife rescue centre. – Veterinaria Italiana 52(2): 139-144. DOI: 10.12834/VetIt.327.1374.2.
[19] Giraud, E., Moulin, L., Vallenet, D., Barbe, V., Cytryn, E., Avarre, J. C., Jaubert, M., et al. (2007): Legume symbioses: absence of *nod* genes in photosynthetic *bradyrhizobia*. – Science 316: 1307-1312.
[20] Griffiths, A. F. J., Miller, J. H., Suzuki, D. T., et al. (2000): An Introduction to Genetic Analysis. 7th Ed. – W. H. Freeman and Company, New York.
[21] Hamilton, T. L., Marcus, L, Ray, D., Eric, S. B., Patricia, C., et al. (2011): Transcriptional profiling of nitrogen fixation in *Azotobzctervinelandii*. – J. Bacteriol. 193(17): 4477-4486.

http://www.aloki.hu ● ISSN 1589 1623 (Print) ● ISSN 1785 0037 (Online)
DOI: http://dx.doi.org/10.15666/aeer/1706_1400914024

[22] Hausner, M., Wuertz, S. (1999): High rates of conjugation in bacterial biofilms as determined by quantitative in situ analysis. – Applied and Environmental Microbiology 65(8): 3710-3713.
[23] Helmut, B. F., Widmer, W., Sigler, V., Zeyer, J. (2004): New molecular screening tools for analysis of free-living diazotrophs in soil. – Appl. Environ. Microbiol. 70: 240-247.
[24] Jones & Bartlett Learning, LLC. (2016): Bacterial Transformation. Chap. 1. – ShutterStock, Inc., New York.
[25] Jones, K. M., Kobayashi, H., Davies, B. W., Taga, M. E., Walker, G. C. (2007): How *rhizobial* symbionts invade plants: the Sinorhizobium–Medicago model. – Nat. Rev. Microbiol. 5: 619-633.
[26] Kennedy, I. R., Islam, N. (2001): The current and potential contribution of a symbiotic nitrogen fixation to nitrogen requirement on farms: a review. – Australian Journal of Experimental agriculture 42: 441-457.
[27] Khider, A. K. (2011): Chromosomal *nif* genes transfer by conjugation in nitrogen fixing *Azotobacter chrococcum* to *Lactobacillus planetarium*. – Current Research Journal of Biological Sciences 3: 155-164.
[28] Khider, A. K. (2012): Molecular study of *nifH1, nifH2, nifH3, nifU, nifV, VF* genes and classical approach cared out to identification of *Azotobacter chrococcum* from soil. – Curr. Res. J. Biol. Sci. 4(5): 570-577.
[29] Kidaj, D., Wielbo, J. (2010): Use of Rhizobial *Nod* Factors as Biofertilizers for Legumes. – M. Curie-Skodowska University, Lublin, Poland. Mikkeli, Finland.
[30] Kumari, S., Sinha, R. P. (2011): Symbiotic and Asymbiotic N2 Fixation. Chap. 5. – In: Sinha, R. P. et al. (eds.) Advances in Life Sciences. I. K. International Publishing House Pvt. Ltd., New Delhi.
[31] Lerouge, P., Roche, P., Faucher, C., Maillet, F., Truchet, G., Promé, J., Dénarié, J. (1990): Symbiotic host-specificity of Rhizobium meliloti is determined by a sulphated and acylated glucosamine oligosaccharide signal. – Nature 344: 781-784.
[32] Marwa, A. S., Elbaz, A. F., Ragab, A. A., Hamza, H. A., El Halafawy, K. A. (2010): Identification and characterization of *Azotobacter chroococcum* isolated from some Egyptian soils. – J. of Agricultural Chemistry and Biotechnology 1(2): 93-104.
[33] Mohamed, A. S. A. (2017): Molecular study on isolated *Azotobacter, Rhizobium* and *Bacillus megaterium var phosphaticum* employment as biofertilizer. – Ph.D. thesis. Salahaddin University-Erbil, Kurdistan.
[34] Moses, P. B. (1987): AppendixGene Transfer Methods Applicable to Agricultural Organisms. – National Center for Biotechnology Information, U.S. National Library of Medicine, Bethesda, MD.
[35] Nosheen, A., Bano, A., Ullah, F., Farooq, U., Yasmin, H., Hussain, I. (2011): Effect of plant growth promoting *rhizobacteria* on root morphology of Saffl ower (*Carthamus tinctorius L.*). – African Journal of Biotechnology 10(59).
[36] Olsen, J., Brown, D., Baggesen, D. L., Bisgaard, M. (1992): Biochemical and molecular characterization of *Salmonella enterica serovar berta*, and comparison of methods for typing. – Epidemiology and Infection 108: 243-260.
[37] Patil, H. S. R., Patil, Naik, T. V., Avin, B. R. V., Sayeswara, H. A. (2013): Isolation and molecular characterization of *Bacillus megaterium* isolated from various agro climatic zones of Karnataka and its effect on medicinal plant *Ruta gradiolus*. – Curr Res Microbiol Biotechnol. 1(4): 173-182.
[38] Pimda, W., Bunnag, S. (2010): Genetic transformation of *Vanda lilacina* Teijsm & Binnend. with a chitinase gene. – AAB Bioflux 2(1): 71-78.
[39] Rossen, L., Shearman, C. A., Johnston, A. W. B., Downiel, J. A. (1985): The *nod*D gene of *Rhizobium leguminosarum* is autoregulatory and in the presence of plant exudate induces the *nod* A, B, C genes. – The EMBO Journal 4(13A): 3369-3373.
[40] Sambrook, J., Fritsch, E., Maniatis, T. (1989): Laboratory Manual of Molecular Cloning. Vol. 3. – Cold Spring Harbor, New York.

http://www.aloki.hu ● ISSN 1589 1623 (Print) ● ISSN 1785 0037 (Online)
DOI: http://dx.doi.org/10.15666/aeer/1706_1400914024

[41] Setubal, J. C., Santos, P. D. Goldman, B. S. Ertesvåg, H. Espin, G. et al. (2009): Genome sequence of *Azotobacter vinelandii*, an obligate aerobe specialized to support diverse anaerobic metabolic processes. – J. Bacteriol. 191: 4534-4545.
[42] Shamseldin, A. (2013): The role of different genes involved in symbiotic nitrogen fixation - review. – Global Journal of Biotechnology & Biochemistry 8(4): 84-94.
[43] Shiva, R. D. M., Mohan, B. K., Nataraja, S., Krishnappa, M., Abhilash, M. (2010): Isolation and molecular characterization of *Bacillus megaterium* isolated from different agro climatic zones of Karnataka and its effect on seed germination and plant growth of *Sesamum indicum*. – RJPBCS 1(3): 614.
[44] Shoukry, A. A., Khattab, A. A. Abou-Ellail, M., El-shabrawy, H. (2013): Molecular and biochemical characterization of new *Rhizobium leguminosarum* bio *viciae* strains isolated from different located of Egypt. – J. Appl. Sci. Res. 9(11): 5864-5877.
[45] Siddiqui, A., Shivle, R., Magodiya, N., Tiwari, K. (2014): Mixed effect of *Rhizobium* and *Azotobacter* as biofertilizer on nodulation and production of *chick pea*, *Cicer arietinum*. – Biosci. Biotech. Res. Comm. 7(1): 46-49.
[46] Slonczewski, J. (2006): Bacterial Gene Exchange and Mobile Genes. – KAP Genetics and Development, Biology Dept., Kenyon College.
[47] Snyder, L., Champness, W. (1997): Molecular Genetic of Bacteria. – AMS Press, Washington, DC.
[48] Spaink, H. P., Kondorosi, A., Hooykaas, P. (1998): Molecular biology of model plant-associated bacteria. – The Rhizobiaceae XXIV: 566.
[49] Tu, Z., He, G., Li, X. K., Chen, J. M., Chang, J., Yao, Q., Liu, P. D. et al. (2005): An improved system for competent cell preparation and high efficiency plasmid transformation using different Escherichia coli strains. – Electronic Journal of Biotechnology 8(1).
[50] Velineni, S., Brahmaprakash, G. P. (2011): Survival and phosphate solubilizing ability of *Bacillus megaterium* in liquid inoculants under high temperature and desiccation stress. – J. Agr. Sci. Tech. 13: 795-802.
[51] www.explorer.bio-rad.com. Biotechnology_Explorer@bio-rad.com. Biotechnology Explorer. pGLO™ Bacterial. Transformation Kit.
[52] www.himedialabs.com.a. mb@himedialabs.com. HiPer® Transformation Teaching Kit. Product Code: HTBM017.
[53] www.himedialabs.com.b mb@himedialabs.com. HiPer® Bacterial Conjugation Teaching Kit. Product Code: HTM004.
[54] www.towson.educse. Version (2016): The transformation Lab. Experiment Using *E. coli* and pFluoroGreen. Based on a kit produced by EDVOTEK®. Adapted by Towson University.
[55] Yoo, L. (2010): The Effect of *rpoH* for heat shock gene expression on plasmid transformation. – Journal of Experimental Microbiology and Immunology (JEMI) 14: 108-111.

http://www.aloki.hu ● ISSN 1589 1623 (Print) ● ISSN 1785 0037 (Online)
DOI: http://dx.doi.org/10.15666/aeer/1706_1400914024

A STUDY OF BODY WEIGHT AND MILK TRAITS OF KARADI EWES – SULAIMANI GOVERNORATE, IRAQ

HAMA KHAN, K. M.[1*] – AL-BARZINJI, Y. M. S.[2**] – MAAROF, N. N.[1]

[1]*Department of Animal Science, College of Agricultural Science, University of Sulaimani, Sulaimani, Iraq*

[2]*Department of Animal Resource, College of Agriculture Engineering Science, Salahaddin University-Erbil, Iraq*

**Corresponding author*
e-mail: karwan.hamakhan@univsul.edu.iq; phone: +964-772-526-3296
***Yousif.Noori@Su.Edu.Krd*

(Received 26th May 2019; accepted 10th Sep 2019)

Abstract. This study was carried out to investigate the effect of some factors on birth weight (BW), weaning weight (WW), marketing weight (MW), average daily gain (ADG), daily milk yield (DMY), total milk yield (TMY), protein and fat percentage. A 135 ewes from three flocks used, 114 of them were lambed. The mean ± SE of BW, WW, MW, ADG, DMY, TMY, protein percentage and fat percentage were 4.14 ± 0.65, 16.37 ± 2.87, 23.60 ± 4.42, 0.12 ± 0.02, 0.236 ± 0.10, 34.07 ± 5.94 kg, and 5.33 ± 0.62% and 5.30 ± 12.93%, respectively. All studied traits were significantly ($P \leq 0.05$) affected by flock except BW, protein and fat percentages. Month of lambing had significant effects ($P \leq 0.05$) on MW, ADG and Post daily gain. Stage of lactation had a significant effect ($P \leq 0.05$) on daily milk yield and protein percentage. The lowest and highest BLUP values for BW, WW, MW, ADG, DMY, TMY, protein and fat percentages were -1.6411, 1.6889kg, -6.5307, 10.1293kg, -9.9775, 13.1725 kg, -10.5293, 10.7504 kg, -31.02, 7.38kg, -2.0546, 2.0097%, -1.703, 1.40% respectively. These results indicated that there are high genetic variations among animals for all above studied traits. It means that selection can play a big role in improving economical traits.
Keywords: *Birth Weight, Weaning Weight, Marketing Weight, Milk Yield, BLUP, Fat %, Protein %*

Introduction

Small ruminants (sheep and goat) are important investments in Iraq. They play a major role in strengthening the backbone of the rural economy. The Karadi sheep which comprises about 18-20% of the total sheep population to the northeastern mountain, villages and undulating dry-farming plain of Kurdistan region of Iraq (Alkass and Juma, 2005). Sheep and goat population in Kurdistan region had been estimated to be around 3,500,000 (Ahmad, 2011). Productivity of this breed is low due to the fact that animals are naturally selected for survival under suboptimal environments. Assessment of the amount of milk produced by ewes provides information for the implementation of optimum management and feeding strategies for female sheep and their lambs (Cardellino and Benson, 2002).

Many studies analyzing the factors affecting ewes' growth performance, milk yield and milk composition were reported (Al-Barzinji and Hassan, 2005; Antonič *et al.,* 2013). The main factors were flock (Meraï *et al.,* 2014; Everett-Hincks, *et al.,* 2014; Rahimi *et al.,* 2014), ewes age (Ramakrishanappa *et al.,* 2015; Sezenler *et al.,* 2016; Siddalingamurthy *et al.,* 2017), sex of lamb (Al-Samarai *et al.,* 2016; Al-Bial *et al.*, 2016; Malik *et al.,* 2016), month of lambing (Al-Samarai *et al.,* 2016; Malik *et al.,*

http://www.aloki.hu ● ISSN 1589 1623 (Print) ● ISSN 1785 0037 (Online)
DOI: http://dx.doi.org/10.15666/aeer/1706_1402514038

2016). The effect of stage of lactation on milk yield and composition were also reported by (Kuchtik *et al.,* 2008; Komprej *et al.,* 2012).

In order to devise effective breeding plans for genetic improvement of Karadi ewes, information on the extent of genetic and environmental factors on performance traits is the pre-requisite. Therefore, this study was planned to generate information on the relative importance of genetic and environmental factors on the growth and milk traits of Karadi ewes in addition to estimating the Best Linear Unbiased Prediction (BLUP) for some growth and milk traits.

Materials and methods

The data were obtained from Karadi ewes in three private flocks (*Fig. 1*) at different location, Arbat District (Latitude, 35° 25' 14", Longitude, 45° 03' 36", W, elevation 681 m), Sharazoor District (Latitude, 35° 15' 27", Longitude, 45° 42' 21", W, elevation 614 m) and Mawat District (Latitude, 35° 52' 34", 45° 24' 35", W, elevation 858 m) around Sulamania governorate in Kurdistan Region of Iraq (*Fig. 2*). All animals were apparently healthy and were fed on pasture under open field conditions. In this study, 114 ewes were utilized. At lambing ewes and lambs were identified with spray in addition to the plastic tags with numbers. Lambing date, birth weight, sex of lambs, and other relevant information were recorded. Body weights of lambs at birth and at age of 90 (Weaning weight) and 150 (Marketing weight) days, were also recorded. Milk yield was recorded monthly starting from the second week of lambing until the 150 days (less than 50 gm milk/ewe/day) post partum using lamb-suckling technique plus hand milking (Mousa and Shetawi, 1994). Lambs were separated from dams at 7.00 pm on the day before measuring test milk production. In the following day, lambs were weighed at 7.00 am., and left to suckle their dams until satisfaction, then reweighed and kept away from their mothers, while the residual milk in the udder of each ewe were hand milked and weighted, and the amount of milk was recorded and then multiplied by 2 to calculate the daily milk yield, which multiplied by 30 then summed to calculate the total milk yield (ICARDA and FAO, 1995). Protein% and fat% of milk were estimated from the milk sample monthly using Milkoscan TM minor machine (P/N 6004 4208, Issue 1 GB, March 2010, FOSS Analytical, 69, Slangerupgade, DK 3400 Hillerod, Denmark).

The PROC GLM (General Linear Model) procedure in SAS programs (2010) was used to analyze the data for weights at different ages, average daily gain as well as milk yield traits. Fixed effects studies were: parity, sex of lamb, the month of birth, and age at weaning were fitted in the following model (1) and (2):

Model I for weight traits

$$Y_{ijklm} = \mu + V_i + N_j + O_k + H_l + E_{ijklm} \quad \text{(Eq.1)}$$

where Yijklm = Weights of lambs at different ages and average daily gain (ADG) of individual lambs; μ = Over all mean; Vi = Fixed effect of flock (i = 1,2,3); Nj = Fixed effect of age of dam (j = 1,2,3,4,5); Ok = Fixed effect of sex of lams (k = male, female); Hl = Fixed effect of month of lambing (l = November, December, January and February); Eijklm = Random/error effect.

http://www.aloki.hu ● ISSN 1589 1623 (Print) ● ISSN 1785 0037 (Online)
DOI: http://dx.doi.org/10.15666/aeer/1706_1402514038

Figure 1. *Sheep photo with flocks*

Figure 2. *Study locations*

http://www.aloki.hu ● ISSN 1589 1623 (Print) ● ISSN 1785 0037 (Online)
DOI: http://dx.doi.org/10.15666/aeer/1706_1402514038

Model II for milk traits

$$Y_{ijklmn} = \mu + Vi + Nj + Ok + Hl + Zm + E_{ijklmn} \quad \text{(Eq.2)}$$

The notation of the second model is similar to the first model except Zm = Fixed effect of stage of lactation (m = 1, 2, 3, 4, 5).

Tukey tests used to compare between means for all traits under study because its suitable test to comparing least square means with this program. For genetics evaluation of ewes for various performance traits, Best Linear Unbiased Prediction (BLUP) procedure described by (SAS, 2010) was applied. The model used for this purpose was the Mixed Model (fixed + random effects) of (SAS, 2010) software.

Results

Growth traits of Karadi lambs

Least square means ± SE of BW, WW, MW, ADG, pre-weaning and post weaning daily gain of the Karadi lambs are presented in *Table 1*. The overall means of BW, WW, MW, ADG pre-weaning and post weaning daily gain were 4.14 ± 0.65 kg, 16.37 ± 2.87 kg, 23.60 ± 4.42 kg and 0.12 ± 0.02 kg, 0.13 ± 0.02 kg and 0.12 ± 0.04 kg, respectively.

Milk traits of Karadi ewes

The least square means ± SE of to identify the effect of fixed effects on the observed milk production performance recorded such as daily milk yield, total milk yield, protein% and fat% are given in *Table 2*. The overall means were 0.236 ± 0.10 kg/day, 34.07 ± 5.94 kg/day, 5.33 ± 0.62% and 5.30 ± 12.93% for DMY, TMY, protein% and fat% respectively.

The BLUP values of ewes for some studied traits are shown in *Table 3*. The lowest BLUP values for BW, WW, MW, DMY, TMY, protein% and fat% were -1.641, -6.530, -9.977, -10.52, -2.054, -34.20 and -1.703 kg respectively. The corresponding values of highest BLUP values were 1.688, 10.12, 13.17, 10.75, 2.009, 7.380 and 1.406 kg.

Discussion

Growth traits of Karadi lambs

The mean of the BW (4.14 ± 0.65 kg) in current study was moderately high and the birth weight have significant effect on other last weights, for that the increase this trait is very importance in sheep breeding. This result was agreement with other studies reported earlier by several investigators in different breeds of sheep (Hussain *et al*., 2006; Jawasreh and Khasawneh, 2007). Also the mean of WW/lamb (16.37 ± 2.87 kg) and MW/Lamb (23.60 ± 4.42 kg) were moderately high and marketing weigh determines the outcome of sheep breeders, for that increases these traits necessary in sheep breeding. The effects of flock on WW, MW, ADG pre-weaning and post weaning were significant ($P \leq 0.05$). The significant differences in weaning weight due to flock was in agreement with results obtained by Baneh *et al*. (2010), Tariq *et al*. (2011), Everett-Hincks *et al*. (2014) and Rahimi *et al*. (2014). The significant differences due to flock on ADG and pre-weaning daily gain were in agreement with resulted reported earlier by Baneh and Hafezian (2009) and Tariq *et al*. (2013). Flock can have a

http://www.aloki.hu ● ISSN 1589 1623 (Print) ● ISSN 1785 0037 (Online)
DOI: http://dx.doi.org/10.15666/aeer/1706_1402514038

significant effect on body weight at different ages and average daily gain and could be attributed mainly to differences in management and environmental conditions. This results show the good management and conditions have significant effect on lambs weight traits, because these type of trait classified as a quantification trait which controlled by each genotypic and environmental effect with interaction between them.

The ewe age seems to have no significant effect on all lambs body weight such effect of ewe age on lambs birth and weaning weight are in agreement with some earlier studies (Al-Barzinji, 2003; Jalil-Sarghale *et al*., 2014; Al-Bial *et al*., 2016). Similar results of pre-weaning daily gain in different breeds have been noticed by other (Khalaf *et al*., 2010; Gokdal, *et al*., 2006). Non significant effect of post-weaning gain due to the age found under the present study was disagreement with that reported by (Baneh and Hafezian, 2009; Marufa *et al*., 2017).

Male lambs were statistically heavier than females at birth, although, this difference was statistically no significant for other growth traits (*Table 1*). Similarly, many authors claimed that sex of lamb had no effect on birth and weaning weight of different breeds of sheep (Al-Bial *et al*., 2016; Siddalingamurthy *et al*., 2017). Moreover, the findings in this study for pre-weaning daily gain was also in agreement with those previously obtained by Gokdal *et al*. (2006) and Abbas *et al*. (2010). Likewise, daily weight gain after weaning stage by sex of lamb observed in the present study was in accordance with reported finding by Marufa *et al*. (2017). Although average daily gain was heavies for male than female lambs, differences between them lacked significance. Their averages were 0.15 ± 0.01 and 0.13 ± 0.00 kg, respectively.

The month of lambing also influences MW, ADG and post daily gain. Lambs born early in the lambing period (December and January) gained weight better than those born late (February) due to the accessibility to the pastures in spring season. Lambs born late will not be able to use pasture in spring because of their young age besides they may have higher exposure to internal parasites which thrive in the high temperature. Thus, their weaning and yearling weights will be lower than those lambed early (Elwakil *et al*., 2009). Heaviest lambs at birth and marketing weight were at December, whereas the lighter lamb's birth weight and marketing weight were at February. It is known that month of birth may cause variations in weight and performance of lambs due to climatic variations and/or management (Bathaei and Leroy, 1997). For weight at marketing age, lambs born at December and January were significantly ($p \leq 0.05$) heaviest than those lambs born at February. However, results of the present study were similar to those reported earlier claiming that month of lambing was not significantly affect birth weight in different breeds of sheep (Khalaf *et al*., 2010; Al-Bial *et al*., 2016) and weaning weight (Mohammed, 2008). The present results for pre-waning daily gain agreed with those reported by Abbas *et al*. (2010) who reported pre-weaning daily gain from birth to weaning did not significantly affected by month of lambing. The differences among different reports may be due to breed, size of the data set or method of estimation used in different studies, production system, climatic conditions and ecological zones, where sheep farming were practiced. The significant influences of environmental factors on body weight in the present study can be explained in part by differences in environment, feeding, grazing resources, male and female endocrine system, limited uterine space, and inadequate availability of nutrients during pregnancy, maternal effects and maternal ability of dam at different ages (Rashidi *et al*., 2008).

http://www.aloki.hu ● ISSN 1589 1623 (Print) ● ISSN 1785 0037 (Online)
DOI: http://dx.doi.org/10.15666/aeer/1706_1402514038

Table 1. *Least square means ± SE (kg) for birth weight, weaning weight, marketing weight, average daily gain, pre-weaning daily gain and post weaning daily gain in Karadi lambs*

Fixed effects	Birth weight	Weaning weight	Marketing weight	Daily gain		
				Average	Pre-weaning	Post-weaning
Overall mean	4.14 ± 0.65	16.37 ± 2.87	23.60 ± 4.42	0.12 ± 0.02	0.13 ± 0.02	0.12 ± 0.04
Flock	NS	*	*	*	*	*
1	4.34 ± 0.13^{a}	15.66 ± 0.60^{a}	19.64 ± 0.93^{a}	0.10 ± 0.01^{a}	0.12 ± 0.01^{a}	0.06 ± 0.01^{a}
2	3.66 ± 0.37^{a}	19.86 ± 1.66^{b}	28.22 ± 2.58^{b}	0.16 ± 0.01^{b}	0.17 ± 0.01^{b}	0.13 ± 0.02^{b}
3	4.17 ± 0.22^{a}	14.80 ± 1.00^{a}	29.48 ± 1.53^{b}	0.16 ± 0.00^{b}	0.11 ± 0.01^{a}	0.24 ± 0.01^{c}
Ewes age (year)	NS	NS	NS	NS	NS	NS
2.5	4.15 ± 0.19^{a}	16.49 ± 0.87^{a}	25.52 ± 1.34^{a}	0.14 ± 0.01^{a}	0.13 ± 0.01^{a}	0.15 ± 0.01^{a}
3.5	3.95 ± 0.18^{a}	16.81 ± 0.82^{a}	25.54 ± 1.26^{a}	0.14 ± 0.01^{a}	0.14 ± 0.01^{a}	0.14 ± 0.01^{a}
4.5	3.73 ± 0.21^{a}	15.56 ± 0.93^{a}	24.01 ± 1.44^{a}	0.13 ± 0.01^{a}	0.13 ± 0.01^{a}	0.14 ± 0.01^{a}
5.5	4.38 ± 0.27^{a}	18.24 ± 1.18^{a}	28.04 ± 1.82^{a}	0.15 ± 0.01^{a}	0.15 ± 0.02^{a}	0.16 ± 0.01^{a}
Sex of lamb	NS	NS	NS	NS	NS	NS
Male	4.20 ± 0.25^{a}	18.03 ± 1.12^{a}	27.12 ± 1.73^{a}	0.15 ± 0.01^{a}	0.15 ± 0.01^{a}	0.15 ± 0.01^{a}
Female	3.91 ± 0.22^{a}	15.53 ± 0.97^{a}	24.44 ± 1.49^{a}	0.13 ± 0.01^{a}	0.12 ± 0.01^{a}	0.14 ± 0.01^{a}
Month of lambing	NS	NS	*	*	NS	*
November	4.06 ± 0.14^{a}	15.60 ± 0.64^{a}	25.06 ± 0.99^{ab}	0.14 ± 0.01^{ab}	0.12 ± 0.01^{a}	0.15 ± 0.01^{a}
December	4.35 ± 0.28^{a}	16.68 ± 1.25^{a}	29.99 ± 1.92^{a}	0.17 ± 0.01^{a}	0.13 ± 0.01^{a}	0.22 ± 0.02^{b}
January	4.11 ± 0.28^{a}	18.06 ± 1.24^{a}	27.02 ± 1.92^{a}	0.15 ± 0.01^{a}	0.15 ± 0.01^{a}	0.14 ± 0.02^{a}
February	3.70 ± 0.32^{a}	16.75 ± 1.40^{a}	21.04 ± 2.16^{b}	0.11 ± 0.01^{b}	0.14 ± 0.01^{a}	0.07 ± 0.02^{c}

Means in the same column for each factor with different letters are significantly ($p \leq 0.05$) different from each other. NS: non significant

Milk traits of Karadi ewes

The least square means ± SE of to identify the effect of fixed effects on the observed milk production performance recorded such as daily milk yield, total milk yield, protein% and fat% are given in *Table 2*. The overall means were 0.236 ± 0.10 kg/day, 34.07 ± 5.94 kg/day, 5.33 ± 0.62% and 5.30 ± 12.93% for DMY, TMY, protein and fat respectively. The average of daily and total milk yield observed in this study were lower than the range reported earlier by several investigators in different breeds of sheep (Oramari, 2009; Abd Allah *et al*., 2011). However, protein and fat percentage were similar to other studies reported earlier by several investigators in different breeds of sheep (Bendelja *et al*., 2009; Abd El-Fatah and Awad, 2014).

Flock significantly ($P \leq 0.05$) affected milk production traits. Daily milk yield and total milk yield produced by ewes that were in the third flock was higher (0.312 ± 0.01 and 45.59 ± 2.05 kg) than those produced by ewes from first and second flock (0.220 ± 0.01, 0.211 ± 0.02 and 32.32 ± 1.24, 33.45 ± 3.40 kg) respectively. Many results are in agreement with the significance effect of flock on daily milk yield (Gardi, 2008; Pérez-Cabal *et al*., 2013). Moreover, similar significance effect of flock on total milk yield was also reported by (Pérez-Cabal *et al*., 2013; Meraï *et al*., 2014).

http://www.aloki.hu ● ISSN 1589 1623 (Print) ● ISSN 1785 0037 (Online)
DOI: http://dx.doi.org/10.15666/aeer/1706_1402514038

Table 2. *Least square means ± SE for daily milk yield (DMY), total milk yield (TMY), protein% and fat% in Karadi ewes*

Fixed effects	DMY (kg)	TMY (kg)	Protein %	Fat%
Overall mean	0.236 ± 0.10	34.07 ± 5.94	5.33 ± 0.62	5.30 ± 12.93
Flock	*	*	NS	NS
1	0.220 ± 0.01[a]	32.32 ± 1.24[a]	5.33 ± 0.06[a]	4.23 ± 1.27[a]
2	0.211 ± 0.02[a]	33.45 ± 3.40[a]	5.15 ± 0.16a	6.81 ± 3.48[a]
3	0.312 ± 0.01[b]	45.59 ± 2.05[b]	5.46 ± 0.10[a]	4.37 ± 2.09[a]
Ewes age (year)	NS	NS	NS	NS
2.5	0.261 ± 0.01[a]	39.77 ± 1.79[a]	5.37 ± 0.08[a]	5.31 ± 1.83[a]
3.5	0.245 ± 0.01[a]	36.75 ± 1.68[a]	5.30 ± 0.08[a]	6.07 ± 1.72[a]
4.5	0.241 ± 0.01[a]	35.90 ± 1.90[a]	5.20 ± 0.09[a]	4.71 ± 1.97[a]
5.5	0.244 ± 0.01[a]	36.06 ± 2.40[a]	5.39 ± 0.12[a]	4.45 ± 2.48[a]
Sex of lambs	NS	NS	NS	NS
Male	0.251 ± 0.01[a]	37.88 ± 2.32[a]	5.42 ± 0.11[a]	5.37 ± 2.36[a]
Female	0.245 ± 0.01[a]	36.36 ± 2.00[a]	5.21 ± 0.09[a]	4.90 ± 2.02[a]
Month of lambing	NS	NS	NS	NS
November	0.247 ± 0.01[a]	34.66 ± 1.26[a]	5.34 ± 0.06[a]	5.26 ± 1.34[a]
December	0.264 ± 0.01[a]	39.27 ± 2.57[a]	5.20 ± 0.12[a]	5.58 ± 2.60[a]
January	0.246 ± 0.01[a]	37.10 ± 2.57[a]	5.50 ± 0.12[a]	4.98 ± 2.59[a]
February	0.234 ± 0.02[a]	37.45 ± 2.89[a]	5.22 ± 0.14[a]	4.72 ± 2.95[a]
Stage of lactation (month)	*		*	NS
1	0.321 ± 0.01[a]	-------	5.33 ± 0.08[a]	4.83 ± 1.83[a]
2	0.339 ± 0.02[a]	-------	5.51 ± 0.08[a]	4.90 ± 1.84[a]
3	0.281 ± 0.01[b]	-------	5.32 ± 0.08[a]	7.62 ± 1.85[a]
4	0.201 ± 0.01[c]	-------	5.31 ± 0.08[a]	4.96 ± 1.84[a]
5	0.100 ± 0.01[d]	-------	4.94 ± 0.09[b]	5.21 ± 2.10[a]

Means in the same column for each factor with different letters are significantly ($p \leq 0.05$) different from each other. NS: non significant

In the present work no significant effect of ewe's age on daily and total milk yield was found, There results were in agreement with those reported earlier by (Merkhan, 2014; Akreyi, 2015). Also, the effect of ewe's age on protein and fat% lacked significance. Such results were also reported earlier by (Abd Allah *et al*., 2011; Oramari and Hermiz, 2012). The effect of sex of lamb and month of lambing on the DMY, TMY, protein and fat% was no significance, these findings were in agreement with those reported on DMY and TMY by (Al-Samarai and Al-Anbari, 2009; Merkhan, 2014 and Akreyi, 2015). Also, an author found that month of lambing had no effect on daily milk yield and total milk yield (Abd-Al-Noor, 2011). Moreover, differences in protein and fat percentage studied in ewes lambed in the four months were not significant (*Table 2*). In an earlier study in Iraq, Gardi (2008) did not detect a significant effect of month of lambing on protein and fat% in milk of Karadi, Awassi and Hamdani ewes. Also, Martini *et al*. (2008) and Augusta *et al*. (2008) observed no remarkable monthly changes in protein%. Stage of lactation has significantly ($P \leq 0.05$) effected DMY and

http://www.aloki.hu ● ISSN 1589 1623 (Print) ● ISSN 1785 0037 (Online)
DOI: http://dx.doi.org/10.15666/aeer/1706_1402514038

protein%. Similar results were also obtained by Pavic *et al*. (2002) and Kuchtik *et al*. (2008). While stages of lactation had no significant effect on fat%, which the lowest percentage (4.83) was obtained in the first stage of lactation and highest (7.62%) during the 3rd stage of lactation. This result was in agreement with results obtained by Sevi *et al*. (2006) and Oravcova *et al*. (2007).

As in *Tables 2* and *3* there are variance differences among fixed effect on all traits under studies, it means there are ability to make selection process among sheep to choices the best parents and mated them altogether to speed up the weight and milk traits in the next generation. To removed the effect of fixed factors mixed model was used to calculate the BLUP value which is one methods used to evaluation the animal upon his performances to obtained the realized value for each animals under study to ranking them according to his BLUP values for each trait to select the best one among all animals to speed up the production in next generation.

Table 3 shows the BLUP values for BW, WW, MW, DMY, TMY, protein% and fat%. The lowest and highest BLUP value was (-1.6411 and 1.6889 kg) for BW, (-6.5307 and 10.1293) for WW, (-9.9775 and 13.1725) for MW, (-10.5293 and 10.7405) for DMY, (-31.02 and 7.38) for TMY, (-2.0546 and 2.0097) for protein% and (-1.7033 and 1.4067) for fat%, respectively. The wide range between the BLUP values of ewes for some above traits indicated that selection of elite ewe will improve all these traits in the present sample. Hussain *et al*. (2006) reported that BLUP value for weaning weight ranged from -1.799 to 2.421 kg/ewe in Thalli sheep. Al-Barzinji (2009) reported that BLUP values for ewes ranged from -12.338 to 11.6023 kg for total weight of lambs weaned. In Hamdani sheep predicted BLUP value for daily milk yield from two flocks was reported by Al-Barzinji (2003), from two flocks. Values ranged from -155.56 to 214.58 gm and from -162.46 to 240.39 gm in the two flocks respectively. BLUP values for top 10% of the ewes to be selected as dam of ram lambs ranged between 102.87 to 214.58 gm and 187.63 to 240.39 gm in first and second flocks, while the values for culling 20% ranged from -155.56 to -66.50 gm and from -162.46 to -98.44 gm for first and second flock, respectively. Al-Rawi *et al*. (2002b) revealed that BLUP values for total milk yield ranged from -28.29 to 82.61 kg in Awassi sheep respectively. In Awassi sheep Abdulnoor (2004) reported that BLUP values for total milk yield for selecting 90, 80, 70, 60 and 50% of ewes were 1.98, 3.64, 5.07, 6.62 and 8.15 kg, respectively. Al-Barzinji (2009) reported that BLUP values for total milk yield in ewes ranged from -68.160 to 139.951 kg.

These results show that the breeder can select 10% from top BLUP value (Male) and 70% from top BLUP value (Female) and mate these parents altogether can speed up improvement of weight and milk traits among this population of sheep under study.

http://www.aloki.hu ● ISSN 1589 1623 (Print) ● ISSN 1785 0037 (Online)
DOI: http://dx.doi.org/10.15666/aeer/1706_1402514038

Table 3. *BLUP values (kg) of BW, WW, MW, DMY, TMY, protein% and fat% in Karadi ewes*

Ewe No.	BLUP (BW)	Ewe No.	BLUP (WW)	Ewe No.	BLUP (MW)	Ewe No.	BLUP (DMY)	Ewe No.	BLUP (TMY)	Ewe No.	BLUP (Protein%)	Ewe No.	BLUP (Fat%)
87	1.688	55	10.12	74	13.17	99	10.75	51	7.380	102	2.009	65	1.406
41	1.678	74	10.06	93	12.62	94	10.58	102	1.440	99	1.919	16	1.066
81	1.658	81	9.569	81	12.42	108	10.09	97	1.200	106	1.795	19	1.006
40	1.648	80	8.219	87	11.47	111	9.768	111	0.480	109	1.784	78	1.006
9	1.558	63	5.919	94	11.27	96	9.640	114	0	101	1.716	70	0.996
43	1.138	89	5.069	55	10.27	106	9.359	109	-0.600	107	1.660	15	0.956
73	0.958	24	5.019	71	10.22	91	8.745	94	-1.500	95	1.562	20	0.956
39	0.878	72	4.719	76	10.07	104	8.417	107	-1.980	97	1.525	27	0.956
1	0.808	69	4.669	90	9.122	105	8.090	108	-2.460	114	1.347	37	0.956
74	0.808	39	4.409	85	9.072	98	7.517	101	-3.300	111	1.338	12	0.916
37	0.778	31	4.219	92	8.672	107	7.272	110	-3.660	94	1.306	41	0.896
38	0.768	64	4.219	72	8.472	103	6.903	106	-4.200	108	1.255	74	0.846
6	0.758	71	4.219	73	8.322	109	6.862	112	-4.260	51	1.124	29	0.676
13	0.758	59	4.019	88	8.172	102	6.371	105	-4.980	92	1.111	88	0.646
42	0.758	73	3.969	80	7.872	17	6.131	88	-6.360	87	1.012	93	0.636
10	0.658	60	3.889	63	7.672	84	6.089	98	-6.420	113	0.914	81	0.596
85	0.658	68	3.819	68	7.622	85	5.430	100	-6.420	21	0.863	31	0.516
55	0.628	66	3.219	64	7.172	95	5.389	113	-6.540	22	0.863	32	0.516
93	0.618	95	3.219	31	6.572	97	5.389	37	-6.900	93	0.861	34	0.516
45	0.608	76	2.969	69	5.672	110	5.307	95	-7.320	112	0.833	35	0.516
46	0.558	79	2.819	41	5.422	37	5.062	99	-7.560	110	0.821	24	0.426
80	0.518	38	2.469	66	5.422	92	4.775	92	-7.860	37	0.807	9	0.406
26	0.468	47	2.469	89	5.422	51	4.734	13	-8.640	86	0.805	13	0.406
25	0.458	92	2.429	39	5.172	89	4.407	93	-9.480	105	0.732	76	0.406
82	0.458	41	2.369	95	4.622	13	3.875	12	-9.840	47	0.721	94	0.406
28	0.418	56	2.109	75	4.322	81	3.833	86	-9.960	33	0.709	38	0.296
31	0.418	15	1.519	91	4.322	39	3.499	47	-10.29	88	0.702	30	0.246
44	0.408	78	1.469	38	4.172	90	3.302	50	-10.47	39	0.646	5	0.216
34	0.378	87	1.469	56	4.172	8	3.081	34	-10.80	98	0.632	98	0.206
83	0.368	65	1.419	15	4.122	12	3.057	85	-11.22	18	0.617	23	0.176
5	0.358	5	1.369	42	3.622	83	2.975	38	-11.88	11	0.582	62	0.176
60	0.358	52	1.319	24	3.422	47	2.750	17	-12.60	34	0.518	10	0.086
92	0.328	29	1.269	86	3.372	86	2.580	87	-12.66	100	0.483	105	0.0667
103	0.288	54	1.219	59	2.672	42	2.454	19	-12.96	17	0.477	1	0
95	0.248	70	1.219	67	2.672	34	2.402	18	-13.02	89	0.375	2	0
23	0.208	42	1.169	62	2.622	82	2.115	30	-13.02	84	0.367	3	0
48	0.208	67	1.169	78	2.272	38	1.665	16	-13.26	8	0.270	6	0
71	0.208	82	1.169	101	2.022	28	0.950	21	-13.50	31	0.224	8	0
33	0.198	46	1.069	60	1.872	19	0.929	22	-13.50	12	0.212	11	0
24	0.178	58	0.919	6	1.472	6	0.909	31	-13.62	42	0.168	14	0
86	0.168	62	0.919	54	1.472	18	0.888	33	-13.62	79	0.121	17	0
97	0.168	75	0.919	70	1.162	30	0.888	24	-13.74	45	0.103	18	0
108	0.168	108	0.819	108	0.772	61	-0.789	29	-13.74	61	-0.185	21	0

http://www.aloki.hu ● ISSN 1589 1623 (Print) ● ISSN 1785 0037 (Online)
DOI: http://dx.doi.org/10.15666/aeer/1706_1402514038

Ewe No.	BLUP (BW)	Ewe No.	BLUP (WW)	Ewe No.	BLUP (MW)	Ewe No.	BLUP (DMY)	Ewe No.	BLUP (TMY)	Ewe No.	BLUP (Protein%)	Ewe No.	BLUP (Fat%)
112	0.168	112	-1.010	112	-0.877	11	-0.298	45	-13.80	103	-0.147	22	0
114	0.168	114	-1.030	114	0.122	9	-0.789	20	-13.98	36	-0.154	25	0
8	0.158	86	0.919	100	0.872	16	0.724	41	-14.22	6	0.084	26	0
27	0.158	6	0.819	79	0.772	21	0.560	46	-14.58	41	0.077	28	0
75	0.158	45	0.819	29	0.372	22	0.560	11	-14.76	16	0.058	33	0
109	0.158	109	0.819	109	0.372	60	0.233	15	-15.36	60	-0.016	36	0
77	0.138	61	0.819	26	0.322	31	0.478	9	-15.48	13	0.057	39	0
35	0.118	50	0.719	58	0.322	33	0.478	44	-15.54	20	0.042	42	0
30	0.088	101	0.719	65	0.272	52	0.449	83	-15.78	3	0.034	48	0
3	0.058	77	0.319	23	0.222	24	0.397	84	-15.90	19	-0.016	52	0
15	0.058	96	0.169	4	0.122	29	0.397	23	-16.08	30	-0.018	54	0
47	0.058	48	0.119	37	0.072	45	0.356	78	-16.14	85	-0.044	56	0
50	0.008	85	0.069	82	0.072	20	0.233	39	-16.38	50	-0.061	57	0
89	-0.011	107	0.019	107	-0.027	41	0.069	40	-16.38	28	-0.120	59	0
59	-0.021	49	-0.280	96	-0.127	44	-0.830	27	-16.56	83	-0.182	60	0
98	-0.021	91	-0.530	98	-0.327	25	-0.845	79	-16.62	104	-0.185	61	0
29	-0.031	27	-0.580	99	-0.427	64	-0.845	32	-16.80	96	-0.190	63	0
7	-0.041	97	-0.580	43	-0.627	80	-0.994	8	-16.98	57	-0.198	67	0
19	-0.041	13	-0.630	40	-0.877	50	-1.157	10	-17.04	25	-0.210	68	0
101	-0.061	83	-0.680	61	-0.877	23	-1.199	36	-17.52	29	-0.213	69	0
94	-0.081	2	-0.730	77	-0.877	75	-1.239	76	-17.52	24	-0.283	64	0
2	-0.091	94	-0.730	97	-0.927	40	-1.403	43	-17.58	78	-0.297	73	0
54	-0.091	100	-0.730	13	-0.977	27	-1.526	89	-17.70	67	-0.307	80	0
69	-0.091	57	-0.750	106	-1.427	76	-1.567	42	-17.88	76	-0.329	75	0
79	-0.101	44	-0.830	2	-1.477	32	-1.690	96	-17.88	27	-0.341	77	0
88	-0.101	1	-0.930	1	-1.727	14	-1.799	49	-18.27	38	-0.348	79	0
90	-0.101	93	-1.010	57	-1.727	10	-1.853	62	-18.48	48	-0.349	82	0
111	-0.101	111	-0.630	111	0.122	46	-0.175	74	-18.48	52	-0.130	71	0
4	-0.141	88	-1.030	103	-1.727	61	-2.015	35	-18.57	15	-0.381	72	0
12	-0.141	12	-1.430	12	-1.927	53	-2.222	73	-18.72	91	-0.394	84	0
20	-0.141	37	-1.130	105	-1.727	36	-2.181	7	-18.78	82	-0.382	86	0
49	-0.141	23	-1.380	5	-1.927	73	-2.181	54	-19.50	40	-0.382	87	0
53	-0.141	26	-1.430	34	-1.927	43	-2.222	65	-19.74	56	-0.394	90	0
96	-0.141	90	-1.430	27	-1.977	87	-2.307	103	-19.74	46	-0.407	95	0
110	-0.141	110	-0.580	110	-0.877	59	-0.830	57	-19.86	59	-0.190	99	0
113	-0.141	113	0.819	113	-1.727	15	-0.707	82	-19.86	1	-0.150	101	0
100	-0.161	10	-1.580	102	-2.377	3	-2.349	28	-20.04	75	-0.419	103	0
52	-0.241	98	-1.780	83	-3.177	93	-2.426	6	-20.10	44	-0.419	104	0
91	-0.251	11	-1.880	47	-3.427	49	-2.692	58	-20.10	73	-0.427	106	0
107	-0.261	43	-1.930	30	-3.477	59	-2.835	60	-20.11	32	-0.443	107	0
72	-0.301	105	-2.080	21	-3.727	71	-2.835	59	-20.12	69	-0.459	113	0
36	-0.321	28	-2.230	28	-3.877	35	-2.897	104	-20.52	71	-0.475	111	-0.033
11	-0.341	40	-2.230	19	-4.127	70	-2.999	52	-20.76	49	-0.507	83	-0.043
99	-0.361	21	-2.430	11	-4.327	7	-3.040	75	-21.12	54	-0.514	109	-0.043
21	-0.391	19	-2.830	52	-4.427	54	-3.531	56	-21.30	68	-0.517	66	-0.083

http://www.aloki.hu ● ISSN 1589 1623 (Print) ● ISSN 1785 0037 (Online)
DOI: http://dx.doi.org/10.15666/aeer/1706_1402514038

Ewe No.	BLUP (BW)	Ewe No.	BLUP (WW)	Ewe No.	BLUP (MW)	Ewe No.	BLUP (DMY)	Ewe No.	BLUP (TMY)	Ewe No.	BLUP (Protein%)	Ewe No.	BLUP (Fat%)
104	-0.391	99	-2.830	25	-4.477	62	-3.695	66	-21.48	14	-0.562	55	-0.213
56	-0.441	106	-2.830	20	-4.527	100	-3.695	62	-21.48	62	-0.606	50	-0.263
65	-0.491	30	-2.980	46	-4.527	57	-3.777	48	-21.54	65	-0.621	91	-0.373
70	-0.491	53	-2.980	35	-4.577	79	-3.777	71	-21.96	9	-0.641	102	-0.413
64	-0.511	34	-3.080	36	-4.627	58	-3.940	5	-22.20	10	-0.651	44	-0.463
22	-0.541	36	-3.130	3	-4.977	1	-4.145	25	-22.62	23	-0.67	112	-0.463
57	-0.541	103	-3.280	50	-5.027	101	-4.227	55	-22.62	64	-0.676	108	-0.473
105	-0.541	102	-3.380	45	-5.127	65	-4.521	67	-22.62	26	-0.690	7	-0.483
102	-0.601	18	-3.430	10	-5.377	72	-4.636	81	-22.86	74	-0.702	97	-0.483
76	-0.631	25	-3.480	104	-5.677	56	-4.759	77	-22.92	72	-0.706	40	-0.593
51	-0.641	4	-3.530	33	-5.877	63	-4.882	90	-23.22	77	-0.832	85	-0.593
16	-0.741	20	-3.580	48	-6.327	48	-4.922	70	-23.94	35	-0.855	4	-0.683
106	-0.761	104	-3.580	53	-6.527	68	-5.209	64	-24.30	90	-0.864	49	-0.703
84	-0.831	51	-3.980	32	-6.877	5	-5.373	3	-24.78	80	-0.921	46	-0.773
14	-0.891	9	-4.380	16	-6.977	55	-5.659	72	-24.93	43	-1.055	114	-0.783
63	-0.901	3	-4.480	14	-7.277	78	-5.823	2	-25.20	2	-1.057	53	-0.793
62	-0.911	35	-4.480	51	-7.327	74	-5.864	69	-26.82	66	-1.057	92	-0.793
78	-0.921	16	-4.530	84	-7.527	60	-6.485	1	-27.36	58	-1.070	51	-0.933
66	-0.931	17	-4.930	8	-7.577	67	-6.559	4	-27.72	5	-1.123	110	-0.933
67	-0.981	14	-4.980	49	-7.727	69	-7.23	68	-27.90	7	-1.199	58	-1.053
61	-1.001	8	-5.030	7	-7.877	2	-7.419	80	-28.38	81	-1.250	47	-1.073
32	-1.121	33	-5.130	22	-7.977	66	-8.524	91	-29.76	70	-1.276	100	-1.093
17	-1.141	7	-5.530	18	-8.527	26	-8.908	63	-30.72	55	-1.386	96	-1.103
18	-1.291	84	-5.630	44	-8.877	4	-9.137	53	-30.78	63	-1.469	43	-1.113
68	-1.321	32	-6.080	9	-9.277	77	-9.588	14	-31.02	4	-1.683	45	-1.593
58	-1.641	22	-6.530	17	-9.977	88	-10.52	26	-34.20	53	-2.054	89	-1.703

Conclusion

In conclusion, some of the fixed effects including the flock and the Month of lambing affect lamb's body weights significantly, as well as, it appears that flock had a significant influence on daily milk yield and total milk yield and stage of lactation affects test-day milk yield as well as protein percentage significantly. The wide range between the BLUP values of ewes for many growth and milk traits and this indicate that selecting ewes according to their records at early ages will improve their later performance. The recording of data in sheep breeding from breeder side is necessary because the availability of large data and information's on animal's gives better and accurate values for animal evaluation in selection process and breeder must select his animals upon the accurate and analyzed data which obtained from good managements.

REFERENCES

[1] Abbas, S. F., Abd Allah, M., Allam, F. M., Abooul-Ella, A. A. (2010): Growth performance of Rahmni and Chios lambs weaned at different ages. – Australian Journal Basic & Applied Science 4: 1583-1589.

http://www.aloki.hu ● ISSN 1589 1623 (Print) ● ISSN 1785 0037 (Online)
DOI: http://dx.doi.org/10.15666/aeer/1706_1402514038

[2] Abd Allah, M., Abass, S. F., Allam, F. M. (2011): Factors affecting the milk yield and composition of Rahmani and Chios sheep. – International Journal of Livestock Production 2(3): 024-030.
[3] Abd El-Fatah, E. N., Awad, E. I. (2014): Bacterial pathogens and somatic cell count in sheep and goat milk. – Journal of Global Biosciences 3(7): 1034-1045.
[4] Abd-Al-Noor, M. J. M. (2011): Some factors effect in milk production and lactation period in local Awassi and Turkish sheep. – Diyala Agricultural Sciences Journal 3(1): 21-29.
[5] Abdulnoor, M. J. (2004): Effect of various selection intensities, based on milk and total lambs' weight weaned of Awassi ewes. – MSc. Thesis, Almusauab Technical College, Iraq.
[6] Ahmad, A. (2011): Animal Production and Veterinary Directorate. – September 8th, 18:23. www.NNA.com.
[7] Akreyi, I. A. I. (2015): Udder measurements of Karadi and Awassi sheep and their relation with milk production under local farm conditions. – MSc. Thesis, Coll. of Agric., Univ. of Duhok, Iraq.
[8] Al-Barzinji, Y. M. (2003): A study of growth and body dimensions of lambs and genetic evaluation for milk production of Hamdani ewes. – MSc. Thesis, Salahaddin University, Iraq.
[9] Al-Barzinji, Y. M. (2009): A study of some economical traits with breeding value in Hamdani sheep using molecular genetics techniques. – PhD Dissertation. Animal Resources Department, College of Agriculture, University of Salahaddin, Iraq.
[10] Al-Barzinji, Y. M., Hassan, M. W. (2005): Study of non-genetic factors affecting milk yield and estimation heritability for milk yield in Hamdani ewes. – Iraqi J. Agri. Sci. 7(2): 25-30.
[11] Al-Bial, A., Alazazie, S., Shami, A., Aldoss, A. (2016): Genetic analysis of growth traits in white Boni sheep under the Central Highlands region of Yemen. – Journal of Basic and Applied Research 2(4): 408-413.
[12] Alkass, J. E., Juma, K. H. (2005): Small Ruminant Breeds of Iraq. (Edi. Lusi Iniguez). Characterization of Small Ruminant Breeds in West Asia and North Africa. – ICARDA (International Center of Agriculture Research in the Dry Areas), Aleppo.
[13] Al-Rawi, A. A., Salman, A. D., Al-Azzawi, W. A., Ibraim, S. S. (2002b): breeding values and genetic response of lambs weight weaned and milk yield for Awassi ewes. – IPAJ Agric. Res. 12(3): 67-79.
[14] Al-Samarai, F. R., Al-Anbari, N. N. (2009): Genetic evaluation of rams for total milk yield in Iraqi Awassi sheep. – ARPN Journal of Agricultural and Biological Science 4(3): 54-57.
[15] Al-Samarai, F. R., Mohammed, F. A., Al-Zaydi, F. H., Al-Anbari, N. N., Abdulrahman, Y. K. (2016): Genetic evaluation of Iraqi Awassi rams for some growth traits of their lambs. – American Journal of Applied Scientific Research 2(1): 1-5.
[16] Antonič, J., Jackuliaková, L., Uhrinčať, M., Mačuhová, L., Oravcová, M., Tančin, V. (2013): Changes in milk yield and composition after lamb weaning and start of machine milking in dairy ewes. – Slovak Journal of Animal Science 46: 93-99.
[17] Augusta, L., Vioara, M., Camella, R., Daniela, L. (2008): Seasonal variation of Turcana sheep milk chemical composition. – Lucrari Stiintifice Zootehnie si Biotehnologii 41(2): 758-761.
[18] Baneh, H., Hafezian, S. H. (2009): Effects of environmental factors on growth traits in Ghezel sheep. – African Journal of Biotechnology 8: 2903-2907.
[19] Baneh, H., Hafezian. S. H., Rashidi, A., Gholizadeh, M., Rahimi, G. (2010): Estimation of genetic parameters of body weight traits in Ghezel sheep. – Asian-Aust. J. Anim. Sci. 23(2): 149-153.

http://www.aloki.hu ● ISSN 1589 1623 (Print) ● ISSN 1785 0037 (Online)
DOI: http://dx.doi.org/10.15666/aeer/1706_1402514038

[20] Bathaei, S. S., Leroy, P. L. (1997): Genetic and phenotypic aspects of the curve characteristics in Mehraban Iranian fat-tailed sheep. – Small Ruminant Research 29(3): 261-269.
[21] Bendelja, D., Antunac, N., Milkulec, N., Vnucec, I. (2009): Urea concentration in sheep's milk. – Mljekarstvo 59(1): 3-10.
[22] Cardellino, R. A., Benson, M. E. (2002): Lactation curves of commercial ewes rearing lambs. – J. Anim. Sci. 80: 23-27.
[23] Elwakil, S. L., ElSayed, M., Ahmed, A. M., Sadek, R. R., Nigm, A. A. (2009): Genetic and phenotypic parameters of birth, weaning and yearling body weights of Barki sheep raised in the North West coast of Egypt. – Egyptian J. Anim. Prod. 46: 43-52.
[24] Everett-Hincks, M. J., Mathias-Davis, H. C., Greer, G. J., Auvray, B. A., Dodds, K. G. (2014): Genetic parameters for lamb birth weight, survival and death risk traits. – J. Anim. Sci. 92: 2885-2895.
[25] Gardi, H. E. A. (2008): Effect of Breed and some environmental fixed factors on milk yield in commercial flocks. – MSc. Thesis, College of Agriculture, University of Sallahaddin, Iraq.
[26] Gokdal, O., Ulker, H., Karakus, F., Cengiz, F. (2006): The growth of Karakas and its crosses lambs (F1) with Ile De France X Akkaraman (G1) under unlimited suckling regime. – Journal of Biology Sci. 6(4): 787-792.
[27] Hussain, P., Akhtar, S. A., Younas, M., Shafiq, M. (2006): Effect of inbreeding on pre-weaning growth traits in Thalli sheep. – Pakistan Vet. J. 26(3): 138-140.
[28] ICARDA, FAO (1995): The Recording of Fat-Tailed Sheep in Syria, Turkey and Jordan. – Consultancy Report, Jordan.
[29] Jalil-Sarghale, A., Kholghi, M., Shahrebabak, M. M., Shahrebabak, H. M., Mohammadi, H., Abdollahi-Arpanah, R. (2014): Model comparisons and genetic parameter estimates of growth traits in Baluchi sheep. – Slovak J. Anim. Sci. 47(1): 12-18.
[30] Jawasreh, K. I. Z., Khasawneh, A. Z. (2007): Studies of some economic characteristics on Awassi lambs in Jordan. – Egyptian Journal of sheep, Goat and Desert Animals Sciences 2(2): 101-110.
[31] Khalaf, A. I., Said, S. I., Edriss, S. M. (2010): Role of some genetic and environmental factors in growth traits of Turkish Awassi, local and crossbred lambs. – The Iraqi Journal of Agricultural Sciences 41(3): 12-22.
[32] Komprej, A., Gorjanc, G., Kompan, D., Kovač, M. (2012): Lactation curves for milk yield, fat, and protein content in Slovenian dairy sheep. – Czech J. Anim. Sci. 57(5): 231-239.
[33] Kuchtik, J., Sustova, K., Urban, T., Zapletal, D. (2008): Effect of the stage of lactation on milk composition, its properties and the quality of rennet curdling in East Friesian ewes. – Czech J. Anim. Sci. 53: 55-63.
[34] Malik, Z. S., Dalal, D. S., Dahiya, S. P., Patil, C. S., Dahiya, R. (2016): Genetic analysis of growth traits in Harnali sheep. – Veterinary World 9(2): 128-132.
[35] Martini, M., Mele, M., Scolozzi, C., Salari, F. (2008): Cheese making aptitude and chemical and nutritional characteristics of milk from Massese ewes. – Ital. J. Anim. Sci. 7: 419-437.
[36] Marufa, E., Taye, M., Abebe, G., Tera, A., Jimma, A. (2017): Effect of non-genetic factors on reproductive and growth performance of Abera sheep under community based breeding program in SNNPRS Ethiopia. – J Adv Dairy Res 5: 196. DOI: 10.4172/2329-888X.1000196.
[37] Meraï, A., Gengler, N., Hammami, H., Rekik, M., Bastin, C. (2014): Non-genetic sources of variation of milk production and reproduction and interactions between both classes of traits in Sicilo-Sarde dairy sheep. – Animal 8(9): 1534-1539.
[38] Merkhan, K. Y. (2014): Milk traits and their relationship with udder measurements in Awassi ewes. – Iranian Journal of Applied Animal Science 4(3): 521-526.

http://www.aloki.hu ● ISSN 1589 1623 (Print) ● ISSN 1785 0037 (Online)
DOI: http://dx.doi.org/10.15666/aeer/1706_1402514038

[39] Mohammed, L. T. (2008): Computing adjustment factors for growth traits in Karadi sheep. – MSc. Thesis, College of Agriculture, University of Duhok, Iraq.
[40] Mousa, M. T., Shetaewi, M. M. (1994): Crossing local Ossimi sheep with imported Chios to improve milk production and pre-weaning lamb gains. – Assuit Vet. Med. J. 30(600): 76-86.
[41] Oramari, R., Hermiz, H. (2012): Non-genetic factors and estimates of repeatability for milk yield traits and compositions in Karadi sheep. – Journal of University of Duhok 15(1): 163-171.
[42] Oramari, R. A. S. (2009): Genetic evaluation of Karadi sheep using some productive traits. – PhD Dissertation. Animal Production Department, College of Agriculture, University of Duhok. Iraq.
[43] Oravcova, M., Margetin, M., Peskovicova, D., Dano, J., Milerski, M., Hetenyi, L., Polak, P. (2007): Factors affecting ewes milk fat and protein content and relationships between milk yield and milk components. – Czech. J. Anim. Sci. 52(7): 189-198.
[44] Pavic, V., Antunac, N., Mioc, B., Ivankovic, A., Havranek, J. L. (2002): Influence of stage of lactation on the chemical composition and physical properties of sheep milk. – Czech, J. Anim. Sci. 47(2): 80-84.
[45] Pérez-Cabal, M. Á., Legaz, E., Cervantes, I., de la Fuente, L. F., Martínez, R., Goyache, F., Gutiérrez, J. P. (2013): Association between body and udder morphological traits and dairy performance in Spanish Assaf sheep. – Archiv Tierzucht 56(42): 430-442.
[46] Rahimi, S. M., Rafat, S. A., Jafari, S. (2014): Effects of environmental factors on growth traits in Makuie sheep. – Biotechnology in Animal Husbandry 30(2): 185-192.
[47] Ramakrishanappa, N., Sreesujatha, R. M., Kumar, S. N., Manju, G. U., Roopa Devi, Y. S. (2015): Growth performance of Mandya lambs under farm management. – Indian Vet. J. 92(10): 30-32.
[48] Rashidi, A., Mokhtari, M. S., Jahanshahi, A. S., Mohammad-Abadi, M. R. (2008): Genetic parameter estimates of pre-weaning growth traits in Kermani sheep. – Small Rumin. Res. 7(4): 165-171.
[49] SAS (2010): Statistical Analysis System. Version 9.1. – SAS Institute Inc., Cary, NC.
[50] Sevi, A., Albenzio, M., Annicchiarico, G., Caroprese, M., Marino, R., Santillo, A. (2006): Effects of dietary protein level on ewe milk yield and nitrogen utilization, and on air quality under different ventilation rates. – J. Dairy Res. 73: 197-206.
[51] Sezenler, T., Ceyhan, A., Yükse, M. A., Koncagül, S., Soysal, M., Yildirir, M. (2016): Influence of year, parity and birth type on milk yield and milk components of Bandırma Sheep (German Black Head Mutton x Kıvırcık). – Journal of Agricultural Sciences 22: 89-98.
[52] Siddalingamurthy, H. K., Manju, G. U., Roopa Devi, Y. S., Manjunatha, S. S., Sreesujatha, R. M. (2017): Non-genetic factors affecting birth and weaning weight in Mandya sheep. – Int. J. Adv. Res. 5(4): 345-348.
[53] Tariq, M. M., Bajwa, M. A., Babar, S., Waheed, A., Bukhari, F. A., Hameed, T., Marghazani, I. B., Javed, Y. (2011): Effect of non-genetic and genetic factors on birth weight of Mengali sheep of Balochistan. – Can. J. App. Sci. 1(3): 121-128.
[54] Tariq, M. M., Bajwa, M. A., Javed, K., Waheed, A., Awan, M. A., Rafeeq, M., Rashid, N., Shafee, M. (2013): Identification of environmental factors affecting pre weaning performance of Mengali sheep of Balochistan. – Journal of Animal & Plant Sciences 23(2): 340-344.

http://www.aloki.hu ● ISSN 1589 1623 (Print) ● ISSN 1785 0037 (Online)
DOI: http://dx.doi.org/10.15666/aeer/1706_1402514038

WATER INFILTRATION OF COVERING SOILS WITH DIFFERENT TEXTURES AND BULK DENSITIES IN GRAVEL-MULCHED AREAS

DONG, Q. G.[1,2,3,4*] – HAN, J. C.[1,2,3,4*] – ZHANG, Y.[1,2,3,4] – LI, N.[1] – LEI, N.[1,2,3,4] – SUN, Z. H.[1,2,3,4] – DU, Y. C.[1,2,3,4] – HE, J.[1,2,3,4]

[1]*Shaanxi Provincial Land Engineering Construction Group Co., Ltd., Xi'an 710075, China*

[2]*Institute of Land Engineering and Technology, Shaanxi Provincial Land Engineering Construction Group Co., Ltd., Xi'an 710075, China*

[3]*Key Laboratory of Degraded and Unused Land Consolidation Engineering, Ministry of Natural Resources, Xi'an 710075, China*

[4]*Shaanxi Provincial Land Consolidation Engineering Technology Research Center, Xi'an 710075, China*

**Corresponding author*
e-mail: dq-guang@163.com; phone: +86-029-8862-5020

(Received 27th May 2019; accepted 10th Sep 2019)

Abstract. To determine the influence of different bulk densities and texture on soil water infiltration after remediation in gravel-mulched areas, we subjected two different soil types were to a battery of tests to determine their soil infiltration characteristics. The results show that the soil infiltration capacity decreases with increasing soil bulk density. A logarithmic negative correlation was identified between stable infiltration rate and the bulk density of the two soils ($R^2 > 95\%$). Moreover, the larger the bulk density, the smaller the cumulative infiltration, and there is a significant linear negative correlation between density and infiltration. The Kostiakov infiltration model better describes the infiltration process of the Lou soil at all stages and the infiltration of Yellow-brown soil before 40 min. Finally, as soil water is redistributed, and its content increases with soil depth, and the greater the bulk density, the greater the water storage capacity of the soil from 0 to 30 cm. Overall, the soil bulk density should be no less than 1.5 g/cm^3 when Lou soil is chosen to cover on gravel-mulched land, and not less than 1.4 g/cm^3 for Yellow-brown soil.
Keywords: *bulk density, infiltration model, infiltration rate, cumulative infiltration, soil moisture*

Introduction

Given the importance of land for development, the shortage of cultivable land resources is an important factor restricting social and economic construction in China. Bringing new land under cultivation is therefore of critical importance, and one type of reserved land that may be suitable for new cultivation are gravel-mulched areas, of which China has about 1.04×10^6 km^2. Such land is widely distributed, and often possesses good light and heat conditions, thereby conferring great potential for development (Yi et al., 2013). Development of gravel-mulched areas involves constructing a new soil layer by covering the existing gravel layer. However, the soil covering process is relatively expensive, and there is a lack of corresponding theoretical research on the desired texture, density, or structure of the source soil. This is a notable limitation, since ineffective soil coverage can result in poor soil cultivation and/or inefficient water usage (Zhang et al., 2017, 2018). In order to solve

http://www.aloki.hu ● ISSN 1589 1623 (Print) ● ISSN 1785 0037 (Online)
DOI: http://dx.doi.org/10.15666/aeer/1706_1403914052

this problem, it is necessary to further clarify the optimal bulk density of the overlying soil on the gravel-mulched areas.

Soil moisture is critical for simulating physical processes affecting soil such as surface runoff, soil erosion, and solute transport (Chen et al., 2007). Soil infiltration capacity is mainly determined by characteristics such as soil bulk density, texture and structure (Hillel, 1998; Tejedor et al., 2013). However, existing studies on the effect of bulk density on soil water infiltration focus on the differences between soil structures with single or different textures (She et al., 2012; Li Z. M. et al., 2009; Zeng et al., 2017; Sun et al., 2017). As basic physical properties of soil, changes in bulk density and pore condition cause changes in soil infiltration performance. Zeng et al. (2017) studied the effect of bulk density on water infiltration of red soil, and found that both the cumulative infiltration and infiltration rates decreased with increasing of soil bulk density. Li et al. (2009a) studied the relationship between soil water infiltration and bulk density in soils of different consistencies and reached a similar conclusion. This relationship is due to the fact that as soil bulk density increases, the aggregate structure of the soil is destroyed, decreasing porosity and making the soil tight and solid, reducing infiltration capacity (Kang et al., 2016; Wang et al., 2017). The studies about water movement in large porous media such as gravel focused on the effects of gravel cover and soil:rock ratio on soil water movement. For example, Mandal et al. (2005) and Cerdà (2001) studied water infiltration in gravel-covered soils from two sites, one in a tropical, semi-arid region of India and another in southeastern Sweden. They found that infiltration rate and humidification peak migration velocity increased with the increasing gravel cover. In addition, Zavala et al. (2010) studied the relationship between gravel coverage, runoff generation, and soil erosion in the Spanish Mediterranean coast. Novák et al. (2012) developed a simulation-based modelling approach to analyze soil water content and water transport at different soil depths, and identified the complexity of the gravel content as a major determinant of water flow. These results agreed with the findings of Zhou et al. (2009), who showed that when the gravel content is < 40%, infiltration rate and hydraulic conductivity decrease with increasing gravel content, although both increase with increasing gravel content when it is > 40%. Most research on the influence of gravel on soil infiltration focuses on the effect of mountain sand and/or gravel cover on water infiltration, or on moisture infiltration characteristics in mixtures of earth and stone.

However, when there is a large porous medium layer such as gravel in the lower part of the soil, a distinct layered interface is formed between the soil and gravel. Moreover, when the textures and bulk density structures of the overlying soil are different from the large-pore gravel layer, gas may be generated there. The ease of formation of water flow channels affects water movement, thereby affecting soil fertility and water retention even after gravel remediation.

Therefore, this study aimed to provide the influence of covering soil texture and bulk density on water infiltration and compare the infiltration process of two typical soils in gravel-mulched areas, which would be beneficial to determine the appropriate soil bulk density based on different soil texture in the grave-mulched land consolidation project. This information would provide a theoretical and technical basis for the development and remediation of gravel-mulched areas, and would thus facilitate to determine the reasonable bulk density of the covering soil.

http://www.aloki.hu ● ISSN 1589 1623 (Print) ● ISSN 1785 0037 (Online)
DOI: http://dx.doi.org/10.15666/aeer/1706_1403914052

Materials and methods

Test soil

Natural soil used in experiments was collected from Lou soil deposits in Fuping County, Guanzhong, Shaanxi Province, and from Yellow-brown soil deposits in Hanzhong City, southern Shaanxi. Soil samples were collected 30 cm below the surface to minimize contamination by organic matter content found in the plough layer. In the actual soil-covering process, the soil is often disturbed, to ensure the same initial conditions of the experiment. Collected soil was naturally air-dried, ground, and passed through a 2 mm sieve. The particle composition of each stage was determined using the sedimentation method. The results of these analyses are shown in *Table 1*.

Table 1. *Test soil particle composition*

Test soil type	Sand (2-0.05 mm)	Silt (0.05-0.002 mm)	Clay (<0.002 mm)	Soil texture
Lou soil	13.37%	77.10%	9.53	Silt loam
Yellow-brown soil	7.09%	65.19%	27.72	Silty clay loam

Test methods

Next, we performed water infiltration tests to compare characteristics of infiltration. The test device has two parts: a soil column and a water supply system (*Fig. 1*). The soil column is a transparent plexiglass column with a diameter of 10 cm and a height of 50 cm, 4 taking soil holes with a diameter of 1 cm are set each layer around the soil column, a total of 6 layers of soil taking holes are set to take soil for determination moisture after infiltration. The lower part of the plexiglass column contains a steel wire mesh that is highly permeable to water. The water supply (Mariotte Bottle) has the same specifications as the soil column device (i.e. a diameter of 10 cm and a height of 50 cm), the water depth is controlled at 4-5 cm. Each test soil sample was examined at four volumetric weight levels of 1.3 g/cm^3, 1.4 g/cm^3, 1.5 g/cm^3, and 1.6 g/cm^3. In order to simulate the gravel, the lower part of each test soil sample was filled with 1 cm diameter glass bead with the thick of 5 cm, a layer of gauze was placed between the glass beads and the soil layer to prevent soil particle migration. Before filling, the inner wall of the pipe was coated with Vaseline. Air-dried soil samples were weighed and hierarchically filled (5 cm/layer) according to the designed bulk density. The total height of the soil was 30 cm. A layer of filter paper was placed on the surface of the soil column to prevent the soil surface from being eroded. Infiltration measurements were made every 1-3 min at the beginning of the test, and every 5 min afterward until 100 min. After this point a measurement was recorded every 10-30 min. The test was performed for 300 min. After completion of the infiltration test, samples were taken every 5 cm under the surface of each soil column and the water content of each layer was determined. Samples were taken through the taking soil holes just after the 300 min had elapsed, as well as 1 d, 3 d, and 10 d after the experiment. To eliminate the confounding influence of temperature, the indoor temperature was maintained in a range from 22 to 24 °C. Each set of experiments was repeated 3 times. The regression was used to fit the measured results.

http://www.aloki.hu ● ISSN 1589 1623 (Print) ● ISSN 1785 0037 (Online)
DOI: http://dx.doi.org/10.15666/aeer/1706_1403914052

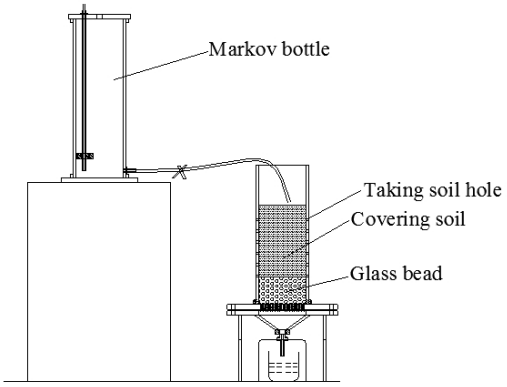

Figure 1. *Schematic diagram of test device*

Infiltration model

Kostiakov and Philip models were used to simulate the soil water infiltration process in gravel soil (Mehuys et al., 1975), and its applicability was evaluated. The Kostiakov model formula is:

$$I_t = K \cdot t^{1-\alpha} \quad \text{(Eq.1)}$$

Here, I_t is the cumulative infiltration amount at time t, cm; t is the infiltration time, min; K is the empirical infiltration coefficient, and its physical meaning is the cumulative amount of infiltration at the end of the first period after the infiltration began. It is also numerically equal to the average infiltration rate of the soil in the first unit period; α is the empirical infiltration index, which reflects the decay rate of the soil infiltration capacity. In the initial stage of infiltration, the parameter K plays a leading role. As the infiltration process continues, the parameter α becomes the main factor affecting the rate of infiltration.

The Philip model formula is:

$$I_t = S \cdot t^{0.5} + A \cdot t \quad \text{(Eq.2)}$$

Here, S is the infiltration rate in cm/min$^{0.5}$; A is the steady infiltration rate (usually less than the saturated hydraulic conductivity), also in cm/min.

Results

The infiltration rate changes over time

The infiltration rate is defined as the amount of water permeating into a unit of soil per unit area through the surface. *Figure 2* reflects the infiltration rate of different soils of different weights in the gravel area over time. The variation of soil infiltration rate over time among soils of different textures and bulk densities shows a rapid decrease followed by stabilization. For the two texture soils, the infiltration rate showed a rapid decrease after 5 min of infiltration, mainly due to a decrease in the absolute value of the matric potential and the rapid decrease of the soil negative pressure. After 10 min of

http://www.aloki.hu ● ISSN 1589 1623 (Print) ● ISSN 1785 0037 (Online)
DOI: http://dx.doi.org/10.15666/aeer/1706_1403914052

infiltration, the soil matric potential gradient begins to decrease slowly, finally approaching zero. The soil infiltration rate is generally stable, but the time required to reach stable infiltration of different soils with different textures differ. The Lou soil reached a stable infiltration state after 20 min, while the Yellow-brown soil gradually reached stable infiltration after 40 min. During the infiltration process of both soils, the larger the bulk density, the smaller the infiltration rate. The curve of the late infiltration is close to a horizontal straight line, indicating that the influence of soil bulk density on the infiltration rate decreases gradually over time.

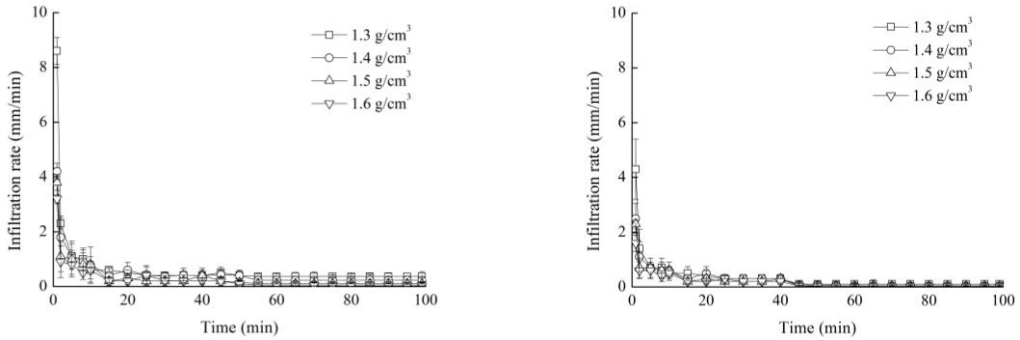

(a) Lou soil (b) Yellow-brown soil

Figure 2. *Infiltration rate over time*

Taken together, our soil infiltration test data suggest that soil bulk density has a significant effect on the stable infiltration rate. The stable infiltration rate in turn characterizes the infiltration capacity of the soil infiltration stage. *Figure 3* shows the relationship between the soil bulk density and the stable infiltration rate of two different textures, and shows that the bulk density of Lou soil increased from 1.3 g/cm^3 to 1.6 g/cm^3, and the steady infiltration rate decreased from 0.365 mm/min to 0.051 mm/min. In contrast, the bulk density of Yellow-brown soil increased from 1.3 g/cm^3 to 1.6 g/cm^3, and the steady infiltration rate declined from 0.065 mm/min to 0.012 mm/min. At the same bulk density, the stable infiltration rate of Yellow-brown soil is less than that of Lou soil, and the decrease in the soil infiltration rate in Lou soil is greater than the corresponding decrease in Yellow-brown soil. We also found that the soil infiltration rate and bulk density showed a highly significant log-negative correlation (equation shown in *Fig. 3*). These results showed that the stable infiltration rate of cover soils above gravel was greatly affected by soil bulk density. The steady infiltration rates of the two types of test soils decreased with increasing bulk density. Moreover, both soils showed nearly linear logarithmic relationships. However, the shape of this linear relationship in Lou soil had a relatively steep slope, while Yellow-brown soil showed a relatively flat linear relationship.

Influence of soil bulk density on cumulative infiltration

The cumulative infiltration amount is defined as the total amount of water infiltrated into the soil through the surface per unit area. Analyses of cumulative infiltration in different soil types under different soil weights over 100 min is shown in *Figure 4*. These results show that the cumulative infiltration of soils with different bulk density increases over time. At the same time, the larger the bulk density, the smaller the

http://www.aloki.hu ● ISSN 1589 1623 (Print) ● ISSN 1785 0037 (Online)
DOI: http://dx.doi.org/10.15666/aeer/1706_1403914052

cumulative infiltration. We found a significant linear negative correlation between permeability and bulk density ($R^2 > 0.95$), and the relationship between bulk density and cumulative infiltration is shown in *Figure 5*. In this figure we see that when the bulk density increased from 1.3 g/cm^3 to 1.6 g/cm^3, the cumulative infiltration decreased from 54.6 mm to 20.3 mm. Moreover, we also see that when the bulk density of Yellow-brown soil increased from 1.3 g/cm^3 to 1.6 g/cm^3, the cumulative infiltration decreased from 29.1 mm to 16.5 mm. The infiltration amount of the two soils was significantly different at 40 min. The process from the initial state to the final stable infiltration of Lou soil was relatively smooth, and the Yellow-brown soil showed an obvious turning after 40 min. This may be due to the differences in soil texture of the two soils.

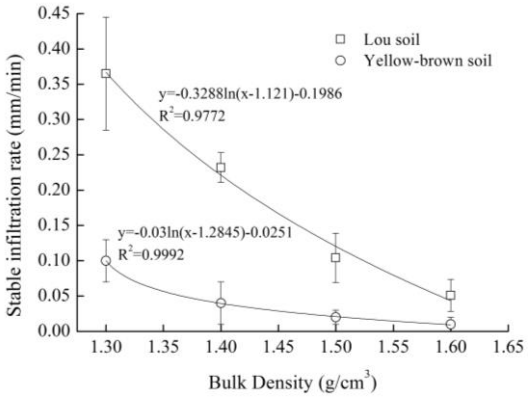

Figure 3. *The relationship between stable infiltration rate and soil bulk density*

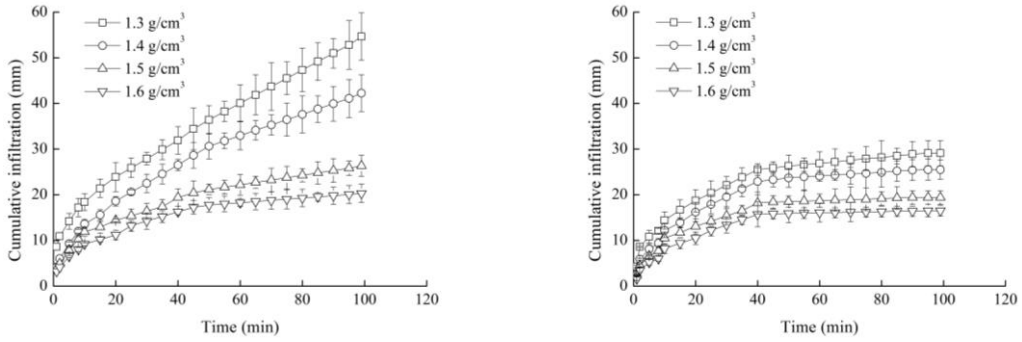

(a) Lou soil (b) Yellow-brown soil

Figure 4. *Cumulative infiltration over time*

Infiltration model for soils with different textures and bulk densities

To further study the influence of covering soil bulk density on soil water infiltration in gravel areas, we used Kostiakov (*Eq. 1*) and Philip models (*Eq. 2*) to simulate soil water infiltration in gravel soil. The results of these simulations for both Lou and Yellow-brown soils are shown in *Tables 2–4*. Lou soil can be better fitted with Kostiakov model. However, fitting of Yellow-brown soil revealed that the infiltration process slowed significantly after 40 min. Neither model simulated Yellow-brown soil well over then 100 min study period, so we then performed model segmentation: the

http://www.aloki.hu ● ISSN 1589 1623 (Print) ● ISSN 1785 0037 (Online)
DOI: http://dx.doi.org/10.15666/aeer/1706_1403914052

Kostiakov and Philip models were used for the first 40 min, then another linear model was fitted after the turning. It can be seen from *Tables 2* and *3* that the Kostiakov model effectively simulates the results of the whole infiltration process of the Lou soil as well as the first 40 min of the Yellow-brown soil infiltration (i.e. $R^2 > 0.98$), while the overall simulation results of the Philip model are poor. Thus the Philip model has poor applicability when describing soil water infiltration processes the gravel cover soil. The infiltration process of the Yellow-brown soil after the first 40 min can be better described by a linear equation ($R^2 > 0.95$). Taken together, our data support the use of the Kostiakov model for further analysis of water infiltration in the two soils.

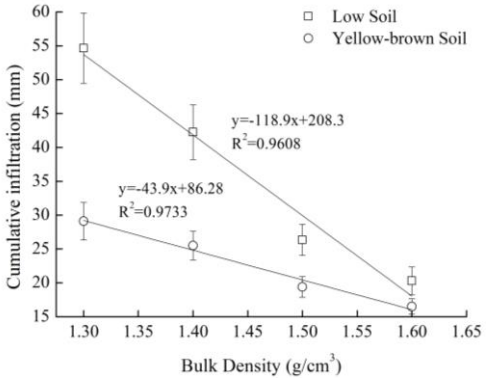

Figure 5. *The relationship between cumulative infiltration and bulk density of test soil*

The K value indicates the cumulative infiltration rate at the end of the first period after the start of soil infiltration—i.e. the initial infiltration rate, which is mainly affected by the soil structure. For samples of the same soil texture type, the main factors affecting the K value are the pore distribution characteristics of the soil, which are mainly determined by soil bulk density. In general, the larger the bulk density, the smaller the porosity and the denser the soil. It can be seen from *Tables 2* and *3* that as the bulk density increases, the K value decreases gradually. When the bulk density of Lou Soil increased from 1.3 g/cm^3 to 1.6 g/cm^3, the K value decreased from 5.776 to 3.953. In Yellow-brown soil the K value decreased from 5.387 to 2.168 in response to the same change, and the K values of the Yellow-brown soil was consistently lower than the K values of Lou soil. In the initial stage of water infiltration, the macropores in the surface soil are first filled with water by the action of the soil matric potential. This water is affected by the gravitational and the matric potentials, and eventually migrates deeper in the soil, given small bulk density and large pores. With increasing bulk density, the soil macropores decrease and the initial infiltration capacity decreases. Therefore, the K value generally decreases as volume density increases.

The empirical infiltration index α reflects the decay rate of the soil infiltration capacity. The larger the α value, the faster the infiltration capacity decays. *Tables 2* and *3* show that the Lou and Yellow-brown soils have opposite relationships between bulk density and the α value. Increasing the bulk density of Lou soil results in an increase in the α value—e.g. when the bulk density of Lou Soil increased from 1.3 g/cm^3 to 1.6 g/cm^3, the α value increased from 0.521 to 0.634. In contrast, increasing the bulk density of Yellow-brown soil resulting in a decrease in the α value—e.g. when the bulk density of Yellow-brown soil increased from 1.3 g/cm^3 to 1.6 g/cm^3, the α value decreased from 0.583 to 0.464. For Lou soil, the larger the bulk density of the

http://www.aloki.hu ● ISSN 1589 1623 (Print) ● ISSN 1785 0037 (Online)
DOI: http://dx.doi.org/10.15666/aeer/1706_1403914052

overburden, the faster the soil water infiltration capacity decays with time. Moreover, the smaller the bulk density of the soil, the slower the decay rate of soil water infiltration capacity with time, resulting in the accumulation of water. This results in a curve that becomes more horizontal as bulk density increases. A change in bulk density causes a large change in the α value, the smaller the soil bulk density and the larger the pores, the better the internal connectivity of the soil, which facilitates moisture penetration. Large pores also result in the discharge of air, thereby reducing the influence of air resistance on the infiltration process. Soil structures with larger bulk densities have less macroporous content, and the pores of such soils are enriched by infill of soil particles, thereby reducing internal connectivity. When soil moisture enters the pores, it often forms due to the surface tension of water. Smaller bubbles cause reduced gas discharge and increase the resistance to soil moisture infiltration. Gas resistance can cause a rapid decay in infiltration capacity. Therefore, the α value increases with increasing bulk density.

Table 2. *Fitting results of infiltration model of Lou Soil*

Bulk density (g/cm^3)	Kostiakov model				Philip model		
	K	α	K/α	R^2	S	A	R^2
1.3	5.776	0.521	11.086	0.988	5.294	6.64E-4	0.987
1.4	4.116	0.494	8.332	0.999	4.157	0.0078	0.999
1.5	4.505	0.613	7.349	0.995	3.591	3.21E-7	0.329
1.6	3.953	0.634	6.235	0.981	3.274	1.02E-9	0.754

Table 3. *Descriptive statistics of an infiltration model of yellow-brown soil before the transition*

Bulk density (g/cm^3)	Kostiakov model				Philip model		
	K	α	K/α	R^2	S	A	R^2
1.3	5.387	0.583	9.249	0.990	4.893	0	0.711
1.4	3.566	0.497	7.174	0.992	3.590	0.00195	0.992
1.5	3.122	0.526	5.942	0.987	3.081	0	0.954
1.6	2.168	0.464	4.670	0.992	2.224	0.04050	0.992

Table 4. *Descriptive statistics of a linear infiltration model of yellow-brown soil after the transition*

Bulk density (g/cm^3)	$I_t = a \cdot t + b$		
	a	b	R^2
1.3	0.06454	22.13329	0.99504
1.4	0.04429	20.98801	0.98907
1.5	0.02237	16.98222	0.98767
1.6	0.01384	15.17097	0.96204

http://www.aloki.hu ● ISSN 1589 1623 (Print) ● ISSN 1785 0037 (Online)
DOI: http://dx.doi.org/10.15666/aeer/1706_1403914052

Yellow-brown soil behaves differently—soil samples of the same texture will show large differences in α value from small changes in bulk density. The α value of Yellow-brown soil showed a slight decrease with increasing bulk density. This is mainly due to the relatively high content of clay in the soil and the low number of macropores present. The initial infiltration rate is small, and the larger the bulk density, the smaller the degree of attenuation of the infiltration velocity; therefore the relationship between the bulk density and the α value differs.

The K/α ratio reflects the whole infiltration process. On the whole, larger K/α ratios indicate stronger infiltration ability. In our data, we found that K/α decreased with increasing bulk density in both soils. At the same time, we also found that there was a significant inflection point in cumulative infiltration of Yellow-brown soil. The variation in cumulative infiltration over time after turning can be described linearly, and the linear slope decreases with increasing bulk density (*Table 4*).

Effect on soil water content and water storage capacity

The redistribution of soil moisture affects the distribution of water content in all layers of soil, and therefore directly affects the availability of soil moisture for plants (Liang et al., 2015). *Figures 6* and *7* show distribution curves of the water content of each layer of soil at the end of the infiltration test, as well as the degree of redistribution at 24 h, 72 h, and 240 h for different soil bulk densities of Lou and Yellow-brown soil. At the end of infiltration, both soils showed the same pattern: the greater the soil bulk density, the smaller the water content at the same soil layer height. This is likely due to greater soil bulk density resulting in weaker water holding capacity. At the bottom of the soil layer, due to the gravel having poor water holding capacity and strong permeability, the soil moisture in contact with the gravel layer moves downward, and the water content is the lowest. Water redistribution, under the joint action of matric and gravity potentials, involves soil moisture migrating to the vertical deep and dry soil. Moreover, we found that the soil bulk density became smaller as the redistribution period progressed. This is because as water migrates downward during redistribution, the gravity potential becomes more influential, causing the soil moisture content to increase with soil depth, thus decreasing bulk density. For instance, in our Yellow-brown soil trials the moisture content of the lower soil layer was low at all bulk density values, and the redistribution process was slower than it was in Lou soil.

Following water infiltration, changing soil water storage capacity varies in response to the redistribution of soil moisture among soil layers, as shown in *Figure 8*. The Bulk density of the soil covering the gravel has a significant effect on the water storage capacity of soil layers up to 30 cm below the surface. At early stages of water redistribution, the smaller the bulk density, the greater the water storage capacity. However, as time progresses, soil types with small bulk density have a high water capacity but lose water quickly. In contrast, soils with slower redistribution phases generally have better water retention. At a bulk density of 1.3 g/cm^3, water storage capacity of Lou soil decreased from an initial volume of 12.2 cm to a volume of 5.8 cm 10 d after infiltration. When the bulk density was 1.6 g/cm^3, the water storage capacity was 9.6 cm at initial infiltration, and was reduced by 17.7% (i.e. to 7.9 cm) after 10 d. This was different in Yellow-brown soil. At a bulk density of 1.3 g/cm^3, its water storage capacity declined from 11.8 cm to 6.4 cm (45.8%) over the same time period. Moreover, at a bulk density of 1.6 g/cm^3, the soil water storage declined from 11.0 cm to 9.7 cm, a reduction of only 11.8%.

http://www.aloki.hu ● ISSN 1589 1623 (Print) ● ISSN 1785 0037 (Online)
DOI: http://dx.doi.org/10.15666/aeer/1706_1403914052

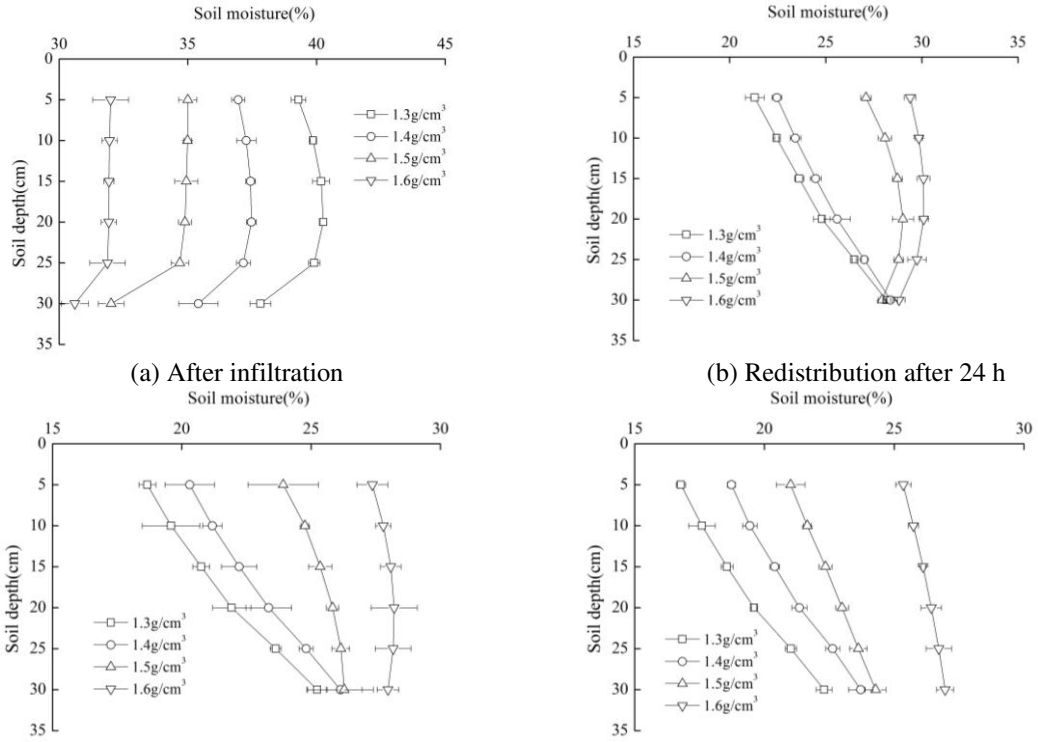

(a) After infiltration (b) Redistribution after 24 h

(c) Redistribution after 72 h (d) Redistribution after 240 h

Figure 6. *Water content distribution of each soil layer under different soil bulk densities of Lou soil*

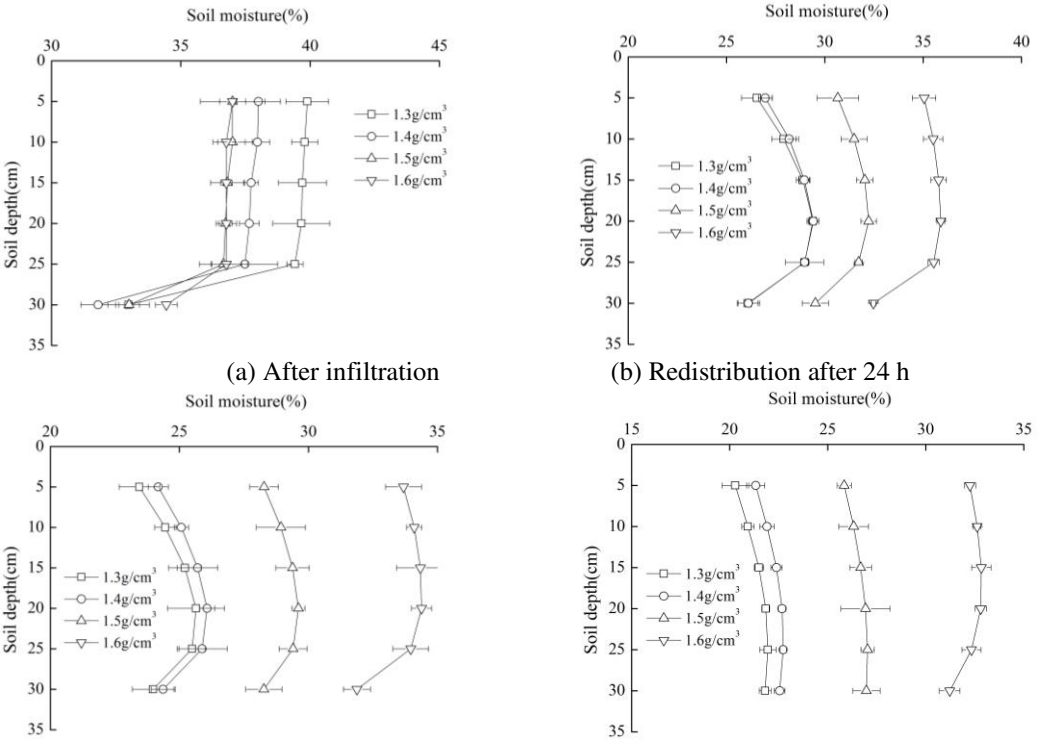

(a) After infiltration (b) Redistribution after 24 h

(c) Redistribution after 72 h (d) Redistribution after 240 h

Figure 7. *Distribution of water content in each soil layer under different soil bulk densities of Yellow-brown soil*

http://www.aloki.hu ● ISSN 1589 1623 (Print) ● ISSN 1785 0037 (Online)
DOI: http://dx.doi.org/10.15666/aeer/1706_1403914052

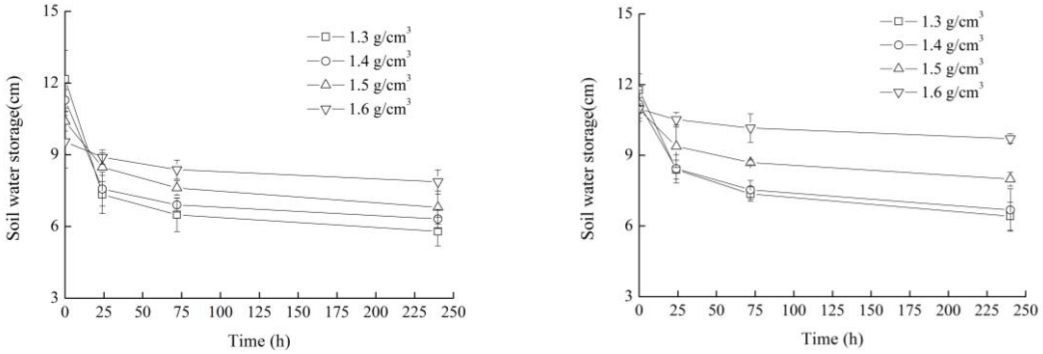

(a) Lou soil (b) Yellow-brown soil

Figure 8. *The effect of bulk density on soil water storage capacity*

Discussion

The infiltration rate reflects the infiltration performance of the soil. When the gravel is covered with soil, it is especially important to consider the soil infiltration performance of the resulting soil mixture. The bulk density structure, which strongly affects the water storage capacity and drainage capacity of the soil, can cause crops to be flooded when infiltration capacity is too low to discharge accumulated water quickly. However, if the infiltration capacity is too high, it is difficult to retain water in the soil. The effect of bulk density on water infiltration capacity is determined by the number of macropores present. According to Darcy's seepage law of unsaturated soil, the infiltration of soil moisture is determined by soil hydraulic conductivity and soil water potential gradient, while soil hydraulic conductivity is mainly determined by soil texture, bulk density, structure, moisture content, and matric potential (Wang et al., 2017). The initial stage of infiltration is mainly affected by the soil matric potential. Due to the low initial soil water content, the soil negative pressure is large and the matric potential gradient at the interface between the accumulated water and the soil column is also large, resulting in a higher initial infiltration rate. The infiltration process is gradually influenced by the gravity potential, and the infiltration rate decreases rapidly. Soil texture and bulk density affect the hydraulic conductivity of soil by affecting the size and distribution of soil pores, especially macropores and conductive pores.

In this study, we examined differences in soil moisture infiltration among different topsoil cover treatments for gravel-mulched areas. Our findings were similar to those of Kang et al. (2016), who confirmed that both the infiltration rate and cumulative infiltration decreased with increasing soil bulk density. The cumulative infiltration amount and its relationship over time is important to analyse the effect of rainfall and irrigation after soil covering in gravel-mulched areas. Soil bulk density had a great influence on cumulative infiltration during the infiltration process, and the cumulative infiltration was negatively correlated with soil bulk density. The infiltration capacity depends on the distribution of macropores in soil, because water migration channels in soil mainly depend on the presence of conductive pores and macropores (Fu et al., 2008). Soil bulk density is determined by the size and quantity of pores in the soil and the degree of soil compaction. The smaller the soil bulk density, the higher the pore content and the stronger the infiltration capacity and the moisture flux (Zhao et al., 2008). At the same time, we also found a negative linear correlation between the stable

http://www.aloki.hu ● ISSN 1589 1623 (Print) ● ISSN 1785 0037 (Online)
DOI: http://dx.doi.org/10.15666/aeer/1706_1403914052

infiltration rate and the logarithm of soil bulk density. This finding is consistent with those of Li et al. (2009b). Water infiltration into soil layers on a gravel base is well described by the widely-used Kostiakov model. However, we also found that the sticky soil texture of Yellow-brown soil has a turning point late in the process of infiltration, which agrees with the findings of Song et al. (2013) on their studies of water retention in water-repellent soils. Finally, we found that as infiltration progresses, the rate of infiltration rate changes slowly before stabilizing. Our results showed that after infiltration, the redistribution of soil moisture proceeded in a way similar to that described by Zeng. The major difference between the findings of that study and our results is that here the middle and lower soil layers were composed of gravel, and the loss of soil moisture at the end of the redistribution process was relatively small.

Conclusions

In this study, indoor simulated soil column tests were used to examine the relationship between soil traits and infiltration performance. We found that covering soil bulk density and texture strongly influenced infiltration and soil moisture levels present in different soil strata in gravel-mulched areas. We also note three key findings from this study.

First, when gravel is covered in soil, the importance of soil weight and textures is larger. This is because the soil porosity of the topsoil layer is smaller than the gravel underneath, reducing the connectivity between soil pores. This results in a lower infiltration rate. Moreover, the stable infiltration rate has a logarithmic negative correlation with soil bulk density. We also found that at the same bulk density, the stable infiltration rate of Yellow-brown soil is lower than that of Lou soil, and the decrease in the soil infiltration rate caused by the increase of bulk density in Lou soil was much greater than the corresponding increase in Yellow-brown soil.

Second, we found that the cumulative infiltration of soil at all bulk densities increases with time. At the same time, the larger the bulk density, the smaller the cumulative infiltration. After 100 min of infiltration, we found a significant linear negative correlation between the degree of infiltration and soil bulk density ($R^2 > 0.95$). Moreover, we used a Kostiakov model to characterize the first 100 min of infiltration in Lou soil and the first 40 min of infiltration in Yellow-brown soil. The Yellow-brown soil showed obvious turning after 40 min of infiltration, and the infiltration process can then be described by a linear equation.

Finally, at the initial moment of the end of infiltration, the soil moisture content of the bottommost layer of soil (30 cm below the surface) was small, even where the soil water content at other depths was close to saturation. Moreover, 10 days after the end of infiltration, the soil moisture of greater bulk density in the same soil layer is larger than it was of smaller bulk density. After infiltration, redistribution causes the soil water content to increase with increasing soil depth, although the redistribution process in Yellow-brown soil lags behind that of Lou soil. In the initial stage of soil water redistribution, smaller bulk density was linked to greater water storage capacity in the soil. As time progresses, soils with smaller bulk densities lose water faster.

Considering that the gravel-mulched land is used for crop planting after covering soils, the soil should stabilize and retain water, we suggest that the soil bulk density should be no less than 1.5 g/cm^3 when Lou soil was chosen to cover on gravel-mulched land, and not less than 1.4 g/cm^3 for Yellow-brown soil.

http://www.aloki.hu ● ISSN 1589 1623 (Print) ● ISSN 1785 0037 (Online)
DOI: http://dx.doi.org/10.15666/aeer/1706_1403914052

In order to further clarify the law of water infiltration after covering soil in the gravel-mulched areas, the effect of gravel particle size on water infiltration and the migration of nutrients may be studied with undisturbed soil in future researches.

Acknowledgements. This study was funded by the Fundamental Research Funds for the Central Universities, CHD (No.300102279502); we also acknowledge TopEdit LLC for linguistic editing and proofreading during the preparation of this manuscript.

REFERENCES

[1] Cerdà, A. (2001): Effects of rock fragment cover on soil infiltration, interrill runoff and erosion. – European Journal of Soil Science 52(1): 59-68.
[2] Chen, L., Huang, Z., Gong, J., Fu, B., Huang, Y. (2007): The effect of land cover/vegetation on soil water dynamic in the hilly area of the Loess Plateau, China. – Catena 70(2): 0-208.
[3] Fu, B., Wang, Y. K., Zhu, B., Wang, D. J., Wang, X. T., Wang, Y. Q., Ren, Y. (2008): Experimental study on rainfall infiltration in sloping farmland of purple soil. – Transactions of the Chinese Society of Agricultural Engineering 24(7): 39-43.
[4] Hillel, D. (1998): Environmental Soil Physics. – Academic Press, New York.
[5] Kang, J. L., Yang, J., Liu, Y. J., Tu, A. G. (2016): Impacts of soil initial water content and bulk density on infiltration law of red soil. – Journal of Soil and Water Conservation 30(1): 122-126.
[6] Li, Z. M., Zhou, Q., Wang, H., Lu, X. (2009a): Influence of bulk density on the characteristic of water solute transport in red soil. – Journal of Soil and Water Conservation 23(5): 101-103.
[7] Li, Z., Wu, P. T., Feng, H., Zhao, X. N., Huang, J., Zhuang, W. H. (2009b): Simulated experiment on effect of soil bulk density on soil infiltration capacity. – Transactions of the Chinese Society of Agricultural Engineering 25(6): 40-45.
[8] Liang, W. L., Kosugi, K., Mizuyama, T. (2015): Soil water redistribution processes around a tree on a hillslope: the effect of stemflow on the drying process. – Ecohydrology 8(8): 1381-1395.
[9] Mandal, U. K., Rao, K. V., Mishra, P. K., Vittal, K. P. R., Sharma, K. L. (2005): Soil infiltration, runoff and sediment yield from a shallow soil with varied stone cover and intensity of rain. – European Journal of Soil Science 56(4): 435-443.
[10] Mehuys, G. R., Stolzy, L. H., Letey, J. (1975): Effect of stones on the hydraulic conductivity of relatively dry desert soil. – Soil Science Society of America Journal 39(1): 37-42.
[11] Novák, V., Kňava, K. (2012): The influence of stoniness and canopy properties on soil water content distribution: simulation of water movement in forest stony soil. – European Journal of Forest Research 131(6): 1727-1735.
[12] She, D. L., Liu, Y. Y., Liu, D. D., Xu, C. L., Qu, X., Chen, Y. L., Deng, L. Y., Yu, S. E. (2012): Study on impact of soil bulk density on infiltration properties of silt soil in coastal reclamation regions. – Research of Agricultural Modernization 33(6): 749-752+761.
[13] Song, H. Y., Li, Y., He, C. S. (2013): Infiltration models for different textures of water-repellent soils. – Journal of Drainage and Irrigation Machinery Engineering 31(7): 629-635.
[14] Sun, Z. H., Zhang, Y., Wang, H. Y. (2017): Effect of soil bulk density on soil infiltration in land or organic reconstruction on based on HYDRUS-1D model. – Land Develop Land Development and Engineering Research 2(7): 20-27.
[15] Tejedor, M., Neris, J., Jiménez, C. (2013): Soil properties controlling infiltration in volcanic soils. – Egu General Assembly 15(1): 202-212.

http://www.aloki.hu ● ISSN 1589 1623 (Print) ● ISSN 1785 0037 (Online)
DOI: http://dx.doi.org/10.15666/aeer/1706_1403914052

[16] Wang, X. Y., Cai, C. F., Li, H., Xie, D. T. (2017): Influence of rock fragments on bulk density and pore characteristics of purple soil in Three-Gorge Reservoir area. – Acta Pedologica Sinica 54(2): 379-386.
[17] Yi, L., Zhang, Z. X., Wang, X., Liu, B., Zuo, L. J., Zhao, X. L., Wang, J. (2013): Spatial-temporal change of major reserve resources of cultivated land in China in recent 30 years. – Transactions of the Chinese Society of Agricultural Engineering 29(6): 1-12.
[18] Zavala, L. M., Jordán, A., Bellinfante, N., Gil, J. (2009): Relationships between rock fragment cover and soil hydrological response in a Mediterranean environment 2010. – Soil Science and Plant Nutrition 56(1): 95-104.
[19] Zeng, J., Fei, L. J., Pei, Q. B. (2017): Influence of soil bulk density on soil water infiltration characteristics in water vertical movement for red loams. – Journal of Drainage and Irrigation Machinery Engineering 35(12): 1081-1087.
[20] Zhang, Y., Li, Z. B., Dong, Q. G. (2017): Effects of covering soil thickness of bare rock gravel land on soil moisture. – Yangtze River 48(24): 52-55.
[21] Zhang, Y., Li, Z. B., Dong, Q. G., Yuan, S. L. (2018): Experimental study on influence of overburden thickness on soil particle transport process in bare rock gravel land. – Journal of Soil and Water Conservation 32(2): 87-91+103.
[22] Zhao, Y. G., Zhao, S. W., Cao, L. H., Liang, X. F. (2008): Soil structural characteristics and its effect on infiltration on abandoned lands in semi-arid typical grassland areas. – Transactions of the Chinese Society of Agricultural Engineering 24(6): 14-20.
[23] Zhou, B. B., Shao, M. A., Shao, H. B. (2009): Effects of rock fragments on water movement and solute transport in a Loess Plateau soil. – Comptes Rendus Geoscience 341(6): 462-472.

http://www.aloki.hu ● ISSN 1589 1623 (Print) ● ISSN 1785 0037 (Online)
DOI: http://dx.doi.org/10.15666/aeer/1706_1403914052

CHANGES IN PHYSICAL, MECHANICAL, SHRINKING AND SWELLING PROPERTIES OF PINE WOOD SPECIES TREATED WITH SALT NATURAL GEOTHERMAL WATERS AS ENVIRONMENTALLY SAFE RESOURCES

VAR, A. A.* – KARDAŞ, İ.

Department of Forest Biology and Wood Preservation Technology, Faculty of Forestry, Isparta University of Applied Sciences, 32260 Cunur, Isparta, Turkey
(phone: + 90-246-211-4986; fax: +90-246-211-3948)

**Corresponding author*
e-mail: alivar@isparta.edu.tr; phone: +90-533-760-2309; fax: + 90-246-211-3948

(Received 27th May 2019; accepted 28th Aug 2019)

Abstract. The purpose of this study was to study the effects of salt natural geothermal water (SNGW) treatment on the physical, mechanical, shrinking and swelling properties of wood materials from two pine species. This study used the SNGW of Eynal, Çitgöl, and Naşa from Kutahya in Turkey on sapwood samples of black pine (*Pinus nigra* Arnold.) and Brutia pine (*Pinus brutia* Ten.). The absorption, retention, density, moisture content, modulus of rupture (MOR), modulus of elasticity in bending (MOE), compression strength parallel to the grain (CSPG), shrinking, and swelling values were measured for the treated and non-treated wood samples. The results showed that the absorption and retention values increased by depending on the concentrations of the dissolved salts in the SNGW used. In addition, the density and moisture content values of the SNGW-treated pine wood species were significantly higher than those of the untreated wood, whereas the values of MOR, MOE, CSPG, shrinking, and swelling were lower. In general, the Eynal treatment had the highest effect on pine species' wood properties, whereas the Naşa treatment had the least effect.
Keywords: *renewable, preservative, impregnation, ecofriendly, treatment*

Introduction

The idea of eliminating the environmentally harmful aspects of industrial processes has led researchers to develop not only new alternative resources but also new environmentally compatible wood preservatives. New alternatives alleviate some environmental problems caused by the wood preservative industry. Hence, natural resources have been used and preferred for worldwide application to limit and control pollution (Bozkurt et al., 1993). SNGW can be considered as an environmentally safe sustainable natural resource for wood preservatives. In recent years, research into wood preservatives has led to the development of several new methods that are able to produce pine wood with properties near those treated by conventional methods. The use of SNGW in the impregnation processes is a new idea and could be a useful approach.

It is well-known that geothermal waters naturally contain high amounts of dissolved chemicals, including various mineral salts; and this resource is valuable for different areas, such as heating, livestock farms, drying of organic materials, recreation, and health tourism, all of which depend on the water temperature and the chemicals contained in the water. In this regard, the use of geothermal waters has expanded appreciably from agriculture, livestock, and medical applications (Ilgar, 2005).

Moreover, wood impregnation with preservatives is a process that often uses synthetic and toxic chemicals that are not environmentally compatible. New

http://www.aloki.hu ● ISSN 1589 1623 (Print) ● ISSN 1785 0037 (Online)
DOI: http://dx.doi.org/10.15666/aeer/1706_1405314068

environmentally safe chemicals are needed to preserve the wood that is used for indoor and outdoor applications. Due to their high levels of dissolved mineral salts, geothermal waters have potential as wood preservatives, in which this resource may resolve some environmental issues facing the wood preservative industry. For this reason, these salt natural waters should be studied as a wood preservative agent.

To date, much research has been conducted on the physical, mechanical, shrinking and swelling properties of various impregnated wood species. Examples of these species are European beech, pine, spruce, Scots pine, yellow poplar, and red oak treated with waterborne preservatives such as chromated copper arsenate (CCA), ammoniacal copper arsenate (ACA), ammoniacal copper zinc arsenate (ACZA), and alkaline copper quaternary (ACQ) compounds (Winandy, 1995); pine treated with linseed oil (Megnis et al., 2002); yellow pine treated with CCA, ACQ-1900, ACQ-2200, Tanalith-E 3491, and Wolmanit CX-8 (Yildiz et al., 2004); oriental beech, oak, Scots pine, oriental spruce, and Uludag fir treated with Imersol-Aqua (Ors et al., 2005); pine and American beech treated with copper chloride, sodium borate, and phenol-formaldehyde resin-pyrolytic oil (Mourant et al., 2007); jack pine and sugar maple treated with copper chloride, copper chloride-sodium borate mixture, and phenol formaldehyde-pyrolytic oil resins (Mourant et al., 2008); beech and pine treated with aqueous solution of borates (Simsek et al., 2010); rowan treated with Tanalith-E, Vacsol Azure, Imersol-Aqua, borax, and boric acid (Keskin et al., 2013); fir treated with citric acid (Ville et al., 2014); oriental beech treated with Turkish sweetgum balsam as an aromatic resinous wood preservative (Degirmentepe et al., 2015); and beech, walnut, poplar, ash, and pine treated with Tanalith-E (Keskin and Daglioglu, 2016); shrinking and swelling minimization of wood treated with the synthetic resin-forming materials (Stamm and Seborg, 1936); beech wood impregnated with NH_3 (Bariska, 1975); Corsican pine wood treated with ammonia (Coles and Walker, 1978); swelling of wood in liquid ammonia (Stamm, 1955). Some of the wood preservatives mentioned above are now prohibited in several countries, and are being used less frequently in other countries due to their negative impacts to the environment. Currently, new research is being conducted to develop new impregnation agents for wood preservation.

In contrast, the economic use of SNGW could only be possible by evaluating the dissolved chemicals in those waters, including various minerals. However, there are few studies that evaluate geothermal water properties. Var (2009) discussed whether geothermal waters could potentially be used for wood preservation. Another study reported results that included absorption, retention, and swelling values of Brutia pine treated with geothermal waters from Izmir, Turkey (Var et al., 2013). A third study examined the effects of condensed geothermal waters from Aydin, Turkey on wood properties (Yaldiz and Var, 2017). In these investigations, which study the wood treated with geothermal waters, a definite result was not obtained regarding the wood's physical and mechanical properties. The potential wood impregnants content in geothermal waters was observed, as well as some properties such as absorption, retention, and swelling of wood treated with such natural saltwater. Also, this observation showed that more than half of the naturally dissolved minerals contained in the SNGW could be used as potential wood preservative in the wood preservation formulations; the absorption and retention properties of treated wood had increased due to the concentration of naturally dissolved salts in the SNGW; the swelling properties of treated wood decreased compared to the untreated control wood. However, it has been noted that there are few studies that have reported the physical, mechanical, shrinking

http://www.aloki.hu ● ISSN 1589 1623 (Print) ● ISSN 1785 0037 (Online)
DOI: http://dx.doi.org/10.15666/aeer/1706_1405314068

and swelling properties of wood that was impregnated with preservatives. For instance, Var et al. (2017) only examined the modulus of elasticity and compressive strength of wood impregnated with hot geothermal waters. Sen et al. (2017) only reported some of the mechanical properties of wood treated with geothermal and mineral waters.

It should be realized that geothermal waters contain diverse mineral salts at various concentrations. These natural resources could be useful as waterborne wood impregnation agents for wood preservation (Var, 2009). It is known that waterborne wood impregnation agents affect the mechanical properties of wood. These effects can be related to many factors, such as types of dissolved mineral salts within the natural water, types of woods treated, sizes and grades of woods being treated, and environmental conditions of wood exposure; other influencing factors include the type of preservative used and its retention. However, the effects of SNGW on wood properties have not been reported. Such studies are needed to determine if SNGW have certain effects on the properties of wood.

In this paper, the goal is to investigate the effects of treatment with various SNGW on the physical, mechanical, shrinking and swelling properties of various pine wood species. The SNGW contain various inorganic ions such as chloride, sodium, calcium, sulfate, potassium, magnesium, silicate, fluoride, boron, ammonia, and borate. These inorganics are used as water-based wood preservatives added to wood preservative formulations (Var, 2009). When pine wood materials are treated with SNGW, such dissolved ions can affix to the cell walls, lumens, and intercellular spaces, or react with wood constituents, to result in precipitates within the wood structure. In contrast, it is still challenging to find natural and environmentally compatible processes for wood protection. Hence, the determination of effects on such properties of pine wood of the natural saltwaters can be useful as an environmentally friendly wood preservative. In this sense, the use of SNGW in the wood protection systems can also reduce the environmental problems related to the health and ecology when compared to other conventional wood preservatives.

Materials and methods

Materials

Preparation of wood specimens

Two different pine wood species, black pine (*Pinus nigra* Arnold.) and Brutia pine (*Pinus brutia* Ten.), were collected from a natural forest located in Isparta, Turkey. The specimens were obtained from air-dried sapwood portions in the radial direction in accordance to ISO 3129 (2012) standard. Clear and defect-free specimens were prepared with the following dimensions: 30 mm radial (R) × 30 mm tangential (T) × 15 mm longitudinal (L) for the absorption and retention tests; 20 mm R × 20 mm T × 30 mm L for the density, moisture content, shrinking and swelling tests; 20 mm R × 20 mm T × 300 mm L for the modulus of rupture (MOR) and modulus of elasticity in bending (MOE) tests; and 20 mm R × 20 mm T × 100 mm L for the compression strength parallel to grain (CSPG) tests. Prior to wood impregnation treatments, 15 samples for each test were placed in a conditioning cabinet, and held at a relative humidity of 65% ± 3% and temperature of 20 °C ± 2 °C until a stable mass was obtained in accordance to the ISO 13061-1 (2014) standard. To avoid potential

http://www.aloki.hu ● ISSN 1589 1623 (Print) ● ISSN 1785 0037 (Online)
DOI: http://dx.doi.org/10.15666/aeer/1706_1405314068

fluctuations in the moisture content, the samples were placed into plastic bags and stored until the treatments were conducted.

Preparation of SNGW

SNGW was obtained from the Eynal (E-6), Çitgöl (C-1), and Naşa (N-1) geothermal fields of Kutahya, Turkey (*Table 1; Fig. 1*). These waters were refrigerated at 23 °C ± 2 °C in 20-L containers. The SNGW was used without filtration and sterilization in the wood impregnation processes. The chemical compositions of SNGW, their concentrations, and their dosage levels have been described in Var et al. (2015). This study reported that SNGW contained boron, sodium, potassium, calcium, magnesium, arsenic, chlorine, fluorine, aluminum, silicon dioxide, sulfate, and ammonia. Also, the study determined that the highest concentration (1930.47 mg/L) was for the E-6 geothermal, and the lowest concentration (1421.56 mg/L) was for the N-1 geothermal.

Table 1. *The GPS coordinates of the survey localities from Turkey's Kutahya province*

Survey localities	GPS coordinates
Eynal	39.126875, 28.995479
Çitgöl	39.132907, 28.967043
Naşa	39.143784, 28.961431

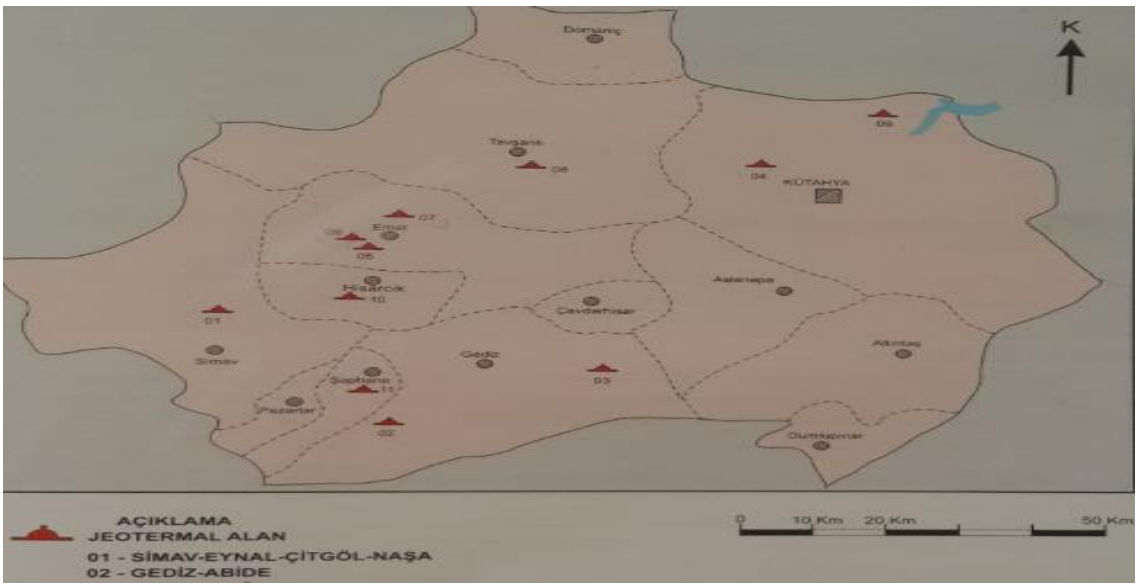

Figure 1. *Geothermal area map of the survey localities in Kutahya, Turkey (Akkuş et al., 2005)*

Methods

Treatment process

The treatment process was performed at room temperature in the laboratory. Wood samples were treated with one of the three SNGW in accordance to the ASTM D1413–07e1 (2007) standard. A dipping treatment was used for the wood impregnation process.

http://www.aloki.hu ● ISSN 1589 1623 (Print) ● ISSN 1785 0037 (Online)
DOI: http://dx.doi.org/10.15666/aeer/1706_1405314068

The samples were immersed in the selected SNGW for 24 h. After the treatment, the excess SNGW was wiped off the surfaces of the sample. The treated specimens were immediately weighed to determine the gross SNGW uptake; afterwards, the specimens were then conditioned at 20 °C ± 2 °C and 60% ± 3% relative humidity prior to physical, mechanical, swelling, and shrinking testing in accordance to ISO 13061-1 (2014).

Measurement of physical properties

The physical properties of the wood samples were determined in accordance to the following international laboratory standards: ASTM D1413-07e1 (2007) for absorption and retention values, ISO 13061-2 (2014), for density measurement, and ISO 13061-1 (2014) for moisture content measurement.

Measurement of mechanical properties

The mechanical properties of the wood samples were determined in accordance to the following international laboratory standards: ISO 13061-3 (2014) for modulus of rupture in bending (MOR), ISO 13061-4 (2014) for modulus of elasticity in bending (MOE), and ISO 13061-17 (2017) for compression strength parallel to the grain (CSPG). Mechanical tests were performed with a 4000 kp universal testing machine (Marestek, Istanbul, Turkey) using a constant 6 $mm \cdot min^{-1}$ crosshead speed.

Measurement of shrinking and swelling properties

The shrinking and swelling properties for the wood samples were determined accordance to the following international laboratory standards: ISO 4469 (1981) for radial and tangential shrinking, ISO 4858 (1982) for volumetric shrinking, ISO 4859 (1982) for radial and tangential swelling, ISO 4860 (1982) for volumetric swelling, and Kantay (1978) and Bozkurt et al. (1993) for anisotropic shrinking and swelling.

Statistical analysis of data

The data collected from the experimental measurements were analyzed using an analysis of variance (ANOVA) at a 95% significance level ($p \leq 0.05$); statistical comparisons among the groups were made using the Duncan test. A computerized program, SPSS 20 Statistics (IBM Corp., New York, NY, USA), was used for the analyses. Statistical evaluations *via* the Duncan test were made using homogeneity groups, in which different letters reflected significant differences among the groups.

Results and discussion

Physical properties

Table 2 shows the physical data for absorption, retention, density, and moisture content tests for both pine species treated with salt natural geothermal waters. It appeared that the SNGW had a clear effect on these physical properties. The E-6 treatment yielded the highest measured physical values for both wood species. For black pine, the highest absorption (2.06 g), retention (0.60 kg/m^3), density (0.56 g/cm^3), and moisture content (9.89%) values were obtained. Likewise, for Brutia pine, the highest values for absorption of 2.41 g, retention of 0.72 kg/m^3, density of 0.59 g/cm^3, and

http://www.aloki.hu ● ISSN 1589 1623 (Print) ● ISSN 1785 0037 (Online)
DOI: http://dx.doi.org/10.15666/aeer/1706_1405314068

moisture content of 10.57% were observed for the E-6 treatment. Furthermore, the N-1 treatment yielded the lowest measured physical values of 1.82 g (absorption), 0.48 kg/m^3 (retention), 0.53 g/cm^3 (density), and 9.44% (moisture content) for black pine, and 2.15 g (absorption), 0.52 kg/m^3(retention), 0.58 g/cm^3 (density), and 9.93% (moisture content) for Brutia pine.

Table 2. *Physical properties of pine wood species treated with SNGW*

Wood species	Geothermal water	Absorption (g)	Retention (kg/m^3)	Density (g/cm^3)	Moisture (%)
Black pine	Control*	-	-	0.52 (0.05) e	9.11 (0.70) h
	N-1	1.82 (0.22**) a	0.48 (0.04) c	0.53 (0.04) ef	9.44 (0.83) h
	C-1	1.96 (0.16) ab	0.56 (0.12) d	0.55 (0.04) ef	9.75 (0.79) i
	E-6	2.06 (0.44) b	0.60 (0.08) d	0.56 (0.06) f	9.89 (0.24) i
Brutia pine	Control*	-	-	0.57 (0.06) p	9.26 (0.48) q
	N-1	2.15 (0.31) j	0.52 (0.07) l	0.58 (0.07) p	9.93 (0.56) r
	C-1	2.24 (0.26) jk	0.63 (0.09) m	0.58 (0.05) p	10.39 (0.38) rs
	E-6	2.41 (0.35) k	0.72 (0.07) n	0.59 (0.05) p	10.57 (1.29) s

*Untreated. **Values in parentheses are the standard deviation; the same letters in each column indicate no statistical difference at the 95% confidence level among treatments

There were no significant differences found between the N-1 and C-1 treatments in the amount of absorption for both wood species, whereas there was a significant difference between E-6 and N-1 (*Table 2*). With regards to retention, there were considerable differences among the SNGW. There was no remarkable difference in density among the control, N-1, and C-1 treatments for black pine, whereas there was a noticeable difference between the E-6 and control. Moreover, there was no substantial difference among the three SNGW used to treat the Brutia pine. With regards to moisture content, there was no significant difference between the control, N-1, and C-1 treatments versus the E-6 treatment for black pine, while there was a significant difference among the E-6, N-1, and control treatments. For Brutia pine, there was no considerable difference between the N-1 versus C-1, and E-6 versus C-1, but there was a remarkable difference among the E-6, control, and N-1 treatments.

Based on these results, it was deduced that SNGW with higher concentrations of dissolved inorganics resulted in higher values of measured physical properties. Hence, the values measured for absorption, retention, density, and moisture content of the treated wood increased depending on which SNGW was used, and the concentration of dissolved salt species the SNGW contained. Such increases in physical properties were attributed to the dissolved salts in the SNGW affixing to the walls and lumens of the wood fibers, which increased the mass, as well as the volume (by swelling) of the wood. In the treatment with chemical preservative solutions it has been reported that chemical substances attached to the cell walls and lumens, resulting in an increase in mass and volume of the treated wood (Ozciftci and Batan, 2009). Ammoniacal-based waterborne wood preservatives are commonly used for wood protection (Yildiz et al., 2004). Ammonia can react with lignin and hemicelluloses of the wood cell wall (Ostmeyer, 1987; Winandy, 1995) to cause the wood to swell, and thereby increase the penetration of chemicals within its structure (Megnis et al., 2002). However, the absorption increase could also have been attributed to the expansion of lumens within the wood fibers,

http://www.aloki.hu ● ISSN 1589 1623 (Print) ● ISSN 1785 0037 (Online)
DOI: http://dx.doi.org/10.15666/aeer/1706_1405314068

which absorb the SNGW into the wood structure (Ors and Keskin, 2001). The retention increase could result from affixation or precipitate of the wood preservatives to the cell walls, lumens, and intercellular spaces due to passage pairs performing the liquid flow within the wood structure (Ozciftci and Batan, 2009). Several investigations have stated that chemical treatments with different water-soluble preservatives, such as copper chrome boron (CCB) (Peker et al., 1999), CCA (Temiz et al., 2004; Sreeja and Edwin, 2013; Gezer and Cooper, 2016), and ammonium tetrafluoroborate (Atilgan and Peker, 2012), increase the retention value of the treated wood sample, which is also related to the concentration of the wood preservatives in the solution. The increase in moisture content of the treated versus the untreated sample may be caused by the absorption of water by the wood structure from the SNGW (Ors and Keskin, 2001). Moisture levels increase upon wood exposure to water-based preservatives, which could be due to the high amount of water that is used as the solvent (Yildiz et al., 2004). In addition, there are hygroscopic salts that absorb and retain water within the wood fiber walls, which causes the wood fibers to swell (Militz, 1993). Moreover, it has been reported that waterborne wood preservatives, such as borate (Simsek and Baysal, 2015), ammonium tetrafluoroborate (Atilgan and Peker, 2012), silicon dioxide (Dong et al., 2015), boric acid, borax, and sodium perborate (Toker, 2007), increase the density of the treated wood when compared to the untreated control. In certain studies, this increase in wood density due to preservative treatment has been shown to be statistically significant (Simsek and Baysal, 2015). Other defined parameters of wood preservatives, such as its toxicity against wood-destroying agents and its leaching, as well as aging, should be examined. Ors et al. (2005) and Var (2013) studied wood that was treated with Imersol-Aqua and SNGW, respectively, and reported that such treatments increased the values of retention, density, and moisture content. Hence, it was concluded that the results in *Table 2* were consistent with the reported data in the literature.

Mechanical properties

The results for MOR, MOE, and CSPG for the pines treated with the SNGW is presented in *Table 3*. For black pine, the highest MOE values were obtained with the N-1 treatment (11175.22 N/mm^2), while the C-1 treatment gave the maximum MOR (91.41 N/mm^2) and CSPG (42.31 N/mm^2). The lowest MOR values were observed for the C-1 treatment (88.05 N/mm^2), whereas the lowest MOE and CSPG values were observed for the E-6 treatment (9759.96 N/mm^2 and 39.71 N/mm^2, respectively). Additionally, the MOR, MOE, and CSPG values of the untreated control samples were observed to be 99.55 N/mm^2, 11365.18 N/mm^2, and 44.54 N/mm^2, respectively. For Brutia pine, the highest CSPG (41.63 N/mm^2) was observed for the C-1 treatment, whereas the N-1 treatment had the highest MOR (86.82 N/mm^2) and MOE (11015.93 N/mm^2). The lowest MOR (79.71 N/mm^2), MOE (10484.65 N/mm^2), and CSPG (37.89 N/mm^2) were noted for the E-6, C-1, and N-1 treatments, respectively.

Statistically significant differences for the MOR and CSPG values were noted for the treatments of both pines versus the untreated controls (*Table 3*). With regards to MOE values for black pine, there were significant differences in the C-1 and E-6 treatments versus the control, but not for the N-1 treatment. There were no significant differences observed among the geothermal water treatments for Brutia pine in the MOE values when compared to the control. Moreover, no significant differences in the MOR were noted among the geothermal water treatments, whereas there were significant differences detected between the E-6 and N-1 treatments for Brutia pine. No significant

http://www.aloki.hu ● ISSN 1589 1623 (Print) ● ISSN 1785 0037 (Online)
DOI: http://dx.doi.org/10.15666/aeer/1706_1405314068

differences in CSPG were observed between the N-1 and E-6 treatments for black pine, and no significant differences were observed between the C-1 and E-6 treatments for Brutia pine. In general, these findings indicated that SNGW treatments significantly decreased the mechanical properties of the two wood species when compared to the respective untreated controls. This observation was attributed to the fact that geothermal salts or minerals tend to increase the equilibrium moisture content of the wood samples.

Table 3. *Mechanical properties of pine wood species treated with SNGW*

Wood species	Geothermal water	MOR (N/mm^2)	MOE (N/mm^2)	CSPG (N/mm^2)
Black pine	Control*	99.55 (5.60**) a	11365.18 (966.70) c	44.54 (2.48) f
	N-1	88.05 (3.68) b	11175.22 (637.15) c	40.16 (1.80) g
	C-1	91.41 (4.27) b	10545.24 (998.78) d	42.31 (0.91) h
	E-6	89.92 (4.84) b	9759.96 (691.44) e	39.71 (1.36) g
Brutia pine	Control*	94.38 (5.76) i	11193.62 (683.80) l	43.23 (2.24) m
	N-1	86.82 (4.05) j	11015.93 (1079.94) l	37.89 (1.30) n
	C-1	83.17 (10.22) jk	10484.65 (1249.53) l	41.63 (0.98) o
	E-6	79.71 (4.07) k	10892.84 (1568.33) l	41.61 (0.91) o

*Untreated. **Values in parentheses are the standard deviation; the same letters in each column indicate no statistical difference at the 95% confidence level among treatments

These results indicated that all of the treated samples had lower mechanical strength values when compared to the untreated control samples. This decrease could also have been due to the acidity of the SNGW, which caused some hydrolysis of the wood structure. Bozkurt and Erdin (1997) reported that if the moisture content of wood increases at temperatures above 0 °C, then the resistance of wood against the forces causing deformation can decrease, and the chemical solutions whose pH value is in the acidic zone can strengthen the hydrolysis of wood polysaccharides, and therefore, lower the mechanical properties of wood materials. The SNGW contain many chemical components that are commonly found in waterborne wood preservation formulations (Var, 2009). Such substances account for more than half (55% to 87%) of the total chemicals contained in SNGW (Var and Yaldiz, 2017). Wood treatments with such chemicals generally decrease the mechanical properties of the substrate because the waterborne preservatives physically react with the cellular wood components (Winandy, 1996). Many acidic substances used in waterborne formulations hydrolyze wood sugar components, which can decrease the strength values of the wood structure (Hamel, 1988). It has been reported that different concentration levels of waterborne wood preservatives result in more than a 20% reduction in CSPG values for Calabrian pine and beech (Toker et al., 2008). It has been determined that waterborne treatments have caused some decreases in other mechanical properties of wood materials (Laks and Palardy, 1990). The effect of different waterborne wood preservatives is related to the chemistry of the system and the severity of the fixation reaction (Winandy, 1996). Waterborne systems, such as borates, decrease the CSPG and MOR values of the impregnated wood. As the borate concentration in this system increases, the CSPG and MOR values of the impregnated wood decrease (Simsek et al., 2010). In other studies, it has been reported that waterborne formulations, such as boric acid (Colakoglu et al., 2003; Ayrilmis et al., 2005), borate (Wu et al., 2002; Simsek et al., 2010), CCA (Hesp

http://www.aloki.hu ● ISSN 1589 1623 (Print) ● ISSN 1785 0037 (Online)
DOI: http://dx.doi.org/10.15666/aeer/1706_1405314068

and Watson, 1964; Yildiz et al., 2004), and boron compounds (Toker et al., 2009), decreased the MOR and MOE of the preserved wood compared to the untreated control.

The measured results in *Table 3* were compared to the results in certain studies; for example, Sen et al. (2017) and Var et al. (2017) studied the properties of wood treated with the geothermal and rich mineral waters, and geothermal hot waters, respectively. It was reported that such treatments decreased the values of MOR, MOE, and CSPG. The data in *Table 3* indicated that the treatment of pine woods with SNGW lowered their mechanical strength values. Hence, it was concluded that these observations are consistent with the findings reported in the aforementioned studies. According to these results, it could be useful that the wood materials from pine woods treated with SNGW are used under the conditions of air-dry moisture content for the potential use areas exposed to the effects of mechanical strengths such as MOR and CSPG. However, for potential applications of wood materials, the users of pine woods should consider the physical and mechanical properties such as strength type and moisture content for pine woods treated with such SNGW.

Shrinking properties

Table 4 presents the data for shrinking tests for both pine wood species treated with SNGW. For black pine, the lowest shrinking values for the tangential of 5.89% and anisotropic of 1.19 were measured for the N-1 treatment, while the C-1 and E-6 treatments gave the minimum shrinking values for the radial (4.49%) and volumetric (10.36%), respectively. Also, the C-1 treatment gave the highest tangential (6.18%) and anisotropic (1.38) shrinking values, while the maximum radial (4.96%) and volumetric (10.77%) shrinking were obtained with the N-1 treatment. For Brutia pine, the lowest radial (5.29%) and volumetric (12.00%) shrinking were observed for the C-1 treatment, whereas the E-6 treatment yielded the lowest tangential (7.02%) and anisotropic (1.13) shrinking. Furthermore, the N-1 treatment gave the highest measured shrinking values of 7.72% (tangential) and 13.17% (volumetric), while the highest radial (6.25%) and anisotropic (1.35) shrinking were noted for the E-6 and C-1 treatments, respectively.

Table 4. *Shrinking properties of pine wood species treated with SNGW*

Wood species	Geothermal waters	Radial shrinking (%)	Tangential shrinking (%)	Volumetric shrinking (%)	Anisotropic shrinking
Black pine	Control*	5.52 (0.18**) a	6.94 (0.22) d	12.20 (0.32) g	1.26 (0.04) j
	N-1	4.96 (0.22) b	5.89 (0.15) e	10.77 (0.28) h	1.19 (0.06) k
	C-1	4.49 (0.10) c	6.18 (0.20) f	10.45 (0.29) i	1.38 (0.05) l
	E-6	4.53 (0.14) c	6.13 (0.17) f	10.36 (0.28) i	1.35 (0.05) l
Brutia pine	Control*	6.08 (0.33) m	7.48 (0.36) p	13.11 (0.59) r	1.23 (0.08) t
	N-1	5.91 (0.31) m	7.72 (0.36) p	13.17 (0.65) r	1.31 (0.10) u
	C-1	5.29 (0.27) n	7.10 (0.38) q	12.00 (0.40) s	1.35 (0.07) u
	E-6	6.25 (0.35) o	7.02 (0.47) q	12.83 (0.50) r	1.13 (0.09) w

*Untreated. **Values in parentheses are the standard deviation; the same letters in each column indicate no statistical difference at the 95% confidence level among treatments

Statistically significant differences for the shrinking values were found for the treatments of black pine versus the non-treated controls, except for the C-1 and E-6

http://www.aloki.hu ● ISSN 1589 1623 (Print) ● ISSN 1785 0037 (Online)
DOI: http://dx.doi.org/10.15666/aeer/1706_1405314068

treatments (*Table 4*). The similar situations were observed between the N-1 treatment and other geothermal water treatments for the black pine. For Brutia pine, the significant differences between the C-1 and E-6 treatments were found for all shrinking values, excluding the N-1 treatment, when compared to the untreated control. With regards to shrinking, for Brutia pine, there were significant differences among all geothermal water treatments in the radial values, while no significant differences in the volumetric values were found between the N-1 and E-6 treatments; no significant differences in the anisotropic values were also observed between the N-1 and C-1 treatments. Furthermore, the significant differences between the C-1 and E-6 treatments were noted for the radial, volumetric, and anisotropic shrinking for Brutia pine, while no significant differences were yielded for the tangential shrinking.

Here results showed that the SNGW treatment significantly decreased the shrinking properties of treated samples versus the non-treated samples for both pine woods. For black pine, the anisotropic shrinking reduced in the N-1 treatment, whereas it increased in the E-6 treatment; but the vice versa was for Brutia pine. Moreover, for black pine, the N-1 treatment significantly reduced the tangential and anisotropic shrinking versus the C-1 and E-6 treatments, while it increased the radial and volumetric shrinking. Also, both the C-1 and E-6 treatments had not indicated a significant effect on the shrinking properties of black pine. For Brutia pine, the E-6 treatment significantly increased the radial shrinking when compared to the N-1 and C-1 treatments, whereas the C-1 treatment significantly had reduced the volumetric shrinking versus the N-1 treatment. However, the N-1 treatment had significantly improved tangential and anisotropic shrinking of Brutia pine when compared to the E-6 treatment.

According to these findings, it was observed that the shrinking values of pine woods treated with the distilled water after the SNGW treatment lowered when compared to the non-treated control wood. This lowing could be due to the following: In the SNGW, the geothermal chemicals that are initially absorbed by pine wood could plasticize the lumen linings and cell walls within the wood structure (Stamm, 1955). The woody cells that are lose its plasticity during evaporation of the SNGW from the lumen system within the wood structure could force the more plastic cells to shrink inwards, towards them, and cause an overall shrinking in the wood volume (Pollisco et al., 1971.

The results in *Table 4* were compared to the findings in some studies; for instance, Bozkurt and Erdin (1997), and Bozkurt et al. (1993) had studied on the wood technology, and wood impregnation technique, respectively. It was reported that the shrinking values of black pine are 5.60% for the radial, 8.20% for the tangential, 13.90% for the volumetric, and 1.46 for the anisotropic. Likewise, it was nopted that the shrinking values of Brutia pine are 4.90% for the radial, 6.80% for the tangential, 12.20% for the volumetric, and 1.39 for the anisotropic. Also, some of earlier studies had investigated the properties of wood impregnated with the ammonia (Bariska, 1975; Coles and Walker, 1978), the liquid ammonia (Stamm and Seborg, 1936), and the ammonia vapor (Pollisco et al., 1971). It was noted that such treatments decreased the shrinking properties of wood. The obtained results in *Table 4* showed that SNGW treatments lowered the shrinking values of pine woods. Hence, it was concluded that these results in *Table 4* were agree with the findings in the aforesaid studies. According to these results, it could be advantageous that the pine woods treated with SNGW is utilized under the low relative humidity conditions for potential uses. Otherwise, in such treated pine woods, it could be an overall volumetric shrinking and dimensional change.

http://www.aloki.hu ● ISSN 1589 1623 (Print) ● ISSN 1785 0037 (Online)
DOI: http://dx.doi.org/10.15666/aeer/1706_1405314068

Swelling properties

The results of swelling tests for both pine wood treated with the SNGW is shown in *Table 5*. For black pine, the lowest radial (4.15%) and volumetric (11.20%) swelling values were obtained with the N-1 treatment, while the E-6 treatment gave the minimum volumetric (11.45%) and anisotropic (1.37) swelling values. The highest tangential and volumetric swelling values were measured for the C-1 treatment (7.08% and 12.00%, respectively), whereas the E-6 and N-1 treatments had the highest radial (4.72%) and anisotropic (1.63) swelling values, respectively. For Brutia pine, for the radial, tangential and volumetric swelling, the C-1 treatment gave the lowest values (5.08%, 7.20%, and 12.65%, respectively), while the highest values were observed to be 5.76%, 7.79%, and 14.00%, respectively (with the N-1 treatment). Additionally, for the anisotropic swelling, the highest value was noted for the C-1 treatment (1.43), whereas it was reported that the minimum value is 1.28 for the E-6 treatment.

Table 5. *Swelling properties of pine wood species treated with SNGW*

Wood species	Geothermal waters	Radial swelling (%)	Tangential swelling (%)	Volumetric swelling (%)	Anisotropic swelling
Black pine	Control*	6.61(0.18**) a	7.57(0.18) d	14.60 (0.30) h	1.15 (0.03) l
	N-1	4.15 (0.09) b	6.76 (0.21) e	11.20 (0.29) i	1.63 (0.06) m
	C-1	4.51 (0.07) c	7.08 (0.23) f	12.00 (0.19) j	1.57 (0.06) n
	E-6	4.72 (0.11) c	6.46 (0.16) g	11.45 (0.28) k	1.37 (0.04) o
Brutia pine	Control*	6.20 (0.27) ö	9.07 (0.34) r	15.85 (0.32) t	1.47 (0.10) v
	N-1	5.76 (0.47) p	7.79 (0.38) s	14.00 (0.76) u	1.36 (0.11) yz
	C-1	5.08 (0.48) q	7.20 (0.37) ş	12.65 (0.67) ü	1.43 (0.15) vy
	E-6	5.72 (0.51) p	7.27 (0.30) ş	13.41 (0.67) w	1.28 (0.10) z

*Untreated. **Values in parentheses are the standard deviation; the same letters in each column indicate no statistical difference at the 95% confidence level among treatments

For the swelling values, the statistically significant differences were observed for the treatments of both pine woods versus the non-treated controls (*Table 5*). For black pine, there were significant differences observed among the SNGW treatments in the swelling values. For Brutia pine, with regards to radial swelling, there were remarkable differences between the N-1 and E-6 treatments *vesus* the C-1 treatment, whereas there was no significant difference between the E-6 and N-1 treatments. Besides, significant differences in the tangential swelling were observed between the C-1 and E-6 treatments *vesus* the N-1 treatment for Brutia pine, while no significant differences were observed between the E-6 and C-1 treatments. Moreover, significant differences in the anisotropic swelling were noted between the E-6 and C-1 geothermal waters used to treat the Brutia pine, whereas there were no considerable difference observed between the N-1 treatment versus the C-1 and E-6 treatments.

The data noted in *Table 5* saw that the swelling values of pine wood samples treated with the distilled water after the SNGW treatment decreased when compared to the untreated control samples. One of the major disadvantages of wood material is also its swelling due to the moisture content of the air. The wood material swells when used under the high moisture content conditions. Likewise, the same cases are also observed in the wood materials treated with the hygroscopic wood preservative salts. But, the

http://www.aloki.hu ● ISSN 1589 1623 (Print) ● ISSN 1785 0037 (Online)
DOI: http://dx.doi.org/10.15666/aeer/1706_1405314068

swelling values of wood treated with the hygroscopic chemicals are less than that of the untreated wood (Bozkurt et al., 1993). The decrease of a general swelling in the volume of wood treated with the SNGW could be from the hygroscopic geothermal chemicals absorbed by the woody cells within the wood structure. The strength of hydrogen bonding could be decrease as the absorption of hygroscopic chemicals increases; consequently, the water sorptive capacity of the cell wall and the volumetric swelling of wood in water could be decrease with increasing of the hygroscopic chemical absorption (Coles and Walker, 1978). Also, the swelling of wood in water could be related to hydrogen bonding and by changes in the cellulose structure (Stamm, 1955). Compared to the untreated wood, this swelling phenomenon could be due to the cellulose chains that are the less swelling within the SNGW-treated wood structure, and the cellulose chains that remain in the less swollen state within this structure after the SNGW evaporation (Stamm and Seborg, 1936).

The results in *Table 5* were compared to the results of earlier studies; for example, some workers had studied the properties of wood treated with the ammonia (Coles and Walker, 1978), the liquid ammonia (Stamm and Tarkow, 1955), and the liquid ammonia-solvent combinations (Pentoney, 1966). It was reported that such treatments decreased the swelling properties of wood. Our own observations in *Table 5* indicated that the SNGW treatments lowered the swelling values of pine woods. Hence, it was concluded that the results of *Table 5* are consistent with these studies. According to the results noted here, it could be helpful that the pine wood species treated with such SNGW is not used under the high moisture content conditions. If not, it could be a general volumetric swelling and dimensional modify for such treated pine wood materials.

Conclusions

This study investigated how the impregnation of black and Brutia pine wood species with three different SNGW from Turkey (as environmentally safe resources) affected the physical, mechanical, shrinking, and swelling properties of the wood. The absorption and retention values for all treated pine wood samples significantly increased depending on the concentration of the mineral salts found in the SNGW. The highest physical values were observed for the E-6 treatment, whereas the lowest physical values were observed for the N-1 treatment.

In general, the SNGW treatments increased the values of density and moisture content of the two pine wood species, but decreased the values of MOR, MOE, CSPG, shrinking, and swelling. The decreases in the MOR, MOE, CSPG, shrinking, and swelling of the treated pine woods were higher compared to the non-treated wood, but the increases in density and moisture content were lower. For the E-6 treatment, the increases in density and moisture content were higher than those of the other treatments. For the N-1 treatment, the decreases in MOR, MOE, and CSPG were less than those of the other SNGW treatments. For example, in the E-6 treatment the density increased 7.69% and 3.51% for black pine and Brutia pine, respectively; for the N-1 and C-1 treatments, the increases in density were 1.92% and 5.77% for black pine, respectively, and were 1.79% and 3.75% for Brutia pine, respectively. Similar increases were also observed for the moisture content values. In the N-1 treatment, the MOR values decreased 11.55% and 8.01% for black pine and Brutia pine, respectively, whereas for the C-1 and E-6 treatments, the decreases were 8.14% and 9.67% for black pine,

http://www.aloki.hu ● ISSN 1589 1623 (Print) ● ISSN 1785 0037 (Online)
DOI: http://dx.doi.org/10.15666/aeer/1706_1405314068

respectively, and the decreases were 11.88% and 15.54% for Brutia pine, respectively. Similar reductions were also observed for the MOE, CSPG, shrinking, and swelling.

Based on these laboratory results, the effects of SNGW on the physical, mechanical, shrinking, and swelling properties of pine woods can be directly related to several important factors related to: wood type and quality; saltwater absorption and mineral retention amounts within the wood; variety and content of chemical compounds within the SNGW; treatment method used; wood drying temperature; and wood treatment processing factor.

The pine wood materials treated with such SNGW can be used in the application areas, where no dense humidity, static bending and pressure parallel to grain effects for long periods. Therefore, for such application areas, the users or designers should consider the loading type and humidity criteria calculation for pine wood materials treated with such natural salt waters.

This study is not an indication that the SNGW can be used as wood preservatives. Therefore, for the examination protective performance of SNGW treatment, some analyzes such as decay test, leaching test, and weathering test could be done. Because those tests could be a requirement to determine the usability of SNGW as a wood preservative.

Acknowledgments. The authors are grateful for the support from the TR Suleyman Demirel University Department of Scientific Research Projects Coordination (Grant No. 3365-YL1-12).

REFERENCES

[1] Akkuş, İ., Akıllı, H., Ceyhan, S., Dilemre, A., Tekin, Z. (2005): Turkey Geothermal Resources Inventory. – General Directorate of Mineral Research and Exploration's Publications, Inventory Series-201, Ankara, Turkey (in Turkish).

[2] ASTM D1413-07e1 (2007): Standard Test Method for Wood Preservatives by Laboratory Soil Block Cultures. – ASTM International, West Conshohocken, PA.

[3] Atilgan, A., Peker, H. (2012): Effects of different wood preservatives on the some physical properties of wood species used in furniture and building industry. – Artvin Coruh Univ. J. of Forestry Faculty 13(1): 67-78.

[4] Ayrilmis, N., Kartal, S. N., Laufenberg, T. L., Winandy, J. E., White, R. H. (2005): Physical and mechanical properties and fire, decay, and termite resistance of treated oriented strandboard. – Forest Products Journal 55(5): 74-81.

[5] Bariska, M. (1975): Collapse Phenomena in Beech wood during and after NH_3-Impregnation. – Wood Science and Technology 9: 293-306.

[6] Bozkurt, A. Y., Erdin, N. (1997): Textbook of Wood Technology. – Istanbul University Faculty of Forestry Publications, Istanbul, Turkey (in Turkish).

[7] Bozkurt, A. Y., Goker, Y., Erdin, N. (1993): Textbook of Wood Impregnation Technique. – Istanbul University Faculty of Forestry Publications, Istanbul, Turkey (in Turkish).

[8] Colakoglu, G., Colak, S., Aydin, I., Yildiz, U. C., Yildiz, S. (2003): Effects of boric acid treatment on mechanical properties of laminated beech veneer lumber. – Silva Fennica 37(4): 505-510. DOI: 10.14214/sf.488.

[9] Coles, R. W., Walker, J. C. F. (1978): Induced shrinkage and structural reorganisation in ammonia-treated wood of Corsican pine. – Wood and Fiber 10 (1): 39-57.

[10] Degirmentepe, S., Baysal, E., Turkoglu, T., Toker, H., Deveci, I. (2015): Some properties of Turkish sweetgum balsam (*Styrax liquidus*) impregnated oriental beech wood. Part II: Decay resistance, mechanical and thermal properties. – Wood Research 60(4): 591-604.

http://www.aloki.hu ● ISSN 1589 1623 (Print) ● ISSN 1785 0037 (Online)
DOI: http://dx.doi.org/10.15666/aeer/1706_1405314068

[11] Dong, Y., Yan, Y., Zhang, S., Li, J., Wang, J. (2015): Flammability and physical-mechanical properties assessment of wood treated with furfuryl alcohol and nano-SiO_2. – European J. of Wood and Wood Prod. 73(4): 457-464. DOI: 10.1007/s00107-015-0896-y.
[12] Gezer, E., Cooper, P. A. (2016): Effects of wood species and retention levels on removal of copper, chromium, and arsenic from CCA-treated wood using sodium hypochlorite. – Journal of Forest Research 27(2): 433-442. DOI: 10.1007/s11676-015-0172-3.
[13] Hamel, M. P. (1988): Wood Protection Techniques and the Use of Treated Wood in Construction. Proceedings. – Forest Products Research Society, Madison, WI, pp. 54-62.
[14] Hesp, T., Watson, R. W. (1964): The effects of water-borne preservatives applied by vacuum pressure methods on the strength properties of wood. – Wood 29(6): 50-53.
[15] Ilgar, R. (2005): The view of dualist approach on geothermal sources. – Electronic Journal of Social Sciences 4(13): 88-98 (in Turkish).
[16] ISO 3129 (2012): Wood-Sampling Methods and General Requirements for Physical and Mechanical Testing of Small Clear Wood Specimens. – International Organization for Standardization, Geneva, Switzerland.
[17] ISO 4469 (1981): Wood-Determination of Radial and Tangential Shrinkage. – International Organization for Standardization, Geneva, Switzerland.
[18] ISO 4858 (1982): Wood-Determination of Volumetric Shrinkage. – International Organization for Standardization, Geneva, Switzerland.
[19] ISO 4859 (1982): Wood-Determination of Radial and Tangential Swelling. – International Organization for Standardization, Geneva, Switzerland.
[20] ISO 4860 (1982): Wood-Determination of Volumetric Swelling. – International Organization for Standardization, Geneva, Switzerland.
[21] ISO 13061-1 (2014): Physical and Mechanical Properties of Wood - Test Methods for Small Clear Wood Specimens - Part 1: Determination of Moisture Content for Physical and Mechanical Tests. – International Organization for Standardization, Geneva, Switzerland.
[22] ISO 13061-2 (2014): Physical and Mechanical Properties of Wood - Test Methods for Small Clear Wood Specimens - Part 2: Determination of Density for Physical and Mechanical Tests. – International Organization for Standardization, Geneva, Switzerland.
[23] ISO 13061-3 (2014): Physical and Mechanical Properties of Wood - Test Methods for Small Clear Wood Specimens - Part 3: Determination of Ultimate Strength in Static Bending. – International Organization for Standardization, Geneva, Switzerland.
[24] ISO 13061-4 (2014): Physical and Mechanical Properties of Wood - Test Methods for Small Clear Wood Specimens - Part 4: Determination of Modulus of Elasticity in Static Bending. – International Organization for Standardization, Geneva, Switzerland.
[25] ISO 13061-17 (2017): Physical and Mechanical Properties of Wood - Test Methods for Small Clear Wood Specimens - Part 17: Determination of Ultimate Stress in Compression Parallel to Grain. – International Organization for Standardization, Geneva, Switzerland.
[26] Kantay, R. (1978): Properties of steamed wood material (Translation from H. Kübler). – Istanbul University Journal of Forestry Faculty B (28): 231-240 (in Turkish).
[27] Keskin, H., Daglioglu, N. (2016): Effects of Tanalith E impregnation substance on bending strengths and modulus of elasticity in bending of some wood types. – Artvin Coruh Univ. J. of Forestry Faculty 17(1): 62-69. DOI: 10.17474/acuofd.90044.
[28] Keskin, H., Atar, M., Erturk, N. S., Colakoglu, M. H., Korkut, S. (2013): Mechanical properties of rowan wood impregnated with various chemical materials. – International Journal of Physical Science 8(2): 73-82. DOI: 10.5897/IJPS12.688.
[29] Laks, P. E., Palardy, R. D. (1990): The development of borate-containing flakeboard. – Proceedings of the First International Conference on Wood Protection with Diffusible Preservatives, Forest Products Research Society, Madison, WI, pp. 76-79.
[30] Megnis, M., Olsson, T., Varna, J., Lindberg, H. (2002): Mechanical performance of linseed oil impregnated pine as correlated to the take-up level. – Wood Science and Technology 36(1): 1-18. DOI: 10.1007/s002260100120.

http://www.aloki.hu ● ISSN 1589 1623 (Print) ● ISSN 1785 0037 (Online)
DOI: http://dx.doi.org/10.15666/aeer/1706_1405314068

[31] Militz, H. (1993): Treatment of timber with water soluble dimethylol resins to improve their dimensional stability and durability. – Wood Science and Technology 27(5): 347-355. DOI: 10.1007/BF00192221.
[32] Mourant, D., Yang, D. Q., Roy, C. (2007): Decay resistance of PF-pyrolytic oil resin treated wood. – Forest Products Journal 57(5): 30-35.
[33] Mourant, D., Yang, D. Q., Rield, B., Roy, C. (2008): Mechanical properties of wood treated with PF-pyrolytic oil resins. – Holz als Roh- und Werkstoff 66: 163-171. DOI: 10.1007/ s00107-007-0221-5.
[34] Ors, Y., Keskin, H. (2001): Textbook of Wood Material Technology. – Nobel Publishing, Ankara, Turkey (in Turkish).
[35] Ors, Y., Atar, M., Keskin, H., Yavuzcan, H. G. (2005): Impacts of impregnation with imersol aqua on the modulus of elasticity in bending. – Journal of Applied Polymer Science 99(6): 3210-3217. DOI: 10.1002/app.22035.
[36] Ostmeyer, J. G. (1987): Chemical and mechanical evaluation of southern pine wood treated with chromated copper arsenate. – Ph.D. Dissertation, Auburn Univ., USA.
[37] Ozciftci, A., Batan, F. (2009): Effect of some mechanical properties on wood materials impregnated with waste boron oil. – Journal of Polytechnic 12(4): 287-292. DOI: 10.2339/2009.12.4, 287-292.
[38] Peker, H., Sivrikaya, H., Baysal, E., Yalınkılıç, M. (1999): Static bending strength of wood treated with fire retardant and water repellent preservation chemicals. – Pamukkale University Journal of Engineering Sciences 5(1): 975-982.
[39] Pentoney, R. E. (1966): Liquid ammonia–solvent combinations in wood plasticization: Properties of treated wood. – Ind. Eng. Chem. 5(2): 105-110.
[40] Pollisco, F. S., Skaar, C., Davidson, R. W. (1971): Some physical properties of maple wood treated with ammonia vapor. – Wood Sciences 4(2): 65-70.
[41] Sen, S., Var, A. A., Oz, A. (2017): The effects of antifungal, antitermitic and some physical-mechanical properties of geothermal and rich mineral waters as environmental protectors in wood material. – Proceedings of the Second International Symposium on Multidisciplinary Studies, Rome, Italy, pp. 153-169.
[42] Simsek, H., Baysal, E. (2015): Some physical and mechanical properties of borate-treated oriental beech wood. – Drvna Industrija 66(2): 97-103. DOI: 10.5552/drind.2015.1356.
[43] Simsek, H., Baysal, E., Peker, H. (2010): Some mechanical properties and decay resistance of wood impregnated with environmentally-friendly borates. – Construction and Building Materials 24(11): 2279-2284. DOI: 10.1016/j.conbuildmat.2010.04.028.
[44] Sreeja, A., Edwin, L. (2013): Physical barriers: an alternative to prevent negative impacts of chemically treated wood. – Indian Academy of Wood Science 10(2): 140-146. DOI: 10.1007/s13196-013-0106-7.
[45] Stamm, A. J. (1955): Swelling of wood and fiberboards in liquid ammonia. – Forest Products Journal 5(6): 413-416.
[46] Stamm, A. J., Seborg, R. M. (1936): Minimizing wood shrinkage and swelling: treating with synthetic resin-forming materials. – Ind. Eng. Chem. 28(10): 1165-1169.
[47] Temiz, A., Yildiz, U. C., Gezer, E. D., Yildiz, S. (2004): Interaction of copper based preservatives with wood. – Artvin Coruh Univ. J. of Forestry Faculty 5(2): 204-211.
[48] Toker, H. (2007): Determination of effects of boron compounds on some physical mechanical and biological properties of wood. – Ph.D. Dissertation, Gazi Univ., Ankara, Turkey (in Turkish).
[49] Toker, H., Baysal, E., Ozcifci, A., Altinok, M., Sonmez, A., Yapici, F. (2008): An investigation on compression parallel to grain values of wood impregnated with some boron compounds. – Wood Research Journal 53(4): 59-68.
[50] Toker, H., Baysal, E., Simsek, H., Senel, A., Sonmez, A., Altinok, M. (2009): Effects of some environmentally-friendly fire-retardant boron compounds on modulus of rupture and modulus of elasticity of wood. – Wood Research Journal 54(1): 77-88.

http://www.aloki.hu ● ISSN 1589 1623 (Print) ● ISSN 1785 0037 (Online)
DOI: http://dx.doi.org/10.15666/aeer/1706_1405314068

[51] Var, A. A. (2009): Quantative of potential wood preservatives in geothermal fluids and their suitableness for wood impregnation treatment. – Suleyman Demirel University Faculty of Forestry Journal A 1: 184-197.
[52] Var, A. A., Yaldiz, M. Y. (2017): Wood impregnants potential of Alangullu, Camkoy and Germencik (Aydin) geothermal resources and their effects on absorption, retention and density of black pine wood. – El-Cezerî J. of Science and Engineering 4(3): 482-496.
[53] Var, A. A., Goncu, D., Karsantiozu, F. (2013): Investigation of absorption, retention and swelling in Izmir-Doğanbey geothermal waters–treated pine wood. – Suleyman Demirel University Faculty of Forestry Journal 14(2): 127-133.
[54] Var, A. A., Kardas, I., Genc, A. (2015): Determination of wood impregnant potential, effects on absorption, retention and density in wooden of Kütahya–Simav geothermal waters. – Turkish Journal of Forestry 16(1): 42-49.
[55] Var, A. A., Yalcin, O. U., Soyguder, A. (2017): Effects of geothermal hot water treatment on rate of water absorption, modulus of elasticity, compressive strength parallel to grain of brutian pine wood: a case study from Sakarya, Turkey. – Turkish Journal of Forestry 18(4): 314-320. DOI: 10.18182/tjf.340453.
[56] Ville, L., Kimmo, H., Timo, K. (2014): The effects of preservatives on the properties of wood after modification. – Baltic Forestry 20(1): 189-203.
[57] Winandy, J. E. (1995): Effects of waterborne preservative treatment on mechanical properties: a review. – Proceedings of the Ninety-First Annual Meeting of American Wood-Preservers' Association, New York, pp. 17-34.
[58] Winandy, J. E. (1996): Effects of Treatment, Incising, and Drying on Mechanical Properties of Timber. – In: Ritter, M. A., Duwadi, S., Lee, P., Hilbrich, D. (eds.) Proceedings of the National Conference on Wood Transportation Structures - New Wood Treatments. Department of Agriculture Forest Products Laboratory, Forest Service, Madison, WI, pp. 371-378.
[59] Wu, Q., Lee, S., Lee, J. N. (2002): Mechanical, physical, and biological properties of borate-modified oriented strandboard. – Proceedings of the International Conference on Advances in Building Technology, Hong-Kong, China, pp. 137-144. DOI: 10.1016/B978-008044100-9/50018-8.
[60] Yaldiz, M. Y., Var, A. A. (2017): Investigation of some properties of black pine (*Pinus nigra* Arnold.) sapwood impregnated with geothermal waters of Turkey's Aydin regional. – Proceedings of the 3rd ASM International Congress of Agriculture and Environment, Abstract Book-1, Antalya, Turkey.
[61] Yildiz, U. C., Temiz, A., Gezer, E. D., Yildiz, S. (2004): Effects of the wood preservatives on mechanical properties of yellow pine (*Pinus sylvestris* L.) wood. – Building and Environment 39(9): 1071-1075. DOI: 10.1016/j.buildenv.2004.01.032.

http://www.aloki.hu ● ISSN 1589 1623 (Print) ● ISSN 1785 0037 (Online)
DOI: http://dx.doi.org/10.15666/aeer/1706_1405314068

TEMPORAL AND SPATIAL CHANGES OF NUTRIENT CONTENT AND EUTROPHICATION CONDITION IN WATERS OF THE ABANDONED YELLOW RIVER DELTA

ZHANG, Y. M.[1] – WANG, J.[2*] – MENG, K.[3] – ZHAO, L.[2]

[1]*School of Environment, Nanjing Normal University, Nanjing 210023, China*

[2]*College of Marine Science and Engineering, Nanjing Normal University, Nanjing 210023, China*

[3]*Jiangsu Yunfan Testing Technology Co., Ltd., Nanjing 210023, China*

**Corresponding author*
e-mail: wangjing0108@njnu.edu.cn

(Received 28th May 2019; accepted 3rd Sep 2019)

Abstract. This study made use of the trophic state index method, the eutrophication index method, and the potential eutrophication evaluation method to analyze temporal and spatial changes of the nutrient content and the eutrophication level in waters of the Abandoned Yellow River Delta from 2010 to 2015. Findings of this study include the following: the average trophic state index in the study area remained above 3 over the years of investigation, so the study area was under eutrophication; the average eutrophication index each year was above 3, so the study area was in a medium-eutrophication state; both the average trophic state index and the average eutrophication index showed fluctuating trends and the indices were higher in each autumn than in each spring. Fourth, the study area showed a surplus of nitrogen and deficiency in phosphorus, but the N/P ratio declined from 176.68 to 32.234. The concentration of nutrients and the level of eutrophication declined from the coast to the sea and from north to south, with the estuaries marking the highest concentration and most severe eutrophication. Pollutants discharged from the rivers and development projects along the coastline are the main contributors to the high concentrations of nutrients and eutrophication.
Keywords: *trophic state index, eutrophication index, potential eutrophication evaluation, distribution, variation, cause*

Introduction

Coastal waters, which connect the continent with the sea, are among the most vibrant areas bustling with human activity and account for some of the world's most important economic belts. The ecology of coastal waters, subject to influence from both the continent and the sea, is susceptible to human interferences and is hence very sensitive and vulnerable. As costal development and ocean exploitation gather pace, and as land-sourced pollution exacerbates, the environment of coastal waters deteriorates and nutrients (especially nitrogen and phosphorus) and organic matter increase, which results in eutrophication in the waters (Pinckney et al., 2001; Peru's et al., 2004; Demit et al., 2018). Eutrophication will disturb the ecological balance of the waters, threatens marine ecosystems (Andersen et al., 2006; Cabrita et al., 2015), alters the original ecological system structure (Telesh et al., 1999; Capriulo et al., 2002), and leads to degradation of ecological functions (Diaz et al., 1995; Richardson et al., 1997). Eutrophication has become a major challenge that impedes the sustainable development of coastal areas.

Located in the north-central coast of Jiangsu province in China, the Abandoned Yellow River Delta features an erosion coast and deep waters, having all the ideal

http://www.aloki.hu ● ISSN 1589 1623 (Print) ● ISSN 1785 0037 (Online)
DOI: http://dx.doi.org/10.15666/aeer/1706_1406914085

conditions to build a large port. Additionally, backed by the rich resources of the adjacent continent, the local government plans to build a port with berths able to accommodate 300,000-tonnage vessels along the northern estuary of the Abandoned Yellow River to facilitate industrial transfer from the Yangtze River economic belt and boost the port economy. This area is expected to become a thriving economic engine along Jiangsu's coastline. Nevertheless, as the port develops and industries there take off, the waters of the delta face growing environmental threats. The major environmental problem now confronting the coastal areas of Jiangsu is eutrophication caused by excessive nutrients. Previous studies on eutrophication along coastal areas in Jiangsu focused on Haizhou Bay (Zhao, et al., 2015; Zhang, et al., 2014), but research on eutrophication in waters of the Abandoned Yellow River Delta is still limited. Using the waters of the Abandoned Yellow River Delta as the study area, this study examined water quality data obtained through investigations in 2010, 2012, 2013, and 2015 to analyze trend changes and distribution of nutrients in this area. Using such methods as the trophic state index method, the eutrophication index method, and the potential eutrophication evaluation method, this work probed the causes of pollution in hopes of providing a basis for environmental management and planning, protocols for pollution control, and policies to support environmental protection.

Materials and methods

Introduction to the study area

Located in the north-central coast of Jiangsu province in China, the study area stretches from the Zhongshan River estuary to the Northern Irrigation Canal of Jiangsu and extends 20 km into the sea (as shown in *Fig. 1*). The study area belongs to the waters of the Abandoned Yellow River Delta. With the headland on the north of the Abandoned Yellow River estuary as the point of inflexion, the coastline which meanders from northwest to southeast then runs from north to south. The coast is a plain erosion silt-muddy coast. The coast is broad and spacious, and the -15 m isobath and -10 m isobath on top of the delta are 3.95 km and 2.0 km away from the coastal baseline, respectively, which means the water is deep along the coast and this area offers ideal conditions to build a large port. Currently, a port with berths able to accommodate 100,000-tonnage vessels is under construction in the northern waters of the Abandoned Yellow River Delta. Rivers that join the sea through the study area include Zhongshan River, Fanshen River, the Abandoned Yellow River, and the Northern Irrigation Canal of Jiangsu. The major coastal development activities in the study area include open marine transportation, culture, and discharge of effluent. The port under construction now runs from the Fanshen River estuary to Erhong River estuary. Along the northern seawall of the study area are coastal industrial parks, the industrial effluent from which are discharged into the sea via outfalls 6 km away from the Zhongshan River estuary and the volume of discharge reaches 20,000 tons per day. The southern part of the industrial park specializes in aquiculture, the wastewater from which is discharged into the sea through the marine outfalls along the coast.

Sampling and sample processing

Sea water quality investigations were conducted from the waters of the Abandoned Yellow River Delta in May 2010, October 2012, May 2013, and October 2015. In

http://www.aloki.hu ● ISSN 1589 1623 (Print) ● ISSN 1785 0037 (Online)
DOI: http://dx.doi.org/10.15666/aeer/1706_1406914085

October 2010, there were 21 investigation sites in total. In May 2013, October 2012 and October 2015, there were 22 investigation sites. The sampling point coordinate range is 34°10′N-34°30′40.45″N, 120°6′E-120°32′41.33″E. The areas of investigation remained essentially the same, so data obtained from the investigations have good comparability in terms of space (*Fig. 1*).

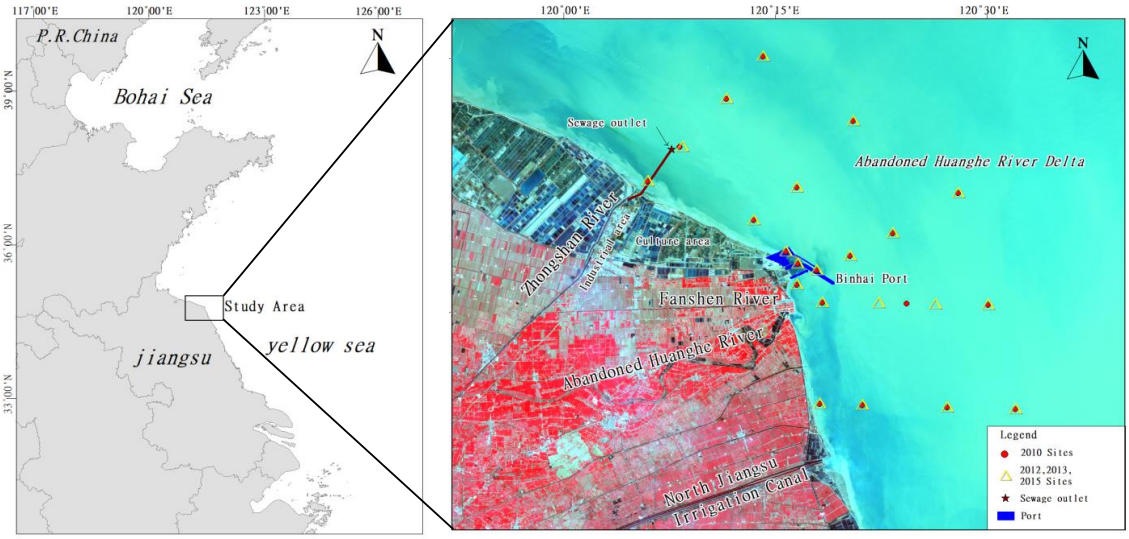

Figure 1. *Location of study area and sample sites*

Items monitored include chemical oxygen demand (COD), dissolved inorganic nitrogen (DIN, including NO_3-N, NO_2-N, NH_4-N), dissolved inorganic phosphorus (DIP), chlorophyll a, and salinity. Collection, storage, and transport of samples were performed according to the "Specifications for Marine Monitoring (GB17378-2007)," "Specifications for Oceanographic Survey (GB/T 12763-2007)," and other standards. The water samples were collected from a 50-cm depth where applicable using an Aqua trap water sampler and were then transported to the laboratory for the water quality investigations.

Methods

Single-factor pollution index method

The single-factor pollution index method (Jiang et al., 1991) uses the ratio of measured concentration of a given pollutant to the standard concentration to reflect how much pollution the pollutant has caused.

$$P_i = \frac{C_i}{L_i} \quad \text{(Eq.1)}$$

where P_i denotes the pollution index of the i-th pollutant, Ci denotes the measured concentration of the i-th pollutant, and Li denotes the concentration of the i-th pollutant in sea water of standard quality. The evaluation standard used in this study refers to Level-I Standard in "Sea Water Quality Standard (GB3097-1997)".

http://www.aloki.hu ● ISSN 1589 1623 (Print) ● ISSN 1785 0037 (Online)
DOI: http://dx.doi.org/10.15666/aeer/1706_1406914085

Trophic state index (TSI) method

The trophic state index (TSI) method (Chen et al., 1999; Bian et al., 2013) is one of most widely used methods to assess eutrophication and its calculation equation is as follows:

$$TSI = \frac{COD}{COD_S} + \frac{TN}{TN_S} + \frac{TP}{TP_S} + \frac{Chl.a}{Chl.a_S} \quad \text{(Eq.2)}$$

where COD, TN, TP, and Chl.a stand for the measured concentrations of the pollutants (mg/L), CODs, TNs, and Chl.as their corresponding standard concentrations (mg/L). According to the Level-II standard in the "Sea Water Quality Standard (GB3091-1997)" and the conditions of nutrients in the study area, the standard concentrations for COD, DIN, DIP, and Chl-a are 3 mg/L, 0.3 mg/L, 0.03 mg/L, and 3 mg/m^3, respectively. *Table 1* presents the levels of nutrition identified according to the TSI.

Table 1. *The levels of nutrition according to the trophic state index (TSI)*

Trophic state index (TSI)	Level of nutrition
Above 3	Eutrophic
2-3	Mesotrophic
Below 2	Oligotrophic

Eutrophication index (EI) method

The eutrophication index (EI) method, first proposed in Japan, was introduced to China by Zou (1983) and has been used according to the "Water Quality Standard for Fisheries" and the "Sea Water Quality Standard" issued by the Chinese government. Its calculation equation is:

$$EI = \frac{COD \times DIN \times DIP \times 10^6}{4500} \quad \text{(Eq.3)}$$

where *EI* denotes the eutrophication index, and COD (Chemical Oxygen Demand), DIN (dissolved inorganic nitrogen), and DIP (Dissolved Inorganic Phosphorus) refer to the measured concentrations of these pollutants (mg/L). If $EI < 1$, the water is considered as oligotrophic; if $EI \geq 1$, it is considered that eutrophication starts in the water, and the larger *EI* is, the more severe eutrophication is. If $EI \geq 1$, the water is identified as eutrophic. When $1 \leq EI \leq 3$, the water is identified as slightly eutrophic. When $3 < EI \leq 9$, the water is identified as moderately eutrophic. When $EI > 9$, the water is identified as severely eutrophic.

Potential eutrophication evaluation method

When pollution of nutrients occurs in sea water, the The concentration ratio of dissolved inorganic nitrogen and dissolved inorganic phosphorus (N/P ratio) does not equal the Redfield ratio of 16 (Redfield, 1963) and even deviates much from the latter. In such cases, there is a surplus of nitrogen (compared with phosphorus limitation) or phosphorus (compared with nitrogen limitation) and the surplus will not be absorbed by

http://www.aloki.hu ● ISSN 1589 1623 (Print) ● ISSN 1785 0037 (Online)
DOI: http://dx.doi.org/10.15666/aeer/1706_1406914085

marine plants. Excess of nutrients does not make a direct contribution to eutrophication, so it is considered a potential source that may induce eutrophication. In other words, only when a proper amount of phosphorus (compared with phosphorus limitation) or nitrogen (compared with nitrogen limitation) is supplemented do the excess of nutrients play a role in eutrophication (Guo et al., 1998). This is in fact a phenomenon of potential eutrophication. *Table 2* displays the division of nutrition levels in potential eutrophication.

Table 2. *Division of nutrition levels in potential eutrophication according to N/P ratio*

Level	Nutrition level	DIN (mg/L)	DIP (mg/L)	N/P
I	Oligotrophic	< 0.2	< 0.03	8-30
II	Mesotrophic	0.2-0.3	0.03-0.045	8-30
III	Eutrophic	> 0.3	> 0.045	8-30
IV_P	Phosphorus-limited mesotrophic	0.2-0.3	—	> 30
V_P	Medium-phosphorus-limited potential eutrophic	> 0.3	—	30-60
VI_P	Phosphorus-limited potential eutrophic	> 0.3	—	> 60
IV_N	Nitrogen-limited mesotrophic	—	0.03-0.045	< 8
V_N	Medium-nitrogen-limited potential eutrophic	—	> 0.045	4-8
VI_N	Nitrogen-limited potential eutrophic	—	> 0.045	< 4

Statistical methods

The DIN and DIP concentrations in water samples were statistically analyzed by SPSS25, the mean, standard deviation and coefficient of variation were calculated. Combining with the spatial information of station location, the data are processed by using Suffer11 software and Kristin interpolation method, and the spatial distribution maps of DIN, DIP, TSI, EI are drawn.

Results and discussion

Concentration changes of nutrients and spatial distribution

The statistical results of dissolved inorganic nitrogen (DIN) and dissolved inorganic phosphorus (DIP) from 2010 to 2015 are shown in *Table 3* and *Figure 2*. The DIN concentration in the delta measured in May 2010 ranged from 0.586 to 1.004 mg/L in May 2010, with a mean concentration of 0.793mg/L. In October 2012, the measured DIN concentration ranged from 0.512 to 1.615 mg/L, with a mean concentration of 0.851 mg/L. In May 2013, the measured range of DIN concentrations was from 0.306 to 1.520 mg/L, with a mean concentration of 0.590 mg/L. In November 2015, the DIN concentration ranged from 0.213 to 0.924 mg/L, with a mean concentration of 0.474 mg/L. From 2010 to 2012, the maximum concentration of inorganic nitrogen in the waters of the delta witnessed a considerable increase and the average concentration rose slightly. From 2012 to 2015, both the maximum concentration and average concentration of inorganic nitrogen in this area declined (*Fig. 2*), and this trend is significant. Data from estuaries (*Table 3; Fig. 3*) show that the DIN concentration of Zhongshan estuary over the years was obviously higher than the average value of the study area, the DIN concentration of Abandoned Yellow River estuary was slightly higher than the average value in 2010 and 2012, the DIN concentration of Northern Jiangsu Irrigation Canal estuary was slightly higher than the average value in 2010.

http://www.aloki.hu ● ISSN 1589 1623 (Print) ● ISSN 1785 0037 (Online)
DOI: http://dx.doi.org/10.15666/aeer/1706_1406914085

Table 3. *Statistical description of dissolved inorganic nitrogen (DIN) and dissolved inorganic phosphorus (DIP) concentrations from 2010 to 2015*

Item			Time			
			2010.5	**2012.10**	**2013.5**	**2015.11**
DIN	Study area	Maximum concentration (mg/L)	1.004	1.615	1.520	0.924
		Minimum concentration (mg/L)	0.586	0.512	0.306	0.213
		Mean concentration (mg/L)	0.793	0.851	0.590	0.474
		Standard deviation	0.124	0.316	0.282	0.184
		Coefficient of variation (%)	15.6%	37.1%	47.8%	38.9%
	Zhongshan River estuary		1.004	1.615	1.520	0.924
	Abandoned Yellow River estuary		0.943	0.856	0.450	0.451
	Northern Jiangsu Irrigation Canal estuary		0.819	0.553	0.604	0.634
DIP	Study area	Maximum concentration (mg/L)	0.019	0.040	0.041	0.106
		Minimum concentration (mg/L)	0.011	0.018	0.014	0.012
		Mean concentration (mg/L)	0.016	0.029	0.021	0.035
		Standard deviation	0.002	0.006	0.007	0.018
		Coefficient of variation (%)	14.2%	21.9%	32.8%	51.2%
	Zhongshan River estuary		0.011	0.04	0.041	0.106
	Abandoned Yellow River estuary		0.019	0.027	0.016	0.036
	Northern Jiangsu Irrigation Canal estuary		0.017	0.035	0.017	0.030

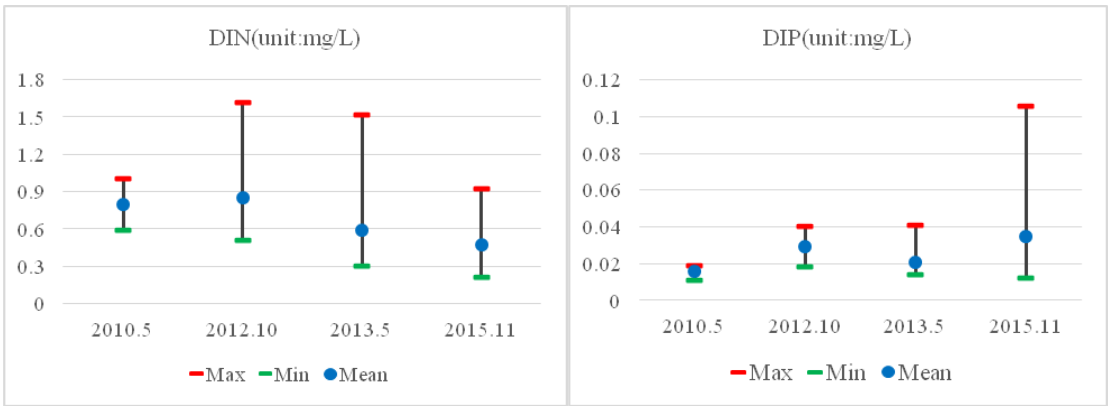

(a) Statistical charts of DIN (b) Statistical charts of DIP

Figure 2. *Statistical charts of DIN and DIP concentrations from 2010 to 2015*

(a) The DIN concentrations of estuaries (b) The DIP concentrations of estuaries

Figure 3. *The DIN and DIP Concentrations of estuaries from 2010 to 2015*

http://www.aloki.hu ● ISSN 1589 1623 (Print) ● ISSN 1785 0037 (Online)
DOI: http://dx.doi.org/10.15666/aeer/1706_1406914085

The DIP concentration in this area ranged from 0.011 to 0.019 mg/L in May 2010, with a mean concentration of 0.016 mg/L; the DIP concentration monitored in October 2012 ranged from 0.018 to 0.040 mg/L, with a mean concentration of 0.029 mg/L; in May 2013, the DIP concentration range was from 0.014 to 0.041 mg/L, with a mean concentration of 0.021 mg/L; in November 2015, the DIP concentration range was from 0.012 to 0.106 mg/L, with a mean concentration of 0.035 mg/L. From 2010 to 2015, the maximum concentration of DIP in the study area kept rising (*Fig. 2*), and this trend is obvious. The average DIP concentration fluctuated, with the concentration higher in autumns than in springs obviously. Data from estuaries (*Table 3; Fig. 3*) show that the DIP concentration of Zhongshan estuary was obviously higher than the average value in2012, 2013 and 2015, the DIP concentration of Northern Jiangsu Irrigation Canal estuary was slightly higher than the average value in 2010 and 2012, the DIP concentration of Abandoned Yellow River estuary was slightly higher than the average value in 2010.

The coefficient of variation can reflect the dispersion degree of data distribution at different sampling points. The larger the coefficient of variation, the greater the degree of dispersion. It can also reflect the degree of influence of human factors on water, the larger the coefficient of variation, the greater the influence of human factors. The coefficient of variation of DIN from 2010 to 2015 ranged from 15.6 to 47.8%, with the largest coefficient of variation in 2013. From 2010 to 2015, the coefficient of variation of DIP ranged from 14.2 to 51.2%, and the coefficient of variation increased over the years. This data reflected the uneven spatial distribution of DIN and DIP concentration, which was obviously influenced by human factors.

Regarding spatial distribution (*Figs. 4* and *5*), the concentrations of DIN and DIP on the surface sea water in the study area declined from the shore outwards and from west to east. It presents a gradient of concentrations in spatial distribution and high concentrations occur near the estuary with the estuary recording the highest. The concentration isolines of DIN in the study area in 2010 are saddle-shaped, with the highest concentrations occurring both at the Zhongshan River estuary and at the Abandoned Yellow River estuary, and the level of pollution in these peak sites was essentially the same. In 2012, the concentration of DIN in these two estuaries remained high, but the concentration at the Zhongshan River estuary far exceeded that at the other estuary. In 2013 and 2015, high DIN concentrations only occurred at the Zhongshan River estuary and the Abandoned Yellow River estuary was no longer a high-concentration area. In 2010 and 2012, the highest concentrations of DIP occurred in areas radiating from the abandoned Yellow River estuary and from the estuary of Northern Irrigation Canal of Jiangsu, but in 2013 and 2015, high DIP concentrations only occurred at the Zhongshan River estuary.

Result of single-factor pollution index evaluation

Table 4 shows the Single-Factor Pollution Index of dissolved inorganic nitrogen and dissolved inorganic phosphorus (*Eq. 1*). According to the Level-I standards detailed in "Sea Water Quality Standard," the pollution index of DIN was between 2.931 and 5.021 in 2010, averaging 3.963. In 2012, this index ranged from 2.562 to 8.073, averaging 4.256. In 2013, the index ranged from 1.531 to 7.598, averaging 2.949. In 2015, the index ranged from 1.067 to 4.622, averaging 2.371. The index in all these years exceeded the standard index and, if calculated by the ratio of measured index to the standard, the index first presented an increase and then later a decline.

http://www.aloki.hu ● ISSN 1589 1623 (Print) ● ISSN 1785 0037 (Online)
DOI: http://dx.doi.org/10.15666/aeer/1706_1406914085

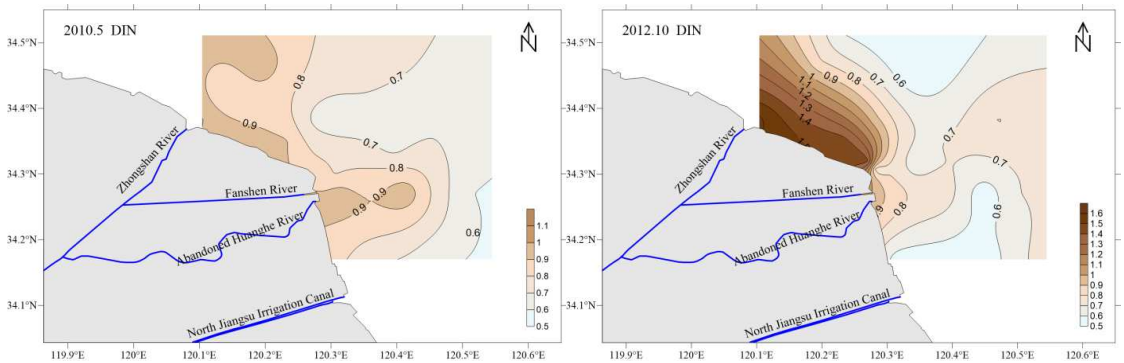

(a) Spatial distribution of DIN in May 2010 (b) Spatial distribution of DIN in October 2012

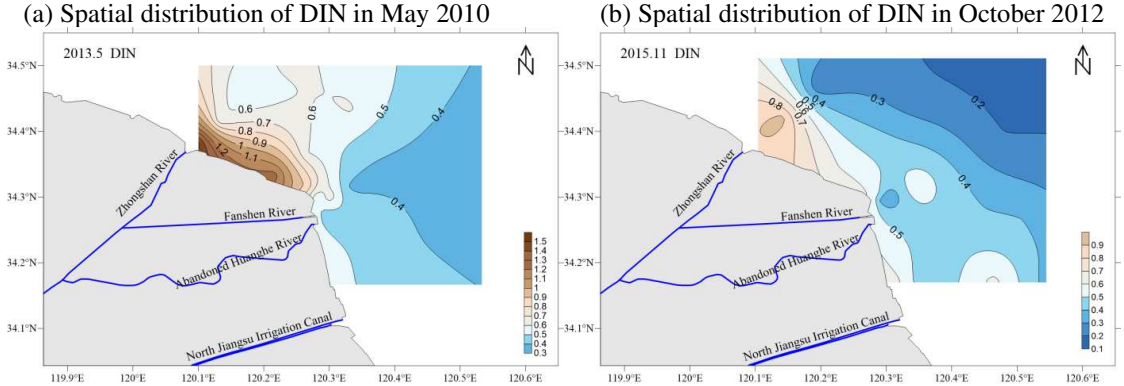

c) Spatial distribution of DIN in May 2013 (d) Spatial distribution of DIN in November 2015

Figure 4. *Spatial distribution of dissolved inorganic nitrogen (DIN) in the study area from 2010 to 2015 (unit: mg/L)*

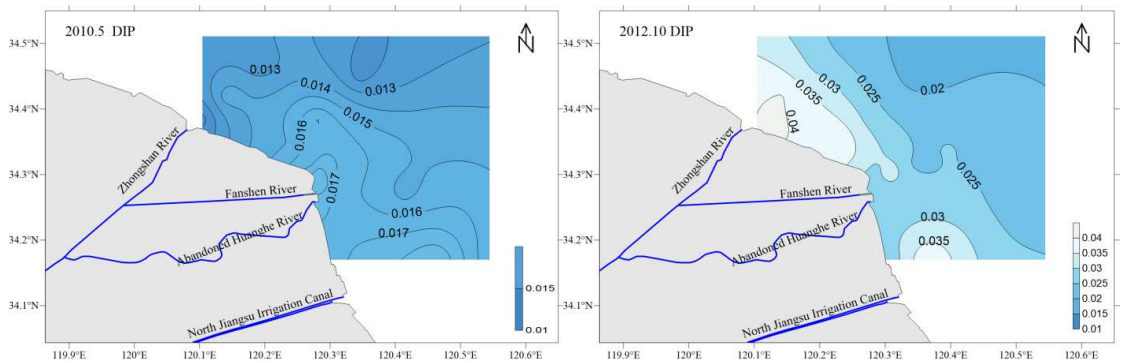

(a) Spatial distribution of DIP in May 2010 (b) Spatial distribution of DIP in October 2012

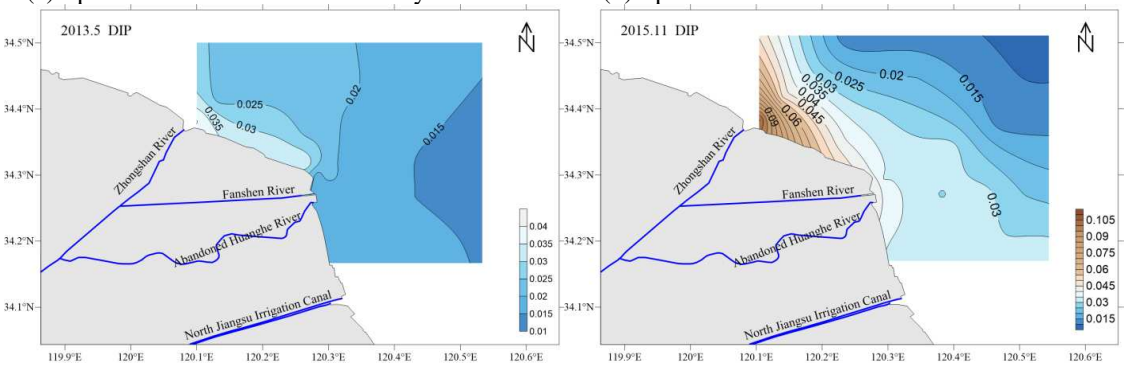

(c) Spatial distribution of DIP in May 2013 (d) Spatial distribution of DIP in November 2015

Figure 5. *Spatial distribution of dissolved inorganic phosphorus (DIP) in the study area from 2010 to 2015 (unit: mg/L)*

http://www.aloki.hu ● ISSN 1589 1623 (Print) ● ISSN 1785 0037 (Online)
DOI: http://dx.doi.org/10.15666/aeer/1706_1406914085

Table 4. *The single-factor pollution index of dissolved inorganic nitrogen (DIN) and dissolved inorganic phosphorus (DIP)*

Item			Time			
			2010.5	**2012.10**	**2013.5**	**2015.11**
DIN	Pollution index	Maximum	5.021	8.073	7.598	4.622
		Minimum	2.931	2.562	1.531	1.067
		Mean	3.963	4.256	2.949	2.371
		Rate of exceeding the standard	100%	100%	100%	100%
DIP	Pollution index	Maximum	1.267	2.687	2.687	7.067
		Minimum	0.707	1.207	0.907	0.793
		Mean	1.037	1.909	1.370	2.310
		Rate of exceeding the standard	61.9%	100%	86.3%	90.9%

According to the Level-I water quality standards detailed in the "Sea Water Quality Standard," the pollution index (*Eq. 1*) of DIP in 2010 ranged from 0.707 to 1.267, averaging 1.037, and the rate of exceeding the standard stood at 61.9%. In 2012, the pollution index ranged from 1.207 to 2.687, averaging 1.909, and the rate of exceeding the standard was 100%. In 2013, the index ranged from 0.907 to 2.760, averaging 1.439, and the rate of exceeding the standard was 87.5%. In 2015, the range of the index was from 0.793 to 7.067, averaging 2.310, and the rate of exceeding the standard was 90.9% (*Table 4*). The ratio of the measured index to the standard presented a fluctuating pattern, with the value in autumns higher than in springs.

Trophic state analysis

Table 5 and *Figure 6* show the analysis results of the trophic state index (TSI, *Eq. 2*) in the study area from 2010 to 2015. In May 2010, the TSI of the study area ranged from 3.314 to 5.015, with a mean index of 4.135, and the area was identified as eutrophic according to the division standard of nutrition levels. In October 2012, the index changed between 2.864 and 7.509, averaging 4.427, and the area was identified as being between mesotrophic and eutrophic, with an overall tendency towards the eutrophic level. In May 2013, the index ranged from 1.928 to 7.027, averaging 3.227, and the area was identified as being between oligotrophic and eutrophic, with an overall tendency towards the eutrophic level. In November 2015, the index ranged from 2.018 to 7.792, with the mean standing at 3.974, and the area was identified as being between the mesotrophic state and the eutrophic state, with an overall evaluation as eutrophic. From 2010 to 2015, the TSI value of Zhongshan estuary was significantly higher than the average value of the study sea area and other estuaries values (*Fig. 7*).

According to the analysis from the angle of time (*Table 5*), it can be seen that from 2010 to 2015, the average TSI fluctuated but remained above 3 and the area was identified as eutrophic. According to analysis from the angle of spatial distribution (*Fig. 8*), the TSI of areas near the shore were higher than those far away in the sea and presented a declining trend from the shore to the sea, with high TSIs occurring in waters close to the estuaries. In 2010, the TSI isolines resembled the shape of a saddle; the Zhongshan River estuary and the Abandoned Yellow River estuary had the highest and similar TSIs. In 2012, areas from the Zhongshan River estuary to the shore of the port had the highest TSIs and the index declined outwards from the estuary to the sea. High TSIs also occurred in the Abandoned Yellow River estuary, but the values were generally

http://www.aloki.hu ● ISSN 1589 1623 (Print) ● ISSN 1785 0037 (Online)
DOI: http://dx.doi.org/10.15666/aeer/1706_1406914085

smaller than those in the Zhongshan River estuary. In 2010 and 2012, the researched waters were essentially eutrophic. In 2013 and 2015, the TSI improved compared with 2012 and severe organic pollution only occurred in Zhongshan estuary and the Abandoned Yellow River estuary no longer showed high organic pollution. The area of eutrophic waters shrank and nearly half of the waters were in a mesotrophic state.

Analysis of eutrophication condition

According to the calculated eutrophication indices of the study area from 2010 and 2015 (as shown in *Table 5* and *Fig. 9*), the eutrophication index (*Eq. 3*) in this area ranged from 2.114 to 7.798, with a mean index of 4.419 in May 2010, and hence the area was identified as in a state between slight-eutrophic and moderate-eutrophic. In October 2012, the index fluctuated between 2.802 and 29.135, with the mean standing at 8.871, so the area as identified as being in a state between slight-eutrophic to severe-eutrophic. In May 2013, the range of the index was from 0.907 to 23.134, with the mean standing at 4.556, so the study area was identified as being in a state between oligotrophic to severe eutrophic. In November 2015, the index fluctuated from 0.717 to 29.229, with the mean standing at 7.252, so the study area was identified as being in a state between oligotrophic and severe eutrophic. From 2012 to 2015, the EI value of Zhongshan estuary was significantly higher than the average value of the study sea area and other estuaries values (*Fig. 7*).

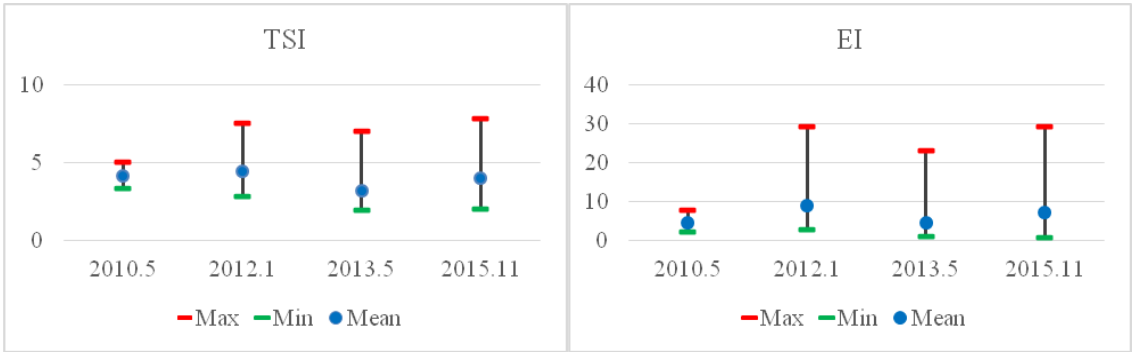

(a) Statistical charts of TSI (b) Statistical charts of EI

Figure 6. *Statistical charts of TSI and EI from 2010 to 2015 in study area*

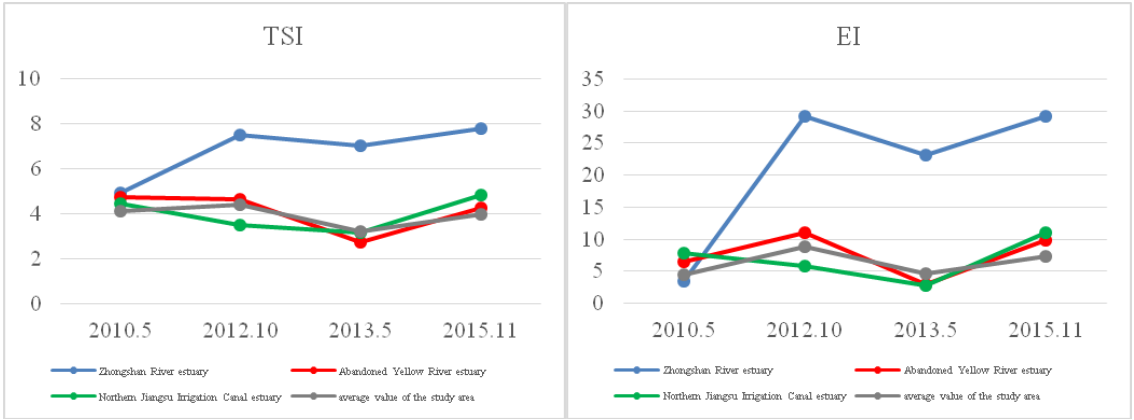

(a) The TSI of estuaries (b) The EI of estuaries

Figure 7. *The TSI and EI of estuaries from 2010 to 2015 in study area*

http://www.aloki.hu ● ISSN 1589 1623 (Print) ● ISSN 1785 0037 (Online)
DOI: http://dx.doi.org/10.15666/aeer/1706_1406914085

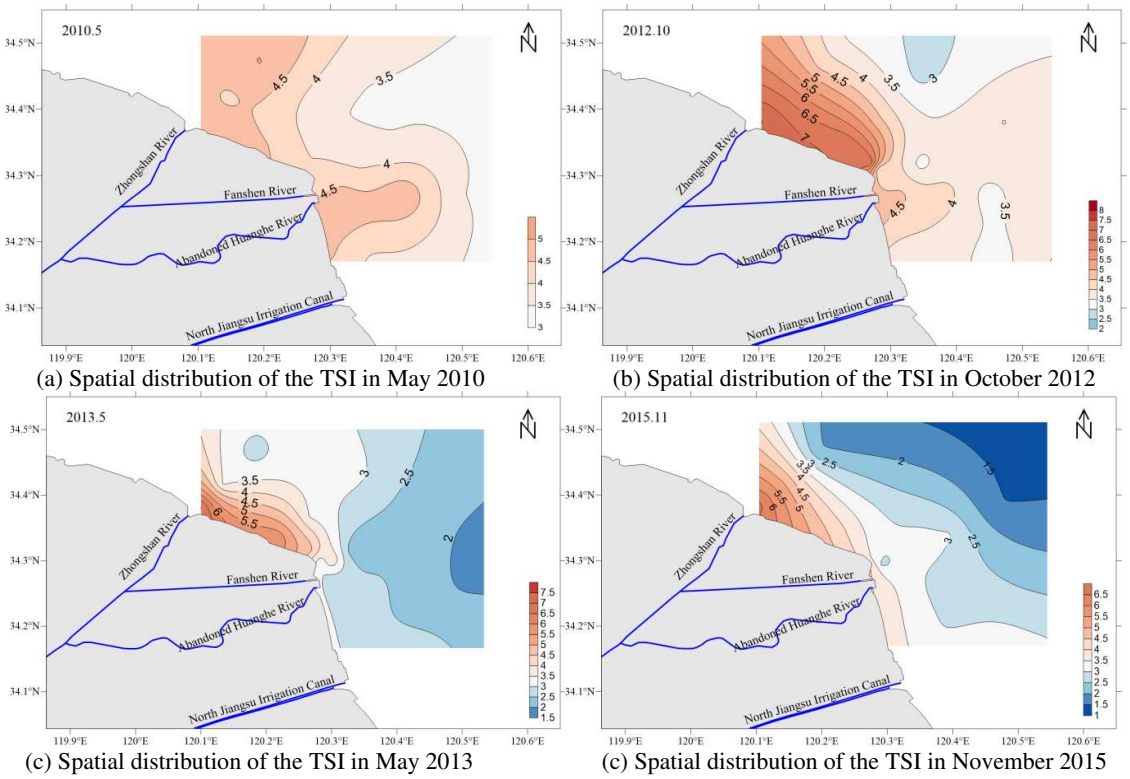

(a) Spatial distribution of the TSI in May 2010
(b) Spatial distribution of the TSI in October 2012
(c) Spatial distribution of the TSI in May 2013
(c) Spatial distribution of the TSI in November 2015

Figure 8. *Spatial distribution of the trophic state index (TSI) in the study area from 2010 to 2015*

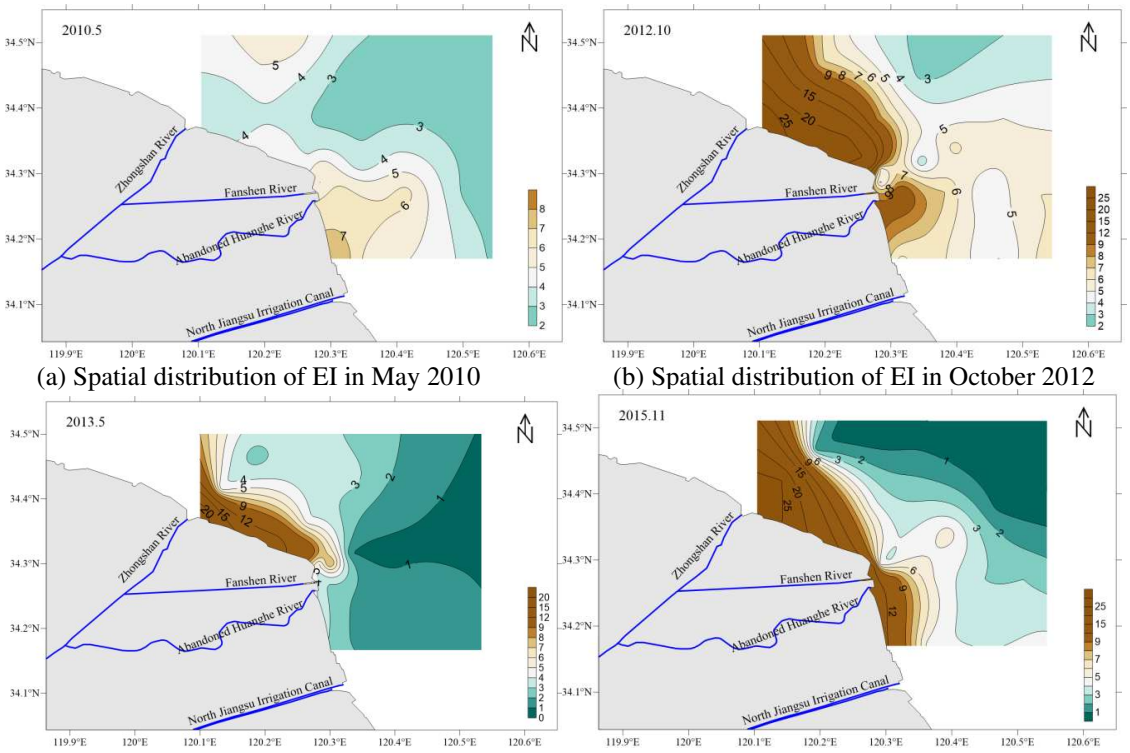

(a) Spatial distribution of EI in May 2010
(b) Spatial distribution of EI in October 2012
(c) Spatial distribution of EI in May 2013
(d) Spatial distribution of EI in November 2015

Figure 9. *Spatial distribution of the eutrophication indices (EI) of the study area from 2010 and 2015*

http://www.aloki.hu ● ISSN 1589 1623 (Print) ● ISSN 1785 0037 (Online)
DOI: http://dx.doi.org/10.15666/aeer/1706_1406914085

Table 5. *Trophic state index (TSI) and eutrophication index (EI) over years*

Time	Category		TSI		EI	
			Scale	Nutrition level	Scale	Eutrophication level
2010.5	Study area	Maximum	5.015	Eutrophic	7.798	Moderate-eutrophic
		Minimum	3.314	Eutrophic	2.114	Slight-eutrophic
		Mean	4.135	Eutrophic	4.419	Moderate-eutrophic
	Zhongshan River estuary		4.954	Eutrophic	3.382	Moderate-eutrophic
	Abandoned Yellow River estuary		4.730	Eutrophic	6.558	Moderate-eutrophic
	Northern Jiangsu Irrigation Canal estuary		4.457	Eutrophic	7.798	Moderate-eutrophic
2012.10	Study area	Maximum	7.509	Eutrophic	29.135	Severe-eutrophic
		Minimum	2.864	Mesotrophic	2.802	Slight-eutrophic
		Mean	4.427	Eutrophic	8.871	Moderate-eutrophic
	Zhongshan River estuary		7.509	Eutrophic	29.135	Severe-eutrophic
	Abandoned Yellow River estuary		4.643	Eutrophic	11.063	Severe-eutrophic
	Northern Jiangsu Irrigation Canal estuary		3.514	Eutrophic	5.811	Moderate-eutrophic
2013.5	Study area	Maximum	7.027	Eutrophic	23.134	Severe-eutrophic
		Minimum	1.928	Oligotrophic	0.907	Oligotrophic
		Mean	3.227	Eutrophic	4.556	Moderate-eutrophic
	Zhongshan River estuary		7.027	Eutrophic	23.134	Severe-eutrophic
	Abandoned Yellow River estuary		2.733	Mesotrophic	2.868	Slight-eutrophic
	Northern Jiangsu Irrigation Canal estuary		3.159	Eutrophic	2.791	Slight-eutrophic
2015.11	Study area	Maximum	7.792	Eutrophic	29.229	Severe-eutrophic
		Minimum	2.018	Mesotrophic	0.717	Oligotrophic
		Mean	3.974	Eutrophic	7.252	Moderate-eutrophic
	Zhongshan River estuary		7.792	Eutrophic	29.229	Severe-eutrophic
	Abandoned Yellow River estuary		4.253	Eutrophic	9.787	Severe-eutrophic
	Northern Jiangsu Irrigation Canal estuary		4.855	Eutrophic	11.092	Severe-eutrophic

From 2010 to 2015, the mean of the eutrophication index indicated a moderate-eutrophic state of the study area, but the highest reading of the index witnessed a significant rise from 2010 to 2012, and the years from 2012 to 2015 marked the largest value of the maximum index, which reflected the fact that part of the researched waters suffered from severe eutrophication. The spatial distribution of the eutrophication index was in alignment with that of the trophic state index.

Potential eutrophication evaluation

The concentration and makeup of nutrients are of significant importance for the growth of phytoplankton and the N/P ratio is a vital indicator of the makeup of nutrients. When the N/P ratio equals 16:1, the waters provide the necessary conditions for the phytoplankton to growth; a smaller ratio will limit the growth of the phytoplankton and a larger ratio will make phosphorus the decisive factor for the phytoplankton's growth.

http://www.aloki.hu ● ISSN 1589 1623 (Print) ● ISSN 1785 0037 (Online)
DOI: http://dx.doi.org/10.15666/aeer/1706_1406914085

According to the observed data regarding concentrations of DIN and DIP from 2010 to 2015, this study analyzed the potential eutrophication conditions of the study area, as shown in *Table 6*. In May 2010, the N/P ratio of the study area stayed between 108.818 and 318.031, with the mean standing at 176.680, so the whole area was in a state of phosphorus-limited potential eutrophication. In October 2012, the N/P ratio of the study area was between 30.654 and 97.282, with the mean standing at 65.433, and the waters was in a state between medium-phosphorus-limited potential eutrophication and phosphorus-limited potential eutrophication. In May 2013, the N/P ratio was between 45.893 to 83.433, with the mean standing at 60.639, so the researched waters were in a state between medium-phosphorus-limited potential eutrophication and phosphorus-limited potential eutrophication. In November 2015, the N/P ratio of the study area was between 18.636 and 54.377, with the mean standing at 32.234, so the study area was in a state of medium-phosphorus-limited potential eutrophication and medium-eutrophication.

Table 6. *Result of potential eutrophication evaluation over years*

Time	Category	DIN (mg/L)	DIP (mg/L)	N/P	Level	Nutrition level
2010.5	Maximum	1.0041	0.019	318.031	VI_P	Phosphorus-limited potential eutrophication
	Minimum	0.5862	0.0106	108.818	VI_P	Phosphorus-limited potential eutrophication
	Mean	0.7926	0.0156	176.680	VI_P	Phosphorus-limited potential eutrophication
2012.10	Maximum	1.6146	0.0403	97.282	VI_P	Phosphorus-limited potential eutrophication
	Minimum	0.5123	0.0181	30.654	V_P	Medium- phosphorus-limited potential eutrophication
	Mean	0.8513	0.0286	65.433	VI_P	Phosphorus-limited potential eutrophication
2013.5	Maximum	1.520	0.041	83.433	VI_P	Phosphorus-limited potential eutrophication
	Minimum	0.306	0.014	49.804	V_P	Medium- phosphorus-limited potential eutrophication
	Mean	0.602	0.022	61.712	VI_P	Phosphorus-limited potential eutrophication
2015.11	Maximum	0.924	0.106	54.377	V_P	Medium- phosphorus-limited potential eutrophication
	Minimum	0.213	0.012	18.636	II	Mesotrophic
	Mean	0.474	0.035	32.234	V_P	Medium- phosphorus-limited potential eutrophication

From 2010 to 2015, the N/P ratio of the researched waters presented a declining trend and the area shifted from phosphorus-limited potential eutrophication to medium-phosphorus-limited potential eutrophication. In the study area, there was excessive nitrogen and deficient phosphorus, but the gap between the content of these two nutrients was narrowing. Once the content of phosphorus rises due to an increased discharge of pollutants from outfalls or rivers, the area will be very likely to suffer from eutrophication.

Analysis of causes

According to the characteristics of the temporal distribution, the content of nutrients and the eutrophication level in the study area were higher in autumns than in springs,

http://www.aloki.hu ● ISSN 1589 1623 (Print) ● ISSN 1785 0037 (Online)
DOI: http://dx.doi.org/10.15666/aeer/1706_1406914085

which was largely because the phytoplankton begins reproduction and consumes nitrogen and phosphorus in springtime (Li et al., 2018; Sun et al., 2016).

According to the spatial distribution of nutrients and the conditions of eutrophication, the nutrient content declined from the shore to the sea and from north to south, with the estuary marking the highest content. Inside the northern seawall of the study area are coastal industrial parks and aquaculture plants, and outside the seawall are outfalls and berths. Effluents of these human activities discharged into the sea influence the water quality along the northern coastline. As for the southern part of the study area, inside the seawall are farmlands, which produce relatively less pollutants.

The eutrophication level of the study area is largely subject to the pollutants discharged to the sea from the rivers. Industrial effluents, urban sewage, and agricultural wastewater that are rich in such nutrients as nitrogen and phosphorus enter the sea from the Zhongshan River, the Abandoned Yellow River, and the Northern Irrigation Canal of Jiangsu, which increases the content of nutrients in the study area, exacerbates eutrophication, and gives rise to high-content areas that radiate from the estuaries.

The area and condition of high content of nutrients at the estuary vary with the conditions of discharge from the river. Channels of the Zhongshan River, the Abandoned Yellow River, and the Northern Irrigation Canal of Jiangsu are all gate-controlled channels, so the monitored content of pollutants in the waters near the estuaries was correlated to the status of the gate (i.e. whether the gate was open or not). The salinity of the sea near the estuary during investigations reflected the conditions of discharge of fresh water from the rivers. According to the result of the salinity investigation performed in 2010 (*Fig. 10*), a low-salinity area occurred in the waters close to the estuaries of these three rivers, which meant that the gates of these three rivers were open at that time. As a result, the estuaries marked the highest content of nutrients and highest level of eutrophication in the study area in 2010. According to the salinity map of 2015 (*Fig. 10*), waters surrounding the Zhongshan River estuary showed low salinity and waters surrounding the other two estuaries did not, which means the gates of the other two rivers were closed at the time of investigation and thus there was no discharge of freshwater into the sea from these two rivers. Consequently, the high content of nutrients only occurred around the Zhongshan River estuary in 2015. In short, pollutants from the rivers and effluents from production activities along the coastline and the nearby continent are major factors that determine the concentration of nutrients and the level of eutrophication in the study area (Hu et al., 2016; Zhang et al., 2018).

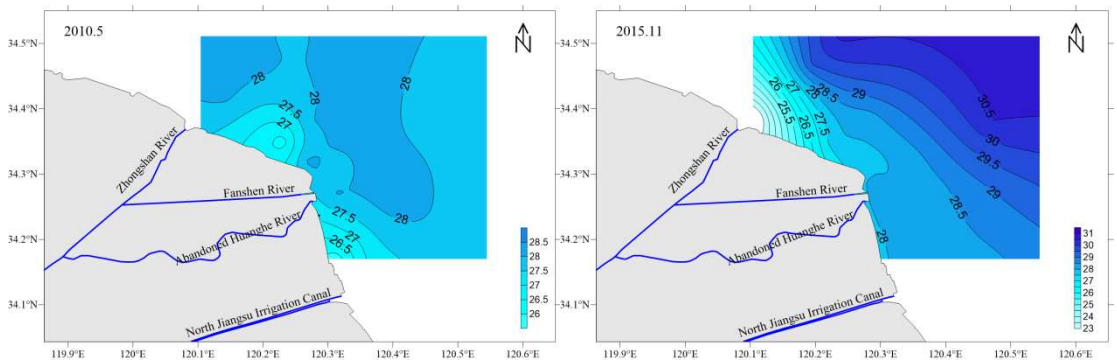

(a) Spatial distribution of salinity in May 2010 (b) Spatial distribution of salinity in November 2015

Figure 10. *Spatial distribution of salinity in the study area in May 2010 and November 2015 (unit: ‰)*

http://www.aloki.hu ● ISSN 1589 1623 (Print) ● ISSN 1785 0037 (Online)
DOI: http://dx.doi.org/10.15666/aeer/1706_1406914085

According to the China Marine Environmental Quality Bulletin of 2015, China's marine pollution areas were mainly distributed in Liaodong Bay, Bohai Bay, Laizhou Bay, Jiangsu coast, Yangtze Estuary, Hangzhou Bay, Zhejiang coast, Pearl River Estuary. The main pollution factors were inorganic nitrogen, active phosphate and petroleum. Inorganic nitrogen and active phosphate had become the main pollution factors in China's coastal areas, and the problem of seawater eutrophication was grim. Areas with serious eutrophication were mainly concentrated in estuaries, bays and coastal waters. Land-source pollutants from rivers entering the sea and coastal development activities were the main reasons for eutrophication (Chen et al., 2017; Dai et al., 2016; Li et al., 2018; Sun et al., 2016). Eutrophication had become a water environment problem in coastal waters of China.

Based on four-time water quality data of the Abandoned Yellow River Delta, this study analyzed the trend and distribution characteristics of nutrients in this area. For long-term eutrophication changes, distribution rules and characteristics, continuous monitoring and further analysis of the water quality are still needed in the abandoned Yellow River Delta. For the reasons of eutrophication, this paper makes a preliminary discussion. In the future, quantitative research should be strengthened on the extent and scope of impacts of human activities especially rivers, on eutrophication in coastal waters. In view of the eutrophication problem in coastal areas, it is necessary to reduce the amount of nutrients into the sea from the river and strengthen the regulation of sewage discharge from coastal development activities.

Conclusion

According to this study, the following conclusions are reached.

First, in 2010, 2012, 2013 and 2015, the average DIN concentration in the study area first increased and then declined, and the average DIP concentration followed a fluctuating trend, with the concentration higher in autumns than in springs. The DIN concentration in all the years of investigation exceeded the standard concentration for Level-I sea water and the rate that the DIP concentration exceeded the standard was between 61.9% and 100%.

Second, the mean of the trophic state index remained above 3 over the years of investigation and the study area was in a eutrophic state. The mean of TSI fluctuated, with the value higher in autumns than in springs.

Third, the mean of the eutrophication index over the years of investigation indicated that the researched waters were in the medium-eutrophic state; the maximum of the eutrophication index increased from 2010 to 2012, and from 2012 to 2015, it remained relatively high, which means that part of the researched waters were subject to severe eutrophication, with the estuaries marking the most eutrophic areas.

Fourth, there is an excess of nitrogen and a deficiency in phosphorus in the study area, but the N/P ratio declined from 176.680 in 2010 to 32.234 in 2015, which means the gap between the content of nitrogen and that of phosphorus narrowed and that the researched waters shifted from a state of phosphorus-limited eutrophication to medium-phosphorus-limited eutrophication. If the content of phosphorus rises due to the discharge of pollutants and effluents from rivers, the study area will in all likelihood suffer from eutrophication.

Lastly, according to the analysis from the perspective of time, the content of nutrients and the level of eutrophication in the study area is higher in autumns than in springs,

http://www.aloki.hu ● ISSN 1589 1623 (Print) ● ISSN 1785 0037 (Online)
DOI: http://dx.doi.org/10.15666/aeer/1706_1406914085

which is largely because the phytoplankton begins reproduction and consumes such nutrients as nitrogen and phosphorus during this time. According to the analysis from the perspective of spatial distribution, the content of nutrients and level of eutrophication declines from the land outwards and from north to south, with the estuaries marking the highest values. Pollutants from rivers and effluents from human activities along the coastline and in the adjacent land to the sea are major factors that determine the temporal and spatial distribution of the content of nutrients and level of eutrophication in the waters of the Abandoned Yellow River Delta.

REFERENCES

[1] Andersen, J. H., Schueter, L., et al. (2006): Coastal eutrophication: recent developments in definitions and implications for monitoring strategies. – Plankton Res 28: 621-628.
[2] Bian, J. Y., Yuan, L., Wang, Q., et al. (2013): Analysis on the trend of seawater quality variation and assessment of eutrophication at Yangshan Deep-water Port. – Marine Science Bulletin 32(1): 107-112.
[3] Cabrita, M. T., Silva, A., et al. (2015): Assessing eutrophication in the portuguese continental exclusive economic zone within the european marine strategy framework directive. – Ecological Indicators 58: 286-299.
[4] Capriulo, G. M., Smith, G., Troy, R., et al. (2002): The planktonic food web structure of a temperate zone estuary and its alteration due to eutrophication. – Hydrobiologia 475/476: 263-333.
[5] Chen, Y. W., Wang, X., Cai, M. H. (1999): Meizhou Bay marine nutrition status evaluation. – Marine Environmental Science 3: 39-42.
[6] Chen, Y., Zhao, Q., Xu, G. P., (2017): Eutrophication assessment of estuary area in the northern part of Liaodong Bay in summer based on artificial neutral network method. – Transactions of Oceanology and Limnology 5: 48-57.
[7] Dai, A. Q., Shi, X. Y., Tang, H. J., et al. (2016): The two-grade entropy maximization model for eutrophication fuzzy assessment: a case study of eutrophication assessment in Yangtze River estuary and its adjacent area. – Journal of Ocean University of Qingdao 2016(9): 59-70.
[8] Desmit, X., Thieu, V., Billen, G., et al. (2018): Reducing marine eutrophication may require a paradigmatic change. – Science of the Total Environment 635: 1444-1466.
[9] Diaz, R. J., Rosenberg, R. (1995): Marine benthic hypoxia: A review of its ecological effects and the behavioural responses of benthic macrofauna. – Oceanography and Marine Biology 33: 245-303.
[10] Guo, W. D., Zhang, X. M., Yang, Y. P., et al. (1998): Evaluation of the potential eutrophication of China's offshore waters. – Taiwan Strait 1: 64-70.
[11] Hu, Q., Qu, L., Huang, B. G., et al. (2016): Status and evaluation on nutrients for the adjacent sea water of the Yellow River estuary in autumn of 2014. – Marine Environmental Science 35(5): 732-738.
[12] Jiang, T. L., Xu, H. D., Pan, H. Z., et al. (1991): Present situation and evaluation of water environment in Southwest Laizhou Bay. – Marine Science Bulletin 10(2): 17-52.
[13] Li, P., Guo, Z., Mo, H. L., Wang, D., et al. (2018): Temporal and spatial distribution of guangxi inshore nutrients. – Transactions of Oceanology and Limnology 3: 148-156.
[14] Perus, J., Bonsdorff, E. (2004): Long-term changes in macrozoobenthos in the Åland archipelago, northern Baltic Sea. – Sea Research 52(1): 45-56.
[15] Pinckney, J. L., Paerl, H. W., Tester, P., et al. (2001): The role of nutrient loading and eutrophication in estuarine ecology. – Environmental Health Perspectives 109(5): 699-706.

http://www.aloki.hu ● ISSN 1589 1623 (Print) ● ISSN 1785 0037 (Online)
DOI: http://dx.doi.org/10.15666/aeer/1706_1406914085

[16] Redfield, A. C. (1963): The influence of organisms on the composition of sea water. – The Sea: 26-77.
[17] Richardson, K. (1997): Harmful or exceptional phytoplankton blooms in the marine ecosystem. – Advances in Marine Biology 31: 301-385.
[18] Sun, W., Tang, X. C., Xu, Y. D., Liu, Y. J., et al. (2016): Characteristics of nutrients and eutrophication assessment of the Laoshan Bay, Qingdao. – Transactions of Oceanology and Limnology 6: 45-52.
[19] Telesh, I. V., Alimov, A. F., Golubkov, S. M., et al. (1999): Response of aquatic communities to anthropogenic stress: a comparative study of Neva Bay and the eastern Gulf of Finland. – Hydrobiologia 393: 95-105.
[20] Zhang, A. Q., Jiang, H. H., Gu, Z. P., et al. (2018): Composition, distribution and seasonal variation of surface seawater nutrients in Jiangsu coastal waters. – Transactions of Oceanology and Limnology 2: 50-59.
[21] Zhang, S., Zhu, Z., Gao, C. M. (2014): The analysis and evaluation of water quality in the artificial reefs areas, Haizhou Bay. – Advanced Materials Research 7: 1368-1375.
[22] Zhao, J. H., Li, F. (2015): The recognition of characteristics and pollution sources of nutrients in Haizhou Bay. – Environmental Science & Technology 38(12Q): 32-35.
[23] Zou, J. Z., Dong, L. P., Qin, B. P. (1983): A preliminary discussion on eutrophication and red tide in Bohai Bay. – Marine Environmental Science 2(2): 42-53.

http://www.aloki.hu ● ISSN 1589 1623 (Print) ● ISSN 1785 0037 (Online)
DOI: http://dx.doi.org/10.15666/aeer/1706_1406914085

DETERMINING LEAF YIELD, SOME PLANT CHARACTERS AND LEAF ESSENTIAL OIL COMPONENTS OF DIFFERENT CULTIVARS OF LAVENDER AND LAVANDIN (*LAVANDULA* SPP.) ON THE HARRAN PLAIN ECOLOGICAL CONDITIONS

ÖZEL, A.

Department of Crop Sciences, Faculty of Agriculture, Harran University, Şanlıurfa, Turkey
(e-mail: hozel@harran.edu.tr; phone: +90-506-316-2859)

(Received 28th May 2019; accepted 31st Oct 2019)

Abstract. This study was conducted to determine the yield and some plant characters of different types of lavender (*Lavandula* spp.) at Harran University, Faculty of Agriculture, in Şanlıurfa, Turkey, during 2015, with Randomized Complete Block Design with three replications. In the study, 5 different types of lavender [*L. angustifolia* (Grosso Tina, English cv.) and *L. x intermedia* (Abriel, Dutch, Grosso cv.)] were used as plant material. This research was determined the plant height (29.30-31.15 and 25.47-30.10 cm), canopy diameter (47.72-56.86 and 44.33-47.60 cm), dry herb yield (91.32-111.80 and 66.17-103.31 g plant^{-1}), dry leaf yield (68.52-83.11 and 53.36-78.99 g plant^{-1}) and essential oil ratio (0.92-0.99% and 0.87-0.99%) of *L. angustifolia* and *L. x intermedia*, respectively. In addition, the major constituents of the essential oils of *L. angustifolia* and *L. intermedia* leaves were determined to be 1.8 cineol (33.11-36.19%), camphor (21.04-22.15%) and borneol (7.33-9.63%).
Keywords: *leaf yields, volatile oil constituents, herb yields, L. angustifolia, L. x intermedia*

Introduction

In recent years, the use and trade of medicinal and aromatic plants has increased significantly. This has made these crops sought after in domestic and foreign markets (Baydar and Erbas, 2007). The *Lavandula* genus belongs to the family of *Lamiaceae* (*Labiatae*) and has perennial species containing aromatic flowers and leaves. There are about 39 lavender species (*Lavandula* spp.), most of which originate from the Mediterranean region. There are three important species of lavender in the world with high commercial value. These are lavender (*Lavandula angustifolia* Mill), lavandin (*Lavandula x intermedia* Emeric ex Loisel) and spike lavender (*Lavandula spica* Medik.). More in the world, lavender and lavandin species are being cultivated (Baydar, 2009). Lavender essential oil quality is the best, while lavandin varieties have higher essential oil yield (Baydar and Erbas, 2007). Lavender and lavandin essential oils have a wide range of uses due to its many properties. It is used in perfumery and cosmetics industry because of its beautiful smell and is used in the pharmaceutical industry due to its sedative and pain-relieving properties (Baydar, 2009). Also, the herb essential oils of lavender and lavandin possible used be in fermentative or enzymatic processes involving various microorganisms, especially filamentous fungi, for the production of antimicrobials, antioxidants and other bio products with pharmaceutical and cosmetic activities, opening up new challenging perspectives in white biotechnology applications (Meessen et al., 2015).

It has been reported that the essential oil components of *Lavandula* species vary according to plant parts (Touati et al., 2011), genotype (Kara and Baydar, 2013), ecological conditions (Khalajee et al., 2017) and cultivation technique (Chrysargyris et al., 2017). The essential oils of *Lavandula* species show different chemotypes. The main

http://www.aloki.hu ● ISSN 1589 1623 (Print) ● ISSN 1785 0037 (Online)
DOI: http://dx.doi.org/10.15666/aeer/1706_1408714094

components of lavender essential oil are linalyl acetate (25.0-47.0%), linalool (25.0-45.0%) and camphor (0.5-1.5%) (ISO 3515), whereas the main components of lavandin essential oil are linalool (28.0-38.0%), linalyl acetate (19.0-29.0%) and camphor (7.0-11.0%) (ISO 3054). Lavender essential oil is included the lower camphor content than the essential oil of lavandin. Therefore, lavender essential oil is better than lavandin essential oil (Kara and Baydar, 2013). For these reasons, we can say that the most important indicator of lavender essential oil quality is the camphor ratio.

The leaves and stems of *Lavandula* plants are contain essential oil like flowers. In commercial lavender essential oil production, flowers are generally used, but contain a significant amount of essential oil of leaves and stems. For this reason, it is important to know the essential oil components of lavender and lavandin leaves.

The aim of this study is to determine the leaf yields, some plant characteristics and leaf essential oil components of lavender and lavandin varieties.

Materials and methods

In the study, *L. angustifolia* (Grosso Tina and English cv.) and *L. x intermedia* Emeric ex Loisel, (Abriel, Dutch and Grosso cv.) obtained from the Atatürk Horticultural Central Research Institute, Yalova, seedlings were used as plant materials.

The trial was carried out in the summer of 2015 in Harran University, Faculty of Agriculture, Eyyübiye Campus, Agricultural Research and Application Field, in Şanlıurfa, Turkey. The experimental field was located in South-eastern Anatolia region (in the Harran Plain) where semi-arid climate conditions are prevail, and some climatic data for the area are given in *Table 1*.

Table 1. *Monthly average some climate data in Şanlıurfa (Anonymous, 2016)*

Mounts	Temperature (°C)			Total Precipitation (mm)	Relative Humidity (%)	Sunshine Duration (h)
	Minimum	Maksimum	Mean			
January	-3.1	17.2	6.2	82.5	68.8	3.7
February	-0.6	18.2	7.6	100.8	74.3	3.5
March	2.5	24.8	11.7	79.0	58.9	5.8
April	4.7	29.9	15.7	24.3	49.7	7.9
May	11.8	36.9	22.8	10.3	38.0	10.4
June	16.7	38.4	27.7	0.7	35.3	12.1
July	21.4	42.8	33.2	0.2	26.5	12.4
August	22.1	43.1	31.5	0.0	37.4	11.1
September	18.7	40.4	29.8	0.0	30.5	9.0
October	12.7	33.0	21.6	58.8	50.5	6.0
November	6.8	24.3	14.0	7.9	48.1	6.1
December	0.5	20.0	8.6	25.3	50.8	4.6
Average/ Total	-3.1	43.1	19.2	389.8	47.4	7.7

In the Sanliurfa province, where the typical continental climate prevails, the summers are hot and dry and the winters are cold and rainy. Throughout vegetation period, totally 389.8 mm precipitation were recorded.

The soils where the experiment was established are deep and flat soils with flat all sides. Typical red profiles have a clayy texture. The whole profile is very calcareous, low organic matter content, high cation exchange capacity (Dinç et al., 1988).

The trial area was plowed deeply before planting, then mixed by a cultivator and made ready for planting. In trail area, before the surface tillage, 150 cc da^{-1} herbicide

http://www.aloki.hu ● ISSN 1589 1623 (Print) ● ISSN 1785 0037 (Online)
DOI: http://dx.doi.org/10.15666/aeer/1706_1408714094

(*trifluralin*), 10 kg da^{-1} N, 10 kg da^{-1} $P_2 0_5$ and 10 kg da^{-1} K_2O composite fertilizer (15.15.15) was applied. The experiment was set up as four rows each was 5 m in length, for each cultivars. The seedlings were planted by hand, in the each plot with 70 x 50 cm distance on May 16, 2014. The trial was planned to the Randomised Block Design with three replicated. Immediately after planting, seedlings were given water. During the growing period, according to the needs of the plant irrigation and weed operation was performed according to the weed condition. The 10 plants were harvested, after the side effects were removed from the middle parts (3 repetitions), with 15 cm high from the ground on November 20, 2015 and the related observations were taken. After harvest *Lavandula* plant samples were separated in leaves and stems. Each samples were naturally dried in shadow and kept at 4°C until analysis. In the trial, plant height (cm), canopy diameter (cm), dry herba yield (g $plant^{-1}$), dry leaf yield (g $plant^{-1}$), volatile oil ratio in dry leaf (%) and volatile oil components (%) were determined to the method proposed by Balyemez (2014). Since the varieties did not bloom in the experimental year, there were no observations about the flowers.

Essential Oil isolation

Each dry *Lavandula* leaf sample (50 g) was hydrodistilled with 500 ml water in a Clevenger type apparatus during 3 h. The essential oil was stored in a dark glass bottle and kept at 4°C until GC-MS analysis.

Gas chromatography-mass spectrometry analysis

Lavandula essential oil was analysed by GC-MS using an Agilent 7890A equipped with an electron impact quadruple, Agilent 5975C mass spectrometer detector. The electron ionization energy was 70 eV, scan range 35-450 amu and scan rate 1 scans $second^{-1}$. The GC column was used an HP Innowax Capillary (A fused silica capillary column 5% phenyl-poly-dimethyl-siloxane), film thickness of 0.25 μm, a length of 60 m, and internal diameter 0.25 mm. The carrier gas was helium with a flow rate 0.8 ml $minute^{-1}$. Inlet temperature was 250°C. The GC oven temperature program was used as follows; 60°C initial temperature, hold for 10 min, raised at 4°C min^{-1} to 220°C and finally hold at 220°C for 10 min. A 1% (v/v) solution of the sample in n-Hexane was prepared and 1μl was injected using a 40:1 split ratio.

The identification of compounds was performed by comparing their mass spectra with data from Adams, US National Institute of Standards and Technology (NIST, USA) and WILEY 1996 Ed. mass spectra library. The identification of compounds was also based on the Kovats retention indices.

The data were subjected to analysis of variance (ANOVA) using Randomized Complete Block Design. The significance of differences among the different cultivars was determined using LSD with 5%.

Results and Discussion

Determined average the plant height, canopy diameter, dry herb yield, dry leaf yield and essential oil ratios of the varieties of different *Lavandula* species was given *Table 2*.

As shown in *Table 2*, the highest plant height, canopy diameter, dry herb yield and dry leaf yield were determined in Grosso Tina cultivar of the *L. angustifolia* and Grosso cultivar of the *L. x intermedia* type. In general, all properties were examined,

http://www.aloki.hu ● ISSN 1589 1623 (Print) ● ISSN 1785 0037 (Online)
DOI: http://dx.doi.org/10.15666/aeer/1706_1408714094

L. angustifolia species was higher than *L. x intermedia*. This difference may be caused by genotypic difference.

As seen in *Table 2*, there was no statistically significant difference between the varieties in terms of essential oil ratio. The ratio of essential oils were varied between 0.91% and 1.01% depended on cultivars. The highst essential oil ratio was determined on the Grosso Tina and the Grosso cultivars.

Table 2. *Average the plant height, canopy diameter, dry herb yield, dry leaf yield and essential oil ratios depending on the varieties of different Lavandula species in 2015*

Species	Cultivars	Plant Height (cm)	Canopy Diameter (cm)	Dry Herb Yield (g plant^{-1})	Dry Leaf Yield (g plant^{-1})	Essential Oil Ratio (%)
L. angustifolia	Grosso Tina	25.90 a*	67.17 a	138.43 a	101.80 a	1.01
	English	32.30 b	57.73 b	111.30 b	84.70 b	0.96
L. x intermedia	Abriel	32.17 b	56.27 b	106.60 b	80.59 b	0.91
	Dutch	28.80 c	54.33 b	82.80 c	64.37 c	0.98
	Grosso	35.10 ab	57.60 b	116.67 b	89.37 b	1.01
Avarege		32.85	58.62	111.17	84.16	0.97
LSD (%5)		**2.96**	**4.18**	**13.74**	**9.60**	**NS.**

*****The mean values with the same letter within variable are not significantly different (LSD P < 0.05); **NS**. No significant

According to *Lavandula* varieties, the ratio of the essential oil components detected in the leaves and the ratio of the chemical groups of the essential oil components are given in *Tables 3* and *4*, as percentage.

In total, between 51-52 components were quantified and characterized in the leaf essential oils of *L. angustifolia* and *L. x intermedia* cultivars, accounting for 97.31-99.55% (by GC peak area) of total oils. The main constituents in the essential oil of *Lavandula* leaves were 1.8 cineol 35.24% (33.11-36.19%), camphor 21.79% (21.04-22.15%), borneol 8.63% (7.33-9.63%), tau-cadinol 3.01% (2.46-3.35%), limonene 2.53% (2.11-2.86%), caryophyllene oxide 2.39% (2.12-2.63%), cumin aldehyde 1.91% (1.56-2.08%), carvone 1.45% (1.23-1.55%), *delta*-terpineol 1.43% (1.39-1.47%), *gamma*-cadinene 1.28% (1.05-1.44%), *trans*-verbenol 1.17% (1.13-1.24%), *trans*-carveol 1.12% (1.10-1.19%), *p*-cymene 1.11% (1.03-1.18%), *alpha*-terpineol 1.02% (0.90-1.11%) and terpinen-4-ol 1.01% (0.81-1.31%) (*Table 3*). However, the leaf essential oil was characterized by the presence of two dominating constituents (1.8 cineol and camphor with more than 54% composed of components). The other compounds detected in the range 0.05-1.00%. Essential oils of *Lavandula* species have been previously investigated by some researchers. In lavender, it was found the main components of the essential oil that in leaves 1,8-cineole 25.70% and borneol 11.32% (Meftahizade et al., 2011), borneol 15.21%, 1,8-cineole 8.50% and geraniol acetate 5.21% (Skwirzyńska et al., 2013), 1,8-cineole 31.9%, borneol 24% and camphor 16.1% (Hassanpouraghdam et al., 2011); in inflorescence β-linalool 18.74-34.43% and linalool acetate 20.68-30.57% (Zagorcheva et al., 2013), 1,8-cineole 64.99-71.08% and limonene 8.58-9.11% (Koleilat et al., 2017), linalool 28.5-43.9%, linalyl acetate 5.38-25.7% and cymene 1.14-11.30% (Kara and Baydar, 2013), linalool 33.7%, 1,8-cineole 17.1% and borneol 14.7% (Hassanpouraghdam et al., 2011).

http://www.aloki.hu ● ISSN 1589 1623 (Print) ● ISSN 1785 0037 (Online)
DOI: http://dx.doi.org/10.15666/aeer/1706_1408714094

Table 3. *The leaves essential oil composition ratio (%) in the cultivars of Lavandula angustifolia and L. intermedia*

R.T.	Components	*L. angustifolia*		*L. intermedia*			Mean
		English	Grs.Tina	Grosso	Dutch	Abriel	
12.420	*alpha*-Pinene	0.99	0.87	0.82	1.03	0.96	0.93
13.528	Camphene	1.63	0.56	0.55	0.65	0.62	0.80
14.461	*beta*-Pinene	0.93	0.94	0.87	1.01	0.98	0.95
14.713	Sabinene	0.46	0.38	0.35	0.41	0.38	0.40
15.278	*delta*-3-Carene	0.19	0.21	0.23	0.25	0.19	0.21
15.480	Myrcene	0.11	0.12	0.18	0.15	0.07	0.13
15.859	*alpha*-Terpinene	0.40	0.12	0.20	0.04	0.08	0.17
16.201	Limonene	2.11	2.62	2.53	2.86	2.54	2.53
16.391	1.8 Cineol	36.19	35.16	33.11	35.78	35.94	35.24
16.936	*gamma*-Terpinene	0.36	0.19	0.19	0.21	0.18	0.23
17.275	*o*-Cymene	0.37	0.34	0.38	0.40	0.40	0.38
17.323	*p*-Cymene	1.09	1.03	1.09	1.18	1.16	1.11
18.426	Tyranton	-	0.46	-	0.48	-	0.19
18.845	Hexyl butanoate	0.07	-	0.05	0.03	0.11	0.05
18.947	Perillene	0.16	0.22	0.21	0.22	0.21	0.20
19.078	1-Octen-3-ol	0.21	0.36	0.27	0.23	0.24	0.26
19.183	*p*-Cymenene	0.15	0.16	0.10	0.14	0.04	0.12
19.321	*trans*-Sabinene hydrate	0.65	0.74	0.75	0.94	0.84	0.78
19.408	*trans*-Limonene oxide	0.13	0.16	0.16	0.18	0.16	0.16
19.694	*alpha*-Campholenal	0.28	0.30	0.36	0.29	0.30	0.31
19.862	Linalool	0.12	0.16	0.16	0.16	0.10	0.14
20.050	Camphor	22.05	21.04	21.87	22.15	21.84	21.79
20.149	cis-p-Menth-2-en-1-ol	0.12	0.17	0.17	0.17	0.11	0.15
20.350	Lavandulyl acetate	0.19	0.25	0.24	0.09	0.15	0.18
20.435	Pinocarvone	0.89	0.94	0.95	0.58	0.88	0.85
20.486	Terpinen-4-ol	1.31	1.01	0.96	0.81	0.95	1.01
20.608	*trans*-p-Menth-2.8-dien-1-ol	0.28	0.37	0.38	0.31	0.35	0.34
20.836	Lavandulol	0.22	0.33	0.35	0.24	0.13	0.25
20.879	Myrtenal	0.67	0.70	0.71	0.67	0.68	0.69
20.925	*delta*-Terpineol	1.40	1.47	1.47	1.39	1.42	1.43
21.001	*trans*-Verbenol	1.14	1.18	1.24	1.13	1.17	1.17
21.085	*alpha*-Terpineol	0.90	1.11	1.06	1.03	0.99	1.02
21.201	Borneol	7.33	9.47	9.63	8.37	8.35	8.63
21.331	Lavandulyl isovalerate	0.15	-	0.39	0.04	0.44	0.20
21.366	Geranyl propanoate	-	0.92	0.22	0.80	0.32	0.45
21.386	Eucarvone	0.43	-	0.27	-	0.12	0.16
21.460	Verbenone	0.23	0.20	0.21	0.13	0.23	0.20
21.551	Carvone	1.23	1.53	1.55	1.48	1.48	1.45
21.699	*gamma*-Cadinene	1.05	1.33	1.44	1.25	1.31	1.28
21.758	Myrtenol	0.39	0.40	0.42	0.38	0.41	0.40
21.894	Cumin aldehyde	1.56	2.08	2.02	2.02	1.89	1.91
21.965	*trans*-Carveol	1.02	1.14	1.19	1.10	1.17	1.12
22.044	*p*-Cymen-8-ol	0.69	0.73	0.77	0.70	0.77	0.73
22.163	*cis*-Calamenene	0.17	0.24	0.24	0.19	0.22	0.21
22.947	*alpha*-Terpinen-7-al	0.34	0.35	0.37	0.29	0.34	0.34
23.446	Caryophyllene oxide	2.42	2.35	2.63	2.12	2.41	2.39
23.628	Ledol	0.25	-	0.07	0.13	0.15	0.12
23.757	1.10-di-epi-Cubenol	0.22	0.23	0.28	0.34	0.26	0.27
23.868	*p*-Cymen-7-ol	0.94	1.01	1.07	0.97	0.99	1.00
24.551	*tau*-Cadinol	2.46	3.10	3.35	3.15	3.01	3.01
24.762	*epi-alpha*-Bisabolol	0.20	0.30	0.27	0.29	0.25	0.26
26.393	*cis*-14-nor-Muurol-5-en-4-one	0.23	0.25	0.26	0.24	0.26	0.25
26.534	Cadina-4.10(15)-dien-3-one	0.23	0.25	0.27	0.24	0.28	0.25
Total		**97.31**	**99.55**	**98.88**	**99.44**	**98.83**	**98.80**

http://www.aloki.hu ● ISSN 1589 1623 (Print) ● ISSN 1785 0037 (Online)
DOI: http://dx.doi.org/10.15666/aeer/1706_1408714094

In lavandin, it was found the main component of the inflorescence essential oil that 1,8-cineole 33.54% and camphor 18.89% (Koleilat et al., 2017), linalool 34.8-43.3%, linalyl acetate 3.76-44.46% and camphor 5.28-19.8% (Kara and Baydar, 2013). In *L. dentata*, it was found the main component of the leaf essential oil that 1,8-cineole 33.54% and camphor 18.89% (Touati et al., 2011). In *L. stoechas*, it was found the main component of the essential oil that fenchone 31.6%, camphor 22.4% and *p*-cymene 6.5% (Dob et al., 2006). Some researchers declared that the essential oil composition of lavender and lavandin varied depending on the genotype of the plant (Kara and Baydar, 2013), fertilization (Arabaci and Bayram, 2005; Chrysargyris et al., 2017), growth stage on the harvesting time (Baydar and Erbas, 2007), parts of the plant (Touati et al., 2011), harvest times at different on the day and year (Zheljazkov et al., 2012), drying conditions (Özgüven et al., 2007) and essential oil isolation technique (Skwirzyńska et al., 2013; Khalajee et al., 2017). Some similarities were recorded between our study and the previous reports. Investigation of our results revealed that the main component of leaves essential oils of lavender and lavandin cultivars were found 1.8 Cineol, like other researchers (Hassanpouraghdam et al., 2011; Meftahizade et al., 2011; Touati et al., 2011; Koleilat et al., 2017).

Table 4. *The leaves essential oil chemical groups ratio (%) in the cultivars of Lavandula officinalis and L. intermedia*

Chemical groups	*L. angustifolia*		*L. intermedia*		
	English	**Grs. Tina**	**Grosso**	**Dutch**	**Abriel**
Monoterpenes	**89.53**	**89.51**	**88.95**	**89.85**	**89.53**
Monoterpene Hydrocarbons	*8.79*	*7.54*	*7.49*	*8.33*	*7.60*
Oxygenated Monoterpenes	*80.74*	*81.97*	*81.46*	*81.52*	*81.93*
Sesquiterpenes	**7.15**	**7.80**	**8.94**	**7.75**	**8.33**
Sesquiterpene Hydrocarbons	*1.22*	*1.57*	*1.68*	*1.44*	*1.53*
Oxygenated Sesquiterpenes	*5.93*	*6.23*	*7.26*	*6.31*	*6.80*
Others	0.63	2.24	0.99	1.84	0.97
Total	**97.31**	**99.55**	**98.88**	**99.44**	**98.83**

Baydar (2009) stated that better quality essential oil was included low camphor content and the camphor content in quality lavender oil must be between 0.5 and 1% in lavenders and between 5.0 and 10.0 in lavandins. Our result show that leaves essential oils of lavender and lavandin were included high camphor content (21.04-22.05% in lavender and 21.79-22.15% in lavandin). In this case, as the percentage of leaves in the plant during harvest increases, the amount of camphor in the volatile oil will also increase. In order to produce quality lavender essential oil, as few leaves as possible should be harvested.

GC/MS examinations of the essential oil indicated that monoterpens (88.95-89.85%) were characterized as the main class of components, followed by a minor rate of sesquiterpens (7.15-8.94%) in leaves of lavender and lavandin cultivars. It consists mainly of oxygenated monoterpenes (80.74-81.97%). Additionally, the leaves essential oil contained 7.49-8.79% monoterpene hydrocarbons, 5.93-7.26% oxygenated sesquiterpenes, 1.22-1.68% sesquiterpene hydrocarbons, and 0.63-2.24% other (*Table 4*). The concentrations of sesquiterpene hydrocarbons were lowest. Higher amounts of oxygen-containing monoterpenes in oils strongly support the dynamic pool of plastidal hydroxylases and dehydrogenases involved in the post-modification of the initial hydrocarbonic compounds (Hassanpouraghdam et al., 2011). Sesquiterpenes had a minor

http://www.aloki.hu ● ISSN 1589 1623 (Print) ● ISSN 1785 0037 (Online)
DOI: http://dx.doi.org/10.15666/aeer/1706_1408714094

share in the component classification, and the oxygenated compounds was higher than that of hydrocarbon sesquiterpenes. The lavender plant was potentiated in the biosynthesis and accumulation of monoterpenes rather than sesquiterpene ones. 1,8-Cineole was characterized as the most important oxidized compound and Camphor was the chief ketonic compounds of leaf essential oil.

Conclusion

Finally, the chemical profile of the leaf essential oil of lavender and lavandin cultivars were similar and showed a high content of 1,8-cineole, borneol and camphor. Camphor ratio was founded to be high in the essential oils of all cultivars leaves. If we are to produce high quality essential oil (low camphor), we must reduce the leaf content in the dry matter. The effect of lavender flower spike axis and stalk essential oil components on commercial lavender oil should be determined.

REFERENCES

[1] Anonymous (2016): Monthly average climate values. – Regional Directorate of Meteorology, Şanlıurfa.
[2] Arabaci, O., Bayram, E. (2005): The effect of nitrogen fertilization and plant density on some agronomic and quality traits of lavender (*Lavandula angustifolia* Mill.) under ecological conditions of Aydin. – Adnan Menderes Uni. J. of Agric. Faculty 2(2): 13-19.
[3] Balyemez, Ö. E. (2014): Determining yield and some plant characters of different types of lavender (Lavandula spp.) under the Harran plain conditions. – MSc thesis, Harran University Natural Sciences Institute, Turkey.
[4] Baydar, H. (2009): Lavender. Medicinal and Aromatic Plant Science and Technology (3th press). – Suleyman Demirel University Press 51: 274-278. Isparta (in Turkish).
[5] Baydar, H., Erbas, S. (2007): Effects of harvest time and drying on essential oil properties in lavandin (*Lavandula x intermedia* Emeric ex Loisel.). – I. International Medicinal and Aromatic Plants Conference on Culinary Herbs, 29 April - 4 May 2007, Antalya-Turkey.
[6] Chrysargyris, A., Drouza, C., Tzortzakis, N. (2017): Optimization of potassium fertilization/nutrition for growth, physiological development, essential oil composition and antioxidant activity of *Lavandula angustifolia* Mill. – Journal of Soil Science and Plant Nutrition 17(2): 291-306.
[7] Dinç, U., Şenol, S., Sayın, M., Kapur, S., Güzel, N., Derici, R., Yeşilsoy, M. Ş., Yeğingil, D., Sari, M., Kaya, Z., Aydın, M., Kettaş, F., Berkman, A., Çolak, A. K., Yılmaz, K., Tunç Göğüs, B., Çavuşgil, V., Özbek, H., Gülüt, K. Y., Karaman, C., Dinç, O., Öztürk, N., Kara, E. E. (1988): The Soils of Southeastern Anatolia Region (GAT) 1. Harran Plain. – TUBİTAK Agriculture and Forestry Group Guided Research Project, Final Result Report. Project Number: TOAG-534. (in Turkish).
[8] Dob, T., Dahmane1, D., Agli1, M., Chelghoum, C. (2006): Essential oil composition of *Lavandula stoechas* from Algeria. – Pharmaceutical Biology 44(1): 60-64.
[9] Hassanpouraghdam, M. B., Hassani, A., Vojodi, L., Asl, B. H., Rostami, A. (2011): Essential oil constituents of *Lavandula officinalis* Chaix. from Northwest Iran. – Chemija 22(3): 167-171.
[10] ISO 3515 (2004): Oil of lavender (*Lavandula angustifolia* Mill.). – French type.
[11] ISO 3054 (2017): Eseential oil of lavandin Abrial (*Lavandula angustifolia* Mill. x *Lavandula latifolia* Medik.). – French type.

http://www.aloki.hu ● ISSN 1589 1623 (Print) ● ISSN 1785 0037 (Online)
DOI: http://dx.doi.org/10.15666/aeer/1706_1408714094

[12] Kara, N., Baydar, H. (2013): Determination of lavender and lavandin cultivars (*Lavandula* sp.) containing high quality essential oil in Isparta, Turkey. – Turkish Journal of Field Crops 18(1): 58-65.
[13] Khalajee, M. B., Jaimand, K., Mozaffari, S., Mirshokraie, S. A. (2017): Comparative study on essential oils of *Lavandula officinalis* L. from three different sites with different methods of distillation. – Journal of Medicinal Plants and By-products 1: 53-58.
[14] Koleilat, M., Raafat, K., El-Lakany, A., Aboul-Ela, M. (2017): Designing monographs for *Rosmarinus officinalis* L. and *Lavandula angustifolia* L.: Two Lebanese species with significant medicinal potentials. – Pharmacogn J. 9(4): 452-474.
[15] Meessen, L. L., Bou, M., Sigoillot, J. C., Faulds, C. B., Lomascolo, A. (2015): Essential oils and distilled straws of lavender and lavandin: a review of current use and potential application in white biotechnology. – Appl Microbiol Biotechnol. 99(8): 3375-3385.
[16] Meftahizade, H., Moradkhani, H., Barjin, A. F., Naseri B. (2011): Application of *Lavandula officinalis* L. antioxidant of essential oils in shelf life of confectionary. – African Journal of Biotechnology 10(2): 196-200.
[17] Özgüven, M., Bux, M., Koller, W. D., Sekeroglu, N., Kirpik, M., Muller, J. (2007): Influence of fluctuating drying conditions during shade, sun and solar drying on the quality of *Lavandula officinalis L.*, O*riganum syriacum* L. and *Thymbra spicata* L. – Zeitschrift fur Arznei- & Gewurzpflanzen 12(2): 80-87.
[18] Skwirzyńska, M. A., Śmist, M., Swarcewicz, M. (2013): Comparison of extraction methods for the determination of essential oil content and composition of lavender leaves. – Chemistry & Chemical Technology, Available online: http://ena.lp.edu.ua:8080/ bitstream/ntb/27086/1/069-180-181.pdf
[19] Touati, B., Chograni, H., Hassen, I., Boussa, M., Toumi, L., Brahima, N. B. (2011): Chemical composition of the leaf and flower essential oils of Tunisian *Lavandula dentata* L. (*Lamiaceae*). – Chemistry & Biodiversity 8: 1560-1569.
[20] Zagorcheval, T., Stanev, S., Rusanov, K., Atanassov, I. (2013): Comparative GC/MS analysis of lavender (*Lavandula angustifolia* Mill.) inflorescence and essential oil volatiles. – Agricultural Science and Technology 5(4): 459-462.
[21] Zheljazkov, V. D., Astatkie, T., Hristov, A. N. (2012): Lavender and hyssop productivity, oil content, and bioactivity as a function of harvest time and drying. – Industrial Crops and Products 36: 222-228.

http://www.aloki.hu ● ISSN 1589 1623 (Print) ● ISSN 1785 0037 (Online)
DOI: http://dx.doi.org/10.15666/aeer/1706_1408714094

[1]H NUCLEAR MAGNETIC RESONANCE SPECTROSCOPY REVEALS SECONDARY METABOLIC VARIATIONS OF SPECIAL TEA (*MONSONIA BURKEANA* PLANCH. EX HARV) POPULATIONS FROM THREE SELECTED LOCATIONS IN SOUTH AFRICA

NNZERU, L. R.* – TSHIKHUDO, P. P. – NTUSHELO, K. – MUDAU, F. N.

Department of Agriculture and Animal Health, University of South Africa, Private Bag X6, Science Campus, Florida 1710, South Africa

**Corresponding author*
e-mail: Lnnzeru@gmail.com

(Received 28th May 2019; accepted 10th Sep 2019)

Abstract. The present study was conducted to assess the secondary metabolite profile differences of *Monsonia burkeana* populations naturally grown at Chuenespoort, Zebediela and Rietondale in South Africa. Three field surveys were conducted on 14 January 2015, 11 January 2016 and 4 May 2016 respectively in Chuenespoort, Zebediela and Rietondale and secondary metabolite profiles of the plants were determined using [1]H nuclear magnetic resonance (NMR) spectroscopy coupled with principal component analysis (PCA). Leaf samples from three plants per locality in the first survey and fourteen plants per site in subsequent samplings were included in the NMR analysis. Based on [1]H NMR spectroscopy and PCA of secondary metabolite profile data no major differences were detected between the populations except for the first survey where the Zebediela and the Chuenespoort populations were more closely related to each other than the Rietondale population. This study has for the first time determined differences between three plant populations of special tea with regards to secondary metabolite profiles.
Keywords: *plant population analysis, Monsonia burkeana, secondary metabolites, nuclear magnetic resonance, principal component analysis*

Introduction

Special tea (*Monsonia burkeana* Planch. ex Harv) (*Fig. 1*) is a prominent medicinal plant which is used to cure minor ailments (Venter, 1979) and it is native to Southern African countries such as Botswana, Lesotho, Mozambique, Namibia, Swaziland and South Africa (Wells et al., 1986; Gibbs Russel et al., 1987). This tea plant was recently reported in Madagascar (Schatz et al., 2011). Over and above indigenous knowledge various studies have uncovered the potential health benefits of special tea, among them, anti-diabetic and anticancer properties (Ngoepe et al., 2018; Mathivha, et al., 2019). Various biological and physical characteristics determine plant growth, plant traits and chemical composition, and therefore plant populations of various habitats are likely to differ in average plant height, average stem diameter, average number of leaves per plant, average dry biomass, leaf fat content, leaf protein content and secondary metabolite profiles (Khokhar and Magnusdottir, 2002; Clayton et al., 2006; Ohno et al., 2011; Von Staszewski et al., 2011; Sabhapondit et al., 2012; Lee et al., 2014a). For a wild tea plant which is harvested and traded it is important to determine if different populations are affected by their habitat characteristics so that productivity can be predicted and the harvested product quality can be standardized. Three populations of *M. burkeana* were selected for the assessment.

http://www.aloki.hu ● ISSN 1589 1623 (Print) ● ISSN 1785 0037 (Online)
DOI: http://dx.doi.org/10.15666/aeer/1706_1409514103

Figure 1. *Special tea (Monsonia burkeana Planch. ex Harv) plant growing in Rietondale, Gauteng Province, South Africa*

Nuclear magnetic resonance (NMR) spectroscopy coupled with principal component analysis (PCA) have been employed to evaluate the quality of foods and drugs and to evaluate drug toxicity (Khokhar and Magnusdottir, 2002; Ohno et al., 2011; Lee et al., 2014a; Martínez-Richa et al., 2003; Morita et al., 2004; Morita et al., 2008; Jiang et al., 2015). The use of this approach has been extended to plant population studies to assess differences as well as gauge various traits like plant population survival. Thus, in this study whose aim was to assess differences between three plant populations of special tea naturally grown in Chuenespoort, Zebediela and Rietondale and secondary metabolites profile differences of special tea populations were revealed using NMR coupled with PCA.

Materials and methods

Study area

Three sites, namely, Zebediela (Long: 24° 11′ 6″ S and Lat: 29° 27′ 42″ E), Chuenespoort (Long: 24° 10′ 56″ S and Lat: 29° 27′ 29″ E) and Riotendale (Long: 25° 43′ 43″ S and Lat: 28° 14′ 19″ E) were selected for the study. Zebediela and Chuenespoort are in the Limpopo province of South Africa about 20 km apart and Rietondale is in the Gauteng province about 300 km from the other two sites (*Figs. 2* and *3*).

These sites are isolated and natural except for Chuenespoort which was a maize field. However, no apparent disturbance took place at these sites, including Chuenespoort, during the survey period. Three field surveys were conducted on 14 January 2015, 11 January 2016 and 4 May 2016 as shown in *Table 1*. The climate data was included to show one of the aspects that vary between the sites but no aspect of climate is part of the investigation.

http://www.aloki.hu ● ISSN 1589 1623 (Print) ● ISSN 1785 0037 (Online)
DOI: http://dx.doi.org/10.15666/aeer/1706_1409514103

Figure 2. *A modified Google map of the north-eastern South Africa showing the study sites, Zebediela, Chuenespoort and Rietondale where the leaf samples of Monsonia burkeana were collected for secondary metabolite profiling. The city of Johannesburg is circled in black*

Table 1. *Average daily rainfall and maximum temperatures in the 90 days before sampling in Zebediela (Z), Chuenespoort (C) and Rietondale (R). Notice that the Rietondale site received more rain and was warmer than the other two sites*

Survey	Average daily rainfall (mm) 90 days before sampling	Average maximum temperature (°C) 90 days before sampling
^{Z}1 14 January 2015	70.0	26.9
^{C}1 14 January 2015	70.0	26.9
^{R}1 14 January 2015	130.0	28.9
^{Z}2 11 January 2016	32.2	29.0
^{C}2 11 January 2016	32.4	29.0
^{R}2 11 January 2016	62.0	31.3
^{Z}3 04 May 2016	50.0	27.0
^{C}3 04 May 2016	50.0	27.0
^{R}3 04 May 2016	102.0	28.7

http://www.aloki.hu ● ISSN 1589 1623 (Print) ● ISSN 1785 0037 (Online)
DOI: http://dx.doi.org/10.15666/aeer/1706_1409514103

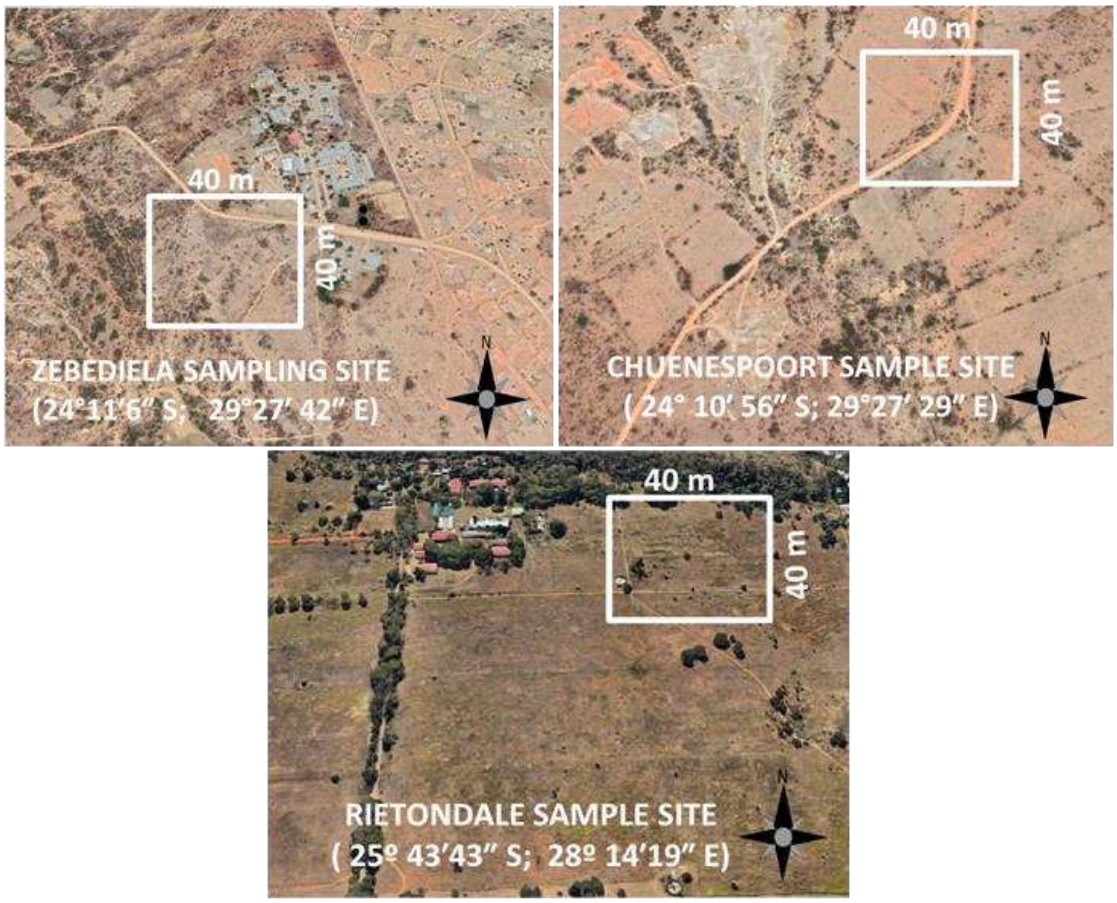

Figure 3. *Study sites Zebediela, Chuenespoort and Rietondale showing the demarcation of unitary quadrats in which leaf samples of Monsonia burkeana were collected for secondary metabolite profiling*

Secondary metabolite profiles of the plants were determined, three plants per locality in the first survey, fourteen plants per site in subsequent samplings. Secondary metabolite profiles were determined by ^{1}H NMR using a 600 MHz NMR Varian spectrometer to obtain magnetic spectra of the samples. Both phase and baseline corrections of the spectra were done using the ACD/NMR Processor. Only the most visibly discriminant range (assessed from spectra) was included in the bucketing for PCA. After processing the spectra, the intensity values represented by the spectra were exported as ASCII files and these intensity values were displayed on MS Excel to form a matrix which was used for PCA. PCA reduces dimensions of a dataset. It works by using an orthogonal transformation to convert a set of possible correlated variables into was is referred to as principal components. The principal components are designed in such a way as to explain as much of the possible variability. The first principal component has the largest possible variance and incrementally from the first principal component to successive principal components the possible variance decreases. For the dataset obtained in this study, the PCA was done using Multibase. Datapoints which represented NMR intensity values of the secondary metabolites extracted from the leaves of the plant samples from each of the localities were spread along PC 1 and PC 2. On the PCA scatterplot ellipses were drawn to show the discrimination between the localities.

http://www.aloki.hu ● ISSN 1589 1623 (Print) ● ISSN 1785 0037 (Online)
DOI: http://dx.doi.org/10.15666/aeer/1706_1409514103

Results

Secondary metabolite profiles which were determined by [1]H NMR spectroscopy, slightly varied or did not vary at all between the populations of Zebediela, Chuenespoort and Rietondale. Zebediela and the Chuenespoort populations were more closely related to each other than the Rietondale population in the first survey as shown by the PCA plot (*Fig. 4*) and the spectra shown in *Figure 5*.

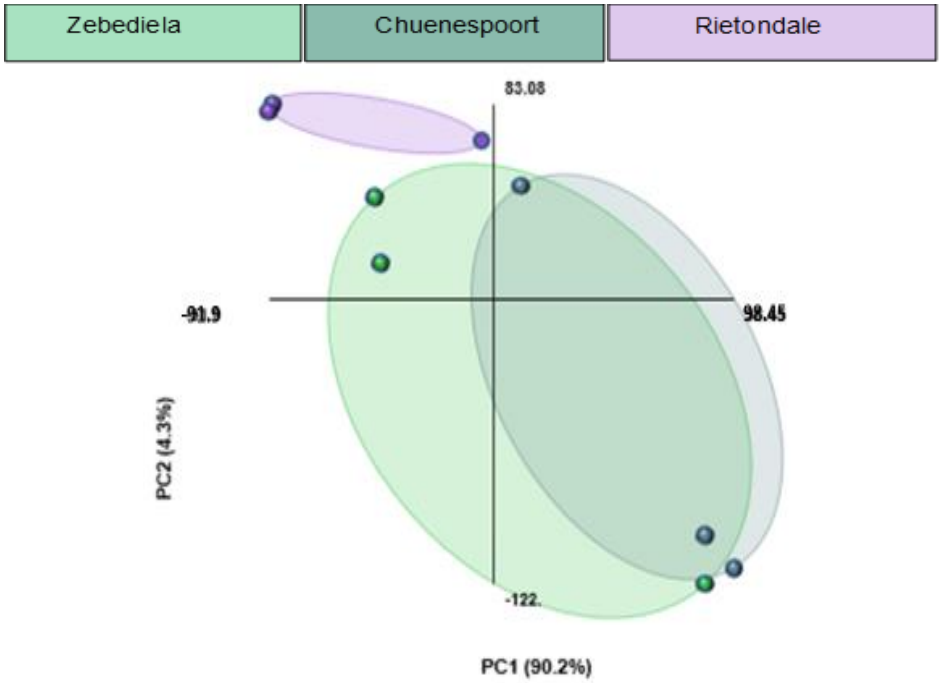

Figure 4. *Principal component analysis plot of [1]H NMR intensity values of secondary metabolites of Monsonia burkeana leaf samples from Zebediela, Rietondale and Chuenespoort. The sampling dates was 14 January 2015. The PCA plots show that the Rietondale site is slightly different from the other two sites which are similar*

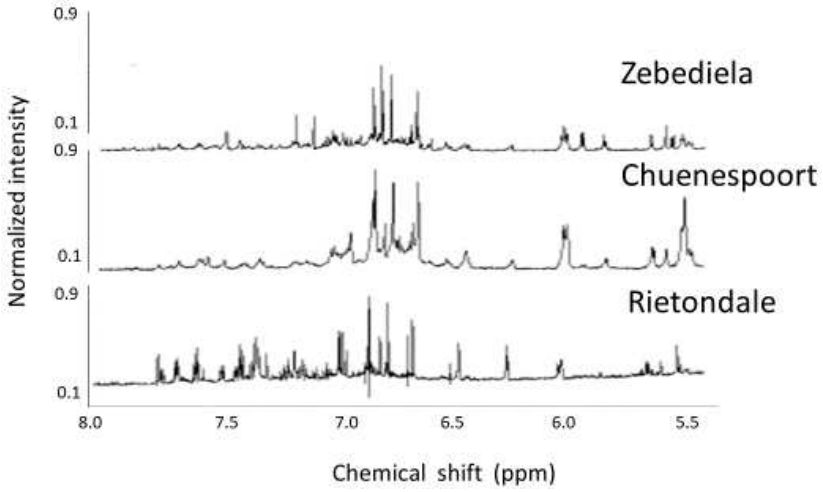

Figure 5. *[1]H NMR spectra of Monsonia burkeana leaf secondary metabolites in the 8.0–5.5 ppm range. Sampling was done in 14 January 2015. Notice that the spectrum of the Zebediela locality and Chuenespoort's are visible different from the Rietondale spectrum*

http://www.aloki.hu ● ISSN 1589 1623 (Print) ● ISSN 1785 0037 (Online)
DOI: http://dx.doi.org/10.15666/aeer/1706_1409514103

In subsequent surveys, no difference in secondary metabolite profiles were detected in the different plant populations. The differences in the ^{1}H NMR spectra of special tea leaves from three plant populations shown in *Figure 5* was clearly as a result of differences in the 5.5–8.0 ppm range which was selected from the original shift scale which was from 0 ppm to 14 ppm. Within this discriminant region, it was obvious that the segregation was further determined by the region between 6.5 ppm and 7.8 ppm. The regions of sharp differences between the Rietondale spectra and either of the spectra, Zebediela and Chuenespoort must have caused the separation of the Zebediela ellipse from the other ellipses in the PCA plot in *Figure 4*.

Discussion

The current study revealed slight differences in the secondary metabolite profiles of three areas in one of three samplings conducted on 14 January 2015, 11 January 2016 and 4 May 2016. Studying natural plant populations is always challenging because of the inability to determine all interacting factors. The authors of this manuscript intended just to assess differences in the secondary metabolomic profiles of *M. burkeana* populations in Zebediela, Chuenespoort and Rietondale without investigating all underlying biophysical factors. However, it was found necessary to obtain rainfall and temperature data since rainfall and temperature are assumed to be major determinants of the growth and survival of the plant. The Rietondale site which is located about 300 km south of the other two sites received a little more rain and was also slightly warmer than the other sites. Despite these observable differences it was not possible to assume that these climatic differences were the main causes of the marked secondary metabolite profile differences observed in the samples collected on the 14 January 2015. A more comprehensive study would be necessary to assess this aspect. The scope of this work was only limited to assess if there are any differences in the secondary metabolomic fingerprint. However, it was unsurprising to find some differences in the secondary metabolite profiles of the study populations given the differences between plant populations caused by factors such as rainfall, temperature, soil type and altitude. The difference in secondary metabolites may be attributed to variation in rainfall received during the sampling periods. It was noted that in the first survey of the current study high rainfall was recorded as compared to the subsequent two surveys where low rainfall was received. A study conducted by Wedeking et al. (2018) indicated that drought stress triggers various physiological and biochemical responses in plants. The exposure of plants to various stress conditions results in modulations in metabolite contents and altered metabolic interactions, caused by alterations in environmental parameters, such as light, temperature and water (Mittler, 2006).

Secondary metabolism of plants may change considerably due to the influence of several biotic and abiotic stress signals (Pavarini et al., 2012). The finding of the current study is in agreement with Lee et al. (2014b) who found that secondary metabolites from the *Curcuma* spp. from different geographical locations using PCA was not different between the locations. However, this is in disagreement with Martin et al. (2016) who found that secondary metabolites from *Galium odoratum* showed clear differences between the plants from nature and those of controlled growth conditions as well as internal variation within the group. Lee et al. (2010) studied the effects of climatic conditions on *C. sinensis* metabolites in three different growing areas of Jeju Island, South Korea using ^{1}H NMR spectroscopy and found the revealed clear

http://www.aloki.hu ● ISSN 1589 1623 (Print) ● ISSN 1785 0037 (Online)
DOI: http://dx.doi.org/10.15666/aeer/1706_1409514103

discriminations of green teas from the three different growing areas. The ^{1}H NMR technique itself provides a solution for the identification and quantification of metabolites in plant cell, tissue, organ and extracts (Halabalaki et al., 2014; Zhou et al., 2017). Both PCA and orthogonal projections to latent structures discriminant analysis (OPLS-DA) revealed clear discriminations of green teas from the three different growing areas in terms of theanine, isoleucine, leucine, valine, alanine, threonine, glutamine, quinic acid, glucose, epicatechin (EC), epigallocatechin (EGC), epigallocatechin-3-gallate (EGCG), and caffeine levels. The PCA revealed a separation between the Longjing type and other Chinese teas in metabolites differences. Changes in seasonal climatic conditions affect flavanol and purine alkaloid contents of two leaves and a bud of tea (Wang et al., 2011). Lengthy period of precipitation decreases EGC, EC, ECG, EGCG and their total content but increases C content, whereas increased daily average temperature decreases the levels of EGC, EC, ECG, EGCG and C in green tea. The EGCG, CG and total catechins (TC) in *C. sinensis* grown at a high altitude are higher than those grown at a low altitude (Chen et al., 2010).

Nchabeleng et al. (2012) determined the chemical composition of wild bush (*Athrixia phylicoides* DC.) tea growing at locations differing in altitude, climate and edaphic factors. There was a positive correlation ($r^2 = 0.55$) between total polyphenol content of *A. phylicoides* and altitude. Samples of *Angelica gigas* collected from different geographical regions were distinguished by Kim et al. (2011) using ^{1}H NMR spectroscopy and ultraperformance liquid chromatography–mass spectrometry (UPLC-MS) followed by multivariate data analyses. The study concluded that ^{1}H NMR and UPLC-MS-based metabolic profiling coupled with chemometric analysis can be used to discriminate the geographical origins of various herbal tea. The variations of the total and individual catechin contents of tea were evaluated among three cultivars grown in 10 locations; the dynamic changes of chlorophyll and catechin contents in two cultivars during young leaf development were also analysed. This study highlights how metabolomics coupled with multivariate statistical analysis can illuminate the metabolic characteristics of *M. burkeana.* This application can be extended to do special tea quality studies.

Conclusion

In conclusion, based on ^{1}H NMR and principal component analysis of secondary metabolite profile data no major differences were detected between the populations except only in the first survey when the Zebediela and the Chuenespoort populations were more closely related to each other than the Rietondale population. Follow-up studies must focus on an in-depth understanding of the various causes of secondary metabolite profile differences between populations in various localities in South Africa. Discriminatory secondary metabolites must be identified using various applications from NMR to chromatography coupled with mass spectrometry. Moreover, future studies should determine the growth potential of *M. burkeana* under controlled conditions, and further metabolomic profiling of the special tea growing under controlled conditions.

Acknowledgements. We thank Mr. Livhuwani Nemutandani and Mr. Mpho Nematswerani for assistance during the field survey. Ms. Kemello Mathe assisted with NMR analysis. Mr. Joe Matsapola from the

http://www.aloki.hu ● ISSN 1589 1623 (Print) ● ISSN 1785 0037 (Online)
DOI: http://dx.doi.org/10.15666/aeer/1706_1409514103

South African Weather Services provided the historical weather data. This study was funded partially by the National Research Foundation (NRF) grant (TTK 1206051038).

Conflict of interests. The authors declared that there is no conflict of interests regarding the publication of this paper.

REFERENCES

[1] Chen, Y., Jiang, Y., Duan, J., Shi, J., Xue, S., Kakuda, Y. (2010): Variation in catechin contents in relation to quality of 'Huang Zhi Xiang' Oolong tea (*Camellia sinensis*) at various growing altitudes and seasons. – Food *C*hem. 119(2): 648-652.

[2] Clayton, T. A., Lindon, J. C., Cloarec, O., Antti, H., Charuel, C., Hanton, G., Provost, J. P., Le Net, J. L., Baker, D., Walley, R. J., Everett, J. R., Nicholson, J. K. (2006): Pharmaco-metabonomic phenotyping and personalized drug treatment. – Nature 440(7087): 1073-077.

[3] Gibbs Russell, G. E. W. G., Welman, E., Reitief, K. L., Immelman, G., Germishuizen, B. J., Pienaar, M. V., Wyk, A., Nicholas, A. (1987): List of species of Southern African plants. – Memoirs Botanical Survey South Africa 2(1-2): 1-152 (pt. 1): 1-270 (pt. 2).

[4] Halabalaki, M., Vougogiannopoulou, K., Mikros, E., et al. (2014): Recent advances and new strategies in the NMR-based identification of natural products. – Curr. Opin. Biotechnol. 25: 1-7.

[5] Jiang, X., Liu, Y., Wu, Y., Tan, H., Meng, F., Wang, Y. S., Li, M., Zhao, L., Liu, L., Qian, Y., Gao, L., Xia, T. (2015): Analysis of accumulation patterns and preliminary study on the condensation mechanism of proanthocyanidins in the tea plant [*Camellia sinensis*]. – Sci. Rep. 5: 8742.

[6] Khokhar, S., Magnusdottir, S. G. (2002): Total phenol, catechin, and caffeine contents of teas commonly consumed in the United Kingdom. – J. Agric. Food Chem. 50: 565-570.

[7] Kim, E. J., Kwon, J., Park, S. H., Park, C., Seo, Y. B., Shin, H. K., Kim, H. K., Lee, K. S., Choi, S. Y., Ryu, D. H., Hwang, G. S. (2011): Metabolite profiling of *Angelica gigas* from different geographical origins using [1]H NMR and UPLC-MS analyses. – J. Agric. Food Chem. 59(16): 8806-8815.

[8] Lee, J., Lee, J., Chung, J., Ahhwang, J., Lee, J., Lee, C., Hong, Y. (2010): Geographical and climatic dependencies of green tea (*Camellia sinensis*) metabolites: a [1]H NMR-based metabolomics study. – J. Agric. Food Chem. 58: 10582-10589.

[9] Lee, L., Kim, S., Kim, Y., Kim, Y. (2014a): Quantitative analysis of major constituents in green tea with different plucking periods and their antioxidant activity. – Molecules 19: 9173-9186.

[10] Lee, J., Jung, Y., Shin, J., Kim, H. K., Moon, B. M., Ryu, D. H., Hwang, G. (2014b): Secondary metabolite profiling of curcuma species grown at different locations using GC/TOF and UPLC/Q-TOF MS. – Molecules 19: 9535-9551.

[11] Martin, B., Frederich, M., de Tullio, P., Tits, M., Wauters, J. N., Choi, Y. H., Bodson, M. (2016): Metabolomics analysis of *Galium odoratum* (L.) scopus: impact of the plant population origin and growth conditions. – Curr. Metabolomics 3(2): 122-129.

[12] Martínez-Richa, A., Joseph-Nathan, P. (2003): Carbon-13 CP-MAS nuclear magnetic resonance studies of teas. – Solid State Nucl. Magn. 3: 119-135.

[13] Mathivha, L. P., Thibane, V. S., Mudau, F. N. (2019): Anti-diabetic and anti-proliferative activities of herbal teas, Athrixia phylicoides DC and *Monsonia burkeana* Planch. ex Harv, indigenous to South Africa. – Br. Food J. 121(4): 964-974.

[14] Mittler, R. (2006): Abiotic stress, the field environment and stress combination. –Trends in Plant Science 11(1): 15-19.

[15] Morita, A., Horie, H., Fujii, Y., Takatsu, S., Watanabe, N., Yagi, A., Yokota, H. (2004): Chemical forms of aluminum in xylem sap of tea plants (*Camellia sinensis* L.). – Phytochemistry 65: 2775-2780.

http://www.aloki.hu ● ISSN 1589 1623 (Print) ● ISSN 1785 0037 (Online)
DOI: http://dx.doi.org/10.15666/aeer/1706_1409514103

[16] Morita, A., Yanagisawa, O., Takatsu, S., Maeda, S., Hiradate, S. (2008): Mechanism for the detoxification of aluminum in roots of tea plant (*Camellia sinensis* (L.) Kuntze). – Phytochemistry 69: 147-153.
[17] Nchabeleng, L., Mudau, F. N., Mariga, I. K. (2012): Effects of chemical composition of wild bush tea (*Athrixia phylicoides* DC.) growing at locations differing in altitude, climate and edaphic factors. – J. Med. Plants Res. 6(9): 1662-1666.
[18] Ngoepe, N. M., Mbita, Z., Mathipa, M., Mketo, N., Ntsendwana, B., Hintsho-Mbita, N. C. (2018): Biogenic synthesis of ZnO nanoparticles using *Monsonia burkeana* for use in photocatalytic, antibacterial and anticancer applications. – Ceram. Int. 44(14): 16999-17006.
[19] Ohno, A., Oka, K., Sakuma, C., Okuda, H., Fukuhara, K. (2011): Characterization of tea cultivated at four different altitudes using [1]H NMR analysis coupled with multivariate statistics. – J. Agric. Food Chem. 59: 5181-5187.
[20] Pavarini, D. P., Pavarin, S. P., Niehues, M., Lopes, N. L. (2012): Exogenous influenceson plant secondary metabolite levels. – Anim Feed Sci. Tech. 176: 5-16.
[21] Sabhapondit, S., Karak, T., Bhuyan, L. P., Goswami, B. C. Hazarika, M. (2012): Diversity of catechin in northeast Indian tea cultivars. – The Scientific World Journal. DOI: 10.1100/2012/485193.
[22] Schatz, G. E. S., Andriambololonera-Andrianarivelo, M. W., Callmander Faranirina, P. P., Lowry, P. B., Phillipson Rabarimanarivo, J. I., Raharilala Rajaonary Rakotonirina, R. H., Ramananjanahary, B., Ramandimbisoa, A., Randrianasolo, N., Ravololomanana, Z. S., Rogers, C. M., Taylor, A., Wahlert, G. A. (2011): Catalogue of the vascular plants of Madagascar. – Monogr. Syst. Bot. Missouri Botanical Garden.
[23] Venter, H. J. T. (1979): A Monograph of Monsonia L. (Geraniaceae). – H. Veenman & Zonen B. V., Wageningen, pp. 26-32.
[24] Von Staszewski, M., Pilosof, A. M. R., Jagus, R. J. (2011): Antioxidant and antimicrobial performance of different Argentinean green tea varieties as affected by whey proteins. – Food Chem. 125(1): 186-192.
[25] Wang, L. Y., Wei, K., Jiang, Y. W., Cheng, H., Zhou, J., He, W., Zhang, C. C. (2011): Seasonal climate effects on flavanols and purine alkaloids of tea (*Camellia sinensis* L.). – Eur Food Res Technol. 233(6): 1049-1055.
[26] Wedeking, R., Maucourt, M., Deborde, C., Moing, A., Gibon, Y., Goldbach, H. E., Wimmer, M. A. (2018): [1]H NMR metabolomic profiling reveals a distinct metabolic recovery response in shoots and roots of temporarily drought-stressed sugar beets. – PLoS One 13(5): e0196102.
[27] Wells, M. J., Balsinhas, V. M., Joffe, H., Engelbrecht, V. M., Harding, G., Stirton, C. H. (1986): A Catalogue of Problem Plants in Southern Africa, Incorporating the National Weed List of South Africa. – Memoirs of the Botanical Survey of South Africa, Botanical Research Institute, Pretoria, South Africa, No. 53.
[28] Zou, P., Song, Y., Lei, W., Li, J., Tu, P., Jiang, Y. (2017): Application of [1]H NMR based metabolomics for discrimination of different parts and development of a new processing workflow for *Cistanche deserticola*. – Acta Pharm. Sin. B. 7(6): 647-656.

http://www.aloki.hu ● ISSN 1589 1623 (Print) ● ISSN 1785 0037 (Online)
DOI: http://dx.doi.org/10.15666/aeer/1706_1409514103

CONTAMINATION, RISK ASSESSMENT OF HEAVY METALS IN SURFACE SEDIMENTS FROM A MARICULTURE BAY IN SOUTH CHINA

SONG, Y. M.[1] – WANG, C.[2#] – LIU, S.[1] – PAN, J. C.[1] – WEI, Y. N.[1] – GUO, P. R.[1*]

[1]Guangdong Provincial Key Laboratory of Emergency Test for Dangerous Chemicals, Guangdong Engineering and Technology Research Center of Online Monitoring for Water Environmental Pollution, Guangdong Institute of Analysis, Guangzhou 510070, China

[2]School of Public Health, Sun Yat-Sen University, Guangzhou 510080, China

[#]Wang,C is co-first author.

**Corresponding author*
e-mail: guopengran@gmail.com

(Received 29th May 2019; accepted 10th Oct 2019)

Abstract. In order to assess the contamination, ecological and biotoxicity risk of heavy metals (Cd, Cr, Cu, Ni, Pb and Zn) in mariculture area of China, the total concentrations and speciation of metals were analysed in the sediments from a typical mariculture bay in 2011 and 2013. The results show that most heavy metal concentrations in 2013 were lower than those in 2011. The residual and sulfide-bound fractions were the primary fractions of heavy metals. The pollution can be described in all the sampling sites of heavy metals (except Cd) with moderate to a very high degree by geo-accumulation index (Igeo), enrichment factor (EF) and pollution load index (PLI). According to the risk assessment code (RAC), Cd, Ni and Pb posed a medium to very high ecological risk. The sampling sites that exhibited the biotoxicity risk in 2013 had higher biotoxicity levels than that in 2011. Based on statistical analysis and environmental investigation, four sites (S1, S2, S4 and S7) were highly affected by the environmental pollutants which primarily resulted from the combustion of gasoline and diesel fuel and the ships protective layer.
Keywords: *ecological risk, biotoxicity risk, Zhelin Bay, speciation, pollution load index, the risk assessment code*

Introduction

Heavy metals in ecosystems have received extensive attention because they are toxic, non-biodegradable, and easily bioaccumulate in organisms (Al-Othman et al., 2012; Dabney et al., 2018; Gao et al., 2012; Ghosh et al., 2018; Islam et al., 2014; Väänänen et al., 2016; Yang et al., 2012). With rapid industrialization and economic development in the coastal region of South China, heavy metals from industrial waste, sewage runoff, and agricultural discharges, are continuously introduced into the estuarine and bay environment through rivers, runoff, dust deposition and land-based point sources (El Nemr et al., 2016; Hyun et al., 2007; Wu et al., 2015; Yu et al., 2008). Due to the adsorption, hydrolysis, and co-precipitation of heavy metals, most of such pollutants deposit in the sediments and only a small part of free metal ions leave in water (Chaudhary et al., 2015; Hu et al., 1997; Nobi et al., 2010; Zwolsman et al., 2013.)

In recent decades, various assessment indices have been applied to assess the environmental pollution and risk of heavy metals in marine sediments. The heavy metal contamination in sediments is evaluated by the geo-accumulation index (Igeo), enrichment factor (EF) and pollution load index (PLI) (Gu et al., 2018; Liu et al., 2014; Varol et al., 2011; Wang et al., 2016;). In particular, the Hakanson risk index is prevalent in evaluating the ecological risk posed by heavy metals in sediments (Wu et al., 2014; Yi

http://www.aloki.hu ● ISSN 1589 1623 (Print) ● ISSN 1785 0037 (Online)
DOI: http://dx.doi.org/10.15666/aeer/1706_1410514120

et al., 2011; Zhuang et al., 2014.). However, the mobility and toxicity of heavy metals in sediment depend not only on their total concentrations, but also on their physicochemical fractions described as "speciation" (Yuan et al., 2004; Zhou et al., 2004.). The sequential extraction (SE) technique is often used to determine heavy metal speciation in sediments, defined operationally as acid soluble, reducible, oxidizable and residual fractions (Gao et al., 2010; Zhang et al., 2013.). Meanwhile, sediment quality guidelines (SQGs) and acid volatile sulfide (AVS)-simultaneous extracted metals (SEM) model are widely applied to analyze the bio-toxicity of heavy metals (Prica et al., 2008; Poot et al., 2009; Sundaray et al., 2011.). The exchangeable and carbonate fractions are usually used in the method of the risk assessment code (RAC) to assess the ecological risk.

Zhelin Bay, a semi-enclosed estuarial bay, which situated in the northeast part of Guangdong Province, is one of the most developed areas in China. Zhelin Bay is the largest cage mariculture areas and a vital culture fish zone in South China (Qiao et al., 2010) with many seaport container terminals for international seafood export. Due to the maritime activities, a lot of phosphorus, nitrogen, and organic wastes are discharged, and consequently result in water eutrophication (Cao et al., 2007; Liang et al., 2011; Wu et al., 2016; Xia et al., 2016). Meanwhile, the heavy metal pollution in the bay area is getting worse (Qiao et al., 2010; Xia et al., 2016). The high concentration of heavy metals in sediments can be directly or indirectly bio-accumulated in benthic invertebrates, as sediments provide the benthic fauna food sources and habitats. Therefore, the environmental hazards in the bay become increasingly severe (Kalantzi et al., 2013). The risk assessment of heavy metals in the sediment of the culture area has gained much attention because of the pollution characteristics and ecological hazards of heavy metals.

Our previous study suggested that the ecological risk level of heavy metals in this area is medium to high, especially at the northwest coastal area of the semi-closed bay (Wang et al., 2016). This study was conducted to consolidate and complement the previous results. PLI was used to assess the metal contamination compared with the EF and I_{geo} results. Based on heavy metal speciation, RAC was used to assess the ecological risk, and the results were compared with the Hakanson risk index. The AVS-SEM model was used to predict the bio-toxicity risk, and the results were compared with the SQGs. The study aims to analyze and evaluate the pollution and risk of heavy metals in this area, and identify the potential sources of high risk. The results could provide crucial information for the monitoring, management and conservation of coastal environments.

Materials and methods

Sampling

Samples of surface sediment from eleven sites were collected using a Petersen grab in September 2011 and August 2013 (*Fig. 1*) from Zhelin Bay in southern China. Temperature, salinity, pH and dissolved oxygen of the bottom water were measured by YSI water quality sensors on site (600R mode, YSI Inc., USA). Triplicate sediment samples were placed in the N_2 filled polypropylene bags rapidly after collection, immediately transported to the laboratory and freeze-dried before chemical analysis.

Chemical analysis

After drying at 70 °C for more than 24 h, the samples were re-weighted for the determination of moisture. Sediment total organic carbon (TOC) contents were estimated

http://www.aloki.hu ● ISSN 1589 1623 (Print) ● ISSN 1785 0037 (Online)
DOI: http://dx.doi.org/10.15666/aeer/1706_1410514120

by the wet oxidation method using $K_2Cr_2O_7$ -H_2SO_4 (Mingorance et al., 2007). The total concentration of heavy metal in sediment samples was analyzed following the EPA 3052 method (Wang et al., 2011). The concentrations of Al, Fe, Mn, Si, Cu, Ni, Pb, Zn, Cr and Cd in the final solutions were measured by microwave plasma-atomic emission spectroscopy (MP-AES, Agilent 4200) and atomic absorption spectrometry (AAS, Hitachi Z-2000). Analytical accuracy was achieved by the use of blanks and certified reference materials including GBW 07314 and GBW 07334, issued by the State Oceanographic Administration of China.

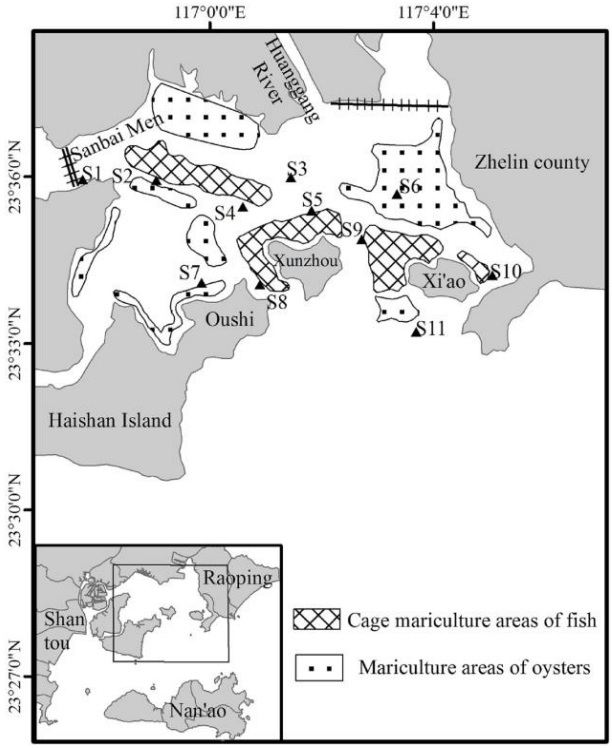

Figure 1. *The study area and sediment sampling sites in Zhelin Bay along the southern coast of China*

Extraction operations were performed by rotary shaking at 20 °C in dark environment with 100 ml of sealed centrifuge tubes. By centrifuging (4000 rpm, 10 min), the separation of the solid from solution was carried out for each step. The supernatant was then thrown away, and the residual was rinsed and centrifuged again. The centrifuge tubs were filled with N_2 in the experimental procedure. After acidifying the metal solutions with HNO_3, the metal concentration was determined by MP-AES and graphite furnace atomic absorption spectrometry (GFAAS, Thermo SOlAAR M6).

Five fractions from 4.5 g wet sediment were extracted using the proposal sequential extraction (PSE) procedure (Wang et al., 2011; Xia et al., 2016). Five fractions were weak acid soluble fraction (F1: pH 5.0, 1 M NaOAc, sample dry weight/extractant volume (SE) 1:15, 5 h), reducible fraction (F2: pH 2.0, 0.2 M NH_2OH•HCl + 0.2 mM EDTA-Na_2, SE 1:15, 5 h), organic matter bound fraction (F3: pH 9.8, 0.1 M $Na_4P_2O_7$, SE 1:10, 5 h), sulfide bound fraction (F4: 6 M HCl, SE 1:10, 1 h) and residual fraction (F5: estimated as the total metal content). F1 was the bioavailable fraction of heavy metals including the exchangeable and carbonates bound fractions.

http://www.aloki.hu ● ISSN 1589 1623 (Print) ● ISSN 1785 0037 (Online)
DOI: http://dx.doi.org/10.15666/aeer/1706_1410514120

The procedure for AVS analyses was protected by N_2 and the same with that by Allen et al. (1993). The suspension in the acidified sediment was filtrated with a 0.45 μm membrane filter (Fang et al., 2005) and analyzed by MP-AES and GFAAS. Standard materials validated the results. By methylene blue method, the sulfide in the trapping solution was analyzed.

Ultra-pure, deionized water (Milli-Q) was boiled and purged with nitrogen to remove dissolved oxygen. All glassware and plastic containers were soaked in 2.7 M HNO_3 for at least 24 h and rinsed with deionized water before use. Standard solutions were prepared by dilution of 1000 μg/mL stock solutions with deionized water. All chemicals used in the experiment were at least of analytical reagent grade (p. A.) or superior purity. The concentrations of sediment components, including AVS, TOC, and metals were expressed as dry weight normalized concentrations.

Assessment of the metal contamination

The index of contamination factor (CF) and the pollution load index (PLI) were used to describe the sediment quality. PLI of the six metals were counted (Islam et al., 2015). The PLI was defined as the nth root of the multiplications of the CF of metals.

$$\mathrm{PLI} = (CF_1 \times CF_2 \times CF_3 \times \ldots \times CF_n)^{1/n} \quad \text{(Eq.1)}$$

where $CF_{metals} = C_{metal}/C_{background}$.

The background values of Cd, Cr, Cu, Ni, Pb and Zn in sediment were 0.15, 28.6, 15.8, 14.8, 32.2 and 57.8 ug/g, respectively (Qiao et al., 2009; Wang et al., 2010). PLI evaluated the overall contamination evaluation for all sites and a contribution consequence of the six metals. Therefore, the PLI value of zero indicated excellence, 1.0 represented only baseline level pollutants, and more than 1.0 indicated gradual deterioration of estuarine environment (Tomilson et al., 1980). The contamination factor (CF) of a given metal was calculated as the ratio of its measured concentration to natural abundance. The CF was then classified into four grades for monitoring the pollution from each metal over a period of time: low degree ($CF < 1$), moderate degree ($1 \leq CF < 3$), considerable degree ($3 \leq CF < 6$), and very high degree ($CF \geq 6$). Thus, the CF values indicated the enrichment of each metal in sediments over a period of time (Islam et al., 2015).

Assessment of risk

Assessment of ecological hazardous risk

In order to assess the risk to the ecological environment, the RAC was applied (Perin et al., 1985; Zhao et al., 2012), which was defined as *Equation 2:*

$$\mathrm{RAC} = \frac{[\mathrm{M}]_{Weak}}{[M]_{Total}} \times 100\% \quad \text{(Eq.2)}$$

where $[M]_{Weak}$ was the concentration of metals in weak acid soluble fraction, and $[M]_{Total}$ was the total concentration of metals. According to the RAC values, each sample falled into one of the five tiers: i) $RAC \leq 1\%$ (no risk); ii) $1\% < RAC \leq 10\%$ (low risk); iii) $10\% < RAC \leq 30\%$ (medium risk); iv) $30\% < RAC \leq 50\%$ (high risk); v) $50\% < RAC$ (very high risk).

http://www.aloki.hu ● ISSN 1589 1623 (Print) ● ISSN 1785 0037 (Online)
DOI: http://dx.doi.org/10.15666/aeer/1706_1410514120

Assessment of biotoxicity risk

The concentrations of AVS, SEM and TOC were used to predict the toxicity (Di Toro et al., 2005). If $(\sum SEM\text{-}AVS)/f_{OC}$ was less than 150 μmol/g_{OC}, adverse effects due to SEM metals were not expected, and if $(\sum SEM\text{-}AVS)/f_{OC}$ was over than 3400 μmol/g_{OC}, suggested acute toxicity, and the range of uncertain effects was 150-3400 μmol/g_{OC} (McGrath et al., 2002).

Quality control and data analysis

The AVS, SEM and speciation analysis in replicates were measured to estimate the precision of the method. The relative standard deviation was less than 12% with the recoveries within 10% for the certified values. Total recoveries as the sum of individual metal fractions from SE compared to total contents were reasonable and ranged from 92.5-110% for Cd, 90.0-112% for Cu, 93.4-110% for Ni, 90.5-108% for Pb, and 96.9%-104% for Zn, respectively.

In this work, factor analysis and correlation analysis were used to elucidate the relationship between metals, parameters and risks, characterize the associated components of heavy metals, and identify the sources of heavy metal contamination. Correlation analysis was performed with two-tailed Pearson test, with $p < 0.05$ and $p < 0.01$ as the significant values. The descriptive statistics were used by SPSS 19.0.

Results and discussion

Distribution of heavy metals in the sediments

Among all sampling sites, no fluctuation was observed in the values of pH, dissolved oxygen (DO) and the moisture content of sediment (*Table 1*). However, the concentrations of TOC, Al, Mn, Fe, and Si show significant differences when comparing the values obtained in 2011 and 2013 ($p > 0.05$). For instance, the average value of TOC, Al, Mn, Fe, and Si was 1.11%, 9.86%, 0.104%, 5.09%, and 22.27%, respectively. In 2013, the average content of the above parameters reached 1.05%, 10.17%, 0.104%, 5.07% and 22.84%, respectively. The dissolved oxygen concentration was 2.88 ~4.72 mg/L in 2011 and 3.94~6.74 mg/L in 2013, indicating that the sampling point was an anoxic area.

The mean concentration of each metal in 2013 was lower than that in 2011 (*Fig. 2*). In 2011, the concentrations of Cd, Cr, Cu, Ni, Pb and Zn were in the ranges of 0.071–0.150, 27–35, 26–45, 31–204, 6–83 and 138–177 μg/g, with the averages of 0.108, 31, 32, 90, 76 and 156 μg/g. In 2013, the respective ranges were 0.057–0.110, 21–30, 23–35, 26–136, 51–64 and 116–196 μg/g, with the averages of 0.082, 26, 28, 55, 56 and 121 μg/g. The average values of Cu, Ni, Pb and Zn were higher than their background values, and close to their background for Cd and Cr. Heavy metal concentrations here generally exceeded the results from earlier studies (Qiao et al., 2010; Xia et al., 2016). There was a big difference on the distribution of Cd and Ni at those sampling sties. According to *Figure 2A* and *C,* Cd was mainly distributed close to the land area (S1, S2, S5, S7 and S11), and Ni near the cage mariculture areas (S2, S4, S5, S8 and S10).

The speciation distribution of heavy metals in the mariculture sediment is shown in *Figure 3.* Cr fractions were not investigated because the valence state is more important than that its bound fraction. Cd mainly was found in F1 33.6~63.8% in 2011 and 47.4~63.6% in 2013 and F4 16.9~43.4% in 2011 and 21.9~34.8% in 2013. The dominant

http://www.aloki.hu ● ISSN 1589 1623 (Print) ● ISSN 1785 0037 (Online)
DOI: http://dx.doi.org/10.15666/aeer/1706_1410514120

phase of Cu was in F5 53.6~69.2% in 2011 and 51.4~69.0% in 2013 and F4 20.0~32.7% in 2011 and 18.9~29.1% in 2013. Additionally, 5.3~12.2% in 2011 and 6.4~14.4% in 2013 of total Cu concentration existed in F3. The dominant proportion 64.0~74.1% in 2011 and 58.7~67.4% in 2011 of Pb was found in F5, and the proportions of other fractions were in the following order: F4 (12.8~19.5%, 2011), (17.1~26.7%, 2013); F1 (5.8~15.8%, 2011), (7.2~17.4%, 2013). The dominant phase of Zn was in F5, which accounted for 59.0~67.2% in 2011 and 53.0~69.6% in 2013. Ni was mostly retained in F5, representing 61.6~77.6% (in 2011), 58.6~72.5% (in 2013) of total concentration, and then F4 accounted for 8.9~23.6% (in 2011), 13.2~18.3% (in 2013) of total concentration. To sum up, Cu, Ni, Pb, Zn from the sediment were mainly present in the residual fractions, followed by the sulfide bound fractions, and then the content of organic matter bound fractions in Cu was higher than that of Cd, Pb, Ni, Zn. The Cd in the sediments was dominated by sulfide and weak acid fractions, followed by the residual fractions. On the whole, the reducing fractions of five heavy metals were low.

Assessment of the metal contamination

Figure 4 shows the CF values of each heavy metal in 2011 and 2013. It was shown that most of the CF values of the heavy metals in 2013 were lower than that in 2011, and the concentrations of heavy metals varied significantly at the eleven sampling sites. According to the CF values of heavy metals, all sites for Cd were in low degree in both years. The most sites for Cr in 2013 were in low degree, but in moderate degree in 2011. All sites for Cu and Pb were in moderate degree. Zn (at S6 in 2011 and at S8 in 2013) were in considerable degree. Half of the sites for Ni (mainly near the cage mariculture areas) were in very high degree, and heavy metal in this figure were arranged by their pollution degrees, Cd < Cr < Cu < Pb < Zn < Ni. The pollution degrees assessed by CF were higher for Zn, Cu, Cd, Pb, Ni than that by EF and Igeo in our previous studies (Wang et al., 2016.), furthermore, there were unpolluted at all sites for Cr by EF and Igeo. In general, based on CF, EF and I_{geo}, Cd at all sampling sites was unpolluted, and other heavy metals (except Cr) at all sampling sites were polluted, especially Ni near the cage mariculture areas was polluted in high degree. The PLI values of each sampling site are shown in *Figure 5*. It was shown that the PLI values in 2013 were lower than that in 2011 at all sites (except S8). At S8, the CF values of Cd, Cu, Zn and Ni in 2013 were higher than that in 2011. In both of 2011 and 2013, the PLI values were over 1.0 at all sites, which indicated that this area was polluted. In this case, despite the comprehensive pollution decreases, heavy metal pollution (especially Cd, Cu, Zn and Ni) at some site of this area should be considered for mariculture actions.

Assessment of risk

Assessment of ecological risk

The weak acid soluble fraction (F1) of Cd, Cu, Pb, Zn and Ni was analyzed, and the spatial distribution of calculated RAC values for those five metals in both two years was shown in *Figure 6* by ArcGIS. The order of ecological risk assessed by RAC was: Cd > Ni > Pb > Cu > Zn. The risk for heavy metals in 2013 was higher than that in 2011 (except Cu), the inconsistency of ecological risk and contamination shown that ecological hazardous risk was heavily affected by bound fractions of heavy metals than by their total concentrations.

http://www.aloki.hu ● ISSN 1589 1623 (Print) ● ISSN 1785 0037 (Online)
DOI: http://dx.doi.org/10.15666/aeer/1706_1410514120

The range of RAC values for Cd was from 33.6% to 68.7%, which indicated high to very high risk. In 2011, very high risks for Cd were found at more than 50% of sites, especially at S5 and S9, where RAC values exceeded 60%. In 2013, very high risks for Cd were found in most of the sites (especially at S3 and S8) except S7. The range of RAC values for Ni and Pb was from 5.0% to 17.8%, from 5.80% to 17.4% respectively, which showed low to medium risk. For Ni, the medium risks existed in more than half site in 2011 and more than 70% sites in 2013, and a higher risk was found on S7 and S9 in 2011 and on S4 and S11 in 2013. For Pb, medium risks were contributed from less than half sites in both two years, and it presented higher risk at the S6 and S11 than other sites in 2011, S7 and S10 sites were higher in 2013. The range of RAC values for Cu and Zn were from 1.80% to 5.60%, from 1.80% to 6.30% respectively, which indicated low risk. For Cu, S9 and S10 showed higher risk than other sites in 2011, and S6 and S9 were higher in 2013. For Zn, S1 and S2 showed higher risk than other sites in 2011, and S1 and S10 were higher in 2013.

The order by Hakanson risk index was: Cd > Pb > Ni > Cu > Zn (Wang et al., 2016). The orders by both RAC and Hakanson risk index were approximately the same. However, assessed by Hakanson risk index, the risk degrees was a little lower than that by RAC, the higher risk occurred in 2011. Furthermore, the spatial distribution of ecological risk for each metal was different in two assessment methods.

Assessment of biotoxicity risk

The AVS and SEM concentrations of heavy metals in mariculture sediments were showed in *Table 2*. The AVS concentrations varied with sites, ranging from 0.005 to 2.012 μmol/g in 2011 and from 0.210 to 1.706 μmol/g in 2013. The average concentrations of Cd, Cu, Ni, Pb and Zn were 0.0002, 0.187, 0.861, 0.150, 0.898 μmol/g in 2011, and 0.0003, 0.166, 0.602, 0.130, 0.992 μmol/g in 2013 respectively. The sums of AVS-SEM, ∑SEM (SEM-Cd + SEM-Cu + SEM-Ni + SEM-Pb + SEM-Zn) at S2 and S8 in 2011 and at S2 and S5 in 2013 were higher than that on the other sampling sites.

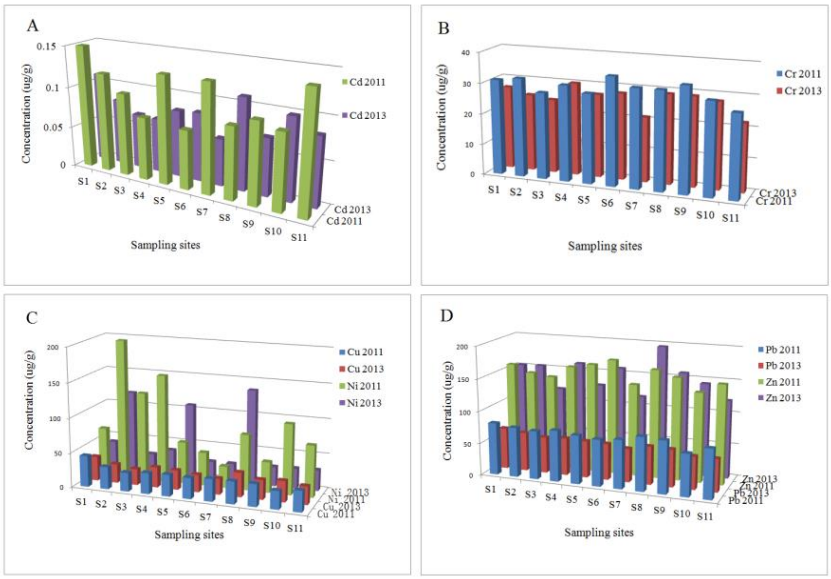

Figure 2. *The total concentration distribution of each metal at sediment sampling sites in Zhelin Bay*

http://www.aloki.hu ● ISSN 1589 1623 (Print) ● ISSN 1785 0037 (Online)
DOI: http://dx.doi.org/10.15666/aeer/1706_1410514120

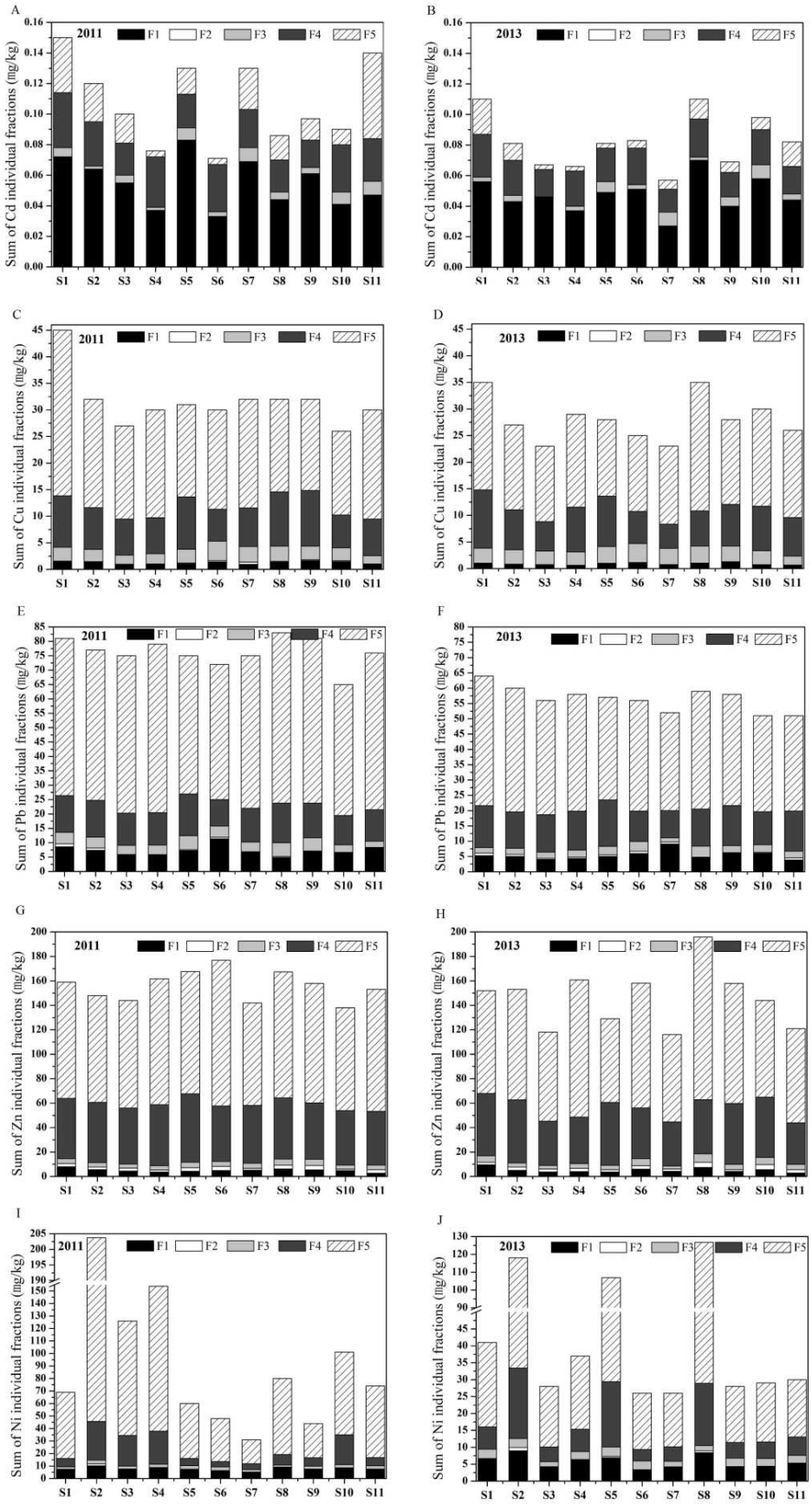

Figure 3. *The speciation distribution of each metal at sediment sampling sites in Zhelin Bay*

http://www.aloki.hu ● ISSN 1589 1623 (Print) ● ISSN 1785 0037 (Online)
DOI: http://dx.doi.org/10.15666/aeer/1706_1410514120

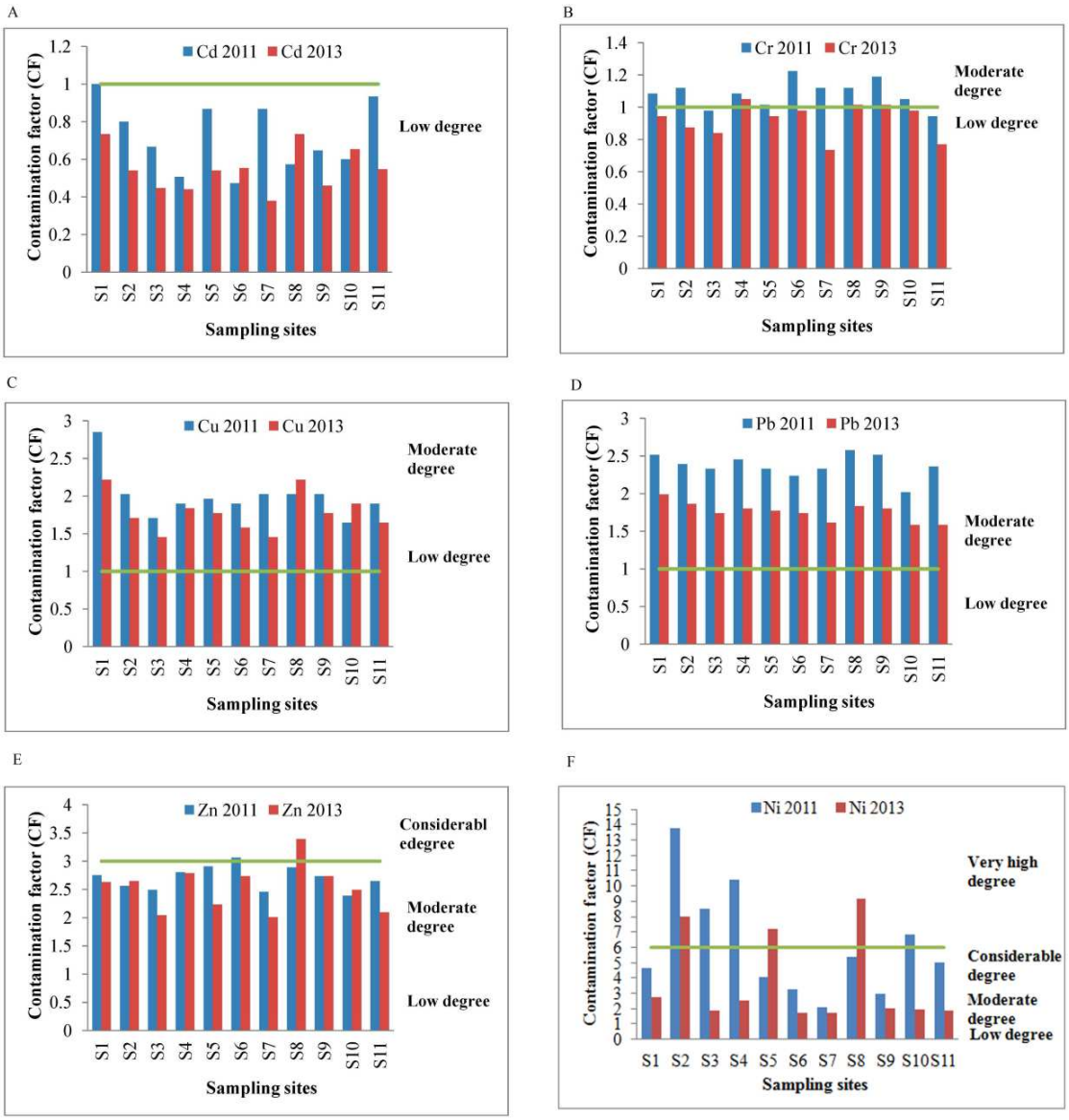

Figure 4. *The CF values of each heavy metal*

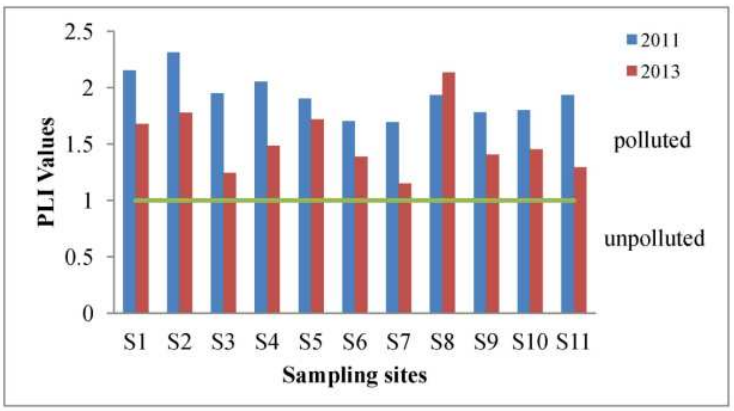

Figure 5. *The PLI values of each sampling site*

http://www.aloki.hu ● ISSN 1589 1623 (Print) ● ISSN 1785 0037 (Online)
DOI: http://dx.doi.org/10.15666/aeer/1706_1410514120

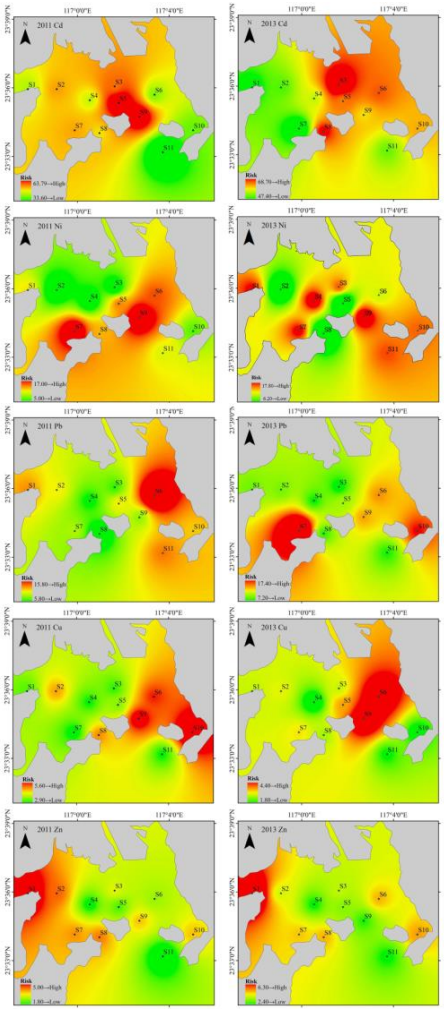

Figure 6. *The ecological hazardous risk of heavy metals from Zhelin bay*

Table 1. *Characterization of sediment (n = 6) and water (n = 2) in sampling sites of the Zhelin Bay*

Site	Sediment												Water			
	TOC (%)		SMC (%)		Al (%)		Mn (%)		Fe (%)		Si (%)		pH		DO (mg/l)	
	2011	2013	2011	2013	2011	2013	2011	2013	2011	2013	2011	2013	2011	2013	2011	2013
S1	1.15	1.14	46.1	49.3	9.64	10.42	0.109	0.135	5.00	5.21	22.4	22.6	8.20	7.33	2.88	4.07
S2	1.04	1.10	50.0	51.3	10.27	9.98	0.102	0.098	5.26	5.18	22.6	22.1	8.36	7.49	3.81	4.01
S3	1.19	0.92	47.9	48.6	10.60	10.73	0.079	0.079	5.16	4.98	22.1	22.9	8.62	7.51	3.97	4.02
S4	0.94	0.96	45.5	46.6	10.14	10.72	0.106	0.117	5.29	5.24	21.8	23.7	8.66	7.64	4.19	3.94
S5	1.12	1.21	43.5	47.9	9.54	10.30	0.117	0.117	5.16	5.24	21.5	23.5	8.70	7.77	4.72	4.92
S6	1.13	0.84	51.6	54.0	9.98	10.13	0.106	0.109	5.24	5.16	22.3	22.1	8.30	7.85	3.60	5.53
S7	1.10	0.78	48.6	50.6	10.23	9.68	0.087	0.090	5.18	4.56	22.7	22.4	8.70	7.86	4.10	6.74
S8	1.11	0.93	44.6	47.9	9.75	9.99	0.113	0.098	5.13	5.08	22.6	21.8	8.23	7.65	3.66	4.60
S9	1.15	1.19	47.0	51.6	9.58	10.24	0.117	0.121	5.00	5.18	21.5	23.2	8.78	7.74	3.45	4.66
S10	1.12	1.34	48.3	50.1	9.26	9.93	0.087	0.087	4.59	5.03	23.1	23.5	8.02	7.90	3.61	4.91
S11	1.12	1.10	52.7	53.0	9.52	9.75	0.125	0.098	5.03	4.90	22.4	23.4	8.30	7.80	3.60	5.83
Avg	1.11	1.05	47.80	50.08	9.86	10.17	0.10	0.10	5.09	5.07	22.27	22.84	8.44	7.69	3.78	4.84
p	0.288		0.000		0.043		0.983		0.760		0.089		0.000		0.004	

AVS = acid volatile sulfides; TOC = total organic carbon; SMC = sediment moisture contents; Avg: average
The data were statistical mean in the table; $p < 0.05$: paired t-test revealed that this difference was no significant

http://www.aloki.hu ● ISSN 1589 1623 (Print) ● ISSN 1785 0037 (Online)
DOI: http://dx.doi.org/10.15666/aeer/1706_1410514120

Table 2. *AVS and SEM concentrations of heavy metals in mariculture sediments in sampling sites of the Zhelin Bay (umol/g)*

Sites	AVS		SEM-Cd		SEM-Cu		SEM-Ni		SEM-Pb		SEM-Zn		∑SEM	
	2011	2013	2011	2013	2011	2013	2011	2013	2011	2013	2011	2013	2011	2013
S1	0.212	1.053	0.0004	0.0004	0.212	0.227	0.415	0.469	0.132	0.121	0.747	0.781	1.506	1.598
S2	0.511	0.991	0.0003	0.0006	0.141	0.222	1.969	1.325	0.109	0.199	0.668	1.918	2.887	3.665
S3	0.797	0.234	0.0002	0.0002	0.129	0.116	1.558	0.315	0.099	0.075	0.742	0.645	2.528	1.151
S4	0.193	0.128	0.0002	0.0002	0.113	0.139	1.681	0.467	0.108	0.097	0.834	0.733	2.736	1.436
S5	2.012	1.216	0.0002	0.0002	0.329	0.235	0.36	1.227	0.265	0.253	1.033	1.556	1.987	3.271
S6	0.007	0.359	0.0002	0.0002	0.101	0.137	0.281	0.218	0.083	0.072	0.797	0.747	1.262	1.174
S7	0.608	1.111	0.0003	0.0001	0.120	0.101	0.306	0.271	0.095	0.067	0.817	0.746	1.338	1.185
S8	1.637	0.538	0.0002	0.0002	0.316	0.141	0.537	1.172	0.304	0.098	1.752	0.684	2.909	2.095
S9	1.181	0.210	0.0001	0.0002	0.339	0.208	0.43	0.315	0.261	0.212	1.088	0.839	2.118	1.574
S10	0.525	1.706	0.0003	0.0002	0.142	0.186	1.514	0.437	0.103	0.148	0.713	1.783	2.472	2.554
S11	0.005	0.234	0.0002	0.0002	0.113	0.112	0.418	0.404	0.084	0.082	0.687	0.482	1.302	1.080

∑SEM = SEM-Cd + SEM-Cu + SEM-Ni + SEM-Pb + SEM-Zn; $f$oc = organic carbon fraction

The ratios of (∑SEM-AVS)/f_{OC} obtained in our study sites were calculated to 113, 228, 145, 271, -2, 111, 66, 115, 81, 174, 116 μmol/gOC in 2011, and 48, 243, 100, 136, 170, 97, 10, 167, 115, 63, 77 μmol/g OC in 2013, respectively (*Fig. 7*). The results indicated that there were no adverse effects, except S2, S4, and S10 in 2011, and except S2, S5 and S8 in 2013.

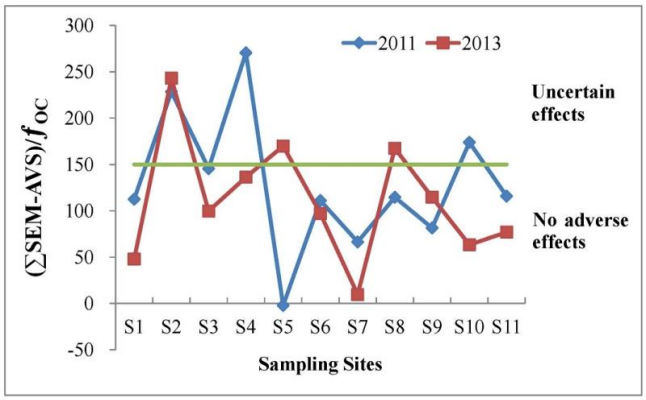

Figure 7. *The ratios of (∑SEM-AVS)/fOC*

The results of no adverse effects by AVS-SEM were in accord with the prediction results by the mean ERL quotients (Wang et al., 2016), which indicated that the ratios of (∑SEM-AVS)/f_{OC} could accurately be used to judge if there were no adverse effects and be of great help for environmental protection. Then, the uncertain risk part by AVS-SEM model could be compensated by other methods and would be discussed in the next step.

Statistical analysis

The average values of metal elements, characterization parameters and risk assessment values from 2011 to 2013 were analyzed by factor analysis and correlation

http://www.aloki.hu ● ISSN 1589 1623 (Print) ● ISSN 1785 0037 (Online)
DOI: http://dx.doi.org/10.15666/aeer/1706_1410514120

analysis. *Figure 8A* was factor loading plot to describe 20 features (six metals, seven characterization parameters and seven risk assessment indexes) from the different sampling sites. *Figure 8B* was factor loading plot for the different sampling sites, each of which was described by 20 features. The correlation analysis was mainly carried out by 15 features (seven risk assessment indexes, six metals, and two characterization parameters), and the results were showed in *Table 3*.

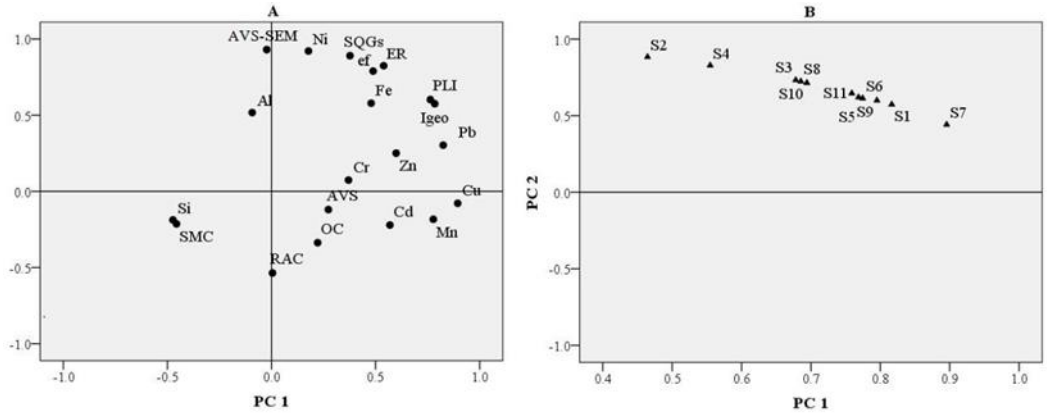

Figure 8. *The principal component analysis diagram for heavy metals and different sampling sites*

Table 3. *Correlation between the risk assessment indexes and the elements in the sediment of Zhelin Bay*

	Igeo	ef	PLI	RAC	ER	SQGs	AVS-SEM	Cd	Cr	Cu	Ni	Pb	Zn	Fe	Si
Igeo	1	0.910**	0.998**	-0.394	0.923**	0.856**	0.519*	0.455*	0.249	0.687*	0.733*	0.734*	0.567*	0.598*	-0.355
ef		1	0.920**	-0.523*	0.958**	0.976**	0.750*	0.265	0.180	0.396	0.933**	0.516*	0.465*	0.524*	-0.229
PLI			1	-0.426	0.936**	0.871**	0.537*	0.454*	0.221	0.675*	0.752*	0.733*	0.548*	0.590*	-0.355
RAC				1	-0.487*	-0.505	-0.502*	-0.329	0.392	-0.143	-0.52*	-0.035	0.020	-0.067	-0.350
ER					1	0.973**	0.731*	0.224	0.144	0.418	0.902**	0.672*	0.445	0.649*	-0.361
SQGs						1	0.820**	0.133	0.139	0.269	0.975**	0.501*	0.390	0.582*	-0.259
AVS-SEM							1	-0.298	0.266	-0.057	0.856**	0.244	0.336	0.545*	-0.052
Cd								1	-0.397	0.662*	0.048	0.241	-0.135	-0.193	0.090
Cr									1	0.314	0.047	0.360	0.819**	0.454	-0.383
Cu										1	0.078	0.703*	0.486*	0.209	-0.214
Ni											1	0.314	0.253	0.482*	-0.147
Pb												1	0.571*	0.645*	-0.665*
Zn													1	0.586*	-0.521*
Fe														1	-0.613*
Si															1

The determinant of coefficient is 0.000; *Correlation is significant at the level of $p < 0.05$; **Correlation is significant at the level of $p < 0.01$

In *Figure 8A,* the first factor described 41.76% of the common variance, and the second factor described 15.44%. Rotation of the factor solution was necessary for better interpretation. The first factor was closely linked to Cu, Pb, As in Igeo, and the second factor was closely linked to Ni in AVS-SEM, SQGs, ER. These results indicated that 1) the ecological impacts of Ni were different from the impacts of Cu, Pb, As; 2) Cu and

http://www.aloki.hu ● ISSN 1589 1623 (Print) ● ISSN 1785 0037 (Online)
DOI: http://dx.doi.org/10.15666/aeer/1706_1410514120

Pb were the major pollutants in the sediments; and 3) Ni was the main toxicity factor for ecological risk. From the correlation analysis, we concluded that: 1) the pollution factors (I_{geo} and PLI) were significantly and positively correlated with Fe and all heavy metals except Cr; 2) Ni was very significantly and positively correlated with SQGs, Hakanson risk index and AVS-SEM, followed by Fe; 3) Pb was significantly and positively correlated with SQGs and Hakanson risk index; 4) Si was negatively correlated with most of the heavy metals, which showed that the metal pollutants were mostly from human activities.

The factor scores were used to analyze the contamination sources. In *Figure 8B,* the first factor for the common variance was 96.39% with high contribution from S1 and S7. The second described 2.70% and highly loaded by S2 and S4. Near to Sanbai Men port that was occupied in fishery and trade, the locations of the four sites were concentrated in the northwest coastal area of the semi-closed bay. It is evident that the wasters from the fishery, trade, port construction and other urban activities resulted in the serious environmental pollution. On the other hand, in the cage area for the fish and maricultrure, vessel activities were frequent, which suggested that the primary pollution sources were from the combustion of gasoline and diesel fuel (Zhu et al., 2016; Yuan et al., 2015).

Conclusions

In this study area, all the sampling sites were polluted by heavy metals (Zn, Cu, Cr, Pb, Ni). The concentrations of heavy metals in 2013 were lower than that of 2011, and the residual fraction and sulfide bound fraction were the primary fractions of heavy metals. For each metal, Ni posed a moderate to very high risk; Zn and As posed a moderate to considerable risk; Cr, Cu and Pb were at a moderate degree; Cd was unpolluted at the sampling sites. From the aspects of ecological risk, a medium to very high risk came from Cd, Ni and Pb. Except for the cage mariculture area (S2, S5 and S8), all the sites would be expected no biotoxicity. Through analyzing the various factors about the heavy metals, four sites (S1, S2, S4 and S7) were profoundly affected by the environmental pollutants which primarily resulted from the combustion of gasoline and diesel fuel and the ship protective layer. The intensive mariculture activity is one of the main reasons for the heavy metal pollution and ecological risk of sediments in Zhalin bay. The exploration of effective strategies is quite necessary in the future for keeping a good quality of the coastal environment and sustainable mariculture development.

Acknowledgments. The project was supported by GDAS'Special Project of Science and Technology Development (No. 2017GDASCX-0104), National Nature Science Foundation of China (21777150, 21307120), Science and Technology Planning Projects of Guangdong Province (2016B02024006, 2017A05040), Science and Technology Planning Projects of Guangzhou (201803030042).Sincere appreciation is expressed to Professor Hong Du from Shantou University for their sampling work and Professor Jingwei Xu from Changchun Institute of Applied Chemistry for language improvement.

http://www.aloki.hu ● ISSN 1589 1623 (Print) ● ISSN 1785 0037 (Online)
DOI: http://dx.doi.org/10.15666/aeer/1706_1410514120

REFERENCES

[1] Al-Othman, Z. A., Ali, R., Al-Othman, A. M., Ali, J., Habila, M. A. (2012): Assessment of toxic metals in wheat crops grown on selected soils, irrigated by different water sources. – Arab. J. Chem. 9(S2): S1555–S1562.

[2] Allen, H. E., Fu, G., Deng, B. (1993): Analysis of acid-volatile sulfide (AVS) and simultaneously extracted metals (SEM) for the estimation of potential toxicity in aquatic sediments. – Environ. Toxicol. Chem. 12: 1441-1453.

[3] Chaudhary, M. Z., Ahmad, N., Mashiatullah, A., Ahmad, N., Ghaffar, A. (2013): Geochemical assessment of metal concentrations in sediment core of Korangi Creek along Karachi Coast, Pakistan. – Environ. Monit. Assess. 185(8): 6677-6691.

[4] Cao, L., Wang, W. M., Yang, Y., Yang, C. T., Yuan, Z. H., Xiong, S. B., Diana, J. (2007): Environmental impact of aquaculture and countermeasures to aquaculture pollution in China. – Environ. Sci. Pollut. R. 14(7): 452-462.

[5] Dabney, B. L., Clements, W. H., Williamson, J. L., Ranville, J. F. (2018): Influence of Metal Contamination and Sediment Deposition on Benthic Invertebrate Colonization at the North Fork Clear Creek Superfund Site, Colorado, USA. – Environ. Sci. Technol. 52(12): 7072-7080.

[6] Di Toro, D. M., McGrath, J. A., Hansen, D. J., Berry, W. J., Paquin, P. R., Mathew, R., Wu, K. B., Santore, R. C. (2005): Predicting sediment metal toxicity using a sediment biotic ligand model: methodology and initial application. – Environ. Toxicol. Chem. 24: 2410-2427.

[7] El Nemr, A., El-Said, G. F., Ragab, S., Khaled, A., El-Sikaily, A. (2016): The distribution, contamination and risk assessment of heavy metals in sediment and shellfish from the Red Sea coast, Egypt. – Chemosphere 165: 369-380.

[8] Fang, T., Li, X. D., Zhang, G. (2005): Acid volatile sulfide and simultaneously extracted metals in the sediment cores of the Pearl River Estuary, South China. – Ecotox. Environ. Saf. 61: 420-431.

[9] Gao, X. L., Chen, C. T. A. (2012): Heavy metal pollution status in surface sediments of the coastal Bohai Bay. – Water Res. 46: 1901-1911.

[10] Gao, X. L., Chen, C. T. A., Wang, G., Xue, Q. Z., Tang, C., Chen, S. Y. (2010): Environmental status of Daya Bay surface sediments inferred from a sequential extraction technique. – Estuar. Coast. Shelf Sci. 86: 369-378.

[11] Ghosh, S. P., Maiti, S. K. (2018): Evaluation of heavy metal contamination in roadside deposited sediments and road surface runoff: a case study. – Environ. Earth Sci. 77(7): 267.

[12] Gu, Y. G., Lin, Q., Jiang, S. J., Wang, Z. H. (2014): Metal pollution status in Zhelin Bay surface sediments inferred from a sequential extraction technique, South China Sea. – Mar. Pollut. Bull. 81: 256-261.

[13] Hu, N. J., Huang, P., Zhang, H., Zhu, A. M., Liu, J. H., Zhang, J., He, L. H. (2015): Anthropogenic Pb input into Bohai Bay, China: evidence from stable Pb isotopic compositions in sediments. – Cont. Shelf. Res. 109: 188-197.

[14] Hyun, S., Lee, C. H., Lee, T., Choi, J. W. (2007): Anthropogenic contributions to heavy metal distributions in the surface sediments of Masan Bay, Korea. – Mar. Pollut. Bull. 54: 1059-1068.

[15] Islam, M. S., Han, S., Masunaga, S. (2014): Assessment of trace metal contamination in water and sediment of some rivers in Bangladesh. – J. Water Environ. Technol.12: 109-121.

[16] Islam, M. S., Ahmed, M. K., Raknuzzaman, M., Habibullah-Al-Mamun, M., Islam, M. K. (2015): Heavy metal pollution in surface water and sediment: a preliminary assessment of an urban river in a developing country. – Ecol. Indic. 48: 285-291.

http://www.aloki.hu ● ISSN 1589 1623 (Print) ● ISSN 1785 0037 (Online)
DOI: http://dx.doi.org/10.15666/aeer/1706_1410514120

[17] Kalantzi, I., Shimmield, T. M., Pergantis, S. A., Papageorgiou, N., Black, K. D., Karakassis, I. (2013): Heavy metals, trace elements and sediment geochemistry at four Mediterranean fish farms. – Sci. Total Environ. 444: 128-137.
[18] Liang, P., Shao, D. D., Wu, S. C., Shi, J. B., Sun, X. L., Wu, F. Y., Lo, S. C. L., Wang, W. X., Wong, M. H. (2011): The influence of mariculture on mercury distribution in sediments and fish around Hong Kong and adjacent mainland China wasters. – Chemosphere 82(7): 1038-1043.
[19] Liu, J. J., Ni, Z. X., Diao, Z. H., Hu, Y. X., Xu, X. R.,(2018): Contamination level, chemical fraction and ecological risk of heavy metals in sediments from Daya Bay, South China Sea. – Mar. Pollut. Bull. 128: 132-139.
[20] McGrath, J. A., Paquin, P. R., Di, Toro, D. M. (2002): Use of the SEM and AVS Approach in Predicting Metal Toxicity in Sediments. – In: Fairbrother, A., Smolders, E. (eds,) Fact Sheet on Environmental Risk Assessment. International Council on Mining and Metals (ICMM), London, 10: 1-6.
[21] Mingorance, M. D., Barahona, E., Fernandez-Galvez, J. (2007): Guidelines for improving organic carbon recovery by the wet oxidation method. – Chemosphere 68(3): 409-413.
[22] Nobi, E. P., Dilipan, E., Thangaradjou, T., Sivakumar, K., Kannan, L. (2010): Geochemical and geo-statistical assessment of heavy metal concentration in the sediments of different coastal ecosystems of Andaman Islands, India. – Estuar. Coast. Shelf Sci. 87(2): 253-264.
[23] Perin, G., Craboledda, L., Lucchese, L., Cirillo, R., Dotta, L., Orio, A. A. (1985): Heavy Metal Speciation in the Sediments of Northern Adriatic Sea. A New Approach for Environmental Toxicity Determination. – In: Lekkas, T. D. (ed.) Heavy Metal in the Environment. CEP Consultant, Edinburgh, 2: 454-456.
[24] Poot, A., Meerman, E., Gillissen, F., Koelmans, A. A. (2009): A kinetic approach to evaluate the associated to acid volatile sulfide and simultaneously extracted metals in aquatic sediments. – Environ. Toxicol. Chem. 28: 711-717.
[25] Prica, M., Dalmacija, B., Roncevic, S., Krcmar, D., Becelic, M. (2008): A comparison of sediment quality results with acid volatile sulfide (AVS) and simultaneously extracted metals (SEM) ratio in Vojvodina (Serbia) sediments. – Sci. Total Env. 389(2-3): 235.
[26] Qiao, Y. M., Huang, C. J., Yang, Y. (2009): A preliminary study of heavy metal background values in Zhelin Bay of eastern Guangdong Province. – J. Trop. Oceanogr. 28(2): 81-85 (in Chinese).
[27] Qiao, Y. M., Huang, C. J., Zhao, J. G. (2010): Heavy metal accumulation and environmental quality assessment for surface sediment in Zhelin Bay. – Environ. Sci. 29(3): 325-327 (in Chinese).
[28] Sundaray, S. K., Nayak, B. B., Lin, S., Bhatta, D. (2011): Geochemical speciation and risk assessment of heavy metals in the river estuarine sediments – a case study: Mahanadi Basin, India. – J. Hazard. Mater. 186(2-3):1837-1846.
[29] Tomilson, D. C., Wilson, D. J., Harris, C. R., Jeffrey, D. W. (1980): Problem in assessment of heavy metals in estuaries and the formation of pollution index. – Helgol. Wiss. Meeresunlter. 33: 566-575.
[30] Väänänen, K., Kauppila, T., Mäkinen, J., Leppänen, M., Akkannen, J. (2016): Ecological risk assessment of boreal sediments affected by metal mining: Metal geochemistry, seasonality, and comparison of several risk assessment methods. – Integr. Environ. Assess. 12(4): 759-771.
[31] Varol, M. (2011): Assessment of heavy metal contamination in sediments of the Tigris River (Turkey) using pollution indices and multivariate statistical techniques. – J. Hazard. Mater. 195(1): 355-364.
[32] Wang, C., Du, H., Yang, Y. Y., Guo, P. R. (2011): Effect of sequential extraction for heavy metals speciation on mineral phases of sediment. – Chin. J. Anal. Chem.39: 1887-1892.

http://www.aloki.hu ● ISSN 1589 1623 (Print) ● ISSN 1785 0037 (Online)
DOI: http://dx.doi.org/10.15666/aeer/1706_1410514120

[33] Wang, F., Huang, X. P., Zhang, J. P., Jiang, Z. J., Shi, Z. (2010): Distribution, accumulation and ecological risk of mercury in the sediment of the mariculture zone at Zhelin Bay of Guangdong province, Asian. – J. Ecotox. 5(2): 184-192 (in Chinese).
[34] Wang, Y., Wei, Y. N., Guo, P. R., Pan, J. C., Wu, Q. H., Liu, N. (2016): Distribution variation of heavy metals in maricultural sediments and their enrichment, ecological risk and possible source-A case study from Zhelin bay in Southern China. – Mar. Pollut. Bull. 113: 240-246.
[35] Wu, Q. H., Tam, N. F. Y., Leung, J. Y. S., Zhou, X. Z., Fu, J., Yao, B. (2014): Ecological risk and pollution history of heavy metals in Nanshan mangrove, South China. – Mar. Pollut. Bull. 104: 143-151.
[36] Wu, Q. H., Leung, J. Y. S., Geng, X. H., Chen, S. J., Huang, X. X., Li, H. Y., Huang, Z. Y., Zhu, L. B., Chen, J. H., Lu, Y. Y. (2015): Heavy metal contamination of soil and water in the vicinity of an abandoned e-waste recycling site: implications for dissemination of heavy metals. – Sci. Total Environ. 506-507(15): 217-225.
[37] Wu, R. S. S., Lam, K. S., Mackay, D. W., Lau, T. C., Yam, V. (1994): Impact of marine fish farming on water quality and bottom sediment a case study in the sub-tropical environment. – Mar. Environ. Res. 38(2): 115-145.
[38] Xia, B., Guo, P. R., Lei, Y. Q., Zhang, T., Qiu, R. L., Knorr, K. H. (2016): Investigating speciation and toxicity of heavy metals in anoxic-marine sediments—a case study from a mariculture bay in Southern China. – J. Soil Sediment. 16(2): 665-676.
[39] Yang, Y. Q., Chen, F. R., Zhang, L., Liu, J. S., Wu, S. J., Kang, M. L. (2012): Comprehensive assessment of heavy metal contamination in sediment of the Pearl River Estuary and adjacent shelf . – Mar. Pollut. Bull. 64(9): 1947-1955.
[40] Yi, Y. J., Yang, Z. F., Zhang, S. H. (2011): Ecological risk assessment of heavy metals in sediment and human health risk assessment of heavy metals in fishes in the middle and lower reaches of the Yangtze River basin. – Environ. Pollut. 159(10): 2575-2585.
[41] Yu, R., Yuan, X., Zhao, Y., Hu, G., Tu, X. (2008): Heavy metal pollution in intertidal sediments from Quanzhou Bay, China. – J. Environ. Sci. 20: 664-669.
[42] Yuan, C. G., Shi, J. B., He, B., Liu, J. F., Liang, L. N., Jiang, G. B. (2004): Speciation of heavy metals in marine sediments from the East China Sea by ICP-MS with sequential extraction. – Environ. Int. 30: 769-783.
[43] Yuan, G. M., He, G. F. (2015): Distribution and environmental geochemistry characteristics of heavy metals in surface sediment from Zhelin Bay to Dacheng Bay, Guangdong Province, China. – Earth and Environment 43(2): 190-197 (in Chinese).
[44] Zhang, R., Zhou, L., Zhang, F., Ding, Y., Gao, J., Chen, J., Yan, H., Shao, W. (2013): Heavy metal pollution and assessment in the tidal flat sediments of Haizhou Bay, China. – Mar. Pollut. Bull. 74: 403-412.
[45] Zhao, S., Feng, C. H., Yang, Y. R., Niu, J. F., Shen, Z. Y. (2012): Risk assessment of sedimentary metals in the Yangtze Estuary: new evidence of the relationships between two typical index methods. – J. Hazard. Mater. 241-242(4): 164-172.
[46] Zhou, Q. X., Kong, F. X., Zhu, L. (2004): Ecotoxicology: Principle and Methods. – Science Press, Beijing.
[47] Zhu, Z. M., Xue, J. H., Deng, Y. Z., Chen, L., Liu, J. F. (2016): Trace metal contamination in surface sediments of intertidal zone from Qinhuangdao, China, revealed by geochemical and magnetic approaches: distribution, sources, and health risk assessment. – Mar. Pollut. Bull. 105(1): 422-429.
[48] Zhuang, W., Gao, X. L. (2014): Integrated assessment of heavy metal pollution in the surface sediments of the Laizhou Bay and the coastal waters of the Zhangzi Island, China: comparison among typical marine sediment quality indices. – PLoS One 9(4): e4145.
[49] Zwolsman, J. J. G., Van Eck, B. T. M., Der Weijden, C. H. (1997): Geochemistry of dissolved trace metals (cadmium, copper, zinc) in the Scheldt estuary, southwestern Netherlands: impact of seasonal variability. – Geochim. Cosmochim. Ac. 61(8): 1635-1652.

http://www.aloki.hu ● ISSN 1589 1623 (Print) ● ISSN 1785 0037 (Online)
DOI: http://dx.doi.org/10.15666/aeer/1706_1410514120

THE RIVERINE FLOOD CATASTROPHE IN AUGUST 2010 IN SOUTH PUNJAB, PAKISTAN: POTENTIAL CAUSES, EXTENT AND DAMAGE ASSESSMENT

SAJJAD, A.[1] – LU, J. Z.[1*] – CHEN, X. L.[1] – CHISENGA, C.[1] – MAHMOOD, S.[2]

[1]*State Key Laboratory of Information Engineering in Surveying, Mapping and Remote Sensing, Wuhan University, Wuhan 430079, China*

[2]*Department of Geography, Government College University, Lahore, Pakistan*

**Corresponding author*
email: lujzhong@whu.edu.cn; phone: +86-27-6877-8755

(Received 29th May 2019; accepted 16th Oct 2019)

Abstract. The paper investigates the causes, magnitude and damage caused by the flood as a result of the breaching of the east marginal embankment of the Taunsa Barrage. The flood frequency in the district of Muzaffar Garh located in south Punjab, Pakistan had serious impacts on human lives and their properties. To pursue this study, we used primary data, collected through questionnaire, formal interviews, field observations and secondary data, obtained through government departments and online open source databases. Furthermore, Landsat ETM+ imageries were used as input in the supervised classification in order to investigate the pre and post flooding land cover and land use. Hydrograph was used to analyze the flood limits and spatiotemporal change in river discharge for barrages. The results show an abnormal rainfall occurring in the month of July in the upper Indus Basin, which resulted in a massive discharge in the central Indus Basin. As a consequence, it exceeded the flood limits at the Taunsa Barrage, which resulted in the breaching of east marginal embankment. The flood caused a high number of human casualties and a total economic loss of 14.23 million US$ including a 6.8 million US$ agricultural loss. The study thus, gives insight on how authorities can devise a flood management plan in such a way to reduce the future impacts of riverine flood disasters in Muzaffar garh.
Keywords: *Indus Basin, east marginal embankment, flood disaster management, supervised classification, abnormal rainfall*

Introduction

Floods are the most frequent and destructive hydrological disasters in the world (Banerjee, 2010; Cann et al., 2013). In recent years, the severity and magnitude of excessive flooding has been experienced by many South Asian countries, including Pakistan, India and Bangladesh (Khan et al., 2009), which caused devastation to greater number of people as compared to other nature hazards(Zhou et al., 2000; Khan et al., 2009; Haq et al., 2012). Generally, floods have been widely caused by certain factors including unpreceded rainfall, melting of ice and snow, breaching of river embankment, improper structural measures and insufficient capacity of reservoirs (Howe and White, 2002; Shah and Gabriel, 2002; Ali, 2013). Similarly, population growth, land use change, deforestation, degradation of ecosystems, human encroachments in floodplains are some of the human escalation factors (Milly et al., 2002). Over the last few decades, the frequency and intensity of riverine flooding have been immensely boosted by various factors, including unusual climatic variability, abrupt sea level rise and extreme rainfall (Tariq and Giesen, 2012; Rehman and Khan, 2013; Dawood et al., 2017). In recent years, a large number of riverine floods have been triggered by the failure of dams, barrages and embankments, which rendered disastrous capacity to disrupt human

http://www.aloki.hu ● ISSN 1589 1623 (Print) ● ISSN 1785 0037 (Online)
DOI: http://dx.doi.org/10.15666/aeer/1706_1412114142

life and their property due to unpredictability and severity (Walder and O'connor, 1997). Moreover, riverine floods in the Indus Basin are induced by various factors, including flat topography, hydrology, climate, demographic and socio-economic catchment characteristic in the proximity of Indus river (Gaurav et al., 2011; Tariq and Giesen, 2012; Laghari et al., 2012). Riverine flooding is extremely destructive in terms of life loss with shattering economic developments to all sectors (Zhou et al., 2000).

Globally, floods produce severe damages to all socio-economic sectors. Every year, flood events have directly claim more than 20,000 lives and affect 1.4 million people (Howe and White, 2002; Messner et al., 2007). Categorically, management of flooding impacts involve three stages: the first stage is the estimation of flood inundation extent, the second stage is the estimation of damage to all socio-economic sectors and the last stage is flood recovery and rehabilitation (Zhou et al., 2000; Shah and Gabriel, 2002). These following marked flood impacts can be tackled down by applying certain structural and non-structural strategies (Rehman and Khan, 2011; Gaurav et al., 2011; Tariq and Giesen, 2012).

In Pakistan, flood is a frequent hydrological hazard (Khan, 2005; Syvitski and Brakenridge, 2013; Mahmood and Rani, 2018; Mahmood et al., 2019). Pakistan is considered as the most flood affected country in the world (Solheim et al., 2001; Natalia et al., 2008). In the last few decades, number of shattering floods of various magnitudes have recurrently been influenced by topographical and geological characteristics and climate change (Gaurav et al., 2011; Geis and Steeves, 1998). In addition, some human escalation factors have worsened the situation, which included urbanization, population growth in the proximity of floodplain, deforestation and ill equipped flood managers (Laghari et al., 2012; Khan, 2005; Ghosh et al., 2015). These factors have increased the risk of flooding in Pakistan and also increased the danger of loss of lives, damages to the infrastructure, standing agriculture crops and other vital properties (FFC, 2010; Hashmi et al., 2012). In this regard, an appropriate structural modifications and non-structural measures are required to efficiently cope with this menace (Khan et al., 2009).

In 2010, Pakistan was hit by the worst flood in the history of the Indo-Pak subcontinent, which was caused by widespread heavy rain spell of more than 250 mm. The rainfall occurred from the 27th to the 31st July with much intense in the catchment area of the upper Indus Basin (Rahman and Khan, 2011, 2013). As a consequence, flash flooding occurred in the upper Indus Basin and riverine flooding has occurred in the central Indus Basin. Over 2000 death tolls and massive acceleration in economic loss of ~43 billion US$ was recorded (PMD, 2010; Rahman and Khan, 2013 Mahmood et al., 2016a, b, 2019). Previous studies have studied the magnitude and intensity of flood damages, as a result of fluvial geomorphology, population density, land use change, structural river embankments, levees and irrigation systems (Syvitski and Brakenridge, 2013; Mahmood et al., 2016a, b). Nevertheless, the destructive effect in the whole Indus Basin was due to breaching of embankments, floodplains coupled with high population density, and economic growth (Ali, 2013; Chaudary and Sarwar, 2016; Mahmood et al., 2019). Furthermore, the flood's high peak runoff of 31149 m^3/s, exceeds the flood limits of various barrages and dams along the River Indus, including the Taunsa Barrage that falls within our study area (FFC, 2010; Chaudary and Sarwar, 2014, 2016; Mahmood et al., 2019).

Since 2010, a number of studies have been conducted to understand the causes and effects of flooding (e.g., Rahman and Khan, 2011, 2013; Syvitski and Brakenridge, 2013; Hashmi et al., 2012; Mahmood et al., 2016a, b, 2019; Khalid et al., 2018).

http://www.aloki.hu ● ISSN 1589 1623 (Print) ● ISSN 1785 0037 (Online)
DOI: http://dx.doi.org/10.15666/aeer/1706_1412114142

However, these studies focused on the upper section of the River Indus with little or no emphasis on the middle section and the contribution caused by a number of series of barrages. The middle section of the river is of paramount importance as it has unique characteristics, one of which is the contribution to flooding pattern as the result of the Taunsa Barrage breach. Thus, this study focused on integrating the effect of the Taunsa Barrage and remote sensing results to better understand the causes, effects and damages caused by the flood in 2010. Remote sensing provides a framework to flood monitoring, depicts fluvial morphological changes, and extracts flood inundation and damages (Haq et al., 2012; El Bastawesy, 2015). We used supervised classification techniques, coupled with multispectral and temporal remote sensing data, to map the flood extent, damages to infrastructure and changes in river courses (e.g., Khalid et al., 2018). The land use and land cover change analysis of pre and post flooding in Muzaffar garh and in downstream areas of the Taunsa Barrage, which have not been done before, thus providing useful information for the implementation of flood protection measures along study area. We then explored the prevailing effects of the monsoon rainfall and the huge discharge over Upstream Indus Basin and the breaching of Taunsa Barrage. Thus, the present study provides a flood management plan framework to authorities on the management of future flood in relation to the control of Barrages and other flood barriers. This framework incorporates the flood generating factors and associated damages, the flood extent in relation to the land use/cover changed as the result of the flood in 2010, the water Inflow of the Taunsa and Chashma barrages to address how future managements of these barrages will reduce the effect of floods. The main objective of this present study is assessing the 2010 flood-causing factors, extent of inundation and associated socio-economic damages in one of the severely flood-affected areas in the south Punjab district Muzaffar garh, Pakistan. Further the study is focusing on filling the afore knowledge gap and introducing the use of combined techniques in Geographical Information System and climate data analysis as a monitoring tool in flood risk management in the future.

Materials and methods

Study area

The district Muzaffar garh is located in south Punjab, central Pakistan within 29.016°N to 30.765°N and 70.537°E to 71.726°E (*Fig. 1*). It is ~34 km away from Multan, which is regarding its population the 5th largest historical city of south Punjab, Pakistan. It is bounded by Layyah and Jhang districts in the north and Rahimyar Khan and Bahawalpur along River Chenab in the south. Dera Ghazi Khan and Rajaun pur along the mighty Indus are located in the west while Multan and Khanewal district lie in the East. Geographically, it is sandwiched between the mighty Indus and Chenab Rivers in the western and eastern borders, approximately 35 km and 8 km from district headquarter, respectively (*Fig. 1*). The total geographical area is 8,250 km², which is administratively divided into four tehsils; Muzaffar garh, Kot addu, Alipur, and Jatoi. Furthermore, it is subdivided into 93 smallest electoral units (Union Councils). In accordance with the latest 2017 census, the total population of the district was 4.32 million with 84% in rural areas and 16% urban population in comparison with the 1998 census with a total population of 2.64 million in 1998 with 88% rural and 12% urban population. The recorded average annual growth rate is 2.63 from 1998 to 2017 (Gop, 1999, 2017).

http://www.aloki.hu ● ISSN 1589 1623 (Print) ● ISSN 1785 0037 (Online)
DOI: http://dx.doi.org/10.15666/aeer/1706_1412114142

Elevation varies from 42 m to 192 m above mean sea level from south to north, respectively (*Fig. 8*). The natural gradual slope in the district is toward the south, which made it possible to build an extensive irrigation canal system (Gop, 1999, 2017). District Muzaffar garh has desert type of climate, which is further classified as BWh, according to Koppen climate model (Mahmood et al., 2019). The highest maximum recorded temperature is 50 °C in the hottest month of June and the lowest is 2 °C recorded in the coldest month of January (PMD, 2010). The annual mean rainfall is 157 mm with a maximum of 45 mm monsoon rainfall in July a minimum of only 2 mm rainfall in October (PMD, 2010) The soil is fertile with the properties of sandy loam, which is suitable for widespread range of crops. In the study area, around 1,020,000 ha (60%) of land is characterized as barren land, which is not suitable for cultivation. The remaining 680,000 ha (40%) of land is cultivated with wide variety of crops including wheat, rice, sugarcane (Gop, 1999, 2017).

This paper emphasized the use of mixed research method approach to understand the flood causes, extent and evaluate the flood damages in the study area. To obtain the required objectives, primary and secondary data sources were used.

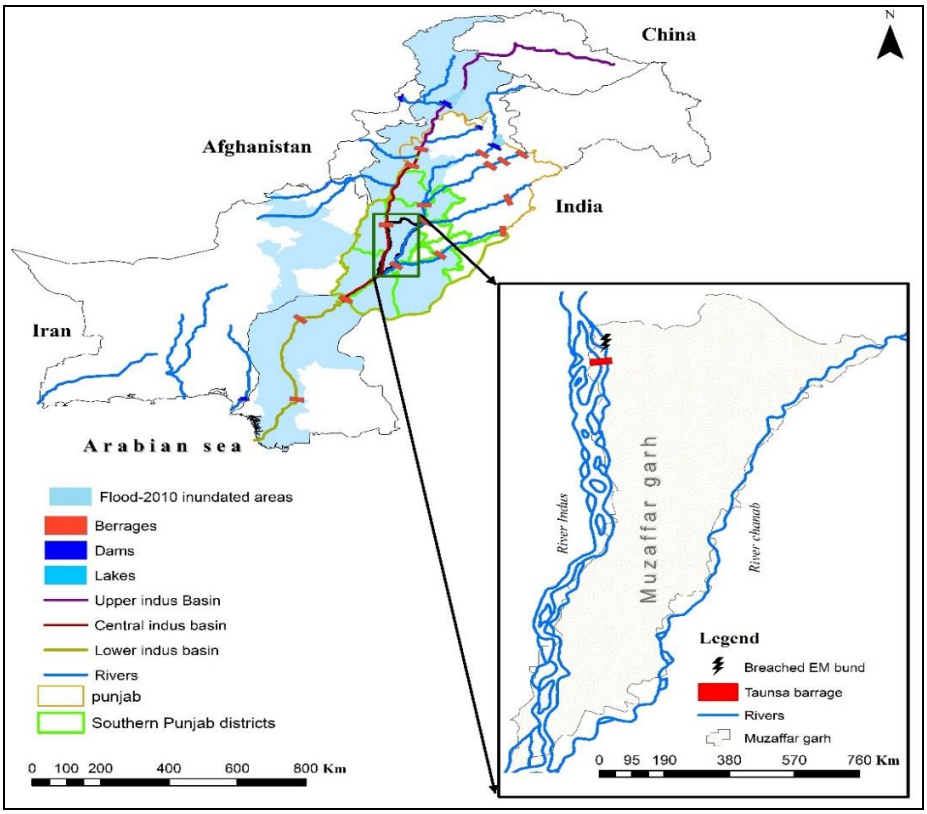

Figure 1. *Pakistan location of study area*

Primary data acquisition

Primary data was acquired through questionnaire-based survey, formal interviews and personal field observation and GPS. Prior to the survey, some frequent spatial field visits were conducted along with certain meetings arranged with different stakeholders, i.e. local communities, local irrigation department officials and farmers. The aim was to identify the most affected areas for conducting field survey. Based on prior field visits,

http://www.aloki.hu ● ISSN 1589 1623 (Print) ● ISSN 1785 0037 (Online)
DOI: http://dx.doi.org/10.15666/aeer/1706_1412114142

comprehensive micro-level flood investigation and damage analysis of flood affected communities were examined. For this purpose, a semi-structured questionnaire was designed for the surveyed households to assess the flood genesis, magnitude and flood damages from three aspects. The first questionnaire was dealing with socio-economic condition of the household's while the second questionnaire was comprised of questions concerning flood causes, magnitude and damages to agricultural crops, livestock's, and houses with estimate loss in US$. Likewise, questionnaire for formal interviews with concerned government officials was designed to get the information of flood causes and damages and estimated rehabilitation cost of flood affected areas in million US$. A total of 500 households were selected on the basis of simple random technique. In the year of 2012, field survey was conducted by asking face to face afore mentioned questions in local language 'Saraiki'. Similarly, Global Positioning System (GPS) has been used to collect a total of 100 flood depth points in the study area, and sample training points of supervised classification classes e.g. water, built up, vegetation and barren land were examined to validate the result. On the other hand, the surveyed household locations were also taken along with infrastructure damages, and site locations were also noted. Field observation was also carried out in the study area to estimate flood extent, duration and depth. Similarly, correlation of flood duration and depth with Extent of damages to standing crops, livestock, housing structures were comprehensively investigated. Furthermore, identification of the most affected sites and the most vulnerable areas to flood in the study area were defined. Formal interviews were arranged with officials of government departments at provincial and district levels to get real time information of flood causes and estimated economic losses to all socio-economic sectors in US$.

Secondary data acquisition

Secondary data was acquired from different concerned government departments of Pakistan, and online open sources databases. In fact, there is no one single operating department to deal comprehensively with flood hazards in Pakistan. Further, flood hazard responsibilities are shared by various government departments. Topographic map of district Muzaffar garh was acquired from the Survey of Pakistan (SOP), Islamabad. Meteorological Rainfall data of 14 stations during 2010 were collected from the Pakistan Meteorology Department (PMD), Regional Office Lahore (PMD, 2010). Demographic statistics of Muzaffar garh district were acquired from the Population Census Organization, Islamabad (Gop, 2017). Economic loss to public roads infrastructures were collected from the Communication and Work Department, Muzaffar garh. Economic damages to electric power lines was collected from the Multan Electric Power Company (MEPCO) and river discharge data were collected from the Water and Power Development Authority (WAPDA), Pakistan.

Remote sensing Landsat 7 Enhanced Thematic mapper (ETM) images were downloaded from the United State Geological Survey (USGS) Landsat archive (https://earthexplorer.usgs.gov/). It was used to monitor pre and post-flood-2010 activities along the central Indus Basin, in district Muzaffar garh, south Punjab. Due to access of extensive spatio-temporal satellite imageries, it was easy to monitor flood extent and assess flood damages. Landsat ETM Image of 03 July, 2010 was used for pre-flood instance while ETM image of 20 August, 2010 was used for post-flood analysis. The effective spatial resolution and spectral sensitivity of Landsat ETM in visible and near infrared portion of electromagnetic spectrum have been useful for the

http://www.aloki.hu ● ISSN 1589 1623 (Print) ● ISSN 1785 0037 (Online)
DOI: http://dx.doi.org/10.15666/aeer/1706_1412114142

extraction of flood inundation, flood damage assessment and monitoring (Chohan et al., 2015; Khalid et al., 2018). Shuttle Radar Topography Mission (SRTM) Digital Elevation Model (DEM) with 30 m resolution was downloaded from USGS open access archive. We have used for an understanding the spatial variations in the elevation in Muzaffar garh district.

Google Earth images of pre-flood 2009 and post-flood 2011 were acquired from Google earth Pro, which were used for observing the breaching points and their reconstruction.

Data methods and preparation

We used supervised classifications to separate different land cover and land use on the Landsat ETM images. The supervised image classification is widely used for the extraction of detailed invisible information from remote sensing data (Melgani and Bruzzone, 2004). It is a well-known automation technique that converts pixels into land use/cover change detection at a same location (Alphan et al., 2009). Maximum likelihood approach of supervised image classification was used for the mapping of pre- and post-flooding occasions in the study area. This technique has also been applied in a similar study by Khalid et al. (2018) and Chohan et al. (2015). Four classes were identified namely, water, built up, vegetation and barren land in the study area. Maximum likelihood approach is widely applied by various studies due to its results reliability and accuracy compared to other approaches. It provides a quantitative decision in which pixels are assigned based on their likelihood spectral signature classes by using sample training points (e.g. Chohan et al., 2015; Khalid et al., 2018). Global positioning system was also used to collect sample training points for the validation of spectral signatures of land use/cover classes (*Table 1*).

Table 1. *Training sites for image classification*

Sr. No	Class type	Latitude	Longitude
1	Water	30.5161	70.8486
2	Built up	30.4899	70.9386
3	Vegetation	30.3946	70.8997
4	Barren land	30.3747	71.3077

Moreover, we used change detection method, based on the classified classes for the pre and post flood images, to investigate the significant land use and land cover changes due to flooding phenomena in the study area. We have applied this change detection method on both images using Raster calculator tool in GIS environment. After that supervised classification of both pre and post images were presented in a map and change statistics results were compiled and presented in graphical form using MS Excel.

Meteorological rainfall data was collected from 14 meteorological stations located in all provinces of Pakistan from 27-31 July, 2010. Geo-database was prepared to store, manipulate, and geo-visualize spatiotemporal rainfall data in GIS environment. Moreover, Rainfall spatial distribution pattern was analyzed and interpolated using Inverse distance weightage (IDW) spatial analysis tool in Arc GIS. This technique (IDW) is ideal to interpolate scattered points, which employ deterministic methods to calculate the values of unknown points using weighed averages (Rehman and Khan, 2011, 2013). In this approach, it assumes that close points are related to each other that

http://www.aloki.hu ● ISSN 1589 1623 (Print) ● ISSN 1785 0037 (Online)
DOI: http://dx.doi.org/10.15666/aeer/1706_1412114142

diminish with distance, hence the inverse distance weighing. Similarly, this IDW technique was also applied to interpolate flood depth in the study area to geo-visualize the spatial pattern of flood depth.

Digital elevation model data files contain spatial terrain altitude at a defined grid interval over the bare Earth. ArcGIS 10.4.1 was used to analyze the spatial variance in terrain elevation in the study area.

Descriptive statistical analysis was applied on the collected socio-economic data and, and flood damages data using MS Excel. Arithmetic mean formula was applied to determine the average estimated economic loss of agriculture crops per ha. The estimated loss to all sectors were calculated in US$ and presented in graphical and tabular form. River Indus discharge data of Chashma and Taunsa stations from 29 July to 06 August, 2010 was collected from the Water and power development authority. Discharge data was prepared and organised in MS excel and presented in a hydrograph. Hydrograph is an ideal method to present any timeline series data. Additionally, the rainfall trends during monsoon rainfall from the years of 2001-2010 were also analyzed, compared and presented in line graph method.

Results and analysis

Socio-economic characteristics

A total of 500 households were surveyed from Kot addu, Muzaffar garh, Ali pur and Jatoi with a total population of 1617 persons. Out of which 915 were male and 702 were females. A total of 36.6% households were from Kot addu, 14% households were from Muzzafar garh, while 16.4% and 33% households were from Jatoi and Ali pur, respectively. The age structure of the respondents was classified into three main age groups; the 1st group (20-40 years) was 37.8% of total respondents, the 2nd group (41-60 years) was 54.2% and the 3rd group (46-60 years) made 8% of the total households. The family size was divided into four categories; Small family size of less than 4 members was 62%, medium size consist of 4 to 8 members was 28% and large family size of above 8 members made 10% of the total surveyed population. The flood in 2010 has induced direct implications on the well-being of these households. It damaged their limited assets and sources of earning, which consequently push them into extreme poverty level. The survey indicated that literacy ratio is 83% in the study area. Most of them were only literate at matric level and only few of them were at graduate and post-graduate level. The survey indicated that more than 60% respondents belong to daily wagers profession with less than 130 US$ earnings monthly.

Perceived causes of flood-2010

The 2010 flood in the central Indus Basin in south Punjab started in early August and continued till early September, following heavy prolong rainfall in the upstream of the Indus. Spatial Analysis of the rainfall data from 27-31 July was published by the Pakistan Metrological Department, which had experienced much higher rainfall in many stations in the monsoon season in 2010 in Khyber Pakhtunkhwa (KPK), Punjab, and Sindh provinces as shown in *Figure 2*. For example, abnormal heavy rainfall over 250 mm in 24 h had been recorded at Saidu sharif station located in KPK province. Similarly, northwestern part of the country had received high concentration of rainfall in

http://www.aloki.hu ● ISSN 1589 1623 (Print) ● ISSN 1785 0037 (Online)
DOI: http://dx.doi.org/10.15666/aeer/1706_1412114142

comparison with the central and southern part of the country, which had received very low rainfall as depicted by rainfall spatial pattern analysis (*Fig. 2*).

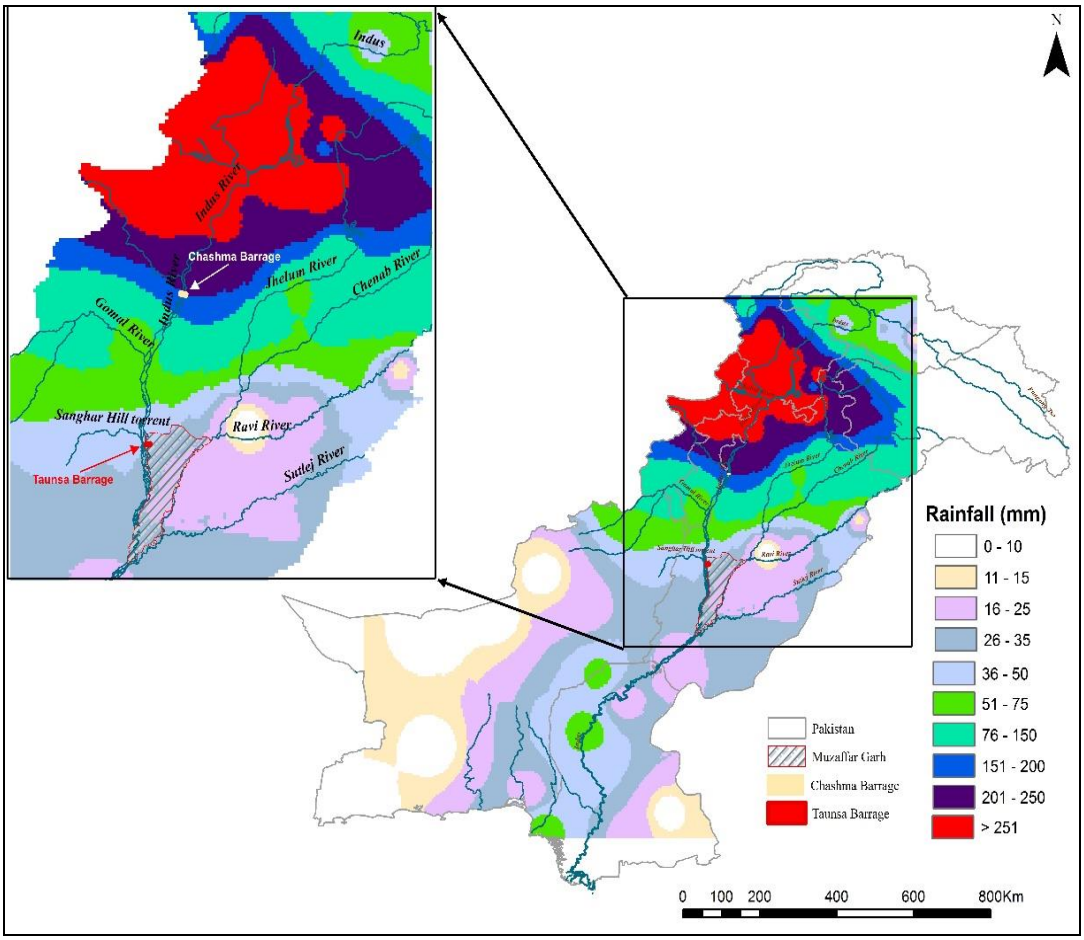

Figure 2. *Spatial pattern of rainfall from 27-30 July, 2010*

As a result of high intensity and continuous downpour in the upstream of the Indus river carried very high surface run off discharge and abnormal flow at several western tributaries of the Indus namely, Swat, Dir, Kabul, Panjkore, Gomal rivers, which caused an adverse flash flooding in KPK province, Pakistan. The hydrological data analysis shows that the unprecedented accumulated flood water recorded discharge of 26546 m^3/s on 30 July at Jinnah Barrage resulted in severe breaches at its left and right Guide Banks and inundated nearby low lying areas. Further, this extreme swollen water flow discharge generated high intense pressure at Chashma Barrage with an alarming level of recorded inflow 29354 m^3/s, and resulted inundation in the floodplain areas of districts Mianwali, Bhakhar and Layyah. The high flow of water with its disastrous consequences rushed down toward Taunsa Barrage and generated intense pressure on both sides of its embankments. Further, the recorded high flood peak of 27184 m^3/s on 2 August, 2010 at Taunsa Barrage not just exceeded the discharges at danger levels but it was also very close to its designed capacity of 28317 m^3/s. This recorded inflow water piled at the barrage and resulting the pressure of the East bank and the protective embankment. As a result, 12 km upstream of Taunsa Barrage, the east marginal embankment (EM) Abbas wala could not sustain the tremendous pressure and breached

http://www.aloki.hu ● ISSN 1589 1623 (Print) ● ISSN 1785 0037 (Online)
DOI: http://dx.doi.org/10.15666/aeer/1706_1412114142

at Rd 32-38 on the 2nd August with 1972 m length. Thereafter, three main secondary breaches of 140 m, 120 m, and 448 m have been formed subsequently to adjacent embankment as a consequence of EM embankment breach (*Fig. 6*). The approximate disastrous flow of more than, 3540 m^3/s roaring flood water through breached embankments, overtopped Taunsa Panjnad Link canal by breaching at Rd 10 and continued its disastrous flow followed by various breaches to Muzaffar garh canal in between Rd 13-14. As a result, the water gushing went on to flood the Muzaffargarh district and its adjoining areas. The hydrological analysis result shows the recorded 6 hourly discharge at Chashma-Taunsa barrages during flood instance that is closely matching with the breaching dates of the embankments (*Fig. 3*).

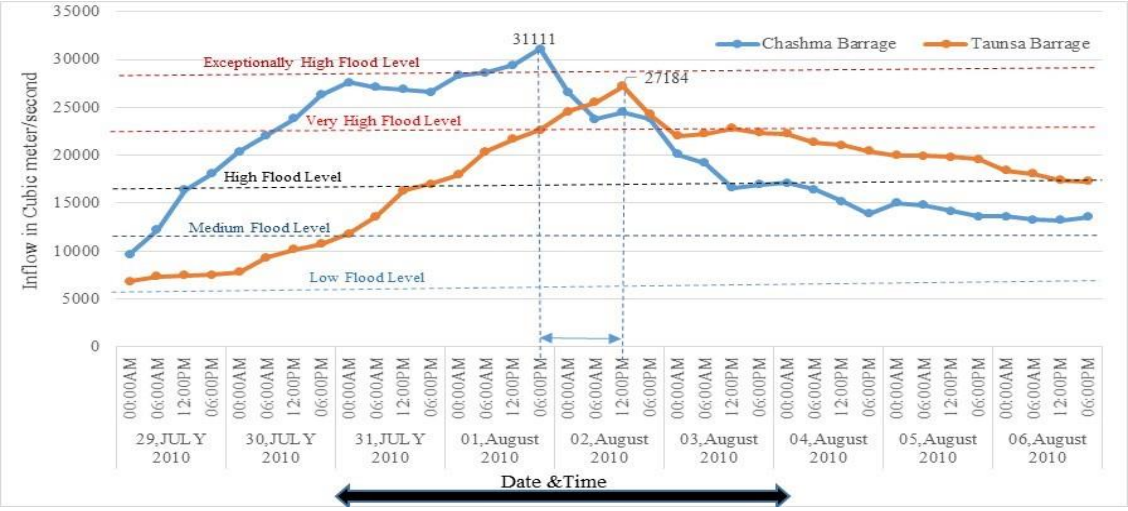

Figure 3. *Inflow m^3/s of Chashma Barrage and Taunsa Barrage from 29 July to 6 August 2010. Chashma–Taunsa reach is ~270 km*

Over the last decade, the analysis revealed that the trend of monsoon rainfall in Pakistan was not uniform, in the year 2003 has received maximum rainfall, which was exceeded in 2010 with an exceptional rainfall above 250 mm as shown in *Figure 4*.

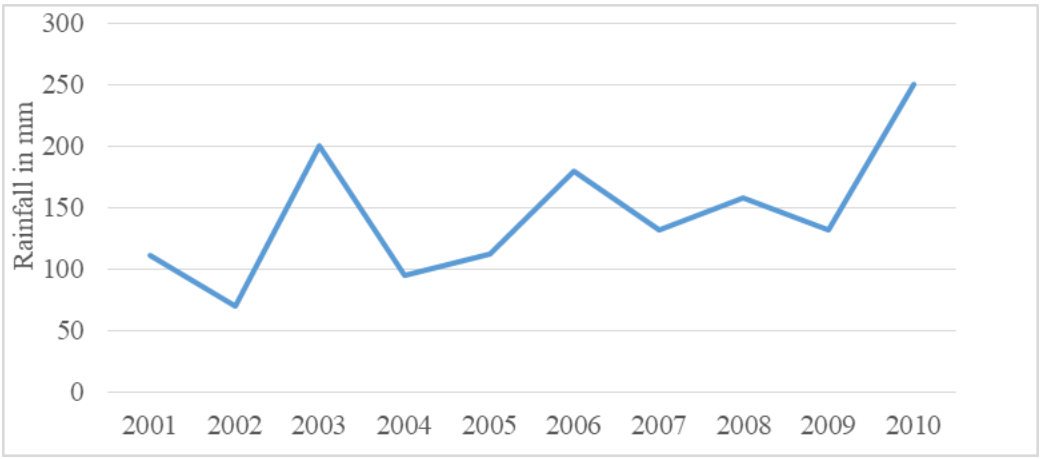

Figure 4. *Monsoon rainfall trend in Pakistan from 2001-2010*

http://www.aloki.hu ● ISSN 1589 1623 (Print) ● ISSN 1785 0037 (Online)
DOI: http://dx.doi.org/10.15666/aeer/1706_1412114142

Taunsa Barrage is located in south Punjab district Muzaffar garh (*Fig. 2*). Taunsa Barrage is considered the most susceptible barrage structures built across the River Indus (Chaudary and Sarwar, 2016). As *Figure 5* shows in the year 2008, for the purpose of diversion structure re-modelling the construction of a sub-weir was completed at Taunsa Barrage which had about 2.5 m vertical and 274 m horizontal length. For this construction work, a massive coffer dam was used. Consequently, after completing the construction work, the coffer dam discarded material remained at the top of sub weir caused a minor blockage at the downstream of the Taunsa Barrage (Chaudary and Sarwar, 2014). As a result, flood-2010 water level remained the same in the upstream and downstream of the barrage. Similarly, the rising riverbed resulted in the deposition of large amount of sediments downstream in head up area that has reduced the discharge capacity of the Taunsa Barrage and triggered the high waves of flood water back to its embankment on the eastern side and breached the protection EM embankment (*Fig. 6*).

Figure 5. *Aerial view of the Taunsa Barrage, construction of sub-weir, sediments in head up during the flood in 2010. (Source URL: https://www.dawn.com/news/1195398)*

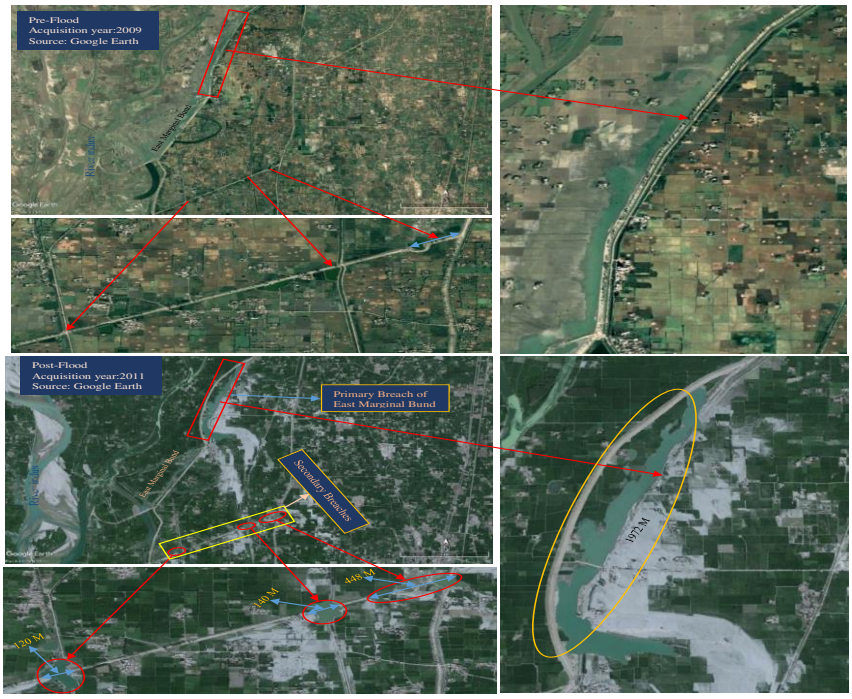

Figure 6. *Pre and post flood images of breached East Marginal Embankment at Rd 32-38*

http://www.aloki.hu ● ISSN 1589 1623 (Print) ● ISSN 1785 0037 (Online)
DOI: http://dx.doi.org/10.15666/aeer/1706_1412114142

According to respondent perceptions regarding flood causing factors, 90% had indicated that breaching of the EM embankment at Rd (*32-38*) Abbas Wala at the Taunsa Barrage had caused this flood menace in the study area. A total of 10% reported heavy monsoon rainfall in upstream areas of the Indus River. Based on indigenous knowledge of this phenomenon and previous experiences forest and irrigation officials described that deforestation along the canal embankment for fuel and timber purposes has weakened the canal banks along with unpaved canal, as a contributing factor of breaching of canal banks, waterlogging and floods in the rainy season in the study area.

Extent of flood-2010

The extent of flood-2010 analysis comprises of supervised classification of flooded areas and depth of inundated surveyed areas. The supervised classification was performed using Landsat ETM Images. The Landsat ETM image of the 3rd July, 2010 was classified for pre-flooding situation whereas image of the 20th August, 2010 was classified for post-flood 2010 instance analysis. Further, we used change detection method, based on the classified classes for the pre and post flood images, to investigate the significance land use and land cover changes due to flooding phenomena as shown in *Figure 7*. The pre-flood image classification of the 3rd July, 2010 shows that only 7% of the area was covered by water, while vegetation, built up and barren land were covered by 39.9%, 30.03% and 22.8%, respectively. Similarly, Post flood image classification of the 20th August, shows that 24% of the area was covered by water while vegetation, built up and barren land were covered by 35%, 22% and 19%, respectively. Both pre and post flood instances classifications show significant clear demarcation of defined classes. Post flood change detection analysis shows dramatic change in water class, with an increase from 7% to about 21% while built up area has decreased by 8.03%, from 30.03% to 22% in post flood analysis. The vegetation decreased by 5%, from 40% in pre-flood instance to 35% in post flood situation and the barren land decreased by 3.8% from an area of 22.8% in pre-flood instance to 19% recorded in post-flood situation (*Fig. 7*). Overall, the significant change was shown in water class in comparison with other classes and inundated an area of around ~1732 km^2 in the study areas. A total number of 1,780,226 people were affected in the 2010 flood (NDMA, 2010; PPDMA, 2010). The resulted inundation depth was found very uneven in the study area measured by GPS and measuring tape. The flood inundation depth was found very high in Kot addu area, due to high proximity to breached EM embankment as shown in *Figure 1*. Similarly, in Ali pur area, moderate flood inundation depth was found, as located in the lower reach of the study area where the Indus and Chenab rivers meet as shown in *Figure 8*. Comparatively, most of the socio-economic damages were reported from these areas.

Damage assessment

Analysis revealed that the flood in 2010 was severely disastrous and devastating in nature, however, it has caused serious damages at large scale to agriculture, human settlements and physical infrastructure in the study area. Flood damage assessment was done through Geo-spatial analysis and statistical analysis.

Damage to agriculture

The study area is one of the fertile floodplains of the Indus. Agriculture is the main source of economic activity, hence local residents are actively engaged in crop

http://www.aloki.hu ● ISSN 1589 1623 (Print) ● ISSN 1785 0037 (Online)
DOI: http://dx.doi.org/10.15666/aeer/1706_1412114142

cultivations, in both Rabi and Kharif crop seasons. The analysis revealed that flood has badly affected the standing crops of Kharif season, including rice, sugarcane, cotton and fodder crop. A total of 4182.8 ha of agriculture standing crops were destroyed with an estimated economic loss of 8.68 million US$ as shown in *Figure 9*. It was further indicated that ~1499.9 ha of rice standing crop was submerged, which resulted in an estimated economic loss of 2.9 million US$. Likewise, sugarcane standing crop on ~1029.1 ha was destroyed, which incurred an estimated economic loss of 2.9 million US$. A total of 479.1 ha of cotton crop was completely destroyed, with an estimated economic loss of 1.1 million US$. Similarly, about 1174.7 ha of fodder crops were inundated with an estimated economic loss of 1.8 million US$ (*Fig. 9*).

According to community perception, an average estimated economic cost of rice crop on per ha was 1934 US$, sugar cane was 2906 US$, cotton was 2325 US$, fodder crop was 1611 US$.

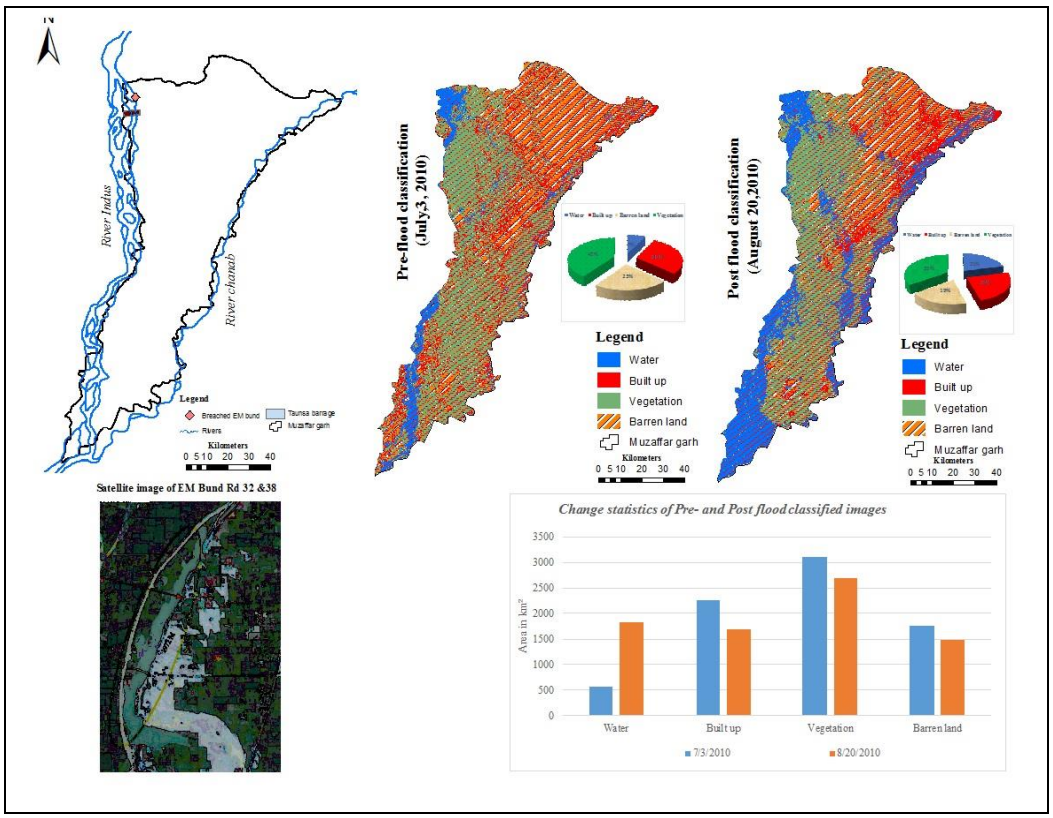

Figure 7. *Pre and post flood change detection statistics and classification*

Damage to livestock

Muzaffar garh is ranked as the 2nd largest district in livestock sector in Punjab province, Pakistan (GoP, 2017). People usually keep subsistence and commercial livestock for their source of earning, which include buffaloes, cows, sheep, goats, oxen, donkeys and camels in the study area. As *Figure 10* shows that a total number of 1172 livestock animals were found dead with an estimated economic loss of 0.761 million US$. The loss of buffaloes has incurred an estimated economic cost of 0.404 million US$ while an estimated economic cost by loss of cows was 0.28 million US$. Whereas

http://www.aloki.hu ● ISSN 1589 1623 (Print) ● ISSN 1785 0037 (Online)
DOI: http://dx.doi.org/10.15666/aeer/1706_1412114142

the loss of goats, sheep and donkeys has imposed a collective estimated economic loss of 0.077 million US$ (*Fig. 10*). The survey indicated that the maximum loss of animals was reported from the Kot addu surveyed area, where the flood depth was maximum revealed by the flood depth spatial analysis as shown in *Figure 8*. During field survey, the average estimated economic cost was determined as per community estimate, the average economic estimated cost of buffalo was 1176 US$, of cow was 823 US$, of goat and sheep was 176.4 US$ and of donkey was 94 US$ per community each.

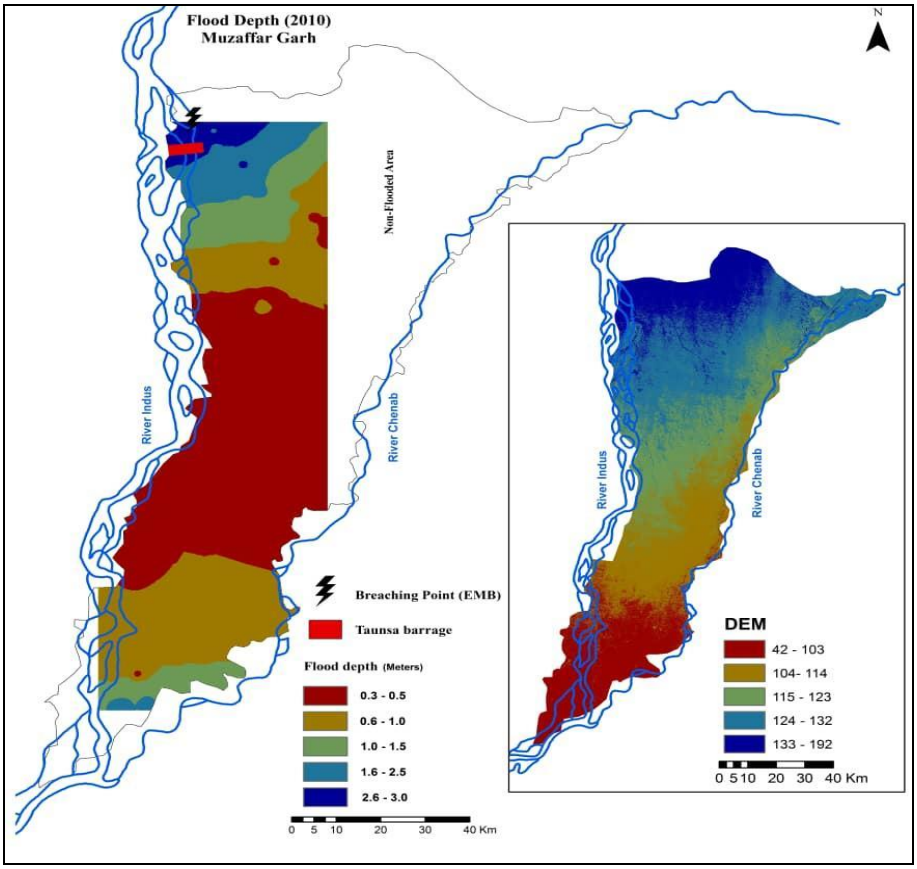

Figure 8. *Spatial pattern of flood depth and Digital Elevation Model (DEM) of Muzaffar garh*

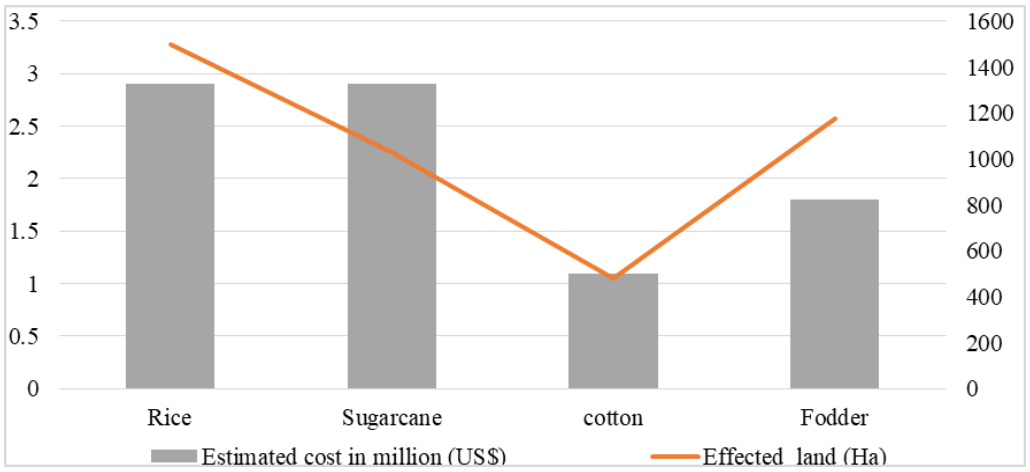

Figure 9. *Damaged agriculture crops and estimated loss in million (US$)*

http://www.aloki.hu ● ISSN 1589 1623 (Print) ● ISSN 1785 0037 (Online)
DOI: http://dx.doi.org/10.15666/aeer/1706_1412114142

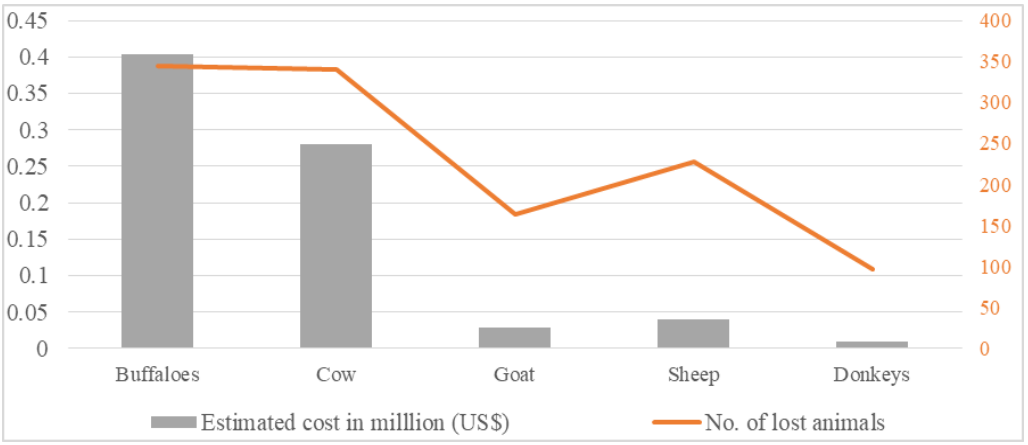

Figure 10. *Number of lost livestocks estimated loss in million US$*

Damages to houses

In the study area, housing structures were very dissimilar with respect to urban and rural areas. Brick houses and mud houses were found in the study area. Field observation and result revealed that the brick houses have more coping capacity in term of flood resilience and structural vulnerability, whereas mud houses have no such flood resilient coping capacity and have high vulnerability to flooding. As *Table 2* shows a total of 2673 houses were located in the study area with 1859 mud houses and 814 brick houses. A total of 776 mud houses were partially damaged with an estimated economic loss of 0.27 million US$, and about 768 mud houses were completely damaged with an estimated economic loss of 0.54 million US$ (*Table 3*). As a result, about 83% mud houses were found partially and completely damaged in the study area. In addition to this, a total of 360 brick houses were found partially damaged with an estimated economic loss of 0.25 million US$. Besides that, 188 brick houses were found fully damaged with an estimated economic loss of 0.26 million US$. The community estimated that the average cost per partially and fully damaged mud house was 353 US$ and 706 US$, respectively. Similarly, they had also indicated that the average rehabilitation cost of partially and fully damaged brick house were 706 US$ and 1412 US$, respectively (*Table 4*).

Damages to infrastructure

Road infrastructure is the main source of transportation link between the study area and the rest of the provinces of Pakistan, which in turn stimulate economic growth. In the flood 2010, major G.T. Roads and intra-district roads were severely damaged. According to Communication and Works Department (C&W) Punjab, a total of 150 km road network was fully damaged with an estimated economic loss of 3 million US$. For example, the road that connects G.T. Road in Taunsa Sharif to Multan via Muzaffar garh was seriously damaged from various places with the width of around 100 km. Further, Pak-Arab Oil Refinery Company (PARCO), which is located along this road, suspended oil supply in the whole country due to this flooding event. As a result, Kot addu power plant and Lalpir thermal power plant in Muzaffar garh, which depends on the oil supply from PARCO, were partially shut down, which meant that only 1600 MW was generated instead of the maximum capacity of 2400 MW.

http://www.aloki.hu ● ISSN 1589 1623 (Print) ● ISSN 1785 0037 (Online)
DOI: http://dx.doi.org/10.15666/aeer/1706_1412114142

Table 2. *Damages to mud and brick houses and estimated loss in million US$*

Sr. no.	Type of houses	Total no. of houses	Partially damaged	Completely damaged	Estimated loss in million US$
1	Brick houses	814	360	188	0.5
2	Mud houses	1859	776	768	0.81

Table 3. *Study area: damages to mud houses*

Surveyed areas	Mud houses			
	Total number of houses	Partially damaged	Completely damaged	Loss in million US$
Kot addu	685	256	308	0.30
Ali pur	594	225	265	0.27
Muzaffar garh	335	180	105	0.14
Jatoi	245	115	90	0.10

Table 4. *Study area: damages to brick houses*

Surveyed areas	Brick houses			
	Total number of houses	Partially damaged	Completely damaged	Loss in million US$
Kot addu	274	126	68	0.18
Ali pur	234	109	55	0.15
Muzaffar garh	175	70	35	0.09
Jatoi	131	55	30	0.08

The railway line is the other source of transportation in the study area. According to railway officials, around 4 km long railway track was burst in various locations. However, the most damaged tracks were in Kot addu due to the gushing water flow from nearby breached EM embankment. The devastated tracks of 1.5 km occurred in between Kot addu station to Taunsa Barrage station and around 2.5 km bursted track was reported in between Bud railway station to Memood kot railway station. The total estimated economic loss was 0.1 million US$.

The analysis revealed that following the collapse of EM embankment, the floodwater roared through Thal Panjnad (T-P) link canal and breached it due to the excessive spillover from the canal capacity. Further this torrent water drained into Muzaffar garh canal, which could not sustain the pressure of a destructive water and resulted in breaching at many points. According to the District Irrigation Department, collectively around 15 km irrigation channels were damaged by flood-2010 in the study area with a total estimated economic loss of 0.32 million US$.

In addition to this, flood had also seriously damaged bridges that were constructed over the irrigation channels for communication and transportation purposes. As *Table 5* shows a total of 15 bridges were completely damaged with an estimated loss of 0.151 million US$. Similarly, the flood has also disrupted electric power supply in the study area for almost two months by damaging more than 100 electric power poles and electric supply lines. According to Multan Electric Power Company (MEPCO), a total

http://www.aloki.hu ● ISSN 1589 1623 (Print) ● ISSN 1785 0037 (Online)
DOI: http://dx.doi.org/10.15666/aeer/1706_1412114142

of 0.15 million US$ economic loss was estimated for rehabilitation to recover the power supply.

The results of this study were supported by recent related research studies. Mahmood et al. (2019) concluded that 2010 flood in the central Indus Basin was devastating in term of agricultural damages and infrastructure. Gaurav et al. (2011) claimed that the Indus flood 2010 was triggered due to engineering structures of barrages and embankments along the Indus Basin. Hashmi et al. (2012) found that flood 2010 in Pakistan was very damaging in terms of infrastructure and agricultural losses. He further explained that the agricultural sector was badly affected by damaging of standing agriculture crops. Mahmood et al. (2016a) concluded that the 2010 flood in Pakistan was destructive in terms of damages to buildings, infrastructure, and huge economic losses to agriculture. Rehman and Khan (2013) found that 2010 flood disaster has triggered huge losses to infrastructure due to damaging of building, roads and canals. He further explained that infrastructure is the most flood affected sector in the upstream areas of the Indus.

Table 5. *Damaged bridges and estimated loss in million US$*

Tehsil	Number of damaged bridges	Estimated loss in million US$
Kot addu	10	0.071
Ali pur	2	0.011
Muzaffar garh	2	0.011
Jatoi	1	0.058

Discussion

The flood 2010 occurred in the study area following the worst weather forecast ever recorded in history by Pakistan meteorological stations in the month of July 2010, with respect to cloud formation incorporated with spatial extent and duration of monsoon rainfall, as a result of the convergence of monsoon winds with upper air jet stream over the North-western regions of KPK province, Pakistan (PMD, 2010; Rehman and Khan, 2013; Mahmood et al., 2016a, b). As *Figure 4* shows the evidence of high rainfall of more than 250 mm recorded during 2010 in comparison with last decade rainfall data that triggered the high inflow of 27184 m^3/s at Taunsa Barrage. This high inflow was somehow equal to the designed capacity of the barrage as shown in *Figure 3*. Despite that the water flow was crossing at an alarming level, no action was timely taken to decide the breaching section at emergency purpose. In addition to this, as *Figure 5* shows that the influence of sub-weir construction and its upstream narrowing embankments certainly decreased the designed carrying capacity of the Taunsa Barrage. Furthermore, the Indus is famous for carrying a high sediment load from the Himalayas foothills and Taunsa Barrage structure has stuck huge sediments within the river belt thus causing the river bed raise in the last few years. Moreover, in the years 2004-2008, with the request of the Government of Pakistan (GOP), the World Bank took initiative and provided 144 Million US$ for the remodelling of a diversion structure at Taunsa Barrage (Chaudary and Sarwar, 2014). They did the remodelling of the structure in such a way that they had constructed a sub-weir of about 2.5 m vertical and 274 m horizontal length downstream of the Taunsa Barrage, as shown in *Figure 5*. The coffer dam material was used for construction work. The coffer dam discarded material remained at

http://www.aloki.hu ● ISSN 1589 1623 (Print) ● ISSN 1785 0037 (Online)
DOI: http://dx.doi.org/10.15666/aeer/1706_1412114142

the top of sub-weir resulted in a minor blockage and an increased sediment in the river bed eventually resulted in the breach of the EM embankment.

The findings regarding flood management at Taunsa Barrage revealed that there was no breaching outlet upstream on either side of the barrage. But in fact, the natural topographical slope and depression in the west side upstream, that can divert the emergency water to the depression areas is missing. As such, once flood peak wave passed to downstream, the emergency water can recede back to the river bed. Furthermore, the west bank is scarcely populated in terms of settlements, and economic developments. This resulted in less loss of life and properties since there was no such defined breaching outlet on the western side. In comparison with recent breached east embankment, there were dense human settlements with intensive agriculture crop cultivations and strong infrastructural developments (*Fig. 6*). The worst in fact is that the flood 2010 overbank water did not return to the river. Rather it was rushed and remained in the cities, towns and agriculture lands for about two months. Further, refilling process took 10 days, overbank bursted water remained destructive in nature with high intensity and destroyed everything that came in its way. Similarly, technical negligence and mismanagement of the Taunsa Barrage was also revealed. The heavy, prolonged rainfall in upstream of the Indus was forecasted by PMD, but there were no pre-flood measures taken to manage or even to reduce the impacts of flood by rapid structural maintenance of the embankments. In addition to this, they were also failed to operate the newly motorized hoisting system, as a result ten barrage gates were not totally opened (Chaudary and Sarwar, 2014, 2016). This led to the sudden pressure at the barrage and caused the collapse of EM embankment at Rd 32-38. Similarly, the Kosi flood 2008, in the eastern part of India also occurred due to a 1.2 km long breach in the eastern embankment at Kusaha, which was located almost 12 km upstream of the Kosi Barrage. Likewise, Indus, the Kosi River carries a very high sediment influx from upstream areas which caused the river bed level raise and a super elevated flowing in condition toward lower reaches in the Kusaha region. Further, negligence and improper maintenance of the embankments were also found which made this Kosi river more disastrous for the affected population in the Kusaha region (Sinha, 2010). In contrast, the Kosi flood disaster 2008 in India occurred due to a breach at eastern embankment with a very low discharge of 4078 m^3/s, whereas in southern Punjab 2010 flood occurred due to the breach of the EM embankment at Rd 32-38 near Taunsa Barrage with the discharge of 27184 m^3/s.

Depth of the flood 2010 in the study area was unevenly located in all surveyed areas with the help of GPS and measuring tape. The result shows the correlation between the flood depth and the nature of damages, which increased the flood magnitude of socio-economic infrastructure damages. During survey, we noticed that a total of 75% of the households indicated that flood depth varied from 1 to 2 m while the remaining 25% households indicated that flood depth varied from 2.1 to 3 m (*Fig. 8*). In addition, flood duration varied due to the slight geographical and topographical variability in the area and soil texture. The most consistent observation was that almost all the respondents indicated that flood water remained stagnant from 2 to 3 months in post flood situation. This increased the magnitude of damages as the mud houses and crop were subjected to adverse conditions.

Supervised classification was used for analyzing the landuse/cover change in the study area**.** Supervised classification result shows that built up areas has been decreased by 8.02% in post-flood situation. Further survey indicated that most of the respondents

http://www.aloki.hu ● ISSN 1589 1623 (Print) ● ISSN 1785 0037 (Online)
DOI: http://dx.doi.org/10.15666/aeer/1706_1412114142

belonged to very poor families and settled in mud houses. Flood had badly destroyed and even washed them away. Similarly, infrastructure and other built up areas were also destroyed in such a way that their materials were dispersed. In some areas, flooded water transported households' material in a different way, such as traction by rolling and suspension. Thus, survey evidences were found consistent with supervised classification result as decrease in built up area was shown in post flood classification (*Fig. 7*). Moreover, vegetation area had decreased by 5% in post flood classification and flood 2010 occurred in the month of July and August during the growing season of Kharif crops including rice, sugarcane, cotton and maize with other fodder crops. Thus, the visible green due to increase in chlorophyll was found in both pre and post flood instances and resulted in vegetation areas having the highest values in comparison with all other classes. Similarly, slight difference found in barren class during pre and post-flood classification (*Fig. 7*). Further, most of the barren land lies in the northern and north-eastern part of the study area characterized by high elevation and far away from the proximity of river which makes it the proposed area for safe evacuation places if flood occurs in future flood risk reduction.

We noticed that more damage and destruction was found in the agricultural sector in comparison with other sectors. Flood was not only very destructive in terms of agriculture standing crops damages, but also destroyed the district government wheat seed stocks. Further, disruption was observed in the forthcoming Rabi season crops, which were cultivated very late due to the presence of flood water for almost 8 weeks. Additionally, most of the damages to agriculture standing crops were found in Kot addu area as it was located very near to the breached EM embankment. Similarly, it was indicated that the maximum livestock damages were also reported from Kot addu, as this area had faced roaring disastrous unpredictable flood water with long duration and maximum depth.

Observations also revealed that an increase in duration and depth of flood is proportional to the increase of sensitivity of livestock. The depth difference influenced the loss numbers of different animals. For example, in areas with high flood depth of above 1.5 m experienced more buffaloes, cows, and donkeys were lost while areas having less than 1.5 m depth experienced the maximum losses of sheep and goat according to the records.

As far as housing structure is concerned, there were two types of houses that were found in the area namely, brick houses and mud houses. The brick houses were more resilient against flood vulnerability, whereas mud house had very little resilient capacity and had high flood vulnerability. In addition to this, a total of 1544 of mud houses were found completely and partially destroyed. We noticed that about 50% of the people have monthly income of less than 130 US$, which limited their capability to build brick houses. That is why, a large number of registered damaged houses were mud houses and mostly reported from the Kot addu survey area. Further, it is highly recommended that there is a need of appropriate financial aid to the vulnerable people to construct their flood resilient houses that can withstand future flooding events.

Conclusion

District Muzaffar garh is one of the unprivileged districts of South Punjab, Pakistan. It is located in a near juxtaposition to the river Indus and Chenab from its both sides which are exposing it to riverine flooding. Almost every year, riverine flooding occurs in the study area from the east bank of the mighty River Indus and the west bank of the River Chenab. In 2010, the worst riverine flooding of the century occurred in the study

http://www.aloki.hu ● ISSN 1589 1623 (Print) ● ISSN 1785 0037 (Online)
DOI: http://dx.doi.org/10.15666/aeer/1706_1412114142

area due to 4-days extra-ordinary amount of monsoon rainfall in the upstream of the Indus Basin that triggered a discharge of about 28317 m^3/s at Taunsa Barrage, which exceeded its capacity. The East Marginal (EM) embankment could not sustain the discharged water and it eventually collapsed. The collapse of the Taunsa Barrage caused inundation in the study area and consequently, agricultural standing crops, livestocks, infrastructure, human settlements were destroyed or damaged. This also led to a temporary shift for most of the local people to safe locations.

The leading majority of above 40% surveyed households were engaged directly and indirectly since the agricultural sector is considered as one of the main sources of earnings. Throughout the study area, flood has badly affected the standing crops of Kharif season with an estimated economic loss was 8.68 million US$ and it is largely one of the most exposed economic sectors to recurrent floods and poor mitigation approaches. Overall, total damages from flood 2010 were about 14.23 million US$. Agriculture and Infrastructure were seriously damaged sectors with an estimated economic losses of 8.68 and 3.48 million US$, respectively. Similarly, the economic damages to housing and livestock sectors were 1.31 and 0.761million US$. Furthermore, most of the surveyed respondents earned less than 130US$, which is not permitting them to build resilient brick houses. Therefore, the majority of them have been living in mud houses, which are highly vulnerable to floods. This circumstance had further intensified and exposed the physical and economic vulnerabilities of local communities to riverine floods. Out of all surveyed areas, the maximum damages to all economic sectors were reported from Kot addu which lies in the proximity of the breached EM embankment. Furthermore, most of the respondents were living in flood plain areas and that has further increased the intensity of massive flooding and imposed the huge economic losses to this vicinity.

The study concludes that, as many previous related studies and forums cited in the year of 2010, high rainfall in upstream Indus was the main cause of flooding in the entire Indus Basin. In comparison to this study, it is defined that the resulting discharge (27184 m^3/s) at Taunsa Barrage did not exceed its proposed designed capacity (28317 m^3/s). However, the obstacle of excessive volumes of water together with a large quantity of sediment deposition in the head up because of structural sub-weir construction in downstream and narrow river bed due to the construction of protective embankments in the upstream, has reduced the designed carrying capacity of the Taunsa Barrage. Moreover, the concerned authority and river management department did not take any measures corresponding to upraise the protective embankments with respect to flood management in 2010. This research study provides effective mixed method approaches to the local, regional and national disaster management authorities for devising the effective flood management plan with the identification of breaching points in any emergency situation to minimize future flood risk, human causalities and socio-economic damages. Moreover, this study will bring the attention of disaster management authorities to divert their obsolete strategy of river control to river management.

It can finally be concluded that this increase of population sprawl in floodplain for socio-economic development is expected to continue in the future in the study region. Similarly, there is an utmost need of effective flood-risk zonation and strategies to reduce the future impacts of riverine flood disasters in the study area. There is a need of effective studies on the human interventions in the river basins in term of cost-benefit approach, including impacts on human and environment. In addition to this, zone-specific flood-risk reduction strategies should be the next step.

http://www.aloki.hu ● ISSN 1589 1623 (Print) ● ISSN 1785 0037 (Online)
DOI: http://dx.doi.org/10.15666/aeer/1706_1412114142

Acknowledgements. This work was funded by the National Key Research and Development Program (2018YFC1506506), the Frontier Project of Applied Foundation of Wuhan (2019020701011502), the Natural Science Foundation of Hubei Province (2019CFB736), the Fundamental Research Funds for the Central Universities (2042018kf0220) and the LIESMARS Special Research Funding.

REFERENCES

[1] Ali, A. (2013): Indus Basin Floods: Mechanisms, Impacts, and Management. – Asian Development Bank, Mandaluyong City, Philippines.
[2] Alphan, H., Doygun, H., Unlukaplan, Y. I. (2009): Post-classification comparison of land cover using multitemporal Landsat and ASTER imagery: the case of Kahramanmaras, Turkey. – Environ Monit Assess 151: 327-336.
[3] Banerjee, L. (2010): Effects of flood on agricultural productivity in Bangladesh. – Oxford Development Studies 38: 339-356.
[4] Cann, K. F., Thomas, D. R., Salmon, R. L., Wyn-Jones, A. P., Kay, D. (2013): Extreme water-related weather events and waterborne disease. – Epidemiology and Infection 141: 671-686.
[5] Chaudary, Z. A., Sarwar, M. K. (2014): Rehabilitated Taunsa Barrage: prospects and concerns. – Science, Technology and Development 33(3): 127-131.
[6] Chaudary, Z. A., Sarwar, M. K. (2016): Catastrophe of flood 2010 at Taunsa Barrage; review of technical findings of Punjab Judicial Tribunal Report. – Science, Technology and Development 35(1): 1-5. DOI: 10.3923/std.2016.1.5.
[7] Chohan, K., Ahmad, S. R., Islam, Z., Adrees, M. (2015): Riverine flood damage assessment of cultivated lands along Chenab River using GIS and remotely sensed data: a case study of district Hafizabad, Punjab, Pakistan. – J Geogr Inf Syst 7: 506-526.
[8] Dawood, M., Mahmood, S., Rahman, G., Rahman, A. (2017): Impact of rain-fall fluctuation on river discharge in Hindu Kush Region, Pakistan. – Abasyn J Soc Sci 10: 246-259.
[9] El Bastawesy, M., Gabr, S., Mohamed, I. (2015): Assessment of hydrological changes in the Nile River due to the construction of Renaissance Dam in Ethiopia. – Egypt. J. Remote Sens. Space Sci. 18(1): 65-75.
[10] Federal Flood Commission (FFC) (2010): Annual Flood Report. – Ministry of Water and Power, Government of Pakistan, Islamabad.
[11] Gaurav, K., Sindha, R., Panda, P. K. (2011): The Indus flood of 2010 in Pakistan: a perspective analysis using remote sensing data. – Nat. Hazards 59: 1815-1826.http://dx.doi.org/10.1007/s11069-011/9569-6.
[12] Geis, D., Steeves, B. (1998): Flood Hazards. – Association of Collegiate Schools of Architecture, Inc. https://www.jstor.org/stable/1424687.
[13] Ghosh, D. D., Mandal, M., Banerjee, M. (2015): Environmental impact of embankment breaching: a case study along lower reaches of Ajay River, West Bengal, India. – International Journal of Arts, Humanities and Management Studies 01: 09.
[14] Government of Pakistan (1999, 2017): District Census and disaster Report of Muzaffar Garh. – Population Census Organization, Islamabad.
[15] Haq, M., Akhtar, M., Muhammad, S., Paras, S., Rahmatullah, J. (2012): Techniques of remote sensing and GIS for flood monitoring and damage assessment: a case study of Sindh province, Pakistan. – Egyptian Journal of Remote Sensing and Space Sciences 15: 135-141.
[16] Hashmi, H. N., Siddiqui, Q. T. M., Ghuman, A. R., Kamal, M. A., Mughal, H. A. (2012): critical analysis of 2010 floods in Pakistan. – African Journal of Agricultural Research 7: 1054-1067.
[17] Howe, J., White, I. (2002): The Geography of the autumn 2000 floods in England and Wales: causes and solution. – Geographical Association 87: 116-124.

http://www.aloki.hu ● ISSN 1589 1623 (Print) ● ISSN 1785 0037 (Online)
DOI: http://dx.doi.org/10.15666/aeer/1706_1412114142

[18] Khalid, B., Cholaw, B., Alvim, D. S. (2018): Riverine flood assessment in Jhang district in connection with ENSO and summer monsoon rainfall over Upper Indus Basin for 2010. – Nat Hazards 92: 971. DOI: https://doi.org/10.1007/s11069-018-3234-y.
[19] Khan, A. N. (2005): An assessment of floods hazard causes for efficient flood plain management: a case of Neelam-Jehlum Valley. – Pakistan Geographical Review 60(1): 42-53.
[20] Khan, B., Iqbal, M. J., Yosufzal, M. A. K. (2009): Flood risk assessment of river Indus of Pakistan. – Arab J Geosci 4: 115-122.
[21] Laghari, A. N., Vanham, D., Rauch, W. (2012): The Indus basin in the framework of current and future water resources management. – Hydrol. Earth Syst. Sci 16: 1063-1083.
[22] Mahmood, S., Rani, R. (2018): Extent of 2014 Flood Damages in Chenab Basin Upper Indus Plain. – In: Antunes Do Carmo, J. S. (ed.) Natural Hazards-Risk Assessment and Vulnerability Reduction. IntechOpen, London. https://doi.org/10.5772/intec hopen.79687.
[23] Mahmood, S., Khan, A. H., Mayo, S. M. (2016a): Exploring underlying causes and assessing damages of 2010 flash flood in the upper zone of Panjkora River, Pakistan. – Nat Hazards 83(2): 1213-1227.
[24] Mahmood, S., Khan, A. H., Ullah, S. (2016b): Assessment of 2010 flash flood causes and associated damages in Dir Valley, Khyber Pakhtunkhwa Pakistan. – Int J Disaster Risk Reduct 16: 215-223.
[25] Mahmood, S., Rahman, A., Sajjad, A. (2019): Assessment of 2010 flood disaster causes and damages in district Muzaffargarh, Central Indus Basin, Pakistan. – Environmental Earth Sciences 78: 63.
[26] Melgani, F., Bruzzone, L. (2004): Classification of hyper spectral remote sensing images with support vector machine. – IEEE Trans. Geosci. Remote Sens. 42(8): 1778-1790.
[27] Messner, F., Penning, R. E., Green, C., Meyer, V., Tunstall, S., Veen, A. (2007): Evaluating flood damages: guidance and recommendations on principles and methods. – Flood Site Project Deliverable. Report no. T09-06-01.
[28] Milly, P. C. D., Wetherald, R. T., Dunne, K. A., Delworth, T. L. (2002): Increasing risk of great floods in a changing climate. – Nature 415: 514-517.
[29] Natalia, K., Shelestov, A., Skakun, S., Kravchenko, O. (2008): Data assimilation technique for flood monitoring and prediction. – International Journal Information Theories & Applications 15: 76-83.
[30] National Disaster Management Authority (NDMA) (2010): annual flood report 2010. – Government of Pakistan, Islamabad.
[31] Pakistan Metrological Department (PMD) (2010): Annual flood report 2010. – Government of Pakistan, Islamabad.
[32] Punjab Provincial Disaster Management Authority (PPDMA) (2010): Annual Flood Report 2010. – Government of Punjab, Lahore.
[33] Rahman, A., Khan, A. N. (2011): Analysis of flood causes and associated socio-economic damages in the Hindu Kush region. – Nat Hazards 59: 1239-1260. http://dx.doi.org/10.1007/s11069-0011-9830-8.
[34] Rahman, A., Khan, A. N. (2013): Analysis of 2010-flood causes, nature and magnitude in the Khyber Pakhtunkhwa, Pakistan. – Nat Hazards 66: 887-904.
[35] Sinha, R. (2010): A river runs through it. – Public Serv Rev Int Dev 17: 20-22.
[36] Shah, S. M. S., Gabriel, H. F. (2002): Floods in Pakistan. – A Country Paper presented in the Regional Media and Policy Workshop on "Fencing Floods in South Asia: Disaster Preparedness Through Risk Communication". Dec. 15-18, 2002, Islamabad, Pakistan.
[37] Solheim, I., Solbo, S., Indregard, M., Lauknes, I.(2001): User requirements and SAR-solutions for flood mapping. – 4th International Symposium on Retrieval of Bio- and Geophysical Parameters from SAR Data for Land Applications, Innsbruck, Austria.
[38] Syvitski, J. P., Brakenridge, G. R. (2013): Causation and avoidance of catastrophic flooding along the Indus River, Pakistan. – GSA Today 23(1): 4-10.

http://www.aloki.hu ● ISSN 1589 1623 (Print) ● ISSN 1785 0037 (Online)
DOI: http://dx.doi.org/10.15666/aeer/1706_1412114142

[39] Tariq, M. A. U. R., Giesen, V. D. N. (2012): Floods and flood management in Pakistan. – Phys. Chem. Earth 47: 11-20. http://dx.doi.org/10.1016/j.pce.2011.08.014.
[40] Walder, J. S., o'connor, J. E. (1997): Methods for predicting peak discharge of floods caused by failure of natural and constructed earthen dams. – Water Resources Research 33: 2337-2348.
[41] Zhou, C., Yang, C. J., Baoiln, L. I., Wang, S. (2000): Flood monitoring using multi-temporal AVHRR and RADARSAT imagery. – Photogramm. Eng. Remote. Sens. 66: 633-638.

http://www.aloki.hu ● ISSN 1589 1623 (Print) ● ISSN 1785 0037 (Online)
DOI: http://dx.doi.org/10.15666/aeer/1706_1412114142

COMPOSITION AND DIVERSITY IN SOIL SAMPLES FROM THE NAPAHAI PLATEAU WETLAND OF SOUTHWESTERN CHINA

CHEN, W.[1] – LI, X. R.[2] – TENG, P. Y.[1] – WEI, Y. L.[2] – JI, X. L.[2*]

[1]*Medical School, Kunming University of Science and Technology, Kunming, Yunnan Province 650500, China*

[2]*Faculty of Life Science and Technology, Kunming University of Science and Technology, Kunming, Yunnan Province 650500, China*

**Corresponding author*
e-mail: jixiuling@126.com

(Received 30th May 2019; accepted 3rd Sep 2019)

Abstract. The Napahai plateau wetland, located in northwestern Yunnan province, China, is a unique seasonal plateau wetland of low-latitude and high-altitude, yet the microbial community is still unknown. To address this shortcoming, MiSeq high-throughput sequencing was used to analyze the composition and diversity of bacteria and archaea. The bacterial community comprised of 64 phyla, 164 classes and 484 genera, in which *Proteobacteria* was the most abundant, followed by *Actinobacteria*, *Chloroflexi* and *Acidobacteria*. Archaea comprised of 3 phyla, 5 classes, and 7 genera, in which *Thaumarchaeota* dominated. The results indicated that the composition and diversity of the bacterial community were more influenced by seasonal changes than by soil types, whereas the archaeal community was mostly resistant to these factors. Additionally, canonical correlation analysis (CCA) showed that the diversity of the bacterial community was closely correlated with nitrogen (N), total nitrogen (TN) and soil organic matter (SOM) in the dry season. However, no significant correlation of any of the factors was observed in the archaeal community. In conclusion, these results indicated that microbial communities in the soil of Napahai plateau wetland have unique diversity and composition, and Napahai plateau wetland as a microbial resource requires protection and restoration.
Keywords: *wetland ecosystem, high throughput sequencing, bacterial community diversity, archaeal community diversity, environmental factors*

Introduction

Wetlands are important links between terrestrial and aquatic systems. They are large reservoirs of biodiversity and ecologically powerful natural ecosystems. Ecological services of wetlands have high social and economic value. In wetland ecosystems, microbial community diversity is much better than vegetation species diversity to reflect environmental changes. The microbial community diversity and composition of wetland soils are more sensitive and comprehensive to reflect the wetland ecological conditions. Also they have a great significance for maintaining the balance of wetland ecosystems, repairing damaged wetlands and carrying out comprehensive environmental management.

Recently, the rapid development of high-throughput DNA sequencing has allowed the detailed study of the diversity of microbial communities in wetland soils, with fruitful results. For instance, soil samples were collected from six wetlands on the Qinghai-Tibetan plateau, and high-throughput 16S rRNA gene sequencing was used to assess the composition and localization of enriched microbial communities. Overall, microbial communities from the Qinghai-Tibetan plateau wetlands showed significant potential in converting cellulose and chitin to methane at low temperatures (Dai et al., 2016). In a subarctic wetland in Russia, the major bacterial groups identified in peat by high-

http://www.aloki.hu ● ISSN 1589 1623 (Print) ● ISSN 1785 0037 (Online)
DOI: http://dx.doi.org/10.15666/aeer/1706_1414314158

throughput sequencing of the 16S rRNA genes were *Acidobacteria* (35.4-41.2%), *Alphaproteobacteria* (19.1-24.2%), and *Gammaproteobacteria* (7.9-11.1%). The distinctive feature of this community was a high proportion of two subdivisions of *Acidobacteria*, which are not characteristic for boreal sphagnum peat bogs (Danilova et al., 2016). In coastal mangrove wetlands, MiSeq high throughput sequencing was used to understand the microbial composition and diversity pattern. The five most abundant phyla within the bacterial and archaeal communities remained stable between two distinctive seasons, suggesting that the microbial community in the Mai Po wetland exhibits a mild seasonal dynamic (Zhou et al., 2017).

In a wetland ecosystem, geographic distance and environmental factors are two important drivers of the distribution of microorganisms (Widder et al., 2014; Savio et al., 2015). However, in the whole space, environmental factors are more important. Previous studies have demonstrated that soil microbial communities can be significantly influenced by mineral nutrients (Su et al., 2015). In Qinghai-Tibet plateau, soil organic matter and pH were the main factors affecting the soil macrofauna communities of composition and diversity. In addition to environmental factors, the sampling site can influence the microbial community. For instance, Cao studied soil samples across a regional scale in China (including Jiangxi, Hubei, and Henan provinces). Henan has the largest amount of bacterial and fungal phospholipid fatty acids (PLFAs), while Jiangxi shows the lowest amount of PLFAs (Cao et al., 2016). Moreover, the dominant microbial communities generally differ in different sites. For instance, the dominant bacterial phyla are *Proteobacteria*, *Bacteroidetes*, and *Actinobacteria* in Beijing (Tian et al., 2014), but they are *Proteobacteria*, *Acidobacteria*, and *Chloroflexi* in Jiangsu (Zhao et al., 2014).

The Napahai plateau wetland, an important water source for the upper reaches of the Yangtze River and located in northwestern of Yunnan Province, China, is a unique, seasonal plateau wetland in low latitude and at high altitude. The Napahai plateau wetland has been listed as an internationally important wetland, and has the significance of being a representative plateau wetland (Xiang et al., 2018). However, the microbial community composition and diversity of this region have not become the subjects of research. Soil microbes have ecological functions of central importance, playing crucial roles in nutrient cycling and soil fertility. Their diversity is a sensitive indicator of soil quality that can determine its ecological function (Anderson et al., 2009). Thus, research on microbial communities in the Napahai plateau wetland has become a fundamental need. To provide new insight into the Napahai plateau wetland microbial resources, six sets of samples from three different soil types were studied, with high-throughput 16S rRNA gene sequencing used to investigate the bacterial and archaeal community diversity in the soil. The major aims of this research were to address the following two key questions. (i) What are the characteristics of the bacterial and archaeal communities, with respect to diversity in the soil of Napahai plateau wetland? (ii) What are the influential factors and their contributions to the compositions of the two communities within the Napahai wetland environments?

Materials and methods

Soil sample sites and collection

Soil samples were collected from the Napahai plateau wetland, where the whole year split between the dry season (October to April) and the rainy season (May to September). According to the region's geomorphology, samples were collected from the areas of three

http://www.aloki.hu ● ISSN 1589 1623 (Print) ● ISSN 1785 0037 (Online)
DOI: http://dx.doi.org/10.15666/aeer/1706_1414314158

different soil types, including bog soil (YN), swamp meadow soil (SD) and peat soil (NT).

Soil samples were collected in November 2014 (dry season) and June 2015 (rainy season) from three sampling areas (YN, SD and NT). For each sampling areas, two samples were collected and for each sample, and eight mixed sample plot soils were selected ("S" distribution) at 10 cm soil layer. *Table 1* shows the general conditions of each sample, and *Figure 1* shows the sampling sites. YN samples were collected from the vicinity of Lalang from areas less disturbed by human activities. The work regarded as the environmental background area. NT soil sample area was overgrazed by livestock, belonging to a tourism hotspot. *Stellera chamaejasme* Linn., a plant that is a sign of wetland degradation, was also found. Therefore, this area was regarded to have significant disturbance by human activities. The soil from YN, SD and NT sampling areas represented the transition from native swamp soil and swamp meadow soil to meadow soil formed due to the degradation of the Napahai plateau wetland. The twelve soil samples were obtained and stored at 4 °C, and then transported to the lab for DNA extraction and property analysis.

Analysis of physical and chemical properties

Soil samples for property analysis were crushed and sifted using sieves with apertures of 1 mm. Physical and chemical factors, including soil organic matter (SOM), total nitrogen (TN), total phosphorus (TP), total potassium (TK) and nitrogen (N), were measured using ion chromatography (Dionex^{TM} ICS-6000, Thermo Scientific, USA) at the Ministry of Agriculture Agricultural Products Quality Supervision and Testing Center (Kunming, China).

DNA extraction and PCR amplification

Total soil DNA was extracted from 0.1 g of each soil sample, which had roots removed and was ground using the Power Soil DNA kit (MoBio Laboratories Inc., CA, USA) according to the manufacturer's instructions (Zhou et al., 2017). The DNA was confirmed using 1.0% agarose gel electrophoresis and a NanoDrop (ND2000, Thermo Fisher, USA), then stored at -80 °C.

For bacterial and archaeal communities, the primer pairs bac-515F 5'GTGCCAGCMGCCGCGGTAA3' and bac-806R 5'GGACTACHVGGGTWTCTAAT3'; arc-U515F 5'CAGYMGCCRCGGKAAHACC3' and arc-U806R 5'GGACTACNSGGGTMTCTAAT3' were used for amplifying the V4 region of the 16S rRNA genes of bacterial and archaeal, respectively, including barcodes and adapters (Peiffer et al., 2013; Shehab et al., 2013). The PCR mixtures (50 μl) contained 25 μl 2×MightyAmp Buffer Ver.2, 1 μl of each primer (10 μmol/L), 1.0 μl MightyAmp DNA Polymerase, and 2.0 μl template DNA (10-200 ng), with nuclease-free water added to 50 μl. The PCR amplifications used an initial denaturation step at 94 °C for 4 min, followed by 30 cycles of 30 s at 94 °C, 45 s at 56 °C and 35 s at 72 °C and were held at 72 °C for 10 min. The 16S rRNA gene PCR products were sequenced using the Illumina platform (Peiffer et al., 2013).

Sequence analysis

For each sample, three amplicons were pooled together and purified according to the Gene JET kit (Thermo Scientific, USA) instructions. Sequencing of the purified

http://www.aloki.hu ● ISSN 1589 1623 (Print) ● ISSN 1785 0037 (Online)
DOI: http://dx.doi.org/10.15666/aeer/1706_1414314158

amplicons was performed on an Illumina MiSeq platform (MiSeq PE300, Illumina, USA) at the Computer Center (Beijing, China). Sequence analysis was performed with Fast Length Adjustment of Short reads (FLASH), discarding the low-quality sequences. Using UPARSE v7.1, sequences were clustered into operational taxonomic units (OTUs) with a 97% similarity cutoff, and Usearch7.1 was used to filtered chimaeras (Edgar, 2013). The remaining sequences, including 530,418 bacterial and 561,217 archaeal, were assigned to OTUs at the 97% similarity level using Mothur v1.34.4 (Schloss et al., 2009). Each representative OUT sequence was assigned to a taxonomic level using the Quantitative Insights into Microbial Ecology (QIIME) pipeline and the RDP classification method (Caporaso et al., 2010).

Table 1. *The overview of Napahai plateau wetland sampling areas*

Soil samples	Sampling points	Longitude	Latitude	Average altitude (m)
YN1	NPH-YN1-YN8	E99°37’43.00”-41.26”	N27°54’26.00”-’24.38”	3290
YN2	NPH-YN1’-YN8’	E99°37’22.88”-20.75”	N27°53’41.21”-36.81”	3282
SD1	NPH-SD1-SD8	E99°38’6.46”-0.67”	N27°51’36.33”-40.22”	3277
SD2	NPH-SD1’-SD8’	E99°38’7.73”-15.63”	N27°50’44.27”-36.02”	3275
NT1	NPH-NT1-NT8	E99°38’7.00”-3.63”	N27°50’1.00”-49’58.92”	3273
NT2	NPH-NT1’-NT8’	E99°38’0.96”-1.97”	N27°49’35.63”-34.87”	3272

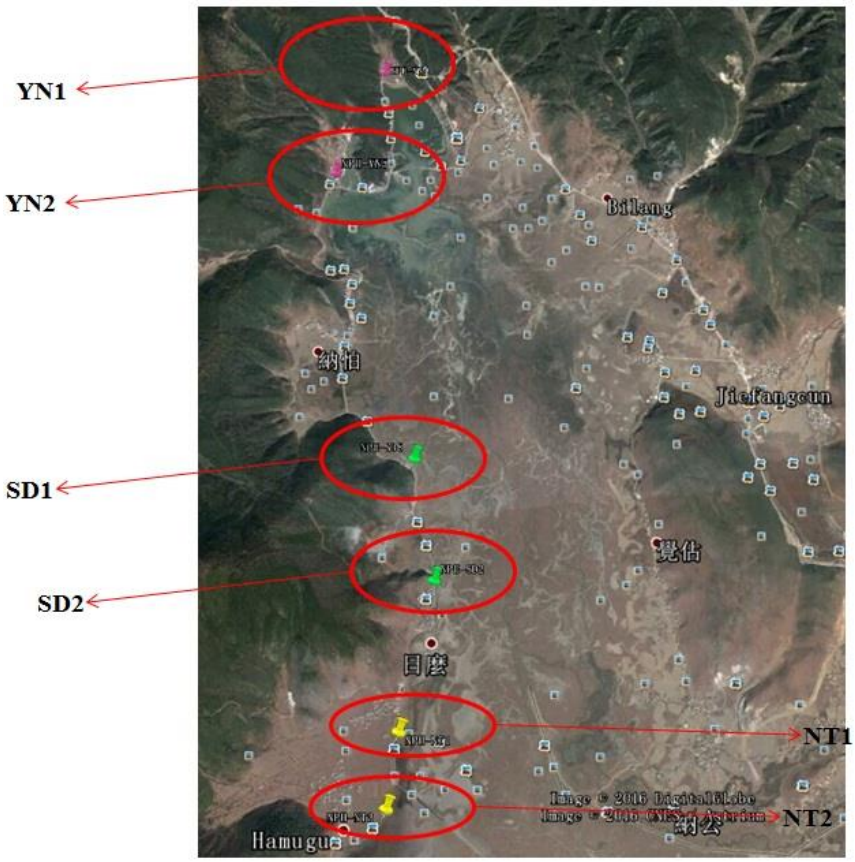

Figure 1. *Distribution of Napahai plateau wetland sampling areas. Each sampling area is composed of eight sampling points and eight sampling points distributed as “S”*

http://www.aloki.hu ● ISSN 1589 1623 (Print) ● ISSN 1785 0037 (Online)
DOI: http://dx.doi.org/10.15666/aeer/1706_1414314158

Statistical analysis

A number of alpha diversity indices were assessed at the 97% similarity level using mothur 1.34.4 including the Shannon-Wiener and Simpson index, the abundance based coverage estimator (ACE), terminal richness estimation (Chao1), and Good's coverage estimator (Schloss et al., 2009). Beta diversity was measured using Bray-Curtis distances among samples, and community differences were assessed using complete-linkage clustering analysis. Based on Weighted_Unifrac, the Unweighted Pair-group Method with Arithmetic Means (UPGMA) was applied. The heatmap and Venn diagrams were generated using the Vegan Package for R v3.0.2 (Oksanen et al., 2013). Canonical correspondence analysis (CCA) was performed using Canoco v4.5.1 to reveal the relationships between microbial community diversity and soil environmental factors (Legendre et al., 2001).

Results

Physical and chemical properties of soil samples

Table 2 shows the physical and chemical properties of the soil. It can be concluded that soil nutrient contents (SOM, TN, TP, TK and N) show no significant differences in different seasons ($p > 0.05$), but are significantly different in different soil types ($p < 0.05$).

Table 2. *Determination of physical and chemical factors of soil samples*

Sample	SOM, g/kg	TN, g/kg	N, mg/kg	TP, g/kg	TK, g/kg
DS.YN1	105.8	0.568	393	0.032	0.416
DS.YN2	117.4	0.624	368	0.062	0.414
DS.SD1	31.2	0.26	121	0.102	0.664
DS.SD2	26.8	0.166	97.9	0.106	0.675
DS.NT1	43.7	0.445	246.3	0.279	0.795
DS.NT2	38.7	0.392	233	0.369	0.806
RS.YN1	145.8	0.659	381	0.088	0.647
RS.YN2	160.9	0.823	346	0.081	0.643
RS.SD1	22.3	0.18	106	0.09	0.732
RS.SD2	17.4	0.156	91.3	0.127	0.764
RS.NT1	59.7	0.435	259	0.12	0.950
RS.NT2	51.2	0.358	227	0.142	0.908

Microbial community alpha-diversity analysis

To estimate the bacterial and archaeal community diversity and richness, the work applied the Shannon-Wiener index and Simpson's index, ACE, Chao1 and Good's coverage estimation (*Table 3*). In general, high OTU richness in both the bacterial and archaeal communities was found. Good's coverage estimator showed high coverage and reasonable sequencing depth. Regarding the seasons, the diversity (Shannon-Wiener and Simpson's) and richness (ACE, Chao1) indices for the bacterial community showed higher diversity in the rainy season than in the dry season, whereas there was no obvious change of index in the archaeal community. The soil type also influenced the

http://www.aloki.hu ● ISSN 1589 1623 (Print) ● ISSN 1785 0037 (Online)
DOI: http://dx.doi.org/10.15666/aeer/1706_1414314158

diversity of the bacterial and archaeal communities. In the NT sampling area, both the bacterial and archaeal communities had higher diversity than in the other sampling areas.

Table 3. *The diversity analysis of bacterial and archaeal community at the 97% similarity level*

	Season	Sample	OTUs	Goods coverage	Alphya diversity			
					Shannon	Simpson	ACE	Chao1
Bacteria	Dry season	DS.YN1	2505	0.84	8.38	0.96	5457.84	4955.89
		DS.YN2	2351	0.83	7.98	0.95	5447.82	4938.42
		DS.SD1	2137	0.86	7.69	0.95	5197.22	4757.14
		DS.SD2	2715	0.84	8.88	0.97	5286.83	4700.81
		DS.NT1	3454	0.77	10.28	0.99	8248.06	7169.99
		DS.NT2	3238	0.78	10.02	0.99	7951.63	7305.19
	Rain season	RS.YN1	5324	0.93	10.14	0.99	8614.29	8058.17
		RS.YN2	6020	0.92	10.78	0.99	9550.27	9129.80
		RS.SD1	4606	0.95	10.11	0.99	6413.36	6067.05
		RS.SD2	6332	0.92	11.12	0.99	9824.72	9371.37
		RS.NT1	5845	0.92	10.57	0.99	9708.51	9282.13
		RS.NT2	5908	0.93	10.87	0.99	8813.01	8408.68
Archaeal	Dry season	DS.YN1	1411	0.98	7.16	0.98	1402.50	1369.08
		DS.YN2	1553	0.99	6.52	0.93	1592.97	1567.33
		DS.SD1	1344	0.99	7.43	0.98	1306.80	1275.64
		DS.SD2	1221	0.99	7.06	0.97	1206.14	1180.20
		DS.NT1	1743	0.98	7.17	0.98	1913.99	1915.81
		DS.NT2	1276	0.99	6.68	0.97	1362.58	1256.25
	Rain season	RS.YN1	1771	0.98	7.71	0.98	1966.28	1922.17
		RS.YN2	1448	0.98	6.61	0.96	1668.68	1627.47
		RS.SD1	1270	0.99	6.58	0.96	1255.94	1215.25
		RS.SD2	1631	0.99	7.77	0.99	1664.68	1562.00
		RS.NT1	1620	0.99	7.63	0.99	1627.14	1553.94
		RS.NT2	1480	0.99	7.25	0.98	1508.16	1476.85

Taxonomic composition of the microbial community

Analysis of the bacterial community composition in the Napahai plateau revealed 64 phyla, 164 classes, 271 orders, 330 families and 484 genera. In addition, 3 archaeal phyla were detected to comprise 5 classes, 8 orders, 7 families and 7 genera. *Figure 2* shows the relative abundances of bacteria and archaea at the phylum and genus levels.

The dominant bacterial phyla across all samples were *Proteobacteria*, *Actinobacteria*, *Chloroflexi* and *Acidobacteria*, accounting for 72.4 to -81.8% of the bacterial sequences. It depended on the season and soil type (*Fig. 3*). The abundance of the phylum *Proteobacteria* was much higher ($p < 0.1$), and that of *Chloroflexi* and *Acidobacteria* was much lower ($p < 0.1$) in the dry season, while *Proteobacteria*, *Chloroflexi* and *Acidobacteria* showed the differences ($p < 0.1$) in soil type. The archaeal sequence information included approximately 40% unknown; the dominant archaeal phylum, *Thaumarchaeota* (*Cenarchaeum*), accounted for 50% without exhibiting differences in seasons and soil types.

http://www.aloki.hu ● ISSN 1589 1623 (Print) ● ISSN 1785 0037 (Online)
DOI: http://dx.doi.org/10.15666/aeer/1706_1414314158

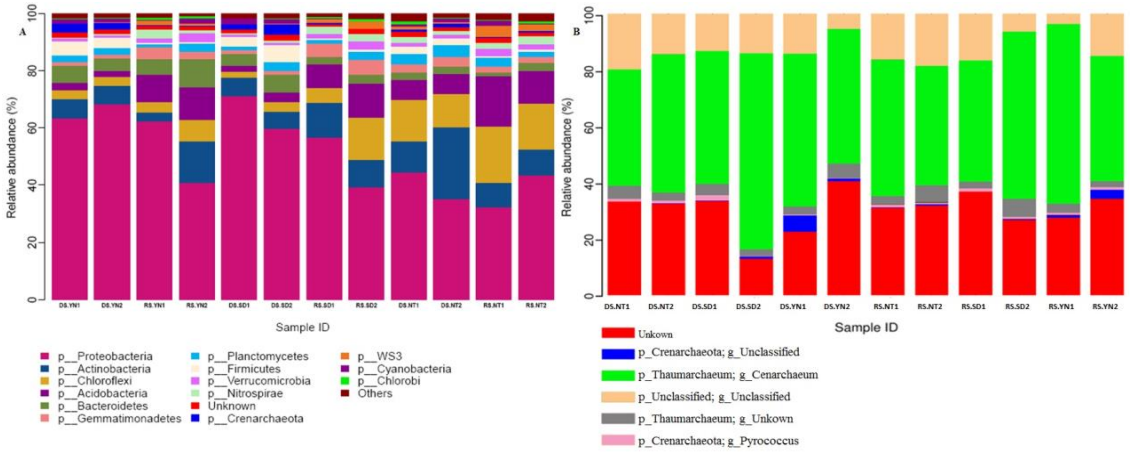

Figure 2. *Relative abundance of bacterial phyla (A) and archaeal phyla (B) detected in soil samples. At different taxonomic levels, the classification of microbial community structure in soil samples to the currently known taxonomic unit is defined as "unknown"; the definition of "others" in which the proportion of microbial community structure is less than 1%; although the microbial community information is aligned to sequences in the database, there is no definitive annotation for the data defined as "unclassified"*

Microbial community analysis of OTU distributions

Based on the statistics of the total OTUs, Venn diagrams were created to display the unique and OTUs were shared among samples (*Fig. 4*). Under a similarity threshold of 0.97, the numbers of overlapping bacterial and archaeal OTUs in the rainy season (2,634 and 828, respectively) were more than in the dry season (1,187 and 741, respectively) in the three soil types. For archaea, the YN sampling area contained more OTUs (1329) than the NT (1020), and SD (935) areas. Each sample contained specific OTUs. For bacteria, the NT sampling area contained more OTUs (2,547) than the SD (1,391) and YN (1,368) areas in the dry season, while the YN sampling area contained more OTUs (4,127) than the SD (3,344) and NT (2,919) areas in the rainy season.

The authors also performed heatmap cluster analysis to discern the community compositional differences (*Fig. 5*). The overall taxonomic diversity of the bacterial community was significantly higher than that of the archaeal community at the genus level. Bacterial and archaeal taxonomic diversity was considerably lower in the dry season compared to the rainy season. The heatmap of bacterial communities showed that *Proteobacteria*, *Actinobacteria* and *Bacteroidetes* were most differentiated between seasons. Additionally, bacterial communities differed slightly in the soil samples from the SD and YN sampling areas in the dry season, but were more irregular in the rainy season. In contrast, *Thaumarchaeota* (*Cenarchaeum*) was the predominant phylum in the archaeal communities. The abundance of archaeal was independent of seasons and soil types.

Microbial community beta-diversity analysis

Based on Weighted_Unifrac distances, the work assessed the similarities and differences in the composition of the microbial communities with respect to seasonal and spatial variations (*Fig. 6*). The UPGMA analysis showed that the diversity and composition of the bacterial community were more impacted by seasonal changes than

http://www.aloki.hu ● ISSN 1589 1623 (Print) ● ISSN 1785 0037 (Online)
DOI: http://dx.doi.org/10.15666/aeer/1706_1414314158

by soil types, the opposite of the low-abundance archaeal community. The archaeal community composition did not differ in soil samples from the SD and YN sampling areas, but dissimilar to the NT sampling area.

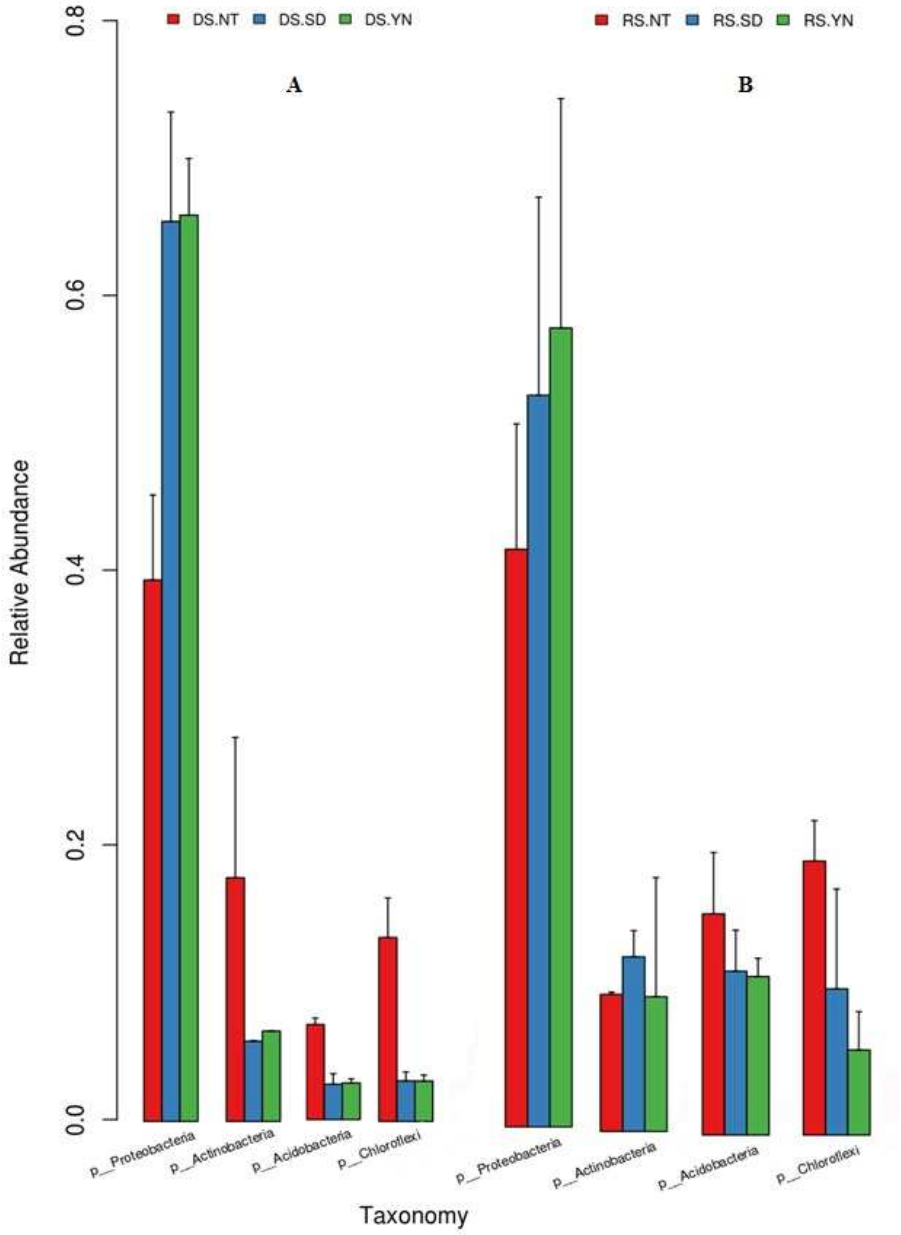

Figure 3. *Comparisons of the bacteria four mainly phyla taxonomy abundance of soil samples (YN, SD and NT) in dry and rainy seasons (DS and RS). The bacteria four mainly phyla taxonomy are Proteobacteria, Actinobacteria, Chloroflexi and Acidobacteria.* ***A*** *The soil samples are collected in dry season (DS).* ***B*** *The soil samples are collected in rainy season (RS)*

Effects of environmental factors on microbial community diversity

CCA was performed to identify the relationships between major environmental factors and microbial community diversity (*Fig. 7*). In the bacterial communities, the first two axes of the CCA plot explained 21.7 and 2.7% (in the dry season) and 77 and

http://www.aloki.hu ● ISSN 1589 1623 (Print) ● ISSN 1785 0037 (Online)
DOI: http://dx.doi.org/10.15666/aeer/1706_1414314158

26.92% (in the rainy season), respectively, of the total variation in the data. These results indicate that the bacterial community is closely correlated with N, TN and SOM in the dry season. In the archaeal community, the first two axes of the CCA plot explained 34.38 and 27.05% (in the dry season) and 35.12 and 23.32% (in the rainy season), respectively, of the total variation in the data. However, no significant correlation of any of the factors was observed for the archaeal community.

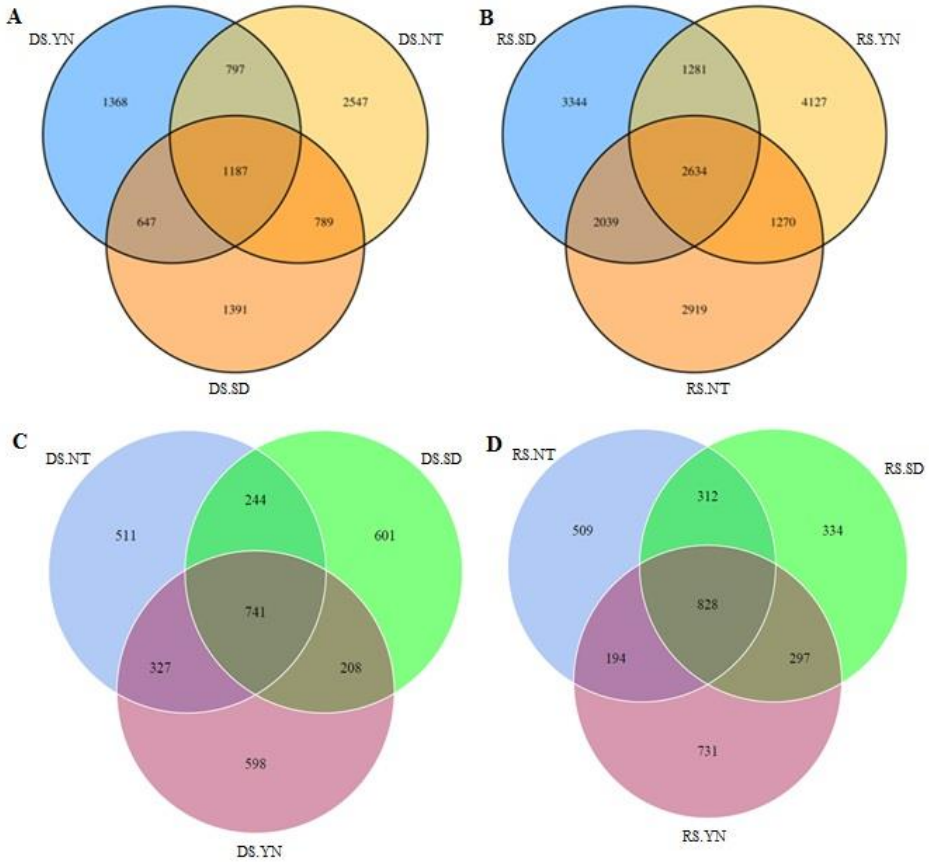

Figure 4. *Venn diagram of microbial community of soil samples (YN, SD and NT) in dry and rainy seasons (DS and RS). The arrangement of the circles indicates the overlaps between the soil samples.* ***A*** *Venn diagram of bacterial community of soil samples in dry season (DS).* ***B*** *Venn diagram of bacterial community of soil samples in rainy season (RS).* ***C*** *Venn diagram of archaeal community of soil samples in dry season (DS).* ***D*** *Venn diagram of archaeal community of soil samples in rainy season (RS)*

Discussion

Plant and animal diversity have been studied over the past decade in the Napahai plateau wetland. The research has been complemented with microbial diversity information through the measurement of the bacterial and archaeal community composition and diversity, allowing for a better assessment of the whole area's ecosystem.

The composition and diversity of the microbial community in the Napahai plateau wetland were investigated using high-throughput sequencing of 16S rRNA V4 genes. *Proteobacteria*, *Actinobacteria*, *Chloroflexi* and *Acidobacteria* were the top four most abundant bacterial phyla (*Fig. 2A*). Similar results have been obtained in different land-

http://www.aloki.hu ● ISSN 1589 1623 (Print) ● ISSN 1785 0037 (Online)
DOI: http://dx.doi.org/10.15666/aeer/1706_1414314158

use types of soils in North and South America (Lauber et al., 2009), agricultural and forest soils in Salta and Jujuy (Montecchia et al., 2015) and soils from Antarctic and Arctic (Teixeira et al., 2010; Yergeau et al., 2010). However, compared with those derived from cucumber rhizosphere soils, *Proteobacteria*, *Bacteroidetes* and *Actinobacteria* in the work were the most abundant phyla, accounting for over 70% (Tian et al., 2013). Nevertheless, *Proteobacteria* is the most common phylum in soils worldwide, consistent with our results (Janssen, 2006; Spain et al., 2009). *Actinobacteria* is not only the dominant phylum in low temperature environments but also the dominant phylum in freshwater ecosystems (Zwart et al., 2002; Johnson et al., 2007). The Napahai plateau wetland has an average temperature of approximate 5 °C with a freshwater lake, and its ecological environment is in line with *Actinobacteria* growth. Thus, *Actinobacteria* was also the most abundant phylum in the region. In contrast, the archaeal community compositions, especially the dominant phylum *Thaumarchaeota*, were clearly different from many other ecosystems, which tend to be dominated by *Crenarchaeota* and *Euryarchaeota*. The difference may be due to special geological features (Porat et al., 2010; Wang et al., 2010). *Thaumarchaeota* was the most abundant phylum accounting for almost 50%, which played an important role in the biochemical cycling of carbon, nitrogen and other elements (Cabello et al., 2004). In the *Thaumarchaeota*, most of the known sequences belong to the ammoxidation archaea, involved in the ammoxidation of soil and affect the nitrogen cycle. Therefore, it is speculated that archaea play a more important role than bacteria in the cycling of nitrogen in this area. How archaea and bacteria coordinate with each other to accomplish biogeochemical cycling in the wetland needs further study.

Moreover, greater biodiversity in soil can lead to a more stable system, providing the enhanced combinations of vital microbial functions and processes (Wagg et al., 2014; Regar et al., 2019). In the work, the difference in microbial community composition in different soil types revealed the feedback mechanism of ecological environmental degradation and microbial composition. *Acidobacteria* distribution in acidic environments is contaminated by heavy metal, belonging to non-original colonies (Diamond et al., 2019). Among the YN, SD and NT sampling areas, no significant differences in *Acidobacteria* abundance were observed (*Fig. 3B*). This may indicate that the whole area is affected by heavy metal pollution. In contrast, *Proteobacteria* and *Chloroflexi* showed differences ($p < 0.1$) in different soil types (*Fig. 3B*). One of the predominant classes of *Proteobacteria* was *Gammaproteobacteria*, which can degrade organic matter and were most abundant in the NT sampling area (Picazo et al., 2019). The authors also observed that the abundance of *Chloroflexi* was significantly higher in the NT sampling area, and these bacteria are known to live in environment with high organic matter content (Denef et al., 2015). These similar results could probably be due to the NT sampling area having more nitrogen oxides caused by serious disturbance of human activities. In the archaeal community, *Methanofollis* only present in the NT sampling area in the rainy season (*Fig. 5B*). *Methanofollis* lived in anaerobic environments such as oceans, lake sediments and the digestive tract of ruminants (Pazinato et al., 2010). In the NT sampling area, there are a large number of animals such as cattle and sheep grazing in the rainy season; therefore, *Methanogenus* has had an ecological balance with host ruminants for a long time. All the results illustrated that from the microbial perspective, the NT sampling area can be regarded as consisting of meadow soil formed due to disruption by human activities. Soil microbial composition is important for soil quality and health.

http://www.aloki.hu ● ISSN 1589 1623 (Print) ● ISSN 1785 0037 (Online)
DOI: http://dx.doi.org/10.15666/aeer/1706_1414314158

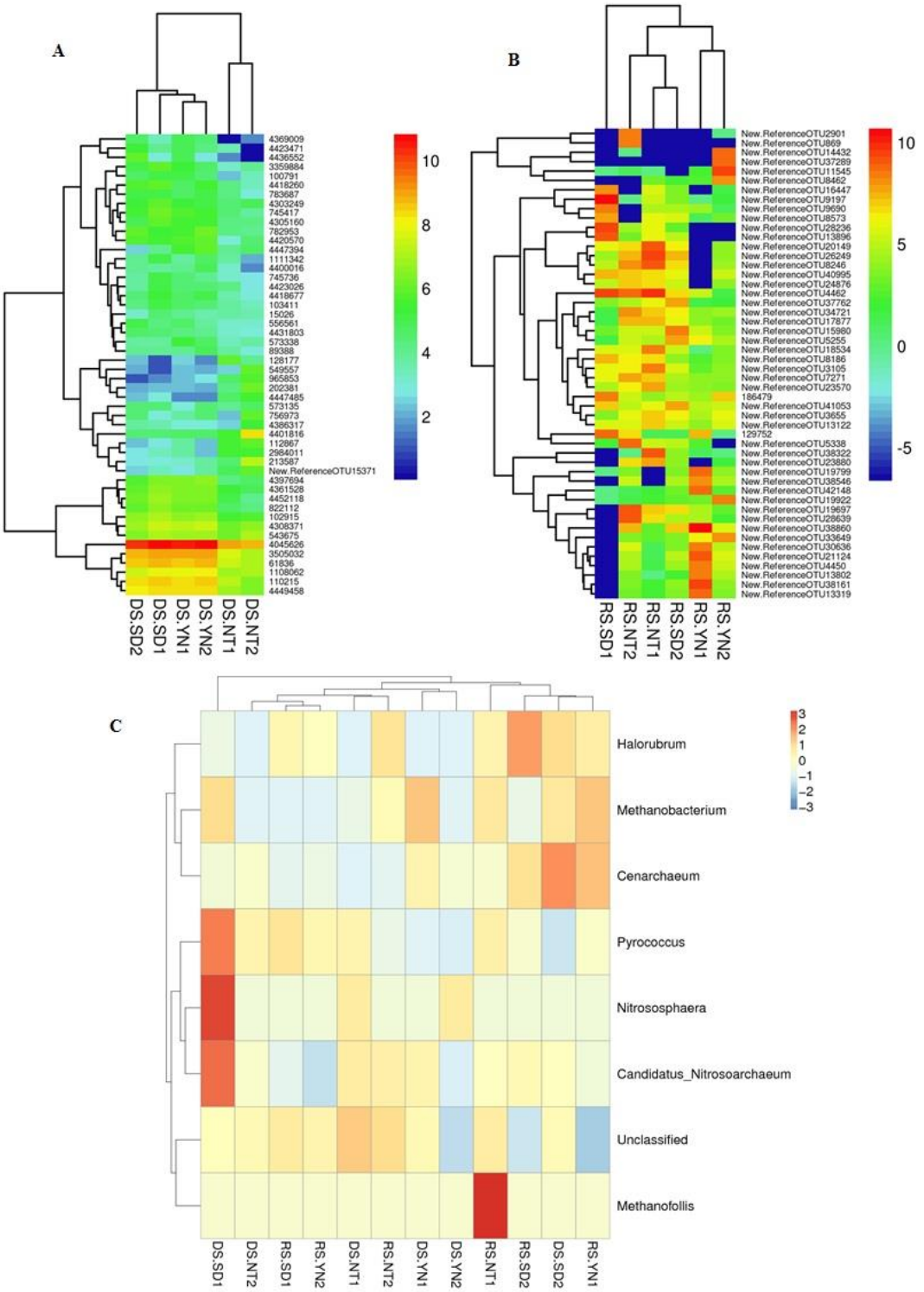

Figure 5. *Heatmap cluster of microbial community of soil samples (YN, SD and NT) in dry and rainy seasons (DS and RS). A show the distribution of community OTUs classified at the genus level. Colors correspond to the relative abundance of each OTU within the community and cluster distance based on Bray-Curtis distances. Only the most abundant 50 bacterial genera based on statistical analysis are shown and the numbers in the plate to stand for in supplement material.* ***A*** *Heatmap cluster of bacterial community of soil samples in dry season (DS).* ***B*** *Heatmap cluster of bacterial community of soil samples in rainy season (RS).* ***C*** *Heatmap cluster of archaeal community of soil samples in dry and rainy seasons (DS and RS)*

http://www.aloki.hu ● ISSN 1589 1623 (Print) ● ISSN 1785 0037 (Online)
DOI: http://dx.doi.org/10.15666/aeer/1706_1414314158

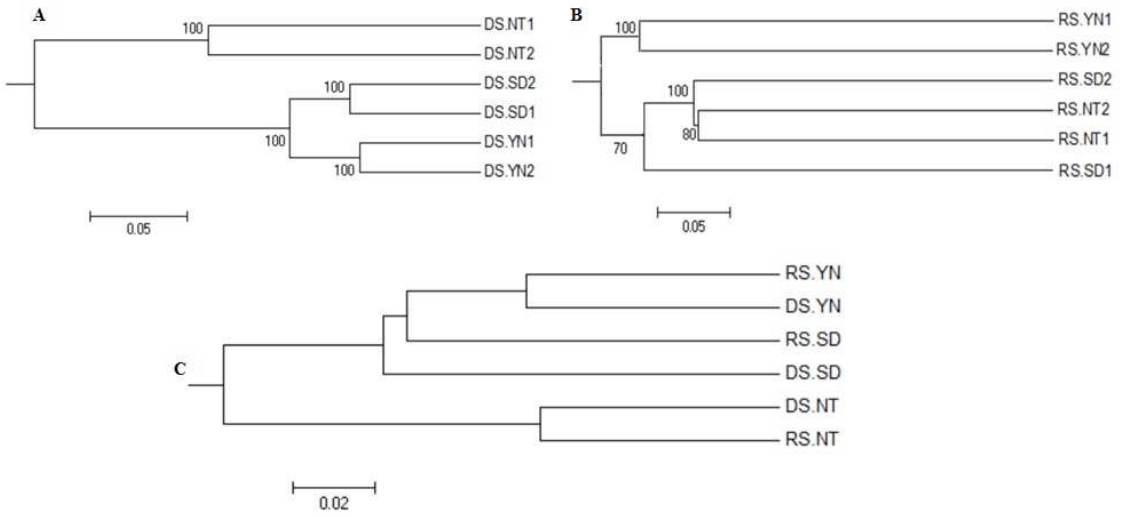

Figure 6. *UPGMA of microbial community of soil samples (YN, SD and NT) in dry and rain seasons (DS and RS).* ***A*** *UPGMA of bacterial community of soil samples in dry season (DS).* ***B*** *UPGMA of bacterial community of soil samples in rainy season (RS).* ***C*** *UPGMA of archaeal community of soil samples in dry and rainy seasons (DS and RS)*

In this work, the effects of seasons and soil types on soil microbial community characteristics were observed. Based on the analysis of OTU distributions (Venn diagrams and heatmap cluster) and beta-diversity analysis, the differences in two factors impact the microbial community (*Figs. 4–6*). Seasonal differences clearly impacted bacterial diversity, consistent with most of the literature reported (Bissett et al., 2007; Kara et al., 2013; Wilhelm et al., 2014). Unlike our result for bacterial diversity, archaeal diversity was affected by neither seasons nor soil types, especially in terms of abundance. Our finding is consistent with the numerous studies on the homogeneous spatial distributions of the archaeal community in various habitats, including field soil (Yuan et al., 2009) and sediment (Keuter et al., 2016); however, in ocean ecosystems, the diversity of archaea was influenced by spatial and temporal differences (Vik et al., 2017). This difference is probably due to unpredictable movements in ocean ecosystems. The soil ecosystem is relatively stable. However, one major drawback of our study was that the small number of sampling sites was in different soils samples, so the changes of microbial community diversity was relatively less convincing.

Our analysis of the relationship between major environmental factors and microbial community diversity showed that TN had the largest effect on bacterial community diversity, but the archaeal community was not significantly affected by environmental factors. This conclusion was also supported by our finding that archaeal diversity was not affected by seasons or soil types (Keuter and Rinkevich, 2016).

Finally, a large number of unclassified microorganisms were detected in the Napahai plateau wetland, with the abundance of unclassified bacteria and archaea at the phylum level being approximate 10 and 25%, respectively. The unclassified bacteria consisted of the novel candidate divisions WPS-2, WS3, GN04, MVP-21 and MVS-104, whereas the archaeal candidate divisions included GA55, VAL11 and FRD15. Their ecological and biological interactions are unknown. Therefore, the isolation of soil microbes combined with traditional methods under laboratory conditions is ongoing, which will help us to identify critical resources in the Napahai plateau wetland.

http://www.aloki.hu ● ISSN 1589 1623 (Print) ● ISSN 1785 0037 (Online)
DOI: http://dx.doi.org/10.15666/aeer/1706_1414314158

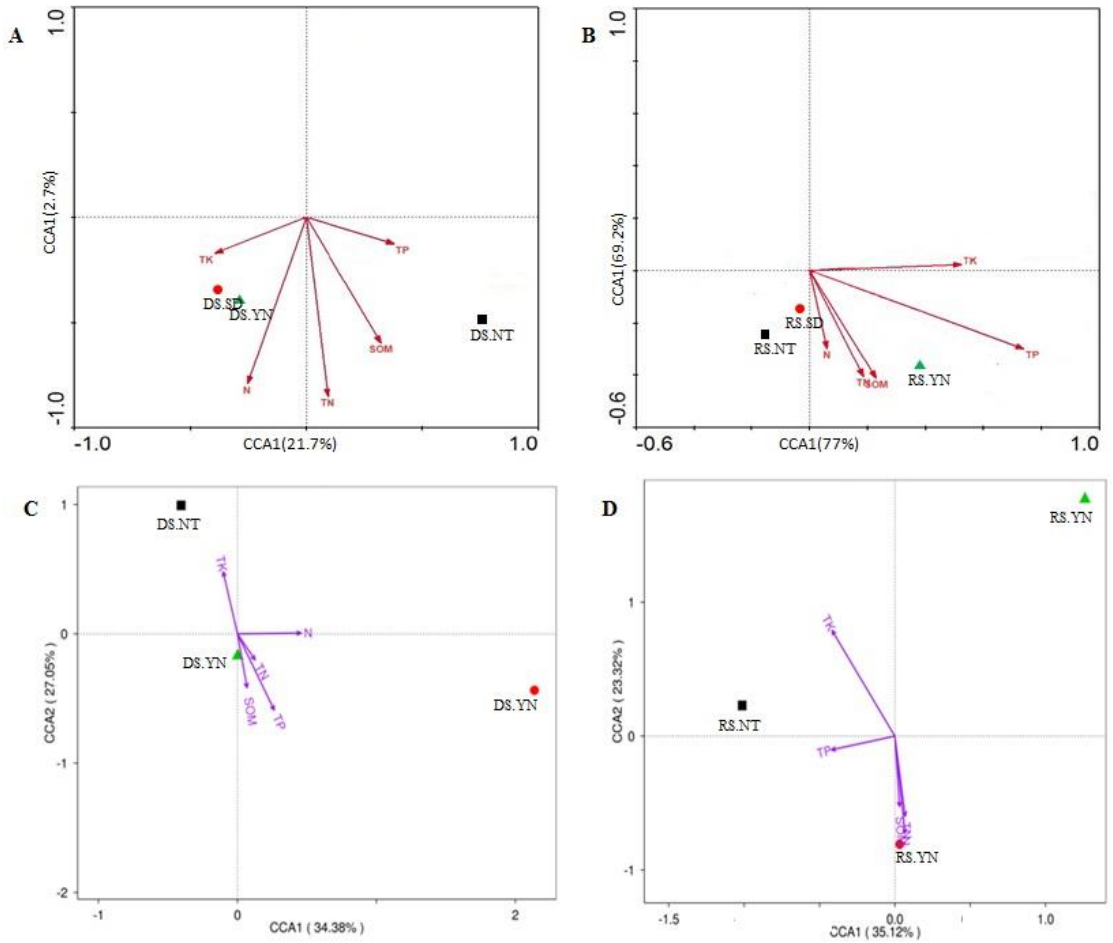

Figure 7. *CCA plot of the relationship between the major environmental factors and microbial community composition of soil samples (YN, SD and NT) in dry and rain seasons (DS and RS). Samples are indicated by dots and environmental factors indicated by color arrows. Arrow vector length represents the strength of the correlation with the axes.* ***A*** *CCA plot of the relationship between the major environmental factors and bacterial composition of soil samples in dry season (DS).* ***B*** *CCA plot of the relationship between the major environmental factors and bacterial composition of soil samples in rainy season (RS).* ***C*** *CCA plot of the relationship between the major environmental factors and archaeal composition of soil samples in dry season (DS).* ***D*** *CCA plot of the relationship between the major environmental factors and archaeal composition of soil samples in rainy season (RS)*

Conclusions

The work examined the composition and diversity of the bacterial and archaeal communities with respect to spatial and temporal distribution and explored the relationships between environmental variables in the Napahai plateau wetland. For the bacterial community, *Proteobacteria* prevailed was the most abundant, followed by *Actinobacteria*, *Chloroflexi* and *Acidobacteria*. Meanwhile, they were more influenced by seasonal changes than by soil types and was closely correlated with N, TN and SOM in the dry season. For the archaea community, *Thaumarchaeota* dominated. Meanwhile, the archaeal community was neither associate with these factors nor significant correlation of physical and chemical factors. The microbial communities showed high and unique microbial diversity and composition, and influence with seasons and soil

http://www.aloki.hu ● ISSN 1589 1623 (Print) ● ISSN 1785 0037 (Online)
DOI: http://dx.doi.org/10.15666/aeer/1706_1414314158

types, which lays a foundation for understanding the microbial and environmental response mechanism of the Napahai plateau wetland.

In the future, we will combine transcriptomics and proteomics to conduct research on microbial communities, and understand how the main bacteria or archaea conduct ecological functions in the particular ecological environment, and also for the discovery of unknown microorganism.

Acknowledgments. This research was funded by the Personnel Training Fund by the Kunming University of Science and Technology (KKSY201632059) and National Natural Science Foundation of China (No. 31700324).

REFERENCES

[1] Anderson, J. A., Hooper, M. J., Zak, J. C., Cox, S. B. (2009): Characterization of the structural and functional diversity of indigenous soil microbial communities in smelter-impacted and nonimpacted soils. – Environ Toxicol Chem 28(3): 534-541.

[2] Bissett, A., Burke, C., Cook, P. L., Bowman, J. P. (2007): Bacterial community shifts in organically perturbed sediments. – Environ Microbiol 9(1): 46-60.

[3] Cabello, P., Roldan, M. D., Moreno-Vivian, C. (2004): Nitrate reduction and the nitrogen cycle in archaea. – Microbiology 150(Pt 11): 3527-3546.

[4] Cao, H., Chen, R., Wang, L., Jiang, L., Yang, F., Zheng, S., Wang, G., Lin, X. (2016): Soil pH, total phosphorus, climate and distance are the major factors influencing microbial activity at a regional spatial scale. – Sci Rep 6: 25815.

[5] Caporaso, J. G., Kuczynski, J., Stombaugh, J., Bittinger, K., Bushman, F. D., Costello, E. K., Fierer, N., Pena, A. G., Goodrich, J. K., Gordon, J. I., Huttley, G. A., Kelley, S. T., Knights, D., Koenig, J. E., Ley, R. E., Lozupone, C. A., McDonald, D., Muegge, B. D., Pirrung, M., Reeder, J., Sevinsky, J. R., Turnbaugh, P. J., Walters, W. A., Widmann, J., Yatsunenko, T., Zaneveld, J., Knight, R. (2010): QIIME allows analysis of high-throughput community sequencing data. – Nat Methods 7(5): 335-336.

[6] Dai, Y., Yan, Z., Jia, L., Zhang, S., Gao, L., Wei, X., Mei, Z., Liu, X. (2016): The composition, localization and function of low-temperature-adapted microbial communities involved in methanogenic degradations of cellulose and chitin from Qinghai-Tibetan Plateau wetland soils. – J Appl Microbiol 121(1): 163-176.

[7] Danilova, O. V., Belova, S. E., Gagarinova, I. V., Dedysh, S. N. (2016): Microbial community composition and methanotroph diversity of a subarctic wetland in Russia. – Mikrobiologiia 85(5): 545-554.

[8] Denef, V. J., Mueller, R. S., Chiang, E., Liebig, J. R., Vanderploeg, H. A. (2015): Chloroflexi CL500-11 populations that predominate deep-lake hypolimnion bacterioplankton rely on nitrogen-rich dissolved organic matter metabolism and C1 compound oxidation. – Appl Environ Microbiol 82(5): 1423-1432.

[9] Diamond, S., Andeer, P. F., Li, Z., Crits-Christoph, A., Burstein, D., Anantharaman, K., Lane, K. R., Thomas, B. C., Pan, C., Northen, T. R., Banfield, J. F. (2019): Mediterranean grassland soil C-N compound turnover is dependent on rainfall and depth, and is mediated by genomically divergent microorganisms. – Nat Microbiol 4: pages1356–1367.

[10] Edgar, R. C. (2013): UPARSE: highly accurate OTU sequences from microbial amplicon reads. – Nat Methods 10(10): 996-998.

[11] Janssen, P. H. (2006): Identifying the dominant soil bacterial taxa in libraries of 16S rRNA and 16S rRNA genes. – Appl Environ Microbiol 72(3): 1719-1728.

[12] Johnson, S. S., Hebsgaard, M. B., Christensen, T. R., Mastepanov, M., Nielsen, R., Munch, K., Brand, T., Gilbert, M. T. P., Zuber, M. T., Bunce, M. (2007): Ancient

http://www.aloki.hu ● ISSN 1589 1623 (Print) ● ISSN 1785 0037 (Online)
DOI: http://dx.doi.org/10.15666/aeer/1706_1414314158

bacteria show evidence of DNA repair. – Proceedings of the National Academy of Sciences of the United States of America 104(36): 14401-14405.
[13] Kara, E. L., Hanson, P. C., Hu, Y. H., Winslow, L. McMahon, K. D. (2013): A decade of seasonal dynamics and co-occurrences within freshwater bacterioplankton communities from eutrophic Lake Mendota, WI. – ISME J 7(3): 680-684.
[14] Keuter, S., Rinkevich, B. (2016): Spatial homogeneity of bacterial and archaeal communities in the deep eastern Mediterranean Sea surface sediments. – Int Microbiol 19(2): 109-119.
[15] Lauber, C. L., Hamady, M., Knight, R., Fierer, N. (2009): Pyrosequencing-based assessment of soil pH as a predictor of soil bacterial community structure at the continental scale. – Appl Environ Microbiol 75(15): 5111-5120.
[16] Legendre, P., Gallagher, E. D. (2001): Ecologically meaningful transformations for ordination of species data. – Oecologia 129(2): 271-280.
[17] Montecchia, M. S., Tosi, M., Soria, M. A., Vogrig, J. A., Sydorenko, O., Correa, O. S. (2015): Pyrosequencing reveals changes in soil bacterial communities after conversion of Yungas forests to agriculture. – PLoS One 10(3): e0119426.
[18] Oksanen, J., Blanchet, F. G., Kindt, R., Legendre, P., O'Hara, R. B., Simpson, G. L., Solymos, P., Stevens, M. H., Wagner, H. (2013): Multivariate Analysis of Ecological Communities in R: package "vegan". – R Package Version 1.
[19] Pazinato, J. M., Paulo, E. N., Mendes, L. W., Vazoller, R. F., Tsai, S. M. (2010): Molecular characterization of the archaeal community in an Amazonian wetland soil and culture-dependent isolation of methanogenic archaea. – Diversity 2(7): 1026-1047.
[20] Peiffer, J. A., Spor, A., Koren, O., Jin, Z., Tringe, S. G., Dangl, J. L., Buckler, E. S., Ley, R. E. (2013): Diversity and heritability of the maize rhizosphere microbiome under field conditions. – Proc Natl Acad Sci USA 110(16): 6548-6553.
[21] Picazo, A., Rochera, C., Villaescusa, J. A., Miralles-Lorenzo, J., Velazquez, D., Quesada, A., Camacho, A. (2019): Bacterioplankton Community Composition Along Environmental Gradients in Lakes From Byers Peninsula (Maritime Antarctica) as Determined by Next-Generation Sequencing. – Front Microbiol 10: 908.
[22] Porat, I., Vishnivetskaya, T. A., Mosher, J. J., Brandt, C. C., Yang, Z. K., Brooks, S. C., Liang, L., Drake, M. M., Podar, M., Brown, S. D., Palumbo, A. V. (2010): Characterization of archaeal community in contaminated and uncontaminated surface stream sediments. – Microb Ecol 60(4): 784-795.
[23] Regar, R. K., Gaur, V. K., Bajaj, A., Tambat, S., Manickam, N. (2019): Comparative microbiome analysis of two different long-term pesticide contaminated soils revealed the anthropogenic influence on functional potential of microbial communities. – Sci Total Environ 681: 413-423.
[24] Savio, D., Sinclair, L., Ijaz, U. Z., Parajka, J., Reischer, G. H., Stadler, P., Blaschke, A. P., Bloschl, G., Mach, R. L., Kirschner, A. K., Farnleitner, A. H., Eiler, A. (2015): Bacterial diversity along a 2600 km river continuum. – Environ Microbiol 17(12): 4994-5007.
[25] Schloss, P. D., Westcott, S. L., Ryabin, T., Hall, J. R., Hartmann, M., Hollister, E. B., Lesniewski, R. A., Oakley, B. B., Parks, D. H., Robinson, C. J., Sahl, J. W., Stres, B., Thallinger, G. G., Van Horn, D. J., Weber, C. F. (2009): Introducing mothur: open-source, platform-independent, community-supported software for describing and comparing microbial communities. – Appl Environ Microbiol 75(23): 7537-7541.
[26] Shehab, N., Li, D., Amy, G. L., Logan, B. E., Saikaly, P. E. (2013): Characterization of bacterial and archaeal communities in air-cathode microbial fuel cells, open circuit and sealed-off reactors. – Appl Microbiol Biotechnol 97(22): 9885-9895.
[27] Spain, A. M., Krumholz, L. R., Elshahed, M. S. (2009): Abundance, composition, diversity and novelty of soil Proteobacteria. – ISME J 3(8): 992-1000.
[28] Su, J. Q., Ding, L. J., Xue, K., Yao, H. Y., Quensen, J., Bai, S. J., Wei, W. X., Wu, J. S., Zhou, J., Tiedje, J. M., Zhu, Y. G. (2015): Long-term balanced fertilization increases the

http://www.aloki.hu ● ISSN 1589 1623 (Print) ● ISSN 1785 0037 (Online)
DOI: http://dx.doi.org/10.15666/aeer/1706_1414314158

soil microbial functional diversity in a phosphorus-limited paddy soil. – Mol Ecol 24(1): 136-150.

[29] Teixeira, L. C., Peixoto, R. S., Cury, J. C., Sul, W. J., Pellizari, V. H., Tiedje, J., Rosado, A. S. (2010): Bacterial diversity in rhizosphere soil from Antarctic vascular plants of Admiralty Bay, maritime Antarctica. – ISME J 4(8): 989-1001.

[30] Tian, Y., Gao, L. (2014): Bacterial diversity in the rhizosphere of cucumbers grown in soils covering a wide range of cucumber cropping histories and environmental conditions. – Microb Ecol 68(4): 794-806.

[31] Tian, Y., Zhang, X., Wang, J., Gao, L. (2013): Soil microbial communities associated with the rhizosphere of cucumber under different summer cover crops and residue management: a 4-year field experiment. – Scientia Horticulturae 150(2): 100-109.

[32] Vik, D. R., Roux, S., Brum, J. R., Bolduc, B., Emerson, J. B., Padilla, C. C., Stewart, F. J., Sullivan, M. B. (2017): Putative archaeal viruses from the mesopelagic ocean. – PeerJ 5: e3428.

[33] Wagg, C., Bender, S. F., Widmer, F. van der Heijden, M. G. (2014): Soil biodiversity and soil community composition determine ecosystem multifunctionality. – Proc Natl Acad Sci USA 111(14): 5266-5270.

[34] Wang, P., Li, T., Hu, A., Wei, Y., Guo, W., Jiao, N., Zhang, C. (2010): Community structure of archaea from deep-sea sediments of the South China Sea. – Microb Ecol 60(4): 796-806.

[35] Widder, S., Besemer, K., Singer, G. A., Ceola, S., Bertuzzo, E., Quince, C., Sloan, W. T., Rinaldo, A., Battin, T. J. (2014): Fluvial network organization imprints on microbial co-occurrence networks. – Proc Natl Acad Sci USA 111(35): 12799-12804.

[36] Wilhelm, S. W., LeCleir, G. R., Bullerjahn, G. S., McKay, R. M., Saxton, M. A., Twiss, M. R., Bourbonniere, R. A. (2014): Seasonal changes in microbial community structure and activity imply winter production is linked to summer hypoxia in a large lake. – FEMS Microbiol Ecol 87(2): 475-485.

[37] Xiang, Y., Wang, S., Li, J., Wei, Y., Zhang, Q., Lin, L., Ji, X. (2018): Isolation and characterization of two lytic cold-active bacteriophages infecting Pseudomonas fluorescens from the Napahai plateau wetland. – Can J Microbiol 64(3): 183-190.

[38] Yergeau, E., Hogues, H., Whyte, L. G., Greer, C. W. (2010): The functional potential of high Arctic permafrost revealed by metagenomic sequencing, qPCR and microarray analyses. – ISME J 4(9): 1206-1214.

[39] Yuan, Y., Conrad, R., Lu, Y. (2009): Responses of methanogenic archaeal community to oxygen exposure in rice field soil. – Environ Microbiol Rep 1(5): 347-354.

[40] Zhao, J., Ni, T., Li, Y., Xiong, W., Ran, W., Shen, B., Shen, Q., Zhang, R. (2014): Responses of bacterial communities in arable soils in a rice-wheat cropping system to different fertilizer regimes and sampling times. – PLoS One 9(1): e85301.

[41] Zhou, Z., Meng, H., Liu, Y., Gu, J. D., Li, M. (2017): Stratified bacterial and archaeal community in mangrove and intertidal wetland mudflats revealed by high throughput 16S rRNA gene sequencing. – Front Microbiol 8: 2148.

[42] Zwart, G., Crump, B. C., Agterveld, M., Hagen, F., Han, S. K. (2002): Typical freshwater bacteria: an analysis of available 16S rRNA gene sequences from plankton of lakes and rivers. – Aquatic Microbial Ecology 28(2): 141-155.

http://www.aloki.hu ● ISSN 1589 1623 (Print) ● ISSN 1785 0037 (Online)
DOI: http://dx.doi.org/10.15666/aeer/1706_1414314158

PERFORMANCE EVALUATION OF NOVEL SELECTION PROCESSES THROUGH HYBRIDIZATION OF K-MEANS CLUSTERING AND GENETIC ALGORITHM

HAQ, E. U.[1] – HUSSAIN, A.[4] – AHMAD, I.[2,3,1]

[1]*Department of Mathematics and Statistics, Faculty of Basic and Applied Sciences, International Islamic University, 44000 Islamabad, Pakistan*

[2]*Department of Mathematics, King Khalid University, Abha 62529, Kingdom of Saudi Arabia*

[3]*Statistical Research and Studies Support Unit, King Khalid University, Abha 62529, Kingdom of Saudi Arabia*

[4]*Department of Statistics, Quaid-e-Azam University, 44000 Islamabad, Pakistan*

**Corresponding author*
e-mail: abid0100@gmail.com; phone: + 92-33-3431-0207

(Received 30th May 2019; accepted 25th Oct 2019)

Abstract. K-means clustering combined with genetic algorithm (GA) techniques are used to improve the accuracy of estimation process and to minimize computational effort for solving nonlinear optimization problems. The main purpose of K-means clustering is to exhibit faster convergence which turns into quick evolution. This paper focuses on newly proposed cluster based GA selection techniques for solving unconstrained optimization problems. The K-means cluster based genetic algorithm (GKA) selection techniques comprise of four major stages: clustering, membership probability indexing, fitness evaluation and selection. The hybridization of genetic algorithm and clustering will effectively cater the problem of population diversity and selection pressure. There are two types of GKA selection techniques that are examined, the first selection technique (GKA_F) includes two proposed selection operators which are linked with a fixed number of clusters while the second technique (GKA_{opt}) is based on the optimum number of clusters. The main focus of these new selection techniques is to preserve population diversity as well as to avoid local optima. The performance of each technique is evaluated through eleven well known benchmark functions. On the whole, the novel cluster based selection techniques are demonstrated to be extremely efficient and effective for achieving optimum solutions which are verified by simulated results.
Keywords: *cluster evaluation, selection operators, benchmarks, selection pressure, population diversity, comparisons*

Introduction

There has been a significant growth in the fields of artificial intelligence, computational analysis, data mining and optimization in recent years. Classical techniques are unable to solve complex problems efficiently in the fields of computational engineering, transportation, energy, and management (Zhang et al., 2014). Hence the edification of optimization algorithms can be classified into stochastic and deterministic approaches (Fister et al., 2013). Mostly, deterministic algorithms are gradient based algorithms that employ the function values with their derivatives. These algorithms are very much useful for smoothing unimodal problems, but in terms of some discontinuous functions, non-gradient algorithms will be preferred (Yang, 2014). Hooke–Jeeves pattern and Nelder–Mead downhill simplex (Rajan and Malakar, 2015) search techniques are some of the examples of non-gradient based algorithms. In regard of stochastic approach, heuristics and meta-heuristics are two types of stochastic

http://www.aloki.hu ● ISSN 1589 1623 (Print) ● ISSN 1785 0037 (Online)
DOI: http://dx.doi.org/10.15666/aeer/1706_1415914177

algorithms. The major focus of stochastic techniques is to obtain feasible solutions at optimum scenario. There is no surety for finding absolute optimum solutions; however, it is presumed that mostly stochastic algorithms will achieve nearly optimal solutions.

Genetic algorithms (GAs) are stochastic based-heuristic search techniques that originated from biological evolution theory and applied in solving practical problems in the field of human developments. In the process of GAs, sometimes the optimal solution may not be feasible due to internal deficiencies such as less computational efficiency and premature convergence (Aibinu et al., 2016). GA does not have much mathematical requirements. Due to their developmental nature, GA will hunt down arrangements without looking to the particular internal working of the issue. It can deal with any sort of target capacities and imperatives (i.e. direct or nonlinear) characterized on discrete, non-stop or blended inquiry spaces. Hence the main focus of genetic algorithm (GA) is to find the best techniques through suitable adjustment between exploration (population diversity) and exploitation (selection pressure/premature convergences) (Haq et al., 2019a).

On the other hand, clustering is an algorithmic technique to organize the numeric information into meaningful groups. It can also be described as an unsupervised arrangement whereby the data values are clustered using specific information that is available in the dataset and also have prior knowledge about the number of clusters 'K'. This method is often used to discover the patterns of a given dataset (Li et al., 2015). The dataset contains information on variables and usually one attempt to reorganize the useful variables that have the same characteristics into the same group or cluster. However, the main challenge with the clustering is that different clustering algorithms may provide different clusters for the same dataset (Rehman and Islam, 2011). A good clustering algorithm is the algorithm that can reflect the natural clusters in a dataset and at the same time, attain the lowest validity index value (Islam et al., 2018). The clustering validity indices usually measure the compactness and the differentiability of the clusters. The detailed summary regarding strength and weakness of GA (Sivanandam and Deepa, 2008; Aibinu et al., 2016) and K means clustering (Islam et al., 2018) is presented in *Table 1*.

Genetic algorithm is one of the well-known optimization algorithms used to overcome K-means weakness. The major focus of GA based algorithm was to generate high quality clusters in minimum time. Some algorithms have also been designed in a multi-objective optimization form to understand and implement problems that are multifarious. In present study, we will focus on the cluster based selection techniques in genetic algorithm (GA), where clustering is used to organize the population of chromosomes/individuals for the process of reproduction and recombination. Hence, these newly proposed K-means cluster based genetic algorithm (GKA) selection techniques are effectively handle unconstraint optimization problems. The GKA method comprises of four major stages: clustering, membership probability indexing, fitness evaluation and selection. Hence the hybridization of genetic algorithm and clustering will effectively cater the problem of population diversity and selection pressure. A membership selection probability to each individual is followed by clustering. Fitness scaling modified the membership results in regard of selection function. Here two versions of (GKA) selection techniques are examined, the first selection technique (GKA_F) has two proposed selection operators which are linked with fixed number of clusters and the second technique (GKA_{opt}) is based on the optimum number of clusters. The performance of each technique is evaluated through eleven well-known benchmark

http://www.aloki.hu ● ISSN 1589 1623 (Print) ● ISSN 1785 0037 (Online)
DOI: http://dx.doi.org/10.15666/aeer/1706_1415914177

functions. The simulated results reveal that the proposed cluster based selection methods outperform as compared to others for achieving optimum solutions.

Table 1. *Detailed summary regarding strength and weakness of algorithms*

Type	Strength	Weakness
Genetic algorithm	• Conceptually easy to understand and execute • Efficiently perform for large scale complex optimization problems • Handle complex and noisy functions easily • Powerfully handle difficulties in evaluation process of the objective function • Require no prior knowledge or gradient information about the problem • Avoid to become stuck at local optima	• Difficulty in identifying fitness function and representation of optimization problems • Occurrence of premature convergence • Difficulty in selection of different parameters like population size, crossover and mutation rate etc. • Population diversity • Configuration is not so simple and straightforward
K-means clustering	• Relatively easy to implement • Computationally faster than other clustering methods with large population size • Clustering process is surely convergent • Easy adaptation for new examples • Easy generalization of clusters to different shapes and sizes	• Number of clusters must be determined before the iterative process begins • Clustering result is extremely sensitive to the initial seed-points • Noise, or outliers and empty clusters decline the superiority of the K-means clustering result • Neglects to recognize non-straight detachable groups in the input space

The remainder portion of this research is presented as: in "Literature review", we comprise of some relevant study for K-means clustering co-integrated with optimization algorithms. Defining problem along with working strategy of genetic algorithm is described in "Defining problem through hybridization of K-means clustering and genetic algorithm". The proposed selection strategy is comprehensively discussed in "Proposed K-means cluster based GA selection operators". A detailed description about the benchmark functions is presented after the proposed work, while simulated results and performance evaluation of proposed methods are demonstrated in "Statistical results and discussion". Finally, "Conclusions and future work" is provided at the end of the study.

Literature review

There are several algorithmic techniques like simulated annealing (Hatamlou et al., 2012) in the literature which are helpful to solve cluster problems. GA is one of the most promising algorithms that have consistently performed well in solving clustering problems. The capability of GA has proven to obtain efficient and effective results and provide appropriate clustering. In the past several years, GA has been extensively used as an optimization method in various domains such as image processing (Loai et al.,

http://www.aloki.hu ● ISSN 1589 1623 (Print) ● ISSN 1785 0037 (Online)
DOI: http://dx.doi.org/10.15666/aeer/1706_1415914177

2008; Younus et al., 2015; Huang and Ma, 2019; Belahbib and Souami, 2011), and clustering (Lin et al., 2005; Maulik et al., 2011; Murty et al., 2008) to name a few examples. There are several literature reviews that focus on the application of GAs to cluster integer data. All of these methods showed good performance and better results when compared to other clustering methods. However, some of these methods have drawbacks and need to be improved to develop a better clustering algorithm.

Genetic K-means Algorithm, GKA is one of the examples of GAs that was proposed to improve the performance of K-means. The main objective of GKA is to find the global optimum of the given dataset and partition the data into a specified number of clusters. In GKA, instead of using a common crossover operator K-means are used (Zeebaree et al., 2017) as search operators. The problem of minimizing the total within cluster variation (TWCV) was also handled successfully by GKA.

Lu et al. (2004) proposed a Fast Genetic K-means Algorithm, FGKA, which was inspired by GKA, by incorporating several improvements over GKA. Both FGKA and GKA achieved the objective of their studies which converged to the global optima, and the study found that FGKA runs faster than GKA. Maulik et al. (2011) proposed a GAs based clustering where chromosomes were represented by the strings of the real numbers and encoded a fixed number of cluster centers in RN. This algorithm was then extended by Maulik et al. (2011) and named as Genetic Clustering for Unknown K (GCUK). To check the performance of the algorithm, Maulik et al. (2011) compared the minimum value of the objective function in the K-means algorithm with the same K, and showed that the GCUK outperform the K-means. In GCUK, Maulik et al. (2011) used the Davies Bouldin (DB) index to measure the validity of the clusters. These two algorithms used the Euclidean distance to calculate the distance from a point to a cluster center. GCUK became the most effective GAs clustering method but due to the real number representation, it took a longer time to converge (Lin et al., 2005).

In a paper by Lin et al. (2005), the cluster centers were selected directly from the data set and they constructed the look-up table to save the distances between all pairs of the data points. This process allowed the algorithm to speed up the evaluation of the fitness value. In GCUK, GAs clustering by Maulik et al. (2011), the string representation was used to encode the variable number of cluster centers, while Lin et al. (2005) used the binary representation. A cluster based genetic algorithm with polygamy and dynamic population control procedure have been suggested by Aibinu et al. (2016) with an application of route optimization problem. Islam et al. (2018) presented an effective genetic algorithm that combines the capacity of genetic operators to conglomerate different solutions of the search space with the exploitation of the hill-climber cycles of K-means.

Defining problem through hybridization of K-means clustering and genetic algorithm

It is very important for any clustering algorithmic to find approximate or global optima for complex nonlinear optimization problems (Maulik et al., 2011). The K-means clustering algorithm is quite likely to converge to a suboptimal position. The key benefit of stochastic optimization approach over deterministic techniques is that they are unable to converge to local optima. Hence, stochastic techniques are able to solve clustering related problems; such as genetic algorithms, ant colony optimization, simulated annealing and other evolutionary techniques.

http://www.aloki.hu ● ISSN 1589 1623 (Print) ● ISSN 1785 0037 (Online)
DOI: http://dx.doi.org/10.15666/aeer/1706_1415914177

Genetic Algorithms (GAs) play with the idea of the evolutionary process where the chromosomes will have to compete with each other to have a place in the next generation. Strong chromosomes have more chance to survive and usually the weak chromosomes have limited chance. GAs are working with a search space that contains all feasible solution. It means that each of the points in the search space represents one feasible solution that will be marked according to its fitness through objective functions. The core processes of GAs are selection, crossover and mutation. All the processes of GAs make this algorithm more unique as compared to other conventional algorithms for the optimization. The selection process aims to select the good chromosomes which will be sent to the mating pool to combine with the other chromosomes where the features of parents are combined to form new offspring through crossover process (Haq et al., 2019b). Crossover process creates offspring with the help of those parents which are selected through the selection operator. Meanwhile the mutation process aims to encourage diversity in the new population with a very small probability.

Normally GA is a deliberately stochastic process, i.e. an ordered chain of well-defined states, whereby suitable solutions to given problems are determined by using a population of selected individuals. These individuals are examined by using some fitness criterion against the specific problem and using some predefined convergence or stopping procedure for the process to be terminated (Devooght, 2010). In Markov Chain, development of problem is based on modelling and analysis of GA (Eiben and Smit, 2011). Therefore, one of the most significant feature of GA is stochastic aspect which demonstrate the selection and formation of new chromosomes.

The conventional GA, may be characterized by the following schematic scheme:

1. Selection of all individuals as parents followed by a randomization approach (Zeebaree et al., 2018).
2. Genetic operators are used for a generation of offspring.
3. The new population of chromosomes are selected from the mixture of the old and newly generated offspring without changing the size of the string.
4. The main features including the fitness value of new chromosomes are examined against the termination criterion, the algorithm either stops or continue to the next step.

Genetic operators have the ability to maintain the genetic diversity throughout the generations. Variability in genetics or genetic diversity is necessary for the evolutionary process. The core intension of the genetic process is the creation of the fittest population which depends on the valuable cooperation between the genetic operators. The initiation of the idea regarding clustering in genetic algorithm is originated in the context to enhance the quality of solutions by avoiding excessive exploitation and restricting local optima instead of global optimum solution (local maximum or minimum solutions). The methodology of clustering is to enhance the selection probability for the convergence to the global optima by adequately covering the solution space, yet ensuring appropriate selection pressure to attain even better solutions from current population.

Moreover, there is not a rule of thumb for evaluating the performance of GA by choosing an appropriate optimization function. Therefore, the performance of the algorithm is based on the nature of the problem regarding variation rate in objective function and the number of local optima etc. (Hussain et al., 2017). A multimodal function has at least two local optima. The efficient search procedure must be proficient in eliminating the region around local optimum in context of the search for global

http://www.aloki.hu ● ISSN 1589 1623 (Print) ● ISSN 1785 0037 (Online)
DOI: http://dx.doi.org/10.15666/aeer/1706_1415914177

optima. The scenario becomes more complex in a situation of random distribution of local optima in search space. By hybridizing the strength of genetic algorithm and clustering of the fitness values, a detailed description of the proposed KGA methodology is revealed in the following section.

Proposed K-means cluster based GA selection operators

In this section, we briefly describe the process of proposed selection operators of genetic algorithm K-means clustering (GKA) for obtaining optimum solution of unconstraint optimization problems. Here, we use a standard genetic algorithm with objective function $f(\vec{x})$ to evaluate the performance of proposed GKA algorithm. These proposed techniques which cater the short comings associated the conventional section (selection) methods by minimizing the distance between centers and individuals by enhancing the search space.

GKA$_F$

The proposed methodology about selection operators of GKA is unique in such a way that the individuals of the population are divided into homogenous groups/clusters. These clusters are internally homogenous and externally heterogeneous as possible. These newly proposed selection techniques will resolve two important issues i.e. exploitation and exploration. Exploration means identifying potential areas of search space and discover new knowledge (Yang et al., 2009). It is also a process of attaining new information by visiting new states. Exploitation generates information and transmission of adaptation, which means optimizing within a promising region. Pure stochastic search is suitable at exploration while hill climbing is best at exploitation (Das et al., 2008). Recombination of the individuals within same cluster reduces population diversity and thus compromising scenario between the exploration and exploitation is mainly determined through clustering within individuals of the population.

The basic aim of the clustering is to explore a specific sequence among the data points that are exploratory in nature (Jain, 2010). The main focus is to organize datasets by using clustering technique which requires some divergence among the nature of the datasets and according to the purpose of analysis. Several types of clustering algorithmic techniques have been proposed (Jain, 2010; Belhaouari et al., 2014; Xu and Wunsch, 2005; Islam et al., 2018) i.e. taxonomy of clustering, discussions on primary short comings and major issues. One of the simplest and most popular clustering algorithmic technique is the K-means algorithm (KMA), and was originated by Steinhaus (1956). Although it was quite long ago, this technique is still the most widely used algorithm for clustering.

Our interest in this study was to cluster the fitness values to observe the same pattern for the selection of individuals. Illustratively, a set of '*n*' variables $X = \{x_1, x_2, x_3 \dots \dots x_n\}$ to be clustered with each of these $X_i \in R^p$is an attribute vector used to describe the variables. These variables will be clustered into a set of clusters, $C = \{C_1, C_2, C_3 \dots \dots C_k\}$ where K is the number of clusters.

The clusters are mutually exclusive $C, C_i \cap C_j = \emptyset \; for \; i \neq j$. The numbers of K may be priori known or not. Let $\bar{x}_k$ be the mean of the cluster C_k. The main objective of clustering is to find the minimum distance between x_i to the closest center $\bar{x}_k$ as follows in *Equation 1*.

$$\sum_{k=1}^{K} \sum_{x_i \in C_k} \| x_i - \bar{x}_k \|^2 \qquad \text{(Eq.1)}$$

http://www.aloki.hu ● ISSN 1589 1623 (Print) ● ISSN 1785 0037 (Online)
DOI: http://dx.doi.org/10.15666/aeer/1706_1415914177

The most familiar clustering technique is K-means (Islam et al., 2018) clustering which is an iterative procedure which is flexible to implement (Jain, 2010).

The procedure of K-means clustering along with inclusion of selection probabilities through GA can be described below:

1. Initially, the cluster centers $\{\bar{x}_1, \bar{x}_2, \bar{x}_3 \dots \dots \dots, \bar{x}_k\}$ are selected for each respective clusters $\{C_1, C_2, C_3 \dots \dots C_k\}$.
2. The new cluster membership is calculated by assigning each data value to the closest centers.
3. After allocation of data value to new cluster, cluster centers are re-computed.
4. If all cluster center stay in its position the algorithmic process is terminated. Otherwise, the procedure will be repeated from Step 2.
5. The selection probabilities are computed from proposed selection operators.
6. The parents are selected through recombination process.

To improve the performance of the GA process, a newly proposed cluster based selection operator through membership probability index that is assigned to each individual after clustering phase. Basically fitness evaluation will be transformed into membership probabilistic scores in range those are appropriate for selection. The membership probability score of an individual is a measurement of its affiliation with respect to both designated and external clusters. Hence proposed cluster based selection techniques create a balance between selection pressure and population diversity. In other words, these techniques are helpful for suitable adjustment between selection pressure and population diversity (Hussain and Muhammad, 2019). It has been also perceived that the mating pool may comprise of all higher proportionate individuals on absolute uniform scaling. These proposed selection techniques will be helpful in minimizing the selection pressure and improving the search space through clustering approach. The initiation of K-means clustering concept with new selection probability indices will definitely introduce greater diversity in the population thus offering better solution with sustainable convergence speed. In fact, new selection techniques create a balance between selection parameters. The mathematical ecology of the two newly proposed selection probability indices are shown in *Equations 2–7:*

Cluster based selection operator-1

$$P_{(i,j,l),1} = \frac{1}{N}\left[\frac{h_j}{N(h_j-1)}\left(\sum_{l=1}^{N} Z_l - NZ_l\right) + 1\right] \quad \text{(Eq.2)}$$

where

$$Z_l = \frac{f(x_i)}{h_j\left(e^{\sum_{i=1}^{h_j} \frac{\ln(f(x_i)}{h_j}}\right)} \quad \text{(Eq.3)}$$

and

$$N = \sum_{l=1}^{K} h_j \quad \text{(Eq.4)}$$

http://www.aloki.hu ● ISSN 1589 1623 (Print) ● ISSN 1785 0037 (Online)
DOI: http://dx.doi.org/10.15666/aeer/1706_1415914177

Cluster based selection operator-2

$$P_{(i,j,l),2} = \left[\frac{W_j}{(h_j - 1)}\left(\sum_{l=1}^{N} Z_l - NZ_l\right) + \frac{1}{N}\right] \quad \text{(Eq.5)}$$

where

$$Z_l = \frac{f(x_i)\left(\sum_{i=1}^{h_j} \frac{1}{f(x_i)}\right)}{h_j^2} \quad \text{(Eq.6)}$$

and

$$W_j = \frac{h_j}{N} \quad \text{(Eq.7)}$$

where N is the size of the population of individuals, K is the number of cluster along with cluster size h_j. W_j is the proportion of the cluster from individuals' population.

Here some theoretical findings associated with cluster based selection probability are given below.

1. The cumulative probabilities of j^{th} clusters with size h_j is equal to W_j, hence clusters with more individuals will be obtained larger probability sum of each cluster. Moreover, an individual with higher fitness value within the cluster allocated lower selection probability to control selection pressure and population diversity increased.
2. By reducing the recombination probability, the cluster will avoid premature convergence and lower selection probability will be awarded to each individuals in larger clusters.
3. The cumulative selection probability is equal to one i.e. $\sum_{i=1}^{N} P_{(i,j,l),1} = \sum_{i=1}^{N} P_{(i,j,l),2} = 1$.

In the process of fitness evaluation, fitness scaling transforms the membership scores in a range appropriate for the selection function which selects the parents for the next generation. The selection function assigns a higher selection probability to individuals with higher scaled values. The range of the scaled values can affect the GA performance. High variation in scaled values result in rapid reproduction and prevent the GA from searching other regions in the search space. On the other hand, lower scaled value variations give the same opportunity for reproduction resulting low search space progress. *Figure 1* depicted the proposed K-means cluster based GA selection scheme framework.

***GKA**$_{opt}$*

It is quite clear that the validation of clusters plays a vital role to improve the performance of cluster based GA. Validity of clusters is done to measure the quality of the clustering methods based on the compactness and separateness of the clusters. There are two major types of approaches for clusters validation:

External index is used to measure the extent to which cluster labels match externally supplied class labels, e.g. Rand and Adjusted Rand index.

http://www.aloki.hu ● ISSN 1589 1623 (Print) ● ISSN 1785 0037 (Online)
DOI: http://dx.doi.org/10.15666/aeer/1706_1415914177

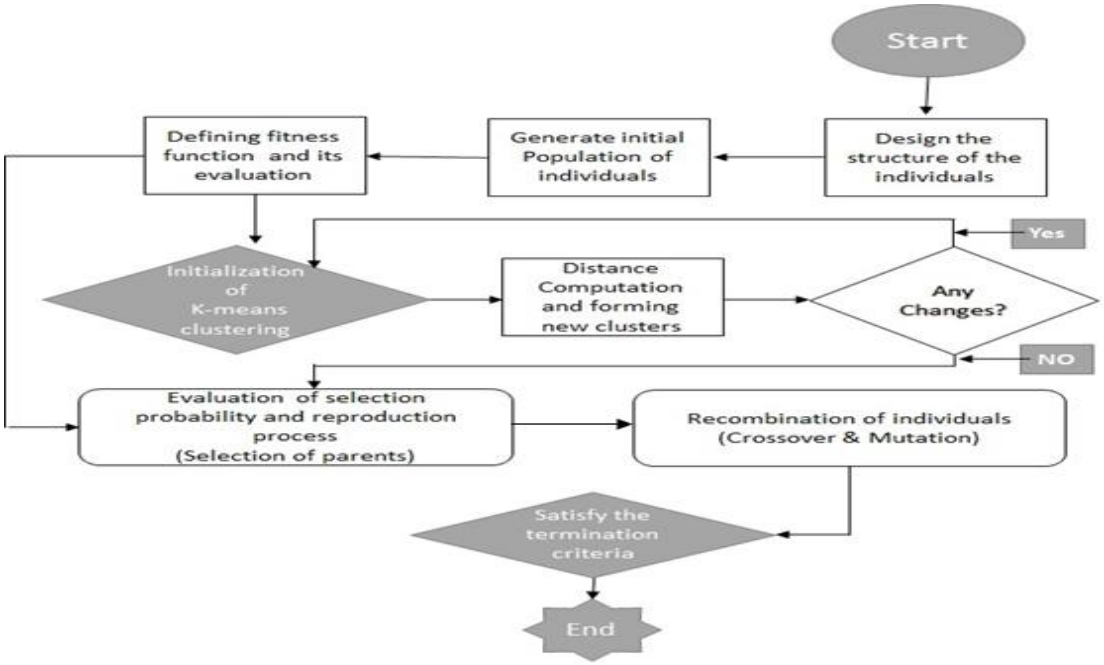

Figure 1. *Frame work of proposed cluster based selection process*

Internal index is used to measure the goodness of a clustering structure without respect to external information e.g. Davies-Bouldin index, Dunn's index, Xie-Beni index, Silhouette index.

The Silhouette index (Mahi, et al., 2018) is one of many cluster indices that can be used to find the number of clusters. The highest value of the average of the Silhouette index s_i indicates a suitable number of clusters. This index is an internal cluster index that can be used as a tool to find the suitable numbers of K with a graphical aid to show the performance of the clustering algorithm.

For each datum i, the Silhouette index can be defined as follows in *Equations 8* and *9:*

$$s_i = \frac{b_{(i)} - a_{(i)}}{max\,(a_{(i)}, b_{(i)})} \qquad \text{(Eq.8)}$$

which is

$$s_i = \begin{cases} 1 - a_{(i)}/b_{(i)}, & \text{if } a_{(i)} < b_{(i)} \\ 0, & \text{if } a_{(i)} = b_{(i)} \\ b_{(i)}/a_{(i)} - 1, & \text{if } a_{(i)} > b_{(i)} \end{cases} \qquad \text{(Eq.9)}$$

where $a_{(i)}$ the average dissimilarities of i with all data points in the same cluster and $b_{(i)}$ the average dissimilarity of i between the other neighbouring cluster. The smallest values of $a_{(i)}$ will indicate the better cluster while the largest values of $b_{(i)}$ will represent a cluster badly matched to its neighbour. If the value of (s_i) is close to 1, then we can say that it is well-clustered. However, if (s_i) is near to 0, then it is not clear in which cluster i belongs to. The larger the average value of the Silhouette index (s_i), the better the performance of the results.

http://www.aloki.hu ● ISSN 1589 1623 (Print) ● ISSN 1785 0037 (Online)
DOI: http://dx.doi.org/10.15666/aeer/1706_1415914177

GKA is a single objective optimization method that use only one fitness function. DB index (Mahi, et al., 2018) is used as their fitness function to measure the validity of the clustering algorithm. This index measured the similarity between the clusters (how separated and compact are the clusters). The lowest values of the index indicate the better clustering and how well the clusters are separated. For these reasons, this study uses the DB index.

The DB index measures the similarity of the clusters by calculating the function of the ratio of the sum within cluster scatter to the between cluster separation. The scatter within the C_i for the i^{th} can be computed as in *Equation 10:*

$$S_{i,q} = \left(\frac{1}{|C_i|}\sum_{x \in C_i} \|x - c_i\|_2^q\right)^{1/q} \quad \text{(Eq.10)}$$

where c_i is the center of the cluster C_i. Usually the choice of q is *2*, where a Euclidean distance measured between the center of the cluster and the individual data points. The $R_{i,qt}$ in *Equation 11* denotes the similarity of C_i to the other clusters. In this study, the Hamming distance is denoted in $d_{ij,t} = d(C_i;C_j)$.

$$R_{i,qt} = \mathrm{Max}_{j,j \neq i}\left\{\frac{S_{i,q}+S_{j,q}}{d_{ij,t}}\right\} \quad \text{(Eq.11)}$$

where $d_{ij,t} = d(C_i, C_j) = \|c_i - c_j\|t$.

Hence the fitness value can be evaluated by:

$$DB_i = \frac{1}{k_i}\sum_{i=1}^{k_i} R_{i,qt} \quad \text{(Eq.12)}$$

From *Equation 10,* the measure of dispersion of a cluster C_i; $i = 1,\ldots\ldots,K_i$ is represented by $S_{i,q}$. The evaluation of the DB index for the chromosome Ch_i is defined in *Equation 12* where the lowest value is indicated the better clustering. The whole process of GKA_{opt} technique focuses on finding optimum number of clusters within a range of clusters through evaluation of validity index functions. Hence the number of clusters K and the searching for k^{th} is constrained to a suitable interval $[K_{min}; K_{max}]$, where $K_{min} > 2$ and $K_{max} \leq n = 10$. The individual has a fixed length of K_{max}. While, the number of K is held to fixed then $K_{min} = K_{max}$. The reason to hold the K constant is to make sure that the best number of clusters has been pre-specified and its validity tested by the Silhouette index, whereas the minimum value of DB determines the optimization of clusters.

Benchmark functions

There are several optimization procedures claiming dominance over other procedures. Hence, to obtain an optimum solution, benchmark functions can be utilized as indicators to authenticate their effectiveness. Many benchmark functions along with their properties have been used to appraise the feasibility of optimization problems. Hence the efficiency of algorithm is based on the nature of the optimization problem regarding variation rate in objective function and the number of local optima etc. (Zhang et al., 2013). A multimodal benchmark function has a minimum of two local optima. The efficient search technique effectively eliminates the region around local optima for searching global optima. Furthermore, the dimensionality of search space is

http://www.aloki.hu ● ISSN 1589 1623 (Print) ● ISSN 1785 0037 (Online)
DOI: http://dx.doi.org/10.15666/aeer/1706_1415914177

another significant factor which makes the problem more complicated. A comprehensive study regarding dimensionality problem and its characteristics were carried out by Friedman. During the search process, the value regarding global optimum needs to be obtained efficiently. Hence the areas close to local minima must be avoided as possible. If the local optima are randomly distributed in the search area, then that is considered to be a more difficult problem. The optimization process is focused on obtaining the global optimum point, consequently the regions nearby local optima should be circumvented because the optimization process might be stuck at local optima and then the local optima is considered as global optima (Deng et al., 2015).

To evaluate the performance and sustainability of the proposed selection operators, we will use eleven unimodal, multi-modal, non-separable, convex and continuous benchmark functions. *Table 2* presents the list of benchmark functions (Surjanovic and Bingham, 2016) utilized to appraise the efficiency of suggested evolutionary methods. Hence the benchmark function name, limit, properties and its fitness function are presented in *Table 2*. These benchmark functions have varying complexities that are most commonly applied in many comparative studies. The necessary detail regarding these benchmarks are given below:

Table 2. *Detail of benchmark functions for comparison*

Benchmark	Fitness function	Search limits	Optimum value	Properties
Axis parallel ellipsoid	$f(x) = \sum_{i=1}^{D} ix_i^2$	[-5.12, 5.12]	0	Continuous, convex, unimodal
Bohachevsky	$f(x) = \sum_{i=1}^{D} (x_i^2 + 2x_{i+1}^2 + 0.3 - 0.3\cos(3\pi x_i + 4\pi x_{i+1}))$	[-100, 100]	0	Multimodal, non-separable
Booth	$f(x) = \sum_{i=1}^{D} ((x_i + 2x_{i+1} - 7)^2 + (2x_i + x_{i+1} - 5)^2)$	[-10, 10]	0	Multimodal, separable
Easom	$f(x) = \sum_{i=1}^{D} \cos(x_i)\cos(x_{i+1})e^{(-(x_i-\pi)^2-(x_{i+1}-\pi)^2)}$	[-100, 100]	-1	Multimodal, non-separable
Ellipsoidal	$f(x) = \sum_{i=1}^{D} (100^{\frac{i-1}{k-1}}x_i)^2$	[-5.12, 5.12]	0	Multimodal, non-separable
Himmelblau	$f(x) = \sum_{i=1}^{D} ((x_i^2 + x_{i+1} - 11)^2 + (x_i + x_{i+1}^2 - 7)^2)$	[-6, 6]	0	Non-convex, multimodal
Six-hump camel	$f(x) = \sum_{i=1}^{D} \{(4 - 2.1x_i^2 + \frac{1}{3}x_i^4)x_i^2 + x_i x_{i+1} + 1 + (-4 + 4x_i^2 + 1)x_i^2\}$	[-3, 3]	(-0.0898, -0.7126, 0.0898, 0.7126)	Multimodal, non-separable
Matyas	$f(x) = \sum_{i=1}^{D} (0.26(x_i^2 + x_{i+1}^2) - 0.48x_i x_{i+1})$	[-10, 10]	0	Non-scalable, Unimodal
Maccormick	$f(x) = \sum_{i=1}^{D} (\sin(x_i + x_{i+1}) + (x_i + x_{i+1})^2 - 1.5x_i + 2.5x_{i+1} + 1)$	[-3,-1.5, 4,4]	-1.91333	Multimodal, Non-separable
Rastrigin	$f(x) = \sum_{i=1}^{D} [10n + \{(x_i^2 - x_{i+1})^2 + (1 - x_i)^2\}]$	[-5.12, 5.12]	0	Multimodal, Separable
Schwefel	$f(x) = \sum_{i=1}^{D} x_i \sin(\sqrt{\lvert x_i \rvert})$	[-500, 500]	0	Multimodal, Non-separable

http://www.aloki.hu ● ISSN 1589 1623 (Print) ● ISSN 1785 0037 (Online)
DOI: http://dx.doi.org/10.15666/aeer/1706_1415914177

Statistical results and discussion

The statistical results of GKA methods (**GKA$_{opt}$** (S-index), **GKA$_{opt}$** (DB-inbex), **GKA$_{P1}$** and **GKA$_{P2}$**) were evaluated at 10, 50 and 100 dimensions and compared with standard GA. In the present experimental study, the performance of optimization techniques is evaluated by fixed parameters such as population size, maximum number of generations, crossover fraction and scaling function. The population size for each experiment is 50 along with 0.8 two-point crossover fraction for 10, 50 and 100 dimensions. Each experiment is executed thirty times to determine the statistical results in terms of means, standard deviation (S.D) and t-test. An independent t-test is obtained to assess the significant difference between standard GA and proposed selection techniques. The performance of these selection methods are evaluated on eleven benchmark functions using MATLAB version R2015a.

The statistical results in *Tables 3–5* reveal that the proposed selection techniques (**GKA$_{P1}$** and **GKA$_{P2}$**) outperform under all benchmark functions from 10 to 100 dimensions. Additionally, the probability values of Bohachevsky, Easom and Schwefel benchmark functions at dimension 10 are ranging 0.0010 to 0.0093 which is significant to some extent but when we increase the dimension of the experiment from 50 to 100, the experimental results turned into highly significant with probability values are tend toward 0.0000. Most of the statistical results demonstrate that **GKA$_{P2}$** perform the best for achieving an optimal solution and **GKA$_{P1}$** is the second best technique because of its closeness to the theoretical optimum value. Overall cluster based selection techniques are broader and more comprehensive for achieving optimum solution and also restrict the individuals to premature convergence. More specifically, there are slight differences between optimum values of **GKA$_{P1}$** and **GKA$_{P2}$** at lower dimension but these differences become highly significant at 50 to 100 dimensions. Results of the above tables are also reveal that the proposed selection techniques perform distinctly better in unimodal and multimodal benchmark functions but rate of the change is slightly high in unimodal functions which turn into highly significant results.

In the context of the above results it is described that the cluster based GA techniques establish a realistic partitioning of the population. These techniques actually extend the population diversity by strengthening the search process and limiting the chance of less fitted individuals. The inclusion of the cluster is also more beneficial for reducing selection pressure, hence the proposed selection schemes authenticate the process of best fitted individuals' selection. Additionally, partitioning of the individuals in the form of clusters endorse that the adequate mixture of individuals is always carried forward to the next generation for obtaining optimum solutions. Above statistical results ensure that clustering is always helpful in exploration process and also minimizing the chance of permute convergence at local optima due to well-adjusted selection pressure.

In order to evaluate the pairwise comparison between the above selection techniques: a non-parametric statistical test is used known as Wilcoxon matched pair signed rank test. The test statistic (T_c) of this test is based on the ranking of absolute difference between two techniques. T^+ is the rank sum with positive signs and T^- is the rank sum with negative signs, the value of Tc depends on the fewer rank sum between T^+ and T^-. A sufficiently small value of T^+ and T^- will cause the rejection of the null hypothesis. The results in *Table 5* represent the pairwise comparison of the following cluster based selection techniques using Wilcoxon matched pair signed rank test at 5% level of significance.

http://www.aloki.hu ● ISSN 1589 1623 (Print) ● ISSN 1785 0037 (Online)
DOI: http://dx.doi.org/10.15666/aeer/1706_1415914177

Table 3. *Statistical comparison of the optimum values for different selection techniques under 10 dimensions*

Selection methods (Dimension 10)						
Benchmark	**Statistics**	**GKA$_{opt}$ (S index)**	**GKA$_{opt}$ (DB index)**	**GKA$_{P1}$**	**GKA $_{P2}$**	**Standard GA**
Axis parallel hyper ellipsoid	Mean	1.64×10^{-7}	1.93×10^{-7}	2.70×10^{-7}	2.66×10^{-7}	5.08×10^{-5}
	S.D	1.93×10^{-7}	2.03×10^{-7}	2.14×10^{-7}	2.10×10^{-7}	7.98×10^{-7}
	T-test	0.0010	0.0006	0.0000	0.0000	---
Bohachevsky	Mean	0.17	0.19	0.20	0.20	0.54
	S.D	0.41	0.44	0.34	0.34	0.61
	T-test	0.0027	0.0026	0.0012	0.0010	---
Booth	Mean	13.30	14.60	14.80	15.00	17.50
	S.D	1.03×10^{-4}	1.07×10^{-4}	1.08×10^{-4}	1.09×10^{-4}	2.01×10^{-1}
	T-test	0.0000	0.0000	0.0000	0.0000	---
Easom	Mean	-0.90	-0.84	-1.08	-1.07	-4.37
	S.D	0.25	0.17	0.39	0.38	1.47
	T-test	0.0028	0.0031	0.0085	0.0079	---
Ellipsoidal	Mean	3.28×10^{-3}	3.37×10^{-3}	3.71×10^{-3}	3.64×10^{-3}	3.56×10^{1}
	S.D	0.01	0.01	0.01	0.01	123.00
	T-test	0.00083	0.00081	0.00053	0.00029	---
Himmelblau	Mean	-1.55×10^{4}	-1.98×10^{4}	-2.25×10^{4}	-2.28×10^{4}	-1.63×10^{8}
	S.D	4.89×10^{3}	5.12×10^{3}	8.06×10^{3}	8.20×10^{3}	2.06×10^{7}
	T-test	0.0000	0.0000	0.0000	0.0000	---
Six-Hump	Mean	-1.03	1.27	-1.70	-1.67	-2.05
	S.D	0.08	0.11	0.14	0.14	0.15
	T-test	0.0000	0.0000	0.0000	0.0000	---
Matyas	Mean	3.21×10^{-3}	2.51×10^{-3}	5.30×10^{-3}	5.21×10^{-3}	3.75×10^{-2}
	S.D	4.89×10^{-3}	5.29×10^{-3}	5.24×10^{-3}	5.15×10^{-3}	5.28×10^{-2}
	T-test	0.0000	0.0000	0.0008	0.0008	---
Maccormick	Mean	-3.81	-4.45	-5.29	-5.38	-6.13
	S.D	0.38	0.44	0.49	0.48	1.71
	T-test	0.0000	0.0000	0.0008	0.0000	---
Rastrigin	Mean	7.90×10^{2}	7.38×10^{2}	9.03×10^{-2}	8.87×10^{-2}	9.90×10^{-2}
	S.D	1.38×10^{-4}	1.07×10^{-4}	1.67×10^{-4}	1.65×10^{-4}	3.33×10^{-1}
	T-test	0.0000	0.0000	0.0000	0.0000	---
Schwefel	Mean	-2.06×10^{3}	-2.41×10^{3}	-2.73×10^{3}	-2.68×10^{3}	-4.02×10^{3}
	S.D	2.15×10^{2}	2.28×10^{2}	2.39×10^{2}	2.35×10^{2}	1.38×10^{2}
	T-test	0.0053	0.0046	0.0029	0.0025	---

http://www.aloki.hu ● ISSN 1589 1623 (Print) ● ISSN 1785 0037 (Online)
DOI: http://dx.doi.org/10.15666/aeer/1706_1415914177

Table 4. *Statistical comparison of the optimum values for different selection techniques under 50 dimensions*

Selection methods (Dimension 50)						
Benchmark	**Statistics**	**GKA$_{opt}$ *(S index)***	**GKA$_{opt}$ *(DB index)***	**GKA$_{P1}$**	**GKA $_{P2}$**	**Standard GA**
Axis parallel hyper ellipsoid	Mean	15.40	13.50	16.00	15.70	315.00
	S.D	7.90	8.12	8.39	8.24	185.00
	T-test	0.0000	0.0000	0.0000	0.0000	---
Bohachevsky	Mean	11.70	11.10	12.50	12.20	78.20
	S.D	2.10	2.02	2.35	2.30	34.00
	T-test	0.0000	0.0000	0.0000	0.0000	---
Booth	Mean	93.10	93.05	91.70	93.50	153.00
	S.D	3.36	3.17	3.45	3.51	25.50
	T-test	0.0000	0.0000	0.0000	0.0000	---
Easom	Mean	-1.25	-1.02	-1.49	-1.47	-10.20
	S.D	0.28	0.19	0.52	0.51	4.08
	T-test	0.0000	0.0000	0.0000	0.0000	---
Ellipsoidal	Mean	0.63×10^{4}	0.56×10^{4}	1.01×10^{4}	0.87×10^{3}	8.18×10^{4}
	S.D	1.02×10^{4}	0.88×10^{4}	1.04×10^{4}	1.02×10^{4}	5.35×10^{4}
	T-test	0.0000	0.0000	0.0000	0.0000	---
Himmelblau	Mean	-1.07×10^{9}	-1.22×10^{9}	-7.05×10^{4}	-7.18×10^{4}	-1.45×10^{9}
	S.D	6.11×10^{7}	6.43×10^{7}	2.50×10^{4}	2.55×10^{4}	1.42×10^{8}
	T-test	0.0000	0.0000	0.0000	0.0000	---
Six-Hump	Mean	-2.79	-3.17	-3.32	-3.38	-7.35
	S.D	0.34	0.38	0.41	0.42	2.79
	T-test	0.0000	0.0000	0.0000	0.0000	---
Matyas	Mean	0.56	0.79	0.90	0.88	2.60
	S.D	0.22	0.28	0.35	0.34	0.81
	T-test	0.0000	0.0000	0.0000	0.0000	---
Maccormick	Mean	35.40	35.60	37.30	36.60	59.90
	S.D	1.73	1.75	1.80	1.76	4.78
	T-test	0.0000	0.0000	0.0000	0.0000	---
Rastrigin	Mean	4.37×10^{3}	$4.42\times\times10^{3}$	4.43×10^{3}	4.52×10^{3}	4.97×10^{3}
	S.D	1.08	1.96	1.98	2.02	2.83
	T-test	0.0000	0.0000	0.0000	0.0000	---
Schwefel	Mean	-6.47×10^{4}	-5.36×10^{4}	-7.92×10^{3}	-7.77×10^{3}	-11.54×10^{4}
	S.D	7.22×10^{2}	6.99×10^{2}	7.39×10^{2}	7.25×10^{2}	8.49×10^{2}
	T-test	0.0000	0.0000	0.0000	0.0000	---

http://www.aloki.hu ● ISSN 1589 1623 (Print) ● ISSN 1785 0037 (Online)
DOI: http://dx.doi.org/10.15666/aeer/1706_1415914177

Table 5. *Statistical comparison of the optimum values for different selection techniques under 100 dimensions*

Selection methods (Dimension 100)						
Benchmark	**Statistics**	**GKA$_{opt}$ (S index)**	**GKA$_{opt}$ (DB index)**	**GKA$_{P1}$**	**GKA $_{P2}$**	**Standard GA**
Axis parallel hyper ellipsoid	Mean	626.00	645.00	664.00	649.00	3050.00
	S.D	103.00	127.00	159.00	155.00	823.00
	T-test	0.0000	0.0000	0.0000	0.0000	---
Bohachevsky	Mean	62.20	55.70	68.40	66.90	239.00
	S.D	11.30	10.70	12.70	12.40	44.40
	T-test	0.0000	0.0000	0.0000	0.0000	---
Booth	Mean	209.00	225.00	265.00	271.00	531.00
	S.D	23.00	24.10	26.00	26.50	130.00
	T-test	0.0000	0.0000	0.0000	0.0000	---
Easom	Mean	-1.20	-1.10	-1.65	-1.61	-12.90
	S.D	0.54	0.31	0.65	0.64	1.81
	T-test	0.0000	0.0000	0.0000	0.0000	---
Ellipsoidal	Mean	1.36×10^{5}	1.45×10^{5}	1.74×10^{5}	1.70×10^{5}	1.37×10^{5}
	S.D	4.24×10^{4}	4.55×10^{4}	4.83×10^{4}	4.73×10^{4}	7.32×10^{5}
	T-test	0.0000	0.0000	0.0000	0.0000	---
Himmelblau	Mean	-1.06×10^{5}	-1.09×10^{5}	-1.12×10^{5}	-1.10×10^{5}	-2.73×10^{9}
	S.D	1.17×10^{4}	1.23×10^{4}	2.73×10^{4}	2.67×10^{4}	2.54×10^{8}
	T-test	0.0000	0.0000	0.0000	0.0000	---
Six-Hump	Mean	3.66	3.29	3.83	3.74	47.10
	S.D	3.38	2.79	4.10	4.01	20.00
	T-test	0.0000	0.0000	0.0000	0.0000	---
Matyas	Mean	3.67	3.40	3.77	3.69	10.90
	S.D	0.58	0.43	0.61	0.60	2.55
	T-test	0.0000	0.0000	0.0000	0.0000	---
Maccormick	Mean	86.00	81.00	84.60	86.50	179.00
	S.D	5.83	4.34	5.80	5.93	27.70
	T-test	0.0000	0.0000	0.0000	0.0000	---
Rastrigin	Mean	8.34×10^{3}	8.13×10^{3}	8.57×10^{3}	8.76×10^{3}	9.95×10^{3}
	S.D	2.17	2.14	2.52	2.58	3.22
	T-test	0.0000	0.0000	0.0000	0.0000	---
Schwefel	Mean	-0.97×10^{4}	-0.93×10^{4}	-1.04×10^{4}	-1.02×10^{4}	-2.41×10^{4}
	S.D	1.19×10^{3}	1.23×10^{3}	1.36×10^{3}	1.33×10^{3}	1.71×10^{3}
	T-test	0.0000	0.0000	0.0000	0.0000	---

According to the results indicated in *Table 6,* there is highly significant difference between most of the pairs of K-means cluster based techniques, when the dimension of the experiment increases from 10 to 100 the p-value turn into highly significant. However, there is also a non-significant difference between GKA$_{P1}$ and GKA$_{P2}$ at lower dimension but when dimension increases difference between them becomes highly significant.

http://www.aloki.hu ● ISSN 1589 1623 (Print) ● ISSN 1785 0037 (Online)
DOI: http://dx.doi.org/10.15666/aeer/1706_1415914177

Table 6. *Pairwise comparison of different selection techniques using Wilcoxon signed rank test*

Comparison	Dimension	T^+	T^-	T_c	P-value
GKA$_{opt}$(S-index) vs **GKA**$_{opt}$(DB-inbex)	10	112	353	112	0.0160
	50	103	362	103	0.0063
	100	87	378	87	0.0010
GKA$_{P1}$ vs **GKA**$_{P2}$	10	187	278	187	0.1799
	50	163	302	163	0.0790
	100	142	323	142	0.0318
GKA$_{opt}$(S-index) vs **GKA**$_{P1}$	10	127	338	127	0.0147
	50	87	378	87	0.0010
	100	45	420	45	0.0000
GKA$_{opt}$(DB-inbex) vs **GKA**$_{P1}$	10	96	369	96	0.0020
	50	45	420	45	0.0000
	100	28	437	28	0.0000
GKA$_{opt}$(S-index) vs **GKA**$_{P2}$	10	119	346	119	0.0093
	50	78	387	78	0.0005
	100	39	426	39	0.0000
GKA$_{opt}$(DB-inbex) vs **GKA**$_{P2}$	10	82	383	82	0.0007
	50	36	429	36	0.0000
	100	24	441	24	0.0000
GA vs **GKA**$_{P1}$ **& GKA**$_{P2}$	10	465	0	0	0.0000
	50	465	0	0	0.0000
	100	465	0	0	0.0000

Conclusions and future work

K-means cluster based genetic algorithm (GKA) selection techniques are proposed to solve optimization problems using unimodal and multimodal benchmark functions. Two distinct types of GKA techniques were proposed, one is using fixed number of clusters GKA_F and other is through optimum number of clusters GKA_{opt}. Hence, Davies-Bouldin and Silhouette index is used to determine optimum number of clusters in the population. The GKA method comprise of four major stages: clustering, membership probability indexing, fitness evaluation and selection. The hybridization of genetic algorithm and clustering of individuals will effectively cater the problem of population diversity and selection pressure. A selection probability is assigned to each individual after the process of K-means clustering. Fitness scaling changes the membership fitness scores in a limit that is suitable for selection function, which select the parents for future generation by the utilization of scaled fitness values. The comparative performance of each cluster based GA technique (GKA_{opt} (S-index), GKA_{opt} (DB-inbex), GKA_{P1} and GKA_{P2} are evaluated on eleven benchmark functions under 10, 50 and 100 dimensions. Usually, the performance of standard GA is good to solve unimodal problem but unable to handle multimodal problems. By the hybridization of GA and K-means clustering, the newly proposed selection techniques efficiently and effectively handle the multimodal problems by obtaining optimum value. The statistical results of present study represent that the performance of GKA_{P1} and GKA_{P2} selection operators are comparatively more superior to standard GA selection techniques. In addition, the

http://www.aloki.hu ● ISSN 1589 1623 (Print) ● ISSN 1785 0037 (Online)
DOI: http://dx.doi.org/10.15666/aeer/1706_1415914177

significance of proposed techniques is also improved by increasing the dimension of the experiment from 50 to 100. In-fact the cluster based selection techniques outperform in solving unimodal and multimodal problems with positive impact.

In the present research study, integrating the strengths of data mining and evolutionary computation were limited to single-objective optimization problems. Future research study could evaluate the performance of GKA in solving constrained optimization problems with multi-objective functions. The efficacy of novel selection procedure should be considered in future research study. It would be compelling to hybridize the K-means cluster with population based optimization schemes such as firefly algorithm (Rajan and Malakar, 2015), ant colony optimization (Gao et al., 2016) and particle swarm optimization (Pednekar, 2019). Finally, another potential avenue for future research is to examine the performance by making comparison of standard K-means clustering with the other clustering methods like Incremental K-means (IKM), Scalable K-means and Online K-means (Saharan et al., 2018) by considering presently proposed selection techniques.

Acknowledgments. Authors are very grateful to deanship of scientific research at King Khalid University, Abha, Saudi Arabia for the financial support through General Research Program under project number GRP-32-41.

Data availability. The data used to support the findings of this manuscript are taken from the website https://www.sfu.ca/~ ssurjano/optimization.html.

Conflict of interests. All authors of this article declare that there is no conflict of interests regarding the publication of this article.

REFERENCES

[1] Aibinu, A. M., Salau, H. B., Rahman, N. A., Nwohu, M. N., Akachukwu, C. M. (2016): A novel clustering based genetic algorithm for route optimization. – Engineering Science and Technology, an International Journal 19(4): 2022-2034.

[2] Belahbib, F. Z. B., Souami, F. (2011): Genetic algorithm clustering for color image quantization. – 3rd European Workshop on Visual Information Processing, IEEE, July 4-6, Paris, pp. 83-87.

[3] Belhaouari, S. B., Ahmed, S., Mansour, S. (2014): Optimized K-means algorithm. – Mathematical Problems in Engineering 2014(2): 1-14.

[4] Das, S., Abraham, A., Konar, A. (2008): Automatic kernel clustering with a multi-elitist particle swarm optimization algorithm. – Pattern Recognition Letters 29(5): 688-699.

[5] Deng, Y., Liu, Y., Zhou, D. (2015): An improved genetic algorithm with initial population strategy for symmetric TSP. – Mathematical Problems in Engineering. http://dx.doi.org/10.1155/2015/212794.

[6] Devooght, R. (2010): Multi-objective genetic algorithm. – https://pdfs.semanticscholar.org/bfee/f4cf230d4db51ef332237dae8530f2b5f613.pdf.

[7] Eiben, A. E., Smit, S. K. (2011): Parameter tuning for configuring and analyzing evolutionary algorithms. – Swarm and Evolutionary Computation 1(1): 19-31.

[8] Fister Jr, I., Yang, X. S., Fister, I., Brest, J., Fister, D. (2013): A brief review of nature-inspired algorithms for optimization. – arXiv preprint arXiv 1307.4186.

[9] Gao, S., Wang, Y., Cheng, J., Inazumi, Y., Tang, Z. (2016): Ant colony optimization with clustering for solving the dynamic location routing problem. – Applied Mathematics and Computation 285: 149-173.

[10] Haq, E., Hussain, A., Ahmad, I., IbrahimM, Almanjahie (2019a): A Novel Selection Approach for Genetic Algorithms for Global Optimization of Multimodal Continuous

http://www.aloki.hu ● ISSN 1589 1623 (Print) ● ISSN 1785 0037 (Online)
DOI: http://dx.doi.org/10.15666/aeer/1706_1415914177

Functions. – Computational Intelligence and Neuroscience. https://doi.org/10.1155/2019/8640218

[11] Haq, E., Hussain, A., Ahmad, I. (2019b): Development a New Crossover Scheme for Traveling Salesman Problem by aid of Genetic Algorithm. – International Journal of Intelligent Systems and Applications (IJISA) 12(2): 46-52.

[12] Hatamlou, A., Abdullah, S., Nezamabadi-Pour, H. (2012): A combined approach for clustering based on K-means and gravitational search algorithms. – Swarm and Evolutionary Computation 6: 47-52.

[13] Huang, H., Ma, Y. (2019): A hybrid clustering approach for bag-of-words image categorization. – Mathematical Problems in Engineering. https://doi.org/10.1155/2019/4275720.

[14] Hussain, A., Muhammad, Y. S., Nauman Sajid, M., Hussain, I., Mohamd Shoukry, A., Gani, S. (2017): Genetic algorithm for traveling salesman problem with modified cycle crossover operator. – Computational Intelligence and Neuroscience. https://doi.org/10.1155/2017/7430125.

[15] Hussain, A., Muhammad, Y. S. (2019): Trade-off between exploration and exploitation with genetic algorithm using a novel selection operator. – Complex & Intelligent Systems. https://doi.org/10.1007/s40747-019-0102-7.

[16] Islam, M. Z., Estivill-Castro, V., Rahman, M. A., Bossomaier, T. (2018): Combining k-means and a genetic algorithm through a novel arrangement of genetic operators for high quality clustering. – Expert Systems with Applications 91: 402-417.

[17] Jain, A. K. (2010): Data clustering: 50 years beyond K-means. – Pattern Recognition Letters 31(8): 651-666.

[18] Li, Z. Y., Yi, J. H., Wang, G. G. (2015): A new swarm intelligence approach for clustering based on krill herd with elitism strategy. – Algorithms 8(4): 951-964.

[19] Lin, H. J., Yang, F. W., Kao, Y. T. (2005): An efficient GA-based clustering technique. – Journal of Tamkang University of Science and Technology 8(2): 113-122.

[20] Loai, L., Lin, T., Li, B. (2008): Mri brain image segmentation and bias field correction based on fast spatially constrained kernel clustering approach. – Pattern Recognition Letters 29(10): 1580-1588.

[21] Lu, Y., Lu, S., Fotouhi, F., Deng, Y., Brown, S. J. (2004): Incremental genetic K-means algorithm and its application in gene expression data analysis. – BMC Bioinformatics 5(1): 172.

[22] Mahi, H., Farhi, N., Labed, K., Benhamed, D. (2018): The silhouette index and the K-harmonic means algorithm for multispectral satellite images clustering. – 2018 International Conference on Applied Smart Systems (ICASS), IEEE, Medea University, Médéa, Algeria, 24-25 November, pp. 1-6.

[23] Maulik, U., Bandyopadhyay, S., Mukhopadhyay, A. (2011): Multiobjective Genetic Algorithms for Clustering: Applications in Data Mining and Bioinformatics. – Springer Science & Business Media, Berlin.

[24] Murty, M., Babaria, R., Chiranjib, B. (2008): Clustering Based on Genetic Algorithms. – In: Ghosh, A. et al. (eds.) Multi-Objective Evolutionary Algorithms for Knowledge Discovery from Databases. Vol. 98 of Studies in Computational Intelligence. Springer, Berlin, pp. 137-159.

[25] Pednekar, A. M. (2019): Optimal initialization of K-means using Particle Swarm Optimization. – arXiv preprint arXiv 1904.09098.

[26] Rahman, A., Islam, Z. (2011): Seed-detective: A novel clustering technique using high quality seed for K-means on categorical and numerical attributes. – Proceedings of the Ninth Australasian Data Mining Conference (Australian Computer Society, Inc.) 121: 211-220.

[27] Rajan, A., Malakar, T. (2015): Optimal reactive power dispatch using hybrid Nelder–Mead simplex based firefly algorithm. – International Journal of Electrical Power & Energy Systems 66: 9-24.

http://www.aloki.hu ● ISSN 1589 1623 (Print) ● ISSN 1785 0037 (Online)
DOI: http://dx.doi.org/10.15666/aeer/1706_1415914177

[28] Saharan, S., Baragona, R., Nor, M. E., Salleh, R. M., Asrah, N. M. (2018): Clustering for binary data sets by using genetic algorithm-incremental K-means. – Journal of Physics: Conference Series 995(1): 012038.
[29] Sivanandam, S. N., Deepa, S. N. (2008): Genetic Algorithms. – In: Sivanandam, S. N. (ed.) Introduction to Genetic Algorithms. Springer, Berlin, pp. 15-37.
[30] Steinhaus, H. (1956): Sur la division des corps materiels en parties. – Bull. Acad. Polon. Sci. C1 II-IV: 801-804.
[31] Surjanovic, S., Bingham, D. (2016): Virtual library of simulation experiments: test functions and datasets (2013). – https://www.sfu.ca/ssurjano/optimization.html.
[32] Xu, R., Wunsch, D. C. (2005): Survey of clustering algorithms. – IEEE Transactions on Neural Networks 16(3): 645-678.
[33] Yang, F., Sun, T., Zhang, C. (2009): An efficient hybrid data clustering method based on K-harmonic means and particle swarm optimization. – Expert Systems with Applications 36(6): 9847-9852.
[34] Yang, X. S. (2014): Nature-Inspired Optimization Algorithms. – Elsevier, Amsterdam.
[35] Younus, Z. S., Mohamad, D., Saba, T., Alkawaz, M. H., Rehman, A., Al-Rodhaan, M., Al-Dhelaan, A. (2015): Content-based image retrieval using PSO and k-means clustering algorithm. – Arabian Journal of Geosciences 8(8): 6211-6224.
[36] Zeebaree, D. Q., Haron, H., Abdulazeez, A. M., Zeebaree, S. R. (2017: Combination of K-means clustering with genetic algorithm: a review. – International Journal of Applied Engineering Research 12(24): 14238-14245.
[37] Zhang, M. X., Zhang, B., Zheng, Y. J. (2014): Bio-inspired meta-heuristics for emergency transportation problems. – Algorithms 7(1): 15-31.
[38] Zhang, X., Zhang, Y., Hu, Y., Deng, Y., Mahadevan, S. (2013): An adaptive amoeba algorithm for constrained shortest paths. – Expert Systems with Applications 40(18): 7607-7616.

http://www.aloki.hu ● ISSN 1589 1623 (Print) ● ISSN 1785 0037 (Online)
DOI: http://dx.doi.org/10.15666/aeer/1706_1415914177

SIMULATION OF SHALLOW GROUNDWATER FLOW FIELD OF A SMALL BEDROCK ISLAND BASED ON REMOTE SENSE: A CASE STUDY IN WAILINGDING ISLAND, CHINA

XU, H. L.[1] – DING, Z. B.[1*] – WANG, D. Q.[1*] – DENG, Z. D.[1] – NI, B. R.[1] – XU, X. G.[2] – LIU, Z. X.[2] – YU, D. H.[3] – ZHAO, X. L.[1]

[1]*Defense Engineering College, Army Engineering University, Nanjing 210007, China*

[2]*School of Resources and Geosciences, China University of Mining and Technology Xuzhou 221116, China*

[3]*Institute of engineering design, Beijing 100043, China*

[*]*Corresponding authors*
e-mail: Njwaterdzb@qq.com (Ding, Z. B.); wangdq_cumt@sina.com (Wang, D. Q.)

(Received 31st May 2019; accepted 16th Oct 2019)

Abstract. In order to overcome the difficulty in obtaining the initial shallow groundwater level of a small bedrock island and build a better geological body model, the assessment of groundwater potential by remote sense (RS) method was introduced into the shallow groundwater flow field modeling of bedrock islands. And the Wailingding Island in China was taken as the study area. The buried depth (h) of water level was fitted with the remote sensing assessment score of shallow groundwater potential, according to the actual water volume. As a result, the study obtained the formula of the fitting curve, which was $S=0.427e^{0.239h}$, $R^2=0.8462$ ($P<0.05$). Then, it used ENVI software to calculate $h=(1/0.239)\ln(S/0.427)$ and evaluate the initial water level of shallow groundwater: D= DEM-h. Moreover, the study introduced the value of D into the GMS software as the initial water level for the simulation of the shallow groundwater flow field, overcoming the difficulty in obtaining the water level of shallow groundwater in the bedrock islands. The GMS software was used to establish a simulation model of shallow groundwater flow field based on the hydrogeological data in this study area. Also, it used ENVI software to convert DEM data into TIF files and import them into the GMS software, improving the precision of island geological body simulation. Next, the study attempted to change the initial conditions of the simulation model of the shallow groundwater flow field, such as rainfall, evaporation capacity and so on, to predict the distribution of shallow groundwater flow field at different times. Finally, the actual water yield of springs and wells and the geophysical data were used to verify the results of the simulation, and the accuracy has met the requirement. Therefore, it is possible complete the simulation of the shallow groundwater flow field of a small bedrock island by RS technology and other techniques.
Keywords: *the bedrock island, simulation of groundwater flow, remote sensing technology, initial water level, geological modeling by using DEM*

Introduction

Water is the source of life. Islands are short of water (McCartney and Houghton-Carr, 2018), and the protection of groundwater is an important factor for environment protection and an indispensable part of environmental assessment. Studying on the flow field distribution and pollutant migration and diffusion of island groundwater, which are helpful to the protection and development of groundwater resources. Due to the different geology, different landform and other factors, there are differences and similarities between the study of terrestrial groundwater and that of islands groundwater. As early as 1995, Li's team used the finite element method of water head and concentration dependence to calculate and simulate the water level, water flow and

http://www.aloki.hu ● ISSN 1589 1623 (Print) ●ISSN1785 0037 (Online)
DOI: http://dx.doi.org/10.15666/aeer/1706_1417914195

water quality of the pyroclastic pore aquifer of Weizhou island and the basalt pore and fracture aquifer (Li et al., 1995). Then, the basis of the groundwater exploitation planning and the control of seawater intrusion was obtained. In 1998, Person studied and predicted the distribution of groundwater in Nantui island (the United States) between 1977 and 2020, using the sharp-interface model, and discussed the intrusion of seawater (McCartney et al., 1998). Subsequently, with the development of computer software, some corresponding groundwater simulation programs and software came out. Liu's team used Modflow-96 to simulate the distribution of groundwater in China's Jinmen island in 2006 (Liu et al., 2006). The eastern part of the island is dominated by granite and gneiss, while the western part is dominated by laterite. Different parameters are set by the program to evaluate the variation level of the groundwater level and provide a scheme for groundwater utilization. In 2008, Barazzuoli et al. used field and experimental data from 1995-2013 in the coastal region of Tuscany, Italy, and used the FEFLOW numerical simulation software to model and analyze the impact of the natural inflow of groundwater into the sea, rivers and man-made wells, and considered the intrusion of seawater, and obtained the water budget. Wen's team studied the groundwater in Leizhou peninsula in 2013 (McCartney et al., 2018). The shallow aquifer in this area is composed of loose rocks and fissure water in volcanic rock cavities. In 2014, Kadi et al. used GMS software to simulate the flow field of Jeju island. And the island is a volcanic, basalts and pyroclastic rocks. For simulating the groundwater situation (Wen et al., 2013), they used the MODFLOW module simulation analysis of groundwater level and spring water, with the SEAWAT module simulating the analysis of seawater intrusion, according to the water level elevation, stream, salinity and other indicators, assessment of the island of groundwater sustainable ability (Alfaro et al., 2017; Mehdizadeh et al., 2017). Subsequently, Lathashri et al. (2016) also studied coastal areas by using the MODFLOW module and proceeds the module of GMS numerical simulation software. Yi et al. (2016) used GMS software to simulate the discharge and seawater intrusion of groundwater in Bohai Bay in Tianjin, China. He used the FEMWATER module to simulate variable density fluid to generalize groundwater and seawater. Li's team built a groundwater simulation model on the east island of Zhanjiang, China (Teng et al., 2015; Zhou et al., 2017). The island was turned into heterogeneous anisotropic, using the Visual MODFLOW software to simulate solution, combining the actual drilling data. The model can better reflect its groundwater hydrogeological situation, and put forward the following island in deep aquifers and deep aquifer groundwater hydraulic ties with China. They discussed the island's sustainability situation of groundwater, and guided the mining of groundwater. Before some integrated programs and software appear, bedrock island groundwater simulation takes analytical calculation as the mainstream, and its visualization effect is not good, and the simulator must have a high level of programming. With the advent of MODFLOW, Visual MODFLOW, GMS, FEFLOW and other software, it seems that the groundwater simulation becomes simple and process-based. It only needs to carry out a detailed investigation on the groundwater recharge and drainage of bedrock islands and seawater intrusion, as well as the experiment and investigation of geological parameters in the region. Then the study used the software to establish a model to simulate. The generalization of bedrock islands of pyroclastic rocks, basalt pore media, highly weathered granite or gneiss, and simulation of other loose rocks is no problem, in accordance with Darcy's law and the equation of motion of groundwater or two-dimensional flow. However, for some bedrock islands, there are mainly bedrock cracks,

http://www.aloki.hu ● ISSN 1589 1623 (Print) ●ISSN1785 0037 (Online)
DOI: http://dx.doi.org/10.15666/aeer/1706_1417914195

such as granite and gneiss. It should conform to the cubic law of groundwater movement. If the geological body is still to be generalized as a pore model, it is similar to the equivalent porous continuous medium model (Long et al., 1982), and it is necessary to modify the parameters such as lithology, water supply and permeability coefficient in local areas. If the geological body is directly considered as a fracture model, the discrete fracture network seepage model (Mao et al., 1984; Wang et al., 2012) is needed to simulate the fracture flow. If the upper strata of the island dominated by bedrock fissures are weathered to a high degree of loose rocks, and the middle and lower strata are still unweathered bedrock fissures, double or multiple media should be considered. If the geological body is still replaced by the pore model and the MODFLOW, Visual MODFLOW, GMS and FEFLOW are used, then the parameters of stratified strata need to be set, which should conform to the properties of each stratum. If the crack model is used, the crack can be simulated with the TOUGH2 software or GMS+TOUGH2 (Tan et al., 2017). At present, the Lawrence Berkeley laboratory in the United States has introduced TOUGH3 software, which is an upgraded version of TOUGH2, adding the function of coding modification and realizing a wider range of simulation. The MODFLOW-SURFACT module is also a program module that can simulate dual media and fracture well (Tan et al., 2017). The CONNETFLOW is a finite element groundwater simulation software for cracks, in which the NAMMU module is for porous media model and the NAPSAC module is for discrete fracture network seepage model. The software can be applied to dual media. Islands of volcanic islands, loose rocks and highly differentiated bedrock are pore type, whose seepage flow conforms to the movement equation of the groundwater of the heterogeneous anisotropy or transverse isotropy, which can be directly simulated by the MODFLOW program, Visual MODFLOW, GMS or FEFLOW software. Bedrock fissures are dominated or with a low degree of bedrock differentiation. They are fracture type. The movement law of groundwater conforms to the cubic law, which can be simulated by the TOUGH2 software, MODFLOW-SURFACT program module and CONNETFLOW finite element simulation software. If the geological body is a pore-crack type (dual medium or multiple medium), we need to simulate the flow geological model based on the MODFLOW, TOUGH2 software, or SURFACT program module. And the study used the CONNETFLOW finite element simulation software to carry out the coupling between pores and cracks. For the intrusion of the bedrock island seawater, its boundary can be directly delineated by combining geophysical and drilling data with its coastline, using SUTRA software, taking into account MODFLOW flow model combined with MT3DMS solute transport model, or using fault module for simulation.

In the past, researchers studied the groundwater flow field of islands in large scale sea areas or mostly studied the distribution of groundwater flow field of sandy islands. However, the simulation of the groundwater flow field in a small bedrock island has not been well studied. This study mainly aimed at the simulation of the shallow groundwater flow field in a small bedrock island. Groundwater in bedrock islands is mostly stored in the form of "freshwater mushroom" (Pang, 1987, 1988), and there are also "freshwater lens", which is different sand islands. The difficulty of shallow groundwater flow field simulation in bedrock islands lies in the acquisition of hydrogeological parameters, especially in small islands which are short of adequate wells or springs. Zhou et al. (2017) used the MODFOLW model to simulate the Donghai island of Zhanjiang, China. Currently, geophysical techniques were also used to detect groundwater throughout the islands (Rosemary et al., 2009). However, it will

http://www.aloki.hu ● ISSN 1589 1623 (Print) ●ISSN1785 0037 (Online)
DOI: http://dx.doi.org/10.15666/aeer/1706_1417914195

cost a lot of work in this method. Therefore, the assessment of the shallow groundwater by remote sensing technology was introduced in this paper to solve the problem that it is difficult to obtain the initial water level of the shallow groundwater flow field in the small bedrock islands. And it combined with geophysical exploration technology and other hydrogeological means. Also, it combined with stratigraphic stratification data, and some hydrogeological parameters of the strata. Furthermore, the shallow groundwater flow field simulation of small bedrock islands was realized.

Material and Methods

Equation of groundwater movement in the bedrock islands

According to the lithologic characteristics of different bedrock islands, there are different theoretical expressions of groundwater movement. Its specific theory should be based on the island's specific bedrock lithology or stratigraphic lithology to choose different forms. If the bedrock island strata are loose strata, such as the east island of Zhenjiang city (Lu, 2007), and granite and gneiss affected by weathering, unloading, and topographic factors, it can be thought that the geological body can be generalized into non-homogeneous anisotropy or transversely isotropy in this paper. The groundwater motion equation (simplified anisotropic medium) or two-dimensional flow motion equation can be used as *(Eq. 1)*:

$$\frac{\partial}{\partial x}[\mathrm{K}_{xx}\frac{\partial H}{\partial x}+\mathrm{K}_{xy}\frac{\partial H}{\partial y}+\mathrm{K}_{xz}\frac{\partial H}{\partial z}]+\frac{\partial}{\partial y}[\mathrm{K}_{yx}\frac{\partial H}{\partial x}+\mathrm{K}_{yy}\frac{\partial H}{\partial y}+\mathrm{K}_{yz}\frac{\partial H}{\partial z}]+\frac{\partial}{\partial z}[\mathrm{K}_{zx}\frac{\partial H}{\partial x}+\mathrm{K}_{zy}\frac{\partial H}{\partial y}+\mathrm{K}_{zz}\frac{\partial H}{\partial z}]=\mathrm{S}_s\frac{\partial H}{\partial t} \quad \text{(Eq.1)}$$

Equation (1) is the general groundwater movement equation of anisotropic media (Wang, 2011). Assuming that x=y is substituted into *Equation (1)*, the groundwater movement equation of transverse isotropic media is obtained, that is *(Eq. 2)*:

$$2\frac{\partial}{\partial x}[2\mathrm{K}_{xx}\frac{\partial H}{\partial x}+\mathrm{K}_{xz}\frac{\partial H}{\partial z}]+\frac{\partial}{\partial z}[2\mathrm{K}_{zx}\frac{\partial H}{\partial x}+\mathrm{K}_{zz}\frac{\partial H}{\partial z}]=\mathrm{S}_s\frac{\partial H}{\partial t} \quad \text{(Eq.2)}$$

Assuming that K_x is the permeability coefficient in the horizontal direction and K_z is the permeability coefficient in the vertical direction, the two-dimensional flow motion equation is shown as follows (*Eq. 3*):

$$\frac{\partial}{\partial x}[\mathrm{K}_x\frac{\partial H}{\partial x}]+\frac{\partial}{\partial z}[\mathrm{K}_z\frac{\partial H}{\partial z}]=\mathrm{S}_s\frac{\partial H}{\partial t} \quad \text{(Eq.3)}$$

In fact, the principle of three-dimensional flow and two-dimensional flow is essentially consistent, as shown in *Figure 1*.

In *Figure 1*, profile 1 is the y-z profile of the geological body, and profile 2 is the x-z profile of the geological body. The permeability coefficients are K_y and K_z, K_x and K_z,

http://www.aloki.hu ● ISSN 1589 1623 (Print) ●ISSN1785 0037 (Online)
DOI: http://dx.doi.org/10.15666/aeer/1706_1417914195

respectively. $K_y=K_x$ indicates that the penetration coefficient of the y-z profile is consistent with that of the x-z profile, indicating that the permeability coefficient of 3 dimension form is consistent with that of 2 dimension, that is, the essence of 3 dimension flow is consistent with that of 2 dimension flow, but only means that the form is different.

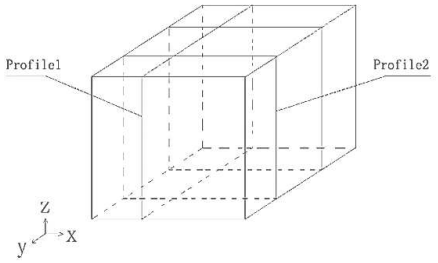

Figure 1. *Two - dimensional, three - dimensional seepage model of the geological body*

The theory of shallow groundwater level based on remote sense groundwater assessment

In this paper, the concept of "shallow layer" in the shallow groundwater is the first aquifer, most of which is the diving layer that is the first stable aquifer below the surface, sometimes the upper stagnant water, sometimes the pressure water, in short, the first aquifer below the surface. In order to obtain the initial groundwater level of bedrock islands, the study used the assessment of groundwater potential by RS method (GRSFAI method) to obtain the initial water level. And lithology index, slope index, relief index, soil humility index, land temperature index, vegetation fraction index and other indexes were selected to establish the model. The equation of score, S, is shown as follows (*Eq. 4*) (Deepesh et al., 2010; Lee et al., 2012; Deng et al., 2013):

$$S = \sum_{i}^{n} W_i \bullet Y_i \qquad \text{(Eq.4)}$$

where S is the score of assessment of groundwater potential, the Y_i values are different kinds of indexes. And the W_i values are the weights of indexes.

The assessment score, S, of shallow groundwater enrichment grade and the water volume, V, in the measured well can be obtained by applying the improved GRSFAI method based on RS-image grayscale statistics and cluster analysis method, and the fitting curve of the two can be finally obtained. And the general formula is $S = a \cdot e^{bV}$. The average the amount of water in a well or spring in terms of its area, the study can get the formula (*Eq. 5*):

$$h = \frac{1}{\Delta s \cdot b} \ln \frac{S}{a} \qquad \text{(Eq.5)}$$

where h is the buried depth per unit water level, as shown in *Figure 2*, and is the elevation from the level groundwater to 2 meters above the groundwater surface. Then, the study can obtain a water level of groundwater: D=DEM-h. The average V water

http://www.aloki.hu ● ISSN 1589 1623 (Print) ●ISSN1785 0037 (Online)
DOI: http://dx.doi.org/10.15666/aeer/1706_1417914195

flow is directly represented by the actual unit water level buried depth h at this point, and the formula (*Eq. 6*) is

$$S = a_1 \cdot e^{b_1 h} \quad \text{(Eq.6)}$$

Next, by fitting the evaluated score, S, with the buried depth, h, of unit water level, the coefficients a_1 and b_1 are obtained. Then, using ENVI software (Duan, 2016), MATLAB software or EXCEL software to calculate the value of h in the entire research area, or the key points of the research area. And the water level of groundwater: DEM-h is used as the initial water level data matrix of the first aquifer in this area. The initial digital, D, is introduced into the GMS software or TOUGH software to simulate and predict the shallow groundwater flow. Thus, the difficulty of obtaining the initial water level elevation of the bedrock islands is overcome.

The specific research route of this paper is shown in *Figure 3*.

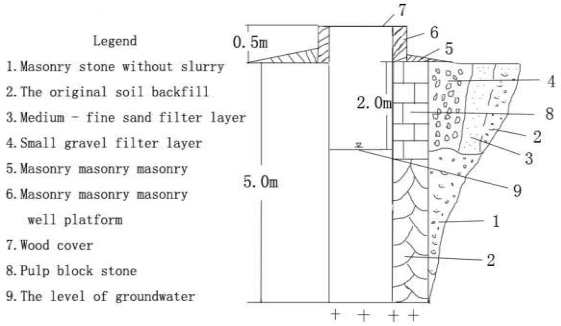

Figure 2. *Diagram of the well*

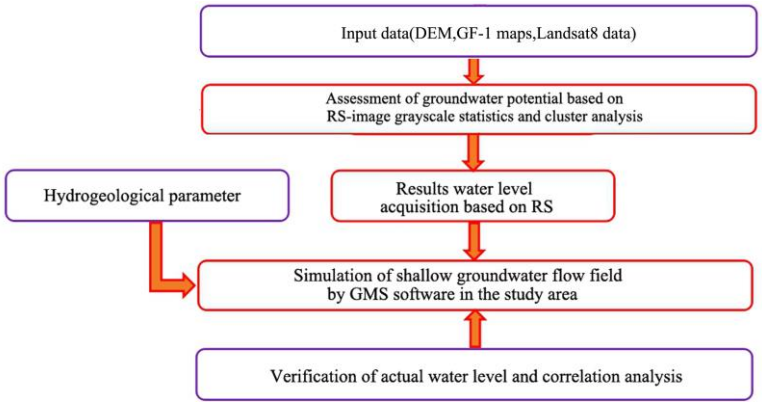

Figure 3. *The research idea flow chart*

Hydrogeological parameters of the study area

Waiilingding island is located in the northeast of Zhuhai city, Guangdong province, China, extending between 22°5′17.16″N and 22°6′57.54″N latitude and 114°1′11.19″E and 114°3′15.40″E longitude, shown as *Figure 4*. Rainfall situation of the island is

http://www.aloki.hu ● ISSN 1589 1623 (Print) ●ISSN1785 0037 (Online)
DOI: http://dx.doi.org/10.15666/aeer/1706_1417914195

following, the rainfall can be divided into high and dry seasons. The rainfall during the period from April to September takes up more than 80% of the annual rainfall. The average monthly rainfall is between 200 and 350 mm. In addition, the whole island is about 3,200 meters long, about 2,400 meters wide, and the narrowest place is only 1,070 meters, with an area of 4.33 km^2. The coastline around the island is 12.3 km. And the coastline is changeable, the geomorphology changes is rich, the island landscape coexists, has many kinds of bay and beach. Wailingding island is very rocky outcrop. In the valley, there are a lot of granite eggs with diameter of 2 to 4 meters.

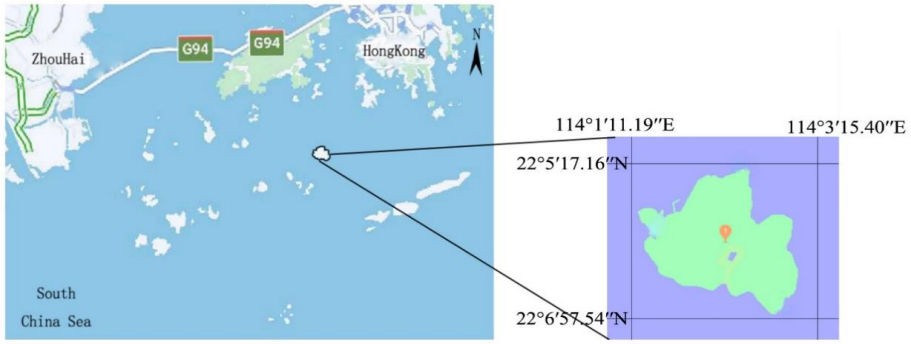

Figure 4. *The map of the study area*

The island's geological structure is simple, mostly granite. From the top to the bottom of the island, it can be divided into three layers, namely the weathered layer soil, vegetation cover, and bare rock, semi-weathered layer and granite bedrock bottom layer. Moreover, the joints of rocks are relatively developed, but the density is not uniform, and there are large faults. The discovery of groundwater in the large sump pit and the wells and springs previously used by people on the island has indicated the existence of groundwater, but the capacity is limited. The islands are surrounded by seawater, and the only source and supply of groundwater is rainwater. Underground cave or fissure, that is, a closed can accumulate a certain amount of water, and also known as island freshwater mushroom body or freshwater lens, forming the groundwater in this island for many years.

Software simulation of shallow groundwater flow field based on remote sense

Setting hydrogeological parameters in GMS software

According to the test values of hydrogeological parameters given in the Hydrogeological handbook (Wang, 2012), the Dam project handbook (Mao, 2009) and the Simulation of pollutant migration in groundwater (Zheng, 2009), The parameters such as horizontal permeability coefficient, vertical permeability coefficient, water availability, water storage coefficient and anisotropic parameters were input into the groundwater simulation software, as shown in *Figure 5*. And the *Figure 6* was a lithological sample of the study area.

Then, the study used the Wailingding island area of Google map as the base of software simulation. Large areas of groundwater on the island were delineated and potholes (or small lakes) were formed, and there were wells and springs in the study area. The recharge in this region is 0.000493 m/d. Due to the particularity of the

http://www.aloki.hu ● ISSN 1589 1623 (Print) ●ISSN1785 0037 (Online)
DOI: http://dx.doi.org/10.15666/aeer/1706_1417914195

bedrock island, the coastal edge of bedrock is in the form of the freshwater mushroom body, which can set the bedrock coastline as the fixed head boundary by the SEAWATER module of GMS software (Pang and Gao, 1988). And the coastline of the island is used as the boundary of bedrock islands.

ID	Name	Color/Pattern	Transparency (%)	Horizontal k (m/d)	Vertical k (m/d)	Horiz. anisotropy	Vert. anisotropy (Kh/Kv)	Specific storage (1/m)	Specific yield	Long. disp.	Porosity
1	Sandy soil		0.0	0.864	0.864	1.0	1.0	0.0013	0.06	0.0	0.3
2	diff granite1		0.0	0.01296	0.01296	1.0	1.0	0.000069	0.0036	0.0	0.3
3	diff granite2		0.0	0.005184	0.005184	1.0	1.0	3.3e-006	0.0021	0.0	0.3
4	granite		0.0	1.728e-007	1.728e-007	1.0	1.0	3.0e-006	0.003	0.0	0.3
5	Shingle		0.0	86.4	864.0	1.0	10.0	3.0e-006	0.03	0.0	0.3

Figure 5. *Various lithologic hydrogeological parameters*

Figure 6. *A lithological sample of the study area*

Water level distribution parameters based on remote sense

Based on the assessment score value, S, of the results of shallow groundwater potential in the study area (Xu et al., 2018) which was shown as *Figure 7* (Xu et al., 2018). And the basal remote sensing data (DEM, GF-1 data, Landsat8 data and so on) can be download from http://www.rscloudmart.com or http://www.gscloud.cn/sources. The actual unit water level depth h of this point is directly expressed according to the average V water volume, that is, $S=a_1 \cdot e^{b1h}$. Subsequently, the evaluated score S was fitted with the buried depth h of unit water level, and the coefficients a_1 and b_1 were obtained. Then, using ENVI software or MATLAB to get the level of groundwater of the first layer, D=DEM-h.

According to *Table 1*, the study can obtain the formula (*Eq. 7*) of fitting curve of h and S (Zheng et al., 2009; Deng et al., 2013):

$$S=0.427E^{0.239H} \quad \text{(Eq.7)}$$

And $R^2=0.8472$. It showed that the fitting degree of h of water level per unit area per unit time in wells or springs and the S of assessment of shallow groundwater potential by remote sensing was good. Next, the formula for calculating h of the evaluated score value S of each point can be deduced reversely according to the formula (*Eq. 8*):

http://www.aloki.hu ● ISSN 1589 1623 (Print) ●ISSN1785 0037 (Online)
DOI: http://dx.doi.org/10.15666/aeer/1706_1417914195

$$h = \frac{1}{0.239} \ln(\frac{S}{0.427}) \quad \text{(Eq.8)}$$

In addition, the water level of shallow groundwater was D, and the surface elevation valued DEM and h were (*Eq. 9*):

$$D=DEM-H \quad \text{(Eq.9)}$$

Then, the study introduced the initial level D of the simulation of the shallow subsurface flow field of the bedrock island into the GMS software. And the study set the parameters of layers and starting heads which were shown in *Figure 8*.

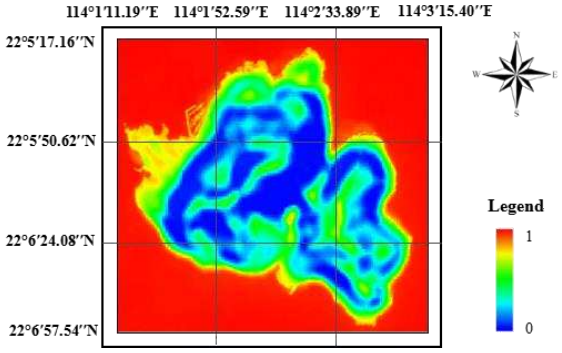

Figure 7. *Level results of assessment of groundwater potential in the study area (Xu et al., 2018)*

Table 1. *Scores of shallow groundwater potential and depth of water level per unit*

Number	Yield of water/(L·s^{-1})	S of assessment	h/(m)	DEM-h = D /(m)
#1	About 1.26	0.655	1.26	1.79
#2	0.20~0.40	0.415	0.30	-0.12
#3	0.20~0.30	0.414	0.25	-0.13
#4	About 1.00	0.620	1.00	1.56
#5	About 3.22	0.830	3.22	2.78
#6	0.55~0.60	0.510	0.59	0.743
#7	0.23~0.30	0.426	0.25	-0.01
#8	About 1.50	0.650	1.50	1.76

Establishment of shallow groundwater model by using GMS software (Liu and Zhang, 2015)

[STEP1]: Setting the basic hydrogeological parameters of the study area as shown in *Figure 5* and setting the parameters of layers and staring heads. Then, setting the supply item and discharge item according to the water level geological data and actual survey data. And the recharge is 0.000493 L/d. The recharge was 0.00603 L/d at the location of puddles and small lakes. And setting up the corresponding well-pumping water. The supply area was shown in *Figure 9*.

http://www.aloki.hu ● ISSN 1589 1623 (Print) ●ISSN1785 0037 (Online)
DOI: http://dx.doi.org/10.15666/aeer/1706_1417914195

[STEP2]: Inputing reproduction, and then inputing the region of the DEM (Dong et al., 2008) which can download freely http://www.gdem.aster.ersdac.or.jp/index.jsp. TIF file was shown in *Figure 10*. And drawing the corresponding CAD reproduction, convenient area of the surface waters in the region, islands area, block partition and edge boundaries.

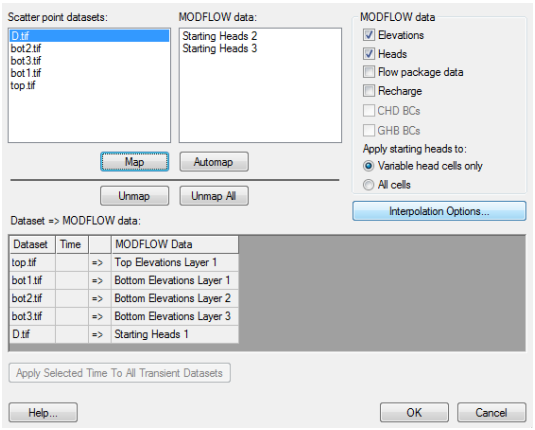

Figure 8. *Setting parameters of layers and starting heads*

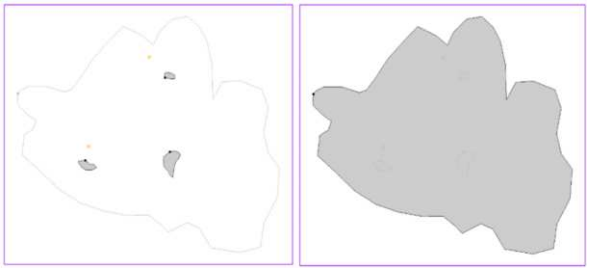

Figure 9. *Setting of the supply area*

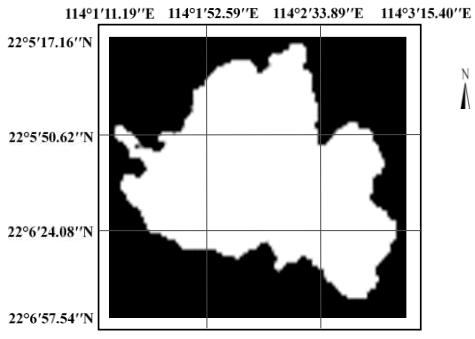

Figure 10. *TIF file of DEM in the study area*

[STEP3]: The mesh generation and model calculation.

The study imported the TIF file of the initial water level, D, into the GMS software and converted it into a scatter in the GMS software, as shown in *Figure 11*. And the study used the direct current method to detect the stratigraphic stratification of the

http://www.aloki.hu ● ISSN 1589 1623 (Print) ●ISSN1785 0037 (Online)
DOI: http://dx.doi.org/10.15666/aeer/1706_1417914195

island, as shown in *Figure 11*. The results showed that the thickness of the blue region with low apparent resistivity was about 1~2 m. The thickness of the medium apparent resistivity area in *Figure 12* was about 2~5 m, that was, 5~7 m underground. It's green and yellow parts that were shown on the *Figure 12*. Moreover, the high apparent resistivity area below, combined with the actual survey data, should correspond to the underlying granite bedrock, and the orange and red parts were shown in *Figure 12*. The ground penetrating radar (GPR) was used to study the stratigraphic stratification results of the direct current method. The results were shown in *Figure 13*. According to the difference in the dielectric constant of the plastid, the thickness range of the surface layer is about 1~2 m, as shown in *Figure 13*.

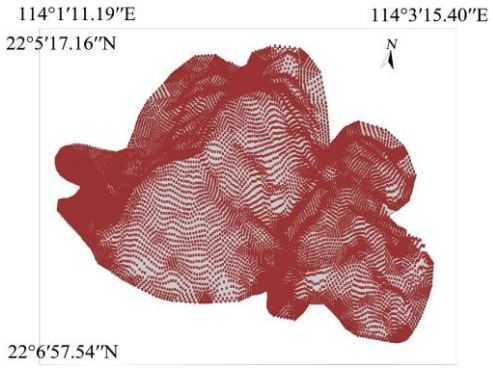

Figure 11. *A scatter diagram of D*

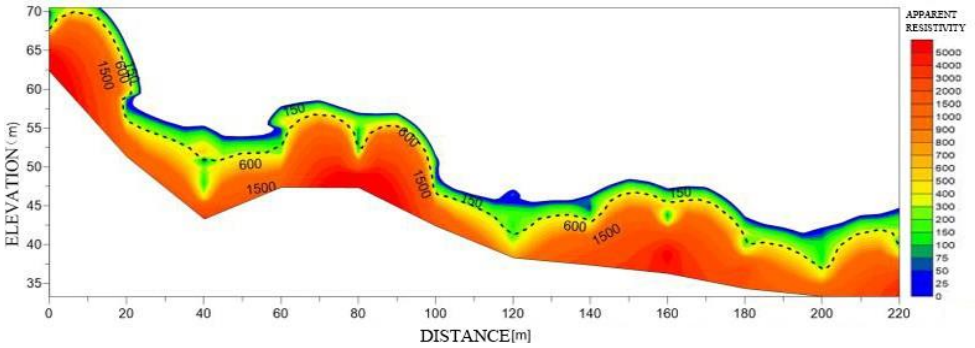

Figure 12. *The result of detection by DC method*

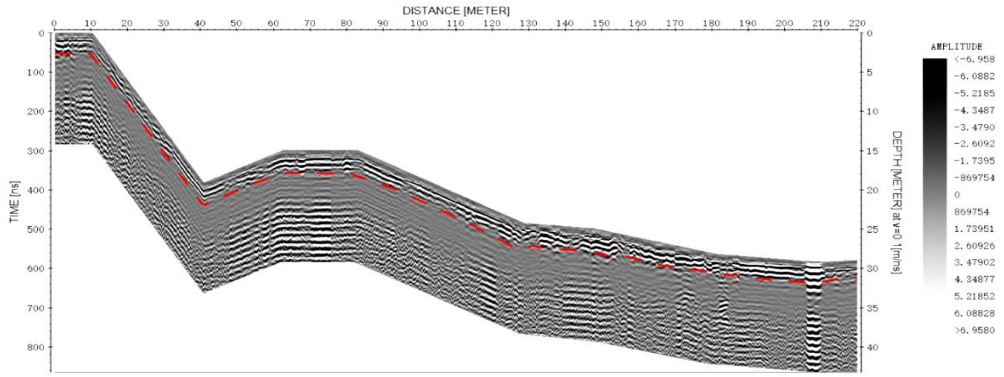

Figure 13. *The result of detection by GPR method*

http://www.aloki.hu ● ISSN 1589 1623 (Print) ●ISSN1785 0037 (Online)
DOI: http://dx.doi.org/10.15666/aeer/1706_1417914195

It is the completely weathering granite layer in the ground. Next, another 5-7 metre underground stratum can be clearly shown in the diagram, combined with the actual survey data, can correspond to partly weathering granite layer. Then, the part below 5~7 m underground is obviously different from the above stratum. Combined with the actual survey data, it can be corresponding to the bottom of the granite bedrock. Thus, the study can set the formation parameters according to the results of *Figure 5*, *Figure 12* and *Figure 13*. Then, the mesh was segmented, as shown in *Figure 14*. Next, the study used the MODFLOW program to calculate the flow field distribution in the study area.

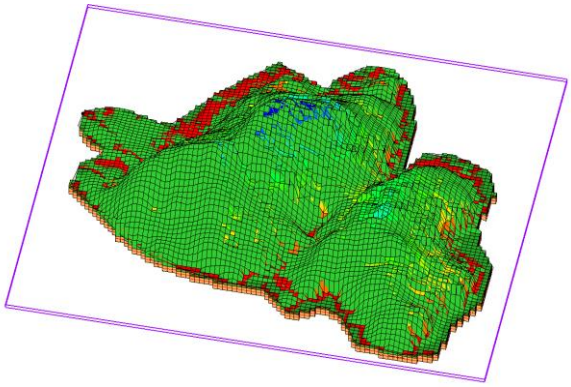

Figure 14. *Schematic diagram of mesh subdivision*

Results and Analysis

Simulation results of shallow groundwater flow field based on remote sense

The results of simulation by using GMS were shown the *Figure 15* and *Figure 16*. They showed that the level of groundwater in this island. The water level around the island was low.

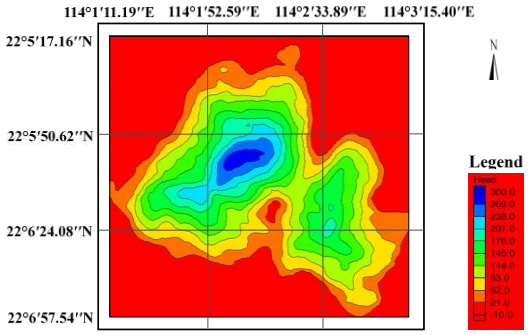

Figure 15. *Simulation results of island shallow groundwater by using GMS software*

High water levels in the middle and southeast of the island indicated a water-storage structure. And the study can see the shallow groundwater flow field that flows outward from the middle of the island, outward from the southeast, and surrounding flow towards the middle of the island. The lower water level in the south-central part of the island and combined with its analysis of water yield showed that the area was easy to fetch water.

http://www.aloki.hu ● ISSN 1589 1623 (Print) ●ISSN1785 0037 (Online)
DOI: http://dx.doi.org/10.15666/aeer/1706_1417914195

Figure 15 can clearly reflect the water level distribution of shallow groundwater. Moreover, *Figure 16* can clearly reflect the simulation results of the shallow groundwater flow field. From the perspective of water level, the water level of this island tends to be high in the middle and southeast and low in the periphery. *Figure 17* can reflect the water level distribution of the whole island in 3 dimensions. *Figure 16* can reflect the flow field trend of shallow groundwater of the island, which flowed from the middle to the outside, from the southeast to the outside, and from the surrounding to the inside of the island. The reason for the trend of the underground flow field to the island should be the existence of seawater. Four points, the first line, about 12 m in length, was located in the puddle above the road next to the first point coordinates: N22.096674°, E114.038623°, H33.2 m. The result is shown as *Figure 18*, which can show there should be bedrock fissure water storage in the underground 5~13 m range by analyzing the different apparent resistivity of this area. Also, spring water emerged about 10 m below this area, N22.097272°, E114.038793°, H21.4 m. It was shown as *Figure 19*.

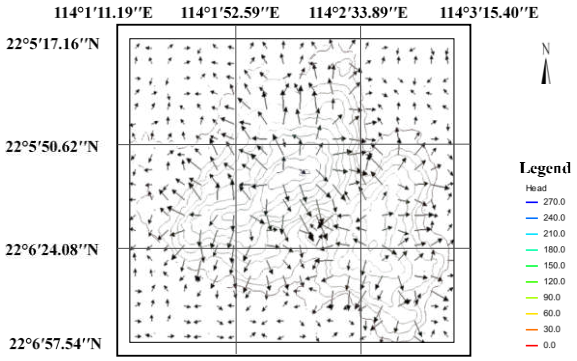

Figure 16. *Simulation results of island shallow groundwater flow*

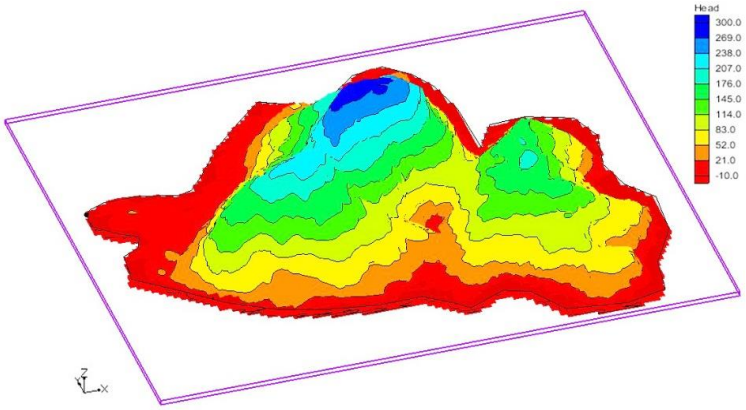

Figure 17. *3D results of simulation groundwater level of the island*

According to the data of springs and wells on the island, and the field survey and the evidence results of DC detection, the unit water level value of the corresponding point can be obtained, and the corresponding relationship between the simulated value and the actual value can be reflected in *Table 2*.

http://www.aloki.hu ● ISSN 1589 1623 (Print) ●ISSN1785 0037 (Online)
DOI: http://dx.doi.org/10.15666/aeer/1706_1417914195

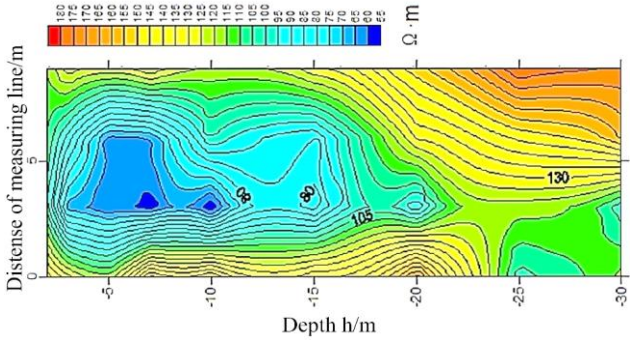

Figure 18. *The profile of DC detection in the study area*

Figure 19. *Actual view of spring water outcropping in the research area*

Table 2. *The results of simulation and the D of points*

Point	S	DEM-h=D/(m)	D of simulation/(m)	Point	S	DEM-h=D/(m)	D of simulation/(m)
1	0.529	29.4	31.79	5	0.483	25.65	20.2
2	0.592	23.1	24.97	6	0.514	22.78	17.1
3	0.640	21.5	22.73	7	0.531	23.69	19
4	0.458	26.2	29.41	8	0.689	17.01	14.3

Correlation analysis of simulation data and the measured water level value

The study analyzed the results of simulation and D more carefully by using a correlation analysis chart between the D and D of simulation that was shown as *Figure 20*. And it was easy to see the two values were positively correlated.

The correlation between the simulated value and the actual water level of unit time and unit area D was positive and linear, and R^2=0.862 (P<0.05), as shown in *Figure 20*, indicating that the simulation results were consistent with the actual water level results and the error accuracy was also good. Therefore, the initial water level obtained based on remote sensing assessment of shallow groundwater was imported into GMS software, and corresponding hydrogeological parameters of islands were added. The model of flow field simulation can reflect the distribution of real shallow groundwater flow field within a certain precision range. Therefore, the difficulty of obtaining the initial water level of bedrock islands was solved based on an assessment of shallow groundwater by RS technology and groundwater simulation technology.

http://www.aloki.hu ● ISSN 1589 1623 (Print) ●ISSN1785 0037 (Online)
DOI: http://dx.doi.org/10.15666/aeer/1706_1417914195

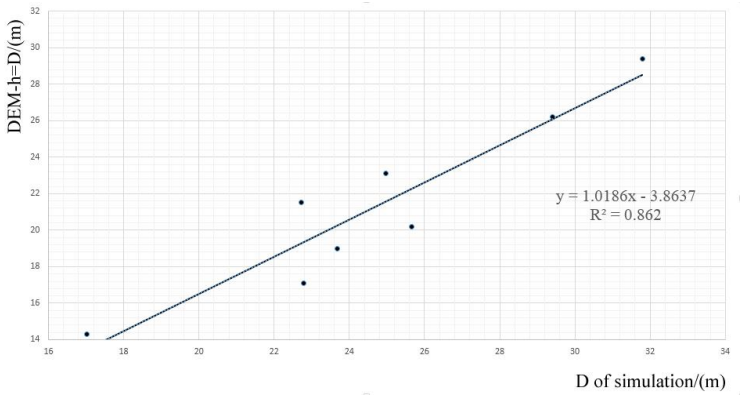

Figure 20. *A correlation analysis chart between the D and D of simulation*

Discussion

This study used ENVI software to convert remote sensing satellite DEM data into TIF files and imported them into GMS software, which improved the accuracy of island geological body model. Using the DEM data to model the geological model of island was more accurate than the traditional method which based on use of some well data. And this paper combined high-precision remote sensing data with shallow groundwater simulation, which was an innovation in methods.

In addition, the score, S, of assessment groundwater potential was fitted to the depth, h, of the unit water level, which was used to obtain the initial water level, D, of shallow groundwater. Then, D was introduced into the GMS software. And using the meteorological and hydrogeological data, geological data and geophysical data of the study area, the simulation of shallow groundwater flow field was carried out, which solved well the difficulty of obtaining the initial water level of shallow groundwater in a small bedrock island and simulated well the shallow groundwater flow of a small bedrock island. Also, the results of the shallow groundwater simulation based on RS are correlated with the actual water level of wells or springs and the geophysical data.

Conclusions

This paper studied the related theories of groundwater in a bedrock island, which proposed to use remote sensing assessment technology of shallow groundwater to get the initial water level of groundwater in the bedrock island so that the study can simulate the flow of groundwater in this island. Finally, the following conclusions can be drawn:

(1) It was concluded that the form of fresh water on the bedrock islands is mainly in the form of "mushroom body", which is accompanied by the form of "lens body". If the groundwater flow field can be simulated, the movement equation of bedrock islands can be expressed as transverse isotropy (isotropy in horizontal direction), and the main recharge of island groundwater is rainfall.

(2) By combining remote sensing data with groundwater simulation, DEM data was transformed into TIF files by ENVI software, which was then introduced into GMS software, and the stratification of island strata determined by geophysical exploration technology combined with actual survey data improved the accuracy of geological body simulation.

http://www.aloki.hu ● ISSN 1589 1623 (Print) ●ISSN1785 0037 (Online)
DOI: http://dx.doi.org/10.15666/aeer/1706_1417914195

(3) The results of assessment shallow groundwater based on remote sensing was fitted with the water level of the area to get the initial water level. This method can solve the problem that the initial water level of the bedrock islands is difficult to obtain, and results the simulation flow groundwater of the island have good accuracy.

Acknowledgements. This work was supported by Development Program of China: research and demonstration of ecological construction of typical islands in the South China Sea and the monitoring technology of ecological things in the South China Sea, NO.2017YFC0506304. And based on remote sensing geology survey, the application information extraction and drawing of national defense construction, NO.DD2016007637.

REFERENCES

[1] Alfaro, P., Liesch, T., Goldscheider, N. (2017): Modelling groundwater over-extraction in the southern Jordan Valley with scarce data. – Hydrogeology Journal 25(5): 1319-1340.
[2] Barazzuoli, P., Nocchi, M., Rigati, R. (2008): A conceptual and numerical model for groundwater management: A case study on a coaster aquifer in southern Tuscany, Italy. – Hydrogeology Journal 16(1): 1557-1576.
[3] Deepesh, M., Madan, K. J., Bimal, C. M. (2010): Assessment of Groundwater Potential in a Semi-Arid Region of India Using Remote Sensing,GIS and MCDM Techniques. – Water Research Management 25: 1359-1386.
[4] Deng, Z. D., Ye, X., Long, F., Yu, D. H., Guan, H. J., Zhang, B. S. (2013): Construction and investigation of groundwater remote sensing fuzzy assessment index. – Chinese Journal of Geophysics 56(11): 3908-3916.
[5] Dong, Y. H., Li, G. M., Guo, Y. H. (2008): Application of SRTM3 DEM in regional groundwater numerical simulation. – Geotechnical Investigation & Surveying 11(1): 41-44.
[6] Duan, H. J., Deng, Z. D., Deng, F. F., Wang, D. Q. (2016): Assessment of groundwater potential based on multicriteria decision making model and decision tree algorithms. – Mathematical Problems in Engineering 1(1): 1-11.
[7] EI-Kadi, A., Tillery, S., Whinier, R. B. (2014): Assessing sustainability of groundwater resources on Jeju Island, South Korea, under climate change, drought, and increased usage. – Hydrogeology Journal 22(3): 625-642.
[8] Lathashri, U. A., Mahesha, A. (2016): Groundwater sustain-ability assessment in coastal aquifers. – Journal of Earth System Science 125(6): 1-16.
[9] Lee, S., Kim, Y. S., Oh, H. J. (2012): Application of a weights-of-evidence method and GIS to regional groundwater productivity potential mapping. – Journal of Environmental Management 96(1): 91-105.
[10] Liu, C. W., Lin, C. N. (2006): Sustainable groundwater management in Kinmen Island. – Hydrological Processes 20(20): 4363-4372.
[11] Liu, L. H., Zhang, S. Q. (2015): Construction of 3D visualization model of groundwater system under multiple constraints based on GMS. – Journal of University of Chinese Academy of Sciences 32(4): 506-511.
[12] Long, J. C. S., Remer, J. S., Wilson, C. R. (1982): Porous media equivalents for networks of discontinuous fractures. – Water Resource Research 18(3): 645-658.
[13] Lu, Y. D. (2007): Report on hydrogeological characteristics of east island new area of Zhanjiang economic and technological development zone. – Zhanjiang: The first team of hydrological engineering geology of Guangdong geological bureau 1(1): 1-12.
[14] Mao, C. X., Chen, P. (1984): Calculation and test of rock fracture seepage flow. – Scientific Research on Water Conservancy and Transportation 1(3): 29-37.

http://www.aloki.hu ● ISSN 1589 1623 (Print) ●ISSN1785 0037 (Online)
DOI: http://dx.doi.org/10.15666/aeer/1706_1417914195

[15] Mao, C. X. (2009): Dam project handbook. – China water conservancy and hydropower press 1(1): 1-105.
[16] McCartney, M. P., Houghton-Carr, H. A. (2018): An assessment of groundwater recharge on the Channel Island of Jersey. – Journal of the Chartered Institution of Water and Environmental Management 12(6): 445-451.
[17] Mehdizadeh, S. S., Karamalipour, S. E., Asoodeh, R. (2017): Sea level rise effffect on seawater intrusion into layered coastal aquifers (simulation using dispersive and sharp-interface approaches). – Ocean & Coastal Management 138: 11-18.
[18] Pang, C. H. (1987): Distribution characteristics of groundwater resources in bedrock islands along the east coast of China: a case study of Miaodao islands. – Geoscience (in Chinese) 7(3): 291-299.
[19] Pang, C. H., Gao, M. (1988): Groundwater resources and environment in bedrock islands: a case study of Miaodao islands. – Survey science and technology (in Chinese) 1(3): 27-30.
[20] Pang, Z. H., Gao, M. (1988): The groundwater resources and environment of the bedrock island-take the temple islands as an example. – Site Investigation Science and Technology 3(1): 27-30.
[21] Rosemary, W. H. C., Greg, M. P., Ronald, L. H. (2009): An unconfined groundwater model of the Death Valley Regional Flow System and a comparison to its confined predecessor. – Journal of Hydrology 5(6): 316-328.
[22] Tan, J. H., Lei, H. W. (2017): Three - dimensional TOUGH2 model and simulation based on GMS. – Journal of Jilin University (geoscience edition) 47(4): 1229-1235.
[23] Teng, J. B., Liu, W. F., Zhou, W. (2015): A numerical simulation study on the groundwater of alluvial continental islands-east island as an example. – Environmental impact assessment 37(1): 59-63.
[24] Tian, K. M., Wang, L. (1989): Study and evaluation of anisotropic fracture medium permeability. – Scholastic press 1(1): 1-89.
[25] Wang, X. S., Wan, L. (2011): Equation for Groundwater Flow. – Beijing: Geological Publishing House 1(1): 1-15.
[26] Wang, H. L. (2012): A review of numerical simulation of fracture water seepage in bedrock. – World nuclear geoscience 29(2): 85-91.
[27] Wang, M., Yin, Y. P., Wen, D. G. (2012): Hydrogeological handbook. – Geological publishing house 1(1): 1-95.
[28] Wen, H. H. (2013): Study on groundwater circulation law and reasonable exploitation and utilization in Leizhou peninsula. – China University of Geosciences 1(1): 1-56.
[29] Xu, H. L., Wang, D. Q., Deng, Z. D., Ding, Z. B., Liu, Z. X., Wang, G. Y., Ni, B. R. (2018): Application of remote sensing fuzzy assessment method in groundwater potential in Wailingding Island. – The Journal of Supercomputing 1(1): 1-13.
[30] Yi, L. X., Ma, B., Liu, L. L. (2016): Simulation of groundwater-seawater interaction in the coastal surficial aquifer in Bohai Bay, Tianjin, China. – Estuarine Coastal & Shelf Science 177(1): 20-30.
[31] Zheng, C. M., Sun, J. Y. (2009): Simulation of pollutant migration in groundwater. – Higher publishing house education 1(1): 1-85.
[32] Zhou, P. P., Li, M., Lu, Y. D. (2017): Study on the groundwater sustainable problem by coastal aquifer numerical simulation in a multi-layered system of Zhanjiang, China. – Indian Academy of Sciences 102(1): 1-26.
[33] Zhou, P. P., Li, M., Lu, Y. D. (2017): Hydrochemistry and isotope hydrology for groundwater sustainability of the coastal multilayered aquifer system (Zhanjiang, China). – Geofluids: 1-19.

http://www.aloki.hu ● ISSN 1589 1623 (Print) ●ISSN1785 0037 (Online)
DOI: http://dx.doi.org/10.15666/aeer/1706_1417914195

RESEARCH ON ATOMIZING MICRO-CLIMATE REGULATION TECHNOLOGIES FOR VINEYARDS IN EXTREMELY ARID AREAS IN SHANSHAN COUNTY, CHINA

YANG, S.[1,4] – BAI, Y.[2*] – YANG, T.[1,3]

[1]*State Key Laboratory of Desert and Oasis Ecology, Xinjiang Institute of Ecology and Geography, Chinese Academy of Sciences, 830011 Urumqi, China*

[2]*Xinjiang Institute of Water Resources and Hydropower Research, 830049 Urumqi, China*

[3]*State Key Laboratory of Hydrology Water Resources and Hydraulic Engineering, Hohai University, Nanjing, 210098 Jiangsu, China*

[4]*University of Chinese Academy of Sciences, 100101 Beijing, China*

**Corresponding author*
e-mail: xjbaiyg@sina.com; phone: +86-99-1852-3145

(Received 1st Jun 2019; accepted 2nd Sep 2019)

Abstract. In response to characteristics of the natural climate in extremely arid areas and the physiological characteristics of grapes in Shanshan County, China, and by relying on micro-spray atomizing regulation technology to change micro-climate environments in vineyards and using methods of contrastive analysis of test data and model calculation analysis, this paper studies changes in grape physiological ecology, photosynthetic characteristics, quality and yield under atomizing regulation action and proposes an optimal technical scheme for atomizing regulation: the atomizing regulation treatment can lower average temperatures by 1.6 °C during grape expansion periods, increase average humidity by 6.6%, and improve grape branch length, internode length, leaf number, leaf area, mid-rib length and oven-dry weight better than conventional drip irrigation (CK) treatment. Fitting calculation analysis of the photosynthetic rate, CO_2 concentration response curve, and light response curve through a mathematical model shows that the atomizing regulation treatment has less influence on photosynthetic characteristics of grapes but helps improve grape quality and provides higher yield than conventional drip irrigation (CK) treatment. Spray water for 1 h a day (WP2) treatment creates optimal quality and the highest yield, 24.0% higher than that of conventional drip irrigation (CK) treatment. All research data indicate that spray water for 1 h a day (WP2) treatment is an optimal technical scheme for atomizing regulation treatment of vineyards in extremely arid areas and creates strong benefits, including a high water resource utilization ratio, enhancement of micro-climates, obvious quality improvement, and yield increase effects.
Keywords: *vineyard, micro-spray atomization, micro-climate physiological ecology, photosynthesis, yield, quality*

Introduction

The Turpan-Hami and Rim-Tarim Basins in Xinjiang enjoy light, heat, water and soil conditions suitable for grape growing, with a wide variety of grapes and high grape quality, thus serving as the main sources of grapes in China (Liu et al., 2019). However, the region is characterized by sparse precipitation, strong evaporation, heavy sandstorms, high temperatures and hot weather during the summer, with the highest temperature in daylight at over 40 °C. Such extreme natural climate conditions heavily influence grape quality and yields. At present, traditional irrigation technology can only address basic water demands for grape growth but cannot fundamentally change climate factors that influence grape quality and yield. For this reason, this research proposes micro-spray

http://www.aloki.hu ● ISSN 1589 1623 (Print) ● ISSN 1785 0037 (Online)
DOI: http://dx.doi.org/10.15666/aeer/1706_1419714215

atomizing regulation technology for vineyards in extremely arid areas to address the issue of micro-climates using the following principle: keeping traditional modes of irrigation, arrange micro-spray heads at different positions in the grape trellis and control the length of spraying time and cycle for each water head, to form new artificial microclimates in the vineyard and research changes in physiological ecology, photosynthetic characteristics, and quality and yield of grapes under the effects of artificial microclimate-influencing factors.

Currently, more attention has been paid to micro-spray atomizing regulation technology by researchers, and some technical studies have been carried out both in China and abroad. For example, a study by Zhang et al. (2000) found that the conditions of active, accumulated temperatures ≥ 10 °C are highly related to grape characteristics during the mature period. Chen et al. (1996) has analyzed the agricultural, meteorological effect of mulberry field spray irrigation and drew the conclusion that micro-spray irrigation makes daylight average water vapor pressure increase by 1.33-1.73 hPa, makes humidity increase by 4-8%, and enhances moisture production efficiency by 10-49%. Liu et al. (2000) researched the influence of micro-spray on wheat field microclimates and found that micro-spray irrigation can influence canopy air temperature and humidity during irrigation and that there are phenomena of increasing inversion times, drops in temperature, and increases in humidity over the canopy. Bai et al. (2016a) researched the influence of micro-spray atomizing regulation irrigation technology on grape physiology and yield and found that this technology can produce high grape yields when the irrigation norm is 9,150 m^3/hm^2 and water is sprayed 1-2 h once a day at a spraying capacity of 105-120 m^3/hm^2 per spray. Koblet addressed the influence of light and temperature on vine performance in cool climates and its application to vineyard management in proceedings of an international symposium on cool climate vatic and enol (Koblet, 1986). Jackson examined aspects of light conditions in apple orchards (Jackson, 1970). Kohl et al. assessed the measurement of low pressure sprinkler poration (Kohl et al., 1987). Srinivas et al. (2000) carried out studies on grape growth and development, as well as moisture utilization efficiency, under different irrigation modes, such as drip irrigation and alternative root area irrigation. Studies by Hui et al. (2007) on main grape physiological indicators of water stress show that under water stress, grape leaf compositions of free proline and malondialdehyde increase with a rise in stress level. Under the influence of high-temperature stress, grape seedlings have a mechanism for quick heat resistance in a short period of time. Temperature has a clear influence on group photosynthesis of Kyoho grapes; high temperatures reduce the initial photochemistry efficiency, but increases maximize photosynthetic rates in Kyoho grapes under low CO_2 concentrations (Xie et al., 1998, 2007; Tang et al., 2006). However, studies on how climate factors in extremely arid areas influence grape physiological ecology, photosynthetic characteristics, quality and quantity are still insufficient. Some key problems remain unsolved, and field management still lacks effective technical support. Therefore, it is of great practical significance to promote comprehensive, harmonious and sustainable development of both society and the economy; research and propose a technical scheme of micro-spray atomizing regulation for grape growth; monitor various grape physiological, ecological indicators under different micro-climate conditions; analyze the relationship between different micro-climate environments and their influences on photosynthetic characteristics, quality, and yield of grapes in extremely arid areas; and explore an optimal technical scheme for atomizing regulation to improve moisture production efficiency, solve problems associated with grape quality improvement, and increase grape yields in extremely arid areas.

http://www.aloki.hu ● ISSN 1589 1623 (Print) ● ISSN 1785 0037 (Online)
DOI: http://dx.doi.org/10.15666/aeer/1706_1419714215

Study area

The study area is in the test base of Xinjiang Shanshan Grape, Fruit and Melon Development and Research Center, 42.91°N, 90.30°E, 419 m above sea level, a soil type of gravel sandy loam, an average annual rainfall of 25.3 mm, an average annual evaporation-pan evaporation of 2,751 mm, yearly sunshine time of 3,122.8 h, a higher-than-10 °C effective accumulated temperature more than 4,525 °C, and a frost-free period of up to 192 d, all features belonging to a typical, extremely arid climate. In the study area, the variety of seedless white grapes is ideal for relevant research. The vine was planted in 1981 in trenches along the east-west run, which is 54 m long, 1.0-1.2 m wide, and 0.5 m deep; the row spacing is approximately 1.2-1.5 m with a row pitch of 3.5 m; the cultivation mode is small-trellis cultivation, with the trellis front end at 1.5 m high and the rear end at 0.8 m high. The experiment was conducted from May 2016 to September 2016.

Data and research methodology

Atomization treatment design

The atomizing regulation test is designed with 7 treatments in total, each of which is arranged with 2 repeats. Each test block has an area of approximately 207 m^2. Micro-spray heads are arranged at 50 cm over the trellis (WP1), 50 cm under the trellis (WP2), and 30 cm above the ground (WP3). In addition, at 50 cm under the trellis, there are three additional treatments with different water spraying time lengths and cycles, namely, WP4, WP5 and WP6. Micro sprinkler working pressure 0.3 mpa (30 m water head), all treatments have a spray diameter of 200 cm, the sprinkler spacing is 200 cm, a flow of 40 L/h, It opens at 12:00 a.m. during the period of grape expansion (May 29, 2016 - July 4, 2016). CK treatment is a traditional treatment lacking micro-spray facilities. The irrigation norm is the total water consumption of grapes within a single mist-spraying growth cycle. The experiment scheme is shown in *Table 1*.

Table 1. *Micro-spray treatment design parameters*

Test treatment	Irrigation water volume (m^3)	Irrigation norm (m^3)	Mist spraying time length (h)	Mist spraying cycle (day)	Micro-spray arrangement mode	Micro-spray head parameters	
						Spray head flow (L/h)	Spray diameter (cm)
WP1	30	610	1	Every day	50 cm over the trellis	40	200
WP2	30	610	1	Every day	50 cm under the trellis		
WP3	30	610	1	Every day	30 cm above the ground		
WP4	60	1220	2	Every day	50 cm under the trellis		
WP5	90	1830	3	Every day			
WP6	60	610	2	Once every 1 day			
WP7	90	610	3	Once every 2 days			
CK	*	610	*	*	*	*	*

Data measurement

Photosynthetic data measurement

On July 1, 2016 (early stage of fruit development), three leaves were selected from each treated vine and vine. From 8:00 a.m. to 20:00 p.m., a portable photosynthetic

http://www.aloki.hu ● ISSN 1589 1623 (Print) ● ISSN 1785 0037 (Online)
DOI: http://dx.doi.org/10.15666/aeer/1706_1419714215

system CIRAS-3 (PP SYSTEMS, USA) was used to measure photosynthetic data of selected leaves of sample trees every 2 h. A total of 7 groups of data were measured in one day. Mean values of photosynthetic data of three leaves were measured at the same time as photosynthetic data at that time.

Measurement of temperature and humidity under 2.2.2 rattan

Under each scaffold, a set of louvers were installed at 10, 20, 30, 40 and 50 cm above the surface, totaling 5 groups. Three groups of HC-2 automatic temperature and humidity recorders were built into each louver to monitor the air temperature and humidity under the scaffold, and the recording interval was 30 min.

Determination of yield and quality

Determination of grape quality: 20 clusters of ears were randomly selected from each treatment, 3 grains were randomly selected from the selected ears, and the content of soluble solids was determined by hand-held refractometer; the content of soluble sugar was determined by anthrone colorimetry; the total acid content was determined by NaOH titration. Tartaric acid, 2,6-dichloroindophenol titration for reducing Vc, sugar-acid ratio: soluble sugar content/total acid content.

During grape harvesting, all the ears in the same treatment were weighed and the total yield was calculated: the total fruit quality in this treatment/the area occupied by the treatment experimental field (hectare).

Determination of physiological indicators in vineyards

During the period of grape germination and leaf development, three sample trees with good growth were selected from each treatment, three branches were selected from each sample tree and marked. From May 6 to June 15, the branch growth was measured once every 7 days with a tape measure of 1 mm accuracy. The length of each node, the number of leaves per branch were recorded, and one branch was selected from the selected branches. A vernier caliper with an accuracy of 0.01 mm was used to measure and record the length of the marker veins. The formula for calculating the leaf area of grape branches is as follows: leaf area = 1.183*X0.456*N, where X is the midrib length of leaves and N is the number of leaves.

During the germination period, a fixed number of new branches of grapevine were selected and marked to avoid pruning of the marked branches. Starting from May 11, 2016, three branches were selected from each treatment every 10 days or so, and then cut from the new parts and put into the corresponding breathable paper bags, using the one set at 85 °C. The oven is baked for 24 h. After natural cooling, the electronic balance with accuracy of 0.1 g is weighed and recorded.

Mathematical model

This research adopts fitted values and actual, measured values of four mathematical models for contrastive analysis, namely, “rectangular hyperbola model (Society et al., 1935), non-rectangular hyperbola model (Thornley et al., 1976), exponential function model (Ye, 2010) and corrected rectangular hyperbola model (Liao et al., 2012)”, with Four kinds of mathematical models simulate the changes of photosynthetic characteristics of CK treatment in vineyard, and compare the simulated values with the

http://www.aloki.hu ● ISSN 1589 1623 (Print) ● ISSN 1785 0037 (Online)
DOI: http://dx.doi.org/10.15666/aeer/1706_1419714215

measured values. The purpose is to screen out more suitable models for simulating the photosynthetic characteristics of the region from many different models. On this basis, the selected models are used to simulate the changes of photosynthetic characteristics under different conditions. It can reduce some repetitive tests and improve work efficiency.

CO2 response curve calculation method

Set effective light radiation intensity (PAR) at 1,200 μmol·m^{-2}·s^{-1} and set reference lab CO_2 concentrations at 50, 100, 150, 200, 400, 600, 800, 1000, 1200, 1400, 1600 and 1800 μmol/mol to carry out two repetitive determinations. The CO_2 response curve fitting equation is the same as the light response curve, and the rectangular hyperbola model is adopted for fitting, namely:

$$A = \frac{\alpha A_{\max} C_i}{\alpha C_i + A_{\max}} - R_p \quad \text{(Eq.1)}$$

where α is the initial carboxylation efficiency, C_i is the intercellular CO_2 concentration, and R_p is the light respiration rate.

The fitting formula of the CO_2 concentration saturation point (CSP) and CO_2 concentration compensation point (CCP) is:

$$A = aC_i - R_p (C_i \leq 200\ umol \cdot mol/mol) \quad \text{(Eq.2)}$$

where, when $A = 0$, C_i is the CO_2 concentration compensation point (CCP); when $A = A_{\max}$, C_i is the CO_2 concentration saturation point (CSP); and the initial carboxylation efficiency (α) is expressed as the slope at the initial, straight-line section when CO_2 concentration is under 200 μmol/mol in the CO_2 response curve.

Light response curve calculation method

Set the temperature at (25 ± 1) °C and the relative air humidity (RH) at 60-70%; use the Model CIRAS-3 portable photosynthesis meter to determine the light response curve and CO_2 response curve by controlling light and CO_2 concentrations. In determining the light response curve, diurnal variation of photosynthesis was selected for the measured leaves. the CO_2 concentration is set at 400 μmol/mol, and the intensity of illumination is set at 0, 50, 100, 150, 200, 300, 400, 600, 800, 1000, 1200, 1400, 1600, 1800 and 2000 μmol·m^{-2}·s^{-1}.

Results

Influence of atomizing regulation technology on vineyard microclimate changes

Temperature change under the trellis

(1) Monthly temperature change: The monthly average temperature is obtained from the daily temperature of the same month. The temperature of micro-spraying treatment is the average temperature of all micro-spraying treatments. The control treatment is the monthly average temperature of CK treatment. As shown in *Figure 1,* during the grape

http://www.aloki.hu ● ISSN 1589 1623 (Print) ● ISSN 1785 0037 (Online)
DOI: http://dx.doi.org/10.15666/aeer/1706_1419714215

expansion period (June - Aug.), atomizing regulation technology can significantly lower the temperature under the vineyard trellis and improve vineyard microclimates compared with CK treatment, with drops in temperature of 1.5, 1.7 and 1.5 °C in June, July and August, respectively, an average drop in temperature of 1.6 °C, and a drop range of 5.6%.

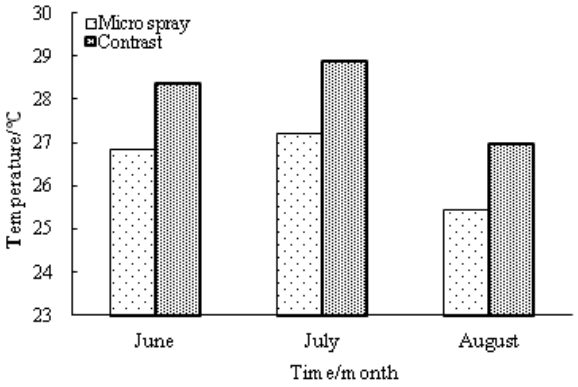

Figure 1. *Monthly temperature change*

(2) Daily temperature change: Daily temperature is obtained from every 30 min recorded by air thermometer and hygrometer during the period of micro-spraying during fruit swelling. As shown in *Table 2,* atomizing regulation treatment produces a daily highest temperature and daily lowest temperature 1.4 °C and 0.4 °C lower than those of CK treatment, respectively, during the grape expansion period. WP1, WP2, WP3, WP4, WP5, WP6, and WP7 daily average temperatures are 27.4, 27.6, 27.3, 27.6, 27.2, 27.4, and 27.4 °C respectively, which, on average, are 0.9 °C lower than the CK treatment average of 28.3 °C.

Table 2. *Temperature change*

Treatment	Temperature (°C)	
	Max value	Min value
WP1	33.1	21.6
WP2	33.7	21.5
WP3	33.0	21.6
WP4	33.3	21.8
WP5	32.7	21.8
WP6	33.1	21.7
WP7	33.2	21.6
CK	34.6	22.0

Humidity change under the trellis

(1) Monthly humidity change: The monthly average humidity is obtained from the daily humidity of that month. The humidity of micro-spraying treatment is the average humidity of all micro-spraying treatments. The control treatment is the monthly average

http://www.aloki.hu ● ISSN 1589 1623 (Print) ● ISSN 1785 0037 (Online)
DOI: http://dx.doi.org/10.15666/aeer/1706_1419714215

humidity of CK treatment. As shown in *Figure 2,* atomizing regulation treatment produces humidity increases by 5, 7.4 and 7.3% in June, July and August, respectively, with an average humidity increase of 6.6% and a range of increase of 13.8%.

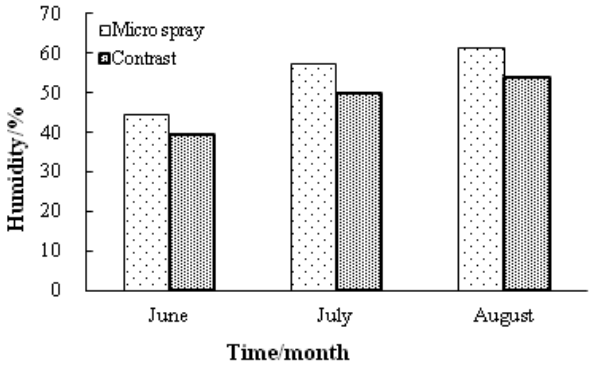

Figure 2. *Monthly humidity change*

(2) Daily humidity change: Daily humidity is the value of humidity every 30 min recorded by air thermometer and hygrometer during fruit expanding period. As shown in *Table 3,* atomizing regulation treatment produces a daily highest humidity and daily lowest humidity 3.0% and 1.0% higher than those of CK treatment, respectively, in June – August. Average daily humidity levels of WP1, WP2, WP3, WP4, WP5, WP6, and WP7 are 57.0, 60.4, 59.6, 57.4, 58.0, 58.3, and 59.6%, respectively, which, on average, are 15.9% higher than the CK treatment average of 56.6 °C.

Table 3. *Daily humidity change*

Treatment	Humidity (%)	
	Max. value	Min. value
WP1	84.9	29.1
WP2	91.5	29.3
WP3	89.7	29.5
WP4	85.0	29.8
WP5	86.3	29.8
WP6	86.2	30.5
WP7	88.3	30.9
CK	84.4	28.9

Influence of atomizing regulation treatment on changes in grape physiological ecology

Change in vine branch length

Length of vine branch under various atomization treatments is shown in *Figure 3,* which shows that the vine branch length continued to increase from May 6 to June 15 and that by Sept. 1, the grape harvesting time, the average vine branch lengths under WP1, WP2, WP3, WP4, WP5, WP6, WP7 and CK treatments were 58.3, 79.7, 79.7, 58.9, 55.5, 60.3, 79.8 and 58.0 cm, respectively.

http://www.aloki.hu ● ISSN 1589 1623 (Print) ● ISSN 1785 0037 (Online)
DOI: http://dx.doi.org/10.15666/aeer/1706_1419714215

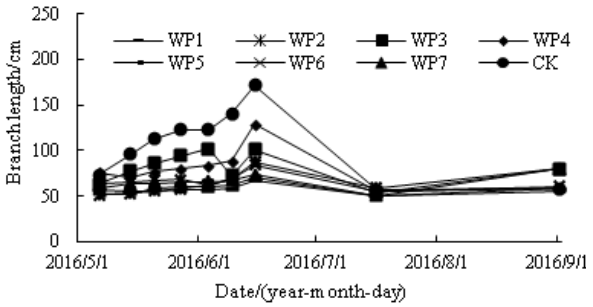

Figure 3. *Change in branch length*

Change in vine internode length

Changes in vine internode length under atomization treatment are shown in *Figure 4,* which shows that vine internode length continued to increase from May 6 to June 15 and that by Sept. 1, the average internode lengths under WP1, WP2, WP3, WP4, WP5, WP6, WP7 and CK treatments were 5.4, 5.4, 5.3, 4.8, 5.0, 5.4, 5.7 and 5.4 cm, respectively.

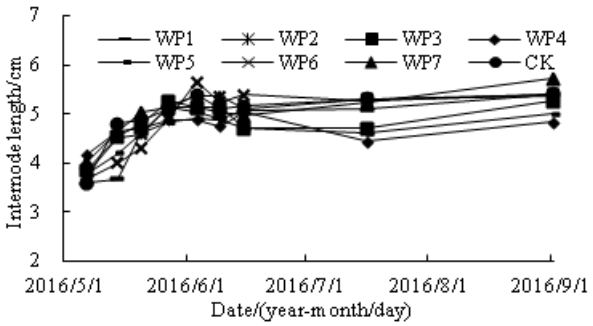

Figure 4. *Change in internode length*

Change in vine leaves

Changes in the number of vine leaves under the atomization treatment are shown in *Figure 5,* which shows that from May 6 to June 15, the number of grape leaves continued to increase and that by Sept. 1, the numbers of leaves under WP1, WP2, WP3, WP4, WP5, WP6, WP7 and CK treatments were 11.0, 15.3, 9.7, 9.5, 8.5, 12.5, 14.0 and 9.5 leaves, respectively.

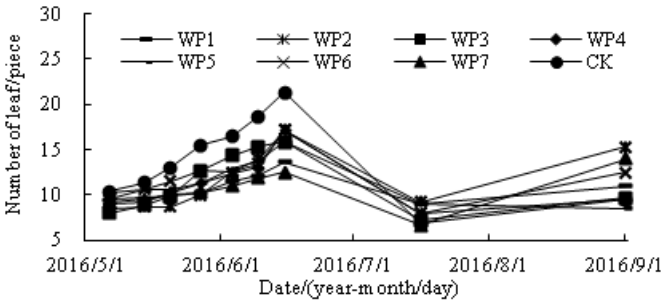

Figure 5. *Change in the number of leaves*

http://www.aloki.hu ● ISSN 1589 1623 (Print) ● ISSN 1785 0037 (Online)
DOI: http://dx.doi.org/10.15666/aeer/1706_1419714215

Change in the length of vine leaf mid-rib

Changes in the length of vine leaf mid-ribs under atomization treatment are shown in *Figure 6,* which shows that from May 6 to May 14, vine leaf mid-ribs grew faster; from May 14 to May 27, vine leaf mid-ribs grew slowly; starting in June, leaves grew rapidly with widely varying changes under different treatments; and by Sept. 1, leaf mid-ribs under various treatments grew relatively slowly and with little variation in growth rates. By Sept. 1, the average lengths of leaf mid-ribs under WP1, WP2, WP3, WP4, WP5, WP6, WP7 and CK treatments were 12.6, 12.8, 13.2, 12.7, 11.7, 12.9, 12.5 and 12.3 cm, respectively.

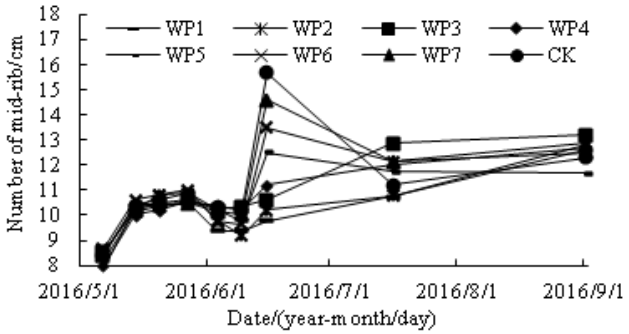

Figure 6. *Change in the length of leaf mid-rib*

Change in vine branch leaf area

Changes in vine branch leaf area under atomization treatment are shown in *Figure 7.* The formula for calculating vine branch leaf area is: leaf area = $1.183 \times X^{0.456} \times N$, where X is the leaf mid-rib length and N is the number of leaves. By Sept. 1, the average leaf areas under WP1, WP2, WP3, WP4, WP5, WP6, WP7 and CK treatments were 41.1, 58.0, 37.1, 35.8, 30.8, 47.5, 52.4 and 32.3 cm^2, respectively.

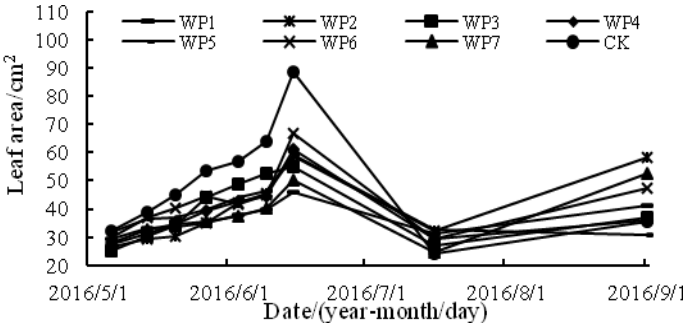

Figure 7. *Change in leaf area*

Changes in the oven-dry weights of new vine branches

Oven-dry weights of new vine branches are shown in *Figure 8*. From the date of initial monitoring, all new vine branches present consistent changes in growth. By Aug. 1, the average oven-dry weights of new branches under WP1, WP2, WP3, WP4, WP5, WP6, WP7 and CK treatments were 17.0, 17.0, 18.5, 17.0, 17.8, 15.8, 17.2 and 15.3 g, respectively.

http://www.aloki.hu ● ISSN 1589 1623 (Print) ● ISSN 1785 0037 (Online)
DOI: http://dx.doi.org/10.15666/aeer/1706_1419714215

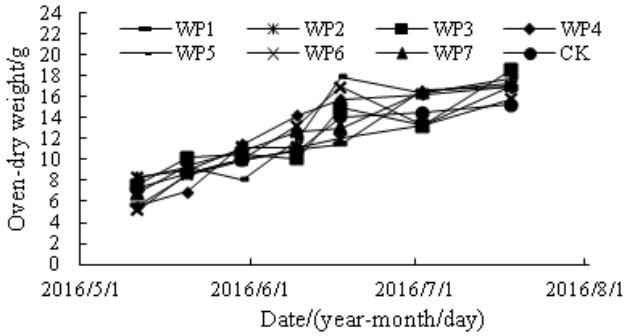

Figure 8. *Change in oven-dry weight*

Influence of atomizing regulation treatment on changes to grape photosynthesis

Change in vine leaf photosynthetic rate

The process of daily changes in vine leaf photosynthetic rate under atomization treatment is shown in *Figure 9,* which shows a consistent law of daily change in photosynthetic rate. Starting at 8:00 am, with a stronger solar radiation intensity and a rising temperature, air holes gradually open, and photosynthetic rates gradually increase until reaching a maximum daily value at 10:00 am. Later in the day, when temperatures continue rising toward the peak daily value, air holes gradually close until they shut off, and photosynthetic rates rapidly drop toward the minimum. At 4:00 pm, when the temperature gradually drops, leaf air holes start to open again, and photosynthetic rates increase once again to reach the second peak daily value. Later in the day, with poorer solar radiation and lower temperatures, photosynthetic rates decrease once again. The law of change under all treatments is consistent, but photosynthetic rates alternate at different time nodes. The average photosynthetic rates under WP1, WP2, WP3, WP4, WP5, WP6, WP7 and CK treatments reach their peak value at 10:00 am, namely, 6.2, 7.2, 7.0, 8.9, 9.2, 6.6, 6.4 and 7.2 μmol m^2s^{-1}, respectively, and the average daily photosynthetic rates of the treatments are 5.4, 6.2, 5.7, 6.4, 6.0, 5.5, 5.6, and 6.1 μmol m^2s^{-1}, respectively.

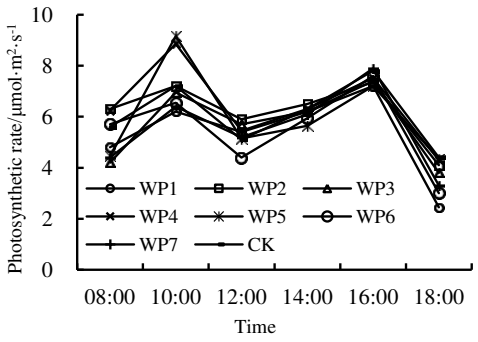

Figure 9. *Daily change of leaf's net photosynthetic rate*

Change in vine leaf transpiration rate

Daily changes in leaf transpiration rate under atomization treatment are shown in *Figure 10,* which demonstrates adherence to the distinctive law of transpiration rate,

http://www.aloki.hu ● ISSN 1589 1623 (Print) ● ISSN 1785 0037 (Online)
DOI: http://dx.doi.org/10.15666/aeer/1706_1419714215

namely, reaching the peak value at approximately 4:00 pm and exhibits a high-low order of WP4 > WP5 > WP3 > WP6 > CK > WP7 > WP2 > WP1.

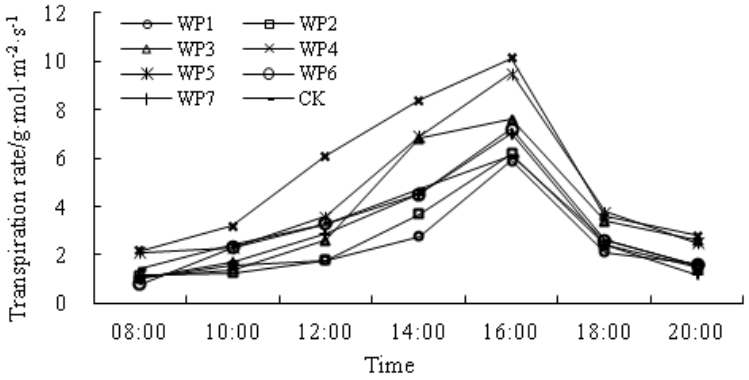

Figure 10. *Daily change in leaf transpiration rate*

Change in vine leaf air hole conductivity

Daily changes in leaf air holes under atomization treatment are shown in *Figure 11,* and basic relationships between air hole conductivity are P2 > WP4 > WP3 > WP7 > CK > WP5 > WP1 > WP6. Starting from 8:00 am, vine leaf air hole conductivity continues to increase until reaching the peak value at approximately 12:00 pm as solar radiation intensity becomes stronger and the temperature rises. After that, the conductivity curve of vine leaf air holes continuously drops.

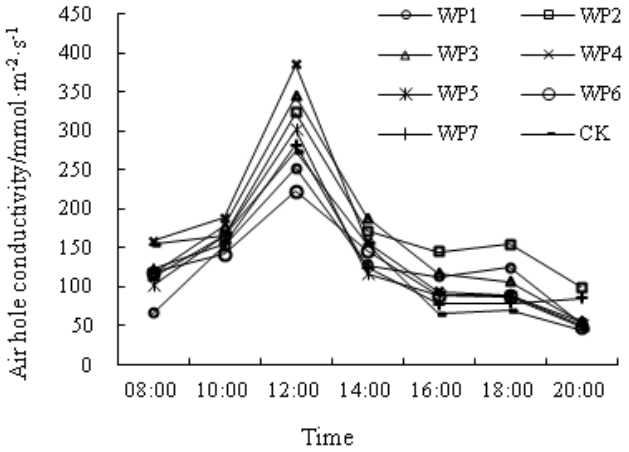

Figure 11. *Daily change of leaf air hole conductivity*

Influence of atomizing regulation technology on changes in grape photosynthesis characteristics

Response of grape photosynthetic rate to CO_2 concentration

The curve representing grape response to low CO_2 concentrations is shown in *Figure 12*. When CO_2 concentrations are under 200 μmol·mol^{-1}, the linear equation fits very well, and the coefficient of determination (R^2) is 0.9773.

http://www.aloki.hu ● ISSN 1589 1623 (Print) ● ISSN 1785 0037 (Online)
DOI: http://dx.doi.org/10.15666/aeer/1706_1419714215

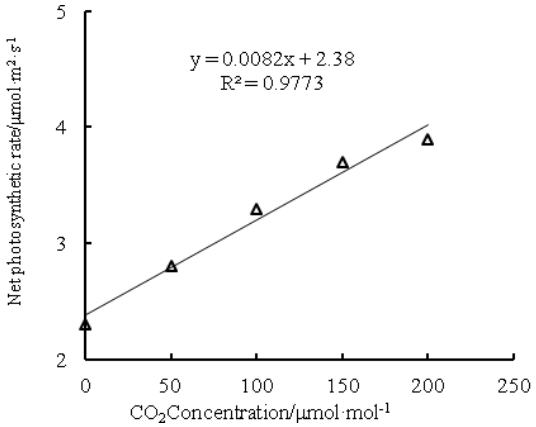

Figure 12. *Curve of response to low CO_2 concentrations*

The curve representing grape response to high CO_2 concentrations is shown in *Figure 13,* which indicates that before CO_2 concentrations reach 800 μmol·mol^{-1}, photosynthetic rates increase rapidly; after 800 μmol/mol, photosynthetic rates increase slowly.

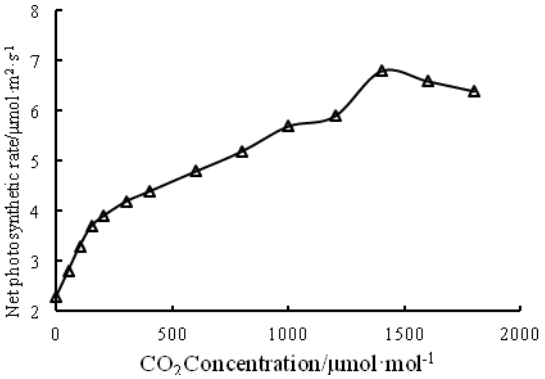

Figure 13. *Curve of response to high CO_2 concentrations*

Using the rectangular hyperbola to fit the curve representing grape response to CO_2, we calculate the maximum net photosynthetic rate, the CO_2 concentration compensation point and the CO_2 concentration saturation point, which are 5.935 μmol·mol^{-1}, 351.67 μmol·mol^{-1} and 1175.97 μmol·mol^{-1}, respectively. The coefficient of determination is 0.967, as shown in *Table 4*.

Table 4. *Characteristics of grape CO_2 response curve*

Characteristic parameters of light response	Fitting value
Max. photosynthetic rate (A_{max})/μmol•m^2•s^{-1}	5.935
CO_2 saturation point (CSP)/μmol·mol^{-1}	1175.97
CO_2 compensation point (CCP)/μmol·mol^{-1}	351.67
Light respiration rate (R_p)/μmol•m^2•s^{-1}	2.532
Carboxylation efficiency (a)	0.0072
R^2	0.967

http://www.aloki.hu ● ISSN 1589 1623 (Print) ● ISSN 1785 0037 (Online)
DOI: http://dx.doi.org/10.15666/aeer/1706_1419714215

Response of grape photosynthesis to light intensity

The curve representing grape photosynthetic response to low light intensity is shown in *Figure 14,* which indicates that when photosynthetic-effective radiation is under 200 μmol·m^{-2}·s^{-1}, the linear equation fits very well, and the coefficient of determination (R^2) is 0.9537.

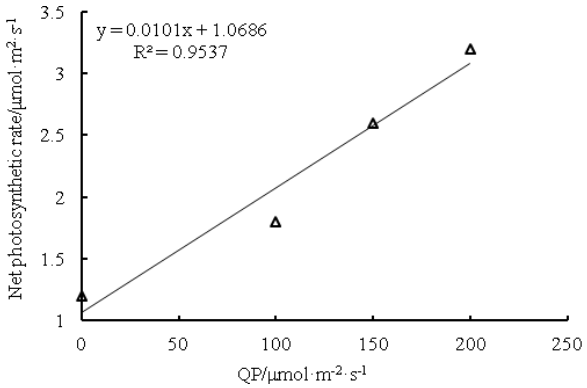

Figure 14. *Curve of photosynthetic response to low light intensity*

The curve representing grape photosynthetic response to high light intensity is shown in *Figure 15,* which indicates that when light intensity is 0-600 μmol·m^{-2}·s^{-1}, net photosynthetic rates rise rapidly, increasing with an increase in intensity of illumination. When the intensity of illumination is 600-1500 μmol·m^{-2}·s^{-1}, the rise in net photosynthetic rate is low. When the intensity of illumination is 1500-2000 μmol·m^{-2}·s^{-1}, net photosynthetic rates decrease with an increase in intensity of illumination, demonstrating the light inhibition phenomenon during which the light energy received by a plant leaf exceeds the light quantity that the leaf can utilize. Long time exposure to strong light can lower leaf photosynthetic activity.

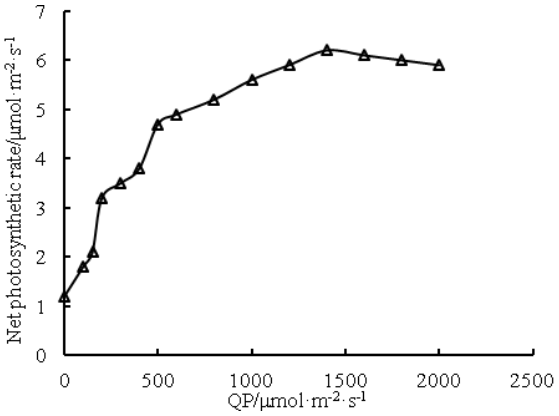

Figure 15. *Light intensity response curve*

Contrastive analysis of fitted values of grape light response curve models

The fitted values of the rectangular hyperbola model, as shown in *Table 5*, show the largest difference from actual measured values, and the net photosynthetic rates of the

http://www.aloki.hu ● ISSN 1589 1623 (Print) ● ISSN 1785 0037 (Online)
DOI: http://dx.doi.org/10.15666/aeer/1706_1419714215

other three models are similar under effective photosynthetic radiation. The fitted values of the corrected rectangular hyperbola model are closest to the actual measured values.

Table 5. *Actual measured value and fitted value of light response curve*

	Net photosynthetic rate A (μmol·m^{2}·s^{-1}))				
Effective photosynthetic radiation (μmol·m^{-2}·s^{-1})	**Actual value**	**Rectangular hyperbola**	**Non-rectangular hyperbola**	**Exponential function**	**Corrected rectangular hyperbola**
0	1.2	0.87	1.10	0.97	1.04
50	1.5	1.55	1.54	1.52	1.55
100	1.8	2.10	1.96	2.01	2.01
150	2.1	2.56	2.36	2.45	2.42
200	3.2	2.94	2.75	2.84	2.80
300	3.5	3.56	3.46	3.51	3.45
400	3.8	4.03	4.05	4.04	3.99
500	4.7	4.40	4.53	4.47	4.44
600	4.9	4.70	4.90	4.81	4.81
800	5.2	5.15	5.38	5.31	5.36
1000	5.6	5.48	5.65	5.62	5.72
1200	5.9	5.73	5.82	5.82	5.94
1400	6.2	5.92	5.93	5.95	6.05
1600	6.1	6.08	6.01	6.04	6.07
1800	6	6.21	6.07	6.09	6.02
2000	5.9	6.32	6.11	6.13	5.92

Photosynthetic parameters of the grape light response curve through the fitting of four models are shown in *Table 6*. The fitted values of the four light response models are highly correlated with the grape light response curve, of which the non-rectangular hyperbola model and the corrected rectangular hyperbola model have the highest coefficients of determination at 0.988 and 0.989, respectively. In the rectangular hyperbola model and the non-rectangular hyperbola model, due to their non-convergence, the light saturation points cannot be obtained but can only be estimated through the linear regression equation under an effective photosynthetic radiation of 200 μmol·m^{-2}·s^{-1} and a maximum net photosynthetic rate (A_{max}). The light saturation points gained in the two models are 544.380 μmol·m^{-2}·s^{-1} and 501.100 μmol·m^{-2}·s^{-1}, respectively, showing a large difference from the actual measured value of 1400 μmol·m^{-2}·s^{-1}. The exponential function model cannot be obtained because the photosynthetic rate is assumed to be 0.9 A_{max}, and the light intensity to which it responds is the saturated light intensity, but the fitted value of 696.80 μmol·m^{-2}·s^{-1} is far lower than the actual measured value; it is assumed that the light intensity to which the photosynthetic rate responds is 0.99 A_{max}. The corrected rectangular hyperbola model can simulate gaining of the light saturation point, with a value of 1557.20 μmol·m^{-2}·s^{-1}, better dealing with the problem of decrease of grape photosynthetic rate in the section of high light intensity, which is closest to the actual measured value. The four models have light compensation points, which is the apparent quantum efficiency and dark respiration rate's simulation value free from significant difference, and the exponential function model's fitted value is closer to the actual measured value; at the highest

http://www.aloki.hu ● ISSN 1589 1623 (Print) ● ISSN 1785 0037 (Online)
DOI: http://dx.doi.org/10.15666/aeer/1706_1419714215

photosynthetic rate, the corrected rectangular hyperbola model's fitted value is 6.072 μmol·m^{-2}·s^{-1}, which is closest to the actual-measured value of 6.1 μmol·m^{-2}·s^{-1}.

Table 6. *Photosynthetic parameters of grape light response curve*

Characteristic parameters of light response	Rectangular hyperbola	Non-rectangular hyperbola	Exponential function	Corrected rectangular hyperbola	Actual measured value
Max photosynthetic rate (A_{max})/μmol·m^2·s^{-1}	6.647	5.330	6.188	6.072	≈6.1
Light saturation point (LSP)/μmol·m^{-2}·s^{-1}	544.380	501.100	696.800	1557.200	≈1500
Light compensation point (LCP)/μmol·m^{-2}·s^{-1}	-87.200	-109.800	65.927	103.020	≈90
Dark respiration rate (R_{day})/μmol·m^{-2}·s^{-1}	-0.872	-1.098	0.842	1.030	
Apparent quantum efficiency (ψ)	0.010	0.010	0.010	0.010	
Initial quantum efficiency (a)	0.015	0.009	0.014	0.011	
R^2	0.980	0.988	0.987	0.989	

Influence of atomizing regulation technology on changes in grape quality and yield

Grape quality change

Grape quality indicators are shown in *Table 7*. CK treatment features a total acid content higher than that under all atomization treatments, but the soluble solid content, soluble sugar content, Vc content and sugar acid ratio are all lower than those under the atomization treatments, showing that atomizing regulation technology can effectively improve grape quality.

Table 7. *Contrast of grape quality indicators under different treatments*

Treatment	Soluble solid content (%)	Soluble sugar content (%)	Total acid content (%)	Reduction Vc content (mg/100 g)	Sugar acid ratio (%)
WP1	23.80	21.20	0.45	6.43	52.89
WP2	24.20	22.30	0.45	6.43	53.78
WP3	23.00	21.00	0.45	4.29	51.11
WP4	23.60	21.40	0.41	5.71	57.21
WP5	22.10	20.00	0.49	2.89	45.33
WP6	20.20	18.10	0.45	3.86	44.89
WP7	21.00	19.20	0.45	3.57	46.67
WP8	19.80	17.50	0.49	2.86	40.62
CK	19.50	16.50	0.49	2.88	39.63

Yield change

Grape yields under atomization treatment are shown in *Figure 16,* and the average yields under WP1, WP2, WP3, WP4, WP5, WP6, WP7 and CK treatments are 2,829.0, 3,432.7, 2,283.0, 2,155.5, 2,880.8, 2,195.8, 3,303.9 and 2767.5 kg/hm^2, respectively.

http://www.aloki.hu ● ISSN 1589 1623 (Print) ● ISSN 1785 0037 (Online)
DOI: http://dx.doi.org/10.15666/aeer/1706_1419714215

Compared with that of CK treatment, yields of the atomization treatments are greater by up to 24.0%, indicating that the atomizing regulation technology plays a clear role in promoting higher yield.

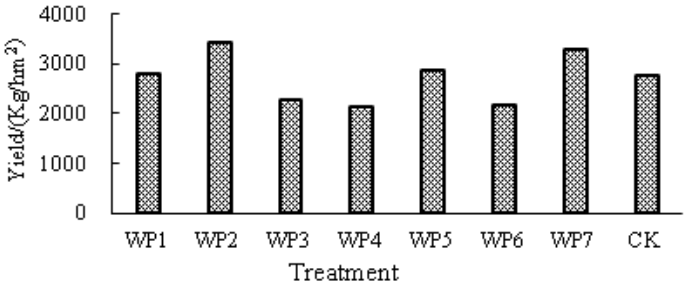

Figure 16. *Yield contrast*

Discussion

This study found that sprinkler treatment had lower temperature and higher humidity than control treatment, which was consistent with the results of Hong, et al. (2016). WP5 treatment should have the shortest spraying period and the longest spraying time, the highest air humidity, but the lowest air humidity. This is because the spraying time of WP5 treatment is longer and its physiological development is relatively inhibited, resulting in shorter branch length, shorter internode length, shorter leaf vein length and relatively fewer branches and leaves. The total leaf area of the branches was smaller and the canopy was sparse compared with other treatments, which increased the air exchange between the air and the atmosphere in the canopy, and eventually resulted in the lowest humidity.

The study also found that the net photosynthetic rate of all treatments in the field decreased at 12:00, that is, the phenomenon of "noon break" of crops, which is consistent with the conclusions of Sun et al. (2017), Wang et al. (2015), but the noon break time is earlier than other studies, the reason may be that the temperature in the experimental area is higher than that in other areas. Comparing the fitting models of photosynthetic response curves of different grapes, the fitting values of the right hyperbola model and the measured values have the greatest error, and the fitting values of the modified right hyperbola model are the closest to the measured values. The net photosynthetic rate decreased with the increase of illumination intensity when the illumination intensity ranged from 1500 to 2000 micromol m^{-2} s^{-1}, which showed the phenomenon of photoinhibition, which was consistent with the results of Bai et al. (2016b).

This study also found that micro-spraying could effectively reduce air temperature and increase humidity in vineyards. The results showed that suitable sprinkler irrigation (WP1, WP2, WP5 and WP7) could improve physiological indexes, photosynthetic characteristics, yield and quality of grapes. Excessive sprinkler irrigation (WP3, WP4 and WP6) could also easily lead to grape yield. Quantity and quality declined. Considering that WP2 treatment is the best treatment among many treatments, but this experiment can only qualitatively screen the best treatment. It is not known how long the spray time (or the amount of spray water) can correspondingly reduce the daily temperature and increase the humidity for grape trees to reach the maximum production capacity under the conditions of temperature and humidity. The numerical value is not clear, so the gradient of sprinkler duration can be set more intensively in future

http://www.aloki.hu ● ISSN 1589 1623 (Print) ● ISSN 1785 0037 (Online)
DOI: http://dx.doi.org/10.15666/aeer/1706_1419714215

experiments. The sprinkler duration is based on the reference crop evapotranspiration on the same day, and is compared with the difference of temperature and humidity in the control group. The yield and quality of each treatment are observed, and the sprinkler duration, temperature and humidity and yield products are discussed. The relationship between quality and yield is to find out the optimal micro-spraying time for maximum yield and quality of grapes.

Conclusions

Field test research during a growth cycle of grapes under different atomizing regulation treatments indicates that atomizing regulation technology leads to various influences on temperature, humidity, physiological ecology, photosynthetic characteristics, and product quality and quantity. The main conclusions are as follows:

(1) Atomizing regulation technology changes vineyard micro-climates. Research data show that atomizing regulation treatment can lower temperatures by an average of 1.6 °C during the entire grape expansion period, with a range in temperature drops of up to 5.6%. Average humidity can increase by 6.6%, with the increase range at up to 13.8%, of which WP2 treatment presents the widest range of change. This is very favorable for grape growth and development.

(2) Atomizing regulation technology changes the physiological ecology of grape plants. In terms of branch length, internode length, leaf number and leaf area under all atomization treatments, WP2 and WP7 treatments are most favorable; in terms of mid-rib length, WP3 and WP6 treatments are most favorable; and in terms of oven-dry weight, WP3 and WP5 treatments are most favorable. All indicators were better than those of CK treatment, demonstrating that regulation technology plays an active role in the physiological ecology of grape plants. In terms of the comprehensive indicator, WP2 treatment presents optimal results.

(3) Atomizing regulation technology slightly influences the photosynthetic characteristics of grapes. Through contrastive analysis of the photosynthetic rate monitoring data, transpiration rates and leaf air hole conductivities of grape plants under various treatments, and fitted calculation analysis of photosynthetic rates, CO_2 concentration response curves and light response curves with the “rectangular hyperbola model, non-rectangular hyperbola model, exponential function model and corrected rectangular hyperbola model”, it is found that atomizing regulation technology has less influence on the abovementioned items.

(4) Atomizing regulation technology influences grape quality and yield. According to contrastive analysis of grape indicators under various treatments, such as soluble solid content, soluble sugar content, Vc content and sugar acid, those under the atomization treatment are all higher than those under CK treatment. Grapes under WP2 treatment showed optimal quality, indicating that atomizing regulation technology effectively improves grape quality. The atomization treatment that produces the highest yield is WP2 treatment, with a yield of up to 3,432.7 kg/hm^2, 24.0% higher than that from CK treatment.

To summarize the abovementioned research conclusions, WP2 treatment is the optimal technical scheme for atomizing regulation treatment of grapes in extremely arid environments, namely, by erecting micro-spray equipment at 50 cm under the trellis, with a water spraying diameter of 200 cm and a spraying cycle of 1 h/day. In addition, WP2 treatment also shows significant benefits, including water resource conservation,

http://www.aloki.hu ● ISSN 1589 1623 (Print) ● ISSN 1785 0037 (Online)
DOI: http://dx.doi.org/10.15666/aeer/1706_1419714215

creation of a more suitable micro-climate for grape growth, improvements to grape quality and significant yield increase effects.

Acknowledgements. The work was jointly supported by grants from the National Natural Science Foundation of China (51569034, 41371051, 51421006, 41561134016), a key grant of Chinese Academy of Sciences KZZD-EW-12, and a grant from Ministry of Water Resources (201501032).

REFERENCES

[1] Bai, Y. G., Liu, H. B., Feng, J. (2016a): Research on the influence of micro-spray atomizing regulation irrigation technology on grape physiology and yield. – Chinese Agricultural Science Bulletin 32(19): 164-169.
[2] Bai, Y. G., Liu, H. B., Zhang, J. H., et al. (2016b): Comparison of light-response curve fitted models for grape. – Water Saving Irrigation 9: 8-11.
[3] Chen, Z. Y. (1996): Analysis of agricultural meteorological effect on mulberry field spray irrigation. – Journal of Zhejiang University Sciences Edition 1: 92-99.
[4] Hong, M., Zhao, J. H., Ma, Y. J., et al. (2016): Micro environmental regulation effect of red jujube trees' canopy in arid oasis region. – Agricultural Research in the Arid Areas 34(1): 16-22.
[5] Hui, Z. M., Fang, Y. L., Guo, Y. Z., et al. (2007): Influences of water stress on 4 major physiological indicators of grape seedling. – Agricultural Research in the Arid Areas 25(3): 146-149.
[6] Jackson, J. E. (1970): Aspects of light climate with apple orchards. – Applied Ecol 7: 207-216.
[7] Koblet, W. (1986): Influence of light and temperature on vine performance in cool climates and application to vineyard management. – In: Heatherbell, D. A., Lombard, P. B., Bodyfelt, F. W., Price, S. F. (eds.) Proc Int Symp on Cool Climate. Vitic Enol. Oregon State University, Oregon.
[8] Kohl, K. D., Kohl, R. A., Deboer, D. W. (1987): Measurement of low pressure sprinklers evaporation loss. – Transactions of the AsAE 30(4): 1071-1074.
[9] Liao, X. F., Liu, Q. M., Zhang, D. K., et al. (2012): Model fitting on light response curve of photosynthesis of wild Drepanostachyum luodianense. – Journal of Central South University of Forestry & Technology 32(3): 124-128.
[10] Liu, H. B., Bai, Y. G., Zhang, J. H., et al. (2019): Effect of water spray duration on SPAD and chlorophyll content of grape leaves. – Chinese Agricultural Science Bulletin 35(12): 107-111.
[11] Liu, H. J., Gong, S. H. (2000): Research on evaporation of water drop in spray irrigation. – Water Saving Irrigation 2: 1620.
[12] Liu, H. J., Kang, Y. H., Wang, Q. G. (2007): Effect of crop canopy on soil water redistribution under sprinkler irrigation: a review. – Agricultural Research in the Arid Areas 2: 137-142.
[13] Society, T. R. (1935): The kinetics of photosynthesis. – Proceedings of the Royal Society of London 149(868): 596-596.
[14] Srinivas, K., Shikhamany, S. D. (2000): Yield and water-use of 'Anab-e-Shahi' grape (Vitis vinifera) vines under drip and basin irrigation. – Indian Journal of Agricultural Science 69(1): 21-23.
[15] Sun, M. S., Li, H., Cheng, P., et al. (2017): Study well type irrigation under different diameter grade prostaglandgray jujube the difference of photosynthetic characteristics. – Journal of Central South University of Forestry & Technology 37(3): 32-38.
[16] Tang, Z., Lv, M., Zhang, X., et al. (2006): Influences of high-temperature stress on three physiological indicators of grape leaf. – Journal of Shihezi University 24(2): 198-200.

http://www.aloki.hu ● ISSN 1589 1623 (Print) ● ISSN 1785 0037 (Online)
DOI: http://dx.doi.org/10.15666/aeer/1706_1419714215

[17] Thornley, J. H. M. (1976): Mathematical Models in Plant Physiology. – Academic Press, London.
[18] Wang, Z. Z., Li, H., Miao, Q. Q., et al. (2015): Photosynthetic characteristics of Chinese jujube under different irrigation conditions in fruit setting period. – Journal of Central South University of Forestry & Technology 35(5): 59-63+69.
[19] Xie, Q., Shi, L., Du, F., et al. (2007): Influences of CO_2 and temperature on grape group photosynthesis. – Journal of Shanghai Jiaotong University 25(2): 110-114.
[20] Xie, Z. (1998): Land-atmosphere coupling mode considering vegetation influences. – Chinese Journal of Theoretical and Applied Mechanics 30(3): 267-276.
[21] Ye, Z. P. (2010): A review on modeling of responses of photosynthesis to light and CO_2. – Chinese Journal of Plant Ecology 34(6): 727-740.
[22] Zhang, J., Li, Y., Cai, X. (2000): Research on mature biomass of vinifera varieties with different mature periods in Yinchun Region, Ningxia. – Journal of Ningxia Agricultural College 21(1): 10-13.

http://www.aloki.hu ● ISSN 1589 1623 (Print) ● ISSN 1785 0037 (Online)
DOI: http://dx.doi.org/10.15666/aeer/1706_1419714215

PREPARATION AND PROPERTIES OF SOLAR COMPOSITE MATERIALS FOR MARINE ENVIRONMENT

XU, J.* – BU, J.

Zhejiang Industry Polytechnic College, Shaoxing 312000, China

**Corresponding author*
e-mail: xujiandeuw1231@163.com

(Received 1st Jun 2019; accepted 2nd Sep 2019)

Abstract. In order to strengthen the advantages of resin matrix composites such as light weight, high strength, fatigue resistance, corrosion resistance and electrical insulation, glass fiber shows great application potential in the field of Marine engineering. Composite profiles were prepared by pull-extrusion process, and the retention rate of mechanical properties was higher after 1000 h test in the neutral salt spray test chamber. The extruded composite profile was used as the frame of the solar module for the Marine environmental test. After a long time of marine environmental testing, the appearance of the component had no obvious defects. The strength retention rate of the composite profile was high, and the maximum power attenuation of the component was less than 5%. The results show that the composite profile can be used as a solar panel frame in marine environment.
Keywords: *vinyl ester resin, resin matrix composites, glass fiber, ocean, solar energy*

Introduction

With the development of science and technology, single material properties cannot meet the needs of production and social development. It has become a trend to combine things with different properties and exert the excellent comprehensive properties of materials by compound effect, and to make such materials become the mainstream of the material industry (Zhang et al., 2017). Composites have emerged at the right moment, and the most widely used composites are glass fiber reinforced resin matrix composites, namely glass fiber reinforced plastics (Huang et al., 2018). Glass fiber reinforced resin matrix composite has the advantages of light weight, high strength, fatigue resistance, corrosion resistance and electrical insulation, etc. Pultrusion preparation process is an important method for the preparation of high performance, high fiber content, fast and low-cost composite profiles (Chen et al., 2017). Marine environmental factors must be considered when pultrusion profiles are used in Marine engineering.

Composite material is a new type of structural material, because of its light weight, high strength, corrosion resistance and other characteristics, and has excellent performance in the long-term use in marine environment. Therefore, composite materials have greater application in ocean engineering, in the mid-1940s, the United States used composites in shipbuilding for the first time, composite materials in our country were first used of military purposes, and then gradually extended to the civilian life, although after rapid development, but the marine environment application still needs more development. Nowadays, the application of composite materials in the marine environment is mainly used in the construction of ships and the production of supporting products, including fishing boats, yachts and lifeboats. At the same time, glass fiber reinforced composite material is used as seawater pipeline, fire and waterproof pipeline in offshore oil and gas development.

The marine environment is complex, mainly including Marine hydrological environment, overhead meteorological conditions, geological environment and other

http://www.aloki.hu ● ISSN 1589 1623 (Print) ● ISSN 1785 0037 (Online)
DOI: http://dx.doi.org/10.15666/aeer/1706_1421714229

environmental factors, which have many influencing factors on the material. In order to apply composite materials more efficiently in the marine environment, research on the performance change of composite materials in the marine environment is a hot topic at present. The main factors of corrosion of materials in marine environment include salt content, temperature, sunshine and pH value. The study of the weather resistance of composite materials mainly refers to the assessment and evaluation of the weather resistance of composite materials by placing them in the outdoor natural environment and making them subject to the comprehensive effect of various factors.

Solar composite material is a new kind of material which is made by using advanced material preparation technology to optimize the composition of materials with different properties. Due to its many advantages, the application of solar composite materials in the Marine environment is increasingly valued. The Marine environment is extremely complex, and multi-traditional metal materials such as air humidity, high salinity and corrosive substances adhesion are a great challenge. Therefore, solar composite materials are of great significance in the application field of Marine engineering. Solar composites in the field of ocean engineering application is of great significance. However, due to the limitations of science and technology and materials, more research efforts are needed. Nachtane et al. (2018) explored and analyzed the properties of glass fiber reinforced composites applied to steel structures. Sutherland et al. (2018) summarized the application of composite riser pipe, coil-able composite pipe, composite mooring cable, underwater weapon shell, propeller and other components, and looked forward to the main technical development direction of composite materials for offshore drilling platforms in the future. Javier et al. (2017) summarized the research progress on accelerated aging of yacht fiber reinforced composites in Marine environment, and analyzed the influence of solar ultraviolet light, thermal oxygen, salt spray, seawater and other factors on their corrosion aging mechanism, material properties and variation rules.

In this paper, based on the research and experiment on the profile of solar composite material, a new material was developed for better marine operation and to provide technical support for the construction of marine engineering.

Experimental materials and methods

Experimental materials and equipment

The grades, models and manufacturers of raw materials required in the experiment are shown in *Table 1*, and the experimental equipment is shown in *Table 2*.

Sample preparation

A certain amount of vinyl vinegar resin liquid (0.5g) should be weighed into a mixing vessel, then according to the proportion of the corresponding mass (according to 1:100 mass ratio) of the additive should be added to the resin, which should be stirred to mix well with a glass rod.Then it should be let stand for deaeration, then mixing liquid should be added into the mould, after curing under 100 °C and a half hours, the samples are bagged for use. Fiberglass reinforced vinyl cool resin composite was prepared by pull-extrusion process. The resin, initiator and flame retardant were mixed according to the weight ratio of 100:1.3 ~1.5:15. The mixture was evenly stirred and injected into the soaking tank. Considering that the composite material surface needs to be protected in practical application, after processing the sample, the surface part of the sample was

http://www.aloki.hu ● ISSN 1589 1623 (Print) ● ISSN 1785 0037 (Online)
DOI: http://dx.doi.org/10.15666/aeer/1706_1421714229

sprayed with fluoropolymer vinegar semi-gloss enamel, which can prevent the corrosion of mold, salt fog and moisture, and there are different colors to choose from.

Table 1. *Experimental materials and manufacturers*

The raw material	Class/model	The manufacturer
Vinyl ester resin	Atlac430	Jinling DSM Resin Co. Ltd
The glass fiber	4800Tex	Shandong Taishan Glass Fiber Co. Ltd
Tert-butyl benzoate peroxide (TBPB)	Industrial-grade	Nobel Peroxide (Tianjin) Co. Ltd
Bis (4-tert-butyl cyclohexyl) carbon peroxide	Industrial-grade	Taiyuan Chemical Co., Ltd. Fine branch factory
Antimony trioxide	Senior pure	Shanghai Aifeng Antimony Trade Co., Ltd
Decabromodiphenyl ether	Senior pure	Shanghai Aifeng Antimony Trade Co., Ltd
Fluorine polyurethane semi-gloss enamel	TS96-61	Tianjin Lighthouse Coating Co. Ltd
Anhydrous ethanol	Analysis of pure	Harbin Yongchang Chemical Company
Sulfuric acid	Analysis of pure	Harbin Yongchang Chemical Company
Hydrochloric acid	Analysis of pure	A chemical distribution station in Harbin
Sodium hydroxide	Analysis of pure	A chemical distribution station in Harbin
Sodium chloride	Analysis of pure	Harbin Yongchang Chemical Company
Acetone	Analysis of pure	A chemical distribution station in Harbin
Acid ester (P16)	Industrial-grade	Taiyuan Chemical Co., Ltd. Fine branch factory

Table 2. *Experimental equipment*

Device name	Model	Origin
Composite pultrusion production line	LJ-1020	Harbin Institute of FRP
Electric blast drying oven	101-2A	Tianjin Taist Industrial Co. Ltd
Infrared spectrometer	Spectrum 100	Perkin Elmer Co., Ltd
Differential scanning calorimeter	Pyris6	Perkin Elmer Co., Ltd
Thermogravimetric analyzer	TGA Q50*	TA Instruments
ZEISS optical microscope	200MAT	Carl Zeiss GmbH
Universal material testing machine	CMT5504	Meister Industrial Systems Co. Ltd
Electronic balance	FA2004A	Shanghai Jingtian Electronic Instrument Co., Ltd
Bar-hardness tester	HBa-1	Wuxi Institute Of Metrology
Salt spray corrosion test chamber	LY W-015	Shanghai Blue Leopard Test Equipment Co., Ltd
Lamp aging test chamber	-	Homemade
Thermostatic water bath	DK-600	Shanghai Jinghong Test Equipment Co., Ltd

Vinyl composite profiles pultrusion speed is 0.1 m/min commonly, it is 0.2 m/min, pultrusion speed when the production efficiency is higher, but too fast pultrusion speed is easy to make the product out of the mold has not fully solidified,in order to guarantee the quality of the products, this study used the pultrusion speed of 0.1 m/min, the traction of 50 kn, and three temperature ranges: 100 ~ 110 °C, 120 ~ 130 °C, 130 ~ 140 °C. In the actual production process, only by adjusting the temperature of the three zones according to the technological conditions a composite with excellent extruded profile properties can be prepared. The pultrusion profile was prepared and then the material was cut into the required size according to the size of the solar module.

http://www.aloki.hu ● ISSN 1589 1623 (Print) ● ISSN 1785 0037 (Online)
DOI: http://dx.doi.org/10.15666/aeer/1706_1421714229

Mechanical performance test

Tensile performance test was performed according to GB/T 3354-1999 “test method for tensile properties of oriented fiber reinforced plastics”. GFRP (Glass Fiber Reinforced Polymer) profile tensile performance test sample size was 230 mm × 15 mm × 2mm, the test was carried out on universal testing machine (Zhao et al., 2018). As the material is easy to be destroyed in the clamping position during the tensile process, aluminum alloy reinforcing sheets should be pasted at both ends of the tensile sample, with the thickness of the reinforcing sheets being 1.5 mm. The adhesive agent used to bond the reinforcing sheets is a mixture of 618 resin and polyphthalein, so as to ensure that the reinforcing sheets do not fall off during the test (Jiao et al., 2018). Tensile properties were tested at room temperature with a loading speed of 2 mm/min (*Fig. 1*).

Figure 1. *Tensile test*

The bending performance test was carried out on the same universal test machine. The bending sample size was 100 mm × 15 mm × 4 mm, and the three-point bending mode is adopted for testing. The loading head radius was R = 5 mm 0.2 mrn, the bearing fillet radius was R = 2 mm 0.2 mrn, and the loading speed was 2 mm/min. The experimental results show that its tensile and bending properties are good and not easily damaged (*Fig. 2*).

Figure 2. *Bending test*

http://www.aloki.hu ● ISSN 1589 1623 (Print) ● ISSN 1785 0037 (Online)
DOI: http://dx.doi.org/10.15666/aeer/1706_1421714229

Corrosion resistance test

According to the provisions of GB/T 10125-2012 "salt fog test for corrosion test of artificial atmosphere", the test of GFRP profile's resistance to neutral salt fog corrosion was conducted in the neutral salt fog test box. See *Figure 3* for the test box. In the neutral salt spray test, the FRP composites were divided into two groups. One group was sprayed with fluorine polyurethane semi-gloss enamel, while the other group was not treated. The two groups were processed according to the tensile sample size and the bending sample size, and tested in the neutral salt spray test chamber (Vimalathithan et al., 2018). Neutral salt spray test for 1000 h was divided into 7 sections in time regarding sampling observations, sampling time were 24 h, 48 h, 72 h, 168 h, 336 h, 672 h, and 1000 h from the test start time, take 3 samples for performance test at each age, including appearance evaluation, the weight test, the tensile strength test, the bending strength test and calculate its strength retention (Lopresto et al., 2018).

Figure 3. *Neutral salt spray test box*

After the test, to reduce the sample on the adhesive and to reduce corrosion,dry the sample in the room for 0.5 h ~ 1 h before cleaning, and then surface should be gently cleaned with flowing water with a temperature below 40 °C, to remove salt on the surface of the sample, then with an air pressure from the sample of about 300 mm less than 200 kpa samples should be blow dried immediately (Alia et al., 2018). The experimental results show that this kind of material has strong corrosion resistance and meets the selection conditions of marine engineering equipment materials.

Marine environmental test of composite profiles

The composite extruded profile was installed on the YGE 145 series solar photovoltaic panels as the frame and applied in the marine environment. The test was conducted at the sanya marine environment test station in China (Barkanov et al., 2017; Tucci et al., 2018). The size of the solar panel is 1470 mm × 680 mm × 25 mm, and the composite frame is prepared according to the size of the solar panel (Barkanov et al., 2018). The test was carried out in three areas: (1) splash platform test area, which can simulate the waves on the deck; (2) offshore platform test area, which can simulate the navigation environment of ships; (3) the atmospheric insolation test area, which is an offshore and coastal area, simulates the ship docking environment. 10 composite frame components and 10 aluminum alloy frame components were installed in each test area.

http://www.aloki.hu ● ISSN 1589 1623 (Print) ● ISSN 1785 0037 (Online)
DOI: http://dx.doi.org/10.15666/aeer/1706_1421714229

During the test, the test environment conditions and the working status of solar photovoltaic modules were monitored in real time. Marine environment test period of 9 months, sampling at different time points, test after test the working characteristic of solar photovoltaic components and mechanical properties of the composite frame, through three areas of the test after the marine environment, the photovoltaic components and the borders of corrosion resistance, prevent ageing, impact resistance, wind resistance, waterproof performance can be evaluated (Barkanov et al., 2018).

Experimental results and analysis

Analysis of mechanical properties

In this paper, the mechanical properties of composite profiles prepared by pultrusion process were tested in accordance with relevant standards. The basic properties of composite profiles are listed in *Table 3*.

Table 3. *Mechanical properties of composite profiles*

The serial number	A pilot project	Test results	Execution standard	Sample size mm
1	The tensile strength MPa	786	GB/T3354-2014	230 × 15 × 2.3
2	The tensile modulus GPa	53.6		
3	The compression strength MPa	312	GB/T 1448-2005	12 × 10 × 4
4	The compression modulus GPa	11.6		
5	The bending strength MPa	1.01×10^3	GB/T3356-2014	100 ×15 × 2.3
6	Bending modulus GPa	40.2		
7	Impact toughness KJ/m2	442	GB/T 1451-2005	120 × 10 × 4
8	The density of kg/m3	2.03×10^3	GB/T 1463-2005	50 × 10 × 2.3

Corrosion resistance analysis

Figure 4 is the change curve of weight gain rate of composite profile after salt spray test. It can be seen from the figure that the quality of the two samples increased gradually from the beginning to 336 h. From 336 h to 1000 h, the weight gain rate of the samples gradually decreased, which was slower than the earlier trend. Because with the extension of the salt spray corrosion time, the absorption of water molecules in the samples was gradually saturated, and the weight gain rate of the two samples was between 0.12% and 0.14%. The reasons for weight gain of composite materials during salt spray test are as follows. First, water molecules in salt spray environment penetrate into the sample through the surface or resin and fiber sections; Another reason is that salt mist is attached to the sample (Baran, 2017).

The maximum stress that the material bears before tensile fracture is the tensile strength of the material， salt fog corrosion test before and after the change of the tensile strength of the sample values to represent composite material corrosion resistance calculation of salt spray test after tensile strength retention rate, neutral salt spray test after surface spraying fluorine polyamine vinegar semifinished enamel the tensile properties of the composite material test results are shown in *Table 4*.

http://www.aloki.hu ● ISSN 1589 1623 (Print) ● ISSN 1785 0037 (Online)
DOI: http://dx.doi.org/10.15666/aeer/1706_1421714229

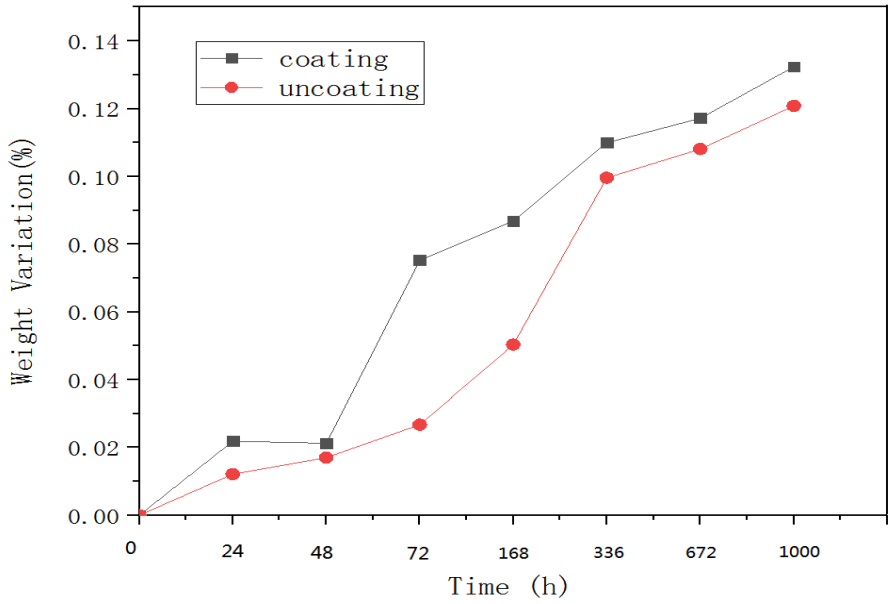

Figure 4. *Quality change of composite profile after salt spray test*

Table 4. *Tensile properties of fluorinated polyurethane semi-gloss enamel composite profiles after salt spray test*

Salt spray test time (h)	The tensile strength (MPa)	Modulus of elasticity (GPa)	Strength retention (%)
0	788.14	53.37	100
168	659.73	49.19	83.71
336	678.75	47.08	86.12
672	711.805	45.31	90.31
1000	678.76	49.18	86.12

Table 5 shows the 1000 h salt spray test for surface treatment of the tensile properties of the composite material. The bending performance shows high bending strength retention at each point in time, basically no bending strength loss, after 1000 h neutral salt fog corrosion specimens, the tensile strength of the composite material and bending strength retention rate was higher, which indicated that the composite material in a neutral salt fog corrosion environment can be used for a long time and able to maintain good tensile and bending properties (Safonov et al., 2017).

Table 5. *Bending properties of untreated composite profiles after salt spray test*

Salt spray test time (h)	The tensile strength (MPa)	Modulus of elasticity (GPa)	Strength retention (%)
0	1378.68	45.03	100
168	1321.12	40.70	95.82
336	1309.05	41.77	94.94
672	1316.18	45.69	95.46
1000	1327.20	41.79	96.26

http://www.aloki.hu ● ISSN 1589 1623 (Print) ● ISSN 1785 0037 (Online)
DOI: http://dx.doi.org/10.15666/aeer/1706_1421714229

Analysis of the influence of marine environment on mechanical properties and photovoltaic characteristics

Will the solar energy components used in ocean environment, respectively in atmospheric exposure test, offshore platform test area and splash experimental zone (*Fig. 5*) experiment platform, and set the aluminum alloy frame component as the control group, the Marine environment test for 9 months, study the mechanical properties of composite frame and through the comparison and analysis of composite frame with aluminium alloy frame's influence on the photovoltaic cell characteristics.

Table 6 shows the results of marine environment test of composite bending performance of solar module frame, after a period of time of test in three experimental areas in Sanya, the bending strength of the composite was increased, the strength retention rate increased, within the scope of the marine environment test time, as the sea trial was the longer the higher bending strength test values were observed (Chadel et al., 2017). This is because in the process of sea trials, composite material solar energy components border were mainly affected by sunlight and salt fog environment, ultraviolet ray is contained in sunlight, Ultraviolet irradiation can cause post-curing of composite material frame and also cause aging damage to the material. According to the test results, during the Marine environment test, the post-curing rate of composite material is higher than the rate of destruction by ultraviolet light, which is manifested as the increase of bending strength.

Table 6. *Component frame bending performance after marine environmental test*

Test area	Trial period of age	The bending strength (MPa)	Strength retention (%)
Splash platform test area	The initial value	1013	100
	Three months	1076	106
	Five months	1200.6	118
Offshore platform test area	The initial value	1013	100
	Six months	1092.4	108
	Nine months	1396.25	137
Atmospheric exposure test area	The initial value	1013	100
	Six months	1074.2	106
	Nine months	1329.8	131

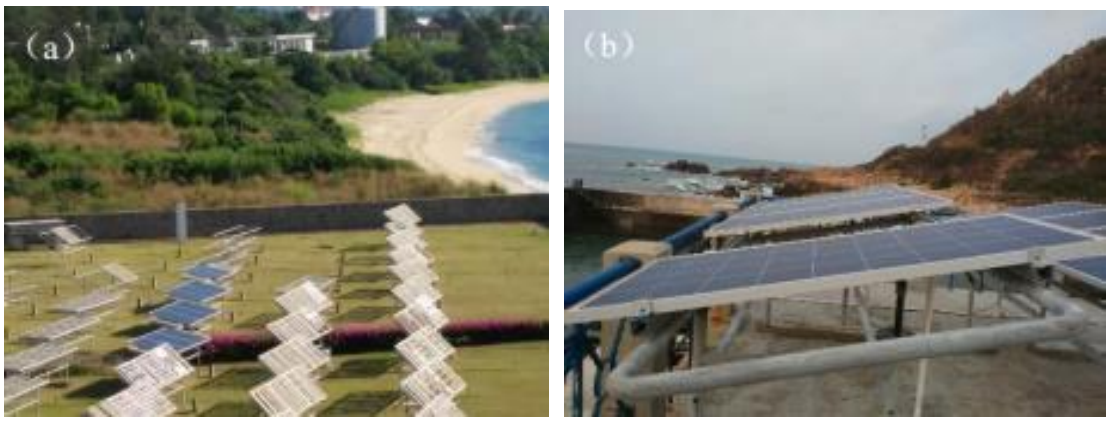

http://www.aloki.hu ● ISSN 1589 1623 (Print) ● ISSN 1785 0037 (Online)
DOI: http://dx.doi.org/10.15666/aeer/1706_1421714229

Figure 5. *Marine environment test platform. (a) Atmospheric exposure test area; (b) offshore platform pilot zones; (c) splash platform test area*

Table 7 shows the tensile properties of composite solar panel frame after the Marine environmental test. According to the experimental results, it can be found that the tensile strength of composite frame varies in different regions.

Table 7. *Tensile properties of component frame after marine environmental test*

Test area	Trial period of age	The tensile strength (MPa)	Strength retention (%)
Splash platform test area	The initial value	690	100
	Three months	673	97.5
	Five months	661	95.8
Offshore platform test area	The initial value	690	100
	Six months	668	96.8
	Nine months	756	109.6
Atmospheric exposure test area	The initial value	690	100
	Six months	716	103.8
	Nine months	716	103.8

Figure 6 for the test during the day some inverter record the change of the components of the power curve, the component rises as the sun began to work, power increased, reached the highest at noon as time extended again after power down, repeat this process every day, and a set of components (20) in the case of the weather is sunny every day capacity up to 18.5 kW/h.

Table 8 shows the component power parameters of solar photovoltaic modules nine months after the marine environment test. In accordance with the relevant standard requirement after Marine environmental testing performance of solar module test, the attenuation of maximum power does not exceed 5% of the experimental measurements before and after the test component of power attenuation is still less than 5%, the component can work normally and no obvious flaw appearance, shows that composite material can be used as a solar module frame used in the marine environment.

http://www.aloki.hu ● ISSN 1589 1623 (Print) ● ISSN 1785 0037 (Online)
DOI: http://dx.doi.org/10.15666/aeer/1706_1421714229

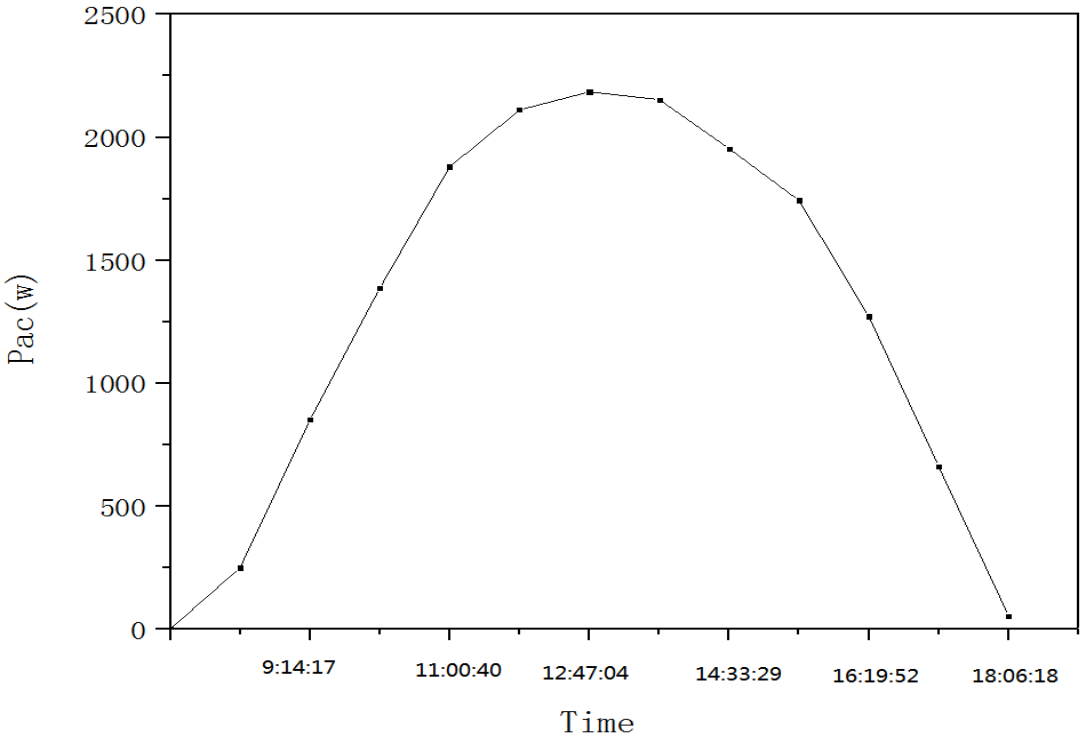

Figure 6. *Power curve of marine environmental test in one day*

Table 8. *Component power parameters nine months after the marine environmental test*

Test area	Component classification	Maximum power before test (w)	Maximum power after test (w)	The power attenuation (%)
Offshore platform	Composite frame	148.529	142.892	4.02
Test area	Aluminium alloy frame	147.551	141.352	4.34
Atmospheric exposure	Composite frame	147.840	141.615	4.25
Test area	Aluminium alloy frame	148.276	141.966	4.08

Discussion

From tensile results, after salt spray test, the tensile strength of the composites decreased, but with the extension of time, the salt fog corrosion did not cause faster strength degradation rate, but in a certain range fluctuations occurred. The reason is that early test of composite profiles in the salt fog environment water absorption, moisture absorption quantity are the important factors influencing the mechanical properties of composite materials, composite materials absorb moisture makes fiber easy to fall off from the substrate, causing internal clearance, and clearance have accelerated the absorption of moisture causing the loss of the performance of composite materials (Safonov et al., 2017). With the extension of time, the moisture absorption quantity saturated. The mechanical properties of the composite material decreased slowly. After 1000 h of neutral salt spray corrosion, the tensile strength retention rate of the composite profile is 86.12%, with a high tensile strength retention rate (Afanasyev et al., 2018).

http://www.aloki.hu ● ISSN 1589 1623 (Print) ● ISSN 1785 0037 (Online)
DOI: http://dx.doi.org/10.15666/aeer/1706_1421714229

The tensile strength of the composite solar panel frame in the splash platform test area decreased slightly after a period of ocean test, but the degree of reduction was not obvious. The tensile strength of the composite solar panel frame in the offshore platform test area decreased at the initial stage, but increased with the extension of the test time. The tensile strength of the frame of the composite solar module in the atmospheric exposure test area increased with the extension of the test time. Similarly, the ultraviolet radiation from the sun may lead to post-curing of the composite frame during the test. When the curing degree is greater than the corrosion degree, the tensile strength of the material increases, which is roughly the same as the change trend of bending strength.

When solar photovoltaic module is used in marine environment, it is easy to accumulate more salinity on the surface of the module because of the large amount of salt fog in the marine environment. When the accumulated particulate matter is mixed with rainwater, sea water or other liquid substances, and then irradiated by sunlight for a long time, it will form a strong spot which is not easy to fall off. If this spot just blocked a series branch of the module, the blocked part could not perform photovoltaic effect and became a load consuming current, forming a “hot spot”. When the temperature of this part rises to a certain extent, it may cause damage to the whole battery assembly. The existence of hot spot will cause the attenuation of the maximum power of the module, and the smaller the size of the hot spot is, the more severe the hot spot effect will be, the more the number of hot spot, the more attenuation of the module will occur. After the marine environment test, the maximum power of the solar module has been attenuated. After nine months test, the maximum power attenuation of the solar module is less than 5%. The module can work normally, which shows that the module with composite frame can be used in the marine environment.

Conclusion

In the research of marine composite materials, it is necessary to pay attention to the coordinated development with marine ecosystem and avoid environmental pollution. On this basis, professional research structures should be established for the research of various materials to provide strong financial and technical support for the innovation of materials. The test results of the mechanical properties of the composite profiles show that the composite insulation has the advantages of light weight and high strength. The corrosion resistance of the composite material was evaluated through the neutral salt spray corrosion test. It can be seen that with the extension of the test time, the quality of the sample increased due to the hygroscopicity of the sample, and its tensile strength and bending strength retention rate were higher, indicating that the composite material had better performance in the salt spray environment. After the marine environment test, the bending and tensile properties of the composite frame were tested. The test results showed that the bending strength of the composite profile increased with the extension of the test time, and the retention rate of its tensile strength was higher, indicating that the composite was suitable for the marine environment. After the Marine environment test, the electrical performance of the solar module was tested. The test results showed that the maximum power of the solar module decreased after the Marine environment test,nine months after the test, the maximum power attenuation is less than 5%, the component can work normally, equipped with composite frame component it can be used in the marine environment.

http://www.aloki.hu ● ISSN 1589 1623 (Print) ● ISSN 1785 0037 (Online)
DOI: http://dx.doi.org/10.15666/aeer/1706_1421714229

REFERENCES

[1] Afanasyev, D. A., Mirzoev, K. Y., Ibrayev, N. K. (2018): Influence of defects of nanostructured zno films on the photovoltaic characteristics of perovskite solar cells. – IOP Conference Series: Materials Science and Engineering, Volume 289, Conference 1.

[2] Alia, C., Jofre-Reche, J. A., Suárez, J. C., Arenas, J. M., Martín-Martínez, J. M. (2018): Characterization of the chemical structure of vinyl ester resin in a climate chamber under different conditions of degradation. – Polymer Degradation & Stability 153: 88-99.

[3] Baran, I. (2017): Analysis of pultrusion process for thick glass/polyester composites: transverse shear stress formations. – Advanced Manufacturing: Polymer & Composites Science. https://doi.org/10.1080/20550340.2016.1269037.

[4] Barkanov, E., Akishin, P., Miazza, N. L., Galvez, S. (2017): Ansys-based algorithms for a simulation of pultrusion processes. – Mechanics of Composite Materials & Structures 24(5): 377-384.

[5] Barkanov, E., Akishin, P., Miazza, N. L., Galvez, S., Pantelelis, N. (2018): Experimental validation of thermo-chemical algorithm for a simulation of pultrusion processes. – Journal of Physics: Conference Series, Volume 991, Conference 1.

[6] Chadel, M., Bouzaki, M. M., Chadel, A., Petit, P., Sawicki, J. P., Aillerie, M., et al. (2017): Influence of the spectral distribution of light on the characteristics of photovoltaic panel. Comparison between simulation and experimental. – AIP Conference Proceedings 1814. https://doi.org/10.1063/1.4976273.

[7] Chen, Y., Yapei, Z. U., Gong, J., Sun, C., Wang, C. (2017): Effect of al film on the electromagnetic properties of glass fiber reinforced resin matrix composite. – Acta Metallurgica Sinica. DOI: 10.11900/0412.1961.2017.00178

[8] He, Y., Xiao, L., Li, L. (2017): Research on the influence of pv cell to thermal characteristics of photovoltaic/thermal solar system. – International Journal of Energy Research 41. DOI: 10.1002/er.3711.

[9] Huang, Q., Qin, W., Garoushi, S., He, J., Lin, Z., Liu, F., et al. (2018): Physicochemical properties of discontinuous s2-glass fiber reinforced resin composite. – Dental Materials Journal 37(1): 95-103.

[10] Javier, C., Leblanc, J., Shukla, A. (2017): Shock Response of Composite Materials Subjected to Aggressive Marine Environments. – In: Sutton, M., Reu, P. L. (eds.) International Digital Imaging Correlation Society. Proceedings of the First Annual Conference, 2016. Springer International, pp 169-171.

[11] Jiao, W., Cai, Y., Liu, W., Fan, Y., Long, J., Jiao, W., et al. (2018): Preparation of carbon fiber unsaturated sizing agent for enhancing interfacial strength of carbon fiber/vinyl ester resin composite. – Applied Surface Science 439: S0169433217338746.

[12] Lopresto, V., Papa, I., Langella, A. (2018): Basalt fibres in vinyl ester resin laminates under low velocity impact conditions. – Journal of Dynamic Behavior of Materials 4(3): 328-335.

[13] Nachtane, M., Tarfaoui, M., Saifaoui, D., Moumen, A. E., Hassoon, O. H., Benyahia, H. (2018): Evaluation of durability of composite materials applied to renewable marine energy: case of ducted tidal turbine. – Energy Reports 4: 31-40.

[14] Safonov, A. A., Carlone, P., Akhatov, I. (2017): Mathematical simulation of pultrusion processes: a review. – Composite Structures 184: S0263822317324212.

[15] Sutherland, L. S. (2018): A review of impact testing on marine composite materials, part iii: damage tolerance and durability. – Composite Structures 185: 512-518.

[16] Tucci, F., Rubino, F., Carlone, P. (2018): Strain and temperature measurement in pultrusion processes by fiber Bragg grating sensors. – AIP Conference Proceedings 1960, https://doi.org/10.1063/1.5034837.

[17] Vimalathithan, P. K., Barile, C., Vijayakumar, C. T. (2018): Investigation of kinetic triplets for thermal degradation of thermally cured vinyl ester resin systems and lifetime predictions. – Journal of Thermal Analysis & Calorimetry 133(3): 1-11.

http://www.aloki.hu ● ISSN 1589 1623 (Print) ● ISSN 1785 0037 (Online)
DOI: http://dx.doi.org/10.15666/aeer/1706_1421714229

[18] Zhang, D., Sun, Y., Wang, Y. (2017): Failure behavior and damage mechanism of multiaxial glass fiber reinforced resin matrix composites. – Acta Materiae Compositae Sinica. DOI: 10.13801/j.cnki.fhclxb.20160606.004.
[19] Zhao, D., Tian, F., Yalin, Y. U., Zhang, B., Meng, B., Feng, Q., et al. (2018): Preparation and performance of lithium ionic liquid/epoxy vinyl ester resin solid electrolyte. – Acta Materiae Compositae Sinica 35(2): 253-259.

http://www.aloki.hu ● ISSN 1589 1623 (Print) ● ISSN 1785 0037 (Online)
DOI: http://dx.doi.org/10.15666/aeer/1706_1421714229

PREDICTION OF MAXIMUM OZONE CONCENTRATION USING BIG DATA MODELS

KAID, Z. – ATTOUCH, M. – MASTEFAOUI, Z. – LAKSACI, A.*

Department of Mathematics, College of Science, King Khalid University
61413 Abha, Kingdom of Saudi Arabia

**Corresponding author*
e-mail: alikfa@kku.edu.sa

(Received 1st Jun 2019; accepted 10th Sep 2019)

Abstract. The air pollution problem which has arisen in developed countries, becoming evident by high levels of smoke from industries or traffic, has forced authorities to search for mechanisms to control the air quality by the real-time monitoring system. For this purpose, in this paper we develop a new procedure able to analyze this real-time data. More precisely, we use the recent development on mathematical Statistics to analyze the relationship between the maximum ozone concentration and the other palling gases such as the Nitric Oxides (NO), Nitrogen Dioxide (NO_2) and Sulphur Dioxide (SO_2). Specifically, we propose three models which are, Functional Nonparametric Regression, Functional Robust Regression and Functional Relative Error Regression. Considering the daily- curve of the concentration of the previous gases collected by the Marylebone road monitoring site in London, we provide statistical models allowing the prediction of the maximum ozone concentration 4 h ahead. We show that the accuracy of our prediction approaches is closely linked to the choice of the regression model and the input variables or the covariates. In particular, the nonparametric regression is more performant than the other models when the regressors are NO_2 and SO_2.
Keywords: *ozone forecasting, air quality data, functional regression, the nitric oxide, nitrogen dioxide, sulphur dioxide, nonparametric statistics, time series analysis, neural network model, Bayesian network models, principal component regression*

Introduction

Analyzing the levels of air pollution is nowadays of primary importance. Indeed the air quality has a great impact on human health as well as natural resources. In the last decades, air pollution is among the leading causes of death. Thus, pollution forecasting allows decision-makers to plan the prevention strategy. For this issue, several mathematical models are used to provide some software to control air quality (see, e.g., Ryan et al., 1995; Slini et al., 2002; Nghiem et al., 2009). Specifically, there exist two kinds of approaches: deterministic and statistical algorithms. The literature on the deterministic models treat the pollutant-formation processes by studying their chemical and physical properties (see Zhang et al., 2012). While the statistical models are based on the historical measurements of air pollution and/or meteorological data. In this context, most statistical models are constructed by using the classical regression method. We cite for instance the neural network models by Yi and Prybutok (1996), Bayesian network models by Gavrila (2013, 2016). We refer the readers to Gong and Ordieres-Meré (2016), Taylan (2017) and Ding et al. (2016) for some recent contributions on the prediction of ozone concentrations by the empirical methods. All the statistical models of these cited works are performed over the observed data in some discrete grid which allows at most making the daily prediction. However, because of the ozone concentration has a faster dynamics the daily prediction is not very important. Furthermore, the recent technological development of the measuring instruments and

http://www.aloki.hu ● ISSN 1589 1623 (Print) ● ISSN 1785 0037 (Online)
DOI: http://dx.doi.org/10.15666/aeer/1706_1423114239

the informatics tools allow the recovery of increasingly bulky data being recorded densely over a thinner discretization grid what make them intrinsically a continuous curve. The manipulation of this kind of data permits the real-time forecasting of the ozone concentration. This is the main purpose of this paper. To do that, we use some new statistical models recently developed of big data analysis. The main advantage of these new models, so-called functional models, is the fact that they take into account the daily- curves in its continuous path, unlike the old models which take only the values of some few hours. Of course, with the functional models, we keep all the information in the sampled data and we predict different horizons. It should be noted that the functional statistics has encountered a strong infatuation in these last years, as evidenced the several special issues dedicated to this topic (see, e.g., Aneiros et al., 2019; Ferraty, 2010). For more discussion on this topic, we refer the reader to Hsing and Eubank (2015), Ling and Vieu (2018) and the references therein.

The present contribution deals with the assessment of functional statistics models for modelling ozone concentrations. More precisely, our main goal is to search accurate prediction methods of the ozone concentration with respect to the other polluting gases. We use for this study a sample of data recorded in the Marylebone road monitoring site in London. It contains the hourly measurements during the 2018-year for the following four variables: Nitric Oxide, Nitrogen Dioxide, Sulphur Dioxide and Ozone. This data is used to predict the maximum ozone concentration 4 h ahead. Let us point out that the considered models come from the recent development of the modern statistics that allow analyzing the big data without reduction of the dimension. These new approaches constitute alternative statistical models to the artificial neural network regression and the principal component regression which are usually employed in this prediction setting. The main feature of our functional models is the possibility to model the environmental date recorded by real-time monitoring. More precisely, we test three regression models that are Functional Nonparametric Regression (FNR), Functional Robust Regression (FRR) and the Functional Relative Regression (FRER) to forecast the maximum ozone concentration given four functional covariates such that the daily curves (one day before) of NO, NO_2, SO_2 and O_3. These models provide predictions, robust, fast and of higher accuracy.

The paper is organized as follows. In the next section, we introduce the functional methodology in the continuous-time prediction problem. The statistical models used are described in the section intituled "Some recent regression models". The predictions results of the three proposed methods are gathered in result's section. The last section is devoted to some conclusions.

Materials and methods

As mentioned in the previous section, the data of this contribution are acquired from real-time measurement by Marylebone road monitoring site. Marylebone Road is an important thoroughfare in central London, within the City of Westminster. It runs north-east to the south-west from the Euston Road at Regent's park to the A40 Westway at Paddington. This road is frequently heavily congested. It carries about 90,000 vehicles a day. The Marylebone Road monitoring site is funded by the Department for Environment, Food and Rural Affairs (Defra) in June 1997. The monitoring cabin is located one meter from the kerb on the southern side of the road. Its geographical

http://www.aloki.hu ● ISSN 1589 1623 (Print) ● ISSN 1785 0037 (Online)
DOI: http://dx.doi.org/10.15666/aeer/1706_1423114239

location are 51.522530 (latitude), -0.154611 (longitude). *Figure 1* shows the location of the site.

Figure 1. *The location of the Marylebone Road*

The data used in this paper are provided by the website https://www.airqualityengland.co.uk/site/data?site_id = MY1. It contains the hourly measurements during the period from January 1st to the 31st December for the year 2018, for the variables NO, NO_2, SO_2 and O_3 (*Fig. 2*).

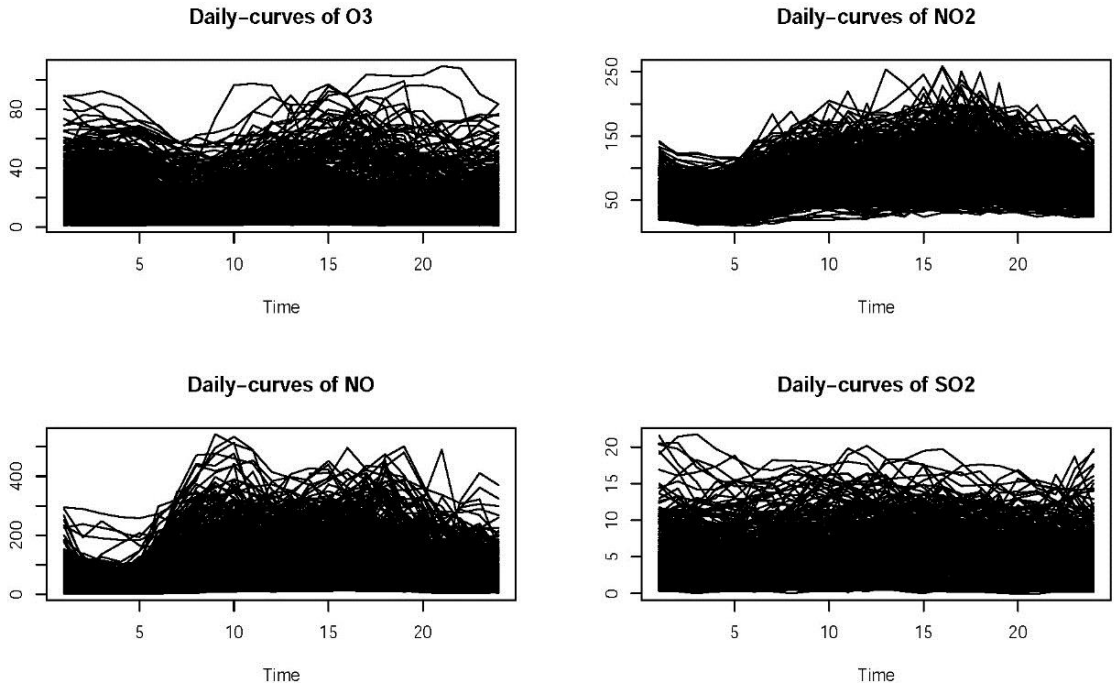

Figure 2. *The curves of the daily emission of the four gases NO, NO_2, SO_2 and O_3 in $\mu g/m^3$*

To fix the ideas, let us present the mathematical formulation of our prediction problem. Indeed, assume that we aim to predict the k-h-ahead prediction of the maximum ozone concentration at hour h_0, denoted by Y, using the curve of the daily emission of the gases observed the day before until $h_0 - k$. Formally, we assume that the output variable Y and the input variables $Z = (X_{NO}, X_{NO_2}, X_{SO_2}, X_{O_3})$ are linked by the following regression formula:

http://www.aloki.hu ● ISSN 1589 1623 (Print) ● ISSN 1785 0037 (Online)
DOI: http://dx.doi.org/10.15666/aeer/1706_1423114239

$$Y = r(Z) + error. \quad \text{(Eq.1)}$$

So, the prediction of Y is based on the determination of the function $r(.)$ in *Equation 1*. Many models are recently developed in mathematical statistics to resolve this kind of big data problem where the data are continuous curves. In this paper, we employ three regression procedures which are described in detail in the next section.

Some recent regression models

Functional nonparametric regression (FNR)

The nonparametric estimation of the functional regression was initially studied by Ferraty and Vieu (2006) and Ferraty et al. (2010). They used the Nadaraya Watson method to estimate this statistical model. Precisely, the function $r(.)$ is explicitly expressed using the least square error criterion by

$$r(x) = argmin_f E[(Y - f)^2 | Z = z]. \quad \text{(Eq.2)}$$

It follows that $r(x) = E[Y|X = z]$.

So, for all fixed curves $x_{NO}, x_{NO_2}, x_{SO_2}, x_{O_3}$ we predict the maximum ozone concentration with respect to the criterion (*Eq. 2*) by

$$\hat{Y} = \hat{r}(z), \text{ where } z = (x_{NO}, x_{NO_2}, x_{SO_2}, x_{O_3})$$

where $\hat{r}(z)$ is the kernel estimator of $r(z)$ defined by

$$\hat{r}(x_{NO}, x_{NO_2}, x_{SO_2}, x_{O_3}) = \frac{\sum_{i=1}^{n} Y_i K\left(\frac{\|x_{NO} - x_{NOi}\| + \|x_{NO_2} - x_{NO2i}\| + \|x_{SO_2} - x_{SO2i}\| + \|x_{O_3} - x_{O3i}\|}{h_n}\right)}{\sum_{i=1}^{n} K\left(\frac{\|x_{NO} - x_{NOi}\| + \|x_{NO_2} - x_{NO2i}\| + \|x_{SO_2} - x_{SO2i}\| + \|x_{O_3} - x_{O3i}\|}{h_n}\right)}$$

with K is a kernel function and h_n is a nonnegative real sequence.

Functional ρ- regression (FRR)

This regression model is obtained by resolving the following optimization problem

$$min_f E[\rho(Y, f)|Z = z], \quad \text{(Eq.3)}$$

ρ is a real-valued Borel function chosen by the user according to the studied data.

The model (*Eq. 3*) has been introduced in functional statistics by Azzedine et al. (2008) independent case and Attouch et al. (2012) for dependent case. The robustness is the main advantage of this model. It permits to analyze the data even in the presence of the outliers. Its functional estimation is expressed by

http://www.aloki.hu ● ISSN 1589 1623 (Print) ● ISSN 1785 0037 (Online)
DOI: http://dx.doi.org/10.15666/aeer/1706_1423114239

$$\bar{\bar{r}}(x_{NO}, x_{NO_2}, x_{SO_2}, x_{O_3}) = argmin_f \frac{\sum_{i=1}^{n} \rho(Y_i f) K\left(\frac{\|x_{NO}-x_{NOi}\|+\|x_{NO_2}-x_{NO2i}\|+\|x_{SO_2}-x_{SO2i}\|+\|x_{O_3}-x_{O3i}\|}{h_n}\right)}{\sum_{i=1}^{n} K\left(\frac{\|x_{NO}-x_{NOi}\|+\|x_{NO_2}-x_{NO2i}\|+\|x_{SO_2}-x_{SO2i}\|+\|x_{O_3}-x_{O3i}\|}{h_n}\right)}.$$

Functional relative error regression (FRER)

This last regression is an alternative nonparametric regression to the least square regression model. It is recently considered in functional statistics by Demongeot et al. (2016) for independent case and Bassoudi and Kaid (2019) for dependent case. It is defined by the following rule

$$min_f E\left[\frac{(Y-f)^2}{Y^2} | Z = x\right]. \quad \text{(Eq.4)}$$

The expression of this regression is explicitly given by

$$\frac{E[Y^{-1}|Z=x]}{E[Y^{-2}|Z=x]}.$$

Its estimator is defined by

$$\ddot{r}(x_{NO}, x_{NO_2}, x_{SO_2}, x_{O_3}) = \frac{\sum_{i=1}^{n} Y_i^{-1} K\left(\frac{\|x_{NO}-x_{NOi}\|+\|x_{NO_2}-x_{NO2i}\|+\|x_{SO_2}-x_{SO2i}\|+\|x_{O_3}-x_{O3i}\|}{h_n}\right)}{\sum_{i=1}^{n} Y_i^{-2} K\left(\frac{\|x_{NO}-x_{NOi}\|+\|x_{NO_2}-x_{NO2i}\|+\|x_{SO_2}-x_{SO2i}\|+\|x_{O_3}-x_{O3i}\|}{h_n}\right)}.$$

Results

Undoubtedly, the accuracy of the three proposed regression models is closely related to the choice of the different parameters involved in these models. Specifically, the leading parameters in this prediction issue are kernel K, the smoothing parameter h_n, and the norm $\| \|$. The letter is equal to the distance between the smoothed curves obtained by interpolation. For basic materials on this notion, we refer the readers to Ferraty and Vieu (2006). Notice that the previous estimators are computed by using a sample of 364 obviations $(Y_i, X_{NOi}, X_{NO_{2i}}, X_{SO_{2i}}, X_{O_{3i}})$. The observations are determined with respect to the aimed prediction horizon. Generally speaking, for k-h-ahead prediction of O_3 at hour h_0 in a day i we denote by $(X_{NOi}, X_{NO_{2i}}, X_{SO_{2i}}, X_{O_{3i}})$ the daily curve of the emission of the gases observed the day before $(i.e.\ (i-1))$ until $h_0 - k$, and we put $Y_i = X_{O_{3\,(i+1)}}(h_0)$. Now, to test the performance of the proposed models, we randomly split the 364 observations into two sub-samples: 200 in learning sample (indexed by i) and 164 in the testing sample (indexed by j). The observations of the learning sample are used to compute the estimators. While the observations of the test sample are employed to evaluate the quality of the models $(\hat{r}, \bar{\bar{r}}, \ddot{r})$. To the end, let us point out that we have used the leave-one-out cross-validation technique to determine the bandwidth parameter h_n. The rule of the used cross-validation procedure is defined by

$$\frac{1}{200}\sum_{i=1}^{200}\left(Y_i - \theta(X_i)\right)^2 \quad \text{(Eq.5)}$$

http://www.aloki.hu ● ISSN 1589 1623 (Print) ● ISSN 1785 0037 (Online)
DOI: http://dx.doi.org/10.15666/aeer/1706_1423114239

where $\theta(.)$ means one of the previous regression models ($\check{r}, \bar{\bar{r}}, \breve{r}$). For the sake of shortness, we fixe $k = 4$ and we give the prediction results for $h_0 = 11\,am$. This hour corresponds to four hours after peak-hour road traffic. For the computational purpose, we use the same kernel and the score function as in Demongeot et al. (2016). To examine the sensitivity of this prediction problem to the input variables we have proceeded with several cases with different covariates. The obtained results are shown in *Figures 3–5*.

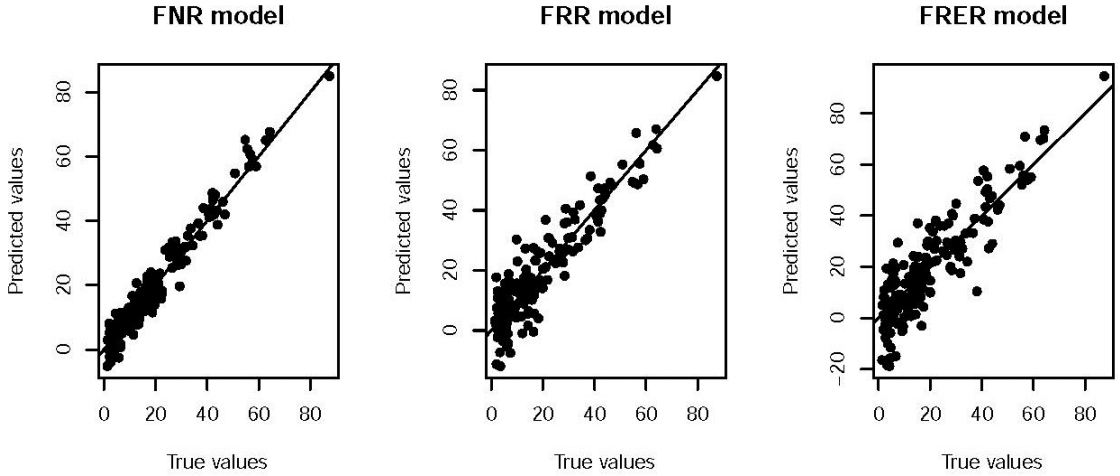

Figure 3. *4-h prediction of the maximum ozone concentration at $h_0 = 11\,am$ using the covariates $X_{NO}, X_{NO_2}, X_{O_3}$*

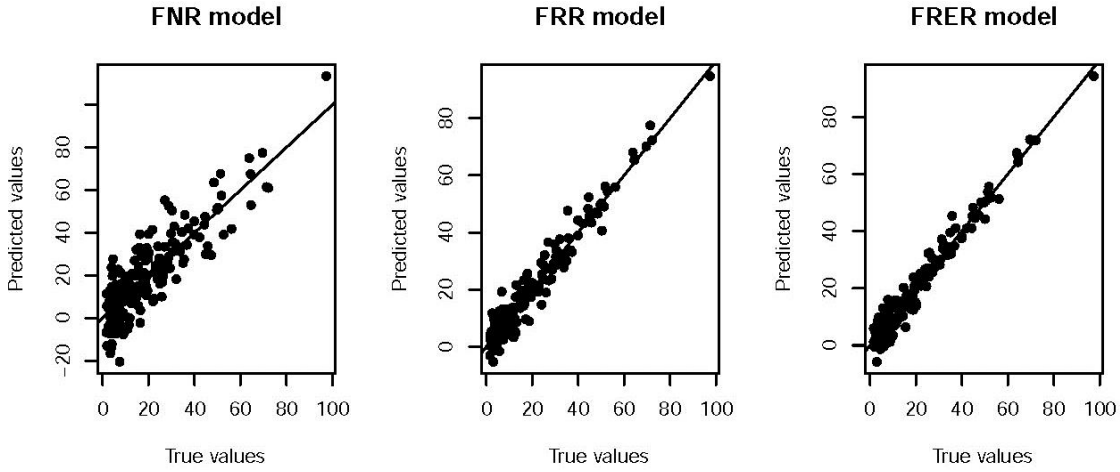

Figure 4. *4-h prediction of the maximum ozone concentration at $h_0 = 11\,am$ using the covariates X_{SO_2}, X_{O_3}*

http://www.aloki.hu ● ISSN 1589 1623 (Print) ● ISSN 1785 0037 (Online)
DOI: http://dx.doi.org/10.15666/aeer/1706_1423114239

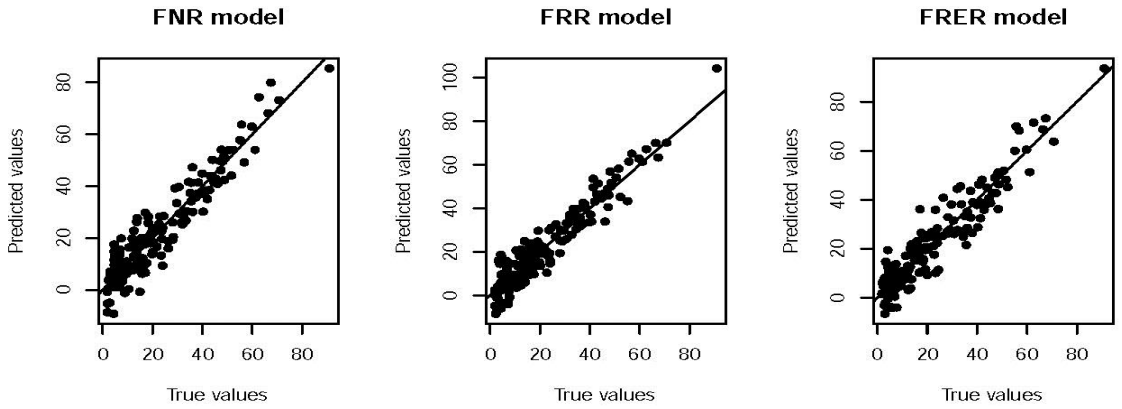

Figure 5. *4-h prediction of the maximum ozone concentration at* $h_0 = 11\ am$ *using the covariates* $X_{NO}, X_{NO_2}, X_{SO_2}, X_{O_3}$

It appears clearly that these new regression models performed well for this prediction problem and they have a fair accuracy. However, the performance of the considered models is varied with respect to the input variables. For instance, the FNR is more accurate when the regressors are $X_{NO}, X_{NO_2}, X_{O_3}$. On the other hand, the FRR and FRER provide better results for the covariates X_{SO_2}, X_{O_3}. All the models have a satisfactory result when the four regressors are considered. Such a conclusion is justified by the mean squared prediction error (MSPE) defined by

$$MSPE = \frac{1}{164}\sum_{j=1}^{164}\left(Y_j - \hat{Y}_j\right)^2. \qquad \text{(Eq.6)}$$

The MSPE errors are summarized in *Table 1*.

Table 1. *The MSPE of the three models*

Covariates	FNR model	FRR model	FRER
$X_{NO}, X_{NO_2}, X_{O_3}$ Case	**2.32**	3.12	2.98
X_{SO_2}, X_{O_3} Case	4.53	**3.09**	3.22
$X_{NO}, X_{NO_2}, X_{SO_2}, X_{O_3}$ Case	3.28	**3.19**	3.53

Discussion

The real time air quality in Marylebone road was analyzed by using the functional statistical models. A sample of 364 observations was used to analyze the impact of the other pollutant gases on the ozone concentration. The results of this statistical analysis are displayed in *Figures 3–5* and the prediction errors are summarized in *Table 1*. According to these prediction results, it appears clearly that the efficiency of this prediction issue is related to two important parameters which are the predictor model and the regressor variables. Precisely, using the three covariates $X_{NO}, X_{NO_2}, X_{O_3}$, Figure 3 shows that the best model is FNR; it gives an MSPE equal to 2.32. However, if we consider as covariates the two variables X_{SO_2}, X_{O_3} or $X_{NO}, X_{NO_2}, X_{SO_2}, X_{O_3}$ the best results were obtained by FRR model. Its prediction error is 3.09 and 3.19, respectively. Overall, it is clear that this functional regression models have satisfactorily performance. The prediction errors evaluated by the rule $MSPE$ is varied between 2.32-3.28 for the FNR, in the interval (3.12, 3.19) and is between 2.98-3.53 for the FRR and

http://www.aloki.hu ● ISSN 1589 1623 (Print) ● ISSN 1785 0037 (Online)
DOI: http://dx.doi.org/10.15666/aeer/1706_1423114239

FRER, respectively. All these predictor models are performed with fixed horizon equal to 4 h. Of course the choice of the prediction horizon is crucial. It should be enough for alarm purposes. Conceptually, our approach can be used for any horizon, but, we focused, here in 4 h ahead prediction, only, to show the easy implementation of the proposed algorithms. Furth more, the prediction results show that the three proposed functional models are fast, robust and accurate in this prediction issue. Moreover, the main feature of these functional models is the modelling of the daily curves of the pollutant gases in theirs continuous path allowing to explore the whole existing information of this time series data. Of course this consideration permits to avoid several drawbacks of the multivariate regression models, such as the curse of dimensionality or the calibration problem. On the other hand, the prediction in advance of the future values of the ozone concentration has a great importance for the decision-makers. They permit to plan the prevention strategy in order to combat the principal cause of the pollution. The present study contribute in this fundamental issue with these flexible models which can be used for various covariates variables and several pollutant factors, such as temperatures, wind (speed and directions), radiations, etc. Thus, the integration of these additional factors in our functional model is one of the natural prospects of this work. In addition, we can, also, predict the ozone concentration using other recent statistical models such as the partial functional linear model or the functional local linear models.

Conclusion

In this work, we have developed a new approach to predict the maximum ozone concentration using other air quality factors. These models are based on real-time measurement of the input data. The main feature of these models is the fact that they allow exploring all the information of these continuous-time observations viewed as curves. They are easily implementable, and their efficiency is related to the choice of the exogenous variables. In the sense that in the function of the considered covariates we can choose the adapted model. Moreover, the proposed models permit to avoid the core drawback of the classical models that is the loss of information after the prediction transformation. Indeed, the classical models induced by the multivariate regression are obtained by discretization of the daily curve in some finite grid or by projection into a finite-dimensional space. All these transformations on the input data are performed independently to the output variables. But, the ozone prediction is very sensitive to the input data. So the classical models are failed in these situations of real-time measured data. Thus, the originality of the functional approach comes from the fact that the prediction problem is performed without any transformation of the data. In conclusion, we can say that the accuracy of air quality prediction is based on both: the choice of the appropriate statistical models and the determination of the covariates. Moreover, the performance of the proposed models can be improved by using other covariates such as the metrological data wind direction, wind speed, humidity, solar radiation, air temperature.

Acknowledgments. Authors greatly thank the Editor in chief, the Associate Editor and the anonymous referees for a careful reading of the paper and for their valuable comments and suggestions which improved the quality of this paper substantially. They also extend their appreciation to the Deanship of Scientific Research at King Khalid University for funding this work through General Research Project under grant number (G.R.P-125-40).

http://www.aloki.hu ● ISSN 1589 1623 (Print) ● ISSN 1785 0037 (Online)
DOI: http://dx.doi.org/10.15666/aeer/1706_1423114239

REFERENCES

[1] Aneiros, G., Cao, R., Fraiman, R., Vieu, P. (2019): Editorial for the special issue on functional data analysis and related topics. – J. Multivariate Anal. 170: 1-3.
[2] Azzedine N., Laksaci A., Ould-Saïd, E. (2008): On robust nonparametric regression estimation for a functional regressor. – Statistics & Probability Letters 78: 3216-3221.
[3] Attouch Mk, Laksaci A., Said, O. (2012): Robust regression for functional time series data. – Journal of the Japan Statistical Society 42: 125-143.
[4] Bassoudi, M., Kaid, Z. (2018): Nonparametric relative error regression for functional ergodic data. – Int. J. Math. Stat. 19: 90-99.
[5] Demongeot J., Hamie A., Laksaci A., Rachdi, M. (2016): Relative-error prediction in nonparametric functional statistics: theory and practice. – Journal of Multivariate Analysis 146: 261-268.
[6] Ding W., Zhang J., Leung Y. (2016): Prediction of air pollutant concentration based on sparse response back-propagation training feedforward neural networks. – Environ Sci Pollut Res 23: 19481-19494.
[7] Ferraty, F. (2010): High-dimensional data: a fascinating statistical challenge. – Journal of Multivariate Analysis 101: 305-306.
[8] Ferraty, F., Vieu, P. (2006): Nonparametric Functional Data Analysis. Theory and Practice. – Springer Series in Statistics, New York.
[9] Ferraty F., Laksaci A., Tadj A., Vieu, P. (2010): Kernel regression with functional response. – Electronic Journal of Statistics 5(140): 335-352.
[10] Gavrila, C., Teodorescu, N., Gruia (2013): Bayesian modelling to the water loss management decisions. – Journal of Water Science and Technology: Water Supply 13: 883-888.
[11] Gavrila, C., Coman, A., Gruia, I., Ardelean, F., Vartires, A. (2016): Prediction method applied for the evaluation of the tropospheric ozone concentrations in Bucharest. – Romanian Journal of Physics 61(5-6): 1067-1078.
[12] Gong B., Ordieres-Meré, J. (2016): Prediction of daily maximum ozone threshold exceedances by preprocessing and ensemble artificial intelligence techniques: case study of Hong Kong. – Environ Model Softw 84: 290-303.
[13] Hsing, T., Eubank, R. (2015): Theoretical Foundations of Functional Data Analysis, with an Introduction to Linear Operators. – Wiley Series in Probability and Statistics. John Wiley & Sons, Chichester, UK.
[14] Ling, N., Vieu, P. (2018): Nonparametric modelling for functional data: selected survey and tracks for future. – Statistics 52: 934-949.
[15] Nghiem, L. H., Oanh, N. T. H. (2009): Comparative analysis of maximum daily ozone levels in urban areas predicted by different statistical models. – Science Asia 35: 276-283.
[16] Ryan, W. F. (1995): Forecasting severe ozone episodes in the Baltimore Metropolitan Area. – Atmospheric Environment 29: 2387-2398.
[17] Slini, T., Karatzas, K., Moussiopoulos, N. (2002): Statistical analysis of environmental data as the basis of forecasting: an air quality application. – The Science of the Total Environment 288: 227-237.
[18] Taylan, O. (2017): Modelling and analysis of ozone concentration by artificial intelligent techniques for estimating air quality. – Atmos Environ 150: 356-365.
[19] Yi, J., Prybutok, V. R. (1996): A neural network model forecasting for prediction of daily maximum ozone concentration in an industrialized urban area. – Environmental Pollution 92: 349-357.
[20] Zhang Y., Bocquet M., Mallet, V., Seigneur C., Baklanov, A. (2012): Real-time air quality forecasting. Part I: History, techniques, and current status. – Atmos Environ 60: 632-655.

http://www.aloki.hu ● ISSN 1589 1623 (Print) ● ISSN 1785 0037 (Online)
DOI: http://dx.doi.org/10.15666/aeer/1706_1423114239

ASSESSMENT OF WATER QUALITY IN TAIHU LAKE USING A RADIAL BASIS FUNCTION NETWORK, STRUCTURE INDEX, AND PRINCIPAL COMPONENT ANALYSIS

HANG, X. – GAO, H.* – JIA, S.

College of Information and Electrical Engineering, China Agriculture University
Beijing 100083, China
(phone: +86-10-6273-8830; fax: +86-10-6273-6746)

**Corresponding author*
e-mail: hjgao@cau.edu.cn

(Received 3rd Jun 2019; accepted 11th Oct 2019)

Abstract. A novel integrated approach was used to assess water quality in Taihu Lake in real-time using a radial basis function (RBF) network, structure index (SI) and principal component analysis (PCA). A total of eight sampling points covering an area of 2,338 km^2 were sampled once weekly from 2000 to 2005, except for 2003 and 2004. An RBF network was developed with 23 water quality parameters used as inputs. Then SI was applied to investigate main parameters. Parameters affecting water quality were also determined using PCA. The water quality of Taihu Lake was estimated by synthesizing the results of SI and PCA. Total nitrogen, with a weight of 0.34 for the first component, had the greatest negative effect on Taihu Lake water quality, being slighter than that of ammonia nitrogen, which had a weight of 0.324 for the first component. Conductivity, total phosphorus and alkalinity had weights of 0.322 0.292 and 0.267 for the first component, respectively. It is possible to identify potential sources of water pollution and the results indicated that the water quality of Taihu Lake in the study period was generally graded as Class V according to Environmental quality standards for surface water (GB 3838-2002).
Keywords: *PCA, RBF neural network, SI, water quality assessment, Taihu*

Introduction

Environmental sustainability is among the most serious global issues being addressed by planners, policy analysts, political scientists and others (Gleeson, 2001). Water pollution is an increasing concern, threatening the ecological integrity and sustainability of some of the world's largest water bodies (Havens et al., 2001). Lake water pollution is of particular concern because of its impact on fish habitats (Scavia et al., 2014) and human and animal health (Utah, 2016), and the fact that these are areas where there are complex interconnections between anthropogenic and climatic factors (Richards, 2010; Brooks, 2016). Harmful cyanobacterial blooms are one of the most significant markers of impaired lake water quality, especially in eastern China, a region with a rapidly growing economy (Paerl, 2011).

Taihu Lake (*Fig. 1*), situated in the Yangtze delta with an area of 2,338 km^2, is the most industrialized area in China, having a high population density and significant urbanization and economic development (Qin et al., 2002). The lake supports 10 million people working in tourism, fisheries, shipping and other industries. Taihu Lake also collects waste from urban, agricultural and industrial areas of surrounding cities, helping rapid growth in local economies (Qin et al., 1999; Qin, 2008). However, the increase of nutrients coming from urban and agricultural development in the watershed, has accelerated eutrophication (James et al., 2009; Duan et al., 2009). Cyanobacterial blooms, indicators of advanced eutrophication, in freshwater lakes impact fish,

http://www.aloki.hu ● ISSN 1589 1623 (Print) ● ISSN 1785 0037 (Online)
DOI: http://dx.doi.org/10.15666/aeer/1706_1424114258

recreational lake users, and the drinking water supply (Fogg, 1969; Paeral,1988). The water quality of the lake is closely related to public health in the local area.

Prior to the 1970s, average water quality of Taihu Lake was classified as Grade II according to GB3838-88 (Groundwater Environmental Quality Standard. China: GB. 2003). Since the 1980s, discharge of industrial waste water and domestic sewage has increased yearly while the water quality of Taihu Lake has dropped, on average, by one grade every 10 years. In the 1980s, the water quality was graded between the second and third levels; in the 1990s, the water quality decreased to the fifth level, and eutrophication had increased. Since the late 1990s, water quality deterioration has slowed and some key indicators, including TP, ammonia nitrogen and chemical oxygen demand of permanganate (Permanganate index), have improved (China Taihu Ecosystem Positioning Observation Data Query System. Taihu Lake Water Quality Inquiry System. Accessed 1990-2018, http://lake.data.ac.cn/taihu).

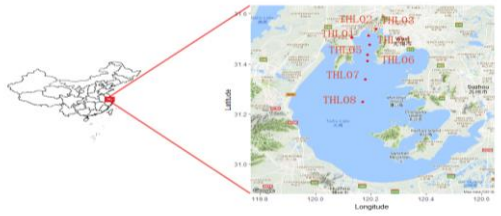

The name of observation station	East longitude (°)	North latitude (°)
THL01	120.13117	31.50383
THL02	120.19067	31.51317
THL03	120.21944	31.53968
THL04	120.19433	31.47633
THL05	120.18796	31.43609
THL06	120.18733	31.41117
THL07	120.18017	31.33833
THL08	120.17062	31.24816

Figure 1. *Location of the study area*

Statistical techniques, visual modeling, prediction algorithms, and time-series analyses have been used to evaluate and monitor water quality, and inform policy-makers (Junli et al., 2019; Jun et al.,2019; Taufiq et al., 2019; Dutta et al., 2018; Jabbar et al., 2018; Meng et al.,2018; Tong et al.,2018; Drakard et al., 2018; Shengli et al., 2018; Omar et al., 2018; Putri et al., 2018; Kellner et al., 2018; Islam et al., 2018; Skowron et al., 2018; Masindi et al., 2018; Meifang et al., 2018; Guilin et al., 2018; Zhi-Qiang et al., 2018; Ju et al., 2018; Cecconello et al., 2018). Methods that have been proposed to assess water quality include Roveda's water quality index (Roveda et al., 2013), EFER (Aminravan et al., 2013) and use of ships with deliberative control architecture (Halal et al., 2014). A RBF network algorithm is commonly used because of its ability to learn, generalize, and adapt (Garrett, 1994). The RBF network algorithm used in this study combines several lake water quality parameters, enabling the most important parameters to be identified based on analysis of the neighboring nodes. It can efficiently describe the non-linear relationships among complex water quality datasets (Adel et al., 2018; Zheng et al., 2017; Alizamir et al., 2017; Asadollahfardi et al., 2017; Wu et al., 2016; Zounemat-Kermani et al., 2016; Shiau et al., 2016; Bagheri et al., 2016).

Combining RBF with SI and PCA (Dutta et al., 2018; Prusty, 2018; Sun et al., 2018; Xiaohu et al., 2018; Wang et al., 2019; Xiao et al., 2019; Zhaoxue et al., 2018) yields more accurate results and provides sufficient evidence to characterize lake water

http://www.aloki.hu ● ISSN 1589 1623 (Print) ● ISSN 1785 0037 (Online)
DOI: http://dx.doi.org/10.15666/aeer/1706_1424114258

quality. In this study, RBF, SI and PCA were applied to identify the main parameters affecting water quality. The primary objectives of this study were to assess water quality in Taihu Lake, identify the main parameters that damage the water quality, and investigate possible sources of pollution.

Material and methods

This study focused on Taihu Lake, which is located in the southern border of the Yangtze River Delta (*Fig. 1*). Taihu Lake is the third largest freshwater lake in China, covering an area of 2,338 km^2. It has a length of 68.5 km from north to south, an average length of 34 km from east to west, and a coastline of 405 km.

Taihu Lake has a complicated river and channel network, with a mean depth of 1.9 m and a maximum depth of 2.6 m. Pen fish is the main form of aquaculture in Taihu Lake. Marsh development occurs primarily along the eastern shoreline. Taihu Lake has many functions, including supplying drinking water, supporting fisheries, tourism and shipping, and retaining flood water.

To evaluate the water quality of Taihu Lake, monthly data from eight sampling points in Taihu Lake were collected for the period 2000 to 2005, except for 2003 and 2004. The data used in this study are from "Lake-Watershed Science Data Center, National Earth System Science Data Sharing Infrastructure, National Science & Technology Infrastructure of China" (http://lake.geodata.cn). Parameters evaluated included pH, total nitrogen, total phosphorus, Chlorophyll a, Demagnesium chlorophyl, permanganate index, dissolved oxygen, ammonia nitrogen, nitrite nitrogen, nitrate, phosphate, alkalinity, potassium, sodium ion, calcium ion, magnesium ion, fluorine ion, chloride, sulfate, silicate, Dissolved total nitrogen, Dissolved total phosphorus, and conductivity. The abbreviations of words used in this paper are shown in *Table 1*.

This study combined RBF, SI and PCA to derive accurate results. Many parameters were included in our assessment of Taihu Lake water quality. Changes in parameter values were captured and analyzed in the MATLAB environment (MathWorks, Natick, MA, USA) using RBF algorithms to derive an accurate results. A novel three-layer RBF network was developed for this study. A confusion matrix was used to assess the performance of the RBF algorithm.

After the RBF network was built, the weights of and links between nodes were ascertained. SI was used to determine the parameters contributing most significantly to the output neurons. SI shows a high value when a parameter makes a great contribution to the RBF network, even if it has a less weight.

Following the above steps, the main parameters affecting each output neuron were determined. SPSS software (ver. 21.0; IBM Corp., Armonk, NY, USA) was used to compute the principal components, that is to seek projection directions with maximal variances which occupy bigger quantity (Flury, 1990; Joliffe, 2011). By investigating the principal components, the most important parameters affecting water quality can be identified using the RBF algorithm. A flow diagram illustrating the analysis process is shown in *Figure 2*.

Assessment model of water quality based on RBF algorithm was used to estimate the percentage amounts of each measured parameter in the lake. All data were pre-processed and separated into three data sets: training, test and verification sets. MATLAB was used for construction and analysis of the RBF network. There were 23 input layer neurons and 1 neuron in the output layer was used to represent the actual

http://www.aloki.hu ● ISSN 1589 1623 (Print) ● ISSN 1785 0037 (Online)
DOI: http://dx.doi.org/10.15666/aeer/1706_1424114258

water quality shown in *Figure 3*. There can be up to 71 hidden layers in this network. The nodes in the input and output layers are arranged in one line. A confusion matrix was used to assess the performance of the network and indicated that most of the predicted data fit, or nearly fit, the actual results.

The SI for the whole network was calculated as

$$\sum_{j}^{n} \sum_{k=1}^{j=1} \frac{|Wij - Wik|}{Djk} \quad \text{(Eq.1)}$$

where W_{ij} and W_{ik} are the connection weights of input variable i in neurons, and j and k of the RBF network, respectively; $\|D_{jk}\|$ is the topological distance between neurons j and k; and N is the total number of output neurons in the RBF network.

Table 1. *The abbreviations of words used in this paper*

Words	Abbreviation	Unit
pH	pH	/
Total nitrogen	TN	mg/L
Total phosphorus	TP	mg/L
Chlorophyll a	CHLA	μg/L
Demagnesium chlorophyl	DC	μg/L
Permanganate index	PI	mg/L
Dissolved oxygen	DO	mg/L
Ammonia nitrogen	NH3-N	mg/L
Nitrite nitrogen	NN	mg/L
Nitrate	NNA	mg/L
Phosphate	PO	mg/L
Alkalinity	ALKY	mmol/L
Potassium ion	K	mg/L
Sodium ion	Na	mg/L
Calcium ion	Ca	mg/L
Magnesium ion	Mg	mg/L
Fluorine ion	F	mg/L
Chloride	Cl-	mg/L
Sulfate	SO4	mg/L
Silicate	SiO	μmol/L
Dissolved total nitrogen	Dissolved TN	mg/L
Dissolved total phosphorus	Dissolved TP	mg/L
Conductivity	EC	μS/cm

The SI of each input node is presented in *Table 2*. Input layer 14, which represents Na, was the parameter most critical to the performance of the whole network. Dissolved TP and F were the second and third most important parameters, respectively. Ca, with an SI of 21.437 was next, followed by TN, PI and DO. Dissolved TN, Mg, NH3-N,

http://www.aloki.hu ● ISSN 1589 1623 (Print) ● ISSN 1785 0037 (Online)
DOI: http://dx.doi.org/10.15666/aeer/1706_1424114258

NNA, NN, pH, EC, ALKY, and TP had SIs above 5; SiO, Cl-, CHLA, PO, DC, K, and SO4 had SIs below 5. Garson's Algorithm (Garson, 1991) and Connection weights approach (Olden, 2002b) are also presented as methods to study the relative importance of inputs on the output. The results are displayed in *Table 2*. Seven factors affecting water quality were identified by developing the network and analyzing the weight of each node by SI as well as synthesizing the results of Garson and Connection weights which was in the order of: TP, SiO, Ca, SO4, Na, K, and F.

Table 2. *The weight of each input node by different methods*

Input layer(s)	Parameter(s)	Weight(s) by SI algorithm	Weight(s) by Garson's algorithm	Weight(s) by connection weights approach
1	pH	6.556	589.59	0.801
2	TN	20.016	247.61	0.300
3	TP	5.145	9.663	0.012
4	CHLA	3.521	1661.71	2.028
5	DC	1.291	374.09	0.459
6	PI	16.219	400.97	0.523
7	DO	13.787	608.08	0.847
8	NH3-N	8.251	80.472	0.086
9	NN	6.644	5.041	0.006
10	NNA	7.739	59.17	0.073
11	PO	3.050	137.11	0.181
12	ALKY	5.658	2558.9	3.323
13	K	1.025	2160.1	2.897
14	Na	43.750	603.89	0.809
15	Ca	21.437	39.15	0.053
16	Mg	8.386	3094.08	4.049
17	F	23.735	4489.51	5.887
18	Cl-	4.632	4050.9	5.185
19	SO4	0.362	32.35	0.044
20	SiO	4.880	2609.58	3.581
21	Dissolved TN	9.444	0.933	0.001
22	Dissolved TP	25.069	314.82	0.418
23	EC	5.959	30309	39.439

PCA was conducted to investigate the impacts of TN, NH3-N, PI, and ALKY. TN, TP, NN, K, SO4, SiO and PI were used to assess lake water quality according to *Tables 3* and *4*.

Table 3. *Relative importance of the studied components to water quality*

	Comp.1	Comp.2	Comp.3	Comp.4	Comp.5	Comp.6	Comp.7	Comp.8	Comp.9	Comp.10
Proportion of variance	0.3009486	0.1968562	0.1087038	0.07997529	0.06654579	0.0451578	0.03621469	0.03031488	0.02527567	0.02249223
Cumulative proportion	0.3009486	0.4978047	0.6065085	0.68648383	0.75302961	0.7981874	0.83440210	0.86471699	0.88999266	0.91248488

http://www.aloki.hu ● ISSN 1589 1623 (Print) ● ISSN 1785 0037 (Online)
DOI: http://dx.doi.org/10.15666/aeer/1706_1424114258

Table 4. *Component matrix*

	Comp.1	Comp.2	Comp.3	Comp.4	Comp.5	Comp.6	Comp.7	Comp.8
pH	0.179	0	0.41	0	-0.22	0	0.252	0.114
TN	-0.34	-0.124	0	0	0.167	0	0	0
TP	-0.292	0	0	0	0	-0.332	0	0.218
CHLA	0	-0.421	0.37	0	-0.104	0	0	0
DC	-0.101	-0.381	0.223	0	-0.158	0.111	-0.28	0.108
PI	-0.199	-0.345	0.216	0	0	-0.18	0	0.158
DO	0.173	0	0.225	-0.419	0	0.202	0	0.238
NH3-N	-0.324	0	-0.151	0	0.102	-0.125	0.131	0
NN	-0.201	-0.258	0	0.156	0.129	0.259	0	-0.257
NNA	-0.213	0	0.111	0	0.318	-0.204	-0.288	-0.288
PO	-0.23	0	-0.173	-0.105	-0.388	0.564	0.232	0
ALKY	-0.267	0	-0.138	0	0	-0.105	0	0
K	-0.241	0.292	0.263	0.159	-0.146	0	0	-0.104
Na	-0.247	0.276	0.255	0.103	0	0	0	0
Ca	-0.177	0.296	0	0.11	-0.347	0.136	-0.333	0.263
Mg	-0.217	0.377	0.253	0	-0.142	0	0	-0.1
F	0	0	0	0.363	0.396	0.339	0.314	0.656
Cl-	-0.27	0.122	0	-0.467	0	0	0.113	0
SO4	-0.258	0.109	0	-0.486	0.127	0	0	0
SiO	-0.104	0	-0.383	0	-0.237	0	-0.475	0.382
Dissolved TN	0	-0.104	-0.173	-0.105	-0.338	0.564	0.232	0
Dissolved TP	0	0	-0.232	0	-0.435	0.137	0.491	-0.132
EC	-0.322	0	0	0	0	0	0	-0.274

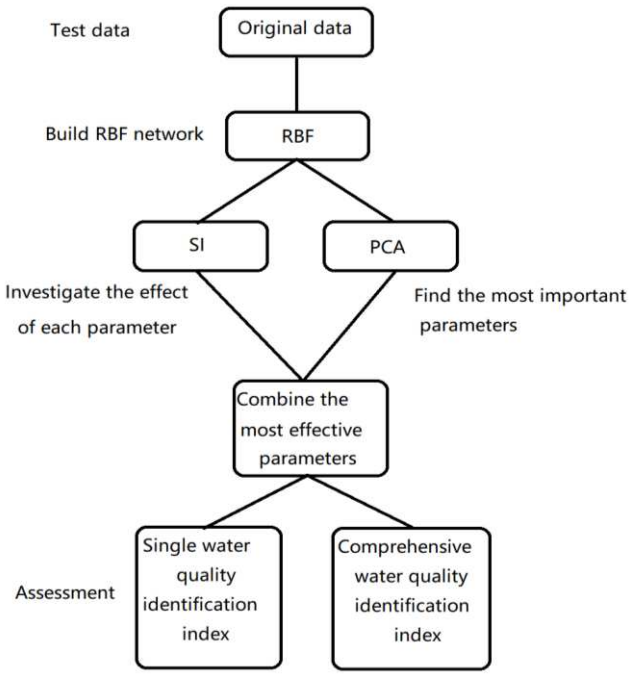

Figure 2. *Process flow diagram*

http://www.aloki.hu ● ISSN 1589 1623 (Print) ● ISSN 1785 0037 (Online)
DOI: http://dx.doi.org/10.15666/aeer/1706_1424114258

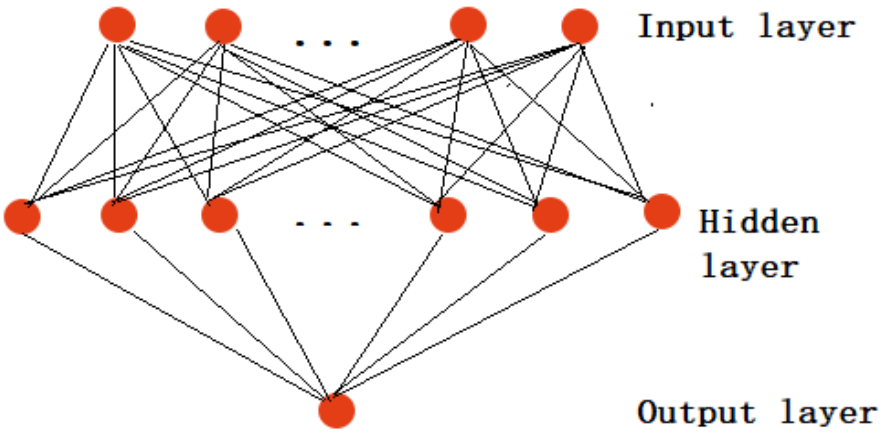

Figure 3. *Basic network structure*

Some criteria were used to evaluate the performance of the RBF model. The sum-squared error which can be calculated in *Equation 2* show the total epochs (iterations) required for the function to converge on parameters. Fitness value, indicators used to measure the quality of individuals in a population, can be calculated in *Equation 3*. Mean square error calculated in *Equation 4* was used to assess performance of each model.

$$\text{Sum - squared - error} = \sum (\text{actual value} - \text{predicted value})^2 \quad \text{(Eq.2)}$$

$$\text{Fittting} = \frac{1}{\text{Sum - squared - error}} \quad \text{(Eq.3)}$$

$$\text{mean square error} = \frac{\text{Sum - squared - error}}{n} \quad \text{(Eq.4)}$$

Results

Analysis of the main parameters affecting water quality

During the study period, TP concentrations in the samples ranged from 0.013 to 2.133 mg/L, with an average of 0.145 mg/L (*Table 5*). The peak concentrations in the third quarter of 2000 and 2002 may be due to the construction of new factories and the associated increase in the quantity of polluted water entering Taihu Lake during this period.

Increasing temperatures in spring promote the release of TP and increase its concentration in water. Throughout the summer, the concentration of TP in water may decrease because aquatic plants consume nutrients (*Fig. 4-1a*). TP peaks in 2000 and 2005 occurred in February, while the peaks in 2001 and 2002 occurred in July.

The dissolution of SiO was relatively stable, ranging from 0 to 157 mg/L and with an average of 77.27 mg/L (*Fig. 4-1b*). The low SiO concentration observed in the fourth quarter of 2000 may have been related to diatom activity. However, the variation in SiO concentrations seen in 2002 and 2005 indicates that diatom activity is likely not the

http://www.aloki.hu ● ISSN 1589 1623 (Print) ● ISSN 1785 0037 (Online)
DOI: http://dx.doi.org/10.15666/aeer/1706_1424114258

main factor affecting SiO concentrations; values were high all year round, particularly in the autumn and winter. Organic pollution of the water body is another possible factor influencing SiO concentrations, which were at an acceptable level for drinking water.

Table 5. *Statistical analysis of the main parameters affecting water quality in Taihu Lake*

Parameter	Max	Min	Avg	Var
pH	9.44	7.25	8.20	6.43
TN	13.34	0.39	6.32	309.40
TP	2.133	0.013	0.145	0.35
CHLA	521.73	0	33.77	16455.58
DC	58.03	0	5.60	505.23
PI	13.6	2.69	6.10	54.23
DO	14.74	0.47	6.72	241.88
NH3-N	6.95	0.001	3.33	230.21
NN	10.54	0.002	0.10	0.13
NNA	4.28	0.001	1.22	12.11
PO	0.162	0	0.015679688	0.000690782
ALKY	3.35	0.147	2.41	10.63
K	10.33	1.73	5.72	65.93
Na	210	4.4	77.65	16111
Ca	125.4	14.3	32.14	2860
Mg	49	2.2	10.58	159.4
F	10.37	0	1.09	81.51
Cl-	114.2	12	44.15463542	241.4987941
SO4	174.6	24.1	58.12	10915.91
SiO	157	0	77.27	8390.89
Dissolved TN	11.31	0.2	1.673229167	3.581032365
Dissolved TP	0.245	0.003	0.035744792	0.0015636
EC	1100	195	195	121.74

Ca concentrations ranged from 14.3 to 125.4 mg/L; Na concentrations ranged from 4.4 to 210 mg/L; K concentrations ranged from 1.73 to 10.33 mg/L; and Flu concentrations ranged from 0 to 10.73 mg/L.

Ca concentrations are expected to show opposite trends to SiO concentrations; this was observed in 2000 and 2001 in *Figure 4-1c*. The decrease in Ca concentration in 2003 may have been caused by polluted water emanating from factories and a nearby residential development. By 2005, the effect of human and diatom activity had reached a balance, and minimal variation Ca concentrations was observed.

SO4 is toxic to human health even at low concentrations. Over the study period, the SO4 concentration in Taihu Lake ranged from 24.1 to 174.6 mg/L, with an average value of 58.12 mg/L. SO4 concentrations declined through the middle part of the year, except in 2005 (*Fig. 4-1d*). The high SO4 concentration during the winter and spring from 2000 to 2002 may have been due to coal mine emissions. The peak SO4 concentration was observed from 2000 to 2002, with the appearance of the peak varied from January to April. SO4 concentrations were consistent with SiO concentrations (*Fig. 4-1b* and *d*, respectively).

http://www.aloki.hu ● ISSN 1589 1623 (Print) ● ISSN 1785 0037 (Online)
DOI: http://dx.doi.org/10.15666/aeer/1706_1424114258

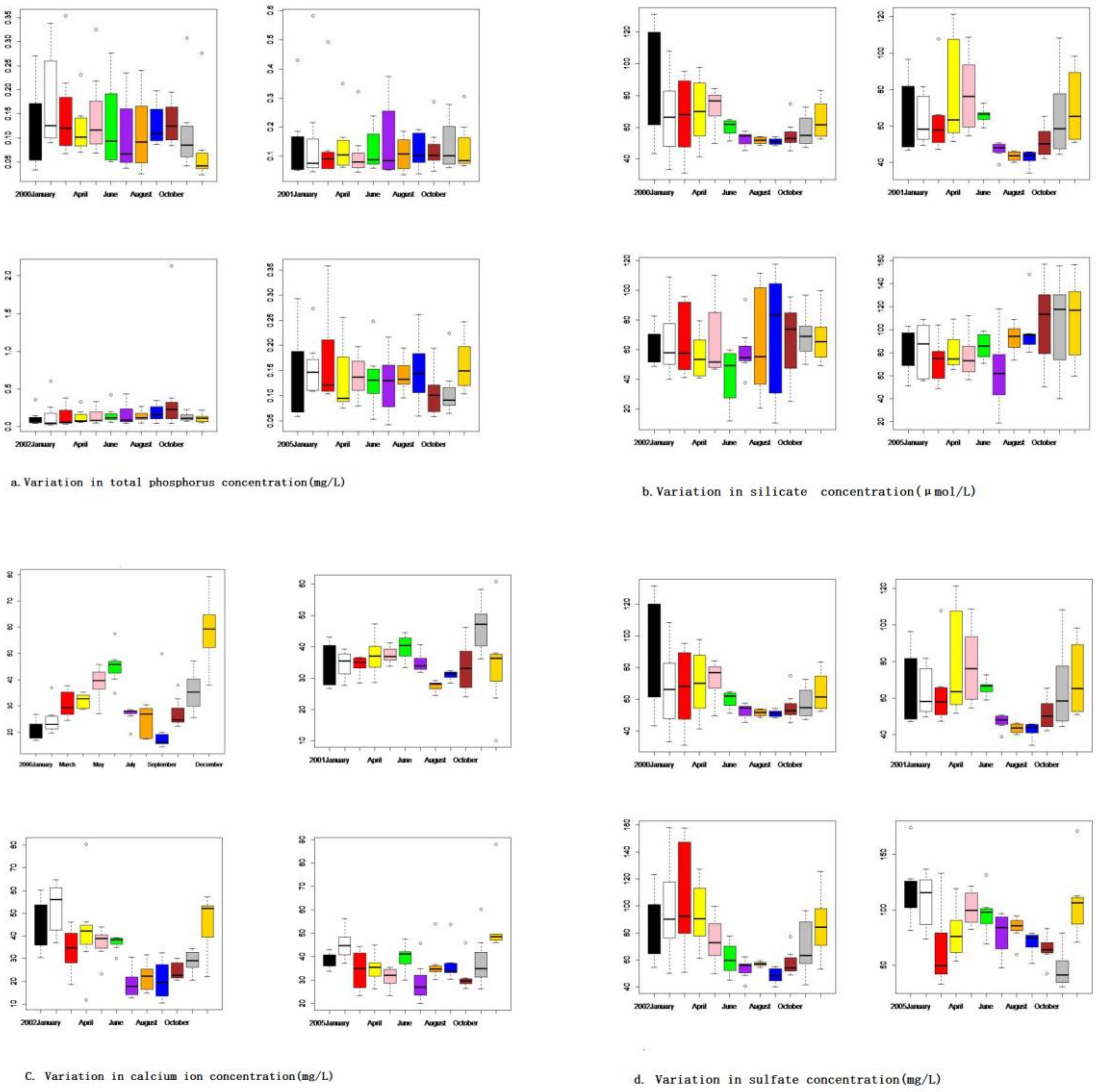

Figure 4-1. *Variation in different parameters' values by study year*

Nas are a common component of natural waterways. The most important characteristic of Nas in natural waterways is the wide variation in concentration under different conditions. *Figure 4-2e* shows that Na concentrations were low during the wet seasons. In the Earth's crust, K and Na are similarly abundant (2.60% and 2.64%, respectively). Although they have similar chemical properties, K concentrations are generally much lower than Na concentrations in natural waterways. K and Na concentrations decreased from 10% to 4% from 2000 to 2005 (*Fig. 4-2e* and *f*, respectively). The K to Na quality ratio was 0.1028 in 2005, while the ratio was 0.118, 0.120, 0.128 in 2003, 2001 and 2000 respectively. Ks are more mobile than Nas due to soil colloid adsorption, but are absorbed by plants. Increases in Na concentrations were mainly due to the drainage of sewage into the basin.

An acceptable F concentration in drinking water is 0.5 - 1.0 mg/L; the F concentration in Taihu Lake was within this range (*Fig. 4-2g*). The peak high and low points in 2000 and 2001 were similar, although the peak occurred later in 2001. The F concentration trend in 2002 was opposite to that in 2001.

http://www.aloki.hu ● ISSN 1589 1623 (Print) ● ISSN 1785 0037 (Online)
DOI: http://dx.doi.org/10.15666/aeer/1706_1424114258

TN and SO4 concentration trends were opposite which are illustrated in *Figures 4-2h* and *4-1d*. TN concentration was highest in the middle part of 2000, while in the following years there were low TN concentrations in the middle of the year.

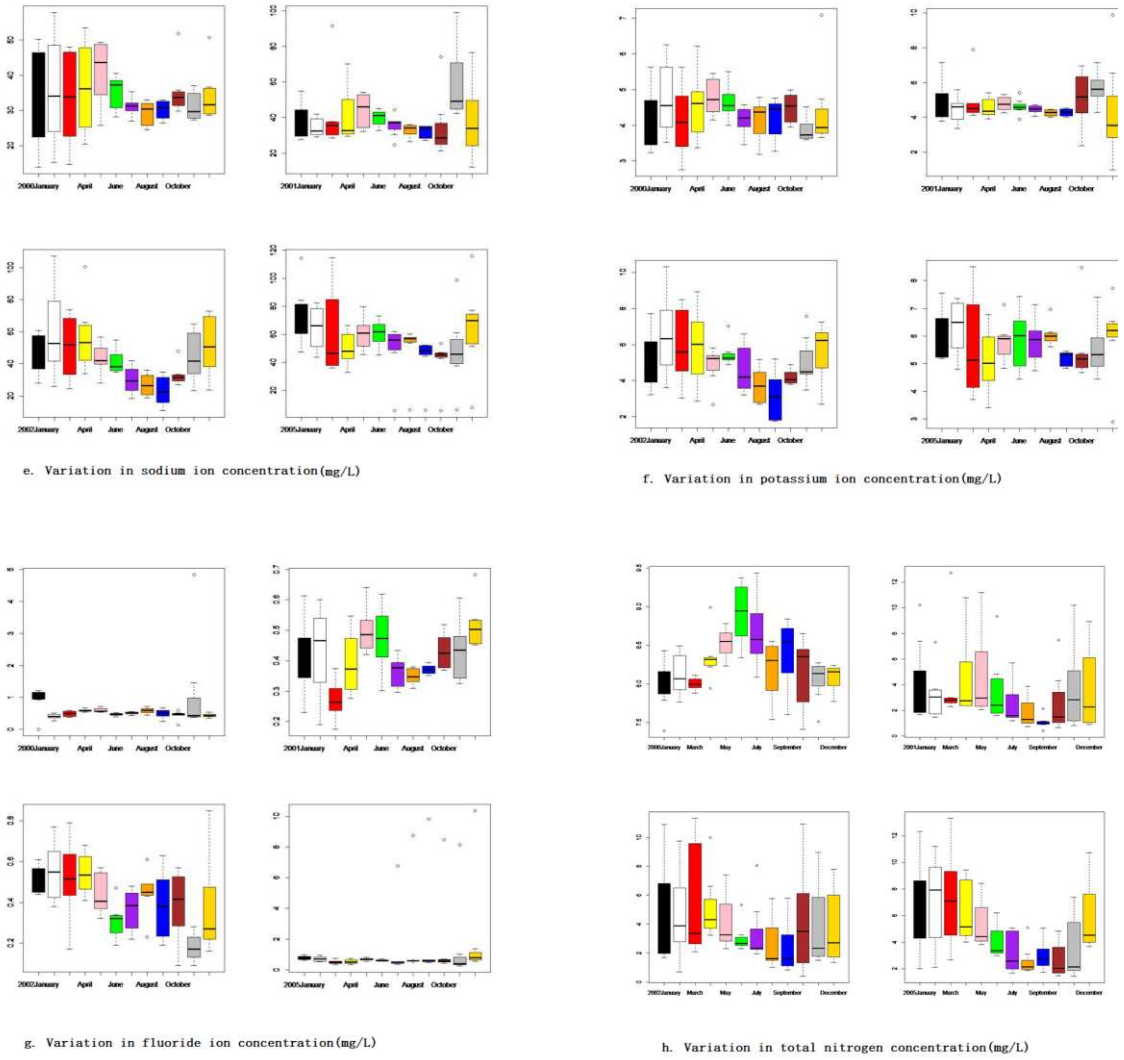

Figure 4-2. *Variation in different parameters' values by study year*

Formation of NH3-N is due to a lack of oxygen during the conversion of ammonia to nitrate. Over the study period, the NH3-N concentration varied from 0.001 mg/L to 6.95 mg/L, with an average of 0.10 mg/L. The NH3-N concentration was high during autumn and winter (*Fig. 4-3i*) and has increased in recent years in Taihu Lake; this is directly related to the lack of oxygen in the water caused by eutrophication of the water body.

PI is commonly used as a comprehensive indicator of the degree of contamination of surface water by organic and inorganic matter. The PI values ranged from 2.69 to 13.6 over the study period. In 2000, the PI concentration was low but exhibited relatively large variation in the following years (*Fig. 4-3j*). In addition, in 2005, the PI concentrations were relatively high.

http://www.aloki.hu ● ISSN 1589 1623 (Print) ● ISSN 1785 0037 (Online)
DOI: http://dx.doi.org/10.15666/aeer/1706_1424114258

ALKY indicates that a water body contains a substance that can accept hydrogen ions. The ALKY of Lake Taihu in summer and autumn was lower than in winter and spring (*Fig. 4-3k*). Over the study period, the minimum value was 0.147, with an overall upward trend in recent years and a peak value of 3.35. The temperature in the Taihu Lake basin is relatively high in summer and autumn. When there are large numbers of plants, microorganisms will produce acidic substances that neutralize some alkaline substances. Additionally, the use of coal for heating in the winter and spring seasons has greatly increased.

EC trends were consistent from 2000 to 2005 (*Fig. 4-3l*). In the spring and summer, as temperature increased, so too did EC. During the wet season, EC decreased due to density loss.

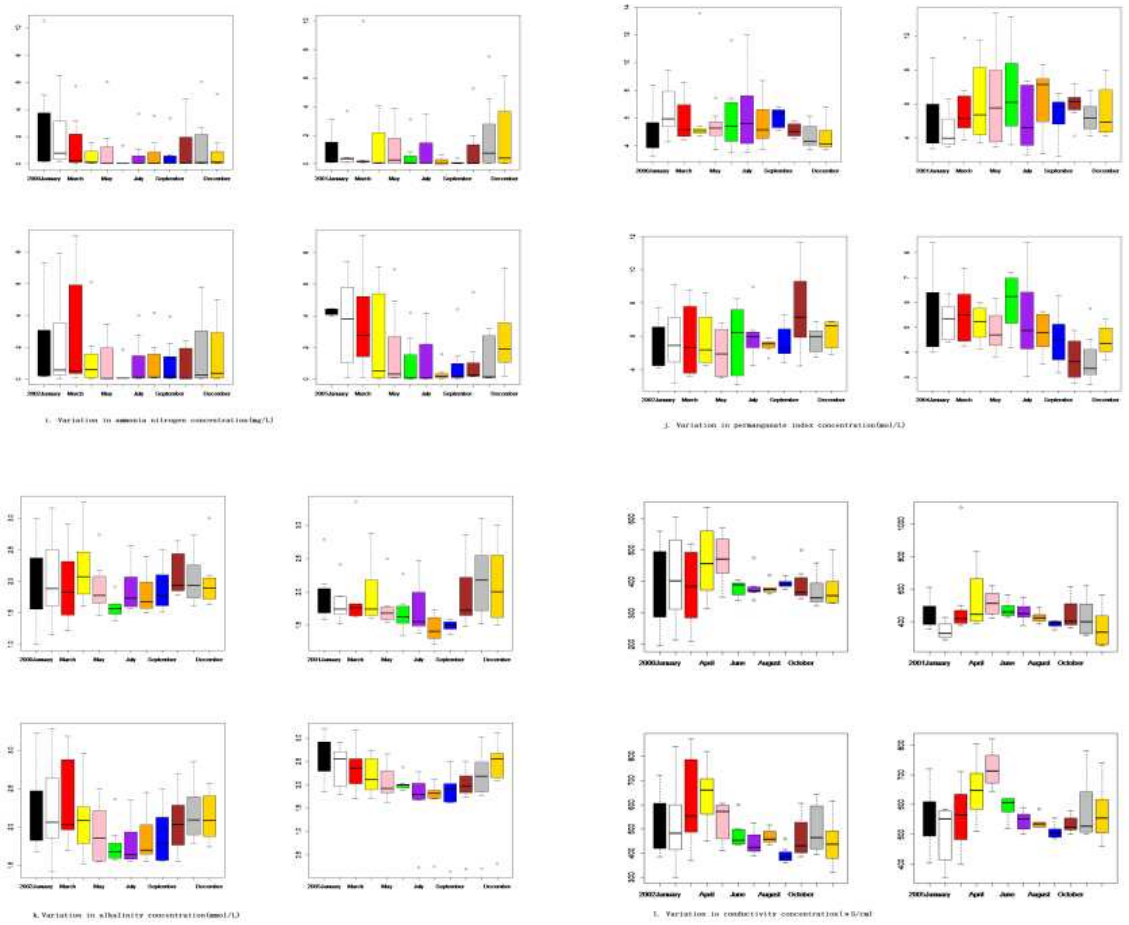

Figure 4-3. *Variation in different parameters' values by study year*

Difference in the water quality index over time

Differences in water quality parameters in Taihu Lake from 2000 to 2005, except for 2003 and 2004

Of the 23 chosen water quality indicators, 4 exhibited little variation over the study period, while 4 exhibited significant variation (*Table 5*). The factors affecting water quality showed similarities as well as differences; the difficulty of assessing water quality can be reduced by focusing only on the factors exhibiting significant changes.

http://www.aloki.hu ● ISSN 1589 1623 (Print) ● ISSN 1785 0037 (Online)
DOI: http://dx.doi.org/10.15666/aeer/1706_1424114258

Water quality index

The main factors influencing water quality, as calculated by the RBF network algorithm, PCA and SI algorithm, were included in the water quality index formula. This yielded a simple water quality index based on single water quality parameters, and a comprehensive index - water quality identification index of water samples which is the worst water quality index (*Table 6*).

Table 6. *Water quality index*

Model number	Feature(s)	Evaluation result
1	Single index – TP	IV
2	Single index – K	V
3	Single index – SO4	V
4	Single index – SiO	V
5	Single index – TN	V
6	Single index NN	IV
7	Single index – PI	II
8	Comprehensive index - water quality identification index	V

Discussion

The sum-squared error graphs (*Fig. 5*) show the total epochs (iterations) required for the function to converge on TP, SO4, SiO and Ca. The red line indicates the ideal objective function evolution curve, and the blue line represents the objective function curve. Graphs of TP, total SO4, SiO and K were produced using BP-GA. 40 epochs (iterations) were required for TP, SO4, SiO and Ca to converge (*Fig. 5*). In *Figure 6,* the blue line indicates the ideal fitness evolution curve, and the other line indicates the actual fitness evolution curve. The fitness of individuals tends to plateau after 70 generations, indicating that they have reached fitness. *Figure 7* shows the performance of each model. The goal is set to 1e-028. All parameters reach their goals at 5 epochs (iterations).

The error rate of the RBF algorithm used to assess the water quality of Taihu Lake in this study was compared to those of other prediction methods (Random Forest and LASSO) applied to the same data sets. The RBF network data were more accurate than those of the other methods. Under identical conditions and using the same data sets, the error rate was 0.032 for the RBF network, 0.093 for Random Forest, and 0.352 for LASSO. Random Forest is commonly used to make predictions and its results are generally accurate; however, the RBF method used in this study was significantly more accurate (*Table 7*).

Table 7. *RBF model error rate compared with other methods*

Method	RBF network	Random forest	LASSO
Error rate	0.032	0.093	0.352

http://www.aloki.hu ● ISSN 1589 1623 (Print) ● ISSN 1785 0037 (Online)
DOI: http://dx.doi.org/10.15666/aeer/1706_1424114258

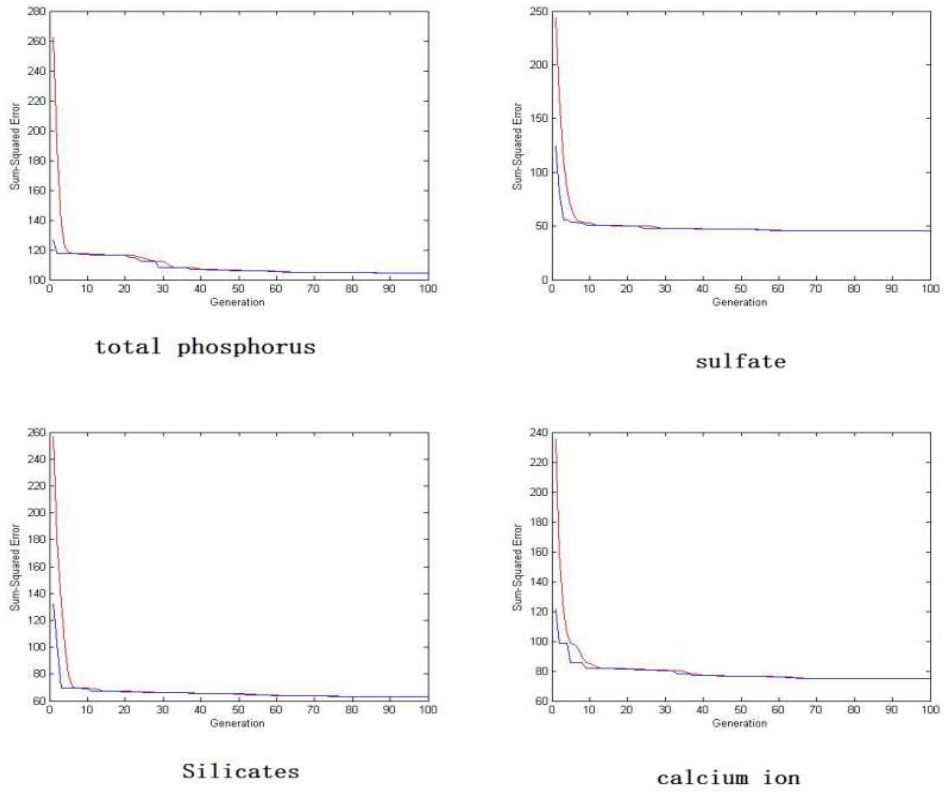

Figure 5. *Sum-squared error of TP, SO4, SiO and Ca affecting water quality*

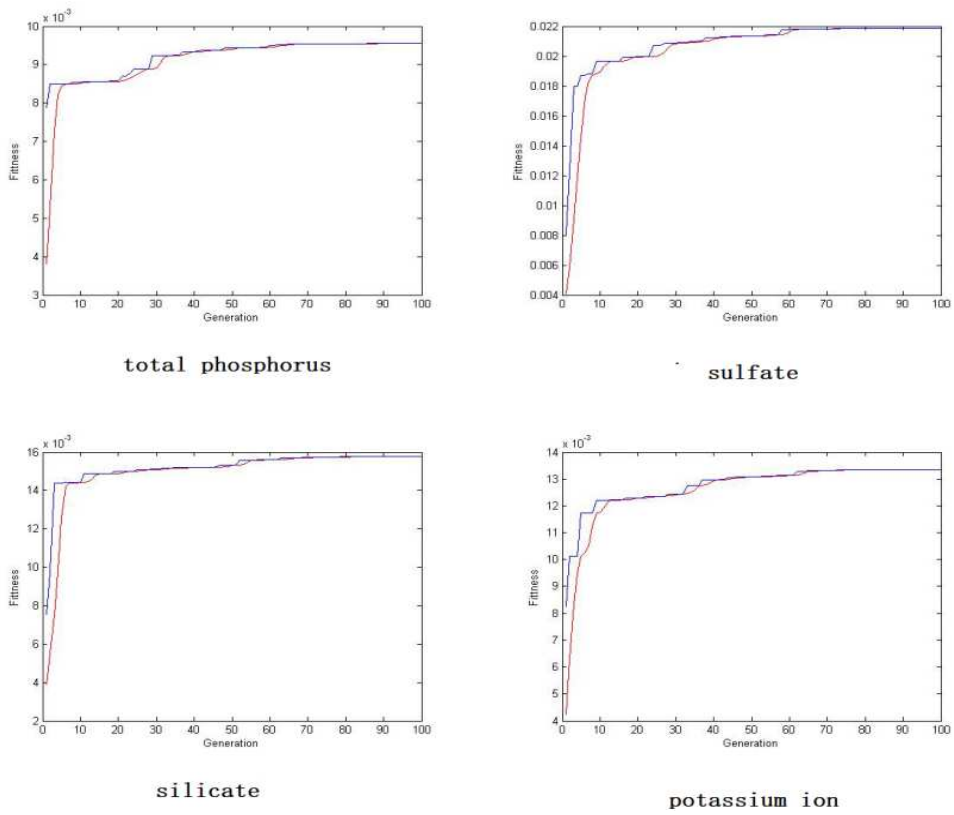

Figure 6. *Fitness of TP, SO4, SiO and Ca affecting water quality*

http://www.aloki.hu ● ISSN 1589 1623 (Print) ● ISSN 1785 0037 (Online)
DOI: http://dx.doi.org/10.15666/aeer/1706_1424114258

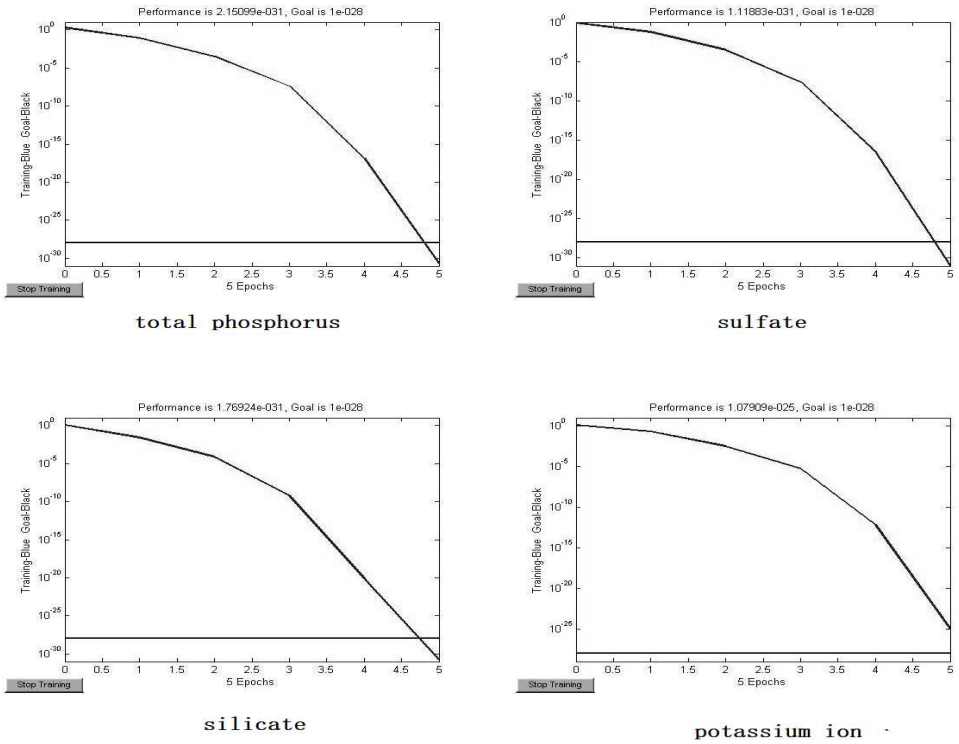

Figure 7. *Performance and goal for TP, SO4, SiO and Ca*

Conclusions

This study proposed a lake water quality assessment method based on an RBF network, SI and PCA. The method is suitable for water quality assessment of large areas over a long period and can identify the most important factors damaging water quality via a comprehensive evaluation. Water quality can be evaluated over time and space and evaluation indexes comprising single and multiple factors can be generated, which avoids over-generalization and better reflects the overall water quality.

The water quality of Taihu Lake for the period 2000 to 2005, except for 2003 and 2004 was between Grade 4 and Grade 5. Thus, water quality satisfied established standards based on our evaluation results. Future water quality control and protection efforts directed toward Taihu Lake should focus on improving management and supervision, as well as water treatment technology; such treatments are expected to improve the water quality of Taihu Lake.

The major environmental issue affecting Taihu Lake concerns control of pollution sources, particularly of Cl-, sulfides, etc. Control of pollution sources is a prerequisite for managing eutrophication in the lake. Ensuring safe drinking water requires point and non-point source pollution control, including a reduction in pollution from sewage. And adjustment of industrial practices and environmental management policies are necessary.

In this study, we investigated the factors affecting the quality of Taihu Lake in the view of data miner. But it is really important to find the very pollution sources, the process in which pollution sources affect the water quality and the cause of pollution sources.

http://www.aloki.hu ● ISSN 1589 1623 (Print) ● ISSN 1785 0037 (Online)
DOI: http://dx.doi.org/10.15666/aeer/1706_1424114258

Acknowledgements. This work was supported by the National Natural Science Foundation of China (grant number 31371531). The authors acknowledge data support from "Lake-Watershed Science Data Center, National Earth System Science Data Sharing Infrastructure, National Science & Technology Infrastructure of China." (http://lake.geodata.cn).

REFERENCES

[1] Adel, Z. H., Mazen, H., Shady, M. (2018): A comparative study of ANN for predicting nitrate concentration in groundwater wells in the southern area of Gaza Strip. – Applied Artificial Intelligence 32(7-8): 727-744. https://doi.org/10.1080/08839514.2018.1506970.

[2] Alizamir, M., Kisi, O., Zounemat, K. M. (2018): Modelling long-term groundwater fluctuations by extreme learning machine using hydro-climatic data. – Hydrological Sciences Journal/Journal Des Sciences Hydrologiques 63(1): 63-73. https://doi.org/10.1080/02626667.2017.1410891.

[3] Aminravan F., Sadiq R., Hoorfar M., et al. (2013): Enhanced fuzzy evidential reasoning using an optimization approach for water quality monitoring. – IFSA World Congress and NAFIPS Meeting, Edmonton, Canada, pp. 1143-1148. https://doi.org/10.1109/IFSA-NAFIPS.2013.6608561.

[4] Asadollahfardi, G., Zangooei, H., Aria, S. H., et al. (2017): Application of Artificial Neural Networks to Predict Total Dissolved Solids at the Karaj Dam. – Environmental Quality Management 26(3): 55-72. http://doi.org/10.1002/tqem.21493.

[5] Bagheri, M., Mirbagheri, S. A., Kamarkhani, A. M., et al. (2016): Modeling of effluent quality parameters in a submerged membrane bioreactor with simultaneous upward and downward aeration treating municipal wastewater using hybrid models. – Desalination & Water Treatment 57(18): 8068-8089. http://doi.org/10.1080/19443994.2015.1021852.

[6] Brooks, B. W., Lazorchak, J. M., Howard, M. D., et al. (2016): Are harmful algal blooms becoming the greatest inland water quality threat to public health and aquatic ecosystems. – Environ. Toxicol. Chem. 35(1): 6. https://doi.org/10.1002/etc.3220.

[7] Cecconello, S. T., Centeno, L. N., Guedes, H. A. S. (2018): Índice de qualidade de água modificado pela análise multivariada: estudo de caso do Arroio Pelotas, RS, Brasil. (Water quality index modified by using multivariate analysis: a case study of Pelotas Stream, RS, Brazil.) – Engenharia Sanitaria e Ambiental 23(5): 973-978. http://dx.doi.org/10.1590/S0103-90162002000100026.

[8] Duan, H., Ma, R., Xu, X., Kong, F., Zhang, S., Kong, W., Hao, J., Shang, L. (2009): Two decode restruction of algal blooms in China's Lake Taihu. – Environ. Sci. Technol. 43(10): 3522-3528. http://pubs.acs.org/doi/abs/10.1021/es8031852.

[9] Dutta, S., Dwivedi, A., Suresh, K. M. (2018): Use of water quality index and multivariate statistical techniques for the assessment of spatial variations in water quality of a small river. – Environmental Monitoring and Assessment 190(12): 718. http://dx.doi.org/10.1007/s10661-018-7100-x.

[10] Drakard, V. F., Lanfranco, S.; Schembri, P. J. (2018): Macroalgal fouling communities as indicators of environmental change: potential applications for water quality monitoring. – Journal of the Marine Biological Association of the United Kingdom 98(7): 1581-1588. https://doi.org/10.1017/S0025315417001102.

[11] Flury, B. (1990): Common Principal Components and Related Multivariate Models. – Journal of the American Statistical Association 85(409): 259-260. https://doi/10.2307/2289562.

[12] Fogg, G. E. (1969): The physiology of an algal nuisance. – Proc. Royal Soc. London, B. 173: 175-189. https://doi.org/10.1098/rspb.1969.0045.

[13] Garrett, J. H. (1994): Where and why artificial RBF networks are applicable in civil engineering. – ASCE, J. Comp. Civ. Engng. Special Issue 8(2): 129-39. https://doi.org/10.1061/(ASCE)0887-3801(1994)8:2(129).

http://www.aloki.hu ● ISSN 1589 1623 (Print) ● ISSN 1785 0037 (Online)
DOI: http://dx.doi.org/10.15666/aeer/1706_1424114258

[14] Garson, G. D. (1991): Interpreting neural-network connection weights. – Artif. Intell. Expert 6: 47-51. http://doi.org/10.1207/s15327752jpa8502.
[15] Gleeson, B. (2001): Governing for the Environment. – In: Low, N., Gleeson, B. (eds.) The Challenge of Ethical Environmental Governance. Palgrave Macmillan, London, pp. 1-26.
[16] Guilin, L., Linfeng, T., Yuexia, C. (2018): Statistics based study on the seasonal variation of main pollutants in Shahu Lake, Ningxia. – Huanjing Huaxue-Environmental Chemistry 37(9): 2071-2080. https://doi/10.7524/j.issn.0254-6108.2017102602.
[17] Kellner, E., Jason, H., Kirsten, S. (2018): Characterization of sub-watershed-scale stream chemistry regimes in an Appalachian mixed-land-use watershed. – Environmental Monitoring and Assessment 190(10): 586. http://doi/10.1007/s10661-018-6968-9.
[18] Halal, F., Pedrocca, P., Hirose, T., et al. (2014): Remote-sensing based adaptive path planning for an aquatic platform to monitor water quality. – IEEE International Symposium on Robotic and Sensors Environments, Timişoara, Romania, pp.43-48. http://doi.org/.10.1109/ROSE.2014.6952981.
[19] Havens, K. E., Kukushima, T., Xie, P., Iwakuma, T., James, R. T., Takamura, N., Hanazato, T., Yamamoto, T. (2001): Nutrient dynamics and the eutrophication of shallow lakes Kasumigaura (Japan), Donghu (PR China), and Okeechobee (USA). – Environ Pollut. 111(2): 263. https://doi.org/10.1016/s0269-7491(00)00074-9.
[20] Islam, A. R. M. T., Shen, S., Haque, M. A. (2018): Assessing groundwater quality and its sustainability in Joypurhat district of Bangladesh using GIS and multivariate statistical approaches. – Environment Development and Sustainability 20(5): 1935-1959. https://doi.org/10.1007/s10668-017-9971-3.
[21] Jabbar, F. K., Grote, K. (2018): Statistical assessment of nonpoint source pollution in agricultural watersheds in the Lower Grand River watershed, MO, USA. – Environmental science and pollution research international 26(2): 1487-1506. https://doi/10.1007/s11356-018-3682-7.
[22] James, R. T., Havens, K., Zhu, G. W., Qin, B. Q. (2009): Comparative analysis of nutrients, chlorophyll and transparency in two large shallow lakes (Lake Taihu, P. R. China and Lake Okeechobee, USA). – Hydrobiologia 627(1): 211-231.https://doi.org/10.1007/s10750-009-9729-5.
[23] Joliffe, I. (2011): Principal Component Analysis. – Springer, New York, pp. 41-64. https://doi.org/10.1007/0-387-22440-8_7.
[24] Ju, Y., Kaown, D., Lee, K. -K. (2018): A three-pronged approach for identifying source and extent of nitrate contamination in groundwater. – Journal of Soil and Water Conservation 73(5): 493-503. https://doi/10.2489/jswc.73.5.493.
[25] Jun, X., Lingqing, W., Li, D. (2019): Characteristics, sources, water quality and health risk assessment of trace elements in river water and well water in the Chinese Loess Plateau. – Science of the Total Environment 650: 2004-2012. https://doi/ 10.1016/j.scitotenv.2018.09.322.
[26] Junli, W., Zishi, F., Hongxia, Q. (2019): Assessment of eutrophication and water quality in the estuarine area of Lake Wuli, Lake Taihu, China. – Science of The Total Environment 650: 1392-1402. https://doi/10.1016/j.scitotenv.2018.09.137.
[27] Masindi, K., Abiye, T. (2018): Assessment of natural and anthropogenic influences on regional groundwater chemistry in a highly industrialized and urbanized region: a case study of the Vaal River Basin, South Africa. – Environmental Earth Sciences 77(20). https://doi.org/10.1007/s12665-018-7907-3.
[28] Meifang, Z., Huayong, Z., Xuewei, S. (2018): Analyzing the significant environmental factors on the spatial and temporal distribution of water quality utilizing multivariate statistical techniques: a case study in the Balihe Lake, China. – Environmental Science and Pollution Research 25(29): 29418-29432. https://doi/ 10.1007/s11356-018-2943-9.

http://www.aloki.hu ● ISSN 1589 1623 (Print) ● ISSN 1785 0037 (Online)
DOI: http://dx.doi.org/10.15666/aeer/1706_1424114258

[29] Meng, L., Rui, Z., Jin-sheng, W. (2018): Apportionment and evolution of pollution sources in a typical riverside groundwater resource area using PCA-APCS-MLR model. – Journal of Contaminant Hydrology 28: 70-83. https://doi/10.1016/j.jconhyd.2018.10.005.
[30] Olden, J. D., Jackson, D. A. (2002b). Illuminating the "black box": a randomization approach for understanding variable contributions in artificial neural networks. – Ecol. Model 154: 135-150. http://doi.org/10.1016/s0304-3800(02)00064-9.
[31] Omar, R. H., Julia, R., Teresa, M., Fulvio, A. (2018): Physicochemical characterization and sources of the thoracic fraction of road dust in a Latin American megacity. – The Science of the Total Environment 652: 434-446. https://doi.org/10.1016/j.scitotenv.2018.10.214.
[32] Paerl, H. W., Hall, N. S., Calandrino, E. S. (2011): Controlling harmful cyanobacterial blooms in a world experiencing anthropogenic and climatic-induced change. – Sci. Tot. Environ. 409(10): 1739. https://doi.org/10.1016/j.scitotenv.2011.02.001.
[33] Paeral, H. W. (1988): Nuisance phytoplankton blooms in coastal, estuarine, and inland waters. – Limnol. Oceanog. 33: 823-847. https://doi.org/10.4319/lo.1988.33.4_part_2.0823.
[34] Prusty, P., Farooq, S. H., Zimik, H. V., et al. (2018): Assessment of the factors controlling groundwater quality in a coastal aquifer adjacent to the Bay of Bengal, India. – Environ Earth Sci. 77: 762. https://doi.org/10.1007/s12665-018-7943-z.
[35] Putri, M. S. A., Lou, C. H., Syai'in, M. (2018): Long-term river water quality trends and pollution source apportionment in Taiwan. – Water 10(10): 1394. https://doi.org/10.3390/w10101394.
[36] Qin, B., Wu, Q., Gao, J. (2002): Water environmental issues in Taihu Lake of China: problems, causes and management. – J. Nat. Res. 17(2): 221-228. https://doi/10.3321/j.issn: 1000-3037.2002.02.015.
[37] Qin, B. Q. (1999): Hydrodynamics of Lake Taihu, China. – Hydrobiologia 28(8): 669-673. https://www.jstor.org/stable/4314980.
[38] Qin, B. Q. (2008): Lake Taihu, China, Dynamics and Environmental Change. – Springer, New York. https://doi/10.1007/978-1-4020-8555-0.
[39] Tong, Q., Pingheng, Y., Groves, C. (2018): Natural and anthropogenic factors affecting geochemistry of the Jialing and Yangtze Rivers in urban Chongqing, SW China. – Applied Geochemistry 98: 448-458.https://doi.org/10.1016/j.apgeochem.2018.10.009.
[40] Richards, R. P., Baker, D. B., Crumrine, J. P., Stearns, A. M. (2010): Unusually large loads in 2007 from the Maumee and Sandusky Rivers, tributaries to Lake Erie. – J. Soil Water Conserv.,65(6): 450-462. http://doi.org/10.2489/jswc.65.6.450.
[41] Roveda, J. A. F., Arashiro, L. T., Roveda, S. R. M. M., et al. (2013): Fuzzy index for public supply water quality. – IFSA World Congress and NAFIPS Meeting, Edmonton, Canada, pp.1155-1159. http://doi.org/10.1109/IFSA-NAFIPS.2013.6608563.
[42] Scavia, D., Allan, J. D., Arend, K. K., et al. (2014): Assessing and addressing the re-eutrophication of Lake Erie: Central basin hypoxia. – Journal of Great Lakes Research 40(2): 226-246. http://dx.doi.org/10.1016/j.jglr.2014.02.004.
[43] Skowron, P., Skowronska, M., Bronowicka, M. U. (2018): Anthropogenic sources of potassium in surface water: the case study of the Bystrzyca river catchment, Poland. – Agriculture Ecosystems & Environment 265: 454-460. https://doi.org/10.1016/j.agee.2018.07.006.
[44] Shengli, Z., Zheng, W., Tianyi, C. (2018): Transcriptomic analysis of zebrafish (Danio rerio) embryos to assess integrated biotoxicity of Xitiaoxi River waters. – Environmental Pollution 242: 42-53. https://doi// 10.1016/j.envpol.2018.06.060.
[45] Shiau, J. T., Hsu, H. T. (2016): Suitability of ANN-based daily streamflow extension models: a case study of Gaoping River basin, Taiwan. – Water Resources Management 30(4): 1499-1513. http://doi.org/10.1007/s11269-016-1235-8.
[46] Sun, Q., Sun, F., Xia, X., et al. (2018): The comparison of ultrasound-assisted immersion freezing, air freezing and immersion freezing on the muscle quality and physicochemical

http://www.aloki.hu ● ISSN 1589 1623 (Print) ● ISSN 1785 0037 (Online)
DOI: http://dx.doi.org/10.15666/aeer/1706_1424114258

properties of common carp (Cyprinus carpio) during freezing storage. – Ultrasonics Sonochemistry 51: 281-291. http://dx.doi.org/10.1016/j.ultsonch.2018.10.006.

[47] Taufiq, A., Effendi, A. J., Iskandar, I. (2019): Controlling factors and driving mechanisms of nitrate contamination in groundwater system of Bandung Basin, Indonesia, deduced by combined use of stable isotope ratios, CFC age dating, and socioeconomic parameters. – Water Research 148: 292-305. https://doi.org/10.1016/j.watres.2018.10.049.

[48] Utah Department of Environmental Quality (2016): Potential health risks force closure of Utah Lake from harmful Algal bloom--Lab tests confirms a high probability of health risks. – https://deq.utah.gov/harmful-algal-blooms/harmful-algal-blooms-home/.

[49] Wang, J., Fu, Z., Qiao, H., et al. (2019): Assessment of eutrophication and water quality in the estuarine area of Lake Wuli, Lake Taihu, China. – Science of The Total Environment 650: 1392-1402. https://doi/10.1016/j.scitotenv.2018.09.137.

[50] Wu, W., Du, W., Zhong, J. (2016): Using Radial Basis Function Neural Networks to identify river water data parameters. – Automatic Control and Computer Sciences 50(4): 285-292. http://doi.org/.10.3103/s0146411616040088.

[51] Xiao, J., Wang, L., Deng, L., et al. (2019): Characteristics, sources, water quality and health risk assessment of trace elements in river water and well water in the Chinese Loess Plateau. – Science of the Total Environment 650: 2004-2012. https://doi/ 10.1016/j.scitotenv.2018.09.322.

[52] Xiaohu, W., Jian, L., Jun, W., et al. (2019): Influence of coastal groundwater salinization on the distribution and risks of heavy metals. – Science of The Total Environment 652(20): 267-277. https://doi.org/10.1016/j.scitotenv.2018.10.250.

[53] Zhaoxue, Z., Yi, L., Haipu, L., et al. (2018): Assessment of heavy metal contamination, distribution and source identification in the sediments from the Zijiang River, China. – Science of The Total Environment 645: 235-243. https://10.1016/j.scitotenv.2018.07.026.

[54] Zheng, J. F., Jiao, J. D., Zhang, S., et al. (2017): An optimization model for water quantity and quality integrated management of an urban lake in a water deficient city. – Urban Water Journal 14(3): 1-8. http://doi.org/10.1080/1573062X.2017.1301500.

[55] Zhi-Qiang, Y., Hiroki, A., Kei, N. (2018): Hydrogeochemical evolution of groundwater in a Quaternary sediment and Cretaceous sandstone unconfined aquifer in Northwestern China. – Environmental Earth Sciences 77: 18. https://doi/ 10.1007/s12665-018-7816-5.

[56] Zounemat, K. M., Özgür Kişi, A. J., et al. (2016): Evaluation of data driven models for river suspended sediment concentration modeling. – Journal of Hydrology 535: 457-472. http://doi.org/10.1016/j.jhydrol.2016.02.012.

http://www.aloki.hu ● ISSN 1589 1623 (Print) ● ISSN 1785 0037 (Online)
DOI: http://dx.doi.org/10.15666/aeer/1706_1424114258

SUPER-RESOLUTION RECONSTRUCTION OF CROP DISEASE IMAGES BASED ON DEPTH LEARNING

WANG, X.

College of Teacher Education, Pingdingshan University, Pingdingshan 467000, China
(e-mail: aaabbbw211@126.com)

(Received 3rd Jun 2019; accepted 11th Oct 2019)

Abstract. Current image reconstruction has some problems, such as low image segmentation and denoising precision, slow convergence speed, and poor image integrity after reconstruction. In this regard, this study proposed a super-resolution reconstruction of crop disease images based on deep learning. The improved neighborhood averaging method is used to denoise the low frequency subband image, and the enhanced wavelet coefficients are replaced by the wavelet inverse transform to realize the high frequency subband image denoising. The image enhancement results are introduced, and the image initial segmentation area is obtained by using the color roughness concept and the incremental region growth method. When the stop condition is satisfied, the best result is presented. The small feature extraction of image segmentation results is carried out, and the feature vectors are transformed from low resolution space to high resolution space by nonlinear mapping. Feature extraction, nonlinear mapping and image reconstruction are fused into a deep convolution neural network, and the final reconstruction results are obtained. The experiment showed that the method improves the image segmentation and denoising precision, and that the integrity coefficient of the image reconstruction is high and the reliability is strong.
Keywords: *reconstruction, wavelet inverse transform, image denoising, nonlinear mapping*

Introduction

The determination and control of crop diseases and insect pests play an important role in the development of agriculture in China. In actual production, most farmers only rely on experience and their own senses to diagnose crop diseases. Although it has achieved some results, it also has harmed the growth status of crops (Burgess et al., 2017). Therefore, early diagnosis is the key to accurately identify disease. It is not scientific to achieve the accurate recognition of all kinds of diseases only by human visual observation and experience (Gao et al., 2017; Fu and Liu, 2017). The symptoms of common crop diseases are mainly expressed by the color and texture of leaves (Mo et al., 2018; Kniat, 2017; Sanchez et al., 2017). At present, the treatment of agricultural diseases is mainly through expert diagnosis, and then taking corresponding measures (Wei, 2017). The symptoms of some diseases are not obvious at the initial stage, their symptoms become more pronounced with time, enabling precise diagnosis. This delays prevention and the time treatment can begin. The symptoms of some diseases are similar to those of other diseases. At this time, the experts have difficulties confirming the diagnosis, and other auxiliary methods should be used. Based on the research situation of crop diseases and insect pests, the following outstanding research results have appeared (Roy et al., 2018; Nongqwenga and Modi, 2017).

Mao et al. reconstruct the SEM (Sitemap) image by using the image edge gradient information. It used Kirsch operator to analyze the gradient information of the image, and then classified each region by using the feature that the gradient of the outer edge of the image is greater than the gradient of the inner edge, and filled the final image according to the statistical information. Experimental results showed that this method has high stability and high automation in high-resolution images, but the accuracy of

http://www.aloki.hu ● ISSN 1589 1623 (Print) ● ISSN 1785 0037 (Online)
DOI: http://dx.doi.org/10.15666/aeer/1706_1425914275

image segmentation is not enough, resulting in image reconstruction effect is not very ideal (Mao and Shi, 2016). Song proposed the 3D (3 Dimensions) reconstruction of images based on compressed sensing. By establishing the mathematical model of the image reconstruction of the SRM section, the principle of the algebraic reconstruction is analyzed. Based on the analysis of ART (Algebra Reconstruction Technique), SART (Simultaneous Algebraic Reconstruction Technique) and SIRT (simultaneous iterative reconstruction technique) method and its iterative formula, the CSART (compressive sensing Algebra Reconstruction Technique) algorithm combining the compressed sensing theory with ART is put forward to test the SRM (Switched Reluctance Moto) structure simulation model. According to the obtained projection data, several algorithms are analyzed and compared. The results showed that the CSART algorithm has the fastest convergence rate, but the reconstructed image integrity is not guaranteed (Song, 2016). Yu proposed a Tabu search based image reconstruction of capacitance tomography. The Tabu algorithm is referenced to the ECT (Emission Computed Tomography) image reconstruction. By constructing the target function, the neighborhood and Tabu table are set to constrain the image reconstruction. The image reconstruction problem is converted to the global optimal solution based on the contempt criteria and the ad hoc criteria and used termination criteria to jump out of Tabu Search. The simulation results showed that the reconstructed image is more fidelity, but the speed of reconstruction is slower (Yu et al., 2016). Li proposed the super-resolution image reconstruction based on support vector machine. The sparse characteristic of the image block is calculated, and the sparse representation coefficient is obtained. Then the sparse representation coefficient is used to train the support vector machine, and the super-resolution image reconstruction model is established. Finally, the simulation is used to analyze its performance. The results showed that the method can effectively maintain the speed of reconstruction, but the noise in the image is larger (Li, 2016). Guo proposed the super-resolution image reconstruction based on wavelet denoising and neural network. The wavelet transform is used to remove the noise in the image, improve the image quality, and obtain the learning samples needed for the network training. The learning samples are trained by neural network, and the artificial fish swarm algorithm is used to determine the key parameters of the neural network. Finally, the effectiveness of the super-resolution image reconstruction algorithm is tested, and its superiority is analyzed by comparison experiment. The experimental results showed that the proposed method can achieve an ideal image denoising effect, but there is also a low segmentation precision (Guo and Cen, 2016).

At present, there are various problems in image reconstruction methods of crop diseases, so we proposed to use deep learning to reconstruct super-resolution images of crop diseases. It can solve the problem that the traditional method does not accurately classify images. The detailed structure is as follows:

1. Using the improved neighborhood averaging method and the wavelet inverse transform respectively, the low frequency subband image and the high frequency subband image are de-noised to improve the image quality.
2. The initial segmentation area of the image is obtained by using the concept of color roughness and the incremental region growth method. Then the initial segmentation region is classified and merged to achieve high precision segmentation.
3. According to the application process of deep learning, we combine small feature extraction, nonlinear mapping and image reconstruction into a deep

http://www.aloki.hu ● ISSN 1589 1623 (Print) ● ISSN 1785 0037 (Online)
DOI: http://dx.doi.org/10.15666/aeer/1706_1425914275

convolution neural network system, and get the final disease image super-resolution reconstruction results.
4. Experimental results and analysis to verify the effectiveness of the reconstruction.
5. Discussion.
6. Summarize the content of the full text and look forward to the future.

According to the above method, the problem that the human eye cannot distinguish the pests and diseases of similar crops can be avoided, the accuracy of the identification of pests and diseases is effectively improved, and the economic benefit is improved.

Materials and methods

Image enhancement of crop disease

In order to effectively remove impulse noise in crop disease image, wavelet transform can be used to decompose the noisy image into low frequency subband and high frequency subband image, and then process them separately.

In the low frequency subband image denoising, the improved neighborhood averaging method is used to filter the low frequency subband image after the wavelet transform. Assuming that the gray value of pixels of crop disease pixels is $w(i,j)$, then the fuzzy distortion can be reduced as far as possible in the denoising process, so that the gray mean value of the original pixel in the window is as follows:

$$\overline{w(i,j)} = \begin{cases} w'(i,j) \left| w(i,j) - w'(i,j) \right| > T \\ w(i,j) \quad else \end{cases} \tag{Eq.1}$$

Among them,

$$w'(i,j) = \frac{1}{MN} \sum_{i=1}^{M} \sum_{j=1}^{N} w(i,j) \tag{Eq.2}$$

where $w'(i,j)$ representative is centered on the pixel $w(i,j)$, the size is the average value of pixels in a window of $M*N$, and T represents the adaptive threshold. M and N represent the length and width of the window, respectively.

According to the calculation of *Equations 1* and *2,* the improved neighborhood averaging method is used to filter the low frequency subband image after the wavelet transform, and the denoised image is obtained as follows:

$$f(x,y) = \frac{1}{M*N} * \frac{\overline{w(i,j)} * T}{w'(i,j) * \kappa} \tag{Eq.3}$$

Among them, $f(x,y)$ represents the image of crop disease after the low-frequency subband image denoising, and κ represents the image enhancement parameters.

http://www.aloki.hu ● ISSN 1589 1623 (Print) ● ISSN 1785 0037 (Online)
DOI: http://dx.doi.org/10.15666/aeer/1706_1425914275

In the high frequency subband image denoising, considering each subband image in a certain direction, so the horizontal high frequency subband image is filtered by the horizontal window, vertical high frequency subband image is filtered by vertical window, high frequency subband images is filtered by using a shaped window (Giuliani et al., 2016). The local energy method of pixel neighborhood is used to judge the pulse noise point, and the point which is larger than the local energy is regarded as the impulse noise point.

Taking the 3*3 window as an example, the pixel $w(i,j)$ neighborhood of the crop disease image is shown in the following case, as shown in *Figure 1*.

	$(i-1,j)$	
$(i,j-1)$	(i,j)	$(i,j+1)$
	$(i+1,j)$	

(a)

$(i-1,j-1)$		$(i-1,j+1)$
	(i,j)	
$(i+1,j-1)$		$(i+1,j+1)$

(b)

Figure 1. *Pixel* $w(i,j)$ *neighborhood of crop disease image*

When the image pixel $w(i,j)$ neighborhood of the crop disease image pixel in the case of *Figure 1a,* the local energy in the neighborhood of the pixel $w(i,j)$ is:

$$E_1(i,j)=\left|\begin{Bmatrix}2[w(i,j)-w'(i,j)]^2-[w(i-1,j)-w'(i,j)][w(i+1,j)-w'(i,j)]-\\[w(i,j-1)-w'(i,j)][w(i,j+1)-w'(i,j)]\end{Bmatrix}\right| \quad \text{(Eq.4)}$$

When the image pixel $w(i,j)$ neighborhood of the crop disease image pixel is in the case of *Figure 1b,* the local energy in the neighborhood of the pixel $w(i,j)$ is:

$$E_2(i,j)=\left|\begin{Bmatrix}2[w(i,j)-w'(i,j)]^2-[w(i-1,j+1)-w'(i,j)][w(i+1,j-1)-w'(i,j)]-\\[w(i-1,j-1)-w'(i,j)][w(i+1,j+1)-w'(i,j)]\end{Bmatrix}\right| \quad \text{(Eq.5)}$$

According to *Equations 4* and *5,* the local energy $E(i,j)$ of the center pixel of the crop disease image center in the neighborhood window is to select the maximum value of $E_1(i,j)$ and $E_2(i,j)$ as follows:

http://www.aloki.hu ● ISSN 1589 1623 (Print) ● ISSN 1785 0037 (Online)
DOI: http://dx.doi.org/10.15666/aeer/1706_1425914275

$$E(i,j)=\max\left[E_1(i,j),E_2(i,j)\right] \quad \text{(Eq.6)}$$

It is assumed that the local energy threshold in the neighborhood window is as follows:

$$TH=\frac{k}{M*N}\sum_{i}^{M}\sum_{j}^{N}E(i,j) \quad \text{(Eq.7)}$$

The k in *Equation 7* represents the empirical constant. Then it is possible to judge whether a point is a pulse noise point.

$$E(i,j)>TH \quad \text{(Eq.8)}$$

The pulse noise of the satisfying *Equation 8* is filtered out by a median filter. An adaptive wavelet threshold is set as follows:

$$TH_l=C_h\sigma_l\sqrt{\frac{2\log l+1}{l}}*2^{\frac{l+1}{2}} \quad \text{(Eq.9)}$$

Among them, l represents the decomposition scale, C_h represents the constant, h value is 1, 2, 3, respectively, which indicates that the horizontal and vertical directions are all high frequency sub-band images, the horizontal direction is the high frequency subband image and the vertical direction is the low frequency subband image, and the horizontal direction is the low frequency subband image and the vertical direction is the high frequency subband image. σ_l represents the standard deviation of the image noise of crop diseases at various scales, and the wavelet coefficients within each sub window of each scale are as follows:

$$\sigma_l=\left\{\frac{TH_l}{M*N}*\sum_{i}^{M}\sum_{j}^{N}w'(i,j)-E\left[w_l'(i,j)\right]\right\}^{\frac{1}{2}} \quad \text{(Eq.10)}$$

Among them, $E\left[w_l'(i,j)\right]$ represents the mean value of the medium and small wave coefficients of each sub window.

Based on the above content, the wavelet coefficients are obtained by using the wavelet soft threshold function to get the enhanced wavelet coefficients.

$$\eta\left[w(i,j)\right]=\operatorname{sgn}\left[w(i,j)\right]\left[\left|w(i,j)\right|\right]*\sigma_l*\left|TH_k\right| \quad \text{(Eq.11)}$$

Among them, η represents the enhanced wavelet coefficients. The setting of the coefficient can effectively improve the effect of image enhancement.

http://www.aloki.hu ● ISSN 1589 1623 (Print) ● ISSN 1785 0037 (Online)
DOI: http://dx.doi.org/10.15666/aeer/1706_1425914275

According to the enhanced wavelet coefficients obtained by *Equation 11,* the image $f'(x,y)$ of high frequency sub-band crop disease after de-noising is obtained by using the inverse wavelet transform *Equation 11.*

$$f'(x,y) = E(i,j) * TH_k * \frac{\eta[w(i,j)]}{TH} \quad \text{(Eq.12)}$$

Image segmentation of crop disease

According to the image enhancement results of crop disease, the image segmentation algorithm of crop disease is realized by using the image segmentation algorithm of color and image spatial information. The image used in the segmentation is color image, and the whole process is divided into initial segmentation and hierarchical region merging.

The initial segmentation of the image is done by color quantization and incremental regional growth, which will be described in detail below. In order to make the algorithm for the definition of color distance conforms to the human visual characteristics, we choose LUV color space, and the color distance is measured by Euclidean distance (Lal et al., 2016).

For color quantization, it is assumed that a crop disease image contains M windows of $w_1 * w_2$, and each window contains n pixels. S_m represents the roughness of the image color, which is used to represent the intensity of the color change in the current window. The color quantization series of the current image is determined by the average color roughness S_{avg} of the entire image. There are:

$$S_m = \left(\frac{1}{n} \sum_{i=0}^{n-1} \left\| \vec{x_i} - \vec{x}_{mean}^{(m)} \right\| \right)^{\frac{1}{2}} * f'(x,y) \quad \text{(Eq.13)}$$

$$S_{avg} = \frac{1}{M} \sum_{i=0}^{M-1} S_m \quad \text{(Eq.14)}$$

where $\vec{x_i}$ represents the color of the i pixel in the $w_1 * w_2$ window, $\vec{x}_{mean}^{(m)}$ represents the mean color in a window, and $\|\cdot\|$ represents the Euclidean distance. Based on *Equation 14,* the quantity of the color quantization of a crop disease image is calculated by using *Equation 15.*

$$N_{Quan} = \beta * S_{avg} + 1 \quad \text{(Eq.15)}$$

Among them, β represents the image color quantization threshold, depending on the accuracy of image segmentation, it can be divided into high, medium and low grades, respectively, and is set to 2, 1, and 0.5, respectively.

After determining the number of color quantization, we use vector quantization to divide the crop disease image pixels into color space, and get the image $\gamma(x,y)$ after color quantization. The formula is as follows:

http://www.aloki.hu ● ISSN 1589 1623 (Print) ● ISSN 1785 0037 (Online)
DOI: http://dx.doi.org/10.15666/aeer/1706_1425914275

$$\gamma(x, y) = VQ * \sqrt{\frac{N_{Quan}}{w_1 * w_2}} \quad \text{(Eq.16)}$$

Among them, VQ represents vector quantization.

Being divided into the same class of pixels in the color space does not necessarily belong to the same region (Olafsson et al., 2017). These color-classified pixels also need to combine space information to form meaningful segmentation areas. An incremental regional growth algorithm is used to discover the spatial connectivity between pixels. The pixels that conform to the following conditions to form the seed region are defined as:

1. The color is the same after the color is quantified.
2. Four neighborhoods are connected in space.
3. Connected pixels reach a certain area (according to the segmentation precision (that is, high, medium, low), set the original image area of 0.001%, 0.01% and 0.1% respectively).

The pixels in the image that are not in the seed region will be allocated by a regional growth method to the region that is adjacent to the color and is the closest to the color. For a seed area, if the newly grown pixels meet the following conditions, the algorithm divides the newly growing connected pixels into an independent new seed area. A new region growing method, which can generate new seed regions in growth process is defined as incremental region growing. This growth algorithm is more conducive to some details in the process of growth.

1. The newly grown pixels are connected in the four neighborhoods in space.
2. The average distance between the newly grown pixels is less than the average distance between the pixels and the current region.
3. The newly grown connected pixels reach the requirement of the seed area. (According to the segmentation accuracy (high, middle and low), they are set to 0.001%, 0.01% and 0.1% of the original image area, respectively).

Through the above calculation and analysis, regional merger is carried out. After the initial segmentation, there are still a lot of similarities between the regions (Katsevich and Katsevich, 2017). The ensemble is combined by a hierarchical region merging algorithm to merge the divided area, and an automatic stop region merging rule is proposed.

For region merging, region distance measurement is an important criterion for region merging. Distance metric determines the result of region merging and the final segmentation result of image. This study considers that the necessary conditions for merging two regions are: two regions are similar in color and adjacent in space, and there is no significant edge on their adjacent areas (Pagnanelli and Borgesneto, 2016). Then the edge, color and adjacency information are fused, and *Equation 17* gives the distance definition of the two regions.

$$D_{ij}^{r} = \left(D_{ij}^{c}\right)^{p} * \left(D_{ij}^{e}\right)^{q} * \Delta_{ij} * \gamma(x, y) \quad \text{(Eq.17)}$$

http://www.aloki.hu ● ISSN 1589 1623 (Print) ● ISSN 1785 0037 (Online)
DOI: http://dx.doi.org/10.15666/aeer/1706_1425914275

Among them, p and q are used to adjust the color distance and the distance from the edge of the effect size threshold, Δ_{ij} represents the adjacency relation, that is, the existence of adjacency relation between representatives of r_i and r_j, there is relationship between adjacent assumptions, the Δ_{ij} value is 1, whereas the value is $+\infty$, and the region distance is $+\infty$. D_{ij}^c and D_{ij}^c represent the color distance and edge distance of two regions, defined as *Equations 18* and *19*.

$$D_{ij}^c = \frac{|r_i| * |r_j|}{|r_i| + |r_j|} * \|\mu_i - \mu_j\| * \sqrt{D_{ij}^r} \quad \text{(Eq.18)}$$

$$D_{ij}^e = \frac{1}{|E_{ij}|} \sum \|x_a - x_b\| * \sqrt{D_{ij}^c} \quad \text{(Eq.19)}$$

Among them, $|r_i|$ and $|r_j|$ represent the number of pixels contained in the i region and the j region, μ_i and μ_j represent the two regional color mean, and the $\|\mu_i - \mu_j\|$ represents the Euclidean distance. The product of the molecular part $|r_i|$ and $|r_j|$ in *Equation 18* is beneficial to the priority merging of the cell domain, making the segmentation results more consistent with the visual characteristics of the masses. E_{ij} represents the pixels on the edge of two regions, and $|E_{ij}|$ represents the number of pixels on the edge. x_a and x_b represent the color values of the a and b points on both sides of the edge, respectively.

For the initial segmentation area, the classification region merging algorithm is used to complete the final segmentation. That is, each time we merge the two regions with the closest distance in the image, form a new area, and the adjacency and distance between the new area and other regions will also be adjusted.

In the process of regional merger, it is a very critical question when to stop the regional merger to get a reasonable combination result, and directly decide the result of image segmentation (Wu et al., 2016). The threshold method is used to terminate the region merging, and the merging is affected by the distance between the local regions. The threshold selection also needs to be adjusted according to different images. It is necessary to manually adjust the number of regions according to different requirements, using the method of specifying the number of areas to terminate the merger. Considering the relationship between the information loss in the process of image merging and the number of areas retained in the image, a new automatic stopping region merging criterion is proposed. The detailed process is as follows:

A function that represents the color divergence of the image region is defined to indicate the degree of disunity of the total color in each region of the image. When the area of the image is merged to K, the color divergence can be defined as:

$$J = \frac{\sum_{r=0}^{K} J_w^r}{J_t} = \frac{\sum_{r=0}^{K} \sum_{i=0}^{N_r} \left\| x_i^r - x_{mean}^r \right\|}{\left\| x_i^r - x_{mean}^r \right\|} \quad \text{(Eq.20)}$$

http://www.aloki.hu ● ISSN 1589 1623 (Print) ● ISSN 1785 0037 (Online)
DOI: http://dx.doi.org/10.15666/aeer/1706_1425914275

where J_w^r represents the color divergence within a region, and J_t represents the total color divergence in the image. N_r represents the number of pixels in the r region, and x_i^r represents the color value of the i pixel in the r region, and x_{mean}^r represents the color mean of the r region.

Each initial region that defines an image contains only one color, and the color value of all the pixels in each region is equal to the mean color of the region. At this point, the region color of the image is 0, that is, $J=0$. With the continuous consolidation of the region, that is, the K continues to decrease, and the region color dispersion of the image is increasing in J. When all areas in the image are merged into one area, J is 1. Assuming that k_l represents the number of remaining regions in the merging process, the relationship curve between J and k_l is shown as shown in *Figure 2.*

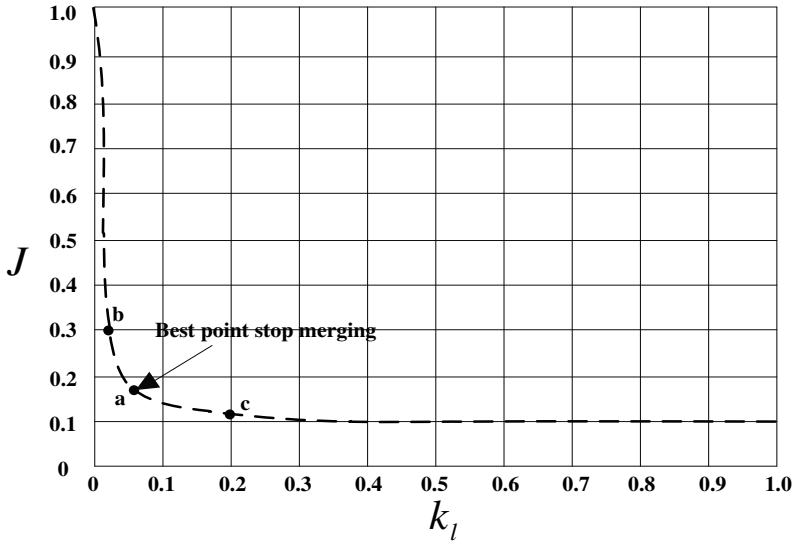

Figure 2. *Relation curve between* J *and* k_l

As shown in *Figure 2,* from the point of view, it is hoped that the least area can be used to represent the information in an image, that is, the smaller the better the k_l. From the point of view of the segmentation, the smaller the better the information loss in each region after the segmentation, that is, the smaller the area of the image is, the smaller the J, the better. The two values cannot be minimized at the same time, because each area merge will cause the increase of J. In order to get the most reasonable segmentation results, the minimum value of $J+k_l$ is obtained, that is, the ratio of reserved regions and the color dispersion J of the image area to achieve the best compromise when the k_l is terminated. According to the above analysis, the best combination point in *Figure 2* is a.

According to the above calculation and analysis, the optimal segmentation results are as follows:

$$F(x,y)=\min\left(k_l+J\right) \quad \text{(Eq.21)}$$

http://www.aloki.hu ● ISSN 1589 1623 (Print) ● ISSN 1785 0037 (Online)
DOI: http://dx.doi.org/10.15666/aeer/1706_1425914275

Super-resolution reconstruction of crop disease images

Deep learning is a new field in machine learning research. Its motive is to establish and simulate the human brain's analysis and learning neural network. It simulates the mechanism of human brain to interpret data, such as image, voice and text (Zhou et al., 2016). Based on the image enhancement of 2.1 and the image segmentation of 2.2, the high resolution reconstruction of the crop disease image is realized by the depth learning method. The concrete process of reconstruction is as follows.

Small feature extraction and representation: it is the first layer of network. The operation will input low resolution image Y to extract small blocks densely, and use high-dimensional feature vectors to represent small blocks. The equivalent is to convolution the image through a set of filters. Assuming that the first layer, the small block feature extraction result is set to F_1, by using the image segmentation of 2.2, F_1 can be expressed as:

$$F_1(Y) = \max(0, W_1 \partial Y + B) \quad \text{(Eq.22)}$$

Among them, W_1 and B represent the bias vector of the filter combination neuron, and ∂ represents the convolution operation. Suppose that d represents the number of channels to enter crop disease image. f_1 represents the spatial size of a single filter, and n_1 represents the number of filters. The size of W_1 is $d * f_1 * n_1$.

Through the calculation of *Equation 22,* n_1 dimensional feature vector were extracted from each image block, in the second layer nonlinear mapping, each high dimensional vector is mapped to a vector of another dimension n_2, that is, to transform feature vectors from low resolution space to high resolution space, the output characteristics is $F_2(Y)$. Then the mapping results of the second layers can be expressed as:

$$F_2(Y) = \max(0, W_2 \partial F_1(Y) + B_1) \quad \text{(Eq.23)}$$

Among them, W_2 represents convolution kernel, B_1 represents a n_2 bias vector, and each output n_2 dimension vector represents the reconstructed high resolution block.

Using the above calculation, the image block reconstruction layer is reconstructed to form the output image after the mapping. The average can be considered as a predefined filter on a set of feature images, thereby defining the following reconstruction layer to produce high resolution images:

$$F(Y) = W_3 \partial F_2(Y) + B_2 \quad \text{(Eq.24)}$$

where W_3 contains d linear filters, and B_2 represents a bias vector with a dimension of d.

Convolution neural network is essentially a mapping from input to output. It can learn a lot of mapping relationships between input and output without any precise mathematical expression between input and output (Salehi et al., 2017). Therefore, as

http://www.aloki.hu ● ISSN 1589 1623 (Print) ● ISSN 1785 0037 (Online)
DOI: http://dx.doi.org/10.15666/aeer/1706_1425914275

long as the convolution network is trained with a known pattern, the network has the ability to map the input and output. The purpose of the convolution neural network is to estimate and optimize the parameters in essence. From the above, the parameters that need to be trained can be expressed as $\theta = \{W_1, W_2, W_3, B, B_1, B_2\}$. When the error between the reconstructed image $F(Y;\theta)$ and the real image X is small, the optimal solution of the parameters can be obtained.

A set of original crop disease image $\{X_i\}$ and its corresponding low resolution image set $\{Y_i\}$ are given, and the loss function is used to indicate the error between them. The mean square error (MSE) is considered to represent the loss function $L(\theta)$. As shown in *Equation 25:*

$$L(\theta) = \frac{1}{n}\sum \left\| F(Y;\theta) - X_i \right\|^2 \quad \text{(Eq.25)}$$

According to the calculation by *Equation 25,* we can see that the error between original crop disease image $\{X_i\}$ and its corresponding low resolution image set $\{Y_i\}$ is the smallest, that is, when the loss function is minimum $\min L(\theta)$, the image reconstruction accuracy of crop disease is the highest. The result of the final image super-resolution reconstruction using the minimum loss function is as follows:

$$Best(X,Y) = \min L(\theta) * \left(\{X_i\} \Leftrightarrow \{Y_i\} \right) * \varpi * \vartheta \quad \text{(Eq.26)}$$

Among them, ϖ represents the threshold of super resolution reconstruction for crop disease image, which is controlled between 0.4-0.5. After image reconstruction, integrity is kept the best and the reconstruction result is the best. ϑ represents the speed factor of the image reconstruction convergence speed, which can improve the speed of image reconstruction efficiently.

Results

In order to verify the effect of reconstruction, the experiment was completed by the contrast of different image reconstruction methods. Taking into account the fairness of comparison, the experiment used a data set of a domestic agricultural production base on crop disease image as a training sample, and the experimental platform was built on Matlab7.0. After training the samples, the experimental objects were tested with the trained parameters, this result is obtained from a real agricultural planting shed and *Figure 3* is the test sample.

According to the experimental platform and the experimental data, the experiment is carried out under the following experimental indexes.

1. Image enhancement effect of crop disease, that is, image clarity.
2. The accuracy of image segmentation.
3. The integrity of the reconstructed image.
4. The convergence rate of image reconstruction.

http://www.aloki.hu ● ISSN 1589 1623 (Print) ● ISSN 1785 0037 (Online)
DOI: http://dx.doi.org/10.15666/aeer/1706_1425914275

Figure 3. *Test examples*

The experimental results are as follows:

Figure 4 showed that image reconstruction based on support vector machine has low clarity and low color division, and texture area is poor. The image reconstruction method based on depth learning is very effective, the texture is clear and the color is distinct. The overall definition of the image is better than the image reconstruction method based on support vector machine.

(a) Image enhancement effect based on support vector machine image reconstruction

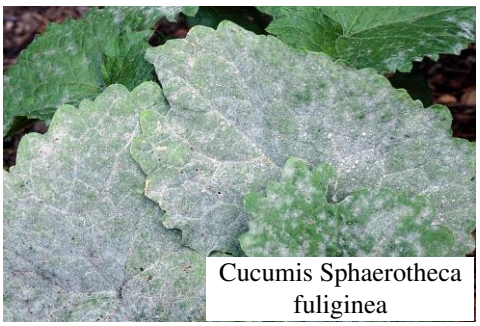

(b) Image enhancement effect based on deep learning image reconstruction

Figure 4. *Enhancement of image reconstruction with different image reconstruction methods*

According to the analysis of *Figure 5,* the image segmentation accuracy of image reconstruction based on edge gradient information is gradually low with the increase of image number. The maximum segmentation precision is 56% and the lowest is 33%, which indicates that the reliability of the method is low. The image segmentation accuracy based on wavelet denoising and neural network image reconstruction has a downward trend, the maximum segmentation precision is 63%, and the lowest is 50%.

http://www.aloki.hu ● ISSN 1589 1623 (Print) ● ISSN 1785 0037 (Online)
DOI: http://dx.doi.org/10.15666/aeer/1706_1425914275

The image segmentation precision curve of the image reconstruction method based on depth learning is increasing gradually, the maximum segmentation precision is 96% and the minimum segmentation precision is 75%, which is more reliable compared with image reconstruction method based on the edge gradient information.

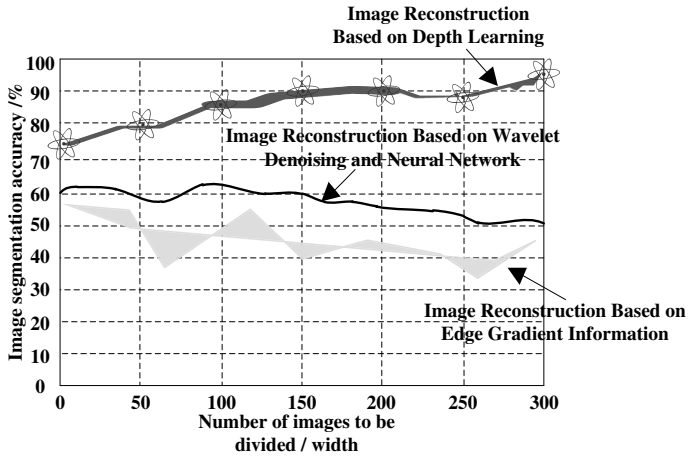

Figure 5. *Image segmentation precision comparison of different image reconstruction methods*

From the contrast result of *Figure 6,* we can see that the integrity coefficient of image reconstruction based on compressed sensing is low, the highest is 0.48. This data indicates that the integrity of image reconstruction is not guaranteed. The integrity coefficient of the reconstruction method based on depth learning is 0.98 and the lowest is 0.7. According to the data comparison, it is obvious that the image reconstruction based on depth learning can be practicable and useful for reference.

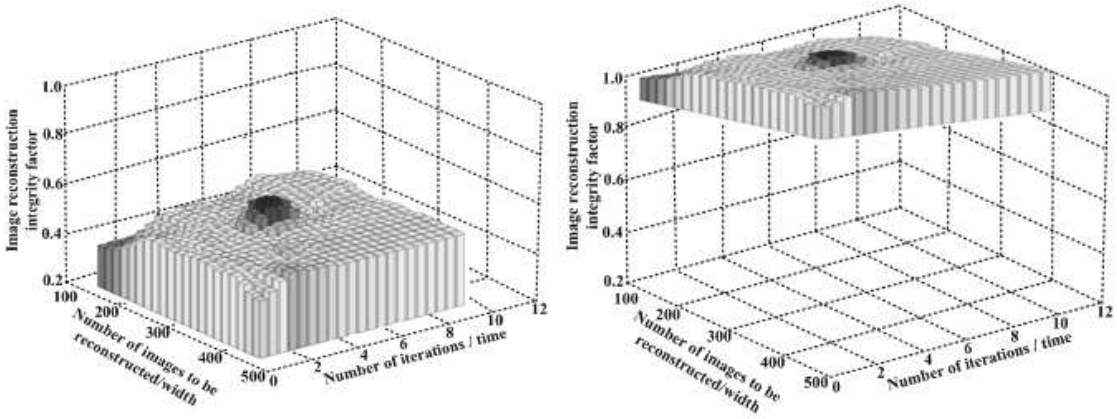

(a) Integrity of image reconstruction based on compressed sensing

(b) Integrity of image reconstruction based on deep learning

Figure 6. *Reconstruction integrity comparison of different image reconstruction methods*

In *Figure 7,* the time-consuming curve of the image reconstruction convergence based on Tabu search showed an unstable state, which is fluctuate up and down, and the average convergence time is about 0.5 s. The time-consuming curve stability of the image reconstruction based on depth learning is better, the maximum time of

http://www.aloki.hu ● ISSN 1589 1623 (Print) ● ISSN 1785 0037 (Online)
DOI: http://dx.doi.org/10.15666/aeer/1706_1425914275

convergence is 0.35 s, and the time of average convergence is 0.3 s. Compared with the two image reconstruction methods, the time dependent data is convergent, and the image reconstruction method based on depth learning occupies a significant advantage and is reliable.

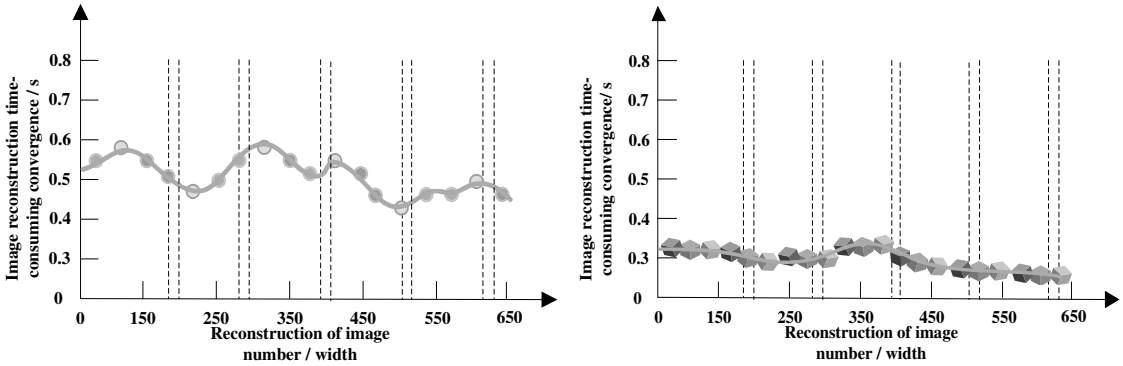

(a) Time consuming of image reconstruction based on Tabu Search

(b) Time consuming of image reconstruction based on deep learning

Figure 7. *Time consuming comparison of reconstruction of different image reconstruction methods*

The identification of crop diseases is accurately compared, and the results are as follows:

Analysis of *Figure 8* shows that the accuracy of the identification of disease and insect information in three different methods is different. The accuracy of this method is significantly higher than the other two methods, and has a high promotion value.

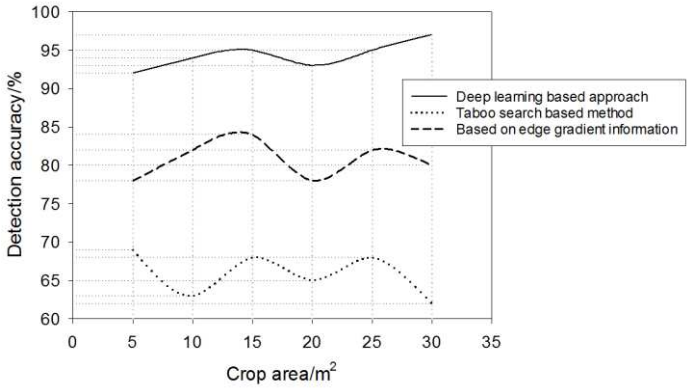

Figure 8. *Comparison of information recognition accuracy under different methods*

Discussion

In the discussion part, the ϖ threshold of super resolution reconstruction of crop disease image is used to observe and verify the influence of the value range on the super resolution reconstruction of crop image.

In order to make the results of the discussion more comprehensive, the ϖ values of 0.3, 0.4 and 0.45 are considered as the scope of discussion, respectively. The discussion environment is selected as follows: Intel (R) Core (TM) i5-3210M CPU@2.50 GHz;

http://www.aloki.hu ● ISSN 1589 1623 (Print) ● ISSN 1785 0037 (Online)
DOI: http://dx.doi.org/10.15666/aeer/1706_1425914275

6.00 GB memory; Win7x64; Matlab; Caffe. And the Matlab interface of Caffe is used to achieve image super resolution reconstruction.

The graphs in *Figure 9* represent the effects on image reconstruction when the ϖ values are 0.3, 0.4, and 0.45.

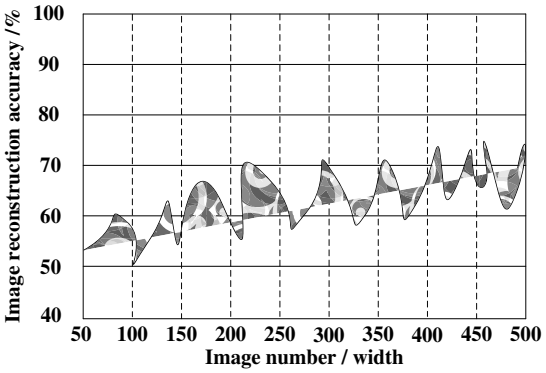

(a) Image reconstruction accuracy when ϖ is 0.3

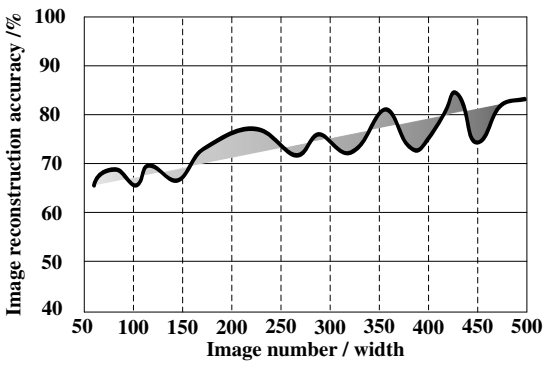

(b) Image reconstruction accuracy when ϖ is 0.4

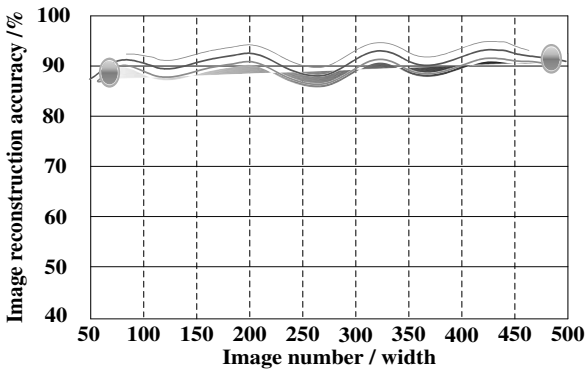

(c) Image reconstruction accuracy when ϖ is 0.45

Figure 9. *The impact of different values of* ϖ *on image reconstruction results*

According to the results of *Figure 9,* we can see that when ϖ is 0.3, the accuracy of image reconstruction is 73%, and the accuracy of reconstruction accuracy is not good, but it shows a rising trend. When the ϖ is 0.4, the accuracy of image reconstruction is obviously superior to that of when ϖ is 0.3, the precision of the reconstruction is 83%, and the whole fluctuation of the precision curve is stable. When the ϖ is 0.45, the accuracy of the image reconstruction is the highest and the transformation of the precision curve is the smallest. When the reconstructed image is 425, the reconstruction precision is 95%. The above data show that when ϖ is 0.45, the image reconstruction results are most significant.

Conclusions

At present, there are many problems in the algorithms and methods of image reconstruction. In order to solve these problems, an image super-resolution reconstruction based on deep learning is proposed. Image reconstruction is completed by three links of image enhancement, image segmentation and image reconstruction. In the process of image reconstruction, the speed of reconstruction and the accuracy of

http://www.aloki.hu ● ISSN 1589 1623 (Print) ● ISSN 1785 0037 (Online)
DOI: http://dx.doi.org/10.15666/aeer/1706_1425914275

reconstruction are the difficult problems. In order to solve such problems, the threshold of image super-resolution reconstruction and the speed factor of image reconstruction convergence are set up respectively. Two parameters are used to control the accuracy and speed of the reconstruction. The effectiveness of the proposed image reconstruction method is verified by experiments and discussions. It is also proved that the threshold of reconstruction and the speed of convergence play a very important role in the whole process of image reconstruction, which effectively solves the problems of image reconstruction.

In the future, the efficiency of image reconstruction will be further studied while compressing reconstruction costs.

REFERENCES

[1] Burgess, A. J., Retkute, R., Pound, M. P., Mayes, S., Murchie, E. H. (2017): Image-based 3D canopy reconstruction to determine potential productivity in complex multi-species crop systems. – Annals of Botany 119: 517-532.

[2] Fu, H., Liu, X. (2017): A Study on the impact of environmental education on individuals' behaviors concerning recycled water reuse. – Eurasia Journal of Mathematics Science and Technology Education 13(10): 6715-6724.

[3] Gao, W., Baig, A. Q., Ali, H., Sajjad, W., Farahani, M. R. (2017): Margin based ontology sparse vector learning algorithm and applied in biology science. – Saudi Journal of Biological Sciences 24(1): 132-138.

[4] Giuliani, M., Vissa, A., Driouchi, A., et al. (2016): Effect of data pre-processing on super-resolution reconstruction and pattern recognition. – Biophysical Journal 110(3): 331a.

[5] Guo, B. H., Cen, Z. S. (2016): Super resolution image reconstruction based on wavelet denoising and neural network. – Laser Journal 37: 61-64.

[6] Katsevich, A., Katsevich, A. (2017): A local approach to resolution analysis of image reconstruction in tomography. – Siam Journal on Applied Mathematics 77: 1706-1732.

[7] Kniat, A. (2017): Visualization of a lifeboat motion during lowering along ship's side. – Polish Maritime Research 24(4): 42-46.

[8] Lal, A., Shan, C., Xi, P. (2016): Structured illumination microscopy image reconstruction algorithm. – IEEE Journal of Selected Topics in Quantum Electronics 22: 50-63.

[9] Li, C. (2016): Super resolution image reconstruction based on support vector machine. – Laser Journal 37: 138-141.

[10] Mao, X. D., Shi, Z. (2016): Method about reconstruction of SEM image based on gradient. – Computer Science 43: 297-301.

[11] Mo, S., Li, Z., Gou, K., Qin, L., Shen, B. (2018): Quantifying the effects of climate variability and direct human activities on the change in mean annual runoff for the Bahe River (Northwest China). – Journal of Coastal Research 34(1): 81-89.

[12] Nongqwenga, N., Modi, A. T. (2017): Phosphorus and potassium quantity/intensity properties of selected South African soils (Kwazulu-Natal) and their correlation with selected soil parameters. – Applied Ecology and Environmental Research 15(3): 1-14.

[13] Olafsson, V. T., Noll, D. C., Fessler, J. A. (2017): Fast spatial resolution analysis of quadratic penalized least-squares image reconstruction with separate real and imaginary roughness penalty: application to fMRI. – IEEE Transactions on Medical Imaging. DOI: 10.1109/TMI.2017.2768825.

[14] Pagnanelli, R., Borgesneto, S. (2016): Technical aspects of resolution recovery reconstruction. – Journal of Nuclear Cardiology 23: 149-152.

http://www.aloki.hu ● ISSN 1589 1623 (Print) ● ISSN 1785 0037 (Online)
DOI: http://dx.doi.org/10.15666/aeer/1706_1425914275

[15] Roy, S., Handique, G., Bora, F. R., Rahman, A. (2018): Evaluation of certain non-conventional plant based oils against red spider mite of tea. – Journal of Environmental Biology 39(1): 1-4.
[16] Salehi, B., Daneshfar, B., Davidson, A. M. (2017): Accurate crop-type classification using multi-temporal optical and multi-polarization SAR data in an object-based image analysis framework. – International Journal of Remote Sensing 38: 4130-4155.
[17] Sanchez Camacho, E. A., Martinez Morales, M. (2017): Estimation of the volume of underground water for a coastal wetland. – Revista Internacional De Contaminacion Ambiental 33(SI): 65-76.
[18] Song, J. H. (2016): Image reconstruction of SRM cross-section based on compressed sensing. – Computer Simulation 33: 132-137.
[19] Wei, D. (2017): Image super-resolution reconstruction using the high-order derivative interpolation associated with fractional filter functions. – Iet Signal Processing 10: 1052-1061.
[20] Wu, G. H., Zhang, H. D., Li, X. K., Dai, J. Y. (2016): FR-CoSaMP image reconstruction algorithm based on improved measurement. – Computer Engineering and Design 37: 1555-1559.
[21] Yu, J. P., Chen, D. Y., Wang, L. L. (2016): A Novel image reconstruction algorithm based on improved taboo search for electrical capacitance tomography. – Journal of Harbin University of Science and Technology 21: 51-56.
[22] Zhou, L. Y., Su, C. X., Cao, Y. F. (2016): Image super-resolution via sparse representation. – Computer Engineering and Design 37: 3290-3294.

http://www.aloki.hu ● ISSN 1589 1623 (Print) ● ISSN 1785 0037 (Online)
DOI: http://dx.doi.org/10.15666/aeer/1706_1425914275

LANDSCAPE SENSITIVITY ANALYSIS AS AN ECOLOGICAL KEY: THE CASE OF DUZCE, TURKEY

KARADAĞ, A. A.* – ŞENIK, B.

Department of Landscape Architecture, Faculty of Forestry, Düzce University, Konuralp Campus, 81620 Duzce, Turkey

**Corresponding author*
e-mail: ayferkaradag@duzce.edu.tr

(Received 2nd Jun 2019; accepted 10th Sep 2019)

Abstract. Landscape sensitivity is one of the ways that give us the opportunity to exhibit ecology-based approaches to the world we live in. Landscape sensitivity refers to areas where landscape is sensitive to natural or human-based pressures. This study aims to develop a model for revealing and mapping the landscape sensitivity of Duzce province in Turkey. The model was developed by evaluating four parameters (ecologic process). These are erosion risk, landslide susceptibility, water infiltration and habitat fragmentation. Within the scope of the study, sensitivity data related to each parameter has first been formed within the framework of expert opinions and then all data has been analyzed by ArcGIS 9.3 software and a Duzce Province Landscape Sensitivity Map has been produced. When the landscape sensitivity map obtained within the scope of the model is evaluated, it is seen that the sensitivity in 38.6% of the area is low while it is medium with 30.6%, very low with 21.7%, high with 8.2% and very high with 8.2%. These findings are easily visualized on the map. As a result, the landscape sensitivity map produced is a data that is compatible with ecological principles, produced by scientific methods, compatible with technological tools and can be integrated with similar analyses. In addition it is an important element to develop ecological based decisions related to the space. Therefore, its usage as a basis map for spatial planning is a need beyond desire.
Keywords: *ecological sensitivity, vulnerability, risk analysis, suitability analysis, land use decision, landscape planning*

Introduction

The coexistence of nature and man is an existential necessity. Indeed, there is no other space in the known universe where human beings can survive. On the other hand, nature has no such obligation. For nature can realize its cycle on its own. Such that, the quite short history of mankind in the world is the clearest indication of our need for nature and not its need for us. In the simplest sense, man is born and raised within nature; he grows up and builds his culture and civilization there. However, human beings' disposition on nature varies according to historical periods (İlboğa and Aygül, 2015). This differentiation has been rapidly moving towards a humanistic approach that sees nature as an object exploitable for its own interests and commodifies it. Scientists who realized this strived to reveal the discomforts caused by this commoditization process and to identify its sensitivity to solve the problems. Landscape sensitivity is one of the studies conducted in this context.

The landscapes arose from the unity of man and nature. The landscape is a combination of rocks, surface deposits, soils, plants, animals, people, etc. together with the earth itself, and each of these is a component of the landscape. The landscapes do not only contain objects, they also include dynamic earth surface systems. In this context, they are energy and material stores maintained with growth, decay, flow and transformation processes. The landscapes exhibit spatial mosaics forming a "complex

http://www.aloki.hu ● ISSN 1589 1623 (Print) ● ISSN 1785 0037 (Online)
DOI: http://dx.doi.org/10.15666/aeer/1706_1427714296

combination" at different characters and scales on the earth's surface (Thomas, 2001). In this context, the landscape is a heterogeneous land area consisting of similarly replicated and interrelated ecosystem clusters, i.e. habitat patches (Forman and Godron, 1986; Dunning et al., 1992; Turner et al., 2001; Boström et al., 2011). While maintaining growth, decay, flow and transformation processes of landscaping, the landscape is also dynamical earth surface systems containing not only objects but also energy and material stores (Thomas, 2001). The landscape which consists of many superimposed environments or components is the semiotic interface between sources and organisms, and it is shaped by ecological processes (Farina, 2001, 2008; Farina and Pieretti, 2012). In fact, landscaping refers to two natural systems (physical and biological) and processes that constitute this system. Physical systems are composed of landform, surface deposits, rock components and are formed as a result of processes such as rock erosion and sediment transportation etc. Biological systems are composed of plants, animals and people, and have many ecological processes. Soil is the other component of landscape which these two systems closely interact with. In short, landscaping is an area on which action, interaction and various relationships between natural and/or cultural resources take place (Demir, 2019). Therefore, it is a dynamic and multidimensional concept.

With its components and ecological processes, the landscape has become key to defining the relationship between nature and human beings, and the common evolution between natural and human processes (Mazzino and Burlando, 2010). For, the landscape is the product of a long history of evolution that reflects the interactions of landscape, geology, topography, climate, geomorphologic processes and their transformations over time (Gordon and Sutherland, 1993). All aspects of landscaping (ecological, economic, social) also arise with historical processes (Turner, 2018). This process is in fact related to the history of Quaternary. The history of the Quaternary has evidence related to the occurrence rate of natural processes (especially geomorphologic processes) and plant communities' response to both climatic changes and improvements. Furthermore, this evidence provides information on the development of the natural environment before and after the human impact (Gordon and Sutherland, 1993). This information provides important clues to the understanding landscape formation and change. These clues can contribute to the identification of red lines related to human life in the landscape. As Usher (2001) argues, human is also a part of this landscape and as natural as plants, but due to its non-conscientious nature, it is necessary to determine its boundaries of movement in the landscape, to provide the nature with an opportunity to renew the nature and to ensure its sustainability. In this context, it is very important to determine the landscape sensitivity, in other words to determine the sensitive areas in the landscape. The result is an open system; any interference from outside may affect this structure. These effects on the landscape can be realized in such a way as to contribute to the sustainability of the landscape or change its very structure (Steffen et al., 2011; Lewis and Maslin, 2015).

Landscape sensitivity is not easy to define. It requires considering the main natural systems that determine the landscape, its structure and the processes that change these natural systems (Usher, 2001). Based on this idea, the concept comes from geomorphology (Miles, 2001). Biostasisve and rexistasis concepts used by Erhart in 1955 to define the transition from biogeochemical equilibrium to the conditions of erosion and clastic sedimentation that refer to the basic idea of landscape sensitivity concept. However, the "landscape sensitivity" concept was first used in 1979 by

http://www.aloki.hu ● ISSN 1589 1623 (Print) ● ISSN 1785 0037 (Online)
DOI: http://dx.doi.org/10.15666/aeer/1706_1427714296

Brunsden and Thornes to help think about geomorphological systems and understand especially episodes of erosion and sedimentation (Thomas, 2001). The first definition of the concept of landscape sensitivity was as "landscape's capacity to absorb the effects of changes and disturbances." Since then, the meanings of landscape sensitivity have been constantly explored and developed (Chia et al., 2019). For example, landscape sensitivity is expressed as the ratio of change in a system in a landscape component. The higher the ratio is, the greater is the sensitivity (Usher, 2001). Due to perturbations in controlling environmental processes, landscape sensitivity is defined as conditional instability in the system with the possibility of a rapid and irreversible change. It has also been used to describe the response of landscape systems to perturbations at different time and spatial scales (Thomas, 2001). Landscape sensitivity was also defined as landscape's exposure to external stressors of the natural components of the landscape and thus, their capacity to change or to be affected or harmed (Aretano et al., 2015; Kesoretskikh et al., 2015).

Usually, there is a need for landscape sensitivity for three reasons. These include: (i) determining which environmental conditions require a major change in the landscape; (ii) identifying which parts of the landscape are affected in what proportions; (iii) demonstrating how long the transition of landscape features will be before the semi-equilibrium state is reached (Knox, 2001). For, the landscape can give different responses to anthropogenic pressures or ecological processes. As stated by Brunsden, when a landscape is in a state of stability with respect to controlling environment and its minor perturbations, the change will be incremental and at rates that allow mutual readjustment between all the components of the landscape complex. But when instability results from increases in the magnitude and rate of stress applied to landscape components, a period of readjustment will take place, as the various subsystems respond by attempting to establish new equilibria. These equilibria will not be attained if the frequency of high magnitude events, enough to cause further disturbance, is greater than the 'relaxation time' of the system. The stability of ecosystems has been considered both in terms of their resistance to displacement by disturbing forces, and their ability to recover after disturbance (Thomas, 2001). At this point, it is important to distinguish between concepts of sustainability/adaptive capacity, resilience and vulnerability in understanding landscape sensitivity. Sustainability or adaptation capacity is the capacity of a system to withstand external influences/pressures, to manage the risks and effects, to respond to the challenges by developing effective approaches, and to adapt (Turner et al., 2003; Damiano et al., 2014; Kesoretskikh et al., 2015). Resilience is defined as the ability of a system to improve, reorganize and develop against stresses and disturbances (Aretano et al., 2015). Resilience can also be expressed as the capacity to adapt (Vaillant et al., 2016). Vulnerability is generally referred to as sensitive landscapes' exposure to the stressor and their inability to absorb the change and failure to adapt. In this context, vulnerability has three primary components: exposure to the stressor, sensitivity to a range of stressor variability, and resilience following exposure (Adger, 2006; Birkmann and Wisner, 2006; Golobič and Žaucer, 2010; Damiano et al., 2014; Aretano et al., 2015; Campbell et al., 2016; Vaillant et al., 2016; Menezes et al., 2018). In this context, low adaptation capacity and resilience increase the landscape sensitivity. High sensitivity and these areas' failure to adapt due to constant pressure causes vulnerability. Therefore, the relationship between sensitivity and vulnerability is very important in understanding the process.

http://www.aloki.hu ● ISSN 1589 1623 (Print) ● ISSN 1785 0037 (Online)
DOI: http://dx.doi.org/10.15666/aeer/1706_1427714296

The aim of this study is to reveal the landscape sensitivity based on ecological processes and to identify the sensitive areas. In addition, the properties and importance of sensitivity maps are revealed.

Materials and methods

Study case

The study was conducted in Duzce province in the Black Sea region located in 64685.081-613754.468 and 572602.468-766623.408 UTM coordinates (ED-1950-utm-zone 36N) (*Fig. 1*). The study area covers approximately 2487 km^2 area, and this area constitutes 0.3% of Turkey (Tatar, 2003; Anonymous, 2019a). Water resources, vegetation cover, rich biodiversity and ecologically sensitive qualities were effective in determining the study area.

Figure 1. *The location of the study area*

The study area has a landscape view surrounded by the plain of Duzce near the south-west border and mountains in the north, south and east. Approximately 14.5% of the area is Duzce plain and its 85.5% is mountainous areas surrounding this plain. The mountain heights are 1388-1380 in the south and east, and they reach to the Black Sea as the heights reduce northward. The mountains are generally divided into deep valleys (Tatar, 2003). 64.2% of the area has more than 20% slopes. Urbanization and settlements are concentrated in Duzce plain and other plains due to high slopes. The flat areas are located in the plateaus in the mountains, Duzce plain and Black Sea coasts (Anonymous, 2000). The area is located in North Anatolian Fault line, 1st-degree seismic zone. It has 22 various rock formations with different names such as sandstone, shale, conglomerate, siltstone, limestone, ophiolitic rocks, granite, gabbro, tuff,

http://www.aloki.hu ● ISSN 1589 1623 (Print) ● ISSN 1785 0037 (Online)
DOI: http://dx.doi.org/10.15666/aeer/1706_1427714296

andesite, basalt, agglomerate, gneiss, metagranite, amphibolite, migmatite, marble, phyllite etc. Duzce plain is covered with thick and loose alluvium (Anonymous, 2002; Tatar, 2003). The hydrological structure of the area consists of 6 large streams, ranging in length from 4.5 km to 17 km; 7 natural lakes, reservoirs, groundwater and geothermal resources (Anonymous, 2019a). 79.8% of the area is in VI., VII. and VIII. degree land use capability class which have limited agricultural potential. Most of the fertile agricultural land is located in Duzce plain (Anonymous, 2010). The study area is located in the flora of Euxine and Xsero-Euxine transition zone and the vegetation cover is very rich. In the area, there are 14 taxon rare plants located under 11 families. There are also 66 endemic species. 5 of them are in critically endangered (CR), 2 in endangered (EN), 3 in vulnerable (VU), 12 in near threat (NT) and 44 in the least concern (LC) category. The area is ranked 15th in terms of its forest density. In addition, there is one protection area (430 ha), four nature parks (340.71 ha), 4 natural monuments (10 ha) and 3 wildlife development areas in the study area. The wildlife in the area is also very rich (Anonymous, 2019a). According to the climatic parameters of the area, the average annual temperature is 13.2 °C, the average humidity is 77.5% and the rainfall is 87.7 mm/month (Anonymous, 2019b). 50% of the area is forest and heathland, 30% is agricultural area, 9% is other areas (settlement, industry, etc.) and 1% is meadows and pastures (Anonymous, 2019a).

Duzce province has 7 districts, 279 villages and 2 towns. The population of the area in 2018 is 387844. Its population has increased by 65.4% from the day it became a province in 2000 (130632). The number of people per square kilometer in Duzce is 156 (Anonymous, 2019c-d). The economic structure the area is based on tourism, agriculture and industry. Due to the widespread forests, the study area is rich in the forestry industry and has also developed rapidly in other industrial areas as well thanks to industrial incentives to support development in the aftermath of 1999 earthquake. In 2017, in order to protect agricultural areas against urbanization and industry, Duzce Plain and its vicinity were declared agricultural protection sites. The most important issue to be mentioned about the agricultural activities in Duzce is the transformation of forest areas into hazelnut agricultural area for years (Anonymous, 2019a). Furthermore, the Büyük Melen Dam still under construction is planned to cover 75% of the water demand of Istanbul, which is 170 km away. The project was prepared in 1997 and construction started in 2001, the first phase was completed in 2007 and the work is still in progress (Anonymous, 2019e). The project is significant since it is the largest water supply project in Turkey. In this context, the study area is a very important drinking water basin.

The study area has an ecologically sensitive structure. The earthquake, landslide, erosion, flood and habitat fragmentation clearly reveal this fact. One of the most important examples is 17 August and 12 November 1999 earthquakes in 7.4 and 7.2 density according to the Richter scale. In these earthquakes, approximately 18 thousand 374 people were killed, and 48 thousand 901 people were injured (Anonymous, 2019d). There are also natural disaster risks such as mass movements, landslides, and floods along with earthquakes. Mass movement around the Duzce basin is widespread due to its abundant rainy climatic characteristics and geological and geomorphologic structure. In 1998, various mass movements occurred due to excessive precipitation. In this context, Duzce-Akçakoca Highway in Yazlık Dere, Melen River basin in the north of Cumayeri and Almacık Mount slopes are areas with landslide risks (Özaslan et al., 2001). In this context, it is stated that 12.8% of the area has high risk, 21.7% has high,

http://www.aloki.hu ● ISSN 1589 1623 (Print) ● ISSN 1785 0037 (Online)
DOI: http://dx.doi.org/10.15666/aeer/1706_1427714296

23.6% has medium, 16.8% has low, and 15.6% has very low landslide susceptibility. Furthermore, data on 9.5% of the area has not been produced (Anonymous, 2016). There is no significant difference between the north and south of Duzce in terms of landslide susceptibility. In the central part, landslide sensitivity is quite low. The main reason for this is the increase in height and slope as progressed north and south from the middle section. The landslide susceptibility is increased along the Çilimli Fault and the Duzce Fault in the East-West direction along the North Anatolian Fault. The landslide sensitivity is high on the slopes facing the north, northwest and northeast. A little more rainfall on the north-facing slopes makes the sensitivity higher. The landslide sensitivity is high on slopes with 10-30% inclination. Vegetation is often forest depending on climate and recently transformed into hazelnut areas; thus, the natural balance of the slopes deteriorates and the landslide sensitivity increases (Kocabaş, et al., 2016). The rivers in the study area are mainly in the form of meanders and are quite twisted and the stream beds are very shallow. This situation constitutes the flood risk for Duzce basin (Özaslan et al., 2001). As a matter of fact, flood incidents that caused considerable loss of property occurred in 1995, 1997 and 1998, and similar cases are experienced every year (Tatar, 2005). Also, 21.4% of the area has very severe, 18.2% has severe, 11.4% has medium; 19.5% has mild and 29.5% has very mild erosion risk (Anonymous, 2018). The human spread in the area (urbanization, industrialization, transportation, etc.) ignoring the habitats causes habitat fragmentation (Aydın et al., 2016), threatening both forest areas and biodiversity.

Materials

The main material of the study is composed of the maps, which are evaluated in order to reveal the natural and cultural characteristics of Duzce province, and which are used to create the sensitivity map. The other study materials consist of institutional reports on Duzce province and the scientific literature on landscape sensitivity. Maps used in the study are:

- 1/25000 scale digital Duzce Topographic Map produced by The Ministry of Defense, the General Directorate of Maps in 2000 (Anonymous, 2000) and updated road network map based on this map.
- 1/25000 scale digital Duzce Geological Map produced by Ministry of Energy and Natural Resources, General Directorate of Mineral Research and Exploration in 2002 (Anonymous, 2002).
- 1/25000 scale Digital Duzce Soil Map produced by the Ministry of Agriculture and Forestry, General Directorate of Agricultural Research and Policies in 2008-2010 (Anonymous, 2010).
- 1/25000 scale digital Duzce Forest Management Map produced by the Ministry of Agriculture and Forestry, General Directorate of Forestry in 2008 (Anonymous, 2008).
- 1/25000 scale digital Duzce Landslide Susceptibility Map produced by the Ministry of Internal Affairs Disaster and Emergency Management in 2016 (Anonymous, 2016).
- 1/125000 scale Duzce Erosion Risk Map produced by the Ministry of Agriculture and Forestry in 2018 (Anonymous, 2018).
- In the study, ArcGIS 9.3 software was utilized to create some thematic maps and sensitivity maps.

http://www.aloki.hu ● ISSN 1589 1623 (Print) ● ISSN 1785 0037 (Online)
DOI: http://dx.doi.org/10.15666/aeer/1706_1427714296

The theoretical basis of methods

As Brunsden states, landscape sensitivity should be sought in landscapes resistance against and their responses to the forces of change (Thomas, 2001). Barabas et al. (2014) defined the sensitivity analysis as the examination of how ecological variables of interest respond to changes in external conditions. Usher (2001) emphasized that starting to think primarily about the landscape; the main natural systems that determine the structure of the landscape; and then about actions that change the natural systems are the best ways to determine sensitivity. In addition, it was also emphasized that changes and their magnitudes have both spatial and temporal components and that these components are an integral part of the sensitivity (Usher, 2001). In this context, to determine the sensitivity of landscape, some researchers are interested in related landscape components (inclination, aspect, proximity to water resources, etc.); some researchers consider ecological processes (erosion, landslide, desertation, climate change, habitat fragmentation, etc.); some others consider both as a combination parameter (Gordon and Sutherland, 1993; Thomas, 2001; Penghua et al., 2007; Mingwu, 2010; Wang and Bian, 2011; Aretano et al., 2015; Kesoretskikh et al., 2015; Bede-Fazekas et al., 2017; Haara et al., 2017; Hussain et al., 2018; Shi et al., 2018; Chia et al., 2019). The reason for the holistic evaluation of the parameters is that "anyone or more landscape components/ecological processes may be sensitive to change in certain situations and that the change in a component may trigger instability in any part of the system." For, the landscape is an intrinsically complex system, and the sub-systems can exhibit concurrent but opposite behaviours (Phillips, 1999; Usher, 2001; Thomas, 2001).

In the study, it was decided to conduct a sensitivity analysis based on the landscape processes including the components of the landscape. Landscape processes indicate a process depending on landscape components. Therefore, the analysis of processes will also allow the components to be analyzed at the same time. In addition, the spatial heterogeneity will be ensured, and excessive data will be avoided, and landscape systems will be evaluated with a reductionist approach.

Erosion risk, landslide susceptibility, water infiltration and habitat fragmentation processes were evaluated as parameters within the scope of the study. The efficiency of these processes and the existence of reliable spatial data related to these processes or the possibility of being produced were effective in the selection of the parameters and the landscape of the study area

The erosion sensitivity evaluated in the study is a parameter that has been evaluated since the first studies on landscape sensitivity (Thomas, 2001; Penghua et al., 2007; Mingwu, 2010; Wang and Bian, 2011). Erosion refers to the movement of upper soil due to various factors. Erosion is also important in terms of exploring the relationship between landscape pattern and ecological process. Landscape pattern, type of vegetation, soil properties, precipitation, etc. are some of the factors for erosion (Fu and Bruce Jones, 2013). In addition, as Thomas (2001) states, the soil has the clearest expression of landscape complexity, and it is sensitive to many landscape components such as rocks, precipitation, slope, aspect etc.

The landslide is another parameter that affects the landscape and is important for landscape sensitivity (Thomas, 2001). The landslide is a sudden mass movement of soil and substrate in the sloping areas. Landslides can cause many changes in landscape hydrology, vegetation cover, habitat, sediment load, biodiversity, organism movement, etc. Landslides, especially in mountainous landscapes, are one of the common problems

http://www.aloki.hu ● ISSN 1589 1623 (Print) ● ISSN 1785 0037 (Online)
DOI: http://dx.doi.org/10.15666/aeer/1706_1427714296

along with precipitation and steep slope and should be accordingly evaluated in sensitivity process (Walker and Shiels, 2013).

Water is an important component of life and hence, landscape. In this context, the hydrologic cycle is one of the important processes in the landscape. The water is in continuous motion inside atmosphere, hydrosphere and lithosphere layers. Precipitation water's passing through vegetation cover, soil and rock layers to reach the impermeable layers thanks to gravity and slope effects is called the water process in the landscape or landscape's water function (Karadağ, 2019). This infiltration of water is important for landscape sensitivity and is considered as a parameter (Aydın et al., 2018).

Habitat fragmentation is one of the other important sensitivity criteria in the landscape (Thomas, 2001; Penghua et al., 2007; Mingwu, 2010; Wang and Bian, 2011; Aretano et al., 2015; Bede-Fazekas et al., 2017; Chiet et al., 2019). For, habitat loss and/or fragmentation have been identified as perhaps the most important driving force of the global biodiversity crisis. Landscape connectivity is critical to the viability of many types of species (Forman and Godron, 1986; Cushman et al., 2010). Habitat fragmentation decreases disintegration, increases mortality and decreases genetic diversity (Cushman et al., 2010; Kosydar, 2014). In addition, the vegetation cover destroyed by habitat fragmentation ceases its duty to protect soil and water resources, (Babalık et al., 2019) and changes the landscape pattern. Landscape pattern is a concrete reflection of the spatial heterogeneity of the landscape (Penghua et al., 2007). It is also the result of ecological processes affecting different spatial and temporal scales (Bolliger, 2005).

Earthquake risk zones are not taken into consideration in the study. For, the whole area is within the 1st-degree earthquake zone.

Methods (data acquisition and analyses)

The study consists of three stages. These are; determination of parameters to be evaluated in sensitivity analysis; obtaining the parameter data and making the necessary analysis in this process; holistic analysis of selected parameters on the basis of sensitivity analysis (*Fig. 2*).

Düzce Erosion Risk map was obtained from the relevant unit of the Ministry of Agriculture and Forestry. The map was created by Revised Universal Soil Loss Equation (RUSLE) method. The average soil loss per year hectare with RUSLE method is generally determined by the holistic evaluation of six different parameters. These parameters are; rainfall-runoff erosivity, soil erosion erodibility, slope length, slope steepness and support practice. Erosion risk status in the map is classified as very severe, severe moderate, mild and very mild (Erpul et al., 2018). Also, erosion risk map has been considered as an erosion sensitivity map within the scope of this study. Because risk maps are produced in order to reveal the loss of life and property to be affected by the change in landscape. Therefore, in this study, erosion risk maps were used to determine areas sensitive to erosion. This classification was evaluated using a scale between 1 and 5 according to expert opinions. According to the evaluation, the areas with very severe erosion risk had 5 points (too high sensitivity) followed by severe with 4 points (high sensitivity); moderate with 3 points (medium sensitivity); mild with 2 points (low sensitivity) and very mild with 1 point (too low sensitivity). Later, these scores were added to the database of erosion risk maps with ArcGIS 9.3 software and an erosion sensitivity map was created.

http://www.aloki.hu ● ISSN 1589 1623 (Print) ● ISSN 1785 0037 (Online)
DOI: http://dx.doi.org/10.15666/aeer/1706_1427714296

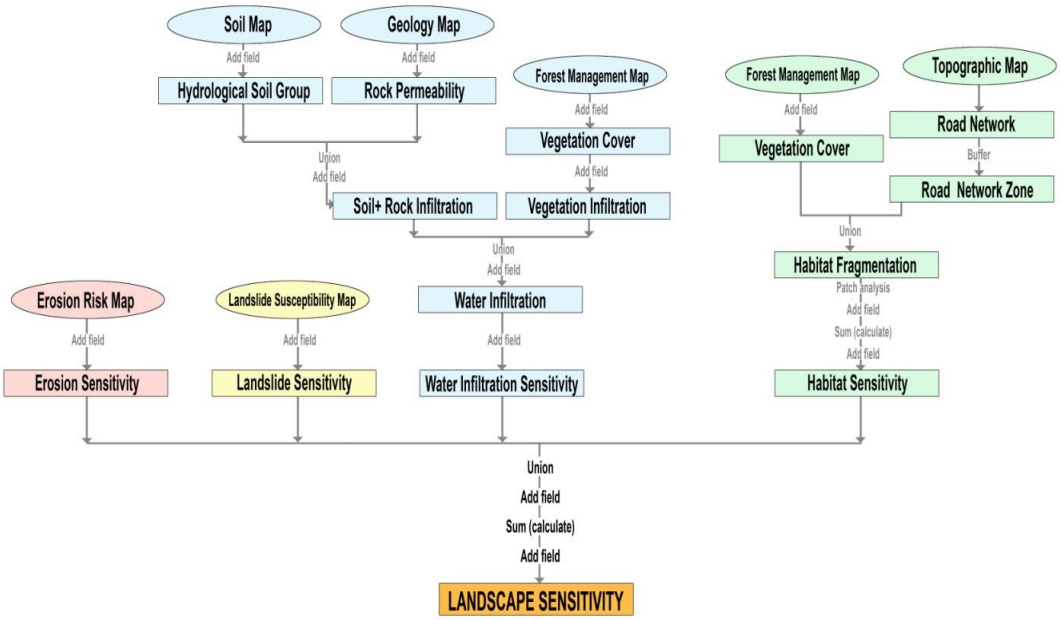

Figure 2. *Landscape sensitivity analysis model (parameters, data, and analysis process)*

Düzce Landslide Susceptibility Map was obtained from the relevant unit of the Ministry of Internal Affairs. The map was generated by the Frequency Ratio method. In this method, after the determination of the parameters which come out as a result of the field observations, the parameter maps and the landslide polygons are coupled. It provides the proportional landslide possibility in other areas based on the characteristics of the corresponding parameters. In determining landslide sensitivity, lithology, height, curvilinearity, aspect and slope were considered holistically. Landslide susceptibility status is classified as very high, high, medium, low, very low on the map (Kocabaş et al., 2016). This classification was evaluated by using a scale between 1 and 5 according to 3 expert opinions. According to the evaluation, the areas with very high landslide susceptibility have 5 points (very high sensitivity); high areas have 4 points (high sensitivity); medium areas have 3 points (medium sensitivity), low areas have 2 points (low sensitivity) and very low areas have 1 point (very low sensitivity). These points were then added to the database of the landslide susceptibility map with the ArcGIS 9.3 software and a landslide sensitivity map was created.

Water infiltration map was created within the scope of the study. Water process analysis method was used to create the water infiltration map of the study area. Within the scope of the method, 1/25000 scaled digital soil map, geology map and forest management map were used (Anonymous, 2002; Anonymous, 2008; Anonymous, 2010). Hydrological soil groups from the soil map; the rock permeability from the geology map, vegetation cover from the forest management map, and then vegetation infiltration data were produced. These data are then were analyzed according to the water process analysis method used by Uzun et al. (2015) and Karadağ (2019), and water infiltration data were generated (*Table 1*). Then, hydrological soil groups and rock permeability data were evaluated by union analysis and soil + rock infiltration data were obtained in the first stage. In the second stage, this data was subjected to union analysis with vegetation infiltration, and water infiltration data consisting of five classes were formed. This map was then evaluated by using a scale between 1 and 5 according

http://www.aloki.hu ● ISSN 1589 1623 (Print) ● ISSN 1785 0037 (Online)
DOI: http://dx.doi.org/10.15666/aeer/1706_1427714296

to 3 expert opinions. According to the evaluation, areas with very high water infiltration have 5 points (very high sensitivity); high areas have 4 points (high sensitivity); medium areas have 3 points (medium sensitivity); low areas have 2 points (low sensitivity) and very low areas have 1 point (too low sensitivity). These points were later added to water infiltration map database with ArcGIS 9.3 software and a water infiltration sensitivity map was created.

A habitat fragmentation map was created within the scope of the study. The data obtained by using the patch-corridor-matrix model in the creation of the habitat fragmentation map of the study area were analyzed and interpreted by the Patch Analysis 4 software, an interface of ArcGI9.3 developed by Rempel (2010). In this context, Düzce Forest Management Map was used, and vegetation cover data were prepared from this map. In this data, the forest cover was examined and four spots (coniferous forest, leafy forest, mixed forest and pasture) were defined. The data were subjected to union analysis with the road map in order to reveal the fragmentation. The road map was prepared from 1/25000 scaled digital topographic map. However, before the analysis, 4 m effect zones were formed on the roads by way of proximity (buffer) analysis in order to involve the effects of the roads on the environment. The data obtained from the Union analysis were accepted as the base data of the habitat fragmentation. These data were then analyzed at class level with the Patch Analysis module, which was developed by Rempel (2010) as an interface to ArcGIS 9.3. The analysis was carried out in two stages. In the first stage, patch size and number, patch shape and edge properties of patches were determined by spatial statistics based on patch analysis. As a result of the analysis, No of Patches (NumP) Related to patch size and number, Class Area (CA) and Mean Patch Size (MPS), Mean Shape Index (MSI) related to patch shape, Mean Perimeter-area Ratio (MPR), Mean Patch Fractal (MPFD) values, and Edge Density (ED) values were obtained. In the second stage, core areas related to patches were determined on the basis of patch analysis. During the analysis, a 100 m edge zone was identified in order to assess fragmented forest edges and their effects on the living creatures in the inner habitats. Then, total core area (TCA), total core area index (TCAI) and Core Area Density (CAD) values were obtained by spatial statistics on the basis of patch analysis. All obtained spatial values were evaluated on the basis of the studies by Forman and Godron (1986), Rempel (2010) and Uzun (2012). In this context, the result was that "NumP increased, MPS and CA decreased, fragmentation decreased; MPAR and MSI values decreased, MPFD value closed to 1 and fragmentation decreased; ED increased, fragmentation increased; TCAI and CAD increased, fragmentation decreased." Decreased of that fragmentation was evaluated as an increase in sensitivity. For, in larger patches, biodiversity and forest cover is high and these areas should be considered a priority in conservation. In order to map this condition, first, the sensitivity status of each patch was scored between 1 and 5. Then, the scores obtained from these four parameters were totalized, and the habitat total sensitivity score was determined and reclassified. In this context, the total score for each patch from four parameters is maximum 20 and minimum 4. These scores are divided into five classes (very high, high, medium, low, very low) according to the sensitivity status. The range of points used in the formation of the classes was found to be about 3, calculated by "subtracting the lowest score from the highest, and dividing the sum into six." According to this assessment, areas with very high sensitivity have 20-19 points; high sensitivity have 19-16 points; moderate sensitivity have 15-12 points; low sensitivity have 11-8, and too low sensitivity has 4-7 points. Finally, by calculating the

http://www.aloki.hu ● ISSN 1589 1623 (Print) ● ISSN 1785 0037 (Online)
DOI: http://dx.doi.org/10.15666/aeer/1706_1427714296

total scores obtained from four parameters of each patch, sensitivity scores according to the class range were determined. Then, the total habitat sensitivity score was calculated with ArcGIS 9.3, which was processed in a new field in the patch map database and a habitat vulnerability map was created. Uzun's (2012) study was used in the analysis and evaluation process.

The final analysis within the scope of the study is the union analysis performed to ensure a holistic assessment of all data, after the creation of the four data sensitivity parameters to be evaluated in the sensitivity analysis. Four data are subjected to union analysis. A new field is added to the database of the resulting map. Later, calculation of landscape sensitivity total score of each polygon is done with the following formula:

$$\text{Landscape sensitivity total score} = \text{Erosion sensitivity score} + \text{Landslide sensitivity score} + \text{Water infiltration sensitivity score} + \text{Habitat sensitivity score} \quad \text{(Eq.1)}$$

The total score of each polygon was written to the new field. Then the maximum and minimum scores are determined, and the difference is divided into six so that the sensitivity can be defined by a scale of 5 (sensitivity is very high, sensitivity is high, sensitivity is medium, sensitivity is low, sensitivity is very low). The score interval of these 5 classes is defined with the number obtained. Finally, the total sensitivity score received by each polygon is determined based on specific sensitivity state, and this detection is processed in the new data added to the database of the data obtained from the union analysis and a total sensitivity map is generated.

Results

In this study, firstly, data sensitivity parameter maps in *Figure 3* are produced. When the database of the maps was examined, the data given in *Table 1* was obtained.

When the erosion sensitivity map was examined, it was seen that the erosion sensitivity increases in the mountainous areas to the north of the area. In the southern and inner parts of the area, erosion sensitivity decreases (*Fig. 3*). When the erosion sensitivity map database was evaluated, it was seen that the sensitivity in 21.4% of the area was very high while it was high in 18.2%, medium in 11.4%, low in 19.5% and very low in 29.5% (*Table 1*).

Table 1. *Sensitivity (sen.) parameter areas in the study area, (%)*

Sensitivity degree	Sensitivity parameters			
	Erosion sen. area (%)	**Landslide sen. area (%)**	**Water infiltration sen. area (%)**	**Habitat sen. area (%)**
Very high	*21.4*	12.8	0.4	-
High	*18.2*	21.7	11.6	*33.1*
Medium	*11.4*	23.6	80.6	*3.4*
Low	*19.5*	16.8	4.2	*16.8*
Very low	*29.5*	15.6	3.2	-

When the landslide sensitivity map was examined, it was seen that the landslide sensitivity increases in the mountainous areas to the north of the area. This is due to the high slope, elevation, fault lines and habitat fragmentation in these areas. In the inner

http://www.aloki.hu ● ISSN 1589 1623 (Print) ● ISSN 1785 0037 (Online)
DOI: http://dx.doi.org/10.15666/aeer/1706_1427714296

parts of the area, landslide sensitivity is low (*Fig. 3*). When the landslide sensitivity map database was evaluated, it was seen that the sensitivity in 12.8% of the area was very high while it was high in 21.7%, medium in 23.6%, low in 16.8% and very low in 15.6% (*Table 1*). Data for 9.5% of the area was not produced

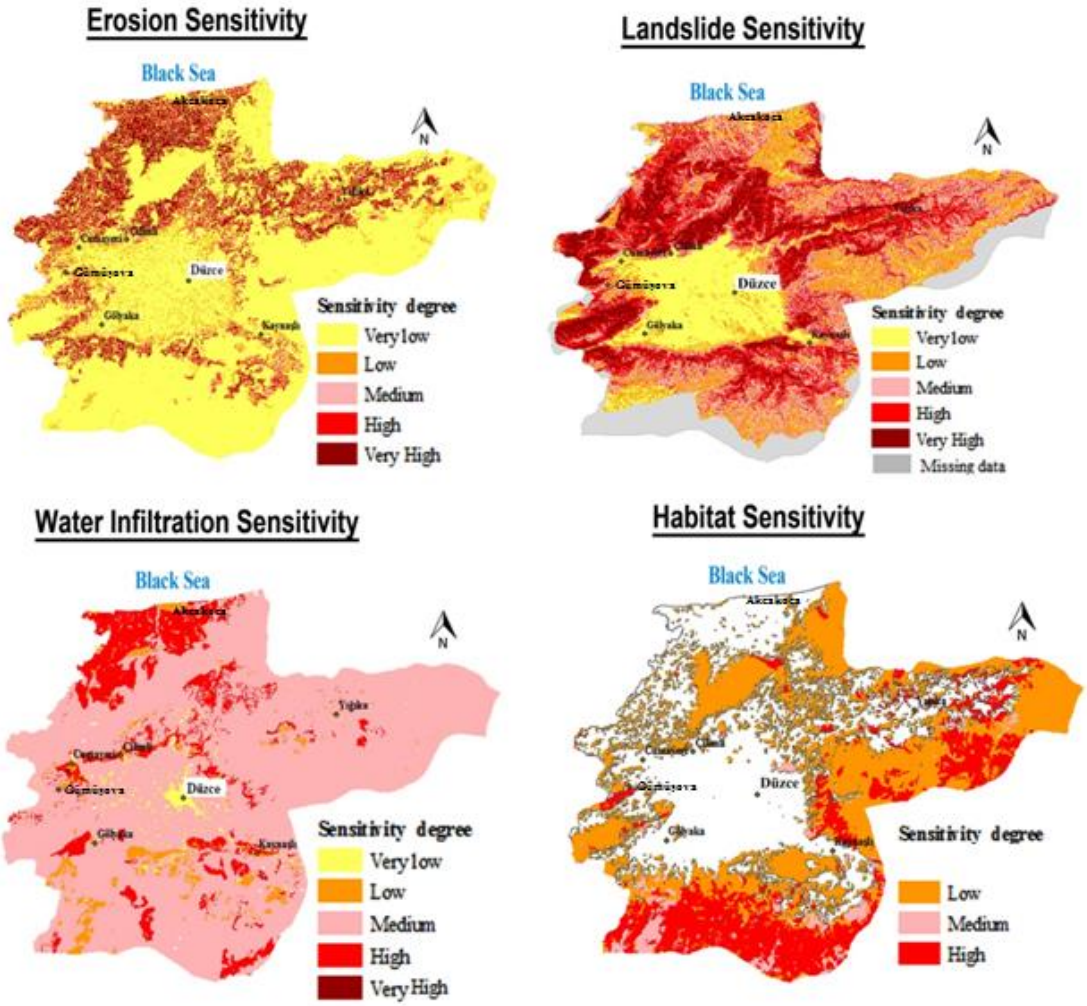

Figure 3. *Maps of landscape sensitivity parameters*

When the water infiltration sensitivity map was examined, it was seen that the water infiltration sensitivity in the area is generally moderate (except for residential areas/artificial surfaces). Only the Black Sea coast and from the coast to the inland increase sensitivity (*Fig. 3*). When the water infiltration sensitivity map database is evaluated, it was seen that the sensitivity in 0.1% of the area was very high while it was high in 11.6%, moderate in 80.6%, low in 4.5% and very low in 3.2% (*Table 1*).

The habitat sensitivity map of the area was produced based on vegetation cover. The habitat patches in the area were evaluated as "coniferous forest, leafy forest, mixed forest, pastures" and the breaks in these spots were analyzed based on conservation priority. In order to reveal the fragmentation in the patches, the destructive power of the roads was evaluated and a total of 3158 patches were detected in the area by union analysis. Patch size and number, patch shape, patch edge and core area parameters

http://www.aloki.hu ● ISSN 1589 1623 (Print) ● ISSN 1785 0037 (Online)
DOI: http://dx.doi.org/10.15666/aeer/1706_1427714296

related sub-criteria values were determined. These values were scored based on the studies by Forman and Godron (1986), Rempel (2010) and Long (2012) and expert opinions as the increase of fragmentation is accepted as a sensitivity-lowering effect; and mixed forests received 16 points, pastures 14 points, coniferous forests 12 points and leafy forests 10 points. When these scores were evaluated according to the sensitivity classification in the area, it was determined that mixed forests had high sensitivity while coniferous forests and pastures had moderate, and leafy forests had low sensitivity. When the habitat sensitivity map was examined, it was seen that the sensitivity decreased in the eastern and southern parts of the area. This situation shows that habitat fragmentation occurs in this area (*Fig. 3*). When the habitat sensitivity map database was evaluated, it was seen that the sensitivity in 33.1% of the area was high while it was low in 16.8% and moderate in 3.4% (*Table 1*). 46.7% of the area has not been evaluated as patch.

As a result of overlay analysis of four sensitivity parameter data related to the study area, Duzce Province landscape Sensitivity Map in *Figure 4* was obtained. When the sensitivity map database was examined, it showed that the maximum landscape sensitivity total score in the field was 18 and the min total score was 4. When scores are ranked according to their sensitivity, 16-18 points were considered very high sensitivity, 13-15 points were considered high, 10-12 points was considered moderate, 7-9 points was considered low and 4-6 points was considered very low. When the landscape sensitivity map database was evaluated, it was seen that the sensitivity in 38.6% of the area is low while it is medium with 30.6%, very low with 21.7%, high with 8.2% and very high with 8.2%. These findings indicate that 39.7% of the area is sensitive (medium, high and very high) (*Fig. 4*).

When the landscape sensitivity map is examined, it is seen that very low sensitivity areas are located in Duzce plain. In these areas, especially water infiltration has affected sensitivity. There are intense land uses like settlements, agriculture, and industry in these areas. Low sensitivity areas are located in the south and southeast of the area. In these areas, habitat fragmentation and water infiltration have affected sensitivity and the settlement is not dense. Medium sensitivity areas are spread throughout the study area. Erosion, landslide and water infiltration are effective in sensitivity in these areas. There are especially rural settlements and forests in these areas. High sensitivity areas are concentrated, especially located in the northwest of the area. In these areas, erosion, landslide and water infiltration sensitivity is high. Very high precision areas are located in the north of the area. These areas take up very little space in the area. Erosion, landslides, water infiltration and habitat sensitivity are high in these areas (*Fig. 4*).

Discussion

The deterioration of the ecological balance has been a common problem in the world since the industrial revolution. Many researchers in different disciplines have done various researches on this concept (Shi and Tong, 2019). Landscape sensitivity analysis is one of these studies.

Landscape studies has a significant public interest in cultural, ecological, environmental and social areas and is a resource that is conducive to economic activity and that can contribute to job creation, conservation, management and planning. In this context, it is one of the key elements of individual and social welfare (Anonymous, 2017). Therefore, understanding and recognizing the landscape is very important. In the

http://www.aloki.hu ● ISSN 1589 1623 (Print) ● ISSN 1785 0037 (Online)
DOI: http://dx.doi.org/10.15666/aeer/1706_1427714296

process of recognizing and understanding the landscape, sensitive landscapes are very important. This is because sensitive landscapes are the most intensively associated with ecological-environmental changes and tend to be most prone to ecological problems (Forman, 1995; Hong et al., 2017). In this context, it is aimed to reveal areas which are sensitive to natural/anthropogenic factors, have a high potential for change under external factors and have priority in spatial development (Thomas, 2001; Shi et al., 2018; Chia et al., 2019). In this study, mapping of landscape sensitivity areas is the main objective. In this study, an ecology based sensitivity map has been created for spatial planning. This map is practical data for many occupational disciplines. Uzun et al. (2015), Demiroğlu (2016), Cengiz et al. (2017) and Karadağ (2019) emphasize that such practical data is necessary for ecology-based planning.

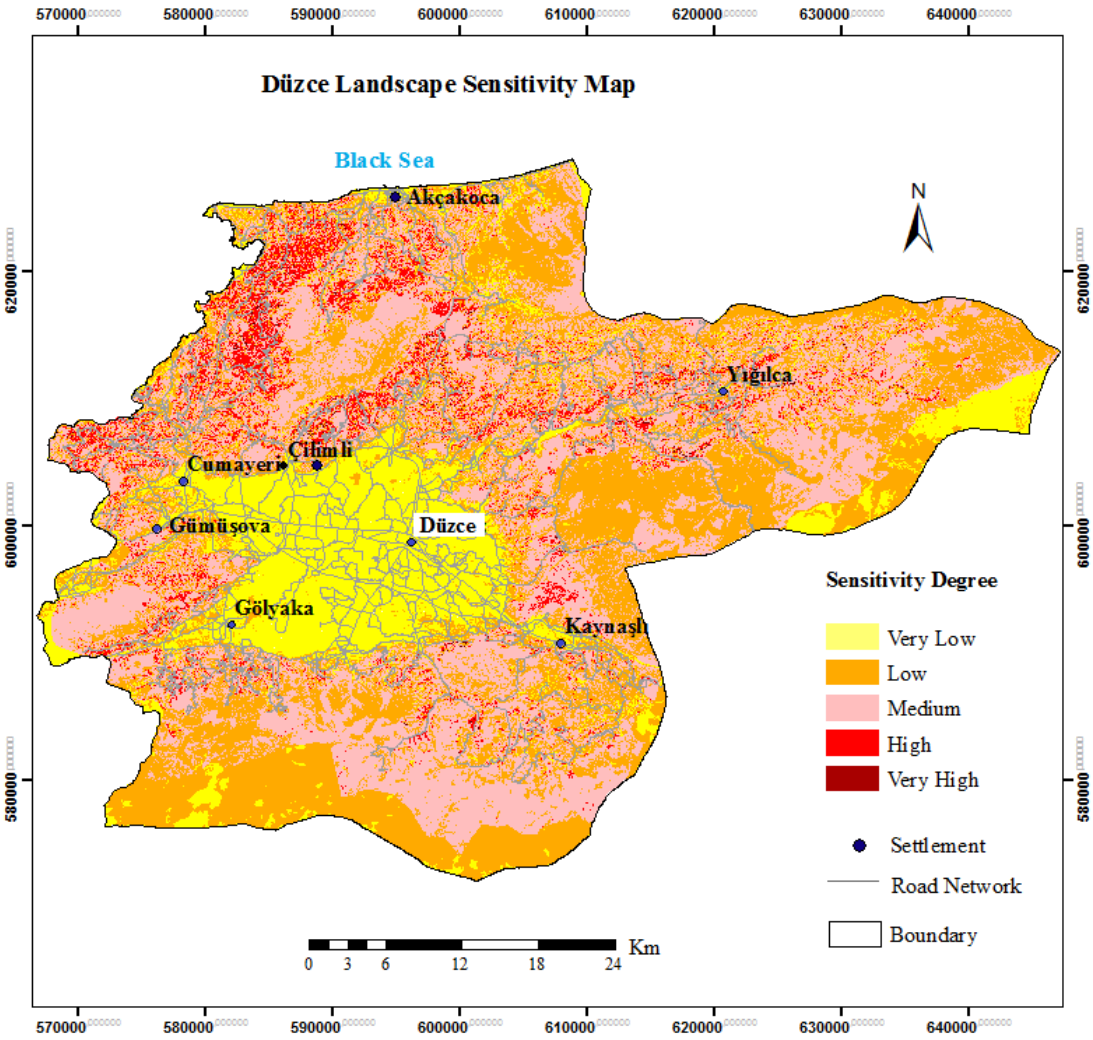

Figure 4. *Duzce landscape sensitivity map*

In this study, landscape sensitivity map is presented as a result of sensitivity analysis. In the sensitivity analysis, like many researchers (e.g., Thomas, 2001; Penghua et al., 2007; Mingwu, 2010; Wang and Bian, 2011; Fu and Bruce Jones, 2013; Walker and Shiels, 2013; Aretano et al., 2015; Bede-Fazekas et al., 2017; Aydın et al., 2018; Chia et

http://www.aloki.hu ● ISSN 1589 1623 (Print) ● ISSN 1785 0037 (Online)
DOI: http://dx.doi.org/10.15666/aeer/1706_1427714296

et al., 2019) ecological processes were evaluated holistically. Ecological processes to be included in the analysis are shaped according to the purpose of the study. In this study, four different ecological processes (erosion sensitivity, water infiltration sensitivity, habitat fragmentation sensitivity) were considered as parameters. The processes were selected on the basis of the basic processes that have an impact on the landscape character of the study area. In addition, these parameters and natural and cultural landscape components could be evaluated together.

Sensitivity parameter maps and landscape sensitivity map obtained in the study showed that the sensitivity structure of the study area has a complex structure. Mapping of this complex structure is very important in terms of spatial planing and land use. Aydın et al. (2018) have reached similar results and map regarding the landscape sensitivity of the study area. They also emphasized the importance of landscape sensitivity map for spatial planning.

The study area has significant ecological sensitivities. However, the land uses in the study area were not developed with ecology-based plan decisions. The creation of the sensitivity map is necessary in order to determine the sensitive areas/ecosystems in the area and to determine the protection priority compared to others. For, areas with high landscape sensitivity are areas that need to be protected. The exposure to human uses and their severity may cause vulnerability issues and may pose risk situations. In this context, sensitivity maps can be considered as a basis for suitable analysis used in the development of land-use decisions. For, space use should be considered on the basis of sensitivity due to its effects on the loss of ecosystems as stated by Saran et al. (2019).

In this study, the reduction of the data to be analyzed with the evaluation of ecological processes and a reductionist approach was exhibited. However, many researchers like Gordon and Sutherland (1993), Penghua et al. (2007), Wang Mingwu (2011), and Bian (2011), Aretano (2015), Haara et al. (2017) Hussain et al. (2018), Shi et al. (2018), Chia et al. (2019) evaluated ecological process and landscape components together. As Thomas (2001) points out, landscape sensitivity is more easily analyzed with reductionist approaches. In addition, the performance of the ArcGIS program was not forced by the reduction of data.

Conclusion

In this study, a model for the development of landscape sensitivity areas is presented and the reasons for this approach are explained. The most important result of the study is to produce a map describing the landscape sensitivity of the study area. The landscape sensitivity map of the study area is a data that is compatible with ecological principles, produced by scientific methods, compatible with technological tools and can be integrated with similar analyzes. It is an ecological guide for various spatial plans (landscape planning, construction planning, open and green space planning, green infrastructure planning, etc.). It may contribute to the development of policies for ecology-based protection, usage, planning, management, etc. They can be legally defended due to their scientific and transparent nature during production/preparation. In addition, sensitivity maps are base data that provide the exposure of field uses, vulnerability and risk analysis.

In the study, only four parameters were evaluated in determining landscape sensitivity. However, a wide range of parameters (habitat sensitivity, earthquake sensitivity, etc.) can be included in the analysis to further enhance landscape sensitivity.

http://www.aloki.hu ● ISSN 1589 1623 (Print) ● ISSN 1785 0037 (Online)
DOI: http://dx.doi.org/10.15666/aeer/1706_1427714296

Increasing parameters will change the total landscape sensitivity in the area. Thus, a more accurate result will be achieved. The landscape sensitivity map in spatial planning processes is an impressive guide. However, it should be noted that each parameter map should be included in the decision-making process and evaluated.

Determination of parameters is very important in sensitivity analysis. The selection of sensitivity parameters should take into account the ecological processes that direct the formation of the area or ecological sensitivities in the area.

The spatial data used in the study are digital maps with a scale of 1/25000. These data are of a higher scale and might be more directives for planning decisions. For decisions on a local scale, sensitivity maps developed using smaller-scale maps should be used. For this reason, further sub-scale data should be used to make decisions on local scale (cities, rural settlements, etc.).

In the assessment of the sensitivity of the maps used in the production of the sensitivity map, a scale of sensitivity (1-5) was created and scoring was made by applying 3 expert opinions. In order to increase objectivity, the number of experts can be increased, and the scores can be analyzed by statistical methods (e.g. analytic hierarchy process, Delphi technique) and transferred to the mapping process. Thus, objectivity is further increased.

Intensive land use in the study area has developed in very low sensitivity area. These areas are not sensitive in terms of erosion and landslides. There is also no vegetation cover. However, they are sensitive areas for water infiltration. But these plans were not developed on the basis of landscape sensitivity and the necessary measures were not taken. Because there is no such legal justification in the spatial planning processes of the study area. Therefore spatial planning related to the study area should be developed on the basis of landscape sensitivity maps. For example, in areas with high sensitivity, necessary protection decisions should be made and appropriate planning made. The rationale for these decisions should be clearly demonstrated on the basis of scientific and technological data.

As a result, landscape sensitivity map is one of the important keys in order to develop ecologically-based decisions related to space. Therefore, its usage as a basis map for spatial planning is a need beyond desire. In addition, the preparation and use of these maps as a base should be made legally mandatory.

REFERENCES

[1] Adger, W. N. (2006): Vulnerability. – Global Environmental Change 16(3): 268-281.
[2] Anonymous (2000): 1/25000 Scale Digital Düzce Topographic Map. – Republic of Turkey Ministry of National Defense, General Directorate of Mapping, Ankara, Turkey (in Turkish).
[3] Anonymous (2002): 1/25000 Scale Digital Düzce Geological Map and Report. – Republic of Turkey Ministry of Energy and Natural Resources, General Directorate of Mineral Research and Exploration, Ankara, Turkey (in Turkish).
[4] Anonymous (2008): 1/25000 Scale Digital Düzce Soil Map and Report. – Republic of Turkey Ministry of Agriculture and Forestry, General Directorate of Agricultural Research and Policies, Ankara, Turkey (in Turkish).
[5] Anonymous (2010): 1/25000 Scale Digital Düzce Forest Cover Map and Report. – Republic of Turkey Ministry of Agriculture and Forestry, General Directorate of Forestry. Ankara, Turkey.

http://www.aloki.hu ● ISSN 1589 1623 (Print) ● ISSN 1785 0037 (Online)
DOI: http://dx.doi.org/10.15666/aeer/1706_1427714296

[6] Anonymous (2016): 1/25000 Scale Digital Düzce Landslide Susceptibility Map. – Republic of Turkey Ministry of Interior, Disaster and Emergency Management Presidency, Ankara, Turkey (in Turkish).
[7] Anonymous (2017): Presentation of the European Landscape Convention of the Council of Europe. – www. rm.coe.int/CoERMPublicCommonSearchServices/DisplayDCTMContent?documentId=09000016802f7dfd (date of access: 19.02.2019).
[8] Anonymous (2018): 1/25000 Scale Digital Düzce Erosion risk Map. – Republic of Turkey Ministry of Agriculture and Forestry, General Directorate of Combating Desertification and Erosion Ankara, Turkey (in Turkish).
[9] Anonymous (2019a): Duzce Province Environmental Situation Report in 2017. – Duzce Provincial Directorate of Environment and Urbanization. www.webdosya.csb.gov.tr (date of access: 23.01.2019) (in Turkish).
[10] Anonymous (2019b): Duzce Province Clean Air Action Plan in 2015. – Duzce Provincial Directorate of Environment and Urbanization. www.webdosya.csb.gov.tr (date of access: 23.01.2019) (in Turkish).
[11] Anonymous (2019c): Duzce Address Based Population Registration System 2018. – Duzce Provincial Directorate of Population and Citizenship. www.duzcenufus.gov.tr (date of access: 23.01.2019) (in Turkish).
[12] Anonymous (2019d): Duzce Geological Structure. – Düzce Governorship. http://www.duzce.gov.tr/jeolojik-yapi (date of access: 11.04.2019) (in Turkish).
[13] Anonymous (2019e): Melen Dam. – Duzce Municipality. http://www.duzce.bel.tr/detay.asp?id=29919 (date of access: 11.04.2019) (in Turkish).
[14] Aretano, R., Semeraro, T., Petrosillo, I., De Marco, A., Pasimeni, M. R., Zurlini, G. (2015): Mapping ecological vulnerability to fire for effective conservation management of natural protected areas. – Ecological Modelling 295: 163-175.
[15] Aydın, B., Tezer, A., Turkay, Z., Yılmaz Kaya, M., Kutay Karacor, E., Guler, İ., Uzun, O, Okay, N., Terzi, F., Köylü, P., Satilmis, E., Kara, D. (2018): Resilience through participatory planning for the integrated ecological risks in Duzce. – Resilience Journal 2(2): 105-121.
[16] Babalık, A. A., Yazıcı, N., Fakır, H., Dursun, I. (2019): Determination of the certain vegetation characteristics of Kizilova forest pasture located in the south of Turkey. – Applied Ecology and Environmental Research 17(1): 521-532.
[17] Barabas, G., Pasztor, L., Meszena, G., Ostling, A. (2014): Sensitivity analysis of coexistence in ecological communities: theory and application. – Ecology Letters 17: 1479-1494.
[18] Bede-Fazekas, A., Czúcz, B., Somodi, I. (2017): Vulnerability of natural landscapes to climate change - a case study of Hungary. – Quarterly Journal of the Hungarian Meteorological Service 121(4): 393-414.
[19] Birkmann, J., Wisner, B. (2006): Measuring the un-measurable the challenge of vulnerability. – www. d-nb.info/1029694141/34 (date of access: 19.02.2019).
[20] Bolliger, J. (2005): Simulating complex landscapes with a generic model: sensitivity to qualitative and quantitative classifications. – Ecological Complexity 2: 131-149.
[21] Boström, C., Pittman, S. J., Simenstad, C., Kneib, R. T. (2011): Seascape ecology of coastal biogenic habitats: advances, gaps, and challenge. – Marine Ecology Progress Series 427: 191-217.
[22] Campbell, C., Conger, S., Gould, B., Haegeli, P., Jamieson, B., Statham, G. (2016): Technical aspects of snow avalanche risk management. – Canadian Avalanche Association, Revelstoke, BC, Canada.
[23] Chia, Y., Zhang, Z., Gao, J., Xie, Z., Zhao, M., Wanga, E. (2019): Evaluating landscape ecological sensitivity of an estuarine island based on landscape pattern across temporal and spatial scales. – Ecological Indicators 101: 221-237.

http://www.aloki.hu ● ISSN 1589 1623 (Print) ● ISSN 1785 0037 (Online)
DOI: http://dx.doi.org/10.15666/aeer/1706_1427714296

[24] Cegiz, A. E., Karadağ, A. A., Demiroğlu, D. (2017): Importance of landscape planning for sustainable spaces. – International Congress of the New Approaches and Technologies for Sustainable Development, Isparta, Turkey, Congress Book 1(1): 4-16.
[25] Cushman, S. A., Landguth, E., L., Flather, C., H. (2010): Climate change and connectivity: assessing landscape and species vulnerability. – Phase 1-Final Report. www.fws.gov/southwest/es/documents/R2ES/LitCited/LPC_2012/Cushman_et_al_2010.pdf (date of access: 19.02.2019).
[26] Damiano, H. R., Umberger, M., Monitz, G., Friedman, J., Hariri, M., Tehranifar, R., Grassi, C., Lindsey, E. (2014): NYC's Risk Landscape: A Guide to Hazard Mitigation. – The NYC Department of City Planning & The NYC Mayor's Office of Recovery and Resiliency. www1.nyc.gov/assets/em/downloads/pdf/hazard_mitigation/nycs_risk_landscape_a_guide_to_hazard_mitigation_final.pdf (date of access: 26.03.2019).
[27] Demir, S. (2019): Landscape dynamics changes of the protected Mary Valley, Turkey. – Applied Ecology and Environmental Research 17(2): 3591-3613.
[28] Demiroğlu, D., Pekin Timur, U. Karadağ, A. A., Cegiz, A. E. (2014): Ecology Based Contemporary Urbanism Approaches. – In: Efe, R., Onay, T. T., Sharuho, I., Atasoy, E. (eds.) Urban and Urbanization. St. Kliment Ohridski Universty Press, Bulgaria.
[29] Dunning, J. B., Danielson, B. J., Pulliam, H. R. (1992): Eco-logical processes that affect populations in complex landscapes. – Oikos 65: 169-175.
[30] Erpul, G., Şahin, S., Küçümen, A., Akdağ, M. A., Demirtaş, İ., Çetin, E., İnce, K. (2018): Erosion Model and Dynamic Monitoring System (DEMIS) Turkey Water Erosion Statistics. – Technical Report. Republic of Turkey Ministry of Agriculture and Forestry General Directorate of Combating Desertification and Erosion, Turkey (in Turkish).
[31] Farina, A. (2001): Landscapes and their ecological components. – www3.udg.edu/cgpt/Almo%20Farina/Biosphere.PDF (date of access: 19.02.2019).
[32] Farina, A. (2008): The landscape as a semiotic interface between organisms and resources. – Biosemiotics 1(1): 75-83.
[33] Farina, A., Pieretti, N. (2012): The soundscape ecology: a new frontier of landscape research and its application to islands and coastal system. – Journal of Marine and Island Cultures 1(1): 21-26.
[34] Forman, R. T. (1995): Some general principles of landscape and regional ecology. – Landscape Ecology 10(3): 133-142.
[35] Forman, R. T., Godron, M. (1986): Landscape Ecology. – John Wiley & Sons, New York.
[36] Fu, B., Bruce Jones, K. (2013): Landscape Ecology for Sustainable Environment and Culture. – Springer Science, London.
[37] Godrdon, J. E., Sutherland, D. G. (1993): Quaternary of Scotland. – Geological Conservation Review Series (No: 6). Chapman and Hall, London.
[38] Golobič, M., Žaucer, L. B. (2010): Landscape planning and vulnerability assessment in the Mediterranean. – Regional Activity Centre for the Priority Actions Programme, Croatia. www.pap-thecoastcentre.org/pdfs/Landscape%20Vulnerability.pdf (date of access: 19.02.2019).
[39] Haara, A., Store, R., Leskinen, P. (2017): Analyzing uncertainties and estimating priorities of landscape sensitivity based on expert opinions. – Landscape and Urban Planning 163: 56-66.
[40] Hong, W., Guo, R., Su, M., Tang, H., Chen, L., Hu, W. (2017): Sensitivity evaluation and land-use control of urban ecological corridors: a case study of Shenzhen, China. – Land Use Policy 62: 316-325.
[41] Hussain, A., Singh, G., Rawat, G., S. (2018): Landscape Vulnerability Assessment Using Remote Sensing and GIS Tools in the Indian Part of Kailash Sacred Landscape. – The International Archives of the Photogrammetry, Remote Sensing and Spatial Information Sciences, Volume XLII-5, 20-23 November 2018, Dehradun, India.

http://www.aloki.hu ● ISSN 1589 1623 (Print) ● ISSN 1785 0037 (Online)
DOI: http://dx.doi.org/10.15666/aeer/1706_1427714296

[42] İlboğa, M., Aygül, H. H. (2015.): Culture of living together in the context of human-nature dialectic. – Academic Overview International Refereed Journal of Social Science 52: 64-78 (in Turkish).
[43] Karadağ, A. A. (2019): A Research on determination of vulnerable landscapes in terms of groundwater: Duzce case, Turkey. – Fresenius Environmental Bulletin 28(4A): 3231-3241.
[44] Kesoretskikh, I., Zotov, S, Drobiz, M. (2015): Assessing spatial and temporal changes in the landscape vulnerability in the Kaliningrad Region as an element of sustainable spatial planning. – Baltic Region 4(26): 122-136.
[45] Knox, J. C. (2001): Agricultural influence on landscape sensitivity in the upper Mississippi river valley. – Catena 42: 193-224.
[46] Kocabaş, S., Çelik, F., Aksoy, Ö., Kiriş, C. (2016): Landslide Sensitivity Analysis Report. – Düzce Provincial Directorate of Disaster and Emergency, Düzce, Türkiye (in Turkish).
[47] Kosydar, A. J., Conquest, L. L., Tewksbury, J. J. (2014): Can life histories predict the effects of habitat fragmentation? A meta-analysis with terrestrial mammals. – Applied Ecology and Environmental Research 12(2): 505-521.
[48] Lewis, S. L., Maslin, M. A. (2015): Defining the anthropocene. – Nature 519(7542): 171-180.
[49] Mazzino, F., Burlando, P. (2010): Cultural landscapes: negotiation between global and local. – A-Z ITU Journal of the Faculty of Architecture 7(2): 14-20.
[50] Menezes, J. A., Confalonieri, U., Madureira, A. P., Duval, I. B., Santos, R. B. D. (2018): Mapping human vulnerability to climate change in the Brazilian Amazon: the construction of a municipal vulnerability Index. – PLoS One 13(2): 1-30.
[51] Miles, J., Cummins, R. P., French, D. D., Fardner, S., Orr, J. L. (2001): Landscape sensitivity: an ecological view. – Catena 42: 125-141.
[52] Mingwu, Z., Haijiang, J., Desuo, C., Chunbo, J. (2010): The comparative study on the ecological sensitivity analysis in Huixian karst wetland, China. – Procedia Environmental Sciences 2: 386-398.
[53] Özaslan, M., Erşahin, G., Akkahve, D., Sabuncu, A. (2001): Duzce Province Report. – State Planning Organization General Directorate of Regional Development, Ankara, Turkey.
[54] Penghua, Q., Songjun, X., Genzong, X., Benan, T., Hua, B., Longshi, Y. (2007): Analysis of the ecological vulnerability of the Western Hainan Island based on its landscape pattern and ecosystem sensitivity. – Acta Ecologica Sinica 27(4): 1257-1264.
[55] Phillips, J. D. (1999): Earth Surface Systems. – Blackwell Publishers Ltd, Oxford, UK.
[56] Rempel, R. (2010): Centre for Northern Forest Ecosystem Research. – www. www.flash.lakeheadu.ca/~rrempel/ecology/papers/patchanalyst.pdf (date of access: 12.04.2019).
[57] Saran, E., Dusza Zwolińska, E., Gamrat, R. (2019): Plant species richness in fragmented agricultural landscape-meta-analysis. – Applied Ecology and Environmental Research 17(1): 53-83.
[58] Shi, S. X., Tong, P. S. (2019): Evaluation system and spatial distribution pattern of ecological city construction-based on dpsir-topsis model. – Applied Ecology and Environmental Research 171: 601-616.
[59] Shi, Y., Lib, J., Xie, M. (2018): Evaluation of the ecological sensitivity and security of tidal flats in Shanghaı. – Ecological Indicators 85: 729-741.
[60] Steffen, W., Grinevald, J., Crutzen, P., McNeill, J. (2011): The anthropocene: conceptual and historical perspectives. – Mathematical, Physical and Engineering Sciences 369(1938): 842-867.
[61] Tatar, Y. (2003): Duzce Province Development Plan: Environment and Spatial Development. – www.duzce.edu.tr (date of access: 23.01.2019) (In Turkish).

http://www.aloki.hu ● ISSN 1589 1623 (Print) ● ISSN 1785 0037 (Online)
DOI: http://dx.doi.org/10.15666/aeer/1706_1427714296

[62] Thomas, M. F. (2001): Landscape sensitivity in time and space - an introduction. – Catena 42: 83-98.
[63] Turner, M. G., Gardner, R. H., O'Neill, R. V. (2001): Landscape Ecology in Theory and Practice. – New York: Springer-Verlag.
[64] Turner II, B. L., Kasperson, R. E., Matson, P. A., Mc Carthy, J. J., Corell, R. W., Christensen, L., Eckley, N., Kasperson, J. X., Luers, A., Martello, M. L., Polsky, C., Pulsipher, A., Schiller, A. (2003): A framework for vulnerability analysis in sustainability science. – Proceedings of the National Academy of Sciences of the United States of America 100(14): 8074-8079.
[65] Turner, S. (2018): Historic Landscape Characterisation. – In: Fairclough, G., Sarlöv Herlin, I., Swanwick, C. (eds.) Routledge Handbook of Landscape Character Assessment Current Approaches to Characterisation and Assessment. Routledge, Abingdon. www.routledge.com (date of access: 13.03.2019).
[66] Usher, M. B. (2001): Landscape sensitivity: from theory to practice. – Catena 42: 375-383.
[67] Uzun, O., İlke, E. F., Cetinkaya, G., Erduran, F., Acıksoz, S. (2012): Landscape Planning: Bozkir-Seydisehir-Ahirli-Yalihüyük District of Konya and Sugla Lake Village Landscape Management Conservation and Planning Project. – The Ministry of Forestry and Water Affairs, Ankara, Turkey (in Turkish).
[68] Uzun, O., Muderrisoglu, H., Demir, Z., Kaya, L., G., Gultekin, P., Gunduz, S. (2015): Yesilirmak Basin Landscape Atlas Project (II. Report). – The Ministry of Forestry and Water Affairs, Ankara, Turkey (in Turkish).
[69] Vaillant, N. M., Kolden, C. A., Smith, A. M. S. (2010): Assessing landscape vulnerability to wildfire in the USA. – Current Forestry Reports 23: 201-213.
[70] Walker, L. R., Shiels, A. B. (2013): Landslide Ecology. – Cambridge University Press, New York.
[71] Wang, X., Bian, Z. (2011): The implications of ecological sensitivity on exploitation of unutilized land: a case study in Ji'Nan City, China. – Procedia Environmental Sciences 10: 275-281.

http://www.aloki.hu ● ISSN 1589 1623 (Print) ● ISSN 1785 0037 (Online)
DOI: http://dx.doi.org/10.15666/aeer/1706_1427714296

ANNOTATION AND ANALYSIS OF THE TRANSCRIPTOME OF BEARING BRANCH

ZHU, B.[1] – ZHANG, L.[1*] – XU, X. B.[1] – ZOU, B. Y.[2] – GUAN, Q. M.[2] – YANG, J. J.[2] – YU, Z.[2]

[1]*Forestry College, Jiangxi Agricultural University, Nanchang 330045, China*

[2]*Jiangxi BoJun Agriculture Holding Limited, Nancheng 344700, China*

[*]*Corresponding author*
e-mail: LLPPMM222@163.com

(Received 4th Jun 2019; accepted 16th Oct 2019)

Abstract. The analysis of the Transcriptome of different jujube, and the mining of their functional genes was performed. And the genes were annotated and analyzed, and the difference gene was screened out to provide the theoretical basis for the fresh jujube. The sequencing of the cDNA library was performed using synthesis technology and the Illumina HiSeq platform. The sequencing results of splicing and functional annotation. A total of 29402 Unigenes were annotated, while in the Nr, Swiss-Prot, GO, COG, KEGG and Pfam databases 29330, 24358, 21771, 11028, 6962 and 28940 Unigenes, respectively. At the same time, 355 new genes were annotated. The 50 functional groups in the Go database gene function annotation, 14608 metabolic processes in biological processes, accounting for 67.1%; reference KEGG database, 110 metabolic pathways, the number of annotations, gene function ribosomes, amino acid biosynthesis. Human embryonic stem cells, carbon metabolism, and plant hormone signaling are more abundant; it is noted that COD in 11028 single-gene distribution families has general function prediction, transcription, replication, recombination and repair, and secondary metabolites in 25 genes. Biosynthesis, transport and catabolism. This study is the first time to use RNA-seq high-throughput sequencing technology to perform transcriptome sequencing and functional analysis of transcriptome results in fresh-eating jujube leaves, to explore genes for biological processes, cell components and molecular functions, and to study different functional genes, effective biosynthetic pathways and regulatory mechanisms.

Keywords: *fresh jujube, Bearing branch, RNA-seq, differential gene expression, gene ontology, transcriptomics*

Introduction

Ziziphus jujuba Mill is a plant belonging to the Rhamnaceae family. It's the main cultivated species in China. Cultivation and distribution all over the country. The species has recently been introduced to Asia, Europe, America, Africa and Oceania, but is generally not cultivated economically (Qu et al., 1993). *Jujube* are different from other fruits. Its branches can be divided into once branch of jujube, jujube stock and bearing branch. The Bearing branch is the basic unit of the result of the jujube tree. It is also known as the result branch, the exfoliative branch, the falling branch, and the two type

http://www.aloki.hu ● ISSN 1589 1623 (Print) ●ISSN1785 0037 (Online)
DOI: http://dx.doi.org/10.15666/aeer/1706_1429714313

branch (Tang et al., 2012). Bearing branch can be divided into lignification jujube hoists and shedding jujube cranes (Yang et al., 2007, 2014). Recently, many studies have been made on the lignification of jujube cranes. Scholars believe that lignification jujube is better in result performance. Study on the cultivation of fresh Chinese jujube in the South. Study on the performance, photosynthetic efficiency, nutrient transport and nutrient accumulation of lignification jujube hoist (Yan et al., 2013; Wang et al., 2014). The majority of jujube stock is formed by the accessory bud. In practice, callus or pruning of jujube head is easy to form jujube crane. The jujube cranes can also be lifted on the base of the jujube head and the two branches of the year. Most jujube cranes are able to blossom, and the small part of the jujube is suspended from the top of the jujube head (Shi et al., 1999; Tang et al., 2012; Wang et al., 2014). In fact, jujube crane can be divided into fruit jujube crane and non-fruiting jujube crane from its form, bear fruit Jujube cranes are divided into lignification jujube cranes and non-lignification jujube cranes. The study of jujube crane is directly related to the value of the breeding and breeding of jujube trees. It is also related to the economic and production value of jujube trees. Study the development rule of jujube crane to provide basic theory for production management (Sun et al., 1996; Chen et al., 2015).

RNA-Seq can respond to the expression of genes at the transcriptional level (Reich et al., 2018). High energy sequencing can be used to better study the expression of different genes in different jujube cranes. Thus, the molecular formation mechanism of the flower bud differentiation and results of jujube crane is described better.

Materials and methods

Experimental materials

Sample from Jiangxi Xianlv modern agricultural demonstration garden Magu jujube No. 1, Take 3 different jujube cranes: first is Lignification jujube hanging leaf (A1, A2, A3), Non lignification jujube hanging leaf (B1, B2, B3). Non lignification jujube leaves without flower bud differentiation (C1, C2, C3). Lignification leaves of jujube leaves on 3 jujube trees (A1, A2, A3), B1 and C1 are the same trees, B2 and C2 are the same trees, B3 and C3 are the same trees. A total of 9 samples (3 Biological duplicates). Rapid freezing of liquid nitrogen after sampling. Put in the -80℃ refrigerator and spare.

Construction of cDNA library and sequencing of Transcriptome

RNA sequencing is commissioned by Hangzhou Jing Jie Biological Technology Co., Ltd. After testing the sample. Magnetic beads with Oligo (dT). Complementary pairing through A-T and use The combination of mRNA's ployA tail enriching the mRNA of eukaryotes. Then add fragmentation buffer to break mRNA into short segments. Take mRNA as a template. Synthesis of a chain cDNA with six base random primers. And then add the buffer, *dNTPs* and *DNA* polymerase I. Synthesis of two chain cDNA. Then using

http://www.aloki.hu ● ISSN 1589 1623 (Print) ●ISSN1785 0037 (Online)
DOI: http://dx.doi.org/10.15666/aeer/1706_1429714313

AMPure XP beads to purify double stranded cDNA. Purification of double stranded cDNA for terminal repair. Adding A tail and connecting sequenced joint. Then AMPure XP beads is used to select the size of the fragment. Finally, the final PCR library is enriched and the final cDNA library is obtained (Qi et al., 2011; Ding et al., 2017).

Statistics and comparison of sequencing

The original data reads of the machine. Clean Data was filtered after removing the reads containing the joint, repeated and low quality of the sequencing. Sequence alignment with the specified reference genome. The obtained Mapped Data. Quality evaluation of insert fragment length test, randomness test and so on. This project uses the specified genome as a reference for sequence alignment and subsequent analysis. Using *TopHat2* (Kim et al., 2013) Alignment of Clean Reads with the reference genome. Obtaining location information on the reference genome or gene. And sequence characteristic information of sequence samples. *TopHat2* is based on the comparison of software *Bowtie2* (Langmead et al., 2012). Comparison of the transcriptome sequence Reads to the genome, Recognition of splice points between exons by analyzing comparison results (Splicing Junction).

Discovery of new genes

Based on the selected reference genome sequence. Using Cufflinks software to splice Mapped Reads. And compare with the original genome annotation information. Looking for the original unnoted transcriptional area. Discovery of the new transcript and new genes of the species. So as to supplement and improve the original genome annotation information. Filtering the encoded peptide chain is too short or contains only a single exon sequence (less than 50 amino acid residues). Using BLAST software to compare the new genes that are excavated with the *NR, Swiss-Prot, GO, COG, KOG, Pfam, KEGG* database, KEGG Orthology results of new genes were obtained by using KOBAS2.0, Using HMMER software compared with Pfam database after predicting the amino acid sequence of the new gene. Annotated information of new genes (Zhu et al., 2018).

Functional annotation and analysis of the Transcriptome

Filtering and assembly of Unigenes. Based on the selected reference genome sequence. Using *Cufflinks* software to splice Mapped Reads. And compare with the original genome annotation information. Looking for the original unnoted transcriptional area. Discovery of the new transcript and new genes of the species. So as to supplement and improve the original genome annotation information. Filtering the encoded peptide chain is too short or contains only a single exon sequence (less than 50 amino acid residues). Using *BLAST* software to compare the new genes that are excavated with the *NR, Swiss-Prot, GO, COG, KOG, Pfam, KEGG* database. KEGG Orthology results of new genes were obtained by using *KOBAS2.0*. Using *HMMER* software compared with Pfam database after predicting

http://www.aloki.hu ● ISSN 1589 1623 (Print) ●ISSN1785 0037 (Online)
DOI: http://dx.doi.org/10.15666/aeer/1706_1429714313

the amino acid sequence of the new gene, Obtain annotated information of the measured genes (Liu et al., 2017; Niu et al., 2018; Zhang et al., 2018; Chen et al., 2018).

Results and analysis

Sequencing data output statistics

Repeat sequencing of 3 material samples with high energy sequencing technology. The total number of pair-end Reads of clean Data in the ReadSum of A2 is maximum. Up to 28708241. The total base number of Clean Data in BaseSum is 8612472300. The minimum of A3's ReadSum in all the samples is 21709049. The BaseSum 6512714700 of A3. The percentage of two bases of G and C in Clean DataGC is more than 44%. The percentage of Clean Data with a mass greater than or equal to 30 of a base is greater than 88%. The percentage of Clean Data with a mass greater than or equal to 20 of a base is greater than 94%. The above analysis indicates that the quality of sequencing is good, and the data can be used for subsequent All-Unigenes database establishment, gene function annotation, classification and same-sex analysis. The output statistics of the sample data in this project are shown in *Table 1*.

Table 1. *Sequencing data statistics table*

SampleID	ReadSum	BaseSum	GC(%)	Q20(%)	Q30(%)
A1	24, 974, 459	7, 492, 337, 700	45. 18%	95. 07%	88. 88%
A2	28, 708, 241	8, 612, 472, 300	44. 78%	95. 25%	89. 25%
A3	21, 709, 049	6, 512, 714, 700	44. 34%	94. 81%	88. 42%
B1	26, 961, 553	8, 088, 465, 900	44. 44%	95. 25%	89. 25%
B2	26, 875, 609	8, 062, 682, 700	45. 00%	95. 27%	89. 26%
B3	27, 843, 858	8, 353, 157, 400	44. 96%	95. 28%	89. 30%
C1	22, 799, 545	6, 839, 863, 500	44. 79%	95. 25%	89. 24%
C2	24, 859, 991	7, 457, 997, 300	45. 08%	95. 34%	89. 41%
C3	24, 962, 466	7, 488, 739, 800	45. 00%	95. 32%	89. 35%

Ratio of transcriptional data to reference genome sequence

This not only provides a data base for variable splicing analysis, but also enables more Reads to be compared to the reference genome, and improves the utilization of sequencing data.

Comparison efficiency refers to the percentage of Mapped Reads that accounts for Clean Reads, which is the most direct manifestation of the data utilization of the transcriptional group. The efficiency of comparison is not only affected by the quality of data sequencing, but also related to the advantages and disadvantages of the reference genome assembly, and the biological classification relationship between reference genome and sequencing samples. By comparing efficiency, it is possible to assess whether the selected reference genome assembly can meet the needs of information analysis (*Table 2*).

http://www.aloki.hu ● ISSN 1589 1623 (Print) ●ISSN1785 0037 (Online)
DOI: http://dx.doi.org/10.15666/aeer/1706_1429714313

Table 2. *A statistical table of sequence alignment of the sample sequence and the selected reference genome*

sampleID	total_read	reads_mapped (%)	multi_mapped (%)	uniq_mapped (%)	reads_plus (%)	reads_minus (%)
A1	49948918	34289534 (68. 6)	486538 (1. 42)	33802996 (98. 58)	37956271 (62. 85)	22435941 (37. 15)
A2	57416482	39460995 (68. 73)	484144 (1. 23)	38976851 (98. 77)	42123971 (63. 49)	24220188 (36. 51)
A3	43418098	29243769 (67. 35)	362679 (1. 24)	28881090 (98. 76)	32184159 (64. 11)	18019123 (35. 89)
B1	53923106	36479830 (67. 65)	477714 (1. 31)	36002116 (98. 69)	39978099 (64. 07)	22423068 (35. 93)
B2	53751218	36611439 (68. 11)	487630 (1. 33)	36123809 (98. 67)	40024889 (63. 69)	22814098 (36. 31)
B3	55687716	38058734 (68. 34)	524265 (1. 38)	37534469 (98. 62)	41600309 (63. 49)	23922692 (36. 51)
C1	45599090	31073411 (68. 14)	426693 (1. 37)	30646718 (98. 63)	34299648 (63. 54)	19678520 (36. 46)
C2	49719982	33687509 (67. 75)	499050 (1. 48)	33188459 (98. 52)	37803787 (63. 55)	21683112 (36. 45)
C3	49924932	34395909 (68. 90)	478825 (1. 39)	33917084 (98. 61)	37594222 (63. 12)	21969233 (36. 88)

More than 67% samples in total percentage of Reads compared to the reference genome Reads number in Clean Reads accounted for the percentage of the number of Reads, compared to the reference genome at various locations in the Clean Reads accounted for less than 2%, the number of Reads percentage compared to the reference genome location in Clean Reads only accounted for more than 98%, the percentage ratio the number of Reads positive reference genome chains in Clean Reads accounted for more than 62% (including more than reads), compared to the number of Reads and percentage of negative strand genome reference in Clean Reads accounted for less than 38% (including more than reads).

Discovery of new genes

The total number of newly discovered genes obtained from corresponding database annotation information was 355, of which 196 were 300-1000bp in length and 155 in length 1000bp. COG notes to 37, of which there are 19 300-1000bp in length, length of more than 1000bp 18; GO notes to 205, of which there are 123 300-1000bp in length, length of more than 1000bp 79; KEGG notes to 65, of which there are 38 300-1000bp in length, length of more than 1000bp there are 27; KOG notes to 155, of which there are 77 300-1000bp in length, length of more than 1000bp 77; Pfame notes to 138, of which there are 68 300-1000bp in length, length of more than 1000bp 68; Swissprot notes to 196, of which there are 100 300-1000bp in length a length of more than 1000bp, 95; NR notes to 344, of which there are 188 300-1000bp in length, length of more than 1000bp 152. The specific distribution of the genes for each data annotation is shown in *Table 3* and *Figure 1*.

http://www.aloki.hu ● ISSN 1589 1623 (Print) ●ISSN1785 0037 (Online)
DOI: http://dx.doi.org/10.15666/aeer/1706_1429714313

Table 3. *New discovery of gene functional annotation results*

Anno_Database	Annotated_Number	300<=length<1000	length>=1000
COG	37	19	18
GO	205	123	79
KEGG	65	38	27
KOG	155	77	77
Pfam	138	68	68
Swissprot	196	100	95
nr	344	188	152
All	355	196	155

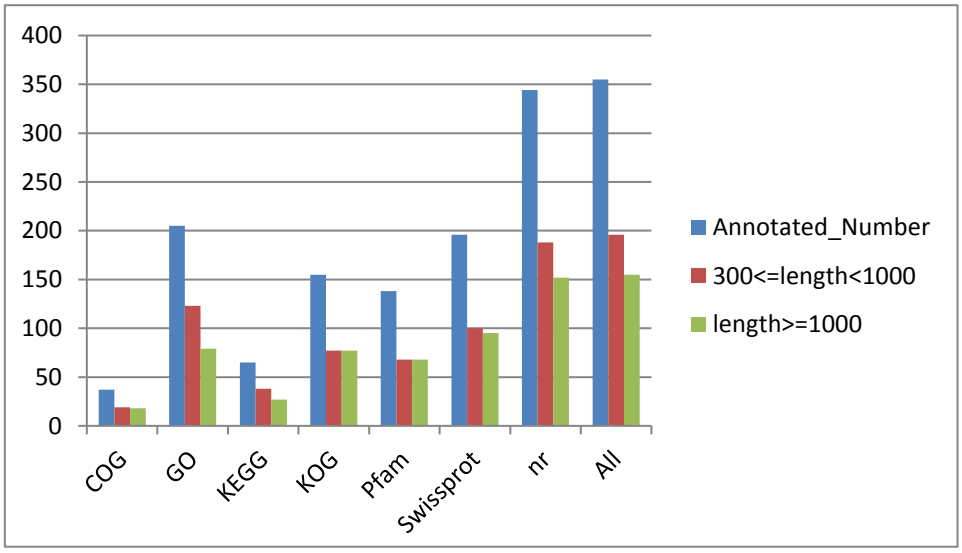

Figure 1. *New gene annotation distribution*

Annotation and functional classification of genes

The total number of genes in the annotation was 29402, of which 12539 were 300-1000bp in length and 16307 in length greater than that of 1000bp. COG notes to 11028, of which there are 3757 300-1000bp in length, length of more than 1000bp 7172; GO notes to 21771, of which there are 8900 300-1000bp in length, length of more than 1000bp 12413; KEGG notes to 6962, of which there are 2683 300-1000bp in length, length of more than 1000bp there are 4154; KOG notes to 16821, of which there are 6294 300-1000bp in length, length of more than 1000bp 10278; Pfame notes to 28940, of which there are 12273 300-1000bp in length, length of more than 1000bp 16115; Swissprot note to 24358, which is 300-1000bp in length 9435, length of more than 1000bp 14589; NR notes to 29330, of which there are 12491 300-1000bp in length, length of more than 1000bp 16286.

The number of functional genes that are ultimately annotated by each database is shown in *Table 4*.

http://www.aloki.hu ● ISSN 1589 1623 (Print) ●ISSN1785 0037 (Online)
DOI: http://dx.doi.org/10.15666/aeer/1706_1429714313

Table 4. *Statistical analysis of functional annotation of gene*

Anno_Database	Annotated_Number	300<=length<1000	length>=1000
COG	11028	3757	7172
GO	21771	8900	12413
KEGG	6962	2683	4154
KOG	16821	6294	10278
Swissprot	24358	9435	14589
Pfam	28940	12273	16115
nr	29330	12491	16286
All	29402	12539	16307

Gene GO classification

GO database is a structured standard biological annotation system built by GO Organization (Gene Ontology Consortium) in 2000, aiming at establishing standard vocabulary system of genes and their product knowledge, which is suitable for all kinds of species. The GO annotation system is a directed acyclic graph, which contains three main branches, namely Biological Process, Molecular Function and Cellular Component. In this study, the Unigene obtained from three samples of fresh jujube was compared in the GO functional database. A total of 21771 annotations were selected in 50 functional groups of GO biology. The metabolic processes involved in biological processes (14608, 67.1%), cell processes (12146, 55.79%), and single biological processes (10464, 48.06%). The main components related to annotation of cell components were cells (9818, 45.09%), membrane (8930, 41.02%), cell components (9760, 44.83%), and membrane (6609, 30.36%). The main parts of the molecular functional annotations are catalytic activity (11882, 54.57%), and binding (9688, 44.5%). This result also shows the main distribution of the annotation function. See *Table 5*.

Classification of KEGG metabolic pathways

To KEGG database as a reference, there are 6962 notes to the KEGG database, can be classified into 110 groups of gene transcription in the metabolic pathways (*Table 6*), which notes to the biosynthesis of ribosomes, amino acid biosynthesis, carbon metabolism, plant hormone signaling, plant pathogen interaction, splicing, RNA transport, and starch sucrose metabolism, endoplasmic reticulum protein processing, phenylpropanoid is relatively high. Glucosinolate biosynthesis and degradation of aromatic compounds, sulfur relay systems, non-homologous termination, glycosphingolipid biosynthesis - ganglion series, beet red pigment biosynthesis, lipoic acid metabolism, other types of O-glycan biosynthesis and Vancomycin resistance, caffeine metabolic pathways is to compare notes low.

http://www.aloki.hu ● ISSN 1589 1623 (Print) ●ISSN1785 0037 (Online)
DOI: http://dx.doi.org/10.15666/aeer/1706_1429714313

Table 5. *GO annotation classification of Unigene in jujube leaf transcriptional group*

#GO_classify1	GO_classify2	Trans gene
cellular component	extracellular region	594
cellular component	cell	9818
cellular component	nucleoid	17
cellular component	membrane	8930
cellular component	virion	81
cellular component	cell junction	431
cellular component	extracellular matrix	11
cellular component	membrane-enclosed lumen	413
cellular component	macromolecular complex	2218
cellular component	organelle	6339
cellular component	extracellular region part	48
cellular component	organelle part	2962
cellular component	virion part	81
cellular component	membrane part	6609
cellular component	cell part	9760
molecular function	protein binding transcription factor activity	108
molecular function	nucleic acid binding transcription factor activity	502
molecular function	catalytic activity	11882
molecular function	receptor activity	153
molecular function	guanyl-nucleotide exchange factor activity	30
molecular function	structural molecule activity	512
molecular function	transporter activity	1435
molecular function	binding	9688
molecular function	electron carrier activity	154
molecular function	antioxidant activity	207
molecular function	channel regulator activity	1
molecular function	metallochaperone activity	4
molecular function	enzyme regulator activity	228
molecular function	protein tag	6
molecular function	translation regulator activity	1
molecular function	nutrient reservoir activity	44
molecular function	molecular transducer activity	303
biological process	reproduction	337
biological process	cell killing	3
biological process	immune system process	234
biological process	metabolic process	14608
biological process	cellular process	12146
biological process	reproductive process	827
biological process	biological adhesion	49
biological process	signaling	1087
biological process	multicellular organismal process	1343
biological process	developmental process	1785
biological process	growth	281
biological process	locomotion	9
biological process	single-organism process	10464
biological process	rhythmic process	26
biological process	response to stimulus	3905
biological process	localization	3404
biological process	multi-organism process	525
biological process	biological regulation	4495
biological process	cellular component organization or biogenesis	2970

http://www.aloki.hu ● ISSN 1589 1623 (Print) ●ISSN1785 0037 (Online)
DOI: http://dx.doi.org/10.15666/aeer/1706_1429714313

Table 6. *KEGG metabolic pathway annotation table*

#pathway	pathway_id	Gene_number
Glycolysis / Gluconeogenesis	ko00010	102
Citrate cycle (TCA cycle)	ko00020	39
Pentose phosphate pathway	ko00030	45
Pentose and glucuronate interconversions	ko00040	66
Fructose and mannose metabolism	ko00051	54
Galactose metabolism	ko00052	57
Ascorbate and aldarate metabolism	ko00053	40
Fatty acid biosynthesis	ko00061	44
Fatty acid elongation	ko00062	35
Fatty acid degradation	ko00071	38
Synthesis and degradation of ketone bodies	ko00072	8
Cutin, suberine and wax biosynthesis	ko00073	21
Steroid biosynthesis	ko00100	19
Ubiquinone and other terpenoid-quinone biosynthesis	ko00130	18
Oxidative phosphorylation	ko00190	89
Photosynthesis	ko00195	36
Photosynthesis - antenna proteins	ko00196	12
Purine metabolism	ko00230	128
Caffeine metabolism	ko00232	1
Pyrimidine metabolism	ko00240	101
Alanine, aspartate and glutamate metabolism	ko00250	44
Glycine, serine and threonine metabolism	ko00260	60
Cysteine and methionine metabolism	ko00270	65
Valine, leucine and isoleucine degradation	ko00280	59
Valine, leucine and isoleucine biosynthesis	ko00290	25
Lysine biosynthesis	ko00300	12
Lysine degradation	ko00310	20
Arginine and proline metabolism	ko00330	72
Histidine metabolism	ko00340	16
Tyrosine metabolism	ko00350	42
Phenylalanine metabolism	ko00360	92
Tryptophan metabolism	ko00380	27
Phenylalanine, tyrosine and tryptophan biosynthesis	ko00400	38
beta-Alanine metabolism	ko00410	46
Taurine and hypotaurine metabolism	ko00430	9
Selenocompound metabolism	ko00450	25
Cyanoamino acid metabolism	ko00460	85
Glutathione metabolism	ko00480	94
Starch and sucrose metabolism	ko00500	166
N-Glycan biosynthesis	ko00510	39
Other glycan degradation	ko00511	16
Other types of O-glycan biosynthesis	ko00514	2
Amino sugar and nucleotide sugar metabolism	ko00520	106
Glycosaminoglycan degradation	ko00531	17
Glycerolipid metabolism	ko00561	47
Inositol phosphate metabolism	ko00562	58
Glycosylphosphatidylinositol(GPI)-anchor biosynthesis	ko00563	19
Glycerophospholipid metabolism	ko00564	74
Ether lipid metabolism	ko00565	28
Arachidonic acid metabolism	ko00590	10
Linoleic acid metabolism	ko00591	11
alpha-Linolenic acid metabolism	ko00592	37
Sphingolipid metabolism	ko00600	20
Glycosphingolipid biosynthesis - globo series	ko00603	14
Glycosphingolipid biosynthesis - ganglio series	ko00604	5

http://www.aloki.hu ● ISSN 1589 1623 (Print) ●ISSN1785 0037 (Online)
DOI: http://dx.doi.org/10.15666/aeer/1706_1429714313

#pathway	pathway_id	Gene_number
Pyruvate metabolism	ko00620	78
Glyoxylate and dicarboxylate metabolism	ko00630	51
Propanoate metabolism	ko00640	26
Butanoate metabolism	ko00650	20
C5-Branched dibasic acid metabolism	ko00660	11
One carbon pool by folate	ko00670	16
Carbon fixation in photosynthetic organisms	ko00710	52
Thiamine metabolism	ko00730	9
Riboflavin metabolism	ko00740	9
Vitamin B6 metabolism	ko00750	9
Nicotinate and nicotinamide metabolism	ko00760	14
Pantothenate and CoA biosynthesis	ko00770	30
Biotin metabolism	ko00780	17
Lipoic acid metabolism	ko00785	3
Folate biosynthesis	ko00790	11
Porphyrin and chlorophyll metabolism	ko00860	45
Terpenoid backbone biosynthesis	ko00900	46
Monoterpenoid biosynthesis	ko00902	11
Limonene and pinene degradation	ko00903	8
Diterpenoid biosynthesis	ko00904	21
Brassinosteroid biosynthesis	ko00905	9
Carotenoid biosynthesis	ko00906	33
Zeatin biosynthesis	ko00908	28
Sesquiterpenoid and triterpenoid biosynthesis	ko00909	24
Nitrogen metabolism	ko00910	29
Sulfur metabolism	ko00920	35
Phenylpropanoid biosynthesis	ko00940	143
Flavonoid biosynthesis	ko00941	23
Anthocyanin biosynthesis	ko00942	13
Flavone and flavonol biosynthesis	ko00944	9
Stilbenoid, diarylheptanoid and gingerol biosynthesis	ko00945	13
Isoquinoline alkaloid biosynthesis	ko00950	23
Tropane, piperidine and pyridine alkaloid biosynthesis	ko00960	23
Betalain biosynthesis	ko00965	5
Glucosinolate biosynthesis	ko00966	8
Aminoacyl-tRNA biosynthesis	ko00970	54
Biosynthesis of unsaturated fatty acids	ko01040	33
Carbon metabolism	ko01200	199
2-Oxocarboxylic acid metabolism	ko01210	55
Fatty acid metabolism	ko01212	68
Degradation of aromatic compounds	ko01220	8
Biosynthesis of amino acids	ko01230	206
Vancomycin resistance	ko01502	2
ABC transporters	ko02010	15
Ribosome biogenesis in eukaryotes	ko03008	83
Ribosome	ko03010	230
RNA transport	ko03013	167
mRNA surveillance pathway	ko03015	109
RNA degradation	ko03018	103
RNA polymerase	ko03020	41
Basal transcription factors	ko03022	40
DNA replication	ko03030	45
Spliceosome	ko03040	171
Proteasome	ko03050	45
Protein export	ko03060	41
Base excision repair	ko03410	43
Nucleotide excision repair	ko03420	49

http://www.aloki.hu ● ISSN 1589 1623 (Print) ●ISSN1785 0037 (Online)
DOI: http://dx.doi.org/10.15666/aeer/1706_1429714313

#pathway	pathway_id	Gene_number
Mismatch repair	ko03430	33
Homologous recombination	ko03440	49
Non-homologous end-joining	ko03450	7
Phosphatidylinositol signaling system	ko04070	56
Plant hormone signal transduction	ko04075	188
Ubiquitin mediated proteolysis	ko04120	96
Sulfur relay system	ko04122	8
SNARE interactions in vesicular transport	ko04130	27
Regulation of autophagy	ko04140	21
Protein processing in endoplasmic reticulum	ko04141	157
Endocytosis	ko04144	135
Phagosome	ko04145	67
Peroxisome	ko04146	74
Plant-pathogen interaction	ko04626	180
Circadian rhythm - plant	ko04712	46

COG functional classification

In this study, 11028 Unigenes, annotated into COG, were distributed in 25 gene families (*Table 7*).

Table 7. *The function table annotated in the COG Library*

ID	Class_Name	Numbers
R	General function prediction only	3500
K	Transcription	1767
L	Replication, recombination and repair	1749
T	Signal transduction mechanisms	1669
O	Posttranslational modification, protein turnover, chaperones	960
G	Carbohydrate transport and metabolism	821
J	Translation, ribosomal structure and biogenesis	797
Q	Secondary metabolites biosynthesis, transport and catabolism	749
E	Amino acid transport and metabolism	740
S	Function unknown	615
C	Energy production and conversion	562
P	Inorganic ion transport and metabolism	530
I	Lipid transport and metabolism	457
M	Cell wall/membrane/envelope biogenesis	417
D	Cell cycle control, cell division, chromosome partitioning	310
V	Defense mechanisms	244
H	Coenzyme transport and metabolism	235
A	RNA processing and modification	185
Z	Cytoskeleton	182
U	Intracellular trafficking, secretion, and vesicular transport	180
F	Nucleotide transport and metabolism	147
B	Chromatin structure and dynamics	87
N	Cell motility	25
Y	Nuclear structure	1
W	Extracellular structures	0

Such as general function prediction, transcription, replication, recombination and repair, signal transduction, signal transduction, signal transduction, post-translational modification, protein turnover, mate, sugar transport and metabolism, translation,

http://www.aloki.hu ● ISSN 1589 1623 (Print) ●ISSN1785 0037 (Online)
DOI: http://dx.doi.org/10.15666/aeer/1706_1429714313

ribosome structure and biosynthesis of secondary metabolites biosynthesis, transport and catabolism and other functions (Allen et al., 2018; Astaneh et al., 2018; Li et al., 2018; Nisavic et al., 2018; Wang et al., 2018; Wu et al., 2018).

Conclusion

The sequence of cDNA library using Using Illumina HiSeq platform, the sequencing results were linked and functional annotations were analyzed to reveal the overall functional expression pattern of transcripts from different leaves of jujube. In recent years, there have been many studies based on high-energy sequencing, including Daphne *odora Thunb* (Yang et al., 2017), *Michelia macclurei Dandy* (Li et al., 2017), Rhododendron calvescens Balf.f. (Li et al., 2017), *Carthamus tinctorius L.* (Dong et al., 2017), *Penthorum chinense Pursh* (Yuan et al., 2017) and other plants. Transcriptome genes are classified into 110 metabolic pathways, including ribosome, amino acid biosynthesis, carbon metabolism, plant hormone signal transduction, plant pathogen interaction, splicer, RNA transport, starch and sucrose metabolism, endoplasmic reticulum protein processing, phenylpropanoid biosynthesis and so on. This study is the first time to use RNA-seq high-throughput sequencing technology to perform transcriptome sequencing and functional analysis of transcriptome results in fresh-eating jujube leaves, to explore genes for biological processes, cell components and molecular functions, and to study different functional genes, effective biosynthetic pathways and regulatory mechanisms.

Analysis of lignin-related genes in lignified jujube suspension

The results showed that the expression of lignin-related genes was more active in comparison with non-lignified jujube suspension, all of which were up-regulated genes. There were 11 up-regulated genes: *gene 29690, gene 4518, gene 30089, gene 1272, gene 21988, gene 16475, gene 16475, gene 14268, gene 14269, gene 10082 and gene 29495.*

The main functional genes in *gene 29690* family are monooxygenase activity and lignin metabolism. In *gene 14269* gene family, it includes the functions to be expressed in almost other gene families. Meristem growth regulation, chitin decomposition, glycolysis, cytokinin response, abscisic acid response, lignin biosynthesis, polar transport of auxin, cell tip growth.

The up-regulation of gene expression related to Lignin Metabolism in lignified jujube suspension also confirms that the cause of lignified jujube suspension is related to the synergy of gene expression mentioned above. Jiang et al. (2018) found that 16 lignin genes, including *2 PAL*, *5 CCR*, *3 4CL*, *2 CADH2* and *4 LAC*, were up-regulated with shoot development, suggesting that they may be related to developmental lignin accumulation. Lin et al. (2018) studied the characteristics and rules of Lignin Metabolism in okra fruits and found that the significant increase of lignin and cellulose content was

http://www.aloki.hu ● ISSN 1589 1623 (Print) ●ISSN1785 0037 (Online)
DOI: http://dx.doi.org/10.15666/aeer/1706_1429714313

related to phenylalanine ammonia lyase (*PAL*), cinnamyl alcohol 4-hydroxylase (*C4H*), 4 coumarin acyl-CoA ligase, protopectin and flavonoid enzymes.

PRX52 is a major lignin and secondary cell wall biosynthetic gene, especially in xylem vessel. The mutant of Arabidopsis thaliana showed a 70-80% decrease in lignin content, which was syringyl lignin (Fernandez-Perez et al., 2015). Previous studies have investigated its possible role in ABA-mediated plant defense against bacterial and fungal responses (Mohr et al., 2007). *TCP3* and *MYB12* were found to be involved in the regulation of *PRX52* (Arro et al., 2017) in grape tendril transcriptome studies. During lignification, *PRX52* interacts with TCP3 more extensively than it responds to adversity. *PRX52* also shares the phenylpropane metabolic pathway in lignin biosynthesis with *MYB12* (response switch gene for flavonol metabolism) (Czemmel et al., 2012). Phenylalanine aminolytic enzyme (*PAL*) is a rate-limiting enzyme in the metabolic pathway of lignin phenylpropane, which catalyzes the conversion of phenylalanine to cinnamic acid and coenzyme lipids, and is one of the most important enzymes in lignin synthesis (Matus et al., 2008). In this experiment, homologous genes were expressed in the transcripts of lignified jujube suspension.

Differential gene expression analysis of lignified jujube suspension related to photosynthesis

The results showed that the genes annotated in GO were up-regulated in *gene 4228*, *gene 10305* and *gene 42934*, down-regulated in *gene 6204*, *gene 29074*, *gene 24178*, *gene 15775*, *gene 2674*, *gene 4496* and *gene 296156*. In the annotation of metabolic pathway in KEGG database, three genes participated in photosynthesis expression, of which *gene 4496*, *gene 24178* were down-regulated and *gene 4293* was up-regulated.

In the *gene 4496* gene family, there are reactive oxygen species, photosynthesis and redox processes involved in biological processes. Molecular function is involved in iron oxidase activity and iron binding. Chloroplasts are involved in cell components. In gene 24178 expression, serine cysteine biosynthesis, photosynthetic adaptation, regulation of hydrogen peroxide metabolism, regulation of superoxide metabolism, photosynthesis and so on. The molecular functions include transferase activity, pyridoxal phosphate binding activity and cysteine synthetase activity. The thylakoid cavity is involved in the up-regulation of cell composition. *Gene 4293* family genes are up-regulated, including sulfur amino acid metabolism, glycine metabolism, vitamin metabolism, cell amino acid biosynthesis, aromatic amino acid metabolism, lipid metabolism, coenzyme biosynthesis, cold reaction, biological stimulation detection, blue light response. High light intensity response, red light response, far red light response, PSII related light capture complex II catabolism process, regulation of hydrogen peroxide metabolism process, chlorophyll biosynthesis process, starch biosynthesis process. Only the chloroplast envelope is involved in the expression.

Liu (2008) studied the temporal and spatial expression of *cab-PhE3, cab-PhE1, cab-PhE5, cab-PhE8, cab-PhE10* and *cab-PhE11* genes in Phyllostachys heterocycla (Carr.)

http://www.aloki.hu ● ISSN 1589 1623 (Print) ●ISSN1785 0037 (Online)
DOI: http://dx.doi.org/10.15666/aeer/1706_1429714313

Mitford cv. Pubescens under photosynthesis (Zhang et al., 2009). Through proteomics, bioinformatics and *VIGS* analysis, it was found that *TYLCCNV/TYLCCNB* invasion was involved in stress and defense, energy production, photosynthesis, protein homeostasis, metabolism, cell structure, signal transduction, transcription, transport and cell growth/division. Effective methylation of N-methyl was promoted through N-adenosine-L-methionine cycle II pathway (Zhang, 2014). Molecular mechanism of carbon flux regulation is fixed carbon expression in photosynthesis in different wild-type algae and Arabidopsis thaliana. Arabidopsis thaliana is used as a model to study the transformation of genetic regulation from vegetative growth to reproductive growth (Khan et al., 2014; Carrieri et al., 2018). The study also proved that both lignified and non-lignified jujube suspension had gene expression, and more up-regulated genes were expressed in lignified jujube suspension.

Summary

By comparing lignified jujube suspension with non-lignified jujube suspension, using GO and KEGG database annotations, the differential functional genes were analyzed from three database systems.

For lignified jujube suspension analysis, 11 genes were up-regulated with lignin gene expression, and there was no up-regulated with non-lignified jujube suspension. The results showed that lignified jujube suspension was related to lignin synthesis. There are 42 genes involved in lignin biosynthesis. They have synergistic effects on Chitinase activity, polysaccharide binding, cell wall tissue, root hair elongation, regulation of carbohydrate biosynthesis, cellulose biosynthesis and meristem growth. The formation of lignified jujube suspension is related to the co-regulation of photosynthesis and endogenous hormones.

REFERENCES

[1] Allen, D. T., Carrier, D. J., Gong, J. L., Hwang, B. J., Licence, P., Moores, A., Pradeep, T., Sels, B., Subramaniam, B., Tam, M. K. C., Zhang, L., Williams, R. M. (2018): Advancing the Use of Sustainability Metrics in ACS Sustainable Chemistry & Engineering. – ACS Publications 6(1): 1.

[2] Arro, J., Cuenca, J., Yang, Y. Z., Liang, Z. C., Cousins, P., Zhong, G. Y. (2017): A transcriptome analysis of two grapevine populations segregating for tendril phyllotaxy. – Horticulture Research 4: 17032.

[3] Astaneh, R. K., Bolandnazar, S., Nahandi, F. Z., Oustan, S. (2018): The Effects of Selenium On some Physiological Traits and K, Na Concentration of Garlic (Allium Sativum L.) Under Nacl Stress. – Information Processing in Agriculture 5(1): 156-161.

[4] Carrieri, D., Lombardi, T., Paddock, T., Cano, M., Goodney, G. A., Nag, A., Old, W., Maness, P.-C., Seibert, M., Ghirardi, Yu, J. P. (2017): Transcriptome and proteome

http://www.aloki.hu ● ISSN 1589 1623 (Print) ●ISSN1785 0037 (Online)
DOI: http://dx.doi.org/10.15666/aeer/1706_1429714313

analysis of nitrogen starvation responses in Synechocystis 6803 Δ glgC, a mutant incapable of glycogen storage. – Algal Research 21: 64-75.

[5] Chen, Z. L., Liu, S. P., Liu, C. H. (2015): Discussion on growth and development of jujube and jujube crane. – Chinese agronomy bulletin 31(28): 104-111.

[6] Chen, H., Wu, Y. G., Yang, Y. Z. (2018): The data assembly of the young leaves and mature leaves of patchouli and the gene function annotation. – Molecular Plant Breeding 16(7): 2139-2154.

[7] Czemmel, S., Heppel, S. C., Bogs, J. (2012): R2R3 MYB transcription factors: key regulators of the flavonoid biosynthetic pathway in grapevine. – Protoplasma 249: 109-118.

[8] Ding, Y. H. (2017): High-throughput sequencing of small RNA and functional verification of microRNA in cotton male sterility induced by high temperature stress. – Huazhong Agricultural University.

[9] Dong, Y. Y., Liu, X. M., Yao, N., Li, H. Y. (2017): Transcription factor analysis based on transcriptome data of different tissues of Safflower. – Chinese herbal medicine 48(21): 4515-4522.

[10] Fernandez-Perez, F., Pomar, F., Pedreno, M. A., Novo-Uzal, E. (2015): The suppression of AtPrx52 affects fibers but not xylem lignification in Arabidopsis by altering the proportion of syringyl units. – Physiol Plant 154: 395-406.

[11] Jiang, H. G., Wang, S. G., Liu, Y. (2018): Screening and expression analysis of lignin genes in shoots of Cizhu bamboo based on transcriptome sequencing. – Plant studies 38(03): 415-421.

[12] Khan, M. R., Ai, X. Y., Zhang, J. Z. (2014): Genetic regulation of flowering time in annual and perennial plants. – Wiley Interdiscip. Rev. 5: 347-359.

[13] Kim, D., Pertea, G., Trapnell, C., Pimentel, H., Kelley, R., Salzberg, S. L. (2013): TopHat2: accurate alignment of transcriptomes in the presence of insertions, deletions and gene fusions. – Genome Biology 14(4): R36.

[14] Langmead, B., Salzberg, S. L. (2012): Fast gapped-read alignment with bowtie. – Nature Methods 9(4): 357-359.

[15] Li, Q. Y., Zhong, C. L., Jiang, Q. B. (2017): Molecular Plant Breeding 15(11): 4396-4404.

[16] Li, T. Q., Liu, X. F., Wanyou, M. (2017): Transcriptome analysis of wild plant Rhododendron longstalk based on high-throughput sequencing. – Plant studies 37(06): 825-834.

[17] Li, Z., Han, C. G. (2018): Economics of Biomass Gasification: A Review of the Current Status. – Energy Sources Part B Economics Planning & Policy 13(2): 137-140.

[18] Lin, X., Pan, X., Kang, X. (2018): Effects of picking time on Lignin Metabolism and related enzyme activities of Chuanqiu okra. – Zhejiang Agricultural Journal 09: 1519-1525.

[19] Liu, Y. L. (2008): Isolation and expression of light-harvesting pigment binding protein gene in Phyllostachys pubescens photosystem. – Chinese Academy of Forestry Sciences.

[20] Liu, J. T., Zhu, H. S., Wen, Q. F. (2017): Separation and browning of WRKY transcription factor gene of silk gourd. – Journal of Agricultural Biotechnology 25(12): 1950-1960.

http://www.aloki.hu ● ISSN 1589 1623 (Print) ●ISSN1785 0037 (Online)
DOI: http://dx.doi.org/10.15666/aeer/1706_1429714313

[21] Matus, J. T., Aquea, F., Arce-Johnson, P. (2008): Analysis of the grape MYB R2R3 subfamily reveals expanded wine quality-related clades and conserved gene structure organization across Vitis and Arabidopsis genomes. – BMC Plant Biol. 8: 83.

[22] Mohr, P. G., Cahill, D. M. (2007): Suppression by ABA of salicylic acid and lignin accumulation and the expression of multiple genes, in Arabidopsis infected with Pseudomonas syringae PV. Tomato. – Funct Integr Genomics 7: 181-191.

[23] Nisavic, M., Stoiljkovic, M., Crnolatac, I., Milosevic, M., Rilak, A., Masnikosa, R. (2018): Highly Water-Soluble Ruthenium(Ii) Terpyridine Coordination Compounds Form Stable Adducts with Blood-Borne Metal Transporting Proteins. – Arabian Journal of Chemistry 11(3): 291-304.

[24] Niu, J. Q., Su, J. M., Wang, X. M. (2018): Data analysis of Dendrobium nobile leaves transcriptome based on high throughput sequencing. – Molecular Plant Breeding 16(03): 747-756.

[25] Qi, Y. X., Liu, Y. B., Rong, W. H. (2011): rRNA-Seq and its applications:a new technology for transcriptomics. – Yichuan(Hereditas) 33(11): 1191-1202.

[26] Qu, Z. Z., Wang, Y. H. (1993): Fruit tree of China. Jujube volume. – China Forestry Publishing House.

[27] Reich, I., Ijaz, U. Z., Gormally, M., Smith, C. J. (2018): 16s rRNA sequencing reveals likely beneficial core microbes within faecal samples of the eu protected slug geomalacus maculosus. – Scientific Reports 8(1): 10402.

[28] Sun, Q. H., Cheng, Z. Y., Qi, H. R. (1996): Observation and report on the growth and fruiting habit of Jinzao jujube crane. – Shaanxi forestry science and technology 3: 10-11.

[29] Tang, Z. J., He, M., Gao, J. P. (2012): Influence of pinching and sprouting on the formation of lignification jujube crane. – North horticulture 22: 26-28.

[30] Wang, S., Yan, C. (2014): Comparison of accumulation capacity of Photosynthate from 2 types of jujube crane in southern China. – Forestry Science 50(06): 90-97.

[31] Wang, S., Yan, C., Deng, B. L. (2014): Comparison of nutrient transport and accumulation ability of two types of jujube crane in southern China. – Journal of Central South University of Forestry and Technology 34(12): 35-39.

[32] Wang, M., Zhang, D. Q., Su, J., Dong, J. W., Tan, S. K. (2018): Assessing Hydrological Effects and Performance of Low Impact Development Practices Based On Future Scenarios Modeling. – Journal of Cleaner Production 179: 12-23.

[33] Wu, X., Song, M., Qiu, P., Li, F., Wang, M., Zheng, J., Wang, Q., Xu, F., Xiao, H. (2018): A Metabolite of Nobiletin, 4 '-Demethylnobiletin and Atorvastatin Synergistically Inhibits Human Colon Cancer Cell Growth by Inducing G0/G1 Cell Cycle Arrest and Apoptosis. – Food & Function 9(1): 87-95.

[34] Yan, C., Wang, S., Shao, F. X. (2013): Comparison of photosynthetic efficiency between leaves of lignification and non lignification of jujube leaves in southern jujube. – Economic Forest Research 31(02): 113-117.

[35] Yang, Y. R., Zhao, J., Liu, M. J. (2007): Research progress of jujube crane. – Acta agronomica Sinica S2: 53-57.

http://www.aloki.hu ● ISSN 1589 1623 (Print) ●ISSN1785 0037 (Online)
DOI: http://dx.doi.org/10.15666/aeer/1706_1429714313

[36] Yang, L., Zhang, W., Xu, Y. T. (2014): Effects of dormant pruning on Germination of ash dates, Jun jujube and date jujube crane. – Xinjiang Agricultural Sciences 51(11): 1984-1989.

[37] Yang, Y., Liu, H., Qiu, D. (2017): Transcriptome data analysis of Stellera chamaejasme based on high-throughput sequencing. – Chinese herbal medicine 48(22): 4740-4747.

[38] Yuan, C., Fang, P., Zhong, W. J. (2017): Transcriptome sequencing and analysis of Phellodendron chinensis. – Chinese herbal medicine 48(21): 4507-4514.

[39] Zhang, D., Li, W., Li, D. (2009): The relationship between isoflavone content in soybean leaves and relative expression of PAL gene. – Soybean Science 28(4): 670-673.

[40] Zhang, Y., Zhou, Y., Chen, Q. (2014): Molecular basis of flowering time regulation in Arabidopsis. – China. Bull. Bot. 49: 469-482.

[41] Zhang, S. P., Zhang, S. H., Qiu, S. L. (2018): Based on the transcriptional sequence analysis of the related genes of sunflower green anthocyanin in purple back. – Acta Agriculturae Nucleatae Sinica 32(04): 639-645.

[42] Zhu, L. S., Liu, G., He, S. E. (2018): Analysis of the transcriptional characteristics of Eucalyptus grandis based on Illumina HiSeq 2000 sequencing technology. – Molecular Plant Breeding 13: 1-13.

http://www.aloki.hu ● ISSN 1589 1623 (Print) ●ISSN1785 0037 (Online)
DOI: http://dx.doi.org/10.15666/aeer/1706_1429714313

FIRST STUDY OF THE ECOLOGICAL STATUS IN THE ATLANTIC COAST OF MOROCCO USING THE BROWN SEAWEED *CYSTOSEIRA TAMARISCIFOLIA*

BOUNDIR, Y.[1,2,3*] – HASNI, M.[4,5] – RAFIK, F.[2] – SABRI, H.[1,3] – BAHAMMOU, N.[1,3] – CHEGGOUR, M.[5] – ACHTAK, H.[2] – CHERIFI, O.[1,3]

[1]*Laboratory of Hydrobiology, Ecotoxicology, Sanitation and Global Changes (LHEAC-URAC33), Faculty of Sciences Semlalia, Cadi Ayyad University*
Bd. Prince My Abdellah, PO Box 2390, 40000 Marrakesh, Morocco

[2] *Environment and Health Team, Polydisciplinary Faculty, Cadi Ayyad University*
Route Sidi Bouzid PO Box 4162 Avenue Mohamed Belkhadir, 46000 Safi, Morocco

[3]*National Center for Studies and Research on Water and Energy (CNEREE), Cadi Ayyad University*
Avenue Abdelkrim Khattabi, PO Box 511, 40000 Marrakesh, Morocco

[4]*Faculty of Sciences, Ibn Zohr University, PO Box 8106, 80000 Agadir, Morocco*

[5]*Biology department, Ecology unit, Ecole Normale Supérieure, Cadi Ayyad University*
Hay Hassani Route d'Essaouira, PO Box 2400, 40000 Marrakesh, Morocco

[*]*Corresponding author*
e-mail: younes.boundir@ced.uca.ma; phone: +21-263-884-6052; fax: +21-205-433-170

(Received 5th Jun 2019; accepted 25th Oct 2019)

Abstract. This study is a first attempt to evaluate the toxic effects of prominent aquatic pollutants (nutrients and toxic metals) on the brown seaweed *Bushy Rainbow Wrack (Cystoseira tamariscifolia)* physiology along the Atlantic coast of Morocco. The physicochemistry (nutrients) of seawater, toxic metals (Chromium, Lead, Copper and Cadmium) and physiological parameters (Chlorophyll contents, Proline, Glycinebetaine and Total Phenolic Compounds) of the brown macroalgae *Bushy Rainbow Wrack* were studied in order to assess the pollution degree of 8 coastal areas. The results show that the toxic metal contents of *Bushy Rainbow Wrack* (especially Cadmium) and the concentration of phosphorus are correlated with stress physiological parameters, and inversely correlated with pigment contents. It shows that while these brown algae exist in the less polluted areas, their physiology is significantly affected. However, in the highly polluted areas, this brown seaweed disappears. Thus, this specie could be used for monitoring the pollution degree in coastal areas.
Keywords: *environmental pollution, heavy metals, physicochemical parameters, algal physiology*

Introduction

Cystoseira is a genus of brown macroalgae. Most of the species of this genus are very sensitive to pollution and to other anthropogenic pressures, and their numbers have diminished considerably during the last decades (Cormaci et al., 1999; Thibaut et al., 2005). With the rapid industrialization and economic development of coastal regions, heavy metals continue to be introduced into coastal zones, our country's coast must be in such a state that local organisms can live, develop and reproduce without hindrance. To achieve this goal, it is essential that pollutant inputs to water be reduced or even avoided, regardless of their origin: domestic, artisanal, industrial, agricultural or other sources (Blinda et al., 2013). Seaweeds are widely recognized as autogenic "ecosystem

http://www.aloki.hu ● ISSN 1589 1623 (Print) ● ISSN 1785 0037 (Online)
DOI: http://dx.doi.org/10.15666/aeer/1706_1431514331

engineers" (Jones et al., 1994) or "foundation species" (Dayton, 1975). In general, the direct causes of change in marine biodiversity loss and coastal ecosystems, are: pollution, habitat destruction, increases in sedimentation, overexploitation of resources, climate change, and invasive species (Walker and Kendrick, 1998; Claudet and Fraschetti, 2010; Munday et al., 2013). The aim of this study is to portray the decrease of *Bushy Rainbow Wrack* (*Cystoseira tamariscifolia* (Hudson) Papenfuss) and to clarify the source and the conceivable reasons of its decrease in the Atlantic coast of Morocco.

Materials and Methods

Location

Eight (8) stations located on rocky substrates along the Atlantic coast of Morocco were chosen:

- Eljadida city with 2 stations: Sidi Bouzid coast: 33°13'N-8°55'W as a control area (S1). According to Moroccan beaches position, this station is ranked each year among the beaches called "Blue Flag". The Mohammed VI Foundation for the Protection of the Environment awards this distinction each year to beaches that fit the international standard norms of cleanliness (F.M.6, 2018). Jorf Lasfar: 33°07'N -8°37'W (S2) known as a polluted one. This area is characterized by the presence of multiple industrial units including a phosphate complex and a power thermal plant (Essedaoui et al., 2001; Kaimoussi et al., 2001; Ferssiwi et al., 2004).
- Safi city with 3 stations: Beddouza: 32°54'N-9°27'W (S3), less polluted station located 34 km from the industrial city of Safi (Goumri et al., 2018); Industrial Area: 32°28'N-9°24'W (S4) and Phosphate Area: 32°18'N-9°26'W (S5).
- Essaouira city where 3 stations were selected: Moulay Bouzerktoun (31°63'N-9°67'W) (S6); located approximately 15 km from the enclosure of the city, it is less affected by anthropogenic activities, just an ephemeral tourism activity during the summer. Bab Doukala: 31°51'N-9°76'W (S7) and the port: 31°51'N-9°77'W (S8), receive domestic and some industrial releases (Sabri et al., 2017; Cherifi et al., 2018). Among them, 3 stations less polluted and 5 more polluted near to industrial factories (*Fig. 1*).

Sampling

Algal Samples were collected during Autumn 2017 to Summer 2018 at 0-5 meter depth depending on the geomorphology of the stations (*Fig. 2*) and following the principle of the quadrats. Then, washed in seawater, put in plastic packs and transported to the research center in a cooler for metal analysis. The samples expected for identification are preserved into alcohol at 10% while samples for physiology analysis are kept dry. Those of ocean water were collected during the same period, placed in a cooler and were conveyed fresh to the research center.

Physicochemical parameters

Concentration of inorganic nutrients of seawater (Phosphorus and Nitrogenous compounds) was measured according to AFNOR norms: T90-012 for Nitrate, T90-015 for Ammonium, T90-061 for Total nitrogen, T90-022 for Orthophosphate and T90-023 for Total phosphorus. Metal Concentrations of Cd, Cu, Pb and Cr were measured in seawater and the dried *Bushy Rainbow Wrack* according to Blinda et al (2013) and

http://www.aloki.hu ● ISSN 1589 1623 (Print) ● ISSN 1785 0037 (Online)
DOI: http://dx.doi.org/10.15666/aeer/1706_1431514331

Topcuoglu et al (2003) methods, respectively. The samples were digested with concentrated nitric acid and analyzed using Atomic Absorption Spectrophotometer.

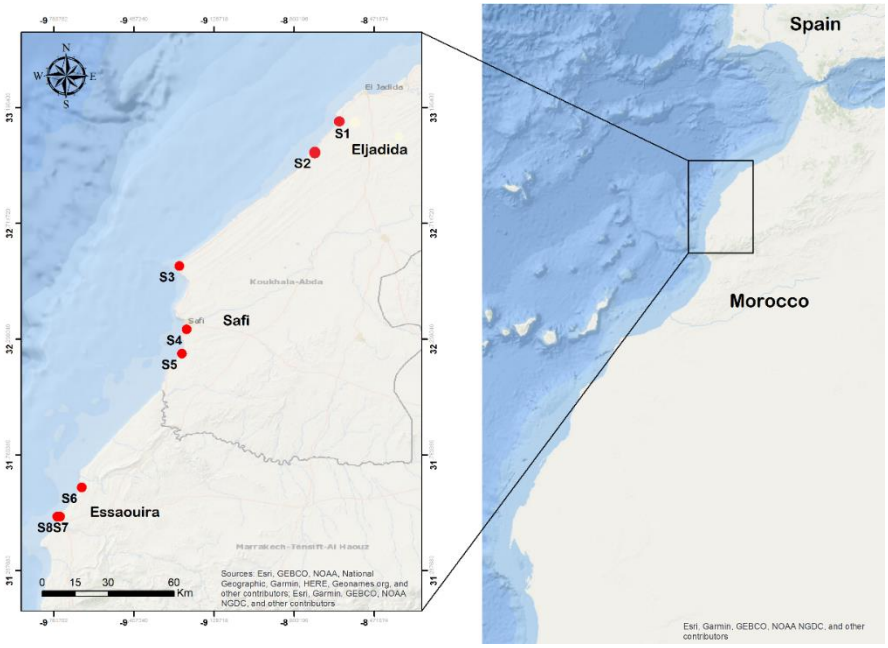

Figure 1. *The location of the sampling points using ArcGIS, version 10.7. (S1) Sidi Bouzid: 33°13'N-8°55'W, (S2) Jorf Lasfar: 33°07'N-8°37'W, (S3) Beddouza: 32°54'N-9°27'W, (S4) Industrial Area: 32°28'N-9°24'W, (S5) Phosphate Area: 32°18'N-9°26'W, (S6) Moulay Bouzerktoun: 31°63'N-9°67'W, (S7) Bab Doukala: 31°51'N-9°76'W, (S8) The port: 31°51'N-9°77'W*

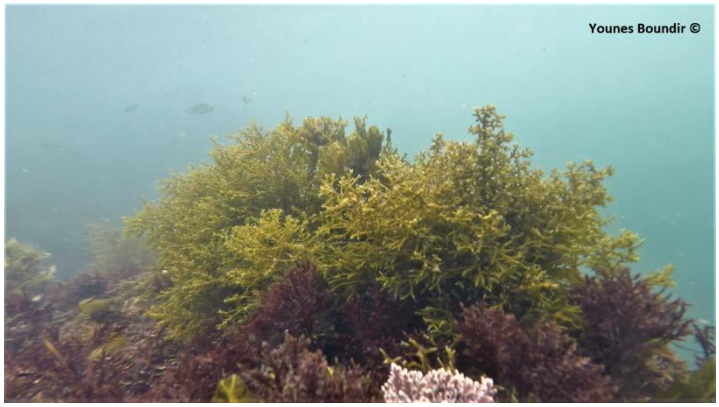

Figure 2. *Bushy Rainbow Wrack captured with underwater camera from (S1) Sidi Bouzid coast near Eljadida city at 5m depth. Picture: Younes Boundir © June 2018*

Biochemical and physiological parameters

Chlorophyll

The contents of chlorophyll a, c were estimated using the method of Jeffrey and Humphrey (1975). Pigment concentrations are expressed as µg/g FW (Fresh Weight) and calculated according to the following equations:

http://www.aloki.hu ● ISSN 1589 1623 (Print) ● ISSN 1785 0037 (Online)
DOI: http://dx.doi.org/10.15666/aeer/1706_1431514331

$$\text{Chlorophyll a} = 11.47 \times \text{O.D.}664 - 0.40 \times \text{O.D.}630 \quad \text{(Eq.1)}$$

$$\text{Chlorophyll c} = 24.36 \times \text{O.D.}630 - 3.73 \times \text{O.D.}664 \quad \text{(Eq.2)}$$

The pigments were extracted from 1 g seaweed *Bushy Rainbow Wrack* with 10 mL of acetone in the presence of calcium carbonate. Then put in 4°C for 24 hours in the dark. The chlorophyll content was determined in triplicate.

Total carotenoids were calculated according to the equation of Lichtenthaler (1987):

$$\text{Carotenoid} = \frac{1000 \times \text{O.D.}470 - 1.9 \times \text{Cha} - 63.14\,\text{Chb}}{214} \quad \text{(Eq.3)}$$

Glycinebetaine (GB)

Analysis of GB was performed according to the method of Grieve and Grattan (1986). 0.5 g DW (dry weight) of the seaweed *Bushy Rainbow Wrack* prepared in 20 mL test tubes was mechanically shaken with 20 mL of deionized H_2O at 25°C for 24 h. The extracts then were diluted 1:1 with 2N H_2SO_4. 0.5 ml of this solution were measured into heavy walled glass centrifuge tubes and cooled in ice water for about 1 hour. A preparation of 0.2 ml KI-I2 was made by dissolving 20 g of KI and 15.7 g of iodine in 100 ml. Then, water was added and the reactants were gently stirred with a vortex mixer. The tubes were stored for 16h at 0-4°C and then centrifuged at 10000 rpm at 0°C for 15 min. The supernatant was aspirated and dissolved in 9 ml of 1,2-dichloroethane. Vortex mixing was made to effect complete solution in the developing solvent. The absorbance was measured after 2 h at 365 nm. The concentration was estimated by using a standard curve developed with different concentration of GB in triplicate.

Proline

The method used is the one of Monneveux and Nemmar (1986). 100 mg of the seaweed *Bushy Rainbow Wrack* are directly weighed and then placed in a test tube. 2 ml of methanol 40% is added to the tubes and placed in a water bath at 85°C for about 1 hour. 1 ml of the solution is added to 25 mg ninhydrin after cooling, 1 ml of acetic acid and 1 ml of the mixture distilled water-acetic, acid-acetic, acid-acid orthophosphoric, of density 1.7 (120, 300, 80: v / v / v). The solution is brought again for 30 minutes in a water bath at 100°C, then cooled and added to 5 ml of toluene. After agitation, a pinch of Na_2SO_4 is added to each tube. Absorbance was measured at 528 nm.

Total phenolic compounds (TPC)

TPC of the extract was estimated by the method of Taga et al. (1984). Dry weight samples of the seaweed *Bushy Rainbow Wrack* were prepared in 60:40 (0.3% HCl) acidified methanol/water. Solutions of 100 µL were added to 2 mL of Na_2CO_3 (2%). 100 µL of Folin-Ciocalteau (50%) reagent were added after 2 min. Absorbance was measured after 2 hours at 750 nm. Gallic acid standards was prepared with a range of concentrations of 10 mg/mL to 200 mg/mL. The phenolic concentrations were determined by comparison with the standard calibration curve. Phenolic content was expressed as gallic acid equivalent (GAE).

http://www.aloki.hu ● ISSN 1589 1623 (Print) ● ISSN 1785 0037 (Online)
DOI: http://dx.doi.org/10.15666/aeer/1706_1431514331

Statistical analysis

All the analyzed parameters were established in triplicate and gave mean values and standard deviation. The values were tested for normality and homogeneity of variance, as well as for significance between parameters using a one-way and two-way analysis of variance with Excel 2016 and SPSS (IBM, USA), version 22. Correlation matrix was used to determine the relation between the physiological parameters, Heavy metals and the physicochemical compounds studied. Principal Component Analysis (PCA) was performed using SPSS (IBM, USA), version 22.

Results

Distribution of Bushy Rainbow Wrack

The preliminary study shows that there is a first presence of Bushy Rainbow Wrack in the control station (S1) at Eljadida coast during the 4 seasons. Essaouira city comes in the second range where this specie is more present in (S5). Safi coast comes in the thirth place where the Bushy Rainbow Wrack is abondant in unpolluted station (S3) (*Table 1*).

Table 1. *Bushy Rainbow Wrack inventory in the studied areas during autumn-summer 2018*

City	Station	Autumn	Winter	Spring	Summer
Eljadida	**S1**	A	A	A	A
	S2	-	-	-	-
Safi	**S3**	R	R	R	R
	S4	-	-	-	-
	S5	-	-	-	-
Essaouira	**S6**	R	R	F	A
	S7	-	-	R	F
	S8	-	-	R	F

-: Absence of Bushy Rainbow Wrack. A: Abundant, F: Frequent, R: Rare

Physicochemical parameters: nitrogenous and phosphorus compounds

Statistical analysis of nitrogenous compounds didn't show significant difference between control and polluted stations ($F= 11.29$; $p<0.01$). Thus, it could not explain the degradation of the species studied. Total nitrogenous concentrations are ranged between 2.52±0.30 and 4.70±0.16 mg/L and those of nitrate between 1.30±0.56 and 2.56±0.46 mg/L (*Table 2*).

Statistical analyses of phosphorus compounds, however, have showed a highly significant difference between the areas studied ($F= 1.65$; $p<<0.01$). The maximum total phosphate concentration was recorded in the Phosphate industrial area (S5), at Safi coast with 2.00±0.13 mg/L and the minimum in the control station (S1), in Sidi Bouzid coast with only 0.04±0.01 mg/L (*Table 2*).

Heavy metals analysis

Heavy metals analysis in seawater

The analysis of metals shows that the mean metal levels in seawater decreased in the following order: Pb > Cd > Cr > Cu (*Table 3*). The results obtained are discussed on the basis of the Moroccan standards for direct discharges of heavy metals into aquatic

http://www.aloki.hu ● ISSN 1589 1623 (Print) ● ISSN 1785 0037 (Online)
DOI: http://dx.doi.org/10.15666/aeer/1706_1431514331

environments (surface water). The maximum concentrations required by the above standard are: 0.5 mg/l for Pb, 2 mg/l for Cr, 0.5 mg/l for Cu and 0.2 mg/l for Cd (FAO, 2006). The highest concentrations of toxic metals were recorded in two polluted stations near to Safi coast: a fish industrial discharges (Cd: 1.12±0.15 µg/L; Pb: 2.563±0.73 µg/L) and phosphate discharge area (Cd: 1.15±0.88 µg/L; Pb: 1.53±0.55 µg/L).

Table 2. *Variation of Phosphorus and Nitrogenous compounds in different stations*

Station	Season	TP	DP	PO_4^{3-}	TN	DN	NO_3^-	NH_4^+
S1	Autumn	$0.06\pm0.03^{C*}$	0.05 ± 0.02^{C}	0.02 ± 0.01^{C}	4.03 ± 0.14^{A}	3.74 ± 0.11^{A}	2.14 ± 0.20^{A}	0.89 ± 0.09^{BC}
	Winter	0.07 ± 0.02^{C}	0.08 ± 0.03^{BC}	0.05 ± 0.02^{C}	4.40 ± 0.13^{A}	4.10 ± 0.14^{A}	2.40 ± 0.16^{A}	1.14 ± 0.04^{A}
	Spring	0.06 ± 0.03^{C}	0.07 ± 0.02^{B}	0.04 ± 0.01^{C}	4.31 ± 0.14^{A}	3.65 ± 0.13^{A}	2.33 ± 0.14^{A}	0.90 ± 0.05^{BC}
	Summer	0.05 ± 0.02^{C}	0.05 ± 0.03^{C}	0.03 ± 0.01^{C}	4.12 ± 0.15^{A}	3.21 ± 0.12^{A}	2.20 ± 0.12^{A}	1.11 ± 0.12^{A}
S2	Autumn	0.04 ± 0.01^{C}	0.05 ± 0.02^{C}	0.05 ± 0.02^{C}	2.15 ± 0.12^{C}	1.23 ± 0.21^{B}	1.30 ± 0.56^{B}	0.74 ± 0.16^{AB}
	Winter	0.09 ± 0.05^{C}	0.08 ± 0.01^{BC}	0.07 ± 0.03^{BC}	2.40 ± 0.14^{C}	2.30 ± 0.23^{B}	1.50 ± 0.20^{B}	1.12 ± 0.13^{A}
	Spring	0.08 ± 0.03^{C}	0.07 ± 0.03^{B}	0.06 ± 0.02^{BC}	2.32 ± 0.15^{C}	1.96 ± 0.17^{B}	1.45 ± 0.23^{B}	1.10 ± 0.16^{A}
	Summer	0.05 ± 0.02^{C}	0.04 ± 0.01^{C}	0.06 ± 0.01^{BC}	2.30 ± 0.13^{C}	1.50 ± 0.12^{B}	1.33 ± 0.12^{B}	0.88 ± 0.18^{A}
S3	Autumn	0.26 ± 0.03^{B}	0.06 ± 0.03^{C}	0.03 ± 0.01^{C}	2.65 ± 0.15^{C}	1.65 ± 0.18^{B}	1.70 ± 0.13^{AB}	1.15 ± 0.13^{A}
	Winter	0.38 ± 0.02^{B}	0.08 ± 0.03^{BC}	0.05 ± 0.02^{C}	2.90 ± 0.12^{BC}	2.40 ± 0.17^{B}	1.90 ± 0.16^{AB}	1.21 ± 0.18^{A}
	Spring	0.25 ± 0.03^{B}	0.05 ± 0.02^{C}	0.04 ± 0.01^{C}	2.85 ± 0.15^{BC}	1.96 ± 0.13^{B}	1.88 ± 0.18^{AB}	1.12 ± 0.22^{A}
	Summer	0.26 ± 0.03^{B}	0.06 ± 0.03^{C}	0.03 ± 0.01^{C}	2.74 ± 0.14^{BC}	1.80 ± 0.12^{B}	1.65 ± 0.14^{B}	1.10 ± 0.17^{A}
S4	Autumn	0.14 ± 0.04^{B}	0.06 ± 0.01^{C}	0.05 ± 0.02^{C}	4.33 ± 0.18^{A}	1.78 ± 0.13^{B}	2.22 ± 0.25^{A}	0.54 ± 0.18^{B}
	Winter	0.29 ± 0.02^{B}	0.10 ± 0.03^{AB}	0.07 ± 0.02^{BC}	4.70 ± 0.16^{A}	2.60 ± 0.14^{B}	2.40 ± 0.24^{A}	0.99 ± 0.17^{AB}
	Spring	0.13 ± 0.03^{B}	0.10 ± 0.02^{AB}	0.06 ± 0.01^{BC}	4.62 ± 0.12^{A}	2.20 ± 0.14^{B}	2.33 ± 0.22^{A}	0.85 ± 0.18^{AB}
	Summer	0.15 ± 0.02^{BC}	0.05 ± 0.02^{C}	0.06 ± 0.02^{BC}	4.56 ± 0.13^{A}	1.96 ± 0.15^{B}	2.10 ± 0.14^{A}	1.23 ± 0.13^{A}
S5	Autumn	1.55 ± 0.08^{A}	0.95 ± 0.04^{AB}	0.11 ± 0.03^{A}	2.33 ± 0.11^{C}	2.90 ± 0.14^{AB}	2.30 ± 0.33^{A}	0.64 ± 0.13^{B}
	Winter	2.00 ± 0.13^{A}	1.58 ± 0.06^{A}	0.11 ± 0.02^{A}	3.10 ± 0.14^{B}	3.00 ± 0.17^{A}	2.60 ± 0.45^{A}	0.65 ± 0.17^{B}
	Spring	1.22 ± 0.12^{A}	1.15 ± 0.08^{A}	0.11 ± 0.03^{A}	2.63 ± 0.17^{B}	2.80 ± 0.20^{A}	2.56 ± 0.46^{A}	0.24 ± 0.18^{C}
	Summer	1.69 ± 1.13^{A}	1.22 ± 0.07^{A}	0.09 ± 0.02^{B}	2.54 ± 0.15^{B}	2.55 ± 0.13^{A}	2.41 ± 0.34^{A}	0.32 ± 0.13^{C}
S6	Autumn	0.25 ± 0.09^{B}	0.03 ± 0.01^{C}	0.03 ± 0.01^{C}	3.21 ± 0.13^{AB}	1.80 ± 0.12^{AB}	1.46 ± 0.21^{B}	0.54 ± 0.21^{C}
	Winter	0.48 ± 0.07^{AB}	0.05 ± 0.02^{C}	0.05 ± 0.02^{C}	4.20 ± 0.15^{A}	2.00 ± 0.16^{B}	1.90 ± 0.12^{B}	1.21 ± 0.12^{A}
	Spring	0.35 ± 0.05^{B}	0.01 ± 0.01^{C}	0.04 ± 0.01^{C}	4.10 ± 0.13^{A}	1.55 ± 0.13^{B}	1.56 ± 0.11^{B}	0.74 ± 0.16^{AB}
	Summer	0.35 ± 0.06^{B}	0.02 ± 0.01^{C}	0.04 ± 0.02^{C}	3.32 ± 0.12^{B}	1.69 ± 0.17^{B}	1.70 ± 0.10^{B}	0.64 ± 0.17^{AB}
S7	Autumn	0.24 ± 0.02^{B}	0.09 ± 0.02^{C}	0.05 ± 0.01^{C}	2.12 ± 0.11^{C}	2.54 ± 0.12^{A}	2.22 ± 0.22^{A}	0.45 ± 0.15^{B}
	Winter	0.30 ± 0.01^{B}	0.17 ± 0.03^{B}	0.07 ± 0.02^{B}	2.90 ± 0.15^{AB}	2.60 ± 0.13^{A}	2.50 ± 0.14^{A}	0.87 ± 0.12^{AB}
	Spring	0.25 ± 0.01^{B}	0.12 ± 0.04^{B}	0.07 ± 0.01^{B}	2.55 ± 0.13^{B}	2.33 ± 0.14^{A}	2.45 ± 0.11^{A}	0.32 ± 0.14^{C}
	Summer	0.23 ± 0.02^{B}	0.14 ± 0.06^{B}	0.06 ± 0.02^{BC}	2.31 ± 0.12^{C}	2.30 ± 0.18^{A}	2.30 ± 0.24^{A}	0.35 ± 0.12^{C}
S8	Autumn	0.26 ± 0.03^{B}	0.21 ± 0.02^{B}	0.11 ± 0.01^{A}	3.31 ± 0.16^{B}	2.50 ± 0.12^{A}	1.30 ± 0.12^{BC}	0.58 ± 0.13^{BC}
	Winter	0.36 ± 0.06^{B}	0.23 ± 0.03^{B}	0.11 ± 0.02^{A}	4.30 ± 0.14^{A}	2.80 ± 0.21^{A}	1.50 ± 0.13^{B}	0.65 ± 0.13^{BC}
	Spring	0.26 ± 0.03^{B}	0.16 ± 0.02^{B}	0.11 ± 0.01^{A}	4.23 ± 0.16^{A}	2.66 ± 0.23^{A}	1.45 ± 0.23^{AB}	0.67 ± 0.16^{B}
	Summer	0.25 ± 0.05^{B}	0.19 ± 0.01^{B}	0.11 ± 0.02^{A}	3.56 ± 0.12^{A}	2.12 ± 0.18^{A}	1.36 ± 0.14^{AB}	0.54 ± 0.11^{B}

*The different upper-case letters in the same row indicate the differences between the studied stations and seasons at the level ($p<0.05$). TP: Total Phosphorus; DP: Dissolved Phosphorus; PO_4^{3-}: Orthophosphate; TN: Total Nitrogenous; DN: Dissolved Nitrogenous; NO_3^-: Nitrate; NH_4^+: Ammonium

Heavy metals analysis in Bushy Rainbow Wrack

The analysis of heavy metals shows that the mean levels in seaweed *Bushy Rainbow Wrack* decreased in the following order: Cu > Pb > Cr > Cd. The results obtained are discussed on the basis of comparaison of these heavy metals levels in seaweed *Cystoseira* sp. from other different locations in the world. The highest concentrations of all heavy metal were recorded in the polluted area (S8), the port station at Essaouira coast (Cd: 2.60±0.15 µg/g during spring; Pb: 4.43±0.73 µg/g during autumn, Cu: 10.60±1.14 µg/g during summer and Cr: 2.90±0.23 µg/g during autumn) (*Table 4*).

http://www.aloki.hu ● ISSN 1589 1623 (Print) ● ISSN 1785 0037 (Online)
DOI: http://dx.doi.org/10.15666/aeer/1706_1431514331

Table 3. *Heavy metals mean concentrations of Cd, Pb, Cu, and Cr in seawater along the studied stations*

Station	Cd	Pb	Cu	Cr
S1	$0.09\pm0.02^{C*}$	0.93 ± 0.28^{B}	0.08 ± 0.02^{C}	0.07 ± 0.02^{C}
S2	0.11 ± 0.04^{BC}	0.98 ± 0.27^{B}	0.12 ± 0.07^{C}	0.09 ± 0.03^{C}
S3	0.17 ± 0.03^{B}	-	0.19 ± 0.06^{C}	0.25 ± 0.06^{BC}
S4	1.12 ± 0.15^{A}	2.56 ± 0.73^{A}	0.20 ± 0.04^{BC}	0.98 ± 0.17^{A}
S5	1.15 ± 0.88^{A}	1.53 ± 0.55^{A}	0.60 ± 0.17^{A}	0.84 ± 0.07^{A}
S6	0.12 ± 0.07^{B}	1.12 ± 0.24^{AB}	0.09 ± 0.04^{C}	0.03 ± 0.01^{C}
S7	0.15 ± 0.09^{B}	0.97 ± 0.26^{B}	0.16 ± 0.08^{C}	0.04 ± 0.02^{C}
S8	0.17 ± 0.06^{B}	0.87 ± 0.19^{B}	0.13 ± 0.03^{C}	0.05 ± 0.01^{C}

*The different upper-case letters in the same row indicate the differences between the studied stations and seasons at the level ($p<0.05$)

Table 4. *Heavy metal mean concentrations (µg/g Dry Weight) of Cd, Pb, Cu, and Cr in Bushy Rainbow Wrack collected during autumn - summer 2018 along the stations studied*

Station	Season	Cd	Pb	Cu	Cr
S1	Autumn	$0.10\pm0.02^{C*}$	2.30 ± 0.32^{AB}	0.21 ± 0.05^{C}	0.11 ± 0.02^{C}
	Winter	0.22 ± 0.05^{BC}	1.20 ± 0.08^{C}	3.07 ± 0.19^{BC}	0.20 ± 0.05^{C}
	Spring	0.39 ± 0.09^{BC}	1.30 ± 0.05^{C}	0.36 ± 0.05^{C}	0.36 ± 0.03^{C}
	Summer	0.10 ± 0.03^{C}	0.50 ± 0.04^{C}	0.17 ± 0.09^{C}	0.14 ± 0.01^{C}
S2	Autumn	-	-	-	-
	Winter	-	-	-	-
	Spring	-	-	-	-
	Summer	-	-	-	-
S3	Autumn	0.20 ± 0.06^{C}	2.51 ± 0.08^{B}	4.00 ± 0.18^{BC}	0.14 ± 0.04^{C}
	Winter	0.42 ± 0.05^{BC}	2.14 ± 0.04^{BC}	2.72 ± 0.07^{C}	0.25 ± 0.06^{C}
	Spring	0.17 ± 0.04^{BC}	1.25 ± 0.08^{C}	0.45 ± 0.05^{C}	0.24 ± 0.03^{C}
	Summer	0.20 ± 0.02^{C}	1.22 ± 0.06^{C}	1.90 ± 0.09^{C}	0.36 ± 0.02^{C}
S4	Autumn	-	-	-	-
	Winter	-	-	-	-
	Spring	-	-	-	-
	Summer	-	-	-	-
S5	Autumn	-	-	-	-
	Winter	-	-	-	-
	Spring	-	-	-	-
	Summer	-	-	-	-
S6	Autumn	0.50 ± 0.07^{C}	1.20 ± 0.06^{C}	2.10 ± 0.14^{C}	0.28 ± 0.04^{C}
	Winter	0.60 ± 0.05^{C}	2.00 ± 0.05^{BC}	4.55 ± 0.08^{B}	0.58 ± 0.08^{BC}
	Spring	0.20 ± 0.06^{C}	1.13 ± 0.09^{C}	4.10 ± 0.05^{B}	0.26 ± 0.05^{C}
	Summer	0.15 ± 0.04^{C}	1.11 ± 0.06^{C}	6.10 ± 0.10^{B}	0.12 ± 0.07^{C}
S7	Autumn	1.22 ± 0.13^{B}	3.20 ± 0.45^{A}	4.62 ± 0.12^{B}	2.66 ± 0.13^{A}
	Winter	1.21 ± 0.18^{B}	1.05 ± 0.07^{C}	5.78 ± 0.13^{B}	0.98 ± 0.11^{BC}
	Spring	1.90 ± 0.17^{AB}	2.25 ± 0.23^{B}	7.50 ± 0.07^{B}	1.85 ± 0.13^{B}
	Summer	1.70 ± 0.16^{AB}	2.20 ± 0.30^{B}	8.80 ± 0.09^{A}	1.50 ± 0.18^{B}
S8	Autumn	2.50 ± 0.15^{A}	4.43 ± 0.73^{A}	5.60 ± 0.11^{BC}	2.90 ± 0.23^{A}
	Winter	2.26 ± 0.13^{A}	1.90 ± 0.20^{AB}	4.32 ± 1.23^{BC}	1.99 ± 0.16^{A}
	Spring	2.60 ± 0.15^{A}	2.54 ± 0.32^{AB}	10.41 ± 1.56^{A}	2.23 ± 0.17^{A}
	Summer	1.60 ± 0.13^{B}	1.90 ± 0.24^{AB}	10.60 ± 1.14^{A}	2.89 ± 0.18^{A}

-: Absence of Bushy Rainbow Wrack.
*The different upper-case letters in the same row indicate the differences between the studied stations and seasons at the level ($p<0.05$)

http://www.aloki.hu ● ISSN 1589 1623 (Print) ● ISSN 1785 0037 (Online)
DOI: http://dx.doi.org/10.15666/aeer/1706_1431514331

Biochemical and physiological parameters

Chlorophyll contents

Maximum value of chlorophyll a were recorded at (S1) Sidi Bouzid coast near Eljadida city with 586±167 µg/g FW during spring season, and reached its minimum at (S8) The port station in Essaouira city with 59±14 µg/g FW during autumn season. Values of chlorophyll c has its maximum as well at (S1) Sidi Bouzid coast near Eljadida city with 387±93 µg/g FW during spring and summer season, and its minimum also at (S8) The port station in Essaouira city with 34±13 µg/g FW during spring season. The same thing for carotenoid that shown a maximum value at (S1) Sidi Bouzid coast near Eljadida city with 399±175 µg/g FW during summer season and a minimum likewise at (S8) The port station in Essaouira city with 34±0.9 µg/g FW during summer season (*Table 5*).

Table 5. *Concentrations of Chlorophyll a, c, carotenoid and proline (µg/g Fresh Weight), GB and TPC (mg/g Dry Weight) of Bushy Rainbow Wrack in different stations during the 4 seasons of 2018*

Station	Season	Chl a	Chl c	Carotenoid	Proline	GB	TPC
S1	Autumn	$475\pm133^{A*}$	267 ± 97^{AB}	255 ± 76^{A}	69.06 ± 24.22^{C}	2.06 ± 0.25^{C}	0.56 ± 0.14^{C}
	Winter	567 ± 128^{A}	267 ± 86^{AB}	276 ± 94^{A}	69.06 ± 13.03^{C}	2.06 ± 0.53^{C}	0.52 ± 0.12^{C}
	Spring	586 ± 167^{A}	387 ± 93^{A}	376 ± 146^{A}	71.94 ± 18.13^{C}	2.15 ± 0.33^{C}	0.56 ± 0.23^{C}
	Summer	489 ± 120^{A}	387 ± 56^{A}	399 ± 175^{A}	112.23 ± 14.50^{BC}	3.35 ± 0.45^{C}	0.73 ± 0.15^{C}
S2	Autumn	-	-	-	-	-	-
	Winter	-	-	-	-	-	-
	Spring	-	-	-	-	-	-
	Summer	-	-	-	-	-	-
S3	Autumn	393 ± 117^{AB}	143 ± 75^{AB}	129 ± 87^{B}	57.55 ± 15.11^{C}	1.72 ± 0.12^{C}	0.72 ± 0.17^{C}
	Winter	398 ± 128^{AB}	176 ± 86^{AB}	175 ± 95^{B}	120.86 ± 45.16^{B}	3.61 ± 0.15^{C}	0.74 ± 0.14^{C}
	Spring	498 ± 127^{A}	198 ± 95^{AB}	176 ± 84^{B}	94.96 ± 34.00^{BC}	2.83 ± 0.45^{C}	0.68 ± 0.12^{C}
	Summer	373 ± 57^{AB}	187 ± 97^{AB}	183 ± 77^{AB}	112.23 ± 43.12^{B}	3.35 ± 0.36^{C}	0.72 ± 0.16^{C}
S4	Autumn	-	-	-	-	-	-
	Winter	-	-	-	-	-	-
	Spring	-	-	-	-	-	-
	Summer	-	-	-	-	-	-
S5	Autumn	-	-	-	-	-	-
	Winter	-	-	-	-	-	-
	Spring	-	-	-	-	-	-
	Summer	-	-	-	-	-	-
S6	Autumn	487 ± 156^{A}	276 ± 74^{AB}	166 ± 83^{B}	92.08 ± 15.00^{BC}	2.752 ± 0.14^{C}	0.65 ± 0.17^{C}
	Winter	476 ± 186^{A}	387 ± 59^{A}	276 ± 75^{A}	129.49 ± 34.65^{B}	3.87 ± 0.56^{C}	0.90 ± 0.27^{BC}
	Spring	492 ± 94^{A}	254 ± 122^{AB}	285 ± 86^{A}	115.10 ± 54.66^{B}	3.44 ± 0.76^{C}	0.72 ± 0.26^{C}
	Summer	530 ± 82^{A}	376 ± 110^{A}	236 ± 93^{A}	109.35 ± 45.56^{B}	3.268 ± 1.78^{BC}	0.58 ± 0.17^{C}
S7	Autumn	183 ± 56^{BC}	45 ± 12^{C}	98 ± 24^{B}	460.43 ± 176.76^{A}	13.76 ± 1.54^{AB}	1.36 ± 0.28^{B}
	Winter	287 ± 86^{B}	98 ± 16^{C}	176 ± 37^{B}	215.82 ± 76.44^{AB}	6.45 ± 1.76^{B}	1.04 ± 0.93^{AB}
	Spring	287 ± 89^{B}	65 ± 18^{C}	111 ± 30^{BC}	330.93 ± 165.66^{AB}	9.89 ± 1.77^{B}	1.11 ± 0.28^{AB}
	Summer	245 ± 112^{B}	57 ± 14^{C}	123 ± 34^{BC}	503.59 ± 164.43^{A}	15.05 ± 2.65^{A}	1.20 ± 0.17^{A}
S8	Autumn	59 ± 14^{C}	35 ± 09^{C}	96 ± 12^{C}	517.98 ± 174.11^{A}	15.48 ± 3.17^{A}	1.54 ± 0.28^{A}
	Winter	165 ± 87^{BC}	76 ± 29^{C}	54 ± 15^{C}	546.76 ± 145.19^{A}	16.34 ± 4.75^{A}	1.10 ± 0.16^{AB}
	Spring	156 ± 75^{BC}	34 ± 13^{C}	87 ± 17^{C}	566.90 ± 175^{A}	16.94 ± 07.56^{A}	1.14 ± 0.27^{A}
	Summer	74 ± 19^{C}	76 ± 33^{C}	34 ± 09^{C}	647.48 ± 198^{A}	19.35 ± 14.97^{A}	1.51 ± 0.37^{A}

-: Absence of Bushy Rainbow Wrack.
*The different upper-case letters in the same row indicate the differences between the studied stations and seasons at the level ($p<0.05$)

http://www.aloki.hu ● ISSN 1589 1623 (Print) ● ISSN 1785 0037 (Online)
DOI: http://dx.doi.org/10.15666/aeer/1706_1431514331

Glycinebetaine (GB), proline and total phenolic compounds (TPC)

GB parameter reaches a high value of 19.35±14.97 mg/g DW at (S8) The port station in Essaouira city during summer season, and achieved its minimum at (S3) Beddouza station near Safi city with 1.72±0.12 mg/g DW during autumn season. In the same way, the proline parameter has the same result as GB. The maximum value is recorded at (S8) The port station in Essaouira city with 647.48±198 µg/g DW during summer season, and a minimum value of 57.55±15.11 µg/g DW at (S3) Beddouza station near Safi city during autumn season. Moreover, TPC parameter has given the same result as GB and proline parameters which we have found a maximum value of 1.54±0.28 mg/g DW during autumn season at (S8) The port station in Essaouira city, as well as a minimum value of 0.52±0.12 mg/g DW at (S1) Sidi Bouzid coast near Eljadida city during winter season (*Table 5*).

Statistical analysis

A tow-way mixed ANOVA was conducted to investigate the impact of seasons, the sampling sites and Heavy metals concentrations in sea water. There was a significant main effect of sampling sites and seasons, $F(1, 66) = 183.397$, $p<0.001$ (*Table 6*). Moreover, there was a significant interaction between Heavy metals, Sampling sites and seasons, $F(1, 66) = 2.197$, $p<0.001$ (*Table 7*).

Table 6. *Tests of Within-Subjects Contrasts*

Source	Seasons_Sites	Type III Sum of Squares	df	Mean Square	F	Sig.
Seasons_Sites	Linear	298.239	1	298.239	183.397	0.000
Seasons_Sites * HM	Linear	316.802	66	4.800	2.952	0.000
Error(Seasons_Sites)	Linear	99.198	61	1.626		

Table 7. *Tests of Between-Subjects Effects*

Source	Type III Sum of Squares	df	Mean Square	F	Sig.
Intercept	2251.892	1	2251.892	1114.998	0.000
HM	292.802	66	4.436	2.197	0.000
Error	123.198	61	2.020		

By performing the Principal Component Analysis (PCA) on the physiological parameters (Chlorophyll a, Chlorophyll c, Carotenoid, Proline, Glycinebetaine (GB) and Total Phenolic Compounds (TPC)) combined with the physicochemical parameters (Phosphorus and Nitrogenous compounds) and heavy metals (Cu, Cd, Pb and Cr) under study, two principal components have been extracted by covering 74.085 % of the cumulative variance (*Table 8*).

Discussion

Based on the online Algaebase data which includes marine algal species, Guiry and Guiry (2019) provided information about *Cystoseira* species diversity and discussed the description of new taxa and distribution. In Morocco, some authors have discussed the

http://www.aloki.hu ● ISSN 1589 1623 (Print) ● ISSN 1785 0037 (Online)
DOI: http://dx.doi.org/10.15666/aeer/1706_1431514331

geographic distribution of *Bushy Rainbow Wrack* in the Mediterranean sea of Morocco (Ribera et al., 1992; Báez et al., 2005; Taskin et al., 2012; Bermejo et al., 2018; Moussa et al., 2018). However, no studies have been made in the Atlantic coast of Morocco concerning these species. Some authors have mentioned their sensitivity (Ballesteros et al., 1984; Thibaut et al., 2005). In contrast, the situation is more critical at Safi coast where only *Bushy Rainbow Wrack* seems to be more tolerant but all *Cystoseira* species have disappeared in 3 polluted stations (S2, S4 and S5). Many authors have showed the sensitivity of these brown seaweeds in polluted coasts (Cormaci et al., 1999; Thibout et al., 2005; Sales and Ballesteros, 2009). Furthermore, *Cystoseira* species are used as indicators of good water quality (Ballesteros et al., 2007).

Table 8. *Varimax with Kaiser Normalization rotated loading for 2 components. converged in 3 iterations with Principal Component Analysis extraction method according to heavy metals, physiological parameters in Bushy Rainbow Wrack and physicochemical compounds for the stations studied*

Parameter	Component	
	1	2
Cd	0.951	-0.059
Pb	0.645	-0.177
Cu	0.735	-0.327
Cr	0.961	-0.097
TP	0.101	-0.797
DP	0.912	0.093
PO_4^{3-}	0.905	-0.034
TN	-0.113	0.569
DN	0.084	0.965
NO_3^-	-0.215	0.528
NH_4^+	-0.653	0.162
Chl a	-0.940	0.240
Chl c	-0.824	0.279
Carotenoid	-0.753	0.509
Proline	0.967	-0.104
TPC	0.915	-0.220
GB	0.967	-0.104
Variance (%)	57.500	16.858
Cumulative (%)	57.500	74.085

The values of nitrogenous compounds are higher in comparison with the other ocean areas (Sverdrup et al., 1943). It is widely accepted that nitrogen may be an important factor in limiting marine algal productivity. Although the need to examine macroalgal-nitrogen relationships has long been recognized (Haas and Hill, 1933). Efforts with benthic marine algae have not paralleled those with phytoplankton.

The highly concentration of phosphorus was due to the huge amount of phosphogypsum used by the industrial factory. Inorganic nutrients are present in natural environments but their concentration near urban areas is usually enhanced (Nixon, 1995; Scavia and Bricker, 2006). The overloading of inorganic nutrients stimulates algal production and increases turbidity leading to changes in the species composition and the structure of littoral communities (Mcglathery et al., 2007). In addition, increased nutrient concentration in seawater favors opportunistic species, while long-lived species such as seagrasses and perennial macroalgae gradually decline (Munda, 1982; Schramm et al., 1999). Thus. the high phosphorus concentration in (S5) could explain the disappearance

http://www.aloki.hu ● ISSN 1589 1623 (Print) ● ISSN 1785 0037 (Online)
DOI: http://dx.doi.org/10.15666/aeer/1706_1431514331

of *Cystoseira* species. It is known according to Celis-Plá et al. (2014) that nitrate and phosphate represent important macronutrients for macroalgae development and can protect the algae against stress. Moreover, highly concentrations of nutrients in seaweeds can reduce photoinhibition, as it has been observed in *Bushy Rainbow Wrack*. Other observations showed that nutrient enrichment could also have effects on photosynthesis, photo-protection and biochemical responses (Celis-Plá et al., 2016). Nonetheless, stress biology studies on heavy metal in brown seaweeds has demonstrate different results of molecular, biochemical and physiological effects, as it has been studied in *Ascophyllum nodosum* (Connan and Stengel, 2011a,b), *Fucus vesiculosus* (Nielsen and Nielsen, 2010) and *Ectocarpus siliculosus* (Roncarati et al., 2015; Sáez et al., 2015).

The comparison of our data with those previously studied by some authors (*Table 9*) shows that the concentrations of heavy metals: Cd, Pb, Cu and Cr for *Bushy Rainbow Wrack* in the present study recorded higher values in *Cystoseira* sp obtained by Akcali and Kucuksezgin (2011) of the Aegean Sea in Turkey, Al-Masri et al. (2003) at the Syrian Coast, Schintu et al. (2010) at Sardinia coast in Italy and Caliceti et al. (2001) at the Venice lagoon in Italy. Nonetheless, lower level of Pb and Cu than those reported by Schintu et al. (2010) and Caliceti et al. (2001), respectively.

Table 9. *Comparison of heavy metal levels (µg/g dry weight) in seaweed Cystoseira sp. from other different locations in the world*

	Cd	Pb	Cu	Cr	Location	References
***Cystoseira* sp.**	0.18	0.003	6.00	-	Aegean Sea, Turkey	(Akcali and Kucuksezgin, 2011)
	1.72	10.3	1.80	-	Sardinia, Italy	(Schintu et al., 2010)
	0.1-0.5	1.31	7.21	-	Syrian Coast	(Al-Masri et al., 2003)
	0.2	5.6	21	1.5	Venice lagoon, Italy	(Caliceti et al., 2001)
	2.6	4.43	10.6	2.9	Atlantic coast of Morocco	Present study

The relatively high levels of Lead in seawater could be attributed to discharges from industries near the study sites that could increase directly this element (leaching from gas stations), as well as leaching at the dump, traffic and leaching of farmlands, can contribute to the highly lead concentration at these stations. However, the lead concentrations at all stations are below the Moroccan standard 500 µg/l (FAO, 2006). For Cadmium detected in polluted waters, concentrations indicate a non-contamination by this element. Indeed, they are all below the limit value of 200 µg/l (FAO, 2006) (*Table 10*). The concentrations found at these sites, lead us to assume the presence of one or several sources of pollution near the stations above.

Table 10. *Comparison of heavy metal levels in seawater (µg/l) for the studied stations with the Moroccan standards for seawater (FAO, 2006)*

Heavy metals	Sea water	Moroccan norm FAO, 2006
Cd	1.151	200
Pb	2.563	500
Cu	0.604	500
Cr	0.987	2000

The resultant PCA (*Fig. 3*) presenting the loading of the variables on the two principal components demonstrate that Cd, Pb, Cu, Cr, DP, PO_4^{3-}, Proline, TPC and GB were the

http://www.aloki.hu ● ISSN 1589 1623 (Print) ● ISSN 1785 0037 (Online)
DOI: http://dx.doi.org/10.15666/aeer/1706_1431514331

dominant correlated positive variables on the PC1 (0.951; 0.645; 0.735; 0.961; 0.912; 0.905; 0.967; 0.915; 0.967, respectively) while Chla, Chlc and Carotenoid the negatif correlated ones (-0.940; -0.824; -0.753, respectively), in addition to TN, DN and NO_3^-, the dominant variables on the PC2 (0.569; 0.965; 0.528, respectively). Indeed, according to PCA results, an important positive correlation and proportionate augmentation in proline, GB and TPC contents was recorded with increase in concentration of heavy metals and excessive Phosphorus in polluted stations mentioned, in addition to a negative correlation with pigments. It is proved by Alia et al. (1999) that Cadmium is the strongest inducer for proline and GB accumulation. Moreover, TPC can be released in stressful conditions from algal thalli and could react rapidly with carbohydrates and proteins to form UV-absorbing exudates (Koivikko et al., 2005). It has also been shown that proline, GB and TPC are the stress-induced substances in plants and algae under different kind of stress (Anbazhangan et al., 1988; Fadma et al., 2007; Abdel Latef and Sallam, 2015). Proline and GB concentrations in *Bushy Rainbow Wrack* in polluted areas are much higher than those found in other green, brown and red seaweeds (Fleurence, 2004). Furthermore, the maximum value of TPC in this study (1.54 mg/g dry weight during autumn season at (S8) The port station in Essaouira city) is higher than that found by Pereira and Yoneshigue (1999) in brown seaweed *Sargassum furcatum* (0.2-0.5 mg/g DW). According to this author, TPC may also be present in brown seaweed for reasons other than defense, as they have been considered to have a number of physiological and ecological functions.

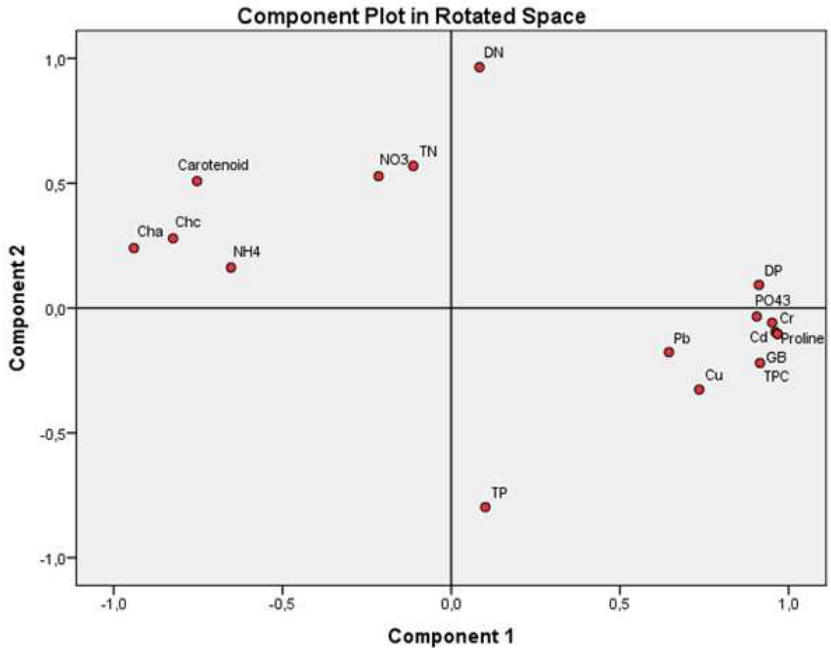

Figure 3. *Component Plot in Rotated Space for the parameters studied*

In the basis of the Conceptual framework of Mineur et al. (2014), anthropogenic local stressors create additional disruption often altering dramatically assemblage's structure. Global stressors are not manageable locally, but have local impacts and may indirectly affect local stressors. All stressors are affecting seaweed diversity (populations and communities), and directly impacting coastal ecosystems (*Fig. 4*) (Mineur et al., 2014).

http://www.aloki.hu ● ISSN 1589 1623 (Print) ● ISSN 1785 0037 (Online)
DOI: http://dx.doi.org/10.15666/aeer/1706_1431514331

At the Industrial area (S4) and Phosphate area (S5) in Safi city and Jorf Lasfar area (S2) near Eljadida city, these stressors are due to increased nutrient inputs, heavy metal pollution and mostly derived from the industrial activity out there. According to Ferreira et al. (2011), marine biota living in coastal waters are under constant threat from exposure to elevated concentrations of pollutants, such as metals and nutrients, mostly derived from domestic, industrial and farming activities.

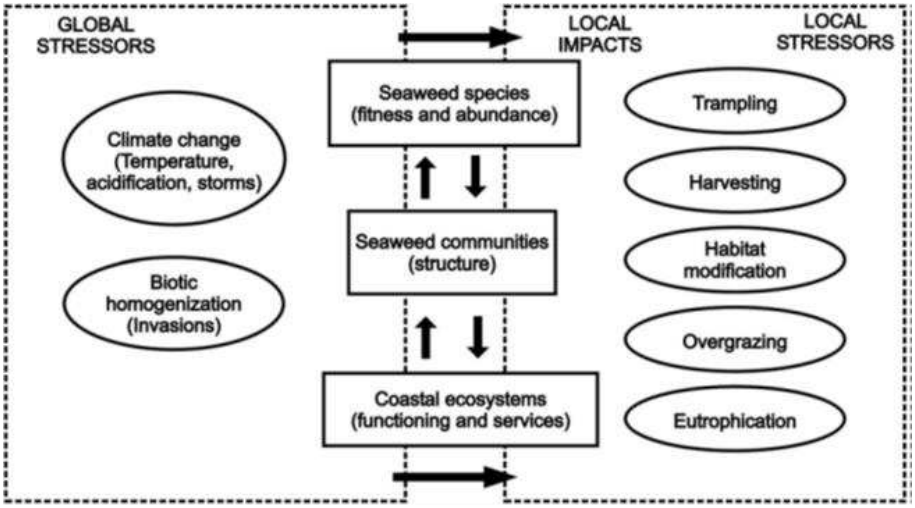

Figure 4. *Conceptual framework of Mineur et al. (2014)*

Changes in the composition of *Bushy Rainbow Wrack* through these stressors in polluted stations (S2, S4 and S5) has resonated through entire coastal ecosystems in this area. Furthermore, anthropogenic activities on these coastal areas, such as industrialization and urbanization create increasing anthropogenic stress. *Cystoseira* and seaweed biodiversity in general of the Moroccan coastlines need more attention to predict how they are affected by human activities.

Conclusion

To conclude, we have found a regular element variety in species lavishness with least qualities in winter and an auxiliary least top in spring, and most extreme qualities in summer. The regularity is for the most part because of the adjustment in biomass of the overwhelming species. Just *Bushy Rainbow Wrack* is by all accounts progressively tolerant to the contamination in polluted stations. Nitrogenous compounds did not clarify the decay of the species around there, yet the highly phosphorus concentration in the phosphate station and highly values of heavy metal concentrations could affect the physiology and clarify the vanishing of *Bushy Rainbow Wrack*, notwithstanding the nearness of dangerous components like Pb, Cd, Cu and Cr.

Thus, the investigation on the combined effects of nutrients, metals and biochemical parameters studied in this brown seaweed would provide relevant information about their capacity to withstand the future pollution scenarios. The interaction between metals and nutrients excess is still not well understood for macroalgae. Further examinations ought to be done to characterize different parameters that lead to *Bushy Rainbow Wrack* debasement.

http://www.aloki.hu ● ISSN 1589 1623 (Print) ● ISSN 1785 0037 (Online)
DOI: http://dx.doi.org/10.15666/aeer/1706_1431514331

For future research, we aim to develop the culture experiments under controlled laboratory conditions on *Bushy Rainbow Wrack* as well as the genetic characterization of this brown seaweed based upon DNA barcoding of the cytochrome oxidase subunit 1 (COI), 23S rDNA (23S), and 23S-tRNAVal intergenic spacer (mt-spacer).

REFERENCES

[1] Abdel Latef, A. A., Sallam, M. M. (2015): Changes in Growth and Some Biochemical Parameters of Maize Plants Irrigated with Sewage Water. – Austin Journal of Plant Biology 1: 1004.
[2] AFNOR NF T90-012. Août (1975): Dosage des nitrates.
[3] AFNOR NF T90-015-2. Janvier (2000): Qualité de l'eau. Dosage de l'ammonium. – Partie 2: méthode spectrométrique au bleu d'indophénol.
[4] AFNOR NF T90-022. Avril (2005): Dosage des orthophosphates.
[5] Akcali, I., Kucuksezgin, F. (2011): A biomonitoring study: heavy metals in macroalgae from eastern Aegean coastal areas. – Marine Pollution Bulletin 62: 637-645.
[6] Alia, F., Saradhi, P. P. A. (1991): Proline Accumulation Under Heavy Metal Stress. – Plant Physiology 138: 554-558.
[7] Al-Masri, M. S., Mamish, S., Budier, Y. (2003): Radionuclides and trace metals in eastern Mediterranean Sea algae. – Journal of Environmental Radioactivity 67: 157-168.
[8] Anbazhagan, M., Krishnamurthy, R., Bhagwat, K. A. (1988): Proline: an enigmatic indicator of air pollution tolerance in rice cultivars. – Journal of Plant Physiology 133: 122-123.
[9] Báez, J. C., Olivero, J., Real, R., Vargas, J. M., Flores-Moya, A. (2005): Analysis of geographical variation in species richness within the genera Audouinella (Rhodophyta). Cystoseira (Phaeophyceae) and Cladophora (Chlorophyta) in the western Mediterranean Sea. – Botanica Marina 48: 30-37.
[10] Ballesteros, E., Perez, M., Zabala, M. (1984): Aproximacion al conocimiento de las comunidades algales de la zona infralitoral superior en la costa catalana. – Collectane A Botanica 15: 69-100.
[11] Ballesteros, E., Torras, X., Pinedo, S., Garcia, M., Mangialajo, L., De Torres, M. (2007): A new methodology based on littoral community cartography for the implementation of the European Water Framework Directive. – Marine Pollution Bulletin 55: 172-180.
[12] Bermejo, R., Chefaoui, R. M., Engelen, A. H., Buonomo, R., Neiva, J., Ferreira-Costa, J., Pearson, G. A., Marbà, N., Duarte, C. M., Airoldi, L., Hernández, I., Guiry, M. D., Serrão, E. A. (2018): Marine forests of the Mediterranean-Atlantic Cystoseira tamariscifolia complex show a southern Iberian genetic hotspot and no reproductive isolation in parapatry. – Science Reports 8: 1-13.
[13] Blinda, M., Bellaouchou, A., Fekhaoui, M., Barcha, S.-E., El Morhit, M. (2013): Assessment of metal contamination of the sediments and superficial waters in the northwest coast of Morocco. – Bulletin de l'Institut Scientifique 35: 43-49.
[14] Caliceti, M., Argese, E., Sfriso, A., Pavoni, B. (2001): Heavy metal contamination in the seaweeds of the Venice lagoon. – Chemosphere 47: 443-454.
[15] Celis-Plá, P. S. M., Bouzon, Z. L., Hall-Spencer, J. M., Schmidt, E. C., Korbee, N., Figueroa, F. L. (2016): Seasonal biochemical and photophysiological responses in the intertidal macroalga Cystoseira tamariscifolia (Ochrophyta). – Marine Environmental Research 115: 89-97.
[16] Celis-Plá, P. S. M., Martínez, B., Quintano, E., García-Sánchez, M., Pedersen, A., Navarro, N. P., Copertino, M. S., Mangaiyarkarasi, N., Mariath, R., Figueroa, F. L., Korbee, N. (2014): Short-term ecophysiological and biochemical responses of Cystoseira

http://www.aloki.hu ● ISSN 1589 1623 (Print) ● ISSN 1785 0037 (Online)
DOI: http://dx.doi.org/10.15666/aeer/1706_1431514331

tamariscifolia and Ellisolandia elongata to environmental changes. – Aquatic Biology 22: 227-243.
[17] Cherifi, O., Sabri, H., Gharmali, A., Maarouf, A., Hasni, M., Cherifi, K., Ait-Hman, A., Derhem, A., Bahammou, N., Sbihi, K. (2018): Variation spatio-temporelle des métaux traces (Cr, Cu, Pb, Zn) chez la laminariale Saccorhiza polyschides au niveau du littoral de la région d'Essaouira. – SMETox Journal 1: 53-58.
[18] Claudet, J., Fraschetti, S. (2010): Human-driven impacts on marine habitats: a regional meta-analysis in the Mediterranean Sea. – Biological Conservation 143: 2195-2206.
[19] Connan, S., Stengel, D. B. (2011a): Impacts of ambient salinity and copper on brown algae: 2. Interactive effects on phenol pool and assessment of metal binding capacity of phlorotannin. – Aquatic Toxicology 104: 1-13.
[20] Connan, S., Stengel, D. B. (2011b): Impacts of ambient salinity and copper on brown algae: 1. Interactive effects on photosynthesis. growth. and copper accumulation. – Aquatic Toxicology 104: 94-107.
[21] Cormaci, M., Furnari, G. (1999): Changes of the benthic algal flora of the Tremiti Islands (southern Adriatic) Italy. – In: Kain, J. M., Brown, M. T., Lahaye, M. (eds.) Sixteenth International Seaweed Symposium. Developments in Hydrobiology. Springer. Dordrecht.
[22] Dayton, P. K. (1975): Experimental evaluation of ecological dominance in a rocky intertidal algal community. – Ecological Monographs 45: 137-159.
[23] Essedaoui, A., Sif, J. (2001): Bioaccumulation des métaux lourds et induction des métallo-protéines au niveau de la glande digestive de Mytilus galloprovincialis. – Revue Marocaine des Sciences Agronomiques et Vétérinaires 21: 17-25.
[24] F.M.6. (2018): The Mohammed VI Foundation for the Protection of the Environment. – Annual report, Morocco.
[25] FAO. (2006): Projet de gestion des ressources en eau : Elaboration des dossiers techniques relatifs aux valeurs limites des rejets industriels dans le Domaine Public Hydraulique. Elaboration des fiches techniques des valeurs limites des rejets industriels. – Convention FAO/UTF/MOR019/MOR.
[26] Fatma, T., Khan, M. A., Choudhary, M. (2007): Impact of environmental pollution on cyanobacterial proline content. – Journal of Applied Phycology 19: 625-629.
[27] Ferreira, J. G., Andersen, J. H., Borja, A., Bricker, S. B., Camp, J., Cardoso da Silva, M., Garcés, E., Heiskanen, A. Z., Humborg, C., Ignatiades, L., Lancelot, C., Menesguen, A., Tett, P., Hoepffner, N., Claussen, U. (2011): Overview of eutrophication indicators to assess environmental status within the European Marine Strategy Framework Directive. – Estuary Coastal Shelf Science 93: 117-131.
[28] Ferssiwi, A., Sif, J., El Hamri, H., Rouhi, A., Amiard, J. C. (2004): Contamination par le cadmium de l'Annélide Polychète Hediste diversicolor dans la région d'El Jadida (Maroc) implication des protéines type métallothionéines. – Journal de recherche océanographique 29: 59-64.
[29] Fleurence, J. (2004): Seaweed proteins. – University of Nantes, France.
[30] Goumri, M., Cheggour, M., Maarouf, A., Mouabad, A. (2018): Preliminary data on the composition and spatial distribution patterns of echinoderms along Safi rocky shores (NW Morocco). – AACL Bioflux 11(4): 1193-1202.
[31] Grieve, C. M., Grattan, S. R. (1986): Rapid assay for determination of water soluble quaternary ammonium compounds. – Plant and Soil 70: 303-307.
[32] Guiry, M. D, Guiry, G. M. (2019): AlgaeBase. – World-wide electronic publication, National University of Ireland, Galway.
[33] Haas, P., Hill, T. G. (1933): Observations on the metabolism of certain seaweeds. – Annals of Botany 47: 55-67.
[34] Jeffrey, S. W., Humphry, G. F. (1975): New Spectrophotometric Equations for Determining Chlorophylls a, b, c1 and c2 in Higher Plants, Algae and Natural Phytoplankton. – Biochimie und Physiologie der Pflanzen (BPP) 167: 191-194.
[35] Jones, A. (1997): Environmental biology. – Routledge, London.

http://www.aloki.hu ● ISSN 1589 1623 (Print) ● ISSN 1785 0037 (Online)
DOI: http://dx.doi.org/10.15666/aeer/1706_1431514331

[36] Kaimoussi, A., Chafik, A., Mouzdahir, A., Bakkas, S. (2001): The impact of industrial pollution on the Jorf Lasfar coastal zone (Morocco, Atlantic Ocean): the mussel as an indicator of metal contamination. – Comptes Rendus, Academie des Sciences, Paris 333: 337-341.
[37] Koivikko, R., Loponen, J., Honkanen, T., Jormalainen, V. (2005): Contents of soluble cell-wall-bound and exuded phlorotannins in the brown alga Fucus vesiculosus with implications on their ecological functions. – Journal of Chemical Ecology 31(1): 195-212.
[38] Lichtenthaler, H. K. (1987): Chllorphyls and carotenoids: Pigments of photosynthetic biomembranes. – Methods in Enzymology 148: 350-380.
[39] Mcglathery, K. J., Sundbäk, K., Anderson, I. C. (2007): Eutrophication in shallow coastal bays and lagoons: the role of plants in the coastal filter. – Marine Ecology Progress Series 348: 1-18.
[40] Mineur, F., Arenas, F., Assis, J., Davies, A. J., Engelen, A. H., Fernandes, F., Malta, E. J., Thibaut, T., Nguyen, T. V., Vaz-Pinto, F., Vranken, S., Serrão, E. A., De Clerck, O. (2014): European seaweeds under pressure: Consequences for communities and ecosystem functioning. – Journal of Sea Research 98: 91-108.
[41] Monneveux, P., Nemmar, M. (1986): Contribution à l'étude de la résistance à la sécheresse chez le blé tendre (Triticum aestivum L.) et chez le blé dur (Triticum durum Desf.): étude de l'accumulation de la proline au cours du cycle de développement. – Agronomie 6: 583-590.
[42] Moussa, H., Hassoun, M., Salhi, G., Zbakh, H., Riadi, H. (2018): Checklist of seaweeds of Al-Hoceima National Park of Morocco (Mediterranean Marine Protected Area). – Acta Botanica Malacitana 43: 91-109.
[43] Munda, I. M. (1982): The effects of organic pollution on the distribution of fucoid algae from the Istrian coast (vicinity of Rovinj). – Acta Adriatica 23: 329-337.
[44] Munday, P. L., Warner, R. R., Monro, K., Pandolfi, J. M., Marshall, D. J. (2013): Predicting evolutionary responses to climate change in the sea. – Ecology Letters 16: 1488-1500.
[45] NF EN ISO 11905-1. Juillet (1998): Qualité de l'eau. Dosage de l'azote. – Partie 1: Méthode par minéralisation oxydante au peroxodisulfate (indice de classement T 90-061).
[46] NF EN ISO 6878. Avril (2005): Qualité de l'eau. Dosage du phosphore: méthode spectrophotométrique au molybdate d'ammonium (indice de classement T90-023).
[47] Nielsen, H. D., Nielsen, S. L. (2010): Adaptation to high light irradiances enhances the photosynthetic Cu^{2+} resistance in Cu^{2+} tolerant and non-tolerant populations of the brown macroalgae Fucus serratus. – Marine Pollution Bulletin 60: 710-717.
[48] Nixon, S. W. (1995): Coastal marine eutrophication: a definition, social causes and future concerns. – Ophelia 41: 199-219.
[49] Pereiraa, R. C., Yoneshigue, V. Y. (1999): The Role of Polyphenols from the Tropical Brown Alga Sargassum furcatum on the Feeding by Amphipod Herbivores. – Botanica Marina 42: 441-448.
[50] Ribera, M. A., Gómez-Garreta, A., Gallardo, T., Cormaci, M., Furnari, G., Giaccone, G. (1992): Check-list of Mediterranean Seaweeds. I. Fucophyceae (Warming 1884). – Botanica Marina 35: 109-130.
[51] Roncarati, F., Sáez, C. A., Greco, M., Gledhill, M., Bitonti, M. B., Brown, M. T. (2015): Response differences between Ectocarpus siliculosus populations to copper stress involve cellular exclusion and induction of the phytochelatin biosynthetic pathway. – Aquatic Toxicology 159: 167-175.
[52] Sabri, H., Cherifi, O., Maarouf, A., Cheggour, M., Bertrand, M., Mandi, L. (2017): Wastewater impact on macroalgae biodiversity in Essaouira coast (Morocco). – Journal of Materials and Environmental Sciences 8: 857-862.
[53] Sáez, C. A., Roncarati, F., Moenne, A., Moody, A. J., Brown, M. T. (2015): Copper-induced intra-specific oxidative damage and antioxidant response of the brown alga Ectocarpus siliculosus with different pollution histories. – Aquatic Toxicology 159: 81-89.

http://www.aloki.hu ● ISSN 1589 1623 (Print) ● ISSN 1785 0037 (Online)
DOI: http://dx.doi.org/10.15666/aeer/1706_1431514331

[54] Sales, M., Ballesteros, E. (2009): Shallow Cystoseira (Fucales: Ochrophyta) assemblages thriving in sheltered areas from Menorca (NW Mediterranean): relationships with environmental factors and anthropogenic pressures. – Estuarine Coastal and Shelf Science 84: 476-482.

[55] Scavia, D., Bricker, S. B. (2006): Coastal eutrophication assessment in the United States. – Biogeochemistry 79: 187-208.

[56] Schintu, M., Marras, B., Durante, L., Meloni, P., Contu, A. (2010): Macroalgae and DGT as indicators of available trace metals in marine coastal waters near a lead–zinc smelter. – Environmental Monitoring and Assessment 167: 653-661.

[57] Schramm, W. (1999): Factors influencing seaweed responses to eutrophication: some results from EU-project EUMAC. – In: Kain, J. M., Brown, M. T., Lahaye, M. (eds.) Sixteenth International Seaweed Symposium. Developments in Hydrobiology. Springer. Dordrecht.

[58] Sverdrup, H. U., Johnson, M. W., Fleming, R. H. (1943): The Oceans, their physics, chemistry, and general biology. – Physiological Zoology 16: 322-323.

[59] Taga, S. M., Miller, E. E., Pratt, D. E. (1984): Chia seeds as a source of natural lipid antioxidants. – JAOCS 61: 928.

[60] Taskin, E., Jahn, R., Öztürk, M., Furnari, G., Cormaci, M. (2012): The Mediterranean Cystoseira (with photographs). – Photographs. Celar Bayar University. Manisa. Turkey.

[61] Thibaut, T., Pinedo, S., Torras, X., Ballesteros, E. (2005): Long-term decline of the populations of Fucales (Cystoseira spp. and Sargassum spp.) in the Albères coast (France north-western Mediterranean). – Marine Pollution Bulletin 50: 1472-1489.

[62] Topcuoglu, S., Güven, K.C., Balkis, N., Kibasoglu, C¸., 2003. Heavy metal monitoring of marine algae from the Turkish Coast of the Black Sea, 1998–2000. – Chemosphere 52: 1683–1688.

[63] Walker, D. I., Kendrick, G. A. (1998): Threats to macroalgal diversity: Marine habitat destruction and fragmentation, pollution and introduced species. – Botanica Marina 41: 105-112.

http://www.aloki.hu ● ISSN 1589 1623 (Print) ● ISSN 1785 0037 (Online)
DOI: http://dx.doi.org/10.15666/aeer/1706_1431514331

MODERN STATISTICAL ANALYSIS OF FORAGE QUALITY ASSESSMENT WITH NIR SPECTROSCOPY

ALMANJAHIE, IBRAHIM M.[1,2] – AHMAD, I.[1,2,3] – CHIKR ELMEZOUAR, Z.[1,2,4*] – LAKSACI, A.[1,2]

[1]*Department of Mathematics, College of Science, King Khalid University, 62529 Abha, Kingdom of Saudi Arabia*

[2]*Statistical Research and Studies Support Unit, King Khalid University, Abha, Kingdom of Saudi Arabia*

[3]*Department of Mathematics and Statistics, International Islamic University, Islamabad, Pakistan*

[4]*Department of Mathematics, University Tahri Mohamed, Bechar, Algeria*

**Corresponding author*
e-mail: chikrtime@yahoo.fr

(Received 5th Jun 2019; accepted 9th Sep 2019)

Abstract. Recently, the statisticians have developed a new approach called functional Statistics to treat the data as curves or images. In parallel, the Near-Infrared Reflectance (NIR) spectroscopy approach has been used in modern Chemistry being a fast, inexpensive and accurate procedure to characterize chemical properties for an object. In this paper, we study the forage quality by analysing the spectroscopy procedure with some modern statistical models. Our contribution leads to the prediction of chemical components of Chinese ryegrass forage by analysing its spectral data using some functional models. Precisely, the functional linear quantile regression (FLQR), the functional nonparametric quantile regression (FNQR), the functional local linear quantile regression (FLLQR) and the functional local linear model regression (FLLMR) are implemented to predict the quantities of acid detergent fiber (ADF), neutral detergent fiber (NDF), and crude protein (CP) contents. The choice of these functional models is motivated by the fact that they can construct a predictive region with a given confidence level. We show that the considered models improve the prediction results significantly as compared to conventional models such as the classical partial least squares regression (PLSR) and the principal component regression (PCR). Moreover, we also show that the proposed models are more robust than their competitive models like PLSR and PCR in the sense that their efficiency is not much affected by non-homogeneity of the data.

Keywords: *Leymus chinensis, functional quantile regression, principal component regression (PCR), neutral detergent fiber, predictive regions, crude protein, neutral detergent fiber, acid detergent fiber*

Introduction

The analysis of the forage quality is crucial for livestock producers. It usually measured by its ability to provide livestock high amounts of nutrients and all kinds of livestock feeds. The forage quality depends on the composition of different chemical and biological components present in it. Precisely, the amounts of crude protein (CP), acid detergent fiber (ADF) and neutral detergent fiber (NDF) are the most critical parameters to determine the forage quality (see Mott and Moore, 1970). While the CP content increases the quantity of protein in milk and meat which is essential for dairy producers. On the other hand, NDF and ADF are also crucial for the digestibility of livestock animals (see Agnihotri et al., 2003 or Suksombat, 2004). Accurate prediction of the nutrients present in forage permits the producers to harvest, store and inventory the feed resource optimally way for both grazing and confinement fed ruminants. To get ideal results before

http://www.aloki.hu ● ISSN 1589 1623 (Print) ● ISSN 1785 0037 (Online)
DOI: http://dx.doi.org/10.15666/aeer/1706_1433314346

selling, it is highly needed to apply rapid and accurate methods to evaluate the chemical properties of forage without its destruction. In literature, two methods are commonly used to analyze the quality of forage samples in a laboratory. First, one is the traditional wet chemistry analysis, and the other one is near-infrared reflectance Spectroscopy (NIRS) analysis. First, one is based upon well-established chemical principles, with the help of chemicals and drying agents to find the quality of different components present in the forage.

On the other hand, NIRS analysis is a computerized method to determine the quality of the forage using near-infrared light. However, the traditional approaches are costly, non-ecological and require a great number of samples (Yu et al., 2010; Yu et al., 2011; Albrecht et al., 2008). Alternatively, the NIRS is precise technology, rapid, inexpensive and nondestructive nature of the analysis (see for example Kamruzzaman et al., 2012; De Marchi et al., 2012; Stuth et al., 2003; Foley et al., 1998). The NIR spectroscopy assessment of the forage quality is widespread in the last few years. It was introduced by Norris et al. (1976). This approach has significant advantages over the classical chemical analyses in the form of minimal sample in the laboratory, short time for analysis, less cost in case of a single sample or large batches of samples, many constituents can be found simultaneously, non-destruction of the samples during analysis, no need of skilled operator during analysis, elimination of use of hazardous chemical reagents, and the results are usually more precise and accurate as compared with the methods usually employed. Being the responsibility of the analyst, it is utmost important not only to choose the most appropriate analytical technique but also to follow standard procedures for accurate and precise results. In the last decade this technology has received a growing interest in forage quality assessment (see Bai et al., 2004; Nie et al., 2007; Chen et al., 2007; En et al., 2009 for previous studies and Asekova et al., 2016; Monrroy et al., 2017; Yang et al., 2017 for recent advances). In all these previous studies, the spectral data are analyzed by some classical statistical methods such as the partial least regression (PLSR) or the Principal Component Regression (PCR). However, these old approaches have some drawbacks, which affect their efficiency. Indeed, in these two models the spectral data is not taken into account. The users are required to reduce the dimension of the data by transforming it over some directions. But this transformation can lead inaccurate prediction and results because the direction is chosen independently of the prediction problem. In particular, the variable of interest does not intervene in the choice of the optimal direction reduction. In order to avoid this drawback, we implemented some alternatives models recently developed in modern Statistics. Such models allow analyzing the big data without dimension reduction. These new models are based on the notion of functional Statistics that allows to model the data as curves instead of some numerical numbers which permit to explore the total information of the data. For an overview on recent developments in this topic, we cite, some special issues dedicated to this topic by various statistical journals such as Gonzalez-Manteiga and Vieu (2007), Valderrama (2007), Goia and Vieu (2016) and Aneiros et al. (2019).

More precisely, the main aim of this paper is to combine the Near Infrared Spectroscopy (NIRs) methodology (as modern Chemistry tools) with the recent development of big-data analysis in order to provide a new prediction approaches for the forage quality to circumvent the drawbacks of the previous model. For this study, we consider a sample of 151 size of Chinese ryegrass (Leymus Chinensis) forage and we examine the performance of NIR spectroscopy in estimating the CP, ADF and NDF quantities present in this sample. For this purpose, we use four statistical models the

http://www.aloki.hu ● ISSN 1589 1623 (Print) ● ISSN 1785 0037 (Online)
DOI: http://dx.doi.org/10.15666/aeer/1706_1433314346

functional linear quantile regression (FLQR), the functional nonparametric quantile regression (FNQR), the functional local linear quantile regression (FLLQR) and the functional local linear model regression (FLLMR). The main feature of these models is to make two kinds of prediction namely, pointwise prediction and predictive regions. Moreover, it is well known in statistics that these predictors are more robust than the classical regression models.

Materials and methods

Sample collection and chemical analysis

The samples for this study were taken of the sites ranging from the west to east across the grassland situated in Heilongjiang Province of Northeast China. To accomplish the task 151 samples of sheepgrass hay were chosen at random from different sheepgrass fields of hay factories in 2013 with longitudes from 123.209°E to 132.944°E and latitudes from 44.475°N to 51.728°N. These sampling sites are rich in production of sheepgrass fields and also comprise of wide range of soils and climate. All of the samples were taken at the stage of blooming, recognized and collected before being cutting and packaging. Total of 151 samples from 21 different sites were distributed over 8 regions in Heilongjiang province and tested in the lab and stored at 4 °C for further process. For good quality, every sample consisted of one quarter square meter trimmed at 4 cm, oven dried (65 °C, for 48 h), ground (1 mm sieve), and finally mixed. The chemical and microbiological properties of this data set have been described in Chen et al. (2015). They state that the CP was being measured using the Kjeldahl method for nitrogen (N) determination such as (%CP = %N × 6.25) with the help of methods recommended by Association of Official Analytical Chemists-AOAC (AOAC, 1990). Similarly, the ADF and NDF were treated with the help of the methods proposed by Van Soest et al. (1991). As discussed in the introduction the core feature of the prosed models is their insensitivity to the outliers. To highlight this point, we compare their resistances to outliers to the classical models (PLS and PCR). For this aim, we have used the MAD-Median rule (Wilcox, 2005) to detect the outliers in the endogenous variables CP, ADF and ANF. Thus we observe that there is wide variability in the ADF variable compared to the others variables. This variable is ranged between 23.81% and 47.86% and MAD-test detect 11 outliers. The CP and the NDF values are more homogenous than the CP concentration. Specifically, the CP is ranged from 5.59% to 15.76%, and the MAD-test report 3 outliers in this variable. While the NDF values are between 62.96% and 81.41% and have 5 outliers from the MAD-test.

Spectroscopic analysis

NIR spectrometer Model (DA7200, Perten Corporation, Hagersten, Sweden) was used to collect the spectra of the given sample. The NIR spectra were taken at 5 nm intervals in a range from 950 to 1,650 nm. A dried sample with a weight of 50 g was scanned in a sample cell with a diameter of 7.5 cm, with a quartz window maintained at room temperature of 25 °C. Further, using DA7200 software with reflectance mode (R mode) the samples were scanned from 950 to 1,650 nm. The obtained measurements were transformed into the logarithms of the reflectance reciprocal (absorbance). To minimize or eliminate an error caused by loading the sample, each sample was repeated to scan three times. Then the average of three spectral scanning recordings was considered as the final value, which was further treated to final calculation with the help of Grams32

http://www.aloki.hu ● ISSN 1589 1623 (Print) ● ISSN 1785 0037 (Online)
DOI: http://dx.doi.org/10.15666/aeer/1706_1433314346

software (Perten Corporation, Hagersten, Sweden). Because of the fineness of the grid, we can consider each subject of the spectral data as a continuous curve (see *Fig. 1*).

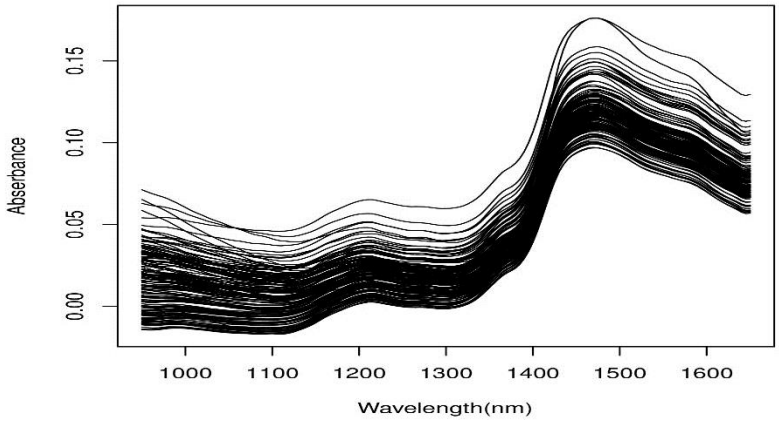

Figure 1. *The NIR spectroscopy curves of the data*

A first preliminary study with the multivariate factorial analysis shows that there is no visible structure of the data (see *Fig. 2*). This fact confirms that the spectral data cannot be summarized by a discretization on small number of grides. In sense that for this prediction issue, it would be more interesting if we incorporate the whole curve of the spectral data.

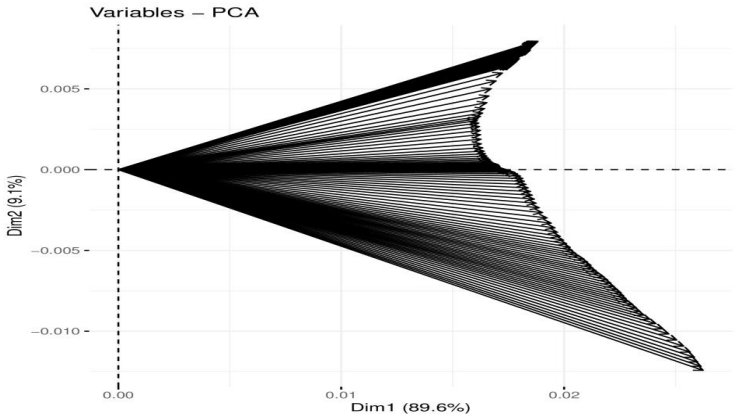

Figure 2. *Factorial analysis of the data*

Notice that the shape of the spectra contains some peaks and valleys which indicated the different chemical component characteristics of Chinese ryegrass samples.

Using this NIR sample, Chen et al. (2015) have considered three standard models (MLR, PCR and PLSR) to predict the chemical quality of this sheepgrass. However, the implementation of these models requires some pretreatment of the spectral data such as dimension reduction, linearity correlation, outliers removing, calibration etc. Such pretreatment modifies the structure of the spectral data independently to the chemical parameters CP, ADF or NDF, which ultimately influence the prediction results negatively. Alternatively, in this paper, we use some new statistical models in order to investigate the forage quality without any transformation. The main advantage of this approach is the fact

http://www.aloki.hu ● ISSN 1589 1623 (Print) ● ISSN 1785 0037 (Online)
DOI: http://dx.doi.org/10.15666/aeer/1706_1433314346

that it takes into account the whole curve in its continuous path. Of course, with this consideration, we keep all the information in the sampled data and we accelerate the prediction process by avoiding the initial pretreatment and related drawbacks.

Statistical analysis

Recall that, in the previous works (see, for instance, Chen et al., 2015; Asekova et al., 2016; Monrroy et al., 2017; Yong et al., 2017) the correlation between the NIR spectroscopy and the chemical components of the forage is assumed to be linear. In this contribution, we consider the general case that covers not only the linear and nonlinear models but also the parametric and nonparametric situations. Indeed, to fix the ideas, let us present the mathematical formulation of the equation describing the relationship between the spectral data and the chemical properties of the sheepgrass:

$$Y = r(X) + error, \quad \text{(Eq.1)}$$

where Y is a real variable means either the CP, ADF or NDF. The functional variable X is the curve of the NIR spectroscopy (950-1,650 wavelength). Therefore, the prediction of Y given $X = x$ is based on the determination of the function $r(.)$. The latter is obtained by minimizing the following criterion

$$r(x) = argmin_f E[\rho(Y, f)|X = x] \quad \text{(Eq.2)}$$

Where ρ is a given loss function.

In the modern statistics, there exist various approaches which can be used to model this prediction issue. In this paper, we focus on some models related to the conditional distribution of Y given X which is constructed from the quantile regression and the modal regression. Of course, the conditional distribution of Y given X has the advantage of completely characterizing the relationship between Y and X. Thus, the two used regression models are more informative than the standard regression for analyzing the link between the spectral data and the chemical components of the hay. Furthermore, to provide to NIR spectroscopy users, we present in the rest of this section a varied collection of statistical predictors with mathematical formalism which is recently developed in functional statistics.

The functional linear quantile regression (FLQR)

The FLQR was first introduced in functional Statistics by Cardot et al. (2005). Since this pioneer work, this model had been widely studied in the context of functional Statistics (see, for instance, Qingguo and Linglong, 2017). Mathematically, the quantile regression of order α is the quantity t_α such that$P(Y \leq t_\alpha|X = x) = \alpha$. It is well known that the quantile regression can be also expressed by *Equation 2* using loss function $\rho_\alpha(z) = (2\alpha - 1)z + |z|$ (see the proof in Laksaci et al., 2009). Based on the linear formulation of the quantile regression obtained by Koenker et al. (1978) and Cardot et al. (2005) constructed an conditional quantile estimator of order α for a given sample $(X_i, Y_i)_{i=1,...,n}$ as below

$$\widehat{t_\alpha} = argmin_f \sum_{i=1}^{n}[(2\alpha - 1)(Y_i - < f, X_i >) + |Y_i - < f, X_i >| \quad \text{(Eq.3)}$$

http://www.aloki.hu ● ISSN 1589 1623 (Print) ● ISSN 1785 0037 (Online)
DOI: http://dx.doi.org/10.15666/aeer/1706_1433314346

It is well established that the conditional median which corresponds to $\alpha = \frac{1}{2}$ constitutes an alternative predictor than the classical regression. Thus, for all given spectra curves x, we can predict CP, ADF and NDF contents by

$$\hat{Y} = \hat{r}(x) = argmin_f \sum_{i=1}^{n} |Y_i - < f, X_i >| \quad \text{(Eq.4)}$$

Notice that one of the main advantage of the quantile regression is to make prediction with predictive region being informative than a single-point prediction, It allows the predictions for thorough contingency planning. Indeed, for a fixed confidence level, for example $\gamma = 0.95$ the theoretical confidence interval is expressed $(t_{0.025}, t_{0.975})$. From the estimator given in *Equation 3,* we can write the interval of predictive region as

$$(\widehat{t_{0.025}}, \widehat{t_{0.975}}) \quad \text{(Eq.5)}$$

The functional nonparametric quantile regression (FNQR)

The nonparametric version of the quantile regression is defined by

$$\tilde{t_\alpha} = argmin_f \sum_{i=1}^{n} [(2\alpha - 1)(Y_i - f) + |Y_i - f|] K\left(\frac{\|x - x_i\|}{h_n}\right) \quad \text{(Eq.6)}$$

This estimator was constructed by Laksaci et al. (2009). In fact, there exist several versions of the FNQR, the natural one is the inverse of the cumulative distribution function estimator. This last estimator was studied by Ferraty et al. (2006) and Dabo-Niang and Laksaci (2012). In this work, we have opted the estimator presented in *Equation 6* being more fast and robust. Similar to the previous case, for single-point prediction, we use the conditional median to predict the CP, ADF or NDF contents denoted by Y. So for all given spectra curves x, Y is approximated by

$$\tilde{Y} = \tilde{r}(x) = argmin_f \sum_{i=1}^{n} |Y_i - f|] K\left(\frac{\|x - x_i\|}{h_n}\right) \quad \text{(Eq.7)}$$

while for the predictive region we use the following nonparametric confidence interval

$$(\widetilde{t_{0.025}}, \widetilde{t_{0.975}}) \quad \text{(Eq.8)}$$

The functional local linear quantile regression (FLLQR)

The study of the local linear estimation of the quantile regression is more recent than the other models. It was introduced by Al-Awadhi et al. (2018). This version of the quantile regression inherits the advantages of the both of the previous models. In particular, from the linear property of this model, we reduce the convergence rate and from the nonparametric one we explore the local structure of the curves. Recall that as a local linear approach, the FLLQR is obtained by assuming that the function $t_\alpha(x)$ has a linear form in the neighbourhood of a given spectra curve x. Mathematically, this assumption is expressed by

$$\forall\, x_0 \; in \; neigborhood \; of \; x \;\; t_\alpha(x) \approx a + b\beta(x, x_0) \quad \text{(Eq.9)}$$

http://www.aloki.hu ● ISSN 1589 1623 (Print) ● ISSN 1785 0037 (Online)
DOI: http://dx.doi.org/10.15666/aeer/1706_1433314346

Where the quantities a *and* b are obtained by minimizing

$$min_{f,g} \sum_{i=1}^{n} [(2\alpha - 1)(Y_i - f - g\beta(X_i, x)) + |Y_i - f - g\beta(X_i, x)|] K\left(\frac{\|x - X_i\|}{h_n}\right) \quad \text{(Eq.10)}$$

with $\beta(x,x)$ is known function used to measure the proximity among the curves. Thus, for fixed spectra curve x, FLLQR is estimated by $\widehat{t_\alpha}(x) = a$ (where a is solution of *Eq. 4*). Furthermore, for the pointwise prediction, we approximate the contents of CP, ADF and NDF by the conditional median $\bar{r}(x) = \bar{a}$ as solution of *Equation 11*

$$min_{f,g} \sum_{i=1}^{n} |Y_i - f - g\beta(X_i, x)| K\left(\frac{\|x - X_i\|}{h_n}\right) \quad \text{(Eq.11)}$$

Once again this estimator can be used to construct the 95% confidence interval that is

$$(\widehat{t_{0.025}}(x), \widehat{t_{0.975}}(x)) \quad \text{(Eq.12)}$$

The functional local linear modal regression (FLLMR)

The modal regression or the conditional mode is an old alternative model introduced by Collomb (1986). It is well established that this model is more pertinent than the classical regression where the white noise has a Chi-squared distribution. In functional Statistics there exist several nonparametric estimators for conditional mode. In this work we consider more recent one that is proposed by Almanjahie et al. (2018). This estimator is attractive and more robust and fast. With this model, the response variable CP, ADF and NSDF is approximated for a given spectral curve x as in *Equation 13*

$$\ddot{Y} = \ddot{r}(x) = argmin_y \hat{f}(y|X = x) \quad \text{(Eq.13)}$$

where $\hat{f}(.|X = x)$ is the local linear estimator of the conditional density of Y given $X = x$ (see Almanjahie et al., 2018 for more details on this topic). From this estimator, we construct a predictive region so-called the maximum conditional density predictive region introduced by Hyndman (1995). It is defined for a given spectral curve x as in *Equation 14*

$$R = \{y \quad such\ that \quad \hat{f}(y|X = x) > l_{0.95}\} \quad \text{(Eq.14)}$$

with

$$l_{0.95} = max\{l > 0\ such\ that \int_{f(y|X=x)>l} \hat{f}(y|X = x)dy > 0.95\}. \quad \text{(Eq.15)}$$

Results

The performance of all above mentioned models is closely linked with the use of different parameters involved in the estimation of $\hat{r}, \tilde{r}, \bar{r}$ *and* $\ddot{r}$. In fact, the distance between the curves $\|.\|$ and the smoothing parameter h_n are the most influencing parameters in this prediction issue. Concerning the norm $\|.\|$, it is observed that the most of the metrics are obtained by expanding the curve on some basis functions such as

http://www.aloki.hu ● ISSN 1589 1623 (Print) ● ISSN 1785 0037 (Online)
DOI: http://dx.doi.org/10.15666/aeer/1706_1433314346

spline basis, trigonometric basis or the interpolation by wavelet basis functions see for example, Ferraty and Vieu (2006). Formally, we write

$$x(t) \approx \sum_{i=1}^{k} c_i B_i(t) \quad \text{(Eq.16)}$$

where $(B_i(.))_i$ is a given orthonormal basis function. Thereafter, the distance between the curves is computed between their interpolation functions. We refer the readers to Ferraty and Vieu (2006) for more details on the mathematical formulation for the functional metric. Meanwhile, we use the leave-one-out Cross-Validation (CV) technique to select the parameter k and the bandwidth parameter h_n. We point out that the CV procedure is implemented with respect to the Mean Square Error (MSE) defined by *Equation 17*

$$MSE = \frac{1}{n}\sum_{i=1}^{n}\left(Y_i - \theta(X_i)\right)^2 \quad \text{(Eq.17)}$$

where $\theta(.)$ Refers to one of the previous models $\hat{r}, \tilde{r}, \bar{r}$ *and* $\ddot{r}$. On the other hand, we choose the same locative function β and the same kernel K as Rachedi et al. (2014). To evaluate the efficiency of the proposed model in this prediction issue, we divide random sample of 151 into two parts as learning sample (size = 100) and testing sample (size = 51). Further, in *Figures 3–5* we draw the box-cox plots of the absolute errors of the testing sample curves of CP, ADF and NDF respectively for four proposed regression models along with previous classical models namely PLS and PCR. The prediction results are shown in *Figures 3–5*.

It is depicted in *Figures 3–5* that there is a significant gain among the functional models as compared to the classical ones. The models FLQR, FNQR, FLLQR, and FLLMR are giving small absolute errors followed by PLS and PCR (*Table 1*).

Table 1. *Absolute error (AE) of crude protein (CP), acid detergent fiber (ADF) and neural detergent fiber (NDF) contents using proposed functional models and classical models*

Models	FLQR	FNQR	FLLQR	FLLMR	PCR	PLS
CP	0.73	1.11	0.73	0.62	2.95	1.45
ADF	0.82	1.24	0.81	1.12	7.08	2.03
NDF	0.67	1.17	0.77	0.71	5.24	1.78

The same fact is confirmed by *Table 2,* where we present the root mean squares error (RMSE) expressed by *Equation 18*

$$RMSE = \sqrt{\frac{1}{25}\sum_{j=1}^{25}\left(Y_i - \theta(X_i)\right)^2} \quad \text{(Eq.18)}$$

Table 2. *Root mean square errors (RMSE) of crude protein (CP), acid detergent fiber (ADF) and neural detergent fiber (NDF) contents using proposed functional models and classical models*

Models	FLQR	FNQR	FLLQR	FLLMR	PCR	PLS
CP	0.85	1.04	0.88	0.69	2.83	1.54
ADF	0.96	1.11	0.97	1.04	6.87	1.91
NDF	0.89	1.09	0.90	0.83	5.08	1.72

http://www.aloki.hu ● ISSN 1589 1623 (Print) ● ISSN 1785 0037 (Online)
DOI: http://dx.doi.org/10.15666/aeer/1706_1433314346

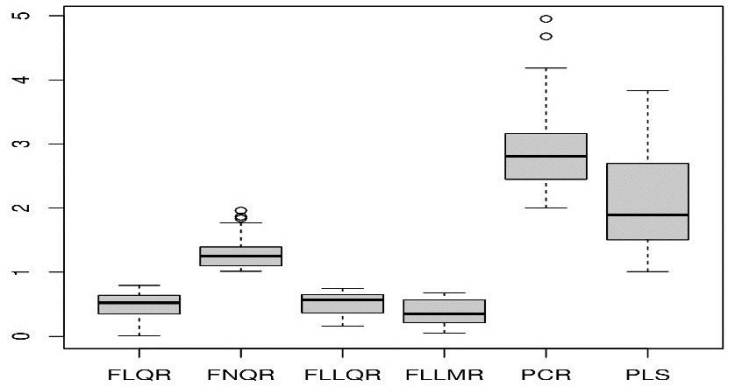

Figure 3. *Box-cox plots of absolute errors of crude protein (CP) contents using functional models and classical models*

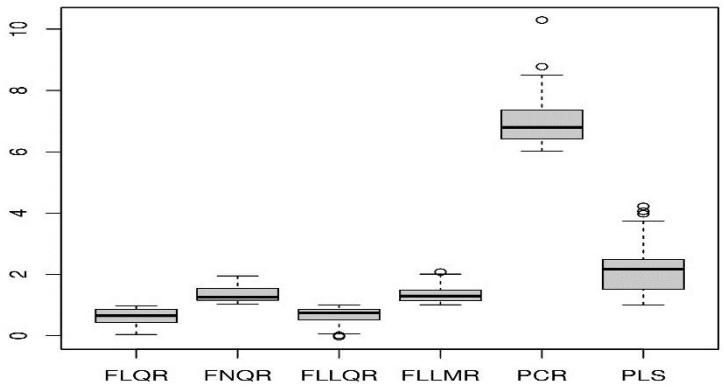

Figure 4. *Box-cox plots of absolute errors of acid detergent fiber (ADF) contents using functional and classical models*

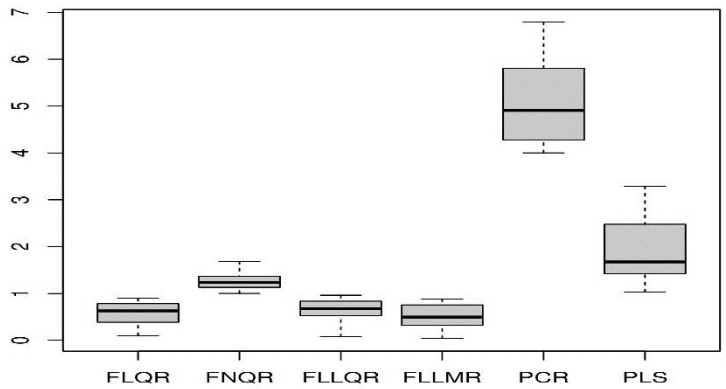

Figure 5. *Box-cox plots of absolute errors of neural detergent fiber (NDF) contents using functional models and classical models*

The values of RMSE is relatively stable and smaller for the four proposed functional models namely FLQR, FNQR, FLLQR and FLLMR as compared to the classical models namely PLS and PCR.

http://www.aloki.hu ● ISSN 1589 1623 (Print) ● ISSN 1785 0037 (Online)
DOI: http://dx.doi.org/10.15666/aeer/1706_1433314346

Although the performance of the studied models is varied, the variability of the RMSE is relatively stable for the four proposed models FLQR, FNQR, FLLQR and FLLMR as compared to that of the classical models such as PLS and PCR (see *Table 3*).

Table 3. *The broader range of the RMSE*

Models	FLQR	FNQR	FLLQR	FLLMR	PCR	PLS
Range for CP	(0.7, 0.97)	(0.9, 1.93)	(0.35, 0.84)	(0.37, 0.76)	(2.21, 4.95)	(1.01, 3.82)
Range for ADF	(0.4, 0.98)	(1.15, 1.81)	(0.09, 0.99)	(0.97, 1.76)	(6.01, 10.25)	(1.15, 1.81)
Range for NDF	(0.5, 0.91)	(1.03, 1.68)	(0.11, 0.96)	(0.33, 0.88)	(4.11, 6.97)	(1.02, 3.29)

In addition, we also evaluate the performance of NIRS to determine the predictive region using four functional models. The accuracy of these predictive intervals is evaluated with the help of two statistical measures namely the coverage in probability (Co-P) and the mean length of the interval (ML).

In *Table 4,* we summarize the (Co.P) and the M.L of 95% confidence intervals as mentioned in *Equations 3, 6, 10* and *13*.

Table 4. *Accuracy measures in terms of coverage in probability (Co-P) and mean length (ML) for predictive intervals using functional models*

Models	FLQR	FNQR	FLLQR	FLLMR
Co.P-CP	0.97	0.94	0.97	0.98
Co.P-ADF	0.95	0.91	0.93	0.94
Co.P-NDF	0.96	0.94	0.95	0.97
M.L-CP	0.41	0.65	0.34	0.28
M. L.-ADF	0.49	0.75	0.47	0.34
M.L-NDF	0.38	0.69	0.42	0.30

Discussion

The principal forage quality parameters were evaluated using a sample of 151 observations and the results summarized in *Tables 1–3*. The analyzed parameters are CP, ADF and NDF which are ranged between 5.59%-15.76%, 23.81%-47.86% and 62.96%-81.41%, respectively. Such a data analysis was operated using four functional models: FLQR, FNQR, FLLQR and FLLMR.

Based on the results from *Tables 1–3,* it is clear that the best model (having a small AE and RMSE) is the FLQR; it has an absolute error between 0.85-0.96 and its RMSE is valued between 0.67-0.82. Overall, it appears clearly that efficiency of the NIR Spectroscopy to predict the chemical properties differs from one parameter to another and also from one model to another. In particular, the best result is obtained by the FLLMR model in the prediction of the CP quantities. The model FLLQR is more adequate for the ADF parameter as well as for the NDF. On the other hand, both RMSE and AE emphasize the superiority of the functional model against the multivariate models (represented by the PCR and PLS regressions). Furthermore, the best multivariate model is the PCR for which RMSEs are respectively 2.83, 6.87 and 5.08 of CP, ADF and NDF. Moreover, the prediction results confirm that the robustness of the proposed functional models over the multivariate ones have lower variability in the

http://www.aloki.hu ● ISSN 1589 1623 (Print) ● ISSN 1785 0037 (Online)
DOI: http://dx.doi.org/10.15666/aeer/1706_1433314346

prediction error (RMSE and AE). Undoubtedly, the performance of the functional algorithms over that for the multivariate model is justified by the adequate exploration of the information based on the NIR data. Whilst the efficiency of the multivariate model is linked to several uncontrolled arguments such as the number of regressors, number of factors, the regression equation, etc. Furthermore, the functional approach has also satisfactorily performance for the prediction by the confidence interval as shown in *Table 4*. Precisely, the results of *Table 4* show that there is no substantial difference among the four models for the Co.P parameter as well as for ML. Nevertheless, by taking into account the ratio of Co.P and ML, we can say that the most suitable model in the sense of accuracy measure for the CP is FLLMR while for ADF and NDF is the FLQR model.

Conclusion

In this work, we have developed a new approach to predict the forage quality of Chinese ryegrass in term of its chemical components. We are interested to the prediction the CP, NDF and ADF contents. The proposed approaches combine the recent development in Chemistry and the modern Statistics. Specifically, from the Chemistry, we use the NIR spectroscopy technology which is inexpensive, rapid, reliable and accurate method. Moreover, it reduces the need for conventional wet Chemistry procedures. On the other hand, form the modern statistics we use some functional models which allow to explore all the information of the spectroscopy analysis where the spectral data are viewed as curves. These models are easily implementable and improve substantially of the prediction results. Moreover, the proposed models permit to avoid the core drawback of the PLS and PCR models that is the loss of information after the predictors transformation. Indeed, it is well known that the prediction by the PLS or the PCR regressions requires some transformation of the exogenous variable to reduce the dimension, get the linearity or remove the effect of the outliers. However, all these transformations are carried out through some directions chosen independently to the prediction problem. In particular, the endogenous variable does not intervene in the choice of the optimal direction which can affect the performance of the prediction. Thus, the originality of the functional approach comes from the fact that the prediction problem is performed without any transformation of the data. In conclusion, we can say that this combination of modern Chemistry and modern Statistics is very beneficial ecologically, economically and is more flexible, robust and fast. To the end, let us point out that in addition to pointwise, the proposed models offer the possibility to precise a predictive interval with a given confidence level which being more informative than a single-point prediction in certain situations.

We mention that the NIR analysis of the forage data is a promising analysis technique. It has been regarded as a new fast and reliable method compared to traditional analytical methods. In the last decade, this kind of technique is becoming more and more popular for the screening of forage quality parameters. See, for instance, Asekova et al. (2016) for a list of references). In this study, we combine this modern chemical technique together with the recent development of mathematical statistics in order to provide performance prediction procedures permits to use the whole spectroscopy curves as regressors.

http://www.aloki.hu ● ISSN 1589 1623 (Print) ● ISSN 1785 0037 (Online)
DOI: http://dx.doi.org/10.15666/aeer/1706_1433314346

Acknowledgments. Authors greatly thank the Editor in chief, the Associate Editor and the anonymous referees for a careful reading of the paper and for their valuable comments and suggestions which improved the quality of this paper substantially. They also extend their appreciation to the Deanship of Scientific Research at King Khalid University for funding this work through research groups program under the project number R.G.P1/102/40.

REFERENCES

[1] Agnihotri, R. K., Palni, L. M. S., Singh, B., Pangtey, Y. P. S. (2003): Evaluation of fodder quality of straw of different landraces of rice (Oryza sativa L.) under cultivation in the Kumaun Region of Indian Central Himalaya. – International Journal of Sustainable Development and World Ecology 10: 391-400.

[2] Al-Awadhi, F., Kaid, Z., Laksaci, A., Ouassou, I., Mustapha, R. (2018): Functional data analysis: local linear estimation of the L1-conditional quantiles. – Statistical Methods & Applications 28(2): 217-240.

[3] Albrecht, R., Richard, J., Jean, L., Gerard, T., Claude, P. (2008): Calibration of chemical and biological changes in composting of biowastes using near-infrared Spectroscopy. – Environnemental Science & Technology 43(3): 804-811.

[4] Aneiros, G., Cao, R., Fraiman, R., Vieu, P. (2019): Special issue on functional data analysis and related topics. – J. Multivariate Anal. 170: 1-336.

[5] AOAC (1990): Protein (Crude) Determination in Animal Feed: Copper Catalyst Kjeldahl Method 984.13. 15th Ed. – Official Methods of Analysis of AOAC International, Maryland.

[6] Asekova, S., Sang-Ik, H., Hong-Jib, C., Sang-jo, P., Dong-Hyun, S., Chan-Ho, K., Grover Shannon, J., and Jeong Dong, L. (2016): Determination of forage quality by near-infrared reflectance spectroscopy in soybean. – Turkish Journal of Agriculture and Forestry 40(1): 45-52.

[7] Bai, Q. L., Chen, S. J., Dong, X. L., Meng, Q. X., Yan, Y. L., Dai, J. R. (2004): Prediction of NDF and ADF concentrations with near infrared reflectance spectroscopy (NIRS). – Guang Pu Xue Yu Guang Pu Fen Xi = Guang Pu 24(11): 1345-1347.

[8] Cardot, H., Crambes, C., Sarda, P. (2005): Quantile regression when the covariates are fonctions. – Nonparametric Statistics 17(7): 841-856.

[9] Chen, J., Zhu, R., Xu, R., Zhang, W., Shen, Y., Zhang, Y. (2015): Evaluation of Leymus chinensis quality using near-infrared reflectance spectroscopy with three different statistical analyses. – Peerj 3: e1416. DOI: 10.7717/peerj.1416.

[10] Chen, P. F., Rong, Y. P., Han, J. G., Wang, J. H., Zhang, L. D., Xu, X. Y. (2007): Evaluation of fresh sample of alfalfa silage through near infrared reflectance spectroscopy (NIRS). – Guang Pu Xue Yu Guang Pu Fen Xi = Guang Pu 27(7): 1304-1307.

[11] Chikr-Elmezouar, Z., Almanjahie, I., Laksaci, A., Rachdi, M. (2018): FDA: strong consistency of the k NN local linear estimation of the functional conditional density and mode. – Journal of Nonparametric Statistics 1-21.

[12] Collomb, G., Härdle, W., Hassani, S. (1986): A note on prediction via estimation of the conditional mode function. – Journal of Statistical Planning and Inference 15: 227-236.

[13] Dabo-Niang, S., Laksaci, A. (2012): Nonparametric quantile regression estimation for functional dependent data. – Communications in Statistics - Theory and Methods 41(7): 1254-1268.

[14] De Marchi, M., Riovanto, R., Penasa, M., Cassandro, M. (2012): At-line prediction of fatty acid profile in chicken breast using near infrared reflectance spectroscopy. – Meat Science 90(3): 653-657.

[15] En, X. Z., Guo, H. R., Jia, Y. S., Ge, G. T., Wang, K. (2009): Application and prospect of near infrared reflectance spectroscopy in forage analysis. – Spectroscopy and Spectral Analysis 29: 635-640.

http://www.aloki.hu ● ISSN 1589 1623 (Print) ● ISSN 1785 0037 (Online)
DOI: http://dx.doi.org/10.15666/aeer/1706_1433314346

[16] Ferraty, F., Vieu, P. (2006): Nonparametric Functional Data Analysis: Theory and Practice. – Springer Science & Business Media, New York.
[17] Ferraty, F., Laksaci, A., Vieu, P. (2006): Estimating some characteristics of the conditional distribution in nonparametric functional models. – Statistical Inference for Stochastic Processes 9(1): 47-76.
[18] Foley, W. J., McIlwee, A., Lawler, I., Aragones, L., Woolnough, A. P., Berding, N. (1998): Ecological applications of near infrared reflectance spectroscopy–a tool for rapid, cost-effective prediction of the composition of plant and animal tissues and aspects of animal performance. – Oecologia 116(3): 293-305.
[19] Goia, P., Vieu, P. (2016): An introduction to recent advances in high/infinite dimensional statistics. – J. Multivariate Anal. 146: 1-6.
[20] Hyndman, R. J. (1995): Highest-density forecast regions for nonlinear and non-normal time series models. – Journal of Forecasting 14(5): 431-441.
[21] Kamruzzaman, M., ElMasry, G., Da-Wen, S., Allen, P. (2012): Non-destructive prediction and visualization of chemical composition in lamb meat using NIR hyperspectral imaging and multivariate regression. – Innovative Food Science & Emerging Technologies 16: 218-226.
[22] Koenker, R., Bassett, G. Jr. (1978): Regression quantiles. – Econometrica: Journal of the Econometric Society 46(1): 33-50.
[23] Laksaci, A., Lemdani, M., Ould-Saïd, O. (2009): A generalized L1-approach for a kernel estimator of conditional quantile with functional regressors: consistency and asymptotic normality. – Statistics & Probability Letters 7998: 1065-1073.
[24] Manteiga, W. G., Vieu, P. (2007): Statistics for functional data. – Computational Statistics & Data Analysis 51(10): 4788-4792.
[25] Monrroy, M., Dehylis, G., Marissa, M., Karla, H. (2017): Determination of brachiaria spp. forage quality by near-infrared spectroscopy and partial least squares regression. – Journal of the Chilean Chemical Society 62(2): 3472-3477.
[26] Mott, G., Moore, J. (1970): Forage evaluation techniques in perspective. – Proceedings Natn Conf Forage Qual Eval Util., Univ Nebraska.
[27] Nie, Z. D., Han, J. G., Zhang, L. D., Li, J. H. (2007): Applications of near infrared reflectance spectroscopy technique (NIRS) to grassland ecology research. – Guang Pu Xue Yu Guang Pu Fen Xi Guang Pu 27(4): 691-696.
[28] Norris, K. H., Barnes, R. F., Mooret, J. E., Shenk, J. S. (1976): Predicting forage quality by infrared reflectance spectroscopy. – J. Anim. Sci. 43: 889-897.
[29] Qingguo, T., Linglong, K. (2017): Quantile regression in functional linear semiparametric model. – Statistics 51(6): 1342-1358.
[30] Stuth, J., Abdi, J., Doug, T. (2003): Direct and indirect means of predicting forage quality through near infrared reflectance spectroscopy. – Field Crops Research 84(1-2): 45-56.
[31] Suksombat, W. (2004): Comparison of different alkali treatment of bagasse and rice straw. – Asian Australasian Journal of Animal Sciences 17: 1430-1433.
[32] Valderrama, M. J. (2007): An overview to modelling functional data. – Comput Stat 22: 331-334.
[33] Van Soest, P. J., Robertson, J. B., Lewis, B. A. (1991): Methods for dietary fiber, neutral detergent fiber, and nonstarch polysaccharides in relation to animal nutrition. – Journal of Dairy Science 74: 35833597.
[34] Wilcox, R. (2005): Introduction to Robust Estimation and Hypothesis Testing (Statistical Modeling and Decision Science). Vol. 2. – Academic Press, San Diego, CA.
[35] Yan, R., Chen, S., Zhang, X., Han, J., Zhang, Y., Undersander, D. (2011): Effects of replacing part of corn silage and alfalfa hay with Leymus chinensis hay on milk production and composition. – American Dairy Science Association 94(7): 3605-3608 DOI: 10.3168/jds.2010-3536.

http://www.aloki.hu ● ISSN 1589 1623 (Print) ● ISSN 1785 0037 (Online)
DOI: http://dx.doi.org/10.15666/aeer/1706_1433314346

[36] Yang, Z., Gang, N., Ling, P., Yan, Z., Linkai, H., Xiao, M., Xinquan, Z. (2017): Development and validation of near-infrared spectroscopy for the prediction of forage quality parameters in Lolium multiflorum. – PeerJ 5: e3867.
[37] Yu, G., Min-Jie, W., Yi-Hong, L., Xing-Ming, Y., Wei, R., Qi-Rong, S. (2011): Fluorescence excitation–emission spectroscopy with regional integration analysis for assessment of compost maturity. – Waste Management 31(8): 1729-1736.

http://www.aloki.hu ● ISSN 1589 1623 (Print) ● ISSN 1785 0037 (Online)
DOI: http://dx.doi.org/10.15666/aeer/1706_1433314346

THE ROLE OF LAND TENANCY IN RICE FARMING EFFICIENCY IN UPLAND KARST MOUNTAINOUS GUNUNGKIDUL INDONESIA

KHOTIMAH, Y. K.[1] – ANTRIYANDARTI, E.[2*] – SUPARDI, S.[2]

[1]*Master Program of Agribusiness, Postgraduate School, Universitas Sebelas Maret*
Jl Ir Sutami 36A, Kentingan, Surakarta 57126, Indonesia

[2]*Study Program of Agribusiness, Faculty of Agriculture, Universitas Sebelas Maret*
Jl Ir Sutami 36A, Kentingan, Surakarta 57126, Indonesia

**Corresponding author*
e-mail: ernoiz_a@staff.uns.ac.id

(Received 6th Jun 2019; accepted 11th Oct 2019)

Abstract. The land area of paddy has decreased every year. Karst as one of the most extensive dry land areas in Indonesia is used to raise paddy as well. This study aims to determine the role of land tenancy in rice farming efficiency and the determining factors of the efficiency of rice farming in the karst mountainous Gunungkidul. The research is located in karst mountainous area of Gunung Sewu, Gunungkidul. This study uses the stochastic frontier analysis with cost function approach. The result shows that the estimated parameter of land rent, price of urea fertilizer, labor wage, and production are significantly correlated with the cost production of rice farming. In addition, land tenancy plays an important role in increasing the efficiency of rice farming in the karst mountainous Gunungkidul. Farmers prefer to lease land in the long term between 1-4 years due to the fact that the price offered is cheaper. Other factors that improve the efficiency of rice farming are the number of household members and farm size, while the household head age decreases the efficiency of rice farming.
Keywords: *paddy, land tenancy, stochastic frontier analysis, cost function, farm size*

Introduction

Indonesia is classified as the third largest rice consumer in the world with an average of 38.41 million tons per year (Ministry of Agriculture, 2016). Rice as the primary food of the Indonesian people with a population of 258, 705 million in 2016 (Central Bureau of Statistics Republic of Indonesia, 2017). Compared to other food commodities, per capita rice consumption is the highest (Central Bureau of Statistics Republic of Indonesia, 2017) with an average of 98.01 kg/year (Ministry of Agriculture, 2016).

Due to high consumption of rice, Indonesian rice production is not able to meet the demand and the commodity must be imported. During the 1983-2016 period the value of trade's balance of rice became deficits every year (Ministry of Agriculture, 2016). Even though Indonesia is also the third largest paddy producing in the world (8.11%) reaching 77.29 million tons (FAO, 2018). The cultivated of rice in Indonesia are lowland paddy and dry paddy.

The increasing productivity of dry paddy is higher than lowland paddy. During the period of 2010-2013 dry paddies reached 3.43%/year (Irawan, 2015). The success of increasing productivity of paddy on dry land is not only because of increasing land area, but also caused by technological innovation and an intensification program approach. In fact, the land area has decreased every year. In the period of 2010-2016 the total area of

http://www.aloki.hu ● ISSN 1589 1623 (Print) ● ISSN 1785 0037 (Online)
DOI: http://dx.doi.org/10.15666/aeer/1706_1434714357

agricultural land was decreased by more than 3,202,560.55 ha (Ministry of Agriculture, 2015a, 2017).

Rice farmers in Indonesia actually have economies of scale which is being able to enlarge their farmland (Antriyandarti and Fukui, 2016). However, the average land area is still stagnant around 0.3 hectares. This is due to several obstacles in the process of enlarging (Antriyandarti and Fukui, 2016; Antriyandarti, 2018). The recommended alternative policy to expand the land is by increasing land liquidation. According to Antriyandarti (2018) liquidation of agricultural land in Indonesia has not gone well, only a small percentage of farmers are renting out their land. Land liquidation is a condition of land market through rent (lease) or sale. In rural Java, land is part of social status and inheritance that must be maintained. Sale of farmland is very rare and in many cases when sale does happen, it is a difficult process.

The potential of availability agricultural land in Indonesia is quite large and has not been utilized optimally. There are 95.81 million hectares which are potential for agriculture, with 70.59 million hectares of which are located on dry land (Ministry of Agriculture, 2015b). Karst is one of the most extensive dry land areas in Indonesia. Indonesia classified as a country that uses the largest karst waters in the world (Margat and Gun, 2013; Younos et al., 2019). The karst region in Indonesia is also the largest karst region in Southeast Asia (Clements et al., 2006). Indonesian karst is estimated at ± 15.4 million hectares (National Development Planning Agency, 2016). One of the karstic areas that become a prototype of karst in tropical regions in Indonesia is karst Gunungsewu, Gunungkidul (Adji et al., 1999).

Gunung Sewu is one of two UNESCO Global Geoparks in Indonesia (UNESCO, 2017). Gunung Sewu as a karst terrain that is geologically, geomorphologically and hydrogeologically shows unique phenomena. It is a classic tropical karst landscape in the south central part of Java Island well-known in the world, and dominated by limestone. Typical formation of “conical hills” is the formation of a series of small hills which are estimated to be 40,000 hills it can be called “gunung sewu”. The Javanese word “sewu” translates into “thousand”.

Geology of Gunungsewu expresses tracks of tectonic, erosion, denudation, and deposition occurred since Miocene epoch. Gunungsewu displays a specific Tropical landform, characterized by the existence of hills, closed depressions, and caves (Kusumayudha et al., 2015). Groundwater systems in this area are dominated by gaps resulting from dissolution which cause dry conditions on the surface. So that for agricultural production is less optimal. This condition causes low crop productivity and causes high poverty (Retnowati et al., 2014; Central Bureau of Statistics of Yogyakarta Province, 2017).

According to (Liu et al., 2017) agricultural land rent increases productivity from households with low productivity to high productivity. The land leasing market to bring land to more productive uses while at the same time providing development of rural non-agricultural economies (Deininger and Jin, 2003; Deininger et al., 2006). According to Zhang (2008), the tenancy increases efficiency in agriculture, because households that acquire land use it more productively. On the other hand (Roger, 1998), productivity and efficiency have a relationship with each other, namely productivity growth includes changes in efficiency and increased efficiency can increase productivity. If technically the production process is carried out inefficiently, it will have an impact on the failure to realize maximum productivity. Therefore, the factors that cause the efficiency of rice farming need to be known. This paper has significant

http://www.aloki.hu ● ISSN 1589 1623 (Print) ● ISSN 1785 0037 (Online)
DOI: http://dx.doi.org/10.15666/aeer/1706_1434714357

contributions. This is the first study that aims to determine the role of land tenancy on the efficiency of rice farming in the Gunungkidul Karst Mountainous. Then, the recommendation of this study will be useful for Indonesian government to set the alternative policies and strategies to enlarge farmland in Java which has the largest contribution to the national rice production. Expanding farmland on Java Island would improve the national productivity of rice.

Materials and methods

This research was conducted in the karst mountainous, Gunungsewu area Gunungkidul district located in the coordinates 110°19'48"-110°50'24" BT and 7°52'48"- 8°12'36" LS (see *Fig. 1*). Gunungsewu karst region is a prototype of karst in the tropical region in Indonesia (Kusumayudha et al., 2015; Adji et al., 1999). The focus of the study was carried out in the Girusubo sub-district where the area is in the south which occupies a large part of the Gunungsewu karst region (Regional Development Planning Agency of Gunungkidul, 2013; Tjia, 2013; Retnowati et al., 2014).

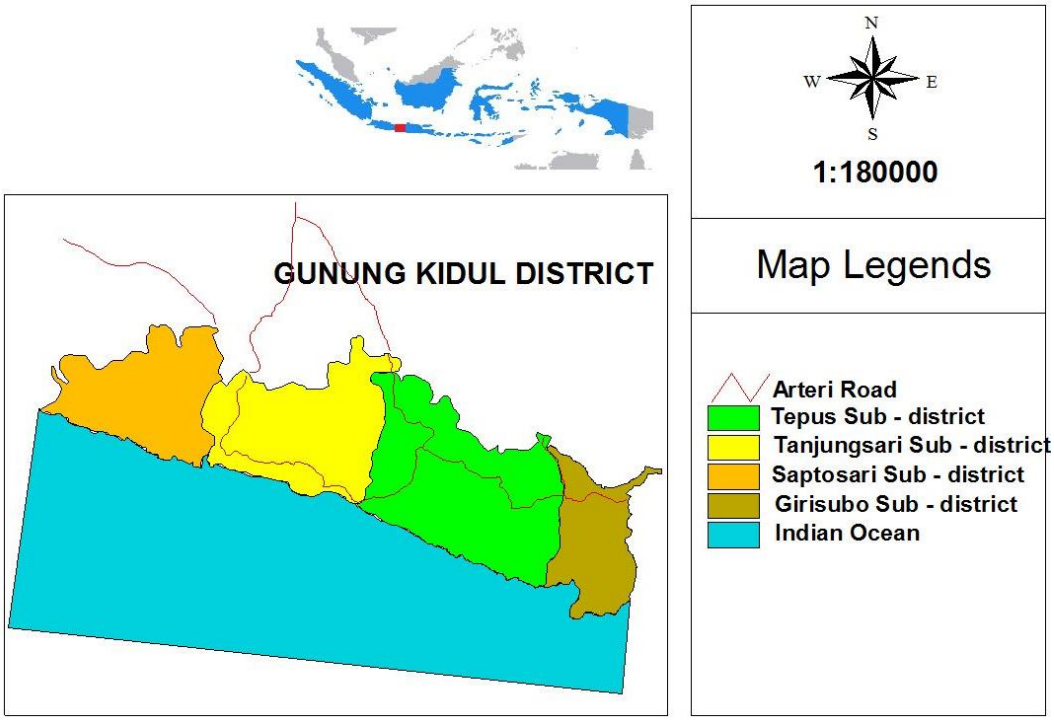

Figure 1. *The Gunung Sewu Karst Area in Gunungkidul District*

The farmers in the study area use karst groundwater as groundwater system. The characteristics of this karst region are influenced by secondary porosity (groundwater flow through dissolving gaps) which causes water to enter the underground flow system and cause dry conditions on the ground (Ford and William, 2007; Cahyadi et al., 2013). So that rice cultivation is not optimal. Because of that reason, the cultivation of rice uses rain to get water or can be called rainfed rice. Where it can only be planted once a year when the rainy season arrives. It cannot be planted for other planting seasons since rice requires a lot of water.

http://www.aloki.hu ● ISSN 1589 1623 (Print) ● ISSN 1785 0037 (Online)
DOI: http://dx.doi.org/10.15666/aeer/1706_1434714357

The soil condition in this karst region is classified as dry. So it causes the condition of infertile land that has an impact on agricultural cultivation in this region is less optimal (Regional Development Planning Agency of Gunungkidul, 2013). The income of farmers in the Gunungkidul karst area is very small due to the land in this area is not fertile and only relies on rainwater. This condition causes low crop productivity and causes high poverty (Retnowati et al., 2014; Central Bureau of Statistics of Yogyakarta Province, 2017). The survey was conducted in July 2018. The research was collected from household farmers selected as samples using the in-depth interview method with a structured questionnaire prepared. The questionnaire contains characteristic of respondents, farming system, inputs and outputs of crops, farmland liquidation. The sample used was 60 households of rice farmers using the random sampling method.

One method for estimating a production frontier using such data is to envelop the data points using an arbitrarily-chosen function. This approach was used Cobb-Douglas production frontier of the form:

$$Ln\, q_i = x_i\, \alpha - u_i \; i = 1,\ldots,I \qquad \text{(Eq.1)}$$

where q_i represents the output of the i-th firm; x_i is a K x 1 vector containing the logarithms of inputs; α is a vector of unknown parameters; and w, is a non-negative random variable associated with technical inefficiency.

The production frontier (*Eq. 1*) is *deterministic* insofar as q_i is bounded from above by the non-stochastic (i.e., deterministic) quantity $\exp(x_i\alpha)$. A problem with frontiers of this type (and with the DEA frontier) is that no account is taken of measurement errors and other sources of statistical noise - all deviations from the frontier are assumed to be the result of technical inefficiency. An obvious solution to the problem is to introduce another random variable representing statistical noise. The resulting frontier is known as a stochastic production frontier. The stochastic frontier production function model of the form

$$Ln\, q_i = x_i\, \alpha + v_i - u_i \qquad \text{(Eq.2)}$$

Equation 2 is identical to the model *Equation 1* except we have added a symmetric random error, V/, to account for statistical noise. Statistical noise arises from the inadvertent omission of relevant variables from the vector x_i, as well as from measurement errors and approximation errors associated with the choice of functional form. The model defined by *Equation 2* is called a stochastic frontier production function because the output values are bounded from above by the stochastic (random) variable $\exp(x_i\alpha + v_i.)$. The random error v, can be positive or negative and so the stochastic frontier outputs vary about the deterministic part of the model, $\exp(x_i\alpha)$.

These important features of the stochastic frontier model can be illustrated graphically. To do so it is convenient to restrict attention to firms that produce the output qt using only one input, x. In this case, a Cobb-Douglas stochastic frontier model takes the form:

$$Ln\, q_i = \alpha_0 + \alpha\, ln\, x_i + v_i - u_i \qquad \text{(Eq. 3)}$$

This study uses a stochastic frontier analysis with cost function approach. The method of the stochastic frontier cost function which is a derivative of the Cobb-

http://www.aloki.hu ● ISSN 1589 1623 (Print) ● ISSN 1785 0037 (Online)
DOI: http://dx.doi.org/10.15666/aeer/1706_1434714357

Douglas production function. The cost function of the stochastic frontier according to (Kumbhakar et al., 2015; Coelli et al., 2005) the equation is as follows:

$$Ln\, C = \alpha_0 + \alpha_1 lnPx_1 + \alpha_2 lnPx_2 + \alpha_3 lnPx_3 + \alpha_4 lnPx_4 + \alpha_5 lnPx_5 + (v_i - u_i) \quad \text{(Eq.4)}$$

C = Total cost production (USD)
Px_1 = Land rental (USD/ha)
Px_2 = Labor wage (USD/HOK)
Px_3 = Seed price (USD/kg)
Px_4 = Fertilizer price (USD/kg)
Px_5 = Production (kg)
U_i = Farmer specific characteristics related to cost inefficiency
V_i = Statistical disturbance term

Variable total cost production expresses cost as a function of input prices and outputs (Coelli et al., 2005). Examples of variable costs include the costs associated with the purchase of inputs such as seeds, fertilizers, wages of labor, land rent, herbicides, insecticides, and so on (Debertin, 2004). Land Rental is costs incurred by farmers to rent land during one crop rotation be counted in (USD/ha). Labor wages is costs incurred to pay labor used in the production process for various types of activities farming system, from land preparation to post-harvest during one crop rotation be counted in (USD/HOK). Price of seeds, fertilizers is costs incurred to buy seeds and fertilizers used in a crop rotation be counted in (USD/kg). According to Antriyandarti (2015) seed prices, labor costs, tractor fees, land rental, irrigation costs significantly correlated with total cost in some rice producing areas in Indonesia. Cost is the total cost including land cost, labor cost and material cost, materials include seed, water, fertilizer, chemicals, mulch and other agricultural production materials and services (Liu et al., 2017).

To identify the determinants of cost inefficiency, we estimate the following regression *Equation 2.*

$$U_i = \delta_0 + \delta_1 Z_1 + \delta_2 Z_2 + \delta_3 Z_3 + \delta_4 Z_4 + \delta_5 Z_5 + e \quad \text{(Eq. 5)}$$

U_i = Cost inefficiency effects
Z_1 = Land tenure (if rented land = 1; others = 0)
Z_2 = Number of household member (people)
Z_3 = Education of household head (years)
Z_4 = Age of household head (years)
Z_5 = Farm size (ha)
e = Error term

Efficiencies are observed among rice farmers to examine factors that explain why some farmers are more efficient than others. The source of inefficiency in rice farming concerns the characteristic of the farm and farmers (Villano and Fleming, 2004). Furthermore, efficiency will imply to raise the productivity (Okoruwa, et al., 2006). The base for determining this variable is because of that variable influencing technical inefficiency must be a farmer characteristic or socioeconomic. Variable of age, education, family member, kind of land, location of land, land tenure, off farm occupation, farm size plot significantly correlated with inefficiency in some rice producing areas in Indonesia (Antriyandarti, 2015). Fukui et al. (2002) that the

http://www.aloki.hu ● ISSN 1589 1623 (Print) ● ISSN 1785 0037 (Online)
DOI: http://dx.doi.org/10.15666/aeer/1706_1434714357

production efficiency under tenancy land is not lower than that of the owned land. Variable of renting land, renting out land, head age, education, agricultural labor, block size, soil fertility, landform significantly correlated with cost inefficiency components in wheat and maize in Gansu, China (Liu et al., 2017). Variable of farmers' age, frequency of participation in counseling, frequency of participation in training, the role of institution, farming system management significantly correlated with inefficiency in organic rice farming in Boyolali Indonesia (Sudrajat et al., 2017). Variable of age, education, training, farm size has effect on inefficiency in rice farmers in Bangladesh (Rahman, 2013).

Results and discussion

Efficiency of cost is the possibility of the minimum cost ratio with the level of specific inefficiencies to the actual total cost (Coelli et al., 2005; Kumbhakar and Lovell Knox, 2000). Therefore, efficiency of cost is defined as the percentage of achieving production costs with best practices. Thus, estimation of the cost efficiency index is calculated from the frontier analysis function. *Table 1* presented the input prices, production and potential determinants of cost inefficiency in the study area.

Table 1. *Input prices, production and potential determinants of cost inefficiency*

Variable	Min	Max	Mean	Amount (percentage)
Total cost (USD)	150.697	545.494	309.926	
Land rent (USD/ha)	59.653	596.525	230.077	
Labor wage (USD/HOK)	3.190	4.052	3.686	
Seed (USD/kg)	0.522	0.969	0.699	
Fertilizer (USD/kg)	0.137	0.164	0.153	
Production (kg/ha)	200.000	2,700.000	967.000	
Family member (person)	1.000	7.000	3.183	
Education of household head (year)	0.000	16.000	7.066	
Age of household head (year)	23.000	85.000	53.500	
Farm size (ha)	0.250	1.000	0.450	
Land Tenure: % of land is HH's owned land				
- All owned (person)				28(47%)
- Mixed (owned and rent) (person)				0
- All rent (person)				32 (53%)

HOK = Workday of labor

This study uses the Cobb Douglas stochastic frontier cost function model. Cost function analysis is carried out to examine the factors that influence the total cost of rice farming in study area. In the initial cost function it is suspected that there are five variables, namely production, land rent, seed price, fertilizer price, and labor wage. The result can be shown by *Table 2.*

The estimation results illustrate the best performance of the respondent farmers at the level of existing technology. This study uses half model with heteroscedasticity, so the standard error is the white standard error (Baum, 2006). The coefficient of all variables is positively significant, except the seed price is negative but not significant. Thus, the results are mostly plausible and consistent with the theory. The estimated parameter of land rent, fertilizer price, production and labor wage are positively significant to the

http://www.aloki.hu ● ISSN 1589 1623 (Print) ● ISSN 1785 0037 (Online)
DOI: http://dx.doi.org/10.15666/aeer/1706_1434714357

total production cost. While, the estimated parameter of seed price is not significant the total production cost. This is in line with the Rachmat (1985) variable of seed prices do not have a significant effect on total costs and coefficients are negative. Antriyandarti (2015) seed price variables had no effect on the total cost production and coefficient values were negative in rice farming in North Sumatra, West Java and Central Java.

Table 2. *Estimation of Cobb–Douglas frontier cost function*

Variable	Coefficient	S.E
Land rent	0.102*	0.053
Labor wage	1.272**	0.555
Seed price	-0.060^{ns}	0.096
Fertilizer price	0.819*	0.467
Production	0.259***	0.050
Constant	-7.282	7.206
Number of obs	60	
Log likelihood	20.7156	
Sigma_v	0.171	0.015
Sigma_u	0.004	0.208
Sigma2	0.029	0.005
Lamda	0.025	0.210

*Significant at 10% level; **significant at 5% level; ***significant at 1% level, ^{ns}not significant

Variable of production is positively significant to total cost production at 1% level. An increase in rice production by 1% lead to increase the total cost production of rice farming by 0.25%. Variable of land rent has positive effect on the total cost production of rice farming at 10% level, with a coefficient of 0.102 it is mean that an increase in land rent by 1% lead to increase the total cost by 0.1%. In addition, the frontier cost elasticity of the variables of fertilizer and labor is 0.81 and 1.27, respectively. This result is consistent with Antriyandarti (2015).

The result of the determinants of cost inefficiency is presented in *Table 3*. The estimated parameter of land tenure as dummy variable is negatively significant to the inefficiency of rice production cost at 5% level. The status of 'tenant' land will decrease inefficiency compared to the status of non-tenant land. In other words, land tenancy will increase the efficiency of rice farming in the karst mountainous, Gunungkidul. This is highly related to the behavior of farmers. The farmer who rent land has higher motivation to take care for their land so that productivity is higher compared to the owned land farmers. The tenant farmers strive to manage production in a professional manner and are receptive to new technology; therefore, they can improve their production and increase their income. This result is in accordance with Antriyandarti (2015) that land rent has a positive effect on the efficiency of rice farming costs in most parts of Indonesia. This finding is also consistent with Mailena et al. (2014) and the result in Central Java by Fukui et al. (2002) that production efficiency on rented land is not lower than that of the owner's own land.

Tenancy of land in the karst mountainous Gunungkidul, originated from the farmers who rent land to other farmers, the land of the village treasury managed by village officials to fund the construction of infrastructure or village needs, and the land which is right of the village officials to compensate for their salary called "*tanah lungguh*". The contract of land tenancy term is ranging from 1-4 years. If the farmer rents in the long run the price offered is cheaper. This finding is the main highlight of this study. Land

http://www.aloki.hu ● ISSN 1589 1623 (Print) ● ISSN 1785 0037 (Online)
DOI: http://dx.doi.org/10.15666/aeer/1706_1434714357

tenancy plays an important role on improving the efficiency of rice farming in karst mountainous Gunungkidul which is an unproductive area with a high poverty rate. Poverty alleviation effort in this area is very urgent (Antriyandarti et al., 2018). The improvement of efficiency of rice farming would improve rice farm income. Thus, the poverty in karst mountainous Gunungkidul can be reduced.

Table 3. *Potential determinants of cost inefficiency*

Variable	Coefficient	Std. Err
Land tenure	-0.074**	0.031
Household member	-0.095**	0.041
Education	-0.017**	0.006
Age	0.020**	0.007
Farm size	-0.110***	0.002
Constant	0.522*	0.276
F-stat	52.57***	
Number of observations	60	
R^2	0.792	

*Significant at 10% level; **significant at 5% level; ***significant at 1% level

The estimated parameter of number of household member is negatively significant to the inefficiency of rice farming at 5% level. The larger number of household members will reduce the inefficiency of rice farming in the karst mountainous Gunungkidul. This indicates that efficiency will increase if the number of households increases. This finding is contrast with Antriyandarti (2015) which states that the number of family members influences the increase in inefficiency of rice farming in West Java and North Sumatra, Indonesia. The rice farming in Gunungkidul is dominated by the use of family labor for land preparation, transplanting, fertilization, weeding, and harvesting.

The education of household head is also negatively significant to inefficiency of rice farming. It is suggested that the higher education can manage rice farming more efficiently. This is in line with the (Antriyandarti, 2015; Rahman, 2013; Sudrajat et al., 2017) that education has a positive effect on the cost efficiency of rice farming. The education is an important variable that can improve efficiency. Conditions in the field prove that farmer education is still low, so that it becomes a problem in efficiency. Therefore, this finding has policy implementation for government to improve education and managerial skills of farmers. Meanwhile, the variable of age is positively significant to inefficiency of rice farming. This indicates that the older the farmer, the greater inefficiency of rice farming or in other word, the younger farmer will produce more efficient farming. This finding is contrast with Antriyandarti (2015). The younger household head in the study area suggests more adaptable to accept and implement the new innovation technology of rice farming that can achieve high efficiency. Thus, farmer regeneration is strongly needed, particularly family member in the farm household. However, degeneration in agricultural sector is serious problems in most countries since young people are uninterested in farming or in rural futures.

The estimated coefficients of farm size are significantly negative to inefficiency of rice farming in karst mountainous Gunungkidul**.** This shows that the larger farm size will increase the efficiency of rice farming (Antriyandarti, 2015).

http://www.aloki.hu ● ISSN 1589 1623 (Print) ● ISSN 1785 0037 (Online)
DOI: http://dx.doi.org/10.15666/aeer/1706_1434714357

Conclusion

The results show that land tenancy and farm size increases the efficiency of rice farming in the karst mountainous, Gunungkidul. This is much related to the behavior of farmers where renting land have the motivation to care for their land so that productivity is higher compared to farmers who own their own land. Land tenancy has important role in increasing efficiency and improving farmland liquidation in dryland area. Farm size can be enlarged by improving land tenancy system. Farmers in the study area need to enlarge their farm size by leasing land from others because rice farmers in upland Gunungkidul are not willing to sell their land. This prompted the government to facilitate leasing of land in rural areas to increase rice production. Moreover, local government can facilitate transaction in rental market and promote farmland liquidation. Enlarging farm size not only increases efficiency but also increases farm household income. Therefore, the poverty in the karst mountain region in Gunungkidul can be reduced (Antriyandarti, 2018).

REFERENCES

[1] Adji, T., Haryono, E., Woro, S. (1999): Karst area and its development prospects in Indonesia. – Seminar PIT IGI in Universitas Indonesia, 26-27 Oktober 1999 (in Indonesian).
[2] Antriyandarti, E. (2015): Competitiveness and cost efficiency of rice farming in Indonesia. – Journal of Rural Problems 51(2): 74-85.
[3] Antriyandarti, E. (2018): Constraints of farm size enlargement in the rice sector of Central Java: A case study. – Bulgarian Journal of Agricultural Science 24(6): 949-958.
[4] Antriyandarti, E., Fukui, S. (2016): Economies of scale in Indonesian rice production: an economic analysis using PATANAS data. – Journal of Rural Problems 52(4): 259-264.
[5] Antriyandarti, E., Fajarningsih, R. U., Agustono, Darsono, Marwanti, S., Supardi, S., Sutrisno, J., Ferichani, M., Barokah, U., Rahayu, W., Ani, S. W., Khairiyakh, R. (2018): Poverty alleviation system of dryland farm community in karst mountains Gunungkidul, Indonesia. – IOP Conf. Ser: Earth Environ. Sci. 200: 012062.
[6] Baum, C. F. (2006): An Introduction to Modern Econometrics Using Stata. – Stata Press, Texas.
[7] Cahyadi, A., Ayuningtyas, E. A., Prabawa, B. A. (2013): Urgence of management of effort sanitation water resources conservation in karst area Gunungsewu Gunungkidul Region. – Indonesian Journal of Conservation 2(1): 23-32 (in Indonesian).
[8] Central Bureau of Statistics of DIY Province (2017): Daerah Istimewa Yogyakarta in Figures. – BPS-Statistic of D. I. Yogyakarta Province, Indonesia.
[9] Central Bureau of Statistics Republic of Indonesia (2017): Statistic Year Book of Indonesia 2017. – BPS-Statistics, Indonesia.
[10] Clements, R., Sodhi, N. S., Schilthuizen, M., Ng, P. K. L. (2006): Limestone karsts of Southeast Asia: imperilled arks of biodiversity. – Journal of Bio Science 56(9): 733-742.
[11] Coelli, T. J., Rao, D. S. P., O'Donnell, C., Battese, G. E. (2005): An Introduction to Efficiency and Productivity Analysis. – Springer International Publishing, New York.
[12] Debertin, D. L. (2004) : Agricultural Production Economics. – Pearson Education, New Jersey.
[13] Deininger, K., Jin, S. (2003): Land Sales and Rental Markets in Transition: Evidence from Rural Vietnam Policy Research. – The World Bank, Washington, DC.
[14] Deininger, K., Jin, S., Nagarajan, H. K. (2006): Equity and efficiency impacts of rural land rental restrictions: Evidence from India. – Policy Research, Working Paper 4324, The World Bank, Washington, DC.

http://www.aloki.hu ● ISSN 1589 1623 (Print) ● ISSN 1785 0037 (Online)
DOI: http://dx.doi.org/10.15666/aeer/1706_1434714357

[15] Food and Agricultural Organization (2018): faostat.org. – Accessed on July 29, 2018.
[16] Ford, D., Williams, P. (2007): Karst Geomorphology and Hydrology. – John Wiley & Sons Ltd, Chichester.
[17] Fukui, S., Hartono, S., Iwamoto, N. (2002): Risk and rice farming intensification in Rural Java. – The Japanese Journal of Rural Economics 4: 32-43.
[18] Irawan, B. (2015): Dynamics of Paddy Rice and Upland Rice Production: Implications for Rice Production Improvement Policies. – In: Pasadaran, E. (ed.) Strengthening Food Self-Sufficiency Capability. Indonesian Agency for Agricultural Research and Development (IAARD) Press, Jakarta, pp. 68-87 (in Indonesian).
[19] Kumbhakar, S. C., Lovell Knox, C. A. (2000): Stochastic Frontier Analysis. – Cambridge University Press, Cambridge.
[20] Kumbhakar, S. C., Wang, H. J., Horncastle, A. P. (2015): Stochastic Frontier Analysis Using STATA. – Cambridge University Press, Cambridge.
[21] Kusumayudha, S. B., Setiawan, J., Ciptahening, A. N., Septianta, P. D. (2015): Geomorphologic model of Gunungsewu Karst, GunungKidul Regency, Yogyakarta Special Territory, Indonesia: the role of lithologic variation and geologic structure. – Journal of Geology Resource Eng. 3: 1-7.
[22] Liu, Y., Wang, C., Tang, Z., Nan, Z. (2017): Farmland rental and productivity of wheat and maize: an empirical study in Gansu, China. – Journal of Sustainability (9) 1678: 1-18.
[23] Mailena, L., Shamsudin, M. N., Radam, A., Latief, I. (2014): Rice farms efficiency and factors affecting the efficiency in MADA Malaysia. – Journal of Applied Sciences 14: 2177-2182.
[24] Margat, J., Gun, J. (2013): Groundwater around the World: A Geographic Synopsis. – CRC Press, Taylor and Francis Group.
[25] Ministry of Agriculture (2015a): Statistic of Agricultural Land 2011-2014. – Center for Agriculture Data and Information System Secretariat General, Jakarta.
[26] Ministry of Agriculture (2015b): Ministry of Agriculture's Strategic Plan for 2015-2019. – Government of Indonesia, Jakarta.
[27] Ministry of Agriculture (2016): Outlook for Agricultural Crops for Rice Food Crops. – Center for Agriculture Data and Information System Secretariat General, Jakarta.
[28] Ministry of Agriculture (2017): Statistic of Agricultural land 2012-2016. – Center for Agriculture Data and Information System Secretariat General, Jakarta.
[29] National Development Planning Agency (2016): Indonesian Biodiversity Strategy and Action Plan 2015-2020. – NDPA, Jakarta
[30] Okoruwa, V. O., Ogundele, O., Oyewusi, B. O. (2006): Efficiency and productivity of farmers in North Central Nigeria. – Paper presented at the International Association of Agricultural Economists Conference, August 12-18, 2006, Australia.
[31] Rahman, M. C., Siddique, M. A. B., Salam, M. A., Islam, M. A., Al-faisal, M. S. (2013): Assessment of technical efficiency of rice farmers in a selected empoldered area of Bangladesh. – European Journal of Agricultural Sciences 10: 2668-3547.
[32] Regional Development Planning Agency of Gunungkidul (2012): Regional Profile of Gunungkidul Regency. – Regional Development Planning Agency of Gunungkidul, Indonesia.
[33] Retnowati, A., Anantasari, E., Marfai, M. A., Dittmann, A. (2014): Environmental ethics in local knowledge responding to climate change: an understanding of seasonal traditional calendar pranotomongso and its phenology in karst area of GunungKidul, Yogyakarta, Indonesia. – Procedia Environmental Sciences 20: 785-794.
[34] Roger, M. (1998): The definition and measurement of productivity. – The University of Melbourne Institute of Applied Economics and Social Research, Working Paper 9/98.
[35] Sudrajat, I. S., Rahayu, E. S., Kusnandar, K., Supriyadi (2017): Effect of social factors in stochastic frontier profit of organic rice farming in Boyolali. – Bulgarian Journal of Agricultural Science 23(4): 551-559.

http://www.aloki.hu ● ISSN 1589 1623 (Print) ● ISSN 1785 0037 (Online)
DOI: http://dx.doi.org/10.15666/aeer/1706_1434714357

[36] Tjia, H. D. (2013): Morphostructural development of Gunungsewu Karst, Java Island. – Indonesian Journal of Geology 8(2): 75-88.
[37] UNESCO (2017): UNESCO global geoparks celebrating earth heritage, sustaining local communities. – www.globalgeopark.org (accessed on January 30, 2019).
[38] Villano, R., Fleming, E. (2004): Analysis of technical efficiency in a rainfed lowland rice environment in Central Luzon Philippines using a stochastic frontier production function with a heteroskedastic error structure. – Working Paper Series in Agricultural and Resource Economics, University of New England.
[39] Wang, H., Riedinger, J., Jin, S. (2015): Land documents, tenure security and land rental development: panel evidence from China. – China Economic Review 36: 220-235.
[40] Younos, T., Schreiber, M., Ficco, K. K. (2019): Karst Water Environment Advances in Research, Management and Policy. – In: Stevanovic, Z. (ed.) Karst Aquifers in the Arid World of Africa and the Middle East: Sustainability or Humanity? Springer International Publishing, Switzerland, pp. 2-40.
[41] Zhang, Q. F. (2008): Retreat from equality or advance towards efficiency? Land markets and inequality in Rural Zhejiang. – Journal of the China Quarterly 195: 535-557.

http://www.aloki.hu ● ISSN 1589 1623 (Print) ● ISSN 1785 0037 (Online)
DOI: http://dx.doi.org/10.15666/aeer/1706_1434714357

RESEARCH ON COMPREHENSIVE EVALUATION INDEX SYSTEM OF PERFORMANCE AUDITING OF GOVERNMENTAL ECOLOGICAL ENVIRONMENT

LIU, X. J.[1,2] – PAN, Y.[1*] – YANG, J.[2] – ZHU, L. Z.[1] – YING, L. M.[2]

[1]*School of Economics and Management, Fuzhou University, 350116 Fuzhou, PR China*

[2]*School of Management, Wenzhou Business College, 325000 Wenzhou, PR China*

[*]*Corresponding author*
e-mail: panyan_fzdx@126.com

(Received 6th Jun 2019; accepted 24th Oct 2019)

Abstract. A performance auditing evaluation problem of governmental ecological environment belongs to a Multiple Criteria Decision Making (MCDM) problem. However, we must use quantitative data to avoid inconsistency as well as to ensure the science and correctness of the decision in an evaluation index system of performance auditing. In this paper, we present a comprehensive evaluation index system of performance auditing of governmental ecological environment based on fuzzy Analytic Hierarchy Process (AHP) and Technique for Order Preference by Similarity to Ideal Solution (TOPSIS). Firstly, a comprehensive evaluation index system of performance auditing is approved from the literature related to governmental ecological environment. Secondly, the relative weights of the chosen evaluation indexes of performance auditing are calculated by fuzzy AHP method. Furthermore, TOPSIS method is adopted to rank the performance auditing and improve the gaps with five local governments as an empirical example. As a new data analysis method, the results show that fuzzy AHP theoretical model and TOPSIS method has become suitable for use in the evaluation of performance auditing of governmental ecological environment.
Keywords: *performance auditing, evaluation index system, decision model, governmental ecological environment, TOPSIS, analytic hierarchy process*

Introduction

In response to accelerating global clean-energy race, governmental ecological environment has been heavily advocated over the past decade. Many different theories and methods of performance auditing of governmental ecological environment for conducting a scientific and reasonable valuation have been applied in various academic circles in the last several years (Paydar et al., 2017). Today organizations operate in an ecological environment where performance auditing is continuously changing and increasing in the process of incidental development (Ivanova et al., 2016). Thus, dealing with qualitative information is quite common in various fields such as decision making and prediction (Fero et al., 2013). The fact of the matter is that evaluation process of performance auditing of governmental ecological environment is costly and its adaptation takes too much time so the evaluation cost is too high in many countries (Zanardo et al., 2018). The performance auditing evaluation has become the certain tendency for the government ecological environment (Shi, 2017). With the development of economic reforms, remarkable progress has been made in the efficient use of resources and ecological environment by using performance auditing in the past years in China. Thus, an effective intelligent decision method which automates and integrates evaluation processes and allows information sharing in governmental ecological environment needs to be researched in in-depth (Minichilli et al., 2017; Manzoor et al., 2018). Moreover, making some research on performance auditing of the governmental ecological

http://www.aloki.hu ● ISSN 1589 1623 (Print) ● ISSN 1785 0037 (Online)
DOI: http://dx.doi.org/10.15666/aeer/1706_1435914374

environment is of great significance to find a way to evaluate performance auditing accurately.

On the other hand, it is necessary to supervise and improve the situation of performance auditing by government, and the evaluation of governmental ecological environment is becoming more and more important. The research of comprehensive evaluation index system of performance auditing has been theoretical and practical as the development of scientific technology and economic reform (Gutierrez, 2015). So a theoretical analysis of the objectiveness for evaluation of performance auditing was used to protect the whole governmental ecological environment. Although local governments can develop their own evaluation index system, other ones may prefer ready systems to shorten application cycle and reduce human resource cost (Johansen and Christoffersen, 2017). Therefore the evaluation index system of performance auditing is an important decision making problem of local governments and effects directly the governmental ecological environment (Mueller, 2011). The overall performance auditing must be verified by environmental checkers in the following aspects of implementation measures of governmental ecological environment, environmental monitoring and auditing arrangement and other environmental protection system (Nehme, 2017). Because governmental ecological environment entries propagate to performance auditing, the comprehensive evaluation index system would require more attention and time (Stephenson, 2015). This paper focuses on structuring a decision aid mechanism on the basis of fuzzy AHP and TOPSIS under fuzzy environment in order to route useful decisions with respect to the public satisfaction evaluation of governmental sectors. Furthermore, the fuzzy algorithms are integrated into the decision-making framework in order to involve quantitative information into the performance auditing evaluation.

The remainder of this paper is organized as follows. A comprehensive evaluation index system of performance auditing of governmental ecological environment is built in Section 2. And the concepts of fuzzy AHP and TOPSIS are introduced in this section. In Section 3, the performance auditing evaluation framework and the analytical methods are proposed. The detailed implementation of the evaluation model and process by using fuzzy AHP and TOPSIS method is also given in this section. An empirical example for performance auditing evaluation indexes and the result analyses is presented to illustrate the approved evaluation model and method with five local governments in Section 4. Lastly, concluding remarks and proposals for further research are given in Section 5.

Comprehensive evaluation index system of performance auditing

In this paper, a fuzzy theory and AHP method is adopted to implement the evaluation process. To use AHP model for the evaluation of performance auditing of governmental ecological environment for a new tool, a new group of expert's opinions are needed as input to the decisions process. The comprehensive evaluation index system of performance auditing is shown in *Fig. 1*.

At present, the research on a systematic and complete performance auditing evaluation system is not perfect in practice. This study has attempted to establish a decision mechanism towards the execution of shipping investment decisions based on customer satisfaction levels in different markets. The comprehensive evaluation index system of performance auditing is presented with the analysis of governmental ecological environment affecting factors. As an effective decision tool, the proposed comprehensive evaluation index system of performance auditing is expected to provide invaluable decision for governmental ecological environment. In addition, multi-level

http://www.aloki.hu ● ISSN 1589 1623 (Print) ● ISSN 1785 0037 (Online)
DOI: http://dx.doi.org/10.15666/aeer/1706_1435914374

comprehensive evaluation index system of performance auditing of governmental ecological environment was expounded from the model.

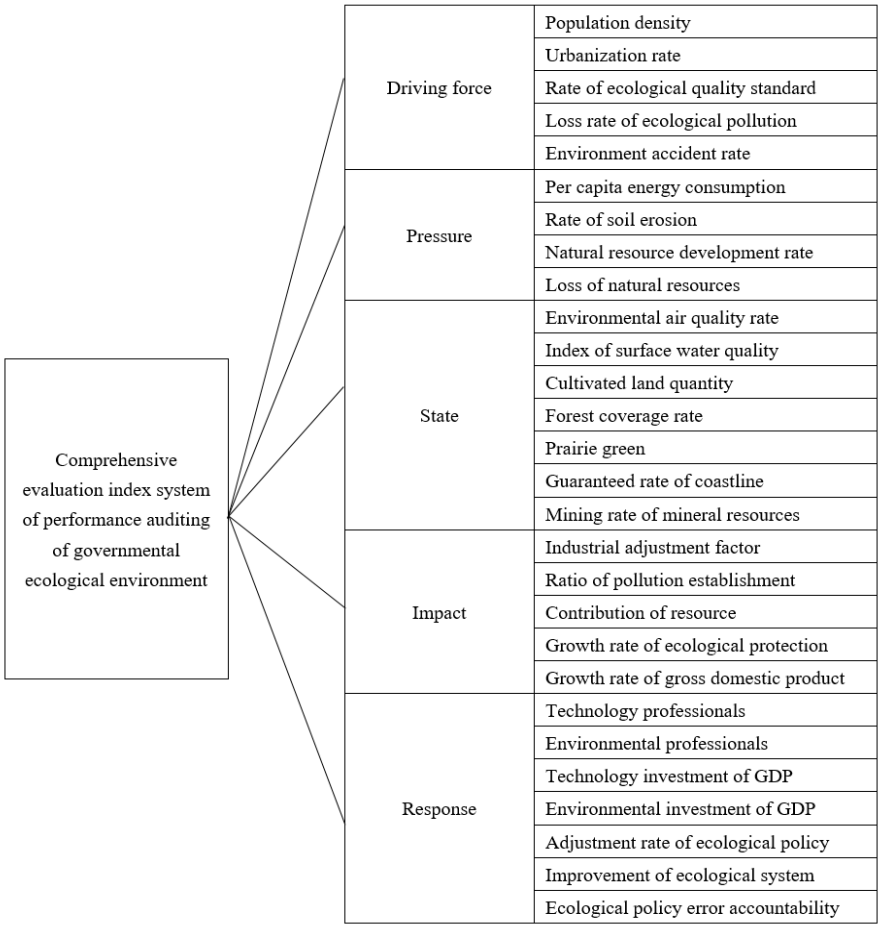

Figure 1. *The comprehensive evaluation index system of performance auditing*

Research methodology

Fuzzy analytic hierarchy process

In this paper, we propose a comprehensive evaluation method of performance auditing consists of integration of fuzzy AHP and TOPSIS. The Analytic Hierarchy Process (AHP) was firstly devised by Wind and Saaty in 1980. It is a useful tool to solve complex decision problems in many fields (Groselj and Stirn, 2018). The relative importance of a list of indexes was presented by using a pairwise comparison amongst the factors by relevant experts (Ahmadipari et al., 2018). In past years, the AHP method has been used often for decision problem, but recently years fuzzy AHP method has been preferred more than AHP method for MCDM problem (Kumar et al., 2017). Moreover, the fuzzy theory has become a useful tool for automating human activities in the decision-making process (Nazari et al., 2018). Fuzzy numbers are often convenient to work with triangular fuzzy numbers in promoting representation and information processing of system theory in a fuzzy environment (Hategekimana, 2018). For example, the decision makers cannot provide a satisfaction value precisely such as ‘quite satisfactory’ and ‘not very

http://www.aloki.hu ● ISSN 1589 1623 (Print) ● ISSN 1785 0037 (Online)
DOI: http://dx.doi.org/10.15666/aeer/1706_1435914374

satisfactory' (Tahri et al., 2017). In here, it is suggested that the decision makers use the different variables to evaluate the importance of the criteria combined with the actual condition.

The evaluation criteria and alternatives as regards the problems of performance auditing of governmental ecological environment presented in this paper have been modeled by using fuzzy AHP. Next, this paper describes the relevant elements of computational steps and the main method of calculating process.

Step 1. Structuring fuzzy judgment matrix

Triangular fuzzy number M is presented as (l, m, u), and $\mu_{\mathrm{M}}(x)$ is given as:

$$\mu_{\mathrm{M}}(x)=\begin{cases}\dfrac{1}{m-u}x-\dfrac{u}{m-u} & x\in[m,u]\\ \dfrac{1}{m-x}x-\dfrac{l}{m-l} & x\in[l,m]\\ 0 & other\end{cases} \quad \text{(Eq.1)}$$

where l≤ m ≤u, l and u is the lower and upper bound values of M respectively, which is shown in *Fig. 2*.

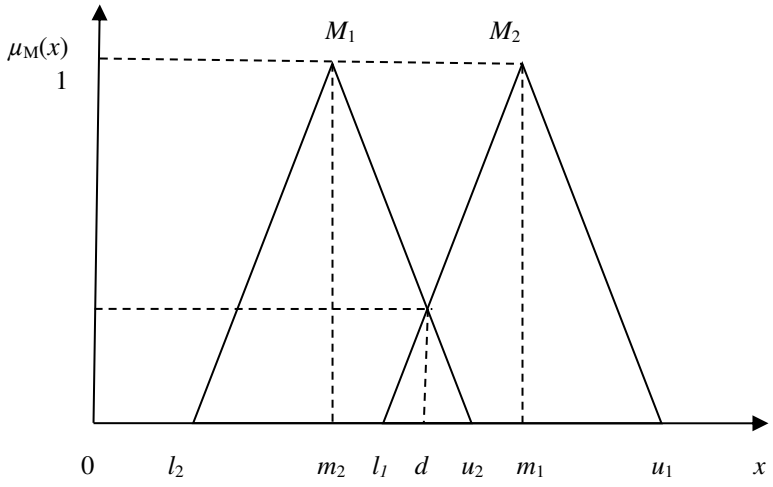

Figure 2. *Relationship between fuzzy number M1 and M2*

As $M_1=(l_1,m_1,u_1)$ and $M_2=(l_2,m_2,u_2)$ are two triangular fuzzy numbers, the operation methods of two trigonometric fuzzy numbers are presented in the following:

$$M_1+M_2=(l_1+l_2,m_1+m_2,u_1+u_2) \quad \text{(Eq.2)}$$

$$M_1\otimes M_2\approx(l_1l_2,m_1m_2,u_1u_2) \quad \text{(Eq.3)}$$

$$1/M\approx(1/u,1/m,1/l) \quad \text{(Eq.4)}$$

http://www.aloki.hu ● ISSN 1589 1623 (Print) ● ISSN 1785 0037 (Online)
DOI: http://dx.doi.org/10.15666/aeer/1706_1435914374

Step 2. Determining fuzzy number

In order to get the interval solution of the model, all the comparison matrix numbers would be turn into a fuzzy number. The formula to transform various kinds of fuzzy number into triangular ones are given as:

$$(\frac{l_1 + l_2 + \cdots + l_i}{i}, \frac{m_1 + m_2 + \cdots + m_i}{i}, \frac{u_1 + u_2 + \cdots + u_i}{i}) \quad \text{(Eq.5)}$$

With algorithms, a fuzzy variable will transform the fuzzy number into interval number by using the basic theory of fuzzy numbers.

Step 3. Calculating fuzzy value

In this paper, the definition of a fuzzy value is presented in the following:

$$\boldsymbol{D}_{\mathrm{i}}^{k} = \sum_{j=1}^{n} a_{ij}^{k} / (\sum_{i=1}^{n} \sum_{j=1}^{n} a_{ij}^{k}) \quad \text{(Eq.6)}$$

where $i = 1,2,...,n$.

Step 4. Definition of trigonometric fuzzy functions

As M1 ≥ M2, the probability of the triangular fuzzy function is defined as:

$$V(M_1 \geq M_2) = sup_{x \geq y}[\min(\mu_{M1}(x), \mu_{M2}(y))] \quad \text{(Eq.7)}$$

$$V(M_1 \geq M_2) = \mu(d) = \begin{cases} (l_2 - u_1) / ((m_1 - u_1) - (m_2 - l_2)) & m_1 \leq m_2, \ u_1 \geq l_2 \\ 1 & m_1 \geq m_2 \\ 0 & otherwise \end{cases} \quad \text{(Eq.8)}$$

Step 5. Determining weights of the level indicators

If a fuzzy number is greater than the probability of other fuzzy numbers, it is given in the following:

$$V(M \geq M_1, M_2, ..., M_n) = \min V(M \geq M_i) \quad \text{(Eq.9)}$$

Step 6. Calculating the weight vectors

Assume that d(Ai) = minV(Si≥ Sk), and k=1, 2, . . ., n. the fuzzy theory was used to determine the weight vector of each index, which can be defined by

$$W' = (d'(A_1), d'(A_2), \cdots, d'(A_n))^T \quad \text{(Eq.10)}$$

where Ai (i=1, 2, …, n) are n elements of a situation.

Next, the normalized weight vectors with different optimum indicators are expressed as follows:

$$W = (d(A_1), d(A_2), \cdots, d(A_n))^T \quad \text{(Eq.11)}$$

Thus, the calculation method obtained from above results can be used to accurately determine the comprehensive weight of each index.

http://www.aloki.hu ● ISSN 1589 1623 (Print) ● ISSN 1785 0037 (Online)
DOI: http://dx.doi.org/10.15666/aeer/1706_1435914374

Technique for order preference by similarity to ideal solution

TOPSIS (Technique for Order Preference by Similarity to Ideal Solution) is one of the useful tools to solve real-world problems of quantitative and qualitative factors including economic and social factors (Deveci et al., 2018). TOPSIS makes it possible to appraise the distances of each indicators from the positive and negative ideal solutions by comparing the difference among many schemes (Wang et al., 2017; Korucu et al., 2018). The positive ideal solution is composed of all best values in the decision making process (Hussain and Yang, 2018). Furthermore, the sorting of schemes and weights are very straight forward and clear. In the process of TOPSIS method, the performance ratings and the weights of each criteria are given more verbose output (Kaur et al., 2018). The TOPSIS is an extensive and thorough decision tool to evaluate the performance auditing in different fields (Lourenzutti et al., 2017; Gupta, 2018). With respect to MCDM problem in which both the attribute weights and attribute values are fuzzy numbers, a new method of TOPSIS is presented in this paper.

Assume that a multiple criteria decision-making problem with m alternatives $A_1, A_2, \cdots, A_m$ and n decision attributes $D_1, D_2, \cdots, D_n$, and the decision matrix is defined in *Table 1*.

Table 1. *The decision matrix of multiple criteria decision-making problem*

No.	D_1	D_2	$\cdots$	D_n
A_1	x_{11}	x_{12}	$\cdots$	x_{1n}
A_2	x_{21}	x_{22}	$\cdots$	x_{2n}
$\cdots$	$\cdots$	$\cdots$	$\cdots$	$\cdots$
A_m	x_{m1}	x_{m2}	$\cdots$	x_{mn}

Step 1. Computing canonical decision matrix

The multilevel matrix is modeled and simulated in the following:

$$y_{ij}^{'} = \begin{cases} y_{ij} & income-type\,inde \\ -y_{ij} & cost-type\,ind \\ 1-y_{ij} & others \end{cases} \quad \text{(Eq.12)}$$

The indexes are evaluated by each decision maker, and are converted into proper variables, which can be defined by

$$Z_{ij} = x_{ij} / \sqrt{\sum_{i=1}^{m} x_{ij}^2} \quad \text{(Eq.13)}$$

Step 2. Calculating weighted canonical decision matrix

With the help of the object weight vector, the weighted canonical decision matrix of the alternatives is defined as

http://www.aloki.hu ● ISSN 1589 1623 (Print) ● ISSN 1785 0037 (Online)
DOI: http://dx.doi.org/10.15666/aeer/1706_1435914374

$$V_{ij} = W_j \cdot n_{ij} \quad \text{(Eq.14)}$$

where $\sum_{j=1}^{n} W_j = 1$, which can be determined by using fuzzy AHP method.

Step 3. Determining positive ideal solution (PIS) and negative ideal solution (NIS)

$$A^+ = \left\{V_1^+, V_2^+, \cdots, V_n^+\right\} = \left\{\left(\max V_{ij} \,|\, j \in I\right), \left(\min V_{ij} \,|\, j \in I\right)\right\} \quad \text{(Eq.15)}$$

$$A^- = \left\{V_1^-, V_2^-, \cdots, V_n^-\right\} = \left\{\left(\min V_{ij} \,|\, j \in I\right), \left(\max \upsilon_{ij} \,|\, j \in I\right)\right\} \quad \text{(Eq.16)}$$

where, I belongs to benefit attribute, j belongs to cost attribute.

Step 4. Calculating the distance of each alternative from PIS and NIS

The distance of each alternative from PIS and NIS are determined:

$$d_i^+ = \sqrt{\sum_{j=1}^{n} \left(V_{ij} - V_j^+\right)^2} \quad \text{(Eq.17)}$$

$$d_i^- = \sqrt{\sum_{j=1}^{n} \left(V_{ij} - V_j^-\right)^2} \quad \text{(Eq.18)}$$

Step 5. Calculating the closeness coefficient of each alternative

The closeness coefficient of each alternative is given by

$$C_i^* = \frac{d_i^-}{d_i^+ + d_i^-} \quad \text{(Eq.19)}$$

where $i = 1, 2, \cdots, m.$.

Then, the ranking of alternatives can be designed by comparing C*i values.

In this paper, we present TOPSIS method and fuzzy AHP to analyze decision objects, it would make the result to be more reasonable and accurate.

Results

The aim of this paper is to evaluate the performance auditing of governmental ecological environment of five local governments in Fujian Province of China. The comprehensive evaluation index system and method are applied to assessing performance auditing in part of the local government of Fujian province administrative cities as one example. Firstly, the comprehensive evaluation index system was set up in allusion to the ecological environment of the five local governments by using the method of multifactorial evaluation method of fuzzy mathematics. Based on analysis mode and characteristics of comprehensive evaluation index system, the hierarchy structure of comprehensive evaluation index system was established in a very powerful way. Then,

http://www.aloki.hu ● ISSN 1589 1623 (Print) ● ISSN 1785 0037 (Online)
DOI: http://dx.doi.org/10.15666/aeer/1706_1435914374

many decision makers from different areas evaluate the importance of evaluation indexes with the help of questionnaires. Next, the performance auditing was built and the traditional method of AHP is improved with fuzzy theory, which was also utilized for determining the weights of main evaluation criteria. Finally, TOPSIS method was presented for evaluating the performance auditing of governmental ecological environment by considering ecological efficiency and weights of the criteria. According to above methods, the ranking of the performance auditing can be obtained by improvement of the given model and method in the numerical example.

Based on fuzzy AHP method, the hierarchical structure of performance auditing of model in application is shown in *Fig. 3*.

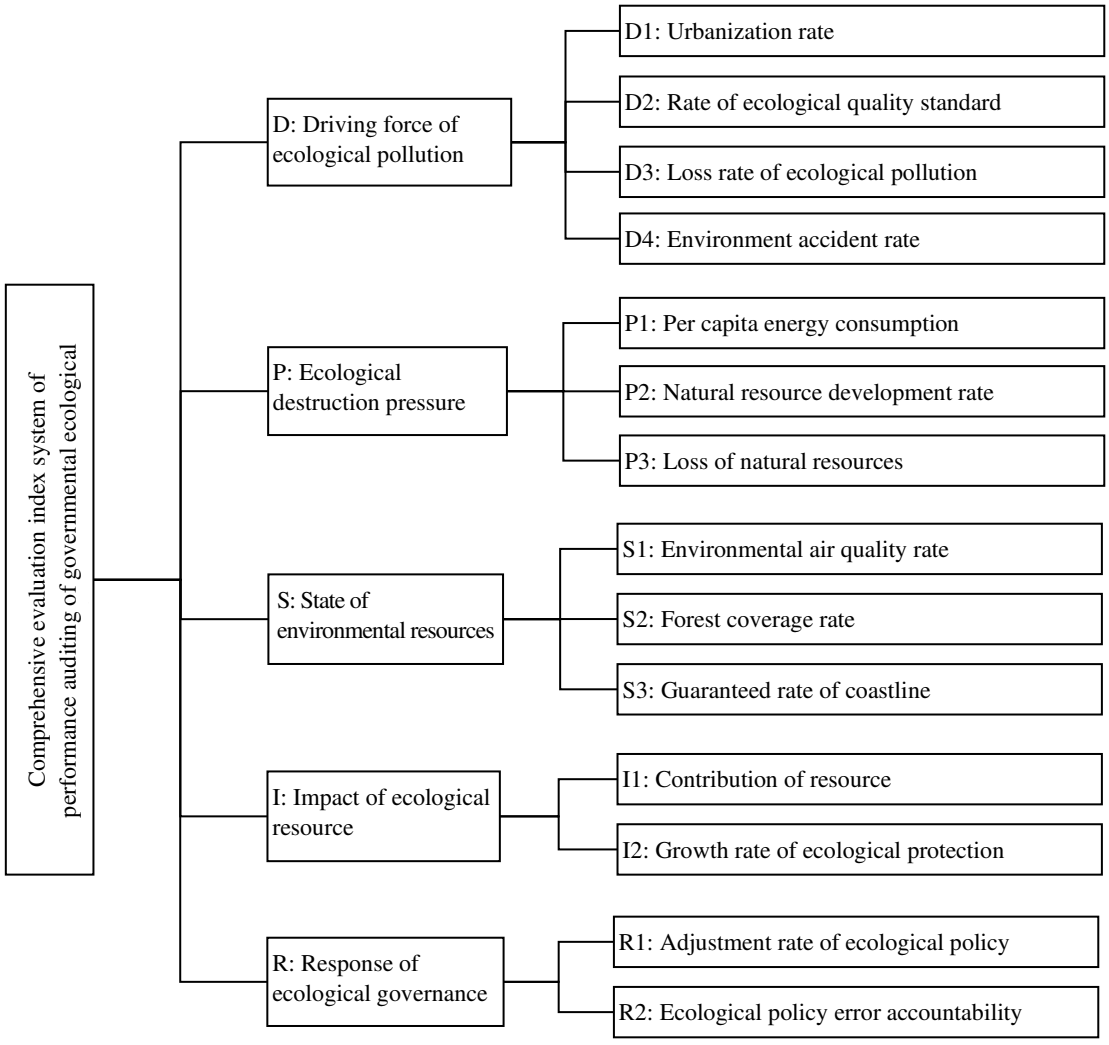

Figure 3. *Hierarchical structure of performance auditing of model in application*

The decision of fuzzy AHP is an interactive evaluation system intended to help decision makers from different backgrounds compile useful information from different weight vectors to make decisions. The data extraction process includes combinations of qualitative and quantitative data analysis, questionnaires, interviews, scoring by many experts from Fujian province administrative cities in China. For the purpose of

http://www.aloki.hu ● ISSN 1589 1623 (Print) ● ISSN 1785 0037 (Online)
DOI: http://dx.doi.org/10.15666/aeer/1706_1435914374

determining the correlation between evaluation criterions more accurately and faster than ever before, we determine relative importance of each criteria over another based on pair-wise comparison by a group decision. Thus, each decision maker individually can make out pair-wise comparison by using 1–9 scale.

In this paper, we take the evaluation index of ecological destruction pressure (P) as example, the mathematical model and solution procedure for performance auditing of governmental ecological environment are briefly depicted, which includes sub-indicator of per capita energy consumption (P1), natural resource development rate (P2) and loss of natural resources (P3). The pair-wise comparison matrix is show by using *Eq. 1* in the following:

1	1	1	3	2	2	1	1	2
1	1	1	2	3	4	2	1	2
1	1	1	4	1	2	1	2	3
1/2	1/2	1/3	1	1	1	1	1	2
1/4	1/3	1/2	1	1	1	1	2	3
1/2	1	1/4	1	1	1	8	1	7
1/2	1	1	1/2	1	1	1	1	1
1/2	1	1/2	1/3	1/2	1	1	1	1
1/3	1/2	1	1/7	1	1/8	1	1	1

Based on triangular fuzzy number judgment matrix theory and priority method, the fuzzy pair-wise comparison matrix is transformed into triangular fuzzy numbers by using *Eq. 2*, *Eq. 3* and *Eq. 4*, which is given as

1.000	1.000	1.000	3.000	2.000	2.667	1.333	1.333	2.333
0.417	0.611	0.361	1.000	1.000	1.000	3.333	1.333	4.000
0.444	0.833	0.833	0.325	0.833	0.708	1.000	1.000	1.000

By using fuzzy pair-wise comparison matrix, the synthesis values of different evaluation indexes can be calculated in the following:

5.333	4.333	6.000
4.750	2.944	5.361
1.770	2.667	2.542

Next, the complementary index set is composed of the evaluation indexes, which is given as

0.384	0.436	0.506
0.342	0.296	0.452
0.127	0.268	0.214

http://www.aloki.hu ● ISSN 1589 1623 (Print) ● ISSN 1785 0037 (Online)
DOI: http://dx.doi.org/10.15666/aeer/1706_1435914374

Then, the synthesis values respect to main goal can be calculated using the system and load characteristics in the following:

V(S1≥S2)= 1.000, V(S1≥S3)= 1.000.

Then, d'(C1)=min(1.000, 1.000)=1.0000.

V(S2≥S1)= 0.330, V(S2≥S3)= 1.000.

Then, d'(C2)=min(0.330, 1.000)=0.3296.

V(S3≥S1)= 106.446, V(S3≥S2)= 1.281.

Then, d'(C3)=min (106.446, 1.281)=1.281.

Thus, we can obtaine the values priority weights respect to main goal, which is given as

W=(0.383,0.126,0.491).

In the same way, we can calculate other weights of evaluation index of performance auditing of governmental ecological environment with similarity calculation method. So weights of sub-criteria to illustrate the steps used to evaluate five local governments are shown in *Table 2*.

Table 2. *The weights of multiple evaluation criteria*

Evaluation criteria	Local weights	Over weights	Rank
(D) Driving force of ecological pollution	0.358	0.358	1
(D1) Urbanization rate	0.138	0.049	10
(D2) Rate of ecological quality standard	0.187	0.067	8
(D3) Loss rate of ecological pollution	0.372	0.133	1
(D4) Environment accident rate	0.303	0.108	2
(P) Ecological destruction pressure	0.217	0.217	2
(P1) Per capita energy consumption	0.383	0.083	5
(P2) Natural resource development rate	0.126	0.027	14
(P3) Loss of natural resources	0.491	0.107	4
(S) State of environmental	0.106	0.106	5
(S1) Environmental air quality rate	0.273	0.029	13
(S2) Forest coverage rate	0.321	0.034	12
(S3) Guaranteed rate of coastline	0.406	0.043	11
(I) Impact of ecological resource	0.173	0.173	3
(I1) Contribution of resource	0.384	0.066	9
(I2) Growth rate of ecological protection	0.616	0.107	3
(R) Response of ecological governance	0.146	0.146	4
(R1) Adjustment rate of ecological policy	0.473	0.069	7
(R2) Ecological policy error accountability	0.527	0.077	6

Thus, the weights of multiple criteria of the comprehensive evaluation index system of performance auditing of governmental ecological environment is shown in *Fig. 4*.

In subsequent sections, we discuss how TOPSIS method is used for comprehensive evaluation of performance auditing of governmental ecological environment. Based on the survey of five local governments in China, this paper sums up the document data and makes some summary statistics, which is shown in *Table 3*.

Based on TOPSIS method, the establishing process includes constructing the fuzzy judgment matrix and integrating the weight vector is given in the following.

http://www.aloki.hu ● ISSN 1589 1623 (Print) ● ISSN 1785 0037 (Online)
DOI: http://dx.doi.org/10.15666/aeer/1706_1435914374

By using *Eq. 12*, we can get the index data after transformed and processed of five local governments, which is shown in *Table 4*.

Next, data normalization of index classification during system modeling has been given in *Table 5*.

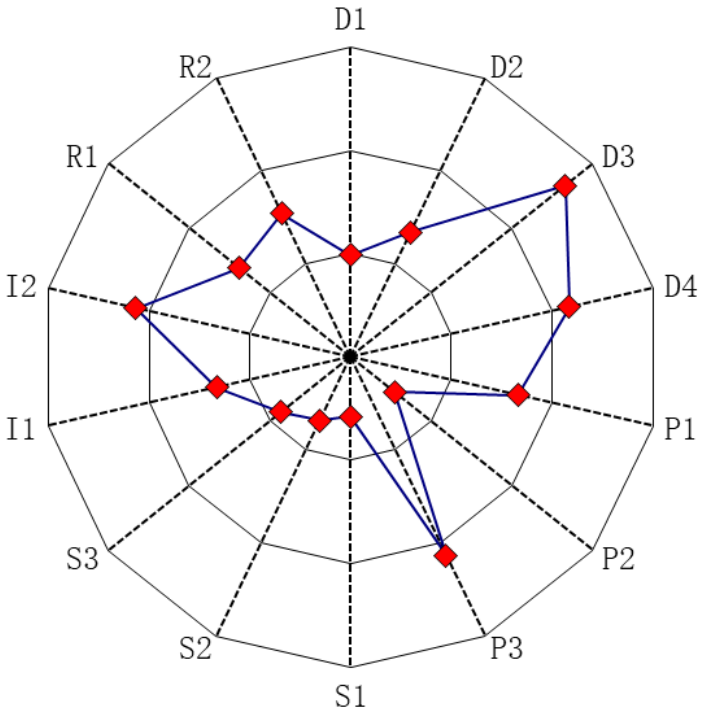

Figure 4. *The Spider chart of the weights of comprehensive evaluation indexes*

Table 3. *The summary statistics of five local governments*

Indexes	A local government	B local government	C local government	D local government	E local government
D1	87%	85%	76%	90%	82%
D2	98%	92%	94%	88%	94%
D3	15%	10%	18%	11%	19%
D4	18%	9%	21%	22%	16%
P1	2.756	2.213	2.451	2.346	2.524
P2	21%	25%	18%	28%	22%
P3	7%	10%	15%	17%	11%
S1	95%	90%	91%	89%	96%
S2	78%	70%	82%	72%	86%
S3	9.5	7.6	8.2	6.4	8.8
I1	90%	87%	95%	91%	93%
I2	81%	88%	78%	85%	82%
R1	12%	9%	10%	7%	8%
R2	91%	94%	96%	88%	92%

http://www.aloki.hu ● ISSN 1589 1623 (Print) ● ISSN 1785 0037 (Online)
DOI: http://dx.doi.org/10.15666/aeer/1706_1435914374

Table 4. *The index data after transformed and processed of five local governments*

Indexes	A local government	B local government	C local government	D local government	E local government
D1	0.870	0.850	0.760	0.900	0.820
D2	0.980	0.920	0.940	0.880	0.940
D3	0.850	0.900	0.820	0.890	0.810
D4	0.820	0.910	0.790	0.780	0.840
P1	2.756	2.213	2.451	2.346	2.524
P2	0.790	0.750	0.820	0.720	0.780
P3	0.930	0.900	0.850	0.830	0.890
S1	0.950	0.900	0.910	0.890	0.960
S2	0.780	0.700	0.820	0.720	0.860
S3	9.500	7.600	8.200	6.400	8.800
I1	0.900	0.870	0.950	0.910	0.930
I2	0.810	0.880	0.780	0.850	0.820
R1	0.880	0.910	0.900	0.930	0.920
R2	0.910	0.940	0.960	0.880	0.920

Table 5. *The data normalization of five local governments*

Indexes	A local government	B local government	C local government	D local government	E local government
D1	0.462	0.452	0.404	0.478	0.436
D2	0.470	0.441	0.451	0.422	0.451
D3	0.445	0.471	0.429	0.466	0.424
D4	0.442	0.491	0.426	0.421	0.453
P1	0.500	0.402	0.445	0.426	0.458
P2	0.457	0.434	0.475	0.417	0.451
P3	0.472	0.457	0.432	0.421	0.452
S1	0.461	0.436	0.441	0.431	0.465
S2	0.448	0.402	0.471	0.414	0.494
S3	0.520	0.416	0.449	0.350	0.482
I1	0.441	0.426	0.466	0.446	0.456
I2	0.437	0.475	0.421	0.459	0.443
R1	0.433	0.448	0.443	0.458	0.453
R2	0.441	0.456	0.465	0.427	0.446

Then, the distance of each local government from PIS and NIS with respect to each criterion are calculated with the help of basic principles and methods of TOPSIS.

The ranking of the five local governments is shown as

C*=(0.804, 0.475, 0.361, 0.197, 0.652).

Moreover, the ranking result of the five local governments is shown in *Fig. 5*.

http://www.aloki.hu ● ISSN 1589 1623 (Print) ● ISSN 1785 0037 (Online)
DOI: http://dx.doi.org/10.15666/aeer/1706_1435914374

Based on C* values, the ranking of the evaluation alternatives in descending order are A, E, B, C and D. Proposed model results indicate that A local government is the best alternative with C* value of 0.804. The result is a fundamental measure for raising the evaluation quality, which auditors can also put forward adequate audit findings and audit conclusions.

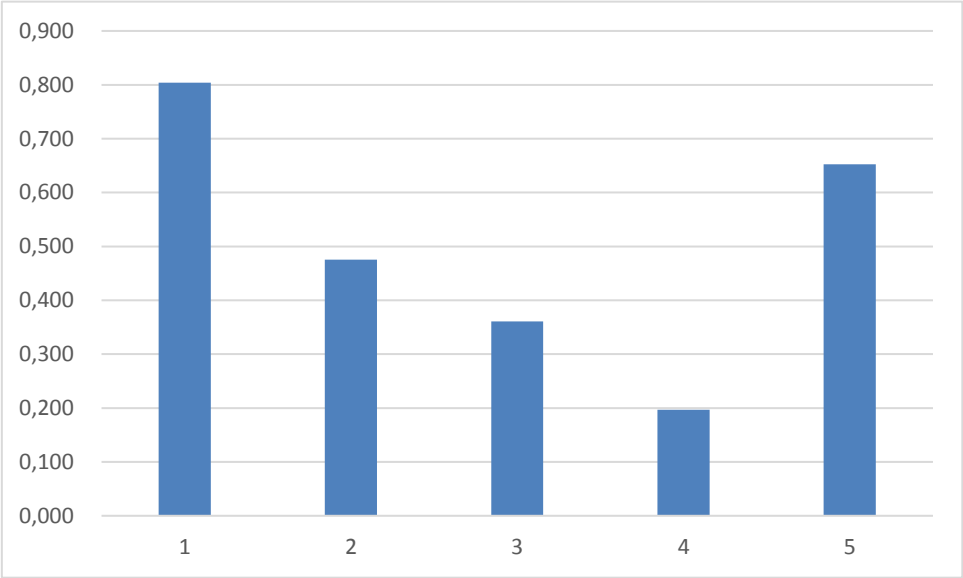

Figure 5. *The ranking results of the five local governments*

Discussion and implications

This Innovative Comprehensive Evaluation Index System is an Effective Means to the Performance Auditing of Governmental Ecological Environment in China

In this paper, we find that the comprehensive evaluation index system of performance auditing can better solve the dilemmas faced by China's governmental ecological environment. A comprehensive index system based on fuzzy AHP model is presented in this paper. AHP can be used to solve MCDM problem in many areas, so it has good applicability. Based on establishment of evaluation index system, AHP model is applied to realize the scientific computation on performance auditing of governmental ecological environment in china. This paper also based upon the comprehensive evaluation index system of fuzzy AHP model to come to a good conclusion, which corresponds to the actual case.

This Innovative Method Can Enrich the Evaluation Veracity and Efficiency of Performance Auditing

Based on fuzzy AHP and TOPSIS method to analyze and solve the evaluation problem is an innovative way to enrich the quality of performance auditing scientifically. The evaluation index system is put forward and the expert system based on AHP is established, so as to solve the evaluation problem of performance auditing combined with TOPSIS method effectively. And the evaluation process are divides into five levels and associates them with evaluating values to solve the problem of index standards for different policies governmental ecological environment. Finally, the result of the case in

http://www.aloki.hu ● ISSN 1589 1623 (Print) ● ISSN 1785 0037 (Online)
DOI: http://dx.doi.org/10.15666/aeer/1706_1435914374

Fujian Province of China shows that the improved method, this innovative method with fuzzy AHP and TOPSIS method increases the evaluation's veracity and efficiency of the comprehensive evaluation system.

This New Model of Performance Auditing Contributes to the Sustainable Development of Governmental Ecological Environment in China

Through our investigations, we can see that government and people have indicated that it gains the great benefits to take action to solve the ecological environment in China. Constructed intelligent evaluation technology that combines together of performance auditing and governmental ecological environment, it has extensive application prospects in sustainable development status on the scales of the Fujian Province and the whole country. This paper explains the meaning of sustainable development, analyses the importance of evaluating performance auditing of governmental ecological environment, and proposed the corresponding countermeasure.

Conclusions

The performance auditing evaluation of governmental ecological environment has become the important part of government auditing in many developed countries. This study mainly focused on discussing the theory feasibility by using the comprehensive evaluation index system of governmental ecological environment in performance auditing evaluation process. The performance auditing evaluation of governmental ecological environment is a synthetic analysis process from the macro-point of view. This paper gives some useful suggestion in the application of performance auditing evaluation system. Moreover, the solution is performed by using decision-making algorithms under fuzzy evaluation environment. In this paper, we extended the concept of fuzzy AHP and TOPSIS to develop a new method for solving MCDM problems in fuzzy environment. The comprehensive evaluation index system is built by using the concept and trait of performance auditing. Therefore, the proposed evaluation framework overcomes the various difficulties during the decision process of decision-making. In this paper, the illustrative application of the approved model was performed on the base of complex classification and processing. Moreover, the research methodology of this paper is established on the basis of fuzzy theory, AHP theoretical model and TOPSIS method. The results show that the comprehensive approach of evaluation index system has better decision precision and adaptability. This research is of significance not only to performance auditing of the governmental ecological environment, but also to performance auditing of other government environment protection policy. For future work, if the approved methods combining with other intelligent decision making techniques can be successfully applied to the evaluation system, then the decision efficiency and accuracy will be effectively increased.

Acknowledgements. This work was supported by the National Social Science Foundation in China (19BJY033); Ministry of Education Industry and Education Integration Project in China (201802154075); Major Social Science Planning Projects in Fujian Province (FJ2018JDZ014);Wenzhou Basic Scientific Research Project (R20190019 and R20190023); Zhejiang Social Sciences Planning Project (18NDJC128YB); Soft Science Project of Zhejiang Province (2020C35025); Wenzhou Social Sciences Planning Project (19wsk215 and 19wsk216); The Project of Culture Department in Zhejiang Province (zw2018052).

http://www.aloki.hu ● ISSN 1589 1623 (Print) ● ISSN 1785 0037 (Online)
DOI: http://dx.doi.org/10.15666/aeer/1706_1435914374

REFERENCES

[1] Ahmadipari, M., Hoveidi, H., Jafari, H. R., Pazoki, M. (2018): An integrated environmental management approach to industrial site selection by genetic algorithm and fuzzy analytic hierarchy process in geographical information system. – Global Journal of Environmental Science and Management-Gjesm 4(3): 339-350.

[2] Deveci, M., Canitez, F., Gokasar, I. (2018): WASPAS and TOPSIS based interval Type-2 fuzzy MCDM method for a selection of a car sharing station. – Sustainable Cities and Society 41: 777-791.

[3] Fero, J., Duncan, D. H., Spry, S. (2013): Evaluating the performance of a centralised government geodatabase in capturing publicly-funded natural resource management activities in Victoria, Australia. – Australasian Journal of Environmental Management 20(2): 101-115.

[4] Fleming, R. A., Barclay, H. J., Candau, J. N. (2002): Scaling-up an autoregressive time-series model (of spruce budworm population dynamics) changes its qualitative behaviour. – Ecological Modelling 149(1-2): 127-142.

[5] Groselj, P., Stirn, L. Z. (2018): Evaluation of several approaches for deriving weights in fuzzy group analytic hierarchy process. – Journal of Decision Systems 27: 217-226.

[6] Gupta, H. (2018): Assessing organizations performance on the basis of GHRM practices using BWM and fuzzy TOPSIS. – Journal of Environmental Management 226: 201-216.

[7] Gutierrez, L. A. (2015): The supreme audit at subnational level in Mexico: a performance's evaluation of the local supreme audit institutions (SAIs). – Revista Mexicana De Analisis Politico Y Administracion Publica 4(2): 141-165.

[8] Hategekimana, Y., Yu, L., Nie, Y., Zhu, J., Liu, F., Guo, F. (2018): Integration of Multi-Parametric fuzzy analytic hierarchy process and GIS along the UNESCO world heritage: a flood hazard index, Mombasa County, Kenya. – Natural Hazards 92(2): 1137-1153.

[9] Hussain, Z., Yang, M. S. (2018): Entropy for hesitant fuzzy sets based on Hausdorff metric with construction of hesitant fuzzy TOPSIS. – International Journal of Fuzzy Systems 20(8): 2517-2533.

[10] Ivanova, D., Haradinova, A., Vasileva, E. (2016): Environmental performance of companies with environmental management systems in Bulgaria. – Quality-Access to Success 17(152): 61-66.

[11] Johansen, T. R., Christoffersen, J. (2017): Performance evaluations in audit firms: evaluation Foci and dysfunctional behaviour. – International Journal of Auditing 21(1): 24-37.

[12] Kaur, R., Singh, S., Kumar, H. (2018): AuthCom: authorship verification and compromised account detection in online social networks using AHP-TOPSIS embedded profiling based technique. – Expert Systems with Applications 113: 397-414.

[13] Korucu, H., Simsek, B., Yartasi, A. (2018): A TOPSIS-based Taguchi design to investigate optimum mixture proportions of Graphene Oxide powder synthesized by hummers method. – Arabian Journal for Science and Engineering 43(11): 6033-6055.

[14] Kumar, K. A., Kumar, P. S., Madhusudanan, S., Pasupathy, V., Vignesh, P. R., Sankaranarayanan, A. R. (2017): A simplified model for evaluating best biodiesel production method: fuzzy analytic hierarchy process approach. – Sustainable Materials and Technologies 12: 18-22.

[15] Lourenzutti, R., Krohling, R. A., Reformat, M. Z. (2017): Choquet based TOPSIS and TODIM for dynamic and heterogeneous decision making with criteria interaction. – Information Sciences 408: 41-69.

[16] Manzoor, R., Zhang, T., Zhang, X., Wang, M., Pan, J. F., Wang, Z., Zhang, B. (2018): Single and combined metal contamination in coastal environments in China: current status and potential ecological risk evaluation. – Environmental Science and Pollution Research 25(2): 1044-1054.

http://www.aloki.hu ● ISSN 1589 1623 (Print) ● ISSN 1785 0037 (Online)
DOI: http://dx.doi.org/10.15666/aeer/1706_1435914374

[17] Minichilli, F., Santoro, M., Bianchi, F., Caranci, N., De Santis, M., Pasetto, R. (2017): Evaluation of the use of the socioeconomic deprivation index at area level in ecological studies on environment and health. – Epidemiologia & Prevenzione 41(3-4): 187-196.
[18] Mueller, P. (2011): Performance audit and evaluation similarities and differences between the performance audits of the German federal court of audit and evaluations on active labour market policies. – Zeitschrift Fur Evaluation 10(1): 17-38.
[19] Nazari, S., Fallah, M., Kazemipoor, H., Salehipour, A. (2018): A fuzzy inference-fuzzy analytic hierarchy process-based clinical decision support system for diagnosis of heart diseases. – Expert Systems with Applications 95: 261-271.
[20] Nehme, R. (2017): Performance evaluation of auditors: a constructive or a destructive tool of audit output. – Managerial Auditing Journal 32(2): 215-231.
[21] Paydar, L., Firouzi, S., Aminpanah, H. (2017): Energy audit of organic and non-organic olive (Olea europaea L.) production agro-ecosystems in Rudbar region, iron. – Revista De La Facultad De Agronomia De La Universidad Del Zulia 34(4): 497-517.
[22] Podani, J. (1994): Multivariate Data Analysis in Ecology and Systematics. – SPB Publishing, The Hague.
[23] Shi, S. X. (2017): Performance evaluation of urban ecological environment construction with interval-valued intuitionistic fuzzy information. – Journal of Intelligent & Fuzzy Systems 32(1): 1119-1127.
[24] Stephenson, P. (2015): Reconciling audit and evaluation? the shift to performance and effectiveness at the European court of auditors. – European Journal of Risk Regulation 6(1): 79-89.
[25] Tahri, M., Maanan, M., Maanan, M., Bouksim, H., Hakdaoui, M. (2017): Using fuzzy analytic hierarchy process multi-criteria and automatic computation to analyse coastal vulnerability. – Progress in Physical Geography 41(3): 268-285.
[26] Thompson, J. N. (1984): Insect Diversity and the Trophic Structure of Communities. – In: Huffaker, C. B. (ed.) Ecological Entomology. Wiley-Interscience, New York.
[27] Tóthmérész, B. (1995): Comparison of different methods for diversity ordering. – Journal of Vegetation Science 6: 283-290.
[28] Wang, J., Tang, L., Luo, Y., Ge, P. (2017): A weighted EMD-based prediction model based on TOPSIS and feed forward neural network for noised time series. – Knowledge-Based Systems 132: 167-178.
[29] Wind, Y., Saaty, T. L. (1980): Marketing applications of the analytic hierarchy process. – Management Science 26(7): 641-658.
[30] Zanardo, R. P., Mairesse Siluk, J. C., Savian, F. d. S., Smith Schneider, P. (2018): Energy audit model based on a performance evaluation system. – Energy 154: 544-552.

http://www.aloki.hu ● ISSN 1589 1623 (Print) ● ISSN 1785 0037 (Online)
DOI: http://dx.doi.org/10.15666/aeer/1706_1435914374

THE IMPACT OF THE GENETICALLY MODIFIED CROP'S VALUE ON THE SUSTAINABILITY OF AN ECOSYSTEM'S BIOMASS

HUANG, W. L.

School of Finance and Trade, Wenzhou Business College, 325000 Wenzhou, PR China
e-mail: huangwl@wzbc.edu.cn

(Received 6th Jun 2019; accepted 24th Oct 2019)

Abstract. This study uses the discrete-time optimal control models and numerical simulations of different scenarios to explore the impact of Genetically Modified (GM) Crop' value on the sustainability of an ecosystem's biomass. The results indicate that profit-maximizing farmers and a welfare-maximizing government would plant GM crops regardless of whether the biomass of the ecosystem remains sustainable (the ecological or evolutionary loss of GM crops) or not. However, the slightest loss of biomass (ecological loss) caused by the ecological mechanism of GM crops, due to their evolution mechanism, may become significant (evolutionary loss). Furthermore, the sustainability problem of biomass would become more severe due to the impact on identity preservation, improvement in planting technology and biotechnology, and climate change. However, conservation activities may help solve this problem.
Keywords: *genetically modified crop, bioeconomics, biodiversity, discrete-time optimal control model, the value of genetically modified crop*

Introduction

A genetically modified (GM) crop is the fastest developing crop, and it is governed by many regulatory systems dictated by international groups and countries. The focus of these regulatory systems should be the economic or ecological values of GM crops; however, the existing literature does not discuss all the value categories of GM crops. Thus, this paper proposes a numerical approach to evaluate GM crops, which combines economic value, ecological loss and evolutionary loss (Mutuc et al., 2013; Bradshaw, 2016). Many countries have discussed the values of GM crops and pronounced their regulations, as the regulation of GM crops in Belgium focuses on authorizing their production, use, and distribution (economic value), and limiting the potential release of GM crops into non-GM crop fields (ecological loss). Brazil has established rules for the production and marketing of GM crops and their release into the environment. The production and sale of GM crops are subject to very restrictive rules in France, and French legislation focuses on the potential release of GM crops into the environment and on labeling requirements (The Law Library of Congress, 2014).

The economic value of GM crops is defined as the additional profit of a crop-mix (with non-GM and GM crops) compared to a non-GM crop. Many studies have proved that profit from GM crops is higher than that from non-GM crops, as the former has larger yields. This is after considering its sustainability, health, and other related issues (James, 2005; Jacobsen et al., 2013; Mutuc et al., 2013; Blahova et al., 2014; Brookes and Barfoot, 2015; The International Service for the Acquisition of Agri-biotech Applications, 2016). As Qaim and Zilberman (2003) show that the pest-resistant GM crops substantially reduces pest damage and increases yields. Klümper and Qaim (2014) found the adoption of GM crops has reduced chemical pesticide use by 37%, increased crop yields and farmer profits by 22% and 68%.

http://www.aloki.hu ● ISSN 1589 1623 (Print) ● ISSN 1785 0037 (Online)
DOI: http://dx.doi.org/10.15666/aeer/1706_1437514390

The ecological and evolutionary loss of GM crops are defined as the negative value from the reduced biomass in the present and last stages of an evolutionary ecosystem with a crop-mix compared to a scenario with a non-GM crop. A GM crop negatively affects the biomass of ecosystems because it may increase the mortality of other species. The impact on this biomass by GM crops could follow the competition or predation of the evolution mechanism and produce an uncertain result of this biomass. The evolution mechanism consists of elements such as monoculture, mutation, natural selection, genetic drift, recombination, and gene flow. The United Nations (2010) and Jesse and Obrycki (2000) show that the promotion of superior breeds (e.g., a GM crop) can have side effects (Brock and Xepapadeas, 2003; Noailly, 2008).

We argue that the value of a GM crop could be the sum of its economic value and ecological and evolutionary loss. Therefore, this study will discuss these three perspectives through numerical simulations of discrete-time optimal control models on the biomass of an ecosystem with crop-mix and pest interactions. Moreover, the impact of identity preservation, the improvement in planting technology and biotechnology, and climate change on the value of GM crops and the biomass of an ecosystem would be discussed (Weitzman, 1998; Kouser and Qaim, 2013).

In short, the goal of this study is to analyze and simulate the effect of a GM crop' value on biomass sustainability. The remainder of this paper is organized as follows. In Section 2, we develop the Materials and Methods. The points are Farmer's GM crop management (FGM) Model and Government's GM crop Management (GGM) Model. In Section 3, we develop their results, the points are to perform the numerical simulations of FGM and GGM numerical simulations. The last two sections contain our discussions and concluding remarks.

Materials and methods

To develop an integrated valuation model of farmer's GM crop management, this study considered an ecosystem with crop-pest interactions, and this theoretical model should be adapted to many countries. The crops could be divided into GM, and non-GM crops, i=1, 2, and there was only one type of pests (Ives and Andow, 2002).

At time t, let $Q_{i,t}$ denote the farmer' s harvest of crop i, $D_i(Q_{i,t})$ and $S_i(Q_{i,t})$ be the inverse demand and supply function of crop i, so that the farm's revenue and cost function would be $R(Q_{1,t}, Q_{2,t}) = D_1(Q_{1,t})Q_{1,t} + D_2(Q_{2,t})Q_{2,t}$, and $C(Q_{1,t}, Q_{2,t}) = S_1(Q_{1,t})Q_{1,t} + S_2(Q_{2,t})Q_{2,t}$, respectively.

The objective of a representative farmer is to choose time paths $Q_{i,t}$ to maximize the farmer's profit function:

$$\sum_{t=1}^{T} \rho^t [D_1(Q_{1,t})Q_{1,t} + D_2(Q_{2,t})Q_{2,t} - S_1(Q_{1,t})Q_{1,t} + S_2(Q_{2,t})Q_{2,t}] \quad \text{(Eq.1)}$$

The time [0, T] is assumed fixed, and the discount factor is $\rho = (1+\eta)^{-1}$, where $\eta>0$ is the discount rate.

The biomass of this ecosystem (B_t) is defined as the sum of the biomass of the crop and pest at time t ($B_{c,t}, B_{p,t}$). In the existing literature, B_t could be measured by its biodiversity from different hierarchical categories. World Resources Institute et al. (1992)

http://www.aloki.hu ● ISSN 1589 1623 (Print) ● ISSN 1785 0037 (Online)
DOI: http://dx.doi.org/10.15666/aeer/1706_1437514390

divided biodiversity into three hierarchical categories: genetic diversity, species diversity, and ecosystem diversity (Vatn and Bromley, 1994; Mainwaring, 2001).

The amount of land for crop-mix is limited, and crops in the initial stage are all crop 2. The biomass of the ecosystem depends on the farmer's harvests of the crop-mix, and the growth and death rates of crop and pest. Biomass corresponds to the quantity of crop 2, based on the assumption that the genetic makeup of every individual in crop 1 is the same. Although GM crops can be planted in higher densities than conventional crops, for the sake of simplicity, this study does not consider this situation (Stanger and Lauer, 2006).

Based on the above assumptions, as in Brock and Xepapadeas (2003), the biomass evolution of the crop, pest, and ecosystem could be characterized as follow:

$$\begin{gathered} B_{c,t} - B_{c,t-1} = \left(B_{c,t-1} - Q^*_{1,t}\right)\left(g_c p_{c,t-1} - m_c p_{p,t-1}\right) - Q^*_{1,t} - Q^*_{2,t} \\ B_{c,t=0} = B_{c,0} \\ t=1, \ldots T \end{gathered} \tag{Eq.2}$$

$$\begin{gathered} B_{p,t} - B_{p,t-1} = B_{p,t-1}\left[g_p p_{p,t-1} - m_p \left(p_{c,t-1}\right)^{-1}\right] \\ B_{p,t=0} = B_{p,0} \\ t=1, \ldots T \end{gathered} \tag{Eq.3}$$

where:

$$\begin{gathered} p_{c,t} = B_{c,t}(B_{c,0})^{-1},\ p_{p,t} = B_{p,t}(B_{p,0})^{-1} \\ B_t = B_{c,t} + B_{p,t} \\ t=1, \ldots T \end{gathered} \tag{Eq.4}$$

$$\begin{aligned} B_t - B_{t-1} = {} & \left(B_{c,t-1} - Q^*_{1,t}\right)\left(g_c p_{c,t-1} - m_c p_{p,t-1}\right) \\ & + B_{p,t-1}\left[g_p p_{p,t-1} - m_p \left(p_{c,t-1}\right)^{-1}\right] - Q^*_{1,t} - Q^*_{2,t} \\ B_{t=0} = {} & B_{c,0} + B_{p,0} \end{aligned} \tag{Eq.5}$$

where g_c, g_p, m_c and m_p are the constant growth and death rates of the crop and pest. The pest biomass is exogenously assumed to be negatively related to the quantity of the GM crop.

For numerical simulations of the above model, this study assumes $D_1\left(Q_{1,t}\right) = P_1$, $D_2\left(Q_{2,t}\right) = P_2$, $S_1\left(Q_{1,t}\right) = \alpha + \beta Q_{1,t}$, $S_2\left(Q_{2,t}\right) = \alpha + \gamma Q_{2,t}$, and $\gamma > \beta > 0$. The optimal harvest quantity of crop 1 and crop 2 at time t ($Q^*_{1,t}$, $Q^*_{2,t}$) are derived from *Equation (1)*, which are $Q^*_{1,t} = (P_1 - \alpha)(2\beta)^{-1}$ and $Q^*_{2,t} = (P_2 - \alpha)(2\gamma)^{-1}$. These equations are used in combination with the growth *Equation (5)* of the ecosystem's biomass to obtain a measure of biomass in time [0, T].

Moreover, this study uses the GGM model which assess the value of biomass to discuss the economic, ecological, and evolutionary value of GM crops. In the GGM model, the welfare function on the biomass of an ecosystem is defined as $W(B_t) = W(B_{c,t}, B_{p,t})$. The social welfare function of the government is defined as follows:

http://www.aloki.hu ● ISSN 1589 1623 (Print) ● ISSN 1785 0037 (Online)
DOI: http://dx.doi.org/10.15666/aeer/1706_1437514390

$$\sum_{t=1}^{T} \rho^{t-1}\Big[\int_0^{Q_{1,t}} D_1(x)dx + \int_0^{Q_{2,t}} D_2(x)dx + W(B_{t-1}) - \int_0^{Q_{1,t}} S_1(x)dx - \int_0^{Q_{2,t}} S_2(x)dx - D_1(Q_{1,t})Q_{1,t} - D_2(Q_{2,t})Q_{2,t} + S_1(Q_{1,t})Q_{1,t} + S_2(Q_{2,t})Q_{2,t} \quad \text{(Eq.6)}$$

This study uses the Bellman state valuation function as a welfare measure of biomass, and it assumes that the welfare function in t is affected by the ecosystem's biomass in t-1. Brock and Xepapadeas (2003) obtained an endogenous measure (Bellman state valuation function) of the biomass' value, which is linked to ecologically/biologically oriented biomass metrics. There are more than 100 empirical papers that positively evaluate the biodiversity of indigenous cattle, threatened mammals, native plants, forests, wetlands, marine sanctuaries, ecosystems (Martin-Lopez et al., 2007; Matero and Saastamoinen, 2007; Siikamaki and Layton, 2007; Baral et al., 2008; Garcia et al., 2009; Yi et al., 2014). Many studies argue that the value of biodiversity includes the market value (a source of new industrial, agricultural, or pharmaceutical products) and non-market value (option, existence, and bequest values, culture and spiritual), as in Weitzman (1998), Polasky and Solow (1995), Nehring and Puppe (2002), and Brock and Xepapadeas (2003).

The purpose of the government is to maximize social welfare function, and the present value of the social welfare function at time t is $V(BS_{t-1}, C_t)$. Let $BS_{t-1} = (B_{c,t-1}, B_{p,t-1})$, $C_t = (Q_{1,t}, Q_{2,t})$ be the state and control vector associated with the maximization of (6), and $f(BS_{t-1}, C_t)$ be the vector of (5). The Hamiltonian function is as follows:

$$H_c(BS_{t-1}, C_t) = V(BS_{t-1}, C_t) + \rho\lambda_{p,t+1} f_p(BS_{t-1}, C_t),$$

For the sake of simplicity and comparability, we follow the assumptions in Section 2: $W(B_t) = W(BS_t) = \delta(B_{c,t} + B_{p,t})$, and δ is a constant value for a unit of biomass.

As the optimality conditions of the Hamiltonian function derived from (2), (3), (4) and (6) are self-referred, ($B_{c,t}$, $B_{p,t}$) could not be simulated by repeating the process. Thus, the assumptions of (2) and (3) are modified as:

$$B_{c,t} - B_{c,t-1} = \left(B_{c,t-1} - Q^*_{1,t}\right) - Q^*_{1,t} - Q^*_{2,t},\ B_{c,t=0} = B_{c,0}, \qquad t=1, \ldots T,$$
$$B_{p,t} - B_{p,t-1} = B_{p,t-1}(g_p - m_p),\ \ B_{p,t=0} = B_{p,0}, \qquad t=1, \ldots T,$$

The Hamiltonian function is:

$$H_c(BS_{t-1}, C_t) = P_1 Q_{1,t} + P_2 Q_{2,t} + \delta\left(B_{c,t-1} + B_{p,t-1}\right) - \alpha Q_{1,t} - \beta Q_{1,t}^2 - \alpha Q_{2,t} - \gamma Q_{2,t}^2 + \rho\lambda_{c,t+1}\left[\left(B_{c,t-1} - Q_{1,t}\right)(g_c - m_c) - Q_{1,t} - Q_{2,t}\right] + \rho\lambda_{p,t+1} B_{p,t-1}\left(g_p - m_p\right),$$

with the optimality conditions:

$$\partial H_c/\partial Q_{1,t} = P_1 - \alpha - 2\beta Q_{1,t} - \rho\lambda_{c,t+1}(1 + g_c - m_c) = 0,\ t=1, \ldots T, \quad \text{(Eq.7)}$$

$$\partial H_c/\partial Q_{2,t} = P_2 - \alpha - 2\gamma Q_{2,t} - \rho\lambda_{c,t+1} = 0,\ t=1, \ldots T, \quad \text{(Eq.8)}$$

http://www.aloki.hu ● ISSN 1589 1623 (Print) ● ISSN 1785 0037 (Online)
DOI: http://dx.doi.org/10.15666/aeer/1706_1437514390

$$\rho(\lambda_{c,t+1} - \lambda_{c,t}) = -\partial H_c/\partial B_{c,t-1} = \rho\lambda_{c,t+1}(g_c - m_c) - \delta,\ t=1, \ldots T, \quad \text{(Eq.9)}$$

$$\rho(\lambda_{p,t+1} - \lambda_{p,t}) = -\partial H_c/\partial B_{p,t-1} = \rho\lambda_{p,t+1}(g_p - m_p) - \delta,\ t=1, \ldots T, \quad \text{(Eq.10)}$$

$$\lambda_{c,T+1} = \lambda_{p,T+1} = 0, \quad \text{(Eq.11)}$$

$$B_{c,t} - B_{c,t-1} = \rho^{-1}\,\partial H_c/\partial\lambda_{c,t-1} = (B_{c,t-1} - Q_{1,t})(g_c - m_c) - Q_{1,t} - Q_{2,t},\ t=1, \ldots T \quad \text{(Eq.12)}$$

$$B_{p,t} - B_{p,t-1} = \rho^{-1}\,\partial H_c/\partial\lambda_{p,t-1} = B_{p,t-1}(g_p - m_p),\ t=1, \ldots T, \quad \text{(Eq.13)}$$

$$g_c = g_p = G,\ m_c = 0.5m_p = M,\ B_{c,0} = B_{p,0} = 0.5B_0 \quad \text{(Eq.14)}$$

To derive all the necessary information, the process begins in the final period (T = 20, in this case) and proceeds backward. From (7) and (8), the optimal harvest quantity of the GM crop and non-GM crop at time t ($Q_{1,t}^{**}$, $Q_{2,t}^{**}$) are $[P_1 - \alpha - \rho\lambda_{c,t+1}(1 + g_c - m_c)]/(2\beta)$ and $(P_2 - \alpha - \rho\lambda_{c,t+1})/(2\gamma)$, respectively. Since $\lambda_{c,21} = \lambda_{p,21} = 0$, (9) is used to solve $\lambda_{c,20} = \lambda_{p,20} = \delta/\rho$. The process is repeated and ($B_{c,t}$, $B_{p,t}$) is derived.

Results

Table 1 reports the values of the parameters obtained through the FGM model. We consider six cases to study the value of GM crops and the biomass of the ecosystem in time [0, 20]. The parameters in *Tables 1 and 3* are set as the existing literature, and the minor modification of the assumptions in the FGM and GGM model does not affect the findings of this study as many simulation results have been obtained from various parameter values. Many studies have discussed the higher price of the non-GM crop in Case 2. Lusk et al. (2001) and Chern et al. (2003) discussed consumer acceptance and willingness to pay for the non-GM crop. Many studies have also discussed the lower fixed cost of the two crops in Case 3, such as Marra et al. (2003). Raymond Park et al. (2010) examine the lower variable cost of GM crops in Case 4. McDowell et al. (2011) discussed the lower growth rate and higher death rate of the two crops in Case 5 and Case 6.

Case 0 is the initial scenario with Crop 2, and Case 1 is used as the baseline for the crop-mix. In Case 2, the non-GM crop is segregated by identity preservation and has a higher price. Case 3 is characterized by a lower fixed cost of the two crops for the improvement of planting technology, and Case 4 by the lower variable cost of GM crops for the improvement of biotechnology. Case 5 and Case 6 are characterized by the lower growth rate and higher death rate of the two crops due to climate change. Crop 1 and Crop 2 sell at the same price in all cases (except Case 2, for identity preservation), as in most cases, it is hard to distinguish GM crops from non-GM crops.

http://www.aloki.hu ● ISSN 1589 1623 (Print) ● ISSN 1785 0037 (Online)
DOI: http://dx.doi.org/10.15666/aeer/1706_1437514390

The solutions of Cases 0 ~ 6 are reported in *Table 2* and *Figure 1*. Our main conclusions on the value of the GM crop are as follows. First, the value of the GM crop is equal to its economic value in the FGM model, as farmers do not consider the value of biomass. Second, profit-maximizing farmers are likely to plant more GM crops than non-GM crops, as the value of GM crops is higher. Third, the improvement of planting technology and biotechnology increases the value of GM crops. Moreover, identity preservation and climate change do not affect the value of GM crops. These conclusions are in line with Brookes and Barfoot (2015), James (2005) and The International Service for the Acquisition of Agri-biotech Applications (2016).

Table 1. *Values of the Parameters obtained with the FGM Model*

	P_1	P_2	α	β	γ	G	M	B_0	η
Case 0	0	5.00	1.00	0	0.04	0.04	0.02	10,000.00	0.05
Case 1	5.00	5.00	1.00	0.02	0.04	0.04	0.02	10,000.00	0.05
Case 2	5.00	6.00	1.00	0.02	0.04	0.04	0.02	10,000.00	0.05
Case 3	5.00	5.00	0.50	0.02	0.04	0.04	0.02	10,000.00	0.05
Case 4	5.00	5.00	1.00	0.01	0.04	0.04	0.02	10,000.00	0.05
Case 5	5.00	5.00	1.00	0.02	0.04	0.02	0.02	10,000.00	0.05
Case 6	5.00	5.00	1.00	0.02	0.04	0.04	0.04	10,000.00	0.05

Note: these results are based on simulated data

Table 2. *Simulation using the FGM Model*

	The value of GM crop	**The value of non-GM crop**	**The biodiversity at T=20**		
			Crop	**Pest**	**Ecosystem**
Case 0	0	1,308.53	6,891.52	5,631.04	12,522.56
Case 1	2,617.06	1,308.54	3,320.71	4,211.80	7,532.51
Case 2	2,617.06	2,044.59	2,951.07	3,993.74	6,944.80
Case 3	3,312.22	1,656.11	2,765.40	3,875.60	6,641.01
Case 4	5,234.13	1,308.53	629.45	1,785.07	2,414.52
Case 5	2,617.06	1,308.54	1,954.48	1,968.84	3,923.32
Case 6	2,617.06	1,308.54	2,433.38	759.69	3,193.08
Mean	2,716.37	1,463.34	2,992.29	3,175.11	6,167.40

Note: these results are based on simulated data

Furthermore, our main conclusions about the impact of the introduction of a GM crop on the biomass of an ecosystem are as follow. First, the biomass of an ecosystem is decreased by the introduction of a GM crop. Second, the impact on the biomass of an ecosystem caused by a GM crop in the initial stage might be negligible, but even the slightest change could follow the evolution mechanism and lead to a considerable loss of an ecosystem's biomass. Third, climate change and the improvement in planting technology and biotechnology would decrease the biomass of an ecosystem. Fourth, the biomass of an ecosystem would not be improved and may even be worsened by identity preservation. These conclusions mean the sustainability of an ecosystem's biomass might not exist by the impact of the GM crop's economic value and are in line with Gregory et al. (2009), and the United Nations (2010).

http://www.aloki.hu ● ISSN 1589 1623 (Print) ● ISSN 1785 0037 (Online)
DOI: http://dx.doi.org/10.15666/aeer/1706_1437514390

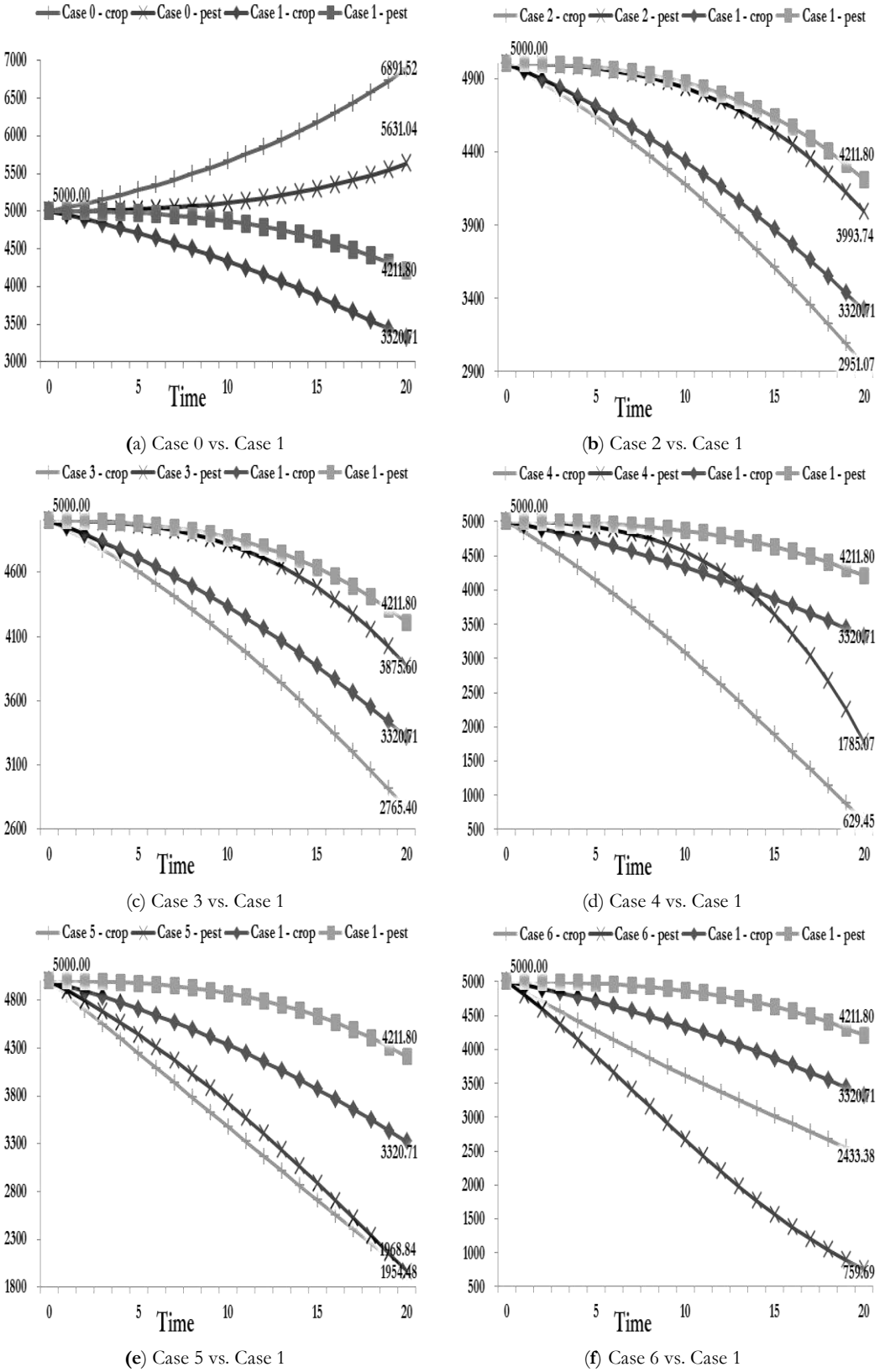

Figure 1. *The biodiversity of crop and pest at t = 0~20 for (a) Case 0 vs. Case 1, (b) Case 2 vs. Case 1, (c) Case 3 vs. Case 1, (d) Case 4 vs. Case 1, (e) Case 5 vs. Case 1, and (f) Case 6 vs. Case 1*

http://www.aloki.hu ● ISSN 1589 1623 (Print) ● ISSN 1785 0037 (Online)
DOI: http://dx.doi.org/10.15666/aeer/1706_1437514390

Table 3 reports the values of the parameters obtained through the GGM model. This study uses these cases to study the value of the GM crop, welfare, and the biomass in the GGM model. A non-GM crop characterizes Case 7, and Case 8 uses a crop-mix to discuss its effect of the increment of P_2 (Case 9), α (Case 10), β (Case 11), M (Case 13), δ (Case 14), and the decrement of G (Case 12). Case 14 can be explained by the growing recognition and activities of the public and private sector to conserve biomass (Bishop et al., 2008). A discount rate of 5 percent means that the discount factor (ρ) is about 0.95.

Table 3. *Values of the Parameters with the government's bit-crop management model*

	P_1	P_2	α	β	γ	G	M	δ	η	B_0
Case 7	0.00	5.00	1.00	0.00	0.04	0.04	0.02	1.00	0.05	10,000.00
Case 8	5.00	5.00	1.00	0.02	0.04	0.04	0.02	1.00	0.05	10,000.00
Case 9	5.00	6.00	1.00	0.02	0.04	0.04	0.02	1.00	0.05	10,000.00
Case 10	5.00	5.00	0.50	0.02	0.04	0.04	0.02	1.00	0.05	10,000.00
Case 11	5.00	5.00	1.00	0.01	0.04	0.04	0.02	1.00	0.05	10,000.00
Case 12	5.00	5.00	1.00	0.02	0.04	0.02	0.02	1.00	0.05	10,000.00
Case 13	5.00	5.00	1.00	0.02	0.04	0.04	0.04	1.00	0.05	10,000.00
Case 14	5.00	5.00	1.00	0.02	0.04	0.04	0.02	2.00	0.05	10,000.00

Note: these results are based on simulated data

The value of biomass is set far below the price of GM crops. The reason for this is that people's willingness to pay for conserving the biomass is lower than its market value. The solutions of Cases 7~14 are reported in *Table 4*, *Table 5*, and *Figure 2*.

Table 4. *Simulation of welfare and biodiversity in the GGM model*

	The present value of Welfare	**The biodiversity of the ecosystem in T=20**
Case 7	2,791.33	13,671.94
Case 8	5,176.34	8820.74
Case 9	5,897.93	8,517.03
Case 10	6,197.10	8,359.09
Case 11	7,677.02	6,399.28
Case 12	4,987.48	5,409.29
Case 13	4,912.35	4,281.26
Case 14	6,431.81	8,904.95
Mean	5,494.46	7,741.73

Note: these results are based on simulated data

Our main conclusions on the social welfare and value of GM crops are as follows. First, a welfare-maximizing government is likely to plant more GM crops than non-GM crops, as the welfare associated with GM crops is higher than that of non-GM crops. Second, identity preservation, improvement in planting technology and biotechnology, and biomass conservation activities could improve social welfare, but climate change could not. Third, the improvement in planting technology and biotechnology and biomass

http://www.aloki.hu ● ISSN 1589 1623 (Print) ● ISSN 1785 0037 (Online)
DOI: http://dx.doi.org/10.15666/aeer/1706_1437514390

conservation activities could improve the value of GM crops, but identity preservation and biomass conservation activities could not. Finally, the impact of climate change on the value of GM crops depends on the ability of species to migrate or cope with new scenarios.

Our conclusions about the impact of the introduction of a GM crop on the biomass of an ecosystem are as follows. First, the approaches of simulated biomass in each case of the GGM and FGM models are similar, the conclusions are in line with the solutions of the FGM model, and the modification of the assumptions in the GGM model does not affect the findings of this paper. Second, biomass conservation activities slow down the decline rate of biomass. These conclusions imply the sustainability of an ecosystem's biomass might not exist by the impact of the GM crop's economic value considering its ecological or evolutionary loss.

Table 5. *Simulation of the Value of GM crop in the GGM Model*

	The economic value of GM crop (B)	**The ecological value of GM crop (C)**	**The evolutionary value of GM crop (D=A-B-C)**	**The value of GM crop (A)**
Case 7	0.00	0.00	0.00	0.00
Case 8	2,615.07	-12.76	-217.30	2,385.01
Case 9	2,615.07	-12.76	-217.30	2,385.01
Case 10	3,310.22	-14.39	-230.41	3,065.42
Case 11	5,230.13	-25.52	-318.93	4,885.69
Case 12	2,614.53	-12.72	-180.17	2,421.64
Case 13	2,614.53	-12.72	-255.30	2,346.51
Case 14	2,609.08	-24.87	-428.06	2,156.15
Mean	2,701.08	-14.47	-230.93	2,455.68

Note: these results are based on simulated data

The simulated value of GM crops in previous studies (e.g., FGM model solution) is more significant than that in this study (e.g., GGM model solution), as the ecological and evolutionary loss of GM crops would decrease the optimal planned harvest of the welfare-maximizing government. Thus, the legal restrictions should consider the ecological and evolutionary loss of GM crops. Owing to public hostility and legal restrictions, no GM crops are currently planted in France (The Law Library of Congress, 2014). Based on the findings of FGM model are in line with previous studies, the differences between the presented approach and the referred literature are: 1. Their methods are different: the method of this paper is to use the numerical calculus and derivation of the hypothetic theory model which is the optimal control models with crop-mix and pest interactions, and the methods of the referred literature are most the statistical analysis of the different empirical models. 2. Their influencing factors are different: their influencing factors which discussed by this paper are identity preservation, improvement in planting technology and biotechnology, and climate change; their influencing factors of the referred literature are most the developing degree of country. As Klümper and Qaim (2014) use meta-analysis to prove that yield and profit gains for farmers of GM crops are higher in developing countries than those in developed countries.

http://www.aloki.hu ● ISSN 1589 1623 (Print) ● ISSN 1785 0037 (Online)
DOI: http://dx.doi.org/10.15666/aeer/1706_1437514390

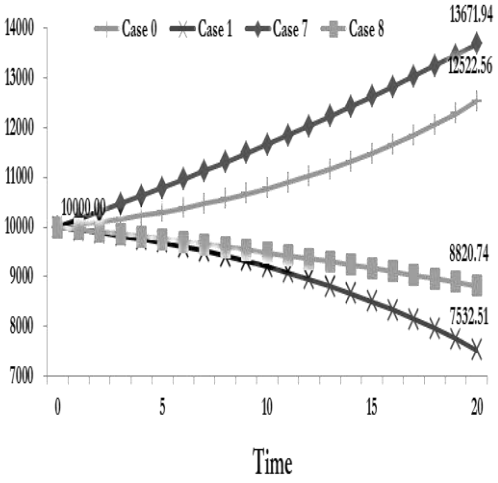

(a) Case 0 and Case 1 vs. Case 7 and Case 8

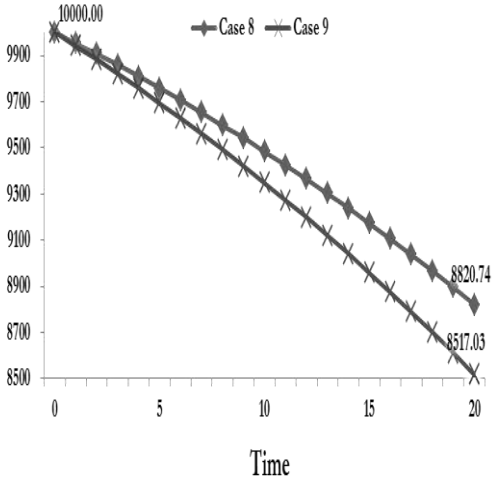

(b) Case 9 vs. Case 8

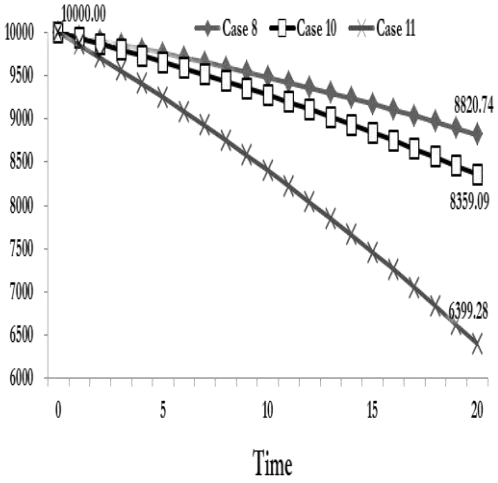

(c) Case 10 and Case 11 vs. Case 8

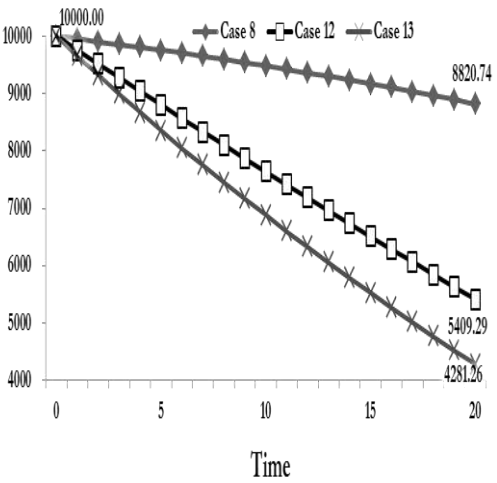

(d) Case 12 and Case 13 vs. Case 8

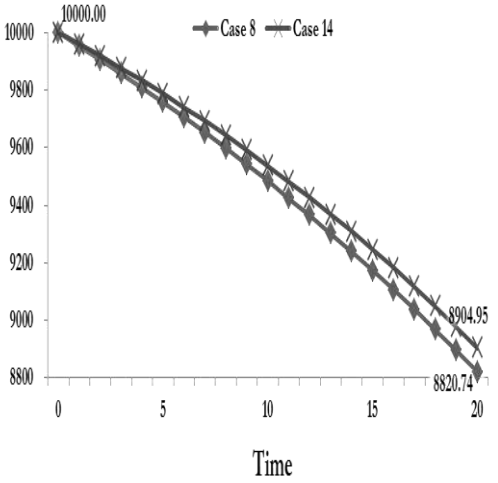

(e) Case 14 vs. Case 8

Figure 2. *The biodiversity of the ecosystem at t = 0 ~ 20 for (a) Case 0 and Case 1 vs. Case 7 and Case 8, (b) Case 9 vs. Case 8, (c) Case 10 and Case 11 vs. Case 8, (d) Case 12 and Case 13 vs. Case 8, and (e) Case 14 vs. Case 8*

http://www.aloki.hu ● ISSN 1589 1623 (Print) ● ISSN 1785 0037 (Online)
DOI: http://dx.doi.org/10.15666/aeer/1706_1437514390

Discussion

The major contributions of this study are as follows. First, this paper discussed the economic value and ecological and evolutionary loss of GM crops in agricultural systems simultaneously. Most existing studies discuss the economic value of GM crops as Klümper and Quaim (2014). Some studies discuss the ecological loss of GM crops as in Sanvido et al. (2007). Moreover, the only study discussing the evolutionary loss of GM crops is Flynn et al. (2010).

Second, this paper employs a discrete-time optimal control model and its numerical simulations to discuss the value of GM crops. We have not seen much research discussing the value of GM crops by the economic model and its numerical simulations. Therefore, this paper could increase the completeness of the theory on the value of GM crops. Third, this paper found that ecological loss of GM crops would be due to the mortality of its natural enemies, its monoculture, and competition with non-GM crops. The ecological loss of GM crops, which is the mortality of its natural enemies affected by GM crops, has been discussed in many previous studies. This paper also develops the ecological effect of GM crops to its monoculture and competition with non-GM crops. For the value of biodiversity is underestimated, government subsidies and fines for bioconservation are far below the market value of biology. As Chan et al. (1995) reported, the fine for illegal hunting is USD 50 (Kalmykia) and USD 60 (Kazakhstan) for one male Saiga antelope. However, the antelope can be sold at USD 764 (Hong Kong), USD 885 (Mainland China) and USD 920 (Taiwan) per kilogram.

Jose et al. (2006) studied the economic impact of GM crop in the Philippines by a Cobb-Douglas production function and a two-step econometric procedure where the initial stage consists of GM crop adoption decision and the second stage estimates the impact of GM crop adoption on net returns. The results showed that the yields of GM crop farmers (4,850 kg/ha) were significantly higher than those of the non-GM crop farmers (3,610 kg/ha) and there was a significant welfare effect (PhP 43.48 million) of using GM crop among farmers. James (2010) stated that the first 500 million GM crop hectares in 2005 took 10 years to reach, but only 5 years were needed to plant the second 500 million GM crop hectares (a total of 1 billion GM crop hectares) in 2010.

Fourth, this paper found that the evolutionary loss of GM crops is an aggregated ecological loss through the evolutionary mechanism. Also, this paper is one of the first to establish models to prove the reason why its existence. Fifth, this paper found that small ecological loss would develop into substantial evolutionary loss and might result in crop species rapidly becoming purebred. So the sustainability of an ecosystem's biomass might not exist by the impact of the GM crop's economic value regardless of considering its ecological or evolutionary loss or not. Very few studies focus on the relationship between the ecological loss of GM crops and its evolutionary loss, and how the relationship affects crops. Hence, this paper builds models to fill this research gap. Craft and Simpson (2001) used two models of competition between differentiated products to derive the value of biodiversity for use in new product development, and found the private value of marginal species (as biodiversity) is small, and its social value could be very model-dependent and parameter-specific. However, these findings would undervalue biodiversity, due to the static models and negligible nonmarket value of biodiversity. The Secretariat of the Convention on Biological Diversity (2010) shows that the promotion of superior breeds (like GM crop) would reduce biodiversity.

Magg et al. (2001) found greater European corn borer larval mortality observed for GM maize (84.6% after 4 days) when compared to non-GM maize (50.4% after 4 days).

http://www.aloki.hu ● ISSN 1589 1623 (Print) ● ISSN 1785 0037 (Online)
DOI: http://dx.doi.org/10.15666/aeer/1706_1437514390

Jesse and Obrycki (2000) proved that GM corn pollen naturally deposited on milkweed in a corn field (lethal effect) cause significantly higher mortality of monarch butterflies (20±3% at 48 h) than with no pollen (3±3% at 48 h) or with non-GM corn pollen (0%). Hilbeck et al. (1998) proved that the mortality rate for chrysopid larvae raised on GM corn-fed prey was 62.25±5.97% compared with 36.88±4.57% when raised on non-GM corn-fed prey.

Last but not least, this paper simulated the impact of the value of GM crops due to identity preservation, improvement in planting technology and biotechnology, climate change, and conservation activities. Therefore, this paper fills another significant research gap as there is a lack of studies on the impact of the value of GM crops by the change of external factors. Specifically, this paper selected and observed the changes in external factors to understand how that related to the value of GM crops. The impacts on the value of GM crops are also considered.

Conclusions

This paper introduces optimal control models and numerical analysis to analyze the value of GM crops, seen as the sum of economic value, and ecological, and evolutionary loss. In the FGM model, which does not consider the value of biomass, a profit-maximizing farmer plant more GM crops. However, even the slightest loss of biomass caused by GM crops in the initial stage may become significant following the evolution mechanism. Furthermore, the biomass of the crop, pest, and ecosystem worsens by identity preservation, improvement in planting technology and biotechnology, and climate change in the FGM and GGM model. In the GGM model, which takes into consideration the value of biomass, the welfare-maximizing government plants the GM crop. Moreover, the social welfare could be improved by identity preservation, the improvement in planting technology and biotechnology, and biodiversity conservation activities.

Based on the simulation results, our conclusions are as follow. First, a GM crop raises not only the mortality of its natural enemies and species on the same food chain or ecosystem, as reported by previous studies, but also causes the ecological loss resulting from monoculture of the GM crop and competition between GM and non-GM crops, as well as evolutionary loss, which is ecological loss determined by the evolutionary mechanism. Second, the biomass of the ecosystem has been over-damaged by the introduction of GM crops, and market mechanisms alone cannot determine the efficient use of GM crops. Third, using GM crops for profit maximization induces species to become purebred quickly (Noailly, 2008). Thus, the impact of Genetically Modified Crop' value on the sustainability of an ecosystem's biomass might be significantly negative.

The several limitations of this study may provide useful ideas for future researchers. The main limitation of this study is the simplification of the GGM model for the simulations. As this paper takes into consideration of the value of a GM crop is highly simplified for the GM crops are not homologous. The future study could take the discussion on the different transgene or the different type of genetic modification could have influenced the value of the GM crop. Or as the government's target for ecosystem biomass, which should be its sustainability, could be utilized for a discussion of its impact on the government's behavior. Moreover, the model can consider the risk of GM crops, as a single pathogen could wipe out entire species and their predators (Martin, 2000). Capellesso et al. (2016) proved that GM crops increase environmental impacts without

http://www.aloki.hu ● ISSN 1589 1623 (Print) ● ISSN 1785 0037 (Online)
DOI: http://dx.doi.org/10.15666/aeer/1706_1437514390

changing economic performance. Researchers can also study the impact of GM crops on the biomass of other species (as non-target insects). For example, they can study farm size for managing conventional corn-soybean rotation in a larger area than organic rotation (Lu et al., 2012; Delbridge et al., 2013). Finally, the bifurcation theory could be employed to assess the ecological and evolutionary value of GM crops, as it involves a complicated evolution mechanism and cannot be represented by an optimal control model.

REFERENCES

[1] Baral, N., Stern, M. J., Bhattarai, R. (2008): Contingent valuation of ecotourism in Annapurna conservation area, Nepal: implications sustainable park finance and local development. – Ecological Economics 66(2-3): 218-227. DOI: 10.1016/j.ecolecon. 2008.02.004.

[2] Bishop, J., Kapila, S., Hicks, F., Mitchell, P., Vorhies, F. (2008): Building Biodiversity Business. Shell International Limited and the International Union for Conservation of Nature: London, UK, and Gland, Switzerland. – International Union for Conservation of Nature, Switzerland. ISBN: 978-2-8317-1019-8.

[3] Blahova, P., Janda, K., Kristoufek, L. (2014): The perspectives for genetically modified Cellulosic Biofuels in the central European conditions. – Agricultural Economics 60(6): 247-259. EID: 2-s2.0-84903314070.

[4] Bradshaw, J. E. (2016): Plant Breeding: past, present, and future. – Springer: Berlin, Germany. ISBN: 978-3-319-23285-0.

[5] Brock, W. A., Xepapadeas, A. (2003): Valuing biodiversity from an economic perspective: a unified economic, ecological and genetic approach. – American Economic Review 93(5): 1597-1614. DOI: 10.1257/000282803322655464.

[6] Brookes, G., Barfoot, P. (2015): Environmental Impacts of Genetically Modified (GM) Crop Use 1996–2013: Impacts on Pesticide Use and Carbon Emissions. – GM Crops & Food 6(2): 103-133. DOI:10.1080/21645698.2015.1025193.

[7] Capellesso, A. J., Cazella, A. A., Schmitt Filho, A. L., Farley, J., Martins, D. A. (2016): Economic and environmental impacts of production intensification in agriculture: comparing transgenic, conventional, and agroecological maize crops. – Agroecology and Sustainable Food Systems 40(3): 215-236. DOI: 10.1080/21683565.2015.1128508.

[8] Chan, S., Maksimuk, A. V., Zhirnov, L. V., Nash, S. V. (1995): From Steppe to Store: The Trade in Saiga Antelope Horn. – TRAFFIC International, Cambridge, UK.

[9] Chern, W. S., Rickertsen, K., Tsuboi, N., Fu, T.-T. (2003): Consumer acceptance and willingness to pay for genetically modified vegetable oil and salmon: a multiple-country assessment. – AgBioForum 5(3): 105-112. Available online: http://agbioforum.org/v5n3/ v5n3a05-chern.pdf (accessed on 09/12/2017).

[10] Craft, A. B., Simpson, R. D. (2001): The value of biodiversity in pharmaceutical research with differentiated products. – Environmental and Resource Economics 18(1): 1-17. DOI: 10.1023/A:1011170024649.

[11] Delbridge, T. A., Fernholz, C., King, R. P., Lazarus, W. (2013): A whole-farm profitability analysis of organic and conventional cropping systems. – Agricultural systems 122: 1-10. DOI: 10.1016/j.agsy.2013.07.007.

[12] Flynn, K. J., Greenwell, H. C., Lovitt, R. W., Shields, R. J. (2010): Selection for fitness at the individual or population levels: modelling effects of genetic modifications in microalgae on productivity and environmental safety. – Journal of Theoretical Biology 263(3): 269-280. DOI: 10.1016/j.jtbi.2009.12.021.

[13] Garcia, S., Harou, P., Montagne, C., Stenger, A. (2009): Models for sample selection bias in contingent valuation: application to forest biodiversity. – Journal of Forest Economics 15(1-2): 59-78. DOI: 10.1016/j.jfe.2008.03.008.

http://www.aloki.hu ● ISSN 1589 1623 (Print) ● ISSN 1785 0037 (Online)
DOI: http://dx.doi.org/10.15666/aeer/1706_1437514390

[14] Gregory, R. D., Willis, S. G., Jiguet, F., Voříšek, P., Klvaňová, A., Van Strien, A., Huntley, B., Collingham, Y. C., Couvet, D., Green, R. E. (2009): An indicator of the impact of climatic change on European bird populations. – PLoS ONE 4(3): e4678. DOI: 10.1371/journal.pone.0004678.

[15] Hilbeck, A., Baumgartner, M., Fried, P. M. (1998): Effects of transgenic bacillus thuringiensis corn-fed prey on mortality and development time of immature Chrysoperla Carnea (Neuroptera: Chrysopidae). – Environmental Entomology 27(2): 480-487. DOI: 10.1093/ee/27.2.480.

[16] Ives, A., Andow, D. A. (2002): Evolution of resistance to Bt crops: directional selection in structured environments. – Ecology Letters 5(6): 792-801. DOI: 10.1046/j.1461-0248.2002.00392.x.

[17] Jacobsen, S. E., Sørensen, M., Pedersen, S. M., Weiner, J. (2013): Feeding the world: genetically modified crops versus agricultural biodiversity. – Agronomy for Sustainable Development 33(4): 651-662. DOI:10.1007/s13593-013-0138-9.

[18] James, C. (2005): Global Status of Commercialized Biotech/GM Crops: 2005. – ISAAA: NY, USA. ISBN 1-892456-38-9.

[19] James, C. (2010): Global Status of Commercialized Biotech/GM Crops: 2010. – ISAAA Brief No. 42. ISAAA: Ithaca, NY.

[20] Jesse, L. C. H., Obrycki, J. J. (2000): Field deposition of Bt transgenic corn pollen: Lethal effects on the Monarch butterfly. – Oecologia 125(2): 241-248. DOI: 10.1007/s004420000502.

[21] Jose, M., Yorobe, Jr., Cesar, B. Q. (2006): Economic impact of Bt corn in the Philippines. – The Philippine Agricultural Scientist 89(3): 258-267.

[22] Klümper, W., Qaim, M. (2014): A meta-analysis of the impacts of genetically modified crops. – PloS one 9(11): e111629. DOI: 10.1371/journal.pone.0111629.

[23] Kouser, S., Qaim, M. (2013): Valuing financial, health, and environmental benefits of Bt cotton in Pakistan. – Agricultural Economics 44(3): 323-335. DOI: 10.1111/agec.12014.

[24] Lu, Y., Jiang, K., Wu, Y., Guo, Y., Desneux, N. (2012): Widespread adoption of Bt cotton and insecticide decrease promotes Biocontrol services. – Nature 487(7407): 362-365. DOI: 10.1038/nature11153.

[25] Lusk, J., Daniel, M. S., Mark, D., Lusk, C. (2001): Alternative calibration and auction institutions for predicting consumer willingness to pay of Nongenetically modified corn chips. – Journal of Agricultural and Resource Economics 26(1): 40-57. Available online: http://www.waeaonline.org/jareonline/archives/26.1%20-%20July%202001/JARE,Jul2001,pp40, Lusk.pdf (accessed on 09/12/2017).

[26] Magg, T., Melchinger, A. E., Klein, D., Bohn, M. (2001): Comparison of Bt maize hybrids with their non-transgenic counterparts and commercial varieties for resistance to European corn borer and for agronomic traits. – Plant Breeding 120(5): 397-403. DOI: 10.1046/j.1439-0523.2001.00621.x.

[27] Mainwaring, L. (2001): Biodiversity, biocomplexity, and the economics of genetic dissimilarity. – Land Economics 77(1): 79-83. DOI: 10.2307/3146982.

[28] Marra, M., Pannell, D. J., Ghadim, A. A. (2003): The economics of risk, uncertainty, and learning in the adoption of new agricultural technologies: where are we on the learning curve? – Agricultural systems 75(2): 215-234. DOI: 10.1016/s0308-521x(02)00066-5.

[29] Martin, S. W. (2000): Crop strength through diversity. – Nature 406(6797): 681-682. DOI: 10.1038/35021152.

[30] Martin-Lopez, B., Montes, C., Benayas, J. (2007): Influence of user characteristics on valuation of ecosystem services in Doñana natural protected area (South-West Spain). – Environmental Conservation 34(3): 215-224. DOI: 10.1017/s0376892907004067.

[31] Matero, J., Saastamoinen, O. (2007): In search of marginal environmental valuations - ecosystem services in Finnish forest accounting. – Ecological Economics 61(1): 101-114. DOI: 10.1016/j.ecolecon.2006.02.006.

http://www.aloki.hu ● ISSN 1589 1623 (Print) ● ISSN 1785 0037 (Online)
DOI: http://dx.doi.org/10.15666/aeer/1706_1437514390

[32] McDowell, N. G., Beerling, D. J., Breshears, D. D., Fisher, R. A., Raffa, K. F., Stitt, M. (2011): The interdependence of mechanisms underlying climate-driven vegetation mortality. – Trends in Ecology & Evolution 26(10): 523-532. DOI: 10.1016/j.tree.2011.06.003.

[33] Mutuc, M., Rejesus, R. M., Yorobe Jr., J. M. (2013): Which farmers benefit the most from Btcorn adoption? estimating heterogeneity effects in the Philippines. – Agricultural Economics 44(2): 231-239. DOI:10.1111/agec.12006.

[34] Nehring, K., Puppe, C. (2002): A theory of diversity. – Econometrica 70(3): 1155-1198. DOI: 10.1111/1468-0262.00321.

[35] Noailly, J. (2008): Coevolution of economic and ecological systems: an application to agricultural pesticide resistance. – Journal of Evolutionary Economics 18(1): 1-29. DOI: 10.1257/000282803322655464.

[36] Polasky, S., Solow, A. R. (1995): On the value of a collection of species. – Journal of Environmental Economics and Management 29(3): 298-303. DOI: 10.1006/jeem.1995.1048.

[37] Qaim, M., Zilberman, D. (2003): Yield effects of genetically modified crops in developing countries. – Science 299(5608): 900-902. DOI: 10.1126/science.1080609.

[38] Raymond Park, J., McFarlane, I., Hartley Phipps, R., Ceddia, G. (2010): The role of transgenic crops in sustainable development. – Plant Biotechnology Journal 9(1): 2-21. DOI: 10.1111/j.1467-7652.2010.00565.x.

[39] Sanvido, O., Romeis, J., Bigler, F. (2007): Ecological Impacts of Genetically Modified Crops: Ten Years of Field Research and Commercial Cultivation. – In: Fiechter, A., Sautter, C. (eds.) Green Gene Technology. Advances in Biochemical Engineering/Biotechnology 107. Springer; Berlin, Heidelberg, Germany. ISBN: 978-3-540-71323-4.

[40] Siikamaki, J., Layton, D. F. (2007): Discrete choice survey experiments: a comparison using flexible methods. – Journal of Environmental Economics and Management 53(1): 122-139. DOI: 10.1016/j.jeem.2006.04.003.

[41] Stanger, T. F., Lauer, J. G. (2006): Optimum plant population of Bt and non-Bt corn in Wisconsin. – Agronomy Journal 98(4): 914-921. DOI: 10.2134/agronj2005.0144.

[42] The International Service for the Acquisition of Agri-biotech Applications (2016): Global Status of Commercialized Biotech/GM Crops: 2016. – ISAAA: NY, USA. ISBN 978-1-892456-66-4.

[43] The Law Library of Congress (2014): Restrictions on Genetically Modified Organisms: Argentina, Belgium, Brazil, Canada, China, Egypt, England and Wales, European Union, France, Germany, Israel, Italy, Japan, Lebanon, Mexico, Netherlands, New Zealand, Norway, Russian Federation, South Africa, South Korea, Sweden, United States. – International Protocols, Bibliography. Available online: https://www.loc.gov/law/help/restrictions-on-gmos/restrictions-on-gmos.pdf (accessed on 09/12/2017).

[44] The Secretariat of the Convention on Biological Diversity (2010): Global Biodiversity Outlook 3. – Montréal (http://gbo3. cbd. int/) Phil. Trans. R. Soc. B (Vol. 9).

[45] United Nations (2010): Global Biodiversity Outlook 3. – United Nations: NY, USA. ISBN: 978-9-292-25220-5.

[46] Vatn, A., Bromley, D. W. (1994): Choices without prices without apologies. – Journal of Environmental Economics and Management 26(2): 129-148. DOI: 10.1006/jeem.1994.1008.

[47] Weitzman, M. L. (1998): The Noah's ark problem. – Econometrica 66(6): 1279-1298. DOI: 10.2307/2999617.

[48] World Resources Institute; the World Conservation Union; United Nations Environment Program (1992): Global Biodiversity Strategy: Guideline for Action to Save, Study and Use Earth's Wealth Sustainably and Suitably. – World Resources Institute: Washington, D. C. USA. ISBN: 0-915825-74-0.

http://www.aloki.hu ● ISSN 1589 1623 (Print) ● ISSN 1785 0037 (Online)
DOI: http://dx.doi.org/10.15666/aeer/1706_1437514390

[49] Yi, Z. F., Cannon, C. H., Chen, J., Ye, C. X., Swetnam, R. D. (2014): Developing indicators of economic value and biodiversity loss for rubber plantations in Xishuangbanna, southwest China: a case study from Menglun township. – Ecological Indicators 36: 788-797. DOI: 10.1016/j.ecolind.2013.03.016.

http://www.aloki.hu ● ISSN 1589 1623 (Print) ● ISSN 1785 0037 (Online)
DOI: http://dx.doi.org/10.15666/aeer/1706_1437514390

IDENTIFICATION OF PHOSPHORUS SPECIES AND BIO-AVAILABILITY IN PRIMARY, SECONDARY AND DIGESTED SLUDGE

ZHANG, S. X.[1] – CUI, W. Z.[1] – LIU, D. F.[2] – HUANG, W. L.[2,3*]

[1]*School of Civil Engineering, Shijiazhuang Tiedao University, Shijiazhuang 050043, China*

[2]*Key Laboratory of Pollution Process and Environmental Criteria, Ministry of Education, College of Environmental Science and Engineering, Nankai University, Tianjin 300350, China*

[3]*Graduate School of Life and Environmental Sciences, University of Tsukuba, 1-1-1 Tennodai, Tsukuba, Ibaraki 305-8572, Japan*

**Corresponding author*
e-mail: huangwenli@nankai.edu.cn; phone: +86-22-2350-1117

(Received 7th Jun 2019; accepted 10th Oct 2019)

Abstract. The species and bio-availability of phosphorus (P) in primary, secondary and digested sludge were fractionated and further analyzed in this study. Results showed that inorganic P (IP) was the primary P fraction in the secondary sludge and digested sludge, in which non-apatite IP (NAIP) amounted to 91.6% and 69.3% of total IP, respectively. Organic P (OP), accounting for about 71.7% of total P (TP), was the dominant P composition in primary sludge. The content of bio-available P was about 9.7, 43.4, 29.8 mg-P/g-TS in primary sludge, secondary sludge and digested sludge, respectively, suggesting secondary sludge is the optimal choice when land application of sewage sludge is taken into consideration, followed by digested sludge and primary sludge. Polyphosphate and orthophosphate, comprising approximately 54.3% and 89.2% of TP, were the dominant P species in the secondary sludge and digested sludge, respectively. Monoester-P (54.6% of TP in extract) and diester- P (24.1%) were identified as OP species in primary sludge by Phosphorus-31 nuclear magnetic resonance (^{31}PNMR). The present results would be helpful for P recovery and recycling from sewage sludge in wastewater treatment plants.
Keywords: *sewage sludge, P bio-availability, P species, SMT protocol*

Introduction

Phosphorus (P) is one of the essential mineral elements for all living organisms, which accounts for around 2 - 4% of the dry weight of most cells (Karl, 2000). The extensive application of P fertilizers is one of the main reasons that the current crop production has been able to meet the food demand and security associated with an ever-expanding world population. It is estimated that approximately 90% of the P derived from phosphate rock is used in agriculture as fertiliser (Christen, 2007). However, on one hand, phosphate rock is a non-renewable resource which is estimated to be exhausted in 50 - 100 years with a peak in its production occurring in 2030s if the growth of demand for fertilizers remains at 3% per year (Cordell et al., 2009; Gilbert, 2009; Hao et al., 2013). On the other hand, according to the statistics of the US Geological Survey (USGS, 2014), eight countries or areas including United States, Algeria, China, Jordan, Morocco and Western Sahara, Russia, South Africa and Syria control 93.9% of global phosphate rock reserves. In order to secure domestic raw materials, some major producer countries have designated phosphorous as a strategic resource and restricted export of the P rock or in the form of processed

http://www.aloki.hu ● ISSN 1589 1623 (Print) ● ISSN 1785 0037 (Online)
DOI: http://dx.doi.org/10.15666/aeer/1706_1439114402

and chemical products with added value in recent years (Cordell et al., 2009). With these trends, the price of P rock has been increasing in the international trade market. Therefore, P resource protection and P recycling is prerequisite for a sustainable agriculture and society on a global scale, especially for the countries that lack P resources.

Sewage sludge, a by-product of biological wastewater treatment process, is regarded as a potential P reservoir due to its high production and P content (Xu et al., 2012). Various P recovery technologies from sewage sludge have been developed, including incineration, alkaline/acid extraction, thermal treatment, phosphorous crystallization as HAp (hydroxylapatite) and MAP (magnesium ammonium phosphate) (Arakane et al., 2006; Hao et al., 2013; Hosni et al., 2008). However, the costs of these projects are too high due to their complex processes for phosphorus recovery. Land application of sewage sludge as P fertilizer is now very attractive, because it not only solves the sludge disposal problem but also benefits crop production (Singh and Agrawal, 2008). In US and EU-15, land application of sludge now is the predominant choice for sludge management (41% in US and 53% in EU-15) (Catallo and Comeaux, 2008; He et al., 2018; Kelessidis and Stasinakis, 2012; Zhang et al., 2018). In China, about 45% and 3.5% of sludge is applied to agriculture and gardening, respectively. It is a well-known fact that Japan is a P resource- poor country. While the percentage of treated sewage sludge for farmland and green areas has been stable at around 14% for many years in Japan, it is much lower than those in other countries (UN-HABITAT, 2009). Thus land application of sewage sludge as P fertilizer has great development potential to alleviate P resource shortage to a certain extent in Japan.

Generally, P content in sewage sludge accounts for about 0.3-4.8% of total solid (Fytili and Zabaniotou, 2008). But it is well known that not all the forms of P exhibit similar mobility and bio-availability in the sludge, identification of the P fraction and species in the sludge is beneficial for both land application of sewage sludge as P fertilizer and understanding the characteristics and function of P in different sludge. Primary sludge, secondary sludge and digested sludge are the three main types of sludge produced from WWTP. Previous study mainly focus on investigate the bio-availability of P in secondary sludge and P species in secondary sludge and digested sludge. Xie et al. (2011) reported that 75%-88.7% of TP in secondary sludge possesses high mobility and bio-availability. Poly-P and ortho-P was the major P in enhanced P removal activated sludge and digested sludge, respectively (Hinedi et al., 1989; Uhlmann et al., 1990; Lalmi and Hadef, 2017). However, to date, little detailed and comprehensively information could be found about the P fractions and species in primary sludge, secondary and digested sludge.

This study aimed to investigate the P bio-availability and species in primary sludge, secondary and digested sludge. The Standards, Measurements and Testing (SMT) protocol was applied to analyze the fractionation of P in sewage sludge and to evaluate the mobility and bio-availability of P in various sludge. Solution 31P nuclear magnetic resonance (^{31}P NMR) spectroscopy is employed to characterize the inorganic and organic phosphorus species in sewage sludge. It is expected that this work will be useful for P utilization and recovery from sewage sludge, especially when agriculture utilization of sludge is taken into consideration.

http://www.aloki.hu ● ISSN 1589 1623 (Print) ● ISSN 1785 0037 (Online)
DOI: http://dx.doi.org/10.15666/aeer/1706_1439114402

Materials and methods

Sewage sludge sample

Sludge samples were collected from a WWTP treating domestic wastewater in Shimodate, Ibaraki Prefecture, Japan, on October, 2018. The process flow diagram of the WWTP is shown in *Figure 1*. 50 L sludge samples were collected from the primary tank, secondary sedimentation tank and digestion tank, respectively. The collected sludge was kept in a refrigerator at 4 °C and analyzed within 2 days.

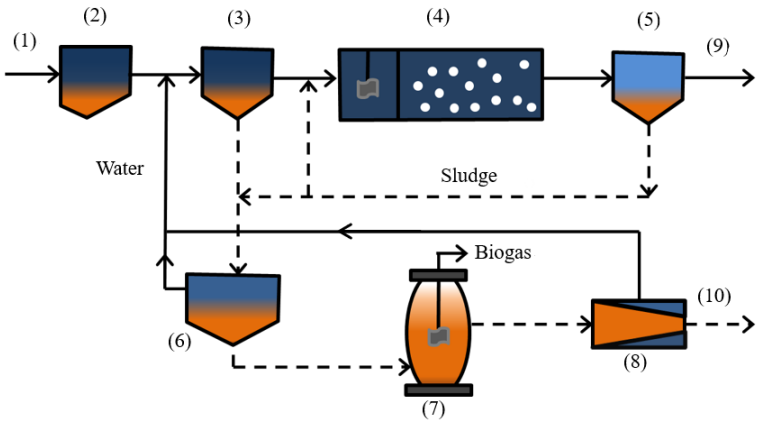

Figure 1. *Process flow diagram of wastewater treatment plant in Shimodate, Ibaraki Prefecture, Japan. (1) influent, (2) grid, (3) primary settling tank, (4) aeration tank, (5) secondary settling tank, (6) sludge concentration tank, (7) digestion tank, (8) sludge dewatering, (9) effluent, (10) sludge disposal*

Phosphorus fractionation in sludge

In this study, the SMT programme extraction protocol was applied to analyze P fractions in all sludge samples (*Fig. 2*), which has been widely used in soil, sediment and sewage sludge samples (Ruban et al., 1999; Medeiros et al., 2005; Zhao, 2012).

After sequential extraction based on the SMT method, P in sludge was fractionated into the following 5 categories: (1) concentrated HCl-extractable P, namely total P (TP), (2) organic P (OP), (3) inorganic P (IP), (4) non-apatite inorganic P (NAIP, the P fraction associated with oxides and hydroxides of Al, Fe and Mn), and (5) apatite P (AP, the P fraction associated with Ca). In order to avoid the transformation of P species in sludge during preparation, the samples centrifuged at 6000×g for 10 min at 4 °C, and then the residue were frozen immediately at -80 °C, lyophilized at -50 °C for 48 h and stored at -20 °C until analysis. The P concentration in the supernatant collected after extraction was determined with molybdenum blue method. All of the experiments were done in triplicate, and the average data was reported.

Extraction of P from sludge

PCA and NaOH extraction methods have been efficiently used for IP and OP extraction from sludge, soil and sediment samples (Ahlgren et al., 2005; Daumer et al., 2008; Vestergren et al., 2012; Saric et al., 2016). In this study, the PCA-NaOH extraction procedure was applied to fractionate and characterize P in the sludge samples according to the schematic diagram shown in *Figure 3*. Before extraction, a certain

http://www.aloki.hu ● ISSN 1589 1623 (Print) ● ISSN 1785 0037 (Online)
DOI: http://dx.doi.org/10.15666/aeer/1706_1439114402

amount of sludge was washed twice with 100 mM NaCl solution (4 °C) with the supernatant being discharged. After extraction, neutralization was conducted immediately to minimize P transformation. 2 ml of the resultant supernatant was taken for TP, IP and OP analysis. The remaining extracts were freeze-dried at -50 °C for 48 h, and the dried PCA-NaOH extracts were uniformly mixed and them stored at -20 °C till 31P NMR analysis.

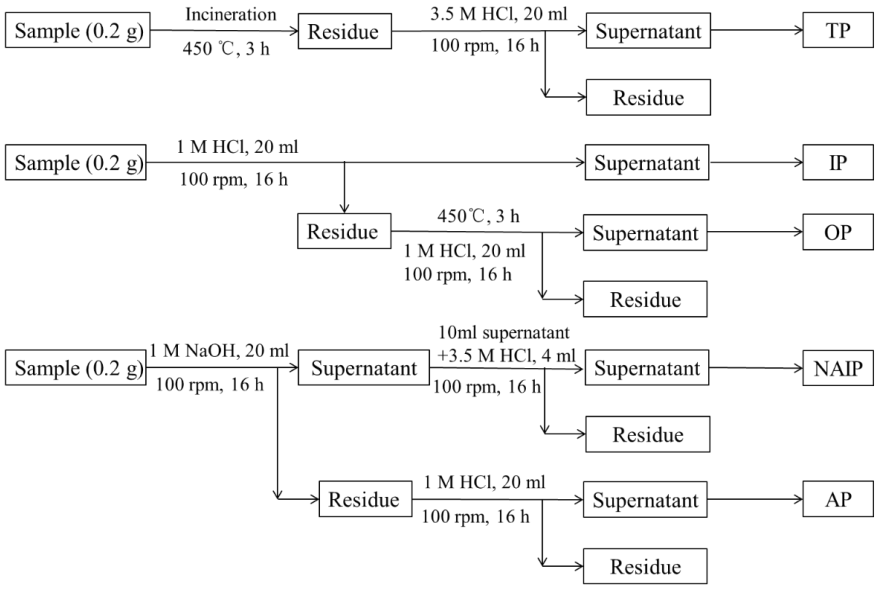

Figure 2. *The schematic diagram of the SMT protocol*

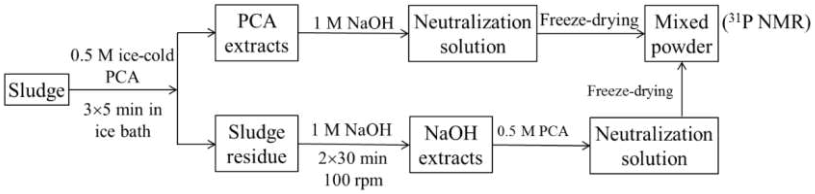

Figure 3. *Schematic diagrams for the fractionation and characterization of various forms of P in sewage sludge*

Chemical analysis

Mixed liquor (volatile) suspended solids (ML(V)SS), chemical oxygen demand (COD), ammonia nitrogen (NH_4-N), and phosphorus (PO_4-P) were measured in accordance with the standard methods (APHA, 2012). Total concentration of phosphorus in the liquid was determined with molybdenum blue method after digestion by potassium persulfate at 120 °C. Metal ions in sludge samples were quantified after the sludge samples being digested and filtered through 0.22 μm cellulose nitrate membrane filters (Nalgene). 0.1 g of dried sludge was digested in a mixture of 3 ml hydrochloric acid (37%, Wako), 1 ml nitric acid (70%, Wako), and 1 ml perchloric acid (60%, Wako) on an electric heating plate for 10 min. The concentration of each metal was measured by inductively coupled plasma mass spectrometry (ICP-MS, ELAN DRC-e, Perkin Elmer, USA).

http://www.aloki.hu ● ISSN 1589 1623 (Print) ● ISSN 1785 0037 (Online)
DOI: http://dx.doi.org/10.15666/aeer/1706_1439114402

^{31}P NMR analysis

To obtain the ^{31}P NMR spectrum, 200 mg of freeze-dried sludge extracts were re-dissolved in 0.8 ml of 1 M NaOH and 0.2 ml D_2O and then 0.2 ml of 100 mM EDTA solution was added. The dose of EDTA and NaOH solutions was to minimize the interference of divalent/trivalent cations and to adjust pH above 12.0, respectively, to ensure consistent chemical shifts and optimal spectral resolution during the ^{31}P NMR measurement.

The ^{31}P NMR spectrum was obtained by using a Bruker Avance-600 MHz NMR Spectrometer at 242.94 MHz. 90 °C of pulse width, 25 °C of regulated temperature, and acquisition time of 0.67 s (with relaxation delay of 2 s) were applied in the experiments. To obtain accurate phosphorus forms, spectra were collected immediately after preparation and the process was finished within 2 h to minimize transformation of phosphorus species. Chemical shifts of signals were determined relatively to an external standard of 85% H_3PO_4 via signal lock. The peaks were assigned to P species according to the reports in literature with peak areas calculated by integration (Turner, 2003; Turner et al., 2004; Zhang et al., 2013; Reis et al., 2017).

Statistical analysis

All values presented are the means of independent triplicates ± standard deviation. One-way analysis of variance was used to compare the experimental results using SPSS statistics 19.0 (IBM, US). And statistical significance was declared when $p < 0.05$.

Results

Characterization of sludge

TS, TVS and TVS/TS ratio of sludge were shown in *Figure 4*.

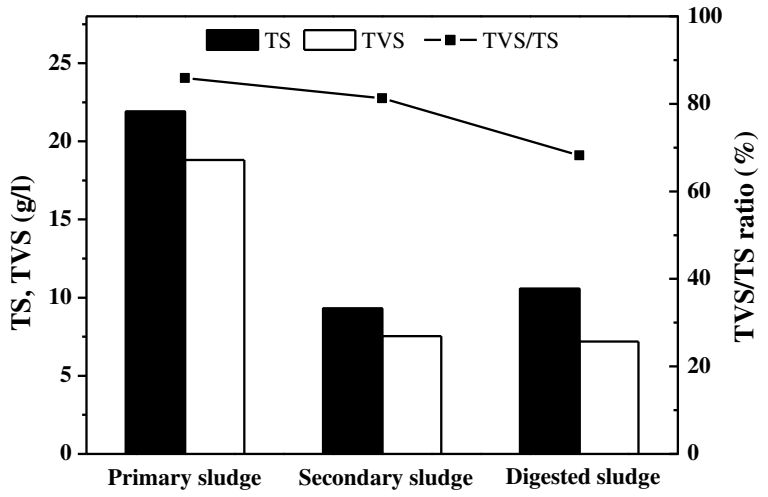

Figure 4. *Changed in TS, TVS and TVS/TS ratio of the sludge sample*

The concentration of TS in primary sludge is about 21.9 g/L, which is approximately 2 times of that in secondary and digested sludge. The TVS concentration is insignificant with TS concentration in the three kinds of sludge ($p = 0.362 > 0.05$). The TVS/TS ratio

http://www.aloki.hu ● ISSN 1589 1623 (Print) ● ISSN 1785 0037 (Online)
DOI: http://dx.doi.org/10.15666/aeer/1706_1439114402

of primary sludge, secondary sludge and digested sludge were 85.9%, 81.2% and 68.1%, respectively. In anaerobic digestion stage, biodegradable organic substances can be converted to biogas, leaving most inorganic and recalcitrant materials in the digested sludge. This can be explained the lower TVS/TS ratio of digested sludge than those of primary sludge and secondary sludge. Mineral element analysis showed that K, Mg, Fe and Ca were the major ions in all sludge samples (*Table 1*). In addition, the concentration of mineral elements in digested sludge was much higher than that in primary sludge and secondary sludge, proved previously explanation.

Table 1. *Average metal content in sewage sludge (unit: mg/g-TS)*

Sample	Na	K	Mg	Ca	Fe
Primary sludge	1.6	2.3	1.4	1.7	0.6
Secondary sludge	4.3	12.4	9.6	7.2	6.4
Digested sludge	6.2	22.7	17.1	13.1	11.5

P fractionation in sludge by SMT protocol

TS, total solids; TP, total P; OP, organic P; IP, inorganic P; NAIP, non-apatite P; AP, apatite P; Bio-availability, the percentage of OP + NAIP to TP. *Table 2* summarized the P fractions of primary sludge, secondary sludge and digested sludge, respectively. The concentration of different P fractions in primary sludge varied were significant with that in secondary sludge and digested sludge ($p = 0.010\text{-}0.015 < 0.05$), and the P contents between secondary sludge and digested sludge were insignificant ($p = 0.338 > 0.05$). The TP concentration in secondary sludge was about 46.1 mg/g-TS, which was around 4.3 times of that in primary sludge. This result may be brought about by the secondary sludge, which accumulated high concentration of P and responsible for P removal from wastewater. While the primary sludge directly settled from wastewater is mainly suspended solid contaminants. Compared to secondary sludge, lower concentration of TP in digested sludge was also detected, most probably due to parts of P in the secondary sludge was released to the effluent in digestion tank (*Table 3*). The percentage of OP to TP were 71.7%, 41.4% and 16.3% in primary sludge, secondary sludge and digested sludge, respectively, indicating OP is the dominant P in primary sludge. The concentration of OP varied similarly with TP content in the three types of sludge ($p = 0.166 > 0.05$). Ahlgren et al. (2011) claimed that OP can be released from sediments and utilized by algae. Moreover, OP in soil can be hydrolyzed by phosphatase and then used by the rhizosphere of plants (George et al., 2006; Mesmoudi et al., 2017). Thus high content of OP in sludge may play an important role in P recycle when land application of sludge as P fertilizer is taken into consideration.

Table 2. *Average contents of each P fraction in sludge by using the SMT extraction protocol*

Sludge	TP (mg-P/g-TS)	OP (mg-P/g-TS)	IP (mg-P/g-TS)	NAIP (mg-P/g-TS)	AP (mg-P/g-TS)	OP + NAIP (mg-P/g-TS)	Bio-availability (%)
Primary sludge	10.6±3.2	7.6±2.4	3.1±1.6	1.7±0.8	1.4±0.6	9.3	87.7
Secondary sludge	46.1±5.6	19.1±3.5	26.9±2.8	24.6±3.1	2.6±1.1	43.7	94.8
Digested sludge	31.9±5.1	5.2±2.9	26.7±3.4	19.1±2.3	8.2±2.7	24.3	76.2

http://www.aloki.hu ● ISSN 1589 1623 (Print) ● ISSN 1785 0037 (Online)
DOI: http://dx.doi.org/10.15666/aeer/1706_1439114402

Table 3. *Variation of COD, NH_4-N, TP, and PO_4-P in the influent and effluent from the treatment units of the WWTP*

Treatment units	COD (mg/l)	NH_4-N (mg/l)	TP (mg/l)	PO_4-P (mg/l)
Influent	205.3	28.3	3.0	2.3
Primary settling tank effluent	248.8	30.2	3.5	3.4
Digestion tank effluent	714.2	636.9	241.4	211.8
Effluent	19.3	1.3	0.2	0.1

COD: chemical oxygen demand; TP: total phosporus

On the other hand, IP was the major P fraction in secondary sludge and digested sludge, in which IP accounted for 58.4% and 77.5% of TP, respectively. Only about 3.1 mg/g IP (about 28.8% of TP) was detected in primary sludge (*Table 2; Fig. 5*). Statistical significances analysis indicated that the IP has a similar trend with TP in the three kinds of sludge ($p = 0.459 > 0.05$). NAIP was the dominant IP in primary sludge, secondary sludge and digested sludge, accounting for 55.8%, 91.6% and 69.3% of IP, respectively. In addition, NAIP was about 16.0%, 53.4% and 59.9% of TP in primary sludge, secondary sludge and digested sludge, respectively. Compared with OP and NAIP, AP content was relatively low, about 13.2% of TP in primary sludge and 5.6% of TP in secondary sludge. However, a high content and percentage of AP was founded in digested sludge (8.2 mg/g-TS and 25.7% of TP), most probably due to the formation of Ca-P precipitates in the digestion tank resulting from the saturation status of co-existing calcium phosphate. AP content was significant different with TP content in the three kinds of sludge ($p = 0.042 < 0.05$).

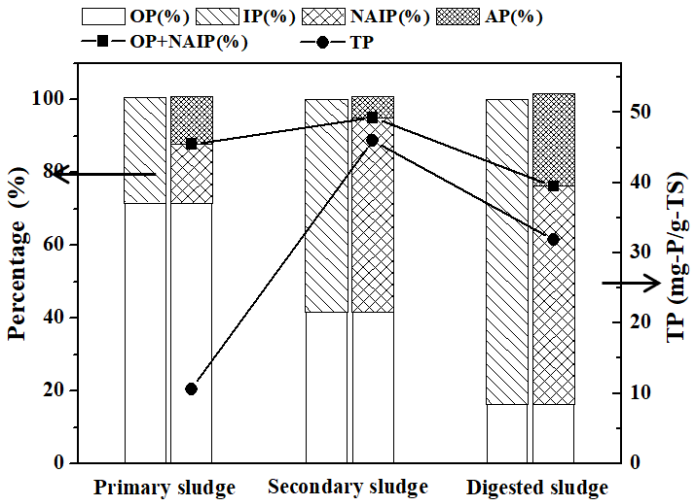

Figure 5. *TP concentrations and percentage of each P fraction to TP in the sludges by using the SMT extraction protocol. TS, total solids; TP, total phosphorus; OP, organic phosphorus; IP, inorganic phosphorus; NAIP, non-apatite inorganic phosphorus; AP, apatite phosphorus*

OP and NAIP were considered to be releasable and bio-available P. In this study, the concentration of NAIP + OP were 9.3, 43.7 and 24.3 mg/g-TS, accounting for about 87.7%, 94.8% and 76.2% of TP in primary sludge, secondary sludge and digested sludge, respectively. It was obviously that secondary sludge not only has the highest

http://www.aloki.hu ● ISSN 1589 1623 (Print) ● ISSN 1785 0037 (Online)
DOI: http://dx.doi.org/10.15666/aeer/1706_1439114402

NAIP + OP content but also has the highest percentage of NAIP + OP among the three sludge samples. Although digested sludge has the lowest percentage of NAIP + OP, its NAIP + OP contents are much higher than those in primary sludge. Thus digested sludge should be reused in preference to primary sludge when utilization of sewage as P fertilizer is taken into consideration. These indicated the content of bio-available P was a more intuitive and better parameter than TP concentration and proportion of bio-available P to assess the bio-availability of P in sewage sludge.

Identification of P species in sludge by ^{31}P NMR analysis

Quantification of various P fractions by integrating the peak areas in NMR spectra has been widely used to estimate the relative proportions of P fractions. All NMR-spectra show peaks in the areas for ortho-P, monoester-P, diester-P, pyro-P, poly-P (*Fig. 6*). *Table 4* summarizes the contents of these compounds and their relative proportions (% TP) in primary sludge, secondary sludge and digested sludge extracts identified by ^{31}P NMR. The average TP contents in the PCA + NaOH extracts from primary sludge, secondary sludge and digested sludge were 9.7, 43.4 and 29.8 mg-P/g-TS with average extraction rate of approximately 91.5-94.1% of TP, respectively, indicating the high efficiency of PCA + NaOH procedure for P extraction from sludge samples.

In primary sludge extracts, ortho-P, monoester-P and diester-P were identified as the major P species, accounting for approximately 21.3, 54.6 and 24.1% of TP, respectively. Obviously, the monoester-P and diester-P were the dominant OP species in primary sludge extracts. Generally, monoester-P and diester-P are regarded as potential bio-available P due to that they can be hydrolyzed and utilized by plants and algal in certain conditions. In the secondary sludge, poly-P was the major form of P species, comprising 54.2% of the extractable TP from sludge (*Table 4*). The high content of poly-P in secondary sludge signals the high amount and bioactivity of PAOs in activated sludge in the aeration tank during sampling period. Specifically, pyro-P was only identified in the secondary sludge, around 2.4% of extractable TP. The presence of pyro-P could reflect microbial activity in sludge due to it was directly related to adenosine triphosphate (ATP) hydrolysis in cells. Ortho-P, a main nutrient for living organisms, was about 89.2% of TP in the digested sludge and much higher than that in the primary sludge and the secondary sludge. These results indicated that most of poly-P, pyro-P, monoester-P and diester-P in primary sludge and secondary sludge were converted to ortho-P or reused by anaerobic bacteria during digestion process.

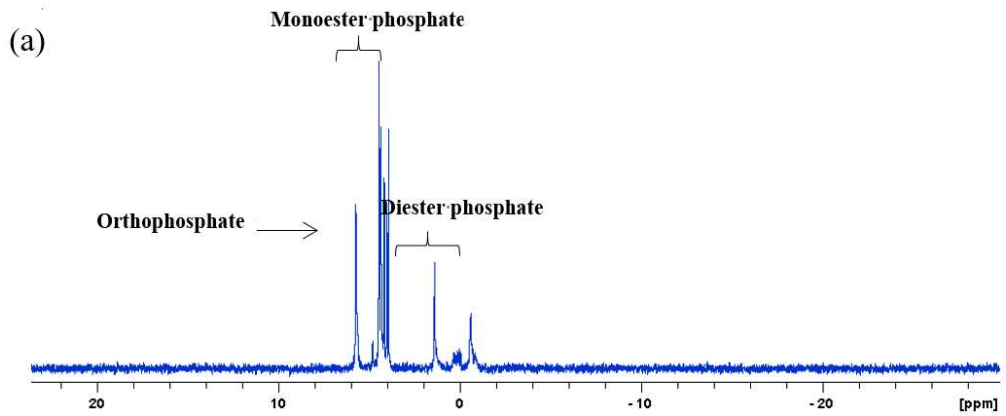

http://www.aloki.hu ● ISSN 1589 1623 (Print) ● ISSN 1785 0037 (Online)
DOI: http://dx.doi.org/10.15666/aeer/1706_1439114402

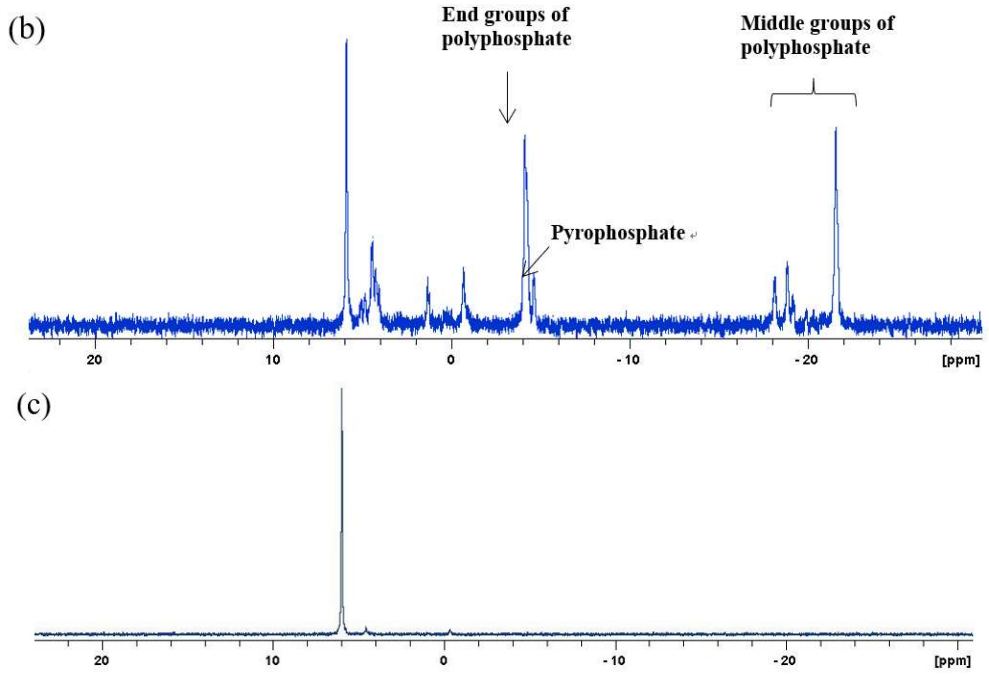

Figure 6. *Typical ^{31}P NMR spectra of PCA + NaOH extracts from (a) primary sludge, (b) secondary sludge and (c) digested sludge*

Table 4. *Contents of different P fractions extracted by PCA + NaOH method and their relative proportions (%TP) identified by ^{31}P NMR in the sludge samples*

Sample	$TP_{Extract}$ (mg-P/g-TS)	IP			OP	
		Ortho-P (%)	Pyro-P (%)	Poly-P (%)	Monoester-P (%)	Diester-P (%)
Primary sludge	9.7±2.8	21.3±3.1	-	-	54.6±5.7	24.1±4.2
Secondary sludge	43.4±4.7	17.6±6.5	2.4±1.2	54.2±5.7	16.1±4.9	9.7±2.2
Digested sludge	29.8±4.1	89.2±5.8	-	-	6.6±3.3	4.3±3.6

Discussion

The TP content in primary sludge, secondary sludge and digested sludge was about 10.6, 46.1 and 31.9 mg/g-TS, respectively. Obviously, secondary sludge has the highest concentration of P, followed by digested sludge and primary sludge. In primary sludge, OP was the dominant P fractions and accounting for about 71.7% of TP. IP was the major P fraction in secondary sludge and digested sludge, in which IP accounted for 58.4% and 77.5% of TP, respectively. Monoester-P, poly-P and ortho-P, accounting for 54.6%, 54.3% and 89.2% of TP, were the dominant P species in the primary sludge, secondary sludge and digested sludge, respectively. The concentrations of NAIP + OP were 9.3, 43.7 and 24.3 mg/g-TS, accounting for about 87.7%, 94.8% and 76.2% of TP in primary sludge, secondary sludge and digested sludge, respectively, indicating the high mobile and bio-available P stored in those sludge samples.

Some studies have been conducted to investigate the P in sewage sludge, but most have only focused on the concentration of TP and ignoring the bio-available P in sludge. The content of bio-available P may provide a more intuitive and convenient parameter

http://www.aloki.hu ● ISSN 1589 1623 (Print) ● ISSN 1785 0037 (Online)
DOI: http://dx.doi.org/10.15666/aeer/1706_1439114402

to evaluate the P in sewage sludge. The results of the present study indicated that secondary sludge not only contains the highest concentration and proportion of TP among different sludge samples, but also has the highest content of potential mobile and bio-available P. In this study, secondary sludge was the optimal choice for land application of sewage sludge as P fertilizer source. Although the proportion of bio-available P in primary sludge was slightly higher than that in digested sludge, digested sludge is more suitable for land application as it contains much more bio-available P content. This study proved that land application of sewage sludge as P fertilizer should be in the order secondary sludge > digested sludge > primary sludge.

Conclusions

In this study, the P species and bio-availability in primary sludge, secondary sludge and digested sludge were identified and evaluated. The following results can be obtained:

(1) IP was the primary P fraction in the secondary sludge and digested sludge, in which NAIP amounted to 91.6% and 69.3% of TP, respectively. OP content (about 7.6 mg/g-TS) was the dominant P in the primary sludge.

(2) Two OP fractions (monoester-P and diester-P) and three IP compounds (ortho-P, poly-P and pyro-P) were identified P species in the secondary sludge. Poly-P was the dominant P species in the secondary sludge, comprising approximately 54.3% of TP. Monoester-P and ortho-P, accounting for 54.6% and 89.2% of TP, were the major P species in the primary sludge and digested sludge, respectively.

(3) The content of bio-available P is a good parameter to evaluate the bio-availability of P in sewage sludge. About 9.3, 43.7 and 24.3 mg/g-TS bio-available P were stored in primary sludge, secondary and digested sludge, respectively.

These results revealed that P species and bio-availability were different in primary sludge, secondary sludge and digested sludge, which is much meaningful for P removal and recovery from wastewater and sludge in WWTPs. As secondary sludge has high P concentration and bio-available P, future researches should pay more attention to how to effectively utilize and recover P from secondary sludge.

Acknowledgements. The authors would like to thank the financial support from National Natural Science Foundation of China (No. 51608279), Natural Science Fund of Hebei Province (No. E2017210094) and the Japan Society for the Promotion of Science (JSPS), Grants-in-Aid for Scientific Research (No. 15K00599).

REFERENCES

[1] Ahlgren, J., Tranvik, L., Gogoll, A., Waldeback, M., Markides, K., Rydin, E. (2005): Sediment depth attenuation of biogenic phosphorus compounds measured by 31P NMR. – Environmental Science & Technology 39(3): 867-872.

[2] Ahlgren, J., Reitzel, K., Brabandere, H. D., Gogoll, A., Rydin, E. (2011): Release of organic P forms from lake sediments. – Water Research 45(2): 565-572.

[3] APHA (2012): Standard methozds for the zexamination of wazter and wasztewater. 20th Ed. – American Public Health Association/American Water Work Association/Water Environment Federation, Washington, DC.

http://www.aloki.hu ● ISSN 1589 1623 (Print) ● ISSN 1785 0037 (Online)
DOI: http://dx.doi.org/10.15666/aeer/1706_1439114402

[4] Arakane, M., Imai, T., Murakami, S., Takeuchi, M., Ukita, M., Sekine, M., Higuchi, T. (2006): Resource recovery from excess sludge by subcritical water combined with magnesium ammonium phosphate process. – Water Science and Technology 54: 81-86.
[5] Catallo, W. J., Comeaux, J. L. (2008): Reductive hydrothermal treatment of sewage sludge. – Waste Management 28(11): 2213-2219.
[6] Christen, K. (2007): Closing the phosphorus loop. – Environmental Science & Technology 41(7): 2078-2078.
[7] Cordell, D., Drangert, J. O., White, S. (2009): The story of phosphorus: global food security and food for thought. – Global Environmental Change 19(2): 292-305.
[8] Daumer, M. L., Béline, F., Spérandio, M., Morel, C. (2008): Relevance of a perchloric acid extraction scheme to determine mineral and organic phosphorus in swine slurry. – Bioresource Technology 99(5): 1319-1324.
[9] Fytili, D., Zabaniotou, A. (2008): Utilization of sewage sludge in EU application of old and new methods - a review. – Renewable and Sustainable Energy Reviews 12(1): 116-140.
[10] George, T. S., Turner, B. L., Gregory, P. J., Menun, C. B. J., Richardson, A. E. (2006): Depletionoforganic phosphorus from oxisols in relation to phosphatase activities in the rhizosphere. – European Journal of Soil Science 57(1): 47-57.
[11] Gilbert, N. (2009): The disappearing nutrient. – Nature 461: 716-718.
[12] Hao, X., Wang, C., van Loosdrecht, M. C. M., Hu, Y. (2013): Looking beyond struvite for P –recovery. – Environmental Science & Technology 47(10): 4965-4966.
[13] He, F., Wang, J., Chen, W. (2018): Numerical simulation and analysis of the effect of baffle distance and depth on solid-liquid two-phase flow in circular secondary clarifier. – International Journal of Heat and Technology 36(1): 111-117.
[14] Hinedi, Z. R., Chang, A. C., Lee, R. W. K. (1989): Characterization of phosphorus in sludge extracts using phosphorus-31 nuclear magnetic resonance spectroscopy. – Journal of Environmental Quality 18(3): 323-329.
[15] Hosni, K., Ben Moussa, S., Chachi, A., Ben Amor, M. (2008): The removal of PO43 + by calcium hydroxide from synthetic wastewater: Optimization of the operating conditions. – Desalination 223(1-3): 337-343.
[16] Karl, D. M. (2000): Aquatic ecology: phosphorus, the staff of life. – Nature 406: 31-33.
[17] Kelessidis, A., Stasinakis, A. S. (2012): Comparative study of the methods used for treatment and final disposal of sewage sludge in European countries. – Waste Management 32(6): 1186-1195.
[18] Lalmi, D., Hadef, R. (2017), Numerical study of the swirl direction effect at the turbulent diffusion flame characteristics. – International Journal of Head and Technology 35(3): 520-528.
[19] Medeiros, J. J. G., Cid, B. P., Gomez, E. F. (2005): Analytical phosphorus fractionation in sewage sludge and sediment samples. – Analytical and Bioanalytical Chemistry 381(4): 873-878.
[20] Mesmoudi, K., Meguellati, K., Bournet, P. E. (2017): Thermal analysis of greenhouses installed under semi arid climate. – International Journal of Head and Technology 35(3): 474-486.
[21] Reis, A. N., Pitombeira-Neto, A. R., Rolim, G. A. (2017): Simulation of tank truck loading operations in a fuel distribution. – International Journal of Simulation Modelling 16(3): 435-447.
[22] Ruban, V., Lopez-Sanchez, J. F., Pardo, P., Rauret, G., Muntau, H., Quevauviller, P. (1999): Selection and evaluation of sequential extraction procedures for the determination of phosphorus forms in lake sediment. – Journal of Environmental Monitoring 1(1): 51-56.
[23] Saric, T., Simunovic, G., Simunovic, K., Svalina, I. (2016): Estimation of machining time for CNC manufacturing using neural. – International Journal of Simulation Modelling 15(4): 663-675.

http://www.aloki.hu ● ISSN 1589 1623 (Print) ● ISSN 1785 0037 (Online)
DOI: http://dx.doi.org/10.15666/aeer/1706_1439114402

[24] Singh, R. P., Agrawal, M. (2008): Potential benefits and risks of land application of sewage sludge. – Waste Management 28(2): 347-358.
[25] Turner, B. L. (2004): Optimizing phosphorus characterization in animal manures by solution phosphorus- 31 nuclear magnetic resonance spectroscopy. – Journal of Environmental Quality 33(2): 757-766.
[26] Turner, B. L., Mahieu, N., Condron, L. M. (2003): Phosphorus-31 nuclear magnetic resonance spectral assignments of phosphorus compounds in soil NaOH–EDTA extracts. – Soil Science Society of America Journal 67(2): 497-510.
[27] Uhlmann, D., Röske, I., Hupfer, M., Ohms, G. (1990): A simple method to distinguish between polyphosphate and other phosphate fractions of activated sludge. – Water Research 24(11): 1355-1360.
[28] UN-HABITAT (2009): Global Atlas of Excreta Wastewater Sludge, and Biosolids Management: Moving Forward the Sustainable and Welcome Uses of a Global Resource (Local Economic Development Series). – United Nations Human Settlements Programme, New York.
[29] USGS (2014): Phosphate Rock in Mineral Commodity Summaries. – U.S. Geological Survey, Washington, DC.
[30] Vestergren, J., Vincent, A. G., Jansson, M., Persson, P., Ilstedt, U., Gröbner, G., Giesler, R., Schleucher, J. (2012): High-resolution characterization of organic phosphorus in soil extracts using 2D 1H−31P NMR correlation spectroscopy. – Environmental Science & Technology 46(7): 3950-3956.
[31] Xie, C., Zhao, J., Tang, J., Xu, J., Lin, X., Xu, X. (2011): The phosphorus fractions and alkaline phosphatase activities in sludge. – Bioresource Technology 102(3): 2455-2461.
[32] Xu, H., Zhang, H., Shao, L., He, P. (2012): Fraction distributions of phosphorus in sewage sludge and sludge ash. – Waste and Biomass Valorization 3: 355-361.
[33] Zhang, H. L., Fang, W., Wang, Y. P., Sheng, G. P., Xia, C. W., Zeng, R. J., Yu, H. Q. (2013): Species of phosphorus in the extracellular polymeric substances of EBPR sludge. – Bioresource Technology 142: 714-718.
[34] Zhang, J. X., Sun, W. G., Niu, F. S., Wang, L., Zhao, Y. W., Han, M. M. (2018): Atmospheric sulfuric acid leaching thermodynamics from metallurgical zinc-bearing dust sludge. – International Journal of Heat and Technology 36(1): 229-236.
[35] Zhao, R. (2012): Simulation-based environmental cost analysis for work-in-process. – International Journal of Simulation Modelling 4: 211-224.

http://www.aloki.hu ● ISSN 1589 1623 (Print) ● ISSN 1785 0037 (Online)
DOI: http://dx.doi.org/10.15666/aeer/1706_1439114402

CONTRIBUTION OF ETHYLENE TO THE CADMIUM RESISTANCE OF THALE CRESS (*ARABIDOPSIS THALIANA*)

LU, X. Y.[1] – CHEN, Q.[2] – CUI, X. Y.[1*] – ZU, Y. G.[1] – TANG, Z. H.[1]

[1]*Institution Northeast Forestry University, Harbin 150040, China*

[2]*School of Life Sciences, Nantong University, Nantong 226010, China*

**Corresponding author*
e-mail: c_xiaoyang@126.com; phone: +86-451-8219-2198

(Received 7th Jun 2019; accepted 10th Oct 2019)

Abstract. Ethylene was reported to be important in the response to cadmium (Cd). It is generally agreed that ethylene could improve Cd resistance, but the specific mechanism is not yet clear. To make up for this gap, this paper explores the antioxidant capacity, malondialdehyde (MDA), hydrogen peroxide (H_2O_2) content, Cd content and the expression of relevant genes in *Arabidopsis thaliana* seedlings, and examines the effect of ethylene on the physiological performance of Cd-stressed seedlings. The results show that ethylene could greatly improve the Cd resistance of plants by suppressing the translocation of Cd ions. In addition, ethylene can ease the metal phytotoxicity of Cd by lowering the MDA content and H_2O_2 generation, and regulate the over-expression of AtATM3 and APDR8 to enhance Cd resistance. To sum up, ethylenecould enhance Cd resistance by enhancing antioxidant activity and inhibiting the translocation of Cd ions.
Keywords: *ethylene, cadmium (Cd), resistance, gene expression, translocation factor*

Introduction

Cadmium (Cd) is ubiquitously distributed in the environment, it is non-essential and toxic to the human body. Because of its high-water solubility, the element can easily be absorbed by plants from Cd-contaminated soil, and can interfere in nutrient absorption and translocation, leading to nutrient imbalance (Järup and Akesson, 2009). The uptake of Cd by plants is accelerated under Cd stress. A high content of Cd ions may inhibit plant growth, reduce biomass accumulation and even cause cell death. The Cd can also affect membrane function by inducing lipid peroxidation. In addition, the element tends to boost the production of oxygen free radicals and suppress that of enzymatic antioxidants, leading to oxidative stress (Gratão et al., 2012; Monteiro et al., 2011).

Many scholars have proved that Cd stress has the potential to cause the following issues: the accumulation of reactive oxygen species (ROS), the inactivation of antioxidant enzymes, damages protein and DNA and negatively influences lipid peroxidation (Mishra et al., 2006; Ranieri et al., 2005; Schützendübel et al., 2002). Focusing on the Cd-resistance of ethylene, Zhang et al. (2010) investigated the effect of ethylene on the Cd uptake and accumulation of plants at different Cd contents, and found that plants with high translocation factor are less tolerable to Wang et al. (2011) observed that Cd and Cd-containing toxic compounds were excluded from the cytoplasm of *Arabidopsis*, with the increase in the expression of AtPDR8, indicating that transport gene is contributing to Cd resistance. The studies of Chen et al. (2018) showed that exogenous application of Cu, Zn or Ca to plant medium could alleviated the Cd stress to *Catharanthus roseus*.

http://www.aloki.hu ● ISSN 1589 1623 (Print) ● ISSN 1785 0037 (Online)
DOI: http://dx.doi.org/10.15666/aeer/1706_1440314414

It has been reported that lipid peroxidation, a sensitive response to metal stress, is usually characterized by the contents of Malondialdehyde (MDA) and hydrogen peroxide (H_2O_2). Some scholars discovered immediate generation of H_2O_2 when plants were exposed to high Cd content, and thus considered H_2O_2 as the key molecule that stimulates signal transduction after metal exposure of plants (Mithöfer et al., 2004; Smeets et al., 2008, 2009). Some concluded that the roots of plants, especially the plasma membranes of root cells, are the primary targets of metal action under Cd stress (Cuypers et al., 2009; Vangronsveld and Clijsters, 1994). Because the toxicity of Cd^{2+} is exerted through membrane damage and inactivation of enzymes. The antioxidation power of cells mainly comes from antioxidants like catalases (CAT), glutathione reductase (GR) (Mittler et al., 2004). The CAT and the GR can detoxify H_2O_2 into H_2O (Gratao et al., 2005; Passardi et al., 2007), and control cellular redox homeostasis within certain limits (Mittler et al., 2004).

Ethylene is an endogenous regulator for plant growth. The hydrocarbon has a strong impact on ripening, abscission and senescence, as well as many other aspects of vegetative growth. The existing studies have shown that ethylene is involved in the plant's response to metal stress (Cao et al., 2007; Iakimova et al., 2005). Under metal stress, the plants will produce much more ethylene than that under normal conditions. This surge in ethylene production occurs when the Cd content exceeds 1 mM (Chen, 2017). Many scholars held that ethylene regulates cellular and developmental processes responding to abiotic stress, highlighting how ethylene is involved in stress responses of plants (Achard et al., 2006; Ahmadi et al., 2018; Ali et al., 2018; Cao et al., 2007; Jung et al., 2009; Wang et al., 2007). Furthermore, ethylene is considered as a stress hormone (Kende, 1993) and ethylene signalling regulates multiple stress responses (Cao et al., 2009). However, it is not clear what specific roles it plays in signalling of stress responses (Cao et al., 2008).

In light of the above, this paper probes deep into the relationship between ethylene and plant resistance to heavy metal stress, aiming to enhance crop yield, improve the crop resistance to heavy metal stress and remediate the soil polluted by heavy metals.

Materials and methods

Plant and Cd treatment

Arabidopsis thaliana (Columbia ecotype) (Col-0) seeds were surface sterilized by 10%(v/v) sodium hypochlorite (NaClO), then washed with water and dried under sterile conditions. The sterilized seeds were then placed on agar plates containing Murashige and Skoog (MS) basal salt mixture, 1% sucrose, pH 5.7, 0.8% Agar. Next, the plates were respectively added 0 μM, 10 μM, 20 μM, 40 μM, 50 μM, 60 μM and 100 μM $CdCl_2$. The plates were kept in the dark at 4 °C for a 4d-long synced germination, before being relocated to light (photosynthetically active radiation (PAR) = 160 μM photons m^{-2} s^{-1}) at 23 °C with a 16:8 h light: dark regime.

Assay of seedling growth

To measure the growth of *Arabidopsis thaliana*, the root lengths of at least 15 seedlings were measured daily after the seedlings were transferred to light. The measurements were carried out with an SMZ 1500 stereomicroscope (Nikon, Japan) and the measured data were analysed on NIS-Elements Basic Research (Nikon, Japan).

http://www.aloki.hu ● ISSN 1589 1623 (Print) ● ISSN 1785 0037 (Online)
DOI: http://dx.doi.org/10.15666/aeer/1706_1440314414

Assay of antioxidative enzyme activity

To evaluate antioxidative enzyme activity, 0.3 g seedling were ground in liquid nitrogen and extracted in 5 mL phosphate-buffered saline (PBS) buffer (50 mM, pH7.0), containing 1mM ethylenediaminetetraacetic acid (EDTA), 1mM acetylsalicylic acid (ASA) and 1% (w/v) soluble polyvinylpyrrolidone (PVP). The homogenates were centrifuged (10,000g) for 30 min at 4 °C, and then the supernatant was collected for the assay of enzyme activities.

The CAT activity was measured by the method of Lin et al. (2013). The H_2O_2 (extinction coefficient: 0.04nM-1cm-1) was decomposed at 240nm for 3min in a quartz cuvette. The reaction mix consists of 2.7mL 0.1M PBS buffer (pH7.0), 0.1mL 300mM H_2O_2 solution and 0.2mL extract. All experiments were performed in triplicate for each treatment.

The GR activity was determined by the method of Kaya and Yigit (2012). The glutathione disulphide (GSSG) and reduced nicotinamide adenine dinucleotide phosphate (NADPH) were reduced into glutathione and nicotinamide adenine dinucleotide phosphate ($NADP^+$) in the presence of GR. The reaction mix consists of 0.5mL PBS buffer (pH7.8), 0.1mL 20mM EDTA-Na_2 solution, 0.1mL 5mM GSSG solution, 0.1mL 1.5mM NADPH solution and 0.2mL extract. The absorbance of the mixture was measured at 340nm. The reaction lasted for 3min. All experiments were performed in triplicate for each treatment.

Determination of H_2O_2

The content H_2O_2 was determined by the method of Satterfield and Bonnell (1955) with a little modification. Firstly, about 0.3g plant tissue was frozen in liquid nitrogen and then ground into powder. Then, 3mL precooled propanone was added and mixed with the powder. After centrifugation, the supernatant was collected for further use. Next, 2mL supernatant was taken, and added with 0.1mL 5% titanium sulphate and 0.2mL concentrated ammonia. After centrifugation, the precipitate was collected and washed with propanone, and then added with 5mL 2M sulfuric acid. The absorbance of the mixture was measured at 415nm. All experiments were performed in triplicate for each treatment.

Determination of lipid peroxidation

The lipid peroxidation was determined by the method of Ashraf et al. (2015). The thiobarbituric acid reactive substances (TBARS) were taken as the measure of lipid peroxidation. Firstly, 300 mg plant tissue was homogenized with 3 mL 10% precooled trichloroacetic acid (TCA) buffer. After centrifugation (8,000 g) for 10 min at 4 °C, 2 mL 0.5% TBA was added to 2 mL extract. Then, the mixture was heated for 30 min at 95 °C and centrifuged. Finally, the absorbance of the supernatant was measured at 532 nm and corrected for unspecific absorbance at 600 nm.

Analysis on gene expression

The total ribonucleic acid (RNA) was extracted from 100~200 mg samples (both leaves and roots), using TRIzol reagent, and quantified by a Nanodrop ND-1000 spectrophotometer (Thermo Fisher Scientific, US) with absorbance at 260 nm. Next, 2 μg RNA was adopted for reverse transcription with a Revert Aid Reverse Transcriptase

http://www.aloki.hu ● ISSN 1589 1623 (Print) ● ISSN 1785 0037 (Online)
DOI: http://dx.doi.org/10.15666/aeer/1706_1440314414

and Oligo (dT) primers (Takara, Japan). The quantitative reverse transcription-polymerase chain reaction (qRT-PCR) was analysed on a RealMasterMix Kit (TIANGEN Biotech, China). The initial denaturation lasted 30 s at 94 °C, 30 s at 60 °C and 30 s at 72 °C, followed by a 5 min-long process at 92 °C. All quantifications were normalized to the amplification of Actin2 gene. The primer sequences of all genes used for qRT-PCR are listed in *Table 1*. All experiments were performed in triplicate for each treatment.

Statistical analysis

In the present study, there were three replicates arranged in a randomized block design manner for each treatment including control. All the data were presented as mean ± standard error (SE) and comparison of means were performed using SPSS (SPSS 17.0, SPSS Inc., USA). The one-way ANOVA with the Duncan's post hoc test was performed to test the difference significance ($p < 0.05$) of means.

Table 1. *The primer sequences of all genes used for qRT-PCR*

Gene	GeneBankaccession no.	Primers
aco2	ACO2 R	TGCAGGAGGCATCATCTTGTT
	ACO2 F	AACGATGCAACCGACATCCT
acs2	ACS2 R	AGGCAATTGCACATTTCATGG
	ACS2 F	CTGTCCGCCACCTCAAGTCT
ein3	EIN3 R	AGGCAGAGACCTTTTTCATCA
	EIN3 F	CAGGCTCAGCTTGTGGAACA
atm3	ATM3 R	TGCTCGGACATTTTTGAAATC
	ATM3 F	GTCCATAGCTGCGCATATCTC
pdr8	PDR8 R	CTCTTGATTGGTACAGTCTTCTG
	PDR8 F	CCATAATGGTCCTCAATGTATTGC
actin2	Actin2 R	TGAGCAAAGAAATCACAGCACT
	Actin2 F	CCTGGACCTGCCTCATCATAC

Experimental results

Ethylene synthesis and signal related gene expression

Figure 1 illustrates the expression of ACO2, ACS2 and EIN3 genes in *Arabidopsis thaliana* under elevated Cd content. Obvious changes were seen in the expression of all three genes from the figure. Specifically, ACO2 was expressed more strongly under Cd stress, except at the Cd content of 10 μM; ACS2 had a strong expression at the Cd content of 60 μM; EIN3 expression increased with Cd content. Overall, the strongest synthesis and signal of ethylene gene expressions were observed at the Cd content of 60 μM. This means ethylene is involved to maintain the normal growth of plants under Cd stress.

Altered element uptake in Arabidopsis thaliana under Cd stress

Several macro- and micro-nutrients were analysed to disclose the nutrient acquisition in *Arabidopsis thaliana* seedlings under Cd stress. The seedlings were placed in nutrient solutions with different Cd contents for 14 d. Then, the Cd contents in the shoot and the

http://www.aloki.hu ● ISSN 1589 1623 (Print) ● ISSN 1785 0037 (Online)
DOI: http://dx.doi.org/10.15666/aeer/1706_1440314414

root of the seedlings were measured one by one. The results show that, under Cd stress, the Cd contents in both the shoot and the root are positively correlated with the Cd content in the solution, while the translocation factor of the shoot is negatively correlated with the Cd content in the solution.

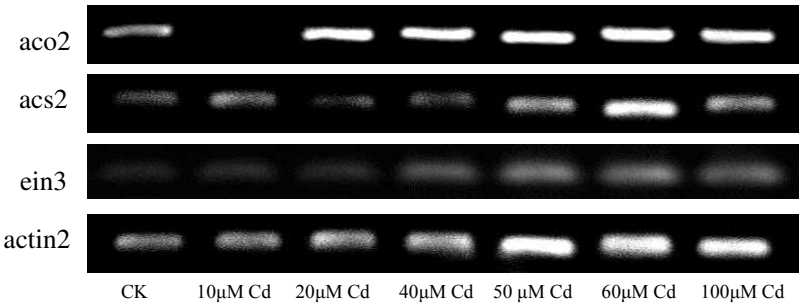

Figure 1. *Expression of ACO2, ACS2 and EIN3 in Arabidopsis thaliana under elevated Cd content*

Effect of ethylene on Cd content in Arabidopsis thaliana under Cd stress

The effect of ethylene on Cd content in *Arabidopsis thaliana* were explored at three Cd contents. The experimental results are displayed in *Figure 2*. Compared with the seedlings treated with Cd alone, the seedings treated with 30 μM aminocyclopropane-l-carboxylic acid (ACC) had a low Cd content in the shoots. The same trend was observed in the roots. The translocation factor of seedlings added with ethylene was lower than that of those treated with Cd alone. To sum up, the ethylene could reduce the Cd content and translocation factor in *Arabidopsis thaliana* seedlings under Cd stress.

Effect of ethylene on MDA content in Arabidopsis thaliana under Cd stress

Plasma membranes are the primary targets for metal stress in both roots and leaves. The membrane damage can be deduced through the TBA assay on lipid peroxidation products. Here, several *Arabidopsis thaliana* seedlings are treated with different contents of Cd. The results show that the Cd treatment consistently promoted the MDA contents in leaves of *Arabidopsis thaliana* seedlings. Hence, three Cd contents were selected to treat the seedlings, and used to detect the effect of ethylene on MDA contents in leaves. As shown in *Figure 3,* the seedlings added with ethylene contained fewer MDA than those treated by Cd alone. Under Cd stress, the application of ethylene suppressed the MDA content, easing the membrane damage caused by lipid peroxidation.

Effect of ethylene on H_2O_2 content in Arabidopsis thaliana under Cd stress

H_2O_2 is a common product under metal exposure. Thus, the H_2O_2 contents in leaves of *Arabidopsis thaliana* seedlings were measured at different Cd contents. The measured results in *Figure 4* show that the leaves of seedlings treated with Cd produced more H_2O_2 than the control. Thus, the Cd content can greatly impact the production of H_2O_2 in seedlings. With the increase of Cd content, the H_2O_2 content in leaves of *Arabidopsis thaliana* gradually increased (*Fig. 4*). Then, the effect of ethylene on H_2O_2 content in the leaves was determined at the Cd content of 60 μM. The results indicate that the ethylene inhibited the H_2O_2 content in *Arabidopsis thaliana* seedlings under Cd stress.

http://www.aloki.hu ● ISSN 1589 1623 (Print) ● ISSN 1785 0037 (Online)
DOI: http://dx.doi.org/10.15666/aeer/1706_1440314414

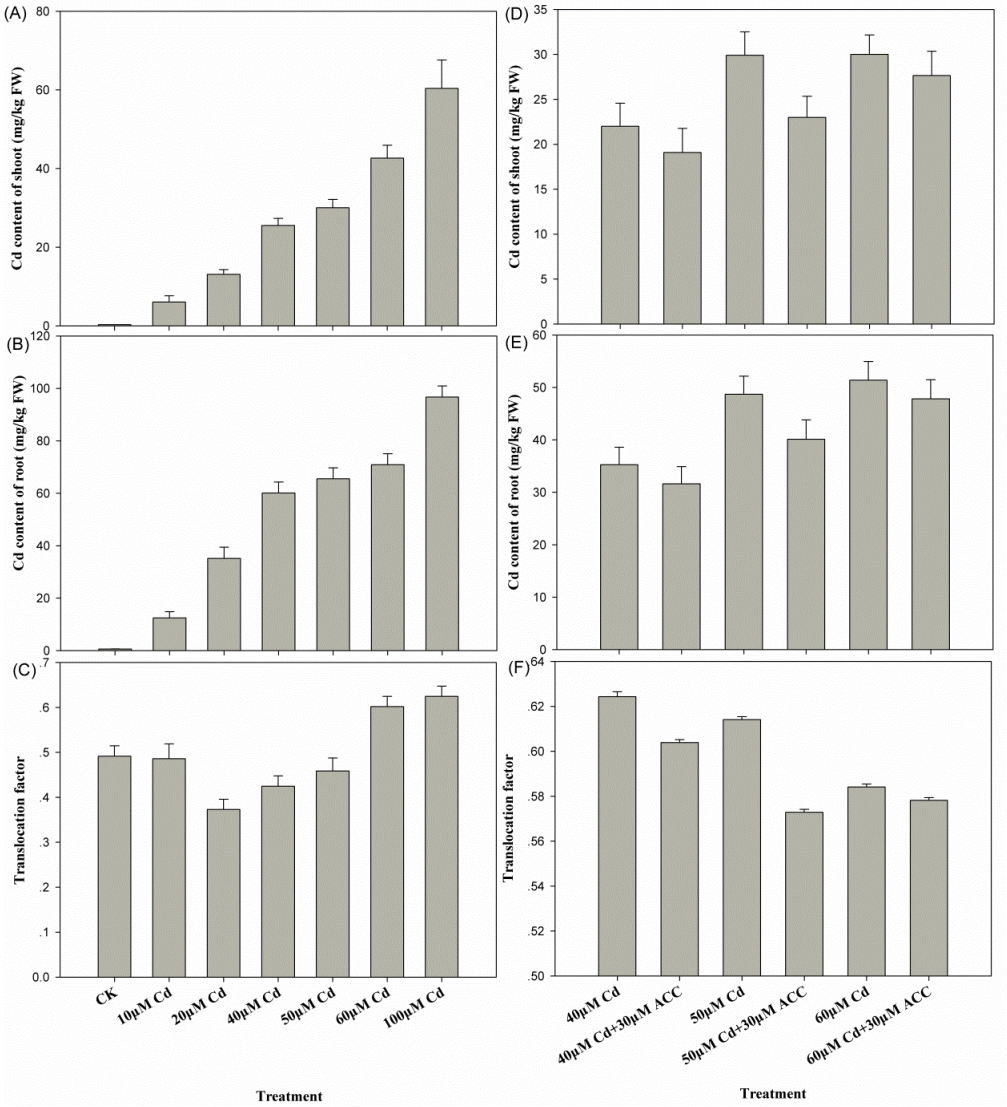

Figure 2. *Effect of ethylene on Cd contents of shoots (A and D), roots (B and E) and Cd translocation factors (C and F)*

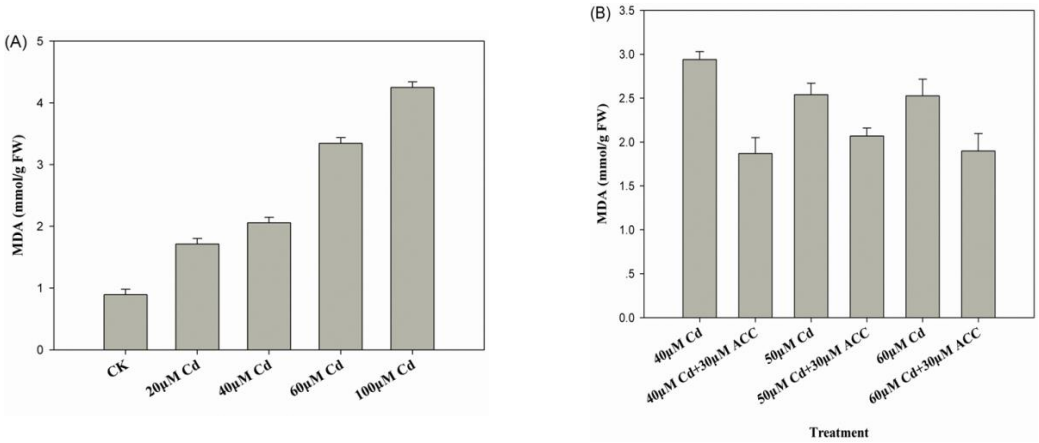

Figure 3. a *Effect of Cd on MDA contents in leaves of Arabidopsis thaliana seedlings.* ***b*** *Effect of ethylene on MDA contents in leaves of Arabidopsis thaliana seedlings under Cd stress*

http://www.aloki.hu ● ISSN 1589 1623 (Print) ● ISSN 1785 0037 (Online)
DOI: http://dx.doi.org/10.15666/aeer/1706_1440314414

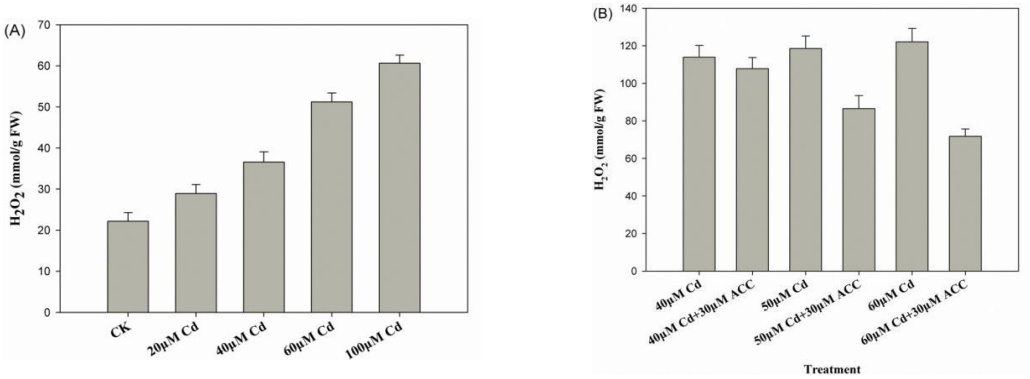

Figure 4. a *Effect of Cd on H_2O_2 contents in leaves of Arabidopsis thaliana seedlings.* ***b*** *Effect of ethylene on H_2O_2 contents in leaves of Arabidopsis thaliana seedlings under Cd stress*

Antioxidative enzyme activities

The effects of Cd and ethylene on CAT and GR activities in leaves of *Arabidopsis thaliana* seedlings were tested, and the results were plotted in *Figure 5*. Obviously, the Cd content exhibited a great impact on the antioxidative enzyme activities. The CAT activities in seedlings treated with Cd were greatly affected. Compared with the control, the CAT activities in all seedlings treated with Cd were relatively low. Next, the Cd content of 60 μM was selected to detect how ethylene affects CAT activity. The detection results show that the ethylene significantly boosted the CAT activities in seedlings under Cd stress. In addition, the Cd content greatly promoted the GR activities in seedlings, while the growth in ethylene content led to a decline and then increase in the GR activities.

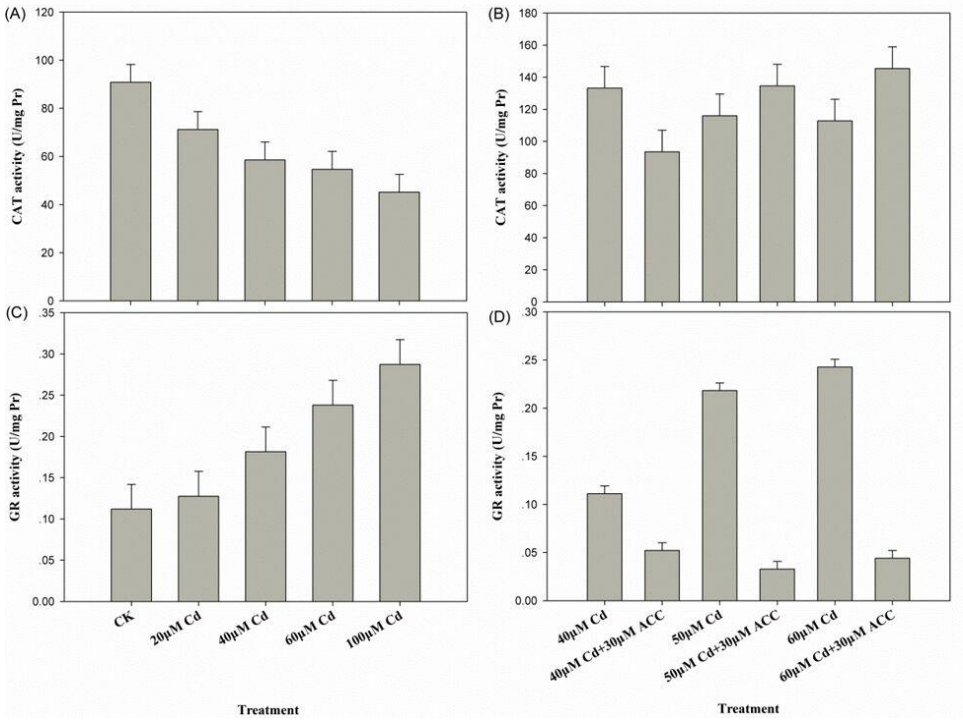

Figure 5. *Effect of Cd and ethylene on the activities of CAT (A and B) and GR (C and D) in leaves of Arabidopsis thaliana seedlings*

http://www.aloki.hu ● ISSN 1589 1623 (Print) ● ISSN 1785 0037 (Online)
DOI: http://dx.doi.org/10.15666/aeer/1706_1440314414

Expression of AtATM3 and AtPDR8 in Arabidopsis thaliana seedlings under Cd stress

The AtATM3 gene is involved in Cd transporter proteins in the roots of *Arabidopsis thaliana* seedlings. If this gene is overexpressed, the plant will be more resistant to Cd. Meanwhile, the AtPDR8 gene has been identified as a transporter of ATP-binding cassette (ABC) that contributes to Cd resistance in *Arabidopsis thaliana*, as it excludes Cd or Cd-containing toxic compounds from the cytoplasm. The author tested the expression of AtATM3 and AtPDR8 in *Arabidopsis thaliana* seedlings treated with different Cd contents. The results (*Fig. 6*) show that both AtATM3 and AtPDR8 were expressed more stronger with the growth in Cd content, indicating that the two genes contribute to Cd resistance.

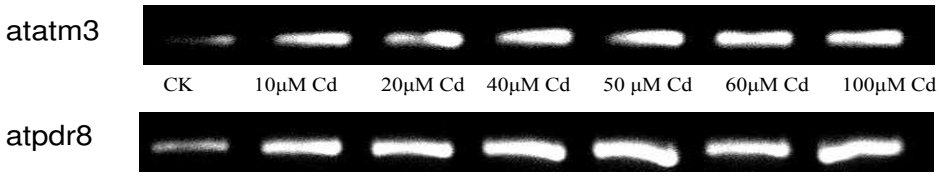

Figure 6. *Expression of AtATM3 and AtPDR8 in Arabidopsis thaliana seedlings under different Cd contents*

Figure 7 presents how ethylene content affects the expression of AtATM3 and AtPDR8 in *Arabidopsis thaliana* seedlings under Cd stress. It can be seen that the two genes were expressed more strongly with the Cd content and with the ethylene content. This means ethylene contributes to Cd resistance by enhancing the expression of AtATM3 and AtPDR8 (*Fig. 7*).

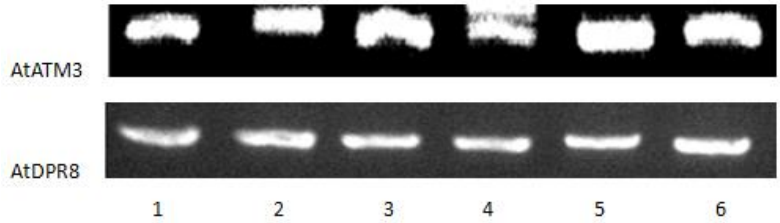

Figure 7. *The effect of ethylene content on expression of AtATM3 and AtPDR8 in Arabidopsis thaliana seedlings under Cd stress. Note: The treatments are 60 μM Cd(1), 60 μM Cd+ 2 μM ACC(2), 60 μM Cd+ μM ACC(3), 60 μM Cd+ 10 μM ACC(4), 60 μM Cd+ 30 μM ACC(5) and 60 μM Cd+ 50 μM ACC(6)*

Discussion

This research uses *Arabidopsis thaliana* seedlings to test the effect of ethylene on Cd resistance. Ethylene, an important regulator of plant physiology under stress, is deeply involved in the response to abiotic response. In recent years, several reports claim that ethylene could improve Cd resistance (Fuhrer, 1982). In these reports, it is confirmed that ethylene takes part in modulating the cadmium response, but the modulation mechanism is not explained. Therefore, our research attempts to verify the hypothesis that the modulation mechanism works thanks to the ability of ethylene to reduce Cd

http://www.aloki.hu ● ISSN 1589 1623 (Print) ● ISSN 1785 0037 (Online)
DOI: http://dx.doi.org/10.15666/aeer/1706_1440314414

translocation from roots to shoots in Cd-stressed *Arabidopsis thaliana*. The research results prove the validity of the hypothesis.

With the increase in metal content in the environment, plants worldwide are suffering from metal phytotoxicity (Chen, 2018). The roots, which are in direct contract with the nutrient solution, often accumulate lots of Cd. Under the stress, there is a cumulative effect on the inhibition and phytotoxicity of roots. Our research results also show that Cd stress could greatly boost the expression of ACO2, ACS2 and EIN3 genes in *Arabidopsis thaliana* seedlings. Hence, ethylene may play an important role in resistance to Cd.

Over the time, the heavy amount of Cd accumulated in roots under Cd stress will gradually move to the shoots. With the growth in Cd content, both shoots and roots will witness an increase in their Cd contents. In our research, the root-shoot Cd transport is measured by the translocation factor. Our results show that the translocation factor of shoots first decreased and then increased with the increase in Cd content. Under a high translocation factor, lots of heavy metals were transported from roots to shoots. Thus, a high translocation factor does not contribute to the Cd resistance. After adding ethylene to Cd-stressed seedlings, it is observed that the Cd content in the seedlings decreased. Besides, the addition of ethylene significantly suppressed the translocation factor under the 50 μM Cd stress.

The cellular redox state is an important determinant of metal phytotoxicity (Kranner et al., 2010). Lipid peroxidation could be the first indication of oxidative damage and was observed under Cd exposure. There is a mutual promotion relationship between lipid peroxidation and the production of hydroxyl radicals. In our experiment, when seedlings were treated with Cd alone, the MDAs in roots and leaves increased gradually with the Cd content. Comparatively, the roots had higher MDA than leaves, and thus suffered more injuries under Cd stress. When ethylene of different contents was applied to the Cd-stressed seedlings, the MDA contents dropped across the board. This means ethylene could ease the membrane injury caused by lipid peroxidation in Cd-stressed plants. During lipid catabolism, H_2O_2 is generated as a by-product of fatty acid oxidation (Sharma et al., 2012). However, excess H_2O_2 may bring oxidative damage to plants. In our experiment, the H_2O_2 content in the leaves of *Arabidopsis thaliana* seedlings gradually increased with the Cd content. The trend is the same with that of the MDA. Thus, the addition of ethylene could suppress the H_2O_2 content in Cd-stressed seedlings.

In leaves, the H_2O_2-scavenging enzymes are key weapons of the antioxidative defence system (Skulachev, 1997). Major H_2O_2-scavenging enzymes of plants include the CAT, the GR, the ascorbate peroxidase (APX), the superoxide dismutase (SOD), and the peroxidase (POD). Among them, the CAT and the GR were selected for our research. The experiment shows that the CAT ability in seedlings treated by Cd alone was poorer than that of the control, indicating that the Cd-exposure suppressed the activity of the H_2O_2-scavenging enzyme, and boosted the production of H_2O_2. However, the CAT ability improved after the addition of ethylene, revealing the promotional effect of ethylene on the CAT. With the growth in Cd content, the GR activity exhibited an increasing trend. This is because the GR can produce the GSH to eliminate H_2O_2 and combine with Cd to yield PC_S. As a result, heavy metals are combined with proteins, malic acid and other substances in the cells. However, the GR activity was weakened after ethylene was added, meaning ethylene could suppress GR ability.

http://www.aloki.hu ● ISSN 1589 1623 (Print) ● ISSN 1785 0037 (Online)
DOI: http://dx.doi.org/10.15666/aeer/1706_1440314414

AtATM3 is a transporter protein involved in the root-shoot Cd transport in *Arabidopsis thaliana* (Kim et al., 2006). Our research shows that the AtATM3 was upregulated in the roots of seedlings with the increase of Cd content, and overexpression of the gene could enhance Cd resistance. Besides, it is learned that ethylene can enhance AtATM3 expression to resist the Cd. Specifically, the ethylene retains the Cd ions in roots, lowering the translocation factor. In some plants, about 90% of the Cd ions are combined with PC_S. In our experiment, about 60% absorbed in the roots existed as PC-Cd compounds. Meanwhile, AtPDR8 is an ABC transporter capable of excluding Cd or Cd-containing toxic compounds from the cytoplasm (Kim et al., 2010). Our research shows that the overexpression of this gene enhances Cd resistance, and that ethylene improves AtPDR8 gene expression to resist Cd.

Conclusions

Our research results demonstrate the key role of ethylene in alleviating the metal phytotoxicity of Cd stress. Ethylene is involved in plant responses to Cd stress, ensuring the normal growth of plants. The application of ethylene is an effective way to enhance the Cd resistance. Taking *Arabidopsis thaliana* for example, ethylene reduces the root-shoot translocation of Cd ions, leading to stronger Cd resistance. In addition, ethylene can ease the metal phytotoxicity of Cd by lowering the MDA content and H_2O_2 generation, and regulate the over-expression of AtATM3 and APDR8 to enhance Cd resistance. To sum up, the ethylene mainly bolsters Cd resistance of plants by enhancing antioxidant activity and suppressing the root-shoot translocation of Cd ions. It is worthing that related antioxidative substance should be further studied in the future.

Acknowledgements. This work was supported by Nantong Science and Technology Foundation of China (JC2018159) and the Research Initiation Funds for Nantong University (03081171).

REFERENCES

[1] Achard, P., Cheng, H., De Grauwe, L., Decat, J., Schoutteten, H., Moritz, T., Van Der Straeten, D., Peng, J., Harberd, N. P. (2006): Integration of plant responses to environmentally activated phytohormonal signals. – Science 311(5757): 91-94.

[2] Ahmadi, M. H., Hajizadeh, F., Rahimzadeh, M., Shafii, M. B., Chamkha, A. J., Lorenzini, G., Ghasempour, R. (2018): Application GMDH artificial neural network for modeling of Al2O3/water and Al2O3/Ethylene glycol thermal conductivity. – International Journal of Heat and Technology 36(3): 773-782.

[3] Ali, F., Arif, M., Khan, I., Sheikh, N. A., Saqib, M. (2018): Natural convection in polyethylene glycol-based molybdenum disulfide nanofluid with thermal radiation, chemical reaction and ramped wall temperature. – International Journal of Heat and Technology 36(2): 619-631.

[4] Ashraf, M. A., Rasheed, R., Hussain, I., Iqbal, M., Haider, M. Z., Parveen, S., Sajid, M. A. (2015): Hydrogen peroxide modulates antioxidant system and nutrient relation in maize (Zea mays L.) under water-deficit conditions. – Archives of Agronomy & Soil Science 61(4): 507-523.

[5] Cao, S., Chen, Z., Liu, G., Jiang, L., Yuan, H., Ren, G., Bian, X., Jian, H. Y., Ma, X. (2009): The Arabidopsis ethylene-insensitive 2 gene is required for lead resistance. – Plant Physiology & Biochemistry 47(4): 308-312.

http://www.aloki.hu ● ISSN 1589 1623 (Print) ● ISSN 1785 0037 (Online)
DOI: http://dx.doi.org/10.15666/aeer/1706_1440314414

[6] Cao, W. H., Liu, J., He, X. J., Mu, R. L., Zhou, H. L., Chen, S. Y. (2007): Modulation of ethylene responses affects plant salt-stress responses. – Plant Physiology 143(2): 707-719.
[7] Cao, Y. R., Chen, S. Y., Zhang, J. S. (2008): Ethylene signaling regulates salt stress response: an overview. – Plant Signaling & Behavior 3(10): 761-763.
[8] Chen, Q., Wu, K., Tang, Z., Guo, Q. X., Guo, X., Wang, H. (2017): Exogenous ethylene enhanced the cadmium resistance and changed the alkaloid biosynthesis in Catharanthus roseus seedlings. – Acta Physiologiae Plantarum 39(12): 267-272.
[9] Chen, Q., Lu, X., Guo, X., Pan, Y., Yu, B., Tang, Z. (2018): Differential responses to cd stress induced by exogenous application of Cu, Zn or Ca in the medicinal plant Catharanthus roseus. – Ecotoxicol Environ Saf 157: 266-275.
[10] Cuypers, A., Smeets, K., Vangronsveld, J. (2009): Heavy Metal Stress in Plants. – In: Hirt, H. (Ed.) Plant stress Biology: From Genomics to Systems Biology; Wiley-VCH: Verlag: Weinheim, Germany, 161-178.
[11] Fuhrer, J. (1982): Ethylene biosynthesis and cadmium toxicity in leaf tissue of beans (Phaseolus vulgaris l.). – Plant Physiology 70(1): 162-167.
[12] Gratao, P. L., Polle, A., Lea, P. J., Azevedo, R. A. (2005): Making the life of heavy metal-stressed plants a little easier. – Functional Plant Biology 32(6): 481-494.
[13] Gratão, P. L., Monteiro, C. C., Carvalho, R. F., Tezotto, T., Piotto, F. A., Peres, L. E. (2012): Biochemical dissection of diageotropica and never ripe tomato mutants to cd-stressful conditions. – Plant Physiol Biochem 56: 79-96.
[14] Iakimova, E., Kapchinatoteva, V., Jong, A. D., Atanassov, A., Woltering, E. (2005): Involvement of ethylene, oxidative stress and lipid-derived signals in cadmium-induced programmed cell death in tomato suspension cells. – BMC Plant Biology 5(S1): S19-S19.
[15] Järup, L., Akesson, A. (2009): Current status of cadmium as an environmental health problem. – Toxicology & Applied Pharmacology 238(3): 201-208.
[16] Jung, J. Y., Shin, R., Schachtman, D. P. (2009): Ethylene mediates response and tolerance to potassium deprivation in Arabidopsis. – Plant Cell 21(2): 607-621.
[17] Kaya, A., Yigit, E. (2012): Interactions among glutathione s-transferase, glutathione reductase activity and glutathione contents in leaves of Vicia faba, L. subjected to flurochloridone. – Fresenius Environmental Bulletin 21(6): 344-350.
[18] Kende, H. (1993): Ethylene biosynthesis. – Annual Review of Plant Biology 44(44): 283-307.
[19] Kim, D. Y., Bovet, L., Kushnir, S., Noh, E. W., Martinoia, E., Lee, Y. (2006): AtATM3 is involved in heavy metal resistance in Arabidopsis. – Plant Physiology 140(3): 922-932.
[20] Kim, D. Y., Bovet, L. M., Martinoia, E., Lee, Y. (2010): The ABC transporter AtPDR8 is a cadmium extrusion pump conferring heavy metal resistance. – Plant Journal 50(2): 207-218.
[21] Kranner, I., Roach, T., Beckett, R. P., Whitaker, C., Minibayeva, F. V. (2010): Extracellular production of reactive oxygen species during seed germination and early seedling growth in Pisum sativum. – Journal of Plant Physiology 167(10): 805-811.
[22] Lin, Y., Chen, D., Paul, M., Zu, Y., Tang, Z. (2013): Loss-of-function mutation of ein2 in arabidopsisexaggerates oxidative stress induced by salinity. – Acta Physiologiae Plantarum 35(4): 1319-1328.
[23] Mishra, S., Srivastava, S., Tripathi, R. D., Govindarajan, R., Kuriakose, S. V., Prasad, M. (2006): Phytochelatin synthesis and response of antioxidants during cadmium stress in Bacopa monnieri L{lozenge, open. – Plant Physiology and Biochemistry 44(1): 25-37.
[24] Mithöfer, A., Schulze, B., Boland, W. (2004): Biotic and heavy metal stress response in plants: evidence for common signals. – Febs Letters 566(1): 1-5.
[25] Mittler, R., Vanderauwera, S., Martin, G., Van Breusegemb, F. (2004): Reactive oxygen gene network of plants. – Trends in Plant Science 9(10): 490-498.
[26] Monteiro, C. C., Carvalho, R. F., Gratão, P. L., Carvalho, G., Tezotto, T., Medici, L. O. (2011): Biochemical responses of the ethylene-insensitive never ripe, tomato mutant

http://www.aloki.hu ● ISSN 1589 1623 (Print) ● ISSN 1785 0037 (Online)
DOI: http://dx.doi.org/10.15666/aeer/1706_1440314414

subjected to cadmium and sodium stresses. – Environmental & Experimental Botany 71(2): 306-320.

[27] Passardi, F., Theiler, G., Zamocky, M., Cosio, C., Rouhier, N., Teixera, F. (2007): Peroxibase: the peroxidase database. – Phytochemistry 68(12): 1605-1611.

[28] Ranieri, A., Castagna, A., Scebba, F., Careri, M., Zagnoni, I., Predieri, G. (2005): Oxidative stress and phytochelatin characterisation in bread wheat exposed to cadmium excess. – Plant Physiology & Biochemistry Ppb 43(1): 45-54.

[29] Satterfield, C. N., Bonnell, A. H. (1955): Interferences in titanium sulfate method for hydrogen peroxide. – Analytical Chemistry 27(7): 1174-1175.

[30] Schützendübel, A., Nikolova, P., Rudolf, C., Polle, A. (2002): Cadmium and H_2O_2 - induced oxidative stress in populus × canescens, roots. – Plant Physiology & Biochemistry 40(6): 577-584.

[31] Sharma, P., Jha, A. B., Dubey, R. S., Pessarakli, M. (2012): Reactive oxygen species, oxidative damage, and antioxidative defense mechanism in plants under stressful conditions. – Journal of Botany 2012: 1-26.

[32] Shen, L. (2008): Improvement in cadmium tolerance of tomato seedlings with an antisense dna for 1-aminocyclopropane-1-carboxylate synthase. – Journal of Plant Nutrition 31(5): 809-827.

[33] Skulachev, V. P. (1997): Membrane-linked systems preventing superoxide formation. – Bioscience Reports 17(3): 347-366.

[34] Smeets, K., Ruytinx, J., Semane, B., Belleghem, F. V., Remans, T., Sanden, S. V. (2008): Cadmium-induced transcriptional and enzymatic alterations related to oxidative stress. – Environmental & Experimental Botany 63(1): 1-8.

[35] Smeets, K., Opdenakker, K., Remans, T., Van, S. S., Van, B. F., Semane, B. (2009): Oxidative stress-related responses at transcriptional and enzymatic levels after exposure to cd or cu in a multipollution context. – Journal of Plant Physiology 166(18): 1982-1992.

[36] Vangronsveld, J., Clijsters, H. (2008): Toxic Effects of Metals. – In: Farago, M. E. (ed.) Plants and the Chemical Elements: Biochemistry, Uptake, Tolerance and Toxicity. Wiley, New York, pp. 149-177.

[37] Wang, Y., Liu, C., Li, K., Sun, F., Hu, H., Li, X., Zhao, Y., Han, C., Zhang, W., Duan, Y., Liu, M., Li, X. (2007): Arabidopsis ein2 modulates stress response through abscisic acid response pathway. – Plant Molecular Biology 64(6): 633-644.

[38] Wang, Y., Zong, K., Jiang, L., Sun, J., Ren, Y., Sun, Z. (2011): Characterization of an Arabidopsis cadmium-resistant mutant cdr3-1d reveals a link between heavy metal resistance as well as seed development and flowering. – Planta 233(4): 697-706.

[39] Zhang, Z. H., Meney, Z. R. K. (2010): Cadmium accumulation and translocation in four emergent wetland species. – Water Air & Soil Pollution 212(1-4): 239-249.

http://www.aloki.hu ● ISSN 1589 1623 (Print) ● ISSN 1785 0037 (Online)
DOI: http://dx.doi.org/10.15666/aeer/1706_1440314414

PREDICTION BASED ON COPULA ENTROPY AND GENERAL REGRESSION NEURAL NETWORK

HUANG, C. Y.[1] – ZHANG, Y. P.[2*]

[1]*School of Mathematics and Statistics, North China University of Water Resources and Electric Power, Zhengzhou, Henan 450011, China*

[2]*North China University of Water Resources and Electric Power, Zhengzhou, Henan 450011, China*

**Corresponding author*
e-mail: zhangyunpeng@ncwu.edu.cn; phone: +86-139-3826-4486

(Received 7th Jun 2019; accepted 10th Oct 2019)

Abstract. Drought prediction is the premise of effective response to the hazards of drought, a serious water-deficit phenomenon resulting from the complex interaction between climatic factors. Considering the high non-linearity of drought, this paper establishes a drought prediction model based on copula entropy and general regression neural network (GRNN). The climate indices that directly affect the formation of drought were selected as the inputs of the GRNN. The established model was applied to predict droughts for Lanzhou site of the middle reaches of the Yellow River. The results show that our model can effectively predict drought occurrence in the study area. With a strong predictive ability for drought, the proposed model is an ideal tool to forecast meteorological disasters based on climate factors.
Keywords: *Hampel, intelligence algorithms, SPI, neural network, prediction*

Introduction

Drought as one of the major natural disasters the human race faces directly threatening human life. It is now a serious factor that can restrict the sustainable development of community economy. Intensifying drought monitoring and prediction is significant for the relative authorities, in order to prevent drought and reduce losses caused by drought. However, the route that leads to drought is extremely complex, but it often develops and occurs as the result of a relatively slow process. Impacted by many factors, there has not been a relatively mature, accurate and universal model for drought prediction. The study is still in its infancy (Liu et al., 2019; Mossad and Alazba, 2018).

To predict drought, the regression model in time series is mostly used to construct future drought prediction model (Mokhtarzad et al., 2017) since it has a certain practicability. However, the meteorological forecast features significant nonlinearity. There is a highly complex nonlinear relationship between the predicted object and the predictor, but the regression model in the time series ignores this complex relationship.

By far, the Artificial Neural Network (ANN) model have been widely applied in the field of hydrology (Bello and Mamman, 2018; Garai et al., 2018; Isah et al., 2017; Mostefa et al., 2018; Qi et al., 2019; Sánchez-Escalona and Góngora-Leyva, 2018). When it is used to establish a drought prediction model, there is problem on how to select the predictors and the network models. To select predictive input factors, the practice is to consider the correlation between relevant drought predictors and drought indices, based on which to effectively predict the drought. As there is a highly complex nonlinear relationship between drought indices and prediction factors, it is considered the copula entropy can be used to determine the prediction factors; for the specific

http://www.aloki.hu ● ISSN 1589 1623 (Print) ● ISSN 1785 0037 (Online)
DOI: http://dx.doi.org/10.15666/aeer/1706_1441514424

network model, the Generalized Regression Neural Network (GRNN) with strong nonlinear mapping is used (Ladlani et al., 2012; McKee et al., 1993).

Based on all above, GRNN coupled with copula entropy (CE) is used to construct a drought prediction model based on CE-GRNN. The drought prediction correlation factor was selected by CE, and the GRNN was used for prediction to achieve drought prediction results.

This paper includes the following parts: Part 1 is the Introduction; Part 2 discusses the basic method and theory, including: the selection of predictors, the establishment of neural networks and the flow chart of the hybrid model. Part 3 is the Analysis of the results of the relevant sites; Part 4 gives the discussion, and the last part gives the Conclusion.

Materials and methods

Standard precipitation index

Standard Precipitation Index (SPI) (McKee et al., 1995; Shiau and Chiu, 2019) as one of drought indices was proposed by American scholar McKeed in 1993. It represents the standard deviation of the precipitation from the mean, similar to that in mathematical statistics.

SPI is defined as follows (Sharma, 2000):

Assume that the precipitation in an area is x, the probability density function is:

$$g(x) = \frac{1}{\beta^{\gamma}} x^{\gamma-1} e^{-x/\beta} \quad \text{(Eq.1)}$$

where: $\beta > 0$ is the scale, but $\gamma > 0$ is the shape parameter; β and γ can be obtained by the maximum likelihood estimation method:

$$\gamma = \frac{1 + \sqrt{1 + 4A/3}}{4A} \quad \text{(Eq.2)}$$

$$\beta = \frac{\bar{x}}{\gamma} \quad \text{(Eq.3)}$$

where:

$$A = \lg \bar{x} - \frac{1}{n} \sum_{i=1}^{n} \lg x_i \quad \text{(Eq.4)}$$

where: x_i represents the precipitation; $\bar{x}$ represents the mean of precipitation; n represents the length of the sequence.

After determining the parameters for the probability density function of the distribution, the cumulative probability function is expressed as

http://www.aloki.hu ● ISSN 1589 1623 (Print) ● ISSN 1785 0037 (Online)
DOI: http://dx.doi.org/10.15666/aeer/1706_1441514424

$$G(x) = \int_0^x g(x)dx = \int_0^x \frac{1}{\beta^\gamma} x^{\gamma-1} e^{-x/\beta} dx \quad \text{(Eq.5)}$$

Since the *Gamma* function is undefined when $x = 0$, the precipitation value 0 can be transformed by the following formula:

$$H(x) = q + (1-q)G(x) \quad \text{(Eq.6)}$$

where: q is the probability of occurrence of value 0 in the precipitation sequence, and then $H(X)$ is normalized by a Gaussian function. The normal normalization is performed on *Gamma* distribution probability, so that an approximated solution can be obtained:

$$SPI = S(t - \frac{2.52 + 0.8t + 0.01t^2}{1 + 1.43t + 0.19t^2 + 0.001t^3}) \quad \text{(Eq.7)}$$

where:, $t = \sqrt{ln\frac{1}{H(x)^2}}$, $H(x)$ is the probability obtained by the *Equation 6,* when $H(x) > 0.5$, $S = 1$; when $H(X) \leq 0.5$, $S = -1$.

Option of prediction factors based on copula entropy

Copula Entropy, as a new entropy concept defined by Ma and Sun (Chen et al., 2015; Chen and Guo, 2019; Fernando et al., 2009; Hao and Singh, 2012; Ma and Sun, 2011) in 2008, can be used to measure the full order correlation between random variables. Here, Copula entropy can describe the correlation between the target and the predictive factors. How to use the copula entropy to select predictive factors requires an effective and reliable standard. That is to say, at the time of what the copula entropy value is, relevant prediction factors can be used as the input set of the prediction model. Here, the Hampel test recommended by Fernando and May, et al. is used as the stopping criterion of the algorithm (May et al., 2008).

The Hampel test algorithm is expressed as:

$$H_j = \frac{d_j}{1.4826 d_j^{(50)}} \quad d_j = \left| C_{PMI} - C_{PMI}^{(50)} \right| \quad \text{(Eq.8)}$$

where: H_j- Hampel distance; 1.4826 - normalization factor such that H_j is equal to the standard deviation σ of the data sequence; $d_j^{(50)}$- median of d_j; $C_{PMI}^{(50)}$- median of the values C_{PMI} in a set of data; $C_{PMI}^{(50)}$- copula entropy.

According to the standard deviation 3σ criterion, when the Hampel distance is greater than 3, the input variable will be included into the set of input variables, that is, determined as the prediction factors of the model.

According to the selection criteria of copula entropy, the prediction factors of the neural network model are determined by the following procedure:

1. Filter out all possible input variables;.

http://www.aloki.hu ● ISSN 1589 1623 (Print) ● ISSN 1785 0037 (Online)
DOI: http://dx.doi.org/10.15666/aeer/1706_1441514424

2. Construct a joint distribution of individual factors and the predicted target, and select the optimal Copula function.
3. Determine the Copula density function with the selected Copula function, calculate the Copula entropy value of each factor and the predicted target.
4. Calculate the Hampel distance between the predicted target and the factor with the Hampel algorithm.
5. According to the test criteria, the determined factors are included in the input variable set as the last input factor for the neural network.

Establishment of NN model

The neural network is a new type of intelligent algorithm that can imitate the animal's nervous system. It depends on the neurons to link each other. there are three layers: the input layer, the hidden layer, and the output layer, each of which has its own special functions: the input layer performs factor input and processing; since input data must not be linear in real world, and sometimes is multidimensional. It is required to allow data to be trained via the hidden layer to make data visible, in order to obtain data as required. The hidden layer is therefore the core of the neural network; after the training via the hidden layer, data basically is what we want to be. Then it is required to output data via the output layer. These three layers are independent of each other, and the state of neurons in each layer can only affects those in the next layer. In this paper, the input variables are various factors related to drought prediction, and the output variables is drought prediction result. The framework of neural network is shown in *Figure 1*.

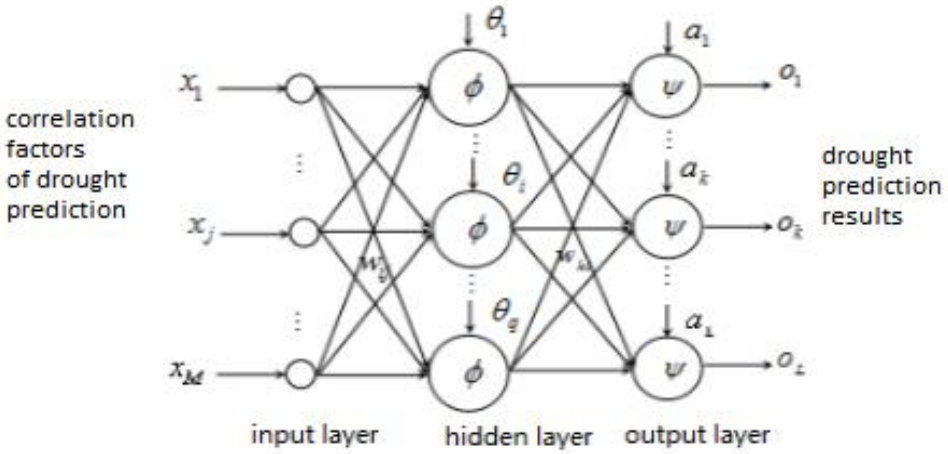

Figure 1. *Framework of neural network*

Hybrid prediction model based on Copula entropy and GRNN

When the GRNN is used to carry out the correlation prediction algorithm, the correlation between individual factors and drought object is first calculated based on the Copula entropy, and then the last input factor selected is chosen as the input layer of the neural network according to the Hampel distance. The drought prediction is also explored when appropriate. The relevant prediction process is shown in *Figure 2*.

In the process of establishing the GRNN model, more attention should be paid to the analysis of the physical meaning between prediction objects and the selection of

http://www.aloki.hu ● ISSN 1589 1623 (Print) ● ISSN 1785 0037 (Online)
DOI: http://dx.doi.org/10.15666/aeer/1706_1441514424

predictors. Undoubtedly, precipitation and drought are the most closely related. The SPI drought index is calculated from precipitation. Therefore, when the predictor is considered, the correlation between the nine related factors other than precipitation is studied. Among these related factors, CE method is used to select four factors which are most closely related to drought as prediction factors according to HAMPLE criterion. This coincides with the prediction content of the climate dynamics model proposed by Zeng Qingcun, an academician at the Institute of Atmospheric Physics of Chinese Academy of Sciences (Zeng, 1998).

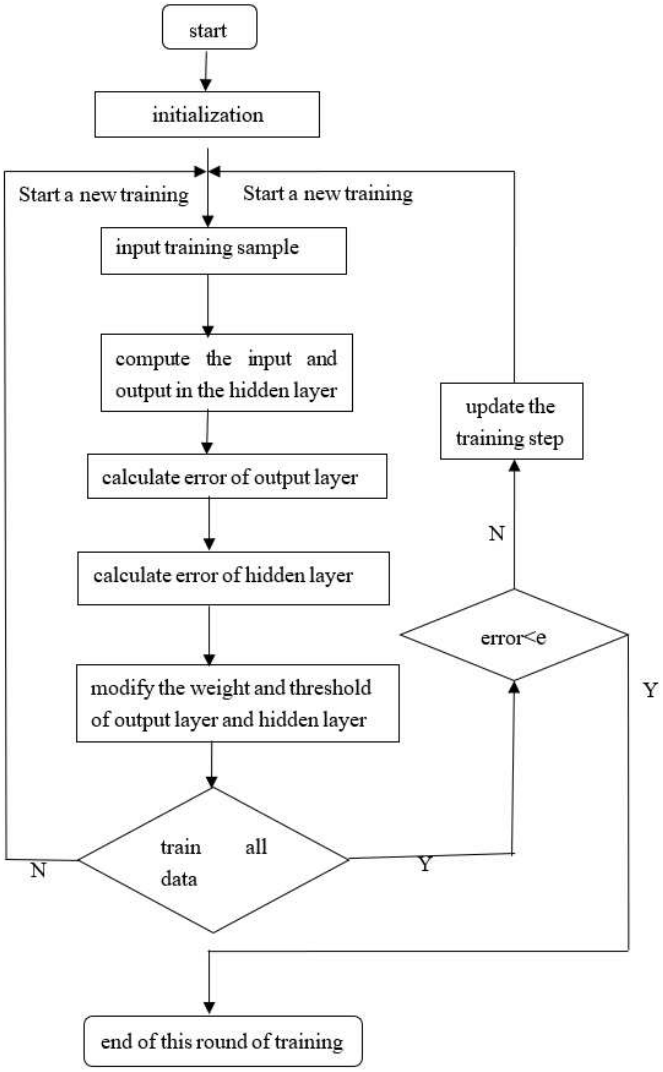

Figure 2. *Flow chart of prediction of neural network*

Results

Selection of input set

In order to verify the effectiveness of the algorithm of drought prediction in practice, the Lanzhou site in the middle reaches of the Yellow River basin of China is taken as study sample. The Lanzhou site is located at 34.29° north latitude and 110.05° east longitude. The distribution map of Lanzhou site and nearby sites is shown in *Figure 3*.

http://www.aloki.hu ● ISSN 1589 1623 (Print) ● ISSN 1785 0037 (Online)
DOI: http://dx.doi.org/10.15666/aeer/1706_1441514424

For some reasons, only some relevant data are obtained. Therefore, meteorological data from 1957 to 2010 are used for analysis. In order to eliminate the inconsistency of data, normalization processing for homogenize data is adopted, and at the same time, interpolation method is used to process the abnormal value.

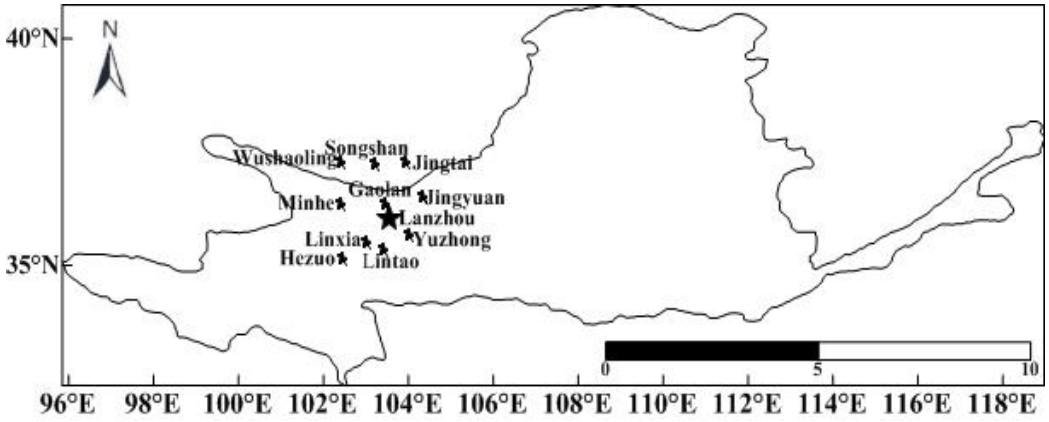

Figure 3. *Distribution map of Lanzhou site*

For selecting drought prediction factors, the following nine meteorological drought indices: wind speed, wind direction, air temperature, precipitation anomaly, temperature departure, vapor pressure, relative humidity, percentage of sunshine, sunshine hours, are used as initial factors and labeled as independent variables to calculate the Copula entropy, then n factors closely related to drought index of SPI were screened out based on the Hampel test which value is greater than 3 as the last set C. Finally, the variables of last set *C* are used as an input variable into the neural network for training. *Table 1* lists the copula value and the associated Hampel distance calculated by the above method from meteorological data of Lanzhou site.

Table 1. *Entropy value and Hampel list*

Factor (SPI)	Mutual entropy	Copula entropy	Hampel distance
Precipitation nomaly	0.29	-0.29	2.82
Wind speed	0.16	-0.16	3.05
Air temperature	0.39	-0.39	3.47
Temperature nomaly	0.09	-0.09	2.89
Vapor pressure	0.45	-0.45	3.31
Sunshine hours	0.07	-0.07	2.82
Relative humidity	0.29	-0.29	3.41
Percentage of sunshine	0.16	-0.16	2.77
Wind direction	0.01	-0.01	1.65

According to the Hampel test criteria, when the Hampel distance is greater than 3, the selected factors are used as the last input factors. As shown in *Table 1,* there are meteorological factors with Hampel distance greater than 3, including four factors: wind speed, air temperature, vapor pressure, and relative humidity. Therefore, these four factors are used as the last input set of variables of GRNN for drought prediction.

http://www.aloki.hu ● ISSN 1589 1623 (Print) ● ISSN 1785 0037 (Online)
DOI: http://dx.doi.org/10.15666/aeer/1706_1441514424

Predicted results

The predictive analysis of drought is made with the Lanzhou site SPI as the prediction target, and the selected factors, i.e. wind speed, air temperature, vapor pressure and relative humidity, are input into the input layer of the neural network for correlation prediction. And in his paper, the error of the actual value and the predicted value is used to test the performance of the algorithms. The image of predicted results is shown in *Figure 4*. The error map for the actual and predicted values of the drought indices is shown in *Figure 5,* and the violin plot of the predicted results is shown in *Figure 6*.

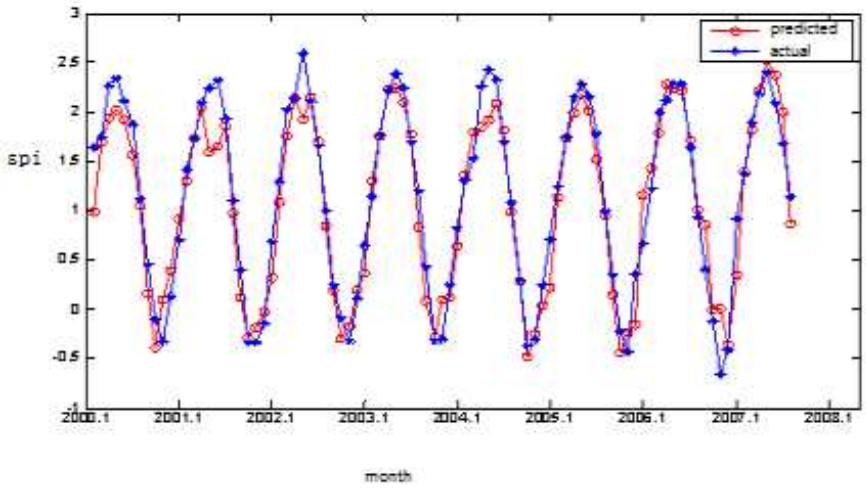

Figure 4. *Actual and predicted SPI value*

The red line in *Figure 4* represents the predicted value output, and the blue line represents the actual value. As shown in *Figure 4,* the fitting effect is better at most points, but the prediction effect at the critical values is relatively poor. In *Figure 5,* the value of the horizontal coordinate corresponds to the time coordinate in *Figure 4,* and it describes the error value of the corresponding time. As seen from the error results in *Figure 5,* the prediction effect is better.

Figure 5. *Error of actual drought and predicted values*

http://www.aloki.hu ● ISSN 1589 1623 (Print) ● ISSN 1785 0037 (Online)
DOI: http://dx.doi.org/10.15666/aeer/1706_1441514424

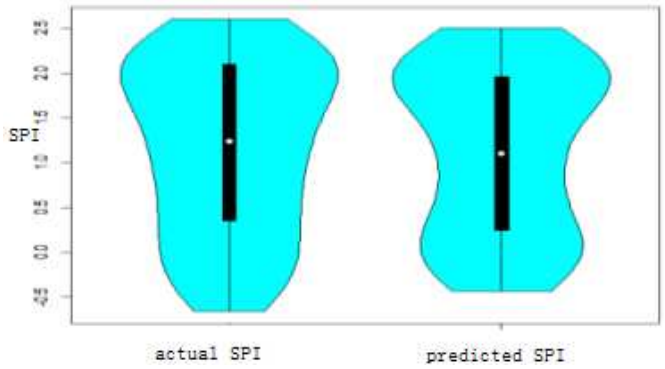

Figure 6. *Violin plot of actual and predicted results*

As shown in *Figure 6,* the simulated and actual values for the drought indices of Lanzhou site can well fit the nuclear density and box plot. The median of the simulated values is slightly lower than but substantially consistent with the actual value. It lies in half-way down the box, basically to be consistent with the actual situation. The maximum of the simulated values is substantially equal to that of the actual values, and the minimum value is relatively low.

As shown in *Figures 4, 5* and *6,* the results simulated for the drought prediction in Lanzhou site further show that the hybrid algorithm based on Copula entropy and GRNN has better prediction effect.

Discussion

Traditional prediction method is designed for linear sequences, while predicted results from methods for nonlinear drought sequences are often unsatisfactory. It is extremely important to improve the prediction accuracy of nonlinear time series. Copula entropy can well describe how well the correlation between nonlinear drought sequences and drought predictors, and the neural network is also proven to be effective in predicting nonlinear drought time series.

Conclusion

Since the drought presents a complex nonlinearity, the traditional drought prediction algorithm has a relatively wide error. In contrast, the GRNN has a good nonlinear approximation performance, so that it features high robustness and fault tolerance. With copula entropy, the nonlinear dependence between factors and objects can be depicted. Therefore, this paper predicts the meteorological drought indices by establishing a hybrid model based on Copula entropy and GRNN. The results reveal that the well-established drought prediction model can directly predict the drought time sequence at a high accuracy rate. This model has a favorable generalization performance.

Although GRNN improves the prediction accuracy to some extent, but it is easy to fall into the extreme value, and the mapping ability of the non-stationary sequence is insufficient, which affects the accuracy of prediction to a certain extent. Therefore, some relevant parameter optimization algorithm (for example, the fruit fly optimization algorithm) can be considered to optimize the parameters of the neural network to further improve the prediction accuracy.

http://www.aloki.hu ● ISSN 1589 1623 (Print) ● ISSN 1785 0037 (Online)
DOI: http://dx.doi.org/10.15666/aeer/1706_1441514424

Acknowledgements. This research was supported by Key Scientific Research Projects Plan of Henan Higher Education Institutions (19A120008). Sincere gratitude is extended to the editor and anonymous reviewers for their professional comments and corrections, which greatly improved the presentation of the paper.

REFERENCES

[1] Bello, A. A., Mamman, M. B. (2018): Monthly rainfall prediction using artificial neural network: A case study of Kano, Nigeria. – Environmental and Earth Sciences Research Journal 5(2): 37-41.
[2] Chen, L., Guo, S. (2019): Copulas and Its Application in Hydrology and Water Resources. Chap. 10. – Springer Water Series. Springer, Singapore, pp. 237-271.
[3] Chen, L., Singh, V. P., Guo, S., Zhou, J. Z., Zhang, J. H. (2015): Copula-based method for multisite monthly and daily streamflow simulation. – Journal of Hydrology 528: 369-384.
[4] Fernando, T. M. K. G., Maier, H. R., Dandy, G. C. (2009): Selection of input variables for data driven models: an average shifted histogram partial mutual information estimator approach. – Journal of Hydrology 367: 165-176.
[5] Garai, D., Agrawal, H., Mishra, A. K., Kumar, S. (2018): Influence of initiation system on blast-induced ground vibration using random forest algorithm, artificial neural network, and scaled distance analysis. – Mathematical Modelling of Engineering Problems 5(4): 418-426.
[6] Hao, Z., Singh, V. P. (2012): Entropy-copula method for single-site monthly streamflow simulation. – Water Resources Research 48(6): 6604.
[7] Isah, O. R., Usman, A. D., Tekanyi, A. M. S. (2017): A hybrid model of PSO algorithm and artificial neural network for automatic follicle classification. – International Journal Bioautomation 21(1): 43-58.
[8] Ladlani, I., Houichi, L., Djemili, L., Heddam, S. (2012): Modeling daily reference evapotranspiration (ET0) in the north of Algeria using generalized regression neural networks (GRNN) and radial basis function neural networks (RBFNN): a comparative study. – Meteorology & Atmospheric Physics 118(3-4): 163-178.
[9] Liu, Q., Zhang, G. L., Ali, S., Wang, X. P., Wang, G. D., Pan, Z. K., Zhang, J. H. (2019): SPI-based drought simulation and prediction using ARMA-GARCH model. – Applied Mathematics and Computation 355: 96-107.
[10] Ma, J., Sun, Z. (2011): Mutual information is copula entropy. – Tsinghua Science and Technology 16(1): 51-54.
[11] May, R. J., Maier, H. R., Dandy, G. C., Fernando, T. M. K. G. (2008): Non-linear variable selection for artificial neural networks using partial mutual information. – Environmental Modeling & Software 23: 1312-1326.
[12] McKee, T. B., Doesken, N. J., Kleist, J. (1993): The relationship of drought frequency and duration to time scales. – 8th Conference on Applied Climatology, Anaheim, CA, pp. 179-184.
[13] Mckee, T. B. N., Doeskin, N. J., Kleist, J. (1995): Drought Monitoring with Multiple Time Scales. – American Meteorological Society, Dallas, TX, pp. 233-236.
[14] Mokhtarzad, M., Eskandari, F., Vanjani, N. J., Arabasadi, A. (2017): Drought forecasting by ANN, ANFIS, and SVM and comparison of the models. – Environmental Earth Sciences 76(21): 729-735.
[15] Mossad, A., Alazba, A. A. (2018): Determination and prediction of standardized precipitation index (SPI) using TRMM data in arid ecosystems. – Arabian Journal of Geosciences 11(6): 132-139.

http://www.aloki.hu ● ISSN 1589 1623 (Print) ● ISSN 1785 0037 (Online)
DOI: http://dx.doi.org/10.15666/aeer/1706_1441514424

[16] Mostefa, T., Tarak, B., Hachemi, G. (2018): An automatic diagnosis method for an open switch fault in unified power quality conditioner based on artificial neural network. – Traitement du Signal 35(1): 7-21.
[17] Qi, J. X., Jiang, G. Z., Li, G. F., Sun, Y. (2019): Surface EMG hand gesture recognition system based on PCA and GRNN. – Neural Computing and Applications (4): 1-9.
[18] Sánchez-Escalona, A. A., Góngora-Leyva, E. (2018): Artificial neural network modeling of hydrogen sulphide gas coolers ensuring extrapolation capability. – Mathematical Modelling of Engineering Problems 5(4): 348-356.
[19] Sharma, A. (2000): Seasonal to interannual rainfall probabilistic forecasts for improved water supply management: Part 1 - A strategy for system predictor identification. – Journal of Hydrology 239(1): 232-239.
[20] Shiau, J. T., Chiu, Y. F. (2019): Wavelet-based detection of time-frequency changes for monthly rainfall and SPI series in Taiwan. – Asia-Pacific Journal of Atmospheric Sciences 55(4): 657-667.
[21] Zeng, Q. C. (1998): A mathematic model of climate dynamics suitable for modern mathematical analysis. – Scientia Atmospherica Sinica 22(4): 408-417.

http://www.aloki.hu ● ISSN 1589 1623 (Print) ● ISSN 1785 0037 (Online)
DOI: http://dx.doi.org/10.15666/aeer/1706_1441514424

EVOLUTIONARY GAME ANALYSIS OF ECOLOGICAL COMPENSATION IN THE ECONOMIC TRANSITION OF STATE-OWNED FOREST AREAS

GUO, J. Y.* – CHEN, S. L.

Forest Road and Structural Engineering, Civil Engineering College, Central South University of Forestry and Technology, Changsha 410000, China

**Corresponding author*
e-mail: lydiagjy@163.com

(Received 7th Jun 2019; accepted 10th Oct 2019)

Abstract. The excessive consumption of forest resources has severely challenged the sustainable development of society, economy and resources in state-owned forest areas, so it is urgent to explore the economic transformation of forest areas. In the process of economic transformation and development in forest areas, a large amount of social capital is needed to make up for the shortage of national financial investment. The implementation of an ecological compensation mechanism is of great significance to attract social capital to the economic transformation and development of forest areas and to realize the sustainable development of the ecological environment. However, ecological compensation involves the direct interests of many parties, and it is easy to form a game situation. The evolutionary game model between government's ecological compensation behavior and social capital's ecological protection behavior is constructed to study the selection strategies of ecological problems under different circumstances by both sides, obtaining stability strategy and evolution path of both sides within different range of parameters. The research shows that the necessary condition to realize the optimal and stable equilibrium strategy is that the project investment profit of social capital should be larger than speculative profit under the government's ecological non-compensation, and the supervision cost of government departments should be less than ecological profit.
Keywords: *ecological protection, ecological compensation, evolutionary strategy, evolutionary trend, ecological benefit*

Introduction

During the inspection of state-owned forest areas in China, some scholars have pointed out that new ways for industrial development should be explored after the commercial logging has been completely stopped in the state-owned forest areas. It is necessary to shift from the extensive strategy of resource development and economic development to the ecological development strategy of rational protection, intensive resource development and economic development. At this stage, the research achievements on the economic transformation of state-owned forest areas are as follows: the current situation of the transformation is analyzed, and the measures for the coordinated development of ecological construction and economic transformation are put forward (Li et al., 2019; Tong et al., 2018; Wen et al., 2017). Through the analysis of the interest game among the central government, local government and state-owned forestry enterprises in the process of the construction of the ecological function zones in the Daxiaoxingan Mountains, the strategies for improving the economic transformation in the state-owned forestry areas are put forward (Zhong et al., 2017). In the reform of the state-owned forest ownership, the game model of the stakeholders' responsibility of the government, forestry enterprises and workers is established, and the measures for the three parties to obtain reasonable interests according to their responsibilities are put

http://www.aloki.hu ● ISSN 1589 1623 (Print) ● ISSN 1785 0037 (Online)
DOI: http://dx.doi.org/10.15666/aeer/1706_1442514434

forward (Sun et al., 2018). To sum up, it is an arduous task to protect both ecology and the people's livelihoods in the transformation and development of forest areas. We should broaden our thinking and take multiple measures simultaneously. Therefore, finding a balance between ecological protection and economic transformation has become the key to the reform of state-owned forest areas in China. Introducing the mechanism of ecological compensation and adjusting the ecological interest relations among ecological stakeholders by economic means are of great significance for protecting the forest ecosystem and promoting the economic transformation and upgrading of forest areas.

The existing research on ecological compensation mainly includes two aspects: one is the construction of ecological compensation mechanism. On the basis of systematic analysis of the elements of ecological compensation for forest tourism, the specific mechanism of taking ecological protection and economic development into account simultaneously through ecological compensation is put forward (Fang et al., 2018; Liu et al., 2018). The other is that the evolutionary game theory is used to solve the problem of ecological compensation in many fields. In China's non-resident islands, the dynamic evolution process of the influence of various elements of the main stakeholders of ecological compensation on decision-making behavior is analyzed by using the evolutionary game theory (Liu et al., 2016). The strategic selection between ecological compensation of mineral resources development enterprises and government supervision is discussed from the perspective of evolutionary game theory (Zhang, 2016). The game behavior of upstream and downstream governments in the process of implementing ecological protection and compensation is analyzed, and the effective ways to protect the ecological environment of the basin is obtained (Zhou et al., 2018). The conflict of interest and game in ecological compensation for coal mining is analyzed, and some measures and suggestions for coordinating and balancing the interests of all parties in ecological compensation is put forward (Guo et al., 2018). In summary, no scholars have explored the ecological compensation problems for the economic transformation of the state-owned forest areas in China from the perspective of the Public-Private Partnership model and the evolutionary game. Therefore, this paper introduces evolutionary game theory to construct a game model between the social capital side's ecological protection behavior and government's ecological compensation behavior, which provides theoretical basis and decision support for the realization of high-quality coordinated development of ecological construction and economic transformation.

Materials and methods

Research subject

This paper takes Lutou forest farm in Pingjiang County, Yueyang City, Hunan Province, China, as a specific research object. The construction of Lutou forest farm needs a large amount of financial support. The Public-Private Partnership model should be adopted to encourage and guide the participation of social capital, which is conducive to promoting the economic transformation of the forest farm. However, in the process of cooperation, there is a certain conflict between the social capital's goal of maximizing economic benefits and the government's goal of pursuing environmental benefits, which leads to the game between them in the process of ecological protection implementation. In the process of game, when the investment income of the social

http://www.aloki.hu ● ISSN 1589 1623 (Print) ● ISSN 1785 0037 (Online)
DOI: http://dx.doi.org/10.15666/aeer/1706_1442514434

capital side decreases due to the protection of the ecological environment, they tend to prefer not to protect the ecological environment. For this kind of behavior of the social capital side, when the government takes incentive measures to compensate for the ecological expenditure of enterprises, they will restore the ecological environment; and when the government relaxes the incentive of their ecological protection behavior, the social capital side will produce acts of destroying the environment. In this way, the social capital side and governments play games according to their respective goals until they reach equilibrium.

Therefore, the main stakeholders involved in the evolutionary game model of the ecological compensation are the social capital side and government departments. The social capital side and government departments conduct strategy selection for ecological protection. The strategic space for social capital side is ecological protection and non-ecological protection, and the strategic space for government departments is ecological compensation and non-ecological compensation. During the whole process of cooperation, the two sides are bounded rationality and they constantly adjust their own decision-making according to their own benefits and strategies of the other side.

Basic assumptions

The following assumptions are made on the evolutionary game model of ecological compensation:

(1) Benefits and cost of social capital side: I is the project investment; R is the benchmark rate of return; b_s is the for the distribution rate of benefits; L_1 is the environmental benefits obtained by carrying out the ecological protection measures; e is the extra benefits by pursuing the pure economic interests but failing to implement the ecological protection measures, which is related to the degree of speculation of the social capital side. c_1 is the cost paid by social capital to achieve the project economic and environmental benefits; K is the ecological compensation given by government departments when social capital side performs ecological protection measures; S is the punishment imposed by government departments on the social capital side which does not perform ecological protection measures.

(2) P_1 ($0 \leq P_1 \leq 1$) is the ecological protection level of the social capital side. In the case of ecological protection measures in place, $P_1 = 1$; the smaller the value of P_1, the weaker the ecological protection, which is reflected in the decline in ecological protection costs, increase in the extra benefits and punishment cost.

(3) Benefits and cost of government departments: the benefits of government departments come from the distribution of the income of the social capital side and punishment imposed on the social capital side. The cost includes the cost c_2 of supervising whether the social capital side implement ecological protection measures and the incentive cost of ecological subsidy for the social capital side.

(4) P_2 ($0 \leq P_2 \leq 1$) is the ecological compensation level of government departments. The smaller the value of P_2, the less the compensation, which is reflected in the decline of supervision cost and punishment cost.

Establishment of evolutionary game model

The evolutionary game is based on bounded rationality, which assumes that due to the bounded rationality of the economic subjects, it is impossible for the economic

http://www.aloki.hu ● ISSN 1589 1623 (Print) ● ISSN 1785 0037 (Online)
DOI: http://dx.doi.org/10.15666/aeer/1706_1442514434

subjects to clearly understand their own state and thus they will follow the most favorable strategy to imitate until reaching the equilibrium.

Based on the above assumptions, the income matrix of the ecological compensation can be obtained, as is shown in *Table 1*.

Table 1. *Income matrix of the evolutionary game model of ecological compensation*

Social capital side	**Government departments**	
	Ecological compensation	**Non-ecological compensation**
Ecological protection	$(b_sIR+L_1-C_1+K,$ $(1-b_s)IR+L_1-C_2-K)$	$(b_sIR+P_2L_1-C_1+P_2K,$ $(1-b_s)IR+P_2L_1-P_2C_2-P_2K)$
Non-ecological protection	$b_sIRP_1+P_1L_1+e(1-P_1)-$ $P_1C_1+K-(1-P_1)S,$ $(1-b_s)IRP_1+P_1L_1-$ $C_2-K+(1-P_1)S$	$b_sIRP_1+P_1P_2L_1+e(1-P_1)-$ $P_1C_1+P_2K-(1-P_1)S,$ $(1-b_s)IRP_1+P_1P_2L_1-$ $P_2C_2-P_2K+(1-P_1)S$

Assuming that ratio of adopting "ecological protection" by the social capital side is x and the ratio of adopting "non- ecological protection" is $1-x$ ($0 \le x \le 1$); the ratio of adopting "ecological compensation" by government departments is y and the ratio of adopting "non-ecological compensation" is $1-y$ ($0 \le y \le 1$). In this way, the benefits θ_{11} and θ_{12} when adopting "ecological protection" and "non-ecological protection" and the group average benefit $\bar{\theta}_1$ are showed in *Equations 1–3:*

$$\theta_{11}=y(b_sIR-C_1+K)+(1-y)(b_sIR-C_1+P_2K) \quad \text{(Eq.1)}$$

$$\theta_{12}=y(b_sIRP_1+e(1-P_1)-P_1C_1+K-(1-P_1)S)+(1-y)(b_sIRP_1+e(1-P_1)-P_1C_1+P_2K-(1-P_1)S) \quad \text{(Eq.2)}$$

$$\bar{\theta}_1=x\theta_{11}+(1-x)\theta_{12} \quad \text{(Eq.3)}$$

The replicated dynamic equation of the social capital side is showed in *Equations 4* and *5:*

$$G(x)=\frac{dx}{dt}=x(\theta_{11}-\bar{\theta}_1)=x(1-x)\begin{pmatrix}(b_sIR-e-C_1+S+L_1P_2)(1-P_1)\\+L_1y(1-P_1)(1-P_2)\end{pmatrix} \quad \text{(Eq.4)}$$

$$G'(x)=(1-2x)\begin{pmatrix}(b_sIR-e-C_1+S+L_1P_2)(1-P_1)\\+L_1y(1-P_1)(1-P_2)\end{pmatrix} \quad \text{(Eq.5)}$$

In the same way, the replicated dynamic equation of local government department is showed in *Equations 6* and *7:*

http://www.aloki.hu ● ISSN 1589 1623 (Print) ● ISSN 1785 0037 (Online)
DOI: http://dx.doi.org/10.15666/aeer/1706_1442514434

$$G(y)=\frac{dy}{dt}=y(\theta_{21}-\bar{\theta}_2)=y(1-y)\begin{pmatrix}(-C_2-K+L_1P_1)(1-P_2)\\+L_1x(1-P_2)(1-P_1)\end{pmatrix} \quad \text{(Eq.6)}$$

$$G'(y)=(1-2y)\begin{pmatrix}(-C_2-K+L_1P_1)(1-P_2)\\+L_1x(1-P_2)(1-P_1)\end{pmatrix} \quad \text{(Eq.7)}$$

Make $G(x)=0$, $G(y)=0$, and obtain the five local equilibrium points in this evolutionary game system is $A(0,0)$, $B(1,0)$, $C(0,1)$, $D(1,1)$. When $0\le x^*\le 1$ and $0\le y^*\le 1$, the $E(x^*,y^*)$ is also the local equilibrium point in this evolutionary game system. In *Equations 8* and *9:*

$$x^*=\frac{C_2+K-L_1P_1}{L_1(1-P_1)} \quad \text{(Eq.8)}$$

$$y^*=-\frac{b_sIR-e-C_1+S+L_1P_2}{L_1(1-P_2)} \quad \text{(Eq.9)}$$

The Jacobian matrix corresponded to *Equations 4* and *6* is shown in *Equation 10:*

$$J=\begin{bmatrix}\frac{\partial G(x)}{\partial x} & \frac{\partial G(x)}{\partial y}\\ \frac{\partial G(y)}{\partial x} & \frac{\partial G(y)}{\partial y}\end{bmatrix}=\begin{bmatrix}(1-2x)\begin{pmatrix}(b_sIR-e-C_1+S+L_1P_2)(1-P_1)\\+L_1y(1-P_1)(1-P_2)\end{pmatrix} & x(1-x)L_1(1-P_1)\\ y(1-y)L_1(1-P_2) & (1-2y)\begin{pmatrix}(-C_2-K+L_1P_1)(1-P_2)\\+L_1x(1-P_2)(1-P_1)\end{pmatrix}\end{bmatrix} \quad \text{(Eq.10)}$$

The determinant and trace of this Jacobian matrix can be obtained from *Equation 10,* see *Equations 11* and *12:*

$$\det.J\left(\det e\min ant.Jacobian,\det.J\right)=\frac{\partial F(x)}{\partial x}\square\frac{\partial F(y)}{\partial y}-\frac{\partial F(y)}{\partial x}\square\frac{\partial F(x)}{\partial y} \quad \text{(Eq.11)}$$

$$trJ\left(trace\,Jacobian,trJ\right)=\frac{\partial F(x)}{\partial x}+\frac{\partial F(y)}{\partial y} \quad \text{(Eq.12)}$$

If $\det.J>0$ and $trJ<0$ are satisfied, then the equilibrium point of the replicated dynamic equation is evolutionary stable strategy.

Results

Make $\pi_1=(b_sIR-e-c_1+S+L_1)(1-P_1)$ as the net income of social capital side who implement the ecological protection measures under the ecological compensation of government departments, $\pi_2=(b_sIR-e-c_1+S+L_1P_2)(1-P_1)$

http://www.aloki.hu ● ISSN 1589 1623 (Print) ● ISSN 1785 0037 (Online)
DOI: http://dx.doi.org/10.15666/aeer/1706_1442514434

as net income of social capital side who implement the ecological protection measures under the non- ecological compensation of government departments, $\pi_3 = (-c_2 - K + L_1)(1 - P_2)$ as the net income of government departments who perform ecological compensation when social capital side implement the ecological protection measures, and $\pi_4 = (-c_2 - K + L_1 P_1)(1 - P_2)$ as the net income of government departments who perform ecological compensation when social capital side fails to implement the ecological protection measures. From the formulas, $\pi_1 > \pi_2$ and $\pi_3 > \pi_4$.

The local equilibrium point stability of the Jacobian matrix of the system in Case (1) ($\pi_1 < 0$, $\pi_3 < 0$) were analyzed as shown in *Table 2*. Similarly, the evolutionary stable strategy of the system with different parameter value ranges, as shown in *Table 3*.

Table 2. *Analysis of equilibrium point stability in case (1)*

Equilibrium point	det. J	trJ	$\pi_1 < 0, \pi_4 < 0$		
			det. J	trJ	**Stability**
$A(0,0)$	$\pi_2 \cdot \pi_4$	$\pi_2 + \pi_4$	+	-	ESS (evolutionary stable strategy, ESS)
$B(1,0)$	$-\pi_2 \cdot \pi_3$	$-\pi_2 + \pi_3$	-	±	Saddle point
$C(0,1)$	$-\pi_1 \cdot \pi_4$	$\pi_1 - \pi_4$	-	±	Saddle point
$D(1,1)$	$\pi_1 \cdot \pi_3$	$-\pi_1 - \pi_3$	+	+	Instability

Table 3. *Analysis of equilibrium point stability with different parameter values*

	Parameter value range		**Evolutionary stability strategy**
(1)	$\pi_1 < 0, \pi_3 < 0$	$A(0,0)$	{no protection, no compensation}
(2)	$\pi_1 < 0, \pi_3 > 0, \pi_4 < 0$	$A(0,0)$	{no protection, no compensation}
(3)	$\pi_1 < 0, \pi_3 > 0, \pi_4 > 0$	$C(0,1)$	{no protection, compensation }
(4)	$\pi_1 > 0, \pi_2 < 0, \pi_3 < 0$	$A(0,0)$	{no protection, no compensation}
(5)	$\pi_1 > 0, \pi_2 > 0, \pi_3 < 0$	$B(1,0)$	{protection, no compensation}
(6)	$\pi_1 > 0, \pi_2 > 0, \pi_3 > 0, \pi_4 < 0$	$D(1,1)$	{protection, compensation}
(7)	$\pi_1 > 0, \pi_2 > 0, \pi_3 > 0, \pi_4 > 0$	$D(1,1)$	{protection, compensation}
(8)	$\pi_1 > 0, \pi_2 < 0, \pi_3 > 0, \pi_4 > 0$	$D(1,1)$	{protection, compensation}
(9)	$\pi_1 > 0, \pi_2 < 0, \pi_3 > 0, \pi_4 < 0$	$D(1,1)$	{protection, compensation}

Discussion

Analysis of the system stability strategy

In line with comparison and analysis of the data in *Table 3:*

(1) It can be concluded from Cases (1), (2) and (4) that only when $\pi_2 < 0$ and $\pi_4 < 0$, namely $b_s IR - c_1 + L_1 P_2 < e - S$ and $c_2 > L_1 P_1 - K$, the point $A(0,0)$ refers to the evolution stable strategy of the system, namely non- ecological protection by social capital side and non-ecological compensation by government departments. And the rest of the points are in a temporarily stable state, which means that once affected by factors, they will deviate from this state.

(2) It can be concluded from Cases (3) that only when $\pi_1 < 0$ and $\pi_4 > 0$, namely $b_s IR - c_1 + L_1 < e - S$ and $c_2 < L_1 P_1 - K$, ESS is $C(0,1)$, referring to non-ecological

http://www.aloki.hu ● ISSN 1589 1623 (Print) ● ISSN 1785 0037 (Online)
DOI: http://dx.doi.org/10.15666/aeer/1706_1442514434

protection by social capital side and ecological compensation by government departments.

(3) From Cases (5), it can be concluded that only when $\pi_2 > 0$ and $\pi_3 < 0$, namely $b_s IR - c_1 + L_1 P_2 > e - S$ and $c_2 > L_1 - K$, ESS is $B(1,0)$, indicating ecological protection by social capital side and non-ecological compensation by government departments.

(4) From Cases (6), (7), (8) and (9), it can be told that only when $\pi_1 > 0$ and $\pi_3 > 0$, namely $b_s IR - c_1 + L_1 > e - S$ and $c_2 < L_1 - K$, ESS is $D(1,1)$, referring to ecological protection by social capital side and ecological compensation by government departments.

Analysis of the system evolutionary trend

In line with the stability theorem of the differential equation and the nature of the evolutionary stable strategy, the value of y under $G'(x) < 0$ and the value of x under $G'(y) < 0$ can constitute the evolutionary stable strategy. Therefore, if $G(x) = 0$, $x_1 = 0$ and $x_2 = 1$ are the two stable state points of the dynamic equation of the social capital side. When $y = y^*$, $G(x) \equiv 0$, indicating all x refer to the stable state of the social capital side. When $y > y^*$, $G'(x) < 0$ shall be met. As $G'(1) < 0$, $x_2 = 1$ is the evolution stable strategy, when government departments choose "ecological compensation" strategy with the $y > y^*$ level, the social capital side tends to choose the strategy of ecological protection. When $y < y^*$, $G'(x) < 0$ shall be met. As $G'(0) < 0$, $x_1 = 0$ is the evolution stable strategy, when government departments choose "ecological compensation" strategy with the $y < y^*$ level, the social capital side tends to not choose the strategy of ecological protection.

If $G(y) = 0$, $y_1 = 0$ and $y_2 = 1$ are the two stable state points of the dynamic equation of government departments. When $x = x^*$, $G(y) \equiv 0$, indicating all y are in the stable state. When $x > x^*$, $G'(y) < 0$ shall be met. As $G'(1) < 0$, $y_2 = 1$ is the evolution stable strategy, when the social capital side choose "ecological protection" strategy at the $x > x^*$ level, the government departments tends to choose the strategy of ecological compensation. When $x < x^*$, $G'(x) < 0$ shall be met. As $G'(0) < 0$,$y_1 = 0$ is the evolution stable strategy, when the social capital side choose "ecological protection" strategy with the $x < x^*$ level, the government departments tends not to choose the strategy of ecological compensation.

Based on the above analysis, the evolution trends of the system under different parameter values are as shown in *Figure 1* (value ranges).

The strategic choice of the social capital side

Define $b_s IR - c_1 + L_1$ and $b_s IR - c_1 + L_1 P_2$ as the project investment profits of the social capital side under the ecological compensation and non- ecological compensation strategy of government departments, with $b_s IR - c_1 + L_1 > b_s IR - c_1 + L_1 P_2$. $e - S$ are defined as the speculative profits of the social capital side. For the social capital side, when $y^* > 1$ (the value range in cases (1) (2) (3)), $b_s IR - c_1 + L_1 < e - S$. The trend of evolution is that as long as the project investment profit is less than the speculative profit under the ecological compensation by the government, no matter what kind of strategy the government department adopts, the social capital side will tend to adopt the non- ecological protection strategy. When $y^* < 0$ (the value range in cases (5) (6) (7)), $b_s IR - c_1 + L_1 P_2 > e - S$. And the evolution trend is that as long as the

http://www.aloki.hu ● ISSN 1589 1623 (Print) ● ISSN 1785 0037 (Online)
DOI: http://dx.doi.org/10.15666/aeer/1706_1442514434

investment profit of the project is greater than the speculative profit under the non-ecological compensation of the government, the social capital side will tend to adopt the strategy of ecological protection regardless of the strategy adopted by the government. When $0 < y^* < 1$ (the value range in cases (4) (8) (9)), $b_s IR - c_1 + L_1 P_2 < e - S < b_s IR - c_1 + L_1$, and the strategy choice of the social capital side is related to the selection of government departments. When the proportion of government departments adopting the strategy of " ecological compensation" is large enough ($y > y^*$), the social capital side will eventually choose to implement the ecological protection strategy after evolution. However, if the government at this time fails to strengthen compensation ($y < y^*$), then the social capital side will be more likely to choose not to implement the ecological protection strategy.

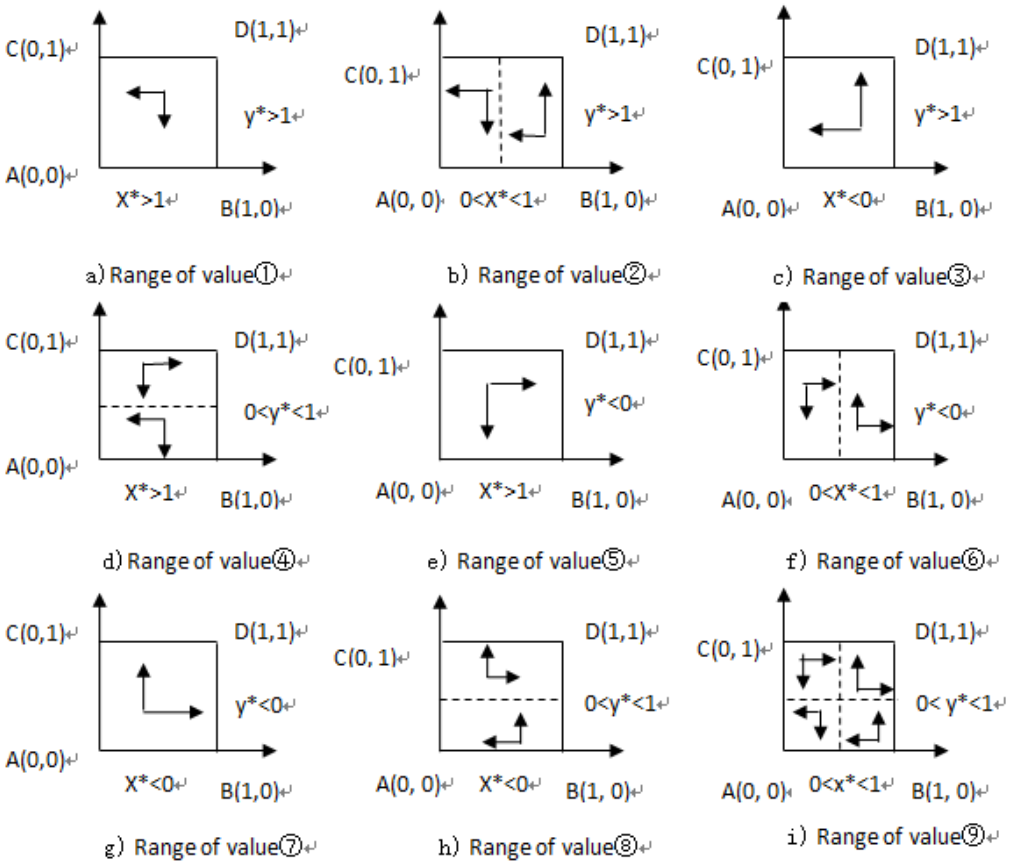

Figure 1. *Game evolution phase diagram of ecological compensation*

The strategic choice of government departments

Define $L_1 - K$ and $L_1 P_1 - K$ as the ecological benefits of government departments under the ecological protection and non-ecological protection strategy of the social capital side. For the government, when $x^* > 1$ (the value range in cases (1) (4) (5)), $c_2 > L_1 - K$. In this case, the evolution trend is that as long as the supervision cost is greater than the ecological benefits, the government department will tend to adopt the non-ecological compensation strategy regardless of the strategy adopted by the social capital side. When $x^* < 0$ (the value range in cases (3) (7) (8)), $c_2 < L_1 P_1 - K$, and the evolution trend is that as long as the supervision cost is less than the ecological benefits,

http://www.aloki.hu ● ISSN 1589 1623 (Print) ● ISSN 1785 0037 (Online)
DOI: http://dx.doi.org/10.15666/aeer/1706_1442514434

the government departments will tend to adopt the ecological compensation strategy regardless of the strategy adopted by the social capital side. When $0 < x^* < 1$ (the value range in cases (2) (6) (9), $L_1P_1 - K < c_2 < L_1 - K$, and the government departments' strategy choice is related to the selection of the social capital side. As long as the social capital party increases the proportion of the strategy of "ecological protection"($x > x^*$), the government department will eventually choose ecological compensation strategy after evolution. However, if the ratio is lowered in this case ($x < x^*$), government departments are more likely to choose non-ecological compensation strategy.

The evolutionary game characteristics of ecological compensation in state-owned forest areas

The evolutionary game analysis of ecological compensation in state-owned forest areas is different from that in other fields. This paper is based on the Public-Private Partnership model. The role of the government is no longer a supervisor, but a cooperator. In the process of setting model parameters, three characteristics of Public-Private Partnership model should be embodied: partnership, benefit sharing and risk sharing. Therefore, in the process of the economic transformation of state-owned forest areas, the government departments and the social capital side can actively use the results of this study to achieve the consistency of project objectives. At the same time, the model construction in this paper is a theoretical analysis under a series of basic assumptions, but the reality is more complex. For example, the dishonest behavior of the government, the high financing cost of the social capital, and the complexity of the transaction structure, and so on. All of these have a certain impact on the strategic choice of the government departments and the social capital side on ecological protection.

Conclusions

(1) In this paper, evolutionary game tools were used to study the decision-making of ecological compensation strategies by government departments and the social capital side in the process of economic transformation of Lutou forest farm. The motivation and interaction between the two sides are emphasized. The government's guidance and support and the leading and coordinating role of the social capital side are used to protect the ecological environment, improve economic, social and ecological benefits, and realize the sustainable development of forestry.

(2) The income matrix of different selection of ecological compensation strategies by government departments and the social capital side was established through introducing social capital's ecological protection strength and cost, government's ecological compensation strength and supervision cost, opportunity benefit, penalty quota, ecological subsidy and profit distribution ratio.

(3) In order to achieve the coordinated development of ecological construction and economic transformation, the ecological protection by social capital and the ecological compensation by government departments were the best strategies. Only when the investment profit of the project was greater than the speculative profit under the non-ecological compensation of the government departments and the supervision cost of

http://www.aloki.hu ● ISSN 1589 1623 (Print) ● ISSN 1785 0037 (Online)
DOI: http://dx.doi.org/10.15666/aeer/1706_1442514434

government departments is less its ecological profit, the optimal strategy could be achieved in the game evolution.

(4) Through the analysis of the evolvement trend of government departments and social capital side, we could draw that: reducing the ratio threshold y^* of ecological compensation by government departments, it is conducive for the social capital side to select the ecological protection strategy; reducing the ratio threshold x^* of ecological protection strategy by the social capital side, it is conducive for government departments to select the ecological compensation strategy.

(5) In order to make the ecological compensation strategies of government departments and the social capital side evolve smoothly to a satisfactory state, we should clarify the dominant position of the government, actively promote the ecological compensation systems and reward and punishment restraint mechanisms, Give full play to the key role of the social capital side, coordinate their interests distribution and conflict, build the reasonable mechanism of cost sharing and benefit sharing, improve their initiative to protect the ecological environment, and reduce the risk of participating in the economic transformation of the state-owned forest areas.

REFERENCES

[1] Fang, S. Q., Ma, H. Y., Xu, S. G. (2018): Analysis on ecological compensation mechanism of the forest tourism and its countermeasures. – Ecological Economy 34(5): 207-211.

[2] Guo, B., Hou, D. (2018): Study of ecological compensation of coal enterprises based on evolutionary game theory. – Coal Technology 37(5): 333-334.

[3] Li, C. H., Zhao, X. H. (2019): Study on the coordinated development of ecological construction and economic transformation in state-owned forest region of forest industry in Heilongjiang Province. – Journal of Nanjing Forestry University (Natural Sciences Edition) 43(2): 144-147.

[4] Liu, C., Cui, W. L. (2016): On ecological compensation mechanism of evolutionary game-based uninhabited islands. – Journal of Zhejiang Ocean University (Humanities Science 33(4): 24-30.

[5] Liu, M. M., Lu, Q. Q., Yang, J. C. (2018): Problems and improvement of compensation system for forest ecological benefits in China. – Issues of Forestry Economic 38(5): 1-7.

[6] Sun, W. Q., Sun, L. (2018): A study on the responsibility game of the interest subject in the reform of state-owned forest right from the perspective of the new development concepts. – Ecological Economy 34(6): 139-143.

[7] Tong, G. J., Geng, X. X. (2018): A survey and analysis on economic transformation in state-owned forest regions–taking Yichun city as an example. – Forestry Economics (2): 19-20.

[8] Wen, W., Tian, G. S. (2017): Research on the inter-regional ecological compensation coordination path of ecological function region in Heilongjiang province from the perspective of the game theory. – Forestry Economics (2): 16-20.

[9] Zhang, Q. (2016): Research on ecological compensation of mineral resources exploitation based evolutionary game theory. – Resource Development & Market 32(2): 165-169.

[10] Zhong, W. W., Zhang, B., Zhang, H. R. (2017): The game analysis on the economic transition in state-owned forest regions-based on the construction of Daxiaoxingan mountains ecological function districts. – Forestry Economics (12): 46-49.

[11] Zhou, C. F., Zhang, X., Liu, B. (2018): Research on basin ecological compensation based on evolutionary game theory: case of Chishui River Basin in Guizhou Province. – Yangtze River 49(23): 38-41.

http://www.aloki.hu ● ISSN 1589 1623 (Print) ● ISSN 1785 0037 (Online)
DOI: http://dx.doi.org/10.15666/aeer/1706_1442514434

COMPARATIVE ANALYSIS OF SPALTED *AQUILARIA SINENSIS* SPECIES WITH ZONE LINES PREPARED WITH *XYLARIA VENOSULA*

PAN, Z. H.[1] – HE, H. S.[2] – LI, Q. D.[3] – QIU, J.[2*]

[1]*Zhongshan Polytechnic, Zhongshan 528400, China*

[2]*College of Material Engineering, Southwest Forestry University, Kunming 6500224, China*

[3]*Foshan University, Foshan 528000, China*

**Corresponding author*
e-mail: qiujianswfu@foxmail.com; phone: +86-137-5951-2363

(Received 7th Jun 2019; accepted 10th Oct 2019)

Abstract. In this paper, *Xylaria venosula* strains were inoculated separately into wood blocks of *Alnus nepalensis*, *Betula alnoides*, *Aquilaria sinensis* and *Pinus kesiya*, and induced artificially to create spalted woods with zone lines. The results showed that: (1) *Aquilaria sinensis* could easily form black zone lines, where the mycelia were denser than elsewhere. (2) The zone lines on and within *Aquilaria sinensis* were the most obvious when the wood blocks contained 50% water. In this case, zone lines were rich and beautiful and the wood was not severely rotten. (3) The largest spalt was observed on *Aquilaria sinensis* blocks. This type of wood underwent the most serious spalting, with 6.64% of its surface and 1.84% of its interior covered by spalts. As the wood blocks rotted over time, the weight loss rates of spalted woods were on the rise, while the compressive strengths parallel to grain were gradually falling. The unitary linear regression shows significant correlation between the mass loss ratio and the compressive strength parallel to grain. It can be concluded that *Xylaria venosula* did not destroy the cell walls within the woods, and had little effect on the strength of the woods.
Keywords: *Xylaria venosula strains, water content, weight loss rate, compressive strength, regression analysis*

Introduction

Spalting is a manifestation of fungi causing discoloration of wood. The wood after discoloration is called Spalted wood. The spalting generally manifests in four types: white rot, stains, zone lines, and brown rots, and actually the first three have practical values. It mainly occurs on the felled wood, and also on the standing timbers under harsh environmental conditions. Generally, one or more of the above three types can be formed on the same piece of wood. Currently, spalted wood with rich zone lines are the most valuable in the foreign market. *Xylaria venosula*, making the wood coloring to form the mottling pattern, is onekindoffungususedtoformthe line-patterned varietal wood, which can form a unique decorative effect and a certain medicinal value.

The fungi that can form spalted pattern are mainly basidiomycetes and a few ascomycetes, and the polymorpha charcoal which can form the striatum line alone is often used in the laboratory to study the planting of *Aquilaria sinensis*. According to previous studies and speculations, Robinson et al. of the College of Forestry, University of Toronto, Canada, believe that the zone lines are the spalts formed as a defensive mechanism against the obstacle between the strains (Robinson et al., 2009); in their experiment, 25 species of fungi were isolated from the wood, and then incubated on an agar medium in pairs; where they produced a distinct pigment on the agar medium

http://www.aloki.hu ● ISSN 1589 1623 (Print) ● ISSN 1785 0037 (Online)
DOI: http://dx.doi.org/10.15666/aeer/1706_1443514454

between the two fungi and the line of resistance between the two strains, the two fungi that formed zone lines on the medium were inoculated separately at both ends of the sugar maple block, for a total of 21 pairs of fungi combinations, two of which produced stable zone lines and white rot, that is, *Bjerkandera adusta/Trametes versicolor* and *Polyporusbrumalis/Trametes Versicolor*, while the fungi of the remaining 22 woody plants did not form stable spalts. In addition, Robinson et al. believe that the zone lines can be formed on any wood species. The broadleaf woods are whiter in colour, and the trees with low content of extracts are more likely to form spalting, such as *Acer* spp., *Betula* spp. and *Fagus* spp. (Xu et al., 2013). Robinson and Turnquist studied the *Xylari polymorpha*, which can form zone lines independently by inoculating it on *Populus tremuloides*, *Acer saccharum*, *Betulaalleghaniensis* and *Tilia Americana*; with the time extension on the medium, it is observed through the amount of spalts that *Populus tremuloide*s and *Acer saccharum* produced more zone lines than the other two (Robinson et al., 2009).

Based on the concept of the spalted wood, this paper probes into the artificial preparation of spalted wood using the *Xylaria venosula* strain to infect the wood block, and then studies the related ways and characteristics of the strain infection. By inoculating *Xylaria venosula* strain on different kinds of woods, it focuses on comparing the similarities and differences of the formed zone lines, the influence of water content, wood property, weight loss, and spalting formation etc. Besides, it studies the formation and mechanism of the zone lines in spalted woods. Thus, the random variation of the surface lines on the spalted wood can help to produce the green, low-carbon, environmentally-friendly and beautifully crafted products and attaching veneers, and improve the comprehensive utilization and added value of the wood. This is of high economic value and social significance, and also lays a theoretical foundation for the stably and continuously acquiring the spalted wood.

Materials and methods

Experimental materials

Main material:

(1) The *Xylaria venosula* strain: purchased from the China Forestry Culture Collection Centre, and prepared by the screening test of fungal strains in the same genus or the same species, as shown in *Figure 1*.

(2) Wood specimens: they were collected from variety of trees such as *Alnus nepalensis*, *Betula alnoides*, *Aquilaria sinensis*, and *Pinus kesiya* on April 9 and 29, 2017 in Jindian Park, Kunming City, Yunnan Province, China, and nearby forests.

(3) Filtered water: It is filtered by YJD laboratory water purifier (Yongjieda Purification Technology Co., Ltd., Hangzhou, China) filter.

Cultivating the fungus of spalted wood

First, the liquid potato-Dextrose-agar (PDA) culture medium was placed into a 250 ml triangle flask or culture bottle, for about 100 ml per bottle, then autoclaved and sterilized for 30 min under high pressure. Afterwards, the *Xylaria venosula* was inoculated into the bottle, and cultured for 7-12 days using the thermostat oscillator SHA-B (A) (Chengdu Yike Instrument Equipment Co., Ltd., Sichuan, China), to obtain

http://www.aloki.hu ● ISSN 1589 1623 (Print) ● ISSN 1785 0037 (Online)
DOI: http://dx.doi.org/10.15666/aeer/1706_1443514454

the bacterial suspension with a large number of agglomerated mycelia inside (Fournier et al., 2011; Osono et al., 2011; Zink and Fengel, 1988).

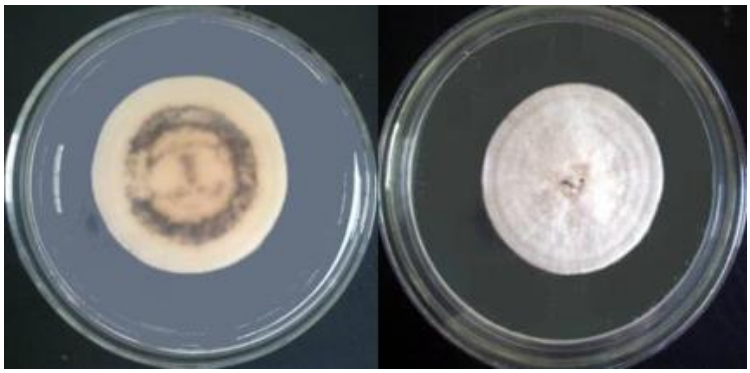

Figure 1. *Morphological characteristics of the Xylaria venosula strain*

Pre-treating the inoculated wood block

From the four easily spalted tree species of *Alnus nepalensis*, *Betula alnoides, Aquilaria sinensis*, and *Pinus kesiya*, 60 pieces of 30 mm × 20 mm × 20 mm wood blocks were taken respectively, for a total of 240, and placed into the bottle (Robinson and Laks, 2010), which was filled with appropriate amount of filtered water and then sterilized for 45 min in the YM30Z vertical autoclave (Sanshen Medical Instrument Factory, Shanghai, China), together with the cultural medium and the medium vermiculite.

Inoculation of wood blocks

First, cut the plate PDA strain into 10 mm × 20 mm pieces, clip it with the tweezers and stick it on the wooden block, put it into the culture bottle and cover it with vermiculite, and add 10-25 ml of filtered water to wet the vermiculite and the wood block before fastening the cap. Then, for liquid inoculation, use the tweezers to clamp the wood block and cover the bacteria solution, cover it with vermiculite, add 10-25 ml of water to wet the vermiculite and wood block. Next, the inoculated wood blocks were placed in a constant temperature and humidity chamber (produced by Blue Sky Laboratory Instrument Factory, Hangzhou, China) at 27 °C under dark conditions (Robinson and Laks, 2010), cultivating for about 80 days. Finally, take out the wooden block, scrape off its surface mycelium, wash and dry it, and observe whether there has formed a clear zone line inside and outside the block.

Observing the characteristics of the spalted wood with zone lines

The 10 mm × 10 mm × 10 mm blocks with rotten zones were taken from the four wood species of *Alnus nepalensis*, *Betula alnoides*, *Aquilaria sinensis*, and Pinus kesiya. They were sliced with German Leica 2000R slicer (Leica Microsystems Nussloch GmbH, NuBloch, Germany), and stained by double staining to better observe mycelia (Pearce, 1984), then observed and recorded using an Eclipse 80i microscope. Besides, electron microscopy (HC300X type Shengtian Instrument Co., Ltd., Shenzhen, China) was used to observe the morphology and distribution of mycelia inside and outside the rotten area.

http://www.aloki.hu ● ISSN 1589 1623 (Print) ● ISSN 1785 0037 (Online)
DOI: http://dx.doi.org/10.15666/aeer/1706_1443514454

Analysis of wood microstructure

From the four kinds of woods, namely, *Alnus nepalensis, Betula alnoides, Aquilaria sinensis, and Pinus kesiya*, 5 mm × 5 mm × 5 mm cubes were made, ensuring that the transverse section, radial section, and tangential section can be found on each wood block as much as possible. In our experiment, the wood block was softened first at a certain extent with hot water, then cut evenly at each face with a sharp blade without leaving any scratches, and finally undergo air drying at room temperature. Since the dried wood is basically non-conductive, in order to clearly observe the ultrastructure of the wood cell wall and the rotting degree of the strain *Xylaria venosula* in the wood tissue, it is necessary to metallize the surface of the wood block (Passarini et al., 2013). For the gold-coated wood blocks, the SEM-EDXA scanning electron microscopy (FEI Company, Eindhoven, the Netherlands) was adopted to observe the extent of damage to the wood cell wall by the activity of mycelium in the rotten area (Læssøe et al., 2013; Robinson et al., 2011).

Experimental steps of wood water content

The four types of wood blocks mentioned above were made into 2 cm × 2 cm × 2 cm squares with CS70EB precision woodworking table saw (FESTOOL, Germany). They were dried in a blast drying oven at 60 °C ± 5 °C, and then weighed. The vermiculite was dried to absolute dryness at 60 °C ± 5 °C. Through preliminary experiments, the relationship between the amount of water added and the water content of the wood block was obtained. Then, one specimen from each tree species, 10 g vermiculite, and unequal amount of filtered water were added to each culture bottle respectively. 5 pieces of blocks were prepared repeatedly for each gradient, sterilized in autoclave, and cooled for 6-8 h and weighed again. Then, the blocks containing the 10%, 30%, 50%, 70%, 90% of water were prepared. The water content calculation formula is shown as (Tian et al., 2013):

$$M_c = [(m_1 - m_2)/m_2]\ 100\% \quad \text{(Eq.1)}$$

M_c-water content; m_1-mass at the end of the test (g); m_2-mass (g) at the start of the test.

Determining the average mass loss percentage

Before inoculation, all the blocks were placed in a blast drying oven at 60 °C for 48-60 h until reaching constant weight, and the mass m_2 was weighed; after they're autoclaved at high temperature, inoculated and placed in a constant temperature and humidity chamber, infected by fungi for 4, 6, 8, 10, and 12 weeks, the blocks were taken out and the surface mycelium were scraped off, and then dried in a blast drying oven at 60 °C to a constant weight (Passarini et al., 2013; Læssøe et al., 2013), thus the mass m_3 was weighed. Then, the average mass loss rate of the rotted wood block was calculated as (Robinson et al., 2007):

$$L = [(m_3 - m_2)/m_3]\ 100\% \quad \text{(Eq.2)}$$

L-mass loss rate; m_2-mass at the start of the test (g); m_3-mass (g) at the end of the test.

http://www.aloki.hu ● ISSN 1589 1623 (Print) ● ISSN 1785 0037 (Online)
DOI: http://dx.doi.org/10.15666/aeer/1706_1443514454

Determining compressive strength

The blocks with the mass loss rate measured and the untreated healthy wood were dried in a blast drying oven at a temperature of 103 °C for more than 48 h until constant weight in an absolute dry state. The RGT-20A versatile experimental machine (REGER Instrument Co., Ltd., Shenzhen, China) was used to determine the compressive strength of the blocks. The experimental results are the average of 5 specimens according to the experimental standard ISO 3787-1976 *Wood-Test Method-Determination of Ultimate Stress in Compression Parallel to Grain* (Liers et al., 2006).

Unitary linear recursive analysis

Unitary linear recursive analysis was conducted about the weight loss rate and compressive strength of the four tree species using SPSS18.0 software. The Pearson correlation coefficient between the two variables is less than 1, indicating a highly linear correlation between the two.

Results and discussion

Morphology and distribution of mycelium in wood

From the successfully cultivated spalted woods with black zone lines in the four species of trees, four samples were selected, as shown in *Figure 2.*

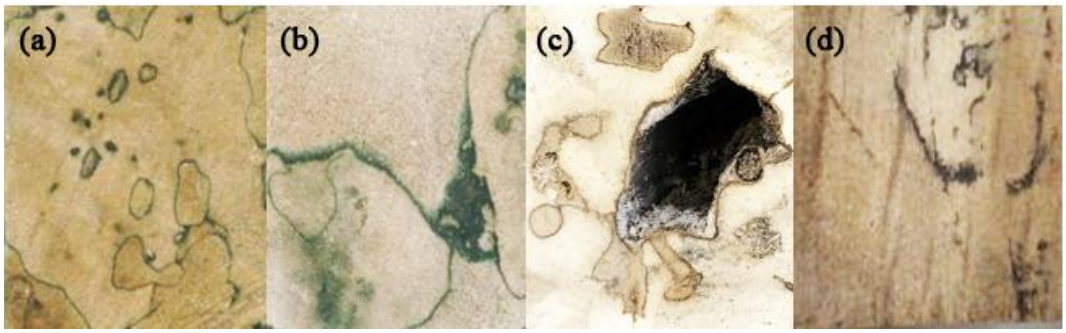

Figure 2. *Visual characteristics of the artificially formed spalted woods' macrostructure. (a) Alnus nepalensis, (b) Betula alnoides, (c) Aquilaria sinensis, (d) Pinus kesiya*

Figure 2 shows the micrograms of the spalted woods artificially cultivated from the four species of trees. The linear parts in dark colour were spalts. When the *Xylaria venosula* strain infected the woods, a large amount of melanin was excreted in their respective areas of the woods for mutual defences, producing black short lines, small spots, and irregular strips and forming bands, thereby forming the zone lines. Due to the extremely fineness of mycelium, it is easily damaged during slicing and cleaning, but the zone lines formed are still obvious. Therefore, if properly controlled, the sap stain fungi could be used to secrete the pigment, and colour the surrounding wood tissue. Thus, a beautiful natural pattern can be formed.

The micro-structure of artificially cultivated spalted wood was observed by light microscopy. 6 pictures in transverse section, radial section and tangential section were selected for research analysis, as shown in *Figure 3.*

http://www.aloki.hu ● ISSN 1589 1623 (Print) ● ISSN 1785 0037 (Online)
DOI: http://dx.doi.org/10.15666/aeer/1706_1443514454

Figure 3 shows the morphology and distribution of mycelium in wood block under light microscope: a represents an area of distinct black zone lines in the radial section of *Alnus nepalensis* under 10-fold light microscope, and the area around the line was shallow in wood colour, significantly different from the area outside; one obvious feature was that the black zone lines extends outward at the wood ray. b represents the black zone lines in the radial section of *Alnus nepalensis* under the 40-fold light microscope, which was formed by the melanin secreted by the fungus in each wood tissue; the arrow refers to the mycelium filled in the duct within the zone line area, and the area outside the zone lines on the right has no difference from the normal wood, only with a small amount of mycelium distributed near the black zone line area. c indicates the V-shaped black zone lines in the tangential section of *Alnus nepalensis* under the 4-fold light microscope, and the V-shaped inner area was light yellow, and the wood colour outside the V-shaped area was normal. d represents the mycelial distribution at the black zone lines in the tangential section of *Alnus nepalensis* under the 40-fold light microscope, which clearly indicates that the mycelia were mainly distributed in ray parenchyma cells, axial parenchyma, and wood fibre connected with parenchyma cells, and the black zone lines were the macroscopic performance of the mycelia that are entangled into a group. However, in the wood fibre cells closely spaced from the mycelium (the area between the two arrows in the figure), there was very little mycelium distribution, which is more common in white rot fungi (Robinson et al., 2011; Tudor et al., 2012, 2013). This may be because there are fewer nutrients in the fibre cells, and the parenchyma cells are the tissues that transport nutrients in the wood, containing more starch, polysaccharides and oils; the fungus will not decompose the cell walls to absorb nutrients until these substances are completely decomposed. e represents the distribution of the black zone line in the transverse section of the *Betula alnoides* under the 4-fold light microscope. f represents the mycelial distribution of the black zone lines in the transverse section of the *Betula alnoides* under the 40-fold light microscope; it can be observed that there were many mycelia distributed in the fibre cells and wood ray cells, and a large amount of melanin was accumulated in the wood ray cells and cell walls.

Microstructure analysis of spalted wood

In the experiment, the black zone lines were successfully cultivated from the four species of trees. For each species, several sections were scanned and analysed.

Figure 4 shows the growth of *Xylaria venosula* in the *Alnus nepalensis*, where a represents the mycelial distribution in the duct lumen and wood fibre lumen, and b is the mycelial distribution on the pits inside the vessel element, c and d are the mycelial distribution of the vessel element and the wood ray in the tangential section of *Alnus nepalensis.*

Figure 5 shows the growth of Xylaria venosula in the wood of *Betula alnoides*, where a and b represent the mycelial distribution in the lumen of the duct and wood fibre, and c represents the mycelial distribution on the pit in the radial section, d represents the mycelial distribution of vessel element and wood ray on the tangential section of *Betula alnoides*.

Figure 6 shows the growth of *Xylaria venosula* in the wood block of *Aquilaria sinensis*, where a and b represent the mycelial distribution in the lumen of the duct and wood fibre, and c represents the mycelial distribution on the pit inside the radial section, d represents the mycelial distribution of vessel element and wood ray.

http://www.aloki.hu ● ISSN 1589 1623 (Print) ● ISSN 1785 0037 (Online)
DOI: http://dx.doi.org/10.15666/aeer/1706_1443514454

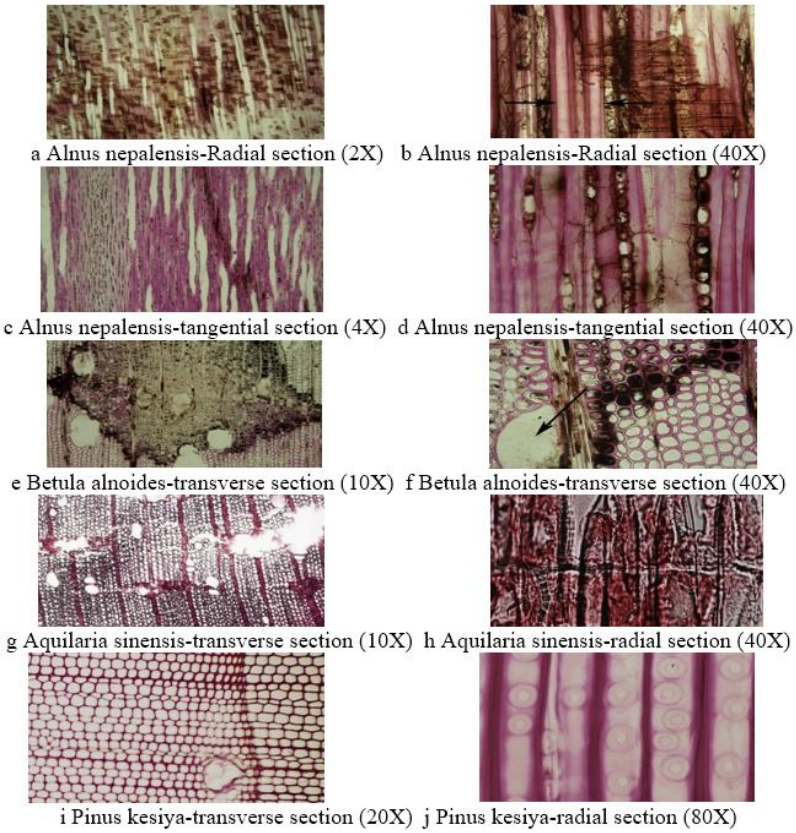

Figure 3. *Morphology and distribution of mycelium in wood under light microscope*

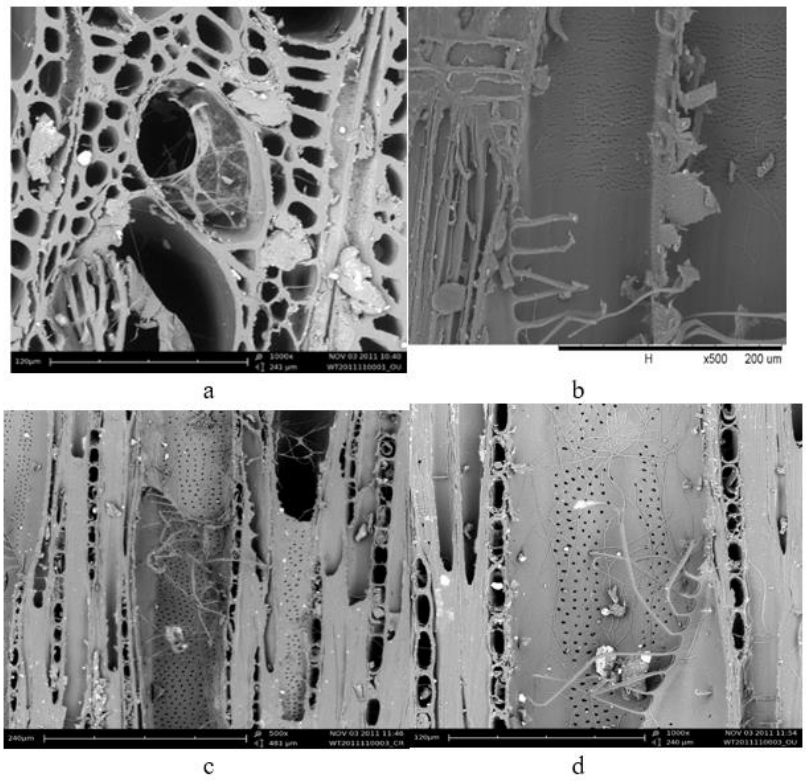

Figure 4. *Influence of Xylaria venosula on wood structure of Alnus nepalensis*

http://www.aloki.hu ● ISSN 1589 1623 (Print) ● ISSN 1785 0037 (Online)
DOI: http://dx.doi.org/10.15666/aeer/1706_1443514454

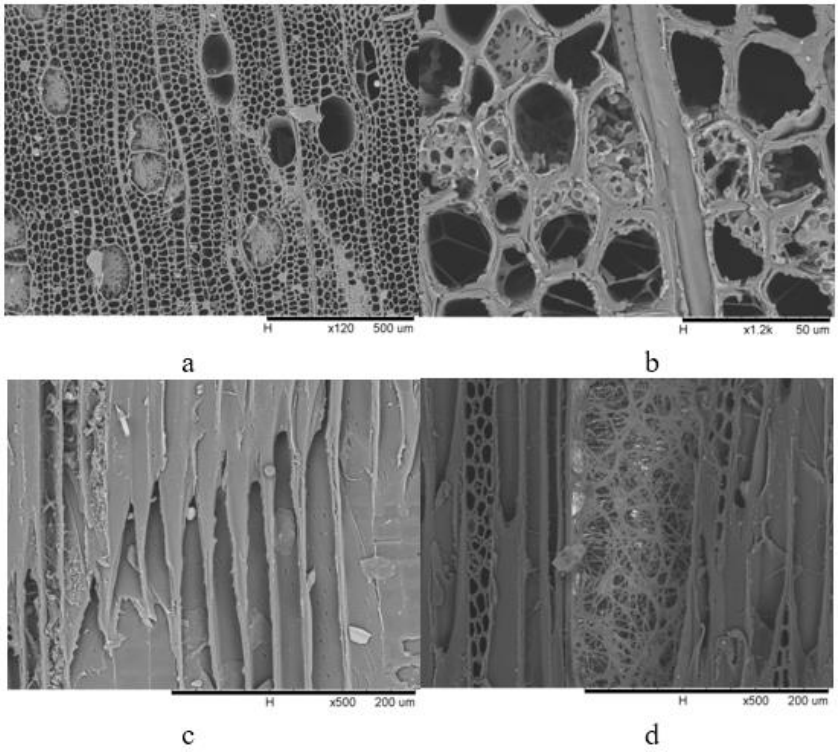

Figure 5. *Influence of Xylaria venosula on wood structure of Betula alnoides*

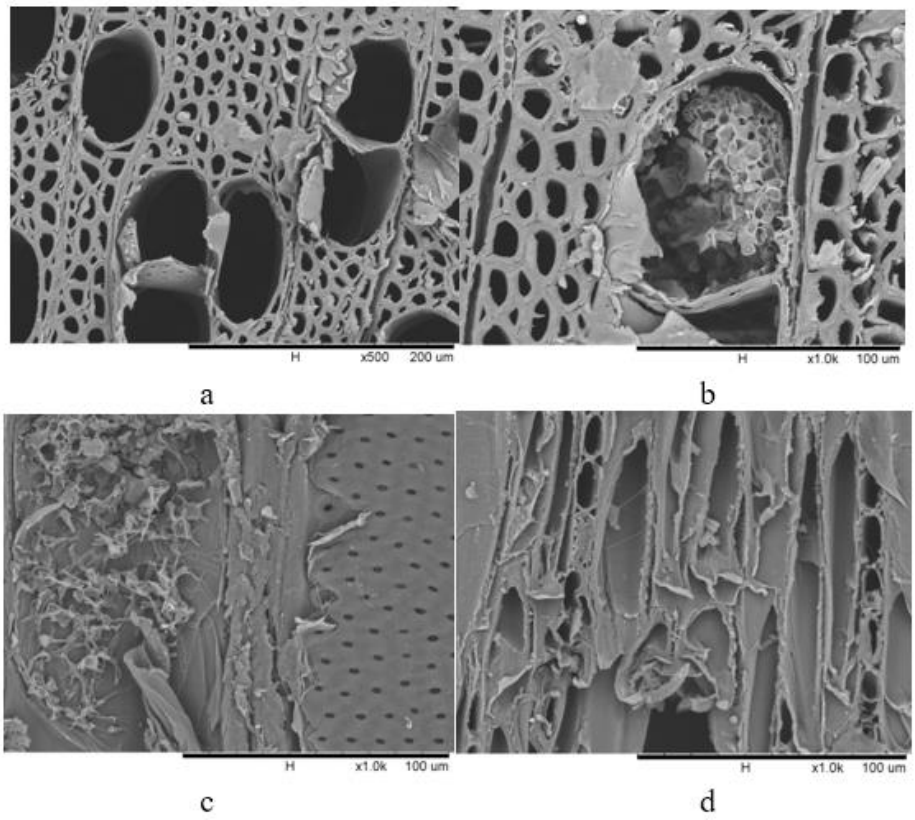

Figure 6. *Influence of Xylaria venosula on wood structure of Aquilaria sinensis*

http://www.aloki.hu ● ISSN 1589 1623 (Print) ● ISSN 1785 0037 (Online)
DOI: http://dx.doi.org/10.15666/aeer/1706_1443514454

Figure 7 shows the growth of Xylaria venosula in the wood of *Pinus kesiya*, where a and b represent the mycelial distribution in the lumen of the duct and wood fibre, and c represents the mycelial distribution on the pit in the radial section, d represents the mycelial distribution of the vessel element and wood ray on the tangential section of *Pinus kesiya*.

Based on the results in *Figures 3–7,* no obvious rot was found in the samples, and the strain *Xylaria venosula* was grown along natural cavities such as wood ducts, wood fibres, and parenchyma cells, even crossing between adjacent cells with the pits as the passages. A large amount of mycelial distribution was seen in the lumen of the duct, but no signs of disrupting the cell wall. Xylaria venosula is a white rot fungus. It is an initial rot from the mycelial distribution and morphology, and has little effect on the strength of wood.

The mycelia were mainly concentrated in the duct, parenchyma cells and the fibre cells connected to the parenchyma cells. Some of the fibre cells were close to the mycelia but have few mycelia, mainly due to a small number of nutrients inside. These characteristics indicate that these fungal infestations on specimens are performed by means of minimal resistance and the fastest access to nutrients anatomically (Dai, 2012).

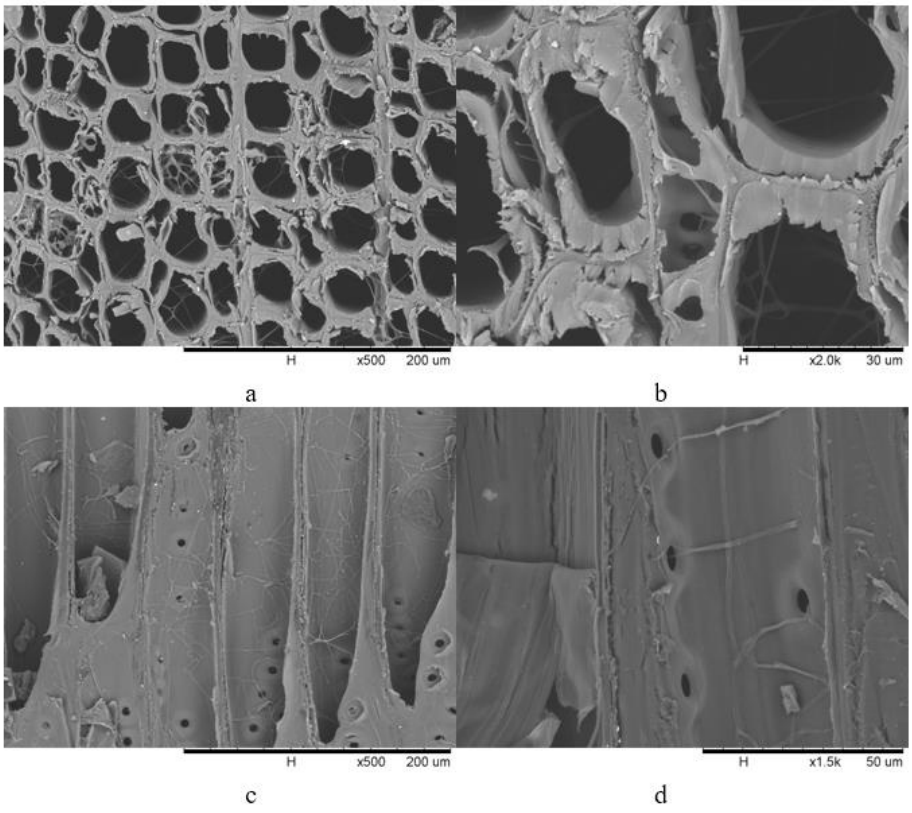

Figure 7. *Influence of Xylaria venosula on the wood structure of Pinus kesiya*

There is a certain amount of mycelium inside the zone lines, but significantly less than the centre of the zone lines; outside the zone lines the mycelium may exist or not. The zone lines appear in the same colour as the mycelium itself entangled in a group and they're formed by the secreted pigment layer in the cell cavity and cell wall. One

http://www.aloki.hu ● ISSN 1589 1623 (Print) ● ISSN 1785 0037 (Online)
DOI: http://dx.doi.org/10.15666/aeer/1706_1443514454

common feature is the mycelia in the rotten area were denser than outside, and the peak density appeared at the centre of decayed area. This just proves that the formation of the zone lines is closely related to the water content of wood rot fungi, especially white rot fungus. There were some closed areas at the zone lines, which could provide the most suitable humidity for the fungi in the wood incubated area, because pseudo-bacterial nucleus produced by the fungus restricts the evaporation of water on the surface of the closed region, or maybe the boundary formed by the contact of two different mycelium also plays the same role (Nagy et al., 2012; Dai et al., 2012). The melanin secreted by the fungus has certain toxicity and is resistant to attack of other microorganisms. Thus, the rotten area in the wood is a barrier that the fungus uses to resist the invasion of other microorganisms so that it can keep utilizing the resources in the enclosed area. Almost all mycelia enter the adjacent cells through the pits of the wood's natural channel, which does not cause a significant decrease in the strength of the wood so that the 8-month-old spalted wood can fully meet the requirements for the production of handicrafts.

Effect of wood water content on the formation of spalts

Statistical analysis of the percentage of the spalts in the area of wood block

Figure 8 shows the percentage of external spalts on the four types of wood blocks infected by the strain *Xylaria venosula* under different water contents. Wood water content was evaluated using *Equation 1*. The SPSS one-way analysis of variance (ANOVA) ($\alpha = 0.05$, $n = 30$) showed that their external spalts were significantly different; when the water content reached 10%, the area of spalts on the *Aquilaria sinensis* block by the strain *Xylaria venosula* was 3.72%, which was the most serious spalting; when the water content reached 50%, the spalt on the four wood blocks reached the largest, and that of *Alnus nepalensis, Betula alnoides, Aquilaria sinensis* and *Pinus kesiya* reached 6.35%, 5.81%, 6.64%, and 6.23% respectively; but with the increase in water content, the external spalt on the blocks decreased, which is consistent with Yan Huang's research results (Huang et al., 2017); when the water content reached 90%, the spalt area of *Alnus nepalensis, Betula alnoides, Aquilaria sinensis* and *Pinus kesiya* was reduced to 5.03%, 4.42%, 5.18% and 4.57%. Studies have shown that when the water content of the wood block reaches 50%, the living environment is most suitable for the growth of the strain *Xylaria venosula*, and the surface spalting is the most serious. Through comparing the four types of wood blocks, it is found that the external spalt on the *Aquilaria sinensis* wood block was the largest, and its spalting was the most serious, followed bythe *Alnus nepalensis* wood block, only 0.29% lower than that of *Aquilaria sinensis*.

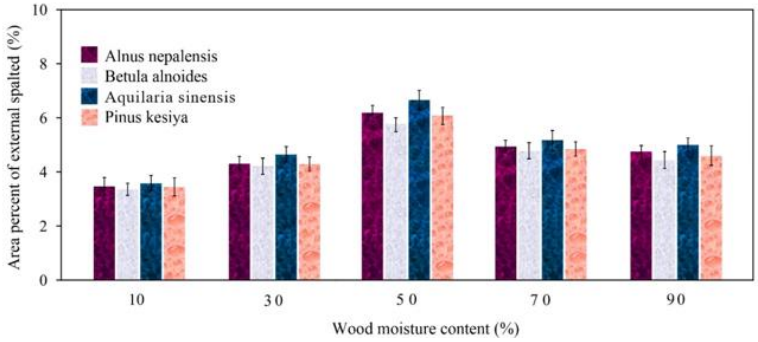

Figure 8. *Percentage of surface spalts area formed by strains under different water contents*

http://www.aloki.hu ● ISSN 1589 1623 (Print) ● ISSN 1785 0037 (Online)
DOI: http://dx.doi.org/10.15666/aeer/1706_1443514454

Figure 9 shows the area percentage of the internal spalts in the four wood blocks formed by the strain *Xylaria venosula* under different water contents. The SPSS ANOVA ($\alpha = 0.05$, $n = 30$) indicates that the area percentage of the internal zone lines was significantly different; when the water content reached 10%, the percentage of the internal zone lines formed by the strain *Xylaria venosula* in the *Aquilaria sinensis* block was 0.4%; when the water content reached 50%, the area percentage of the internal spalts of the four blocks was the largest, the spalts percentage of *Alnus nepalensis, Betula alnoides, Aquilaria sinensis* and *Pinus kesiya* was 1.75%, 1.61%, 1.84%, and 1.67%, respectively; as the water content increases, the internal spalt area of blocks was reduced; when the water content reached 90%, the spalt area of *Alnus nepalensis, Betula alnoides, Aquilaria sinensis* and *Pinus kesiya* decreased to 1.23%, 1.09%, 1.28% and 1.17%. Studies have shown that when the water content of the wood block is 50%, this living environment is most suitable for the growth of the strain *Xylaria venosula*, and the internal zone line is the largest; among the four types of blocks, the internal spalts of *Aquilaria sinensis* are most obvious; that of the *Alnus nepalensis* block was second, 0.19 lower than *Aquilaria sinensis*.

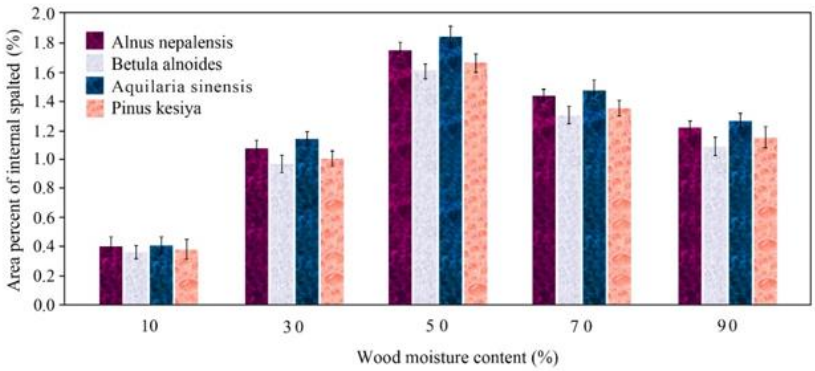

Figure 9. *Percentage of internal spalts formed by strains at different water contents*

The average mass loss percentage was evaluated using *Equation 1*. The fibre saturation point of the wood block is generally 30%. When the water content of the wood block exceeded 30%, free water molecules were present in the cell cavity for fungal growth and utilization; when it was below 30%, there were very few free water molecules in the cell cavity, which is not conducive to fungal growth; when it was too high, the free water of the cell cavity occupied the lumen of the wood cell, with an extremely low air content, which is also unfavourable for the growth of the fungus.

When the water content of the wood block was 30-50%, there was certain free water in the cell cavity, but still more air inside. The cell cavity was like a capillary tube, in which the free water keeps moving. In order to maintain the moisture required for its own growth, the fungus forms zone lines or stains to prevent the moisture movement, which is the main reason for the formation of large spalts.

Mass loss rate of wood block

Figure 10 shows the mass loss rates of the spalted woods obtained by the strain *Xylaria venosula* under different water contents of four wood specimens. It is found that the maximum value was 6.39%, the minimum value was 4.36%, and the average mass

http://www.aloki.hu ● ISSN 1589 1623 (Print) ● ISSN 1785 0037 (Online)
DOI: http://dx.doi.org/10.15666/aeer/1706_1443514454

loss was 5.15%, with little mass loss. The following results were obtained using the SPSS one-way analysis of variance ($\alpha = 0.05$, $n = 5$).

The strain *Xylaria venosula* has the highest mass loss rate under the water content 50% of wood blocks, and the lowest mass loss rate under the water content of 10%. The strain *Xylaria venosula* had certain differences in mass loss rate under the different water contents of the four wood specimens. The mass loss rate of the *Betula alnoides* block was the highest, reaching 6.69%, which exceeded that of *Aquilaria sinensis* block by 0.62%, while the mass loss rate of *Aquilaria sinensis* was second to it.

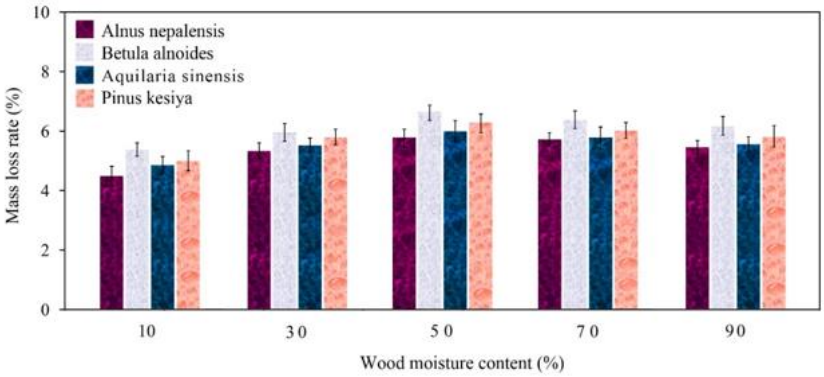

Figure 10. *Average mass loss rate of spalted wood under the condition of different water contents*

Effect of strain Xylaria venosula on the mass loss rate and the parallel-to-grain compressive strength

Result of the experimental was evaluated using *Equation 3*. *Table 1* shows the results of weight loss rate and compressive strength parallel to grain of the spalted woods varying with the rotted time through the experiment, in which these four types of wood blocks were infested with *Xylaria venosula* strain for 4, 6, 8, 10, and 12 weeks at a water content of 50%, and 12 pieces were weighed every 2 weeks, for a total of 240 pieces. It can be seen that with the increase of rotten time, the weight loss rate of the spalted wood was on the rise, and its compressive strength parallel to grain was correspondingly reduced, which is consistent with the research results of Daniela Tudor (Hladki and Romero, 2010).

Unitary linear recursive analysis was conducted about the weight loss rate and compressive strength of the four tree species using SPSS18.0 software. *Table 2* lists the correlation coefficients of *Alnus nepalensis*, in which the Pearson correlation coefficient between the two variables was -0.986, indicating a highly linear correlation between the two. *Table 3* lists the linear equation coefficients. It can be seen that the regression coefficients in the regression model are: the constant of 67.739, and the independent variable mass loss rate of -3.613. Then, the regression equation is given as:

$$y = -3.613x + 67.73 \quad \text{(Eq.3)}$$

Table 1 also indicates that the weight loss rate of the four tree species has a linear relationship with the compressive strength. Their regression equation is shown in *Figure 11*.

http://www.aloki.hu ● ISSN 1589 1623 (Print) ● ISSN 1785 0037 (Online)
DOI: http://dx.doi.org/10.15666/aeer/1706_1443514454

Table 1. *Effect of the spalted wood on the weight loss rate and the compressive strength parallel to grain*

Tree species	Character	Decay time/week					
		0	**4**	**6**	**8**	**10**	**12**
Alnus nepalensis	Weightlessness rate /%	0	2.49	2.89	3.35	3.76	3.83
	Compressive strength /MPa	68.18	57.25	56.87	56.72	54.15	54.02
Betula alnoides	Weightlessness rate /%	0	1.59	2.11	2.55	2.97	3.34
	Compressive strength /MPa	117.69	99.62	95.10	92.12	91.19	90.91
Aquilaria sinensis	Weightlessness rate /%	0	2.18	2.97	3.31	3.75	4.01
	Compressive strength /MPa	96.28	93.67	93.36	89.49	81.31	77.84
Pinus kesiya	Weightlessness rate /%	0	1.32	1.70	1.98	2.11	2.35
	Compressive strength /MPa	117.48	113.04	112.54	108.21	108.01	105.91

Table 2. *Correlation coefficients*

Character		Compressive strength of *Alnus nepalensis*	Weightlessness rate of *Alnus nepalensis*
Pearson correlation	Compressive strength of *Alnus nepalensis*	1.000	-.986
	Weightlessness rate of *Alnus nepalensis*	-.986	1.000
Sig. (single side)	Compressive strength of *Alnus nepalensis*	.	.000
	Weightlessness rate of *Alnus nepalensis*	.000	.
N	Compressive strength of *Alnus nepalensis*	6	6
	Weightlessness rate of *Alnus nepalensis*	6	6

Table 3. *Model coefficients*

Model		Non-standardized coefficient		Standard coefficient	t	Sig.	The 95.0% confidence interval of B	
		B	**Standard error (SE)**				**Lower bound**	**Upper bound**
1	(Constant)	67.739	.909		74.549	.000	65.216	70.262
	Weightlessness rate of *Alnus nepalensis*	-3.613	.300	-.986	-12.036	.000	-4.447	-2.780

The significant level of regression was 0.000, indicating that the probability for regression coefficient equal to 0 in T-statistic test was 0.000, and also that the linear correlation between the two variables is extremely significant, and the established regression equation is valid.

Figure 12 shows the measured cumulative probability p-p chart in the regression analysis, in which the scatter points are roughly scattered around the oblique line, so it can be approximated that the residual distribution is subject to a normal distribution.

Result of the experimental was evaluated using *Equation 4*. *Table 4* shows the correlation coefficients of the *Betula alnoides*, in which the Pearson correlation coefficient between the two variables was -0.968, indicating a highly linear correlation between the two. *Table 5* lists the linear equation coefficients. It can be seen that the

http://www.aloki.hu ● ISSN 1589 1623 (Print) ● ISSN 1785 0037 (Online)
DOI: http://dx.doi.org/10.15666/aeer/1706_1443514454

regression coefficients in the regression model are: 115.232 for constant, and -8.297 for the independent variable mass loss rate. Then, the regression equation is given as:

$$y = -8.297x + 115.232 \quad \text{(Eq.4)}$$

The significant level of regression was 0.002 for the weight loss rate of the *Betula alnoides*, and it was 0.000 for the compressive strength, indicating that the probability of regression coefficient equal to 0 in the t-statistical test that was 0.002 and 0.000, respectively, and also the linear correlation between the two variables is extremely significant and the established regression equation is valid.

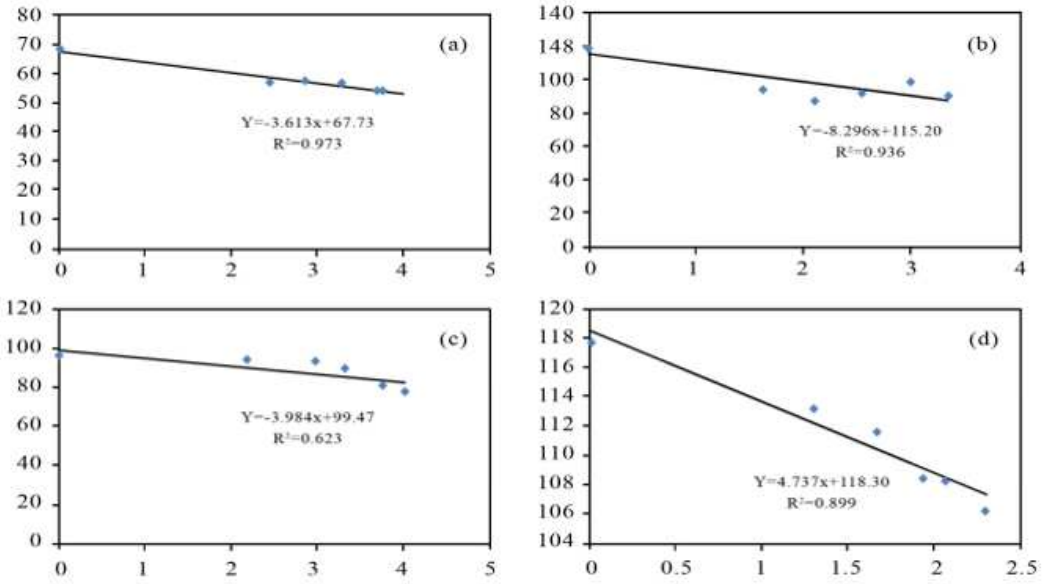

Figure 11. *Regression analysis for weight loss rate and compressive strength of tree species*

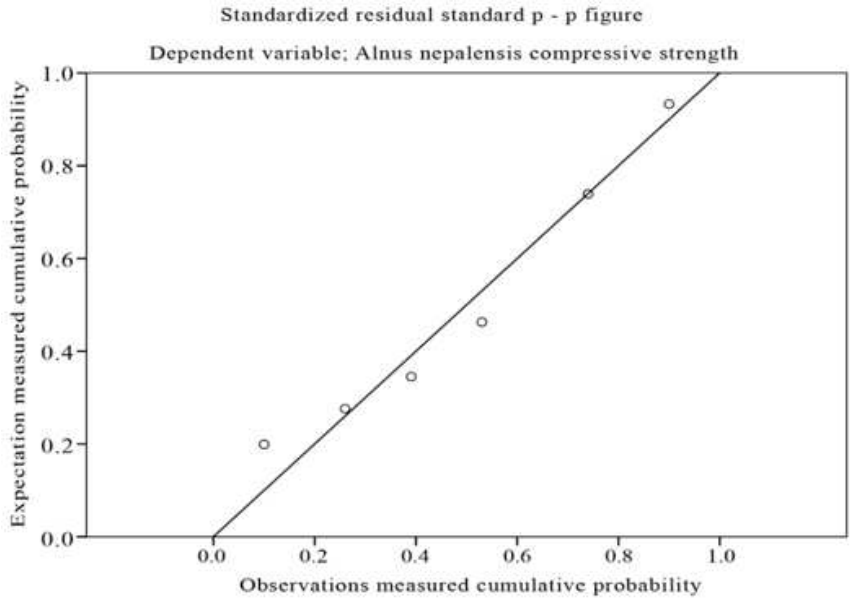

Figure 12. *Measured cumulative probability*

http://www.aloki.hu ● ISSN 1589 1623 (Print) ● ISSN 1785 0037 (Online)
DOI: http://dx.doi.org/10.15666/aeer/1706_1443514454

Table 4. *Correlation coefficients*

Character		Compressive strength of *Betula alnoides*	Weightlessness rate of *Betula alnoides*
Pearson correlation	Compressive strength of *Betula alnoides*	1.000	-.968
	Weightlessness rate of *Betula alnoides*	-.968	1.000
Sig. (single side)	Compressive strength of *Betula alnoides*	.	.001
	Weightlessness rate of *Betula alnoides*	.001	.
N	Compressive strength of *Betula alnoides*	6	6
	Weightlessness rate of *Betula alnoides*	6	6

Figure 13 shows the measured cumulative probability p-p chart in the regression analysis, in which the scatter points are roughly scattered around the oblique line, so it can be approximated that the residual distribution is subject to a normal distribution.

Result of the experimental was evaluated using *Equation 5*. *Tables 6* and *7* show the correlation coefficients of the *Aquilaria sinensis*, in which the Pearson correlation coefficient between the two variables was -0.790, indicating a highly linear correlation between the two. *Table 5* lists the linear equation coefficients. It can be seen that the regression coefficients in the regression model are: 99.472 for constant, and -3.985 for the independent variable mass loss rate. Then, the regression equation is given as:

$$y = -3.985x + 99.472 \quad \text{(Eq.5)}$$

The significant level of regression was 0.062 for the weight loss rate of the *Aquilaria sinensis*, and it was 0.000 for the compressive strength, indicating that the probability of regression coefficient equal to 0 in the t-statistical test that is 0.062 and 0.000, respectively, and also the linear correlation between the two variables is extremely significant and the established regression equation is valid.

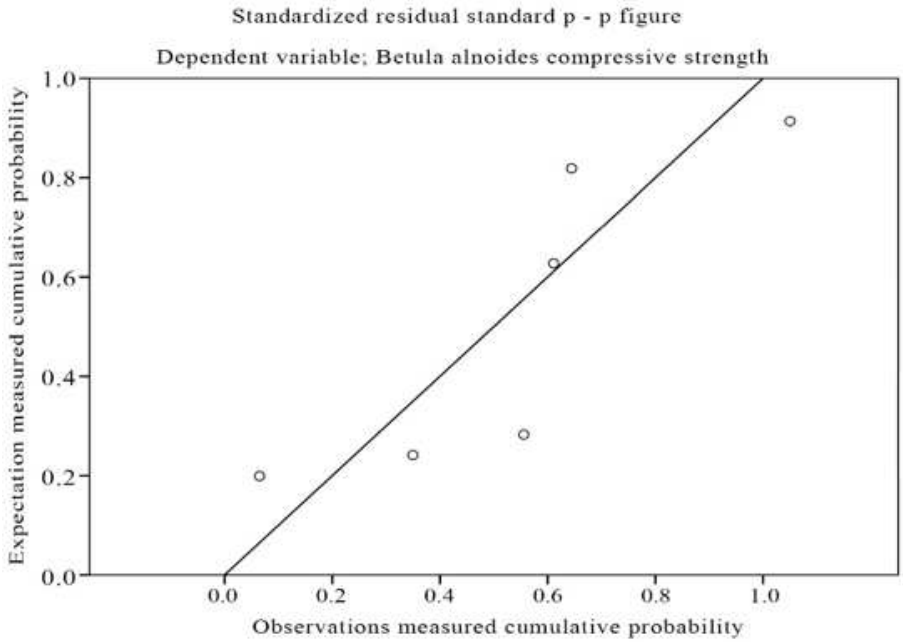

Figure 13. *Measured cumulative probability*

http://www.aloki.hu ● ISSN 1589 1623 (Print) ● ISSN 1785 0037 (Online)
DOI: http://dx.doi.org/10.15666/aeer/1706_1443514454

Table 5. *Model coefficient*

Model		Non-standardized coefficient		Standard coefficient	t	Sig.	The 95.0% confidence interval of B	
		B	Standard error (SE)				Lower bound	Upper bound
1	(Constant)	115.232	2.561		44.996	.000	108.122	122.342
	Weightlessness rate of *Betula alnoides*	-8.297	1.080	-.968	-7.683	.002	-11.295	-5.298

Dependent variable: compressive strength of *Betula alnoides*

Table 6. *Correlation and checklist*

Character		Compressive strength of *Aquilaria sinensis*	Weightlessness rate of *Aquilaria sinensis*
Pearson correlation	Compressive strength of *Aquilaria sinensis*	1.000	-.790
	Weightlessness rate of *Aquilaria sinensis*	-.790	1.000
Sig. (single side)	Compressive strength of *Aquilaria sinensis*	.	.031
	Weightlessness rate of *Aquilaria sinensis*	.031	.
N	Compressive strength of *Aquilaria sinensis*	6	6
	Weightlessness rate of *Aquilaria sinensis*	6	6

Table 7. *Model coefficient*

Model		Non-standardized coefficient		Standard coefficient	t	Sig.	The 95.0% confidence interval of B	
		B	Standard error (SE)				Lower bound	Upper bound
1	(Constant)	99.472	4.685		21.234	.000	86.465	112.478
	Weightlessness rate of *Aquilaria sinensis*	-3.985	1.547	-.790	-2.575	.062	-8.281	.311

Dependent variable: compressive strength of *Aquilaria sinensis*

Figure 14 shows the measured cumulative probability p-p chart in the regression analysis, in which the scatter points are roughly scattered around the oblique line, so it can be approximated that the residual distribution is subject to a normal distribution.

Result of the experimental was evaluated using *Equation 6*. *Tables 8* and *9* shows the correlation and coefficients of the Pinus kesiya, in which the Pearson correlation coefficient between the two variables is -0.948, indicating a highly linear correlation between the two. *Table 9* lists the linear equation coefficients. It can be seen that the regression coefficients in the regression model are: 118.381 for constant, and -4.738 for the independent variable mass loss rate. Then, the regression equation is given as:

$$y = -4.738x + 118.381 \quad \text{(Eq.6)}$$

The significant level of regression was 0.004 for the weight loss rate of the *Pinus kesiya*, and it was 0.000 for the compressive strength, indicating that the probability of

http://www.aloki.hu ● ISSN 1589 1623 (Print) ● ISSN 1785 0037 (Online)
DOI: http://dx.doi.org/10.15666/aeer/1706_1443514454

regression coefficient equal to 0 in the t-statistical test that is 0.004 and 0.000, respectively, and also the linear correlation between the two variables is extremely significant and the established regression equation is valid.

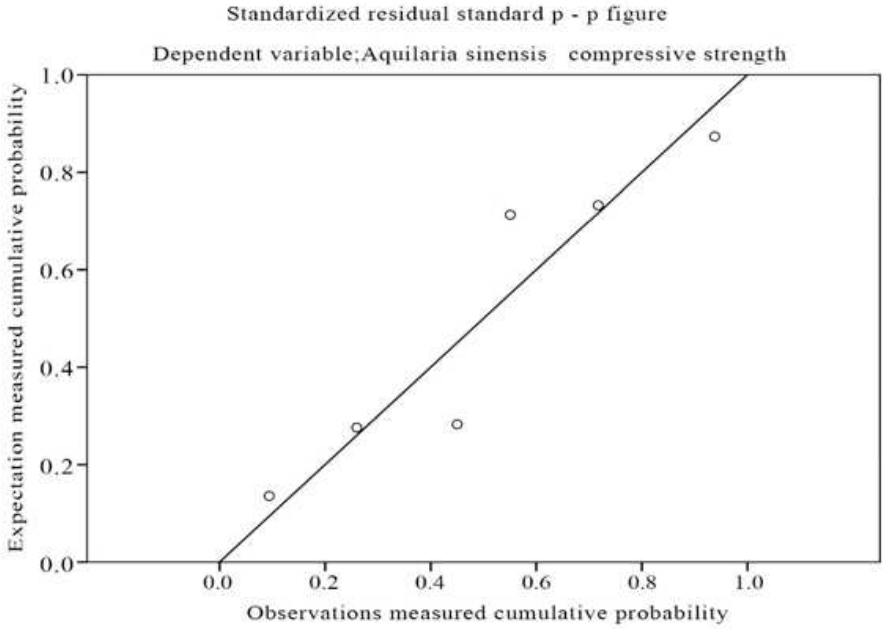

Figure 14. *Measured cumulative probability*

Figure 15 shows the measured cumulative probability p-p chart in the regression analysis, in which the scatter points are roughly scattered around the oblique line, so it can be approximated that the residual distribution is subject to a normal distribution.

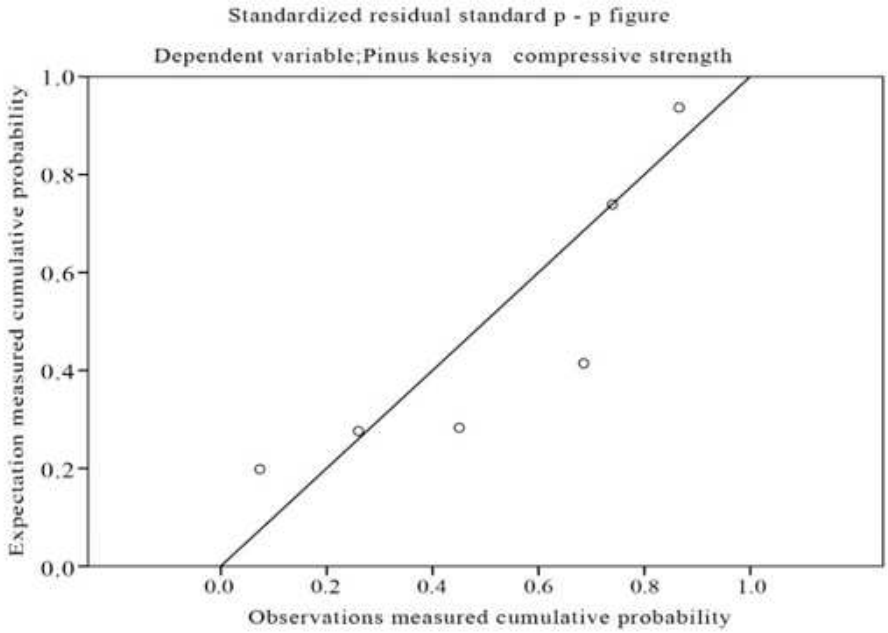

Figure 15. *Measured cumulative probability*

http://www.aloki.hu ● ISSN 1589 1623 (Print) ● ISSN 1785 0037 (Online)
DOI: http://dx.doi.org/10.15666/aeer/1706_1443514454

Table 8. *Correlation coefficients*

Character		Compressive strength of *Pinus kesiya*	Weightlessness rate of *Pinus kesiya*
Pearson correlation	Compressive strength of *Pinus kesiya*	1.000	-.948
	Weightlessness rate of *Pinus kesiya*	-.948	1.000
Sig. (single side)	Compressive strength of *Pinus kesiya*	.	.002
	Weightlessness rate of *Pinus kesiya*	.002	.
N	Compressive strength of *Pinus kesiya*	6	6
	Weightlessness rate of *Pinus kesiya*	6	6

Table 9. *Model coefficients*

Model		Non-standardized coefficient		Standard coefficient	t	Sig.	The 95.0% confidence interval of B	
		B	Standard error (SE)				Lower bound	Upper bound
1	(Constant)	118.381	1.402		84.442	.000	114.489	122.274
	Weightlessness rate of *Pinus kesiya*	-4.738	.794	-.948	-5.969	.004	-6.942	-2.534

Dependent variable: compressive strength of *Pinus kesiya*

In summary, the unitary linear regression analysis shows that the correlation between the weight loss rate and the compressive strength parallel to grain is very significant, and both are highly negatively correlated. The weight loss rate of the specimens did not change much; with the increase of rotten time, the weight loss rate of the specimens was on the rise; while the compressive strength parallel to grain of the spalted woods was gradually reduced. The strain *Xylaria venosula* does not destroy the internal cell wall of the spalted wood, and has little effect on the strength of the wood, since it is an initial decay in terms of the mycelial distribution and morphology.

Conclusions

Spalting is the coloration of wood caused by fungal colonization with beautiful patterns, it can be made into green, low-carbon, environmentally friendly and nice decorative crafts and wood veneer products, so as to enhance the rate of multipurpose utilization and additional value, it is provided with a very high economic value.

This paper aims to carry out a preliminary study and discussion on the spalted woods with zone lines induced artificially by fungi and the related mechanism. For this purpose, the strain *Xylaria venosula* was selected and inoculated into the wood blocks for preparing the spalted wood. Then, using the light and electron microscopy, it analyses the microfeatures of the spalted wood, and conducts experiments on the measurement of compressive strength and the influence of wood water content on the spalt formation. Finally, the following conclusions were drawn:

(1) The microfeatures of the spalted woods were analysed by light and electron microscopy, revealing that *Aquilaria sinensis* could easily form black zone lines, which are mainly distributed in ducts, parenchyma cells and fibroblasts connected with

http://www.aloki.hu ● ISSN 1589 1623 (Print) ● ISSN 1785 0037 (Online)
DOI: http://dx.doi.org/10.15666/aeer/1706_1443514454

parenchyma cells, indicating that these fungal infestations on specimens are performed by means of minimal resistance and the fastest access to nutrients anatomically; the mycelia inside the zone lines were denser than outside, and the peak density appeared at the centre of each zone line; the black zone lines in the wood is a barrier that the fungus uses to resist the invasion of other microorganisms, so that the resources in the enclosed area can be utilized continuously.

(2) Analysis for the effect of wood water content on the spalts formed by *Xylaria venosula* showed that when the water content of the wood was 50%, the amount of external and internal spalts formed was the most and the most obvious, and the surface spalts formed on the four wooden blocks reached the maximum; The largest spalt was observed on *Aquilaria sinensis* blocks; this type of wood underwent the most serious spalting, with 6.64% of its surface and 1.84% of its interior covered by spalts. In this case, zone lines were rich and beautiful and the wood was not severely rotten. Thus, this wood and the water content offer the most suitable conditions for the growth of *Xylaria venosula* strains.

(3) The measured results of mean mass loss percentage and compressive strength show that as the wood blocks rotted over time, the weight loss rates of spalted woods were on the rise, while the compressive strengths parallel to grain were gradually falling. When the water content was 10%, the mass loss rate of the specimen was the smallest; when it was 50%, the mass loss rate of *Aquilaria sinen*sis was large, reaching 6.07%, but lower than Alnus nepalensis.

(4) The compressive strength measurement showed that the weight loss rate of *Alnus nepalensis* was increased with rotten time, and the compressive strength of the spalted wood was correspondingly reduced. A linear regression analysis was conducted about the weight loss rate and the compressive strength parallel to grain of the artificially prepared spalted wood, to find that the correlation between the two was very significant and also highly negatively correlated. Also, there was no sign of destroying the cell wall inside the spalted wood formed by the strain *Xylaria venosula*. In terms of distribution and morphology, the mycelium was an initial decay and had little effect on the strength of the wood.

To sum up, the spalted wood cultivated by artificially inoculated *Xylaria venosula* has good stability, natural and beautiful pattern, and low corrosiveness. It has no big effect on mass loss rate and the compressive strength of wood blocks. Therefore, it has a good prospect for the use of the strain *Xylaria venosula* to prepare the spalted wood has a good prospect which is suitable for application and promotion.

These contents will become the next study. First, directional generation of zone lines. Then, the generation time of zone lines will shorted.

Acknowledgements. This work was financially supported by the National Natural Science Foundation of China (Grant No. 31570555)

REFERENCES

[1] Dai, Y. C. (2012): Polypore diversity in China with an annotated checklist of Chinese polypores. – Mycoscience 53(1): 49-80.

[2] Fournier, J., Flessa, F., Peršoh, D., Stadler, M. (2011): Three new Xylaria species from southwestern Europe. – Mycological Progress 10(1): 33-52.

http://www.aloki.hu ● ISSN 1589 1623 (Print) ● ISSN 1785 0037 (Online)
DOI: http://dx.doi.org/10.15666/aeer/1706_1443514454

[3] Hladki, A. I., Romero, A. I. (2010): A preliminary account of Xylaria in the Tucuman Province, Argentina, with a key to the known species from the Northern Provinces. – Fungal Diversity 42(1): 79-96.
[4] Huang, Y., Finell, M., Larsson, S., Wang, X., Zhang, J., Wei, R., Liu, L. (2017): Biofuel pellets made at low moisture content-Influence of water in the binding mechanism of densified biomass. – Biomass and Bioenergy 98: 8-14.
[5] Læssøe, T., Srikitikulchai, P., Luangsa-ard, J. J. D., Stadler, M. (2013): Theissenia reconsidered, including molecular phylogeny of the type species T. Pyrenocrata and a new genus Durotheca (Xylariaceae, Ascomycota). – IMA Fungus 4(1): 57-69.
[6] Liers, C., Ullrich, R., Steffen, K. T., Hatakka, A., Hofrichter, M. (2006): Mineralization of 14 C-labelled synthetic lignin and extracellular enzyme activities of the wood-colonizing ascomycetes Xylaria hypoxylon and Xylaria polymorpha. – Applied Microbiology and Biotechnology 69(5): 573-579.
[7] Nagy, N. E., Ballance, S., Kvaalen, H., Fossdal, C. G., Solheim, H., Hietala, A. M. (2012): Xylem defense wood of Norway spruce compromised by the pathogenic white-rot fungus Heterobasidion parviporum shows a prolonged period of selective decay. – Planta 236(4): 1125-1133.
[8] Osono, T., To-Anun, C., Hagiwara, Y., Hirose, D. (2011): Decomposition of wood, petiole and leaf litter by Xylaria species from northern Thailand. – Fungal Ecology 4(3): 210-218.
[9] Passarini, M. R., Santos, C., Lima, N., Berlinck, R. G., Sette, L. D. (2013): Filamentous fungi from the Atlantic marine sponge Dragmacidon reticulatum. – Archives of Microbiology 195(2): 99-111.
[10] Pearce, R. B. (1984): Staining fungal hyphae in wood. – Transactions of the British Mycological Society. https://doi.org/10.1016/S0007-1536(84)80029-7.
[11] Robinson, S. C., Laks, P. E. (2010): Culture age and wood species affect zone line production of Xylaria polymorpha. – Mycological Research in Review 4: 18-21.
[12] Robinson, S. C., Richter, D. L., Laks, P. E. (2007): Colonization of sugar maple by spalting fungi. – Forest Products Journal 57(4): 24.
[13] Robinson, S. C., Laks, P. E., Turnquist, E. J. (2009): A method for digital color analysis of spalted wood using Scion Image software. – Materials 2(1): 62-75.
[14] Robinson, S. C., Tudor, D., Cooper, P. A. (2011): Feasibility of using red pigment producing fungi to stain wood for decorative applications. – Canadian Journal of Forest Research 41(8): 1722-1728.
[15] Tian, J. J., Gao, X. X., Zhang, W. M., Wang, L., Qu, L. H. (2013): Molecular identification of endophytic fungi from Aquilaria sinensis and artificial agarwood induced by pinholes-infusion technique. – African Journal of Biotechnology 12(21).
[16] Tudor, D., Robinson, S. C., Cooper, P. A. (2012): The influence of moisture content variation on fungal pigment formation in spalted wood. – AMB Express 2(1): 69.
[17] Tudor, D., Robinson, S. C., Cooper, P. A. (2013): The influence of pH on pigment formation by lignicolous fungi. – International Biodeterioration & Biodegradation 80: 22-28.
[18] Xu, Y., Zhang, Z., Wang, M., Wei, J., Chen, H., Gao, Z., Meng, H. (2013): Identification of genes related to agarwood formation: Transcriptome analysis of healthy and wounded tissues of Aquilaria sinensis. – BMC Genomics 14(1): 227.
[19] Zink, P., Fengel, D. (1988): Studies on the colouring matter of blue-stain fungi. Part 1. General characterization and the associated compounds. – Holzforschung - International Journal of the Biology, Chemistry, Physics and Technology of Wood 42(4): 217-220.

http://www.aloki.hu ● ISSN 1589 1623 (Print) ● ISSN 1785 0037 (Online)
DOI: http://dx.doi.org/10.15666/aeer/1706_1443514454

COMPREHENSIVE ECO-ENVIRONMENTAL IMPACT ASSESSMENT OF URBAN PLANNING BASED ON PRESSURE-STATE-RESPONSE MODEL

LIU, L.[1,2] – ZHANG, Q.[1,2*] – WANG, C. L.[1] – ZHANG, K.[1] – ZHANG, X.[1]

[1]*School of Art and Design of Zheng Zhou University of Light Industry, Zhengzhou 450002, China*

[2]*Henan Cultural Industry Development Research Base, Zhengzhou 450002, China*

**Corresponding author*
e-mail: 27412397@qq.com

(Received 7th Jun 2019; accepted 10th Oct 2019)

Abstract. Considering the irreversible impacts of urban master plan on the eco-environment, the specific impacts must be evaluated in a comprehensive manner before preparing the plan. As a result, this paper studies the impacts of urban planning on eco-environment, sets up an assessment system for it based on the pressure-state-response (PSR) model, and applies the system to assess the eco-environment before and after the implementation of an urban master plan. The evaluation results show that the medium to long-term urban master plan promoted the eco-environment of the city. The research results shed new light on the eco-environmental impact assessment of urban master plans.
Keywords: *urban planning, eco-environmental impact assessment, pressure-state-response (PSR) model, analytic hierarchy process (AHP), eco-environmental pressure*

Introduction

In recent years, following the rapid development of China's urban economic level, the urbanization process has continued to advance (Wang et al., 2008). The extensive economic development model with high resource consumption brings not only the rapid urban development, but also "urban diseases" such as resource wasting, population expansion, and environmental damage (Crainic et al., 2009). All these affect the city's sustainable development, which will inevitably lead to irreversible problems for the city if not valued (Mancini et al., 2010; Liu et al., 2011). Therefore, it is necessary to design a master plan of urban land use and resource allocation for the healthy, orderly and harmonious development of the city.

Eco-environmental impact assessment was first proposed by American scholars in 1969, accompanied by an increasing environmental problem (Elena et al., 2008). After 40 years of development, it has been further verified that an urban master plan must consider its impact on the eco-environment under the condition of not destroying and improving the eco-environment (Pang et al., 2015). Only the environmentally friendly urban planning can ensure the sustainable development of the city, provide long-term benefits for environmental protection and the city, and further promote the decision-making system for environmental protection (Seenivasaperumal et al., 2010). For this, a study on comprehensive impact assessment of urban planning on eco-environment should be conducted, which not only helps the public to obtain effective information about the environmental impact of urban planning, but also enables government departments to realize the top-priority environmental indicators needed in plan implementation (Fitzpatrick et al., 2008).

http://www.aloki.hu ● ISSN 1589 1623 (Print) ● ISSN 1785 0037 (Online)
DOI: http://dx.doi.org/10.15666/aeer/1706_1445514463

Over the years, China has attached more importance to environmental protection, and its research results on environmental impact assessment have become increasingly abundant (Shiojiri et al., 2010; Muthu et al., 2010). However, environmental impact assessment is mostly limited to engineering construction, and the research on eco-environmental impact assessment of urban master plan is still at the exploratory stage (Maj, 2015; Boulay et al., 2015). Thus, in order to ensure the coordinated and sustainable development of the overall city, the eco-environment should be improved in a scientific, orderly, efficient and reasonable manner, which can truly alleviate the pressure of eco-environment in urban planning (Zhou et al., 2013).

Therefore, this paper firstly introduces the connotation of PSR model. Based on this, an eco-environment evaluation system under the impact of urban planning was constructed. Then, the author proposed eco-environment improvement measures through comprehensive evaluation of the eco-environment of one city. The research results demonstrate feasibility of the comprehensive eco-environment impact assessment in urban master plan for the sustainable and harmonious development of cities, and also the objectivity and feasibility of the PSR model.

Materials and methods

The eco-environmental impact assessment of urban planning means to analyse and evaluate the impacts of the eco-environment and its ecosystems after urban planning of the structure, layout and land use, and then propose measures to mitigate the adverse effects (Wolfslehner and Vacik et al., 2008). The impact assessment system of urban planning on eco-environment is shown in *Figure 1*.

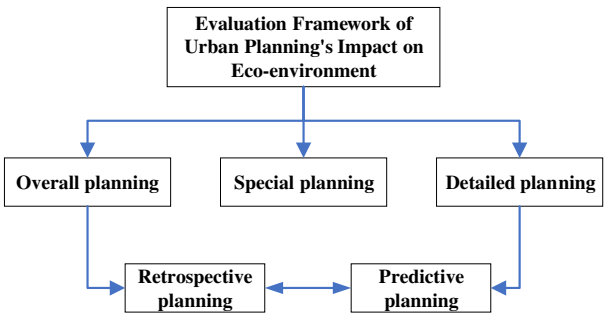

Figure 1. *Urban planning impact assessment system on eco-environment*

It should be noted that due to the different eco-environment conditions in different cities, the water environment, soil, plant diversity, natural disasters, etc. must be selected according to the environmental characteristics.

Pressure-state-response model

The PSR model is used for comprehensive assessment of eco-environmental impacts (Korol et al., 2016). It aims to construct one assessment system in three aspects: what the problems are, why the problems happen, and how to deal with these problems. *Figure 2* shows the framework of the PSR model.

http://www.aloki.hu ● ISSN 1589 1623 (Print) ● ISSN 1785 0037 (Online)
DOI: http://dx.doi.org/10.15666/aeer/1706_1445514463

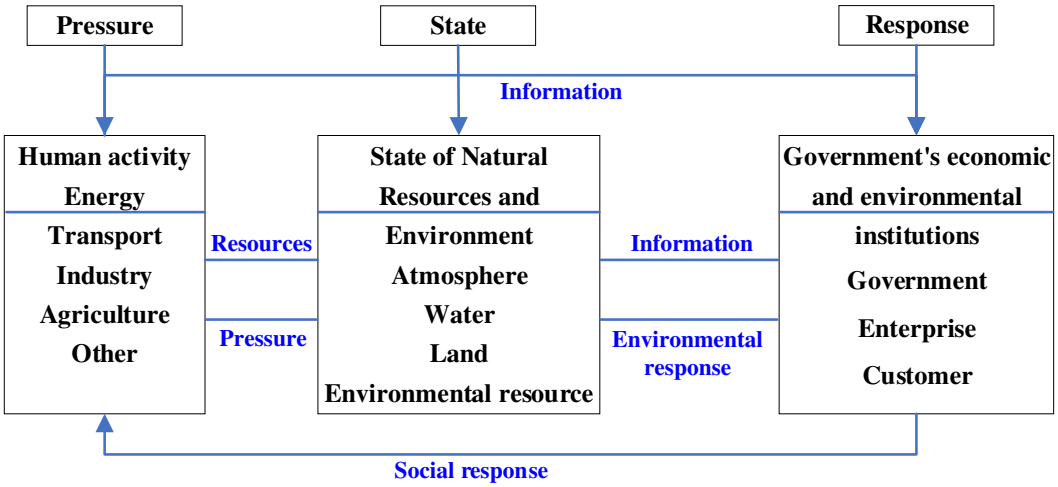

Figure 2. *PSR framework*

It can be further seen from *Figure 2* that the PSR model contains a strong logical causality. First, it shows the degree of improvement or even deterioration for the eco-environment by describing the "state" of the eco-environment. Secondly, it discusses the impact degree of the eco-environment on social and economic development under the economic and social "pressure". Finally, through the "response" at the institutional and policy levels, the measures are taken for the "state" of the eco-environment.

Eco-environmental impact assessment system based on PSR model

With reference to the relevant research literature (Jr et al., 2013; Prestrelo and Monteiro-Neto, 2016), the eco-environmental impact assessment indicators based on the PSR model were established, as shown in *Table 1*.

Table 1. *Eco-environmental impact assessment indicators based on PSR model*

Target layer	Criterion layer	Indicator layer
Eco-environmental status index	Socio-economic pressure (P)	Per capita GDP
		Urbanization level
		Traffic network density
	Ecological environment state (S)	Vegetation coverage
		Plant and biodiversity
		Water resources abundance and deficiency index
	Policy response (R)	Protection index of ecologically sensitive areas
		Indicators of land reclamation
		Intensive utilization of rural residential areas

Different indicators vary in their dimensions, making it impossible to compare the indicators and to truly reflect the current relationship between the indicators. So, it is necessary to standardize the assessment indicators. When these indicators and the eco-environment shows a positive and negative relationship, the standardized values of indicators are expressed in *Equations 1* and *2* below, respectively. The research data on

http://www.aloki.hu ● ISSN 1589 1623 (Print) ● ISSN 1785 0037 (Online)
DOI: http://dx.doi.org/10.15666/aeer/1706_1445514463

urban planning were collected through statistical survey and published on the *China Statistical Yearbook* released by National Bureau of Statistics, China.

$$PI_i = \frac{X_i - X_{\min}}{X_{\max} - X_{\min}} * 100\% \quad \text{(Eq.1)}$$

$$PI_i = \left(1 - \frac{X_i - X_{\min}}{X_{\max} - X_{\min}}\right) * 100\% \quad \text{(Eq.2)}$$

where PI_i is the normalized value of the i th indicator, X_{min} is its minimum value, X_i is its actual value, and X_{max} is its maximum value.

Among them, with PI_i being closer to 100%, it indicates a better eco-environment reflected by this indicator.

Furthermore, it is necessary to analyse the correlation of the indicators and screen out the highly correlated indicators, as shown in *Equation 3*.

$$r = \frac{\sum(X - \bar{X}) \cdot (Y - \bar{Y})}{\sqrt{\sum(X - \bar{X})^2 \cdot \sum(Y - \bar{Y})^2}} = \frac{\sum XY - \frac{\sum X \sum Y}{n}}{\sqrt{\left[\sum X^2 - \frac{(\sum X)^2}{n}\right]\left[\sum Y^2 - \frac{(\sum Y)^2}{n}\right]}} \quad \text{(Eq.3)}$$

where r is the correlation coefficient between the indicators; X and Y are the normalized value of the different indicators.

r is usually between -1 and + 1; the degree of correlation between indicators is positively correlated with the absolute value of r.

Determination of indicator weights

Analytic Hierarchy Process (AHP) can decompose the relevant factors of the problem into three layers: goals, criteria and alternatives. As shown in *Figure 3,* the goal layer A lists the goal of problem solving, i.e. the overall objective of the AHP; the criterion layer B gives the criteria that affect the realization of the goal; the alternative layer C provides the various indicators that promote the achievement of the goal.

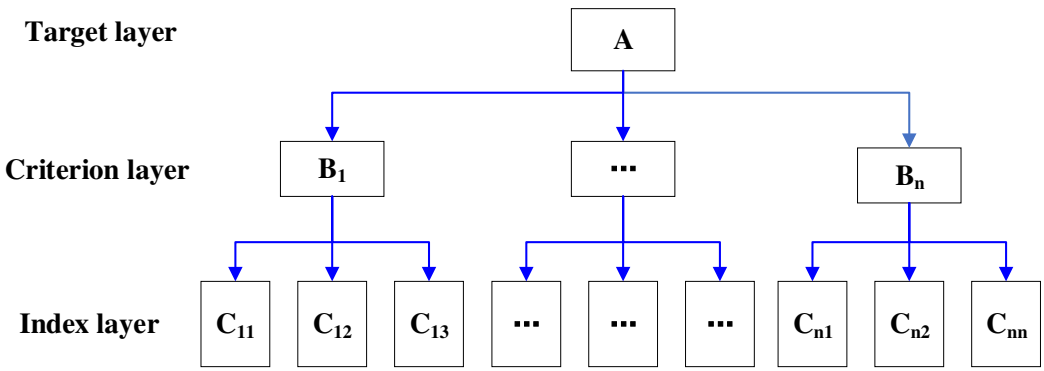

Figure 3. *AHP structural model*

http://www.aloki.hu ● ISSN 1589 1623 (Print) ● ISSN 1785 0037 (Online)
DOI: http://dx.doi.org/10.15666/aeer/1706_1445514463

The AHP was used to construct a judgment matrix (*Eq. 4*) by pairwise comparison between indicators, perform a consistency test (*Eq. 5*), and then determine the weight of each indicator.

$$\begin{pmatrix} A & B_1 & B_2 & \cdots & B_n \\ B_1 & c_{11} & c_{12} & \cdots & c_{1n} \\ B_2 & c_{21} & c_{22} & \cdots & c_{2n} \\ \vdots & \vdots & \vdots & \ddots & \vdots \\ B_n & c_{n1} & c_{n2} & \cdots & c_{nn} \end{pmatrix} \quad \text{(Eq.4)}$$

$$CR = \frac{\sum_{j=1}^{m} CI(j)c_j}{\sum_{j=1}^{m} RI(j)c_j} \quad \text{(Eq.5)}$$

In *Equation 5,* CI is the consistency indicator, and CR is the consistency ratio.

Classification of eco-environment indicators

The eco-environment evaluation is shown in *Equation 6*.

$$EI = \sum_{i=1}^{n} w_i \cdot c_i \quad \text{(Eq.6)}$$

where w_i is the indicator weight; c_i is the normalized value of the indicator.

Generally, the eco-environment indicators can be classified into four grades, namely excellent, good, fair, and poor, as shown in *Table 2*.

Table 2. *Classification of eco-environment indicators*

Level	Excellent	Good	Commonly	Bad
Index	$EI \geq 80$	$60 \leq EI < 80$	$40 \leq EI \leq 60$	$EI < 40$

The extent of the eco-environment changes before and after urban planning can be divided into: significant change, obvious change, slight change, and almost no change. The specific changes and the corresponding values of each level are shown in *Table 3*.

Table 3. *Different impact degrees of urban planning on the eco-environment*

Level	Significant change	Obvious change	Slight change	Almost invariable
Index	$\|\Delta EI\| \geq 10$	$5 \leq \|\Delta EI\| < 10$	$2 \leq \|\Delta EI\| < 5$	$\|\Delta EI\| < 2$
Description	The ecological environment has changed significantly. If ΔEI is positive, it shows a significant improvement, and vice versa, a significant deterioration	The ecological environment has been greatly changed. If ΔEI is positive, it shows a marked improvement, and vice versa, a marked deterioration	The ecological environment has changed slightly. If ΔEI is positive, it means slightly better, and vice versa, slightly worse	The state of ecological environment has hardly changed

http://www.aloki.hu ● ISSN 1589 1623 (Print) ● ISSN 1785 0037 (Online)
DOI: http://dx.doi.org/10.15666/aeer/1706_1445514463

Results

One certain city was selected to plot the urban master plan for its three districts and six counties during the period of 2020-2040. The base data were collected from 2009 to 2018, with 2018 being the base year. The actual values of various eco-environment indicators are shown in *Table 4,* where B1~B6 are productivity, stability, protection, economic vitality, social acceptance, and policy response, respectively; C1~C20 are land utilization rate, area ratio of basic farmland, ratio of non-agricultural construction land, per unit area yield of grain, diversity of land use, land development rate, land consolidation rate, land reclamation rate, farmland conversion rate, area ratio of ecological land, forest coverage, water surface index, per capita public green area in urban areas, output index of construction land, output index of agricultural land, per capita GDP, economic density, expert satisfaction, protection index of ecologically sensitive area, intensive utilization of rural residential areas.

Table 4. *Actual values of various eco-environment indicators*

Index/Year		2018	2020	2025	2030	2035	2040
B1	C1	0.58	0.70	1.04	1.39	2.07	12.99
	C2	240	244	247	251	256	269
	C3	4.22	4.23	4.26	4.32	4.53	5.28
	C4	0.26	0.03	0.26	0.03	0.27	0.05
B2	C5	802	673	723	784	853	1118
	C6	1296	1362	1389	1409	1847	2462
	C7	76.00	91.89	80.85	81.85	94.87	125.24
B3	C8	887	875	858	847	829	8785
	C9	402	462	1144	1084	1191	1370
	C10	0.38	0.33	0.28	0.25	0.26	0.23
B4	C11	10.41	38.75	51.91	57.96	65.01	80.01
	C12	91.07	91.65	92.44	101.78	101.01	102.01
B5	C13	30.20	31.63	33.37	34.63	35.97	47.45
	C14	1.37	1.34	1.33	1.32	1.30	1.27
	C15	63.75	72.62	60.82	83.41	86.01	92.01
	C16	57.12	52.57	74.90	72.01	73.23	79.79
B6	C17	84.10	85.75	88.81	90.14	89.89	109.99
	C18	3.44	4.66	3.87	5.13	6.01	9.01
	C19	561510	555524	528519	527736	506461	458601
	C20	17.42	21.85	30.50	40.92	56.07	291.30

Based on the PSR model, the evaluation value of the urban planning impact on the eco-environment was obtained (*Fig. 4*).

Figure 4 indicates the overall upward trend of the eco-environment under the influence of the urban master plan for this City from 2018 to 2040, of which 2018-2025 is a slowly rising process, which is consistent with the development trend of this city, and also the city's environmental protection facilities and economic base are in a slow development stage; from the mid-term planning of 2025 to the long-term 2035, the city's ecological situation has made a qualitative leap and reached a new level in 2040.

http://www.aloki.hu ● ISSN 1589 1623 (Print) ● ISSN 1785 0037 (Online)
DOI: http://dx.doi.org/10.15666/aeer/1706_1445514463

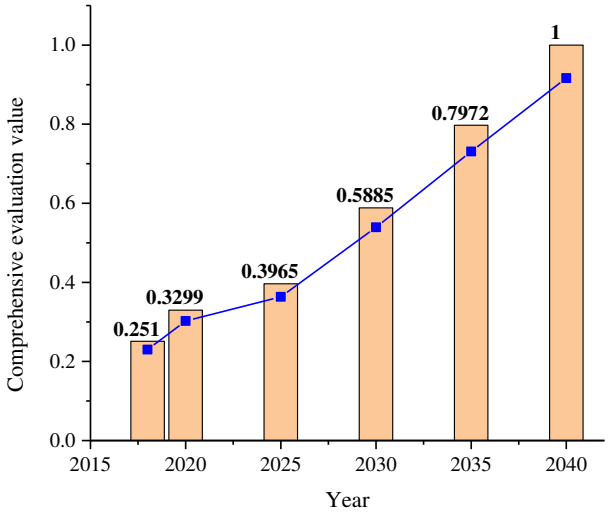

Figure 4. *Evaluation value of the urban planning impact on the eco-environment for one certain city*

Discussion

Figure 5 shows the variation trend of all indicators at the criterion layer from 2018-2040. *Table 5* lists the grading levels of different indicators.

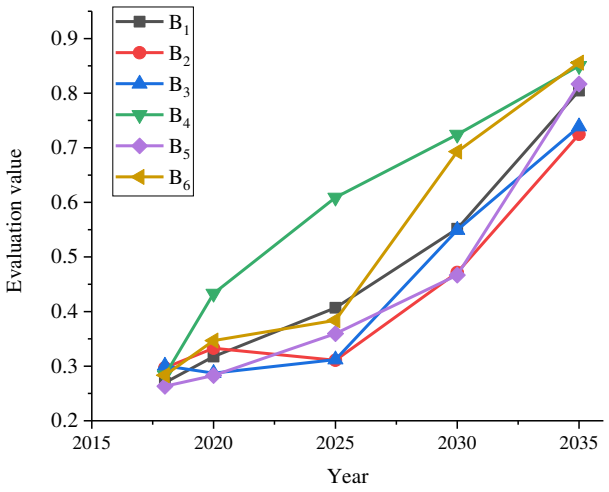

Figure 5. *Variation trends of the primary indicators during the period 2018-2035*

Table 5. *Classification of eco-environment levels of primary indicators during the period 2018-2040*

Index/Year	2018	2020	2025	2030	2035	2040
B1	Relatively low	Relatively low	Secondary	Secondary	Relatively high	High
B2	Relatively low	Secondary	Secondary	Relatively low	Relatively high	High
B3	Relatively low	Relatively low	Relatively low	Secondary	Relatively high	Relatively high
B4	Relatively low	Secondary	Secondary	Secondary	Relatively high	High
B5	Relatively low	Relatively low	Secondary	Relatively high	Relatively high	High
B6	Relatively low	Relatively low	Secondary	Secondary	Secondary	Relatively high

http://www.aloki.hu ● ISSN 1589 1623 (Print) ● ISSN 1785 0037 (Online)
DOI: http://dx.doi.org/10.15666/aeer/1706_1445514463

From the 6 primary indicators in *Figure 5* and *Table 5,* it can be seen that all these indicators in 2018 were at a relatively low development level, but after several years of construction until 2025, most of the indicators have reached a medium level, and by 2035 it reaches a high level.

In order to accelerate the improvement of the eco-environment, it is recommended to continuously improve the internal driving force for urban development by appropriately increasing the related planned value of the indicators to economic development; to relieve the impact of urban planning on the environment, such as reducing the emissions of carbon dioxide and sulphur dioxide, control the discharge of water pollution etc.

Conclusions

This paper studies the urban planning impact assessment on the eco-environment. The main conclusions are as follows:

(1) With the purpose of realizing the urban planning impact assessment on eco-environment, a comprehensive analysis of the urban master planning process was conducted, and then a system diagram for this impact assessment was established.

(2) Based on the PSR model, an indicator system for impact assessment of urban planning on the eco-environment was constructed, including the goal layer, the criterion layer l and the alternative layer.

(3) AHP was used to determine the weight of each indicator, and evaluate the eco-environment of one certain city. The evaluation results show that under the current urban planning, the variation trend of eco-environment is consistent with the sustainable development of this city.

The complete eco-environmental impact assessment of urban planning should cover the predictive assessment in the preparation phase of the urban master plan, the inspective assessment in the implementation phase, and the retrospective assessment after the implementation. This paper only deals with the predictive assessment of the eco-environmental impacts of urban planning. The future research will tackle the inspective and retrospective assessments of the eco-environmental impacts of urban planning during and after the implementation of the urban master plan.

Acknowledgements. (1) Henan provincial department of science and technology key research and development and promotion special project (tackling key problems in science and technology): research on the analysis and reconstruction technology of parametric spatial texture characteristics in the development of traditional villages in central China (182102310963), 2018/01-2019/12, presided over and under research; (2) Research project of Henan science and technology think tank in 2018: research on regional feature extraction and activation path of traditional villages in central China under the background of rural revitalization (HNKJZK-2019-54b), 2019/01-2019/12, presided over and under research; (3) 2016 Zheng Zhou Institute of Light Industry doctoral research fund funded project: research on the restoration and activation strategy of traditional village texture in the area with remnants and debris-taking Henan province as an example (2016BSJJ061), 2017/01-2019/12, presided over and under research. Research project of humanities and social sciences of Henan provincial department of education, Research on the promotion of spatial features of landscape features of traditional villages in southern Henan under the protection and early warning strategy (2020-ZZJH-519).

http://www.aloki.hu ● ISSN 1589 1623 (Print) ● ISSN 1785 0037 (Online)
DOI: http://dx.doi.org/10.15666/aeer/1706_1445514463

REFERENCES

[1] Boulay, A. M., Camillo de Camillis, J. B., Döll, P., et al. (2015): Consensus building on the development of a stress-based indicator for LCA-based impact assessment of water consumption: outcome of the expert workshops. – International Journal of Life Cycle Assessment 20(5): 577-583.
[2] Crainic, T. G., Ricciardi, N., Storchi, G. (2009): Models for evaluating and planning city logistics systems. – Transportation Science 43(4): 432-454.
[3] Elena, D., Díaz, C. M., Baquero, R. A. (2008): Effects of landscape complexity on the ecological effectiveness of agri-environment schemes. – Landscape Ecology 23(2): 135-148.
[4] Fitzpatrick, P., Sinclair, A. J., Mitchell, B. (2008): Environmental impact assessment under the Mackenzie valley resource management act: deliberative democracy in Canada's north. – Environmental Management 42(1): 1-18.
[5] Jr, G. R., Kawamura, A., Medina, R., Amaguchi, H., Nakagawa, N., Bui, D. D. (2013): Environmental impact assessment of structural flood mitigation measures by a rapid impact assessment matrix (RIAM) technique: a case study in metro Manila, Philippines. – Science of the Total Environment 456-457(7): 137-147.
[6] Korol, J., Burchart-Korol, D., Pichlak, M. (2016): Expansion of environmental impact assessment for eco-efficiency evaluation of biocomposites for industrial application. – Journal of Cleaner Production 113(4): 144-152.
[7] Liu, X., He, B., Li, Z., Zhang, J., Wang, L., Wang, Z. (2011): Influence of land terracing on agricultural and ecological environment in the Loess Plateau regions of China. – Environmental Earth Sciences 62(4): 797-807.
[8] Maj, G. (2015): Diversification and environmental impact assessment of plant biomass energy use. – Polish Journal of Environmental Studies 24(5): 2055-2061.
[9] Mancini, V., Micarelli, R., Pizziolod, G. (2010): The relational project: a goal for the ecology of city designing and planning. – Annals of the New York Academy of Sciences 879(1): 416-421.
[10] Muthu, S., Hans, J. F., Kálmán, J. (2010): Mechanism of the asymmetric sulfoxidation in the esomeprazole process: effects of the imidazole backbone for the enantioselection. – Advanced Synthesis Catalysis 351(6): 903-919.
[11] Pang, B., Yang, P., Wang, Y., Kendall, A., Xie, H., Zhang, Y. (2015): Life cycle environmental impact assessment of a bridge with different strengthening schemes. – International Journal of Life Cycle Assessment 20(9): 1300-1311.
[12] Prestrelo, L., Monteiro-Neto, C. (2016): Before-after environmental impact assessment of an artificial channel opening on a south-western Atlantic choked lagoon system. – Journal of Fish Biology 89(1): 735-752.
[13] Seenivasaperumal, M., Federsel, H.-J., Szabó, K. J. (2010): Mechanism of the asymmetric sulfoxidation in the esomeprazole process: effects of the imidazole backbone for the enantioselection. – Advanced Synthesis & Catalysis 351(6): 903-919.
[14] Shiojiri, K., Yamasaki, A., Fujii, M., Kiyono, F., Yanagisawa, Y. (2010): Life cycle impact assessment of various treatment scenarios for sulfur hexafluoride (sf6) used as an insulating gas. – Environmental Progress and Sustainable Energy 25(3): 218-227.
[15] Wang, Y. S., Lou, Z. P., Sun, C. C., Sun, S. (2008): Ecological environment changes in Daya Bay, China, from 1982 to 2004. – Marine Pollution Bulletin 56(11): 1871-1879.
[16] Wolfslehner, B., Vacik, H. (2008): Evaluating sustainable forest management strategies with the analytic network process in a pressure-state-response framework. – Journal of Environmental Management 88(1): 1-10.
[17] Zhou, J., Chang, V. W. C., Fane, A. G. (2013): An improved life cycle impact assessment (lcia) approach for assessing aquatic eco-toxic impact of brine disposal from seawater desalination plants. – Desalination 308(1): 233-241.

http://www.aloki.hu ● ISSN 1589 1623 (Print) ● ISSN 1785 0037 (Online)
DOI: http://dx.doi.org/10.15666/aeer/1706_1445514463

IMPACTS OF URBAN EVOLUTION ON BIODIVERSITY CONSIDERING THE SUSTAINABLE DEVELOPMENT OF THE ECOSYSTEM

DONG, X. M.[1,2*] – XU, S. N.[1]

[1]*School of Architecture, Harbin Institute of Technology; Key Laboratory of Cold Region Urban and Rural Human Settlement Environment Science and Technology, Ministry of Industry and Information Technology, Harbin 150000, China*

[2]*School of Architecture, Inner Mongolia University of Technology, Hohhot 010051, China*

**Corresponding author*
e-mail: 57126970@qq.com

(Received 7th Jun 2019; accepted 10th Oct 2019)

Abstract. The life of urban residents demands sufficient material supply and a good eco-environment. The rapid expansion of cities has stimulated the urban population and economy, exerting irreversible changes on the eco-system. During the urban evolution, it is of great importance to evaluate the overall impacts of urban development on biodiversity. The evaluation aims to integrate biodiversity protection into urban development and maintain it in a harmonious and stable state. Focusing on ecosystem sustainability, this paper designs the architecture to evaluate the impacts of urban evolution on plant diversity, and creates an integrated evaluation system for biodiversity from five perspectives, namely, species richness, species diversity, species evenness, species importance and population diversity. On this basis, the proposed system was applied to assess the biodiversity in a city. The assessment results show that continuous biodiversity evaluations can ensure the sustainable development of species during urban evolution. The research findings provide new insights into the diversity and sustainability of urban species.
Keywords: *urban evolution, ecosystem, biodiversity, sustainable development, structure of plant community*

Introduction

In recent years, following the rapid advancement of urbanization, human society has been facing unprecedented problems such as environmental damage, increased pollution, over-exploitation of resources, reduction of green spaces, and shortage of water resources, which urgently require the protection of the diversity of the city and improvement of the city's ecological environment while promoting the living standards of human beings (Olofson et al., 2009). Also, with the current urban development, the biodiversity and ecological stability are seriously threatened. Therefore, the issues of protecting the environment, rationally utilizing biological resources, and ensuring the biodiversity for sustainable development have gradually attracted people's attention (Hunter and Philip, 2007; Karmaker et al., 2018).

Multi-level, sustainable and stable use of ecological resources is an important part of biodiversity protection (Kaushal et al., 2014). With the acceleration of urban evolution, the natural appearance has also undergone great changes. In particular, the destruction of ecosystems has greatly affected the living space of biological species, seriously threatening the biodiversity closely related to urban ecological environment and human settlements (Crawford and Goldstein, 2010). Therefore, it's of great significance to protect the biodiversity for ecological cities in development, continuously improving

http://www.aloki.hu ● ISSN 1589 1623 (Print) ● ISSN 1785 0037 (Online)
DOI: http://dx.doi.org/10.15666/aeer/1706_1446514474

ecosystems, and the overall level of urban construction, and achieving sustainable urban development.

Over the years, during the process of urban development, the rural population has gradually moved into the city, increasing the urban population rapidly (Loreau, 2001), which resulted in the excessive exploitation and utilization of various biological resources, and the continuous destruction of the soil and microbial environment, and even pushed some species to the verge of extinction. All these have further challenged the diversity of protected organisms (Lavorel, 2002; Reiss et al., 2009). Therefore, it is necessary to carry out a comprehensive evaluation study on the impact of urban development on biodiversity in the process of urban evolution, which not only enables the public to obtain effective information on the impact of urban development on biodiversity, but also makes the government departments to well realize the top-priority biodiversity indicators in the decision-making process of urban development (Miki, 2009).

As more emphasis is gradually put on ecological environment and biodiversity conservation in China, research results on biodiversity conservation have been also becoming more abundant (Tscharntke et al., 2005). But the research on the impact of urban evolution on biodiversity is still in the exploratory stage (Weiland et al., 2008; Lubbe et al., 2012). In order to develop the city and urban ecosystems sustainably together, it is necessary to ensure the biodiversity and the harmony of the ecological environment (Anstead et al., 2003; Burd et al., 2006).

As above, this paper constructs a comprehensive evaluation system of biodiversity based on urban evolution in order to understand the relationship between biodiversity and urban development. Then, taking the evaluation of a city as an example, it proposes relevant measures to further improve biodiversity. The research results indicate that during the urban evolution, a comprehensive evaluation considering the impacts of biodiversity is feasible for the conservation and sustainable development of biodiversity.

Materials and methods

The green space types of urban vegetation include residential green space, ecological landscape green space and public green space (Symstad et al., 2003). In order to study the impact of urban evolution on plant diversity, an evaluation system considering the impact of urban evolution on plant diversity was established (*Fig. 1*).

Evaluation index of species diversity

The index of species diversity mainly includes species richness, diversity, evenness, importance and population diversity (Gamfeldt et al., 2006), as shown below.

(1) Richness index

$$R = \frac{S-1}{\ln N} \qquad \text{(Eq.1)}$$

where S and N respectively, indicate the number of species and the number of individuals.

http://www.aloki.hu ● ISSN 1589 1623 (Print) ● ISSN 1785 0037 (Online)
DOI: http://dx.doi.org/10.15666/aeer/1706_1446514474

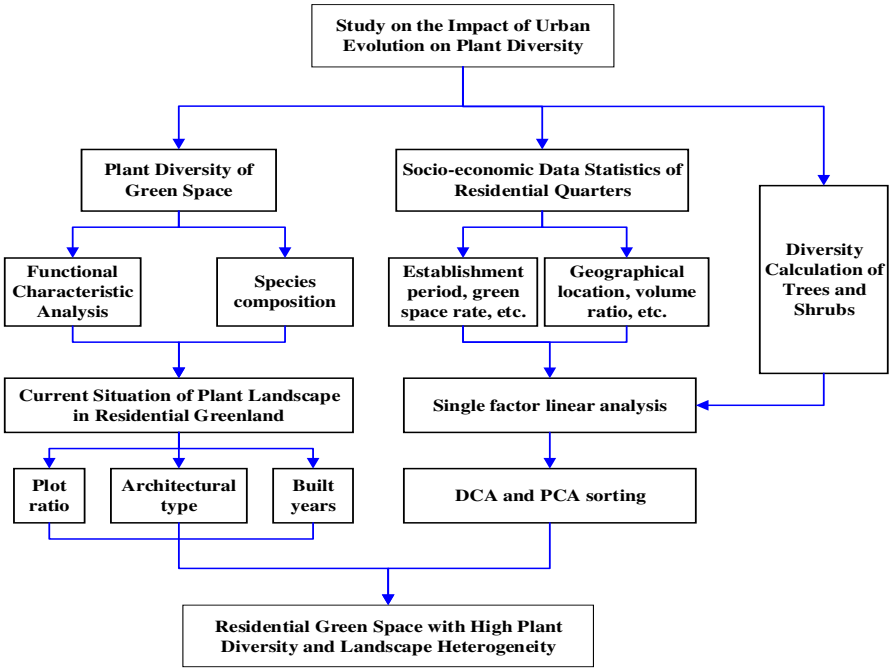

Figure 1. *Evaluation system considering the impact of urban evolution on plant diversity*

(2) Diversity index

$$H = -\sum_{i=1}^{S} P_i \ln P_i \quad \text{(Eq.2)}$$

$$D = 1 - \sum_{i=1}^{S} P_i^2 \quad \text{(Eq.3)}$$

where H, D respectively, refers to the *Shannon-Wiener* index and *Simpson* index; N_i is the number of individuals for the i-th species, and P_i is the proportion of the species.

(3) Evenness index

$$J = \frac{H}{\ln S} \quad \text{(Eq.4)}$$

J is *Pielou* index.

(4) Importance index

$$I_i = \frac{(DR_i + FR_i + CR_i)}{3} \quad \text{(Eq.5)}$$

where DR_i, FR_i, and CR_i are the relative density, relative frequency, and relative coverage of the i-th plant respectively.

http://www.aloki.hu ● ISSN 1589 1623 (Print) ● ISSN 1785 0037 (Online)
DOI: http://dx.doi.org/10.15666/aeer/1706_1446514474

(5) Population diversity index

It is divided into arbors, shrubs, and herbs. The population diversity refers to the average diversity of the three plants.

$$D = \frac{W_1 D_1 + W_2 D_2 + W_3 D_3}{3} \quad \text{(Eq.6)}$$

In *Equation 6,* D_1, D_2, and D_3 respectively refer to the diversity index of the arbor, shrub, and herb; W_1, W_2, W_3 are the weight coefficient corresponding to the three plants.

An integrated evaluation system of plant diversity

In order to objectively and comprehensively evaluate the impact of plant diversity in urban evolution, it is necessary to build the evaluation index from the three aspects of species such as the biological characteristics (ornamental value, anti-pollution, pest-resistance, etc.), ecological properties (light tolerance, drought tolerance, cold endurance etc.), combined greening effects (humidification, bactericidal, cooling, air purification, etc.) (Breton et al., 2007; Sun and Xu, 2010), as shown in *Figure 2*.

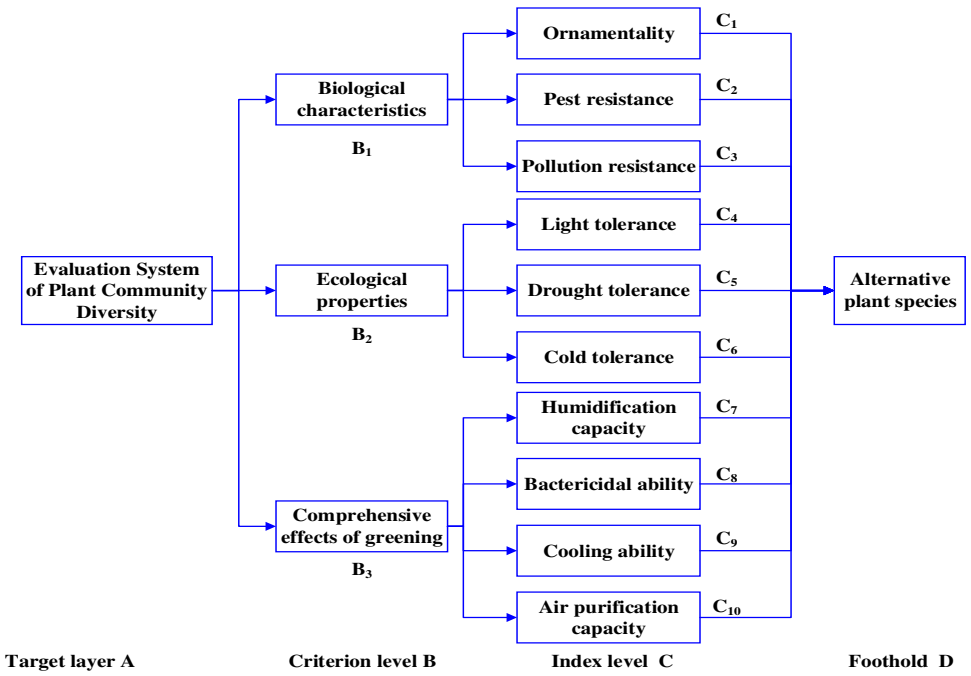

Figure 2. *Evaluation system of plant diversity*

Determination of index weights

Analytic hierarchy process (AHP) was adopted to construct the judgment matrix. Let

$$a_{ji} = 1/a_{ij} \, (a_{ij} > 0) \quad \text{(Eq.7)}$$

Use 1-9 and its reciprocal as the scale to determine the value of a_{ij}. The composition of the Judgement Matrix *(JM)* is shown in the *Equation 8* below.

http://www.aloki.hu ● ISSN 1589 1623 (Print) ● ISSN 1785 0037 (Online)
DOI: http://dx.doi.org/10.15666/aeer/1706_1446514474

$$JM = \begin{pmatrix} A & B_1 & B_2 & \cdots & B_n \\ B_1 & c_{11} & c_{12} & \cdots & c_{1n} \\ B_2 & c_{21} & c_{22} & \cdots & c_{2n} \\ \vdots & \vdots & \vdots & \ddots & \vdots \\ B_n & c_{n1} & c_{n2} & \cdots & c_{nn} \end{pmatrix} \quad \text{(Eq.8)}$$

Further, the square root method was used to solve the weights of each index, and the consistency test was performed. The single-layer consistency test is shown in *Equations 9* and *10,* and the comprehensive consistency test is shown in *Equation 11*.

$$CI = \frac{(\lambda_{\max} - N)}{N - 1} \quad \text{(Eq.9)}$$

$$CR = CI / RI \quad \text{(Eq.10)}$$

$$CR = \frac{\sum_{j=1}^{m} CI_j c_j}{\sum_{j=1}^{m} CR_j c_j} \quad \text{(Eq.11)}$$

where λ_{max} is the largest eigenvalue of *JM*, *CI* is the consistency indicator, and *CR* is the consistency test indicator.

Results

Taking the centre of Nanning as the sampling origin, a grid with a spacing of 1 km was adopted, and the intersection point was the sampling point for analysis of urban green space and plant diversity. Nanning City is located in the southwest of Guangxi Zhuang Autonomous Region, about 50 km south of the Tropic of Cancer, and in the transitional zone from south subtropics to northern tropics. It belongs to the south subtropical monsoon climate. Its geographical coordinates are at 22°40'-23°06' north latitude, and 107°45'-108°27' east longitude. Facing Southeast Asia, it is backed by the southwest, bordering Hong Kong, Macao, and Hainan in the east, and Indian Peninsula in the west. It is the junction of the two major economic zones of the South China coastal region and the southwestern coastal region, and the connecting point of the Southeast Asian economic circle.

Through the comprehensive survey of selected survey sites, the representative plant communities in the survey sites were selected, and the 10 m × 10 m samples were prepared respectively using typical sampling methods. The survey was conducted on January 1st to December 31st, 2018 in six types of green spaces such as the comprehensive park, theme park, roadside green space, residential green space, public facilities green space, and road green space: the survey sites of the comprehensive parks include People's Park, Binjiang Leisure Park and Nanhu Park, with 14 sampling points; those of theme parks include Nanning Zoo and Guangxi Medicinal Botanical Garden, with 19 sampling points; those of roadside green space include Nanhu Square and Chaoyang Square, with 17 sampling points; those for residential green space include

http://www.aloki.hu ● ISSN 1589 1623 (Print) ● ISSN 1785 0037 (Online)
DOI: http://dx.doi.org/10.15666/aeer/1706_1446514474

Beihu Anju Community, Cuihu New City, Hengda New City, Mingxiu Community, and Zhenning Cuifeng community, with 18 sampling points; those of public facilities green space include Guangxi University, Guangxi Sports General Administration, Nanning Theater, tand he First Affiliated Hospital of Guangxi Medical University, with 13 sampling points; those of road green space include Minzu Avenue, Zhonghua Road, Chaoyang Road, and University Road, with 9 sampling points. According to statistics, there were 90 effective sampling points and 476 plant species, including 127 genera and 349 species. *Table 1* lists the specific composition. *Table 2* shows the ratios of population to vegetation land in the urban, suburban, and remote suburbs.

Table 1. *Composition of plant species at sampling points*

Classification		Section		Genus		Species	
		Quantity	Proportion	Quantity	Proportion	Quantity	Proportion
Fern		10	7.9%	9	2.6%	19	4.0%
Gymnosperm		10	7.9%	10	2.9%	20	4.2%
Plant	Monocotyledons	85	66.9%	233	318	66.8%	65.6%
	Dicotyledons	22	17.3%	97	119	25.0%	28.1%
	Subtotal	107	84.3%	330	437	91.8%	93.7%
Total		127	100%	349	100%	476	100%

Table 2. *Proportion of population and vegetation land in urban, suburban and remote suburbs*

Region	Area	Population density	Population growth rate (%, 2000~2018)	Proportion of vegetation land
Urban	1405	5321	76	63
Suburban	3581	764	65	27
Outer suburbs	9860	213	38	11

Through the judgment matrix, the weights of biological characteristics, ecological performance and greening effects were derived as W = (0.32, 0.22, 0.46). 5 experts with a certain reputation in the industry were selected to score the above 10 indicators using 10-points system, and obtain the weights of each indicator (*Table 3*). The consistency test results are shown in *Table 4*.

Table 3. *Index weights*

Index	C_1	C_2	C_3	C_4	C_5	C_6	C_7	C_8	C_9	C_{10}
Weight	0.127	0.112	0.081	0.037	0.117	0.066	0.113	0.145	0.076	0.126

Table 4. *Consistency test of indicators*

Consistency test	A-B	B_1-C	B_2-C
λ_{max}	3.0195	4.0445	3.0105
CI	0.0107	0.0157	0.0067
RI	0.5815	0.9015	0.5815
CR	0.0177	0.0177	0.0097

http://www.aloki.hu ● ISSN 1589 1623 (Print) ● ISSN 1785 0037 (Online)
DOI: http://dx.doi.org/10.15666/aeer/1706_1446514474

At these sampling points, the top 10 vegetations in terms of importance degree were selected respectively from the three plants of arbor, shrub and herb for evaluation. According to the weights shown in *Table 3,* the comprehensive scores were finally obtained (*Table 5*).

Table 5. *Rankings of three plants (arbors, shrubs and herbs)*

Arbor name	Score	Shrub name	Score	Herbs	Score
Grid wood	4.392	Chinese wolfberry	4.885	Cricket grass	4.772
Rag leaf	4.251	Bush clovers	4.764	Field spinning	4.544
White cicada	4.107	Wild jujube	4.652	Dandelion	4.346
Juglans mandshurica	4.029	Patrinia	4.498	Duchesnea indica	4.207
Pu Shu	4.004	Lygodium microphyllum	4.442	Black jujube	4.156
Acer mon	3.989	Three white grass	4.299	Bletilla striata	4.056
Seven leaf lotuses	3.974	Centella asiatica	4.094	White Ginger Lily	4.036
Tilia amurense	3.981	Vitex negundo	4.091	Madder	4.028
Wood butterfly	3.910	Leptopus chinensis	3.905	Kerosene	3.905
Pistacia chinensis Bunge	3.917	Crabgrass	3.513	Light bamboo leaves	3.759

It can be seen from *Table 5* that the top 3 plants in the arbors are: Grid wood, Rag leaf, White cicada; the top 3 in the shrub plants are: Chinese wolfberry, Bush clovers, Wild jujube; the top 3 of herbs are: Cricket grass, Field spinning, and dandelion.

Based on the principle of "sustainable development" and "ecological priority", it is necessary to first select plants that are easy to cultivate, adaptable, and easy to promote, and give priority to the five plants with higher scores in *Table 5* as garden species and green resources, in order to continuously enrich the diversity of plants.

Discussion

The relationship between plant species distribution and population density is shown in *Figure 3,* and the relationship between plant species distribution and cultivated land area is shown in *Figure 4*. The 10 regions in the figure represent People's Park, Binjiang Leisure Park, Nanhu Park, Chaoyang Square, Cuihu New City, Mingxiu Community, Zhenning Cuifeng Community, Minzu Avenue, Chaoyang Road and University Road.

Figure 3 shows that the population density is negatively correlated with the distribution of plant species, and the region with smaller population density is richer in plant diversity, indicating that human activities directly affect the distribution of plant species, such as logging directly destroying plant species, land clearing, etc.

Figure 4 shows that the area of cultivated land is negatively correlated with the distribution of plant species, and the area with larger cultivated land area is richer in plant diversity, indicating that the area with high forest coverage has a certain protective effect on the diversity of plant species due to the small artificial disturbance.

Therefore, in order to ensure the sustainable development of plant diversity, the following countermeasures were proposed:

(1) In the planting area, the plant species needs should be selected according to local conditions such as local soil, climate, and water quality etc.;

http://www.aloki.hu ● ISSN 1589 1623 (Print) ● ISSN 1785 0037 (Online)
DOI: http://dx.doi.org/10.15666/aeer/1706_1446514474

(2) When introducing new varieties, more emphasis needs to be put on species adaptability and pest control, so as to ensure that new species can adapt well to local natural ecosystems;

(3) It is necessary to achieve the proper management and maintenance of plants, and establish a scientific management system. In particular, the education and guidance should be strengthened to protect plant diversity.

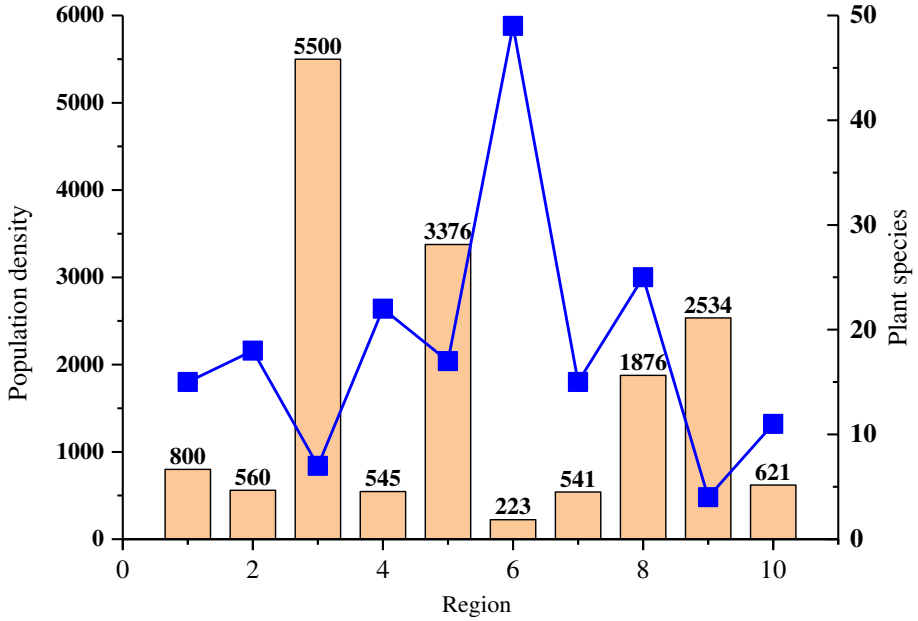

Figure 3. *The relationship between plant species distribution and population density in each region*

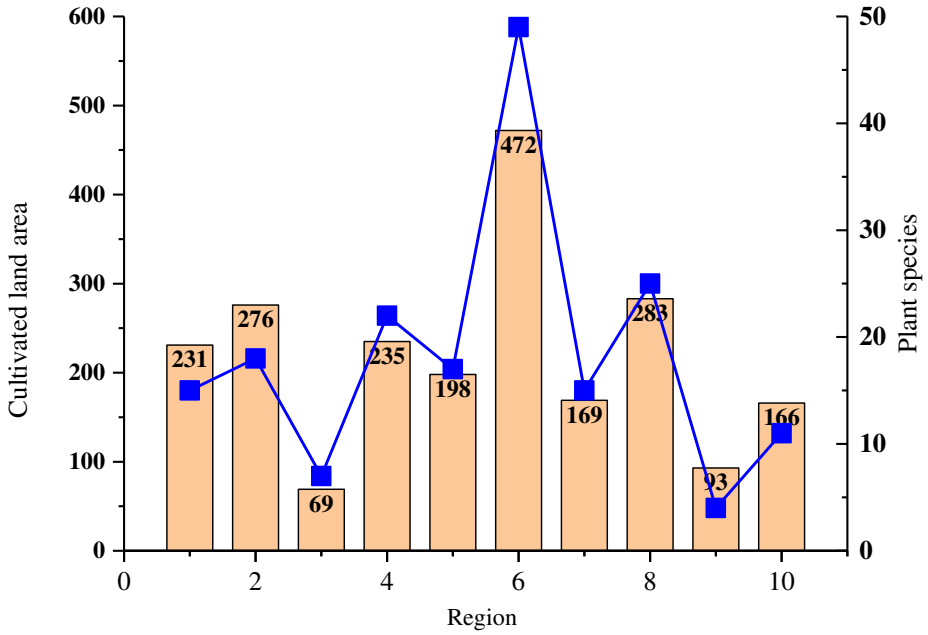

Figure 4. *The relationship between plant species distribution and cultivated land area in each region*

http://www.aloki.hu ● ISSN 1589 1623 (Print) ● ISSN 1785 0037 (Online)
DOI: http://dx.doi.org/10.15666/aeer/1706_1446514474

The result analyses of this study were based on data from the one-year Nanning plant diversity survey. These data are currently the most comprehensive, widely, and convincing among the plant diversity surveys in Nanning. Through related analysis, the overall situation of different species of plants in Nanning was obtained, and the key distribution areas of alien invasive plants in Nanning were proposed, which provide the main scientific basis for the plant protection in Nanning and invasive plants prevention (Huangfu et al., 2019).

Conclusion

This paper studies the impact pf urban development on plant diversity. The main conclusions are as follows:

(1) An evaluation system on the impact of urban evolution on plant diversity was established, to solve the related impact evaluation problem of plant diversity;

(2) An integrated evaluation system consisting of five evaluation indicators of plant diversity from the perspectives, namely, species richness, species diversity, species evenness, species importance and population diversity, and three layers: target layer, criteria layer and alternative layer (biological characteristics, ecological performance and greening combined effect) were established; AHP method was used determine the weight of each index;

(3) Taking a city as an example, the plant diversity in the urban evolution process was assessed. The assessment results can provide an important scientific basis for the protection of urban biodiversity and the sustainable development of ecosystems.

In the comparative analysis of the diversity for plants, only the data in each unit sample of the same type of green space was used for comprehensive analysis, rather than the overall information of the same type of green land such as its number of species. In the subsequent study, it is a problem worthy of further discussion on how to use this information for comprehensive evaluation.

REFERENCES

[1] Anstead, J. A., Burd, J. D., Shufran, K. A. (2003): Over-summering and biotypic diversity of schizaphis graminum (homoptera: aphididae) populations on noncultivated grass hosts. – Environmental Entomology 32(3): 662-667.

[2] Breton, J., Bart-Delabesse, E., Biligui, S., Carbone, A., Seiller, X., Okome-Nkoumou, M. (2007): New highly divergent rrna sequence among biodiverse genotypes of Enterocytozoon bieneusi strains isolated from humans in Gabon and Cameroon. – Journal of Clinical Microbiology 45(8): 2580-2589.

[3] Burd, J. D., Porter, D. R. (2006): Biotypic diversity in greenbug (Hemiptera: Aphididae): characterizing new virulence and host associations. – Journal of Economic Entomology 99(3): 959-965.

[4] Crawford, M. H., Goldstein, E. (2010): Demography and evolution of an urban ethnic community: Polish Hill, Pittsburgh. – American Journal of Physical Anthropology 43(1): 133-140.

[5] Gamfeldt, L., Lefcheck, J. S., Byrnes, J. E. K., Cardinale, B. J., Duffy, J. E., Griffin, J. N. (2015): Marine biodiversity and ecosystem functioning: what's known and what's next? – Oikos 124(3): 252-265.

http://www.aloki.hu ● ISSN 1589 1623 (Print) ● ISSN 1785 0037 (Online)
DOI: http://dx.doi.org/10.15666/aeer/1706_1446514474

[6] Huangfu, C., Hui, D., Qi, X., Li, K. (2019): Plant interactions modulate root litter decomposition and negative plant-soil feedback with an invasive plant. – Plant and Soil 437(1-2): 179-194.
[7] Hunter, P. (2007): The human impact on biological diversity. How species adapt to urban challenges sheds light on evolution and provides clues about conservation. – Embo Reports 8(4): 316-318.
[8] Karmaker, S., Ruhi, F. Y., Mallick, U. K. (2018): Mathematical analysis of a model on guava for biological pest control. – Mathematical Modelling of Engineering Problems 5(4): 427-440.
[9] Kaushal, S. S., Mcdowell, W. H., Wollheim, W. M. (2014): Tracking evolution of urban biogeochemical cycles: past, present, and future. – Biogeochemistry 121(1): 1-21.
[10] Lavorel, G. (2002): Predicting changes in community composition and ecosystem functioning from plant traits: revisiting the holy grail. – Functional Ecology 16(5): 545-556.
[11] Loreau, M. (2001): Biodiversity and ecosystem functioning: current knowledge and future challenges. – Science 294(5543): 804-808.
[12] Lubbe, S. J., Di, B. M., Broderick, P., Chandler, I., Houlston, R. S. (2012): Comprehensive evaluation of the impact of 14 genetic variants on colorectal cancer phenotype and risk. – American Journal of Epidemiology 175(1): 1-10.
[13] Miki, T. (2009): A new graphical model for untangling complex relationships among environment, biodiversity, and ecosystem functioning. – Ecological Research 24(4): 937-941.
[14] Olofson, K. F. G., Andersson, P. U., Hallquist, M., Ljungstr, M. E., Tang, L., Chen, D. (2009): Urban aerosol evolution and particle formation during wintertime temperature inversions. – Atmospheric Environment 43(2): 340-346.
[15] Reiss, J., Bridle, J., Montoya, J., Woodward, G. (2009): Emerging horizons in biodiversity and ecosystem functioning research. – Trends in Ecology & Evolution 24(9): 505-514.
[16] Sun, Q., Tan, J., Xu, Y. (2010): An ERDAS image processing method for retrieving lst and describing urban heat evolution: a case study in the pearl river delta region in South China. – Environmental Earth Sciences 59(5): 1047-1055.
[17] Symstad, A. J., Chapin, F. S., Wall, D. H., Gross, K. L., Huenneke, L. F., Mittelbach, G. G. (2003): Long-term and large-scale perspectives on the relationship between biodiversity and ecosystem functioning. – Bioscience 53(1): 89-98.
[18] Tscharntke, T., Klein, A. M., Kruess, A., Steffan-Dewenter, I., Thies, C. (2005): Landscape perspectives on agricultural intensification and biodiversity – ecosystem service management. – Ecology Letters 8(8): 857-874.
[19] Weiland, A. A., Peairs, F. B., Randolph, T. L., Rudolph, J. B., Haley, S. D., Puterka, G. J. (2008): Biotypic diversity in Colorado Russian wheat aphid (Hemiptera: Aphididae) populations. – Journal of Economic Entomology 101(2): 569-574.

http://www.aloki.hu ● ISSN 1589 1623 (Print) ● ISSN 1785 0037 (Online)
DOI: http://dx.doi.org/10.15666/aeer/1706_1446514474

CURRENT STATUS AND INTEGRATED POLLUTION CONTROL OF BLACK AND ODOROUS WATER BODIES IN DONGXINKAI RIVER BASIN OF CHINA

ZHAO, S. Y.[1] – WANG, D. D.[1] – WANG, Y. L.[2] – CHEN, L.[1*]

[1]*College of Municipal and Environmental Engineering, Jilin Jianzhu University Changchun 130000, China*

[2]*Urban and Rural Planning and Design Institute of Jilin Province Changchun 130000, China*

**Corresponding author*
e-mail: coffeezsy@163.com

(Received 7th Jun 2019; accepted 10th Oct 2019)

Abstract. This paper monitors and analyzes the surface water and sediments in the Dongxinkai (DXK) River basin. The analysis shows that the water bodies mainly suffer from aerobic pollution, with chemical oxygen demand (COD) and ammonia nitrogen (NH_3-N) being the primary causes of pollution. Considering the main causes of the pollution, the author put forward an integrated pollution control plan for the basin focusing on pollutant interception, source control, and ecological construction. After the treatment, the dissolved oxygen (DO) values at all sampling points were greater than 2 mg/L, the NH_3-N values were all smaller than 8 mg/L and the water transparency values were all above 25 cm, indicating that the river is no longer black or odorous. The implementation of the entire plan costs RMB 26.2×10^8 yuan. The research findings shed important new lights on pollution control in other rivers across China.
Keywords: *black and odorous waterbody, chemical oxygen demand (COD), ammonia nitrogen (NH_3-N), wetland, sponge city*

Introduction

As urbanization has been picking up speed in China, a lot of sewage have been discharged into rivers without any treatment. As a result, water quality indices like chemical oxygen demand (COD), ammonia nitrogen (NH_3-N) and total phosphorus (TP) have greatly surpassed limits in many rivers, making the water bodies black and odorous (Wang et al., 2014, 2016a; Corsino et al., 2016). In 2015, the State Council, China's cabinet, unveiled its *Action Plan for Water Pollution Prevention and Control*, setting out the goal to control the proportion of black and odorous water bodies in urban built-up regions at prefecture-level and push it below 10% by 2020 (Chi et al., 2019; Li et al., 2018).

In light of the above, this paper attempts to prepare an integrated plan to solve the water pollution in the basin of Dongxinkai (DXK) River, northeastern China's Jilin Province, aiming to control the water quality indices within the limits. The prepared plan would promote the construction of sponge cities and provide reference to river pollution control across China.

With a basin of 98.12 km^2, the DXK River is a 16.5-km-long primary tributary of Yitong River, which crisscrosses Jilin Province. The mean slope of the river is about 1.5‰. The main tributaries include Xibaizi (XBZ) Ditch, Dabaizi (DBZ) Ditch, Baizi (BZ) Ditch, Weizi (WZ) Ditch, Jinqian (JQ) Ditch, etc. Currently, the water bodies are of poor quality in the river basin. The COD and nutrient salts (nitrogen and phosphorus)

http://www.aloki.hu ● ISSN 1589 1623 (Print) ● ISSN 1785 0037 (Online)
DOI: http://dx.doi.org/10.15666/aeer/1706_1447514486

far exceed their respective limits. As a typical black and odorous water bodies, the river and its tributaries cannot even reach Class V specified in China's environmental quality standard for surface water, which seriously affects the life quality of nearby residents. This calls for immediate pollution control and regulation.

Materials and methods

Sampling and analysis method

During 11:00-15:00 on March 22- 25, 2016, the project team collected water samples from 50 cm of obvious flow on both Banks and river center in each monitoring section at the same time. After fully mixing, 500 ml of mixed water samples were taken, sealed with polyethylene bottles, and brought back to the laboratory for physical and chemical determination within 24 h. Each indicator of each water sample was measured three times and averaged. The surface water and sediment samples were collected from 29 points (*Fig. 1*) in the DXK River and its main tributaries. During the collection, a YSI (Yellow Springs Instrument Co) water quality meter and other portable water quality analyzers were adopted to measure the following indices of the surface water samples: temperature, pH, oxidation reduction potential (ORP), conductivity and dissolved oxygen (DO) (Moungar et al., 2018; Uddin et al., 2017; Zhao et al., 2016, 2019). Meanwhile, the surface sediments were collected with a gravity column sampler (Behaddya and Hadjel, 2014; Bhuiyan et al., 2010; Wang et al., 2016).

The sediments were analyzed to determine their water content, organic content, particle size and heavy metal content. Specifically, the distribution of particle size was determined by a laser particle size analyzer, while the heavy metal content was measured by inductively coupled plasma optical emission spectrometry (ICP-OES). Before the ICP-OES, the sediment samples were freeze-dried by a freeze dryer, and then digested by microwave (Zhou et al., 2011).

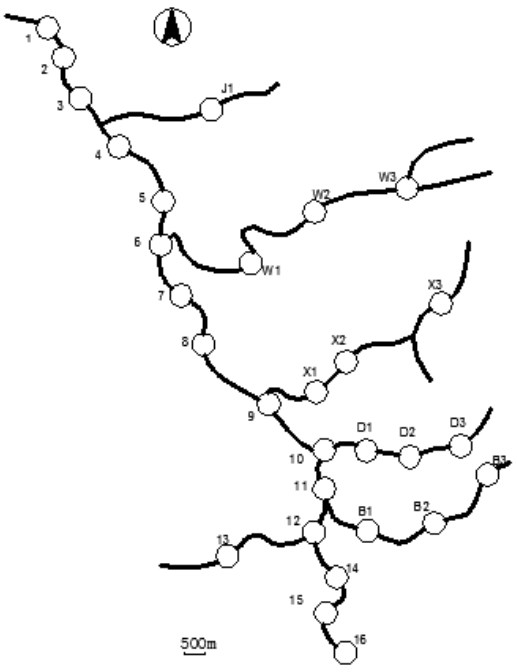

Figure 1. *Distribution of sampling points*

http://www.aloki.hu ● ISSN 1589 1623 (Print) ● ISSN 1785 0037 (Online)
DOI: http://dx.doi.org/10.15666/aeer/1706_1447514486

Water quality analysis

The results of water quality and sediment analysis are listed in *Table 1*. In general, the surface water COD in the river basin fell in 13~222 mg/L, averaging at 106.9 mg/L. The WZ Ditch and DBZ Ditch had relatively high mean CODs, respectively, 166 mg/L and 148 mg/L. The values were 4 and 5 times that for Class V in China's environmental quality standard for surface water. In the main stream, the COD at about 82% of sampling points was greater than the Class V level.

Table 1. *Results of surface water quality and sediment analysis*

	Results of surface water quality analysis						**Results of sediment analysis**				
Sampling point	**COD mg/L**	**NO_3-N mg/L**	**NH_3-N mg/L**	**TN mg/L**	**TP mg/L**	**SRP mg/L**	**TN mg/kg**	**TP mg/kg**	**TC %**	**TS %**	**LOI %**
1	100	0.05	14.2	28.13	1.87	1.98	3218.4	1456.8	5.2	0.21	0.083
2	98	0.28	14.1	28.10	5.16	5.46	898.5	500.3	0.2	0.03	0.064
3	122	0.97	15.1	28.11	2.13	2.13	1998.6	478.6	1.8	0.07	0.072
4	120	0.55	16.2	39.24	1.71	1.88	3048.5	1639.6	3.7	0.22	0.058
5	126	0.68	17.2	23.52	3.69	3.78	3128.7	1586.9	3.6	0.18	0.046
6	118	0.57	15.2	30.26	1.54	1.63	2082.3	456.9	2.9	0.16	0.135
7	130	0.60	16.3	21.68	1.62	1.67	2278.6	698.3	2.8	0.07	0.033
8	126	0.62	15.4	20.96	1.60	1.65	789.9	121.6	3.9	0.31	0.065
9	25	1.08	5.9	4.61	0.17	0.26	2001.9	689.7	3.5	0.25	0.054
10	96	0.28	11.8	18.15	3.06	3.52	1978.6	498.6	3.8	0.26	0.057
11	119	0.34	20.4	28.74	4.79	5.03	438.6	396.5	0.9	0.04	0.051
12	32	3.45	1.04	13.11	0.43	0.63	1847.7	452.3	2.1	0.06	0.047
13	220	4.57	51.3	77.61	6.05	5.92	5875.1	426.9	2.3	0.05	0.049
14	220	4.01	46.7	60.41	5.82	5.63	431.6	415.6	0.3	0.03	0.028
15	30	4.98	1.97	15.84	0.36	0.42	3568.7	894.6	5.1	0.14	0.084
16	121	0.04	6.87	17.26	1.12	1.44	1894.5	487.7	2.9	0.08	0.048
J1	78	0.28	9.87	13.27	0.71	0.65	3248.6	600.1	3.1	0.16	0.063
W1	220	2.88	81.2	107.7	10.12	8.82	214.9	587.6	1.6	0.02	0.028
W2	222	2.65	70.6	44.91	6.73	6.12	1846.5	189.6	1.5	0.03	0.025
W3	196	0.78	0.91	18.79	2.61	2.63	5876.4	689.1	6.6	0.12	0.011
X1	26	0.58	3.12	11.54	0.52	0.29	687.6	220.3	4.3	0.06	0.016
X2	20	0.50	1.25	12.83	0.13	0.13	690.5	497.6	2.4	0.09	0.009
X3	71	2.98	5.37	13.69	0.68	0.33	246.8	498.9	1.6	0.11	0.008
D1	39	0.58	0.08	12.16	0.50	0.24	278.6	396.5	1.4	0.07	0.010
D2	197	5.83	10.16	70.61	11.24	10.21	428.7	788.6	3.9	0.05	0.011
D3	188	0.57	24.5	36.83	0.48	0.21	528.6	758.3	4.1	0.06	0.013
B1	39	2.87	2.01	14.21	0.51	0.23	2000.2	425.3	5.1	0.31	0.014
B2	40	2.45	6.37	16.53	0.54	0.35	398.3	345.6	1.7	0.05	0.135
B3	13	3.31	0.09	15.64	0.41	0.01	401.2	754.6	3.0	0.21	0.012

*NO_3-N: nitrate nitrogen. TC: total carbon. SRP: soluble reactive phosphorus. TS: total sulfur. LOI: loss on ignition. COD: chemical oxygen demand. TN: total nitrogen. TP: total phosphorus. NH_3-N: ammonia nitrogen

http://www.aloki.hu ● ISSN 1589 1623 (Print) ● ISSN 1785 0037 (Online)
DOI: http://dx.doi.org/10.15666/aeer/1706_1447514486

The NH_3-N in the water bodies ranged between 0.04 mg/L and 5.83 mg/L. In the main stream and each tributary, the NH_3-N gradually decreased streamwise. The mean NH_3-N was the highest in the BZ Ditch, while that of the WZ Ditch and the DBZ Ditch were 36 mg/L and 13.1 mg/L respectively. In the main stream, the NH_3-N exhibited an obvious spatial difference. In the downstream, the NH_3-N obeyed a relatively uniform distribution and all exceeded the Class V level. This is attributable to the industrial wastewater and domestic sewage discharged from cities, towns and villages.

The total nitrogen (TN) fluctuated between 4.61 mg/L and 107.7 mg/L across the river basin, and always stayed above the Class V level. The peak TN was observed at the sampling point W1, about 54 times the Class V level. This means all water bodies in the basin have been seriously polluted by nitrogen.

The mean TP in the basin stood at 2.4 mg/L, more than 7 times the Class V level (0.4 mg/L).

The soluble reactive phosphorus (SRP) of the basin averaged at 2.26 mg/L, indicating that an average of 84% phosphorus in the water bodies mainly exist in the dissolved state. The SRP proportion of the main stream even surpassed 90%.

Sediment analysis

The analysis results in *Table 1* show that the TP of surface sediments in the basin averaged at 613.03 mg/kg, far above the internationally accepted TP threshold (500 mg/kg) for sediments. The TN of surface sediments in the basin averaged at 1,951.3 mg/kg. This level greatly surpassed the internationally accepted TN threshold (1,000 mg/kg) for sediments, posing the risk of pollutant release.

The sediment samples differed greatly in total carbon (TC), which ranged between 0.27% and 6.6%. The peak TC belonged to the sampling point W3. The distribution of TC changed significantly from place to place in the tributaries.

The total sulfur (TS) of sediment samples, an indicator of pollutant content, averaged at 0.113%, and peaked at sampling points 8 and B1. The spatial distribution of TS was relatively stable.

The loss on ignition (LOI) characterizes how much organic matter exists in the sediments, and how much gaseous products come from the thermal decomposition of sediments. The analysis results demonstrate an obvious difference in organic content between sediment samples. The highest organic content was discovered at sampling points 6 and B2. Therefore, TC and LOI must have similar pollution sources.

The author monitored 29 sampling points with 4 indicators including TN, TP, COD and NH_3-N for a total of 4 times in March 2016, and extracted 3 samples from each sampling point for a total of 1392 ($29 \times 4 \times 12$) monitoring samples for laboratory analysis. The specific statistical description of the results is shown in *Table 2*. According to the statistical data, the flowing water of this river is seriously polluted. TN, NH_3-N and TP all seriously exceed the category V of surface water environmental quality standards. Normal test was carried out on the average data set of sampling points, and the results showed that all monitoring indexes except TN followed normal distribution with 95% or higher reliability.

Diagnosis of water environment problems

The water bodies in the river basin mainly suffers from aerobic pollution, with COD and NH_3-N being the primary pollutants. According to the analysis on surface water

http://www.aloki.hu ● ISSN 1589 1623 (Print) ● ISSN 1785 0037 (Online)
DOI: http://dx.doi.org/10.15666/aeer/1706_1447514486

quality indices, the surface water is severely polluted by nutrient salts. On average, the surface water samples exceeded the standard level by 7.3 times, 13.6 times, 5.8 times and 2.6 times in terms of NH_3-N, TN, TP and COD. Considering the current states of pollution and sewage pipe network, the blackness and odor of the water bodies can be attributed to the following reasons:

(1) Our survey shows that agricultural land (63.02 km^2) takes up 64.2% of the river basin (98.12 km^2); For the pollution load of the basin, 70% comes from agricultural non-point source pollution and 5% from scattered discharge of rural sewage. Thus, the rural area is the main contributor to non-point source pollution of the basin. The non-point source pollution load in the river basin is specified in *Table 3*.

(2) There is no sewage treatment plant in the river basin. Neither has any sewage treatment plant been planned for this region. The sewage is mainly collected by the pipe network, and transported to the Beijiao Sewage Treatment Plant in the downstream. As a result, the water flow in the middle and lower reaches of the DXK River is not stable. The river often dries up in the dry season.

(3) The runoff is seriously polluted in rainy days. In the basin, the rainwater and sewage are still discharged in the same pipe network. During rainstorms, the sewage often flows over and carry garbage into the river.

(4) The rivers have weak self-purification ability due to ecological degradation. The river basin does not have enough ecological space (Podani, 1994; Xu, 2005). Many river channels are illegally occupied by buildings and lots of beaches are turned into farmland, leaving a narrow watercourse for flood discharge (Lazaro, 1979). These behaviors severely undermine the regional flood control and discharge, water regulation and storage, river self-purification and river landscape. This is the main threat to the ecological space of the river basin.

Table 2. *Statistical description of water quality variables and the environmental guideline of national quality standards for surface waters*

Parameter	TN mg/L	NH_3-N mg/L	TP mg/L	COD mg/L
Mean value	29.154	17.442	2.658	7.352
Standard deviation	2.48	2.16	0.34	0.98
Standard error	0.13	0.11	0.02	0.09
Least value	4.61	0.09	0.13	13
Maximum value	107.7	81.2	11.24	222
I*	0.2	0.15	0.02	2
II	0.5	0.5	0.1	4
III	1.0	1.0	0.2	6
IV	1.5	1.5	0.3	10
V	2.0	2.0	0.4	15

*State Environmental Protection Administration (2002)

Results

The cause analysis of the black and odorous river bodies indicates that the river basin is mainly affected by agricultural non-point source pollution. Considering the segmented features of the pollution status, the author put forward a pollution control

http://www.aloki.hu ● ISSN 1589 1623 (Print) ● ISSN 1785 0037 (Online)
DOI: http://dx.doi.org/10.15666/aeer/1706_1447514486

plan focusing on pollutant interception, source control, and ecological construction. The plan mainly covers five areas, namely, sewage treatment plant, sponge city, garbage treatment and sediment cleaning, rural water pollution control and wetland construction.

Table 3. *Non-point pollution load in the river basin*

Land use	Area km^2	Percentage %	TSS*	COD	TN t/a	TP	NH_3-N
Farmland	53.47	54.5	2491.7	498.3	74.8	7.5	24.9
Rural construction land	13.39	13.6	1559.9	468.0	31.2	3.1	12.5
Urban factory land	7.6	7.7	929.7	796.9	18.6	1.9	5.3
Urban residential land	11.36	11.6	1032.3	894.6	24.1	2.4	6.9
Forest land	3.72	3.8	26	13.0	1.3	0.1	0.3
Grass land	5.83	5.9	54.3	27.2	2.7	0.3	0.5
Water body	2.75	2.8					
Total	98.12	100	6093.9	2698	152.6	15.3	50.4

*TSS: total suspended solids. COD: chemical oxygen demand. TN: total nitrogen. TP: total phosphorus. NH3-N: ammonia nitrogen

(1) The sediment and garbage were removed from 46.4-km-long river channels. In total, 8.4×10^4 m^3 of sludge was cleaned away, which effectively reduces the sediment release and boosts the flood discharge ability. The sediments being removed were separated from water through a five-stage coagulative precipitation tank, dried in open air, and finally backfilled (Bohn, 2002). After dredging, COD and NH_3 - N index of the river cut nearly 50%, after dredging, adding the volcanic debris (size 6 ~ 10 mm) and pebbles on the bottom of the riverbed sediment improvement, on the microorganism immobilized bacterium agent, the bacteria agent by photosynthetic bacteria, spores, bacteria, to produce alkali bacteria, yeast and other 10 genera and more than 120 kinds of microorganism distribution and slow release cycle for 3 ~ 6 months.

(2) The sponge city project was implemented in view of the following facts: the surface runoff coefficient (0.7) and surface runoff is obviously higher in the built-up area than other areas in the basin, the water quality is greatly affected by surface runoff, and the ecosystem is serious undermined. Specifically, a 0.8 km^2 wetland park was built in the upstream of the DXK River and another 5.4 km^2 one was constructed in the downstream of the JQ Ditch. The two parks were constructed to restore the natural water system and wetlands, which can retain, regulate and purify the surface runoff pollution, reduce the load of non-point pollution from the upstream, and ensure the ecological flow in the river basin. In addition, a pilot program of sponge city was implemented in the middle reaches of the WZ Ditch. The 4.7 km^2 sponge city could cut down the surface runoff load by 50~75%.

(3) The 82 ponds in the basin were expanded into a pond-wetland system. To maintain the water volume and purify the water in the basin, the following key wetlands were constructed: two reservoir wetlands, three pond wetlands, one estuary wetland and one artificially enhanced wetland (using the tail water from sewage treatment plant) (Ascelin et al., 2002; Zhu et al., 2019; Barinova, 2017). The area, pondage, and pollution reduction amount of each wetland are listed in *Table 4*. The locations of the wetlands are shown in *Figure 2*.

(4) The urban sewage was carried by lift pump stations to the sewage treatment plant for centralized treatment. The plant was newly constructed, with a capacity of

http://www.aloki.hu ● ISSN 1589 1623 (Print) ● ISSN 1785 0037 (Online)
DOI: http://dx.doi.org/10.15666/aeer/1706_1447514486

1×10^4 t·d^{-1}. Using the Anaerobic/Anoxic/Oxic (A/A/O) process, the sewage treated by the plant can reach the IA level in the *Discharge Standard of Pollutants for Municipal Wastewater Treatment Plant* (GB18918-2002). The pollutant interception pipe network was constructed as an auxiliary project of the plant. The quality of the treated sewage is illustrated in *Figure 3*.

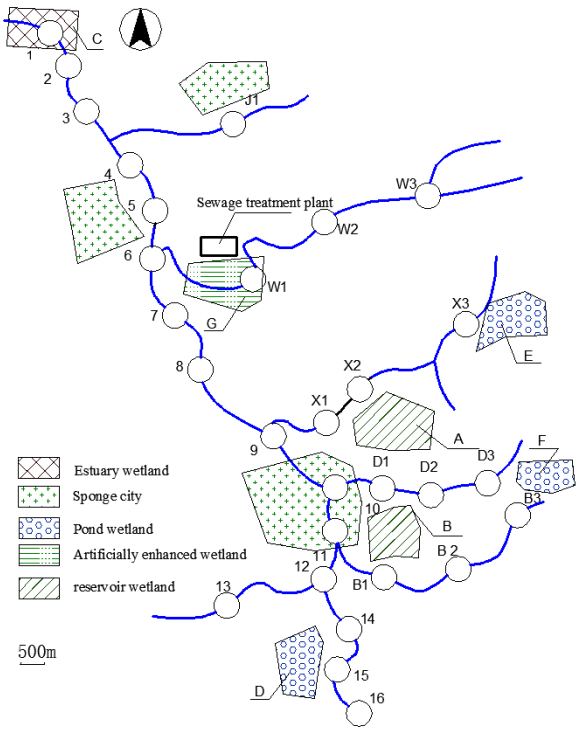

Figure 2. *Distribution of different types of wetlands and sponge cities. (J: JQ Ditch, W: WZ Ditch, X: XBZ Ditch, D: DBZ Ditch, B: BZ Ditch)*

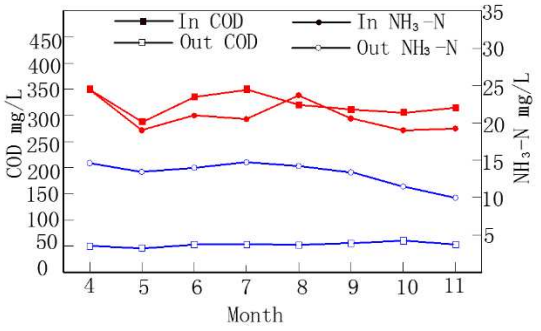

Figure 3. *Comparison between inlet and outlet water of the A/A/O sewage treatment plant*

(5) In light of the scattered discharge of rural sewage in the basin, the author developed a system to utilize and purify domestic sewage and rainwater. The system, encompassing rainwater and sewage collectors, sewage purifier, and ecological pools, can collect and purify domestic sewage and rainwater separately, and discharge them after they reached the relevant standard. In this way, the proposed system makes full use

http://www.aloki.hu ● ISSN 1589 1623 (Print) ● ISSN 1785 0037 (Online)
DOI: http://dx.doi.org/10.15666/aeer/1706_1447514486

of water resources, and opens up a new way to replenish the groundwater. As shown in *Figure 4,* the sewage purifier consists of such four parts as sewage collector, primary purification tank, secondary purification tank and tertiary purification tank. The primary purification tank has three layers, which respectively filters coal cinder, medium-coarse sand and fine sand. The secondary purification tank mainly relies on a fiber filter layer consists of bio-fiber straws extracted from corn and wheat. This layer provides the function of biological purification. The tertiary purification tank works with an activated carbon filter layer. After entering the sewage purifier, the sewage passes through the three purification tanks in turn, and undergoes thorough purification.

Table 4. *Statistics of multi-level pond-wetland system in the basin*

No.	Type of project	Longitude	Latitude	River	Area (10^4 m^2)	Pondage (10^4 m^3)	COD reduction (t/a)	NH_3-N reduction (t/a)	Function
1	Reservoir wetland A	125.443561	43.892365	XBZ Ditch	4	6	9.8	2.4	Water storage and purification
2	Reservoir wetland B	125.444718	43.873799	DBZ Ditch	4.9	8.1	11.2	3.1	Water storage and purification
3	Estuary wetland C	125.366975	43.957737	DXK River - Yitong River	16.1	6.1	64	12	Water purification
4	Pond wetland D	125.426149	43.861221	DXK River	6.5	9.8	43.1	6.9	Water storage and purification
5	Pond wetland E	125.460136	43.885143	XBZ Ditch	5.5	8.3	38.4	5.9	Water storage and purification
6	Pond wetland F	125.4700	43.871532	DBZ Ditch	8.7	13.1	57.6	9.2	Water storage and purification
7	Artificially enhanced wetland G	125.410269	43.912186	WZ Ditch	7.8	5	18.2	2.3	Purification of tail water from sewage treatment plant

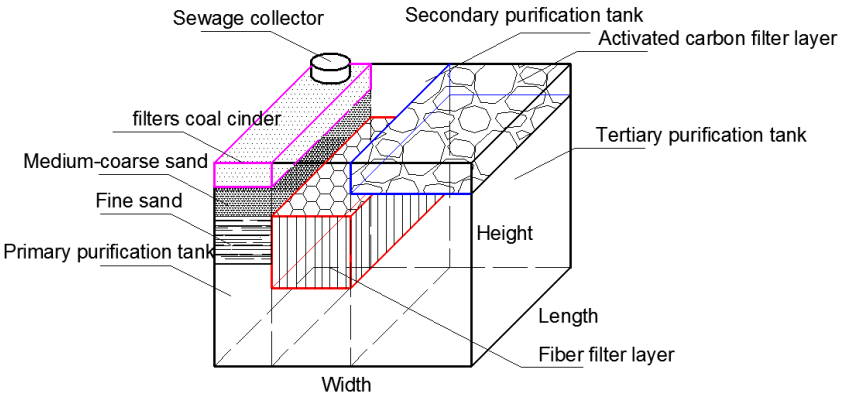

Figure 4. *Sewage purifier*

Discussion

The treatment of black and odorous waterbody should be adapted to local conditions and different treatment schemes should be adopted in different areas. The lower reaches of Fuchuangxi River in HaiNan province of China are tidal river sections with high salinity. Therefore, sewage interception, wastewater treatment, aeration and mangroves ecosystem were used to remediate the black and odorous waterbody of Fuchuangxi River (Chi et al., 2019). Yitng river of JiLin province, black and odorous waterbody is

http://www.aloki.hu ● ISSN 1589 1623 (Print) ● ISSN 1785 0037 (Online)
DOI: http://dx.doi.org/10.15666/aeer/1706_1447514486

caused by farming and agriculture, so the construction of biogas greenhouse ecological system, heat storage and utilization of the manure, straw compost renewal, on the one hand, can make use of biogas technology in biochemical treatment, on the other hand can purify livestock farming aquaculture wastewater, reduce its pollution material such as COD, nitrogen, phosphorus content, reach discharge standards to reduce the surface water pollution (Zhao et al., 2019). Considering the segmented features of the pollution status, the author put forward a pollution control plan focusing on pollutant interception, source control, and ecological construction. The pollution control plan mainly covers five areas, namely, sewage treatment plant, sponge city, garbage treatment and sediment cleaning, rural water pollution control and wetland construction.

The pollution control plan was fully implemented by October 2017. From May to November, 2018, the author collected water samples from the DXK River at sampling points 5, 11 and 14, and analyzed the DO, ORP, NH_3-N and transparency of the samples. The results in *Figure 5* show that, through the seven months, the DO values at all three points were greater than 2 mg/L, the NH_3-N values were all smaller than 8 mg/L and the water transparencies were all above 25 cm, indicating that the river is no longer black or odorous. The implementation of the entire plan costs USD 3.47×10^8. The investment is break down in *Table 5*.

Table 5. *Main workloads and investment breakdown of the pollution control plan*

No.	Name of project	Project contents	Workload	Investment (USD thousand)
1	Drainage system and sewage treatment plant	Main sewage pipes ng the rivers	Pollutant interception pipes (49 km)	45714
		Rainwater and sewage interception wells	Interception wells (39)	55714
		Sewage treatment plant	10^4 m^3/d	29997
2	Sponge city	Green rainwater foundation	0.8 km^2	14286
		Green road construction	5.9 km × 45 m	8286
		Green communities and squares	4 km^2	28571
3	Sediment cleaning	Mechanical dredging	30 places	214
		Dehydration and capacity reduction	84514 m^3	1207
		Transport and disposal	94514 m^3	714
4	Rural water pollution control	Village demolition	3500 J[3]	5000
		Domestic sewage treatment	20000 J[3]	2857
		Fecal composting	1 station	2143
		Others	/	571
5	Wetland construction	Estuary wetland	100,000 m^2	571
		Artificially enhanced wetland	78,000 m^2	1114
		Reservoir wetlands	106,000 m^2	1514
		Pond wetlands	65,000 m^2	650
6	Water ecological project	Rubber dams	4	929
		Ecological revetment	Soil and earthworks 52,600 m^3	511
		River landscape	990,000 m^2	28285
		Parks	1160,000 m^2	82857
		Wetland spaces	170,000 m^2	7286
		Riverfront landscape belt	810,000 m^2	40500
		Leisure nodes	210,000 m^2	13500
Total				3.74×10^8

http://www.aloki.hu ● ISSN 1589 1623 (Print) ● ISSN 1785 0037 (Online)
DOI: http://dx.doi.org/10.15666/aeer/1706_1447514486

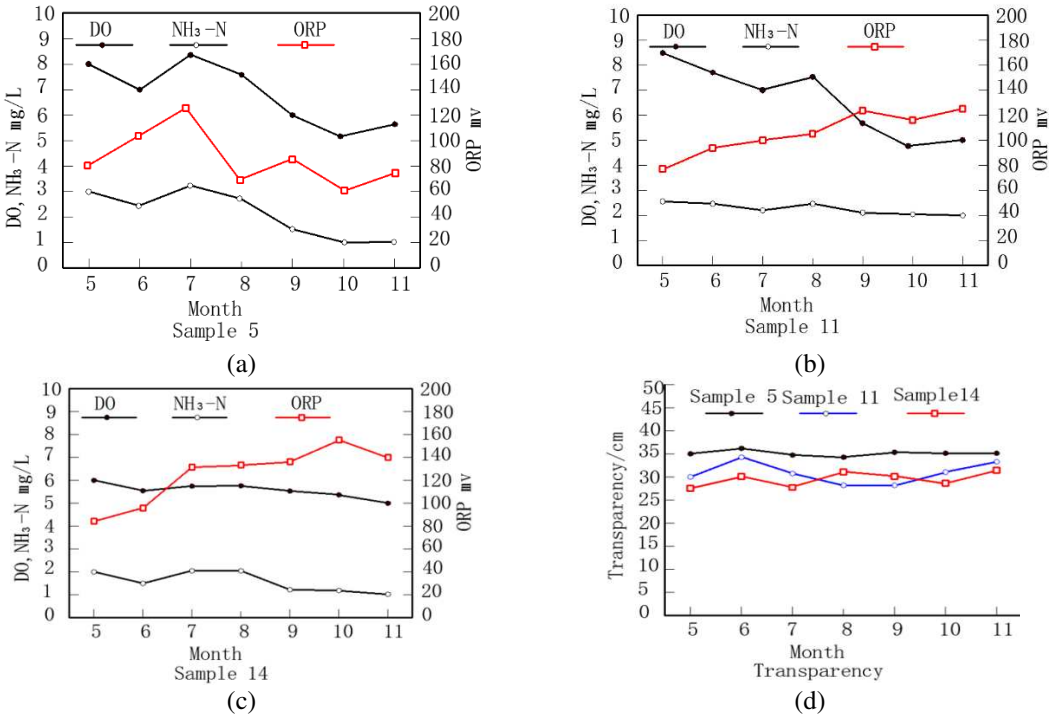

Figure 5. *Analysis results on water sample quality*

Conclusions

This paper monitors and analyzes the surface water and sediments in the DXK River basin, and discovers that the water bodies mainly suffer from aerobic pollution, with COD and NH3-N being the primary pollutants. Agricultural non-point source pollution accounts for 70% of the pollution load, and scattered discharge of rural sewage accounts for 5% of the pollution load, which is the main source of water pollution.

Considering the main causes of the pollution, the author put forward an integrated pollution control plan for the basin focusing on pollutant interception, source control, and ecological construction.

Removing the sediment and garbage from the river can reduce COD, NH3-N and other indicators in the river by nearly 50%. The immobilized microbial agent was used to remove NH_3-N and COD in black and odorous waterbody. The construction of wetland park, the ponds in the basin were expanded into a pond-wetland system, can significantly reduce NH_3-N and COD.

After the treatment, the DO values at all sampling points were greater than 2 mg/L, the NH_3-N values were all smaller than 8 mg/L and the water transparencies were all above 25 cm, indicating that the river is no longer black or odorous. The implementation of the entire plan costs USD 3.47×10^8. The research findings shed important new lights on pollution control in other rivers across China.

Also suggested that the basin water pollution comprehensive treatment to pollution load distribution in the process, on the one hand, it can realize basin within the scope of reasonable layout and the load sharing ratio of the control area, on the other hand, within the scope of the basin can be unequal distribution of technical and economic investment, implement the specific implementation of total amount control load index, the governance effect is better.

http://www.aloki.hu ● ISSN 1589 1623 (Print) ● ISSN 1785 0037 (Online)
DOI: http://dx.doi.org/10.15666/aeer/1706_1447514486

Acknowledgment. This paper is made possible thanks to the generous supports from Science and Technology Department, Jilin Province (Grant No.: 20180101339JC and 20190303022SF), Education Department, Jilin Province (Grant No.: JJKH20180575KJ and JJKH20180600KJ), Laboratory of Geo-Exploration Instrumentation, Jilin University (Grant No.: ERCGR201704) and the National Natural Science Foundation of China (Grant No.: 51878316).

REFERENCES

[1] Ascelin, G., David, S., Matt, W., Atte, M., Sarah, A. B. (2008): Integrating conservation planning and landuse planning in urban landscapes. – Landscape and Urban Planning 91(4): 183-194.
[2] Barinova, S. S. (2017b): Empirical model of the functioning of aquatic ecosystems. – International Journal of Oceanography and Aquaculture 1(3): 1-9.
[3] Behaddya, M. L., Hadjel, M. (2014): Spatial distribution and contamination assessment of heavy metals in surface soils of Hassi Messaoud, Algeria. – Environmental Earth ciences 71(3): 1473-1486.
[4] Bhuiyan, M. A., Parvez, L., Isiam, M. A., Dampare, S. B., Suzukia, S. (2010): Heavy metal pollution of coal mine-affected agricultural soils in the northern part of Bangladesh. – Journal of Hazardous Materials 173(1-3): 384-392.
[5] Bohn, B. A., Kershner, J. L. (2002): Establishing aquatic restoration priorities using a watershed approach. – Journal of Environmental Management 64(4): 355-363.
[6] Chi, J., Jiang, Y., Yuan, X. K. (2019): Remediation project of black and odorous waterbody of Fuchuangxi and Dapaigou with one river and one policy. – Chinese Journal of Environmental Engineering 13(2): 496-504.
[7] Corsino, S. F., Capodici, M., Morici, C. (2016): Simultaneous nitritation-denitritation for the treatment of high-strength nitrogen in hypersaline wastewater by aerobic granular sludge. – Water Res. 88: 329-336.
[8] Lazaro, T. (1979): Urban Hydrology. – Ann Arbor Science Publishers, Michigan.
[9] Li, S., Shi, W., Li, H. (2018): Antibiotics in water and sediments of rivers and coastal area of Zhuhai City, Pearl River estuary, south China. – Science of the Total Environment 636: 1009-1019.
[10] Moungar, H., Azzi, A., Sahli, Y., Haida, A. (2018): Monthly fresh water yield analysis of three solar desalination units a comparative study in the south Algeria climatic condition. – International Journal of Heat and Technology 36(4): 1330-1335.
[11] Podani, J. (1994): Multivariate Data Analysis in Ecology and Systematics. – SPB Publishing, The Hague.
[12] State Environmental Protection Administration (2002): Water and Wastewater Detection and Analysis Method. – China Environmental Science Publishing House, Beijing.
[13] Uddin, M. J., Halim, M. A., Mohiuddin, M. (2017): Copper oxide-water nanofluid flow within an annulus shaped cavity: a numerical study on natural convective heat transfer. – Annales de Chimie - Science des Matériaux 41(3-4): 239-260.
[14] Wang, G. F., Li, X. N., Fang, Y., Huang, R. (2014): Analysis on the formation condition of the algae-induced odorous black water agglomerate. – Saudi Journal of Biological Sciences 21(6): 597-604.
[15] Wang, X., Wang, Y. G., Sun, C. H. (2016a): Formation mechanism and assessment method for urban black and odorous water body: a review. – Chinese Journal of Applied Ecology 27(4): 1331-1340.
[16] Wang, Y. Q., Bai, Y. R., Wang, J. Y. (2016b): Distribution of urban soil heavy metal and pollution evaluation in different functional zones of Yinchuan City. – Environmental Sciene 37(2): 710-716.

http://www.aloki.hu ● ISSN 1589 1623 (Print) ● ISSN 1785 0037 (Online)
DOI: http://dx.doi.org/10.15666/aeer/1706_1447514486

[17] Xu, Z. X. (2005): Comprehensive water quality identification index for environmental quality assessment of surface water. – Journal of Tongji University: Natural Science 33(4): 482-488.
[18] Zhao, S. Y., Su, X., Zhao, S. (2016): A study on the water pollution of poultry and livestock breeding and the resource utilization of the wastewater in Sonln Village. – Chemical Engineering Transactions 55: 469-474.
[19] Zhao, S. Y., Qin, Y. Q., Zheng, H. N., Chen, L. (2019): Construction of the biogas heat strorage greenhouse ecosystem under the context of water pollution resulting from livestock breeding. – Environmental Engineering and Management Journal 18(3): 757-763.
[20] Zhou, S. L., Li, R. H., Wu, S. H. (2011): Study on Relations between the Economic Development and the Spatial and Temporal Variation of Heavy Metals in Agricultural Land. – China Land Press, Beijing.
[21] Zhu, W. T., Liu, Y. Y., Wang, S. T., Yu, M., Qian, W. (2019): Development of microbial community–based index of biotic integrity to evaluate the wetland ecosystem health in Suzhou, China. – Environmental Monitoring and Assessment 191(6): 1-11.

http://www.aloki.hu ● ISSN 1589 1623 (Print) ● ISSN 1785 0037 (Online)
DOI: http://dx.doi.org/10.15666/aeer/1706_1447514486

CONSTRUCTION AND ANALYSIS OF CHINA'S INDUSTRIAL NETWORK OF CARBON CORRELATION

HU, W.[1] – HU, Y. W.[1*] – WANG, C. L.[2] – CHEN, X. Z.[2]

[1]*School of Economics and Management, Shanghai University of Electric Power, Shanghai 200090, China*

[2]*School of Business, Shandong Normal University, Ji'nan 250014, China*

**Corresponding author*
e-mail: 99030411@qq.com

(Received 7th Jun 2019; accepted 10th Oct 2019)

Abstract. Increasing concern about carbon emission reduction demands knowledge on the industrial structure of carbon linkages in an economy. Based on sectorial input-output analysis and network analysis, this paper develops a combined method to construct the industrial network of carbon correlation (INCC) serving as an essential tool to provide insight about carbon emission transfer and emission responsibility. Using China's 2005, 2010 and 2015 Input-Output Tables and China Energy Statistical Yearbook, China's INCCs under the transition period were constructed and the relationship structures were analyzed. Research shows that carbon emission has a decreasing trend as a whole in the transition period in China. The main consumer responsibility sectors and the critical emission transfer paths were identified to provide the analysis basis for decision makers and planners in industrial carbon management. In addition, the industry group analysis provided useful analytical techniques for carbon emission reduction policies.

Keywords: *Weaver-Thomas index, carbon correlation coefficient, CO_2 emission reduction, carbon transfer path, carbon cycle correlation*

Introduction

Concerns over climate and environment makes the public more and more aware of the problem of greenhouse gas emissions most of which is in the form of carbon dioxide. China is currently the world's largest emitter of carbon dioxide (Lin and Sun, 2010). So the production sectors in China (including electric power production and metal smelting) became the first the focus of emission reduction. The fact that the production sectors received more attention was warranted due to the fact that these sectors account for more than half of the total carbon emissions. (Sonis et al., 1995). However, further analysis shows that carbon emissions from an industrial sector include not only direct emissions, but also indirect emissions (Chang, 2015). Some consumption sectors which have less direct emissions have a higher carbon responsibility because of their intermediate inputs, including various equipment and services. However, people pay less attention to them just because the direct emission is small (Zhang et al., 2017).

Production cannot be separated from consumption. Consumption sectors cannot be excluded to committing carbon emissions responsibilities because of their required massive intermediate inputs. As we know, industrial linkages among varied sectors can be explored by the Input-Output Table. So, Input-Output analysis is a good perspective to describe industrial linkages. Scholars (Chang and Lin, 1998; Machado et al., 2001; Labandeira and Labeaga, 2002; Jain and Gupta, 2019; Xu et al., 2019; Kaivo-oja and Luukkanen, 2004; Tahara et al., 2005; Mongelli et al., 2006; Lixon et al., 2008; Lin and Sun, 2010; Seppälä et al., 2011; Brown et al., 2012; Cadarso et al., 2012) have taken

http://www.aloki.hu ● ISSN 1589 1623 (Print) ● ISSN 1785 0037 (Online)
DOI: http://dx.doi.org/10.15666/aeer/1706_1448714503

advantage of Input-Output of various countries or cities to track Carbon footprint. Most of their works in early discussions have found that the production sectors (such as electric power production and metal smelting) were the focus of emission reduction. Their works also established some important linkages between vary sectors, making understructure for emission responsibility and assessment in economic structures. Later, scholars gradually realized that industrial linkages would shift the responsibility of carbon emissions among the industrial sectors (Egilmez et al., 2013; Mózner, 2013; Arto et al., 2014). So we cannot explore low-carbon development in the isolated production sectors. Carbon metabolic (Baccini, 1996; Chen and Chen, 2012; Zhang et al., 2014; Wu et al., 2016; Zhang Du and Wang, 2018; Zhang et al., 2018) is then raised to investigate carbon flow and carbon transfer in social economic system. Most of these works were based on international trades and the primary target was to find the discharging countries and districts. However, carbon flows within different sub-systems or sectors were scare (Zhao et al., 2014; Zhang et al., 2018).

Carbon related responsibility can be divided into two parties, emission responsibility and requirement responsibility. In most of the study of CO_2 emission problems, the direct emission factors are targeted and some main factors can be found by the Factor Decomposition Method. In view of indirect factors of carbon emissions, Structural Decomposition Method is used to study the issue of carbon emission reduction. Most of the researchers pay close attention to emission responsibility and the potential methods of reduction of high carbon emission sectors. These studies enrich the carbon emission theory and provide a reference for carbon emission reduction from the view of emission responsibility. However, existing literatures have not analyzed the main requirement responsibility of carbon emissions, this is to say, which sectors' requirement lead to the increase of emission responsibilities, and in which path industrial sectors are transmitting these responsibilities.

Network is often used to express the nodes and the relationships in group study. Analyzing network structure can excavate the deep inner structure relationships among individuals. Defining the industrial network of carbon correlation (INCC) needs to clarify all kinds of sector structures and their effects. The INCC consists of the high carbon emission sectors and some closely related consumption sectors. According to the comprehensive analysis of the INCC, we can determine which sectors are the high carbon emission sectors and which sectors are committed directly or indirectly requirement responsibilities. We can also determine which linkages are the primary transmission paths and which industrial sectors have grouped together in carbon emissions. The clarity of these problems provides the basis for adjusting policy for better developing industrial correlation structure and constructing low carbon industrial system.

This paper firstly analyzes the carbon relationships among industrial sectors, defining the concept and calculation method of industrial carbon correlation coefficient. Secondly, regarding industrial sector as node and carbon relationship as edge, this paper designs the method of constructing INCC. Thirdly, based on the Input-Output Table and the Energy Statistic Yearbook of China in 2005, 2010 and 2015, this paper constructs and analyzes the INCCs of China. Finally, through the paths and sub-graphs analysis, the main carbon emission responsibility sectors and consumption responsibility sectors are identified for industrial reduction management.

http://www.aloki.hu ● ISSN 1589 1623 (Print) ● ISSN 1785 0037 (Online)
DOI: http://dx.doi.org/10.15666/aeer/1706_1448714503

Materials and methods

Analysis of the carbon correlation between industrial sectors

As we all know, production process often release CO_2 directly by burning fossil fuels. An industrial sector requires a variety of intermediate inputs which probably emit a lot of CO_2 in their production processes. Therefore, the production activities of an industrial sector often lead to other sectors emitting CO_2 by intermediate demand. When sector *i* supplies intermediate products to sector *j*, sector *i* transfers CO_2 emissions responsibility to sector *j*, and these two sectors form a carbon linkage due to industrial linkage. Similarly, sector *j* may establish a carbon linkage with sector *k*. In this way, the industrial sectors in a region have formed carbon correlations due to industrial linkages, which lead to a network of industrial sectors, i.e., the industrial network of carbon correlation (INCC). According to INCC, the main responsible sectors for CO_2 emission and the path of responsibility transmission can be identified, which provide the basis for CO_2 emission reduction.

From the view of investment, the production of an industrial sector *i* requires various intermediate inputs from multiple sectors, which emit CO_2 directly in producing these inputs. All of the CO_2 emitted directly by those inputs is caused by the sector *i*, so the requirement responsibility should be attributed to sector *i*. From the view of distribution, the products of sector *i* can be divided into two parts, one part as intermediate inputs for other sectors, and the other as final product. The emission responsibility of sector *i* should also transfer to demand sectors or final consumers with product distribution. When sector *j* demands the product of sector *i* which discharges CO_2, it is considered that sector *i* transfer emission responsibility to sector *j*, so there is a carbon correlation between sector *i* and sector *j*.

In order to express the carbon correlation between industrial sectors, we define the industrial carbon correlation coefficient as: To manufacture one unit product of sector *j* need to be directly invested in a certain number products of sector *i*, the direct CO_2 emission quantity of sector *i* in producing such products is called the carbon correlation coefficient of sector *i* to sector *j*. The greater the coefficient, the higher is the carbon correlation strength between these two sectors. Obviously, when the amount of utilization from sector *i* to sector *j* increases, the industrial carbon correlation coefficient c_{ij} increases. Also, when the amount of CO_2 produced in one unit by sector *i* increases, c_{ij} increases, so

$$c_{ij} = d_i \times a_{ij} \quad \text{(Eq.1)}$$

In *Equation 1,* a_{ij} is the direct consumption coefficient of sector *j* from sector *i*; d_i is the CO_2 amount directly discharged from sector *i* for one unit.

We assume that *C* is the carbon correlation coefficient matrix, *A* represents the direct consumption coefficient matrix, and *D* is generated by the diagonal matrix d_i. So,

$$C = DA \quad \text{(Eq.2)}$$

In *Equation 1,* the direct consumption coefficient a_{ij} can be calculated from the Input-Output table. The emission amount per unit in production of sector *i*, i.e., d_i can be calculated by combining the Energy Statistical Yearbook with the Input-Output Table according to the following method.

http://www.aloki.hu ● ISSN 1589 1623 (Print) ● ISSN 1785 0037 (Online)
DOI: http://dx.doi.org/10.15666/aeer/1706_1448714503

In order to calculate d_i, it is necessary to calculate the total amount of CO_2 emitting directly from this sector. Direct emission CO_2 from an industrial sector occurs at the stage of burning fossil fuels, in which fossil fuels contain three primary energy sources (coal, crude oil and natural gas) and five secondary energy sources (coke, gasoline, kerosene, diesel, fuel oil). So the direct emissions of each industrial sector can be calculated according to the consumption of fossil fuels. For the non-secondary petrochemical energy conversion sector i, the total direct emissions CO_2 from the production process are the total emissions CO_2 from the consumption of various fossil fuels. Let it be D_i, then

$$D_i = \sum_{s=1}^{8} u_s(i) \times e_s \quad \text{(Eq.3)}$$

In the *Equation 3,* $u_s(i)$ is the total amount of energy s consumed by sector i, and e_s is the CO_2 emission coefficient of energy s.

Unlike the general sector, petroleum processing, coking and nuclear fuel processing consume primary energy for obtaining secondary energy. In those productive process most of the primary energy has not changed to CO_2, but has been transformed into secondary energy. However, the CO_2 emissions from the secondary energy burning have already been taken into respective user sector. Therefore, in calculating the direct CO_2 emission of petroleum processing, coking and nuclear fuel processing sectors, it is necessary to use *Equation 1* to subtract the secondary fuels CO_2 produced by them.

From the total output of each industrial sector and the total amount of CO_2 emissions, we can calculate the amount d_i of CO_2 emissions per unit in sector i. Let the total output of sector i be X_i and the total direct CO_2 emission be D_i, the unit output of sector i is calculated by *Equation 4:*

$$d_i = D_i / X_i \quad \text{(Eq.4)}$$

Construction of industrial network of carbon correlation

The industrial network is a directed graph constructed by the industrial sectors and the relationships between these sectors. This graph can describe the structure of industrial sectors, revealing characteristics and laws of industrial correlation. Similarly, the INCC takes the industrial sector as the vertex and the inter-departmental carbon correlation as the edge to construct a directed graph to reveal characteristics of a given industrial carbon correlation. There are many ways to build industrial networks (Wang and Yang, 2015; Yan et al., 2017; Zhao and Yang, 2016). Here we use Weaver-Thomas index to calculate the threshold and build INCCs.

The production of an industrial sector requires different inputs from multiple sectors which vary greatly in CO_2 emitting in manufacturing process. In order to find the main carbon linkages among industrial sectors, it is necessary to find the inflection point as the critical value from many carbon correlation coefficients. When the carbon correlation coefficient between the two sectors is greater than the critical value, it is considered that there exists a carbon linkage between them; otherwise there is no carbon linkage. By this way, The Weaver-Thomas index can find the key connections. So, we calculate the Weaver-Thomas index for building INCCs.

http://www.aloki.hu ● ISSN 1589 1623 (Print) ● ISSN 1785 0037 (Online)
DOI: http://dx.doi.org/10.15666/aeer/1706_1448714503

By comparing the observed distribution with the hypothetical distribution, the best fitting approximate distribution is established to identify the key elements in the numerical sequence. For the industry including n sectors, c_{ij} is the carbon correlation coefficient of sector j to sector i. If we arrange the carbon correlation coefficients c_{1j}, c_{2j}, ..., c_{nj} from the large to the small for sector j, the Weaver-Thomas index of sector i is:

$$w(i,j)=\sum_{i=1}^{n}\left[s(k,i)-100\times\frac{c_{kj}}{\sum_{l=1}^{n}c_{lj}}\right]^2 \quad \text{(Eq.5)}$$

Here, $s(k,i)=\begin{cases}100/i,(k\le i)\\ 0,(k>i)\end{cases}$.

Now we set, $k=\min\{w(1,j),w(2,j),\cdots,w(n,j)\}$.

So, the corresponding coefficient c_{kj} of sector j is the critical value of sector k.

By calculating the Weaver-Thomas index of each sector, we can obtain n independent critical values. If the carbon correlation coefficient between two sectors is greater than the critical value, it means that here exists a carbon correlation edge, and the corresponding element in the adjacency matrix is 1. Otherwise, it means that there is no correlation edge, and the corresponding element in the adjacency matrix is 0. Similar to the industrial network, the INCC focuses on the correlation among various sectors and not the ring in the network, so the diagonal element of the adjacency matrix is set to 0.

Analysis and expansion of INCC

The INCC describes the carbon linkages between various industrial sectors. When there is a directed edge from sector i to sector j in an INCC, sector i emits CO_2 by providing input for sector j. It also can be considered that sector i transfers CO_2 emission responsibility to sector j at the same time. This transmission make sector j taking on more carbon emission requirement responsibility, as shown in *Figure 1a.* When there is no directed edge from sector i to sector j, sector i does not have CO_2 emission responsibility transmitted directly to sector j. However, it is possible there existing a directed path in the INCC, such as, sector i passes to other sectors (e.g., sector l, k, *etc.*), which in turn passes to sector j. Like this, there is an indirect carbon correlation between sector i and sector j, as shown in *Figure 1b.*

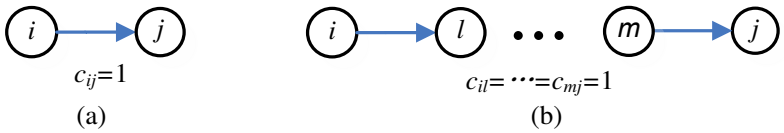

Figure 1. *A directed edge and a directed path in an INCC*

If all the directed edges and paths in an INCC are connected along the directed road, the extended INCC can be obtained. The degree of vertices in the extended INCC reflects the number of all other sectors linked with a sector, including direct and indirect linages. The in-degree of a sector reflects its degree of accepted requirement responsibility. When an in-degree of a sector is large, it means many sectors

http://www.aloki.hu ● ISSN 1589 1623 (Print) ● ISSN 1785 0037 (Online)
DOI: http://dx.doi.org/10.15666/aeer/1706_1448714503

transmitting CO_2 emission responsibility to this sector. It is a recipient and a major consumer responsibility sector. Out-degree reflects the degree of a sector transmitting emission responsibility. When an out-degree of a sector is large, it means that it is a main sector of emission responsibility source.

China's industrial network of carbon correlations (INCCs)

According to the Input-Output Table and the Statistical Yearbook of China in 2005, 2010 and 2015, we construct China INCCs for these three years. For facilitating comparison, the Input-Output Tables of each year and the division of sectors in the Energy Statistics Yearbook are unified, in which some industrial sectors are merged. In the Input-Output Table of 2015, "general equipment" and "professional equipment" are divided into two, while in the other two years they are unified, so we merged them. In the Input-Output Tables in 2005 and 2015, "other manufacturing" and "waste scrap" are two sectors, while in the Table of 2010 these two sectors are one, so they are merged. In the Statistical Yearbook, "transportation, warehousing and postal", "wholesale, retail and accommodation, catering" and "other industries" are combined to one into correspondence with the Input-Output Table. The correspondence between the specific industrial sector and the code is shown in *Table 1*.

Table 1. *Industry sectors and codes after merger*

Code	Industrial sector	Code	Industrial sector
1	Agriculture, forestry, animal husbandry and fishery	15	Metal products sector
2	Coal mining and washing sector	16	General purpose and special equipment manufacturing sector
3	Petroleum and natural gas extraction sector	17	Transportation equipment manufacturing sector
4	Metal mining sector	18	Electrical machinery and equipment manufacturing sector
5	Nonmetallic ores and other mining and mineral processing sectors	19	Communications equipment, computers and other electronic equipment manufacturing sector
6	Food manufacturing and tobacco processing sector	20	Instrumentation and cultural office machinery manufacturing sector
7	Textile sector	21	Crafts and other manufacturing sectors (including waste products)
8	Textile, clothing, shoes, hats, leather, feather and its products sector	22	Production and supply of electricity and heat
9	Wood processing and furniture manufacturing	23	Gas production and supply sector
10	Paper making, printing, cultural, educational, sporting goods manufacturing	24	Water production and supply
11	Petroleum processing, coking and nuclear fuel processing sector	25	Construction business
12	Chemical sector	26	Transportation, storage and post
13	Nonmetallic mineral products industry	27	Wholesale, retail, accommodation and catering sectors
14	Metal smelting and calendering processing sector	28	Other sectors

http://www.aloki.hu ● ISSN 1589 1623 (Print) ● ISSN 1785 0037 (Online)
DOI: http://dx.doi.org/10.15666/aeer/1706_1448714503

According to the second part of the analysis and *Equations 1-4,* the correlation coefficient of INCCs is calculated. According to the third part of the modeling method, we build China's INCCs and the extended INCCs.

Results

Correlation coefficient analysis of INCCs

According to *Equations 1-4,* the industrial carbon correlation coefficients among different sectors in China' INCCs in 2005, 2010 and 2015 are calculated. The number of correlation edges in these three years 85, 76 and 83 were found significant respectively of all the 784 linkages, which means about 10% (10.8%, 9.7% and 10.6%) of the linkages pass the critical values. The top 30 in each year are listed in *Table 2*.

Table 2. *China's top 30 INCC coefficients in 2005, 2010 and 2015*

	2005 year			2010 year			2015 year		
Sequencing	**INCC coefficient c_{ij}**	**Sector *i***	**Sector *j***	**INCC coefficient c_{ij}**	**Sector *i***	**Sector *j***	**INCC coefficient c_{ij}**	**Sector *i***	**Sector *j***
1	3.2831	22	24	3.6311	22	22	2.9632	22	22
2	2.0365	22	4	3.3776	3	11	1.1517	22	24
3	1.7465	22	2	2.8110	3	23	0.7816	14	14
4	1.6622	11	26	2.4814	22	24	0.7114	11	11
5	1.4222	14	15	1.4247	22	4	0.6760	22	4
6	1.3298	22	3	1.1869	11	26	0.6490	14	15
7	1.2000	14	14	1.0930	14	15	0.6420	11	26
8	1.1515	11	23	0.9280	22	5	0.6251	11	3
9	1.1060	22	12	0.9153	14	14	0.6074	2	2
10	1.0513	22	5	0.8369	14	18	0.5151	14	18
11	1.0489	22	22	0.7921	2	2	0.4618	22	14
12	1.0387	2	22	0.7603	2	22	0.4471	22	5
13	0.9994	2	23	0.7211	22	3	0.4263	2	22
14	0.9365	22	13	0.6692	14	16	0.3670	22	3
15	0.9154	22	14	0.6377	22	13	0.3601	11	12
16	0.8986	11	4	0.6137	22	15	0.3550	22	2
17	0.8677	14	18	0.5172	22	14	0.3332	22	13
18	0.8054	14	16	0.5137	13	25	0.3283	22	15
19	0.6924	22	23	0.4729	12	12	0.3084	11	14
20	0.6829	22	15	0.4627	22	12	0.3083	12	12
21	0.5883	11	22	0.4336	13	13	0.3046	14	16
22	0.5723	3	11	0.3993	14	25	0.3007	22	12
23	0.5376	12	12	0.3980	11	12	0.2911	11	5
24	0.5226	11	5	0.3931	11	11	0.2830	13	13
25	0.5200	11	12	0.3776	11	4	0.2724	22	11
26	0.4445	14	17	0.3496	22	2	0.2681	13	25
27	0.4377	14	25	0.3411	14	17	0.2598	14	25
28	0.4092	22	10	0.3178	2	13	0.2417	11	4
29	0.4049	22	16	0.3082	11	5	0.2307	2	23
30	0.4019	22	27	0.3052	22	9	0.2193	22	23

http://www.aloki.hu ● ISSN 1589 1623 (Print) ● ISSN 1785 0037 (Online)
DOI: http://dx.doi.org/10.15666/aeer/1706_1448714503

We can see from *Table 2,* in these three years of China's transition period the correlation coefficients rise in the first and then decline. The means of carbon correlation coefficients of the top 5, 12, and 30 in also show this trend. In 2010 the coefficient is the highest, indicating that carbon emissions may reach a high peak during this period (*Fig. 2*). This is in line with the accelerated investment of Chinese traditional industries in this period. In 2005 the coefficient is in the second place, maybe because the quantities of various industrial outputs were not so vast. After 2010, the carbon correlation coefficients show a decreasing trend from 2010 to 2015, indicating dynamic energy conversion of economic development may be acting up. To further and more comprehensive observe this trend, the first 50 carbon correlation coefficients are represented in *Figure 3*.

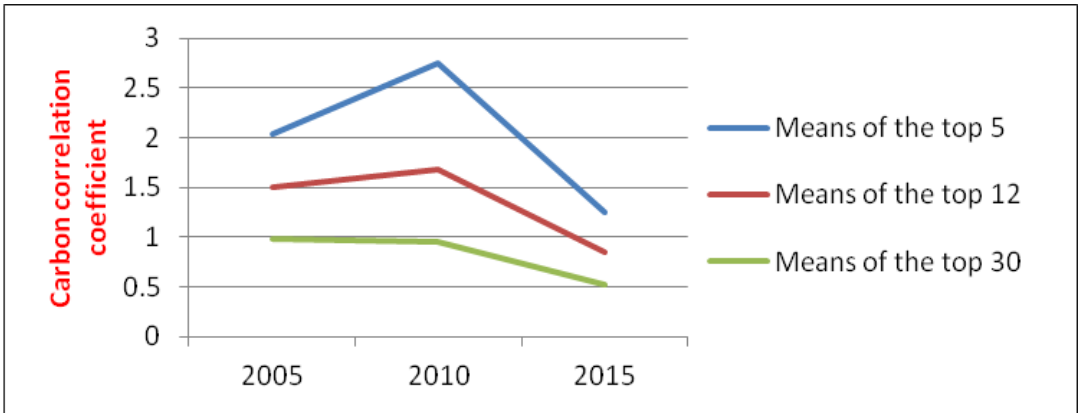

Figure 2. *The means of INCC coefficients in China in 2005, 2010 and 2015*

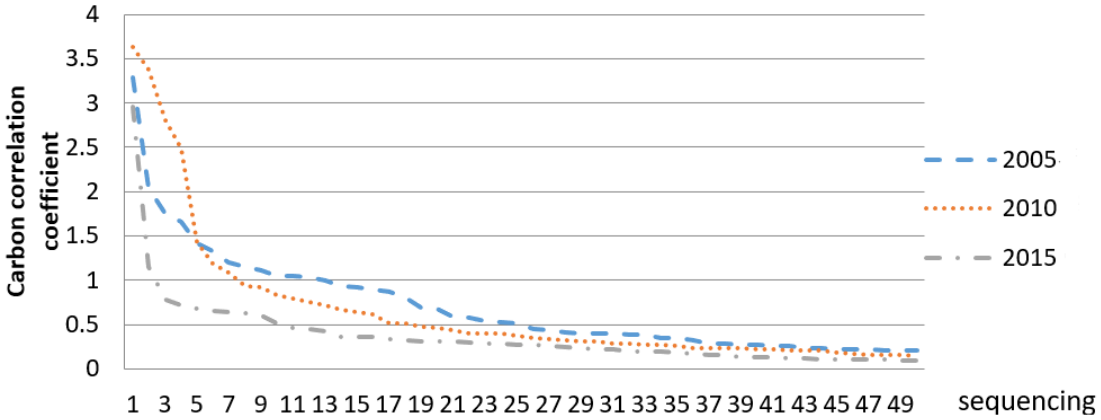

Figure 3. *The top 50 INCC coefficients in China in 2005, 2010 and 2015*

In each year of these transition periods, these carbon correlation coefficients show the same unbalanced state, which is the power law distribution. Among the significant coefficients which were though tested, only a few coefficients were higher, and most of them were lower. Further analysis of *Table 2* and *Figure 3* shows that in the first 50 carbon correlation coefficients, the main direct emission sector possessing the highest coefficients is the production and supply of electricity and heat (22), possessing 13, 11 and 13 edges in each year, nearly half of the highest carbon emission coefficients

http://www.aloki.hu ● ISSN 1589 1623 (Print) ● ISSN 1785 0037 (Online)
DOI: http://dx.doi.org/10.15666/aeer/1706_1448714503

coming from this sector. The main indirect discharging sectors possessing the highest coefficients are water production and supply (24), metal mining and dressing, and electricity (4) and thermal production and supply (22), which emit a lot of carbon by using products from other sectors.

Analysis of China's INCCs

Analyzing the structural characteristics can excavate the intrinsic characteristics of carbon linkages among China's various industrial sectors. The basic statistical characteristics of China's INCCs in 2005, 2010 and 2015 are shown in *Table 3*. It is particularly interesting that, contrary to correlation coefficients trend, significant edge numbers decline in the first and then rise. In 2010, there were 76 linkages, less than 85 linages in 2005 and 83 linages in 2015. Why the carbon correlation coefficients becoming greater and the significant numbers becoming less happened at the same time in 2010? Further analysis shows that this was probably related to China's large-scale investment into some special industries in 2008.

Table 3. *Basic characteristics of China' INCCs in 2005, 2010 and 2015*

	Significant numbers	**Self-circulation sectors numbers**	**Sector numbers with more than 5 in-degrees**	**Sector numbers with 0 out-degree**	**Sectors of the top five out-degree**
2005	85	9	3	16	22, 11, 12, 14, 13
2010	76	8	3	16	22, 11, 12, 14, 26
2015	83	10	1	14	22, 11, 12, 14, 26

We can see there were existing 9, 8 and 10 sectors with self-recycling in these three years, that is, nearly one-third of the industrial sectors possess self-recycling carbon emissions. So, self-circulation problem in INCCs were prominent. We have also noticed that there were 7 sectors (6, 7, 10, 12, 13, 14, 22) always possessing self-recycling in these three years and there were 2 sectors (2, 11) possessing self-recycling in these two years. So most self-recycling sectors have always kept stable. About half of the sectors (16, 16 and 14 in these three years) having zero out-degree show that these sectors do not transmit emission responsibility to other sectors. They just accept carbon transmission to them and become carbon consumption sectors. These sectors are not "innocent". It is just because of their requirements that the carbon emission sector excludes a large amount of carbon, so they should bear the responsibility of carbon transfer. We have listed the sector numbers with more than 5 in-degrees for a special purpose. They were sector 8, 9 and 21 in 2005, sector 6, 8 and 20 in 2010, and sector 20 in 2015. High in-degree means these sectors bear more responsibility of carbon transfer. And the sectors with more than 5 in-degrees changed from sector 8, 9 and 21 in 2005 to sector 6, 8 and 20 in 2010 and to sector 20 in 2015. The sectors had changed considerably during this transition period. Contrary to the sectors with more in-degrees, the sectors of the top five out-degrees had remained broadly consistent over the past ten years. Sector 22, 11, 12 and 14 maintained the top four in these three interval years, and the order remained unchanged. Only the fifth changed from sector 13 in 2005 to sector 26 in 2010 and 2015. From the perceptive of in-degree and out-degree, there were typical star nodes and strong sub-graphs in China's INCC graphs of these three years. The INCC graphs of these three years are shown in *Figure 4*.

http://www.aloki.hu ● ISSN 1589 1623 (Print) ● ISSN 1785 0037 (Online)
DOI: http://dx.doi.org/10.15666/aeer/1706_1448714503

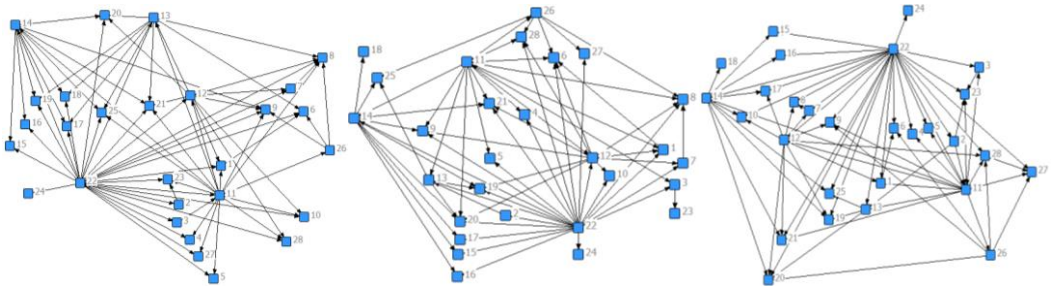

Figure 4. *China's INCCs in 2005/2010/2015. (Please refer to Table 1 for the meanings of the sector numbers in the figure)*

Star node sector in INCC

Out-degree star topology

As shown in *Figure 4,* there is a common prominent feature in these three network diagrams. Each network diagram has showed 4 or 5 star topologies, in which node sectors transmit emission responsibility to other sectors, as presented in *Figure 4.* According to the number of out-degree, the same top four sectors, namely, power, thermal production and supply (22), petroleum processing, coking and nuclear fuel processing (11), chemical sector (12) and metallurgical smelting and calendaring (14), have constructed a sub-network with maximum out-degree of 27 and minimum out-degree of 10 in these three years. The non-metallic mineral products sector (13) ranked fifth in 2005, with an out-degree of 9, falling to 4 in 2010 and 2015. At the same time, transportation, storage and postal service (26) increased from 3 in 2005 to 5 in 2010 and 2015. It can be seen that these sectors were the main emission sectors and that they pass the emission responsibility to other sectors through industrial linkages. *Figure 5* showed the carbon emission sub-graphs of electricity and thermal production and supply (22) in these three years. Almost all connections to 22 passed the significant test.

It is of great significance to study the sub-network which constructed by the emission sectors and their consumption sectors. As the cores of these sub-networks, these sectors act as responsibility transfer source and have immediately responsibility for carbon emission. For these sub-networks, the most important thing is controlling key nodes. Although the utilization efficiency of fossil fuels, such as in electricity and thermal production and supply, is an old problem, it is also a common problem. Research and development of common technologies for carbon emission reduction is the management emphasis of out-degree star topology.

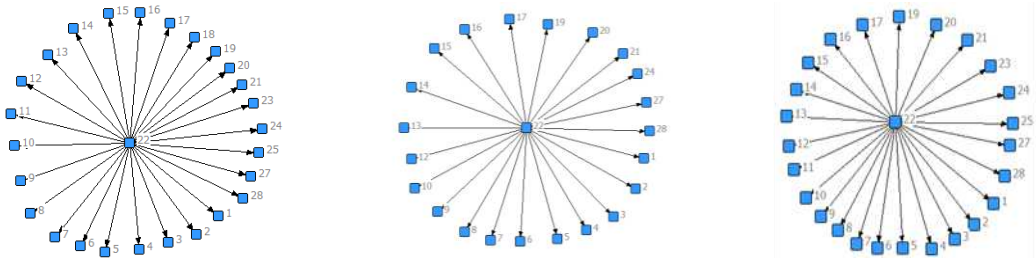

(a) 2005 (b) 2010 (c) 2015

Figure 5. *Carbon emission sub-graphs of electricity and thermal production and supply (22). (Please refer to Table 1 for the meanings of the sector numbers in the figure)*

http://www.aloki.hu ● ISSN 1589 1623 (Print) ● ISSN 1785 0037 (Online)
DOI: http://dx.doi.org/10.15666/aeer/1706_1448714503

In-degree star topology

Different from the out-degree star topology, the in-degree star topology have smaller degrees, the maximum in-degree being 6, and a few sectors being 4, 5 or 6. Since the beginning of the 21st century, China's economic growth mode has changed from extensive to intensive, and the focus of economic development has gradually shifted from textile manufacturing, food manufacturing to machinery manufacturing. The development of key industries requires many other sectors' products, resulting in Changes in the in-degree star node sector. The largest in-degree sectors in 2005, 2010 and 2015 were respectively Textile, clothing, shoes, hats, leather, feather and its products industry (8), Food manufacturing and tobacco processing industry (6) and Instrumentation and cultural office machinery manufacturing industry (20), as shown in *Figure 6*. These sectors do not necessarily emit a lot of carbon in the process of producing their own products. However, these sectors have to bear indirect carbon responsibility because they receive products from other sectors that emit a lot of carbon in manufacturing process. Careful analysis of these three sectors in *Figure 6* shows that these three highest in-degree sectors all receive carbon emissions from electricity, thermal production and supply sectors (22), chemical sector (12) and transportation, warehousing and postal services (26).

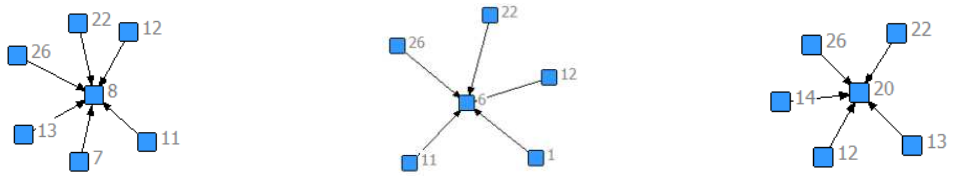

(a) sector 8 in 2005 (b) sector 6 in 2010 (c) sector 20 in 2015

Figure 6. *Carbon emissions graphs of the in-degree star node sector. (Please refer to Table 1 for the meanings of the sector numbers in the figure)*

The research about in-degree star topology is a meaningful job that few scholars have done before. First of all, we can identify the main demand responsibility sectors, which define the transfer destination of carbon emissions from the demand side. From the perspective of the social responsibility system, the complete responsibility system of carbon emissions needs perfecting analysis from both demand side and supply side. Secondly, study about in-degree star topology lays the foundation for the construction of carbon supply chain network. Carbon emissions from the demand side and the supply side can constitute a complete chain network. Thirdly, from the perspective of management regulation, In the formulation of industrial policies on carbon emissions, besides strengthening the supervision of direct carbon emission sectors, we also need to strengthen the management and control of more carbon receiving sectors.

Carbon cycle correlation in INCC

Further analysis of China's INCCs of each year reveals that there is a cyclic structure among industrial sectors. Among this cycle, the first sector provides significant carbon emissions for the second sector, while the second sector provides significant carbon emissions for the first sector directly or by other(s). Those sectors and these significant linkages form a cycle which expands the role of individual sector in carbon emissions.

http://www.aloki.hu ● ISSN 1589 1623 (Print) ● ISSN 1785 0037 (Online)
DOI: http://dx.doi.org/10.15666/aeer/1706_1448714503

We can see from these three years, the cycles always embraced petroleum and natural gas extraction sector (3) and petroleum processing, coking and nuclear fuel processing sector (11). The difference was, these two sectors interflowed through production and supply of electricity and heat (22) in 2005, while in 2010 and 2015 these two sectors directly formed the main body of mutual carbon consumption. However, due to the sparse linkages in China's INCCs and the existence of typical star node sectors, there are not many sectors entering the circular structure, as shown in *Figure 7*.

(a) In 2005 (b) In 2010 and 2015

Figure 7. *Industry carbon cycle structure. (Please refer to Table 1 for the meanings of the sector numbers in the figure)*

Although the structure of carbon correlation cycle among industrial sectors is rare, self-cycling exists in many sectors. There were respectively nine, eight and ten sectors with self-cycling correlations of carbon emissions in 2005, 2010 and 2015. There are seven common industrial sectors in these three years, namely, food manufacturing and tobacco processing (6), textile (7), paper making, printing, cultural, educational, sporting goods manufacturing (10), chemical (12), nonmetallic mineral products (13), metal smelting and calendering processing (14), production and supply of electricity and heat (22). It can be seen that these sectors bear significant carbon emission responsibility because of the use of products in their own sectors.

Both the circular structures and self-cycling sectors in INCC deserve great attention. Because these sectors related these bidirectional overflow structures are always establishing high carbon driving force in INCCs, including propulsive force and pulling force. Finding these micro-structures and self-circulation within and outside the sectors can help us to explore the carbon trajectory in a more subtle way. These studies also contribute to the construction of industrial balance and carbon ecosystem.

Carbon emission transmission path

The directed path in the INCCs shows the transmission path of carbon emission responsibility. In one path, the starting sector transfers the carbon emission responsibility to the intermediate sectors, while the intermediate acts as a transmitter and the terminal sector receives the responsibility from multiple sectors through multi-step transmission. As shown in *Figure 8,* in 2005 the longest carbon transmission path consists of six steps: 2→22→3→11→12→1(13)→6(17\18\19\20\21\25). In 2010, the longest carbon transport path is five steps: 22→3(2)→11→12→1(7)→6(8). In 2015, the longest carbon transmission path is also five steps, but there are two main paths: 22→3(2)→11→12(26)→17(28)→6(8\27). In 2005 the carbon emission transmission paths were longer and wider than in 2010 and 2015. Sector 13 (nonmetallic mineral products) has greatly broadened the width of the path. The transmission paths in 2010 and 2015 are similar, but the transmission paths in 2015 are more complex, adding some new branches and connections.

http://www.aloki.hu ● ISSN 1589 1623 (Print) ● ISSN 1785 0037 (Online)
DOI: http://dx.doi.org/10.15666/aeer/1706_1448714503

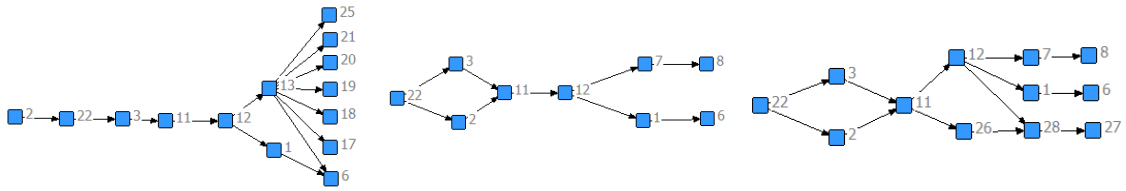

(a) In 2005 (b) In 2010 (c) In 2015

Figure 8. *Carbon emission transmission path. (Please refer to Table 1 for the meanings of the sector numbers in the figure)*

Path study not only emphasizes the source and destination of carbon emissions, but also emphasizes the role of "bridge" and "intermediary". Some sectors, such as sector 3 (Petroleum and natural gas extraction sector), sector 11(petroleum processing, coking and nuclear fuel processing sector) and sector 12(chemical), undertakes a strong channel role. They digest and absorb products that contain large amounts of carbon emissions, and transfer products that emit large amounts of carbon to other sectors.

Analysis of extended INCC

According to previous defining, we can also build three extended INCCs diagrams for these three years, as shown in *Figure 9*. As we know, in these extended INCCs, all the directed edges and paths are connected along the directed road. Directed edges are connected between two nodes with paths in the extended INCC graph. That is to say, if only there is a carbon transmission responsibility between two sectors, there is a linkage. Therefore, the significance of node degree in the extended INCC graph is more obvious. The degree of a vertice in the extended INCC reflects the number of all other sectors linked with the sector, including direct and indirect linages. So the degree of a sector in the extended INCC can be more comprehensively demonstrated the carbon linkages.

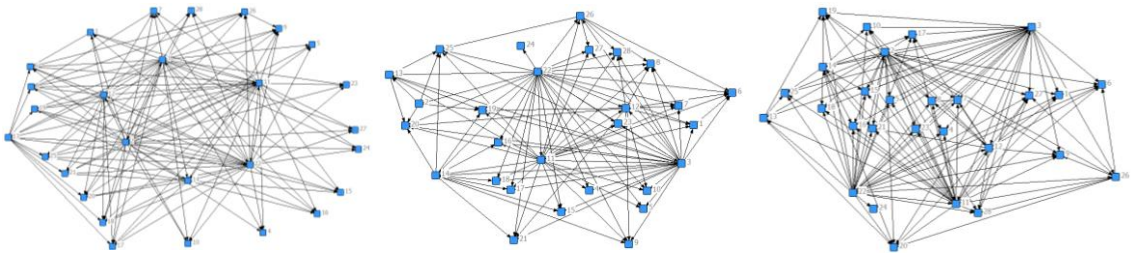

2005 2010 2015

Figure 9. *China's extended INCC in 2005\2010\2015 (Please refer to Table 1 for the meanings of the sector numbers in the figure)*

Out-degree in the extended INCCs reflects the overall emission responsibility of a sector transmitting to others. When an out-degree of a sector is large, it means that it is a main sector of emission responsibility source. As shown in *Figure 9* in the extended INCC in 2005, there were four sectors (2, 3, 11 and 22) which possess 28 out-degrees, which can transmit carbon emission responsibilities to all other sectors. In the extended INCCs in 2010 and 2015, there were four sectors possessing more than 25-outdegree

http://www.aloki.hu ● ISSN 1589 1623 (Print) ● ISSN 1785 0037 (Online)
DOI: http://dx.doi.org/10.15666/aeer/1706_1448714503

(sector 2, 3, 11 having 25, sector 22 having 27), which can transmit carbon emission responsibility to almost all other sectors. We contrast the extended INCCs and the customary INCCs, discovering sector 2 and 3 is the hidden emission source.

The in-degree in the extended INCCs reflects its overall accepted requirement responsibility of a sector. When an in-degree of a sector is large, it means many sectors transmitting CO_2 emission responsibility by varied paths to this sector. It is a recipient and a major consumer responsibility sector. In all industrial sectors of three years, the largest in-degree was 7. these sectors are food manufacturing and tobacco processing (6), textile, clothing, shoes, hats, leather, feather and its products (8), wood processing and furniture manufacturing (9), communications equipment, computers and other electronic equipment manufacturing (19) and instrumentation and cultural office machinery manufacturing industry (20). It can be seen that these sectors accept carbon emission responsibilities directly or indirectly from 7 sectors. We contrast the large in-degree sectors in the extended INCCs and the customary INCCs, finding that little change is found and the carbon consumption sectors sustain stable.

Discussion

Based on Weaver-Thomas index, we combine sectorial input-output analysis and network analysis to construct the industrial network of carbon correlation (INCC) for carbon emission management. We also use the data of China's 2005, 2010 and 2015 to analysis the developmental trajectories of transition period. The contribution of this paper lies in the following.

On the theoretical side, we apply network analysis to the carbon correlation study, and the carbon flow laws among industrial sectors are sorted out as a whole. Carbon correlations have formed transmission responsibilities of carbon emission between industrial sectors. We use Industrial Carbon Correlation Coefficient to describe the amount of carbon directly emitted by an industry sector in producing a unit product for another sector. The greater the coefficient, the stronger is the carbon correlation between these two sectors. Base on Industrial Carbon Correlation Coefficient, we construct INCC which is a directed graph among various industrial sectors, to describe the transmission structure of carbon emission responsibilities among industrial sectors. Constructing a national or regional INCC and analyzing the structural characteristics of the network can excavate the characteristics of carbon emissions among these national or regional industrial sectors, thus providing an analytical basis for emission reduction and other decisions.

On the practical side, we use the INCCs to find that there are typical significantly characteristics in China's INCC graphs of this transition period. First, in recent years, the carbon correlation coefficient of the same ranking has become smaller, in which 2015 is almost half of 2005. It can be seen that with the development of societies, emission reduction has been gained more effective. Secondly, these three years' INCCs indicate that there are relatively sparse significant carbon correlations between sectors and there are obvious star nodes in the INCC graphs. Star nodes are divided into out-degree type and in-degree type. As for the out-degree node, we can see that these sectors are relatively unified, and that the most prominent is the power and thermal production and supply sectors which transmit emission responsibility to almost all other sectors. Most of transmissions are direct, while some are indirect. The following sectors are petroleum processing, coking and nuclear fuel processing (11), chemical (12) and

http://www.aloki.hu ● ISSN 1589 1623 (Print) ● ISSN 1785 0037 (Online)
DOI: http://dx.doi.org/10.15666/aeer/1706_1448714503

metal smelting and calendering (14). As for in-degree node type, more than half of all industrial sectors are in-degree nodes which only accept emissions responsibility from other sectors. The maximum in-degree sectors are food manufacturing and tobacco processing (6), textile, clothing, shoes, hats, leather, feather and its products (8), and instrumentation and cultural office machinery manufacturing sector (20). Third, there are only a few correlation cycles among transmission responsibility which involve fewer sectors in INCCs. We can see that there is only but always a cycle in the three INCCs between petroleum and natural gas extraction sector (3) and petroleum processing, coking and nuclear fuel processing sector (11). Fourth, the path in these INCCs are not very long, only 5-6 steps. There is a stable carbon emission path in the three INCCs. That is, the production and supply of electricity and heat (22) → oil and natural gas extraction (3) → oil processing, coking and nuclear fuel processing (11) → chemical (12) → agriculture, forestry, animal husbandry and fishery (1) → food manufacturing and tobacco processing (6).

The EU's carbon trading system is a leader in the global carbon trading market, and in January 2005, the EU officially launched the Greenhouse Gas Emissions Trading System (EUETS), it is the world's first greenhouse gas emissions quota trading market, using the "total limit and trading" rule. New Zealand and Australia are actively promoting the carbon trading market, New Zealand introduced mandatory carbon trading in 2008 in a step-by-step approach, Australia is one of the first countries in the world to implement mandatory greenhouse gas reduction programmes, and on July 1, 2012, Australia began implementing carbon trading nationwide.

Conclusions

In order to reduce greenhouse gas emissions such as CO_2, different measures should be taken for different sectors. As the research reveals, the industrial carbon correlation coefficient between sectors is not only related to the direct input between sectors, but also related to the carbon emissions per unit. For the main out-degree sectors, such as power, thermal production and supply industries, relevant measures should be taken to reduce their direct CO_2 emissions, such as reducing thermal power and increasing other forms of electricity, promoting the use of geothermal, improving energy conversion rate and so on. For the main in-degree sectors, the important ways to reduce CO_2 emissions are taking measures to change the proportion of their inputs, reducing the demand of high carbon emission sectors, and trying to reduce the final demand for these products. As circle can enlarge carbon emissions, changing one or two linkages in this circle can greatly reduce carbon emissions. For long transmission paths, reducing their length can cut down carbon emissions for the whole system. In overall, Discussions about correlations, key sectors and paths allow us to look deeply into the internal productive linkages within an economy with implications for CO_2 emission. They provide valuable information for planners and decision makers in formulating feasible and practical industrial polices with implications for CO_2 emissions.

In the future research, we should focus on how to reduce the direct carbon emission and interrupt the correlation of carbon emission between sectors, so as to achieve the goal of energy conservation and emission reduction. How to reduce carbon dioxide emissions from industrial sector units into products; How to accurately position the responsibility of carbon emission, and can give relevant solutions.

http://www.aloki.hu ● ISSN 1589 1623 (Print) ● ISSN 1785 0037 (Online)
DOI: http://dx.doi.org/10.15666/aeer/1706_1448714503

Acknowledgements. This work is supported by the Humanities and Social Sciences Project of Chinese Ministry of Education (Grant No.: 17YJCZH062).

REFERENCES

[1] Arto, I., Rueda-Cantuche, J. M., Peters, G. P. (2014): Comparing the GTAP-MRIO and WIOD databases for carbon footprint analysis. – Economic Systems Research 26(3): 327-353.

[2] Baccini, P. (1996): Understanding regional metabolism for a sustainable development of urban systems. – Environmental Science and Pollution Research 3(2): 108-111.

[3] Brown, H. L., Buettner, G. P., Canyon, V. D., Mac Crawford, J., Judd, J. (2012): Estimating the life cycle greenhouse gas emissions of Australian ambulance services. – Journal of Cleaner Production 37: 135-141.

[4] Cadarso, M., Lopes, L., Gomez, N., Tobarra, M. (2012): International trade and shared responsibility by sector. An application to the Spanish economy. – Ecological Economics 83: 221-235.

[5] Chang, N. (2015): Changing industrial structure to reduce carbon dioxide emissions: A Chinese application. – Journal of Cleaner Production 103: 40-48.

[6] Chang, Y. F., Lin, S. J. (1998): Structural decomposition of industrial CO2 emission in Taiwan: an input-output approach. – Energy Policy 26(1): 5-12.

[7] Chen, S., Chen, B. (2012): Network environ perspective for urban metabolism and carbon emissions: a case study of Vienna, Austria. – Environment Sciences & Technology 46(8): 4498-4506.

[8] Egilmez, G., Kucukvar, M., Tatari, O. (2013): Sustainability assessment of U.S. manufacturing sectors: an economic input output-based frontier approach. – Journal of Cleaner Production 53: 91e102.

[9] Jain, S., Gupta, P. (2019): Entropy generation analysis of carbon nanotubes nanofluid 3d flow along a nonlinear inclined stretching sheet through porous media. – International Journal of Heat and Technology 37(1): 131-138.

[10] Kaivo-oja, J., Luukkanen, J. (2004): The European Union balancing between CO2 reduction commitments and growth policies: decomposition analyses. – Energy Policy 32: 1511-1530.

[11] Labandeira, J., Labeaga, J. (2002): Estimation and control of Spanish energy-related CO2 emissions: an input-output approach. – Energy Policy 30(7): 597-611.

[12] Lin, B. Q., Sun, C. W. (2010): Evaluating carbon dioxide emissions in international trade of China. – Energy Policy 38(1): 613-621.

[13] Lixon, B., Thomassin, P. J., Hamaide, B. (2008): Industrial output restriction and the Kyoto Protocol: an input-output approach with application to Canada. – Ecological Economics 68(1): 249-258.

[14] Machado, G., Schaeffer, R., Worrell, E. (2001): Energy and carbon embodied in the international trade of Brazil: an input-output approach. – Ecological Economics 39: 409-424.

[15] Mongelli, I., Tassielli, G., Notarnicola, B. (2006): Global warming agreements, international trade and energy/carbon embodiments: an input-output approach to the Italian case. – Energy Policy 34(1): 88-100.

[16] Mózner, V. Z. (2013): A consumption-based approach to carbon emission accounting - sectoral differences and environmental benefits. – Journal of Cleaner Production 42: 83-95.

[17] Seppälä, J., Mäenpää, I., Koskela, S., Mattila, T., Nissinen, A., Katajajuuri, J., Härmä, T., Korhonen, M., Saarinen, M., Virtanen, Y. (2011): An assessment of greenhouse gas emissions and material flows caused by the Finnish economy using the ENVIMAT model. – Journal of Cleaner Production 19(16): 1833-1841.

http://www.aloki.hu ● ISSN 1589 1623 (Print) ● ISSN 1785 0037 (Online)
DOI: http://dx.doi.org/10.15666/aeer/1706_1448714503

[18] Sonis, M., Guilhoto, J. J. M., Hewings, G. J. D., Martins, E. B. (1995): Linkages, key sectors, and structural change: some new perspectives. – SSRN Electronic Journal XXXIII(3): 233-270.
[19] Tahara, K., Sagisaka, M., Ozawa, T., Yamaguchi, K., Inaba, A. (2005): Comparison of "CO2 efficiency" between company and industry. – Journal of Cleaner Production 13(13): 1301-1308.
[20] Wang, Z., Yang, J. (2015): Study on the evaluation and selection of strategic emerging industries based on the entropy right method and Weaver-Thomas model: taking the Lujiang City belt as an example. – Science and Technology Management Research 35(20): 84-89+94.
[21] Wu, J., Qi, H., Wang, R. (2016): Insight into industrial symbiosis and carbon metabolism from the evolution of iron and steel industrial network. – Journal of Cleaner Production 135: 251-262.
[22] Xu, L. J., Wang, G. Y., Liu, T. Y., Liu, N. Z., Zhang, S. C., Sun, S. Y. (2019): A new leakoff analysis approach for acid fracturing in naturally fractured carbonate gas reservoirs. – International Journal of Heat and Technology 37(1): 139-147.
[23] Yan, X. H., Gong, H., Wang, B. C., Xie, K. C. (2017): Analysis of industrial green development countermeasures in Xi'an city based on Weaver-Thomas model. – Ecological Economy 33(12): 72-76+118.
[24] Zhang, B., Du, Z., Wang, Z. (2018): Carbon reduction from sustainable consumption of waste resources: an optimal model for collaboration in an industrial symbiotic network. – Journal of Cleaner Production 196: 821-828.
[25] Zhang, Y., Zheng, H., Fath, B. D. (2014): Analysis of the energy metabolism of urban socioeconomic sectors and the associated carbon footprints: model development and a case study for Beijing. – Energy Policy 73: 540-551.
[26] Zhang, Y., Li, Y., Liu, G., Hao, Y. (2017): CO2 metabolic flow analysis in global trade based on ecological network analysis. – Journal of Cleaner Production 170: 34-41.
[27] Zhang, Y., Li, Y., Liu, G., Hao, Y. (2018): CO2 metabolic flow analysis in global trade based on ecological network analysis. – Journal of Cleaner Production 170: 34-41.
[28] Zhao, R., Huang, X., Zhong, T., Liu, Y., Chuai, X. W. (2014): Carbon flow of urban system and its policy implications: the case of Nanjing. – Renewable and Sustainable Energy Reviews 33: 589-601.
[29] Zhao, Y. Y., Yang, Q. S. (2016): Analysis of innovative industrial leaders in Zhongguancun – based on the Weaver-Thomas Index. – The World of Survey and Research 9: 32-37.

http://www.aloki.hu ● ISSN 1589 1623 (Print) ● ISSN 1785 0037 (Online)
DOI: http://dx.doi.org/10.15666/aeer/1706_1448714503

ANALYSIS TECHNOLOGY OF ENVIRONMENTAL MONITORING DATA BASED ON INTERNET OF THINGS ENVIRONMENT AND IMPROVED NEURAL NETWORK ALGORITHM

ZHAI, W.

Xi'an Aeronautical University, Xi'an 710077, China
(e-mail: 2587842805@qq.com)

(Received 7th Jun 2019; accepted 10th Oct 2019)

Abstract. With the development of industrialization, the problem of environmental pollution has become increasingly serious. Environmental monitoring data, as a measurement index of environmental quality, is increasingly valued by governments and citizens. However, the environmental data accumulated through real-time monitoring at the current stage is mostly used to write basic reports, while the hidden laws or values still need to be further explored. This paper proposes two original environmental prediction models and improves upon these two methods separately to predict the quality of the atmospheric environment. The following research results are obtained: the multivariate linear equation is optimized through stepwise linear regression, which can accurately predict the short-term atmospheric environmental quality; the improved BP neural network can predict the mid-term and long-term atmospheric environmental quality through short-term training.
Keywords: *environmental monitoring, neural network, environmental quality, data analysis, prediction*

Introduction

With the rapid advancement of industrialization and the rapid increase of urban population, the environmental pollution problem is becoming more and more serious (Beck et al., 1961; Jeffrey et al., 2000), including atmospheric pollution, such as acid rain and fog; water environment pollution, such as black odorous water, water bloom and red tide; solid waste pollution, such as construction waste and tailings pond pollution. In recent years, the atmospheric pollution has been particularly prominent. It directly leads to a decline in the quality of people's living environment, affecting human health and causing huge economic losses (Lauth et al., 2010; Abramovitch et al., 2015). In order to avoid the occurrence of air pollution, large funds have been invested in the prevention of air pollution at various levels in our country (Bey et al., 2017) and an atmospheric environment monitoring Internet of Things has been established. Through the monitoring of the quality of the atmospheric environment, it can be controlled in real time, which guides the industrial production and the construction of related pollution prevention facilities (Rodgers et al., 2015; Lochner et al., 2011; Zhang et al., 2018a). At present, almost all atmospheric environmental monitoring data is used to prepare environmental reports such as daily newspapers and annual reports (Arsie et al., 2010; Marino et al., 2017) while the value of data needs to be further explored (Li et al., 2014). For example, through historical monitoring data, the future trend of atmospheric environmental quality can be predicted so as to better guide people's production activities (Chien et al., 2005, 2010). Meanwhile, it provides relevant scientific evidence for government decision-making and management departments in the formulation of systems concerning this area (Chien et al., 2003).

http://www.aloki.hu ● ISSN 1589 1623 (Print) ● ISSN 1785 0037 (Online)
DOI: http://dx.doi.org/10.15666/aeer/1706_1450514516

At present, the methods for predicting the quality of atmospheric environment mainly include numerical prediction and statistical prediction. However, the model precision of numerical prediction is lower than that of statistical prediction and the scope of application is limited (Chien et al., 2007; Song, 2018; Cooper and Ekström, 2005; Reifman et al., 2000; Zhang et al., 2018b; Zhao et al., 2018). Therefore, this paper adopts the statistical prediction with easy data acquisition and high prediction precision, including the back propagation (BP) neural network and multiple linear regression equation for the analysis of atmospheric environment prediction.

Materials and methods

Multiple regression model

When there is a linear relationship between two or more independent variables and dependent variables, it is a multiple linear regression. Its mathematical model is shown in *Equation 1:*

$$y = a_1 + a_2 x_1 + a_3 x_2 + \cdots\cdots + a_{m+1} x_m + \varepsilon \quad \text{(Eq.1)}$$

In this formula, $a_1, a_2, a_3, \ldots a_{m+1}$, are regression coefficients; ε is a random error.

The estimated value of regression coefficient is shown in *Equation 2:*

$$Q = \sum_{t=1}^{n} [y_1 - (a_1 + a_2 x_{1t} + a_3 x_{2t} + \cdots\cdots a_{m+1} x_{mt})]^2 \quad \text{(Eq.2)}$$

After obtaining the multiple linear regression equation, it needs to be tested to determine its precision. The commonly used test methods include correlation coefficient test, F test and t test.

(1) Correlation coefficient test

The correlation coefficient is an index used to measure the fitting degree of the linear models. The mathematical expression is the ratio of the regression sum of squares to the total sum of squares, as is shown in *Equation 3:*

$$R^2 = \frac{SSR / p}{SST / n - p - 1} \quad \text{(Eq.3)}$$

(2) F test

The F test is used to test whether the relationship between the independent variable and the dependent variable is significant in the linear model and it is expressed by *Equation 4:*

$$F = \frac{\sum_{i=1}^{n} (\hat{y}_1 - \bar{y})^2 / p}{\sum_{i=1}^{n} (y_i - \hat{y}_1)^2 / (n - p - 1)} = \frac{SSR}{SSE / (n-2)} = \frac{R^2}{1 - R^2} (N-2) \sim F(1, n-2) \quad \text{(Eq.4)}$$

http://www.aloki.hu ● ISSN 1589 1623 (Print) ● ISSN 1785 0037 (Online)
DOI: http://dx.doi.org/10.15666/aeer/1706_1450514516

(3) T test

The t test can be used to determine whether a variable is retained as an independent variable in the model and it is expressed by *Equation 5:*

$$t = \frac{\frac{\hat{\beta}_1}{\sigma} \sim t(n-p-1)}{\sqrt{\sum_{j=1}^{n}(x_{ij} - \overline{x_{11}})^2}} \quad \text{(Eq.5)}$$

In this equation:

$$\hat{\beta} \sim N\left[\frac{\sigma^2}{\sum_{j=1}^{n}(x_{ji} - \bar{x})}\right], \quad \hat{\sigma}^2 = \frac{SSE}{(n-p-1)}.$$

In *Equations 3–5,* SST represents the deviation sum of squares of the difference between the observed value and the mean value of the dependent variable. SSR is the deviation caused by the independent variable, which is the regression sum of squares. SSE is the residual sum of squares caused by the experimental error. The relationship is shown in *Equation* 6*:*

$$SST = \sum_{i=1}^{n}(y_i - \bar{y})^2 = \sum_{i=1}^{n}(\hat{y}_1 - \bar{y})^2 + \sum_{i=1}^{n}(y_i - \hat{y}_i)^2 = SSR + SSE \quad \text{(Eq.6)}$$

BP neural network

BP neural network is a neural network of error inverse propagation, as is shown in *Figure 1:* after the data is input, it is forwardly propagated from the input layer to the output layer via the hidden layer. According to the set error, the output layer corrects the weight through the hidden layer, which is the error inverse propagation, thereby achieving a stepwise improvement of the precision of the output value of the neural network.

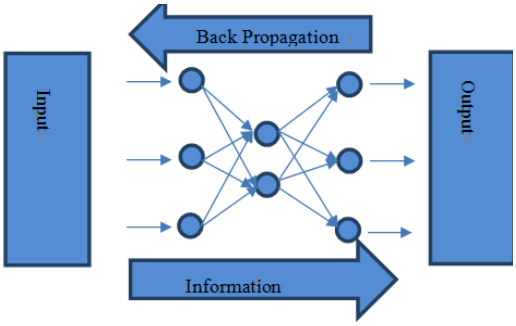

Figure 1. *BP neural network topology*

http://www.aloki.hu ● ISSN 1589 1623 (Print) ● ISSN 1785 0037 (Online)
DOI: http://dx.doi.org/10.15666/aeer/1706_1450514516

Genetic algorithm

The genetic algorithm is developed from the Darwin's theory of evolution and Mendel's genetics. It uses the imitation of biological gene coding to encode individuals, serving as the initial population. The selection, crossover and mutation are completed according to the principle of survival of the fittest. The new population is formed and the above operation is repeated, thereby realizing the retention of excellent genes and inheriting these genes to the offspring. Therefore, the population can better adapt to the environment and continue to breed and evolve.

Data collection and processing

We adopt the GB3095-2012 standard to evaluate the atmospheric environmental quality in the suburbs of Shijiazhuang. The air quality automatic monitor was used to measure the PM2.5, PM10, CO, SO2, O3 and NO2 in the air; temperature-humidity sensor, anemometer and barometer were used to measure meteorological conditions such as temperature, humidity, wind speed, wind direction and air pressure, etc. For example, when the humidity is high, the degree of air pollution will increase. Therefore, this paper will collect 6 indexes of atmospheric pollutants and corresponding 5 meteorological indexes.

Data collection

This paper downloads the monitoring data of atmospheric environment of the environmental protection bureau in the Shi Jiazhuang by writing the crawler software. The data collection process is shown in *Figure 2*.

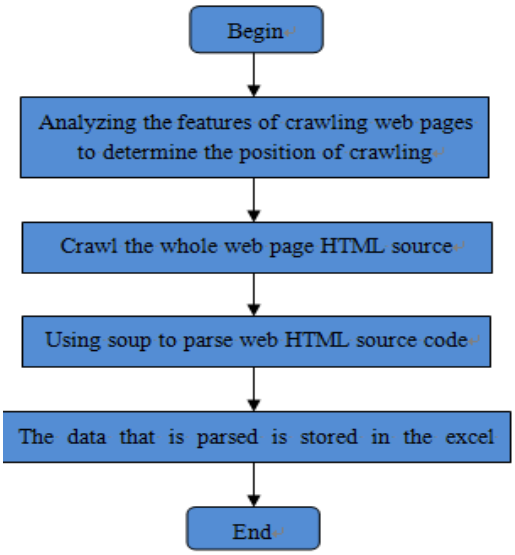

Figure 2. *Flow chart of web crawler*

Data processing

Data preprocessing plays an important role in the in-depth, accurate mining and analysis of data. In this paper, the collected data is preprocessed in the following two ways.

http://www.aloki.hu ● ISSN 1589 1623 (Print) ● ISSN 1785 0037 (Online)
DOI: http://dx.doi.org/10.15666/aeer/1706_1450514516

(1) Eliminating abnormal data

According to the reasonable distribution range and mutual relationship of each atmospheric data, it is checked whether there is abnormal or contradictory value in the data and the abnormal data is eliminated. In addition, the collected data may be invalid or missing and the mean value of variables is used for the estimation and supplement.

(2) Data normalization

In order to reduce the deduction in the precision of the prediction model caused by the difference in magnitude and dimension between the atmospheric monitoring data, the normalization is conducted on the data. The following two normalization methods are adopted for the multiple linear regression model and the neural network model respectively:

1) Normalized to the interval of [0, 1]

Set x_{max} and x_{min} represent the maximum and minimum value of the original data respectively; x_i is the actual data; and $\hat{x}_i$ represents the normalized value. The normalization equation is:

$$\hat{x}_t = \frac{x_i - x_{\max}}{x_{\max} - x_{\min}} \quad \text{(Eq.7)}$$

The output value is then converted using the formula $x_i = (x_{max} - x_{min})\hat{x}_t + x_{min}$.

2) Normalized to zero mean and unit variance

After all the raw data is calculated as the mean value of each dimension, the mean is subtracted from each dimension and finally each dimension of the data is divided by the standard deviation of the dimension. The equation is:

$$\hat{x}_i = \frac{x_i - \mu}{\sigma^2} \quad \text{(Eq.8)}$$

Then, the output value is then converted using the formula $x_i = \hat{x}_t\sigma^2 + \mu$.

Results and discussion

The crawler software is used to obtain atmospheric pollutants such as PM2.5, PM10, CO, SO_2, O_3, NO_2, as well as the meteorological data such as temperature, humidity, wind speed, wind direction and pressure. There are 22,000 pieces of PM10 concentration data, of which 20,000 pieces of data are used as training data and the rest 2,000 pieces of data are used as test data at the monitoring point.

Traditional multivariate model

The preprocessed data is constructed into a multiple linear regression model, and correlation coefficient test, F test and t test are performed. The predicted result is then compared to the test data.

http://www.aloki.hu ● ISSN 1589 1623 (Print) ● ISSN 1785 0037 (Online)
DOI: http://dx.doi.org/10.15666/aeer/1706_1450514516

Traditional multiple linear regression prediction model

The dependent variable is PM10 and the independent variable is five types of meteorological data such as temperature and pressure. The modeling method is all input.

1) The correlation coefficient test results are shown in *Table 1* and R2 represents the fitting effect. The larger the value, the better the fitting effect.

Table 1. *Test of correlation coefficient*

Model	R	R2	R2 adjusted	Standard deviation rate error
1	0.438	0.509	0.507	26.73%

2) The result of the F test is shown in *Table 2*. As it can be seen from the table, the result of F test is < 0.01. Therefore, five meteorological indexes have a significant impact on the concentration of PM10.

Table 2. *Test of significance*

Model	Square	Df	Mean square	F	Significance
Regression	237971.932	5	475897.746	80.792	0.00
Residual	3424801.21	579	5883.049		
Statistics	5804671.02	596			

3) The result of the t test is shown in *Table 3*. The non-normalized coefficient is used to list the regression equation. The normalization coefficient is used to reflect the degree of influence of the independent variable on the dependent variable; the partial regression coefficient is used to determine whether the influence of an independent variable on the dependent variable is statistically significant. When it is < 0.05, it indicates significant statistical significance; when it is < 0.01, the statistical significance is extremely significant.

Table 3. *T-test*

Model	Unstandardized coefficients	Standardized coefficient	T	Significance
constant	398.212		5.461	0.00
Pressure/Pa	-3.796	-0.248	-5.377	0.00
Temperature/°C	-1.296	-0.0497	-0.981	0.032
Moisture/%	2.223	0.379	9.201	0.00
Wind speed/m/s	-55.059	-0.228	-7.068	0.00
Wind direction	-0.207	-0.179	-5.425	0.00

4) The linear regression equation of the prediction model is:

$$y = -3.796 \times 1 - 1.296 \times 2 + 2.223 \times 3 - 55.059 \times 4 - 0.207 \times 5 + 398.212.$$

The comparison between the true value and the predicted data is shown in *Figure 3*.

http://www.aloki.hu ● ISSN 1589 1623 (Print) ● ISSN 1785 0037 (Online)
DOI: http://dx.doi.org/10.15666/aeer/1706_1450514516

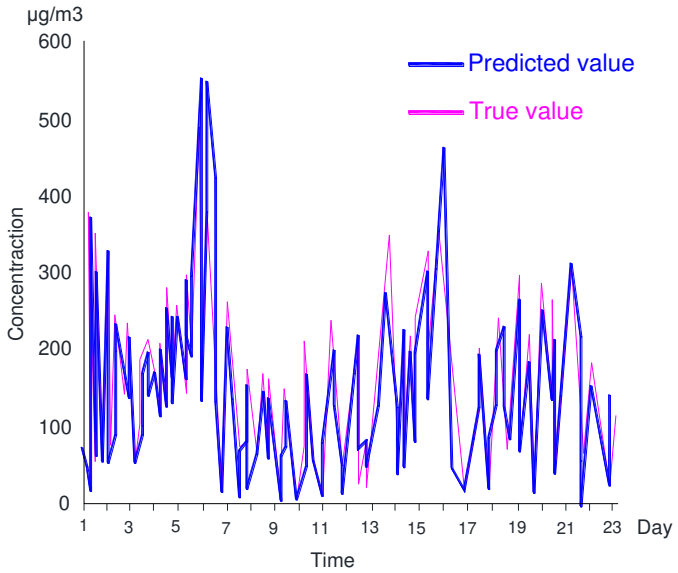

Figure 3. *Comparison of predicted value by traditional multiple linear regression model and true value*

Improved multiple linear regression prediction model

Considering the physical and chemical reactions between pollutants and the significant impact of seasonal factors on pollutants, other pollutants and seasonal factors are included in the multivariate equation for the optimization. The seasonal variables are: spring 108.1 μg/m^3, weight 0.25; summer 97.8 μg/m^3, weight 0.2; autumn 112.3 μg/m^3, weight 0.25; winter 121.9 μg/m^3, weight 0.3.

The significance test is performed by introducing independent variables one by one into the regression model until all significant independent variables are introduced into the regression model. The result of the stepwise regression model is shown in *Table 4*.

Table 4. *Model abstract*

Model	R	R2	R2 adjusted	Standard deviation rate error	Introduce variable
1	0.781	0.739	0.821	20.89%	Constant, PM2.5, season
2	0.813	0.769	0.825	20.75%	Constant, PM2.5, season, temperature, O_3
3	0.836	0.808	0.825	20.17%	Constant, PM2.5, season, wind speed, temperature, O_3
4	0.852	0.817	0.827	19.964%	Constant, PM2.5, season, wind speed, temperature, O_3, pressure
5	0.863	0.842	0.829	19.697%	Constant, PM2.5, season, wind speed, temperature, O_3, pressure, moisture
6	0.881	0.842	0.828	19.603%	

It can be seen from *Table 4* that PM2.5 has the most significant impact on PM10, while the impact of atmospheric pollutants SO_2, NO_2, CO and the meteorological factor, wind direction on PM10 can be negligible. Therefore, after eliminating these indexes, *Table 5* can be obtained.

http://www.aloki.hu ● ISSN 1589 1623 (Print) ● ISSN 1785 0037 (Online)
DOI: http://dx.doi.org/10.15666/aeer/1706_1450514516

Table 5. *Test of correlation coefficient*

Model	Unstandardized coefficients	Standardized coefficient	T	Significance
Constant	-90.087		-4.875	0.00
PM2.5/ppm	30.304	0.937	89.851	0.00
Temperature/°C	19.729	0.113	8.	0.032
O_3/ppm	-0.359	-0.10	-7.61	0.00
Wind speed/m/s	8.541	0.038	4.31	0.00
Pressure/Pa	0.897	0.059	5.081	0.00
Moisture	5.184	0.029	2.857	0.003
Season	10.280	0.269	20.351	0.005

The regression equation can be obtained:

$$y = 30.304 \times 1 + 19.729 \times 2 - 0.359 \times 3 + 8.541 \times 4 + 0.897 \times 5 + 5.184 \times 6 + 10.28 \times 7 - 90.087.$$

Using this model, the true value and the predicted value are shown in *Figure 4.*

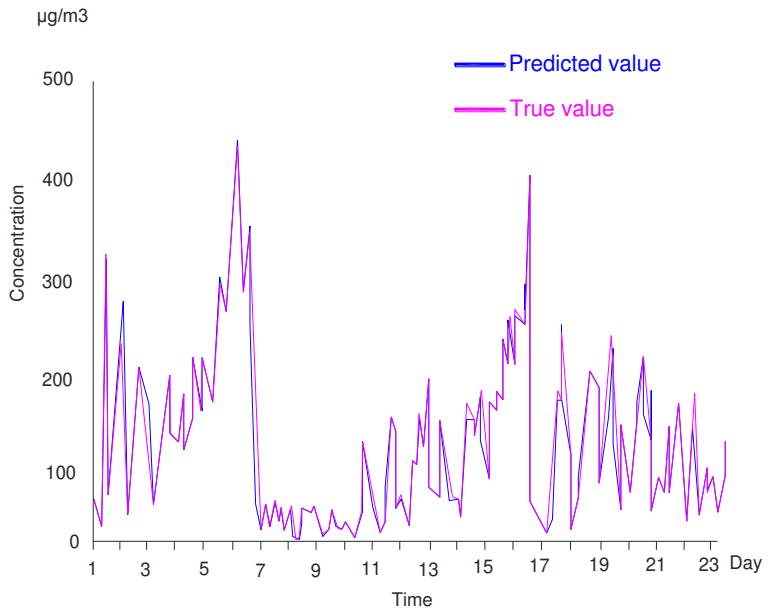

Figure 4. *Comparison of predicted value by optimal multiple linear regression model and true value*

It can be seen from *Figure 4* that the fitting degree of the optimized model reaches 0.828, which is significantly higher than that of the original model, indicating that the prediction for PM10 by the stepwise linear regression method is more precious after considering meteorological factors and other pollutants.

In addition, it can also be seen from *Figure 4* that the prediction error in the short term (4 days) is the smallest. At the same time, PM2.5, wind speed, air pressure, humidity and season have an enhancing effect on PM10 concentration. The impact of PM2.5 on PM10 is the greatest; while O_3 and temperature has a weakening effect on PM10.

http://www.aloki.hu ● ISSN 1589 1623 (Print) ● ISSN 1785 0037 (Online)
DOI: http://dx.doi.org/10.15666/aeer/1706_1450514516

Traditional BP neural network model

The neural network structure needs to be determined by the number of hidden layers, the number of nodes in the input layer, the number of nodes in the hidden layer, the number of nodes in the output layer, the activation function, training method and training parameters. In this paper, a three-layer neural network with a layer of hidden layer is used and it is set to be 11 and 1 according to the principle that the number of input and output nodes is as small as possible. The number of neurons in the hidden layer is determined by formula $M = \sqrt{n+m} + a$. In the formula, a is a constant between 0 and 10, and m and n are the number of neurons in the input layer and the output layer respectively. The number of hidden layers in this paper is 6. The input function in the hidden layer is $f(x) = \frac{1}{1+e^{-x}}$ and the linear activation function is used on the output layer. The learning rate is 0.01.

The fitting relationship between the predicted value and the true value of the BP neural network is shown in *Figure 5*.

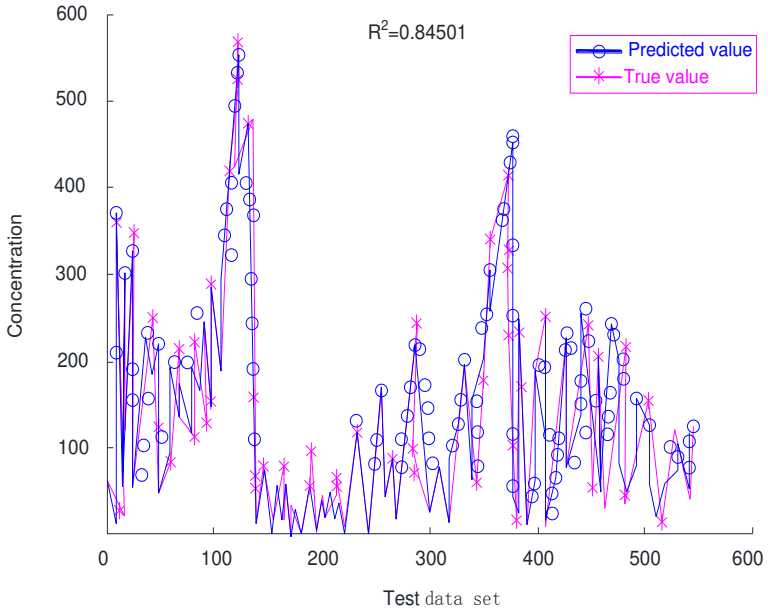

Figure 5. *Comparison of predicted value of BP neural network and true value μg/m³*

It can be seen from the *Figure 5* that the traditional BP neural network can better reflect the variation trend of atmospheric pollution in the future and can relatively accurately predict the concentration of atmospheric pollutants. Its goodness of fit is 0.84501.

Improved BP neural network prediction model

The traditional BP neural network uses the gradient descent method to train the neural network, which may lead to problems such as insufficient neural network search ability and slow training speed. This problem can be solved by genetic algorithm. By calculating the fitness value of each individual, it can conduct three genetic operations of selection, crossing and mutation to improve its global search ability and find the individual with the best fitness.

http://www.aloki.hu ● ISSN 1589 1623 (Print) ● ISSN 1785 0037 (Online)
DOI: http://dx.doi.org/10.15666/aeer/1706_1450514516

The number of input and output layers in the neural network are 11 and 1, respectively. It is found through the experiment that when the number of nodes in the hidden layer is 11, the prediction effect is the best. There are a total of 120 weights and 11 thresholds in the optimized neural network. The individual coding length is 131; the population size is 22; the evolution number is 57; the crossover probability is 0.22; and mutation probability is 0.1, as is shown in *Table 6*.

Table 6. *Learning and training of GA-BP*

Network structure	Population size	Evolution times	Initial crossover probability	Initial mutation probability
11-11-1	22	57	0.22	0.1

The fitting of the predicted value in the optimized BP neural network is shown in *Figure 6*. The goodness of fitness in the optimized BP neural network is 0.87925.

The comparison of the effect of these four types of neutral network prediction model is shown in *Table 7*.

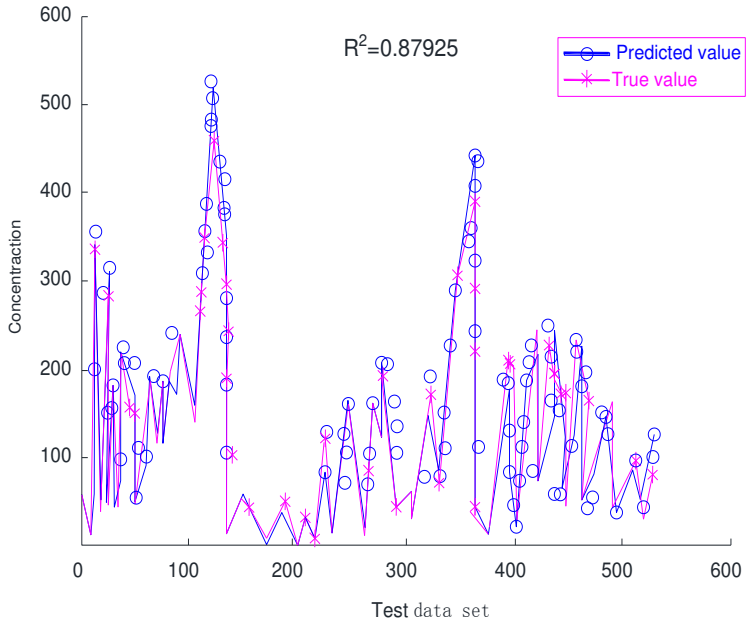

Figure 6. *Comparison of predicted value of optimized BP neural network model and true value* $\mu g/m^3$

Table 7. *Comparison of prediction results of four models*

	Traditional multiple regression model	Multiple regression model after optimization	Traditional BP neural network model	Optimized BP neural network model
Goodness of fit	0.509	0.819	0.862	0.882
PM10 mean square error	30.27	12.31	8.81	5.38
PM10 mean absolute error	0.163	0.085	0.069	0.047

http://www.aloki.hu ● ISSN 1589 1623 (Print) ● ISSN 1785 0037 (Online)
DOI: http://dx.doi.org/10.15666/aeer/1706_1450514516

Conclusions

With the increase of people's requirement for environmental quality, the prediction for the variation trend of environmental quality using the monitoring data becomes increasingly important. In this paper, the original multiple linear regression model, the original BP neural network and the optimized model are used to predict the atmospheric environmental quality. The following research conclusions are drawn:

(1) The traditional multiple linear regression model can only predict the variation trend of atmospheric environmental quality coarsely; while the other three models can predict the concentration of future atmospheric pollutants accurately.

(2) The stepwise linear regression can be used to predict PM_{10} more accurately after considering meteorological factors and other pollutants. The prediction error for the short term (4 days) is the smallest.

(3) The prediction for the mid-term and long-term atmospheric environmental quality is the best using the optimized BP neural network model.

(4) This paper applied the IoT environment and the improved neural network algorithm to the analysis of environmental monitoring data, which had improved the analysis accuracy and provided a theoretical basis for subsequent data management, atmospheric environment prediction and map management.

REFERENCES

[1] Abramovitch, A., Pizzagalli, D. A., Geller, D. A., Reuman, L., Wilhelm, S. (2015): Cigarette smoking in obsessive-compulsive disorder and unaffected parents of OCD patients. – European Psychiatry 30(1): 137-144.

[2] Arsie, I., Marra, D., Pianese, C., Sorrentino, M. (2010): Real-time estimation of engine nox emissions via recurrent neural networks. – IFAC Proceedings Volumes 43(7): 228-233.

[3] Beck, A. T., Ward, C. H., Mendelson, M., Mock, J., Erbaugh, J. (1961): An inventory for measuring depression. – Arch Gen Psychiatry 4(6): 561-571.

[4] Bey, K., Lennertz, L., Riesel, A., Klawohn, J., Kaufmann, C., Heinzel, S. (2017): Harm avoidance and childhood adversities in patients with obsessive-compulsive disorder and their unaffected first-degree relatives. – Acta Psychiatrica Scandinavica 135(4): 328-338.

[5] Chien, C. F., Chen, W. C., Lo, F. Y., Lin, Y. C. (2007): A case study to evaluate the productivity changes of the thermal power plants of the Taiwan Power Company. – IEEE Transactions on Energy Conversion 22(3): 680-88.

[6] Chien, T. W., Chu, H., Hsu, W. C., Tseng, T. K., Hsu, C. H., Chen, K. Y. (2003): A feasibility study on the predictive emission monitoring system applied to the Hsinta power plant of Taiwan Power Company. – Air Repair 53(8): 1022-28.

[7] Chien, T. W., Chu, H., Hsu, W. C., Tu, Y. Y., Tsai, H. S., Chen, K. Y. (2005): A performance study of PEMS applied to the Hsinta power station of Taipower. – Atmospheric Environment 39(2): 223-30.

[8] Chien, T. W., Hsueh, H. T., Chu, H., Hsu, W. C., Tu, Y. Y., Tsai, H. S. (2010): A feasibility study of a predictive emissions monitoring system applied to Taipower's Nanpu and Hsinta power plants. – Air Repair 60(8): 907-13.

[9] Cooper, D. A., Ekström, M. (2005): Applicability of the PEMS technique for simplified NOx monitoring on board ships. – Atmospheric Environment 39(1): 127-37.

[10] Jeffrey, B. H., Richard, J. D. (2000): Decreased responsiveness to reward in depression. – Cognition & Emotion 14(5): 711-24.

[11] Lauth, B., Arnkelsson, G. B., Magnússon, P., Skarphéðinsson, G. Á., Ferrari, P., Pétursson, H. (2010): Validity of k-sads-pl (schedule for affective disorders and

http://www.aloki.hu ● ISSN 1589 1623 (Print) ● ISSN 1785 0037 (Online)
DOI: http://dx.doi.org/10.15666/aeer/1706_1450514516

schizophrenia for school-age children - present and lifetime version) depression diagnoses in an adolescent clinical population. – Nordic Journal of Psychiatry 64(6): 409-409.

[12] Li, P. K., Pan, R., Chen, C. (2014): A novel neural network based modeling for control of NOx emission in power plant. – Applied Mechanics & Materials 643(643): 385-90.

[13] Lochner, C., Serebro, P., Van, D. M. L., Hemmings, S., Kinnear, C., Seedat, S. (2011): Comorbid obsessive-compulsive personality disorder in obsessive-compulsive disorder (OCD): a marker of severity. – Progress in Neuropsychopharmacology & Biological Psychiatry 35(4): 1087-92.

[14] Marino, C., Nucara, A., Nucera, G., Pietrafesa, M. (2017): Economic, energetic and environmental analysis of the waste management system of Reggio Calabria. – International Journal of Heat and Technology 35(S1): S108-S116.

[15] Reifman, J., Feldman, E. E., Wei, T. Y., Glickert, R. W. (2000): An intelligent emissions controller for fuel lean gas reburn in coal-fired power plants. – Air Repair 50(2): 240-51.

[16] Rodgers, S., Ajdacic-Gross, V., Kawohl, W., Müller, M., Rössler, W., Hengartner, M. P. (2015): Comparing two basic subtypes in OCD across three large community samples: a pure compulsive versus a mixed obsessive-compulsive subtype. – European Archives of Psychiatry & Clinical Neuroscience 265(8): 719-34.

[17] Song, S. L. (2018): Application of gray prediction and linear programming model in economic management. – Mathematical Modelling of Engineering Problems 5(1): 46-50.

[18] Zhang, J., Li, Y. B., Liu, B. X., Wu, Y. Q., Yi, H. C. (2018a): Forward modelling of circular loop source and calculation of whole area apparent resistivity based on TEM. – Traitement du Signal 35(2): 183-198.

[19] Zhang, J. X., Sun, W. G., Niu, F. S., Wang, L., Zhao, Y. W., Han, M. M. (2018b): Atmospheric sulfuric acid leaching thermodynamics from metallurgical zinc-bearing dust sludge. – International Journal of Heat and Technology 36(1): 229-236.

[20] Zhao, W., Li, Y. J., Ren, J. Y., Chen, S. G., Li, Y. Q. (2018): A novel operation state prediction method for servers in smart grids. – European Journal of Electrical Engineering 20(3): 379-392.

http://www.aloki.hu ● ISSN 1589 1623 (Print) ● ISSN 1785 0037 (Online)
DOI: http://dx.doi.org/10.15666/aeer/1706_1450514516

INVERSION OF TOTAL SUSPENDED SEDIMENT IN TAIHU LAKE BASED ON MEASURED SPECTRAL DATA

XU, J. J.

Taizhou College, Nanjing Normal University, Taizhou 225300, China
(e-mail: x_j_j1981@126.com; phone: +86-181-3665-8696)

(Received 7th Jun 2019; accepted 10th Oct 2019)

Abstract. The concentration of suspended sediments is an important indicator of the water quality of inland water bodies. Several single sensitive bands were employed to locate the bands in the mixed spectrum on water surface (WS-MS) that are sensitive to the TSS. However, this approach was proved wrong, for a high concentration of suspended sediment was derived from the WS-MS measured in the same water area under strong sunlight (i.e. high surface reflectivity). As a result, the single sensitive bands were replaced with the reflectivity ratio between the two bands most correlated with the TSS (the reflectivity ratio), such as to eliminate the impact of sunlight intensity. Correlation analysis shows that (R639 + R544)/(R639/R544) had closer correlation with the TSS than any other band combination. Based on the measured reflectivity ratio and concentration of suspended sediments, the TSS in the target water body was inverted separately by the least squares method and fuzzy regression. The results show that the inversion by fuzzy regression was not affected by measurement uncertainties or error, indicating that the fuzzy regression inverse model is more applicable than the least squares inverse model.
Keywords: *sediment remobilization, reflectivity ratio, mixed spectrum on water surface (WS-MS), least squares method, fuzzy regression*

Introduction

Background and significance

The SS concentration is a critical indicator for water environment evaluation. The SS (Suspended Sediment) refers to all particulate matters suspended in water, including organic detritus resulting from dead phytoplankton and inorganic suspension particles produced by resuspending terrestrial or lake sediments (Cai, 1998). In inland water, it is a more common phenomenon that there are the SSs, mainly seen in estuaries, coastal waters and shallow lakes with a high or low concentration affecting the sunlight transmission, the growth of underwater crops and the use of light by phytoplankton, and worse, the SSs may also change the aquatic ecological environment and restrict the primary productivity of the whole waters (Yang et al., 2002).

Foreign scholars have studied this area long ago. Traditional water quality monitoring in Lake Erie has been conducted using in situ and laboratory observations. The USEPA Great Lakes National Program Office (GLNPO) has conducted spring and July water quality sampling on Lake Erie since the early 1980s (Barbiero et al., 2018) and the NOAA Great Lakes Environmental Research Laboratory (GLERL) has been conducting weekly monitoring for over five years. Liu et al. (2019) also found in the study of hyperspectral remote sensing inversion that spectral reflectance ratio is more suitable for hyperspectral remote sensing inversion than single-band spectrum. The study of Binding et al. (2003) has shown that the optical parameters (backscatter coefficient and absorbance) in the water body are the most principal factors affecting the water reflectivity, affording a theory reference for quantitatively exploring suspended sediments. Suspended particles play an important role in coastal waters by controlling to a large extent the variability of the water inherent optical properties

http://www.aloki.hu ● ISSN 1589 1623 (Print) ● ISSN 1785 0037 (Online)
DOI: http://dx.doi.org/10.15666/aeer/1706_1451714528

(IOPs). In this study, focused on the complex waters of the Southern North Sea, the relationships between the concentration, composition and size of suspended particles and their optical properties (light absorption, and attenuation in the visible and near-infrared spectral regions) are investigated.

Some scholars in China have also attempted to explore the remote sensing inversion on suspended sediments since the 1980s. Shi et al. (2015) found that the spectral reflectance and total suspended solids had a strong correlation at 645 nm wavelength from the measured data of water body. Based on this, an empirical inversion model of total suspended solids with strong adaptability was developed and good results were achieved. Zhang et al. (2016) developed an analytical method to retrieve the total suspended solids by remote sensing in view of the complex situation of the turbidity and optical factors of Xinanjiang Reservoir, and achieved good results. Li et al. (2002) created the suspended sediment inversion model for the Yangtze River estuary at band ratio (R555 + R670)/(R555/R670). These studies have shown that the inversion of suspended sediment concentration using the remote sensing method is feasible. Cao et al. (2016) studied Nansi Lake and found that there was a relationship between the measured spectra and suspended matter concentration.

Owing to uneven distribution of TSSs in vertical space, it is difficult to measure TSS concentration with conventional water sample unable to timely reflect current water quality due to a manually realtime field inspection at a long cycle. In this study, given spectrum data as measured and the concentration at local sampling point, a TSS concentration inversion model can be built to monitor how the TSS changes in time and space in a timely manner.

Materials and methods

Survey of study area

Situated in the southern margin of the Yangtze River Delta, 30°55’40”~31°32’58” latitude North and 19°52’32”~120°36’10” East longitude, Taihu Lake is one of the five largest freshwater lakes in China. With the lakeshore line of 393.2 km in total length, the average water depth of 1.9 m and the maximum water depth of 2.6 m, Taihu Lake has an average annual runoff of 7.5 billion m^3, water storage capacity of 4.4 billion m^3, and annual average water temperature of 17.1 °C, that is, 4 °C in January, 25 °C in July. The Taihu Lake covers a lake area of 2427.8 km^2, the water area of 2338.1 km^2. There are hilly mountains in the west and southwest sides, and plains and water net in the east.

As a shallow-water inland lake, Taihu Lake has suspended sediments mostly dominated by inorganic sediments and organic carbonized particles. Inorganic sediments derive from branch river system, and organic carbonized particles mainly come from some eutrophic remains of dead algae. Analyzing the curves of surface sediment fining and volume concentration as a function of time, we find that the suspended sediment particles are dominated by silt and clay.

Taihu Lake is open with strong wind, but moderate in the average depth. Therefore, the lakebed sediments are easily agitated, resulting in a higher concentration of suspended sediments in the water body. Over many years’ water sample monitoring at the hydrological station, the concentration of suspended sediments in Taihu Lake varies in different times and spaces. In horizontal space, it is higher in the estuary area and the wind-agitating lake center, and low in the closed arm of lake (such as Meiliang Bay),

http://www.aloki.hu ● ISSN 1589 1623 (Print) ● ISSN 1785 0037 (Online)
DOI: http://dx.doi.org/10.15666/aeer/1706_1451714528

but the minimum is in Dongtai Lake, mainly because there are lush hydrophytes, and less agitated suspended sediments.

Data sample

Data

The measured concentration used hereof is available from the lab, where the water sample is filtered and weighed after collecting at a sampling point preset (as shown in the figure), see *Table 1* for specific data.

Here, water sample is available by the hierarchical collection method, namely, water is divided into three layers in depth: 0.2D, 0.5D, D (D is the water depth at the time of measurement), each takes 1/3 of the water yield. Water samples collected from three layers are mixed.

In the lab, water sample is filtered and weighed by the following way: put 0.45 μm filter membrane into an oven at 40 °C, let it dry for 24 h at a constant temperature, and then remove the dried filter membrane from the oven and place it in a drying bottle to be stable, weigh it with a one ten-thousandth balance, then, number the filter membrane, and filter the water sample. The sediment available by filtration is placed in an oven at 40 °C and weighed with the above balance.

Sample SS concentration analyzed in the lab

The concentrations measured for SS samples available on November 13, 2017 (*Fig. 1*) and July 27, 2018 (*Fig. 2*) are shown in *Tables 1* and *2*.

Table 1. *Concentration of SS samples (13/11/2017)*

Sample number	SS (mg/L)	Sample number	SS (mg/L)	Sample number	SS (mg/L)
1	31.40	9	23.35	17	30.56
2	49.90	10	10.32	18	24.55
3	39.33	11	54.08	19	36.72
4	29.19	12	63.26	20	35.76
5	28.34	13	33.61	21	29.43
6	53.71	14	30.59	22	76.17
7	69.21	15	48.74		
8	60.92	16	39.94		

Table 2. *Concentration of SS samples (27/07/2018)*

Sample number	SS (mg/L)	Sample number	SS (mg/L)
1	54.15	9	66.05
2	76.25	10	91.55
3	81.35	11	72
4	75.4	12	77.1
5	81.35	13	72.85
6	31.2	14	94.1
7	97.5		
8	89		

http://www.aloki.hu ● ISSN 1589 1623 (Print) ● ISSN 1785 0037 (Online)
DOI: http://dx.doi.org/10.15666/aeer/1706_1451714528

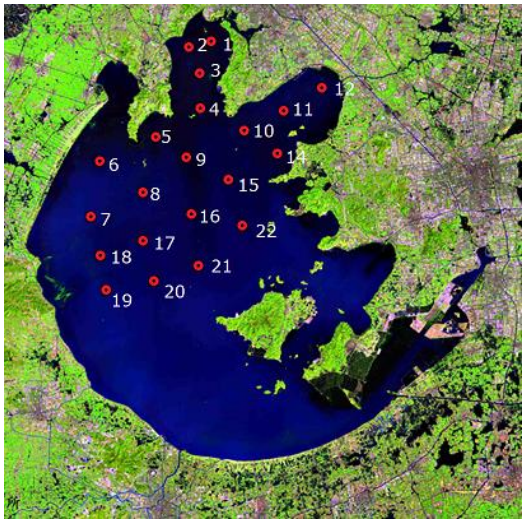

Figure 1. *Distribution of samples (23/11/2017)*

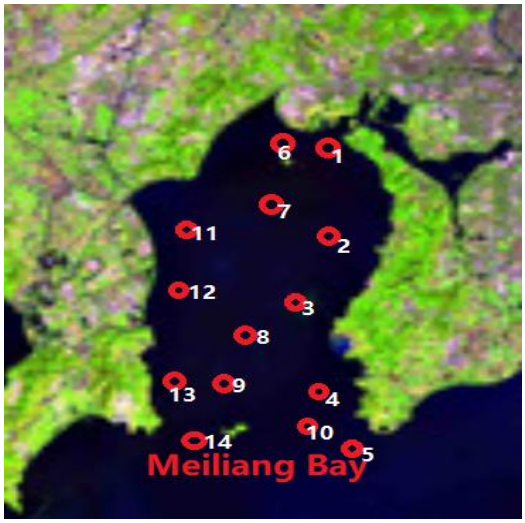

Figure 2. *Distribution of samples (27/07/2018)*

As seen from data measured in the lab, the concentration of suspended sediments in autumn is low, for example, the maximum in *Table 1* is 76.17 mg/L, the minimum is 9.44 mg/L; the concentration of suspended sediments in July is high, for example, the maximum in *Table 2* is 94.1 mg/L, and the minimum is 66.05 mg/L. However, due to the concentrated sampling points, there is a small gap between the maximum and the minimum.

Hybrid spectrum signature measured on water surface

On November 13, 2017, the hybrid spectrum on water surface was measured by a handheld ASD spectrometer of the United States at 22 points of the Meiliang Bay in North Taihu Lake (after removing the anomaly points, 16 points can be available), and treated by the ASD ViewSpec. During hyperspectral measurement, impacted by other external factors, the available SS spectrum has many tiny peaks, which makes it

http://www.aloki.hu ● ISSN 1589 1623 (Print) ● ISSN 1785 0037 (Online)
DOI: http://dx.doi.org/10.15666/aeer/1706_1451714528

difficult to extract and analyze the spectral signature of suspended sediment. For this purpose, the characteristic wavelength corresponding to each reflection peak is analyzed. It is preferred to smooth spectral data (moving average, namely, five bands are chosen every time, and averaged as the center band value). Smoothing not only effectively eliminates the noise, but also retains useful information. The resulting spectrum curve is shown below.

In this area, 22 samples (14 out of them are available) are measured for remote sensing reflectance spectra using the same device on July 27, 2018, and the curve are shown in *Figure 4.*

As shown in *Figures 3* and *4,* two spectral curves available in November and in July differ a lot since chlorophyll spectrum features the reflectance peaks at around 550 nm, around 620 nm, around 700, and 820 nm. Most strikingly, there is a reflectance peak appeared at around 700 nm. Whether it appears or not is generally considered as the basis for determining whether there are lots of algae chlorophylls. These spectral signatures get blur when the algae concentration is low. Otherwise, water surface reflectivity sharply increases due to the strong reflectance of algae cells in the near-infrared band if the algae bloom, as shown in *Figure 4.* In *Figure 3,* there is no similar signature (8# sample is removed as anomaly point because there is phytoplankton on the lake). The too high concentration of chlorophyll has a effect on the overall spectral reflectance, so that the monodrome inversion will have a error.

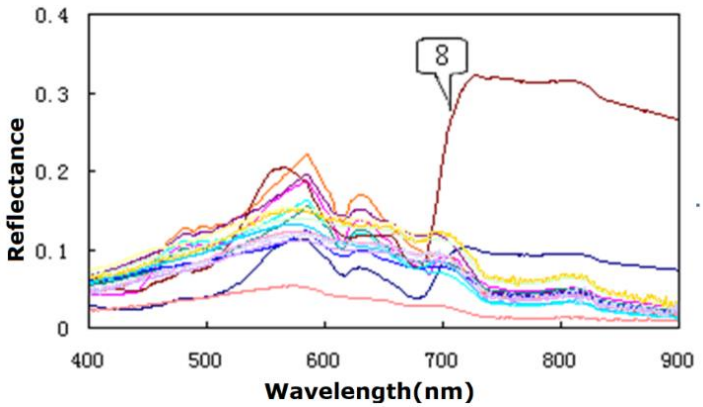

Figure 3. *Curve of sample water surface reflectance spectrum in North Taihu lake (13-11-2017)*

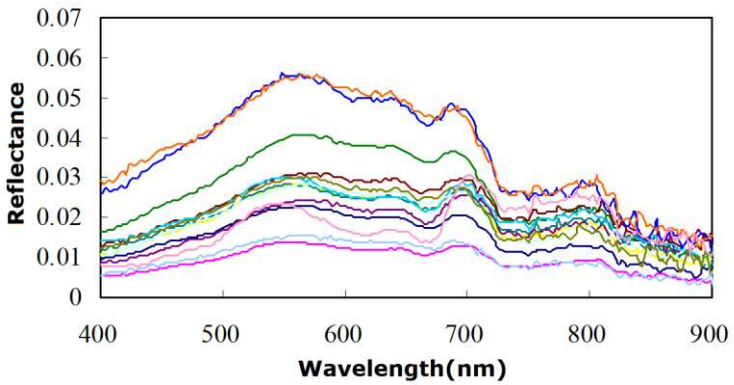

Figure 4. *Curve of sample water surface reflectance spectrum in Meiliang Bay (29-07-2018)*

http://www.aloki.hu ● ISSN 1589 1623 (Print) ● ISSN 1785 0037 (Online)
DOI: http://dx.doi.org/10.15666/aeer/1706_1451714528

SS-sensitive band analysis and inversion model construction

Establishment of linear regression model

To extract the characteristic wavelength of the suspended sediment, the spectral curve, if used directly, will make it impossible to identify it. Introductory spectrum theory is used here. Based on the derivative spectrum theory, the second derivative of suspended sediment spectrum is preferentially obtained. Here, the wavelength in the visible light range is chosen for the following reasons: the "red shift phenomenon" will occur in the infrared band when the suspended sediment concentration is higher. As shown in *Figure 5,* the reflection peaks appear at 447 nm, 500 nm, 544 nm, 585 nm, 593 nm, 623 nm, 639 nm, and 695 nm. The existing theory holds that the characteristic spectrum of suspended sediment is at 510-600 nm, 630-700 nm, and derivative analysis concludes the characteristic wavelength that roughly coincides with the existing conclusion (Doxaran et al., 2002; Xue et al., 2012).

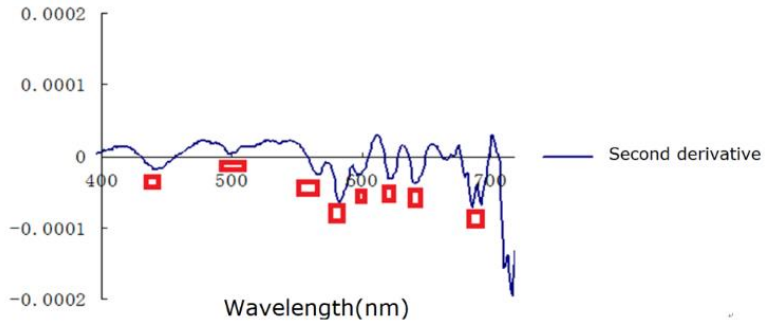

Figure 5. *Second derivative and characteristic peak of suspended sediment spectrum*

Since the second derivative of suspended sediment spectrum is very sensitive, some fine impure peaks are also erroneously assumed as characteristic peaks of the suspended sediment concentration. As a result, the correlation between the flux concentration and the measured spectral reflectivity is analyzed to further determine the characteristic peaks of suspended sediment spectrum. As shown in *Figures 6* and *7,* the characteristic peaks at 447 nm, 544 nm, 593 nm, 623 nm, 639 nm and 695 nm still exist, but are not highly correlated with the concentration of suspended sediments. In particular, it is almost irrelevant in the curve of the spectrum as a function of the concentration of sample (27-07-2017), mainly because the solar rays are too strong.

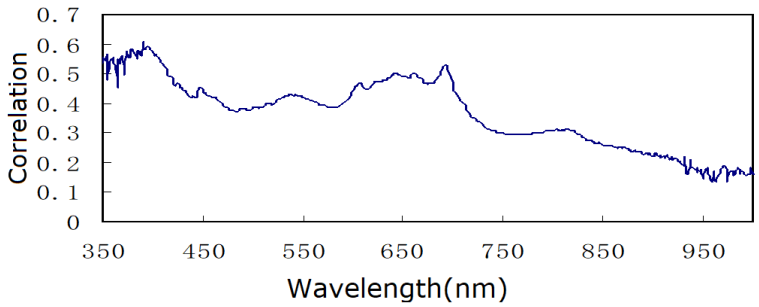

Figure 6. *Correlation between spectrum reflectivity and suspended sediment concentration of sample (13-11-2017)*

http://www.aloki.hu ● ISSN 1589 1623 (Print) ● ISSN 1785 0037 (Online)
DOI: http://dx.doi.org/10.15666/aeer/1706_1451714528

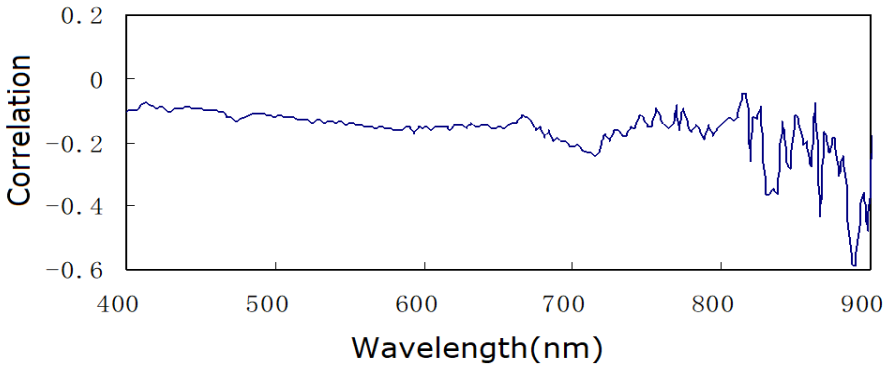

Figure 7. *Correlation between remote sensing reflectivity and suspended sediment concentration of sample (13-11-2017)*

To eliminate the interferences of solar ray intensity, ambient environment, water surface smoothness and other background factors, the characteristic spectrum ratio can be used (Pulliainen, 2011). The Chen et al. (1991) found that the natural logarithm of suspended sediment concentration is well correlated with water surface spectrum reflectivity, as shown in *Figures 8* and *9*.

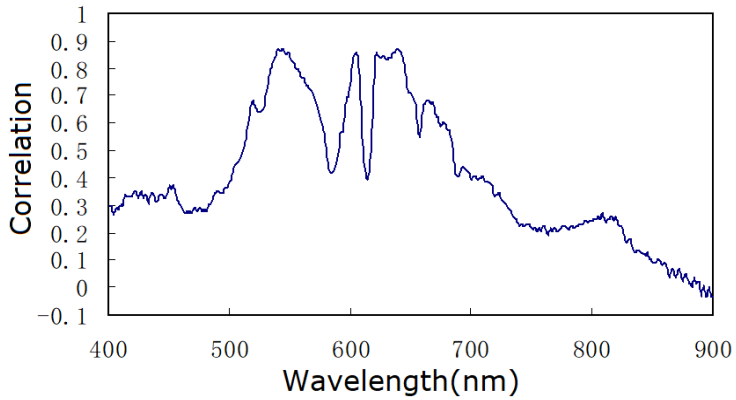

Figure 8. *Correlation of the concentration (13-11-2017) logarithm with reflectivity ratio*

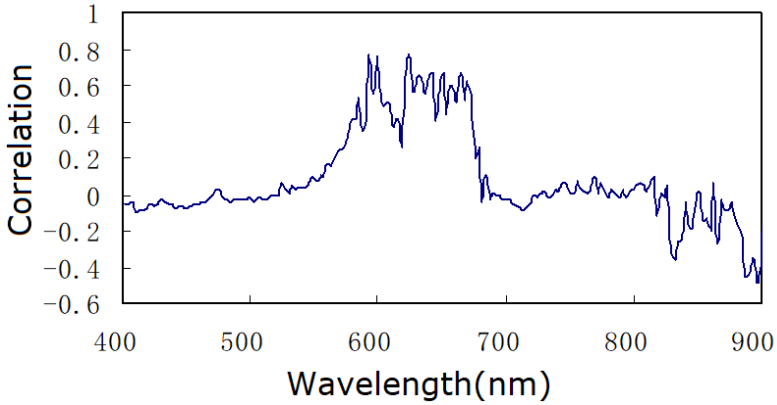

Figure 9. *Correlation of the concentration (27-07-2018) logarithm with reflectivity ratio*

http://www.aloki.hu ● ISSN 1589 1623 (Print) ● ISSN 1785 0037 (Online)
DOI: http://dx.doi.org/10.15666/aeer/1706_1451714528

As shown in *Figure 8,* there is a high correlation between 530 nm and 680 nm, and the first two values at which the correlation is higher are chosen to obtain the ratio. It is found that the maximum value in *Figure 8* appears at R639 and R544 (consistent with the previous single-band characteristic peaks), i.e. R639/R544; in *Figures 2–9,* there is a high correlation between 580 nm and 680 nm, and the first two values at which the correlation is higher are chosen to obtain the ratio. The maximum values appear at R623 and R593 nm (consistent with the previous single-band characteristic peaks), i.e. R623/R593; the hybrid spectra measured on the surface of water bodies on 13-11-2017 and 27-07-2018 are respectively correspond to the lnSS (natural logarithm of the SS) to plot a scatter diagram and find the appropriate linear regression equation, as shown in *Figure 10.*

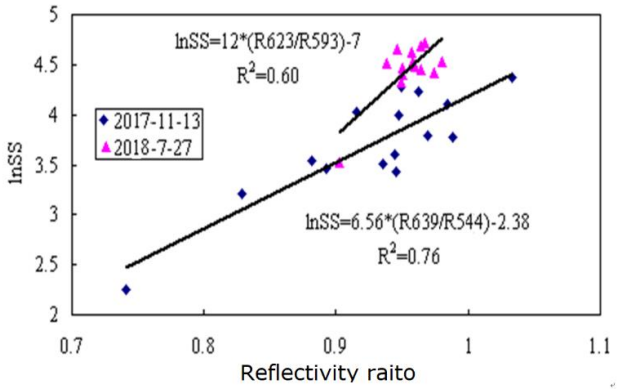

Figure 10. *Relationship between reflectivity ratio and InSS*

With the regression equation (see *Fig. 1*) fitted by the reflectivity ratio and lnSS, the RMSEs (Root Mean Square Error) between the inverted SS concentration and the concentration of the sample in the lab are 10.79 mg/L (13-11-2017) and 14.99 mg/L (27-07-2018).

As seen from the RMSEs, the sample in November is significantly better than that in July. The main reason is that the solar intensity in July has an effect on the overall reflectance of the measured spectrum on the water surface. Next, in July, the phytoplanktons bloom in Taihu Lake due to the eutrophication of water bodies, blocking the projection of the SS spectrum onto the spectrometer. Therefore, the significance of the model in November ($R^2 = 0.76$) is better than that in July ($R^2 = 0.60$).

Although the regression model in *Figure 10* can be applied, there are still some errors due to the uncertainty of spectrometer and the laboratory SS quality error measured by Hu et al. (2004) and so on. However, this kind of error always changes around the model, so that the fuzzy regression method is used to establish the model hereof since it can eliminate the error caused by measurement and weighing. In fuzzy regression, spectral measurement and SS weighing errors are the inherent ambiguity of the system. The SS concentration inverted by the ratio of the measured spectra is not a value, but an interval (with the upper and lower bounds), i.e. it can take any value in this interval. Therefore, the fuzzy regression model focuses on the possibility rather than a specific value.

http://www.aloki.hu ● ISSN 1589 1623 (Print) ● ISSN 1785 0037 (Online)
DOI: http://dx.doi.org/10.15666/aeer/1706_1451714528

Establishment of fuzzy regression model

The fuzzy regression model was first proposed by Tanaka and Watada (1998) in 1982, and the specific model is as follows:

$$\tilde{Y}_i = \tilde{A}_0 x_{i0} + \tilde{A}_1 x_{i1}, (i = 1, 2, 3, \ldots n) \quad \text{(Eq.1)}$$

Let $x_i = (x_{i0}, x_{i1}) = (1, x_{i1})$, the fuzzy coefficients $\tilde{A}_0$, $\tilde{A}_1$ are usually the symmetric triangular fuzzy numbers, i.e. $\tilde{A}_j = (m_j, w_j), j = 0,1$.

Its membership function is:

$$\mu_{\tilde{A}_j}(n_j) = \begin{cases} 1 - \frac{|m_j - n_j|}{w_j} & , m_j - w_j \leq n_j \leq m_j + w_j \\ 0 & , other \end{cases} \quad \text{(Eq.2)}$$

where m_j is the center value $\tilde{A}_j$; w_j is the span value. Then the membership function of $\tilde{Y}_i$ can be obtained using the extension principle, expressed as:

$$\mu_{\tilde{Y}_i}(y_i) = \begin{cases} 1 - \frac{|y_i - x_i m|}{w^T |x_i|}, x_i \neq 0 \\ 1 \quad x_i \neq 0, y_i \neq 0, \forall i = 1, 2, \ldots . M \\ 0 \quad , x_i = 0, y_i = 0 \end{cases} \quad \text{(Eq.3)}$$

The last is to convert the fuzzy regression model into the following optimal model.

$$\begin{cases} \min \sum_{j=0}^{1} \left[w_j \sum_{i=1}^{M} |x_{ij}| \right] \\ 1 - \frac{|y_i - x_i m|}{w^T |x_i|} \geq h, \end{cases} \quad \text{(Eq.4)}$$

where $0 \leq \square \leq 1, w \geq 0, w^T = (w_0, w_1), m^T = (m_0, m_1)$.

Results

The fuzzy level *h* is arbitrarily set based on the number of samples, and the size of preset *h* determines the model fitting degree. In general, when there are sufficient samples, *h* should be set to as small as possible; the lower the fuzzy level, the smaller the span; when the number of samples is not enough, *h* should be set to be as large as possible. In this case, the fitting degree builds up regardless of the rising fuzzy level. There are lesser samples collected in this project, so that the fuzzy level *h* is set to 0.1. With the natural logarithm of the SS concentration of laboratory measurement sample as the dependent variable, and R639 and R544 spectrum values as the independent variables, the fuzzy regression equation of the suspended sediment is available as below:

http://www.aloki.hu ● ISSN 1589 1623 (Print) ● ISSN 1785 0037 (Online)
DOI: http://dx.doi.org/10.15666/aeer/1706_1451714528

$$\ln \tilde{S} = (1.1678, 0.9269) + (18.587, 0) * (R639 + R544) / （R639 / R544） \quad \text{(Eq.5)}$$

Discussion

The built model should be tested for its fitness. In this study, the least square method is compared with the established fuzzy regression model. For the least square method as the statistical regression model, it is required to try to minimize the sum of the squares of the error between the inversion concentration and the observation value. A good fuzzy regression model should try to minimize the sum of absolute value of difference between the inversion concentration fuzz scope (the upper and lower bounds of the interval) and the observation value. The inversion results between the two are shown in *Table 3*.

Table 3. *Least squares and fuzzy regression inversion of SS concentration*

Sample number	Measurement of suspended solids concentration (mg/L)	Prediction results of least squares method (mg/L)	Prediction results of fuzzy regression (lower bounds) (mg/L)	Prediction results of fuzzy regression (central value) (mg/L)	Prediction results of fuzzy regression (upper bounds) (mg/L)	Absolute error of least square prediction (mg/L)	Absolute error of forecasting lower boundary value of fuzzy regression (mg/L)	Absolute error of fuzzy regression center value prediction (mg/L)
1	28	44	26	50	108	-16	2	-34
2	29	47	27	54	117	-18	2	-38
3	169	84	54	114	256	85	115	82
4	169	128	90	198	447	41	79	-43
5	98	86	55	118	264	12	43	-31
6	169	212	168	381	869	-43	1	-318
7	218	146	106	234	532	72	112	-25
8	104	142	102	227	515	-38	2	-185
9	22	24	14	24	46	-2	8	-2
10	18	33	18	34	70	-15	0	-23
12	134	129	91	201	455	5	43	-100
13	106	128	89	198	446	-22	17	-137
14	113	124	86	191	431	-11	27	-117
15	25	24	14	23	44	1	11	3
16	18	20	12	18	34	-2	6	0
17	78	36	20	38	78	42	58	61
18	24	17	10	15	27	7	14	13

As shown in *Table 3:* (1) Intuitively, it seems that the inversion of the least square regression model is better. In fact, that is not the case. The fuzzy regression reflects a concentration range, such as 1# sample, absolute error predicted by the least squares is -16. Although the absolute error of center value in the fuzzy regression model is high, the absolute error between the measured value and the lower bound is only 2; for 6# sample, for example, the absolute error of the center value in the fuzzy regression model reaches -318, but the deviation from lower bound error is only 1. (2) Overall, the inversion effects of the least squares and the fuzzy regression are better. Fuzzy regression reflects a range of an interval, so is more flexible and greater in the information content. (3) There is a bit error in the high SS concentration area since original data for the model is mainly concentrated in the low concentration area, so that the high concentration has a poor fitness to the model that needs to be optimized later.

http://www.aloki.hu ● ISSN 1589 1623 (Print) ● ISSN 1785 0037 (Online)
DOI: http://dx.doi.org/10.15666/aeer/1706_1451714528

Conclusion

Based on the measured spectra measured on the water surface and the SS concentration of the sample at different times, here draw the following conclusions:

(1) The model is built with spectrum data measured on the water surface and the SS concentration, the inversion effect is poor since single reflectivity value is greatly affected by the background factors. This paper uses the reflectivity ratio and the optimal bands R639/R544, R623/R593 and the SS concentration to build the inversion model for samples, for example, in July and November, respectively.

(2) Due to the uncertainty of spectrameter and the error of laboratory weighing on suspended sediment, the linear regression inversion model established has a poor significance. As a result, this paper attempts the fuzzy regression inversion model for suspended sediment concentration and compares it with the least squares method. It is found that the fuzzy regression model established herein gives not only the inversion concentration but also the interval in which the inverted concentration changes. The model features strong significance and fitness.

Outlook

The measured spectrum has great application potential in the monitoring of water quality in inland lakes. Because some theories and methods are still immature, its application is limited in water quality monitoring. In the study of the inversion model of total suspended solids in Taihu Lake, there are still some problems that need to be further solved.

(1) The particle size, mineral composition, surface roughness and color of the suspended solids cause significant differences in the spectral characteristics of the suspended solids. Therefore, in the estimation of suspended solids, the influence of different types of suspended solids should also be considered. Secondly, although the spectral characteristics of individual water quality parameters such as chlorophyll, suspended matter, and yellow matter are currently well understood by experimental means, the interaction between them is not well understood, so it is necessary to strengthen the analysis of the effects of chlorophyll and yellow matter on the concentration estimation of suspended solids in the future. It is only possible to establish a more accurate and effective model after separating the water quality parameters and clarifying the interaction between them.

(2) Since the sample data is still relatively small, the stability and representativeness of the model need further verification. In future works, the number of samples can be increased and the representativeness of the samples improved.

Acknowledgements. Research on network scheduling optimization model and method for monitoring camera in complex geographic scene (No. 18KJB170007).

REFERENCES

[1] Astoreca, R., Doxaran, D., Ruddick, K., Rousseau, V., Lancelot, C. (2012): Influence of suspended particle concentration, composition and size on the variability of inherent optical properties of the Southern North Sea. – Continental Shelf Research 1(7): 117-128.

http://www.aloki.hu ● ISSN 1589 1623 (Print) ● ISSN 1785 0037 (Online)
DOI: http://dx.doi.org/10.15666/aeer/1706_1451714528

[2] Barbiero, R. P., Lesht, B. M., Hinchey, E. K. (2018): A brief history of the US EPA Great Lakes National Program Office's water quality survey. – Journal of Great Lakes Research 44(4): 539-546.
[3] Binding, C. E., Bowers, D. G., Mitchelson-Jacob, E. G. (2003): An algorithm for the retrieval of suspended sediment concentrations in the Irish Sea from SeaWiFS ocean color satellite imagery. – International Journal Remote Sensing 24(19): 3791-3860.
[4] Cao, Y., Yan, Y. T. (2016): Analysis of the relationship between hyperspectral measurements and suspended solids concentration and turbidity in Nansi Lake. – Water Resources and Power 36(1): 40-41.
[5] Doxaran, D., Froidefond, J. M., Lavender, S. (2002): Spectral signature of highly turbid waters: Application with SPOT data to quantify suspended particulate matter concentrations. – Remote Sensing of Environment 81: 149-161.
[6] Gordon, H. R., Wang, M. (1994): Retrieval of water leaving radiance and aerosol optical thicken Concentration of suspended solids over the oceans with SeaWiFS: a preliminary algorithm. – Applied Optics 33(3): 443-452.
[7] Hu, S. W., Xu, H., Yu, Z. Z. (2004): On the fuzzy uncertainty of remote sensing data. – Mine Survey 4: 19-21.
[8] Li, S. H., Tang, J. W., Yun, C. X. (2002): Study on SeaWiFS remote sensing quantitative model of suspended sediment concentration in estuary. – Journal of Oceanography 24(2): 51-58.
[9] Liu, E. H., Zhou, G. S., Zhou, L. (2019): Fraction of absorbed photosynthetically active radiation over summer maize canopy estimated by hyperspectral remote sensing under different drought conditions. – Chinese Journal of Applied Ecology 6: 2021-2029.
[10] Pulliainen, J., Kallio, K., Eloheimo, K. (2011): A semi-operative approach to lake water quality retrieval Fuzzy regression remote sensing data. – The Science of the Total Environment 268: 79-93.
[11] Shi, K., Zhang, Y., Zhu, G. (2015): Long-term remote monitoring of total suspended matter concentration in Lake Taihu using 250 m MODIS-Aquadata. – Remote Sensing of Environment 164: 43-56.
[12] Tanaka, H., Watada, J. (1998): Possibilistic linear systems and their application to the linear regression model. – Fuzzy Sets and Systems 27(3): 275-289.
[13] Xue, Z. J., Jiang, C., Xu, L. G. (2012): The flocculation of fine-grained suspended sediment and its impact on spectral characteristics based on in situ measurement in the Changjiang Estuary, China. – Canadian Journal of Remote Sensing 49: 404-412.
[14] Yang, D. T., Chen, W. M., Zhang, Y. L. (2002): Distribution characteristics of suspended matter and spectra in Meiliang Bay of Taihu Lake. – Ecology Science 21(4): 289-293.
[15] Zhang, Y. B., Zhang, Y. L., Shi, K. (2016): A Landsat 8 OLI-Based, semi-analytical model for estimating the total suspended matter concentration in the slightly turbid Xin'anjiang reservoir (China). – IEEE 9(1): 398-413.

http://www.aloki.hu ● ISSN 1589 1623 (Print) ● ISSN 1785 0037 (Online)
DOI: http://dx.doi.org/10.15666/aeer/1706_1451714528

SEDIMENTARY SEQUENCE ANALYSIS ON THE NORTHERN MARGIN OF THE ORDOS BASIN BASED ON MARKOV PROCESS

WANG, J.[1,3] – LU, L. J.[1*] – DING, R.[2]

[1]*Digital Geoscience of Institution, Jilin University, Jilin University, Changchun 130000, China*

[2]*Institute of Special Education, Changchun University, Changchun 130000, China*

[3]*School of Electronic Information Engineering, Changchun University, Changchun, 130000, China*

**Corresponding author*
e-mail: lulj@jlu.edu.cn

(Received 7th Jun 2019; accepted 10th Oct 2019)

Abstract. Uranium is of great importance to China's nuclear energy and national defense. As a clean energy, the nuclear energy helps to adjust and optimize the energy structure, improve the eco-environment, and reduce the CO_2 and S emissions, paving the way to sustainable development and ecological civilization. The sandstone-type uranium deposit, one of the four types of uranium deposits for industrial use, is an important supplier in China. This type of uranium deposit mainly exists in sandstone basins. And the basin is a complex space of different sedimentary strata and facies. Hence, basin analysis is an essential approach to determine the distribution and variation law of uranium resources. This paper mainly studies the sandstone-type uranium deposits on the northern margin of the Ordos Basin, China. Firstly, the author collected typical data of the geological features on the basin, and sorted data gathered from typical boreholes. Next, the Markov process model was adopted to analyze the sedimentary sequence and evolution in the basin. Finally, the relationship was clarified between the spatial distribution of uranium resources and the stratum evolution of the sedimentary basin.
Keywords: *uranium, spatial distribution, sandstone-type, deposit, strata*

Introduction

Uranium resources is a very important strategic material in China's nuclear energy strategic objectives and national defense construction. It is also an important guarantee for China's nuclear energy development. The national medium and long-term development plan for nuclear power (2011-2020) states that carbon dioxide emissions per unit of GDP will drop by 40% to 45% by 2020 compared with 2005, and the proportion of non-fossil energy in primary energy consumption will reach around 15%. The proportion of nuclear energy in most developed countries in the world has exceeded 20%, while that in China is less than 2%. In order to ensure the long-term stable supply and strategic reserve of uranium resources in China, it is necessary to have enough natural uranium supply and reserve resources as guarantee (Jin et al., 2015). Therefore, it is of great significance to adjust and optimize China's energy structure, improve the ecological environment, and reduce CO_2 and S emissions.

There are two giant uranium metallogenic belts in the world, one is the giant uranium metallogenic belt running through north and South America, the other is the giant uranium metallogenic belt in Europe and Asia. The sandstone uranium metallogenic belt in northern China is located in the eastern section of the Eurasian uranium metallogenic belt. It indicates that China has superior geological conditions and

http://www.aloki.hu ● ISSN 1589 1623 (Print) ● ISSN 1785 0037 (Online)
DOI: http://dx.doi.org/10.15666/aeer/1706_1452914541

resource potential for uranium mineralization. Sandstone-type uranium deposit has many advantages such as large scale, low cost of in-situ leaching and environmental protection, at present, it has become the main type of ore deposit in the world and the main type of uranium resources in China. Sandstone-type uranium deposit is one of the four major industrial uranium mine types in China. As we know the majority of uranium mine in China is sandstone type deposits, and it plays a very important role in the supply of uranium resources in China. The formation conditions of such a deposit are relatively stable, so it is easy to form large and ultra-large deposits (Liu et al., 1997). Sandstone uranium deposit is a major uranium resource type around the world, it mainly exists in sandstone basins (Adler, 1974), and the basin which are complex formation spaces for different sedimentary strata and facies. As studies indicated sandstone uranium deposits in the north of China is very huge (Wang et al., 2019). Therefore, sedimentary basin analysis has become an important area of the study of the distribution and variation law of uranium resources, and the analysis of ore-bearing space involves the analysis of these dimentary sequence of strata (Zhang and Han, 2008), the sedimentary phase change law, and the localization of redox environment. And now, quantitative analysis and digital simulation of basins have become an important direction and trend for the researches in this field at home and abroad (Brookins, 1976; Cohenour, 1960; Elmasour and Elseed, 2018; Fu et al., 2018; Liu et al., 2006; Liu and Jiao, 2013; Miao and Jiao, 2010; Wyborn et al., 1995).

Materials and methods

Basic geological conditions of the Ordos Basin

The Ordos Basin is located in the western part of the North China Plate and is one of the large inland depression sedimentary basins in China (Zhang and Chen, 2010). The basin is rectangular-shaped and spreads from north to south direction, covering an area of about 250,000 km^2. It is an important basin containing coal, oil, natural gas, uranium and other resources, as shown in *Figure 1*.

The Ordos Basin has a two-layer structure. The basement layer consists mainly of metamorphic rocks of the Archaean Eonothem and the Paleoproterozoic Erathem, together with marine facies limestone and clastic sedimentary rocks of the Mesoproterozoic Erathem (Chen and Li, 2003; Chen and Xiang, 2010), the Neoproterozoic Erathem, and the Paleozoic Erathem. The caprock layer is continental facies clastic sedimentary rocks of the Mesozoic Erathem and the Cenozoic Erathem. The Dongsheng sandstone-type uranium deposit is located in the eastern part of the Ordos Basin. The ore-bearing stratum is the gray medium sandstone and medium-coarse sandstone in the lower section of the Middle Jurassic Series Zhiluo Formation, and these sandstones are composite watercourse sands of multi-stage braided river in deeply incised valley under humid climate conditions (Adler et al., 1974). The erosion surface of the sandstone was developed, where in the Middle Jurassic Series Zhiluo Formation in the ore-bearing stratum conformably or disconformably capped on the coal-bearing stratum of the Middle Jurassic Series Yan'an Formation (Miao and Jiao, 2010; Lin et al., 2007). In terms of geotectonic structure, it belongs to the Ikh Juu League uplift zone. In the Early Paleozoic Era, the basin accepted the shallow marine clastic rocks and carbonate sedimentary rocks, and in the Late Paleozoic Era, the marine facies and continental facies deposited stably and alternately. In the Late Triassic Epoch, the inland depression formed, and very thick Mesozoic Erathem fluviatile-lacustrine facies

http://www.aloki.hu ● ISSN 1589 1623 (Print) ● ISSN 1785 0037 (Online)
DOI: http://dx.doi.org/10.15666/aeer/1706_1452914541

clastic rocks deposited, then the later Yanshan movement caused the Upper Jurassic Series and the Upper Cretaceous Series missing from the Mesozoic Erathem. During the development of the basin, paleogeographic conditions such as the climate changed from wet to dry and several regional sediments had been interrupted, had laid a basis for the formation of sandstone-type uranium deposits.

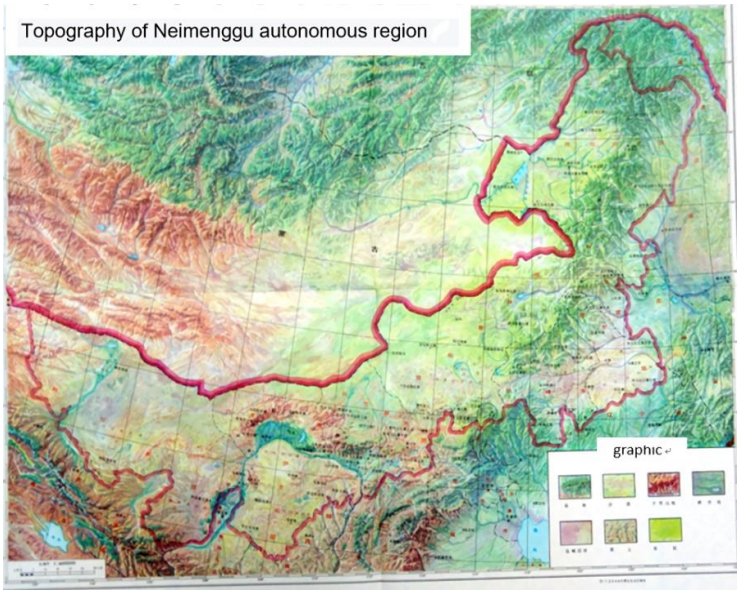

Figure 1. *Terrain of the Ordos Basin*

Borehole data of the Ordos Basin

This study collected several dozens of the sandstone uranium samples from the Dongsheng sandstone uranium mine area in the Ordos Basin and from several wells in the Huanglong area. The rock type of the uranium-bearing minerals is mainly variegated grayish-green sandstones of the Middle Jurassic Series Zhiluo Formation, with medium-grained sand-like structures. Thin section identification results indicate that the sandstones are mainly composed of plagioclase, quartz, muscovite, chlorite and epidote (Chen and Li, 2003), and the cement consists of clay minerals, carbonates and a small part of limonite.

The sampling of sandstone uranium was completed in the 28th Brigade of the Ministry of Nuclear Industry, which is a subordinate unit of the geology and minerals department of the CNNC (China National Nuclear Corporation), it is a deputy-department level national secondary public institution with 1,500 employees and 6 Grade-A qualification certificates such as the regional geological survey certificate. Since 2000, it has made major breakthroughs in uranium mines and made important contributions to rapidly improving the uranium resources capacity of China.

To ensure the uranium content of the samples, detailed geological and geophysical exploration and cataloging of the newly constructed boreholes was carried out to deepen our macroscopic understanding of the ore-bearing sandstones. The boreholes of the uranium industry were selected as research objects. The surrounding rocks (including gray sandstones and grayish-green sandstones) at different positions around the ore-bearing stratum, mineralized sandstones and uranium ore samples were collected, and every sample was subject to the radioactivity measurement on the site. The well logging

http://www.aloki.hu ● ISSN 1589 1623 (Print) ● ISSN 1785 0037 (Online)
DOI: http://dx.doi.org/10.15666/aeer/1706_1452914541

borehole samples are shown in *Figure 2,* and the well logging data are shown in *Table 1* and *Figure 3*.

Figure 2. *Borehole samples of the Ordos Basin*

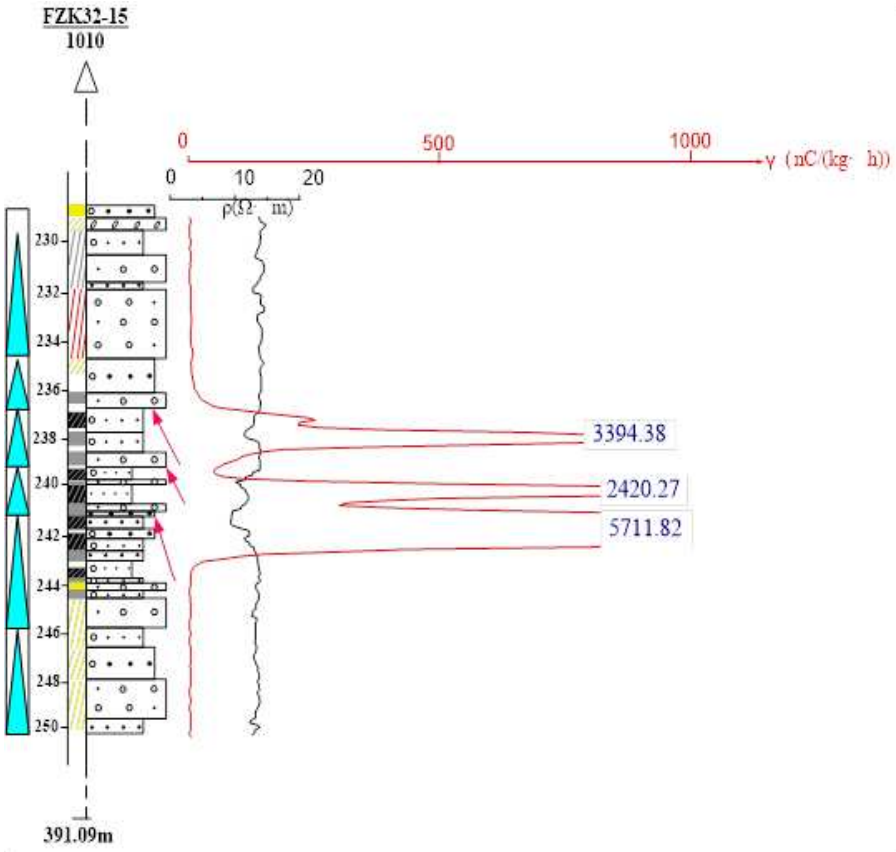

Figure 3. *Borehole data of the Ordos Basin*

Table 1. *Well logging data of the Ordos Basin*

Well logging	Burial depth of the ore block (m)	Thickness (m)	Grade %	Uranium content per square meter (kg/m^2)
Middle well logging	236.37-243.27	6.90	0.4449	65.70
Basic well logging	236.23-243.03	6.80	0.4383	63.77
Inspection well logging	236.23-243.23	7.00	0.4162	62.34

http://www.aloki.hu ● ISSN 1589 1623 (Print) ● ISSN 1785 0037 (Online)
DOI: http://dx.doi.org/10.15666/aeer/1706_1452914541

According to the identified sandstone-type uranium mines and the collected coalfield radioactive well logging data we can know that, the uranium-bearing strata in the northeastern Ordos Basin are mainly the Zhiluo Formation, followed by the Yan'an Formation.

The Yan'an Formation is a set of sedimentary stratum dominated by fluviatile-lacustrine delta facies, which are mainly dark-colored sandstones, mudstone and shale interbeds, and stably developed coal seams, containing rich animal and plant fossils and organic matters. Generally (Zhang and Li, 2010), it is composed of two lithologic sections that are tapered upwards; the lower section consists of gray medium-grained and fine-grained mingled sandstones and mudstones. The sand body is rich in reducing media such as charcoal and pyrite; nonuniform thickness, the sandstones' cementation matter is mainly the mud, and the consolidation degree is relatively loose; the upper section is dominated by grayish-white medium- or fine-grained sandstones, followed by gray or black mudstones, quartz sandstones are seen locally, and grayish-white kaolinized sandstones are seen at the top, with mud as cementation matter and high degree of consolidation, local sections were altered and became kaolin, which is a unique weathering product when the Yan'an Formation is exposed on the surface. The currently found mineralized uranium is mainly concentrated in this section, as shown in *Figure 4.*

Figure 4. *Rock core of the Yan'an Formation*

According to the characteristics of well logging curve, lithology, cycle and color, the Zhiluo Formation can be divided into the lower section and the upper section. The lower section of the Zhiluo Formation is stable throughout the whole area, and it is mainly composed of primary gray clastic rocks, and the sand body of fluviatile facies had developed. *Figure 5* shows the stratigraphic division and logging response of the Zhiluo Formation.

Markov probability

If a process is given a "present", then its "future" is independent of its "past", and such a random process is called a Markov process. The Markov chain is a time-discrete, state-discrete Markov process. In a Markov chain, the transfer of system states can be represented by a transition probability matrix, namely $P = [P_{ij}]$. The elements in the transition matrix are called transition probabilities. The transition matrix has two important properties, that is, all elements are non-negative and the sum of the elements is equal to 1, namely $P_{ij} \geq 0$, $\sum P_i = 1, 2, 3, \ldots, n$. Therefore, the formula is as follows:

http://www.aloki.hu ● ISSN 1589 1623 (Print) ● ISSN 1785 0037 (Online)
DOI: http://dx.doi.org/10.15666/aeer/1706_1452914541

$$(P_{ij})_{n\times n} = \begin{bmatrix} P_{11} & P_{12} & \cdots & P_{1n} \\ P_{21} & P_{22} & \cdots & P_{2n} \\ \vdots & \vdots & \ddots & \vdots \\ P_{n1} & P_{n2} & \cdots & P_{nn} \end{bmatrix} \underline{\Delta} P, \sum_{j=1}^{n} P_{ij} = 1 \qquad \text{(Eq.1)}$$

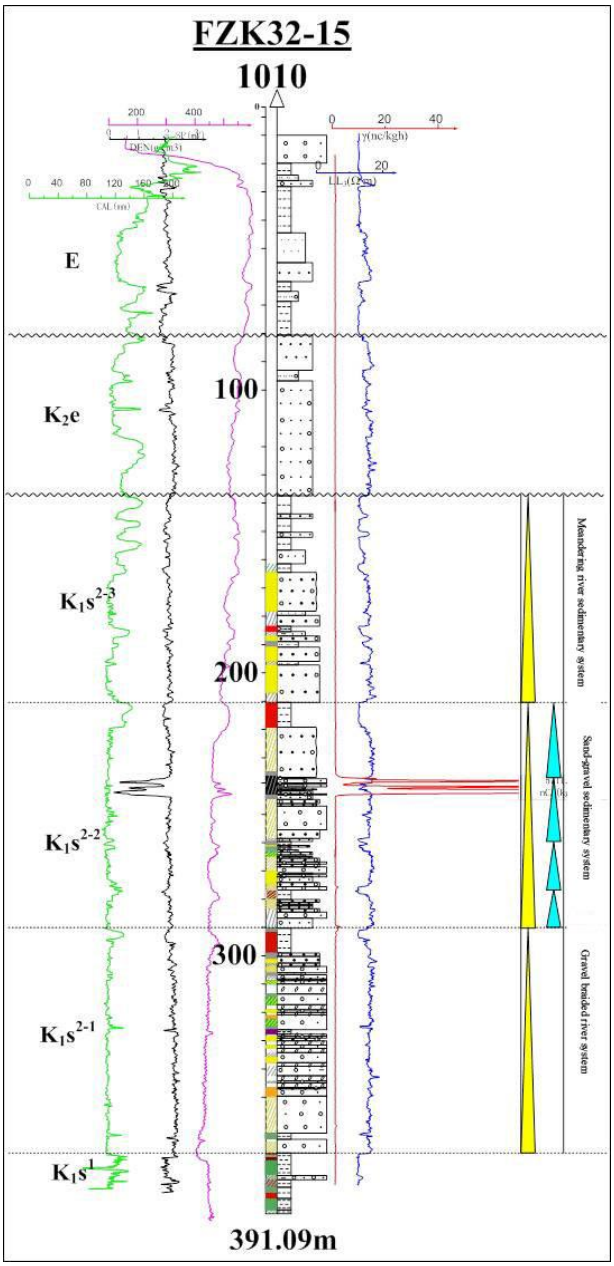

Figure 5. *Stratigraphic division and logging response of the Zhiluo Formation*

When the system state starts from any fixed state i, goes through a transition and reaches the state j, then it will generates states $E_1, E_2, E_3, \cdots, E$, so P_{ij} would constitute a probability matrix, which is a first-order transition probability matrix. Therefore, accordingly, there are also second-order, third-order, and n-order (high-order) transition probability matrices. And high order transition probability matrix can be obtained by matrix multiplication: $P^{(n)} = P^{(1)} \cdot P^{(n-1)}$, and the formula is as follows:

http://www.aloki.hu ● ISSN 1589 1623 (Print) ● ISSN 1785 0037 (Online)
DOI: http://dx.doi.org/10.15666/aeer/1706_1452914541

$$(P_{ij}(k))_{n\times n} = \begin{bmatrix} P_{11}(k) & P_{12}(k) & \cdots & P_{1n}(k) \\ P_{21}(k) & P_{22}(k) & \cdots & P_{2n}(k) \\ \vdots & & & \\ P_{n1}(k) & P_{n2}(k) & \cdots & P_{nn}(k) \end{bmatrix} \triangleq P(k) \quad \text{(Eq.2)}$$

Therefore, the k-th transition probability matrix is equal to the k-th power of one-time transition, namely:

$$P(k) = (P_{ij}(k))_{n\times n} = P(1)^k = \begin{bmatrix} P_{11} & P_{12} & \cdots & P_{1n} \\ P_{21} & P_{22} & \cdots & P_{2n} \\ \vdots & & & \\ P_{n1} & P_{n2} & \cdots & P_{nn} \end{bmatrix}^k \quad \text{(Eq.3)}$$

Markov prediction model

Assume the system has n mutually incompatible states, and the initial state vector of the system is:

$$S(0) = [S_1(0), S_2(0), \cdots, S_j(0), \cdots, S_n(0)] \quad \text{(Eq.4)}$$

where, $S_j(0)$ is the initial probability that the system is in the state j.

Since after *k*-steps transition the probability that the system is in state *j* is S_j(k), then after *k*-steps transition, the state vector is:

$$S(k) = [S_1(k), S_2(k), \cdots, S_j(k), \cdots, S_n(k)] \quad \text{(Eq.5)}$$

where, $S_j(k)$ is the probability that the system is *j* in a state at the moment k.

Therefore, the Markov prediction model is:

$$\begin{aligned} S(k) &= S(k-1)\cdot P = S(k-1)\begin{bmatrix} P_{11} & P_{12} & \cdots & P_{1n} \\ P_{21} & P_{21} & \cdots & P_{2n} \\ \cdots & \cdots & \cdots & \cdots \\ P_{n1} & P_{n2} & \cdots & P_{nn} \end{bmatrix} \\ &= S(0)\cdot P^k = S(0)\cdot \begin{bmatrix} P_{11} & P_{12} & \cdots & P_{1n} \\ P_{21} & P_{21} & \cdots & P_{2n} \\ \cdots & \cdots & \cdots & \cdots \\ P_{n1} & P_{n2} & \cdots & P_{nn} \end{bmatrix} \end{aligned} \quad \text{(Eq.6)}$$

The spatial distribution of the basin sediment formation is multicomponent, heterogeneous, periodic and extensive, and the distribution in each stratum layer is regular. The research results show that the distribution of the sedimentary strata in the basin has Markov characteristics. The sedimentary strata have the characteristics of complexity and cyclicity. In the structure of the basin, the uranium-bearing stratum is only one of the sections. If each stratum is regarded as a state, then the probability of the stratum can be represented by the number of times the stratum appears in the entire sedimentary strata, and a Markov probability matrix can be constructed with the probabilities of all strata. Therefore, the Markov process can be used to clarify the

http://www.aloki.hu ● ISSN 1589 1623 (Print) ● ISSN 1785 0037 (Online)
DOI: http://dx.doi.org/10.15666/aeer/1706_1452914541

sequence of the sedimentary process of the strata and even the cyclic or the phase change law, thus establishing a Markov process model for stratum sediment.

According to the collected logging data, part of the borehole data is shown in *Figure 6*. The basin stratum sequence can be sorted from bottom to top. According to the borehole data, there were a total of 55 stratum samples, which can be divided into 36 lithologic states after repeated screening, and some lithology states after screening are shown in *Table 2*.

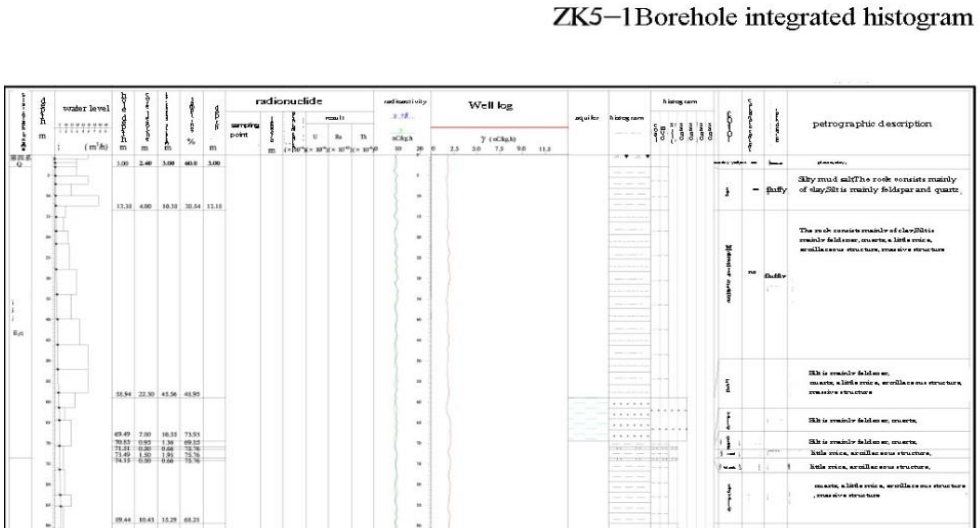

Figure 6. *Partial comprehensive histogram of the Ordos Basin*

Table 2. *Partial lithology states after screening*

Layer	Petrographic description	Type	Layer	Petrographic description	Type
1	Coarse gravel sandstone (light grayish green)	1	15	Coarse gravel sandstone (light brown yellow)	10
2	Carbonaceous mudstone (grayish black)	2	16	Silty mudstone (blue gray)	3
3	Silty mudstone (blue gray)	3	17	Coarse gravel sandstone (gray, off-white)	12
4	Coarse gravel sandstone (off-white)	4	18	Oil sand salt (gray, off-white)	12
5	Fine gravel salt (off-white)	5	19	Coarse gravel sandstone (off-white)	4
6	Coarse gravel sandstone (off-white)	6	20	Medium pebbled sandstone (off-white)	13
7	Silty mud salt (blue grey)	3	21	Fine sand salt (off-white)	5
8	Carbonaceous mud salt (gray black)	2	22	Oil sand salt (light brown yellow)	14

Therefore, the one-step probability matrix of the mutual transition of 36 lithology is calculated by MATLAB:

$$P_{36}=\begin{bmatrix}0 & 1 & 0 & 0 & 0 & 0 & 0 & 0 & \cdots & 0\\ 0 & 0 & 0.33 & 0 & 0 & 0 & 0.33 & 0.33 & \cdots & 0\\ 0 & 0.33 & 0 & 0.33 & 0 & 0 & 0 & 0 & \cdots & 0\\ 0 & 0 & 0 & 0 & 0.25 & 0 & 0 & 0 & \cdots & 0\\ \vdots & \vdots & \vdots & \vdots & \vdots & \vdots & \vdots & \vdots & \vdots & \vdots\\ 0 & 0 & 0 & 0 & 0 & 0 & 0 & 0 & \cdots & 1\\ 0 & 0 & 0 & 0 & 0 & 0 & 0 & 0 & \cdots & 0\end{bmatrix} \quad \text{(Eq.7)}$$

http://www.aloki.hu ● ISSN 1589 1623 (Print) ● ISSN 1785 0037 (Online)
DOI: http://dx.doi.org/10.15666/aeer/1706_1452914541

The probability of two-time transitions is:

$$P_{36}{}^{2} = \begin{bmatrix} 0 & 0 & 0.33 & 0 & 0 & 0 & 0.33 & 0.33 & \cdots & 0 \\ 0 & 0.43 & 0 & 0.27 & 0 & 0 & 0 & 0 & \cdots & 0 \\ 0 & 0 & 0.1 & 0 & 0.08 & 0 & 0.1 & 0.1 & \cdots & 0 \\ 0 & 0 & 0.25 & 0.25 & 0.12 & 0 & 0 & 0 & \cdots & 0 \\ \vdots & \vdots & \vdots & \vdots & \vdots & \vdots & \vdots & \vdots & \vdots & \vdots \\ 0 & 0 & 0 & 0 & 0 & 0 & 0 & 0 & \cdots & 0 \\ 0 & 0 & 0 & 0 & 0 & 0 & 0 & 0 & \cdots & 0 \end{bmatrix} \quad \text{(Eq.8)}$$

According to the modeling process, if the initial state of an event at moment (or period) K is known, then by using *Equation 2* we can obtain its possible variation trend at the first moment (or period) after one-time state transition, as shown in *Figure 7.* Therefore, through calculation, we can get the probabilities of various possible states after one-time transition, as shown in *Figure 8.* And so on, we can also obtain the variation trend of the event's two-time state transition at the second moment (or period), as shown in *Figure 9*. And the prediction of the probability of two-time transition is shown as *Figure 10.*

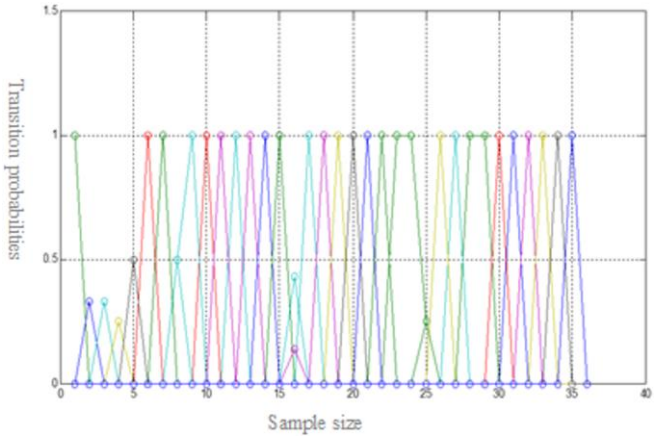

Figure 7. *Variation trend of one-time state transition*

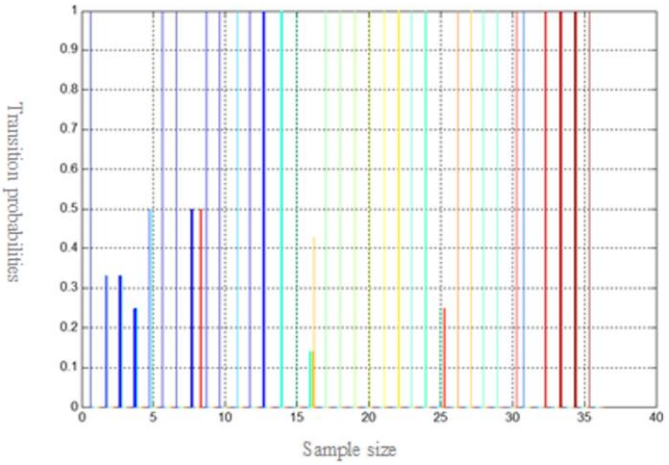

Figure 8. *Probability of one-time state transition*

http://www.aloki.hu ● ISSN 1589 1623 (Print) ● ISSN 1785 0037 (Online)
DOI: http://dx.doi.org/10.15666/aeer/1706_1452914541

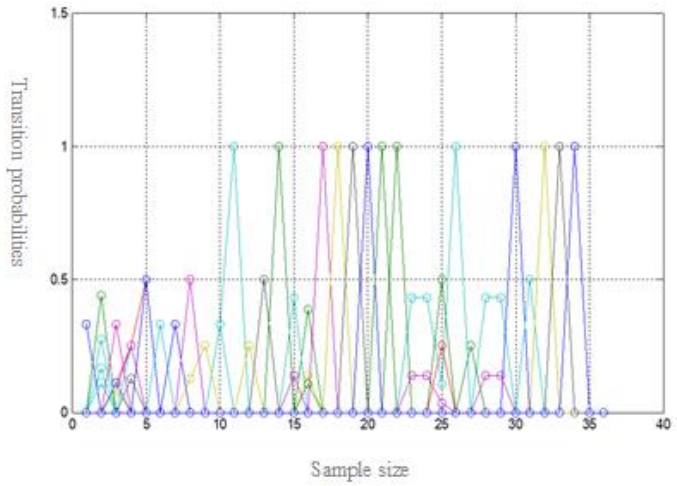

Figure 9. *Variation trend of two-time state transition*

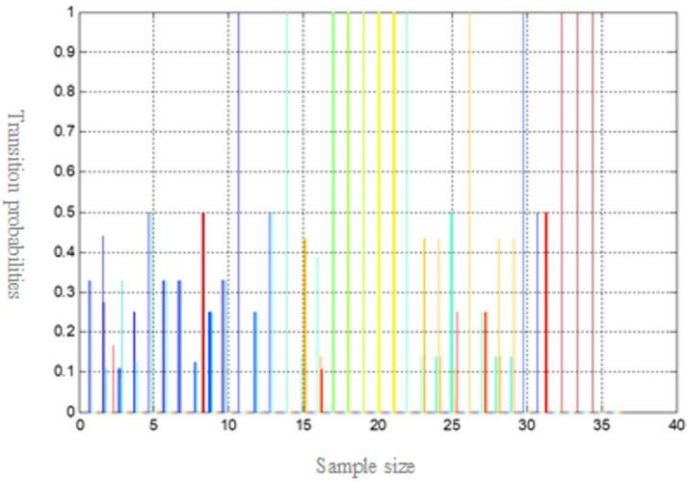

Figure 10. *Probability of two-time state transition*

Results

Therefore, through the Markov probability modeling process we can know that, regardless of the one-time transition probability or the two-time transition probability, the transition probability of all lithology does not exceed 1. Color is a simple and direct feature mark of rocks. Color is usually used to describe rocks and distinguish mineral components, and the color change of rock surface is an important basis for obtaining and identifying rock and mineral information. By looking up the lithology transition states we can see that, in the one-time transition probabilities, the probability of transferring from carbonaceous mudstone (grayish black) to silty mudstone (blue-gray) is 33%, the probability of transferring from carbonaceous mudstone (grayish black) to coal (black) is 33%, the probability of transferring from carbonaceous mudstone (grayish black) to mudstone (dark grayish green) is 33%. The probability of transferring from silty mudstone (blue-gray) to carbonaceous mudstone (grayish black) is 33%, the probability of transferring from silty mudstone (blue-gray) to coarse-grained sandstone (gray-white) is 33%, the probability of transferring from silty mudstone (blue-gray) to

http://www.aloki.hu ● ISSN 1589 1623 (Print) ● ISSN 1785 0037 (Online)
DOI: http://dx.doi.org/10.15666/aeer/1706_1452914541

coarse-grained sandstone (gray, grayish white) is 33%. They have the same transition probability. Therefore, it can be seen that the organic matter is not oxidized and the uranium signal reaches the normal background value.

Discussion

In the two-time transition probabilities, the probability of transferring from carbonaceous mudstone (grayish black) to carbonaceous mudstone (grayish black) is 43.9%. There are usually accompanying elements such as molybdenum, selenium, vanadium, plumbum in the sandstone-type uranium deposits. For the radioactive elements such as uranium and thorium contained in the grayish green and grayish-black lithic feldspar sandstone, there is data show that the content of uranium in the grayish-green sandstones is significantly lower than that in the grayish-black sandstones. The average uranium content in the former is 3.38×10^{-6}, while in the latter this number is 14.33×10^{-6}. In the two kinds of sandstones, the content of thorium varies little, therefore, for the thorium/uranium ratio, the former is larger, with an average ratio of 1.78, and the latter is smaller, with an average ratio of 0.31. The uranium content, thorium content and strontium/uranium ratio in the grayish-green sandstone indicate that uranium has obvious outward migration, which also indicates that the grayish-green sandstones were subject to strong oxidation. Molybdenum and vanadium often co-migrate with uranium during oxidation and precipitate and enrich in a reducing environment. It can be seen from the transition probability and the variation trend that the probability of transferring from carbonaceous mudstone (grayish black) to silty mudstone (blue-grey) is 33%, and grayish-black carbonaceous mudstones have higher yttrium, zirconium and niobium contents than blue-grey silty mudstones, and the enrichment of these alkaline elements is due to the introduction of alkaline fluids. The geochemical characteristics of trace elements in grayish-black sandstones also indicate that they experienced a slightly acidic oxidation at an earlier time, and then were subject to the alkaline chloritization alteration. In view of the two giant uranium mineralization belts in the world, Russia attaches great importance to and pays close attention to the search of uranium mineralization resources, and applies the most commonly used geological distribution rules to search. In this paper, Markov process model is applied to analyze the sedimentary sequence and evolution relationship of the basin by means of transfer probability, which is of great importance to the distribution law of sand-salt uranium ore.

Conclusion

The study area of this paper is the northern margin of the Ordos Basin. Through the derivation of the Markov one-time transition and two-time transition probabilities, it can be seen that the black organic veins in the target sandstone layer of the study area have the mixed sources of coal-generated gas and oil gas, which also indicates that a strong oil-gas effect occurred after the formation of the sandstones. Studies have shown that there are also good conditions for oil and gas traps in the northern part of the Ordos Basin. The oil and gas fluids are generally alkaline and have a strong reduction effect; high-valent iron is reduced to low-valent iron, under such reductive and alkaline fluid conditions, the indication significance of the grayish-green sandstone for the uranium mineralization are well known, and the grayish-green sandstone indicates the reductive

http://www.aloki.hu ● ISSN 1589 1623 (Print) ● ISSN 1785 0037 (Online)
DOI: http://dx.doi.org/10.15666/aeer/1706_1452914541

geochemical environment. After recognizing that it is a product of ancient oxidation and re-reduction, we can realize the essence through the appearance. In the northern part of the Ordos Basin, the grayish-green sandstones indicate a strong ancient oxidation effect, that is, a strong inter-layer oxidized uranium mineralization effect had occurred. The contact position between the grayish-black sandstones and the grayish-green sandstones, namely the pinch-out of the front of the ancient inter-layer oxidation zone, is the most favorable position for uranium mineralization. The obvious changes of sedimentary rhythm or sedimentary microfacies of river sand bodies, the transition zone of grayish-black sandstones and grayish-green sandstones, and the abnormal diffusion halo of uranium are caused by the different formation causes of the upper and lower sub-sections of the Zhiluo Formation, which resulted in significant differences in the sand body, structure and scale. The lower sub-section sand body has a larger scale and better connectivity, while the upper sub-section sand body has a smaller scale and a stronger heterogeneity. This law has an important guiding effect in understanding the expansion of sandstone uranium mineralization in the northern Ordos Basin, and it has important practical guiding significance for the exploration of similar deposits, especially sandstone uranium deposits in basins with rich oil, gas or coal resources. With the continuous development and progress of prospecting and exploration technology in the future, a variety of high-tech analytical and testing technologies can be applied to predict and evaluate the rules of uranium diagenesis and mineralization.

Acknowledgement. This paper was assisted by "evaluation of uranium resource potential based on big data", project No.2015CB453005 of project 973 "continental basin sedimentary environment and large-scale mineralization in the giant sandstone uranium mineralization belt in northern China", project No. 2015CB453000.

REFERENCES

[1] Adler, H. H. (1974): Concepts of uranium ore formation in reducing environments in sandstones and other sediments. – Formation of Uranium Ore Deposits 7: 141-168.
[2] Brookins, D. G. (1976): Position of uraninite and/or coffinite accumulations to the hematite-pyrite interface in sandstone-type deposits. – Economic Geology 5: 944-948.
[3] Chen, D. S., Li, S. X. (2003): A discussion on research situation and development direction of and stone-type uranium deposits in the meso-cenozoic basin of China. – Acta Sedimentologica Sinica 1: 113-117.
[4] Chen, Z. Z., Xiang, W. D. (2000): Uranium provinces in China. – Acta Geologica Sinica (3): 587-594.
[5] Cohenour, R. E. (1960): Geology and Uranium Occurrences near Lakeview. – Atomic Energy Comm., RME-2070, Oregon, US.
[6] Elmansour, A. A., Elseed, E. G. (2018): Groundwater dynamics in Ennuhud Basin, Kordofan Region, Sudan. – Environmental and Earth Sciences Research Journal 5(4): 94-100.
[7] Fu, X. G., Tang, Z. H., Lv, W. B., Wang, X. M., Yan, B. Z. (2018): Exploitation potential of groundwater in Yangzhuang Basin, China under recharge enhancement. – International Journal of Heat and Technology 36(2): 483-493.
[8] Glass, L., Mackey, M. C. (1989): From Clocks to Chaos: The Rhythms of Life. – Princeton University Press, Princeton, pp. 72-80.

http://www.aloki.hu ● ISSN 1589 1623 (Print) ● ISSN 1785 0037 (Online)
DOI: http://dx.doi.org/10.15666/aeer/1706_1452914541

[9] Jin, R. S., Deng, J. (2015): Sedimentary environment and large-scale mineralization in continental basin of giant sandstone uranium metallogenic belt in north China. – World Nuclear Geology 5: 79-84.
[10] Lin, T., Luo, J. L., Liu, X., H., Zhang, S. (2007): Characteristics and genesis of sandstone type uranium inclusions in Zhiluo formation. – Acta Petrolei Sinica 5: 72-78.
[11] Liu, Y. Q., Feng, Q., Yang, R. C. (2006): Genesis of sandstone-type uranium deposits in Dongsheng area of Ordos Basin. – Geological Journal (5): 761-769.
[12] Martell, M. I. (2013): Introduction to discrete dynamical systems and chaos. – John Wiley & Sons 5: 205-210.
[13] Mather, J. D. (2014): The Geochemistry of boron and its isotopes in groundwaters from marine and non-marine sandstone aquifers. – Applied Geochemistry 16: 821-834.
[14] Miao, A. S., Jiao, Y. Q. (2016): Fine anatomy of interlayer oxidation zone of Dongsheng uranium deposit in the northeast of Ordos Basin. – Frontiers of Geology 3: 55-61.
[15] Mclennan, S. M., Talyor, S. R. (2012): Sedimentary rocks and crustal evolution. – Tectonic Setting and Secular Trend 99: 1-5.
[16] Wang, J. L., Zhang, J. H. (2019): Guided by the integration and innovation of Chinese uranium mineralization theories. Innovation and practice of management mode of geoscience and technology. – Geological Review 3: 772-773.
[17] Wyborn, L. A. I., Gallagher, R., Mernagh, T. P. (1995): Using GIS for mineral potential evaluation in areas with few known mineral occurrences. – Proceedings of the Second National Forum on GIS in the Geosciences. Australian Geological Survey Organisation Record 46: 6-24.
[18] Zhang, C. J., Chen, Y. L. (2010): Discovery and genetic significance of vertical Zoning of uranium deposits at 510-1. – Geology and Exploration 3: 434-441.
[19] Zhang, Z. L., Han, Y. Z. (2008): Geochemical characteristics and uranium mineralization in Zhiluo formation of Ordos Basin. – World Nuclear Geology 2: 79-84.
[20] Zhang, Z. L., Li, S. X. (2010): Lower member sedimentary facies of middle Jurassic Zhiluo formation in northeastern Ordos Basin and its control on uranium mineralization. – Acta Palaeogeography 6: 749-758.

http://www.aloki.hu ● ISSN 1589 1623 (Print) ● ISSN 1785 0037 (Online)
DOI: http://dx.doi.org/10.15666/aeer/1706_1452914541

DEMOLITION DUST FORMATION, DIFFUSION MECHANISM AND MONITORING QUANTITATIVE RESEARCH ON DEMOLITION OF EXISTING BUILDINGS

LIU, W.* – TANG, P. T. – LI, K. – JIANG, T.

School of Civil Engineering and Architecture, East China Jiaotong University, Nanchang 330013, China

**Corresponding author*
e-mail: liuweijx13@163.com; phone: +86-138-7061-8920

(Received 7th Jun 2019; accepted 10th Oct 2019)

Abstract. By monitoring the change of dust fall concentration at the same height and different distances near the boundary of a building demolition site, this paper tries to study the law of dust formation and diffusion in the area site. In order to conduct quantitative analysis on the raise dust distribution in the construction site at the demolition stage, the amount of fine particulate matter $PM_{2.5}$ and inhalable particle PM_{10} in such a site where an experimental demolition is performed measured. The data measurement is carried out with the help of logarithm conversion, so as to reduce the data variability and enable it to approach normal distribution, and the data with the confidence coefficient of 95% is selected. The main components of $PM_{2.5}$ and PM_{10} emissions are extracted to indicate the emission intensity. According to the emission intensity, a construction site can be divided into three categories for analysis by hierarchical clustering, so as to obtain the desired results. Through the comparison and analysis of the monitoring quantitative and discrete phase model, the motion, diffusion and settlement equations of the dust of the demolition site are verified, indicating that the simulation results using the discrete phase model are credible.

Keywords: *raise dust in construction, formation mechanism, discrete phase model, diffusion mechanism, monitoring quantification*

Introduction

In recent years, the value orientation of the public policy making in China has gradually transformed from emphasizing the pursuit of economic efficiency to focusing more on social equity, with an expectation of balancing the, dual goals of economic development and social welfare. With the acceleration of the urbanization process, the demolition of old buildings is increasing day by day. As a way to the old buildings in an unprecedented manner, the building demolition project is also included in one of the important tasks of the construction project. The demolition of old buildings has produced a lot of construction waste. "The amount of construction waste in China already accounts for 30 to 40% of the total amount of urban waste," said Qiu Baoxing, a former vice-minister of housing and urban-rural development. According to the rough statistics of the loss of construction materials of brick and concrete structure, whole cast-in-situ structure and frame structure, in the construction process of every 10,000 m^2 of buildings, only the construction waste will produce 500 to 600 tons; Every 10,000 m^2 of old buildings demolished will generate 7,000 to 12,000 tons of construction waste, and 40% of the old buildings demolished in China each year. Wang Guangtao, former minister of construction, said that by 2020, China will add 30 billion m^2 of construction area, and the total amount of construction waste will be 1.8 billion tons. This poses a huge environmental threat to China. These construction units or individuals usually do not carry out any treatment on the muck, spoil, waste, mud and other waste generated in

http://www.aloki.hu ● ISSN 1589 1623 (Print) ● ISSN 1785 0037 (Online)
DOI: http://dx.doi.org/10.15666/aeer/1706_1454314559

the demolition of various buildings, structures and pipe networks. Moreover, the raise dust, sand dust and other problems generated in waste transportation and stacking have caused serious environmental pollution. Raise dust can be hazardous human health and it is likely to cause dust pollution, which in turn leads to deterioration of the surrounding environment. Studies have shown that air pollution can be divided into two types: gaseous pollution and particulate pollution. Particles with a diameter of less than 10 μm are called inhalable particles (PM_{10}), which are rather harmful to human health. Inhalable particles can be divided into fine particles ($PM_{2.5}$) and coarse particles according to the particle size. In recent years, the $PM_{2.5}$ index has attracted a lot of people's attention. The main reason is that fine particles (also known as microparticles) can directly enter and precipitate in human lungs. Its impact on human health is permanent. If a large amount of building raise dust enters the lung, it will cause obstructive damage to the respiratory system, reduce the ventilatory function of the bronchus, and lose the air exchange function the alveoli. In the meanwhile, fine particles adsorbed in the lungs stimulate the cell wall, causing bronchitis, asthma and other diseases. In addition, the increased concentration of PM_{10} and $PM_{2.5}$ in the atmosphere will lead to cardiovascular disease, resulting in an increase in the incidence rate of cancer. The increase of particles in the air easily leads to the appearance of haze weather condition and affects people's normal travel. Acidic substances in the air have a certain corrosive effect on buildings. If the amount of acidic substances increases, the corrosion degree is improved, and the hazard is rather serious especially after rainfall. Therefore, the research on the generation, movement law and concentration of raise dust in the demolition construction site of existing buildings is the basis for the construction site employees to make preparations and control in advance, an important means to protect the health and life of employees, and an important prerequisite for ecological environmental protection.

For many years, various researches have been carried out on raise dust pollution in building construction at home and abroad, including the exploration of raise dust emission factors for building construction (Muleski et al., 2005; Toropov et al., 2018). Raise dust is an open pollution source entering the atmosphere and it is an important component of total suspended particulates in the ambient air. According to the dust research, the causes of dust mainly come down to the following two aspects: The powder is separated from the powder flow because of the influence of the surrounding air during the falling process, and it suspends in the transition layer of the powder flow (Ansart et al., 2009), thus generating the dust cloud. The falling powder particles collide with particles and walls in the bag to produce impact dust and suspend in the air (Wang et al., 2014). The essence of the phenomenon that powders take up air and the air affects particles is gas-solid collaboration effect (Alekhfne, 2012; Cerecedo et al., 2009). Fan et al. (2019) conducted accumulated dust load sampling and laboratory screening analysis on typical roads, measured the road dust particle size distribution and particle size multiplier by resuspension system and particle size spectrometer, investigated the road vehicle composition and calculated the vehicle weight, and applied the model method to establish a localized road raise dust $PM_{2.5}$ emission factor. Based on the survey data of architecture and municipal construction projects in Xi'an, Xiao et al. (2019) combined with two sets of emission factors of typical cities in northern China measured by different institutions to estimate the emission amount and emission strength of the architecture construction raise dust PM_{10} and $PM_{2.5}$ in Xi'an in 2017, so as to construct a list of particulate matter emissions from county-level buildings in Xi'an, and analyze

http://www.aloki.hu ● ISSN 1589 1623 (Print) ● ISSN 1785 0037 (Online)
DOI: http://dx.doi.org/10.15666/aeer/1706_1454314559

the spatial distribution characteristics. All local governments have attached great importance to this and have issued a series of guidelines and policies to monitor the raise dust pollution. However, the current construction raise dust pollution monitoring still relies on manual patrol and fixed-point monitoring, which is inefficient and ineffective, and there is no more effective monitoring techniques. The construction environment monitoring mainly focuses on the raise dust and material waste and so on at the construction site (Kohlman et al., 2014), in which, the construction raise dust control is a research hotspot. In terms of monitoring methods, instrument sampling is the main method and video monitoring is feasible as well (Wu et al., 2015). However, although the above methods have high precision, they are not efficient because of being easily interfered. In recent years, UAV (Unmanned Aerial Vehicle) images have been used for water pollution monitoring, chemical gas pollution monitoring, vehicle identification, building deformation monitoring and so on (Chen et al., 2016). Construction dust is the main source of atmospheric pollutants and the key object of construction environment monitoring, but the traditional monitoring methods have limited efficiency and effectiveness. For this purpose, Ma et al. (2018) integrated the use of UAV and image recognition technology, designed the structure, function and operation process of the construction dust pollution source automatic monitoring system with HSV (Hue, Saturation, Value) feature extraction, histogram comparison, nonzero pixel calculation as the core, and tested the operation test. It is found that the pollution source characteristic comparison effect is relatively stable, basically meeting the construction dust pollution source monitoring demand Wu et al. (2017) designed a construction site environmental monitoring system to achieve real-time monitoring of the construction site environment. In order to propose a targeted construction dust prevention and control measure, ensure the occupational health and safety of construction workers, Li et al. (2014) selected two main residential projects in Beijing and arranged the raise dust concentration monitoring sites in the main construction activity areas at the second structure and indoor rough decoration stages to analyze the emission characteristics and main distribution laws of raise dust. Huang et al. (2013) considered that the screening of dust source samples is an elementary test for studying the dust pollution characteristics. It has a wide application. The screen test is required whether it is to determine the critical friction wind speed of wind erosion dust, road dust load and other parameters, or to prepare a dust source resuspension test sample for studying the particle size distribution and source composition spectrum of total suspended particulate matter. Shi et al. (2013) applied laser demand technology to find that the non-structured particles in the near-surface atmosphere have important theoretical and practical values. The laser demand technology is used to detect the raise dust of urban construction sites, and the outer wall of the building is utilized to conduct relatively calibration of the laser demand signal. Afterwards, according to the laser demand equation, the extinction coefficient of the raise dust particles along the optical path is solved, and the extinction coefficient distributions of multiple paths are obtained through the process control scanning station. In the end, the two-dimensional mass concentration distribution condition is achieved by combining with the mass extinction efficiency factor.

Dong et al. (2019) such as using the positive definite matrix factorization model (PMF) - the health risk assessment model (HMHR) explores the Yangzhou fine particulate matter (PM2.5) in heavy metal pollution sources and little pollution, and combine the health risk assessment model (heavy metal health risk, HMHR) to calculate

http://www.aloki.hu ● ISSN 1589 1623 (Print) ● ISSN 1785 0037 (Online)
DOI: http://dx.doi.org/10.15666/aeer/1706_1454314559

the influence of different pollution on human health, to reveal the different sources of pollution potential harm to human body health to provide scientific information. Atmospheric fine particulate matter (PM2.5) (aerodynamic equivalent diameter < 2.5 micron) has an impact on human health and environmental air quality. Among them, heavy metals have a particularly significant impact on human health, which can enter the human body through hand ingestion, breathing and skin contact, and further lead to functional dysfunction and irreversible injury. Elements Cr and Pb are elements with the highest potential health risks in cities, which can cause diseases of the nervous system and blood system, especially for infants and young children (Thomas et al., 2009). PM2.5 receptor samples were collected, positive matrix factorization (PMF) was used to analyze the contribution of different pollution sources to PM2.5 and different heavy metals, and the heavy metal health risk HMHR was combined to calculate the impact of different pollution sources on human health (Peng et al., 2016). Li et al. (2015) evaluated the pollution of construction workers by dust at different construction stages by establishing a model of health damage caused by construction dust. Chou et al. (2015) calculated the economic loss caused by CO2 emission to construction workers in the construction process by establishing Monte Carlo simulation model. However, most of these studies only focus on the occupational health damage to construction workers, which to some extent cannot accurately reflect the impact scope and degree of construction dust.

Sung et al. (2006) observed that building demolition was one of the most common activities in the construction industry. The commonly used demolition techniques are mechanical demolition, demolition and mixed demolition. Although deconstruction is advocated in an environmentally friendly way, the cost comparison of demolition projects with different technologies is rarely studied. Mohamed et al. (2008) proposed a new framework for building pollution control based on multi-objective optimization. The method used in the proposed framework is based on the calculation of pollution from dust, hazardous gases and noise to each activity involved in the project. Madelyn et al. (2010) proposed a new method based on the building cost system (BCS) to deal with the costs associated with construction and demolition waste management, which improves accuracy and produces estimates independent of the general budget. Water suppression to mitigate the spread of dust is the most popular and a universal method to deal with construction dust (Zuo et al., 2017). However, countries or regions which experience water shortage find this technique to be expensive and morally incorrect. Maintaining standard heights for stockpiling, wetting objects before cutting or grinding, wetting while sweeping are very easy methods to control some of the dust generated at sites. Use of chemical agents, electrical sweepers, dust screens, local exhaust ventilation, *etc*., are some technologies that are available for the construction companies to manage dust pollution (Wu et al., 2016).

At present, China has carried out rather sufficient research on the raise dust pollution in construction projects and storage yards, but there is indeed insufficient research on raise dust in demolition projects. The raise dust emission law of the demolition project is rather complicated. Up to now, China has not published any feasible management method with the emission limit as the basis, which can be used to quantitatively evaluate the raise dust emission strength of the demolition projects. Although some provinces and municipalities have published a series of prescribed measures for the raise dust of demolition projects and put forward corresponding controls to the generated raise dust in heavy demolition area, most of these regulations are behavioral

http://www.aloki.hu ● ISSN 1589 1623 (Print) ● ISSN 1785 0037 (Online)
DOI: http://dx.doi.org/10.15666/aeer/1706_1454314559

regulations, which are lack of quantitative understanding and control, and researches on the emission characteristics of demolition raise dust pollution, so it is difficult to accurately grasp the emission intensity of dust emission in demolition projects. This study takes the formation and diffusion of raise dust in the demolition process of existing buildings as the research object, explores the relevant laws of dust formation and diffusion, regards green construction environmental protection as the objective, provides theoretical and practical basis for the raise dust monitoring quantification of the construction site. Based on the gas-solid two-phase flow theory, the method of simulation, monitoring and quantification of the movement, diffusion and settlement equation of demolition construction dust is used to study the formation and diffusion of dust in the demolition construction.

Methods

Variable selection and model establishment

Confirmation of raise dust formation and diffusion impact factor

This research selects the falling dust as the inspection index of analyzing the laws of raise dust formation and diffusion. Falling dust refers to particulates that naturally settle to the surface by gravity under airborne conditions. The amount of dust generated in the demolition construction is not only related to the construction stage and construction strength factors, but also has a certain correlation with the climatic conditions in demolishing the building. Through literature research and consultation with experts, it has been determined that the raise dust formation and diffusion impact factors include: dust particle diameter, gas density, dust particle density, dust moisture content, construction strength, wind speed, temperature, humidity, height and other factors.

Equation of motion of the dust in the air

The dust unmooring load refers to the force overcoming the gravity of the dust particles, the gravitation and adhesion force among particles to fly the dust. The critical load that causes the dust to rise is called the ultimate unmooring force. However, according to Zhi et al. (2018), the VWD (Visual Web Developer) force is used to calculate the gravitational attraction between dust particles, which is negligible under normal conditions. In studying the dust in this paper, it is assumed to be a spherical particle. The stress of the dust is very complicated at the construction site. The force of the dust particles in demolishing the existing buildings is analyzed, and the dust is found to be affected by gravity, buoyancy force, air resistance and other external forces. The resultant force $F_{\alpha 0}$ of the dust is determined by the following equation:

$$F_{\alpha 0} = F_g + F_f + F_d + F_{un} \quad \text{(Eq.1)}$$

In the equation, $F_{\alpha 0}$ is the resultant force of the dust, with the unit of N. F_g is the weight of the powder particle, with the unit of N. F_f is the adhesion force among powder particles, with the unit of N. F_d is the air resistance of the dust particles, with the unit of N. F_{un} is other forces of the dust particles, with the unit of N.

The movement law of dust in the air essentially belongs to the research area of gas-solid two-phase flow (Zhu et al., 2017). The volume of dust particles is much smaller than the volume of air. In order to simplify the equation of motion of dust at the

http://www.aloki.hu ● ISSN 1589 1623 (Print) ● ISSN 1785 0037 (Online)
DOI: http://dx.doi.org/10.15666/aeer/1706_1454314559

construction site, the volume occupied by dust particles can be neglected. In gas-solid two-phase flow, solid particles are exerted with more and complex forces. For the convenience of calculation, it is assumed that the dust is not affected by other forces, but only the force caused by the relative motion of the gas-solid two phases, the equation of motion of the dust is established in Cartesian coordinates according to Newton's second law (Sun et al., 2016):

$$m_p \frac{dv_p}{dt} = \frac{\pi}{6} d_p^3 \rho_p g + \frac{\pi}{6} d_p^3 \rho_g g + \frac{\pi C_d d_p^2 v_p^2 \rho_p}{8} \quad \text{(Eq.2)}$$

After simplification, it can be expressed as:

$$\frac{dv_p}{dt} = \frac{3C_d \rho_g \left(v_g - v_p\right)^2}{4 d_p \rho_p} \quad \text{(Eq.3)}$$

In the equation: m_p is the dust mass, with the unit of mg; v_p is the dust movement speed, with the unit of m/s; t is the movement time, with the unit of s; d_p is the dust particle diameter, with the unit of m; ρ_P is the dust particle density, with the unit of $kg \cdot m^{-3}$; g is the gravitational acceleration, with the unit of m/s^2; ρ_g is the gas density, with the unit of $kg \cdot m^{-3}$; C_d is the air resistance coefficient; v_p is the moving speed of the dust particles, with the unit of $m \cdot s^{-1}$; v_g is the gas movement speed, with the unit of $m \cdot s^{-1}$; π is valued as 3.14.

Diffusion equation of dust in air

The dust particles with smaller particle diameter generated in the demolition process of the existing building have small gravity and low sedimentation speed. Due to the impact of the Brownian motion of the air molecules, irregular movements are generated accordingly. The research shows that the smaller the particle size of the dust particles, the more intense the dust particles move. This movement is named as the dust diffusion movement.

Any particle fluid unit in the space (as shown in *Fig. 1*) is used to analyze the dust diffusion motion (Li et al., 2006), assuming that the volume of the particle unit is $\Delta V = \Delta x \cdot \Delta y \cdot \Delta z$. The mass flux of a substance (called as flux for short) refers to the mass of a substance that flows through.

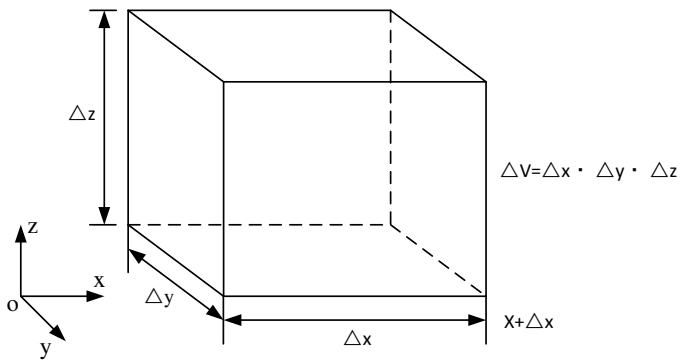

Figure 1. *Diagram of dust diffusion model*

http://www.aloki.hu ● ISSN 1589 1623 (Print) ● ISSN 1785 0037 (Online)
DOI: http://dx.doi.org/10.15666/aeer/1706_1454314559

According to the gradient conveying theory, the amount of dust passing through a unit area along the x direction for the dust unit time suspended in the air is proportional to the dust mass concentration gradient in the x direction. The flux of dust in the x direction is:

$$Q_x = -K_x \frac{\partial c}{\partial x} \quad \text{(Eq.4)}$$

In the equation: Q_x is the flux of dust in the x direction, with the unit of $mg \cdot m^{-3} \cdot s^{-1}$; K_x is the diffusion coefficient of dust in the x direction; c is the mass concentration of dust, with the unit of $mg \cdot m^{-3}$; $\frac{\partial c}{\partial x}$ is the dust mass concentration gradient along the x direction.

Under the action of the wind flow at the construction site, the dust particles will move along the wind flow direction under the action of the wind flow. Combined with the diffusion action of the dust, the dust concentration in the wind flow movement direction will keep on changing. The wind speeds in the x, y, and z directions are set as v_x, v_y, and v_z, respectively. According to the mass conservation equation, the net inflow in three directions is equal to the cumulative rate, then:

$$\frac{\partial c}{\partial t} = -v_x \frac{\partial c}{\partial x} - v_y \frac{\partial c}{\partial y} - v_z \frac{\partial c}{\partial z} + K_x \frac{\partial^2 c}{\partial x^2} + K_y \frac{\partial^2 c}{\partial y^2} + K_z \frac{\partial^2 c}{\partial z^2} \quad \text{(Eq.5)}$$

In practical applications, in order to simplify the calculation, a one-dimensional stationary diffusion equation can be selected for the research in the three-dimensional coordinate system. When the x-axis direction in the three-dimensional coordinate system is selected for the calculation, $v_y = v_z = 0$. The above equation (*Eq. 5*) can be simplified as:

$$\frac{\partial c}{\partial t} + v_x \frac{\partial c}{\partial x} = K_x \frac{\partial^2 c}{\partial x^2} + K_y \frac{\partial^2 c}{\partial y^2} + K_z \frac{\partial^2 c}{\partial z^2} \quad \text{(Eq.6)}$$

When the wind speed and turbulence intensity are in a steady state, $\frac{\partial c}{\partial t} = 0$. When the ambient wind speed is high, the diffusing capacity of the dust in the x direction $K_x \frac{\partial^2 c}{\partial x^2}$ can be negligible. In such condition, the above equation (*Eq. 6*) can be further simplified as:

$$v_x \frac{\partial c}{\partial x} = K_y \frac{\partial^2 c}{\partial y^2} + K_z \frac{\partial^2 c}{\partial z^2} \quad \text{(Eq.7)}$$

The diffusion coefficients of the dust particles with the same property in the x, y, and z directions are equal, which are uniformly expressed by K_p (Chen et al., 2015). The

http://www.aloki.hu ● ISSN 1589 1623 (Print) ● ISSN 1785 0037 (Online)
DOI: http://dx.doi.org/10.15666/aeer/1706_1454314559

differential equation (*Eq. 7*) is solved by Gauss formula, so as to obtain the diffusion equation of dust in air as follows:

$$c = kx^{-1} \exp\left[-\frac{v_x}{4K_p x}\left(y^2 + z^2 \right) \right] \quad \text{(Eq.8)}$$

In the equation, k is the Boltzmann constant, which is valued as 1.38×10^{-23} J·K^{-1}.

Sedimentation equation of the dust in the air

Dust particles settle under gravity during the process of demolishing existing buildings. During the sedimentation process, the particle velocity changes continuously, and the resistance transforms accordingly. When the gravity, buoyancy and air resistance reach a balance, the dust particles settle at a constant speed, and the sedimentation velocity also reaches a maximum value at this moment. Such a speed is called Stokes velocity.

When the dust settles gradually, it is in the stress equilibrium status, and it is $F = F_g - F_f = F_d$ at this moment. Hence, the following equation is obtained:

$$\frac{\pi}{6} d_p^3 \left(\rho_p - \rho_g \right) g = \frac{\pi C_d d_p^2 v^2 \rho_p}{8} \quad \text{(Eq.9)}$$

When the dust begins to settle evenly, the sedimentation velocity also reaches a maximum value, that is, $v = v_t$. The dust sedimentation speed is as follows:

$$v_t = \sqrt{\frac{4(\rho_p - \rho_g) g d_p}{3 \rho_g C_d}} \quad \text{(Eq.10)}$$

(a) When $Re_p \leq 1$, the movement of the dust particles is in a laminar flow state, $C_d = \frac{24}{\mathrm{Re}_p}$. (b) When $1 < Re_p < 500$, the movement of the dust particles belongs to the turbulent transition state. (c) When $500 < Re_p < 2 \times 10^5$, the movement of dust particles belongs to the turbulent state, and C_d hardly changes with Re_p, which is approximately $C_d \approx 0.44$. The Reynolds number of the dust particles Re_p is a dimensionless number reflecting the relationship between the inertial force and the viscous force in fluid flowing process. Its value is related to the flow velocity, feature size and fluid viscosity. Reynolds number $Re_p = \frac{d_p \rho_g v}{\mu_g}$. In the formula, μ_g is the dynamic viscosity of air, with the unit of *Pa·s*.

Empirical analysis

Profile of demolition project

The demolished buildings in the demolition project include 107, 107A, 107C, 107D buildings and some demolition projects above the ground surface, with a total floor area of about 5000 m^2 and a total construction area of about 13798.95 m^2. Among them, 107

http://www.aloki.hu ● ISSN 1589 1623 (Print) ● ISSN 1785 0037 (Online)
DOI: http://dx.doi.org/10.15666/aeer/1706_1454314559

is a teaching building with five-story frame structure, 107A is a hospital with two-story brick-and-mortar structure, 107C is a dormitory building with four-story frame structure, and 107D is an auditorium with two-story brick-concrete. The demolition of the building is required to be completed in September 11, 2018~October 5, 2018. The construction site is completely enclosed by iron sheets, with a height of no less than 1.8 m. The safe distance of the building enclosing structure away from the building is 1.5 times of the building height, with its east side connected with the wall (refer to *Figure 2:* construction site planar graph for the building enclosing structure).

Monitoring quantification method

The research results show that particles with a particle size of less than 50 μm will float in the atmosphere for a long time because of the buoyancy and eddy functions, and will be transported to a distant place. Particles with a particle size of 50-100 μm can be kept in suspension, but settle down soon. Particles with a particle size larger than 100 μm can only roll on the ground under the action of wind.

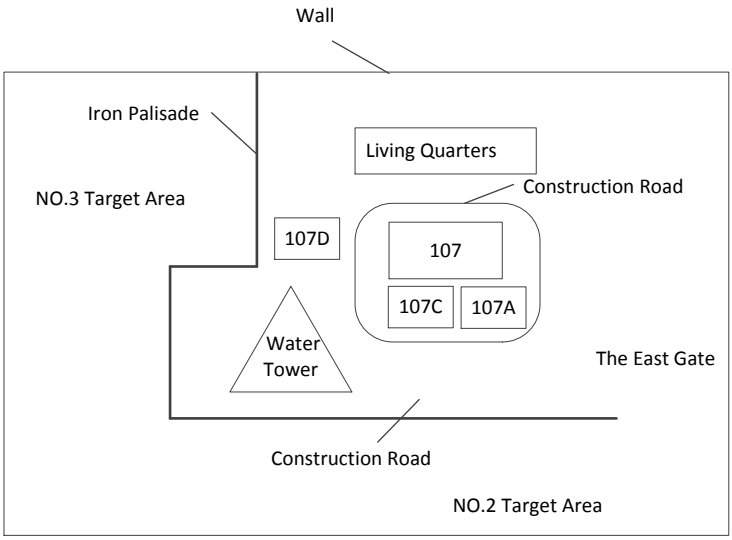

Figure 2. *Construction site planar graph*

In this research, monitoring is carried out by combining dust removal cylinder collection and weighing and $PM_{2.5}$ automatic detector. The dust removal cylinder is mainly located at the boundary of the construction site, and the height is no less than 3 m. The particles collected in the dust removal cylinder have a diameter of below 100 μm, mainly 50-100 μm particles. The instrument for measuring the concentration of particles adopts Xinsite handheld $PM_{2.5}$ laser dust concentration detector, with the model of HT-9600. The instrument employs the $PM_{2.5}$ photoelectric sensor principle, and the pumping sampling method is more accurate. The measuring height is about 1.5 m and the measuring time of each measuring point is 50 s. At the demolition stage, each measurement point shall be recorded of the reading for every 1 h. The monitored data includes: temperature, relative humidity, $PM_{2.5}$ concentration, PM_{10} concentration, dust particle size (0.3 μm, 2.5 μm, 10 μm) and time record. The hourly mean value of $PM_{2.5}$ and PM_{10} measured by the air quality real-time monitoring station at the location

http://www.aloki.hu ● ISSN 1589 1623 (Print) ● ISSN 1785 0037 (Online)
DOI: http://dx.doi.org/10.15666/aeer/1706_1454314559

of building demolition was selected as the background value. This study only conducted raise dust monitoring to the demolition project of 107 teaching building. 16 measuring points were selected around the 107 teaching building, and 16 dust removal cylinders were placed in the measuring points to collect dust. The position of the measuring point is shown in *Figure 3*. According to the measuring point arrangement method in the similar literature, the wind speed measuring points and the dust mass concentration measuring points were respectively arranged at the demolition site, which were arranged with a certain interval along the wind flow direction. The wind speed measuring points were arranged to have a space of 20 m, and a total of 7 measuring points were arranged. Each measurement point was conducted with the data measurement of no less than 3 times, and then an average value was calculated.

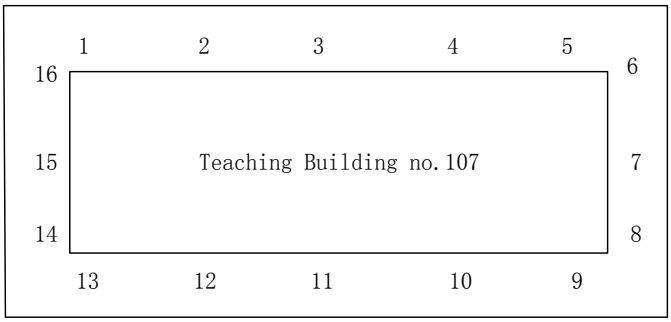

Figure 3. *Measuring point position diagram*

Data preprocessing

SPSS22.0 and Excel are used to process the data, logarithmically transform the obtained $PM_{2.5}$ and PM_{10} data, so as to reduce the data variability of the original data, and enable the data distribution to approach the normal distribution. Cases with a confidence coefficient of 95% were selected for the analysis, namely, cases with the data exceeding ($\mu - 1.96\sigma$, $\mu + 1.96\sigma$) were eliminated (μ and σ are the mean and standard values of the normal distribution, respectively). Afterwards, the original data and the logarithmic data are analyzed, and the inspection level a is valued as 0.05. Through conducting correlation analysis to the two groups of data after logarithmic transformation, it shows that the Pearson correlation coefficients of the data after the logarithmic transformation and the original data are 0.898 and 0.941, respectively, presenting an extremely strong correlation. In other words, the logarithmic transformation process is reasonable. 325 measured data is obtained during the demolition phase, and 296 is selected, showing a data efficiency of 91.08%. After the completion of the demolition phase, there is a total of 120 measured data, in which, 112 is selected, showing a data efficiency of 93%. The statistical description of the cases after screening is shown in *Table 1*.

Quantitative data analysis

Emission intensity index

Correlation analysis is conducted to $PM_{2.5}$ and PM_{10} emissions. The Pearson correlation coefficient of the two variables is obtained through analysis: 0.950, showing that the two variables have an extremely strong correlation. The principal component

http://www.aloki.hu ● ISSN 1589 1623 (Print) ● ISSN 1785 0037 (Online)
DOI: http://dx.doi.org/10.15666/aeer/1706_1454314559

analysis can be used to extract a principal component to achieve variable dimension reduction. Refer to *Table 2* for the index characteristic values and contribution rates of the component extraction process obtained by principal component analysis. The factor load matrix is shown in *Table 3*.

Table 1. *Case selection and statistical description*

Category	Demolition stage		After completing the staged work of demolition	
	$PM_{2.5}/(\mu g \cdot m^{-3})$	$PM_{10}/(\mu g \cdot m^{-3})$	$PM_{2.5}/(\mu g \cdot m^{-3})$	$PM_{10}/(\mu g \cdot m^{-3})$
Minimum	10.18	49.36	10.01	28.91
Maximum	432.30	495.40	189.24	202.20
Mean	94.409	156.521	59.511	92.881
Standard deviation	60.573	81.404	33.220	35.444

Table 2. *Index characteristic values and contribution rates*

Times	Initial characteristic value	Variance percentage /%	Accumulated variance percentage
1	1.904	95.189	95.189
2	0.096	4.811	100

Table 3. *Factor load matrix*

Project	Principal component 1 load
$PM_{2.5}$ emission	0.955
PM_{10} emission	0.955

It can be seen from *Table 2* that the contribution rate of the first principal component extracted is 95.189%. This principal component is selected to reflect the emission intensity of $PM_{2.5}$ and PM_{10} on the site. If it is recorded as *Z*, the emission intensity *Z* can be prepared combined with the component matrix:

$$Z = 0.512 \times \Delta PM_{2.5} + 0.512 \times \Delta PM_{10} \quad \text{(Eq.11)}$$

The principal component values of each measured case can be calculated according to the principal component equation. Refer to *Table 4* for the average principal component value of each measured position.

Table 4. *The average principal component value of each measured position*

Location	Average principal component value	Location	Average principal component value
Road side	69.854	Living quarter of the workers	59.003
Waste recycling area	77.315	Gunnery area	145.951
Working passage	227.444	Out of the construction wall	48.080
Excavator	159.201	Loading vehicle	109.694
Plane transport corridor	91.343	Construction waste dump	133.256

http://www.aloki.hu ● ISSN 1589 1623 (Print) ● ISSN 1785 0037 (Online)
DOI: http://dx.doi.org/10.15666/aeer/1706_1454314559

In order to identify the location of raise dust emissions to be concentrated during the construction process, and understand the sources and influencing factors of dust at different locations, the locations are classified according to emission intensity. The SPSS self-contained system clustering method is used to classify the locations. After standardizing the emission intensity, the square Euclidean distance is used for classification, so as to draw the system clustering spectrum shown in *Figure 4*.

According to the diagram, the sixteen positions are divided into three categories: the first category is the outer wall of the construction site, and the average value of the main component *Z* is 10.416, indicating that the dust amount at this position is only slightly higher than the background value. It shows that the construction wall has a good restraining effect on dust diffusion. The second category includes the plane transport corridors, the living quarter of the workers, road side, waste recycling area, and around the load vehicle. The third category includes the construction waste dump, gunnery area, excavator area, and working passage. These positions have the highest raise dust emissions and the strongest construction intensity on the construction site. An independent sample T test is performed on the classification results, obtaining a T-test P-value matrix among the three categories as shown in *Table 5*.

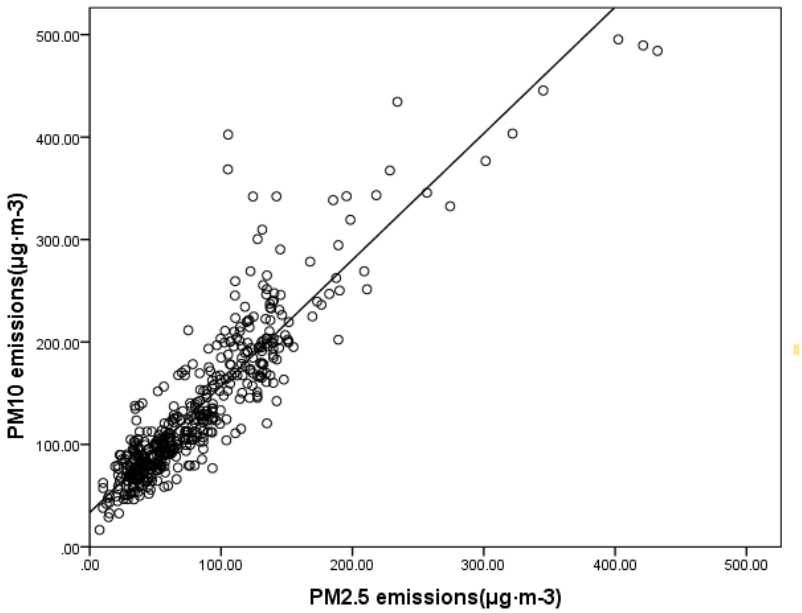

Figure 4. *Linear fitting of PM_{10} and $PM_{2.5}$ emission*

Table 5. *Independent sample T test on the classified result*

T test	The first category	The second category	The third category
The first category	1	0.019	9.5×10^{-5}
The second category	0.019	1	2.4×10^{-5}
The third category	9.5×10^{-5}	2.4×10^{-5}	1

According to the test standard $P < 0.05$, it can be seen that the classification of the measuring points into three categories has a good effect.

http://www.aloki.hu ● ISSN 1589 1623 (Print) ● ISSN 1785 0037 (Online)
DOI: http://dx.doi.org/10.15666/aeer/1706_1454314559

$PM_{2.5}$ and PM_{10} emission correlation

A linear fitting is conducted to PM_{10} and $PM_{2.5}$ emissions of each region. The R^2 fitting between two types of particle emissions in the region of the first category is 0.806, while the R^2 of linear fitting in the region of the second category is 0.481. The two has a good linear relationship in the third region with the highest emission intensity.

The linear fitting of PM_{10} and $PM_{2.5}$ emissions is shown in *Figure 5,* with a confidence coefficient of $R^2 = 0.817$. The following equation can be obtained for linear fitting:

$$\Delta PM_{10} = 1.234 \times \Delta PM_{2.5} + 33.496 \quad \text{(Eq.12)}$$

It can be seen from the fitting equation R^2 that the linear relationship between the two variables is good, indicating that the $PM_{2.5}$ and PM_{10} emissions have the same emission source in the region of the third category. The paired sample T test is used to test the two emissions, thus obtaining the significance coefficient $4.1^{-12} < 0.05$, that is, the PM_{10} emission is significantly larger than that of $PM_{2.5}$ in the demolition stage, and the particles discharged are mainly larger than 10 μm. When the demolition machinery in the region of the third category is working, the construction dust will be generated in the construction area, and the measured dust produces a large amount of $PM_{2.5}$ and PM_{10}. An independent sample T test is performed on the emission intensity in doing the demolition work and completing the demolition staged work, obtaining the double-tailed significance coefficient between the two categories is $0.025 < 0.05$. In other words, the dust emission in the demolition process is significantly higher the dust emission after completing the demolition staged work.

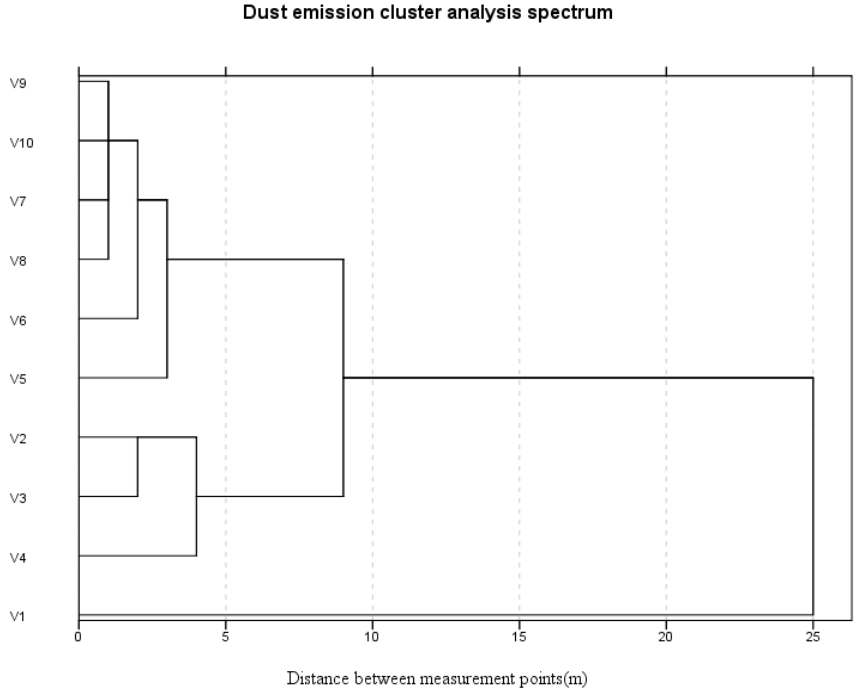

Figure 5. *Clustering analysis spectrum. V1: the working channel passage; V2: excavator working area; V3: the hydraulic crushing hammer working area; V4: the construction waste dump; V5: loading vehicle; V6: the plane transport corridor; V7: the waste recycling area; V8: the road side; V9: living quarter of the workers; V10: out of the construction wall*

http://www.aloki.hu ● ISSN 1589 1623 (Print) ● ISSN 1785 0037 (Online)
DOI: http://dx.doi.org/10.15666/aeer/1706_1454314559

Correlation between emission intensity and temperature and humidity

Based on the classification result of system clustering, the correlation analysis of emission intensity, temperature and humidity for the location of each category is conducted. The analysis result is shown in *Table 6*.

Table 6. *Correlation between emission strength and climate factor*

Factor	The first category	The second category	The third category
Temperature	0.296	0348**	0.091
Humidity	-0.353	-0.352**	-0.15

** indicates the significant correction in 0.01

According to the results of the correlation analysis, it can be seen that only the emission intensity in the region of the first category is significantly correlated with temperature and humidity. The region of the second category has the largest area in the construction site, and the dust emission intensity is negatively correlated with humidity and positively correlated with temperature. A higher relative humidity in the air enables the particles in the construction site to combine into the larger particles with waters and gases, and promotes PM_{10} to be converted into larger particles, reducing the content of inhalable particles in the air, and decreasing the dust diffusion capacity, so as to decline the emission intensity index in the region of the second category. The emissions of the planar transport corridor, living quarter of the workers, roadside, waste collection area and loading vehicle in the region of the second category is mainly caused by the diffusion of particles.

As the area with the largest amount of dust emission on the construction site, the emission intensity in the region of the third category is mainly affected by the construction intensity, and the particles mainly come from themselves. It has a greater impact on the surrounding area and is less affected by temperature and humidity, so the correlation between emission intensity and these two factors is not significant. The emission intensity outside the wall is low, which is greatly affected by other factors such as the dust of the vehicle, thus reducing the correlation.

Results

It can be seen from *Figure 6* that during the demolition process, the simulation result of the dust mass concentration is basically consistent with the measured data, and the distribution and variation laws are basically the same. The slight deviation between the two values is due to some errors in the field measurement, geometric model establishment and parameter setting process. Through comparative analysis, the movement, diffusion and settlement equations of demolition dust are verified, proving that it is feasible to use the discrete phase model to monitor and quantify the demolition construction dust distribution, and the simulation result is credible.

The region with the highest emission strength in the construction site is the operation channel, excavator working area, gunnery working area and construction dump. An independent sample T test is used to inspect the classification effect, a sound classification result has been obtained.

http://www.aloki.hu ● ISSN 1589 1623 (Print) ● ISSN 1785 0037 (Online)
DOI: http://dx.doi.org/10.15666/aeer/1706_1454314559

In the region with the highest emission intensity, PM_{10} emission has a strong positive correlation with $PM_{2.5}$ emission ($R^2 = 0.817$), namely, both pollutants have the same source of pollution.

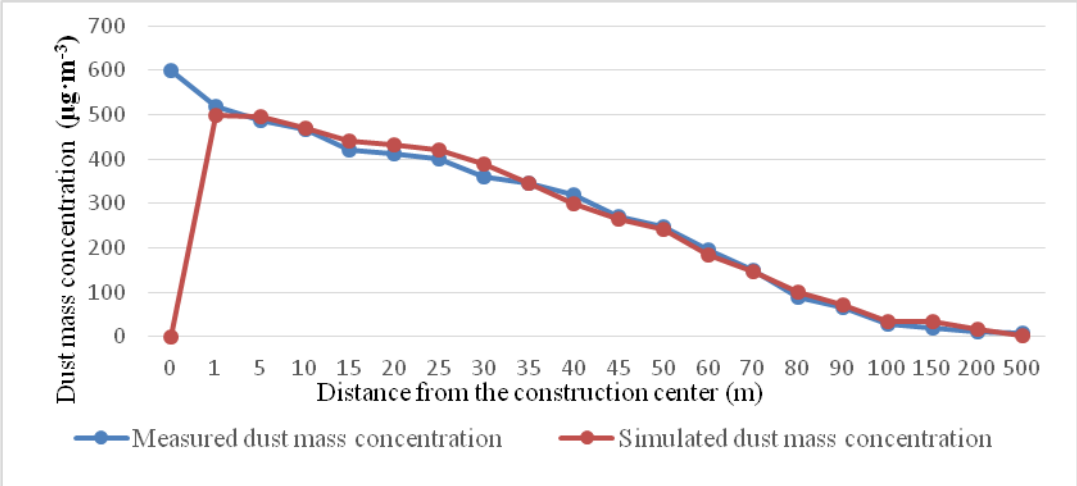

Figure 6. *Comparative analysis of dust mass concentration simulation and actual measurement*

Discussion

After analyzing the correlation between emission intensity and meteorological factors, it is concluded that the emission intensity of the plane transport corridor, living quarter of the workers, roadside, waste collection area and loading vehicle has a significant positive relationship with the temperature and a significant negative relationship with the humidity.

Moisture content of the dust: The higher the moisture content of the dust, the less likely the dust is to be raised.

Air temperature: When the temperature is low, the phenomenon of temperature inversion will probably occur, which hinders the convective movement of the air, so that the dust particles near the ground layer are not easily diffused, causing dust pollution. In the same condition, a lower temperature will lead to the probability of a higher dust concentration.

Air humidity: When the humidity of the air is high, the dust particles suspended in the air collide with the water molecules in the air, increasing the volume and mass of the dust particles, and enhancing the probability that the fine particles are mutually combined into large particles, thereby facilitating the sedimentation of dust particles.

Conclusion

Dust pollution during demolition operations creates a huge challenge for companies involved in such operations with regards to health and safety of workers and the neighboring community. By monitoring the change of dust concentration at the same height and at different distances near the boundary of the blasting site, this paper studied the dust diffusion law and formation law of the case study site in detail.

The main factors affecting the generation of construction dust include: (1) Moisture content of the dust. The higher the moisture content of the dust, the less likely the dust

http://www.aloki.hu ● ISSN 1589 1623 (Print) ● ISSN 1785 0037 (Online)
DOI: http://dx.doi.org/10.15666/aeer/1706_1454314559

is to be raised. (2) Air temperature. When the temperature is low, the phenomenon of temperature inversion will probably occur, which hinders the convective movement of the air, so that the dust particles near the ground layer are not easily diffused, causing dust pollution. In the same condition, a lower temperature will lead to the probability of a higher dust concentration. (3) Air humidity. When the humidity of the air is high, the dust particles suspended in the air collide with the water molecules in the air, increasing the volume and mass of the dust particles, and enhancing the probability that the fine particles are mutually combined into large particles, thereby facilitating the sedimentation of dust particles.

Due to the limitations in the theory, there is no unified method or quantitative analysis possible to derive demolition intensity. Therefore, the influence of demolition intensity on dust emission intensity was not considered in this study. It could be a very useful further research as demolition intensity was found to be a deciding factor on dust generation. As a further research area, developing a quantitative tool to represent demolition intensity would facilitate an in-depth study of the relationship between the demolition method, its intensity and dust generation and diffusion.

Acknowledgements. This work is supported by A Value-added Research of EPC Project Based on Value Chain, Jiangxi Provincial Department of Education Science and Technology Project (GJJ180367); Spatial Effect, Realization Mechanism and Path of New Urbanization Inclusive Development in Underdeveloped Areas, Jiangxi Science and Technology Plan Project (20181BAA208017).

REFERENCES

[1] Alekhfne, F. (2012): Gas-particles flow transitions for high density powder. – Lecture Notes in Engineering and Computer Science 1: 1820-1825.
[2] Ansart, R., Ryck, A., Dodds, J. A., Roudet, M., Fabre, D., Charru, F. (2009): Dust emission by powder handling: comparison between numerical analysis and experimental results. – Powder Technology 190(1-2): 274-281.
[3] Cerecedo, L. M., Aisa, L., Ballester, J. (2009): Experimental study on a non-dilute two-phase coflowing jet: Dynamics of particles in the near flow field. – International Journal of Multiphase Flow 35(5): 468-483.
[4] Chen, B., Chen, Z., Deng, L. (2016): Building change detection with RGB-D map generated from UAV images. – Neuro Computing 208: 350-364.
[5] Chen, J. S., Jiang. L., Jiang, Z. G. (2015): Numerical simulation of dust distribution and its influencing factors in slope drilling. – Journal of Engineering Science 37(6): 685-692.
[6] Chou, J. S., Yeh, K. C. (2016): Life cycle carbon dioxide emissions simulation and environmental cost analysis for building construction. – Journal of Cleaner Production 101: 137-147.
[7] Dong, S. H., Xie, Y., Huang, F. Y. Q., Shi, X. R., Yi, R., Shi, G. L., Feng, Y. (2019): Assessment of heavy metal sources and potential health risks of $PM_{2.5}$ in Yangzhou. – Environmental Science 2: 1-10.
[8] Fan, S. B., Yang, T., Wang, K., Li, X. F. (2019): Establishment method and application of road raise dust emission factor establishment. – Environmental Study 4: 1-13.
[9] Huang, Y., Qu, S., Song, G., Li, G., Tian, G. (2013): Comparison of dust source particle composition screening method. – Environmental Science Research 26(5): 522-526.
[10] Kohlman, R. E. R., Shapira, A., Martins, A. R. B. (2014): Characterization and evaluation dust on building construction sites in Brazil. – Neurochemistry International 5(1): 1-8.
[11] Li, M., Wu, C. (2006): Visualization of dust point pollution diffusion model. – Environmental Science and Technology 11(12-14): 115-116.

http://www.aloki.hu ● ISSN 1589 1623 (Print) ● ISSN 1785 0037 (Online)
DOI: http://dx.doi.org/10.15666/aeer/1706_1454314559

[12] Li, X. D., Su, S., Huang, T. J. (2014): Monitoring and analysis of raise dust of the building in secondary structure and indoor rough decoration stages. – Journal of Chinese Safety Sciences 24(8): 103-106.
[13] Li, X. D., Su, S., Huang, T. J. (2015): Quantitative evaluation of health damage caused by construction dust. – Journal of Tsinghua University (Natural Science Edition) 55(1): 50-55.
[14] Ma, G. X., Han, Y., Lu, J. F., Yao, J., You, S. D. (2018): Design and achievement of automatic monitoring system for dust pollution sources based on UAV. – Environmental Monitoring in China 34(1): 151-156.
[15] Madelyn, M., Antonio, R. D. A. (2010): The building cost system in Andalusia: application to construction and demolition waste management. – Construction Management and Economics 28(5): 495-507.
[16] Mohamed, M., Magdy, M., Azza, A. Z., Ei-said, M. (2008): Handling construction pollutions using multi-objective optimization. – Construction Management and Economics 26(10): 1113-1125.
[17] Muleski, G. E., Cowherd, C. J., Kinsey, J. S. (2005): Particulate emission from construction activities. – Journal of the Air & Waste Management Association 55: 772-783.
[18] Peng, X., Shi, G., Liu, G., Xu, J., Tian, Y., Zhang, Y., Feng, Y., Russell, A. G. (2016): Source apportionment and heavy metal health risk (HMHR) quantification from sources in a southern city in China, using an ME2-HMHR model. – Environmental Pollution 221: 335-342.
[19] Shi, P., Du, K., Mu, C., Wang, K., Wang, Y. (2013): Vertical scanning radar observation method for unorganized raise dust of the construction site. – Optical Journal 33(3): 39-45.
[20] Sun, Z. Q., Fang, B. J. (2016): Analysis of dust stress and its movement in construction tunnel. – Coal Technology 35(5): 176-178.
[21] Sung, K. P., Liu, C. L., Craig, L. (2006): Case study of demolition costs of residential buildings. – Construction Management and Economics 24(9): 967-976.
[22] Thomas, L. D., Hodgson, S., Nieuwenhuijsen, M., Jarup, L. (2009): Early kidney damage in a population exposed to cadmium and other heavy metals. – Environmental Health Perspectives 117(2): 181-184.
[23] Toropov, E. V., Osintsev, K. V., Aliukov, S. V. (2018): Analysis of the calculated and experimental dependencies of the combustion of coal dust on the basis of a new methodological base of theoretical studies of heat exchange processes. – International Journal of Heat and Technology 36(4): 1240-1248.
[24] Wang, R., Chen, B. (2014): Three-dimensional lattice vortex method for simulating free falling particle groups. – Engineering Thermophysics 35(3): 499-502.
[25] Wu, F. B., Zhang, H. K., Lv, Q. T. (2017): Design of environmental monitoring system based on embedded construction site. – Modern Electronic Technique 40(20): 72-76.
[26] Wu, Z., Zhang, X., Wu, M. (2015): Mitigating construction dust pollution: state of the art and the way forward. – Journal of Cleaner Production 112: 1658-1666.
[27] Xiao, H., Yang, X., Wu, Q., Bai, Q., Chen, H., Chen, X., Xue, R., Du, M., Huang, L., Wang, R., Wang, H. (2019): Estimate emissions of construction fugitive dust in Xi'an. – Chinese Journal of Environmental Science 1: 222-228.
[28] Zhi, X., Jiang, Z., Tang, M., Jiang, X (2018): Force analysis of settling dust on dust collecting plate and secondary flying research. – Coal Journal 33(3): 310-313.
[29] Zhu, P., Zhang, C., Li, D. M., Bai, S. (2017): Research on numerical simulation of dust distribution in belt conveyer lane. – Journal of North China Institute of Science and Technology 14(6): 40-46.
[30] Zuo, J., Raufdeen, R., Matthew, H. (2017): Dust pollution control on construction site: awareness and self-responsibility of managers. – Journal of Cleaner Production 166: 312-320.

http://www.aloki.hu ● ISSN 1589 1623 (Print) ● ISSN 1785 0037 (Online)
DOI: http://dx.doi.org/10.15666/aeer/1706_1454314559

UNPACKING THE INFLUENCE OF MAJOR CITIES ON CORPORATE ENVIRONMENTAL PERFORMANCE IN CHINA: A PERSPECTIVE OF SPATIAL KNOWLEDGE SPILLOVER

WANG, T.[1,2] – TIAN, M.[1,3*] – LIU, Z. R.[1,2]

[1]*Business School, Hohai University, Nanjing 211100, China*

[2]*Institute of International River in Hohai University, Nanjing 211100, China*

[3]*World Water Valley Institute, Nanjing 211100, China*

**Corresponding author*
e-mail: hhutm@hhu.edu.cn; phone: + 86-138-0518-2774

(Received 7th Jun 2019; accepted 10th Oct 2019)

Abstract. As one of the most concerned topics in environmental and ecological research, the environmental performance of firms is extensively studied while little notices the relationship between firms' geo-location and major cities. Focusing on the spatial agglomerations of corporate environmental performance (CEP) surrounding major cities in China, we examine the research question of "How could major cities affect firms' environmental performances". We propose that major cities affect CEP through knowledge spillover, while the strength of influences depends on firms' spatial proximity to the central area of major cities. Besides, we argue that CEP knowledge spillover principally consists of knowledge transfer and knowledge conversion, the two modes via which CEP knowledge spills over. Based on a sample of 193 Chinese firms, we find that Firms in spatial proximity to major cities centers could obtain more knowledge transfer and conversion on CEP, and thereby improving their environmental performance. Finally, we discuss the research findings, limitations, and future research directions.
Keywords: *spatial proximity, major cities, corporate environmental performance, knowledge spillover, knowledge transfer, knowledge conversion*

Introduction

With the rapid development of China's economy, environmental and ecological issues constantly snowball and draw attention. As one of the most influential economic entities, firms significantly affect the environment and ecology while their environmental performance gradually turns into a crucial concern in theory and practice. In recent years, while overall corporate environmental performance (CEP) has improved in many countries, the distributions show obvious spatial imbalances, such as the prominent CEP agglomeration around major cities. For example, in the United States, firms closer to New York and Chicago are significantly more active in environmental performance, while those in other locations are relatively mediocre (Husted et al., 2016). Extant wisdom shows that major cities could significantly impact corporate environmental performance in both form and content while the impact is tightly related to firms' spatial closeness to major cities (Marquis and Tilcsik, 2016). However, how do firms' spatial proximities to major cities affect their environmental performances? Extant literature lacks a unified and detailed explanation (Marquis and Battilana, 2009; Husted et al., 2012). Thus, correctly clarifying the influence of major cities on CEP and identifying the potential factors that explains the effect of geo-location on firms' environmental performance have become the primary concern.

http://www.aloki.hu ● ISSN 1589 1623 (Print) ● ISSN 1785 0037 (Online)
DOI: http://dx.doi.org/10.15666/aeer/1706_1456114576

In extant literature, most scholars have studied the mechanisms between firms' spatial proximity to major cities and CEP from the institutional perspective. Based on the neo-institutional theory, researchers suggest that institution is the key reason that a firm's geo-location affects its environmental performance (DeBoer et al., 2017). Similar to industry-related organizational fields (DiMaggio and Powell, 1983), space-related stakeholders could form geographic fields. To obtain legitimization positions in local fields, companies conduct and adjust environmental strategies to meet the legitimacy demands of local stakeholders (Marquis et al., 2007; Hoi et al., 2018). Since the legitimacy requirements in geographic fields are often different, firms' environmental performance vary by locations (Attig and Brockman, 2017; Marquis et al., 2013). In the meantime, related literature suggests that geo-location could influence a firm's organizational practices through efficiency mechanisms, not only in innovation but also in many other organizational practices, including internationalization (Lejpras, 2015), competitive strategy choice (Liarte and Forgues, 2008), legislation resistance behaviors (Simons et al., 2016), stock backdating (Audia and Yao, 2017), and so forth. In such cases, some scholars focus on the efficiency perspective and seek for other theoretical explanations that could bridge proximity to major cities and CEP.

Despite the prevalence of institutional perspective, a few scholars argue that local resources also matter in the influence of geo-location on firms' environmental performances. They propose that firms' geo-locations determine the local resources that are necessary for organizational practices, such as local labor, news media, and information (Sorenson and Baum, 2003). Among those local resources, knowledge resource is of particular importance to corporate environmental performance. Through knowledge spillover, CEP knowledge could significantly promote firms' environment-friendly actions. For instance, Nyuur argues that knowledge spillover from FDI could increase domestic firms' uptake of environment-protection activities (Nyuur et al., 2016). Ning and Wang propose that environmental knowledge spillover could improve local firms' environmental performances (Ning and Wang, 2018). Although a few scholars have noticed the influence of knowledge spillover on CEP, the corresponding research is quite limited, leaving critical issues unanswered. Specifically, how proximity to major cities influence corporate environmental performance through knowledge spillover.

To address the gap mentioned, this study integrates stakeholder theory and knowledge spillover theory to study the mediating role of knowledge spillover between firms' spatial proximity to major cities and environmental performance. We initially analyze the dimension of CEP knowledge spillovers and identify two modes - knowledge transfer and knowledge conversion- via which CEP knowledge spills over. Then we construct the theoretical model that consists of the "spatial proximity-knowledge transfer-CEP" path and the "spatial proximity-knowledge conversion-CEP" path. We hypothesize that knowledge transfer and knowledge conversion are the two potential mediating roles between proximity to major cities and CEP. Furthermore, we empirically test the research hypotheses. Finally, we discuss research findings, limitations, and future research directions.

Materials and methods

Study area

The study area includes multiple major cities from different regions in China mainland, including eastern coastal regions and western inland regions. *Figure 1* shows the location

http://www.aloki.hu ● ISSN 1589 1623 (Print) ● ISSN 1785 0037 (Online)
DOI: http://dx.doi.org/10.15666/aeer/1706_1456114576

of the study area, the gray area represents the administrative boundary of China mainland, the blue labeled area represents the cities that our sample firms located in.

Those cities typically inhabit more population and other stakeholders, which derives the influence in social, economic, cultural, and political aspects, on the national or regional scale. For instance, Beijing (21.54 million), Shanghai (24.24 million), Guangzhou (14.9 million), and Shenzhen (13.03 million) are the top four cities in China, while Nanjing (8.44 million), Hangzhou (9.81 million), Xining (2.37 million), Hefei (8.09 million), and Zhengzhou (10.13 million) are provincial capital (population in the brackets).

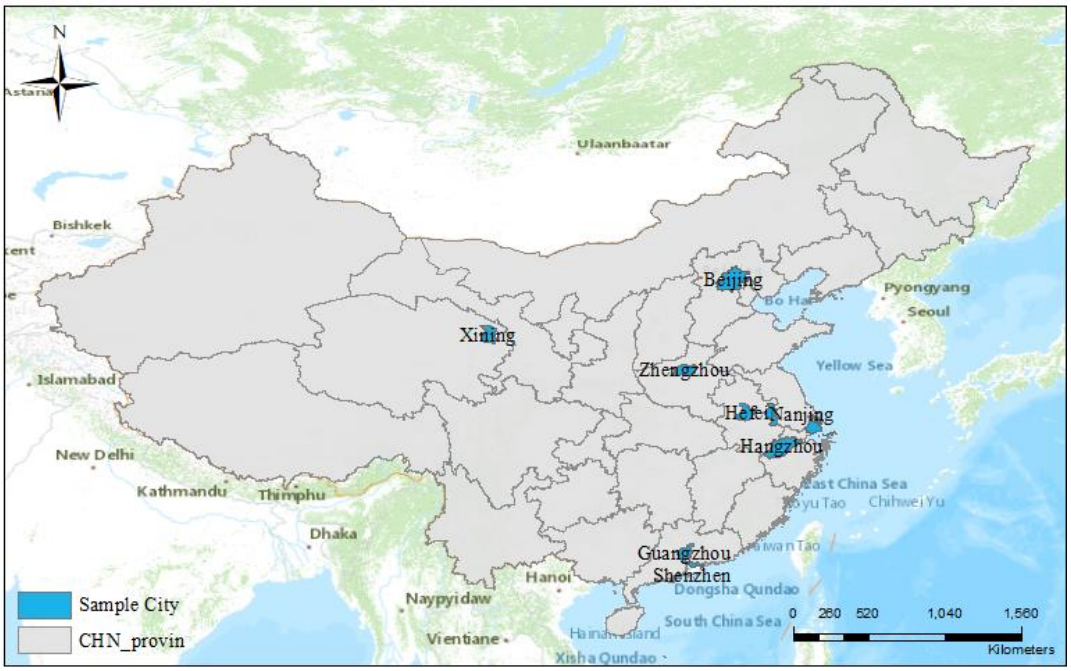

Figure 1. *Location of study area*

Theories and hypotheses

CEP knowledge spillover: knowledge transfer and conversion

As an essential concept in economic geography, knowledge spillover is controversial in its definition (Stanko and Olleros, 2013; Yang and Steensma, 2014; Qiu et al., 2017). Relevant literature extensively diverges on various facets in the process that knowledge spills over. For instance, the intentionality of knowledge providers (Fallah and Ibrahim, 2004), the content of knowledge (Lejpras, 2015; Simons et al., 2016; Wang and Wu, 2016), and whether receivers adjust the knowledge they gained (Eapen, 2012; Battke et al., 2016). Despite the above disputes, we follow Ko and Liu that define knowledge spillover as 'the process that firms receive information, technique, and experience from knowledge providers, and improve the action efficiencies' (Ko and Liu, 2015).

In early research, knowledge spillover mostly is correlated to the efficiencies of production or innovation (Krugman, 1991; Glaeser et al., 1992; Fukugawa, 2017). However, with the extension of application extent, this concept has been gradually employed in other fields. Knowledge attribute embeds not only in innovation which is knowledge-intensive but also in many other organizational practices, such as

http://www.aloki.hu ● ISSN 1589 1623 (Print) ● ISSN 1785 0037 (Online)
DOI: http://dx.doi.org/10.15666/aeer/1706_1456114576

international expansion (Lejpras, 2015), entrepreneurship (Dahl and Sorenson, 2012), and stock backdating (Audia and Yao, 2017), etc. Similarly, CEP practices also require different types and extent of knowledge, which could make CEP practices more cost-efficient, encouraging firms to further engage in CEP (Mcwilliams and Siegel, 2001). For instance, managers who received ethic knowledge training are more likely to integrate ethics codes into corporate's strategic decisions, because they know how to fulfill environmental performance efficiently and thus be encouraged to do more (Stevens et al., 2005). Similarly, FDI could promote the environmental performance of local firms, since foreign companies could provide local firms CEP knowledge (Nyuur et al., 2016).

How can firms obtain CEP knowledge? Besides the endogenous growth from learning by doing (Arrow, 1962), firms could acquire CEP knowledge from the external as well. While CEP knowledge spillover differs from other knowledge spillovers in terms of knowledge content, they are fundamentally similar in other aspects. Therefore, based on the two modes of knowledge spillover and context-specific trait of CEP (Williams, 2007; Aguinis and Glavas, 2012), we define CEP knowledge spillover as 'the process that firms receive information, technique, and experience that are related to CEP, and thereby improve CEP efficiencies.' Furthermore, we propose that CEP knowledge spillover happens via two modes: knowledge transfer and knowledge conversion.

In CEP knowledge spillover, knowledge receivers acquire knowledge from different providers, such as local or industrial peers, NGOs, academic institutes and even governments (Miles, 2015). In some cases, receivers would find the acquired knowledge fits the CEP practices and can be applied without modification. Based on Fallah's definition of knowledge transfer (Fallah and Ibrahim, 2004), we define this dimension as CEP knowledge transfer. Meanwhile, not all the CEP knowledge spills over via this mode because the external CEP knowledge is often not completely applicable. Since firms' environmental performance is context-specific organizational actions and policies, successful applications of CEP knowledge are often bounded within specific contexts, such as national context (Matten and Moon, 2008; Kim et al., 2013), industrial context (Wanderley et al., 2008; Cordeiro and Tewari, 2015), and organizational context (Aguinis and Glavas, 2012). In this case, the external CEP knowledge should be conversed according to receivers' external environment and internal conditions, which is termed as knowledge conversion.

Spatial proximity, major cities and corporate environmental performance

Recent studies have discovered the influence of major cities on CEP. Drawing on the neo-institutional theory, scholars argue that major cities could form geo-institutional communities, which exert institutional pressures on firms and drive them to engage in CEP (Ning and Wang, 2018). The primary logic is, the three pillars of institutional pressures-regulatory pressure, normative pressure, and cognitive pressure originates from the different type of stakeholders, which intensively resident in major cities. In the meantime, compared with the peripheral areas, the central areas of major cities inhabit much more stakeholders, including residents, universities, local communities, and NGOs, and so forth.

Besides residents, the other stakeholders also tend to locate concentrated in the central areas of major cities (Taylor, 2005). While the major cities' influence on CEP majorly results from those stakeholders, the influence would be stronger in those areas

http://www.aloki.hu ● ISSN 1589 1623 (Print) ● ISSN 1785 0037 (Online)
DOI: http://dx.doi.org/10.15666/aeer/1706_1456114576

populated with more stakeholders. Therefore, compared with the peripheral areas, the central areas of major cities are more likely to function as the influences sources and affect firms' environmental performances. Meanwhile, the influences from stakeholders in major cities centers could transmit across geographic distance via face-to-face interactions (Sorper and Venables, 2004), which means the remote firms could also be affected by major cities centers and engage in CEP. However, the influence would decade with distance due to the economic and time cost of interactions, which means firms close to the major cities centers would be influenced more and thereby engage in CEP more. The following hypotheses are therefore proposed:

Hypothesis 1: Firms in spatial proximity to major cities centers engage in CEP more than their more remote counterparts.

Proximity to major cities centers and knowledge spillover

According to Boschma (2005), geographic proximity is "the spatial or physical distance between economic actors". In this study, spatial proximity to major cities centers refers to "the spatial distance between the focal firm and the central area of the nearest major city". Urban economists argue that knowledge spillover happens more intensively in major cities, no matter inter- or intra- industries (Jacobs, 1969; Carlino et al., 2007). In the meantime, we argue that knowledge spillover happens more intensively in the central areas of major cities than the peripheral areas, which would be further explained in the following.

In economic geography, knowledge is an important resource that could boost firms' efficiencies, which is arduous to transport (Krugman, 1991). Stakeholders in the major cities centers could be viewed as CEP knowledge reserve, from which firms could acquire CEP knowledge by interacting (Porter and Kramer, 2011). Through direct or indirect, pro-active or passive interactions, companies can obtain CEP knowledge from nearby non-peer stakeholders (Miles et al., 2006). *Figure 2* is created by utilizing diagramming software Visio 2016, as the figure shows, local peers are also an important source to obtain CEP knowledge via inter-firm knowledge spillover (Appleyard, 1996). Comparing to those remote peers, nearby firms are more convenient to contact, while the CEP knowledge from them is regarded as more legitimate and proper (Haveman, 1993). For those knowledge receivers, CEP knowledge would be beneficial to the CEP practices by bettering the cost-efficiencies. Therefore, because of knowledge spillovers from local stakeholders, a firms' geo-location could influence its accessible CEP knowledge and thereby the cost-efficiency of CEP practices.

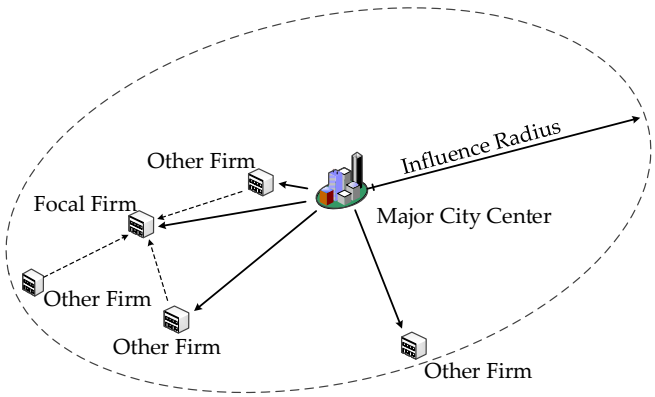

Figure 2. *The model of major cities centers' influence on knowledge spillover*

http://www.aloki.hu ● ISSN 1589 1623 (Print) ● ISSN 1785 0037 (Online)
DOI: http://dx.doi.org/10.15666/aeer/1706_1456114576

Although CEP knowledge flows from major cities centers toward nearby firms, its spatial-bounded trait limits the long-distance transmission (Boschma, 2005), which means effective knowledge spillover only happen within a limited geographic extent. Although IT technologies could help explicit knowledge flows beyond geographic limits, face-to-face interaction is still an important channel for knowledge spillovers, especially tacit knowledge (Storper, 2004). Besides, the interpretation and absorption of explicit knowledge might still need implicit knowledge (Howells, 2002). Hence, the spillover of codified CEP knowledge could also be spatial-bounded. In this case, the spatial closeness between knowledge receiver and provider would be a must for effective CEP knowledge spillover, no matter knowledge transfer or knowledge conversion. The following hypotheses are therefore proposed:

Hypothesis 2a: Firms in spatial proximity to major cities centers obtain more knowledge transfer on CEP than their more remote counterparts.

Hypothesis 2b: Firms in spatial proximity to major cities centers obtain more knowledge conversion on CEP than their more remote counterparts.

Knowledge spillover and corporate environmental performance

Despite the disputes of available conceptualizations, we avoid confusion by following Aguinis and Trumpp (Aguinis and Glavas, 2012; Trumpp et al., 2015), and define CEP as "context-specific organizational actions and policies that take into account stakeholders' expectations in environmental performance". In the past decades, due to the limited role of knowledge in CEP practices, studies about knowledge spillovers and CEP were carried out independently, and few scholars noticed the connections. With the evolution of CEP in theory and practice, the importance of knowledge on firms' environmental performance gradually draws attention.

As a significant channel that knowledge spills over, training programs can deepen the financial supervisors' understanding of ethical regulations, who thereafter consider more environment-friendly action in decision-making. Stevens finds that financial executives who received relevant training are more inclined to integrate ethic codes into strategic activities because they know how to do so effectively (Stevens et al., 2005). The dialogue between firms and stakeholders contribute to the flow of tacit knowledge and help firms make better decisions about CEP (Miles et al., 2006). When other conditions remain unchanged, obtaining knowledge makes CEP practices more cost-efficient, and firms that receive CEP knowledge will be more environment-friendly (Stevens et al., 2005). For instance, FDI could promote local firms in host countries to engage in CEP more. In most developing countries, because of more knowledge and experience in CEP foreign companies function as important CEP knowledge sources for domestic companies (Nyuur et al., 2016). During communication with foreign peers, local domestic firms could acquire CEP knowledge as well as technological knowledge.

Knowledge spillover enables firms to acquire knowledge, increasing cost-efficiency in the same practice. Similarly, CEP knowledge can guide firms to know how to effectively perform CEP, encouraging firms to further engage in CEP activities (McWilliams and Siegel, 2001). Driven by different motives such as organizational interest, institutional pressure or managerial preference, firms would increase the CEP engagements to a certain extent. However, the influences of these drivers are usually limited. Similar to the other organizational practice such as internationalization, the

http://www.aloki.hu ● ISSN 1589 1623 (Print) ● ISSN 1785 0037 (Online)
DOI: http://dx.doi.org/10.15666/aeer/1706_1456114576

decreasing marginal profits restrict firms to participate in CEP unconditionally but stay at a certain cost-benefit equilibrium point (Kim et al., 2015). For firms that gain operational efficiency from CEP knowledge spillover, the CEP capabilities are further enhanced, enabling those firms to reduce the cost or improve the revenue when performing environment-friendly actions. Those firms could break the initial equilibrium point and further participate in CEP until reaching the new equilibrium point. In this process, no matter knowledge transfer or knowledge conversion, CEP knowledge spillover always follow the "knowledge-efficiency-action" path, providing firms with CEP knowledge to enhance the CEP efficiencies, and further promotes firms to engage in CEP activities. The following hypotheses are therefore proposed:

Hypothesis 3a: Obtaining knowledge transfer on CEP promotes firms' CEP engagements.

Hypothesis 3b: Obtaining knowledge conversion on CEP promotes firms' CEP engagements.

The mediating role of knowledge spillover

The recent study shows that proximity to major cities should promote firms to engage in CEP more (Husted et al., 2012, 2016). The arguments overwhelmingly derive from the belief that various stakeholders in major cities centers could exert institutional pressures on nearby firms, driving them to improve environmental performance and obtain legitimacy in local communities (Marquis and Tilcsik, 2016; Marquis et al., 2007; Attig and Brockman, 2017). Meanwhile, some scholars argue that the influence of major cities centers on firms' practices is usually comprehensive, including not only legitimacy mechanism of institutional pressures but also efficiency mechanism of knowledge spillover (Jacobs, 1969; Carlino, 2001). On this basis, we argue that legitimacy mechanism maybe not the unique channel that links major cities to CEP. One alternative is that proximity to major cities may influence CEP through the efficiency mechanism that typically derives from knowledge spillover.

Based on knowledge spillover theory, we argue that firms close to major cities could benefit from local knowledge reserve via knowledge spillover, which enhances the efficiency of environmental actions and encourages firms to engage in CEP more (Lejpras, 2015; Audia and Yao, 2017). During the process of CEP knowledge spillover, firms could obtain CEP knowledge through knowledge transfer or knowledge conversion from the local knowledge reserve embedded in major cities. Knowledge transfer offers firms proper CEP knowledge that could be applied directly, and knowledge conversion offers firms partially proper CEP knowledge that is applicable after adaptation. Because of knowledge transfer and knowledge conversion, firms close to major cities could access CEP knowledge spillover more, and thus more actively engage in CEP. Furthermore, whether knowledge transfer and knowledge conversion mediate the relationship between proximity to major cities and CEP warrants an empirical test. The following hypotheses are therefore proposed:

Hypothesis 4a: Firms in spatial proximity to major cities centers obtain more knowledge transfer on CEP than their more remote counterparts, and thereby engage in CEP more.

Hypothesis 4b: Firms in spatial proximity to major cities centers obtain more knowledge conversion on CEP than their more remote counterparts, and thereby engage in CEP more.

http://www.aloki.hu ● ISSN 1589 1623 (Print) ● ISSN 1785 0037 (Online)
DOI: http://dx.doi.org/10.15666/aeer/1706_1456114576

Research design

Sample and procedures

In this research, we collect data primarily through a questionnaire survey. A total of 474 questionnaires are distributed with 278 returned, which means a 58.65% response rate. After discarding questionnaires that contain missing information, 193 questionnaires are usable. To ensure the diversity and reliability of our sample, in our survey three principles are followed.

First, we manage to ensure the diversity of firms' regions and industries. This study examines the connection between major cities and corporate environmental performance from a spatial proximity perspective, hence the dispersion of geography and industry is particularly important. Considering the actual influence radius of major cities centers, in this study we only distribute questionnaires to those firms located in the administrative areas of major cities. The research samples include major cities in the eastern coastal areas such as Beijing, Shanghai, Nanjing, Hangzhou, Guangzhou, Shenzhen, and those in the inland provinces such as Xining, Hefei, and Zhengzhou. In terms of industry distribution, the research samples' industry includes manufacturing (51.30%), financial (8.80%), real estate (12.95%) and others (26.94%).

Second, we manage to ensure the diversity of firms' age and size. Extant literature suggests that a firm's age, size, and ownership could significantly affect its environmental performance [238, 261]. Therefore, we pay particular attention to those corporate characteristics in sample selection. Based on the survey results, the research sample of this study has good representativeness in terms of age, scale, and ownership, including 22.80% for less than eight years, 45.60% for 8 to 15 years, and 31.6% for 15 years or more. In terms of firm size, 100 or less accounted for 31.61%, 101 to 500 people accounted for 26.94%, 501 to 1000 people accounted for 10.88%, and more than 1,000 people accounted for 30.57%.

Third, to ensure the reliability of data acquired, we invite senior executives and key management personnel to fill out the questionnaire to obtain comprehensive and accurate survey results. We distribute questionnaires through channels including social networks, economic development zone management committees, and college MBA centers to ensure the participation of senior managers or CEP-related managers.

Measures

Except for the "proximity to major cities" variable, all other variables were measured by multi-item scales with a five-point Likert scale (1 = strongly disagree, 5 = strongly agree).

Spatial proximity to major cities. We utilize the instrumental variable "driving distance" to measure "spatial proximity to major cities". The calculation involves two coordinate points, including the coordinates of the target enterprise and the coordinates of the center point of the nearest major city. Following DeBoer, this study utilizes Google Map software to calculate the driving distance between target firm and the central point of the major city, the driving distance could reflect the accessibility and convenience of communication between socio-economic entities (Husted et al., 2016; DeBoer et al., 2017). Based on the operational definition from Mahafzaa (Mahafza et al., 2017), we adopt the logarithm of the driving distance between the firm's location and the city center point as the measurement of proximity to major cities. Also, in case

http://www.aloki.hu ● ISSN 1589 1623 (Print) ● ISSN 1785 0037 (Online)
DOI: http://dx.doi.org/10.15666/aeer/1706_1456114576

that the target firm's distance to the central point is less than 1 km, we increase all the measured distance by 1 km before taking the logarithm (Broekel and Boschma, 2011).

Knowledge transfer. Knowledge transfer is measured by adopting a four-item scale developed by modifying the relevant scale and theoretical arguments (Ko and Liu, 2015; Tho and Trang, 2015). Sample items include: "Our company obtains entirely suitable CEP knowledge from local peers, governments, NGOs or academic institutions", and "Our company improves the efficiency of CEP practices by directly applying acquired CEP knowledge". The Cronbach's α is 0.899.

Knowledge conversion. Knowledge conversion is measured by adopting a four-item scale developed by modifying the relevant scale and theoretical arguments (Williams, 2007; Islam et al., 2017). Sample items include: "Our company obtains entirely suitable CEP knowledge from local peers, governments, NGOs or academic institutions", and "Our company improves the efficiency of CEP practices by adjusting or improving acquired CEP knowledge". The Cronbach's α is 0.926.

Corporate environmental performance. Corporate environmental performance is measured by a 4-item scale developed by modifying extant scales to fit our research context and purpose (Turker, 2009; Moneva and Ortas, 2010). Sample items include: "Our company participates in activities which aim to protect and improve the quality of the natural environment", "Our company implements special programs to minimize its negative impact on the natural environment", "Our company conducts environmental training of employees", and "Our company supports environmental NGOs working in problematic areas". The Cronbach's α is 0.876.

Control variables. Due to the potential effects of firm demographics (e.g., firm size, age, region, and industry) on corporate environmental performance (Brik et al., 2011; Wu et al., 2015), we control for firm size, firm age, firm industrial type, and firm region type. We collect the data of control variables through a questionnaire survey, firm size (employee number, 1 = less than 100, 2 = 101 – 500, 3 = 501 – 1000, 4 = more than 1000), firm age (establishment years, 1 = 1 – 7, 2 = 8 – 15, 3 = more than 15), and firm industry (1 = manufacture, 2 = finance, 3 = real estate, 0 = others) are represented by category variables, while a dummy variable represents firm region (1 = coastal cities, 0 = non-coastal cities).

Methods and models

To examine hypothesis 1 and 2, this study utilizes the following regression model 1 (*Eq. 1*), model 2 (*Eq. 2*), and model 3 (*Eq. 3*). Symbol *i* represents each firm, *CEP* represents the dependent variable corporate environmental performance, *Distance* represents the independent variable spatial proximity to major cities centers, *Transfer* represents the mediator knowledge transfer, and *Conversion* represents the mediator knowledge conversion. *Controls* represents the control variables, including firm size, firm age, firm region, and firm industry. ε represents random error terms. β represents parameters to be estimated.

$$CEP_i = \beta_0 + \beta_1\, Distance_i + \beta_2\, Controls_i + \varepsilon_i, \quad \text{(Eq.1)}$$

$$Transfer_i = \beta_0^{'} + \beta_1^{'} Distance_i + \beta_2^{'} Controls_i + \varepsilon_i, \quad \text{(Eq.2)}$$

$$Conversion_i = \beta_0^{''} + \beta_1^{''} Distance_i + \beta_2^{''} Controls_i + \varepsilon_i, \quad \text{(Eq.3)}$$

http://www.aloki.hu ● ISSN 1589 1623 (Print) ● ISSN 1785 0037 (Online)
DOI: http://dx.doi.org/10.15666/aeer/1706_1456114576

To examine hypothesis 3 about the relationship between knowledge spillover (knowledge transfer and conversion) and CEP, we construct model 4 (*Eq. 4*) and model 5 (*Eq. 5*), meanwhile, we integrate the above models and construct the regressions model 6 (*Eq. 6*) and model 7 (*Eq. 7*) to further examine the mediating effects of knowledge transfer and knowledge conversion.

$$CEP_i = \beta_0''' + \beta_1''' Transfer_i + \beta_2''' Controls_i + \varepsilon_i, \quad \text{(Eq.4)}$$

$$CEP_i = \beta_0'''' + \beta_1'''' Conversion_i + \beta_2'''' Controls_i + \varepsilon_i, \quad \text{(Eq.5)}$$

$$CEP_i = \beta_0''''' + \beta_1''''' Transfer_i + \beta_2''''' Distance_i + \beta_3''''' Controls_i + \varepsilon_i, \quad \text{(Eq.6)}$$

$$CEP_i = \beta_0'''''' + \beta_1'''''' Conversion_i + \beta_2'''''' Distance_i + \beta_3'''''' Controls_i + \varepsilon_i, \quad \text{(Eq.7)}$$

Results

Descriptive statistics

Table 1 presents the means, standard deviations, and correlations of all critical variables. As shown in the table, proximity to the major city significantly correlates with knowledge transfer (r = -.469, p < .01), knowledge conversion (r = -.606, p < .01) and CEP (r = -.700, p < .01). Besides, both knowledge transfer (r = .428, p < .01) and knowledge conversion (r = .544, p < .01) are positively associated with CEP. The above results provide primary support to our hypotheses.

Table 1. *Means, standard deviations, and correlations*

Variable	1	2	3	4	5	6	7	8
1. Distance	1							
2. Transfer	-.469**	1						
3. Conversion	-.606**	.419**	1					
4. CEP	-.700**	.428**	.544**	1				
5. Firm size	-.485**	.195**	.243**	.365**	1			
6. Firm age	-.533**	.347**	.385**	.437**	.250**	1		
7. Industry	-.032	.018	.019	.026	-.128	.104	1	
8. Region	-.041	.109	.059	.056	-.027	-.004	-.022	1
Mean	3.642	2.763	3.505	2.404	2.088	1.078	.777	.780
S.D.	.819	.913	.725	1.222	.734	.935	.417	.415

N = 193; **p < .01; *p < .05 (two-tailed)

Confirmatory factor analyses

We first examined a four-factor model, in which distance, knowledge transfer, knowledge conversion, and corporate environmental performance are included. Following suggestions by Hair (Wu et al., 2015; Hair et al., 2006), we utilize the overall model's Chi-square, the comparative fit index (CFI), the Tucker-Lewis Index (TLI), and the root mean square error of approximation (RMSEA) to assess the model fit. A cutoff value closes to or above .90 for CFI and TLI, and a cutoff value below .08 for RMSEA

http://www.aloki.hu ● ISSN 1589 1623 (Print) ● ISSN 1785 0037 (Online)
DOI: http://dx.doi.org/10.15666/aeer/1706_1456114576

indicate a relatively acceptable fit between the proposed model and the observed data. Our theoretical model consists of two mediating structures, including SP→KT→CEP path and SP→KC→CEP path, and the results suggest that our model fits the data well (χ^2 / df = 1.468 < 3; RMSEA = 0.049 < 0.08; CFI = 0.978 > 0.9; TLI = 0.983 > 0.9). Besides, all the factor loadings were significant, providing evidence for convergent validity.

Hypotheses testing

In the above, we raise hypotheses to predict that knowledge transfer mediates the relationship between spatial proximity to major cities centers (measured by instrumental variable distance) and corporate environmental performance. We conduct hierarchical multiple regression analysis to test those hypotheses by entering the control variables, the independent variable (distance), and mediator variable (knowledge transfer) on separate steps.

The results in *Table 2* show that (1) distance is negatively related to knowledge transfer (β = -0.409, p < 0.01, model 2), which supports H2a; (2) distance is negatively related to corporate environmental performance (β = -0.632, p < 0.01, model 4), which supports H1; (3) knowledge transfer is positively related to CEP (β = 0.281, p < 0.01, model 5), which supports H3a; and (4) the relationship between distance and corporate environmental performance remains significant (β = -0.584, p < 0.01, model 6) when knowledge transfer presents (β = 0.119, p < 0.05, model 6), which indicates the partial mediation of knowledge transfer and supports H4a.

Table 2. *Regression analysis on the mediation of knowledge transfer*

	Transfer		**Corporate environmental performance**			
	Model 1	**Model 2**	**Model 3**	**Model 4**	**Model 5**	**Model 6**
Control variables						
Firm size	.118	-.038	.279**	.037	.246**	.042
Firm age	.318**	.141+	.365**	.091	.276**	.074
Firm industry	.002	-.013	.026	.002	.025	.004
Firm region	.113	.091	.065	.031	.033	.020
Independent var.						
Distance		-.409**		-.632**		-.584**
Mediators						
Transfer					.281**	.119*
R^2	.146	.243	.266	.498	.333	.508
ΔR^2	.146	.097	.266	.232	.067	.011
F	8.017	11.982**	17.000	37.056**	18.665**	32.051**
ΔF	8.017	23.930**	17.000	86.393**	18.863**	4.027*

β, standardized regression weight; + p < .1, *p < .05, **p < .01

Table 3 shows the results of hierarchical multiple regression analysis on the mediation of knowledge conversion. The results show that (1) distance is negatively related to knowledge conversion (β = -0.590, p < 0.01, model 2), which supports H2b; (2) distance is negatively related to corporate environmental performance (β = -0.632, p < 0.01, model 4), which supports H1; (3) knowledge conversion is positively related

http://www.aloki.hu ● ISSN 1589 1623 (Print) ● ISSN 1785 0037 (Online)
DOI: http://dx.doi.org/10.15666/aeer/1706_1456114576

to CEP ($\beta = 0.401$, $p < 0.01$, model 5), which supports H3b; and (4) the relationship between distance and CEP remains significant ($\beta = -0.524$, $p < 0.01$, model 6) when knowledge conversion presents ($\beta = 0.184$, $p < 0.01$, model 6), which supports the mediation of knowledge conversion and H4b.

Table 3. *Regression analysis on the mediation of knowledge conversion*

	Conversion		**Corporate environmental performance**			
	Model 1	**Model 2**	**Model 3**	**Model 4**	**Model 5**	**Model 6**
Control variables						
Firm size	.159*	-.067	.279**	.037	.215**	.049
Firm age	.345**	.089	.365**	.091	.226**	.074
Firm industry	.005	-.017	.026	.002	.024	.005
Firm region	.062	.033	.065	.031	.039	-.025
Independent var.						
Distance		-.590**		-.632**		-.524**
Mediators						
Conversion					.401**	.184**
R^2	.175	.377	.266	.498	.399	.519
ΔR^2	.175	.202	.266	.232	.133	.021
F	9.984	22.640**	17.000	37.056**	41.330**	33.422**
ΔF	9.984	60.603**	17.000	86.393**	24.783**	8.160**

β, standardized regression weight; + p < .1, *p < .05, **p < .01

Discussion

As interest in the topic of geo-location and CEP steadily grows (Marquis and Tilcsik, 2016; Attig and Brockman, 2017), the lack of understanding of the influence mechanism of major cities on CEP emerges. Drawn on knowledge spillover theory and stakeholder theory, we seek to unravel the hidden path that links major cities and CEP. Based on empirical tests, the evidence from China supports our proposals, which we would further discuss in the following.

First, we find a strong correlation between proximity to major cities and CEP practices in China ($\beta = -0.743$, $p < .01$), which is consistent with extant research findings that based on U.S. samples (Husted et al., 2016). As a significant geographical element that could shape firms' environmental performances, major cities inhabitant varieties of stakeholders, including firms, residents, NGO, and governments (Marquis et al., 2007). In the meantime, this influence decays with distance, which means nearer firms are affected more. Answering Husted's call (Husted et al., 2016), our study finds that this particular relationship holds across different national contexts, not only in developed economies like the U.S. but also in emerging economies like China.

Second, in the relationship of proximity to major cities and CEP in China, knowledge transfer and knowledge conversion function as essential mediators. As independent channels via which firms acquire CEP knowledge, both of them are negatively correlated with proximity to major cities ($\beta = -0.396$, $p < 0.01$; $\beta = -0.576$, $p < 0.01$), which means firms that are more proximal could acquire more CEP knowledge. Despite the different ways of obtaining knowledge, both knowledge transfer and conversion significantly affect corporate environmental performance ($\beta = 0.303$, $p < 0.01$;

http://www.aloki.hu ● ISSN 1589 1623 (Print) ● ISSN 1785 0037 (Online)
DOI: http://dx.doi.org/10.15666/aeer/1706_1456114576

$\beta = 0.360$, $p < 0.01$). Besides, both knowledge transfer ($\beta = -0.107$, $p < 0.01$) and conversion ($\beta = -0.077$, $p < 0.1$) remain significant when present simultaneously with independent variable in affecting CEP, indicating their mediating effects.

Third, based on the mediating role of knowledge transfer and knowledge conversion, via which CEP knowledge spills over, we also argue that knowledge spillover mediates the relationship between proximity to major cities and CEP. Besides the prevalent legitimacy mechanism based on institutional pressure (Marquis and Tilcsik, 2016; Marquis et al., 2013), major cities also promote firms to engage in CEP by offering relevant knowledge and efficiency mechanism. For nearby firms, major cities play as the sources of both institutional pressures and knowledge spillovers, and firms could absorb CEP knowledge while bearing pressures. It is noticeable that CEP knowledge providers include local peers and non-peer stakeholders, such as local governments, NGOs or academic institutions.

Conclusion

As the forms that firms participate in environmental actions being more diversified, the related capability gradually plays more significant roles when firms perform environment-friendly actions. Despite its importance in boosting firms' ability, the influence of knowledge on CEP is still not adequately recognized. Therefore, in the research about the impact of major cities on CEP, few scholars examine the connections from the knowledge perspective, leaving this critical path undiscovered. Based on stakeholder theory and knowledge spillover theory, this study conducts a theoretical and empirical analysis of the mediating role of knowledge spillovers between firms' proximity to major cities and CEP engagements. The research not only enriches the front-end research of corporate environmental performance, but also further expands the application scope of knowledge spillover theory.

As with any study, our study is not without limitations. There are boundaries to our theorizing and limitations to our approach, which future research could address. In this study, we introduce and build connections between knowledge spillover and CEP; meanwhile, we notice that there are some puzzles left unsolved. For example, the impact of FDI knowledge spillovers on CEP, the effect of implicit and explicit knowledge spillovers on CEP, and whether absorptive capacity moderates the relationships. Those questions worth further studies to fully discover the links between knowledge spillover and CEP.

Besides, future research could extend the logic chain and test the influence of knowledge-driven CEP engagements on financial performance. So far, our findings support that knowledge spillover could facilitate firms' CEP engagements, but we still know little about the financial outcomes of those CEP engagements. Will the knowledge-driven CEP practices benefit corporates' financial performance? Future research may incorporate financial performance into the analytical framework, follow the "S-C-P" paradigm and construct "space-behavior-performance" framework, and thereby strengthen its instructive value on CEP practices.

Acknowledgements. This research was funded by National Social Science Foundation of China, grant number 16ZDA046.

http://www.aloki.hu ● ISSN 1589 1623 (Print) ● ISSN 1785 0037 (Online)
DOI: http://dx.doi.org/10.15666/aeer/1706_1456114576

REFERENCES

[1] Aguinis, H., Glavas, A. (2012): What we know and don't know about corporate social responsibility. – Journal of Management 38: 932-968.
[2] Appleyard, M. M. (1996): How does knowledge flow? Interfirm patterns in the semiconductor industry. – Strategic Management Journal 17: 137-154.
[3] Arrow, K. (1962): The economic implications of learning by doing. – Review of Economic Studies 29: 155-173.
[4] Attig, N., Brockman, P. (2017): The local roots of corporate social responsibility. – Journal of Business Ethics 142: 479-496.
[5] Audia, P. G., Yao, F. K. (2017): The spatial diffusion of an invisible corporate practice: revisiting stock backdating, 1981–2005. – Geography, Location, and Strategy 36: 309-339.
[6] Battke, B., Schmidt, T. S., Stollenwerk, S., Hoffmann, V. H. (2016): Internal or external spillovers—which kind of knowledge is more likely to flow within or across technologies. – Research Policy 45: 27-41.
[7] Boschma, R. A. (2005): Proximity and innovation: a critical assessment. – Regional Studies 39: 61-74.
[8] Brik, A. B., Rettab, B., Mellahi, K. (2011): Market orientation, corporate social responsibility, and business performance. – Journal of Business Ethics 99: 307-324.
[9] Broekel, T., Boschma, R. (2011): Knowledge networks in the Dutch aviation industry: the proximity paradox. – Journal of Economic Geography 12: 409-433.
[10] Carlino, G. A. (2001): Knowledge spillovers: cities' role in the new economy. – Business Review Q 4: 17-24.
[11] Carlino, G. A., Chatterjee, S., Hunt, R. M. (2007): Urban density and the rate of invention. – Journal of Urban Economics 61: 389-419.
[12] Cordeiro, J. J., Tewari, M. (2015): Firm characteristics, industry context, and investor reactions to environmental CSR: a stakeholder theory approach. – Journal of Business Ethics 130: 833-849.
[13] Dahl, M. S., Sorenson, O. (2012): Home sweet home: entrepreneurs' location choices and the performance of their ventures. – Management Science 58: 1059-1071.
[14] DeBoer, J., Panwar, R., Rivera, J. (2017): Toward a place-based understanding of business sustainability: the role of green competitors and green locales in firms' voluntary environmental engagement. – Business Strategy and the Environment 26: 940-955.
[15] DiMaggio, P., Powell, W. W. (1983): The iron cage revisited: collective rationality and institutional isomorphism in organizational fields. – American Sociological Review 48: 147-160.
[16] Eapen, A. (2012): Social structure and technology spillovers from foreign to domestic firms. – Journal of International Business Studies 43: 244-263.
[17] Fallah, M. H., Ibrahim, S. (2004): Knowledge spillover and innovation in technological clusters. – Proceedings of IAMOT 2004 Conference, Washington, DC, pp. 1-16.
[18] Fukugawa, N. (2017): University spillover before the national innovation system reform in Japan. – International Journal of Technology Management 73: 206-234.
[19] Glaeser, E. L., Kallal, H. D., Scheinkman, J. A., Shleifer, A. (1992): Growth in cities. – Journal of Political Economy 100: 1126-1152.
[20] Hair, J. F., Black, W. C., Babin, B. J., Anderson, R. E., Tatham, R. L. (2006): Multivariate Data Analysis. – Pearson Prentice Hall, Upper Saddle River; NJ.
[21] Haveman, H. A. (1993): Follow the leader: mimetic isomorphism and entry into new markets. – Administrative Science Quarterly 38(4): 593-627.
[22] Hoi, C. K., Wu, Q., Zhang, H. (2018): Community social capital and corporate social responsibility. – Journal of Business Ethics 152: 647-665.
[23] Howells, J. R. (2002): Tacit knowledge, innovation and economic geography. – Urban Studies 39: 871-884.

http://www.aloki.hu ● ISSN 1589 1623 (Print) ● ISSN 1785 0037 (Online)
DOI: http://dx.doi.org/10.15666/aeer/1706_1456114576

[24] Husted, B. W., Jamali, D., Saffar, W. (2012): Location, clusters, and CSR engagement: the role of information asymmetry and knowledge spillovers. – Academy of Management Proceedings 2012(1). DOI: 10.5465/AMBPP.2012.72.
[25] Husted, B. W., Jamali, D., Saffar, W. (2016): Near and dear? The role of location in CSR engagement. – Strategic Management Journal 37: 2050-2070.
[26] Islam, M. Z., Jasimuddin, S. M., Hasan, I. (2017): The role of technology and socialization in linking organizational context and knowledge conversion: the case of Malaysian service organizations. – International Journal of Information Management 37: 497-503.
[27] Jacobs, J. (1969): The Life of Cities. – Random House, New York.
[28] Kim, C. H., Amaeshi, K., Harris, S., Suh, C. J. (2013): CSR and the national institutional context: the case of South Korea. – Journal of Business Research 66: 2581-2591.
[29] Kim, H., Hoskisson, R. E., Lee, S. H. (2015): Why strategic factor markets matter:"New" multinationals' geographic diversification and firm profitability. – Strategic Management Journal 36: 518-536.
[30] Ko, W. W., Liu, G. (2015): Understanding the process of knowledge spillovers: learning to become social enterprises. – Strategic Entrepreneurship Journal 9: 263-285.
[31] Krugman, P. (1991): Increasing returns and economic geography. – Journal of Political Economy 99: 483-499.
[32] Lejpras, A. (2015): Knowledge, location, and internationalization: empirical evidence for manufacturing SMEs. – Economics of Innovation and New Technology 24: 734-754.
[33] Liarte, S., Forgues, B. (2008): Location strategies of multiunit service businesses: spatial differentiation and agglomeration among hamburger restaurants in Paris, 1984–2004. – Service Business 2: 233-248.
[34] Mahafza, Z. B., Stoutenborough, J. W., Vedlitz, A. (2017): The role of proximity in problem identification: risk of water scarcity in Texas. – Water Policy 19: 86-98.
[35] Marquis, C., Battilana, J. (2009): Acting globally but thinking locally? The enduring influence of local communities on organizations. – Research in Organizational Behavior 29: 283-302.
[36] Marquis, C., Tilcsik, A. (2016): Institutional equivalence: how industry and community peers influence corporate philanthropy. – Organization Science 27: 1325-1341.
[37] Marquis, C., Glynn, M. A., Davis, G. F. (2007): Community isomorphism and corporate social action. – Academy of Management Review 32: 925-945.
[38] Marquis, C., Davis, G. F., Glynn, M. A. (2013): Golfing alone? Corporations, elites, and nonprofit growth in 100 American communities. – Organization Science 24: 39-57.
[39] Matten, D., Moon, J. (2008): "Implicit" and "explicit" CSR: a conceptual framework for a comparative understanding of corporate social responsibility. – Academy of Management Review 33: 404-424.
[40] McWilliams, A., Siegel, D. (2001): Corporate social responsibility: a theory of the firm perspective. – Academy of Management Review 26: 117-127.
[41] Miles, M. P., Munilla, L. S., Darroch, J. (2006): The role of strategic conversations with stakeholders in the formation of corporate social responsibility strategy. – Journal of Business Ethics 69: 195-205.
[42] Miles, S. (2015): Stakeholder theory classification: a theoretical and empirical evaluation of definitions. – Journal of Business Ethics 142: 437-459.
[43] Moneva, J. M., Ortas, E. (2010): Corporate environmental and financial performance: a multivariate approach. – Industrial Management & Data Systems 110: 193-210.
[44] Ning, L., Wang, F. (2018): Does FDI bring environmental knowledge spillovers to developing countries? The role of the local industrial structure. – Environmental and Resource Economics 71(2): 381-405.
[45] Nyuur, R. B., Ofori, D. F., Debrah, Y. A. (2016): The impact of FDI inflow on domestic firms' uptake of CSR activities: the moderating effects of host institutions. – Thunderbird International Business Review 58: 147-159.

http://www.aloki.hu ● ISSN 1589 1623 (Print) ● ISSN 1785 0037 (Online)
DOI: http://dx.doi.org/10.15666/aeer/1706_1456114576

[46] Porter, M. E., Kramer, M. R. (2011): The big idea: creating shared value. – Harvard Business Review 89: 2.
[47] Qiu, S., Liu, X., Gao, T. (2017): Do emerging countries prefer local knowledge or distant knowledge? Spillover effect of university collaborations on local firms. – Research Policy 46: 1299-1311.
[48] Simons, T., Vermeulen, P. A., Knoben, J. (2016): There's no beer without a smoke: community cohesion and neighboring communities' effects on organizational resistance to antismoking regulations in the Dutch hospitality industry. – Academy of Management Journal 59: 545-578.
[49] Sorenson, O., Baum, J. A. C. (2003): Editors' introduction: geography and strategy: the strategic management of space and place. – Geography and Strategy 20: 1-19.
[50] Stanko, M. A., Olleros, X. (2013): Industry growth and the knowledge spillover regime: does outsourcing harm innovativeness but help profit? – Journal of Business Research 66: 2007-2016.
[51] Stevens, J. M., Steensma, H. K., Harrison, D. A., Cochran, P. L. (2005): Symbolic or substantive document? The influence of ethics codes on financial executives' decisions. – Strategic Management Journal 26: 181-195.
[52] Storper, M., Venables, A. J. (2004): Buzz: face-to-face contact and the urban economy. – Journal of Economic Geography 4: 351-370.
[53] Taylor, P. J. (2005): Leading world cities: empirical evaluations of urban nodes in multiple networks. – Urban Studies 42: 1593-1608.
[54] Tho, N. D., Trang, N. T. M. (2015): Can knowledge be transferred from business schools to business organizations through in-service training students? SEM and fsQCA findings. – Journal of Business Research 68: 1332-1340.
[55] Trumpp, C., Endrikat, J., Zopf, C., Guenther, E. (2015): Definition, conceptualization, and measurement of corporate environmental performance: a critical examination of a multidimensional construct. – Journal of Business Ethics 126: 185-204.
[56] Turker, D. (2009): Measuring corporate social responsibility: a scale development study. – Journal of business ethics 85: 411-427.
[57] Wanderley, L. S. O., Lucian, R., Farache, F., de Sousa Filho, J. M. (2008): CSR information disclosure on the web: a context-based approach analysing the influence of country of origin and industry sector. – Journal of Business Ethics 82: 369-378.
[58] Wang, C. C., Wu, A. (2016): Geographical FDI knowledge spillover and innovation of indigenous firms in China. – International Business Review 25: 895-906.
[59] Williams, C. (2007): Transfer in context: replication and adaptation in knowledge transfer relationships. – Strategic Management Journal 28: 867-889.
[60] Wu, L. Z., Kwan, H. K., Yim, F. H. K., Chiu, R. K., He, X. (2015): CEO ethical leadership and corporate social responsibility: a moderated mediation model. – Journal of Business Ethics 130: 819-831.
[61] Yang, H., Steensma, H. K. (2014): When do firms rely on their knowledge spillover recipients for guidance in exploring unfamiliar knowledge? – Research Policy 43: 1496-1507.

http://www.aloki.hu ● ISSN 1589 1623 (Print) ● ISSN 1785 0037 (Online)
DOI: http://dx.doi.org/10.15666/aeer/1706_1456114576

ANALYSIS OF URBAN LANDSCAPE PATTERN AND ECO-ENVIRONMENT BENEFIT BASED ON HEAT ISLAND EFFECT – WITH BEIJING, CHINA AS AN EXAMPLE

LEI, L. J.[1] – WANG, W. C.[2]

[1]*Jinzhong University, Jinzhong 030600, China*

[2]*Shanxi Urban and Rural Planning Design Institute Engineering Design Center, Taiyuan 030000, China*

**Corresponding author*
e-mail: Leilingjia@163.com; phone: +86-187-0344-7111

(Received 7th Jun 2019; accepted 10th Oct 2019)

Abstract. As urbanization picks up speed, great changes have taken place in the Urban Landscape Pattern (ULP), which in turn causes variation in urban climate. The Heat Island Effect (HIE), a prominent feature of the changing urban climate, poses a huge threat to our life and health. Starting with HIE and with the aid of geographic information system (GIS) and remote sensing (RS), this paper studies the remote sensing images of Beijing from 1995 to 2015, which were captured by Landsat Thematic Mapper (TM) and infrared technology. Specifically, the author analyzed the evolution laws of the ULP and the HIE in Beijing, discussed the relationship between the two factors, and disclosed the controlling effect of the ULP on the HIE. The results show that: the accelerated urbanization has fragmented the landscapes in Beijing dramatically; the HIE can be alleviated by increasing the greenery coverage, reducing the spacing between green lands, and enhancing their density. Finally, several suggestions were put forward to construct a secure and ecological ULP in Beijing from the angle of adjusting the green land landscape pattern. This research sheds new light on the relationship between the ULP and the HIE and lays a basis for the planning and construction of eco-cities.
Keywords: *heat island effect (HIE), urban landscape pattern (ULP), eco-environment benefit (EEB), Beijing, secure and ecological ULP*

Introduction

With the rapid growth of population and economy, the urbanization process is accelerating, and the cities are gradually expanding over surrounding areas. As a result, the changes in landscape pattern and land use, and the environmental pollution have caused ecological problems such as the soil property variation (e.g. unbalanced soil acid-base property and poor adsorption), urban heat island effect, etc. (Connors et al., 2013), which pose threats to people's health, and even influence the sustainable development of the cities. Therefore, analyzing the ULP and the evolution of the ecological environment is of great significance for constructing a secure and ecological ULP (Goward, 1981).

The city is a human-centered landscape ecosystem (Estoque et al., 2017). Urban ecosystems are composed of two ecosystems, or more precisely, it is dominated by the artificial ecosystem and supplemented by the natural ecosystem (Li et al., 2014). Land use is a main factor affecting the artificial ecosystem, so the research on the changes in land use is the focus of urban ecological security research (Yang et al., 2017). In the landscapes, the evolution of ecological processes such as biological migration, surface temperature, and local air flow, as well as the spatial distribution will all be influenced by the changes in landscape patterns. HIE is a phenomenon in which the urban temperature is significantly higher than the surrounding areas, it occurs as a result of the the process of urbanization and

http://www.aloki.hu ● ISSN 1589 1623 (Print) ● ISSN 1785 0037 (Online)
DOI: http://dx.doi.org/10.15666/aeer/1706_1457714586

is caused by the destruction of vegetation and water bodies, the increment of residential land construction, and the aggregation of population (Bao et al., 2016). HIE is one of the main consequences of the changes in ULP, it changes the urban climate and produces adverse effects on the health of residents and the ecological environment of the city (Chen et al., 2016). Xiao Rongbo adopted correlation analysis to study the actual surface temperature and related influencing factors of urban land in Beijing, and the results showed that ULP and land use situation are closely related to HIE (Chen et al., 2014). Cao Liping proposed through research that the human impact on the climate shows a trend from weak to strong with the progress of urbanization (Mohajerani et al., 2017). However, currently there are few researches on the correlation between ULP and HIE, and no unified conclusion has been formed yet.

Based on the above analysis, this paper carries out research on the HIE-based ULP and the EEB, and selects the data of Beijing city from 1995 to 2015 to analyze and study the evolution of ULP, the heat island spatial distribution and the causes of formation, as well as the heat island areas and green land patterns in Beijing. From the perspective of adjusting the green land landscape pattern, this paper proposes suggestions for constructing a secure and ecological ULP in Beijing, in the hopes of providing a reference for the planning and building of eco-cities.

Materials and methods

Data source of the evolution of ULP in Beijing and the research methods

This paper selected the GIS and RS data of Beijing from 1995 to 2015, and divided the landscapes within the Sixth Ring Road of Beijing into five categories: urban land, agricultural land, green land, water-area land and unused land (Xie et al., 2016). The study used the landscape index method and the gradient analysis to conduct quantitative analysis on the evolution of ULP in Beijing, and adopted the Fragstats landscape index calculation software to calculate the selected indices such as the SHDI (diversity index), the Contagion index, the MN-SHAPE (mean shape of the plaque) index, and the PD (Plaque Density) index, etc.

Shannon's diversity index (SHDI):

$$SHDI = \sum_{i=1}^{m} (P_i \times \ln P_i) \quad \text{(Eq.1)}$$

Contagion index (Contagion):

$$Contagion = \left[1 + \sum_{i=1}^{m} \sum_{j=1}^{n} \frac{P_{ij} \ln(P_{ij})}{2 \ln(m)} \right] (100) \quad \text{(Eq.2)}$$

Mean shape of the plaque (MN-SHAPE):

$$MN - SHAPE = \frac{\sum_{i=1}^{m} \sum_{j=1}^{n} \left(\frac{0.25 P_{ij}}{\sqrt{a_{ij}}} \right)}{N} \quad \text{(Eq.3)}$$

http://www.aloki.hu ● ISSN 1589 1623 (Print) ● ISSN 1785 0037 (Online)
DOI: http://dx.doi.org/10.15666/aeer/1706_1457714586

Plaque density (PD):

$$PD = \frac{n_i}{A} \quad \text{(Eq.4)}$$

where: P_i is the occurrence probability of the i-type plaque, m is the total number of plaque types, P_{ij} is the probability that two adjacent grid cells belong to types i and j, A is the total area of all landscapes, n_i is the total area of the i-type landscape elements.

Data source of HIE in Beijing and research methods

Although the data of surface temperature obtained by the field measurement method is accurate, it requires to set up a large number of meteorological stations in reasonable layout, which would consume huge financial resources and time (Chang et al., 2011), the development and application of thermal infrared remote sensing technology enable us to obtain the surface temperature of large areas, which has overcome the shortcomings of the traditional field measurement method. Therefore, this paper selected the Landsat TM/ETM + images from 2000, 2005, 2010 and May 2015 to study the relationship between the built areas of Beijing and the heat island spatial distribution changes.

Generally, the temperature of the black body that radiates radiation energy equal to the observed object is called the brightness temperature, which is slightly less than the real temperature, and its relationship with the real temperature is $T = \varepsilon^{\frac{1}{4}} t$ (Huang et al., 2013). Using *Equation 1,* we can unify the range of surface brightness temperature to 0-1, meanwhile, the density segmentation method was applied to eliminate the time-phase differences in the images of the four seasons as much as possible (Zhang et al., 2013). *Figure 3* shows the distribution of brightness temperature in Beijing in 2000, 2005, 2010 and 2015. According to historical statistics, the meteorological conditions of the dates selected in this paper are basically the same and comparable. According to the temperature, the brightness temperatures are divided into seven levels: very-high temperature (44-47 °C), high temperature (40-44 °C), sub-high temperature (36-40 °C), medium temperature (32-36 °C), sub-medium temperature (28-32 °C), low temperature (24-28 °C) and very-low temperature (20-24 °C). The seven levels are indicated by brown, red, orange, yellow, light green, green and blue.

$$N_i = \frac{T_i - T_{\min}}{T_{\max} - T_{\min}} \quad \text{(Eq.5)}$$

Data source of urban heat island and urban green land pattern and research methods

Urban green land can increase the value of real estate, provide people with leisure and entertainment places, moreover, they have multiple important ecological functions such as reducing surface runoff, alleviating urban heat islands, cooling and humidifying (Cannistraro et al., 2017; Gehrt and Chelsvig, 2003; Jiao and Fang, 2018), as well as reducing ecological and environmental damages caused by urbanization. However, if we want to achieve the goal of improving the urban ecological environment through the urban green land system, we must not only ensure large areas of green land, but also scientifically plan the shape and spatial distribution of urban green land (Dai et al.,

http://www.aloki.hu ● ISSN 1589 1623 (Print) ● ISSN 1785 0037 (Online)
DOI: http://dx.doi.org/10.15666/aeer/1706_1457714586

2010; Dong et al., 2018). Therefore, this paper selected the urban images of Beijing taken by SPOT5 satellite in 2015, and adopted the gradient analysis and landscape index method (main landscape indices are calculated according to *Eqs. 1-4*) to analyze heat island areas in Beijing and the green land pattern on the main extension axes.

Table 1 shows the green landscape pattern of districts with different interference intensities.

Table 1. *Greenland landscape pattern in districts with different interference intensities*

Landscape index	Urban heat island area	Urban cold island area
Greenery coverage %	30.2	13.6
Average nearest neighbor distance (m)	41.62	56.45
Aggregation index	93.27	89.88
Average plaque area (h m^2)	0.86	0.53
Plaque density (/k m^2)	195	108

Results

Evolution of ULP in Beijing

Figure 1 shows the overall landscape dynamic changes of urban districts in Beijing from 1995 to 2015.

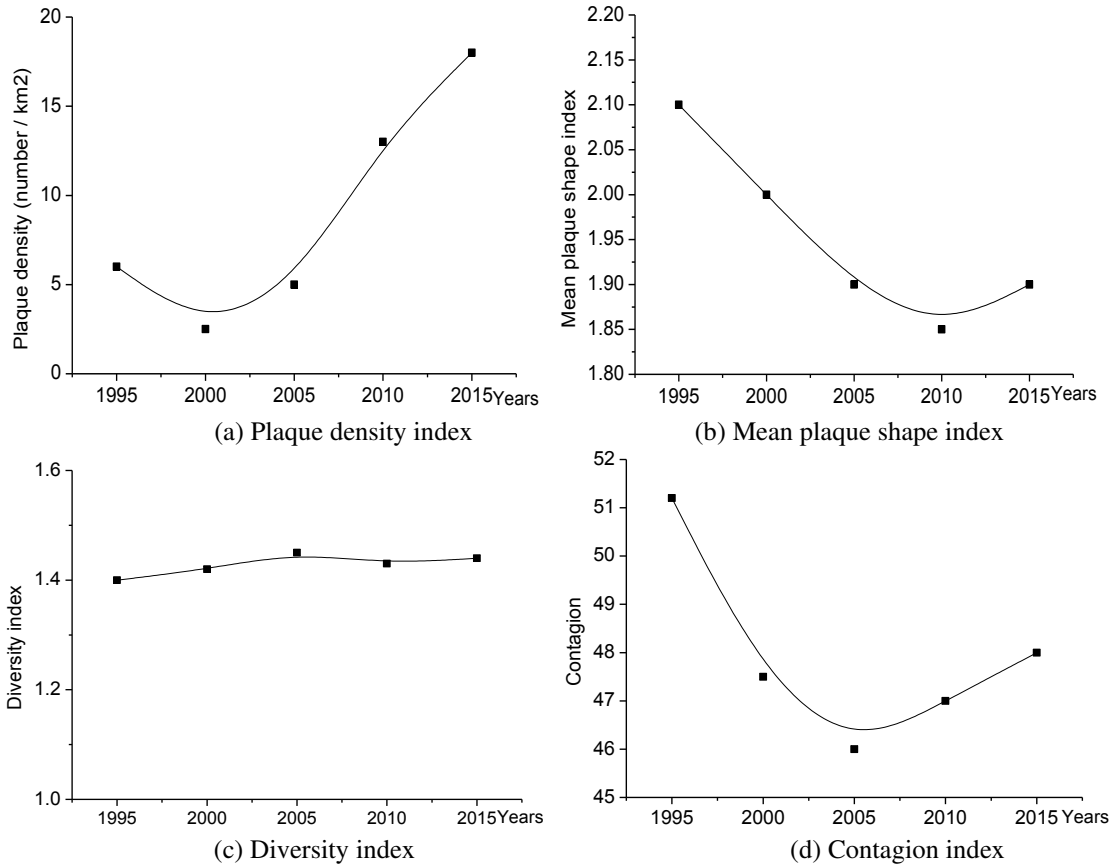

Figure 1. *Dynamic changes of overall landscape in urban districts of Beijing*

http://www.aloki.hu ● ISSN 1589 1623 (Print) ● ISSN 1785 0037 (Online)
DOI: http://dx.doi.org/10.15666/aeer/1706_1457714586

Figure 1 shows the dynamic changes of the overall landscape of urban districts in Beijing from 1995 to 2015, it can be seen from the figure that the density of plaques has shown a downward trend from 1995 to 2000, and a rapid upward trend after 2000. The landscape diversity index has shown a linear increase with the year, and for the MN-shape index and the Contagion index, both have presented a large downward trend at first, then hit the bottom in 2010 and 2005, respectively, after that, both rebounded, indicating that as the urbanization in Beijing has sped up, the degree of landscape fragmentation has intensified.

Figure 2 shows the proportion of urban land in Beijing in the four directions from 1995 to 2015. In terms of the distance from the city center, the south and west directions are negative, and the north and east directions are positive.

It can be seen from *Figure 2* that in the past 20 years, Beijing has shown a comprehensive and large-scale expansion of urban land from the city center to the surroundings in different directions, with a largest increase of about 50%, the expansion mainly concentrated in the plain area in the southeast, it is because the mountains in the west and north of Beijing have played a certain role in hindering the development of the city, so the development is relatively slow.

The rapid growth of Beijing's economy and population has led to an increase in urban residential construction land and related infrastructures such as the roads, and the conversion of suburban land into urban land has destroyed the original landscape pattern, which is the main reason for the evolution of ULP in Beijing.

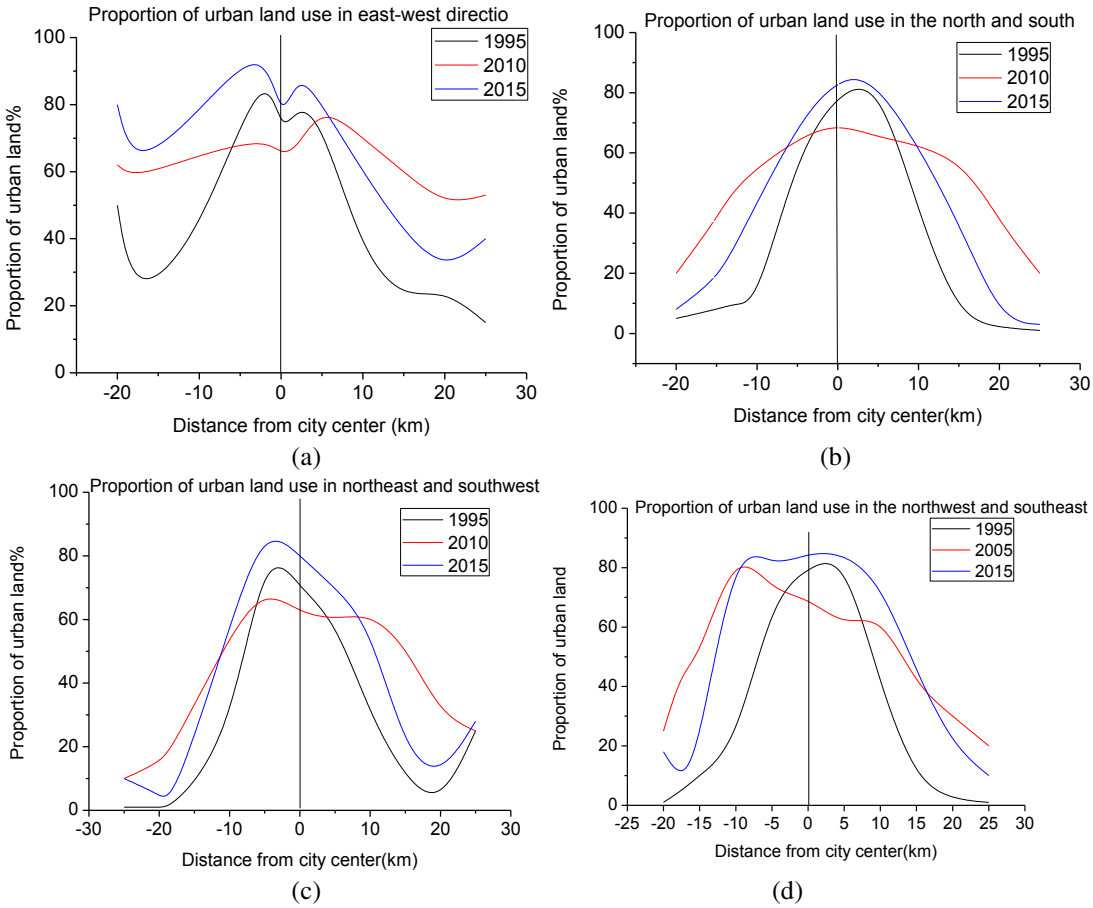

Figure 2. *Proportion of urban land in Beijing from 1995 to 2015*

http://www.aloki.hu ● ISSN 1589 1623 (Print) ● ISSN 1785 0037 (Online)
DOI: http://dx.doi.org/10.15666/aeer/1706_1457714586

Spatial distribution and formation causes of urban heat islands in Beijing

Figure 3 shows the heat island brightness temperature distribution in Beijing, it can be seen from the figure that, the very-high temperature area (brown), the high temperature area (red) and the sub-high temperature area (orange) in Beijing have spread to the surroundings and increased year by year from 2000 to 2015. Wherein, the Shougang Plant Area, the Dashilan and the Yongdinghe River have been in high temperature areas for many years, while Yuyuantan Lake, Kunminghu Lake, Beihai, Shichahai and other water areas have been in the low temperature areas for many years. In the city center areas, there are vegetation and water body areas, as well as scattered low temperature areas, and the brightness temperature areas present a tendency to gradually increase from the center to the periphery. In addition, by 2015, the HIE in the downtown area within the Third Ring Road had been alleviated significantly, while the intensity of HIE around the Fourth Ring and the Fifth Ring roads had increased, this is because the newly-developed residence and technology parks are concentrated near the Fourth Ring and the Fifth Ring roads, while the green land construction had been strengthened within the Third Ring Road, so the isolation belt had separated the Third Ring Road from other high temperature areas.

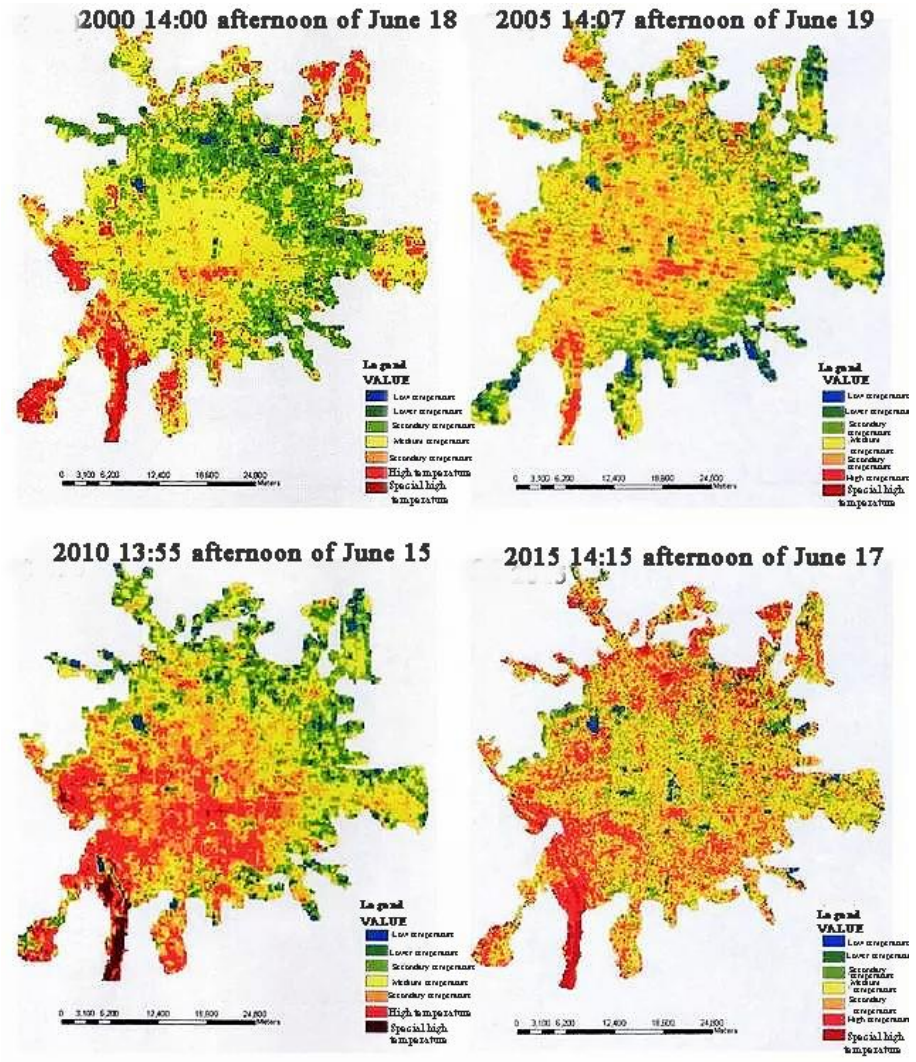

Figure 3. *Bright temperature distribution map of Beijing in 2000, 2005, 2010 and 2015*

http://www.aloki.hu ● ISSN 1589 1623 (Print) ● ISSN 1785 0037 (Online)
DOI: http://dx.doi.org/10.15666/aeer/1706_1457714586

Figure 4 shows the comparison of the areas of urban districts in Beijing. It can be seen from the figure that since 2000, the area occupied by the urban heat island had decreased slightly, and the proportion of the low temperature area had gradually increased, indicating that the HIE had been alleviated.

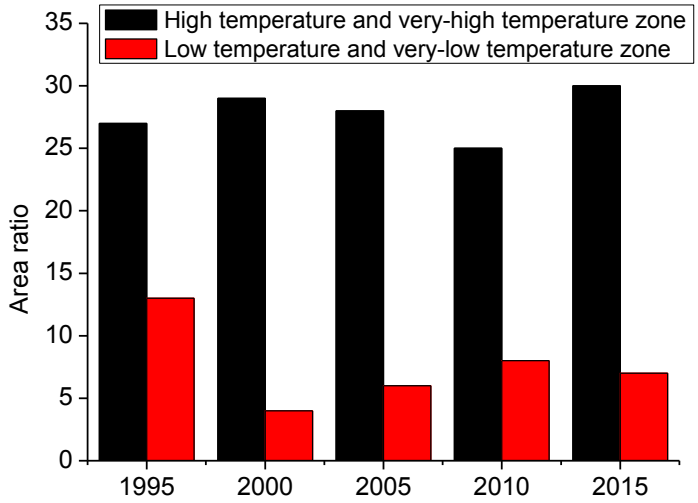

Figure 4. *Comparison of the areas of urban districts in Beijing*

Analysis of the heat island area and green land pattern in Beijing

Figure 5 shows the area ratio of green land plaques of different area levels and in different directions.

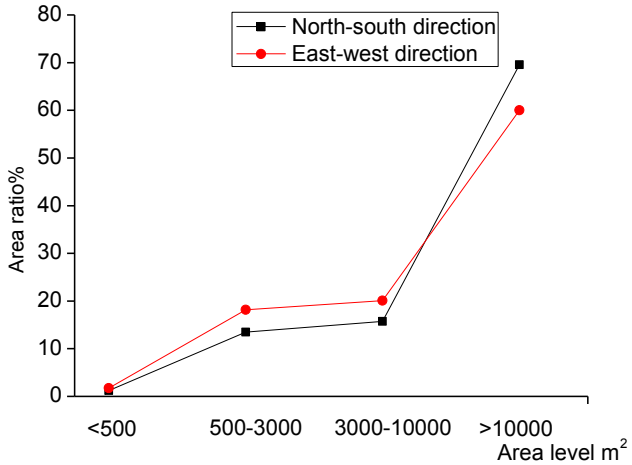

Figure 5. *Area ratio of green land plaques of different area levels and in different directions*

Figure 6 shows the changes of greenery coverage in the east-west and north-south directions.

It can be seen from *Figures 5* and *6* that the greenery coverage in all directions of the urban extension axes has no obvious correlation with the distance, and fluctuates between 10 and 30%. Overall, the north-south direction is slightly higher than the east-

http://www.aloki.hu ● ISSN 1589 1623 (Print) ● ISSN 1785 0037 (Online)
DOI: http://dx.doi.org/10.15666/aeer/1706_1457714586

west direction. In the east, west, south-north directions, peaks appeared at the positions of 4 km, 6 km, and 12 km, respectively, by analysis it is found that it is mainly due to the existence of park green land such as Yuyuantan Park, and the Olympic Park near these spots. In areas that have no park, the greenery coverage is below 15%, and the number of large plaque areas with a plaque area of more than 60% is less than 10%. These plaques are mainly concentrated in government units and urban parks, indicating that the distribution of large park green land determines the size of greenery coverage. It can be found from the data in *Table 1* that the anti-interference intensity of the landscape pattern increases with the increase of greenery coverage, plaque spacing and density, therefore, the artificial interferences can be eliminated by increasing the greenery coverage, reducing the spacing, and increasing the density.

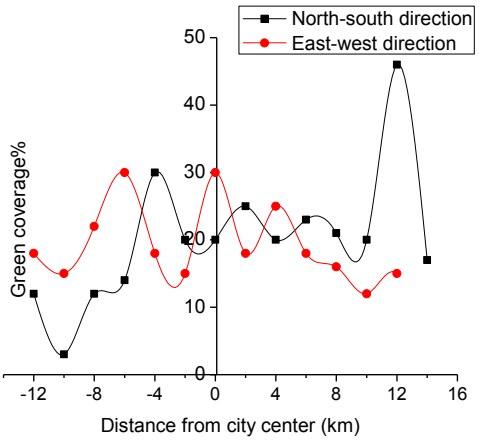

Figure 6. *Greenery coverage changes in two directions*

Discussion

In order to alleviate the HIE in Beijing and construct a secure and ecological ULP in Beijing, this paper combines with the evolution of ULP, the HIE, and the green land pattern in Beijing to analyze the results, and proposes countermeasures and suggestions from the following three aspects:

Plan the development pattern scientifically

Change Beijing's current development pattern which is circle-shaped and single-centered; use evacuation and integration methods to alleviate the problem that the human activities often gather in the center of the city. To achieve the goal of multi-center development, relevant policies should be adopted to encourage and guide the migration of economy, population and industrial belt. In addition, the density of buildings is also one of the main factors of HIE. Therefore, in order to avoid the distribution of urban buildings from distributing in clusters and blocks, the spacing between buildings should be properly arranged and the density of the buildings should be strictly controlled.

Save energy, reduce emission, and develop ecological buildings

Previous research results (Oberndorfer et al., 2007) have confirmed that greenhouse gases from vehicle exhaust and industrial production, and heat emission caused by

http://www.aloki.hu ● ISSN 1589 1623 (Print) ● ISSN 1785 0037 (Online)
DOI: http://dx.doi.org/10.15666/aeer/1706_1457714586

human activities are important factors for the formation of HIE, therefore, we should make full use of renewable green resources such as wind energy and solar energy to reduce the use of gasoline and diesel, and meanwhile adopt new thermal insulation equipment, heating and ventilation equipment, and other energy-saving technologies to develop green buildings and reduce heat emissions caused by human activities.

Increase water body, greenery coverage, and improve the natural ecosystem

According to the research results of this paper, the green land and water body inside the city can effectively alleviate and reduce the HIE. Therefore, we can build heat island green belt inside the city, adjust the current green land pattern, and construct corridors between the central green land and other middle and small green land, so as to achieve the ideal status in which there are both scattered and concentrated green land, and at the same time, protect the suburb farmland and river surface from pollution and damage.

Conclusion

- The evolution of ULP in Beijing showed that the urbanization level of Beijing increased significantly between 1995 and 2015, mainly concentrated in the plain area in the southeast direction, due to the acceleration of urbanization and the changes in urban land use structure, the landscape pattern of Beijing had been fragmented more dramatically.
- The research results of Beijing's heat island spatial distribution and the cause of formation showed that, the very-high temperature area (brown), the high temperature area (red) and the sub-high temperature area (orange) in Beijing had spread to the surroundings and increased year by year from 2000 to 2015. Since 2015, the HIE within the Third Ring Road had alleviated significantly. In term of spatial distribution, we can see that in spots where the industry and population are gathered and the greenery coverage is low, the HIE is stronger.
- The analysis results of the heat island area and green land pattern in Beijing showed that the distribution of large park green land determines the size of greenery coverage, and the anti-interference intensity of landscape pattern increases with the increase of greenery coverage, plaque spacing and density.
- This paper proposed countermeasures and suggestions for constructing a secure and ecological ULP from three aspects: plan the development pattern scientifically; save energy, reduce emission, and develop ecological buildings; and increase water body, greenery coverage, and improve the natural ecosystem.
- The study of ULP and HIE requires to combine factors of various aspects to conduct case study and evaluation. This paper only discussed from the two aspects of urban land use and landscape pattern change, so it is not comprehensive enough, in future researches, we should also analyze other ecological process types and scales as well.

REFERENCES

[1] Bao, T., Li, X. M., Zhang, J., Zhang, Y. J., Tian, S. Z. (2016): Assessing the distribution of urban green spaces and its anisotropic cooling distance on urban heat island pattern in Baotou, China. – ISPRS International Journal of Geo-Information 5(2): 12.

http://www.aloki.hu ● ISSN 1589 1623 (Print) ● ISSN 1785 0037 (Online)
DOI: http://dx.doi.org/10.15666/aeer/1706_1457714586

[2] Cannistraro, G., Cannistraro, M., Trovato, G. (2017): Islands "Smart Energy" for eco-sustainable energy a case study "Favignana Island". – International Journal of Heat and Technology 35(S1): S87-S95.
[3] Chang, H., Li, F., Li, Z., Wang, R., Wang, Y. (2011): Urban landscape pattern design from the viewpoint of networks: a case study of Changzhou City in Southeast China. – Ecological Complexity 8(1): 51-59.
[4] Chen, A., Yao, X. A., Sun, R., Chen, L. (2014): Effect of urban green patterns on surface urban cool islands and its seasonal variations. – Urban Forestry & Urban Greening 13(4): 646-654.
[5] Chen, A., Zhao, X., Yao, L., Chen, L. (2016): Application of a new integrated landscape index to predict potential urban heat islands. – Ecological Indicators 69: 828-835.
[6] Connors, J. P., Galletti, C. S., Chow, W. T. L. (2013): Landscape configuration and urban heat island effects: assessing the relationship between landscape characteristics and land surface temperature in Phoenix, Arizona. – Landscape Ecology 28(2): 271-283.
[7] Dai, X., Guo, Z., Zhang, L., Wu, J. (2010): Spatio-temporal pattern of urban land cover evolvement with urban renewal and expansion in shanghai based on mixed-pixel classification for remote sensing imagery. – International Journal of Remote Sensing 31(23): 6095-6114.
[8] Dong, J. H., Xu, M., Wan, S. M., Xie, F. H., Wu, Q. H. (2018): Stability analysis of accumulation body based on monitoring results of deep displacement. – Instrumentation Mesure Métrologie 17(4): 563-572.
[9] Estoque, R. C., Murayama, Y., Myint, S. W. (2017): Effects of landscape composition and pattern on land surface temperature: an urban heat island study in the megacities of Southeast Asia. – Science of the Total Environment 577: 349-359.
[10] Gehrt, S. D. D., Chelsvig, J. E. E. (2003): Bat activity in an urban landscape: patterns at the landscape and microhabitat scale. – Ecological Applications 13(4): 939-950.
[11] Goward, S. (1981): Thermal behavior of urban landscapes and the urban heat island. – Physical Geography 2(1): 19-33.
[12] Huang, Y. X., Yin, X. Q., Ye, G. F., Lin, J. M., Huang, R., Wang, N., Wang, L., Sun, Y. (2013): Spatio-temporal variation of landscape heterogeneity under influence of human activities in Xiamen City of China in recent decade. – Chinese Geographical Science 23(2): 227-236.
[13] Jiao, H., Fang, Y. C. (2018): Simulation and prediction of urban heat island effect of urban high-speed rail construction. – International Journal of Heat and Technology 36(4): 1438-1442.
[14] Li, C. F., Shen, D., Dong, J. S., Yin, J. Y., Zhao, J. J., Xue, D. (2014): Monitoring of urban heat island in Shanghai, China, from 1981 to 2010 with satellite data. – Arabian Journal of Geosciences 7(10): 3961-3971.
[15] Mohajerani, A., Bakaric, J., Jeffrey-Bailey, T. (2017): The urban heat island effect, its causes, and mitigation, with reference to the thermal properties of asphalt concrete. – Journal of Environmental Management 197: 522-538.
[16] Oberndorfer, E., Lundholm, J., Bass, B., Coffman, R. R., Doshi, H., Dunnett, N., et al. (2007): Green roofs as urban ecosystems: ecological structures, functions, and services. – Bioscience 57(10), 823-833.
[17] Xie, Y., Yu, M., Bai, Y., Xing, X. (2006): Ecological analysis of an emerging urban landscape pattern—Desakota: a case study in Suzhou, China. – Landscape Ecology 21(8): 1297-1309.
[18] Yang, Q., Huang, X., Li, J. (2017): Assessing the relationship between surface urban heat islands and landscape patterns across climatic zones in China. – Scientific Reports 7(1): 9337.
[19] Zhang, C., Wu, J., Grimm, N. B., Mchale, M., Buyantuyev, A. (2013): A hierarchical patch mosaic ecosystem model for urban landscapes: model development and evaluation. – Ecological Modelling 250(1753): 81-100.

http://www.aloki.hu ● ISSN 1589 1623 (Print) ● ISSN 1785 0037 (Online)
DOI: http://dx.doi.org/10.15666/aeer/1706_1457714586

ECOLOGICAL ECONOMICS FOR ENERGY CONSERVATION AND EMISSION REDUCTION OF HIGH ENERGY CONSUMING INDUSTRIES BASED ON THEORY OF CIRCULAR ECONOMY

LI, X. L.[1*] – YANG, C. Z.[2]

[1]*School of Civil Engineering, Qinghai University, Xining 810016, China*

[2]*Qinghai Provincial Institute of Geography and National Situation Monitoring, Xining 810001, China*
(phone: +86-133-8329-3867)

**Corresponding author*
e-mail: lxlsource@163.com; phone: +86-136-1371-1818

(Received 7th Jun 2019; accepted 10th Oct 2019)

Abstract. The high energy consumption and the large amount of pollutants discharged by high-energy-consuming industries in the production process have posed a great threat to the ecological environment. This paper takes the theory of circular economy and the basic concept of sustainable development as the research foundation to study energy conservation, emission reduction and eco-economic construction of high-energy-consuming industries; and then it proposes countermeasures and suggestions for the ecological construction and development of such industries. The research shows that the reduction of energy consumption has contributed a lot to the reduction in the total energy consumption and the comparable energy consumption; In recent years, the energy consumption per one ton of steel has been decreasing year by year, and the energy conservation and emission reduction measures such as technological reform, policy regulation and economic coordination have played a major role in it; the energy-conservation and emission-reduction eco-economic system based on circular economy can mitigate improve the high energy consumption of the industries, which has laid a foundation for their ecological development. This paper has provided theoretical support and guidance for the energy conservation, emission reduction and the eco-economic construction of high-energy-consuming industries.
Keywords: *circular economy, high energy-consuming industry, ecological economy, energy conservation and emission reduction, analytic hierarchy process*

Introduction

Protection of the global environment, energy conservation and emission reduction, and the concept of sustainable development have become development strategies for industries around the globe (Price et al., 2011; Tu and Ma, 2018; Krishna, 2018; Liao, 2011). In recent years, the rapid development of the world economy, resources and industries has damaged to the environment. In order to build an environment-friendly and resource-saving society, countries have implemented energy conservation, emission reduction and the development of circular economy into the economic construction, in the hopes of maintaining the balance of environment and ecology, and controlling the severe pollution and high energy consumption in industrial development, thus improving the utilization of resources around the globe and building an ecological society (Lei et al., 2009; Tao et al., 2014; Cheng et al., 2012). In recent years, the demand for oil and coal resources has increased year by year, and the domestic resource supply cannot meet the demand in actual economic development (Algaba et al., 2012; Habib et al., 2016). In addition, at present, China's energy utilization rate is not high, and our mining and utilizing technology is not mature enough, which has caused

http://www.aloki.hu ● ISSN 1589 1623 (Print) ● ISSN 1785 0037 (Online)
DOI: http://dx.doi.org/10.15666/aeer/1706_1458714598

adverse effects on the environment to a certain extent in the process of resource exploitation. Therefore, the research and practice of energy conservation, emission reduction and ecological development of high-energy-consuming industries is one of the main issues to be solved urgently.

Among various industries, the metallurgical industry is one of the industrial types that have high energy consumption and high pollutant emissions (Danza et al., 2018; Mostafaei et al., 2019; Trica et al., 2019; Jonas et al., 2018; Hobson and Lynch, 2016; Rudra and Chakraborty, 2017). The energy consumption in steelmaking and other metal smelting processes accounts for nearly a quarter of the total industrial energy consumption (Murray et al., 2017; Cordova-Pizarro et al., 2019; Rigueiro-Rodríguez et al., 2018). Although the country's energy consumption control policies and administrative measures have improved the problem of energy consumption and pollution emission to some extent, the efforts on energy conservation and emission reduction still unable to catch up with the control level in the developed countries. And the main reasons for the unsatisfactory control effects include: low energy utilization rate, inadequate control of pollutant emissions, low level of waste recycling technology, and lacking of effective control measures (Tiening and Jimei, 2018; Gallagher et al., 2017; Peters et al., 2007; Tomi and Schneider, 2017).

Based on the above-mentioned issues, the theory of circular economy and the basic concept of sustainable development, this paper starts from the perspective of energy conservation and emission reduction of metallurgical industry, and combines the development characteristics and overall trend of today's high energy-consuming industries to study the energy conservation, emission reduction and the ecological and economic construction of high-energy-consuming industries, and proposes countermeasures and suggestions for the ecological construction and development of high-energy-consuming industries, in the hopes of providing theoretical support for the energy conservation, emission reduction and the ecological and economic construction and development of high-energy-consuming industries.

Materials and methods (related theories of circular economy)

Circular economy theories

In the development of traditional economic, production activities such as ecological resource development, energy utilization, agricultural and industrial production, and waste generation have produced serious damages and environmental pollutions to our ecological environment. In today's society, environmental problems are becoming increasingly prominent, and countries around the world are gradually realizing that only by optimizing the economic development mode can we achieve coordinated construction and sustainable development of environment and social economy. In such social context, circular economy emerges as a new type of economic development mode.

The emergence of circular economy has alleviated or eliminated the conflicts and contradictions between environment and economic and social development to a certain extent, and realized the harmonious coexistence of the natural environment and human beings. The concept of circular economy refers to transform the traditional economic mode into an economic mode with resource recycling and energy conservation as the development goals within a complex system of nature, human, and technological development. The circular economy mode is a process of value re-creating, economy

http://www.aloki.hu ● ISSN 1589 1623 (Print) ● ISSN 1785 0037 (Online)
DOI: http://dx.doi.org/10.15666/aeer/1706_1458714598

developing and environment coordinating with minimizing input costs and achieving maximal economic and environmental benefits through high resource utilization rate and low emission of exhaust pollutants as the goals.

In order to realize the ecological construction and development of the economy, the economic mode follows three principles: resource reduction, that is, reduce resource consumption, waste generation and reducing environmental damages during the production process; product recycling, that is, re-cycle and re-use the products, renovate or remould the old products and re-use them, so as to prolong the life cycle of the products; waste recycling, that is, convert the wastes generated during production into resources as much as possible with the highest conversion rate, thereby reducing consumption of natural resources and energy.

Basic concepts of energy conservation and emission reduction

Speaking from a micro level, the concept of energy conservation and emission reduction is to save energy and reduce pollutant emissions; while speaking from a macro level, this concept refers to save natural resources and energy sources, and reduce harmful substances and pollutant emissions. Studies have shown that the economic development process needs to be able to meet the requirements of humans and kept within a bearable range of the environment. If the regeneration ability of the nature and the self-coordination ability of the environment are destroyed during the development process, it will cause extremely serious ecological problems, and the social economy could not develop effectively and sustainably

The proposal of energy conservation and emission reduction stems from the problems of environmental degradation and resource crisis emerged from the traditional economic development mode, so countries around the globe have begun to adopt energy conservation and emission reduction measures. The above problems and the motivations for energy conservation and emission reduction can be attributed to the following reasons: the needs of human survival and social development, the decrease of non-renewable resources, the deterioration of ecological environment and the requirements of sustainable social development. Therefore, environmental and energy issues are not only problems for the development of human beings, but also the premise for human to live in harmony with the nature.

Development of high energy-consuming industries

In recent years, high-energy-consuming industries such as the metallurgical industry are developing gradually, and the entire production processes (mining, smelting, processing, molding, etc.) consume a large amount of energy and discharge a large amount of wastes. The manufacturing procedures of steelmaking and the generated wastes are shown in *Figure 1*.

Due to the nature of the data in this paper, the complexity and cumbersomeness of the data such as the steel industry's energy consumption and types, this paper obtained some data from the public agency management department and the China Iron and Steel Association (CISA). Then, based on the statistical data of the CISA, further analysis was performed to achieve the development trends and internal laws. In addition, a combination of literature survey and data report analysis was applied in this study to summarize the data analyzed below for enhancing the use value and statistical significance of the data.

http://www.aloki.hu ● ISSN 1589 1623 (Print) ● ISSN 1785 0037 (Online)
DOI: http://dx.doi.org/10.15666/aeer/1706_1458714598

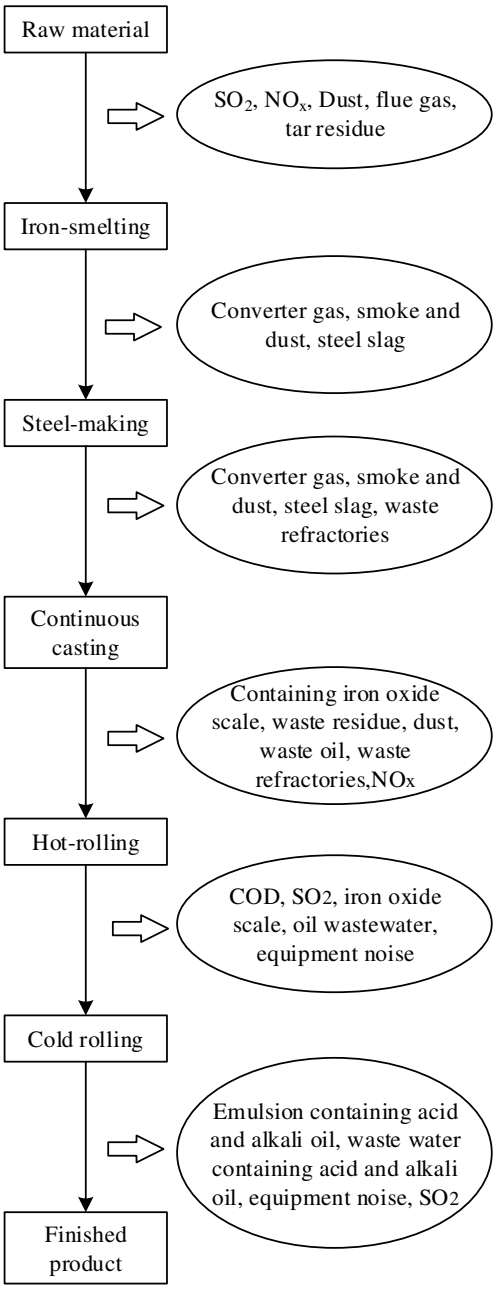

Figure 1. *Manufacturing procedures of steelmaking and the generated wastes*

According to the survey results obtained from public agency management and CISA, the energy consumption of major steelmaking companies in 2016 and 2017 is counted and shown in *Table 1,* and the statistical results are shown in *Figure 2*. Compared with the energy consumption in 2016, the energy consumption of the steelmaking industry decreased by about 3%, and the electricity and water consumption of per ton steel production had been significantly reduced, which had brought great benefits to the economic development and energy-saving of the companies. In addition, the reduction in energy consumption of the manufacturing procedures has made great contributions to the reduction of total energy consumption and comparable energy consumption in steelmaking.

http://www.aloki.hu ● ISSN 1589 1623 (Print) ● ISSN 1785 0037 (Online)
DOI: http://dx.doi.org/10.15666/aeer/1706_1458714598

Table 1. *Energy consumption in steelmaking industry (kgce/t)*

	Energy consumption	Sinter	Pelletizing	Coking	Furnace	Steel rolling	Power consumption (kWh/t)	Water consumption (m^3/t)
2016	668.7	48.6	27.1	98.5	434.7	59.8	451.4	3.12
2017	648.4	46.8	25.4	94.8	425.1	56.3	438.9	3.09
Reduction	20.3	1.8	1.7	3.7	9.6	3.5	12.5	0.03
Reduction rate (%)	3.04	3.70	6.27	3.76	2.21	5.85	2.77	0.96

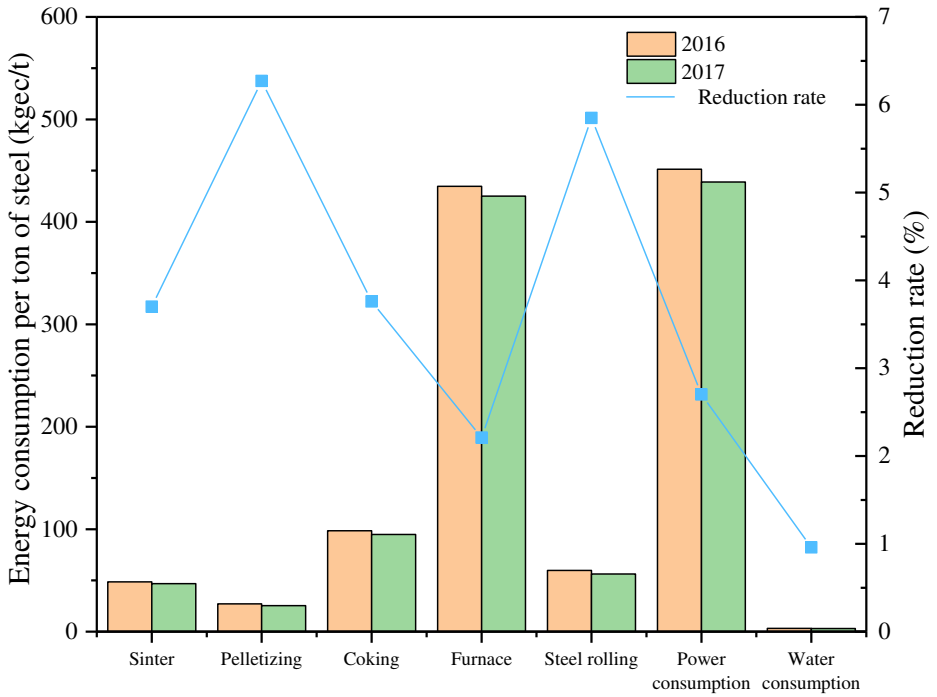

Figure 2. *Energy consumption of per ton steel in each process (kgce/t)*

In the past 7 years, the change trend of energy consumption of per ton steel production of major steelmaking companies is shown as *Figure 3*. It can be seen that the energy consumption of per ton steel production is decreasing year by year, indicating that the processing technologies of the metallurgic industry has made new progress, which is closely related to the policy control of energy conservation and emission reduction of high-energy-consuming industries and the develop of technology. However, from the perspective of circular economy, steel production still consumes a lot of energy, so the strategy of energy conservation and emission reduction still needs to be further implemented.

The CISA provides the data about the energy consumption per ton of steel in key steel industries in the past seven years. It can be seen from *Figure 3* that the comprehensive energy consumption and comparable energy consumption of the per ton steel produced by the metallurgical industry are decreasing year by year, indicating that the technology of the steel enterprises is improving continuously, and the energy consumption of each process is also reduced to varying degrees, which has provided support for the reduction of comprehensive energy consumption and the emission of the

http://www.aloki.hu ● ISSN 1589 1623 (Print) ● ISSN 1785 0037 (Online)
DOI: http://dx.doi.org/10.15666/aeer/1706_1458714598

waste. However, the energy consumption of these enterprises is still at a high level worldwide, and there is still room for improvement. If such enterprises can combine multiple aspects such as economy, government policy and technology to carry out the improvement, they will be able to realize further-level energy conservation and emission reduction, and build an ecological economy.

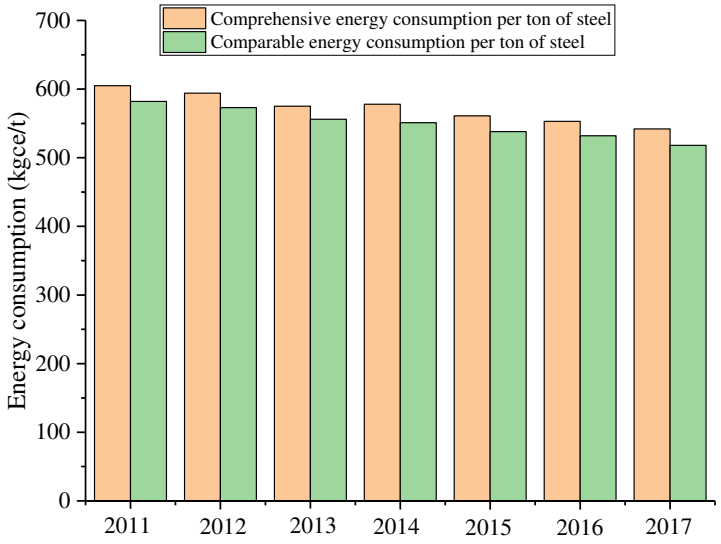

Figure 3. *Changes in energy consumption of per ton steel in steelmaking companies*

At present, in order to further implement energy conservation, emission reduction and develop ecological economy, the high-energy-consuming industries represented by the metallurgical industry have gradually transformed from economic benefit-oriented companies to harmonious enterprises, constantly rethinking the relationship between economic development, ecological environment and resources; in addition, these high-energy-consuming enterprises have also changed the traditional extensive management, and gradually improved to intensive management, thereby improving their unit output, and increasing social and economic benefits by optimizing resource allocation and elements of various links.

Results (eco-economics of high energy-consuming industries)

Construction of energy conservation and emission reduction system

The development of high-energy-consuming industries such as the metallurgical industry consumes a large amount of energy and resources. Therefore, based on the basic theory and principle of circular economy, we should adopt a comprehensive approach combining economy, policy and laws to implement energy conservation and emission reduction, and systematically build a comprehensive energy-saving and emission-reducing system. Therefore, based on the basic mechanism of energy conservation and emission reduction, combining with relevant theories of circular economy, this paper proposes the Best management Practices (BMP) comprehensive system for the energy conservation and emission reduction of high-energy-consuming industries, the basic processes are shown in *Figure 4*. Based on information platform,

http://www.aloki.hu ● ISSN 1589 1623 (Print) ● ISSN 1785 0037 (Online)
DOI: http://dx.doi.org/10.15666/aeer/1706_1458714598

human resources and management, it adopts policy incentives, index constraints, target assessment and other approaches to guarantee the implementation, thereby achieving the goal of energy conservation and emission reduction of high-energy-consuming enterprises.

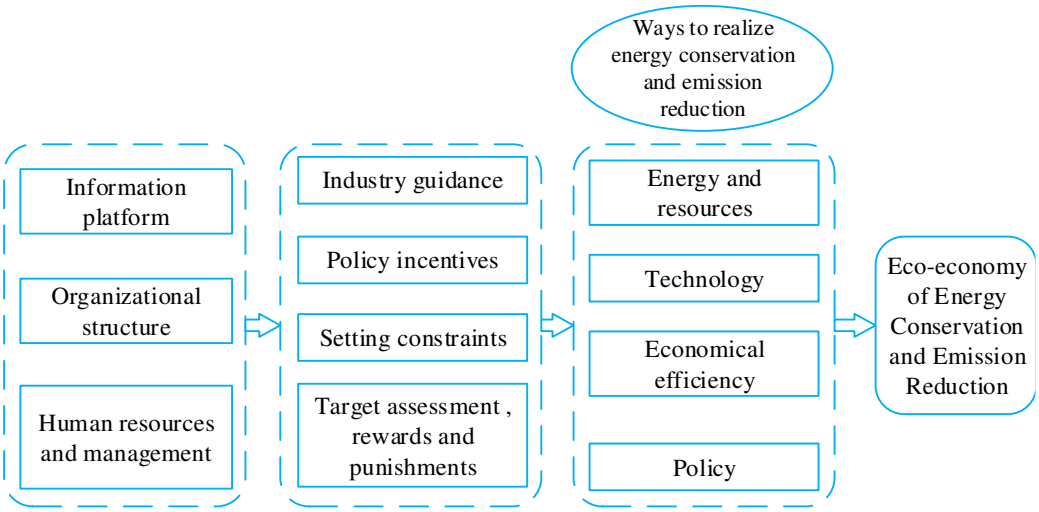

Figure 4. *Energy conservation and emission reduction system*

Structure of energy conservation and emission reduction system

When building the energy-conservation emission-reduction system, the construction of the system is guaranteed from three aspects: information platform, organizational structure and human resources. The information platform for energy conservation and emission reduction can integrate informationization and industrialization in depth, through information collection, processing, analysis and sharing of the energy conservation and emission reduction and the whole production process of the high-energy-consuming enterprises, it conducts dynamic monitoring and optimization processing on the whole production process, resource utilization, allocation of equipment and materials, and the condition of energy consumption, balances the economic benefits and energy, and finally achieves industrialized energy conservation and emission reduction. The management of the organizational structure is a comprehensive management system with government policies and regulations as guidance, production enterprises as subjects, and public and third parties as supervisors. The first is the government's guidance and control of the companies' production, energy conservation and emission reduction according to laws, regulations, and relevant economic policies, while within the companies, through hierarchical management and internal strategies, assessment system and reward and punishment policies for energy conservation and emission reduction are set up, and relevant liability system are established, so as to ensure the realization of the goal of energy conservation and emission reduction. And the human resources are to enable enterprises to cultivate professional and compound talents for energy conservation and emission reduction, learn the related theoretical knowledge of energy conservation and emission reduction and apply it to the actual production. The operation mechanism of the energy-conservation emission-reduction system is shown in *Figure 5,* mainly including fiscal policies, rewards and punishments, and taxation policies.

http://www.aloki.hu ● ISSN 1589 1623 (Print) ● ISSN 1785 0037 (Online)
DOI: http://dx.doi.org/10.15666/aeer/1706_1458714598

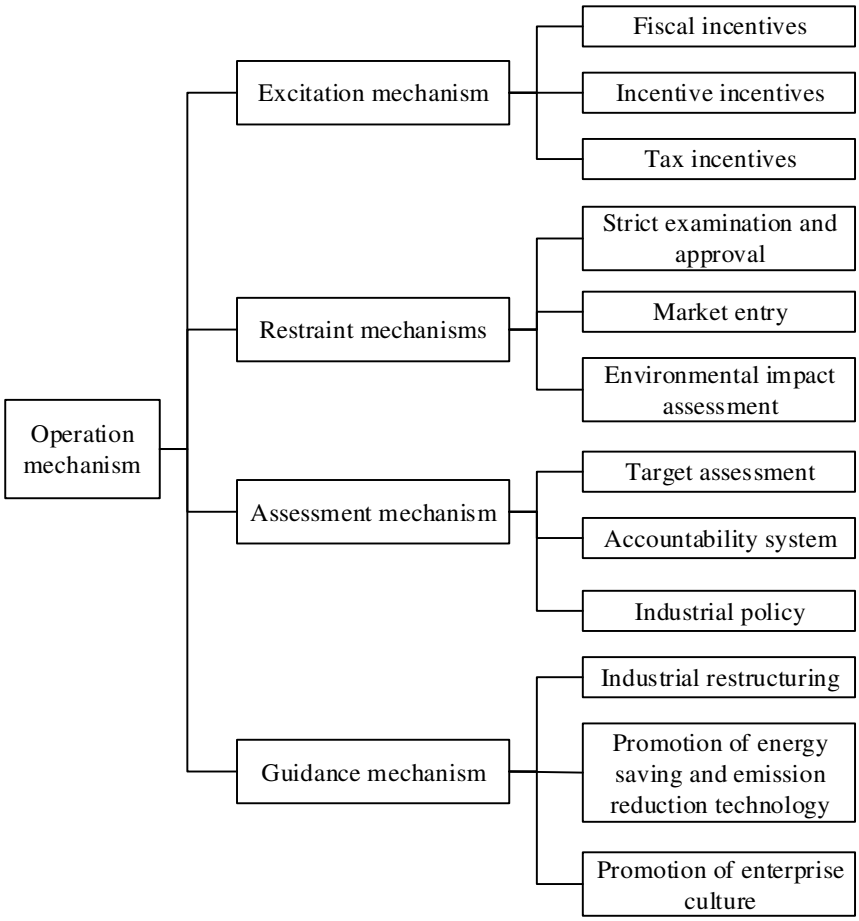

Figure 5. *Operation mechanism of energy conservation and emission reduction system*

Discussion (analytic hierarchy process (AHP) of energy conservation and emission reduction)

This paper first adopted the AHP to decompose the problem, as shown in *Figure 6,* the problem of circular economy development and energy conservation and emission reduction of high energy-consuming industries was divided into four layers (target layer, standard layer, index layer and scheme layer). The corresponding judgment matrix established is shown in *Table 2*. For the judgment matrix results, the value assignment was made according to the importance of factors, as shown in *Table 3*.

Based on the above judgment matrix, the relative weights of the elements were calculated using the sum method. For the inconsistent judgment matrix, the weights of the vectors in each column were calculated according to *Equation 1,* as for the consistent judgment matrix, after normalizing the vectors in each column, the corresponding weights could be obtained.

$$W_i = \frac{1}{n}\sum_{j=1}^{n}\frac{a_{ij}}{\sum_{k=1}^{n} a_{ki}} \quad \text{(Eq.1)}$$

After the relative weights of the elements were calculated, the consistency of the judgment matrix was tested, and the specific steps are as follows: calculate the

http://www.aloki.hu ● ISSN 1589 1623 (Print) ● ISSN 1785 0037 (Online)
DOI: http://dx.doi.org/10.15666/aeer/1706_1458714598

consistency indicator *C.I.* according to *Equation 2,* and determine the average random consistency indicator *R.I.* according to *Table 4;* then according to *Equation 3,* use the consistency indicator and the average random consistency indicator to calculate the consistency ratio *C.R.*, thereby determining the consistency of the judgment matrix. When the value of *C.R.* is less than 0.1, the judgment matrix is considered to be consistent; otherwise, it is inconsistent and needs to be modified.

$$C.I. = \frac{\lambda_{\max} - n}{n - \mathbf{1}} \quad \text{(Eq.2)}$$

$$C.R. = \frac{C.I.}{R.I.} \quad \text{(Eq.3)}$$

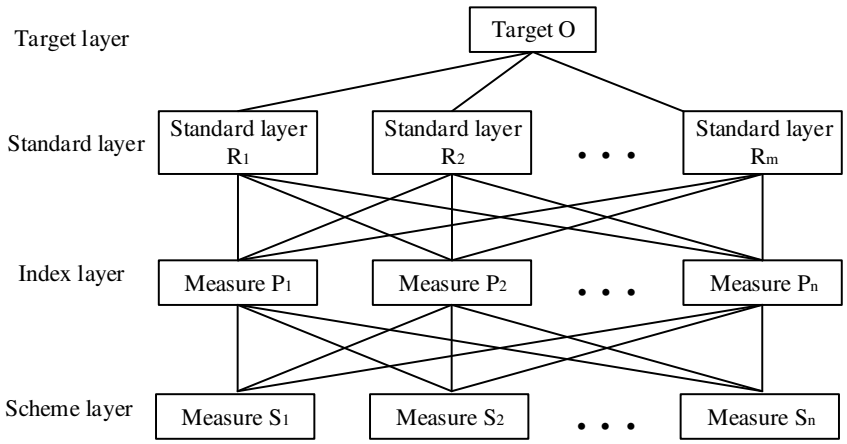

Figure 6. *Model structure of analytic hierarchy process for green economy development*

Table 2. *The judgement matrix of green economy development level*

$\mathbf{M_x}$	$\mathbf{N_1}$	$\mathbf{N_2}$	$\mathbf{N_3}$	$\mathbf{N_4}$
N_1	n_{11}	n_{12}	n_{13}	n_{14}
N_2	n_{21}	n_{22}	n_{23}	n_{24}
N_3	n_{31}	n_{32}	n_{33}	n_{34}
N_4	n_{41}	n_{42}	n_{43}	n_{44}

Table 3. *The implication of importance assignment scale*

Assignment scale	Implication
1	The two elements are equally important
3	The former is slightly more important than the latter
5	The former is obviously more important than the latter
7	The former is strongly more important than the latter
9	The former is extremely more important than the latter
2, 4, 6, 8	The intermediate value of the above judgment
Reciprocal	If the ratio of importance between elements I and j is m_{ij}, the ratio of importance between elements J and I is $m_{ij} = 1/m_{ji}$

http://www.aloki.hu ● ISSN 1589 1623 (Print) ● ISSN 1785 0037 (Online)
DOI: http://dx.doi.org/10.15666/aeer/1706_1458714598

Table 4. *Random consistency indicators*

Order of matrix	1	2	3	4	5	6	7	8
R.I.	0	0	0.52	0.89	1.12	1.26	1.36	1.41
Order of matrix	9	10	11	12	13	14	15	-
R.I.	1.46	1.49	1.52	1.54	1.56	1.58	1.59	-

Finally, the weights of factors in each layer relative to the upper layer factors were calculated top-down layer by layer, and sorted according to the weight, and then subject to the consistency check according to *Equation 4*. If the value of $C.R.^{(m+1)}$ of the total elements in (m + 1) layer is less than 0.1, then the total sorting is considered to be consistent, otherwise, it is not consistent.

$$C.R.^{(m+1)} = \frac{C.I.^{(m+1)}}{R.I.^{(m+1)}} \quad \text{(Eq.4)}$$

where:

$$C.R._j^{(m+1)} = \left(C.R._1^{(m+1)}, C.R._2^{(m+1)}, ..., C.R._n^{(m+1)}\right) W^m \quad \text{(Eq.5)}$$

$$R.I._j^{(m+1)} = \left(R.I._1^{(m+1)}, R.I._2^{(m+1)}, ..., R.I._n^{(m+1)}\right) W^m \quad \text{(Eq.6)}$$

Based on the AHP and above steps, the weights of the high-energy-consuming enterprises' energy conservation, emission reduction, and circular economy development level can be calculated, analyzed and evaluated comprehensively. According to the above-mentioned energy-conservation emission-reduction economic comprehensive system and the AHP, the eco-economic development of energy-conservation and emission-reduction of several high-energy-consuming industries had been evaluated, and it is found that the effects of energy-conservation and emission-reduction of such enterprises are obvious, which is conducive to the development of eco-economy.

Conclusion

Based on the theory of circular economy and the basic concept of sustainable development, combining with data research and analysis, this paper carried out researches on the energy conservation and emission reduction and eco-economic construction of high-energy-consuming industries. The main conclusions are as follows:

- The energy consumption data of the metallurgical industry in the past 7 years shows that the energy consumption and comparable energy consumption of per ton steel are decreasing year by year, indicating that technological reform, policy regulation, economic coordination and other countermeasures have exerted positive effects on reducing energy consumption and pollutant emission and improving economic benefits of the industries during the production process.

http://www.aloki.hu ● ISSN 1589 1623 (Print) ● ISSN 1785 0037 (Online)
DOI: http://dx.doi.org/10.15666/aeer/1706_1458714598

- For the energy conservation and emission reduction of high-energy-consuming industries, this paper constructed an energy conservation and emission reduction eco-economic system based on circular economy, which gradually achieved energy conservation and emission reduction through policy, technology, organizational structures, resources, and other approaches, it promoted the upgrade of the industries, and combined with the policies and economic countermeasures, and implemented the energy conservation and emission reduction of the industries from two aspects of inside and outside.
- The energy conservation and emission reduction eco-economic system of high-energy-consuming industries based on circular economy is conductive to the improvement of the high energy consumption of the industries, and it laid a foundation for the eco-economic development of high-energy-consuming industries and the sustainable development of the society.
- This paper conducts a preliminary study on the energy reduction of high-energy-consuming industries from a macro perspective. However, at the micro level, it still requires more in-depth and systematic research on how the high-energy-consuming industries coordinate economic interests and social interests by organically combining them to effectively improve the level of ecological economic construction in energy conservation and emission reduction.

Acknowledgements. Qinghai Social Science Fund Project, Project number: 17001; Ministry of Education "Chunhui Plan" project, Project number: Z2017041.

REFERENCES

[1] Algaba, A., Fernández Sánchez, F., Merino, M., Rodríguez Luis, A. J. (2012): Comments on analysis and application of a novel three-dimensional energy-saving and emission-reduction dynamic evolution system. – Energy 40(1): 291-299.
[2] Cheng, C. T., Shen, J. J., Wu, X. Y., Chau, K. W. (2012): Operation challenges for fast-growing China's hydropower systems and respondence to energy saving and emission reduction. – Renewable & Sustainable Energy Reviews 16(5): 2386-2393.
[3] Cordova-Pizarro, D., Aguilar-Barajas, I., Romero, D., Rodriguez, C. A. (2019): Circular economy in the electronic products sector: material flow analysis and economic impact of cellphone e-waste in Mexico. – Sustainability 11(5): 1631.
[4] Danza, L., Belussi, L., Floreani, F., Meroni, I., Piccinini, A., Salamone, F. (2018). Application of model predictive control for the optimization of thermo-hygrometric comfort and energy consumption of buildings. – Instrumentation Mesure Métrologie 17(3): 375-391.
[5] Gallagher, J., Basu, B., Browne, M., Kenna, A., Mccormack, S., Pilla, F., Styles, D. (2017): Adapting stand-alone renewable energy technologies for the circular economy through eco-design and recycling. – Journal of Industrial Ecology 23(1): 133-140.
[6] Habib, M. A., Hasanuzzaman, M., Hosenuzzaman, M., Salman, A., Mehadi, M. R. (2016): Energy consumption, energy saving and emission reduction of a garment industrial building in Bangladesh. – Energy 112: 91-100.
[7] Hobson, K., Lynch, N. (2016): Diversifying and de-growing the circular economy: radical social transformation in a resource-scarce world. – Futures 82: 15-25.
[8] Jonas, M., Michael, J., Claudia, B. (2018): Transition of the Swiss Phosphorus System towards a circular economy—part 1: current state and historical developments. – Sustainability 10(5): 1479.

http://www.aloki.hu ● ISSN 1589 1623 (Print) ● ISSN 1785 0037 (Online)
DOI: http://dx.doi.org/10.15666/aeer/1706_1458714598

[9] Krishna, V. M. (2018): Emissions control and performance evaluation of spark ignition engine with oxy-hydrogen blending. – International Journal of Heat and Technology 36(1): 118-124.
[10] Lei, J. Y., Xie. J., Gan. D. Q. (2009): Optimization of distributed energy system and benefit analysis of energy saving and emission reduction. – Automation of Electric Power Systems 33(23): 29-36.
[11] Liao, G. C. (2011): A novel evolutionary algorithm for dynamic economic dispatch with energy saving and emission reduction in power system integrated wind power. – Energy 36(2): 1018-1029.
[12] Mostafaei, A., Mirrzaei, M., Ghazvini, M., Ahmadi, M. H., Lorenzini, G. (2019): Investigation of energy saving in building by using phase-change materials (PCM). – Mathematical Modelling of Engineering Problems 6(1): 47-51.
[13] Murray, A., Skene, K., Haynes, K. (2017): The circular economy: an interdisciplinary exploration of the concept and application in a global context. – Journal of Business Ethics 140(3): 369-380.
[14] Peters, G. P., Weber, C. L., Guan, D., Hubacek, K. (2007): China's growing CO_2 emissions - a race between increasing consumption and efficiency gains. – Environmental Science & Technology 41(17): 5939-5944.
[15] Price, L., Levine, M. D., Zhou, N., Fridley, D., Aden, N., Lu, H., McNeil, M., Zheng, N., Qin, Y. N., Yowargana, P. (2011): Assessment of China's energy-saving and emission-reduction accomplishments and opportunities during the 11th five year plan. – Energy Policy 39(4): 2165-2178.
[16] Rigueiro-Rodríguez, A., Amador-García, A., Ferreiro-Domínguez, N., Muñoz, N., Santiago-Freijanes, J. J., Mosquera-Losada, M. R. (2018): Proposing policy changes for sewage sludge applications based on zinc within a circular economy perspective. – Land Use Policy S0264837718300425.
[17] Rudra, J. P., Chakraborty, M. (2017). Increase in lifetime by harvested energy and analysis of RC5 along with efficient energy consumption in WBAN. – Environmental and Earth Sciences Research Journal 4(2): 39-44.
[18] Tao, F., Zuo, Y., Xu, L. D., Lv, L., Zhang, L. (2014): Internet of things and BOM-based life cycle assessment of energy-saving and emission-reduction of products. – IEEE Transactions on Industrial Informatics 10(2): 1252-1261.
[19] Tiening, C., Jimei, Z. (2018): Bibliometric and review of the research on circular economy through the evolution of Chinese public policy. – Scientometrics 116(2): 1013-1037.
[20] Tomi, T., Schneider, D. R. (2017): Municipal solid waste system analysis through energy consumption and return approach. – Journal of Environmental Management 203: 973-987.
[21] Trica, C. L., Banacu, C. S., Busu, M. (2019): Environmental factors and sustainability of the circular economy model at the European Union level. – Sustainability 11: 1114.
[22] Tu, J. Z., Ma, D. L. (2018): A spatial economics perspective on convergence research of carbon emissions performance in China. – International Journal of Heat and Technology: 36(3): 962-972.

http://www.aloki.hu ● ISSN 1589 1623 (Print) ● ISSN 1785 0037 (Online)
DOI: http://dx.doi.org/10.15666/aeer/1706_1458714598

INFLUENCE OF ENVIRONMENTAL LANDSCAPE STRUCTURE ON THE DISTRIBUTION FEATURES OF PLANT COMMUNITIES IN GREEN PARKS

PENG, Y.

Hunan International Economics University, Changsha 410006, China
(e-mail: 451058850@qq.com; phone: +86-186-8495-1668)

(Received 7th Jun 2019; accepted 10th Oct 2019)

Abstract. Green parks are indispensable to urban ecosystem, and critical to living environments, urban greening and city development. Based on the theory of landscape ecology, this paper explores how environmental landscape structure (ELS) affects the distribution features of plant communities in several green parks in Jiangmen, southern China's Guangdong Province. The study was carried out with analytical hierarchy process (AHP), geographic information system (GIS) and remote sensing (RS). The research results show that: Compared to the other two parks, Penglai Park, a downtown park surrounded by residential buildings and highways, boasts a high overall temperature, and witnesses limited variations in temperature and PM10. In addition, this park outperforms the other two parks in plant height, the density/overall height/mean coverage of shrub and herb layers, as well as the ecological benefit. In contrast, Jiangbin Park, which is greatly affected by wind from the nearby river, saw great variations in the temperatures inside and outside plant communities and the PM10. As a result, this park lags behind the other two parks in the following aspects: the average height/average coverage of shrub and herb layers, and the mean diameter at breast height (DBH) of arbor layer. The research findings provide a good reference to optimizing the plant communities in green parks and promoting urban ecology.
Keywords: *environmental landscape structure (ELS), urban park, plant community, distribution features, temperature changes, PM10, urban green park protection*

Introduction

Green parks are an important part of urban ecosystems and the most concentrated areas of urban biodiversity and green spaces (Kruess, 2003). They provide citizens with recreation and fitness places, and have the ecological functions of conserving water, purifying air, reducing noise, and regulating the local climate of the city (Schmucki et al., 2012). The collection of all plants living in a certain area is called a plant community (Svenning et al., 2004). Plant communities are basic components of green parks, and a reasonable plant community layout is the basis for maintaining a green park and exerting its ecological role (Wallgren et al., 2009). In the plant communities, there are certain correlations between the plants and the environment, and between the plants; the surrounding environment has a strong influence on the growth of plants. Therefore, studying the influence of ELS on the distribution features of park plant communities is of great significance.

At the end of the 18th century, in order to solve the problem of urban development and the quality of urban living environment, foreign countries began to study the construction of urban green parks, and the Regent's Park and the Birkenhead Park in England were built in this context (Miller et al., 2016). Subsequently, ecological design has become a main trend for green parks in western countries. In the 19th century, designers chose different tree species and designed a number of green parks according to the structure of the natural communities (José et al., 2016). In the 1920s, designers and ecologists such as Broerse and Springer imitated the natural plant communities and

http://www.aloki.hu ● ISSN 1589 1623 (Print) ● ISSN 1785 0037 (Online)
DOI: http://dx.doi.org/10.15666/aeer/1706_1459914609

their habitats to create urban ecological gardens (Chiron et al., 2014). China's research on landscape ecology and urban green parks started relatively late, but in recent years, as people are paying more attention to the urban ecological environment, Chinese landscape architects have also applied the ecological concept to the design of urban green parks (Davidson et al., 2011). In 1998, in order to effectively transform an urban garbage dump, designers used native plants to build artificial plant communities and construct the Shimen Park in Dashiba, Chongqing city (Amici et al., 2015). Ding Fenghua et al. took the Changsha Martyrs Park as an example and analyzed its current plant landscaping situations (Wrbka et al., 2008). Liu Yanhong et al. investigated the biodiversity characteristics and plant species of urban green parks in Beijing (Goodwin and Fahrig, 2002). Zhang Jing et al. classified the typical plant communities of green parks in Shanghai (Moebiusclune et al., 2013). Concerning the researches on plant communities and environmental factors, current domestic and foreign studies focus mostly on the landscape functions, maintaining biodiversity, cooling and humidifying, and other aspects (Rodrigo León Cordero et al., 2016). The comprehensive effect of plant community structure, the structure model of plant communities and environmental factors based on 3S technology, the dynamic monitoring of plant community structure, and the quantitative analysis of their correlations, will be the main trends and focuses of researches in the future (Bouasria et al., 2012).

Based on the above analysis, this paper aims to study the influence of environmental landscape structure on the distribution features of plant community in green parks by selecting Jiangbin Park, Penglai Park and Donghu Park in Jiangmen city as the research area, and analyzes the plant community structure features of these parks according to the three layers: arbor layer, shrub layer and herb layer; three indices of diversity index, ecological advantage index and richness index have been selected to analyze the structure features of the plant communities in the three parks; meanwhile two ecological factors of temperature and PM10 which are largely affected by the environmental landscape structure have also been selected to analyze the influence of ELS on the ecological factor features of plant communities in the park; then this paper comprehensively compares the plant community distribution features of each park under different ELS conditions and proposes related suggestions for the optimization of plant communities in the parks, in the hopes of providing relevant references for the construction of eco-cities.

Materials and methods

Research objects and methods of plant community structure in major regions

Research object

The distribution of plant communities is largely interfered by the surrounding landscape pattern and human factors, which leads to large differences between plant communities in parks and in natural state. This study used GIS and RS technology to obtain the overall plan of Jiangmen City, Guangdong Province, China. After systematic investigation of the vegetation in the parks of Jiangmen City, this paper selects Jiangbin Park (sample area 135,772 m^2), Penglai Park (sample area 68,732 m^2) and Donghu Park (sample area 87,521 m^2) in Jiangmen city as the research areas. *Figure 1* shows the specific location of these three parks in Pengjiang District: 1 for Penglai Park, 2 for Jiangbin Park, 3 for Donghu Park. In addition, it uses AHP to conduct sampling and

http://www.aloki.hu ● ISSN 1589 1623 (Print) ● ISSN 1785 0037 (Online)
DOI: http://dx.doi.org/10.15666/aeer/1706_1459914609

survey on the target areas. The sampling area of Jiangbin Park was 1,800 m^2 (east longitude 113.118431, north latitude 22.602591), Penglai Park sampling area was 1,800 m^2 (east longitude 113.08728, north latitude 22.581711), and Donghu Park sampling area was 2,100 m^2 (east longitude 113.087898, north latitude 22.591829). Excel software and landscape pattern analysis software were used for calculation.

Founded in 1958 and opened to the public in July 2014, Donghu Park is located in the center of Jiangmen with the green ecology as the theme. It covers an area of 53 ha, including 17 ha of lake area. It has the elegant restaurant and tea house, as well as the specialties of the hometown. Jiangbin Park is located on the Xijiang River in the North Street of Jiangmen City, covering an area of 3.8 ha. It was built in 1984 as the only park in the city for barbecue. It also has an open-air lounge. Penglai Park was built in 1983 and covers an area of 0.95 ha. It is located at the intersection of Penglai Road and Jianshe Road in Jiangmen City. It was first built with plant landscaping and was renamed as Children's Park in 1990.

Calculation methods

(1) Diversity index (D_1)

$$D_1 = 1 - \sum_{i=1}^{s} \frac{N_i(N_i - 1)}{N(N-1)} \quad \text{(Eq.1)}$$

The larger the D_1 value, the higher the diversity (Ames et al., 2016).

(2) Ecological advantage index (D_2)

$$D_2 = \sum_{i=1}^{s} \frac{N_i(N_i - 1)}{N(N-1)} \quad \text{(Eq.2)}$$

The smaller the D_2 value, the higher the diversity and the smaller the ecological advantage (Brunzel et al., 2004).

(3) Richness index (R)

$$R = \frac{S-1}{\ln N} \quad \text{(Eq.3)}$$

where: N is the number of individuals of all species, N_i is the number of individuals of species i, and S is the number of plant species within the sampling area.

Selection of ecological factors

The various environmental factors that affect biological organisms are called ecological factors, and there are many types of ecological factors. No matter which type, all ecological factors would influence the survival, reproduction and various functions of plant individuals and the whole plant community, moreover, there are interactions among the ecological factors, which would also have an impact on the plant

http://www.aloki.hu ● ISSN 1589 1623 (Print) ● ISSN 1785 0037 (Online)
DOI: http://dx.doi.org/10.15666/aeer/1706_1459914609

community; on the one hand, ecological factors are related to season, climate and other factors in the nature, on the other hand, they are also affected by the landscape of surrounding environment. In order to study the influence of ELS on the distribution features of plant communities in green parks, this paper selects two ecological factors, temperature and PM10 (Herrera et al., 2016), which are strongly influenced by environmental landscape, as the objects of measurement to measure the ecological factors of plant communities inside and outside the parks.

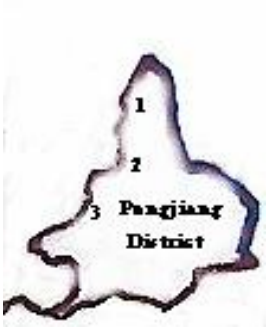

Figure 1. *The specific location of the three parks in the Pengjiang District*

The temperature and PM10 were measured using the Testto608-H2 dual-purpose thermometer and the hand-held PM10 hand-held dust meter respectively. The measuring instruments were placed at a height of 1.5 m from the ground. For the external ecological factors of plant community the measuring instruments were mainly placed in the park square and lawn, while for the internal ecological factors of the plant community, the instruments were placed in a sample plot with rich community, with the central position of the shade as the main measurement point. *Figure 2* shows the pictures of the measured temperature and PM10 at the experimental site of Donghu Park.

Figure 2. *Temperature and PM10 picture of the experimental site of Donghu Park*

http://www.aloki.hu ● ISSN 1589 1623 (Print) ● ISSN 1785 0037 (Online)
DOI: http://dx.doi.org/10.15666/aeer/1706_1459914609

Results

Analysis of plant community structure features

Through investigation, the plant communities in green parks in Jiangmen city were divided into three community layers: the arbor layer, the shrub layer and the herb layer. *Figures 3–5* show the statistical results of the structure features of plant communities in the three parks (number of plants, average height, average coverage). *Figure 6* shows the average DBH of the arbor layer.

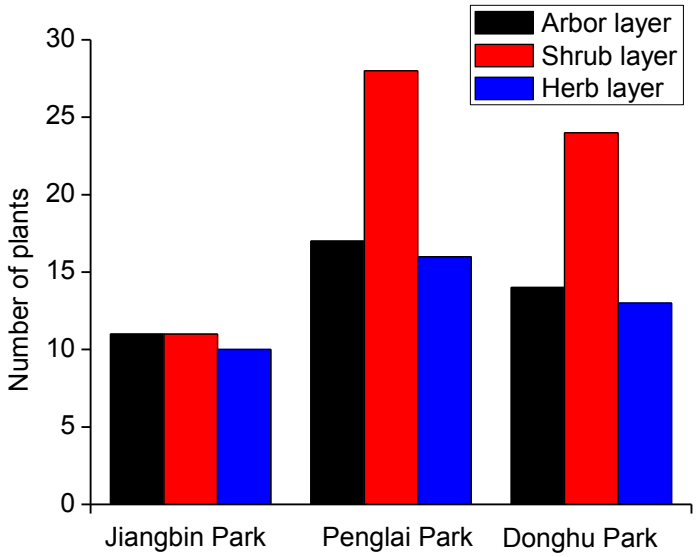

Figure 3. *Number of plants of each community layer in the three parks*

It can be seen from *Figure 3* that the number of shrub layer plants in the three parks is the largest, and the number of herb layer plants is the smallest; in the Jiangbin Park, the number of arbor layer plants, shrub layer plants, and herb layer plants are basically the same, and are much less than those of the Penglai Park and the Donghu Park.

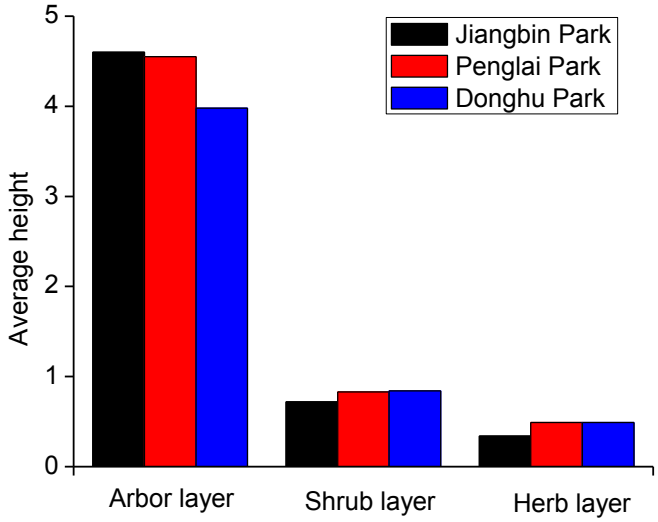

Figure 4. *Average height of plant communities in the three parks*

http://www.aloki.hu ● ISSN 1589 1623 (Print) ● ISSN 1785 0037 (Online)
DOI: http://dx.doi.org/10.15666/aeer/1706_1459914609

As can be seen from *Figure 4,* for the Jiangbin Park, the average height of the arbor layer is the highest, and the average heights of shrub layer and the herb layer are the lowest; for the Donghu Park, the average height of the arbor layer is the lowest; There is a small difference in the average height of shrub layer and herb layer between the Penglai Park and Donghu Park, which can be considered to be basically the same.

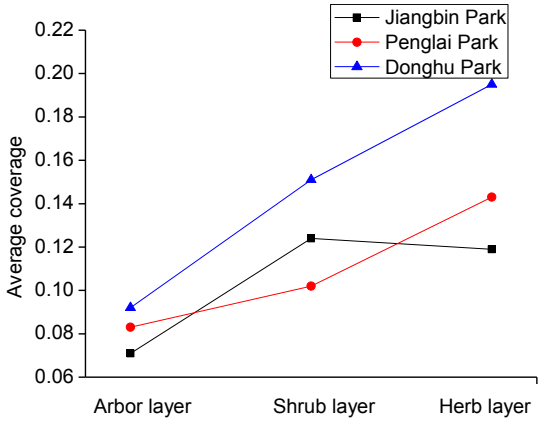

Figure 5. *Average coverage of each plant community layer in the three parks*

It can be seen from *Figure 5* that the average coverages (Average coverage = the sum of the vertical projection areas of all plants of a tree species/the total area of the sample) of the arbor, shrub and herb layers of Donghu Park are much higher than the other two parks. The average coverage of the shrub layer in Jiangbin Park is higher than that of the Penglai Park, while the average coverages of arbor and herb layers of Jiangbin Park are lower than those of the Penglai Park.

Calculate the average DBH of the arbor layer according to *Equation 4:*

$$DBH = \frac{D_1 \times K_1 + D_2 \times K_2 + D_3 \times K_3 + \cdots D_n \times K_n}{K_1 + K_2 + K_3 + \cdots K_n} \quad \text{(Eq.4)}$$

where: DBH is the average DBH, D_1 is the first diameter grade value, and K_1 is number of trees in the first diameter grade.

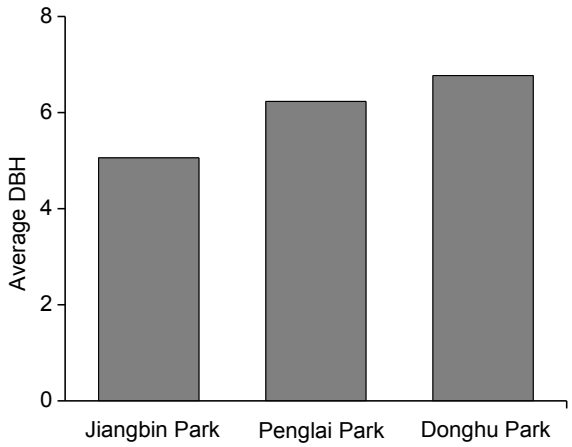

Figure 6. *Average DBH of the arbor layer in the three parks*

http://www.aloki.hu ● ISSN 1589 1623 (Print) ● ISSN 1785 0037 (Online)
DOI: http://dx.doi.org/10.15666/aeer/1706_1459914609

It can be seen from *Figure 6* that the order of the average DBH of arbor layer is: Donghu Park > Penglai Park > Jiangbin Park.

Based on the above analysis, it can be seen that the density and overall height of the shrub layer and the herb layer in Penglai Park are higher and its ecological benefit is better.

Analysis of structure feature indices of plant communities in the parks

According to *Equations 1, 2* and *3,* the diversity index (D_1), ecological dominance index (D_2) and richness index (R) of park plant community structure were calculated. *Figure 7* shows structure features of plant communities in the three parks, it can be seen from the figure that in the three parks, the diversity index (D_1) and richness index (R) of the arbor layer, shrub layer and herb layer of the Penglai Park are the highest, while its ecological advantage index (D_2) is the lowest; the ecological advantage index (D_2) of the arbor layer, shrub layer and herb layer of the Jiangbin Park is the highest.

Influence of ecological factors of plant communities in parks

Temperature changes inside and outside the plant communities in parks

Table 1 shows the statistics of temperature changes inside and outside the plant communities of each park. It can be seen from the table that the highest temperature of each park appeared in the three months of July, August and September, and the lowest temperature appeared in March and December. Wherein the internal and external temperatures of Jiangbin Park fluctuated greatly, the highest internal and external temperatures were 34 °C and 35 °C, and the lowest internal and external temperatures were 8 °C and 6 °C. This is mainly because the Jiangbin Park is located by the riverside near the Jiangbei Bridge, so the temperature is greatly affected by the wind from the river. In the summer, the inside of the plant community is influenced by the evaporation of the river water, so the temperature rises, while in the winter, the influence is smaller, and there are fewer plant types in the plant community, so the warming effect of the plant community is not obvious, plus the influence of the wind from the river, so the temperature is very low in winter. As for the Penglai Park, the internal and external temperature fluctuations were relatively small, its highest temperature and lowest temperatures were 1 °C lower than that of the Jiangbin Park, respectively, and its external temperature was about 1–2 °C higher than the internal temperature, this is mainly because the Penglai Park is located in the center of the Jiangmen city, and surrounded by roads and buildings, therefore, its external temperature is higher; inside the park, due to the rich structure of the plant community, and the distribution is reasonable, so the cooling function in the summer and the warming function in the winter are significant.

PM10 inside and outside the plant communities in the parks

Figure 8 shows the changes of PM10 inside the plant communities of each park, and *Figure 9* shows the changes of PM10 outside the plant communities of each park. It can be seen from the figures that the PM10 inside the plant communities of each park was about 10-15 $\mu g/m^3$ lower than the external PM10 level, wherein, the PM10 in the Penglai Park in autumn was as low as 80 $\mu g/m^3$. As for the Jiangbin Park, since it is near the river and the wind is strong in winter, so the PM10 values in summer and winter are much higher than that in the autumn; for the Donghu Park, it is in the leeward

http://www.aloki.hu ● ISSN 1589 1623 (Print) ● ISSN 1785 0037 (Online)
DOI: http://dx.doi.org/10.15666/aeer/1706_1459914609

of production forest farms, so the PM in autumn is higher than that in summer and winter; and for the Penglai Park, its surroundings are mostly residence, plus the distribution of plant community inside the park is reasonable, so the PM10 varies little in summer, autumn and winter.

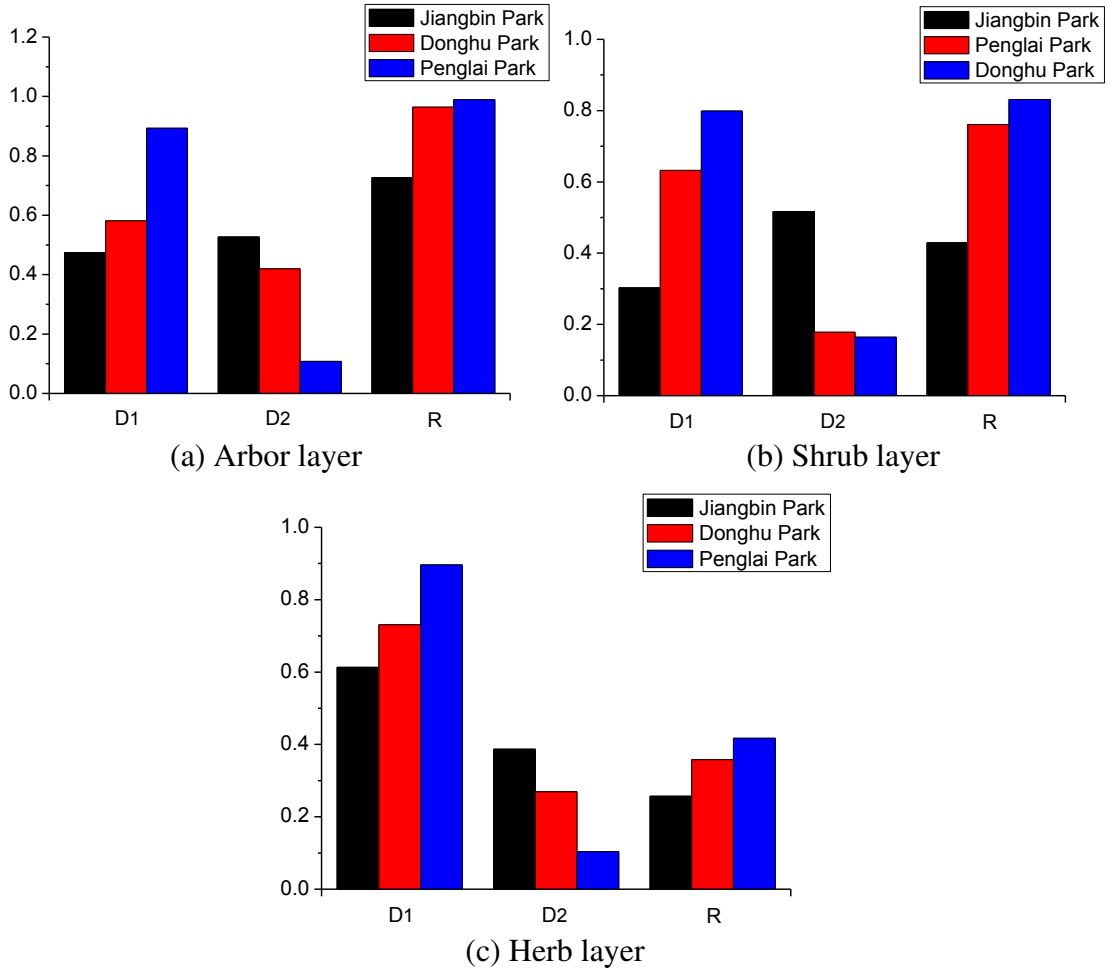

Figure 7. *Structure features of plant communities in the three parks*

Table 1. *Statistics of temperature (°C) changes inside and outside the plant communities of each park*

Month	Jiangbin Park		Penglai Park		Donghu Park	
	Internal	External	Internal	External	Internal	External
3	15	15	23	23	18	18
4	19	19	26	27	21	19
5	22	22	30	29	22	21
6	31	33	31	32	24	24
7	34	35	32	34	31	32
8	32	34	32	33	32	35
9	33	34	31	33	32	33
10	28	29	27	28	26	27
11	14	16	16	14	15	15
12	8	6	9	7	8	7

http://www.aloki.hu ● ISSN 1589 1623 (Print) ● ISSN 1785 0037 (Online)
DOI: http://dx.doi.org/10.15666/aeer/1706_1459914609

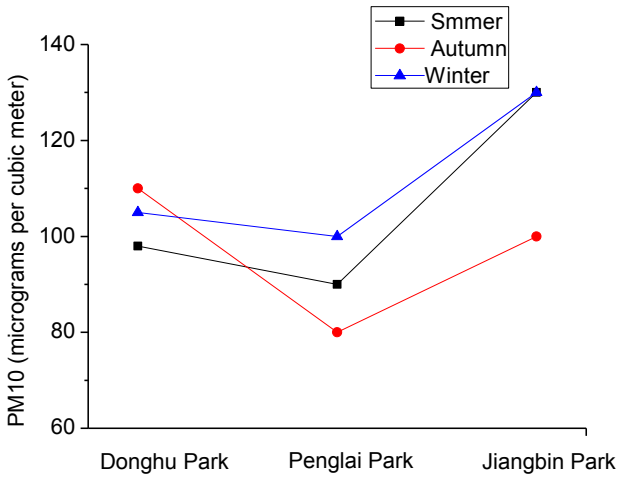

Figure 8. *PM10 variation inside the plant communities of each park*

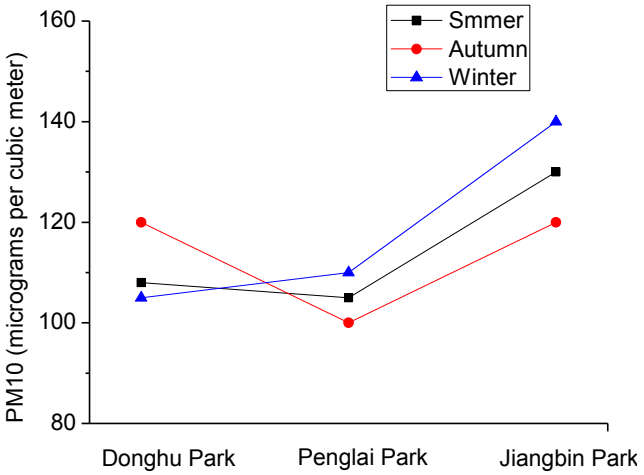

Figure 9. *PM10 variation outside the plant communities of each park*

Discussion

Influence of ELS on the distribution features of plant communities in green parks

According to above analysis results we can see that, the Penglai Park is located in the center of the city, and surrounded by residential buildings and highways, the temperature changes little, and the overall temperature is higher than the other two parks; its fluctuation of PM10 is small, the density, overall height and average coverage of the shrub layer and herb layer, and the ecological benefit of the Penglai Park are all higher than the other two parks, which is basically in line with the previous research results. As for the Jiangbin Park, since it is near the river and greatly affected by the wind from the river, the temperature inside and outside the plant community and the PM10 vary greatly, therefore, its average height and average coverage of the shrub layer and the herb layer, and the average DBH of the arbor layer are all lower than the other two parks. In the past, there have been few studies on the distribution features of plant communities by ecological factors. This study is expected to provide reference for future research in this regard.

http://www.aloki.hu ● ISSN 1589 1623 (Print) ● ISSN 1785 0037 (Online)
DOI: http://dx.doi.org/10.15666/aeer/1706_1459914609

Countermeasures and suggestions for green park protection in Jiangmen City

Improve urban green space system planning

Green parks are only a part of the urban green space system, to make the distribution of park plant communities more reasonable, we should reduce damages and development of urban green space and enhance green land construction along highway, in squares and tourist attractions, make use of every single space, form a complete urban green space system, and provide a good ELS for green parks.

Strengthen the design of plant communities in green parks and enrich the diversity of plant communities

When designing the green parks, we should introduce more native tree species and landscapes, enrich the diversity of plant community by planting plants of different heights, and afforest reasonably outside the plant communities, so as to conserve water, lower the temperature and increase relative humidity, thereby improving and exerting the overall ecological benefits of the plant community.

Conclusion

- The analysis of plant community structure features showed that the order of the average DBH of the arbor layer in the three parks is: Donghu Park > Penglai Park > Jiangbin Park. The density and overall height of the shrub layer and the herb layer in Penglai Park are higher, indicating that the overall ecological benefit of the Penglai Park is better.
- The analysis results of the indices of the plant community structure features showed that, the diversity index (D_1) and richness index (R) of the arbor layer, shrub layer and herb layer in the Penglai Park are the highest, and its ecological advantage index (D_2) is the lowest.
- The analysis results of the influence of ELS on the distribution features of plant communities in green parks showed that, the Penglai Park is located in the center of the city, and surrounded by residential buildings and highways, both the temperature and the PM10 change little, and its overall temperature is higher than the other two parks; the density, overall height and average coverage of the shrub layer and herb layer, and the ecological benefit of the Penglai Park are all higher than the other two parks. As for the Jiangbin Park, since it is near the river and greatly affected by the wind from the river, the temperature inside and outside the plant community and the PM10 vary greatly, therefore, its average height and average coverage of the shrub layer and the herb layer, and the average DBH of the arbor layer are all lower than the other two parks.
- Taking the urban green parks of Jiangmen City as examples, this paper studies the influence of environmental landscape structure on the distribution features of plant communities in green parks. It comprehensively compares the distribution features of plant communities in different parks under different environmental landscape structures, and proposes relevant suggestions for the optimization of park plant communities. This shall provide a theoretical reference for urban ecological construction.

http://www.aloki.hu ● ISSN 1589 1623 (Print) ● ISSN 1785 0037 (Online)
DOI: http://dx.doi.org/10.15666/aeer/1706_1459914609

REFERENCES

[1] Ames, G. M., Anderson, S. M., Wright, J. P., Baltzer, J. (2016): Multiple environmental drivers structure plant traits at the community level in a pyrogenic ecosystem. – Functional Ecology 30(5): 789-798.
[2] Amici, V., Rocchini, D., Filibeck, G., Bacaro, G., Santi, E., Geri, F., Landi, S., Scoppola, A., Chiarucci, A. (2015): Landscape structure effects on forest plant diversity at local scale: exploring the role of spatial extent. – Ecological Complexity 21: 44-52.
[3] Bouasria, A., Mustafa, T., Bello, F. D., Zinger, L., Choler, P. (2012): Changes in root-associated microbial communities are determined by species-specific plant growth responses to stress and disturbance. – European Journal of Soil Biology 52(9): 59-66.
[4] Brunzel, S., Elligsen, H., Frankl, R. (2004): Distribution of the cinnabar moth Tyria jacobaeae L. at landscape scale: use of linear landscape structures in egg laying on larval hostplant exposures. – Landscape Ecology 19(1): 21-27.
[5] Chiron, F., Chargé, Rémi, Julliard, R., Jiguet, F., Muratet, A. (2014): Pesticide doses, landscape structure and their relative effects on farmland birds. – Agriculture, Ecosystems & Environment 185: 153-160.
[6] Cordero, R. L., Torchelsen, F. P., Overbeck, G. E., Anand, M. (2016): Invasive gorse (Ulex europaeus, Fabaceae) changes plant community structure in subtropical forest–grassland mosaics of southern Brazil. – Biological Invasions 18(6): 1629-1643.
[7] Davidson, J. M., Patterson, H. A., Wickland, A. C., Fichtner, E. J., Rizzo, D. M. (2011): Forest type influences transmission of, Phytophthora ramorum, in California oak woodlands. – Phytopathology 101(4): 492-501.
[8] Goodwin, B. J., Fahrig, L. (2002): Effect of landscape structure on the movement behaviour of a specialized goldenrod beetle, Trirhabda borealis. – Canadian Journal of Zoology 80(1): 24-35.
[9] Herrera, J. M., Isa de Sá Teixeira, Rodríguez-Pérez, J., Mira, A. (2016): Landscape structure shapes carnivore-mediated seed dispersal kernels. – Landscape Ecology 31(4): 731-743.
[10] Kruess, A. (2003): Effects of landscape structure and habitat type on a plant-herbivore-parasitoid community. – Ecography 26(3): 283-290.
[11] Miller, J. E. D., Damschen, E. I., Harrison, S. P., Grace, J. B. (2016): Landscape structure affects specialists but not generalists in naturally fragmented grasslands. – Ecology 96(12): 3323-3331.
[12] Moebiusclune, D. J., Moebiusclune, B. N., Harold, M. van Es, Pawlowska, T. E. (2013): Arbuscular mycorrhizal fungi associated with a single agronomic plant host across the landscape: community differentiation along a soil textural gradient. – Soil Biology & Biochemistry 64(64): 181-190.
[13] Schmucki, R., Reimark, J., Lindborg, R., Cousins, S. A. O. (2012): Landscape context and management regime structure plant diversity in grassland communities. – Journal of Ecology 100(5): 1164-1173.
[14] Svenning, J. C., Kinner, D. A., Stallard, R. F., Wright, B. M. J. E. J. (2004): Ecological determinism in plant community structure across a tropical forest landscape. – Ecology 85(9): 2526-2538.
[15] Wallgren, M., Bergstrom, R., Danell, K., Skarpe, C. (2009): Wildlife community patterns in relation to landscape structure and environmental gradients in a Swedish boreal ecosystem. – Wildlife Biology 15(3): 310-318.
[16] Wrbka, T., Schindler, S., Pollheimer, M., Schmitzberger, I., Peterseil, J. (2008): Impact of the Austrian agri-environmental scheme on diversity of landscapes, plants and birds. – Community Ecology 9(2): 217-227.

http://www.aloki.hu ● ISSN 1589 1623 (Print) ● ISSN 1785 0037 (Online)
DOI: http://dx.doi.org/10.15666/aeer/1706_1459914609

SMALL-SCALE SPATIAL OPTIMIZATION OF NATURAL GEOGRAPHIC REGIONS FOR BIODIVERSITY AND ECO-SUSTAINABILITY

SHANG, M. – CHEN, H. – CHEN, J. Y.*

College of Geography and Land Engineering, Yuxi Normal University, Yuxi 653100, China

**Corresponding author*
e-mail: chenjingyi@yxnu.net; phone: +86-135-0940-5239

(Received 7th Jun 2019; accepted 10th Oct 2019)

Abstract. The current scale of space division cannot effectively protect and manage the biodiversity in different natural geographic regions across China. To solve the problem, this paper optimizes natural geographic regions on a small scale based on the eco-sustainability and biodiversity in China, and prepares an optimized layout plan for China's ecological nature reserve system. The research results show that different natural geographic regions require different division scales, e.g. small-scale spatial layout is suitable for forest ecology and wild plants; the reduction in spatial scale has varied impacts on the protection of the different; the optimization of spatial scale is affected by vertical and horizontal gradients, e.g. the vegetation system is better protected in a region with small spatial scale; the small-scale spatial optimization of natural geographic regions makes the division of eco-environmental protection grids more effective; the regions with high biodiversity should be divided into denser grids to promote eco-sustainability. The research findings lay the theoretical basis for the planning of natural geographic regions and the maintenance of eco-diversity.
Keywords: *eco-environment, biodiversity, sustainability, spatial layout, spatial optimization*

Introduction

Today, the man-nature relationship gets increasingly strained, and the huge inputs in biodiversity protection have created an enormous social and economic burden on China. Protection for natural geographical areas has yielded an indistinctive result, especially for small and medium-sized ecological environments (Cochrane and Perrella, 2012). To study the best way to scientifically optimize the geographical regionalization grid, it is significant to effectively protect natural ecosystems and their biodiversity, and also improve it (Senator, 2017). The spatial optimization layout of China's natural geographical areas focuses primarily on the lists of protected species and important ecosystems, but lacks the integrated geographical regionalization on natural reserves, and never includes comprehensive and systematic protection of biodiversity (Maiano et al., 2006; Matchanov et al., 2016). Spatial optimization of natural geographic areas renders important basic data for regional biodiversity and eco-environmental protection and system construction of nature reserves. This lays a broad scientific foundation for developing regional biodiversity policies (Liu et al., 2014).

In recent years, scholars at home and abroad have made extensive studies on the spatial optimization of geographical areas, but the optimization methods vary according to different backgrounds, regionalization, bio-communities and other reference indicators. In response to the local geomorphological pattern, a small-scale spatial layout suitable for reserves has not yet been proposed (Sperry et al., 2016; Hübner and Schaal, 2017a). The principles of spatial optimization for natural geographic areas include relative consistency, the integration and the integrity. According to the regional

http://www.aloki.hu ● ISSN 1589 1623 (Print) ● ISSN 1785 0037 (Online)
DOI: http://dx.doi.org/10.15666/aeer/1706_1461114619

geomorphology, the natural geographic areas can be divided into tier-1, 2, 3 and 4 spaces (Dyck and Willems, 2013). The regional spaces should be divided and optimized aiming at the construction of nature reserve systems with definite purposes, and the hierarchical regionalization system should overall be improved and more scientific (Hübner and Schaal, 2017b). Based on the sustainability of the ecological environment, this paper makes a spatial optimization for the natural geographical areas on a small-scale according to the biodiversity in China, and gives the optimal layout program for the ecological nature reserve system in China.

Materials and methods

Through the course of eco-environment protection, there are still many common problems. To reasonably protect the eco-environment, the best practice is to correctly evaluate current situation of the reserves and identify the existing key issues (Kaufmann and Banerjee, 2014). There are many types of small spaces included in natural geographic areas, including the natural reserves, wilderness reserves, the national parks, the natural monument museums, the habitat and species management reserves, the terrestrial and marine landscapes, etc. (Jiang and Liu, 2012). The spatial scale of natural geographical areas can be determined according to spatial acreage of the nature reserves. In general, the area greater than 10,000 km^2 is called a large-scale space, and the area less than 100 km^2 is called a small-scale space (Krasnov et al., 2015). According to the incomplete statistics, China's nature reserves cover an area of more than 106 km^2, and the layout of most spaces are statistically designed as required by the provinces as the large scales, thus leading the statistical species to averaging (Jiang et al., 2013).

Using statistical survey method, according to data from the Bureau of Land and Resources, currently, there are 2392 nature reserves having been divided in China, among which, there are more than 400 small-scale ones. As shown in *Figure 1,* different types of national nature reserves as percentage of the total areas are figured out, where the desert ecology ranks the first, followed by the wild animals and inland wetlands. The desert ecology is suitable for large-scale spatial layout in natural geographical areas, and for the forest ecology and wild plants, they are suitable for small-scale spatial layout. *Figure 2* illustrates the number of different types of the national nature reserves. It is obvious that there is a great difference in the construction layout in different times between various nature reserves. There are even more layouts for the forest ecology due to the fact that forest ecology is mostly divided on a small scale.

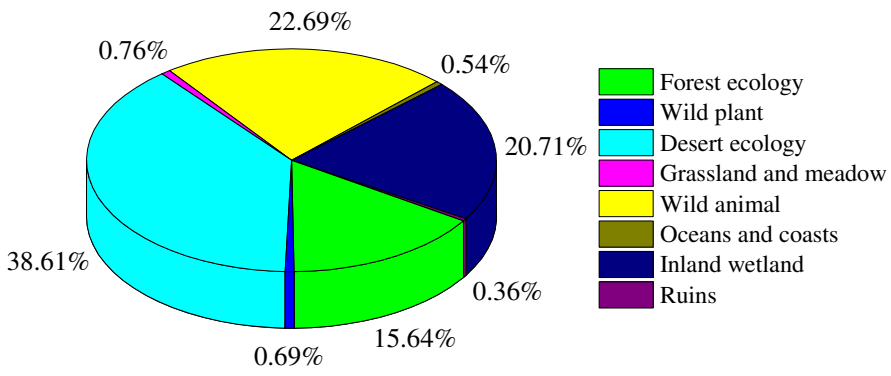

Figure 1. *Area ratio of different types of national nature reserves*

http://www.aloki.hu ● ISSN 1589 1623 (Print) ● ISSN 1785 0037 (Online)
DOI: http://dx.doi.org/10.15666/aeer/1706_1461114619

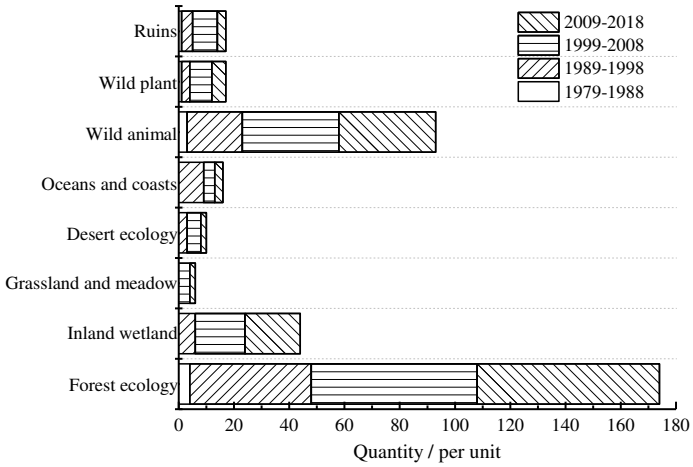

Figure 2. *Number of national nature reserves of different types*

Results

Small-scale spatial division for regional system

To divide the small-scale spaces in natural geographical areas, it is conducive to safeguard the ecosystems, rare and endangered animals and plants, as well as the sites and relics. According to the existing areas as divided, the number of national nature reserves in different natural geographical areas and the corresponding upland areas are not directly proportional to each other, and there are disparities in the scale division between the natural geographical areas. For the number and the area of small-scale spaces in the nature reserves, see *Figure 3*. It is obvious that the number of small-scale spaces in China increases year by year, but their mean area calculated by the ratio of the area to the number gradually decreases.

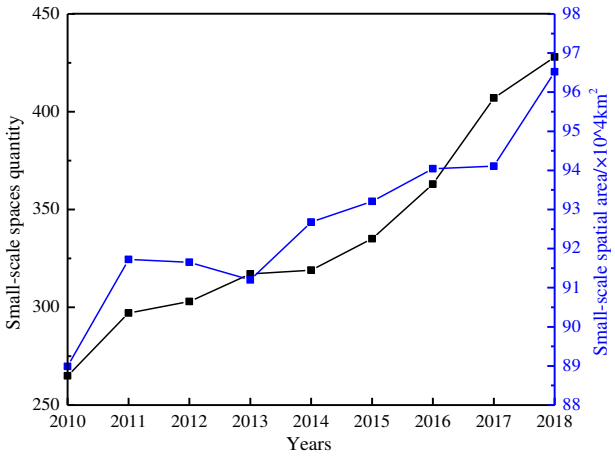

Figure 3. *Quantity and area of small-scale space in nature reserves*

The small-scale spaces as percentage of the natural geographical areas at different protection ratios are shown in *Figure 4,* more than 30% of them are protected at less than 5%. Among them, there are the maximum small-scale spaces in the unprotected natural geographic areas in the northwest warm temperate zone, exceeding 70% of the

http://www.aloki.hu ● ISSN 1589 1623 (Print) ● ISSN 1785 0037 (Online)
DOI: http://dx.doi.org/10.15666/aeer/1706_1461114619

total. Further, except for the Qinghai-Tibet Plateau, a natural geographical area, the protective area of small-scale spaces in other geographical areas is generally 3% lower than that of other land areas. The total small-scale spaces as percentage of the natural geographical areas at different protection ratios are shown in *Figure 5*. In the east and south China, the small-scale spaces as percentage of the natural geographical areas at the protection ratio below 5% is the maximum, followed by those in the north China and in the northwest China. As the scale spaces diminish, the effective protection in different natural geographic areas varies from unit to unit.

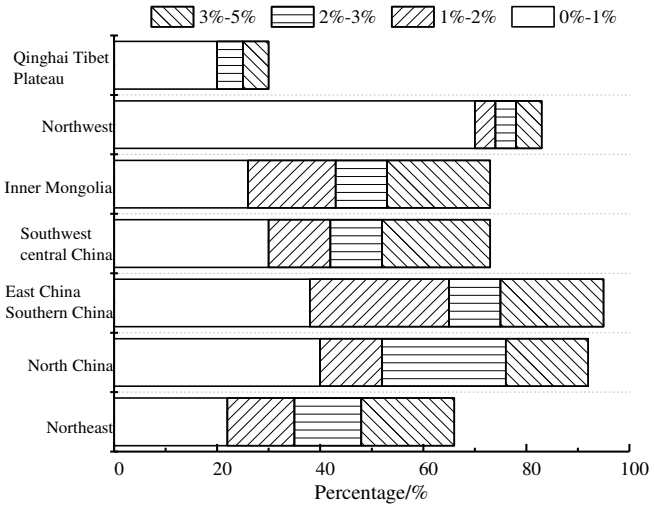

Figure 4. *The proportion of the total number of small-scale space in different conservation proportions of natural geographical regions*

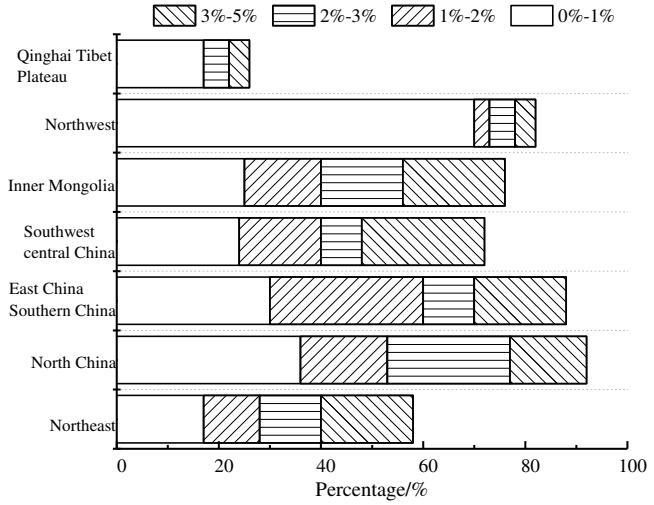

Figure 5. *The proportion of the total area of small-scale space in the natural geographical regions with different protection ratios*

Analysis of vegetation ecosystem protection potency

Investigation research shows that the vegetation system is suitable for dividing small-scale spaces in the natural geographical areas. The regional biodiversity may be subject

http://www.aloki.hu ● ISSN 1589 1623 (Print) ● ISSN 1785 0037 (Online)
DOI: http://dx.doi.org/10.15666/aeer/1706_1461114619

to the spatial layout of vegetation. It is impossible to make up for the gap in the conservation of existing reserves by evaluating biodiversity distribution data with divided scale spaces. The vegetation ecosystem may be subjected to the topography, altitude and climatic environment. Vegetation distribution pattern and its conservation have a significant impact on global biodiversity and the protection of natural ecosystems. Vegetation systems in small-scale spatial areas will be protected at a higher rate. In different natural geographical areas, some reserves have a concentrated layout, and the coverage of upland areas as they did in different areas varies greatly. The current situation of small-scale spaces as percentage of the total conserved vegetation systems is illustrated in *Figure 6*. As we can see, more than 60% of the vegetation systems are conserved at a rate of less than 5%.

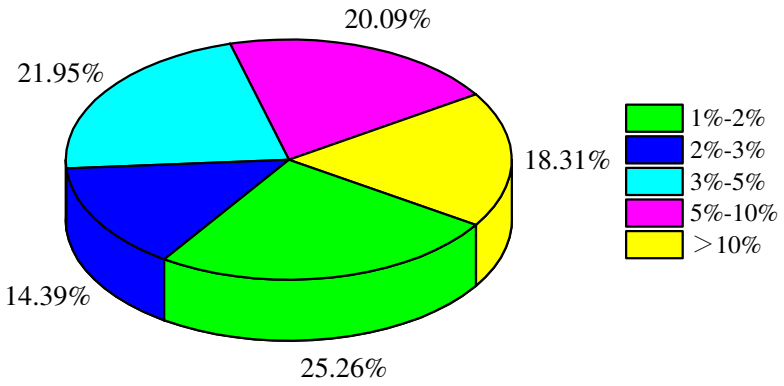

Figure 6. *Current status of small-scale spatial conservation proportion of vegetation system*

Figure 7 illustrates the small-scale spaces as percentage of natural geographical areas at different altitudes. As can be seen, the small-scale spaces are mainly distributed at low altitude (<200 m) and 1000-3000 m altitude in North China (*Fig. 7a*); at 1000-3000 m altitude in the southwest of central China (*Fig. 7b*); and relatively uniform in the northeast areas (*Fig. 7c*), presenting the tendency to decrease with the increase of altitude height. The small-scale spaces of the natural geographical area in the Qinghai-Tibet Plateau (*Fig. 7d*) are all centralized in the high altitude areas (>3000 m).

Discussion

Evaluation on biodiversity conservation value by small-scale spatial optimization

The small-scale space divided in the natural geographical areas is an important form for biodiversity conservation. The priority and biodiversity of small-scale spaces particularly value the typicality and non-substitutability of species and their habitats. There are some main evaluation indicators for biodiversity conservation value, including diversity, representative, scarcity, natural type, area suitability and vulnerability, etc. Great attention should be paid to the diversity of habitat types, while in different scale spaces, the evaluation indicators for biodiversity conservation values vary, but they all focus on the rare and endangered features, protection classes and geographical distribution tendencies of the species. For example, in Jilin Changbai Mountain, there are large chunks of rare animals and plants in the natural geographical areas, so that its diversity protection value is high.

http://www.aloki.hu ● ISSN 1589 1623 (Print) ● ISSN 1785 0037 (Online)
DOI: http://dx.doi.org/10.15666/aeer/1706_1461114619

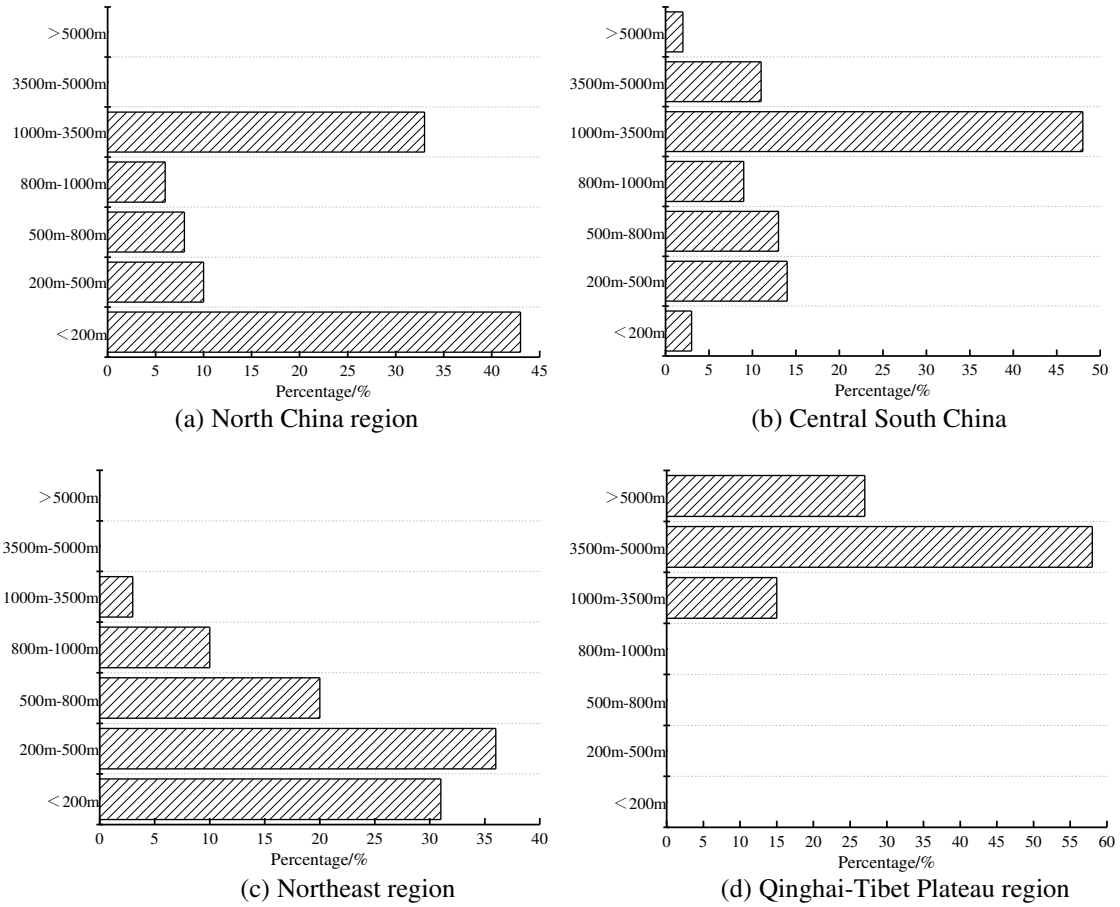

Figure 7. *Proportion of small-scale space in natural geographical regions at different altitudes*

To evaluate how the biodiversity conservation values are susceptible to small-scale spatial optimization, 39 small-scale spaces in the northeastern areas are chosen for study, and different attributes of individual species in the scale space grid are assigned the values at different levels. Those scale spaces with the highest protection value index mainly concentrate in the deciduous broad-leaved forest area of the Taihang Mountain, while those with the maximum protection value index of wild plant diversity fall in the cultivated vegetation and wetland area of Haihe Plain.

Optimized layout plan for China's ecological nature reserve system

On the whole, China has divided the natural geographical areas, but the optimization for small-scale spaces is a complex process involving multiple protection targets and strategies, habitat quality. The existing large-scale space is divided into several small-scale spaces to establish a more effective eco-environmental protection network. It is preferable to divide the area with high biodiversity conservation value into a spatial grid for small-scales, or connect several reserves near each other into a reserve network, this is an important strategy for realizing the natural conservation. Specifically speaking, it is to set up eco-environmental lag zones, and divide them into two categories according to the optimization difficulty: the barely-coordinated ecological optimization zone and the nearly-uncoordinated ecological optimization zone. The land types that need to be renovated are adjusted to forest land, garden land, wetland and other ecological

http://www.aloki.hu ● ISSN 1589 1623 (Print) ● ISSN 1785 0037 (Online)
DOI: http://dx.doi.org/10.15666/aeer/1706_1461114619

environments so as to improve the land types that can produce positive effects. According to the existing natural geographical division grid and the preferred biodiversity reserves, the scale space optimization program is designed based on the layout principle of building the areas with low diversity conservation value into the large-scale spaces, and preferentially optimizing the national or international important nature geographical areas into small-scale spaces. In the key natural areas, the species should be highly protected. Those mall-scale spaces with higher conservation values can be preferentially promoted to the national nature reserves.

Figure 8 shows the comparison of the national nature reserves at the protection ratios after small-scale spaces are optimized. As we can see, the bio-conservation coverage in natural geographical areas increases after the spatial optimization layout for small-scale spaces. *Figure 9* shows the optimal composition of small-scale spaces in natural geographic areas. The small-scale spaces in the natural geographical areas are mainly composed of forest ecology, inland wetlands and wild animals. Small-scale spatial layout can effectively fulfill the protection and management targets to more quickly make management measures and tools.

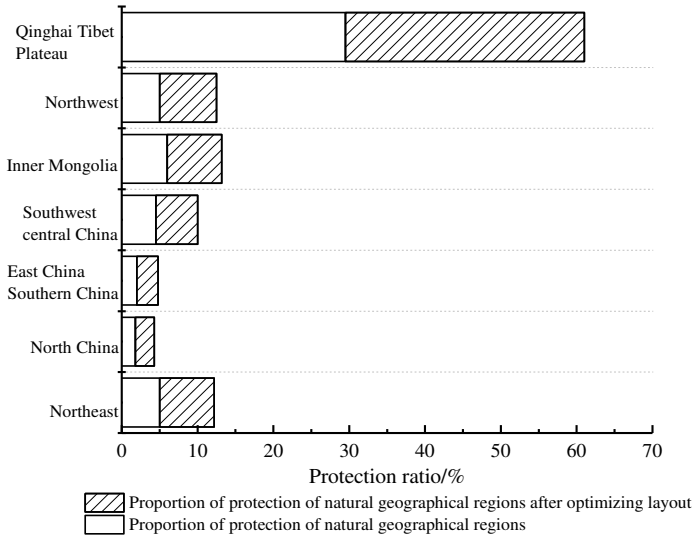

Figure 8. *Proportion of national nature reserves after small-scale space optimization*

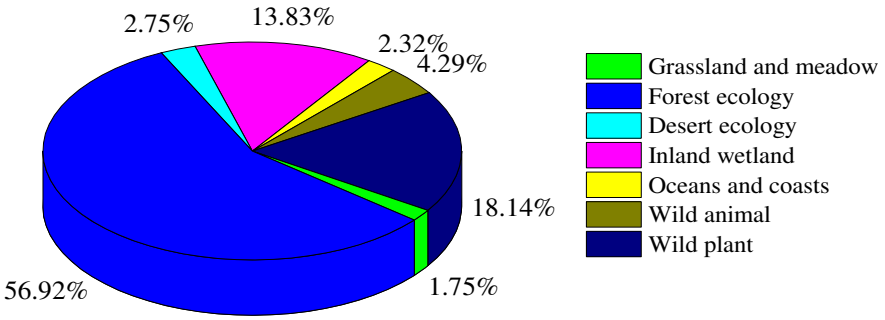

Figure 9. *Small-scale spatial optimization composition of natural geographical regions*

http://www.aloki.hu ● ISSN 1589 1623 (Print) ● ISSN 1785 0037 (Online)
DOI: http://dx.doi.org/10.15666/aeer/1706_1461114619

Conclusion

Based on the sustainability of the ecological environment, this paper optimizes the small-scale spaces in the natural geographical areas in line with the biodiversity of China. In doing so, the optimal layout program is given for the ecological nature reserve system in China. Here come specific conclusions:

- The number of small-scale spaces in China increases year by year, but the mean area of small-scale spaces gradually decreases. In the east and south China, the small-scale spaces as percentage of the total at a protection ratio of less than 5% in the natural geographical area 5% is the highest, followed by those in north China and in north-west region.
- The vegetation system in the small-scale spaces will be protected at a higher ratio. In different natural geographical areas, some protected areas have a concentrated spatial layout, quite different from coverage ratio of the land area in different zones.
- The existing large-scale space is divided into several small-scale ones to establish a more effective eco-environmental protection network. It is preferable to divide the area with high biodiversity conservation value into a small-scale spatial grid, or connect the reserves near each other into a reserve network. This is an important strategy for realizing ecological environmental protection and species diversity.
- This paper analyzed the advantages of spatial optimization for ecosystem development based on actual data. With the sustainable and coordinated development of ecological environment reserves as the principle, it optimized the allocation of ecological spaces and provided a reference for natural geography and land use.

Acknowledgements. This research has been financed by Educational Science Planning Project in Yunnan Province in 2018 “Practical Research on Constructing School-based Course of Innovative GIS Experiment Based on Skills Contests and Teaching” (GJZ171813).

REFERENCES

[1] Cochrane, C., Perrella, A. (2012): Regions, regionalism and regional differences in canada. – Canadian Journal of Political Science 45(4): 829-853.
[2] Dyck, V. J., Willems, P. (2013): Probabilistic flood risk assessment over large geographical regions. – Water Resources Research 49(6): 3330-3344.
[3] Hübner, A., Schaal, K. (2017a): An integrated assortment and shelf-space optimization model with demand substitution and space-elasticity effects. – European Journal of Operational Research 261(1): 302-316.
[4] Hübner, A., Schaal, K. (2017b): Effect of replenishment and backroom on retail shelf-space planning. – Business Research 10(1): 123-156.
[5] Jiang, B., Liu, X. (2012): Scaling of geographic space from the perspective of city and field blocks and using volunteered geographic information. – International Journal of Geographical Information Science 26(2): 215-229.
[6] Jiang, B., Liu, X., Jia, T. (2013): Scaling of geographic space as a universal rule for map generalization. – Annals of the Association of American Geographers 103(4): 844-855.
[7] Kaufmann, R. K., Banerjee, S. (2014): A unified world oil market: regions in physical, economic, geographic, and political space. – Energy Policy 74: 235-242.

http://www.aloki.hu ● ISSN 1589 1623 (Print) ● ISSN 1785 0037 (Online)
DOI: http://dx.doi.org/10.15666/aeer/1706_1461114619

[8] Krasnov, B. R., Shenbrot, G. I., Khokhlova, I. S., Stanko, M., Morand, S., Mouillot, D. (2015): Assembly rules of ectoparasite communities across scales: combining patterns of abiotic factors, host composition, geographic space, phylogeny and traits. – Ecography 38(2): 184-197.

[9] Liu, X. C., Zhang, J. Q., Li, X. Z. (2014): Geographical information system-based assessment of ecological security in Changbai Mountain region. – Journal of Mountain Science 11(1): 86-97.

[10] Maiano, C., Ninot, G., Stephan, Y., Morin, A. J. S., Florent, J.-F., Vallée, P. (2006): Geographic region effects on adolescent physical self: an exploratory study. – International Journal of Psychology 41(2): 73-84.

[11] Matchanov, M., Teodoro, A., Schroder, C. (2016): Criterion definition for the identification of physical-geographical boundaries of Khorezm oasis through remotely sensed data. – Environmental Monitoring and Assessment 188(1): 35.

[12] Senator, S. A. (2017): Flora diversity of physical-geographical regions and a scheme of floristic zoning of middle Povolzh'e. – Biology Bulletin 44(10): 1208-1214.

[13] Sperry, M. M., Telesford, Q. K., Klimm, F., Bassett, D. S. (2016): Rentian scaling for the measurement of optimal embedding of complex networks into physical space. – Journal of Complex Networks 5(2): 199-218.

http://www.aloki.hu ● ISSN 1589 1623 (Print) ● ISSN 1785 0037 (Online)
DOI: http://dx.doi.org/10.15666/aeer/1706_1461114619

EFFECT OF TREE IDENTITY, TEMPORAL VARIATION AND EDAPHIC PARAMETERS ON THE STRUCTURE OF THE EDAPHIC COMMUNITY OF ORIBATID MITES IN AN EVERGREEN TROPICAL FOREST OF MEXICO

VILLAGOMEZ, F.[1,2*] – PALACIOS-VARGAS, J. G.[1] – CASTAÑO-MENESES, G.[3] – CASTELLANOS-VARGAS, I.[4]

[1]*Laboratorio de Ecología y Sistemática de Microartrópodos, Facultad de Ciencias, Universidad Nacional Autónoma de México, 04510 Cd. Mx., México*

[2]*Posgrado en Ciencias Biológicas, Unidad de Posgrado, Edificio D. Universidad Nacional Autónoma de México, 04510 Cd. Mx., México*

[3]*Unidad Multidisciplinaria de Docencia e Investigación, Facultad de Ciencias, Universidad Nacional Autónoma de México, Campus UNAM 3001, Juriquilla, 76230 Querétaro, México*

[4]*Grupo de Interacciones y Procesos Ecológicos, Departamento de Ecología y Recursos Naturales, Facultad de Ciencias, Universidad Nacional Autónoma de México, 04510 Cd. Mx., México*

**Corresponding author*
e-mail: lfvilagomez@gmail.com; phone: +52-55-5622-4902

(Received 7th Jun 2019; accepted 16th Oct 2019)

Abstract. This paper analyzes the community structure of edaphic oribatid mites from the tropical forest at Los Tuxtlas, Veracruz, showing its monthly variation during only one year, considering two contrasting tree species and their relation with abiotic edaphic parameters. Randomly, five *Astrocaryum mexicanum* and *Guarea glabra* plants were chosen and near the stem of each one, a sample of soil was taken and processed in the same biological station with Berlese-Tullgren funnels. The most abundant families were Scheloribatidae, Oppiidae, Xylobatidae, Arceremaeidae, and Galumnidae. The Kruskall-Wallis test showed that structure of oribatid mite community is not significative related to tree identity, which they are associated. Pearson's multiple correlation showed that the edaphic temperature is one of the most important abiotic factors in the structuring of oribatid mites communities. The abiotic variables explained 58% of oribatid community variance in its first two axes, with temporality and CO_2 being the factors with most influence over the community. It is concluded that tree identity is not a factor that affects the structuring of oribatid mite communities in this tropical forest, while temporality, soil temperature and CO_2 are the factors that most influence its establishment, this last factor as an indirect indicator of system productivity.
Keywords: *arboreal identity, community diversity, temporality, Astrocaryum mexicanum, Guarea glabra*

Introduction

From several decades edaphic communities have been observed to have a high value of biotic diversity, it is even estimated that our current knowledge covers less than 10% of the total number of species worldwide, due in part to the lack of studies, low efficiency in extraction methods and methodological issues (André et al., 2002). Together with the canopy, the need to study edaphic communities to understand the functioning of ecosystems has been evidenced, considering the soil as one of the last biotic frontiers (André et al., 1994). Anderson (1975) mentions that the mechanisms by which such diverse communities exist are poorly understood, and he named it as the

http://www.aloki.hu ● ISSN 1589 1623 (Print) ● ISSN 1785 0037 (Online)
DOI: http://dx.doi.org/10.15666/aeer/1706_1462114639

"enigma of animal diversity in the soil". Since then, multiple factors associated with this phenomenon have been proposed, although most of them are focused on the litter diversity, reporting the environmental heterogeneity, content of organic matter, temperature, soil pH, humidity and altitude as some of the determining factors of the communities (Perdue and Crossley, 1989; Urhan et al., 2006; Mumladze et al., 2015). Nielsen et al. (2010) hypothesized that small-scale environmental heterogeneity in respect to organic and mineral soil can be responsible of this high species richness, and recently Bernier (2018) emphasizes the importance of the type of humus for the establishment of the edaphic fauna, not only as a transition point between the soil and litter, but also as a kind of habitat with particular characteristics.

Forest soils are ecosystems characterized by being extremely fertile, in addition to having a great biodiversity in their first 20 cm, which contributes in the cycle of nutrients and decompositions of organic matter (Gessner et al., 2010). In the edaphic communities of tropical forests, oribatid mites are numerically dominant organisms, and species richness of their biotic community is generally around 70 species (Kaneko et al., 2005; Mumladze et al., 2015). Wunderle (1992) reports 82 species of oribatids with an average density of 61,500 individuals per m^2 for a low rain forest in Peru, while Ferreira et al. (2012) recorded 143 species of oribatids and up to 460 morphospecies for the Brazilian Amazon. In Mexico, there have been communities in tropical forests up to 120 species for the state of Quintana Roo (Vázquez, 2006).

It has been reported that abundance of oribatid mites show spatial and temporal (seasonal) variations, which reflects different dynamics of the microhabitat, although the taxonomic composition often does not reflect this pattern (Irmler, 2006; Wehner et al., 2018). Temporal variations in abundance are usually related to parameters such as temperature, humidity and even the availability of food, although sometimes these effects tend to influence particular species but frequently not all the community in general (Gergócs et al., 2011). Despite registering patterns of seasonal variation in his abundances, little is known about the role of the leaf litter and identity of the plants in relation to the stability of the community of mites that inhabit the soil near them.

Although the incorporation of leaf litter into the soil of ecosystems contribute with elements such as nitrogen, phosphorous and carbon differentially in relation to the plant species and senescent phase (Fonte and Schowalter, 2004), the diversity of oribatids on the litter is not much influenced by plant richness, nor by the accumulation of organic matter from different species (Kaneko et al., 2005), even with plants with allelochemical attributes that directly influence the chemical composition of the soil by the production of metabolites and other substances, are not capable of altering the structure of his communities (Osler and Beattie, 2001). However, in other papers this group has responded positively in relation to the increase in plant richness and diversity of litter (Kaneko and Salamanca, 1999; Hansen, 2000). Because most of the investigations are focused on analyzing the structure of the community in upper litter of the forest soils, it is not known if the community has this same behaviour belowground.

The tropical rain forest of Los Tuxtlas in the state of Veracruz is one of the last relicts of high tropical evergreen forest in Mexico. The Sierra of Los Tuxtlas is a mountain formation of volcanic origin, located in the coastal plain of the Gulf of Mexico, within this region is the Los Tuxtlas Tropical Field Station (hereafter referred to as LTS), this station was founded in 1968 and is operated by the Universidad Nacional Autonóma de México, actually has an area of 640 ha and its elevation range goes from 150 to 720 m asl (Dirzo et al., 1997).

http://www.aloki.hu ● ISSN 1589 1623 (Print) ● ISSN 1785 0037 (Online)
DOI: http://dx.doi.org/10.15666/aeer/1706_1462114639

The palm *Astrocaryum mexicanum* Leibm. is the most abundant plant species of LTS, can register from 300 to 1,230 individuals per hectare and constitutes 20 to 61% of the total density of plants (Piñero et al., 1977), it has a longevity of 140 years and have heights of 1.5 to 6 meters (Piñero et al., 1984). This plant is favoured by disturbance, since its population grew from 1975 to 2013 with an average of 2.9% per year due to habitat alteration, edge effect and anthropogenic impact (Martínez-Ramos et al., 2016).

This palm is characterized by a monocaule stem of 10 cm thick and spiny leaves up to one and a half meters that have a development of 1.6 to 5 leaves per year in relation to the degree of light which they are exposed (Núñez-Castillo and Álvarez-Sánchez, 2003). Due to architecture, form of growth and the large number of thorns up to 6 cm that present in the stem, fruit and leaves, this plant has the ability to store a large amount of organic matter in its petioles, mainly of leaf litter from other trees, which gives an extra contribution of nitrogen and phosphorous by means of the decomposition on the plant that later reaches the soil by cauline flow (Raich, 1983; Álvarez-Sánchez et al., 2016).

Guarea glabra Vahl., also abounds in LTS (Álvarez-Sánchez and Guevara, 1999). It reaches heights of 25 m and has up to 30 cm in diameter (Coronado, 2006). It can persist for periods close to 100 years (Ibarra-Manríquez et al., 1997), has a strong trunk that begins to branch from near three meters and all the year constantly generates leaves, the fruits typically occur from May to July (Wenny, 1999) in reproductive season, its fruits cover small regions of soil, being a strong contribution of nutrients and organic matter to it.

Both plant species are part of different functional groups: *A. mexicanum* has a lower contribution of organic matter to the litter and soil and presents a slow decomposition rate (León, 2003) compared to *G. glabra* which is constantly generating and releasing leaves to the soil, also the genus *Guarea* present a quick green-leaf decomposition rate (Fonte and Schowalter, 2004). They have a different architecture and the first one enriches the soil by means of the continuous decomposition of organic matter that it captures in its leaves and petioles, incorporating nutrients into the soil by caulinar flow (Álvarez-Sánchez et al., 2016), while the contribution of nutrients and organic matter by *G. glabra* comes from the decomposition of leaves and temporarily from its fruits, incorporating magnesium, sodium and potassium mainly in the superior edaphic profiles (Barrantes and Ortiz, 2011).

The objective of this work is to analyze the effect of tree identity of two species of taxonomic and morphologically contrasting plants, monthly variation and soil abiotic parameters (pH, organic matter, organic carbon, CO_2, porosity and soil moisture) on the diversity and structure of the belowground oribatid mite community in this Mexican tropical forest.

Our first hypothesis is that tree species will have a significant effect on the structure of the belowground oribatid community, we infer that in the soil associated with *G. glabra* the diversity, richness and abundance of oribatids will be greater due to the abundant and constant contribution of organic matter by this plant to the soil. *A. mexicanum* releases few leaves and most of the nutrients it contributes to the soil come from captured organic matter that decomposes on it, so that the amount of plant material and decomposition rate is lower, also we assume a different species composition in oribatid communities of both plants soils, with more species inhabiting soil related with *G. glabra* due to a bigger thickness of soil organic horizon in comparison of *A. mexicanum*. Our second hypothesis is that the community will show a significant variation in its richness, abundance, diversity and composition in relation to temporality

http://www.aloki.hu ● ISSN 1589 1623 (Print) ● ISSN 1785 0037 (Online)
DOI: http://dx.doi.org/10.15666/aeer/1706_1462114639

(months), and soil abiotic parameters, being the families Galumnidae, Scheloribatidae, Haplozetidae, Oppidae, Phthiracaridae and Carabodidae more abundant as reported in literature for others tropical rainforest (Franklin et al., 2006; Caruso et al., 2019).

Materials and methods

Study area and description

LTS geographically is located in state of Veracruz, Mexico, between 18°34' to 18°36'N and 95°04' to 95°09'W (see *Fig. 1*). This station is mostly covered by evergreen tropical rain forest favoured by a warm climate with rainfall throughout the year, rainfall in the driest month is above 60 mm and are accentuated in the months of June to February marking a season of "rains" and one of "dry" in March to May, being September the month with greater precipitation. In addition, presents a scarce thermal variation, keeping mostly between 24 and 26 °C (Soto and Gama, 1997).

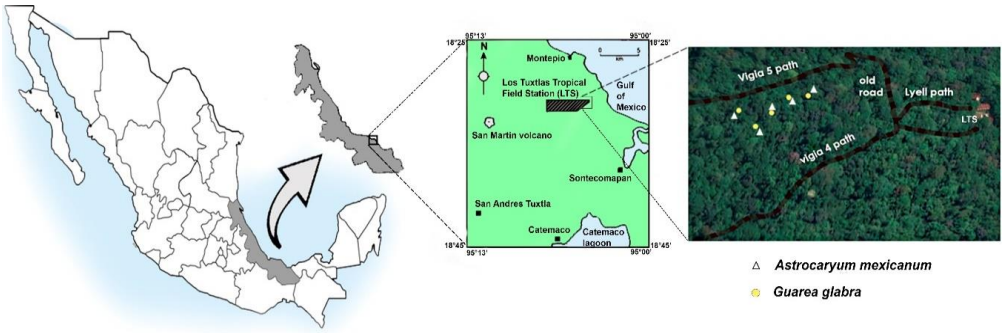

Figure 1. *Location of Los Tuxtlas Tropical Field Station (LTS) in Veracruz, Mexico, and position of sampling sites within LTS (modified from Flores et al., 2014)*

Sampling method

To analyze the effect of the leaf litter on the structure of belowground oribatid mite community, at random in a non-traveled area outside the walking paths Vigia 4 and 5 within the LTS (*Fig. 1*) five plants of *G. glabra* and another five of *A. mexicanum* were chosen in a paired design, the litter near the trunk was removed manually and immediately five samples of soil were taken associated with different arboreal individuals of *A. mexicanum* and five more with *G. glabra* with soil nucleators (11 cm wide and 5 cm deep) (see *Fig. 2*). The material was collected monthly from March 2016 to February 2017 and processed *in situ* the same day of collection in Berlese-Tullgren funnels during six days (three days without light and three days with 25-watt bulbs).

The record of environmental parameters of temperature, relative humidity and CO_2 was made by using a thermo-hygrometer IAQ-Calc^{TM}, model 8760 at ground level. Additionally, 100 g of soil were taken to determine the gravimetric humidity of the soil, porosity, pH, percentage of carbon (%C) and organic matter (%O.M.).

Laboratory techniques

The soil pH was measured with 10 g of sifted soil diluted in distillate H_2O with a pH meter. %O.M. was obtained by Walkey-Black method (Walkey, 1947) with 0.2 g of sifted soil, percentage of carbon (%C) was calculated as in *Equation 1:*

http://www.aloki.hu ● ISSN 1589 1623 (Print) ● ISSN 1785 0037 (Online)
DOI: http://dx.doi.org/10.15666/aeer/1706_1462114639

$$\%C = (\%O.M.)(0.58) \quad \text{(Eq.1)}$$

For obtaining soil porosity (Jackson, 1976; Van Reeuwijk, 2002) we first measured apparent density (*Ad*) of soil by weighting a test tube of 10 ml, then added soil until 10 ml, using a funnel and hit above-down from 20 cm ten times softly, posteriorly added again soil to refill 10 ml and weight again the test tube, by resting the test tube weight and dividing it in test tube volume we obtain de apparent density (g/cm^3), the density of solid particles of soil was obtained by pycnometer method (Blake and Hartge, 1986). First the dry pycnometer was weighted (*S*), then 5 g of soil was added and the pycnometer is filled with water (*s* + *a*), finally the soil is removed and the pycnometer is filled with water and weighted (*S* + *A*). We calculate the of soil particles density (*Sd*) with *Equation 2*.

$$Sd = \frac{S}{S+A} - s + a \quad \text{(Eq.2)}$$

The total porosity (*Ptotal*) was obtained using the apparent density and density of soil particles with *Equation 3*.

$$Ptotal = \frac{(1-Ad)(100)}{Sd} \quad \text{(Eq.3)}$$

The mites were separated and quantified manually under the stereoscopic microscope (Zeiss^{TM}, Stemi 2000), later they were mounted in semi-permanent preparations in Hoyer´s solution. Identifications were made at the finest taxonomic level possible by dichotomous keys (Balogh and Balogh, 1992) and specialized literature for each family, those with identification problems were assigned to morphospecies, the specimens are deposited in the collection of Collembola and edaphic mites of the Laboratory of Ecology and Systematics of Microarthropods (LESM), Faculty of Sciences, UNAM, Mexico.

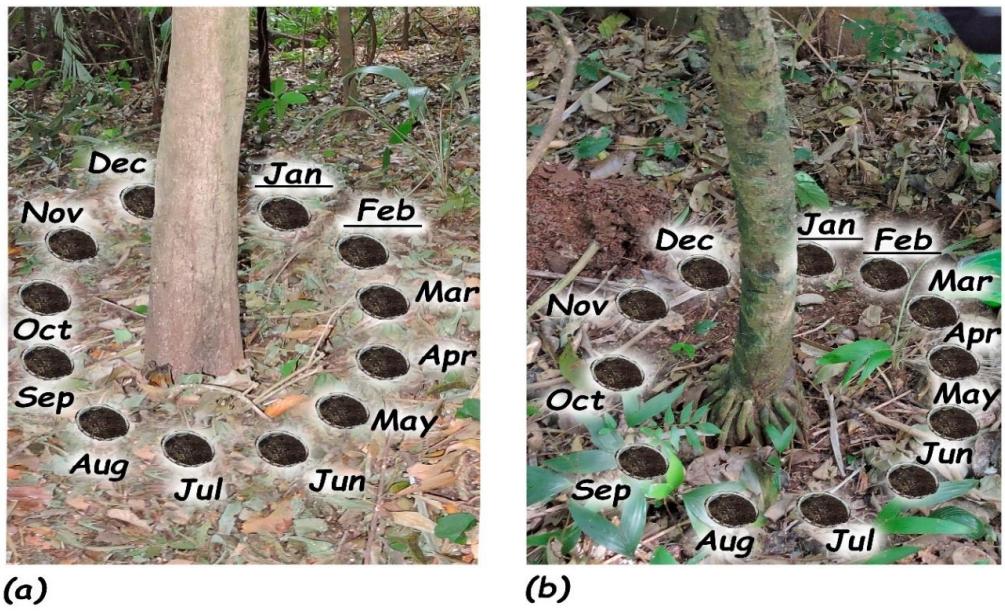

Figure 2. *Schematic diagram of experimental setup.* ***a*** *Soil samples taken around Guarea glabra.* ***b*** *Soil samples taken around Astrocaryum mexicanum. Months underlined correspond to 2017 year, all others from 2016*

http://www.aloki.hu ● ISSN 1589 1623 (Print) ● ISSN 1785 0037 (Online)
DOI: http://dx.doi.org/10.15666/aeer/1706_1462114639

Numerical and statistical analysis of the community

To observe the fit of data and type of analysis to be performed, its normality was tested with Kolmogorov-Smirnov test in software R (R Core Team, 2016), and homoscedasticity with Statistica v.8.0. (Statsoft Inc, 2007). For each sample of tree species was obtained the abundance and oribatid species richness (S) by direct count, also, Pielou´s equitativity (*J´*), Simpson´s dominance (*D*) and Shannon diversity index (*H´*) were calculated in PAST 3.22 software (Hammer et al., 2001) with *Equations 4*, *5* and *6,* respectively.

$$J' = \frac{H}{\ln(S)} \quad \text{(Eq.4)}$$

$$D = \left(\frac{n_i}{n}\right)^2 \quad \text{(Eq.5)}$$

$$H' = -\sum \frac{n_i}{n} \ln \frac{n_i}{n} \quad \text{(Eq.6)}$$

The effective species number (^1D) was obtained through Shannon exponential with *Equation 7* (e^H; Jost, 2006).

$$^1D = \exp(H') \quad \text{(Eq.7)}$$

To determine the effect of the identity of the plant species on the abundance, density, species richness, dominance and equity of the community of oribatid mites a nonparametric Kruskall-Wallis test was carried out between each plant community data in R software. Also, a t test with Shannon diversity index (*H´*) were performed in PAST 3.22 software for analyze possible variations in this community attribute between plants.

The relationship and significance between the community structure and soil abiotic factors was tested by a multiple correlation analysis of Pearson in software R with $\alpha = 0.05$, including factors as abundance, density of individuals, richness (*S*), diversity (*H'*), effective species number (^1D), equity (*J´*), dominance (*D*) and soil parameters like CO_2, pH, temperature, moisture, %O.M., %C and porosity. We performed a Canonical correspondence Analysis (CCA) using the CCorA function in vegan package (Oksanen et al., 2016) with Software R (R Core Team, 2016) to detect interactions between the community of oribatid mites and abiotic parameters, the envfit function ("Fits an Environmental Vector or Factor Onto An Ordination) was used with 999 permutations, to get the p-value or correlation of each variable with overall oribatid community, samples with total absence of specimens was removed from the analysis.

Results

A total of 2577 Oribatid mites with a mean monthly density of 289.49 ind/m^2, belonging to 41 families and 72 species (see *Table 1* and *Appendix 1*). Most abundant families were Scheloribatidae (320 specimens), Oppiidae (288), Oripodidae (285), Protoribatidae (266), Arceremaeidae (222), Galumnidae (186) and Haplozetidae (148). Total abundance of oribatid present in soil of *G. glabra* (1,321) was slightly higher than that recorded in *A. mexicanum* (1,256). Most abundant species throughout the study

http://www.aloki.hu ● ISSN 1589 1623 (Print) ● ISSN 1785 0037 (Online)
DOI: http://dx.doi.org/10.15666/aeer/1706_1462114639

were *Scheloribates ca. grandiporosus*, *Tecteremaeus cornutus*, *Brasilobates* sp. nov. and *Benoibates* sp. nov. with 9.5%, 8.6%, 8.4% and 8% respectively from the total of individuals.

Specific composition of oribatids between soils from trees was shared in 78%, with 56 species in common between both communities, while seven were exclusively in *G. glabra* soils and nine in soils of *A. mexicanum*, although most of these records were made through the presence of a single specimen. *Acrotritia ardua* (March, April, May and August) and *Rostrozetes cubanus* (October, November and December) were the only species that present records in at least three months in soil of *G. glabra* and *A. mexicanum* respectively. Most abundant species related to *G. glabra* were *Benoibates* sp. nov. and *Scheloribates* ca. *grandiporosus*, while in *A. mexicanum* they were *Tecteremaeus cornutus* and *Brasilobates* sp. nov.

No homoscedasticity was found in the samples corresponding to both plant species, the Kolmogorov-Smirnof test showed that oribatids abundance was not a normal distribution ($D = 0.166$, $p = 0.0026$), making it necessary to use nonparametric methods for its analysis.

No significant differences were found between the community of oribatids associated to *G. glabra* and *A. mexicanum* through the analysis of Kruskall-Wallis in relation to abundance ($X^2 = 0.203$; $p = 0.651$), density ($X^2 = 0.204$; $p = 0.651$), richness (S) ($X^2 = 0.117$; $p = 0.733$), dominance (D') ($X^2 = 0.008$; $p = 0.927$) and equity (J') ($X^2 = 1.8162$; $p = 0.178$). The t-test for diversity between the community associated with these two plants using the Shannon entropy index (H') showed no significant differences ($t_{22} = 1.7691$, $p = 0.077$). Due to the lack of significant effects of tree species to the edaphic community of oribatids, their abundance from both plants was grouped for the analysis of temporal variation and its relationship with abiotic soil factors.

The highest abundance was recorded in March 2016 (*Table 1*), while the lowest was presented in February 2017; there is a second period of population increase in July and August 2016 with 372 and 305 specimens respectively. In March 2016, there were four species with the greatest abundance: *Brasilobates* sp. nov., *Scheloribates* ca. *grandiporosus*, *Rostrozetes foveolatus* and Galumnidae gen. nov. In July 2016 three species that showed high abundance in March again increase their population numbers; however, five different species increased their abundance in this season (*Tecteremaeus cornutus*, *Benoibates* sp. nov., Multio*ppia* sp., *Mesoplophora longisetosa*, and *Scheloribates praeincisus*), which shows a temporal differentiation in relation to the specific composition of the oribatid community. The variation of the abundance of the oribatid species was very evident in some months (see *Appendix 1*), with families which live throughout the year (Arceremaeidae, Protoribatidae, Galumnidae, Epactozetidae, Neoliodidae, Oppiidae), others that are only temporary (Epilohmannidae, Mesoplophoridae, Malaconothridae) and some circumstantial like Cymbaeremaeidae, which normally can be found inhabiting in the trunk or canopy of trees.

The highest richness (S) was presented in August (*Table 1*), followed by July and June, the lowest richness was recorded in February. The average diversity of all months according to the Shannon index was high ($H' = 2.96$), the greatest true diversity (^1D) was reported in November and July, while the lowest was in February and May, with an average of 20.24 effective species number per month. The highest dominance (D) was registered in February due to the low number of specimens and the big abundance of a member of *Truncozetes sturmi* (Epactozetidae), and in May mainly due to the high abundance of three species of families Oppiidae (*Multioppia* sp.), Scheloribatidae (*Scheloribates praeincisus*) and Protoribatidae (*Brasilobates* sp. nov.). The values of the

http://www.aloki.hu ● ISSN 1589 1623 (Print) ● ISSN 1785 0037 (Online)
DOI: http://dx.doi.org/10.15666/aeer/1706_1462114639

equity index (*J′*) showed quite homogeneous communities, because they were always above $J' = 0.75$, the month with the greatest equity were January and November, while the least equitable was May. Statistically significant differences between each collecting month and numerical attributes of oribatid mites community can be found in *Appendix 2*.

Table 1. *Monthly numerical attributes of oribatid mites community in Los Tuxtlas, Veracruz*

Year	**2016**										**2017**	
Month	**Mar**	**Apr**	**May**	**Jun**	**Jul**	**Aug**	**Sep**	**Oct**	**Nov**	**Dec**	**Jan**	**Feb**
N	**495**	297	185	243	372	305	197	116	166	113	49	**39**
Ind/m^2	**1061**	344.1	214.3	281.57	431	353.4	228.3	134.4	192.3	131	56.8	**45.2**
S	35	36	32	41	46	**50**	39	36	39	28	24	**13**
H′	3.06	2.85	2.70	3.16	3.26	3.18	2.87	3.20	**3.32**	2.83	2.92	**2.22**
^1D	21.52	17.34	14.99	23.66	26.23	24.07	17.63	24.68	**27.91**	17.03	18.54	**9.29**
D′	0.06	0.09	0.11	0.05	0.05	0.07	0.09	0.06	**0.04**	0.08	0.07	**0.14**
J′	0.86	0.79	**0.78**	0.85	0.85	0.81	**0.78**	0.89	0.90	0.85	**0.92**	0.86

Maximum and minimum values of each parameter in bold
Abundance (N) = total number of individuals; density (Ind/m^2) = monthly mean of individuals/m^2; Species richness (S) = Number of species; Shannon diversity index (H′) = Shannon entropy index using ln; true diversity (^{1}D) = Effective number of species with rank 1 ($^q = 1$); D′ = Dominance index; J′ = Pielou′s equity (evenness)

Kruskall-Wallis analysis showed a significant relation between collecting month with abundance and density ($X^2 = 56.53$; $p < 0.001$), Richness (*S*) ($X^2 = 51.99$; $p < 0.001$), diversity (*H′*) and effective species number (^1D) ($X^2 = 48$; $p < 0.001$) and marginally significative with Dominance (*D′*) ($X^2 = 19.52$; $p = 0.052$), only the relation with equity (*J′*) was not significative ($X^2 = 14.653$; $p = 0.199$). With which the monthly seasonality showed to be a key factor in the structuring of the community of oribatids in this jungle (*Appendix 2*).

For the Pearson′s correlations between the edaphic parameters and the structural attributes of the community, only the relation between soil temperature with the density ($r = 0.641$, $p = 0.0009$), richness ($r = 0.621$, $p = 0.0022$), dominance ($r = 0.524$; $p = 0.0420$) and true diversity ($r = 0.604$, $p = 0.004$) were significative and positive, so the soil temperature is one of the factors that most influence the communities structure of these mites in the jungle; while porosity, percentage of organic matter, pH, humidity and organic carbon did not have a significant interaction with the community of oribatids (*Table 2*).

The canonical correspondence analysis for the soil abiotic variables (*Fig. 3*) explains in its first two axes 58% of the variance in the community of oribatids (axis 1, 36%, axis 2, 22%). The monthly temporality shows a high negative correlation with axis 1 ($r = -0.9222$); similarly, the percentage of soil CO_2 shows a high negative correlation with axis 2 ($r = -0.7211$); CO_2 is indicative of the high primary productivity of the system and therefore of the high amount of food available for the oribatids (Herrera et al., 2001). The variables that correlate significantly with the ordination were temporality, soil temperature, CO_2, soil relative humidity, percentage of organic matter and organic carbon (*Table 3*). The species most related to axis 1 are *Licneremaeus discoidalis* (Ld),

http://www.aloki.hu ● ISSN 1589 1623 (Print) ● ISSN 1785 0037 (Online)
DOI: http://dx.doi.org/10.15666/aeer/1706_1462114639

Kaliptrazetes desaussurei (Kd) and *Berlesezetes peruensis* (Bp), these last two species are also related positively to axis 2, *Klappericheș* sp. nov., *Protoribates capucinus* and *Epilohmannia pallida* are the species more related negatively to this axis (*Table 4*).

Table 2. *Pearson correlation coefficients and p-values of structural attribute of oribatid mites community and soil abiotic factors*

	N	ind/m2	S	H´	^{1}D	Month	CO_2	pH	Por	sT	%C.O.	%M.O.	%RH
N		<.0001	<.0001	<.0001	<.0001	<.0001	ns	ns	ns	ns	ns	ns	ns
ind/m2	0.836		<.0001	<.0001	<.0001	<.0001	ns	ns	ns	0.0009	ns	ns	ns
S	0.975	0.729		<.0001	<.0001	<.0001	ns	ns	ns	0.002	ns	ns	ns
H´	0.935	0.735	0.97		<.0001	0.0003	ns	ns	ns	0.0035	ns	ns	ns
^{1}D	0.878	0.835	0.877	0.929		0.0008	ns	ns	ns	0.0004	ns	ns	ns
Month	-0.741	-0.69	-0.693	-0.667	-0.646		ns	ns	ns	<.0001	ns	ns	ns
CO_2	-0.021	-0.144	0.006	0.01	-0.092	-0.009		0.042	ns	ns	ns	ns	ns
pH	-0.1	0.05	-0.099	-0.046	0.029	0.314	-0.534		ns	ns	ns	ns	ns
Por	-0.141	-0.542	-0.159	-0.173	-0.154	-0.07	-0.152	-0.08		ns	ns	ns	ns
sT	0.681	0.641	0.621	0.608	0.604	-0.883	0.231	-0.375	-0.101		ns	ns	ns
%O.C.	-0.11	-0.111	-0.116	-0.086	-0.082	0.31	0.1	0.029	-0.263	-0.278		ns	ns
%O.M.	-0.11	-0.111	-0.116	-0.086	-0.082	0.31	0.1	0.029	-0.263	-0.278	1		<.0001
%RH	-0.138	-0.147	-0.101	-0.092	-0.105	0.035	0.114	-0.288	0.199	-0.145	-0.063	0.063;	

Scores below diagonal, p-value above diagonal
Abundance (N) = total number of individuals; density (Ind/m^2) = monthly mean of individuals/m^2; Species richness (S) = Number of species; Shannon diversity index (H´) = Shannon entropy index using ln; true diversity (^{1}D) = Effective number of species with rank 1 (^{q} = 1); D´ = Dominance index; J´ = Pielou's equity index (evenness)
Por = soil porosity; sT = soil temperature; %O.C. = percentage of organic Carbon; %O.M. = percentage of organic matter; %RH = percentage of soil relative humidity; ns = non significant

Table 3. *Envfit, CCA squared correlation coefficients (r^2) and significance levels of the oribatid mites species abundance with respect to abiotic soil parameters*

	CCA1	CCA2	r^2	p-value
Month	-0.995	-0.091	0.75	0.001***
sT	-0.992	-0.125	0.404	0.002**
CO_2	0.473	-0.880	0.516	0.001***
% RH	0.719	-0.694	0.353	0.006**
% O.M.	0.687	0.726	0.249	0.050*
% O.C.	0.687	0.726	0.249	0.050*
gH	-0.653	-0.756	0.104	0.318
pH	-0.876	0.482	0.160	0.137
rD	-0.393	-0.919	0.199	0.100
aD	-0.368	0.929	0.060	0.493
Por	-0.292	-0.956	0.153	0.132
Tree	0.218	0.975	0.014	0.865

*Significance level
%O.C. = percentage of organic carbon; %O.M. = percentage of organic matter; sT = soil temperature; gH = gravimetric humidity; rD = real density of soil; Por = soil porosity; aD = apparent density; %RH = relative humidity of soil

http://www.aloki.hu ● ISSN 1589 1623 (Print) ● ISSN 1785 0037 (Online)
DOI: http://dx.doi.org/10.15666/aeer/1706_1462114639

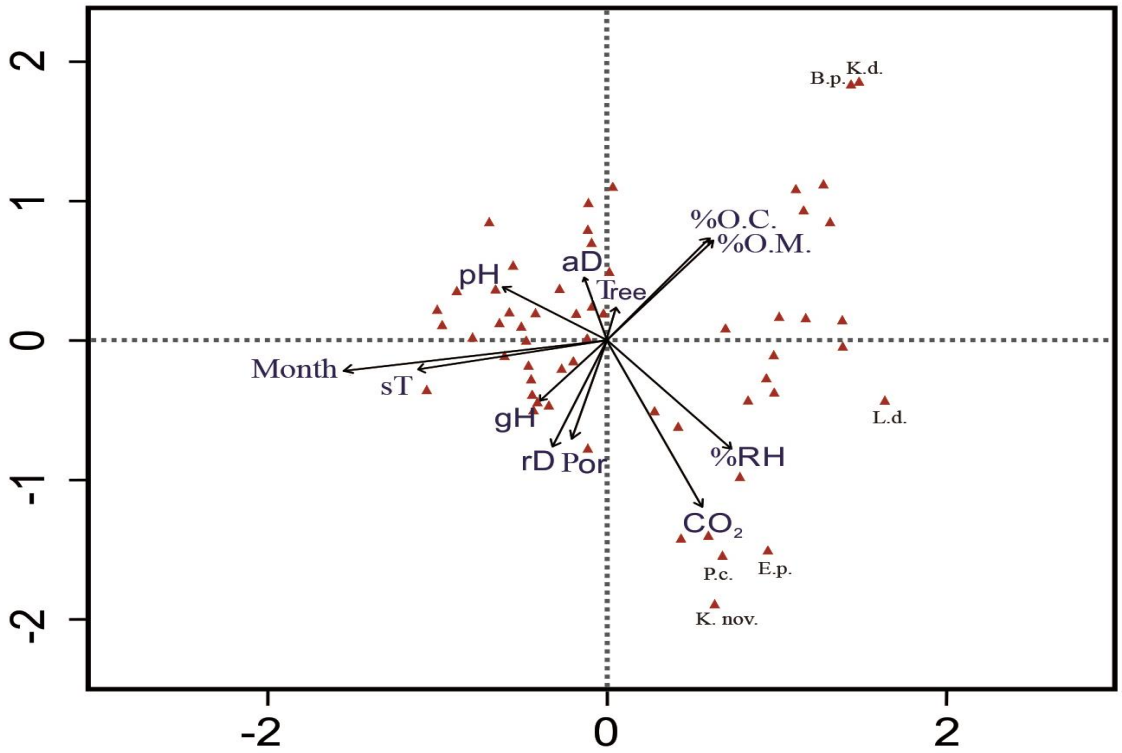

Figure 3. *Canonical correspondence analysis between oribatid species abundance and edaphic abiotic parameters. Factors abbreviations: %O.C. = percentage of organic carbon; %O.M. = percentage of organic matter; sT = soil temperature; gH = gravimetric humidity; rD = real density of soil; Por = soil porosity; aD = apparent density; %RH = relative humidity of soil. Species abbreviations: L.d. = Licneremaeus discoidalis; K.nov. = Klappericheś* sp. nov.*; K.d. = Kalyptrazetes desaussurei; B.p. = Berlesezetes peruensis; P.c. = Protoribates capucinus; E.p. = Epilohmannia pallida*

Table 4*. CCA species scores of the species more related with Axis 1 and 2*

Family	Genus and species	CCA axis 1	CCA axis 2
Licneremaeidae	*Licneremaeus discoidalis*	**1.640062**	-0.420947
Microzetidae	*Kalyptrazetes desaussurei*	**1.474698**	1.849525
Microzetidae	*Berlezesetes peruensis*	**1.468658**	1.846099
Carabodidae	*Klapericches* sp. nov.	0.639038	**-1.902672**
Protoribatidae	*Protoribates capucinus*	0.684869	**-1.551144**
Epilohmannidae	*Epilohmannia pallida*	0.9484	**-1.513977**

Bold number denotes to which axis are more related

Discussion

There is a large amount of information about the close interaction between the community of edaphic fauna and plant species, especially because they provide a large amount of organic matter and their roots exudates to the soil, which are captured by litter and reintegrated into the soil with the help of degrading organisms (Bardgett and Wardle, 2010). This litter has mainly a structural function for oribatids, maintaining habitat heterogeneity necessary to sustain their complex communities, without significant influence

http://www.aloki.hu ● ISSN 1589 1623 (Print) ● ISSN 1785 0037 (Online)
DOI: http://dx.doi.org/10.15666/aeer/1706_1462114639

of the identity of the litter (even with more than 25 species of leaves) on the community of these mites (Kaneko et al., 2005), this is due to the decrease of leaf litter quality as the decomposition process progresses, and also to the high range of food resources that can be consumed by the oribatids (Scheu, 2005; Kaneko et al., 2005).

Contrary to our first hypothesis, specific identity of the trees studied (*A. mexicanum* and *G. glabra*) is not a determinant factor on the communities structure of soil oribatids in this tropical forest, so there are no significant differences in abundance, richness, dominance, equity and diversity; also, a similarity of 72% was observed among their species, and many of them were represented by a single specimen (*Appendix 1*). This can be because the litter under these plants in natural conditions is still heterogeneous and the decomposition process and abundant rains unmasks the possible differences between types of litter and generates a redistribution of organic matter and nutrients (Donoso et al., 2013). Finally, because the low evolutionary relationship between these mites and the plant resources they ingest, is common to find oribatids with general food habits (Wardle, 2006; Donoso et al., 2010, 2013) feeding indistinctly of any type of organic matter.

It is known that the abundance of mites depends on the seasonality of the ecosystems, since the quantity and quality of the organic matter in litter varies with the season and climate. In a tropical forest in Panama, a decrease in the abundance and richness of oribatids was observed in the last months of the year (November) since litter tended to be shallower (Donoso et al., 2013).

In this study, the total abundance (2,577 specimens) and richness (72 spp.) was lower than that reported by Minor et al. (2017a), who registered 10,585 specimens and 139 spp. in a tropical forest of Vietnam. Also the density of oribatids per sample in this forest goes from 12 to 984 ind/m^2, with a monthly mean of 289.5 ind/m^2 (see *Table 1*) which was low compared to the records (between 4,000 and 40,000 ind/m^2) for other tropical forests (Bluhm et al., 2016; Minor et al., 2017a); although there are records at the soil of rainforest Vietnam, with densities lower than 180 ind/m^2 (Minor et al., 2017b). The densities found in LTS are still below even compared with a dry forest in western Mexico, where densities greater than 8,000 ind/m^2 have been recorded (Palacios-Vargas et al., 2007).

In respect to our second hypothesis, our results show a similar tendency in the decrease of oribatids abundance at winter season, which is generally related to a reduction in the specific richness and diversity in the community, registering the three lowest abundances in December, January and February, and the highest in March, which is explained by the presence of a large number of tropical and northern cyclones that naturally occur in the region in the winter season from November to January (Soto and Gama, 1997), and that during our sampling, they were present very intensively from October to February, flooding large areas of the jungle and part of our collection points (University Network of Atmospheric Observatories, RUOA, http://www.ruoa.unam.mx), which generates a large number of soils oribatids perish, migrate vertically, or they resort to some morphophysiological strategy to survive, however the success and survival time to the floods is dependent on each species (Bardel and Pfingstl, 2018; Smrž, 1996; Pequeno et al., 2017), also only the families Scheloribatidae, Oppidae, Oripodidae, Protoribatidae and Arceremaeidae were abundant in this forest which possess generalist feeding habits, contrary to our expectations Phthiracaridae and Carabodidae was low abundant families.

The edaphic temperature result one of the main determinants of community structure of oribatids, since there is a great dependence of poikilothermic animals with this

http://www.aloki.hu ● ISSN 1589 1623 (Print) ● ISSN 1785 0037 (Online)
DOI: http://dx.doi.org/10.15666/aeer/1706_1462114639

parameter for physiology (mainly metabolic and respiratory) throughout their life cycle (Stamou et al., 1995); this relationship is generally reported as negative, so that as the temperature increases, the abundance of many groups of the mesofauna decreases, among them the oribatid mites. Maximum lethal temperatures for them are close to 40 °C (Wehner et al., 2018; Ermilov and Lochynska, 2008; Bezci et al., 2017), other factors that significantly influence these communities are content of organic matter, soil pH, porosity and humidity (Urhan et al., 2006; Wissuwa et al., 2013); however, in our study none of these parameters were significant, suggesting that among the factors analyzed, only the soil temperature plays a key role in structuring oribatids in this rainforest.

The analysis of canonical correspondence explains about 60% of the variance of the community of oribatids in relation to temporality and the percentage of CO_2, the temporality has been previously addressed as a structuring character of the communities of these mites; however the CO_2 has been used as a measure of the productivity of the system, observing that the greater amount of this compound, tropical plant species increase their photosynthetic rate, increasing their productivity and possibly their hydric status (Herrera et al., 2001). However, high levels of CO_2 generate changes in the edaphic flora and microbiota, which in short-term studies do not show enough interaction to modify the structure of the oribatid mites (Haimi et al., 2005), although in studies of modification of the amount of CO_2 in soil in the long term, after 18 months in plots with increase of this compound with 200 ppm above the environmental values, there are significant differences in the decrease of the populations of these mites in up to 61%, due to the variation in the microbiota and litter quality (Hansen et al., 2001).

Conclusions

No significant effect of tree identity was found on the structure of the oribatid mite community in Los Tuxtlas rainforest. Soil constitutes a continuum in conditions and resources as proposed by Wehner et al. (2016) in its hypothesis about litter, being considered as a connecting bridge between the organisms; besides that litter quality decreases as the decomposition process advances and therefore they end up masking the differential properties of leaves (Scheu, 2005; Kaneko et al., 2005); however, it is relevant to mention that contrary cases have been reported for temperate forests (Eissfeller et al., 2013).

The community structure of oribatids mites showed significant differences in relation to collecting months, finding in general terms two large demographic increases in March 2016 and July 2016, which show a differentiation in the specific composition and allow a greater richness in the community.

Within the soil abiotic factors only soil temperature had a significant relationship with soil community according to Pearson correlation analysis; however, in the CCA ordination with envfit, additionally to temporality and edaphic temperature, the % of CO_2, the edaphic relative humidity, percentage of O.M. and O.C. was also significant and have an effect on the structuration. Even so, analyzed factors are insufficient to explain the whole variation in the community structure of the Oribatid mites.

Subsequent analyzes are necessary to know if the plant identity does not affect the communities of oribatid mites inhabiting the litter or even the trunks or canopy of morphological and functionally contrasting trees in this tropical ever-green forest, and also compare these results with others tropical forest for the world.

http://www.aloki.hu ● ISSN 1589 1623 (Print) ● ISSN 1785 0037 (Online)
DOI: http://dx.doi.org/10.15666/aeer/1706_1462114639

Acknowledgments. We thank to the Postgraduate doctoral program in Biological Sciences of the UNAM for all the support given during the realization of this work. CONACyT gave a scholarship to the senior author for this doctoral study. This project was supported by the project PAPIIT (DGAPA, UNAM) IN214816: "Microarthropod ecology of Los Tuxtlas forest, Veracruz" in charge of José G. Palacios Vargas. We had logistic help from the personal of Tropical Biology Station of Los Tuxtlas, Veracruz, mainly from Rosamond Coates and Martha Madora, Maira Montejo gave assistance in the ecological analyzes, Ricardo Iglesias supported the taxonomic determination of oribatid mites, Tila Pérez support with valuable suggestion for the improvement of this paper.

REFERENCES

[1] Anderson, J. M. (1975): The Enigma of Soil Animal Species Diversity. – In: Vanek, J. (ed.) Progress in Soil Ecology. Academia, Prague.
[2] André, H. M., Noti, M.-I., Lebrun, P. (1994): The soil fauna: the other last biotic frontier. – Biodiversity and Conservation 3: 45-46.
[3] André, H. M., Ducarme, X., Lebrun, P. (2002): Soil biodiversity: myth, reality or conning? – Oikos 96: 3-24.
[4] Álvarez-Sánchez, J., Guevara, S. (1999): Litter interception on *Astrocaryum mexicanum* Liebm. (Palmae) in a Tropical Rain Forest. – Biotropica 31(1): 89-92.
[5] Álvarez-Sánchez, J., Barajas-Guzmán, G., Campo, J., León, R. (2016): Inorganic nitrogen and phosphorous in stemflow of the palm *Astrocaryum mexicanum* Liebm. located in Los Tuxtlas, Mexico – Tropical Ecology 57(1): 45-55.
[6] Balogh, J., Balogh, P. (1992): The Oribatid Mites Genera of the World. – Hungarian Natural History Museum, Budapest.
[7] Bardel, L., Pfingstl, T. (2018): Resistance to flooding of different species of terrestrial oribatid mites (Acari, Oribatida) – Soil Organisms 90(2): 71-77.
[8] Bardgett, R. D., Wardle, D. A. (2010): Aboveground-Belowground Linkages: Biotic Interactions, Ecosystem Processes, and Global Change. – Oxford University Press, Oxford, UK.
[9] Barrantes, T., Ortiz, R. (2011): Nutrient distribution in *Guarea glabra* Vahl. in San Lorencito river basin at Alberto ML Brenes Biological Reserve of San Ramón, Alajuela, Costa Rica. – Biocenosis 25(1-2): 68-78.
[10] Bernier, N. (2018): Hotspots of biodiversity in the underground: a matter of humus form? – Applied Soil Ecology 123: 305-312.
[11] Bezci, T., Altun, A., Barán, Ş. (2017): Monthly variation of oribatid subspecies *Eremaeus hepaticus cordiformis* Grandjean, 1934 (Acari). – Sakarya Üniversitesi Fen Bilimleri Enstitüsü Dergisi 21(6): 1331-1335.
[12] Blake, G. R., Hartge, K. H. (1986): Particle Density. – In: Kutle, A. (ed.) Methods of Soil Analysis. Part I. Physical and Mineralogical Methods. ASA, Madison, WI.
[13] Bluhm, C., Scheu, S., Maraun, M. (2016): Temporal fluctuations in oribatid mites indicate that density-independent factors favour parthenogenetic reproduction. – Experimental and Applied Acarology 68: 387-407.
[14] Caruso, T., Schaefer, I., Monson, F., Keith, A. M. (2019): Oribatid mites show how climate and latitudinal gradients in organic matter can drive large-scale biodiversity patterns of soil communities. – Journal of Biogeography 46: 611-620.
[15] Coronado, I. M. (2006): Five new species of *Guarea* (Meliaceae), two from the *Guarea glabra* Vahl complex, in Central America. – Novon 16(4): 462-467.
[16] Dirzo, R., Gónzalez-Soriano, E., Vogt, R. C. (1997): General Introduction. – In: Gónzalez-Soriano, E., Dirzo, R., Vogt, R. C. (eds.) Natural History of Los Tuxtlas. National Autonomous University of Mexico, México D. F. (in Spanish).
[17] Donoso, D. A., Johnston, M. K., Kaspari, M. (2010): Trees as templates for tropical litter arthropod diversity. – Oecologia 164: 201-211.

http://www.aloki.hu ● ISSN 1589 1623 (Print) ● ISSN 1785 0037 (Online)
DOI: http://dx.doi.org/10.15666/aeer/1706_1462114639

[18] Donoso, D. A., Johnston, M. K., Clay, N. A., Kaspari, M. E. (2013): Trees as templates for trophic structure of tropical litter arthropod fauna. – Soil Biology and Biochemistry 61: 45-51.
[19] Eissfeller, V., Langenbruch, C., Jacob, A., Maraun, M., Scheu, S. (2013): Tree identity surpasses tree diversity in affecting the community structure of oribatid mites (Oribatida) of deciduous temperate forests. – Soil Biology and Biochemistry 63: 154-162.
[20] Ermilov, S., Łochyńska, M. (2008): The influence of temperature on the development time of three oribatid mites species (Acari, Oribatida). – North-Western Journal of Zoology 4(2): 274-281.
[21] Ferreira, R. N. C., Franklin, E., Pereira de Souza, J. L., de Moraes, J. (2012): Soil oribatid mite (Acari: Oribatida) diversity and composition in semi-deciduous forest in eastern Amazonia and comparison with the surrounding savanna matrix. – Journal of Natural History 46(33-34): 2131-2144.
[22] Flores, J. J., Coates, R. I., Sánchez-Cordero, V., Mendieta, V. J. (2014): Terrestrial mammals of the Tropical Biology Station of Los Tuxtlas. – University Digital Magazine 15(4): 1-10 (in Spanish).
[23] Fonte, S. J., Schowalter, T. D. (2004): Decomposition of greenfall vs. senescent foliage in a tropical forest ecosystem in Puerto Rico. – Biotropica 36(4): 474-482.
[24] Franklin, E., Santos, E. M. R., Albuquerque, M. I. C. (2006): Diversity and distribution of oribatid mites (Acari:Oribatida) in a lowland rain forest in Peru and in several environments of the Brazilians states of Amazonas, Rondônia, Roraima and Pará. – Brazilian Journal of Biology 66(4): 999-1020.
[25] Gergócs, V., Garamvölgyi, A., Homoródi, R., Hufnagel, L. (2011): Seasonal change of oribatid mite communities (Acari, Oribatida) in three different types of microhabitats in an oak forest. – Applied Ecology and Environmental Research 9(2): 181-195.
[26] Gessner, M. O., Swan, M. S., Dang, C. K., McKie, B. G., Bardgett, R. D., Wall, D. H., Hättenschwiler, S., Gasser, P. (2010): Soil animals alter plant litter diversity effects on decomposition. – Proceedings of the National Academy of Sciences of the United States of America 102: 1519-1524.
[27] Haimi, J., Laamanen, J., Penttinen, R., Räty, M., Koponen, S., Kellomäki, S., Niemelä, P. (2005): Impacts of elevated CO2 and temperature on the soil fauna of boreal forests. – Applied Soil Ecology 30(2): 104-112.
[28] Hammer, Ø., Harper, D. A. T., Ryan, P. D. (2001): PAST: Paleontological Statistics software package for education and data analysis. – Paleontologia Electronica 4(1): 1-9.
[29] Hansen, R. A. (2000): Effects of habitat complexity and composition on a diverse litter microarthropod assemblage. – Ecology 81(4): 1120-1132.
[30] Hansen, R. A., Williams, R. S., Degenhardt, D. C., Lincoln, D. E. (2001): Non-litter effects of elevated CO2 on forest floor microarthropod abundances. – Plant and soil 236: 139-144.
[31] Herrera, A., Fernández, M. D., Rengifo, E., Tezara, W. (2001): Effect of high concentration of CO2 on photosynthesis in tropical species. – Interciencia 26(10): 469-471 (in Spanish).
[32] Ibarra-Manríquez, G., Martínez-Ramos, M., Dirzo, R., Núñez-Farfán, J. (1997): The Vegetation. – In: Gónzalez-Soriano, E., Dirzo, R., Vogt, R. C. (eds.) Natural History of Los Tuxtlas. National Autonomous University of Mexico, Mexico, D. F.
[33] Irmler, U. (2006): Climatic and litter fall effects on collembolan and oribatid mite species and communities in a beech wood based on a 7 years investigation. – European Journal of Soil Biology 42(1): 51-62.
[34] Jackson, M. L. (1976): Chemical Analysis of Soils. – Omega, Barcelona (in Spanish).
[35] Jost, L. (2006): Entropy and diversity. – Oikos 113: 363-374.
[36] Kaneko, N., Salamanca, E. F. (1999): Mixed leaf litter effects on decomposition rates and soil microarthropod communities in an oak-pine stand in Japan. – Ecological Research 14: 131-138.
[37] Kaneko, N., Sugawara, Y., Miyamoto, T., Hasegawa, M., Hiura, T. (2005): Oribatid mite structure and tree species diversity: a link? – Pedobiologia 49: 521-529.

http://www.aloki.hu ● ISSN 1589 1623 (Print) ● ISSN 1785 0037 (Online)
DOI: http://dx.doi.org/10.15666/aeer/1706_1462114639

[38] León, R. (2003): Effects of Decomposition, Frugivorous and Removal of Fruits and Seeds of Tree Species on Patterns of Decomposition in Situ in Rainforest Soil. – In: Álvarez-Sánchez, J., Naranjo-García, E. (eds.) Soil Ecology in the Tropical Humid Forest of Mexico. National Autonomous University of Mexico, Mexico, D. F.
[39] Martínez-Ramos, M., Ortiz-Rodríguez, I. A., Piñero, D., Dirzo, R., Sarukhán, J. (2016): Anthropogenic disturbances jeopardize biodiversity conservation within tropical rainforest reserves. – Proceedings of the National Academy of Sciences 113(19): 5323-5328.
[40] Minor, M. A., Babenko, A. B., Ermilov, S. G. (2017a): Oribatid mites (Acari: Oribatida) and springtails (Collembola) in alpine habitats of southern New Zealand. – New Zealand Journal of Zoology 44(1): 65-85.
[41] Minor, M. A., Ermilov, S. G., Anichkin, A. E. (2017b): Biodiversity of soil oribatid mites (Acari: Oribatida) in a tropical highland plateaux, Bi Doup-Nui Ba National Park, Southern Vietnam. – Tropical Ecology 58(1): 45-55.
[42] Mumladze, L., Murvanidze, M., Maraun, M., Salakaia, M. (2015): Oribatid mite communities along an elevational gradient in Sairme Georgia (Caucasus). – Experimental and Applied Acarology 66(1): 41-51.
[43] Nielsen, U. N., Osler, G. H. R., Campbell, C. D., Neilson, R., Burslem, D. F. R. P., van der Wal, R. (2010): The enigma of soil animal species diversity revisited: the role of small-scale heterogeneity. – PLoS One 5(7): e11567.
[44] Núñez-Castillo, O., Álvarez-Sánchez, F. J. (2003): Arbuscular mycorrhizae of the palm *Astrocaryum mexicanum* in disturbed and undisturbed stands of a Mexican tropical forest. – Mycorrhiza 13: 271-276.
[45] Oksanen, J., Blanchet, F. G., Friendly, M., Kindt, R., Legendre, P., McGlinn, D., Minchin, R., O'Hara, R. B., Simpson, L., Solymos, P., Stevens, M. H. H., Szoecs, E., Wagner, H. (2016): Vegan: Community Ecology Package. R package. Version 2.4-1. – https://CRAN.R-project.org/package=vegan.
[46] Osler, G. H. R., Beattie, A. J. (2001): Contribution of oribatid and mesostigmatid soil mites in ecologically based estimates of global species richness. – Austral Ecology 26: 70-79.
[47] Palacios-Vargas, J. G., Castaño-Meneses, G., Gómez-Anaya, J. A., Martínez-Yrizar, A., Mejía-Recamier, B. E., Martínez-Sánchez, J. (2007): Litter and soil arthropods diversity and density in a tropical dry forest ecosystem in western Mexico. – Biodiversity and Conservation 16: 3703-3717.
[48] Pequeno, P. A. C. L., Franklin, E., Norton, R. A., Wellington de Morais, J., Guilherme, D. R. (2017): Spatial abundance pattern of a common soil arthropod changes suddenly with season in a tropical rainforest. – Pedobiologia 63: 46-51.
[49] Perdue, J. C., Crossley, D. A. (1989): Vertical distribution of soil mites (Acari) in conventional and no-tillage agricultural systems. – Biology and Fertility of Soils 9(2): 135-138.
[50] Piñero, D., Sarukhán, J., González. E. (1977): Demographic studies in plants. *Astrocaryum mexicanum* Liebm. I. Populations structure. – Bulletin of the Botanical Society of Mexico 37: 69-118 (in Spanish).
[51] Piñero, D., Martínez-Ramos, M., Sarukhán, J. (1984): A population model of *Astrocaryum mexicanum* and a sensitive analysis of its finity rate of increase. – The Journal of Ecology 72: 977-991.
[52] Raich, J. W. (1983): Understory palms as nutrient traps: a hypothesis. – Brenesia 21: 119-129.
[53] R Core Team (2016): R: A Language and Environment for Statistical Computing. – R Foundation for Statistical Computing, Vienna, Austria. http://www.R-project.org/.
[54] Scheu, S. (2005): Linkages between Tree Diversity, Soil Fauna and Ecosystem Processes. – In: Scherer-Lorenzen, M., Korner, C., Schulze, E. (eds.) Forest Diversity and Function Temperate and Boreal Systems. Springer, Berlin.

http://www.aloki.hu ● ISSN 1589 1623 (Print) ● ISSN 1785 0037 (Online)
DOI: http://dx.doi.org/10.15666/aeer/1706_1462114639

[55] Soto, M., Gama, L. (1997): Climes. – In: Gónzalez-Soriano, E., Dirzo, R., Vogt, R. C. (eds.) Natural History of Los Tuxtlas. National Autonomous University of Mexico, México D. F. (in Spanish).
[56] Smrž, J. (1996): Some Aspects of the Life Strategy of Oribatid Mites (Oribatida). – In: Mitchell, R., Horn, D. J., Needham, G. R., Welbourn, W. C. (eds.) Acarology IX: Vol. 1, Proceedings. Ohio Biological Survey, Columbus, USA.
[57] Stamou, G. P., Asikidis, M. D., Argyropoulou, M. D., Iatrou, G. D. (1995): Respiratory responses of oribatid mites to temperature changes. – Journal of Insect Physiology 41(3): 229-233.
[58] Statsoft, Inc. (2007): STATISTICA Data Analysis Software System, Versión 8.0. – Statsoft, Inc., Tulsa, OK.
[59] Urhan, R., Katilmis, Y., Kahveci, A. Ö. (2006): Vertical distribution of oribatid mites (Acari: Oribatida) and some ecological parameters affecting the distribution pattern in south-west Turkey. – Zoology in the Middle East 37: 99-105.
[60] Van Reeuwijk, L. P. (1998): Procedures for soil analysis. – International Soil Reference and Information Center (ISRIC), Wageningen, Netherlands.
[61] Vázquez G., M. M. (2006): Oribatid mites from tropical jungles of Mexico and Belice. – Caos Conciencia 1: 19-23 (in Spanish).
[62] Walkey, A. (1947): A critical examination of a repid method for determining organic carbon in soils: effect of variations in digestion conditions and of inorganic soil costituents. – Soil Science 63: 251-264.
[63] Wardle, D. A. (2006): The influence of biotic interactions on soil biodiversity. – Ecology Letters 9: 870-886.
[64] Wehner, K., Heethoff, M., Bruckner, A. (2018): Seasonal fluctuation of oribatid mite communities in forest microhabitats. – PeerJ 6: e4863.
[65] Wehner, K., Norton, R. A., Blüthgen, N., Heethoff, M. (2016): Specialization of oribatid mites to forest microhabitats - the enigmatic role of litter. – Ecosphere 7(3): e01336
[66] Wenny, D. G. (1999): Two-stage dispersal of *Guarea glabra* and *G. kunthiana* (Meliaceae) in Monteverde, Costa Rica. – Journal of Tropical Ecology 15: 481-496.
[67] Wissuwa, J., Salamon, J. A., Frank, T. (2013): Oribatida (Acari) in grassy arable fallows are more affected by soil properties than habitat age and plant species. – European Journal of Soil Biology 59: 8-14.
[68] Wunderle, I. (1992): Arboricolous and edaphic oribatids (Acari) in the lowland rainforest of Panguana, Peru. – Amazoniana 12: 119-142.

APPENDIX

Appendix 1. *Taxonomic list, occurrence and abundance of oribatid mites from the Los Tuxtlas Tropical Field Station related to A. mexicanum (A) and G. glabra (G)*

Taxonomic classification	Genus and species	Mar	Apr	May	Jun	Jul	Aug	Sep	Oct	Nov	Dec	Jan	Feb	N total	N relative
Enarthronota															
Cosmochthoniidae	*Cosmochthonius* sp. nov.										G			1	NA
Hypochthoniidae	*Eohypochthonius beckii*					G	A	A		A			G	9	0.003
Haplochthonidae	*Haplochthonius clavatus*							G						1	NA
Mesoplophoridae	*Mesoplophora longisetosa*	G,A	G	G,A		G,A								64	0.025
Mesoplophoridae	*Mesoplophora* ca. *silvaticus*						A							1	NA
Lohmanniidae	*Lohmannia* sp. nov.							A						1	NA
Lohmanniidae	*Torpacarus* sp.	G,A	A	G,A		A	G				A			37	0.014
Lohmanniidae	*Torpacarus ommitens*		G,A		A	G,A	G,A	G,A	A	G,A	A	G,A	G	45	0.017
Mixonomata															
Dichosomata															

http://www.aloki.hu ● ISSN 1589 1623 (Print) ● ISSN 1785 0037 (Online)
DOI: http://dx.doi.org/10.15666/aeer/1706_1462114639

Epilohmannidae	*Epilohmannia minuta*					G,A	A	G						4	0.002
Epilohmannidae	*Epilohmannia pallida*			G,A		G,A		G		G,A				9	0.003
Euphthiraridae	*Acrotritia ardua*	A	G,A	A	G		G							8	0.003
Euphthiraridae	*Euphthiracarus* ca. *breviculus*							G	G		G			5	0.002
Phthiracaridae	*Hoplophorella* sp.1		G,A	G,A	G	G,A	G				A	G,A		25	0.010
Phthiracaridae	*Hoplophorella scapellata*	G,A	G,A	G,A	A	A	A		A	G				24	0.009
Phthiracaridae	*Hoplophorella* ca. *eximia*		G	A	G,A	G	G,A					G		8	0.003
Holosomata															
Trhypochthoniidae	*Archegozetes magnus*		G	A				G,A	G					31	0.012
Crotoniidae	*Camisia* ca. *horrida*		G,A											6	0.002
Malaconothridae	*Malaconothrus* ca. *silvaticus*	G			G									2	0.001
Brachypylina															
Pycnonoticae															
Arceremaeidae	*Tecteremaeus cornutus*	G,A	G,A	G,A	G,A	G,A	G,A	G,A	G,A	G,A	A	A	G	222	0.086
Basilobelbidae	*Basilobelba* sp.	G,A	A	G	A	G					A			10	0.004
Compactozetidae	*Reticulocepheus* ca. *grandis*	G,A	G,A	G	G	G,A	G	G,A	A					38	0.015
Charassobatidae	*Charassobates tuberosus*	G,A	G,A		G	G,A	G			G	A	G		17	0.007
Carabodidae	*Cubabodes verrucatus*	G,A	G,A	G,A	G,A	G,A	G,A	G	G	G,A	G,A	G		65	0.025
Carabodidae	*Carabodes (Klapericches)* sp. nov.				G		G							2	0.001
Carabodidae	*Carabodes (Phyllocarabodes)* sp.			G		A								4	0.002
Ceratoppiidae	*Ceratorchestes baloghi*	A	A	A	G	G	G		A	G	A			17	0.007
Cymbaeremaeidae	*Scapheremaeus tonathiu*			G										1	NA
Damaeidae	*Epidamaeus* sp. nov.	G,A			G	G	G	G						10	0.004
Dampfiellidae	*Dampfiella procera*	A			G	A	G	A	G,A					8	0.003
Eremulidae	*Eremulus rigidisetosus*	G,A			G,A	G,A	G	G	G,A	G,A				25	0.010
Tetracondylidae	*Flagellocepheus sagittatus*		A						A					3	0.001
Damaeoliodidae	*Fosseremus* ca. *laciniatus*							G						1	0.001
Hermanniellidae	*Hermaniella* sp. nov.				G	A	A							6	0.002
Hermanniellidae	*Sacculobates* ca. *heterotrichus*						G			G				3	0.001
Hermanniellidae	*Sacculobates horologiorum*	G,A	G,A	A	G,A	G,A	G,A	G	G	G		G		39	0.015
Heterobelbidae	*Heterobelba oxapampensis*	A												1	NA
Xenillidae	*Xenillus* ca. *fazendae*	G,A	A			G,A	A	A						8	0.003
Microtegeidae	*Microtegeus similis*					A								2	0.001
Microtegeidae	*Microtegeus borhidii*	G,A	A			G	G,A	G	A	G,A	A	A		56	0.022
Nanhermannidae	*Cyrthermannia simplex*	G,A	G,A	A	G,A	G,A	A	G		G		A	G	30	0.012
Nanhermannidae	*Cyrthermannia* ca. *florens*								A					1	NA
Neoliodidae	*Teleioliodes madininensis*	G,A	G,A	G	G	G,A	G,A	A	G,A	A	G	A	G	44	0.017
Oppiidae	*Multioppia* sp.	G,A	G,A	G,A	G,A	G,A	G	G	A	G,A	G,A	A	G	129	0.050
Oppiidae	*Stachyoppia curvispina*		A	A	G,A	G,A	G,A	G,A	G,A	G,A	G,A	G		112	0.043
Oppiidae	*Arcoppia* sp.				G,A		G	G,A	A	G,A	A			47	0.018
Poronoticae															
Ceratozetidae	*Fuscozetes* sp. nov.	G,A	A	A	A		G			A	A			26	0.010
Epactozetidae	*Truncozetes sturmi*	G,A	A	G,A	G	G,A	G,A	G,A	G,A	G,A	G,A	A	G	94	0.036
Galumnellidae	*Galumnopsis* sp. nov.	G,A	A			A	G	A		A				26	0.010
Galumnidae	*Galumna (Orthogalumna)* sp. nov.						G	G	G,A					4	0.002
Galumnidae	*Notogalumna* sp. nov.				A									1	NA
Galumnidae	*Pergalumna dactylaris*	G	A	G,A	G,A	A	G,A	G,A		G,A		A		27	0.010
Galumnidae	*Pergalumna hypergranulosa*	G,A		A	A	G,A	G	A		G				21	0.008
Galumnidae	*Pergalumna obsidiana*	G	G			G		A	G,A	G,A				14	0.005
Galumnidae	*Pergalumna ekaterinae*	G,A	G,A	G,A	G,A	G,A	G,A	G	G,A	A	A	A	A	59	0.023
Galumnidae	Galumnidae gen. nov.	G,A	G,A	G,A	G,A	G,A	A	A	G,A	G,A	A	A	G	60	0.023
Haplozetidae	*Rostrozetes.* ca. *dimorphochartes*				G		A		G	G,A				7	0.003
Haplozetidae	*Rostrozetes cubanus*								A	A	A			3	0.001
Haplozetidae	*Rostrozetes foveolatus*	G,A	G,A	G,A	G,A	G,A	G,A	G,A	A	G,A	G,A	G,A		138	0.054

http://www.aloki.hu ● ISSN 1589 1623 (Print) ● ISSN 1785 0037 (Online)
DOI: http://dx.doi.org/10.15666/aeer/1706_1462114639

Licneremaeidae	*Licneremaeus discoidalis*				G		G	G				G,A	G	9	0.003
Microzetidae	*Berlesezetes peruensis*					A				A				2	0.001
Microzetidae	*Kalyptrazetes desaussurei*		A			G,A			A	A	A			14	0.005
Microzetidae	*Schalleria* ca. *mexicana*	G,A			G	G,A	G,A	G	A					12	0.005
Oripodidae	*Benoibates* sp. nov.				G,A	G,A	G,A	G,A	G,A	G,A	G,A	G,A	G,A	208	0.081
Oripodidae	*Benoibates* sp.1							G						1	NA
Oripodidae	*Oripoda lobata*				G,A		G,A	G	G,A	G,A	A	G		43	0.017
Oripodidae	*Oripoda scissurata*				G,A		A			A				6	0.002
Oribatellidae	*Oribatella szaboi*	G				G,A				G				5	0.002
Phenopelopidae	*Eupelops suramericanus*						A		G					2	0.001
Protoribatidae	*Protoribates capucinus*		A	G,A	G,A	G,A	G,A		A		A	A		49	0.019
Protoribatidae	*Brasilobates* sp. nov.	G,A	G,A	G,A	G,A	G,A	G,A	G,A	G,A	G,A	A	G,A	G	217	0.084
Scheloribatidae	*Scheloribates praeincisus*				G,A	G,A	G,A	G,A	A	A	A	G	G	75	0.029
Scheloribatidae	*Scheloribates* ca. *grandiporosus*	G,A	G,A	G,A	G,A	G,A	G,A	G	G,A	G,A				245	0.095

N total = total abundance; N relative = relative abundance

Appendix 2. *Kruskall-Wallis Post-hoc comparisons of collecting month with structural parameters of oribatid mites community from Los Tuxtlas, Veracruz. Dunn´s test with Bonferroni adjustment. Scores below diagonal, p-value above diagonal. In bold in each side the significant values with α = 0.05. Abundance (N) and density (ind/m²) registered the same tendency, for which only one is reported; Species richness (S); Dominance (D´); Shannon diversity (entropy) index (H') and true diversity (¹D) registered the same tendency, for which only one is reported; J´ = Pielou's equity (evenness)*

Ind/m²	**Mar**	**Apr**	**May**	**Jun**	**Jul**	**Aug**	**Sep**	**Oct**	**Nov**	**Dec**	**Jan**	**Feb**
Mar		1	1	1	1	1	**0.0215***	**0.0154***	0.071	**0.0024***	**0.0001***	**0.0000***
Apr	1.483		1	1	1	1	1	1	1	0.427	0.035	**0.0107***
May	2.148	0.666		1	1	1	1	1	1	1	0.301	0.112
Jun	1.830	0.347	-0.318		1	1	1	1	1	1	0.113	0.038
Jul	0.839	-0.643	-1.309	-0.990		1	0.336	0.258	0.853	0.058	**0.0030***	**0.0007***
Aug	1.180	-0.302	-0.968	-0.650	0.341		0.853	0.674	1	0.175	**0.0115***	**0.0032***
Sep	**3.409**	1.926	1.261	1.579	2.569	2.229		1	1	1	1	1
Oct	**3.499**	2.016	1.351	1.669	2.660	2.319	0.090		1	1	1	1
Nov	3.068	1.585	0.920	1.238	2.229	1.888	-0.341	-0.431		1	1	1
Dec	**3.968**	2.486	1.820	2.139	3.129	2.788	0.560	0.470	0.900		1	1
Jan	**4.756**	3.274	2.608	2.926	**3.917**	**3.576**	1.347	1.257	1.688	0.788		1
Feb	**5.078**	**3.595**	2.930	3.248	**4.239**	**3.898**	1.669	1.579	2.010	1.109	0.322	

S	**Mar**	**Apr**	**May**	**Jun**	**Jul**	**Aug**	**Sep**	**Oct**	**Nov**	**Dec**	**Jan**	**Feb**
Mar		1	0.5017	1	1	1	0.0401	0.1228	0.4348	**0.0061***	**0.0006***	**0.0000***
Apr	1.526		1	1	1	1	1	1	1	0.8904	0.1894	0.0288
May	2.428	0.901		1	1	1	1	1	1	1	1	0.5017
Jun	1.668	0.142	-0.760		1	1	1	1	1	1	0.2896	0.0474
Jul	0.338	-1.188	-2.089	-1.330		1	0.1241	0.3427	1	**0.0223***	**0.0026***	**0.0002***
Aug	0.863	-0.663	-1.565	-0.805	0.525		0.5826	1	1	0.1333	**0.0202***	**0.0022***
Sep	3.236	1.710	0.808	1.568	2.898	2.373		1	1	1	1	1
Oct	2.901	1.375	0.473	1.233	2.563	2.038	-0.335		1.0000	1.0000	1.0000	1
Nov	2.479	0.953	0.052	0.811	2.141	1.616	-0.757	-0.422		1.0000	1.0000	0.5776
Dec	**3.738**	2.212	1.310	2.070	**3.400**	2.875	0.502	0.837	1.259		1.0000	1
Jan	**4.288**	2.762	1.861	2.621	**3.950**	**3.426**	1.053	1.388	1.809	0.551		1
Feb	**4.855**	3.329	2.428	3.187	**4.517**	**3.992**	1.619	1.954	2.376	1.117	0.567	
D´	**Mar**	**Apr**	**May**	**Jun**	**Jul**	**Aug**	**Sep**	**Oct**	**Nov**	**Dec**	**Jan**	**Feb**
Mar		1	0.6354	1	1	1	1	0.6922	1	0.1044	0.1619	0.9349
Apr	-1.489		1	1	1	1	1	1	1	1	1	1

http://www.aloki.hu ● ISSN 1589 1623 (Print) ● ISSN 1785 0037 (Online)
DOI: http://dx.doi.org/10.15666/aeer/1706_1462114639

May	-2.341	-0.852		1	1	1	1	1	1	1	1	1
Jun	-1.858	-0.370	0.482		1	1	1	1	1	1	1	1
Jul	-0.511	0.977	1.829	1.347		1	1	1	1	0.4844	0.7041	1
Aug	-0.752	0.736	1.588	1.106	-0.241		1	1	1	0.9197	1	1
Sep	-0.871	0.617	1.469	0.987	-0.360	-0.119		1	1	1	1	1
Oct	-2.308	-0.820	0.032	-0.450	-1.797	-1.556	-1.437		1	1	1	1
Nov	-1.743	-0.254	0.598	0.116	-1.231	-0.990	-0.871	0.566		1	1	1
Dec	-2.951	-1.463	-0.611	-1.093	-2.440	-2.199	-2.080	-0.643	-1.209		1	1
Jan	-2.813	-1.325	-0.473	-0.955	-2.302	-2.061	-1.942	-0.505	-1.071	0.138		1
Feb	-2.193	-0.704	0.148	-0.334	-1.681	-1.440	-1.321	0.116	-0.450	0.759	0.621	

H´	**Mar**	**Apr**	**May**	**Jun**	**Jul**	**Aug**	**Sep**	**Oct**	**Nov**	**Dec**	**Jan**	**Feb**
Mar		1	0.4656	1	1	1	0.0484	0.3261	1	**0.0051***	**0.0019***	**0.0001***
Apr	1.628		1	1	1	1	1	1	1	1	0.5414	0.0679
May	2.454	0.827		1	1	1	1	1	1	1	1	0.7964
Jun	1.776	0.148	-0.679		1	1	1	1	1	1	0.8031	0.1105
Jul	0.338	-1.290	-2.117	-1.438		1	0.1472	0.8234	1	**0.0188***	**0.0074***	**0.0004***
Aug	0.804	-0.824	-1.650	-0.971	0.466		0.5756	1	1	0.0955	0.0418	**0.0031***
Sep	3.181	1.554	0.727	1.406	2.844	2.377		1	1	1	1	1
Oct	2.580	0.952	0.125	0.804	2.242	1.776	-0.602		1	1	1	1
Nov	2.126	0.499	-0.328	0.351	1.789	1.322	-1.055	-0.454		1	1	0.3231
Dec	**3.783**	2.155	1.329	2.007	**3.445**	2.979	0.602	1.203	1.657		1	1
Jan	**4.027**	2.400	1.573	2.252	**3.690**	3.223	0.846	1.448	1.901	0.244		1
Feb	**4.709**	3.082	2.255	2.934	**4.372**	**3.905**	1.528	2.130	2.583	0.926	0.682	

J´	**Mar**	**Apr**	**May**	**Jun**	**Jul**	**Aug**	**Sep**	**Oct**	**Nov**	**Dec**	**Jan**	**Feb**
Mar		1	1	1	1	1	1	1	1	1	1	1
Apr	-0.405		1	1	1	1	1	1	1	1	1	1
May	-0.109	0.296		1	1	1	1	1	1	1	1	1
Jun	-0.084	0.322	0.026		1	1	1	1	1	1	1	1
Jul	-0.354	0.051	-0.245	-0.270		1	1	1	1	1	1	1
Aug	-0.595	-0.190	-0.486	-0.512	-0.241		1	1	1	1	1	1
Sep	0.885	1.290	0.994	0.968	1.239	1.480		0.9938	0.3508	1	0.56	1
Oct	-1.284	-0.878	-1.174	-1.200	-0.930	-0.689	-2.169		1	1	1	1
Nov	-1.670	-1.264	-1.560	-1.586	-1.316	-1.075	-2.555	-0.386		1	1	0.4734
Dec	0.171	0.576	0.280	0.254	0.524	0.766	-0.714	1.454	1.840		1	1
Jan	-1.503	-1.097	-1.393	-1.419	-1.149	-0.907	-2.387	-0.219	0.167	-1.673		0.7438
Feb	0.779	1.184	0.888	0.862	1.133	1.374	-0.106	2.062	2.448	0.608	2.281	

http://www.aloki.hu ● ISSN 1589 1623 (Print) ● ISSN 1785 0037 (Online)
DOI: http://dx.doi.org/10.15666/aeer/1706_1462114639

DISTRIBUTION AND GENETIC DIVERSITY OF TOBACCO ETCH VIRUS IN TURKEY AND RESISTANCE OF IMPROVED CAPSICUM LINES

ARPACI, B. B.

Department of Horticulture, Faculty of Agriculture, University of Kilis 7 Aralik, 79100 Kilis, Turkey
(e-mail: bbarpaci@kilis.edu.tr; phone: +90-348-814-2666; fax: +90-348-814-2667)

(Received 9th Jun 2019; accepted 10th Sep 2019)

Abstract. Tobacco etch virus (TEV) belonging to *Potyviridae* is among the most destructive viruses and widespread Worldwide but it has been found only Turkey in Mediterranean Basin. Both dominant and recessive pvr alleles contribute resistance against potyviruses. Prevalence of TEV in main pepper cultivation areas in Turkey and phylogenetic diversity of the isolates based on their coat protein region were determined in this study. Transferring resistance genes both recessive and dominant to susceptible chilli pepper lines was aimed with a breeding program including CM334 and Perennial known as resistance sources against several potyviruses. Two geographically and genetically distinct TEV isolates 1002 and 774 were inoculated to pepper genotypes carrying *Pvr4*, *pvr2*$^{+}$, *pvr2*^{1}, *pvr2*^{2}, *pvr2*^{3} alleles and 15 lines improved from CM334 carrying *Pvr4*, *pvr2*^{3} and Perennial carrying *pvr6* allele and QTLs. None of the pvr alleles contribute to resistance to isolate 774 while *pvr2*^{2} provides resistance to isolate 1002. All the pepper cultivation areas are infected by TEV in Turkey mainly Aegean Region and the isolates found in Turkey are close to those from Chinese isolate. Polygenic resistance was transferred by breeding program to line 4 could resist to both Turkish isolates.
Keywords: *polygenic resistance, pvr2 alleles, coat protein, pepper, phylogenetic analysis*

Introduction

Due to widespread cultivation of pepper in the World, harmful pests and diseases caused by fungi, viruses and bacteria of this plant have become prevalent. Capsicum spp. widely grown in the world is exposed to 70 viruses and more than 20 important viruses limit its production (Moury and Verdin, 2012; Green and Kim, 1991; Florini and Zitter, 1986). Among these viruses, the most prevalent ones are Tobamoviruses; Potyviruses, Cucumoviruses; and thrips-transmitted tospoviruses and Potyviruses (Moury and Verdin, 2012). Tobacco etch virus (TEV; genus *Potyvirus*; family *Potyviridae*) is an important pathogen in solanaceous crops with 10 described species that are very destructive and distributed with regard to continental pattern (Moury et al., 2005; Janzac et al., 2008). Potyviruses is characterized by flexuous, rod-shaped particles with approximately 10 kb in length single-stranded, positive sense RNA encapsidated coat protein (CP). Tobacco etch virus (TEV) causes up to 70% yield loss in pepper and spread mainly in North and Central America and the Caribbean (Nutter et al., 1989; Ariyaratne et al., 1996; Green and Kim, 1991). The use of resistant genotypes is one of the most efficient methods to protect crops from the yield losses caused by viruses. Using resistant varieties reduce incidence of TEV in pepper cultivated fields and increase fruit yield (Padgett et al., 1990).

Pepper resistance genes and alleles whether dominant or recessive are efficient against several potyviruses. The dominant gene *Pvr4* which originates from *Capsicum annuum* Criollo de Morelos 334 (CM334) confers to a broad range resistance of potyviruses (Kim et al., 2017). *Pvr4* gene provides resistance to PepSMV (Pepper severe mosaic virus) and PTV (Peru tomato mosaic virus), but carrying genotypes this gene are susceptible to ChiVMV (Chilli veinal mottle virus), PVMV (Pepper veinal mottle virus) and TEV

http://www.aloki.hu ● ISSN 1589 1623 (Print) ● ISSN 1785 0037 (Online)
DOI: http://dx.doi.org/10.15666/aeer/1706_1464114651

(Janzac et al., 2009). Recessive genes *pvr1* and *pvr2* in pepper have been observed for resistance to potyviruses including tobacco etch virus but many virulent strains of TEV overcome most of these recessive genes (Parrella et al., 2002). Two main alleles from *Capsicum annuum* at the *pvr2* locus have been transferred to modern pepper cultivars (Kyle and Palloix, 1997) and *pvr1* from *C. chinense* (PI 152225) (Venkatesh et al., 2017) so that to provide resistance against potyviruses. Digenic recessive resistance to another potyvirus PVMV has successed by combination of recessive allelic series *pvr2* and *pvr6* allele corresponding to the eIF4E and eIF(iso)4E, respectively (Moury et al., 2005; Rubio et al., 2009).

In this study, spreading of TEV in the main open-field and protected pepper cultivation areas in Turkey has been determined and genetic diversity of CP region of some isolates compared with World isolates. Improved pepper lines from Perennialand CM334 resistance sources carrying pvr alleles were selected as resistant to two isolates determined distinct both genetically and geographically in this study. The genetic diversity of TEV infecting pepper was analysed in Turkey, to understand the diversity of TEV populations and to estimate the response of improved pepper genotype transferred both recessive resistance allele *pvr2*^{3}, *pvr6* and dominant gene *Pvr4* from resistant donors and the impact of geographic location on that structure. Transferring resistance genes against potyviruses both recessive and dominant to susceptible chili pepper lines was aimed with a breeding program including CM334 and Perennial as resources of resistance and Sena chili pepper variety which were commercial and susceptible to pathogen.

Materials and methods

Breeding population

First four years of breeding program resistant sub-populations were improved so that collecting resistance alleles. These populations were derived from crosses between the resistant donor Criollo de Morelos 334 (CM334) and Perennial inbred lines resistant to several potyviruses. CM334 (male) carrying *Pvr4* and *pvr2*^{3} genes and Perennial (female) carrying *pvr2*^{3} and *pvr6 genes* were crossed and 106 F_2 individuals were self-pollinated for three years. Selected as new resistant sources were crossed by Sena which was suitable for paprika production but susceptible variety against infections of TEV. F_1 progeny were not backcrossed to susceptible recipient (Sena) but self-pollinated and resistant individuals backcrossed to susceptible recipient and self-pollinated again. After two backcrossing and self-pollination alternately, selected 15 lines were mechanically inoculated by two TEV isolates 1002 and 774.

Field surveys and collecting of TEV isolates

TEV isolates were collected from June to August in 2013 and 2014 (open field) and March to May 2013 and 2014 (protected cultivation) with hierarchical (nested) sampling method (Ben Khalifa et al., 2009; d'Urso et al., 2003) from important pepper growing areas in Turkey. The factors was assessed by hierarchically partitioning the sample population among region, (West, South and East), cultivation system (open and protected) and sites (11 provinces) and samples were collected from 51 fields and 39 greenhouses. The pepper production values and sampling number of provinces were given in *Table 1*. Totally 1525 leaf samples and/or small pepper fruits were randomly collected from plants having symptoms related with viral infection.

http://www.aloki.hu ● ISSN 1589 1623 (Print) ● ISSN 1785 0037 (Online)
DOI: http://dx.doi.org/10.15666/aeer/1706_1464114651

Table 1. *Prevalence of tobacco etch virus infections determined by DAS-ELISA and RT-PCR in the main pepper-growing areas, Turkey*

Province	Pepper production of sampled provinces (tons)	Number of samples [b]	ELISA		RT-PCR	
			Number	%	Number	%
Antalya[a]	270,127	193 (21)	9	5	0	0.0
Balikesir	61,046	39 (4)	0	0	2	5.1
Bursa	133,438	183 (7)	42	22.9	70	38.2
Çanakkale	130,063	256 (8)	52	20.3	49	19.1
Hatay	102,665	294 (5)	36	18.6	9	3.0
Izmir	132,519	131 (7)	0	0.0	2	1.5
Kilis	55,000	93 (4)	2	2.1	4	5.3
Manisa	169,787	143 (8)	0	0.0	8	5.5
Mersin[a]	227,086	75 (18)	8	10.6	5	6.7
Samsun	257,306	60 (4)	3	5.0	0	0.0
Şanliurfa	67,583	58 (4)	0	0.0	2	3.4
Total	1,606,620	1525 (90)	152	9.9	151	9.9

[a]Protected cultivation areas
[b]Number of visited sampling areas in the bracket

Serological analysis and molecular characterization of TEV pathotypes

Samples were analyzed by DAS-ELISA (double antibody sandwich enzyme-linked immunosorbent assay) with antibodies against TEV (Agdia, France) and sequenced CP cistrons. Total RNAs were extracted with the Tri-Reagent kit (Molecular Research Centre Inc.) from fruit flesh or leaf (0.5 g) of collected pepper plants. Viral populations were characterized by two steps reverse transcription-polymerase chain reaction (RT-PCR) amplified with Avian myeloblastosis virus reverse transcriptase (Promega Corp., Madison, WI, USA) and Taq DNA polymerase (Promega Corp.) and primers reported by Buzkan et al. (2015). Degenerated primers were designed as reverse primer positions from 9273 to 9297 (CCCTAATAGTGTGTGCATGTTACGG) and the forward primer positions from 8538 to 8560 (TGCTGAYGCYGGYAAGAAGAAAG) produced a 760 nucleotide amplicon for TEV CP cistron. RT-PCR products were sequenced with primers corresponding to viral polarity by Medsantek (İstanbul, Turkey). CLUSTAL W program (Thompson et al., 1994) were used to align nucleotide sequences of CP coding regions of TEV and sequences retrieved from databanks were compared with Turkish isolates. MEGA version 6.06 software (Tamura et al., 2013) was used to select appropriate nucleotide substitution model with MODELTEST (Posada and Crandall, 1998). Neighbor joining, maximum likelihood and maximum parsimony methods were used to estimate nucleotide diversity and phylogenetic construction and evaluation with 1000 bootstrap resampling.

Biological characterization of TEV pathotypes, inoculation and screening improved pepper lines

Selected two different TEV isolates in relation to their geographical origin (774 from Hatay and 1002 from Gaziantep) and corresponding to phylogenetic tree (*Fig. 2*) were mechanically inoculated on the pepper genotypes possessing *pvr2* alleles Yolo Wonder (YW), Yolo Y (YY), Florida VR2 (VR2) and W4. YW genotypes. YY, VR2 and W4

http://www.aloki.hu ● ISSN 1589 1623 (Print) ● ISSN 1785 0037 (Online)
DOI: http://dx.doi.org/10.15666/aeer/1706_1464114651

are homozygous for the *pvr2*$^{+}$, *pvr2*^{1}, *pvr2*^{2} and *Pvr4* resistance genes, respectively. Isolate 774 was selected as viral material because of its resistance breaking ability over *pvr2*^{2} allele from Florida VR2 confers resistance to TEV isolates (Caranta et al., 1997). Isolate 1002 is not be able to overcome *pvr2*^{2} allele. Two TEV isolates were multiplied on Nicotiana to obtain high titer inoculum for tests on *C. annuum*. Nicotiana leaves showing severe symptoms of the TEV were weighed as 1 g and homogenized in 4 ml of 0.03 M phosphate buffer (pH 7.0) supplemented with 2% (wt/vol) diethyldithiocarbamate, active charcoal at 20 mg/ml, and Carborundum at 20 mg/ml. Inoculum multiplied on tobacco plants were inoculated on the two cotyledons of 15 seedlings from each pepper genotype. *C. annuum* test plants were inoculated manually at cotyledon leaf stage with same as well as in tobacco plants. Symptoms were recorded between 14 and 30 days postinoculation (dpi) and genotypes without symptoms were re-inoculated by two isolates 1002 and 774. Virus multiplication in the pepper genotypes were assessed by DAS-ELISA after one month post-inoculation (Moury et al., 2004). Genotypes were considered as positive and susceptible when their absorbance values at 405 nm was higher than three times that of negative control (Murphy et al., 1998).

Results and discussion

Distribution of tobacco etch virus in main pepper cultivation areas in Turkey

DAS-ELISA and two-steps reverse transcription polymerase chain reactions (RT-PCRs) were used to assess Tobacco etch virus both open field and protected pepper cultivation areas in Turkey (*Fig. 1*). Total 1525 fruit and/or leaf samples from different provinces of Turkey were tested. Tobacco etch virus was most prevalent in Bursa and Çanakkale provinces in open field pepper cultivation areas. According to ELISA signals TEV did not spread through Balıkesir, İzmir and Şanlıurfa provinces. But RT-PCR results indicated that TEV was also prevalent in these provinces. Assessing both ELISA and RT-PCR results TEV was widespread all the pepper cultivation areas both open field and protected (*Table 1*). In Mediterranean Basin TEV was only presence in Turkey (Moury and Verdin, 2012). Americas, Africa and Asia especially China also were infected with TEV (Green and Kim, 1991). Some of the pepper cultivation areas with local varieties nearly whole of the field infected with TEV in Çanakkale province located western side of the Turkey. Benner et al. (1985) and Abdalla et al. (1991) indicated that the incidence of the TEV can be reach nearing %100.

Genetic diversity of tobacco etch virus

The phylogenetic tree of the CP coding region displayed that the Turkey was clustered three subgroups. Isolate 1002 from Gaziantep province and 774 from Hatay were distinct (0.025 p distance) from each other based on their CP (coat protein) sequences (*Fig. 2*). This distinction was sourced from threonine to alanine substitutions on 57th position on CP region (T57A). Two haplotypes were defined according to the amino acid sequence of the CP corresponding to isolate 1002 (KR024266.1) and 774. Other distinction based on amino acid substitutions were originated by A49S (isolate 1496), N6S (isolate 851), and S1T (isolate 861) among the Turkish isolates. Clustering of other Turkish isolates was based on synonymous substitutions of nucleotides. All of the survey area only isolates of Hatay (774 to 1506) could be sequenced. Single amino

http://www.aloki.hu ● ISSN 1589 1623 (Print) ● ISSN 1785 0037 (Online)
DOI: http://dx.doi.org/10.15666/aeer/1706_1464114651

acid substitution of CMV-CP (Cucumber mosaic virus-Coat Protein) induced chlorosis on tobacco (Shintaku, 1991; Shintaku et al., 1992). Mochizuki et al. (2008) reported that substitution of the amino acid in the coat protein of Melon necrotic spot virus preventing from transmitting by *Olpidium bornovanus* zoospores. Dolja et al. (1994) indicated that mutation of CP of TEV affects movement of the virus in the plant.

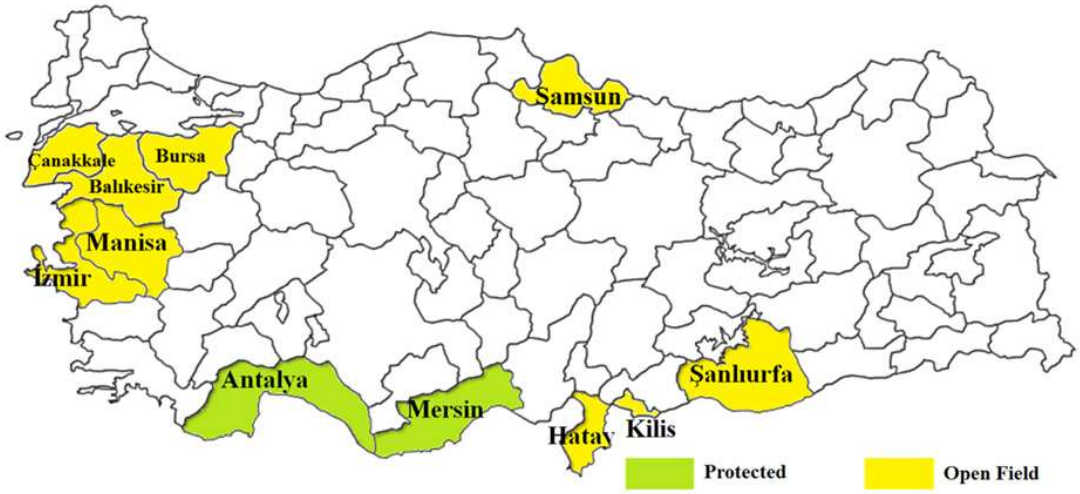

Figure 1. *Survey area of tobacco etch virus isolates on open and protected cultivation field in Turkey*

The TEV virus infections in surveyed regions are widespread through Turkey in main pepper grown fields. They are built a distinct phyletic group from the other isolates in the World related with CP regions. This group is clustered to three subgroups because of amino acid substitution. TEV was presence in only Turkey among the Mediterranean countries (Moury and Verdin, 2012). Americas (USA, Canada, El Salvador, Puerto Rico, Jamaica, Mexico) Africa (Nigeria) and Asia especially China also were infected with TEV (Olawale et al., 2015; Ariyaratne et al., 1996; Green and Kim, 1991). The nucletide sequences of isolates from these countries except Nigeria have been registered in GenBank. Potato virus Y (PVY) is widespread in the World, while TEV isolates occur mainly in North and Central America and in the Caribbean (Caranta and Palloix, 1996). Bootstrap values associated to the branches of the tree supported the existence of three major clades (*Fig. 1*). The first clade includes TEV isolates from Turkey and SD1 isolate AY787757 from China. The second one includes Chinese, Jamaican and Mexian TEV isolates. Several Chinese and Jamaican isolates grouped in same cluster but also they built distant clades. Complete sequences of the TEV isolates (MK688996, MK688997 and MK680813) from Trinidad and Tobago have been recorded recently. These isolates clustered more distantly from Turkish isolates in the third clade. However the closest isolate to Turkish ones from the world was SD1 registered as AY787757 from China (*Fig. 2*).

Virulence properties TEV isolates against resistance sources and improved pepper lines

Two isolates (774 and 1002) clustered different group both molecular related their CP region and geographic origin were evaluated against improved pepper lines and

http://www.aloki.hu ● ISSN 1589 1623 (Print) ● ISSN 1785 0037 (Online)
DOI: http://dx.doi.org/10.15666/aeer/1706_1464114651

homozygous reference pepper genotypes for the *Pvr4*, *pvr2*^{1}, *pvr2*^{2} and *pvr2*$^{+}$ genes (or alleles) (*Fig. 3*). On the basis of ELISA results assessed one month post-inoculation on apical leaves, both TEV isolates multiplied in and infected to susceptible Yolo Wonder carrying *pvr2*$^{+}$ Yolo Y; *pvr2*^{1} and W4; *Pvr4* and many of the improved lines selected as resistant. Florida VR2 carrying *pvr2*^{2} alleles resisted to isolate 1002 but infected by isolate 774. Improved lines 62 and 63 also resisted to isolate 1002 but resistance failed by inoculation of isolate 774 except two plants of line 63 (*Table 2*). Only one improved line 4, showed resistance to both isolates. *pvr2*^{2} contributes resistance to TEV but virulent strains are overcome resistance *pvr2* alleles providing restriction of cell-to-cell movement or inhibition of viral coat protein accumulation (Pallard et al., 2002). *Pvr4* did not provide any resistance against TEV (Janzac et al., 2009).

Table 2. *Numbers of resistant and susceptible individuals of improved lines and genotypes carrying pvr alleles to tobacco etch virus infections determined by DAS-ELISA*

Improved Lines and genotypes carrying pvr alleles	TEV isolate 1002		TEV isolate 774	
	R	S	R	S
3	0	15	0	15
4	15	0	15	0
6	0	15	0	15
8	0	15	0	15
11	0	15	0	15
23	0	15	0	15
25	0	15	0	15
27	0	15	0	15
54	0	15	0	15
61	0	15	0	15
62	15	0	0	15
63	15	0	2	14
64	0	15	0	15
69	0	15	0	15
W4 (*Pvr 4*)	0	15	0	15
Florida VR2 (*pvr2*^{2})	15	0	0	15
Yolo Y (*pvr2*^{1})	0	15	0	15
Yolo Wonder (*pvr2*$^{+}$)	0	15	0	15

Related with resistance provided by the *Pvr4* dominant gene to potyviruses is not effective to prevent TEV (Janzac et al., 2009; Moury and Verdin, 2012). CM334 originated *Pvr4* and *pvr2*^{3} resistance also is not effective for TEV (Janzac et al., 2009). Line 4 was improved from CM334 and Perennial which was carrying recessive alleles *pvr2*^{3} and *pvr6* (Caranta et al., 1997) expressing resistance to TEV. Caranta and Palloix (1996) reported that resistance to several potyviruses can be controlled by recessive alleles and/or by a dominant allele from Criollo de Morelos 334 and by polygenic resistance in Perennial. In this study Line 4 which has been improved as resistant to both 1002 and 774 TEV isolates probably has *pvr2*^{3} alleles from CM334 and *pvr6* Perennial along with some QTL (Quantitative trait loci).

http://www.aloki.hu ● ISSN 1589 1623 (Print) ● ISSN 1785 0037 (Online)
DOI: http://dx.doi.org/10.15666/aeer/1706_1464114651

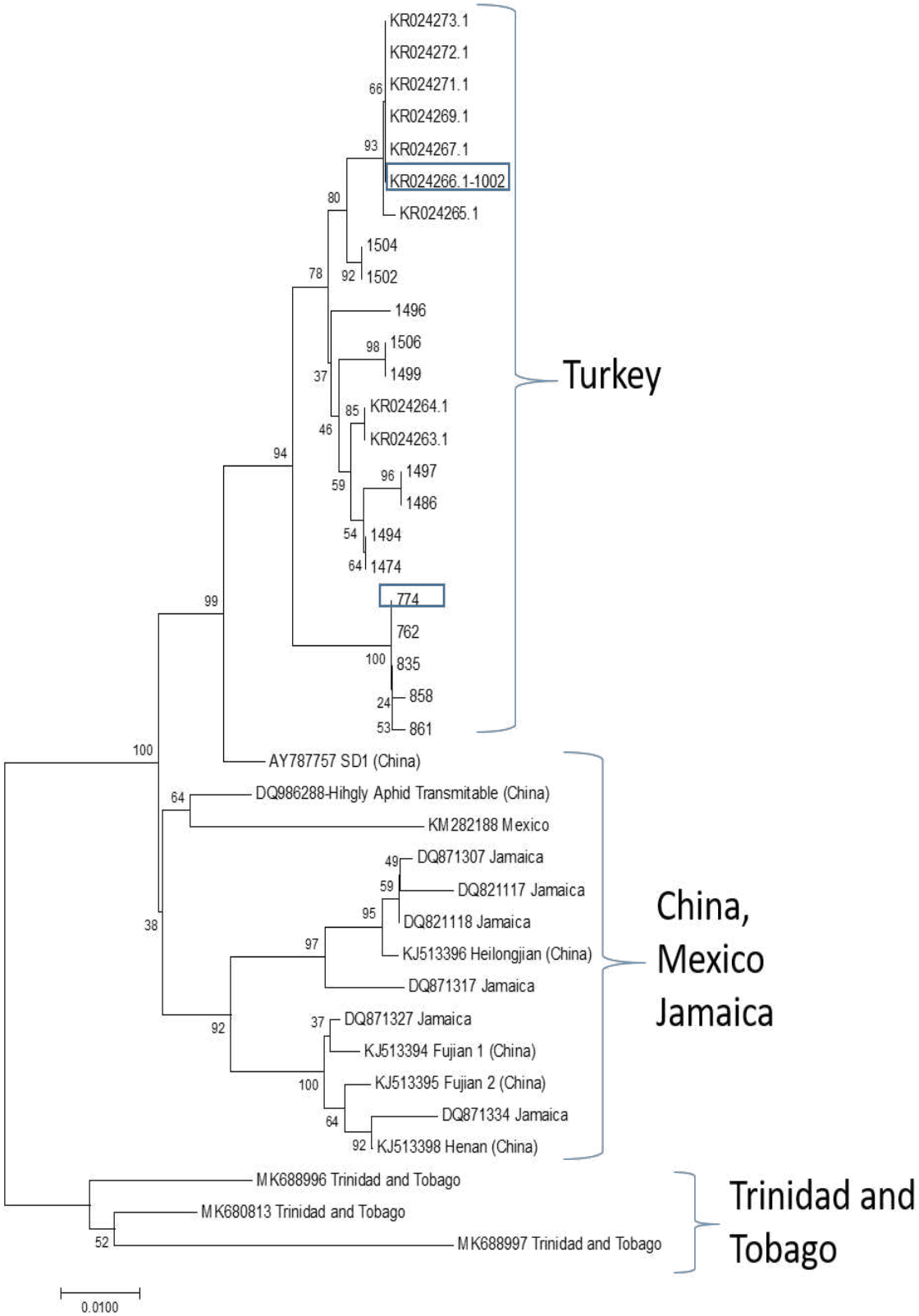

Figure 2. *Phylogenetic tree of Turkish Tobacco etch virus (TEV) isolates and registered nucleotides in NCBI corresponding to 687 nucleotides of the CP coding region with 1000 bootstrap replicates. Isolates 1002 and 774 in the frame were used to determine resistance of the improved lines*

http://www.aloki.hu ● ISSN 1589 1623 (Print) ● ISSN 1785 0037 (Online)
DOI: http://dx.doi.org/10.15666/aeer/1706_1464114651

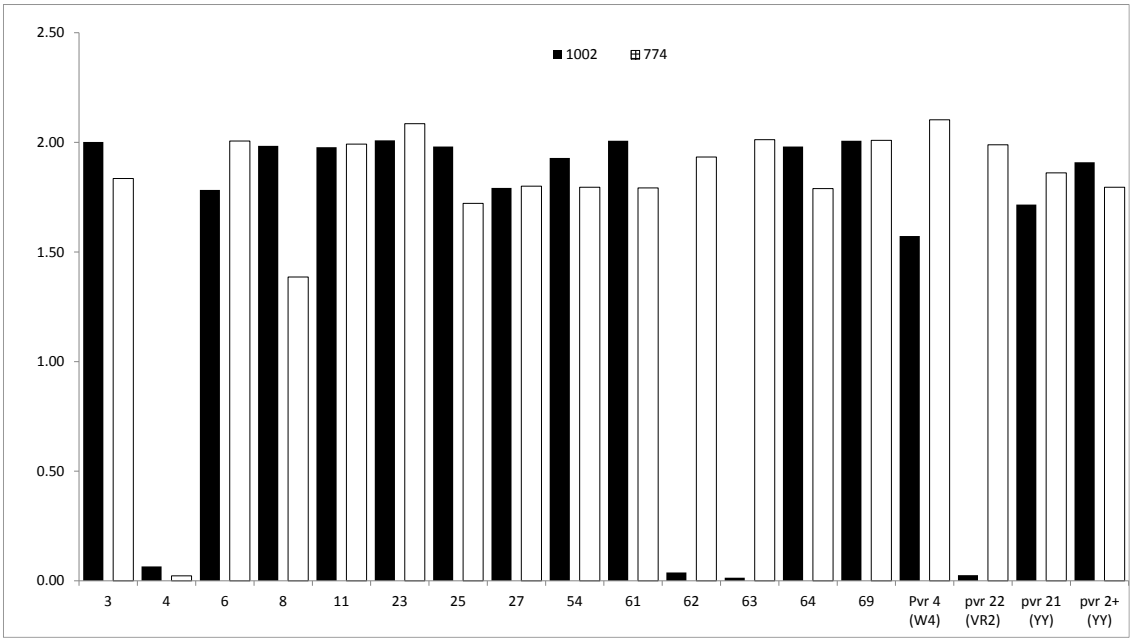

Figure 3. *ELISA optical density absorbance at 405 nm of improved lines to 1002 and 774 isolates one month post inoculation*

pvr2^2 and *pvr6* allele combinations were identified as providing resistance source to another potyvirus PVMV (Rubio et al., 2009). Systemic infection of TEV isolate 774 breaking down *pvr2*^{2}-mediated resistance could be prevented by the combination between *pvr2*^{3} and *pvr6* alleles. Lines possessing the *pvr2*^{2} and *pvr6* genes resist to systemic infection by PVMV or ChiVMV potyviruses (Moury et al., 2005). Because of the lack of resistance ability of the *pvr2*^{2} allele against isolate 774 it is suggested that TEV resistance resulted from complementary effects between recessive alleles transferred both resistant and susceptible parents. With respect to the pepper-TEV interaction, not much more alleles were characterized that confer complete resistance to TEV while eleven chromosomal regions were found to be associated with quantitative resistance to PVY (Caranta et al., 1997). Also heterozygoty of *pvr2* alleles has been found to increase resistance efficiency against potyviruses (Moury et al., 2005; Rubio et al., 2009). Kang et al. (2005) demonstrated that TEV (both highly transmitted by aphids and non wilting isolates) infectivity could be blocked by wild-type eIF4E in *pvr1* (234) and *pvr1*^{2}. Murphy et al. (1998) indicated that *pvr1* does not confer resistance to Mex21 TEV isolate. Finally, pathogenic processes of TEV and potyviral resistance interactions determine resistance of improved lines.

Conclusion

Viral pathogens threaten to crop production world wide as a consequence of the evolution of viral genomes to overcome resistance genes in plants and to adapt vector organisms causing epidemics. In the last decade resistance breaking Tomato spotted wilt virus isolates have overcome *Tsw* (Tentchev et al., 2011), a local strain of Paprika mild mottle virus have broken *L3* mediated resistance (Luria et al., 2018) and poleroviruses exclusively transmitted by aphid have adapt to whiteflies (*Bemisia tabaci*)

http://www.aloki.hu ● ISSN 1589 1623 (Print) ● ISSN 1785 0037 (Online)
DOI: http://dx.doi.org/10.15666/aeer/1706_1464114651

as a vector (Ghosh et al., 2019) and Zucchini yellow mosaic virus has appeared in peppers (Verma et al., 2019).

Potyviruses is in the top ten list of plant viruses (Rybicki, 2015) and pepper (*Capsicum annuum* L.) affected by five major potyviruses including tobacco etch virus which has resistant breaking abilities on both many recessive *pvr* alleles and dominant *Pvr* genes. Conclusively, our results further emphasize the threat to pepper breeders and growers around the world especially in Turkey that evolvement of virulent TEV isolates and the possibility of combining recessive alleles will be able to provide resistance to infection of tobacco etch virus. The mechanisms of multigenic resistance can be explored further and combination of resistance alleles against TEV need to be searched by associating host pathogen interactions.

Acknowledgements. This project was supported by General Directorate of Agricultural Research and Policies with TAGEM/13/ARGE/21 project number. Thanks to anonymous reviewers for their constructive comments.

REFERENCES

[1] Abdalla, O. A., Desjardins, P. R., Dodds, J. A. (1991): Identification, disease incidence, and distribution of viruses infecting peppers in California. – Plant Disease 75(10): 1019-1023.

[2] Ariyaratne, I., Hobbs, H. A., Valverde, R. A., Black, L. L., Dufresne, D. J. (1996): Resistance of Capsicum spp. – genotypes to tobacco etch potyvirus isolates from the Western Hemisphere Plant Dis. 80: 1257-1261.

[3] Ben Khalifa, M., Simon, V., Marrakchi, M., Fakhfakh, H., Moury, B. (2009): Contribution of host plant resistance and geographic distance to the structure of Potato virus Y (PVY) populations in pepper in northern Tunisia. – Plant Pathology 58(4): 763-772.

[4] Benner, C. P., Kuhn, C. W., Demski, J. W., Dobson, J. W., Colditz, P., Nutter Jr. F. W. (1985): Identification and incidence of pepper viruses in northeastern Georgia. – Plant Disease (USA) 69: 999-1001.

[5] Buzkan, N., Arpacı, B. B., Görsoy, G., Zencirkıran, M., Moury, B. (2015): Genetic variability of Potato virus Y (PVY) and Tobacco etch virus (TEV) from naturally infected pepper fields in the Hatay region of Turkey. – Archives of Phytopathology and Plant Protection 48(7): 588-600.

[6] Caranta, C., Palloix, A. (1996): Both common and specific genetic factors are involved in polygenic resistance of pepper to several potyviruses. – Theoretical and Applied Genetics 92(1): 15-20.

[7] Caranta, C., Lefebvre, V., Palloix, A. (1997): Polygenic resistance of pepper to potyviruses consists of a combination of isolate-specific and broad-spectrum quantitative trait loci. – Molecular plant-microbe interactions 10(7): 872-878.

[8] d'Urso, F., Sambade, A., Moya, A., Guerri, J., Moreno, P. (2003): Variation of haplotype distributions of two genomic regions of Citrus tristeza virus populations from eastern Spain. – Molecular Ecology 12(2): 517-526.

[9] Dolja, V. V., Haldeman, R., Robertson, N. L., Dougherty, W. G., Carrington, J. C. (1994): Distinct functions of capsid protein in assembly and movement of tobacco etch potyvirus in plants. – The EMBO Journal 13(6): 1482-1491.

[10] Florini, D. A., Zitter, T. A. (1986): Cucumber mosaic-virus (CMV) in peppers (Capsicum-annuum-l) in New-York, and associated yield losses. – Phytopathology 76(6): 652-652.

http://www.aloki.hu ● ISSN 1589 1623 (Print) ● ISSN 1785 0037 (Online)
DOI: http://dx.doi.org/10.15666/aeer/1706_1464114651

[11] Ghosh, S., Kanakala, S., Lebedev, G., Kontsedalov, S., Silverman, D., Alon, T., Mor, N., Sela, N., Luria, N., Dombrovsky, A., Mawassi, M., Haviv, S., Czosnek, H., Ghanima, M. (2019): Transmission of a new polerovirus infecting pepper by the whitefly Bemisia tabaci. – Journal of Virology JVI-00488. DOI: 10.1128/JVI.00488-19.
[12] Green, S. K., Kim, J. S. (1991): Characteristics and Control of Viruses Infecting Peppers: A Literature Review. – In: Technical Bulletin 18. Asian Vegetable Research and Development Center, Taipei.
[13] Janzac, B., Fabre, M. F., Palloix, A., Moury, B. (2008): Characterization of a new potyvirus infecting pepper crops in Ecuador. – Archives of Virology 153(8): 1543.
[14] Janzac, B., Fabre, M. F., Palloix, A., Moury, B. (2009): Phenotype and spectrum of action of the Pvr4 resistance in pepper against potyviruses, and selection for virulent variants. – Plant Pathology 58(3): 443-449.
[15] Kim, S. B., Kang, W. H., Huy, H. N., Yeom, S. I., An, J. T., Kim, S., Kang, M. Y., Kim, H. J., Jo, H. D., Ha, Y., Choi, D., Kang, B. C. (2017): Divergent evolution of multiple virus-resistance genes from a progenitor in Capsicum spp. – New Phytologist 213(2): 886-899.
[16] Kyle, M. M., Palloix, A. (1997): Proposed revision of nomenclature for potyvirusresistance genes in Capsicum. – Euphytica 97(2): 183-188.
[17] Luria, N., Smith, E., Sela, N., Lachman, O., Bekelman, I., Koren, A., Dombrovsky, A. (2018): A local strain of Paprika mild mottle virus breaks L 3 resistance in peppers and is accelerated in Tomato brown rugose fruit virus-infected Tm-2 2-resistant tomatoes. – Virus Genes 54(2): 280-289.
[18] Mochizuki, T., Ohnishi, J., Ohki, T., Kanda, A., Tsuda, S. (2008): Amino acid substitution in the coat protein of Melon necrotic spot virus causes loss of binding to the surface of Olpidium bornovanus zoospores. – Journal of General Plant Pathology 74(2): 176-181.
[19] Moury, B., Verdin, E. (2012): Viruses of Pepper Crops in the Mediterranean Basin: A Remarkable Stasis. – In Series: Advances in Virus Research (Vol. 84). Academic Press, Amsterdam, pp. 127-162.
[20] Moury, B., Morel, C., Johansen, E., Guilbaud, L., Souche, S., Ayme, V., Caranta, C., Palloix, A., Jacquemond, M. (2004): Mutations in Potato virus Y genome-linked protein determine virulence toward recessive resistances in Capsicum annuum and Lycopersicon hirsutum. – Molecular Plant-Microbe Interactions 17(3): 322-329.
[21] Moury, B., Palloix, A., Caranta, C., Gognalons, P., Souche, S., Selassie, K. G., Marchoux, G. (2005): Serological, molecular, and pathotype diversity of Pepper veinal mottle virus and Chili veinal mottle virus. – Phytopathology 95(3): 227-232.
[22] Murphy, J. F., Blauth, J. R., Livingstone, K. D., Lackney, V. K., Jahn, M. K. (1998): Genetic mapping of the pvr1 locus in Capsicum spp. and evidence that distinct potyvirus resistance loci control responses that differ at the whole plant and cellular levels. – Molecular Plant-Microbe Interactions 11(10): 943-951.
[23] Nutter Jr. F. W., Kuhn, C. W., All, J. N. (1989): Models to estimate yield losses in bell pepper caused by tobacco etch virus epidemics. – Phytopathology 79z: 1213.
[24] Olawale, A., Samuel, B. O., Solomon, A. S. O., Kumar, P. L. (2015): Surveys of virus diseases on pepper (Capsicum spp.) in South-west Nigeria. – African Journal of Biotechnology 14(48): 3198-3205.
[25] Padgett, G. B., Nutter Jr. F. W., Kuhn, C. W., All, J. N. (1990): Quantification of disease resistance that reduces the rate of tobacco etch virus epidemics in bell pepper. – Phytopathology 80(5): 451-455.
[26] Parrella, G., Ruffel, S., Moretti, A., Morel, C., Palloix, A., Caranta, C. (2002): Recessive resistance genes against potyviruses are localized in colinear genomic regions of the tomato (Lycopersicon spp.) and pepper (Capsicum spp.) genomes. – Theoretical and Applied Genetics 105(6-7): 855-861.

http://www.aloki.hu ● ISSN 1589 1623 (Print) ● ISSN 1785 0037 (Online)
DOI: http://dx.doi.org/10.15666/aeer/1706_1464114651

[27] Posada, D., Crandall, K. A. (1998): Modeltest: testing the model of DNA substitution. – Bioinformatics (Oxford, England): 14(9): 817-818.
[28] Rubio, M., Nicolaï, M., Caranta, C., Palloix, A. (2009): Allele mining in the pepper gene pool provided new complementation effects between pvr2-eIF4E and pvr6-eIF (iso) 4E alleles for resistance to pepper veinal mottle virus. – Journal of General Virology 90(11): 2808-2814.
[29] Rybicki, E. P. (2015): A Top Ten list for economically important plant viruses. – Archives of Virology 160(1): 17-20.
[30] Shintaku, M. (1991): Coat protein gene sequences of two cucumber mosaic virus strains reveal a single amino acid change correlating with chlorosis induction. – Journal of General Virology 72(10): 2587-2589.
[31] Shintaku, M. H., Zhang, L., Palukaitis, P. (1992): A single amino acid substitution in the coat protein of cucumber mosaic virus induces chlorosis in tobacco. – The Plant Cell 4(7): 751-757.
[32] Tamura, K., Stecher, G., Peterson, D., Filipski, A., Kumar, S. (2013): MEGA6: molecular evolutionary genetics analysis version 6.0. – Molecular Biology and Evolution 30(12): 2725-2729.
[33] Tentchev, D., Verdin, E., Marchal, C., Jacquet, M., Aguilar, J. M., Moury, B. (2011): Evolution and structure of Tomato spotted wilt virus populations: evidence of extensive reassortment and insights into emergence processes. – Journal of General Virology 92(4): 961-973.
[34] Thompson, J. D., Higgins, D. G., Gibson, T. J. (1994): CLUSTAL W: improving the sensitivity of progressive multiple sequence alignment through sequence weighting, position-specific gap penalties and weight matrix choice. – Nucleic Acids Research 22(22): 4673-4680.
[35] Venkatesh, J., An, J., Kang, W. H., Jahn, M., Kang, B. C. (2017): Fine mapping of the dominant potyvirus resistance gene Pvr7 reveals a relationship with Pvr4 in Capsicum annuum. – Phytopathology 108(1): 142-148.
[36] Verma, R., Tripathi, S., Gorane, A. T., Naik, A. A., Nikam, T. D., Ade, A. A., Mahapatro, G. K. (2019): First report of zucchini yellow mosaic virus in bell pepper, Capsicum annum L., in India. – Plant Disease. https://doi.org/10.1094/PDIS-04-19-0740-PDN.

http://www.aloki.hu ● ISSN 1589 1623 (Print) ● ISSN 1785 0037 (Online)
DOI: http://dx.doi.org/10.15666/aeer/1706_1464114651

INTRA- AND INTERSPECIFIC RECOMBINATION IN THE NATURAL CONDITION OF PEPPER VEIN YELLOWS VIRUS AND RESPONSE OF *PVR* ALLELES IN PEPPER

ARPACI, B. B.

Department of Horticulture, Faculty of Agriculture, University of Kilis 7 Aralik, 79100 Kilis, Turkey
(e-mail: bbarpaci@kilis.edu.tr; phone: +90-348-814-2666; fax: +90-348-814-2667)

(Received 9th Jun 2019; accepted 10th Sep 2019)

Abstract. Since their first observing in Japan, poleroviruses have threatened pepper cultivation all around the World. Symptoms of vein yellowing originating from poleroviruses have become widespread in both open field and protected pepper cultivation areas recently. In this work samples collected from highly infected pepper fields in South East Turkey have been determined as Pepper Vein Yellows Virus (PVYV) and Beet Western Yellows Virus (BWYV) (genus *Polerovirus*, family *Luteoviridae*). Recombinant PVYV isolates have been observed from intra and interspecific combination in relation to part of the RNA-dependent RNA polymerase coding region subjected to recombination detection methods. One of the PVYV isolates has induced recombination between BWYV and PVYV and located middle of the PVYV and BWYV isolates. Another isolate recombined from intraspecific combination has been transferred onto pepper genotypes carrying pvr alleles and landraces under both artificial and natural conditions to determine their response. None of the pvr alleles in pepper genotypes used in this study could contribute to resistance to PVYV isolates.
Keywords: *poleroviruses, capsicum, resistance, Luteoviridae, genetic diversity*

Introduction

Pepper crops are exposed to many pests and diseases because of their wide geographical distribution and cultivation areas. Mono-cultivation of pepper intensively along with climate changes increase the vector and virus infection in Mediterranean Basin. Capsicum spp. is exposed to over 70 viruses and pepper production is limited by more than 20 important plant viruses (Florini and Zitter, 1986; Green and Kim, 1991; Moury and Verdin, 2012). The new viruse causing interveinal yellowing symptoms was recently sequenced and identified by Murakami et al. (2011) as Pepper vein yellowing virus (PeVYV). Denomination and identification starts in Japan with Pepper vein yellows virus (PeVYV) (Yonaha et al., 1995) and continue Pepper yellow leaf curl virus (PYLCV) in Israel (Dombrovsky et al., 2010), Pepper vein yellowing virus (PeVYV) in Japan (Murakami et al., 2011), Pepper vein yellows virus (PVYV) in Turkey and Tunisia (Buzkan et al., 2013) and Pepper Yellows Disease (PYD) in Greece (Lotos et al., 2017). Regardless of nomenclature many researcher reported causing yellowing symptoms in pepper having similar genome organization in Spain (Villanueva et al., 2013), India, Indonesia, Mali, Philippines, Thailand and Taiwan (Knierim et al., 2013), Sudan (Alfaro-Fernández et al., 2014), China (Tan et al., 2015), Australia (Maina et al., 2016) and Saudi Arabia (Kamran et al., 2017).

Poleroviruses belonging *Luteoviridae* have icosahedral virions in 26–30 nm diameter including about 6.2 kb positive-sense single-stranded RNA without envelope (Kenyon et al., 2014). *Luteoviridae* family tends to recombination related their nucleotide substitution of coat protein region (Pagán and Holmes, 2010). Recombination and mutation are main factor to generate genetic variability for the

http://www.aloki.hu ● ISSN 1589 1623 (Print) ● ISSN 1785 0037 (Online)
DOI: http://dx.doi.org/10.15666/aeer/1706_1465314664

viruses (Desbiez et al., 2011). Buzkan et al. (2013) emphasized the recombinant nature of PVYV compared different countries related their RNA-dependent RNA polymerase region. Fiallo-Olivé et al. (2018) confirmed recombinant structure of PVYV by phylogenetic analysis of full length genome and classified the virus from PeVYV-1 to PeVYV-5 related their genome organization.

Breeding sweet and large-fruited blocky-type peppers has been limited because of undesirable traits exist among wild accessions. Wild accessions of *Capsicum annuum* species differ in many yield and quality characters comprising cultivated varieties (Ben-Chaim and Paran, 2000). Disease resistance genes from wild accessions have been transferred by many researchers into sweet blocky types (Lefebvre et al., 1995; Daubeze et al., 1995; Caranta et al., 1997; Lapidot et al., 1997; Paran et al., 1998).

In this study the recombination events of PVYV isolates were determined from one location highly infected by poleroviruses. Both PVYV and BWYV (Beet western yellows virus) were determined in the same location and recombination evidence was calculated intra- and interspecific combination. Response of local pepper landraces, varieties and genotypes possessing *pvr* alleles to PVYV were also determined.

Materials and methods

Plant material

Pepper genotypes including different genotypes and varieties were used to test resistance against PVYV in natural and artificial aphid transmission conditions. PVYV isolate 24 were inoculated by aphid (*Myzus persicae*) transmission on the pepper plants carrying *pvr2* alleles in Yolo Wonder (YW), Yolo Y (YY), Florida VR2 (VR2) and W4. YY, VR2 and W4 are homozygous for the $pvr2^{+}$, $pvr2^{1}$, $pvr2^{2}$, and *Pvr4* resistance genes, respectively. Criollo de Morelos 334 was also used as control plants in the experiment. Şahinbey variety and eleven inbred line having blocky pod type were used for resistance experiment.

Virus detection

The presence of PVYV in leaf samples was determined both reverse transcription polymerase chain reaction (RT-PCR) and Double antibody sandwich enzyme-linked immunosorbent assay (DAS-ELISA) with cucurbit aphid-borne yellows virus (CABYV) antibodies which are strongly cross reacted poleroviruses (Buzkan et al., 2013). Total RNAs were extracted from symptomatic pepper leaf samples and aphids fed on leaves using TRI Reagent (Sigma) according to the instructions. RT-PCR method was carried out with Moloney murine leukemia virus (M-MuLV) reverse transcriptase and Taq DNA polymerase (Invitrogen).

Two-step reverse transcription polymerase chain reactions (RT-PCRs) were performed by using primers Pol-G-F (5′-GAYTGCTCYGGYTTYGACTGGAG-3′) and Pol-G-R (5′-GATYTTATAYTCATGGTAGGCCTTGAG-3′) designed by Knierim et al. (2010) from conserved regions from all poleroviruses. PCR conditions were at 60 °C for annealing temperature and 90 min for extension time. RT-PCR amplification products at 1.1-kb (RNA-dependent RNA polymerase coding region, the intergenic noncoding region and part of the coat protein coding region) were directly sequenced with primer Pol-G-F by MEDSANTEK (Istanbul, Turkey).

http://www.aloki.hu ● ISSN 1589 1623 (Print) ● ISSN 1785 0037 (Online)
DOI: http://dx.doi.org/10.15666/aeer/1706_1465314664

Recombination analysis

Aligned sequences by ClustalW program were implemented in the software MEGA 7 (Kumar et al., 2016) and confirmed Blastn program. Neighbor-joining, Tamura-Nei model was implemented with 500 bootstrap resampling to assess the robustness of branches (Saitou and Nei, 1987). Recombination events between sequences were predicted using RDP4 software and confirmed by boot scan analysis using SimPlot software (http://sray.med.som.jhmi.edu/SCRoftware) with the Kimura 2-parameter distance model (Lole et al., 1999).

PVYV isolates and inoculation

Thirty pepper plants showing inter-veinal yellowing and curling symptoms on leaves were collected diagonally in one highly infected field with poleroviruses (Bogazkirim, Dorucak/Musabeyli/Kilis/Turkey 36° 49' 49.9" N and 36° 51' 47.2" E) in Kilis province (southeastern Turkey) in August 2015 (*Fig. 1a, b* and *c*). The plants were numbered, potted and transferred from field to insect proof greenhouse. The PVYV isolates were detected as described at virus detection section by reverse transcription polymerase chain reaction (RT-PCR) and Double antibody sandwich enzyme-linked immunosorbent assay (DAS-ELISA) and isolate 24 determined as recombinant isolate was used as viral material.

Artificial inoculation

Aphids (*Myzus persicae*) collected from upper leaves of peach trees were propagated on sweet pepper (cv. Yolo Wonder) plants at the true leaf stage to use aphid transmission. Isolate 24 was used to determine response of pepper genotypes to PVYV. Aphids propagated on Yolo Wonder leaves were allowed a 48-h acquisition access feeding period on plant infected by isolate 24. Two aphids were transferred from infected plants to lower leaf surface of healthy ten pepper plants of each genotype at four-leaf stage for artificial inoculation. Plants were treated with the insecticide after inoculation access feeding of 48 h. PVYV could be transmitted efficiently by at least two aphid vectors *M. persicae* (Dombrovsky et al., 2010).

Transmission on greenhouse conditions

Artificially infected ten Yolo Wonder plants by isolate 24 were transplanted in greenhouse along with the genotypes which will have been tested. Fifteen plants of each genotype were transplanted at four true leaves stage between 70 and 50 cm spaces in rows. Twenty aphids were placed on each infected Yolo Wonder plants. Three months after planting PVYV were detected on genotypes both DAS-ELISA and RT-PCR. Isolate 24 was re-isolated from plants (*Fig. 1e*) and confirmed by sequencing (*Fig. 2a*).

Results and discussion

Because of the lack of specific antibodies to PVYV and presence of serological cross-reactions between these viruses, CABYV antibodies were used in DAS-ELISA (Buzkan et al., 2013). Twenty-nine of the collected plants strongly reacted to CABYV antibodies. Pol-G-F and Pol-G-R primers designed by Knierim et al. (2010) from conserved regions in the polerovirus genome were used and 1.1-kbp amplicons were

http://www.aloki.hu ● ISSN 1589 1623 (Print) ● ISSN 1785 0037 (Online)
DOI: http://dx.doi.org/10.15666/aeer/1706_1465314664

produced after two-step reverse transcription polymerase chain reactions. Fifteen of the twenty-nine samples reacted CABYV antibodies were shown similarity with PVYV and seven of the samples were identified as BWYV after using the Blastn program after aligned using the ClustalW software. Six of the RT-PCR products directly sequenced by Pol-G-F primer could not been identified because of low sequencing quality (*Table 1*). Aphids fed on pepper plants infected isolate 24 was also confirmed by RT-PCR and sequence analysis.

Table 1. *Total number of samples and number of isolates determined belonging polerovirus genus*

Number of samples cross-reacted CABYV antisera	Number of samples determined as PVYV	Number of samples determined as BWYV	Number of samples not detected any *Polerovirus*	Total number of samples
29	15	7	8	30

Figure 1. *Highly infected pepper plants by poleroviruses in open field condition in Kilis (a, b, c) Physalis spp. infected by PVYV at the border of the pepper cultivation area (d) Blocky type landrace of Kilis infected by recombinant PVYV isolate 24 in greenhouse (e) Aphid transmitted PVYV isolate 24 on Yolo Wonder pepper plant (f, g)*

http://www.aloki.hu ● ISSN 1589 1623 (Print) ● ISSN 1785 0037 (Online)
DOI: http://dx.doi.org/10.15666/aeer/1706_1465314664

Intergenic noncoding region and part of ORF3 (open read frame 3: the coat protein coding region) of sequences were trimmed and aligned by ClustalW (Thompson et al., 2003) and converted the file format to detect recombination events. Part of the RNA-dependent RNA polymerase coding region subjected to recombination detection methods by RDP4 software (Martin et al., 2015). Two of seven different methods implemented in the software RDP4 showed small recombination evidence ($P = 10^{-2}$ to 10^{-5}) in isolate 24 (*Fig. 2*). This recombination event would involve isolate 15 as a major parent while isolate 21 used to infer unknown parents (*Fig. 3*). Recombination event confirmed by SimPlot software (Lole et al., 1999) with the Kimura 2-parameter with 100 replicates (*Fig. 4*).

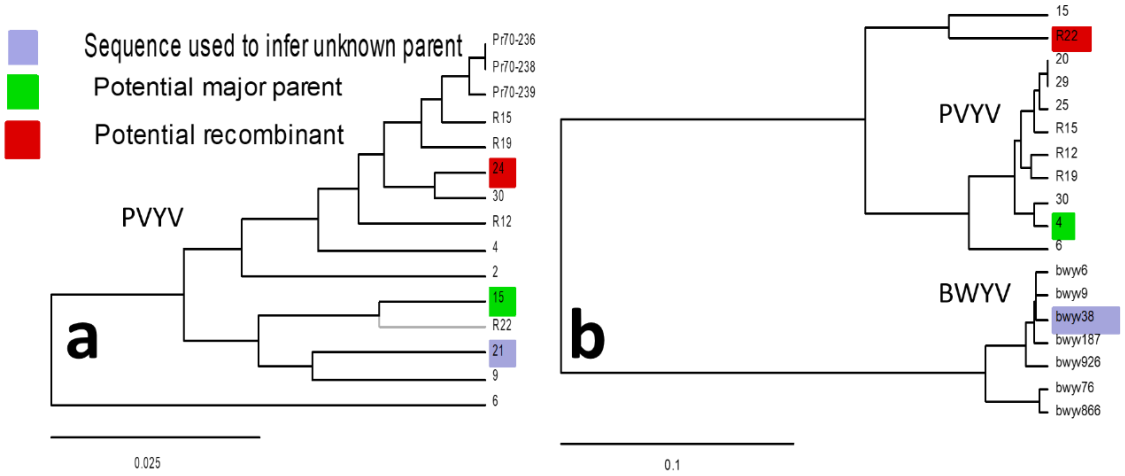

Figure 2. *Tree topology test for recombinant and parental isolates for PVYV isolates (a) and tree topology test for recombinant and parental isolates for both PVYV and BWYV (b)*

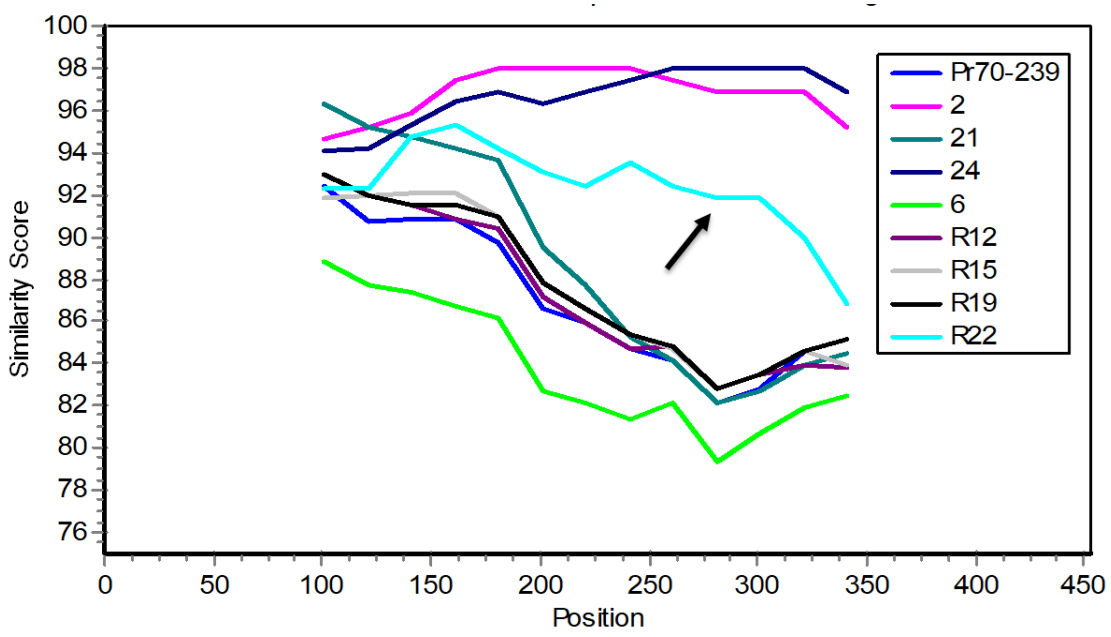

Figure 3. *Similarity plot diagram comparing the nucleotide sequence of PVYV isolate from one pepper cultivation field. Recombinant isolate R22 was indicated with arrow*

http://www.aloki.hu ● ISSN 1589 1623 (Print) ● ISSN 1785 0037 (Online)
DOI: http://dx.doi.org/10.15666/aeer/1706_1465314664

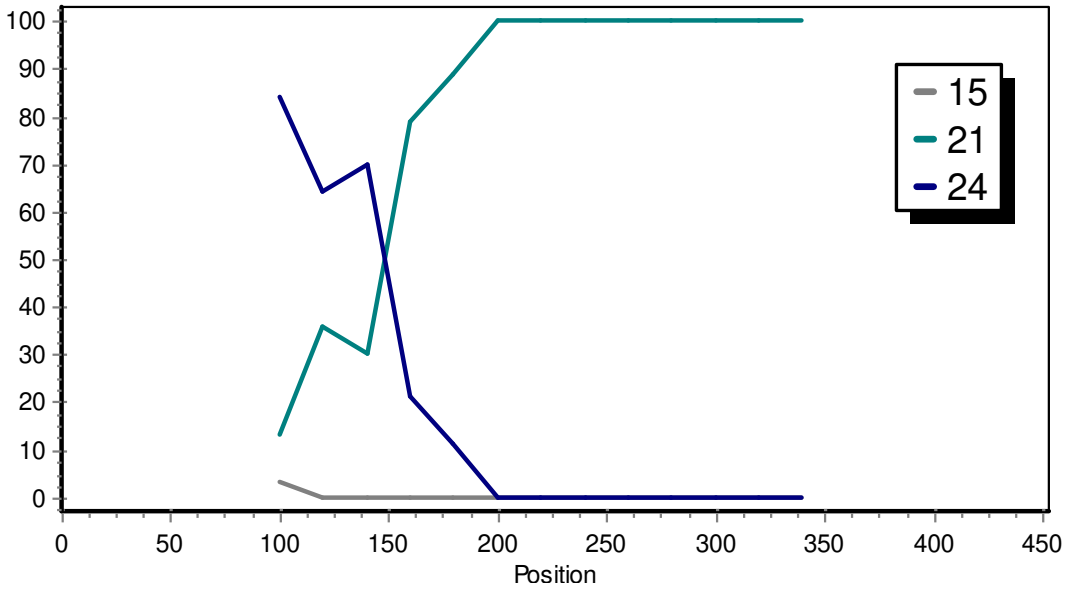

Figure 4. *Recombination position of the nucleotide sequence of parental isolates*

Recombination event was also detected between BWYV and PVYV. Recombination evidence was confirmed by GENECONV (1.292×10^{-2}) using RDP4 software (*Fig. 5*).

Isolate R22 was recombined by PVYV isolate 4 and BWYV isolate 38. Putative recombinant isolate 24 rooted different groups from their estimated parents isolate 15 and 21. PVYV isolates have shown between 79 and 98% similarity (*Figs. 2* and *3*) Neighbor-Joining phylogeny implemented in MEGA 7 using Tamura–Nei distance with 500 bootstrap re-samplings grouped BWYV and PVYV in different clades. Recombinant PVYV isolate R22 was placed between BWYV and PVYV in relation to part of the RNA-dependent RNA polymerase coding region (*Fig. 6*). Fiallo-Olivé et al. (2018) declared that PeVYV was a recombinant of CABYV and TVDV concerning with whole genome sequencing.

Buzkan et al. (2013) found a high prevalence of poleroviruses in open field pepper cultivation areas both Turkey and Tunisia. They showed an evidence PVYV-like isolate recombined from another region of Tunisia. Dombrovsky et al. (2010) hypothesized that PeVYV was a recombinant of Tobacco vein distorting virus (TVDV) while Fiallo-Olivé et al. (2018) were declared it as distinct from other poleroviruses. They proposed the name of the virus as Pepper vein yellows virus and classified from 1 to 5 corresponding to their complex genome organization due to recombination events. In this study, recombinant isolates corresponding C-terminal part of the RNA-dependent RNA polymerase were determined only one location pepper cultivation area widespread infected by poleroviruses (*Fig. 1*). Pagán and Holmes (2010) determined the occurrence of recombination within and between the RdRp and CP genes for each of the *Luteoviridae* species.

Pleiotropic effects of both viral and coat protein genome mutations have been observed on Capsicum. Pepper resistance genes and alleles whether dominant or recessive are efficient against several potyviruses. Sacchi et al. (2003) identified potyviruses in Brazil and improved resistant progenies to Potato Virus Y. Dominant *Pvr4* gene provides resistance to PepSMV (Pepper severe mosaic virus) and PTV (Peru tomato mosaic virus), but carrying genotypes this gene are susceptible to ChiVMV

http://www.aloki.hu ● ISSN 1589 1623 (Print) ● ISSN 1785 0037 (Online)
DOI: http://dx.doi.org/10.15666/aeer/1706_1465314664

(Chilli veinal mottle virus), PVMV (Pepper veinal mottle virus) and TEV (Tobacco etch virus) (Janzac et al., 2009). Recessive genes *pvr1* and *pvr2* in pepper have been observed for resistance to potyviruses including TEV but many virulent strains overcome most of these recessive genes (Parrella et al., 2002). Yolo Wonder ($pvr2^{+}$), Yolo Y ($pvr2^{1}$), Florida VR2 ($pvr2^{2}$) and W4 (*Pvr4*) did not resist to PVYV isolate 24 at greenhouse condition. CM334 originated *Pvr4* and $pvr2^{3}$ resistance also was not effective for PVYV both aphid transmission and under protected cultivation experiments. Şahinbey variety selected from blocky type pepper population in Gaziantep and other blocky type lines also did not resist to PVYV under both inoculation methods (*Table 2*).

PVYV transmitted by grafting and aphids persistent circulative manner not through seed or by mechanical inoculation (Yonaha et al., 1995) except mix infection with umbraviruses like as Potato leaf roll virus (Ryabov et al., 2001). Restriction of mechanical inoculation and absence of infectious clone of PVYV obstructs to determine response of pepper genotypes to the agent wide spreading Worldwide. The evolutionary period of the poleroviruses has been estimated as with in the last 4000 years. This evolutionary change is shorter than that proposed for the Potyviridae which is including species causing the most destructive diseases on plants (Pagán and Holmes, 2010).

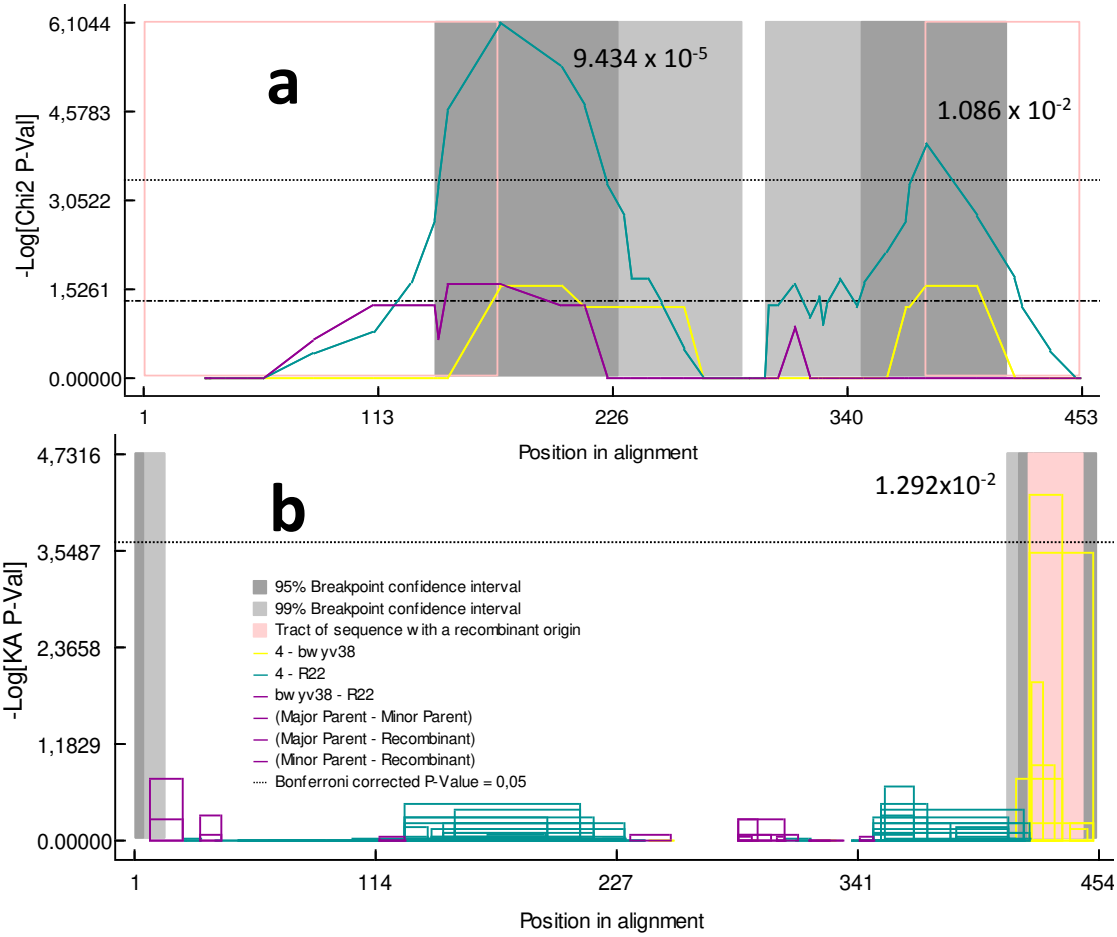

Figure 5. *The main putative recombination event of major parent: PVYV isolate 15 and minor parent: PVYV isolate 21 by MaxChi (9.434 x 10-5) for PVYV isolate 24 and 3Seq (1.086 x 10-2) (a) and PVYV isolate 4 and BWYV isolate 38 by GENECONV (1.292 x 10-2) for PVYV isolate R22*

http://www.aloki.hu ● ISSN 1589 1623 (Print) ● ISSN 1785 0037 (Online)
DOI: http://dx.doi.org/10.15666/aeer/1706_1465314664

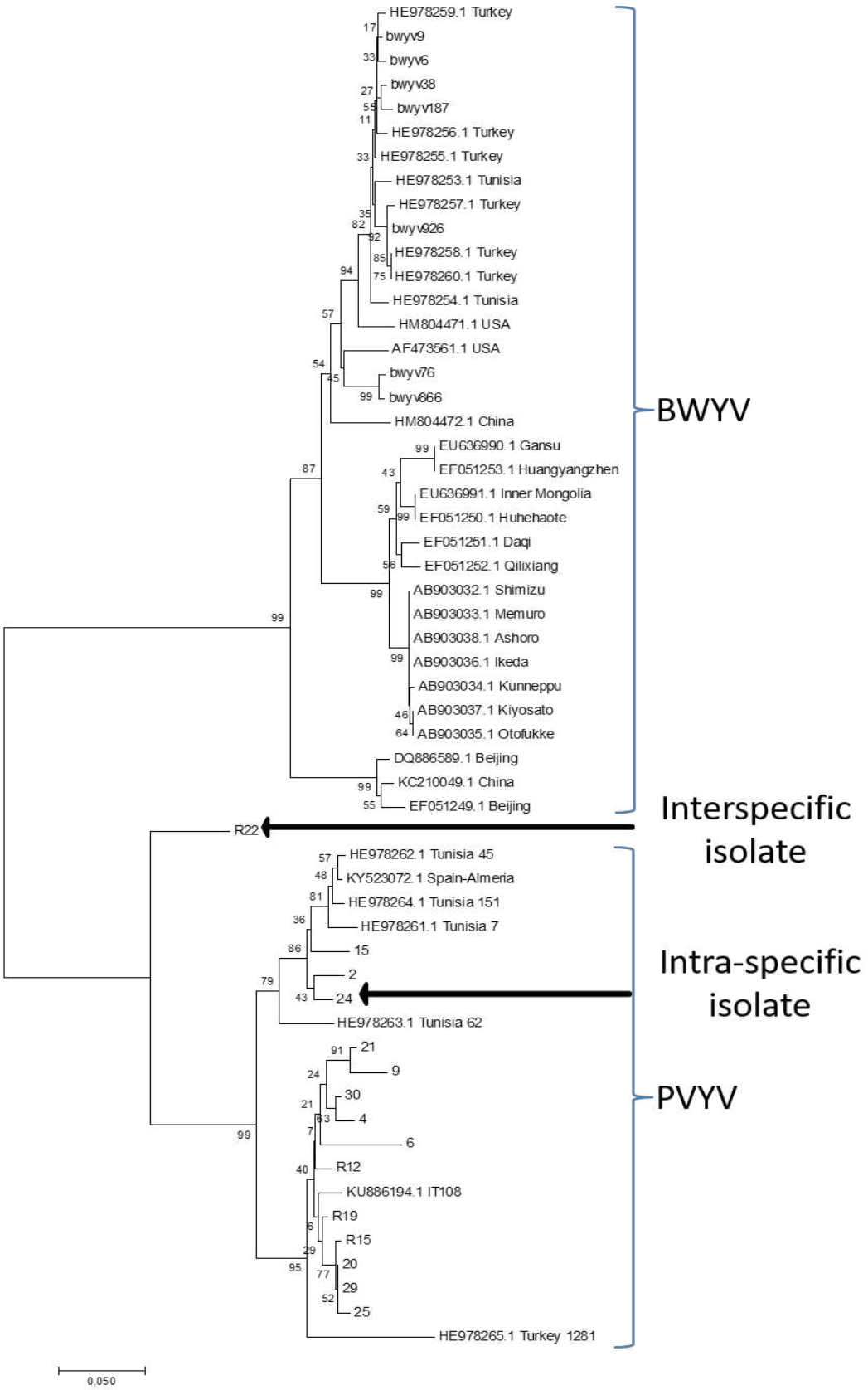

Figure 6. *Phylogenetic tree of PVYV and BWYV using the neighbor-joining method clustered together in the bootstrap test (500 replicates) conducted in MEGA7*

http://www.aloki.hu ● ISSN 1589 1623 (Print) ● ISSN 1785 0037 (Online)
DOI: http://dx.doi.org/10.15666/aeer/1706_1465314664

Table 2. *Response of the pepper genotypes to PVYV. (S: susceptible nt: not tested)*

Pepper genotype	Aphid transmission	Greenhouse conditions
Yolo Wonder (*pvr2*$^{+}$)	S	S
Yolo Y (*pvr2*^{1})	S	S
Florida VR2 (*pvr2*^{2})	nt	S
W4 (*Pvr4*)	nt	S
CM 334 (*Pvr4*$^{+}$ *pvr2*^{3})	S	S
Er Fu Tou	nt	S
Şahinbey	S	S
E01	S	S
E04	S	S
E07	S	S
E14	S	S
E17	S	nt
E26	S	S
E29	S	S
E32	S	S
E34	S	S
Y08	S	S
Y32	S	S

Gibbs et al. (2008) indicated that the evolution of potyvirus CP region has been occurred in the last 6,560 years. The high evolution rate of the Luteoviruses and Poleroviruses can be change their host selectiveness. As a matter of fact that Pepper vein yellows virus has been detected on *Physalis spp.* (*Fig. 1d*) a weed host in this study. Adnyani (2018) detected the PVYV on cucurbit plants in Bali. Ghosh et al. (2019) reported whitefly (Bemisia tabaci)-transmitted polerovirus known as exclusively transmitted by aphids, and named the new virus as Pepper whitefly-borne vein yellows virus (PeWBVYV) highly homologous to Pepper vein yellows virus.

Conclusion

Recently described poleroviruses Pepper vein yellows virus and Beet western yellows virus has been spreading on pepper cultivation areas in Turkey and other countries in the World. The isolates of the PVYV can be easily changing their genetic structure even restricted geographical region because of its high recombination ability. PVYV can be evolved both intra and interspecific recombination. Pvr alleles are not contributing any resistance to PVYV.

Because of appearance new vectors such as insect resistance whitefly for their transmission and reported new host range of PVYV along with their relative viruses will threaten both pepper and other crops cultivated in the world in the future. The epidemiology of PVYV and biological, serological and pathological properties of isolates should be investigated in next studies. The improvement of infectious clone can be enabled to determine response of pepper genotype to PVYV. The availability of infectious clones will facilitate investigation of resistance genes whether dominant or recessive in pepper and other crops.

http://www.aloki.hu ● ISSN 1589 1623 (Print) ● ISSN 1785 0037 (Online)
DOI: http://dx.doi.org/10.15666/aeer/1706_1465314664

Acknowledgements. This project was partly supported by Scientific Research Department of Kilis 7 Aralik University with 2013/1/MAP/04 project number. Thanks to anonymous reviewers for their constructive comments.

REFERENCES

[1] Adnyani, N. N. P. (2018): Deteksi Pepper vein yellows virus yang berasosiasi dengan penyakit yellow vein banding pada tanaman mentimun di tabanan-BALI. – Dwijenagro 8(2).

[2] Alfaro-Fernández, A., ElShafie, E. E., Ali, M. A., El Bashir, O. O. A., Córdoba-Sellés, M. C., Ambrosio, M. F. S. (2014): First report of pepper vein yellows virus infecting hot pepper in Sudan. – Plant Disease 98(10): 1446-1446.

[3] Ben-Chaim, A., Paran, I. (2000): Genetic analysis of quantitative traits in pepper (Capsicum annuum). – Journal of the American Society for Horticultural Science 125(1): 66-70.

[4] Buzkan, N., Arpaci, B. B., Simon, V., Fakhfakh, H., Moury, B. (2013): High prevalence of poleroviruses in field-grown pepper in Turkey and Tunisia. – Archives of Virology 158(4): 881-885.

[5] Caranta, C., Palloix, A., Lefebvre, V., Daubeze, A. M. (1997); QTLs for a component of partial resistance to cucumber mosaic virus in pepper: restriction of virus installation in host-cell. – Theor. Appl. Genet. 94: 431-438.

[6] Daubeze, A. M., Hennart, J. W., Palloix, A. (1995): Resistance to Leveillula taurica in pepper (Capsicum annuum) is oligogenically controlled and stable in Mediterranean regions. – Plant Breeding 114: 327-332.

[7] Desbiez, C., Joannon, B., Wipf-Scheibel, C., Chandeysson, C., Lecoq, H. (2011): Recombination in natural populations of watermelon mosaic virus: new agronomic threat or damp squib? – Journal of General Virology 92(8): 1939-1948.

[8] Dombrovsky, A., Glanz, E., Pearlsman, M., Lachman, O., Antignus, Y. (2010): Characterization of Pepper yellow leaf curl virus, a tentative new Polerovirus species causing a yellowing disease of pepper. – Phytoparasitica 38(5): 477-486.

[9] Fiallo-Olivé, E., Navas-Hermosilla, E., Ferro, C. G., Zerbini, F. M., Navas-Castillo, J. (2018): Evidence for a complex of emergent poleroviruses affecting pepper worldwide. – Archives of Virology 163(5): 1171-1178.

[10] Florini, D. A., Zitter, T. A. (1986): Cucumber mosaic-virus (CMV) in peppers (*Capsicum annuum* L) in New-York, and associated yield losses. – Phytopathology 76(6): 652-652.

[11] Ghosh, S., Kanakala, S., Lebedev, G., Kontsedalov, S., Silverman, D., Alon, T., Mor, N., Sela, N., Luria, N., Dombrovsky, A., Mawassi, M., Haviv, S., Czosnek, H., Ghanima, M. (2019): Transmission of a new polerovirus infecting pepper by the whitefly Bemisia tabaci. – Journal of Virology JVI-00488. DOI: 10.1128/JVI.00488-19.

[12] Gibbs, A. J., Ohshima, K., Phillips, M. J., Gibbs, M. J. (2008): The prehistory of potyviruses: their initial radiation was during the dawn of agriculture. – PLoS One 3(6): e2523.

[13] Green, S. K., Kim, J. S. (1991): Characteristics and Control of Viruses Infecting Peppers: A Literature Review. – In: Technical Bulletin 18. Asian Vegetable Research and Development Center, Taipei.

[14] Janzac, B., Fabre, M. F., Palloix, A., Moury, B. (2009): Phenotype and spectrum of action of the Pvr4 resistance in pepper against potyviruses, and selection for virulent variants. – Plant Pathology 58(3): 443-449.

[15] Kamran, A., Lotos, L., Amer, M. A., Al-Saleh, M. A., Alshahwan, I. M., Shakeel, M. T., Ahmad, M. H., Umar, M., Katis, N. I. (2018): Characterization of pepper leafroll chlorosis virus, a new polerovirus causing yellowing disease of bell pepper in Saudi Arabia. – Plant Disease 102(2): 318-326.

http://www.aloki.hu ● ISSN 1589 1623 (Print) ● ISSN 1785 0037 (Online)
DOI: http://dx.doi.org/10.15666/aeer/1706_1465314664

[16] Kenyon, L., Kumar, S., Tsai, W. S., Hughes, J. D. A. (2014): Virus Diseases of Peppers (Capsicum spp.) and Their Control. – In Series: Advances in Virus Research (Vol. 90). Academic Press, Amsterdam, pp. 297-354.
[17] Knierim, D., Deng, T. C., Tsai, W. S., Green, S. K., Kenyon, L. (2010): Molecular identification of three distinct Polerovirus species and a recombinant Cucurbit aphid-borne yellows virus strain infecting cucurbit crops in Taiwan. – Plant Pathology 59(5): 991-1002.
[18] Knierim, D., Tsai, W. S., Kenyon, L. (2013): Analysis of sequences from field samples reveals the presence of the recently described pepper vein yellows virus (genus Polerovirus) in six additional countries. – Archives of Virology 158(6): 1337-1341.
[19] Kumar, S., Stecher, G., Tamura, K. (2016): MEGA7: Molecular Evolutionary Genetics Analysis version 7.0 for bigger datasets. – Molecular Biology and Evolution 33: 1870-1874.
[20] Lapidot, M., Paran, I., Ben-Joseph, R., Ben-Harush, S., Pilowsky, M., Cohen, S., Shifriss, C. (1997): Tolerance to cucumber mosaic virus in pepper: development of advanced breeding lines and evaluation of virus level. – Plant Dis. 81: 185-188.
[21] Lefebvre, V., Palloix, A., Caranta, C., Pochard, E. (1995): Construction of an intra-specific integrated linkage map of pepper using molecular markers and doubled-haploid progenies. – Genome 38: 112-121.
[22] Lole, K. S., Bollinger, R. C., Paranjape, R. S., Gadkari, D., Kulkarni, S. S., Novak, N. G., Sheppard, H. W., Ray, S. C. (1999): Full-length human immunodeficiency virus type 1 genomes from subtype C-infected seroconverters in India, with evidence of intersubtype recombination. – Journal of Virology 73(1): 152-160.
[23] Lotos, L., Olmos, A., Orfanidou, C., Efthimiou, K., Avgelis, A., Katis, N. I., Maliogka, V. I. (2017): Insights into the etiology of polerovirus-induced pepper yellows disease. – Phytopathology 107(12): 1567-1576.
[24] Maina, S., Edwards, O. R., Jones, R. A. (2016): First complete genome sequence of Pepper vein yellows virus from Australia. – Genome Announc. 4(3): e00450-16.
[25] Martin, D. P., Murrell, B., Golden, M., Khoosal, A., Muhire, B. (2015): RDP4: detection and analysis of recombination patterns in virus genomes. – Virus Evolution 1(1). https://doi.org/10.1093/ve/vev003.
[26] Moury, B., Verdin, E. (2012): Viruses of Pepper Crops in the Mediterranean Basin: A Remarkable Stasis. – In Series: Advances in Virus Research (Vol. 84). Academic Press, Amsterdam, pp. 127-162.
[27] Murakami, R., Nakashima, N., Hinomoto, N., Kawano, S., Toyosato, T. (2011): The genome sequence of pepper vein yellows virus (family Luteoviridae, genus Polerovirus). – Archives of Virology 156(5): 921-923.
[28] Pagán, I., Holmes, E. C. (2010): Long-term evolution of the Luteoviridae: time scale and mode of virus speciation. – Journal of Virology 84(12): 6177-6187.
[29] Paran, I., Aftergoot, E., Shifriss, C. (1998): Variation in Capsicum annuum revealed by RAPD and AFLP markers. – Euphytica 99: 167-173.
[30] Parrella, G., Ruffel, S., Moretti, A., Morel, C., Palloix, A., Caranta, C. (2002): Recessive resistance genes against potyviruses are localized in colinear genomic regions of the tomato (Lycopersicon spp.) and pepper (Capsicum spp.) genomes. – Theoretical and Applied Genetics 105(6-7): 855-861.
[31] Ryabov, E. V., Fraser, G., Mayo, M. A., Barker, H., Taliansky, M. (2001): Umbravirus gene expression helps Potato leafroll virus to invade mesophyll tissues and to be transmitted mechanically between plants. – Virology 286(2): 363-372.
[32] Sacchi, H., Melo, A. M. T., Colariccio, A. (2003): Reação de progênies de pimentão ao Potato Virus Y. – Bragantia 62(1): 53-60.
[33] Saitou, N., Nei, M. (1987): The neighbor-joining method: a new method for reconstructing phylogenetic trees. – Molecular Biology and Evolution 4: 406-425.

http://www.aloki.hu ● ISSN 1589 1623 (Print) ● ISSN 1785 0037 (Online)
DOI: http://dx.doi.org/10.15666/aeer/1706_1465314664

[34] Tan, W. P., Dong, Y. Z., Sun, X. H., Liang, Y. C., Liu, H. X., Zhu, X. P. (2015): The first identification of Pepper vein yellows virus in Shandong Province, China. – Plant Disease 99(9): 1288.
[35] Thompson, J. D., Gibson, T. J., Higgins, D. G. (2003): Multiple sequence alignment using ClustalW and ClustalX. – Current Protocols in Bioinformatics 1: 2-3.
[36] Villanueva, F., Castillo, P., Font, M. I., Alfaro-Fernández, A., Moriones, E., Navas-Castillo, J. (2013): First report of Pepper vein yellows virus infecting sweet pepper in Spain. – Plant Disease 97(9): 1261-1261.
[37] Yonaha, T., Toyosato, T., Kawano, S., Osaki, T. (1995): Pepper vein yellows virus, a novel luteovirus from bell pepper plants in Japan. – Japanese Journal of Phytopathology 61(3): 178-184.

http://www.aloki.hu ● ISSN 1589 1623 (Print) ● ISSN 1785 0037 (Online)
DOI: http://dx.doi.org/10.15666/aeer/1706_1465314664

EFFECTS OF DIFFERENT DEVELOPMENT STAGES AND STRESS GRADIENT ON DENSITY-BIOMASS EXPONENT AND SIZE INEQUALITY OF *HALOXYLON AMMODENDRON* (C.A. MEY)

ZHAO, Z. L. – HU, X. J. – SONG, Y. Y.*

Department of Forestry, Agricultural College, Xinjiang Shihezi University
Road of North 4th, Shihezi City, Xinjiang 832003, China

**Corresponding author*
e-mail: syy.agr.shzu@126.com

(Received 10th Jun 2019; accepted 11th Oct 2019)

Abstract. Quantifying the biomass–density (M–N) exponent and size inequality in plant communities has become a long-standing issue in both theoretical and empirical studies. The biomass–density (M–N) exponent and size inequality of the tree populations have not been studied so widely as that of herbaceous plants. we studied the variation of biomass–density (M–N) exponent and size inequality at different stages of development clusters along erosion gradient in *Haloxylon ammodendron* populations. The results showed that the value of the M-N exponent ranged from 1.21 to 1.73 in sapling stages, -0.691 to -0.437 in Adult stages and -0.934 to -0.812 in senescence phase along a erosion gradient, the M-N exponents at different stages of development showed an downward trend, and indicated that when the density of the cluster increases, which is a process of self-thinning. Moreover, the populations size inequality in different locations decreased with the increase of wind erosion intensity. The size inequality also showed a downward trend in various stages of development, that of the first two stages of development were significantly greater than the later development stages. Our study showed that interactions among individuals at different stages of development have an important impact on the population structure.
Keywords: *density, interaction, Haloxylon ammodendron, Severe environment, cluster*

Introduction

Mass–density (M–N) scaling relationship describes variation in population density with body size in the plant community and can be described as $M = K \times N^{\gamma}$. In past 40 years, many ecological scientists have devoted themselves to research M–N scaling relationship, and most of these researches proved the -3/2 (Yoda et al., 1963) or -4/3 M–N scaling relationship (Equist et al., 1998; Brian et al., 2003). However, -3/2 and -4/3 exponents of M–N scaling relationship were also criticized on theoretical and empirical grounds (Kozlowski and Konarzewski, 2004; Deng et al., 2006), controversy continues over the underlying value and variability of the M–N scaling exponent. Many literatures indicate that γ varies with soil fertility (Morris, 2003), water availability (Deng et al., 2006), aridity gradient (Bai et al., 2010), hormone response (Zhang et al., 2006, 2016) and salinity gradient (Zhang et al., 2010), all of the above experiments showed γ is an exponent that increases as the pressure gradient increases or vary with different forest types (Zhang et al., 2011). Chu found that the density regulation of plant populations is actually affected by the positive and negative effects among individuals (Chu et al., 2008), which think that environmental factors can affect the law of density regulation by affecting the interaction between plants. The law of density regulation is the external performance of interaction between plants and plants, between plants and the

http://www.aloki.hu ● ISSN 1589 1623 (Print) ● ISSN 1785 0037 (Online)
DOI: http://dx.doi.org/10.15666/aeer/1706_1466514677

environment. The result of plant competition leads to a decrease in the growth rate of the individual, which in turn affects biomass accumulation and ultimately affects the biomass-density relationship. If the interaction between individuals is not competition, but reciprocity, it is inevitable that the average individual biomass will increase with the increase of density (Chu et al., 2008; Lin et al., 2012). Therefore, it can be assumed that the interaction among individual plants and density regulation exponent is closely related.

A lot of studies have shown that the balance of competition and facilitation shifts among the various life stages of two interacting species (Chapin et al., 1994; Long et al., 2014; Zhang et al., 2012; Lin et al., 2012). However, facilitative and competitive mechanisms do not act in isolation from each other in nature, and by co-occurring within the same community, and even between the same individuals, they may produce complex and variable effects. Some studies have shown that life stages (e.g. seed, seedling, juvenile, pre-reproductive adult, reproductive adult, senescent adult) may affect the outcome of interactions between plant species (Rousset et al., 2000). Since the positive and negative interactions are different at different stages of development, is the M–N scaling exponent different? Or how does it change in different stages of development? It seems to attract little attention.

Large variation in individual size is a ubiquitous feature of natural plant populations and this variation has major implications for plant ecology and evolution. There have been a few studies on size inequality among individuals (Weiner et al., 2001; Chu et al., 2009). They found that the different spatial patterns, different density gradients of plant populations (Weiner et al., 2001) and different pressure gradients (Zhang et al., 2012) have a significant impact on population size inequality, Weiner (Weiner et al., 2001) showed that at low densities and early in growth, spatial pattern played a more important role than size asymmetry of competition in generating size inequality, but at high densities or after longer periods of growth, the size asymmetry of competition was more important than spatial pattern. Zhang et al.'s (2012) experiments on the growth of mung bean with different intensity of ultraviolet radiation found that the balance among positive interactions, stress, and mortality driven by competition determined the size inequality of the populations (Zhang et al., 2012). However, studies on the variation of size inequality in developmental stages of tree populations are rare.

Haloxylon ammodendron, which belongs to genus *Haloxylon*, is a typical desert plant, primarily found on shifting or semi-shifting sand dunes of the narrow sub-desert areas in middle and western Asia (Zou et al., 2010). The species is also termed a super xerophyte due to its particular drought tolerance that enables it to survive in prohibitive environments (Gao et al., 2010). This species had been selected as a pioneer plant for sand dune stabilization, and it is an excellent plant for evaluating disturbance and vegetation restoration in Gurbantunggut Desert (Bedunah and Schmidt, 2000). However, the area of natural *Haloxylon ammodendron* forest is decreasing because of land development, groundwater mining, excessive deforestation, and overgrazing. Hence, *Haloxylon ammodendron* has been listed as a national grade 3 endangered plant in China (Guo et al., 2005). A 35-yr-old replacement series of *Haloxylon ammodendron* clusters in the Gurbantunggut Desert has provided a condition to study the density change of cluster under severe stress environments. The *Haloxylon ammodendron* is distributed in the form of cluster on top of sand dunes in the desert, which suffer from strong wind erosion and they grows in aggregate pattern. There is no more aggregation pattern to be found except at the top of the hill. Interestingly, there is a significant phase

http://www.aloki.hu ● ISSN 1589 1623 (Print) ● ISSN 1785 0037 (Online)
DOI: http://dx.doi.org/10.15666/aeer/1706_1466514677

difference in the density change process of *Haloxylon ammodendron* clusters, therefore, it provides us with a convenient way to study the variation of the M–N scaling exponent and changes in size inequality in different developmental stages. Thus we will ask the following three questions: (1) How does the M–N exponent change in different developmental stages of *Haloxylon ammodendron*? (2) How does the size inequality of *Haloxylon ammodendron* change during different developmental stages? (3) Is there a positive self-thinning exponent and how much is its size?

Materials and methods

Description of the study site

This study has been conducted along a natural wind speed gradient at five sites (Xinhu, Shihezi, Kuitun, Guertu and Jinghe) in the Gurbantunggut Desert, Xinjiang, which is located in the hinterland of the Junggar Basin in northwest China (44°11′ to 46°20′N, 84°31′ to 90°00′E), with an area of up to 48,800 km^2. The Gurbantunggut Desert is the second largest desert in China. Due to its long distance from any ocean, it has a temperate arid desert climate. The annual precipitation is 80 mm to 190 mm. The annual average temperature is 5.0 to 5.7 °C. *Haloxylon ammodendron* is the dominant species in this desert, and the ephemeral plant layer is well-developed (*Figs. 1* and *2*).

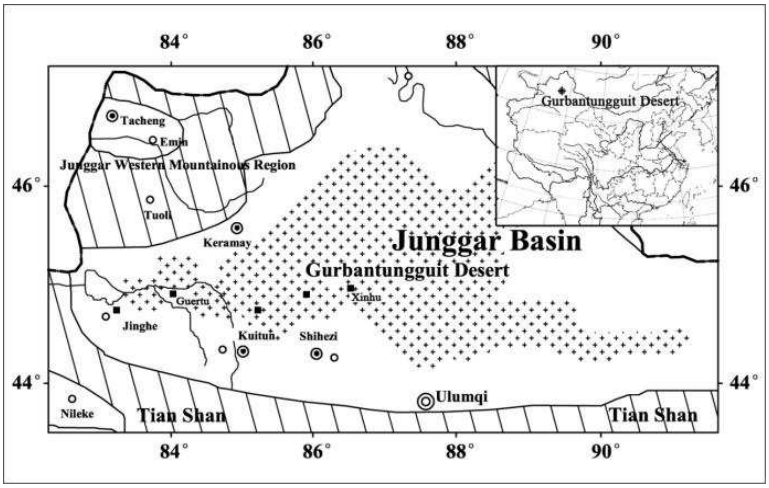

Figure 1. *The maps of different sampling sites*

Figure 2. *Research sites and species*

http://www.aloki.hu ● ISSN 1589 1623 (Print) ● ISSN 1785 0037 (Online)
DOI: http://dx.doi.org/10.15666/aeer/1706_1466514677

Field surveying

At the beginning of 2016, we chose five sites at the study area, and all the sites were located in different spot from low wind speed to high wind speed (*Table 1*), since the difference in height and shape of sand dunes at each location is not large, the influence of different shapes on wind speed can be ignored, in addition, the rainfall in the entire Gurbantunggut desert is almost the same. Data were collected from local weather stations respectively. A 40 × 40 m plot was selected at different research sites and the clusters of five development stages were selected for each plot, to avoid sample size inhomogeneity, we initially selected 10-15 clusters for each stage of development, then selected three representative clusters from among them. According to the distribution situations of the age of *Haloxylon ammodendron* clusters, we only need to find the maximum age for each cluster because each *Haloxylon ammodendum* cluster is composed of uneven-aged individuals. *Haloxylon ammodendron* is divided into five developmental stages, which can be expressed as follows, sapling: 1-6 yr; Adult phase I: 7-13 yr; Adult phase II: 14-20 yr; senescence phase: 21-27 yr; death phase: 28-34 yr; Age formula comes from previous research results (Song et al., 2011), and they are used to determine the age of the cluster. In addition, we selected 1 × 1 m quadrat in each cluster to collect the basal diameter, crown width and tree height data of each *Haloxylon ammodendum*. Moreover, in order to reduce difference of sample scale and avoid edge effects, each plot is close to the middle of the clusters and each quadrat was replicated three times, meanwhile, the number of *Haloxylon ammodendron* per square meter was measured to calculate the density.

Table 1. *Descriptions of the five experimental sites*

Parameters	Site				
	Xinhu	**Shihezi**	**Kuitun**	**Guertu**	**Jinghe**
Latitude	45°13	45°26′	44°89′	45°41	44°75′
Longitude	86°55	85°88′	85°47′	84°26	83°35′
Altitude (m)	454	443	460	442	436
Annual mean temperature (°C)	5.2	5.1	5.5	5.6	5.4
Annual mean precipitation (mm)	230	210	182	173	144
Annual mean potential evaporation (mm)	1280	1300	1810.7	1960	2000
Wind speed (m/s)	1.9	2.1	2.8	3.2	3.7
Spring mean wind speed (m/s)	4	5.4	6.5	7	9.5

The above data are from the local monitoring result from 1975 to 2015

Biomass estimation

To picks representative *Haloxylon ammodendron* individuals of each age to measure his above-ground biomass, height, basal diameter for deriving the biomass calculation formula, three representative *Haloxylon ammodendron* plants were selected for each age, the whole tree (above the ground) was excavated and weighed, and adopt the age separation excavation method, a total of 45 *Haloxylon ammodendron* plants were dug at each site. Parts of the samples were brought back to the laboratory to be dried and weighed, and then above ground biomass (ATB) was calculated accordingly. The biomass calculation formulas of Xinhu, Shihezi, Kuitun, Guertu and Jinghe are respectively:

http://www.aloki.hu ● ISSN 1589 1623 (Print) ● ISSN 1785 0037 (Online)
DOI: http://dx.doi.org/10.15666/aeer/1706_1466514677

$$B_{Xin} = 0.2012(d^2h)^{0.8231} \quad \text{(Eq.1)}$$

$$B_{Shi} = 0.1965(d^2h)^{0.7953} \quad \text{(Eq.2)}$$

$$B_{Kui} = 0.1834(d^2h)^{0.7826} \quad \text{(Eq.3)}$$

$$B_{Gu} = 0.1238(d^2h)^{0.7492} \quad \text{(Eq.4)}$$

$$B_{Jing} = 0.1107(d^2h)^{0.7223} \quad \text{(Eq.5)}$$

where B were the individual biomass weight, d were basal diameter, h were tree height.

Calculation of the size inequality of individual Haloxylon ammodendron

We analysed the size inequality of different parameters which can be expressed by the coefficient of variation (CV) of basal diameter, height, individual mass of *Haloxylon ammodendron*. To quantify size inequality in *Haloxylon ammodendron* clusters, the CV used is $CV = SD/X_{mean}$ (Weiner et al., 2001; Chu et al., 2009), SD is the standard deviation, X_{mean} is the sample mean.

Collection of stress factors

The collected field data are supposed to contain the five different wind erosion intensity which are to be used as abiotic stress factors, usually from March to May, the average wind speeds of Xinhu, Shihezi, Kuitun, Guertu and Jinghe are 4 m/s, 5.4 m/s, 6.5 m/s, 7 m/s, 9.5 m/s respectively, which show a trend of decreasing from west to east. Wind speed at the top of the dune is greater than that of the sand-driving wind velocity (6 m/s) and the top of the sand hill is exposed to the process of wind erosion, the above data are from the local monitoring result from 1975 to 2015.

Data analysis

All data were analyzed by spss 22 and Excel 2016, the plotted results was conducted via Origin 8.0 software, the scaling exponents and intercepts of M–N relationships were estimated by the standard major axis (SMA) regression of log-transformed data. Significance between the CV value (coefficient of variation) of different stages of development are expressed by the means of the Duncan's test, $p > 0.05$.

Results

Density changes

For the trend of the density changes of *Haloxylon ammodendron* clusters in five sites with wind erosion, a rapidly increased is found firstly in Sapling phase while a rapid decrease is found in Adult phase I, after that, a slow decline trend appears (*Fig. 3*). In Xinhu, *Haloxylon ammodendron* reaches its maximum density (30 trees/m^2) at the ninth age, subsequently, the density is in rapid decline from age 9 to age 13, after that the decline in density enters a relatively slow process. The Kuitun site reached its maximum density (41 trees/m^2) in the seventh year. Seven to eleventh years is regarded as a rapid decline period, which is slightly steeper than that Shihezi and Xinhu (*Fig. 3*). In Jinghe,

http://www.aloki.hu ● ISSN 1589 1623 (Print) ● ISSN 1785 0037 (Online)
DOI: http://dx.doi.org/10.15666/aeer/1706_1466514677

the density reach its maximum (60 trees/m^2) in the fourth year. Similarly, in the period from fourth to eighth year, a rapid decline period can be seen, this stage in Jinghe has the steepest change compared with the change other four location. After that the downward trend began to be slower (*Fig. 3*). Compared to the other four locations at the same time, obviously, the density of *Haloxylon ammodendron* increased with the increase of wind erosion and showed a more intense pattern of aggregation. Another fact is that wind erosion significantly accelerated the onset of *Haloxylon ammodendron* density-dependent mortality, especially at the Jinghe site, the density-dependent mortality occurred earlier than that in other four locations. However, the density of the five sites during the death phase is similar (*Fig. 3*).

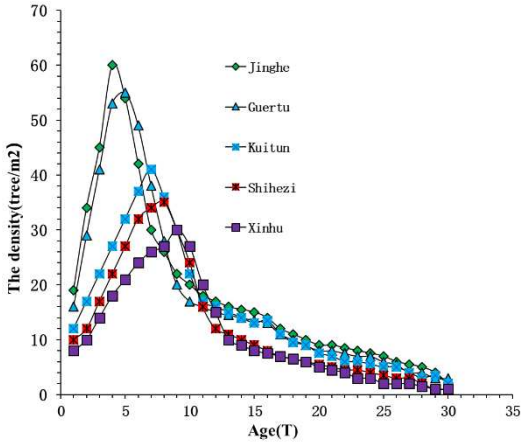

Figure 3. *The trend of the density change of Haloxylon ammodendron at five different locations, respectively*

The M-N exponents

There are three parts of density changes concerning rise and rapid fall, slow decline during self-thinning period (*Fig. 4*), so we calculate the M-N exponents in three sections respectively. The value of the M-N exponent ranged from 1.73 to 1.21 for phase along a erosion gradient (*Table 2*), the density exponent of the sapling phase were significantly larger than the traditional -3/2 and -4/3 ($p > 0.05$) based on the 95% CI; the density exponent of the adult phase were also significantly different from -3/2 and -4/3. In the senescence phase, the density exponent of Xinhu, Kuitun and Jinghe had no significant difference with -4/3, which indicates that the relationship between the average individual biomass and density on the ground during the senescence phase follows the -4/3 M-N exponent rule, meanwhile, in the same sites, with the increase of *Haloxylon ammodendron* age, the M-N exponents at different stages of development showed a downward trend.

Size inequality

At the top of the dune, different wind speed significantly influenced the size inequality of the *Haloxylon ammodendron* different parameters. For the basal diameter, High, Crown width and biomass, the CV value (coefficient of variation) of size inequality at Jinghe (strong wind) was lower than those in other four places, the highest CV value (coefficient of variation) is found at Xinhu site (*Fig. 5*). The CV Values

http://www.aloki.hu ● ISSN 1589 1623 (Print) ● ISSN 1785 0037 (Online)
DOI: http://dx.doi.org/10.15666/aeer/1706_1466514677

(coefficient of variation) of various parts under different wind erosion conditions in the same developmental stage are also significantly different (*Fig. 5*), The CV values (coefficient of variation) of size inequality of the sapling stage and Adult phase I was significantly higher than those in other stages of development.

Table 2. *Self-thinning exponents (γ) and intercepts (K) for above-ground across different developmental stages as estimated by SMA regression of log-transformed data*

Developmental stage	Sites	Regression relationship	Slope(γ)	95% CI	Intercept(k)	95% CI	R^2	n
Sapling phase	Xi hu	M:D	1.73	1.34, 2.24	-0.1083	-0.735, 0.376	0.932	8
	Shi he zi	M:D	1.94	1.34, 2.81	-0.606	-1.7, 0.1528	0.926	6
	Kui tun	M:D	1.73	1.54, 2.15	-0.19	..-1.27,-0.411	0.968	5
	Guertu	M:D	1.27	0.992, 1.62	-0.609	-1.13, -0.199	0.994	4
	Jinghe	M:D	1.21	0.93, 1.57	-0.712	-1.27, -0.281	0.996	4
Adult phase	Xi hu	M:D	-0.691	-1.031, -0.463	3.5	3.21, 3.93	0.95	5
	Shi he zi	M:D	-0.739	-1.16, -0.469	3.38	3.12, 4.04	0.935	5
	Kui tun	M:D	-0.467	-0.774, -0.282	2.82	2.55, 3.26	0.918	5
	Guertu	M:D	-0.422	-0.559, -0.318	2.44	2.28, 2.69	0.976	5
	Jinghe	M:D	-0.437	-1.015, -0.1883	2.43	2.04, 3.36	0.735	5
Senescence phase	Xi hu	M:D	-0.934	-1.09, -0.801	3.98	3.9, 4.08	0.922	17
	Shi he zi	M:D	-0.782	-0.901, -0.679	3.78	3.72, 3.84	0.918	20
	Kui tun	M:D	-1.021	-1.18, -0.881	3.95	3.84, 4.08	0.905	21
	Guertu	M:D	-1.1	-1.31, -0.925	3.74	3.59, 3.92	0.858	22
	Jinghe	M:D	-0.812	-1, -0.659	3.5	3.35, 3.68	0.798	22

M is aboveground average individual biomass, N is density. M:N is log M : log N. 95% CIs are confidence intervals for λ and K, n is the number of samples

Discussion

The density changes with developmental stages

Our natural *Haloxylon ammodendron* clusters show there is a pattern of hump-shaped density change, apparently, *Haloxylon ammodendron* cluster density in the Sapling phase showed a rapid growth trend. The survival rate of clusters was significantly higher than the mortality rate when the maximum density is reached, but due to the fact that individual clusters are too dense, some smaller individuals do not receive sufficient light and other nutrition so that the mortality rate has increased dramatically, resulting in a large number of individual deaths during the adult I period. Experience observation suggests that light is an important factor in the growth of *Haloxylon ammodendron*, subsequently, the trend of decreasing density has gradually become more moderate. Moreover, the worse the environmental gradient is, the sooner the *Haloxylon ammodendron* cluster enters self-thinning period (*Fig. 3*). This phenomenon was inconsistent with the previous model study in which the asymmetric facilitation delays the onset of density-dependent mortality (Lin et al., 2015), this situation may be caused by the fact that the cluster is trying to resist wind erosion, a large number of individuals colonize the top of the dune in high density, resulting in density-dependent deaths. The initial density is proportionally related to the environmental stress gradient (*Fig. 3*), in order to compete limited resources, the higher the initial density is, the more fierce the density-dependent death among individual will be. Moreover, the density decreasing degree in Adult phase I is significantly different from that of subsequent periods. So we speculate that the essential cause of phase

http://www.aloki.hu ● ISSN 1589 1623 (Print) ● ISSN 1785 0037 (Online)
DOI: http://dx.doi.org/10.15666/aeer/1706_1466514677

change of the density of cluster during different development period is the result of the transformation of the interactions between individuals (Chu et al., 2008). Therefore, it is very meaningful to study the characteristics of density variation between different developmental stages of tree populations under extreme conditions. How to changes the interaction among *Haloxylon ammodendron* individuals with the density and development stage will be an important direction for future study.

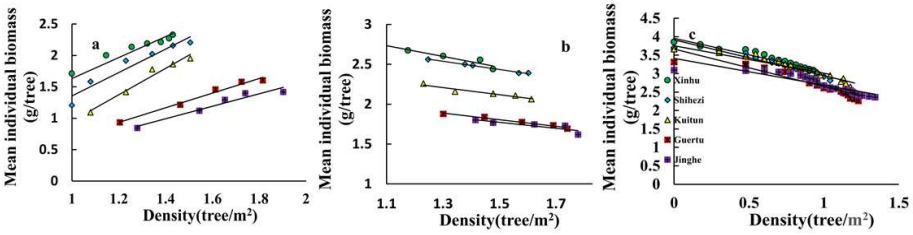

Figure 4. *Density-biomass exponents along wind erosion gradient at different development stages. The self-thinning line of sapling phase (a), the self-thinning line of adult phase I (b), the self-thinning line of adult (c)*

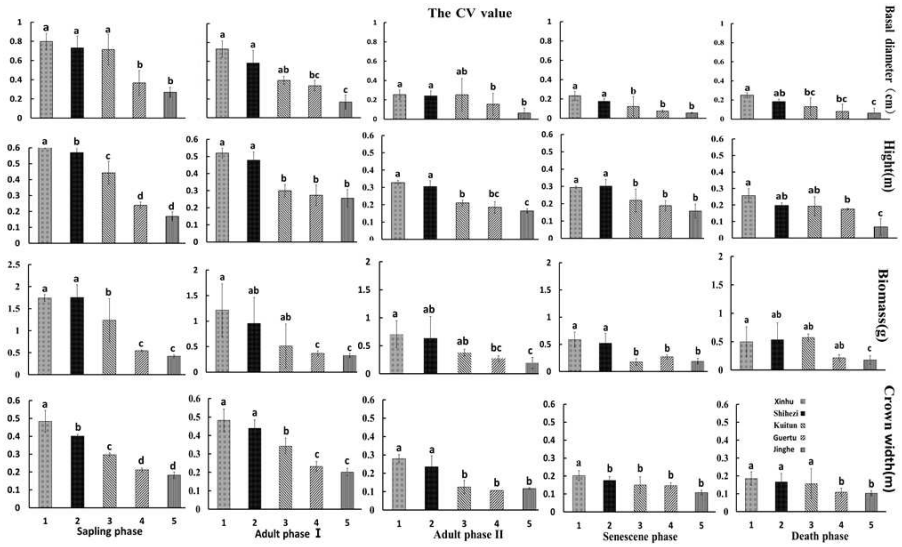

Figure 5. *The CV value of the stem, High, Crown width and the whole Haloxylon ammodendron biomass were calculated under different wind erosion stress gradient in the different stages of growth. Different places represent different wind erosion. 95% confidence intervals for unbiased values were determined by using the Duncan's test*

The M-N (self-thinning) exponents and size inequality

In our study, there was no general predicted value that can describe all the M–N relationships exponents for different stages development across different wind erosion gradient, also different from the -3/2 and -4/3 "law" (Deng et al., 2006; Zhang et al., 2011, 2017). According to the definition of population self-thinning, when the mortality rate within the population reaches 20%, it indicates that density dependent death has occurred (Maina et al., 2015). The *Haloxylon ammodendron* cluster we studied was originally planted on top of a dune in the form of a small area, in order to resist the

http://www.aloki.hu ● ISSN 1589 1623 (Print) ● ISSN 1785 0037 (Online)
DOI: http://dx.doi.org/10.15666/aeer/1706_1466514677

erosion of wind, the density of *Haloxylon ammodendron* seedlings reaches dozens, so that the intertwined roots fix the sand in a higher density, as the *Haloxylon ammodendron* cluster grows, the clusters expand radially around the center of the initial colonization site and grow usually in high density and seeds added in subsequent years, except for falling inside the clusters, must fall near the initial settlement, and if they are far away, they will not survive. So when the clusters grow to 2 to 3 years, the competition among individuals is more intense, a lot of individuals begin to die and can beyond 25% mortality rate (*Table 3*), at the same time, the occurrence of this process is accompanied by a higher survival rate and the survival rate is much greater than the mortality rate, therefore, the essential reason for the increase in density is that the new planting individual counteracts the death individual, resulting in a "trend of increasing density". This phenomenon is different from the tree population self-thinning in the traditional sense that is generally colonized in a certain area in a random distribution, the occurrence of self-thinning is often accompanied by a decrease in population density (Xu et al., 2018; Zhang et al., 2011; Deng et al., 2006; Chu et al., 2010). Moreover, although a small number of individuals die in the early stages of population development, but the death is not density-dependent death, but is caused by other external causes, such as disease, weakness or harsh environmental conditions, so self-thinning can be a process of increasing density, which proves that there is a positive self-thinning exponents in nature. The self-thinning exponent of three-phase decreases monotonously as the different developmental stages increases (*Fig. 4*). Self-thinning exponent was positive in the previous one to five years, after the cluster reaches the highest density, self-thinning has become very fierce, especially in Adult phase I. Later it shows a negative Self-thinning exponent, which may be caused by the fact that there is strong wind erosion stress at the top of dune, thus there may be a strongly facilitation effects among *Haloxylon ammodendron* individuals (Bertness et al., 1994; Callaway and Walker et al., 1997; Callaway et al., 2002, 2007). The strong positive effect promotes the individual average biomass of cluster to increase with the density in Sapling phase. In fact, this situation has been predicted by previous research, which suggested that the allometric exponents (or regression slopes) might even become positive under the most extreme conditions where facilitation is commonly observed, the above study predicted this result, but it was not confirmed in reality yet (Deng et al., 2006). The results of this paper has just verified the existence of positive M-N exponents and proved the complexity of the self-thinning patterns of different species. It can be seen herbs have a shorter developmental history, but not long enough for us to observe its phase effects. As for arbor plants with long developmental history, it is more convenient to observe a series of change characteristics during the developmental stage. Therefore, it is very meaningful to discover the characteristics of different interacting species and natural stress factors (Maestre et al., 2009).

In addition, the coefficient of variation of different parameters of *Haloxylon ammodendron* at different developmental stages also decreases with increasing wind erosion in this same location, however, previous study (Zhang et al., 2012) showed that size inequality (coefficient of variation) was simply monotonic decreases in Mung beans growing phase 1 with the increase of UV-B stress strength, but non-monotonic decreases is with UV-B radiation increased in phase 2 and 3. They attribute the result to the spatial pattern of plant growth and the symmetry of competition (Chu et al., 2009; Weiner et al., 2001). Our study does not need to consider these factors, because the entire process of cluster development is in a state of self-thinning, so there is no effect

http://www.aloki.hu ● ISSN 1589 1623 (Print) ● ISSN 1785 0037 (Online)
DOI: http://dx.doi.org/10.15666/aeer/1706_1466514677

of spatial patterns. It can more accurately reflect with environmental pressure gradient how the size inequality (coefficient of variation) changes for each developmental stage. For each parameter, sapling, We speculate, this may be related to the predominance of facilitation in the previous period, in the same facilitation patterns sapling stage and adult phase I, the clusters are constantly recruit new individuals and accompanied by the death of some individuals. *Haloxylon ammodendron* individuals that are constantly settled and death exacerbate the size inequality of clusters, lead to a relatively high size variation, in the adult phase II, senescene phase, death phase the changes in density have slowed and subsequent supplements can only survive for 1-3 years. The difference in the age of surviving individuals at this stage is much smaller than that in the previous period, thus clusters show a more neat trend.

Table 3. *Changes of Haloxylon ammodendron clusters plants number during sapling phase*

Age		Jinghe	Guertu	Kuitun	Shihezi	Xinhu
One year	Survival	19	16	12	10	8
	Deaths/current year	0	0	0	0	0
	Mortality rate	0	0	0	0	0
Two year	Survival	34	29	17	12	10
	Deaths/current year	12 (9)	10 (8)	8 (5)	6 (4)	4 (3)
	Mortality rate	26%	25%	32%	33%	28%
Three year	Survival	45	41	22	17	14
	Deaths/current year	34 (15)	26 (11)	16 (6)	14 (5)	12 (5)
	Mortality rate	33%	28%	26%	32%	36%
Four year	Survival	60	53	27	22	18
	Deaths/current year	60 (18)	56 (13)	31 (10)	23 (8)	18 (6)
	Mortality rate	30%	25%	37%	35%	33%
Five year	Survival	54	55	32	27	21
	Deaths/current year	98 (22)	83 (18)	35 (19)	43 (8)	29 (7)
	Mortality rate	41%	33%	60%	29%	34%
Six year	Survival	42	49	37	32	24
	Deaths/current year	107 (14)	100 (14)	77 (14)	67 (14)	40 (7)
	Mortality rate	35%	29%	37%	43%	31%

The survival number and death number in the table are cumulative values, and all death individuals will disappear due to wind erosion two to three years after death. Current Year is the number of deaths is the number of individuals who died in the current year. When calculating the mortality rate, the number of deaths is the number of individuals who died in the current year

Conclusion

(1) The density of clusters increased rapidly at the sapling stage, decreased rapidly at the adult stage, and then decreased slowly at the later stage. By comparing five different wind erosion sites, we can clearly find that the density of *Haloxylon ammodendron* increases with the increase of wind erosion intensity, showing a denser growth pattern. Wind erosion significantly accelerated density-dependent death of *Haloxylon ammodendron*.

(2) the self-thinning indexes of *Haloxylon ammodendron* clusters along different wind erosion gradients were all positive at the rapid rising stage, it is significantly

http://www.aloki.hu ● ISSN 1589 1623 (Print) ● ISSN 1785 0037 (Online)
DOI: http://dx.doi.org/10.15666/aeer/1706_1466514677

different from the traditional -3/2 and -4/3 self-thinning indices; in the stage of rapid density decline, the negative value presents an upward trend along the wind erosion gradient, which is significantly different from the traditional -3/2 and -4/3 self-thinning indexes; the difference between the -4/3 self-thinning index and self-thinning index of Xinhu, Kuitun and Jinghe in the stages of aging and death is not obvious, indicating that the self-thinning stage conforms to the -4/3 self-thinning rule. With the growth and development of cluster, the self-thinning index of the same location showed a decreasing trend.

(3) The CV values of the cluster size inequality of the sapling stage and adult phase I was significantly higher than those in other stages of development.

Future research should explicitly evaluate how to incorporate different developmental stages of arbor species into current conceptual and mathematical models, which can be used to improve the SGH (stress-gradient hypothesis) framework. The computer models of tree species need to be made to explore the changing patterns of positive and negative interactions among individuals, the facilitative effect from key species is essential for ecological system diversity and stability (Brooker et al., 2008; Vellend, 2008), which help us extend the SGH (stress-gradient hypothesis) framework and foster research on facilitation in ecology (Brooker et al., 2005, 2008; Maestre et al., 2009).

REFERENCES

[1] Bai, Y., Zhang, W., Jia, X., et al. (2010): Variation in root: shoot ratios induced the differences between above and belowground mass–density relationships along an aridity gradient. – Acta Oecologica 36(4): 393-395.
[2] Bertness, M. D., Callaway, R. (1994): Positive interactions in communities. – Trends in Ecology & Evolution 9(5): 191-193.
[3] Brian, J. E., Evan, P. E., Travis, E. H., Huxman, T. E., Allen, A. P., Ignace, D. D., Gillooly, J. F. (2003): Scaling metabolism from organisms to ecosystems. – Nature 423: 639-642.
[4] Brooker, R., Kikvidze, Z., Pugnaire, F. I., et al. (2005): The importance of importance. – Oikos 109(1): 63-70.
[5] Brooker, R. W., Maestre, F. T., Callaway, R. M., et al. (2008): Facilitation in plant communities: the past, the present, and the future. – Journal of Ecology 96(1): 18-34.
[6] Callaway, R. M. (2007): Positive Interactions and Interdependence in Plant Communities. – Springer, Dordrecht.
[7] Callaway, R. M., Walker, L. R. (1997): Competition and facilitation: a synthetic approach to interactions in plant communities. – Ecology 78(7): 1958-1965.
[8] Callaway, R. M., Brooker, R. W., Choler, P., et al. (2002): Positive interactions among alpine plants increase with stress. – Nature 417(6891): 844-848.
[9] Chapin, F. S., Walker, L. R., Sharman, F. L. C. (1994): Mechanisms of primary succession following deglaciation at Glacier Bay, Alaska. – Ecological Monographs 64(2): 149-175.
[10] Chu, C. J., Maestre, F. T., Xiao, S., et al. (2008): Balance between facilitation and resource competition determines biomass–density relationships in plant populations. – Ecology letters 11(11): 1189-1197.
[11] Chu, C. J., Weiner, J., Maestre, F. T., et al. (2009): Positive interactions can increase size inequality in plant populations. – Journal of Ecology 97(6): 1401-1407.

http://www.aloki.hu ● ISSN 1589 1623 (Print) ● ISSN 1785 0037 (Online)
DOI: http://dx.doi.org/10.15666/aeer/1706_1466514677

[12] Chu, C. J., Weiner, J., Maestre, F. T., et al. (2010): Effects of positive interactions, size symmetry of competition and abiotic stress on self-thinning in simulated plant populations. – Annals of Botany 106(4): 647-652.
[13] Deng, J., Wang, G., Morris, E., et al. (2006): Plant mass-density relationship along a moisture gradient in north-west China. – Journal of Ecology 94(5): 953-958.
[14] Gao, S., Su, P. X., Yan, Q. D., et al. (2010): Canopy and leaf gas exchange of Haloxylon ammodendron under different soil moisture regimes. – Science China Life Sciences 53(6): 718-728.
[15] Koz Owski, J., Konarzewski, M. (2004): Is West, Brown and Enquist's model of allometric scaling mathematically correct and biologically relevant? – Functional Ecology 18(2): 283-289.
[16] Lin, Y., Berger, U., Grimm, V., et al. (2012): Differences between symmetric and asymmetric facilitation matter: exploring the interplay between modes of positive and negative plant interactions. – Journal of Ecology 100(6): 10.
[17] Long, Y., Zhang, J., Tian, X., et al. (2014): De novo assembly of the desert tree Haloxylon ammodendron (C. A. Mey.) based on RNA-Seq data provides insight into drought response, gene discovery and marker identification. – BMC Genomics 15(1): 1111.
[18] Maestre, F. T., Callaway, R. M., Valladares, F., et al. (2009): Refining the stress-gradient hypothesis for competition and facilitation in plant communities. – Journal of Ecology 97(2): 199-205.
[19] Maina, J. N., Wang, Q. (2015): Seasonal response of chlorophyll a/b ratio to stress in a typical desert species: Haloxylon ammodendron. – Arid Land Research and Management 29(3): 321-334.
[20] Morris, E. C. (2003): How does fertility of the substrate affect intraspecific competition? Evidence and synthesis from self-thinning. – Ecological Research 18(3): 287-305.
[21] Rousset, O., Lepart, J. (2000): Positive and negative interactions at different life stages of a colonizing species (*Quercus humilis*). – Journal of Ecology 88(3): 401-412.
[22] Song, Y. Y., Chu, G. M., Xiao-Jing, H. U. (2011): Relationship of diameter-class and age-class of *Haloxylon ammodendron* population in Gurbantonggut Desert. – Acta Botanica Boreali - Occidentalia Sinica 31(4): 808-814.
[23] Vellend, M. (2008): Effects of diversity on diversity: consequences of competition and facilitation. – Oikos 117(7): 1075-1085.
[24] Weiner, J., Stoll, P., Mullerlandau, H., et al. (2001): The effects of density, spatial pattern, and competitive symmetry on size variation in simulated plant populations. – The American Naturalist 158(4): 438-450.
[25] Xu, S., Yu, Z., Zhang, K., et al. (2018): Simulating canopy conductance of the, Haloxylon ammodendron, shrubland in an arid inland river basin of northwest China. – Agricultural and Forest Meteorology 249: 22-34.
[26] Yoda, K. (1963): Self-thinning in overcrowded pure stands under cultivated and natural conditions (Intraspecific competition among higher plants XI). – J. Biol. Osaka City Univ. 14: 107-129.
[27] Zhang, H., Wang, G. X., Shen, Z. X., et al. (2006): Effect of sensitivity to abscisic acid on scaling relationships for biomass production rates and body size in Arabidopsis thaliana. – Acta Physiologiae Plantarum 28(4): 373-379.
[28] Zhang, H., Wang, G., Zheng, K., et al. (2010): Mass–density relationship changes along salinity gradient in Suaeda salsa L. – Acta Physiologiae Plantarum 32(6): 1031-1037.
[29] Zhang, R. C., Lin, Y., Yue, M., et al. (2012): Effects of ultraviolet-B irradiance on intraspecific competition and facilitation of plants: self-thinning, size inequality, and phenotypic plasticity. – PLoS One 7(11): e50822.
[30] Zhang, W. P., Jia, X., Bai, Y. Y., et al. (2011): The difference between above-and below-ground self-thinning lines in forest communities. – Ecological Research 26(4): 819-825.

http://www.aloki.hu ● ISSN 1589 1623 (Print) ● ISSN 1785 0037 (Online)
DOI: http://dx.doi.org/10.15666/aeer/1706_1466514677

[31] Zhang, W. P., Jia, X., Wang, G. X. (2017): Facilitation among plants can accelerate density-dependent mortality and steepen self-thinning lines in stressful environments. – Oikos. https://doi.org/10.1111/oik.03983.
[32] Zhang, Y., Xie, J. B., Li, Y. (2016): Effects of increasing root carbon investment on the mortality and resprouting of, *Haloxylon ammodendron*, seedlings under drought. – Plant Biology. https://doi.org/10.1111/plb.12511.
[33] Zou, T., Li, Y., Xu, H., et al. (2010): Responses to precipitation treatment for Haloxylon ammodendron growing on contrasting textured soils. – Ecological Research 25(1): 185-194.

http://www.aloki.hu ● ISSN 1589 1623 (Print) ● ISSN 1785 0037 (Online)
DOI: http://dx.doi.org/10.15666/aeer/1706_1466514677

ALLEVIATION OF CADMIUM STRESS IN THAI RICE CULTIVAR (PSL2) BY INOCULATION OF INDIGENOUS CADMIUM-RESISTANT MICROBIAL CONSORTIA

SEANG-ON, L.[1] – MEEINKUIRT, W.[2] – SAENGWILAI, P.[3,4] – SAMINPANYA, S.[5] – KOEDRITH, K.[1,6*]

[1]*Faculty of Environment and Resource Studies, Mahidol University, 999 Phuttamonthon District, Nakhon Pathom 73170, Thailand*

[2]*Mahidol University, Nakhonsawan Campus, Nakhonsawan 60130, Thailand*

[3]*Department of Biology, Faculty of Science, Mahidol University, Rama VI, Bangkok 10400, Thailand*

[4]*Center of Excellence on Environmental Health and Toxicology (EHT), CHE, Ministry of Education, Bangkok, Thailand*

[5]*Department of General Science, Faculty of Science, Srinakharinwirot University, 114 Sukhumvit 23 Road, Bangkok 10110, Thailand*

[6]*Institute of Environmental Medicine for Green Chemistry, Department of Life Science, Dongguk University Biomedical Campus, 32, Dongguk-ro, Ilsandong-gu, Goyang-si, Gyeonggi-do 820-410, South Korea*

**Corresponding author*
e-mail: preeyaporn.koe@mahidol.edu

(Received 11th Jun 2019; accepted 25th Oct 2019)

Abstract. This study was aimed at isolating indigenous soil bacteria exhibiting cadmium (Cd)-resistance, and characterizing their ability to improve growth and reduce Cd bioaccumulation of Thai rice (*Oryza sativa* L.) PSL2 seedlings. Repeated enrichment, microorganisms were selectively propagated from agricultural soils receiving dredged sediments that contained Cd at 30-50 mg kg^{-1}, in Western Thailand. Over a range of 0-1,000 ppm, the enriched bacterial consortia had a maximum tolerance to Cd at 800 ppm. In batch cultures containing 50 or 100 ppm Cd, they exhibited 53-56 and 69-78% Cd removal, respectively. The inoculation of enriched consortia ameliorated Cd phytotoxicity by promoting rice biomass and growth, and lowering tissue Cd content upon high Cd exposure (50-100 ppm). 16S metagenomic analysis showed that at least the top bacterial phyla of *Proteobacteria, Firmicutes,* and *Bacteroidetes* were enriched in the naturally polluted topsoil microorganisms with dominant bacterial phyla including *Planctomycetes, Proteobacteria, Acidobacteria, Verrucomicrobia, Bacteroidetes, Chloroflexi, Actinobacteria, Firmicutes,* and *Gemmatimonadetes*. In the enriched consortia, certain predominant detoxifiers (e.g., *Acinetobacter* sp.*, Comamonas* sp.*, Enterococcus* sp., and *Pseudomonas* sp.) were explored at a finer taxonomic level among other detected genera. These results emphasized that indigenous soil Cd-resistant microorganisms have potential to cope with metal stress and improve crop plant growth and yield for agricultural benefits.
Keywords: *bioremediation, Cd-resistant bacteria, food safety, microbial community, rice seedling*

Introduction

Biosphere pollution by heavy metals has risen due to industrial activities and extensive use of agrochemicals. Particularly in developing countries, unorganized industrialization and waste management significantly accelerate the release of heavy metals into the soil and water bodies (Sharma et al., 2008). Toxic metals such as cadmium (Cd) have been deposited on the surface soil via industrial operations such as mining and alkaline battery manufacturing.

http://www.aloki.hu ● ISSN 1589 1623 (Print) ● ISSN 1785 0037 (Online)
DOI: http://dx.doi.org/10.15666/aeer/1706_1467914697

Cadmium confers carcinogenicity and mutagenicity, even at low concentrations. In addition, Cd can interfere with renal function by its accumulation in the proximal tubular cells and also cause bone demineralization (Bernard, 2008). In addition to its adverse health effects, excessive Cd levels in the soil cause plant growth retardation, symbiosis interference, and crop yield reduction (Wani et al., 2007).

Soil pollution is one of the main factors causing Cd contamination in rice grains and human exposure via the food chain, indicating that a key point is to remedy Cd pollution from the paddy area, in order to minimize plant Cd uptake from soil and reduce its bioaccumulation in rice grains (Deng et al., 2014). Remarkably high levels of Cd in agricultural soils have been detected in the Padaeng zinc mining area of the southeast region of Mae Sot District, Tak Province, Thailand (Simmons et al., 2003, 2005). This has become a major concern since the International Water Management Institute demonstrated significant Cd contamination in rice grains and paddy soils in this province (Simmons et al., 2003). These Cd levels (ranging from 3.4-284.0 mg kg^{-1} in the agricultural areas) are much higher than the European Community limit of 3 mg kg^{-1}, posing high risk to the environment and human health (Swaddiwudhipong et al., 2012). Therefore, it is essential to remediate Cd-polluted soil in order to alleviate phytotoxicity, improve crop yield, and ultimately prevent direct human exposure.

A number of physicochemical approaches have been utilized for the reduction of toxicity and recovery of polluted agricultural sites. Nevertheless, bioremediation with use of indigenous heavy metal-resistant microorganisms conferring heavy metal removal and plant growth promoting potential would be a cost-effective choice for sustainable agricultural benefits (Govindasamy et al., 2011). The main issue is selection of indigenous heavy metal resistant microorganisms and their implementation in the contaminated area in a sustainable, ecologically friendly manner. Some soil microorganisms playing a dual role in both Cd resistance and plant growth promotion would be greatly in demand when applied in agricultural areas contaminated with heavy metal, as has been described for example, *Variovorax, Rhodococcus, Flavobacterium, Pseudomonas, Klebsiella, Bacillus, Stenotrophomonas, Serratia, Leifsonia* and *Enterobacter* (Ahmad et al., 2014, 2015; Belimov et al., 2005; Etesami, 2018; Mitra et al., 2018; Sharma and Archana, 2016). Metal tolerance of plants can be improved by selection of the crop species; however, microorganisms conferring metal immobilizing abilities would be potentially applied to minimize pollutant uptake (Kuffner et al., 2010).

Rather than a single microbial isolate, biofilm-like indigenous soil microorganisms having relatively high Cd tolerance and rice growth promotion would be useful for long-term management and recovery of the metal-polluted rice paddy. The objective of the present study was to isolate indigenous Cd-resistant microbial consortia from the contaminated agricultural soils by repeated enrichment culture, characterizing their Cd-tolerance and -removal capacities, and assessing their effects on the seed germination and seedling growth of Thai rice cultivar (*Oryza sativa* L.) PSL2, as well as tissue Cd content upon high Cd stress.

Materials and methods

Study site

Soil samples were collected from a Cd and zinc (Zn)-contaminated agricultural area in Pha Dei Village, Mae Sot District, Tak Province, Thailand (N 16° 40′ 35.9″ E 98° 37′ 37.4″) at an altitude of 197 m. The study site is controlled by the subtropical monsoon

http://www.aloki.hu ● ISSN 1589 1623 (Print) ● ISSN 1785 0037 (Online)
DOI: http://dx.doi.org/10.15666/aeer/1706_1467914697

climate with average annual temperature of 26 °C and average annual precipitation of 1,448 mm. This rice paddy is usually cultivated either with rice-corn or rice-bean crops in a cropping year. For enrichment and isolation of indigenous Cd resistant microorganisms, soil samples were collected from the agricultural area and alongside an irrigation streamline adjacent to the rice paddy in a single site (the sampling site is shown in *Fig. A1* in the *Appendix*). Thirty-six samples of topsoil (<20 cm in depth, ca. 1 kg in weight each) were collected from May to July 2016 (rainy season) and January to March 2017 (dry season).

Physicochemical studies of Cd-contaminated soil

The topsoil samples were collected as described above. Soil samples were divided into 2 main portions: one for physicochemical analyses and another one for the culture enrichment. The following soil properties were determined: pH (1:5 soil/water suspensions) using field-moist samples and a pH meter; electrical conductivity (EC) using an EC meter; organic matter (OM) content by wet oxidization and titration according to the modified Walkley-Black procedure (Nelson and Sommers, 1996); and oxidation-reduction potential (ORP) using field-moist samples and an ORP meter; and cation exchange capacity (CEC) was tested after leaching with 1N ammonium acetate (NH_4OAc) buffer.

The collected soil samples were oven-dried and crushed using an agate mortar before being passed through a 200-mesh sieve. The samples then were analyzed for total Cd concentration in a flame atomic absorption spectrophotometer (FAAS, AAnalyst 200, PerkinElmer®) after HNO_3 digestion (APHA, AWWA, and WEF, 2005). Bioavailable soil Cd was determined by FAAS after extraction with 0.05 M diethylene triamine pentaacetic acid (DTPA) (APHA, AWWA, and WEF, 2005). Total nitrogen (N) was measured by the Kjeldahl method (Blake, 1965). Extractable phosphorus (P) and potassium (K) were determined by the Bray II method and extraction with neutral NH_4OAc buffered to pH 7.0, respectively (Bray and Kurtz, 1945). Soil texture was examined with the hydrometer (Allen et al., 1974). Physicochemical characteristics of soil samples are listed in *Table 1*.

Table 1. *Selected physicochemical properties of the contaminated agricultural soil*

Parameter	Rainy season		Dry season	
	#1	#2	#3	#4
Temperature (°C)	24	25	26	27
pH	7.22	7.44	5.39	6.73
ORP (mV)	400	300	100	200
EC (dS m^{-1})	0.48	0.38	0.28	0.34
CEC (cmol kg^{-1})	18.2	19.4	13.8	12.6
OM (%)	1.99	1.85	1.38	1.49
Total N (mg kg^{-1})	2943	2846	2445	2628
Extractable P (mg kg^{-1})	11.0	13.0	9.0	8.0
Extractable K (mg kg^{-1})	210.0	190.0	170.0	150.0
Total Cd (mg kg^{-1})	52	45	28	41
Extractable Cd (mg kg^{-1})	5.5	4.9	4.6	3.8

Enumeration of total cells and of cultivable microorganisms in the polluted soils

http://www.aloki.hu ● ISSN 1589 1623 (Print) ● ISSN 1785 0037 (Online)
DOI: http://dx.doi.org/10.15666/aeer/1706_1467914697

The total microbial cells isolated from the original soil samples were enumerated by fluorescent blue dye Hoechst® 33342 staining method, as previously described by Brunk et al. (1979) with some modifications. Ten grams of each soil sample was resuspended with 90 ml PBS buffer. The suspension was stirred for 30 min at 200 rpm, sonicated in a sonication bath for 5 min, and then centrifuged at 3,000 rpm for 5 min. The supernatant was subjected for enumeration of total cells.

To determine the cell concentration of cultivable bacteria by the viable plate count technique, they were first inoculated in nutrient broth and incubated at 30 °C, 100 rpm for 18 h. Each serially diluted cell suspension was subsequently spread on nutrient agar plates without and with $CdCl_2$ at 50 and 100 ppm. After 24 h incubation at 30 °C, colonies of Cd-resistant bacteria were counted and referred to as colony forming units per ml (CFU ml^{-1}).

Enrichment and isolation of Cd-resistant bacteria

For enriching the Cd-resistant bacteria, the first 5 g of each sample was added to 95 ml of nutrient broth (NB, 0.5% peptone, 0.3% meat extract, pH7.0) containing 50 or 100 ppm cadmium chloride ($CdCl_2$). After 2 weeks of incubation at 30 °C, the bacteria were cultured on nutrient agar plates (NA, nutrient broth and 1.5% agar) supplemented with $CdCl_2$ for 72 h at 30 °C. The colonies of Cd-resistant bacteria were quantified as colony forming units per ml (CFU ml^{-1}). Each single bacterial colony with different morphology was then streaked onto agar medium for 24 h at 30 °C.

16S-Metagenomic analysis of the Cd-resistant consortia

Bacterial diversity and composition of the enriched consortia in comparison to the originally polluted soil consortia were analyzed using 16S rRNA gene Illumina MiSeq sequencing. Total genomic DNA was extracted from 0.5 g of frozen soils and 10 ml of the enriched culture (three replicates per treatment) using QIAamp® DNA Stool Mini Kit (Qiagen, Germany) according to the manufacturer's instructions with some modifications. The 16S rDNA (V3-V4) universal bacterial primers containing the Illumina overhang adapter sequences (as underlined) 341F (5' - TCGTCGGCAGCGTCAGATGTGTATAAGAGACAGCCTACGGGNGGCWGCAG) and 805R (5'- GTCTCGTGGGCTCGGAGATGTGTATAAGAGACAGGACTACHVGGGTATCTAATCC) were utilized for PCR amplification (Herlemann et al., 2011). The PCR mixtures (25 µl) contained 12.5 µl of 2x KAPA HiFi Hot Start Readymix (KAPA Biosystems, USA), 5 µl of each primer (1 µmol l^{-1}) and 2.5 µl of target DNA (5 ng μl^{-1}). The PCR cycling conditions consisted of an initial denaturation step at 94 °C (3 min), followed by 25 cycles of 98 °C (20 s), 55 °C (30 s) and 72 °C (30 s) and a final elongation at 72 °C (5 min). The PCR products were cleaned-up on AMPure XP beads (Agencourt Bioscience, USA). The purified amplicons (550-bp fragments) were submitted to the Omics Sciences and Bioinformatics Center (Chulalongkorn University, Bangkok, Thailand) for paired-end sequencing on the Illumina MiSeq platform.

Subsequently, the purified 16S amplicons were then indexed using 2X KAPA hot-start ready mix and 5 µl of each Nextera XT index primer in a 50 µl PCR reaction, followed by 8-10 cycles of PCR amplification. The PCR cycling was set as aforementioned. Next, the indexed 16S amplicons were purified on AMPure XP beads (Agencourt Bioscience, USA), pooled and diluted to a final loading concentration of 4 pM. Cluster generation and 250-bp paired-end read sequencing were done on an Illumina MiSeq using the MiSeq Reagent Kit at the Omics Sciences and Bioinformatics Center (Chulalongkorn University, Bangkok,

http://www.aloki.hu ● ISSN 1589 1623 (Print) ● ISSN 1785 0037 (Online)
DOI: http://dx.doi.org/10.15666/aeer/1706_1467914697

Thailand). Amplicon sequence analysis was performed with QIIME version 1.9.0. (Caporaso et al., 2010). All sequence reads were sorted based on their unique barcodes, trimmed for sequence quality, and clustered at 97% identity for operational taxonomic units (OTUs). The UCHIME algorithm was used to discard chimera sequences (Edgar et al., 2011). The microbial diversity index in terms of diversity (Shannon index) and richness (Chao1 index) were then computed using the MOTHUR (Schloss et al., 2009). To study the microbial composition and diversity, the Shannon diversity index, an estimator of species richness and diversity using a natural logarithm, accounts for both abundance and evenness of the taxa present, while Chao1 richness estimator is used to estimate diversity from abundance data and number of rare taxa missed from under-sampling.

Determination of maximum tolerance concentration (MTC) of Cd

In brief, the enriched consortia and isolated strains were inoculated in nutrient broth supplemented with $CdCl_2$ (50 to 1,000 ppm). After 18 h incubation at 30 °C, each culture was then spread on nutrient agar plates with $CdCl_2$ at the same concentrations. The highest concentration of metal ions at which growing colonies of bacteria were observed was defined as the maximum tolerance concentration (MTC) of Cd for the tested bacteria. Media without $CdCl_2$ serves as controls. All experiments were performed in triplicate.

Determination of Cd removal capacity of the enriched consortia in batch culture

Effect of the enriched Cd-resistant microbial consortia on reduction of water-soluble Cd concentration in culture medium was examined according to the method of Chen et al. (2008) with some modifications. In brief, the enriched consortia were initially cultivated in nutrient broth, harvested by centrifugation, and washed twice with sterile deionized water. Cell pellets were then resuspended in the sterile water. Triplicate flasks of nutrient broth supplemented with 50 or 100 ppm $CdCl_2$ were inoculated with microbial suspension of either the enriched consortium or the selected single strain, compared to microbial-inoculated culture without Cd and the control (uninoculated culture with Cd addition). After 24 h incubation at 30 °C, the microbial growth in the cultures was measured at the optical density (OD_{600}) for quality control (data not shown). The cell pellets were harvested by centrifugation and their dry cell weight were measured while the water-soluble Cd concentration in the supernatant was then determined with an AAnalyst 200 Perkin-Elmer® FAAS. The percentage of Cd removal of each culture was calculated using *Equation 1:*

$$\%\ Cd\ removal = \frac{CI-CF}{CI} x\ 100 \qquad \text{(Eq.1)}$$

where CI is the initial Cd concentration in the medium; CF is the Cd concentration that remains in the supernatant.

Effect of Cd-resistant bacteria on rice seedlings using the filter paper system

The plant root/shoot elongation promoting ability of the enriched consortia was assessed using the modified root elongation assay of Belimov et al. (2001). Bacteria were grown on nutrient broth containing Cd for 48 h at 30 °C and resuspended to 5×10^7 cells ml^{-1} in sterile deionized water. Six milliliters of the bacterial suspensions at final concentration 1×10^6 cells ml^{-1} or sterile water (uninoculated control) were added to glass Petri dishes containing filter paper that was soaked with 50 or 100 ppm $CdCl_2$ (final concentration) in comparison to bacterial inoculation without $CdCl_2$ as control. The seeds of rice cultivar (*Oryza sativa*

http://www.aloki.hu ● ISSN 1589 1623 (Print) ● ISSN 1785 0037 (Online)
DOI: http://dx.doi.org/10.15666/aeer/1706_1467914697

L.) PSL2 were surface-sterilized with a mixture of ethanol and 30% H_2O_2 (1:1) for 20 min, washed twice with sterile water and placed on the wetted filter paper. Root/shoot length and number of fibrous roots of seedlings were measured after incubation at 28 °C for 7 and 14 days in the dark. Dry biomass was determined after plant materials were oven-dried at 80 °C for 4 days prior to weight determination. The assay was repeated two times with six dishes (20 seeds $dish^{-1}$) for each treatment.

Effect of Cd-resistant bacteria on Cd accumulation of rice tissues

The plant root/shoot Cd content was measured according to the method of Ihnat (2000). After 14 days of incubation at 28 °C in the dark, rice seedlings grown in Cd with or without bacteria inoculation were washed twice with sterile water, oven-dried at 80 °C for 2 h, and weighed prior to Cd quantification. The Cd concentration of 30 rice seedlings per treatment was measured using an AAnalyst 200 Perkin-Elmer® FAAS after HNO_3 digestion (APHA, AWWA, and WEF, 2005). The assay was performed in triplicate.

Statistical analysis

Data were subjected to the statistical analysis using the student's t-test. The treatment means were compared by setting the significant difference at the 5% probability level (*P*-value ≤ 0.05).

Results

Enrichment and isolation of Cd-resistant soil microorganisms

During the selection of Cd-resistant microorganisms, thousands of growing colonies were observed on nutrient agar plates containing 50-100 ppm $CdCl_2$. Fluorescent nuclear staining revealed that total microbial abundance in the naturally polluted soils ranged from 1.8×10^8-8.9×10^9 cells ml^{-1} after Hoechst® 33342 dye blue staining (*Fig. 1*). The direct cultivable microbial abundance in the polluted soils ranged from 1-5 $\times 10^7$ CFU ml^{-1} after cultivation on nutrient agar plates without $CdCl_2$. After 2 weeks of repeated enrichment culture, the average number of enriched microorganisms was found to be 1.5-7.5 $\times 10^8$ CFU ml^{-1} on nutrient agar plates with 50 ppm $CdCl_2$. Thereby, indigenous Cd-resistant microbial consortia were successfully isolated by the repeated enrichment method and sequential dilution technique.

Relative abundance and composition structure of the enriched consortia

The relative abundance and composition of the enriched consortia were assessed and compared to the originally polluted topsoil consortia by a 16S metagenomic sequencing approach. *Table 2* shows the alteration in the functional diversity indices of the enriched consortia, in comparison to the polluted topsoil consortia. Diversity indices of the enriched consortia were altered when compared to the naturally polluted topsoil samples, as shown by the decrease in the Shannon diversity index and the Chao1 richness estimator.

http://www.aloki.hu ● ISSN 1589 1623 (Print) ● ISSN 1785 0037 (Online)
DOI: http://dx.doi.org/10.15666/aeer/1706_1467914697

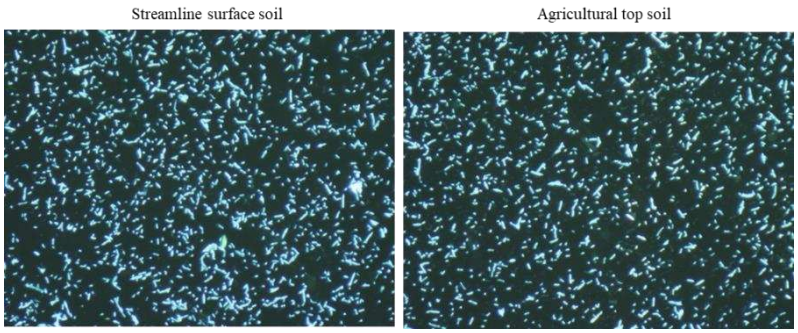

Figure 1. *Representative images showing total cellular abundance of indigenous soil microbial consortia. Total microbial cells were directly collected from the Cd polluted soils: streamline surface soil (left panel) and agricultural top soil (right panel). Microbial DNA was stained with Hoechst 33342 fluorescent dye, and observed under a fluorescence microscope at 1,000× magnification*

Table 2. *Summary of bacterial 16S sequencing data and diversity estimates for each sample*

Sample	Season	Reads	OTUs	Coverage	Chao1	Shannon
TS#1	Rainy	62157 ± 6091	2698 ± 319	0.998	7740.87	10.86
TS#2	Rainy	65129 ± 5982	2749 ± 258	0.998	7772.27	10.98
TS#3	Dry	63269 ± 7081	2643 ± 321	0.997	5700.46	10.84
TS#4	Dry	61709 ± 7109	2763 ± 289	0.997	6759.19	10.85
BC#1	Rainy	60987 ± 8305	3019 ± 196	0.996	491.35**	4.69**
BC#2	Rainy	61268 ± 7949	2991 ± 362	0.995	551.72**	4.75**
BC#3	Dry	60106 ± 8104	3026 ± 234	0.995	470.77**	4.42**
BC#4	Dry	61232 ± 7756	2987 ± 265	0.996	474.97**	4.60**

**Indicates respective significant difference at P-value ≤ 0.05, by comparing the selected parameters (Chao1 richness or Shannon diversity estimator) of the bacterial enriched consortia (BC) to that of the original polluted topsoil (TS) samples. OTUs represent operational taxonomic units. BC indicates Cd-resistant bacterial consortia after Cd-added culture enrichment, and TS indicates topsoil samples originally contaminated with Cd

Figure 2a presents the relative abundances of the bacterial phyla in the polluted topsoil and the enriched consortia. *Planctomycetes, Proteobacteria, Acidobacteria, Verrucomicrobia, Bacteroidetes, Chloroflexi, Actinobacteria, Firmicutes* and *Gemmatimonadetes* were the most dominant phyla, accounting for 90% of the total bacterial 16S rRNA gene sequences in the polluted topsoil. *Planctomycetes* occupied the highest proportions (47.5%) of the bacterial sequences. *Proteobacteria, Acidobacteria, Verrucomicrobia, Bacteroidetes, Chloroflexi, Actinobacteria, Firmicutes* and *Gemmatimonadetes* were identified in all topsoil samples at cumulative relative abundance (ca.42.5%). Approximately 2% of bacterial phyla were unassigned.

The consecutive addition of Cd at increasing concentrations (20-100 ppm) could select population of Cd-resistant bacterial phyla among other Cd-sensitive phyla. The 16S metagenomic result showed that the 3 top phyla including *Proteobacteria* (47.7%) *Firmicutes* (36.5%) and *Bacteroidetes* (15.5%) were markedly enriched relative to the original topsoil (P-value ≤ 0.05) (*Fig. 2a*). The relative abundances of *Proteobacteria, Firmicutes*, and *Bacteroidetes* increased across the culture enrichment period, while those

http://www.aloki.hu ● ISSN 1589 1623 (Print) ● ISSN 1785 0037 (Online)
DOI: http://dx.doi.org/10.15666/aeer/1706_1467914697

of *Acidobacteria, Actinobacteria, Chloroflexi, Gemmatimonadetes, Planctomycetes,* and *Verrucomicrobia* decreased. In the enriched consortia, predominant detoxifiers at finer taxonomic level of *Proteobacteria* (including *Arcobacter* sp., *Comamonas* sp., *Pseudomonas* sp., *Acinetobacter* sp., *Stenotrophomonas* sp., and *Delftia* sp.), *Firmicutes* (including *Leuconostoc* sp., *Enterococcus* sp., *Lactobacillus* sp., and *Lactococcus* sp.), and *Bacteroidetes* (including *Wautersiella* sp., *Myroides* sp., *Cloacibacterium* sp., *Paludibacter* sp.) were uncovered among other genera (*Fig. 2b*). The enriched microbial consortia were successfully established and subjected to subsequent characterization.

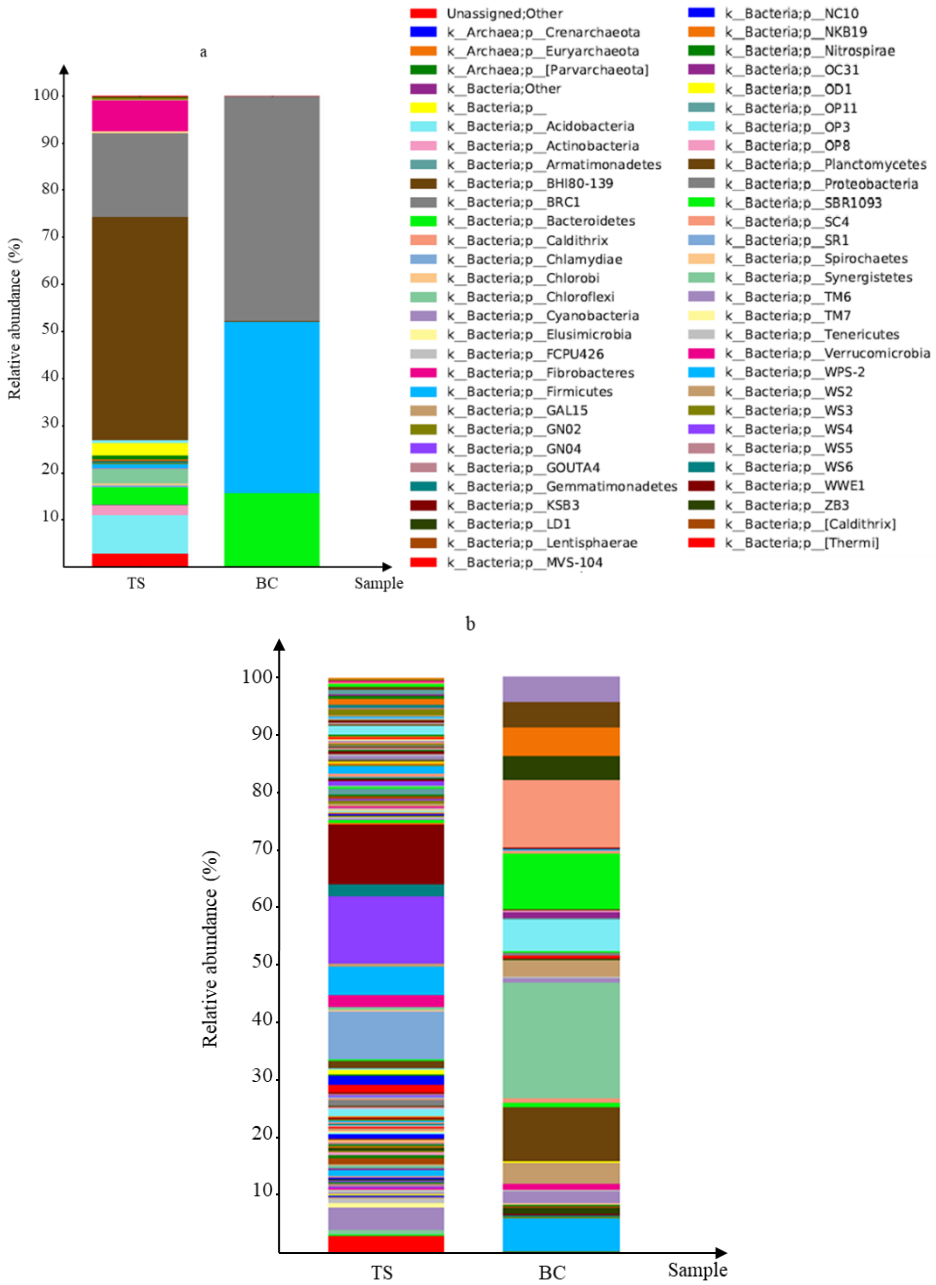

Figure 2. *Representative images showing relative abundance levels of dominant bacterial phyla (a) and genera (b) in the contaminated topsoil (TS) and the enriched cadmium-resistant bacterial consortia (BC) (cultivable Cd) based on 16S metagenomic sequencing*

http://www.aloki.hu ● ISSN 1589 1623 (Print) ● ISSN 1785 0037 (Online)
DOI: http://dx.doi.org/10.15666/aeer/1706_1467914697

Determination of maximum Cd tolerance and Cd removal capacity of the enriched consortia

The maximum tolerance of the enriched microbial consortia toward $CdCl_2$ (0-1,000 ppm) were determined in comparison to that of selected single strains. Viable plate counts showed that the enriched consortia grew well and survived on nutrient agar containing $CdCl_2$ up to 800 ppm (*Fig. A2* in the *Appendix*), while most of the isolated single strains could only grow on the media with much lower $CdCl_2$ up to 200 ppm (*Fig. A3* in the *Appendix*).

Furthermore, the effect of enriched consortia on immobilization of toxic Cd in the batch culture was investigated. After 24 h incubation, the water-soluble Cd concentration in each supernatant was remarkably decreased upon inoculation of either enriched consortia or single isolates. In presence of 50 ppm Cd, the enriched consortia had Cd removal capacities ranging from 19.3 ± 0.9 to 25.5 ± 0.8 mg g^{-1} cell dry weight, equivalent to 52.8-56.3% Cd removal (*Table 3*). At a higher Cd concentration of 100 ppm, the Cd removal capacities ranged from 37.4 ± 1.2 to 48.6 ± 0.6 mg g^{-1} cell dry weight, equivalent to 68.7-77.5% Cd removal (*Table 3*). This indicated that the inoculation of Cd-resistant microorganisms could reduce water-soluble level of toxic Cd in order to possibly overcome Cd toxicity in the culture, and that the exogenous addition of Cd affected Cd removal capacities of the enriched consortia.

Table 3. *Cadmium removal capacity of indigenous Cd-resistant bacterial consortia (BC) after batch culture in nutrient broth containing $CdCl_2$ at 50-100 ppm*

Microbial culture sample	Cd concentration (ppm)	Percentage of Cd removal (%)	Cell dry weight (g)	Cd removal capacity (mg g^{-1} cell dry weight in average)
BC#1	0	0	0.22	-
	50	52.8**	0.25	19.3 ± 0.9
	100	71.9**	0.19	37.4 ± 1.2
BC#2	0	0	0.20	-
	50	56.3**	0.22	25.4 ± 0.8
	100	68.7**	0.14	48.6 ± 0.6
BC#3	0	0	0.23	-
	50	55.8**	0.26	21.2 ± 0.4
	100	76.7**	0.21	36.2 ± 0.7
BC#4	0	0	0.20	-
	50	53.2**	0.24	22.1 ± 0.9
	100	77.5**	0.17	45.3 ± 0.7
Bacillus cereus	0	0	0.21	-
	50	14.9**	0.19	8.6 ± 0.5
	100	24.5**	0.12	19.7 ± 0.4

**Indicates respective significant difference at P-value ≤ 0.05, by comparing the selected parameters of Cd-treated group to that of control (untreated group) at indicated concentrations of $CdCl_2$. BC indicates Cd-resistant bacterial consortia after Cd-added culture enrichment

Effect of Cd-resistant microbial consortia on rice germination and seedling growth toward high-concentration Cd in vitro

Cadmium usually impairs plant growth, which is one indicator for evaluating plant ability in response to Cd stress. Inoculation with the enriched consortia was applied for

http://www.aloki.hu ● ISSN 1589 1623 (Print) ● ISSN 1785 0037 (Online)
DOI: http://dx.doi.org/10.15666/aeer/1706_1467914697

germination and growth studies at seedling stage of the Thai rice cultivar PSL2 in the presence or absence of Cd. After 7 days of incubation, the length of roots and shoots and number of fibrous roots were measured in rice seedlings treated with or without the enriched consortia inoculant, in comparison to a soil bacterium *Bacillus*-inoculated group and non-metal treated group (control) upon Cd exposure (either 50 or 100 ppm). The control rice exhibited normal growth (*Fig. 3a; Table 4*), while the Cd-treated groups exhibited symptoms of toxicity; showing inhibited primary root growth and reduced shoot length (*Fig. 3a; Table 4*). Indeed, the obvious effect of Cd toxicity on rice roots rather than shoots was observed. Seedlings treated with the bacterial inoculant at 1×10^6 CFU ml^{-1}, in the absence of $CdCl_2$, exhibited normal root elongation and somewhat enhanced fibrous root number. Upon Cd exposure, the enriched consortia-inoculated seedlings markedly enhanced root length and fibrous root number, and moderately increased shoot length, compared with uninoculated seedlings (*Fig. 3a, b*). Particularly, the addition of enriched consortia inoculant obviously enhanced the length of roots and number of fibrous roots by 2.1- and 12-times, and by 1.9- and 18-times, respectively, in rice seedlings exposed to 50 ppm and 100 ppm Cd when compared to the uninoculated group, but the addition of *Bacillus cereus* did not (*Table 4*). A bacterial inoculant at 1×10^6 CFU ml^{-1} could alleviate phytotoxicity, as evidenced by promoted rice germination and seedling growth even under Cd stress.

Table 4. *Effect of indigenous Cd-resistant bacterial consortia (BC) on 7-day rice germination of the Thai rice PSL2 on filter paper system containing $CdCl_2$ at 50 or 100 ppm, with Bacillus cereus as control*

Treatment	Root length (cm in average)	Shoot length (cm in average)	No. of fibrous root (in average)
Control	7.5 ± 2.8	4.6 ± 2.6	28 ± 7.4
Bacillus cereus	6.2 ± 2.2	4.2 ± 2.3	26 ± 7.2
50 ppm $CdCl_2$	2.8 ± 0.8**	3.2 ± 0.6**	2 ± 1.1**
50 ppm $CdCl_2$ + *B. cereus*	1.8 ± 0.5**	3.1 ± 0.7**	2 ± 1.4**
Control	7.5 ± 2.8	4.6 ± 2.6	28 ± 7.4
Cd-resistant BC	7.1 ± 2.2	4.5 ± 2.4	35 ± 9.8
50 ppm $CdCl_2$	2.8 ± 0.8**	3.2 ± 0.6**	2 ± 1.1**
50 ppm $CdCl_2$ + BC	5.9 ± 1.6##	4.0 ± 2.4	24 ± 9.2##
100 ppm $CdCl_2$	2.2 ± 0.6**	3.6 ± 0.4 **	1 ± 1.8**
100 ppm $CdCl_2$ + BC	4.1 ± 1.3##	3.9 ± 2.1	18 ± 8.3##

**Indicates significant difference at P-value ≤ 0.05, by comparing the selected parameters of Cd-treated group to that of control (untreated group), and ## indicates significant difference at P-value ≤ 0.05, by comparing the selected parameters of bacteria inoculated group to that of uninoculated group in presence of $CdCl_2$ at indicated concentrations. BC indicates Cd-resistant bacterial consortia after Cd-added culture enrichment

Effect of Cd-resistant consortia on biomass and Cd accumulation of rice tissues toward high-concentration Cd in vitro

In absence of Cd, the enriched consortia enhanced biomass production of shoot and particularly root of Thai rice PSL2 seedlings. The exogenous addition of Cd at 100 ppm decreased root and shoot dry biomass of rice by 16.1 and 44.5%, respectively, compared to control (*Table 5*). However, within 14 days of exposure the microbial consortia-

http://www.aloki.hu ● ISSN 1589 1623 (Print) ● ISSN 1785 0037 (Online)
DOI: http://dx.doi.org/10.15666/aeer/1706_1467914697

inoculated seedlings significantly ($p > 0.05$) increased both root and shoot dry biomass at least at one concentration of $CdCl_2$ (50 or 100 ppm) as compared to the Cd-treated group alone (*Table 5*). Our result indicated that the inoculation with enriched consortia at 1×10^6 CFU ml^{-1} positively affected root biomass production and moderately influenced the shoot length upon high Cd exposure level.

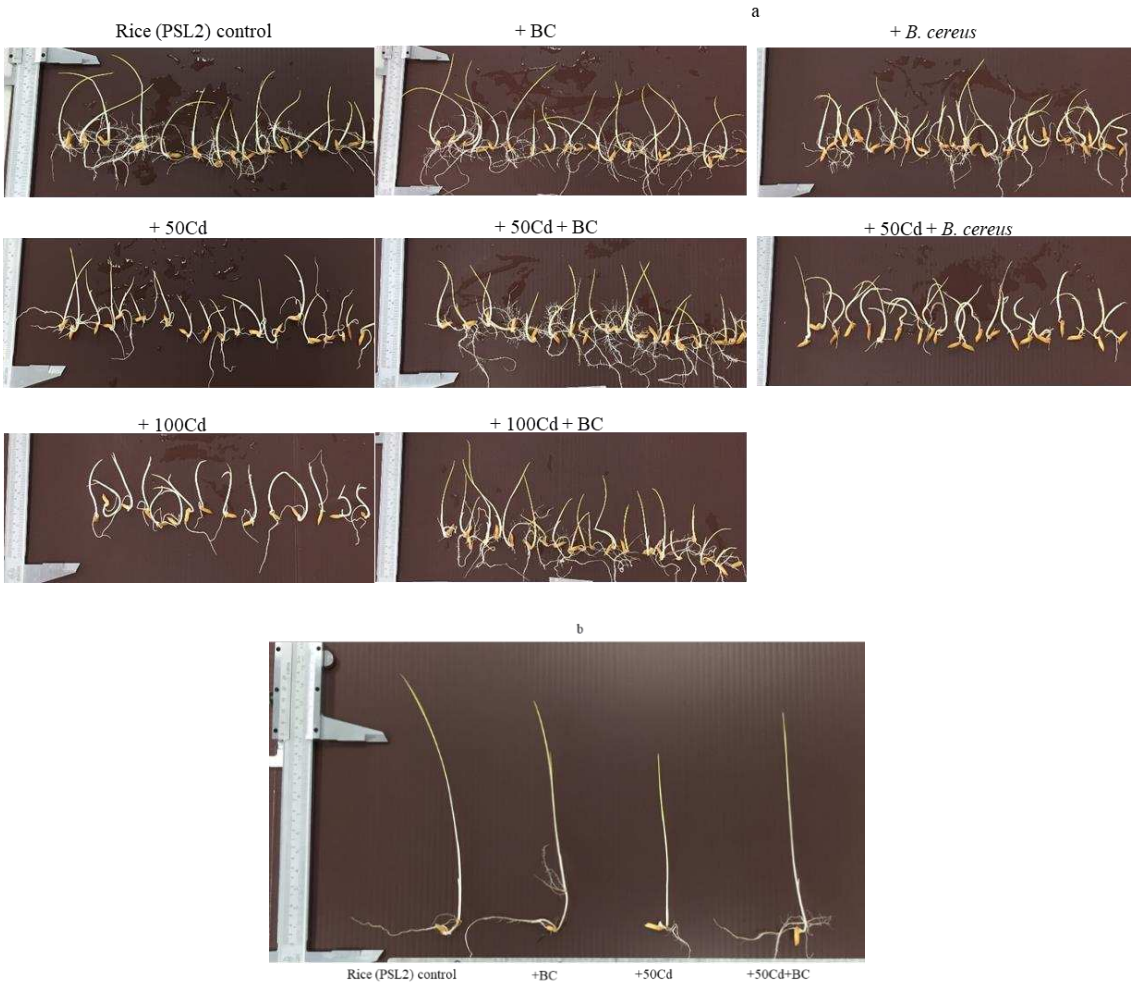

Figure 3. *Effect of indigenous Cd-resistant bacterial consortia (BC) on (a) 7-day rice germination in filter paper cultures containing $CdCl_2$ at 50 or 100 ppm, with use of Bacillus cereus as control bacteria, and on (b) 14-day representative growth of rice seedling inoculated with the bacterial consortia in absence or presence of Cd at 50 ppm, as compared to the uninoculated bacterial consortia*

Cadmium content in rice root and shoot was influenced by exogenous addition of Cd; however, the inoculation of enriched consortia remarkably ameliorated Cd accumulation in rice tissues even at the initial seedling stage (*Table 5*). Cadmium accumulation in rice root and shoot significantly ($p > 0.05$) decreased when the treatment with enriched consortia at both levels of Cd exposure (50 and 100 ppm). Notably, the inoculation with enriched consortia at 1×10^6 CFU ml^{-1} led to mitigated metal phytotoxicity due to reduced Cd bioconcentration and promoted biomass production in rice seedlings toward high Cd exposure level, as summarized in *Figure 4*.

http://www.aloki.hu ● ISSN 1589 1623 (Print) ● ISSN 1785 0037 (Online)
DOI: http://dx.doi.org/10.15666/aeer/1706_1467914697

Table 5. *Effect of indigenous Cd-resistant bacterial consortia (BC) on 14-day rice shoot and root dry biomass and Cd content in solution system containing $CdCl_2$ at 50 or 100 ppm, with Bacillus cereus as control*

Treatment	Root dry biomass (mg)	Shoot dry biomass (mg)	Root Cd content (mg kg^{-1})	Shoot Cd content (mg kg^{-1})
Rice (PSL2) control	14.2 ± 2.0	41.4 ± 4.8	-	-
Bacillus cereus	13.3 ± 1.4	38.2 ± 1.7	-	-
50 ppm $CdCl_2$	13.9 ± 1.9 (1.3%)	31.2 ± 3.5 (24.6%)	85.3 ± 1.3	43.2 ± 1.7
50 ppm $CdCl_2$ + *B. cereus*	14.0 ± 2.6	33.0 ± 1.7	90.8 ± 1.4	45.3 ± 1.4
Control	14.2 ± 2.0	41.4 ± 4.8	-	-
Cd-resistant BC	25.4 ± 4.4	44.4 ± 3.2	-	-
50 ppm $CdCl_2$	13.9 ± 1.9 (1.3%)	31.2 ± 3.5 (24.6%)	85.3 ± 1.3	43.2 ± 1.7
50 ppm $CdCl_2$ + BC	23.9 ± 3.5$^{\#\#}$	35.5 ± 2.7	51.2 ± 1.9$^{\#\#}$	30.5 ± 1.6$^{\#\#}$
100 ppm $CdCl_2$	11.9 ± 0.7 (16.1%)	23.0 ± 5.3 ** (44.5%)	162.1 ± 1.5	72.6 ± 2.0
100 ppm $CdCl_2$ + BC	19.8 ± 1.8$^{\#\#}$	34.07 ± 1.6$^{\#\#}$	99.9 ± 2.2$^{\#\#}$	54.0 ± 1.1$^{\#\#}$

**Indicates significant difference at P-value ≤ 0.05, by comparing the selected parameters of Cd-treated group to that of control (untreated group), and ## indicates significant difference at P-value ≤ 0.05, by comparing the selected parameters of bacteria inoculated group to that of uninoculated group in presence of $CdCl_2$ at indicated concentrations. Numbers in bracket represents percentage of decrease in plant dry biomass of Cd-treated group relative to control. BC indicates Cd-resistant bacterial consortia after Cd-added culture enrichment

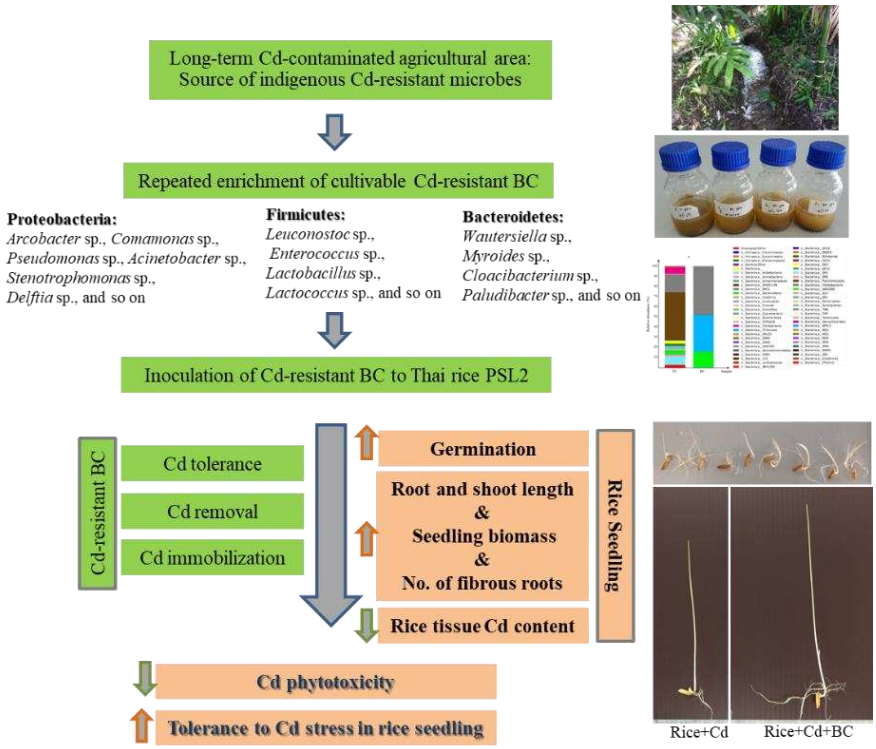

Figure 4. *Scheme illustrating the mitigation of Cd stress by inoculation of indigenous Cd-resistant soil bacterial consortia (BC) in seedlings of Thai rice cultivar PSL2 under high Cd exposure level. Due to the Cd tolerance and removal properties of microbial inoculants, Cd phytotoxicities were alleviated as evidenced by increased seedling germination and growth as well as lower Cd accumulation in rice tissues. The top phyla including Proteobacteria (47.7%) Firmicutes (36.5%) and Bacteroidetes (15.5%) were enriched accounting for 99.7% of total bacterial sequences*

http://www.aloki.hu ● ISSN 1589 1623 (Print) ● ISSN 1785 0037 (Online)
DOI: http://dx.doi.org/10.15666/aeer/1706_1467914697

Discussion

Inoculation of plant inhabiting extreme environments (such as Cd-polluted soils) with specific metal resistant microorganisms could allow them to be more tolerant to high metal stress (Sharma and Archana, 2016). Selection of these metal resistant microorganisms which are capable of promoting plant growth in contaminated environments and minimizing accumulation of metal in edible parts is our intention. Out of concern for the Cd contamination in agricultural areas of Western Thailand and its effects on human health, indigenous soil microbial consortia with high Cd tolerance were herein screened for potential application to reduce Cd accumulation in rice tissues. This experiment was designed with the idea that these indigenous Cd-resistant microorganisms have high intrinsic fitness to the local area, and cause minimum disturbance to the local micro-ecological niche.

In this study, indigenous Cd-resistant soil microbial consortia that were successfully enriched on media successively supplemented with Cd had a maximum tolerance to Cd of 800 ppm while the selected single strains mostly exhibited much lower tolerance to Cd. Microbial growth was primarily inhibited upon Cd exposure, but the consecutive addition of Cd could induce microbial tolerance to this metallic element. The tolerance to higher Cd levels might be attributed to several tolerance mechanisms, including biosorption, intracellular/extracellular sequestration, complexation, and active efflux (Gadd, 2004; Sharma and Archana, 2016). Indeed, microbial consortia in microenvironments are mostly present as biofilms, which promotes resistance of microbial cells by forming a protective sheath, as well as transforming toxic metal ions into non-toxic forms after biosorption (Hall-Stoodley et al., 2004). Certain metal resistant plant-growth promoting microorganisms can excrete extracellular polymeric substances (e.g., polysaccharides, glycoproteins and lipopolysaccharide) and consequently stimulate biofilm formation in response to toxic metal, as well as facilitating the plant to obtain more water and nutrients. In addition to biosorption, bioaccumulation has a major role in heavy metal uptake and further detoxification by metal-resistant plant-growth promoting microorganisms. Moreover, the enriched consortia had much higher Cd removal capacities. They also showed *in vitro* ability to promote rice germination, growth, and biomass production at the seedling stage; however, whether these traits would be active in the paddy field depends on their survival in the natural conditions and capability to colonize rice roots.

Upon high Cd exposure (50 or 100 ppm), the inoculation with enriched Cd-resistant microbial consortia to PSL2 rice (*Oryza sativa* L.) enhanced root length and biomass and fibrous root number particularly, and moderately increased shoot length and biomass, compared with the uninoculated seedlings. The increase in root biomass and development of numerous fibrous roots might improve plant performance by extracting more water and nutrients, and consequently promote plant growth under Cd stress (Ahmad et al., 2014). As previously evidenced by the root and shoot biomass data, the inoculation of a metal-resistant *Pseudomonas* sp. bacterium was regarded as an effective approach for protecting plants against toxic metals (Rajkumar and Freitas, 2008). *Pseudomonas* spp. belonging to the plant growth-promoting bacterial group is capable of heavy metal biosorption and bioaccumulation, consequently reducing the metal phytotoxicity to the plant (Zaidi and Musarrat, 2004). Similar to our study, the inoculation by enriched Cd-resistant microbes ameliorated Cd toxicity and promoted germination of rice seedlings. The microbial load at 1×10^6 CFU ml^{-1} could enhance rice germination and seedling growth even at high Cd exposure level.

http://www.aloki.hu ● ISSN 1589 1623 (Print) ● ISSN 1785 0037 (Online)
DOI: http://dx.doi.org/10.15666/aeer/1706_1467914697

Our finding was consistent with a previous study that reported that monocotyledonous plants under stressful conditions generally develop a shallow and fibrous root network, enabling them to anchor and efficiently collect surface water (Uraguchi and Fujiwara, 2012). Siripornadulsil and Siripornadulsil (2013) demonstrated that *Cupriavidus taiwanensis* isolates enhanced fibrous root growth and shoot length in rice seedlings, as well as enhancing germination under Cd exposure. Notably, the enriched consortia had significant ($p > 0.05$) ability to reduce metal phytotoxicity in terms of root and shoot elongation, even at high Cd level (50 ppm). Lee et al. (2010) have revealed increased levels of Glutathione (GSH) and oxidative stress-responsive proteins in the rice root in response to Cd stress. Furthermore, the enriched consortia increased metal tolerance in rice seedlings, as shown by the increase in root and shoot biomass production. Our study demonstrated that the indigenous Cd-resistant microbial consortia isolated from long term Cd-contaminated agricultural area of Western Thailand performed well with the Thai rice PSL2 cultivar widely-cultivated in this area. The inoculation of high metal-resistant and bioaccumulating microorganisms might hold promise to improve plant tolerance to metal stress.

Using 16S next generation sequencing, 3 top phyla including Proteobacteria (47.7%) Firmicutes (36.5%) and Bacteroidetes (15.5%) were detected across the culture enrichment period and accounted for 99.7% of total bacterial sequences. In the enriched consortia, predominant genera of detoxifiers of Proteobacteria (including *Arcobacter* sp., *Comamonas* sp., *Pseudomonas* sp., *Acinetobacter* sp., *Stenotrophomonas* sp., and *Delftia* sp.), Firmicutes (including *Leuconostoc* sp., *Enterococcus* sp., *Lactobacillus* sp., and *Lactococcus* sp.), and Bacteroidetes (including *Wautersiella* sp., *Myroides* sp., *Cloacibacterium* sp., *Paludibacter* sp.) were identified, among other genera. Bacteroidetes is regarded as a soil health indicator, and the prevalence of certain Proteobacteria and Firmicutes is positively associated with soil-borne disease suppressiveness (Sanguin et al., 2009). Previous reports have documented Cd resistance, bioaccumulation and biotransformation in microorganisms belonging to the *Acinetobacter, Agrobacterium, Arthrobacter, Bacillus, Cupriavidus, Flavobacterium, Mycobacterium, Pseudomonas, Rhotococcus, Aspergillus,* and *Trichoderma* genera (Belimov and Dietz, 2000; Belimov et al., 2005; Roane and Pepper, 2000; Siripornadulsil and Siripornadulsil, 2013). Certain metal-resistant microorganisms, such as *Pseudomonas, Cupriavidus, Bacillus* and *Acinetobacter*, confer beneficial properties for plant growth and development (e.g., nitrogen fixation, phosphate solubilization, and phytohormones production). Recently, an isolated strain of *Delftia* sp. could stabilize Cd by intracellular bioaccumulation, and thereby decrease Cd accumulation in rice grains (Liu et al., 2018). Above mentioned microbial strains would be potentially appropriate for Cd detoxification and bioremediation of Cd-contaminated soils, as well as sustainable plant growth.

Bacteria habituating in different microenvironments have varying adaptabilities to heavy metals. The currently recognized fundamental mechanisms of heavy metal resistance are: 1) metal biosorption on the bacterial cell wall; 2) intracellular sequestration of metal by thiol-rich proteins; 3) extracellular sequestration on biosurfactants; 4) metal complexation by sulfur and phosphate; and 5) metal efflux (Sharma and Archana, 2016). Cadmium resistance of soil bacteria primarily relies on active efflux of metal ions by P-type ATPases, cation diffusion facilitator (CDF) transporters, (cobalt/zinc/cadmium) CzcCBA transporters belonging to the resistance, nodulation, cell division (RND) type efflux pump, and chemiosmotic transporters. P-type ATPases and CDF transporters are

http://www.aloki.hu ● ISSN 1589 1623 (Print) ● ISSN 1785 0037 (Online)
DOI: http://dx.doi.org/10.15666/aeer/1706_1467914697

widely present in various bacterial species, while CBA transporter likely acts as determinant for a high-degree of heavy metal tolerance (Nies, 2003). In Gram-negative bacteria, such as *Pseudomonas aeroginosa*, Cd efflux is mediated by Czc-based zinc efflux and (nickel/cobalt/cadmium) Ncc-based nickel efflux systems in combination with the proton pump ATPase (Das et al., 2016; Hrynkiewicz et al., 2015). In Gram-positive bacteria, Cd efflux occurs by Cd-exporting P-type ATPase, so called CadA pump, first identified in *Staphylococcus aureus* (Silver et al., 1989). In addition, CadA-like proteins exist in other Gram-positive bacteria, such as *Bacillus* sp. and *Listeria* sp (Bruins et al., 2000). In this respect, detailed mechanistic studies underlying metal-immobilizing and plant growth-promoting capabilities of the target enriched microorganisms under various rice stages would be meaningful for optimization and further achievement of their efficient field performance.

The beneficial effect of these Cd-resistant microbial consortia was obvious, even at the high concentration Cd, as they could remove a certain amount of Cd (ca. 50% and higher) and had tolerance to Cd (up to 800 ppm). Thus, the utilization of these consortia will be a practical, cost-effective, biotechnological approach, which is an alternative to the hugely difficult or expensive and laborious physicochemical treatment of Cd-polluted paddy soil at a large scale. Regarding our findings, the indigenous Cd-resistant microbial consortia with bioremediating and plant-growth promoting potential would be useful to improve rice crop yield and quality in a sustainable, ecologically friendly manner.

Conclusions

Taken together, our findings demonstrated that the indigenous Cd-resistant microbial consortia were successfully propagated by repeated enrichment culture. They exhibited good performance on alleviating Cd phytotoxicity and lowering Cd bioaccumulation in the Thai rice cultivar (*Oryza sativa* L.) PSL2, resulting in better plant growth upon high Cd exposure level. The 3 top phyla represented in the detoxifying consortia included *Proteobacteria, Firmicutes,* and *Bacteroidetes* (e.g., *Acinetobacter* sp., *Comamonas* sp., *Enterococcus* sp., and *Pseudomonas* sp.) but other genera were also present. The enriched consortia showed Cd-removal capacities upon high Cd exposure level. These results highlight the great promise that such Cd-resistant microbial consortia hold for bioremediation of soils for producing low Cd-accumulating rice; however, further studies of the mechanisms underlying their metal-stabilizing effects resulting in healthy plants and field performance studies should be further undertaken for better understanding and appropriate implementation.

Acknowledgements. This work was supported by a grant from Mahidol University, Thailand under the program titled “Stabilization and bioremediation of cadmium and zinc contaminated soil for sustainable rice cultivation” from the National Research Council of Thailand. Thanks to Faculty of Graduate Studies, Mahidol University, Thailand for English proofreading.

REFERENCES

[1] Ahmad, I., Akhtar, M. J., Zahir, Z. A., Naveed, M., Mitter, B., Sessitsch, A. (2014): Cadmium-tolerant bacteria induce metal stress tolerance in cereals. – Environmental Science and Pollution Research 21: 11054-11065.

http://www.aloki.hu ● ISSN 1589 1623 (Print) ● ISSN 1785 0037 (Online)
DOI: http://dx.doi.org/10.15666/aeer/1706_1467914697

[2] Ahmad, I., Akhtar, M. J., Asghar, H. N., Ghafoor, U., Shahid, M. (2015): Differential effects of plant growth-promoting Rhizobacteria on maize growth and cadmium uptake. – Journal of Plant Growth Regulation 35: 303-315.
[3] Allen, S. E., Grimshaw, H. M., Parkinson, H. M., Quarmby, J. A. (1974): Chemical Analysis of Ecological Materials. – Blackwell, Oxford.
[4] APHA, AWWA, WEF (2005): Standard Methods for the Examination of Water and Wastewater. – Public Health Association, Washington, DC.
[5] Belimov, A., Dietz, K. (2000): Effect of associative bacteria on element composition of barley seedlings grown in solution culture at toxic cadmium concentrations. – Microbiology Research 155: 113-121.
[6] Belimov, A. A., Safronova, V. I., Sergeyeva, T. A., Egorova, T. N., Matveyeva, V. A., Tsyganov, V. E., Borisov, A. Y., Tikhonovich, I. A., Kluge, C., Preisfeld, A., Dietz, K. J., Stepanok, V. V. (2001): Characterisation of plant growth-promoting rhizobacteria isolated from polluted soils and containing 1-aminocyclopropane-1-carboxylate deaminase. – Canadian Journal of Microbiology 47: 642-652.
[7] Belimov, A. A., Hontzeasb, N., Safronovaa, V. I., Demchinskayaa, S. V., Piluzzac, G., Bullittac, S., Glick, B. R. (2005): Cadmium-tolerant plant growth-promoting bacteria associated with the roots of Indian mustard (*Brassica juncea* L. Czern.). – Soil Biology and Biochemistry 37: 241-250.
[8] Bernard, A. (2008): Cadmium and its adverse effects on human health. – Indian Journal of Medical Research 128: 557-564.
[9] Blake, G. R. (1965): Bulk Density. – In: Black, C. A. (ed.) Methods of Soil Analysis. Part I: Physical and Mineralogical Properties, including Statistics of Measurement and Sampling. American Society of Agronomy, Madison, WI, pp. 374-395.
[10] Bray, R. H., Kurtz, L. T. (1945): Determination of total, organic and available forms of phosphorus in soil. – Soil Science 59: 39-45.
[11] Bruins, M. R., Kapil, S., Oehme, F. W. (2000): Microbial resistance to metals in the environment. – Ecotoxicology and Environmental Safety 45: 198-207.
[12] Brunk, C., Jones, K., James, T. (1979): Assay for nanogram quantities of DNA in cellular homogenates. – Analytical Biochemistry 92: 497-500.
[13] Caporaso, J. G., Kuczynski, J., Stombaugh, J., Bittinger, K., Bushman, F. D., Costello, E. K., Fierer, N., Peña, A. G., Goodrich, J. K., Godron, J. I. (2010): QIIME allows analysis of high-throughput community sequencing data. – Nature Methods 7: 335-336.
[14] Chen, W. M., Wu, C. H., James, E. K., Chang, J. S. (2008): Metal biosorption capability of *Cupriavidus taiwanensis* and its effects on heavy metal removal by nodulated *Mimosa pudica*. – Journal of Hazardous Material 151: 364-371.
[15] Das, S., Dash, H. R., Chakraborty, J. (2016): Genetic basis and importance of metal resistant genes in bacteria for bioremediation of contaminated environments with toxic metal pollutants. – Applied Microbiology and Biotechnology 100: 2967-2984.
[16] Deng, Z., Zhang, R., Shi, Y., Hu, L., Tan, H., Cao, L. (2014): Characterization of Cd-, Pb-, Zn-resistant endophytic *Lasiodiplodia* sp. MXSF31 from metal accumulating *Portulaca oleracea* and its potential in promoting the growth of rape in metal-contaminated soils. – Environmental Science and Pollution Research 21(3): 2346-2357.
[17] Edgar, R. C., Haas, B. J., Clemente, J. C., Quince, C., Knight, R. (2011): UCHIME improves sensitivity and speed of chimera detection. – Bioinformatics 27: 2194-2200.
[18] Etesami, H. (2018): Bacterial mediated alleviation of heavy metal stress and decreased accumulatio of metals in plant tissues: mechanisms and future propects. – Ecotoxicology and Environmental Safety 147: 175-191.
[19] Gadd, G. M. (2004): Microbial influence on metal mobility and application for bioremediation. – Geoderma 122: 109-119.
[20] Govindasamy, V., Senthilkumar, M., Bose, P., Kumar, L. V., Ramdoss, D., Annapurna, K. (2011): Acc Deaminase Containing PGPR for Potential Exploitation in Agriculture. – In:

http://www.aloki.hu ● ISSN 1589 1623 (Print) ● ISSN 1785 0037 (Online)
DOI: http://dx.doi.org/10.15666/aeer/1706_1467914697

Maheshwari, D. K. (ed.) Bacteria in Agrobiology: Plant Nutrient Management. Springer-Verlag, Berlin.

[21] Hall-Stoodley, L., Costerton, J. W., Stoodley, P. (2004): Bacterial biofilms: from the natural environment to infectious diseases. – Nature Reviews Microbiology 2: 95-108.

[22] Herlemann, D. P. R., Labrenz, M., Jurgens, K., Bertilsson, S., Waniek, J. J., Andersson, A. F. (2011): Transitions in bacterial communities along the 2000 km salinity gradient of the Baltic Sea. – ISME Journal 5: 1571-1579.

[23] Hrynkiewicz, K., Ztoch, M., Kowalkowski, T., Baum, C., Niedojadto, K., Buszewki, B. (2015): Strain-specific bioaccumulation and intracellular distribution of Cd^{2+} in bacteria isolated from the rhizosphere, ectomycorrhizae, and fruitbodies of ectomycorrhizal fungi. – Environmental Science and Pollution Research 22: 3055-3067.

[24] Ihnat, M. (2000): Metal and Other Elements at Trace Levels in Foods. – In: Horwitz, W. (ed.) Official Methods of Analysis of AOAC International. AOAC International, Maryland.

[25] Kuffner, M., De Maria, S., Puschenreiter, M., Fallmann, K., Wieshammer, G., Gorfer, M., Strauss, J., Rivelli, A. R., Sessitsch, A. (2010): Culturable bacteria from Zn- and Cd-accumulating *Salix caprea* with differential effects on plant growth and heavy metal availability. – Journal of Applied Microbiology 108: 1471-1484.

[26] Lee, K., Bae, D. W., Kim, S. H., Han, H. J., Liu, X., Park, H. C., Lim, C. O., Lee, S. Y., Chung, W. S. (2010): Comparative proteomic analysis of the short-term responses of rice roots and leaves to cadmium. – Journal of Plant Physiology 167: 161-168.

[27] Liu, Y., Tie, B., Li, Y., Lei, M., Wei, X., Liu, X., Du, H. (2018): Inoculation of soil with cadmium-resistant bacterium *Delftia* sp. B9 reduces cadmium accumulation in rice (*Oryza sativa,* L.) grains. – Ecotoxicology and Environmental Safety 163: 223-229.

[28] Mitra, S., Pramanik, K., Ghosh, P. K., Soren, T., Sarkar, A., Dey, R. S., Pandey, S., Maiti, T. K. (2018): Characterization of Cd-resistant *Klebsiella michiganensis* MCC3089 and its potential for rice seedling growth promotion under Cd stress. – Microbiological Research 210: 12-25.

[29] Nelson, D. W., Sommers, L. E. (1996): Total Carbon, Organic Carbon, and Organic Matter. – In: Sparks, D. L. (ed.) Methods of Soil Analysis. Part 3: Chemical Methods. SSSA Book Series No. 5. SSSA and ASA, Madison, WI.

[30] Nies, D. H. (2003): Efflux-mediated heavy metal resistance in prokaryotes. – FEMS Microbiology Reviews 27: 313-339.

[31] Rajkumar, M., Freitas, H. (2008): Influence of metal resistant-plant growth-promoting bacteria on the growth of *Ricinus communis* in soil contaminated with heavy metals. – Chemosphere 71: 834-842.

[32] Roane, T. M., Pepper, I. L. (2000): Microbial responses to environmentally toxic cadmium. – Microbiol Ecology 38: 358-364.

[33] Sanguin, H., Sarniguet, A., Gazengel, K., Moënne-Loccoz, Y., Grundmann, G. L. (2009): Rhizosphere bacterial communities associated with disease suppressiveness stages of take-all decline in wheat monoculture. – New Phytology 184: 694-707.

[34] Schloss, P. D., Westcott, S. L., Ryabin, T., Hall, J. R., Hartmann, M., Hollister, E. B., Lesniewski, R. A., Oakley, B. B., Parks, D. H., Robinson, C. J., Sahl, J. W., Stres, B., Thallinger, G. G., Van Horn, D. J., Weber, C. F. (2009): Introducing mothur: open-source, platform-independent, community-supported software for describing and comparing microbial communities. – Applied and Environmental Microbiology 75(23): 7537-7541.

[35] Sharma, P. K., Frenkel, A., Balkwill, L. D. (2008): A new *Klebsiella planticola* strain (cadmium-1) grows anaerobically at high cadmium concentrations and precipitates cadmium sulphide. – Applied and Environmental Microbiology 66: 3083-3087.

[36] Sharma, R. K., Archana, G. (2016): Cadmium minimization in food crops by cadmium resistant plant growth promoting rhizobacteria. – Applied Soil Ecology 107: 66-78.

[37] Silver, S., Misra, T. K., Laddaga, R. A. (1989): DNA sequence analysis of bacterial toxic heavy metal resistances. – Biological Trace Element Research 21: 145-163.

http://www.aloki.hu ● ISSN 1589 1623 (Print) ● ISSN 1785 0037 (Online)
DOI: http://dx.doi.org/10.15666/aeer/1706_1467914697

[38] Simmons, R. W., Pongsakul, P., Chaney, R. L., Saiyasitpanich, D., Klinphoklap, S., Nobuntou, W. (2003): The relative exclusion of zinc and iron from rice grain in relation to rice grain cadmium as compared to soybean: implications for human health. – Plant and Soil 257: 163-170.
[39] Simmons, R. W., Pongsakul, P., Saiyasitpanich, D., Klinphoklap, S. (2005): Elevated levels of cadmium and zinc in paddy soils and elevated levels of cadmium in rice grain downstream of a zinc mineralized area in Thailand: implications for public health. – Environmental Geochemistry and Health 27: 501-511.
[40] Siripornadulsil, S., Siripornadulsil, W. (2013): Cadmium-tolerant bacteria reduce the uptake of cadmium in rice: potential for microbial bioremediation. – Ecotoxicology and Environmental Safety 94: 94-103.
[41] Swaddiwudhipong, W., Limpatanachote, P., Mahasakpan, P., Krintratun, S., Punta, B., Funkhiew, T. (2012): Progress in cadmium-related health effects in persons with high environmental exposure in northwestern Thailand: a five-year follow-up. – Environmental Research 112: 194-198.
[42] Uraguchi, S., Fujiwara, T. (2012): Cadmium transport and tolerance in rice :perspectives for reducing grain cadmium accumulation .– Rice 5(1): 5. http//:dx.doi.org /10.1186/1939-8433-5-5.
[43] Wani, P. A., Khan, M. S., Zaidi, A. (2007): Cadmium, chromium and copper in greengram plants. – Agronomy for Sustainable Development 27: 145-153.
[44] Zaidi, S., Musarrat, J. (2004): Characterisation and nickel sorption kinetics of a new metal hyper-accumulator *Bacillus* sp. – Journal of Environmental Science Health A 39: 681-691.

APPENDIX

Figure A1. *Representative map showing the location of the single site for topsoil sampling at Pha Dei village, Phra That Pha Daeng, Mae Sot District, Tak Province, Thailand (N 16° 40′ 35.9″ E 98° 37′ 37.4″) and its surrounding with 1:500,000 ratio*

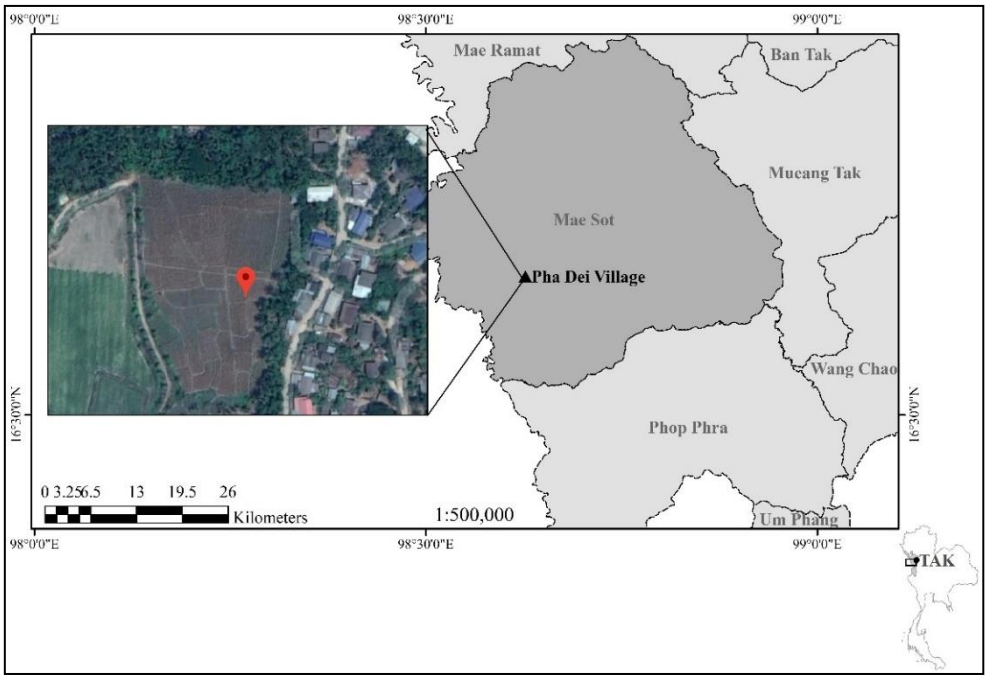

http://www.aloki.hu ● ISSN 1589 1623 (Print) ● ISSN 1785 0037 (Online)
DOI: http://dx.doi.org/10.15666/aeer/1706_1467914697

Figure A2. *Representative images showing maximum tolerance concentration (MTC) of cadmium of the enriched cadmium-resistant microbial consortia (Cultivable cadmium) on nutrient agar plates with different cadmium chloride concentrations (0, 100, 200, 300, 400, 500, 600, 700, 800, and 1000 ppm)*

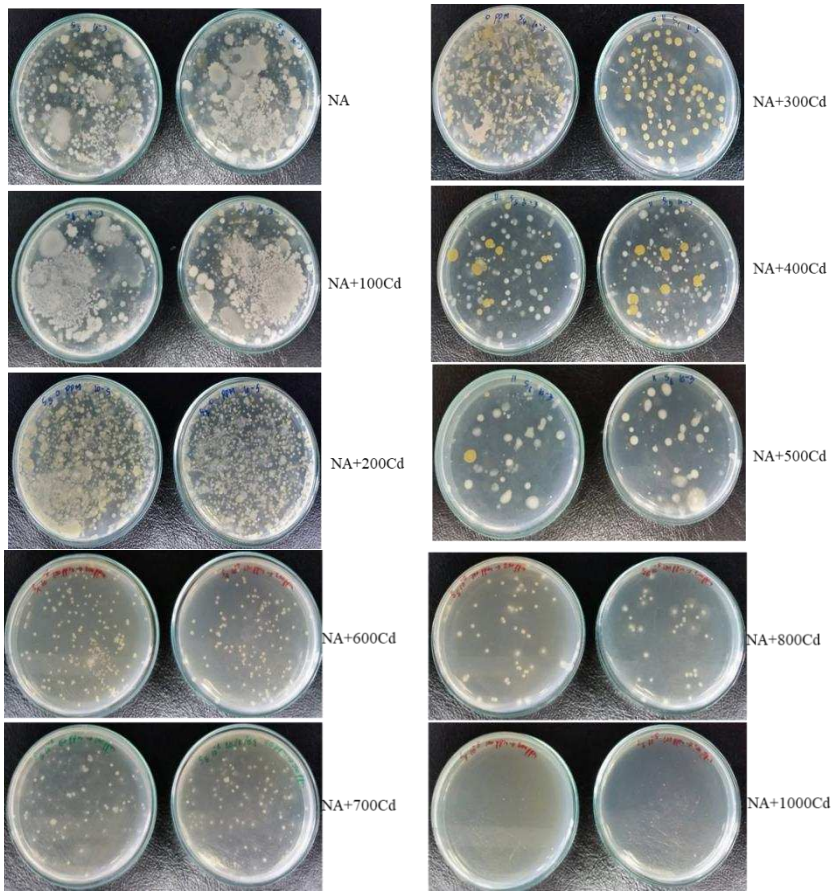

Figure A3. *Colony forming and morphology of each cadmium-resistant single strain (Cultivable cadmium) on nutrient agar plates containing 200 ppm cadmium chloride*

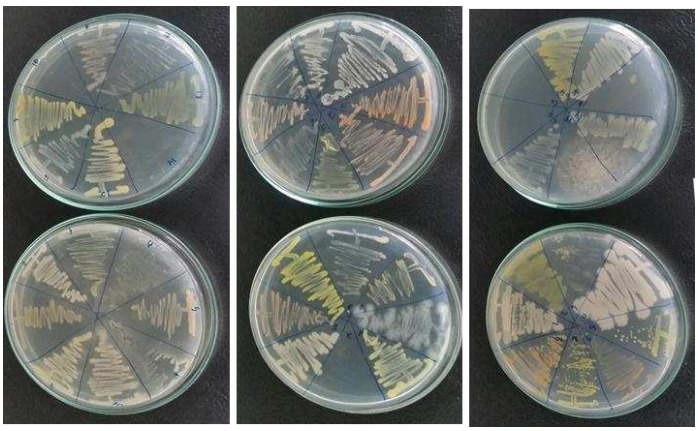

http://www.aloki.hu ● ISSN 1589 1623 (Print) ● ISSN 1785 0037 (Online)
DOI: http://dx.doi.org/10.15666/aeer/1706_1467914697

EFFECTS OF CEFAN MELON *(CUCUMIS MELO* L.*)* SEED EXTRACTS ON HUMAN ERYTHROCYTE CARBONIC ANHYDRASE I-II ENZYMES

AKKEMIK, E.[1,2*] – AYBEK, A.[1] – FELEK, I.[1]

[1]*Department of Food Engineering, Faculty of Engineering, Siirt University, 56100 Siirt, Turkey*

[2]*Science and Technology Research and Application Center, Siirt University, 56100 Siirt, Turkey*

**Corresponding author*
e-mail: eakkemik@siirt.edu.tr; phone: +90-484-223-1224/3020)

(Received 11th Jun 2019; accepted 11th Oct 2019)

Abstract. Carbonic anhydrases (CAs, E.C.4.2.1.1) are an important metalloenzyme family that catalyzes reversible CO_2 hydration and HCO_3^- dehydration in organisms. CA inhibitors can be used in the treatment of many diseases such as glaucoma, epilepsy, obesity, and cancer. This study aimed to determine the effects of oil and methanol extracts of Cefan melon (*Cucumis melo* L.) seed (CMS) on CA enzyme activity. While both extracts activated hCA-I isoenzyme, they inhibited hCA-II. In order to determine the active substance causing inhibition or activation in CMS, essential oil content, phenolic substance profile and macro-micronutrient elements were investigated. Dominant fatty acids were identified as linoleic and oleic acid, while the dominant phenolic compound was gallic acid. Besides, it was found that CMS contained high concentrations of Ca, K and Na, and was rich in Se. Results demonstrated that essential oil and phenolic compounds in Cefan melon have potential applications as alternative natural products for pharmaceutical industries. In addition, Cefan melon seed has a wide range of applications for food and cosmetic industries based on the research into the fatty acid, phenolic content, and nutrient elements.
Keywords: *inhibition, activation, fatty acid, phenolic compound, ICP MS*

Introduction

Carbonic anhydrase enzymes (CAs, E.C.4.2.1.1), containing Zn^{2+} ion as a cofactor in their structure, belonging to the metalloenzyme class, alternately catalyze the hydration of CO_2 and dehydration of HCO_3^- (Supuran, 2008). CAs are encoded by different genes in many families. The class of α CAs which includes high vertebrate organisms contains 16 different isoenzymes. These isoenzymes are tissue-specific and could be seen in different compartments of cells, and they could be used as disease markers (Lehtonen et al., 2004; Cankaya et al., 2007; Uymaz, 2017; Akkemik et al., 2018). CAs are very important in terms of their physiological roles, and besides their role as being pH regulator enzyme, they are involved in many physiological and pathological events such as calcification, tumor growth and biosynthetic reactions such as urea synthesis, lipogenesis and gluconeogenesis (Scozzafava et al., 2006; Supuran, 2008). Inhibition or activation of these isoenzymes is of paramount importance in many diseases such as glaucoma, epilepsy, gastric, neurological disorders, obesity and cancer (Scozzafava et al., 2006; Supuran, 2008; Aggarwal et al., 2013; Uymaz, 2017). Also, it has been stated that CA activators could be used in the treatment of Alzheimer's disease (AD) (Dilek, 2017; Akkemik et al., 2018).

hCA-I in cell cytosol is involved in the process of pH homeostasis, respiration and erythroid differentiation (Chegwidden et al., 2000; Picaud et al., 2009; Hassan et al.,

http://www.aloki.hu ● ISSN 1589 1623 (Print) ● ISSN 1785 0037 (Online)
DOI: http://dx.doi.org/10.15666/aeer/1706_1469914713

2013). What makes this isoenzyme important is its relationship with some pathological processes such as chronic acidosis, diabetic macular edema, proliferative diabetic retinopathy and vasogenic edema (Chegwidden et al., 2000; Picaud et al., 2009; Hassan et al., 2013). Furthermore, it has been stated that it is a biomarker for many cancer types such as colorectal cancer (Woolley, 1975), non-small cell lung cancer (Dodgson and Forster, 1985) and prostate cancer (Gay et al., 1984). The function of CA II is necessary for bone resorption, osteoclast differentiation and liquid secretion regulation to the ophthalmic anterior chamber. Recent findings suggest that CA II activity functions in connection with several ion carriers, and CA II act as mediators of certain metabolic pathways through providing additional substrates to balance cytosolic pH of carriers. As a result of these interactions, CA II is involved in the pathogenesis of various diseases such as glaucoma, renal tubular acidosis, cerebral calcification, hypertrophy of cardiomyocytes, growth retardation and osteoporosis (Coleman, 1975; Nishimori et al., 2007; Casey et al., 2009; Torring et al., 2009). Lack of expression and reduced or abnormal expression of these isoenzymes disrupt the balance of the system, which could lead to various diseases. Many synthetic drugs are used to reestablish and sustain this balance. However, synthetic drugs involve expensive synthesis and characterization procedures, and have many side effects. Phytotherapy using natural products has gained importance recently. However, a study examining the effects of melon on CA enzyme activity is not available in the literature.

Melon (*Cucumis melo*) belongs to the Cucurbitaceae family and is consumed commonly because of its pleasant aroma and flavor. Not only melon fruit but also its peel and seed are consumption material. Moreover, sufficient consumption of melon is beneficial for health. Given the 2017 data of FAO, 75% of melon production is realized in the Asia continent (FAOSTAT, 2018). While China ranks in the first place in world melon production with 17,082,608 tons, Turkey ranks second with 1,813,422 tons (FAOSTAT, 2018). There are many melon varieties grown in Turkey. Among the known medical uses of melon are the elimination of kidney stones, treatment of alcohol intoxication and even prevention of heart attacks (Van Wyk and Gericke, 2000; Nyam et al., 2009).

Therefore, In the present study, the effects of the oil and methanol extracts of Cefan melon on the activity of hCA-I and hCA-II isoenzymes were investigated the first time. We hypothesized that oil and methanolic extracts of Cefan melon seeds could exhibit different effects on two isoenzymes in a manner that will keep the system in balance to prevent the onset of diseases. Moreover, in order to determine the active substance causing inhibition or activation in Cefan melon seed, essential oil content, phenolic substance profile, and macro-micronutrient elements were investigated using GC-MS, HPLC, and ICP-MS.

Materials and methods

Melon seed material

Cefan melon (CM) is a melon variety growing in TRC3 region covering Siirt, Mardin, Batman and Şırnak in Turkey. Cefan melon was commercially purchased from markets, and maintained in Siirt University, Science and Technology Application and Research Center throughout the study. Dried seeds constituted approximately 6.6% of Cefan melon.

http://www.aloki.hu ● ISSN 1589 1623 (Print) ● ISSN 1785 0037 (Online)
DOI: http://dx.doi.org/10.15666/aeer/1706_1469914713

Extraction of phenolic compounds and oil

Extraction of oil was performed based on Malićanin method (Malićanin et al., 2014). This method was modified according to our laboratory conditions. For oil extraction, approximately 30 g of dried and the ground sample was wrapped in a filter paper and placed in Soxhlet extractor. 400 ml of petroleum ether was added in volumetric flasks which were placed on a hot plate. The condenser was adjusted, and the process was started. The extraction continued for 60 min at 23°C. Oil was purified by evaporating petroleum ether of oil mixture obtained at the end of the process in an evaporator (Hei Polphl/Heilbad-hei-vap evaporator). **The** extraction of phenolic compounds was performed according to method described by Xu et al. (2010). For the preparation of methanol extract, 5 g granulated melon seed was taken into a volumetric flask. 20 mL 1:1 distilled water: methanol mixture was added, and the flask was taken to a shaking water bath (Julabo/SW22) with 200 rpm at 50 °C for 2 h. After the incubation, centrifugation was performed at 5,000 rpm for 5 min (Thermo Scientific/Megafuge 16R). The supernatant was taken and used in furthers analyses. All analyses were replicated three times.

In vitro effects of phenolic compounds and oil extracts on human erythrocyte carbonic anhydrase I-II isoenzymes

Purification of CA I and II isozymes from human erythrocyte was performed in a single step by sepharose-4B-L tyrosine-sulfonamide affinity column. Erythrocyte was hemolyzed with iced pure water at 1:5 (v:v) ratio. The hemolysis solution was centrifuged at 10.000×g for 30 min and the upper layer of hemolysate was collected. The pH of the hemolysate was adjusted to 8.7 with solid Tris. Then, the hemolysate was applied to the affinity column pre-equilibrated with 25 mM Tris-HCl/0,1 M Na_2SO_4 (pH 8.7) and the column was washed with 25 mM Tris-HCl/22 mM Na_2SO_4 buffer (pH 8.7). The washing process was continued until the absorbance difference of eluate and equilibration buffer reached to 0.05 at 280 nm. Then 1 M NaCl/25 mM Na_2HPO_4 (pH 6.3) and 0.1 M $NaCH_3COO$/0.5 M $NaClO_4$ (pH: 5.6) buffers were used to elute the hCA-I and hCA-II isoenzymes, respectively. All experiments were carried out at +4 °C (Akkemik et al., 2018). The presence of the enzymes in tubes was determined by measuring the absorbance at 280 nm using elution buffers as blind samples. Then, the enzyme solution was dialyzed against 0.05 M Tris-SO_4 (pH 7.4). The enzyme purity was checked with 3-10% SDS-PAGE in accordance with Laemmli procedure (Protein Standard; Abcam Inc USA, ab48854) (Laemmli, 1970). Protein determination was performed using the Bradford assay (Bradford, 1976). The esterase activity assay of the hCA isozymes was conducted spectrophotometrically by following the change in absorbance at 348 nm of 4-nitrophenol produced from 4-nitrophenylacetate by CA catalyzed reaction. The reaction mixture contained 0.05 M Tris-SO_4 (pH 7.4), 3 mM p-nitrophenol acetate, distilled water and enzyme solution (Verporte et al., 1967; Akkemik, et al., 2018). To determine the inhibitory effect of samples on hCA isoenzymes I and II, esterase activity was measured on samples at five different concentrations. Control cuvette activity was accepted as 100% in the absence of inhibitor. An Activity % − [Extract] graph was drawn for each extract. Calculation of K_i constants was performed using the Cheng–Prusoff equation (Cheng and Prusoff, 1973). VWR UV-6300PC double beam spectrophotometer was used in all spectrophotometric analyses. All analyses were replicated three times.

http://www.aloki.hu ● ISSN 1589 1623 (Print) ● ISSN 1785 0037 (Online)
DOI: http://dx.doi.org/10.15666/aeer/1706_1469914713

Essential oil, phenolic acid and nutrient element composition analyses of Cefan melon

All content analyses in this study were performed in Siirt University, Science and Technology Application and Research Center.

Analysis of essential oil content by GC-MS

The fatty acid analysis was performed using a GC-MS Thermo/ISQLT series Gas chromatograph-mass spectroscopy (GC-MS, Thermo Fisher Scientific, the US) based on the method described by Kılıçoğlu (2018) with a slight modification. **The** GC-MS analysis was conducted with helium gas (1.2 mL/min) in the Thermo Scientific TG-WAXMS column (60 m-0.25 mm, 0.25 µm film thickness). GC furnace temperature was kept at 70 °C for 6 min, then increased to 230 °C at a rate of 4 °C/min and was finally kept stable for 15 min at this temperature. Purge flow was adjusted to 5.0 mL/min. The split flow was adjusted to 6.0 mL/min and injection volume was 1 µL. Mass spectrometer scan range was adjusted to m/z 50-550 atomic mass unit (amu) and screening time was adjusted to 0.2 s. NIST and Wiley GC-MS libraries were used in the determination of the components. The relative percentages of the separated components were calculated from the total ion chromatography through the digital integrator. These analyses were replicated twice.

Analysis of phenolic acid composition by HPLC

The methanol extract was added to vials using 0.22 µm filters. The phenolic composition analysis was performed by a Thermo/DIONEX Ultimate 3000 series high-performance liquid chromatography (HPLC-DAD, Thermo Fisher Scientific, the US) based on the method described by Duran (2014) with a slight modification (Montealegre et al., 2006; Duran, 2014). HPLC was performed with a C-18 Inertsil ODS-3 column (5 µm particle, 4.6 × 250 mm ID) which was equipped with a UV detector. The UV detector absorbance was monitored at 280 nm. The mobile phases consisted of solvent A (98: 2 (Water: Formic Acid)) and solvent B (78: 20: 2 (water: Acetonitrile: Formic Acid)). The flow rate was set at 0.75 ml/min, and the column temperature was maintained at 28 °C throughout the test. Gallic acid (60 ppm), chlorogenic acid (40 ppm), caffeic acid (38 ppm), 4-hydroxybenzoic acid (50 ppm) and vanillic acid (56 ppm) were used as standards (*Table 1*). The sample injection volume was 20 µL. The concentrations of phenolic acids in the sample were calculated using standard curves from a plot of peak areas versus levels for a series of standard solutions. The results were multiplied by the dilution factor. These analyses were replicated three times.

Table 1. *Analytical parameters for HPLC-DAD analysis*

No	Compounds	UV	Coeff. det %	Linearity range (ppm)	Slope
1	Gallic acid	280	99.9039	60-6.0	0.8979
2	Chlorogenic acid	280	99.7478	40-4.0	0.6237
3	Caffeic acid	280	99.9179	38-3.8	0.5663
4	4-Hydroxy benzoic acid	280	99.9734	50-5.0	1.3758
5	Vanillic acid	280	99.9868	56-5.6	0.6652

http://www.aloki.hu ● ISSN 1589 1623 (Print) ● ISSN 1785 0037 (Online)
DOI: http://dx.doi.org/10.15666/aeer/1706_1469914713

Determination of nutrient elements by ICP-MS

For the inductively coupled plasma-mass spectrometry (ICP-MS) technique, 0.2-0.4 g of Cefan melon seeds were dissolved in 6 mL of concentrated nitric acid (65%) and 2 mL hydrogen peroxide (30%), digested in a microwave system (Berghof Microwave Digestion Speedwave MWS-2), and then decomposed 15 min at 180 °C. After cooling, the preparation was filtered. One milliliter of each filtrate was pipetted into a falcon tube and diluted to 25 mL with ultrapure water. All samples were then placed in the ICP-MS autosampler unit (Thermo Scientific iCAP Q, 02878R ICP-MS; Plasma power, 1550 W; nebulizer flow, 1.17/min; cooling flow, 14/min; auxiliary flow, 0.8/min). These analyses were replicated at least three times (Kuru et al., 2019). The mean values of three measurements were calculated. Calibration solutions were prepared at six different concentrations ranging from 25.00 to 1000.00 ppb using standard solution (ICP Multielement Standard; Sigma Aldrich-1.11355) (*Table 2*).

Results and discussion

CAs that are the subject of the present study have roles in pH regulation in living organisms, and they serve as one of the major buffering systems. Further, they take part in biosynthetic reactions such as urea synthesis, lipogenesis and gluconeogenesis (Scozzafava et al., 2006; Supuran, 2008). However, enzymes of this family are disease markers or disease factors in many physiological and pathological processes such as calcification, tumor formation and Alzheimer's (Scozzafava et al., 2006; Supuran, 2008; Aggarwal, 2013; Akkemik et al., 2018). For this reason, inhibition or activation of these isoenzymes is of high importance in many diseases. For example, currently, CA inhibitors are used in the treatment of various diseases such as glaucoma, epilepsy, gastric and neurological disorders, obesity and cancer (Scozzafava et al., 2006; Supuran, 2008; Aggarwal et al., 2013). There are many studies reporting that activators can be used in AD treatment (Dilek, 2017; Uymaz, 2017; Akkemik et al., 2018). Considering the side effects and high costs of synthetic drugs, demand for natural products has been increasing. Therefore, effects of Cefan melon seed extracts on hCA-I and hCA-II isoenzymes have been investigated in the present study.

The undesirable side effects of synthetic drugs have started to direct many people to natural products. Therefore, research on treatment with natural products has begun to gain popularity. Furthermore, inhibition or activation effects of many plant extracts on carbonic anhydrase enzyme activity have been investigated. In a study the effects of black, green and white, and herbal teas on bovine and human erythrocyte carbonic anhydrase were investigated (Karaçelik, 2018). In a different study, inhibition effects of *Artemisia dracunculus* L. extracts were investigated against hCA I-II (Yurtvermez, 2016). In another study effects on hCA I-II enzymes activities of *Ferula rigidula*, *Eremurus spectabilis*, *Rheum ribes* and *Prangos ferulacea* taxa were determined (Sevim, 2018). There are many studies wherein the effects of plant extracts on different enzymes or properties are investigated (Oluba et al., 2007; Bangou, 2011; Sacan, and Yildiz, 2014; El-Hadary and Ramadan, 2019).

Cefan melon was chosen as the subject of the present study because it is a lesser known type of melon, although it is common in a small geographic region. Moreover, it has a sour taste in contrast to other melon species. To our best knowledge, inhibition or activation effects of Cefan melon seed on hCA I-II were determined first time. Two isoenzymes of carbonic anhydrase enzyme were initially purified. For this purpose, sepharose 4B-L-tyrosine-sulfonamide activated with cyanogen bromide affinity column was used. Enzyme purity was checked with SDS-PAGE (*Fig. 1*).

http://www.aloki.hu ● ISSN 1589 1623 (Print) ● ISSN 1785 0037 (Online)
DOI: http://dx.doi.org/10.15666/aeer/1706_1469914713

Table 2. *Standards information used during elemental analysis by ICP-MS (Thermo Scientific iCAP Q)*

Element	Concentration range (ppb)	Standard curve equation	R^2	Background equivalent concentrations (BEC) ppb	Limits of detection (LOD) ppb
^{7}Li	25.00-1000.00	f(x) = 46839.1204x + 31857.5472	0.9992	0.680	0.0934
^{11}B	25.00-1000.00	f(x) = 11634.3811x + 62806.0377	0.9990	5.398	0.5031
^{23}Na	25.00-1000.00	f(x) = 71266.8556x + 721554.0481	0.9994	10.125	0.6556
^{24}Mg	25.00-1000.00	f(x) = 44262.8717x + 209231.0649	0.9992	4.727	0.8755
^{27}Al	25.00-1000.00	f(x) = 66001.7287x + 281798.3539	0.9949	4.270	0.4715
^{39}K	25.00-1000.00	f(x) = 83729.4407x + 3887583.5973	0.9995	46.430	0.6893
^{44}Ca	25.00-1000.00	f(x) = 3999.0021x + 341506.9113	0.9943	85.398	5.8430
^{52}Cr	25.00-1000.00	f(x) = 87177.3340x + 114923.2662	0.9937	1.318	0.1398
^{55}Mn	25.00-1000.00	f(x) = 122306.5132x + 128449.2444	0.9993	1.050	0.0784
^{57}Fe	25.00-1000.00	f(x) = 2568.9864x + 64650.7997	0.9993	25.166	1.6484
^{59}Co	25.00-1000.00	f(x) = 81035.0866x + 67606.4554	0.9988	0.834	0.0611
^{60}Ni	25.00-1000.00	f(x) = 17630.2008x + 14131.3861	0.9996	0.802	0.0714
^{63}Cu	25.00-1000.00	f(x) = 38817.8017x + 34323.9999	0.9996	0.884	0.0395
^{66}Zn	25.00-1000.00	f(x) = 13461.0977x + 237646.1776	0.9962	17.654	2.1606
^{74}Se	25.00-1000.00	f(x) = 111.5321x + -630.3276	0.9995	-5.652	1.5789
^{75}As	25.00-1000.00	f(x) = 9679.9289x + 6428.3363	0.9991	0.664	0.0984
^{76}Se	25.00-1000.00	f(x) = 1263.8109x + 122312.6551	0.9995	96.781	3.2944
^{77}Se	25.00-1000.00	f(x) = 1059.7189x + 1533.4352	0.9993	1.447	0.4007
^{88}Sr	25.00-1000.00	f(x) = 122465.8524x + 102090.6547	0.9990	0.834	0.0172
^{95}Mo	25.00-1000.00	f(x) = 17197.3209x + 10427.7554	0.9994	0.606	0.0367
^{105}Pd	25.00-1000.00	f(x) = 25.4574x + 2746.9880	0.8436	107.905	44.2970
^{111}Cd	25.00-1000.00	f(x) = 10842.5299x + 8492.9498	0.9993	0.783	0.0706
^{121}Sb	25.00-1000.00	f(x) = 33942.0002x + 18991.2024	0.9987	0.560	0.0205
^{137}Ba	25.00-1000.00	f(x) = 13617.5973x + 13997.9311	0.9989	1.028	0.2084
^{209}Bi	25.00-1000.00	f(x) = 81754.9691x + 54245.2449	0.9992	0.664	0.1297

http://www.aloki.hu ● ISSN 1589 1623 (Print) ● ISSN 1785 0037 (Online)
DOI: http://dx.doi.org/10.15666/aeer/1706_1469914713

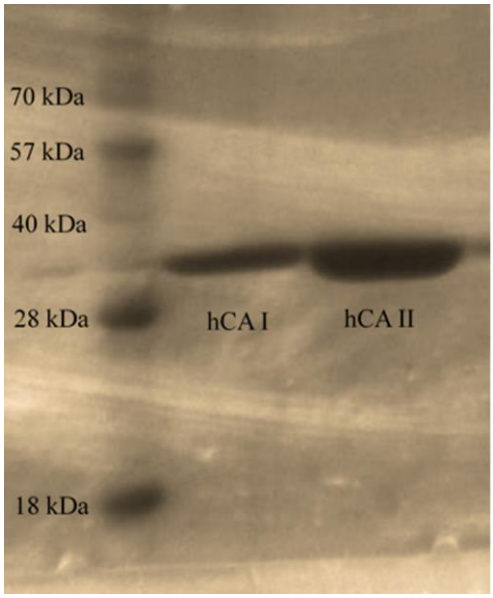

Figure 1. *SDS-PAGE bands of hCA I and hCA II*

The effects of oil and methanol extracts of melon seed on hCA-I and hCA-II were investigated *in vitro* conditions (*Fig. 2*). While both extracts activated hCA-I isoenzyme (AC_{50} 0.333 ng/mL and 80.369 µg/mL, respectively), they inhibited hCA-II isoenzyme (IC_{50} 0.497 ng/mL and 10.98 µg/mL, respectively) (*Table 3*).

Furthermore, the active substance causing inhibition and activation effect in the Cefan melon seeds was also investigated in the present study. Therefore, the oil content was determined by GC-MS, while phenolic substance content was analyzed using HPLC and nutrient content using ICP-MS.

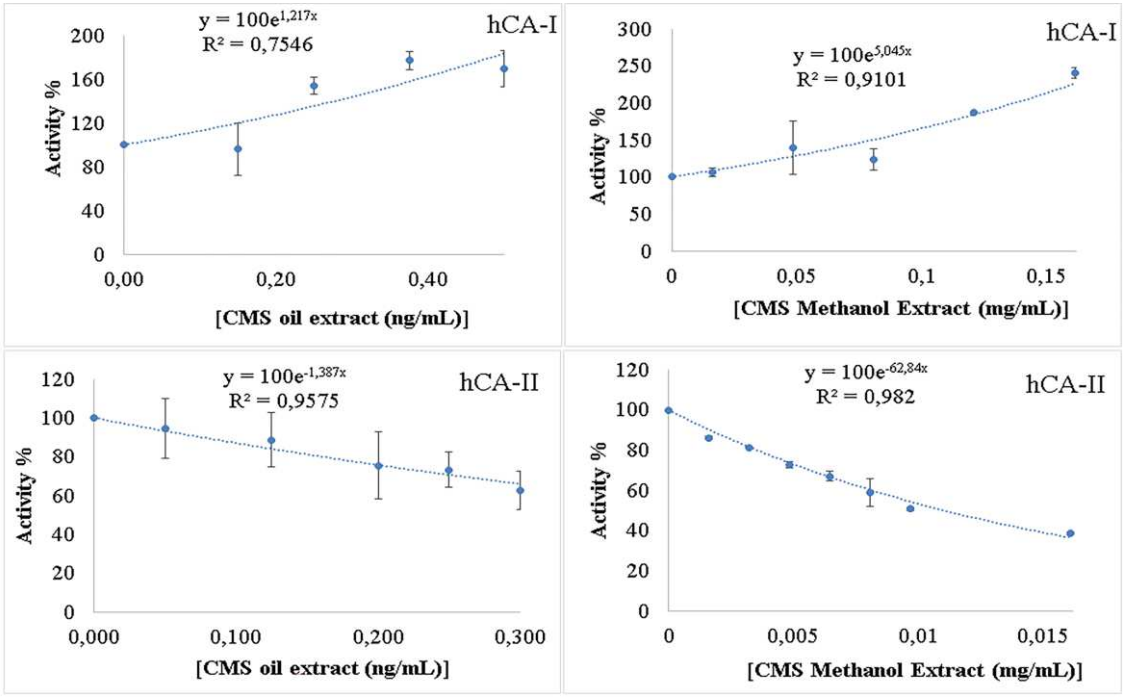

Figure 2. *Effects on hCA I and hCA II of melon seed oil and methanol extracts*

http://www.aloki.hu ● ISSN 1589 1623 (Print) ● ISSN 1785 0037 (Online)
DOI: http://dx.doi.org/10.15666/aeer/1706_1469914713

Table 3. *Effect of extracts on isoenzymes of human carbonic anhydrides I and II*

Sample	Melon seed oil extract		Methanol extract	
Enzyme	**hCA-I**	**hCA-II**	**hCA-I**	**hCA-II**
AC_{50}	0.333 (ng/mL)	-	80.369 µg/mL	-
IC_{50}	-	0.497 ng/mL	-	10.98 µg/mL
R^2	0.7546	0.9575	0.9101	0.9820
K_i	-	0.369±0.166 ng/mL	-	7.25±0.400 µg/mL

In the present study, Cefan melon seed was found to contain approximately 25.00 ± 0.01% crude oil. Seeds of different melon cultivars contain about 33.0% crude oil (Ramakrishna et al., 1970; Teotia and Ramakrishna, 1984; Mello et al., 2001; Kale, 2017). Crude oil extracts obtained were analyzed for fatty acid contents in the GC-MS device. It was found out that the dominant fatty acids in melon seed oil were linoleic and oleic acids (*Table 4*). Unsaturated fatty acids constituted 67.09% of total fatty acids in melon seed oil extract.

Table 4. *GC-MS data of melon seed oil extract*

Seed oil acids	Retention time (min)	%
Linoleic acid (18:2)	48.33	33.13
Oleic acid (18:1)	47.13	26.24
Palmitic acid (16:0)	42.03	12.24
Stearic acid (18:0)	46.59	7.96
N-decylbenzene ($C_{16}H_{26}$)	35.69	7.76
γ-Linolenic acid (18:3)	50.84	4.48
Dimethylamine, N(Neopentyloxy)	44.31	3.29
α-Linolenic acid (18:3)	58.02	3.24
Octadecanoic-D4 acid	48.91	33.13

Inhibitors of hCA-II are used in the treatment of diseases such as glaucoma and epilepsy. Inhibition of hCA-II by very low concentration of both extracts in the present study indicates that both extracts could be efficiently used in the treatments of these diseases. However, an evaluation of IC_{50} value revealed that oil extract was more effective compared to methanolic extract, possibly because Cefan melon seeds contain a considerable amount of unsaturated fatty acids. Most of these unsaturated fatty acids were essential fatty acids. They are the fatty acids that must be taken through food. Inadequate unsaturated fatty acid intake through food may lead to many diseases such as cardiovascular disease, AD, depression, osteoporosis, and prostate, breast, intestinal and lung cancers (Liperoti et al., 2009; Lee and Park, 2014; Bentsen, 2017). Therefore, Cefan melon seed oil extract may provide a cure for diseases like glaucoma, epilepsy, etc.

The predominant fatty acids in the extracted Kalahari melon seed oil were linoleic (62.2–63.1%), oleic (16.8–17.1%), palmitic (11.4–12.4%), stearic (7.5–8.1%), linolenic (0.7–1.2%), and eicosenoic acids (0.3%) (Nyam et al., 2009). Another study mentioned that although the seeds of a different melon variety contained unsaturated fatty acids such as palmitic and stearic acids, the dominant fatty acid was unsaturated ones,

http://www.aloki.hu ● ISSN 1589 1623 (Print) ● ISSN 1785 0037 (Online)
DOI: http://dx.doi.org/10.15666/aeer/1706_1469914713

especially linoleic and oleic acids (Mehra et al., 2015). Similarly, as a result of the analysis conducted in the seed oil of 10 different kinds of melon, it was stated that they contained 57.14-74.66% linoleic acid, 12.95-28.37% oleic acid, and 6.98-10.07% palmitic acid (Kale, 2017). Comparing the data from the present study and results in the literature, we could say that the fatty acids are similar. However, they vary in terms of amount. For example, Cefan melon seed contained relatively less linoleic acid.

An *in vitro* study was performed to investigate the effect of oil extract of melon seeds on serum lactate dehydrogenase, alanine transaminase, aspartate transaminase and γ-glutamyl transpeptidase levels in rats. It was reported that activities of the specified enzymes were lower in rats fed with melon seed oil extract (Oluba et al., 2007). Their results demonstrated that melon seed oil extract has a regulatory role in metabolism and this finding supports our results.

The methanolic extract showed an activation effect on hCA-I activity, whereas its effect on hCA-II activity was inhibitory. There was an 8-fold difference in the concentration range at which methanolic extract was effective on hCA-I and hCA-II. Different effects in different doses of both isoenzymes lead to selective inhibition. This finding showed that the inhibition effect was more pronounced.

In our study, the main phenolic compound in Cefan melon seed was found to be gallic acid. According to the HPLC results, Cefan melon seed contained 247.401 ± 5.9816 ppm gallic acid, 50.1811 ± 8.8379 ppm chlorogenic acid, 3.6850 ± 1.5866 ppm 4-hydroxybenzoic acid and 2.7173 ± 1.8528 ppm vanillic acid while caffeic acid was not detected (*Fig. 3*). In a study where a phenolic analysis was conducted both in peel and seeds of a kind of melon grown in Brazil, it was stated that gallic acid was the dominant phenolic compound in both samples, which also contained catechins, salicylic acid, and eugenol (Rolim, et al., 2018). Furthermore, they also found that the peel extract contained more phenolic acid compared to seeds (Rolim et al., 2018). In a different study, it was stated that gallic acid, caffeic acid, and catechins were dominant phenolic compounds in melon seed extract (Zeb, 2016). In a study where a phenolic analysis was conducted in peel, fruit, and seeds of Cefan melon, it was stated that gallic acid was the dominant phenolic compound in all samples (Özbek, 2019). A comparison of the results from the present study with the data in the literature showed that the content and concentration of the phenolic compounds vary in different varieties grown in different areas of the world, which could be due to climatic conditions (Zeb, 2016; Rolim et al., 2018).

While phenolic compounds were suggested to cause inhibition by interacting (through hydrogen bonding) with water molecules around Zn^{2+} in the active region of the carbonic anhydrase enzyme (Durdagi et al., 2011), no clear mechanism for the activation was proposed. In our study, the gallic acid was dominant compared to other phenolic compounds in methanol extract. Therefore, although oil and methanol extracts were expected to inhibit both isoenzymes, they activated hCA-I isoenzyme. These results were somewhat surprising. Gallic acid was dominant in the methanol extract in CMS, but the activation or inhibition effect was not necessarily related to that compound since no purified gallic acid was used in the experiments. This effect could be due to the mixing of phenolic compounds. However, given the selective inhibition or activation effect, these findings are very important.

In a study where mineral content was conducted in peel, fruit, and seeds of Cefan melon, it was seen that different the results were obtained from our study. There were some deficiencies in Özbey's (2019) study. For example, the method was not explicitly

http://www.aloki.hu ● ISSN 1589 1623 (Print) ● ISSN 1785 0037 (Online)
DOI: http://dx.doi.org/10.15666/aeer/1706_1469914713

stated in the relevant study. And also results of Özbey (2019) were not explained in detail.

In our study, oil and methanol extracts had different effects on the activities of the two isoenzymes. We believe that this could be caused by the mineral content of the Cefan melon seed extract. For this purpose, elemental content was analyzed by ICP-MS in melon seed extract.

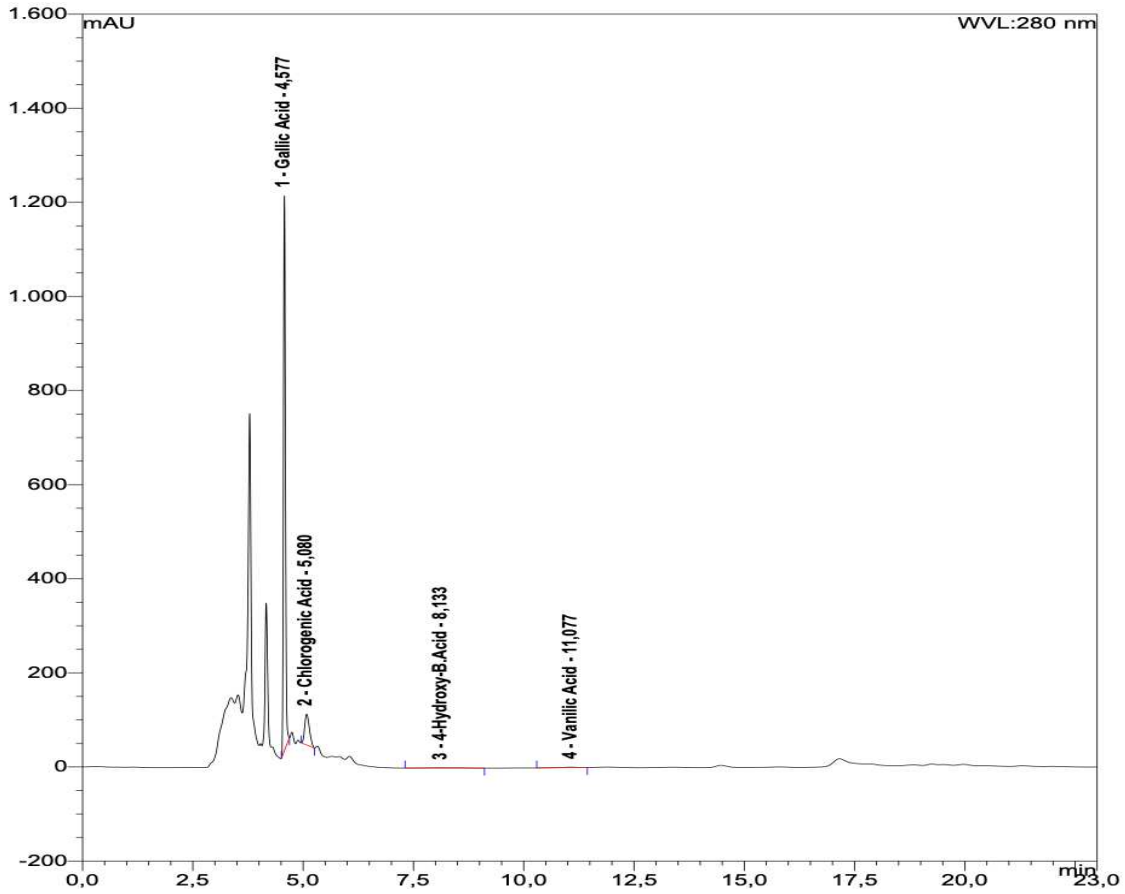

Figure 3. *HPLC chromatogram of Cefan melon seed*

Mineral content was also analyzed using ICP-MS. The mineral analysis of Cefan melon seeds showed that they were rich in calcium (6960.59 ± 220.66 ppm), sodium (4059.93 ± 80.199 ppm), potassium (1291.18 ± 44.49 ppm) and magnesium (858.534 ± 20.173 ppm). Moreover, Cefan melon seeds contained low levels of aluminum (361.247 ± 10.852 ppm), iron (326.523 ± 13.409 ppm), molybdenum (278.718 ± 7.1555 ppm), chrome (143.515 ± 4.3967 ppm) and selenium (141.241 ± 14.824 ppm) (*Table 5*). Data obtained in the present study indicated that 48% of inorganic matter in Cefan melon seed was Ca.

Analysis of Cefan melon seed showed that it contained metals of the 1A and 2A group as well as the transition metals. It was reported that groups containing free OH interact with heavy metals and transition metals, whereas those containing benzene ring interact with alkaline and alkaline earth metals (Çalışır, 2014). hCA-I and hCA-II contain about 260 amino acids, but amino acid sequences show only 60% similarity. (Hassan et al., 2013). In other words, their amino acid sequences are quite different.

http://www.aloki.hu ● ISSN 1589 1623 (Print) ● ISSN 1785 0037 (Online)
DOI: http://dx.doi.org/10.15666/aeer/1706_1469914713

While CA isoenzyme, which has a high number of aromatic amino acids, interacts with alkaline and alkaline earth metals, the isoenzyme which contains a higher amount of amino acids such as serine and threonine interacts with heavy metals and transition metals. Therefore, they may not give the same response to inhibitors and activators.

Table 5. *ICP-MS data of melon seed*

Element	Concentration (ppm)
Ca	6960.59 ± 220.66
Na	4059.93 ± 80.199
K	1291.18 ± 44.491
Mg	858.534 ± 20.173
Al	361.247 ± 10.852
Fe	326.523 ± 13.409
Mo	278.718 ± 7.1555
Cr	143.515 ± 4.3967
Se	141.241 ± 14.824
Ba	38.3107 ± 1.5176
Cu	27.5614 ± 0.7242
B	21.1259 ± 17.028
Sr	13.0292 ± 0.7815
Sb	5.31247 ± 0.2819
Mn	2.41853 ± 0.1566
Ni	1.6246 ± 0.10619

Conclusion

Cefan melon seed is rich in phenolic compounds, unsaturated fatty acids, calcium, sodium, potassium, and magnesium. Thus, Cefan melon seed, which was found to have beneficial *in vitro* effects, could be useful in different food or cosmetic products because of active substances in it. In addition, extracts can also be used as alternative natural sources for the treatment of different diseases. Our study could be evaluated as a preclinical study. Preclinical studies are needed for clinical studies. Therefore, the present study provides the information needed by many researchers conducting *in vivo* studies. In the present study, oil and methanol extracts of Cefan melon seed showed different effects on hCA I-II activity. Synthetic drugs involve expensive synthesis and characterization procedures and have many side effects. Therefore, Cefan melon seed may be preferred instead of synthetic drugs in the treatment of diseases such as glaucoma, epilepsy, gastric, neurological disorders, obesity, cancer, and AD. Clinical trials are needed to indicate the potency of a chemical as a drug. Therefore, it would be useful to conduct clinical studies with melon seed extracts for the treatment of the above-mentioned diseases.

Acknowledgments. We thank Siirt University, Science and Technology Application and Research Center, for their contribution. This research received no specific grant from any funding agency in the public, commercial, or not-for-profit sectors.

Conflict of interests. The authors declare that they have no conflict of interests.

http://www.aloki.hu ● ISSN 1589 1623 (Print) ● ISSN 1785 0037 (Online)
DOI: http://dx.doi.org/10.15666/aeer/1706_1469914713

REFERENCES

[1] Aggarwal, M., Kondeti, B., McKenna, R. (2013): Insights Towards Sulfonamide Drug Specificity in A-Carbonıc Anhydrases. – Bioorganic & Medicinal Chemistry 21(6): 1526-1533. Doi: 10.1016/J. Bmc. 2012.08.019.

[2] Akkemik, E., Cicek, B., Camadan, Y., Calisir, U., Onbasioglu, Z. (2018): The determination of the carbonic anhydrase's activators in vitro effect of mixed donor crown ethers. – Journal of Biochemical and Molecular Toxicology 32(3): e22032. https://doi.org/10.1002/jbt.22032.

[3] Bangou, J. M., Kiendrebeogo, M., Compaore, M., Coulibaly, A. Y., Roland Meda, N. T., Abarka Almaraz, N., Zeba, B., Millogo-Rasolodimby, J., Nacoulma, O. G. (2011): Enzyme inhibiting effect and polphenolic content of medicinal plant extracts from Burkina Faso. – Journal of Biological Sciences 11(1): 31-38. DOI: 10.3923/jbs.2011.31.38.

[4] Bentsen, H. (2017): Dietary polyunsaturated fatty acids, brain function and mental health. – Microbial Ecology in Health and Disease 28: 1281916 DOI: http://Dx.Doi.Org/10.1080/16512235.2017.1281916.

[5] Bradford, M. M. (1976): A rapid and sensitive method for the estimation of microgram quantities of protein utilizing the principle of protein-dye binding. – Analytical Biochemistry 72: 248-254. PMID: 942051.

[6] Çalışır, U. (2014): Benzo-tiyo crown eterlerin sentezi ve ekstraktif özelliklerinin incelenmesi. – Balıkesir Üniversitesi, Fen bilimleri Enstitüsü, Kimya ABD, Yüksek Lisans Tezi, Balıkesir.

[7] Cankaya, M., Hernandez, A. M., Ciftci, M., Beydemir, S., Ozdemir, H., Budak, H., Gulcin, I., Comakli, V., Emircupani, T., Ekinci, D., Kuzu, M., Jiang, Q., Eichele, G. and Kufrevioglu, O. I. (2007): An analysis of expression patterns of genes encoding proteins with catalytic activities. – BMC Genomics 8: 232.

[8] Casey, J. R., Sly, W. S., Shah, G. N., Alvarez, B. V. (2009): Bicarbonate homeostasis in excitable tissues: role of AE3 Cl-/HCO3- exchanger and carbonic anhydrase XIV interaction. – American Journal of Physiology 297(5): C1091-102. DOI: 10.1152/ajpcell.00177.2009.

[9] Chegwidden, W. R., Dodgson, S. J., Spencer, I. M. (2000): The roles of carbonic anhydrase in metabolism, cell growth and cancer in animals. – EXS 90: 343-63 PMID: 11268523.

[10] Cheng, Y., Prusoff, W. H. (1973): Relationship between the inhibition constant (KI) and the concentration of inhibitor which causes 50 per cent inhibition (I50) of an enzymatic reaction. – Biochemical Pharmacology 22(23): 3099-108. DOI: 10.1016/0006-2952(73)90196-2.

[11] Coleman, J. E. (1975): Chemical reactions of sulfonamides with carbonic anhydrase. – Annual Review of Pharmacology 15: 221-242. https://doi.org/10.1146/annurev.pa.15.040175.001253.

[12] Dilek, E. (2017): Activation of two different drugs used in Alzheimer's disease treatment on human carbonic anhydrase isozymes I and II Activity: an in vitro study. – Turk J Pharm Sci 14(2): 164-168. DOI: 10.4274/tjps.43434.

[13] Dodgson, S. J., Forster, R. E. (1985): 2nd. Carbonic anhydrase: inhibition results in decreased urea production by hepatocytes. – J Appl Physiol 60(2): 646-52. DOI: 10.1152/jappl.1986.60.2.646.

[14] Duran, Z. (2014): Malatya ve Elâzığ illerinde Yetiştirilen Bazı Üzüm Çeşitlerinin Organik Asit, Seker Ve Fenolik Madde Bileşikleri ile Antioksidan Aktivitelerinin Belirlenmesi. – İnönü Üniversitesi Fen Bilimleri Enstitüsü, Yüksek Lisans Tezi, Gıda Mühendisliği Anabilim Dalı, Malatya, Türkiye.

[15] Durdagi, S., Sentürk, M., Ekinci, D., Balaydin, H. T., Göksu, S., Küfrevioglu, Ö. I., Innocenti, A., Scozzafava, A., Supuran, C. T. (2011): Kinetic and docking studies of

http://www.aloki.hu ● ISSN 1589 1623 (Print) ● ISSN 1785 0037 (Online)
DOI: http://dx.doi.org/10.15666/aeer/1706_1469914713

phenol-based inhibitors of carbonic anhydrase isoforms I, II, IX and XII evidence a new binding mode within the enzyme active site. – Bioorg. Med. Chem. 19: 1381.

[16] El-Hadary, A. E., Ramadan, M. F. (2019): Phenolic profiles, antihyperglycemic, antihyperlipidemic, and antioxidant properties of pomegranate (Punica granatum) peel extract. – Journal of Food Biochemistry e12803. https://doi. org/10.1111/jfbc.12803.

[17] FAOSTAT (2018): Production quantities of melons, other (inc.cantaloupes) by country average 1994–2017. – http://www.fao.org/faostat/en/#data/QC/visualize.05.02.2018-21: 18.

[18] Gay, C. V., Schraer, H., Anderson, R. E., Cao, H. (1984): Current studies on the location and function of carbonic anhydrase in osteoclasts. – Annals of the New York Academy of Sciences 429: 473-8. PMID: 6430184.

[19] Hassan, M. I., Shajee, B., Waheed, A., Ahmad, F., Sly, W. S. (2013): Structure, function and applications of carbonic anhydrase isozymes. – Bioorganic & Medicinal Chemistry 21(6): 1570-1582. DOI: 10.1016/j.bmc.2012.04.044.

[20] Kale, S. (2017): Farklı Kavun Çeşitlerinin Bazı Fizikokimyasal Özelliklerinin Belirlenmesi. – Selçuk Üniversitesi, Fen Bilimleri Enstitüsü, Gıda Mühendisliği Ana Bilim Dalı, Yüksek Lisans Tezi, Konya, Türkiye.

[21] Karaçelik, A. A. (2018): Effect of carbonic anhydrase activity of the herbal tea components and food additives. – Karadeniz Teknik Üniversitesi, Fen Bilimleri Enstitüsü, Kimya Anabilim Dalı, Biyokimya Bilim Dalı, Yüksek Lisans Tezi, Trabzon, Türkiye.

[22] Kılıçoğlu, F. M. (2018): Güneydoğu Anadolu Bölgesinde Yetişen Farklı Nıcotıana Spp. Tiplerinin Yağ Asidi, Fenolik Flavonoid Ve Nikotin İçeriklerinin Belirlenerek Kemometrik Yönden İncelenmesi. – Batman Üniversitesi, Fen Bilimleri Enstitüsü, Biyoloji Anabilim Dalı, Yüksek Lisans Tezi, Batman, Türkiye.

[23] Kuru, R., Yilmaz, S., Tasli, N, P., Yarat, A., Sahin, F. (2019): Boron content of some foods consumed in Istanbul, Turkey. – Biol Trace Elem Res 187: 1. https://doi.org/10.1007/s12011-018-1319-9.

[24] Laemmli, U. K. (1970): Cleavage of structural proteins during the assembly of the head of bacteriophage T4. – Nature 227: 680-685 PMID: 5432063.

[25] Lee, H., Park, J. W. (2014): Unsaturated fatty acids, desaturases, and human health. – Journal of Medicinal Food 17(2): 189-197. DOI: 10.1089/jmf.2013.2917.

[26] Lehtonen, J., Shen, B., Vihinen, M., Casini, A., Scozzafava, A., Supuran, C. T., Parkkila, A. K., Saarnio, J., Kivelä, A. J., Waheed, A., Sly, W. S., Parkkila. S. (2004): Characterization of CA XIII, a novel member of the carbonic anhydrase isozyme family. – The Journal of Biological Chemistry 279(4): 2719-27. DOI: 10.1074/jbc.M308984200.

[27] Liperoti, R., Landi, F., Fusco, O., Bernabei, R., Onder, G. (2009): Omega-3 polyunsaturated fatty acids and depression: a review of the evidence. – Current Pharmaceutical Design 15: 4165-4172. DOI: 10.2174/138161209789909683.

[28] Malićanin, M., Rac, V., Antic, V., Antić, M., Palade, M., Kefalas, P., Rakic, V. (2014): Content of antioxidants, antioxidant capacity and oxidative stability of grape seed oil obtained by ultrasound assisted extraction. – JAOCS, Journal of the American Oil Chemists' Society 91. 989-999. 10.1007/s11746-014-2441-2.

[29] Mehra, M., Pasricha, V., Gupta, RK. (2015): Estimation of nutritional, phytochemical and antioxidant activity of seeds of musk melon (Cucumis melo) and watermelon (Citrullus lanatus) and nutritional analysis of their respective oils. – Journal of Pharmacognosy and Phytochemistry 3(6): 98-102.

[30] Mello, M. L. S., Bora, P. S., Narendra, N. (2001): Fatty and amino acids composition of melon (Cucumis melo Var. saccharinus) seeds. – Journal of Food Composition and Analysis 14: 69-74. DOI: 10.1006/jfca.2000.0952.

[31] Montealegre, R. R., Peces, R. R., Vozmediano, J. L. C., Gascuena, J. M., Romero, E. G. (2006): Phenolic compounds in skin and seeds in ten grape Vitis vinifera varieties grown

http://www.aloki.hu ● ISSN 1589 1623 (Print) ● ISSN 1785 0037 (Online)
DOI: http://dx.doi.org/10.15666/aeer/1706_1469914713

in a warm climate. – Journal of Agricultural and Food Chemistry 19: 687-693. DOI: 10.3390/ijms13033492.

[32] Nishimori, I., Innocenti, A., Vullo, D., Scozzafava, A., Supuran, C. T. (2007): Carbonic anhydrase inhibitors. Inhibition studies of the human secretory isoform VI with anions. – Bioorg Med Chem Lett. 17(4): 1037-42. DOI: 10.1016/j.bmcl.2006.11.028.

[33] Nyam, K. L., Tan, C. P., Man, Y. B. C., Lai, O. M., Long, K. (2009): Physicochemical properties of Kalahari melon seed oil following extractions using solvent and aqueous enzymatic methods. – International Journal of Food Science and Technology 44: 694-701. https://doi.org/10.1111/j.1365-2621.2008.01828.x.

[34] Oluba, O., Adeyemi, O., Ojieh, G., Isiosio, I. (2007): Fatty acid composition of Citrullus lanatus (Egusi melon) oil and its effect on serum lipids and some serum enzymes. – The Internet Journal of Cardiovascular Research 5(2): 1-7.

[35] Özbek, A. (2019): Siirt İlinde Yetiştirilen "Cefan" Kavunu'nun (Cucumis Melo L. C. V./Cucurbitaceae) Bazı Biyokimyasal Özelliklerinin Belirlenmesi. – Van Yüzüncü Yıl Üniversitesi, Fen Bilimleri Enstitüsü, Biyoloji Anabilim Dalı, Yüksek Lisans Tezi, Van, Türkiye.

[36] Picaud, S. S., Muniz, J. R., Kramm, A., Pilka, E. S., Kochan, G., Oppermann, U., Yue, W. W. (2009): Crystal structure of human carbonic anhydrase-related protein VIII reveals the basis for catalytic silencing. – Proteins 76(2): 507-11. DOI: 10.1002/prot.22411.

[37] Ramakrishna, G., Viswanadnam, R. K. S., Rao, T. (1970): Pilot plant oil production from muskmelon. – Oil Mill Gazette 75: 8.

[38] Rolim, P. M., Fidelis, G. P., Padilha, C. E. A., Santos, E. S., Rocha, H. A. O., Macedo, G. R. (2018): Phenolic profile and antioxidant activity from peels and seeds of melon (Cucumis melo L. var. reticulatus) and their antiproliferative effect in cancer cells. – Brazilian Journal of Medical and Biological Research 51(4): e6069. DOI: 10.1590/1414-431X20176069.

[39] Sacan, O., Yildiz, E. (2014): Turhan, lipoxygenase inhibitory activities of some plant extracts and chemical compounds. – The Journal of Biological Chemistry 73(2): 47-52.

[40] Scozzafava, A., Mastrolorenzo, A., Supuran, C. T. (2006): Carbonic anhydrase inhibitors and activators and their use in therapy. – Expert Opinion on Therapeutic Patents 16(12): 1627-1664. https://doi.org/10.1517/13543776.16.12.1627.

[41] Sevim, O. (2018): Determination of some macro and micro element contents of multi-medical plants growed in agri and the effects of these elements on metabolic enzyme. – Ağrı İbrahim Çeçen Üniversitesi, Fen Bilimleri Enstitüsü, Kimya Anabilim Dalı, Yüksek Lisans Tezi, Ağrı, Türkiye.

[42] Supuran, C. T. (2008): Carbonic anhydrases as drug targets. – Current Pharmaceutical Design 14(7): 601-2. DOI:10.2174/138161208783877910.

[43] Teotia, M. S., Ramakrishna, P. (1984): Chemistry and technology of melon seeds. – Journal of Food Science and Technology 21: 332-340.

[44] Torring, M. S., Holmgaard, K., Hessellund, A., Aalkjaer, C., Bek, T. (2009): The vasodilating effect of acetazolamide and dorzolamide involves mechanisms other than carbonic anhydrase inhibition. – Investigative Ophthalmology & Visual Science 50(1): 345-51. DOI: 10.1167/iovs.08-2435.

[45] Uymaz, Y. (2017): Karbonik Anhidraz Enziminin Afinite Kromatografisiyle Saflaştırılması Ve Biyoteknolojik Uygulamaları. – Eskişehir Anadolu Üniversitesi, Fen Bilimleri Enstitüsü, Eskişehir.

[46] Van Wyk, B. E., Gericke, N. (2000): People's Plants. A Guide to Useful Plants of South Africa. – Briza Publications, Pretoria.

[47] Verporte, J. A., Mehta, S., Edsall, J. T. (1967): Esterase activities of human carbonic anhydrases B and C. – The Journal of Biological Chemistry 242(422): 1-9.

[48] Woolley, P. (1975): Models for metal ion function in carbonic anhydrase. – Nature 258(5537): 677-82.

http://www.aloki.hu ● ISSN 1589 1623 (Print) ● ISSN 1785 0037 (Online)
DOI: http://dx.doi.org/10.15666/aeer/1706_1469914713

[49] Xu, C., Zhang, Y., Cao, L., Lu, J. (2010): Phenolic compounds and antioxidant properties of different grape cultivars grown in China. – Food Chemistry 119: 1557-1565. 10.1016/j.foodchem.2009.09.042.
[50] Yurtvermez, B. (2016): Isolation of bioactive secondary metabolites from tarragon (Artemisia dracunculus L.) and identification of their chemical structures. – Ağrı İbrahim Çeçen Üniversitesi, Fen Bilimleri Enstitüsü, Kimya Anabilim Dalı, Yüksek Lisans Tezi, Ağrı, Türkiye.
[51] Zeb, A. (2016): Phenolic profile and antioxidant activity of melon (Cucumis melo L.) seeds from Pakistan. – Foods 5: 67. DOI: 10.3390/foods5040067.

http://www.aloki.hu ● ISSN 1589 1623 (Print) ● ISSN 1785 0037 (Online)
DOI: http://dx.doi.org/10.15666/aeer/1706_1469914713

CURING THE DRUG RESISTANCE PLASMID IN *E. COLI* O157:H7

OZDEMIR, K.

Department of Basic Science, Faculty of Engineering and Natural Science, Bandırma Onyedi Eylül University, Balikesir, Turkey
(e-mail: keremozdemir@bandirma.edu.tr; phone: +90-532-609-0335)

(Received 12th Jun 2019; accepted 25th Oct 2019)

Abstract. In this study, twenty five isolates of *E. coli* O157:H7 were identified among 200 samples taken from children under ten years old suffer from diarrhea. Isolates were identified from stool sample by using cultural, morphological, biochemical characteristics and serological test. The plasmid profile has been conducted by using gel electrophoresis. To control the antibiotic resistance of the tested *E. coli* O157:H7 isolates, curing of plasmid DNA was conducted using Ethidium bromide (EB) and elevated temperature (ET) at 46 °C. One of the most resistance isolate was chosen for this purpose E15 then treated with Ethidium bromide at 125 μg/ml. The results revealed that the genes encoded resistance to AK (Amikacin), CIP (Ciprofloxacin), CN (Gentamicin) and TMP + SXT (Trimethoprim + Sulphamethoxazole) (were cured from E15 and the percentage of curing was 28.57%. The results confirmed by conducting gel electrophoresis and showed that EB removed three plasmid of E15, while two plasmids remained. On the other hand, elevated temperature used also as curing agent for the same isolate and the results revealed that resistance to AK, CIP, CN and TMP + SXT genes were cured from E15 and the curing percent was 35.71% after incubating the isolate at 46 °C. The results confirmed by conducting gel electrophoresis and showed that tested isolate lost three plasmids after incubation at 46 °C.
Keywords: *E. coli O157:H7, antibiotic resistance, plasmid profile, plasmid curing*

Introduction

The human large intestine ordinarily harbors a huge microbial population, most bacterial, protozoan, and viral agent of diarrhea are not members of this normal gut flora but are acquired through contaminated food or water (Talaro and Talaro, 2002). *Escherichia coli* O157:H7 is an emerging public health concern in most countries of the world (Schlundt, 2001). It is an important cause of foodborne human disease. Complications related to infection include diarrhea, hemorrhagic colitis, and hemolytic uremic syndrome (Nataro and Kaper, 1998). The constant increase in the antibiotic resistance of clinical bacterial strains has become an important clinical problem (Adamus-Bialek et al., 2013). This is a major problem in the world now "antibiotics resistance", so the medicine manufactures which yearly produced new generations of antibiotic to solute this problem, specially there are some bacteria considered a multiple antibiotic resistance as *Escherichia coli*, *Klebsiella* and others (Al-Faisal, 1999). Plasmids allow the movement of genetic material, including antimicrobial resistance genes between bacterial species and genera (Hamad, 2009). Antimicrobial resistance (AMR) is a global problem hindering treatment of bacterial infections, rendering many aspects of modern medicine less effective. AMR genes (ARGs) are frequently located on plasmids, which are self-replicating elements of DNA. They are often transmissible between bacteria, and some have spread globally. Novel strategies to combat AMR are needed, and plasmid curing and anti-plasmid approaches could reduce ARG prevalence, and sensitise bacteria to antibiotics (Michelle et al., 2018).

Antibiotic resistance increases the likelihood of death from infection by common pathogens such as Escherichia coli and Klebsiella pneumoniae in developed and developing countries alike. Most important modern antibiotic resistance genes spread

http://www.aloki.hu ● ISSN 1589 1623 (Print) ● ISSN 1785 0037 (Online)
DOI: http://dx.doi.org/10.15666/aeer/1706_1471514727

between such species on self-transmissible (conjugative) plasmids. These plasmids are traditionally grouped on the basis of replicon incompatibility (Inc), which prevents coexistence of related plasmids in the same cell. These plasmids also use post-segregational killing ('addiction') systems, which poison any bacterial cells that lose the addictive plasmid, to guarantee their own survival (Kamruzzaman et al., 2017).

Between 2000 and 2010, global human use of antibiotics increased by 36%, and the use of two last-resort antibiotics, carbapenems and polymyxins, increased by 45% and 13%, respectively (Van Boeckel et al., 2014). Antimicrobials have many non-human uses including in animals for growth promotion, veterinary treatment and aquaculture (Vyas and Piddock, 2015; Van Boeckel et al., 2015). In 2013, an estimated 131 109 tons of antimicrobials were used globally in food animals; by 2030 this is expected to increase to 200 235 tons (Van Boeckel et al., 2017). However, there is a growing trend to improve antimicrobial stewardship in many countries. For example, in Switzerland veterinary antimicrobial sales increased between 2006 and 2008, but then steadily decreased, reaching a 26.2% reduction in 2013 (Carmo et al.2017). In addition to human and animal use, many cleaning and personal hygiene products contain biocides, such as triclosan, which can select for mutants resistant to biocides, and in some cases to antibiotics used in medicine (Vyas and Piddock, 2015; Webber et al., 2015, 2017).

Plasmid curing is the process by which plasmids are removed from bacterial populations. This is an attractive strategy to combat AMR (antimicrobial-resistant) as it has the potential to remove ARGs (AMR genes) from a population while leaving the bacterial community intact. This means, for example, that the structure of the gastrointestinal microbiome of a chicken treated with a plasmid curing agent might remain largely unchanged, but potentially pathogenic bacteria which may unfortunately be transmitted into the food chain would be susceptible to antibiotics. Alternatively, a plasmid curing agent could be given to a patient prior to surgery, to reduce the likelihood of a resistant hospital acquired infection. Plasmid curing agents could also be taken by international travellers to reduce the global spread of AMR. Unfortunately, at the moment no such treatment options are in use. In fact, there are very few curing mechanisms that have been tested in vivo, even in experimental models. Therefore, research in this area is urgently needed. Recently, it was shown that 24% of non-antibacterial drugs impact growth of members of the human microbiome (Maier et al., 2018). Studies such as this would be important for determining any impact of anti-plasmid compounds on the microbiome.

The risk of *E. coli* O157:H7 occurs in its plasmid, because of its ability to transfer plasmids to other bacteria or other strains of *E. coli* by transformation, conjugation and transduction processes (Jawetz et al., 2004). Therefore, controlling and elimination of the resistance that conferred by R -plasmid by using biological mutagen, physical and chemical or other curing agents will be quite useful to eliminate such resistance (Jawetz et al., 2007). For this reasons this study concerned with the isolation and identification of *E. coli* O157:H7 from children suffering from diarrhea, study the antimicrobial resistance patterns of the isolated *E. coli* O157:H7 to different antibiotics, characterization of the plasmid DNA profile pattern of the isolates using gel electrophoresis technique, and elimination of the bacterial resistance to antibiotic for some isolates by curing using ethidium bromide and elevated temperature.

http://www.aloki.hu ● ISSN 1589 1623 (Print) ● ISSN 1785 0037 (Online)
DOI: http://dx.doi.org/10.15666/aeer/1706_1471514727

Materials and methods

Specimen collection

The samples were collected during the period 20st May 2013 to 1th November 2013. A total of two hundred (200) stool specimens were collected from infants and children (68 males and 132 females), aged one day- 10 years attending Rapareen Teaching Hospital for Children in Erbil City (Iraq) and the relevant information were recorded from each patient including age and sex. All stool samples were collected in clean disposable plastic containers from diarrheal patient**.** The specimens were transferred to the laboratory and processed within half an hour of collection.

Bacterial identification

Bacterial isolates were identified by performing morphological, cultural, biochemical, and serological test.

Antibiotic susceptibility test

To study the effect of different antibiotics on the isolates of *E. coli* 0157:H7, Mueller-Hinton agar was used as growth media (Wayne, 2005). Antibiotic resistance patterns of the isolates were determined using the Disc diffusion (Kirby Bauer) method; bacterium inoculate was adjusted to 0.5 McFarland standard of Clinical and Laboratory standards institute (Clinical and Laboratory Standard Institute, 2007). The test inoculums were spread onto Muller-Hinton agar using a sterile cotton swab. The tested antimicrobial agents were aseptically placed on the inoculated Muller Hinton agar and incubated overnight. The zones of inhibition were measured and interpreted according to (Clinical and Laboratory Standard Institute, 2007).

Plasmid DNA extraction (Gene Aid Company) laboratory protocol

Plasmid DNA was extracted and purified from 5 ml overnight culture of the selected isolates of the *P. mirabilis* grown in LB broth medium containing 100 µg/ml Ampicillin using a plasmid DNA purification kit, according to the manufacturer's instructions. A single bacterial colony was used to inoculate 5 ml LB, which was incubated overnight in a shaker incubator at 37 °C. A volume of 3 or 5 ml of each isolate in an eppendorf tube was centrifuged for 30 s at 13,000 rpm and the supernatant discarded. The bacterial pellet resuspended by vortexing in 250 µl of resuspension buffer (RNase A solution was added), until no clumps of the cell pellet remain. Two-hundred and fifty µl of lysis buffer added to resuspended cells and the tube closed and gently mixed by inverting the tube several times without vortexing. Three-hundred fifty µl of neutralization buffer was added and gently mixed by inverting the tube several times. Resuspended cells centrifuged at 13,000 rpm for 10 min at 4 °C, then a column inserted into collection tube. After centrifugation, supernatant transferred promptly into the column, and centrifuged at 13,000 rpm for 60 s. The column removed from the collection tube, the filtrate in collection tube discarded. The spin column placed back in the same collection tube. Five hundred µl of washing buffer A added and centrifuged at 13,000 rpm for 60 s. The column removed from collection tube, the filtrate discarded in collection tube, and then placed the spin column back in the same collection tube. Seven-hundred µl of washing buffer B was added, centrifuged at 13,000 rpm for 60 s. The filtrate discarded in collection tube and column placed back in the same collection tube, Centrifuged at

http://www.aloki.hu ● ISSN 1589 1623 (Print) ● ISSN 1785 0037 (Online)
DOI: http://dx.doi.org/10.15666/aeer/1706_1471514727

13,000 rpm for 60 s to dry the filter membrane. The column put in a clean and sterile eppendorf. Fifty µl of elution buffer added to the upper reservoir of the column, and let stand for 1 min. Then, the tube centrifuged at 13,000 rpm for 60 s. The purified DNA plasmid used immediately in downstream applications or store at -20 °C (Manufacturer protocol).

Plasmid profile

The extracted plasmids were electrophoresed in 0.7% agarose gel with Tris-borate ethylene diamine tetra-acetic acid (TBE), Agarose gel electrophoresis was used to separate DNA fragments according to size, 0.7% (w/v) agarose gel was made by adding 0.7 gm of agarose to 100 ml of 1X TBE buffer solubilized by heating at boiling temperature in microwave oven for 2 min, then the agarose was left to cool down at 55 °C before pouring in a tray to solidify. A comb was placed near one edge of gel, and gel was left to harden. After gel solidification, the comb was removed gently and the gel was soaked in a gel tank contain 1X TBE buffer and the placement of the gel in the tank should be in a way that the wells located on the negative (cathode) pole. The amount of TBE buffer had to be sufficient to cover about 2-3 mm of the gel, 1 kb DNA ladder (Fermentas) was used as molecular size marker of DNA fragment, 3µl of loading buffer was mixed with 10 µl plasmid DNA extract, and then samples were added carefully to individual wells. After loading the samples into wells, the power supply was set on 45 V for 15 min. Then the voltage changed to 75 V and the gel was run for 90 min. until the bromophenol blue dye migrated to the other end of the gel. The gel was immersed in ethidium bromide (0.5 µg/ml of D.W.) for 30-45 min. The gel was visualized by UV-trans illuminator and then photographed (Sambrook and Russella, 2001).

Ethidium bromide as a curing agent

Curing by ethidium bromide was done by the procedure mentioned by (Tomoeda et al., 1974). Five ml of LB broth containing appropriate antibiotic at final concentration inoculated with single colony of *E. coli* O157:H7 isolate, incubated at 37 °C for 24 h, after overnight 0.1 ml of the broth bacterial culture were inoculated into 5 ml LB broth containing 125 µg/ml of ethidium bromide agents and incubated with shaking at 37 °C for 48 h. Serial dilutions were prepared up to 10^{-6}, 0.1 ml from the last three dilutions were spread onto nutrient agar plates and incubated at 37 °C for 24 h. After incubation time, fifty colonies were transferred to nutrient agar plate and incubated over night at 37 °C representing the master plate. Five colonies were randomly chosen, picked up and transferred to Muller Hinton agar plates and tested for antibiotic sensitivity pattern, incubated at 37 °C for 24 h. After overnight incubation the percentages of curing colonies for antibiotic sensitivity pattern were calculated.

Curing of plasmid DNA by elevated temperature

This curing was carried out according to (Baldwin and Strickland, 1969). Ten ml of LB broth inoculated with single colony of *E. coli* isolate, after inoculation for 24 h at 37 °C, 10 ml LB broth culture inoculated with 0.2 ml of bacterial culture, incubated with shaking (100 rpm at 46 °C for 24 h), serial dilutions were prepared up to 10^{-7}, then 0.1 ml from last three dilutions spread on nutrient agar plates and incubated at 37 °C for 24 h. After incubation time, fifty colonies were transferred to nutrient agar plate and incubated over night at 37 °C representing the master plate. Five colonies were

http://www.aloki.hu ● ISSN 1589 1623 (Print) ● ISSN 1785 0037 (Online)
DOI: http://dx.doi.org/10.15666/aeer/1706_1471514727

randomly chosen, picked up and transferred to Muller Hinton agar plates and tested for antibiotic sensitivity pattern incubated at 37 °C for 24 h. After overnight incubation the percentages of curing colonies for antibiotic sensitivity pattern were calculated.

Antibiotic resistance pattern after plasmid curing

The colonies were screened for antibiotic resistance by the disk diffusion method after curing. Cured markers were determined by comparison between the pre- and post-curing resistance pattern of isolates. Loss of resistance markers gave an indication that those markers were probably located on plasmid and not on the chromosome.

Results and discussion

Identification of E. coli O157 isolates

They produce bright metallic green sheen colonies on Eosin Methylene Blue (EMB) agar and on Sorbitol MacConkey agar colonies of *E. coli* O157:H7 appear as colorless colony due to non sorbitol fermenting which consider as a selective media (Wistreich and Lechtman, 1980). Bacterial cells from smear preparation are gram negative short rods, motile, non-spore forming and presumptively are *E. coli* O157:H7 which in accordance with previous observations (Sharma et al., 2007). The biochemical tests for all bacterial isolates were negative for citrate, oxidase and urease production test, but they were positive for catalase and indole test. On Kligler Iron Agar (KIA) medium, all isolates of *E. coli* understudy produce a yellow slant and a yellow butt A/A reaction due to the fermentation of lactose and glucose and negative for H_2S production (Wistreich and Lechtman, 1980).

Serological test

Samples serotyped by application of solid agglutination test, using anti *Escherichia coli* O157:H7. Once the agglutination was detected, the reaction was considered positive according to the materials used. Three drops of physiological normal saline were added on a clean slide, and then with the aid of the loop, a small piece of fresh bacterial growth was mixed with the 3 drops in order to obtain a homogenous mixture. After that a drop of polyvalent antisera was added to the two drops (mixture) while the third drop was considered as control test. The appearance of clear agglutination within 1 min indicates a positive result.

Antibiotic sensitivity test

Antibiotic sensitivity testing was done for all isolates by using fourteen antibiotic types which include amikacin (AK), ampicillin (AMP), chloramphenicol (C), cephalothin (KF), ciprofloxacin (CIP), cefepime (FEP), ceftriaxone (CRO), cefotaxime (CTX), gentamicin (CN), imipenem (IPM), metronidazole (MET), tetracycline (TE), trimethoprim (TMP) and trimethoprim + sulphamethoxazole (SXT). Antibiotic discs of Amikacin (30 μg), Imipenem (10 μg), Ampicilin (25 μg), Gentamicin (30 μg), Chloramphenicol (30 μg), Cephalothin (30 μg), Ciprofloxacin (10 μg), Cefepime (30 μg), Cefotaxime (30 μg), Ceftriaxone (30 μg), Metronidazole (5 μg), Tetracycline (30 μg), Trimethoprim (5 μg) and Sulphamethoxazole (25 μg) were applied on the plates. The resistance rate of the isolates toward these antibiotics were 100% for AMP,

http://www.aloki.hu ● ISSN 1589 1623 (Print) ● ISSN 1785 0037 (Online)
DOI: http://dx.doi.org/10.15666/aeer/1706_1471514727

96% for MET, 76% for CTX, 72% for TE and KF, 68% for TMP, 56% for FEP, 52% for C and SXT, 48% for CRO, 28% for AK, 20% for CIP, while the lowest percent 16% was for CN, and all isolates were sensitive for IPM (*Table 1*).

Table 1. *Percentages of resistance of bacterial isolates to different antibiotics*

Antibiotics	Abbreviation	No. of Isolates	Resistant percentage of resistance %
Amikacin	AK	7	28
Ampicillin	AMP	25	100
Chloramphenicol	C	13	52
Cephalothin	KF	18	72
Ciprofloxacin	CIP	5	20
Cefepime	FEP	14	56
Cefotaxime	CTX	19	76
Ceftriaxone	CRO	12	48
Gentamicin	CN	4	16
Imipenem	**IMP**	**0**	**0**
Metronidazole	MET	24	96
Tetracycline	TE	18	72
Trimethoprim	TMP	17	68
Sulphamethoxazole	SXT	13	52

IPM was the most effective antibiotic against isolates of *E. coli O157* and 100% of these isolates were susceptible to IPM, this result was agree with Hadi (2008), Al-Hilali (2010), and Shamki et al. (2012). They reported that all *E. coli* isolated from different clinical source were sensitive for IPM. The high efficiency of these antibiotics may be the usage rarely in studied area and it is expensive drug. In the present work, 68% of the isolates were resistant to TMP, this result was in agreement with Nanakaly (2013) who stated that 52% of *E. coli* isolates were resistant for TMP, also Salah (2007) and Al-Hilali (2010) found that 59.03% and 72.2% of *E. coli* isolates were resistant to TMP. This may be result from mutational changes that lead to over production of the bacterial dihydrofolatereductase (Salah, 2007). Regarding to C resistance, 52% of isolates was resistant to it. Taye et al. (2013) mentioned that 100% of the *E. coli* O157:H7 isolates were resistant to C and Salah (2007) who found that 97.59% of isolates were resistant to C, while in a study conducted by Shamki et al. (2012) and Momtaz et al. (2012), it was found that 32.14% and 29.8% *E. coli* isolates were resistant to C. In the current study, it has been shown that the resistance raised to the third generation of cephalosporin 3GC such as CTX, and the results were 76% for CTX. These results were agreed with Al-Hilali (2010). Shamki et al. (2012) and Nanakaly (2013) they mentioned that (68.2, 96.4% and 87%) respectively of the isolates resistant for the CTX. High resistance pattern for AMP reported with a percentage of 100%, similar result obtained by Zinnah et al. (2008), Shamki et al. (2012) and Taye et al. (2013) whom found the resistance to AMP as 90%-100%, and 100% while Albert et al. (2009) reported 45.9%. This was explained by the overuse of antibiotics especially AMP in Erbil Hospitals, and also to the misuses of these antibiotic as they are prescribed without sensitivity test (Decre et al., 2002). On detecting the resistance of *E. coli* O157:H7 for KF, it was found that 72%

http://www.aloki.hu ● ISSN 1589 1623 (Print) ● ISSN 1785 0037 (Online)
DOI: http://dx.doi.org/10.15666/aeer/1706_1471514727

of the isolates was resistant to it, Shamki et al. (2012) and Dehkordi et al. (2014) reported that 100% and 48% respectively, of *E. coli* isolates showed resistance for KF, while Bekele et al. (2014) showed that the resistance of the isolates for KF was 12.8%. In our work, 56% of the isolates were resistant to FEP, this result agree with Kalantar et al. (2010) who found that 40.5% of the isolates resistance for FEP while Al-Hilali et al. (2010) and Shamki et al. (2012) mentioned that 77.3%, 92.85%of the isolates resistance for FEP. The resistance to CIP was 20%, this result in agreement with (Shamki et al., 2012; Bekele et al., 2014) recorded 25% and 17.9% respectively but the result that mentioned by Zinnah (2008) and Al-Hilali (2010) disagree who reported that all isolates were sensitive to CIP. This is due to that the ciprofloxacin is newly used in treatment in comparison with other antibiotics. Moreorever, Rice et al. (1992) showed that increasing uses of antibiotics was associated with development of resistance against them. The clinical use of fluoroquinolone in children should be restricted because of potential cartilage damage that occurred in research with immature animals, the safety and efficacy of oral ciprofloxacin in children is understudy (Elder, 2004). Jalal et al. (2010) showed that the resistance in bacterial population can be spread either by transfer of bacteria between people or transfer of resistance genes between bacteria (usually on plasmids) and by transfer of resistance genes between genetic elements within bacteria, on transposons or may chromosomally located. Susceptibility to antibiotics is changing in general and increase in antibiotic resistance has been shown worldwide. The main reason for this trend is the increase in antibiotic consumption, the abuse of board spectrum antibiotics or self medication (Younis et al., 2009).

Plasmid profile of E. coli O157:H7

Extracted plasmids analyzed by gel electrophoresis on 0.7% agarose gel as shown in *Figure 1*. The results revealed that most isolates have one band with molecular weight more than 10 kb while (E11, E13 and E21) have two bands with molecular weight more than 10 kbp, E16, E20 and E24 have three bands but E15 which is resistant for 13 antibiotics have 5 bands with molecular weight ranging between (2 kbp- more than 10 kbp) bp in size.

Analysis of plasmid DNA content by agarose gel electrophoresis showed variation in their size and more than one DNA bands appeared in many isolates. These results revealed that among 25 *E. coli* O157:H7 isolates, the size of the bands ranged from 2 Kbp to more than 10 Kbp. The presence of more than one DNA band in the agarose gel is a good indication for existence of more than one plasmid DNA species. The variation in the molecular weights of plasmids might be a result of these plasmids carrying different gene cassettes for resistance against different classes of antibiotics (Khan et al., 2007). The reported results indicate the dissemination of plasmids among *E. coli* O157:H7 isolates which may be carrying resistant genes against wide spectrum of clinically used antibiotics, which may explain the reason of evolution antibiotic resistant patterns in studied bacterial cultures. The study of Ehywarieme (2011) showed that some *E. coli* O157:H7 isolates had plasmid bands with sizes > 1.5 kbp. Aibinu et al. (2007) mentioned that all isolates of *E. coli* O157:H7 had harbored plasmids ranging in size between 21,563 and 27,444 kb. In a research conducted by Malkawi (1998) on *E. coli,* he demonstrated that the plasmid sizes were from (1.5–54) kbp. Tsen (1996) reported that a range of (2 – 22) kbp for plasmid sizes among *E. coli* isolates. Danbara et al. (1987) have also reported plasmid size variations between 3.9 kbp and 50 kbp in *E. coli* strains. As ampicillin showed the most resistance, therefore we have suggested

http://www.aloki.hu ● ISSN 1589 1623 (Print) ● ISSN 1785 0037 (Online)
DOI: http://dx.doi.org/10.15666/aeer/1706_1471514727

that the gene coding for ampicillin resistance could be located on the plasmid. Possibly, some antibiotic resistance genes may not be located on the plasmid but may be on the bacterial chromosome or on transposable elements (Transposon) (Farshad et al., 2012). This indicates that plasmids allow the movement of genetic materials, including antimicrobial resistance genes between bacterial species and strains.

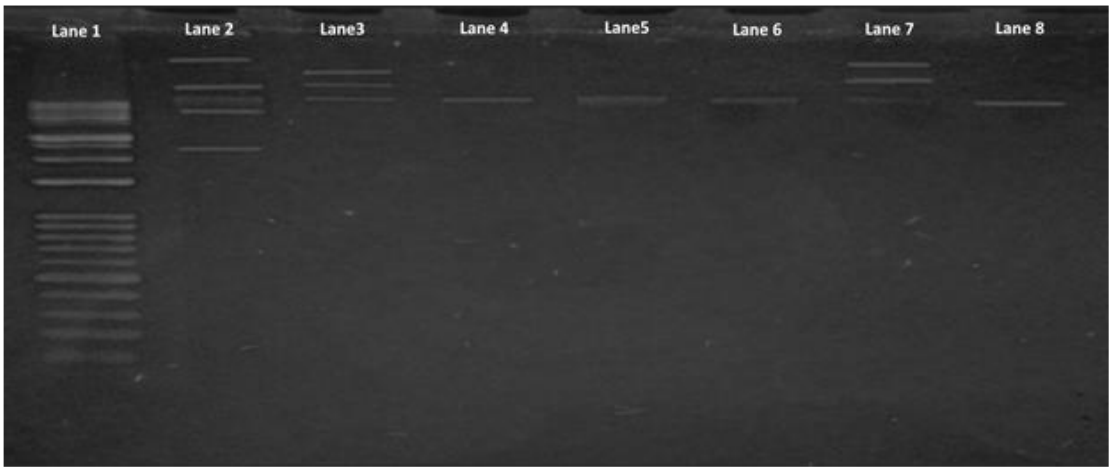

Figure 1. *Plasmid profile of E. coli O157:H7 isolates. (Lane 1: 10 000 bp DNA ladder, Lane 2: Plasmid content of E15, Lane 3: Plasmid content of E16, Lane 4: Plasmid content of E17, Lane 5: Plasmid content of E18, Lane 6: Plasmid content of E19, Lane 7: Plasmid content of E20, Lane 8: Plasmid content of E21)*

Curing of plasmid in E. coli O157:H7 isolate E15 by ethidium bromide

Table 2 demonstrates the curing percent of plasmid DNA from *E. coli* O157:H7 isolates by ethidium bromide. For E15 isolate, ethidium bromide affect AK, CIP, CN and SXT genes with (28.57%). *Figure 2* shows the plasmid DNA profile for *E. coli* O157:H7 isolate (E15) and it is clear that two plasmid DNA were remain in the E15 isolate after treating with ethidium bromide.

Table 2. *Curing of plasmid DNA from E. coli O157:H7 (E15) isolate by using ethidium bromide (EtBr)*

Treatment	Antibiotic resistance pattern														
	AK*	AMP	C	KF	CIP	FEP	CTX	CRO	CN	IPM	MET	TE	TMP	SXT	
E15	R	R	R	R	R	R	R	R	R	S	R	R	R	R	28.57%
EtBr + E15	S	R	R	R	S	R	R	R	S	S	R	R	R	S	

Among various plasmids present in bacterial strains, R plasmids are very significant as they confer resistance to one or more antibiotics, thus possess a threat to chemotherapy. Treatment of cells with certain chemical and physical agents enhances the elimination of plasmids from host cells. This phenomenon is referred to as curing and has been used to ascertain the plasmid associated nature of genes. Susceptibility to curing agent also varies among plasmids (Madigan et al., 2000). Hamad (2009) study the effect of plasmid curing on the drug resistance determinants of MDR *E. coli*, the results revealed that some of the resistance markers (chloramphenicol and nalidixic

http://www.aloki.hu ● ISSN 1589 1623 (Print) ● ISSN 1785 0037 (Online)
DOI: http://dx.doi.org/10.15666/aeer/1706_1471514727

acid) were stably lost in all isolates, thereby confirming their location on plasmid that showed missing of 15 Kbp plasmid band after treating MDR *E. coli* with ethidium bromide, the results also showed losing of all resistant markers for (ampicillin, ceftazidime, cefotaxime, chloramphenicol, nalidixic acid and tetracycline) in some strains of MDR *E. coli,* no plasmid band obtained when these strain subjected to electrophoresis**.**

Ehywarieme (2011) study the impact of plasmid curing on the drug resistance determinant of *E. coli* O157:H7 by using acridine orange*,* the results showed that some of antibiotic resistance marker (Ciprofloxacin and Nalidix acid) were equally observed to be lost in all isolates except E4. The effect of ethidium bromide as curing agent might be due to their action as intercalating agent. This mutagen became inserted between two abnormal conformation can lead to insertion or deletion, thus can induce frameshift mutation (Nariman et al., 1998). On the other hand, the unsuccess of ethidium bromide in curing process for certain antibiotic genes may be attributed to their failure in inhibition of plasmid replication that carry resistance to these antibiotics due to incapability to create mutation in the original replication that specific for this plasmid, or because of their disability to prevent plasmid distribution mechanism on daughter cell as a result remaining of these plasmids in these isolates.

Curing of plasmid DNA by elevated temperature

Elevated temperature at 46 °C was used to cure the plasmid DNA that confers resistance to antibiotics in *E. coli* O157:H7 (E15) isolate and the main results are represented in *Table 3*. *Table 3* indicates that the E15 when treated with elevated temperature at 46 °C AK, CN, CIP, CRO and SXT genes were affected and the curing percent was (35.71%). *Figure 2* shows that E15 tested isolate missing three bands of plasmid DNA after incubation at 46 °C.

Table 3. *Curing of plasmid DNA from E. coli O157:H7 (E15) isolates by using elevated temperature*

Treatment	Antibiotic resistance pattern														
	AK*	AMP	C	KF	CIP	FEP	CTX	CRO	CN	IPM	MET	TE	TMP	SXT	
E15	R	R	R	R	R	R	R	R	R	S	R	R	R	R	35.71 %
Elevated temperature 46 °C + E15	S	R	R	R	S	R	R	S	S	S	R	R	R	S	

Nariman et al. (1998) studied the effect of elevated temperature on eliminating plasmid from *E. coli* isolates and the results indicated that CEP, CTX and CRO determinant were plasmid encoding and they concluded that this may due to the existence of two separate R-plasmids or one plasmid is carrying these antibiotic resistance genes. Nanakaly (2013) performed curing of plasmid DNA by elevated temperature (46 °C) for uropathogenic *E. coli*, she mentioned that E3 when treated with elevated temperature at 46 °C, the ciprofloxacin, ceftriaxone, nitrofurantoin, chloramphenicol, Cefotaxime sodium, gentamycin, sulfamethoxazole/trimethoprim and amikacin genes were affected and the curing percent was (66.6%), while when E25 isolate treated with elevated temperature at 46 °C, genes which responsible for ciprofloxacin, ceftriaxone, nitrofurantoin, cefotaxime, gentamycin,

http://www.aloki.hu ● ISSN 1589 1623 (Print) ● ISSN 1785 0037 (Online)
DOI: http://dx.doi.org/10.15666/aeer/1706_1471514727

sulfamethoxazole/trimethoprim and amikacin resistance were affected with the percentages of (58.3%). From the obtained results, a conclusion can be made that curing by elevated temperature is efficient method for plasmid curing, and this may be due to the fact that the enzymes which contribute to the DNA replication processes are more affected by this high temperature. The inactivation of these enzymes may be due to the change in the folding of polypeptide at this temperature, i.e. the enzymes are sensitive to elevated temperature (Khder, 2002). These results also agree with Radi and Rahman (2010) they concluded that curing by elevated temperature is the most efficient method among others. Furthermore, enzymatic activity declines above the optimum temperature that is characteristic of the heat stability of the particular enzyme (Hardy, 1986). However, plasmids appear to be dependent on host enzymes for their replication, therefore, most of the proteins synthesized during changing of temperature might be utilized for cell division, by that, chance of plasmid replication decreases then curing occurred (Radi and Rahman, 2010). Many researchers demonstrated the mechanism by which the elevated temperature create curing of plasmid DNA, of these, the effect of elevated temperature on plasmid curing may be due to decreasing the amount of synthesized DNA.

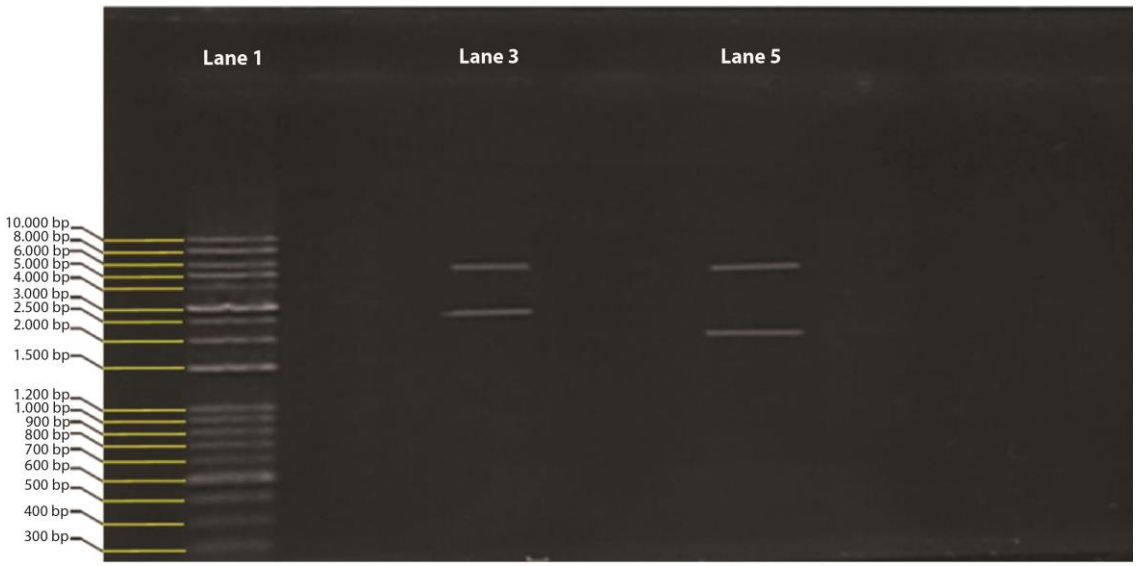

Figure 2. *Plasmid profile of cured E15 by ethidium bromide and elevated temperature. (Lane 1: 10 000 bp DNA ladder, Lane 3: E15 after curing with ethidium bromide, Lane 5: E15 after curing with elevated temperature)*

Conclusion

The article aimed to cure the drug resistance genes twenty-five isolates of E. coli O157:H7 obtained from 200 child stool samples, using using cultural, morphological, biochemical characteristics and serological test to identify the bacteria, and gel electrophoresis to register the plasmid profile, and utilizing Ethidium bromide and elevated temperature to cure the plasmid DNA.

For this purpose, two different types of curing methods were used and the results obtained was a preliminary indication of association of drug resistance of the clinical isolate of *E. coli* O157:H7 (E15*)* with plasmids. Among the two curing method used, elevated temperature displayed greater success rate than the ethidium bromide.

http://www.aloki.hu ● ISSN 1589 1623 (Print) ● ISSN 1785 0037 (Online)
DOI: http://dx.doi.org/10.15666/aeer/1706_1471514727

REFERENCES

[1] Adamus-Bialek, W., Zajac, E., Parniewski, P., Kaca, W. (2013): Comparison of antibiotic resistance patterns in collections of Escherichia coli and *Proteus mirabilis uropathogenic* strains. – Mol. Biol Rep. 40: 3429-3435.

[2] Aibinu, I. E., Peters, R. F., Amisu, K. O., Adesida, S. A., Ojo, M. O., Odugbemi, T. (2007): Multidrug resistance in *E. coli* 0157 strains and the public health implication. – Journal of American Science 3(3): 33-45.

[3] Albert, M. J., Rotimi, V. O., Dhar, R., Silpikurian, S., Pacsa, A. S., Molla, A. M., Szucs, G. (2009): Diarrheagenic *Escherichia coli* are not a significant cause of diarrhea in hospitalized children in Kuwait. – BMC Microbiol. 9: 62-67.

[4] Al-Faisal, A. (1999): Genetic Engineering. – Dar Al-shrooq for Publishing, Amman (in Arabic).

[5] Al-Hilali, Z. B. (2010): Dissemination of β-lactamases in Escherichia coli and Klebsiella spp. isolated from Merjan teaching hospital in Hilla city. – M. Sc. Thesis. Kufa University, College of Science.

[6] Baldwin, J. N., Strickland, R. H. (1969): Some properties of the β-lactamase genes in *S. epidermidis*. – J. Microbiol. 18: 628-630.

[7] Bekele, T., Zewde, G., Tefera, G., Feleke, A., Zerom, K. (2014): *Escherichia coli* O157:H7 in raw meat in Addis Ababa, Ethiopia: prevalence at an abattoir and retailers and antimicrobial susceptibility. – International Journal of Food Contamination 1(4): 45-55.

[8] Carmo, L. P., Schüpbach-Regula, G., Müntener, C. et al. (2017): Approaches for quantifying antimicrobial consumption per animal species based on national sales data: a Swiss example, 2006 to 2013. – Euro Surveill 22: 30458.

[9] Clinical and Laboratory Standard Institute (2007): Performance standard for antimicrobial susceptibility testing. – Fifteenth Informational Supplement 26(3): CLSI-M100-S16.

[10] Danbara, H., Komase, K., Yasuyuki Kirii, K., Shinohara, M., Arita, H., Makino, S., Yoshikawa, M. (1987): Analysis of the plasmids of *Escherichia coli* 0148:H28 from travelers with diarrhoea. – Microbial Pathолog. 3: 269-278.

[11] Decre, D., Verdet, C., Raskine, L., Blanchard, H., Brughoffer, B., Philippon, A., Sanson-Le-Pors, M. J., Petit, J. C., Arlet, G. (2002): Characterization of CMY-type β-lactamases in clinical strains of *Proteus mirabilis* and *Klebsiella pneumonia* isolated in four hospitals in the Paris area. – J Antimicrob. Chemother. 50: 681-688.

[12] Dehkordi, F. S., Yazdani, F., Mozafari, J., Valizadeh, Y. (2014): Virulence factors, serogroups and antimicrobial resistance properties of *Escherichia coli* strains in fermented dairy products. – BMC Res Notes 7: 217.

[13] Ehywarieme, D. A. (2011): R-plasmids amongst *E. coli* O157:H7 isolated from Nigerian currency notes. – International Journal of Tropical Medicine and Public Health 1(1): 123-134.

[14] Elder, J. S. (2004): Urologic Disorders in Infants and Children. – In: Behrman, R. E., Kliegman, R. M., Jenson, H. B., Stanton, B. E. (eds.) Nelson Textbook of Pediatrics. 17th Ed. Saunders, Philadelphia, pp. 1621-788.

[15] Farshad, S., Ranjbar, R., Japoni, A., Hosseini, M., Anvarinejad, M., Mohammadzadegan, R. (2012): Microbial susceptibility, virulence factors, and plasmid profile of uropathogenic *E. coli* strains isolated from Jahrom, Iran. – Arch. Iran Med. 15(5): 312-316.

[16] Hadi, Z. J. (2008): Detection of extended-spectrum beta-lactamases of Escherichia coli and *Klebsiella spp*. isolated from patients with significant bacteriuria in Najaf. – M. Sc. Thesis, College of Medicine, Kufa University.

[17] Hamad, I. S. (2009): Distribution of *E. coli* strains isolated from patients of teaching hospital in Sulaimani City. – J. Duhok Univ. 12(1): 282-287.

[18] Hardy, K. (1986): Bacterial Plasmid. 2nd Ed. – Am. Soc. Microbial., USA.

http://www.aloki.hu ● ISSN 1589 1623 (Print) ● ISSN 1785 0037 (Online)
DOI: http://dx.doi.org/10.15666/aeer/1706_1471514727

[19] Jalal, K. C. A., Nur Fatin, U. T., Mardiana, M. A., Akbar John, B., Kamaruzzaman, Y. B., Shahbudin, S., Omar, M. N. (2010): Antibiotic resistance microbes in tropical mangrove sediments in east coast peninsular, Malaysia. – African Journal of Microbiology Research 4(8): 640-46.
[20] Jawetz, E., Melnick, J. L., Adelberg, E. A., Brooks, G. F., Butel, J. S., Morse, S. A. (2004): Medical Microbiology. 23rd ed. – McGraw-Hill, USA.
[21] Jawetz, E., Melnick, E., Adelberg's, E. (2007): Medical Microbiology. 24th Ed. – McGraw Hill Companies, USA.
[22] Kalantar, D., Mansouri, S. (2010): Emergence of multiple β-lactamases produced by *Escherichia coli* clinical isolates from hospitalized patient in Kerman, Iran. – Jundishapur J. Microbiol. 3(4): 137-45.
[23] Kamruzzaman, M., Shoma, S., Thomas, C. M., Partridge, S. R., Iredell, J. R. (2017): Plasmid interference for curing antibiotic resistance plasmids in vivo. – PLoS One 12(2): e0172913.
[24] Khan, A. U., Sultan, A., Tyagi, A., Zahoor, S., Akram, M., Kaur, S., Shahid, M, Vaishnavi, C. V. (2007): Amplification of mecA gene in multi-drug resistant *Staphylococcus aureus* strains from hospital personnel. – J. Infect. Developing Countries 1(3): 289-295.
[25] Khder, A. K. (2002): Studies on antibiotic resistance by plasmids of *Pseudomonas aeruginosa*. – Ph.D. Thesis, College of Science Education, Salahaddin University, Erbil, Iraq.
[26] Madigan, M. J., Martinlo, J. M., Parker, J. (2000): Brock Biology of Microorganisms. 9th Ed. – Prentice-Hall, Inc., USA.
[27] Maier, L., Pruteanu, M., Kuhn, M. et al. (2018): Extensive impact of nonantibiotic drugs on human gut bacteria. – Nature 555: 623-8.
[28] Malkawi, H. I., Youssef, M. T. (1998): Antibiotic susceptibility testing and plasmid profile of *Escherichia coli* isolated from diarrhoeal patients. – J. Trop. Ped. 44: 128-132.
[29] Michelle, M. M. C., Ciusa, M. L., Piddock, L. J. V. (2018): Strategies to combat antimicrobial resistance: anti-plasmid and plasmid curing. – FEMS Microbiology Reviews 42: 781-804.
[30] Momtaz, H., Rahimi, E., Moshkelani, S. (2012): Molecular detection of antimicrobial resistance genes in *E. coli* isolated from slaughtered commercial chickens in Iran. – Veterinarni Medicina 57(4): 193-197.
[31] Nanakaly, Z. G. A. (2010): Characterization of plasmid DNA content and antimicrobial effect of bile salts on *Esherichia coli* isolated from urinary tract infection of pregnant woman. – Higher Diploma Thesis, College of Education/Scientific, University of Salahaddin, Iraq.
[32] Nariman, A. H., Amany, T., El-Baz, W. F. (1998): Plasmids-mediated antibiotic resistance in *E. coli*. – Arab Journal of Biotechnology 1(1): 17-27.
[33] Nataro, J. P., Kaper, J. B. (1998): Diarrheagenic *Escherichia coli*. – Clinical Microbiology Reviews 11: 142-201.
[34] Radi, R. O. and Rahman, H. (2010): Study the effect of ethidium bromide, SDS and elevated temperature on stability of multiple antibiotic resistances plasmids of *P. aeruginosa*. – Iraqi J. Biotechnol. 9(4): 797-811.
[35] Rice, L. B., Marshal, S. H., Carias, L. L. (1992): Tn5381, a conjugative transposon identifiable as a circular from in *Enterococcus feacalis*. – J. Bacterio. 174: 7308-7315.
[36] Salah, H. F. (2007): Effect of some medicinal plant extracts on antibiotic resistance by plasmids of *Escherichia coli* isolated from different sources in Erbil City. – M.Sc. Thesis, College of Science Education, Salahaddin University, Erbil, Iraq.
[37] Sambrook, J., Russella, D. W. (2001): Molecular Cloning: A Laboratory Manual. 3rd Ed. – Herbour Lab., Cold Spring, New York.
[38] Schlundt, J. (2001): Emerging food-borne pathogens. – Biomed. Enviro. Sci. 14(1-2): 44-52.

http://www.aloki.hu ● ISSN 1589 1623 (Print) ● ISSN 1785 0037 (Online)
DOI: http://dx.doi.org/10.15666/aeer/1706_1471514727

[39] Shamki, J. A., Al-Charrakh, A. H., Al-Khafaji, J. K. (2012): Detection of ESBLs in enteropathogenic, *E. coli* (EPEC) isolates associated with infantile diarrhea in Kut City, Iraq. – Medical Journal of Babylon 9(2): 45-55.
[40] Sharma, S., Bhat, G. K., Shenoy, S. (2007): Virulence factors and drug resistance in *Escherichia coli* isolated from extraintestinal infections. – Indian J. Med. Microbiol. 25(4): 369-373.
[41] Talaro, K., Talaro, A. (2002): Foundation in Microbiology. 4th Ed. – Times Mirror Higher Education Group, Inc, Dubuque, Iowa.
[42] Taye, M., Berhanu, T., Berhanu, Y., Tamiru, F., Terefe, D. (2013): Study on carcass contaminating *Escherichia coli* in apparently healthy slaughtered cattle in Haramaya University slaughter house with special emphasis on Escherichia coli O157:H7, Ethiopia. – J. Veterinar. Sci. Tech. 4: 132-140.
[43] Tomoeda, M., Anto, S., Konishi, M. (1974): Curing action of sodium dodocylsulfate on a *P. aerogenosa* R + strain. – J. Bacteriol. 130: 1158-1163.
[44] Tsen, H. Y., Chi, W. R. (1996): Plasmid profile analysis for enterotoxigenic *E. coli* and detection for heat stable enterotoxin I (ST1) gene by polymerase chain reaction. – J. Food Drug Analysis. 4: 215-222.
[45] Van Boeckel, T. P., Gandra, S., Ashok, A., Caudron, Q., Grenfell, B.T., Simon, A., Levin, S. A., Laxminarayan, A. (2014): Global antibiotic consumption 2000 to 2010: an analysis of national pharmaceutical sales data. – Lancet Infect. Dis. 14: 742-50.
[46] Van Boeckel, T. P., Brower, C., Gilbert, M., Grenfell, B. T., Levin, S. A., Robinson, T. P., Teillant, A., Laxminarayan, R. (2015): Global trends in antimicrobial use in food animals. – Proceedings of the National Academy of Sciences 112(18): 5649-5654.
[47] Van Boeckel, T. P., Glennon, E. E., Chen, D., Gilbert, M., Robinson, T. P., Grenfell, B. T. (2017): Reducing antimicrobial use in food animals. Consider user fees and regulatory caps on veterinary use. – Science 357: 1350-1352.
[48] Wayne, P. A. (2005): Clinical and Laboratory Standard Institute. Performance Standard for Antimicrobial Susceptibility Testing. 15th Ed. – Information Supplement CLSI/NCCLS M 100-S15.
[49] Webber, M. A., Whitehead, R. N., Nick, M. M., Loman, J., Pallen, M. J., Piddock, L. J. V. (2015): Parallel evolutionary pathways to antibiotic resistance selected by biocide exposure. – Journal of Antimicrobial Chemotherapy 70(8): 2241-2248.
[50] Wistreich, G. A., Lechtman, M. D. (1980): Laboratory Exercises in Microbiology. 4th Ed. – Glencoe Publishing Co., Inc. New York.
[51] Woodford, N., Johnson, A. P. (1998): Molecular Bacteriology. Protocols and Clinical Applications. – Humana Press Inc, Totowa, NJ.
[52] Younis, N., Quaol, K., Al-Momani, T., Al-Awaisheh, F., Al-Kayed, D. (2009): Antibiotic resistance in children with recurrent or complicated urinary tract infection. – J. Nepal Med. Assoc. 48(173): 14-9.
[53] Zinnah, M. A., Haque, M. H., Islam, M. T., Hossain, M. T., Bari, M. R., Babu, S. A. M., Rahman, M. T., Islam, M. A. (2008): Drug sensivity pattren of *Escherichia coli* isolated from samples of different biological and environmental sources. – Bangl. J. Vet. Med. 6(1): 13-18.

http://www.aloki.hu ● ISSN 1589 1623 (Print) ● ISSN 1785 0037 (Online)
DOI: http://dx.doi.org/10.15666/aeer/1706_1471514727

IMPACT OF DAY LENGTH AND TOTAL PROTEIN CONTENT IN THE DIET OF FARMED FALLOW DEER (*DAMA DAMA*) ON THEIR PLASMA MINERAL LEVEL AND HAEMATOLOGICAL INDICES

TAJCHMAN, K.[1*] – BOGDASZEWSKI, M.[2] – KOWALCZUK-VASILEV, E.[3] – DĄBROWSKI, R.[4]

[1]*Department of Ethology and Animal Welfare, Faculty of Biology, Animal Sciences and Bioeconomy, University of Life Sciences in Lublin, Akademicka 13, 20-950 Lublin, Poland*

[2]*Institute of Parasitology of the Polish Academy of Sciences, Research Station in Kosewo Górne, 11-700 Mrągowo, Poland*
(e-mail: kosewopan@kosewopan.pl; phone: +48-89-742-4380)

[3]*Institute of Animal Nutrition and Bromatology, Faculty of Biology, Animal Sciences and Bioeconomy, University of Life Sciences in Lublin, Akademicka 13, 20-950 Lublin, Poland*
(e-mail: edyta.kowatczuk@up.lublin.pl; phone: +48-81-445-6914)

[4]*Department and Clinic of Animal Reproduction, Faculty of Veterinary Medicine, University of Life Sciences in Lublin, Głęboka 30, 20-612 Lublin, Poland*
(e-mail: roman.dabrowski@up.lublin.pl; phone: +48-81-445-6168)

**Corresponding author*
e-mail: katarzyna.tajchman@up.lublin.pl; phone: +48-81-445-6848

(Received 12th Jun 2019; accepted 11th Oct 2019)

Abstract. Blood is the main carrier of nutrients and the first indicator of changes occurring in an organism. Hence, the aim of the study was to demonstrate the effect of the day length and the total protein content in the diet for farmed fallow deer (*Dama dama*) on the selected mineral contents of the plasma and blood haematology. The investigation of farmed fallow deer revealed an increase in the level of red blood cells (RBC) and haemoglobin (HGB) induced by altered light conditions, which may the evidence stimulation of erythropoiesis by an increased concentration of androgens. The level of white blood cells (WBC) changed significantly in the control group, which was kept in the least favourable conditions, as indicated by leukocytosis. In the present study, animals exposed to a changed day length exhibited a significant increase in the plasma concentrations of most minerals (phosphorus - P, magnesium - Mg, copper - Cu, calcium - Ca, iron - Fe) after the winter period in the first year of studies, which indicates accelerated development of antlers in farmed fallow deer. However, there was no equally intensive increase in the plasma mineral content (except for Ca) in the same group of animals in the second year of the study. This probably resulted from the administration of adequate nutrition, which prevented changes in the blood mineral concentration despite the antler growth.
Keywords: *Dama dama, wintering conditions, photoperiodism, nutrition, haematology, minerals*

Introduction

Blood is a living tissue composed of different cells which are suspended in the liquid part of the blood called plasma. Its components form a highly developed defense and transport system on which animal body health highly depend. It is, among others, a transporter of various compounds that provides cells with oxygen, nutrients, removes carbon dioxide and other unnecessary or harmful by-products of metabolism, but is also a carrier of hormones, chemical messenger substances, and thus participates in the transmission of information throughout the body. In addition, blood is involved in the

http://www.aloki.hu ● ISSN 1589 1623 (Print) ● ISSN 1785 0037 (Online)
DOI: http://dx.doi.org/10.15666/aeer/1706_1472914750

regulation of body temperature, performs defense functions, protects against pathogens, cures the body - thanks to its coagulation properties (Weiss and Wardrop, 2010).

All this makes so blood is the main and the first indicator of changes occurring in the organism (Weiss and Wardrop, 2010). All factors that can affect an animal are reflected by basic blood tests. Adequate nutrition and enhanced light conditions are often used in farm breeding. The impact of the photoperiod and an appropriate composition of the feed ration have been extensively investigated in cervids, but insufficient attention has been devoted to the closely related fallow deer (*Dama dama*). It is difficult to find literature with data on the influence of an altered day length on the basic haematological parameters in European fallow deer. The day length is extremely important in the life of cervids (Jaczewski, 1954; Pollock, 1975) especially in their hormonal economy (Asher et al., 1989; Suttie et al., 1984; Sempere et al., 1992; Elliott et al., 1996), which may affect the basic haematological parameters.

One of the most important stages in the life of deer is the growth of the antlers regulated by among other things, the hormonal economy which is affected by the daily photoperiod as demonstrated by Jaczewski (1954). Goss (1969) subsequently demonstrated that acceleration of antler cycles can be induced by increasing the frequency of annual daylight cycles with up to four complete antler growth cycles being achieved in 12 months. Changes in food intake, behaviour and plasma hormone concentrations of red deer stags were also fully entrained to a 6-monthly photoperiod cycle (Goss, 1969).

Growing Cervids require an additional 14–20% protein (Ullrey et al., 1967) especially during the growth of antlers. However, Dryden (2016) showed antler growth in adult stags is little affected by diet protein concentrations over 7%, but supplements of protected protein or methionine may improve antler growth. Richardson et al. (2008) research has shown growing antlers consist almost entirely of protein (collagen) and typically consist of 35–45% protein once they harden or "mineralize." While antlers are growing, bucks require a diet of 13–16% protein for optimum development, along with other required nutrients. Only 6–10% protein is required for maintenance of adult deer (Richardson et al., 2008). Antler development in deer results from the collective contribution of nutrition, genetics and age (Ullrey, 1982). It was shown that, white-tailed deer require a diet containing 13 to 16% crude protein (including adequate levels of carbohydrates, fats, minerals and vitamins) in order to express their genetic potential for antler development. In the other studies showed wild cervids require roughly 5% crude protein of dry matter intake for maintenance, but up to 25% for reproduction (Dryden, 2011; Felton et al., 2018). Natural forage for northern cervids typically contains 5–15% crude protein, with rare extremes of 25–30% (Marell et al., 2006; Wam et al., 2016). The objective of protein diet and supplementation is therefore to provide additional nutrients to the deer's natural diet during times when native forage is thought to be inadequate in quantity or quality (especially winter months in the temperate climate zone). Moreover Felton et al. (2018) revealed a lack of evidence that cervids more strongly select for protein in summer than they do in winter. In addition, under farm conditions, the amount of feed consumed by cervids can be controlled only in winter (outside the pasture period).

It has been proven that changes in animal nutrition affect the basic haematological parameters and the concentration of minerals in the blood (Kováč et al., 1997). Also blood is a very sensitive indicator of metabolic changes in both the physiological and pathological status of animals (Weiss and Wardrop, 2010). Thus, the aim of the study

http://www.aloki.hu ● ISSN 1589 1623 (Print) ● ISSN 1785 0037 (Online)
DOI: http://dx.doi.org/10.15666/aeer/1706_1472914750

was to demonstrate the effect of the day length and total protein content in the diet for farmed fallow deer on the plasma level of selected minerals and haematological blood indices.

Materials and methods

Experimental design

The research was carried out at the Research Station of the Institute of Parasitology, Polish Academy of Sciences, Kosewo Górne (Region of Warmia and Mazury; Poland; N: 53°48'; E: 21°23'). All analyses were performed with the consent of the Local Ethics Committee 0069, Resolution No. 42/2016. The study involved 36 male stags in the 3rd-6th year of life divided on an analogous basis into three equal groups (n = 12) receiving different nutrition and provided with different daily photoperiods in winter months (from January to the end of March 2016 and from December 2016 to the end of March 2017):

Experimental group I: Standard farm nutrition with a total protein level of 16% (each animal ingested on average 600 g of the mixture per day with the following composition: 70% of crushed oats in 15% of universal rapeseed concentrate (producer: Eko-pasz, Mońki, Poland) containing 33% of crude protein and in 15% of universal soybean concentrate (producer: Eko-pasz, Mońki, Poland) with 45% crude protein content). The diet included hay and grass silage provided *ad libitum* and a mineral feed mixture Opas Ekstra 7669 from LNB (producer: Cargill, Polska) (*Table 1*). The supplement constituted 2.5% of the standard farm nutrition - 15 g. The experimental group I animals were kept on a run between 7:00 and 15:00 and spent the rest of the day inside the shelter; they were exposed to the natural length of the daylight.

Table 1. *Composition of the diet supplement provided to all groups farmed fallow deer*

Premix composition	Components	Content (in 1 kg)
Macronutrients (%)	Calcium (Ca)	21
	Phosphorus (P)	3
	Sodium (Na)	10
	Magnesium (Mg)	4
Micronutrients (mg)	Manganese (Mn)	3 000
	Zinc (Zn)	6 000
	Iron (Fe)	4 000
	Copper (Cu)	1 000
	Cobalt (Co)	25
	Iodine (I)	100
	Selenium (Se)	25
Vitamins	A (j.m.)	500 000
	D3 (j.m.)	100 000
	E (mg)	1 000
	B1 (mg)	4 000

http://www.aloki.hu ● ISSN 1589 1623 (Print) ● ISSN 1785 0037 (Online)
DOI: http://dx.doi.org/10.15666/aeer/1706_1472914750

Experimental group II: Nutrition was identical as in the experimental group I. Group II was subjected to changed photoperiod conditions, i.e. the day length was artificially prolonged in relation to natural conditions. The experimental group II animals were kept on a run adjacent to the shelter between 7:00 and 15:00 and spent the rest of the day inside. The shelter was equipped with electric LED lamps with a nominal power of 18 W and a declared light stream of 1850 lumens. The emitted light was cold white (colour temperature 6000 K). Light intensity in the shelter and outside was measured using an AB-8809A luxometer (producer: Abatronic, Radom, Poland).

In accordance with the adopted assumptions, the day length was extended by illumination of the shelter from January to the end of March 2016 and from December to the end of March 2017. Unfortunately, the same length of the artificial illumination plan was not used in both years, because in the first one the work associated with the breeding treatment performed annually was delayed by a month. The light in the shelter was turned on and off automatically. The comparison of the length of the natural daylight and the applied photoperiod regime are presented in *Figure 1*.

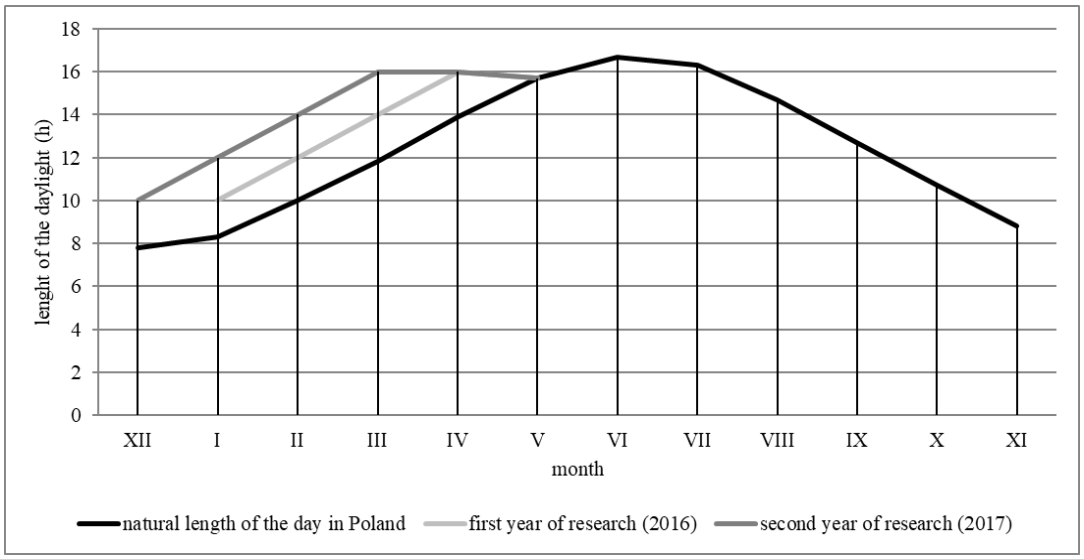

Figure 1. *Comparison of the natural day length in Poland and the photoperiod regime in 2016 and 2017*

Control group III: Standard farm nutrition with a total protein content of 10%. The diet included hay and grass silage provided *ad libitum* and a mineral feed mixture Opas Ekstra 7669 from LNB (producer: Cargill, Poland) (*Table 1*). The supplement constituted 2.5% of the standard farm nutrition - 15 g. The group was kept on a run throughout the day and exposed to the natural length of the daylight.

Observations and measurements

The animals from groups I and II spent the winter (December - March) under a shelter situated in the wintering ground divided into two identical rooms so that it was possible to control the amount of consumed feed. The walls of the shelter were constructed of horizontal wooden boards and provided protection against the adverse impact of weather conditions. Under the shelter, there was a feeding rack for haylage, water containers, and feeding troughs for concentrated feed. The concentrate was

http://www.aloki.hu ● ISSN 1589 1623 (Print) ● ISSN 1785 0037 (Online)
DOI: http://dx.doi.org/10.15666/aeer/1706_1472914750

provided once daily. The animals had free access to water over the entire winter period. After the winter period, the animals stayed on the available pasture without supplementation (April - October) (*Fig. 2*). Body weight was measured with the use of a set of MP 800 sensors coupled with a Tru-Test DR 3000 weight reader LNB (producer: Tru-Test Group, Auckland, New Zealand). As declared by the manufacturer, the accuracy of this set is +/- 1% and the minimum resolution is 100 g.

Figure 2. *Farm fallow deer during the pasture period*

In accordance with the routine zootechnical practice adopted on the farm, antlers were cut at a height of 1 cm above the rose, which is the minimum height in technical terms. This treatment not only does not affect the welfare of experimental animals but also enhances their safety during the mating season, as a high density of relatively large groups of males on farms with limited space increases the risk of serious injuries and even deaths. After removal of dried velvet and mineral impurities and after final drying (in natural conditions) for 30 days, the antlers were weighed (each beam separately) on an electronic balance WLC F1/K with an accuracy of +/- 0.5 g (producer: Radwag, Poland).

Sampling

Samples were collected while the fallow deer were standing inside a small handling box (2 m × 2 m × 0.6 m) (*Fig. 3*) with no need of sedation. Blood samples were collected from *vena jugularis externa* always at the same time (from 1 to 3 h after dawn) to avoid variations associated with circadian rhythms as in research of Gáspar-López et al. (2011). For haematological analyses, 5-ml blood samples were collected into vacuum tubes containing an anticoagulant agent (EDTA) and into tubes with heparin as an anticoagulant. The samples were chilled (4-8 °C) within 15 min after collection. Haematological analysis was carried out within 2 or 3 h after extraction with the use of an automated haematological analyzer Mythic 18 (producer: Orphee S.A.,

http://www.aloki.hu ● ISSN 1589 1623 (Print) ● ISSN 1785 0037 (Online)
DOI: http://dx.doi.org/10.15666/aeer/1706_1472914750

Switzerlan). The device was calibrated each time before the analysis of the samples. The blood was analysed for the content of white blood cells (WBC), red blood cells (RBC), haemoglobin (HGB), and haematocrit (HCT).

Figure 3. *Farm fallow deer in the handling box*

Concurrently, plasma for analysis of the biochemical parameters was obtained by centrifugation of whole blood at 3000 rpm for 10 min in a laboratory centrifuge MPW-350R (producer: MPW Medical Instruments, Warsaw, Poland) at a temperature of 4 °C. After centrifugation, plasma zinc (Zn), phosphor (P), magnesium (Mg), copper (Cu), calcium (Ca), iron (Fe) levels were determined using reagent kits (BioMaxima, Lublin, Poland) according to the manufacturer's protocols and a random access biochemical analyser Metrolab 2300 GL (producer: Metrolab SA, Buenos Aires, Argentina).

The haematological parameters and the plasma content of selected minerals were determined in two terms: before and after the winter in 2016 and 2017, because in these times all animals were kept in the handling box and where weighed. After the procedure, they are moved to a suitable room (before winter) depending on the group to which they belong or to the pasture (after winter). The article is part of a cycle of research of farmed fallow deer. These animals have participated too in study in which we examined some hematological parameters (Tajchman, 2019).

Statistical analysis

The results were analysed statistically. The values were presented as a mean value and standard deviation in the case of measurable parameters and as cardinality and percentage in the case of non-measurable variables.

http://www.aloki.hu ● ISSN 1589 1623 (Print) ● ISSN 1785 0037 (Online)
DOI: http://dx.doi.org/10.15666/aeer/1706_1472914750

The normality of the distribution of variables in the analysed groups was verified with the Shapiro-Wilk test. The differences between the two measurement terms were assessed with the Student's t-test or with the Mann-Whitney test for dependent samples and with the paired-samples Wilcoxon test when the conditions for application of the former test were not met. The differences between the three experimental groups were evaluated with the ANOVA analysis of variance and the post-hoc RIR Tukey test. When the conditions for application of the former analysis were not fulfilled, the Kruskal-Wallis test was used. In order to analyze the interaction of the effect of various factors (diet, lighting, time/year), a mixed multivariate ANOVA analysis of variance was performed. In the case of sphericity disorders (tested by the Meuchly test), the Greenhouse-Geisser correction was applied to the *F* statistics. A significance level of $P < 0.05$ was assumed, which indicated the presence of statistically significant differences or correlations. The database was compiled and statistical analyses were carried out in the Statistica 9.1 software (StatSoft, Polska).

Results

The investigations consisted in comparison of the haematological parameters and mineral concentration in the blood plasma of the farmed fallow deer assessed before the winter period in the first year (2016) of the study and before the winter period in the second year (2017). There was a significant decline from 5.288 to 3.638 $\times 10^9$ L^{-1} ($P = 0.041$) in WBC in group I and on average from 14.397 to 11.564 $\times 10^{12}$ L^{-1} ($P < 0.05$) in RCB in all experimental groups (*Table 2*). In turn, the Zn content increased significantly, on average by 19.11 μmol L^{-1} ($P < 0.05$), in all groups. The highest increase, i.e. by 30.559 umol L^{-1} was noted in group I. A significant increase by 0.267 ($P = 0.034$) in the plasma P content was noted in group I, while the level of Mg increased by 0.174 mmol L^{-1} ($P = 0.0015$) in group II. The plasma Ca content increased significantly in all study groups assessed in the pre-wintering period in 2016 and 2107, with the highest increase by 0.685 ($P < 0.05$) observed in the control group. The Fe concentration also increased significantly in all groups, and the highest increase was noted in group II, i.e. by 13.046 ($P = 0.004$) (*Table 2*).

A statistical analysis of differences between the haematological parameters and the plasma mineral content recorded after the winter period in the first (2016) and second (2017) years of the study was carried out. The data showed a significant increase by 0.657 $\times 10^9$ L^{-1} ($P = 0.049$) in WBC only in the control group and a significant reduction of RBC, on average by 2.404 $\times 10^{12}$ L^{-1} ($P < 0.05$), in all groups (*Table 3*). The plasma Zn concentration increased in group I and in the control, with a higher value in the control group (III), i.e. by 16.970 umol L^{-1} ($P < 0.05$). The plasma P concentration declined on average by 0.875 mmol L^{-1} ($P < 0.05$) after the winter period. There was a significant reduction on the Mg level (by 0.145 mmol L^{-1}) in group II. The levels of Ca and Fe in group I significantly increased by 0.381 mmol L^{-1} and 16.024 umol L^{-1}, respectively (*Table 3*).

We also compared the haematological parameters and plasma mineral content recorded before and after the wintering periods in 2016 and 2017. In the first year of the research, RBC and HCT significantly decreased by 1.031 $\times 10^{12}$ L^{-1} and 2.239% ($P < 0.05$), respectively, after the winter period. In group I, a higher level of only Cu (by 5.168 umol L^{-1}) was observed. With the exception of Zn, the plasma concentrations of all minerals increased significantly in group II. There was an increase in the level of P from 2.448 to

http://www.aloki.hu ● ISSN 1589 1623 (Print) ● ISSN 1785 0037 (Online)
DOI: http://dx.doi.org/10.15666/aeer/1706_1472914750

2.812 mmol L^{-1}, Mg from 0.682 to 0.880 mmol L^{-1}, Cu from 12.438 to 16.437 umol L^{-1}, Ca from 2.301 to 2.596 mmol L^{-1}, and Fe from 32.386 to 36.106 umol L^{-1} ($P < 0.05$). A significant increase in the control group was only noted in the case of P, Mg, and Cu. The content of P increased from 1.988 to 2.442 mmol L^{-1}, Mg from 0.641 to 0.747 mmol L^{-1}, and Cu from 12.277 to 15.754 μmol L^{-1} ($P < 0.05$) (*Table 4*).

In the second year of the investigations, there was a significant decrease (by 0.61 × 10^9 L^{-1}) in WBC in the control group (III) after the winter period, whereas RBC and HGB significantly increased by 0.896 × 10^{12} L^{-1} and 1.200 g L^{-1}, respectively, ($P < 0.05$). The plasma Zn and P concentration in group I decreased after the winter period from 49.979 to 29.697 umol L^{-1} and from 2.802 to 1.629 mmol L^{-1}, respectively ($P < 0.05$). In turn, the Mg and Cu content increased from 0.675 to 0.766 mmol L^{-1} and from 11.867 to 15.063 umol L^{-1}, respectively ($P < 0.05$). In the other groups (II and III), the content of Ca declined statistically significantly after the winter period, i.e. by 0.349 mmol L^{-1} (*Table 5*).

Additionally, the antler and body weight was compared in the study groups. In all groups, the weight of the animals' antlers increased significantly between 2016 and 2107. The increase was substantially higher in group I (from 941.176 to 1558.235 g) and III (from 1064.706 to 1450.588 g) than in group II (from 1062.437 to 1185.000 g) ($P < 0.05$). The body weight of the fallow deer before and after the winter period significantly increased in all groups as well (*Table 6*). Furthermore, the cycle of antler growth, velvet loss, and antler shedding was accelerated by on average 3 weeks in group II.

The changes in the haematological parameters and plasma mineral content in the farmed fallow deer were analysed statistically. A statistically significant difference was found in the magnitude of the change in the Zn level between the groups analysed in the pre-wintering period in the first and second year of the study ($F = 11.653$, $P = 0.003$). Statistically significant differences were found between groups I and II (a mean increase by 30.559 umol L^{-1} in group I and by 12.609 umol L^{-1} in group II) and between groups I and III (a mean increase by 12.609 umol L^{-1} in group I and by 14.185 umol L^{-1} in group III) (*Table 7*).

There was a statistically significant difference in the magnitude of the change in the Ca content between the analysed groups ($H = 8.343$, $P = 0.015$) before the wintering period in 2016 and 2017. Statistically significant differences were found for groups I and II (a mean increase by 0.260 mmol L^{-1} in group I and by 0.661 mmol L^{-1} in group II) and between groups I and III (a mean increase by 0.260 mmol L^{-1} in group I and by 0.684 mmol L^{-1} in group III) (*Table 7*).

After the wintering period in the first and second year of the study, there was a statistically significant difference in the magnitude of the change in the levels of Mg ($F = 5.001$, $P = 0.013$) and Ca ($F = 4.041$, $P = 0.027$) between the analysed groups. Statistically significant differences were found between groups I and II. On average, the Mg content increased by 0.114 mmol L^{-1} in group I and declined by 0.144 mmol L^{-1} in group II. Similarly, the content of Ca increased on average by 0.382 mmol L^{-1} in group I and decreased by 0.143 mmol L^{-1} in group II (*Table 7*). There was a statistically significant difference in the magnitude of the changes in the antler weight between the analysed groups ($H = 18.544$, $P = 0.0001$). Statistically significant differences were found between groups I and II (a mean increase in the weight by 617.059 g in group I and by 122.563 g in group II) (*Table 7*).

Statistically significant differences were also found between the measurement terms in the study years. Before and after the wintering periods in 2016, there were

http://www.aloki.hu ● ISSN 1589 1623 (Print) ● ISSN 1785 0037 (Online)
DOI: http://dx.doi.org/10.15666/aeer/1706_1472914750

differences in the magnitude of changes in the levels of Ca ($F = 4.464$, $P = 0.017$) and Fe ($F = 3.727$, $P = 0.032$). Statistically significant differences were noted between groups I and II. On average, the Ca content decreased by Ca o 0.144 mmol L^{-1} in group I and increased by 0.296 mmol L^{-1} in group II. Similarly, the Fa content increased on average by 2.989 umol L^{-1} in group I and increased by 3.720 umol L^{-1} in group II (*Table 8*). Before and after the wintering period in 2017, there were significant differences in the magnitude of the changes in the Zn content only ($F = 4.199$, $P = 0.024$). Statistically significant differences were found between groups I and III. On average, the Zn content decreased by 20.283 umol L^{-1} in group I and decrease by 0.998 umol L^{-1} in group III (*Table 8*).

The research also analyzed the effect of out-object (natural and artificial light length and 10% and 16% protein in the diet) and intra-object (change of results over time). No statistically significant effect of time as well as the effect of protein alone and light on WBC was observed. However, a significant effect of time and protein interaction was noted (F (3, 60) = 3.864, $P = 0.038$, $eta^2 = 0.162$) and the effect of time and light interaction (F (3, 60) = 4.089, $P = 0.032$, $eta^2 = 0.170$) (*Table 9*).

In the case of RBC, only the effect of time (F (3, 60) = 26.913, $P < 0.001$, $eta^2 = 0.574$) was significant, the difference was between the measurements from 2016 and 2017: 1 - 3, 1 - 4, 2 - 3, 2 - 4 (*Table 9*).

No significant effect of time, protein and light, and interaction between them on HGB and HCT was observed (*Table 9*).

In the case of Zn, a significant effect of time alone was demonstrated (F (3, 60) = 32.972, $P < 0.001$, $eta^2 = 0.507$), the significant difference was met between the measurements from 2016 and 2017: 1 - 3, 1 - 4, 2 - 3, 2 - 4. A significant effect of time and protein interaction (F (3, 60) = 5.374, $P = 0.008$, $eta^2 = 0.144$) and time and light interaction (F (3, 60) = 4.793, $P = 0.013$, $eta^2 = 0.013$) were also met for Zn concentration in fallow deer plasma. However, the time effect itself was the strongest ($eta^2 = 0.507$) (*Table 9*).

No significant effect of time, protein and light as well as the relationship between them on the P plasma concentration of animals was observed (*Table 9*).

The plasma Mg content was influenced by the time effect (F (3, 60) = 5.625, $P = 0.001$, $eta^2 = 0.149$), a difference was dependent between measurements from 2016 and 2016 and 2017: 1 - 2, 1 - 3, 1 - 4. A significant effect of time and light was also shown (F (3, 60) = 2.816, $P = 0.043$, $eta^2 = 0.081$). The time effect was stronger ($eta^2 = 0.149$) (*Table 9*).

The plasma Cu content was affected only by the time effect (F (3, 60) = 5.551, $P = 0.005$, $eta^2 = 0.148$), a statistically significant difference was between measurements 1 - 2, 1 - 4 (*Table 9*).

In the case of Ca, a significant effect of time alone was demonstrated (F (3, 60) = 20.736, $P < 0.001$, $eta^2 = 0.393$), the significant difference was between the measurements from 2016 and 2017 and from 2017 alone: 1 - 3, 1 - 4, 2 - 3, 3 - 4. In addition, a significant effect of time and light interaction (F (3, 60) = 4.923, $P = 0.003$, $eta^2 = 0.133$) on the fallow deer plasma Ca content was also demonstrated. The time effect itself was again stronger in this case (*Table 9*).

Demonstrated a significant effect of time alone on plasma Fe concentration (F (3, 60) = 12.506, $P < 0.001$, $eta^2 = 0.281$), a significant difference was between the measurements: 1 - 3, 1 - 4, 2 - 3, 2 - 4 (*Table 9*).

http://www.aloki.hu ● ISSN 1589 1623 (Print) ● ISSN 1785 0037 (Online)
DOI: http://dx.doi.org/10.15666/aeer/1706_1472914750

Table 2. *Comparison of some haematological parameters and mineral concentration in the plasma of farmed fallow deer before the winter period in 2016 and 2017*

Analyzed variable	Group I						Group II						Group III					
	Before wintering 2016		Before wintering 2017		2016-2017		Before wintering 2016		Before wintering 2017		2016-2017		Before wintering 2016		Before wintering 2017		2016-2017	
	M	SD	M	SD	t^a/Z^b	*P*	M	SD	M	SD	t^a/Z^b	*P*	M	SD	M	SD	t^a/Z^b	*P*
Haematological parameters																		
WBC (10^9 L^{-1})	5.288	2.772	3.638	0.753	2.039[b]	0.041*	3.380	1.010	3.874	0.607	-1.308[a]	0.232	3.807	0.625	4.442	0.876	-2.145[a]	0.085
RBC (10^{12} L^{-1})	15.008	0.878	11.916	0.826	14.909[a]	< 0.005*	14.050	0.872	11.140	1.348	8.429[a]	< 0.005*	14.133	1.015	11.637	1.127	10.485[a]	< 0.005*
HGB (g L^{-1})	17.700	0.773	17.658	0.867	0.275[b]	0.784	17.887	0.356	16.925	1.801	1.581[a]	0.158	17.850	0.493	17.450	1.508	0.737[a]	0.494
HCT (%)	49.750	2.385	48.500	2.938	1.077[a]	0.304	50.275	2.111	47.650	5.261	1.451[a]	0.190	48.633	1.311	48.400	5.230	0.123[a]	0.907
Content of minerals in plasma																		
Zn (umol L^{-1})	19.420	2.811	49.979	11.053	3.059[b]	0.002*	22.237	4.501	34.846	11.800	-3.534[a]	0.004*	22.258	4.510	36.442	10.661	-3.949[a]	0.002*
P (mmol L^{-1})	2.535	0.338	2.802	3.154	2.118[b]	0.034*	2.507	0.424	2.165	0.529	1.707[a]	0.116	1.864	0.852	5.631	11.956	0.978[b]	0.328
Mg (mmol L^{-1})	0.594	0.225	0.675	0.064	-1.101[a]	0.294	0.680	0.063	0.854	0.206	2.432[b]	0.015*	0.647	0.094	0.787	0.262	1.529[b]	0.126
Cu (umol L^{-1})	11.231	1.762	11.867	3.439	0.314[b]	0.754	12.269	2.516	13.991	2.629	-1.860[a]	0.089	12.344	2.508	13.352	3.862	-0.925[a]	0.375
Ca (mmol L^{-1})	2.576	0.218	2.836	0.425	2.628[b]	0.008*	2.234	0.134	2.895	0.326	-6.805[a]	< 0.005*	2.213	0.250	2.898	0.411	-5.090[a]	< 0.005*
Fe (umol L^{-1})	31.903	3.522	38.552	7.983	-2.672[b]	0.0217*	32.835	4.274	45.881	12.144	-3.619[a]	0.004*	29.863	5.638	36.689	6.201	-3.523[a]	0.004*

a – the Student's *t*-test result, b – Mann-Whitney test results, M-mean, SD- standard deviation, *values statistically significant $P < 0.05$

http://www.aloki.hu ● ISSN 1589 1623 (Print) ● ISSN 1785 0037 (Online)
DOI: http://dx.doi.org/10.15666/aeer/1706_1472914750

Table 3. *Comparison of some haematological parameters and mineral concentration in the plasma of farmed fallow deer after the winter period in 2016 and 2017*

Analyzed variable	Group I						Group II						Group III					
	After wintering 2016		After wintering 2017		2016-2017		After wintering 2016		After wintering 2017		2016-2017		After wintering 2016		After wintering 2017		2016-2017	
	M	SD	M	SD	t^a/Z^b	*P*	M	SD	M	SD	t^a/Z^b	*P*	M	SD	M	SD	t^a/Z^b	*P*
Haematological parameters																		
WBC (10^9 L^{-1})	3.868	0.769	3.912	0.781	-0.176[a]	0.864	4.053	0.918	3.761	0.816	0.917[a]	0.379	3.904	0.885	4.561	0.733	-2.211[a]	0.049*
RBC (10^{12} L^{-1})	14.140	0.899	12.375	0.242	6.144[a]	< 0.005 *	14.675	3.135	12.060	0.559	2.667[b]	0.007*	15.042	2.059	12.209	0.496	3.059[b]	0.002*
HGB (g L^{-1})	17.640	1.265	18.300	0.558	-2.199[a]	0.055	18.425	1.835	18.067	0.943	0.039[b]	0.969	18.300	1.467	18.192	0.640	0.470[b]	0.638
HCT (%)	47.860	3.739	47.740	2.737	0.127[a]	0.902	49.333	8.564	47.200	2.676	0.789[a]	0.446	50.975	6.039	47.133	2.319	1.647[b]	0.099
Content of minerals in plasma																		
Zn (umol L^{-1})	19.455	3.286	28.737	11.581	-3116[a]	0.008*	21.614	2.725	32.013	16.466	-1.914[a]	0.085	18.475	4.549	35.445	11.924	-4.674[a]	< 0.005 *
P (mmol L^{-1})	2.603	0.520	1.609	0.558	4.652[a]	< 0.005 *	2.834	0.296	1.777	0.369	9.862[a]	< 0.005 *	2.400	0.328	1.821	0.355	3.760[a]	0.003*
Mg (mmol L^{-1})	0.656	0.168	0.770	0.111	-1.814[a]	0.094	0.885	0.099	0.740	0.160	2.856[a]	0.017*	0.735	0.139	0.746	0.125	-0.192[a]	0.852
Cu (umol L^{-1})	16.888	8.093	14.718	4.032	0.834[a]	0.420	16.273	1.563	15.318	7.690	0.403[a]	0.695	15.305	3.712	16.192	7.361	-0.356[a]	0.729
Ca (mmol L^{-1})	2.391	0.344	2.772	0.441	-3.562[a]	0.0048	2.616	0.242	2.474	0.443	0.809[a]	0.437	2.415	0.378	2.625	0.239	-1.889[a]	0.085
Fe (umol L^{-1})	29.747	4.733	45.773	13.085	-4.819[a]	< 0.005 *	37.888	4.956	54.575	32.823	-1.671[a]	0.125	31.997	7.776	46.989	25.171	-1.900[a]	0.083

a – the Student's *t*-test result, b – Mann-Whitney test results, M-mean, SD- standard deviation, *values statistically significant $P < 0.05$

http://www.aloki.hu ● ISSN 1589 1623 (Print) ● ISSN 1785 0037 (Online)
DOI: http://dx.doi.org/10.15666/aeer/1706_1472914750

Table 4. *Comparison of some haematological parameters and mineral concentration in the plasma of farmed fallow deer before and after the winter period in 2016*

Analyzed variable	Group I						Group II						Group III					
	Before wintering 2016		After wintering 2016		Before-after		Before wintering 2016		After wintering 2016		Before-after		Before wintering 2016		After wintering 2016		Before-after	
	M	SD	M	SD	t^a/Z^b	*P*	M	SD	M	SD	t^a/Z^b	*P*	M	SD	M	SD	t^a/Z^b	*P*
Haematological parameters																		
WBC (10^9 L^{-1})	4.841	2.535	3.809	0.689	0.804[b]	0.422	3.240	0.879	3.761	0.599	-1.707[a]	0.119	3.564	0.775	3.764	0.898	-1.068[a]	0.316
RBC (10^{12} L^{-1})	15.054	0.855	14.023	0.891	3.640[a]	0.414 *	14.218	0.785	14.518	2.749	0.000[b]	1.000	14.322	0.960	15.789	2.996	0.533[b]	0.594
HGB (g L^{-1})	17.585	0.779	17.515	1.152	0.278[a]	0.786	17.873	0.307	18.291	1.566	0.509[b]	0.610	17.911	0.521	18.955	2.186	0.889[b]	0.374
HCT (%)	49.600	2.475	47.361	3.381	2.359[a]	0.036 *	50.009	1.844	49.627	7.37	0.157[a]	0.878	49.056	1.859	53.267	8.841	0.886[b]	0.374
Content of minerals in plasma																		
Zn (umol L^{-1})	19.680	2.720	18.348	3.655	1.126[a]	0.277	27.563	4.257	21.707	3.822	-0.096[a]	0.925	21.234	4.597	18.911	4.924	1.706[b]	0.088
P (mmol L^{-1})	2.471	0.365	2.496	0.528	-0.170[a]	0.867	2.448	0.493	2.812	0.326	-2.475[a]	0.026*	1.988	0.742	2.442	0.351	2.499[b]	0.012 *
Mg (mmol L^{-1})	0.569	0.228	0.636	0.168	-0.865[a]	0.399	0.682	0.0567	0.880	0.106	-6.736[a]	< 0.00 5*	0.641	0.084	0.747	0.135	2.508[b]	0.012 *
Cu (umol L^{-1})	10.884	1.780	16.052	7.694	-2.485[b]	0.013 *	12.438	2.282	16.437	2.287	-4.913[a]	< 0.00 5*	12.277	2.286	15.754	3.516	-3.459[a]	0.003 *
Ca (mmol L^{-1})	2.506	0.244	2.362	0.516	1.107[a]	0.284	2.301	0.182	2.596	0.253	-3.339[a]	0.004*	2.222	0.236	2.406	0.364	-1.819[a]	0.088
Fe (umol L^{-1})	31.691	3.716	28.701	4.848	1.902[a]	0.075	32.386	4.412	36.106	5.837	-2.327[a]	0.034*	29.413	5.785	32.178	8.324	-1.136[a]	0.274

a – the Student's *t*-test result, b – Mann-Whitney test results, M-mean, SD- standard deviation, *values statistically significant $P < 0.05$

http://www.aloki.hu ● ISSN 1589 1623 (Print) ● ISSN 1785 0037 (Online)
DOI: http://dx.doi.org/10.15666/aeer/1706_1472914750

Table 5. *Comparison of some haematological parameters and mineral concentration in the plasma of farmed fallow deer before and after the winter period in 2017*

Analyzed variable	Group I						Group II						Group III					
	Before wintering 2017		After wintering 2017		Before-after		Before wintering 2017		After wintering 2017		Before-after		Before wintering 2017		After wintering 2017		Before-after	
	M	SD	M	SD	t^a/Z^b	*P*	M	SD	M	SD	t^a/Z^b	*P*	M	SD	M	SD	t^a/Z^b	*P*
Haematological parameters																		
WBC (10^9 L^{-1})	3.638	0.753	4.042	0.745	-1.281[a]	0.226	3.962	0.655	3.761	0.816	0.353b	0.724	3.951	0.917	4.561	0.733	-2.211[a]	0.049*
RBC (10^{12} L^{-1})	11.916	0.826	12.374	0.359	1.490[b]	0.136	11.164	1.181	12.060	0.559	-3.442[a]	0.005*	11.943	1.189	12.209	0.496	-1.103[a]	0.293
HGB (g L^{-1})	17.658	0.867	18.350	0.620	1.579[b]	0.114	16.867	1.598	18.067	0.943	-3.035[a]	0.011*	17.633	1.536	18.192	0.640	-1.582[a]	0.142
HCT (%)	48.500	2.938	48.050	2.800	0.549[b]	0.583	47.391	4.631	47.200	2.675	0.177[a]	0.862	49.058	4.744	47.133	2.329	1.858[a]	0.090
Content of minerals in plasma																		
Zn (umol L^{-1})	49.979	11.053	29.697	11.542	6.867[a]	< 0.005 *	35.599	12.069	32.013	16.467	0.522[a]	0.613	36.442	10.661	35.444	11.924	0.191[a]	0.852
P (mmol L^{-1})	2.802	3.154	1.629	0.578	2.118[b]	0.034*	2.128	0.539	1.777	0.369	2.094[a]	0.063	5.631	11.956	1.812	0.371	1.689[b]	0.091
Mg (mmol L^{-1})	0.675	0.064	0.766	0.115	-2.547[a]	0.027*	0.873	0.204	0.740	0.160	1.274[b]	0.202	0.786	0.262	0.746	0.124	0.157[b]	0.875
Cu (umol L^{-1})	11.867	3.439	15.063	4.008	-2.309[a]	0.041*	14.022	2.756	15.318	7.690	-0.493[a]	0.632	13.352	3.862	16.192	7.361	-1.180[a]	0.263
Ca (mmol L^{-1})	2.836	0.425	2.811	0.437	0.156[a]	0.879	2.899	0.341	2.473	0.443	3.104[a]	0.011*	2.898	0.411	2.625	0.239	2.400[a]	0.035*
Fe (umol L^{-1})	38.552	7.983	47.158	12.632	-1.692[a]	0.119	46.684	12.399	54.575	32.824	0.000[b]	1.000	36.689	6.201	46.989	25.171	-1.349[a]	0.204

a – the Student's *t*-test result, b – Mann-Whitney test results, M-mean, SD- standard deviation,*values statistically significant $P < 0.05$

http://www.aloki.hu ● ISSN 1589 1623 (Print) ● ISSN 1785 0037 (Online)
DOI: http://dx.doi.org/10.15666/aeer/1706_1472914750

Table 6. *Comparison of the antler and body weight before and after the winter period in 2016 and 2017 (calculations are given only for factors that were statistically significant)*

Group I						Group II						Group III					
2016		2017				2016		2017				2016		2017			
M	SD	M	SD	t^a/Z^b	*P*	M	SD	M	SD	t^a/Z^b	*P*	M	SD	M	SD	t^a/Z^b	*P*
Weight of the antler (g)																	
941.176	418.418	1558.235	300.317	3.621[b]	< 0.005*	1062.437	461.535	1185.000	327.088	-2.490[a]	0.025*	1064.706	492.368	1450.588	506.439	-6.346[a]	< 0.005*
Body weight before wintering (October) (kg)																	
72.588	11.847	79.824	9.105	-3.289[a]	0.004*	70.125	6.459	78.250	6.618	-6.889[a]	< 0.005*	72.705	10.110	84.353	6.509	2.769[b]	0.005*
Body weight after wintering (April/May) (kg)																	
57.235	10.047	66.941	6.932	-8.349[a]	< 0.005*	59.500	10.857	69.125	5.488	3.181[b]	0.001*	57.000	8.374	63.705	5.643	-6.638[a]	< 0.005*

a – the Student's *t*-test result, b – Mann-Whitney test results, M-mean, SD- standard deviation, *values statistically significant $P < 0.05$

Table 7. *Statistical analysis of the magnitude of changes in the haematological parameters, plasma mineral levels, and body and antler weight in the fallow deer before wintering period in 2016 and 2017 and after the winter periods in 2016 and 2017 (calculations are given only for factors that were statistically significant)*

Compare terms	Analyzed variable	Group I		Group II		Group III		F^a/H^b	*P*	Intergroup differences
		M	SD	M	SD	M	SD			
Before wintering 2016-2017	**Content of minerals in plasma**									
	Zn (umol L^{-1})	30,559	10,787	12,609	12,360	14,185	12,441	11.653[b]	0.003*	I-II, I-III
	Ca (mmol L^{-1})	0,260	0,349	0,661	0,336	0,684	0,466	8.343[b]	0.015*	I-II, I-III
After wintering 2016-2017	Mg (mmol L^{-1})	0.114	0.226	-0.144	0.168	0.011	0.196	5.001[a]	0.013*	I-II
	Ca (mmol L^{-1})	0.382	0.387	-0.143	0.585	0.209	0.385	4.041[a]	0.027*	I-II
After wintering 2016-2017	**Mass of antler and body weight**									
	mass of antler (g)	617.059	281.930	122.563	196.885	385.882	440.000	18.544[c]	0.0001*	I-II

a - ANOVA variance analysis, b - Kruskal-Wallis test, M-mean, SD- standard deviation, *values statistically significant $P < 0.05$

http://www.aloki.hu ● ISSN 1589 1623 (Print) ● ISSN 1785 0037 (Online)
DOI: http://dx.doi.org/10.15666/aeer/1706_1472914750

Table 8. *Statistical analysis of the magnitude of changes in the haematological parameters, plasma mineral levels in the fallow deer before and after the winter periods in 2016 and before and after the winter periods in 2017*

Compare terms	Analyzed variable	Group I		Group II		Group III		F^a/H^b	*P*	Intergroup differences
		M	SD	M	SD	M	SD			
	Content of minerals in plasma									
Before - after wintering 2016	Ca (mmol L^{-1})	-0,144	0,537	0,296	0,354	0,184	0,404	4.464[a]	0.017*	I-II
	Fe (umol L^{-1})	-2,989	6,479	3,720	6,394	2,764	9,731	3.727[a]	0.032*	I-II
Before - after wintering 2017	Zn (umol L^{-1})	-20,283	10,231	-3,586	22,799	-0,998	18,051	4.199[a]	0.024*	I-III

a - ANOVA variance analysis, b - Kruskal-Wallis test, M-mean, SD- standard deviation, *values statistically significant $P < 0.05$

Table 9. *The effect of the influence of time, protein level in the diet, light day length and interaction between the analyzed variables on selected haematological parameters and the concentration of minerals in plasma of fallow deer (calculations are given only for factors that were statistically significant)*

Analyzed variables			Estimated marginal averages				$F(3, 60)$	*P*	eta^2
			(1) Before wintering	(2) After wintering	(3) Before wintering	(4) After wintering			
			2016		2017				
Haematological parameters									
WBC (10^9 L^{-1})	Protein	10%	3.333	3.833	4.000	4.000	3.864	0.038*	0.162
		16%	3.826	3.340	3.250	3.396			
	Daylight	Natural	4.056	3.694	3.500	3.833	4.089	0.032*	0.170
		Artificial elongated	2.875	3.125	3.500	3.125			

http://www.aloki.hu ● ISSN 1589 1623 (Print) ● ISSN 1785 0037 (Online)
DOI: http://dx.doi.org/10.15666/aeer/1706_1472914750

RBC (10^{12} L^{-1})	Time		14.439	14.741	11.586	12.156	26.913	< 0.001*, Intergroup differences: 1-3, 1-4, 2-3, 2-4	0.574
Content of minerals in plasma									
Zn (umol L^{-1})	Time		20.970	20.068	40.674	32.385	32.972	< 0.001*, Intergroup differences: 1-3, 1-4, 1-3, 1-4	0.507
	Protein	10%	22.257	18.476	36.442	35.445	5.374	0.008*	0.144
		16%	20.326	20.864	42.789	30.855			
	Daylight	Natural	20.839	19.195	43.211	32.571	4.793	0.013*	0.130
		Artificial elongated	21.232	21.814	35.599	32.013			
Mg (mmol L^{-1})	Time		0.637	0.761	0.778	0.751	5.625	0.001, Intergroup differences: 1-2, 1-3, 1-4	0.149
	Daylight	Natural	0.621	0.700	0.731	0.756	2.816	0.043	0.081
		Artificial elongated	0.668	0.885	0.874	0.740			
Cu (umol L^{-1})	Time		11.754	16.309	13.080	15.524	5.551	0.005*, Intergroup differences: 1-2, 1-4	0.148
Ca (mmol L^{-1})	Time		2.339	2.477	2.877	2.636	20.736	< 0.001, Intergroup differences: 1-3, 1-4, 2-3,3-4	0.393
	Daylight	Natural	2.395	2.408	2.867	2.718	4.923	0.003	0.133
		Artificial elongated	2.227	2.616	2.899	2.474			
Fe (umol L^{-1})	Time		31.495	33.359	40.641	49.574	12.506	< 0.001*, Intergroup differences: 1-3, 1-4, 2-3, 2-4	0.281

F- ANOVA variance analysis, *P* - statistically significant values, *correct epsilon Greenhouse-Geisser

http://www.aloki.hu ● ISSN 1589 1623 (Print) ● ISSN 1785 0037 (Online)
DOI: http://dx.doi.org/10.15666/aeer/1706_1472914750

Discussion

There are only few studies on the effect of nutrition and altered day length on haematological parameters and plasma mineral concentrations in farmed fallow deer. Studies on various temperate cervid species conducted with the use of artificial manipulations of the daily photoperiod have shown that light has a significant impact on cervids (Jaczewski, 1954; French et al., 1960; Goss, 1969; Pollock, 1975; Simpson et al., 1983/84; Snyder et al., 1983).

Changing breeding conditions exert an effect on animal physiology, as evidenced by the results of the present study. The level of WBC in the farmed fallow deer usually had lower values in all groups (except for group I before the winter period in 2016 when the values were similar) than values reported in investigations of farmed deer (Gaspar-López et al., 2011) in the respective months. It was shown in the fallow deer that the WBC count changed significantly in the control group, especially in 2017. This group was provided with the least favourable conditions, as reflected in the elevated plasma WBC levels. In the other research groups, the WBC count did not change significantly after the wintering period, as shown by Landete-Castillejos et al. (2002) or Landete-Castillejos et al. (2007), although that was the beginning of the antler development period. Another factor contributing to the slight reduction of WBC and the increase in RBC can be ascribed to the diet, as shown in the present study and investigations reported by Tomkins et al. (1991). The level of leukocytes varies seasonally and may constitute an adaptation to anticipated immune challenges by variation of the use of day length by animals (Nelson, 2004). Unfortunately, the present investigations do not confirm this finding. The RBC level in the farmed fallow deer was usually higher (especially in 2016); it was similar to the values noted in April by Gaspar-López et al. (2011) only after the winter period in 2017. Similarly, the HGB level was higher in the farmed fallow deer than those reported in investigations of farmed deer (Gaspar-López et al., 2011). HCT was higher in the farmed fallow deer, with the exception of group I, in which the value was similar to that reported by Gaspar-López et al. (2011) only after the winter period. The investigations conducted by Gaspar-López et al. (2011) demonstrated characteristic fluctuations in the RCB, HGB and HCT levels, which were substantially lower in November-December than in March-April. As suggested by DelGiudice et al. (1992), changes in nutrition may be a cause of seasonal fluctuations, which could explain the differences related to the altered light conditions in the present study. However, Gaspar-López et al. (2011) suggested another cause of these changes. The high testosterone level during the mating period (Gaspar-López et al., 2010) may be associated with high levels of the haematological parameters described in this study. Available literature provides evidence for stimulation of erythropoiesis by androgens (Gordon et al., 1970). Contrasting data were presented by Bubenik (2006), who suggested that antlers grow during a period of low concentrations of reproductive hormones. Interestingly, the RCB and HGB levels in the present study increased under the impact of the altered light conditions in the second year of the study, which may confirm stimulation of the erythropoiesis process probably by the increased estradiol content during this time. The investigations conducted by Bubenik et al. (1979) demonstrate an increase in the concentration of this hormone in spring and autumn in male white-tailed deer (*Odocoileus virginianus*). Estradiol blocks of the activity of testes and its high levels in spring prevent premature stimulation of spermatogenesis in

http://www.aloki.hu ● ISSN 1589 1623 (Print) ● ISSN 1785 0037 (Online)
DOI: http://dx.doi.org/10.15666/aeer/1706_1472914750

a period that is unsuitable for deer reproduction. This was confirmed by Bubenik et al. (2005) by analysis of blood collected from growing antlers and velvet, where this hormone was present in high concentrations.

The plasma concentration of Ca, P, and Mg in the farmed fallow deer in the analysed months was higher than or similar to the values reported by Kuba (2014). In the present study, the animal group exposed to the altered day length regime exhibited a significant increase in the plasma concentration of most minerals (P, Mg, Cu, Ca, Fe) after the winter period in 2016, which indicates accelerated development of antlers in the farmed fallow deer. Only the Cu content increased in group I and higher Mg and Cu levels were observed in group III. However, as early as in 2017, such an intensive increase in the mineral content (except for Ca) was not noted in the plasma of the group exposed to the greater day length. This was probably associated with the proper and constant level of nutrition, which prevented changes in the blood mineral concentration despite the period of antler growth (Gaspar-López et al., 2011). Interestingly, group I only, which was supplemented with a higher amount of protein in the diet, exhibited lower Zn and P content and a higher Mg and Cu level in the plasma after the winter period in 2017.

Additionally, high Zn concentrations in the plasma of the farmed fallow deer were observed before the winter period in all groups in 2017. This was probably related to the fact that the animals were subjected to the experimental conditions a month earlier than in 2016. Zn is responsible for the normal testosterone concentration and proper function of the immune system (Bartoskewitz et al., 2007). After antler growth and mating periods, the immune system of cervids can return to homeostasis, hence the increased uptake of this mineral in the blood (Kun et al., 2015). This may also be a result of supplementation, as shown by Suresh et al. (2013).

The concentration of P and Mg in the plasma of the farmed fallow deer was in the range reported by Kučer et al. (2013). The Cu content in the fallow deer plasma significantly increased after the winter period in all groups in 2016 and only in group I in 2017. This indicates a high demand for Cu after the pasture period as well as a need for adequate supplementation and the necessity to provide the animals with appropriate conditions in winter to compensate for nutritional deficiencies caused by the decline in the nutritional value of pastures in late autumn (Padilla et al., 2000; Bao et al., 2010).

The fallow deer body weight in the pre-wintering period was evidently higher than after the winter, which was reported in investigations of other cervid species as well. Increased liveweight gain during summer in comparison to winter has been recorded in all arctic, boreal and temperate deer so far studied (McEwan, 1968; Bandy et al., 1970; Pollock, 1975; Asher, 1993). The deer voluntarily reduce their appetite during winter (McEwan, 1968). The cycle of voluntary food intake and growth are known to be under photoperiodic control (Suttie and Simpson, 1985). Whereas for reproductive seasonality the short days of autumn are thought to provide a stimulatory cue for reproduction in temperate deer.

The body weight increased on average by 9.6 kg in the groups with higher protein content in the diet and with the modified day length and by only 6.7 kg in the control group (III). Appropriate conditions provided to animals during winter are essential, as confirmed by experiments conducted by Olguin et al. (2013), Gaspar-López et al. (2011), Janiszewski et al. (2008) and in the present study.

Similarly, the antler weight depended on the conditions provided to the animals during the winter period. However, the greatest effect was exerted by the protein content in the diet, adequate supplementation, and milder wintering conditions. In turn,

http://www.aloki.hu ● ISSN 1589 1623 (Print) ● ISSN 1785 0037 (Online)
DOI: http://dx.doi.org/10.15666/aeer/1706_1472914750

the extended day length accelerated development of antlers and velvet loss; hence, the antlers in this group exhibited the lowest weight. This phenomenon was confirmed by Suttie et al. (1991) as well as Suttie and Webster (1995).

Conclusion

In conclusion, an appropriate level of total protein and supplementation of the stag nutrition had a positive effect on animal fitness and antler growth. Time had the greatest effect on selected haematological parameters and mineral content in farm fallow deer plasma. The differences were mainly observed between the 2016 and 2017 measurements for RBC, Zn, Mg, Cu, Ca and Fe. In contrast, the equations between the measurements were in the first year of testing only in the case of Mg concentration, while in the second year in the case of Ca. Generally, prolonged repeated of breeding treatments give a greater effect. The effect of time and protein interaction had on WBC and Zn, while the effect of time and light interaction on WBC, Zn, Mg, Ca. Increased protein supply, separately, in the fallow deer diet causes an increase in the concentration of P, Mg, Cu and Ca in their plasma, while the extension of the light day has a positive effect on the content of RCB, HGB, P, Mg, Cu and Ca. On the other hand, the reduction in the quality of wintering conditions for animals was marked by an increase in WBC (*Table 10*). Therefore it can be assumed that the results of the present study have not only a theoretical but also application value.

Table 10. *Summary of results obtained*

Analyzed variable	Group I Total protein content of 16%, natural length of the daylight		Group II Total protein content of 16%, artificially extended daylight		Group III Total protein content of 10%, natural length of the daylight	
	2016	2017	2016	2017	2016	2017
WBC	≈	≈	≈	≈	≈	▲
RBC	▼	≈	≈	▲	≈	≈
HGB	≈	≈	≈	▲	≈	≈
HCT	▼	≈	≈	≈	≈	≈
Zn	≈	▼	≈	≈	≈	≈
P	≈	▼	▲	≈	▲	≈
Mg	≈	▲	▲	≈	▲	≈
Cu	▲	▲	▲	≈	▲	≈
Ca	≈	≈	▲	▼	≈	▼
Fe	≈	≈	≈	≈	≈	≈
Body weight	▲		▲		▲	
Mass of antler	▲		▲		▲	

▲- significant increase, ▼- significant decrease, ≈- no significant change

In future research, it is planned to take blood from deer more often and determine hematology and mineral levels to capture more accurate changes over time. In addition, an identical artificial lighting plan should be used. In addition, as recommended by other researchers (Felton et al., 2018) to assess digestibility protein and energy both in

http://www.aloki.hu ● ISSN 1589 1623 (Print) ● ISSN 1785 0037 (Online)
DOI: http://dx.doi.org/10.15666/aeer/1706_1472914750

vivo and in vitro. Estimations of protein- and energy-digestibility are problematic to extrapolate to the population level, because of complex interactions between diet and individual, and many of the studies were compiled at the population level. Furthermore, in the case of research into small ruminants, a constant supply of drinking water should be ensured in pasture management (Fischer et al., 2017), which would also be worth to check in moderate climate conditions.

REFERENCES

[1] Asher, G. W. (1993): Growth and Feeding Management of farmed Fallow Deer in New Zealand. – In: Asher, G. W. (ed.) Procs. First World Forum on Fallow Deer Farming. Mudgee, NSW, Australia.

[2] Asher, G. W., Peterson, A. J., Bass, J. J. (1989): Seasonal pattern of LH and testosterone secretion in adult male fallow deer (*Dama dama*). – Journal of Reproduction and Fertility 85: 657-665.

[3] Bandy, P. J., Mc, T. I., Cowan Wood, A. J. (1970): Comparative growth in four races of black tailed deer (*Odocoileus hemionus*). Part 1. Growth in body weight. – Canadian Journal of Zoology 48: 1401-1410.

[4] Bao, K., Li, G. Y., Cui, X. Z. (2010): Effects of different copper sources on serum biochemical parameters and nutrient digestibilities in growing male sika deer (*Cervus nippon*). – Chinese Journal of Animal Nutrition 22: 717-722.

[5] Bartoskewitz, M. L., Hewitt, D. G., Laurenz, J. C. (2007): Effect of dietary copper and zinc concentrations on white-tailed deer antler growth, body size, and immune system function. – Small Ruminant Research 73: 87-94.

[6] Bubenik, G. A. (2006): Seasonal regulation of deer reproduction as related to the antler cycle - a review. – Veterinarski Arhive 76: 275-285.

[7] Bubenik, G. A., Bubenik, A. B., Zamecnik, J. (1979): The development of circannual rhythm of estradiol in plasma of male white-tailed deer (*Odocoileus virginianus*). – Comparative Biochemistry and Physiology Part A: Physiology 62A: 869-872.

[8] Bubenik, G. A., Miller, K. V., Lister, A. L., Osborn, D. A., Bartoš, L., Van Der Kraak, G. J. (2005): Testosterone and estradiol concentrations in serum, velvet skin and growing antler bone of male white-tailed deer. – Journal of Experimental Zoology 303A: 186-192.

[9] DelGiudice, G. D., Mech, L. D., Kunkel, K. E., Gese, E. M., Seal, U. S. (1992): Seasonal patterns of weight, hematology and serum characteristics of free-ranging female white-tailed deer in Minnesota. – Canadian Journal of Zoology 70: 974-983.

[10] Dryden, G. M. (2011): Quantitative nutrition of deer: energy, protein and water. – Animal Production Science 51(4): 292-302.

[11] Dryden, G. M. (2016): Nutrition of antler growth in deer. – Animal Production Science 56(6): 962-970.

[12] Elliott, J. L., Oldham, J. M., Asher, G. W., Molan, P. C., Bass, J. J. (1996): Effect of testosterone on binding of Insulin - like growth factor I (IGF-1) nad IGF - II in growing antlers of fallow deer (*Dama dama*). – Growth Regulation 6(4): 214-21.

[13] Felton, A. M., Wam, H. K., Stolter, C., Mathisen, K. M., Wallgren, M. (2018): The complexity of interacting nutritional drivers behind food selection - a review of northern cervids. – Ecosphere 9(5): e02230. DOI: 10.1002/ecs2.2230.

[14] Fischer, A., Kaiser, T., Pickert, J., Behrendt, A. (2017): Studies on drinking water intake of fallow deer, sheep and mouflon under semi-natural pasture conditions. – Grassland Science 63(1): 46-53.

[15] French, C. E., McEwen, L. C., Magruger, N. D., Rader, T., Long, T. A., Swift, R. W. (1960): Responses of white-tailed bucks to added artificial light. – Journal of Mammalogy 41: 23-29.

http://www.aloki.hu ● ISSN 1589 1623 (Print) ● ISSN 1785 0037 (Online)
DOI: http://dx.doi.org/10.15666/aeer/1706_1472914750

[16] Gaspar-López, E., Landete-Castillejos, T., Estevez, J. A., Ceacero, F., Gallego, L. (2010): Biometrics, testosterone, cortisol and antler growth cycle in Iberian red deer stags (*Cervus elaphus hispanicus*). – Reproduction in Domestic Animals 45: 243-249.
[17] Gaspar-López, E., Landete-Castillejos, T., Estevez, J. A., Ceacero, F., Gallego, L., Garcia, A. J. (2011): Seasonal variations in red deer (*Cervus elaphus*) hematology related to antler growth and biometric measurements. – Journal of Experimental Zoology 315: 242-249.
[18] Gordon, A. S., Zanjani, E. D., Levere, R. D., Kappas, A. (1970): Stimulation of mammalian erythropoiesis by 5β-H steroid metabolites. – Proceedings of the National Academy of Sciences of the United States of America 65: 919-924.
[19] Goss, R. J. (1969): Photoperiodic control of antler cycles in deer. 1. Phase shift and frequency changes. – Journal of Experimental Zoology 170: 311-324.
[20] Jaczewski, Z. (1954): The effect of changes in length of daylight on the growth of antlers in deer (*Cervus elaphus* L.). – Folia Biologica 2: 133-143.
[21] Janiszewski, P., Dmuchowski, B., Gugołek, A., Żełobowski, R. (2008): Body weight characteristics of farm-raised fallow deer (*Dama dama* L.) over the winter period. – Journal of Central European Agriculture 9(2): 337-342.
[22] Kováč, G., Ciberej, J., Paulíková, I., Seidel, H. (1997): Haematological indices in fallow deer. – Acta Veterinaria Brno 66: 203-211.
[23] Kuba, J. (2014): Analysis of changes in the concentration of Ca, P and Mg in blood serum of red deer (*Cervus elaphus*) immature males in farm breeding. – Acta Scientiarum Polonorum Zootechnica 13(2): 31-40.
[24] Kučer, N., Kuleš, J., Barić Rafaj, R., Tončić, J., Vicković, I., Štokovic, D., Potočnjak, D., Šoštaric, B. (2013): Mineral concentrations in plasma of young and adult red deer. – Veterinarski Arhive 83(4): 425-434.
[25] Kun, B., Weili, S., Chunyi, L., Kaiying, W., Zhipeng, L., Shidan, B., Guangyu, L. (2015): Effects of dietary zinc supplementation on nutrient digestibility, haematological biochemical parameters and production performance in male sika deer (*Cervus nippon*). – Animal Production Science 56(6): 997-1001.
[26] Landete-Castillejos, T., García, A. J., Gómez, J. A., Laborda, J., Gallego, L. (2002): Effects of nutritional stress during lactation on immunity costs and indices of future reproduction in Iberian red deer (*Cervus elaphus hispanicus*). – Biology Reproduction 67: 1613-1620.
[27] Landete-Castillejos, T., Estévez, J. A., Martínez, A., Ceacero, F., García, A. J., Gallego, L. (2007): Does chemical composition of antler bone reflect the physiological effort made to grow it? – Bone 40: 1095-1102.
[28] Marell, A., Hofgaard, A., Danell, K. (2006): Nutrient dynamics of reindeer forage species along snowmelt gradients at different ecological scales. – Basic and Applied Ecology 7: 13-30.
[29] McEwan, E. H. (1968): Growth and development of barren-ground caribou. – Canadian Journal of Zoology 46: 1023-1029.
[30] Nelson, J. E. (2004): Infrared methods for daylight acquisition of leo satellites. – Thesis. Captain, USAF, Washington, DC.
[31] Olguin, C. A., Landete-Castillejos, T., Ceacero, F., García, A. J., Gallego, L. (2013): Effects of Feed Supplementation on Mineral Composition, Mechanical Properties and Structure in Femurs of Iberian Red Deer Hinds (*Cervus elaphus hispanicus*) – PLoS One 8(6): e65461.
[32] Padilla, S., Bouda, J., Quiroz-Rocha, G. F., Davalos, J. L., Sanches, A. (2000): Biochemical and haematological values in venous blood of captive red deer (*Cervus elaphus*) at high altitude. – Acta Veterinaria Brno 69: 327-331.
[33] Pollock, A. M. (1975): Seasonal changes in appetite and sexual condition in red deer stags maintained on a six month photoperiod. – The Journal of Physiology 244: 95P–96P.

http://www.aloki.hu ● ISSN 1589 1623 (Print) ● ISSN 1785 0037 (Online)
DOI: http://dx.doi.org/10.15666/aeer/1706_1472914750

[34] Richardson, C., Lionberger, J., Miller, G. (2008): White-Tailed Deer Management in the Rolling Plains of Texas. – Texas Parks and Wildlife Department, Austin, TX.
[35] Sempere, A. J., Mauget, R., Bubenik, G. A. (1992): Influence of photoperiod on the seasonal pattern of secretion of luteinizing hormone and testosterone and on the antler cycle in roe deer (*Capreolus capreolus*). – Journal of Reproduction and Fertility 95: 693-700.
[36] Simpson, A. M., Suttie, J. M., Kay, R. N. B. (1983/84): The influence of artificial photoperiod on the growth, appetite and reproductive status of male red deer and sheep. – Animal Reproduction Science 6: 291-299.
[37] Snyder, D., Cowan, R., Hagen, D. R., Schanbacher, B. D. (1983): Effect of pinealectomy on seasonal changes in antler growth and concentration of testosterone and prolactin in white-tailed deer. – Biology of Reproduction 29: 63-71.
[38] Suttie, J. M., Simpson, A. M. (1985): Photoperiodic Control of Appetite, Growth, Antlers and Endocrine Status of Red Deer. – In: Fennessy, P. F., Drew, K. R. (eds.) Biology of Deer Production. The Royal Society of New Zealand, Wellington.
[39] Suttie, J. M., Webster, J. R. (1995): Extreme seasonal growth in Arctic deer: comparisons and control mechanisms. – American Zoologist 35: 215-221.
[40] Suttie, J. M., Lincoln, G. A., Kay, R. N. B. (1984): Endocrine control of antler growth in red deer stags. – Journal of Reproduction and Fertility. 71: 7-15.
[41] Suttie, J. M., Fennesy, P. F., Crosbie, S. F., Corson, I. D., Laas, F. J., Elgar, H. J., Lapwood, K. R. (1991): Temporal changes in LH and testosterone and their relationship with the first antler in red deer (*Cervus elaphus*) stags from 3 to 15 months of age. – Journal of Endocrinology 131(3): 467-74.
[42] Suresh, C., Das, A., Katole, S., Saini, M., Swarup, D. (2013): Effect of concentrate supplementation on feed consumption, nutrient utilization and blood metabolite profile in captive spotted deer (*Axis axis*) fed oat (*Avena sativa*) and berseem (*Trifolium alexandrinum*) fodders based diet. – Zoo Biology 32(2): 195-203.
[43] Tajchman, K. (2019): Selected haematological indices in farmed male fallow deer (*Dama dama*) depending on the different conditions during the wintering period. – Veterinarni Medicina 64: 379–385.
[44] Tomkins, N. W., McMeniman, N. P., Daniel, R. C. W. (1991): Voluntary feed intake and digestibility by red deer (*Cervus elaphus*) and sheep (*Ovis ovis*) of pangola grass (*Digitaria decumbens*) with or without a supplement of leucaena (*Leucaena leucocephala*). – Small Ruminant Research 5(4): 337-345.
[45] Ullrey, D. E. (1982): Nutrition and Antler Development in White-Tailed Deer. – In: Brown, R. D. (ed.) Antler Development in Cervidae. Caesar Kleberg Wildlife Research Institute, Kingsville, TX.
[46] Ullrey, D. E., Youatt, W. G., Johnson, H. E., Fay, L. D., Bradley, B. L. (1967): Protein requirements of white-tailed deer fawns. – Journal of Wildlife Management 31: 679-685.
[47] Wam, H. K., Histol, T., Nybakken, L., Solberg, E. J., Hjeljord, €. O. (2016): Transient nutritional peak in browse foliage after forest clearing advocates cohort management of ungulates. – Basic and Applied Ecology 17: 252-261.
[48] Weiss, D. J., Wardrop, K. J. (2010): Schalm's Veterinary Hematology. Sixth Ed. – Blackwell Publishing, Ames, IA.

http://www.aloki.hu ● ISSN 1589 1623 (Print) ● ISSN 1785 0037 (Online)
DOI: http://dx.doi.org/10.15666/aeer/1706_1472914750

INVESTIGATION OF INLAND POLLUTION USING TOTAL CARBON (TC), TOTAL ORGANIC CARBON (TOC), INORGANIC CARBON (IC), TOTAL NITROGEN (TN) AND TOC/TN RATIOS

DINÇER, A. R.[1*] – YÜMÜN, S.[2] – ÖNCE, M.[3] – YÜMÜN, Z. Ü.[1]

[1]*Department of Environmental Engineering, Namık Kemal University, Corlu, Tekirdağ, Turkey*
(e-mail: zyumun@nku.edu.tr)

[2]*Saray Vocational High School, Poliza Endüstri A.Ş Çerkezköy, Tekirdağ, Turkey*
(e-mail: sevinc.yumun@gmail.com)

[3]*Namık Kemal University, Corlu, Tekirdağ, Turkey*
(e-mail: melike21once@gmail.com)

[*]*Corresponding author*
e-mail: adincer@nku.edu.tr

(Received 12th Jun 2019; accepted 25th Oct 2019)

Abstract. In this study, sediment samples were taken at three different points in Edremit Bay at different depths from the sea floor. In Edremit Bay, it was investigated whether the pollution was marine or terrestrial. According the results of measurement of TOC (Total Organic Carbon) values have been yielded results between 10.35-20.36 (Küçükkuyu), 8.14-16.40 (Güre), and 2.71-12.60 g/kg (Dikili) in the marine sediments. The fact that first and second regions are susceptible to mountainous and intra-continental erosion (sedimentation 5.743 and 7.509 mm/year) increased the TOC value. The highest TOC/TN ratio (12.33-46.89) was found in the second region. No linear change in TOC and TOC/TN (Total Nitrogen) ratios was observed at all three points depending on the depth. At results of compared all carotes, the low TOC/TN (2.82-14.48) ratio have been observed in the BH1 carotes, probably the result of small stream beds and low intra-continental erosion. This study shows that TOC and TOC/TN ratios in different parts of Edremit Gulf show inconsistency and this inconsistency arises not only from the marine contribution their natural organic matter, but also from the continent.
Keywords: *inland pollution, marine pollution, TOC, TN, TOC/TN*

Introduction

In this study, total organic carbon (TOC), inorganic carbon (IC), total carbon (TC) and total nitrogen (TN) concentrations in the sea sediments of Edremit Bay (Balıkesit/Turkey) were investigated. Stable isotopes, such as carbon (C) and nitrogen (N), are the tools used to assess the geochemical processes in the environment and to determine the anthropogenic effect. C and N, the major constituents their organic matter, can bear the footprints of their hydrological flows and sediment processes, including anthropogenic modifications in the natural system (Zetsche et al., 2011; De Souza et al., 2017). Elemental composition and C/N ratios are frequently used as markers for organic carbon sources in sediments (Jacob et al., 2009). Soil, sediments, organic carbon, and nitrogen are mainly the result of the decomposition of plants and animals or plankton or anthropogenic sources such as chemical contaminants, fertilizers, or organic-rich wastes (Avramidis et al., 2015). Hydrocarbons in sediments are considered effective tracers because they correlate well with the sources of their formation (Meyers et al.,1984). The atomic TOC/N ratio separates the organic matter from marine or terrestrial. The terrestrial organic matter is enriched in carbon relative to nitrogen and shows a high TOC/N ratio

http://www.aloki.hu ● ISSN 1589 1623 (Print) ●ISSN1785 0037 (Online)
DOI: http://dx.doi.org/10.15666/aeer/1706_1475114765

(Hecky et al., 1993). Terrestrial plants are rich in cellulose, and algae contain nitrogen-rich compounds. The TOC/N ratio of terrestrial organics ranges from 12 to 14 (Meyers et al., 1984). TOC/N ratios in vascular land plants and mangrove leaves were higher than 20 (Lallier-Verges et al., 1998; Azevedo, 2003). If the TOC/N ratio is between 6 and 8, it reflects the nature of planktonic marine origin organic matter (Venkatesan et al., 1987). An intermediate value of TOC/N = 10 reflects the characteristic of the mixing zones between marine and terrestrial sources (Stein, 1991). Allochthonous (ice-fed) and autochthonous (in-situ) carbonates can be distinguished by assuming that carbonates are glacial or biogenic in their origin and that the organic matter is biologically derived (organic carbon is negligible in glacial source material) (Koziorowska et al., 2016). TOC value varies between 1 mg/L in sea waters, 2-10 mg/L in lake or river waters, and up to 10 g/L in swamps (Bayram et al., 2011). Accumulation of OC in marine sediments as a result of biological degradation is known to contribute significantly to the reduction of atmospheric CO_2. Changes in total alkalinity increase or decrease CO_2 emissions from the atmosphere. In contrast, the formation of biogenic carbonates reduces alkalinity and leads to the opposite effects (Koziorowska et al., 2016). Most of the metals in the aquatic systems are associated with the particle phase, and more than 99% of the pollutants are present in fine-grained precipitates in complex with organic matter and oxides (Bartoli et al., 2012; Martínez-Santos et al., 2015).

In the marine environment, organic matter (OM) is composed of compounds that are resistant to biochemical oxidation. In non-contaminated natural waters, TOC results from humic substances and partially degraded plants or animal substances (Visco et al., 2005; Bayram et al., 2011). In a study conducted by Yümün and Önce (2017), heavy metal pollution and foraminiferal populations were determined in the samples obtained from the sea floor soundings in Küçükkuyu (Çanakkale) region. Refractory compounds (humic and fulvic acids), structural carbohydrates, and black carbon usually form the majority of sedimentary organic matter and are often brought to sea from land (Winogradow et al., 2018). C_{org}/TN ratios indicate the greater availability of paleolakes-combined nitrogen and possibly loading of algae-derived organic matter. In order to understand biogeochemical cycles, the formation of organic matter and accumulation in sediments are very important (Waterson et al., 2008; Sampaio et al., 2010). The results of studies to date show that 60-80% of C_{org} originates from land (allochthonous), but other studies show that marine organisms play an important role in OM in sediments (Koziorowska et al., 2016).

In this study, analyses of the total carbon (TC), the total inorganic carbon (IC), the total nitrogen (TN), and C/N were performed in the sludge samples taken from the seabed. It was concluded that the inland pollution dominated in the sediment samples taken from the sea floor in the Küçükkuyu, Güre, and Dikili regions.

Material and Methods

In the Bay of Edremit (Güre, Küçükkuyu, and Dikili), three drillings with an average depth of 20 m were made using a pontoon drilling machine that was modularly constructed on the sea. The sediment cores obtained from the drillings were preserved in special core boxes and analyzed in this study. The depth of the samples was calculated from the top of the sediments.

The Dikili district is located on the northern coast of the Aegean Region in the west of the Aegean Sea, northeast of the Madra Mountains, and south of Çandarlı Bay. Güre is a

http://www.aloki.hu ● ISSN 1589 1623 (Print) ●ISSN1785 0037 (Online)
DOI: http://dx.doi.org/10.15666/aeer/1706_1475114765

town on the Edremit Bay in the Edremit district, Balıkesir. The town of Edremit is 12 km away. The district is located in the Aegean region between Edremit Bay and Kazdağı. Küçükkuyu is a tourist town in Ayvacık, Çanakkale. Güre is located in the west of Altınoluk with Behramkale in the east and Ayvacık in the northeast. There is no river in the Güre-Küçükkuyu region, but there are the Edremit-Zeytinli, Kızılkeçili, Güre, and Altınoluk streams with a length of 6-10 km in this area. From these streams to the coastal section, mostly domestic wastewaters are present (Önce, 2014).

The location and location map of the study area are given in *Figure 1*. Three sea drilling samples were taken from the Güre (13.20 m - 16.00 m), Küçükkuyu (13.00 m - 28.00 m), and Dikili (10.00 m - 19.00 m) area with a modular sea bottom and semi-hydraulic drilling machine (*Figure 2*). The samples were brought to the laboratory in corrugated boxes which were not exposed to sunlight. A total of three samples were taken from the top, bottom and center sections of each drilling core. Total of 15 samples were examined from three drillings. The samples were analyzed in duplicate. The precision for TOC, TN, IC and TC was ± 0.02 wt%, ± 0.01 wt%, ± 0.01 wt% and ± 0.01 wt%, respectively (n=5). The range of TOC-LCSH/CPH is 4 µg/L (ppb) - 30,000 mg/L (ppm).

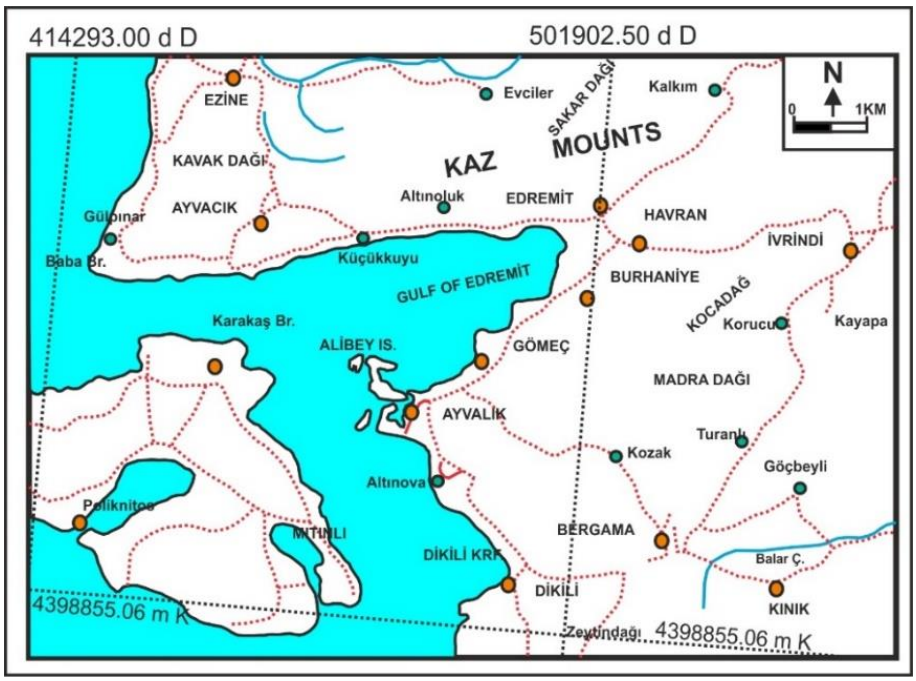

Figure 1. *Map of study area and sampling points (Dikili BH-1, Güre BH-3, and Küçükkuyu BH-3)*

The coordinates of the sample points were shown in *Table 1*. For the analysis of organic matter, 200 grams of sediment samples were taken from the cores with an average of 50 cm spacing (a long depth) and sent to Namık Kemal University Central Research Laboratory (NABİLTEM). A TOC-L series analyzer (Model SSM 5000 A) was used for the analysis of the total organic carbon in 15 samples collected along the drilling depth. TC, TOC, and IC measurements were made with this device. The concentrations of the samples collected at each 50 cm depth were divided by the number of samples collected along the selected depth to find the mean concentrations in each depth range. Total nitrogen (TN) measurements were performed to determine the C/N ratio in the samples.

http://www.aloki.hu ● ISSN 1589 1623 (Print) ●ISSN1785 0037 (Online)
DOI: http://dx.doi.org/10.15666/aeer/1706_1475114765

Nitrogen measurement was performed with a Vapodest VAP 20s model device. In the measurement of TOC, both total carbon (TC) and inorganic carbon (IC) were measured. The total amount of organic carbon can be obtained by subtracting the amount of inorganic carbon from the total carbon content.

Figure 2. *A view of Küçükkuyu BH3 and drilling machine*

Table 1. *The Coordinates of Bore Hole (BH1-Dikili, BH3-Güre and BH3-Küçükkuyu)*

Sample No	Coordinates (WGS-84, 6 Deegre), 2016		Driling depth (m)	Length Of sample (m)
	East (Y)	North (X)		
Dikili (BH-1)	490060.55	4324738.74	10.00 - 19.00	9.00
Güre (BH-3)	489776.20	4381514.27	13.20 - 16.00	2.80
Küçükkuyu (BH-3)	466009.22	4377155.44	13.00 - 28.00	15.00

Results and Discussion

Three soundings were made in the Aegean Sea by Yümün Mühendislik in Dikili (İzmir), Güre (Balıkesir), and Küçükkuyu (Çanakkale) regions, and cores obtained from drilling were used in this study. Five samples of sediment were collected from each core samples at the base, middle, and upper levels, and TOC, OC, IC, and TN concentrations were measured in the laboratory. Inland and marine pollutions were determined by taking into consideration the formation time of the precipitate.

Based on these analyzes, the TOC values were found to be high in Küçükkuyu and Güre. In Dikili, the TOC values obtained at the highest level of drilling were higher than at the lower part. Nitrogen values were generally high at the intermediate levels of the drillings. Previous studies have used the C/N ratios used to monitor dominant carbon resources accumulated in coastal deposits (Zhang et al., 2007; Pan et al., 2019). Hence,

http://www.aloki.hu ● ISSN 1589 1623 (Print) ●ISSN1785 0037 (Online)
DOI: http://dx.doi.org/10.15666/aeer/1706_1475114765

we used C/N ratios to characterize organic matter sources. In the samples taken from Edremit Bay, the TOC/N ratio was variable throughout the depth (increase/decrease), indicating that there was no pollution the result of the population concentration. The organic matter in the sediments is a mixture of materials. It is derived from particles caused by intra-continental erosion, and organic matter is produced from biological activity in the aquatic environment (Chen et al., 2008).

As can be seen in *Figure 3*, the samples taken from the sea bottom near Güre show the TC, IC, TOC, and TN analysis results. There was no linear relation between the TC, TOC, and IC parameters and depth. The TOC concentration varied between 8.14-16.40 g/kg (0.814-1.64%). Walinsky et al. (2009) found that the TOC content of sediments on the coast of Southeast Alaska ranged from 0.3-8% by weight.

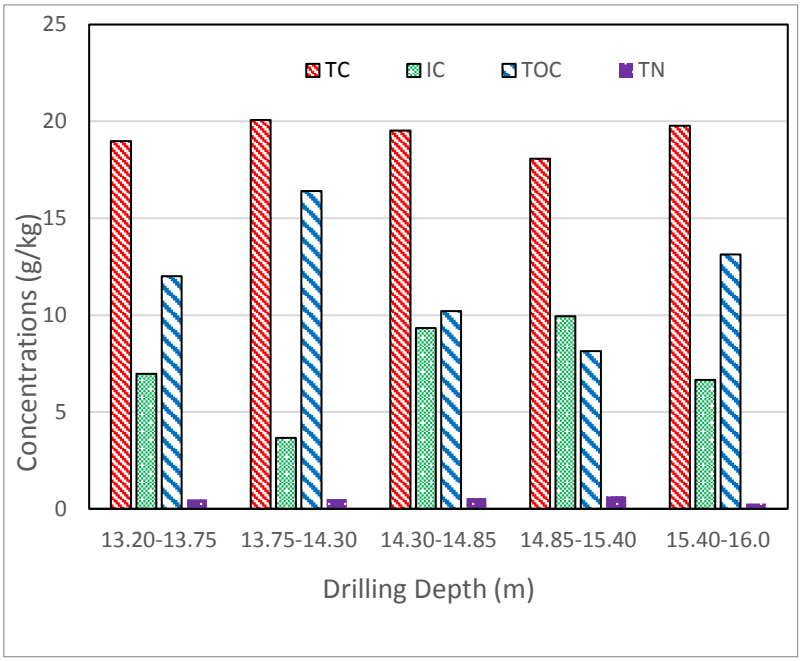

Figure 3. *Total Carbon, Inorganic Carbon, Total Organic Carbon and Total Nitrogen concentration change depending on depth in Güre seabed drilling*

When the surface and deeper samples were compared, no standard increase or decrease was found. Many researchers have reported that fine and coarse-grained clay and sand deposits were effective in changing TOC and TN concentrations (Keil et al.,1994; Ogrinc et al., 2005). The TOC concentration in the sample from the top layer was found to be 12.01 g/kg. The sediment deposition rate was 7.509 mm/year. As a result of the analysis of core samples taken from 13.75-14.30 m depth, the TOC concentration was found to be 16.40 g/kg. Considering the annual amount of sedimentation (Vs=7.509 mm/year) and the population and agricultural structure of the region, this region was not contaminated by humans approximately 100 years ago. In this case, it was concluded that there is natural intra-continental pollution the result of total precipitation intensity. The lowest TOC concentration was measured in the sediment sample taken in the range of 14.85-15.40 m. The TOC concentration increased to 13.13 g/kg in the sample taken at a depth of 15.40-16 m. High TOC showed that pollution was of inland origin (plant origin). Irizuki et al. (2015) conducted a study in Kasado Bay, all samples were below 20 mg/g TOC

http://www.aloki.hu ● ISSN 1589 1623 (Print) ●ISSN1785 0037 (Online)
DOI: http://dx.doi.org/10.15666/aeer/1706_1475114765

content and stated that eutrophication was not severe. At the same point, a very low total nitrogen concentration (0.28) showed that pollution was not from organic matter of algae and marine plants. Algae contain high levels of nitrogen. At this sample point, the concentration of inorganic carbon in the samples taken at the depth was between 3.67-9.94 g/kg. IC concentrations did not show a linear increase or decrease over depth. The low total nitrogen (0.28-0.49 g/kg) (0.028-0.049%) and TOC values compared to the other regions indicate that this area has greater biological activity in the seabed. The concentration of TC in the samples taken from the Güre BH-3 point varied between 18.08-20.07 g/kg. The total carbon values throughout the depth were 18.98 g/kg (13.20-13.75 m), 20.07 g/kg (13.75-14.30), 19.53 g/kg (14.30-14.85 m), 18.08 g/kg (14.85-15.40 m) and 19.78 g/kg (15.40-16 m). The region was stable in terms of TC ratio (mean 19.288 g/kg). In the study conducted by Xu et al. (2017), TOC and TN values were found to be between 0.19-0.67 and 0.03-0.09. In another study conducted by Gao et al. (2008), the TOC content ranged from 0.86 to 1.60% of dry sediment weight and ranged from 1.25% on average. In a different study by Gao et al. (2008), total nitrogen content averaged 0.146% in the range 0.096-0.206% by weight of dry sediment.

At the Küçükkuyu BH-3 point, carrot samples were taken from the seabed at a depth of 13-28 m (*Figure 4*). Total nitrogen concentrations in this point were measured as 1.09, 1.34, 1.12, 1.57 and 1.2 g/kg at 13-16, 16-19-22, 22-25 and 25-28 m depths, respectively. The total nitrogen concentrations (1.09-1.57 g/kg) were found to be highest in this region.

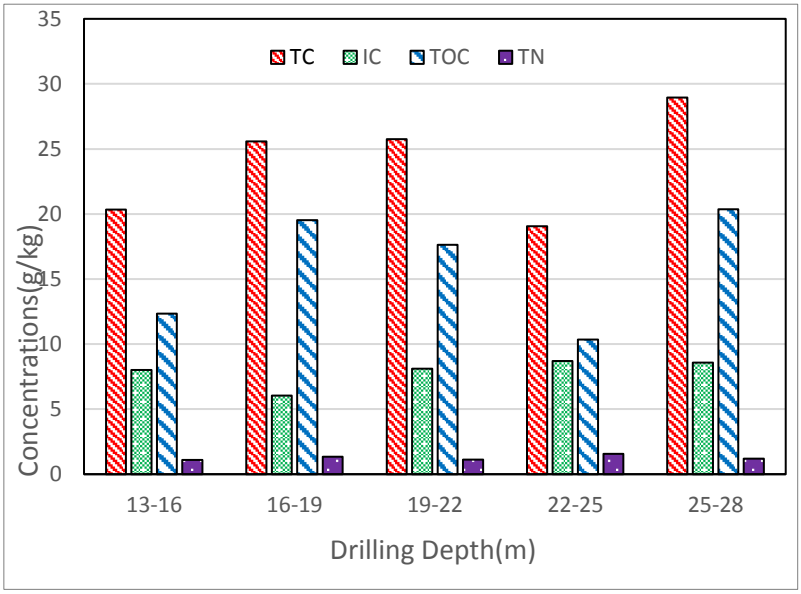

Figure 4. *Total Carbon, Inorganic Carbon, Total Organic Carbon and Total Nitrogen concentration change depending on the depth of Küçükkuyu seabed drilling*

The sedimentation rate at the Küçükkuyu BH-3 point was 5.743 mm/year. The TOC concentration ranged from 10.35 to 20.36 g/kg. The lowest and highest TOC values were in the last two layers. The high total nitrogen and TOC in this region indicated that both marine and continental pollution were present. Higher C/N values may represent a greater portion of terrestrial organic matter (Chen et al., 2008). The inorganic carbon concentration varied between 6.05-8.71 g/kg. Güre and Küçükkuyu regions were similar in terms of IC concentrations. The TOC/TN ratio was greater than 10, except for one

http://www.aloki.hu ● ISSN 1589 1623 (Print) ●ISSN1785 0037 (Online)
DOI: http://dx.doi.org/10.15666/aeer/1706_1475114765

point. The high nitrogen and carbon concentrations in the sediment indicated that the biodegradation of carbonaceous and nitrogenous substances is slow, and, in this area, the nitrification and denitrification rate in the seabed is low. Otherwise, the nitrogen concentration should be lower. The TOC concentration in the sample taken from 13-16 m (top layer) was 12.34 g/kg. In the samples taken between 16-19 m and 19-22 m, the TOC value was measured as 19.54 and 17.64 g/kg, respectively. The lowest TOC value (10.35 g/kg) was found in the sample taken between 22-25 m. In parallel with the current studies (Irizuki et al., 2015), it has been found that eutrophication has not occurred in this field. The TOC/TN ratio was found to be 6.53 at this point. In this period, it was concluded that there was no intra-continental pollution and limited biological activity at the sea bottom (high concentration of total nitrogen). The limited number of agricultural areas in the Küçükkuyu region indicated that high nitrogen concentrations measured in the sediments were the result of algae. Total carbon concentrations along the depth in the Küçükkuyu region were 20.35 g/kg (13-16 m), 25.59 g/kg (16-19 m), 25.76 g/kg (19-22 m), 19.06 g/kg (22-25m) and 28.95 g/kg (25-28 m). The highest total carbon concentration was found in this region (mean 23.94 mg/kg). Küçükkuyu region contains higher concentrations of TOC than Güre region. Küçükkuyu sediments contain less stabilized sludge than Güre region. The TOC and TN values measured in Küçükkuyu region were higher than those of Xia et al. (2019).

Figure 5 shows the variation of the TC, IC, TOC, and TN values in the samples taken from the BH3 point. Sediment samples were taken from the sea floor at depths of 10 to 19.0 m.

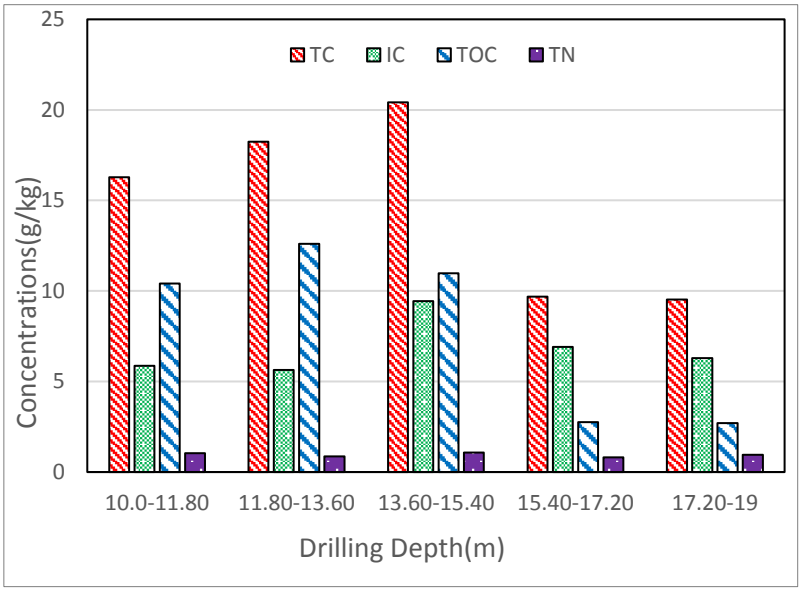

Figure 5. *Total Carbon, Inorganic Carbon, Total Organic Carbon and Total Nitrogen concentration change depending on the depth of Dikili seabed drilling*

The TOC value ranged between 2.71-12.60 g/l. The value here is in good agreement with the findings of Gao et al. (2008) and Xu et al. (2017). The TOC concentration was found to be 2.71 and 2.76 for 15.40-19 meters. Normally, a value of 6-8 represents a root of predominantly marine origin for the organic matter (Aitkenhead et al., 2000). It was very low compared to the upper sediment layers, showing that terrestrial and marine

http://www.aloki.hu ● ISSN 1589 1623 (Print) ●ISSN1785 0037 (Online)
DOI: http://dx.doi.org/10.15666/aeer/1706_1475114765

pollution was minimum. The lowest IC concentration (5.64-9.43 g/kg) was found at this point. Sedimentation rate in this area was 1.217 mm/year. The high levels of TOC in the upper layers indicated that intra-continental (carbon from high plants) and marine pollution (marine plants) is high. Low TOC concentration (<20 mg/g) indicated that there was no eutrophication in this area (Irizuki et al., 2015). The main mechanism for algae growth was the nutrient increase caused by river currents and floods. As a result of nutrient growth, excessive algae growth occurs. Algae growth results in an increase in organic carbon in sediments (Yamamuro et al., 2005; Zhang et al., 2009). The time of formation of the top two layers corresponded to 2958 years. TC concentration increases as the depth increases and decreases again after a certain point. Total carbon concentrations along the depth were 16.28 g/kg (10-11.80 m), 18.24 g/kg (11.80-13.60 m), 20.41 g/kg (13.60-15.40 m), 9.678 g/kg (15.40-17.20 m), and 9.52 g/kg (17.20-19.0 m), respectively. This is the result of the high IC concentration at this point. The total nitrogen concentration has different values throughout the depths. A specific increase or decrease in these sample points was not noted. The TN concentration ranged from 0.81 to 1.89 g/kg. Inland pollution originating from the continent (high plant carbon) was dominant at the depth of 11.80-13.60 (1479 years). High nitrogen concentrations at the sample points indicated that biological degradation (nitrification and denitrification) was poor. Previous studies have shown that degradation of organic matter is most active near the water sludge interface (Middelburg et al., 1993; Niggemann et al., 2006). In region Dikili, higher TOC values were found in the upper layers and decreased towards the lower layers.

In order to make a regional comparison, the correlation graphs of the percentages of TN, TC, IC, and TOC values of the drilling samples taken in Dikili, Güre, and Küçükkuyu were given along with their depths in *Figure 6*.

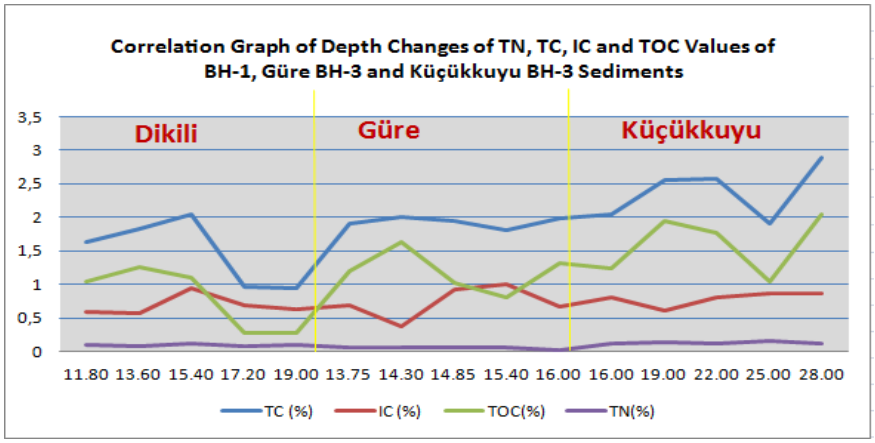

Figure 6. *Correlation Graph of Depth Variations of TN, TC, IC and TOC Values of Dikili BH-1, Gure BH-3 and Küçükkuyu BH-3 Sediments*

As can be seen in *Figure 6*, TOC values were higher in the Küçükkuyu region (10.35-20.36 g/kg) than Dikili (2.71-12.6 g/kg) and Güre (8.14-16.4 g/kg). In terms of heavy metal concentrations, these sample points represent a clean environment when compared to the Pollution Index (PI) map made by Yümün and Önce (2017). In the Küçükkuyu, Dikili, and Güre regions, it was observed that the terrestrial and marine nitrogen sources were similar over a long period of time. When the BH1 (Dikili) (0.81-1.08 g/kg), BH3

http://www.aloki.hu ● ISSN 1589 1623 (Print) ●ISSN1785 0037 (Online)
DOI: http://dx.doi.org/10.15666/aeer/1706_1475114765

(Küçükkuyu) (1.09-1.57 g/kg) and BH3 (Güre) (0.28-0.66 g/kg) regions were compared, the lowest nitrogen concentrations were found in the BH3 (Güre) region. Unlike Chen et al. (2008), there was no linear relationship between TOC and nitrogen exchange in this study. Total nitrogen, total organic carbon and inorganic carbon concentrations increased in Küçükkuyu region and therefore the increase in total carbon concentration was highest in this area (*Figure 6*). As seen from the curve, the total carbon concentration increased gradually from Dikili to Güre and Küçükuyu. Küçükkuyu region has steep mountainous and rich vegetation. TOC and total nitrogen concentrations were considered to be high due to the high intra-continental transport.

Unlike organic carbon, inorganic carbon (IC) values were seen equally in all three regions. The similarity of these values shows that the sources of inorganic carbon from the terrestrial area are similar. Considering that the seabed sediments were formed over more than 2000 years, it was determined that organic pollution was not related to the existing industry and population.

As a result of drilling on the sea floor in the Güre region, the TOC/TN ratios were found to be 24.61 at a drilling depth of 13.20-13.75 meters (*Figure 7*).

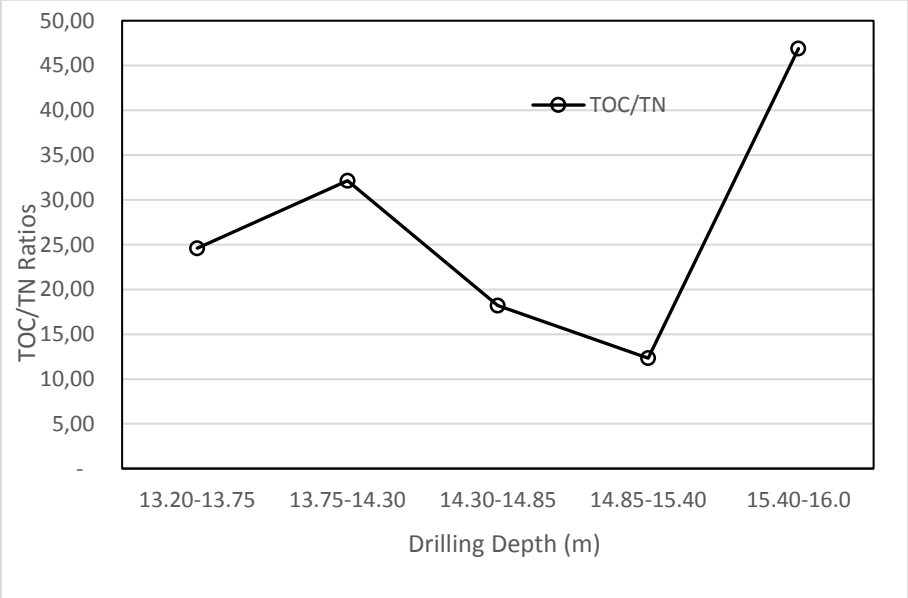

Figure 7. *Change of TOC/TN ratios depending on the depth of drilling in the deep sea bottom(Güre)*

It was found that intra-continental pulural (plant origin) was intense in this area. The intra-continental organic pollution (TOC/TN = 32.16) in the sediment layer of 13.75-14.30 meters increased. At 14.85-15.40 meters sediment thickness, the TOC/TN ratio decreased to 12.33. In the 220-year period required for precipitation formation in this thickness, the transport of intra-continental organic matter (plant origin) decreased considerably. In the 15.40 - 16.0 meter sediment range (80 years), the increase in intra-continental organic matter was found to be very high (TOC/TN = 46.89). Intracurrent contamination increased towards the upper layers of the sediment. Higher C/N values may represent the proportion of organic matter originating mainly from terrestrial areas (Chen et al., 2008). As a result, it was thought that transport of organic matter was carried out in certain periods of time although there were no rainfall records for that period. The

http://www.aloki.hu ● ISSN 1589 1623 (Print) ●ISSN1785 0037 (Online)
DOI: http://dx.doi.org/10.15666/aeer/1706_1475114765

TOC/TN (12.33-46.89) ratios measured in this area (Güre) were much higher than similar studies (Xu et al., 2017; Xia et al., 2019). In the Güre region, the TOC/TN ratios were measured 24.61 (13.20-13.75 m), 32.16 (13.75-14.30 m), 18.21 (14.30-14.85 m), 12.33 (14.85-15.40 m) and 46.89 (15.40-16.0 m) along the depth, respectively. In this area (Güre), the TOC/TN ratio varied between 12.33-46.89. On the coast of Southeast Alaska, these values (C/N) ranged from 7.7 to 12.7 (Walinsky et al., 2009). The average TOC/TN ratio in the Güre region (26.84) was much higher than in the seas such as Jiaozhou Bay (11.48) (Kang et al., 2017), Yellow Sea (7.99) (Limin et al., 2013), East China Sea (7.14) (Limin et al., 2012; Dong et al., 2015). The TOC/TN ratio of the samples taken at 13-16 meters depth in Küçükkuyu region was approximately the same as the samples taken at depths of 14.85-15.40 m in Güre region.

TOC/TN values in the Küçükkuyu region were measured as 11.32 (13-16 m), 14.58 (16-19 m), 14.46 (19-22 m), 6.52 (22-25 m), 16.97 (25-28 m). The TOC/TN ratio was found to be 11.32 at the 13-16 meter sediment depth in Küçükkuyu Bay (*Figure 8*).

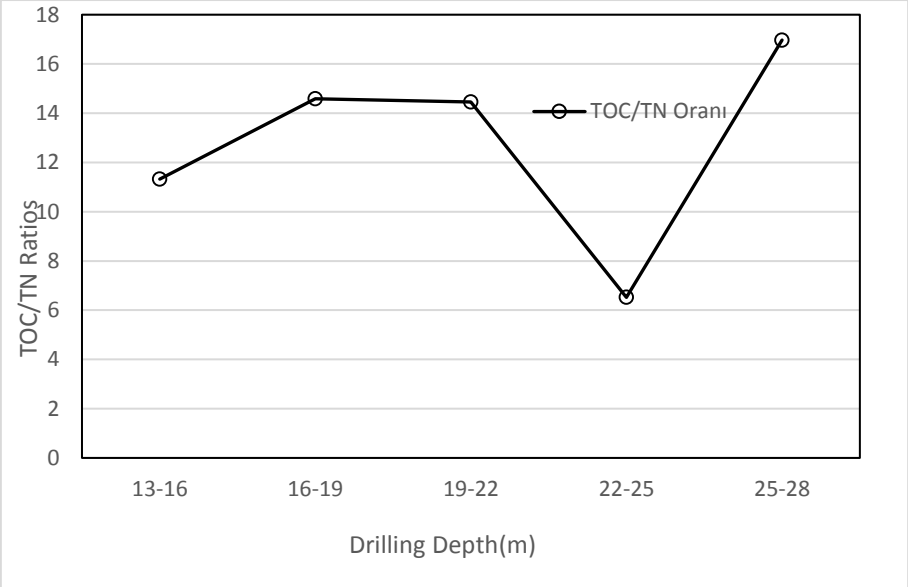

Figure 8. *Change of TOC/TN ratios depending on drilling depth in Küçükkuyu seabed*

The TOC/TN ratio in the sediment range of 16-22 meters remained constant at 14. The C/N ratio in sediments was used to investigate the sources and cycles of organic materials (Azevedo, 2003; Chen et al., 2008). A TOC/TN ratio of 14 indicates continental pollution (Meyers et al., 1984). In accordance with the current literature, this period of precipitation was dominated by inland organic matter (plant origin). The TOC/TN ratio decreased rapidly in the time of 22-25 m precipitate formation. The TOC/TN ratio was 6.52. Since the sedimentation rate was 5.743 mm/year in this region, the organic matter transport remained constant over a period of 500 years. Bacteria play a critical role in the transformation and mineralization of organic carbon and nitrogen in marine sediments (Kawasaki et al., 2006). For the drilling depth of 25-28 m, the TOC/TN ratio was measured as 16.97. In this time period, it was concluded that intra-continental organic matter transport (from high plants) was more dominant than the marine environment. The average TOC/TN ratio in the Küçükkuyui region (12.77) was similar to the Jiaozhou Bay (11.48) (Kang et al., 2017). The TOC/TN ratio in this region was higher than in the seas

http://www.aloki.hu ● ISSN 1589 1623 (Print) ●ISSN1785 0037 (Online)
DOI: http://dx.doi.org/10.15666/aeer/1706_1475114765

such as Yellow Sea (7.99) (Limin et al., 2013) and East China Sea (7.14) (Limin et al., 2012; Dong et al., 2015). At this point, intra-continental pollution increased towards the upper layers of the sediment. The TOC/TN ratio of the samples taken at 13-22 meters depth in Küçükkuyu region was approximately the same as the samples taken at depths of 11.80-13.60 m in Dikili region.

The TOC/TN change in the Dikili area depending on the drill depth was shown in *Figure 9*. The TOC/TN ratio was found to be high in the precipitated upper layers. The TOC/TN ratio decreased as the sample depth increased.

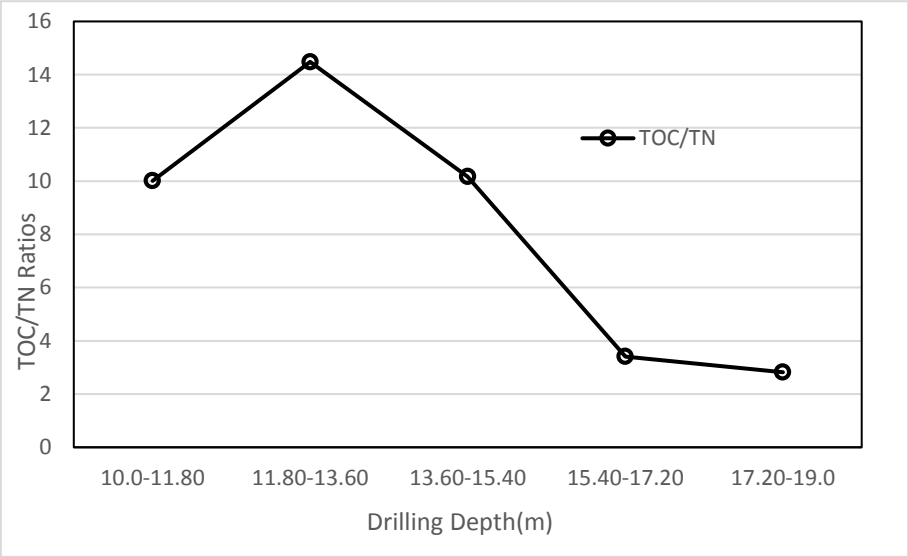

Figure 9. *Change of TOC/TN ratios depending on drilling depth in Dikili seabed*

The TOC/TN ratio was found to be 10.01 at the drilling depth of 10-11.80 meters. In the upper section, it was determined that the source of organic matter originated from the sea's own structure (biological activity). The TOC/TN ratio was measured as 14.48 at the drilling depth of 11.80-13.60 m. C/N ratios showed different distribution ratios depending on depth. The source of organic matter was found to be marine and terrestrial (Venkatesan et al., 1987). Since the sediment deposition rate in this area was 1.217 mm/year, 1479 years was required for 1.8 meters of sediment formation. In this period, intra-continental pollution caused by terrestrial plants increased. The TOC/TN ratio was found to be 2.82 at a drilling depth of 17.20-19.0 meters. It has been found that the transport of intra-continental organic matter in this period of precipitation was very low. The decrease in TOC/TN ratios was the result of the contribution of marine algae (Liu et al., 2012). In this area, the TOC/TN ratios measured in deeper layers were found to be lower than other researchers (Walinsky et al., 2009; Xia et al., 2019). The average TOC/TN ratio in the Dikili region (8.178) was similar to that in the seas such as Jiaozhou Bay (11.48) (Kang et al., 2017), Yellow Sea (7.99) (Limin et al., 2013), East China Sea (7.14) (Limin et al., 2012; Dong et al., 2015). At this point, although the TOC/TN ratio increases towards the upper layers, the TOC/TN ratio does not show intra-continental pollution. Dikili district has less rugged terrain compared to the other two sample areas. Therefore, the sediment formation rate was quite small compared to other regions due to the low intra-continental transport.

http://www.aloki.hu ● ISSN 1589 1623 (Print) ●ISSN1785 0037 (Online)
DOI: http://dx.doi.org/10.15666/aeer/1706_1475114765

Conclusion

TC, TOC, IC and total nitrogen measurements were carried out in Edremit Bay (Küçükkuyu, Güre, and Dikili). As a result of these measurements, TOC/TN ratios were found depending on the depth of the drilling. The total nitrogen concentrations in the Küçükkuyu region ranged from 1.09 to 2.1 g/kg. The total nitrogen concentration increased throughout the drilling depth. It was concluded that this was the result of nitrogen-rich algae activity in the marine environment. TOC concentrations were 12.34-20.36, 12.01-13.13, and 2.71-10.41 gr/kg in Küçükkuyu, Güre, and Dikili marine sediments, respectively. The biodegradation of organic matter and the nitrogen accumulated in the sea floor in Kucukkuyu Bay was low. It was thought that nitrogen-containing organic substances could not be converted to nitrate the result of the oxygen limitation in Küçükkuyu sediments, and, thus, denitrification did not take place.

The decrease in total nitrogen concentration along the depth of the seabed in the Güre region indicated that nitrification and denitrification reactions occur. The decrease of TOC and TN in the depth in the Dikili region indicated that denitrification is performed in the base sediments. The highest TOC/TN ratio was measured at 46.89 at a 15.40-16.0 m depth at the Güre DS3 point. The lowest TOC/TN ratio was found to be 2.82 in Dikili BH1. At the BH3 point in Güre, the TOC/TN increased throughout the depth indicating organic pollution from terrestrial high plants. According to Meyers et al. (1984), if the TOC/TN ratio is between 12-14, it is a terrestrial source of organic matter. It can be concluded that terrestrial pollution prevails in the Güre region. Venkatesan et al. (1987) indicated that organic matter had a planktonic origin if the ratio of TOC/TN was between 6 and 8. At the depth of 15-19 m at the Dikili BH1 point, the organic matter was found to be of marine origin. At other points, terrestrial and marine organic matter formation was observed.

The TC concentration is equal to the sum of IC and TOC. The highest total carbon content was observed in Küçükkuyuda and the lowest in the Dikili region. TC content was found between 19.06-28.95 in the Küçükkuyu region, between 18.08-20.07 in the Güre region, and between 9.52-20.41 in the Dikili region. In the future study, δ13C, and δ15N isotopic parameters should be measured in this area. In addition, in-continental soil samples should also be examined. The research area should be carried out in a wider area and at more sample points.

REFERENCES

[1] Aitkenhead, J. A., McDowell, W. H. (2000): Soil C: N ratio as a predictor of annual riverine DOC flux at local and global scales. – Global Biogeochemical Cycles 14: 127-138.

[2] Avramidis, P., Nikolaou, K., Bekiari, V. (2015): Total Organic Carbon and Total Nitrogen in Sediments and Soils: A Comparison of the Wet Oxidation – Titration Method with the Combustion-Infrared Method. – Agriculture and Agricultural Science Procedia 4: 425-430.

[3] Azevedo, D. A. (2003): A preliminary investigation of the polar lipids in recent tropical sediments from aquatic environments at Campos dos Goytacazes. – Journal of the Brazilian Chemical Society 14: 97-106.

[4] Bartoli, G., Papa, S., Sagnella, E., Fioretto, A. (2012): Heavy metal content in sediments along the Calore river: relationships with physical–chemical characteristics. – Journal of Environmental Management 95: 9-14.

http://www.aloki.hu ● ISSN 1589 1623 (Print) ●ISSN1785 0037 (Online)
DOI: http://dx.doi.org/10.15666/aeer/1706_1475114765

[5] Bayram, A., Önsoy, H., Akinci, G., Bulut, V. N. (2011): Variation of total organic carbon content along the stream Harsit, Eastern Black Sea Basin, Turkey. – Environmental Monitoring and Assessment 182(1-4): 85-95.
[6] Chen, F., Zhang, L., Yang, Y., Zhang, D. (2008): Chemical and isotopic alteration of organic matter during early diagenesis: Evidence from the coastal area off-shore the Pearl River estuary, south China. – Journal of Marine Systems 74: 372-380.
[7] De Souza, J. R. B., de Rosario Zucchi, M. R., Costa, A. B., Azevedo, A. E. G., Spano, S. (2017): Geochemical markers of sedimentary organic matter in Todos os Santos Bay, Bahia – Brazil. Indicators of sources and preservation. – Marine Pollution Bulletin 119: 239-246.
[8] Dong, L., Peng,Y., Bianchi, T. S. (2015): Historical reconstruction of organic carbon inputs to the East China Sea inner shelf: Implications for anthropogenic activities and regional climate variability. – The Holocene 25(12): 1869-1881.
[9] Gao, X., Chen, S., Long, A. (2008): Composition and sources of organic matter and its solvent extractable components in surface sediments of a bay under serious anthropogenic influences: Daya Bay, China. – Marine Pollution Bulletin 56: 1066-1075.
[10] Hecky, R. E., Campbell, P., Hendzel, L. L. (1993): The stoichiometry of carbon, nitrogen, and phosphorus in particulate matter of lakes and oceans. – Limnology and Oceanography 38(4): 709-724.
[11] Irizuki, T., Ito, H., Sako, M., Yoshioka, K., Kawano, S., Nomura, R., Tanak, Y. (2015): Anthropogenic impacts on meiobenthic Ostracoda (Crustacea) in themoderately polluted Kasado Bay, Seto Inland Sea, Japan, over the past 70years. – Marine Pollution Bulletin 91: 149-159.
[12] Jacob, J., Jayaraj, K. A., Rehman, H. H., Chandramohanakumar, N., Balachandran, K. K., Raveendran, T. V., Joseph, T., Nair, M., Achuthankutty, C. T. (2009): Biogeochemical characteristics of the surface sediments along the western continental shelf of India. – Chemistry and Ecology 25(2): 135-149.
[13] Kang, X., Song, J., Yuan, H., Li, X., Li, N., Duan, L. (2017): The sources and composition of organic matter in sediments of the Jiaozhou Bay: implications for environmental changes on a centennial time scale. – Acta Oceanologica Sinica 36(11): 68-78.
[14] Kawasaki, N., Benner, R. (2006): Bacterial release of dissolved organic matter during cell growth and decline: molecular origin and composition. – Limnology and Oceanography 51: 2170-2180.
[15] Keil, R. G., Tsamakis, E., Fuh, C. B., Giddings, J. C., Hedges, J. I. (1994): Mineralogical and texture controls on the organic composition of coastal marine sediments: Hydro-dynamic separation using SPLITT-fractionation. – Geochemica et Cosmochimica Acta 58: 879-893.
[16] Koziorowska, K., Kuliński, K., Pempkowiak, J. (2016): Sedimentary organic matter in two Spitsbergen fjords: Terrestrial and marine contributions based on carbon and nitrogen contents and stable isotopes composition. – Continental Shelf Research 113: 38-46.
[17] Lallier-Verges, E., Perrussel, B. P., Disnar, J. R., Baltzer, F. (1998): Relationships Between Environmental Conditions and The Diagenetic Evolution of Organic Matter Derived from Higher Plants İn A Modern Mangrove Swamp System (Guadeloupe, French West Indies). – Organic Geochemistry 29(5-7): 1663-1686.
[18] Limin, H., Xuefa, S., Zhigang, Y. (2012): Distribution of sedimentary organic matter in estuarine-inner shelf regions of the East China Sea: implications for hydrodynamic forces and anthropogenic impact. – Marine Chemistry 142-144: 29-40.
[19] Limin, H., Xuefa, S., Zhigang, G. (2013): Sources, dispersal and preservation of sedimentary organic matter in the Yellow Sea:the importance of depositional hydrodynamic forcing. – Marine Geology 335: 52-63.
[20] Liu, X., Ge, C. (2012): Spatial and temporal variations of sedimented organic matter in Xiaohai Lagoon, Hainan Island. – Acta Oceanologica Sinica 31(3): 74-86.
[21] Martinez-Santos, M., Probst, A., García-García, J., Ruiz-Romera, E. (2015): Influence of anthropogenic inputs and a high-magnitude flood event on metal contamination pattern in

http://www.aloki.hu ● ISSN 1589 1623 (Print) ●ISSN1785 0037 (Online)
DOI: http://dx.doi.org/10.15666/aeer/1706_1475114765

surface bottom sediments from the Deba River urban catchment. – Science of the Total Environment 514: 10-25.

[22] Meyers, P. A., Leenheer, M. J., Eaoie, B. J., Maule, S. J. (1984): Organic Geochemistry of Suspended and Settling Particulate Matter İn Lake Michigan. – Geochim. Cosmochim Acta 48: 443-452.

[23] Middelburg, J. J., Vlug, T., Jaco, F., Van der Nat, W. A. (1993): Organic matter mineralization in marine systems. – Global and Planetary Change 8(1-2): 47-58.

[24] Niggemann, J., Schubert, C. J. (2006): Fatty acid biogeochemistry of sediments from the Chilean coastal upwelling region: sources and diagenetic changes. – Organic Geochemistry 37: 626-647.

[25] Ogrinc, N., Fontolan, G., Faganeli, J., Covelli, S. (2005): Carbon and nitrogen isotope compositions of organic matter in coastal marine sediments (the Gulf of Trieste, N Adriatic Sea): indicators of sources and preservation. – Marine Chemistry 95(3-4): 163-181.

[26] Önce, M. (2014): Güre (Edremit/Balıkesir) ile Küçükkuyu (Ayvacık/Çanakkale) Arasında Ege Denizi'ndeki Ağır Metal Kirliliğinin Yayılımı ve Foraminiferler Üzerindeki Etkilerinin Araştırılması. – Namık Kemal Üniversitesi Fen Bilimleri Enstitüsü Yüksek lisans Tezi, Tekirdağ.

[27] Pan, Z., Gao, Q. F., Dong, S. L., Wang, F., Li, H. D., Zhao, K., Jiang, X. Y. (2019): Effects of a balone (HaliotisdiscushannaiIno) andkelp (Saccharinajaponica) mariculture on sources, distribution, and preservation of sedimentaryorganic carbon in Ailian Bay, China: Identified by coupling stable isotopes (δ13C and δ15N) with C/N ratio analyses. – Marine Pollution Bulletin 141: 387-397.

[28] Sampaio, L., Rodrigues, A. M., Quintino, V. (2010): Carbon and Nitrogen Stable İsotopes İn Coastal Benthic Populations Under Multiple Organic Enrichment Sources. – Marine Pollution Bulletin 60: 1790-1802.

[29] Stein, R. (1991): Accumulation of Organic Carbon in Marine Sediments. – Lecture Notes in Earth Sciences 34, Springer -Verlag.

[30] Venkatesan, M. I., Kaplan, I. R. (1987): The Lipid Geochemistry of Antarctic Marine Sediments: Bransfield Strait. – Marine Chemistry 21: 347-375.

[31] Visco, G., Campanella, L., Nobili, V. (2005): Organic carbons and TOC in waters: an overview of the international norm for its measurements. – Microchemical Journal 79(1-2): 185-191.

[32] Walinsky, S. E., Prahl, F. G., Mix, A. C., Finney, B. P., Jaeger, J. M., Rosen, G. P. (2009): Distribution and composition of organic matter in surface sediments of coastal Southeast Alaska. – Continental Shelf Research 29: 1565-1579.

[33] Waterson, E. J., Canuel, E. A.(2008): Sources of Sedimentary Organic Matter İn The Mississippi River and Adjacent Gulf of Mexico As Revealed by Lipid Biomarker and $D^{13}C_{toc}$ Analyses. – Organic Geochemistry 39: 422-439.

[34] Wei, W., Shiqi, Z., Youliang, J. (2006): Evolution and controlling factor of the circum-Jiaozhou Bay coastline. – Marine Geology Letters (in Chinese) 22(9): 7-10.

[35] Winogradow, A., Pempkowiak, J. (2018): Characteristics of sedimentary organic matter in coastal and depositional areas in the Baltic Sea. – Estuarine, Coastal and Shelf Science 204: 66-75.

[36] Xia, B., Han, Q., Chen, B., Sui, Q., Jiang, T., Sun, X., Zhu, L., Chai, C., Qu, K. (2019): Influence of shellfish biodeposition on coastal sedimentary organic matter: A case study from Sanggou Bay, China. – Continental Shelf Research 172: 12-21.

[37] Xu, G., Liua, J., Hu, G., Jonell, T. N., Chen, L. (2017): Distribution and source of organic matter in surface sediment from the muddy deposit along the Zhejiang coast, East China Sea. – Marine Pollution Bulletin 123: 395-399.

[38] Yamamuro, M., Kanai, Y. (2005): A 200-year record of natural and anthropogenic changes in water quality from coastal lagoon sediments of Lake Shinji, Japan. – Chemical Geology 218(1-2): 51-61.

http://www.aloki.hu ● ISSN 1589 1623 (Print) ●ISSN1785 0037 (Online)
DOI: http://dx.doi.org/10.15666/aeer/1706_1475114765

[39] Yümün, Z. Ü., Önce, M. (2017): Monitoring heavy metal pollution in foraminifera from the Gulf of Edremit (northeastern Aegean Sea) between Izmir, Balıkesir and Çanakkale (Turkey). – Journal of African Earth Sciences 130: 110-124.
[40] Zetsche, E., Thornton, B., Midwood, A. J., Witte, U. (2011): Utilization of different carbon sources in a shallow estuary identified through stable isotope techniques. – Cont. Shelf Res 31: 832-840.
[41] Zhang, J., Wu, Y., Jennerjahn, T. C., Ittekkot, V., He, Q. (2007): Distribution of organic matter in the Changjiang (Yangtze River) Estuary and their stable carbon and nitrogen isotopic ratios: Implications for source discrimination and sedimentary dynamics. – Marine Chemistry 106: 111-126.
[42] Zhang, L., Yin, K., Wang, L., Chen, F., Zhang, D., Yang, Y. (2009): The sources and accumulation rate of sedimentary organic matter in the Pearl River Estuary and adjacent coastal area, Southern China. – Estuarine, Coastal and Shelf Science 85: 190-196.

http://www.aloki.hu ● ISSN 1589 1623 (Print) ●ISSN1785 0037 (Online)
DOI: http://dx.doi.org/10.15666/aeer/1706_1475114765

THE ENHANCED TOLERANCE OF INVASIVE *ALTERNANTHERA PHILOXEROIDES* OVER NATIVE SPECIES UNDER SALT-STRESS IN CHINA

JAVED, Q.[1] – SUN, J.[1*] – AZEEM, A.[1] – ULLAH, I.[1] – HUANG, P.[1] – KAMA, R.[1] – JABRAN, K.[3] – DU, D.[1,2*]

[1]*School of the Environment and Safety Engineering, Jiangsu University, Zhenjiang 212013, China*

[2]*Key Laboratory of Modern Agricultural Equipment and Technology, Ministry of Education, Institute of Agricultural Engineering, Jiangsu University, Zhenjiang, Jiangsu, China*

[3]*Department of Plant Production and Technologies, Faculty of Agricultural Sciences and Technologies, Niğde Ömer Halisdemir University, Niğde, Turkey*

**Corresponding authors*
e-mail: ddl@ujs.edu.cn (D. L. Du), zxsjf@ujs.edu.cn (J. F. Sun); phone/fax: +86-511-8879-0955

(Received 13th Jun 2019; accepted 2nd Sep 2019)

Abstract. Effects of environmental stress (e.g. salt stress) on the plant invasions are still relatively unknown. Therefore, we analyzed the physiological characteristics of *Alternanthera philoxeroides* (Mart.) Griseb. as an invasive plant and *Alternanthera sessilis* (L.) R.Br. ex DC. as a native plant under single and mixed planting, in green house, Jiangsu University, China. Plants were subjected to four different levels of salt stress treatments "i.e.", control, low (0.8%), medium (1.6%) and high (2.4%) that were made with equal proportion of NaCl and $CaCl_2$ followed by rewatering. The results showed, that different levels of salt stress affect the plant growth of both species differently. The net photosynthetic rate (Pn) for *A. philoxeroides* was higher from low to high stress of both single and mixed planting that of *A. sessilis*. Afterwards, during rewatering, the increments in Pn from low to high salt stress were also found higher in *A. philoxeroides*. In addition, the reduction in photosynthetic activity in *A. sessilis* under mixed planting during salt stress markedly affected the plant growth. After rewatering the comparative increments in plant growth parameter were also noted higher in *A. philoxeroides* than *A. sessilis*. Our results thus suggest that *A. philoxeroides* may possess a better adaptability to salt stress, which results in a successful competitive dominance.
Keywords: *invasiveness, growth, mixed planting, physiological responses, salt tolerance*

Introduction

Biological invasions are among the major global environmental challenges that can cause disturbing effects on the ecosystems (Quinet et al., 2015; Ricciardi et al., 2017; Zenni et al., 2017; Vitousek et al., 1997). Invasive plants may change the ecosystems by threatening the native biodiversity (Schweiger et al., 2010; Vilà et al., 2011). Certain non-native plant species possess some opportunistic characteristics that increase their probability to become invasive. It is related to their ability to proliferate, grow rapidly from germination to reproductive stage, and particularly, their tolerance to the environmental stresses (Van Kleunen et al., 2010). Invasive species compete with natives through a strategy known as jack-of-all-trades, which states that, the invasive species has an ability to maintain their fitness in unfavorable and stressful conditions (Richards et al., 2006), and under favorable conditions they maximize their fitness (Gioria and Osborne, 2014). It has also been well known that invasive plants have a stronger ability for adaptation than native species to heterogeneous environments (Keser

http://www.aloki.hu ● ISSN 1589 1623 (Print) ● ISSN 1785 0037 (Online)
DOI: http://dx.doi.org/10.15666/aeer/1706_1476714785

et al., 2015; Drenovsky et al., 2012). Nonetheless, our knowledge is still limited about the survival, tolerance and competitive dominance of invasive plants over native plants regarding why and how they adapt to heterogeneous abiotic factors.

Among heterogeneous abiotic factors, salt stress is one of the major abiotic concerns, threatening crop productivity (Asrar et al., 2017). Salinity may play an imperative part in the plant invasiveness. Up to now, limited research work has been conducted in the area of the impact of salt stress on plant invasion, and some contradictory results were revealed by a few researchers. As Kolb and Alpert (2003) exhibited high salt stress significantly decreased the relative-competitive-ability of the native species. Whereas, Noe and Zedler (2001) pointed out that salt stress was affecting the invasion by invasive species. The two key principals through which high-salt-levels stressed the plants are: (i) increase in osmotic potential imposed water-stress on plants by the result of high solute concentrations in the soil, and (ii) oxidative stress caused by high-concentration of nonessential-ions is poisonous to plants (Flexas et al., 2012).

Stress causes the changes in cell-water relationships and the ability of the plant to absorb water from the root zone decreases gradually (Ashraf and Foolad, 2007). The decrease in the amount of available water affects the plant growth development (Memon et al., 2010; Habib et al., 2012). In saline-conditions, salinity disturbed the plants' morphological, physiological and biochemical processes. Particularly, its limiting the plant growth (Meloni et al., 2004; Sekmen et al., 2007; Amirjani, 2010) by damaging the net photosynthetic rate (Pn), stomatal conductance (gs), transpiration (E) and leaf water potential (Ψ^{LW}) (Van Kleunen et al., 2010; Azeem et al., 2017b; Zheng et al., 2009). Each parameter which is affected, influenced by many factors up to some extent, including the stress severity and the total duration (Nawaz et al., 2010), the plants species and genotypes (Croser et al., 2001; Morais et al., 2012), the concentration of saline solution (Kosma and Jenks, 2007).

The effects of salt stress on physiological features can be alleviated and recovered through rewatering. Rewatering of saline water is a good approach for a plant to recover and sustain its growth and improve plant survival under salinity stressed environment (Javed et al., 2018). Invasive plants may become more competitive than their co-occurring native plants due to their better adaptation under increasing salt stress (Ozaslan et al., 2016) following rewatering. Therefore, we selected invasive and native species for this research to find out the physiological responses under salt stresses which are rarely tested before. *Alternanthera philoxeroides* (Mart.) Griseb. was taken as invasive species for this research. It mainly spreads by stem and root sprouts and causes serious environmental problems globally. *A. philoxeroides* is a clonal invasive weed, native to South America but growing in both riparian strip and terrestrial zones (You et al., 2018; Schooler, 2012). While, *Alternanthera sessilis* (L.) known as sessile joyweed, was considered as native species. It is a very common plant found in Brazil and in many tropical and subtropical areas of Africa, South Asia, Japan, New Zealand, Pacific Islands, Central America and South America. *A. sessilis* prefers wet surroundings but can grow under a variety of soil conditions (Gunasekera, 2008). Consequently, this study could be a little contribution to our knowledge about the invasiveness of *A. philoxeroides* in saline conditions. To justify this statement, the purpose of this research was to examine how *A. philoxeroides* and *A. sessilis* respond to salt stress followed by rewatering based on physiological properties. Meanwhile, the study also focused on the competitive growth among *A. philoxeroides* and *A. sessilis* under stress and rewatering during mixed planting.

http://www.aloki.hu ● ISSN 1589 1623 (Print) ● ISSN 1785 0037 (Online)
DOI: http://dx.doi.org/10.15666/aeer/1706_1476714785

Materials and methods

Species

Alternanthera philoxeroides (Mart.) Griseb is native to the high temperate region of South America . Except from the temperature zones, it has been also found in both aquatic and as well as in dry terrestrial habitats, and it continues to expand its range around the world. *A. philoxeroides* is considered as an invasive species in China, has phenotypic plasticity, high growth rate and more vegetative propagation (Chen et al., 2008, 2010; Yang et al., 2019). It mainly reproduces through stem and root splitting (Dong et al., 2010).

Alternanthera sessilis (L.) is native to Brazil, broadly distributed all over the tropic and sub-tropic regions of the word. *A. sessilis* prefers wetland areas and grows up to 1 m tall with white flowers. *A. sessilis* is a common leafy-vegetable, and is used as a medicinal plant in South-East- Asia. While, in many places of the world like Sri Lanka, the stems and leaves of *A. sessilis* are cooked and eaten as a vegetable (Hemakanthi de Alwis et al., 2006). In Tropical-Africa, *A. sessilis* is used in different ways, such as sauces and soup in Benin, as soup in Nigeria, as herb in Madagascar and as vegetable in Guinea. *A. sessilis* is also used for simple stomach problem, diarrhea, and as a plaster for diseased or wounded skin (Gunasekera, 2008; Niraimathi et al., 2013; Sun et al., 2010).

Site, culture condition and plant material

The experiment was carried out at Jiangsu University, China (32.20°N, 119.45°E) (*Fig. 1*) under greenhouse conditions in early September 2018. The greenhouse had natural lighting with (25/18) ± 2 °C (day/night) temperature and 70% relative humidity. *A. philoxeroides* and *A. sessilis* were chosen for this experiment, and about 360 ramets per species were collected from the same habitat at the main campus of Jiangsu University. Afterwards, the ramets of both species were grown in nutrient soil filled plastic pots. The chemical and physical characteristics of the nutrient soil were: pH 7.0, organic matter 38%, total nutrients 3.8%, water content 20% and electrical conductivity of 2 ds/m. while, the size of experimental pots were: outer diameter 21 cm, inner diameter 17.7 cm, bottom diameter 11.4 cm and height 12 cm. All pots were randomly arranged and the plant of both species were planted with different densities in mono (2: 0, 0: 2) and mixed planting (2: 2). Each group was irrigated with strengthen Hoagland solution as compound fertilizer to meet the basic requirements and healthy growth of seedlings for a week to keep the plants at full water level without shortage level to a total of seven weeks. After one-week plants were irrigated with fresh water every two days up to saturation levels. In the 2nd week of September, 2019, homogenous seedlings showing a healthy growth about 240 ramets per species were selected for treatments' implementation.

Treatments

Plants were treated with different concentrations of salted water for two weeks, which were prepared by mixing equal quantities (1:1) of NaCl and $CaCl_2$ in fresh water. Salt concentrations were i) control (0%), ii) 0.8%, iii) 1.6%, and vi) 2.4% per liter of fresh water. The division of the treatments for *A. philoxeroides* and *A. sessilis* under single and mixed planting were; AP0: Control received 0% of NaCl and $CaCl_2$;

http://www.aloki.hu ● ISSN 1589 1623 (Print) ● ISSN 1785 0037 (Online)
DOI: http://dx.doi.org/10.15666/aeer/1706_1476714785

AP1 received 0.8% of NaCl and $CaCl_2$; AP2 received 1.6% of NaCl and $CaCl_2$; AP3 received 2.4% of NaCl and $CaCl_2$; AS0: control received 0% of NaCl and $CaCl_2$; AS1 received 0.8% of NaCl and $CaCl_2$; AS2 received 1.6% of NaCl and $CaCl_2$; AS3 received 2.4% of NaCl and $CaCl_2$; MAP0: control received 0% of NaCl and $CaCl_2$; MAP1 received 0.8% of NaCl and $CaCl_2$; MAP2 received 1.6% of NaCl and $CaCl_2$; MAP3 received 2.4% of NaCl and $CaCl_2$; MAS0: received 0% of NaCl and $CaCl_2$; MAS1 received 0.8% of NaCl and $CaCl_2$; MAS2 received 1.6% of NaCl and $CaCl_2$; MAS3 received 2.4% of NaCl and $CaCl_2$, respectively following rewatering. Control treatment received only the fresh water (*Table 1*).

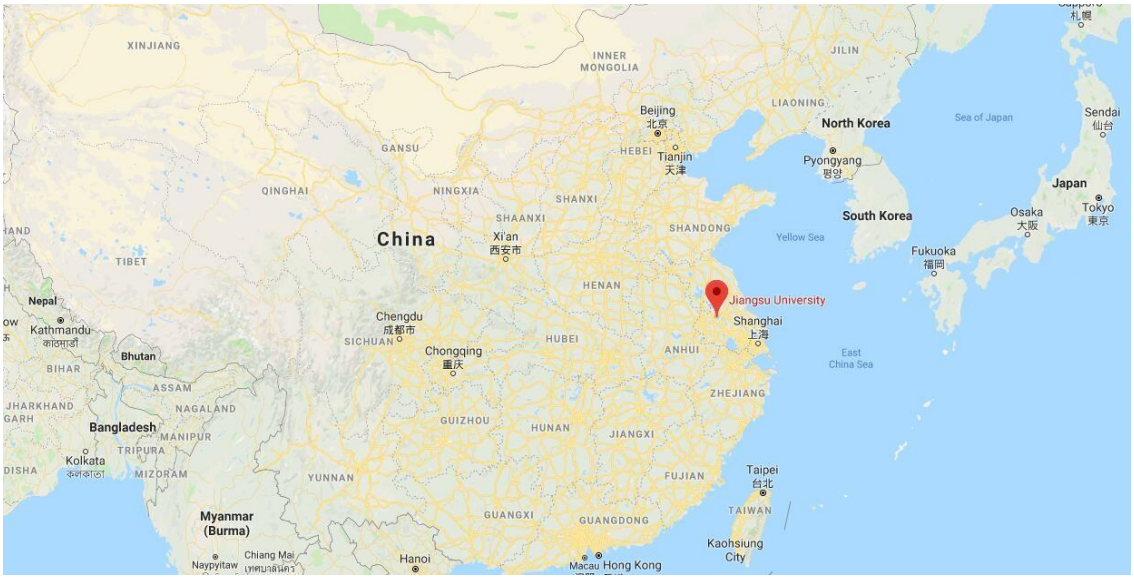

Figure 1. *A map indicating the location of the sampling site*

Rewatering was done on the 5th week from the onset of salt-stress treatments. The order of rewatering is shown in *Figure 2*. The experiment was conducted in randomized-block-design and a total of five replicates were chosen for each physiological measurement.

Photosynthetic traits and growth parameter measurements

Net photosynthetic rate (Pn), stomata conductance (gs), and transpiration rate (E) were measured by using a portable LI-6400XT photosynthesis measurement system (*LI-COR, Lincoln*, NE, USA. We prefer the growing young leaves from the top rather than mature old leaves to check photosynthesis response and growth traits of *A. philoxeroides* and *A. sessilis* in salt-stress phase following rewatering. All these data were recorded during full-sunshine at 9:30–11:30 a.m. after every four days in both salt stress and rewatering phase, respectively. Five plants from each treatment group were selected for the measurement. The following settings were noted during data collection: photosynthetic active radiation (PAR) was 800 µmol m^{-2} s^{-1}, temperature 28 °C and CO_2 concentration was 500 µmol mol^{-1}.

Growth measurements were considered after salt stress and after rewatering in both cases. The measurements chosen for growth traits analysis were: plant's height (PH); stem-diameter (SD), root-length (RL), fresh-weight of shoot (FW^S), dry-weight of shoot

http://www.aloki.hu ● ISSN 1589 1623 (Print) ● ISSN 1785 0037 (Online)
DOI: http://dx.doi.org/10.15666/aeer/1706_1476714785

(DW^S), fresh-weight of root (FW^R) and dry-weight of root (DW^R). The PH was measured with a tape and SD was measured with the help of digital Vernier caliper. Afterwards, FW^S, DW^S, FW^R and DW^R were measured by using weighing scale.

Table 1. *Concentration of saline water for different treatment levels*

Treatments	Division of treatments' levels	Treatment levels	1 L fresh water medium in the quantity of NaCl (g L^{-1})	1 L fresh water medium in the quantity of $CaCl_2$ (g L^{-1})
0%	Control	AS0 AP0 MAS0 MAP0	0.0	0.0
0.8%	Low	AS1 AP1 MAS1 MAP1	4.0	4.0
1.6%	Medium	AS2 AP2 MAS2 MAP2	8.0	8.0
2.4%	High	AS3 AP3 MAS3 MAP3	12.0	12.0

AS: *A. sessilis*; AP: *A. philoxeroides*; MAS: *A. sessilis* under mixed planting; MAP: *A. philoxeroides* under mixed planting

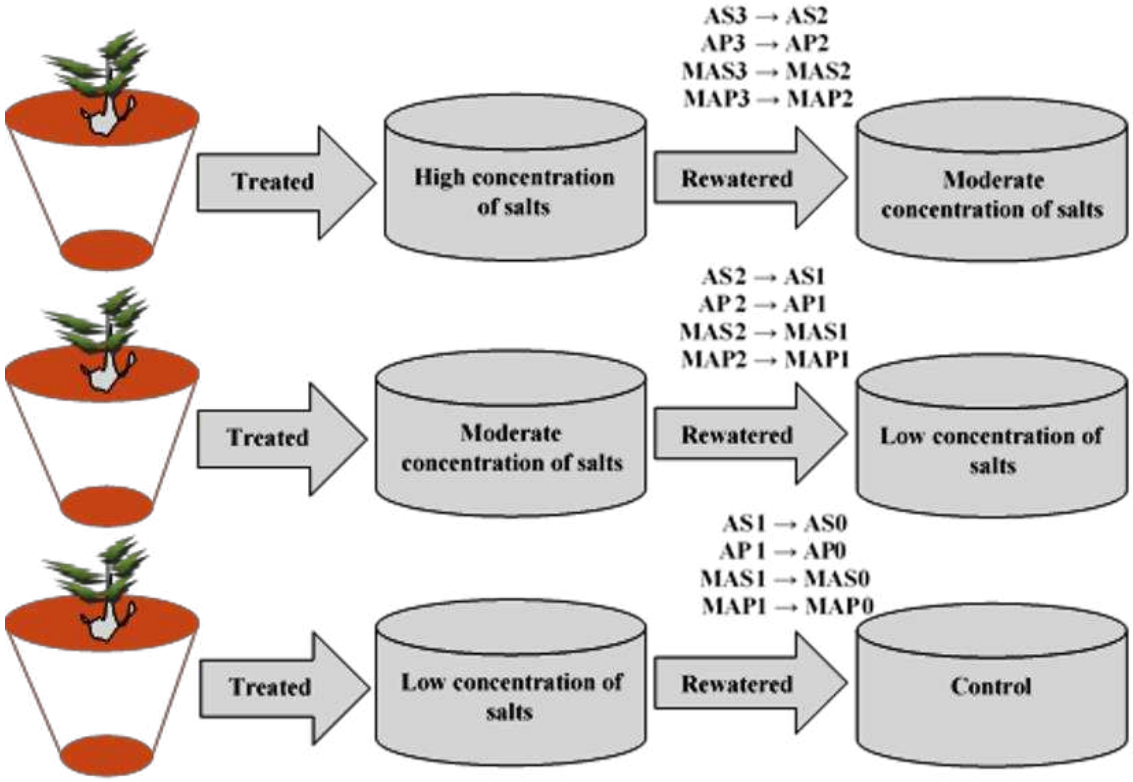

Figure 2. *Rewatering order for plants treated with different concentration of salts*

http://www.aloki.hu ● ISSN 1589 1623 (Print) ● ISSN 1785 0037 (Online)
DOI: http://dx.doi.org/10.15666/aeer/1706_1476714785

Leaf water potential and water use efficiency

Leaf water potential (Ψ^{LW}) of *A. philoxeroides* and *A. sessilis* were measured by using dew point microvolt meter in a C-52-SF universal sample room (Psypro, *Wescor*, USA). The Ψ^{LW} were recorded at 9:30–11:30 a.m. in salt stress subsequently in re-watering phase, respectively. While, water use efficiency (WUE) was calculated according to Javed et al. (2018):

$$WUE = Pn / R_T \quad \text{(Eq.1)}$$

where Pn is the net photosynthetic rate and R_T is the transpiration rate.

Statistical analysis

All measurements were examined statistically through SPSS 22 software (SPSS Inc., Chicago, IL, USA) and Origin Pro 9.0. Variance analysis with two crossed fixed factors was applied to discriminate the effects of species, salt stresses, rewatering and their interaction on physiological characteristics and plant growth properties under mono and mixed planting. The Tukey test was applied to determine the differences at 5% significance level ($P \leq 0.05$) between means (n = 5).

Results

Physiological responses

Net photosynthetic rate, stomatal conductance and transpiration

Net photosynthetic rate and stomatal conductance decreased significantly with increasing salt stress in comparison with the control. The response of the species to salt stress levels are given in *Table 2*. *A. philoxeroides* showed more tolerance from low to high concentration of salts. The values of Pn *for A. philoxeroides* at low concentration levels for single and mixed planting at AP1, MAP1 were 7.63 and 6.64 μmol (CO_2) m^{-2} s^{-1}, higher than the values of Pn for *A. sessilis*, which were 6.68 and 4.90 μmol (CO_2) m^{-2} s^{-1} at AS1 and MS1, respectively. It was found that, Pn was affected more under high stress at AS3, AP3, MAS3 and MAP3 in *A. sessilis* compared to *A. philoxeroides* (*Fig. 3a*). Upon comparing, the average Pn values of *A. sessilis* and *A. philoxeroides*, mixed planting decreased the Pn values more in *A. sessilis* respectively. Similarly, the response of the gs to salt stress levels are given in *Table 2*. The reduction in gs was found higher at high concentration for both *A. philoxeroides* and *A. sessilis* but comparatively less in *A. philoxeroides*. The gs values in mol (H_2O) m^{-2} s^{-1} for both *A. philoxeroides* and *A. sessilis* at high concentration under single and mixed planting were AS3: 0.066 AP3: 0.094 and MAS3: 0.044, MAP3: 0.086, respectively. It was showed that, during competition under mixed planting, *A. sessilis* exhibited maximum reduction in *Np* and afterwards in Cs as compared to single planting (*Fig. 3b*).

The response of Pn and gs during salt stress following rewatering are also shown in (*Table 2; Fig. 3a, b*). It was observed that *A. philoxeroides* exhibited significantly better recovery from stress phase to re-watering phase. During rewatering, by comparing the means under salt stress and rewatering, the increments in Pn from low to high salt concentration (AP1 (1→0), AP2 (2→1), AP3 (3→2)) for single-*A.*

http://www.aloki.hu ● ISSN 1589 1623 (Print) ● ISSN 1785 0037 (Online)
DOI: http://dx.doi.org/10.15666/aeer/1706_1476714785

philoxeroides were 21.50%, 19.95% and 13.70% but for single-*A. sessilis*, increments in Pn at AS1(1→0), AS2(2→1), AS3(3→2) were noted as 16.04%, 10.23% and 5.34%, respectively. The Pn was not recovered well even after rewatering in case of mix-*A. sessilis* and showed less recovery comparatively to mix-*A. philoxeroides* (*Fig. 3a*). In rewatering phase, the increments in gs under low to high salt stress were found lower in *A. sessilis* plants (*Fig. 3b*). Consequently, high salt stresses affected gs and left adverse effect under mixed planting (*Table 2; Fig. 3b*).

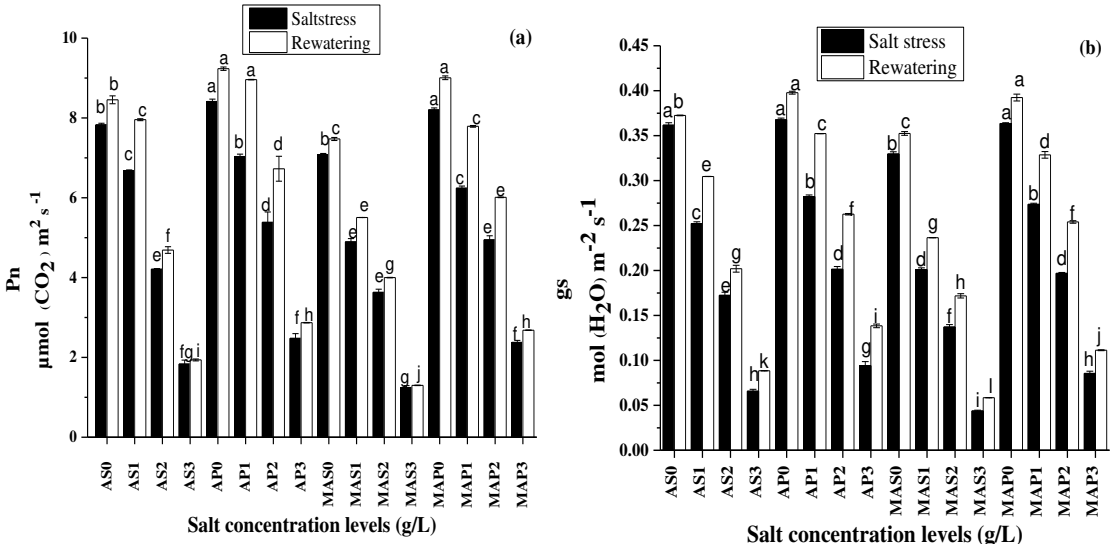

Figure 3. *Subsequent impact of salt stress under rewatering on (a) net photosynthetic rate and (b) stomatal conductance of A. philoxeroides and A. sessilis under single and mixed planting. Mean values sharing different letters are significantly different at $p \leq 0.05$ under different salt treatment levels*

Transpiration, water use efficiency and leaf water potential

Table 2 represented the results of E, WUE and Ψ^{LW}. The results exhibited the significant differences among treatment species and their interactions. The values of E decreased during salt treatments at low to high concentration levels, as compared to control (*Table 2*). Transpiration of *A. sessilis* decreased significantly in the stress and recovered up to moderate level AS2 for single planting during re-watering phase as shown in *Figure 4a*. But the salt stress severely affected *A. sessilis* E at AS3 and it did not recover. The E declined in *A. philoxeroides* throughout salt treatments at low to high concentration levels, as compared to control and recovered well from low to high stress. Therefore, in the rewatering phase, *A. philoxeroides* is also showed better E under mixed planting and was found to be recovering well from low MAP1 (1→0) to moderate level MAP2 (2→1) and less recovered at high level AP3 (3→2) and MAP3 (3→2) (*Fig. 4a*). Recovery of E confirms that *A. philoxeroides* can use more water to decrease the E and can improve plant development after rewatering. On the other hand, rewatering did not leave the positive effect on E recovery of the plant during competition with *A. philoxeroides* under mixed planting. Water potential (Ψ^{LW}) tends to decline as the relative water content of plant leaves decreases under stress condition. According to our results, Ψ^{LW} was affected with increasing salt stress compared with control (*Table 2*).

http://www.aloki.hu ● ISSN 1589 1623 (Print) ● ISSN 1785 0037 (Online)
DOI: http://dx.doi.org/10.15666/aeer/1706_1476714785

Table 2. *Variance analysis of photosynthetic parameters of A. philoxeroides and A. sessilis under salt stress followed by rewatering*

	Salt stress			Rewatering		
	DF	**F**	**P**	**DF**	**F**	**P**
Photosynthesis				**Photosynthesis**		
T	3	3568.091	0.001	3	3997.442	0.001
S	3	299.171	0.001	3	529.100	0.001
T×S	9	15.871	0.001	9	20.350	0.001
Stomatal conductance				**Stomatal conductance**		
T	3	6852.555	0.001	3	1470.533	0.001
S	3	395.100	0.003	3	1366.023	0.001
T×S	9	9.920	0.001	9	52.723	0.001
Transpiration				**Transpiration**		
T	3	3205.679	0.001	3	7551.105	0.001
S	3	486.264	0.004	3	1138.365	0.001
T×S	9	2.368	0.007	9	106.210	0.110
Water potential				**Water potential**		
T	3	2160.235	0.001	3	2345.998	0.001
S	3	244.805	0.001	3	311.879	0.001
T×S	9	22.4554	0.001	9	50.907	0.015
Water use efficiency				**Water use efficiency**		
T	3	2053.659	0.001	3	3601.187	0.001
S	3	1185.221	0.021	3	2054.185	0.105
T×S	9	971.110	0.011	9	814.514	0.132

$T_{=}$ treatments, $S_{=}$ species, $T \times S_{=}$ interaction among the treatments and species, significant at $P \leq 0.001$ and $P \leq 0.005$ according to two-way ANOVA

The WUE showed the significant increase for *A. sessilis* from control to low stress, and the increment after rewatering was found as 31.65% and 23.55% at AS1 and MAS1 followed by medium stress (27.55%, 22.03%) at AS2 and MAS2, respectively. The maximum increments in WUE were recorded under low and medium stress for *A. philoxeroides* (36.16%, 32.13%, 33.53% and 31.90) under AP1, AP2, MAP1 and MAP2, respectively (*Fig. 4b*). However, the stress-persuaded maximum reduction was noted for *A. sessilis* under high stress at AS3 and MAS3. While comparatively, rewatering was reducing the effect of salt stresses significantly, and exposed the significant rise in WUE for *A. philoxeroides* (*Fig. 4b*).

In case of single planting of *A. philoxeroides* and *A. sessilis*, the minimum decrease in Ψ^{LW} was noted as -1.18 MPa and -2.00 MPa under low concentration levels at AP1 and AS1, respectively for both species as compared to moderate and high stress levels. But, the maximum decrease in Ψ^{LW} was noted as -2.82 MPa and -3.10 MPa at AP3 and AS3, respectively. While under mixed planting, *A. sessilis* is becoming more sensitive to salt stress and Ψ^{LW} was affected seriously from moderate to high concentrations (*Fig. 5*). However, in the competition, Ψ^{LW} was severely decreased in *A. sessilis* as compared to *A. philoxeroides*, respectively. As a comparison between single and mixed plantation, salts badly affected the Ψ^{LW} in *A. sessilis* than *A. philoxeroides* (*Fig. 5*).

http://www.aloki.hu ● ISSN 1589 1623 (Print) ● ISSN 1785 0037 (Online)
DOI: http://dx.doi.org/10.15666/aeer/1706_1476714785

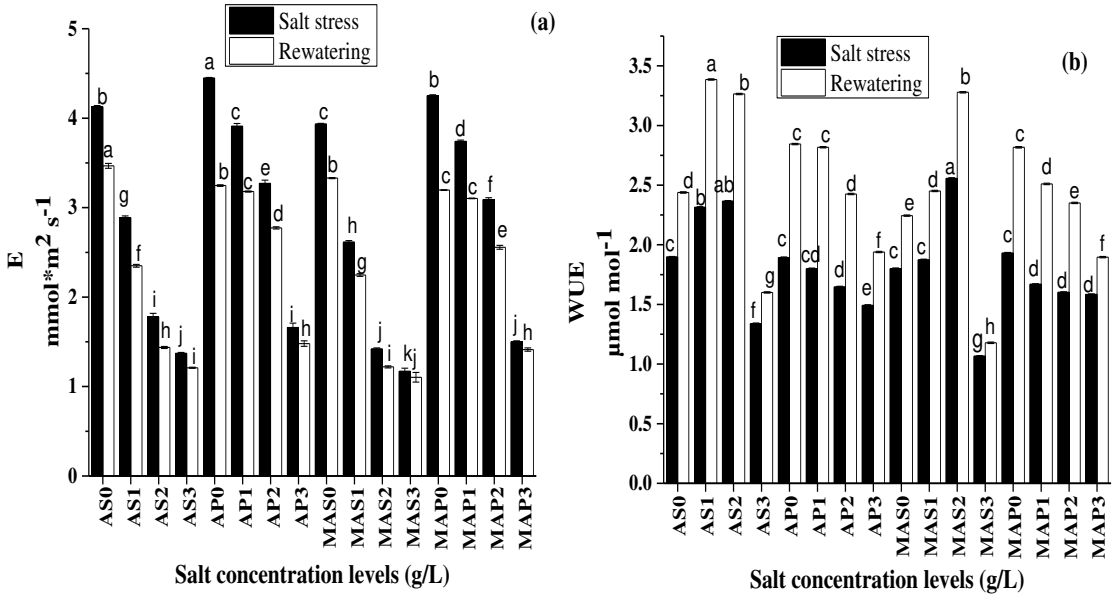

Figure 4. *Subsequent impact of salt stress under rewatering on (a) transpiration rate and (b) water use efficiency of A. philoxeroides and A. sessilis single and mixed planting. Mean values sharing different letters are significantly different at $p \leq 0.05$ under different salts treatment levels*

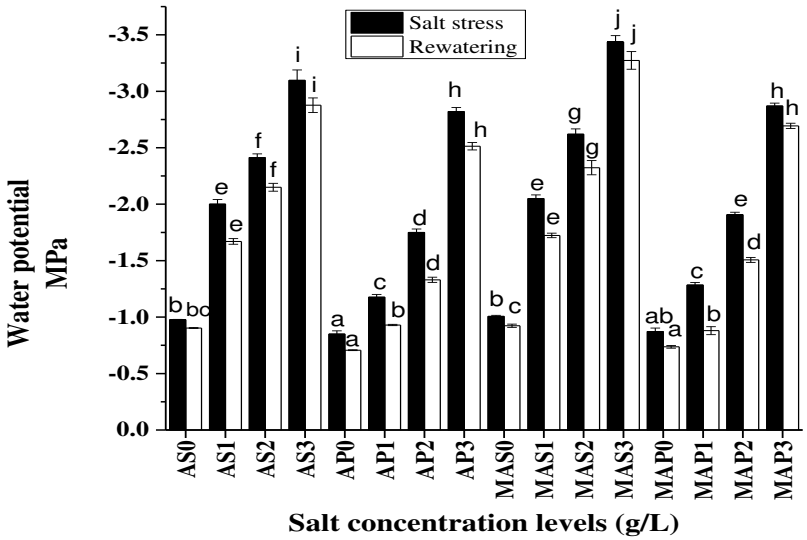

Figure 5. *Subsequent impact of salt stress under rewatering in leaf water potential of A. philoxeroides and A. sessilis under single and mixed planting. Mean values sharing different letters are significantly different at $p \leq 0.05$ under different salts treatment levels*

Table 2 also presents the values of Ψ^{LW} in salt stress following rewatering. The recovery in Ψ^{LW} was found less in single-*A. sessilis* from low to high stress (*Fig. 5*). Water potential was not recovered at high concentration levels for single-*A. sessilis* plants. However, the degree of salts was still showed its adverse effect on *A. sessilis* in the increment of Ψ^{LW} from moderate to high stress even during re-watering under mixed planting (*Fig. 5*).

http://www.aloki.hu ● ISSN 1589 1623 (Print) ● ISSN 1785 0037 (Online)
DOI: http://dx.doi.org/10.15666/aeer/1706_1476714785

Plant growth responses

Plant height and stem diameter

Stresses significantly affected the growth of *A. sessilis* and *A. philoxeroides* through reduction in plant height and stem diameter. The results showed significant differences among treatments, species and their interactions of growth parameters (*Table 3*). Plants growth of *A. sessilis* is more affected in competition under mixed planting as compared to *A. philoxeroides* (*Fig. 6a, b*). *A. philoxeroides* showed more tolerance from low to high stress in single as well as in mixed planting. Plant height and stem diameter were significant as compared to control. Upon comparing *A. philoxeroides* with *A. sessilis* under single and mixed planting, the PH (cm) are AP1: 42.30, AS1: 36.80, AP2: 37.30, AS2: 31.80, AP3: 32.40, AS3: 28, MAP1:40.30, MAS1: 33.80, MAP2: 35.30, MAS2: 28.80, MAP3: 30.60, MAS3: 25.50 (*Fig. 6a*); following SD (mm) which are AP1: 3.71, AS1: 2.98, AP2: 3.42, AS2: 2.39, AP3: 2.97, AS3: 2.23, MAP1: 3.34, MAS1: 2.49, MAP2: 3.16, MAS2: 2.28, MAP3: 2.77, MAS3: 2.00 (*Fig. 6b*). So, the *A. sessilis* exposed its sensitivity during competition under mixed planting, more reduction was found in plant height and stem diameter (*Fig. 6a, b*).

The subsequent PH and SD under salt stress under rewatering are also explained in *Table 3*. It was observed that *A. philoxeroides* exhibited significantly better recovery from stress phase to re-watering phase. While in re-watering phase, by comparing the means, the increments in PH and SD under moderate to high salt stress was found to lower in *A. sessilis*. By comparing, relatively, more increments in PH and SD were found in *A. philoxeroides* (*Fig. 6a, b*). The increments in PH after rewatering are AP1: 24.60%, AS1: 13.62%, AP2: 17.29%, AS2: 12.15%, AP3: 7.95%, AS3: 5.72%, MAP1: 21.44%, MAS1: 12.89%, MAP2: 22.08%, MAS2: 7.99%, MAP3: 6.13%, MAS3: 1.16% (*Fig. 6a*); following by SD as AP1: 19.00%, AS1: 18.36%, AP2: 16.79%, AS2: 13.41%, AP3: 5.41%, AS3: 2.62%, MAP1: 21.60%, MAS1: 17.00%, MAP2: 15.28%, MAS2: 9.52%, MAP3: 4.48%, MAS3: 1.48%, respectively. Rewatering alleviate the effect of salt stress more effectively in *A. philoxeroides* and left positive impact on plant growth.

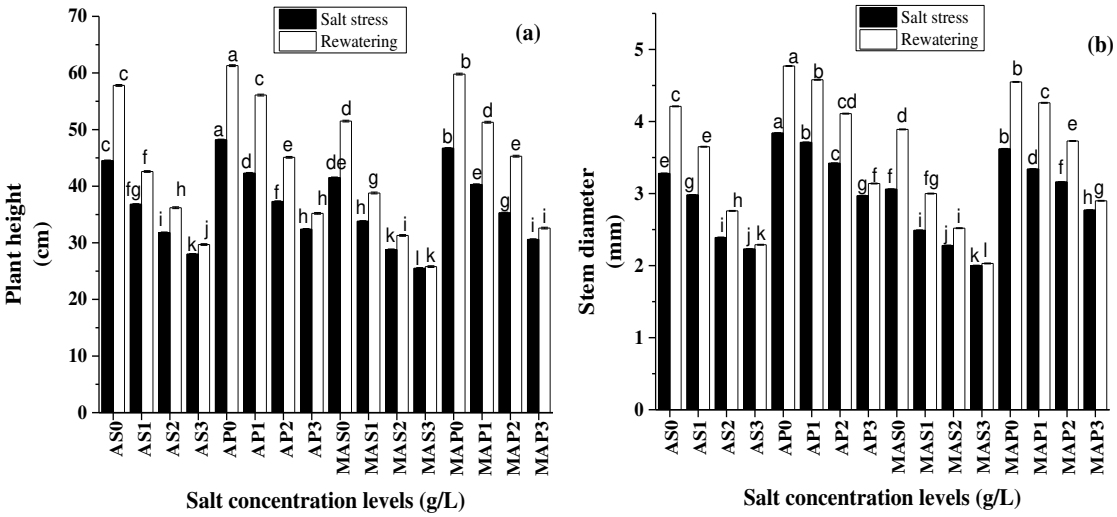

Figure 6. *Subsequent impact of salt stress under rewatering on (a) plant height and (b) stem diameter of A. philoxeroides and A. sessilis under single and mixed planting. Mean values sharing different letters are significantly different at $p \leq 0.05$ under different salts treatment levels*

http://www.aloki.hu ● ISSN 1589 1623 (Print) ● ISSN 1785 0037 (Online)
DOI: http://dx.doi.org/10.15666/aeer/1706_1476714785

Fresh and dry weight of shoot

Fresh and dry weight of shoot of both species for each treatment was presented in *Table 3*. As expected, mean of Fresh and dry weight decreased depending on salt concentration (*Table 3; Fig. 7a, b*). The variations in the results of shoot fresh and dry weight are different in both species. FW^S in single-*A. sessilis* is relatively more affected than mono-*A. philoxeroides* under high salt stress as AS3: 5.60 g, and AP3: 8.93 g following DW^S as AS3: 0.20 g, and AP3: 0.28 g, respectively. While, in competition under mixed planting FW^S and DW^S of *A. sessilis* declined more comparatively with mixed-*A. philoxeroides* (*Table 3; Fig. 7a*). The FW^S under mixed planting are MAS1: 10.30 g, MAP1: 21.27 g, MAS2: 5.20 g, MAP2: 12.43 g, MAS3: 2.57 g, MAP3: 7.97 g (*Fig. 3c*), following DW^S as MAS1: 0.37 g, MAP1: 3.03 g, MAS2: 0.18 g, MAP2: 0.60 g, MAS3: 0.11 g, MAP3: 0.24 g, respectively (*Fig. 7b*). Though, *A. philoxeroides* showed more tolerance from low to high stress in both single and mixed planting.

Table 3. *Variance analysis of plant growth parameters of A. philoxeroides and A. sessilis under salt stress followed by rewatering*

	Salt stress			**Rewatering**		
	DF	**F**	**P**	**DF**	**F**	**P**
Plant height				**Plant height**		
T	3	5598.254	0.001	3	19956.761	0.001
S	3	1355.258	0.001	3	6534.237	0.001
T×S	9	43.666	0.003	9	504.682	0.001
Stem diameter				**Stem diameter**		
T	3	2352.250	0.001	3	70354.187	0.001
S	3	2165.251	0.001	3	5985.843	0.001
T×S	9	71.146	0.005	9	1110.258	0.070
Fresh weight of shoot				**Fresh weight of shoot**		
T	3	3865.307	0.001	3	3813.078	0.001
S	3	887.035	0.001	3	916.774	0.001
T×S	9	11.948	0.171	9	10.115	0.015
Dry weight of shoot				**Dry weight of shoot**		
T	3	2044.585	0.001	3	1669.187	0.001
S	3	407.221	0.005	3	284.552	0.005
T×S	9	6.107	0.071	9	29.741	0.011
Fresh weight of root				**Fresh weight of root**		
T	3	1515.276	0.001	3	726.2045	0.001
S	3	371.399	0.001	3	209.3972	0.001
T×S	9	2.711	0.018	9	2.857	0.008
Dry weight of root				**Dry weight of root**		
T	3	1519.2898	0.001	3	618.984	0.001
S	3	182.1445	0.001	3	160.779	0.001
T×S	9	26.1700	0.001	9	24.602	0.001

$T_=$ treatments, $S_=$ species, $T \times S_=$ interaction among the treatments and species, significant at $P \leq 0.001$ and $P \leq 0.005$ according to two-way ANOVA

http://www.aloki.hu ● ISSN 1589 1623 (Print) ● ISSN 1785 0037 (Online)
DOI: http://dx.doi.org/10.15666/aeer/1706_1476714785

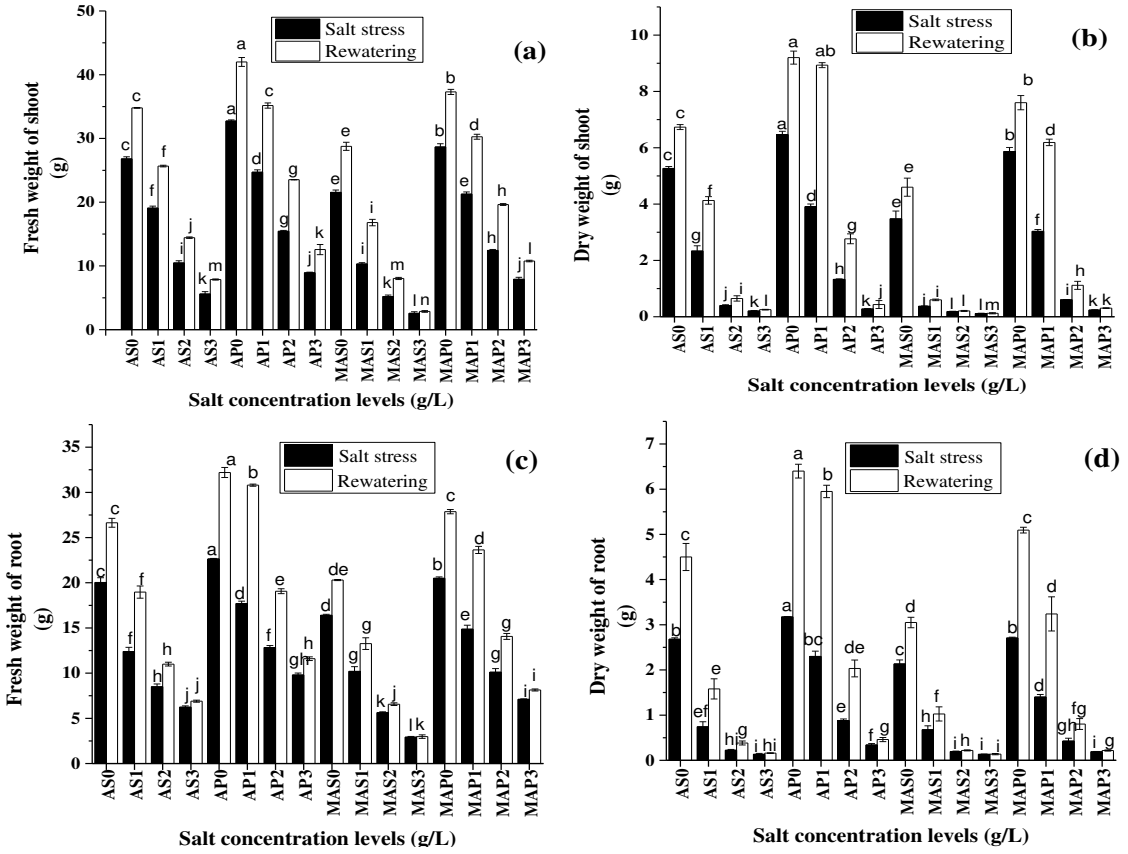

Figure 7. *Subsequent impact of salt stress under rewatering on (a) fresh weight of shoot, (b) dry weight of shoot, (c) fresh weight of root, and (d) dry weight of root of A. philoxeroides and A. sessilis under single and mixed planting. Mean values sharing different letters are significantly different at $p \leq 0.05$ under different salts treatment levels*

Subsequent salt stress under re-watering, is shown in *Table 3* for FW^S and DW^S. The plants showed recovery significantly from stress phase to re-watering phase (*Fig. 7a, b*). During re-watering phase, the increments in FW^S followed by DW^S under moderate to high salt stress were found to lower in *A. sessilis* that are AS2: 33.06%, AP2: 67.47% and AS3: 18.89, < AP3: 30.28%; AS2:38.97%, AP2: 56.27% and AS3:19.74%, AP3: 36.14%, respectively (*Fig. 7a, b*). Relatively, the maximum increment in FW^S and DW^S was observed for single and mixed-*A. philoxeroides* as 87.22%, 71.94%, 56.27%, 51.00% while for mono and mixed *A. sessilis*, it was calculated as 66.67%, 60.28%, 43.52%, 24.42% at AP1, MAP1, AS1, and MAS1, respectively (*Fig. 7a, b*). Comparing with other stress levels after re-watering, relatively, more decrements in FW^S and DW^S were found in *A. sessilis* under mixed planting and minimum recovery found after rewatering.

Fresh and dry weight of root

Fresh and dry weight of root of both species for each treatment was presented in *Table 3*. FW^R and DW^R decrease by increasing salt concentration relatively affected more in *A. sessilis* than *A. philoxeroides* under high salt stress (*Table 3; Fig. 7c, d*). The FW^R under single planting of *A. sessilis* at high concentration was observed as AS3: 6.23 g, and as AP3: 9.80 g (*Fig. 7c*) following DW^R as AS3: 0.13 g, and as AP3: 0.34 g,

http://www.aloki.hu ● ISSN 1589 1623 (Print) ● ISSN 1785 0037 (Online)
DOI: http://dx.doi.org/10.15666/aeer/1706_1476714785

respectively (*Fig. 7d*). Comparatively, the FW^R of *A. sessilis* under mixed planting was affected more following the same trend by DW^R, respectively. Though, *A. philoxeroides* showed more tolerance from low to high stress in both single and mixed planting.

The FW^R and DW^R under salt stress following rewatering for both *A. philoxeroides* and *A. sessilis* is shown in *Table 3*. Recovery in FW^R and DW^R is initiated during re-watering phase (*Fig. 7c, d*). The minimum increments were noted in FW^R under moderate to high salt stress for *A. sessilis* which were AS2: 22.73%, AP2: 32.69% and AS3: 9.66%, AP3: 15.66% (*Fig 7c*), followed by DW^R as AS2: 41.74%, AP2: 56.72% and AS3: 16.69%, AP3: 26.09%, respectively. The maximum increment in FW^R and DW^R were recorded for single and mixed-*A. philoxeroides* as 42.53%, 37.09%, 61.34%, 56.79% and 34.62%, 23.12%, 52.96%, 34.09% were found for single and mixed-*A. sessilis* at AP1, MAP1, AS1, and MAS1, respectively. By comparing with other stress levels after re-watering, relatively, more decrements in FW^R and DW^R were found in *A. sessilis* under mixed planting even after rewatering (*Fig. 7c, d*).

Combined effect of salt stress and invasive plant on native plant

Using the linear regression equation to develop relationship between *A. philoxeroides* and *A. sessilis* under salt stress levels is shown in *Equation 2,* as given below:

$$MAS(FWS) = 0.149Lss + 1.040MAP(FWS) \quad \text{(Eq.2)}$$

where *MAS (FWS)* is shoot fresh weight of *A. sessilis* under mixed planting; $MAP(FWS)$ is shoot fresh weight of *A. philoxeroides* under mixed planting; *Lss* is salt stress levels.

It is well noted that the relationship between fresh weight of *A. philoxeroides* (MAP) under mixed planting, salt stress levels (Lss) and fresh weight of *A. sessilis* (MAS) under mixed planting can well characterize the combined effect of an invasive plant as *A. philoxeroides* and salt stress on its competitor native plant *A. sessilis*. The determination coefficient (R^2 = 0.9310), showed the best relationship between shoot fresh weight, salt stress and species and it is fitted better with the linear regression equation as compared with the other growth parameters.

Discussion

Salinity is a toxic environmental stress and severely influences several growth traits (Ashraf et al., 2012), particularly the photosynthetic rate. Salt stress initially damages the plant roots, disturbs the soil water potential and slows the growth rate of plants (Abbas et al., 2014). In our studies, the interaction between the species and salt stress has shown the significant differences (*Tables 2* and *3*). The salt stress limited the Pn as a result of stomata closure in both *A. sessilis* and *A. philoxeroides*. The Pn *of A. philoxeroides* and *A. sessilis* responded in a different way to different salt stresses (*Fig. 3a*). During the whole period of salt stresses, comparatively, plants kept a lower gs in single and mixed-*A. sessilis* at high salt concentrations (AS3 and MAS3) (*Fig. 3b*) and directly influenced the Pn. Low Pn had an adverse effect on PH and SD in *A. sessilis* (*Fig. 6a, b*), that was the cause of reduction in FW^S, DW^S, FW^R, and DW^R (*Fig. 7a, b, c, d*). It may be because of the disturbed leaf-water-status caused by distribution and accumulation of salts within the plant body that in turn has a marked impact on the plant water and nutrients uptake, resulting in toxicity and low Ψ^{LW} (Ashraf and Foolad, 2007; Zaki, 2016). The variations

http://www.aloki.hu ● ISSN 1589 1623 (Print) ● ISSN 1785 0037 (Online)
DOI: http://dx.doi.org/10.15666/aeer/1706_1476714785

in Ψ^{LW} within tissues (*Fig. 4*) from low (AS1, AP1, MAS1, MAP1), medium (AS2, AP2, MAS2, MAP2) and high stress (AS3, AP3, MAS3, MAP3) in both species under single and mixed planting affected the opening and closing of stomata in *A. sessilis* under mixed planting (*Fig. 3b*). It caused an imbalance in gaseous exchange, and decreased the E (*Fig. 4a*). Under these circumstances, plants have to utilize extra energy to make biochemical adjustments through osmolytes' accumulation for extracting water from the soil. This additional energy is diverted from the processes involved in plant growth, and results in marked reduction in yield and plant growth development (Munns and Tester, 2008; Ashraf et al., 2018), as noted in *A. sessilis* under single and mixed planting at AS3 and MAS3, respectively to *A. philoxeroides* (*Figs. 6* and *7*).

During competition under mixed planting, *A. sessilis* might be suppressed by two factors; one is competition with *A. philoxeroides* and other is its sensitivity to high salt stress. The combined effect of *A. philoxeroides* and salt stress on growth of *A. sessilis* is explained through linear regression (*Eq. 2*). In their meta-analysis, Van Kleunen et al. (2010), demonstrated that invasive species had higher values for numerous beneficial parameters of plant physiology, such as Pn and WUE than native species. Accordingly, *A. philoxeroides* showed photosynthetic tolerance from low stress levels (AP1 and MAP1) to high stress levels (AP3 and MAP3) under both single and mixed planting. Thus, this condition confirmed the best-threshold adaptability of photosynthetic traits and tolerance of *A. philoxeroides* under saline environment. Quinet et al. (2015) have also reported that *Impatiens parviflora* DC. is a better competitor in stress environments characterized by low water availability and shade. *Impatiens parviflora* copes well with shady conditions, it is tolerant to water-stress and maintains the photosynthetic activity under water-stress conditions. Ozaslan et al. (2016) did experiment on two invasive *Physalis species* and found that both species have a potential to withstand against water limited supply and high salinity environment. Although, WUE increased strongly in response to water stress (*Fig. 4b*), and plants adjusted their water potential (*Fig. 4a*) to maintain their water regulation for the fitness and continuation of growth. *A. philoxeroides* also grew well with high FW^S, DW^S, FW^R and DW^R and tolerate salt stresses from low to high concentration of salts at AP1, AP2, AP3 and more effectively and strongly under mixed planting at MAP1, MAP2, and MAP3 relative to its competitor *A. sessilis* (*Fig. 7a, b, c, d*). Liu et al., 2018 examined the response of three invasive and one native species under low, moderate and high water with low or high nitrogen availability. The growth, biomass and development of invasive species were higher relative to the native plant. Besides, higher salt accumulation in leaves of *A. sessilis* lowered the soil-water potential and in high stress at MAS3 prevented water uptake from soil to plant, causing dehydration of plants, with high reduction in PH, SD, (*Fig. 6a, b*). According to Qian and Ricklefs (2006) and Weed and Schwarzländer (2014), invasive plants have competitive advantages over neighboring native species. But these characteristics are varying from species to species and according to the kind of environmental stress (Lorenzo et al., 2010).

Rewatering relieved the stress and left better result on plant growth and development (Javed et al., 2018). But under stress, the variation in plant growth (*Figs. 6a, b, 7a, b, c, d*) did not associate with Pn recovery (*Fig. 3a*) when plant suffered under high stress conditions in *A. sessilis*. The production part of photosynthesis might have been used for the regeneration of ribulose-1,5-disphosphate. Therefore, at that point, an increment in Pn values for *A. sessilis*' plants under mixed planting noted as MAS1: 11.08%, MAS2: 9.25%, MAS3: 4.10%, which was not helpful in recovery of *A. sessilis*' plants (*Fig. 3a*). However, *A. philoxeroides* recovered and maintained its growth and photosynthetic traits

http://www.aloki.hu ● ISSN 1589 1623 (Print) ● ISSN 1785 0037 (Online)
DOI: http://dx.doi.org/10.15666/aeer/1706_1476714785

effectively under single planting (at AP1, AP2, and AP3) subsequent under mixed planting (at MAP1, MAP2, and MAP3) as compared to control levels. Our results supported by findings of Yousfi et al. (2016) for all species of *Medicago laciniata* (L.) and Xing et al. (2018) for *Orychophragmus violaceus*, are proposed that reduction in gs after severe drought-stress, resulted in declined Pn with slow plant growth, as found in *A. sessilis*. Thus, unhealthy growth of *A. sessilis* was observed due to inadequate water-uptake that abruptly decreased the E (*Fig. 4a*). Water regulation through stomata under high stress could not maintain to stable water content and is becoming the reason of reduction in leaf-water-potential. Accordingly, it was hard for *A. sessilis* to improve its growth after rewatering due to the excessive salts-stresses under AS3, MAS2 and MAS3, respectively.

Salt stress following rewatering is found as an important index which specifies the better growth of plant after re-watering and a good method to utilize saline water after dilution in order to safe fresh water resources (Javed et al., 2017a, b; Xing et al., 2018). Because addition in water content after re-watering was directed to the Pn increment comparatively in leaves of *A. philoxeroides* with high growth rate and biomass as PH, SD, FW^S, DW^S, FW^R and DW^R under both single and mixed planting conditions. The massive reduction of water potential by decreasing E under high stress exposed the wilting point, and high demand of water for plants (Azeem et al., 2017a). For that reason, it is also needed for plants to be rewatered before wilting-stage. The relative effect of salts after rewatering, under mono planting of *A. philoxeroides* at AP1 (1→0), AP2 (2→1), AP3 (3→2) was almost the same with mixed planting under MAP1 (1→0), MAP (2→1) and MAP (3→2), respectively. It is concluded that salts were more toxic to plant growth of *A. sessilis* under single-AP3 and all levels of mixed planting, because of its sensitive nature suppressed through competition with *A. philoxeroides* as an invasive plant. It is also demonstrated that *A. philoxeroides* has a good competition ability with its competitive native plant *A. sessilis* and has a stress bearing adaptability to stressful environmental conditions.

Conclusions

In this article, we identified physiological and growth traits linked to salts-stresses tolerance in *A. philoxeroides* and *A. sessilis*. The physiological and growth response confer the competitive capability to both species under stressful environment. Under salt stress followed by rewatering, *A. philoxeroides* had higher values of Pn, gs, Ψ^{LW}, PH and SD with high biomass (FW^S, DW^S, FW^R, and DW^R) than *A. sessilis* in both single and mixed planting. Nevertheless, the competitive ability of the invasive plant *A. philoxeroides* was higher than that of the native species *A. sessilis* under mixed planting. Comparatively, *A. philoxeroides* showed better effect of rewatering with good improvement in plant growth. It can be concluded that, under single and mixed planting, tolerance of *A. philoxeroides* to salt stresses and its restoration after rewatering may aid its invasion success over *A. sessilis* species. Thus this study will be an initial prediction about future distribution of *A. philoxeroides* in the saline environment. In addition for future perspective, the further study could be done by considering different environmental factors based on their biological characteristics. Therefore, investigating the relationship between plant growth and environmental factors is helpful for predicting the invasive potential of non-native plant species.

http://www.aloki.hu ● ISSN 1589 1623 (Print) ● ISSN 1785 0037 (Online)
DOI: http://dx.doi.org/10.15666/aeer/1706_1476714785

Acknowledgements. This work was supported by State Key Research Development Program of China (2017YFC1200100), the National Natural Science Foundation of China (31971427, 31570414, and 31770446), the Priority Academic Program Development of Jiangsu Higher Education Institutions (PAPD), and Jiangsu Collaborative Innovation Center of Technology and Material of Water Treatment.

REFERENCES

[1] Abbas, T., Pervez, M., Ayyub, C., Shaheen, M., Tahseen, S., Shahid, M., Bilal, R., Manan, A. (2014): Evaluation of different Okra genotypes for salt tolerance. – International Journal of Plant, Animal and Environmental Sciences 4: 23-30.

[2] Amirjani, M. (2010): Effect of salinity stress on growth, mineral composition, proline content, antioxidant enzymes of soybean. – American Journal of Plant Physiology 5: 350-360.

[3] Ashraf, M., Foolad, M. (2007): Roles of glycine betaine and proline in improving plant abiotic stress resistance. – Environmental and Experimental Botany 59: 206-216.

[4] Ashraf, M., Shahzad, S. M., Imtiaz, M., Rizwan, M. S., Arif, M. S., Kausar, R. (2018): Nitrogen nutrition and adaptation of glycophytes to saline environment: a review. – Archives of Agronomy and Soil Science 64: 1181-1206.

[5] Ashraf, M. A., Ashraf, M., Shahbaz, M. (2012): Growth stage-based modulation in antioxidant defense system and proline accumulation in two hexaploid wheat (Triticum aestivum L.) cultivars differing in salinity tolerance. – Flora-Morphology, Distribution, Functional Ecology of Plants 207: 388-397.

[6] Asrar, H., Hussain, T., Hadi, S. M. S., Gul, B., Nielsen, B. L., Khan, M. A. (2017): Salinity induced changes in light harvesting and carbon assimilating complexes of Desmostachya bipinnata (L.) Staph. – Environmental and Experimental Botany 135: 86-95.

[7] Azeem, A., Wu, Y., Javed, Q., Xing, D., Ullah, I., Kumi, F. (2017a): Response of okra based on electrophysiological modeling under salt stress and re-watering. – Bioscience Journal 33(5):1219-1229.

[8] Azeem, A., Wu, Y., Xing, D., Javed, Q., Ullah, I. (2017b): Photosynthetic response of two okra cultivars under salt stress and re-watering. – Journal of Plant Interactions 12: 67-77.

[9] Chen, L., Yu, Y., He, X. (2008): Historical invasion and expansion process of Alternaria philoxeroides and its potential spread in China. – Biodiversity Science 16: 578-585.

[10] Chen, Z., Zou, Y., Chen, Y., Zhang, Z., Xu, X. (2010): Effects of fragmentation intensity of perennial roots and their burial depth on sprouting and early growth of Alternanthera philoxeroides (Mart.) Griseb. – Agricultural Science, Technology-Hunan 11: 103-111.

[11] Croser, C., Renault, S., Franklin, J., Zwiazek, J. (2001): The effect of salinity on the emergence and seedling growth of Picea mariana, Picea glauca, and Pinus banksiana. – Environmental Pollution 115: 9-16.

[12] Dong, B.-C., Yu, G.-L., Guo, W., Zhang, M.-X., Dong, M., Yu, F.-H. (2010): How internode length, position and presence of leaves affect survival and growth of Alternanthera philoxeroides after fragmentation? – Evolutionary Ecology 24: 1447-1461.

[13] Drenovsky, R. E., Khasanova, A., James, J. J. (2012): Trait convergence and plasticity among native and invasive species in resource-poor environments. – American Journal of Botany 99: 629-639.

[14] Flexas, J., Loreto, F., Medrano, H. (2012): Terrestrial Photosynthesis in a Changing Environment: A Molecular, Physiological, and Ecological Approach. – Cambridge University Press, New York.

[15] Gioria, M., Osborne, B. A. (2014): Resource competition in plant invasions: emerging patterns and research needs. – Frontiers in Plant Science 5: 501.

http://www.aloki.hu ● ISSN 1589 1623 (Print) ● ISSN 1785 0037 (Online)
DOI: http://dx.doi.org/10.15666/aeer/1706_1476714785

[16] Gunasekera, L. (2008): Sessile joyweed (Alternanthera sessilis): a popular leafy vegetable in South East Asia but federal noxious weed in USA. – Proceedings of the 16th Australian Weed Conference, Cairns, Queensland, 18-22 May 2008.
[17] Habib, N., Ashraf, M., Ali, Q., Perveen, R. (2012): Response of salt stressed okra (Abelmoschus esculentus Moench) plants to foliar-applied glycine betaine and glycine betaine containing sugarbeet extract. – South African Journal of Botany 83: 151-158.
[18] Hemakanthi De Alwis, G., Wijesekera, R., Jayasekera, T. (2006): Use patterns and residue levels of pesticides on mukunuwenna, a leafy vegetable grown in Sri Lanka. – Bulletin of Environmental Contamination and Toxicology 76: 119-125.
[19] Javed, Q., Wu, Y., Azeem, A., Ullah, I. (2017a): Evaluation of irrigation effects using diluted salted water based on electrophysiological properties of plants. – Journal of Plant Interactions 12: 219-227.
[20] Javed, Q., Wu, Y., Xing, D., Azeem, A., Ullah, I., Zaman, M. (2017b): Re-watering: An effective measure to recover growth and photosynthetic characteristics in salt-stressed Brassica napus L. – Chilean Journal of Agricultural Research 77: 78-86.
[21] Javed, Q., Wu, Y., Xing, D., Ullah, I., Azeem, A., Rasool, G. (2018): Salt-induced effects on growth and photosynthetic traits of Orychophragmus violaceus and its restoration through re-watering. – Brazilian Journal of Botany 41: 29-41.
[22] Keser, L. H., Visser, E. J., Dawson, W., Song, Y.-B., Yu, F.-H., Fischer, M., Dong, M., Van Kleunen, M. (2015): Herbaceous plant species invading natural areas tend to have stronger adaptive root foraging than other naturalized species. – Frontiers in Plant Science 6: 273.
[23] Kolb, A., Alpert, P. (2003): Effects of nitrogen and salinity on growth and competition between a native grass and an invasive congener. – Biological Invasions 5: 229-238.
[24] Kosma, D. K., Jenks, M. A. (2007): Eco-physiological and Molecular-Genetic Determinants of Plant Cuticle Function in Drought and Salt Stress Tolerance. – In: Jenks, M. A., Hasegawa, P. M., Jain, S. M. (eds.) Advances in Molecular Breeding toward Drought and Salt Tolerant Crops. Springer, Dordrecht
[25] Liu, Y., Liu, M., Xu, X., Tian, Y., Zhang, Z., Van Kleunen, M. (2018): The effects of changes in water and nitrogen availability on alien plant invasion into a stand of a native grassland species. – Oecologia 188: 441-450.
[26] Lorenzo, P., González, L., Reigosa, M. J. (2010): The genus Acacia as invader: the characteristic case of Acacia dealbata Link in Europe. – Annals of Forest Science 67: 101.
[27] Meloni, D. A., Gulotta, M. R., Martínez, C. A., Oliva, M. A. (2004): The effects of salt stress on growth, nitrate reduction and proline and glycinebetaine accumulation in Prosopis alba. – Brazilian Journal of Plant Physiology 16: 39-46.
[28] Memon, S. A., Hou, X., Wang, L. J. (2010): Morphological analysis of salt stress response of pak choi. – Electronic Journal of Environmental, Agricultural, Food Chemistry 9(1): 248-254.
[29] Morais, M. C., Panuccio, M. R., Muscolo, A., Freitas, H. (2012): Salt tolerance traits increase the invasive success of Acacia longifolia in Portuguese coastal dunes. – Plant Physiology and Biochemistry 55: 60-65.
[30] Munns, R., Tester, M. (2008): Mechanisms of salinity tolerance. – Annual Review of Plant Biology 59: 651-681.
[31] Nawaz, K., Hussain, K., Majeed, A., Khan, F., Afghan, S., Ali, K. (2010): Fatality of salt stress to plants: Morphological, physiological and biochemical aspects. – African Journal of Biotechnology 9(34): 5475-5480.
[32] Niraimathi, K., Sudha, V., Lavanya, R., Brindha, P. (2013): Biosynthesis of silver nanoparticles using Alternanthera sessilis (Linn.) extract and their antimicrobial, antioxidant activities. – Colloids and Surfaces B: Biointerfaces 102: 288-291.

http://www.aloki.hu ● ISSN 1589 1623 (Print) ● ISSN 1785 0037 (Online)
DOI: http://dx.doi.org/10.15666/aeer/1706_1476714785

[33] Noe, G. B., Zedler, J. B. (2001): Spatio-temporal variation of salt marsh seedling establishment in relation to the abiotic and biotic environment. – Journal of Vegetation Science 12: 61-74.
[34] Ozaslan, C., Farooq, S., Onen, H., Bukun, B., Ozcan, S., Gunal, H. (2016): Invasion Potential of Two Tropical Physalis Species in Arid and Semi-Arid Climates: Effect of Water-Salinity Stress and Soil Types on Growth and Fecundity. – PloS one 11: e0164369.
[35] Qian, H., Ricklefs, R. E. (2006): The role of exotic species in homogenizing the North American flora. – Ecology Letters 9: 1293-1298.
[36] Quinet, M., Descamps, C., Coster, Q., Lutts, S., Jacquemart, A.-L. (2015): Tolerance to water stress and shade in the invasive Impatiens parviflora. – International Journal of Plant Sciences 176: 848-858.
[37] Ricciardi, A., Blackburn, T. M., Carlton, J. T., Dick, J. T., Hulme, P. E., Iacarella, J. C., Jeschke, J. M., Liebhold, A. M., Lockwood, J. L., Macisaac, H. J. (2017): Invasion science: a horizon scan of emerging challenges and opportunities. – Trends in Ecology, Evolution 32: 464-474.
[38] Richards, C. L., Bossdorf, O., Muth, N. Z., Gurevitch, J., Pigliucci, M. (2006): Jack of all trades, master of some? On the role of phenotypic plasticity in plant invasions. – Ecology Letters 9: 981-993.
[39] Schooler, S. S. (2012): Alternanthera Philoxeroides (Martius) Grisebach (Alligator Weed). – In: Francis, R. A. (ed.) A Handbook of Global Freshwater Invasive Species. Routledge, London.
[40] Schweiger, O., Biesmeijer, J. C., Bommarco, R., Hickler, T., Hulme, P. E., Klotz, S., Kühn, I., Moora, M., Nielsen, A., Ohlemüller, R. (2010): Multiple stressors on biotic interactions: how climate change and alien species interact to affect pollination. – Biological Reviews 85: 777-795.
[41] Sekmen, A. H., Tuerkan, I., Takio, S. (2007): Differential responses of antioxidative enzymes and lipid peroxidation to salt stress in salt-tolerant Plantago maritima and salt-sensitive Plantago media. – Physiologia Plantarum 131: 399-411.
[42] Sun, Y., Ding, J., Frye, M. (2010): Effects of resource availability on tolerance of herbivory in the invasive Alternanthera philoxeroides and the native Alternanthera sessilis. – Weed Research 50: 527-536.
[43] Van Kleunen, M., Weber, E., Fischer, M. (2010): A meta-analysis of trait differences between invasive and non-invasive plant species. – Ecology Letters 13: 235-245.
[44] Vilà, M., Espinar, J. L., Hejda, M., Hulme, P. E., Jarošík, V., Maron, J. L., Pergl, J., Schaffner, U., Sun, Y., Pyšek, P. (2011): Ecological impacts of invasive alien plants: a meta-analysis of their effects on species, communities and ecosystems. – Ecology Letters 14: 702-708.
[45] Vitousek, P. M., Aber, J. D., Howarth, R. W., Likens, G. E., Matson, P. A., Schindler, D. W., Schlesinger, W. H., Tilman, D. G. (1997): Human alteration of the global nitrogen cycle: sources and consequences. – Ecological Applications 7: 737-750.
[46] Weed, A. S., Schwarzländer, M. (2014): Density dependence, precipitation and biological control agent herbivory influence landscape-scale dynamics of the invasive Eurasian plant Linaria dalmatica. – Journal of Applied Ecology 51: 825-834.
[47] Xing, D., Wu, Y., Yu, R., Wu, Y., Javed, Q. (2018): Determination of appropriate irrigation time based on rewatering water-use efficiency. – Acta Horticulturae. DOI: 10.17660/ActaHortic.2018.1205.43
[48] Yang, C., Yang, X., Zhang, X., Zhou, C., Zhang, F., Wang, X. E., Wang, Q. (2019): Anatomical structures of alligator weed (Alternanthera philoxeroides) suggest it is well adapted to the aquatic–terrestrial transition zone. – Flora 253: 27-34.
[49] You, W.-H., Fang, L.-X., Xi, D.-G., Du, D.-L., Xie, D. (2018): Difference in capacity of clonal integration between terrestrial and aquatic Alternanthera philoxeroides in response to defoliation: implications for biological control. – Hydrobiologia 817: 319-328.

http://www.aloki.hu ● ISSN 1589 1623 (Print) ● ISSN 1785 0037 (Online)
DOI: http://dx.doi.org/10.15666/aeer/1706_1476714785

[50] Yousfi, N., Sihem, N., Ramzi, A., Abdelly, C. (2016): Growth, photosynthesis and water relations as affected by different drought regimes and subsequent recovery in Medicago laciniata (L.) populations. – Journal of Plant Biology 59: 33-43.
[51] Zaki, S. (2016): Effect of compost and nitrogen fertilization on yield and nutrients uptake of rice crop under saline soil. – Modern Chemistry and Application 4: 183.
[52] Zenni, R. D., Ziller, S. R., Pauchard, A., Rodriguez-Cabal, M., Nuñez, M. A. (2017): Invasion science in the developing world: a response to Ricciardi et al. – Trends in Ecology, Evolution 32: 807-808.
[53] Zheng, Y.-L., Feng, Y.-L., Liu, W.-X., Liao, Z.-Y. (2009): Growth, biomass allocation, morphology, and photosynthesis of invasive Eupatorium adenophorum and its native congeners grown at four irradiances. – Plant Ecology 203: 263-271.

http://www.aloki.hu ● ISSN 1589 1623 (Print) ● ISSN 1785 0037 (Online)
DOI: http://dx.doi.org/10.15666/aeer/1706_1476714785

EFFECT OF DIFFERENT IRRIGATION INTERVALS AND TREATMENTS ON YIELD QUANTITY AND QUALITY OF POTATO (*SOLANUM TUBEROSUM* L.) UNDER FIELD CONDITIONS IN SULAIMANI, IRAQI KURDISTAN REGION

BARZNJY, L. G. K.[1] – ALLAWI, M. M.[2] – MAHOOD, N. A.[3]

[1]*Horticulture Department, College of Agricultural Enginerring Sciences, University of Sulaimani, Sulaimani, Kurdistan Region, Iraq*

[2]*Horticulture Department, College of Agricultural Engineering Sciences, University of Baghdad, Iraq*

[3]*Protected Agricultural Department, Bakrajo Technical Agriculture Institute, Sulaimani, Iraq*

**Corresponding author*
e-mail: luqman.karim@univsul.edu.iq; phone: +964-770-143-4161

(Received 13th Jun 2019; accepted 16th Oct 2019)

Abstract. This study was carried out in two growing spring seasons 2017 and 2018 at Kanipanka Agricultural Research Station (Lat. 35°13'12", Long. 45°25'48", 550 MASL) in Shahrazoor valley 35 km east of Sulaimani. The aim was to investigate the effect of two irrigation intervals (5 and 10 days) and thirteen biotic and abiotic treatments on yield quantity and quality of potato under field condition. The results showed that the 5 days irrigation intervals gave the maximum values of total yield, Total Soluble Solute percentage, while 10 days of irrigation intervals obtained the highest values of tuber hardness and all of the amino acids in the tuber seasons 2017 and 2018, while the maximum values of total yield were acquired through mycorrhizal inoculation. Total Soluble Solute and tuber hardness were achieved by potassium chloride treatment. Whereas the maximum values of all amino acid in the tuber were given by the mycorrhizal inoculation treatment with (6 g L^{-1}) of *Glycyrrhiza glabra* extract in the first season 2017. Concerning the second season 2018, the maximum total yield gave by treatment of potassium chloride and (6 g L^{-1}) of *Glycyrrhiza glabra* extract, while the potassium chloride treatment gave the maximum values of Total Soluble Solute in the tuber.
Keywords: *watering period, T.S.S and starch percentage, proline, glycine, lucien, lysine*

Introduction

Potato (*Solanum tuberosum* L.), which belonging to the Solanaceae family, is the fourth most important agronomical feed crop worldwide after winter wheat, maize, and rice. The total world production of potatoes was 388 million t in 2017, (FAOSTA, 2019). The potato production in Iraq was more than 190,000 t with a total cultivated area of 7950 ha on average 23.996 t h^{-1} (Central Statistical Organization, 2016). Regarding the Kurdistan Region, the potato production was estimated to be over 150,000 t in 2016 data to the Ministry of Agriculture and Water Resources in the Iraqi Kurdistan region.

Irrigation aimed for supplying water totally or partially for crop requirements, decreasing soil and plant temperature, leach excess salts, increase storage of groundwater, facilitate continuous cropping, and to enhance fertilizer application. Some other benefits of irrigation include the direct cut on water stress, increasing the investment in inputs such as fertilizers and improving cultivars affected by uncertain crop production under rained conditions (Zotarelli et al., 2009).

http://www.aloki.hu ● ISSN 1589 1623 (Print) ● ISSN 1785 0037 (Online)
DOI: http://dx.doi.org/10.15666/aeer/1706_1478714804

Muthoni and Kabira (2016) reported that water is the most important limiting factor for potato production and it is possible to increase production levels by well-scheduled irrigation programs throughout the growing season in Tigoni, Kenya. Water stress limits crop productivity by affecting photosynthetic processes at the canopy, or by feedback, inhibition if the transport of photosynthesis to sink organs is limited (Murchie et al., 2009). Moisture stress first causes stomatal closure thus reducing CO_2 uptake for photosynthesis; this leads to reduced plant growth and yield (Mafakheri et al., 2010). Sugar concentration within the leaf tissue increases to increase the osmotic potential of the plant, these clues to response inhibition of photosynthesis (Basu et al., 1999). Finkel and Holbrook (2000) found that the water stresses affected to increased accumulation of reactive oxygen species (ROS) in plants such as (O_2^-, H_2O_2). Overproduction of ROS can disrupt normal plant metabolism through impaired enzyme activity due to oxidative damage, protein degradation.

The natural plant extracted can be achieved easily, safely and cheaply. Furthermore, it is considered as highly eco-friendly compounds. Sarby et al. (2009) reported that licorice root extract contains some compounds, which have similar effect to the growth promoters. Also have a wide range of minerals (P, K Zn, Mg, Fe, and Ca), amino acids (alanine, lysine, arginine), vitamins (B_1, B_2, B_6), with carbohydrate and nitrogen addition, It also contains mevalonic acid that can be used in gibberellins synthesis. Matar et al. (2012) found that the spray (5 g L^{-1}) of licorice extract significantly increased protein percentage in tubers with the maximum values of the total and marketable yield of the potato plant. 5% foliar application with licorice extracts resulted in significant increases total tube, and marketable yields and in addition to decreases in physiological disorders and mechanical injury of tomato plants (Fan et al., 2016). EL-Sagan (2015) reported that the mechanism of action of licorice extract in plants is similar to the gibberellic acid action in stimulating of vegetative growth of plants. Moreover, the licorice extract is available, low cost and effective easy to apply. In addition licorice, foliar applications increase the percentages of N, P, and K in plant's leaves, chlorophyll content in the leaves of cucumber (Khalel and Hado, 2011).

The role of potassium in molecular mechanisms and physiological stress resistance, furthermore, ROS damage would be justifying by K under water stress conditions that resulting in the cell death (Wang et al., 2013). Potassium foliar application is another factor that has been used for improved nutrient management and increasing potato growth and yield (Fageria et al., 2016). Asmaa and Magda (2010) concluded that the total yield of potato tubers significantly with the increases of potassium level in tow season growth. In addition, they concluded that the potassium application significantly affected tubers nutritive values. Maximum tuber yield 36.65 t ha^{-1} was obtained from 600 kg K_2SO_4 ha^{-1} for trickle irrigation and 35.23 t ha^{-1} for furrow irrigation. Interaction between irrigation and potassium fertilization were significantly affected in relation to leaf area, the relative water content in leaves, water potential, stomatal resistance and number of the tiny and marketable tuber of potato (Khosravifar et al., 2008). Zelelew et al. (2016) reported that potato needs different plant nutrients for both growth and developments lacking such nutrients caused the reduction in both qualities and quantities of tubers. AL-Alousi (2013) Studied the effect of potassium fertilizer with three levels (0, 200 and 400 kg potassium ha^{-1}) in form of K_2SO_4, also spray with two levels of potassium sulfate (0 and 5000 mg potassium L^{-1}) and spray with organic extract (0 and 10 ml L^{-1}). The results show the addition and spraying of potassium gave the highest values of vegetative day weight, total tuber yields, number of tuber $plant^{-1}$, tuber weight and percentage of starch

http://www.aloki.hu ● ISSN 1589 1623 (Print) ● ISSN 1785 0037 (Online)
DOI: http://dx.doi.org/10.15666/aeer/1706_1478714804

in tuber with 6243.33 kg h^{-1}, 36.07 t h^{-1}, 6.45 tuber $plant^{-1}$,140.33 g $tuber^{-1}$ and 12.41% for treatments K400, F5000 and M10 respectively.

Tuber dry matter is a varietal character; however, growing location, season, climatic conditions and cultural practices greatly affect the accumulation of dry matter in tubers, a dry matter content of more than 20% is considered ideal for making chips (Saran and Chhabra, 2014). As a food, potato ranks second to soybean in protein amount produced per hectare, and second to sugarcane in carbohydrate production (Alavijeh and Yaghmaei, 2016). Chakraborty et al. (2010) showed that potato tuber proteins have been found to be of high nutritional value.

The mycorrhiza's function is enhancing the processes of nutrient absorption from the soil and increase the plant resistance against drought and diseases. Microorganisms are an essential component of the agricultural system. Mycorrhizae are a global soil microbe, can subordinate with the roots of most native crop species (Duc, 2017). Several benefits were observed when arbuscular mycorrhizal (AM) fungi is colonized crops including; increased growth and yield, enhanced plant resistance to environmental adversities, increase the plant resistance to abiotic stress (Birhane et al., 2012). ROS production, and thus antioxidant enzyme activity, is enhanced when plants are exposed to various abiotic stresses, such as drought (Caverzan et al., 2012). Osmosis is a mechanism for maintaining water relations under osmotic pressure. It involves the accumulation of a group of active/osmotic molecules/ions including dissolved sugars, sugar alcohol, proline, glycine betaine, organic acids, calcium, potassium, chloride ions and others under water shortage and due to the dissolved accumulation of the cell, which attracts water to the cell and helps maintain the turgor. Potatoes respond to dehydration and salts accumulated through the accumulation of proline which acts as an endoscopy device (osmoprotector), osmoregulator and ROS scavenger (Vahdati and Lotfi, 2013), they study the effects of different irrigation systems during two stages of growth on total chlorophyll in, total soluble sugars content and antioxidant activity in potato leaves.

The aim of this study was to evaluate the effect of irrigation intervals and some biotic and abiotic treatments on potato yield and quality in two growing spring seasons 2017 and 2018, as well as studding the possibility to reducing water requirements of potato while maintaining the tuber quantities and qualities under the field conditions in Sulaimani – Iraqi Kurdistan region.

Material and methods

This study carried out in two growing spring seasons 2017 and 2018 in Kanipanka Agricultural Research Station which located in North-East of Iraq (Lat. 35°13'12", Long. 45°25'48", 550 MASL) in Shahrazoor valley 35 km east of Sulaimani. GIS software was used to create the study sites shown in *Figure 1*. Generally, the elevation of this region ranges between 5 and 2368 m above sea levels. This study includes the interaction effect of two irrigation intervals (5 and 10 days) and thirteen treatments such as *Glycyrrhiza glabra* extract, potassium chloride (KCl), and mycorrhiza inoculation and their interaction on yield quantity and quality of potato plant under field condition. The climate of the study area is generally characterized by warm, dry summer and cold winters (Najmaddin et al., 2017). Thus, the meteorological data of Kanipanka during both growing seasons are shown in *Table 1*. Some physical and chemical properties of Kanipanka soil are shown in *Table 2*.

http://www.aloki.hu ● ISSN 1589 1623 (Print) ● ISSN 1785 0037 (Online)
DOI: http://dx.doi.org/10.15666/aeer/1706_1478714804

Bio inoculation

The fungal inoculants *Glomus mosseae* was obtained from Al-Zaefaraniya Agricultural Research Station/Ministry of Science and Technology/Baghdad. The inoculants were consisting of mycorrhiza spore with 47 spores g^{-1} dry soil and the residual of the infected roots. Potato tubers were inoculated with the mycorrhiza spores by using 20 g from the mixture of the inoculums and the pet moss inside the pores, which specified for inoculation treatment before planting the tubers where the pad method was used to ensure the infection by touching the inoculums during planting.

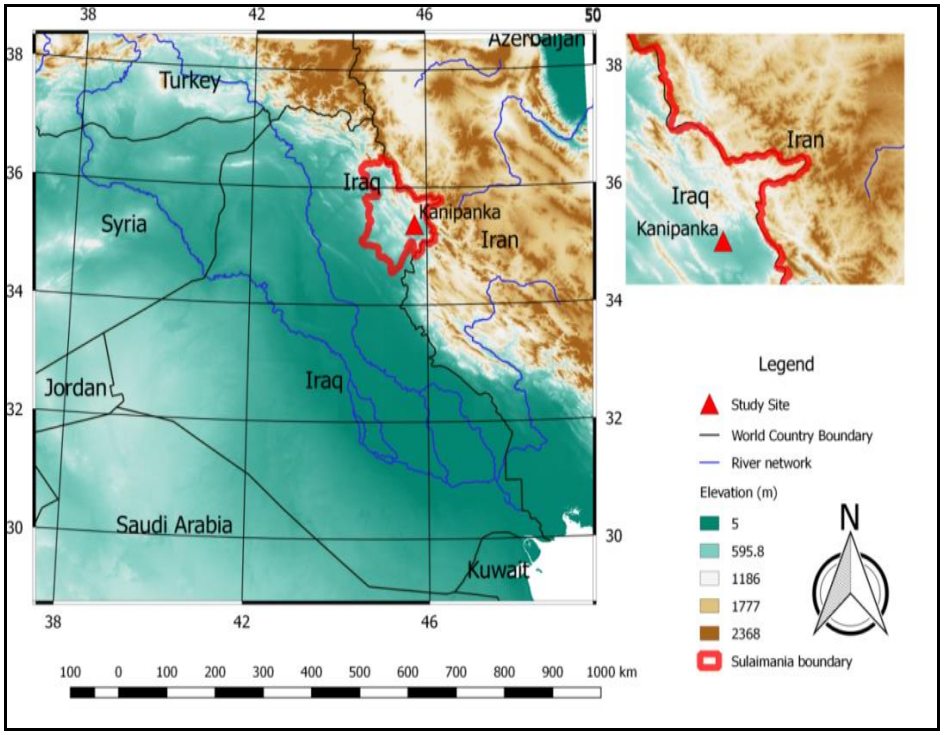

Figure 1. *Regional and local location of the study site*

Table 1. *Meteorological data of Kanipanka location during both growing seasons (2017 and 2018)*

Months	Air temp. (°C)			Humidity (%)			Prec. (mm)	Pan eva. (mm)	Soil temp. (°C)
	Avg.	Max.	Min.	Avg.	Max.	Min.			
First season 2017									
March	12.2	23.0	4.0	49.7	84.0	22.0	107.1	70.2	12.0
April	17.4	31.1	7.0	42.0	79.0	17.0	39.6	119.9	17.6
May	24.6	39.3	12.2	30.3	75.0	16.0	19.3	164.4	23.9
June	30.4	45.7	15.2	21.4	32.0	14.0	0.0	216.0	29.4
Second season 2018									
March	14.7	30.0	2.5	42.3	78.0	18.0	15.5	98.7	11.7
April	17.1	29.7	6.2	38.4	80.0	17.0	82.7	110.5	17.4
May	22.2	37.8	10.0	36.1	84.0	17.0	51.8	135.1	20.6
June	30.3	45.5	17.0	21.7	30.0	13.3	0.0	211.3	27.1

http://www.aloki.hu ● ISSN 1589 1623 (Print) ● ISSN 1785 0037 (Online)
DOI: http://dx.doi.org/10.15666/aeer/1706_1478714804

Table 2. *Some physical and chemical properties of Kanipanka soil*

Soil components	Quantities	Unit
Sand	308.0	g kg^{-1}
Silt	340.0	g kg^{-1}
Clay	352.0	g kg^{-1}
Textured class	Clay loam	
pH	7.10	
EC	0.38	dS m^{-1}
Field capacity	290.0	g kg^{-1}
Wilting point	180.0	g kg^{-1}
Organic matter	8.5	g kg^{-1}
Available nitrogen	32.0	g kg^{-1}
Available phosphate	8.0	g kg^{-1}
Available potassium	73.11	g kg^{-1}
Carbonate minerals	201.2	g kg^{-1}
Bulk density	1.32	g cm^{-3}
CEC	33.0	$cmol_c$ kg^{-1}
Calcium (Ca++)	2.29	meq L^{-1}
Magnesium (Mg++)	2.53	meq L^{-1}
Potassium (K+)	0.93	meq L^{-1}
Sodium (Na+)	2.10	meq L^{-1}
Carbonate (CO3=)	Nil	meq L^{-1}
Bicarbonate (HCO3-)	0.90	meq L^{-1}
Chloride (Cl-)	2.49	meq L^{-1}
Sulfate (SO4=)	2.16	meq L^{-1}

Preparation of Glycyrrhiza glabra extraction

Glycyrrhiza glabra roots powder (3 and 6) g was soaked separately in one litter hot distilled water at 50 °C for 24 h in dark colure bottles with shaking continuously. The solution filtered through several layers of filter papers, to obtained two concentrations of the extraction 3 and 6 g L^{-1} and several drops of Twin20 were added as a spread material to reduce the surface tension. The plants were sprayed two times 45 and 60 days after planting date, after the sun seat in both years 2017 and 2018 (Lazim and Sulaiman, 2012).

Preparation of potassium fertilizer (KCl)

Two half five gram of potassium chloride (KCl) was dissolved in one liter hot distilled water at 40 °C with shaking the potassium completely dissolved and several drops of Twin20 were added as a spreading material to reduce the surface tension. The plants were sprayed at the morning trice 40, 55 and 70 days after planting in both years 2017 and 2018.

Addition of chemical fertilizer

Six hundred kilograms per hectare of Di-Ammonium Phosphate (DAP) 18:18:0 fertilizer was added in two times. The first was during the cultivation of the tubers (spares on the furrows) and the second addition was after one month from the first

http://www.aloki.hu ● ISSN 1589 1623 (Print) ● ISSN 1785 0037 (Online)
DOI: http://dx.doi.org/10.15666/aeer/1706_1478714804

addition as recommended for the chemical fertilizer treatment only (Esho et al., 2009), while half of the recommended were added for the rest of the treatments.

Field practices

Potato tubers (Acterice varieties) which produced by the Agro-plant's Company/Nederland, used in the study, each experimental unit (furrow) was 3 m long and 0.8 m apart (2.4 m^2), each furrow consists of 12 plants in one side. Planting dates were 10 March 2017 and 5 March 2018 at the first and the second season respectively, while the harvesting was accomplished after 100 days on 20 June 2017 and 15 June 2018 at the first and the second season respectively. The land was plowed perpendicularly at 30 cm depth by using moldboard plow then the soil was smoothed by disc harrow then leveled the all the divisions were made to furrow according to the experimental layout (*Fig. 2*). Each experimental units (furrows) within the blocks were divided into four groups, each group consists of four furrows the last one was one furrow, each group were conducted with a 10 cm diameter plastic pipes to feeding them with water from the mainstream. Watering timing from the mainstream to the furrows was calculated according to the field design for furrow irrigation system (*Fig. 3*).

The irrigation timing was computed until the water reached the standardized line in each furrow in order to measure the amount of water that entered each furrow through the plastic pipes in the irrigation intervals (5 and 10 days). The amount of water and its operation time were calculated to estimate the discharge of sub main irrigation pipe. Depending on the knowledge discharge, Furrow area, number of furrow, and operation times for irrigation, the depth of irrigation was calculated as well as it can be used to estimate the amount of irrigation (*Eq. 1*). In 2017, the depth and the amount of irrigation were 369 mm and 0.885 m^3 $furrow^{-1}$ respectively for **I_5**, while the values were 228 mm and 0.547 m^3 $furrow^{-1}$ respectively for **I_{10}**. In 2018, the values were 363 mm and 0.871 m^3 $furrow^{-1}$ respectively for **I_5**, and 287 mm and 0.668 m^3 $furrow^{-1}$ respectively for **I_{10}**.

$$Q\,t = n\,A\,d \qquad \text{(Eq.1)}$$

where: Qt: the amount of irrigation (L), Q: discharge of sub main (L s^{-1}), t: operation time (s), n: No. of the furrows, A: area of the furrow (2.4 m^2), d: depth of irrigation water (mm).

Statistical analysis

A factorial experiment was conducted in a split-plot design with three replicates; the first factor (Irrigation intervals) was implemented in the main plots and conducted with Randomized Complete Block Design (RCBD), while the second factor (Treatments) was implemented in the subplots. All possible comparisons among the means were carried out by using Least Significant Difference (L.S.D) test at a significant level of 5% after they show their significance in the general test (AL-Rawi and Khalafallah, 1980). The study included treatments as specified in *Table 3*.

Quantitative and qualitative yield characters

After tubers maturity harvested were performed manually (100 days from planting date), the yield was calculated (*Eq. 2*).

http://www.aloki.hu ● ISSN 1589 1623 (Print) ● ISSN 1785 0037 (Online)
DOI: http://dx.doi.org/10.15666/aeer/1706_1478714804

$$Total\ Yield\ (t\ ha^{-1}) = \frac{Yield\ of\ the\ Experimental\ Unit\ (t)}{Area\ of\ the\ Experimental\ Unit\ (m^2)} \times 10000\ m^2 \quad \text{(Eq.2)}$$

Total soluble solid (%)

Total soluble solids were measured by Refractometer (LCD DIGITAL BENCH MODEL). In order to measure T.S.S. (%), a drop of the tuber extract was placed on the prism of the digital Refractometer and the total soluble solids were read in Brix (A.O.A.C, 1986).

Tuber starch percentage (%)

The percentage of starch was estimated based on the dry weight of the tuber (A. O. A. C. 1970), according to *Equation 3*.

$$Tuber\ starch\ (\%) = 17.55 + 0.891(Tuber\ dry\ matter\ percentage - 24.18) \quad \text{(Eq.3)}$$

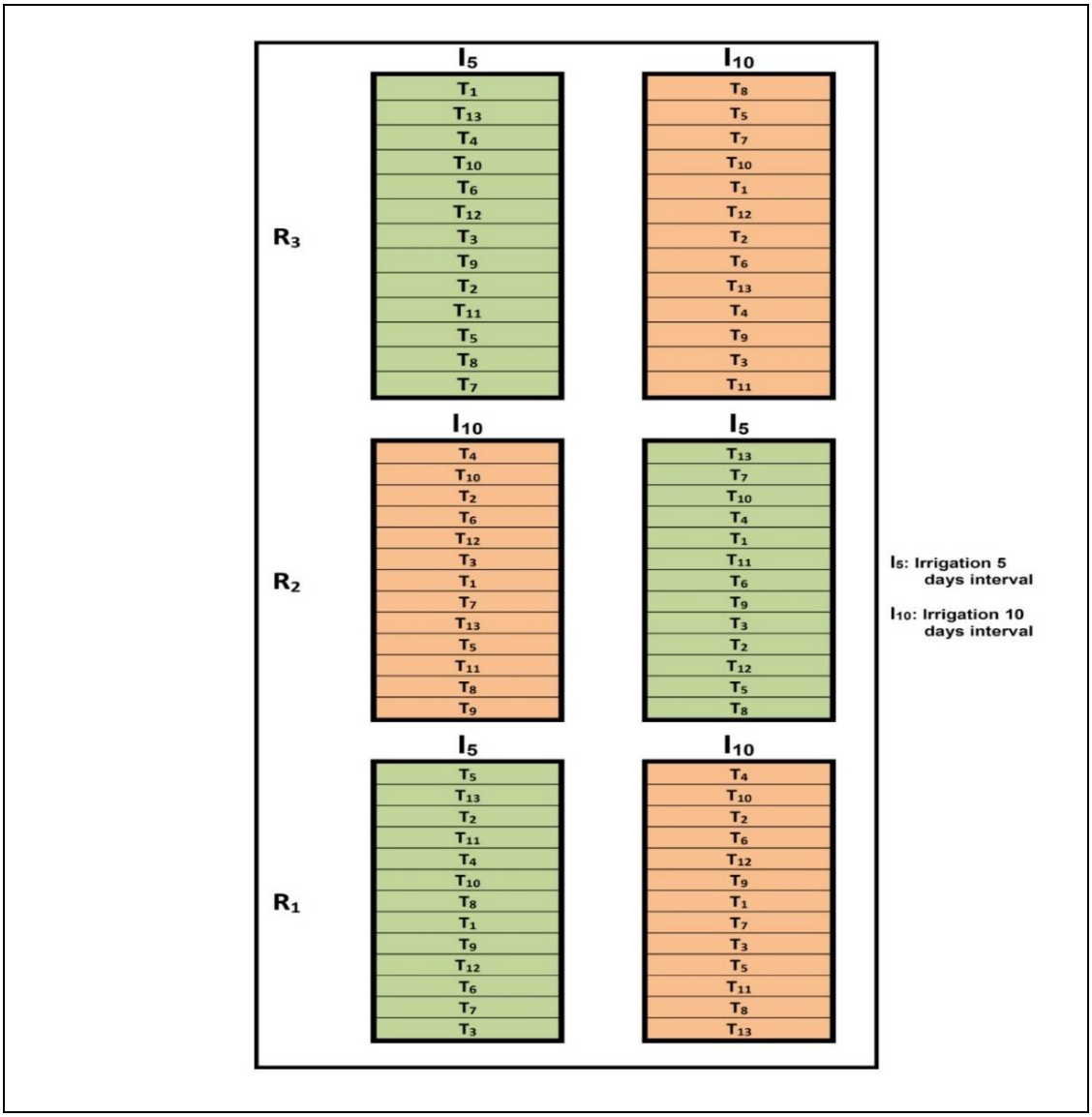

Figure 2. *The experimental layout*

http://www.aloki.hu ● ISSN 1589 1623 (Print) ● ISSN 1785 0037 (Online)
DOI: http://dx.doi.org/10.15666/aeer/1706_1478714804

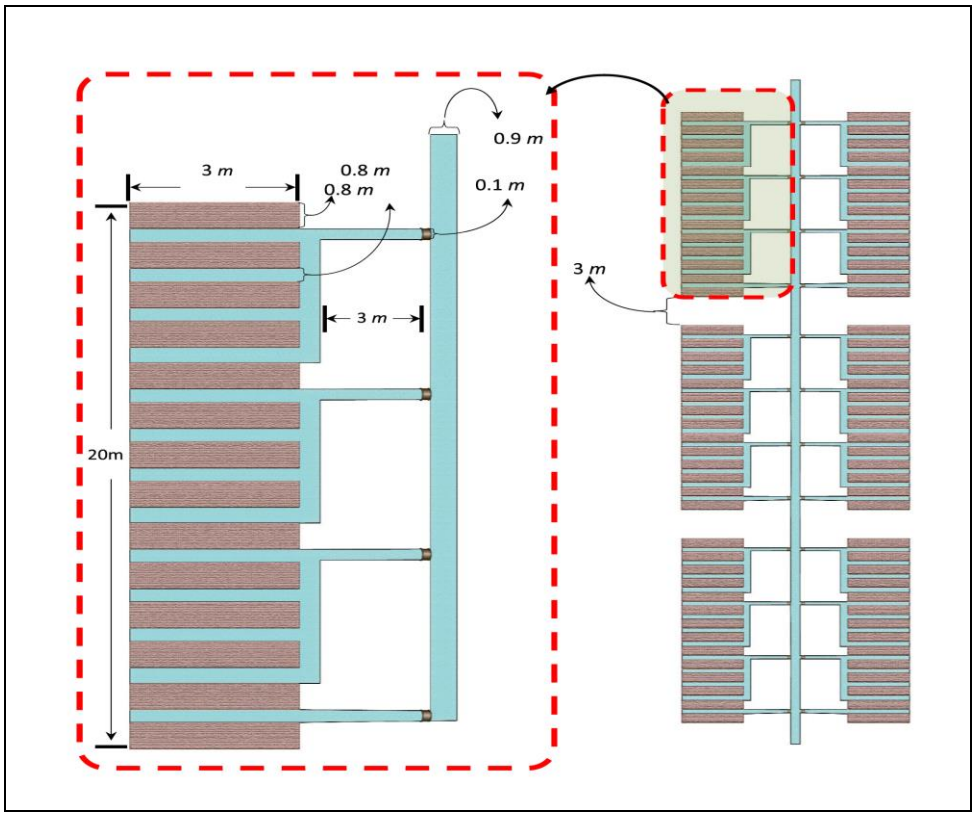

Figure 3. *The field design for furrow irrigation system*

Table 3. *The experimental factors used in the study*

No.	Factors	Levels	Descriptions
First	Irrigation intervals	**I_5**	5 days
		I_{10}	10 days
Second	Treatments	**T_1**	Control (spray with distilled water)
		T_2	Di-Ammonium phosphate (DAP)
		T_3	Mycorrhizal inoculation
		T_4	Spraying with (2.5 g L^{-1}) KCl
		T_5	Spraying with (3 g L^{-1}) *Glycyrrhiza glabra* extract
		T_6	Spraying with (6 g L^{-1}) *Glycyrrhiza glabra* extract
		T_7	Mycorrhizal Inoculation + spraying with (2.5 g L^{-1}) KCl
		T_8	Mycorrhizal Inoculation + spraying with (3 g L^{-1}) *Glycyrrhiza glabra* extract
		T_9	Mycorrhizal Inoculation + spraying with (6 g L^{-1}) *Glycyrrhiza glabra* extract
		T_{10}	Spraying with (2.5 g L^{-1}) KCl + spraying with (3 g L^{-1}) *Glycyrrhiza glabra* extract
		T_{11}	Spraying with (2.5 g L^{-1}) KCl + spraying with (6 g L^{-1}) *Glycyrrhiza glabra* extract
		T_{12}	Mycorrhizal Inoculation + spraying with (2.5 g L^{-1}) KCl + spraying with (3 g L^{-1}) *Glycyrrhiza glabra* extract
		T_{13}	Mycorrhizal Inoculation + spraying with (2.5 g L^{-1}) KCl + spraying with (6 g L^{-1}) *Glycyrrhiza glabra* extract

http://www.aloki.hu ● ISSN 1589 1623 (Print) ● ISSN 1785 0037 (Online)
DOI: http://dx.doi.org/10.15666/aeer/1706_1478714804

Analysis and estimation of some amino acids in potato tubers

Amino acids in tubers were estimated and analyzed using High-Performance Liquid Chromatography (YL9100 HPLC System, Model: YL9101 Vacuum Degasser, S/N: D2714120911, YL: instrument CO. LTD, made in Korea) device in potato tubers. Five grams from the tubers mixed with the methanol and water in 10:40 ratio respectively. The mixture was filtered using fine Tapestry cloth, then the precipitated leach was stored in a sterile bottle (-20 °C) (Itakura et al., 2001). It is worth to mention that the Orethophthalheide derivative (OPA) was prepared according to (Graser et al., 1985). Approximately 5 mg of the sample was weighed into a 10 ml headspace glass vial with crimp cap and 3 ml hydrochloric acid (6 M with 0.1% w/v phenol) was added. The vial was sealed and placed in a preheated oven at 110 °C for 24 h. After hydrolysis, the samples were allowed to cool to handling temperature then neutralized with 3 ml sodium hydroxide (6 M) mixed thoroughly and left to cool to handling temperature. After cooling, an aliquot was filtered through a 0.45 µm, 13 mm diameter nylon filter (*Figs. 4* and *5*).

Mobile phase = acetonitrile: buffer (30: 70), Flow = 1 ml min^{-1}
Injection: injection program, including derivatization steps with OPA
Injected volume = 100 uL
Column = ZORBAX Eclipse-AAA; 3.5 µm; L × i.d. = 150 × 4.6 mm
Detector: fluorescence (Ex = 360 nm, Em = 450 nm)

Results

Table 4 shows the effects of irrigation intervals on yield quantitative and qualitative characters. The irrigation intervals were significant effects on total yield, total soluble solid (T.S.S%) in the tuber and all amino acids in the tuber with an exception for Lucien in the first season 2017. The **I_5** gave the highest values of total yield and T.S.S% in the tubers with 40.418 t ha^{-1} and 9.536%, while the **I_{10}** gave the minimum values of total yield and T.S.S% in the tuber with 32.205 t ha^{-1} and 5.872%, but the **I_{10}** gave the highest values for Proline, Glycine, and Lysine with 2.707, 2.681 and 2.861 mg g^{-1} respectively, and the **I_5** gave the lowest values with 2.060, 2.091, and 1.882 mg g^{-1} respectively.

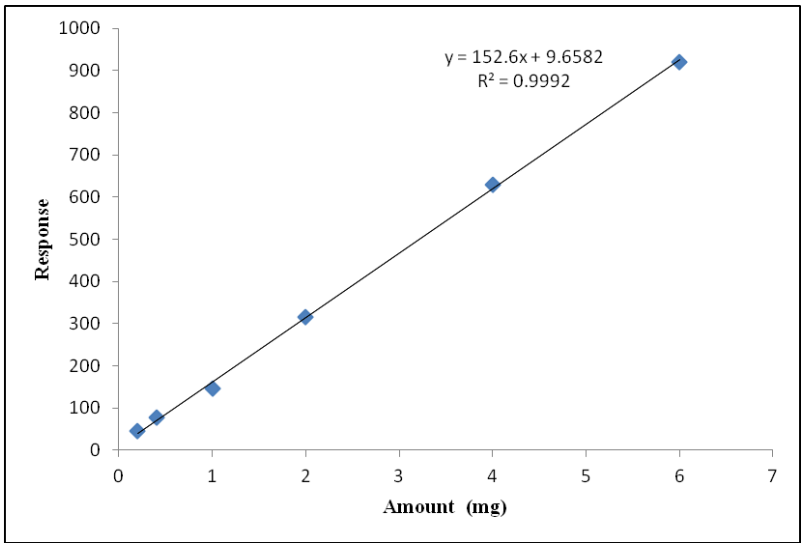

Figure 4. *Calibration standard curve of amino acids*

http://www.aloki.hu ● ISSN 1589 1623 (Print) ● ISSN 1785 0037 (Online)
DOI: http://dx.doi.org/10.15666/aeer/1706_1478714804

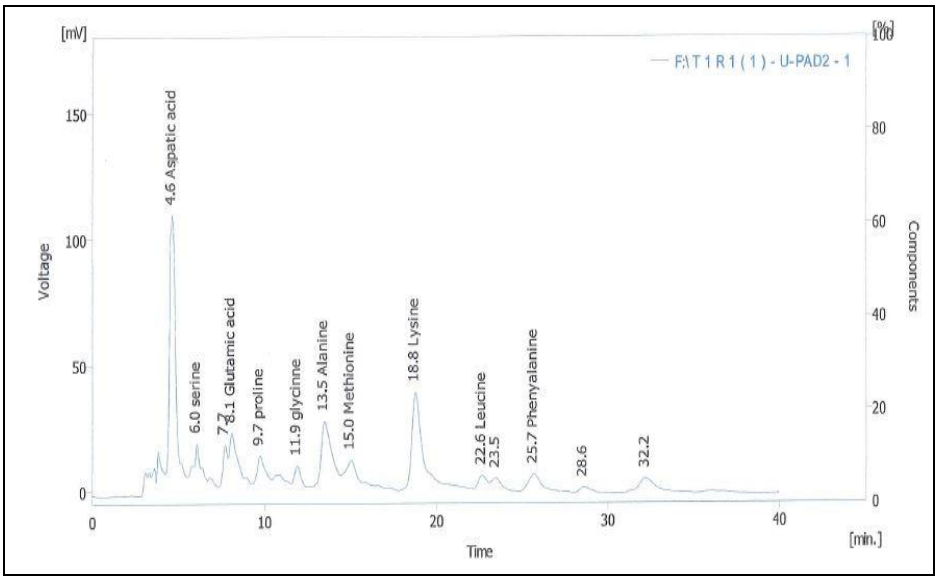

Figure 5. *An example of HPLC chromatogram of amino acid profile in potato tubers*

Table 4. *Effect of irrigation intervals on yield quantitative and qualitative characters at both growing seasons 2017 and 2018*

Irrigation interval (A)	Total yield (t ha^{-1})	T.S.S (%)	Starch (%)	Proline	Glycine	Lucien	Lysine
First season 2017							
I_5	40.418 a	9.536 a	21.392 a	2.060 b	2.091 b	2.659 a	1.882 b
I_{10}	32.205 b	5.872 b	23.570 a	2.707 a	2.681 a	2.778 a	2.861 a
L.S.D $_{(p \leq 0.05)}$	**2.012**	**2.856**	**n.s**	**0.202**	**0.209**	**n.s**	**0.220**
Second season 2018							
I_5	42.886 a	8.479 a	21.751 a	2.091 b	1.991 b	2.656 a	1.942 b
I_{10}	31.431 b	6.954 a	22.281 a	2.681 a	2.988 a	2.816 a	2.951 a
L.S.D $_{(p \leq 0.05)}$	**4.117**	**n.s**	**n.s**	**0.209**	**0.311**	**n.s**	**0.191**

Concerning the second season 2018, the irrigation intervals had a significant effect on total yield, Proline, Glycine, and Lysine character. The **I_5** gave the highest values for total yield with 42.886 t ha^{-1}, while the lowest values gave by **I_{10}** with 31.431 t ha^{-1}. The **I_{10}** achieved the highest values for Proline, Glycine, and Lysine with 2.681, 2.988, and 2.951 mg g^{-1} respectively. The lowest values achieved by **I_5** with 2.091, 1.991 and 1.942 mg g^{-1} respectively.

Table 5A illustrates the effects of treatments on yield quantitative and qualitative characters in the first season 2017; data shows the treatments were significant effect for all characters with the exception of starch% in the tuber. The highest values of total yield gave by **T_3** with 44.912 t ha^{-1}. The minimum values obtained by **T_1** with 25.984 t ha^{-1}**.** And the maximum values of T.S.S% in the tube achieved in **T_4** with 8.925%. The minimum values of T.S.S% in tuber were achieved in **T_{10}** with 6.592%. The highest values of Proline, Glycine, Lucien, and Lysine in the tuber gave by **T_9** with 5.906, 5.823, 6.104 and 6.143 mg g^{-1} respectively. The minimum values were recorded by **T_1** with 0.241, 0.211, 0.293 and 0.126 mg g^{-1} respectively.

http://www.aloki.hu ● ISSN 1589 1623 (Print) ● ISSN 1785 0037 (Online)
DOI: http://dx.doi.org/10.15666/aeer/1706_1478714804

Table 5A. *Effect of the treatments on yield quantitative and qualitative characters in the first season 2017*

T_i	Total yield (t ha^{-1})	T.S.S (%)	Starch (%)	Proline	Glycine	Lucien	Lysine
T_1	25.984 d	7.017 d	23.178 a	0.241 j	0.211 h	0.293 h	0.126 h
T_2	38.984 b	7.875 bc	23.101 a	0.506 hi	0.360 gh	0.462 gh	0.267 h
T_3	44.912 a	8.292 ab	22.359 a	0.559 gh	0.546 gh	0.536 gh	0.408 h
T_4	37.634 b	8.925 ab	20.402 a	0.289 ij	0.286 h	0.414 gh	0.165 h
T_5	31.654 cd	8.658 ab	25.498 a	2.774 e	2.629 e	3.727 d	3.027 e
T_6	37.812 b	7.075 d	23.404 a	3.257 d	3.426 d	4.397 c	3.672 d
T_7	39.331 ab	6.908 d	22.407 a	0.747 g	0.811 g	0.896 g	0.720 g
T_8	36.033 bc	7.225 cd	22.426 a	4.044 c	4.269 c	5.596 b	5.087 b
T_9	33.924 bc	7.892 bc	23.131 a	5.906 a	5.823 a	6.104 a	6.143 a
T_{10}	36.347 bc	6.592 d	23.135 a	1.667 f	1.553 f	1.419 f	1.358 f
T_{11}	36.856 bc	6.992 d	20.470 a	2.279 e	2.184 e	2.256 e	1.620 f
T_{12}	36.293 bc	8.408 ab	21.253 a	4.050 c	4.107 c	3.834 d	3.667 d
T_{13}	36.284 bc	8.292 ab	21.484 a	4.665 b	4.814 b	5.406 b	4.567 c
LSD ($p \leq 0.05$)	**5.940**	**0.799**	**n.s**	**0.225**	**0.453**	**0.496**	**0.305**

Table 5A illustrates the effects of treatments on yield quantitative and qualitative characters in the first season 2017; data shows the treatments were significant effect for all characters with the exception of starch% in the tuber. The highest values of total yield gave by **T_3** with 44.912 t ha^{-1}. The minimum values obtained by **T_1** with 25.984 t ha^{-1}**.** And the maximum values of T.S.S% in the tube achieved in **T_4** with 8.925%. The minimum values of T.S.S% in tuber were achieved in **T_{10}** with 6.592%. The highest values of Proline, Glycine, Lucien, and Lysine in the tuber gave by **T_9** with 5.906, 5.823, 6.104 and 6.143 mg g^{-1} respectively. The minimum values were recorded by **T_1** with 0.241, 0.211, 0.293 and 0.126 mg g^{-1} respectively.

Table 5B shows the effect of the treatments on yield quantitative and qualitative characters in the second season 2018, the statistical analysis reveals a significant difference for all of the characters. The highest values of total yield gave by **T_{11}** with 42.106 t/ha. The minimum values obtained by **T_1** with 29.678 t ha^{-1}**.** And the maximum values for T.S.S% were given by **T_4** with 9.083%. The minimum values were given by **T_5** with 6.450%. Regarding the starch% in the tuber, the **T_1** gave the highest values with 26.948%. The lowest values obtained by treatments **T_{13}** with 18.222%. The maximum values of Proline, Lucien and Lysine were obtained by **T_9** with 5.823, 4.971 and 6.096 mg g^{-1} respectively. Whereas the maximum values for Glycine were recorded by **T_8** with 5.596 mg g^{-1}. The minimum values were recorded by **T_1** with 0.211, 0.222, 0.289 and 0.106 mg g^{-1} for Proline, Glycine, Lucien, and Lysine respectively.

Table 6A shows the interaction effects of irrigation intervals and treatments on yield quantitative and qualitative characters at the first season 2017, the statistical analysis reveals significant difference for T.S.S% and amino acid in the tubers (Proline, Glycine, Lucien, and Lysine). The highest values for T.S.S% was obtained in the interaction of **I_5** × **T_{13}** with 11.200%. The lowest values obtained in interaction **I_{10}** × **T_8** with 4.250%, and the highest values of Proline, Glycine, and Lysine gave by interaction **I_{10}** × **T_{13}** with 6.724, 6.912 and 7.525 mg g^{-1} respectively. But the

http://www.aloki.hu ● ISSN 1589 1623 (Print) ● ISSN 1785 0037 (Online)
DOI: http://dx.doi.org/10.15666/aeer/1706_1478714804

maximum values of Lucien recorded by **I_5 × T_9** with 6.148 mg g^{-1}. The minimum values were recorded by **I_5 × T_1** with 0.143, 0.126, 0.284 and 0.080 mg g^{-1} respectively for Proline, Glycine, Lucien, and Lysine.

Table 5B. *Effect of the treatments on yield quantitative and qualitative characters in the second season 2018*

T_i	Total yield (t ha^{-1})	T.S.S (%)	Starch (%)	Proline	Glycine	Lucien	Lysine
T_1	29.678 e	7.217 cd	26.948 a	0.211 h	0.222 h	0.289 h	0.106 h
T_2	39.809 abc	7.983 bc	23.174 b	0.360 gh	0.371 h	0.477 h	0.290 h
T_3	41.453 ab	8.500 ab	23.725 ab	0.546 gh	0.528 h	0.599 gh	0.385 h
T_4	33.424 cde	9.083 a	21.741 b	0.286 h	0.284 h	0.373 h	0.176 h
T_5	34.799 b-e	6.450 d	21.621 bc	2.629 e	3.317 d	3.759 d	2.855 e
T_6	38.924 a-d	7.833 bc	22.256 b	3.426 d	3.601 d	4.375 c	3.652 d
T_7	41.351 ab	7.367 cd	20.429 bc	0.811 g	0.876 g	0.966 fg	0.865 g
T_8	34.564 b-e	7.367 cd	21.045 bc	4.269 c	5.596 a	5.757 ab	5.458 b
T_9	32.142 de	7.567 bc	22.638 b	5.823 a	5.448 a	6.021 a	6.096 a
T_{10}	40.014 abc	7.850 bc	21.807 b	1.553 f	1.388 f	1.442 f	1.244 g
T_{11}	42.106 a	7.700 bc	21.904 b	2.184 e	2.047 e	2.291 e	1.844 f
T_{12}	36.089 a-e	7.650 bc	20.699 bc	4.107 c	4.079 c	3.842 d	3.916 d
T_{13}	38.709 a-d	7.750 bc	18.222 c	4.814 b	4.604 b	5.376 b	4.918 c
LSD $_{(p \leq 0.05)}$	**7.318**	**0.961**	**3.474**	**0.453**	**0.435**	**0.486**	**0.450**

Data in *Table 6B* illustrates the interaction effects of irrigation intervals and treatments on yield quantitative and qualitative characters at the second season 2018, the interaction had the significant effect on T.S.S, starch and amino acid in the tuber. The highest values of T.S.S were obtained by interaction **I_5 × T_4** with 10.767%. But the lowest values obtained by interaction I_{10} × with 6.167%. Regarding on percentage of starch in the tuber, the highest values were achieved by **I_5 × T_1** with 28.226%, the minimum values achieved by **I_{10} × T_{13}** with 15.964%. The highest values gave by interaction **I_{10} × T_9** Proline, and Lysine with 6.912 and 7.290 mg g^{-1} respectively. And the maximum values for Glycine recorded by interaction with **I_{10} × T_8** with 7.181 mg g^{-1}. The maximum values of Lucien gave by interaction **I_5 × T_9** with 6.094 mg g^{-1}, while the minimum values for all amino acid with exception Glycine were recorded by interaction **I_5 × T_1** with 0.126, 0.252 and 0.079 mg g^{-1} respectively. But the minimum values of Glycine gave by interaction **I_{10} × T_1** with 0.198 mg g^{-1}.

Table 7 shows the effect of seasons on yield quantitative and qualitative characters. The season had no significant effects on yield qualitative characters.

Discussion

Water is one of the most essential elements in growing plants, which constitutes more than 80% of the active cells. Thereby, the amount of applied water during crop irrigation, added time, irrigation methods, quality of added water, and prevailing micro-meteorological conditions have found to play limited roles in yield quality and quantity. In Asia, statistics showed that the yields for most crops have increased 100–400% after

http://www.aloki.hu ● ISSN 1589 1623 (Print) ● ISSN 1785 0037 (Online)
DOI: http://dx.doi.org/10.15666/aeer/1706_1478714804

irrigation. In the first season of irrigation intervals (5 and 10 days) were applied after 50 days from sowing and were ended at 96 days after sowing, since, the amount of irrigation water for 5 days interval was cover the most of depleted water at this time. The cumulative depth of irrigation for 5 and 10 days from (10 May 2017 to 15 June 2017) were practically measured and formed to be (369 and 228 mm) respectively. Since the numbers of irrigation were 10 and 6 times for 5 and 10 days of irrigation intervals respectively, while the amount of actual evapotranspiration for 2017 and 2018 was (529, 423, 515 and 440 mm) respectively, while the cumulate depth of irrigation and precipitation were (535 and 394 mm) respectively.

Table 6A. *Interaction effects of irrigation intervals and treatments on yield quantitative and qualitative characters in the first season 2017*

$I_i \times T_i$ (A×B)	Total yield (t ha^{-1})	T.S.S (%)	Starch (%)	Proline	Glycine	Lucien	Lysine
$I_5 \times T_1$	28.472 a	8.033 fg	23.013 a	0.143 n	0.126 n	0.284 l	0.080 n
$I_5 \times T_2$	44.353 a	9.233 cde	23.473 a	0.228 n	0.186 n	0.388 kl	0.226 mn
$I_5 \times T_3$	52.324 a	10.000 bcd	20.229 a	0.382 mn	0.394 mn	0.502 jkl	0.452 mn
$I_5 \times T_4$	42.859 a	10.500 ab	19.357 a	0.151 n	0.159 n	0.310 l	0.126 mn
$I_5 \times T_5$	33.840 a	9.800 bcd	23.569 a	2.400 h	2.298 ij	3.844 e	2.317 g
$I_5 \times T_6$	43.307 a	9.700 bcd	23.147 a	3.306 f	3.530 fg	4.696 cd	3.476 f
$I_5 \times T_7$	43.763 a	9.000 def	19.040 a	0.592 klm	0.624 mn	0.774 jkl	0.528 lm
$I_5 \times T_8$	38.931 a	10.200 abc	21.967 a	4.114 d	4.334 cde	5.670 a	4.072 e
$I_5 \times T_9$	37.284 a	11.200 a	19.135 a	5.088 bc	4.734 cd	6.184 a	4.762 d
$I_5 \times T_{10}$	38.657 a	8.467 efg	22.443 a	1.837 i	1.772 jk	1.108 ij	0.930 jk
$I_5 \times T_{11}$	45.077 a	8.900 def	21.206 a	1.766 ij	1.869 ijk	1.814 h	1.358 ij
$I_5 \times T_{12}$	39.642 a	9.067 def	20.862 a	3.118 f	3.274 fg	3.104 fg	2.502 g
$I_5 \times T_{13}$	36.923 a	9.867 bcd	20.651 a	3.656 e	3.886 ef	5.894 a	3.632 f
$I_{10} \times T_1$	23.496 a	6.000 jk	23.344 a	0.338 mn	0.296 n	0.302 l	0.172 mn
$I_{10} \times T_2$	33.615 a	6.517 ij	22.730 a	0.784 k	0.534 mn	0.536 jkl	0.308 mn
$I_{10} \times T_3$	37.500 a	6.583 ij	24.489 a	0.736 kl	0.698 lmn	0.570 jkl	0.364 mn
$I_{10} \times T_4$	32.410 a	7.350 ghi	21.447 a	0.428 lmn	0.412 mn	0.518 jkl	0.204 mn
$I_{10} \times T_5$	29.467 a	7.517 ghi	27.426 a	3.147 f	2.960 gh	3.610 ef	3.738 ef
$I_{10} \times T_6$	32.318 a	4.450 l	23.661 a	3.208 f	3.322 fg	4.099 de	3.868 ef
$I_{10} \times T_7$	34.900 a	4.817 l	25.774 a	0.902 k	0.998 lm	1.018 jk	0.912 kl
$I_{10} \times T_8$	33.134 a	4.250 l	22.885 a	3.974 d	4.204 de	5.521 ab	6.102 b
$I_{10} \times T_9$	30.564 a	4.583 l	27.128 a	6.724 a	6.912 a	6.024 a	7.525 a
$I_{10} \times T_{10}$	34.037 a	4.717 l	23.827 a	1.498 j	1.334 kl	1.730 hi	1.786 hi
$I_{10} \times T_{11}$	28.635 a	5.083 kl	19.734 a	2.792 g	2.498 hi	2.698 g	1.882 h
$I_{10} \times T_{12}$	32.943 a	7.750 gh	21.645 a	4.981 c	4.940 c	4.564 cd	4.832 d
$I_{10} \times T_{13}$	35.646 a	6.717 hij	22.318 a	5.674 b	5.742 b	4.918 bc	5.502 c
L.S.D ($p \leq 0.05$)	**n.s**	**1.130**	**n.s**	**0.318**	**0.641**	**0.701**	**0.431**

In the season 2018 the irrigation intervals (5 and 10 days) was applied from the sowing date and were ended at 95 days after sowing, the amount of irrigation water for 5 days interval which cover the most of depleted from (5 March 2018 to 10 June 2018) were practically measured (363 and 287 mm) respectively. Since the numbers of

http://www.aloki.hu ● ISSN 1589 1623 (Print) ● ISSN 1785 0037 (Online)
DOI: http://dx.doi.org/10.15666/aeer/1706_1478714804

irrigation were 9 and 5 times for 5 and 10 days of irrigation intervals respectively, while accumulate depth irrigation and precipitation were (513 and 437 mm) respectively. These results are in agreement with the findings of several other kinds of research (Ati et al., 2013; Ati and Nafaou, 2012). Gander and Tanner (1976) showed that mild water stress of -3 to -5 bars greatly reduce leaf expansion in potatoes, and for best tuber yields, a 120-150 day potato crop requires 508-698.5 mm of the water.

Table 6B. *Interaction effects of irrigation intervals and treatments on yield quantitative and qualitative characters in the second season 2018*

$I_i \times T_i$ (A×B)	Total yield (t ha^{-1})	T.S.S (%)	Starch (%)	Proline	Glycine	Lucien	Lysine
$I_5 \times T_1$	30.886 a	8.267 bcd	28.226 a	0.126 n	0.246 ij	0.252 j	0.079 m
$I_5 \times T_2$	41.377 a	9.167 bc	22.812 b-f	0.186 n	0.365 hij	0.373 j	0.188 m
$I_5 \times T_3$	50.598 a	9.167 bc	22.569 b-f	0.394 mn	0.614 hij	0.526 ij	0.349 lm
$I_5 \times T_4$	38.109 a	10.767 a	19.088 fgh	0.159 n	0.282 ij	0.280 j	0.100 m
$I_5 \times T_5$	37.928 a	6.067 g	17.412 gh	2.298 ij	2.683 de	3.788 e	2.218 gh
$I_5 \times T_6$	46.156 a	9.200 b	20.216 d-h	3.530 fg	2.990 de	4.926 cd	3.578 f
$I_5 \times T_7$	51.678 a	8.233 bcd	20.172 d-h	0.624 mn	0.854 ghi	0.818 hij	0.572 klm
$I_5 \times T_8$	38.385 a	7.933 b-e	22.530 b-f	4.334 cde	4.012 c	5.952 a	4.358 de
$I_5 \times T_9$	35.996 a	8.133 b-e	22.691 b-f	4.734 cd	4.122 c	6.094 a	4.902 cd
$I_5 \times T_{10}$	48.668 a	8.833 bc	22.547 b-f	1.772 jk	1.315 fg	1.276 gh	0.898 jkl
$I_5 \times T_{11}$	48.619 a	8.933 bc	23.130 b-f	1.869 ijk	1.683 f	1.663 g	1.469 ij
$I_5 \times T_{12}$	40.223 a	7.400 d-g	20.890 c-g	3.274 fg	3.032 d	2.954 f	2.658 g
$I_5 \times T_{13}$	48.900 a	8.133 b-e	20.481 d-h	3.886 ef	3.682 c	5.624 ab	3.876 ef
$I_{10} \times T_1$	28.470 a	6.167 g	25.671 abc	0.296 n	0.198 j	0.326 j	0.134 m
$I_{10} \times T_2$	38.241 a	6.800 efg	23.536 a-f	0.534 mn	0.376 hij	0.582 ij	0.392 lm
$I_{10} \times T_3$	32.309 a	7.833 c-f	24.881 a-d	0.698 lmn	0.442 hij	0.672 hij	0.422 klm
$I_{10} \times T_4$	28.739 a	7.400 d-g	24.394 a-e	0.412 mn	0.286 hij	0.466 ij	0.252 m
$I_{10} \times T_5$	31.669 a	6.833 efg	25.830 ab	2.960 gh	3.952 c	3.730 e	3.492 f
$I_{10} \times T_6$	31.692 a	6.467 g	24.296 a-e	3.322 fg	4.212 c	3.824 e	3.726 ef
$I_{10} \times T_7$	31.024 a	6.500 fg	20.686 d-h	0.998 lm	0.898 gh	1.114 ghi	1.158 ijk
$I_{10} \times T_8$	30.742 a	6.800 efg	19.559 e-h	4.204 de	7.181 a	5.562 abc	6.558 b
$I_{10} \times T_9$	28.288 a	7.000 d-g	22.585 b-f	6.912 a	6.774 a	5.948 a	7.290 a
$I_{10} \times T_{10}$	31.360 a	6.867 efg	21.066 b-g	1.334 kl	1.462 fg	1.608 g	1.590 hi
$I_{10} \times T_{11}$	35.594 a	6.467 g	20.678 d-h	2.498 hi	2.412 e	2.920 f	2.218 gh
$I_{10} \times T_{12}$	31.955 a	7.900 b-e	20.508 d-h	4.940 c	5.126 b	4.730 d	5.174 c
$I_{10} \times T_{13}$	28.518 a	7.367d-g	15.964 h	5.742 b	5.526 b	5.128 bcd	5.960 b
L.S.D$_{(p \le 0.05)}$	**n.s**	**1.360**	**4.913**	**0.641**	**0.615**	**0.688**	**0.637**

Table 7. *The effect of seasons on yield quantitative and qualitative characters*

Seasons	Total yield (t ha^{-1})	T.S.S (%)	Starch (%)	Proline	Glycine	Lucien	Lysine
First season 2017	36.311 a	7.704 a	22.481 a	2.383 a	2.386 a	2.718 a	2.371 a
Second season 2018	37.159 a	7.717 a	22.016 a	2.386 a	2.489 a	2.736 a	2.447 a
L.S.D$_{(p \le 0.05)}$	**n.s**	**n.s**	**n.s**	**n.s**	**n.s**	**n.s**	**n.s**

http://www.aloki.hu ● ISSN 1589 1623 (Print) ● ISSN 1785 0037 (Online)
DOI: http://dx.doi.org/10.15666/aeer/1706_1478714804

The treatment of mycorrhizae inoculation gave the highest values for water use efficiency; this may be due to its high ability to produce the glomalin compound, which binds the soil minutes to each other and to the aggregation of aggregates. as well as the mycelium hypha played a major role by increasing the soil mass and stability (Fokom et al., 2012) indicates that there are positive correlations of correlations between organic matter and chlorine associated with Glomalin Related Soil Protein (GRSP). Peng et al. (2013) recorded that the fertilized soil with mycorrhizae increases the stability of its aggregates as a result of the action of the mycorrhizae hypha and the result of its production of glomalin, a watery and insoluble molybdenum protein compound that contributes to the formation and increase stability of the soil complexes where it is released to them and reduce their hydration because it is a glue-absorbing composite. (Martin et al., 2012 and Wu et al., 2013) reported that organic matter also plays an important role in improving the properties of physical, chemical and biological soil. The Glycyrrhiza glabra extract contains various elements such as calcium, iron, silicon, aluminum, magnesium, sulfur, potassium, zinc, and phosphorus, which play an important role in growth (Vispute and Khopade, 2011). Licorice extract also contains mevalonic acid, which enters the synthesis of gibberellins (Moses et al., 2002). AL-Hamdani and AL-Zuhairy (2017) nitrogen enter the formation of chlorophyll as well as the formation of amino acids in the formation of Chloroplast, which increases the leaves content of chlorophyll. Myint et al. (2010) showed that chlorophyll was directly related to the plant content of nitrogen.

Potassium is also associated with many other important phylogenetic functions, including activation of enzymes, regulation of opening and closing of stents, as well as its important role in the synthesis of ATP, where the electrostatic charge in the ATP production sites is closely related to the K^+ (Prajapati and Modi, 2012) and sugars (Van Brunt and Sultenfnss, 1998), water and nutrient transport (Thomas and Thomas, 2009) and protein synthesis and starch (Patil, 2011).

The combination of the licorice extract and the inoculation of the mycorrhizae on the composition of amino acids, especially in the case of a lack of irrigation or dehydration, and the interference of the element nitrogen and potassium religions reduce the presence of amino acids in potato tubers.

Conclusion and recommendation

The 5 days irrigation interval had highly effect on the total yield, while 10 days irrigation period had a significant effect on the tuber hardness, and most of the amino acid content in the tubers. The treatments were significantly affected on all of the studied characters with the exception of starch% in the tubers. The interaction of the 10 days irrigation interval with both of the Mycorrhizal inoculation and Spraying with (2.5 g L^{-1}) KCl + Spraying with (6 g L^{-1}) *Glycyrrhiza glabra* extract recorded significant effects on total soluble solid percentage, tuber hardness and all of the amino acid in the tuber.

Carrying out more investigation on different irrigation intervals as well as more biotic and abiotic treatments to determine their effect on the quantitative and qualitative traits in in different locations and for different years in Sulaimani region to generalize the results and to ensure the potato yield stability. Reduce the use of chemical fertilizers and replace them by increasing the use of different plant extracts at different concentrations according to the recommendations of specialists in that field. The use of

http://www.aloki.hu ● ISSN 1589 1623 (Print) ● ISSN 1785 0037 (Online)
DOI: http://dx.doi.org/10.15666/aeer/1706_1478714804

fungal, bacterial, bio inoculators, and transpiration compounds and potassium salts on potato is recommended to increase the resistance to abiotic stress.

REFERENCES

[1] Al-Alousi, S. A (2013): Effect of adding potassium to soil, spraying and spraying with organic extract in potato growth and yield. – Kufa Journal of Agricultural Sciences 5(1): 120-135.

[2] Alavijeh, M. K., Yaghmaei, S. (2016): Biochemical production of bioenergy from agricultural crops and residue in Iran. – Waste Management 52: 375-394.

[3] Al-Hamdani, S. A., Al-Zuhairy, H. T. H. (2017): Effect of organic, chemical fertilizers and plant density on 2-some growth and yield characteristics of cauliflower *Brassica oleracea* var. botrytis. – Diyala Agricultural Sciences Journal 9 (2): 104-114.

[4] Al-Rawi, K. M., and Khalaf-Allah, A. M. (1980): Design and analysis of agricultural experiments. – El Mousel Univ. Iraq 19: 487.

[5] A.O.A.C. (1970): Official Methods of Analysis. 11th ed. – Association of Official Analytical Chemistry 101, Washington, DC.

[6] A.O.A.C. (1986): Association of Official Agricultural Chemists. Official and Tentative Methods of Analysis. 13th Ed. – Association of Official Agricultural Chemists, Washington, DC.

[7] Asmaa, R. M., Magda, M. H. (2010): Increasing productivity of potato plants (*Solanum tuberosum* L.) By using potassium fertilizer and humic acid application. – International Journal of Academic research (2): 83-88.

[8] Ati, A., Nafaou, S. M. (2012): Effect of potassium fertilization on growth, yield and water use efficiency of irrigated potato. – MISR Journal Agricultural Engineering 29(2): 735-744.

[9] Ati, A., Al-Sahaf, F., Wally, D., Thamer, T. (2013): Effects of potassium humate fertilizers and irrigation rate on potato yield and consumptive use under drip irrigation method. – Journal of Agricultural Science and Technology (3): 803-810.

[10] Basu, P. S., Sharma, A., Garg, I. D., Sukumaran, N. P. (1999): Tuber sink modifies the photosynthetic response in potato under water stress. – Environmental and Experimental Botany (42): 25-39.

[11] Birhane, E., Sterck, F. J., Fetene, M., Bongers, F., Kuyper, T. W. (2012): Arbuscular mycorrhizal fungi enhance photosynthesis, water use efficiency, and growth of frankincense seedlings under pulsed water availability conditions. – Oecologia 169(4): 895-904.

[12] Caverzan, A., Passaia, G., Rosa, S. B., Ribeiro, C. W., Lazzarotto, F., Margis-Pinheiro, M. (2012): Plant responses to stresses: the role of ascorbate peroxidase in antioxidant protection. – Genetics and Molecular Biology 35(4): 1011-1019.

[13] Central Statistical Organization (2016). Ministry of Planning, Republic of Iraq.

[14] Chakraborty, S., Chakraborty, N., Agrawal, L., Ghosh, S., Narula, K., Shekhar, S., Datta, A. (2010): Next-generation protein-rich potato expressing the seed protein gene AmA1 is a result of proteome rebalancing in the transgenic tuber. – Proceedings of the National Academy of Sciences 107(41): 17533-17538.

[15] Duc, N. H., Mayer, Z., Pék, Z., Helyes, L., Posta, K. (2017): Combined inoculation of arbuscular mycorrhizal fungi, Pseudomonas fluorescens, and Trichoderma spp. for enhancing defense enzymes and yield of three pepper cultivars. – Applied Ecology and Environmental Research 15(3): 1815-1829.

[16] El Sagan, M. A. M. (2015): Effect of some natural extracts on the growth and productivity of cucumber under sandy soil conditions. – Int. J. Adv. Res. 3(9): 677-686.

http://www.aloki.hu ● ISSN 1589 1623 (Print) ● ISSN 1785 0037 (Online)
DOI: http://dx.doi.org/10.15666/aeer/1706_1478714804

[17] Esho, T., Enzlin, P., Van Wolputte, S., Temmerman, M. (2010): Female genital cutting and sexual functioning. In search of an alternate theoretical model. – African Identities 8(3): 221-234.
[18] Fageria, N. K. (2016): The Use of Nutrients in Crop Plants. – CRC Press, Boca Raton, FL.
[19] Fan, H., Aubry, S., Arsenlis, A., El-Awady, J. A. (2016): Grain size effects on dislocation and twinning mediated plasticity in magnesium. – Scripta Materialia 112: 50-53.
[20] FAOSTAT (2019). Food and Agricultural Organization of the United Nations, Rome.
[21] Finkel, T., Holbrook, N. J. (2000): Oxidants, oxidative stress and the biology of aging. – Nature 408(6809): 239.
[22] Fokom, R., Adamou, S., Teugwa, M. C., Begoude Boyogueno, A. D.., Nana, W. L., Ngonkeu, M. E. L., Tchameni, N. S., Nwaga, D., Tsala Ndzomo, G., Amvam Zollo, P. H. (2012): Glomalin-related soil protein, carbon, nitrogen and soil aggregate stability as affected by land use variation in the humid forest zone of south Cameroon. – Soil Tillage Res 120: 69-75.
[23] Gander, P. W., Tanner, C. B. (1976): Leaf growth, tuber growth, and water potential in potatoes. – Crop Science 16: 534-538.
[24] Graser, T. A., Godel, H. G., Albers, S., Földi, P., Fürst, P. (1985): An ultra-rapid and sensitive high-performance liquid chromatographic method for the determination of tissue and plasma free amino acids. – Analytical Biochemistry 151(1): 142-152.
[25] Itakura, Y., Ichikawa, M., Mori, Y., Okino, R., Udayama, M., Morita, T. (2001): How to distinguish garlic from the other allium vegetables. – J. Nutr. 131: 955-962.
[26] Khalel, A. M. S., Hado, E. K. (2011): The effect of applying the extract of garlic, liquorice root and algaren on growth and yield of kidney bean (*Phaseolus vulgaris* L). – 5th Scientific Conference of College of Agriculture, Tikrit University, 27-28 April.
[27] Khosravifar, S., Yarnia, M., Khorshidi Benam, M. B., Hosseinzadeh Moghbeli, A. H. (2008): Effect of potassium on drought tolerance in potato cv. Agria. – Journal of Food, Agriculture and Environment 6(3-4): 236-241.
[28] Lazim, Z. S., Sulaiman, S. M. (2012): Effect of gibberellic and liquorice extract on seed germination of black seed (*Nigella sativa* L.). – Iraq. J.Agric. Res. 17(1): 105113.
[29] Mafakheri, A., Siosemardeh, A., Bahramnejad, B., Struik, P., Sohrabi, Y. (2010): Effect of drought stress on yield, proline and chlorophyll contents in three chickpea cultivars. – Australian Journal of Crop Science 4: 580-585.
[30] Martin, S. L., Mooney, S. J., Dickinson, M. J., West, H. M. (2012): Soil structural responses to alterations in soil microbiota induced by the dilution method and mycorrhizal fungal inoculation. – Pedobiologia 55(5): 271-281.
[31] Matar, M. H., Saad, A. M., Ahmad, F. R. (2012): Effect of the treatment by gibberellic acid liquorice extract on growth and yield of potato. – Journal of Diyala for Agriculture Science 4(1): 220-234.
[32] Moses, T. N., Abdul-Jabbar, W. A., Elwy, A. N. (2002): Study of some local licorice root powder components (*Glycyrrhiza glabra* L.). – Iraq. J. of Agric. Sci. 33(4): 30-38.
[33] Murchie, E. H., Pinto, M., Horton, P. (2009): Agriculture and the new challenges for photosynthesis research. – New Phytologist 181(3): 532-552.
[34] Muthoni, J., Kabira, J. N. (2016): Potato production under drought conditions: identification of adaptive traits. – International Journal of Horticulture 6.
[35] Myint, A., Yama Kawa T., Kajihara, Y., Zenmoy, T. (2010): Application of different organic and mineral fertilizers on the growth, yield and nutrient accumulation of rice in a Japanese ordinary paddy field. – Sci. Word. Journal 5(2): 47-54.
[36] Najmaddin, P. M., Whelan, M. J., Balzter, H. (2017): Estimating daily reference evapotranspiration in a semi-arid region using remote sensing data. – Remote Sensing 9(8): 779.
[37] Patil, S. V., Patil, C. D., Salunke, B. K., Salunkhe, R. B., Bathe, G. A., Patil, D. M. (2011): Studies on characterization of bioflocculant exopolysaccharide of Azotobacter

http://www.aloki.hu ● ISSN 1589 1623 (Print) ● ISSN 1785 0037 (Online)
DOI: http://dx.doi.org/10.15666/aeer/1706_1478714804

indicus and its potential for wastewater treatment. – Applied Biochemistry and Biotechnology 163(4): 463-472.

[38] Peng, S., Guo, T., Liu, G. (2013): The effects of arbuscular mycorrhizal hyphal networks on soil aggregations of purple soil in southwest China. – Soil Biology and Biochemistry 57: 411-417.

[39] Prajapati, K. B., Modi, H. A. (2012): Isolation and characterization of potassium solubilizing bacteria from ceramic industry soil. – CIBTech Journal Microbiol 1(2-3): 8-14.

[40] Sabry, G. H., Rizk-Alla, M. S., Abd El-Wahab, M. A. (2009): Influence of effective micro-organisms, seaweed extract and amino acids application on growth, yield and bunch quality of Red globe grapevines. – J. Agric. Sci. Mansoura Univ. 34(6): 5901-5921.

[41] Saran, V. P., Chhabra, P. (2014): Studies on the parameters of potato processing. – Int. Interdisciplinary Research Journal 4: 320-33.

[42] Thomas, T. C., Thomas, A. C. (2009): The vital role of potassium in the osmotic mechanism of stomata aperture modulation and its link with potassium deficiency. – Plant Signal Behaviour 4(3): 240-243.

[43] Van Brunt, J. M., Sultenfuss, J. H. (1998): Better crops with plant food. – Potassium: Functions of Potassium 82(3): 4-5.

[44] Vispute, S., Khopade, A. (2011): *Glycyrrhiza glabra* Linn.-"Klitaka": a review. – Int. Journal Pharma Bio Sci. 2(3): 42-51.

[45] Wang, C., Deng, P., Chen, L., Wang, X., Ma, H., Hu, W., He, G. (2013): A wheat WRKY transcription factor TaWRKY10 confers tolerance to multiple abiotic stresses in transgenic tobacco. – PloS One 8(6): e65120.

[46] Wu, Q. S., Xia, R. X., Zou, Y. N. (2006): Reactive oxygen metabolism in mycorrhizal and non-mycorrhizal citrus (Poncirus trifoliata) seedlings subjected to water stress. – Journal of Plant Physiology 163(11): 1101-1110.

[47] Zelelew, D. Z., Lal, S., Kidane, T. T., Ghebreslassie, B. M. (2016): Effect of potassium levels on growth and productivity of potato varieties. – American Journal of Plant Sciences 7(12): 1629.

[48] Zotarelli, L., Scholberg, J. M., Dukes, M. D., Muñoz-Carpena, R., Icerman, J. (2009): Tomato yield, biomass accumulation, root distribution, and irrigation water use efficiency on sandy soil, as affected by nitrogen rate and irrigation scheduling. – Agricultural Water Management 96(1): 23-34.

http://www.aloki.hu ● ISSN 1589 1623 (Print) ● ISSN 1785 0037 (Online)
DOI: http://dx.doi.org/10.15666/aeer/1706_1478714804

QUANTITATIVE GENES SEQUENCING IN KARADI EWES ASSOCIATED WITH MILK YIELD TRAITS

HAMA KHAN, K. M.[1*] – AL-BARZINJI, Y. M. S.[2*] – MAAROF, N. N.[1]

[1]*Department of Animal Science, College of Agricultural Science, University of Sulaimani, Sulaimani, Iraq*

[2]*Department of Animal Resource, College of Agriculture Engineering Science, Salahaddin University-Erbil, Iraq*

**Corresponding author*
e-mail: karwan.hamakhan@univsul.edu.iq; phone: +964-772-526-3296 (Hama Khan, K. M.)
Yousif.Noori@Su.Edu.Krd (Al-Barzinji, Y. M. S.)

(Received 13th Jun 2019; accepted 10th Sep 2019)

Abstract. The objective of present study was to investigate sequencing of four genes (AlphaS1-casein, alphaS2-casein, beta lactoglobulin and Major histocompatibility complex) that related to milk traits in Karadi sheep. A total of 300 ewes from three flocks were studied. The results revealed which are include effects of lamb's sex, dam's age and month of lambing were not significant on the milk traits except the ewes flock has significant effect on daily milk yield. The Best Linear Unbiased Prediction value for all ewes concerning daily milk yield, protein and fat percentages ranged from -10.5293 to 10.7504, -2.0546 to 2.0097% and -1.7033 to 1.4067%, respectively. The DNA sequencing results show that there are differences between ewes with high and low milk production in AlphaS1-casein, alphaS2-casein, beta lactoglobulin and Major histocompatibility complex loci sequences these differences reflected by milk performance of ewes in two groups, ewes in high group produced 300% more daily milk than ewes in low group (355.8 vs. 102.8 g/day). In conclusion results showed that there are agreements between Best Linear Unbiased Prediction value with DNA sequencing results in the select best animal and the selection process with molecular technique can play a major positive and rapid role to improvement and increasing milk production in this breed of sheep.
Keywords: *Karadi Sheep, BLUP, Daily Milk Yield, Fat%, Protein%, DNA Sequencing*

Introduction

In Kurdistan, there are many native sheep breeds with different productive and reproductive performances. One of the most important of them is the Karadi sheep that reared mainly for milk, meat and wool production. Solid content of ewes milk is a higher than other farm animals (cow and goat), which means the sheep milk is particularly suited to produce cheese and yogurt (Bencini and Johnston, 1997; Gutiérrez-Gil *et al*., 2014). After weaning all milk is used for yogurt and cheese production, for that milk content are very important (Carta *et al*., 2009). The total number of sheep in Iraqi-KRG was 7,722,372 heads (Al-Alaq *et al*., 2011).

The research to locate the gene responsible for the prolificacy in this breed, using molecular genetic markers, may help its use commercially to improve other local breeds. The polymorphism of blood genetic markers gives some useful information in studying the relationships among breeds and their evolution. It can also be used for indirect selection if there were some relationships between these markers and some economically important quantitative traits (Anous *et al*., 2009). Molecular methods have also provided new markers for the study of genetic variation and evolutionary relationships of closely related populations (Visser *et al*., 2004; Iamartino *et al*., 2005;

http://www.aloki.hu ● ISSN 1589 1623 (Print) ● ISSN 1785 0037 (Online)
DOI: http://dx.doi.org/10.15666/aeer/1706_1480514822

Kumar *et al*., 2005). Improvement of livestock has focused on the selection of breeding individuals with superior phenotypes. With the development of increasingly advanced statistical methods that maximize selection for genetic gain, this simple approach has been extremely successful in increasing the quantity of agricultural output and productivity. However, information now available on the organization and functioning of the genome could be used in breeding programmers to improve a range of traits. While genetic markers for QTL that are linked to the trait gene could be used to choose animals for selective breeding programmers, the most effective markers are the functional mutations within the trait genes. Strategies to identify markers for traits and the application of these markers are described by reference to examples of loci that control a range of different traits (Williams, 2005).

Therefore, the objective of the present study is to assess the genetic structure within the Karadi sheep population at the DNA level in order to find molecular genetic markers which can differentiate between females with high and low production and help for the identification of the prolificacy gene in Karadi sheep in Iraqi-KRG.

Materials and methods

Animal and DNA isolated

Experimental done on nearly 300 Karadi ewes (2-5 years old) from three private flocks at different locations of Sulamania governorate Arbat District (Latitude, 35° 25' 14", Longitude, 45° 03' 36", W, elevation 681 m), Sharazoor District (Latitude, 35° 15' 27", Longitude, 45° 42' 21", W, elevation 614 m) and Mawat District (Latitude, 35° 52' 34",45° 24' 35", W, elevation 858 m), Karadi ewes were studied for their milk production with percentage of protein and fat in ewes milk for one season (5 months), milking methods depend on ICARDA (1995). All necessary information was records for each ewe (age of dam, sex of lamb, month of lambing, daily milk production, fat%, and protein %). Protein% and fat% of milk were estimated from the milk sample monthly using milkoscan TM minor machine (P/N 6004 4208, Issue 1 GB, March 2010, FOSS Analytical, 69, Slangerupgade, DK 3400 Hillerod, Denmark).

Whole blood (5 ml) was collected from each ewe from jugular vein into 10 ml Vacutainer tubes containing EDTA for genetic studies. Genomic DNA was extracted from whole blood using Quick-DNATM Miniprep Kit (ZYMO RESEARCH CORP, USA). Following the extraction, the quality and quantity of the extracted DNA samples were assessed using a Nanodrop spectrophotometer 2000 (UK). Laboratory work was done in the postgraduate laboratory at the faculty of agricultural sciences, Sulaimani University, Sulaimani.

PCR amplification and genotyping

Four specific genes were used and the primer sequence and their PCR condition are shown in *Table 1*. PCR reaction was carried out for forward and reverse primers in 50 μL of total volume, containing 10 X PCR buffer (50 mM/L Kcl, 10 mM/L Tris-HCl (pH 8.0), 0.1% Triton X-100), X mM MgCl2, 0.2 mM of each dNTP, 10 pM/L of each primer, 50 ng ewe genomic DNA and 1U Taq DNA polymerase.

The PCR Thermal Cycler (TC9610 /TC9610-230, Applied Bio systems, USA) was done in a final reaction volume of 50 μL. A master mix for all samples for each gene was readied and 40 μL filled in every PCR tube. Ten μL of DNA sample was added to

http://www.aloki.hu ● ISSN 1589 1623 (Print) ● ISSN 1785 0037 (Online)
DOI: http://dx.doi.org/10.15666/aeer/1706_1480514822

each tube to make the last volume 50 µL to accomplish homogeneity of reagents and decrease the risk of contamination, control reaction was situated up without genomic DNA. A GoTaq® Green Master Mix (ADM7122 00000311719, Promega-USA) incorporates with 25 µL Taq DNA polymerase (25 Units/mL, dNTPs 200 µM, and MgCl2 1.5 mM), 4 µL primer (0.1-1 µM, forward and reveres), 5 µL (100 ng) of DNA template and 16 µL DNase free water.

Ewes genotyped were done by using the PCR and direct sequencing. To confirm results, thirty randomly chosen PCR samples of each groups (High, and low milk yield) were sequenced from both directions. Direct sequencing was performed by commercial services using 3100 ABI PRISM sequencer (Applied Bio-systems, USA). Sequences were obtained with the same primers used for PCR amplification.

Table 1. *The sequences and information of primers used in this study*

Gene	Primer sequences 5′ -------- 3′	PCR conditions	PCR product size	References
α-s1 casein	TTGGGTTCAGTGTGAGTCTGG AAAAGCCCTGGGTGGGCAGC	Initial 5 min 95 °C 30 cycles, 95 °C for 30 s,60 °C for 30 s,72 °C for 30 s, final elongation 5 min at 72 °C	452 bp	Corral *et al*. (2010)
α-s2 casein	CTGAAGTTGCCCCAGAGGTA CATTTGGAGAAGAAGCAGTGG	Initial 95 °C for 5 min 35 cycles, 95 °C for 30 s,55 °C for 30 s, 72 °C for 1 min, final 72 °C for 5 min	225 bp	Rozen and Skaletsky (2000)
β-LG	TTGGGTTCAGTGTGAGTC TGG AAAAGCCCTGGGTGG GCAGC	33 cycles,95 °C for 1 min,66 °C for 1 min,72 °C for 1 min, final elongation 5 min at 72 °C	452 bp	Jurate *et al*. (2005)
MCH class II DRB	TCTCTGCAGCACATTTCCTGG CTCGCCGCTGCACAGTGAAAC	35 cycles,95 °C for 1 min,60 °C for 1 min,72 °C for 1 min, final elongation 5 min at 72 °C	258 bp	Ammer *et al*. (1992)

Bioinformatics analysis

Sequences were analyzed using the Chromas version 2.6.5 Technelysium Pty Ltd. Sequence analysis and alignments were carried out using NCBI BLAST: Nucleotide sequence. The nucleotide sequences of the four tested genes in Karadi ewes were submitted to GenBank (NCBI, BankIt).

Statistical and genotypic analysis

The PROC GLM (General Linear Model) procedure (SAS, 2002) was used to analyze the data for daily milk production (g), fat and protein %. Fixed effects studies

http://www.aloki.hu ● ISSN 1589 1623 (Print) ● ISSN 1785 0037 (Online)
DOI: http://dx.doi.org/10.15666/aeer/1706_1480514822

were flock, age of dam, sex of lamb, and month of lambing were fitted in the following model:

$$Y_{ijklm} = \mu + F_i + A_j + S_k + M_l + \varepsilon_{ijklm} \quad \text{(Eq.1)}$$

where: Y ijklm = milk yield, fat and protein% of m^{th} ewe, of i^{th} ewes flock (Fi, i = 1,2 and3), of j^{th} age of ewes (Aj, j = 2,3,4 and 5 years), of k^{th} sex of lambs (Sk, k = 1, male and k = 2, female) and of l^{st} month of lambing (Ml, l = Nov., 2 = Dec., 3 = Jan., and 4 = Feb.), μ = Population mean, ε_{ijklm} = random error. It was assumed to be normally and independently distributed with mean zero and variance $\delta^2 e$.

For genetics evaluation of ewes (High and low milk production) for various performance traits, Best Linear Unbiased Prediction (BLUP) procedure described by (SAS, 2002) was applied. The model used for this purpose was the Mixed Model (Fixed + Random effects) of (SAS, 2002) software. The individuals of the Karadi breed were assembled in three groups; high (30 ewes), medium (240 ewes) and low (30 ewes) production, according to the BLUP value for DMY: where 10% of ewes for the 1st group (Top milk yield group), 80% for 2nd group and 10% for 3th group (low milk yield group). The above *Equation 1* was used to analyze the difference among ewes group after add the groups effect to the equation.

Results

Phenotypic results

Fixed effect

Least square means of milk traits were 236 ± 10 g/day, 5.33 ± 0.62% and 5.30 ± 12.93% for DMY, protein% and fat%, respectively (*Table 2*). The milk traits curve show that the higher milk yield recorded after one month of ewes lambing was arrived 339 g/ewe/day and lowest at end of lactation, while Fat % curve increase linearly after lambing to end of lactation showed the reverse way with milk production, but the protein % look like milk curve along lactation stage (*Fig. 1*).

As in *Figure 2* the ewes flock have significant effect on DMY and Fat %, ewes in 3rd flock yield more milk compared with other two flocks.

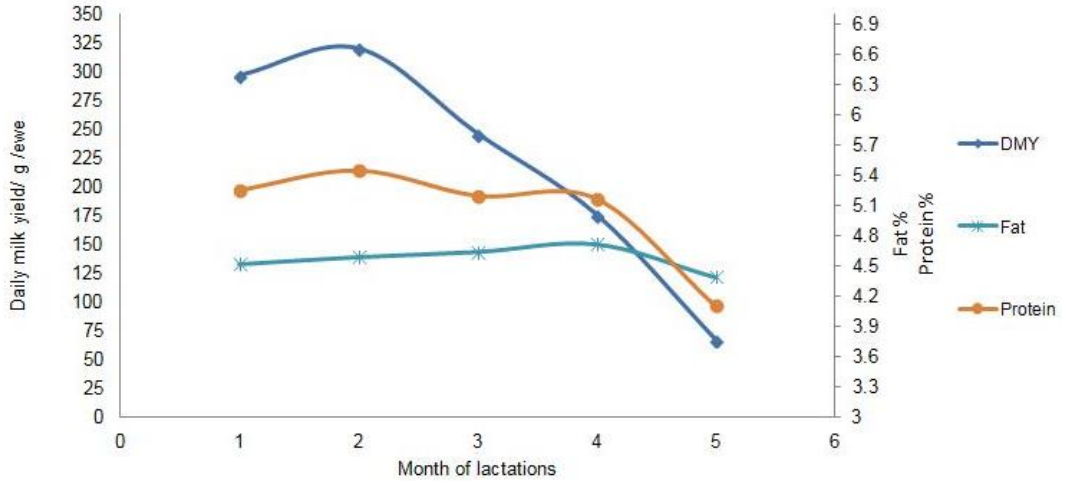

Figure 1. *Daily milk yield (g), fat and protein % in Karadi ewes*

http://www.aloki.hu ● ISSN 1589 1623 (Print) ● ISSN 1785 0037 (Online)
DOI: http://dx.doi.org/10.15666/aeer/1706_1480514822

Table 2. *Least square means ± SE for daily milk yield (DMY), protein% and fat% in Karadi ewes*

Fixed effects	DMY (kg)	Protein %	Fat %
Overall mean	0.236 ± 0.10	5.33 ± 0.62	5.30 ± 12.93
Flock	*	NS	NS
1	0.220 ± 0.01[a]	5.33 ± 0.06[a]	4.23 ± 1.27[a]
2	0.211 ± 0.02[a]	5.15 ± 0.16a	6.81 ± 3.48[a]
3	0.312 ± 0.01[b]	5.46 ± 0.10[a]	4.37 ± 2.09[a]
Ewes age (year)	NS	NS	NS
2.5	0.261 ± 0.01[a]	5.37 ± 0.08[a]	5.31 ± 1.83[a]
3.5	0.245 ± 0.01[a]	5.30 ± 0.08[a]	6.07 ± 1.72[a]
4.5	0.241 ± 0.01[a]	5.20 ± 0.09[a]	4.71 ± 1.97[a]
5.5	0.244 ± 0.01[a]	5.39 ± 0.12[a]	4.45 ± 2.48[a]
Sex of lambs	NS	NS	NS
Male	0.251 ± 0.01[a]	5.42 ± 0.11[a]	5.37 ± 2.36[a]
Female	0.245 ± 0.01[a]	5.21 ± 0.09[a]	4.90 ± 2.02[a]
Month of lambing	NS	NS	NS
November	0.247 ± 0.01[a]	5.34 ± 0.06[a]	5.26 ± 1.34[a]
December	0.264 ± 0.01[a]	5.20 ± 0.12[a]	5.58 ± 2.60[a]
January	0.246 ± 0.01[a]	5.50 ± 0.12[a]	4.98 ± 2.59[a]
February	0.234 ± 0.02[a]	5.22 ± 0.14[a]	4.72 ± 2.95[a]
Stage of lactation (month)	*	*	NS
1	0.321 ± 0.01[a]	5.33 ± 0.08[a]	4.83 ± 1.83[a]
2	0.339 ± 0.01[a]	5.51 ± 0.08[a]	4.90 ± 1.84[a]
3	0.281 ± 0.01[b]	5.32 ± 0.08[a]	7.62 ± 1.85[a]
4	0.201 ± 0.01[c]	5.31 ± 0.08[a]	4.96 ± 1.84[a]
5	0.100 ± 0.01[d]	4.94 ± 0.09[b]	5.21 ± 2.10[a]

Means in the same column for each factor with different letters are significantly ($p \leq 0.05$) different

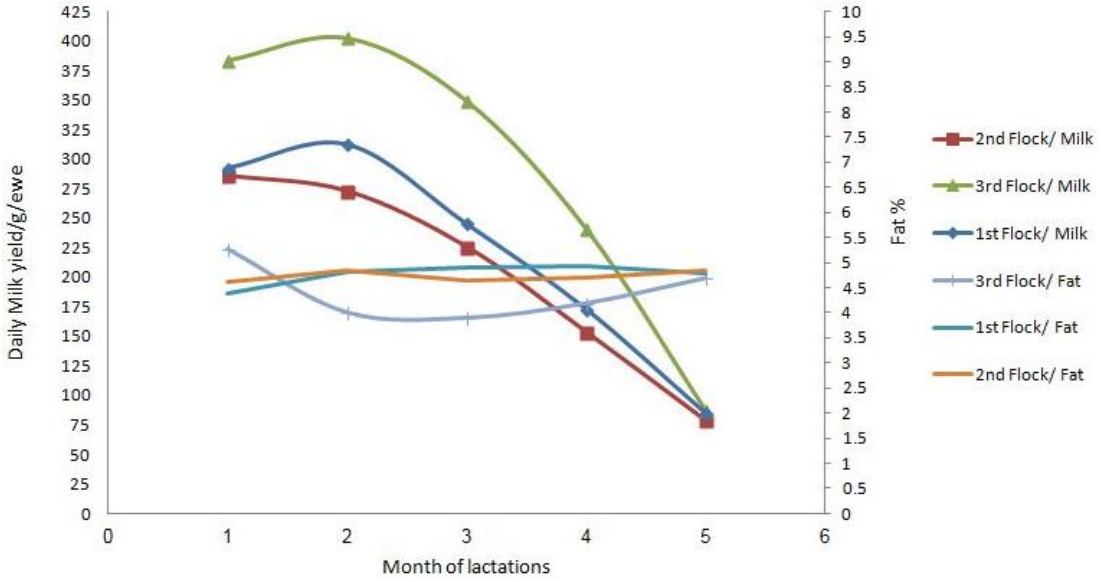

Figure 2. *Effect ewes flock on daily milk yield (g) and fat %*

http://www.aloki.hu ● ISSN 1589 1623 (Print) ● ISSN 1785 0037 (Online)
DOI: http://dx.doi.org/10.15666/aeer/1706_1480514822

The milk traits did not affected by age of ewes, but ewes with 3 years old product more milk compared with another ewes age (*Fig. 3*). This may attributed to the biological condition and physiological maturity of three years old ewes. As well as sex of lamb also did not have significant effect on all milk traits in this study (*Fig. 4*).

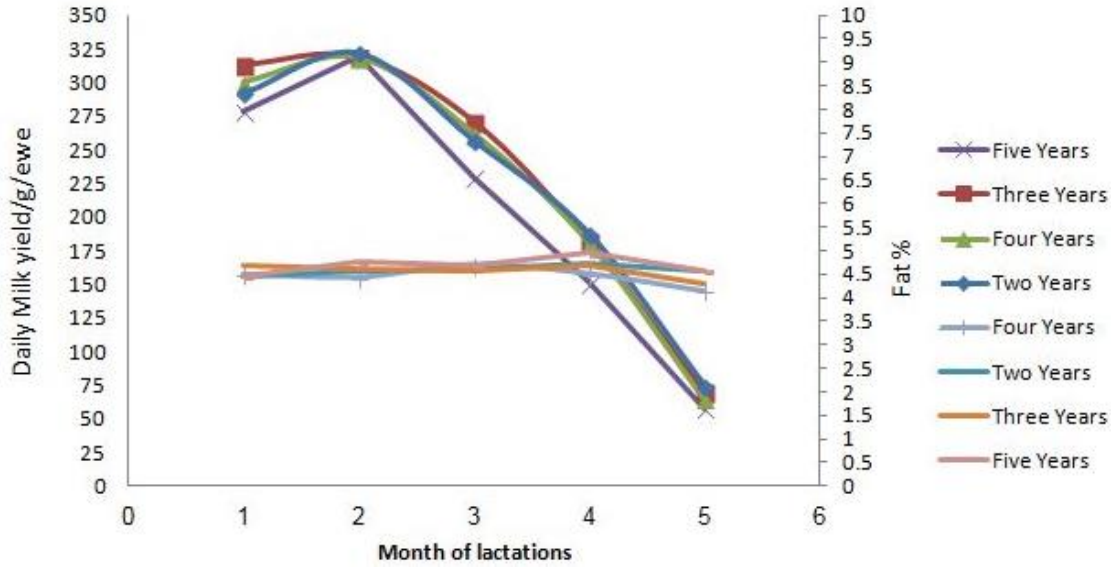

Figure 3. *Effect age of ewes on daily milk yield (g) and fat %*

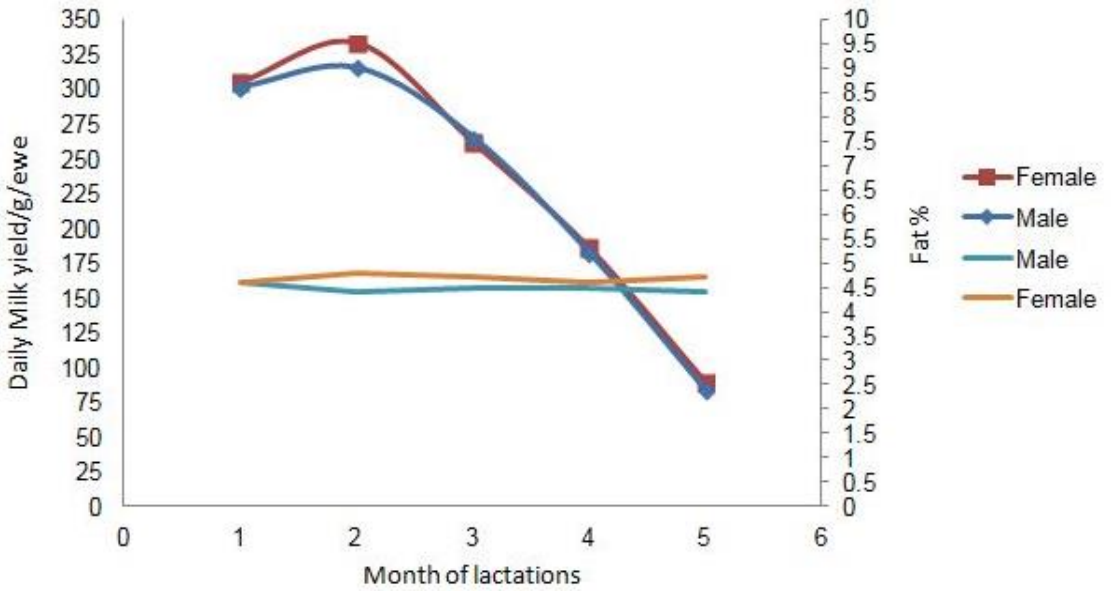

Figure 4. *Effect lamb sex on ewe's daily milk yield (g) and fat %*

Genetic merit (BLUP) of milk traits

Best Linear Unbiased Prediction (BLUP) is generally used to predict animal breeding values, given measurements on progeny, or to predict breeding values of animals with repeated records, or to predict breeding values of all animals in the

http://www.aloki.hu ● ISSN 1589 1623 (Print) ● ISSN 1785 0037 (Online)
DOI: http://dx.doi.org/10.15666/aeer/1706_1480514822

pedigree (Cameron, 1997). Best linear unbiased prediction is one of the current methods of choice for genetic evaluation of quantitative traits. BLUP values overall ewes for DMY, protein and fat% were ranged from -10.52 to 10.75, -2.054 kg to 2.009% and -1.703 to 1.406%, respectively (*Table 3*). According to the BLUP values for high and low groups the results show that there are significant deference's between ewes with high and low milk production group for all traits under studies as in *Figures 5–7*.

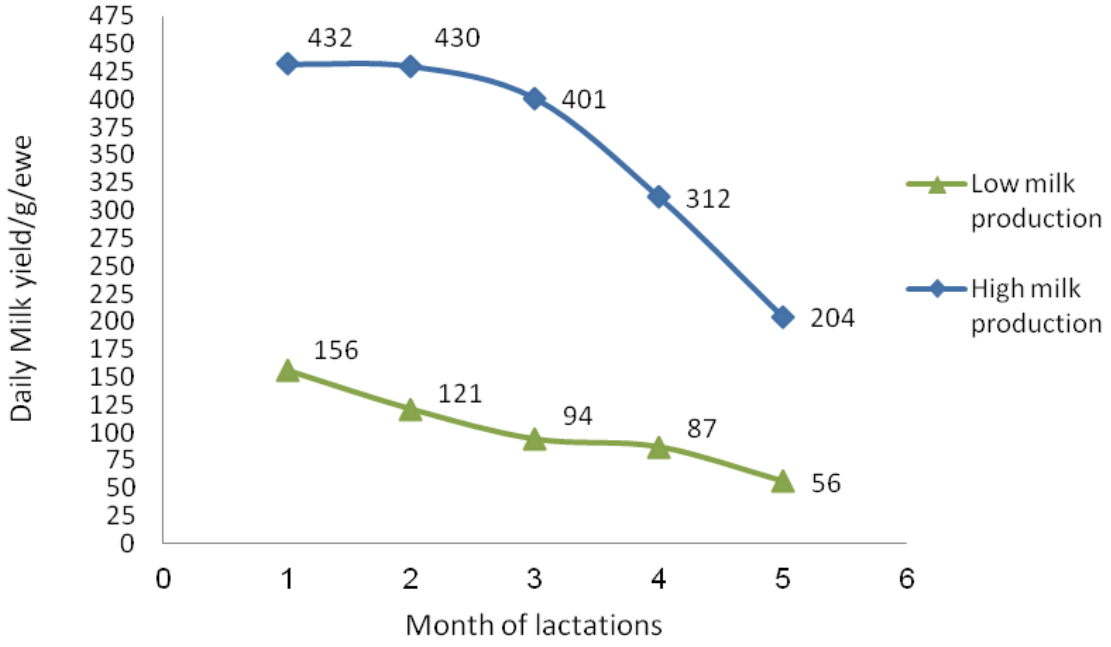

Figure 5. *Daily milk yield (g) curve in high and low ewes group*

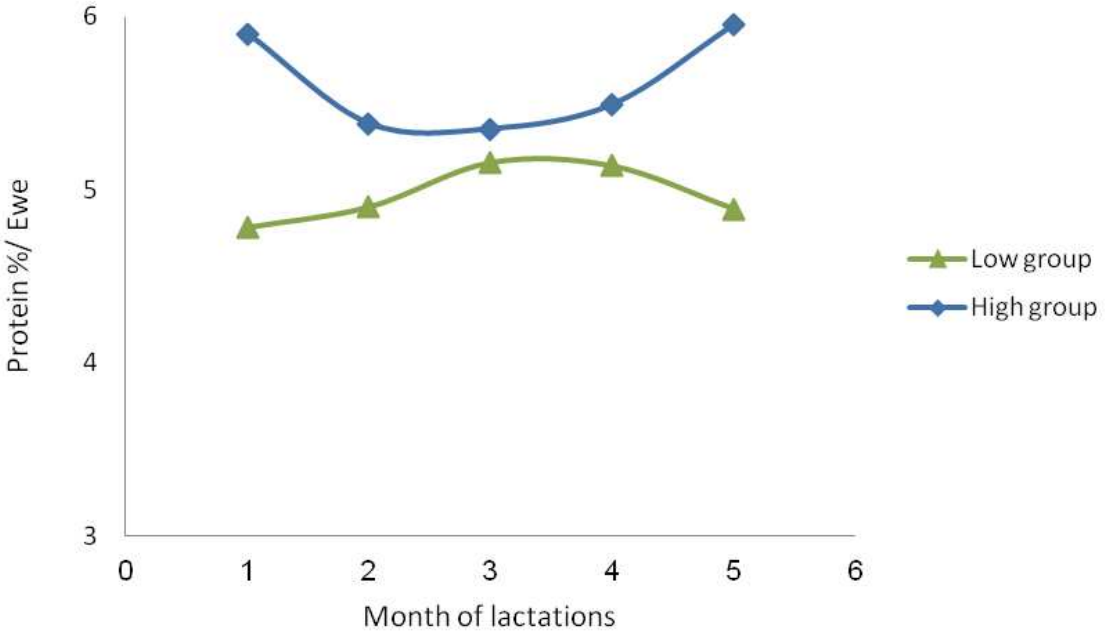

Figure 6. *Protein % curve in high and low ewes group*

http://www.aloki.hu ● ISSN 1589 1623 (Print) ● ISSN 1785 0037 (Online)
DOI: http://dx.doi.org/10.15666/aeer/1706_1480514822

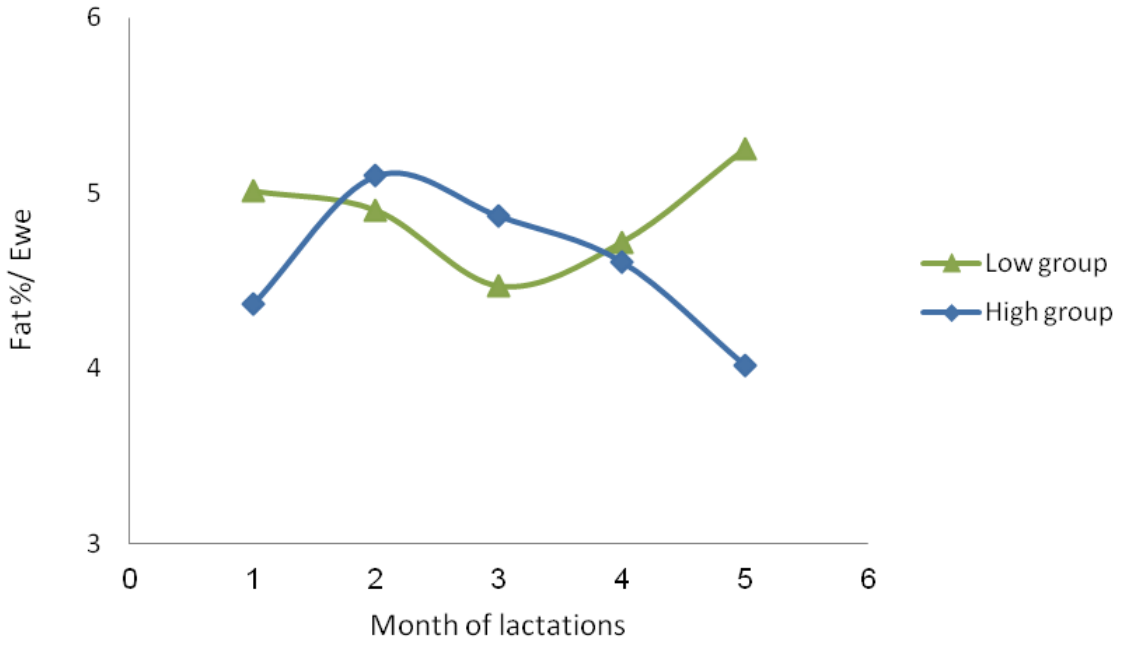

Figure 7. *Fat % curve in high and low ewes group*

Table 3. *BLUP values DMY (kg), protein% and fat% in Karadi ewes*

Ewe No.	BLUP (DMY)	Ewe No.	BLUP (protein%)	Ewe No.	BLUP (fat%)
99	10.75	102	2.009	65	1.406
94	10.58	99	1.919	16	1.066
108	10.09	106	1.795	19	1.006
111	9.768	109	1.784	78	1.006
96	9.640	101	1.716	70	0.996
106	9.359	107	1.660	15	0.956
66	-8.524	70	-1.276	100	-1.093
26	-8.908	55	-1.386	96	-1.103
4	-9.137	63	-1.469	43	-1.113
77	-9.588	4	-1.683	45	-1.593
88	-10.52	53	-2.054	89	-1.703

Genotypic results

In this study, the sequencing analyses for high and low production groups of ewes were done for all genes under study.

AlphaS1-casein (CSN1S1) locus

The results show there are difference between high and low group (*Figs. 8* and *9*) the high group milk production match 100% with NCBI (Sequence ID: JN560175.1) while the low group match 99% with the same NCBI reference which have mutation point at 4298 (T G), this mutation changed the amino acid from cys (UGU) to trp (UGG).

http://www.aloki.hu ● ISSN 1589 1623 (Print) ● ISSN 1785 0037 (Online)
DOI: http://dx.doi.org/10.15666/aeer/1706_1480514822

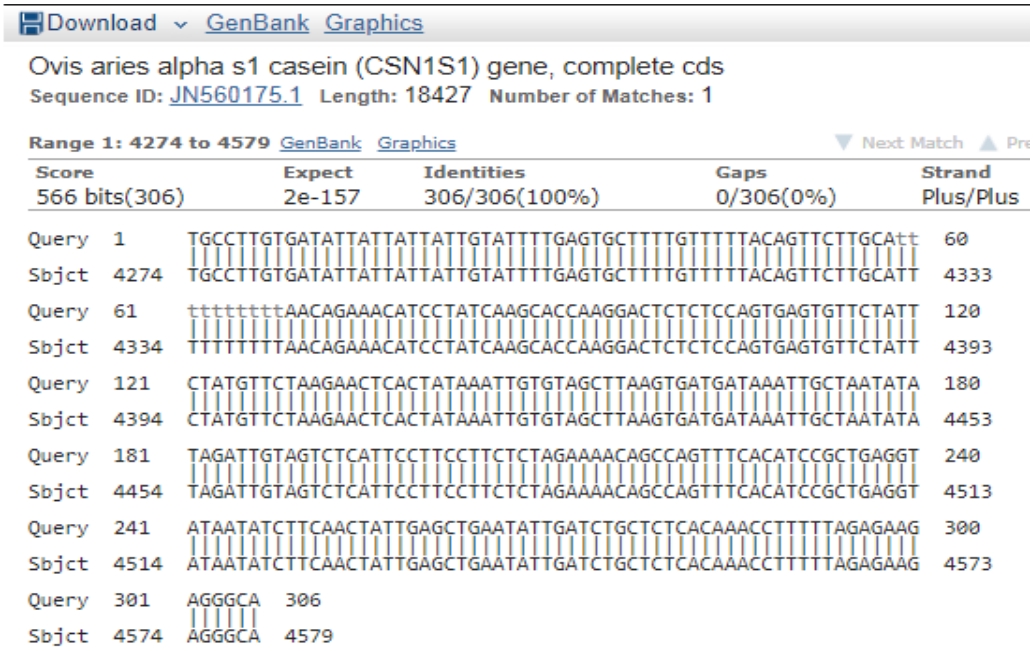

Figure 8. *Sequence alignment of Karadi sheep (high milk production group) CSN1S1with published sequences*

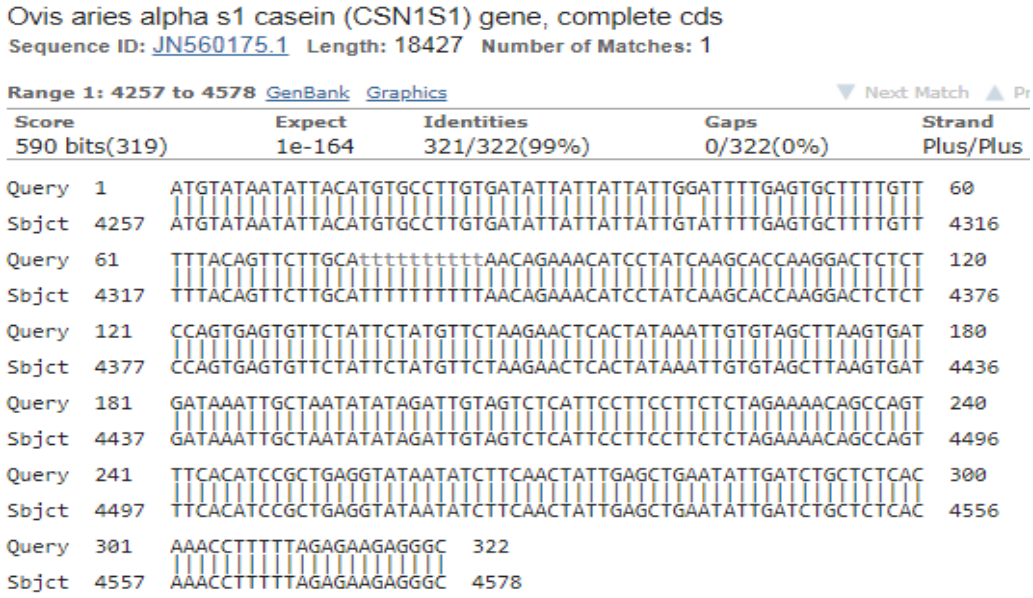

Figure 9. *Sequence alignment of Karadi sheep (low milk production group) CSN1S1with published sequences*

AlphaS2-casein (CSN1S2)

Ewes with low production match 99% with NCBI (Sequence ID: FN601350.1) which have mutation point at 176 (A C) this mutation changed the amino acid from His (CAC) to Pro (CCC), while ewes with high milk production match to the same NCBI 100% (*Figs.10* and *11*).

http://www.aloki.hu ● ISSN 1589 1623 (Print) ● ISSN 1785 0037 (Online)
DOI: http://dx.doi.org/10.15666/aeer/1706_1480514822

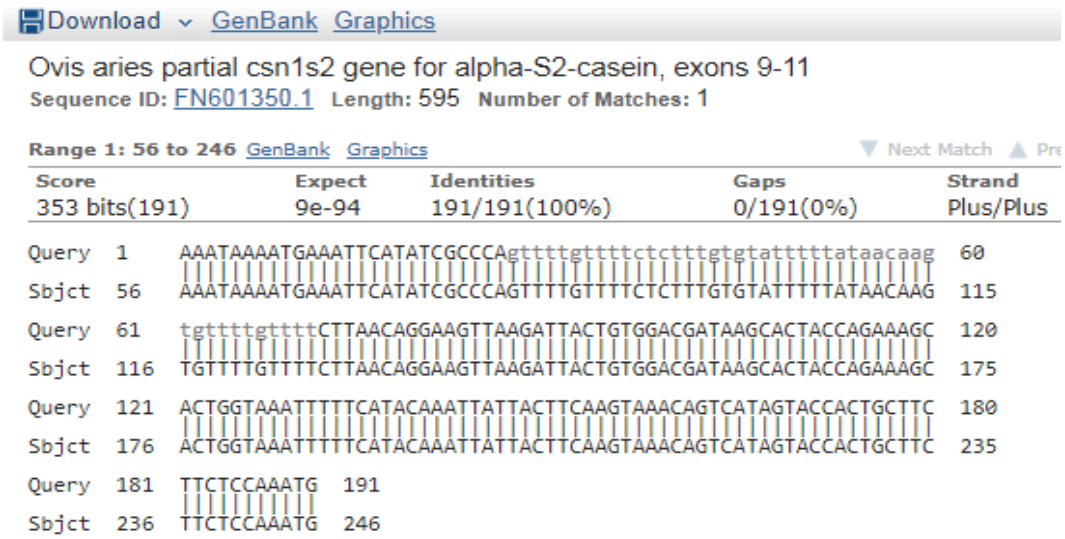

Figure 10. *Sequence alignment of Karadi sheep (High milk production group) CSN1S2 with published sequences*

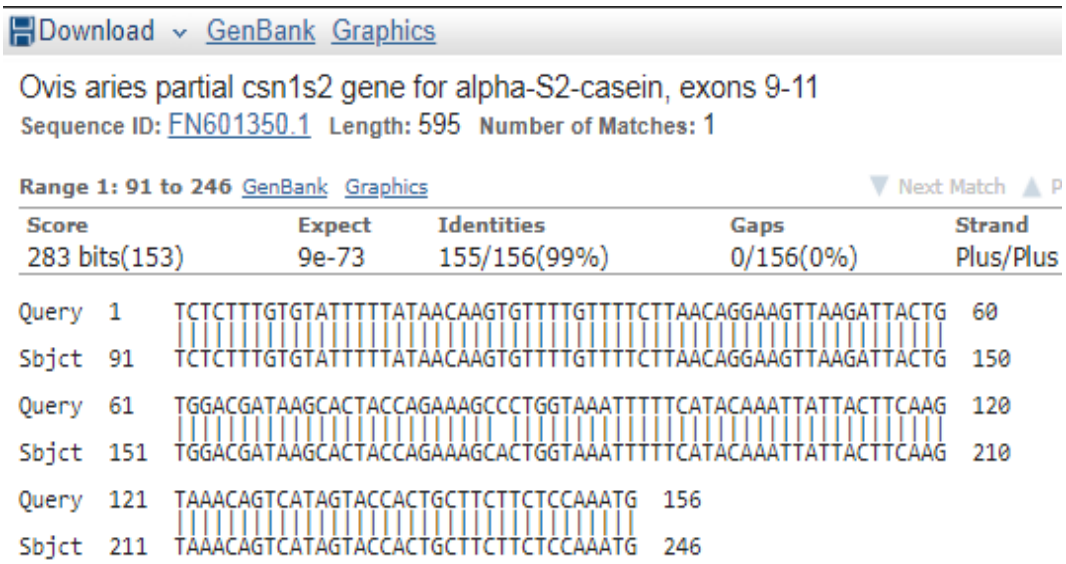

Figure 11. *Sequence alignment of Karadi sheep (low milk production group) CSN1S2with published sequences*

The beta lactoglobulin (β-LG) gene

Both groups was match 100% to the NCBI (Sequence ID: X12817.1) without differences between both groups (*Figs. 12* and *13*).

Major histocompatibility complex (MCH class II DRB)

Ewes in high group milk production match 98% with NCBI (Sequence ID: Z92728.1) for Major histocompatibility complex (MHC- DRB) which have two mutation point, the 1st one found at position 139 (G T) this mutation changed the amino

http://www.aloki.hu ● ISSN 1589 1623 (Print) ● ISSN 1785 0037 (Online)
DOI: http://dx.doi.org/10.15666/aeer/1706_1480514822

acid from arg (CGG) to leu (CUG) and the 2nd one at 244 (G -), this mutation changed the amino acid from ser (AUG) to met (AUG), while low group production match 99% to same NCBI sequence with one mutation point at 244 (G C), this mutation changed the amino acid from ser (AGU) to thr (ACU) (*Figs. 14* and *15*).

As in DNA sequencing results for CSN1S1, CSN1S2, β-LG and MHC-DRB loci there are difference between ewes with high and low milk production groups, this differences in DNA sequencing reflected on milk performance of ewes in two groups, ewes in high group produced DMY 355.8 g/day compared with 102.8 g/day in low group.

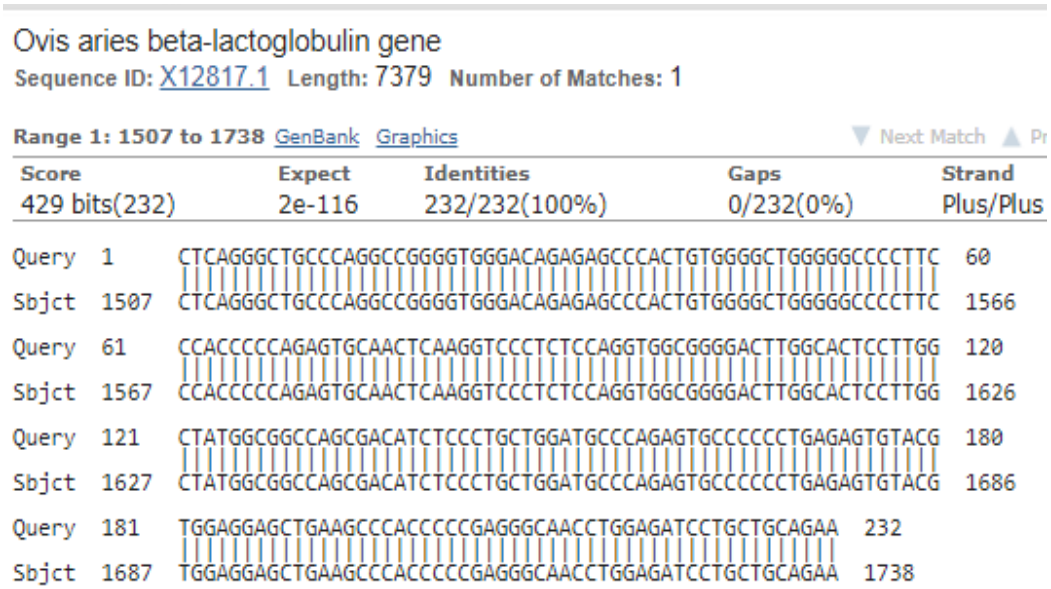

Figure 12. *Sequence alignment of Karadi sheep (high milk production group) beta-lactoglobulin with published sequences*

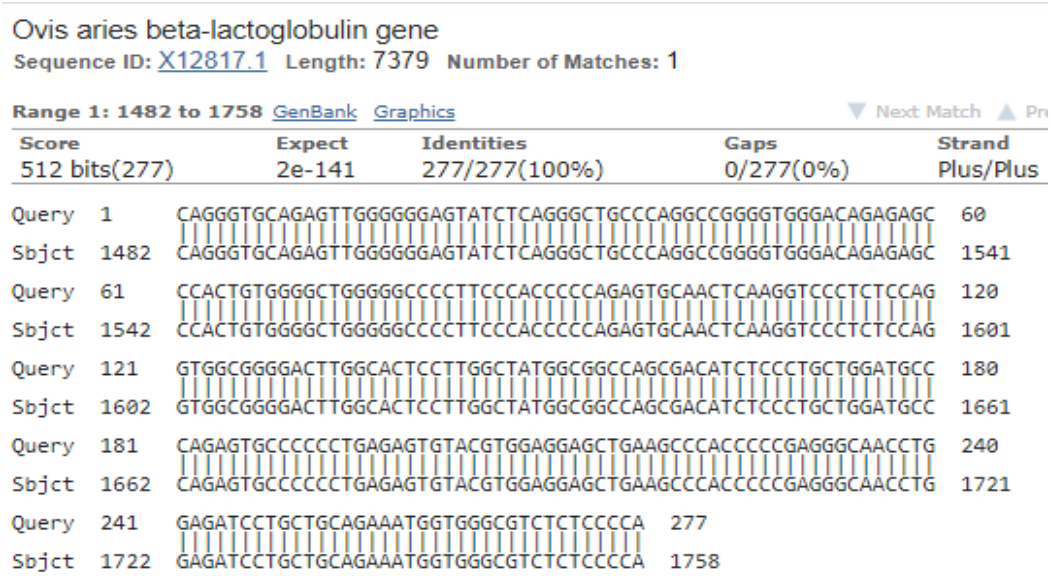

Figure 13. *Sequence alignment of Karadi sheep (low milk production group) beta-lactoglobulin with published sequences*

http://www.aloki.hu ● ISSN 1589 1623 (Print) ● ISSN 1785 0037 (Online)
DOI: http://dx.doi.org/10.15666/aeer/1706_1480514822

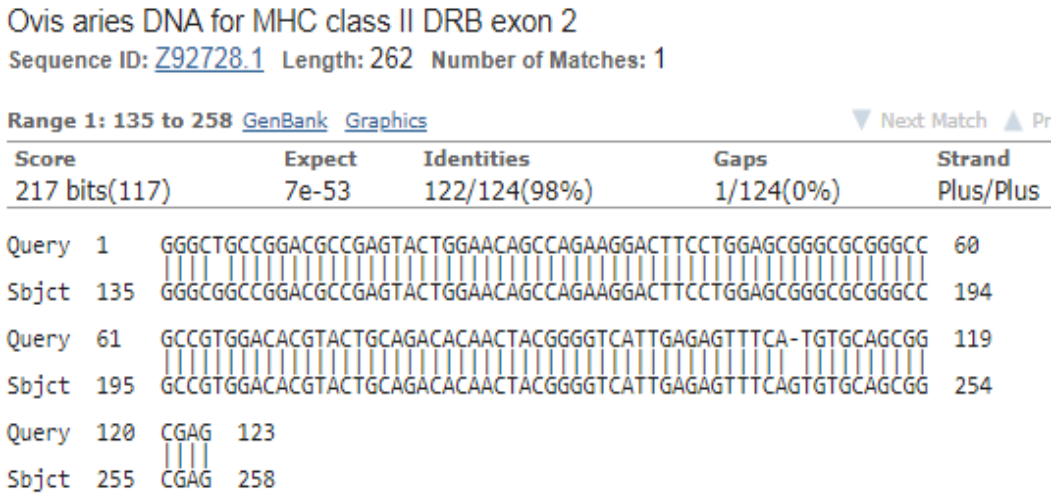

Figure 14. *Sequence alignment of Karadi sheep (high milk production group) MCH class II DRB exon2 with published sequences*

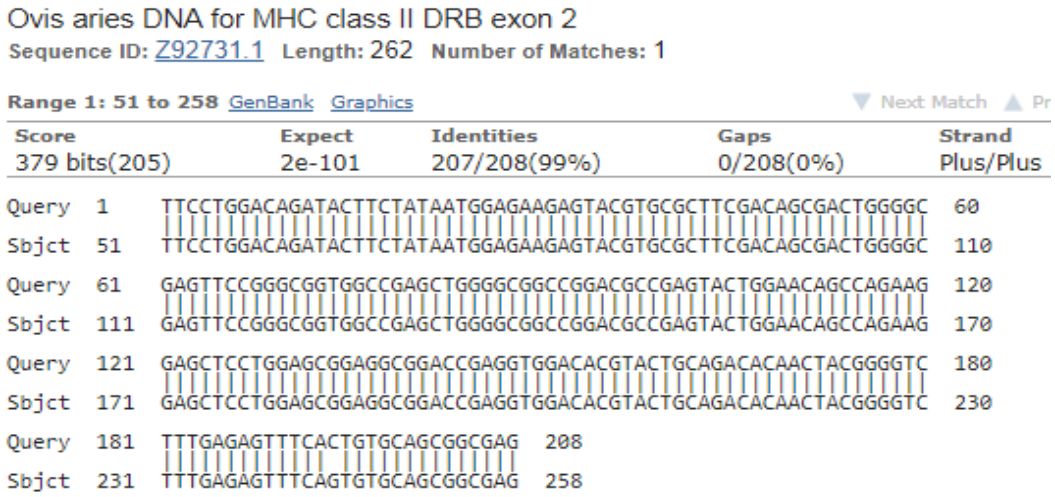

Figure 15. *Sequence alignment of Karadi sheep (low milk production group) MCH class II DRB exon2 with published sequences*

Discussion

Phenotypic results

The average daily milk yield observed in this study was below the range indicated earlier by several researchers for several sheep breeds (Oramari, 2009; Abd Allah *et al*., 2011). However, protein and fat percentage were similar to other studies reported earlier by several investigators in different breeds of sheep (Bendelja *et al*., 2009; Abd El-Fatah and Awad, 2014). Our results showed that flock has significant effect on DMY and fat%. Similar results were recorded by (Maarof *et al*., 1986; Sanna *et al*., 1998; Ruiz *et al*., 2000; Al-Barzinji, 2003, 2009; Raaof, 2005, 2006; Gardi, 2008; Al-Barzinji and Abdul-Rahman, 2012; Al-Barzinji and Al-Rawi, 2012) on Iraqi sheep breeds. According the effect of ewe age our result is in agreement with many research works (Al-Rawi *et al*., 1997; Mavrogenis, 1996; Fuertes *et al*., 1998; Macciotta *et al*., 2000;

http://www.aloki.hu ● ISSN 1589 1623 (Print) ● ISSN 1785 0037 (Online)
DOI: http://dx.doi.org/10.15666/aeer/1706_1480514822

Al-Mohammadi, 2002; Al-Barzinji and Hassan, 2005; Raaof, 2005, 2006; Gardi, 2008; Al-Barzinji, 2009; Al-Barzinji and Al-Rawi, 2012). This result is similar to that reported by (Al-Barzinji, 2009; Al-Barzinji and Abdul-Rahman, 2012; Al-Barzinji and Al-Rawi, 2012) in Hamdani sheep breed which showed that sex of lamb had no significant effect on all milk trait in studied in this study.

The BLUP results in present study are similar to reported by Al-Barzinji and Abdul-Rahman (2012) for DMY and fat % in Hamdani sheep breed in Iraq. The BLUP value ranged from -10.5293 in low milk yield group to 10.7504 in high milk yield group. The BLUP value ranged from -2.0546% in low protein yield group to 2.0097% in high yield group and the BLUP value ranged from -1.7033% in low fat yield group to 1.4067% in high yield group. These results show significant differences among ewes groups, these differences return to genotypic effect among ewes group. The breeder can use these wide ranges of ability to produce more milk among ewes and can make selection process to increase the allele frequency of quantitative loci to speed up the improvement of milk yield which have significant effect on lamb's performance in next generation.

Genotypic results

The results of the study Mroczkowski *et al*. (2004) indicate the superiority of sheep with CC αs1–CN genotypes of the milk yield, fat and protein percentage. Similar results are reported by Chianese *et al*. (1996), who analysed Sarda, Comisana and Delle Lanqhe crosses and observed the milk production level to decrease in the following order: BC > CC > CD. Animals with the CC genotypes were characterized by a higher percentage of fat and casein in milk compared to both the CD and BC genotypes. Piwczyński *et al*. (2002) reported that in a population of Polish Merino × prolific sheep, ewes with BC αs1–CN genotypes were highly significantly better in milk production than animals with AC and CC genotypes. However, CC homozygotes were better in percentage of protein and solids than AC and BC heterozygotes. Ovine milk containing CSN1S1 genotype CC showed a higher protein and/or fat content than AC, CD, DD, or CX milk (Chianese *et al*., 1996; Pirisi *et al*., 1999; Mroczkowski *et al*., 2004; Wessels *et al*., 2004). Therefore, CSN1S1 CC milk had better renneting properties, and better cheese-making characteristics than CD and DD milk (Chianese *et al*., 1997; Pirisi *et al*.,1999).

An investigation was carried out to explain characterize the ovine alphaS2-casein (CSN1S2) by Picariello *et al*. (2009) of three Italy sheep breeds showed that B variant differs from the most common form A with two amino acid exchanges: Asp75 Tyr75 and Ile105 Val105.

Investigations in many countries have shown that β-lactoglobulin is polymorphic in various breeds of sheep. Three co-dominant alleles (A, B and C) have been reported in this species differing by one or more amino acid changes. The genetic variant A differs from variant B in the amino acid sequence at position 20 ($Tyr_{20} \rightarrow His_{20}$) (Bell and Mckenzie, 1967; King, 1969; Kolde and Braunitzer, 1983; Ali *et al*., 1990), the rare variant C is a subtype of A with a single amino acid exchange at position 148 (Arg→Gln) as reported by (Erhardt, 1989).

Pietrolà *et al*. (2000) did not find any direct effect or linkage between milk yield and β-lactoglobulin genotype. Ramos *et al*. (2009) observed higher milk yield in AB heterozygotes in Merino and Serra da Estrela sheep. In addition, the Serra da Estrela AA ewes presented lower milk yield when compared with AB animals with no significant difference AB and BB genotypes Ramos *et al*. (2009). Kawecka and Radko

http://www.aloki.hu ● ISSN 1589 1623 (Print) ● ISSN 1785 0037 (Online)
DOI: http://dx.doi.org/10.15666/aeer/1706_1480514822

(2011) found no associations between β-lactoglobulin genotypes and milk yield and composition in some Polish sheep breeds. Yousefi *et al*. (2013) revealed significant associations between AB genotypes and higher milk fat percentage in indigenous Zel sheep. Finally, in Portuguese sheep breeds, a study was conducted to investigate the effect of the genetic variants at the β-lactoglobulin and α_{S1}-casein loci and milk yield. The genetic variants of β-Lactoglobulin was identified by using PCR-RFLP, which in Portuguese sheep breeds β-Lactoglobulin genotype AA was associated with lower milk yield in Serra da Estrela and Merino ewes (Ramos *et al*., 2009). This marker also affected milk fat content in Serra da Estrela and protein content in Merino. A suggestive effect of the αS1-casein locus on milk yield was detected in Serra da Estrela, but no associations were found between the variants of this marker with milk fat and protein content (Ramos *et al*., 2009).

Major histocompatibility complex (MHC), an organized cluster of tightly-linked genes, encodes the molecules that bind processed peptide antigens including parasite-derived peptides and presents them to T-lymphocytes, thereby triggering antigen-specific immune responses (Millot, 1978). In sheep, the MHC gene family includes two major subfamilies: class I and class II genes (Klein, 1986). Among sheep MHC class II genes, the expressed DRB1 and DQB1 loci have been found to be highly polymorphic (Woodal *et al*., 1997; Konnai *et al*., 2003b; Sun *et al*., 2004). In particular, a high polymorphism level is present in exon 2, which encodes the antigen-binding site (Outteridge *et al*., 1996; Konnai *et al*., 2003a, b). Variation in these genes may impact immune responses to pathogens, which may lead to variation in disease resistance.

The molecular profiles for ewes in high group milk yield show that there are differences between high group ewes with low group ewes in both DNA profile and phenotypic profile, this point can be used by breeder to make or select the parents in future upon these DNA profiles and mate them altogether to increase the allele frequency for marker assisted selection which have high effect on economical traits to increase animals performance in the next generation as well as the outcome of breeder and sheep breeding in Iraqi Kurdistan region.

Conclusion

The molecular and phenotypic results show that there are differences between ewes groups for milk traits ewes in high group produced 355.8 g/ewe/day milk compared with 102.8 g/ewe/day in low group, these values show the ability to increase the breeder outcome about 300% when breeder select the superior animals according to the animal ranking base on molecular and phenotypic profiles. These results showed that there are agreements between BLUP values with DNA sequencing and the selection process with DNA sequencing technique can speed up the improvement and increase milk production in this breed of sheep in Iraqi Kurdistan. For future the bulk sergeant analysis can be performed on various flocks of sheep in Kurdistan which gives more about molecular markers and verification of the result of the present study through selection (and mating) of rams and ewes using the molecular marker investigated in the present study which related to quantitative traits and follow the performance of their progeny in well defined experiment.

http://www.aloki.hu ● ISSN 1589 1623 (Print) ● ISSN 1785 0037 (Online)
DOI: http://dx.doi.org/10.15666/aeer/1706_1480514822

REFERENCES

[1] Abd Allah, M., Abass, S. F., Allam, F. M. (2011): Factors affecting the milk yield and composition of Rahmani and Chios sheep. – International Journal of Livestock Production 2(3): 024-030.
[2] Abd El-Fatah, E. N., Awad, E. I. (2014): Bacterial pathogens and somatic cell count in sheep and goat milk. – Journal of Global Biosciences 3(7): 1034-1045.
[3] Al-Alaq, M. M., Al-Fahad, Y., Abass, T. (2011): The Statistical Atlas Agricultural Roadmap for Agricultural Development (Green Economy). – The Ministry of Planning (Central Organization of Statistics) and Agriculture, Iraq, Baghdad, Iraq (Arabic Reference).
[4] Al-Barzinji, Y. M. (2003): A study of growth and body dimensions of lambs and genetic evaluation for milk production of Hamdani ewes. – M. Sc. Thesis, Salahaddin University, Iraq.
[5] Al-Barzinji, Y. M. (2009): A study of some economical traits with breeding value in Hamdani sheep using molecular genetics techniques. – Ph. D. Dissertation, College of Agriculture, Salahaddin University, Iraq.
[6] Al-Barzinji, Y. M., Abdul-Rahman, F. Y. (2012): Estimated of genetic and non genetic parameters for daily test milk yield and fat percentage in Hamdani ewes. – Mesopotamia J. of Agriculture 40(3): 107-115.
[7] Al-Barzinji, Y. M., Al-Rawi, A. A. (2012): Microsatellite DNA polymorphisms and relation with economical traits in Hamdani ewes. – The 1st Scientific Agricultural Conference, 10-12th April, University of Duhok 15(1): 100-112.
[8] Al-Barzinji, Y. M., Hassan, M. W. (2005): Study of some non-genetic factors affecting milk yield and estimation repeatability for milk yield in Hamdani ewes. – Zanco J. of Pure and Applied Sciences, Salahaddin University, Hawler 17(2): 25-30.
[9] Ali, S., McGlenaghan, M., Simons, J. P., Clark, A. J. (1990): Characterization of the alleles encoding ovine-lactoglobulin A and B. – Gene 91: 202-207.
[10] Al-Mohammadi, D. S. (2002): Genetic evaluation of Awassi sheep in several commercial flocks for test day milk yield. – M. Sc. Thesis, College of Agriculture, University of Baghdad, Iraq (in Arabic).
[11] Al-Rawi, A. A., Al-Haboby, A., Al-Saman, M. H. (1997): Small Ruminants Breeding and Reproductive Physiology Research and Technology Transfer in Iraqi the Development of Integrated Crop-Livestock Production in the Low Rain Fall Areas of WANA (Mashreq/Maghreb project). – W. Mourrani and N. Haddad, Amman, Jordan.
[12] Ammer, H., Schwaiger, F. W., Kammerbauer, C., Gomolka, M., Arriens, A., Lazary, S., Epplenj, T. (1992): Exonic polymorphism vs. intronic simple repeat hypervariability in MHC-DRB genes. – Immunogenetics 35: 332-340.
[13] Anous, M. R., Rashed, M. A., Motaoa, H. R., Sadek, M. H., Saad, Y. M., Osman, M. A., Shath, E. M. (2009): Identification of fecundity gene in Egyptian goat using genetic markers. – Egyptian Journal of Sheep and Goat Sciences 4(1): 1-19.
[14] Bell, K., Mckenzie, H. A. (1967): The whey proteins of ovine milk: β-lactoglobulins A and B. – Biochim Biophys Acta 147: 123-134.
[15] Bencini, R., Johnston, K. (1997): Factors affecting the clotting properties of sheep milk. – Proceedings of the International Dairy Federation Seminar on Production and Utilization of Sheep and Goat's Milk. Hersonissos, Crete, Greece, 19-21 October.
[16] Bendelja, D., Antunac, N., Milkulec, N., Vnucec, I. (2009): Urea concentration in sheep's milk. – Mljekarstvo 59(1): 3-10.
[17] Cameron, N. D. (1997): Selection Index and Prediction of Genetic Merit in Animal Breeding. – CAB International, UK.
[18] Carta, A., Casu, S., Salaris, S. (2009): Invited review: current state of genetic improvement in dairy sheep. – J. Dairy Sci. 92: 5814-5833.

http://www.aloki.hu ● ISSN 1589 1623 (Print) ● ISSN 1785 0037 (Online)
DOI: http://dx.doi.org/10.15666/aeer/1706_1480514822

[19] Chianese, L., Garro, G., Mauriello, R., Laezza, P., Ferranti, P., Addeo, F. (1996): Occurrence of five αs1-casein variants in ovine milk. – Journal of Dairy Research 63: 49-59.
[20] Chianese, L., Mauriello, R., Ferranti, P., Tripaldi, C., Taibi, L., Dell'aquila, S. (1997): Relationship between αs1-casein variants and clotting capability of ovine milk. – In: Proceedings of the IDF Seminar "Milk Protein Polymorphism II", held in Palmerston North, New Zealand, February 1997. International Dairy Federation, Brussels, pp. 316-323.
[21] Corral, J. M., Padilla, J. A., Izquierdo, M. (2010): Associations between milkprotein genetic polymorphisms and milk production traits in Merinosheep breed. – Livest. Sci. 129: 73-79.
[22] Erhardt, G. (1989): Genetic polymorphisms of β-lactalbumin and β-lactoglobulin in sheep milk. – Anim Genet 20: 76-77.
[23] Fuertes, J. A., Gonzalo, C., Carriedo, J. A., San Primitivo, F. (1998): Parameters of test day milk yield and milk components for dairy ewes. – J. Dairy Sci. 81: 1300-1307.
[24] Gardi, H. E. A. (2008): Effect of Breed and some environmental fixed factors on milk yield in commercial flocks. – M.Sc. Thesis, College of Agriculture, University of Sallahaddin, Iraq.
[25] Gutiérrez-Gil, B., Arranz, J. J., Pong-Wong, R., García-Gámez, E., Kijas, J., Wiener, P. (2014): Application of selection mapping to identify genomic regions associated with dairy production in sheep. – PLoS ONE 9(5): e94623. https://doi.org/10.1371/journal.pone.0094623.
[26] Iamartino, D., Bruzzone, A., Lanza, A., Blasi, M., Pilla, F. (2005): Genetic diversity of Southern Italian goat populations assessed by microsatellite markers. – Small Rumin. Res. 57: 249-255.
[27] ICARDA, FAO (1995): The Recording of Fat-Tailed Sheep in Syria, Turkey and Jordan. – Consultancy Report, Jordan.
[28] Jurate, K., Gediminas, V., Jolanta, M., Ilma, T. (2005): Genetic polymorphism of b-lactoglobulin in Lithuanian Blackface and Lithuanian Native Coarsewooled sheep. – Vet. Zootech. 29(51): 90-92.
[29] Kawecka, A., Radko, A. (2011): Genetic polymorphism of β-lactoglobulin in sheep raised for milk production. – J Appl Anim Res 39: 68-71.
[30] King, J. W. B. (1969): The distribution of sheep b-lactoglobulins. – Anim Prod 11: 53-57.
[31] Klein, J. (1986): The Natural History of the Major Histocompatibility Complex. – Wiley, New York, pp. 56-79.
[32] Kolde, H. J., Braunitzer, G. (1983): The primary structure of ovine β-lactoglobulin. – Milchwissenschaft 38: 70-72.
[33] Konnai, S., Nagaoka, Y., Takesima, S., Onuma, M., Aida, Y. (2003a): DNA typing for ovine MHC-DRB1 using polymerase chain reaction restriction fragment length polymorphism (PCR-RFLP). – J. Dairy Sci. 86: 3362-3365.
[34] Konnai, S., Takesima, S., Tajima, S., Yin, S. A., Okada, K., Onuma, M., Aida, Y. (2003b): The influence of ovine MHC class II DRB1 alleles on immune response in bovine leukemia virus infection. – Microbiol. Immunol. 47: 223-232.
[35] Kumar, D., Dixit, S. P., Sharma, R., Pandey, A. K., Sirohi, G., Patel, A. K., Aggarwal, R. A. K., Verma, N. K., Gour, D. S., Ahlawat, S. P. S. (2005): Population structure, genetic variation and management of Marwari sheeps. – Small Ruminant Research 59: 41-48.
[36] Maarof, N. N., Juma, K. H., Arafat, E. A., Chkmakchy, A. M. (1986): Evaluation of factor affecting birth and weaning weight and milk production in Hamdani sheep. – Wld. Rev. Anim. Prod. 22(1): 51-55.
[37] Macciotta, N. P., Cappio-Borlino, A., Pulina, G. (2000): Time series autoregressive integrated moving average modeling of test-day milk yields of dairy ewes. – J. Dairy Sci. 83: 1094-1103.

http://www.aloki.hu ● ISSN 1589 1623 (Print) ● ISSN 1785 0037 (Online)
DOI: http://dx.doi.org/10.15666/aeer/1706_1480514822

[38] Mavrogenis, A. P. (1996): Estimates of environmental and genetic parameters influencing milk and growth traits of Awassi sheep in Cyprus. – Small ruminant Res. 20: 141-146.
[39] Millot, P. (1978): The major histocompatibility complex of sheep (OLA) and two minor loci. – Anim. Blood Groups Biochem. Genet. 9: 115-121.
[40] Mroczkowski, S., Korman, K., Erhardt, G., Piwczynski, D., Borys, B. (2004): Sheep milk protein polymorphism and its effect on milk performance of Polish Merino. – Arch. Tierz. 47(SI): 114-121.
[41] Oramari, R. A. S. (2009): Genetic evaluation of Karadi sheep using some productive traits. – PhD Dissertation. Animal Production Department, College of Agriculture, University of Duhok, Iraq.
[42] Outteridge, P. M., Andersson, L. Douch, P. G., Green, R. S., Gwakisa, P. S. Hohenhaus, M. A., Mikko, S. (1996): The PCR typing of MHC-DRB genes in the sheep using primers for an intronic microsatellite: application to nematode parasite resistance. – Immunol. Cell Biol. 74: 330-336.
[43] Picariello, G., Rignanese, D., Chessa, S., Ceriotti, G., Trani, A., Caroli, A., Di Luccia, A. (2009): Characterization and genetic study of the ovine aS2-casein (CSN1S2) allele B. – Protein Journal 28: 333-340.
[44] Pietrolà, E., Carta, A., Fraghi, A., Piredda, G., Pilla, F. (2000): Effect of β-lactoglobulin locus on milk yield in Sarda ewes. – Zoot. Nutr. Anim. 26: 131-135.
[45] Pirisi, A., Piredda, G., Papoff, C. M., Di Salvo, R., Pintus, S., Garro, G., Ferranti, P., Chianese, L. (1999): Effects of sheep _s1-casein CC, CD and DD genotypes on milk composition and cheesemaking properties. – Journal of Dairy Research 66: 409-19.
[46] Piwczyński, D., Borys, B., Mroczkowski, S., Erhardt, G., Jarzynowska, A. (2002): Charakterystyka polimorfizmu białek i produkcji mleka owiec mieszańców merynosa polskiego z rasami plennymi. – Prace i Materiały Zootechniczne, Zeszyt Specjalny 14: 151-162.
[47] Raaof, S. O. (2006): Genetic evaluation of Hamdani sheep in some flocks for test-day milk yield. – Proc. 4th Int. Con. Biol. Sci. (Zool.), pp. 197-200.
[48] Raaof, S. O. (2005): Estimation of genetic and phenotypic parameters for lambs growth and evaluation of Hamdani ewes for productive traits. – Ph. D. Dissertation, Salahaddin University, Iraq.
[49] Ramos, A. M., Matos, C. A. P., Russo-Almeida, P. A., Bettencourt, C. M. V., Matos, J., Martins, A., Pinheiro, C., Rangel-Figueiredo, T. (2009): Candidate genes for milk production traits in Portuguese dairy sheep. – Small Ruminant Research 82: 117-121.
[50] Rozen, S., Skaletsky, H. J. (2000): Primer3 on the WWW for General Users and for Biologist Programmers. – In: Misener, S. Krawetz, S. A. (eds.) Bioinformatics Methods and Protocols: Methods in Molecular Biology. Humana Press, Totowa, NJ, pp. 365-386.
[51] Ruiz, R., Oregui, L. M., Herrero, M. (2000): Comparison of models for describing the lactation curve of Latxa sheep and an analysis of factors affecting milk yield. – J. Dairy Sci. 83: 2709-2719.
[52] Sanna, S. R., Carta, A., Cause, S. (1998): Comparison between on-farm and nucleus – flock estimated breeding values in Sarda dairy sheep. – 6th World Congress on Genetics Applied to Livestock Production, 12-16, Jan. Armidale, NSN Australia, 23: 141-145.
[53] SAS, Statistical analyses system. (2002): SAS/STAT User's Guide, Version 8. First Ed. – Cary, NC.
[54] Sun, D. X., Zhang, Y. (2004): Polymorphism of the second exon of MHC-DRB gene in Chinese local sheep and goat. Biochem. – Genet. 42: 385-390.
[55] Visser, C., Hefer, C. A., van Marle-Köster, E., Kotze, A. (2004): Genetic variation of three commercial and three indigenous goat populations in South Africa. – South African Journal of Animal Science (34): 24-27.
[56] Wessels, G., Hamann, H., Erhardt, G., Distl, O. (2004): Genotypeffekte von Milchprotein- Polymorphismen auf die Milchleistung beim Ostfriesischen Milchschaf. – Berl. Münch. Tierärztl. Wochenschr. 117: 414-419.

http://www.aloki.hu ● ISSN 1589 1623 (Print) ● ISSN 1785 0037 (Online)
DOI: http://dx.doi.org/10.15666/aeer/1706_1480514822

[57] Williams, J. L. (2005): The use of marker-assisted selection in animal breeding and biotechnology. – Revue Scientifique et Technique, International Office of Epizootics 24(1): 379-391.
[58] Woodal, C. J., Maclaren, L. J., Watt, N. J. (1997): Differential levels of mRNAs for cytokines, the interleukin-2 receptor and class II DR/DQ genes in ovine interstitial pneumonia induced by maedi visna virus infection. – Vet. Pathol. 34: 204-211.
[59] Yousefi, S., Ahani Azari, M., Zerehdaran, S., Samiee, R., Khataminejhad, R. (2013): Effect of β-lactoglobulin and -casein genes polymorphism on milk composition in indigenous Zel sheep. – Arch Tierz 56: 216-224.

http://www.aloki.hu ● ISSN 1589 1623 (Print) ● ISSN 1785 0037 (Online)
DOI: http://dx.doi.org/10.15666/aeer/1706_1480514822

TRACE ELEMENTS AND METAL CONTENT IN THE FEATHERS OF THE NORTHERN BALD IBIS (*GERONTICUS EREMITA*)

DINÇ, H.[1*] – YIĞIN, A.[2] – BOZKAYA, F.[2]

[1]*Department of Pharmacology and Toxicology, Veterinary Faculty, Harran University, Şanlıurfa, Turkey*

[2]*Department of Genetics, Veterinary Faculty, Harran University, Şanlıurfa, Turkey (e-mails:akinyigin@yahoo.com, farukbozkaya@yahoo.com)*

**Corresponding authors*
e-mail: hikmetdnc@gmail.com; phone: +90-414-318-3859

(Received 13th Jun 2019; accepted 25th Oct 2019)

Abstract. Long-lived bird species, such as the Northern Bald Ibis (*Geronticus eremita*), are exposed to heavy metals through air, water and food because they are at the highest point in the food supply chain. Birds accumulate heavy metals in their bodies, organs, and in their feathers. The article aimed to investigate the trace element and heavy metal content of Northern bald ibis feathers using ICP-MS, as an endangered sentinel species, in order to both determine the contamination level of the area and evaluate the risk the species is facing. The study included 34 samples of feathers obtained from bald ibises released into their natural habitat. The results of the study showed that the average values of the trace elements ($^{11}Na^+$, ^{24}Mg, $^{20}Ca^+$, $^{39}K^+$, P, $^{27}Al^+$, $^{56}Fe^+$) which are necessary for the survival of living organisms were above 100 µg g-1, the second group of metals ($^{205}Ti^+$, ^{55}Mn, $^{63}Cu^+$, $^{66}Zn^+$, ^{82} Br) which are toxic to the body in high amounts were between 8.24-22.4 µg g^{-1} and those which are highly toxic at very low doses ($^{51}Sb^+$, ^{60}Ni, As, ^{60}Co, $^{138}Ba^+$, $^{208}Pb^+$, $^{111}Cd^+$, Mo, ^{75} Se) were lower than 1 µg g^{-1}. This study of the Northern Bald Ibis species, animals threatened by extinction due to environmental pollution, investigated their levels of heavy metal pollution in the feathers and indicates that Bald Ibis are possible bioindicators of environmental trace element contamination.
Keywords: *bioindicator, environmental pollution, heavy metal toxication*

Introduction

As a result of human activities, pesticides, industrial products and waste materials containing heavy metals impair the biological integrity of the ecosystem in various ways. Heavy metal pollution of the soil occurs in industrial and mining areas, through the use of fertilizers, drain waters, pesticides, waste products of the coal or oil industry and air pollution. These metals include $^{24}Mg^+$, $^{31}P^+$, $^{39}K^+$, $^{56}Fe^+$, $^{11}Na^+$, $^{20}Ca^+$, $^{63}Cu^+$, $^{66}Zn^+$, ^{75} Se and Ag, which are essential for the human body, but can be toxic in high amounts. Other metals, such as $^{60}Ni^+$, $^{111}Cd^+$, $^{138}Ba^+$, $^{27}Al^+$, $^{52}Cr^+$, ^{55}Mn, $^{208}Pb^+$, ^{82}Br, ^{60}Co, ^{205}Ti and $^{51}Sb^+$ are toxic even at very low amounts.

Animals ingest heavy metals by consuming feedstuffs, grass, and water, or from the application of veterinary drugs, or by licking mineral blocks, or paints containing heavy metals (Kara et al., 2016; Govind and Madhuri, 2014; Das et al., 2009). Due to higher sensitivity levels, birds are usually considered to be bio-indicators for monitoring the effects of environmental pollution (Yohannes et al., 2017).

Since long-living bird species such as the Bald Ibis are at the top of the food chain, they are more exposed to heavy metals through air, water and food. When the metals are digested they are either stored in or excreted from the body. Metals that accumulate in the organs or feathers of the birds may also be passed on to eggs (Dauwe et al., 2000).

http://www.aloki.hu ● ISSN 1589 1623 (Print) ● ISSN 1785 0037 (Online)
DOI: http://dx.doi.org/10.15666/aeer/1706_1482314834

Feathers contain blood vessels during the growth period and heavy metals in the blood are passed to the feathers and then become isolated there after keratinization. Thus feathers provide valuable information on the level of heavy metals in birds' blood. Since the 1960s, feathers have been used as bio-indicators for monitoring heavy metal exposure of birds, and it has been reported that feathers which are directly exposed to environmental pollution may have higher heavy metal contents due to exogenous contamination (Rutkowska et al., 2018).

Thus, there is a need for studies to determine the toxic effects of environmental pollution in order to maintain biological diversity and protect sentinel species such as the Bald Ibis (Bauerová, 2017; Da Silva et al., 2017; Dolan et al., 2017; Borgesi et al., 2016).

Numerous studies have been conducted on birds of prey to determine the residuals of environmental pollutants such as Pb, Cd, and Hg and pesticides (İnangi et al., 2019; Carneiro et al., 2018; Espín et al., 2016). The ingestion of heavy metals by animals has been reported to cause intoxication, resulting in behavioral disorders, impairment of feathering or decreased breeding and hatchability (Kara et al., 2016).

The Bald Ibis population in Turkey declined to a size near extinction due to the intensive use of pesticides (Dichlorodiphenyltrichloroethane - DDT) against grasshoppers between 1955 and 1960. Survivors did not lay eggs for several years and nestlings hatched were weak. In the offspring of subsequent generations, deformations of the beak and feet were observed (Akyıldız et al., 2005). In the red list published by the International Union for the Conservation of Nature (IUCN), the Bald Ibis was classified as an endangered species. There are three different breeding centers in different locations of the world, including the Birecik district of Turkey, Fas in Morocco and Palmyra in Syria (*Fig. 1*). The life span of the Bald Ibises is about 25-30 years. Bald Ibises in Birecik district are housed in wooden nests or in nests carved into calcite rocks (Tel and Keskin, 2012).

The General Administration of Nature Conservation and National Parks, with the support of the World Wildlife Foundation, established a breeding station in the Birecik district of Sanliurfa province. The Bald Ibises are kept semi-captive, eating pests such as snakes, grasshoppers, insects, scorpions, snails, lizards or snapdragons in the fields near the Euphrates River, when they are out of the breeding station in the summer. They are fed on a diet of raw lean meat, whey, cooked egg, and carrot when they enter the breeding station in winter (Mundan and Cetin, 2012).

There have been few studies on the factors threatening the survival of the Bald Ibis. Tel and Keskin (2012) investigated the prevalence of Yersinia spp. and Aeromonas hydrophyla, while Tel et al. (2013) reported the presence of Salmonella spp. Campylobacter spp. and the absence of Chlamydia psitaci in feces samples of Bald Ibisies. Recently, Spergser et al. (2018) reported the cultivable microbiota isolated from different organs of Northern Bald Ibises. As exposure to heavy metals, even at low concentrations, may negatively affect reproduction of birds by decreasing egg production and hatchability, and increasing the mortality of hatchlings (Malik and Zeb, 2009; Scheuhammer, 1987), it is important to monitor the heavy metal exposure status of endangered species, such as the Bald Ibis. However, to the best of our knowledge, there has been no previous report on the heavy metal exposure status of Bald Ibises.

Therefore, the objective of this study was to determine metal and heavy metal contents of feather samples of Bald Ibises raised in the Birecik District of Sanliurfa, Turkey, in order to estimate predict the risk of heavy metal exposure of this species. In

http://www.aloki.hu ● ISSN 1589 1623 (Print) ● ISSN 1785 0037 (Online)
DOI: http://dx.doi.org/10.15666/aeer/1706_1482314834

the future, Bald Ibises might be an ecological indicator for trace element exposure in pollinated ecosystems and studies determining the source of exposure might help develop conservation strategies for protecting this important and charismatic wildlife species

Materials and methods

This study was carried out with the permission and support of the Turkish General Directorate of Nature Conservation and National Parks (Approval No: 72784983.04-42845).

Sample collection

Feather samples of 34 individual birds (17 male and 17 female) were obtained from the wings or tails of birds raised semi-captive at the Bald Ibis breeding station in Birecik district of Şanliurfa province, Turkey (37.01.29 N:37.58.38 E). The feather samples were placed in plastic bags and stored at -20 °C until analysis. Whole feather samples were used for chemical analysis after the removal of dust or feces residues with distilled water. (Costa et al., 2013) Collection of the feather samples was approved by the General Directorate of Nature Conservation and National Parks in the framework of the protocol signed by Harran University and the General Directorate of Nature Conservation and National Parks (Protocol No: 26130895-030.03)

Figure 1. *Settlement and habitat of the bald ibis and map image of Birecik (Turkey) and Palmira (Syria)*

Chemicals and standard solutions

Chemicals including 60% hydrogen peroxide (H_2O_2), 37% hydrochloric acid (HCl) and 65% nitric acid (HNO_3) were purchased from Merck (Darmstad, Germany). Stock standard solutions for each element were purchased from Agilent Technologies, Japan (Lot number: 10-160YPYZ). The 99.9980% Argon gas was supplied by Linde Gases (Linde Group, Turkey)

http://www.aloki.hu ● ISSN 1589 1623 (Print) ● ISSN 1785 0037 (Online)
DOI: http://dx.doi.org/10.15666/aeer/1706_1482314834

Microwave acid digestion

After the feather samples were weighed they were washed with distilled water. The samples were put into a Teflon microwave vessel and 2 ml 60% H_2O_2, 3 ml 37% HCl and 1 ml 65% nitric acid (HNO_3) were added to each sample. The samples were left overnight at room temperature for slow digestion. The samples were treated in a microwave oven (Cem Mars 5) at 180 °C and 800 W for 1 h, then transferred to a 50 mL tube and distilled water was added up to 50 mL.

Analysis of essential element and heavy metal content on ICP-MS

Essential element and heavy metal content of the digest was assessed using an ICP-MS device inductively coupled plasma-mass spectrometer with an Auto Sampler and nebulizer (Agilent, 7500ce Octopole Reaction System, Japan) (Mikoni et al., 2017). Calibration of the method was applied using an internationally validated standard. The accuracy of the device and the method was achieved by measuring a certified reference.

Statistical analyses

Statistical calculations were performed using SPSS 22.0 software (SPSS Inc., Chicago, USA). Conformity of the data to normal distribution was assessed with the Shapiro Wilk test. The Mann-Whitney-U test was applied to variables not showing normal distribution. Correlations between numerical variables were determined using the Spearman rank correlation coefficient. The result of the hierarchical clustering was presented in a dendrogram (*Fig. 2*). A value of $p < 0.05$ was considered statistically significant. The correlations between the elements found in the samples were calculated while the significance value was evaluated.

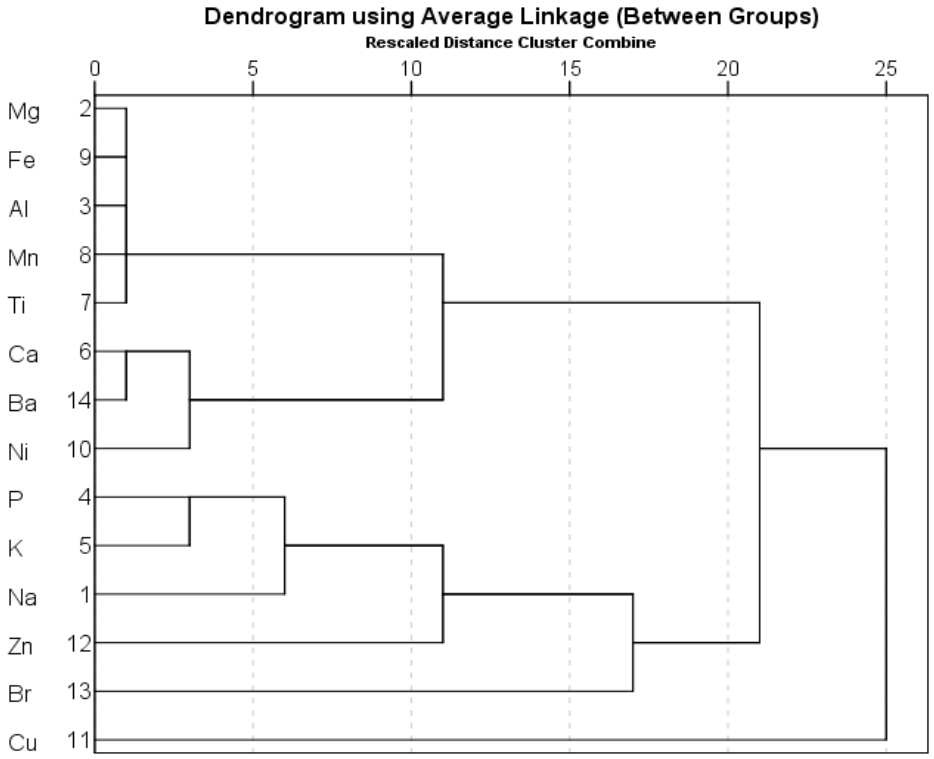

Figure 2. *Hierarchical clustering results of feather samples (dendrogram)*

http://www.aloki.hu ● ISSN 1589 1623 (Print) ● ISSN 1785 0037 (Online)
DOI: http://dx.doi.org/10.15666/aeer/1706_1482314834

Results

The mean concentrations of the essential elements and heavy metals measured in the feather samples are presented in *Table 1.*

Table 1. *Concentrations of essential elements and heavy metals in the feather samples (μg g^{-1}, dw, a dry weight basis)*

Elements	Minimum	Maximum	Mean	Std. error	Std. deviation	CV (%)
Na	1151.90	4601.24	2048.83	124.74	727.25	35.49
Mg	194.87	1181.50	365.96	28.64	167.00	45.63
Al	11.37	1160.74	246.52	34.73	202.50	82.14
P	87.37	1238.64	248.78	32.41	188.97	75.958
K	0.13	2178.72	168.31	70.57	411.41	244.43
Ca	850.62	7486.56	2200.42	217.01	1265.12	57.49
Ti	6.67	72.69	22.74	1.96	11.41	50.17
Mn	1.13	46.12	8.54	1.33	7.76	90.87
Fe	53.93	1664.62	337.58	48.10	280.44	83.07
Ni	0.06	23.37	1.86	0.68	3.94	211.83
Cu	0.09	6.10	2.89	0.21	1.22	42.21
Zn	16.07	210.57	67.88	7.57	44.15	65.04
Br	0.02	35.03	8.24	1.31	7.66	92.96
Ba	0.26	21.01	3.48	0.62	3.61	103.74

Concentrations of the essential elements (Na, Mg, Ca, K, P, Al, Fe) were detected to be higher than 100 μg g^{-1} while those of Ti, Mn, Cu, Zn and Br were between 8.24 and 22.4 μg g^{-1}. Of the heavy metals, As was detected in 5 samples with concentrations varying from 44.77 to 2083.05 μg g^{-1} while Co was found in only 2 samples with concentrations of 344.24 and 848.31 μg g^{-1}. Se and Pb were detected in 1 sample each, at concentrations of 447.01 and 119.66 μg g^{-1}, respectively. Detectable concentrations of Sb, Ni, Mo and Pb were not observed. A significant difference in the metal contents between the sexes was observed only for Cu ($p = 0.024$) while no difference was observed in the contents of other metals ($p > 0.05$)

Other toxic elements were found in the values of Co (227-842 μg g^{-1}), As (45-30 836 μg g^{-1}), Se (0-447 μg g^{-1}), and Pb (0-119 μg g^{-1}). The Sb, Cd and Mo values were determined under the measurable value.

The correlation coefficients between individual metal contents of the samples are shown in *Table 2*. High and significant correlations were observed especially among Mg, Al, Ti, Mn, Fe and Ni contents. The hierarchical clustering results among the metal contents are presented in *Figure 2.*

In this study, significant correlations from moderate to high correlation coefficients between essential elements were observed. For example, moderate positive correlations were determined between Na and Br and between Na and P ($r = 0.473$ $p = 0.01$) ($r = 0.566$, $p = 0.001$) and a weak positive correlation was determined between Na and K content (r: 0.388; p: 0.023). In addition, Ca content was moderately correlated with Ni ($r = 0.518$, $p = 0.02$) and Ba ($r = 0.861$, $p = 0.001$) and with Fe ($r = 0.401$, $p = 0.019$) and Mn ($r = 0.412$, $p = 0.016$) and a weak significant negative correlation with Cu ($r = -0.378$ $p = 0.027$).

http://www.aloki.hu ● ISSN 1589 1623 (Print) ● ISSN 1785 0037 (Online)
DOI: http://dx.doi.org/10.15666/aeer/1706_1482314834

Table 2. *Correlations between the metal contents of the feather samples*

	Na	Mg	Al	P	K	Ca	Ti	Mn	Fe	Ni	Cu	Zn	Br
Mg	0.026	1											
Al	-0.103	0.947**	1										
P	0.566**	-0.079	-0.206	1									
K	0.388*	0.205	0.195	0.072	1								
Ca	0.313	0.480**	0.395*	0.176	-0.035	1							
Ti	0.094	0.920**	0.948**	-0.099	0.204	0.565**	1						
Mn	-0.233	0.889**	0.896**	-0.199	0.111	0.412*	0.819**	1					
Fe	-0.081	0.960**	0.971**	-0.219	0.22	0.401*	0.909**	0.939**	1				
Ni	-0.022	0.906**	0.872**	-0.061	0.246	0.518**	0.844**	0.942**	0.903**	1			
Cu	-0.221	-0.341*	-0.233	-0.113	0.073	-0.378*	-0.297	-0.374*	-0.314	-0.444**	1		
Zn	0.106	-0.246	-0.224	-0.107	-0.202	-0.203	-0.142	-0.209	-0.21	-0.23	-0.255	1	
Br	0.473**	0.118	0.079	0.215	0.425*	0.293	0.197	0.051	0.144	0.138	0.048	-0.243	1
Ba	0.162	0.571**	0.582**	0.029	0.033	0.861**	0.717**	0.557**	0.547**	0.608**	-0.292	-0.108	0.272

Fe is a trace element found in complex with other metals. In this study, Fe showed a positively strong correlation with Ni (r = 0.903, p = 0.01), a medium correlation with Ba (r = 0.547; p = 0.01), and weak negative correlation with Cu (r = -374 P: 0.029).

When the correlations of Mg were examined, there was a weak negative correlation with Cu values (r = -0.342; p = 0.049), while there was a moderate positive correlation with Ca values (r = 0.480 p = 0.04), and a strong positive correlation with Al, Ti, Mn, Fe, Ni, and B (r = 0.947 p = 0.01, r = 0.920; 0.881; 0.960; 0.904; 0.571, p = 0.001, respectively).

A strong positive correlation was found between Mn and Fe and Ni (r = 0.939; 0.942 and p = 0.01). There was a moderate positive correlation with Ba (r = 0.55; p = 0.01).

A strong positive correlation was found between Al, Mn, Fe, Ni and Ba (r = 0.971; 0.948; 0.872; 0.582; p = 0.001 respectively). There was a moderate positive correlation with Ca (r = 0.395; p = 0.021).

As all birds were between 1 and 4 years of age, no statistically significant difference was found between age and heavy metal levels (p > 0.05). In addition, gender analyzes in bald ibises can only be performed genetically by Realtime PCR and RFLP-PCR. No statistically significant difference was found between the genders and heavy metal levels in the analyses (p > 0.05).

Discussion

Due to the accumulation of metals in feathers they reflect both the physiological status of the animal and the environmental conditions. Therefore, feathers are valuable materials for monitoring the effect on birds of environmental pollution with heavy metals. This study reports for the first time the metals and heavy metals contents of feather samples from the Bald Ibis.

The natrium (1151-4601, 2048 ± 727 μg g^{-1}) and K (0.13-2178 μg g^{-1}, 168 ± 70.57) content detected in the feather samples of Bald Ibises were similar to those reported for Na (1087-3950 μg g^{-1}) and K (84-285 μg g^{-1}) in the Greater Flamingo (Borgessi et al., 2016).

http://www.aloki.hu ● ISSN 1589 1623 (Print) ● ISSN 1785 0037 (Online)
DOI: http://dx.doi.org/10.15666/aeer/1706_1482314834

Calcium plays a role in muscle contractions, enzyme activation and cardiac rhythm (Zamberlin et al., 2012). The mean Ca content in the feather samples of Bald Ibises were higher than that reported by Hanson and Jones (1968) for geese (600-2800 μg g^{-1}) from different localities of USA and lower than that (3151.87–4087.67) in red-breasted flycatchers (*Ficedula parva*) as reported by Hanc et al. (2017). The higher level of Ca in the present study could have been due to the higher Ca content of the rocks where the Bald Ibises are housed. Bald Ibises are housed either in wooden nests or in holes carved into limestone rocks within the breeding station. Limestone found around Sanliurfa mostly consists of formations of middle upper Eocene age, comprising limestone (Fonsi Formation) or clayey and chalky limestone (Gaziantep Formation) (Richardson, 1991, cited by Canakci et al., 2007). Turgut et al. (2008) reported that Sanliurfa stone samples contain a high amount of Ca and lower amounts of Al, Fe, Mg, S and Si, while they contain no Na, K and Cl.

Mg plays an important role in protein metabolism, blood pressure regulation and neuromuscular transmission. The Mg content in the feather samples (365.96 ± 28.65 μg g^{-1}) in the present study was lower than that reported by Borghesi et al. (2016) for the Greater Flamingo (463-1843) and higher than that reported by Hanc et al. (2017) in red-breasted flycatchers (*Ficedula parva*) (174.58 μg g^{-1}).

This difference may be related to the feeding patterns of the bird species studied and the environment in which they live. Flamingos feed on small plankton-like animals in wetlands. The Bald Ibises (*Geranticus eremita*) outside of the breeding station feed on insects, snails, etc, and the nesting area includes calcium-rich limestone rocks. This difference might also be related to the age of the bird as the basic elements were expected to be higher because the birds in this study were younger and still in the growth and development period.

Potassium plays an active role in cellular activities, in nerve conduction and bone metabolism. The higher K content of the Bald Ibis feathers associated with environmental pollution, demonstrated that the water, soil and plants in the habitats. Sodium plays a role in the acid-base balance in extracellular fluid. Mean content of Fe in the feather samples in the present study (337.58 ± 48.10) was found to be higher than the reported values of 48.9 ± 5.8, 185.84 ± 18.47 and 52.79 ± 50.69 μg g^{-1} for Common moorhens (*Gallinula chloropus*) (López-Perea et al., 2019), Italian Sparrows (*Passer italiae*) (Innangi et al., 2019) and Anna's humming birds (*Calypte anna*) (Mikoni et al., 2017) respectively. No significant difference in the Fe content between the sexes was observed ($p > 0.05$). The higher Fe content of the Bald Ibis feathers could be attributed to species differences associated with nutritional behavior. For example, moorhens eat plant seeds and invertebrates (Zamani-Ahmadmahmoodi, 2010) while the Bald Ibises in this study consumed both small vertebrates and invertebrates in addition to the diet supplied in the breeding station which contained lean meat. However, the differences may also arise from the geographical distribution of the same species. Innangi et al. (2019) reported that the feathers of Italian Sparrows contained a 9-fold lower level of Fe than those of House Sparrows in Southern Africa.

Based on the observation that Mn together with Zn and Ca is abundant in black-coloured feathers, and that healthier birds have more coloured feathers, Innangi et al. (2019) suggested that higher levels of Mn might indicate a healthier bird. The higher Mn content in the feather samples in this study could therefore be attributed to the black-coloured plumage of Bald Ibises.

http://www.aloki.hu ● ISSN 1589 1623 (Print) ● ISSN 1785 0037 (Online)
DOI: http://dx.doi.org/10.15666/aeer/1706_1482314834

The mean Ba content detected in this study (3.48 ± 0.62 μg g^{-1}) was lower than the value reported by Adout et al. (2007) for Feral Pigeons (4.84 ± 1.31-16.7 ± 8.1) and Hooded Crows (*Corvus corone cornix*) in rural (15.6 ± 7.36) or industrial areas (18.3 ± 6.8). This can be thought to be due to industry in the regions close to the study area. Barium can pharmacologically replace Ca (John et al., 2005) ions in the keratin structure of bird feathers and high Ba levels can result in health problems in young birds (Hanc et al., 2011).

The results of this study showed a high correlation between Ba content and Ca content in the feather samples ($r = 0.861$, $p = 0.001$). It has been suggested that environmental pollution with Ba is caused by dust from road aggregate material (Brumbaugh et al., 2006). The lower Ba content in the Bald Ibis feather samples could therefore be explained by the distance of the breeding station from main roads.

The mean Zn content (67.88 ± 7.57 μg g^{-1}) in this study was found to be similar to that reported for birds raised in regions near to industrial areas. López-Perea et al. (2019) reported a mean Zn level of 71.11 μg g^{-1} in the feather samples of common moorhens living in wetlands irrigated with industrial waste water. Dolan et al. (2017) observed the highest levels of Zn (82.1 mg/kg) in the feathers of Northern Goshawks living in regions near to industrial areas in Norway and Spain. Mikoni et al. (2017) found 123.79 mg g^{-1} on the feathers of free-flying Anna's humming birds in California, which was approximately double the values in the current study. The authors attributed the high level of Zn in this species to the pollution of the nectar and flies they eat by Zn contained in dish washing detergents. Innangi et al. (2019) reported Zn content of 106.26 μg g^{-1} in the feather samples of free-flying birds in a region close to an industrial zone in southern Italy. Borghesi et al. (2016) reported levels of 77.44 mg kg^{-1} in bird colonies living near industrial zones in France, Spain and Italy Zinc is an important and necessary element for the keratinization process in birds, and is also used in veterinary medicine as an emetic and antiseptic drug or as an antagonist drug against copper sulphate toxicity. As excessive ingestion of Zn is toxic, environmental pollution with Zn represents a risk for wildlife (Sundaresan et al., 2008; Honda et al., 1986)

The mean value Ni found in the current study (1.86 ± 0.67 μg g^{-1}) was higher than the values found by Borghesi et al. (2016) (1.058 μg g^{-1}) and López-Perea (2019) (0.087 μg g^{-1}) and lower than that reported by Mikoni et al. (2017) (3.28 μg g^{-1}). Thus, the Ni content reported in this study was within the range previously reported in literature. However, Ni is a metal extensively used in industry and industrial activities, and isa major source of environmental pollution. The town of Birecik, where the study was conducted, is close to the industrial city of Gaziantep. The mean concentration of Ni in the sediments at different locations of the Euphrates River has been reported to be 0.16-0.35 μg g^{-1} (Oymak et al., 2009). Therefore, disposal of industrial waste in the Euphrates River may be the cause of Ni exposure of the birds.

Al can be transmitted from the environment to both natural and anthropogenic sources and its toxicity varies according to the target organ. The mean Al content found in the present study (246.52 ± 34.73) was higher than the values found by Borghesi et al. (2016) (3.71 μg g^{-1}) and Dolan et al. (2017) (23 μg g^{-1}). Mn was determined in the range of 20- 491 μg g^{-1} and these values were higher than all other studies [Lopez et al., 2019, (3.93-89 μg g^{-1}), İnnangi et al., 2019, (0.33-23.83 μg g^{-1}) and Mikoni et al., 2019, (0.33-23.83 μg g^{-1}]. Excessive amounts of Mn have been reported to be life-threatening and high amounts of Mn taken by ingesting sediments can cause acute and chronic toxicity (Sánchez-Virosta et al., 2015).

http://www.aloki.hu ● ISSN 1589 1623 (Print) ● ISSN 1785 0037 (Online)
DOI: http://dx.doi.org/10.15666/aeer/1706_1482314834

In some studies, the Cu content of feather samples gas been found to be 1.97-149.9 μg g^{-1} (Mikoni et al., 2017), 5.04-17.04 μg g^{-1} (López et al., 2019), 6.59 ± 4.72 μg g^{-1} (Bauerová et al., 2017), and 2.68 μg g^{-1} (İnnangi et al., 2019). In this study, the Cu value was determined between 5 -500 μg g^{-1}. This value is higher than those reported by other study groups. Cu is widely used in veterinary medicine as an anthelmintic antiperspirant. Pollution from water, sediment and industrialization affects the amount of Cu in birds. The high Cu concentration determined in this study may reflect the pollution of the habitat in which the animal lives.(Custer et al., 2008) This shows that there is a continuing risk of environmental contamination for the Bald Ibis, which is at risk of extinction.

Arsenic is a toxic element. Acute and chronic intoxication may be seen with excessive intake of this metal (Borghesi et al., 2016; Sanches Virost et al., 2015). In the current study, the mean arsenic levels in the feather samples were 486 ng/g in males and 1451 ng g^{-1} in females although the differences between the sexes were not significant. Bauerová et al. (2017) reported cyanide levels of 1510 ng g^{-1}, Borghesi et al. (2016), 819 ng g^{-1}, and López-Perea et al. (2019) 378 ng g^{-1}. Arsenic is bound to sulphur-rich proteins in feathers (Murphy et al., 1990).

Other toxic elements determined in the current study were Se 447.01 ng g^{-1}, Pb 119.66 ng g^{-1}, and Co 227.96 -848.31 ng g^{-1}. The presence of toxic heavy metals in bird feathers may be due to the contamination of their feathers with external pollution. It has also been reported in other studies that pollution can occur with these metals (Al, Co, Ni, Cu, Fe, Zn, Mn, Ag, Tl, Pb and Cd) during the growth period of feathers (Dauwe et al., 2003). Exposure of birds to Pb, Se, Cd, Zn and As causes reproductive failure, growth disorder, and behavioral changes (Binkowski et al., 2013; Govind and Madhuri, 2014; Alvárez et al., 2013). With the exception of Cu, no significant difference was observed in terms of other elements. Most studies on different bird species have reported no significant difference between the sexes in the metal content of feather samples (Markowski et al., 2013; Squadroneet al., 2016).

The fact that high and significant correlations were observed among Mg, Al, Ti, Mn, Fe and Ni contents might indicate a common physiological or environmental basis. Given that trace elements can move though food chains by a variety of routes.

Conclusion

This is the first study to determine heavy metal pollution in the feathers of the Bald Ibis, which is an endangered bird. In this study, the presence of heavy metals such as Pb, As, Br, Ni, Zn, which are important for the determination of environmental pollution, demonstrated that the water, soil and plants in the habitats of the people are exposed to metal pollution because of industrial, domestic and agricultural activities. The heavy metal limits determined in this study, are at a level that threatens the life of the Bald Ibis and reflects the pollution of the habitat they live in, and that the continued risk of environmental contamination threatens the continuation of the species. This study indicates that Bald Ibis are possible bioindicators of environmental trace element contamination. The only way to ensure the continuity of the species of Bald Ibis and transfer them to future generations is to protect the ecosystem they live in and eliminate or reduce the threats such as the heavy metal elements identified. In order to do this, there is a need for national and international co-operation with local people so that habitat and birds will be protected together in the local community.

http://www.aloki.hu ● ISSN 1589 1623 (Print) ● ISSN 1785 0037 (Online)
DOI: http://dx.doi.org/10.15666/aeer/1706_1482314834

As a result, we recommend further studies to understand the effects of the heavy metals on the population of the species Bald Ibis.

Acknowledgements. The authors thank the Turkish General Directorate of Nature Conservation and National Parks for technical support of the study.

REFERENCES

[1] Adout, A., Hawlena, D., Maman, R., Paz-Tal, O., Karpas, Z. (2007): Determination of trace elements in pigeon and raven feathers by ICP-MS. – International Journal of Mass Spectrometry 267(1-3): 109-116.

[2] Akyıldız, D., Parmak, B., Çetin, İ. T., Arık, B. M., Başak, E. (2006): Bald Ibis. Nature Education Guide for Teachers. – Nature Association, Ankara, Turkey.

[3] Alvárez, C. R., Moreno, M. J., Alonso, L. L., Gómara, B., Bernardo, F. G., Martín-Doimeadios, R. R., González, M. J. (2013): Mercury, methylmercury, and selenium in blood of bird species from Doñana National Park (southwestern Spain) after a mining accident. – Environmental Science And Pollution Research 20(8): 5361-5372.

[4] Bauerová, P., Vinklerová, J., Hraníček, J., Čorba, V., Vojtek, L., Svobodová, J., Vinkler, M. (2017): Associations of urban environmental pollution with health-related physiological traits in a free-living bird species. – Science of the Total Environment 601: 1556-1565.

[5] Binkowski, Ł. J., Sawicka-Kapusta, K., Szarek, J., Strzyżewska, E., Felsmann, M. (2013): Histopathology of liver and kidneys of wild living mallards (Anas platyrhynchos) and coots (Fulica atra) with considerable concentrations of lead and cadmium. – Science of the Total Environment 450: 326-333.

[6] Borghesi, F., Migani, F., Andreotti, A., Baccetti, N., Bianchi, N., Birke, M., Dinelli, E. (2016): Metals and trace elements in feathers: a geochemical approach to avoid misinterpretation of analytical responses. – Science of the Total Environment 544: 476-494.

[7] Brumbaugh, W. G., Mora, M. A., May, T. W. (2006): Assessment of metals exposure and sub-lethal effects in voles and small birds captured near the Delong Mountain Regional Transportation System Road, Cape Krusenstern National Monument, Alaska, 2006. – U.S. Geological Survey Scientific Investigations Report 2008-5211: 21.

[8] Çanakcı, H., Demirboğa, R., Karakoc, M. B., Şirin, O. (2007): Thermal conductivity of limestone from Gaziantep (Turkey). – Building and Environment 42(4): 1777-1782.

[9] Carneiro, M., Oliveira, P., Brandão, R., Soeiro, V., Pires, M. J., Lavin, S., Colaço, B. (2018): Assessment Of the exposure to heavy metals and arsenic in captive and free-living black kites (Milvus migrans) nesting in Portugal. – Ecotoxicology and Environmental Safety 160: 191-196.

[10] Costa, R. A., Eeva T., Eira C., Vaqueiro J., Vingada, J. V. (2013): Assessing heavy metal pollution using great tits (Parus major): feathers and excrements from nestlings and adults. – Environ. Monit. Assess. 185: 5339-5344.

[11] Custer, T. W., Golden, N. H., Rattner, B. A. (2008): Element patterns in feathers of nestling black-crowned night-herons, Nycticorax nycticorax L., from four colonies in Delaware, Maryland, and Minnesota. – Bulletin of Environmental Contamination and Toxicology 81(2): 147-151.

[12] Da Silva, L. T. R., De Oliveira Filho, E. F., De Holanda Kunst, T., Rolim, V. P. M., De Alcântara, J. S., Regueira, R. F. S., Da Fonseca Oliveira, A. A. (2017): Heavy metal concentrations in free-living southern caracaras (Caracara plancus) in the northeast region of Brazil. – Acta Scientiae Veterinariae 45: 1-8.

http://www.aloki.hu ● ISSN 1589 1623 (Print) ● ISSN 1785 0037 (Online)
DOI: http://dx.doi.org/10.15666/aeer/1706_1482314834

[13] Das, Y. K., Aksoy, A., Baskaya, R., Duyar, H. A., Guvenc, D., Boz, V.(2009): Heavy metal levels of some marine organisms collected in Samsun and Sinop coasts of Black Sea, in Turkey. – J Anim Vetadvan 8(3): 496-9.
[14] Dauwe, T., Bervoets, L., Blust, R., Pinxten, R., Eens, M. (2000): Can excrement and feathers of nestling song birds be used as biomonitors for heavy metal pollution. – Archives of Environmental Contamination and Toxicology 39(4): 541-546.
[15] Dauwe, T., Bervoets, L., Pinxten, R., Blust, R., Eens, M. (2003): Variation of heavy metals within and among feathers of birds of prey: effects of molt and external contamination. – Environmental Pollution 124(3): 429-436.
[16] Dolan, K. J., Ciesielski, T. M., Lierhagen, S., Eulaers, I., Nygård, T., Johnsen, T. V., Jaspers, V. L. (2017): Trace element concentrations in feathers and blood of northern goshawk (Accipiter gentilis) nestlings from Norway and Spain. – Ecotoxicology and Environmental Safety 144: 564-571.
[17] Espín, S., García-Fernández, A. J., Herzke, D., Shore, R. F., Vanhattum, B., Martínez-López, E., Jaspers, V. L. B. (2016): Tracking pan-continental trends in environmental contamination using sentinel raptors—what types of samples should we use? – Ecotoxicology 25(4): 777-801.
[18] Govind, P., Madhuri, S.(2014): Heavy metals causing toxicity in animals and fishes. – Res J Anim Vet fish Sci 2(2): 17-23.
[19] Hanć, A., Zduniak, P., Erciyas-Yavuz, K., Sajnóg, A., Barałkiewicz, D. (2017): Laser ablation-ICP-MS in search of element pattern in feathers. – Microchemical Journal 134: 1-8.
[20] Honda, K., Min, B. Y., Tatsukawa, R. (1986): Distribution of heavy metals and their age-related changes in the eastern great white egret, Egretta alba modesta, in Korea. – Archives of Environmental Contamination and Toxicology 15(2): 185-197.
[21] Innangi, M., De Rosa, D., Danise, T., Fozzi, I., Giannotti, M., Izzo, M., Fioretto, A. (2019): Analysis of 11 trace elements in flight feathers of Italian Sparrows in southern Italy: a study of bioaccumulation through age classes, variability in three years of sampling, and relations with body condition. – Science of the Total Environment 651: 2003-2012.
[22] John, P., Kaore, S., Singh, R. (2005): Effects of calcium, strontium, and barium on isolated phrenic nerve-diaphragm preparation of rat and their interactions with diltiazem and nifedipine. – Indian Journal of Physiology and Pharmacology 49: 72-76.
[23] Kara, H., Das, Y. K., Aksoy, A.(2016): The toxicity of mercury, lead, cadmium, arsenic and copper in the veterinary medicine. – Turkiye Klinikleri J Vetsci Pharmaco Toxicol - Special Topics 2.3: 30-7.
[24] López-Perea, J. J., Laguna, C., Jiménez-Moreno, M., Martín-Doimeadios, R. C. R., Feliu, J., Mateo, R. (2019): Metals and metalloids in blood and feathers of common moorhens (Gallinula chloropus) from wetlands that receive treated wastewater. – Science of the Total Environment 646: 84-92.
[25] Markowski, M., Kaliński A., Skwarska J., Wawrzyniak J., Bańbura M., Markowski J. P., Zieliński P., Bańbura J. (2013): Avian feathers as bioindicators of the exposure to heavy metal contamination of food. – Bull. Environ. Contam. Toxicol. 91: 302-305.
[26] Malik, R. N., Zeb, N. (2009): Assessment of environmental contamination using feathers of Bubulcus ibis L., as a biomonitor of heavy metal pollution. – Pakistan Ecotoxicology 18: 522-536.
[27] Mikoni, N. A., Poppenga, R., Ackerman, J. T., Foley, J., Hazlehurst, J., Purdin, G., Tell, L. A. (2017): Trace element contamination in feather and tissue samples from Anna's humming birds. – Ecological Indicators 80: 96-105.
[28] Mundan, D., Çetin, İ. T. (2012): Bald ibis, world natural heritage. – Harran Üniversitesi Veteriner Fakültesi Dergisi 1(1): 61-67.

http://www.aloki.hu ● ISSN 1589 1623 (Print) ● ISSN 1785 0037 (Online)
DOI: http://dx.doi.org/10.15666/aeer/1706_1482314834

[29] Murphy, M. E., King, J. R., Taruscio, T. G., Geupel, G. R. (1990): Amino acid composition of feather barbs and rachises in three species of pygoscelid penguins. Nutritional implications. – Condor 1990: 913-921.
[30] Richardson, B. A. (1991): The durability of porous stone. – Stones Industries 26(10): 22-25.
[31] Rutkowska, M., Płotka-Wasylka, J., Lubinska-Szczygeł, M., Różańska, A., Możejko-Ciesielska, J., Namieśnik, J. (2018): Birds' feathers - suitable samples for determination of environmental pollutants. – TrAC Trends in Analytical Chemistry. https://doi.org/10.1016/j.trac.2018.09.022.
[32] Sánchez-Virosta, P., Espín, S., García-Fernández, A. J., Eeva, T. (2015): A Review On Exposure And Effects Of Arsenic İn Passerine Birds. – Science of the Total Environment 512: 506-525.
[33] Scheuhammer, A. M. (1987): The chronic toxicity of aluminium, cadmium, mercury, and lead in birds: a review. – Environmental Pollution 46(4): 263-295.
[34] Spergser, J., Loncaric, I., Tichy, A., Fritz, J., Scope, A. (2018): Correction: the cultivable autochthonous microbiota of the critically endangered Northern bald ibis (Geronticus eremita). – PloS One 13(5): e0197236.
[35] Sundaresan, N. R., Anish, D., Sastry, K. V. H., Saxena, V. K., Nagarajan, K., Subramani, J., Ahmed, K. A. (2008): High doses of dietary zinc induce cytokines, chemokines, and apoptosis in reproductive tissues during regression. – Cell and Tissue Research 332(3): 543-554.
[36] Squadrone, S., Abete, M. C., Brizio, P., Monaco, G., Colussi, S., Biolatti, C., Modesto, P., Acutis, P. L., Pessani, D., Favaro, L. (2016): Sex- and age-related variation in metal content of penguin feathers. – Ecotoxicology 25: 431-438.
[37] Tel, O. Y., Keskin, O. (2012): Investigation of Yersinia Spp. and Aeromonas hydrophila prevalences in northern bald ibis (*Geronticus eremita*). – Ankara Üniversitesi Veteriner Fakültesi Dergisi 59(2): 147-149.
[38] Tel, O. Y., Bozkaya, F., Keskin, O. (2013). Salmonella, Campylobacter, and Chlamydophila in bald ibis (Geronticus eremita) feces in Turkey. – Journal of Zoo and Wildlife Medicine 44(1): 21-26.
[39] Turgut, P., Yesilnacar, M. I., Bulut, H. (2008): Physico-thermal and mechanical properties of Sanliurfa limestone, Turkey. – Bulletin of Engineering Geology and the Environment 67(4): 485-490.
[40] Oymak, S. A., Karadede-Akin, H., Dogan, N. (2009): Heavy metal in tissues of Tor grypus from Atatürk dam lake, Euphrates River-Turkey. – Biologia 64(1): 151-155.
[41] Yohannes, Y. B., Ikenaka, Y., Nakayama, S. M., Mizukawa, H., Ishizuka, M. (2017): DDTS and other organochlorine pesticides in tissues of four bird species from the Rift Valley Region, Ethiopia. – Science of the Total Environment 574: 1389-1395.
[42] Zamani-Ahmadmahmoodi, R., Esmaili-Sari, A., Savabieasfahani, M., Ghasempouri, S. M., Bahramifar, N. (2010): Mercury pollution in three species of waders from Shadegan Wetlands at the head of the Persian Gulf. – Bulletin of Environmental Contamination and Toxicology 84(3): 326-330.
[43] Zamberlin S., Antunac N., Havranek J., Samarzija D. (2012): Mineral elements in milk and dairy products. – Mljeskarstvo 62(2): 111.

http://www.aloki.hu ● ISSN 1589 1623 (Print) ● ISSN 1785 0037 (Online)
DOI: http://dx.doi.org/10.15666/aeer/1706_1482314834

CONTRIBUTION OF ENVIRONMENTAL FACTORS TOWARD DISTRIBUTION OF TEN MOST DANGEROUS WEED SPECIES GLOBALLY

WAN, J.-Z.[1] – WANG, C.-J.[1,2*]

[1]*State Key Laboratory of Plateau Ecology and Agriculture, Qinghai University, Xining 810016, China*

[2]*College of Agriculture and Animal Husbandry, Qinghai University, Xining 810016, China*

**Corresponding author*
e-mail: wangchunjing00@163.com

(Received 14th Jun 2019; accepted 25th Oct 2019)

Abstract. Weeds can be a global threat to biodiversity and ecosystems. Understanding the contribution of environmental factors toward weed distribution can vastly improve the effectiveness of the methods adopted for the prevention and control of weed expansion on a large scale. Through multiple studies, we are now aware of the top 10 most dangerous weed species (in terms of endangering biodiversity). However, few studies have paid attention to the contribution of environmental factors toward the distribution of these weed species globally. In this study, we used species distribution modelling to project weed distribution based on occurrence records and environmental factors. We then used the jackknife estimation to assess the contribution of environmental factors toward weed distribution globally. Our results showed that climatic factors coupled with the human ecological footprint significantly contributed toward the distribution of these weed species. However, annual mean temperature made the largest contribution toward the distribution, except in the case of *Sorghum halepense.* Concerning distribution, different weed species respond differently to the annual mean temperature. However, the human ecological footprint can enhance their global distribution. We suggest that climate change and human influence should be analyzed together to realize methods for the prevention and control of the 10 most dangerous weed species globally.
Keywords: *climatic factor, human ecological footprint, risk monitoring, soil, species distribution modelling, weed management, worldwide*

Introduction

Weeds have a high potential to threaten biodiversity and ecosystem functions around the world (Holm, 1969; Tilman et al., 2006; Bajwa et al., 2016; Krak et al., 2019). Owing to their generally broad physiological niches and/or specific traits, weeds can invade human-mediated ecosystems with relative ease (Holm, 1969; Tilman et al., 2006; Shimono and Konuma, 2008; Panetta, 2015). Weed expansion can affect biodiversity across different spatial scales; for example, they can spread widely in disturbed or degraded environments (Shimono and Konuma, 2008). Thus, weed species could be dominant in such habitats and deplete the resources available to native plants, resulting in decreased biodiversity (Holm, 1969; Tilman et al., 2006; Shimono and Konuma, 2008). Furthermore, weed invasion could significantly decrease the ecosystem functions (e.g., nutrient cycling and biomass productivity) (Tilman et al., 2006; Bajwa et al., 2016; Zhang et al., 2018). Such negative effects on biodiversity and ecosystem functions may be due to the wide distribution of weeds as well as the spatial changes observed in environmental factors (Holm, 1969; Tilman et al., 2006; Shimono and Konuma, 2008; Panetta, 2015; Zhang et al., 2018).

http://www.aloki.hu ● ISSN 1589 1623 (Print) ● ISSN 1785 0037 (Online)
DOI: http://dx.doi.org/10.15666/aeer/1706_1483514846

Holm (1969) listed the 10 most dangerous weed species globally. These species have large distribution ranges and can expand widely across different environmental conditions. Ervin and Holly (2011) used species distribution modelling (SDM) to project the distribution of *Imperata cylindrica* in the United States based on pertinent environmental factors. Through further analysis of the results, they made some relevant suggestions on the prevention and control of this particular species (Ervin and Holly, 2011). Goncalves et al. (2014) showed that the climatic niche is conserved across continents for the expansion of *Lantana camara*. Based on a large amount of previous evidence (Holm, 1969; Ervin and Holly, 2011; Goncalves et al., 2014; Ray and Quader, 2014; Wan et al., 2019), we now know that environmental changes affect weed expansion, particularly for these 10 species. Therefore, it is necessary to explore the contribution of environmental factors toward the global distribution of these weed species; this will help us realize more effective methods for their prevention and control.

Here we discuss the following two scientific aspects: 1) which environmental factors could affect the distribution of the 10 most dangerous weed species globally, and 2) how could different environmental factors affect weed distribution. To address these questions, we used SDM to model the global distribution of these weed species. Then, the jackknife estimation was used to assess the contribution of environmental factors toward global weed distribution. Finally, we quantified the changing trends in weed distribution based on the relationship between the distribution probability and environmental factors.

Materials and methods

Species data

The following 10 weed species are termed as the most dangerous, as per Holm's study (1969): *Cynodon dactylon*, *Cyperus rotundus*, *Echinochloa colona*, *Echinochloa crus-galli*, *Eichhornia crassipes*, *Eleusine indica*, *Imperata cylindrica*, *Lantana camara*, *Panicum maximum*, and *Sorghum halepense*. These 10 species are dangerous weeds nowadays (Chandramohan and Charudattan, 2001; Punia et al., 2004; Vila-Aiub et al., 2007; Chauhan and Johnson, 2010; Ervin and Holly, 2011; Patel, 2012; Goncalves et al., 2014; Palma-Ordaz and Delgadillo-Rodríguez, 2014). The global occurrence records of these species were downloaded from the Global Biodiversity Information Facility (GBIF; https://www.gbif.org/; assessed on 19th March, 2019). The cleaning facilities of ModestR were used to minimize the frequently appearing errors in GBIF (García-Roselló et al., 2014). Duplicate occurrence records were removed on a 10.0 arc-minutes (~16.0 km) spatial resolution grid. The number of occurrence records ranged from 1795 to 7931 to support the good performance of SDM in our study.

Environmental data

The environmental data of our study included four climatic factors [annual mean temperature (°C*10); temperature seasonality (standard deviation*100); annual precipitation (mm); and precipitation seasonality], eight soil factors [bulk density (kg/m^3); cation exchange capacity (cmolc/kg); soil texture fraction clay (%); coarse fragments volumetric (%); soil organic carbon stock (tonnes per ha); soil pH; soil texture fraction silt (%); and soil texture fraction sand (%)] (Hengl et al., 2014), and one

http://www.aloki.hu ● ISSN 1589 1623 (Print) ● ISSN 1785 0037 (Online)
DOI: http://dx.doi.org/10.15666/aeer/1706_1483514846

human ecological footprint (Sanderson et al., 2002). Non-standard units of temperature were used because this allows for much reduced file sizes, which is important as, for many, downloading large files remains difficult (https://www.worldclim.org). Climate data of 10.0 arc-minutes was downloaded from the WorldClim database (averaged from 1950 to 2000; https://www.worldclim.org), and soil data of 0.5 arc-minutes was downloaded from SoilGrids (https://www.soilgrids.org). The human ecological footprint data was detailed in the study of Sanderson et al. (2002). We chose these environmental factors because they can potentially have a large effect on the distribution of weed species (Holm, 1969; Chicoine et al., 1986; Ervin and Holly, 2011; Goncalves et al., 2014). The four climatic factors, mean and standard deviation temperature and precipitation, were selected because they are widely used in SDMs based on previous studies (Ervin and Holly, 2011; Goncalves et al., 2014; Qin et al., 2014; Wan et al., 2016; Wan and Wang, 2019). Hageer et al. (2017) showed that the eight selected soil factors should be applied to predict distributions of plant species at large spatial scales. The human ecological footprint could explain the the global distribution of plant invaders (Beans et al., 2012; Gallardo et al., 2015). We used ArcGIS 10.6 (https://www.esri.com/software/arcgis/arcgis-for-desktop) to resample the resolution of the soil and human ecological footprint data from 0.5 arc-minutes to 10.0 arc-minutes. Hence, the value ranges of soil and human ecological footprint data were different from the previous studies (i.e., Sanderson et al., 2002; Hengl et al., 2014).

Species distribution modelling and jackknife estimation

We used Maxent modelling to project the global distribution of these weed species based on species data and environmental factors (Phillips et al., 2017). The Maxent modelling sets were as follows: 1) the regularization multiplier (beta) was kept at 2.0 to produce a smooth and general response shape, which represented a biologically realistic behaviour (Radosavljevic and Anderson, 2014); 2) the maximum number of background points was set to 10,000, while maintaining the same bias as the buffer of occurrence records of species on a global scale (Phillips et al., 2017); 3) a four-fold cross-validation approach was used (75% and 25% of occurrence records for training and testing modellings, respectively, in each run) to remove bias with respect to occurrence records (Merow et al., 2013); 4) a complementary log–log (cloglog) transformation was applied for the output of Maxent modelling (Phillips et al., 2017); and 5) the other sets were the same as the study of Merow et al. (2013). The cloglog output format gave each grid cell a value between 0.0 and 1.0, with 0.0 representing the lowest distribution probability of weed species and 1.0 the highest (Phillips et al., 2017). We evaluated the predictive precision of the species distribution models by using the area under the curve (AUC) of the receiver operating characteristic, treating each value of the prediction result as a possible threshold and then obtaining the corresponding sensitivity and specificity values to calculate the curve. Here, the modelling performance was satisfactory for these weed species because the AUC was over 0.7 (Merow et al., 2013).

A jackknife approach was used to assess the percentage contribution (PC) of environmental factors to the distribution probability of weed species using Maxent modelling (Merow et al., 2013; Shcheglovitova and Anderson, 2013; Oke and Thompson, 2015). The output of the jackknife estimation gave each environmental factor a value between 0.0% and 100.0%, representing the increasing PC of environmental factors to the distribution probability (Shcheglovitova and Anderson, 2013; Oke and Thompson, 2015). Response curves of the environmental factors to the

http://www.aloki.hu ● ISSN 1589 1623 (Print) ● ISSN 1785 0037 (Online)
DOI: http://dx.doi.org/10.15666/aeer/1706_1483514846

distribution probability could be quantified using Maxent modelling (Shcheglovitova and Anderson, 2013). We summed up the values of PC based on the groups of climatic and soil factors. In our study, the contribution of environmental factors toward the species distribution was high when the PC was at least 15.00% of the modelling for each weed species (Oke and Thompson, 2015).

Results

Distribution of weed species

The 10 most dangerous weed species were distributed primarily in Europe, Southeast Asia, Australia, southern regions of North America, central and eastern regions of South America, and central and southern regions of Africa (*Fig. 1*). Specifically, *C. dactylon*, *C. rotundus*, and *E. colona* cover most regions of Australia (*Fig. 1*). Compared to other species, *E. crus-galli* and *S. halepense* cover only small areas in the central and southern regions of Africa (*Fig. 1*).

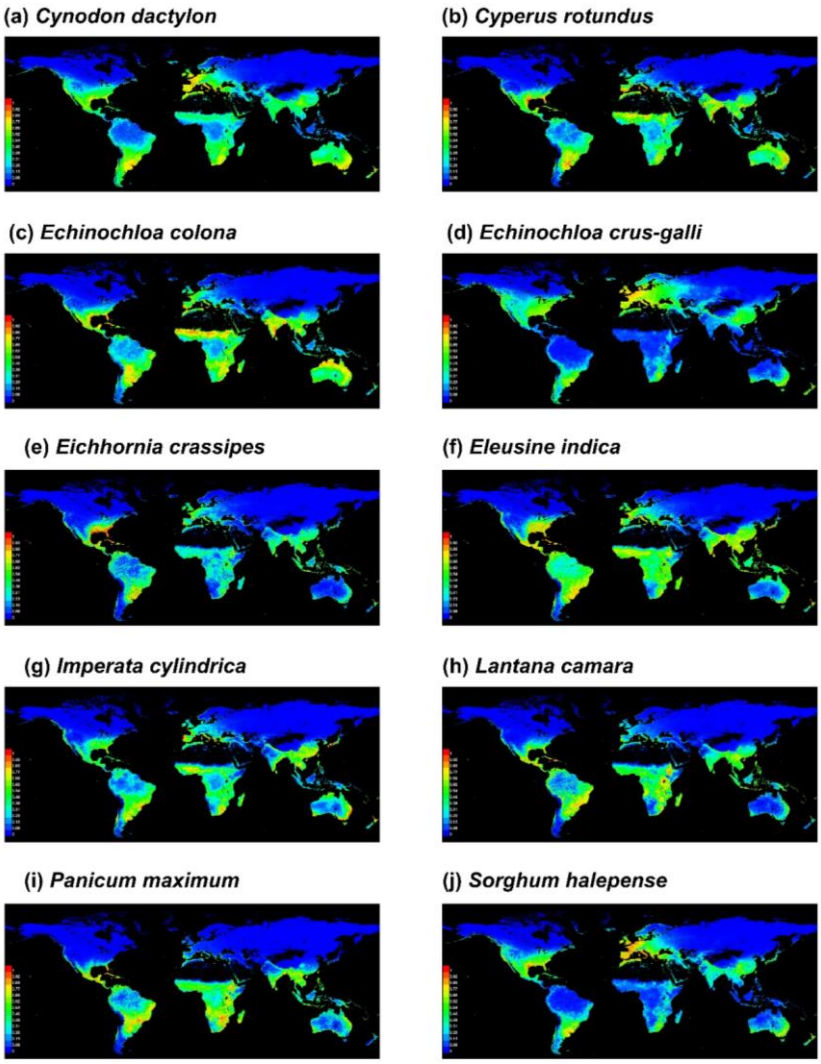

Figure 1. *The distribution of 10 most dangerous weed species on a global scale. The colour of maps from blue to red represents the distribution probability of the 10 most dangerous weed species from low to high levels*

http://www.aloki.hu ● ISSN 1589 1623 (Print) ● ISSN 1785 0037 (Online)
DOI: http://dx.doi.org/10.15666/aeer/1706_1483514846

Contribution of environmental factors to weed distribution

PCs for all climatic factors were over 50% across all these species, thus indicating that the climatic factor made the largest contribution toward the global distribution (*Table 1*). Among the climatic factors, annual mean temperature made the largest contribution toward the distribution, except for *S. halepense*. Further, temperature seasonality and annual precipitation played an important role in the distribution of seven weed species, i.e., *C. dactylon*, *E. colona*, *E. crus-galli*, *E. crassipes*, *E. indica*, *P. maximum*, and *S. halepense* (PC over 15.00%; *Table 1*). Although the distribution ranges were similar among the species, temperature and precipitation made different contributions toward the distribution, and the response curves of the climatic factors to the distribution varied among different weed species (*Fig. 2*). The response curves of climatic factors to the distribution were simply unimodal for *E. crus-galli*, *E. crassipes*, *L. camara*, *P. maximum*, and *S. halepense*. Also, an obvious increasing trend was observed in the unimodal changes for *C. dactylon*, *C. rotundus*, *E. colona*, *E. indica*, and *I. cylindrica* (*Fig. 2*). We found that soil factors made a small contribution toward the global distribution (*Table 1*). At large spatial scales, climatic factors made a larger contribution toward weed distribution than soil factors (*Table 1*). PC was higher than 15.00% for the human ecological footprint for the global distribution of *E. crus-galli*, *E. crassipes*, *E. indica*, *L. camara*, and *S. halepense* (*Table 1*). Furthermore, the distribution probability enhanced with an increased human ecological footprint (*Fig. 3*).

Discussion

We found that the distribution range of the 10 most dangerous weed species included Europe, Southeast Asia, Australia, southern regions of North America, central and eastern regions of South America, and central and southern regions of Africa, indicating that these weed species have great potential to expand widely around the world. Hence, as per Holm (1969), the threat that these species pose to the ecosystem and biodiversity should be a global issue. It is therefore important to explore the drivers behind the wide distribution of these weeds so that the effectiveness of the preventive and control methods can be improved (Panetta, 2015; Bajwa et al., 2016; Wan and Wang, 2019).

Contribution of climatic factors to weed distribution

We found that PCs for all climatic factors were over 50% across all these species, thus indicating that the climatic factor made the largest contribution toward the global distribution (*Table 1*). Among the climatic factors, annual mean temperature made the largest contribution toward the distribution, except for *S. halepense* (PC over 15.00%; *Table 1*). Although the distribution ranges were similar among the species, temperature and precipitation made different contributions toward the distribution, and the response curves of the climatic factors to the weed distribution varied among different weed species (*Fig. 2*). These results indicated that suitable climatic conditions could drive the global expansion of weed species. Previous studies (e.g., Holm, 1969; Tilman et al., 2006; Shimono and Konuma, 2008; Ervin and Holly, 2011; Panetta, 2015; Wan et al., 2017; Zhang et al., 2018) have shown that weeds can strongly adapt to rapid environmental changes and could grow exponentially in the near future. Weeds have a high level of phenotypic plasticity, and are capable of relatively rapid genetic change to enhance their ability to invade new areas in response to climate change (Clements and

http://www.aloki.hu ● ISSN 1589 1623 (Print) ● ISSN 1785 0037 (Online)
DOI: http://dx.doi.org/10.15666/aeer/1706_1483514846

Ditommaso, 2011). Hence, it is important to understand the changing trends in weed distribution along with the variation in global climate changes (Ervin and Holly, 2011; Wan et al., 2016; Zhang et al., 2018; Wang et al., 2019). *Figure 2* shows us the importance of monitoring weed expansion under different climatic conditions.

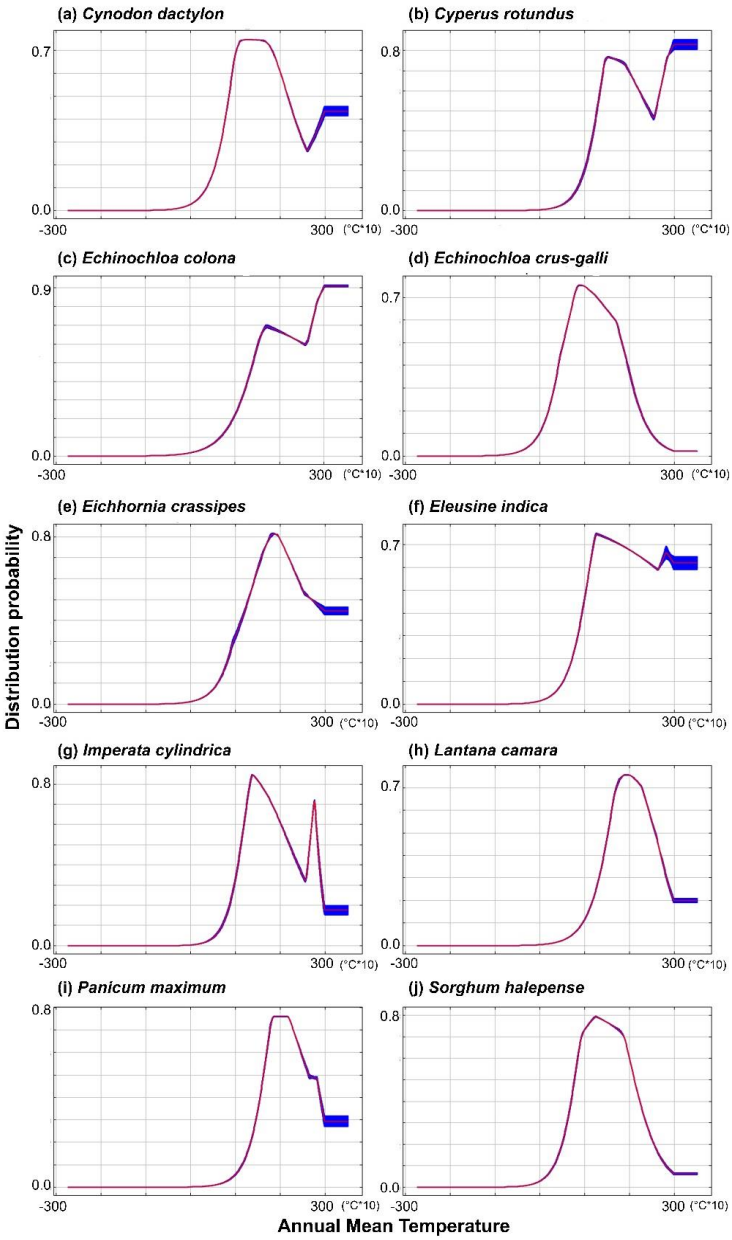

Figure 2. *Response curves of annual mean temperature to weed distribution on a global scale*

Contribution of soil factors toward weed distribution

Our results showed that soil factors made a negligible contribution toward global distribution (PC less than 15.00%; *Table 1*), thus indicating that soil factors solely could not drive weed expansion on a global scale. Numerous experimental studies (Tilman et al., 2006; Ramakrishna et al., 2006; Welch et al., 2016; Zhang et al., 2018) have shown that small-scale soil conditions play an important role in the spatial distribution of weed

http://www.aloki.hu ● ISSN 1589 1623 (Print) ● ISSN 1785 0037 (Online)
DOI: http://dx.doi.org/10.15666/aeer/1706_1483514846

species. However, based on our results, climatic factors made a larger contribution toward weed distribution than soil factors at large spatial scales. At small spatial scales, biotic factors (e.g., soil microorganisms) make a large contribution to weed physiology and weed seed banks (Kremer, 1993; Kennedy et al., 1999). Attention was paid to abiotic factors in our study. This difference may have been due to the effects of the spatial scale on the relationship between soil factors and weed distribution (Ervin and Holly, 2011; Goncalves et al., 2014). However, we should still pay attention to the effects of soil factors because a weed monitoring strategy should be based on different spatial scales, from something as large as a continent to as small as a micro-habitat (Buhler et al., 1997; Dekker et al., 1999; Gallandt, 1999; Wallace et al., 2018).

Contribution of human ecological footprint toward weed distribution

The human ecological footprint made a large contribution toward the global distribution of *E. crus-galli*, *E. crassipes*, *E. indica*, *L. camara*, and *S. halepense* (PC higher than 15.00%; *Table 1*). Furthermore, the distribution probability enhanced with an increased human ecological footprint (*Fig. 3*). The human ecological footprint is a good indicator of human influence in that it estimates the quantity of nature necessary to support the consumption habits of one individual, population, product, activity, or service (Sanderson et al., 2002; Wan et al., 2018). Our results provide clear evidence that human influence could drive the expansion of the above-mentioned 5 species on a global scale, although previous studies (e.g., Young and Evans, 1976; Treier and Müller-Schärer, 2011; Alvarado-Serrano et al., 2019; Krak et al., 2019) have shown that weeds could expand in lands degraded by human influence. Such influences of the human ecological footprint include global trade and transportation (Sanderson et al., 2002; Wiedmann and Lenzen, 2018). Therefore, we should consider making provisions for better control of global trade and transportation if we are to restrict the global distribution of these five species (Holm, 1969; Panetta, 2015; Zhang et al., 2018).

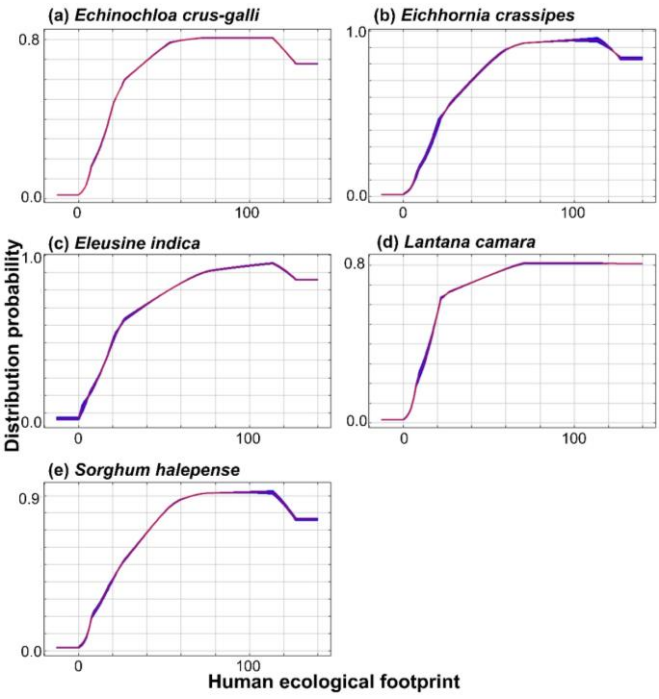

Figure 3. *Response curves of human ecological footprint to weed distribution on a global scale*

http://www.aloki.hu ● ISSN 1589 1623 (Print) ● ISSN 1785 0037 (Online)
DOI: http://dx.doi.org/10.15666/aeer/1706_1483514846

Table 1. *Contribution of environmental factors toward the distribution of 10 most dangerous weed species on a global scale*

Species	Bio1	Bio4	Bio12	Bio15	BLD	CEC	CLYPPT	CRFVOL	ORCDRC	PHIHOX	SLTPPT	SNDPPT	Climate	Soil	HF
Cynodon dactylon	**44.30**	**43.94**	1.08	2.90	0.43	0.03	0.00	0.04	0.00	2.14	0.14	0.06	**92.22**	2.86	4.93
Cyperus rotundus	**68.17**	14.30	1.89	1.94	0.79	0.10	0.81	0.14	0.00	2.32	1.00	0.66	**86.30**	5.82	7.88
Echinochloa colona	**62.00**	**24.92**	2.62	0.93	1.20	0.58	0.23	0.07	0.05	4.14	0.60	0.08	**90.47**	6.94	2.59
Echinochloa crus-galli	**21.01**	**20.00**	1.79	14.15	0.08	0.08	0.17	0.10	0.02	0.15	0.12	0.04	**56.94**	0.75	**42.31**
Eichhornia crassipes	**30.17**	6.09	**15.13**	3.16	0.80	1.59	0.95	2.85	0.00	2.30	2.12	0.34	**54.55**	10.95	**34.50**
Eleusine indica	**46.77**	3.26	**25.21**	0.67	0.49	0.45	1.03	0.34	0.03	2.36	0.09	0.12	**75.91**	4.92	**19.17**
Imperata cylindrica	**64.08**	10.31	13.42	3.48	0.61	0.17	0.04	2.02	0.01	1.23	0.08	1.50	**91.29**	5.65	3.06
Lantana camara	**50.71**	11.86	11.88	0.80	0.68	0.36	0.73	0.16	0.04	1.26	0.94	0.50	**75.25**	4.66	**20.09**
Panicum maximum	**56.35**	**24.40**	2.57	2.47	0.05	0.68	0.58	0.01	0.07	3.18	0.39	0.37	**85.78**	5.33	8.89
Sorghum halepense	**23.69**	**31.78**	0.55	3.86	1.18	1.01	0.18	0.16	0.03	1.22	1.61	0.03	**59.88**	5.43	**34.69**

Climate, soil, and HF denote the total contribution of climate, soil, and human ecological footprint toward weed distribution. The bold values denote the large contribution of environmental variables toward weed distribution. The environmental codes were following: Bio1: annual mean temperature (°C*10); Bio4: temperature seasonality (standard deviation*100); Bio12: annual precipitation (mm); Bio15: precipitation seasonality (coefficient of variation); BLD: bulk density (kg/cubic meter); CEC: cation exchange capacity (cmolc/kg); CLYPPT: soil texture fraction clay (%); CRFVOL: coarse fragments volumetric (%); ORCDRC: soil organic carbon stock (tonnes per ha); PHIHOX: soil pH; SLTPPT: soil texture fraction silt (%); SNDPPT: soil texture fraction sand (%)

http://www.aloki.hu ● ISSN 1589 1623 (Print) ● ISSN 1785 0037 (Online)
DOI: http://dx.doi.org/10.15666/aeer/1706_1483514846

Conclusions

We conclude that climatic factors coupled with the human ecological footprint made a significant contribution toward the distribution of the 10 most dangerous weed species globally. The contribution of the annual mean temperature was the largest for all the species, except for *S. halepense*. Various weed species respond differently to the annual mean temperature, but the human ecological footprint could enhance global expansion. Hence, we should analyze climate change and human influence together for the global prevention and control of these 10 most dangerous weed species. The spatial pattern of climates and the human ecological footprint should be closely monitored in Europe, Southeast Asia, Australia, southern regions of North America, central and eastern regions of South America, and central and southern regions of Africa. Future studies should attach importance to the contribution of environmental factors towards more weed species at the global scale. Weed control and management is increasingly becoming a global issue due to global human activities (e.g., global transportation and trade; Beans et al., 2012; Gallardo et al., 2015; Alvarado-Serrano et al., 2019). More and more weed species have a high potential to expand around the world. Furthermore, future studies also should pay attention to the importance of biotic factors (e.g., soil microorganisms) to the distribution of weed species globally. Therefore, studies on more weed species and biotic factors should be conducted for weed species worldwide.

Acknowledgements. Many thanks are due to the editor and two reviewers for their useful and constructive comments, which helped improve an earlier version of our manuscript. This work was supported by the National Natural Science Foundation of China (NSFC; 31800464 and 31800449), and the Basic Research Project of Qinghai Province, China (2019-ZJ-960Q).

REFERENCES

[1] Alvarado-Serrano, D. F., Van Etten, M. L., Chang, S. M., Baucom, R. S. (2019): The relative contribution of natural landscapes and human-mediated factors on the connectivity of a noxious invasive weed. – Heredity 122: 29.

[2] Bajwa, A. A., Chauhan, B. S., Farooq, M., Shabbir, A., Adkins, S. W. (2016): What do we really know about alien plant invasion? A review of the invasion mechanism of one of the world's most dangerous weeds. – Planta 244: 39-57.

[3] Beans, C. M., Kilkenny, F. F., Galloway, L. F. (2012): Climate suitability and human influences combined explain the range expansion of an invasive horticultural plant. – Biological Invasions 14: 2067-2078.

[4] Buhler, D. D., Hartzler, R. G., Forcella, F. (1997): Implications of weed seedbank dynamics to weed management. – Weed Science 45: 329-336.

[5] Chandramohan, S., Charudattan, R. (2001): Control of seven grasses with a mixture of three fungal pathogens with restricted host ranges. – Biological Control 22: 246-255.

[6] Chauhan, B. S., Johnson, D. E. (2010): Implications of narrow crop row spacing and delayed *Echinochloa colona* and *Echinochloa crus-galli* emergence for weed growth and crop yield loss in aerobic rice. – Field Crops Research 117: 177-182.

[7] Chicoine, T. K., Fay, P. K., Nielsen, G. A. (1986): Predicting weed migration from soil and climate maps. – Weed Science 34: 57-61.

[8] Clements, D. R., Ditommaso, A. (2011): Climate change and weed adaptation: can evolution of invasive plants lead to greater range expansion than forecasted? – Weed Research 51: 227-240.

http://www.aloki.hu ● ISSN 1589 1623 (Print) ● ISSN 1785 0037 (Online)
DOI: http://dx.doi.org/10.15666/aeer/1706_1483514846

[9] Dekker, J. (1999): Soil weed seed banks and weed management. – Journal of Crop Production 2: 139-166.
[10] Ervin, G. N., Holly, D. C. (2011): Examining local transferability of predictive species distribution models for invasive plants: an example with cogongrass (*Imperata cylindrica*). – Invasive Plant Science and Management 4: 390-401.
[11] Gallandt, E. R., Liebman, M., Huggins, D. R. (1999): Improving soil quality: implications for weed management. – Journal of Crop Production 2: 95-121.
[12] Gallardo, B., Zieritz, A., Aldridge, D. C. (2015): The importance of the human footprint in shaping the global distribution of terrestrial, freshwater and marine invaders. – PloS One 10: e0125801.
[13] García-Roselló, E., Guisande, C., Heine, J., Pelayo-Villamil, P., Manjarrés-Hernández, A., González Vilas, L., González-Dacosta, J., Vaamonde, A., Granado-Lorencio, C. (2014): Using ModestR to download, import and clean species distribution records. – Methods in Ecology and Evolution 5: 708-713.
[14] Goncalves, E., Herrera, I., Duarte, M., Bustamante, R. O., Lampo, M., Velasquez, G., Sharma, G. P., García-Rangel, S. (2014): Global invasion of *Lantana camara*: has the climatic niche been conserved across continents?. – PLoS One 9: e111468.
[15] Hageer, Y., Esperón-Rodríguez, M., Baumgartner, J. B., Beaumont, L. J. (2017): Climate, soil or both? Which variables are better predictors of the distributions of Australian shrub species?. – PeerJ 5: e3446.
[16] Hengl, T., de Jesus, J. M., MacMillan, R. A., Batjes, N. H., Heuvelink, G. B., Ribeiro, E., Samuel-Rosa, A., Kempen, B., Leenaars, J. G. B., Walsh, M. G., Gonzalez, M. R. (2014): SoilGrids1km–global soil information based on automated mapping. – PloS One 9: e105992.
[17] Holm, L. (1969): Weeds problems in developing countries. – Weed Science 17: 113-118.
[18] Kennedy, A. C. (1999): Soil microorganisms for weed management. – Journal of Crop Production 2: 123-138.
[19] Krak, K., Habibi, F., Douda, J., Vít, P., Lomonosova, M. N., Wang, L., Mandák, B. (2019): Human-mediated dispersal of weed species during the Holocene: a case study of *Chenopodium album* agg. – Journal of Biogeography 46: 1007-1019.
[20] Kremer, R. J. (1993): Management of weed seed banks with microorganisms. – Ecological Applications 3: 42-52.
[21] Merow, C., Smith, M. J., Silander Jr, J. A. (2013): A practical guide to MaxEnt for modeling species' distributions: what it does, and why inputs and settings matter. – Ecography 36: 1058-1069.
[22] Oke, O. A., Thompson, K. A. (2015): Distribution models for mountain plant species: the value of elevation. – Ecological Modelling 301: 72-77.
[23] Palma-Ordaz, S., Delgadillo-Rodríguez, J. (2014): Distribución potencial de ocho especies exóticas de carácter invasor en el estado de Baja California, México. – Botanical Sciences 92: 587-597.
[24] Panetta, F. D. (2015): Weed eradication feasibility: lessons of the 21st century. – Weed Research 55: 226-238.
[25] Patel, S. (2012): Threats, management and envisaged utilizations of aquatic weed *Eichhornia crassipes*: an overview. – Reviews in Environmental Science and Bio/Technology 11: 249-259.
[26] Phillips, S. J., Anderson, R. P., Dudík, M., Schapire, R. E., Blair, M. E. (2017): Opening the black box: an open-source release of Maxent. – Ecography 40: 887-893.
[27] Punia, S. S., Malik, R. S., Yadav, A., Rinwa, R. S. (2004): Effect of varying density of *Cyperus rotundus, Echinochloa colona* and *Trianthema portulacastrum* on mungbean. – Indian Journal of Weed Science 36: 280-281.
[28] Qin, Z., DiTommaso, A., Wu, R. S., Huang, H. Y. (2014): Potential distribution of two A mbrosia species in C hina under projected climate change. – Weed Research 54: 520-531.

http://www.aloki.hu ● ISSN 1589 1623 (Print) ● ISSN 1785 0037 (Online)
DOI: http://dx.doi.org/10.15666/aeer/1706_1483514846

[29] Radosavljevic, A., Anderson, R. P. (2014): Making better Maxent models of species distributions: complexity, overfitting and evaluation. – Journal of Biogeography 41: 629-643.
[30] Ramakrishna, A., Tam, H. M., Wani, S. P., Long, T. D. (2006): Effect of mulch on soil temperature, moisture, weed infestation and yield of groundnut in northern Vietnam. – Field Crops Research 95: 115-125.
[31] Ray, A., Quader, S. (2014): Genetic diversity and population structure of Lantana camara in India indicates multiple introductions and gene flow. – Plant Biology 16: 651-658.
[32] Sanderson, E. W., Jaiteh, M., Levy, M. A., Redford, K. H., Wannebo, A. V., Woolmer, G. (2002): The human footprint and the last of the wild: the human footprint is a global map of human influence on the land surface, which suggests that human beings are stewards of nature, whether we like it or not. – BioScience 52: 891-904.
[33] Shcheglovitova, M., Anderson, R. P. (2013): Estimating optimal complexity for ecological niche models: a jackknife approach for species with small sample sizes. – Ecological Modelling 269: 9-17.
[34] Shimono, Y., Konuma, A. (2008): Effects of human-mediated processes on weed species composition in internationally traded grain commodities. – Weed Research 48: 10-18.
[35] Tilman, D., Reich, P. B., Knops, J. M. H. (2006): Biodiversity and ecosystem stability in a decade-long grassland experiment. – Nature 441: 629.
[36] Treier, U. A., Müller-Schärer, H. (2011): Differential effects of historical migration, glaciations and human impact on the genetic structure and diversity of the mountain pasture weed *Veratrum album* L. – Journal of Biogeography 38: 1776-1791.
[37] Vila-Aiub, M. M., Balbi, M. C., Gundel, P. E., Ghersa, C. M., Powles, S. B. (2007): Evolution of glyphosate-resistant johnsongrass (Sorghum halepense) in glyphosate-resistant soybean. – Weed Science 55: 566-571.
[38] Wallace, J. M., Keene, C. L., Curran, W., Mirsky, S., Ryan, M. R., VanGessel, M. J. (2018): Integrated weed management strategies in cover crop–based, organic rotational no-till corn and soybean in the mid-Atlantic region. – Weed Science 66: 94-108.
[39] Wang, C. J., Yin, G. J., Song, Z. M., Wan, J. Z. (2019): Evaluating the spread of 10 invasive weeds in Chinese nature reserves under climate change scenarios in consideration of different scales. – Applied Ecology and Environmental Research 17: 3513-3533.
[40] Wan, J. Z., Wang, C. J. (2019): Determining key monitoring areas for the 10 most important weed species under a changing climate. – Science of the Total Environment 683: 568-577.
[41] Wan, J. Z., Wang, C. J., Yu, F. H. (2016): Risk hotspots for terrestrial plant invaders under climate change at the global scale. – Environmental Earth Sciences 75: 1012.
[42] Wan, J. Z., Wang, C. J., Tan, J. F., Yu, F. H. (2017): Climatic niche divergence and habitat suitability of eight alien invasive weeds in China under climate change. – Ecology and Evolution 7: 1541-1552.
[43] Wan, J. Z., Wang, C. J., Yu, F. H. (2018): Human footprint and climate disappearance in vulnerable ecoregions of protected areas. – Global and Planetary Change 170: 260-268.
[44] Wan, J. Z., Wang, C. J., Yu, F. H. (2019): Large-scale environmental niche variation between clonal and non-clonal plant species: roles of clonal growth organs and ecoregions. – Science of the Total Environment 652: 1071-1076.
[45] Welch, R. Y., Behnke, G. D., Davis, A. S., Masiunas, J., Villamil, M. B. (2016): Using cover crops in headlands of organic grain farms: effects on soil properties, weeds and crop yields. – Agriculture, Ecosystems & Environment 216: 322-332.
[46] Wiedmann, T., Lenzen, M. (2018): Environmental and social footprints of international trade. – Nature Geoscience 11: 314-321.
[47] Young, J. A., Evans, R. A. (1976): Responses of weed populations to human manipulations of the natural environment. – Weed Science 24: 186-190.

http://www.aloki.hu ● ISSN 1589 1623 (Print) ● ISSN 1785 0037 (Online)
DOI: http://dx.doi.org/10.15666/aeer/1706_1483514846

[48] Zhang, Y., Wang, L., Yuan, Y., Xu, J., Tu, C., Fisk, C., Zhang, W. J., Chen, X., Ritchie, D., Hu, S. (2018): Irrigation and weed control alter soil microbiology and nutrient availability in North Carolina Sandhill peach orchards. – Science of the Total Environment 615: 517-525.

http://www.aloki.hu ● ISSN 1589 1623 (Print) ● ISSN 1785 0037 (Online)
DOI: http://dx.doi.org/10.15666/aeer/1706_1483514846

CHARACTERISTICS OF A CONTINUOUS HAZE PROCESS IN THE CHANG-ZHU-TAN REGION OF CHINA AND ITS INFLUENCING FACTORS

ZHU, Y. F.[1,2] – GAO, J.[1] – LIAO, J. Y.[3*]

[1]*College of Science, Central South University of Forestry and Technology, Changsha 410004, China*

[2]*Key Laboratory for Digital Dongting Lake Basin of Hunan Province, Changsha 410004, China*

[3]*Hunan Forest Botanical Garden, Changsha 410116, China*

**Corresponding author*
e-mail: liaojuyang@163.com

(Received 17th Jun 2019; accepted 16th Oct 2019)

Abstract. Based on the surface meteorological observation data collected by meteorological stations 57687 (Changsha), 57773 (Xiangtan) and 57780 (Zhuzhou) of Hunan province from January 14 to 20, in 2017, and the air monitoring data of Changsha City, Zhuzhou City and Xiangtan City provided by The National Environment Monitoring Station, this paper analyzed the stage characteristics of a continuous haze process in the Chang-Zhu-Tan Region of China and its influencing factors in late January of 2017. The results show that the haze process has stage characteristics with the fog and the haze alternating. Through correlation analysis, it is concluded that PM2.5 concentration, vapor pressure of water, dew point temperature and relative humidity are the four key factors determining visibility. Through analyzing main components, a meteorological factor consisting of vapor pressure of water, dew point temperature and relative humidity is established. A linear model featuring PM2.5 concentrations and visibility and a cubic curve model featuring the meteorological factor and visibility are set up. During the continuous haze process, the average concentration of PM2.5 is greater than 88 ug/m^3 and is inversely related to the visibility. Accumulation of highly concentrated PM2.5 causes low visibility. With the changes of humidity and dew point temperature, fog and haze appear alternatively.
Keywords: *PM2.5 concentration, meteorological factors, visibility, Chang-Zhu-Tan Region*

Introduction

With the rapid development of urban construction, industry and transportation in Changsha, Zhuzhou and Xiangtan (Chang-Zhu-Tan), the increase in the concentration of fine particles such as pollutants and dust in the near-surface layer has led to a decrease in visibility and more severe urban air pollution. Haze weather has become a danger to our living environment and the atmosphere. Major disasters have had serious negative impacts on the environment, health, climate, and economy. Foreign scholars have long been studying the climate characteristics of haze and its impact on regional climate. Elias et al. (2009) studied the effects of particles (smoke and fog) on visible light radiation. Jansen (2014) used the hourly measurement method to explore the role of secondary inorganic aerosols in Particulate Matter 2.5 (PM2.5) in the haze in Hangzhou, China.

Singh and Giri (2011) studied the properties of the interannual changes of fog and smoke and their impact on agricultural production. Domestically, Guo et al. (2015) analyzed the durative heavy fog weather such as aerosols, cloud condensation nuclei (CCN), fog droplets spectrum and micro physical characteristics such as moisture

http://www.aloki.hu ● ISSN 1589 1623 (Print) ● ISSN 1785 0037 (Online)
DOI: http://dx.doi.org/10.15666/aeer/1706_1484714858

content, atmospheric visibility and vertical structure characteristics of boundary layer. They explored the characteristics and mechanism of the formation, evolution and transformation of haze weather. Xie et al. (2015) analyzed the meteorological elements, PM2.5 concentration and atmospheric boundary layer characteristics of a large-scale continuous heavy haze process in central and eastern China, and concluded that PM2.5 concentration is inversely related to visibility and relative humidity. Hu et al. (2013) analyzed the characteristics and influencing factors of haze weather in Xi'an area by using the data from Xi'an meteorological station gathered since its establishment. Zhao et al. (2013) studied the characteristics of PM2.5 pollution on Beijing's autumn smoggy days using observation data such as PM2.5 concentration in Beijing's urban and suburban areas in 2011. Li et al. (2017) studied the causes and hazards of urban haze. Sun (2016) and Liu et al. (2013) analyzed the causes of continuous haze weather from the optical perspective. Zhu et al. (2015), Dai and Cheng (2008), Yin et al. (2014) Morones Esquivel et al. (2017) and Hou et al. (2017) all studied the meteorological causes of persistent haze.

At present, the domestic research on smog is mainly concentrated on the weather in the Beijing-Tianjin-Hebei region, Yangtze River delta, the Pearl River delta and other regions, though there are also some researches on the haze weather in Hunan province some other cities. For example, Yuan et al. (2015) and Leura Vicencio et al. (2017) analyzed daily visibility and relative humidity data from 1970 to 2012 of 76 ground meteorological observation stations, and obtained the daily fog and haze conditions in various regions of Hunan, using linear trend to analyze the characteristics of fog and haze years; Zhang et al. (2014) used the meteorological observation data and environmental monitoring data of the Changsha area from 1970 to 2012 to analyze the characteristics and influencing factors of smog in Changsha area over the past 43 years, but an analysis on the cause of the continuous smog process in Chang-Zhu-Tan region has not been reported. In this paper, hourly meteorological and environmental data from January 14 to 20, 2017 are used to study the occurrence and evolution of a persistent haze process in Chang-Zhu-Tan region, and corresponding mathematical models are established based on the influencing factors. The conclusion can provide a strong theoretical basis for optimizing environmental management and preventing haze scientifically in Chang-Zhu-Tan region.

Materials and methods

The research site, Chang-Zhu-Tan region, is located in the central and eastern part of Hunan Province in China, as shown in *Figure 1*. It is an important part of the urban agglomeration in the middle reaches of the Yangtze River, including Changsha, Zhuzhou and Xiangtan cities.

The conventional meteorological data used in this paper comes from the China Meteorological Data Network, which mainly includes ground and high-altitude data from January 14 to January 20, 2017 in Changsha, Zhuzhou and Xiangtan of China. The ground data includes air pressure, visibility, temperature, dew point temperature, and relative Humidity, wind direction and wind speed. Except dew-point temperature, all data is hourly data. Visibility data is obtained by referring to the method of obtaining visibility data in the paper (Cao et al., 2013). The altitude data are from the altitude data of Ma-Po-Ling station once a day (12 o'clock). The air pollutant data are from the environmental quality monitoring station, mainly including Particulate Matter 2.5

http://www.aloki.hu ● ISSN 1589 1623 (Print) ● ISSN 1785 0037 (Online)
DOI: http://dx.doi.org/10.15666/aeer/1706_1484714858

(PM2.5) and Air Quality Index (AQI) data of the three cities of Chang-Zhu-Tan region, all of which are hourly average data.

Based on the meteorological and environmental data of Changsha-Zhuzhou-Xiangtan, this paper analyzes the internal relations among the influencing factors by correlation analysis, principal component analysis and regression analysis, and establishes the corresponding mathematical model.

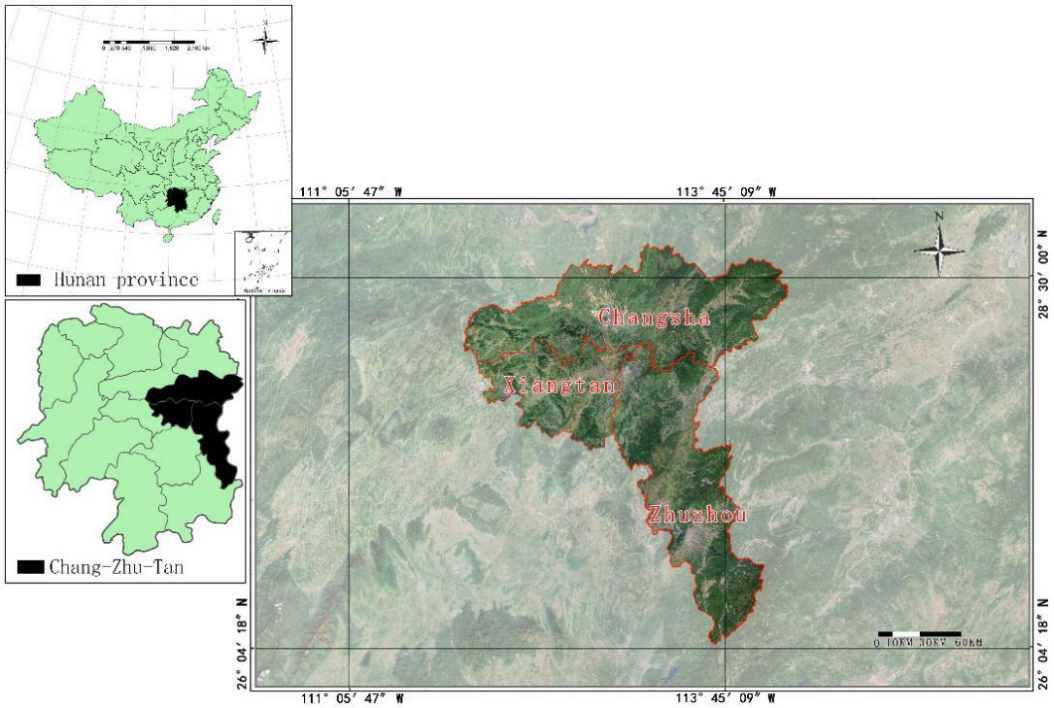

Figure 1. *Location of research site*

Results

Process analysis

Air quality changes in Chang-Zhu-Tan region

Chang-Zhu-Tan metropolitan area is the demonstration zone of the construction of "two-oriented society" and the core growth pole of Hunan province's economic development. Industrialization has accelerated in recent years, and environmental pollution has followed. During this haze, the average AQI and PM2.5 concentrations in Zhuzhou are the highest, respectively, 133 and 101 ug/m^3. The average AQI and PM2.5 concentrations of Changsha are 112 and 87 ug/m^3, respectively. The lowest is Xiangtan city, with average AQI and PM2.5 concentrations of 106 and 80 ug/m^3, respectively. The AQI and PM2.5 concentrations in the three cities all reach peak in the afternoon of the 17th. The changes of AQI and PM2.5 concentration are shown in *Figure 2.*

According to the air quality standards uniformly regulated by the State Environmental Protection Administration, Zhuzhou City has 43 h of moderate pollution and 107 h of light pollution. Changsha has 115 h of light pollution and above. Xiangtan city has 95 h of light pollution and above. The pollution is most serious in Zhuzhou City.

http://www.aloki.hu ● ISSN 1589 1623 (Print) ● ISSN 1785 0037 (Online)
DOI: http://dx.doi.org/10.15666/aeer/1706_1484714858

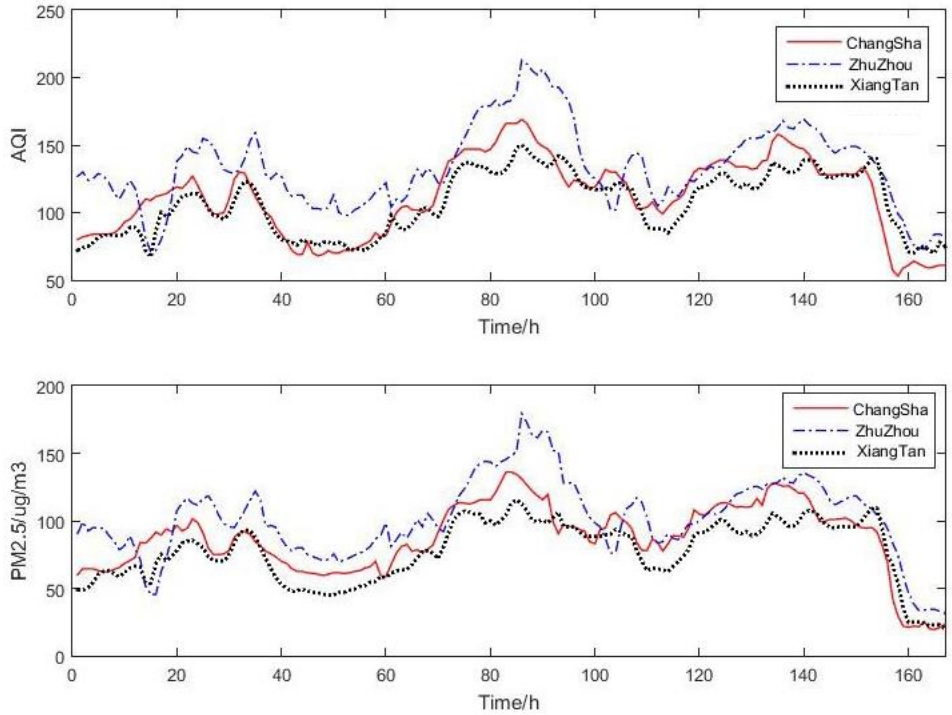

Figure 2. *Variation of AQI and PM2.5 concentration in Chang-Zhu-Tan region*

Evolution of ground visibility

During the smog process from January 14 to 20, 2017, the visibility is less than 1000 m. The visibility is less than 800 m in nearly 136 h, and the visibility is less than 500 m in 20 h. The dense fog process with visibility less than 500 m is 4 h. The minimum visibility of the haze process is 294 m, as shown in *Figure 3*.

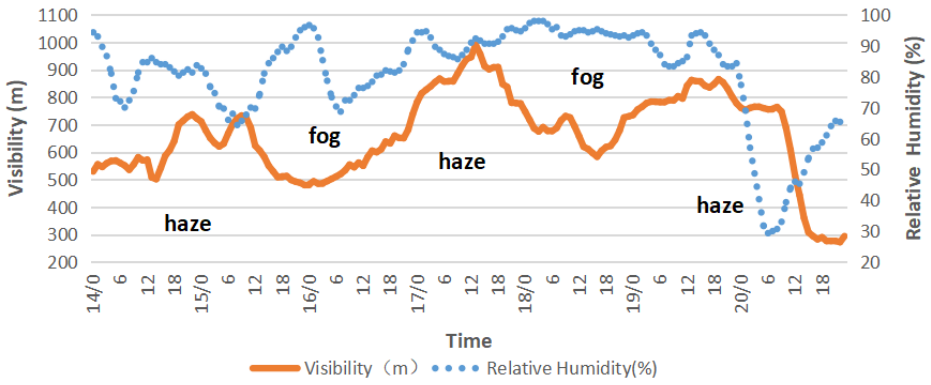

Figure 3. *Variation trend of visibility and relative humidity*

As shown in *Figure 3,* during the haze weather, many transitions and alternations between fog and haze occurred. According to the new haze standards issued by the China Meteorological Administration, atmospheric turbidity with a relative humidity greater than 95% is defined as fog, and atmospheric turbidity with a relative humidity less than 95% is defined as haze. According to the different visibility of haze weather, it is divided into four grades (Xie et al., 2015; *Table 1*).

http://www.aloki.hu ● ISSN 1589 1623 (Print) ● ISSN 1785 0037 (Online)
DOI: http://dx.doi.org/10.15666/aeer/1706_1484714858

Table 1. *Classification of haze levels*

Visibility (km)	[5,10)	[3,5)	[1,3)	[0,1)
Haze levels	Slight haze	Mild haze	Moderate haze	Heavy haze

According to this standard, the haze process in Chang-Zhu-Tan region is divided into five stages. The first, the third and the fifth stages are haze, and the second and fourth stages are fog.

Changes in ground meteorological elements

According to the collected ground meteorological data, the variation trend chart of wind direction, wind speed, maximum temperature, minimum temperature, visibility, relative humidity and dew point temperature is drawn, and the results are shown in *Figure 4.*

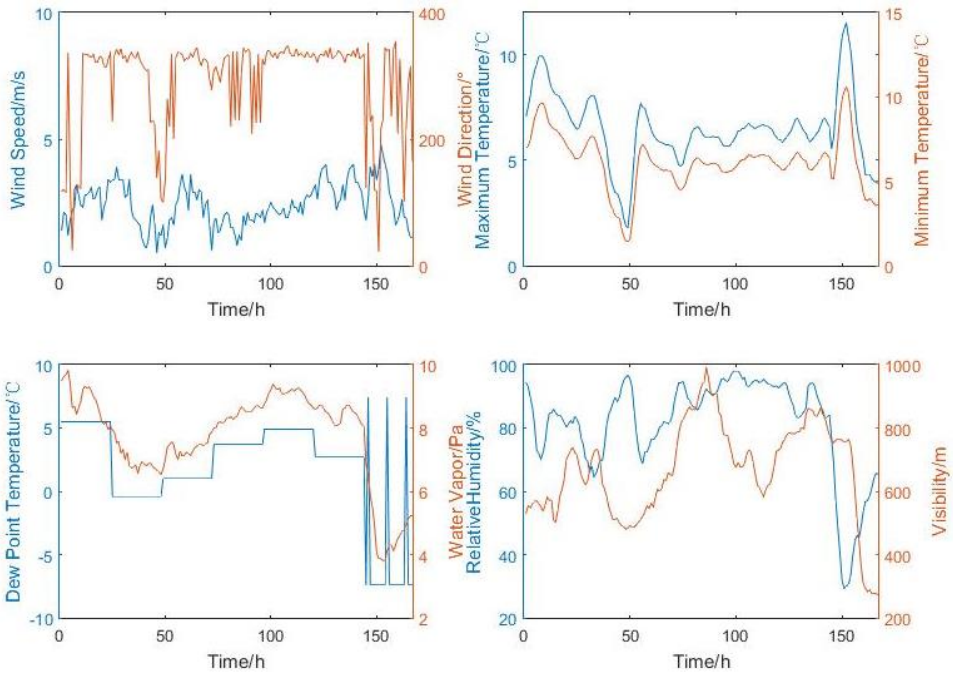

Figure 4. *The trend chart of meteorological factors*

The changes in meteorological elements near the surface of the continuous smog process in Changsha, Zhuzhou and Xiangtan are relatively obvious. The relative humidity increases with the decrease of the dew point and the temperature drop at night, which is conducive for the water vapor to condense to form fog; during the daytime, the opposite is true. In the second and fourth stages, the ground relative humidity increases to more than 95%, corresponding to fog (Torres-Martinez et al., 2017). When relative humidity decreases, fog turns to haze. It can be seen that the increase of relative humidity is conducive to the increase of the hygroscopic growth of aerosol particles suspended in the air. When the air reaches a saturated state, haze will change into fog. As can be seen from the changes in wind speed, the wind speed during the haze is less than 4.8 m/s, and the wind speed during the fog process is mostly between 1.5 m and

http://www.aloki.hu ● ISSN 1589 1623 (Print) ● ISSN 1785 0037 (Online)
DOI: http://dx.doi.org/10.15666/aeer/1706_1484714858

2.5 m/s. In the process of haze occurrence, the wind speed is larger than that of fog, and the wind speed is between 2 m/s and 4.8 m/s (Bremer Bremer et al., 2016). It can be seen from the change of wind direction that when fog occurs, it is mostly southerly wind. When haze occurs, the wind direction is mainly north wind and northwest wind.

Analysis of factors influencing visibility in haze weather process

Visibility is closely related to ground meteorological elements and aerosol concentration in haze weather. In order to determine the main factors that influence the fog haze weather process at different stages, air pressure, wind direction, wind speed, temperature, dew point temperature, vapor pressure, relative humidity, the visibility and PM2.5 concentrations in this haze process are analyzed by Statistical Product and Service Solutions (SPSS) through Pearson correlation analysis on both sides. Pearson correlation coefficient formulas as shown in *Equation 1*. The correlation results are shown in *Table 2*.

$$r = \frac{\sum_{i=1}^{n}(x_i - \bar{x})(y_i - \bar{y})}{\sum_{i=1}^{n}(x_i - \bar{x})^2 \sum_{i=1}^{n}(y_i - \bar{y})^2} \quad \text{(Eq.1)}$$

Table 2. *Correlation analysis of visibility and influence factors*

		Air pressure	Wind direction	Wind speed	Temperature	Dew point temperature	Vapor pressure	Relative humidity	PM2.5
vis	Correlation	-0.020	0.274**	0.222**	0.269**	0.352**	0.400**	0.293**	1.000**
	Significance	0.799	0.000	0.004	0.000	0.000	0.000	0.000	0.000

**Significantly correlated at 0.01 level (bilateral)

It can be seen from *Table 2* that in addition to the air pressure, the visibility is strongly correlated with wind direction, wind speed, temperature, dew point temperature, vapor pressure, relative humidity, the visibility and concentrations of PM2.5 are strong correlation, and the correlation is confirmed at 99% by reliability test. Since the average wind speed during the whole haze weather is about 2.4 m/s, the wind speed provides a relatively stable weather background that enables small horizontal transportation, reflecting the consistency of wind speed and visibility on the weather scale. In comparison, PM2.5 concentration, vapor pressure of water, dew point temperature and relative humidity are more closely related to visibility, with correlation coefficients of 1.00, 0.400, 0.352 and 0.293 respectively (Perez-Sicairos et al., 2016). It indicates that PM2.5 concentration, vapor pressure of water, dew point temperature and relative humidity are the four main factors that directly affect the visibility level during the haze.

Establishment of relationship model between visibility and major factors

Correlation analysis is conducted on PM2.5 concentration, vapor pressure of water, dew point temperature and relative humidity, and the results are shown in *Table 2*. It can be seen from the table that dew point temperature, vapor pressure of water, relative humidity and visibility have strong correlation, and passed the 99% confidence interval.

http://www.aloki.hu ● ISSN 1589 1623 (Print) ● ISSN 1785 0037 (Online)
DOI: http://dx.doi.org/10.15666/aeer/1706_1484714858

In order to study the main factors affecting the visibility and avoid the overlapping effects among the factors, the correlation analysis of the influencing factors is conducted. The results are shown in *Table 3*.

Table 3. *Correlation analysis of influencing factors*

Control variables		The dew point temperature	Vapor pressure	Relative humidity	PM2.5
The dew point temperature	Correlation	1.000	0.834	0.687	0.000
	Significance (bilateral)		0.000	0.000	1.000
Vapor pressure	Correlation	0.834	1.000	0.841	0.000
	Significance (bilateral)	0.000		0.000	1.000
Relative humidity	Correlation	0.687	0.841	1.000	0.000
	Significance (bilateral)	0.000	0.000		1.000
PM2.5	Correlation	0.000	0.000	0.000	1.000
	Significance (bilateral)	1.000	1.000	1.000	

It can be seen from *Table 3* that there is a strong correlation between dew point temperature, vapor pressure of water and relative humidity. Therefore, correlation analysis is conducted again on dew point temperature, vapor pressure of water and relative humidity, and correlation matrix A is obtained. Kaiser-Meyer-Olkin (KMO) and Bartlett tests are carried out, and the results are shown in *Table 4*.

$$A = \begin{bmatrix} 1.000 & 0.856 & 0.718 \\ 0.856 & 1.000 & 0.854 \\ 0.718 & 0.854 & 1.000 \end{bmatrix}$$

Table 4. *KMO and Bartlett inspection*

Sample enough Kaiser-Meyer-Olkin		0.688
Bartlett's sphericity test	Approximate chi-square	434.334
	df	3
	Sig.	0.000

From *Table 4,* the KMO test coefficient is 0.688 > 0.5, and the data have structural validity above 99% confidence interval, so dew point temperature, vapor pressure of water and relative humidity can be used for the principal component analysis. Through principal component analysis, the results are shown in *Table 5*.

As shown in *Table 5,* the cumulative percentage of dew point temperature, vapor pressure of water and relative humidity is 100%. Therefore, dew point temperature, vapor pressure of water and relative humidity can be aggregated into a meteorological factor. As for the component score coefficient matrix, the dew point temperature is 0.350, the vapor pressure is 0.369, the relative humidity is 0.350. Through the score matrix the weight of each factor is calculated, and they are 0.327, 0.345, 0.327, respectively. If the meteorological factor is f, the dew point temperature, vapor pressure of water and relative humidity are x1, x2 and x3 respectively, then *Equation 2* is satisfied.

http://www.aloki.hu ● ISSN 1589 1623 (Print) ● ISSN 1785 0037 (Online)
DOI: http://dx.doi.org/10.15666/aeer/1706_1484714858

$$f = 0.327x_1 + 0.345x_2 + 0.327x_3 \quad \text{(Eq.2)}$$

Table 5. *Principal component analysis of influencing factors*

Component	Initial eigenvalue			Extract the squares and load		
	Summation	Variance's %	Accumulation %	Summation	Variance's %	Accumulation %
1	2.620	87.345	87.345	2.620	87.345	87.345
2	0.282	9.404	96.749			
3	0.098	3.251	100.000			

Model prediction

Meteorological factors and PM2.5 concentration are the main factors affecting visibility. In order to explore the objective relationship between meteorological factors and visibility and that between PM2.5 concentration and visibility, two models are established. First, the model with the highest fitting degree is found through curve fitting. The result is shown in *Figure 5.*

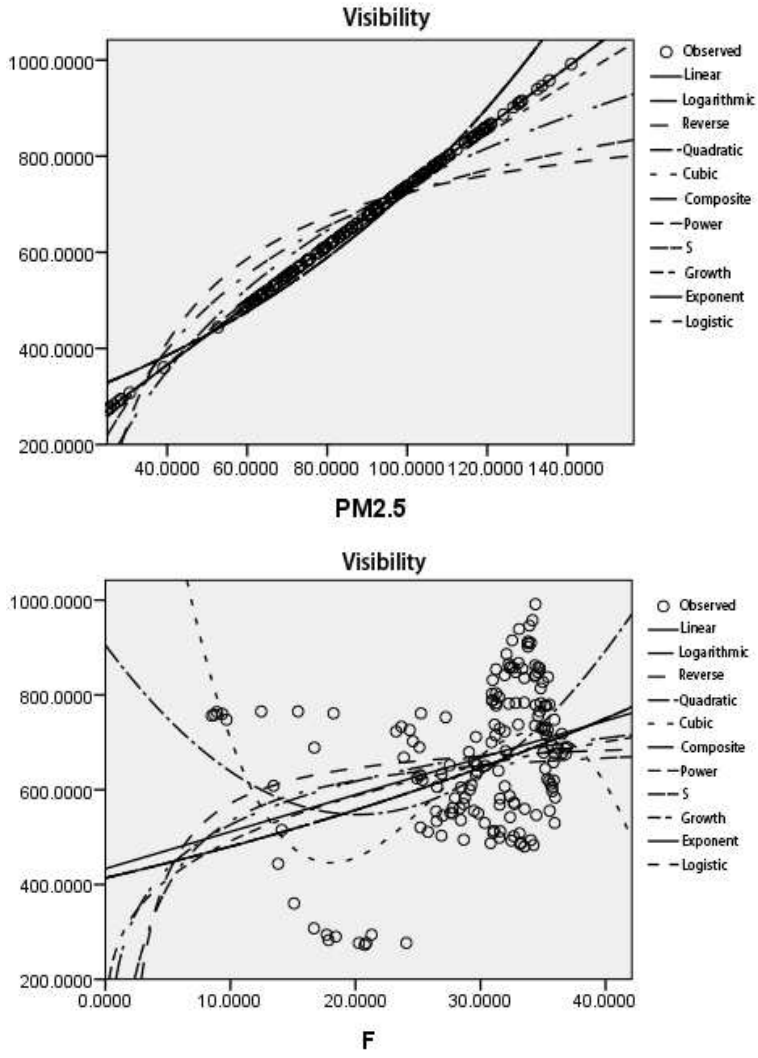

Figure 5. *Model curve estimation*

http://www.aloki.hu ● ISSN 1589 1623 (Print) ● ISSN 1785 0037 (Online)
DOI: http://dx.doi.org/10.15666/aeer/1706_1484714858

As can be seen from *Figure 5,* the relationship between PM2.5 concentration and visibility fits the linear model best. The relationship between meteorological factor F and visibility fits the three models best. Therefore, visibility is set as V (m), PM2.5 concentration is P (ug/m^3), and meteorological factor is F. The linear model between PM2.5 concentration and visibility, and the cubic model between meteorological factors and visibility are respectively established.

Model establishment

Establishment of a linear model between PM2.5 concentration and visibility

(1) Regression analysis

It can be seen from *Figure 5* that of the relationship between PM2.5 concentration and visibility fits the linear model best, so the linear model is established. The results of linear regression analysis of PM2.5 concentration and visibility are shown in *Table 6*.

Table 6. *PM2.5 concentration and visibility linear regression analysis*

	Coefficient	**Standard error**	**Precision**	**Significance**
(Constant)	117.400	.000	7.974E7	.000
PM2.5	6.200	.000	3.867E8	.000

The linear model between PM2.5 concentration and visibility is established by using the data in the table, as shown in *Equation 3*.

$$v = 6.2p + 117.4 \quad \text{(Eq.3)}$$

(2) Model test

The linear model between PM2.5 concentration and visibility is tested, as shown in *Figures 6* and *7*.

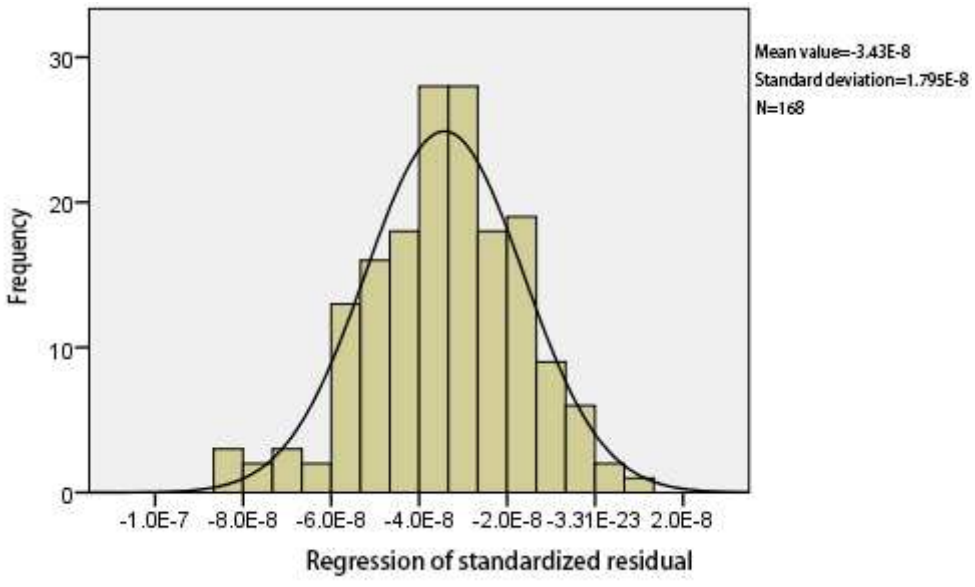

Figure 6. *Visibility standard residual histogram*

http://www.aloki.hu ● ISSN 1589 1623 (Print) ● ISSN 1785 0037 (Online)
DOI: http://dx.doi.org/10.15666/aeer/1706_1484714858

It can be seen from *Figure 6* that the distribution of standardized residual is basically normal distribution, so the resulting regression equation has practical significance.

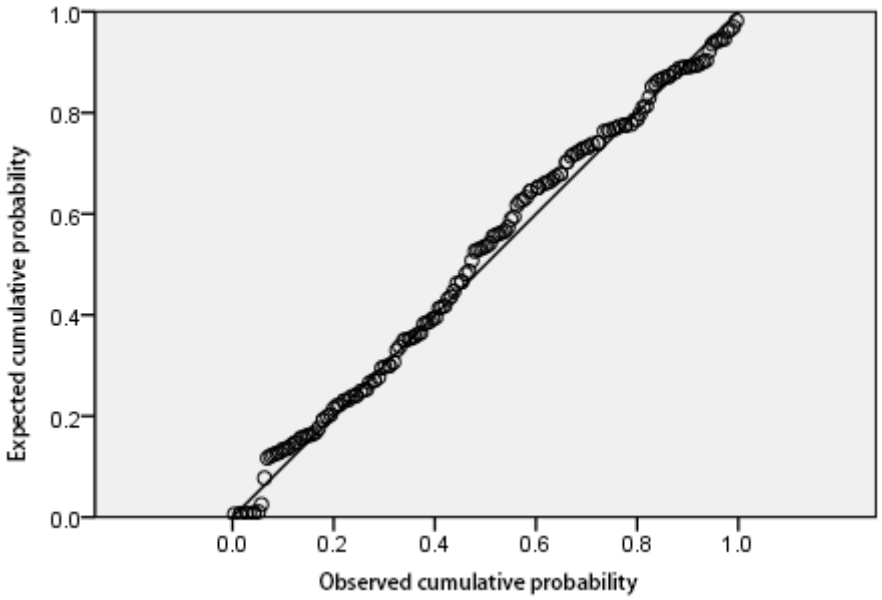

Figure 7. *Visibility standard residual P-P diagram*

It can be seen from *Figure 7* that points in the figure can form approximately a straight line, so the data conforms to the specified distribution after verification.

Establishment of cubic model between meteorological factors and visibility

It can be seen from *Figure 5* that the curve estimation of meteorological factors and visibility has the highest degree of fitting with the third-order model, so the cubic model is established. The results are shown in *Table 7*.

Table 7. *Summary and parameter estimation of meteorological factors and visibility models*

Equation	Model summary					Estimate of parameter			
	R^2	F	df1	df2	Sig.	Constant	b1	b2	b3
Cubic	0.288	22.089	3	164	0.000	2169.164	-231.267	9.755	-0.124

From the data in *Table 6* it can be seen that the fitting degree of the model is 0.288 and the confidence interval of more than 99% passes. Therefore, the three-order curve model between meteorological factors and visibility is established as shown in *Equation 4.*

$$v = -231.267 f^3 + 9.755 f^2 - 0.124 f + 2169.164 \quad \text{(Eq.4)}$$

Description:

$f = 0.327x_1 + 0.345x_2 + 0.327x_3$ and x_1 x_2 x_3 denotes dew point temperature (°C), vapor pressure of water (Bpa) and relative humidity (%), respectively.

http://www.aloki.hu ● ISSN 1589 1623 (Print) ● ISSN 1785 0037 (Online)
DOI: http://dx.doi.org/10.15666/aeer/1706_1484714858

Discussion and conclusion

(1) There are stage characteristics in this haze process. Although the time of haze occurrence is relatively short compared with that of haze occurrence, it still presents the phenomenon of haze and fog alternation.

(2) Low ground wind speed, rising PM2.5 concentration and fluctuation of relative humidity provide favorable conditions for the formation and development of haze weather alternation. PM2.5 concentration, vapor pressure of water, dew point temperature and relative humidity are four key factors that determine visibility.

(3) During the haze, PM2.5 concentration is linearly related to visibility, and meteorological factors formed by vapor pressure of water, dew point temperature and relative humidity are correlated with visibility in the cubic curve.

(4) In future studies, more factors such as wind direction and temperature will be considered to establish a more comprehensive mathematical model to predict trends in the ongoing smog process that may occur in the future.

Acknowledgments. The work was financially supported by Key Research & Development Plan in Hunan (2017SK2272) and Hunan Forestry Science and Technology Plan (XLK201738).

REFERENCES

[1] Bremer Bremer, M. H., Lozano Garcia, D. F., Rodriguez Garcia, M., Hori Ochoa, M. D. C. (2016): Characterization of the pollution levels in a sulfur mine using high resolution satellite imagery to optimize the sampling plan. – Revista Internacional De Contaminacion Ambiental 32: 165-176.

[2] Cao, W. H., Liang, X. D., Li, Q. C. (2013): A study of the stageful characteristics and influencing factors of a long-lasting fog/haze event in Beijing. – Acta Meteorologica Sinica 71(5): 940-951.

[3] Dai, J., Cheng, Y. X. (2008): Analysis on the first haze weather process in Beijing in July 2016. – Environmental Science Guide 37(01): 34-41.

[4] Elias, T., Haeffelin, M., Drobinski, P., Gomes, L., Rangognio, J., Bergot, T., Chazette, P., Raut, J., Colomb, M. (2009): Particulate contribution to extinction of visible radiation: pollution, haze, and fog. – Atmospheric Research 92(4): 443-454.

[5] Guo, L. J., Guo, X. L., Gang, C. G., Zhu, S. C. (2015): Observation and analysis on the occurrence, evolution and transformation characteristics of a persistent severe haze weather in north China. – Scientia Sinica (Terrae) 45(4): 427-443.

[6] Hou, Y. H., Xu, F. S., Zhang, R., Zhao, M., Ming, H. Q. (2017): Analysis on the meteorological causes of persistent haze in a sub-region of Liaoning province. – Meteorological Technology 45(04): 710-716.

[7] Hu, L., Cao, H. L., Zhang, W. J., Wang, Q., Mu, J. (2013): Characteristics of air quality change and its relationship with meteorological conditions in Xi'an city. – Journal of Meteorology and Environment 29(06): 150-153.

[8] Jansen, R. C., Shi, Y., Chen, J., Hu, Y., Xu, C., Hong, S., Li, J., Zhang, M. (2014): Using hourly measurements to explore the role of secondary inorganic aerosol in PM 2.5 during haze and fog in Hangzhou, China. – Advances in Atmospheric Sciences 31(6): 1427-1434.

[9] Leura Vicencio, A. K., Carrizales Yanez, L., Razo Soto, I. (2017): Mercury pollution assessment of mining wastes and soils from former silver amalgamation Area in North-Central Mexico. – Revista Internacional De Contaminacion Ambiental 33: 655-669.

http://www.aloki.hu ● ISSN 1589 1623 (Print) ● ISSN 1785 0037 (Online)
DOI: http://dx.doi.org/10.15666/aeer/1706_1484714858

[10] Li, L. M., Li, L. G., Li, N. W. (2017): Research progress on the causes and hazards of urban smog. – Environmental Engineering 35(12): 92-97 + 104.
[11] Liu, H. M., Fang, C. L., Huang, J. J., Zhu, X. D., Zhou, Y., Wang, Z. B., Zhang, Q. (2013): Analysis on the spatial and temporal characteristics and influencing factors of air pollution in Beijing-Tianjin-Hebei area. – Journal of Geography 73(01): 177-191.
[12] Morones Esquivel, M. M., Pantoja Espinoza, J. C., Proal Najera, J. B., Chairez Hernandez, I., Gurrola Reyes, J. N., Avila Santos, M. (2017): Use of a plate reactor (TiO2/GLASS) for the degradation of 2,5-diclorofenol by solar photocatalisis. – Revista Internacional De Contaminacion Ambiental 33: 605-616.
[13] Perez-Sicairos, S., Alejandro Corrales-Lopez, K., Martin Hernandez-Calderon, O., Israel Salazar-Gastelum, M., Maria Felix-Navarro, R. (2016): Photochemical degradation of nitrobenzene by S2o8-2 ions and Uv radiation. – Revista Internacional De Contaminacion Ambiental 32: 227-236.
[14] Singh, J., Giri, R. K. (2011): Inter-Annual Variation of Fog, Mist, Haze and Smoke at Amritsar and Its Impact on Agricultural Production. – In: Attri, S. D. et al. (eds.) Challenges and Opportunities in Agrometeorology. Springer, Berlin, pp. 409-419.
[15] Sun, R. (2016): Analysis on the optical characteristics and cause of a persistent haze weather process. – The 33rd Annual Meeting of the Chinese Meteorological Society - S10 City, Precipitation and Fog Haze - The Fifth City Meteorological BBS, Chinese Meteorological Society 14.
[16] Torres-Martinez, A., Sanchez, A. J., Alvarez-Pliego, N., Amalia Hernandez-Franyutti, A., Carlos Lopez-Hernandez, J., Bautista-Regil, J. (2017): Gonadal histopathology of fish from La Polvora Urban Lagoon in the Grijalva Basin, Mexico. – Revista Internacional De Contaminacion Ambiental 33: 713-717.
[17] Xie, Z. Z., Fan, X. L., Wang, Y. L., Zha, H. H., Wang, T. F., Sun, Y. (2015): Phase characteristics of a persistent fog and haze process and its influencing factors in Huaian area. – Journal of Meteorology and Environment 31(5): 79-85.
[18] Yin, C. M., Yu, L. J., Zhang, Y. J., Cai, Z., Gao, F. (2014): Analysis on characteristics of haze in Jinan City. – Population Resources and Environment in China 24(S3): 68-70.
[19] Yuan, Z. S., Chen, T., Xiao, L., Li, C. (2015): Analysis on characteristics of haze climate change in Hunan province in the last 43 years. – Journal of Disaster Prevention and Technology Institute (04).
[20] Zhang, X. H., Liu, L. Y., Chen, X. H. (2014): Analysis of haze characteristics and influencing factors in Changsha. – Journal of Environmental Engineering 8(08): 3361-3366.
[21] Zhao, X. J., Pu, W. W., Meng, W., Ma, Z. Q., Dong, F., He, D. (2013): Analysis on the optical characteristics of pollution and aerosol in autumn haze days in Beijing. – Environmental Science 34(02): 416-423.
[22] Zhu, Y. Q., Hu, S. Q., Cao, Z. C. (2015): Analysis on the periodic causes of a persistent haze in Linyi City. – Journal of Environmental Engineering 9(12): 5979-5986.

http://www.aloki.hu ● ISSN 1589 1623 (Print) ● ISSN 1785 0037 (Online)
DOI: http://dx.doi.org/10.15666/aeer/1706_1484714858

JUKES-CANTOR EVOLUTIONARY MODEL BASED PHYLOGENETIC RELATIONSHIP OF ECONOMICALLY IMPORTANT ORNAMENTAL PALMS USING MAXIMUM LIKELIHOOD APPROACH

IJAZ, S.[1*] – HAQ, I. U.[2] – BABAR, M.[1]

[1]*Centre of Agricultural Biochemistry and Biotechnology (CABB), University of Agriculture, University Road, Faisalabad, Pakistan*

[2]*Department of Plant Pathology, University of Agriculture, University Road, Faisalabad, Pakistan*

**Corresponding author*
e-mail: siddraijazkhan@yahoo.com

(Received 17th Jun 2019; accepted 28th Aug 2019)

Abstract. Ornamental palms are famous for their patterned leaves, which make them quite suitable for indoor and outdoor decors. Hitherto, palms were identified morphologically resulting in ambiguous identification. Hence, to stitch this loophole in phylogenetic studies, DNA barcoding is a remarkable way for correct identification and evolutionary study of ornamental palms. We investigated phylogenetic relationship of commonly used ornamental palms in Pakistan. We focused on two genetic regions, rbcL and matK, which had been proved as potential DNA barcodes for species identification and phylogenetic studies. In this study, fifteen ornamental palms were investigated for their evolutionary relationship and molecular identification. This study resolved their evolutionary history using Maximum Likelihood method based on Jukes-Cantor evolutionary model. Among them, nine ornamental palm shared evolutionary history, though four showed evolutionary distinctness from the rest. *Chamaedorea seifrizii* and *Chamaedorea costaricana* revealed close residence in the evolutionary tree with 70% bootstrap support. *Syagrus romanzoffiana* resolved as independent lineage with distinct and highly diverse evolutionary history. Furthermore, *Wodyetia bifurcata* and *Dypsis lutescens* nested together with 61% bootstrap though, they belong to different genera. This showed that the genus Wodyetia and Dypsis had very close evolutionary history. The evolutionary forces either geographical isolation or genetic drift could be the reason for the divergence of these palms into two distinct genera, though being the lineages of the same parent.
Keywords: *ornamental palm, DNA barcoding, Bayesian information criterion, maximum likelihood method, Jukes-Cantor evolutionary model*

Introduction

Arecaceae family, also known as Palmae family, is well known for its ornamental palm members. It consists of 240 genera and 27000 species (Lorenzi et al., 2010). It is a monotypic family of Arecales order. Palms are thought to be originated in Australasia and their fossil records reveal their distribution in early Cenzoic era. In present era, palms are mostly distributed in tropical regions and some species are reported in subtropical regions as well (Henderson et al., 1995). Palmae family comprised of commercially and horticulturally famous landscape ornamental palms which are famous for their palmate patterned evergreen leaves and bright, colorful flowers. Palms are noticeably used in outdoor and indoor house decors. Since many decades, the taxonomy of these ornamental palms is poorly understood due to lack of information about their character identification. These problems are caused because of their morphological

http://www.aloki.hu ● ISSN 1589 1623 (Print) ● ISSN 1785 0037 (Online)
DOI: http://dx.doi.org/10.15666/aeer/1706_1485914865

similarities with each other and difficulties in hybrid discrimination (Pintaud, 2008). High evolutionary rate has been observed in palm trees and the evaluation of genetic evolution through botanical characters is quite difficult task as morphological traits distinguish the plant at specific life stage. The discrimination based upon such characters results in either ambiguous or wrong identification of palm (Sedra et al., 1996) which made them pseudo palms.

To overcome these problems, botanists have moved towards molecular approach for species identification and discrimination. For this purpose, DNA barcodes are used suggested by CBOL (Consortium of Barcode of Life) in 2009. DNA barcodes consists of conserved short DNA sequences which are unique for every species. In case of animals, well known barcode in COI (Cytochrome oxidase gene) while for plants, many plastid sequences have been studied and confirmed as barcode loci (Kress et al., 2005; Ford et al., 2009). Out of many barcodes, two plastid genes namely maturase K (*matK*) and Ribulose-1,5-bisphosphate carboxylase/oxygenase large subunit (*rbcL*) have been recommended and standardized as potential plant barcodes by PWG (International body of Plant Working Group) of CBOL (2009). The barcodes suggested by CBOL group have great potential for discrimination, authentication and identification for international/foreign as well as native plant species (Maloukh et al., 2017). The discriminatory power of *rbcL* is lower than *matK* but it offers many advantages like its unambiguous and clear alignment power, high sequencing frequency and its universality (Dong et al., 2014). In this study, 15 ornamental palms were investigated for their phylogenetic relationship to unravel their evolutionary history and ancestral inference for assessing their divergence as distinct lineages.

Materials and methods

Sample collection and molecular processing

The leave samples of 15 economically important ornamental palms in Pakistan (*Table 1*) were collected for DNA extraction. Genomic DNA was extracted using Plant DNA extraction kit (Favorgen Biotech Corp.). For the amplification of *matK* and *rbcL* regions, their universal primer pairs suggested by Consortium of Barcode of Life (CBOL, 2009) were used in PCR analysis. The total volume of a reaction mixture for PCR was 25 µl containing 50 ng/µl DNA template, 10 µM each primer in a pair, 2 µl dNTPs, 2.5 µl of HF buffer, 0.25 µl of high fidelity polymerase and nuclease free water for volume makeup. PCR product was resolved on 2% high resolution agarose with gel electrophoresis. The required amplicons were eluted by gel purification mini kit (Favorgen Biotech Corp.) and then sequenced through Eurofins Genomics DNA sequencing services, USA. The sequences were trimmed with BioEdit v7.2.6.1. The success frequency of PCR amplification of each target regions (rbcl and matK) was determined as the proportion of total No. of amplified individuals to the total No. of individuals analyzed in study while successful sequencing was evaluated as the percentage of number of good quality sequences to the total number of sequences of studied individuals.

Data analysis

The good quality trimmed sequences were *in silico* characterized and submitted to NCBI database. The homology search of each sequence was performed using BLASTn

http://www.aloki.hu ● ISSN 1589 1623 (Print) ● ISSN 1785 0037 (Online)
DOI: http://dx.doi.org/10.15666/aeer/1706_1485914865

tool. Each sequence was identified based on the 100% identity with the reference sequences of type materials in the NCBI database. The obtained sequences were aligned using ClustalW and then were submitted to NCBI database. For phylogenetic analysis, version 7.0 (Molecular Evolutionary Genetics Analysis) was used to employing Maximum Likelihood (ML) method based on best-fit evolutionary model to generate optimal topology in an evolutionary tree.

Table 1. *Ornamental palm with their native and scientific name along with GenBank accession numbers*

Serial#	Common name	Scientific name	GenBank accession no.	
			rbcL	***matK***
1	Alexandra palm	*Archontophoenix alexandrae*	MK947439	----------
2	Bamboo palm	*Chamaedorea seifrizii*	MK639602	MK639603
3	Bismarckia palm	*Bismarckia nobilis*	MK947440	----------
4	Bottle palm	*Hyophorbe lagenicaulis*	MK947437	----------
5	Cluster palm	*Chamaedorea costaricana*	MK947436	MN047253
6	Clustering fishtail palm	*Caryota mitis*	MK947435	----------
7	Foxtail palm	*Wodyetia bifurcata*	MK947442	----------
8	Golden palm	*Dypsis lutescens*	MK947441	----------
9	Lady palm	*Rhapis excelsa*	MK947443	----------
10	Queen palm	*Syagrus romanzoffiana*	MK650287	MN047252
11	Dwarf Majesty palm	*Ravenea hildebrandtii*	MK947438	MN047254
12	Royal palm	*Roystonea regia*	MK947434	----------
13	Washingtonia palm	*Washingtonia robusta*	MK940273	----------
14	Dioon palm	*Dioon spinulosum*	----------	----------
15	Kangi palm	*Cycas revolute*	----------	----------

Results

Ornamental palms are the pillars of horticultural industry. However, their accurate taxonomic identification is challenging. Hence, in this study, *matK* and *rbcL* regions were targeted to taxonomic investigation of 15 economically important ornamental palm in Pakistan for resolving their phylogenetic topology unequivocally. The universal barcode primers of both genetic regions were used in DNA barcoding analysis.

These two barcode genes *rbcL* and *matK* showed 100% PCR amplification. The sequencing frequency showed that the sequencing success of *rbcL* was comparatively higher than *matK*. The low sequencing rate of *matK* is due to high heterozygosity in the respective regions, which may result in polymerase slippage during Sanger sequencing method. The sequencing rate of *rbcL* was recorded as 86.66% while for *matK* it was recorded as 26.66%. However, the species discriminating power of *matK* is much greater than *rbcL.* The phylogenetic tree for rbcl region of 13 ornamental palm was constructed through Mega 6 software (Tamura et al., 2013) by using maximum likelihood algorithm, which was based upon Jukes-Cantor evolutionary model with Gamma distribution (JC + G) 1 (*Fig. 1*). The best substitution pattern is described the models with lowest Bayesian Information Criterion scores. Akaike Information Criterion (AICc), No. of parameters along with branch lengths and Maximum Likelihood value (lnL) along with estimated values of transversion bias (R), rate of nucleotide substitution (r) and nucleotide frequencies for each nucleotide pair is shown (*Table 2*).

http://www.aloki.hu ● ISSN 1589 1623 (Print) ● ISSN 1785 0037 (Online)
DOI: http://dx.doi.org/10.15666/aeer/1706_1485914865

The constructed tree showed highest log likelihood of -387.1215 with trees percentage is showed next to the branches. Through neighbor joining method, the pairwise distance matrix was assessed by MCL (Maximum Composite Likelihood) approach. The level of evolutionary differences was estimated by discrete Gamma distribution as + G 0.1000 parameter. The branch lengths of the constructed tree were calculated with the No. of substitutions per sites. The analyses were based upon 13 nucleotide sequences with 1st, 2nd, 3rd and noncoding codon positions. A total of 225 positions were included in final dataset with all missing gaps eliminated (*Table 2*).

Table 2. *Maximum likelihood fits of 24 different nucleotide substitution models on 13 ornamental palms using rbcL barcode*

Model	Parameters	BIC	AICc	lnL	(+I)	(+G)	R	f(A)	f(T)	f(C)	f(G)	r(AT)	r(AC)	r(AG)	r(TA)	r(TC)	r(TG)	r(CA)	r(CT)	r(CG)	r(GA)	r(GT)	r(GC)
JC+G	24	965.423	822.292	-386.939	n/a	0.05	0.50	0.250	0.250	0.250	0.250	0.083	0.083	0.083	0.083	0.083	0.083	0.083	0.083	0.083	0.083	0.083	0.083
JC+G+I	25	969.110	820.032	-384.792	0.46	0.05	0.50	0.250	0.250	0.250	0.250	0.083	0.083	0.083	0.083	0.083	0.083	0.083	0.083	0.083	0.083	0.083	0.083
JC	23	969.704	832.520	-393.070	n/a	n/a	0.50	0.250	0.250	0.250	0.250	0.083	0.083	0.083	0.083	0.083	0.083	0.083	0.083	0.083	0.083	0.083	0.083
K2+I	25	969.768	820.690	-385.121	0.84	n/a	1.20	0.250	0.250	0.250	0.250	0.057	0.057	0.136	0.057	0.136	0.057	0.057	0.136	0.057	0.136	0.057	0.057
JC+I	24	970.073	826.941	-389.264	0.62	n/a	0.50	0.250	0.250	0.250	0.250	0.083	0.083	0.083	0.083	0.083	0.083	0.083	0.083	0.083	0.083	0.083	0.083
K2+G	25	971.320	822.242	-385.897	n/a	0.05	1.19	0.250	0.250	0.250	0.250	0.057	0.057	0.136	0.057	0.136	0.057	0.057	0.136	0.057	0.136	0.057	0.057
T92+G	26	975.573	820.550	-384.033	n/a	0.05	1.19	0.290	0.290	0.210	0.210	0.065	0.047	0.116	0.065	0.116	0.047	0.065	0.160	0.047	0.160	0.065	0.047
K2	24	975.685	832.554	-392.070	n/a	n/a	1.18	0.250	0.250	0.250	0.250	0.057	0.057	0.135	0.057	0.135	0.057	0.057	0.135	0.057	0.135	0.057	0.057
K2+G+I	26	978.378	823.355	-385.435	0.12	0.05	1.20	0.250	0.250	0.250	0.250	0.057	0.057	0.136	0.057	0.136	0.057	0.057	0.136	0.057	0.136	0.057	0.057
T92	25	979.778	830.700	-390.126	n/a	n/a	1.18	0.290	0.290	0.210	0.210	0.066	0.048	0.115	0.066	0.115	0.048	0.066	0.159	0.048	0.159	0.066	0.048
T92+G+I	27	980.977	820.011	-382.744	0.29	0.05	1.20	0.290	0.290	0.210	0.210	0.065	0.047	0.116	0.065	0.116	0.047	0.065	0.160	0.047	0.160	0.065	0.047
HKY+I	28	982.633	815.724	-379.582	0.95	n/a	1.21	0.255	0.324	0.193	0.228	0.072	0.043	0.127	0.057	0.107	0.051	0.057	0.180	0.051	0.142	0.072	0.043
T92+I	26	983.797	828.774	-388.145	0.40	n/a	1.18	0.290	0.290	0.210	0.210	0.065	0.047	0.115	0.065	0.115	0.047	0.065	0.159	0.047	0.159	0.065	0.047
HKY+G	28	989.541	822.632	-383.036	n/a	0.05	1.19	0.255	0.324	0.193	0.228	0.073	0.043	0.126	0.057	0.106	0.051	0.057	0.179	0.051	0.141	0.073	0.043
TN93+I	29	990.587	817.738	-379.568	0.95	n/a	1.21	0.255	0.324	0.193	0.228	0.072	0.043	0.130	0.057	0.105	0.051	0.057	0.176	0.051	0.145	0.072	0.043
HKY	27	993.797	832.831	-389.155	n/a	n/a	1.18	0.255	0.324	0.193	0.228	0.073	0.043	0.125	0.057	0.106	0.051	0.057	0.178	0.051	0.140	0.073	0.043
HKY+G+I	29	997.540	824.691	-383.045	0.00	0.05	1.19	0.255	0.324	0.193	0.228	0.073	0.043	0.126	0.057	0.106	0.051	0.057	0.179	0.051	0.141	0.073	0.043
TN93+G	29	997.552	824.703	-383.051	n/a	0.05	1.19	0.255	0.324	0.193	0.228	0.073	0.043	0.129	0.057	0.104	0.051	0.057	0.174	0.051	0.145	0.073	0.043
TN93	28	1001.80	834.891	-389.165	n/a	n/a	1.18	0.255	0.324	0.193	0.228	0.073	0.043	0.129	0.057	0.103	0.051	0.057	0.174	0.051	0.144	0.073	0.043
TN93+G+I	30	1005.53	826.745	-383.051	0.00	0.05	1.19	0.255	0.324	0.193	0.228	0.073	0.043	0.129	0.057	0.104	0.051	0.057	0.174	0.051	0.145	0.073	0.043
GTR+G	32	1014.97	824.312	-379.791	n/a	0.05	0.66	0.255	0.324	0.193	0.228	0.035	0.169	0.054	0.027	0.101	0.024	0.224	0.169	0.055	0.060	0.035	0.047
GTR+G+I	33	1017.30	820.709	-376.966	0.73	0.07	0.71	0.255	0.324	0.193	0.228	0.036	0.159	0.056	0.028	0.107	0.025	0.210	0.179	0.055	0.062	0.036	0.047
GTR	31	1019.22	834.493	-385.904	n/a	n/a	0.65	0.255	0.324	0.193	0.228	0.037	0.167	0.055	0.029	0.098	0.026	0.221	0.166	0.055	0.062	0.037	0.047
GTR+I	32	1019.76	829.102	-382.186	0.62	n/a	0.65	0.255	0.324	0.193	0.228	0.036	0.168	0.054	0.028	0.099	0.025	0.223	0.167	0.055	0.061	0.036	0.047

The phylogenetic topology of the constructed tree revealed the evolutionary history of 13 ornamental palms. Of these thirteen ornamental palms, nine showed evolutionary relatedness. These nine ornamental palms viz., *Chamaedorea seifrizii*, *Chamaedorea costaricana, Roystonea regia, Caryota mitis, Ravenea hildebrandtii Wodyetia bifurcata, Dypsis lutescens, Archontophoenix alexandrae* and *Hyophorbe lagenicaulis* revealed divergence from the same parent in the evolutionary tree (*Fig. 1*) as nested in a clade. This phylogenetic tree showed that they are independent lineages that had been evolutionary diverged. *Chamaedorea seifrizii* and *Chamaedorea costaricana* showed closeness to each other with 70% bootstrap support. They resolved as two different species of the same genus. However, the other ornamental palms resolved as diverse evolutionary history. *Caryota mitis* and Ravenea *hildebrandtii* showed the divergence from the same parent but longer branch length of *Caryota mitis* supported that it is more evolutionary diverse than Ravenea *hildebrandtii* from their parents. Moreover, *Wodyetia bifurcata* and *Dypsis lutescens* nested closely with 61% bootstrap though, they belong to different genera. This showed genus Wodyetia and Dypsis had very close evolutionary history. The geographical isolation and genetic drift during evolution could be the reason of divergence of these palms into two distinct genera, though being lineages of the same parent. Although, *Syagrus romanzoffiana*, *Bismarckia nobilis, Washingtonia robusta* and *Rhapis excelsa* resolved different evolutionary history from nine ornamental palm of a clade. *Washingtonia robusta* and *Rhapis excelsa* showed evolutionary divergence from the same parent by 53% bootstrap support. However, *Bismarckia nobilis* and parent lineage of *Washingtonia robusta* and *Rhapis excelsa* showed close evolutionary history with 44% bootstrap support.

http://www.aloki.hu ● ISSN 1589 1623 (Print) ● ISSN 1785 0037 (Online)
DOI: http://dx.doi.org/10.15666/aeer/1706_1485914865

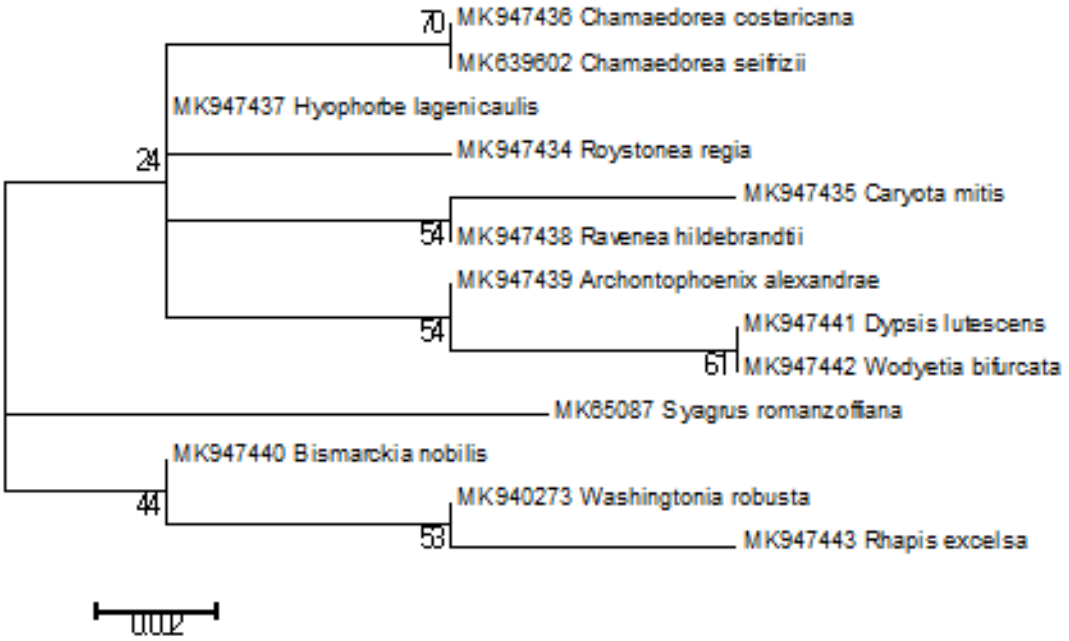

Figure 1. *Chloroplast region, rbcL, based phylogenetic tree of 13 ornamental palms*

Discussion

Ornamental palms, belong to Arecaceae family, are quite important landscape plants of tropical, subtropical and warm climate regions. These are famous for their palmate patterned leaves, and colorful flowers, which makes these plants noticeable in indoor and outdoor decors. High rate of plastid DNA evolution has been observed in palm trees (Asmussen et al., 2000; Dransfield et al., 2008). The determination of genetic evolution and variation through morphological characters is quite tedious in ornamental palm as morphological traits discriminates the plants at particular life stage which results in either wrong or ambiguous identification (Sedra et al., 1996). Taking these problems in account, genetic variability is determined through molecular approaches. DNA barcoding is an efficient molecular approach for efficient species identification based upon the conserved regions as a barcode/marker. For the evaluation of DNA barcode, the success rate of PCR amplification and sequencing are quite important parameters. In the present study, two conserved regions of chloroplast genome, *matK* and *rbcL* were successfully amplified for 15 ornamental palm plant identification. However, the sequencing rate of matK (26.66%) was comparatively lower than rbcL (86.66%) because of its complex heterozygosity nature. The universality of *rbcL* region have been proved by high amplification and sequencing rate as already explained by Huang et al. (2015) and Kang et al. (2017) while studying the Asian tropical trees and tropical cloud forest trees, respectively. The evolutionary tree of thirteen ornamental palms were constructed using Maximum likelihood algorithm whose nodes were supported by bootstrap values. Sequence evolution model, JC + G model, with lowest BIC value (965.423) was selected to generate a tree under maximum likelihood (ML) algorithm. In the respective tree, *Wodyetia bifurcata* and *Dypsis lutescens* are supported by 61%bootstrap, which make them closer to each other although these belong to different genera. This may be due to the less resolving power of *rbcL* genetic region of these two ornamental palm due to less evolution.

http://www.aloki.hu ● ISSN 1589 1623 (Print) ● ISSN 1785 0037 (Online)
DOI: http://dx.doi.org/10.15666/aeer/1706_1485914865

Conclusion

The present evolutionary study helped in identifying the ornamental palms of Pakistan through molecular approaches as morphological characterization was not enough for correct identification due their high similarity nature. This phylogenetic study showed that nine ornamental palm shared evolutionary history, though four showed evolutionary distinctness from the rest. *Chamaedorea seifrizii* and *Chamaedorea costaricana* revealed close residence in the evolutionary tree. However, *Syagrus romanzoffiana* resolved as independent lineage with distinct and highly diverse evolutionary history. Furthermore, *Wodyetia bifurcata* and *Dypsis lutescens* showed cladding though they belong to different genera. This showed that the genus Wodyetia and Dypsis had very close evolutionary history.

REFERENCES

[1] Asmussen, C. B., Baker, W. J., Dransfield, J. (2000): Phylogeny of the Palm Family (Arecaceae) Based on rps16 Intron and trnL-trnF Plastid DNA Sequences. – In: Wilson, K. L., Morrison, D. A. (eds.) Monocuts: Systematics and Evolution: Proceedings of the 2. International Conference on the Comparative Biology of the Monocuts, Sydney. CSIRO, Collingwood.

[2] Dong, W., Cheng, T., Li, C., Xu, C., Long, P., Chen, C., Zhou, S. (2014): Discriminating plants using the DNA barcode rbc L b: an appraisal based on a large data set. – Mol. Ecol. Resour. 14: 336-43. DOI: 10.1111/1755-0998.12185.

[3] Dransfield, J., Uhl, N. W., Asmussen, C. B., Baker, J. W., Harley, M. M., Lewis, C. E. (2008): Genera Palmarum: The Evolution and Classification of Palms. – Kew Publishing, Richmond, UK.

[4] Ford, C. S., Ayres, K. L., Toomey, N., Haider, N., Van, A. S. J., Kelly, L. J., Wikström, N., Hollingsworth, P. M., Duff, R. J., Hoot, S. B., Cowan, R. S. (2009): Selection of candidate coding DNA barcoding regions for use on land plants. – Botanical Journal of the Linnean Society 159(1): 1–11.

[5] Huang, X. C., Ci, X. Q., Conran, J. G., Li, J. (2015): Application of DNA barcodes in Asian tropical trees–a case study from Xishuangbanna Nature Reserve, Southwest China. – PLoS One 10. DOI: 10.1371/journal.pone.0129295.

[6] Henderson, A., Galeano, A. G., Bernal, R. (1995): Field Guide to the Palms of the Americas. – Princeton University Press, Princeton, NJ.

[7] Kang, Y., Deng, Z., Zang, R., Long, W. (2017): DNA barcoding analysis and phylogenetic relationships of tree species in tropical cloud forests. – Scientific Reports 7. DOI: 10.1038/s41598-017-13057-0.

[8] Kress, W. J., Wurdack, K. J., Zimmer, E. A., Weigt, L. A., Janzen, D. H. (2005): Use of DNA barcodes to identify flowering plants. – Proc. Natl. Acad. Sci. 102: 8369-74. DOI: 10.1073/pnas.0503123102.

[9] Lorenzi, H., Larry, R., Noblick, Kahn, F., Ferreira, E. (2010): Brazilian Flora: Arecaceae (Palms). – Instituto Plantarum de Estudos da Flora, Nova Odessa, Brazil.

[10] Maloukh, L., Kumarappan, A., Jarrar, M., Salehi, J., El-Wakil, H., Lakshmi, T. R. (2017): Discriminatory power of *rbcL* barcode locus for authentication of some of United Arab Emirates (UAE) native plants. – 3 Biotech 7: 144. DOI: 10.1007/s13205-017-0746-1.

[11] Pintaud, J. C. (2008): An overview of the taxonomy of Attalea (Arecaceae). – Revista Peruana de Biología 15: 53-62.

[12] Sedra, M., El, F. H., Benzine, A., Allaoui, M., et al. (1996): La palmeraie dattiere marocaine: evaluation du patrimoine phenicicole. – Fruits 1: 247-259.

http://www.aloki.hu ● ISSN 1589 1623 (Print) ● ISSN 1785 0037 (Online)
DOI: http://dx.doi.org/10.15666/aeer/1706_1485914865

[13] Tamura, K., Stecher, G., Peterson, D., Filipski, A., Kumar, S. (2013): MEGA6: molecular evolutionary genetics analysis version 6.0. – Mol. Biol. Evol. 30: 2725-9. DOI: 10.1093/molbev/mst197.

http://www.aloki.hu ● ISSN 1589 1623 (Print) ● ISSN 1785 0037 (Online)
DOI: http://dx.doi.org/10.15666/aeer/1706_1485914865

HEAVY METAL POLLUTION OF SURFACE SEDIMENTS IN THE NORTHERN WATERS OF THE ABANDONED YELLOW RIVER DELTA IN JIANGSU PROVINCE OF CHINA AND ECOLOGICAL RISK ASSESSMENT

WANG, J.[1] – ZHANG, Y. M.[2*] – XU, M.[1] – LIU, B. Q.[1]

[1]*College of Marine Science and Engineering, Nanjing Normal University, Nanjing 210023, China*

[2]*School of Environment, Nanjing Normal University, Nanjing 210023, China*

**Corresponding author*
e-mail: 09352@njnu.edu.cn

(Received 18th Jun 2019; accepted 16th Oct 2019)

Abstract. We studied the distribution, pollution characteristics, and ecological risk of heavy metal pollutants in the northern waters of the abandoned Yellow River Delta in Jiangsu Province of China in the surface sediments in May 2018. The results show that the average content of As, Cu, Pb, Zn, and Cd, exceeds their respective background concentration in the tidal marshes of Jiangsu. Analysis of the pollution load index shows that the pollution level is rated as medium pollution; analysis of the composite potential ecological risk index indicates that the level is medium-high, and the waters from the Zhongshan River estuary to the Abandoned Yellow River estuary have the highest level of heavy metal pollution and are most susceptible to ecological risk. Heavy metal content increases from the Guan River estuary to the Abandoned Yellow River estuary, as well as from the shore to the sea with the estuaries and near-shore port areas having the highest content of heavy metals. The content of Cr is mainly derived from natural sources, while other heavy metals primarily originate from the pollutants discharged into the sea from rivers, marine outfalls and marine development activities like port construction and wind-power development.
Keywords: *pollution characteristics, potential ecological risk, spatial distribution, correlation analysis, clustering analysis*

Introduction

As sensitive regions that connect the continent with the sea, estuaries and coasts are areas where both life and production thrive and where pollutants and sediments from rivers accumulate (Li et al., 2007; Wang et al., 2008; Reddy et al., 2016). Heavy metals are toxic, durable, bio-accumulative, contributive to ecological risks, and hard to decompose (Nguyen et al., 2016; Harikrishnan et al., 2017; Jahan and Strezov, 2018; Zhao et al., 2018). Therefore, heavy metal pollution is receiving considerable attention from researchers because it threatens marine ecology and human health (Phillips et al., 2016; Keshavarzi et al., 2018; Wang et al., 2018). Due to the rapid economic development along coastlines in recent years, marine heavy metal pollution has exacerbated, and human activities are primarily responsible for the majority of this pollution in estuaries and coastal areas throughout the world (Begy et al., 2016; Guan et al., 2016; Monferran et al., 2016). Marine sediments act as a repository of heavy metals in the sea. Moreover, because of the absorption and sedimentation of suspended matters, most heavy metals in the sea get deposited in marine sediments; however, when the environment changes, these heavy metals are released into the sea again and cause pollution (Singh et al., 2005; Guan et al., 2016). Compared to sea water and marine

http://www.aloki.hu ● ISSN 1589 1623 (Print) ● ISSN 1785 0037 (Online)
DOI: http://dx.doi.org/10.15666/aeer/1706_1486714882

organisms, marine sediments usually contain more heavy metals and can provide more accurate detection results (Liang et al., 2018); therefore, the concentration of heavy metals in sediments is an important environmental indicator.

Located in the central and northern coastal areas of Jiangsu province in China (*Fig. 1*), the abandoned Yellow River Delta has an erosion coast and the –15 m isobath and –10 m isobath on top of the delta are 3.95 km and 2.0 km away from the coastal baseline, respectively, which indicates that the water is deep along the coast. Therefore, this area offers ideal conditions for building a large port. The rivers joining the sea in the study area include the Guan River, Zhongshan River and the abandoned Yellow River, with average discharge of 475 m^3/s, 175 m^3/s and 103 m^3/s respectively. Furthermore, because of the rich resources from the adjacent continent and the strategy of developing coastal areas of Jiangsu province, the development of the northern waters of the Abandoned Yellow River Delta is gaining pace. The primary activities in the area are port development, waste discharge, aquaculture, and wind power development. The Guan River Port is located at the estuary of Guan River, whereas another port is under construction along the coastline from the abandoned Yellow River to Erhongkou. Within the eastern seawall of the Zhongshan River estuary, an industrial park is being developed (occupied primarily by chemical plants). The industrial waste water from this park is discharged into the sea via outfalls that are 6 km away from the Zhongshan River estuary with the daily volume of discharge reaching 20,000 tons. Toward the south of the industrial park is an aquaculture area, and the wastewater from this area is discharged into the sea through gated channels. Furthermore, there are three marine wind-power stations in the study area (A, B and C in *Fig. 1*).

As the coastal economy takes off, the development activities along the coastline will increase, which will lead to additional environmental problems in the delta. Note that the concentration of heavy metals in marine sediments can reflect the level of pollution in the sea. Previous studies on heavy metal concentration in coastal sediments in Jiangsu, such as studies on pollution characteristics, sources, and ecological risks of heavy metals in surface sediments in Haizhou Bay and the radiating shoals, have focused on certain regions. There have been no studies on the sources and ecological risks of heavy metals in sediments of the northern waters of the Abandoned Yellow River delta. In this study, we focused on this region as the study area and used the sediment statistics of 2018 to analyze the concentration of heavy metals in surface sediments in this area. The aims of this study are as follows: i) to analyze the concentration and distribution characteristics of seven heavy metals in surface sediments in the northern waters of the Abandoned Yellow River Delta; ii) to assess the pollution level and ecological risks of seven heavy metals in surface sediments in the study area; and iii), to identify the possible sources of heavy metal pollution in the study area via correlation and clustering analyses. The results revealed heavy metal pollution in the surface sediments of the northern waters of the Abandoned Yellow River Delta, and the effect of human activities on the sediment environment, which would provide a scientific basis for environmental protection and pollution treatment in the study area.

Materials and methods

Study area description

Located in the central and northern waters of Jiangsu province in China, the study area extends from the Zhongshan River estuary to the abandoned Yellow River estuary

http://www.aloki.hu ● ISSN 1589 1623 (Print) ● ISSN 1785 0037 (Online)
DOI: http://dx.doi.org/10.15666/aeer/1706_1486714882

and extends 50 km outward into the sea (*Fig. 1*). The study area belongs to the northern waters of the Abandoned Yellow River Delta. With the headland on the north of the Abandoned Yellow River estuary as the point of inflexion, the coastline meanders from northwest to southeast, and then runs from north to south. The coast is a plain erosion silt-muddy coast.

The substrate of the Abandoned Yellow River Delta primarily comprises clayey silt, silt, and sandy silt with a median grain size of 6–8 μm. Clayey silt accounts for 80% of the total fine particles in the study area, whereas silt accounts for 10%–20%; therefore, the study area is the best in Jiangsu in terms of the concentration of fine particles (Hu, 2014). The grain size of sediments in the Abandoned Yellow River Delta decreases from west to east with the major type of sediments changing from sandy silt to clayey silt (Chen, 2014; Hu, 2014). Guan River, which is to the north of the Abandoned Yellow River, is the largest river that joins the sea in Jiangsu, and because of the sediments it carries to the estuary, the grain size of particles in the estuary is relatively big (Hu, 2014; Zhang, 2016). The distribution of sediments is consistent with the change in water depth and landform. From the Guan River estuary to the Zhongshan River estuary, the major particles are sandy silt; however, from the Zhongshan River estuary to the port, the major particles are silt and clayey silt (Hu, 2014).

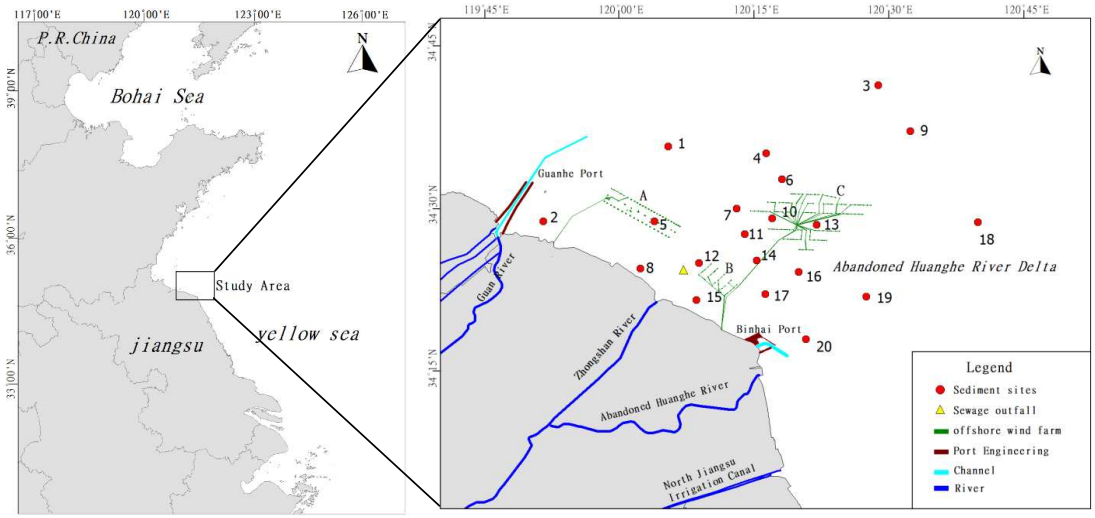

Figure 1. *Location of sample sites*

Sampling and sample processing

We conducted the on-site sampling in May 2018. A total of 20 surface-sediment samples were collected from the sampling sites (*Fig. 1*). The sampling point coordinate range is 34°18′56.34″N–34°42′32.61″N, 119°52′11.18″E–120°40′20.99″E. The test subjects were seven heavy metals, i.e., Hg, As, Cu, Pb, Zn, Cd, and Cr. We conducted the sampling was according to technical regulations established by "Specifications of Marine Monitoring (GB17378-2007)" and "Specifications for Oceanographic Survey (GB/T 12763-2007)". To remove the overlying water, the sediment samples were collected through a grab sampler on the deck. In particular, to test for Cu, Zn, Pb, and Cd, we obtained 500–600 g of wet sample and added it into a clean polyethylene bag, and then sealed the bag. Similarly, to test for petroleum pollutants, organic carbon, and

http://www.aloki.hu ● ISSN 1589 1623 (Print) ● ISSN 1785 0037 (Online)
DOI: http://dx.doi.org/10.15666/aeer/1706_1486714882

total mercury, we obtained 500–600 g of wet sample and added it to a 500 ml wide-mouth bottle, which was then sealed. All wide-mouth bottles were filled with nitrogen, placed in shady areas, and frozen at a low temperature. The frozen samples were wind-dried, and then placed in shady but well-ventilated indoor sites. From these samples, we removed gravels and large debri-like particles (obtained from plants and animals) before they were placed into the agate mortar where these samples were grinded till they were able to pass through a 160-mesh sieve. The mixture was then used for further characterization of chemical elements. We analyzed the test results according to "Specifications of Marine Monitoring – Part 5: Sediment Analysis (GB17378.5-2007)". The atomic fluorescence method was used in order to determine the As and Hg concentrations by AFS-930 Atomic Fluorescence Spectrometer. Flameless atomic absorption spectrophotometry method was used to determine the Cu, Pb and Cr concentration and flame atomic absorption spectrophotometry method was used to determine the Zn and Cd levels and all by VARIAN AA240FS Atomic Absorption Spectrophotometer.

Methods

Pollution load index (PLI)

The pollution load index was first proposed by Tomlinson in 1980 to assess pollution by different chemical elements at different sites. The equations for calculation are:

$$C_f^i = C_{\mathrm{n}}^i / C_0^i \quad \text{(Eq.1)}$$

$$PLI = \sqrt[n]{C_f^1 \times C_f^2 \times C_f^3 \times \ldots \times C_f^{\mathrm{n}}} \quad \text{(Eq.2)}$$

where PLI refers to the pollution load index of a certain site, C_f^i the pollution index of one element, C_{n}^i the value obtained through actual measurement, and C_0^i the background value. The grading standard for PLI (Tomlinson et al., 1980; Zhu et al., 2013) is shown in *Table 1*.

Geo-accumulation index

Geo-accumulation Index (Igeo) was first proposed by G. Müller, a German scientist. It is a quantitative index for assessment of heavy metal contents in sediments and can be used to assess pollution caused by heavy metal contents. The calculation equation is:

$$I_{\mathrm{geo}} = \log_2 \frac{C_n}{1.5B_n} \quad \text{(Eq.3)}$$

where Cn denotes the content of Element n in actual measurement, and Bn is the background value of this element on earth which, in this research, specifically refers to the background value of the content of the researched element in the tidal marsh of Jiangsu province measured in the 1980s by Chen et al. (1985). 1.5 is a coefficient identified by considering possible changes caused by differences of rocks in different places. The grading standard of geo-accumulation index (Müller, 1969) is also shown in *Table 1*.

http://www.aloki.hu ● ISSN 1589 1623 (Print) ● ISSN 1785 0037 (Online)
DOI: http://dx.doi.org/10.15666/aeer/1706_1486714882

Potential ecological risk index

The potential ecological risk index was first proposed by a Swedish environmentalist named Hakanson in 1980 to assess the potential ecological hazards of heavy metal contents in sediments. This method combines the ecological impact, environmental impact and toxicologic research of heavy metal contents to reflect the potential ecological risks of heavy metals. The calculation equations are:

$$E_r^i = T_r^t \times C_f^i \quad \text{(Eq.4)}$$

$$RI = \sum (E_r^i) \quad \text{(Eq.5)}$$

where RI is the value of comprehensive potential ecological risks, E_r^i the value of potential risks of one element. T_r^t denotes the toxicological coefficient of an element which, in this research, adopts the standard toxicological coefficients of heavy metal contents proposed by Hakanson (1980): the respective toxicological coefficients of Cd, As, Cu, Pb, Cr and Zn are 30, 10, 5, 5, 2, and 1. C_f^i is the pollution coefficient of a certain element, $C_n{}^i$ the value obtained through actual measurement and $C_0{}^i$ the background value. The grading standard for the potential ecological risk index of a given element and for the comprehensive potential ecological risk index is also presented in *Table 1*.

Table 1. *Grading standard for geo-accumulation index and potential ecological risk index of heavy metal contents*

Geo-accumulation index (I_{geo}) value	Pollution level	Pollution load index (PLI) value	Pollution level	Single-factor potential ecological risk (E_r^i)	Single-factor potential ecological risk level	Comprehensive potential ecological risk value (RI)	Comprehensive potential ecological risk level
≤ 0	No pollution	< 1	No pollution	< 40	Low	< 110	Low
0~1	Mild pollution	1~2	Medium pollution	40~80	Medium	110~220	Medium
1~2	Mild-medium pollution	2~3	Heavy pollution	80~160	Medium-high	220~440	High
2~3	Medium pollution	≥ 3	Severe pollution	160~320	High	≥ 440	Extremely high
3~4	Serious pollution			≥ 320	Extremely high		
4~5	Heavy pollution						
> 5	Severe pollution						

Statistical and mapping methods

We performed Pearson correlation coefficients between each pair of heavy metals and clustering analysis for the seven heavy metals obtained data from 20 sampling sites by using SPSS. Combining with the spatial information of station location, the data are processed by using Suffer11 software and Kristin interpolation method, and the spatial

http://www.aloki.hu ● ISSN 1589 1623 (Print) ● ISSN 1785 0037 (Online)
DOI: http://dx.doi.org/10.15666/aeer/1706_1486714882

distribution maps of heavy metal contents in surface sediments, pollution load index, and the comprehensive ecological risk index.

Result and discussion

Heavy metal concentration and distribution

Table 2 shows the concentration of different heavy metals in the surface sediments of the study area in May 2018. The concentration range of heavy metals (mg/kg) in the surface sediments of the study area are as follows. The concentration of Hg was 0.0064–0.0287 mg/kg (average of 0.0177 mg/kg); that of As was 5.72–18.1 mg/kg (average of 12.635 mg/kg); that of Cu was 17.9–27.7 mg/kg (average of 22.28 mg/kg); that of Pb was 17.4–25.8 mg/kg (average of 21.77 mg/kg); that of Zn was 60.4–80.2 mg/kg (average of 70.89 mg/kg); that of Cd was 0.137–0.264 mg/kg (average of 0.18 mg/kg); and that of Cr was 35.8–56.7 mg/kg (average of 40.86 mg/kg).

In comparison with the heavy metal contents in sediments obtained by studies in other areas of China (*Table 2*), the average content of Hg, As, Cu, Pb, Zn, Cd, Cr in sediments in the study area stayed at a medium level.

Table 2. *Heavy metal contents of surface sediments in the study area and comparison with other areas (mg/kg)*

		Mercury (Hg)	Arsenic (As)	Copper (Cu)	Lead (Pb)	Zinc (Zn)	Cadmium (Cd)	Chromium (Cr)	Source
Contents in the study area	Maximum	0.0287	18.1	27.7	25.8	80.2	0.264	56.7	This study
	Minimum	0.0064	5.72	17.9	17.4	60.4	0.137	35.8	
	Mean	0.0177	12.635	22.28	21.77	70.89	0.18	40.86	
First category standard of "Marine Sediment Quality Standard (GB 18668-2002)"		0.20	20.0	35.0	60.0	150.0	0.50	80.0	Marine Sediment Quality Standard (GB 18668-2002)
Soil background value of tidal marsh in Jiangsu province		0.023	7.38	15.02	11.40	47.15	0.042	60.11	Chen et al. (1985)
Eastern China intertidal zone		0.03	8.11	18.9	23.05	69.61	0.09	70.03	Zhang et al.(2017)
Jiangsu coastal areas		0.023	14.8	18.3	20.7	53.0	0.113	64.0	Zheng et al.2017
Guangdong coastal region		0.13	20.83	43.83	44.29	139.93	0.38	86.97	Zhao et al.(2016)
Laizhou Bay, China		n.d.	4.84	6.89	14.01	n.d.	0.08	17.10	Zhang et al. (2017)
Bohai Bay		n.d.	n.d.	38.5	44	206.3	0.22	101.4	Wu et al. (2014)
Sheyang Estuary		0.02	12.84	23.51	16.87	62.16	0.15	37.19	Zhao et al. (2018)
Haizhou Bay		n.d.	6.62	19.41	18.23	73.29	0.17	74.18	LI et al. (2014)
Ganyu port		n.d.	11.6	25.6	16	56	0.08	40	LI et al. (2014)
Dafeng port		n.d.	12.1	10.3	14.7	48.7	0.1	74.5	LI et al. (2014)

Note: n.d. means not detected

In 2018, the average contents of seven heavy metal in sediment did not go beyond the first category standard of "Marine Sediment Quality Standard (GB 18668-2002)". The average concentration of five heavy metals, i.e., As, Cu, Pb, Zn, and Cd, exceeded the background concentration in the tidal marshes in Jiangsu, and the ratios of their

http://www.aloki.hu ● ISSN 1589 1623 (Print) ● ISSN 1785 0037 (Online)
DOI: http://dx.doi.org/10.15666/aeer/1706_1486714882

average concentration to the background concentration were 1.71, 1.48, 1.91, 1.50, and 4.29 (*Table 3*), respectively. Among the abovementioned metals, Cd has the highest single-factor pollution index.

Figure 2 shows the distribution of heavy metal in the northern waters of abandoned Yellow River delta. The concentration of Cr is below the background value, which indicates that the presence of this metal is less subject to human activities and its natural level can be maintained. Related studies show that Cr is primarily derived from nature and is subject to properties of the soil form in the parental material, making it a heavy metal of low pollution (Lv et al., 2013; Sun et al., 2013). The concentration of Cr increases from the Guan River estuary to the abandoned Yellow River estuary, and then from the shore towards the sea. The distribution of heavy metal concentration is consistent with the changes in the grain size of sediments. In the study area, the grain size of sediments reduces from the Guan River estuary to the abandoned Yellow River estuary, and then from the shore to the sea (Chen, 2014; Hu, 2014). Many studies have reported that the concentration of heavy metals is closely correlated to the grain size of sediments (Li et al., 2015): if the surface area of the particle sediments is large, more heavy metals will be absorbed, while if the grain size of the particles is large, the concentration of heavy metals will be lesser. Generally, the concentration of the other heavy metals increased from the Guan River estuary to the abandoned Yellow River estuary, and then from the shore to the sea with the estuary and the port area showing the highest values of concentration.

Heavy metal pollution characteristics

Table 4 shows the pollution load indices (*Eqs. 1* and *2*) of heavy metals in sediments in the study area. *Figure 3* shows the distribution of pollution load indices of each sampling site. Note that the pollution load indices in these sampling sites ranged from 1.04 to 1.61 (average of 1.47); hence, according the grading standard for Pollution Load Index shown in *Table 1,* the study area was identified to have medium pollution. However, the pollution load index increased from the Guan River estuary to the abandoned Yellow River estuary with waters from the Zhongshan River estuary to the Abandoned Yellow River estuary showing the largest indices.

Table 5 shows the geo-accumulation index (*Eq. 3*) of heavy metals in the surface sediments in the study area. The I_{geo} for the tested heavy metals are as follows: −2.42 to −0.27 for Hg (average of −1.03); −0.95 to 0.71 for As (average of 0.10); −0.33 to 0.30 for Cu (average of −0.02); 0.03–0.59 for Pb (average of 0.34); −0.23 to 0.18 for Zn (average of 0.00); 1.12–2.07 for Cd (average of 1.50); and −1.33 to −0.67 for Cr (average of –1.15). In terms of I_{geo}, the seven heavy metals are ranked as follows: Cd > Pb > As > Zn > Cu > Hg > Cr. According the grading standard of geo-accumulation index shown in *Table 1,* Cd is marked at the level from mild-medium pollution to medium pollution; Pb is marked as mild pollution; As, Cu, and Zn are marked as clean- mild pollution; and Hg and Cr are marked as clean.

Table 3. *Single-factor pollution index of heavy metal in surface sediments*

	Mercury (Hg)	**Arsenic (As)**	**Copper (Cu)**	**Lead (Pb)**	**Zinc (Zn)**	**Cadmium (Cd)**	**Chromium (Cr)**
Maximum	1.25	2.45	1.84	2.26	1.70	6.29	0.94
Minimum	0.28	0.78	1.19	1.53	1.28	3.26	0.60
Mean	0.77	1.71	1.48	1.91	1.50	4.29	0.68

http://www.aloki.hu ● ISSN 1589 1623 (Print) ● ISSN 1785 0037 (Online)
DOI: http://dx.doi.org/10.15666/aeer/1706_1486714882

Table 4. *Pollution load index (PLI) and pollution level of heavy metals in surface sediments of the study area*

Sampling site	Pollution load index (PLI) value	Sampling site	Pollution load index (PLI) value
1	1.54	11	1.55
2	1.04	12	1.58
3	1.21	13	1.55
4	1.54	14	1.51
5	1.25	15	1.57
6	1.46	16	1.53
7	1.58	17	1.61
8	1.36	18	1.61
9	1.25	19	1.57
10	1.50	20	1.57
Maximum	1.61	Minimum	1.04
Mean	1.47	Pollution level	Medium pollution

Table 5. *Geo-accumulation index and potential ecological risk index of heavy metals in surface sediments of the study area*

		Mercury (Hg)	Arsenic (As)	Copper (Cu)	Lead (Pb)	Zinc (Zn)	Cadmium (Cd)	Chromium (Cr)
Geo-accumulation index (I_{geo})	Maximum	-0.27	0.71	0.30	0.59	0.18	2.07	-0.67
	Minimum	-2.42	-0.95	-0.33	0.03	-0.23	1.12	-1.33
	Mean	-1.03	0.10	-0.02	0.34	0.00	1.50	-1.15
	Degree of pollution	Clean	Clean-mild pollution	Clean-mild pollution	Mild pollution	Clean-mild pollution	Mild-medium pollution - medium pollution	Clean
Single-factor potential ecological risk (E_r^i)	Maximum	49.91	24.53	9.22	11.32	1.70	188.57	1.89
	Minimum	11.18	7.75	5.96	7.63	1.28	97.86	1.19
	Mean	30.80	17.12	7.42	9.55	1.50	128.82	1.36
	Ecological risk	Low - medium	Low	Low	Low	Low	Medium-high - high	Low
Comprehensive potential ecological risk (*RI*)	Maximum	247.33						
	Minimum	146.68						
	Mean	196.57						
	Ecological risk	Medium - High						

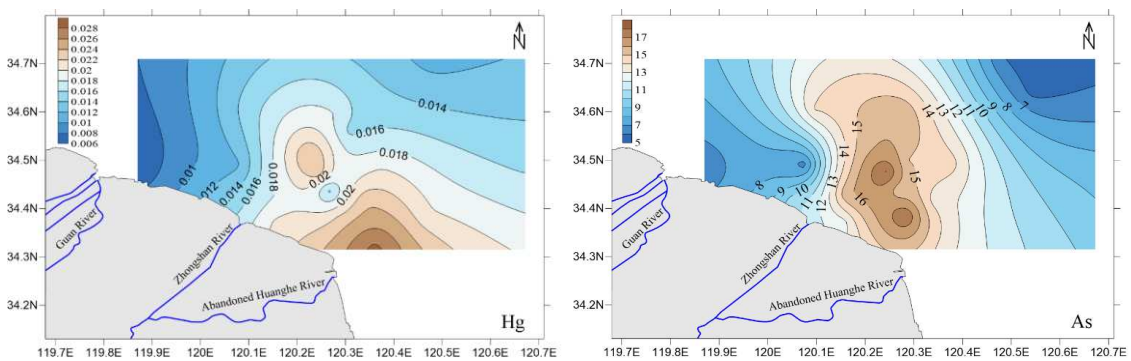

http://www.aloki.hu ● ISSN 1589 1623 (Print) ● ISSN 1785 0037 (Online)
DOI: http://dx.doi.org/10.15666/aeer/1706_1486714882

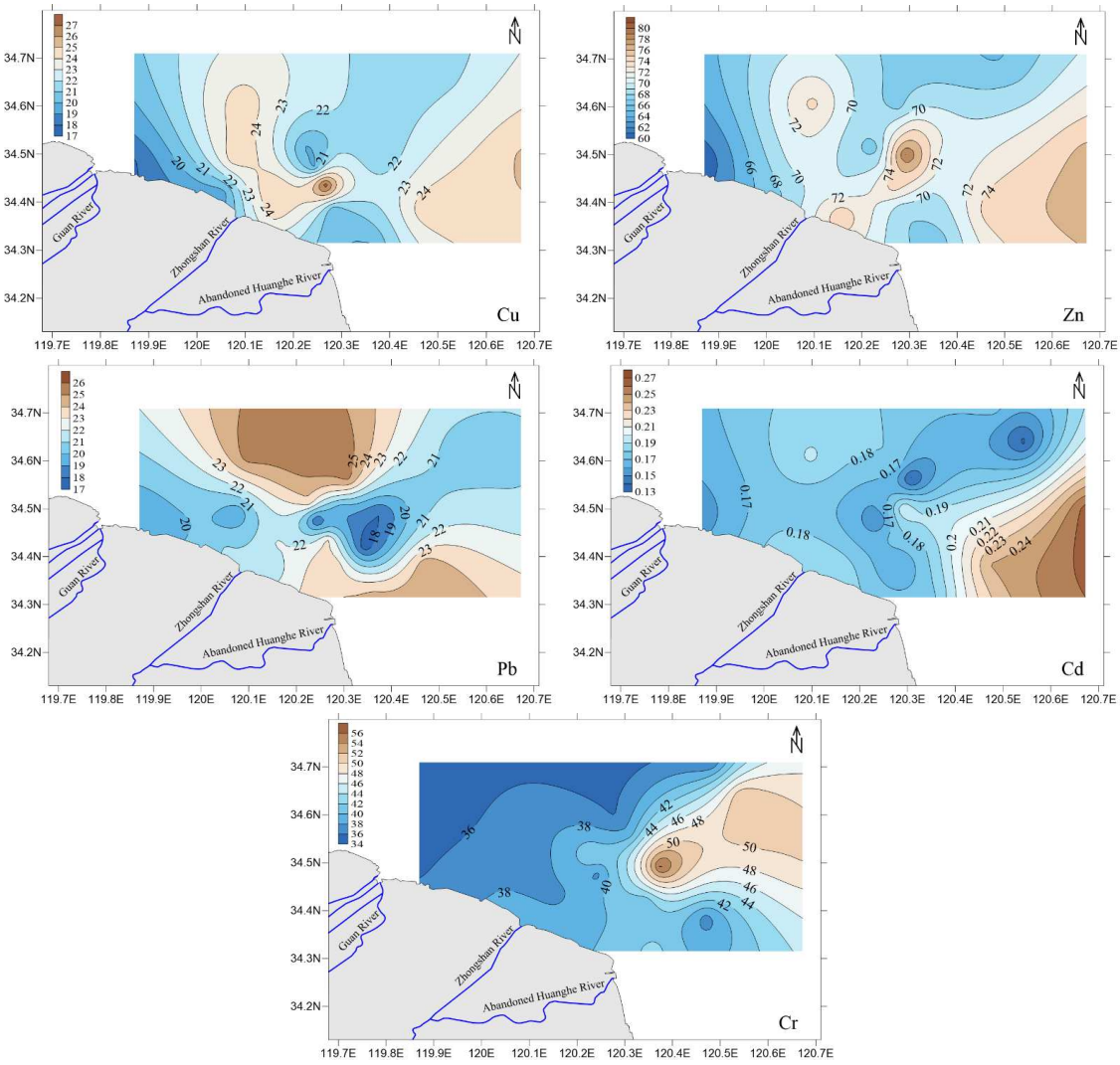

Figure 2. *Spatial distribution of heavy metal contents in 2018 (unit: mg/kg)*

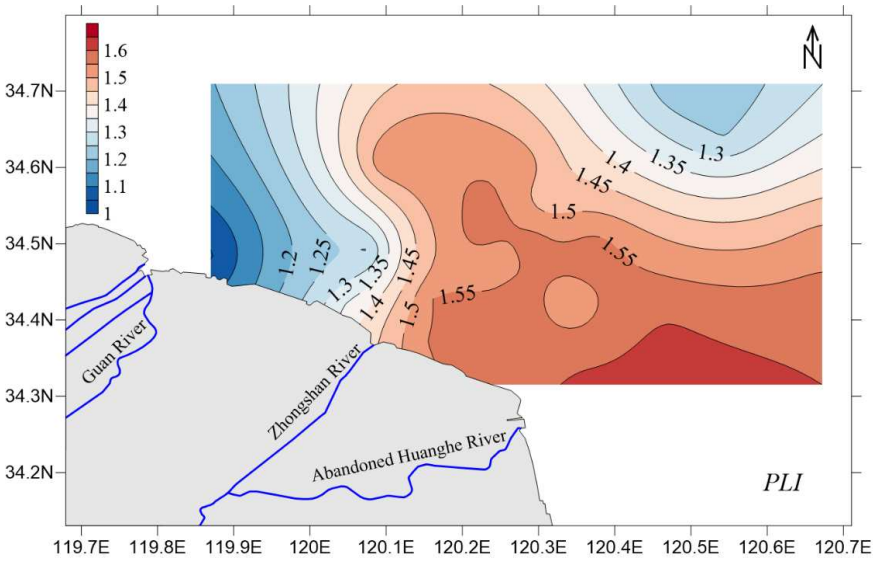

Figure 3. *The distribution of the pollution load index (PLI) of heavy metals in surface sediments*

http://www.aloki.hu ● ISSN 1589 1623 (Print) ● ISSN 1785 0037 (Online)
DOI: http://dx.doi.org/10.15666/aeer/1706_1486714882

Potential ecological risk assessment

Table 5 shows the potential ecological risk index of each heavy metal (*Eq. 4*) and their composite potential ecological risk index (*Eq. 5*). *Figure 4* shows the distribution of composite ecological risk indices. In May 2018, the ranges of ecological risk indices of the tested heavy metals are as follows. For Hg, the index fluctuates between 11.18 and 49.91 with the mean standing at 30.80; for As, the index fluctuates between 7.75 and 24.53 with the mean standing at 17.12; for Cu, the index fluctuates between 5.96 and 9.22 with the mean standing at 7.42; for Pb, the index fluctuates between 7.63 and 11.32, with the mean standing at 9.55; for Zn, the index fluctuates between 1.28 and 1.70, with the mean standing at 1.50; for Cd, the index fluctuates between 97.86 and 188.57, with the mean standing at 128.82; and for Cr, the index fluctuates between 1.19 and 1.89, with the mean standing at 1.36. In terms of the average potential ecological risk index, the seven heavy metals are ranked as Cd > Hg > As > Pb > Cu > Zn > Cr. According the grading standard of Potential ecological risk index shown in *Table 1,* Cd is marked as at the level of medium high and high ecological risk; Hg is marked as at the level of low and a medium ecological risk; and other heavy metals are marked as at the level of low ecological risks. The composite potential ecological risk index of the study area is between 146.68 and 247.33 (average of 196.57); hence, the study area is under medium-high ecological risks with Cd and Hg being the major contributors.

The composite potential ecological risk index increases from the Guan River estuary to the abandoned Yellow River estuary, with the waters near the latter estuary showing the highest indices. This distribution is similar to the distribution of the heavy metal pollution load index.

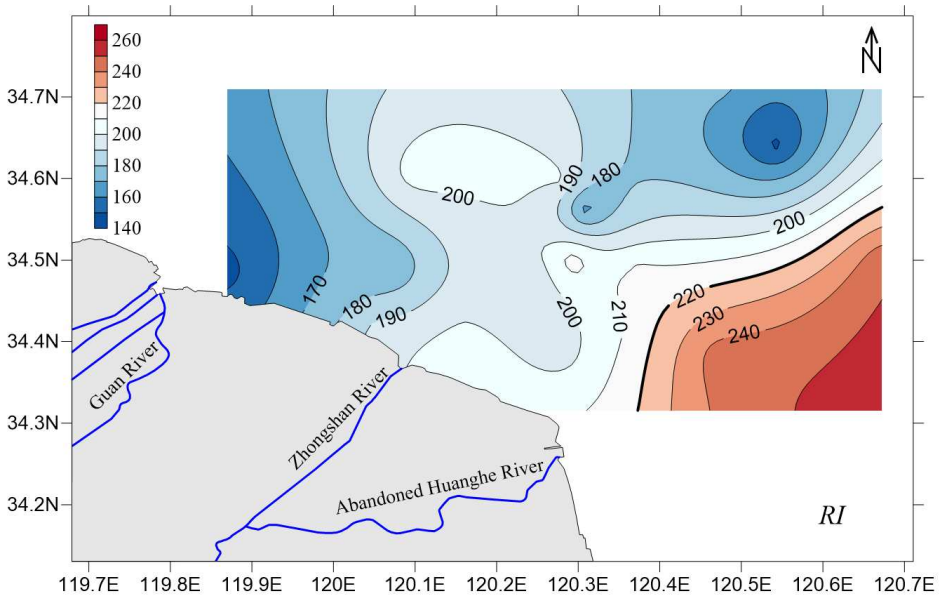

Figure 4. *The distribution of the comprehensive ecological risk index*

Source of heavy metal

Analysis of heavy metals in surface sediments

Correlation among heavy metals reflects the correlation among different elements, which will help recognize the sources of heavy metals (Lv et al., 2015). *Table 6* shows

http://www.aloki.hu ● ISSN 1589 1623 (Print) ● ISSN 1785 0037 (Online)
DOI: http://dx.doi.org/10.15666/aeer/1706_1486714882

the Pearson correlation coefficients between each pair of heavy metals. Hg and As (the Pearson coefficient is 0.694), as well as Zn and Cu (the Pearson coefficient of which is 0.681) are positively correlated, which indicates the correlation between Hg and As and that between Zn and Cu is strong and that elements in each pair are highly homogenous.

Table 6. *Correlation coefficient of heavy metal elements*

	Hg	As	Cu	Pb	Zn	Cd	Cr
Hg	1						
As	0.694**	1					
Cu	-0.080	0.000	1				
Pb	0.133	0.263	0.201	1			
Zn	0.170	0.244	0.681**	0.055	1		
Cd	0.104	-0.122	0.439	0.038	0.531*	1	
Cr	0.145	-0.079	0.001	-0.308	0.166	0.197	1

**Significant correlation at 0.01 level (bilateral). *Significant correlation at 0.05 level (bilateral)

Clustering analysis of heavy metals in surface sediments

We performed clustering analysis using SPSS for the seven heavy metals and obtained data from 20 sampling sites, and the analysis of the results is shown in *Figure 5*. The results show that the heavy metals can be divided into three categories. The first category includes Cu, Zn, and Pb; the second category includes Cd and Cr; and the third category includes Hg and As. Hg and As and Cu and Zn fall into the same category, which is consistent with the correlation analysis result. This indicates a high degree of homology between Hg and As and between Cu and Zn.

The 20 monitoring stations can be divided into two clusters. Stations 1, 4, 6, 7, 12, 14, 15, 17, 19, and 20 are located in waters near the shore from the Zhongshan River estuary to the port are part of the first cluster. Stations 2, 3, 5, 8, 9, and 18 are located in the coastal waters from the Guan River estuary to the Zhongshan River estuary, as well as in the distant waters from the shore are part of the second cluster.

Analysis of source of heavy metals in surface sediments

The results from Pearson correlation coefficient and the cluster analysis show a high level of homology between Zn and Cu. Given the distribution of heavy metal concentration, the distribution of Zn and that of Cu is very similar because the high concentration area of both metals occurs at the waters near the Zhongshan River estuary. Therefore, the concentration of Zn and Cu may be subject to the influence of land-sourced pollutants discharged into the sea from Zhongshan River and from outfalls of the chemical industrial parks near the Zhongshan River estuary. The highest concentration of Zn is observed near the wind-power stations; therefore, the wind-power stations along both sides of the Zhongshan River estuary may be contributors to the increase in the concentration of Zn. The sacrificial anode anticorrosion method used by marine wind power stations releases Zn, which will eventually increase the concentration of Zn in sediments.

Zn, Cu, and Pb are chalcophiles and they share similar geochemical processes in terms of the source, transportation, and concentration. Clustering analysis shows that Pb

http://www.aloki.hu ● ISSN 1589 1623 (Print) ● ISSN 1785 0037 (Online)
DOI: http://dx.doi.org/10.15666/aeer/1706_1486714882

can be classified into the same category as Zn and Cu. However, the distribution diagram and the Pearson coefficients indicate that Pb differs from these other two metals in terms of the source. A high concentration of Pb is observed near the Guan River port and outer waters of the port, which indicates that port development is the major contributor to the increasing concentration of Pb. Pb gets concentrated in the waters of the port, and related studies have confirmed that engine oil containing Pb increases the concentration of Pb (Blake and Goulding, 2002; Wilcke et al., 1998; Lv et al., 2015). As the port sees a lot of traffic of ships and vessels, the constant combustion of engine oil is very likely to cause Pb pollution.

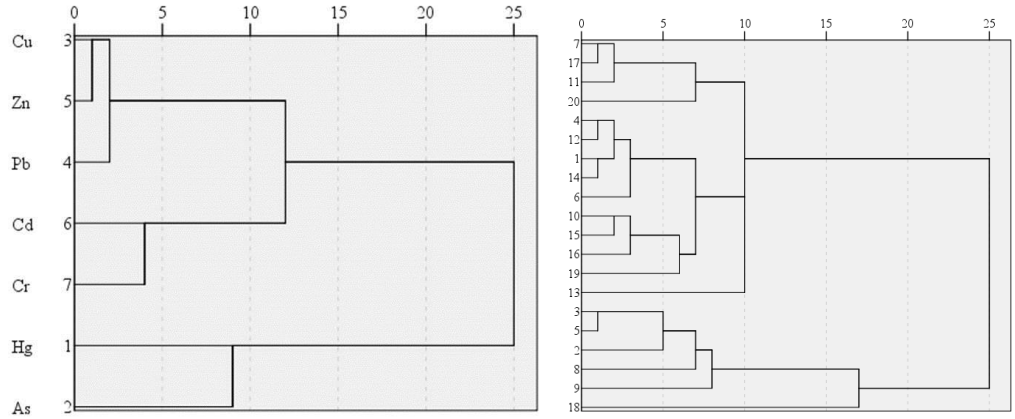

Figure 5. *Heavy metal contents and sample sites location cluster analysis results*

Hg and As share similar distribution characteristics with a high concentration of both metals being observed at the Zhongshan River estuary, the coastal port, and the outer waters of the abandoned Yellow River estuary. In general, Hg and As are obtained from human activities (Liu et al., 2003; Lv et al., 2013); therefore, their concentration is influenced by the discharge of pollutants from rivers, the outfalls of industrial parks, and port development activities.

Based on clustering analysis, we can group Cd and Cr into the same cluster; however, this categorization differs from the correlation analysis results. The Pearson correlation coefficient between Cd and Cr is not high, which indicates that these two metals have no obvious correlation. The concentration of Cr is below the background value and is primarily derived from nature; however, the concentration of Cd is higher than the background value and is primarily derived from human activities. These two metals share similar spatial distribution features as their concentration increases from the Guan River estuary to the Abandoned Yellow River estuary, and then from the shore to the sea. This distribution is consistent with the grain size of surface sediments in the study area. However, it differs in terms of the high-concentration area: the high concentration of Cd occurs in then outer waters from the Zhongshan River estuary to the abandoned Yellow River estuary, particularly in the waters around the abandoned Yellow River estuary. Cd is a standard element in chemical fertilizers (Lv et al., 2015), and the abandoned Yellow River is banked by crop fields; therefore, the high concentration of Cd in the outer waters, a bit far away from the abandoned Yellow River estuary, is possibly caused by the agricultural wastewater discharged from crop fields into the river. However, the high concentration of Cd is not seen in the estuary of the abandoned Yellow River estuary, but in the outer waters far away from the estuary

http://www.aloki.hu ● ISSN 1589 1623 (Print) ● ISSN 1785 0037 (Online)
DOI: http://dx.doi.org/10.15666/aeer/1706_1486714882

because the abandoned Yellow River estuary is highly corrosive. Moreover, in the waters with an isobath of –5 m, the shallow waves corrode the seabed, which takes away the fine particles and leaves large-size particles behind; therefore, the surface sediments are large in grain size (Hu, 2014). Note that sediments outside the abandoned Yellow River estuary are large in grain size, which makes it difficult for heavy metals to attach; therefore, there is a high concentration of Cd in the outer waters that are far away from the estuary.

Clustering analysis of the monitoring stations indicates that the distribution of heavy metals is subject to the joint impact of human activities and natural factors. The sources of heavy metals in surface sediments near the shore from the Zhongshan River estuary to the abandoned Yellow River estuary are identical such as pollutants discharged into the sea from rivers, sewage outfalls, and ports and wind-power stations. In the study area, the grain size of sediments is small, which makes it very easy for heavy metals to attach themselves; therefore, the concentration of heavy metals is high. The coastal waters from the Guan River estuary to the Zhongshan River estuary suffer from lesser heavy metal pollution because there are fewer development activities in this area. Moreover, there is a 10-km-long seawall on both sides of Guan River, which directs pollutants from the river to the sea and hence reduces the pollution in waters near the shore. Furthermore, the coastal areas from the Guan River estuary to the Zhongshan River estuary have the largest grain sizes of surface sediments in the study area, so the concentration of heavy metals in this area is low, and the outer waters away from the shore in this area have low concentration of heavy metals because human activities are lesser.

Based on one-tine heavy metal contents in sediments of the Abandoned Yellow River Delta, this study analyzed the status, distribution characteristics and ecological risk of heavy metal pollution, and speculated the sources of pollution. For long-term heavy metal contents changes, distribution rules and characteristics, continuous monitoring and further analysis of the water quality are still needed in the abandoned Yellow River Delta. In the follow-up study, on basis of long-term and multiple monitoring, it is necessary to analyze the risk of heavy metal content and the correlation between water, sediment and organism. In the future, it is necessary to strengthen the accurate study of the sources of heavy metals by more means and methods.

Conclusion

Based on the results, the following conclusions can be drawn.

The average concentration of Hg, As, Cu, Pb, Zn, Cd, and Cr in the surface sediments in the northern waters of the abandoned Yellow River delta in May 2018 is 0.0177, 12.635, 22.28, 21.77, 70.89, 0.18, and 40.86 mg/kg. Among these metals, the average concentration of As, Cu, Pb, Zn, and Cd exceeds the background value of tidal marshes in Jiangsu by a factor of 1.71, 1.48, 1.91, 1.50, and 4.29, respectively.

In terms of spatial distribution, the heavy metal concentration in the study area increases from the Guan River estuary to the abandoned Yellow River estuary, and then from the shore to the sea. Such a distribution pattern is consistent with that of the grain size of sediments in the study area. Except Cr, all other heavy metals show the highest concentration at either the estuaries or the port.

The heavy metal pollution load index of surface sediments in the study area fluctuates within between 1.04 and 1.61 (average of 1.47), and the study area is marked

http://www.aloki.hu ● ISSN 1589 1623 (Print) ● ISSN 1785 0037 (Online)
DOI: http://dx.doi.org/10.15666/aeer/1706_1486714882

as medium-level pollution. The index increases from the Guan River estuary to the abandoned Yellow River estuary, with the outer waters from the Zhongshan River estuary to the abandoned Yellow River estuary marking the highest indices. The analysis of the geo-accumulation index shows that Cd has the highest geo-accumulation index and is rated as mild-medium pollution to medium pollution; Pb is rated as mild pollution; As, Cu, and Zn are rated as clean or mild pollution; and Hg and Cr are rated as clean.

The analysis of the single-factor potential ecological risk index shows that Cd is at the level of medium-high and high ecological risks, Hg is at the level of low-medium ecological risks, and other heavy metals are at the level of low ecological risks. The composite ecological risk index shows that the study area is at the level of medium-high ecological risks with Cd and Hg being the primary contributors to ecological risks. The composite ecological risk index increases from the Guan River estuary to the Abandoned Yellow River estuary, and the outer waters of the Abandoned Yellow River estuary marks the largest indices. Waters from the Zhongshan River estuary to the abandoned Yellow River estuary are most susceptible to heavy metal ecological risks.

The distribution of heavy metal concentration in the study area is influenced by both human and natural factors. The concentration of Cr is lower than the background value and is mainly derived from natural sources, while other heavy metals are mainly derived from human activities. Heavy metals in surface sediments in the near-shore waters from the Zhongshan River estuary to the abandoned Yellow River estuary share the same sources such as pollutants discharged into the sea from rivers, sewage outfalls, and ports and wind-power stations. The grain size of sediments in this area is small, which makes it easy for heavy metals to attach themselves, so the concentration of heavy metals in this area is high. The near-shore waters from the Guan River estuary to the Zhongshan River estuary suffer from lesser heavy metal pollution because there are fewer development activities and the grain size of sediments in this area is large. Consequently, the concentration of heavy metals in this area is low, and the concentration of heavy metals in the outer waters of the study area is also relatively low because of fewer human activities.

REFERENCES

[1] Begy, R. C., Preoteasa, L., Timar, G. A., Mihaiescu, R., Tanaselia, C., Kelemen, S., Simon, H. (2016): Sediment dynamics and heavy metal pollution history of the cruhlig lake (Danube delta, Romania). – J. Environ. Radioact. 153: 167-175.

[2] Blake, L., Goulding, K. W. T. (2002): Effects of atmospheric deposition, soil pH and acidification on heavy metal contents in soils and vegetation of semi-natural ecosystems at Rothamsted Experimental Station, UK. – Plant and Soil 240(2): 235-251.

[3] Chen, B. B., Hu, R. Q., Chen, M. D. (1985): Natural background values of environmental elements in coastal soil in Jiangsu. – Journal of Nanjing Agricultural University 8(3): 54-60.

[4] Chen, H. Q., Peng, J., Chen, S. L., et al. (2014): Spatial variability characteristics of sediment grain size in sea area of the abandon Yellow River Delta, north of Jiangsu Province. – Journal of Applied Oceanography 33(4): 574-580.

[5] Guan, Q., Wang, L., Pan, B., et al. (2016): Distribution features and controls of heavy metals in surface sediments from the riverbed of the Ningxia-Inner Mongolian reaches, Yellow River, China. – Chemosphere 144: 29-42.

http://www.aloki.hu ● ISSN 1589 1623 (Print) ● ISSN 1785 0037 (Online)
DOI: http://dx.doi.org/10.15666/aeer/1706_1486714882

[6] Hakanson, L. (1980): An ecological risk index for aquatic pollution control. A sedimentological approach. – Water Research 14(8): 975-1001.
[7] Harikrishnan, N., Ravisankar, R., Chandrasekaran, A., et al. (2017): Assessment of heavy metal contamination in marine sediments of East Coast of Tamil Nadu affected by different pollution sources. – Marine Pollution Bulletin 121: 418-424.
[8] Hu, J. (2014): East China Normal University coastal evolution process and nearshore suspended sediment research of the abandoned Yellow River Delta. – Thesis for Master's degree in 2014, East China Normal University.
[9] Jahan, S., Strezov, V. (2018): Comparison of pollution indices for the assessment of heavy metals in the sediments of seaports of NSW, Australia. – Marine Pollution Bulletin 128: 295-306.
[10] Keshavarzi, B., Hassanaghaei, M., Moore, F., et al. (2018): Heavy metal contamination and health risk assessment in three commercial fish species in the Persian Gulf. – Marine Pollution Bulletin 129(1): 245-252.
[11] Li, C., Song, C., Yin, Y., et al. (2015): Spatial distribution and risk assessment of heavy metals in sediments of Shuangtaizi estuary, China. – Marine Pollution Bulletin 98(1): 358-364.
[12] Li, F., Xu, M. (2014): Source characteristics and contamination evaluation of heavy metals in the surface sediments of Haizhou Bay. – Environmental Science 35(3): 1035-1040.
[13] Li, G. H., Cao, Z. M., Lan, D. Z., Xu, J., Wang, S. S., Yin, W. H. (2007): Spatial variations in grain size distribution and selected metal contents in the Xiamen Bay, China. – Environ. Geol. 52: 1559-1567.
[14] Liang, X., Song, J., Duan, L., et al. (2018): Source identification and risk assessment based on fractionation of heavy metals in surface sediments of Jiaozhou Bay, China. – Marine Pollution Bulletin 128: 548-556.
[15] Liu, R. H., Wang, Q. C., Lu, X. G., et al. (2003): Distribution and speciation of mercury in the peat bog of Xiaoxing'an Mountain, northeastern China. – Environmental Pollution 124(1): 39-46.
[16] Lv, J., Liu, Y., Zhang, Z., et al. (2015): Identifying the origins and spatial distributions of heavy metals in soils of Ju country (Eastern China) using multivariate and geostatistical approach. – Journal of Soils and Sediments 15(1): 163-178.
[17] Lv, J. S., Liu, Y., Zhang, Z. L., et al. (2013): Factorial kriging and stepwise regression approach to identify environmental factors influencing spatial multi-scale variability of heavy metals in soils. – Journal of Hazardous Materials 261: 387-397.
[18] Monferran, M. V., Garnero, P. L., Wunderlin, D. A., de los Angeles Bistoni, M. (2016): Potential human health risks from metals and as via Odontesthes bonariensis consumption and ecological risk assessments in a eutrophic lake. – Ecotoxicol. Environ. Saf. 129: 302-310.
[19] Müller, G. (1969): Index of geoaccumulation in sediments of the Rhine River. – Geojournal 2(3): 108-118.
[20] Nguyen, T. T. H., Zhang, W., Li, Z., et al. (2016): Assessment of heavy metal pollution in Red River surface sediments, Vietnam. – Marine Pollution Bulletin 113(1-2): 513.
[21] Phillips, D. P., Human, L. R., Adams, J. B., et al. (2015): Wetland plants as indicators of heavy metal contamination. – Marine Pollution Bulletin 92(1): 227-232.
[22] Reddy, B. C., Jayaraju, N., Sreenivasulu, G., et al. (2016): Heavy metal pollution monitoring with foraminifera in the estuaries of Nellore coast, East coast of India. – Marine Pollution Bulletin 113(1): 542-551.
[23] Singh, K. P., Mohan, D., Singh, V. K., et al. (2005): Studies on distribution and fractionation of heavy metals in Gomti river sediments—a tributary of the Ganges, India. – Journal of Hydrology 312(1): 14-27.

http://www.aloki.hu ● ISSN 1589 1623 (Print) ● ISSN 1785 0037 (Online)
DOI: http://dx.doi.org/10.15666/aeer/1706_1486714882

[24] Sun, C. Y., Liu, J. S., Wang, Y., et al. (2013): Multivariate and geostatistical analyses of the spatial distribution and sources of heavy metals in agricultural soil in Dehui, Northeast China. – Chemosphere 92(5): 517-523.
[25] Tomlinson, D. L., Wilson, J. G., Harris, C. R., Jeffery, D. W. (1980): Problems in the assessment of heavy-metal levels in estuaries and the formation of a pollution index. – Helgoländer Meeresuntersuchungen 33: 566-575.
[26] Wang, M., Tong, Y., Chen, C., et al. (2018): Ecological risk assessment to marine organisms induced by heavy metals in China's coastal waters. – Marine Pollution Bulletin 126: 349-356.
[27] Wang, Y. S., Lou, Z. P., Sun, C. C., Sun, S. (2008): Ecological environment changes in Daya Bay, China, from 1982 to 2004. – Marine Pollution Bulletin 56: 1871-1879.
[28] Wilcke, W., Muller, S., Kanchanakool, N., et al. (1998): Urban soil contamination in Bangkok: heavy metal and aluminium partitioning in topsoils. – Geoderma 86(3): 211-228.
[29] Wu, G., Shang, J., Pan, L., Wang, Z. (2014): Heavy metals in surface sediments from nine estuaries along the coast of Bohai bay, northern China. – Marine Pollution Bulletin 82(1-2): 194-200.
[30] Zhang, J. P., Jiao, X. M., Fang, N., J., et al. (2017): Sources and risk assessment of heavy metals in sediments in Jiangsu coastal areas. – China Environmental Science 37(4): 1514-1522.
[31] Zhang, L. (2015): The coastal erosion-deposition evolution and controlling factors of the abandoned Yellow River delta in northern Jiangsu province. – Doctoral Dissertation in 2016, East China Normal University.
[32] Zhang, M., Bao, Z. Y., Chen, G. G., Yong, T. J., et al. (2017): Characteristics and risks of heavy metals content in surface sediment of tidal flat areas in eastern China. – Environmental Science 38(11): 4513-4524.
[33] Zhang, P., Hu, R., Zhu, L., et al. (2017): Distributions and contamination assessment of heavy metals in the surface sediments of western Laizhou Bay: implications for the sources and influencing factors. – Marine Pollution Bulletin 119(1): 429-438.
[34] Zhao, G., Lu, Q., Ye, S., Yuan, H., Ding, X., Wang, J. (2016): Assessment of heavy metal contamination in surface sediments of the west Guangdong coastal region, China. – Marine Pollution Bulletin 108(1-2): 268-274.
[35] Zhao, Y. F., Xu, M., Liu, Q., et al. (2018): Study of heavy metal pollution, ecological risk and source apportionment in the surface water and sediments of the Jiangsu coastal region, China: A case study of the Sheyang Estuary. – Marine Pollution Bulletin 137: 601-609.
[36] Zhu, Z. M., Li, Z. G., Bi, X. Y., Han, Z. X., Yu, G. H. (2013): Response of magnetic properties to heavy metal pollution in dust from three industrial cities in China. – Hazardous Materials 246-247: 189-198.

http://www.aloki.hu ● ISSN 1589 1623 (Print) ● ISSN 1785 0037 (Online)
DOI: http://dx.doi.org/10.15666/aeer/1706_1486714882

CONTAMINATION OF SOIL WITH TOXOCARA AND OTHER HELMINTHS IN SOILS OF AMADYIA DISTRICT, DUHOK GOVERNORATE, KURDISTAN REGION - IRAQ

GOLEK, H. I.[1] – AL-SAEED, A. T. M.[2*]

[1]*Department of Microbiology, Medical Technical Institute, Polytechnic University, Duhok, Kurdistan Region, Iraq*
(phone: +964-750-767-6474)

[2]*Department of Microbiology, College of Medicine, University of Duhok, Kurdistan Region, Iraq*

**Corresponding author*
e-mail: adelalsaeed@uod.ac; phone: +964-750-450-1898

(Received 18th Jun 2019; accepted 16th Oct 2019)

Abstract. In Amadyia District, Duhok Governorate, Kurdistan Region of Iraq, where there is a high population of people, domestic and stray animals, in addition to the presence of vegetation, grasses and large numbers of pastures. This study was conducted to determine of the soil's contamination with ova of *Toxocara* and other helminths in different areas of Amadyia district. A total of 700 soil samples were collected from different places such as public parks, private gardens, dog shelters, near pastures, parks of schools and around a slaughter house. The soil samples were examined using saturated zinc sulphate with specific gravity 1.2. Helminth ova were found in 593 (84.71%) of the examined soil samples. Ova of *Taenia* were the most frequent helminths and found in 117 (16.71%), followed by ova of *Hymenolepis nana* in 107 (15.28%), *Toxocara* ova in 106 (15.14%), *Ancylostoma* ova in 95 (13.57%), *Ascaris* ova in 71 (10.14%), *Hymenolepis diminuta* ova in 51 (7.28%), and *Trichuris* ova in 46 (6.57%). It is concluded that soils in areas of Amadyia district is contaminated with different helminths. The contamination of soil with *Toxocara* and other helminth ova is relatively high, the population are at a high risk to acquire infection through contact with environment and soil.
Keywords: *environmental contamination, ova, zoonosis, zinc sulphate, Duhok, Iraq*

Introduction

Humans acquire helminth infection by accidental swallowing of infective stages of parasites contaminating the soil (Blaszkowska et al., 2013; Cassenote et al., 2011). Humans are at the highest risk of infection because of outdoor activities and contact with contaminated soils (Al-Megrin, 2010). The poor sanitary condition in developing countries including Iraq leads to the presence of infective stages of parasites in the soils (Mahdi and Ali, 1993). Most often human become infected with helminths by contact with soil, water or food and grasses that contaminated either with ova or other stages of these parasites (Motazeddian et al., 2006; Sadjjadi et al., 2000). Infection rate in certain part of the world is related to poor environmental hygiene such as lack of clean water supply, contamination of the environment by human and animal wastes and bad habits (Anh et al., 2007).

A number of studies in the world have demonstrated the presence of pathogenic parasite in contaminated drinking water (Sprenger et al., 2014), soil (Tavalla et al., 2012), air (Ahmed, 2006) and socio-cultural, such as contact with animals (Thomas and Jeyathilakan, 2014), and lack of public education (Zibaei et al., 2010). In Northern Iraq (Erbil Province), the prevalence of parasitic infections among school aged children have been found to be high (Faraj, 2000). The awareness on the risk of contamination soil is still low (De-Moura et al., 2013).

http://www.aloki.hu ● ISSN 1589 1623 (Print) ● ISSN 1785 0037 (Online)
DOI: http://dx.doi.org/10.15666/aeer/1706_1488314891

The parasites that cause helminth infections are naturally present in the environment, most often human and animals become infected with helminths by coming in contact with soil, water or food that contains the ova or other stages of these parasites (Soulsby, 1986).

Humans, particularly children are at the highest risk of infection because of their outdoor activities and playing on soils contaminated with animal feces.

The current study aimed to analyze soil samples collected in Amadyia district, Duhok Governorate, Kurdistan Region, Iraq, to determine their rate of infection by *Toxocara* and other helminth ova using saturated zinc sulphate, in order to conclude the infection risk of the local populace.

Materials and methods

Amadyia district (*Fig. 1*) is located in the North of Duhok Governorate – Kurdistan Region of Iraq. The city is situated 4,600 feet (1,400 m) above sea level. Total of human population 11,000. Climate of Amadyia has a hot-summer Mediterranean climate with long, hot summers and cool, wet winters. A total of 700 soil samples were collected from different locations of Amadyia district during the period of the year 2016-2017.

The soil samples were collected from different places of Amadyia district such as private gardens, dogs shelters, public park, parks of schools, near pasture and around slaughter house. During soil samples collection, many children were seen playing in the soil with their hands and not wearing shoes, in addition to that presence of dogs and their puppies around them (*Fig. 2*). The soil samples were collected in plastic bags and examined with some modification according to method of Mandarino-Pereira et al. (2010) and Zibaei et al. (2010). Amount ranging 25-50 g of soil from a depth of 3 cm ground was collected from each place and grinded, dissolved in normal saline, mixed well and filtered by sieving method, then centrifuged in 2000 rpm for 5 min. The supernatant was discarded and the sediment was re-suspended in normal saline. Then, centrifuged again and the supernatant was discarded and saturated zinc sulphate with specific gravity 1.2 was added to the sediment in a test tube and centrifuged in 1500 rpm for 15 min, then few drops of saturated zinc sulphate was added to filling the top of the test tube.

Figure 1. *Map of Duhok Governorate showing Amadyia (Amedi) District*

http://www.aloki.hu ● ISSN 1589 1623 (Print) ● ISSN 1785 0037 (Online)
DOI: http://dx.doi.org/10.15666/aeer/1706_1488314891

Figure 2. *Children playing in the soil and puppy with hands and not wearing shoes (famous in rural areas of Kurdistan Region)*

The cover slip was placed on the upper surface of tube in touch with the solution and was kept in the rack for 45 min, then the coverslip was removed gently in a horizontal position and placed on a glass slide, examined under the light microscope. The ova of parasites were diagnosed according to their morphological features (Soulsby, 1986). The limitations of the current study are not studied the mean number of ova and the association between infection rate and, type of soils, pH of soils and habitats. Analysis of data was carried out using the Chi Square test and Statistical Package for Social Science (SPSS).

Results

Out of 700 soil samples examined, helminth ova were found in 593 (84.71%). *Taenia* eggs 117 (16.71%) were the most frequent helminth, followed by *Hymenolepis nana* ova in 107 (15.28%), *Toxocara* ova in 106 (15.14%), *Ancylostoma* ova in 95 (13.57%), *Ascaris* ova in 71 (10.14%), *Hymenolepis diminuta* ova in 51 (7.28%), and *Trichuris* ova in 46 (6.57%) as shown in *Table 1*.

It was clear from *Table 2,* that the ova of *Taenia* were positive in 17/130 (13.07%) samples of soil obtained from dogs shelters, 20/127 (15.74%) in private gardens, 25/106 (23.58%) in parks of schools, 15/165 (9.09%) near pastures, 29/64 (45.31%) around slaughter houses and 11/108 (10.18%) in public parks. There were statistically non - significant (p = 0. 033) when compared with other helminths.

http://www.aloki.hu ● ISSN 1589 1623 (Print) ● ISSN 1785 0037 (Online)
DOI: http://dx.doi.org/10.15666/aeer/1706_1488314891

Table 1. *Contamination of soil samples with helminth ova in Amadyia District (n = 700)*

Ova of parasites	Number of contaminated soil samples	Percentage
Taenia	117	16.71
Hymenolepis nana	107	15.28
Toxocara	106	15.14
Ancylostoma	95	13.57
Ascaris	71	10.14
Hymenolepis diminuta	51	7.28
Trichuris	46	6.57
Total	593	84.71

Table 2. *Contamination of soil samples with helminth ova in according to different places in Amadyia District (n = 700)*

Place and no. of examined soil samples	Number of contaminated soil samples and percentage						
	Ta.	Hn.	To.	An.	As.	Hd.	Tr.
Dogs shelters (130)	17 (13.07)	5 (3.84)	30 (23.07)	13 (10.0)	4 (3.07)	1 (0.76)	2 (1.53)
Private gardens (127)	20 (15.74)	16 (12.59)	13 (10.23)	15 (11.81)	15 (11.81)	10 (7.87)	8 (6.29)
Parks of schools (106)	25 (23.58)	34 (32.07)	15 (14.15)	28 (26.41)	21 (19.81)	15 (14.15)	21 (19.81)
Near pastures (165)	15 (9.09)	20 (12.12)	28 (16.96)	7 (4.24)	11 (6.66)	15 (9.09)	3 (1.81)
Around slaughter houses (64)	29 (45.31)	2 (3.12)	9 (14.06)	12 (18.75)	15 (23.43)	3 (4.68)	5 (7.81)
Public park (108)	11 (10.18)	30 (27.77)	11 (10.18)	20 (18.51)	5 (4.62)	7 (6.48)	7 (6.48)
Total (700)	117 (16.71)	107 (15.28)	106 (15.14)	95 (13.57)	71 (10.14)	51 (7.28)	46 (6.57)
P value ($p < 0.01$)	0.033 NS.	0.00 HS.	0.005 S.	0.115 NS.	0.083 NS.	0.002 HS.	0.008 HS.

Ta (Taenia), Hn (Hymenolepis nana), To (Toxocara), An (Ancylostoma), As (Ascaris), Hd (Hymenoleis diminuta), Tr (Trichuris)

Ova of *H. nana* were positive in 5/130 (3.84%) samples of soil examined from dogs shelters, 16/127 (12.59%) in private gardens, 34/106 (22.07%) in parks of schools, 20/165 (12.12%) near pastures, 2/64 (3.12%) around slaughter houses and 30/108 (27.77%) in public parks. There were statistically highly significant differences ($p = 0.00$) when compared with other helminths.

Toxocara ova were positive in 30/130 (23.07%) samples of soil were collected from dogs shelters, 13/127 (10.23%) in private gardens, 15/106 (14.15%) in parks of schools, 28/165 (16.96%) near pastures, 9/64 (14.06%), around slaughter houses and 11/108 (10.18%) in public parks. There were statistically highly significant differences *(*$p = 0.00$*)* when compared with other helminths.

Regarding to *Ancylostoma* ova were positive in 13/130 (10.0%) samples of soil were examined from dogs shelters, 15/127 (11.81%) in private gardens, 28/106 (26.41%) in

http://www.aloki.hu ● ISSN 1589 1623 (Print) ● ISSN 1785 0037 (Online)
DOI: http://dx.doi.org/10.15666/aeer/1706_1488314891

parks of schools, 7/165 (4.24%) near pastures, 12/64 (18.75%) around slaughter houses and 20/108 (18.51%) in public parks. There were statistically non - significant differences ($p = 0.115$) when compared with other helminths.

Ascaris ova were positive in 4/130 (3.07%) samples of soil were obtained from dogs shelters, 15/127 (11.81%) in private gardens, 21/106 (19.81%) in parks of schools, 11/165 (6.66%) near pastures, 15/64 (23.43%) around slaughter houses and 5/108 (4.62%) in public parks. There were statistically non-significant differences ($p = 0.083$) when compared with other helminths.

The ova of *H. diminuta* were positive in 1/130 (0.76%) samples of soil were collected from dogs shelters, 10/127 (7.87%) in private gardens, 15/106 (14.15%) in parks of schools, 15/165 (9.09%) near pastures, 3/64 (4.68%) around slaughter houses and 7/108 (6.48%) in public parks. There were statistically highly significant differences ($p = 0.002$) when compared with other helminths.

Trichuris ova were positive in 2/130 (1.53%) samples of soil were collected from dogs shelters, 8/127 (6.29%) in private gardens, 21/106 (19.81%) in parks of schools, 3/165 (1.81%) near pastures, 5/64 (7.81%) around slaughter houses and 7/108 (6.48%) in public parks. There were statistically highly significant differences ($p = 0.008$) when compared with other helminths.

Discussion

Out of 700 soil samples examined, 593 (84.7%) were positive for different species of helminth ova. The present study revealed high levels of contamination of soil by parasites. These results concerning the contamination of soil are in agreement with studies in many cities worldwide which also showed that the soils are contaminated with ova of helminth parasites.

In the current study the distribution of *Toxocara* ova was 15.14%, as 23.07% in dogs shelters, 16.96% near pastures, 14.15% in parks of schools, 14.06% around slaughter houses, 10.18% in public park and 10.23% in private gardens. These results agree with the results of Fathailah (1988) which found 16% prevalence of *Toxocara* ova in vegetables collected from different markets in Baghdad city. A study of Molan and Faraj (1989) reported 13.6% prevalence of *Toxocara* ova in Erbil city. A study of Al-Barazanjey (1992) found 14% the prevalence of *Toxocara* ova in Erbil city. In Basra Mahdi and Ali (1993) recorded contamination rate of soil with *Toxocara* ova was 12.2%. A study of Hussein (1997) found 18.1% the prevalence of *Toxocara* ova in Erbil city. A study done by Faraj (2000) reported 16% the prevalence of *Toxocara* ova in Erbil city. A study of Ahmed (2006) found the prevalence of *Toxocara* ova in Erbil city was 13%. In Alnassiriyah city center, southern Iraq, Al-Kassar (2009) found 16.43% prevalence of *Toxocara* ova in public places and children play grounds, A study of Saida and Khder (2014) found that the prevalence of *Toxocara* ova in Erbil city, 12.2% in leafy vegetables. On the other hand, the result of the current study is lower than that observed by Woodruff (1981) in Mosul district Iraq that reported the prevalence of *Toxocara* ova 25%. A study of Nooraldeen (2015) in Erbil city, Iraq found the prevalence of *Toxocara* ova 50% in public squares and parks. In northern and central of Jordan *Toxacara* ova were found in 15.45% of soils collected from school playgrounds and public places (Abo-Shehada, 1989). A study done by Al-Megrin (2010) in Riyadh, Saudi Arabia reported 20% prevalence of *Toxocar*a ova in leafy vegetables. In Turkey,

http://www.aloki.hu ● ISSN 1589 1623 (Print) ● ISSN 1785 0037 (Online)
DOI: http://dx.doi.org/10.15666/aeer/1706_1488314891

Ge and Ge (2000) reported that 8.25-60.9% of public parks was contaminated with *Toxocara* ova.

In Iran, Motazedian et al. (2006) reported that the contamination rate of public places in Shiraz, Iran was 6.3% with *Toxocara* ova. A study done by Tavassoli et al. (2008) reported that the contamination rate of public places with *Toxocara* ova 7.8% in Urmia, Iran. A study of Zibaei et al. (2010) reported soil contamination with *Toxocara* eggs was 22.2% in Khorram Abad, Iran. A study of Tavalla et al. (2012) found that 79.3% the rate of *Toxocara* ova in public place in Tehran. In Italy, Habluetzel et al. (2003) reported 24% prevalence of soil contamination with *Toxocara* ova. In Brazil, several studies were conducted, and the soil contamination rate with *Toxocara* ova was 22.4% (Mandarino-Pereira et al., 2010), 30.2% (Cassenote et al., 2011) and 36% (Sprenger et al., 2014). A study done by Bojar and Káapeü (2012) in Poland found that 18.6% was prevalence of *Toxocara* ova. Another studies conducted in Brazil by De -Moura et al. (2013) and Marchioro et al. (2013) recorded 44% and 78.6% were prevalence of *Toxocara* ova in soils respectively. In Slovakia, the prevalence of *Toxocara* ova was 79.2% (Rudohradská et al., 2011). In Poland, Blaszkowska et al. (2013) reported that prevalence of *Toxocara* ova was10.6%, while in Portugal 63.3% (Otero et al., 2014). A study done in India, 12.84% (Sudhakar et al., 2013), while Thomas and Jeyathilakan (2014) reported 4.75%, in Philippines 32% (Paller and de Chavez, 2014). In the present study, the rate of soil contamination with *Toxocara* ova was 15.1% and statistical analysis showed the presence of highly significant difference. The differences between the results of all those studies mentioned may be attributed to a wide range of factors, such as climatic conditions, the population of dogs, soil type, number and volume of samples tested, the season in which sampling was performed, the mode of storage of soil samples, and the methods used for examination. In the current study, the public schools included did not keep their areas enclosed and allowing dogs to enter the school grounds.

The presence of ova in the soil samples collected suggests the dogs living around the school may be infected with *Toxocara* ova. During sample collection, children were seen playing in the soil with their bare hands and not wearing shoes or slipper, thus increasing the risk of acquiring *Toxocara* infection. In the current study, parasite ova were identified in almost all places that were not fenced and also in dog shelters. Fenced places specially arranged for dogs recreation were free of helminth ova, this means that the animals which had received anthelmintic drugs. Moreover, in this places have access only dogs with their owners. The explanation is that although the place was initially arranged for recreation of dogs subsequently the fence was broken and the access of stray dogs was free, suggesting a potential route of contamination of places.

In the present study the rate of some other helminth ova was reported as 15.28% of *Hymenolepis nana*, 7.28% *Hymenolepis diminuta*, 6.57% *Trichuris trichuria*, 13.57% was prevalence of *Ancylostoma*, 16.71% for *Taenia* and 10.14% for *Ascaris*. All these types of parasitic ova were recovered from soils in many studies. In Baghdad, Fathailah, (1988) reported the prevalence of ova of some helminths as 22% *Ascaris*, 26% *Hymenolepis nana*, 12.57% *Ancylostoma*, 22% *Toxoplasma gondii*, 14% *Hymenolepis diminuta*. Also in Baghdad Guirges and Al-Mofti (2005) found the prevalence of ova of some helminth eggs as 20% *Hymenolepis nana*, 25% *Ascaris*, 21%, *Hymenolepis diminuta*, 19% of *Ancylostoma* and 15% *Trichuris*. In Erbil city, Saida and Nooraldeen (2014) reported the prevalence of ova of some helminths as follow as: ova of *Echinococcus granulosus* 22.4%, *Ascaris* 18.3%, *Hymenolepis nana* 10.2%,

http://www.aloki.hu ● ISSN 1589 1623 (Print) ● ISSN 1785 0037 (Online)
DOI: http://dx.doi.org/10.15666/aeer/1706_1488314891

Hymenolepis diminuta 4.0%, *Trichostrongylus* 8.1%, *Enterobius vermicularis* 4.0% and *Dipylidium caninum* 6.1%, the cysts of each of *Entamoeba histolytica* 20.4%, *Entamoeba coli* 22.4%, *Giardia* 16.3% and oocyst of *Toxoplasma gondii* 18.3%. A study done by Nooraldeen (2015) in Erbil city was found ova of *Hymenolepis diminuta* in 75%, *Ascaris* in 33.3%, *Taenia* in 25%, *Ancylostoma* in 25% and 16.7% for *Trichuris*. A study of Anh et al. (2007) reported the prevalence of *Ancylostoma* 19%, *Ascaris* spp 27%, *Hymenolepis nana* 22%, *Hymenolepis diminuta* 20% *Echinococcus granulosus* 23%, in Cambodia. It is not possible to make an accurate comparison between the results of all those studies because the recovery of parasitic ova from different localities was obviously vary depending on environmental conditions, soil types, choice of sampling sites, the number of animals defecating in the sampled area, recovery methods and the increased prevalence of some of those helminth eggs in soil might be due to using of the humans and animals waste for fertilizing the farms in some countries, which is widely used in Iraqi farms.

Contamination of soil may result from poor environmental sanitation specially the presence of large stray dogs population. The cause of that may be return to the preference of these places by stray dogs in addition to that this area was always humid and helminth ova can remain viable at least few months in humid soil. While prolonged exposure to the sun in poor vegetation and dry soil may cause quick disintegration of the eggs. Climate conditions and other factors (temperature, humidity and rain, soil pH and soil type) were important factors for viability and development of ova, therefore, the differences in climate conditions from place to place and from year to year in the same place may lead to differences in contamination rate of soil which recorded along the months of year in different places or even in the same place during different years. In Iraq climatic conditions such as mild temperature, humidity and rain for maintenance and dispersion may be found in winter and spring seasons therefore, highest contamination rate obtained during the months of these seasons.

Sometimes the number of helminth ova per soil sample was not enough to cause infection and there was a positive correlation between the intensity of ova in soil and the prevalence of infection.

Conclusions

This study has shown that there is high level of contamination of soil of different parts of Amadyia district with *Toxocara* and other helminth ova and that examination of soil samples can be used as a strategy to determine the level of contamination of soil with helminth ova. The present study concluded that more consideration is necessary to improve personal and food hygiene particularly in children to avoid transmitting the infective stages of parasites for human through contaminated soils.

It is important that a further study needed to determine the relationship between the infection rate of helminth ova, soil types, soil pH and seasonal climatic variation.

REFERENCES

[1] Abo-Shehada, M. N. (1989): Prevalence of Toxocara ova in some schools and public grounds in northern and central Jordan. – Annals Tropical Medicine & Parasitology 83(1): 73-75.

http://www.aloki.hu ● ISSN 1589 1623 (Print) ● ISSN 1785 0037 (Online)
DOI: http://dx.doi.org/10.15666/aeer/1706_1488314891

[2] Ahmed, Q. M. (2006): Prevalence of intestinal parasites among food handlers and primary school children in Erbil province with initial cultivation of E. histolytica. – MSc Thesis, Salahaddin University, Erbil.
[3] Al-Megrin, W. A. I. (2010): Prevalence intestinal parasites in leafy vegetables in Riyadh, Saudi Arabia. – International Journal of Tropical Medicine 5(2): 20-23.
[4] Al-Kassar, N. R. (2009): Prevalence of Toxocara species eggs in public places and childrens play grounds of Anassiriyah city. – Journal of Thiqar University 5(2).
[5] Al-Barazanjey, R. K. A. (1992): Epidemiological study of Giardia sp. in Arbil governorate. – MSc Thesis, Salahaddin University, Erbil.
[6] Anh, V. T., Tram, N. T., Klank, L. T., Cam, P. D., Dalsgaard, A. (2007): Faecal and protozoan parasite contamination of water spinach (Ipomoea aquatica) cultivated in urban wastewater in Phnom Penh, Cambodia. – Tropical Medicine & International Health 12(2): 73-81.
[7] Blaszkowska, J., Wojcik, A., Kurnatowski, P., Szwabe, K. (2013): Geohelminth egg contamination of children's play areas in the city of Lodz (Poland). – Veterinary Parasitology 192(1-2): 228-233.
[8] Bojar, H., Káapeü, T. (2012): Contamination of soil with eggs of geohelminths in recreational areas in the Lublin region of Poland. – Annals of Agricultural Environmental Medicine 19(2): 267-270.
[9] Cassenote, A. J. F., Neto, J. M. P., Lima-Catelani, A. R. A., Ferreira, A. W. (2011): Soil contamination by eggs of soil-transmitted helminths with zoonotic potential in the town of Fernandópolis, State of São Paulo, Brazil, between 2007 and 2008. – Revista da Sociedade Brasiliera de Medicina Tropica 44(3): 371-374.
[10] De-Moura, M. Q., Jeske, S., Vieira, N. J., Corrêa, G. T., Berne, A. M. E., Villela, M. M. (2013): Frequency of geohelminths in public squares in Pelotas, RS, Brazil. – Revista Brasileira de Parasitologia Veterinari 22(1): 175-178.
[11] Fathailah, Z. I. (1988): The presence of human parasites in vegetables collected from different markets in Baghdad city. – MSc thesis. University of Baghdad.
[12] Faraj, A. M. (2000): Prevalence of intestinal parasites in some kindergartens in the center of Erbil Northern Iraq. – Journal of Dohuk University 3(1): 7-12.
[13] Ge, S., Ge, H. (2000): Prevalence of Toxocara spp. eggs in the soil of public parks in Ankara, Turkey. – Dtsch tierarztl Wschr (107):72-75.
[14] Guirges, Y., Al-Mofti, A. (2005): The presence of protozoal cysts and helminthic ova on vegetables collected from Baghdad markets. – Journal of Faculty of Medicine, University of Baghdad 47(1): 70-72.
[15] Habluetzel, A., Traldi, G., Ruggieri, S., Attili, A. R., Scuppa, P., Marchetti, R., Menghini, G., Esposito, F. (2003): An estimation of *Toxocara canis* prevalence in dogs environmental egg contamination and risk of human infection in the Marche region of Italy. – Veterinary Parasitology 113: 243-252.
[16] Hussein, M. M. S. (1997): Prevalence of intestinal parasites in children up to 6 years old in Erbil province, Iraq. – Zanco Special Issue 1: 59-65.
[17] Mahdi, N. K., Ali, H. A. (1993): Toxocara eggs in the soil of public places and school in Barsah, Iraq. – Annals of Tropical Medicine and Parasitology 87:201-205.
[18] Mandarino-Pereira, A., de Souza, F. S., Lopes, C. W., Pereira, M. J. (2010): Prevalence of parasites in soil and dog feces according to diagnostic tests. – Veterinary Parasitology 170: 176-181.
[19] Marchioro, A., Colli, C. M., Ferreira, C. E., Tiyo, R., Mattia, S., de Souza, W. F., Falavigna-Guilherme, A. L. (2013): Identification of public areas with potential toxocariasis transmission risk using geographical information. – Acta Parasitologica 58(3): 328-333.
[20] Molan, A. L., Faraj, A. M. (1989): Prevalence of intestinal parasites in school children in Arbil, northern Iraq. – Saudi Medical Journal 10(2): 107-110.

http://www.aloki.hu ● ISSN 1589 1623 (Print) ● ISSN 1785 0037 (Online)
DOI: http://dx.doi.org/10.15666/aeer/1706_1488314891

[21] Motazedian, H., Mehrabani, D., Tabatabaee. S. H. R., Pakniat, A., Tavalali, M. (2006): Prevalence of helminth ova in soil samples from public places in Shiraz. – Eastern Mediterranean Health Journal 12(5): 562-565.
[22] Nooraldeen, K. (2015): Contamination of public squares and parks with parasites in Erbil city, Iraq. – Annals Agriculture Environmental Medicine 22(3):418-420.
[23] Otero, D., Nijsse, R., Gomes, L., Alho, A., Overgaauw, P., Hoek, D., Madeira de Carvalho, L. M. (2014): Prevalência de ovos de Toxocara spp., no solo de parques publicos da area da Grande Lisboa, Portgal - resultados preliminares. – Acta Parasitologica Portuguesa 20(1/2): 47-50 (in Portuguese).
[24] Paller, V. G. V., de Chavez, E. R. C. (2014): Toxocara (Nematoda: Ascaridida) and other soil-transmitted helminth eggs contaminating soils in selected urban and rural areas in the Philippines. – The Scientific World Journal. DOI: 10.1155/2014/386232.
[25] Rudohradská, P., Papajová, I., Juriš, P. (2011): Pets as a source of parasitic soil contamination in the settlements of marginalised groups of inhabitants. – Folia Veterinaria 55(1): 33-35.
[26] Sadjjadi, S. M., Khosravi, M. B., Mehrabani, D. C., Oryan, C. D. (2000): Seroprevalence of *Toxocara* infection in school children in Shiraz, southern Iran. – Journal of Tropical Pediatric 46(6): 327-330.
[27] Saida, L. A., Nooraldeen, K. (2014): Prevalence of parasitic stages in six leafy vegetables in markets of Erbil City, Kurdistan Region, Iraq. – Zanco Journal of Pure and Applied Sciences 26(2): 25-30.
[28] Soulsby, E. J. I. (1986): Examination of Faeces. – In: Soulsby, E. J. L. (ed.) Helminths, Arthropods and Protozoa of Domesticated Animals. 7th Ed. William Clones Limited, Beccles and London, pp. 137-145.
[29] Sudhakar, N. R., Samanta, S., Sahu, S., Raina, O. K., Gupta, S. C., Madhu, D. N., Kumar, A.(2013): Prevalence of *Toxocara* species eggs in soil samples of public health importance in and around Bareilly, Uttar Pradesh, India. – Veterinary World 6(2): 87-90.
[30] Sprenger, L. K., Green, K. T., Molento, M. B. (2014): Geohelminth contamination of public areas and epidemiological risk factors in Curitiba, Brazil. – Brazilian Journal of Veterinary Parasitology 23(1):69-73.
[31] Tavalla, M., Oormazdi, H., Akhlaghi, L., Razmjou, E., Moradi, Lakeh, M., Shojaee, S., Hadighi, R., Meamar, A. R. (2012): Prevalence of parasites in soil samples in Tehran public places. – African Journal of Biotechnology 11(20): 4575-4578.
[32] Tavassoli, M., Hadian, M., Charesaz, S., Javadi, S. (2008): *Toxocara* spp. eggs in public parks of Urmia city, west Azebaijan province Iran. – Iranian J Parasitology (3):24-29.
[33] Thomas, D., Jeyathilakan, N. (2014): Detection of Toxocara eggs in contaminated soil from various public places of Chennai City and detailed correlation with literature. – Journal of Parasitic Diseases 38(2): 174-180.
[34] Woodruff, A. W., Salih, S. Y. D., De Savigny, Baya, E. Z., Shah, A. I.(1981): Toxocariasis in Sudan. – Annals Tropical Medicine Parasitology 75(5): 559-561.
[35] Zibaei, M., Abdollahpour, F., Birjandi, M., Firoozeh, F. (2010): Soil contamination with Toxocara spp. eggs in the public parks from three areas of Khorram Abad, Iran. – Nepal Medical College Journal 12(2): 63-65.

http://www.aloki.hu ● ISSN 1589 1623 (Print) ● ISSN 1785 0037 (Online)
DOI: http://dx.doi.org/10.15666/aeer/1706_1488314891

LAND USE AND TEA PLANTATION LANDSCAPE CHARACTERISTICS AND CORRELATION ANALYSIS ALONG THE ELEVATION GRADIENTS IN LANCANGJIANG CATCHMENT OF YUNNAN IN CHINA

ZENG, W. J.[1,2] – FAN, K.[1,2] –ZHANG, J. S.[1,2] –WANG, J. X.[1] – ZHENG, H. G. [1,2] – CHEN, Y. C. [1,2] – LI, J. H.[1,2*]

[1]*College of Water Conservancy, Yunnan Agricultural University, Kunming, China*

[2]*Engineering Research Center of Science and Technology of Land and Resources, Yunnan Agricultural University, Kunming, China*

**Corresponding author*
e-mail: 28038071@qq.com

(Received 19th Jun 2019; accepted 16th Oct 2019)

Abstract. Land use in this study of the landscape, the spatial, statistical and comparative analysis is carried out on the tea plantation in Lancangjiang Catchment of Yunnan in China and its other main land use typesin perspective of the elevation gradient by using the GIS and data analysis software. The result shows that the landscape index is invert "V" or invert "U"-shaped, or decreasing linearly along the elevation gradient. The peak appears between 1200 and 1800 m with the highest concentration and spatial heterogeneity. Therefore, the tea plantation area is the largest and the tea planting is most active in this range. On the contrary, the bottom value appears at the elevation below 600 m or above 2600 m. Therefore, it holds the least area of the tea plantation. The four main land use types are weakly correlated with the tea plantation landscape, and the construction land use has the weakest correlation. Except for the grassland, the correlation between the tea plantation and other land use types is mainly reflected in the landscape area, the landscape shape index and the landscape agglomeration index. The research might be helpful for optimizing the land use landscape and improving the ecological conditions in the catchment.
Keywords: *land use, tea plantation, landscape index, development trend, correlation*

Introduction

Land is an important resource and a requisite for our living and development. In recent years, with the rapid increase of the world population and the accelerated urbanization, the land use by human beings is expanding in scope and depth. The socio-economic development is accompanied by the big change of the land cover, and it leads to a series of ecological problems. With the development of the landscape ecology, the landscape pattern analysis has become one of the effective technical ways to study the spatial structure and evolution of the land use (Chen, 2014). Tea is the traditional and main cash crop in Yunnan, and the Lancangjiang Catchment has the longest history of planting tea due to its preferable natural conditions. It also has the largest area of the tea plantation. With the rapid development of Pu'er Tea and increasing tea price, the tea production and the scale of the tea plantation has been expanding. It brings great impact on the ecological environment of the catchment. At the macro level, it disturbs and influences the number, area, shape and distribution of the patches of the land use landscape. Therefore, it is of great significance to carry out the tea plantation landscape research in order to optimize the land use landscape and improve the ecological conditions in the catchment.

http://www.aloki.hu ● ISSN 1589 1623 (Print) ● ISSN 1785 0037 (Online)
DOI: http://dx.doi.org/10.15666/aeer/1706_1489314910

The current land use research in the world covers the relationship of the land use and the climate change (Pavani, 2018; Furlanetto, 2018), the significance of the land use research to the (paleo) environment research (Jaeschke, 2018), the land use scheme (Martyn et al., 2017), and the drivers of the land use (Cattarino, 2014). The tea garden research is more focused on the livelihoods of the tea farmers (Biggs, 2018). There has been a lot of the tea research being done in the Lancangjiang Catchment, but most is about the main ingredients of the tea (Tan, 2012; Gong, 2010), heavy metal pollution (Chen, 2011; Liu, 2008), spectroscopic identification (Ning, 2013, 2010; Zheng, 2013), soil nutrients in the tea plantation (Gao, 2013; Yi, 2011; Li, 2011), and so on. Many of the research are aimed to improve the tea production and quality, so they focus on its quality control, physio-chemical properties of the soil and its impact on the tea. More research has been done on the vegetation cover (Fan, 2012) and land use (Wang, 2008) of the catchment than the spatial distribution and landscape of the tea plantation. For the landscape research, more is done on the land use, the urban area (Chu, 2018), the green park (Fan, 2018), lakes and wetlands (Zhai, 2018; Pu, 2018; Zhang, 2019), much less about the tea plantation. The change with time is more studied than the change with the elevation gradients for the land use and the landscape characteristics.

In this paper, the landscape study is carried out on the tea plantation and other main land use types (farmland, forest land, grassland, construction land) in Lancangjiang Catchment (Yunnan Section), in perspective of the elevation gradient by using the GIS and data analysis software, and by conducting the spatial, statistical and comparative analysis. The research might be helpful for optimizing the land use landscape, adjusting the agricultural structure and improving the ecological conditions in the catchment.

Materials and methodologies

Brief introduction of the study area

Lancang-Mekong River is a famous international river, and the only one river connecting the six countries in Asia. It originates in the northwest of Zaduo County of Yushu Tibetan Autonomous Prefecture of Qinghai Province in China (*Fig. 1*). The Yunnan Section of the river sets between N21°08′41″~29°14′04″ (*Fig. 1*). Lancangjiang River flows 1240 km long in Yunnan Province, with a catchment area of 90,000 km^2, covering Diqing, Lijiang, Dali, Baoshan, Lincang, Pu'er and Xishuangbanna prefectures. The catchment is going from north down to the south, and its water system is shaped as a broom. The difference of the elevation in the Catchment is big, and the temperature and precipitation are increasing from the north to the south. The dry and wet seasons are distinctive, the wet season starting from May to October, and the dry season starts from November to April of the next year. More than 85% of the rainfall concentrates in the wet season. There are various vegetation types in the catchment, including the tropical rainforest, monsoon forest and mountainous grassland. The topographic landform and climate of the catchment provides the preferable natural conditions for the tea production. The increasing tea plantation brings great economic benefits for the local society, but the unplanned expansion of the tea plantation brings many environmental issues as well.

Data source and processing

The current land use data for the research is obtained from the remote sensing images of Landsat8, taken in 2017, with a resolution of 30 m. DEM (Digital Elevation Model)

http://www.aloki.hu ● ISSN 1589 1623 (Print) ● ISSN 1785 0037 (Online)
DOI: http://dx.doi.org/10.15666/aeer/1706_1489314910

data is the original data from SRTMDEM 90M. The original images come from the Geospatial Data Cloud Platform of Chinese Academy of Science, and the land use and elevation data is drawn out by ENVI5.1 and ArcGIS10.0. The zoning maps of the latitude, elevation and climate are the research outputs of the Land Resources Science, Technology and Engineering Research Center of Yunnan Agricultural University. The downloaded 13 images are calibrated by ENVI5.1 and the Band 5, 4, 3 images are fused with standard false color based on the enhanced processing. The training samples are selected based on the terrain feature in the field to supervise the classification and its accuracy. Except for the main research target – the tea plantation, the other six land use types are interpreted according to the Current Land Use Classification Standard (GB/T 21010-2007) such as farmlands, forest lands, grasslands, construction lands, water and other land uses (including idle land, barren rocky land, garden). The final classification is finished after blurring, mosaic method processing and range-cutting (*Figs. 2* and *3*). Then the land use type and area data are furthermore extracted by ARCGIS10.0 (*Table 1*).

In order to differentiate the tea garden from the forest land, a modified decision tree classification method is applied. The elevation and slope degree which affect the tea garden growth have been used as decision principles, combined with the spectral characteristics of the tea garden and forest land. The ratio index, NDVI value and the texture index are introduced into the decision classification, and the decision tree remote sensing data extraction model is established to improve the accuracy of the remotely sensed image classification.

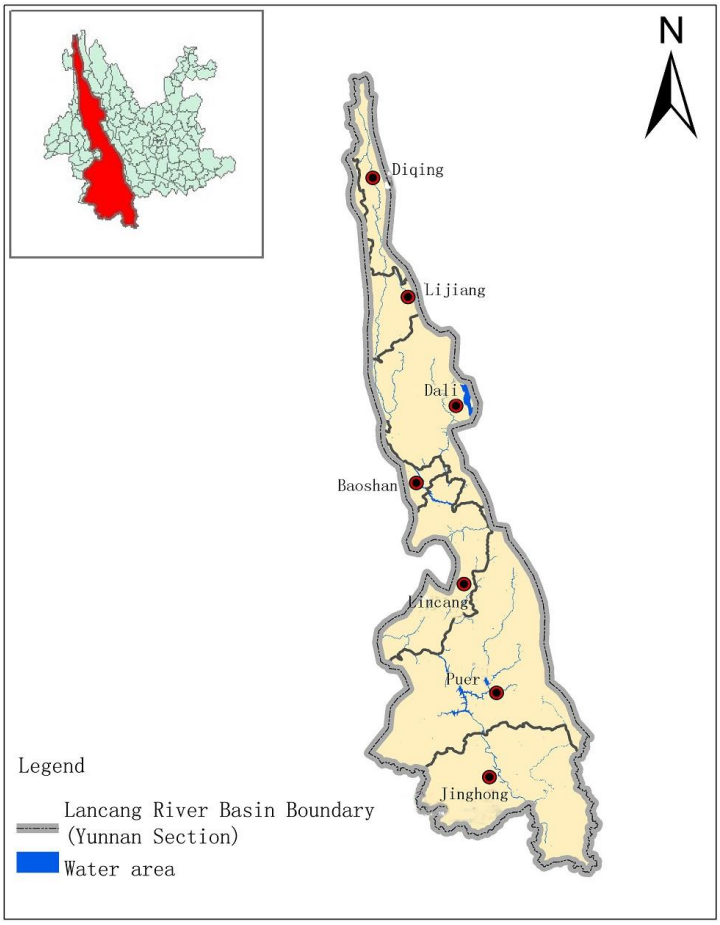

Figure 1. *Location of the study*

http://www.aloki.hu ● ISSN 1589 1623 (Print) ● ISSN 1785 0037 (Online)
DOI: http://dx.doi.org/10.15666/aeer/1706_1489314910

Figure 2. *The map of remote sensing classification*

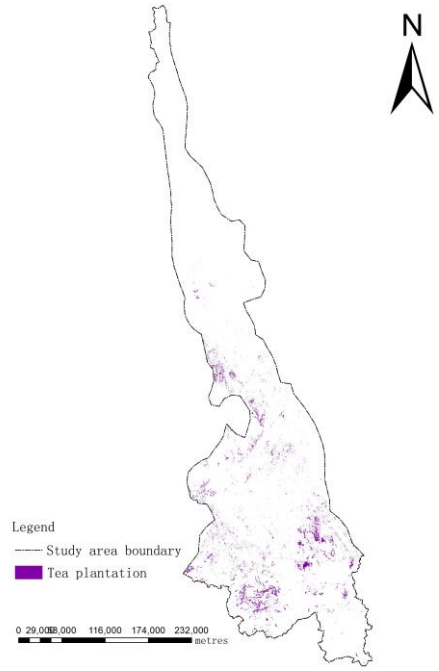

Figure 3. *The map of tea garden distribution*

Research methods

According to the landscape pattern theory, the landscape pattern index is calculated and the pattern of the tea plantation under different elevation gradient and land use is analyzed by spatially overlaying the different map layers. The Fragstats4.2 is applied in this process.

http://www.aloki.hu ● ISSN 1589 1623 (Print) ● ISSN 1785 0037 (Online)
DOI: http://dx.doi.org/10.15666/aeer/1706_1489314910

Table 1. *The information of the remote sensing classification*

Land type	Patch quantity	Patch ratio (%)	Area/hm^2	Area ratio (%)
Farmland	64729	25.65	1198777.76	13.64
Forest land	31724	12.57	6061472.32	68.96
Grassland	71281	28.25	803689.18	9.14
Constn land	19671	7.8	82587.01	0.94
Water area	2234	0.89	101375.14	1.15
Other land	29141	11.55	327609.13	3.73
Tea plant	**33542**	**13.29**	**214282.95**	**2.44**
Total	252322	100	8789793.49	100

There are tens of indexes currently used for studying the landscape pattern (Zhao, 2007), out of which, eight indexes are selected. They are landscape type area (CA), proportion of landscape type area (PLAND), average patch area (AREA_MN), patch area standard deviation (AREA_SD), largest patch index (LPI), patch density (PD), landscape shape index (LSI), landscape agglomeration index (AI).

(1) Class area

CA is the total area of a certain landscape patches, with measurement unit of hm^2. In ecological terms, it reflects the energy storage and energy flow of a certain landscape type. The bigger the patch area the more abundant its species, and the faster energy flow. The formula is as follows (*Eq. 1*):

$$CA = \sum_{j=1}^{n} a_{ij} \quad \text{(Eq.1)}$$

in which, a_{ij} is the area of Patch j of Type i, n is the quantity of the patches.

(2) Proportion of landscape type area (PLAND)

PLAND is the proportion of the patch area of certain landscape in the whole landscape area, expressed by "%", showing the dominance or importance of certain landscape type in the whole landscape. The formula is shown as follows (*Eq. 2*):

$$PLAND = \frac{\sum_{j=1}^{n} a_{ij}}{A} \times 100 \quad \text{(Eq.2)}$$

In this equation, "A" is the total area of the landscape; "a_{ij}" is the area of the Patch j of the Landscape Type i; "n" is the number of the patches.

(3) Average patch area (AREA_MN)

AREA_MN is the average area of all the patches of a certain landscape type. The change of its value gives more ecological information of the landscape, and it is a critical index in reflecting the landscape heterogeneity. The formula is shown as follows (*Eq. 3*):

http://www.aloki.hu ● ISSN 1589 1623 (Print) ● ISSN 1785 0037 (Online)
DOI: http://dx.doi.org/10.15666/aeer/1706_1489314910

$$AREA\_MN = \frac{A_i}{N_i} \quad \text{(Eq.3)}$$

In this equation, "Ai" is the total area of the Landscape Type i; "Ni" is the number of the patches of the Landscape Type i.

(4) Patch area standard deviation (AREA_SD)

AREA_ SD is the standard deviation of all the patch area of a certain landscape type. It reflects the diffusion degree of the patch area of a certain landscape type and the variation degree of the landscape patch scale. The bigger the value, the higher degree of the variation. The formula is as follows (*Eq. 4*):

$$AREA\_SD = \sqrt{\frac{\sum_{j=1}^{n}(a_{ij} - \frac{A_i}{N_i})}{N_i}} \quad \text{(Eq.4)}$$

In this equation, "a_{ij}" is the area of Patch j of the landscape type i; "n" is the number of the patches. "Ai" is the total area of the Landscape type I; "Ni" is the total number of the patches of the Landscape type i.

(5) Largest patch index (LPI)

LPI is the proportion of the largest patch area of a certain landscape type in the whole landscape area. It shows the dominance of a certain landscape type in the whole landscape. Its value reflects the intensity of the human activity. The formula is as follows (*Eq. 5*):

$$LPI = \frac{Max(a_{ij})}{A} \times 100 \quad \text{(Eq.5)}$$

In this equation, "Max(a_{ij})" is the area of the largest patch of the landscape type i; "A" is the total area of the whole landscape.

(6) Patch density (PD)

PD is the ratio of the patch number of a certain landscape type in the whole landscape area, in other words, the patch quantity in each hectare. It shows the fragmentation of the landscape. The bigger the value, the more fragmented the landscape, thus the more complicated spatial structure of the landscape. The formula is as follows (*Eq. 6*):

$$PD = \frac{N_i}{A} \quad \text{(Eq.6)}$$

In this equation, "A" is the total area of the whole landscape, and "N" is the patch quantity of the landscape type i.

http://www.aloki.hu ● ISSN 1589 1623 (Print) ● ISSN 1785 0037 (Online)
DOI: http://dx.doi.org/10.15666/aeer/1706_1489314910

(7) Landscape shape index (LSI)

LSI is the shape of a certain landscape type, and is generally used to indicate the complexity and stability of the landscape. When the landscape patch shape is close to a square, the value of LSI is close to 1. When the shape is complex or becoming elongated, the value will be increased infinitely. The formula is as follows (*Eq. 7*):

$$LSI = \frac{0.25E}{\sqrt{A}} \quad \text{(Eq.7)}$$

In this equation, "A" is the total area of the whole landscape, and "E" is the total length of all the patch boundaries in the landscape.

(8) Agglomeration index of landscape (AI)

"AI" is the agglomeration degree of the patches in a certain landscape type. Its value ranges from 0 to 100. The bigger the value, the higher degree of agglomeration of the patches. The formula is as follows (*Eq. 8*):

$$AI = \frac{g_{ii}}{Max \rightarrow g_{ii}} \times 100 \quad \text{(Eq.8)}$$

In this equation, "g_{ii}" is the number of similar patches jointing each other of the landscape type i.

When the index values of the landscape pattern are obtained, the correlation between the tea plantation and other land use types is analyzed, in other words, the relative variants are analyzed to find out to which extent they are related to each other. Pearson correlation coefficient is used for the analysis and the formula is shown below (*Eq. 9*) (Zhang, 2014):

$$r = \frac{l_{XY}}{\sqrt{l_{XX} l_{YY}}} = \frac{\sum (X - \overline{X})(Y - \overline{Y})}{\sqrt{\sum (X - \overline{X})^2 \sum (Y - \overline{Y})^2}} \quad \text{(Eq.9)}$$

In which, r is correlation coefficient of variants; $|r|$ is the degree the two variants are related, when $r > 0$ means positive correlation, $r < 0$ for negative, $r = 0$ means zero correlation. The closer the value of $|r|$ to 1, the higher the correlation degree. More specifically, when $|r|$ is 0.8~1, very strong correlation; 0.6～0.8 is strong; 0.4~0.6 is medium; 0.2~0.4 is weak; 0.0~0.2 is very weak or no relation.

The correlation coefficient needs to be tested by the prominence value (P). When $P \leq 0.05$, it has prominent correlation. SPSS 22 is used in this process. In the "r" value results, "*" means at $p \leq 0.05$, and "**" means at $p \leq 0.01$. There exists certain deviation in the correlation results due to the limited amount of the data sample, so the prominence of the correlation is only done for those at $p \leq 0.01$.

Results and analysis

Table 1 shows that as far as the patch quantity is concerned, grassland > farmland > tea plantation > forest land > other land > construction land > water area, and the grassland is

http://www.aloki.hu ● ISSN 1589 1623 (Print) ● ISSN 1785 0037 (Online)
DOI: http://dx.doi.org/10.15666/aeer/1706_1489314910

the most, holding a proportion of 0.2825; and the water area is the least, holding 0.0089. The tea plantation patches, preceded by the grassland and farmland, is ranked the third, holding 0.1329. In respect of the type area, it is forest land > farmland > grassland > other land use > tea plantation > water area > construction land. The forest land has the largest area in the whole catchment, its proportion is as high as 0.6896. The construction land has the least area with a portion of 0.0094. The tea plantation, with a portion of 0.0244, stands at the fifth place (*Figs. 2* and *3*).

Tea plantation landscape pattern features under different elevation gradients and land use

There is a wide elevation range in Lancangjiang Catchment (Yunnan Section) running from 460 to 6456 m. In order to accurately display the change of the tea plantation landscape pattern under different elevation gradients and land uses, the elevation is graded every 200 m by equal- or non-equal spacing methods to include 14 gradients. They are below 600 m, 600~800 m, 800~1000 m, 1000~1200 m, 1200~1400 m, 1400~1600 m, 1600~1800 m, 1800~2000 m, 2000~2200 m, 2200~2400 m, 2400~2600 m, 2600~2800 m, 2800~3000 m, above 3000 m (*Fig. 4*). The statistical data of the land types is collected after graphic overlaying of the RS image classification map and latitude change map. Then after cutting and transferring to the grid data, they are introduced to Fragstats for the landscape pattern index. It is exhibited in *Table 1* that there is no tea plantation above 2800 m, so it is only needed to analyze the pattern features below 2800 m.

Landscape pattern features of main land use types at different elevation

By overlaying the land use map and elevation map with Arcgis 10.0, each level is converted into ESRI grid format, and the land use landscape pattern index under different elevation is calculated with Fragstats4.2 (*Fig. 5*).

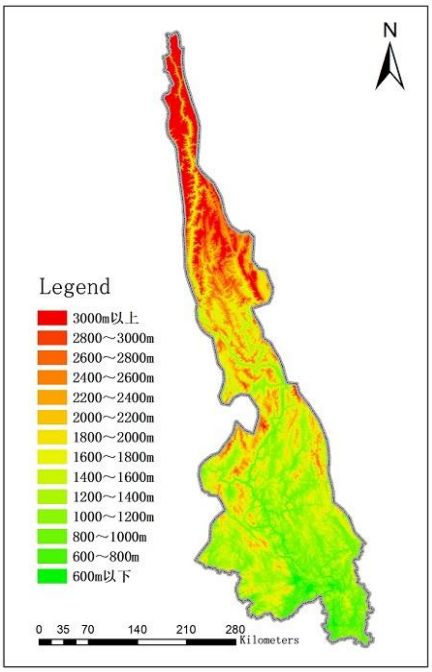

Figure 4. *The map of altitude gradient*

http://www.aloki.hu ● ISSN 1589 1623 (Print) ● ISSN 1785 0037 (Online)
DOI: http://dx.doi.org/10.15666/aeer/1706_1489314910

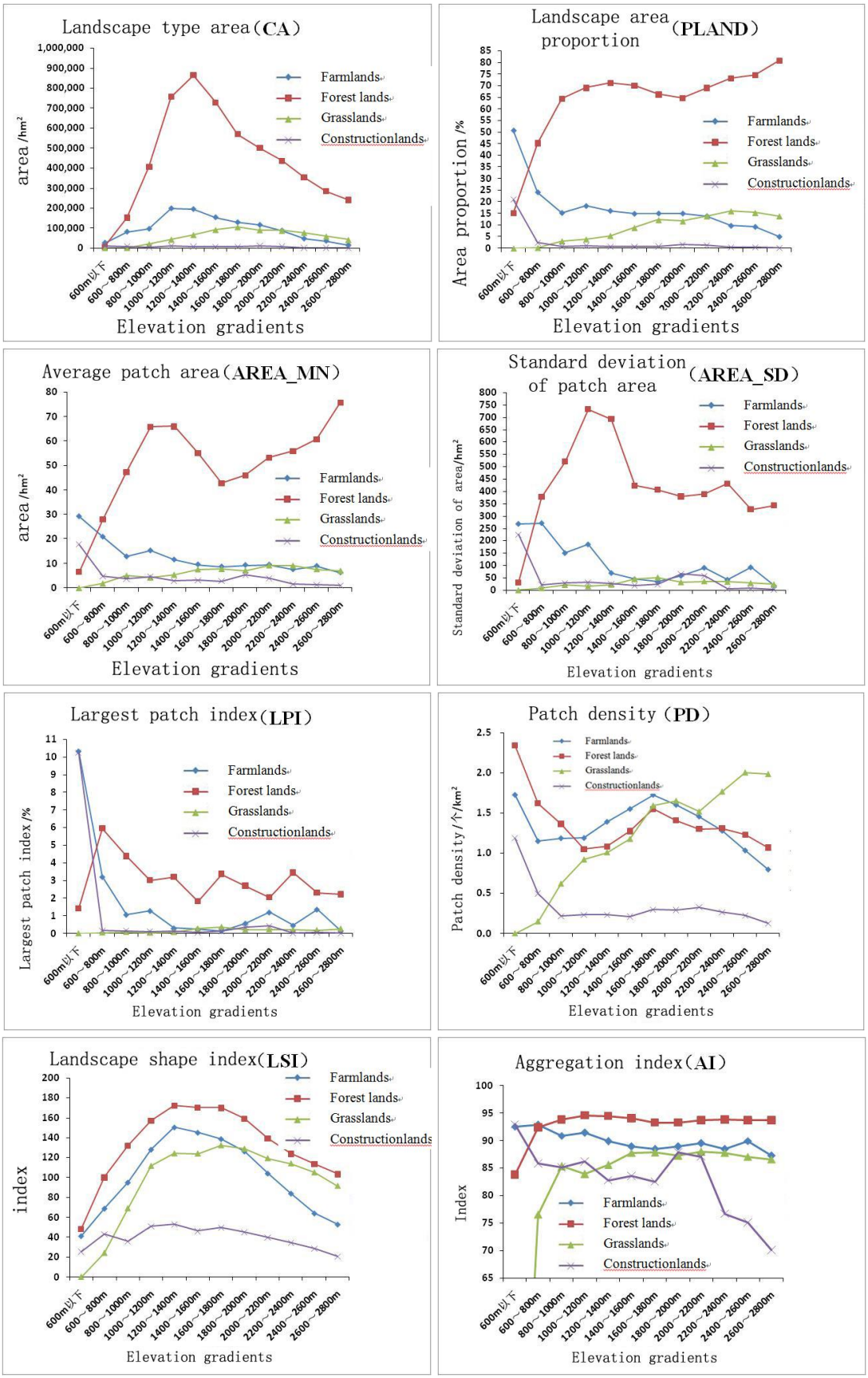

Figure 5. *Landscape pattern index of land use type in different altitude gradient*

http://www.aloki.hu ● ISSN 1589 1623 (Print) ● ISSN 1785 0037 (Online)
DOI: http://dx.doi.org/10.15666/aeer/1706_1489314910

As far as the landscape area (CA) is concerned, when the elevation is increasing, the farmland, forest land and the grassland is going up and down, and the construction land use is generally decreasing. In respect of landscape area proportion (PLAND), the forest land experiences rapid increase first and then gradual decrease, while the grassland keeps going up mildly, and the farmland and the construction land use experience the slow and then the fast climb-up. For the average area of the patch (AREA_MN), the forest land fluctuates but keeps going up; the grassland is increasing gradually; the farmland and the construction land keep declining from a fast to a slow speed. In respect of the standard deviation of the patch area (AREA_SD), the forest land stays stable after an up-and-down; the farmland is declining with a wave shape; the construction land experiences a steep downward and then keeps stable, and the grassland generally stays constant with little change. In respect of LPI, the forest land fluctuates, the farmland and the construction land experience a steep downward and then keeps stable, and the grassland has little change. In respect of the patch density (PD), the forest land, the farmland and the construction land go from a fast to a gentle downward, the grassland is fluctuating to an upward. The landscape shape index (LSI) shows that the farmland, the forest land, the grassland and the construction land first go up and then down, and the construction land is generally declining. In respect of the agglomeration index (AI), the forest land and the grassland go from upward to a stable status, the farmland goes down mildly, and the construction land fluctuates to a downward.

The landscape pattern index of the tea plantation under different elevation

By overlaying the tea plantation distribution map and the elevation map with Arcgis 10.0, each level is converted into ESRI grid format, and the tea plantation landscape pattern index under different elevation is calculated with Fragstats4.2. The result is shown in *Figure 6*.

(1) In respect of the landscape type area (CA), with the increasing elevation, the area of the tea plantation goes upward and then downward. The tea plantation area is larger between 1000 and 2000 m, and it is 18.93×10^4 hm^2, covering 88% of the tea plantation area under the research. It is a main area for tea planting. Between 1200 and 1400 m, the tea plantation area is the largest, which is 5.48×10^4 hm^2, accounting for 25.71%. The area is reducing below 800 m or above 2200 m, accounting for only 2.03%. The smallest area of 20.97 hm^2 is distributed below 600 m, accounting for only 0.01% of the tea plantation area in the whole catchment.

(2) In respect of the landscape type area proportion (PLAND), with the increasing elevation, the area of the tea plantation goes upward and then downward. The proportion of the tea plantation area is bigger between 1000 and 2000 m, covering 2%~5%. Between 1200 and 1400 m, it is the biggest, accounting for 4.52%, so the tea plantation is dominant in this range. The tea area proportion is decreasing below 800 m or above 2200 m, accounting for less than 0.5%. The smallest tea area proportion is distributed below 600 m, accounting for only 0.04%.

(3) In respect of the mean area of the patch (AREA_MN), with the increasing elevation, the mean patch area of the tea plantation goes upward and then downward, with mild fluctuation. The larger mean patch area occurs between 800-2000 m, nearly all above 4 hm^2. It is decreasing below 800 m, nearly all less than 2 hm^2. The least mean patch area is distributed below 600 m, being only 0.62 hm^2. It goes up between 2400 and 2600 m, mainly because of the less number of the patches.

http://www.aloki.hu ● ISSN 1589 1623 (Print) ● ISSN 1785 0037 (Online)
DOI: http://dx.doi.org/10.15666/aeer/1706_1489314910

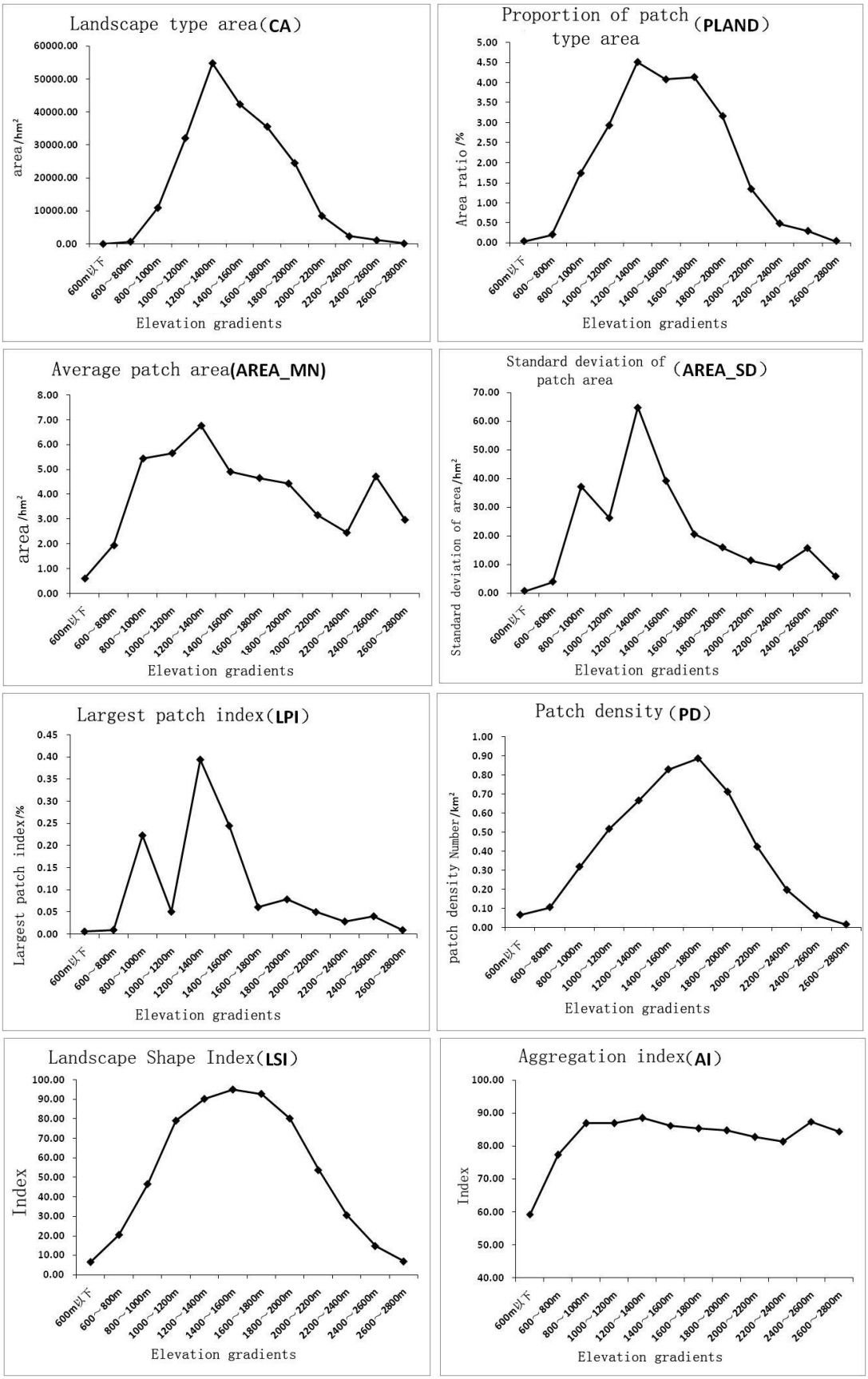

Figure 6. *Landscape pattern index of tea garden in different altitude gradient*

http://www.aloki.hu ● ISSN 1589 1623 (Print) ● ISSN 1785 0037 (Online)
DOI: http://dx.doi.org/10.15666/aeer/1706_1489314910

4) In respect of the standard deviation of the patch area (AREA_SD), it generally goes from upward to downward with small fluctuation, when the elevation is increasing. The standard deviation is bigger between 800-2000 m, nearly all above 20 hm^2. It means that, in this range, the patch size is with a higher dispersion, the patch scale is more varied with high spatial heterogeneity. It reaches the highest level between 1200 and 1400 m, getting to 64.87 hm^2. Then it goes down below 800 m, nearly all less than 4 hm^2. The least deviation is distributed below 600 m, being only 0.70 hm^2.

(5) In respect of the largest patch index (LPI), with the increasing elevation, the development trend of the proportion of the largest patch is similar to the standard deviation of the patch area. The LPI is bigger between 800-1000 m and 1200-1600 m, all above 0.2%, so in these ranges the scale of the tea plantation is larger and more dominant. The index is less for the other elevation ranges, less than 0.05%. The least is found below 800 m or above 2600 m, being only 0.01%.

(6) In respect of the patch density (PD), the density is going up and then down with the increasing elevation. The patches are most densely distributed between 1000 and 2000 m, all above 0.5. In this range, there are most tea plantation patches with the biggest fragmentation and most complex spatial structure. The density is reducing below 600 m or above 2400 m, all less than 0.1. The least patch density appears above 2600 m, being only 0.02.

(7) The landscape shape index (LSI) is going up and then down with the increasing elevation. The shape index has the highest value between 1000 and 2000 m, all above 50. In this range, the tea plantation patch shape is most complex and irregular. So it is mostly disturbed by est the human activity and has the weakest stability, deviating furthest from the square shape. The lowest index value occurs below 600 m or above 2400 m, being respectively 6.71 and 6.99, mainly because of the smallest area of the tea plantation and more regular shape.

(8) The agglomeration index (AI) is going up and then down with the increasing elevation. Its downward trend is not obvious, and the agglomeration degree is generally high. The agglomeration degree is lower below 800 m, being less than 80. It goes steadily up with little variation above 800 m, with a higher agglomeration degree, being more than 80.

Correlation of land use type and tea plantation landscape pattern under elevation gradient

The correlation analysis of the two variants is conducted when the elevation gradient land use type and the tea plantation landscape pattern index are input in SPSS 22 software.

(1) The correlation of the farmland and tea plantation landscape pattern is shown in *Table 2*. The bolded data with means the variants have closer relation at the layer of $p \leq 0.01$. From *Tables 4* and *5* it is shown that as the elevation changes, the farmland area (CA), the shape index (LSI) and the tea plantation area (CA), the proportion of the tea plantation area (PLAND), the tea patch density (PD) and its shape index (LSI) have strong positive relation, and they have the same relation with the tea average patch area (AM) and the standard deviation of the tea patch area (ASD). So, at the elevation gradient, the farmland area and its shape have similar characteristics of the area, patch density and shape of the tea plantation; they influence each other. The farmland area proportion (PLAND), the farmland patch density (PD) and the average farmland patch area (AM) have strong negative relation with the agglomeration index (AI) of the tea plantation. It means with the increasing farmland area, the patch density is increasing and its average area is bigger, but the agglomeration of the tea plantation is lower and lower.

http://www.aloki.hu ● ISSN 1589 1623 (Print) ● ISSN 1785 0037 (Online)
DOI: http://dx.doi.org/10.15666/aeer/1706_1489314910

Table 2. *Correlation analysis results between arable land and tea garden landscape pattern landscape class area (CA), proportion of landscape type area (PLAND), average patch area (AREA_MN), patch area standard deviation (AREA_SD), largest patch index (LPI), patch density (PD), landscape shape index (LSI), landscape agglomeration index (AI)*

		Farmlands CA	Farmlands PLAND	Farmlands PD	Farmlands LPI	Farmlands LSI	Farmlands AM	Farmlands ASD	Farmlands AI
Tea plantation CA	r	**0.907****	-0.139	0.415	-0.406	**0.930****	-0.233	-0.342	-0.187
	p	**0.000**	0.667	0.179	0.190	**0.000**	0.467	0.277	0.560
Tea plantation PLAND	r	**0.883****	-0.181	0.498	-0.457	**0.966****	-0.298	-0.395	-0.244
	p	**0.000**	0.574	0.099	0.135	**0.000**	0.346	0.204	0.445
Tea plantation PD	r	**0.800****	-0.175	0.619*	-0.447	**0.951****	-0.326	-0.425	-0.297
	p	**0.002**	0.587	0.032	0.145	**0.000**	0.301	0.168	0.348
Tea plantation LPI	r	0.637*	-0.142	0.158	-0.324	0.646*	-0.179	-0.253	-0.079
	p	0.026	0.660	0.624	0.304	0.023	0.577	0.428	0.806
Tea plantation LSI	r	**0.896****	-0.223	0.511	-0.501	**0.990****	-0.333	-0.386	-0.239
	p	**0.000**	0.486	0.089	0.097	**0.000**	0.291	0.216	0.455
Tea plantation AM	r	**0.756****	-0.512	-0.065	-0.667*	**0.766****	-0.501	-0.422	-0.246
	p	**0.004**	0.089	0.841	0.018	**0.004**	0.097	0.171	0.441
Tea plantation ASD	r	**0.764****	-0.235	0.103	-0.430	**0.743****	-0.253	-0.284	-0.096
	p	**0.004**	0.463	0.749	0.163	**0.006**	0.428	0.371	0.766
Tea plantation AI	r	0.492	**-0.888****	-0.361	**-0.949****	0.608*	**-0.828****	-0.646*	-0.528
	p	0.104	**0.000**	0.249	**0.000**	0.036	**0.001**	0.023	0.077

r: correlation coefficient; p: significance

(2) The correlation of the forest land and the tea plantation landscape pattern is shown in *Table 3*. The bolded data means the variants have obvious relation at the layer of $p \leq 0.01$. From *Table 3,* it is shown that as the elevation changes, the forest land area (CA), the shape index (LSI) and the tea plantation area (CA), the proportion of the tea plantation area (PLAND), the tea patch density (PD) and its shape index (LSI) have strong positive relation, and they have the same relation with the tea average patch area (AM) and the standard deviation of the tea patch area (ASD). So the forest land area and its shape have similar development trends of most tea plantation landscape index. They have strong influence on the landscape pattern of the tea plantation. The forest land area proportion (PLAND) and the agglomeration index (AI) of the tea plantation has strong negative relation, and the largest patch index (LPI) of the forest land is irrelevant with the AI of the tea plantation. Except the two negative relations, the other forest landscape indexes have very strong or strong positive relation with the AI of the tea plantation.

(3) The correlation of the grassland and the tea plantation landscape pattern is shown in *Table 4*. The bolded data means the variants have prominent relation at the layer of $p \leq 0.01$. From *Table 4,* it is shown that as the elevation changes, the grass land area (CA) and the tea patch density (PD) have strong positive relation. It implies that the bigger the grassland area is, the denser and more fragmented the tea garden patches. The shape index and the agglomeration index of the grassland have strong positive relation with the agglomeration index of the tea garden. They influence each other and keep the same development trend.

http://www.aloki.hu ● ISSN 1589 1623 (Print) ● ISSN 1785 0037 (Online)
DOI: http://dx.doi.org/10.15666/aeer/1706_1489314910

Table 3. *Correlation analysis results between forest land and tea garden landscape pattern landscape class area (CA), proportion of landscape type area (PLAND), average patch area (AREA_MN), patch area standard deviation (AREA_SD), largest patch index (LPI), patch density (PD), landscape shape index (LSI), landscape agglomeration index (AI)*

		Forestlands CA	Forestlands PLAND	Forestlands PD	Forestlands LPI	Forestlands LSI	Forestlands AM	Forestlands ASD	Forestlands AI
Tea plantation CA	r	**0.922****	0.285	-0.356	-0.080	**0.829****	0.304	0.633*	0.380
	p	**0.000**	0.370	0.256	0.804	**0.001**	0.336	0.027	0.223
Tea plantation PLAND	r	**0.901****	0.302	-0.322	-0.058	**0.882****	0.255	0.587*	0.406
	p	**0.000**	0.340	0.308	0.857	**0.000**	0.424	0.045	0.190
Tea plantation PD	r	**0.818****	0.267	-0.228	-0.089	**0.872****	0.155	0.454	0.371
	p	**0.001**	0.401	0.476	0.784	**0.000**	0.631	0.138	0.236
Tea plantation LPI	r	0.695*	0.246	-0.342	0.034	0.571	0.284	0.549	0.328
	p	0.012	0.441	0.277	0.916	0.052	0.371	0.065	0.297
Tea plantation LSI	r	**0.907****	0.335	-0.352	-0.032	**0.919****	0.259	0.615*	0.466
	p	**0.000**	0.288	0.262	0.922	**0.000**	0.416	0.033	0.127
Tea plantation AM	r	**0.864****	0.624*	-0.696*	0.054	**0.827****	0.628*	**0.810****	0.697*
	p	**0.000**	0.030	0.012	0.868	**0.001**	0.029	**0.001**	0.012
Tea plantation ASD	r	**0.826****	0.364	-0.476	0.049	0.693*	0.414	**0.712****	0.455
	p	**0.001**	0.244	0.118	0.881	0.012	0.181	**0.009**	0.137
Tea plantation AI	r	0.704*	**0.918****	**-0.913****	0.177	**0.810****	**0.837****	**0.762****	**0.962****
	p	0.011	**0.000**	**0.000**	0.582	**0.001**	**0.001**	**0.004**	**0.000**

r: correlation coefficient; p: significance

Table 4. *Correlation analysis results between forest grassland tea garden landscape pattern landscape class area (CA), proportion of landscape type area (PLAND), average patch area (AREA_MN), patch area standard deviation (AREA_SD), largest patch index (LPI), patch density (PD), landscape shape index (LSI), landscape agglomeration index (AI)*

		Grasslands CA	Grasslands PLAND	Grasslands PD	Grasslands LPI	Grasslands LSI	Grasslands AM	Grasslands ASD	Grasslands AI
Tea plantation CA	r	0.515	-0.101	0.017	0.146	0.588*	0.153	0.405	0.312
	p	0.087	0.755	0.958	0.650	0.044	0.634	0.192	0.323
Tea plantation PLAND	r	0.607*	-0.030	0.074	0.260	0.643*	0.239	0.525	0.368
	p	0.037	0.926	0.819	0.414	0.024	0.455	0.080	0.240
Tea plantation PD	r	**0.713****	0.071	0.127	0.403	0.665*	0.330	0.647*	0.368
	p	**0.009**	0.825	0.694	0.194	0.018	0.295	0.023	0.239
Tea plantation LPI	r	0.203	-0.211	-0.124	-0.095	0.326	0.075	0.174	0.250
	p	0.526	0.510	0.700	0.770	0.301	0.817	0.588	0.432
Tea plantation LSI	r	0.662*	0.020	0.100	0.288	0.689*	0.313	0.576*	0.434
	p	0.019	0.951	0.757	0.363	0.013	0.322	0.050	0.159
Tea plantation AM	r	0.419	0.082	0.262	0.117	0.677*	0.342	0.393	0.623*
	p	0.175	0.800	0.410	0.718	0.016	0.276	0.206	0.030
Tea plantation ASD	r	0.268	-0.168	-0.043	-0.071	0.453	0.128	0.228	0.360
	p	0.399	0.602	0.896	0.826	0.139	0.692	0.476	0.251
Tea plantation AI	r	0.552	0.451	0.596*	0.434	**0.804****	0.671*	0.603*	**0.942****
	p	0.063	0.141	0.041	0.159	**0.002**	0.017	0.038	**0.000**

r: Correlation coefficient; p: Significance.

http://www.aloki.hu ● ISSN 1589 1623 (Print) ● ISSN 1785 0037 (Online)
DOI: http://dx.doi.org/10.15666/aeer/1706_1489314910

(4) The correlation of the construction land and the tea plantation landscape pattern is shown in *Table 5*. The bolded data means the variants have more prominent relation at the layer of $p \leq 0.01$. From *Table 5,* it is shown that with the elevation change, the shape index (LSI) of the construction land has a very strong positive relation with the area (CA), the area proportion (PLAND), the patch density (PD) and the shape index (LSI) of the tea garden. The agglomeration index (AI) of the grassland has strong negative relation with most landscape indexes of the construction land.

Table 5. *Correlation analysis results between forest construction tea garden landscape pattern landscape class area (CA), proportion of landscape type area (PLAND), average patch area (AREA_MN), patch area standard deviation (AREA_SD), largest patch index (LPI), patch density (PD), landscape shape index (LSI), landscape agglomeration index (AI)*

		Construction lands CA	Construction lands PLAND	Construction lands PD	Construction lands LPI	Construction lands LSI	Construction lands AM	Construction lands ASD	Construction lands AI
Tea plantation CA	r	0.425	-0.291	-0.330	-0.289	**0.828****	-0.194	-0.204	0.193
	p	0.168	0.358	0.294	0.362	**0.001**	0.545	0.525	0.549
Tea plantation PLAND	r	0.449	-0.333	-0.361	-0.331	**0.847****	-0.217	-0.212	0.238
	p	0.143	0.291	0.249	0.293	**0.001**	0.498	0.507	0.456
Tea plantation PD	r	0.479	-0.316	-0.319	-0.318	**0.831****	-0.193	-0.171	0.299
	p	0.115	0.316	0.312	0.313	**0.001**	0.549	0.594	0.345
Tea plantation LPI	r	0.113	-0.251	-0.313	-0.237	0.502	-0.199	-0.203	0.093
	p	0.728	0.431	0.322	0.458	0.096	0.535	0.527	0.775
Tea plantation LSI	r	0.491	-0.390	-0.397	-0.394	**0.890****	-0.252	-0.244	0.286
	p	0.105	0.210	0.201	0.205	**0.000**	0.429	0.444	0.368
Tea plantation AM	r	0.070	-0.620*	-0.691*	-0.603*	0.613*	-0.537	-0.533	-0.126
	p	0.829	0.032	0.013	0.038	0.034	0.072	0.074	0.696
Tea plantation ASD	r	0.134	-0.363	-0.430	-0.349	0.610*	-0.300	-0.312	0.041
	p	0.678	0.246	0.163	0.267	0.035	0.343	0.323	0.899
Tea plantation AI	r	-0.281	**-0.942****	**-0.968****	**-0.926****	0.438	**-0.899****	**-0.877****	-0.487
	p	0.377	**0.000**	**0.000**	**0.000**	0.154	**0.000**	**0.000**	0.108

Notes: r: correlation coefficient; p: significance

Discussion

For the first time, the tea garden landscape pattern change under different land use and altitude gradient is studied for Lancangjiang Catchment (Yunnan Section). It lays a foundation for further research on the ecological environmental effect, and provides scientific basis for optimizing the land use landscape pattern in the catchment and improving the ecological environment of the catchment. However, there is some limitation of this study. Influenced by the resolution of the original remote sensing images, certain interpretation errors exist compared with the actual conditions. The temporal change is not studied due to large research area and time constraints, and only one-year data is studied at the macro level. More field investigation will be done in the future research to collect more information and data to make more accurate research results.

Conclusions

The landscape pattern characteristics of the tea garden under the four main types of the land use (farmland, forest land, grassland and the construction land) is studied from the aspect of the elevation gradient for the Lancangjiang Catchment (Yunnan Section). The study is done through the spatial, statistical and comparative analysis, and by the

http://www.aloki.hu ● ISSN 1589 1623 (Print) ● ISSN 1785 0037 (Online)
DOI: http://dx.doi.org/10.15666/aeer/1706_1489314910

use of such geographical information and data analysis softwares as ENVI5.1, Arcgis10.0, Fragstats4.2 and Office 2007. The conclusions are made as follows:

(1) The eight landscape pattern indexes of the four main land use types express certain regularity with the altitude change. Their development trend is diverse and different.

(2) The landscape indexes of the tea plantation climb up first and then go down along the elevation gradient, with an invert "V" or invert "U"-shape. The peak appears between 1200 and 1800 m where the tea planting is most active, and it implies that in this range, the tea garden is most extensively distributed, and it has the densest patches, the biggest scale change, the most complicated shapes and the highest spatial heterogeneity. The bottom value occurs below 600 m or above 2600 m, and it implies that in this range, the tea garden is least distributed, and it has the least dense patches, the smallest scale change, the simpler shapes, the lowest agglomeration degree and the weaker spatial heterogeneity.

(3) Along the altitude gradient, there is a relatively strong correlation between the four main land use types and the tea garden landscape pattern, of which, the farmland and the forest land is most strongly correlated to the tea garden landscape, while the grassland is the weakest. Their correlation reflects in the characteristics of the three indexes such as the landscape area (CA), the landscape shape index (LSI) and the landscape agglomeration index (AI).

The next study will combine the temporal and spatial research and discuss the drivers of the change, to better comprehend the temporal change of the tea garden landscape, and its development trend and relationship with the ecological environment, and to provide the scientific basis for the ecological planting of the tea garden and improve the ecological environment of the catchment.

Acknowledgements. The research was supported by The National Natural Science Foundation Regional Science Foundation Project of China (No.41961040).

REFERENCES

[1] Biggs, E. M., Gupta, N., Saikia, S. D. (2018): The tea landscape of Assam: multi-stakeholder insights into sustainable livelihoods under a changing climate. – Environmental Science & Policy 82: 9-18.

[2] Cattarino, L., McAlpine, C. A., Rhodes, J. R. (2014): Land-use drivers of forest fragmentation vary with spatial scale. – Global Ecology and Biogeography 23(11): 1215-1224.

[3] Chen, B., Pu, H., Jiang, D., et al. (2011): Content and evaluation of heavy metal in soil of tea garden in Pu'er city. – Journal of Yunnan University (Natural Science Edition) 33(S2): 470-473 + 476.

[4] Chen, L., Wang, R., Gao, M., et al. (2014): A GIS-based gradient analysis of land use landscape pattern changes. – Journal of Southwest University (Natural Science Edition) 36(5): 136-143.

[5] Chu, L., Zhang, X., Wang, T., et al. (2018): Spatial-temporal evolution and prediction of urban landscape pattern and habitat quality based on CA-Markov and in VEST model. – Chinese Journal of Applied Ecology 29(12): 4106-4118.

[6] Fan, C., Tian, L., Shen, S., et al. (2018): Analysis on the landscape pattern change of the urban and green ecological space in Suzhou-Wuxi-Changzhou metropolitan area from 1990 to 2015. – Urban Research 11: 13-19.

http://www.aloki.hu ● ISSN 1589 1623 (Print) ● ISSN 1785 0037 (Online)
DOI: http://dx.doi.org/10.15666/aeer/1706_1489314910

[7] Fan, N., Xie, G., Zhang, C., et al. (2012): Spatial-temporal dynamic changes of vegetation cover in Lancang River basin during 2001-2010. – Resources Science 34(7): 1222-1231.
[8] Furlanetto, L. M., Palma-Silva, C., Perera, M. B. (2018): Potential carbon gas production in southern brazil wetland sediments: possible implications of agricultural land use and warming. – Wetlands 38(3): 485-495.
[9] Gao, F., Li, G., Zhou, P., et al. (2013): Analysis on soil nutrients of tea gardens in Pu'er City of Yunnan Province. – Chinese Journal of Soil Science 44(2): 398-402.
[10] Gong, J., Hu, X., Peng, C., et al. (2010): The molecular composition and spectral properties of polysaccharide isolated from Pu-erh tea and its material. – Spectroscopy and Spectral Analysis 30(7): 1960-1964.
[11] Jaeschke, A., Rethemeyer, J., Lappe, M. (2018): Influence of land use on distribution of soil n-alkane delta D and brGDGTs along an altitudinal transect in Ethiopia: implications for (paleo) environmental studies. – Organic Geochemistry124: 77-87.
[12] Li, Y., Liang, M., Xia, L., et al. (2011): Study on soil chemical constituents of the tableland tea garden in Yunnan Province. – Chinese Agricultural Science Bulletin 2: 171-174.
[13] Liu, X., Gao, X., Gao, X., et al. (2008): Monitoring and pollution evaluation of heavy metals in the tea garden soils from main tea areas of Yunnan. – Journal of Anhui Agricultural Sciences 36(33): 14727-14728 + 14819.
[14] Martyn, A., Barvinsky, A., Tykhenko, R. (2017): Problems of conceptual apparatus in environmental economics: relationship between the systems and mechanism of land use. – Zemleustrìj, Kadastr ì Monìtorìng Zemel 17(4): 21-28.
[15] Ning, J., Zhang, Z., Gu, X., et al. (2010): Fingerprint identification method of Pu'er raw tea based on high performance liquid chromatography profiles. – Transactions of the Chinese Society of Agricultural Engineering 26(3): 243-248.
[16] Ning, J., Wan, X., Zhang, Z., et al. (2013): Discriminating fermentation degree of Pu'er tea based on NIR spectroscopy and artificial neural network. – Transactions of the Chinese Society of Agricultural Engineering 29(11): 255-260.
[17] Pavani, B. F., Sousa, J., Wilson, C., Inouye, C. E. N. (2018): Estimating and valuing the carbon release in scenarios of land-use and climate changes in a Brazilian coastal area. – Journal of Environmental Management 226: 416-427.
[18] Pu, J., Zhao, X. , Gu, Z., et al. (2018): Landscape patterns and water quality changes in Qilu Lake basin of Yunnan Plateau. – Journal of Hydroecology 5: 13-21.
[19] Tan, C., Peng, C., Gao, B., et al. (2012): Spectroscopic and structural characteristics of the main components of theabrownin in Pirerh tea. – Spectroscopy and Spectral Analysis 32(4): 1051-1056.
[20] Wang, J., Cui, B., Liu, J., et al. (2008): The effect of land use and its change on ecological risk in the Lancang River watershed of Yunnan province at the landscape scale. – Journal of Environmental Sciences 28(2): 269-277.
[21] Yi, M., Li, X., Li, Y. (2011): Physical and chemical properties of soil in Pu-erh tea farms in Yunnan Province. – Journal of Beijing Normal University (Natural Science) 47(1): 80-84.
[22] Zhai, J., Hou, P., Zhao, Z., et al. (2018): An analysis of landscape pattern spatial grain size effects in Qinghai Lake watershed. – Remote Sensing for Land & Resources 30(3): 159-166.
[23] Zhang, J., Gao, R., Hu, J., et al. (2014): Application comparison of grey correlation degree and Pearson correlation coefficient. – Journal of Chifeng University (Natural Science Edition) 30(11): 1-2.
[24] Zhang, Y., Cai, X., Yang, C., et al. (2019): Driving force analysis of landscape pattern changes in Honghu Wetland Nature Reserve in recent 40 years. – Journal of Lake Science 31(1): 171-182.

http://www.aloki.hu ● ISSN 1589 1623 (Print) ● ISSN 1785 0037 (Online)
DOI: http://dx.doi.org/10.15666/aeer/1706_1489314910

[25] Zhao, X., Liu, K., Qin, Y. (2007): Urban landscape pattern of Xi'an City based on GIS. – Chinese Journal of Ecology 5: 706-711.
[26] Zheng, L., Zhao, Y., Feng, Y. (2013): Identification of Pu'er ripe teas with different origins and fermentation years by surface-enhanced Raman spectroscopy. – Spectroscopy and Spectral Analysis 6: 1575-1580.

http://www.aloki.hu ● ISSN 1589 1623 (Print) ● ISSN 1785 0037 (Online)
DOI: http://dx.doi.org/10.15666/aeer/1706_1489314910

THE IMPACT OF SURFACE WAVE ON THE SEDIMENT EROSION AND DEPOSITION NEAR THE WELLOW RIVER MOUTH, CHINA

WANG, Z. F.[1] – CAO, X. D.[1] – LI, Q. J.[2*] – LIU, Y. L.[2]

[1]*Shandong Province Key Laboratory of Ocean Engineering, Ocean University of China Qingdao 266100, China*

[2]*Yantai Oceanic Environmental Monitoring Central Station of State Oceanic Administration Yantai 264006, China*

[*]*Corresponding author*
e-mail: lqjwainxl@126.com

(Received 19th Jun 2019; accepted 16th Oct 2019)

Abstract. In this paper, the numerical simulation of sediment erosion and siltation near the Yellow River estuary is carried out by using wave, tidal current and sediment coupling model. A fine triangular mesh is used in the pattern to improve the spatial resolution of numerical calculations. Comparing the measured water depth data with the simulation results, the result shows that the simulation results are in good agreement with the actual situation. In order to analyze the influence of waves on sediment erosion and siltation, the paper carried out wave influence experiments under four conditions: no wind, north wind, easterly wind and south wind. The experimental results show that the wave has a great influence on the erosion and siltation of the seabed in the study sea area. Under the northward wave condition, an erosion zone is distributed in the SE-NW direction, and the maximum erosion thickness is about 1.9 m. Under the eastward wave condition, the erosion zone is north-south. The maximum scouring thickness is about 1.7 m; the scouring and silting effect under the southward wave condition is relatively weak.
Keywords: *sediment movement, wind wave, tidal current, numerical simulation*

Introduction

The large amount of sediment brought by the Yellow River into the sea has changed the trend of the shoreline of the Yellow River estuary, affected the spatial and temporal distribution of the seabed erosion and siltation in the nearby sea, and affected the protection of land and ecological resources, the exploitation of offshore oil and gas, and the construction of other marine projects. The modern Yellow River delta is formed near the estuary of the Yellow River with the characteristics of short formation time, efficient sedimentation rate and loose structure which make sediments prone to be compacted and consolidate under the geo-static stress and overburden stress. It is one of the areas most susceptible land subsidence disasters in China, bringing a series of safety hazards to production and living (Liu et al., 2018).

Li et al. (2004) calculated the coastal erosion/accumulation rates from 1964 to 1976 using Landsat TM imagery. With the combination of historical data, field observations and satellite remotely sensed images, changes in Yellow River estuary since 1996 when were studied by Fan et al. (2005), mainly including water and sediment discharge from the river, tides, tidal currents, suspended sediment diffusion, coastline changes and seabed development. Liu et al. (2011) analyzed the temporal changes of water discharge and sediment load of the Yellow River into the sea based on hydrological data observed at Lijin gauging station from 1950 to 2008. Huang et al. (2018) investigated the distribution of

http://www.aloki.hu ● ISSN 1589 1623 (Print) ●ISSN1785 0037 (Online)
DOI: http://dx.doi.org/10.15666/aeer/1706_1491114926

estuarine salinity and suspended sediment by a three dimensional with numerical simulation under different flow rates. Wang et al. (2019) demonstrated that the shape and length of the Yellow River Delta coastline has changed dramatically since 1976 using the general high-tide line method, which combines remote sensing and geographic information system technology, using multi-spectral scanner, thematic mapper, and enhanced thematic mapper plus images from 1976 to 2014. Yang et al. (2017) investigated water and sediment changes by using coastline and suspended sediment concentration methods, indicate the inter-annual and intra-annual variations of the sediment concentration from 1986 to 2013.

Waves have a vitally important effect on erosion and siltation of shore beach. With the rise of coastal engineering, foreign scholars began to study the sediment movement under the action of waves, and obtained some achievements. Putting forward a variety of sediment starting formulas are mostly limited to the coarser particles of non-cohesive sediment. Because of the complexity of wave motion, the lack of understanding of the oscillating boundary layer flow caused by surface waves and the turbulent mixing mechanism inside the water body, coupled with the randomness of the sediment movement itself, brings a lot of difficulties on theoretical research about sediment movement under wave action. Xu (2003) established a multiple regression equation between the sediment flux to the sea and the influencing factors to estimate the change in the sediment flux to the sea when the influencing variables are further changed. Wang et al. (2005) use a two-dimension numerical model to reveal the tidal and wave dynamics in 2012, and conducts comparative analysis of the changes from 1996 to 2012. Kong et al. (2009) established a numerical model with the application of environmental fluid dynamics code to the Yellow River Delta. The simulation indicates that most of the sediment deposited just out of the Mouth which makes the mouth move forward into the sea 2.5 km per year. Zhan (2017) developed the novel cubic model, which used the ratio of a near-infrared band (740–900 nm) to a visible band (400–600 nm) as factors, for the retrieval of SSSC from Yellow River Estuary. Wang et al. (2019) used a three dimensional current-wave-sediment coupled model to examine the seasonal suspended sediment transport. Yao et al. (2018) developed a new multi-fractional, depth-averaged sediment transport module and embedded into a morph dynamic model for a sand-silt mixed shallow water environment. Comparisons with measurements over two successive tidal cycles indicate that the present model produces very good results on short-time scales.

Due to the complex natural environment, it is a difficult problem to simulate calculation of the sediment erosion and deposition in the sea area of the Yellow River estuary. It is of great significance and practical value to improve the accuracy and precision of sediment numerical simulation by using effective mode. The aim of this paper is to study the impact of surface wave on the sediment erosion and deposition near the Yellow River Mouth by numerical simulation method. The paper is devised into 5 sections. The section 2 is numerical simulation. The section 3 studies the tidal current characteristics and the impact of surface waves is analyzed in section 4. Finally, the conclusion is given in the section 5.

Materials and Method

Measurement data

Research area is near the Yellow River estuary, China, 37.5-38°N, 118.8-119.6°E. The position of the stations is shown in *Figure 1*.

The measured data of tidal level is selected from May 9 to 13, 2004. The measured data of tidal current is taken from May 5 to 6. And the measured data of sediment

http://www.aloki.hu ● ISSN 1589 1623 (Print) ●ISSN1785 0037 (Online)
DOI: http://dx.doi.org/10.15666/aeer/1706_1491114926

concentration is taken from May 1 to 2. Because the various elements are measured separately and the measurement time is dispersed, only the current trend is carried out the measurement of tidal current, tidal level and sediment concentration.

The data of tidal level is measured by RBR in tidal level station, and the data is recorded every 10 min. Tidal currents are measured every 1 hour. The current direction is measured in true north position. The current level of each vertical line is determined by the water depth. The three-point is adopted when the vertical depth is less than 5.0 m that is, the surface layer, the 0.6H layer and the bottom layer are observed. The six-point is adopted when the vertical depth is greater than 5.0 m that is the surface layer, 0.2H layer, 0.4H layer, 0.6H layer, 0.8H layer and the bottom layer are observed.

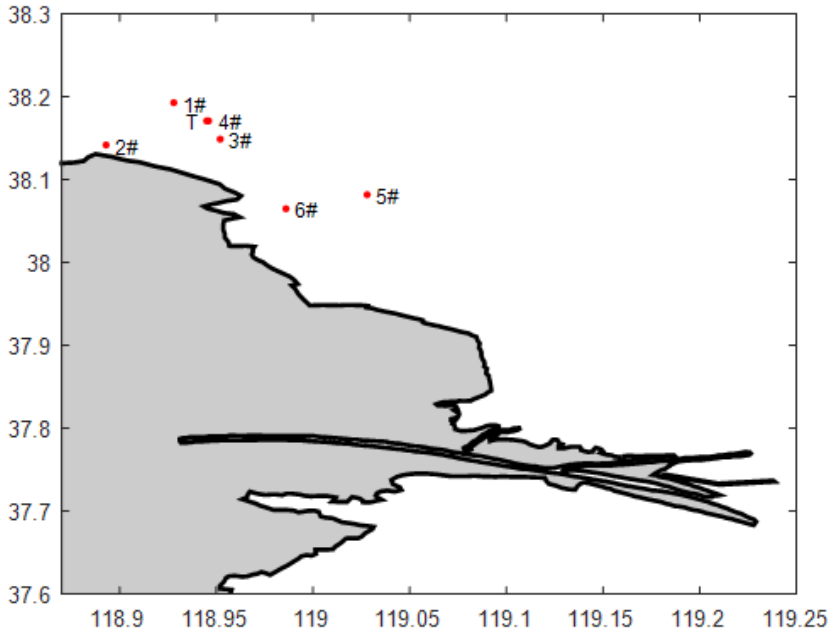

Figure 1. *The Locations of observation stations*

The specific levels are divided as follows:

- Surface layer: 0.5 ~ 1.0 m below the sea surface;
- 0.2H: 0.2×H below the sea surface;
- 0.4H: 0.4×H below the sea surface;
- 0.6H: 0.6×H below the sea surface;
- 0.8H: 0.8×H below the sea surface;

The bottom layer: 0.5 ~ 1.0 meter above the sea floor. Where H is the depth of the vertical water depth during observation, in meters.

Water depth is recorded and water sample are collected for suspended sediment analysis layer by layer when measuring the current.

According to the stratified sediment concentration measured by indoor cup-dry method and weighted by stratified current rate, the average vertical sediment concentration was calculated according to the following formula:

$$\bar{\rho} = \frac{\rho_{surface} \cdot v_{surface} + 2(\rho_{0.2} \cdot v_{0.2} + \rho_{0.4} \cdot v_{0.4} + \rho_{0.6} \cdot v_{0.6} + \rho_{0.8} \cdot v_{0.8}) + \rho_{bottom} \cdot v_{bottom}}{v_{surface} + 2(v_{0.2} + v_{0.4} + v_{0.6} + v_{0.8}) + v_{bottom}} \quad \text{(Eq.1)}$$

http://www.aloki.hu ● ISSN 1589 1623 (Print) ●ISSN1785 0037 (Online)
DOI: http://dx.doi.org/10.15666/aeer/1706_1491114926

Numerical Model

Numerical simulation is an effective method to study the sediment moment and the model in this paper has been also applied and confirmed reliable by Wang et al. (2019). The hydrodynamic model is based on the two-dimensional planar incompressible Reynolds average Navier-Stokes shallow water equation, in which the Boussinesq hypothesis and the hydrostatic pressure hypothesis are used, so that the tide surface can be more accurately Curves and tidal fluxes are simulated. The following two-dimensional depth-average shallow water equations can be obtained by integrating the horizontal momentum equation and the continuous equation in the range:

$$\frac{\partial h}{\partial t}+\frac{\partial h\bar{u}}{\partial x}+\frac{\partial h\bar{v}}{\partial y}=hS \tag{Eq.2}$$

$$\frac{\partial h\bar{u}}{\partial t}+\frac{\partial h\bar{u}^2}{\partial x}+\frac{\partial h\overline{vu}}{\partial y}=f\bar{v}h-gh\frac{\partial \eta}{\partial x}-\frac{h}{\rho_0}\frac{\partial p_a}{\partial x}-\frac{gh^2}{2\rho_0}\frac{\partial \rho}{\partial x}+\frac{\tau_{sx}}{\rho_0}-\frac{\tau_{bx}}{\rho_0}-\frac{1}{\rho_0}\left(\frac{\partial s_{xx}}{\partial x}+\frac{\partial s_{xy}}{\partial y}\right)+\frac{\partial}{\partial x}\left(hT_{xx}\right)+\frac{\partial}{\partial y}\left(hT_{xy}\right)+hu_s s \tag{Eq.3}$$

$$\frac{\partial h\bar{v}}{\partial t}+\frac{\partial h\bar{v}^2}{\partial x}+\frac{\partial h\bar{v}\bar{u}}{\partial y}=f\bar{u}h-gh\frac{\partial \eta}{\partial x}-\frac{h}{\rho_0}\frac{\partial p_a}{\partial y}-\frac{gh^2}{2\rho_0}\frac{\partial \rho}{\partial y}+\frac{\tau_{sy}}{\rho_0}-\frac{\tau_{by}}{\rho_0}-\frac{1}{\rho_0}\left(\frac{\partial s_{yx}}{\partial x}+\frac{\partial s_{yy}}{\partial y}\right)+\frac{\partial}{\partial x}\left(hT_{xy}\right)+\frac{\partial}{\partial y}\left(hT_{yy}\right)+hv_s s \tag{Eq.4}$$

Among them: the first item on the left is the local item, the second and third items are the horizontal convection items, t is the time, x and y are the Cartesian plane coordinates, d is the still water depth, η is the water level, h=η + d is the total water depth, and f is the Coriolis parameters $\bar{u}$ and $\bar{v}$ are respectively the components of the depth average flow velocity in the x and y directions, g is the acceleration of gravity, ρ is the water density.

The equations for sediment transport are following:

$$\frac{\partial \bar{c}}{\partial t}+u\frac{\partial \bar{c}}{\partial x}+v\frac{\partial \bar{c}}{\partial y}=\frac{1}{h}\frac{\partial}{\partial x}\left(hD_x\frac{\partial \bar{c}}{\partial x}\right)+\frac{1}{h}\frac{\partial}{\partial y}\left(hD_y\frac{\partial \bar{c}}{\partial y}\right)+Q_L C_L\frac{1}{h}-S \tag{Eq.5}$$

where $\bar{c}$ is the suspended sediment concentration, D_x and D_y are diffusion coefficient, Q_L is the point source emission per unit level area, C_L is point source emission concentration, S is the source of deposition or erosion.

The sedimentation rate could be expressed as

$$SD=w_s\cdot c_b\cdot p_d \tag{Eq.6}$$

where w_s is the sedimentation velocity; c_b is the bottom sediment concentration; p_d is the settlement probability.

http://www.aloki.hu ● ISSN 1589 1623 (Print) ●ISSN1785 0037 (Online)
DOI: http://dx.doi.org/10.15666/aeer/1706_1491114926

In the case of limited water depth, the fluctuation velocity of water quality points can be expressed by the following formula:

$$u = \frac{\pi H}{T} \frac{\cosh[k(z+h)]}{\sinh kh} \cos(kx - \sigma t) \quad \text{(Eq.7)}$$

$$v = \frac{\pi H}{T} \frac{\sinh[k(z+h)]}{\sinh kh} \sin(kx - \sigma t) \quad \text{(Eq.8)}$$

In the formula, k is wave number, σ is angular frequency, t is time, h is water depth, L is wavelength, u and v *r*epresent horizontal and vertical velocity of fluctuating water quality points.

The equation of unbalanced transport of suspended sediment under the combined action of tidal current and wave can be expressed as follows:

$$\frac{\partial(hS)}{\partial t} + \frac{\partial[hS(U_c + U_w)]}{\partial x} + \frac{\partial[hS(V_c + V_w)]}{\partial y} - \varepsilon_S h(\frac{\partial^2 S}{\partial x^2} + \frac{\partial^2 S}{\partial y^2}) + aw(S - S_*) = 0 \quad \text{(Eq.9)}$$

where S is sediment content, S_* *i*s sediment carrying capacity of current, ε_s is sediment diffusion coefficient, σ is recovery saturation coefficient, w is sediment settling velocity.

The reciprocating sediment transport process of waves is generally reflected in a tidal current cycle (half a day or one day). Because the wave period is relatively small (usually only a few seconds, the wave height greater than 10 seconds in the sea area near the Yellow River Estuary is very rare), the tidal current cycle is relatively large. Therefore, as long as the calculated time step is much longer than the wave period (e.g. more than 200 seconds for dt), the transport equation can be averaged in time. When a wave particle rotates elliptically or circularly, its average velocity in the wave period is equal to zero, and it is also zero when the time step is longer than the wave period, so only the current tide velocity is considered. The results of the above equation are as follows:

$$\frac{\partial(hS)}{\partial t} + \frac{\partial(hSU_c)}{\partial x} + \frac{\partial(hSV_c)}{\partial y} - \varepsilon_S h(\frac{\partial^2 S}{\partial x^2} + \frac{\partial^2 S}{\partial y^2}) + aw(S - S_*) = 0 \quad \text{(Eq.10)}$$

Because the imbalanced transport of suspended sediment causes the erosion and siltation of the seabed, the deformation equation can be expressed as follows:

$$\frac{\partial(hS)}{\partial t} + \frac{\partial(hSU_c)}{\partial x} + \frac{\partial(hSV_c)}{\partial y} - \varepsilon_S h(\frac{\partial^2 S}{\partial x^2} + \frac{\partial^2 S}{\partial y^2}) + \gamma \frac{\partial \eta}{\partial t} = 0 \quad \text{(Eq.11)}$$

Among them, γ is the dry density of sediment deposited on the seafloor, η is the change of the thickness of the seafloor, h is the erosion and siltation.

It can be seen from the above that when calculating the sediment erosion and siltation changes in estuaries and coasts on a large time scale, the short-period wave flow field is not needed to be taken into account, and only the effect of tidal current is considered. However, it cannot be concluded that the effect of wave on erosion and siltation can be time-averaged, because the wave will affect the sediment carrying capacity of seawater.

http://www.aloki.hu ● ISSN 1589 1623 (Print) ●ISSN1785 0037 (Online)
DOI: http://dx.doi.org/10.15666/aeer/1706_1491114926

Results

Model validation

The Yellow River Delta locates in the Bohai Sea, which is a shallow semi-enclosed sea that exchanges with the Yellow Sea through the Bohai Strait between Shan Dong and Liao Dong Peninsulas. The topography datasets used in this paper are shown in *Fig. 2*. The modeling range includes the whole of the Bohai Sea (*Fig. 2a*). The triangular mesh is adopted with the resolution 5 km at the open boundary and 700 m at Yellow River Delta nearshore. The model domain is 117.5°E-122.5°E, 37°N-41°N (*Fig. 2b*). On the open boundary the amplitudes and phases of the four main tidal constituents (M_2, S_2, K_1, O_1) are used as the surface elevation forcing on the open boundaries. At the lateral land boundary, a condition of no normal flux is applied to velocity.

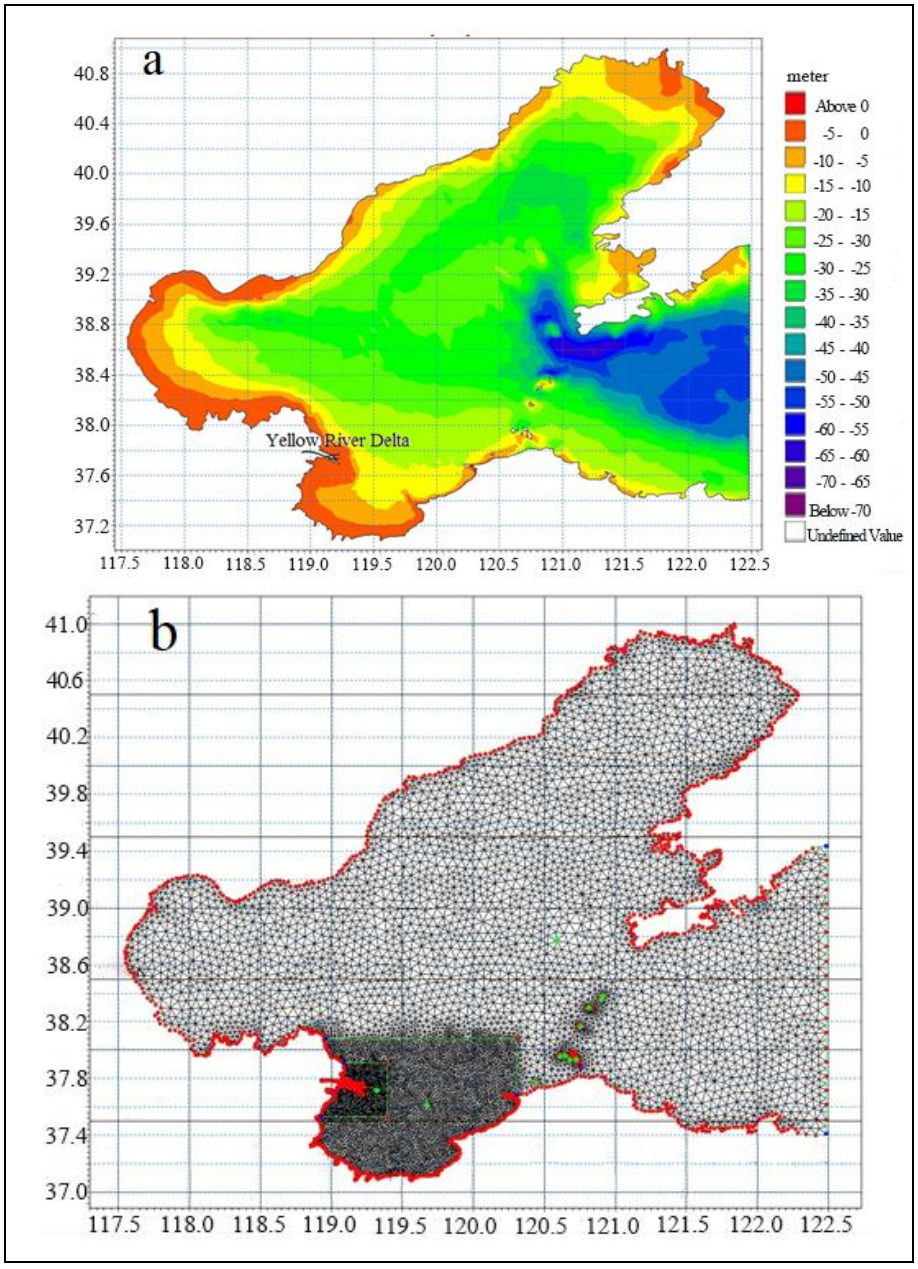

Figure 2. *The topography of Bohai Sea (a) and the model grid (b)*

http://www.aloki.hu ● ISSN 1589 1623 (Print) ●ISSN1785 0037 (Online)
DOI: http://dx.doi.org/10.15666/aeer/1706_1491114926

The measured data of tidal level, tidal current and sediment concentration are collected. The distribution of station positions is shown in *Table 1*. The tidal level, tidal current and sediment concentration in May 2004 were simulated and compared with the measured data. The results are shown from *Figure 3* to *Figure 5*. The comparison shows that it is reasonable to use this model to simulate the hydrodynamic and sediment scouring in the sea near the Yellow River Mouth.

Table 1. *Locations of observation stations*

No.	Longitude	Latitude	Elements
T	118°56.733′	38°10.233′	Tidal Level
1#	118°55.650′	38°11.600′	Tidal Currents
2#	118°53.553′	38°8.547′	Tidal Currents
3#	118°57.100′	38°8.933′	Tidal Currents
4#	118°56.733′	38°10.233′	Tidal Currents
5#	119°01.685′	38°04.909′	Tidal Currents and Sediment
6#	118°59.200′	38°3.920′	Tidal Currents and Sediment

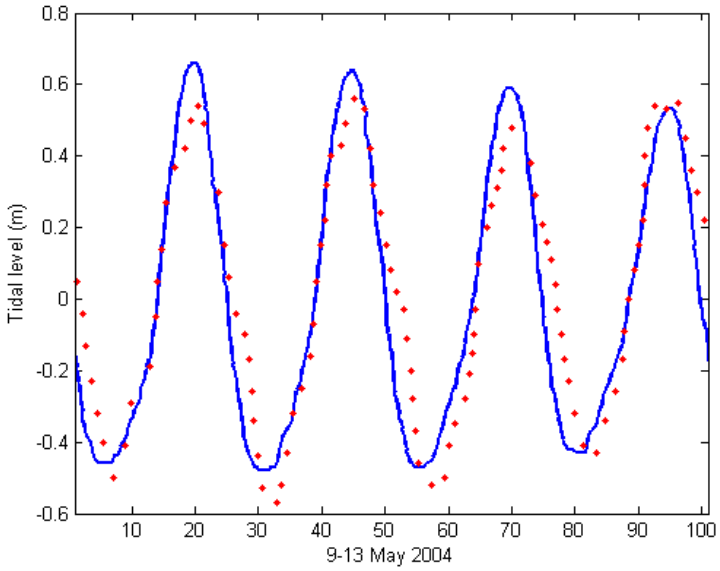

Figure 3. *Comparison of observation tidal level (red dot) and simulation result (blue line)*

The accuracy of the model is estimated by the average absolute error. The average absolute error is calculated as follows:

$$AMEAN = \frac{1}{N}\sum_{i=1}^{N}\left|X_{\text{mod}}^{i} - X_{obs}^{i}\right| \qquad \text{(Eq.12)}$$

Where N is the number of observing stations, X_{mod}^{i} is the value of the mode result interpolated to the i-th station, X_{obs}^{i} is the measured value of the i-th observatory.

The average absolute error of each element of each measurement point is shown in *Table 2*.

http://www.aloki.hu ● ISSN 1589 1623 (Print) ●ISSN1785 0037 (Online)
DOI: http://dx.doi.org/10.15666/aeer/1706_1491114926

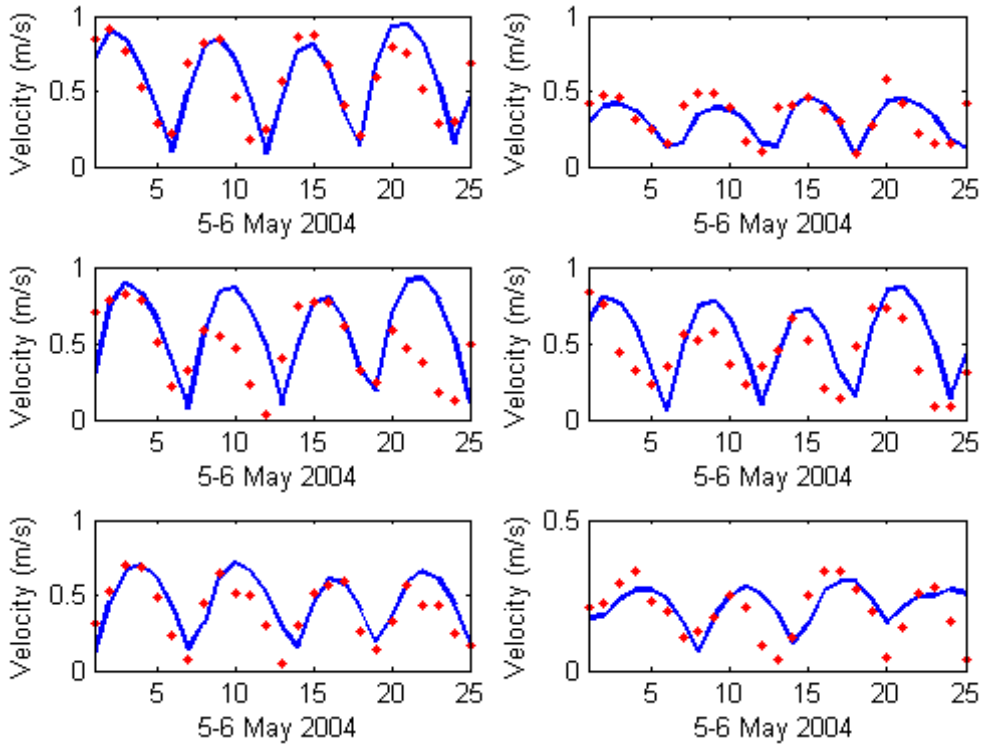

Figure 4a. *Comparison of observation tidal current velocity (red dot) and simulation result (blue line)*

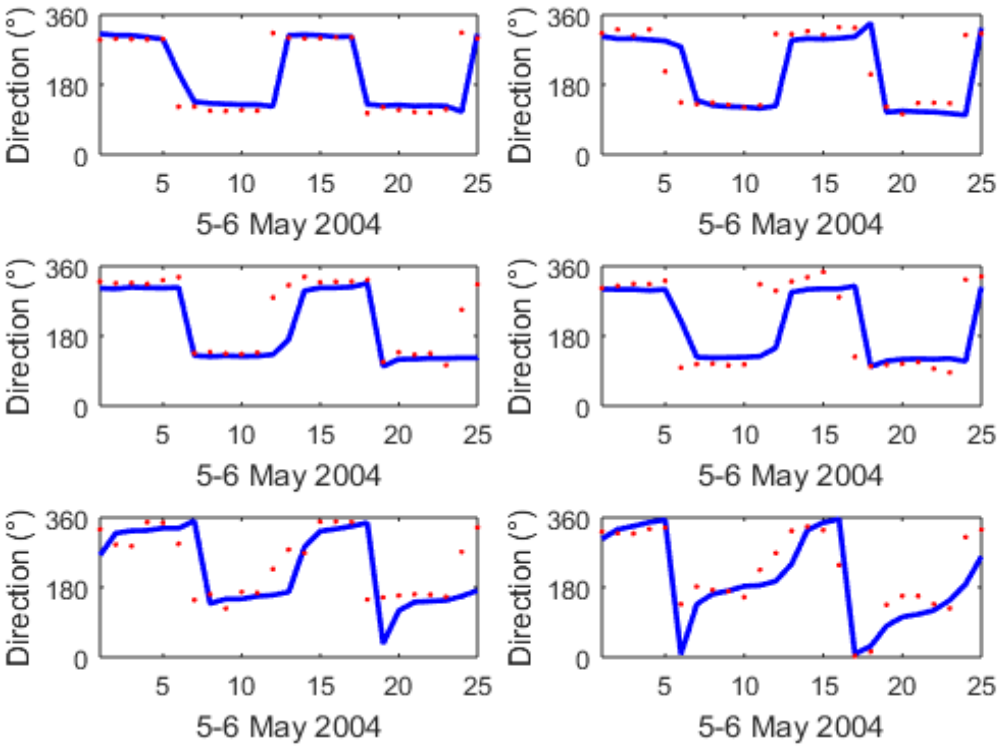

Figure 4b. *Comparison of observation tidal current direction (red dot) and simulation result (blue line)*

http://www.aloki.hu ● ISSN 1589 1623 (Print) ●ISSN1785 0037 (Online)
DOI: http://dx.doi.org/10.15666/aeer/1706_1491114926

Tidal current characteristics

Figure 6 shows the flow field diagram from May 5 to 6, 2004. Overall, the results calculated by the model basically reflect the state of the measured flow rate. The tide of studying the sea area is a regular semidiurnal tide. The tidal waves entering the Bohai Sea are affected by the semi-closed bay form, forming complex rotating tidal waves. During the flood tide, the direction of the tidal current moves from north to south, forming a large clockwise vortex in the east and south sea areas of the old Yellow River estuary and then flowing to the western and central sea areas of Laizhou Bay. During the ebbtide, the sea in the southern part of the old Yellow River estuary (west of Laizhou Bay) was rotated counterclockwise and transported northward. The study of the ebbtide of the sea area lasts longer than the flood tide, and the average flow rate of the ebb tide is greater than the average flow rate of the flood trend, showing an imbalance of fluctuations in the current flow.

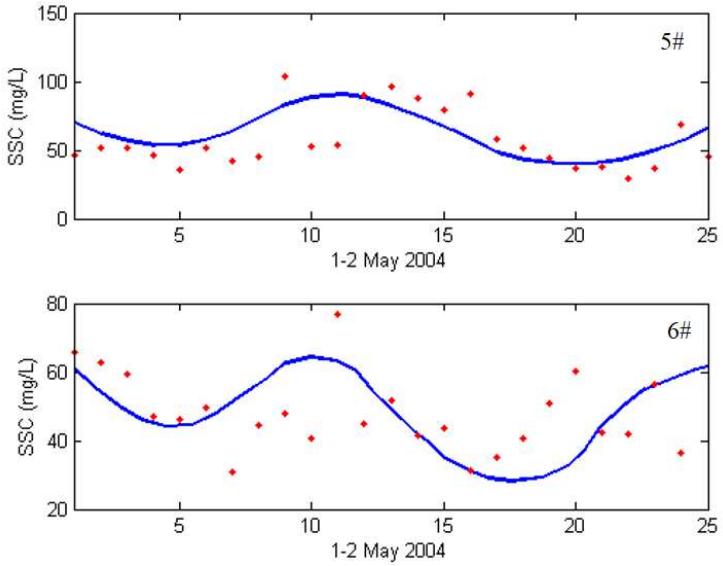

Figure 5. *Comparison of observation sediment concentration (red dot) and simulation result (blue line)*

Table 2. *The mean absolute error of simulation and observation*

T	0.11	-	-	-
1#	-	0.13	10.9	-
2#	-	0.09	14.8	-
3#	-	0.24	13.9	-
4#	-	0.20	19.0	-
5#	-	0.11	22.1	14.9
6#	-	0.07	20.1	11.0

Figure 7 shows the maximum flow velocity distribution of the study sea area in a full tide in May 2004. The contour of the northern Yellow River estuary is basically parallel to the shoreline. The flow velocity is from 0.5 m/s increased to 1 m/s in the 2-15 m isobath. In the southeast direction of the old Yellow River estuary, the maximum flow velocity

http://www.aloki.hu ● ISSN 1589 1623 (Print) ●ISSN1785 0037 (Online)
DOI: http://dx.doi.org/10.15666/aeer/1706_1491114926

increases rapidly from 0.5 m/s, forming a high value zone with a maximum flow velocity of 1.4 m/s. According to historical data, there are two large flow velocity areas in the Yellow River estuary, one of which is in the southeast of Laohekou. The maximum possible flow velocity is 1.8 m/s.

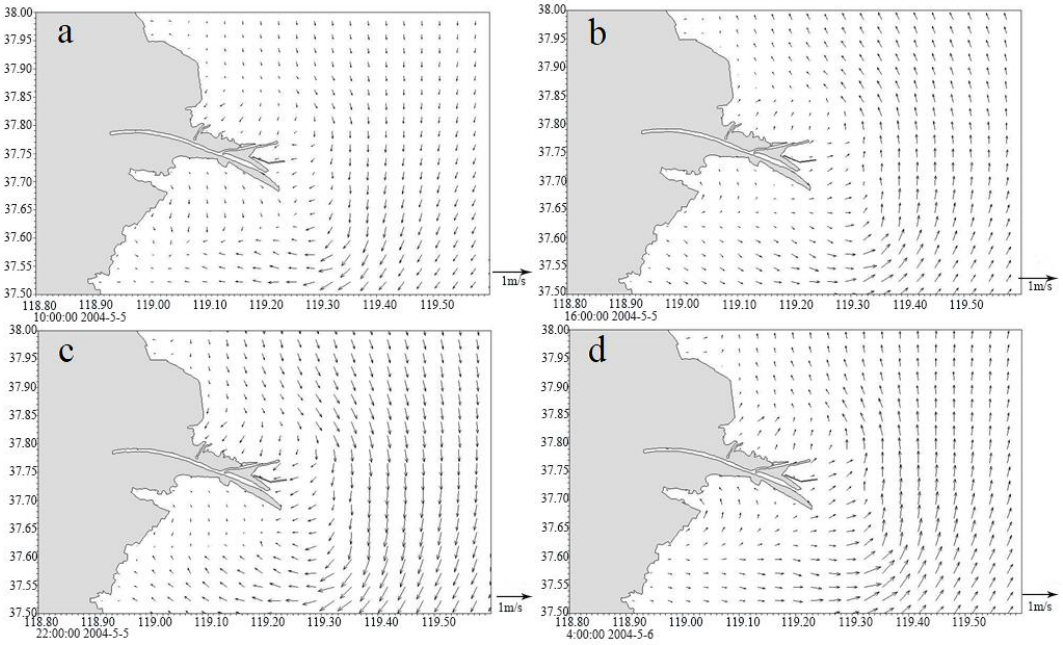

Figure 6. *Distribution of tidal current during 10:00 5th - 4:00 6th May 2004*

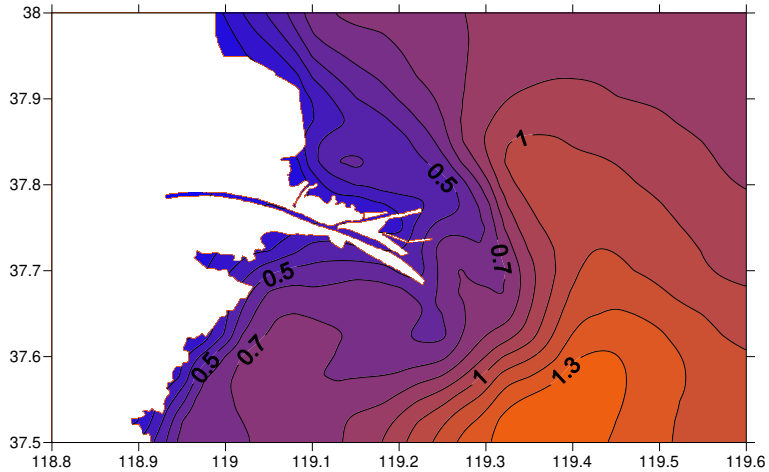

Figure 7. *Maximum velocity distribution (m/s) of the study sea area*

Sediment movement influenced by tidal current

Under the influence of no waves, sediment movement is mainly affected by the trend. The numerical simulation of suspended load concentration and sedimentation and siltation in the absence of wind is shown in *Figure 8*. The northern part of the sea is affected by sediment from the Yellow River and is weakly silted. The concentration of

http://www.aloki.hu ● ISSN 1589 1623 (Print) ●ISSN1785 0037 (Online)
DOI: http://dx.doi.org/10.15666/aeer/1706_1491114926

suspended load is generally 0.6 kg/m3, and the southern part is scouring. In the strong tidal zone in the southeast of the old Yellow River estuary, the scouring is the strongest.

Without considering the influence of waves, the stability of the particles is actually mainly controlled by the water pressure of the film and the adhesion between the particles and the performance of gravity is not dominant. From this point of view, in the absence of waves, the finer the sediment particles, the more difficult it is to reach the conditions of suspension. It can be seen that the effect of waves on the sediment, especially the fine sediment, is more obvious. The waves in the Yellow River estuary are basically wind and waves. Although the average wave energy intensity is not large, due to the fine sediment of the Yellow River underwater delta, the levitation force of the waves on the seabed sediment is relatively large.

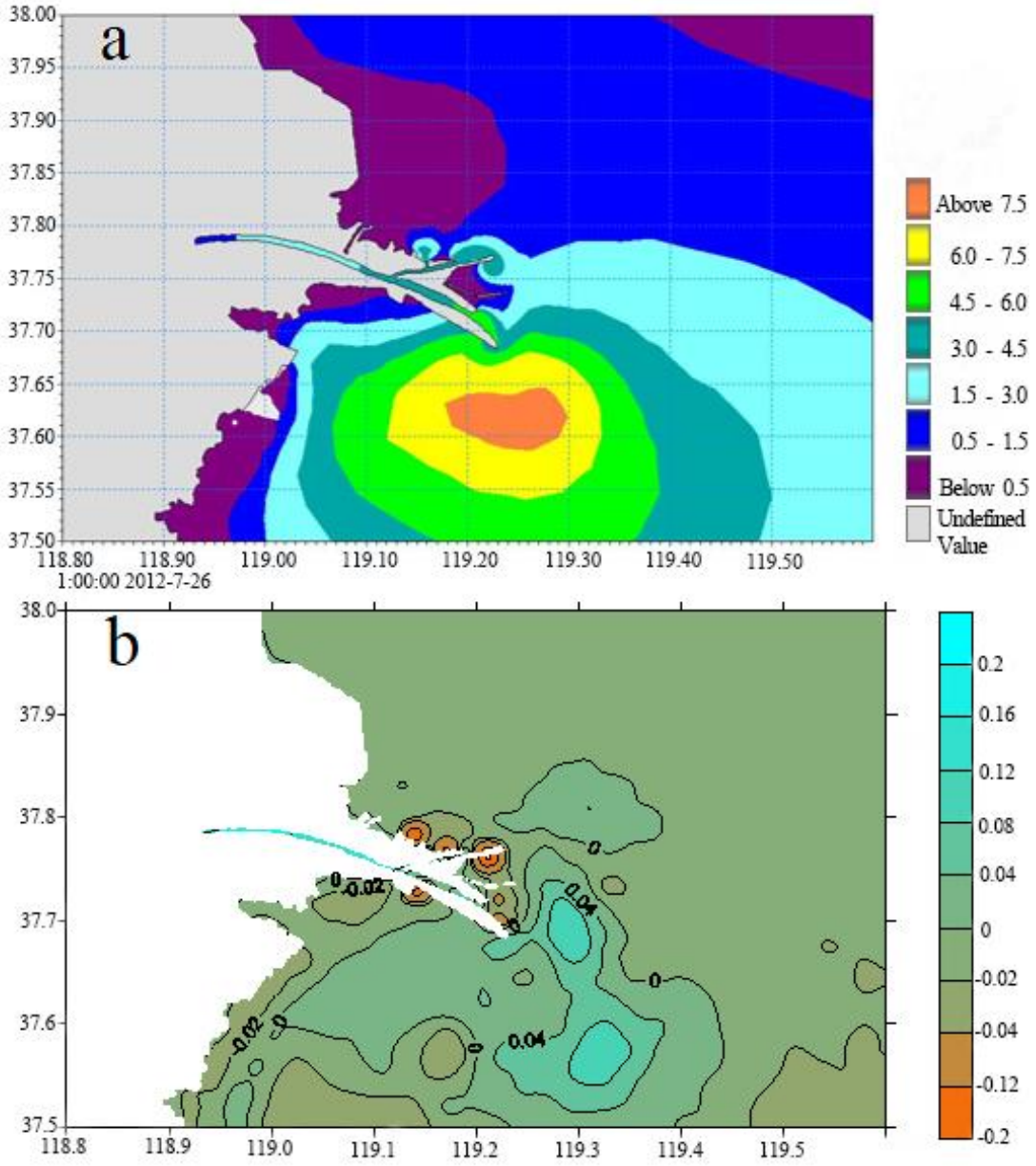

Figure 8. *Distribution of suspended load concentration (a) and distribution of scouring and silting under no-wave action (b, unit: m, positive value is scouring)*

http://www.aloki.hu ● ISSN 1589 1623 (Print) ●ISSN1785 0037 (Online)
DOI: http://dx.doi.org/10.15666/aeer/1706_1491114926

Discussion

Zhang (2011) examined coastline changes in the Modern Yellow River delta in China on the basis of remote sensing and GIS techniques, the Landsat data obtained in 1987, 1996, and 2008. Peng et al. (2010) found that the water discharge and sediment load into the sea were decreasing from 1950 to 2007 with serious fluctuation at Lijin. Cui et al. (2011) extract mean high tide lines of the Yellow River estuary from 1976 to 2005, and explored relationships between the accretion–erosion of land and the runoff and sediment load of the Yellow River. Li et al. (2010) diagnosed the effects of different hydrodynamic factors on the transport of suspended sediment discharged from the Yellow River in the Bohai Sea. Peng et al. (2013) analyzed temporal and spatial evolution of coastline and subaqueous geomorphology in muddy coast of the Yellow River Delta based on measured data of coastline and bathometry.

The coast near the Yellow River estuary is mucky, and the sediment movement is generally dominated by the suspended load. The waves cause the sediment to enter a suspended state, and even if the suspended load is superimposed with the velocity of the smaller water, a large amount of sediment transport will occur. Studies have shown that, without considering the influence of waves, the stability of particles is actually mainly controlled by the water pressure of the film and the adhesion between particles, and the performance of gravity is not dominant. From this point of view, in the absence of waves, the finer the sediment particles, the more difficult it is to reach the conditions of suspension. It can be seen that the effect of waves on the sediment, especially the fine sediment, is more obvious. The waves in the Yellow River estuary are basically wind and waves. Although the average wave energy intensity is not large, due to the fine sediment of the Yellow River underwater delta, the levitation force of the waves on the seabed sediment is relatively large.

Impact of north wave

The north wind in the research area is the strongest, the north wind is the least in summer and the most in spring, autumn, and winter. The average wind speed is 12.3 m/s, and it is stronger at sea. In the cold wave wind on March 3-5, 2007, the average wind speed at sea reached 9-10, and the extreme wind speed is 21.5 m/s. Therefore, in this compromise, the wind speed of the north wind is designed to be 18 m/s and the direction is straight north.

In the process of northbound wind, 2.3 m waves can be formed in the sea near the Yellow River estuary, and the suspended sediment concentration reaches 13 kg/m^3, 20 times higher than that in the case of no waves. Under the influence of northbound waves, the east sea area of Laohekou river presents scour on the whole. There are two high value centers in the northeast and southeast, and the maximum net scour value is up to 1.8m. Inshore waves are small, and the sand-lifting capacity of waves is weak, showing weak deposition of about 0.2 m. The wave action in the new and old Yellow River estuary is mainly reflected by erosion. Erosion in the old Yellow River estuary is caused by both waves and currents.

The distribution of wave field under the action of northbound wind, the distribution of suspended sediment concentration under northbound wave action, the distribution of erosion and deposition under the influence of north waves and the change of scour and silt caused by the north wind waves are shown in *Figure 9*.

http://www.aloki.hu ● ISSN 1589 1623 (Print) ●ISSN1785 0037 (Online)
DOI: http://dx.doi.org/10.15666/aeer/1706_1491114926

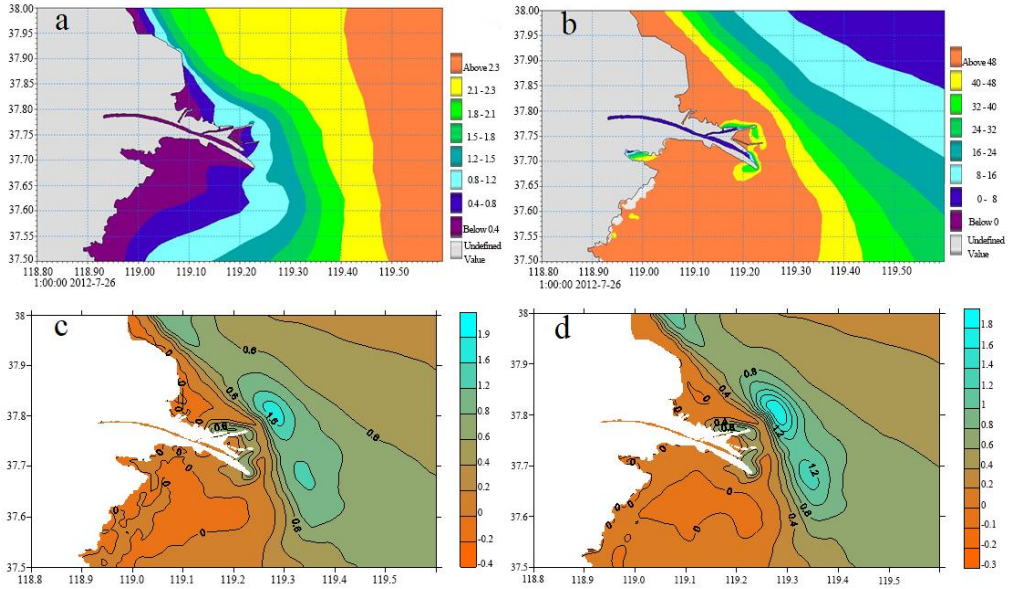

Figure 9. *a Distribution of wave field under the action of northbound wind (significant wave height, m), b Distribution of suspended sediment concentration under northbound wave action, c The distribution of erosion and deposition under the influence of north waves (m, positive for scour) d The change of scour and silt caused by the north wind waves (m, positive for scour)*

Impact of east wave

Under the influence of monsoon climate, the sea area is mainly dominated by south wind and north wind, and the direction is mostly east, forming southeast wind or northeast wind. In a year, 17 out of 33 north wind processes occur in the form of northeast wind, and the average wind is between north wind and south wind. At 21 o 'clock on October 11, 2003, affected by the typhoon, the wind speed of easterly wind increased to 20 m/s and then slowly decreased, and the extreme value is smaller than the maximum value of northerly wind. Therefore, the wind speed of easterly wind is designed to be 15 m/s.

The east wind formed a wave of 2 m in the research area, and the suspended sediment concentration at the depth of 10 m reached 10 kg/m^3, which is 16 times the concentration without waves. The distribution of net scour and silt under the influence of eastbound waves is similar to that of northbound waves, but the scour zone located in the east of the estuary has a smaller scope and intensity, and the net wave erosion depth is 1.7 m, while the direction of scour zone also changes to north-south direction.

The distribution of wave field under the action of eastbound wind, the distribution of suspended sediment concentration under eastbound wave action, the distribution of erosion and deposition under the influence of east waves and the change of scour and silt caused by the east wind waves are shown in *Figure 10*.

Impact of south wave

In the process of the south wind, sea and land breeze wind speed difference is small, the mouth observed port south winds only 3 times a year, with an average of 11.6 m/s, maximum value is 15.6 m/s, appeared in the July 29, 2006, considering the south wind frequency is low, the aerodynamic probability is less, so take the average wind speed for reference, the design wind speed 11.6 m/s, and set this direction due south.

http://www.aloki.hu ● ISSN 1589 1623 (Print) ●ISSN1785 0037 (Online)
DOI: http://dx.doi.org/10.15666/aeer/1706_1491114926

The south wind process can generate 1 m waves, and the suspended sediment concentration at 10 m reaches 2.7 kg /m^3, which is four times larger than the suspended sediment concentration under no wind condition. Compared with northbound and eastbound waves, southbound waves have weak erosion capacity, with maximum erosion thickness of less than 1 m.

The distribution of wave field under the action of southbound wind, the distribution of suspended sediment concentration under southbound wave action, the distribution of erosion and deposition under the influence of south waves and the change of scour and silt caused by the south wind waves are shown in *Figure 11*.

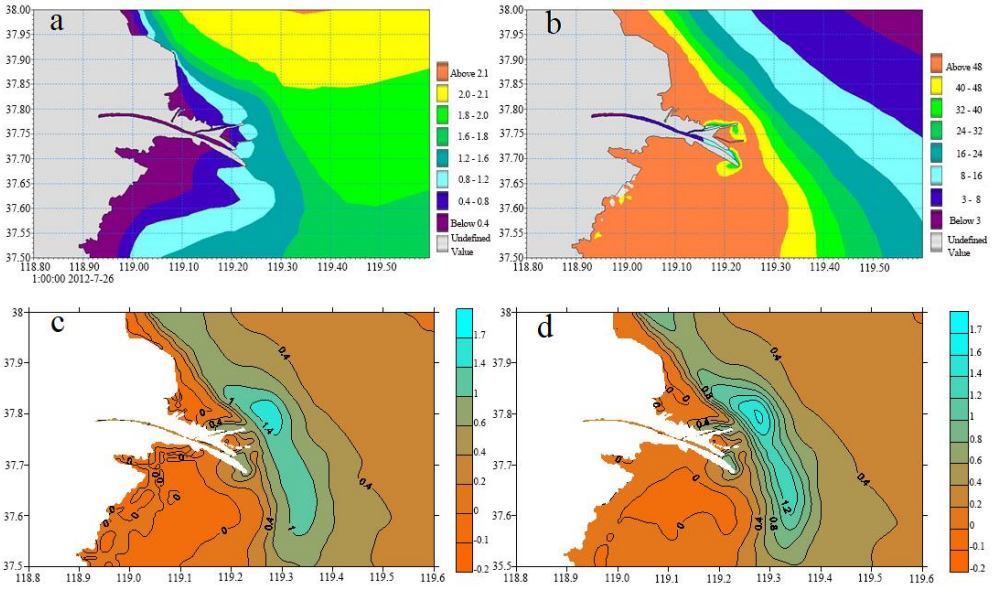

Figure 10. *Same like Fig. 9 but under east wave conditions*

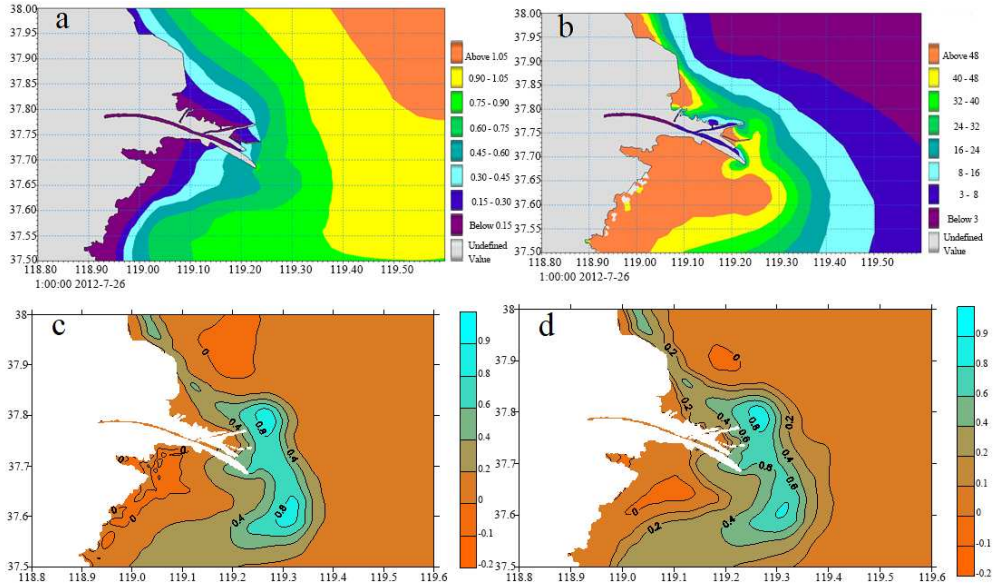

Figure 11. *Same like Fig. 9 but under south wave conditions*

http://www.aloki.hu ● ISSN 1589 1623 (Print) ●ISSN1785 0037 (Online)
DOI: http://dx.doi.org/10.15666/aeer/1706_1491114926

Conclusion

Sediment movement is influenced by runoff, tide, wave, sediment particle size, cumulative siltation area and the specific gravity and composition of the sediment. Wave is an important dynamic factor in the process of erosion and deposition of sediment, which plays an important role in the transport of river sediment into the sea, the re-suspension of seabed sediment and the formation of delta coast.

The suspended sediment concentration in the wave action is much higher than the concentration of the tidal current. The sediment concentration is 20, 16 and 4 times of that without wind wave under north, east and south wind condition respectively. The resuspension is strongest under north wind condition and weakest under south wind condition. The erosion is very strong at the north side slope of Yellow River influenced by north and east waves, and the erosion is relative weak at the south side.

The erosion of the shallow sea floor by waves is very obvious. Wind and waves cause strong scour zone to the east of the estuary. Under the condition of northbound waves, the scour zone is distributed in SE-NW direction, with the maximum scour thickness of 1.9 m. Under easterly wave condition, the scour range is more intense, and the scour zone shows a north-south trend, with the maximum scour thickness up to 1.7 m. The scour and silting action of southward wave is weak.

Acknowledgements. This work is financially supported by the National Key R&D Program of China (2018YFB0504904), National Natural Science Foundation of China (51779236) and Open Fund of Shandong Province Key Laboratory of Ocean Engineering.

REFERENCES

[1] Cui, B. L., Li, X. Y. (2011): Coastline change of the yellow river estuary and its response to the sediment and runoff (1976–2005). – Geomorphology 127(1-2): 0-40.

[2] Fan Hui, Haijiun, H. (2005): Changes in huanghe (yellow) river estuary since artificial re-routing in 1996. – Chinese Journal of Oceanology and Limnology 23(3): 299-305.

[3] Huang, S., Yin, X., Zhao, X. (2018): The effects of saltwater intrusion on suspended sediment movement in estuary. – IOP Conference Series: Earth and Environmental Science 121: 052012.

[4] Kong, Q. R., Jiang, C. B., Qin, J. J., Guo, B. (2009): Sediment transportation and bed morphology reshaping in yellow river delta. – Science in China 52(11): 3382-3390.

[5] Li, A., Li, G. X., Cao, L. H., Zhang, Q. D., Deng, S. G. (2004): The coastal erosion and evolution of the yellow river delta abandoned lobe. – Journal of Geographical Sciences 14(4): 465-472.

[6] Li, G., Xue, X., Liu, Y., Wang, H., Liao, H. (2010): Diagnostic experiments for transport mechanisms of suspended sediment discharged from the yellow river in the bohai sea. – Journal of Geographical Sciences 20(1): 49-63.

[7] Liu, F., Chen, S., Peng, J., Chen, G. (2011): Temporal variability of water discharge and sediment load of the yellow river into the sea during 1950-2008. – Journal of Geographical Sciences 21(6): 1047-1061.

[8] Liu, X., Liu, J., Feng, X. (2018): Inversion and Prediction of Consolidation Settlement Characteristics of the Fluvial Sediments Based on Void Ratio Variation in the Northern Modern Yellow River Subaqueous Delta, China. – Oceanic and Coastal Sea Research 17(3): 545-554.

http://www.aloki.hu ● ISSN 1589 1623 (Print) ●ISSN1785 0037 (Online)
DOI: http://dx.doi.org/10.15666/aeer/1706_1491114926

[9] Peng, J., Chen, S. L. (2010): Response of delta sedimentary system to variation of water and sediment in the Yellow River over past six decades. – Journal of Geographical Sciences 20(04): 613-627.
[10] Peng, J., Ma, S., Chen, H., Li, Z. (2013): Temporal and spatial evolution of coastline and subaqueous geomorphology in muddy coast of the yellow river delta. – Journal of Geographical Sciences 23(3): 490-502.
[11] Peng, Y., Su, M., Wang, Z. B., van Rijn, L. C., Zhang, C. K., Stive, M. J. F. (2018): Modelling tidal-induced sediment transport in a sand-silt mixed environment from days to years: Application to the Jiangsu coastal water, China. – Coastal Engineering 141: 86-106.
[12] Wang, N., Li, G. X., Xu, J. S., Qiao, L., Dada, O. A., Zhou, C. (2005): The Marine Dynamics and Changing Trend off the Modern Yellow River Mouth. – Journal of Ocean University of China 14(03): 433-445.
[13] Wang, K. F. (2019): Evolution of yellow river delta coastline based on remote sensing from 1976 to 2014, China. – Chinese Geographical Science 29(02): 3-13.
[14] Wang, N., Qiao, L., Li, G., Zhong, Y., Song, D., Ding, D., Gao, F., Ji, F. Y. (2019): Numerical study on seasonal transportation of the suspended sediments in the modern yellow river mouth effected by the artificial water and sediment regulation. – Journal of Ocean University of China 18(1): 20-30.
[15] Xu, J. X. (2003): Sediment flux to the sea as influenced by changing human activities and precipitation: example of the yellow river, China. – Environmental Management 31(3): 0328-0341.
[16] Yang, H. B., Li, E. C., Zhao, Y., Liang, Q. H. (2017): Effect of water-sediment regulation and its impact on coastline and suspended sediment concentration in yellow river estuary. – Water Science and Engineering S1674237017301084.
[17] Zhan, C., Yu, J. B., Wang, Q., Li, Y. Z., Zhou, D., Xing, Q. H., Chu, X. J. (2017): Remote Sensing Retrieval of Surface Suspended Sediment Concentration in the Yellow River Estuary. – Chinese Geographical Science 27(06): 934-947.
[18] Zhang, Y. (2011): Coastal environmental monitoring using remotely sensed data and GIS techniques in the modern yellow river delta, China. – Environmental Monitoring & Assessment 179(1-4): 15-29.

http://www.aloki.hu ● ISSN 1589 1623 (Print) ●ISSN1785 0037 (Online)
DOI: http://dx.doi.org/10.15666/aeer/1706_1491114926

PHENOTYPIC AND GENOTYPIC CHARACTERIZATION OF *PSEUDOMONAS SAVASTANOI* PV. *SAVASTANOI* CAUSING OLIVE KNOT DISEASE IN TURKEY

BASIM, H.[1*] – BASIM, E.[2] – ERSOY, A.[3]

[1]*Department of Plant Protection, Akdeniz University, Antalya, Turkey*

[2]*Department of Organic Agriculture, Akdeniz University, Antalya, Turkey*

[3]*Antalya Directorate of Agricultural Quarantine, Antalya, Turkey*

**Corresponding author*
e-mail: hbasim@akdeniz.edu.tr; phone: +90-242-310-2432; fax: +90-242-227-4564

(Received 20th Jun 2019; accepted 16th Oct 2019)

Abstract. Olive knot disease caused by *Pseudomonas savastanoi* pv. *savastanoi* (*Psv*) is one of the major diseases influencing olive (*Oleae europaea* L.) production in Turkey. The disease incidence rate was found to range between 4 and 80% according to the 2015 and 2018 surveys. A total of 67 isolates were recovered from 7 symptomatic Turkish olive cultivars on a semi-selective medium, PVF-1, and then identified as *Psv* by biochemical and molecular tests. The isolates produced characteristic gall symptoms on olive plants and were consistently re-isolated. Fatty acid methyl ester (FAME) analysis indicated that the major fatty acid components were oleic acid (18:1), palmitoleic acid (16:1), and palmitic acid (16:0), and also clustered the olive strains into 2 groups. The repetitive element palindromic PCR (rep-PCR) primer, the BOXA1R primer, produced the discriminatory profile, with amplicon sizes ranging from ~ 200 bp to 2 kb, and categorized the olive strains into 2 separate groups. Pulsed-Field Gel Electrophoresis (PFGE) differentiated the olive *Psv* isolates into 3 discrete haplotype groups after the genomic DNA was digested with *Spe*I. This is the first study using PFGE to determine the genetic diversity of the *Psv* olive population.
Keywords: *FAME, Rep-PCR, olive knot, PFGE, Psv*

Introduction

The olive tree (*Olea europaea* L.) is a standout amongst the most significant and transcendent organic product trees found in western and focal Italy and Spain, southern Morocco and Tunisia, and western Turkey, and Greece (Loumou and Giourga, 2003). It serves as a source of edible fruit and oil for millions of people in various parts of Turkey. At present, global olive oil production exceeds 2,500,000 tons. In 2015, the aggregate production by the member states of the International Olive Oil Council (IOC) was 2,964,500 tons, 94% of the global production. EU production was 2,322,000 tons, whereas the individual IOC member state production showed Spain to be leading with 1,401,600 tons, followed by Italy with 474,600 tons, and then by Greece with 320,000 tons. Turkey produced 143,000 tons, Tunisia 140,000 tons, Morocco 130,000 tons, Algeria 83,500 tons, and Iran 5,000 tons (International Olive Oil Council, 2015). Olive knot disease is perhaps the earliest plant disorder to be specifically reported in ancient times, and is regarded as one of the most critical diseases that affects olive trees.

Olive knot disease is characterised by the production of hyperplastic galls on several plant parts (Nester and Kosuge, 1981). The disease is a serious threat to olive production in the Mediterranean basin, including Turkey, where several climatic conditions including rain, wind, humidity, and temperature favour pathogen

http://www.aloki.hu ● ISSN 1589 1623 (Print) ● ISSN 1785 0037 (Online)
DOI: http://dx.doi.org/10.15666/aeer/1706_1492714944

dissemination, growth, development, and infection processes. In Turkey, the disease is known to be infect olive (*Olea* sp.), oleander (*Nerium oleander*), fontanesia (*Fontanesia phillyreoides*), myrtle (*Myrtus communis*), and jasmine (*Jasminium officinale*) in Çanakkale, Muğla, Antalya, Samsun, Şanlıurfa, Bursa, Izmir, Tekirdağ, Adana, Mersin, and Hatay provinces (Basım and Ersoy, 2000; Tatlı and Benlioğlu 2004; Kavak and Üstün 2009; Mirik et al., 2011).

The development of olive knots relies on the ability of *Psv* to synthesise and secrete cytokinins and indolacetic acid (IAA) (Surico et al., 1985; Perez-Martínez et al., 2007; Quesada et al., 2010) as well as the functionality of its Type Three Secretion System (Sisto et al., 2004; Perez-Martinez et al., 2010; Tegli et al., 2011). Moreover, the capacity of *Psv* to actuate olive knot arrangement depends on the quorum sensing intercellular communication system moderated by N-acyl homoserine lactone (Hosni et al., 2011). The disease affects the yield and vegetative parts of the olive plants, and quality of olive oil (Schroth et al., 1973).

Members of *P. syringae,* including *Psv*, have been previously identified based on plasmid fingerprints (King, 1989), fatty acid fingerprinting (Stead, 1992), and analysis of protein (Van Zyl and Steyn, 1990). Recently, DNA profiling techniques such as Restriction Fragment Length Polymorphism (RFLP) (Manceau and Horvais, 1997), Amplified Fragment Length Polymorphism (AFLP), (REP)-REP1-1/REP2-1 (Sharples and Lioyd, 1990), Enterobacterial Repetitive Intergenic Consensus (ERIC)-ERIC1R/ERIC2 (Hulton et al., 1991), and BOXA1R (Louws et al., 1994), Randomly Amplified Polymorphic DNA (Krid et al., 2009), Pulsed-field gel electrophoresis (PFGE) (Chu et al., 1986), Multi Locus Sequence Typing (MLST) analysis of housekeeping genes (Berge et al., 2014), and a set of primers (Guilbaud et al., 2016) have been applied in genotyping and investigating strains and pathovars of *P. syringae*. The whole genome of *Psv* has also been sequenced and annotated (Rodriguez-Palenzuela et al., 2010). Although there are reports of the presence and identification of *Psv* in west Mediterranean region of Turkey (Basım and Ersoy 2000, 2001), few studies have been conducted to characterize this pathogen in detail.

The objective of this study was to evaluate the phenotypic and genotypic features of the *Psv* olive population in west Mediterranean region of Turkey by gas chromatographic analysis of fatty acid methyl esters (GC-FAME), repetitive element palindromic PCR (rep-PCR), and PFGE. To our knowledge, this is the first study of using PFGE to determine the genetic diversity of the *Psv* olive population.

Materials and methods

Sample collection

Samples were collected from olive trees showing symptoms of suspected knot disease by random sampling of different olive orchards in the districts of Antalya Center (7 orchards; 82 olive trees), Serik (3 orchards; 49 olive trees), Aksu (4 orchards; 35 olive trees), Kaş (6 orchards; 96 olive trees) and Döşemealtı (3 orchards; 58 olive trees) in the Western Mediterranean district of Turkey during May–August of 2015 and May–August of 2018. Samples from different local cultivars of olive trees such as Gemlik, Memeli, Ayvalık, Edinciksu, Edremit, Kan, and Memecik were collected for bacterial isolation. Approximately 320 olive trees in 23 orchards in total were surveyed. The samples were packaged and transported to the Department of Plant Protection of Akdeniz University, where the putative pathogen was isolated. *Psv* isolates (*Pss*I2,

http://www.aloki.hu ● ISSN 1589 1623 (Print) ● ISSN 1785 0037 (Online)
DOI: http://dx.doi.org/10.15666/aeer/1706_1492714944

*Pss*I7, *Pss*I21, *Pss*I24, *Psn*9) obtained from surveys in Antalya province of Turkey in 2000 (Basım and Ersoy, 2000) were also included in this study (*Table 2*). The Myrtus strain, *Pss*I24, and Nerium strain, *Psn*9, were used for clustering. The disease rates within the olive plantations from which the contaminated samples were collected were assessed utilizing the equation as defined by Bansal et al. (1994):

$$\text{Disease incidence } (DI)\ (\%) = (\text{Number of diseased plants / Total number of plants}) \times 100$$

Isolation and identification of bacteria

Bacterial isolation was carried out on olive knots present on two-year-old twigs. Plant surfaces were disinfected using paper towel saturated with 96% ethanol; the decayed sections within the hyperplastic knot tissues were then cut off and grounded in sterile phosphate buffer (0.05 M Na_2HPO_4, 4.26 g; K_2HPO_4, 2.72 g; 1000 ml sterile dH_2O). A loop of bacterial suspension was streaked onto semi-selective PVF-1 medium (glycerol, 10 ml; sucrose, 30 g; casamino acid, 2.5 g; $K_2HPO_4.3H_2O$, 1.96 g; $MgSO_4.7H_2O$, 0.4 g; SDS, 0.4 g; agar, 16 g; 1000 ml dH_2O; pH 7.1) (Surico and Lavermicocca, 1989), King's B medium (KB; protease peptone, 20 g; Bacto agar, 20 g; glycerol, 10 ml; K_2HPO_4, 1.5 g; $MgSO_4$, 1.5 g; 1000 ml dH_2O, pH 7.2) (King et al., 1954) and Nutrient Sucrose Agar (NSA) (Nutrient Broth, 4.8 g; Bacto agar, 9 g; sucrose, 30 g; 600 ml dH_2O) (Surico and Lavermicocca, 1989). The *Psv* isolates utilized in this study are listed in *Table 2*. The bacteria were incubated at 28 °C on PVF-1, KB, and NSA media. Bacterial fluorescent pigment production was examined under UV light at 364 nm. In all, 67 isolates identified as *Psv* were recovered, then freezed in glycerol (30%) at -86 °C for long term storage and further analysis.

Putative *Psv* isolates were identified by several biochemical tests, including LOPAT, according to Schaad et al. (2001). The tests were carried out using flat, greyish-white, irregular margins or semi-translucent colonies grown on PVF-1 medium. The identity of the *Psv* isolates was confirmed by GC-FAME analysis (Stead, 1992) and PCR. The *Psv* isolates were identified directly from bacterial suspension as well as from purified genomic DNA by PCR utilizing primers, IAALN1/IAALN2 (Pelyaver et al., 2000) and PSS1/PSS2; PSS3/PSS4 (Basım and Ersoy, 2001). The polymerase chain reaction (PCR) conditions are given in *Table 1.*

Pathogenicity test

For putative *Psv* isolates, pathogenicity tests were carried out by inoculating the stems of a one-year-old Gemlik olive cultivar. The bark of the stem was wounded with a sterilized needle dipped in bacterial suspension, which contained ~10^8 CFU/ml, and the wounds were then covered with Parafilm for 3 days. The inoculated olive plants were kept in a controlled-room at 25 ± 2 °C and 80-85% RH and monitored for symptom development according to Surico and Lavermicocca (1989). Olive plants similarly treated with reference strains or sterile dH_2O were utilized as positive and negative controls, respectively.

GC-FAME analysis

GC-FAME analyses were performed on each *Psv* isolate as stated in the manufacturer's specifications to determine the phenotypic characteristic of the isolates. The *Psv* isolates were growth on tryptic soy broth agar at 27 °C for 24 h. The each *Psv*

http://www.aloki.hu ● ISSN 1589 1623 (Print) ● ISSN 1785 0037 (Online)
DOI: http://dx.doi.org/10.15666/aeer/1706_1492714944

isolate (a loopful) was blended within a glass tube containing 1.2 N NaOH in methanol: H_2O. The tubes were shortly vortexed, kept in a bubbling water bath for 5 min. The tubes firmly vortexed once more for 10 s and were exchanged to the bubbling water bath for 30-min warming to finish reaction. Two ml methylation arrangement (325 ml 6.0 N hydrochloric acid, 275 ml methyl solution) was included to the tubes after the tubes were cooled to room temperature. The samples were without further ado vortexed, warmed at 80 °C for 10 min. The samples were cooled quickly on ice, and afterward 1.25 ml the extraction arrangement (N-hexane/methyl tert-butyl ether (1:1; v/v) was included. The samples were tenderly blended utilizing a tube revolver for 10 min. The under aqueous phases of the samples were discarded by a micropipette. Three milliliters of the sample clean up solution (10.8 g NaOH dissolved in 900 ml H_2O) was included into the sample, and tenderly blended for 5 min. And after that ~ 2/3 of natural period of the examples was moved into a dull GC vial. These final extracts were analysed with the HP 6980 GC System (Agilent Technologies, CA, USA), and the MIDI system (Microbial ID Inc., USA) with a 25 m × 0.2 mm silica capillary column was performed. The 67 isolates of *Psv* were identified, and phenotypically characterized based on FAME composition by dendrogram analysis using the MIDI software version 6.0.

Table 1. *PCR primers used in this study*

Locus	Primers	Sequence (5'→3')	Size (bp)	References	Conventional PCR conditions
Ptz	PSS1	TGGGGTGCTACTTGTACCGGA	684	Basım and Ersoy (2001)	5 min at 95 °C, followed by 35 cycles, 30 s at 95 °C, 30 s at 62 °C, 45 s at 72 °C, 5 min at 72 °C
	PSS2	CCGTGTACTACGTTCAGCGAG			
*iaa*L	PSS3	CAGGACTTCAGAACCCACGT	1064	Basım and Ersoy (2001)	5 min at 95 °C, followed by 35 cycles, 30 s at 95 °C, 30 s at 62 °C, 45 s at 72 °C, 5 min at 72 °C
	PSS4	CGGTCGATGATGTAGAGCAT			
*iaa*L	IAALF	GGCACCAGCGGCAACATCAA	454	Pelyalver et al. (2000)	5 min at 94 °C, followed by 35 cycles, 30 s at 94 °C, 30 s at 62 °C, 30 s at 72 °C, 5 min at 72 °C m
	IAALR	CGCCCTCGGAACTGCCATAC			
BOX-PCR	BOXA1R	CTACGGCAAGGCGACGCTGACG		Louws et al. (1994)	7 min at 95 °C, followed by 30 cycles, 1 min at 94 °C, 1 min at 53 °C, 8 min at 65 °C, 15 min at 65 °C

DNA extraction

Genomic DNA from *Psv* isolates was extracted based on a modified CTAB method (Doyle and Doyle, 1990), and was dissolved in 50 µl TE buffer. The concentration of DNA was adjusted to 100 ng/µl with TE, using a Nanodrop (Thermo Fisher Scientific, Waltham, MA, USA) and after which the DNA solution was stored at 4 °C.

Rep-PCR

Evaluation of genetic differences among *Psv* was performed by Rep-PCR using primer based on repetitive extragenic palindromic (REP) sequences, BOXA1R (Louws

http://www.aloki.hu ● ISSN 1589 1623 (Print) ● ISSN 1785 0037 (Online)
DOI: http://dx.doi.org/10.15666/aeer/1706_1492714944

et al., 1994). The reaction mixture consisted of 4 µl DNA, 27.8 µl ddH_2O, 5 µl 10x *Taq* buffer, 3 µl $MgCl_2$, 8 µl 0.1 mM dNTPs, and 3.5 U *Taq* Pol. The BOX-PCR conditions are given in *Table 2*. PCR products (10 µl) were fractionated by gel electrophoresis (75 V, for 7 h) on 0.5% standard and 0.5% NuSieve agarose. A 1 kb DNA size marker (Fermantas, Vilnius, Lithuania) was used. The agarose gels were stained with ethidium bromide (0.5 µg/ml) for 20 min., and pictured using a imaging system (Vilber Lourmat transilluminator, France). The outcomes were analysed by Bio-gene gel analysing software (VilberLourma, France). UPGMA (Sneath and Sokal, 1973) and Dice coefficient (2a/(2a + b + c) (Dice, 1945) were utilized for the DNA fingerprint matching and dendrogram analyses.

Table 2. *Bacterial isolates used for the study*

Haplotype groups	Strain designation	Host plant of isolation/cultivar	Geographical origin	Isolation date	Haplotype groups	Strain designation	Host plant of isolation/cultivar	Geographical origin	Isolation date
1	*Pss* 1	Olive/Gemlik	Aksu	2015	2	*Pss* 13	Olive/Gemlik	Antalya	2015
1	*Pss* 2	Olive/Gemlik	Aksu	2015	2	*Pss* 16	Olive/Kan	Antalya	2015
1	*Pss* 3	Olive/Kan	Aksu	2015	2	*Pss* 20	Olive/Edinciksu	Kaş	2015
1	*Pss* 4	Olive/Gemlik	Serik	2015	2	*Pss* 22	Olive/Edremit	Kaş	2015
1	*Pss* 6	Olive/Gemlik	Dösemaltı	2015	2	*Pss* 24	Olive/Memecik	Kaş	2015
1	*Pss* 7	Olive/Kan	Dösemaltı	2015	2	*Pss* 25	Olive/Kan	Antalya	2015
1	*Pss* 9	Olive/Kan	Dösemaltı	2015	2	*Pss* 26	Olive/Gemlik	Antalya	2015
1	*Pss* 10	Olive/Edinciksu	Kaş	2015	2	*Pss* 29	Olive/Ayvalık	Antalya	2015
1	*Pss* 11	Olive/Memeli	Kaş	2015	2	*Pss* 34	Olive/Memecik	Antalya	2015
1	*Pss* 14	Olive/Gemlik	Dösemaltı	2015	2	*Pss* 38	Olive/Edremit	Antalya	2015
1	*Pss* 15	Olive/Gemlik	Antalya	2015	2	*Pss* 41	Olive/Kan	Kaş	2016
1	*Pss* 17	Olive/Kan	Antalya	2015	2	*Pss* 46	Olive/Memecik	Kaş	2016
1	*Pss* 18	Olive/Edinciksu	Antalya	2015	2	*Pss* 50	Olive/Gemlik	Kaş	2016
1	*Pss* 27	Olive/Gemlik	Antalya	2015	2	*Pss* 54	Olive/Memeli	Antalya	2016
1	*Pss* 28	Olive/Gemlik	Kaş	2015	2	*Pss* 58	Olive/Edinciksu	Kaş	2016
1	*Pss* 31	Olive/Gemlik	Dösemaltı	2015	2	*Pss* 59	Olive/Edinciksu	Kaş	2016
1	*Pss* 32	Olive/Edinciksu	Serik	2015	2	*Pss* 62	Olive/Ayvalık	Antalya	2016
1	*Pss* 33	Olive/Memecik	Serik	2016	2	*Pss* 65	Olive/Gemlik	Antalya	2018
1	*Pss* 35	Olive/Gemlik	Serik	2016	2	*Pss* 67	Olive/Gemlik	Antalya	2018
1	*Pss* 36	Olive/Gemlik	Kaş	2016	3	*Pss* 12	Olive/Gemlik	Serik	2015
1	*Pss* 37	Olive/Memeli	Kaş	2016	3	*Pss* 19	Olive/Edremit	Aksu	2015
1	*Pss* 39	Olive/Kan	Aksu	2016	3	*Pss* 21	Olive/Memeli	Kaş	2015
1	*Pss* 40	Olive/Edinciksu	Dösemaltı	2016	3	*Pss* 23	Olive/Kan	Aksu	2015
1	*Pss* 42	Olive/Kan	Dösemaltı	2016	3	*Pss* 30	Olive/Gemlik	Serik	2015
1	*Pss* 44	Olive/Edremit	Dösemaltı	2016	3	*Pss* 43	Olive/Gemlik	Serik	2015
1	*Pss* 45	Olive/Edremit	Serik	2016	3	*Pss* 49	Olive/Gemlik	Kaş	2016
1	*Pss* 47	Olive/Kan	Serik	2016	3	*Pss* 53	Olive/Gemlik	Kaş	2016
1	*Pss* 48	Olive/Gemlik	Kaş	2016	3	*Pss* 60	Olive/Kan	Serik	2016
1	*Pss* 51	Olive/Gemlik	Kaş	2016	3	*Pss* 61	Olive/Ayvalık	Dösemaltı	2016
1	*Pss* 52	Olive/Gemlik	Antalya	2016	3	*Pss* 66	Olive/Gemlik	Dösemaltı	2018
1	*Pss* 55	Olive/Gemlik	Aksu	2016	1	*Pss*I2	Olive/Kan	Aksu	2000
1	*Pss* 56	Olive/Edinciksu	Aksu	2016	1	*Pss*I7	Olive/Kan	Serik	2000
1	*Pss* 57	Olive/Memecik	Kaş	2016	1	*Pss*I21	Olive/Kan	Kaş	2000
1	*Pss* 63	Olive/Memecik	Dösemaltı	2018	4	*Pss* I24	Myrtus	Döşemaltı	2000
1	*Pss* 64	Olive/Kan	Dösemaltı	2018	3	*Psn* 9	Nerium	Serik	2000
2	*Pss* 5	Olive/Kan	Aksu	2015	1	NCPPB639	Olive	Yugoslavia	1908
2	*Pss* 8	Olive/Gemlik	Antalya	2015					

http://www.aloki.hu ● ISSN 1589 1623 (Print) ● ISSN 1785 0037 (Online)
DOI: http://dx.doi.org/10.15666/aeer/1706_1492714944

PFGE

The *Psv* isolates were cultured in 5 ml Nutrient Broth at 28 °C at 140 rpm shaking for 24 h. Cell suspensions were adjusted to an OD of 0.3 A (approximately 1×10^8 CFU/ml) at 600 nm by utilizing a spectrophotometer (Eppendorf, Hamburg, Germany). The bacterial suspensions (1.5 ml) were centrifugated at 14,000 rpm for 2 min, pelleted, and resuspended in 1 ml sterile dH_2O. This procedure was repeated twice. After suspension of the cells in 500 µl TE buffer (10 mM Tris-HCl, pH 8.0; 10 mM $MgCl_2$; 25 mM EDTA, pH 8.0),1×10^8 CFU/ml cells were encapsulated in 500 µl 2% (w/v) low melting point agarose (Bio-Rad Laboratories, Hercules, CA, USA), and transferred into sterile fitting-molds (Bio-Rad Laboratories, Hercules, CA, USA). The hardened agarose fittings at 4 °C for 20 min were returned to a 1.5 ml microfuge tube. Agarose fittings with 1 mg/ml Proteinase K in 250 mM EDTA (pH 9.5) and 25% (w/v) N-laurylsarcosine were incubated overnight at 50 °C. The agarose plugs were returned to a sterile tube containing 1.5 ml sterile 250 mM EDTA (pH 8.0) at 4 °C until used. Complete restriction digestion of 1/5 of agarose fittings was performed with 15 U of *Spe* I, *Ase* I, and *Xba* I (Hacıoğlu et al., 1997) at 37 °C for 7 h. The fittings were inserted into 0.9% (w/v) agarose gel in 0.5x TBE buffer [44.5 mM Tris-HCl, 44.5 mM Boric Acid, 1 mM EDTA (pH 8.0)] at 14 °C all through the kept running by utilizing a pulsed field gel electrophoresis unit (CHEF-DR III) (Bio-Rad Laboratories Hercules, CA, USA).

The optimal migration condition was used, depending on DNA size, at 200 V with an angle of 120°, with an underlying switch time of 5 s and a last switch time of 45 s for 22 h. The gel was stained with 0.5x TBE buffer containing 0.5 µg/ml ethidium bromide for 200 min. Low–Range (New England Biolabs, MA, USA) and Yeast Chromosomal PFGE (*Saccharomyces cerevisiae*) markers were utilized as molecular size markers. The gel image was obtained by using a VilberLourma Monochrome ½" IT CCD camera. DNA fingerprint patterns and sizes were analysed by Bio-gene gel imaging programming (Vilber Lourma, France). UPGMA (Sneath and Sokal, 1973) and Dice coefficient (2a/(2a + b + c) (Dice, 1945) were utilized for the DNA fingerprint matching and dendrogram analyses.

Results

Isolation and identification of bacteria

The isolates and their locations are given in *Figure 1* and *Table 2*. The pathogens were characterized after isolation from infected olive trees, thereby establishing their presence across the various districts of Antalya province in Turkey. The incidence of the olive knot disease reported for each district by Bansal et al. (1994) are: 80% in Serik, 20% in Döşemealtı-Kırkgöz, 17% in Aksu-Topallı, 10% in Kaş-Dalyan, and 4% in Antalya-Center.

Psv grew well and produced unique levan-negative colonies on selective PVF-1, KB, and NSA media. The colonies grown on KB medium were flat, with a diameter ranging from 1–3 mm, greyish to white colour, and irregular margins. The bacteria produced fluorescence pigment on both KB and PVF-1 media under UV light. The colonies grown on PVF-1 were greyish white, slightly raised, smooth, and relatively small (2–3 mm). The colonies grown on NSA medium were grey or pale yellow, slightly raised or flat with a diameter of 3–5 mm. LOPAT indicated negative levan, oxidase, potato

http://www.aloki.hu ● ISSN 1589 1623 (Print) ● ISSN 1785 0037 (Online)
DOI: http://dx.doi.org/10.15666/aeer/1706_1492714944

soft rot, and arginine dehydrolase tests, but all isolates showed positive hypersensitive reaction in the tobacco plant. In all, 67 isolates were recovered from diseased olive trees in Turkey and identified by PCR. The numbers of groups and strains in each group are presented in *Table 2*.

The pathogenicity of the isolates on the one-year-old Gemlik olive seedlings produced characteristic knot symptoms with variable sizes. The healthy olive seedling treated with sterile dH_2O as a control did not show any symptoms (*Fig. 2a*). The pathogen was reliably re-isolated from the knots in the repeated tests, establishing *Psv* as the causal agent of the knot or gall disease in olive plants, thereby satisfying Koch's postulates (*Fig. 2b* and *c*).

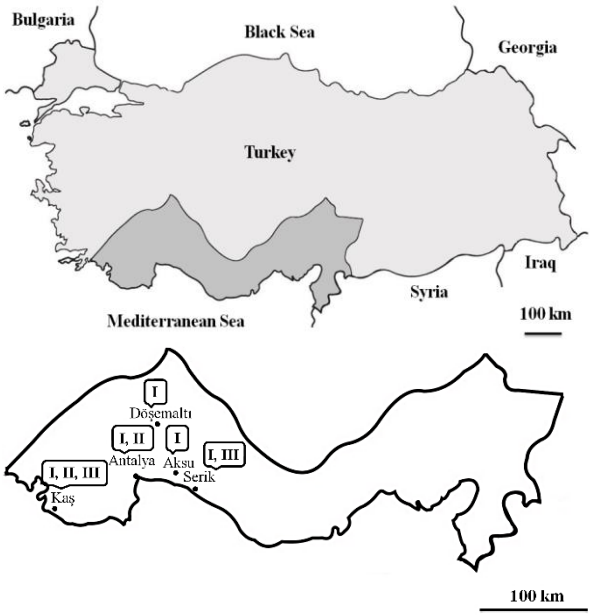

Figure 1. *Distribution of Psv in the western Mediterranean region of Turkey as determined by PFGE analysis. Schematic map of the region showing the 5 districts studied. Letters next to the district names indicate the haplotype groups (I–III)*

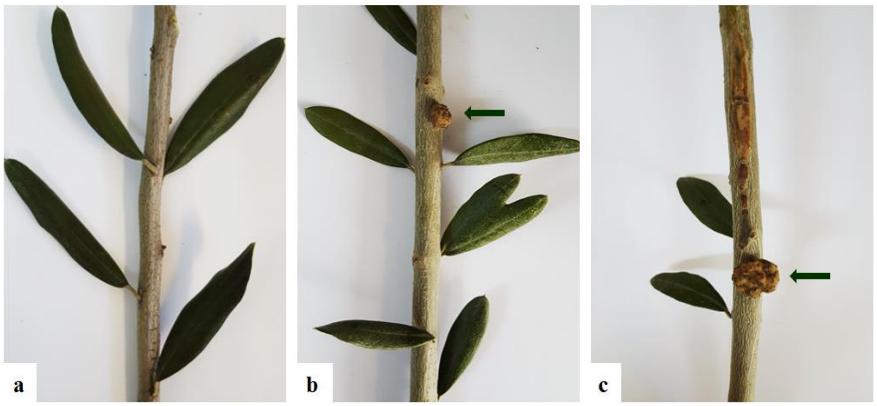

Figure 2. *The pathogenicity of the isolates on a one-year-old Gemlik cultivar of olive seedlings; (a) healthy olive seedling treated with sterile dH_2O used as a control, (b) seedling inoculated with the reference strain (NCPPB 639) showing knot symptoms, (c) seedling inoculated with the Turkish isolate (Pss 2) showing knot symptoms*

http://www.aloki.hu ● ISSN 1589 1623 (Print) ● ISSN 1785 0037 (Online)
DOI: http://dx.doi.org/10.15666/aeer/1706_1492714944

The relationships among the *Psv* strains were established based on FAME analysis. All 67 isolates recovered from the olive plant hosts in Antalya province and the reference strains were analysed. The results show percent similarities of 78.50–100% to the MIS library. The major fatty acids were palmitic acid (16:0), palmitoleic acid (16:1), and oleic acid (18:1) (*Table 3*). The FAME cluster analysis based on the Euclidean distance categorized the Turkish olive strains into 2 groups (*Fig. 3*). Each clade is unique, showing a close relationship among each other.

Table 3. *The percentage values* of total fatty acid methyl esters (FAME) of Psv and Psn isolates*

FAME	Strain groups			
	I	II	III	*Psn* 9
10:0	0.0 ± 0.07	0.0 ± 0.02	0.17 ± 0.03	0.0 ± 0.01
10:0 3OH	4.50 ± 1.20	4.38 ± 1.04	2.66 ± 0.24	4.28 ± 0.11
12:00	2.00 ± 0.31	6.07 ± 0.52	4.69 ± 0.32	2.59 ± 0.04
11:00 iso 3HO	0.0 ± 0.05	0.0 ± 0.06	0.35 ± 0.05	0.0 ± 0.01
12:0 2OH	6.41 ± 0.32	4.40 ± 0.01	3.40 ± 0.92	5.88 ± 0.68
12:0 3OH	4.70 ± 1.21	5.27 ± 1.12	4.19 ± 0.59	4.21 ± 0.67
14:0	0.42 ± 0.03	0.0 ± 0.01	0.18 ± 0.05	0.43 ± 0.07
16:1[a]	34.60 ± 2.58	33.45 ± 2.31	22.98 ± 2.73	35.14 ± 2.99
16:0[b]	27.01 ± 1.47	20.72 ± 1.78	23.19 ± 1.62	26.53 ± 1.25
17:0 iso	0.0 ± 0.04	0.0 ± 0.02	1.61 ± 0.03	0.0 ± 0.01
17:0 cyclo	3.15 ± 0.34	0.0 ± 0.05	4.42 ± 0.37	2.87 ± 0.46
18:1[c]	15.34 ± 3.05	23.02 ± 2.04	27.40 ± 2.81	16.49 ± 3.01
18:0	1.09 ± 0.54	1.53 ± 0.03	2.80 ± 0.89	1.57 ± 0.74
18:1 w7c 11-methyl	0.0 ± 0.03	0.0 ± 0.01	1.13 ± 0.02	0.0 ± 0.05
Sum In Feature 7	0.0 ± 0.40	1.15 ± 0.20	0.37 ± 0.11	0.0 ± 0.02
19:0 cyclo w8c	0.0 ± 0.04	0.0 ± 0.01	0.46 ± 0.02	0.0 ± 0.01

*Each value is an average ± standard deviation of strain groups
I, II: Olive strain groups of *Psv*., III: *Myrtus communis* strain group of *Psv*
[a]Palmitoleic acid, [b]Palmitic acid, [c]Oleic acid

Rep-PCR

The primer, BOXA1R, which was used to amplify the repetitive DNA sequence of *Psv*, showed various genomic fingerprints. The results obtained by the BOXA1R primer pair showed variability among the *Psv* strains. This primer pair produced different polymorphic patterns among the strains with amplification fragments ranging from ~250 to 2250 bp (*Fig. 4*). BOX PCR cluster analysis categorized all the Turkish olive strains into 2 groups (*Fig. 5*).

PFGE

All 67 isolates and reference strains were evaluated by using PFGE. The results showed various discrete DNA patterns of *Psv* after digesting the total genome with *Spe*I. The restriction digestion of the *Psv* genome yielded fragments which ranged from 9 to 1000 kb (*Fig. 6*). *Ase* I and *Xba* I did not effectively digest genomic DNA in this study. The Turkish olive strains were separated into 3 discrete PFGE groups (*Fig. 7*). Based on the cluster analysis, there was nearly identical linkage between the haplotype

http://www.aloki.hu ● ISSN 1589 1623 (Print) ● ISSN 1785 0037 (Online)
DOI: http://dx.doi.org/10.15666/aeer/1706_1492714944

group I and the reference strain. The percentage similarity among the haplotypes as shown by the cluster was 42–100% (*Fig. 7*). Based on the cluster analysis of PFGE, haplotype group I consisted of 38 haplotypes and reference strain NCPPB639; haplotype group II (21 haplotypes): haplotype group III (11 haplotypes), and the myrtus isolate was placed into haplotype group IV as *Figure 7* and *Table 2*.

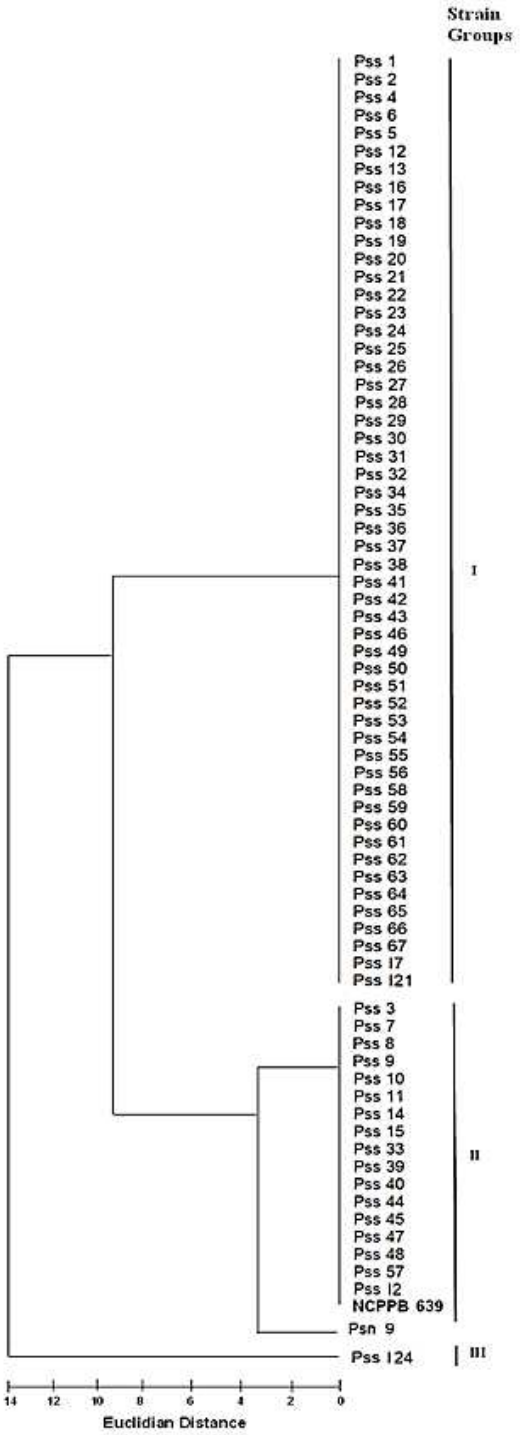

Figure 3. *Dendrogram generated by cluster analysis of Psv strains (Table 2) based on fatty acid composition*

http://www.aloki.hu ● ISSN 1589 1623 (Print) ● ISSN 1785 0037 (Online)
DOI: http://dx.doi.org/10.15666/aeer/1706_1492714944

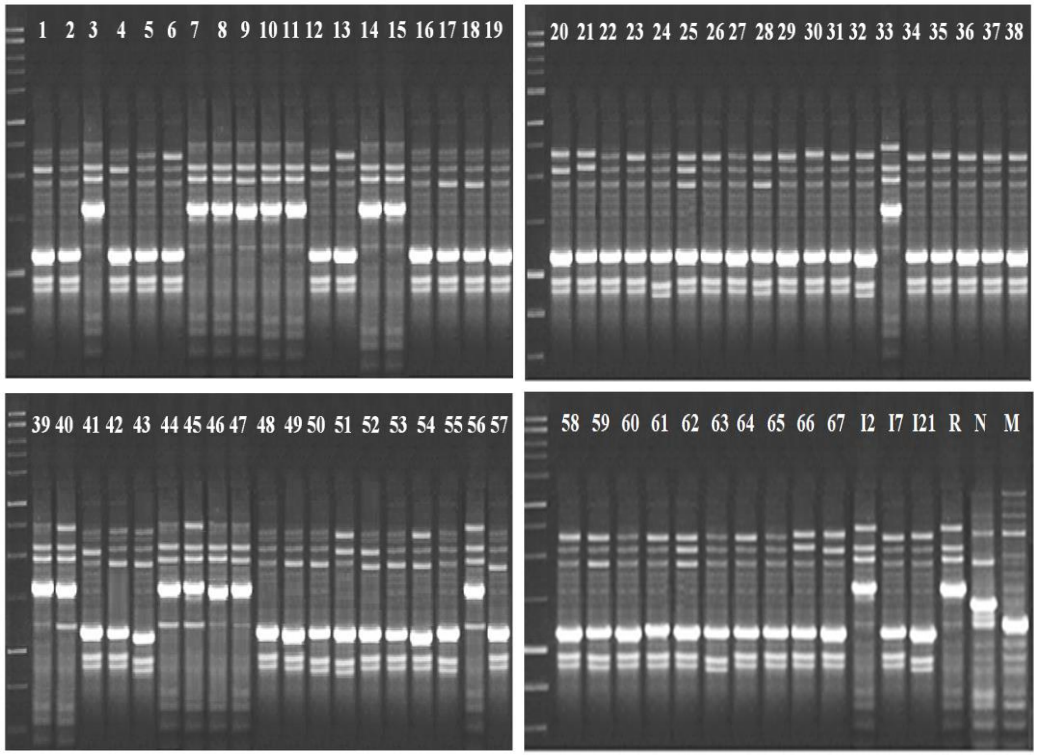

Figure 4. *Agarose gel electrophoresis of repetitive sequence-based BOX-PCR fingerprint patterns obtained from Psv and Psn strains. Lanes: 1–67; Pss 1 – Pss 67, respectively; Lane: I2, I7, I21, R, N, M; Pss I2, Pss I7, Pss I21, NCPPB 639, Psn 9, Pss I24, respectively*

Discussion

Of the isolates collected from diseased olive plants during the 2015–2018 survey, 67 were found to be heterogenic and divided into 3 haplotype groups by PFGE. From the survey results, the highest percentage of the disease and the olive plant cultivars from which the pathogen were isolated were from the Serik district, and the highest infected (80%) or susceptible cultivar from this district was the Gemlik cultivar. The least infected orchard recorded was from the Antalya-center district. When all the collected samples across the various districts were compared, the Gemlik cultivar showed the highest percentage of infection. Some commercial olive cultivars have been found to be considerably tolerant to olive knot disease (Penyalver et al., 2006). The high rate of infection in the Gemlik cultivar could be due to a high susceptibility to this pathogen. It could also be also be attributed to the exposure of these varieties to powerful winds common in the coastal regions of Antalya-center and Kaş-Dalyan. These strong winds create wounds on the plants which allow entrance for the pathogen. Additionally, the fungus, *Cycloconium oleaginum*, a causal agent of olive leaf spot disease that results in defoliation, creates wounds that can serve as entrance point for *Psv*.

The different groups of *Psv* strains according to PFGE occurred in the same districts because of the large olive plant production as well as different cultivars of olive grown in these areas. There was no association of genetic diversity of Turkish *Psv* population with olive cultivars of isolation. The results of Scortichini et al. (2004) were supported by our findings. On the other hand, Moretti et al. (2008) and Krid et al. (2009) reported an association with geography and olive cultivars.

http://www.aloki.hu ● ISSN 1589 1623 (Print) ● ISSN 1785 0037 (Online)
DOI: http://dx.doi.org/10.15666/aeer/1706_1492714944

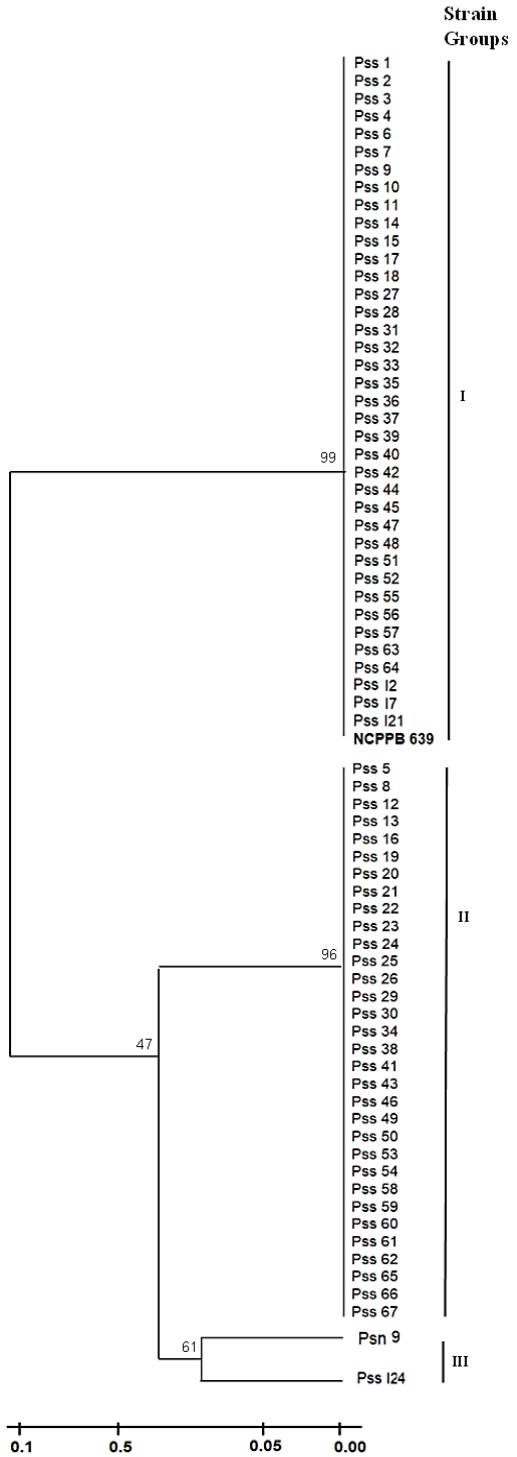

Figure 5. *Unweighted average linkage dendrogram of the cluster analysis of Psv strains (Table 2) based on BOX-PCR analysis*

Understanding the *Psv* population may help to enhance the present control management of olive knot disease. *Psv* isolates obtained from infected olive trees in various geographical region of the world are different. In a few studies, various *Psv* populations were gathered from various parts of the world, including 360 isolates from

http://www.aloki.hu ● ISSN 1589 1623 (Print) ● ISSN 1785 0037 (Online)
DOI: http://dx.doi.org/10.15666/aeer/1706_1492714944

Italy (Scortichini et al., 2004), 71 isolates from Italy, USA, Greece, Portugal, former Yugoslavia, UK, the Netherlands, and France (Sisto et al., 2007), 62 isolates from Spain, Italy, Serbia, France, Portugal, USA, Algeria, Greece, Jordan, and Tunusia (Quesada et al., 2008), 58 strains from Tunusia (Krid et al., 2009), 31 isolates from Italy (Cinelli et al., 2014), 124 isolates from various Mediterranean countries (Moretti et al., 2017), and 19 isolates from Japan (Tsuji et al., 2017)

Scortichini et al. (2004) analysed 360 Italian *Psv* isolates and reported the presence of 20 DNA fingerprint patterns by rep-PCR. The 44 Spanish *Psv* isolates were grouped into 3 different groups, and the only 6 Italian isolates were placed into 3 different groups by the presence of IS*53* (Quesada et al., 2008). The 58 Tunisian *Psv* isolates were clustered into 3 different groups by RAPD (Krid et al., 2009). Recently, Moretti et al. (2017) analysed 124 *Psv* isolates from 15 different countries and grouped the isolates into 2 clusters and 4 subclusters by MLST and rep-PCR. The 19 Japanese isolates were differentiated into 5 different groups by rep-PCR (Tsuji et al., 2017).

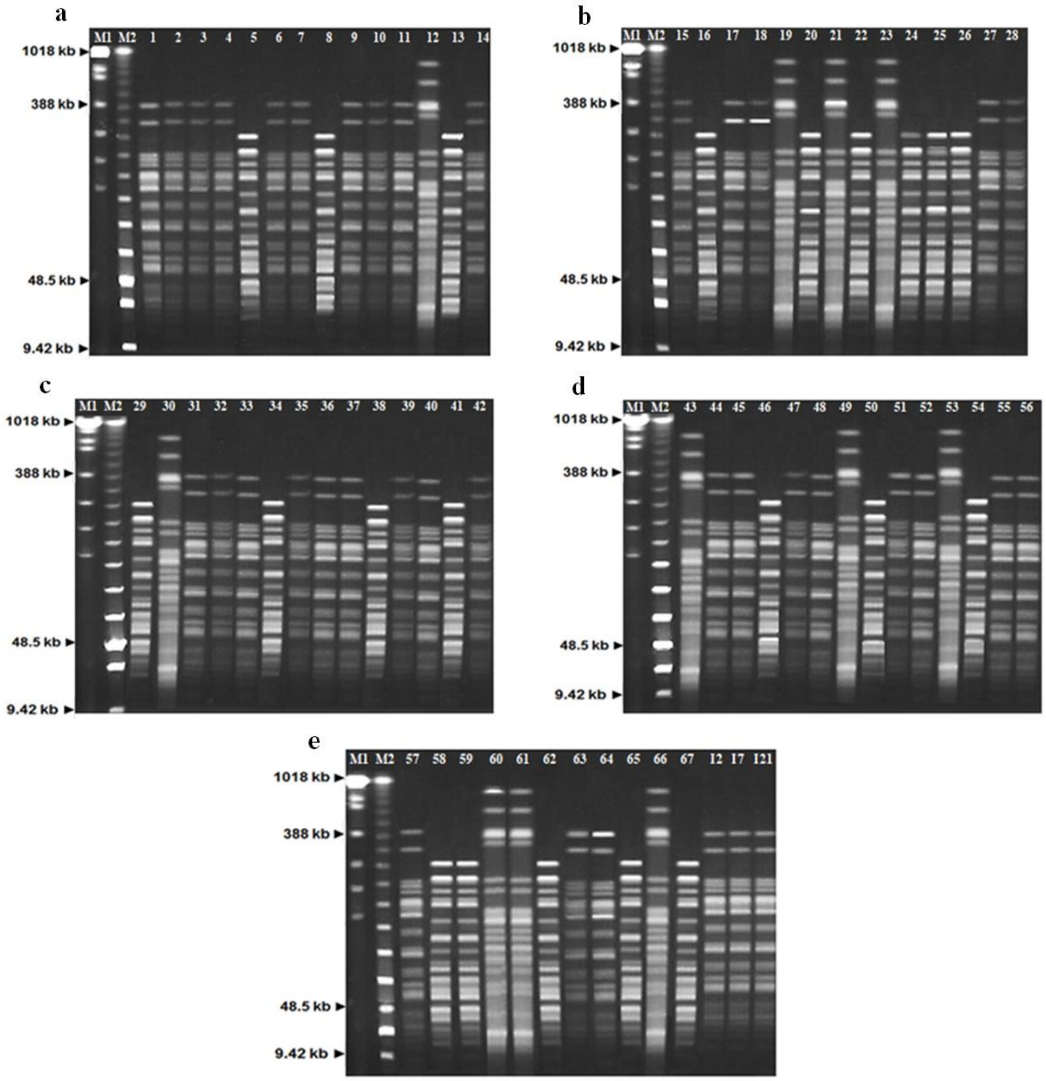

Figure 6. *(a, b, c, d, e) Genomic DNA fingerprints from olive strains of Psv in Turkey by PFGE using Spe I. Lanes: M1 = DNA size standards of Saccharomyces cerevisiae, M2 = Low-range PFGE marker. Lanes: 1–67 = Pss1–Pss67, respectively; Lane: I2, I7, I21 = PssI2, PssI7, PssI21, respectively*

http://www.aloki.hu ● ISSN 1589 1623 (Print) ● ISSN 1785 0037 (Online)
DOI: http://dx.doi.org/10.15666/aeer/1706_1492714944

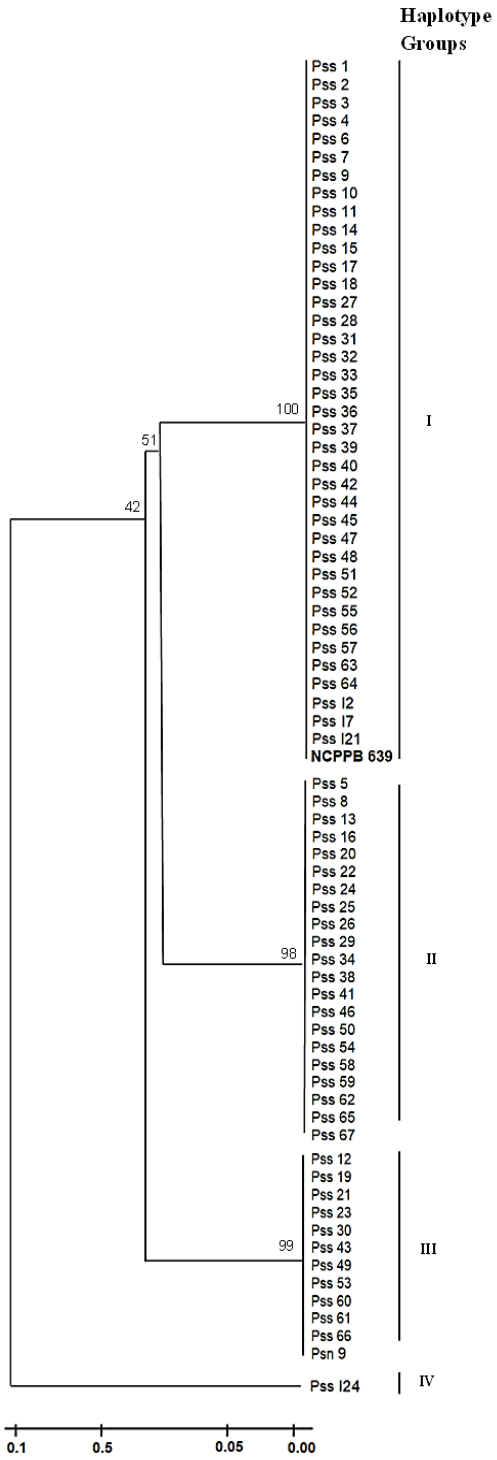

Figure 7. *Unweighted average linkage dendrogram of cluster analysis of Psv (Table 2) haplotype groups generated by PFGE patterns with Spe I. Number of horizontal axes indicates percent similarity as determined by Dice coefficient*

There have been reports of the presence of olive knot disease caused by *Psv* in the Aegean region, which is one of the olive growing provinces of Turkey (Tatlı and Benlioğlu, 2004) and in the western Mediterranean region, specifically in Antalya

http://www.aloki.hu ● ISSN 1589 1623 (Print) ● ISSN 1785 0037 (Online)
DOI: http://dx.doi.org/10.15666/aeer/1706_1492714944

province (Basım and Ersoy, 2000), in oleander plants in the South-eastern Anatolia, specifically in Şanlıurfa (Kavak and Üstün, 2009), and from the Adana, Samsun, and Tekirdağ provinces of Turkey (Mirik et al., 2011).

The morphological and biochemical tests indicated that the 3 media used in this study produced colonies typical of *Psv*. Considerable heterogeneity in the colonies established by *Psv* strains isolated from different cultivars of olive in various localities have been reported in Italy (Surico and Marchi 2003). LOPAT showed isolates to be levan negative, and all isolates produced a positive hypersensitive reaction in tobacco plant. The LOPAT profile (Lelliott et al., 1966) and other tests described by Lelliott and Stead (1987) were used to separate a typical *Psv* strain from *P. syringae* subsp. *syringae*. Janse (1981) observed that some *Psv* strains isolated from various host plants had almost similar physiological and biochemical dispositions. All isolates were confirmed to be pathogenic on a one-year-old olive plant, but not on an oleander plant. Our result is in concordance with the findings reported by Perez-Martinez et al. (2007).

Table 3 indicates the relative (percent) total fatty acid methyl esters as found by FAME analysis of the *Psv* isolates, which were entered into the standard MIDI library. The FAME cluster categorized all the strains isolated from olive plants collected from various districts of Antalya province which were clustered into 2 groups based on Euclidean metrics. The FAME analysis provides useful information with regards to the phenotypic identification of the pathogen, but it is not an effective technique for discriminating between strains.

The diversity study was carried out using rep-PCR with primer pair, BOXA1R, which was found to be informative and discriminatory for all the *Psv* isolates tested in this study, and produced polymorphic patterns corresponding to different amplification fragment sizes (*Fig. 4*). All the strains isolated from olive plants formed 2 groups based on the BOX-PCR. Although the BOX-PCR was found to be effective at differentiating *Psv* isolates, its discriminating ability was less than that of PFGE as observed in this study. Interestingly, it could be seen from the cluster tree that strains from different districts of a province or geographical location showed similar genetic homogeneity and were grouped together in one clade by the BOX-PCR cluster analysis (*Fig. 5*).

The genetic variability among the *Psv* strains was further confirmed by using PFGE after restriction digestion with *Spe* I, a rare-cutting enzyme. Three different haplotype groups were produced based on the DNA fragment patterns generated as compared to FAME and BOX-PCR analyses, which categorized the isolates from olive plant hosts into 2 groups each. The results of this study recommend that the FAME and BOX-PCR strategies were not capable as PFGE to separate *Psv* strains. The PFGE utilizing rare-cutting endonuclease *Spe* I given the foremost comprehensive comes about. The effective discriminatory ability and reproducibility of PFGE makes it one of the foremost broadly utilizied method for comparative fingerprinting of most bacterial species (Sails et al., 2003; Lukinmaa et al., 2004; van Belkum et al., 2007). Based on PFGE, most *Psv* strains were placed in haplotype group I with reference strain NCPPB639. The other strains were separated into 2 haplotype groups, resulting in a total 3 different haplotype groups in the olive *Psv* population. This heterogeneity among the *Psv* population can be clarified by even exchange of plasmids and chromosomal genes as seen in *Xanthomonas* and *Pseudomonas* pathovars (Canteros et al., 1995; Basım et al., 1999; Sundin, 2007). Based on PFGE, the isolate *Pss*9 from *Nerium oleander* was placed in haplotype group II, along with several olive strains. However, the same strain was placed in a different haplotype group by rep-PCR analysis.

http://www.aloki.hu ● ISSN 1589 1623 (Print) ● ISSN 1785 0037 (Online)
DOI: http://dx.doi.org/10.15666/aeer/1706_1492714944

Comparative comes about were found by Moretti et al. (2017). *P. s*. pv. *nerii* and *P. s.* pv. *fraxinii* were plainly isolated from the *Psv* population by utilizing rep-PCR. Based on MLST, isolates of *P. s.* pv. *nerii* and *P. s.* pv. *fraxini* pathovars clearly have a same genetic feature as *Psv*, and may have adjusted to oleander and fraxinus, individually, after *Psv* risen as an olive plant pathogen (Moretti et al., 2017).

Conclusion

Our results show that PFGE using *Spe*I has an effective discriminatory capability for genotypic analysis of *Psv* population. The present study provides important outputs to better comprehension of the genotypic and phenotypic structure of the *Psv* population in Turkey. The results about given an incredible opportunity for following strain shifting in the *Psv* population in future, and for olive breeding programs pointed at the advancement of an olive cultivar safe to the distinctive *Psv* strains.

Acknowledgement. Our sincere gratitude to Scientific Research Projects (BAP) of Akdeniz University for their financial support.

REFERENCES

[1] Bansal, V. K., Kharbanda, P. D., Stringam, G. R., Thiagarajah, M. R., Tewari, J. P. (1994): A comparison of greenhouse and field screening methods for blackleg resistance in doubled haploid lines of *Brassica napus*. – Plant Dis. 78: 276-281.

[2] Basım, H., Ersoy, A. (2000): Identification and spread on *Pseudomonas savastanoi* pv. *savastanoi* caused by knot disease on olive in western Mediterranean region. – Turkish First Olive Symp., Bursa, Turkey, pp. 310-315.

[3] Basım, H., Ersoy, A. (2001): Identification of *Pseudomonas savastanoi* pv. *savastanoi*, olive knot pathogen, by polymerase chain reaction. – Phytopathol. 91: 6.

[4] Basım, H., Stall, R. E., Minsavage, G. V., Jones, J. B. (1999): Chromosomal gene transfer by conjugation in the plant pathogen *Xanthomonas axonopodis* pv. *vesicatoria*. – Phytopathol. 89: 1044-1049.

[5] Berge, O., Monteil, C. L., Bartoli, C., Chandeysson, C., Guilbaud, C., Sands, D. C., Morris, C. E. (2014): A user's guide to a data base of the diversity of *Pseudomonas syringae* and its application to classifying strains in this phylogenetic complex. – PLoS One 9(9): e105547.

[6] Canteros, B. I., Minsavage, G. V., Jones, J. B., Stall, R. E. (1995): Diversity of plasmids in *Xanthomonas campestris* pv. *vesicatoria*. – Phytopathol. 85: 1482-1486.

[7] Chu, G., Vollrath, D., Davis, R. W. (1986): Separation of large DNA molecules by contour-clamped homogeneous electric fields. – Science 234: 1582-1585.

[8] Cinelli, T., Marchi, G., Cimmino, A., Marongiu, R., Evidente, A., Fiori, M. (2014): Heterogeneity of *Pseudomonas savastanoi* populations infecting *Myrtus communis* in Sardinia (Italy). – Plant Pathol. 63: 277-289.

[9] Doyle, J. J., Doyle, J. L. (1990): Isolation of plant DNA from fresh tissue. – Focus 12: 13-15.

[10] Dice, L. R. (1945): Measures of the amount of ecologic association between species. – Ecol. 26: 297-302.

[11] Gardan, L., Bollet, C., Abu, G. M., Grimont, F., Grimont, P. A. D. (1992): DNA relatedness among the pathovar strains of *Pseudomonas syringae* subsp. s*avastanoi* Janse (1991) and proposal of *Pseudomonas savastanoi* sp. nov. – Int. J. Syst. Bacteriol. 42: 606-612.

http://www.aloki.hu ● ISSN 1589 1623 (Print) ● ISSN 1785 0037 (Online)
DOI: http://dx.doi.org/10.15666/aeer/1706_1492714944

[12] Guilbaud, C., Morris, C. E., Barakat, M., Ortet, P., Berge, O. (2016): Isolation and identification of *Pseudomonas syringae* facilitated by a PCR targeting the whole *P. syringae* group. – FEMS Microbiol. Ecol. 92(1): fiv146.
[13] Hacıoğlu, E., Basım, H., Stall, R. E. (1997): Optimized conditions of *Pac* I and *Swa* I for genome analysis of *Xanthomonas axonopodi s*pv. *vesicatoria* by PFGE. – Biotechn. 22: 1026-1028.
[14] Hosni, T., Moretti, C., Devescovi, G., Suarez-Moreno, Z. R., Fatmi, M. B., Guarnaccia, C., Pongor, S., Onofri, A., Buonaurio, R., Venturi, V. (2011): Sharing of quorum-sensing signals and role of interspecies communities in a bacterial plant disease. – ISME J. 5*:* 1857-1870.
[15] Hulton, C. S. J., Higgins, C. F., Sharp, P. M. (1991): ERIC sequences: a novel family of repetitive elements in the genomes of *Escherichia coli*, *Salmonella typhimurium* and other enterobacteria. – Mol. Microbiol. 5: 825-834.
[16] International Olive Oil Council (2015): http://www. internationaloliveoil.org. – Accessed: 15 April 2016.
[17] Janse, J. D. (1981): The bacterial disease of ash (*Fraxinus excelsior*) caused by *Pseudomonas syringae* subsp. *savastanoi* pv. *fraxini,* II etiology and taxonomic considerations. – Eur. J. Forest Pathol. 11: 425-438.
[18] Kavak, H., Üstün, N. (2009): Oleander knot caused by *Pseudomonas savastanoi* pv. *nerii* in Turkey. – J. Plant Pathol. 91: 701-703.
[19] King, E. O., Ward, M. K., Raney, D. E. (1954): Two simple media for the demonstration of pyocyanin and fluorescein. – The J. Lab. Clin. Medic. 44: 301-307.
[20] King, G. J. (1989): Plasmid analysis and variation in *Pseudomonas syringae*. – The J. Appl. Bacteriol. 67: 489-496.
[21] Krid, S., Rhouma, A., Quesada, J. M., Penyalver, R., Gargouri, A. (2009): Delineation of *Pseudomonas savastanoi* pv. *savastanoi* strains isolated in Tunisia by random-amplified polymorphic DNA analysis. – J. Appl. Microbiol. 106: 886-894.
[22] Lelliott, R. A., Stead, D. E. (1987): Diagnostic procedures for bacterial plant diseases. – In: Preece, T. F. (ed.) Methods in Plant Pathology. Vol. 2. Blackwell Scientific Publications, Oxford, UK.
[23] Lelliott, R. A., Billing, E., Hayward, A. C. (1966): A determinative scheme for fluorescent plant pathogenic bacteria. – J. Appl. Bacteriol. 29: 470-489.
[24] Loumou, A., Giourga, C. (2003): Olive groves: "The life and identity of the Mediterranean". – Agric. and Hum. Values 20: 87-95.
[25] Louws, F. J., Fulbright, D. W., Stephens, C. T., De Bruijn, F. J. (1994): Specific genomic fingerprints of phytopathogenic *Xanthomonas* and *Pseudomonas* pathovars and strains generated with repetitive sequences and PCR. – Appl. Environ. Microbiol. 60: 2286-2295.
[26] Lukinmaa, S., Nakari, U. M., Eklund, M., Siitonen, A. (2004): Application of molecular genetic methods in diagnostics and epidemiology of food-borne bacterial pathogens. – APMIS 112: 908-929.
[27] Manceau, C., Horvais, A. (1997): Assessment of genetic diversity among strains of *Pseudomonas syringae* by PCR-restriction fragment length polymorphism analysis of rRNA operons with special emphasis on *P. syringae* pv. *tomato.* – Appl. Environ. Microbiol. 63: 498-505.
[28] Mirik, M., Aysan, Y., Sahin, F. (2011): Characterization of *Pseudomonas savastanoi* pv. *savastanoi* strains isolated from several host plants in Turkey and report of fontanesia as a new host. – J. Plant Pathol. 93*:* 263-270.
[29] Moretti, C., Ferrante, P., Hosni, T., Valentini, F., D'Onghia, A., Fatmi, M. B., Buonaurio, R. (2008): Characterization of *Pseudomonas Savastanoi* pv. *Savastanoi* Strains Collected from Olive Trees in Different Countries. – In: Fatmi, M. et al. (eds) *Pseudomonas Syringae* Pathovars and Related Pathogens - Identification, Epidemiology and Genomics. Springer, New York, pp. 321-329.

http://www.aloki.hu ● ISSN 1589 1623 (Print) ● ISSN 1785 0037 (Online)
DOI: http://dx.doi.org/10.15666/aeer/1706_1492714944

[30] Moretti, C., Vinatzer, B. A., Onofri, A., Valentini, F., Buonaurio, R. (2017): Genetic and phenotypic diversity of Mediterranean populations of olive knot pathogen, *Pseudomonas savastanoi* pv. *Savastanoi.* – Plant Pathol. 66: 595-605.

[31] Nester, E. W., Kosuge, T. (1981): Plasmids specifying plant hyperplasias. – Ann. Rev. Microbiol. 35: 531-565.

[32] Penyalver, R., Garcia, A., Ferrer, A., Bertolini, E., Lopez, M. M. (2000): Detection of *Pseudomonas savastanoi* pv. *savastanoi* in olive plants by enrichment and PCR. – Appl. Environ. Microbiol. 66: 2673-2677.

[33] Penyalver, R., Garcia, A., Ferrer, A., Bertolini, E., Quesada, J. M., Salcedo, C. I., Piquer, J., Pérez-Panadés, J., Carbonell, E. A., del Río, C., Caballero, J. M., López, M. M. (2006): Factors affecting *Pseudomonas savastanoi* pv. *savastanoi* plant inoculations and their use for evaluation of olive cultivar susceptibility. – Phytopathol. 96: 313-319.

[34] Perez-Martínez, I., Rodríguez-Moreno, L., Matas, I. M., Ramos, C. (2007): Strain selection and improvement of gene transfer for genetic manipulation of *Pseudomonas savastanoi* isolated from olive knots. – Res. Microbiol 158: 60-69.

[35] Perez-Martínez, I., Rodríguez-Moreno, L., Lambertsen, L., Matas, I. M., Murillo, J., Tegli, S., Jiménez, A. J., Ramos, C. (2010): Fate of a *Pseudomonas savastanoi* pv. *savastanoi* type III secretion system mutant in olive plants (*Olea europaea* L.). – Appl. Environ. Microbiol. 76: 3611-3619.

[36] Quesada, J. M., Perez-Martinez, I., Ramos, C., Lopez, M. M., Penyalver, R. (2008): IS53: an insertion element for molecular typing of *Pseudomonas savastanoi* pv. *savastanoi*. – Res. Microbiol. 159: 207-215.

[37] Quesada, J. M., Penyalver, R., Perez-Panades, J., Salcedo, C. I., Carbonell, E. A., Lopez, M. M. (2010): Comparison of chemical treatments for reducing epiphytic *Pseudomonas savastanoi* pv. *savastanoi* populations and for improving subsequent control of olive knot disease. – Crop Protect. 29: 1413-1420.

[38] Rodriguez-Palenzuela, P., Matas, I. M., Murillo, J., Lopez-Solanilla, E., Bardaji, L., Perez-Martinez, I., Rodriguez-Moskera, M. E., Penyalver, R., Lopez, M. M., Quesada, J. M., Biehl, B. S., Perna, N. T., Glasner, J. D., Cabot, E. L., Neeno-Eckwall, E., Ramos, C. (2010): Annotation and overview of the *Pseudomonas savastanoi* pv. *savastanoi* NCPPB 3335 draft genome reveals the virulence gene complement of a tumour-inducing pathogen of woody hosts. – Environ. Microbiol. 12: 1604-1620.

[39] Sails, A. D., Swaminathan, B., Fields, P. I. (2003): Utility of multilocus sequence typing as an epidemiological tool for investigation of outbreaks of gastroenteritis caused by *Campylobacter jejuni*. – J. Clinic. Microbiol. 41: 4733-4739.

[40] Schaad, N. W., Jones, J. B., Chun, W. (2001): Initial Identification of Common Genera. – In: Schaad, N. W. et al. (eds.) Laboratory Guide for Identification of Plant Pathogenic Bacteria. 3th Ed. APS Press, St. Paul. MN, pp. 84-120.

[41] Schroth, M. N., Osgood, J. W., Miller, T. D. (1973): Quantitative assessment of the effect of the olive knot disease on olive yield and quality. – Phytopathol. 63: 1064-1065.

[42] Scortichini, M., Rossi, M. P., Salerno, M. (2004): Relationship of genetic structure of *Pseudomonas savastanoi* pv. *savastanoi* populations from Italian olive trees and patterns of host genetic diversity. – Plant Pathol. 53: 491-497.

[43] Sharples, G. J., Lioyd, R. G. (1990): A novel repeated DNA sequence located in the intergenic regions of bacterial chromosomes. – Nucl. Acids Res. 18(22): 6503-6508.

[44] Sisto, A., Cipriani, M. G., Morea, M. (2004): Knot formation caused by *Pseudomonas syringae* subsp. *savastanoi* on olive plants is *hrp*-dependent. – Phytopathol. 94(5): 484-489.

[45] Sisto, A., Cipriani, M. G., Tegli, S., Cerboneschi, M., Stea, G., Santilli, E. (2007): Genetic characterization by fluorescent AFLP of *Pseudomonas savastanoi* pv. *savastanoi* strains isolated from different host species. – Plant Pathol. 56: 366-372.

[46] Sneath, P. H. A., Sokal, R. R. (1973): Numerical Taxonomy: The Principles and Practice of Numerical Classification. – Freeman, San Francisco, CA.

http://www.aloki.hu ● ISSN 1589 1623 (Print) ● ISSN 1785 0037 (Online)
DOI: http://dx.doi.org/10.15666/aeer/1706_1492714944

[47] Stead, D. E. (1992): Grouping of plant pathogenic and some other *Pseudomonas* species by using cellular fatty acid profiles. – Inter. J. System. Evol. Microbiol. 42: 281-295.
[48] Sundin, G. W. (2007): Genomic insights into the contribution of phytopathogenic bacterial plasmids to the evolutionary history of their hosts. – Annu. Rev. Phytopathol. 45: 129-151.
[49] Surico, G., Lavermicocca, P. (1989): A semiselective medium for the isolation of *Pseudomonas syringae* pv. *savastanoi*. – Phytopathol. 79: 185-190.
[50] Surico, G., Marchi, G. (2003): Olive Knot Disease: New Insights into the Ecology, Physiology and Epidemiology of *Pseudomonas Savastanoi* pv. *Savastanoi*. – In: Iacobellis, N. S. (ed.) *Pseudomonas Syringae* and Related Pathogens. Kluwer Academic, Netherlands, pp. 17-28.
[51] Surico, G., Iacobellis, N. S., Sisto, S. (1985): Studies on the role of indole-3-acetic acid and cytokinins in the formation of knots on olive and oleander plants by *Pseudomonas syringae* pv. *savastanoi*. – Physiol. Plant Pathol. 26: 309-320.
[52] Tatlı, B., Benlioğlu, K. (2004): Study on olive knot disease (*Pseudomonas savastanoi* pv. *savastanoi*) occurring olive areas of Aydın and Muğla provinces. – Proceed. 1st Plant Protect. Congr., Samsun, Turkey.
[53] Tegli, S., Gori, A., Cerboneschi, M., Cipriani, M. G., Sisto, A. (2011): Type three secretion system in *Pseudomonas savastanoi* pathovars: does timing matter? – Genes 2: 957-979.
[54] Tsuji, M., Ohta, K., Tanaka, K., Takikawa, Y. (2017): Comparison among Japanese isolates of *Pseudomonas savastanoi* pv. *savastanoi*, causal agent of olive knot disease. – J. General Plant Pathol. 83: 152-161.
[55] van Belkum, A., Tassios, P. T., Dijkshoorn, L., Haeggman, S., Cookson, B., Fry, N. K., Fussing, V., Green, J., Feil, E., Gerner-Smidt, P., Brisse, S., Struelens, M. (2007): Guidelines for the validation and application of typing methods for use in bacterial epidemiology. – Clinical Microbiol. Infect. 3: 1-46.
[56] van Zyl, E., Steyn, P. L. (1990): Differentiation of phytopathogenic *Pseudomonas* and *Xanthomonas* species and pathovars by numerical taxonomy and protein gel electropherogram. – Syst. Appl. Microbiol. 13: 60-71.

http://www.aloki.hu ● ISSN 1589 1623 (Print) ● ISSN 1785 0037 (Online)
DOI: http://dx.doi.org/10.15666/aeer/1706_1492714944

INVESTIGATION OF MILK YIELD FROM CULTURE, CROSS-BRED AND NATIVE CATTLE BREEDS IN TURKEY BY MULTIVARIATE ANALYSIS OF VARIANCE (MANOVA)

AZAK, G. – CELIK, S.*

Department of Animal Science, Faculty of Agriculture, Biometry and Genetics, Bingol University, Bingol, Turkey

**Corresponding author*
e-mail: senolcelik@bingol.edu.tr; phone: +90-505-217-7021

(Received 21st Jun 2019; accepted 16th Oct 2019)

Abstract. In this study, milk yield from culture, cross-bred, and native cattle breeds in 7 geographical regions of Turkey were investigated by multivariate analysis of variance (MANOVA) in 2015. The values of Pillai's Trace, Wilks' Lambda, Hotelling's Trace and Roy's Largest Root statistics used for the MANOVA test were 0.522, 0.546, 0.711 and 0.490, respectively. The corresponding F values for these statistics were found to be 2.422, 2.518, 2.594 and 5.634, respectively. Mean annual milk yield of cross-bred, culture, and native cattle breeds reached to be 3776.355, 2692.803 and 1311.513 kg, respectively. Therefore, the results of these statistics are very close to each other. As a result of the MANOVA test, the difference within milk yield between the regions was not significant for culture and native cattle breeds, whereas a significant difference was found in hybrid breed cattle ($P < 0.001$). As a result of the Bonferroni test, it was found that the milk yield difference in hybrid cattle was due to the difference in yield between Eastern Anatolia-Aegean, Eastern Anatolia-Marmara, Southeast Anatolia-Aegean and Southeast Anatolia-Marmara regions.
Keywords: *Wilks' Lambda, outlier, race, milk yield, geographical region*

Introduction

Production of animal products and per capita consumption of animal products are among the indicators of the development level of a country (Şapdeniz, 1993). Milk is one of the most important animal products. It is an essential nutrient for a sufficient and balanced human diet and for fulfilling the protein need of the ever-growing world population. Milk consumption is significant in the diets of people of all ages. Although milk has a key role in human diet and per capita consumption of milk has been on the rise in Turkey in recent years, it has not reached to a desired level yet (Akman, 2017).

Turkey has a great potential for increasing animal production due to its geographical position and land structure favorable for animal breeding. While Turkey ranks among the leading countries in terms of animal numbers, the yield per animal is not at a desired level. Therefore, researches performed in Turkey aim to improve the yield obtained per animal rather than to increase the number of animals (Yaylak, 2003). In the republican period, culture breeding cattle were imported from abroad for the improvement of the indigenous breeds. Cattle import activities, which started in the republican period, have continued until today. Currently, 88% of the cattle population consists of culture breeds and cross breeds. While the number of indigenous breeds has continuously reduced in the whole cattle population, the number of cross breeds has shown a significant increase. In researches performed to improve the milk yield obtained from cattle in Turkey, culture cattle breeding has been prioritized since 1958 (Kumlu and Akman, 1999).

http://www.aloki.hu ● ISSN 1589 1623 (Print) ● ISSN 1785 0037 (Online)
DOI: http://dx.doi.org/10.15666/aeer/1706_1494514959

In researches on dairy cattle breeding in Turkey, the improvements in milk production, the effects of environmental and genotypic factors and the rate of these factors were emphasized (Alpan and Arpacık, 1998). Milk yield in cattle is affected by two factors, which are; the genotype of the animal and favorable environmental conditions (Tuncel, 1994). Breeding methods and selection are used to improve the milk yield capacity in terms of genetics. On the other hand, environmental factors can lead to long-term and daily changes.

Age, breed, live weight, lactation method, number of daily milking, feeding, ambient temperature, calving season, duration of dry period, diseases and exercises are among the factors that affect milk yield in cows.

In Turkey and in other countries, various researches have been performed on 305-day milk yield of the Holstein Friesian cattle (*Table 1*).

Table 1. *305-day milk yield of the Holstein Friesian cattle in Turkey and in other countries*

Year and authors	Country	Average milk yield	Number of animals
Türkyılmaz (2005)	Turkey	6491	544
Sattar et al. (2005)	Turkey	2772	499
Tekerli and Gündoğan (2005)	Turkey	6404	525
Bakır et al. (2009)	Turkey	6810	1302
Şahin and Ulutaş (2010)	Turkey	6976	536
Keskin and Boztepe (2011)	Turkey	5997	105
Duru et al. (2012)	Turkey	6010	597
Boğakşayan and Bakır (2013)	Turkey	5673	1935
Khattab et al. (2005)	Egypt	4746	2095
Makgahlela et al. (2007)	South Africa	8695	4112
Hashemi and Nayebpoor (2008)	Iran	5123	19885
Oudah and Zainab (2010)	Egypt	2737	1011
Pirzada (2011)	UK	7743	10768
Yousefi-Golverdi et al. (2012)	Iran	5662	1128
Bastin et al. (2013)	Belgium	8851	52147
Irano et al. (2014)	Brazil	9001	5090
Kheirabadi and Alijani (2014)	Iran	9059	763505

According to the Turkish Statistical Institute (TSI), while the number of cattle in Turkey was the highest in 1981 (15 981 000), the number was 13 994 071 in 2015. This indicates that, whereas Turkey had an important cattle potential in the past, this potential has reduced later. According to the statistics of the year 2015; 16 933 520 (90.77%) tones of the 18.654.682 tones milk annually produced in Turkey, were obtained from cattle (TSI, 2015). In this respect, cattle milk has an increased value as it has the highest share.

5.58% of the milk obtained from cattle was from indigenous breeds, 37.30% of it was from cross breeds and 57.12% of it was from culture breeds. As for the annual milk yield from cattle; around 1307 kg was from indigenous breeds, around 2677 kg was from cross breeds, around 3743 was from culture breeds and it was around 2581 kg in general (TSI, 2015).

http://www.aloki.hu ● ISSN 1589 1623 (Print) ● ISSN 1785 0037 (Online)
DOI: http://dx.doi.org/10.15666/aeer/1706_1494514959

According to FAO (2017), cattle breeding is most common in Brazil with 214,889,796 animals. India ranks second with 185,103,532 animals and the USA ranks third with 93,704,600 animals. Turkey ranks twenty third in the world with 14 080 155 cattle. FAO (2017) also reported that, the USA ranks first in cattle milk production with 97 734 736 tones, India ranks second with 83,633,570 tones and Brazil ranks third with 33,490,810 tones. Turkey ranks ninth in the world by producing 18 762 319 tones cattle milk. These indicate that Turkey has a key role in cattle milk production.

The aim of the study is to examine the milk yields from indigenous, cross and culture breeds in 7 geographical regions of Turkey and to analyze the region-based variations in yearly milk yield.

Materials and methods

Material

Research material consisted of information obtained from the website of the Turkish Statistical Institute (TSI) with regards to the number of indigenous, cross and culture breeds cattle and the milk yield from these cattle, as presented on provincial-basis for the year 2015. Turkey Statistical Institute (TSI) of the data compiled by the relevant institutions (Ministry of Agriculture and Forestry) were taken from the records.

The amount of milk obtained from the cities of 7 geographical regions in Turkey was divided by the number of cattle milked, in order to calculate the average yearly milk yield. The values obtained were individually identified and analyzed for indigenous, cross and culture breeds. Statistical evaluations were made using IBM SPSS version 23.

Method

Multivariate analysis is performed when there are 2 or more dependent variables in each group with 2 or more members. In other words, mean vectors of more than 2 groups (in k) are compared (Alpar 2011). Comparison of the mean vector of k population for the MANOVA model (*Eq. 1;* Johnson and Wichern 2002):

$$Y_{ijk} = \mu + \alpha_{ij} + \varepsilon_{ijk} \quad \text{(Eq.1)}$$

here, Y_{ijk} : is the k. observed value of the j. variable in i. population, α_{ij}: is the effect of j. variable in i. population, ε_{ijk}: is the error value in observed k. of the j. variable in i. Population.

Error terms (ε_{ijk}) have a normal distribution that are independent of each other, with zero means and $\sum$ covariance matrix (Jeremy 1974). $\bar{x}_i$: is the mean vector of i. group, $\bar{x}$: is the general mean vector, n_i: is the number of observations in i. group, S_i: is the variance-covariance vector in i. group (*Eqs. 2* and *3*):

$$B = \sum_{i=1}^{k} n_i (\bar{x}_i - \bar{x})\,(\bar{x}_i - \bar{x})' \quad \text{(Eq.2)}$$

$$W = \sum_{i=1}^{k} (n_i - 1) S_i \quad \text{(Eq.3)}$$

http://www.aloki.hu ● ISSN 1589 1623 (Print) ● ISSN 1785 0037 (Online)
DOI: http://dx.doi.org/10.15666/aeer/1706_1494514959

Eigenvalues of the BW^{-1} matrix are λ_i. The largest root test statistics of Roy is the highest λ_i value.

Lawley-Hotelling trace test (*Eq. 4*):

$$T_0^2 = \sum_{i=1}^{s} \lambda_i \quad \text{(Eq.4)}$$

Pillai's Trace statistics (*Eq. 5;* Lehmann 1986):

$$T = \sum_{i=1}^{s} \lambda_i/(1+\lambda_i) \quad \text{(Eq.5)}$$

Here, s is the eigenvalue number. Wilks Lambda statistic is developed by Rao (1973) and is shown as (*Eq. 6*):

$$\Lambda = \prod_{i=1}^{s} 1/(1+\lambda_i) \quad \text{(Eq.6)}$$

One of the key hypotheses needed for the implementation of the multivariate analysis (MANOVA) is the homogeneity of the variance-covariance matrices. This is determined by the 'Box's M' test (*Eq. 7*).

$$M = \sum_{i=1}^{k}(n_i - 1)ln|S| - \sum_{i=1}^{k}(n_i - 1)ln|S_i| \quad \text{(Eq.7)}$$

In this Box's M statistic, S is the covariance matrix, S_i is the covariance matrix of each group (Özdamar 2013). For the multiple comparisons, paired comparisons regarding the Bonferroni approach are made in order to form simultaneous confidence intervals (Hsu 1996; Everitt 2001). Multiple test statistics are used in the multivariate analysis in order to test the H_o hypothesis. The Wilks Lambda test statistic presenting F distribution when the number of variables become 1, 2 for the first time, is the most common among these test statistics and calculated as such:

Wilks Lamda test statistic; *Equation 8* used in the calculation of the test variate F statistic is written as:

$$1 + \frac{\text{G.A.K.O}}{\text{G.İ.K.O}} \quad \text{(Eq. 8)}$$

and inverted for the multivariate B and W matrices, to obtain (*Eq. 9*):

$$\frac{1}{1+\frac{G.A.K.O}{G.İ.K.O}} = \frac{1}{1+\frac{B}{W}} = \frac{|W|}{|B+W|} = \Lambda \quad \text{(Eq.9)}$$

The Λ statistic here is called as the Wilks Lambda statistic.

In multivariate analysis, this ratio is used in place of the F statistic used in univariate analysis and takes a value between 0 and 1. If there is no group effect, Λ value is 1 if B = 0. Accordingly, the Ho hypothesis is accepted when Λ gets a value close to 1. If matrix B is bigger than matrix W, Λ value gets closer to zero (0). In this case, the Ho hypothesis is rejected. As in univariate analysis, there is a correlation between Λ and T^2 in multivariate analysis, too.

When k = 2 (*Eq. 10*):

http://www.aloki.hu ● ISSN 1589 1623 (Print) ● ISSN 1785 0037 (Online)
DOI: http://dx.doi.org/10.15666/aeer/1706_1494514959

$$\Lambda = \frac{1}{1+\frac{T^2}{N-k}} \quad \text{(Eq.10)}$$

When k = 2, Λ and T^2 statistics show p and N-p-1 freedom degree F distribution. When p = 1 (*Eq. 11*):

$$\Lambda = \frac{1}{1+B/W} = \frac{B}{W}\frac{N-k}{k-1} = F \quad \text{(Eq.11)}$$

Results and discussion

Normal distribution of data and covariance matrices homogeneity test were performed based on the hypotheses needed for the covariate analysis (MANOVA). Outlier observations were found in the normality test (*Fig. 1*). Box's Test was performed in the equalities of covariance matrices.

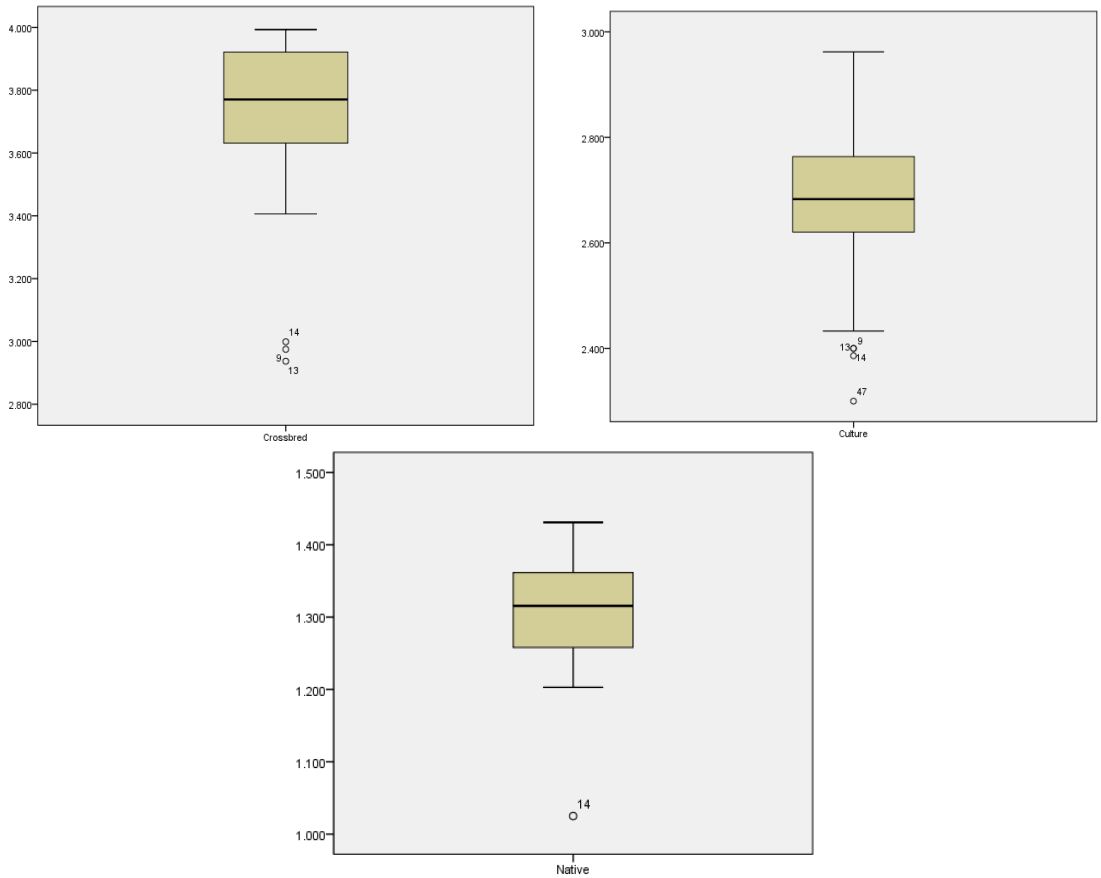

Figure 1. *Outlier observation graph of data (yield-kg)*

As is seen in *Figure 1,* milk yield data of cross, culture and indigenous cattle show a normal distribution. In cross breed group, 9th, 13th and 14th values are the outliers; in culture group, 9th, 13th, 14th and 47th values are the outliers whereas in indigenous group, 14th value is the outlier. As Box's M = 74.391, F = 1.779 and p < 0.01 in Box's M Test as shown in *Table 2*, covariance matrices are not homogenous.

http://www.aloki.hu ● ISSN 1589 1623 (Print) ● ISSN 1785 0037 (Online)
DOI: http://dx.doi.org/10.15666/aeer/1706_1494514959

Following the obtainment of these results, a reanalysis was performed after the removal of 9th, 13th, 14th and 47th outliers from the observed values since they were interrupting normality. The values belonged to the cities of Bingöl, Bitlis, Hakkari and Bartın. For this reason, Kilis, Bingöl, Bitlis, Hakkari and Bartın were excluded from the research and the research was performed with 76 cities. Q-Q Plot and outlier value graphs obtained from the normality tests performed for the new observations are given in *Figure 2.*

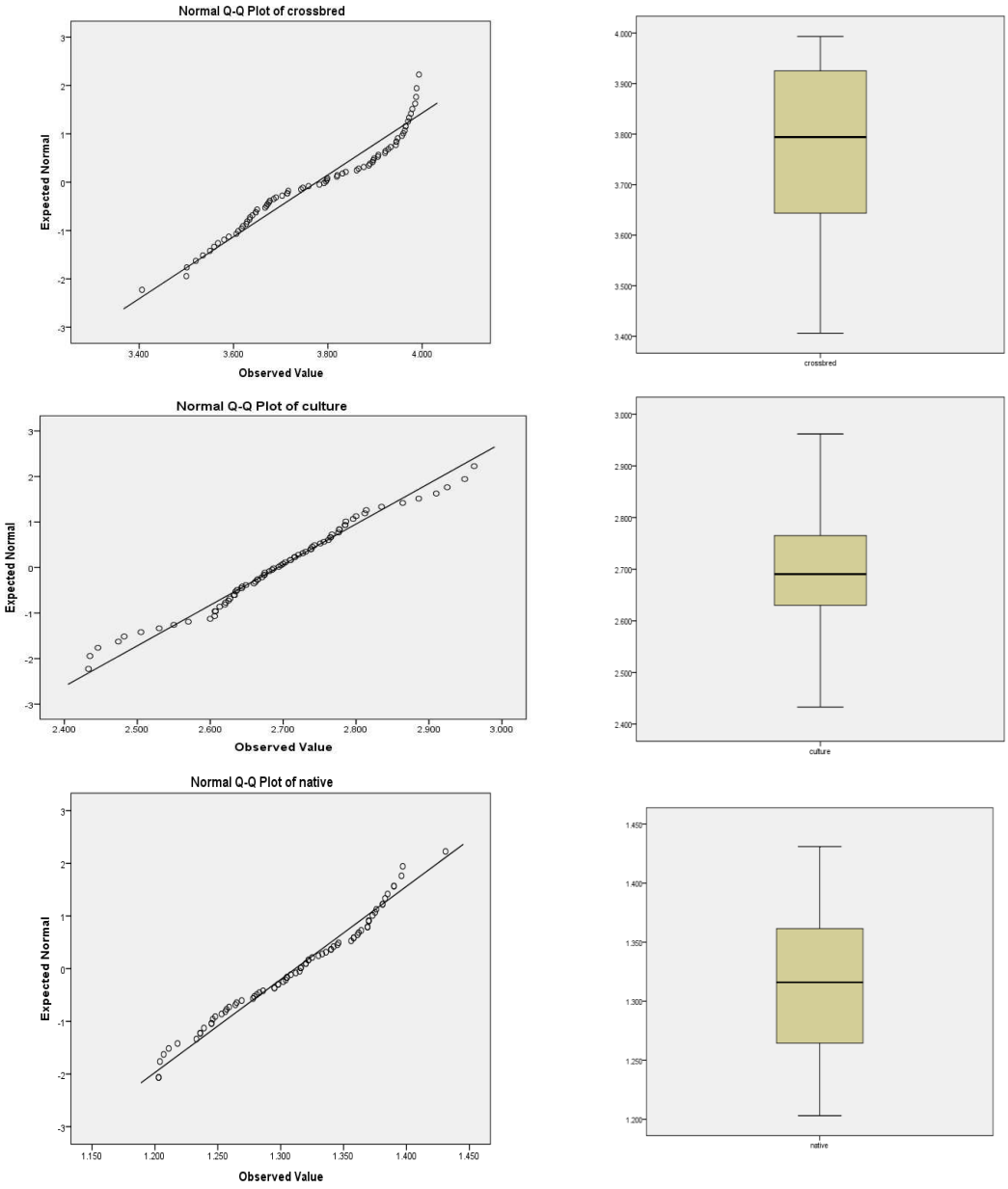

Figure 2. *Normal distribution and outlier observation graph of data*

As is seen in *Figure 2,* milk yield from cross, culture and indigenous cattle breeds show normal distribution according to Q-Q plot graph. This indicates that the outlier value problem has been resolved.

http://www.aloki.hu ● ISSN 1589 1623 (Print) ● ISSN 1785 0037 (Online)
DOI: http://dx.doi.org/10.15666/aeer/1706_1494514959

At this point, homogeneity test for the covariance matrices of these data is presented in *Table 2* and test for sphericity is presented in *Table 3*.

Table 2. *Box's M Test for the equality of the covariance matrices*

Box's M	74.391
F	1.779
df1	36
df2	5667.462
p	0.003

df: degrees freedom

Table 3. *Box's Test for the equality of covariance matrices of groups*

Box's M	57
F	1.356
df1	36
df2	5677.983
p	0.076

H_0: $\Sigma 1 = \Sigma 2 = \Sigma 3$; H_1: At least one of the group mean values is different from the others. Since $p = 0.076 > \alpha{:}0.05$, H_0 cannot be rejected. Which means; group covariance matrices are equal. Therefore, MANOVA can be performed. In *Table 2*, Box's M = 57, F = 1.356 and $p > 0.05$, indicating that covariance matrices are homogenous. Test for sphericity is checked in *Table 4*.

Table 4. *Bartlett's test for sphericity*

Likelihood Ratio	0.000
Approx. Chi-Square	53.611
df	5
p	0.001

In Barlett's test for sphericity shown in *Table 3*, Approx $\chi^2 = 53.611$ and $p < 0.01$, indicating that MANOVA test can be performed. The assumption of normality is provided when the outlier values are omitted. Non-parametric tests are not necessary since appropriate analyzes can be performed with parametric statistics. Descriptive statistics are presented in *Table 5*. The table presenting representative statistics shows that milk yield from cross, culture and indigenous cattle present inter-regional differences.

The highest milk yield from cross breeds is obtained in the Aegean Region whereas the lowest milk yield is obtained in the Eastern Anatolia Region, the highest milk yield from culture breeds is obtained in the Aegean Region whereas the lowest milk is obtained in the Southeastern Anatolia Region, the highest milk yield from indigenous breeds is obtained in the Eastern Anatolia Regions whereas the lowest milk yield is obtained in the Mediterranean Region. MANOVA test results are presented in *Table 6*.

http://www.aloki.hu ● ISSN 1589 1623 (Print) ● ISSN 1785 0037 (Online)
DOI: http://dx.doi.org/10.15666/aeer/1706_1494514959

Table 5. *Descriptive statistics*

Race	Region	$\bar{X}$	Range = Xmax-Xmin	S_X	$S_{\bar{X}}$	N
Culture	Eastern Anatolia	3670.273	163.740	100.480	41.039	11
	Southeastern Anatolia	3677.625	192.002	119.105	48.122	8
	Marmara	3889.182	163.740	79.625	41.039	11
	Aegean	3926.750	192.002	64.913	48.122	8
	Black Sea	3743.412	131.712	147.847	33.011	17
	Central Anatolia	3796.154	150.618	186.853	37.750	13
	Mediterranean	3753.250	192.002	175.830	48.122	8
	General	3776.355	163.740	156.156		76
Cross-bred	Eastern Anatolia	2715.182	135.728	153.598	34.018	11
	Southeastern Anatolia	2624.250	159.156	104.321	39.890	8
	Marmara	2699.818	135.728	137.858	34.018	11
	Aegean	2736.000	159.156	71.544	39.890	8
	Black Sea	2693.235	109.180	113.509	27.364	17
	Central Anatolia	2673.385	124.852	85.381	31.292	13
	Mediterranean	2708.375	159.156	81.703	39.890	8
	General	2692.803	65.058	112.176		76
Native	Eastern Anatolia	1343.455	76.288	26.170	16.306	11
	Southeastern Anatolia	1281.375	65.058	64.790	19.120	8
	Marmara	1298.000	76.288	47.862	16.306	11
	Aegean	1294.250	52.333	64.107	19.120	8
	Black Sea	1324.000	59.845	53.120	13.116	17
	Central Anatolia	1329.077	76.288	60.632	14.999	13
	Mediterranean	1278.500	135.728	59.320	19.120	8
	General	1311.513	159.156	56.576		76

$\bar{X}$: mean, S_X: standard deviation, $S_{\bar{X}}$: standard error

Table 6. *MANOVA test results*

Effect		Values	F	Hypothesis df	Residual df	p	Power of test
Region	Pillai's Trace	0.522	2.422	18	207	0.001	0.993
	Wilks' Lambda	0.546	2.518	18	190	0.001	0.991
	Hotelling's Trace	0.711	2.594	18	197	0.001	0.996
	Roy's Largest Root	0.490	5.634	6	69	0.001	0.995

df: degrees freedom

H_0: $\mu_1 = \mu_2 = \mu_3$; H_1: At least one of the group mean values is different from the others. Since p = Sig:0.001 < α:0.005, H_0 is rejected.

Within the framework of the results of the MANOVA test, Pillai's Trace, Wilks' Lambda, Hotelling's Trace and Roy's Largest Root test results displayed significant inter-regional differences in milk yields from 3 different breeds (indigenous, cross and culture breeds) ($p < 0.01$). (This indicates that group mean vectors are significantly different.) Which means, according to Pillai's Trace statistic: $F = 2.422$, $P < 0.001$;

http://www.aloki.hu ● ISSN 1589 1623 (Print) ● ISSN 1785 0037 (Online)
DOI: http://dx.doi.org/10.15666/aeer/1706_1494514959

according to Wilks' Lambda statistic: $F = 2.518$, $P < 0.001$; According to Hotelling's Trace statistic: $F = 2.594$, $P < 0.001$; according to Roy's Largest Root statistic: $F = 5.694$, $P < 0.001$.

Power of test values were very high. Power of test values for Pillai's Trace, Wilks' Lambda, Hotelling's Trace and Roy's Largest Root tests were 99.3%, 99.1%, 99.6% and 99.5%, respectively. Minimum absolute frequency corresponding to a power rating of 80% is generally favorable (Mendeş 2013). In this respect, the findings of these statistical analyses are favorable. As stated above, it is greater than 80% and the power of the test is high. More than 80% of the power of the test indicates that the analysis is appropriate.

Bonferroni and Tukey Multiple Comparison Tests were performed to determine the inter-regional differences regarding milk yield from each breed. Bonferroni and Tukey test results are presented in *Table 7a, b* and *c*.

According to Bonferroni and Tukey test results, there were significant differences between the Eastern Anatolia-Marmara, Eastern Anatolia-Aegean, Southeastern Anatolia-Marmara and Southeastern Anatolia-Aegean regions with regards to average milk yield ($p < 0.05$ and $p < 0.01$). In this respect, milk yield obtained from culture cattle in the Aegean and Marmara regions was much higher than the milk yield obtained from other regions. Milk yield obtained from culture cattle in the Eastern Anatolia and Southeastern Anatolia regions was lower. The highest milk yield was obtained from the Aegean and Marmara regions, respectively. Conditions of Aegean and Marmara regions in Turkey were observed to be favorable for culture cattle. Inter-regional differences regarding average milk yield from crossbreed and indigenous breed cattle were insignificant, indicating that all regions of Turkey are favorable for crossbreed and indigenous breed cattle.

Likewise, when the present situation (2018 year) can be also analyzed, the obtained results are summarized as follows. The effects of breeds and regions on milk yield in cattle are presented in *Table 8*. MANOVA Tests results for region (*Table 8*): Wilk's Lambda: 0.548, Pillai trace: 0.520, Roy's largest root test: 0.487, Hotelling trace: 0.705. Approximate F test: 12.370* on 36 and 5677 d.f. (degrees freedom).

The results presented in *Table 8* show that the highest mean milk yields were experienced in Aegean, Marmara and Central Anatolia (3926.755, 3889.264 and 3796.178 kg respectively), which are greater than the general mean (3779.394 kg) in culture cattle. The lowest mean milk yield was recorded of 3670.258 kg in Eastern Anatolia. The differences in mean yield owing to region are confirmed by the F-ratio for milk yield ($F = 4.923$ and $P < 0.001$).

Aegean and Eastern Anatolia regions had the highest values for milk yield (2735.997 and 2715.171 kg respectively), while Southeastern Anatolia region recorded the least mean milk yield (2624.235) which is less than the general mean (2696.829 g) in crossbreed cattle. The difference between milk yields in crossbreed cattle by geographical regions was insignificant ($F = 0.997$ and $P > 0.05$).

Eastern Anatolia and Central Anatolia regions had the highest mean milk yield of native cattle (1343.499 and 1328.856 kg respectively) which are greater than the general mean (1309.437 kg), while Mediterranean region had a least mean milk yield of native cattle (1278.477 kg), less than the general mean. The difference between milk yields in native cattle by geographical regions was insignificant ($F = 1.952$ and $P > 0.05$).

Bonferroni Multiple Comparison Test was applied to examine the inter-regional differences regarding milk yield from culture cattle. Bonferroni test results are presented in *Table 9*.

http://www.aloki.hu ● ISSN 1589 1623 (Print) ● ISSN 1785 0037 (Online)
DOI: http://dx.doi.org/10.15666/aeer/1706_1494514959

Table 7a. *Bonferroni and Tukey test results (for Culture)*

Group	Region		Means difference (I-J)	Std. error	P (for Bonferroni)	P (for Tukey)
Culture	Eastern Anatolia	Southeastern Anatolia	-7.352	63.245	0.999	0.999
		Marmara	-218.909*	58.037	0.007	0.006
		Aegean	-256.477*	63.245	0.003	0.002
		Black Sea	-73.139	52.668	0.999	0.806
		Central Anatolia	-125.881	55.760	0.570	0.280
		Mediterranean	-82.977	63.245	0.999	0.844
	Southeastern Anatolia	Marmara	-211.557*	63.245	0.028	0.022
		Aegean	-249.125*	68.055	0.010	0.008
		Black Sea	-65.787	58.357	0.999	0.917
		Central Anatolia	-118.529	61.162	0.999	0.463
		Mediterranean	-75.625	68.055	0.999	0.923
	Marmara	Aegean	-37.568	63.245	0.999	0.997
		Black Sea	145.770	52.668	0.152	0.097
		Central Anatolia	93.028	55.760	0.999	0.639
		Mediterranean	135.932	63.245	0.738	0.336
	Aegean	Black Sea	183.338	58.357	0.052	0.038
		Central Anatolia	130.596	61.162	0.762	0.940
		Mediterranean	173.500	68.055	0.273	0.999
	Black Sea	Central Anatolia	-52.742	50.148	0.999	0.940
		Mediterranean	-9.838	58.357	0.999	0.999
	Central Anatolia	Mediterranean	42.904	61.162	0.999	0.992

Table 7b. *Bonferroni test results (for Cross-bred)*

Group	Region		Means difference (I-J)	Std. error	P (for Bonferroni)	P (for Tukey)
Cross-bred	Eastern Anatolia	Southeastern Anatolia	90.932	52.425	0.999	0.596
		Marmara	15.364	48.109	0.999	0.999
		Aegean	-20.818	52.425	0.999	0.999
		Black Sea	21.947	43.658	0.999	0.999
		Central Anatolia	41.797	46.221	0.999	0.971
		Mediterranean	6.807	52.425	0.999	0.999
	Southeastern Anatolia	Marmara	-75.568	52.425	0.999	0.777
		Aegean	-111.750	56.413	0.999	0.436
		Black Sea	-68.985	48.373	0.999	0.786
		Central Anatolia	-49.135	50.699	0.999	0.959
		Mediterranean	-84.125	56.413	0.999	0.749
	Marmara	Aegean	-36.182	52.425	0.999	0.993
		Black Sea	6.583	43.658	0.999	0.999
		Central Anatolia	26.434	46.221	0.999	0.997
		Mediterranean	-8.557	52.425	0.999	0.999
	Aegean	Black Sea	42.765	48.373	0.999	0.974
		Central Anatolia	62.615	50.699	0.999	0.878
		Mediterranean	27.625	56.413	0.999	0.999
	Black Sea	Central Anatolia	19.851	41.569	0.999	0.999
		Mediterranean	-15.140	48.373	0.999	0.999
	Central Anatolia	Mediterranean	-34.990	50.699	0.999	0.993

http://www.aloki.hu ● ISSN 1589 1623 (Print) ● ISSN 1785 0037 (Online)
DOI: http://dx.doi.org/10.15666/aeer/1706_1494514959

Table 7c. *Bonferroni test results (for Native)*

Group	Region		Means difference (I-J)	Std. error	P (for Bonferroni)	P (for Tukey)
Native	Eastern Anatolia	Southeastern Anatolia	62.080	25.129	0.335	0.186
		Marmara	45.455	23.060	0.999	0.442
		Aegean	49.205	25.129	0.999	0.450
		Black Sea	19.455	20.927	0.999	0.966
		Central Anatolia	14.378	22.155	0.999	0.995
		Mediterranean	64.955	25.129	0.249	0.147
	Southeastern Anatolia	Marmara	-16.625	25.129	0.999	0.994
		Aegean	-12.875	27.040	0.999	0.999
		Black Sea	-42.625	23.187	0.999	0.527
		Central Anatolia	-47.702	24.301	0.999	0.447
		Mediterranean	2.875	27.040	0.999	0.999
	Marmara	Aegean	3.750	25.129	0.999	0.999
		Black Sea	-26.000	20.927	0.999	0.875
		Central Anatolia	-31.077	22.155	0.999	0.799
		Mediterranean	19.500	25.129	0.999	0.987
	Aegean	Black Sea	-29.750	23.187	0.999	0.857
		Central Anatolia	-34.827	24.301	0.999	0.782
		Mediterranean	15.750	27.040	0.999	0.997
	Black Sea	Central Anatolia	-5.077	19.925	0.999	0.999
		Mediterranean	45.500	23.187	0.999	0.448
	Central Anatolia	Mediterranean	50.577	24.301	0.864	0.375

Table 8. *Summary of results of MANOVA test for regions across the milk yield*

Region	Culture, milk yield mean (kg)	Crossbreed milk yield mean (kg)	Native milk yield mean (kg)
Mediterranean	3753.273	2708.339	1278.477
Southeastern Anatolia	3677.567	2624.235	1281.331
Eastern Anatolia	3670.258	2715.171	1343.499
Marmara	3889.264	2699.791	1297.685
Aegean	3926.755	2735.997	1294.120
Black Sea	3756.949	2711.301	1315.155
Central Anatolia	3796.178	2673.365	1328.856
General mean	3779.394	2696.829	1309.437
S.E.D.	17.632	12.325	6.519
F-ratio region	4.923***	0.997 ns	1.952 ns

***, **, *: significant differences at the 0.001, 0.01 and 0.05 level of significance respectively. ns stands for not significant at 5% level of significance. S.E.D stands for standard error for differences. Power of test values for Pillai's Trace, Wilks' Lambda, Hotelling's Trace and Roy's Largest Root tests were 99.3%, 99.1%, 99.6% and 99.5%, respectively. In short, the results of 2018 data and 2015 data were equal to each other

According to Bonferroni test results, there was significant differences between the Eastern Anatolia-Marmara, Eastern Anatolia-Aegean, Southeastern Anatolia-Marmara and Southeastern Anatolia-Aegean regions with regards to average milk yield ($p < 0.05$ and $p < 0.01$). Inter-regional differences regarding average milk yield from crossbreed and native cattle were insignificant.

http://www.aloki.hu ● ISSN 1589 1623 (Print) ● ISSN 1785 0037 (Online)
DOI: http://dx.doi.org/10.15666/aeer/1706_1494514959

Table 9. *Bonferroni test results (for culture)*

	Eastern Anatolia	Southeastern Anatolia	Marmara	Aegean	Black Sea	Central Anatolia	Mediterranean
Eastern Anatolia	---	---	**	**	---	---	---
Southeastern Anatolia	---	---	*	**	---	---	---
Marmara	**	*	---	---	---	---	---
Aegean	**	**	---	---	---	---	---
Black Sea	---	---	---	---	---	---	---
Central Anatolia	---	---	---	---	---	---	---
Mediterranean	---	---	---	---	---	---	---

*P < 0.05, **P < 0.01

Similar results were obtained in the MANOVA test for 2015 and 2018 data. In both data sets, the power of the test gave the same results. Bonferroni test gave the same results for 2015 and 2018 data in determining the difference of milk yield by region.

Çelik (2015) used the MANOVA method to analyze the inter-regional differences with regards to milk yield from small cattle. Research findings presented statistically significant inter-regional differences with regards to milk yield from hair goat and indigenous sheep. As for milk yield from hair goat, there were significant differences between Eastern Anatolia-Southeastern Anatolia, Marmara, Aegean and Mediterranean regions, Southeastern Anatolia-Marmara, Aegean and Mediterranean regions, Marmara-Aegean regions, Middle Eastern Anatolia and Mediterranean regions, Aegean-Mediterranean regions, Middle Eastern Anatolia-Mediterranean regions and Mediterranean-Black Sea regions. As for milk yield from indigenous breed cattle, there were significant differences between Eastern Anatolia-Southeastern Anatolia, Marmara, Aegean, Middle Eastern, Mediterranean and Black Sea regions, Southeastern Anatolia-Marmara, Aegean, Middle Eastern, Mediterranean and Black Sea regions, Marmara-Aegean regions, Middle Eastern Anatolia, Mediterranean and Black Sea regions, Aegean-Middle Eastern, Mediterranean and Black Sea regions and Middle Eastern Anatolia-Black Sea regions.

Indigenous, cross and culture breed animals in Turkey were compared with respect to 11 slaughtering and 18 carcass features and MANOVA analysis was performed. The differences among culture, indigenous and cross breeds were significant with regards to culture breeds (Kızıl and Aydoğan 2014).

In agricultural sciences, MANOVA test has been applied (Engeler and Reyer 2000, Woodward and Bauer 2007, Maposa et al. 2010, Turan 2011).

In this research, studies on other animal breeding data were analyzed using the MANOVA method.

Conclusion

In this research, milk yields from culture, cross and indigenous breed cattle in Turkey were analyzed by multivariate analysis (MANOVA) for 7 geographical regions. In this research, 7 groups (regions) were subjected to MANOVA test on the basis of 3 dependent variables (breeds). The cities of Kilis, Bingöl, Bitlis, Hakkari and Bartın were excluded from the research as they interrupted the observation values of the normality test. Analysis was performed for 76 cities and the observed outlier value was

http://www.aloki.hu ● ISSN 1589 1623 (Print) ● ISSN 1785 0037 (Online)
DOI: http://dx.doi.org/10.15666/aeer/1706_1494514959

eliminated. After this stage, homogeneity test for the covariance matrices and sphericity test were presented with the aim to apply the MANOVA test. As $p = 0.076 > \alpha = 0.05$ according to the results of the test, group covariance matrices were equal. As Approx $\chi^2 = 53.611$ and $p < 0.01$ according to the result of the Barlett's Test for Sphericity, MANOVA test was determined to be suitable for the analyzed data set. Representative statistical analysis was performed to show that milk yield from cross, culture and indigenous breeds varied on regional basis. While a higher milk yield was reported for cross breed cattle in the Aegean Region, the lowest milk yield was reported for the Eastern Anatolia Region. As for culture breed cattle, the highest milk yield was obtained in the Aegean Region whereas the lowest milk yield was obtained in the Southeastern Anatolia Region. As for indigenous breed cattle, the highest milk yield was obtained in the Eastern Anatolia Region whereas the lowest milk yield was obtained in the Mediterranean Region. According to the results of the Bonferroni test, milk yield differences from cross breed cattle were significant between the Eastern Anatolia-Aegean regions, Eastern Anatolia-Marmara regions, Southeastern Anatolia-Aegean regions and Southeastern Anatolia-Marmara regions. The inter-regional differences observed in milk yield obtained from culture breed and indigenous breeds cattle were insignificant. In general, milk yield from cross and culture breeds cattle was higher in Aegean and Marmara regions whereas milk yield from indigenous breed cattle was higher in the Eastern Anatolia region. Statistical methods proved to be favorable in the research, enabling the essential hypotheses. Consequently, MANOVA test can be considered to be a powerful analysis method in this research. The MANOVA test was determined to be good predictors of the difference of milk yield between regions in agriculture. It can be recommended that the use multivariate statistical methods of such as MANOVA method will be beneficial in future studies in agriculture.

Acknowledgements. This study is derived from Mrs. Gamze Azak's master thesis.

REFERENCES

[1] Akman, N., Şen, A. Ö., Cedden, F. (2017): Türkiye'de sığır yetiştiriciliği. – Tarım Haftası 2017 Türkiye'nin Hayvansal Üretimi (Mevcut Durum ve Gelecek) Sempozyumu, 10-11 Ocak 2017, pp. 55-75, Ankara, Türkiye.
[2] Alpan, O., Arpacık, R. (1998): Sığır Yetiştiriciliği. – Medisan, Ankara.
[3] Alpar, R. (2011). Uygulamalı Çok Değişkenli İstatistiksel Yöntemler. – Detay Yayıncılık, Ankara.
[4] Bakır, G., Kaygisiz, A., Çilek, S. (2009): Milk yield of Holstein cattle reared at Tahirova State Farm in Balikesir Province in Turkey. – Journal of Animal and Veterinary Advances 8(11): 2369-2374.
[5] Bastin, C., Soyeurt, H., Gengler, N. (2013): Genetic parameters of milk production traits and fatty acid contents in milk for Holstein cows in parity 1–3. – J. Anim. Breed. Genet. 130: 118-127.
[6] Boğokşayan, H., Bakır, G. (2013): Determination of lifetime yield performance of Holstein cattle raised in Şanlıurfa Ceylanpınar farm. – Atatürk University Journal of the Agricultural Faculty 44(1): 75-81 (Turkish).
[7] Çelik, Ş. (2015): Investigation milk yield in small ruminants by region in Turkey. – International Journal of Innovation Sciences and Research 4(10): 516-519.

http://www.aloki.hu ● ISSN 1589 1623 (Print) ● ISSN 1785 0037 (Online)
DOI: http://dx.doi.org/10.15666/aeer/1706_1494514959

[8] Duru, S., Kumlu, S., Tuncel, E. (2012): Estimation of variance components and genetic parameters for type traits and milk yield in Holstein cattle. – Turk. J. Vet. Anim. Sci. 36(6): 585-591.
[9] Engeler, B., Reyer, H-U. (2000): Choosy females and indiscriminate males: mate choice in mixed populations of sexual and hybridogenetic water frogs (*Rana lessonae, Rana esculenta*). – Behavioral Ecology 12(5): 600-606.
[10] Everitt, B. S. (2001): Statistics for Psychologists. An Intermediate Course. – Lawrance Erlbaum Associates, Inc., New Jersey.
[11] FAO (2017): Food and Agriculture Organization of the United Nations. Live Animal Production. – http://faostat3.fao.org/download/Q/QL/E.
[12] Hsu, J. C. (1996): Multiple Comparisons. – CRS Press LLC, New York.
[13] Jeremy, D. F. A. (1974): General Model for Multivariate Statistical Analysis. – Prentice-Hall International, Inc, USA.
[14] Johnson, R. A., Wichern, D. W. (2002): Applied Multivariate Statistical Analysis. – Prentice Hall, Upper Saddle River, NJ.
[15] Hashemi, A., Nayebpoor, M. (2008): Estimates of genetic and phenotype parameters from milk production in Iran Holstein-Friesian cows. – Research Journal of Biological Sciences 3(6): 678-682.
[16] IBM Corp. Release (2015): IBM SPSS Statistics for Windows, Version 23.0. – IBM Corp, Armonk, NY.
[17] Irano, N., Braga Bignardi, A., El Faro, L., Luiz Santana M, Lúcia, C. V., Albuquerque, L. G. (2014): Genetic association between milk yield, stayability and mastitis in Holstein cows under tropical conditions. – Trop. Anim. Health Prod. 46: 529-535.
[18] Keskin, İ., Boztepe, S. (2011): Estimation of 305 days milk yield using partial milk yield in Holstein cattle. – Tekirdağ Ziraat Fakültesi Dergisi 8(1): 1-7.
[19] Khattab, A. S., Atil, H., Badawy, L. (2005): Variances of direct and maternal genetic effects form milk yield and first calving in a herd of Friesian cattle in Egypt. – Arch. Tierz. 48(1): 24-31.
[20] Kheirabadi, K., Alijani, S. (2014): Genetic parameters for milk production and persistency in the Iranian Holstein population by the multitrait random regression model. – Archiv Tierzucht 57(12): 1-12.
[21] Kızıl, S. H., Aydoğan, M. (2014): Evaluation of major cattle breeds in Turkey for slaughter and carcass traits using MANOVA and multidimensional scaling technique. – Journal of Faculty of Veterinary Medicine, Erciyes University 11(1): 15-22.
[22] Kumlu, S., Akman, N. (1999): Milk yield and reproductive traits of Holstein Friesian breeding herds in Turkey – Lalahan Hayvancılık Araştırma Enstitüsü Dergisi 39(1): 1-15 (Turkish).
[23] Lehmann, E. L. (1986): Testing Statistical Hypotheses. Wiley Series in Probability and Mathematical Statistics. – Wiley, New York.
[24] Makgahlela, M. L., Banga, C. B., Norris, D., Dzama, K., Ng'ambi, J. W. (2007): Genetic correlations between female fertility and production traits in South African Holstein cattle. – South African Journal of Animal Science 37(3): 180-188.
[25] Maposa, D., Mudimu, E., Ngwenya, O. (2010): A multivariate analysis of variance (MANOVA) of the performance of sorghum lines in different agroecological regions of Zimbabwe. – African Journal of Agricultural Research 5(3): 196-203.
[26] Mendeş, M. (2013): Uygulamalı Bilimler İçin İstatistik ve Araştırma Yöntemleri. – Kriter Yayınevi, İstanbul.
[27] Oudah, E. Z. M., Zainab, A. K. (2010): Genetic evaluation for Friesan cattle in Egypt using single-trait animal model. – Journal Animal and Poultry Production, Mansoura University 1(9): 371-381.
[28] Pirzada, R. (2011): Estimation of genetic parameters and variance components of milk traits in Holstein-Friesian and British-Holstein dairy cows. – Kafkas Üniversitesi Veteriner Fakültesi Dergisi 17(3): 463-467.

http://www.aloki.hu ● ISSN 1589 1623 (Print) ● ISSN 1785 0037 (Online)
DOI: http://dx.doi.org/10.15666/aeer/1706_1494514959

[29] Rao, C. R. (1973): Linear Statistical Inference and Its Applications. 2nd. Ed. – John Wiley & Sons Inc, New York.
[30] Şahin, A., Ulutaş, Z. (2010): Genetic parameters of milk production and reproduction traits of Holstein cattle at a Tahirova State Farm conditions. – Kafkas Üniversitesi Veteriner Fakültesi Dergisi 16(6): 1051-1056.
[31] Şapdeniz, İ. (1993): A research on the economic analysis and the physical input requirements on the dairy enterprise of the Agriculture Faculty of Ankara University. – Ankara University Graduate School of Natural and Applied Sciences Department of Agricultural Economics, Master's thesis, Ankara (Turkish).
[32] Sattar, A., Mirza, R. H., Niazi, A. A. K., Laitf, M. (2005): Productive and reproductive performance of Holstein-Friesian cows in Pakistan. – Parkistan Vet. J. 25(2): 75-81.
[33] Tekerli, M., Gündoğan, M. (2005): Effect of certain factors on productive and reproductive efficiency traits and phenotypic relationships among these traits and repeatabilities in West Anatolian Holsteins. – Turk J. Vet. Anim. Sci. (29): 17-22.
[34] Tuncel, E. (1994): Hayvan Islahı. – Uludağ Üniversitesi Ziraat Fakültesi Ders Notları No: 46, Bursa.
[35] Turan, H. (2011): Geometric Morphometric studies Trakya Region honeybees (*Apis mellifera L.).* – Ph.D. Thesis. Namık Kemal University Graduate School of Natural and Applied Sciences Main Science Division of Animal Science (Turkish).
[36] TSI (2015): Animal Production Statistics, Animal Products, Number of Milked Animals and Milk Production Quantity. – Turkish Statistical Institute, Ankara (Turkish). http://www.tuik.gov.tr/PreTablo.do?alt_id=1002 (accessed to 26.10.2016).
[37] Türkyılmaz, M. K. (2005): Reproductive characteristics of Holstein cattle reared in a private dairy cattle enterprise in Aydın. – Turk J. Vet. Anim. Sci. 29: 1049-1052.
[38] Woodward, L. E., Bauer, A. L. (2007): People and their pets: a relational perspective on interpersonal complementarity and attachment in companion animal owners. – Society and Animals 15: 169-189.
[39] Yaylak, E. (2003): Reasons for culling, herd life and productive life in Holstein cows – Akdeniz Üniversitesi Ziraat Fakültesi Dergisi 16(2): 179-185 (Turkish).
[40] Yousefi-Golverdi, A., Hafezian, H., Chashnidel, Y., Farhadi, A. (2012): Genetic parameters and trends of production traits in Iranian Holstein population. – African Journal of Biotechnology 11(10): 2429-2435.

http://www.aloki.hu ● ISSN 1589 1623 (Print) ● ISSN 1785 0037 (Online)
DOI: http://dx.doi.org/10.15666/aeer/1706_1494514959

DETERMINATION OF SOME METAL LEVELS IN WATER, SEDIMENT AND FISH SPECIES OF TERCAN DAM LAKE, TURKEY

GÜNEŞ, M.[1,*] – SÖKMEN, T. Ö.[1] – KIRICI, M.[2]

[1]*Department of Occupational Health and Safety, Vocational School of Tercan, Erzincan Binali Yıldırım University, 24100 Erzincan, Turkey*

[2]*Department of Veterinary Health, Vocational School of Technical Sciences, Bingöl University, 12000 Bingöl, Turkey*

**Corresponding author*
e-mail: gunesmuharrem@hotmail.com; phone: +90-533-318-1454; fax: +90-446-226-6665

(Received 23rd Jun 2019; accepted 16th Oct 2019)

Abstract. This study aimed to determine the metal (Al, As, Cr, Cu, Fe, Mn, Ni, Pb, and Zn) levels in the gill, liver, and muscle tissues of some fish species, water and sediment samples taken from Tercan Dam Lake (Erzincan, Turkey). Initially, some physico-chemical parameters of the water such as temperature, pH, and dissolved oxygen were measured, and the relationship was determined between these parameters and the metal levels detected in the water. According to the analysis conducted on the water and the sediment, the most frequent metal was determined to be Fe. During the analyses conducted in the water, Pb and Zn metals were not detected, and all metals were detected in the sediment. It was determined that metals accumulated to a higher degree in the liver and gill tissues compared to muscle tissues. The harmfulness of the metal amounts determined in the water, sediment, and fish tissues was evaluated by comparing them to the acceptable values determined by national and international institutions.
Keywords: *accumulation, toxicity, Tercan Dam Lake, water contamination, physico-chemical parameters*

Introduction

The aquatic ecosystem, being part of the biosphere, is a receiver and carrier environment for the waste water and used water in the system, it is more exposed to contamination compared to air and soil (Yarsan et al., 2000). Water, which is in a constant cycle on the earth, loses its environment as a result of mostly human activities. Consequently, the water contamination occurs. Undoubtedly, the leading contaminators are the metals, which are common in today's aquatic ecosystem and which cause high rates of toxicity in aquatic organisms. Metals in general have a particular significance among other chemical contaminators since they can emerge from very different sources, cause a vast amount of contamination, continuously affect the biological systems, and—entering the food chain—can simply accumulate in developed living beings with increasing intensities (Erdoğrul and Ates, 2006).

Metals are carried towards waters by rock fragments through erosion, dust particles carried by the wind, volcanic activities, and forest fires. Metals dissolved in the water merge into the sediment by precipitating to the bottom, and thus, the metals accumulate at the sediment (Fergusson, 1990). The concentration of the metals accumulating at the sediment varies based on the ratio of the sediment particles, the size of the particles, and based on whether there are organic substances in the sediments. Since the sediment is an

http://www.aloki.hu ● ISSN 1589 1623 (Print) ● ISSN 1785 0037 (Online)
DOI: http://dx.doi.org/10.15666/aeer/1706_1496114972

important accumulation environment for the metals, it is used in determining the metal contamination of the aquatic environments (Salomans et al., 1987).

The fish take the metals through nutrition, water, gills and skin from the external environment. The amount of the metals accumulating at different tissues of the fish vary according to the amount of metal in the environment, the type of the metal, the interaction duration of metal and the fish, the age and metabolic activities of the fish, the phase of its development, the physico-chemical characteristics of the water, tissues, and organs (Köse and Uysal, 2008). The metals received by the fish reach to the tissues and organs via blood path bonded to the carrier protein, and they reach high concentration levels through being bonded by the metal bonding proteins (Sönmez et al., 2016). Metals show their toxic effects on cell membranes, enzymes, and cell organelles in general (Kirici et al., 2017a). The toxicity of metals involves the interaction between the toxicological target and the free metal ions. Additionally, the cells (liver, renal tubular, gastrointestinal), which make metal transfer during their tasks, are the most toxic-effect-sensitive cells (Elbeshti et al., 2018).

Numerous studies have been conducted on the accumulation of metals in water, sediments, and fish (Moiseenko and Kudryavtseva, 2001; Al-Saadi et al., 2002; Özmen et al., 2004; Tekin-Özan et al., 2007; Tao et al., 2011; Tekin-Özan and Aktan, 2012; Başyiğit and Tekin-Özan, 2013; Kirici et al., 2013a, 2016a, 2017b). In this study, it was aimed at determining the metal (Al, As, Cr, Cu, Fe, Mn, Ni, Pb, and Zn) concentrations in the gills, livers, and muscle tissues of Grass carp (*Ctenopharyngodon idella*), Caner fish (*Barbus capito*), Common carp (*Cyprinus carpio*) and Tigris scraper (*Capoeta umbla*), which live in the Tercan Dam Lake—within the borders of Erzincan province—water, sediment, and lake; it was also aimed at determining the relationship between metal levels in the water and the measured certain physico-chemical parameters of the water.

Materials and methods

Research area

Tercan Dam Lake is located 3 km to the Tercan district of Erzincan province (Turkey). The Dam Lake was inaugurated in 1988 for irrigation and energy. The lake has a surface area of 8.85 km^2, a drainage volume of 178 million m^3, and an irrigation area of 29725 ha. It is located between 39°44’2” north latitude and 40°26’40” east longitudes (*Fig. 1*). Tercan Dam Lake is fed by Tuzla Brook, Çirkiz Brook, Bülbül Brook and Pırnaşil Brook.

Field studies

The research study was conducted through samples taken from 3 stations between March 2018 - May 2018. The water (500 mL water samples were taken from each station) and sediment samples (3 g sediment samples were taken from each station) were taken from each station 3 times in different days, which was repeated 3 times per-month. As per the fish samples (grass carp (n = 22), Caner fish (n = 21), Common carp (n = 25) and Tigris scraper (n = 29)), they were obtained by means of fishermen fishing in the area. During the study, the temperature, pH, and dissolved oxygen amount of the water were measured through the Jenco 6010 (Jenco Instruments Co. China) brand portable multi-parameter. The water, sediment, and fish samples taken from the lake

http://www.aloki.hu ● ISSN 1589 1623 (Print) ● ISSN 1785 0037 (Online)
DOI: http://dx.doi.org/10.15666/aeer/1706_1496114972

were brought to the laboratories after being contained in sample containers under cold storage conditions. The water samples were treated with HNO_3 with a 2% concentration ratio. The water samples were kept at +4 °C until (24 h) they were analyzed. The sediment samples were taken through ekman spoonnet, being brought to the laboratory within propylene containers.

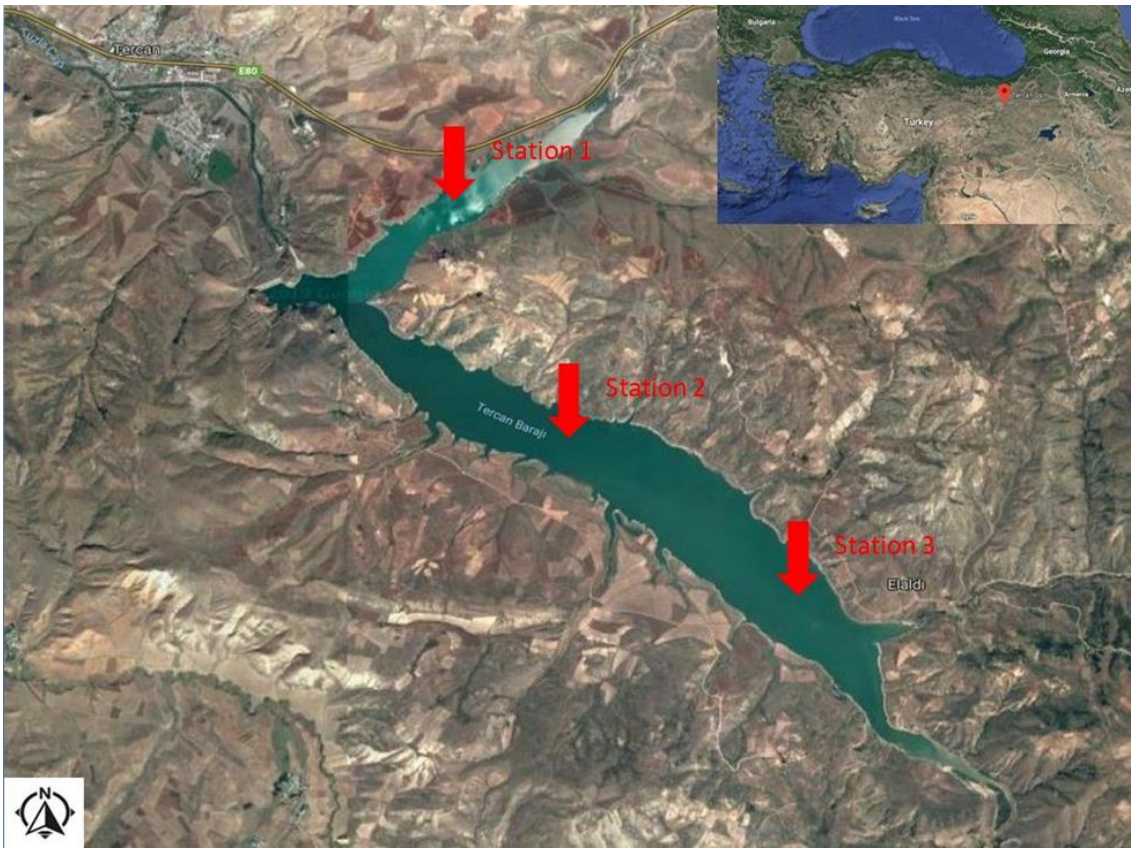

Figure 1. *Tercan Dam Lake*

Laboratory studies

The samples of water, sediment, and fish were brought to the Chemistry Laboratory of Erzincan University Basic Sciences Research and Application Center for laboratory studies. The weights of the fish were measured via scales and their total lengths were measured via measuring board with ± 1 mm precision. Subsequently, muscle, liver, and gill tissue samples of the fish were taken.

In order to determine the Al, As, Cr, Cu, Fe, Mn, Ni, Pb, and Zn accumulation concentrations in the muscle, gill, and liver tissues of the fish, 3-5 g samples were taken from each tissue. The tissue samples were put into heat-proof glass bottles and kept under 105 °C for 24 h in the Drying Oven for drying, and subsequently they were left for cooling down for 24 h. After pulverizing each sample and limiting them to 0.5 g via the precision scale, they were placed into teflon microwave tubes. Adding 7 ml HNO_3 and 1 ml H_2O_2, they were kept at ambient temperature for 24 h. The samples were shaken in the vortex for 10 min, thus, they were mineralized. Placed into microwave tubes, the samples were burnt at 110 °C at 700 W for 45 min. After opening the samples in the fume cupboard, their weights were increased to 200 ml by adding deionized

http://www.aloki.hu ● ISSN 1589 1623 (Print) ● ISSN 1785 0037 (Online)
DOI: http://dx.doi.org/10.15666/aeer/1706_1496114972

water. Filtered through a teflon filter, the samples were made ready for the analysis. The metal analyses of the prepared samples were measured through ICP-MS device (Sökmen et al., 2018).

The sediment samples to be analyzed were taken from the lake via ekman spoonnet and placed into containers, and they were kept in deepfreeze until the analysis. For the measurement, 1 g was taken from each sample and placed into microwave solubilization tubes. Adding 5 ml HNO_3 and 1 ml H_2O_2 into each tube, they were exposed to solubilization process in a microwave oven (Milestone Ethos Plus 2000). Taking the tubes out from the oven, they were cooled down at the ambient temperature and the solutions in the tubes were transferred into 25 ml polypropylene volumetric flasks. The solution amounts in the volumetric flasks were completed to 25 ml by adding distilled water. The metal analysis of the samples was conducted in the (Perkin Elmer, 5300 DV model) ICP-OES device. The metal analyses of the water samples were directly conducted. The detection limits of the elements were Cd 0.0012 ppm, Cr 0.0027 ppm, Cu 0.0069 ppm, Fe 0.0381 ppm, Mn 0.001 ppm, Pb 0.0078 ppm, Zn 0.0015 ppm, Al 0.0057 ppm, and Ni 0.0048 ppm (Tekin-Özan and Kır, 2005).

Statistical analyses

The minimum-maximum values, arithmetic means, and standard deviation values of the results obtained in the study were calculated. Pearson Test was applied to determine the relationship between the physico-chemical parameters (temperature, pH, and dissolved oxygen) of the water and metal amounts. All of the statistical calculations were conducted through SPSS 17 package program.

Results and discussion

In this study, the metal (Al, As, Cr, Cu, Fe, Mn, Ni, Pb, and Zn) concentrations were determined in the gill, liver, and muscle tissues of grass carp, Caner fish, common carp and Tigris scraper fish living in the water, sediment, and lake of the Tercan Dam Lake. Additionally, the relationship between the physico-chemical parameters and metal levels in the water was determined.

During the study, the water temperature, pH value, and dissolved oxygen amounts of the Tercan Dam Lake were measured and given in the *Table 1*. According to the *Table 1*, the highest temperature is 14.2 °C, while the lowest is 8.3 °C, and the mean temperature is 11.4 °C.

The results of the metal analyses conducted in the Tercan Dam Lake are given in the *Table 2*. As the conclusion of the metal analyses conducted in the water, it was determined that the highest accumulated metal in the water was Fe metal. Besides, the Pb and Zn metals were under the analysis limitations. The ranking of the mean values of the accumulation in the water was determined as Fe > Al > Ni > As > Cu > Mn > Cr. Reporting that the highest accumulated metal in the Habbaniyah Lake (Iraq) was Zn, Al-Saadi et al. (2002) stated that it was followed, respectively, by Cu, Pb, Ni, Mn and Cd metals. It was also mentioned that the Cd, Co, Hg, Mo, and Pb were under the AAS analysis limitations. In a study conducted in the Texoma Lake by An and Kampbell (2003) it was mentioned that the highest metal concentrations in the water were Na and Ca, and subsequently Mg and K. In a study conducted in the Kovada Lake by Tekin-Özan et al. (2004), Fe, Zn, and Mn were determined in the waters of the lake, and it was also determined that the levels of Cu, Cr, Pb and Cd were under the AAS analysis

http://www.aloki.hu ● ISSN 1589 1623 (Print) ● ISSN 1785 0037 (Online)
DOI: http://dx.doi.org/10.15666/aeer/1706_1496114972

limitations. Similarly, in a study conducted in the Kovada Lake by Kır et al. (2007), it was determined that the most frequent metal encountered in the water was Fe. In a study conducted in the Taihu Lake (China), it was determined that the highest accumulated metal in the water was Zn, while the least accumulated one was Cd (Tao et al., 2012). Similarly, in a study conducted in the Panjkora River (Pakistan), the highest accumulated metal in the water was Zn, while the least accumulated metal was Cd (Ahmad et al., 2014).

Table 1. *Maximum, minimum, mean and standard deviation values of the temperature, pH, and dissolved oxygen values in the Tercan Dam Lake*

	Temperature	**pH**	**Dissolved oxygen (mg/L)**
Minimum	8.3	7.7	8.3
Maximum	14.2	8.1	9.2
Mean	11.4	7.9	8.7
Standard deviation	2.42	0.17	0.39

Table 2. *Maximum values, minimum values, mean values (ppb), and standard deviation values of the metal concentrations measured in the Tercan Dam Lake*

	Al	**As**	**Cr**	**Cu**	**Fe**	**Mn**	**Ni**	**Pb***	**Zn***
Minimum	2.167	1.430	0.003	0.112	4.737	0.045	0.459	-	-
Maximum	4.152	2.219	0.143	0.460	7.016	0.316	4.568	-	-
Mean	3.466	1.811	0.037	0.268	5.703	0.139	1.896	-	-
Standard deviation	0.921	0.229	0.024	0.089	0.965	0.023	0.743	-	-

*Below the analysis limitations

As the conclusion of the metal analyses conducted in the waters of the Tercan Dam Lake and comparing the metal levels of the study to the acceptable heavy metal amounts in the water determined by the World Health Organization (WHO), Turkish Standards Institute (TSI), and Turkish Ministry of Food, Agriculture, and Livestock (MFAL), and United States Environmental Protection Agency (USEPA), it was determined that all metal levels were under the acceptable values.

Using the Pearson Test, the relationships were determined between the temperature, pH, and dissolved oxygen amounts and the metal levels determined in the water, which are all given in the *Table 3*. According to this, there is a negative relationship between the temperature and the Ph, and there is a positive relationship between temperature and dissolved oxygen. In other words, while the temperature increases, pH value decreases, and the dissolved oxygen amounts increase. There is a negative relationship between the pH and dissolved oxygen, in other words, while pH increases, the dissolved oxygen amounts decrease. The pH value has a negative relationship with Cr, Cu, and Ni; while it has a positive relationship with Al, As, Fe, and Mn. While the dissolved oxygen has a negative relationship with Al, Cr, Cu, and Fe, it has a positive relationship with As, Mn, and Ni. Moreover, there are statistically significant differences between dissolved oxygen and As, between dissolved oxygen and Cu, and between Al and Ni (< 0.05).

http://www.aloki.hu ● ISSN 1589 1623 (Print) ● ISSN 1785 0037 (Online)
DOI: http://dx.doi.org/10.15666/aeer/1706_1496114972

Table 3. *Values of some physico-chemical parameters and metals measured in the waters of Tercan Dam Lake determined via Pearson test*

	Temperature	pH	Dissolved oxygen	Al	As	Cr	Cu	Fe	Mn	Ni
Temperature	1	-0.569	0.457	-0.403	0.433	-0.049	-0.267	-0.221	0.380	0.491
pH		1	-0.035	0.519	0.367	-0.258	-0.106	0.591	0.213	-0.249
Dissolved oxygen			1	-0.647	0.753*	-0.509	-0.731*	-0.473	0.280	0.402
Al				1	-0.211	0.029	0.291	0.656	-0.183	-0.695*
As					1	-0.404	-0.602	0.046	0.421	0.353
Cr						1	0.467	-0.226	0.065	-0.002
Cu							1	0.243	0.050	0.058
Fe								1	0.182	-0.095
Mn									1	0.563
Ni										1

*0.05 significance level

The metal amounts determined in the sediment samples taken from the Tercan Dam Lake are given in *Table 4*. As the conclusion of the metal analyses on the sediment, it was determined that the highest accumulated metal in the lake waters was Fe, and the lowest one was As. According to the ranking of the mean values of the accumulation in the water, it was determined as Fe > Al > Mn > Cr > Ni > Zn > Cu > Pb > As. In the study conducted in the Texoma Lake (USA), An and Kampbell (2003) determined that the metal accumulation mean values ranking was Ca > Al > Fe > K > Mg > Na. Özmen et al. (2004) conducted a research about some certain heavy metal accumulations in the Caspian Sea (Zn, Fe, Mn, Ni, Cu, Cr, Co and Pb). As the conclusion of the study, it was determined that the ranking of the major elements and heavy metal concentrations in the sediment was Fe > Mg > Ca > Mn > Zn > Ni > Cr > Cu > Co > Pb. In another study conducted in Uluabat Lake, Kurtoğlu (2006) detected that the heavy metals had a ranking such as Pb > Cu > Cr > Ni > Cd > Zn in the sediment samples. In another study conducted in the Cauvery River (India), Venkatesha et al. (2012) examined heavy metals such as Fe, Zn, Ni, Mn, Pb, Cu, Co, Cd and Cr in the sediment samples. As the conclusion of the study, it was determined that the highest accumulated metal in the sediment was Fe. It was followed by, respectively, Mn, Cr, Zn, Ni, Cu, Pb, Co, and Cd metals. In a different study conducted in Odiel River (Spain) by Usero et al. (2003), it was determined that the highest accumulated metal in the sediment was Fe. Usero et al. (2003) explained the reason that the metal that existed in the earth's crust at the highest level was Fe, that was why it was at higher levels in the lake, river, and sea sediment compared to other metals.

When the analysis results of the sediment samples taken from the Tercan Dam Lake were compared to the data of the American National Oceanic and Atmospheric Administration (NOAA), it was determined that all the metals were below the acceptable levels.

The number, total length, and weights of the fish caught by the help of the fishermen fishing in the region are given in *Table 5*. In the study, 22 grass carp fish were used with a length of 29.6 ± 1.02 cm, and weighting 409.4 ± 13.64 g, 21 Caner fish fish were used with a length of 43.2 ± 5.11 cm, and weighting 648.6 ± 15.70 g, while 25 common carp fish were used with a length of 31.2 ± 1.46 cm, and weighting 337.2 ± 10.88 g, and 29 Tigris scraper were used with a length of 32.8 ± 2.48 cm, and weighting 385.1 ± 13.5 g.

http://www.aloki.hu ● ISSN 1589 1623 (Print) ● ISSN 1785 0037 (Online)
DOI: http://dx.doi.org/10.15666/aeer/1706_1496114972

Table 4. *Maximum values, minimum values, mean values (mg/kg), and standard deviation values of the metal concentrations measured in the Tercan Dam Lake sediment*

	Al	As	Cr	Cu	Fe	Mn	Ni	Pb	Zn
Minimum	799.091	0.001	2.931	2.149	863.582	31.474	1.169	2.426	1.550
Maximum	1131.294	0.041	66.099	14.533	7731.094	153.228	42.461	7.783	39.148
Mean	936.438	0.015	39.362	5.979	3816.004	102.253	17.944	4.588	17.701
Standard deviation	16.593	0.006	1.684	0.460	22.766	7.160	3.724	0.306	3.948

Table 5. *Weight and length averages of the fish caught*

Fish species	Total length (cm)	Weight (g)	Fish number
Grass carp (*Ctenopharyngodon idella*)	29.6 ± 1.02	409.4 ± 13.64	22
Caner fish (*Barbus capito*)	43.2 ± 5.11	648.6 ± 15.70	21
Common carp (*Cyprinus carpio*)	31.2 ± 1.46	337.2 ± 10.88	25
Tigris scraper (*Capoeta umbla*)	32.8 ± 2.48	385.1 ± 13.53	29

The amounts of metal (Al, As, Cr, Cu, Fe, Mn, Ni, Pb, and Zn) concentrations determined in the gill, liver, and muscle tissues of the Caner fish, Tigris scraper, grass carp and common carp that were caught in the Tercan Dam Lake are given in the *Tables 6, 7, 8* and *9,* respectively.

Table 6. *Maximum, minimum, mean values (mg/kg), and standard deviation values of the metals measured in muscle, liver, and gill tissues of the Caner fish (Barbus capito)*

Tissue	MUSCLE				LIVER				GILL			
Metal	Min	Max	Mean	St. dev.	Min	Max	Mean	St. dev.	Min	Max	Mean	St. dev.
Al	-	-	-	-	0.906	7.817	2.953	0.126	0.145	3.804	1.375	0.144
As	-	-	-	-	0.021	0.187	0.057	0.009	0.032	0.394	0.124	0.028
Cr	0.087	0.192	0.106	0.034	0.031	0.304	0.084	0.005	0.027	1.136	0.398	0.052
Cu	0.008	4.284	0.882	0.013	0.435	57.114	15.888	0.216	0.744	60.003	11.119	2.187
Fe	8.270	124.041	43.638	1.020	16.496	918.684	420.160	8.320	16.496	679.166	195.062	5.792
Mn	0.017	0.571	0.343	0.044	0.562	18.523	7.662	0.672	0.529	16.656	5.714	0.544
Ni	-	-	-	-	0.004	0.173	0.042	0.006	0.028	0.741	0.213	0.016
Pb	-	-	-	-	0.016	0.227	0.090	0.017	0.008	0.067	0.032	0.008
Zn	21.048	237.530	77.936	4.050	0.334	241.328	88.507	3.074	0.334	241.328	91.691	1.935

Table 7. *Maximum, minimum, mean values (mg/kg), and standard deviation values of the metals measured in muscle, liver, and gill tissues of the Tigris scraper (Capoeta umbla)*

Tissue	MUSCLE				LIVER				GILL			
Metal	Min	Max	Mean	St. dev.	Min	Max	Mean	St. dev.	Min	Max	Mean	St. dev.
Al	7.613	57.754	20.009	4.270	37.087	215.078	90.044	11.670	44.105	199.086	96.595	7.749
As	-	-	-	-	0.087	0.479	0.160	0.077	0.045	0.601	0.186	0.091
Cr	0.009	0.054	0.023	0.006	0.753	8.715	2.088	0.723	0.317	12.593	2.455	0.613
Cu	0.108	1.091	0.239	0.082	49.347	358.440	141.470	6.078	0.447	1.928	0.378	0.170
Fe	1.795	43.138	8.986	1.708	117.448	1512.825	486.326	14.719	27.623	122.437	74.916	6.471
Mn	3.186	29.138	9.149	3.485	26.678	120.188	61.528	3.271	9.873	45.415	19.671	2.483
Ni	-	-	-	-	0.953	6.910	2.278	0.240	0.523	7.812	1.667	0.754
Pb	0.316	2.281	0.640	0.150	0.520	3.739	2.074	1.141	0.364	1.733	0.547	0.050
Zn	3.832	54.958	11.703	2.165	3.180	69.201	34.972	5.659	12.385	75.248	37.777	3.762

http://www.aloki.hu ● ISSN 1589 1623 (Print) ● ISSN 1785 0037 (Online)
DOI: http://dx.doi.org/10.15666/aeer/1706_1496114972

Table 8. *Maximum, minimum, mean values (mg/kg), and standard deviation values of the metals measured in muscle, liver, and gill tissues of the Grass carp (Ctenopharyngodon idella)*

Tissue	MUSCLE				LIVER				GILL			
Metal	**Min**	**Max**	**Mean**	**St. dev.**	**Min**	**Max**	**Mean**	**St. dev.**	**Min**	**Max**	**Mean**	**St. dev.**
Al	1.598	8.021	3.069	0.740	2.003	40.217	19.322	3.161	2.714	19.357	10.136	5.983
As	-	-	-	-	-	-	-	-	0.190	1.675	0.774	0.543
Cr	-	-	-	-	0.009	1.136	0.458	0.052	0.012	0.075	0.049	0.026
Cu	0.321	1.723	0.792	0.157	1.122	7.248	4.185	0.251	0.132	2.014	0.882	0.694
Fe	4.170	39.071	27.350	5.412	26.966	104.672	59.277	2.833	7.745	53.402	23.452	3.025
Mn	0.003	0.441	0.014	0.001	0.617	6.218	2.859	0.202	4.021	11.116	7.349	2.596
Ni	-	-	-	-	-	-	-	-	0.019	0.205	0.122	0.065
Pb	0.030	0.991	0.318	0.026	0.013	0.624	0.455	0.146	0.017	0.256	0.116	0.011
Zn	8.763	40.137	18.922	1.257	5.823	61.673	23.709	0.193	79.397	259.631	164.827	5.676

Table 9. *Maximum, minimum, mean values (mg/kg), and standard deviation values of the metals measured in muscle, liver, and gill tissues of the Common carp (Cyprinus carpio)*

Tissue	MUSCLE				LIVER				GILL			
Metal	**Min**	**Max**	**Mean**	**St. dev.**	**Min**	**Max**	**Mean**	**St. dev.**	**Min**	**Max**	**Mean**	**St. dev.**
Al	13.294	266.814	193.973	12.270	456.053	1120.483	807.121	9.627	7.575	97.435	39.624	2.092
As	-	-	-	-	0.057	0.449	0.265	0.146	0.057	0.923	0.383	0.083
Cr	0.198	1.336	0.592	0.445	0.078	2.608	1.409	0.011	0.314	2.692	0.918	0.042
Cu	-	-	-	-	17.069	100.169	46.023	2.831	0.789	6.045	2.695	0.517
Fe	10.766	194.636	87.463	7.210	450.917	1098.847	764.449	4.261	26.848	742.849	330.265	7.924
Mn	6.273	24.114	15.193	6.603	1.749	39.443	26.754	5.254	7.760	104.033	34.735	0.903
Ni	0.025	0.854	0.326	0.092	0.326	3.091	2.584	1.133	0.398	1.300	0.569	0.131
Pb	-	-	-	-	0.279	0.988	0.534	0.253	0.534	1.370	0.962	0.253
Zn	4.219	11.731	8.301	2.490	23.148	109.507	52.752	7.153	11.007	0.945	4.264	1.327

It was determined that the metal accumulation in the muscle tissues of Caner fish was Zn > Fe > Cu > Mn > Cr, while the accumulation in the liver tissues of the same species was Fe > Zn > Cu > Mn > Al > Pb > Cr > As > Ni, and the accumulation in its gill tissues was Fe > Zn > Cu > Mn > Al > Cr > Ni > As > Pb. Additionally, it was determined that the accumulation of Al, As, Ni, and Pb metals in the muscle tissues of the Caner fish were lower than the analysis limitations (*Table 6*). It was determined that the metal accumulation in the muscle tissues of Tigris scraper was Al > Zn > Mn > Fe > Pb > Cu > Cr, while the accumulation in the liver tissues of the same species was Fe > Cu > Al > Mn > Zn > Cr > Ni > Pb > As, and the accumulation in its gill tissues was Al > Fe > Zn > Mn > Cr > Ni > Pb > Cu > As. Additionally, it was determined that the accumulation of As and Ni metals in the muscle tissues of the Tigris scraper were lower than the analysis limitations (*Table 7*). It was determined that the metal accumulation in the muscle tissues of grass carp was Fe > Zn > Cu > Al > Pb > , while the accumulation in the liver tissues of the same species was Fe > Zn > Al > Cu > Mn > Cr > Pb, and the accumulation in its gill tissues was Zn > Fe > Al > Mn > Cu > As > Ni > Pb > Cr. Additionally, it was determined that the accumulation of As, Cr, and Ni metals in the muscle tissues of the grass carp, and those of As and Ni metals in the liver tissues of it were lower than the analysis limitations (*Table 8*). It was determined that the metal accumulation in the muscle tissues of

http://www.aloki.hu ● ISSN 1589 1623 (Print) ● ISSN 1785 0037 (Online)
DOI: http://dx.doi.org/10.15666/aeer/1706_1496114972

common carp was Al > Fe > Mn > Zn > Cr > Ni, while the accumulation in the liver tissues of the same species was Al > Fe > Zn > Cu > Mn > Ni > Cr > Pb > As, and the accumulation in its gill tissues was Fe > Al > Mn > Zn > Cu > Pb > Cr > Ni > As. Additionally, it was determined that the accumulation of As, Cr, and Ni metals in the muscle tissues of the common carp were lower than the analysis limitations (*Table 9*).

There have been numerous research studies conducted in various parts of the world on the accumulation of metals in fish tissues and their detrimental effects on the tissues (Moiseenko and Kudryavtseva, 2001; Uysal et al., 2008; Kirici et al., 2013b, 2016b; El-Moselhy et al., 2014; Baharom and Ishak, 2015; Bosch et al., 2016; La Colla et al., 2017, 2018). For instance, in a study conducted on Avşar Lake (Turkey), Öztürk et al. (2009) examined the metal accumulation concentrations in the muscle, liver, and gill tissues of the Carp, and as the conclusion of the study, it was determined that the Fe metal had the highest accumulation level while Cd had the least. The ranking of metal accumulation in the tissues was determined as Fe > Cu > Pb > Ni > Cr > Cd in the muscle, and Fe > Cu > Ni > Pb > Cr > Cd in the gill and liver. Malik et al. (2010) determined the seasonal changes of some certain heavy metals (Cd, Cr, Cu, Hg, Ni, Pb, Zn) in the muscle, liver, gill, and kidneys of *Labeo rohita* and grass carp species in the Bhopal Lake (India). It was determined that, for the both fish species, the metals accumulated mostly in the livers and at the least levels in the muscles. While the highest accumulated metal in the fish was Zn, it was determined that Hg had the lowest level of accumulation. Taweel et al. (2013), examined the accumulation of Cu, Cd, Ni, Pb, and Zn in the muscle, liver, and gills of Tilapia fish (*Oreochromis niloticus*) living in the Langat River and Engineering Lake. As the conclusion of the study, it was determined that the accumulation ranking of the heavy metals was Cu > Zn > Ni > Pb > Cd in the liver samples, while it was Zn > Ni > Cu > Pb > Cd in the gill and muscle samples. The researchers reported that there was no risk in consumption of Tilapia fish.

The metal amounts determined in the muscle, liver, and gill tissues of the fish were compared to the values determined by the WHO, MFAL, and USEPA. As a result, it was determined that, in the muscle tissue of Caner fish, the Zn amount was higher than the acceptable level determined by the MFAL, the Fe amount in the liver tissue was higher than those of the MFAL and USEPA, the Mn amount was higher than that of the WHO, and the Zn amount was higher than that of the MFAL. Similarly, it was determined that, in the gill tissue of Caner fish, Mn amount was higher than the acceptable level determined by the WHO, and the Zn amount was higher than that of the MFAL. As per the muscle tissue of Tigris scraper, it was determined that the Mn amount was higher compared to the acceptable level determined by the WHO; in the liver tissue of Tigris scraper, it was determined that the Cu amount was higher compared to the acceptable level determined by the WHO, MFAL, and USEPA; as per the gill tissue of Tigris scraper, the Mn amount was higher compared to the level of WHO, and Ni amount was higher compared to the levels determined by the MFAL and WHO.

In the liver tissues of the grass carp, the Mn amount was higher than the acceptable level determined by the WHO, in its gill tissues, the Mn amount was higher than that of the WHO, and Zn amount was higher than those of WHO and MFAL. In the muscle tissues of the common carp, the Mn amount was higher than the acceptable level determined by the WHO for the fish tissues, and the amount of Ni was higher than that of MFAL; in its liver tissues, the Cn amount was higher than that of the WHO, MFAL, and USEPA, and the Mn amount was higher than that of WHO; as per the gill tissues,

http://www.aloki.hu ● ISSN 1589 1623 (Print) ● ISSN 1785 0037 (Online)
DOI: http://dx.doi.org/10.15666/aeer/1706_1496114972

the Zn and Ni amounts were higher than those of WHO and MFAL, Mn amount was higher than that of WHO, and Ni amount than that of MFAL.

Conclusion

As the conclusion of the study, when the metal concentrations determined in the muscle, liver, and gill tissues of fish were compared to the values determined by the WHO, MFAL, and USEPA, it was determined that the metal concentrations determined in the fish tissues were higher than the acceptable levels. It is an important case for the human health, since the muscle, which is consumed by human beings, had a metal concentration over the acceptable levels. Accumulation of metals in tissues directly influences the blood parameters, enzyme activities, growth, and development of the living being. Although numerous factors influence the existence of metals in the waters, undoubtedly the most important factor is the human activities. The water resources are contaminated particularly due to domestic waste, industrial waste, and agricultural activities. At this point, particularly people living around the water resources should be informed by the authorities. Additionally, necessary precautions should be taken against the wastes being released to the water resources from the industrial facilities and these measurements should be supervised by the authorities. Also, a potential danger may exist in the future, depending on the agricultural development in this region. As the Tercan Dam Lake is also used for agricultural irrigation purposes, performance of pollution researches at certain periods is of significance for both environment and public health.

Acknowledgements. This study was supported by the Erzincan Binali Yıldırım University, Scientific Research Projects Unit (Project no: FHD-2017-514). We would like to present our sincere thanks to the Erzincan Binali Yıldırım University, Scientific Research Projects Unit for their supports.

REFERENCES

[1] Ahmad, K., Azizullah, A., Shama, S., Khattak, M. N. K. (2014): Determination of heavy metal contentes in water, sediments, and fish tissues of *Shizothorax plagiostomus* in river Panjkora at Lower Dir, Khyber Pakhtunkhwa, Pakistan. – Environment Monitoring Assessment 186: 7357-7366.

[2] Al-Saadi, H. A., Al-Lami, A. A., Hassan, F. A., Al-Dulymi, A. A. (2002): Heavy metals in water, suspended particles, sediments and aquatic plants of Habbaniya Lake, Iraq. – International Journal of Environmental Studies 59: 589-598.

[3] An, Y. J., Kampbell, D. H. (2003): Total, dissolved, and bioavailable metals at Lake Texoma Marinas. – Environmental Pollution 122: 253-259.

[4] Baharom, Z. S., Ishak, M. Y. (2015): Determination of heavy metal accumulation in fish species in Galas River, Kelantan and Beranang mining pool, Selangor. – Procedia Environmental Sciences 30: 320-325.

[5] Başyiğit, B., Tekin-Özan, S. (2013): Concentrations of some heavy metals in water, sediment and tissues of Pikeperch (*Sander lucioperca*) from Karataş Lake related to physico-chemical parameters, fish size and seasons. – Polish Journal of Fisheries and Aquatic Sciences 22: 11-22.

[6] Bosch, A. C., O'Neill, B., Sigge, G. O., Kerwath, S. E., Hoffman, L. C. (2016): Heavy metal accumulation and toxicity in Smoothhound (*Mustelus mustelus*) shark from Langebaan Lagoon, South Africa. – Food Chemistry 190: 871-878.

http://www.aloki.hu ● ISSN 1589 1623 (Print) ● ISSN 1785 0037 (Online)
DOI: http://dx.doi.org/10.15666/aeer/1706_1496114972

[7] Elbeshti, R. T. A., Elderwish, N. M., Abdelali, K. M. K., Taştan, Y. (2018): Effects of heavy metals on fish. – Menba Journal of Fisheries Faculty 4: 36-47.
[8] El-Moselhy, K. M., Othman, A. I., Abd El-Azem, H., El-Metwally. M. E. A. (2014): Bioaccumulation of heavy metals in some tissues of fish in the Red Sea, Egypt. – Egyptian Journal of Basic and Applied Sciences 1: 97-105.
[9] Erdoğrul, O., Ateş, D. A. (2006): Determination of cadmium and copper in fish samples from Sir and Menzelet Dam Lake, Kahramanmaraş, Turkey. – Environmental Monitoring and Assessment 117: 281-290.
[10] Fergusson, F. E. (1990): The Heavy Elements: Chemistry, Environmental Impact and Health Effects. – Pergamon Press, Oxford, UK.
[11] Kır, İ., Özan, S. T., Tuncay, T. (2007): The seasonal variations of some heavy metals in Kovada Lake's water and sediment. – Ege University Journal of Fisheries and Aquatic 24: 155-158 (in Turkish)
[12] Kirici, M., Taysı, M. R., Bengü, A. Ş., İspir, Ü. (2013a): Determination of some metal levels in *Capoeta capoeta umbla* (Heckel, 1843) caught from Murat River. – Iğdır University Journal of the Institute of Science and Technology 3: 85-90 (in Turkish).
[13] Kirici, M., Taysi, M. R., Bengü, A. Ş., İspir, Ü. (2013b): Determination of some metal concentrations in muscle tissues of *Capoeta trutta* (Heckel, 1843) caught from Murat River. – Erzincan University Journal of Science and Technology 6: 115-124 (in Turkish).
[14] Kirici, M., Kirici, M., Beydemir, Ş., Atamanalp, M. (2016a): Purification of carbonic anhydrase from *Capoeta umbla* (Heckel, 1843) gills and toxicological effects of some metals on enzyme activity. – Turkish Journal of Fisheries and Aquatic Sciences 16: 169-175.
[15] Kirici, M., Kirici, M., Demir, Y., Beydemir, S., Atamanalp, M. (2016b): The effects of Al^{3+} and Hg^{2+} on glucose 6-phosphate dehydrogenase from *Capoeta umbla* kidney. – Applied Ecology And Environmental Research 14: 253-264.
[16] Kirici, M., Atamanalp, M., Kirici, M., Beydemir, Ş. (2017a): *In vitro* effects of some metal ions on glutathione reductase in the gills and liver of *Capoeta trutta*. – Regulatory Mechanisms in Biosystems 8: 66-70.
[17] Kirici, M., Turk, C., Caglayan, C., Kirici, M. (2017b): Toxic effects of copper sulphate pentahydrate on antioxidant enzyme activities and lipid peroxidation of freshwater fish *Capoeta umbla* (Heckel, 1843) tissues. – Applied Ecology and Environmental Research 15: 1685-1696.
[18] Köse, E., Uysal, K. (2008): The comparison of heavy metal accumulation ratios in muscle, skin and gill of non-maturated common carp (*Cyprinus carpio* L., 1758). – Journal of Science and Technology of Dumlupınar University 17: 19-26.
[19] Kurtoğlu, S. (2006): The investigation of some chemical parameters and seasonal variations of sediment in Lake Uluabat. – Master Thesis, Uludağ University, Institute of Science and Technology, Bursa, Turkey (in Turkish).
[20] La Colla, N. S., Botté, S. E., Marcovecchio, J. E. (2018): Metals in coastal zones impacted with urban and industrial wastes: Insights on the metal accumulation pattern in fish species. – Journal of Marine Systems 181: 53-62.
[21] La Colla, N. S., Botté, S. E., Oliva, A. L., Marcovecchio, J. E. (2017): Tracing Cr, Pb, Fe and Mn occurrence in the Bahía Blanca estuary through commercial fish species. – Chemosphere 175: 286-293.
[22] Malik, N., Biswas, A. K., Qureshi, T. A., Borana, K., Virha, R. (2010): Bioaccumulation of heavy metals in fish tissues of a freshwater Lake of Bhopal. – Environmental Monitoring and Assessment 160: 267-76.
[23] Moiseenko, T. I., Kudryavtseva. L. P. (2001): Trace metal accumulation and fish pathologies in areas affected by mining and metallurgical enterprises in the Kola Region, Russia. – Environmental Pollution 114: 285-297.

http://www.aloki.hu ● ISSN 1589 1623 (Print) ● ISSN 1785 0037 (Online)
DOI: http://dx.doi.org/10.15666/aeer/1706_1496114972

[24] Özmen, H., Külahçı, F., Çukurovalı, A., Doğru, M. (2004): Concentrations of heavy metal and radioactivity in surface water and sediment of Hazar Lake (Elazığ, Turkey). – Chemosphere 55: 401-408.
[25] Öztürk, M., Özözen, G., Minareci, O., Minareci, E. (2009): Determination of heavy metals in fish, water and sediments of Avsar Dam Lake in Turkey. – Iranian Journal of Environmental Health Science and Engineering 6: 73-80.
[26] Salomans, W., Rooij, N. M., Kerdijk, H., Bril, J. (1987): Sediments as a source for contaminants. – Hydrobiologia 149: 13-30.
[27] Sökmen, T. Ö., Güneş, M., Kirici, M. (2018): Determination of heavy metal levels in water, sediment and *Capoeta umbla* tissues of Karasu River (Erzincan). – Turkish Journal of Agricultural and Natural Sciences 5: 578-588 (in Turkish).
[28] Sönmez, A. Y., Kadak, A. E., Özdemir, R. C., Bilen, S. (2016): Establishing on heavy metal accumulation in some economically important fish species captured from Kastamonu Costal. – Alınteri 31: 84-90.
[29] Tao, Y., Yuan, Z., Wei, M., Xiaona, H. (2011): Characterization of heavy metals in water and sediments in Taihu Lake, China. – Environmental Monitoring and Assessment 184: 4367-4382.
[30] Taweel, A., Shuhaimi-Othman, M., Ahmad, A. K. (2013): Assessment of heavy metals in Tilapia fish (*Oreochromis niloticus*) from the Langat River and Engineering Lake in Bangi, Malaysia and evaluation of the health risk from Tilapia consumption. – Ecotoxicology and Environmental Safety 93: 45-51.
[31] Tekin-Özan, S., Aktan, N. (2012): Relationship of heavy metals in water, sediment and tissues with total lenght, weight and seasons of *Cyprinus carpio* L., 1752 from Işıklı Lake (Turkey). – Pakistan Journal of Zoology 44: 1405-1416.
[32] Tekin-Özan, S., Kır, İ. (2005): Comparative study on the accumulation of heavy metals in different organs of tench (*Tinca tinca* L., 1758) and plerocercoids of its endoparasite Ligula intestinalis. – Parasitology Research 97: 156-159.
[33] Tekin-Özan, S., Kır, İ., Barlas, M. (2004): Determination of some heavy metals in water of Kovada Lake (Isparta) and Pike Perch (*Stizostedion lucioperca* L., 1758). – 1st National Limnology Workshop, Istanbul University, 16-19 May 2004, Turkey (in Turkish).
[34] Tekin-Özan, S., Kır, İ., Tuncay, Y. (2007): The seasonal variations of some heavy metals in Kovada Lake's water and sediment. – Ege University Journal of Fisheries and Aquatic Sciences 24: 155-158 (in Turkish).
[35] Usero, J., Izquierdo, C., Morillo, J., Gracia, I. (2003): Heavy metals in fish (*Solea vulgaris*, *Anguilla anguilla* and *Liza aurata*) from salt marshes on the Southern Atlantic Coast of Spain. – Environmental International 1069: 1-8.
[36] Uysal, K., Emre, Y., Köse, E. (2008): The determination of heavy metal accumulation ratios in muscle, skin and gills of some migratory fish species by inductively coupled plasma-optical emission spectrometry (ICP-OES) in Beymelek Lagoon (Antalya/Turkey). – Microchemical Journal 90: 67-70.
[37] Venkatesha, R., Somashekar, R. K., Prakash, K. L. (2012): Heavy metal status of sediment in River Cauvery, Karnataka. – Environmental Monitoring and Assessment 184: 361-73.
[38] Yarsan, E., Bilgili, A., Türel, İ. (2000): Heavy metal levels in Mussels (*Unio stevenianus Krynicki*) obtained from Van Lake. – Turkish Journal of Veterinary and Animal Sciences 24: 93-96 (in Turkish).

http://www.aloki.hu ● ISSN 1589 1623 (Print) ● ISSN 1785 0037 (Online)
DOI: http://dx.doi.org/10.15666/aeer/1706_1496114972

COMPARATIVE STUDY OF PHOSPHATE SOLUBILIZATION POTENTIAL OF *TALAROMYCES PINOPHILUS* STRAINS

MAJUMDER, M. S. I.[1,2] – ISLAM, M. K.[1,2,3] – AKAMINE, H.[1,2] – SANO, A.[1,2] – ONJO, M.[1,4] – HOSSAIN, M. A.[1,2*]

[1]*The United Graduate School of Agricultural Sciences, Kagoshima University Kagoshima 890-0065, Japan*

[2]*Faculty of Agriculture, University of the Ryukyus, Okinawa 903-0213, Japan*

[3]*Department of Soil Science, Faculty of Agriculture, Patuakhali Science and Technology University, Bangladesh*

[4]*Faculty of Agriculture, Kagoshima University, Kagoshima 890-0065, Japan*

[*]*Corresponding author*
e-mail: amzad@agr.u-ryukyu.ac.jp; phone: +81-98-895-8824; fax: +81-98-895-8741

(Received 24th Jun 2019; accepted 16th Oct 2019)

Abstract. Phosphorus (P) is one of the most essential macronutrients for plant growth and development. Most of the soils in the world contain insoluble P that cannot be utilized by the plants. Phosphate solubilizing fungi (PSF) including *Talaromyces pinophilus* possess more potential for providing available P in soil for plant nutrition. There is no report regarding P solubilization potential among the different strains of *T. pinophilus*. The article aimed to compare the Phosphorous solubilization capabilities of 17 *Talaromyces pinophilus* fungal strains, in order to determine the best options for environmentally friendly fertilizers. The P solubilization efficiency of the fungal strains was investigated in broth containing insoluble $Ca_3(PO_4)_2$, $AlPO_4$ and $FePO_4$ compounds. Result showed that $Ca_3(PO_4)_2$ was solubilized the most followed by $AlPO_4$ and $FePO_4$. The strains SI-17URAgr, NBRC 6345 and NBRC 100533 have strong abilities to solubilize $Ca_3(PO_4)_2$, but SI-19URAgr could solubilize both $AlPO_4$ and $FePO_4$. These results also imply that the strains SI-4URAgr and JCM 22801 have the potential to solubilize $AlPO_4$ and $FePO_4$, respectively. Although the P solubilization by different strains were source dependent, the strains SI-17URAgr, NBRC 6345 and NBRC 100533 were proved to be potential for solubilizing P from three sources tested. Solubilized P was negatively correlated with pH of the medium. This study suggested that these strains have a great potential as eco-friendly biofertilizers for sustainable soil management and crop production.
Keywords: *fungal strain, phosphorus, insoluble phosphate, eco-friendly biofertilizers, sustainable soil management, soil pH*

Introduction

Phosphorus (P) is the second most important limiting element required for plant growth and development (Chai et al., 2011; Ram et al., 2015). The soluble soil P concentration varies from 0.05 to 10 ppm, and more than 80% of the P becomes fixed and unavailable for absorption by plants due to adsorption, precipitation or conversion to organic forms (Holford, 1997). The fixed form of P in alkaline soils is tricalcium phosphate, $Ca_3(PO_4)_2$, whereas in acidic soils, it is mainly found as $FePO_4$ and $AlPO_4$ (Subba Rao, 1999).

The application of plant growth promoting microorganisms in agriculture could reduce the use of agrochemicals and support eco-friendly crop production (Herrera et al., 1993; Glick, 1995; Requena et al., 1997). It has been reported that a wide range of

http://www.aloki.hu ● ISSN 1589 1623 (Print) ● ISSN 1785 0037 (Online)
DOI: http://dx.doi.org/10.15666/aeer/1706_1497314984

microorganisms, especially bacteria, solubilize insoluble phosphate (Badr El-Din et al., 1986; Gaind et al., 1991) although fungi are more efficient than bacteria (Venkateswarlu et al., 1984). A promising biotechnological strategy in the management of P fertilization is the use of phosphate-solubilizing fungi to solubilize rock phosphates and allow the recovery of unavailable P fixed in the soil.

Talaromyces (Trichocomaceae) is an important fungal genus which is derived from the Greek word for 'basket', which capably describes the body in which ascospores are formed. In the past, species producing sexual stages with *Penicillium* anamorphs have been classified in *Eupenicillium* spp. and *Talaromyces* spp. After July 2011, species formally reclassifies as the *Penicillium* subgenus *Biverticillium* were classified in *Talaromyces*. The situation is complicated by the fact that many species now classified in *Talaromyces* will continue to be sought as *Penicillium* species in identifications (Pitt, 2014).

The habitats of *Talaromyces pinophilus* are global in environment, *T. pinophilus* (Samson et al., 2011); anamorph: *Penicillium pinophilum* (Thom, 1910) and *P. allahabadense* (Mehrotra et al., 1962) currently designated by *T. allahabadensis* (Samson et al., 2011) were prevalently isolated from soil, compost (El-Naggar et al., 2015), seeds grains (Ismail et al., 2016), phyllosphere (Lindow et al., 2002), phylloplane (Abdel-Hafez et al., 2015; Abdel-Gawad et al., 2017) and some medicinal plants (Koul et al., 2016; Yao et al., 2017).

T. pinophilus has received increasing attention in mycological research for its ability to act as a fungal antagonist and plant-growth promoter (Nicoletti et al., 2004; Pandey et al., 2008; Wani et al., 2016). A few categorical studies on phosphate solubilizing abilities of *T. pinophilus* were reported previously by others (Abdul Wahid and Mehana, 2000; Sembiring and Fauzi, 2017) but no studies have been made on the in-depth p-solubilization potential and comparative performance of different *T. pinophilus* strains yet. Therefore, the study aimed to compare the phosphorous solubilization capabilities of 17 *T. pinophilus* fungal strains, in order to determine the best options for environmentally friendly fertilizers.

Materials and Methods

Fungal Isolates and Culture Preparation

The study was carried out in the Mycology Laboratory, Faculty of Agriculture, University of the Ryukyus, Okinawa, Japan during September 2017- March 2019 under a class II biohazard cabinet (BHC-1306IIA/3B, AIRTECH, Tokyo, Japan) followed to the biosafety classification by National Institute of Infectious Disease of Japan, because of possibilities including toxic fungal species treated as BSL2 during the working tenure. Seventeen *T. pinophilus* fungal strains were used in this study where 4 strains isolated from subtropical soils in Okinawa, Japan and 13 strains collected from different institutions in Japan (*Table 1*). The isolates were cultured on potato dextrose agar (PDA; Becton, Dickinson and Company, Sparks, MD, USA) slant at room temperature (25^{o}C) for further study.

Morphological Studies

Morphological studies were done according to the method (Watanabe, 2010). Pigment exudation were investigated on PDA slants. High-temperature resistance and

http://www.aloki.hu ● ISSN 1589 1623 (Print) ● ISSN 1785 0037 (Online)
DOI: http://dx.doi.org/10.15666/aeer/1706_1497314984

pathogenic potential of the isolates were examined. The isolates were cultured on PDA slants in duplicate and incubated at 35^0C, 37^0C and 42^0C for 7 days to evaluate the growth of mycelia. Growth of isolates at 25^0C (room temperature) treated as positive control.

Preparation of Spore Suspension

Sporulated pure fungal cultured slants were selected for preparation of spore suspension followed by standard procedure. A total volume of 5 ml sterile water with 0.02% of tween 80 (Polyoxyethylene sorbitan monooleate, Nacalai Tesque, Inc, Kyoto, Japan) was poured on the culture slants and the fungal colony surface was lightly scraped by a sterile inoculation loop (Thermo Scientific™, Nunc™ Disposable Loops and Needles, Thermo Scientific™ 251586, Fisher Scientific, Tokyo, Japan). The cultures were passing through a syringe with a 4 x 4 cm sheet of a sterile absorbent cotton (Kyualet, Kawamoto Sangyo, Osaka, Japan). Spore count was done by a hemocytometer and the suspension was adjusted to approximately 10^6 spores mL^{-1}.

Table 1. *List of the fungal strains used in the study*

Isolates	Strain in GenBank	Source	Country of origin	Fungi	Institution
1	SI-4URAgr	Soil	Japan	*Talaromyces pinophilus*	Univ. Ryukyus
2	SI-15URAgr	Soil	Japan	*Talaromyces pinophilus*	Univ. Ryukyus
3	SI-17URAgr	Soil	Japan	*Talaromyces pinophilus*	Univ. Ryukyus
4	SI-19URAgr	Soil	Japan	*Talaromyces pinophilus*	Univ. Ryukyus
5	IFM 64651	Sputum	Japan	*Penicillium pinophilum*	Chiba University
6	IFM 57309	Sputum	Japan	*Penicillium pinophilum*	Chiba University
7	NBRC 6345	Radio set	Papua New Guinea	*Talaromyces pinophilus*	NITE BRC
8	NBRC 100533	Polyvinyl chloride plastic	France	*Talaromyces pinophilus*	NITE BRC
9	NBRC 33285	Polyvinyl chloride plastic	France	*Talaromyces pinophilus*	NITE BRC
10	NBRC 106907	Soil	Japan	*Penicillium pinophilum*	NITE BRC
11	NBRC 9575	Polyvinyl chloride plastic	France	*Penicillium allahabadense*	NITE BRC
12	JCM 9928	Soil	India	*Penicillium pinophilum*	RIKEN
13	JCM 5593	Radio set	Papua New Guinea	*Penicillium pinophilum*	RIKEN
14	JCM 22801	Wood stakes	Australia	*Penicillium pinophilum*	RIKEN
15	JCM 22802	Barley grain	Australia	*Penicillium pinophilum*	RIKEN
16	JCM 22803	Moldy sorghum grain	Australia	*Penicillium pinophilum*	RIKEN
17	JCM 23043	Radio set	Papua New Guinea	*Penicillium pinophilum*	RIKEN

NITE; National Institute of Technology and Evaluation, Biological Resource Center, NITE (NBRC), Japan.
RIKEN; is a large scientific research institute in Japan

Determination of TCP Solubilization Index on Solid Medium

All the isolates were tested under *in vitro* condition for their phosphate solubilization activity on Pikovskaya's agar medium containing 0.5% tricalcium phosphate (TSP) as an insoluble phosphorus source. A spot inoculation of each fungal isolate was made onto the plates in triplicate under aseptic condition and incubated at 28°C for 7 days in darkness. At 7^{th} day of incubation, phosphate solubilization index was measured using the following formula (Premono et al., 1996):

Solubilization Index (SI)=[Colony diameter+Halo zone diameter]/Colony diameter

http://www.aloki.hu ● ISSN 1589 1623 (Print) ● ISSN 1785 0037 (Online)
DOI: http://dx.doi.org/10.15666/aeer/1706_1497314984

Quantitative Estimation of Phosphate Solubilization

It was carried out using Erlenmeyer flask containing 40 ml Pikovskaya's broth medium supplemented with 0.5% tricalcium phosphate [$Ca_3(PO_4)_2$], aluminium phosphate ($AlPO_4$) and iron phosphate ($FePO_4$). After sterilization, the medium of each flask was inoculated with the 5% (v/v) spore suspension of a particular fungal isolate containing 10^6 spores mL^{-1}. Sterile distilled water inoculated flaks were treated as control. Three replicates were maintained for each test isolate and mean value was recorded. Incubation was done at 25^0C in an incubator shaker (EYELA Multi Shaker MMS-3010) at 120 rpm for 9 days. The samples were autoclaved and centrifuged (TOMY MX-301) at 5000 rpm for 25 minutes to remove any suspended solids and mycelial parts. Then the cultures were filtered through 0.45 µm pore size syringe filter unit (Advantech, Japan). The filtrates were used for analysis of soluble phosphate and pH value. The pH value of the culture supernatants was determined by a pH meter (HORIBA, Japan) equipped with a glass electrode. The amount of soluble phosphorus in culture supernatants was measured by molybdenum blue method (Murphy and Riley, 1962) and expressed as mg/L. Samples cultured for 3, 6 and 9 days were compared. After calculation of mean phosphate degradation ability from 17 isolates of each day, we selected the adequate period for the comparison depending on the substrate.

Data Analysis

All experiments were conducted in triplicate and data were analyzed using Microsoft Excel program. The mean values were compared by Fisher test and significant differences were detected at $p< 0.05$ level. Correlation between solubilized phosphate and pH of the medium was determined by using Pearson correlation studies.

Results

Pigment Exudation

All isolates were reconfirmed based on morphological studies. Morphological studies results are not shown. The isolates produced various colour in PDA slant, such as coffee, orange, yellow and cream (*Fig. 1*). Differential colour formation by *T. pinophilus* isolates might be attributed to the presence of bioactive metabolites.

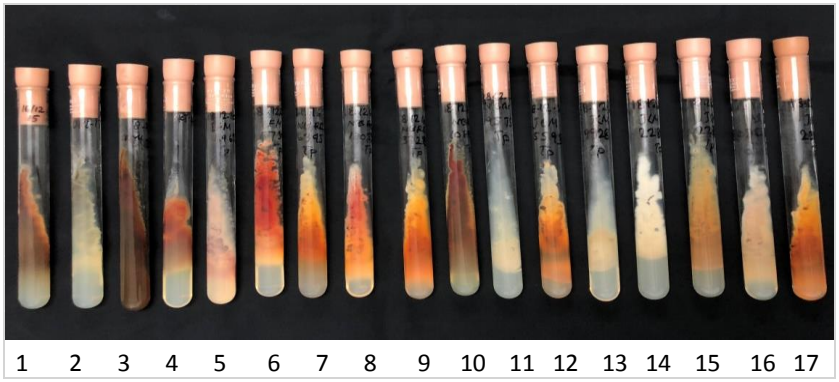

Figure 1. *Talaromyces pinophilus isolates grown on Potato Dextrose Agar (PDA) slant for 7 days at 25^0 C [Coffee: 1, 3, 10; Cream: 2, 5, 11, 13, 14, 16; Orange: 4, 6; Yellow=7, 8, 9, 12, 15, 17]*

http://www.aloki.hu ● ISSN 1589 1623 (Print) ● ISSN 1785 0037 (Online)
DOI: http://dx.doi.org/10.15666/aeer/1706_1497314984

Qualitative Phosphate Solubilization

All isolates showed different levels of phosphate solubilization from inconspicuous to a substantial in Pikovskaya's agar medium using tricalcium phosphate as the substrate. Six isolates produced clear zone, 5 developed translucent and the remaining isolates had inconspicuous zones. All isolates also showed significant phosphate solubilization in Pikovskaya's agar medium using tricalcium phosphate as the substrate. The phosphate solubilization index (PSI) ranged from 1.05 to 1.46 (*Table 2*).

Table 2. *TCP solubilization in Pikovskaya's agar by 17 fungal strains*

Isolate	Fungal strain	Fungi	PSI	Type of zone
1	SI-4URAgr	*Talaromyces pinophilus*	1.31 ± 0.01^{b}	C
2	SI-15URAgr	*Talaromyces pinophilus*	1.46 ± 0.03^{a}	C
3	SI-17URAgr	*Talaromyces pinophilus*	1.09 ± 0.01^{d}	T
4	SI-19URAgr	*Talaromyces pinophilus*	1.12 ± 0.01^{d}	T
5	IFM 64651	*Penicillium pinophilum*	1.07 ± 0.02^{d}	I
6	IFM 57309	*Penicillium pinophilum*	1.09 ± 0.03^{d}	I
7	NBRC 6345	*Talaromyces pinophilus*	1.11 ± 0.02^{d}	T
8	NBRC100533	*Talaromyces pinophilus*	1.21 ± 0.08^{bc}	C
9	NBRC33285	*Talaromyces pinophilus*	1.14 ± 0.08^{cd}	C
10	NBRC 106907	*Penicillium pinophilum*	1.24 ± 0.03^{b}	T
11	NBRC 9575	*Penicillium allahabadense*	1.07 ± 0.03^{d}	I
12	JCM 9928	*Penicillium pinophilum*	1.09 ± 0.06^{d}	T
13	JCM 5593	*Penicillium pinophilum*	1.19 ± 0.09^{bc}	C
14	JCM 22801	*Penicillium pinophilum*	1.05 ± 0.05^{d}	I
15	JCM 22802	*Penicillium pinophilum*	1.08 ± 0.05^{d}	I
16	JCM 22803	*Penicillium pinophilum*	1.09 ± 0.05^{d}	T
17	JCM 23043	*Penicillium pinophilum*	1.06 ± 0.05^{d}	I

PSI: Phosphate solubilization index, Values given are the mean ± standard deviation of three independent replicates, Same letter in the column are not significantly different at $p<0.05$ by Fisher's test, C = clear, T = translucent, I= inconspicuous

Quantitative Phosphate Solubilization

Phosphate solubilization by all isolates were tested in Pikovskaya's broth medium using three substrates of recalcitrant phosphate compounds: tricalcium phosphate $Ca_3(PO_4)_2$, aluminium phosphate ($AlPO_4$) and iron phosphate ($FePO_4$). The phosphate solubilizing ability of fungal isolates varied with incubation period and substrates. The best period of observation was 6 days considering their mean P solubilization for the three substrates (*Table 3*).

All *T. pinophilus* strains were tested for their ability to solubilize hardly soluble phosphate sources [$Ca_3(PO_4)_2$, $AlPO_4$, and $FePO_4$]. All of the *T. pinophilus* strains showed potential P solubilizing in the medium containing $Ca_3(PO_4)_2$ followed by $AlPO_4$ and $FePO_4$ (*Table 4*). The solubilized P ranged between 83.7-574.8 mgL^{-1}, 50.5-192.4 mgL^{-1} and 50.5-192.4 mgL^{-1} from $Ca_3(PO_4)_2$, $AlPO_4$, and $FePO_4$, respectively. Among 17 isolates, 6 isolates (SI-4URAgr, SI-17URAgr, SI-19URAgr, NBRC 6345, NBRC 100533 and JCM 22801) were considered as outstanding isolates because solubilized P was higher than the sum of the mean and standard deviation of P solubilized by 17 isolates. The highest amount of P solubilization from $Ca_3(PO_4)_2$ was shown in NBRC6345 (574.8 mgL^{-1}) followed by NBRC100533 (540.4 mgL^{-1}) and SI-17URAgr (537.2 mgL^{-1}). The highest amount of P solubilization from $AlPO_4$, was

http://www.aloki.hu ● ISSN 1589 1623 (Print) ● ISSN 1785 0037 (Online)
DOI: http://dx.doi.org/10.15666/aeer/1706_1497314984

shown in SI-4URAgr (192.4 mgL^{-1}) followed by SI-19 (153.7 mgL^{-1}). The highest amount of P solubilization from $FePO_4$ was shown in SI-19URAgr (145.2 mgL^{-1}) followed by JCM 22801 (126.1 mgL^{-1}). The strain SI-19URAgr showed outstanding performance in both $AlPO_4$, and $FePO_4$ solubilization (*Table 4*). In case of total solubilized phosphate (mgL^{-1}) from three substrates (TCP, AL-P and Fe-P), the highest amount of P solubilization was shown in NBRC 6345 (829.6 mgL^{-1}) followed by SI-17URAgr (789.2 mgL^{-1}) and NBRC100533 (770.4 mgL^{-1}). The tested isolates produced various colours in broth medium using three P substrates during incubation period (data not shown).

Table 3. *Selection for the best period of phosphate solubilization by 17 isolates*

Solubilized phosphate (mg/L)								
TCP			**Al-P**			**Fe-P**		
3 days	**6 days**	**9 days**	**3 days**	**6 days**	**9 days**	**3 days**	**6 days**	**9 days**
196.2±93.0	354.3±136.1*	343.2±125.1	80.6±29.8	111.6±40.7*	63.6±22.2	55.3±16.3	95.8±28.1*	69.4±20.1

TCP: tricalcium phosphate, Al-P: aluminium phosphate, Fe-P: iron phosphate, Values given are the mean ± standard deviation of P solubilized by 17 fungal isolates, An asterisk (*) indicated the best period of phosphate solubilization

Table 4. *Phosphate solubilization from different substrates by T. pinophilus fungal strains*

Sl. No	**Strain**	**Fungi**	**Solubilized phosphate (mg/L)**			**Total P (mg/L)**
			TCP	**AL-P**	**Fe-P**	
1	SI-4URAgr	*Talaromyces pinophilus*	268.4	192.4*	46.5	507.3
2	SI-15URAgr	*Talaromyces pinophilus*	363.7	132.9	34.8	531.4
3	SI-17URAgr	*Talaromyces pinophilus*	537.2*	135.7	116.3	789.2*
4	SI-19URAgr	*Talaromyces pinophilus*	314.0	153.7*	145.2*	612.8
5	IFM 64651	*Penicillium pinophilum*	324.3	50.5	85.6	460.5
6	IFM 57309	*Penicillium pinophilum*	228.5	51.4	65.6	345.5
7	NBRC 6345	*Talaromyces pinophilus*	574.8*	148.6	106.2	829.6*
8	NBRC100533	*Talaromyces pinophilus*	540.4*	134.7	95.3	770.4*
9	NBRC 33285	*Talaromyces pinophilus*	263.5	135.8	95.4	494.7
10	NBRC106907	*Penicillium pinophilum*	482.5	107.2	106.5	696.3
11	NBRC 9575	*Penicillium allahabadense*	83.7	96.0	116.5	296.2
12	JCM 9928	*Penicillium pinophilum*	135.2	85.1	105.3	325.6
13	JCM 5593	*Penicillium pinophilum*	387.7	137.2	105.3	630.2
14	JCM 22801	*Penicillium pinophilum*	405.7	54.8	126.1*	586.6
15	JCM 22802	*Penicillium pinophilum*	392.2	83.9	85.9	562.1
16	JCM 22803	*Penicillium pinophilum*	397.1	125.2	116.1	638.4
17	JCM 23043	*Penicillium pinophilum*	325.2	71.7	76.6	473.5
		Mean±SD	354.3±136.1*	111.6±40.7	95.8±28.1	561.8±157.8

TCP: tricalcium phosphate, Al-P: aluminium phosphate, Fe-P: iron phosphate, Values given are the mean ± standard deviation of P solubilized by 17 fungal isolates, An asterisk (*) indicated outstanding values of solubilized phosphate, It was higher than sum of mean and standard deviation of P solubilized by 17 fungal isolates

Correlation Between pH and Soluble P

The pH of the culture medium exhibited the opposite changes. It decreased with the increased amount of soluble P in the medium. Correlation studies showed a significant inverse relationship between soluble P and pH of the culture medium (*Fig. 2A, 2B, 2C*).

http://www.aloki.hu ● ISSN 1589 1623 (Print) ● ISSN 1785 0037 (Online)
DOI: http://dx.doi.org/10.15666/aeer/1706_1497314984

The negative correlation was observed in all fermented broth culture and correlation coefficient (r) was -0.88, -0.51 and -0.60 in TCP, Al-P and Fe-P, respectively. The strong negative correlation was observed in TCP containing medium.

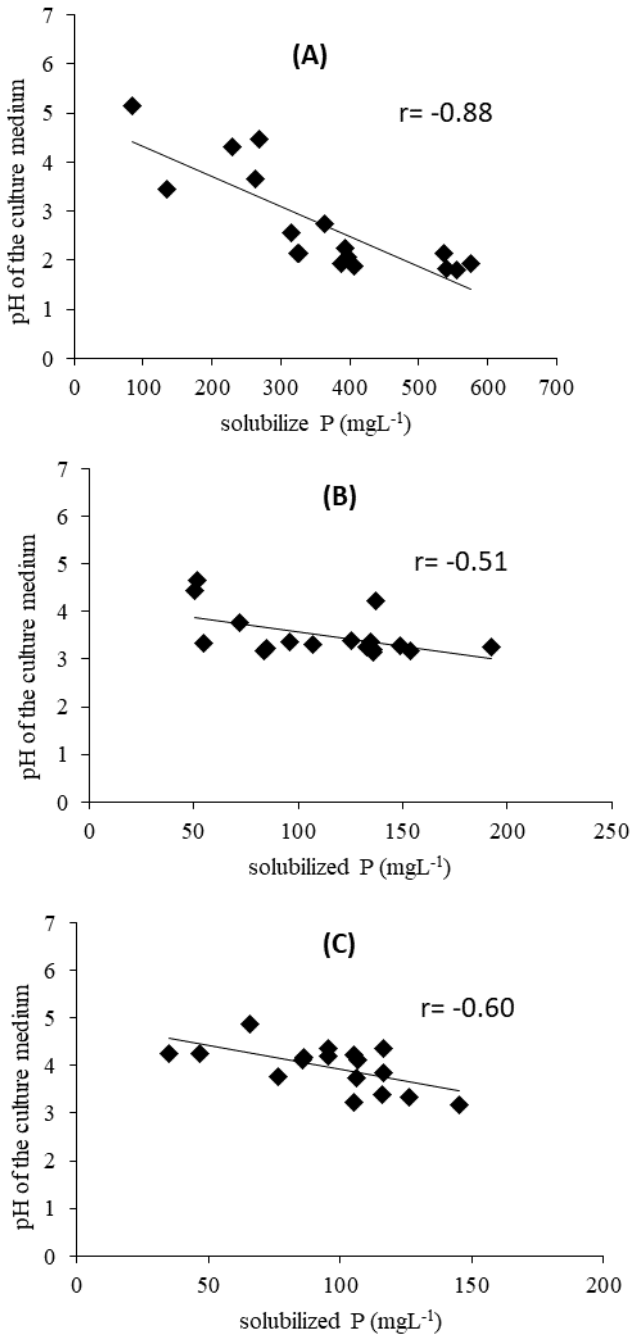

Figure 2. *Pearson's correlation between soluble phosphate and pH of the culture medium supplemented with TCP (2A), $AlPO_4$ (2B) and $FePO_4$ (2C); inoculated by 17 fungal strains. [SI-4URAgr, SI-15URAgr, SI-17URAgr, SI-19URAgr, IFM 64651, IFM 57309, NBRC 6345, NBRC 100533, NBRC 33285, NBRC 106907, NBRC 9575, JCM 9928, JCM 5593, JCM 22801, JCM 22802, JCM 22803, JCM 23043]*

http://www.aloki.hu ● ISSN 1589 1623 (Print) ● ISSN 1785 0037 (Online)
DOI: http://dx.doi.org/10.15666/aeer/1706_1497314984

Temperature Effects on Strains

Survival of the strains at different temperature was investigated (*Table 5*). Most of the strains could grow and survive at 25ºC-37ºC. Strain SI-4URAgr, SI-15URAgr, SI-17URAgr, SI-19URAgr and NBRC 106907 could grow at 25ºC-42ºC. These strains are summer tolerant and they could survive both acidic (low pH) and alkaline environment (high pH).

Table 5. *The growth and survival of T pinophilus strains at different temperature*

SL No.	Strain	Fungi	Growth temperature			
			25^{0}C	**35^{0}C**	**37^{0}C**	**42^{0}C**
1	SI-4URAgr	*Talaromyces pinophilus*	+	+	+	+
2	SI-15URAgr	*Talaromyces pinophilus*	+	+	+	+
3	SI-17URAgr	*Talaromyces pinophilus*	+	+	+	+
4	SI-19URAgr	*Talaromyces pinophilus*	+	+	+	+
5	IFM 64651	*Penicillium pinophilum*	+	+	+	-
6	IFM 57309	*Penicillium pinophilum*	+	+	+	-
7	NBRC 6345	*Talaromyces pinophilus*	+	+	+	-
8	NBRC100533	*Talaromyces pinophilus*	+	+	+	-
9	NBRC 33285	*Talaromyces pinophilus*	+	+	+	-
10	NBRC106907	*Penicillium pinophilum*	+	+	+	+
11	NBRC 9575	*Penicillium allahabadense*	+	+	+	-
12	JCM 9928	*Penicillium pinophilum*	+	+	+	-
13	JCM 5593	*Penicillium pinophilum*	+	+	+	-
14	JCM 22801	*Penicillium pinophilum*	+	+	+	-
15	JCM 22802	*Penicillium pinophilum*	+	+	+	-
16	JCM 22803	*Penicillium pinophilum*	+	+	+	-
17	JCM 23043	*Penicillium pinophilum*	+	+	+	-

(+) indicated growth of fungi, (-) indicated no growth.

Discussion

Morphological studies reconfirmed that all the 17 strains used in this study belong to *Talaromyces pinophilus.* All fungal isolates produced different colours in the medium regardless of the P substrates, but the colour seemed not to have any relation with P solubilization.

T. pinophilus has various applications based on the production of enzymes (Hansen et al., 2015; Li et al., 2017) as well as a renewable source of pigments, colorants (Caro et al., 2017) and bioactive compounds (Wang et al., 2013; Nicoletti et al., 2016) and degrading ability of agricultural waste (El-Naggar et al., 2015). *T. pinophilus* is able to produce a variety of bioactive metabolites, including alkaloids, peptides, lactones, polyketides and miscellaneous structure type compounds, with different chemical and biological activities. *T. pinophilus* produces biomass-degrading enzymes such as α-amylase (Xian et al., 2015), cellulase (Visser et al., 2013), endoglucanase (Pol et al., 2012), xylanase (Visser et al., 2013), laccase (Dhakar et al., 2014) and α-galactosidase (Visser et al., 2013). *T. pinophilus* produces a variety of medically useful metabolites such as 3-O- methylfunicone, which is used to inhibit mesothelioma cell motility, and talaromycolides 1-3,5 and 11 which inhibit the growth of the human pathogen methicillin resistant *Staphylococcus aureus* (Buommino et al., 2012).

In the present study, all isolates showed better P solubilizing activity in liquid medium compared with solid medium. The possible reason for these anomalous behaviors of isolates on liquid and solid media could be attributed to nutrient availability, varying diffusion rate of different organic acids secreted by fungi, and growth requirement of fungi (Jain et al., 2014).

http://www.aloki.hu ● ISSN 1589 1623 (Print) ● ISSN 1785 0037 (Online)
DOI: http://dx.doi.org/10.15666/aeer/1706_1497314984

Alam et al. (2002) reported that some isolates having little clear zone on solid agar medium exhibited higher phosphate solubilization efficiency in liquid medium. Some fungal isolates showed larger clear zones on solid agar medium but low phosphate solubilization in liquid medium. This shows that higher PSI on solid agar medium does not necessarily show solubilization efficiency in liquid medium. Thus, the plate technique is insufficient to screen the best P solubilizers and to detect all phosphate solubilizers mentioned by Nautiyal (1999).

The strongest P solubilization was found in $Ca_3(PO_4)_2$ followed by $AlPO_4$ and $FePO_4$ because $AlPO_4$ and $FePO_4$ have complex structure than $Ca_3(PO_4)_2$ while fungi exhibited low P solubilizing ability in media containing $AlPO_4$ and $FePO_4$ (Son et al., 2006; Zhang et al., 2018). The mechanisms of phosphate solubilization by microorganisms are very complex and are not completely known yet. The very common mechanisms are acidification, chelation and exchange reactions (Chai et al., 2011). Organic acids play an important role in phosphate solubilization processes, which can help the release of P by providing protons and complexing anions, or ligand exchange reactions or complexion of metal ions release to solution. Organic acids production depends on the interaction of P source and fungi (Scervino et al., 2013; Zhang et al., 2018).

In the present study, the isolates (SI-4URAgr, SI-17URAgr, SI-19URAgr, NBRC 6345, NBRC 100533, and JCM 22801) showed the highest efficiency in P solubilization by decreasing pH of the culture medium, which indicated higher amount of organic acid production. Solubilization of the different P sources mostly depended on the amount of organic acids production by fungi (Zhang et al., 2018). Tricarboxylic acids and other lower molecular weight organic acids are considered to be the main contributors to phosphate solubilization and a decrease in pH of the medium (Chai et al., 2011).

It was observed that phosphate solubilization was negatively correlated with pH of the medium. There are several reports where such correlation was documented (Pandey et al., 2008; Jain et al., 2012; Wani et al., 2016). The activities in lower pH indicated that the increase of organic acids in the medium (Pradhan and Sukla, 2005; Saxena et al., 2013). However, soluble P was increased without changing pH in some occasion because of other mechanism (Jain et al., 2012, 2017) such as; chelation and exchange reactions (Chai et al., 2011).

Conclusions

The article aimed to compare the phosphorous solubilization capabilities of 17 *Talaromyces pinophilus* fungal strains, in order to determine the best options for environmentally friendly fertilizers. Findings showed that $Ca_3(PO_4)_2$ was solubilized the most followed by $AlPO_4$ and $FePO_4$. Among the strains tested SI-17URAgr, NBRC 6345 and NBRC100533 were potential for $Ca_3(PO_4)_2$ solubilization but SI-19URAgr could solubilize both $AlPO_4$ and $FePO_4$ whereas SI-4URAgr and JCM 22801 were potential for solubilization of Al-P and Fe-P, respectively. Overall findings suggest that the strains SI-17URAgr, NBRC 6345 and NBRC 100533 could be potent for solubilizing P from different sources. Thus these strains might be used as inoculant in the soil containing various inorganic P. However, further trials are needed to determine the capability of these strains for P solubilization in field experiment, sustainable soil management as well as crop production.

Acknowledgments. We are grateful to Instrumental Research Center (IRC), University of the Ryukyus, Japan for analytical support to this study.

http://www.aloki.hu ● ISSN 1589 1623 (Print) ● ISSN 1785 0037 (Online)
DOI: http://dx.doi.org/10.15666/aeer/1706_1497314984

REFERENCES

[1] Abdel-Gawad, K. M., Abdel-Mallek, A. Y., Hussein, N. A., Abdel-Rahim, I. R. (2017): Diversity of mycobiota associated with onion (*Allium cepa* L.) cultivated in Assiut, with a newly recorded fungal species to Egypt. – J Microbiol Biotech Food Sci 6(5): 1145-1151.

[2] Abdel-Hafez, S. I. I., Abo-Elyousr, K. A., Abdel-Rahim, I. R. (2015): Leaf surface and endophytic fungi associated with onion leaves and their antagonistic activity against *Alternaria porri.* – Czech Mycol. 67(1): 1-22.

[3] Abdul Wahid, O. A., Mehana, T. A. (2000): Impact of phosphate-solubilizing fungi on the yield and phosphorus-uptake by wheat and faba bean plants. – Microbiol Res. 155(3): 221-227.

[4] Alam, S., Khalil, S., Ayub, N., Rashid, M. (2002): *In vitro* solubilization of inorganic phosphate by Phosphate Solubilizing Microorganisms (PSM) from Maize Rhizosphere. – International Journal of Agriculture & Biology 4: 454-458.

[5] Badr El-Din, S. M. S., Khalafallah, M. A., Moawad, H. (1986): Response of soybean to dual inoculation with *Rhizobium japanicum* and phosphate dissolving bacteria. – Z. Pflanzenemaehr. Bodenk. 149: 130-135.

[6] Buommino, E., De Filippis, A., Nicoletti. R., Menegozzo, M., Menegozzo, S., Ciavatta, M. L., Rizzo, A., Brancato, V., Tufano, M. A., Donnarumma, G. (2012): Cell-growth and migration inhibition of human mesothelioma cells induced by 3-O-Methylfunicone from *Penicillium pinophilum* and cisplatin. – Invest New Drug. 30: 1343-1351.

[7] Caro, Y., Venkatachalam, M., Lebeau, J., Fouillaud, M., Dufosse, L. (2017): Pigments and colorants from filamentous fungi. – In: Mérillon, J.-M., Ramawat, K. G. (eds.) Fungal Metabolites. Springer International Publishing, Cham.: 499-568.

[8] Chai, B., Yan, W., Pengming, L., Biao, L., Meiying, G. (2011): Isolation and phosphate solubilizing ability of a fungus, *Penicillium* sp. from soil of alum mine. – JBM 51: 5-14.

[9] Dhakar, K., Jain, R., Tamta, S., Pandey, A. (2014): Prolonged laccase production by a cold and pH tolerant strain of *Penicillium pinophilum* (MCC 1049) isolated from a low temperature environment. – Enzyme Res.: 120708.

[10] El-Naggar, N. E. A., Haroun, S. A., Owais, E. A., Sherief, A. A. (2015): Identification of newly isolated *Talaromyces pinophilus* and statistical optimization of (β-glucosidase production under solid-state fermentation. – Preparative Biochemistry & Biotechnology 45: 712-729.

[11] Gaind, S., Gaur, A. C. (1991): Thermotolerant phosphate solubilizing microorganisms and their interaction with mung bean. – Plant Soil 133: 141-149.

[12] Glick, B. R. (1995): The enhancement of plant growth by free-living bacteria. – Can. J. Microbiol. 41(2): 109-117.

[13] Hansen, G. H., Lübeck, M., Frisvad, J. C., Lübeck, P. S., Andersen, B. (2015): Production of cellulolytic enzymes from ascomycetes: Comparison of solid state and submerged fermentation. – Process Biochem. 50: 1327-1341.

[14] Herrera, M. A., Salamanka, C. P., Barea, J. M. (1993): Inoculation of woody legumes with selected arbuscular mycorrhizal fungi and rhizobia to recover desertified Mediterranean ecosystems. – App. Env. Microbiol. 59: 129-133.

[15] Holford, I. C. R. (1997): Soil phosphorus: its measurement, and its uptake by plants. – Aust. J. Soil Res. 35(2): 227-240.

[16] Ismail, M. A., El-Maali, N. T. A., Omran, G., Nasser, N. M. (2016): Biodiversity of mycobiota in peanut seeds, corn and wheat grains with special reference to their aflatoxigenic ability. – J. Microbiol. Biotechnol. Food Sci. 5: 314.

[17] Jain, R., Saxena, J., Sharma, V. (2012): Solubilization of inorganic phosphates by *Aspergillus awamori* S19 isolated from agricultural soil of semi-arid region. – Annals Microbiol. 62: 725-735.

http://www.aloki.hu ● ISSN 1589 1623 (Print) ● ISSN 1785 0037 (Online)
DOI: http://dx.doi.org/10.15666/aeer/1706_1497314984

[18] Jain, R., Saxena, J., Sharma, V. (2014): Differential effects of immobilized and free forms of phosphate solubilizing fungal strains on the growth and P uptake of mungbean plants. – Annals Microbiol. 64: 1523-1534.
[19] Jain, R., Saxena, J., Sharma, V. (2017): The ability of two fungi to dissolve hardly soluble phosphates in solution. – Mycology 8(2): 104-110.
[20] Koul, M., Meena, S., Kumar, A., Sharma, P. R., Singamaneni, V., Riyaz-Ul Hassan, S., Hamid, A., Chaubey, A., Prabhakar, A., Gupta, P. (2016): Secondary metabolites from endophytic fungus *Penicillium pinophilum* induce ROS-mediated apoptosis through mitochondrial pathway in pancreatic cancer cells. – Planta Med. 82(4): 344-355.
[21] Li, C. X., Zhao, S., Zhang, T., Xian, L., Liao, L. S., Liu, J. L., Feng, J. X. (2017): Genome sequencing and analysis of *Talaromyces pinophilus* provide insights into biotechnological applications. – Sci. Rep. 7: 490.
[22] Lindow, S. E., Leveau, J. H. (2002): Phyllosphere microbiology. – Curr. Opin. Biotechnol. 13: 238-243.
[23] Mehrotra, B. S., Kumar, D. A. (1962): A new species of Penicillium from India. – Canadian Journal of Botany 40(10): 1399-1400.
[24] Murphy, J., Riley, J. P. (1962): A modified single solution method for the determination of phosphate in natural waters. – Anal Chim Acta 27: 31-36.
[25] Nautiyal, C. S. (1999): An efficient microbiological growth medium for screening phosphate solubilizing microorganisms. – FEMS Microbiol Lett. 170(1): 265-270.
[26] Nicoletti, R., De Stefano, M., De Stefano, S., Trincone, A., Marziano, F. (2004): Antagonism against *Rhizoctonia solani* and fungitoxic metabolite production by some *Penicillium* isolates. – Mycopathologia 158: 465-474.
[27] Nicoletti, R., Trincone, A. (2016): Bioactive compounds produced by strains of Penicillium and Talaromyces of marine origin. – Mar. Drugs 14: 37.
[28] Pandey, A., Das, N., Kumar, B., Rinu, K., Trivedi, P. (2008): Phosphate solubilization by Penicillium spp. isolated from soil samples of Indian Himalayan region. – World J Microbiol Biotechnol. 24: 97-102.
[29] Pitt, J. (2014): Penicillium and Talaromyces: Introduction, Penicillium. – Encyclopedia of Food Microbiology (2nd ed.): 6-13.
[30] Pol, D., Laxman, R. S., Rao, M. (2012): Purification and biochemical characterization of endoglucanase from *Penicillium pinophilum* MS 20. – Indian J Biochem Biophys. 49: 189-194.
[31] Pradhan, N., Sukla, L. B. (2005): Solubilization of inorganic phosphate by fungi isolated from agricultural soil. – African J Biotechnol. 5: 850-854.
[32] Premono, M. E., Moawad, A. M., Vlek, P. L. G. (1996): Effect of phosphate-solubilizing *Pseudomonas putida* on the growth of maize and its survival in the rhizosphere. – Indonesian Journal of Crop Science 11: 13-23.
[33] Ram, H., Malik, S. S., Dhaliwal, S. S., Kumar, B., Singh, Y. (2015): Growth and productivity of wheat affected by phosphorus solubilizing fungi and phosphorus levels. – Plant Soil Environ 61(3): 122-126.
[34] Requena, B. N., Jimenez, I., Toro, M., Barea, J. M. (1997): Interactions between plant-growth-promoting rhizobacteria (PGPR), arbuscular mycorrhizal fungi and *Rhizobium* spp. in the rhizosphere of *Anthyllis cytiisoides*, a model legume for revegetation in Mediterranean semi-arid ecosystems. – New Phytol. 136: 667-677.
[35] Samson, R. A., Yilmaz, N., Houbraken, J., Spierenburg, H., Seifert, K. A., Peterson, S. W., Varga, J., Frisvad, J. C. (2011): Phylogeny and nomenclature of the genus Talaromyces and taxa accommodated in Penicillium subgenus Biverticillium. – Studies in Mycology 70: 159-183.
[36] Saxena, J., Basu, P., Jaligam, V., Chandra, S. (2013): Phosphate solubilization by a few fungal strains belonging to the genera *Aspergillus* and *Penicillium.* – Afr J Microbiological Res. 7: 4862-4869.

http://www.aloki.hu ● ISSN 1589 1623 (Print) ● ISSN 1785 0037 (Online)
DOI: http://dx.doi.org/10.15666/aeer/1706_1497314984

[37] Scervino, J. M., Mesa, M. P., Monica, I. D., Recchi, M., Moreno, S., Godeas, A. (2013): Soil fungal isolates produce different organic acid patterns involved in phosphate salts solubilization. – Biol Fertil Soils 49(6): 779-779.
[38] Sembiring, M., Fauzi (2017): Bacterial and fungi phosphate solubilization effect to increase nutrient uptake and potatoes (*Solanum tuberosum* L.) production on Andisol Sinabung area. – J. Agron. 16(3): 131-137.
[39] Son, H. J., Park, G. T., Cha, M. S., Heo, M. S. (2006): Solubilization of insoluble inorganic phosphates by a novel salt- and pH-tolerant *Pantoea agglomerans* R-42 isolated from soybean rhizosphere. – Bioresource Technol. 97(2): 204-210.
[40] Subba Rao, N. S. (1999): Soil Microbiology (Fourth Edition of Soil Microorganisms and Plant Growth). – Oxford & IBH Publishing Co. Pvt. Ltd., New Delhi. 407.
[41] Thom, C. (1910): Cultural studies of species of Penicillium. U.S.D.A. – Bureau of Animal Industry Bulletin 118: 1-107.
[42] Venkateswarlu, B., Rao, A. V., Raina, P. (1984): Evaluation of phosphorus solubilization by microorganisms isolated from arid soil. – J. Ind. Soc. Soil Sci. 23: 273-277.
[43] Visser, E. M., Falkoski, D. L., de Almeida, M. N., Maitan-Alfenas, G. P., Guimarães, V. M. (2013): Production and application of an enzyme blend from *Chrysoporthe cubensis* and *Penicillium pinophilum* with potential for hydrolysis of sugarcane bagasse. – Bioresource Technol. 144: 587-594.
[44] Wang, M. H., Li, X. M., Li, C. S., Ji, N. Y., Wang, B. G. (2013): Secondary metabolites from *Penicillium pinophilum* SD-272, a marine sediment-derived fungus. – Mar. Drugs. 11: 2230-2238.
[45] Wani, Z. A., Mirza, D. N., Arora, P., Riyaz-Ul-Hassan, S. (2016): Molecular phylogeny, diversity, community structure, and plant growth promoting properties of fungal endophytes associated with the corms of saffron plant: An insight into the microbiome of *Crocus sativus* Linn. – Fungal Biol. 120(12): 1509-1524.
[46] Watanabe, T. (2010): Pictorial atlas of soil and seed fungi morphologies of cultured fungi and Key to species, Third Edition. – CRC press, Florida.
[47] Xian, L., Wang, F., Luo, X., Feng, Y-L., Feng, J-X. (2015): Purification and characterization of a highly efficient calcium-independent alpha-amylase from *Talaromyces pinophilus* 1–95. – PLoS ONE 10(3): e0121531.
[48] Yao, Y. Q., Lan, F., Qiao, Y. M., Wei, J. G., Huang, R. S., Li, L. B. (2017): Endophytic fungi harbored in the root of *Sophora tonkinensis* Gapnep: diversity and biocontrol potential against phytopathogens. – Microbiology Open: 1-17.
[49] Zhang, Y., Chen, F-S., Wu, X-Q., Luan, F-G., Zang, L-P., Fang, X-M., Wan, S-Z., Hu, X-F., Ye, J-R. (2018): Isolation and characterization of two phosphate solubilizing fungi from rhizosphere soils of moso bamboo and their functional capacities when exposed to different phosphorus sources and pH environment. – PLoS ONE 13(7): e0199625.

http://www.aloki.hu ● ISSN 1589 1623 (Print) ● ISSN 1785 0037 (Online)
DOI: http://dx.doi.org/10.15666/aeer/1706_1497314984

EFFECT OF DIFFERENT GIBBERELLIC ACID DOSES AND APPLICATION TIMES ON COTTON (*Gossypium hirsutum* L.) IN SOUTHEASTERN ANATOLIA REGION OF TURKEY

COPUR, O.[1*] – DEMIREL, T.[2] – ODABAŞIOĞLU, C.[1]

[1]*Department of Field Crops, Faculty of Agriculture, Harran University, 63190 Sanliurfa, Turkey*

[2]*Department of Field Crops, Graduate School of Natural and Applied Sciences, Harran University, 63190 Sanliurfa, Turkey*

**Corresponding author*
e-mail: ocopur@harran.edu.tr; phone: +90-414-318-3690

(Received 24th Jun 2019; accepted 16th Oct 2019)

Abstract. This study was carried out to determine the impact of different gibberellic acid (GA_3) application times and doses on seed cotton yield and yield components of Stoneville 468 cotton variety in Southeastern Anatolia Region. Experiments were conducted using randomized block design with split plots and with three replications during the 2015 and 2016 growing seasons. Where application times formed the main plots (control, beginning of squaring, beginning of squaring + beginning of flowering and beginning of squaring + beginning of flowering + 14 days after the beginning of flowering one application), application doses formed the sub plots (control, 400, 800, 1200 cc ha^{-1}). Resulting, seed cotton yields varied between 4882.77 kg ha^{-1} and 5557.15 kg ha^{-1}. While the doses of gibberellic acid increased; seed cotton yield, number of bolls per plant, number of sympodia per plant, plant height, seed cotton weight per boll, ginning outturn, seed index, fiber length and fiber uniformity increased, but earliness ratio and fiber fineness decreased. The most suitable GA dose was 1200 cc ha^{-1} and the highest seed cotton yield was obtained from the beginning of squaring + beginning of flowering + 14 days after beginning of flowering administered three times.
Keywords: *plant growth regulator, sympodia, fiber quality, yield, yield components*

Introduction and literature review

Cotton fibers have great economic importance for cotton producing countries with their widely usage areas, added value and created employment opportunities in the textile sector. With the increasing population, increasing interest for natural fibers and living standards increase the demand of cotton fibers. However, because a limited number of countries' ecology allows the cotton farming, about 80% of world production is carried by eight countries including Turkey (Anonymous, 2019a). Cotton farming area in Turkey was 518 000 ha in 2018 and 976 000 tons of cotton fiber were produced from this area. Cotton is grown in Aegean, Mediterranean (Cukurova and Antalya province) and Southeastern Anatolia Regions of Turkey, although 56% of the cotton is produced in Southeastern Anatolia Region, especially 40% of them in the province of Sanliurfa (Anonymous, 2019b). Therefore, Sanliurfa has an important place in the cotton production of Turkey. This ratio is expected to increase with the completion of SAP (Southeastern Anatolian Project) irrigation and energy projects.

Since the cotton is an important industrial product in both export and domestic consumption, many studies are carried out to increase the seed cotton yield and fiber quality characteristics. One of these studies is using and investigating various plant growth regulators in addition to conventional cotton growing techniques. Plant growth

http://www.aloki.hu ● ISSN 1589 1623 (Print) ● ISSN 1785 0037 (Online)
DOI: http://dx.doi.org/10.15666/aeer/1706_1498514999

regulators are important in terms of researching the possibilities of improving yield and quality potential gained by breeding, growing techniques and ecology by affecting mostly the growth physiology of the plant. In recent years, usage of plant growth regulators has become widespread in the application of agricultural chemicals. Plant growth regulators; they are chemical substances that are synthesized by plants or synthetically synthesized and given to the plant from the outside, which can affect growth, development and other physiological events of plants even in very small proportions, and can be effective in the tissues they form as well as in other plant tissues and organs in which they are carried. These chemicals are called hormone when it is synthesized in the plant and called plant growth regulator when they are synthesized artificially outside of the plant (Kurt et al., 1994; Çopur et al., 2010 and Parveen et al., 2017).

It is possible to create suitable conditions for plant growth to achieve high yields for cotton. In addition to suitable environmental conditions, good agronomic practices (soil tillage, fertilization, pest and disease control, irrigation, plant growth regulators, etc.) have important effects in order to obtain the highest yields (Mert et al., 2015). Some adverse environmental conditions (excessive vegetative growth, etc.) that come up during the growing period can be mitigated by good agronomical practices. Squaring, flowering and boll formation periods are the most critical periods for cotton plant. In this period, some wrong practices in plant management are directly reflected in the yield and may cause yield losses. Climatic factors such as high temperature, day length and relative humidity may adversely affect the synthesis of certain hormones that form in the plants. Eventually, physiological events happening in the plant are directly affected by this situation and the plants cannot demonstrate its yield potential. Therefore, in order to minimize or completely eliminate the negative effects of environmental conditions on plants, the application of some phyto-hormones to plants with different formation and effect patterns is important for the continuation of physiological events in the normal course and to find out the maximum yield potential (Güllüoğlu, 2004). One of the plant growth regulators commonly used in agricultural production is gibberellic acid. Gibberellic acid is currently not used commercially as licensed for cotton production in Turkey, but it is observed that producers sometimes apply.

Gibberellic acid, called GA_3, is a natural compound used for flowering and for better growth of bolls in plants. Plants produce about 90 pcs of gibberellins (Davies, 1995). Almost no evidence has been found the Gibberellins to harm human health up to now. Gibberellic acid is a plant growth regulator derived from a fungal species called *Gibberella fujikuroi*. Plant pathologists in Japan discovered this fungus in 1926. The fungus used for the first time in rice seedlings was found to cause very tall and thin growth of plants (Davies, 1995). Gibberellic acid is obtained by fermentation of Gibberella fungus in large barrels. It is sold in powder and liquid forms which are soluble in water. Gibberellic acid has vital importance for plants and increases the growth and development of the plant (Bora and Sarma, 2006). It can also be used to increase flowering, boll formation and size. Gibberellic acid forms naturally in plants and regulates plant growth. Low dose of GA_3 promotes seed growth but does not have a permanent effect on the seed.

In studies of GA_3 in plants; it is reported that different doses study on cotton plant was not affect the yield potential (McCarty et al., 2009); applications of 100 mg L^{-1} and at the 6-7 leaves period for onion plant increased seed yield per umbrella (Mustaq et al., 2018); and olive yield per tree increased by the applications (Ülger et al., 2018).

http://www.aloki.hu ● ISSN 1589 1623 (Print) ● ISSN 1785 0037 (Online)
DOI: http://dx.doi.org/10.15666/aeer/1706_1498514999

The aim of this study is to determine the effect of different gibberellic acid dosages and application times on the yield and yield components of middle early Stoneville-468 cotton variety under Harran Plain with semi-arid climatic conditions and to provide a source for the studies to be carried out on this subject.

Materials and methods

The experiments were conducted in the Eyyubiye Campus experimental area of Agricultural Faculty of Harran University during 2015 and 2016 growing seasons (*Fig. 1*). The average altitude of the trial area is 465 m and it is located at 37^0 08' N latitude and 38° 46' E longitude and close to the Syrian border. The trial area is clay (62%), organic matter is low (0.5-1.2%) and pH is 7.2 (*Table 1*). The trial area is classified as the Ikizce soil series (Vertic Calciorthid Aridisol) (Anonymous, 2006). Southeastern Anatolia region has semi-arid climatic conditions, summers are hot and dry, and winters are temperate and rainy. In summer the temperature can reach up to 44.1 °C (*Table 2*). Total rainfall in the region in 2015 and 2016 were 312.3 and 440.8 mm respectively. For this purpose, the study was carried out under irrigated conditions. The average temperature for long years was 18.3 °C, the average humidity was 50.3% and the average wind speed was 2.2 m s^{-1} (Anonymous, 2017).

The experiments were carried out in randomized block design with split plots and with 3 replications. Application times formed the main plots (beginning of squaring, beginning of squaring + beginning of flowering and beginning of squaring + beginning of flowering + application after 14 days of flowering) and application doses formed the sub plots (*Table 3*). Stoneville-468 cotton (*Gossypium hirsutum* L.) variety was used as plant material. Cotton seeds were sown with cotton trial driller in 4 rows and 10 m in length with 70 cm inter-row spaces on 01 May in 2015 and 03 May in 2016. After emergence, the plants were thinned with a distance of 15–20 cm (50-60 plants in each row) at the time of 4-5 leaves period.

In the experiments, 70 kg ha^{-1} pure nitrogen and 70 kg ha^{-1} pure phosphorus was applied as a 20.20.0 compound fertilizer. The remaining 90 kg ha^{-1} pure nitrogen was applied as a urea fertilizer (46% pure nitrogen) with the lister machine before the first irrigation. A total of 1050 mm of water was applied during growing season. The first irrigation was applied 4 weeks after sowing, and the other irrigations were practiced 10 times in 10-day intervals. Last irrigation was applied when 10% of the bolls in the plots opened.

Table 1. *Some soil properties of the study area (Harran University Research Station, Sanliurfa, Turkey)*

Depth (cm)	BD (g cm^{-3})	OM (%)	Soil particle distribution (%)			pH	N (kg ha^{-1})	P_2O_5 (kg ha^{-1})	K_2O (kg ha^{-1})	FC (%)	PWP (%)
			Sand	Silt	Clay						
0-30	1.37	1.2	7	34	59	7.3	25	27	1280	31.5	22.2
30-60	1.40	0.8	17	25	58	7.2	12	20	900	31.8	22.6
60-90	1.43	0.6	20	21	59	7.2	6	17	810	32.3	21.5
90-120	1.43	0.5	19	20	62	7.2	-	-	-	32.5	21.5

BD: bulk density, OM: organic matter, FC: field capacity, PWP: permanent wilting point

http://www.aloki.hu ● ISSN 1589 1623 (Print) ● ISSN 1785 0037 (Online)
DOI: http://dx.doi.org/10.15666/aeer/1706_1498514999

Table 2. *Climatic data of the experimental area during cotton crop growing season for the years 2015 and 2016*

Climatic parameters	May	June	July	August	September	October
2015						
Min. air temp. (°C)	11.8	16.7	21.4	22.1	18.7	12.7
Max. air temp. (°C)	38.4	42.8	43.1	40.4	33.0	24.3
Average air temp. (°C)	30.1	27.7	33.2	33.5	29.8	21.6
Relative humidity (%)	38.0	40.1	37.9	37.4	42.7	50.5
Wind speed (ms^{-1})	1.6	1.9	1.6	1.3	1.4	1.5
Soil temperature (°C)	24.3	29.0	32.3	32.9	30.7	23.8
Rainfall (mm)	10.3	20.6	---	1.0	30.5	58.8
2016						
Min. air temp. (°C)	10.7	18.9	20.9	21.2	14.7	12.3
Max. air temp. (°C)	35.0	42.0	43.0	43.0	39.3	33.9
Average air temp. (°C)	23.2	29.8	33.0	33.2	26.4	22.1
Relative humidity (%)	38.3	28.0	25.4	30.6	32.1	35.9
Wind speed (ms^{-1})	1.9	1.9	1.7	1.6	1.7	1.2
Soil temperature (°C)	25.5	31.2	34.5	35.1	30.7	24.6
Rainfall (mm)	12.3	0.6	0.2	---	---	17.6
Average temperatures for 46 years period (1970-2016)						
Min. air temp. (°C)	6.0	10.0	16.00	16.0	11.2	2.5
Max. air temp. (°C)	40.0	44.0	46.8	44.8	42.0	36.4
Average air temp. (°C)	22.3	28.2	32.0	31.2	26.8	20.3
Relative humidity (%)	46.2	34.9	32.2	35.3	37.9	47.5
Wind speed (ms^{-1})	1.9	2.4	2.4	2.2	1.9	1.4
Soil temperature (°C)	25.8	33.2	37.4	36.3	31.0	22.6
Rainfall (mm)	25.7	3.6	0.7	1.1	3.2	25.3

Figure 1. *Photography from the experimental field*

http://www.aloki.hu ● ISSN 1589 1623 (Print) ● ISSN 1785 0037 (Online)
DOI: http://dx.doi.org/10.15666/aeer/1706_1498514999

Table 3. *Gibberellic acid doses and application times*

Growing stages	Application doses (cc ha^{-1})			
1. PHS (cc ha^{-1})	WA (T1)	400 (T2)	800 (T3)	1200 (T4)
2. PHS + FF	WA	200 + 200	400 + 400	600 + 600
3. PHS + FF + after two weeks	WA	133 + 133 + 134	266 + 267 + 267	400 + 400 + 400

PHS: pin head square, FF: first flower, T: treatment, WA: water application

During the growing season in the experimental years, the plants were hoed two times by hand and three times by tractor. Before the application of GA_3, the pressure regulated back pump was calibrated with water and the required amount of water was determined and then GA_3 was mixed with water and applied to the plots when the air temperature was 28-30 °C before midday. Control plots were sprayed with water only.

Agronomic practices were applied in the experiment based on the studies conducted in the region. First-hand harvests were carried out by hand on 18 and 20 September, and second-hand harvests on 15 and 20 October in 2015 and 2016 respectively. According to Worley et al. (1976), seed cotton yield, plant height, number of sympodia branches, number of bolls, seed cotton weight per boll, ginning outturn and 100 seed weight were examined; fiber length, fiber fineness, fiber strength and fiber uniformity characteristics were examined by HVI Spectrum instrument (Anonymous, 1997). The data determined according to the methods were analyzed separately each year according to the split plots trial design by using the MSTAT-C package program and the means were compared according to LSD test (Anonymous, 1989).

Results and discussion

Seed cotton yield (kg ha^{-1})

Table 4 shows that the average seed cotton yield in terms of GA_3 application doses ranged from 4800 kg ha^{-1} to 5500 kg ha^{-1} in 2015 and 2016 years. It was determined that the seed cotton yield increased with increasing of GA_3 doses and the highest and lowest seed cotton yield were obtained from 1200 cc ha^{-1} and control plot respectively. In terms of application times, the highest seed cotton yield was obtained from PHS + FF + application after two weeks. According to LSD (Least Significant Difference) test, it was determined that different yield groups were formed in terms of application doses and times in both years, while application times × dose interactions were found insignificant in 2015 but were found significant in 2016 (*Table 4*). Seed cotton yield is a complex character affected by genotypic and environmental conditions (Worley et al., 1974). In addition to genotype and environmental conditions, chemicals that are applied artificially by external cultivation techniques can also affect dry matter production per unit area (Kurt et al., 1994). From *Table 4*, it can be observed that the seed cotton yield was positively affected by increasing doses of gibberellic acid and increased seed cotton yield. Gibberellic acid applications contributed to increase the number of squares, but also increased boll fall, hence had no effect on the seed cotton yield is indicated by Emiroglu and Turan (1974) and McCarty et al. (2009). Eid et al. (1986) in the study of the GA_3 applications during squaring and flowering period increased the seed cotton yield. GA_3 positively affects the formation of new cells by accelerating cell division and elongation in meristematic tissues and as a result, it has been reported that GA_3 have a positive effect

http://www.aloki.hu ● ISSN 1589 1623 (Print) ● ISSN 1785 0037 (Online)
DOI: http://dx.doi.org/10.15666/aeer/1706_1498514999

on plant growth and flax seed yield (Emongor, 2007 and Rastogi et al., 2013). Our results are compatible with the findings of Eid et al. (1986) but were partially contradictory with the findings of Emiroglu and Turan (1974) and McCarty et al. (2009). As indicated above, different results were published by several researchers. This may be due to cotton genotypes used in the study and changing GA doses and application times. As different locations have different climatic and soil characteristics, variable results can occur.

Table 4. *Seed cotton yield, earliness ratio and plant height and its contributions in response to gibberellic acid and growing stages in 2015 and 2016*

GA application doses	Seed cotton yield (kg ha^{-1})		Earliness ratio (%)		Plant height (cm)	
	2015	2016	2015	2016	2015	2016
Control (C)	4882.77 c	4891.71 c	94.23 a	94.63 a	89.63 c	102.73
GA_1 (400 cc ha^{-1})	5146.02 b	5089.33 bc	92.62 ab	89.21 b	96.13 bc	106.09
GA_2 (800 cc ha^{-1})	5400.56 ab	5242.61ab	90.45 bc	89.88 b	102.95 ab	108.02
GA_3 (1200 cc ha^{-1})	5557.15 a	5353.69 a	87.87 c	85.48 c	107.85 a	111.14
Growing stage (GS)						
PHS[1]	5054.64 b	4937.98 b	90.32	90.65	99.63	105.03 b
PHS + FF[2]	5228.85 ab	5095.52 b	91.14	89.89	98.90	106.40 b
PHS + FF + after two weeks	5456.39 a	5399.52 a	90.73	88.87	98.89	109.57 a
Interaction						
$CxGS_1$	4877.21	4747.33 c	94.23	94.65	89.63	102.73
$CxGS_2$	4800.24	4863.97 c	93.34	90.79	100.03	104.37
$CxGS_3$	5204.04	5067.12 bc	89.06	90.74	104.43	105.33
G_1xGS_1	5337.06	5083.48 bc	84.67	86.41	104.43	107.67
G_1xGS	4877.21	4870.70 c	94.23	94.63	89.63	102.73
G_1xGS_3	5277.17	5057.12 bc	91.53	87.78	93.56	105.27
G_2xGS_1	5250.47	5120.35 bc	90.60	90.07	103.33	107.13
G_2xGS_2	5510.55	5333.90 ab	88.20	87.07	109.10	110.47
G_2xGS_3	4893.88	5067.12 bc	94.23	94.62	89.63	102.73
G_3xGS_1	5360.65	5346.90 ab	92.98	89.06	94.80	108.63
G_3xGS_2	5747.18	5550.37 a	91.69	88.83	101.10	111.60
G_3xGS_3	5823.83	5643.70 a	90.73	82.97	110.03	115.30
Grand mean	5246.63	5144.44	91.29	89.80	99.14	106.99
LSD (0.05) (doses)	294.00	286.90	3.06	2.14	7.63	ns
LSD (0.05) (GS)	256.80	230.70	ns	ns	ns	2.01
DxGS interaction	ns	ns	ns	ns	ns	ns
% C.V.	4.94	4.53	3.39	2.41	7.77	7.34

*Means in each column followed by the same letter are not significantly different ($p < 0.05$)
PHS[1]: pin head square, FF[1]: first flower, T: treatment, $GA_{1,2,3}$: gibberellic acid, GS: growing stage, C: control

Earliness ratio (%)

Table 4 shows that the average rate of earliness ratio ranged from 85% to 94% in 2015 and 2016 with an average of 91.29% in 2015 and 89.80% in 2016 in terms of GA_3

http://www.aloki.hu ● ISSN 1589 1623 (Print) ● ISSN 1785 0037 (Online)
DOI: http://dx.doi.org/10.15666/aeer/1706_1498514999

application doses. In terms of application doses, the highest average earliness ratio was obtained from control plot; the lowest earliness ratio was obtained from gibberellic acid dose of 1200 cc ha^{-1}. In terms of application times, it can be observed from *Table 4* that the earliness ratio ranged between 88% and 91% respectively. According to LSD test, different earliness groups were formed in terms of application doses and the earliness ratio was decreased with increasing application doses, but there were no significant differences in terms of application times in both years. Among plant growth regulators, GA_3 and auxins are vital for development of plants (Gou et al., 2010). Gibberellins by helping the development of stem, leaves and other organs of the plant can cause extension of the nodes (Bora and Sarma, 2006). For this reason, maturation of plants is delayed and thus can delay the opening of cotton bolls. Therefore, the earliness ratio may decrease. However, this decrease had not affected the harvesting date, so the plants completed their maturation in time.

Plant height (cm)

Table 4 shows that the average plant height obtained from different application doses ranged from 89 cm to 111 cm in 2015 and 2016, the average plant height was 99.14 cm in 2015 and 107 cm in 2016. In terms of application times, the highest plant height was obtained from 1200 cc ha^{-1} and the lowest plant height was obtained from the control plot. In terms of GA_3 application times, it can be observed from *Table 4* that the average plant height varies between 98 cm and 109 cm. According to LSD test, it was found that different plant height groups were formed according to years in terms of application doses and application times, but application time x application dose interaction was not significant in both experimental years (*Table 4*). GA_3 promotes cell proliferation in plant developmental stages due to their own metabolism regulation and promotes the development of cells by increasing turgor pressure (Davies, 2010). In this case, it is thought that it activates different enzymes and has a positive effect on plant growth and thus causes plant heightening. In addition, GA_3 in flax increases plant height was indicated by Rastogi et al. (2013) and Ayala-Silva et al. (2005). Our results are compatible with the findings of Emiroğlu and Turan (1974), Özdemir (1991) and Öncü (1993), and differ from the findings of İncekara and Turan (1977). This case may be derived due to the use of different GA_3 doses, application times and the cotton varieties in the experiments.

Boll number (no. plant^{-1})

Table 5 shows that the average number of bolls per plant obtained from GA_3 application doses ranged from 10.00 no. $plant^{-1}$ to 16.24 no. $plant^{-1}$ with the average of 12.76 no. $plant^{-1}$ in 2015 and 13.47 no. $plant^{-1}$ in 2016. In terms of application times, the lowest number of bolls was obtained from PHS and the highest number of bolls was obtained from PHS + FF + 14 days application. In the application time × GA_3 dose interaction, while the lowest number of bolls was obtained from the control plot and the highest number of bolls was obtained from 1200 cc ha^{-1} and PHS + FF + 14 days application. According to LSD test, it can be observed that there are different groups of number of bolls in terms of application doses and the number of bolls increased with increasing application dose in both years. Cotton yield is the result of the interaction of genetic and environmental conditions and different yield components can affect the cotton yield (Worley et al., 1974). The main feature that contributes to the cotton yield

http://www.aloki.hu ● ISSN 1589 1623 (Print) ● ISSN 1785 0037 (Online)
DOI: http://dx.doi.org/10.15666/aeer/1706_1498514999

is the number of bolls formed per unit area or per plant (Wilson et al., 1994). GA_3 positively affects the flowering and boll formation (Mathur and Mittal, 1964; Taiz and Zeiger, 2003). Therefore, it was found that the number of bolls per plant increased and had a positive effect on the seed cotton yield.

Number of sympodia (no. plant^{-1})

Table 5 shows that the average number of sympodia branches changed between 11.76 no. plant^{-1} and 17.82 no. plant^{-1} obtained from GA_3 application doses with the average of 13.40 no. plant^{-1} in 2015 and 16.81 no. plant^{-1} in 2016. The highest numbers of sympodia branches were obtained from 1200 cc ha^{-1} and the lowest number of sympodia branches were obtained from control plot. In terms of application times, the number of sympodia branches per plant was increased by dividing the doses into three times and the highest number of sympodia branches was obtained from PHS + FF + application after two weeks. According to LSD test, it was determined that different sympodia branch number groups were formed in terms of application doses and application times in 2015, application time × GA_3 dose interaction was significant, but only application doses were statistically significant in 2016 (*Table 5*). 80-85% of the bolls formed on the sympodia branches of plant. Increase in the number of sympodia branches increasing the number of bolls per plant, which contributes positively to the increase of seed cotton yield per unit area. Similar findings were determined by Çopur et al. (2010). In addition, GA_3 applications increase the number of branches in flax plant (Rastogi et al., 2013). For this purpose, 1200 cc ha^{-1} GA_3 dose and PHS + FF + after two weeks applications yielded the highest number of sympodia.

Seed cotton boll weight (g boll^{-1})

The most important factor affecting yield is a high-yielding cotton variety, favorable environmental conditions as well as boll weight (Mauney et al., 1978). *Table 5* shows that the seed cotton boll weight increased with increasing of GA_3 doses in both years. While the seed cotton weight per boll was 3.8-3.9 g in control plots, increased to 4.2-4.3 g at a dose of 1200 cc ha^{-1} of GA_3. It was also found that seed cotton weight per boll increased by dividing application doses in terms of application times. According to the LSD test, it was determined that different seed cotton boll weight groups were formed in terms of application doses and application times were statistically significant in 2015 and 2016. Also, application time × GA_3 dose interaction was statistically significant in 2015 but not significant in 2016. GA_3 applications increased the seed cotton boll weight by increasing the number of leaves per unit area to promote more photosynthesis and contributed to increase dry matter per unit area. Similar findings were found by Abro et al. (2004). In addition, Çopur et al. (2010) in his study with different plant growth regulators; GA_3 applications contribute to the formation of heavier bolls than other plant growth regulators. McCarty et al. (1987) reported that the application of GA_3 reduces the seed cotton boll weight. This case may be derived due to the use of cotton varieties and the effect of different climate condition on plant growth in the experiments.

Seed index (g)

Table 6 shows that the average seed index was changed between 8.49-9.01 g with the average of 8.80 g in terms of GA_3 application doses in 2015; ranged from 8.65 to 9.20 g with the average of 8.92 g in 2016. In terms of application doses, the highest seed index

http://www.aloki.hu ● ISSN 1589 1623 (Print) ● ISSN 1785 0037 (Online)
DOI: http://dx.doi.org/10.15666/aeer/1706_1498514999

was obtained from 1200 cc ha^{-1} and the lowest seed index was obtained from the control plot. In terms of application times, the average seed index changes between 8.68 and 8.92 g in 2015 and 8.67 and 9.27 g in 2016. When the GA doses and control parcels were compared in terms of application doses according to LSD test, the results obtained from GA_1, GA_2 and GA_3 applications were similar but higher than the control parcel in 2015. In 2016, GA_2 and GA_3 doses were similar but higher than GA_1 and control parcels. It can be seen that seed index was increases with increasing of GA_2 and GA_3 doses. GA_2 and GA_3 applications accelerated the plant growth along with cell division and contributed to the increase of dry matter per unit area and accordingly increased seed weight. Erdemli and Kaya (2015) in the sunflower and Mustaq et al. (2018) in onion reported that an increase in GA_3 doses cause an increase in seed weight. According to these results, it can be said that GA applications had positive effect on seed size.

Table 5. *Boll number, number of sympodia, seed cotton boll weight and its contributions in response to gibberellic acid and growing stages in 2015 and 2016*

GA application doses	Boll number (no. $plant^{-1}$)		Number of sympodia (no. $plant^{-1}$)		Seed cotton boll weight (g $boll^{-1}$)	
	2015	2016	2015	2016	2015	2016
Control (C)	10.00 c	11.10 c	11.76 d	15.23 c	3.95 c	3.81 c
GA_1 (400 cc ha^{-1})	11.96 b	13.44 b	12.90 c	16.86 b	4.12 b	3.95 bc
GA_2 (800 cc ha^{-1})	12.86 b	14.06 b	13.66 b	17.32 ab	4.21 b	4.04 ab
GA_3 (1200 cc ha^{-1})	16.24 a	15.29 a	15.25 a	17.82 a	4.37 a	4.22 a
Growing stage (GS)						
PHS[1]	11.32 c	12.35 b	12.20 b	16.58	4.06 b	3.69 c
PHS + FF[2]	12.43 b	13.02 b	13.56 a	16.82	4.13 b	4.03 b
PHS + FF + after two weeks	14.54 a	13.05 a	14.42 a	17.03	4.31 a	4.29 a
Interaction						
$CxGS_1$	10.00 d	11.10	11.76 d	15.23	3.95	3.81 cd
$CxGS_2$	10.17 cd	12.43	11.70 d	16.70	3.92	3.52 d
$CxGS_3$	10.70 cd	12.23	12.13 d	16.70	4.05	3.63 d
G_1xGS_1	14.40 b	13.63	13.20 c	17.70	4.29	3.82 cd
G_1xGS_2	10.00 d	11.10	11.76 d	15.23	3.95	3.81 cd
G_1xGS_3	11.60 cd	12.27	13.50 c	16.90	4.07	4.09 bc
G_2xGS_1	12.03 c	13.67	13.70 c	17.50	4.15	4.09 bc
G_2xGS_2	16.10 b	15.03	15.30 b	17.63	4.34	4.14 bc
G_2xGS_3	10.00 d	11.10	11.76 d	15.23	3.95	3.81 cd
G_3xGS_1	14.10 b	15.63	13.50 c	16.97	4.37	4.25 b
G_3xGS_2	15.83 b	16.27	15.17 b	17.77	4.43	4.42 ab
G_3xGS_3	18.23 a	17.20	17.26 a	18.13	4.80	4.70 a
Grand mean	12.76	13.47	13.40	16.81	4.17	4.01
LSD (0.05) (doses)	1.56	1.15	0.98	ns	0.15	0.20
LSD (0.05) (GS)	0.78	0.82	0.59	0.57	0.11	0.24
DxGS interaction	2.00	ns	1.02	ns	ns	0.34
% C.V.	9.15	8.59	4.42	3.45	3.60	4.95

*Means in each column followed by the same letter are not significantly different ($p < 0.05$)
PHS[1]: pin head square, FF[1]: first flower, T: treatment, $GA_{1,2,3}$: gibberellic acid, GS: growing stage

http://www.aloki.hu ● ISSN 1589 1623 (Print) ● ISSN 1785 0037 (Online)
DOI: http://dx.doi.org/10.15666/aeer/1706_1498514999

Table 6. *Seed index, ginning outturn, fiber length and its contributions in response to gibberellic acid and growing stages in 2015 and 2016*

GA application doses	Seed index (g)		Ginning outturn (g)		Fiber length (mm)	
	2015	2016	2015	2016	2015	2016
Control (C)	8.49 b	8.65 b	41.02 b	41.49 b	28.49 b	27.62
GA_1 (400 cc ha^{-1})	8.75 ab	8.74 b	41.94 a	42.95 a	29.58 a	27.39
GA_2 (800 cc ha^{-1})	8.93 a	9.08 a	41.76 ab	43.01 a	29.83 a	28.16
GA_3 (1200 cc ha^{-1})	9.01 a	9.20 a	42.36 a	43.35 a	29.91 a	28.51
Growing stage (GS)						
PHS[1]	8.68	8.67 b	41.62	42.70	28.82 b	27.50
PHS + FF[2]	8.78	8.81 b	41.77	42.75	29.54 a	27.86
PHS + FF + after two weeks	8.92	9.27 a	41.93	42.65	30.00 a	28.40
Interaction						
$CxGS_1$	8.49	8.65 b	41.03	41.49	28.49	27.62
$CxGS_2$	8.52	8.68 b	41.54	42.79	28.74	27.37
$CxGS_3$	8.83	8.62 b	41.69	42.98	29.12	27.76
G_1xGS_1	8.89	8.72 b	42.20	43.53	28.91	27.26
G_1xGS_2	8.50	8.65 b	41.02	41.49	28.49	27.62
G_1xGS_3	8.79	8.69 b	42.10	42.97	29.66	27.17
G_2xGS_1	8.88	8.89 b	41.52	43.39	29.76	27.98
G_2xGS_2	8.97	9.03 b	42.42	43.14	30.26	28.65
G_2xGS_3	8.50	8.65 b	41.02	41.49	28.49	27.62
G_3xGS_1	8.94	8.85 b	42.16	43.07	30.33	27.63
G_3xGS_2	9.10	9.73 a	42.07	42.65	30.61	28.74
G_3xGS_3	9.17	9.85 a	42.46	43.39	30.56	29.60
Grand mean	8.80	8.92	41.77	42.70	29.45	27.92
LSD (0.05) (doses)	0.31	0.28	0.80	0.75	0.78	ns
LSD (0.05) (GS)	ns	0.28	ns	ns	0.50	ns
D x GS interaction	ns	0.48	ns	ns	ns	ns
% C.V.	3.52	3.16	1.92	1.77	2.67	3.13

*Means in each column followed by the same letter are not significantly different ($p < 0.05$)
PHS[1]: pin head square, FF[1]: first flower, T: treatment, $GA_{1,2,3}$: gibberellic acid, GS: growing stage, C: control

Ginning outturn (g)

Marketing of cotton in Turkey is done more in ginning enterprises as seed cotton. Ginning enterprises in cotton purchase are taking into account the more ginning outturn as well as the color and the amount of foreign matter for price. For this purpose, ginning outturn is important in the marketing of cotton seed. *Table 6* shows that the average ginning outturn was obtained from the application doses of GA_3 changed between 41-42.36% in 2015 with the average of 41.77%, and between 41-43% with the average of 42.70% in 2016. While the highest ginning outturn was obtained from 1200 cc ha^{-1}, the lowest ginning outturns from the control plot. According to LSD test, it was found that different ginning outturn groups were formed in terms of application doses but there were no significant differences in terms of application times and GA_3 dose x application

http://www.aloki.hu ● ISSN 1589 1623 (Print) ● ISSN 1785 0037 (Online)
DOI: http://dx.doi.org/10.15666/aeer/1706_1498514999

time's interaction in both years. In the findings obtained in GA application doses, GA_1, GA_2 and GA_3 applications were similar in both years but higher results were obtained compared to the control parcels. In the studies of Emiroğlu and Turan (1974) and Özdemir (1991) with different plant growth regulators reported that the gibberellic acid had not affected ginning outturn. This situation differs from our findings. Different results may be observed due to the different climatic conditions of the studies, application time and GA_3 dose and different cotton varieties used in the experiments.

Fiber length (mm)

Table 6 shows that the average fiber length obtained from different GA_3 application doses varied between 28.49 and 29.91 mm in 2015 with the average of 29.45 mm were varied between 27 and 28 mm with the average of 27.92 mm in 2016. While the longest fibers were obtained from 1200 cc ha^{-1} the shortest fibers were obtained from the control plot. In terms of application times, the average fiber length varies between 28.82 and 30.00 mm in 2015 and between 27.50 and 28.40 mm in 2016. In 2016, it can be seen that, GA_1, GA_2 and GA_3 applications were similar but they produce higher results than the control parcel. According to LSD test; fiber lengths were affected by GA_3 applications in 2015 but were not affected in 2016. Although fiber length is an inherited character, it can be affected by environmental conditions and cultivation techniques. In the study of Gokani and Thaker (2002); fiber lengths in both in vitro and in vivo were positively affected from GA_3 applications in three cotton varieties used in the experiment; Oral (1986), Jost and Dolar (2004) and Çopur et al. (2010) reported that GA_3 had no significant effect on fiber length. This may be observed due to the fact that the trials were conducted with different GA_3 doses and cotton varieties under different environmental conditions.

Fiber fineness (micronaire)

Table 7 shows that the average fiber fineness value ranged from 4.18 to 4.55 micronaire (mic) with an average of 4.34 mic in terms of GA_3 application doses in 2015, ranged from 4.77 to 4.91 mic with an average of 4.86 mic in 2016. In terms of application times, the average fiber fineness varies between 4.30 and 4.42 mic with the average of 4.34 mic in 2015, varies between 4.83 and 4.96 mic with an average of 4.86 mic in 2016. In terms of GA_3 doses, it can be observed that the coarser fibers were obtained from 800 cc ha^{-1} and the finest fibers were obtained from the control plot in 2015 but there were no significant differences in terms of application times and GA_3 doses in 2016. It can be seen from *Table 7* that the fiber fineness partially decreased with increasing GA_3 doses.

Although the fiber fineness value is an inherited property, it can be affected by environmental conditions. In particular, temperature and consequently photosynthesis and carbohydrate deposition may affect fiber fineness. Thus, with the dose increases, the maturation of the plants is delayed, and the fibers become coarse due to the increase of dry matter in the plants. Although the fiber fineness is partially getting coarser with increasing of GA_3 dose, the values obtained do not pose a problem in terms of its use in textile (expected values are 3.8-4.6 mic). Our results are partially contradicting with the findings of Özdemir (1991), Zibdieh et al. (1998) and Çopur et al. (2010) and this may be observed due to the differences of GA_3 doses and the cotton varieties used in the trials.

http://www.aloki.hu ● ISSN 1589 1623 (Print) ● ISSN 1785 0037 (Online)
DOI: http://dx.doi.org/10.15666/aeer/1706_1498514999

Table 7. *Fiber fineness, fiber strength, fiber uniformity and its contributions in response to gibberellic acid and growing stages in 2015 and 2016*

GA application doses	Fiber fineness (mic)		Fiber strength (g tex^{-1})		Fiber uniformity (%)	
	2015	2016	2015	2016	2015	2016
Control (C)	4.18 b	4.77	30.70	29.23	83.23 c	82.97 c
GA_1 (400 cc ha^{-1})	4.32 ab	4.82	31.66	28.32	84.58 b	82.86 c
GA_2 (800 cc ha^{-1})	4.55 a	4.93	31.97	29.17	84.98 a	84.16 b
GA_3 (1200 cc ha^{-1})	4.33 ab	4.91	32.37	29.13	85.24 a	85.27 a
Growing stage (GS)						
PHS[1]	4.42	4.83	31.28	28.78	84.27 b	84.02
PHS + FF[2]	4.31	4.78	31.48	29.26	84.55 ab	83.72
PHS + FF + after two weeks	4.30	4.96	32.26	28.86	84.71 a	83.70
Interaction						
$CxGS_1$	4.18	4.77	30.70	29.23	83.23 d	82.97
$CxGS_2$	4.37	4.79	31.06	27.30	84.63 bc	83.33
$CxGS_3$	4.58	4.78	31.60	29.50	84.80 bc	84.87
G_1xGS_1	4.56	4.74	31.73	29.07	84.43 c	84.90
G_1xGS_2	4.18	4.77	30.70	29.23	83.23 d	82.97
G_1xGS_3	4.45	4.73	31.37	29.20	84.33 c	82.67
G_2xGS_1	4.38	5.07	31.73	29.73	84.90 bc	83.67
G_2xGS_2	4.24	4.97	32.13	28.87	85.73 a	85.57
G_2xGS_3	4.18	4.77	30.70	29.23	83.23 d	82.97
G_3xGS_1	4.14	4.94	32.53	28.47	84.77 bc	82.57
G_3xGS_2	4.69	4.95	32.57	28.27	85.27 ab	83.93
G_3xGS_3	4.18	5.04	33.23	29.47	85.57 a	85.33
Grand mean	4.34	4.86	31.67	28.96	84.51	83.81
LSD (0.05) (Doses)	0.25	ns	ns	ns	0.39	1.04
LSD (0.05) (GS)	ns	ns	ns	ns	0.32	ns
D x GS interaction	ns	ns	ns	ns	0.67	ns
% C.V.	5.67	5.07	5.75	6.27	0.46	1.25

*Means in each column followed by the same letter are not significantly different ($p < 0.05$)
PHS[1]: pin head square, FF[1]: first flower, T: treatment, $GA_{1,2,3}$: gibberellic acid, GS: growing stage, C: control

Fiber strength (g tex^{-1})

Table 7 shows that the average fiber strength obtained was 31.67 g tex^{-1} according to GA_3 application doses in 2015 and 28.96 g tex^{-1} in 2016, the highest fiber strength was obtained from 1200 cc ha^{-1} and the lowest fiber strength was obtained from the control plot. According to LSD test; different fiber breakage strength groups has not formed in terms of GA_3 doses, application times and interaction of application doses x application times, but fiber breakage strength increased partially with increasing of GA_3 doses, but it was not statistically significant. This shows that GA_3 applications have no significant effect on the fiber breakage strength. Similar findings were determined by Özdemir (1991), Zibdieh et al. (1998) and Çopur et al. (2010).

http://www.aloki.hu ● ISSN 1589 1623 (Print) ● ISSN 1785 0037 (Online)
DOI: http://dx.doi.org/10.15666/aeer/1706_1498514999

Fiber uniformity (%)

Table 7 shows that the average fiber uniformity ratio obtained from gibberellic acid application doses varies between 83.23% and 85.24% with the average of 84.51% in 2015, and it was varied between 82.97% and 85.27% with the average of 83.81% in 2016. While the highest fiber uniformity was obtained from 1200 cc ha^{-1} and the lowest fiber uniformity was obtained from the control plot. In terms of GA_3 application times, the average fiber uniformity was varied between 84.27 and 84.71% in 2015 and varies between 83.70 and 84.02% in 2016. As a result of the analysis of variance: There were significant differences in all sources of variation in terms of fiber uniformity for 2015, but only a significant difference was found in terms of application times in 2016 (*Table 7*). Fiber uniformity ratio is calculated in the fiber development diagram as 50% fiber length in fiber distribution by comparing to the 2.5% of fiber length. Thus, fiber length is positively affected with increasing doses of GA_3, so that a homogeneous length is obtained with the development of fibers. Increased fiber uniformity is desirable and GA_3 doses have a positive effect on fiber uniformity ratio. Therefore, in GA_3 applications, the dose of 1200 cc ha^{-1} was divided into three as PHS + FF + after two weeks or divided into two as PHS + FF.

Conclusion

In cotton farming, the most important issue that the producers have focused on seed cotton yield. In this study the seed cotton yield varied between 4882.77 kg ha^{-1} and 5557.15 kg ha^{-1}. Cotton yield is the result of interaction of genetic and environmental conditions, and different yield components can affect the seed cotton yield. Therefore, in order to minimize the negative effects of environmental conditions on plants, to maintain normal physiological events in plants and to reach maximum yield potential, it is important to give some phyto hormones to the plant externally. One of the plant growth regulators commonly used in agricultural production is gibberellic acid. Gibberellins promote their growth as they increase the turgor pressure of the cells by promoting cell proliferation during plant developmental stages, thus regulating their own metabolism. Furthermore, GA positively affects flowering, boll formation and number of bolls per plant, thus contributing positively to seed cotton yield. According to our study with different GA doses the most appropriate dose of GA under semi-arid climatic conditions is 1200 cc ha^{-1} and it should be preferred to divide into three doses as beginning of squaring + beginning of flowering + 14 days after beginning of flowering. In addition, it would be useful to carry out more studies related to plant growth regulators at different locations in order to determine the variable dose combinations of GA and the response of different cotton varieties.

REFERENCES

[1] Abro, G. H., Syed, T. S., Zhang, M. S. (2004): Effect of application of a plant growth regulator and micronutrients on insect pest infestation and yield components of cotton. – Journal of Entomology 1(1): 12-16.

[2] Anonymous (1989): MSTAT Development Team. MSTAT User's Guide, A Microcomputer Program for the Design Management and Analysis of Agronomic Research Experiments. – Michigan State University, USA.

http://www.aloki.hu ● ISSN 1589 1623 (Print) ● ISSN 1785 0037 (Online)
DOI: http://dx.doi.org/10.15666/aeer/1706_1498514999

[3] Anonymous (1997): High Volume Instruments (HVI) Catalog. – Costumer Information Service No: 40, May, Sweden.
[4] Anonymous (2006): GAP Agricultural Research Institute. – Soil Analysis Laboratory Results, Sanliurfa, Turkey.
[5] Anonymous (2017): Official record of Meteorology Directory. – Şanlıurfa, Turkey.
[6] Anonymous (2019a): Record of the International Cotton Advisory Committee (ICAC) Report, April Monthly Report. – ICAC, Washington, DC.
[7] Anonymous (2019b): Official Record of Turkish Statistical Institute. – http://www.tuik.gov.tr/bitkiselapp/bitkisel.zul (accessed on 20 April 2019).
[8] Ayala-Silva, T., Akin, D. E., Foulk, J., Dodd, R. B. (2005): Effect of growth regulators on yield and fiber quality and quantity in flax (*Linum usitatissimum* L.). – Plant Growth Regulation Society of America 33: 90-100.
[9] Bora, R. K., Sarma, C. M. (2006): Effect of gibberellic acid and cycocel on growth, yield and protein content of pea. – Asian Journal of Plant Sciences 5: 324-330.
[10] Çopur, O., Demirel, U., Karakus, M. (2010): Effects of several plant growth regulators on the yield and fiber quality of cotton (*Gossypium hirsutum* L.). – Notulae Botanicae Horti Agrobotanici Cluj-Napoca 38(3): 104-110.
[11] Davies, P. J. (1995): Plant Hormones and Their Role in Plant Growth Development. 2nd Ed. – Kluwer, Dordrecht.
[12] Davies, P. J. (2010): The Plant Hormones: Their Nature, Occurrence, and Functions. – In: Davies, P. J. (ed.) Plant Hormones. Springer, Netherlands, pp. 1-15.
[13] Eid, E. T., Aggory, E. A. (1986): Effect of GA_3 different applications on yield, components and mineral status of cotton plant, variety Giza-75 (*G. barbadense* L.). – Field Crops Abs 39(11): 8829.
[14] Emiroğlu, Ş. H., Turan, Z. M. (1974): A research on the effects of cycocel and gibberellin on the anatomical and technological properties of cotton. – Plant 1(13): 415-425 (in Turkish).
[15] Emongor, V. (2007): Gibberellic acid (GA3) influence on vegetative growth, nodulation and yield of cowpea (*Vigna unguiculata* L.) Walp. – Journal of Agronomy 6: 509-517.
[16] Erdemli, H., Kaya, M. D. (2015): The effects of gibberellic acid doses on yield and germination under abiotic stress conditions in sunflower (*Helianthus annuus* L.). – Journal of Field Crops Central Research Institute 24(1): 38-46 (in Turkish).
[17] Gokani, S. J., Thaker, V. S. (2002): Role of gibberellic acid in cotton fibre development. – Journal of Agricultural Science 138: 255-260.
[18] Gou, J., Strauss, S. H., Tsai, C. J., Fang, K., Chen, Y., Jiang, X., Busov, V. B. (2010): Gibberellins regulate lateral root formation in *Populus* through interactions with Auxin and other hormones. – The Plant Cell 22(2): 623-639.
[19] Güllüoğlu, L. (2004): Determination of usage of plant growth regulators in soybean (*Glycine max* L.) farming under Harran plain conditions. University of Harran (Turkey). – Journal of the Faculty of Agriculture (in Turkish) 8(3-4): 17-23.
[20] İncekara, F., Turan, Z. M. (1977): The effect of various gibberellin doses on some agronomic and technological characters in cotton (*G. hirsutum* L.). – Plant 4(2): 161-168 (in Turkish).
[21] Jost, P., Dolar, M. (2004): Comparison of mepiquat pentaborate and mepiquat chloride effects on DP555BR. – Proc. Beltwide Cotton Conf., San Antonio. Natl. Cotton Counc. Am., Memphis, TN, 5-9 January, pp. 2204-2206.
[22] Kurt, O., Leitch, M. H., Avcıoğlu, R. (1994): An investigation into the effects of the application of plant growth regulators (chlor mepiquat and ethaphon) on growth, development and yield of linseed (*Linum usitatissimum* L.). – The First National Field Crops Congress of Turkey. Proceedings of Plant Breeding, University of Ege, Faculty of Agriculture, Department of Field Crops. Izmir, Turkey 2: 219-222 (in Turkish).
[23] Mathur, S. N., Mittal, S. P. (1964): Effect of gibberellin on flowering in cotton. – Physiologia Plantarum 17: 275-278.

http://www.aloki.hu ● ISSN 1589 1623 (Print) ● ISSN 1785 0037 (Online)
DOI: http://dx.doi.org/10.15666/aeer/1706_1498514999

[24] Mauney, J. R., Fry. K. E., Guinn, G. (1978): Relationship of photosynthetic rate to growth and fruiting of cotton, soybean, sorghum and sunflower. – Crop Science 18: 259-263.
[25] McCarty, J. C., Jenkins, J. N., Hedin, P. A., Shepherd, R. L., Parrott, W. L. (1987): The effects of plant growth regulators on cotton yield in two environments. – Miss. Agric. For. Exp. Sta. Res. Rep. 12: 1-4.
[26] McCarty, J. C., Hedin, P. A., Hayes, R. W. (2009): Minimal effects of foliar application of gibberellic acid and carbohydrates on the yield of cotton lint. – Mississippi State University Agricultural and Forestry Experiment Station Report, USA.
[27] Mert, M., Çopur, O., Özek, H. Z. (2015): Changes in the production of fiber crops and new searches. – Turkish Chamber of Agricultural Engineers, 8th Technical Congress, 12-16 January 2015. Ankara, Turkey, pp. 450-482 (in Turkish).
[28] Mustaq, S., Amjad, M., Ziaf, K., Afzal, I. (2018): Gibberellins application timing modulates growth, physiology, and quality characteristics of two onion (*Allium cepa* L.) cultivars. – Environmental Science and Pollution Research 25(25): 25155-25161.
[29] Oral, A. (1986): Effect of some plant growth regulator on shedding in cotton. – Mediterranean University, Faculty of Agriculture, First Turkish Foliar Fertilizers and Plant Hormones Symposium, 23-24 October, Antalya, Turkey (in Turkish).
[30] Öncü, S. (1993): A research on the effect of some growth regulators and harvest aid application in cotton (*Gossypium hirsutum* L.). – Ege University, Graduate School of Natural and Applied Sciences, PhD. Thesis, İzmir, Turkey, pp.45-50 (in Turkish).
[31] Özdemir, M. (1991): The effect of some growth regulators on yield and quality in cotton (*Gossypium hirsutum* L.). – Ege University, Graduate School of Natural and Applied Sciences, MSc Thesis, İzmir, Turkey (in Turkish).
[32] Parveen, S., Iqbal, R. M., Akram, M., Iqbal, F., Tahir, M., Rafay, M. (2017): Improvement of growth and productivity of cotton (Gossypium hirsutum L.) through foliar applications of naphthalene acetic acid. – Semina: Ciências Agrárias, Londrina 38(2): 561-570.
[33] Rastogi, A., Siddiqui, A., Mishra, B. K., Srivastava, M., Pandey, R., Misra, P., Singh, M., Shukla, S. (2013): Effect of auxin and gibberellic acid on growth and yield components of linseed (*Linum usitatissimum* L.). – Crop Breeding and Applied Biotechnology 13: 136-143.
[34] Taiz, L., Zeiger, E. (2003): Plant Physiology. Third Ed. – Sinauer Associates, Sunderland, MA.
[35] Ülger, S., Atmaca, S., Demiral, S. (2018): The effects of GA_3 treatment on yield, carbohydrate, and endogenous hormone changes in Memecik olive cultivar. – Turkish Journal of Agriculture and Forestry 42: 75-81.
[36] Wilson, F. D., Flint, H. M., Deaton, W. R., Buehler, R. E. (1994): Yield, yield components, and fiber properties of insect-resistant cotton lines containing a *Bacillus thuringiensis* toxin gene. – Crop Science 34: s 38-41.
[37] Worley S., Culp, T. W., Harrell, D. C. (1974): The relative contributions of yield components to lint yield of upland cotton, *Gossypium hirsutum* L. – Euphytica 23: 399-403.
[38] Worley, S. J. R., Harmon, H. R., Harrel, D. C., Culp, T. W. (1976): Ontogenetic model of cotton yield. – Crop Science 16: 30-34.
[39] Zibdieh, A., Mouharram, S., Khourı, F. (1998): Effect of growth regulators, PGR IV, cytokin, cytoplex and atonik in Syria in 1996 and 1997 seasons. – FAO Interregional Cooperative Research Network on Cotton, 14-20 July, Bari, Italy, pp. 58-61.

http://www.aloki.hu ● ISSN 1589 1623 (Print) ● ISSN 1785 0037 (Online)
DOI: http://dx.doi.org/10.15666/aeer/1706_1498514999

THE INFLUENCES OF THE SOUTH-TO-NORTH WATER TRANSFER PROJECT ON NITROGEN REMOVAL BY SOIL IN A TERMINAL RESERVOIR IN A CRITICAL STATE IN CHINA

XUE, W.L.[1,2] – LI, F.H.[1*] – ZHAO, H.G.[3*]

[1]*College of Water Resources and Civil Engineering, China Agricultural University, Beijing 10083, PR China*

[2] *Beijing Water Science and Technology Institute, Beijing 100048, PR China*

[3]*Institute of Environment and Sustainable Development in Agriculture, Chinese Academy of Agricultural Sciences, Beijing 100081, PR China*

**Corresponding authors*
e-mail: lifahu@cau.edu.cn, zhaohaigen@caas.cn; phone/fax: +86-010-6273-7706/7796 (F. Li), +86-010-8210-6007/9567 (H. Zhao)

(Received 25th Jun 2019; accepted 15th Nov 2019)

Abstract. Soil in riparian zone can alleviate the risk of nitrogen pollution for water by releasing gaseous nitrogen (N) fluxes. As a critically terminal riparian zone in China, the Miyun Reservoir riparian zone is dramatically submerged by water delivered by the South-to-North Water Transfer Project (SNWTP), which is the largest inter-basin water transfer scheme worldwide. However, few studies have proposed a framework to estimate the effect of SNWTP on N removal by soil at the scale of the riparian catchment. Therefore, a framework that integrates the eco-hydrological model, remote sensing technology, and scenario setting was developed in this study to simulate the spatiotemporal variation of N emissions and to estimate the influences of SNWTP on N removal by soil in the Miyun riparian catchment between April and September of 2015. The simulated results indicate that N removal in the whole catchment ranged from 48.83 t to 290.58 t between April and September and the total N removal was 871.97 t in 2015. With water level exceeding 150 m and 160 m, the riparian soil had about 35%-60% of its original N pollution mitigation ability. Changing farmland and grassland into forestland can effectively offset the impacts of SNWTP.
Keywords: *nitrogen pollution, eco-hydrological model, riparian zone, scenario setting, remote sensing, Miyun reservoir*

Introduction

To relieve the emerging crises of water resource shortage, inter-basin water transfer projects are beginning to be used throughout the world. Prominent examples are the Snowy Mountains Scheme in Australia, the California State Water Project in the United States, the West-to-East Water Transfer Project in Pakistan, the Quebec Water Transfer Project in Canada, the Lesotho Highlands Water Project in Lesotho and South Africa, and the Durance-Verdun Water Transfer Project in France (Chen et al., 2013; Wang et al., 2009; Yang et al., 2018a).

A complete water transfer project needs to draw water from a water source, transport this water via conveyance canals, and inject the water into the terminal reservoir (Yang et al., 2018a). Each part of such a water diversion causes different ecological and environmental problems. Specifically, the supply of adequate water without pollution is the most important item to be considered for the water source region (Gu et al., 2012; Tang et al., 2014; Yang et al., 2016; Zhang, 2009; Zeng et al., 2015); the maintenance of

http://www.aloki.hu ● ISSN 1589 1623 (Print) ● ISSN 1785 0037 (Online)
DOI: http://dx.doi.org/10.15666/aeer/1706_1500115018

adequate water quality and the prevention of disease spread should be the greatest concern in the conveyance canal (Yang et al., 2018a); for the terminal reservoir, protection functions of riparian areas is the main issue due to the drastic increase of the reservoir water level induced by the injection of transferred water (Zhang, 2009; Zhuang, 2016).

So far, the South-to-North Water Transfer Project (SNWTP) that was started to be built in China in 2002 is the largest inter-basin water transfer scheme in the world (Barnett et al., 2015; Li et al., 2016). It includes three independent routines, namely, west, east, and middle routes, where the last two routes have been completed and can deliver about 25 billion m3 of water per year (Liu and Zheng, 2002). At present, a number of studies have reported the ecological and environmental issues related to the SNWTP (Gu et al., 2012; Li et al., 2017; Ma et al., 2014; Tang et al., 2014; Yang et al., 2016, 2012; Zhang et al., 2008, 2018). However, most of these studies focused the water source region and on conveyance canals, while studies on effects of SNWTP on the terminal reservoir are rare.

The riparian zone is the transition region between water and terrace (King et al., 2016). It can intercept non-point source (NPS) pollutants from upland and therefore plays an important role in reducing the pollution risk of the water resource (de Sosa et al., 2018; Shu et al., 2017; Wei et al., 2017). In recent years, NPS N is becoming the key pollutant endangering the water quality safety in the world (Blackburn et al., 2017; Erisman et al., 2013). A number of studies have proposed that the soil in the riparian zone can effectively remove N pollution by releasing gaseous N fluxes (Butterbach-Bahl et al., 2013; de Sosa et al., 2018; Jacinthe and Vidon, 2017; Seitzinger et al., 2006). Furthermore, denitrification, nitrification, and ammonium volatilization have been reported as the three main biochemical processes related to the soil N emission (de Sosa et al., 2018; Groffman et al., 2009; Vymazal, 2007; Wang et al., 2010). In addition, various factors such as soil contents of organic carbon and inorganic nitrogen, moisture, temperature, PH, and microbial activity exert important impacts on soil gaseous N emission fluxes (Brovelli et al., 2012; de Sosa et al., 2018; Figueiredo et al., 2016; Rojas-Oropeza et al., 2010; Si et al., 2018; Wang et al., 2010).

In the past studies, a combination of field sampling and mathematical statistics was usually employed to explore the variance of soil N in the riparian zone (Lind et al., 2013; Shu et al., 2017; de Sosa et al., 2018; Ye et al., 2014; Zhong et al., 2018). This type of method is easy to be conducted; however, it is very difficult to adequately yield an explanation of mechanistic processes and to operate it at the catchment scale (Hoang et al., 2017). In addition, a number of specifically processed models have been developed to simulate the hydrological processes and N dynamics in the riparian, such as the Riparian Soil Model (Brovelli et al., 2012), Wetlands Water Quality Model (Chavan and Dennett, 2008), Soil and Water Assessment Tool-Riparian Ecosystem Management Model (SWAT-REMM, Ryu et al., 2011), Penn State Integrated Hydrological Wetland Model (Zhang et al., 2018), and modified SWAT (SWT-LS, Hoang et al., 2017). In recent years, with the development of remote sensing technology, satellite images with high temporal and spatial resolutions can display the variance of land cover for a large-scale region (Islam and Sado, 2000; Zhao et al., 2018). Moreover, N emissions by the soil at the riparian catchment scale were attempted to be simulated by coupling remotely sensed technology and simple processing models (Wang et al., 2010).

The Miyun reservoir is the terminal reservoir for the middle route of the SNWTP. It is the largest reservoir in North China and its design volume ranges within billion cubic

http://www.aloki.hu ● ISSN 1589 1623 (Print) ● ISSN 1785 0037 (Online)
DOI: http://dx.doi.org/10.15666/aeer/1706_1500115018

meters. Since 1997, it has become the only surface drinking water supply for Beijing and exerts important impacts on the capital's social stability and economic development. Therefore, it is called the "life water" of the capital. After entering the 21st century, the water volume dramatically decreased due to climatic change and human activities and more and more attention are focused on the water quality. As a crucial terminal reservoir, the water volume of the Miyun Reservoir will increase by 0.8 billion m^3 due to water injected by the SNWT between 2015 and 2020. Furthermore, the water level will increase from currently 136 m to 150 m until 2020 (Yang et al., 2018a). As a result, the rapidly increasing water level will extensively inundate the riparian zone and may result in inevitable ecological risks for the water supply from this reservoir. Furthermore, the abilities of pollutant interception and nutrient degradation in the riparian zone may be weakened and the riparian zone may be rendered from a nutrient sink into a nutrient source (Bettez and Groffman, 2012; Schilling et al., 2006). Zhao et al. (2019) and Yang et al.(2018b) have reported that the plants in Miyun reservoir can effectively remove the N pollution, but the study about the N pollution removed by soil in Miyun reservoir under the SNWTP background has not been reported. Therefore, it is necessary to assess the variance of N emissions by soil induced by the SNWT in the Miyun reservoir. However, few studies have proposed a framework with which to estimate the effect of SNWT project on N removal by soil at the riparian catchment scale.

Consequently, the objective of this paper is to provide a useful framework with which to evaluate the SNWTP on N removal by soil in the Miyun riparian zone. Specifically, this study includes three steps: (1) coupling process-originated model and remotely sensed data to simulate the spatio-temporal varieties of N emissions by soil in the Miyun riparian zone between April and September in 2015; (2) dividing the riparian zone into four contour belts from low elevation to high elevation based on the Digital Elevation Model (DEM); (3) using a scenario setting method to estimate the influences of increasing water level induced by the SNWTP on N removal by soil at the Miyun riparian zone catchment scale. The simulated result is useful for the sustainable management of similar catchments than the Miyun riparian zone.

Materials and methods

Study site

This study was conducted in the riparian zone of the Miyun reservoir, which is located in the northeast of Beijing (40°26'N - 40°35'N, 116°47'E - 117°05'E, *Fig. 1*). The riparian buffer in the Miyun reservoir mainly includes the region surrounded by the road that encircles the reservoir and other adjacent regions schemed by local authority. The Miyun reservoir was constructed in September 1960, and has a total storage capacity of 4.375 billion m^3. The region belongs to the continental monsoon climate. The obvious climatic characteristic is an uneven distribution of precipitation and temperature over four seasons. About 70% of the precipitation falls between June and September (Yang et al., 2018a). In addition, the highest temperature during the year also occurs during this season. *Figure 1* shows that the proportions of Calcareous cinnamon soil and Cambisol soil are the largest and smallest, accounting for about 50% and 0.28% of the study area, respectively. Soil types and soil property datasets in this study, including soil texture, soil nutrients content, bulk density, and pH, were obtained based on the Second National Soil Survey and additional field investigation in the study region.

http://www.aloki.hu ● ISSN 1589 1623 (Print) ● ISSN 1785 0037 (Online)
DOI: http://dx.doi.org/10.15666/aeer/1706_1500115018

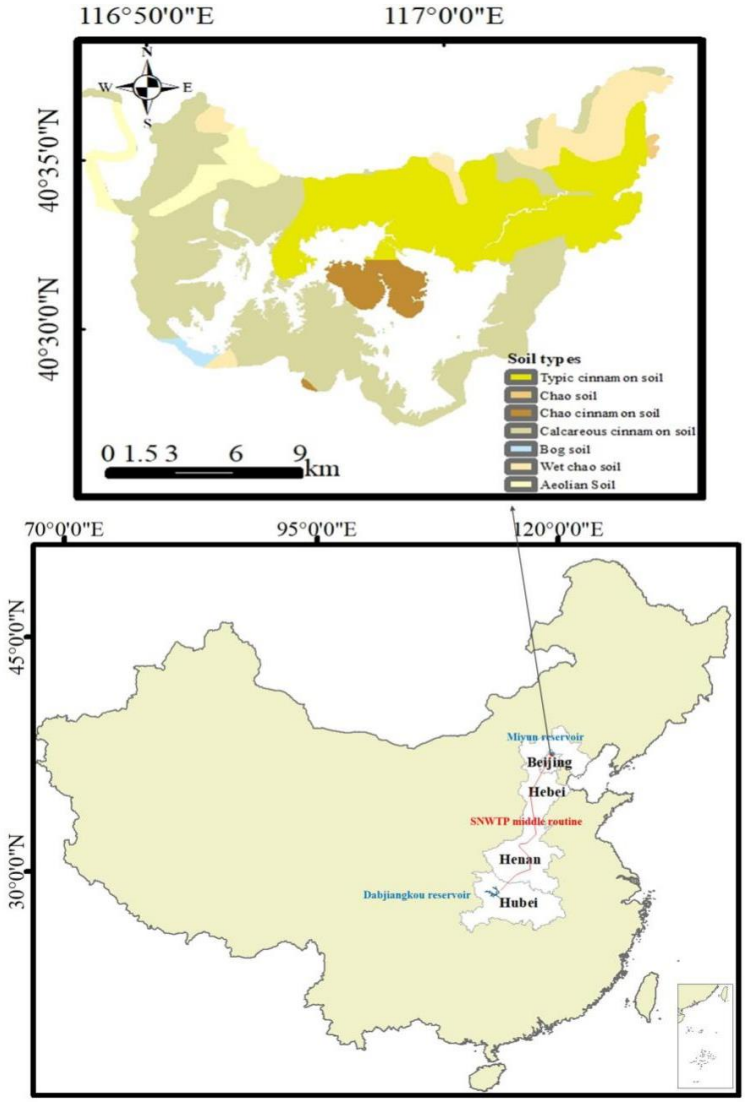

Figure 1. *The study area distribution*

Framework method

This section introduces the framework (*Fig. 2*) that was developed to assess the impacts of the SNWTP on N removal by soil. This framework integrates an ecological model assessment model and scenario setting method, and the specific parts are introduced in the following. Because the ecological model assessment model in *Figure 2* has been successfully used in a Guanting Reservoir that has a similar geographical conditions and climate with Miyun Reservoir, the model parameters of the Guanting Reservoir are used to apply to the Miyun Reservoir simulation (Yang et al., 2018b). Meanwhile, a field experiment in the nearby (39°40.4'-40°27.6'N, 116°28.2'-117°1') of Miyun Reservoir has been conducted (Geng et al., 2018). In this experiment, two typical drilling profiles were selected to determine the denitrification intensity value of the vadose zone at different sampling depths (0-10 m) and analyze the vertical spatial distribution of denitrification in the vadose zone. The experimental results show that the denitrification rate mainly in the soil layer of 0-0.25 m. So, the soil layer depth between 0 and 25 cm was used to simulate the N emissions in this study.

http://www.aloki.hu ● ISSN 1589 1623 (Print) ● ISSN 1785 0037 (Online)
DOI: http://dx.doi.org/10.15666/aeer/1706_1500115018

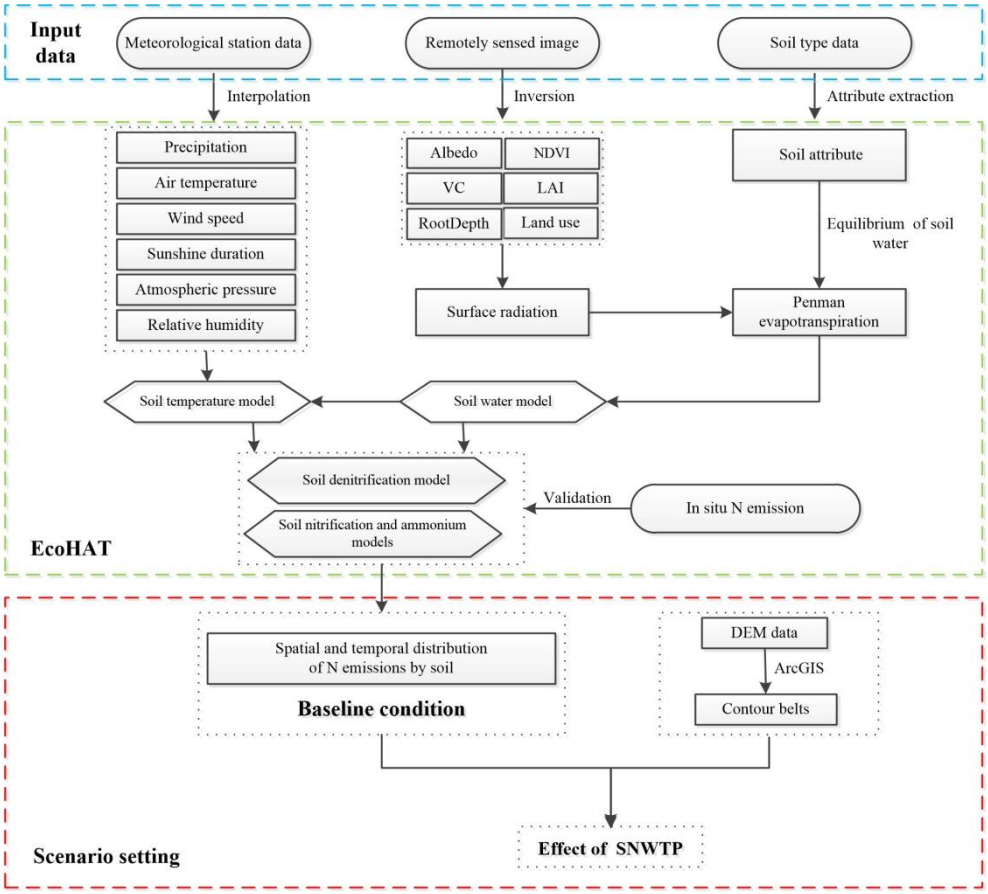

Figure 2. *The framework method in this study. (VC is vegetation coverage, LAI is leaf area index)*

Model inputs

(1) Remotely sensed data

The DEM data with 30-m resolution was obtained from the Advanced Spaceborne Thermal Emission and Reflection Radiometer (ASTER). Land use types (*Fig. 3*) were interpreted using the man-machine interactive method and the GF-1 multispectral data at a resolution of 8 m. The types and proportions of land use in this riparian zone include forestland (28.72%), grassland (24.52%), farmland (13.45%), bottomland (6.27%), residential land (3.17%), and water (23.88%).

Considering the impacts of satellite observation errors and spatio-temporal resolutions, multispectral Landsat 8 OLI satellite images with 30-m resolution between April and September 2015 were chosen. To eliminate the cloud interference with the spectral response to land surface targets, days 106, 138, 154, 186, 234, and 250 in 2015 for Landsat 8 OLI satellite data were chosen to invert the land surface parameters, e.g. VC, LAI, and land surface albedo. Additionally, to invert land surface parameters, a series of preprocessing steps such as radiometric, atmospheric, and geometric corrections were necessary. All of these preprocesses were operated using the ENVI 5.3 software. Finally, all image data mentioned above were re-projected into Albers with the World Geodetic System-84 datum and resampled into 30 m × 30 m spatial resolutions.

http://www.aloki.hu ● ISSN 1589 1623 (Print) ● ISSN 1785 0037 (Online)
DOI: http://dx.doi.org/10.15666/aeer/1706_1500115018

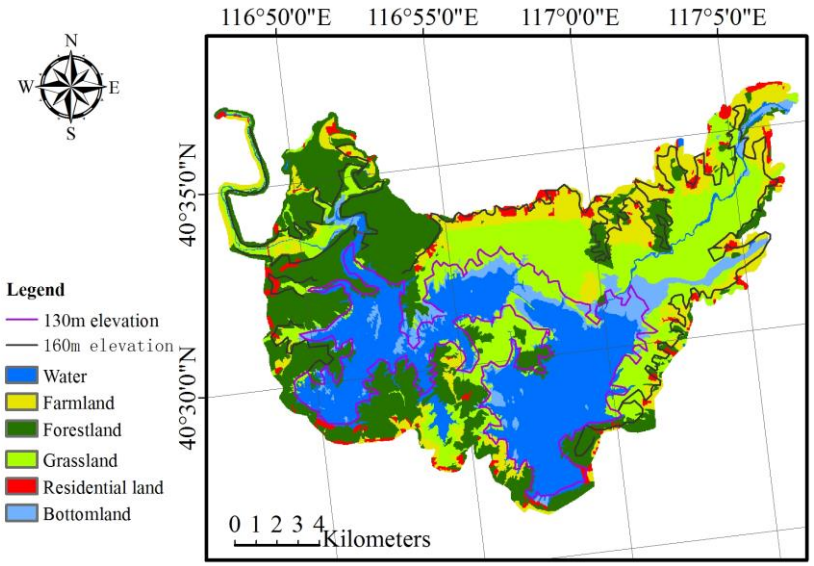

Figure 3. *The land use distribution in Miyun riparian zone*

(2) Meteorological data

The Beijing Meteorological Bureau and National Meteorological Information Center provided the daily observed rainfall data around the Miyun reservoir during the simulated period. Other daily observed climatic data from April to September in 2015 such as wind speed, air temperature, surface temperature, relative humidity, and sunshine duration were downloaded from the National Meteorological Information Center (http://data.cma.cn/site/index.html). The detailed information about the climatic data is listed in *Table A1* in the *Appendix*. All collected site records were generated as raster images using the Inverse Distance to a Power interpolation method using ArcGIS version 9.3.1.

Model descriptions

To simulate nitrogen emissions by the soil of the Miyun riparian zone, an Ecohydrological Assessment Tool (EcoHAT, Liu et al., 2009; Yang et al., 2011) was adopted in this study. EcoHAT was developed based on the mechanism of the ecohydrological processes in the Soil–Plant–Atmosphere Continuum (Dong et al., 2014). It was derived via multi-source data and can simulate hydrological processes, vegetation growth, and nutrient dynamics (Liu et al., 2009). The model used in this study mainly consists of three components: calculations of environmental factors i.e., soil temperature, soil moisture, and soil nitrogen; calculations of soil denitrification; calculations of soil nitrification and ammonia volatilization. *Tables A2* and *A3* (*Appendix*) show the main equations. In addition, model input parameters i.e., NDVI, LAI, and Albedo, were derived from Landsat8 data via remotely sensed inversion. The detailed extraction processes of input parameters and part model principle have been introduced in Zhao et al. (2019) and Yang et al. (2018b). Additionally, Yang et al. (2018b) reported that the EcoHAT has been successfully applied to simulate the N emissions at a region that has similar geographical conditions and climate than the Miyun reservoir; therefore, experimental model parameters in Wang et al. (2010) were chosen for this study.

http://www.aloki.hu ● ISSN 1589 1623 (Print) ● ISSN 1785 0037 (Online)
DOI: http://dx.doi.org/10.15666/aeer/1706_1500115018

Estimation of SNWTP influences

This section describes how to estimate the influences of SNWTP on nitrogen removal by soil in the riparian zone based on the simulated results of the EcoHAT model and the scenario setting method. Before estimating the impacts of the SNWTP, the Miyun riparian zone was first divided into four DEM-based contour belts using ArcGIS software. These four contour belts were respectively 130–140 m, 140–150 m, 150–160 m, and 160–170 m. Then, statistics about N emission of each contour were calculated based on the overlay of these four contour belts and the spatial distribution of N emissions by soil from April to September 2015, and for the simulated period. Finally, this study adopted a scenario setting method to suppose that the four contour belts in the Miyun riparian zone were submerged one by one from lower to higher elevations and gaseous N mission in every flooded soil belt was not included in the N removal by soil in the riparian zone.

Model validation in situ

Because the direct measurement of gaseous N emissions in the field is very difficult, a nitrogen mass conservation method was used to validate the gaseous N emissions by soil induced by denitrification, nitrification, and ammonia volatilization. In this method, the total N variances *in situ* are the sum of leaching N, N-uptake by vegetation, and gaseous N emissions. The following equation shows the nitrogen mass balance:

$$TN_{so} - TN_{sn} = N_{se} + N_{pa} + N_{le} \quad \text{(Eq.1)}$$

where TN_{so} and TN_{sn} are respectively the original total nitrogen content and total nitrogen content left in the soil (mg m^{-2} d^{-1}), N_{se} is the total gaseous N emissions (mg m^{-2} d^{-1}), N_{pa} is the N uptake by plant (mg m^{-2} d^{-1}), N_{le} is the leaching N (mg m^{-2} d^{-1}).

In this study, six sample data from three sample plots with 2 m × 1 m in shrub (116.848°E, 40.547°N), grassland (116.947°E, 40.547°N), and farmland (116.968°E, 40.559°N) were measured during April and May 2015. Every sample plot was divided using an iron plate in the middle, the left and right parts were measured at the beginning and end of April and May, respectively. The N uptaken by plants was calculated using the biomass and N uptake ratio coefficients (Yang et al., 2018b).

Results

Validation of N emissions

In this study, considering the precipitation distribution during the year (*Fig. 4a*), sample plots in April and May were used to validate the simulated results to minimize the influences of leaching N induced by precipitation. *Figure 4b* shows the scatter plots between simulated and in situ gaseous N emission data. Moreover, the correlation coefficient was calculated using the software EXCEL 2010. As shown in *Figure 4b,* the coefficient of determination is $R2 = 0.77$ ($P < 0.05$), which implies that the model has a sound simulation effect. However, the validation result indicates that the observed data is smaller than the simulated data, the reasons may be related to the ignorance of N leaching and the scale effect between observed and simulated data.

http://www.aloki.hu ● ISSN 1589 1623 (Print) ● ISSN 1785 0037 (Online)
DOI: http://dx.doi.org/10.15666/aeer/1706_1500115018

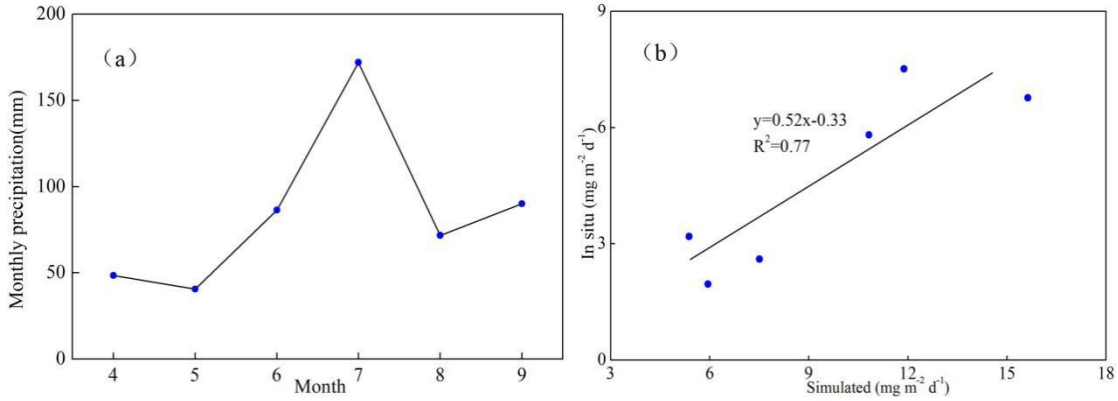

Figure 4. *The monthly precipitation (a) and validation results of N emissions (b)*

Spatio-temporal distribution of N emissions by soil

Figure 5 shows the spatial distributions of the simulated monthly gaseous N emission rate in the Miyun riparian zone from April to September in 2015. *Figure 5* shows that the wetlands distributed near water are nitrogen enrichment regions and have relatively high N emissions by soil. In addition, it is worth mentioning that N emissions by soil in forestland in the north and west clearly exceed those of grassland and farmland in the northeast, especially from June to September. The reasons that explain this phenomenon are related to the soil water content. The soil type in the northeast of this study area is mainly typical cinnamon soil, and the soil type of forestland in this study area is mainly calcareous cinnamon soil (*Fig. 3*). The soil field capacity, soil saturated water content, and soil wilting water content (0.31, 0.45, and 0.11) in typical cinnamon soil are significantly lower than those (0.28, 0.44, and 0.07) of calcareous cinnamon soil based on the experimental analysis. Therefore, for the same rainfall, the calcareous cinnamon regions have higher soil water content, which can further increase the soil dis-anaerobic environment and increase the denitrification rate.

Figure 6 shows the spatial gaseous N emissions in the growing seasons of 2015 for the Miyun riparian zone. The yearly N emission distribution is similar to those of every month. After calculation, the emission distribution in the whole catchment is 871.97 t.

Discrimination of N emission by different soil biochemical processes

Based on the results of model simulation, the contributions of soil N emissions by denitrification, ammonia volatilization, and nitrification were estimated for the simulated period. *Figure 6* shows that the three soil biochemical processes have similar temporal variation trends with a maximum in July and a minimum in April. In addition, *Figure 7* also shows that the proportions of N emissions induced by the three biochemical processes in total gaseous N emissions are significantly different. The soil denitrification process dominated the soil N emissions in this study area; the N emissions ranged from 34.72 t to 260.16 t between April and September and the maximum of 260.16 t of nitrogen occurred in July. In addition, the maximal values for soil nitrification and ammonia volatilization processes were 5.85 t and 24.57 t in July, respectively, and minimal values of 3.18 t and 10.93 t occurred in April. It is worth noting that soil denitrification rates showed dramatic fluctuations during the simulated period in comparison to the other two processes.

http://www.aloki.hu ● ISSN 1589 1623 (Print) ● ISSN 1785 0037 (Online)
DOI: http://dx.doi.org/10.15666/aeer/1706_1500115018

N removal by soil in contour belts

After statistical calculation, *Figure A1* (*Appendix*) shows that the N removal load of soil in the four contour belts were 380.38 t, 342.79 t, 302.72 t, and 981.59 t, respectively, from April to September. Furthermore, *Figure A1* shows the maximum N removals (107.77 t, 112.23 t, 107.18 t, and 384.54 t) and the minimum N removals (26.35 t, 20.63 t, 15.67 t, and 34.75 t) for July and April for the four contour belts. For each month, the N removal loads showed minor fluctuations from 130 m to 160 m; where the elevations exceeded 160 m, the N removal loads all steeply increased.

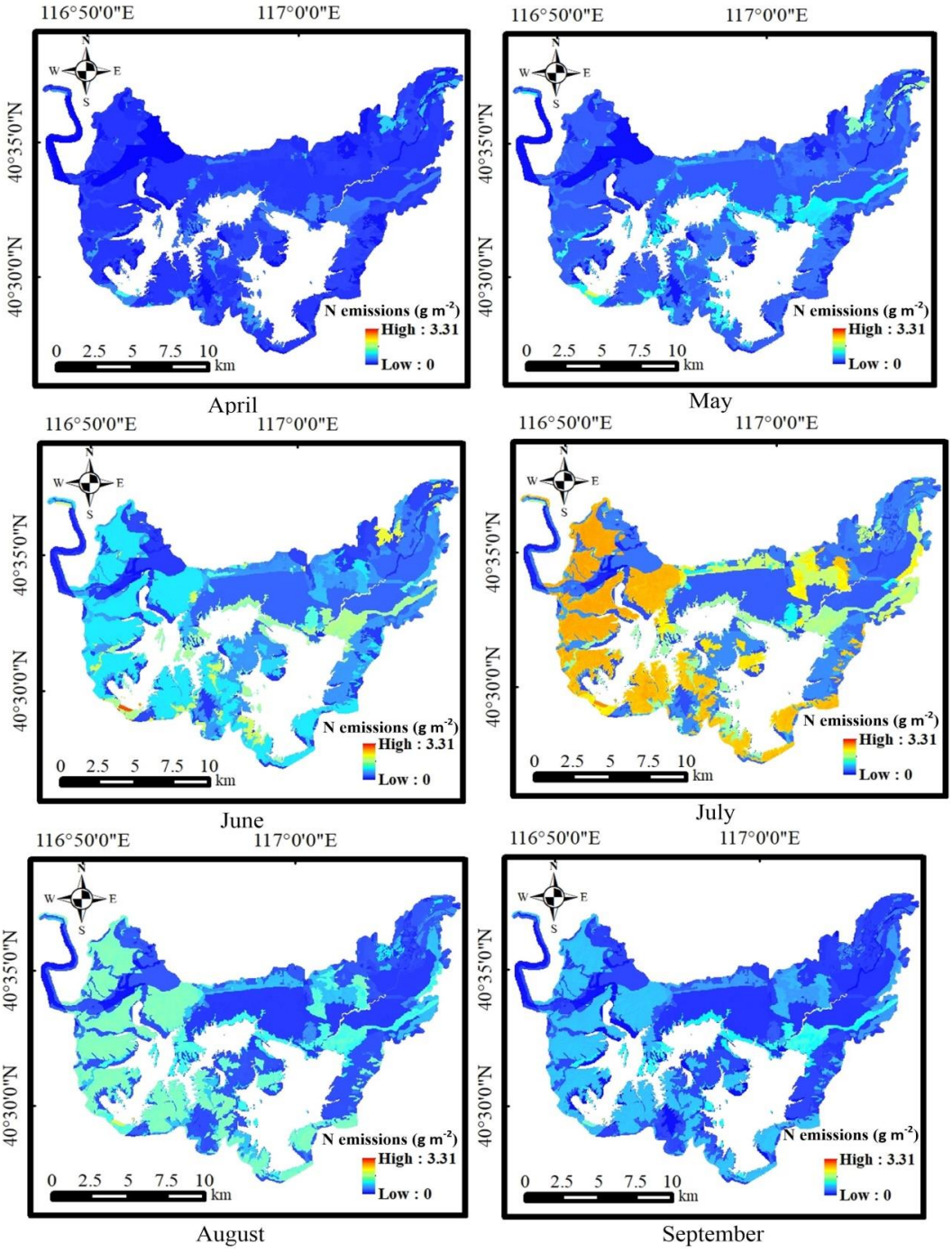

Figure 5. *N emissions rate by soil in study area from April to September*

http://www.aloki.hu ● ISSN 1589 1623 (Print) ● ISSN 1785 0037 (Online)
DOI: http://dx.doi.org/10.15666/aeer/1706_1500115018

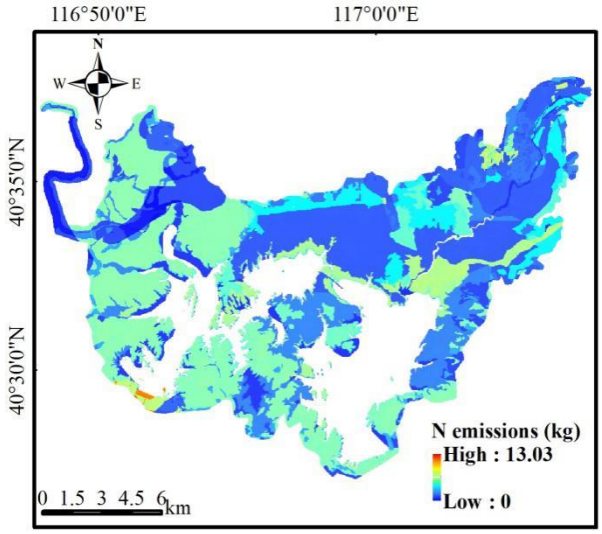

Figure 6. *N emissions amount by soil in study area in 2015*

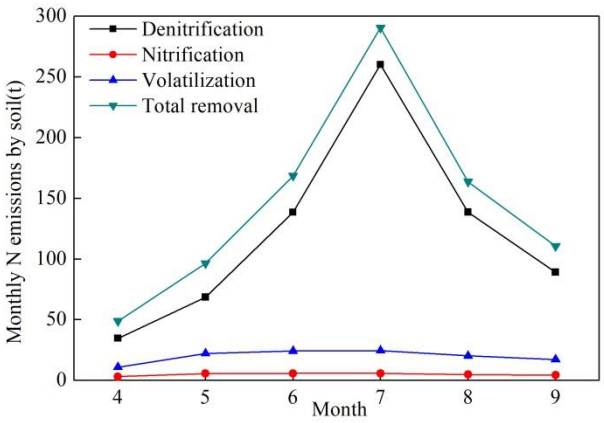

Figure 7. *Monthly N emissions for denitrification, nitrification and volatilization processes*

Influences of SNWTP on N removal by soil in the Miyun riparian zone

When the water transferred by the SNWTP was injected into the Miyun reservoir, the water level dramatically increased and extensively submerged the riparian zone. *Figure A2* (*Appendix*) shows the N pollution by the riparian soil when SNWTP submerged the contour belts. Although the N pollution by soil in the riparian zone decreased for all months, the reduction extent was different for each month. When the water level increased to 150 m, the riparian soil had about 50% of the original N absorption ability in April and May and had about 60% between June and September. With the water level exceeding 160 m, the riparian soil only had about 35% of the original N absorption ability in April and May and about 50% from July to September. Furthermore, these results also imply that the submerged riparian zone may develop into a nutrient source from a nutrient sink (Schilling et al., 2006; Ye et al., 2012) when it became ineffective at removing nitrogen.

http://www.aloki.hu ● ISSN 1589 1623 (Print) ● ISSN 1785 0037 (Online)
DOI: http://dx.doi.org/10.15666/aeer/1706_1500115018

Discussion

Effects of land use types on gaseous N emissions

The N dynamics in riparian soil follow a close relationship to the plant distribution and types (Wu et al., 2016; Ye et al., 2015); therefore, the distribution of land use plays a key role in influencing the N emissions in the riparian zone (Bedard-Haughn et al., 2006; Wang et al., 2010). *Table A4* (*Appendix*) shows the effect of land use type on the N emissions by soil, showing that the forestland has the most N emissions, accounting for 54.38% of the total gaseous N emissions. This is related to the forestland area distribution and soil moisture retention capacity. Furthermore, this study proves that denitrification is the most important way for the removal of N in three soil biochemical process, which is consistent with the results of previous studies (Bedard-Haughn et al., 2006; Kreiling et al., 2011; Ye et al., 2017; Wang et al., 2010). In this study, forestland showed the highest denitrification of the study period, accounting for 47.08% of total N emission; the grassland, farmland, and bottomland accounted for 11.44%, 12.79%, and 12.11%, respectively. In addition, the forestland and grassland dominated the nitrification and volatilization processes, accounting for 43.93% and 27.95% by soil nitrification and 44.06% and 27.66% by volatilization, respectively. The distribution of forest land on the higher elevation in this study has the most N emissions, which can partly be used to explain N removal by soil in contour belts where the elevations exceeded 160 m.

Adjusting riparian structure to improve the defense for N pollution

The results of this study showed that the increasing water level induced by the SNWTP can weaken N removal by soil in the riparian zone (*Figs. A1* and *A2*). A previous study reported that the vegetation restoration is an effective method for the remediation of degraded ecosystems by influencing soil properties in the riparian zone and by up-taking more nitrogen in the riparian (Zhang et al., 2010; Zhao et al., 2019). Consequently, it is necessary to illustrate the unit area N removal of the Miyun riparian zone. *Figure A3* (*Appendix*) shows the monthly average N emission rate variations for different land use types between April and September. There are typical steep increases from April to July in all land use types. However, different land use categories have important effects on the N emission rates. The ranges of the monthly N emission rates for forestland and bottomland are from 0.15 g m^{-2} to 2.23 g m^{-2} and from 0.51 g m^{-2} to 1.45 g m^{-2}, respectively, which exceed those of other types. The monthly soil emission rates for both forestland and bottomland are 0.94 g m^{-2} and 1.07 g m^{-2}, respectively. The soil emission rates for other land use types were 0.32 g m^{-2} for grassland and 0.58 g m^{-2} for farmland.

According to previous studies (Zhang et al., 2010; Zhao et al., 2019) and the results shown in *Figure A3,* the adjustment of land use types can be used to increase the defense ability for N in the riparian zone. Specifically, the farmland and grassland distributed in the lower elevation area around the open reservoir water and the forestland distributed at higher elevation areas in this study. Therefore, this study suggests to change more grassland and farmland into forestland to effectively offset the impacts of SNWTP on the N removal by soil in the Miyun riparian.

http://www.aloki.hu ● ISSN 1589 1623 (Print) ● ISSN 1785 0037 (Online)
DOI: http://dx.doi.org/10.15666/aeer/1706_1500115018

Conclusions

A number of studies reported that the soil in the riparian zones could significantly alleviate the water pollution risk by emitting gaseous N. The SNWTP is the largest inter-basin water transfer scheme in the world, and the Miyun reservoir is the terminal reservoir in the middle route of the SNWTP. With the injection of water since 2015, the riparian zone of the Miyun reservoir was extensively submerged. How to quantitatively assess the effects of increasing water induced by the SNWTP on the N removal in the Miyun riparian has become an important issue.

This study proposed a framework method that integrates the eco-hydrological model, remote sensing technology, and scenario setting to simulate the spatio-temporal varieties of N emissions and to assess influences of SNWTP on N removal by soil in the Miyun riparian zone. The scientificity of the simulated results has been validated by in situ survey data.

The results illustrate that wetlands near the water body are nitrogen enrichment regions and have relatively high N emissions by soil. In addition, the soil N emissions of forestland are higher than those of grassland and farmland, especially from June to September. Moreover, soil denitrification processes dominate soil N emission in this study area. After calculation, N emissions ranged from 48.83 t to 290.58 t between April and September 2015 and the emission distribution in the whole catchment was 871.97 t.

When the water level increased to 150 m, the riparian soil had about 50% of original defense N ability in April and May and had about 60% between June to September. However, the riparian soil had only about 35% of the original defense N ability in April and May and about 50% from July to September with the water level exceeding 160 m. This study demonstrates that changing farmland and grassland to forestland can effectively increase the amount of removed N in this riparian zone.

In summary, the results of this study are helpful for the sustainable management of similar catchment zones than the Miyun riparian zone. However, there are still many follow-up works to be further studied. In this study, the simulation does not consider the effect of groundwater level fluctuation on the removal of non-point pollutants in the Miyun riparian zone. In fact, the depth of groundwater in the riparian zone is shallow, and the water level fluctuates can greatly impact on the soil moisture, and then greatly affects the denitrification and nitrogen release process of the soil. Therefore, it is necessary to increase the simulation module of groundwater level in the future.

Acknowledgments. The China Postdoctoral Science Foundation (Grant No. 2016M591093), the National Key Research and Development Program of China (2017YFD0300400), the National Natural Science Foundation of China (Grant No. 41701517) and Major Science and Technology Program for Water Pollution Control and Treatment (Grant No.2018ZX07101005)provided the financial support for this study.

REFERENCES

[1] Barnett, J., Rogers, S., Webber, M., Finlayson, B., Wang, M. (2015): Sustainability: transfer project cannot meet China's water needs. – Nature 527(7578): 295-297.

[2] Bedard-Haughn, A., Matson, A. L., Pennock, D. J. (2006): Land use effects on gross nitrogen mineralization, nitrification, and N_2O emissions in ephemeral wetlands. – Soil Biology & Biochemistry 38(12): 3398-3406.

http://www.aloki.hu ● ISSN 1589 1623 (Print) ● ISSN 1785 0037 (Online)
DOI: http://dx.doi.org/10.15666/aeer/1706_1500115018

[3] Bettez, N. D., Groffman, P. M. (2012): Denitrification potential in storm water control structures and natural riparian zones in an urban landscape. – Environmental Science & Technology 46(20): 10909-10917.
[4] Blackburn, M., Ledesma, J. L. J., Näsholm, T., Laudon, H., Sponseller, R. A. (2017): Evaluating hillslope and riparian contributions to dissolved nitrogen (N) export from a boreal forest atchment. – Journal of Geophysical Research-Biogeosciences 122: 324-339.
[5] Brovelli, A., Batlle-Aguilar, J., Barry, D. A. (2012): Analysis of carbon and nitrogen dynamics in riparian soils: model development. – Science of the Total Environment 429: 231-245.
[6] Butterbach-Bahl, K., Baggs, E. M., Dannenmann, M., Kiese, R., Zechmeister-Boltenstern, S. (2013): Nitrous oxide emissions from soils: how well do we understand the processes and their controls? – Philosophical Transactions of the Royal Society B-Biological Sciences 368(1621): 20130122.
[7] Chavan, P. V., Dennett, K. E. (2008): Wetland simulation model for nitrogen, phosphorus, and sediments retention in constructed wetlands. – Water Air & Soil Pollution 187(1-4): 109-118.
[8] Chen, Z. S., Wang, H. M., Qi, X. T. (2013): Pricing and water resource allocation scheme for the South-to-North Water Diversion Project in China. – Water Resources Management. 27(5): 1457-1472.
[9] de Sosa, L. L., Glanville, H. C., Marshall, M. R., Williams, A. P., Abadie, M., Clark, I. M., Blaud, A., Deng, K., Wang, J. G., Wang, J. Q. (2018): Treatments to control urban river pollution in water source city of south to north water diversion project. – Polish Journal of Environmental Studies 24(2): 501-504.
[10] Dong, G. T., Yang, S. T., Gao, Y. F., Bai, J., Wang, X. L., Zheng, D. H. (2014): Spatial evaluation of phosphorus retention in riparian zones using remote sensing data. – Environmental Earth Sciences 72(5): 1643-1657.
[11] Erisman, J. W., Galloway, J. N., Seitzinger, S., Bleeker, A., Dise, N. B., Petrescu, A. M. R., Leach, A. M., de Vries, W. (2013): Consequences of human modification of the global nitrogen cycle. – Philosophical Transactions of the Royal Society B-Biological Sciences 368(1621): 20130116.
[12] Figueiredo, V., Enrich-Prast, A., Rütting, T. (2016): Soil organic matter content controls gross nitrogen dynamics and N_2O production in riparian and upland boreal soil. – European Journal of Soil Science 67(6): 782-791.
[13] Geng, H. Z., Huan, Y., Li, M. X., Zhang, Y., Cong, H., Xi, B. D. (2018): Vertical spatial distribution of denitrificatiion intensity in the vadose zone of typical sections of Chaobai River Alluvial Fan. – Environmental Science 39(11): 4972-4980 (Chinese and English abstract).
[14] Groffman, P. M., Butterbach-Bahl, K., Fulweiler, R. W., Gold, A. J., Morse, J. L., Stander, E. K., Tague, C., Tonitto, C., Vidon, P. (2009): Challenges to incorporating spatially and temporally explicit phenomena (hotspots and hot moments) in denitrification models. – Biogeochemistry 93(1-2): 49-77.
[15] Gu, W., Shao, D., Jiang, Y. (2012): Risk evaluation of water shortage in source area of middle route project for South-to-North Water Transfer in China. – Water Resources Management 26(12): 3479-3493.
[16] Hoang, L., van Griensven, A., Mynett, A. (2017): Enhancing the SWAT model for simulating denitrification in riparian zones at the river basin scale. – Environmental Modelling & Software 93: 163-179.
[17] Islam, M. D. M., Sado, K. (2000): Development of flood hazard maps of Bangladesh using NOAA–AVHRR images with GIS. – Hydrological Sciences Journal 45(3): 337-355.
[18] Jacinthe, P. A., Vidon, P. (2017): Hydro-geomorphic controls of greenhouse gas fluxes in riparian buffers of the White River watershed, IN (USA). – Geoderma 301: 30-41.

http://www.aloki.hu ● ISSN 1589 1623 (Print) ● ISSN 1785 0037 (Online)
DOI: http://dx.doi.org/10.15666/aeer/1706_1500115018

[19] King, S. E., Osmond, D. L., Smith, J., Burchell, M. R., Dukes, M., Evans, R. O. (2016): Effects of riparian buffer vegetation and width: a 12-year longitudinal study. – Journal of Environmental Quality 45(4): 1243-1251.
[20] Kreiling, R. M., Richardson, W. B., Cavanaugh, J. C., Bartsch, L. A. (2011): Summernitrate uptake and denitrification in an upper Mississippi River backwater lake: the role of rooted aquatic vegetation. – Biogeochemistry 104: 309-324.
[21] Li, Y., Xiong, W., Zhang, W. L., Wang, C., Wang, P. F. (2016): Life cycle assessment of water supply alternatives in water-receiving areas of the South-to-North Water Diversion Project in China. – Water Research 89: 9-19.
[22] Li, Y. Y., Cui, Q., Li, C. H., Wang, X., Cai, Y. P., Cui, G. N., Yang, Z. F. (2017): An improved multi-objective optimization model for supporting reservoir operation of China's South-to-North Water Diversion Project. – Science of the Total Environment 575: 970-981.
[23] Lind, L. P. D., Audet, J., Tonderski, K., Hoffmann, C. C. (2013): Nitrate removal capacity and nitrous oxide production in soil profiles of nitrogen loaded riparian wetlands inferred by laboratory microcosms. – Soil Biology & Biochemistry 60: 156-164.
[24] Liu, C., Zheng, H. (2002): South-to-North Water Tansfer schemes for China. – International Journal of Water Resources Development 18: 453-471.
[25] Liu, C. M., Yang, S. T., Wen, Z. Q., Wang, X. L., Wang, Y. J., Li, Q., Sheng, H. R. (2009): Development of ecohydrological assessment tool and its application. – Science China-Technological Sciences 52(7): 1947-1957.
[26] Ma, F. B., Li, C. H., Wang, X., Yang, Z. F., Sun, C. C., Liang, P. Y. (2014): A Bayesian method for comprehensive water quality evaluation of the Danjiangkou Reservoir water source area, for the middle route of the South-to-North Water Diversion Project in China. – Front Earth Sci-Prc. 8(2): 242-250.
[27] Rojas-Oropeza, M., Dendooven, L., Garza-Avendano, L., Souza, V., Philippot, L., Cabirol, N. (2010): Effects of biosolids application on nitrogen dynamics and microbial structure in a saline-sodic soil of the former Lake Texcoco (Mexico). – Bioresource Technology 101(7): 2491-2498.
[28] Ryu, J., Cho, J., Kim, I. J., Mun, Y., Moon, J. P., Kim, N. W., Kim, S. J., Kong, D. S., Lim, K. J. (2011): Enhancement of SWAT-REMM to simulate reduction of total nitrogen with riparian buffer. – T Asabe. 54(5): 1791-1798.
[29] Schilling, K. E., Li, Z., Zhang, Y. K. (2006): Groundwater–surface water interaction in the riparian zone of an incised channel, Walnut Creek, Iowa. – Journal of Hydrology 327(1-2): 140-150.
[30] Seitzinger, S., Harrison, J. A., Bohlke, J. K., Bouwman, A. F., Lowrance, R., Peterson, B., Tobias, C., Van Drecht, G. (2006): Denitrification across landscapes and waterscapes: a synthesis. – Ecological Applications 16(-): 2064-2090.
[31] Shu, X., Zhang, K. R., Zhang, Q. F., Wang, W. B. (2017): Response of soil physico-chemical properties to restoration approaches and submergence in the water level fluctuation zone of the Danjiangkou Reservoir, China. – Ecotoxicology And Environmental Safety 145: 119-125.
[32] Si, Z. H., Song, X. S., Wang, Y. H., Cao, X., Zhao, Y. F., Wang, B. D., Chen, Y., Arefe, A. (2018): Intensified heterotrophic denitrification in constructed wetlands using four solid carbon sources: denitrification efficiency and bacterial community structure. – Bioresource Technology 267: 416-425.
[33] Tang, C. L., Yi, Y. J., Yang, Z. F. (2014): Water pollution risk simulation and prediction in the main canal of the South-to-North Water Transfer Project. – Journal of Hydrology 519: 2111-2120.
[34] Vymazal, J. (2007): Removal of nutrients in various types of constructed wetlands. – Science of the Total Environment 380(1-3): 48-65.
[35] Wang, G. Q., Ouyang, Q., Zhang, Y. D., Wei, J. H., Ren, Z. Y. (2009): World' Water Diversion Project. – Publishing Science Press, Beijing.

http://www.aloki.hu ● ISSN 1589 1623 (Print) ● ISSN 1785 0037 (Online)
DOI: http://dx.doi.org/10.15666/aeer/1706_1500115018

[36] Wang, X., Mannaerts, C. M., Yang, S., Gao, Y., Zheng, D. (2010): Evaluation of soil nitrogen emissions from riparian zones coupling simple process-oriented models with remote sensing data. – Science of the Total Environment 408(16): 3310-3318.
[37] Wei, J. B., Feng, H., Cheng, Q. G., Gao, S. Q., Liu, H. Y. (2017): Denitrification potential of riparian soils in relation to multiscale spatial environmental factors: a case study of a typical watershed, China. – Environmental Monitoring and Assessment 189(2): 85.
[38] Wu, H. L., Xu, K. Q., He, X. J., Wang, X. Z. (2016): Removal of nitrogen by three plant species in hydroponic culture: plant uptake and microbial degradation. – Water Air Soil Pollution 227(9): 324.
[39] Yang, Q., Xie, P., Shen, H., Xu, J., Wang, P. L., Zhang, B. (2012): A novel flushing strategy for diatom bloom prevention in the lower-middle Hanjiang River. – Water Research 46(8): 2525-2534.
[40] Yang, S. T., Dong, G. T., Zheng, D. H., Xiao, H. L., Gao, Y. F., Lang, Y. (2011): Coupling Xinanjiang model and SWAT to simulate agricultural non-point source pollution in Songtao watershed of Hainan, China. – Ecological Modelling 222(20-22): 3701-3717.
[41] Yang, S. T., Bai, J., Zhao, C. S., Lou, H. Z., Zhang, C. B., Guan, Y. B., Zhang, Y. C., Wang, Z. W., Yu, X. Y. (2018a): The assessment of the changes of biomass and riparian buffer width in the terminal reservoir under the impact of the South-to-North Water Diversion Project in China. – Ecological Indictor 85: 932-943.
[42] Yang, S. T., Bai, J., Zhao, C. S., Lou, H. Z., Wang, Z. W., Guan, Y. B., Zhang, Y. C., Zhang, C. B., Yu, X. Y. (2018b): Decline of N and P uptake in the inner protection zone of a terminal reservoir during inter-basin water transfers. – Water 10: 178. DOI: 10.3390/w10020178.
[43] Yang, W. H., Liu, Y. B., Ou, C. P., Gabor, S. (2016): Examining water quality effects of riparian wetland loss and restoration scenarios in a southern Ontario watershed. – Journal of Environmental Management 174: 26-34.
[44] Ye, C., Cheng, X. L., Zhang, Y. L., Wang, Z. X., Zhang, Q. F. (2012): Soil nitrogen dynamics following short-term revegetation in the water level fluctuation zone of the Three Gorges Reservoir, China. – Ecological Engineering 38(1): 37-44.
[45] Ye, C., Cheng, X. L., Zhang, Q. F. (2014): Recovery approach affects soil quality in the water level fluctuation zone of the Three Gorges Reservoir, China: implications for revegetation. – Environmental Science And Pollution Research 21(3): 2018-2031.
[46] Ye, C., Cheng, X. L., Liu, W. Z., Zhang, Q. F. (2015): Revegetation impacts soil nitrogen dynamics in the water level fluctuation zone of the Three Gorges Reservoir, China. – Science of the Total Environment 517: 76-85.
[47] Ye, C., Chen, C. G., Du, M., Liu, W. Z., Zhang, Q. F. (2017): Revegetation affects soil denitrifying communities in a riparian ecotone. – Ecological Engineering 103: 256-263.
[48] Zeng, Q., Qin, L., Li, X. (2015): The potential impact of an inter-basin water transfer project on nutrients (nitrogen and phosphorous) and chlorophyll a of the receiving water system. – Science of the Total Environment 536: 675-686.
[49] Zhang, J., Meng, F., Lu, Y., Jing, Y., Zhang, H., Zhang, B. (2008): Ecological assessment of lakeshore wetland rehabilitation on eastern route of South-to-North Water Transfer Project. – Frontiers of Environmental Science & Engineering China 2(3): 306-310.
[50] Zhang, K., Dang, H., Tan, S., Wang, Z., Zhang, Q. (2010): Vegetation community and soil characteristics of abandoned agricultural land and pine plantation in the Qinling Mountains, China. – Forest Ecology and Management 259(10): 2036-2047.
[51] Zhang, M. L., Hu, L. T., Yao, L. L., Yin, W. J. (2018): Numerical studies on the influences of the South-to-North Water Transfer Project on groundwater level changes in the Beijing Plain, China. – Hydrological Process 32(12): 1858-1873.

http://www.aloki.hu ● ISSN 1589 1623 (Print) ● ISSN 1785 0037 (Online)
DOI: http://dx.doi.org/10.15666/aeer/1706_1500115018

[52] Zhang, Q. (2009): The South-to-North water transfer project of China: environmental implications and monitoring strategy 1. – Journal of the American Water Resources Association 45(5): 1238-1247.
[53] Zhao, H. G., Yang, S. T., Huang, Y. C. (2018): Utilizing the MODIS-derived leaf area index to investigate the impact of vegetation processes on hydrological simulation of macroscale catchment. – Environmental Earth Sciences 77(4): 11. DOI: 10.1007/s12665-017-7187-3.
[54] Zhao, H. G., Huang, Y. C., You, S. C., Wu, Y. F., Zheng, F. X. (2019): A framework for assessing the effects of afforestation and South-to-North Water Transfer on nitrogen and phosphorus uptake by plants in a critical riparian zone. – Science of the Total Environment 651: 942-952.
[55] Zhong, R. H., Hu, J. M., Bao, Y. H., Wang, F., He, X. B. (2018): Soil nutrients in relation to vertical roots distribution in the riparian zone of Three Gorges Reservoir, China. – Journal of Mountain Science 15(7): 1498-1509.
[56] Zhuang, W. (2016): Eco-environmental impact of inter-basin water transfer projects: a review. – Environmental Science and Pollution Research International 23(13): 12867-12879.

APPENDIX

Table A1. *Detailed information of observed meteorological stations*

ID	Longitude	Latitude	Resources
1	116.81	40.56	Beijing Meteorological Bureau
2	116.85	40.47	
3	116.85	40.60	
4	116.87	40.62	
5	116.93	40.42	
6	116.97	40.57	
7	117.04	40.58	
8	117.12	40.61	
9	117.13	40.54	
10	116.79	40.62	
11	117.10	40.44	
12	116.38	41.12	National Meteorological Information Center
13	116.52	40.23	
14	117.55	40.58	
15	117.57	40.12	

Table A2. *Main equations in the denitrification process*

No.	Functions	Equations
1	Potential denitrification rate	$D_a = D_P f_N f_S f_T f_{PH}$
2	Actual denitrification rate	$D_P = \frac{4}{5}\frac{\alpha_{om}}{365} C \frac{14}{12} 10^6$
3	Soil nitrate reduction	$f_N = \min[1, \frac{N}{N_{crit}}]$

http://www.aloki.hu ● ISSN 1589 1623 (Print) ● ISSN 1785 0037 (Online)
DOI: http://dx.doi.org/10.15666/aeer/1706_1500115018

4	Soil temperature reduction	$f_T = \begin{cases} 0 & T_s \le 0 \\ Q_{10}^{0.1(T_s - T_r)} & 0 < T_s < T_r \\ 1 & T_r \le T_s \end{cases}$
5	Saturation degree	$S = S_w / (1 - \rho_d / \rho_s)$
6	Soil water content reduction	$f_s = \begin{cases} 0 & S < S_t \\ (\frac{S - S_t}{S_m - S_t})^w & S_t \le S \le S_m \\ 1 & S = S_m \end{cases}$
7	Soil PH reduction	$f_{PH} = \begin{cases} 0 & PH \le 3.5 \\ (PH - 3.5)/3 & 3.5 < PH < 6.5 \\ 1 & PH \ge 6.5 \end{cases}$

D_a is actual denitrification rate (mg N kg^{-1} d^{-1}); D_p is the potential denitrification rate (mg N kg^{-1} d^{-1}); f_N, f_S, f_T *and* F_{PH} respectively represents a dimensionless reduction function for soil nitrate content, soil water content ([0,1]), soil temperature soil pH; α_{om} is the yearly decay rate of organic matter ([0, 1]); C is the soil carbon content (g C g^{-1}); N is the soil nitrate-N content (mg N kg^{-1}); N_{crit} is the critical soil nitrate-N content below which denitrification is assumed to be limited; T_s and T_r are the soil temperature (°C) and reference temperature (°C); Q_{10} is an increase factor in f_T at an increase in T of 10 °C; S is the dimensionless degree of saturation; S_m and S_t are S above which $f_S = 1$ and $f_S = 0$ respectively; SW is the soil water content (cm^3 cm^{-3}); ρ_d and p_s are the dry bulk density (g cm^{-3}) and solids density (g cm^{-3}); w is a measure for the steepness of the curve $(S-S_t)/(S_m-S_t)$

Table A3. *Main equations in the nitrification and volatilization processes*

No.	Functions	Equations
1	NO from nitrification	$NO = 0.0025 \cdot N_{nit/ly} \cdot \eta_{tem,ly}$
2	N removed from NH4 + pool by nitrification	$N_{nit,ly} = [1 - \exp(-\eta_{nit,ly})] / [1 - \exp(-\eta_{nit,ly}) + 1 - \exp(-\eta_{vol,ly})] \times N_{nit/vol,ly}$
3	N production from NH4 + to NH3	$N_{vol,ly} = [1 - \exp(-\eta_{vol,ly})] / [1 - \exp(-\eta_{nit,ly}) + 1 - \exp(-\eta_{vol,ly})] \times N_{nit/vol,ly}$
4	NH4 + converted from nitrification and volatilization	$N_{nit/vol,ly} = NH_{4,ly}^{+} \times [1 - \exp(-\eta_{nit,ly} - \eta_{vol,ly})]$
5	Nitrification regulator	$\eta_{nit,ly} = \eta_{tem,ly} \times \eta_{sw,ly}$
6	Volatilization regulator	$\eta_{vol,ly} = \eta_{tem,ly} \times \eta_{midz,ly} \times \eta_{cec,ly}$
7	Volatilization depth factor	$\eta_{midz,ly} = 1 - \frac{Z_{mid,ly}}{Z_{mid,ly} + \exp[4.706 - 0.0305 \times Z_{mid,ly}]}$

$\eta_{tem,ly}$ and $\eta_{sw,ly}$ is the nitrification/volatilization temperature and soil moisture factors; $\eta_{midz,ly}$ is the volatilization depth factor; $\eta_{cec,ly}$ is cation exchange factor, $\eta_{cec,ly} = 0.15$; $Z_{mid,ly}$ is the depth from the soil surface to the middle of the layer (mm); and η_{cec} is the volatilization cation exchange factor. $N_{nit/vol,ly}$ is the amount of ammonium converted via nitrification and volatilization in layer ly (kg N m^{-2}); $NH_4^{+}{}_{,ly}$ is the amount of ammonium in layer ly (kg N m^{-2}); $\eta_{nit,ly}$ and $\eta_{vol,ly}$ is the nitrification and volatilization regulators; $N_{nit,ly}$ is the amount of nitrogen removed from the ammonium pool by nitrification (kg N m^{-2}); and $N_{vol,ly}$ is the amount of nitrogen removed from the ammonium pool by volatilization (kg N m^{-2})

http://www.aloki.hu ● ISSN 1589 1623 (Print) ● ISSN 1785 0037 (Online)
DOI: http://dx.doi.org/10.15666/aeer/1706_1500115018

Table A4. *Gaseous N emissions by the different soil biochemical processes in different land use (t)*

Land use	Denitrification	Nitrification	Volatilization	Total removal
Forestland	397.84	12.37	49.32	459.53
Farmland	108.05	5.38	21.33	134.76
Bottomland	102.37	2.54	10.34	115.25
Grassland	96.62	7.87	30.96	135.45

Figure A1. *The distributions of N removal by soil in Miyun riparian zone*

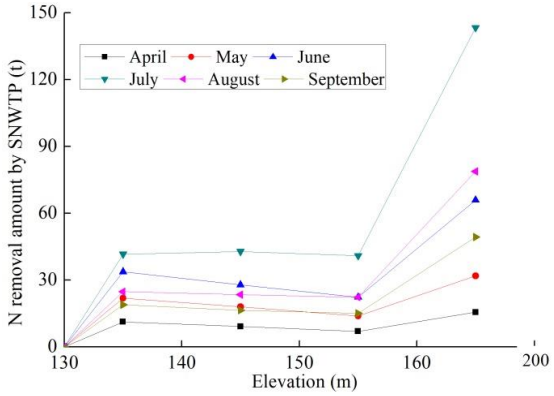

Figure A2. *The defense for N pollution by riparian soil after SNWTP in Miyun riparian zone*

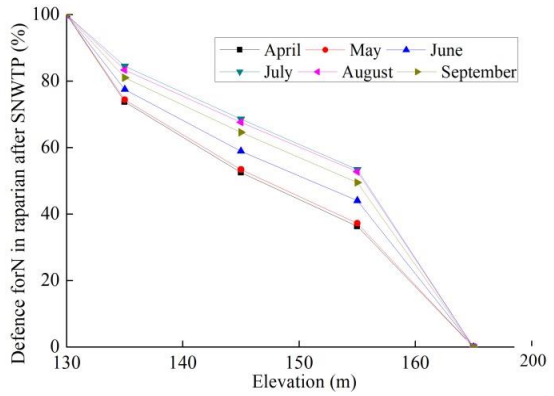

Figure A3. *N emissions rates by soil from April to September in different land use*

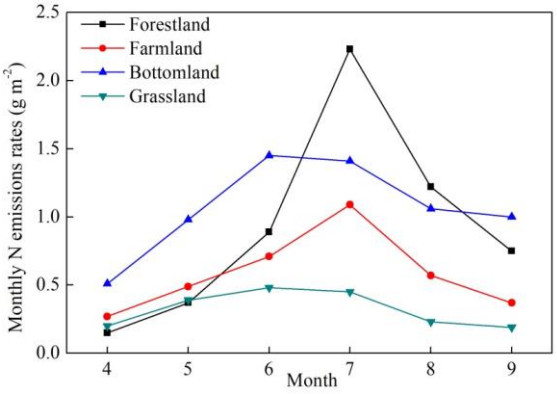

http://www.aloki.hu ● ISSN 1589 1623 (Print) ● ISSN 1785 0037 (Online)
DOI: http://dx.doi.org/10.15666/aeer/1706_1500115018

APPLYING MEMBRANE-LESS ELECTROLYZED WATER FOR INACTIVATING PATHOGENIC MICROORGANISMS

HSU, Y. F.[1] – CHUANG, C. Y.[2] – HUANG, H. C.[1] – YANG, S.[1*]

[1]*Center for General Education, CTBC Business School*
600, Sec. 3, Taijiang Blvd., Annan District, Tainan, Taiwan 709, R.O.C.

[2]*Material and Chemical Research Laboratories, Industrial Technology Research Institute*
195, Sec. 4, Chung Hsing Rd., Chutung, Hsinchu, Taiwan 310, R.O.C.

[*]*Corresponding author*
e-mail: shinhaoyang@ntu.edu.tw; phone: +88-662-873-198

(Received 25th Jun 2019; accepted 24th Oct 2019)

Abstract. The membrane-less electrolyzed water (MLEW) has been reported to possess antimicrobial effects against a variety of microorganisms and is considered as an alternative of traditional disinfectants. In the study, the inactivating efficiency was evaluated by using MLEW with free available chlorine (FAC) at concentrations of 50 and 100 mg/L against food-borne related microorganisms, including *Enterohaemorrhagic Escherichia coli* (ECHC), *Salmonella spp.* and *Staphylococcus aureus* individually. D-value (decimal reduction time) was applied for evaluating the antimicrobial ability of MLEW. D-values of ECHC, *Salmonella*, and *S. aureus* were about 120 sec, 5 sec and 5 sec, respectively. Our study demonstrated that MLEW is very effective in reducing the food-borne microbial contamination.
Keywords: *antimicrobial, free available chlorine, food-borne, disinfectants, microbial contamination*

Introduction

Bacteria induced food-borne illness has had serious impacts on public health. People infected with these food-borne bacteria can suffer from gastroenteritis, including inflammation of gut, diarrhea, abdominal pains and cramps, fever, bloody stool, nausea and vomiting. According to the previous study, the top five food categories linked to food-borne illness in the USA from 1990 to 2003 were seafood, dairy products, eggs, beef, and poultry products (CSPI, 2006). Recently, fresh-cut fruit, vegetables, prewashed and pre-cut salads have become popular eating choices. These food categories are generally eaten without processing. Along with this trend and changes in people's eating habits, the study found that microbial infections associated with fresh-cut fruits and vegetable increased (Qadri et al., 2015; Sureshkumar et al., 2016; Mahfuza et al., 2016).

Investigation of fresh-cut fruit and vegetables have indicated that these producing processes was unable to remove bacteria and also food-borne pathogens such as *Salmonella*, *L. monocytogenes*, *Staphylococcus aureus* and *E. coli* O157:H7 (Upadhyay et al., 2016; Sanchís et al., 2016). *Enterohaemorrhagic Escherichia coli* (EHEC) and *salmonella* have been reported as the causal factor of food-borne illness outbreaks (Switaj et al., 2015; Ebel et al., 2016). *Salmonella* and ECHC were estimated to be the leading cause and should be responsible for 30% of food-borne illness hospitalization in United States individually (CDC, 2013; Jadeja and Hung, 2014). *Staphylococcus aureus* is major pathogen in the food industry and listed among the top 5 pathogens causing food-borne illness (Sun et al., 2012; Giaouris et al., 2015).

Therefore, reducing the contamination caused by these pathogenic bacteria is important for protecting consumers from adverse health exposure in food industry. Many

http://www.aloki.hu ● ISSN 1589 1623 (Print) ● ISSN 1785 0037 (Online)
DOI: http://dx.doi.org/10.15666/aeer/1706_1501915027

previous studies have shown that chlorine-related antimicrobial agent is helpful to reduce the bacterial contamination during food-production process (Rahman et al., 2012; Olaimat and Holley, 2012; Waters and Hung, 2014; Petri et al., 2015).

Electrolyzed water is generated from electrolysis of saline solution in a container within anodic and cathodic electrodes with or without ion-selective permeating membrane. The electrolyzed water contains free available chlorine (FAC) compounds such as hypochlorous acid (HOCl), chlorine gas (Cl_2) and hypochlorite ion (OCl^-) yielding its antimicrobial activity. The distribution of fractions of FAC compounds in electrolyzed water is dependent on pH values and affects biochemical characteristics. Acidic electrolyzed water (AEW) is generated in cathode compartment of electrolysis cell within membrane. It has a strong antimicrobial activity on various microorganisms because of its low pH (2-4) and higher proportion of chlorine gas compared to hypochlorous acid. These characteristics of AEW help destroy cell membrane and disrupt metabolism of microorganisms rapidly. AEW has been widely evaluated for antimicrobial application in recent decades.

Neutral electrolyzed water, has near neutral pH value (6-8), giving similar antimicrobial mechanism but result in less metal surface corrosion or skin irritation as AEW (Huang et al., 2008; Cui et al., 2009). This work chose the membrane-less electrolyzed water (MLEW) as the antimicrobial agent. The MLEW is one of the neutral electrolyzed water. Moreover, the membrane-less electrolytsis container is more productive, stable, convenient and economic because of expendable ion-selective membrane is not utilized during electrolysis (Chuang et al., 2013). MLEW becomes more popular in recent years because of above advantages but revealed less information as the alternative of conventional chlorine-related antimicrobial agents.

Neutral electrolyzed water has been extensively used for inactivating food-borne bacteria (Zhang et al., 2016; Machado et al., 2016). However, the MLEW has not yet been applied to inactivate food-borne bacteria. Thus, this study aims to evaluate antimicrobial activity of MLEW against the selected food-borne illness bacterial microorganism including ECHC, *Salmonella spp.* and *S. aureus* strains. In addition, two commercially available chlorine-related antimicrobial agents including bleach and chlorine dioxide (ClO_2), usually used in the food-processing factory, were applied to inactivate the selected bacterial strains for comparison in our study.

Materials and Methods

Preparation of Membrane-less electrolyzed water (MLEW)

The MLEW used in this study was generated by hand-made membrane-less electrolyzing device (Chuang et al., 2013). The schematic diagram of electrolyzing device is shown in *Figure 1*. The device consists of 850 mL cylinder polycarbonate (PP) container (height: 15 cm; diameter: 10.5 cm) filled with saturated NaCl solution (6.15 M). Two Pt/Ti base electrodes module (10×2 cm^2) was installed inside the PP container as cathode and anode with the gap of 0.8 cm between electrodes, giving 12 A electrical current inputs. The FAC concentration of the MLEW solution was measured with N, N-dimethyl-p-phenylenediamine (DPD) colorimetric method, using portable spectrometer (DR 2800, HACH, Loveland, CO, USA). The pH value of the MLEW solution was measured using pH meter (CyberScan pH 510, Eutech Inc., Singapore).

With 30 minutes of electrolyzing process, FAC concentration of NaCl solution would rise up to over 10,000 mg/L. This 850 mL solution with high FAC concentration was

http://www.aloki.hu ● ISSN 1589 1623 (Print) ● ISSN 1785 0037 (Online)
DOI: http://dx.doi.org/10.15666/aeer/1706_1501915027

subsequently diluted with deionized water (Milli-Q, Millipore, Billerica, MA, USA) to FAC 50 and 100 mg/L as the ready-to-use antimicrobial agent (pH 7.0 ~ 7.2) for further inactivating experiments. In the United States, chlorine-related wash at highest FAC 200 mg/L is allowed to be used sanitizing treatment by the food-production industry (Regulation 21CFR178.1010). Therefore, we applied MLEW with FAC 50 and 100 mg/L in the study for simulate the field application in the factory. Bleaching liquid (NaOCl, Regular-Bleach, Colorox, CA., USA) and chlorine dioxide liquid (ClO_2, CLEAN GOOD, Daisyko Trading Co. Ltd.) were diluted to FAC 50 and 100 mg/L (the same concentrations with MLEW, measured with DPD methos, DR 2800 HACH, Loveland, CO, USA) to inactivate the selected food-borne bacterial strain as the reference antimicrobial agents.

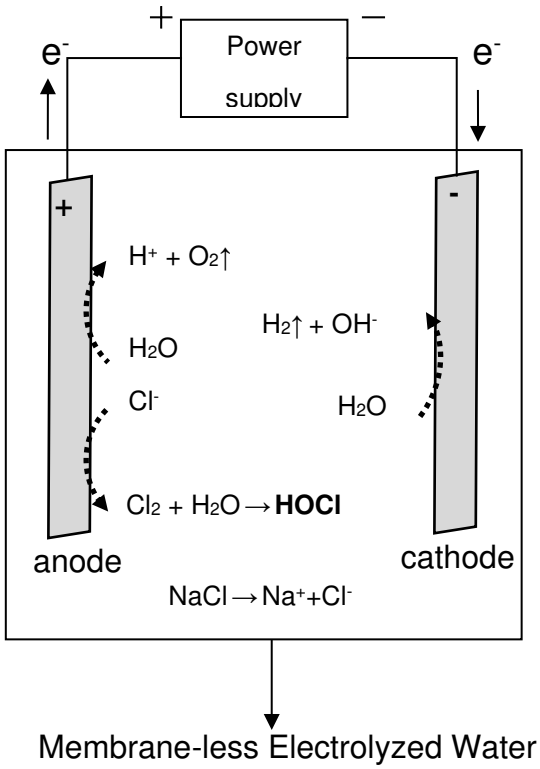

Figure 1. *The schematic diagram of hand-made membrane-less electrolyzing device*

Preparation of test bacterial strains

The bacterial strains used in the study including ECHC, *Salmonella spp.* and *S. aureus* were obtained from Bioresource Collection and Research Center (BCRC, Hsinchu, Taiwan). The preparation and culture of the testing microorganisms based on the previous research (Abadias et al., 2008). ECHC (BCRC 14824), *Salmonella enterica* (BCRC12947) and *S. aureus* (BCRC 10451) pure culture collections were transferred and grown on tryptic soy agar (TSA, BD, N.J., USA) incubating at 37 ± 1℃ for 48 hours. Single bacterial colony was isolated with streaking loop and transferred to tryptic soy broth (TSB, BD, N.J., USA) and incubating at 37 ± 1℃ for 24 hours in order to enrichment. The enriched TSB that respectively contained ECHC, *Salmonella spp.* and *S. aureus* cells were then poured individually into sterile tubes that were then centrifuged

http://www.aloki.hu ● ISSN 1589 1623 (Print) ● ISSN 1785 0037 (Online)
DOI: http://dx.doi.org/10.15666/aeer/1706_1501915027

at 2,500 rpm for 15 minutes. Following the centrifugal process, the supernatant of the TSB were removed. The resulting pellet in the tubes were re-suspended with 30 mL sterilized deionized water as testing suspension. The centrifuge and re-suspension processes were repeated twice to totally remove TSB. Culturable bacterial population of the testing suspensions were determined by tenfold serial dilution of 0.1 mL aliquot on TSA by incubation at 37 ± 1°C for 24 hours. The final bacterial population of the testing suspensions were adjusted to 10^6 ~ 10^7 colony forming unit CFU/mL for subsequent inactivating experiments.

MLEW, bleach and ClO_2 inactivating test against 3 bacterial strains

The experimental system and tests were operating in Taiwan, R.O.C. Quantitative inactivating experiments adapted from Robinson et al. (2010) against 3 bacterial suspensions were performed of MLEW, NaOCl and ClO_2 in the study. 1 mL of MLEW, bleach and ClO_2 with FAC 50 and 100 mg/L were added to 99 mL of 3 bacterial suspensions respectively as inactivating treatment samples (1% v/v contacting). After time interval of 10 and 30 seconds, 0.1 mL aliquot of agents-treated bacterial suspensions were extracted for tenfold serial dilution and spread on TSA, followed with incubation at 37 ±1°C for 24 hours. Each test would spread on three TSA plates. The colonies of the plates were counted and convert to original culturable population in the bacterial suspensions for measuring the survival rate at the inactivating time intervals mentioned above. Sodium thiosulfate ($Na_2S_2O_3$, 217263 Sigma-Aldrich, USA) was used to liberate bacterial aliquot from continuously contact of antimicrobial agents while extracted. The experimental limit of the serial dilution and culture method was 10 CFU/mL. On the other hand, as control sample, another group of 3 bacterial suspensions with neither MLEW, ClO_2 nor NaOCl were added were observed by the same aliquot, serial dilution and incubation process. The experiment was repeated triple.

Inactivating efficiency were evaluated by bacterial strains survival population to the extent of being killed in terms of corresponding decimal reduction times (D-value) of antimicrobial agents. The D-value is the time required, at a given condition, to achieve a log reduction, that is, to kill 90% of relevant microorganisms.

Statistical analysis

The inactivating efficiency of testing bacteria after MLEW, NaOCl and ClO_2 were calculated by subtracting the initial mean bacteria concentration (CFU/mL) from the bacteria concentration (CFU/mL) after each treatment. All experimental values showed the means of three different experiments with 3 replicates of the inactivating treatment per experiment. The Statistical Product and Service Solutions (SPSS version 20) program was utilized for statistical evaluation of measurement data. Significant differences between inactivating test with respect to bacterial reduction were analyzed by one-way ANOVA at a significance level of 0.05.

Results and Discussion

The inactivating efficiency of MLEW, bleach and ClO_2 against 3 bacterial strains

Table 1 shows the inactivating efficiency of MLEW, NaOCl and ClO_2 against ECHC with FAC 50 and 100 mg/L. The ECHC in the test suspension was almost totally inactivated by MLEW and bleach with FAC 50 mg/L after 10 second treatment. However,

http://www.aloki.hu ● ISSN 1589 1623 (Print) ● ISSN 1785 0037 (Online)
DOI: http://dx.doi.org/10.15666/aeer/1706_1501915027

there is still 3.2×10^6 CFU/mL of ECHC remain survival (71%) in test suspension of FAC 50 mg/L ClO_2 after 10 second treatment. It reveals that MLEW and NaOCl performed rapid and effective antimicrobial reaction against ECHC than ClO_2 in the short time contacts ($p<0.05$). It can be expected that longer contact time between antimicrobial agent and bacterial bring better inactivating effect. In our study, 30 seconds treatment of FAC 50 mg/L MLEW and NaOCl did resulted in the same <10 CFU/mL survival population of ECHC. But ClO_2 still could not perform acceptable inactivating efficiency and remain 60% HCHC survival rate (2.7×10^6 CFU/mL) even elongate treatment time to 30 second.

Table 1. *Inactivating efficiency of MLEW, NaOCl and ClO_2 against ECHC*

Time intervals and culturable population of ECHC							
FAC concentration (mg/L)	Control group (CFU/mL)	MLEW		NaOCl		ClO_2	
		10 sec	30 sec	10 sec	30 sec	10 sec	30 sec
50	4.5×10^6	< 10	< 10	< 10	< 10	3.2×10^6	2.7×10^6
100	4.5×10^6	< 10	< 10	< 10	< 10	2.6×10^6	< 10

While treating with FAC 100 mg/L MLEW and bleach, ECHC were also mostly totally inactivated after 10 second contacting. The survival rate of ECHC to FAC 100 mg/L ClO_2 is 58% (2.6×10^6 mg/L) and higher than MLEW and NaOCl ($p<0.05$). In the other way, giving longer treatment time to FAC 100 mg/L ClO_2 cause significant improvement on inactivation. < 10 CFU/mL of ECHC survival was achieved when 30 seconds treatment applied with FAC 100 mg/L ClO_2. Our experimental resulted that ClO_2 does not pose comparable inactivating efficiency to MLEW and bleach in short time contact against ECHC. ClO_2 need longer contact time to present performance the same as MLEW and bleach when treating HCHC.

Table 2 shows the inactivating efficiency of MLEW, bleach and ClO_2 against *Salmonella spp.* with FAC 50 and 100 mg/L. The *Salmonella spp*. in the test suspension was almost totally inactivated by MLEW and ClO_2 with FAC 50 mg/L after 10 second treatment. However, there is still 9.0×10^6 CFU/mL of *Salmonella spp.* remain survived (18%) in test suspension of FAC 50 mg/L NaOCl after 10 second treatment. MLEW and ClO_2 performed rapid and effective antimicrobial reaction against *Salmomnella spp*. than NaOCl in the short time contacts ($p<0.05$). After longer 30 seconds treatment, FAC 100 mg/L of three chlorine-related antimicrobial agents resulted in <10 CFU/mL survival population of *Salmomnella spp*.

Table 2. *Inactivating efficiency of MLEW, bleach and ClO_2 against Salmonella spp.*

Time intervals and culturable population of *Salmonella spp*.							
FAC concentration (mg/L)	Control group (CFU/mL)	MLEW		NaOCl		ClO_2	
		10 sec	30 sec	10 sec	30 sec	10 sec	30 sec
50	5.0×10^7	< 10	< 10	9.0×10^6	< 10	< 10	< 10
100	4.6×10^6	< 10	< 10	< 10	< 10	< 10	< 10

http://www.aloki.hu ● ISSN 1589 1623 (Print) ● ISSN 1785 0037 (Online)
DOI: http://dx.doi.org/10.15666/aeer/1706_1501915027

As to FAC 100 mg/L three chlorine-related antimicrobial agents, all *Salmomnella spp*. survival populations were reduced to <10 CFU/mL condition. MLEW, NaOCl and ClO_2 can present comparable inactivation efficiency once enough contact time was set. The result in here indicates MLEW and ClO_2 are better effective antimicrobial agents against *Salmomnella spp*. while rapid treatment is needed.

Table 3 shows the inactivating efficiency of MLEW, NaOCl and ClO_2 against *S. aureus* with FAC 50 and 100 mg/L. Facing to *S. aureus*, FAC 50 mg/L NaOCl and ClO_2 did not give satisfied inactivation efficiency when treating with 10 second. 71% and 46% of S. aureus were still curturable after the 10 second treatment (4.0×10^7 and 2.6×10^7 CFU/ mL survived for NaOCl and ClO_2 treated samples). On the contrary, the MLEW performed <10 CFU/mL survival rate at the same 10 second contacting. MLEW performed rapid and effective antimicrobial reaction against *S. aureus* than NaOCl and ClO_2 in the short time contacts ($p<0.05$).

Table 3. *Inactivating efficiency of MLEW, NaOCl and ClO_2 against S. aureus*

Time intervals and culturable population of *S. aureus*							
FAC concentration (mg/L)	Control group (CFU/mL)	MLEW		NaOCl		ClO_2	
		10 sec	30 sec	10 sec	30 sec	10 sec	30 sec
50	5.6×10^7	< 10	< 10	4.0×10^7	1.7×10^7	2.6×10^7	< 10
100	5.6×10^7	< 10	< 10	3.2×10^7	1.0×10^7	1.4×10^7	< 10

As to longer 30 second contacting samples, only FAC 50 mg/ L NaOCl did not reach significant inactivating efficiency (30% were still survival). Both MLEW and ClO_2 give performed <10 CFU/mL survival rate in the same time of contacting. For FAC 100 mg/L antimicrobial agents experiments against *S. aureus*, NaOCl did not present significant inactivating efficiency no matter 10 second or 30 second treatment (survival rate were 57% and 17%). ClO_2 bought out satisfied inactivating efficiency after 30 second contact rather than 10 second (25% survived). MLEW presented < 10 CFU/mL survival rate against *S. aureus* both 10 second and 30 second treatment in our experiment. Therefore, ClO_2 and MLEW can be selected to inactive *S. aureus* contamination if longer contact time available.

D-values of MLEW, bleach and ClO_2 against 3 bacterial strains

Table 4 presents D-values (decimal reduction time) of chlorine-related antimicrobial agents applied against 3 bacterial strains in the study. According our experimental results, MLEW were the most suitable antimicrobial agents against ECHC, *Salmonells spp*. and *S. aureus* strains. The inactivating efficiency of NaOCl toward to *S. aureus* is limited. ClO_2 also presented limited inactivation against ECHC.

The MLEW reveals comparable even stronger antimicrobial effects with NaOCl in our study. The same trend could also be observed in previous studies of neutral electrolyzed water (Abadias et al., 2008; Machado et al., 2016). The antimicrobial property of MLEW is contributed to multiple factors. Firstly, at the near-neutral pH chlorinated solution, the predominant FAC species is hypochlorous acid. It has stronger biocidal capacity than hypochlorite ion, which is the predominant species in high pH NaOCl liquid (Rahman et

http://www.aloki.hu ● ISSN 1589 1623 (Print) ● ISSN 1785 0037 (Online)
DOI: http://dx.doi.org/10.15666/aeer/1706_1501915027

al., 2010; Waters and Hung, 2013). Besides, the high oxidation-reduction potential (ORP) in the electrolyzed water is regarded as the primary factor yielding microbial inactivation. ORP can damage the outer and inter membrane of bacterial cell. Then, severely ORP stress can deplete the energy stores and damage the machinery that produced the energy associated with protein structure and cell function. High ORP provides MLEW additional antimicrobial factors apart from FAC species. It may explain the comparative efficacy observed in this study when FAC matched with chlorine dioxide (Thron et al., 2013; Machado et al., 2016). In Thron et al. (2013) study, the 20 minute antimicrobial treatment of electrolyzed water, bleach and ClO_2 against *S. aureus* was conducted. The results showed the order of antimicrobial efficiency was as follows: neutral electrolyzed water > ClO_2 > NaOCl. However, it should be noted there were instances in which no significant difference between agents was observed (Machado et al., 2016). It would going to the same trend if the contact time was elongated to minute level in our experiment. The MLEW did revealed comparable inactivation efficiency against the three common food-borne contagious bacterial strains to ClO_2 and bleach according to our present experimental results.

Table 4. *D-values of MLEW, bleach and ClO_2 against 3 bacterial strains*

D-values and FAC of chlorine-related antimicrobial agents						
Bacterial strains	MLEW		Bleach		ClO_2	
	50 mg/L	100 mg/L	50 mg/L	100 mg/L	50 mg/L	100 mg/L
ECHC	5 sec	5 sec	5 sec	5 sec	144 sec	42 sec
Salmonella spp.	5 sec	5 sec	11 sec	5 sec	5 sec	5 sec
S. aureus	5 sec	5 sec	57 sec	40 sec	5 sec	5 sec

From the standpoint of field usage in food-processing factory and kitchen, MLEW and ClO_2 take the advantages of on-site generation. Since ClO_2 traditionally requires manual mixing of sachets whereas MLEW generation can be automated by device which is simply fabricated and economically maintained. Only water, salt and electrical power are required to generate the MLEW continuously on site. No hazardous matter storage and mixing involved in the MLEW generation (Thorn et al., 2013). Since highly microbial reactive species contained, the disadvantage of MLEW is the rapidly free chlorine loss in the open air. Greatly lost of free chlorine in the electrolyzed water is observed when settled in the open-light environment during several days, following with the significantly decreasing of biocidal efficiency (Han et al., 2018). The generation model comprehend sufficiently supply and using just-in-time is highly demands for the MLEW application in the food-production industry.

Conclusions

Our experimental result indicated that food-borne bacteria inactivation efficiency of MLEW is comparable to conventional chlorine-related agent, including bleach and ClO_2. MLEW even presented more ensuring inactivation to the target strain especially short time treatment set in our study. However, the sanitization in food-production involves

http://www.aloki.hu ● ISSN 1589 1623 (Print) ● ISSN 1785 0037 (Online)
DOI: http://dx.doi.org/10.15666/aeer/1706_1501915027

complicated processes and interfering factors, such as various deploying surface (metal plate, fabric surface or wood cutting board), organic matter reaction (blood, feces or tissue residual), co-existence of microbes (viral and bacterial strains). Therefore, further investigations of broad spectrums and various conditions should be fulfilled to clarify the s and applications of MLEW in the food-production industry.

REFERENCES

[1] Abadias, M., Usall, J., Oliveira, M., Alegre, I., Viñas, I. (2008): Efficacy of neutral electrolyzed water (NEW) for reducing microbial contamination on minimally-processed vegetables. – Int. J. Food Microbiol 123(1-2): 151-158.

[2] Center for Science in the Public Interest (CSPI) (2006): Seafood and produce top food poisoning culprits. – http://www.cspinet.org/foodsafety/OutbreakAlert2006.pdf Accessed 19.12.06.

[3] Centers for Disease Control and Prevention (2013): Surveillance for foodborne disease outbreaks--United States, 2009-2010. – MMWR. Morbidity and mortality weekly report 62: 41-47.

[4] CFR (Code of Federal Regulations) (2011): 21CFR178.1010 – Sanitizing solutions. – Available at: http:// www.gpo.gov/fdsys/pkg/CFR-2011- title21-vol3/xml/CFR-2011-title21- vol3-sec178-1010.xml. Accessed 20 December 2011.

[5] Chuang, C. Y., Yang, S., Huang, H. C., Luo, C. H., Fang, W., Hung, P. C., Chung, P. R. (2013): Applying the membrane-less electrolyzed water spraying for inactivating bioaerosols. – AAQR 13(1): 350-359.

[6] Cui, X., Shang, Y., Shi, Z., Xin, H., Cao, W. (2009): Physicochemical properties and bactericidal efficiency of neutral and acidic electrolyzed water under different storage conditions. – J Food Process Eng 91: 582-586.

[7] Ebel, E. D., Williams, M. S., Cole, D., Travis, C. C., Klontz, K. C., Golden, N. J., Hoekstra, R. M. (2016): Comparing characteristics of sporadic and outbreak-associated foodborne illnesses, United States, 2004–2011. – Emerg Infect Dis 22(7): 1193.

[8] Giaouris, E., Heir, E., Desvaux, M., Hebraud, M., Møretrø, T., Langsrud, S., Doulgeraki, A., Nychas, G. J., Kačániová, M., Czaczyk, K., Ölmez, H., Simões, M. (2015): Intra-and inter-species interactions within biofilms of important foodborne bacterial pathogens. – Front Microbiol 6: 841.

[9] Han, D., Hung, Y. C., Wang, L. (2018): Evaluation of the antimicrobial efficacy of neutral electrolyzed water on pork products and the formation of viable but nonculturable (VBNC) pathogens. – Food Microbiol 73: 227-236.

[10] Huang, Y., Hung, Y., Hsu, S., Huang, Y., Hwang, D. (2008): Application of electrolyzed water in the food industry. – Food Control 19: 329-345.

[11] Jadeja, R., Hung, Y. C. (2014): Efficacy of near neutral and alkaline pH electrolyzed oxidizing waters to control Escherichia coli O157: H7 and Salmonella Typhimurium DT 104 from beef hides. – Food Control 41: 17-20.

[12] Machado, I., Meireles, A., Fulgêncio, R., Mergulhão, F., Simões, M., Melo, L. F. (2016): Disinfection with neutral electrolyzed oxidizing water to reduce microbial load and to prevent biofilm regrowth in the processing of fresh-cut vegetables. – Food Bioprod Process: 333-340.

[13] Mahfuza, I., Arzina, H., Kamruzzaman, M. M., Afifa, K., Afzal, H. M., Rashed, N., Roksana, H. (2016): Microbial status of street vended fresh-cut fruits, salad vegetables and juices in Dhaka city of Bangladesh. – Int. Food Res. J 23(5): 2258-2264.

[14] Olaimat, A. N., Holley, R. A. (2012): Factors influencing the microbial safety of fresh produce: A review. – Food Microbiol 32: 1-19.

http://www.aloki.hu ● ISSN 1589 1623 (Print) ● ISSN 1785 0037 (Online)
DOI: http://dx.doi.org/10.15666/aeer/1706_1501915027

[15] Petri, E., Rodríguez, M., García, S. (2015): Evaluation of combined disinfection methods for reducing escherichia coli o157:H7 population on fresh-cut vegetables. – Int J Environ Res Publ Health 12: 8678-8690.
[16] Qadri, O. S., Yousuf, B., Srivastava, A. K. (2015): Fresh-cut fruits and vegetables: Critical factors influencing microbiology and novel approaches to prevent microbial risks—A review. – Cogent Food Agric 1(1): 1121606.
[17] Rahman, S. M., Ding, T., Oh, D. H. (2010): Effectiveness of low concentration electrolyzed water to inactivate foodborne pathogens under different environmental conditions. – Int J Food Microbiol 139: 147-153.
[18] Rahman, S. M., Park, J., Song, K. B., Al-Harbi. N. A., Oh, D. H. (2012): Effects of slightly acidic low concentration electrolyzed water on microbiological, physicochemical, and sensory quality of fresh chicken breast meat. – J Food Sci 77: M35-41.
[19] Robinson, G. M., Lee, S. W. H., Greenman, J., Salisbury, V. C., Reynolds, D. M. (2010): Evaluation of the efficacy of electrochemically activated solutions against nosocomial pathogens and bacterial endospores. – Lett Appl Microbiol 50: 289-294.
[20] Sanchís, E., González, S., Ghidelli, C., Sheth, C. C., Mateos, M., Palou, L., Pérez-Gago, M. B. (2016): Browning inhibition and microbial control in fresh-cut persimmon (Diospyros kaki Thunb. cv. Rojo Brillante) by apple pectin-based edible coatings. – Postharvest Biol Tec 112: 186-193.
[21] Sun, J. L., Zhang, S. K., Chen, J. Y., Han, B. Z. (2012): Efficacy of acidic and basic electrolyzed water in eradicating staphylococcus aureus biofilm. – Can J Microbiol 58: 448-454.
[22] Sureshkumar, K., Hariharan, B., Vidyalakshmi, R. (2016): Microbiological quality of fresh cut fruit salad sold in Thanjavur City. – J Pure Appl Microbiol 10(2): 1081-1088.
[23] Switaj, T. L., Winter, K. J., Christensen, S. R. (2015): Diagnosis and Management of Foodborne Illness. – Am Fam Physician 92(5): 358-365.
[24] Thorn, R. M. S., Robinson, G. M., Reynolds, D. M. (2013): Comparative antimicrobial activities of aerosolized sodium hypochlorite, chlorine dioxide, and electrochemically activated solutions evaluated using a novel standardized assay. – Am Soc Microbiol 57: 2216-2225.
[25] Upadhyay, A., Chen, C. H., Yin, H., Upadhyaya, I., Fancher, S., Liu, Y., Nair, M. S., Jankelunas, L., Patel, J. R., Venkitanarayanan, K. (2016): Inactivation of Listeria monocytogenes, Salmonella spp. and Escherichia coli O157: H7 on cantaloupes by octenidine dihydrochloride. – Food Microbiol 58: 121-127.
[26] Waters, B. W., Hung, Y.-C. (2013): Evaluation of different methods for determination of properties of chlorine-based sanitizers. – Food Control 30: 41-47.
[27] Waters, B. W., Hung, Y. C. (2014): The effect of ph and chloride oncentration on the stability and antimicrobial activity of chlorine-based sanitizers. – J Food Sci 79: M622-627.
[28] Zhang, C., Li, B., Jadeja, R., Fang, J., Hung, Y. C. (2016): Effects of bacterial concentrations and centrifugations on susceptibility of Bacillus subtilis vegetative cells and Escherichia coli O157: H7 to various electrolyzed oxidizing water treatments. – Food Control 60: 440-446.

http://www.aloki.hu ● ISSN 1589 1623 (Print) ● ISSN 1785 0037 (Online)
DOI: http://dx.doi.org/10.15666/aeer/1706_1501915027

A NATURAL ANTIOXIDANTS OF FOOD PLANT - *CHRYSANTHEMUM NANKINGENSE*, BASED ON ITS ANTIOXIDANT ACTIVITY WITH ACID POLYSACCHARIDES

MA, Y.-P.[1*] – HU, J.[1] – LUO, J.-M.[1] – ZHAO, L.[2]

[1]*College of Life and Health Sciences, Northeastern University*
Shenyang, Liaoning 110004, China

[2]*College of Life Sciences, Northwest A&F University, Yangling, Shaanxi 712100, China*

[*]*Corresponding author*
e-mail: mypluna@sina.com

(Received 25th Jun 2019; accepted 24th Oct 2019)

Abstract. Plant polysaccharides exhibit good antioxidant activity and might represent potential novel antioxidants. Chemical composition, characteristics, and biological activity of plant polysaccharides vary between different species. *Chrysanthemum nankingense*, a vegetable in South China, contains many active chemicals which have been used as materials in medicine to treat various conditions. Here, we extracted crude polysaccharides from *Chrysanthemum nankingense* plant using ultrasonic-assisted extraction with a 1:35 (w/v) ratio of leaf powder to water, extraction time of 1h at 60°C. CNP-1 was isolated, using anion-exchange chromatography on a diethylaminoethyl-cellulose column. We determined molecular weight and chemical composition of the fractions using Fourier transform infrared spectroscopy (FT-IR), high-performance liquid chromatography (HPLC), and nuclear magnetic resonance (NMR) spectrometry. Monosaccharide composition analysis indicated that glucuronic acid was the most abundant unit in CNP-1 polysaccharide fractions. Superoxide radical scavenging assessment, 2, 2-diphenyl-1- picrylhydrazyl (DPPH) assay, and a ferric reducing ability of plasma (FRAP) indicated that CNP-1 has significant antioxidant activity in a dose-dependent manner. In summary, *C. nankingense* contains acidic polysaccharides that may represent a promising natural source of antioxidants for healthy food.

Keywords: *Chrysanthemum nankingense, polysaccharide, structure characterize, antioxidant activities, in vitro*

Introduction

Polysaccharides derived from natural sources are associated with a wide range of therapeutic effects and health-improvement properties (Wang et al., 2016). Polysaccharides are effective antioxidants, and may have antitumor, anticancer and antiviral capabilities, and regulate the immune system (Yang et al., 2014). The natural polysaccharides attracted more and more attention for their potential benefits and perceived safety. Polysaccharides extracted from plants have antioxidant effects on free

http://www.aloki.hu ● ISSN 1589 1623 (Print) ●ISSN1785 0037 (Online)
DOI: http://dx.doi.org/10.15666/aeer/1706_1502915040

radicals, which suggests that they may be helpful, for example, in limiting the effects of aging, lowering blood sugar or adjusting lipid metabolism (Qi et al., 2006; Capek and Turjan, 2009; Chen et al., 2012; Lv et al., 2014). Consequently, the study of naturally occurring polysaccharides in plants might lead to the discovery of a novel source of antioxidants beneficial to humans.

Chrysanthemum nankingense is a perennial herb that belongs to the tribe Anthemideae of Asteraceae (*Figure 1*). Its young leaves are used as a vegetable in South China. Moreover, it is used by traditional medicine to treat various conditions, including stomach heat, bitter taste in the mouth, constipation, headache or red eyes (Dai and Wen, 2015; Wu et al., 2015).

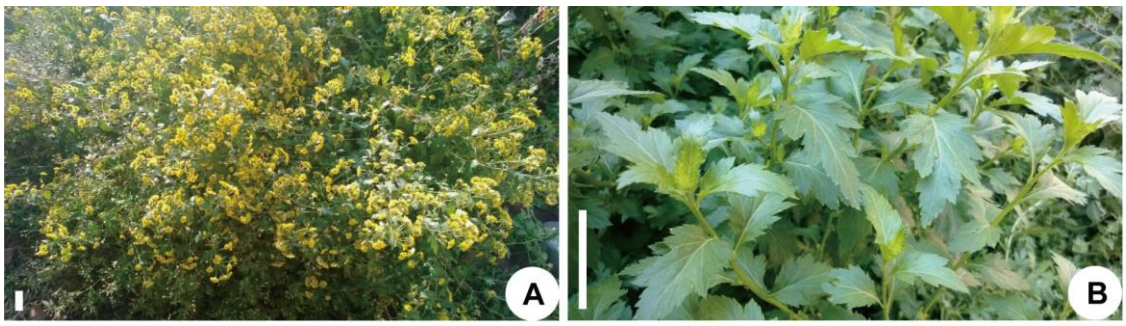

Figure 1. *The Chrysanthemum nankingense plant. A) In flower plant (November). B) Foliage plant (September)*

C. nankingense contains a variety of organic compounds such as flavonoids, polyphenols, alkaloids, organic acids, borneol, and camphor (Yang et al., 2005; Lv et al., 2007; Wu et al., 2015). However, we have little information on the polysaccharides in *C. nankingense*. In this paper, we isolated the polysaccharides present in *C. nankingense* leaves and characterized their properties by Fourier transform infrared (FT-IR) transmission spectroscopy, high performance liquid chromatography (HPLC), and high performance gel permeation chromatography (HPGPC) and nuclear magnetic resonance (NMR) spectrometry. We further explored the polysaccharides antioxidant activity using a variety of in vitro techniques. The objective of this study was to investigate the natural antioxidants fount in *Chrysanthemum nankingense* which may be used as a natural source of antioxidants for healthy food.

Materials and methods

Materials

Chrysanthemum nankingense plants used in this study were collected in the Hubei province, grown in the Nursery Garden of Northeastern University of China. Fresh leaves were collected and washed with distilled water, defatted with two 95% ethanol

http://www.aloki.hu ● ISSN 1589 1623 (Print) ●ISSN1785 0037 (Online)
DOI: http://dx.doi.org/10.15666/aeer/1706_1502915040

washes, and dried in vacuum for 16 h at 60°C. Dry leaves were crushed into powder and filtered with an 80 mesh sieve. The powder was stored in an airtight container at dry place until needed.

All the chemical reagents used were of analytical grade except 2, 2-diphenyl-1-picrylhydrazyl (DPPH), Ascorbic acid (Vc) , 1, 3, 5-tri (2-pyridyl) -2, 4, 6-triazine (TPTZ) and DEAE cellulose DE-52 (DEAE-52) were purchased from the Sinopharm Chemical Reagent Co. (Beijing, China).

Extraction of polysaccharide

About 15 g powder samples were dissolved into deionized water at a 1:35 (w/v) ratio of powder leaves to water, incubated in a water bath at 60°C for 30 min, and subjected to ultrasonic extraction twice for 30 min at a power of 240 W. The mixture was centrifuged at 3000 rpm for 10 min. Then the supernatant was obtained and condensed in a rotating evaporator until a precipitate appeared. The extracts were disposed by activated carbon and Sevag method for decolorizing and removing free proteins. The polysaccharide was precipitate with 80% absolute ethanol overnight at 4°C. The mixture was centrifugated at 3000 rpm for 10 min and lyophilized to obtain raw *C. nankingense* polysaccharides (CNP), which were then stored at −20°C for further use.

Separation and purification of crude CNP

The raw polysaccharides were purified successively by DEAE-52 and Sephadex G-100 chromatography according to the method of Qiao et al. (2009). Five hundred milligrams of crude CNP were dissolved in 10 mL water and applied onto a DEAE-52 column equilibrated with 20 mM phosphate solution (NaH_2PO_4/Na_2HPO_4, pH 6.8). The column was eluted with the 20 mM phosphate solution and sequentially NaCl-phosphate solution gradient (0.05, 0.1, and 0.5 M) with a flow rate of 2 mL/ min. The eluates (5 mL/tube) were collected and monitored by the sulfuric acid anthrone method (Somani et al., 1987). The fraction was collected, concentrated in a rotating evaporator at 50°C, dialyzed in a 21 mm dialysis bag in deionized water for 48 h, and then lyophilized and stored at -20°C till needed.

Characterization of CNPs

FT-IR spectra analysis of CNPs

The infrared spectrum of purified fractions grounded into 1 mm KBr pellets were determined using a FTIR spectrophotometer (Bruker Tensor 27 FT-IR, Bruker Co., Germany) in the frequency range of 4000−400 cm^{-1} (Peng et al., 2012).

http://www.aloki.hu ● ISSN 1589 1623 (Print) ●ISSN1785 0037 (Online)
DOI: http://dx.doi.org/10.15666/aeer/1706_1502915040

Nuclear magnetic resonance (NMR) spectrometric analysis of CNPs

About 30 mg CNP1 was dissolved in 500 μL 99.9% D_2O and analysized using Bruker Advance III 600 MHz spectrometer (Bruker Co., Germany) to obtain ^1H NMR spectra. Chemical shifts were determined in ppm.

Monosaccharide composition analysis of CNPs

Ten milligram of purified CNP were complete hydrolyzed by applying 3 mL trifluoroacetic acid (2 M) at 120°C for 6 hours, then centrifuged at 12000 rpm for 5 min after cooling. 0.2 M NaOH was added to the supernatant to adjust the pH to 7.0. The hydrolysate eluted was aadded to 10 mL and stored in sealed container.

The derivatization was determined following the method of Honda et al. (1989) with some modification. Samples (10 mg/mL) and monosaccharide standards arabinose, glucuronic acid, glucose, rhamnose, mannose, galactose, and xylose were mixed with 0.2 M NaOH and 0.5 M 1-phenyl-3-methyl-5-pyrazolone (PMP) solution in 1 mL test tubes. The solutions were thoroughly mixed and incubated at 70°C for 40 min. Then 0.2 M HCl were used to neutralize the NaOH after the samples cooled. One hundred microliters of trichloromethane were added to the mixture and completed mixed, then centrifuged 5000 rpm for 10 min. The supernatant was extracted for three times with chloroform. The final supernatant was filtered with a 0.45 μm membrane and used for high-performance liquid chromatography (HPLC) with a C18 column (250 mm × 4.6 mm, 5 μm). The mobile phase was 19% (V/V) ammonium acetate buffer solution (pH 5.5) and the flow rate was 1.0 mL/ min.

Determining the molecular weight of CNPs

Molecular weights were measured by high performance gel permeation chromatography (HPGPC) using a Waters HPLC system equipped with two serially linked TSK-GEL G3000 PWXL (7.8 mm × 300 mm) columns and RI and connected to a UV detector. The mobile phase was 0.71% Na_2SO_4 and the flow rate was 0.6 mL/min and the temperature of column was kept at 35°C. Molecular weights of the samples were obtained by comparison with a calibration curve created using the Dextran T-series standards with known molecular weights (23800, 80900, 147600 and 273000). The linear equation of the standard curve was: LogM = −0.34974968tR + 9.75252445, with a correlation coefficient of 0.9981.

Determining the antioxidant activity of CNPs in vitro

Determining CNPs' scavenging activity against oxide anions

The measurement of polysaccharide scavenging activity against superoxide anions were conducted as previously described (Marklund and Marklund, 1974). First, 4.5 mL 0.05 M tris-HCl solution (pH 8.0) was incubated in a water bath at 25°C for 20 min. Then 50, 100, 150, or 200 μL of sample (2 g/L) were added and stirred at 25°C for

http://www.aloki.hu ● ISSN 1589 1623 (Print) ●ISSN1785 0037 (Online)
DOI: http://dx.doi.org/10.15666/aeer/1706_1502915040

20 min. Finally, the reaction was terminated by adding 100 μL 1, 2, 3-phentriol (3 M). The mixture of tris-HCl and 1, 2, 3-phentriol was used as negative control (A_0). The absorbance of the mixture was measured spectrophotometrically at 325 nm and the scavenging activity against superoxide anions was calculated according to the following equation: scavenging effect (%) = (A_0−Asample)/A_0×100%; rate of oxidation (%) = (A_9−A_1)/3×100%, where A_1 is the absorbance of the first detection and A_9 is the absorbance of the ninth detection.

Scavenging ability of DPPH radical

DPPH radical scavenging activity of CNP was measured following the method reported previously (Jia et al., 2014). Two milliliters of sample at various concentrations (0.3, 0.5, and 0.7 mg/mL) were added to 2 mL DPPH ethanol solution (0.06 mM) in a 5 mL cuvetteand mixed completely. The mixture was kept in the dark for 20 min and the absorbance of the sample was measured at 517 nm using a spectrophotometer (721G, China). Ascorbic acid (Vc) was used as the control. The scavenging rate was obtained according the formula: DPPH radical scavenging activity (%) = (1- As/Ab) × 100%, where As is the absorbance of the sample, and Ab is the absorbance of the blank.

Assessment of iron reducing activity

The ferric reducing activity of plasma (FRAP) was measured following the method reported by Jia et al. (2014), with some modifications. Fresh FRAP reaction solution was prepared by mixing 25 mL acetate buffer (300 mM; pH 3.6) with 2.5 mL 1, 3, 5-tri (2-pyridyl) -2, 4, 6-triazine (TPTZ) solutions (10 mM) and 2.5 mL $FeCl_3$•$6H_2O$ (20 mM). Then, 1000 μL of the sample were put into a cuvette to measure the initial absorbance after the sample was warmed to 37°C. The absorption of the solution was measured at 593 nm while 40 μL sample at different concentration (0.2, 0.4, 0.8 or 1.0 mg/mL) were added to the cuvette. The absorption value was recorded at 10 s intervals until it reached a plateau. Iron reducing activity was calculated referencing to the calibration curve prepared of $FeSO_4$•$7H_2O$ solution with several concentrations (100-1000 M). Three technical replicates were conducted for each analysis mentioned above. Three parallel measurements and technical replicates were conducted for each analysis mentioned above. All the data were processed in Origin 8.5.1.

Results and discussion

Purification and segregation of CNP

We obtained the primary polysaccharides from *C. nankingense* using ultrasonic pretreatment with an isolation time of 5 hours, raw materials to water ratio of 1:35 (w/v), power of 240 W, and a combination of activated carbon decolorization and Sevag method to remove the pigment and proteins. The yield of raw polysaccharide from

http://www.aloki.hu ● ISSN 1589 1623 (Print) ●ISSN1785 0037 (Online)
DOI: http://dx.doi.org/10.15666/aeer/1706_1502915040

C. nankingense was about 4.32%. Four elution peaks (CNP-1, CNP-2, CNP-3, and CNP-4) were presented from the crude CNP using a DEAE-52 cellulose anion-exchange chromatogram (*Figure 2*). The major fraction CNP-1 was condensed and lyophilized for next analysis.

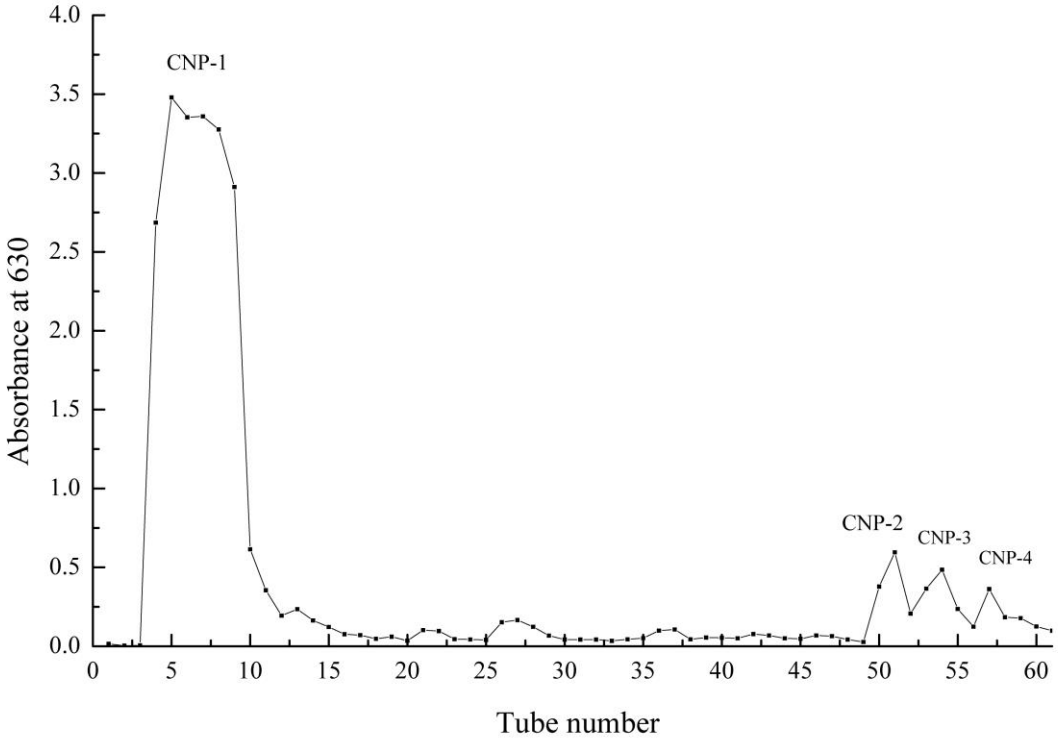

Figure 2. *Elution curve of crude Chrysanthemum nankingense polysaccharide detected by sulfuric acid anthrone method at 490 nm using DEAE52-cellulose column chromatography. CNP-1 was eluted by phosphate solution. CNP-2, CNP-3, and CNP-4 were eluted by 0.5 M NaCl-phosphate solution*

Structure analysis of CNP-1

FT-IR spectra analysis of CNP-1

We characterized the absorption of CNP-1 using FT-IR spectrum (*Figure 3*). This sample showed a wide, intense signals at 3600–3200 cm^{-1}, representing an O-H stretching group, and a weak signal at 3000–2800 cm^{-1}, which we attributed to a C–H stretching vibration (Jia et al., 2014). We also observed peaks in the region of 1630–1510 cm^{-1} and 1420 cm^{-1}, attributed to C=O asymmetric stretching vibration (Cerna et al., 2003), suggesting the carboxyl groups presenting here (Zha et al., 2012). The peaks at 1000–1200 cm^{-1} in the CNP-1 polysaccharide fractions suggests the presence of C–O–C and C–O–H signals, possibly an alduronic acid such as glucuronic acid or mannuronic acid. The CNP-1 fractions presented peaks between 3600 and 3200,

http://www.aloki.hu ● ISSN 1589 1623 (Print) ●ISSN1785 0037 (Online)
DOI: http://dx.doi.org/10.15666/aeer/1706_1502915040

3000 and 2800, 1250 and 1000 cm^{-1}, the typical signals for polysaccharides (You et al., 2014). A characteristic signal at 891±7 cm^{-1} was attribute to glycosidic linkages. CNP-1 has a characteristic signal at 937.3 cm^{-1} induced by asymmetric stretching vibration of pyran ring (Coimbra et al., 1998). Thus, we propose that CNP-1 might be pyranose.

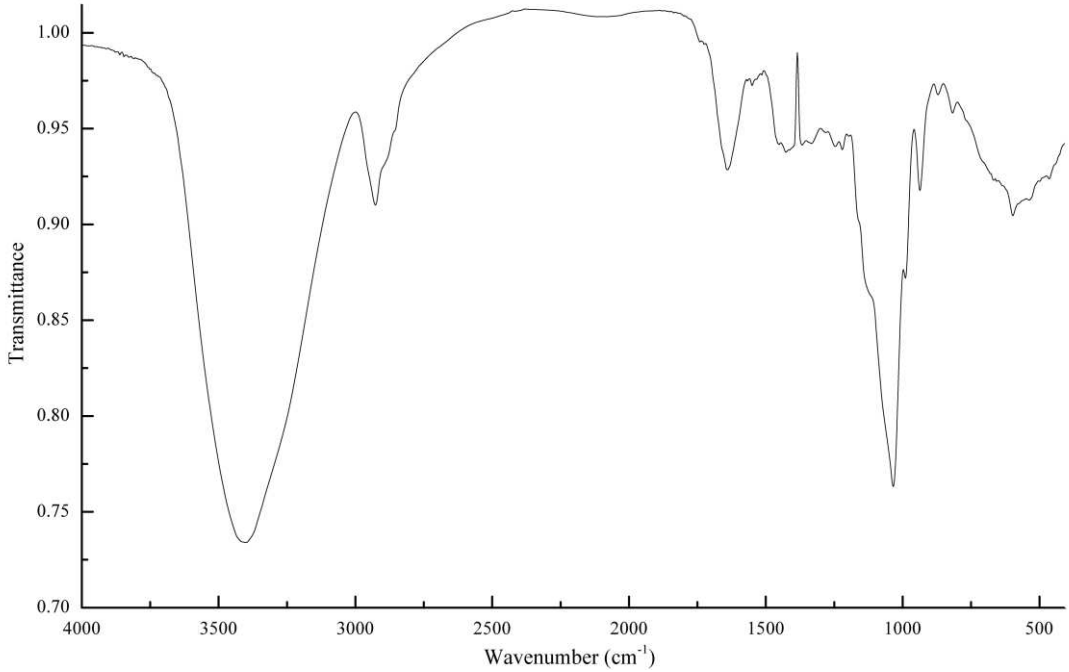

Figure 3. *Fourier transform infrared spectra of CNP-1*

NMR spectra of CNP-1

The structural of CNP-1 was confirmed using ^{1}H-NMR analysis (*Figure 4*). The spectra of CNP was presented between 3.0–5.3 ppm (^{1}H NMR) which were typical signals for polysaccharides (Chen et al., 2016; Wang et al., 2018). The signals induced by protons on sugar rings were present in the region of 3.50–4.50 ppm. We predicted that CNP-1 has a-configuration of saccharide residues for all the resonance signals greater than the shift of 4.8 ppm (Chen et al., 2016). This conclusion further confirmed the results of the infrared spectrum.

Monosaccharide analysis of CNP-1

We characterized the monosaccharide composition of CNP-1 by HPLC (*Figure 5*). Monosaccharide standards of glucuronic acid, mannose, rhamnose, xylose, glucose, galactose, and arabinose produced well separated peaks, with retention times of 16.18, 21.03, 24.47, 26.62, 30.91, 34.12, and 45.69 min. Glucuronic acid was the most abundant monosaccharide in the CNP-1 fraction; mannose and galactose were also

http://www.aloki.hu ● ISSN 1589 1623 (Print) ●ISSN1785 0037 (Online)
DOI: http://dx.doi.org/10.15666/aeer/1706_1502915040

present in trace amounts. These results indicate that CNP-1 is primarily composed of sugar acids, which suggests that it may have deoxidizing activity.

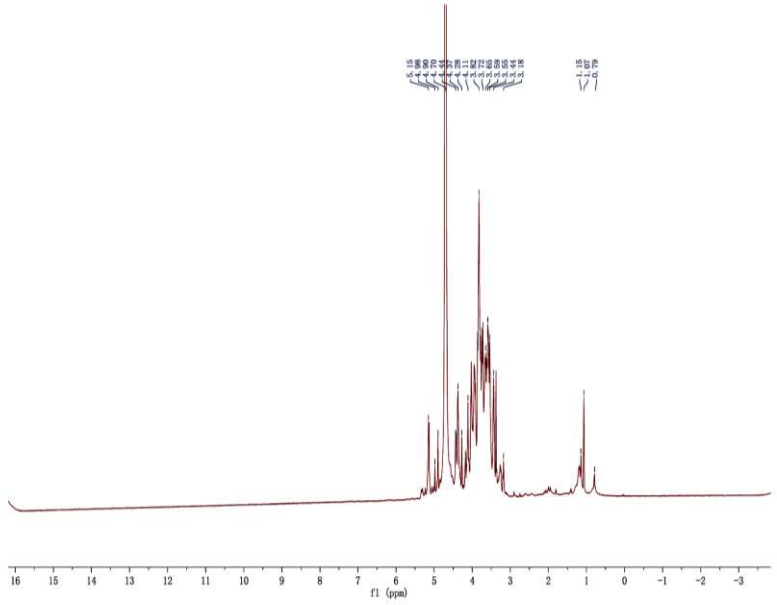

Figure 4. *1H NMR spectra of CNP1*

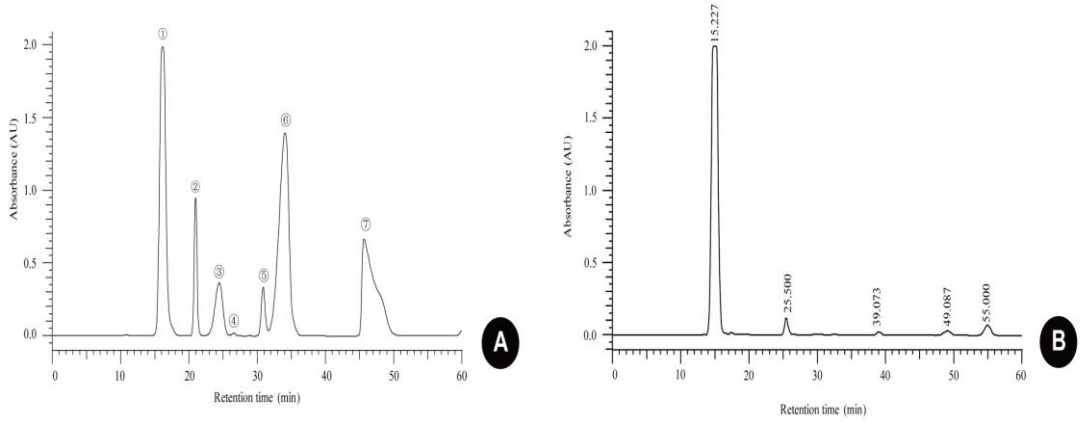

Figure 5. *High-performance liquid chromatograms of three monosaccharide fractions isolated from Chrysanthemum nankingense. Part A shows peaks for the monosaccharide standards glucuronic acid (1), L-mannose (2), D-rhamnose (3), L-xylose (4), L-glucose (5), D-galactose (6), and L-arabinose (7). Parts B shows C. nankingense monosaccharide fractions CNP-1*

Molecular weight of CNP-1

We determined the molecular weight of CNP-1 using the HPGPC method. Based on the reference curve created with dextran standards, we estimated that the average molecular weights of CNP-1 was 4779 Da.

http://www.aloki.hu ● ISSN 1589 1623 (Print) ●ISSN1785 0037 (Online)
DOI: http://dx.doi.org/10.15666/aeer/1706_1502915040

Antioxidant activity of CNP-1 in vitro

Using the DPPH assay, we found that the activity to scavenge free radical of CNP-1 at 0.7 mg mL^{-1} was 21.39%, while that of Vc was 89.00% (*Figure 6A*). The results suggested that CNP-1 had a radicals scavenging effect on DPPH. The FRAP value of CNP-1 increased with the concentration of this fraction (*Figure 6B*). At 0.8 mg/mL, the FRAP value of CNP-1 was 2.726 mmol. These results demonstrate that CNP-1 possesses strong ferric reducing activity.

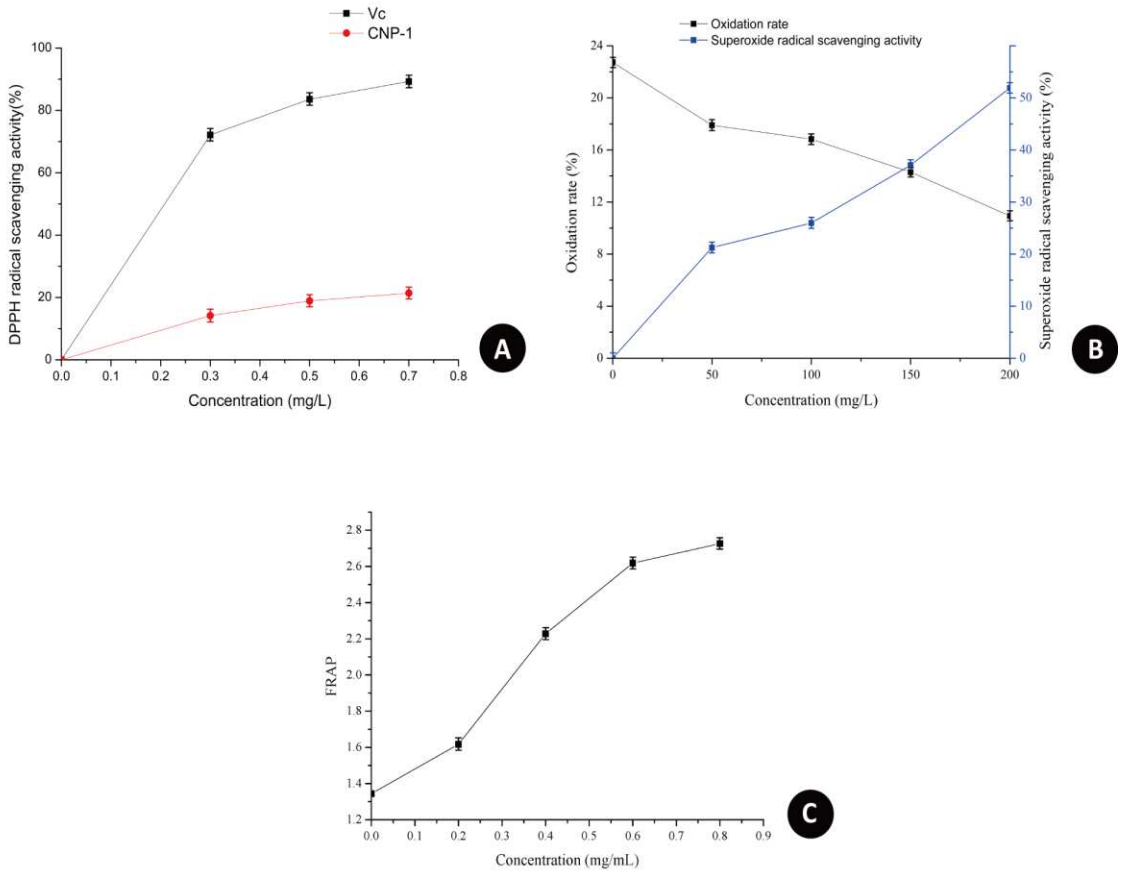

Figure 6. *Antioxidant activity of the purified polysaccharide fraction CNP-1. A. DPPH radical scavenging activity. B. Ferric reducing activity. C. Superoxide radical scavenging activity*

We measured the scavenging activity of CNP-1 on superoxide radical (*Figure 6C*), finding that the oxidation rate of the solution decreased with increases in CNP-1 concentration, while with sample concentration increasing, the scavenging activity of CNP-1 increased also. The scavenging activity of CNP-1 reached 51.91% at the doses of 200 mg L^{-1}. These results demonstrate that CNP-1 is characterized by strong superoxide radical scavenging activity.

http://www.aloki.hu ● ISSN 1589 1623 (Print) ●ISSN1785 0037 (Online)
DOI: http://dx.doi.org/10.15666/aeer/1706_1502915040

Conclusion

In this study, we isolated polysaccharides from *C. nankingense*, and characterized its structural features. Glucuronic acid was the main component of the polysaccharides of this plant by monosaccharide composition analysis. Antioxidant activity analysis demonstrated that CNP-1 had high ferric reducing ability and superoxide radical scavenging activity. These findings suggest the polysaccharides from *C. nankingense* leaves might be a potential source of natural antioxidants in functional foods or pharmacological applications. In addition, the studies showed that most of metabolities were associated with the plant phenotypes (Schauer et al., 2006; Sulpice et al., 2009; Chen et al., 2014; Dan et al. 2016). *Chrysanthemum* is complex taxa with different habitat and various ploidy levels. The phylogeny of *Chrysanthemum* is still not clear. Polysaccharide, as a widely existed metabolite in plant, might be a new way to explore the relationship between *Chrysanthemum* species.

Acknowledgements. This work was supported by the National Natural Science Foundation of China (No. 31872710, 31470699 and 31770200). The authors wish to thank X. G. Sang for assistance with the FTIR analysis.

REFERENCES

[1] Capek, P., Machová, E., Turjan, J. (2009): Scavenging and antioxidant activities of immunomodulating polysaccharides isolated from Salvia officinalis L. – Int J Biol Macromol 44: 75-80.

[2] Cerna, M., Barros, A. S., Nunes, A., Rocha, S. M., Delgadillo, I., Copikova, J., Coimbra, M. A. (2003): Use of FT-IR spectroscopy as a tool for the analysis of polysaccharide food additives. – Carbohyd Ploym 51: 383-389.

[3] Chen, J. J., Zhang, T., Jiang, B., Mu, W. M., Miao, M. (2012): Characterization and antioxidant activity of Ginkgo biloba exocarp polysaccharides. – Carbohyd Ploym 87: 40-45.

[4] Chen, W., Gao, Y., Xie, W., Gong, L., Lu, K., Wang, W. (2014): Genome-wide association analyses provide genetic and biochemical insights into natural variation in rice metabolism. – Science Foundation in China 46: 714-721.

[5] Chen, T., Zhang, M., Li, J., Surhio, M. M., Li, B., Ye, M. (2016): Structural characterization and hypoglycemic activity of trichosanthes, peel polysaccharide. – LWT-Food SCI TE 70: 55-62.

[6] Coimbra, M. A., Barros, A., Barros, M., Rutledge, D. N., Delgadillo, I. (1998): Mul-tivariate analysis of uronic acid and neutral sugars in whole pectic samples byFT-IR spectroscopy. – Carbohyd Ploym 37: 241-248.

[7] Dai, S. L., Wen, X. H. (2015): Efficacy of the medicinal and food Chrysanthemum. – Chin Bull Life Sci 27: 1083-1089.

http://www.aloki.hu ● ISSN 1589 1623 (Print) ●ISSN1785 0037 (Online)
DOI: http://dx.doi.org/10.15666/aeer/1706_1502915040

[8] Dan, Z. W., Hu, J., Zhou, W., Yao, G. X., Zhu, R. S., Zhu, Y. G., Huang, W. C. (2016): Metabolic prediction of important agronomic traits in hybrid rice (Oryza sativa L.). – Scientific Reports 6: 21732.

[9] Honda, S., Akao, E., Suzuki, S., Okuda, M., Kakehi, K., Nakamura, J. (1989): High-performance liquid chromatography of reducing carbohydrates as strongly ultraviolet-absorbing and electrochemically sensitive 1-phenyl-3-methyl-5-pyrazolone derivatives. – Anal. Biochem 180: 351-357.

[10] Jia, X. J., Ding, C. B., Yuan, S., Zhang, Z. W., Chen, Y. E., Du, L., Yuan, M. (2014): Extraction, purification and characterization of polysaccharides from Hawktea. – Carbohyd Ploym 99: 319-32.

[11] Lv, L., Qin, M. J., Wu, G., Han, H. H. (2007): Analysis of essential oil constituents in flower of *Dendranthema indicum* and *D. nankingene* from different provenances. – J Plant Resour Env 16: 53-57.

[12] Lv, L. S., Cheng, Y. H., Zheng, T. S., Li, X. M., Zhai, R. (2014): Purification, antioxidant activity and antiglycation of polysaccharides from Polygonum multiflorum Thunb. – Carbohyd Ploym 99: 765-773.

[13] Marklund, S., Marklund, G. (1974): Involvement of superoxide anion radicals in the autoxidation of pyrogallol and a convenient assay for superoxide dismutase. – Eur J Biochem 47: 469-471.

[14] Peng, Z. F., Liu, M., Fang, Z. X., Wu, J. L., Zhang, Q. Q. (2012): Composition and cytotoxicity of a novel polysaccharide from brown alga (*Laminaria japonica*). – Carbohyd Ploym 89: 1022-1026.

[15] Qi, H. M., Zhang, Q. B., Zhao, T. T., Hu, R. G., Zhang, K., Li, Z. E. (2006): In vitroantioxidant activity of acetylated and benzoylated derivatives of polysaccha-ride extracted from Ulva pertusa (Chlorophyta). – Bioorg Med Chem Lett 16: 2441-2445.

[16] Qiao, D., Hu, B., Gan, D., Sun, Y., Ye, H., Zeng, X. (2009): Extraction optimized by usingresponse surface methodology, purification and preliminary characterization ofpolysaccharides from Hyriopsis cumingii. – Carbohydrate Polymers 76: 422-429.

[17] Schauer, N., Semel, Y., Roessner, U., Gur, A., Balbo, I., Carrari, F. (2006): Comprehensive metabolic profiling and phenotyping of interspecific introgression lines for tomato improvement. – Nature Biotechnology 24: 447-454.

[18] Somani, B. L., Khanade, J., Sinha, R. (1987): A modified anthrone-sulfuric acid method for the determination of fructose in the presence of certain proteins. – Anal. Biochem 167: 327-330.

[19] Sulpice, R., Pyl, E. T., Ishihara, H., Trenkamp, S., Steinfath, M., Witucka-Wall, H. (2009): Starch as a major integrator in the regulation of plant growth. – Proc Natl Acad Sci USA 106: 10348-10353.

[20] Wang, P. C., Zhao, S., Yang, B. Y., Wang, Q. H., Kuanga, H. X. (2016): Anti-diabetic polysaccharides from natural sources: a review. – Carbohyd Ploym 148: 86-97.

http://www.aloki.hu ● ISSN 1589 1623 (Print) ●ISSN1785 0037 (Online)
DOI: http://dx.doi.org/10.15666/aeer/1706_1502915040

[21] Wang, Y., Wei, X., Wang, F., Xu, J., Tang, X., Li, N. (2018): Structural characterization and antioxidant activity of polysaccharide from ginger. – Int J Biol Macromol 111: 862-869.

[22] Wu, S. M., Xu, T., Huang, D. F. (2015): Chemical compositions of the volatile extracts from seeds of Dendranthema nankingense and Borago officinalis. – J Food Drug Anal 23: 253-259.

[23] Yang, N., Ren, A., Hu, W., Qian, S., Duan, J. A., Tian, L. J. (2005): Chemical constituents of Dendranthema nankingense. – J China Pharml University 36: 402-404.

[24] Yang, X. L., Wang, R. F., Zhang, S. P., Zhu, W. J., Tang, J., Liu, J. F., Chen, P., Zhang, D. M., Ye, W. C., Zheng, Y. L. (2014): Polysaccharides from Panax japonicus C. A. – Meyer and their antioxidant activities. – Carbohyd Ploym 101: 386-391.

[25] You, Q. H., Yin, X. L., Zhang, S. G., Jiang, Z. H. (2014): Extraction, purification, and antioxidant activities of polysaccharides from Tricholoma mongolicum Imai. – Carbohyd Ploym 99: 1-10.

[26] Zha, X. Q., Xiao, J. J., Zhang, H. N., Wang, J. H., Pan, L. H., Yang, X. F., Luo, J. P. (2012): Polysaccharides in Laminaria japonica (LP): Extraction, physicochemical properties and their hypolipidemic activities in diet-induced mouse model of atherosclerosis. – Food Chem 134: 244-25.

http://www.aloki.hu ● ISSN 1589 1623 (Print) ●ISSN1785 0037 (Online)
DOI: http://dx.doi.org/10.15666/aeer/1706_1502915040

PERCEPTIONS OF CLIMATE VARIABILITY AND DETERMINANTS OF FARMERS' ADAPTATION STRATEGIES IN THE HIGHLANDS OF SOUTHWEST CAMEROON

NGOE, M.[1] – ZHOU, L.[1*] – MUKETE, B.[2] – ENJEMA, M.[3]

[1]*College of Economics and Management, Nanjing Agricultural University, 1 Weigang, Nanjing 210095, Jiangsu Province, China*

[2]*College of Forestry, Beijing Forestry University, 35 Qinghua Dong Lu, Haidian District, Beijing 100083, China*

[3]*Faculty of Economics and Management, University of Buea, P. O. Box 63, Buea, Cameroon*

**Corresponding author*
e-mail: zhouli@njau.edu.cn; phone: +86-138-5173-1053

(Received 25th Jun 2019; accepted 16th Oct 2019)

Abstract. In Cameroon, climate variability largely controls agriculture related livelihood strategies This variability enhances environmental threats including deforestation, water scarcity and land degradation, which would affect these long and short-term livelihood strategies. This study examined farmers' perceptions of climate variability and the factors that influence various climate adaptation strategies in the highlands of Southwest Cameroon. Using local scale meteorological data from 1974 to 2014 and climate perception data collected from 355 households, in 22 rural villages through household surveys and 12 focus group discussions, descriptive statistics and logit regression model analyses were performed. Results showed 85.1%, 83.9% and 86.2% of the respondents to have observed changes in patterns of temperature, rainfall and number of rainy days. Results further showed household characteristics such as marital status (P-value 0.072) to influence the household decision of increasing in farm size more than gender of household head (P-value 0.221). Also, age of household head (P-value 0.086) influenced adoption of changing planting dates more than gender of household head (P-value 0.207) in a village at the 95% level of significance. This study will help policy makers educate local rural farmers on climate adaptation measures, impacts, and methods for increasing crop yields.
Keywords: *climate variability, perception, adaptation strategies, logit model, smallholder farmers*

Introduction

In Cameroon as in many other sub-Saharan African countries, climate variability exerts varying impacts especially on the agricultural sector. This is probably due to the fact that the majority of the local population mainly relies on rain-fed agriculture for a living (Mukete et al., 2017). Therefore, due to its sensitivity to rainfall and temperature anomalies, the agricultural sector would be adversely affected. These climate effects could likely lead to socioeconomic impacts particularly in the case of farmers whose livelihood (60%-80%) primarily depends on agriculture (Defang et al., 2017). Climate variability is often linked to differential land-maritime interactions which result into various impacts on human lives and livelihoods. Often attributed to changes in rainfall patterns or amount and shifts in thermal and wind regimes, this variation modifies local seasonal and annual water balances. These seasonal and annual water balances in turn influence the periodic distribution for which temperature and moisture conditions permit agricultural crop production (Mongi et al., 2010; Sonwa et al., 2017; Ndiaye et al., 2018).

http://www.aloki.hu ● ISSN 1589 1623 (Print) ● ISSN 1785 0037 (Online)
DOI: http://dx.doi.org/10.15666/aeer/1706_1504115054

In many developing countries, local farmers continue to perceive climate variability as it exerts varying impacts on crop yields. Farmers have therefore developed various adaptation strategies which permit them adapt to this changing climate. But in order to adopt a particular climate adaptation strategy, farmers must first experience climate change before taking measures to adapt to these perceived changes. According to Oluwatusin (2014) and Mukete et al. (2017), these adaptations are interventions and adjustments which occur in order to take advantage of the opportunities or to manage the losses that take place as a result of any external change. From another perspective, IPCC (2012) refers to climate adaptation as the adjustments in natural or man-made systems in response to actual or expected climatic stimuli or their effects. The assessment of farmer adaptation strategies is necessary if the information required for managing climate risks, adaptation enhancement policy analysis and implementation is to be made available (Mukete et al., 2018a).

In this regard, several studies across Africa have examined climate perceptions, variability and farmer adaptation strategies. For instance, Tsegamariam (2018) showed that majority of farmers around Abeshege Woreda in Ethiopia had perceived a decrease in rainfall with an increase in temperatures during the past two decades. Here, farmers applied soil and water conservation, small scale irrigation, changing planting dates, improved crop and livestock varieties as adaptation strategies to climate variability. Using, the logit regression model, the authors observed farmer educational level, farm size, access to credit schemes, and family size to determine a farmer's decision to adopt climate adaptation strategies. Similarly, Gadédjisso (2015) showed about 85% of farmers in Togo, perceived increase in temperature and 85.58% a decrease in rainfall patterns within the past three decades. Farmer adaptation strategies included crop diversification, off-farm jobs, increase in farm size, change of planting date and planting of cycle crops. A multinomial logit analysis showed education level, farming experience, access to extension services, credit schemes, and climate information enhanced a farmer's adaptive capacity to climate variability.

In another study, Seid (2016) observed 96.3% of farmers in Western Ethiopia, had perceived an increase in temperature and 90.7% a decrease in the amount and timing of annual rainfall patterns between 2000 and 2015. In addition, average annual temperatures were found to have increased by about 0.096 °C while annual rainfall had decreased by about 46.75 mm per year. According to the study, over 49.9% of the farmers have adopted climate adaptation approaches such as crop diversification, irrigation, improved crop varieties, adjusting planting dates and various soil conservation techniques like fallowing. In another study around the Vea Catchment of Ghana, Limantol et al. (2016) found, 90% and 94% of farmers believed that temperatures have increased and rainfall amounts, duration, intensity and number of rainy days have decreased. In this catchment area, farmers who rely on rain-fed agriculture adjusted to climate variability by varying crop types, crop rotation without fertilizer. Meanwhile, farmers who rely on irrigation offset climate variability with a greater use of fertilizer application. According to van der Veen (2013), 78%, 69% and 17% of farmers in the Ethiopian Highlands perceived an increased in temperatures and the level of precipitation was declining over the past 20 years. Farmers employed climate adaptation strategies such as crop diversification, various soil conservation methods like planting of trees, fallowing, irrigation, and changing planting dates. Using a multinomial logit (MNL) model, the farmer's level of education, age, wealth, access

http://www.aloki.hu ● ISSN 1589 1623 (Print) ● ISSN 1785 0037 (Online)
DOI: http://dx.doi.org/10.15666/aeer/1706_1504115054

to credit schemes, agricultural extension services and climate change information respectively determined their choice of adaptation strategies.

In Cameroon, agriculture is the main stay of the country's economy, employing over 70% of the population (Kimengsi and Muluh, 2013; Balgah et al., 2016; Tabi et al., 2017). However, agricultural activities have been largely affected by fluctuations in local climate particularly rainfall and temperatures which affect both large scale and subsistence agriculture (Kimengsi and Tosam, 2013; Sonwa et al., 2017). Over the past four decades, lack of reliable quantitative data on agricultural activities and climate variability has been a major challenge for Cameroon's researchers. For instance, and according to Defang et al. (2017), farmers in Southwest Cameroon perceived climate variability as a late start and early cessation of rains, decrease intensity of rainfall, increase temperatures and intensity of the sun. The study also found majority of farmers to have adapted to climate impacts on plantain (*Musa paradisiaca*) and cassava (*Manihot esculenta*) by respectively treating suckers and cuttings with Mocap before and after sowing. MOCAP® is a granular systemic insecticide or nematicide containing 15% w/w ethoprophos which is applied to the soil. It is recommended for the reduction in wireworm damage, potato cyst nematode damage and incidence of Spraing, on all varieties of potatoes. Farmers also changed the cultivated cocoyam variety and planted trees in order to adapt to the impacts of climate change.

Similarly, Darota et al. (2017) observed 92% of the Kaka and 86% of Bulu tribes of Southern Cameroon to have perceived excessive rainfall and which occurs for a short period. Here, 53% of Kaka and 58% Bulu tribes, practiced off-farm activities to compensate for the low income resulting from low harvest due to climate variation. Other adaptation options included, crop diversification, early planting and harvesting as well as cultivating in upland and lowland areas. In another study carried out in the Santa Agrarian Basin of Cameroon's Western Highlands from 2001-2014, Zephania and Bonglam (2016) found farmers to have perceived decreasing rainfall with increasing temperatures and relative humidity trends. The study found over 90% of these local farmers to be aware of climate variability. Meanwhile, about 8.2% were yet to adopt adaptation strategies which would lead to reduced negative impacts, increased crop resilience and integrated animal farming systems. Relatedly, Balgah et al. (2016) found over 97% farmers in North West Cameroon to have demonstrated contextual knowledge of climate variability, as they reported increased rainfall, prolonged dry seasons and changes in rainfall patterns. The study also indicated changing planting dates, and mixed cropping as local farmer adaptation strategies. In another study using primary weather and household livelihood survey data, Mukete et al. (2017) examined the vulnerability and adaptability of women to climate changes in the Rumpi highlands of southwest Cameroon. The study found decreasing amounts of rainfall, receding forests, increasing temperatures, water scarcity, and increasing costs of living. The study also found adjusting sowing dates, adopting petty trading and changing cropping patterns as adaptation strategies applied by these local women.

Although agricultural activity has been largely affected by climate anomalies particularly rainfall and temperature with varying effects on both large and small-scale agriculture, long-term sustainability initiatives and studies are rare. These rare studies such as Defang et al. (2017) and Mukete et al. (2017) have mainly examined farmers' perceptions of climate change and adaptation options without analyzing the various factors that may determine a farmer's choice of climate adaptation measures. Aside farmers' perceptions of climate change and adaptation measures, the present study

http://www.aloki.hu ● ISSN 1589 1623 (Print) ● ISSN 1785 0037 (Online)
DOI: http://dx.doi.org/10.15666/aeer/1706_1504115054

analyzes the various factors that may determine a farmer's choice of climate adaptation measures in the highlands of southwest Cameroon.

This study bridges that knowledge-gap as it assesses farmers' perceptions of climate variability and the factors that determine their choice of adaptation strategies. This baseline information may help improve macro-level poverty estimates and serve as an input into agricultural policy. It may also serve as a knowledge platform for effective collaboration between agriculture dependent communities, stakeholders and policy makers to design effective rural community-based agricultural management and rural development programs aimed at reducing climate change impacts and improve crop yields. This will create the possibility of building a broad knowledge base and offer adaptation and mitigation strategies to help farming households cope with climate changes.

Materials and methods

Study area

This study was carried-out in part of the highlands of Southwest Cameroon located along latitude 4°51′26″ N and longitude 9°07′15″ E in Ndian Division (see *Fig. 1*).

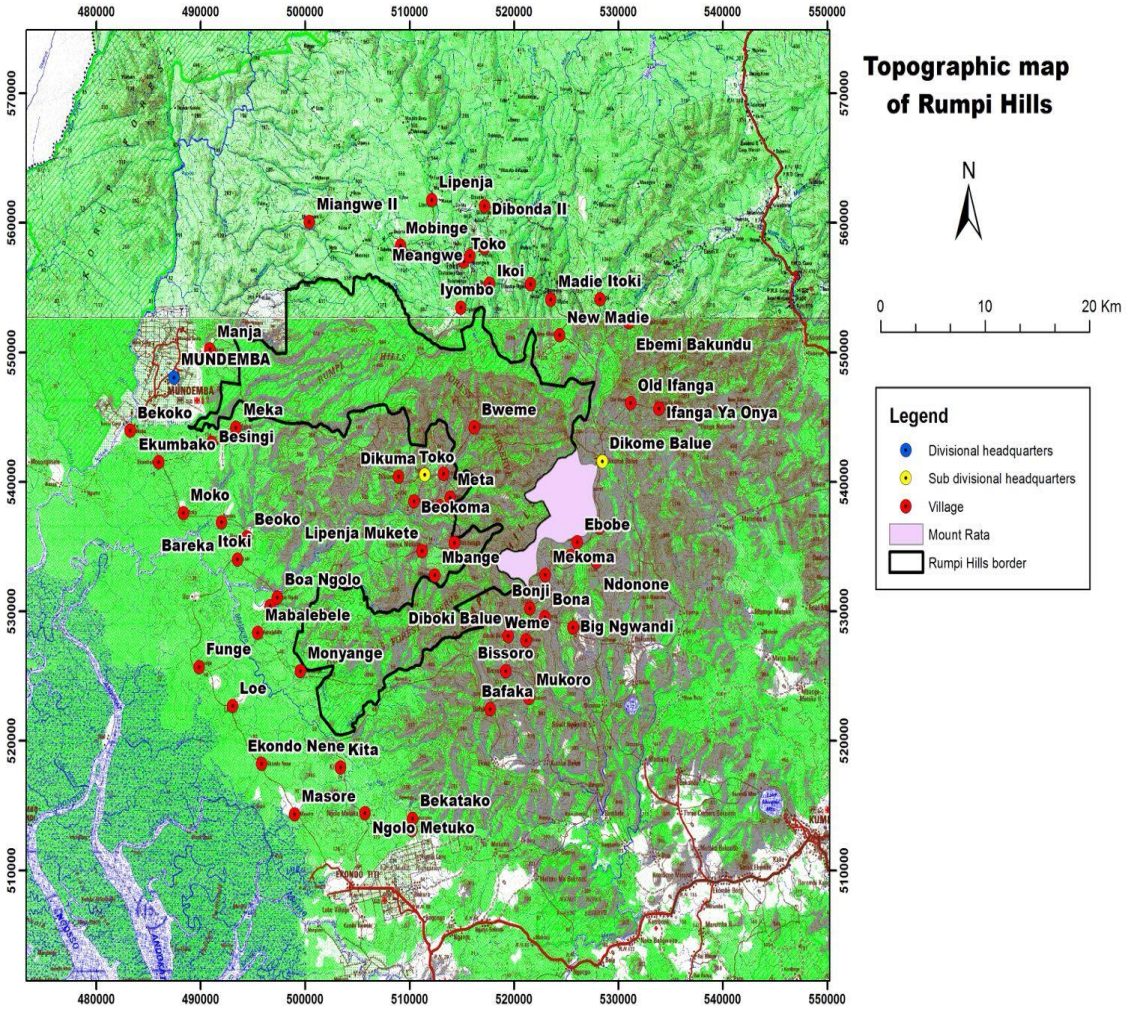

Figure 1. *Map of study area*

http://www.aloki.hu ● ISSN 1589 1623 (Print) ● ISSN 1785 0037 (Online)
DOI: http://dx.doi.org/10.15666/aeer/1706_1504115054

Majority of the population is rural with over 90% involved in agricultural activities growing food crops (cocoyam, plantains, cassava etc.) and cash crops (oil palm, cocoa and rubber tree etc.). Local communities are also engaged in other livelihood activities such as animal husbandry, petit trading and the harvesting of Non-timber forest products (NTFPs) mostly as off-season jobs. NTFPs are items of biological origin which are not timber and wood, obtained from forests, plantations, woods, fallows and other agroforestry systems. In the highlands of southwest Cameroon, NTFPs are primarily land snails, bitter cola, bush mango, njansang, bush pepper and various edible mushrooms (Ofundem et al., 2017; Mukete et al., 2018c).

Data collection

Data were collected between December 2016 and May 2017 through focus group discussions (FGDs) and individual questionnaires. The number of households in each village was obtained from the local village chiefs because official census data are lacking. In villages with less than 25 households, only semi-structured and open-ended questionnaires through a door to door survey were used. Additionally, villages with more than 25 households were divided into groups for easy implementation of FGDs. The number of participants in an FGD was limited to 10 and included volunteers and or randomly selected farmers of at least 18 years old (according to Cameroon Law). Their national identity cards were verified and in cases where this was unavailable, recommendation was sought from the local village chief or his representative. In instances where potential participants were unable to effectively communicate in English language, "Pidgin English" or Oroko dialect was used by the first author to ensure proper understanding. The interview captured at least 90% of the households per village giving a total of 355 interviews of households across the 22 adjacent villages (Mukete et al., 2018c).

The household was the basic unit for this study and it refers *to a group of people living together in the same house who regularly cook and eat from the same pot*. Here, questions were centered on household head demographic characteristics, socioeconomic activities, perception of climate variability and adaptation methods employed. Meteorological data from 1974-2014 were collected from the Pamol Plantations Plc weather station located in Mundemba, Ndian division of southwest Cameroon. Pamol Plantations Plc is an agro-industrial company specialized in palm oil production and growth of natural rubber. Stata 13.0 was used for the logit regression model analysis to identify the determinants of farmer adaptation strategies. Meanwhile, Microsoft Excel for Windows 10 was used to deduce the meteorological data per parameter. The logit model was employed because it considers the relationship between a binary dependent variable and a set of independent variables, be they binary or continuous (*Eqs. 1* and *2;* Greene, 2018).

$$\text{Log } [P_i/(1 - P_i)] = \log (P_i) = \beta_0 + \beta_1 X_i \quad \text{(Eq.1)}$$

where P_i is the probability of perceiving a variability in climate and X_i an independent variable Therefore, the parameter β_1 gives the log odds of the dependent variable and β_0 is a constant.

The probability of occurrence of an event relative to non-occurrence is called odds ratio and is given by

$$P_i/(1 - P_i) = \exp (\beta_0 + \beta_1 X_i) \quad \text{(Eq.2)}$$

http://www.aloki.hu ● ISSN 1589 1623 (Print) ● ISSN 1785 0037 (Online)
DOI: http://dx.doi.org/10.15666/aeer/1706_1504115054

The dependent variables are the adaptation strategies which include increase in farm size, use of external inputs (labour, pesticides, fertilizers, and manure), crop diversification, change of planting dates, off-farm activities and NTFPs harvesting. Meanwhile, the independent variables are the household characteristics such as gender, age, educational level, inhabitants, and marital status of farmer.

Results

Household characteristics of respondents

Household characteristics showed 54.4% of the respondents to be males and 45.6% females. About 10.4% of the respondents were aged 21-30 years, 81.4% aged between 31-60 years and 8.2% were over 60 years. Similarly, 79.7% were indigenous while 20.3% were migrants (*Table 1*). Also, 20.8% had no education, 54.4% had only primary education, 21.7% secondary education and only 3.1% had university education.

Table 1. *Household characteristics of respondents*

Variable	Frequency	Percentage
Gender		
Male	193	54.4
Female	162	45.6
Age		
21-30	37	10.4
31-40	113	31.8
41-50	98	27.6
51-60	78	22
Above 61	29	8.2
Inhabitants		
Indigenous	283	79.7
Migrants	72	20.3
Educational level		
No education	74	20.8
Primary	193	54.4
Secondary	77	21.7
University	11	3.1
Marital status		
Married	205	57.7
Single	102	28.7
Divorce	19	5.4
Widowed	29	8.2

Economic activity

Results showed 51% of the respondents were involved in agricultural activities, 19.4% in petty businesses, and 13.2% in forestry resources harvesting (see *Table 2*).

http://www.aloki.hu ● ISSN 1589 1623 (Print) ● ISSN 1785 0037 (Online)
DOI: http://dx.doi.org/10.15666/aeer/1706_1504115054

Table 2. *Economic activity of respondents*

Sector	Response	Frequency	Percentage
Agricultural	Yes	181	51.0
	No	174	49.0
Public transport	Yes	35	9.9
	No	320	90.1
Petty business	Yes	69	19.4
	No	286	80.6
Forestry	Yes	47	13.2
	No	308	86.8
Other	Yes	23	6.5
	No	332	93.5

Farmer perception of climate variability

About 73.5%, 11.5% and 15% of the respondents had perceived an increase, decrease and no changes in temperature patterns. Similarly, 77.5%, 6.5% and 16% had perceived a decrease, an increase and no change in rainfall patterns respectively. Also, results showed 61.4%, 25.1% and 13.5% thought the number of rainy days had decreased, increased and had not changed (*Table 3*).

Table 3*. Farmers' perception on climate variability*

Climate parameters	Variability	Frequency	Percentage
Temperature patterns	Increase	261	73.5
	Decrease	41	11.5
	No change	53	15
Rainfall patterns	Increase	23	6.5
	Decrease	275	77.5
	No change	57	16
Number of rainy days	Increase	89	25.1
	Decrease	218	61.4
	No change	49	13.5

Variation in mean annual temperature patterns

Mean annual temperature had increased by 0.015 °C per year with 2009 recording the highest mean annual temperatures. The R squared value shows a 16% variation in temperatures (see *Fig. 2*).

Variation in mean annual rainfall

Mean annual rainfall decreases by about 1.7445 mm per year with 1983 having the highest mean annual rainfall and the R squared value shows a 2.5% variation in rainfall indicating that the regression line fits the data as shown in *Figure 3*.

http://www.aloki.hu ● ISSN 1589 1623 (Print) ● ISSN 1785 0037 (Online)
DOI: http://dx.doi.org/10.15666/aeer/1706_1504115054

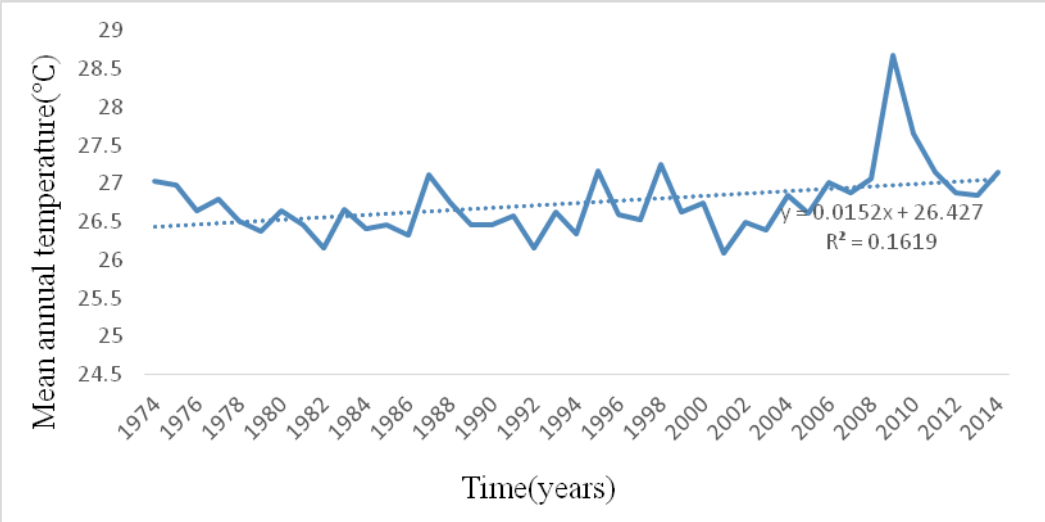

Figure 2. *Mean annual temperature patterns from 1974–2014 (°C)*

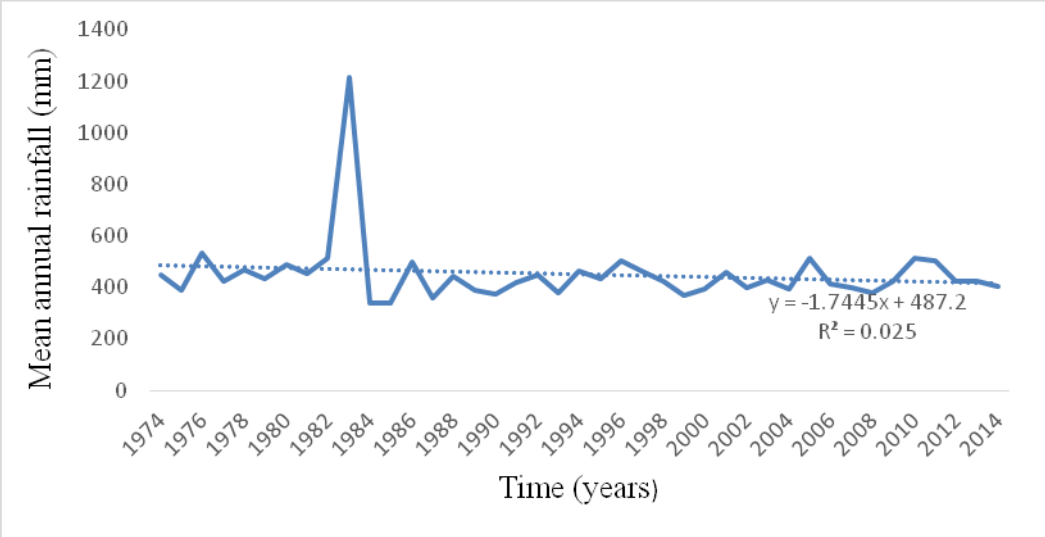

Figure 3. *Trends in mean annual rainfall from 1974–2014*

Variation in mean annual number of rainy days

The number of rainy days from 1974–2014 shows (*Fig. 4*) slight variability and decreases by about 0.0178 days per year with 1993 having the lowest mean annual number of rainy days. The R squared value shows a 2.46% variation in the number of rainy days.

Climate adaptation strategies

The various climate adaptation strategies included increase in farm size (land area under cultivation), use of external inputs (labour, pesticides, fertilizers, and manure), crop diversification, changing of planting dates, off-farm activities such as public transport (commercial motor bikes), and petty businesses (hair beauty salons, barber shops, restaurants), and NTFPs harvesting.

http://www.aloki.hu ● ISSN 1589 1623 (Print) ● ISSN 1785 0037 (Online)
DOI: http://dx.doi.org/10.15666/aeer/1706_1504115054

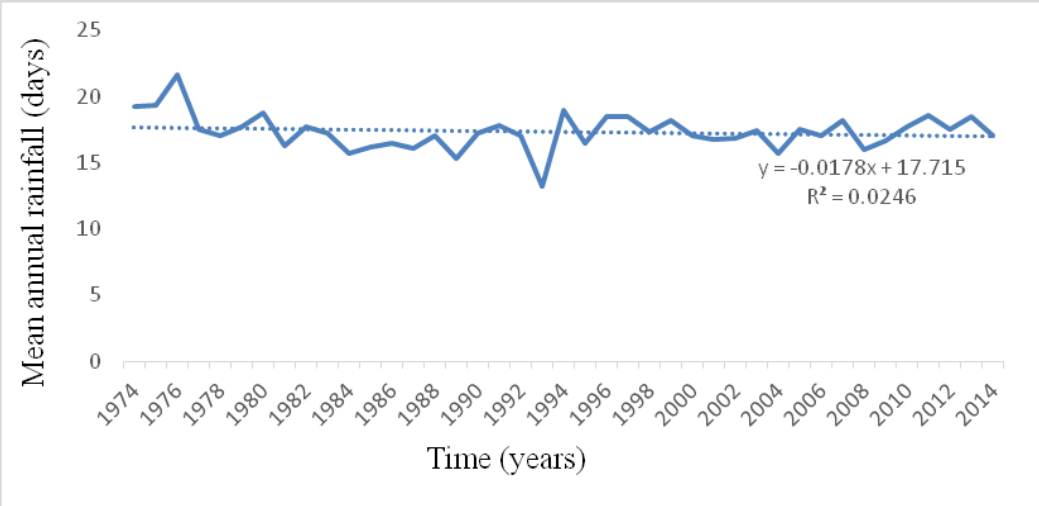

Figure 4. *Mean annual number of rainy days from 1974-2014*

Over 31.8%, 21.7% and 20.6% have adopted crop diversification, off-farm activities and NTFPs harvesting. Meanwhile, 9%, 5.9% and 3.4% had adopted increase in farm size, use of external inputs and changing planting dates as climate adaptation strategies (see *Table 4*).

Determinants of household adaptation strategies

Various determinants of climate adaptation strategies were identified using the logit regression model (*Table 5*). The logit regression model showed marital status (P-value 0.072) to influence a farmer's decision to adopt increase in farm size more than gender of household head (P-value 0.221) in the village at the 95% level of significance. Similarly, age of household head (P-value 0.086) influenced the decision to adopt changing planting dates more than gender (P-value 0.207). Additionally, marital status (P-value 0.128) was more important in the decision to adopt crop diversification than age of household head (P-value 0.187).

Discussion

Household characteristics of respondents

Male headed households were higher than the female headed households due to the tedious nature of farming activity that entails more energy and physical strength. Also, female headed household heads are usually involved in other livelihood activities such as petty businesses and NTFPs harvesting. Majority of the farmers were aged between 31-60 years representing the economically active and working age group. This group has the potential to increase crop productivity by willing to adopt measures aimed at mitigating climate impacts. According to Sofoluwe et al. (2011), individuals in the active working age group have been found to be more knowledgeable about better practices and may be more willing to bear risk and adapt to better farming techniques because of their longer planning horizons. Post primary education was quite low indicating that most youths immediately take up farming after completing primary school. Their choice of selecting climate adaptation practices is usually compromised

http://www.aloki.hu ● ISSN 1589 1623 (Print) ● ISSN 1785 0037 (Online)
DOI: http://dx.doi.org/10.15666/aeer/1706_1504115054

due to lack of access to climate information and knowledge. This is because education increases a farmer's ability and competence in efficient resources use. From another perspective, the allocative effect of education enhances a farmer's ability to obtain, analyze and interpret information (Sofoluwe et al., 2011).

Table 4. *Climate adaptation strategies*

Strategies	Frequency	Percentage
Increase in farm size	32	9.0
NTFP harvesting	73	20.6
Crop diversification	113	31.8
Changing planting dates	12	3.4
Off-farm activities	77	21.7
Use of external inputs	21	5.9
No adaptation	27	7.6

Table 5. *Logit regression of determinants of climate adaptation strategies*

Explanatory variable	NTFPs coef. p-value	Crop diversification coef. p-value	Changing planting dates coef. p-value	Off-farm activities coef. p-value	Use of external inputs coef. p-value	Increase in farm size coef. p-value	No adaptation coef. p-value
Gender	-0.193 0.477	-0.134 0.575	0.804 0.207	-0.060 0.819	-0.146 0.751	0.460 0.221	0.217 0.627
Age of household heads	0.006 0.641	-0.015 0.187	0.065 0.086***	0.004 0.712	-0.005 0.844	0.003 0.864	0.004 0.847
Inhabitants	0.258 0.422	0.007 0.981	-0.263 0.786	-0.119 0.727	0.307 0.588	0.105 0.804	-0.818 0.205
Education	-0.033 0.856	-0.062 0.695	0.353 0.386	0.084 0.648	-0.325 0.233	0.111 0.702	0.052 0.854
Marital status	-0.088 0.572	0.217 0.128	-0.402 0.333	0.001 0.994	-0.006 0.983	-0.324 0.072***	0.114 0.634
Constant	0.780 0.255	1.328 0.068	1.192 0.571	1.197 0.113	4.244 0.000	1.494 0.225	2.714 0.072

***, **, * indicate significant at 1%, 5% and 10% significant level, respectively

Perception of climate variability

Over time, farmers have observed climate changes usually based on recent climatic events which shape their perceptions and hence adaptive decisions. Perception is thus an essential precondition to undertake adaptation measures such as the existence of long-term changes in temperature, rainfall patterns, and number of rainy days.

Climate variability

Trends in temperature and rainfall between 1974 and 2014 have been changing over time. This is may be due to the inter-annual fluctuations of the intertropical convergence zone which causes a shift in the annual alteration of wet and dry seasons in tropical Africa. This intertropical convergence zone (ITCZ) is an area of low atmospheric pressure that forms where the Northeast Trade Winds meet the Southeast Trade Winds near the earth's equator. Climate variability across Africa is further influenced by the

http://www.aloki.hu ● ISSN 1589 1623 (Print) ● ISSN 1785 0037 (Online)
DOI: http://dx.doi.org/10.15666/aeer/1706_1504115054

forces and localizations of the African Easterly Jet (AEJ), the Tropical Easterly Jet (TEJ) and sea-surface temperature (SST), in the Gulf of Guinea (UNFCCC, 2007; Mukete et al., 2017; Sonwa et al., 2017)

Climate variability adaptation strategies

Majority of the farmers were aware of climate variability and had undertaken various adaptation options to cope with these negative climate effects. Major adaptation strategies included increase in farm size, use of external inputs, crop diversification, off-farm activities petty businesses and NTFPs harvesting. For instance, crop diversification provides the farmers with a wider choice of growing a variety of crops within a given area. Wondimagegn and Lemma (2016) also observed that this strategy expands production related activities on various crops, reduces the possible risk of climate variations and enables farmers to change crop types which are better suited to the prevailing climate regimes. Off- farm activities which compensated for the climate related low harvest are supplementary or complimentary activities that farmers engage in either offseason or on-season to support themselves. Studies by Ovwigho (2014) and Darota et al. (2017) also found such off-farm activities to include casual labour, transportation business, traditional dancing, palm wine taping, and petty trading. The switch to NTFPs harvesting and collection is frequent due to the mountainous nature of the area and which is surrounded by lowland and sub-montane forests. Mukete et al. (2018b) also observed that aside being a measure to reduce the negative effects of climate, farmers also depend on the NTFPs harvesting and collection to supplement household income, medicines and fodder for their animals.

Determinants of adaptation strategies

Perception of climate variability is directly proportional to the age of the farmers and older respondents are more efficient in perceiving climate variability than the younger respondents. Therefore, as a farmer aged, his or her ability to correctly describe climatic variations increases. A similar study by van der Veen (2013) observed the likelihood of taking up climate adoption measures to be higher among older farmers. She found the coefficient of marital status to positively correlate with the probability of a farmer selecting increase in farm size as an adaptation strategy. Thus, married farming households with large active household sizes would have more available labour force to extend farm sizes. Similarly, farming households could have access to credit schemes to increase their farm size and pay for hired labour. In Kenya, Korir and Ngenoh (2019) found married household heads to exert a significant and positive influence on the adoption of community-based climate adaptation strategies.

Conclusions

In climate change studies, it is necessary to incorporate local farmer perceptions and meteorological data particularly with respect to its influence on agriculture. As such, these perceptions can be used to examine the impact of climate on crop yield or production and various adaptation strategies employed by farmers after perceiving climate variations. As a result of climate variations, farmers have perceived fluctuations in temperature, rainfall and number of rainy days. These fluctuations have been in the form of decreased rainfall, number of rainy days with an increase in mean annual

http://www.aloki.hu ● ISSN 1589 1623 (Print) ● ISSN 1785 0037 (Online)
DOI: http://dx.doi.org/10.15666/aeer/1706_1504115054

temperatures. Just as observed in farmer perceptions, meteorological data also showed variations. Mean annual rainfall decreased by 1.7445 mm per year with 1983 having the highest mean annual rainfall. Also, mean annual temperature had increased by 0.015 °C per year with 2009 recording the highest mean annual temperatures while the number of rainy days decreased by about 0. 0178 days per year with 1993 having the lowest mean annual number of rainy days. This study also observed that farmers employed various adaptation measures to mitigate perceived aspects of climate change. These strategies included crop diversification, off-farm activities, NTFPs harvesting, increase in farm size, use of external inputs and changing of planting dates.

In addition, household head's characteristics such as marital status and age affected his or her decision to adopt a particular adaptation strategy. The study has also confirmed the importance of combining and including farmer perceptions with climate and meteorological data in climate studies especially in the context of agricultural resilience to climate change as described by many scientific literatures. It has further provided knowledge of the main adaptation strategies used by farmers in the highlands of southwest Cameroon to adapt to climate change. From these adaptation strategies, effective and appropriate policies can be designed and implemented to reduce the effects of climate variability or changes. Areas for further scientific investigation in the study area could include how creating awareness of climate change and variability can influence farmers' choice of adaptation measures.

Acknowledgements. This study was financed by the World Wildlife Fund and Russel Train Fellowship for Nature (WWF/EFN) Grant No. ST60.

Conflict of interests. The authors declare that there is no conflict of interests regarding this paper.

REFERENCES

[1] Balgah, R., Kimengsi, J., Wirbam, B., Antonia, F. (2016): Farmers' knowledge and perceptions to climate variability in North West Cameroon. – World Journal of Social Science Research 3(3): 261-273.

[2] Darota, N., Ngwe, S., Fomekong, L. (2017): Comparative perception and knowledge of smallholder farmers on climate change and variation: case of Kaka (A) and Bulu (B) tribes Eastern Meyomessala sub-Division of Cameroon. – Biodiversity 1(3): 00014. DOI: 10.15406/bij.2017.01.00014.

[3] Defang, T., Amungwa, F., Manu, I. (2017): Farmers' perception of climate change and adaptation options in Southwest Cameroon. – International Journal of Rural Development, Environment and Health Research 1(3): 102-115.

[4] Etongo, D., Glover, K. (2012): Participatory resource mapping for livelihood values derived from the forest in Ekondo-Titi Sub-region, Cameroon: a gender analysis. – International Journal of Forestry Research 2012: 1-10.

[5] Gadédjisso-Tossou, A. (2015): Understanding farmers' perceptions of and adaptations to climate change and variability: the case of the maritime, plateau and savannah region of Togo. – Agricultural Sciences 6: 1441-1454.

[6] Greene, W. (2018): Econometric Analysis. 8th Ed. – Pearson Education Limited, UK.

[7] IPCC (2012): Managing the Risks of Extreme Events and Disasters to Advance Climate Change Adaptation. A Special Report of Working Groups I and II of the Intergovernmental Panel on Climate Change. – Cambridge University Press, Cambridge, UK. https://www.ipcc.ch/site/assets/uploads/2018/03/SREX-Chap5_FINAL-1.pdf.

http://www.aloki.hu ● ISSN 1589 1623 (Print) ● ISSN 1785 0037 (Online)
DOI: http://dx.doi.org/10.15666/aeer/1706_1504115054

[8] Kimengsi, J., Muluh, N. (2013): A comparative assessment of the effect of climatic variations on the crops of the Cameroon Development Corporation (CDC): adaptation options. – Environment and Natural Resources Research 3(1) http://dx.doi.org/10.5539/enrr.v3n1p144.
[9] Kimengsi, J., Tosam, N. (2013): Climate variability and cocoa production in Meme Division of Cameroon: agricultural development policy options. – Greener Journal of Agricultural Sciences 3(8): 606-617.
[10] Korir, J., Ngenoh, E. (2019): Factors influencing the adaptation decisions to impacts of climate change among the Maasai pastoral community in Narok County, Kenya. – Agricultural Sciences 10: 689-705.
[11] Limantol, A., Keith, B., Azabre, B., Lennartz, B. (2016): Farmers' perception and adaptation practice to climate variability and change: a case study of the Vea catchment in Ghana. – Springer Plus 5: 1-38.
[12] Mongi, H., Majule, A., Lyimo, J. (2010): Vulnerability and adaptation of rain fed agriculture to climate change and variability in semi-arid Tanzania. – African Journal of Environmental Science and Technology 4(6): 371-381.
[13] Mukete, B., Sun, Y., Ayonghe, S., Ojong, L., Itoe, C., Tamungang, R. (2017): Adaptation of women to climate variability in the southern slopes of the Rumpi Hills of Cameroon. – Agriculture, Forestry and Fisheries 5: 272-279.
[14] Mukete, B., Sun, Y., Etongo, D., Sajjad, S., Ngoe, M., Tamungang (2018a): Cameroon must focus on SDGs in its economic development plans. – Environment: Science and Policy for Sustainable Development 60(2): 25-32.
[15] Mukete, B., Sun, Y., Etongo, D., Sajjad, S., Abdul, M. (2018b): Assessing the drivers of land use change in the Rumpi Hills Forest protected area, Cameroon. – Journal of Sustainable Forestry. https://doi.org/10.1080/10549811.2018.1449121.
[16] Mukete, B., Sun, Y., Etongo, D., Ekoungoulou, R., Folega, F., Sajjad, S., Ngoe, M., Ndiaye, G. (2018c): Household characteristics and forest resource dependence in the Rumpi Hills of Cameroon. – Applied Ecology and Environmental Research 16(3): 2755-2779.
[17] Ndiaye, G., Shaoyong, F., Mukete, B. (2018): Analysis of market liberalization and the groundnut sector in Senegal. – International Journal of Applied Agricultural Sciences 4(2): 43-51.
[18] Ofundem, T., Nkongho, R., Awono, A., Levang, P. (2017): Bush mango (Irvingia spp.): forest and on-farm resource availability and market chains in the southwest region of Cameroon. – Forests, Trees and Livelihoods 26(3): 170-182.
[19] Oluwatusin, F. (2014): The perception of and adaptation to climate change among cocoa farm households in Ondo State, Nigeria. – Academic Journal of Interdisciplinary Studies 3(1): 147-156.
[20] Ovwigho, B (2014): Factors influencing involvement in non-farm income generating activities among local farmers: the case of Ughelli South local government area of Delta State, Nigeria. – Journal of Sustainable Agriculture Research 3(1): 76-84.
[21] Seid, S (2016): Farmers' perception of and adaptation to climate change and variability: the case of Assosa District, Western Ethiopia. – Journal of Natural Sciences Research 6(17): 117-122.
[22] Sofoluwe, N., Tijani, A., Baruwa, O. (2011): Farmers' perception and adaptations to climate change in Osun State, Nigeria. – African Journal of Agricultural Research 6(20): 4789-4794.
[23] Sonwa, D., Dieye, A., El Mzouri, H., Majule, A., Mugabe, F., Omolo, N., Wouapi, H., Obando, J., Brooks, N. (2017): Drivers of climate risk in African agriculture. – Climate and Development 9(5): 383-398. http://dx.doi.org/10.1080/17565529.2016.1167659.
[24] Tabi, G., Su, Q., Mukete, N. (2017): The economic analysis of resource used efficiency for cocoa production in Cameroon. The case study of Lekie Division. – American Journal of Rural Development 5(5): 123-137.

http://www.aloki.hu ● ISSN 1589 1623 (Print) ● ISSN 1785 0037 (Online)
DOI: http://dx.doi.org/10.15666/aeer/1706_1504115054

[25] Tsegamariam, D (2018): Climate variability and determinants of its adaptation strategies; the case of coffee (Coffea arabica) producer farmers at Abeshege Woreda, Ethiopia. – Agricultural Research and Technology 17(3): 556028. DOI: 10.19080/ARTOAJ.2018.17.556028.
[26] UNFCCC (2007): United Nations framework convention on climate change. Climate change: impacts, vulnerabilities and adaptation in developing countries. – https://unfccc.int/resource/docs/publications/impacts.pdf (accessed: 4 July 2015).
[27] van der Veen, T (2013): Farm level adaptation to climate change: the case of farmer's in the Ethiopian Highlands. – Environmental Management 52: 29-44.
[28] Wondimagegn, T., Lemma, S. (2016): Climate change perception and choice of adaptation strategies. – International Journal of Climate Change Strategies and Management 8(2): 253-270.
[29] Zephania, N., Bonglam, C. (2016): Perception and adaptation adjustments to climate variability within the Santa Agrarian Basin in the western highlands of Cameroon. – Journal of Humanities and Social Science 21(12): 26-34.

http://www.aloki.hu ● ISSN 1589 1623 (Print) ● ISSN 1785 0037 (Online)
DOI: http://dx.doi.org/10.15666/aeer/1706_1504115054

THE POTENTIAL IMPLEMENTATION OF STORMWATER RETENTION PONDS INTO THE BLUE-GREEN INFRASTRUCTURE OF THE SUBURBAN LANDSCAPE OF PILSEN, CZECHIA

KOPP, J.* – PREIS, J.

Department of Geography, Faculty of Economics, University of West Bohemia
Univerzitní 22, 306 14 Pilsen, Czechia
(phone: +420-377-631-111; fax: +420-377-631-112)

**Corresponding author*
e-mail: kopp@kge.zcu.cz; phone: +420-377-633-065

(Received 25th Jun 2019; accepted 25th Oct 2019)

Abstract. This study investigates the requirements for creating blue-green infrastructure (BGI) as an instrument of stormwater management, in which nature-based solutions in urban and suburban landscapes are preferred. This case study of stormwater retention ponds (SWRPs) in the suburban landscape surrounding the city of Pilsen (Czechia) evaluates selected qualitative parametres of SRWPs on private land. Evaluated SWRPs have been classified according to the ownership relations and the potential indicators of their involvement within the BGI. Although the drain control as a primary purpose of SRWPs is a main criterion of their design, the ponds' parameters may differ from each other based on how their nature-based elements are used as well as what their amenity functions in a public space are. Based on the analyses of SRWPs' potential, the case study recommends public administration to provide some tools to support the private sector. The economic tools, motivating private sector, must be enhanced. An example of such an instrument could be the establishment of fees for stormwater drainage taking the ecosystem quality of the water management solutions into account.
Keywords: *ecosystem services, hydro-social system, nature-based solutions, private land, rainwater management, landscape planning*

Introduction

Water management in urban agglomerations has been transforming significantly and systematically in the 21st century: it is characterised by its decentralization (Schmidt, 2009; Rygaard et al., 2011; Elemer and Fraker, 2012; Wong, 2013; Yang et al., 2019). Cities all over the world endeavor to react to climate changes, especially to unbalanced rainfall regime and the increasingly frequent deepening occurrence of temperature extremes. These issues are mainly caused by the relatively high number of artificial and watertight surfaces in both urban and suburban landscapes. In spite of the fact that the hydrological cycle's changes are most obvious in urban landscape, it is necessary to remember a sustainable planning of suburban landscape too (Antrop and Entvelde, 2000). Such a landscape has specific ecological characteristics: It is characterized by a connectivity matrix and a high level of landscape heterogeneity. It means that large number of land covers is present (Antrop and Entvelde, 2000). The areas of the suburban landscape are used with different intensity – on the one hand, there are places strongly transformed by humans, such as industrial or commercial grounds (Spilková and Šefrna, 2010). On the other hand, there are nature-based surfaces, such as residual wetlands (Ehrenfeld, 2000). Historical development of catchment area situated next to urban

http://www.aloki.hu ● ISSN 1589 1623 (Print) ● ISSN 1785 0037 (Online)
DOI: http://dx.doi.org/10.15666/aeer/1706_1505515072

agglomeration generally enhances the proportion of watertight surfaces and thus changes the hydrological regime (Koronkevich and Mel'nik, 2015).

The functions of a suburban landscape, connected to land use categories could be divided into three groups: i) urban functions (residential housing, transport communication, commercial centres, industrial zones); ii) production functions (agricultural and forestry); iii) specific suburban functions (recreational water areas; parks; background of urban infrastructure, such as waterworks or sewerage; dump; mining areas). Changes of water drainage are influenced especially by a significant increase of built up areas as a direct consequence of residential and commercial suburbanization (Miller and Hess, 2017). That's why it is necessary to pay attention to developing blue-green infrastructure (BGI) in localities of suburban landscape. BGI via nature-close remedies should help to mitigate fast water drainage, increase evapotranspiration and replenish groundwater reserves.

The term "blue-green infrastructure" is used rarely in the Czech environment and when the term is used is mostly referring to foreign sources via inaccurate references. From the terminological point of view, there is a discussion about "green infrastructure" in the Czech Republic, which is based on the European Commission's inputs (EC, 2013; Kopp et al., 2017). Czech planning practice has had quite a solid experience with "ecological networking", in Czech terminology known as "Territorial systems of ecological stability" (ÚKRMP, 2016). Unlike foreign countries, where planning of functionally interlinked infrastructure is often considered in expert studies and plans (e.g. Wagner et al., 2013; Faltermaier et al., 2016; Bozovic et al., 2017), in the Czech Republic, there are only plans to broaden ecological networks from undeveloped landscape to the urban landscape. Thus, for our research purposes, we come from of the conceptions of blue-green infrastructure according to foreign studies (Voskamp and Van de Ven, 2015; van Timmeren et al., 2015; DELWP, 2017).

The authors of this paper understand blue-green infrastructure (BGI) primarily as an instrument for stormwater management, in which ecosystem approaches and water management measures are interlinked with green networks' system (Wagner et al., 2013; Voskamp and Van de Ven, 2015; DELWP, 2017). In this sense, the primarily urban concept of BGI (van Timmeren et al., 2015; Bacchin et al., 2016) builds on the more universal concept of green infrastructure, as it is defined by the European Commission (EC, 2013). Implementation of BGI is significant from the water management's perspective, which could be summarized into three main goals (Faltermaier et al., 2016; Bozovic et al., 2017; DELWP, 2017): (1) to retain rainwater and use it efficiently on places where it falls, (2) to reduce the accelerated runoff from surface into integrated sewerage system and via its overflows into watercourses, (3) to help water bodies, wetlands and verdure to evaporate and thus to decrease the effect of overheated urban and suburban areas.

The objective of the study

In the case study of the Pilsen suburban landscape, we deal with stormwater retention ponds (SRWPs) which have been implemented into individual areas as retention elements for rainwater. The water retained in them is not used in the next operational cycle. The objective of this case study is to assess selective qualitative parameters of selected SRWPs and to evaluate their potential to be engaged into the BGI of the suburban landscape. In a subsequent discussion of the results, we bring recommendations for regional and local administration, how to engage a private sector into a sustainable management of the

http://www.aloki.hu ● ISSN 1589 1623 (Print) ● ISSN 1785 0037 (Online)
DOI: http://dx.doi.org/10.15666/aeer/1706_1505515072

suburban landscape. To be more concrete, our goal is to propose instruments that can motivate the private sector to pay attention to SRWPs not only because of their retention function, but also to support their ecosystem services as well.

Review of literature

Hydro-social context of the BGI implementation

The implementation of BGI could be generally understood as a part of systematic changes in water management of the cities: i) a level of new technology's application (e.g. green roofs, water recycling); ii) a level of organization (e.g. building of decentralized water management zones; integration of the water issue in urban and landscape planning) and iii) a level of thinking (Bozovic et al., 2017). From the sustainable development point of view, the BGI benefits are not primarily related just to water management, but have also ecosystem and social aspects (van Timmeren et al., 2015). The BGI tools are targeted to four key issues (Woods Ballard et al., 2015):

1) Quantity of water: to decrease flood risk; to support and protect the hydrologic cycle;

2) Quality of water: to eliminate sources of pollution of water drainage;

3) Amenities: to create better and more sustainable environment for the life of humans;

4) Biodiversity: to create better and more sustainable environment for organisms.

For example, a British concept Blue-Green City is based on requests for flood protection and simultaneously for quality of life in cities with utilization of ecosystem measures. It pays attention to participatory planning process and evaluation of costs and benefits of blue-green infrastructure elements' implementation (Hoang and Fenner, 2015).

To search BGI tools properly, it is necessary to expand the view on the hydrological system. We have to look at it not only from physical and biochemical perspectives but add to them also a level of hydro-social system, in which human activities have a fundamental link to individual parts of water circulation in landscape (Swyngedouw, 2009; Linton and Budds, 2014). To improve BGI management, it is important to study relations between a regional administration and a private sector that could be both potential barriers and opportunities in water management. There are generally three categories of instruments which a regional administration can use to influence the implementation of new sustainable technologies in private sectors (Retzlaff, 2008; Carter and Fowler, 2008; Ferguson et al., 2013; Kabisch et al., 2016):

a) normative instruments (regulatory): e.g. adaptation strategies, urban and landscape plans, regulatory plans, building regulations, city ordinances, territorial protection, water directives, standards, norms,

b) economic instruments (financial): European/national/municipal subsidies, charging of rainwater discharge, tax allowance to properties with eco-labeling, grant schemes, bonuses in the form of favorable construction conditions,

c) ethical instruments (informational and motivational): programs focused on environmental education, awareness raising campaigns, professional training, environmental marketing of cities or developer projects, good practice examples, participatory planning, eco-labeling of companies, services and buildings.

Ethical instruments have also a significant potential. They can be linked with economic advantages if companies acquire eco-certificate for their operations. Regional administration can provide eco-labeling for companies, which carry out nature-based

http://www.aloki.hu ● ISSN 1589 1623 (Print) ● ISSN 1785 0037 (Online)
DOI: http://dx.doi.org/10.15666/aeer/1706_1505515072

solutions beyond compulsory water management measures and thus motivate private sector to enhance their own prestige. In the case of apartment construction, developers use eco-parametres of new residential zones as an instrument for their environmental marketing. Potential of hobby stores as possible epicentres of nature-based promotion of water management on a private land is not used. Despite the fact that they offer their clients artificial ponds for rainwater retention, semi-permeable tiles or a material to build green roofs or green facades, the buildings of these hobby stores unfortunately do not demonstrate any of those solutions.

A more sophisticated level of collaboration between a regional administration and a private sector are partnership projects. The foreign examples show that it is possible to mutually cultivate environmental quality of a territory, if a marketing and conditions for participation are set well. There are several projects that could be examples of joint venture, such as Oeko Business Wien, GreenMoabit Berlin (Pizarro, 2015).

The important instrument to support BGI implementation into practice is Public-Private-Partnership (PPP) (WEF, 2014; Harman et al., 2015; McAllister and Taylor, 2015; Margerum and Robinson, 2015; Koppenjan, 2015). PPP could be drawn up as build-operate-and-transfer (BOTs) arrangements, build-operate-own-transfer (BOOT), design-build-operate (DBO), joint-ventures or voluntary agreements (Hayllar, 2010; Harman et al., 2015). With regard to climate changes, BGI building belongs to PPP projects that are beneficial in terms of both adaptation and mitigation.

Stormwater retention ponds (SWRPs) as a part of BGI

Due to the fact that different instruments are recommended for different areas (e.g. industrial areas, shopping areas, or residential areas), it is necessary to adapt BGI planning in the suburban landscape with regard to land use (Faltermaier et al., 2016). It is appropriate to interconnect suitable elements of BGI with individual types of the landscape in relation to the systems of ecological stability of agricultural areas (Krauze and Wagner, 2019). Stormwater retention ponds (SWRPs) as a frequently used rainwater management instrument is applied in industrial, commercial and residential zones as well as in relation to drainage of roads. (Wong et al., 1998; Scher et al., 2004; USEPA, 2009; Faltermaier et al., 2016).

In spite of the fact that SWRPs are constructed as water management elements, we can sort them to BGI elements too (Hoang and Fenner, 2015). SWRPs, together with wetlands, are classified in methodological manuals about BGI implementation as surface retention elements that are able to clean water and are highly beneficial to the biodiversity of the landscape (Woods Ballard et al., 2015). SWRPs excel in high retention efficiency depending on the retention pond volume. At the same time, both SWRPs and wetlands have the highest initial costs (Hoang and Fenner, 2015). Due to the fact that the hydrological retention function of SWRPs is the top priority, it is also necessary to pay attention to their ecosystem and amenity potentials (Kurilenko and Osmolovskaya, 2007; Chiandet and Xenopoulos, 2011; Noble and Hassall, 2015; Hill et al., 2017).

It is important to deal with a question how to enhance the ecosystem and amenity benefits of SWRPs and how to implement them fully into the BGI of suburban landscape (Moore and Hunt, 2012). Their nature-based qualities determine whether they become a valuable part of the BGI or if they will remain just technical components of a grey infrastructure (Moore and Hunt, 2012; Hoang and Fenner, 2015). There are various types of urban ponds in BGI of urban and suburban landscape. SRWPs, which this paper deals with, are classified as Drainage systems ponds (Hassall, 2014). They differ primarily from

http://www.aloki.hu ● ISSN 1589 1623 (Print) ● ISSN 1785 0037 (Online)
DOI: http://dx.doi.org/10.15666/aeer/1706_1505515072

other categories, such as Garden ponds or Ornamental lakes and ponds by their retention function and possibly cleaning effect of contaminated water. Industrial ponds differ from them by an engagement into water management operation of the enterprise. Drainage system ponds can be classified as "detention" or "retention" ponds (Hill et al., 2017). With regard to a potential ecosystem benefit, retention ponds (SRWPs) are more important. A stable amount of retained water creates an aquatic environment and a design of a bench zone enables littoral vegetation to occur (USEPA, 2009).

Materials and methods

Study area and study sites

The Pilsen city's suburban landscape is currently an area with clearly obvious features of suburbanization, because of the population size of the Pilsen city (170.000 inhabitants in 2018) and its dominant position in the settlement system of the western part of the Czech Republic (Kopp et al., 2015). A significant share of a suburban landscape is located in the frame of the administrative region of the city. Out of 138 km^2, 27.2% is arable land, 7.2% is grassland and 20.6% is forest area (Kopp et al., 2017). The area of production and storage is also a significant feature of urban and suburban landscapes, with a share of 7.2% of the total extent of the administrative region and 17.2% of the built-up area in the urban and suburban landscape. An important category of land use is also shop and service area that makes 1.7% of the total extent of the region and 4.1% of the built up area (Kopp et al., 2017). New studies point out that those production and storage areas as well as shopping and service zones contribute significantly to making heat islands in the area of the Pilsen agglomeration. Building of those kinds of zones as a part of a commercial suburbanization process at the turn of the century brought extension to typically urban problems of hydrological balance in suburban landscape. Studies from other areas point to similar problems as well (Le Viol et al., 2009; Chiandet and Xenopoulos, 2011; Cizek and Hunt, 2013).

Average annual rainfall in 2006–2015 recorded at the Pilsen-Mikulka station was 514.8 mm. If a cadastral area of the city of Pilsen is 137.67 km^2, the total average annual amount of rainwater falling on the city is 74.6 mil. m^3 (Kopp et al., 2017).

According to the standardized values of the Czech Hydrometeorological Institute for the period 2005–2015 for the station Pilsen-Mikulka, a thirty minute rain with a periodicity of repetition n = 1 year causes a direct specific runoff of 115.6 litres per second per hectare (115.6 $l.s^{-1}.ha^{-2}$). A result of such an extreme rainfall event is overloading of the sewerage network and contaminated water overflowing via a drain directly into local watercourses. For example, two consecutive events 5th July 2018 (22 mm) and 6th July 2018 (10 mm) caused disposable pollution of the river. Due to an oxygen deficit, about 3–5 metric tonnes of fish died (Povodí Vltavy, 2018). That's why it is important to enhance a retention ability of both urban and suburban landscapes connected to sewerage.

The private sector in the city of Pilsen has been obliged, according to state law and city regulation, to deal with rainwater drainage from impervious surfaces (roofs, parking sites or roads) in the last decade. They have been responsible to limit drainage into the sewerage system below 4 $l.s^{-1}.ha^{-2}$. Subsurface or surface retention ponds (SWRPs) are allowed if is impossible for rainwater to infiltrate or to use it in another way inside the area of the enterprise (Vítek et al., 2015).

Dozens of SRWPs of different design have been built in the suburban landscape, most of them are located on private land. Our paper focuses on and evaluates five SRWPs in

http://www.aloki.hu ● ISSN 1589 1623 (Print) ● ISSN 1785 0037 (Online)
DOI: http://dx.doi.org/10.15666/aeer/1706_1505515072

detail (PP1–PP5, *Fig. 1, Table 1*), which are located on private land. Their parameters are compared with two other SWRPs (PM1–PM2, *Fig. 1, Table 1*), that were designed for the purpose of private construction, but were handed over to the city administration, whose lands they are located on. They were built to runoff rainwater from the zones of the developer construction projects and their property relations could be classified as "combined" (Freie und Hansestadt Hamburg, 2013). Due to the fact that we compare an ecosystem potential of ponds, we included also one retention pond that the city designed and built as a demonstration project to support BGI during reconstruction of a historic park (MM1, *Fig. 1, Table 1*).

Figure 1. *Different design of surface retention ponds in a case study*

http://www.aloki.hu ● ISSN 1589 1623 (Print) ● ISSN 1785 0037 (Online)
DOI: http://dx.doi.org/10.15666/aeer/1706_1505515072

Table 1. *Location and property relations of surface retention ponds in a case study*

Type by property relations of the retention pond's drainage area	Retention ponds (suburban unit) coordinates WGS84	Land use of the retention pond's drainage area	Type of investment	Property relations of the retention pond's land	Management of the retention pond
private (PP)	PP1 (Černice 1) 49°42'27"N, 13°25'50"E	light industry	private	private	private
	PP2 (Černice 2) 49°42'15"N, 13°25'56"E	light industry	private	private	private
	PP3 (Křimice 1) 49°45'03"N, 13°19'29"E	light industry	private	private	private
	PP4 (Křimice 2) 49°45'01"N, 13°19'37"E	light industry	private	private	private
	PP5 (Borská pole) 49°43'39"N, 13°21'09"E	shopping center	private	private	private
private/ municipal (PM)	PM1 (Černice 3) 49°41'52"N, 13°25'46"E	mixed	private	municipal	municipal
	PM2 (Nová Valcha) 49°42'34"N, 13°19'34"E	residential housing	private	municipal	municipal
municipal (MM)	MM1 (Lochotín) 49°45'37"N, 13°21'56"E	park	municipal	municipal	municipal

Methodology of evaluation of SRWPs'potential

Neither city nor state administrations have systematically recorded SRWPs, which are of interest to this case study. If it is possible to see construction documents (private subjects provide these documents for the research purposes only limited), it is possible to find out technical parameters of the ponds and their planned hydrological functions. When SRWPs are projected and built, the attention toward ecosystem and amenity functions is marginal. No monitoring of their hydrological regime, chemical and hydrobiological status is required, thus it does not exist at all. Some ponds are not accessible due to private property's protection or due to security reasons. The evaluation of SWRPs was primarily based on assessing their spatial parametres using orthophoto maps from different seasons between 2014–2017. We tried to find such pictures, where different levels of replenishment of the pond (and thus different aquatic zone areas) were captured (A_{std}, A_{min}). Another parameter is the detected area of the ponds including safety bench area (USEPA, 2009), which is usually an area of unflooded safety volume (A_{max}). All areas are calculated using orthogonal projection, which was obtained by ortophoto map analysis via geographical information system ArcGIS. The perimeter of a pond is related to a standard area in time, when a pond is normally filled. Out of those parametres, indexes have been calculated:

a) Area amplitude index:

$$I_a = \frac{A_{std}}{A_{min}} \quad \text{(Eq.1)}$$

b) Area unflooded benches index:

$$I_b = \frac{A_{max} - A_{std}}{A_{std}} \quad \text{(Eq.2)}$$

http://www.aloki.hu ● ISSN 1589 1623 (Print) ● ISSN 1785 0037 (Online)
DOI: http://dx.doi.org/10.15666/aeer/1706_1505515072

c) Shape index – ratio of the perimeter area (P_{std}) to the perimeter of a circle with the same area (A_{std}):

$$I_c = \frac{P_{std}}{2\sqrt{\pi} \times \sqrt{A_{std}}} \quad \text{(Eq.3)}$$

These indexes enable us to compare geometrical parameters of the ponds in regard to their ecosystem potential. The ponds with irregular shape with more segmented bench line (*Eq.3*) have a similar quality as natural ponds and have also a potential for higher biodiversity (NJDEP, 2006; Moore and Hunt, 2012). These ponds have also a higher potential of ecological stability in case lower fluctuation of the pond level and area amplitude (*Eq.1, Eq.2*). These features depend on bank's inclination and a set mode of inflow and outflow (Wong et al., 1998; NJDEP, 2006; Blicharska et al., 2016).

Next evaluation of SRWPs has been done according to six criteria that come from recommended features and qualities of ponds included into BGI (Wong et al., 1998; Blicharska et al., 2016). The potential of connection into the BGI network is characterised by a positional feature, which provides a possible link to close elements of green network and water bio-corridors. Ecosystem potential has been distinguished according to the existence and ecological quality of the bench vegetation. A microclimatic significance of ponds has been classified based on a contrast with surrounding areas located nearby, while taking into account the area size. Next two criteria – aesthetic quality and its implementation into a public space – express a social importance of SWRPs as elements of the BGI in a suburban landscape. It is important to distinguish whether a water body is or is not publicly accessible (Li et al., 2019). Even if it is located on a private property, it could be made publicly accessible, as it is obvious in agricultural landscape. The evaluation according to selected criteria has been made via field research and assessment of orthophoto pictures (*Fig. 2*) and documents for city planning. A score for each criterion was made in a scale from 0 to 3 (3 equals the best quality). Rating scales have been derived from particular studies and manuals focusing on the construction of retention ponds according to monitored criteria (Wong et al., 1998; NJDEP, 2006; USEPA, 2009; Moore and Hunt, 2012; Blicharska et al., 2016; Teurlincx et al., 2019) with a request to set the same scale for all parameters. The evaluation of SWRPs was made based on our own assessment in the field. Particular maps and the Master plans' documentation have been used to evaluate certain criteria (potential of connection into the BGI network; microclimatic significance) (ÚKRMP, 2016). Weight for each criterion was not considered, so it was decided that total score equals from 60% ecosystem quality and 40% social quality of SWRPs. Nevertheless, both quality aspects correlate together, for example with an assessment of bank quality or an aesthetic value.

Due to the fact that it was impossible to compare a hydrological regime of ponds using the above-mentioned methodological procedure, our own hydrological monitoring of the water levels in the ponds was used as a material for a follow-up discussion of SWRPs potential. The water level has been realized since mid-2017 on the tank PM2 located in the Nova Valcha site. A primary purpose of this pond is to a course of a runoff from new residential zone's rainwater sewerage. The secondary purpose according to a project documentation is to be a landscaping element in a transitional zone between new buildings and old buildings of the Valcha urban area.

http://www.aloki.hu ● ISSN 1589 1623 (Print) ● ISSN 1785 0037 (Online)
DOI: http://dx.doi.org/10.15666/aeer/1706_1505515072

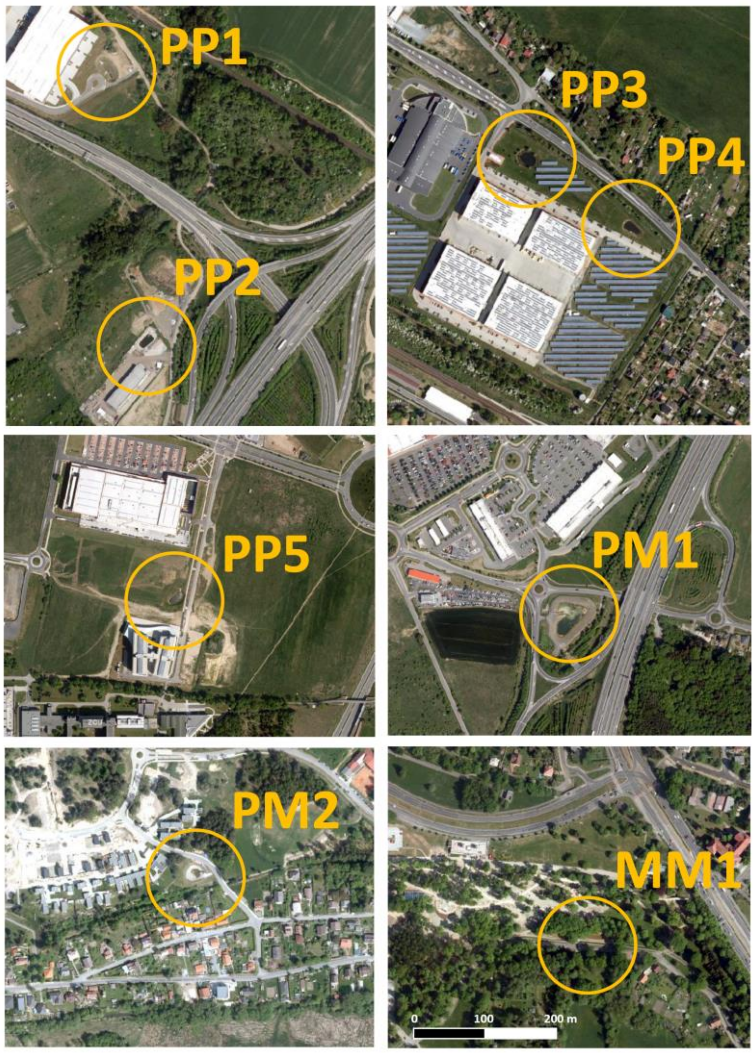

Figure 2. *Location of surface retention ponds in suburban landscape (orthophoto Czech Office for Surveying, Mapping and Cadastre)*

Results

A comparison of area parametres of SWRPs monitored in the suburban landscape proved their different preconditions to be implemented into BGI (*Table 2, Table 3*). Their cubic capacity differs depending on the drainage area. Thus, their sizes differ as well, which directly influences their microclimatic potential. The whole expanse of the tank directly influences the PM1 retention, which drain to a broader zone of a new construction area including impermeable surfaces of surrounding communications (*Table 2*).

A pipeline capacity bringing rainwater corresponds with area and volume of a pond. The pond PP1 has a significant area of unflooded bench slopes, which is in compliance with morphometry and a safety water level of a maximum volume. Consequently, the water level is thus cut deeply under a level of a terrain, which complicates a link of the pond's ecosystem with surrounding areas. From a broader point of view, it also decreases its impact on an aesthetic composition of the landscape. From an aesthetic point of view (*Table 3*), positively influencing aspects are considered not only a quality of vegetation on the benches (PP3) and a morphometry of the bench (MM1), but also adjustment of

http://www.aloki.hu ● ISSN 1589 1623 (Print) ● ISSN 1785 0037 (Online)
DOI: http://dx.doi.org/10.15666/aeer/1706_1505515072

them. These modifications, however, do not have an ecosystem function's potential (PP2). The essential aspects of ecosystem quality (*Table 3*) are predominantly a segmentation of the pond's shape (MM1) and a quality ecosystem of a bank with its woody plants (PP3). Littoral vegetation is scarce at SRWPs, due to a morphometry of ponds, that are primarily focused on a retention volume. In this way, a potential of SRWP is much lower in comparison with constructed wetlands.

Table 2. *Parametres of surface retention ponds*

Retention pond	A_{min} (m^2)	A_{std} (m^2)	A_{max} (m^2)	P_{std} (m)	I_a – Area amplitude index	I_b – Area unflooded banks index	I_c – Shape index
PP1	120	125	758	57	1.04	5.06	1.44
PP2	223	228	500	59	1.02	1.19	1.10
PP3	460	465	664	79	1.01	0.43	1.03
PP4	283	291	364	68	1.03	0.25	1.12
PP5	363	492	910	84	1.36	0.85	1.07
PM1	1677	1710	3145	187	1.02	0.84	1.28
PM2	145	363	658	69	2.50	0.81	1.02
MM1	255	290	529	169	1.14	0.82	2.80

Table 3. *Score of the retention ponds quality*

Retention pond	Potential of connection into the BGI network	Ecological quality of the bank's vegetation	Microclimatic significance (contrast and area)	Aesthetic quality	Accessibility and implementation into a public space	Total score of quality
PP1	1	1	1	2	1	6
PP2	0	0	2	3	0	5
PP3	2	3	2	3	0	10
PP4	1	2	1	2	0	6
PP5	1	1	2	0	1	5
PM1	1	2	3	1	0	7
PM2	1	0	2	1	2	6
MM1	3	2	1	3	3	12

Note: Score for each criterion in a scale from 0 to 3 (3 equals the best quality)

The implementation of SRWPs into BGI results in their position and various conditions of the surrounding suburban landscape (*Table 3*). We found out that SRWPs that we monitored differ in accessibility. From this point of view, not only ponds located on a private property have been inaccessible (PP2, PP3, PP4), but so have a pond in the city administration' ground (PM1). On the other hand, we discovered a few accessible ponds located on a private property (PP1, PP5). These cases prove there is a potential for social and ecological bindings in a landscape, if there is a will to support these bindings.

We discovered significant area fluctuations during standard filling and during a dry season when we compared a level area of ponds PM2 and partly also PP5. It is related with a morphometry of ponds, bank inclinations and also with a pond level amplitude. A significant fluctuation of water level occurred in the PM2 pond that we confirmed our own continuous monitoring, makes some stable pond ecosystem and potential vegetation on the banks difficult to create (*Fig. 3*). Causal precipitation has been measured at the closest meteorological station Pilsen-Mikulka, provided by the Czech meteorological

http://www.aloki.hu ● ISSN 1589 1623 (Print) ● ISSN 1785 0037 (Online)
DOI: http://dx.doi.org/10.15666/aeer/1706_1505515072

institution as a reference station for the territory of the city of Pilsen. Total rainfall for a small new built up area, drained into the pond PM2, have been monitored simultaneously according to other surrounding stations (Stod and University of West Bohemia). After the events have been evaluated, we found out that total rainfalls differed only very little (*Fig. 4*).

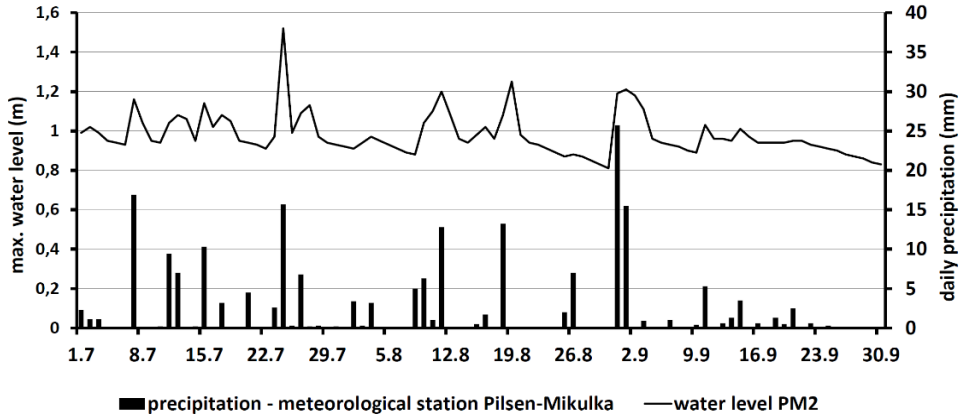

Figure 3. *Maximum daily water levels in the retention pond PM2 (Nova Valcha) and daily precipitation in the weather station Pilsen-Mikulka (July–September 2017). Data of water levels: own monitoring; data for precipitation: Czech Hydrometeorological Institute*

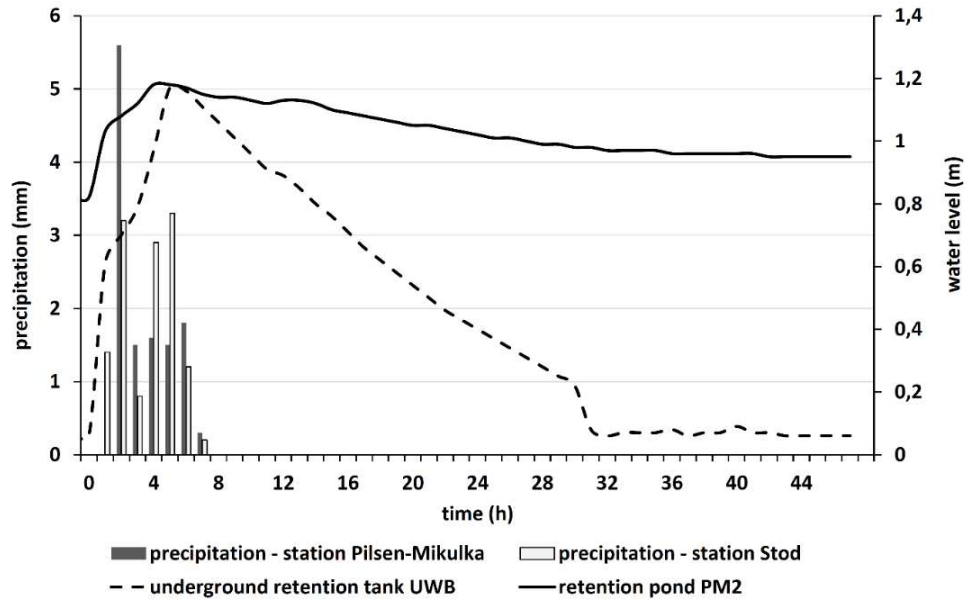

Figure 4. *Development of water levels in retention pond PM2 (Nova Valcha) in comparison with underground retention tank UWB with regulated drain in relation with precipitation event (since 22nd October 2017 at 0:00:00 till 24th October 2017 at 0:00:00)*

According to project documentation, an assumed depth of the PM2 pond during normal regime should be 1.4–0.9 m. However, the water level oscillated between 1.7–0.53 m during the monitoring period (*Table 4*). The lower aggregated average (0.92 m) reflects an especially significantly dry summer in 2018. Based on an analysis of a few

http://www.aloki.hu ● ISSN 1589 1623 (Print) ● ISSN 1785 0037 (Online)
DOI: http://dx.doi.org/10.15666/aeer/1706_1505515072

precipitation events, an outlet (a drainage coefficient of the area drained into sewerage) shares 40% out of total rainfall. This figure, however, has to be confirmed with a following monitoring in compliance with a development of neighbouring built-up areas. Our monitoring of water level in the pond PM2 confirmed a huge dispersion of the water level with a negative impact on environmental conditions. As vegetation on the benches does not occur and the pond warms up during low water level, it all creates favourable conditions for algae growth. Follow-up research will have to be focused on monitoring of hydrobiological conditions in SWRPs.

Table 4. *Total amplitude of the water level in the pond PM2 (Nova Valcha) between 1st July, 2017–31st December, 2018*

Minimal water level	0.53 m (23. 10. 2018)
Maximum water level	1.70 m (10. 06. 2018)
Average	0.92 m
Water level amplitude	1.17 m

We monitored the water level of the underground retention tank located in the campus of the University of West Bohemia (UWB), which collects water from the roof of one campus building, to compare changes of the water level of the pond PM2 (Nova Valcha). The underground retention tank has a total volume 34.5 m^3. Its controlled outflow is according to a request to drain water into common sewerage in a maximum value 4 $l.s^{-1}.ha^{-1}$. At the same time, the regulation is set on the allowed upper speed limit of emptying in order to quickly free up the storage space. These types of tanks are legislatively allowed solutions to drain precipitation water, where infiltration is not possible.

Our monitoring proved that the water level of both retention ponds differ in their reaction rate (*Fig. 4*). This documented event shows how both retention systems responded on total rainfall (13 mm), which was recorded during seven night hours on the 22nd September 2017 from surrounding meteorological stations Pilsen-Mikulka and Stod.

The underground retention tank UWB accumulating water from the roof of the building responds faster when filling or emptying. PM2 retention pond on the surface in the residential zone Nova Valcha empties gradually, which is in compliance with its technical function. Surface retention is desirable to limit too fast fluctuation of the water level due to the fact that ecosystem functions of the pond are supported. On the other hand, the underground retention tank has no ecosystem functions.

Discussion

Based on our SRWPs evaluation, it is possible to specify main adjustments for their successful implementation into the BGI system in suburban landscape. A potential of implementation of SRWPs into BGI is summarized in *Table 5*.

This potential is influenced not only by parameters of the ponds and their location in the landscape, but also by a functional typology of the territory according to a spatial plan (ÚKRMP, 2016). It is highly recommended that spatial planning endeavors to build up green network in areas focused on production and storage as well as in the areas where sales and services are cumulated (Berlin Konkret). Thus, we can achieve much better

http://www.aloki.hu ● ISSN 1589 1623 (Print) ● ISSN 1785 0037 (Online)
DOI: http://dx.doi.org/10.15666/aeer/1706_1505515072

connectivity of nature-based corridors in a suburban landscape, than it is done when only agriculture and forest lands are interlinked.

Norms and methods prefer surface infiltration over a continuous grassy humus layer. If a drain from hard surface enters into green surfaces with a good infiltration, not a huge retention space is necessary. The case study of the Pilsen-city suburban landscape shows, that wherever a surface has a limited ability to soak up water due to the hydrogeological reasons, private entities can fulfill the rainwater management's duty via SWRPs. *Table 5* shows that it is possible to implement SRWPs into BGI, if suitable design principles are applied (Lawrence and Breen, 1998; NJDEP, 2006; Kurilenko and Osmolovskaya, 2007; Blicharska et al., 2016) and relevant implementations into the BGI territorial systems are made, for example in relation to local water bio-corridors.

Table 5. *The potential of implementation of surface retention ponds to the BGI*

Retention pond	Functional type of the territory according to a spatial plan	Land cover of the surrounding area	Potential of implementation
PP1	industrial and storage areas	lawn and roads	to connect to the blue-green infrastructure network
PP2	industrial and storage areas	semi-permeable surfaces and extensive grass	to make a nature-based ecosystem of the pond banks
PP3	industrial and storage areas	lawn	to connect into the blue-green corridor and into a public space
PP4	industrial and storage areas	lawn	to connect into the blue-green corridor and into a public space
PP5	commercial areas	extensive grass	to make nature-based ecosystem of the pond banks and to connect into a public space
PM1	natural areas	roads and extensive grass	to connect into the blue-green corridor and into a public space
PM2	mixed residential areas – potentially built-up	lawn and roads	to connect into the blue-green corridor and into a public space
MM1	parks areas	forest park and roads	to make a nature-based ecosystem of the pond banks

There is so far limited knowledge related to ecologic functions of SRWPs, because there is neither systematic monitoring nor an effort to plan their hydrobiological qualities. Foreign experiences could not be automatically applied, unless a home comparative research is realized. Researches made abroad show that ponds could be influenced by inflowing water that contains a specific pollution depending on a characteristic of a drained surface (Stoianov et al., 2000; Scher et al., 2004). For example, a study in northern Poland showed that small ponds located in agricultural landscape have a higher load of nutrients, than those in urban landscape (Jarosiewicz et al., 2018). Urban ponds have been classified in terms of nutrients on the border of meso- and eutrophy (Jarosiewicz et al., 2018). On the other hand, retention ponds could become tools for a pollution decrease. According to British methodologies, ponds significantly decrease a load of dissolved substances or a concentration of non-ferrous metals in water (Woods Ballard et al., 2015). Macrovegetation of littoral zone plays an important role in detoxifying of water in urban ponds (Kurilenko and Osmolovskaya, 2007).

Besides quality of inflowing water, many different criteria have to be considered when a pond is designed (Lawrence and Breen, 1998; NJDEP, 2006; Blicharska et al., 2016).

http://www.aloki.hu ● ISSN 1589 1623 (Print) ● ISSN 1785 0037 (Online)
DOI: http://dx.doi.org/10.15666/aeer/1706_1505515072

Some criteria depends on handling with rainwater (e.g. appropriateness of hydrogeological environment), other ones deal with specifications of their design (e.g. local spatial and slope ratios or implementation into surrounding landscape) or with economic issues, such as operation and maintenance costs in future, ownership, building costs or aspects influencing the economy of water management of the pond itself. There are more specialized methodological publications dealing in detail with selection of measures (WEF, 2014; Woods Ballard et al., 2015; Faltermaier et al., 2016; Perini and Sabbion, 2017).

Ownership relations influence a potential of SRWPs implementation into BGI, especially in terms of legislation for urban and landscape planning as well as the owners' motivation to support nature-based solutions beyond a duty of rainwater retention. There is currently a low motivation in the private sector to voluntarily support BGI in the Czech Republic. It comes out of a lack of political power to pursue new approaches, underestimation and low public awareness about BGI, inappropriately set legislation and a limited scale of opportunities to take over foreign experience from the past (Stránský and Kabelková, 2015; Slach and Ježek, 2015). The situation, however, has been improving in recent years and new methodologies for practical application have been developed (Vítek et al., 2015). A political support for new approaches grows especially in context with a support of adaptation actions of settlements to climate change. Based on an analysis of potential and opportunities in this case study, it is highly recommended to enhance the private sector's motivation to implement SWRPs to BGI.

In the category of normative tools, it is necessary to make BGI one of the requested elements of a landscape. BGI is neither defined nor legislatively anchored in the Czech law yet. BGI could extend current ecological networks (Territorial system of ecological stability) in build-up landscape as a part of planning practice. Ecological networks as part of landscape and regulatory planning are applied predominantly in rural areas, which is not sufficient for suburban areas. The rainwater management obligation (e.g. defining a specific runoff from the land) of municipalities, which legislatively apply for new construction, should be extended by more detailed specification of how they support building of retention elements and nature-based measures. The law about urban planning enables investors to claim a subsidy for infrastructure in the territory. That could be a way to co-finance related BGI elements on public lands.

It is necessary to strengthen economic instruments motivating private sector to apply nature-based measures (Kabisch et al., 2016). Besides decreasing of fees for rainwater drainage, it is possible to take into consideration an ecosystem quality of the measure via e.g. tax land discounts or "green bonuses". The green construction bonuses make regulatory conditions of an investor more favorable, if the investor proves the ecosystem benefits of the measure that has been accomplished (Retzlaff, 2008; Carter and Fowler, 2008; Ferguson et al., 2013).

Conclusion

The evaluation results of SRWPs in the suburban landscape of Pilsen demonstrated their both positive and negative characteristics, which influence their potential for implementation into BGI. Primary water management functions planned during construction are the same – to control the drain from a residential area during intensive precipitation to temper extremely high discharge waves in rain or common sewerage, or during its drain into a recipient. Parameters of SRWPs are different, especially in terms

http://www.aloki.hu ● ISSN 1589 1623 (Print) ● ISSN 1785 0037 (Online)
DOI: http://dx.doi.org/10.15666/aeer/1706_1505515072

of how their nature-based elements are used or how their amenity functions in a public space are applied. The results based on a few private SRWPs show that their ecological and aesthetic quality could be comparable with those systems built by the city in the public interest and with taking into account their ecosystem functions. It is rarely used a rugged shape of the plan of the ponds when SRWPs are projected. Solidifying of benches with stones should be combined with bench vegetation that can be more beneficial for suburban landscape. The study shows that bench trees and shrub is possible to use around private ponds.

The continuous research should be focused on monitoring of the water quality in SWRPs depending on the season and how the ponds respond to extreme inflows. This is the way how the ponds could be better projected or handled with the pond level. Moreover, our knowledge about the level of fluctuations of SWRPs in compliance with their morphology is insufficient. Missing information about the SWRPs' ecology does not relate only to our case studies region, but to other Czech cities as well. The foreign experience is, however, limited to a few particular studies.

Initial results of the level monitoring of the pond PM2 showed that outflow settings from the pond can significantly influence fluctuations in flooding of its benches as well as other ecological parameters. Still, the surface SWRPs are much more suitable for general improvement of ecological conditions of the landscape than underground SWRPs. Surface SWRPs, besides their ecological, microclimate and aesthetic potentials, play an important role as a part of the BGI network, that can enhance eco hydrological conditions of the suburban landscape, if a proper spatial planning is made. Thus, a city administration must not only register them, but also actively influence their parameters during the construction process of ponds.

Current SWRPs belong objectively between grey- and blue-green infrastructures. This case study shows that it is possible to implement SWRPs located in a suburban landscape into BGI. Water-management practice of the private sector fulfills only obligatory demands for rainwater drain and they have no reason to take into consideration new requirements of society for BGI as a landscape instrument to adapting to climate change. Ecosystem quality of SRWPs differs a lot and is a result of the non-existence of planning and instruments, which could motivate the private sector to carry out nature-based solutions. It is crucial to focus not only normative, but also economic and ethical instruments and pursue a collaboration between private and municipal sectors.

Acknowledgment. This research has been supported by the Technology Agency of the Czech Republic Grant ÉTA TL01000498 "Revitalization of city centers and other public spaces in the Czech Republic: Problems, foreign inspiration, possible solutions".

REFERENCES

[1] Antrop, M., Eetvelde, V. V. (2000): Holistic aspects of suburban landscapes: visual image interpretation nad landscape metrics. – Landscape and Urban Planning 50: 43-58.

[2] Bacchin, T., Ashley, R., Blecken, G., Viklander, M., Gersonius, B. (2016): Green-blue Infrastructure for Sustainable Cities: Innovative Socio-technical Solutions Bringing Multifunctional value. – In: Novatech 2016, Lyon.

[3] Blicharska, M., Andersson, J., Bergsten, J., Bjelke, U., Hilding-Rydevik, T., Johansson, F. (2016): Effects of management intensity, function and vegetation on the biodiversity in urban ponds. – Urban Forestry & Urban Greening 20: 103-112.

http://www.aloki.hu ● ISSN 1589 1623 (Print) ● ISSN 1785 0037 (Online)
DOI: http://dx.doi.org/10.15666/aeer/1706_1505515072

[4] Bozovic, R., Maksimovic, C., Mijic, A., Smith, K. M., Suter, I., van Reeuwijk, M. (2017): Blue Green Solutions. A Systems Approach to Sustainable, Resilient and Cost-Efficient Urban Development. – Climate-KIC Limited, Imperial College London, London.
[5] Carter, T., Fowler, L. (2008): Establishing Green Roof Infrastructure Through Environmental Policy Instruments. – Environmental Management 42: 151-164.
[6] Chiandet, A. S., Xenopoulos, M. A. (2011): Landscape controls on seston stoichiometry in urban stormwater management ponds. – Freshwater Biology 56: 519-529.
[7] Cizek, A. R., Hunt, W. F. (2013): Defining predevelopment hydrology to mimic predevelopment water quality in stormwater control measures (SCMs). – Ecological Engineering 57: 40-45.
[8] DELWP (2017): Planning a Green-Blue City. A how-to guide for planning urban greening and enhanced stormwater management in Victoria. – Department of Environment, Land, Water and Planning, Melbourne.
[9] EC (2013): Green infrastructure (GI) — enhancing Europe's Natural Capital, COM(2013)249. – European Commission, Brussels.
[10] Ehrenfeld, J. G. (2000): Evaluating wetlands within an urban context. – Ecological Engineering 15: 253-265.
[11] Elemer, V., Fraker, H. (2012): Water, neighborhoods nad urban design: micro-utilites and the fifth infrastructure. – In: Howe, C., Mitchell, C. (eds.) Water Sensitive Cities. IWA Publishing, London.
[12] Faltermaier, M., Stock, H., Tonndorf, T. (2016): Stadtentwicklungsplan Klima KONKRET Klimaanpassung in der Wachsenden Stadt. – Senatsverwaltung für Stadtentwicklung und Umwelt, Berlin.
[13] Ferguson, B. C., Fratzeskaki, N., Brown, R. (2013): A strategic program for transitioning to a Water Sensitive City. – Landscape and Urban Planning 117: 32-45.
[14] Freie und Hansestadt Hamburg (2013): Mehr Stadt in der Stadt. Gemeinsam zu mehr Freiraumqualität in Hamburg. – Freie und Hansestadt Hamburg, Behörde für Stadtentwicklung und Umwelt, Hamburg.
[15] Harman, B. P., Taylor, B. M., Lane, M. B. (2015): Urban partnerships and climate adaptation: challenges and opportunities. – Current Opinion in Environmental Sustainability 12: 74-79.
[16] Hassall, Ch. (2014): The ecology and biodiversity of urban ponds. – WIREs Water 1: 187-206.
[17] Hayllar, M. R. (2010): Public-Private Partnerships in Hong Kong: Good Governance – The Essential Missing Ingredient? – The Australian Journal of Public Administration 69(S1): S99-S119.
[18] Hill, M. J., Biggs, J., Thornhill, I., Briers, R. A., Gledhill, D. G., White, J. C., Wood, P. J., Hassall, C. (2017): Urban ponds as an aquatic biodiversity resource in modified landscapes. – Glob Change Biol 23: 986-999.
[19] Hoang, L., Fenner, R. A. (2016): System interactions of stormwater management using sustainable urban drainage systems and green infrastructure. – Urban Water Journal 13(7): 739-758.
[20] Jarosiewicz, A., Radawiec, B., Hetmański, T. (2018): Effect of Catchment Land Use on Trophic State Variables of Small Water Bodies (Northern Poland). – Water Resources 45: 615-623.
[21] Kabisch, N., Frantzeskaki, N., Pauleit, S., Naumann, S., Davis, M., Artmann, M., Haase, D., Knapp, S., Korn, H., Stadler, J., Zaunberger, K., Bonn, A. (2016): Nature-based solutions to climate change mitigation and adaptation in urban areas: perspectives on indicators, knowledge gaps, barriers, and opportunities for action. – Ecology and Society 21(2): 39.
[22] Kopp, J., Frajer, J., Pavelková, R. (2015): Driving forces of the development of suburban landscape – a case study of the Sulkov location west of Pilsen. – Quaestiones Geographicae 34: 51-64.

http://www.aloki.hu ● ISSN 1589 1623 (Print) ● ISSN 1785 0037 (Online)
DOI: http://dx.doi.org/10.15666/aeer/1706_1505515072

[23] Kopp, J., Raška, P., Vysoudil, M., Ježek, J., Dolejš, M., Veith, T., Frajer, J., Novotná, M., Hašová, E. (2017): Ekohydrologický management mikrostruktur městské krajiny (Ecohydrological management of the urban landscape´s microstructures). – University of West Bohemia, Pilsen.
[24] Koppenjan, J. F. M. (2015): Public–Private Partnerships for green infrastructures. Tensions and challenges. – Current Opinion in Environmental Sustainability 12: 30-34.
[25] Koronkevich, N. I., Mel'nik, K. S. (2015): Runoff Transformation under the Effect of Landscape Changes in the Moskva R. Basin and in the Territory of Moscow City. – Water Resources 42: 159-168.
[26] Krauze, K., Wagner, I. (2019): From classical water-ecosystem theories to nature-based solutions — Contextualizing nature-based solutions for sustainable city. – Science of the Total Environment 655: 697-706.
[27] Kurilenko, V. V., Osmolovskaya, N. G. (2007): Bioindication Role of Higher Plants in the Diagnostics of Aquatic Ecosystems: Case Study of Small Water Bodies in St. Petersburg. – Water Resources 34: 718-724.
[28] Lawrence, I., Breen, P. (1998): Design Guidelines: Stormwater Pollution Control Ponds and Wetlands. – Cooperative Research Centre for Freshwater Ecology, Canberra.
[29] Le Viol, I., Mocq, J., Julliard, R., Kerbiriou, Ch. (2009): The contribution of motorway stormwater retention ponds to the biodiversity of aquatic macroinvertebrates. – Biological Conservation 142: 3163-3171.
[30] Li, Z., Xie, C., Lu, H., Che, S. (2019): The rational planning of public open space exploring the effects of environmental factors on human recreation – a case study in Shanghai, China. – Applied Ecology and Environmental Research 17(1): 1247-1260.
[31] Linton, J., Budds, J. (2014): The hydrosocial cycle: Defining and mobilizing a relational-dialectical approach to water. – Geoforum 57: 170-180.
[32] Margerum, R. D., Robinson, C. J. (2015): Collaborative partnerships and the challenges for sustainable water management. – Current Opinion in Environmental Sustainability 12: 53-58.
[33] McAllister, R. RJ., Taylor, B. M. (2015): Partnerships for sustainability governance: a synthesis of key themes. – Current Opinion in Environmental Sustainability 12: 86-90.
[34] Miller, J. D., Hess, T. (2017): Urbanisation impacts on storm runoff along a rural-urban gradient. – Journal of Hydrology 552: 474-489.
[35] Moore, T. L. C., Hunt, W. F. (2012): Ecosystem service provision by stormwater wetlands and ponds – a means for evaluation? – Water Research 46(20): 6811-6823.
[36] NJDEP (2006): New Jersey Stormwater Best Management Practices Manual. – Department of Environmental Protection, New Jersey.
[37] Noble, A., Hassall, Ch. (2015): Poor ecological quality of urban ponds in northern England: causes and consequences. – Urban Ecosystems 18(2): 649-662.
[38] Perini, K., Sabbion, P. (2017): Urban Sustainability and River Restoration. Green and Blue Infrastructure. – WILEY Blackwell, Chichester.
[39] Pizarro, R. E. (2015): Challenges of implementing sustainable urban design plans through community – university partnerships: lessons from Colombia, China, and Germany. – Current Opinion in Environmental Sustainability 17: 48-56.
[40] Povodí Vltavy (2018): Možnost eliminace vzniku kyslíkových deficitů v toku Berounky pod Plzní (Possibility of elimination of oxygen deficits in the Berounka river under the Pilsen). – Povodí Vltavy, State Enterprise, Pilsen.
[41] Retzlaff, R. C. (2008): Green Building Assessment Systems: A Framework and Comparison for Planners. – Journal of the American Planning Association 74(4): 505-519.
[42] Rygaard, M., Binning, P. J., Albrechtsen, H.-J. (2011): Increasing urban water self-sufficiency: New era, new challenges. – Journal of Environmental Management 92: 185-194.
[43] Scher, O., Chavaren, P., Despreaux, M., Thiéry, A. (2004): Highway stormwater detention ponds as biodiversity islands? – Arch.Sci. 57: 121-130.

http://www.aloki.hu ● ISSN 1589 1623 (Print) ● ISSN 1785 0037 (Online)
DOI: http://dx.doi.org/10.15666/aeer/1706_1505515072

[44] Schmidt, M. (2009): Rainwater Harvesting for Mitigating Local and Global Warming. – In: Cities and Climate Change: Responding to an Urgent Agenda. Fifth Urban Research Symposium, Marseille.
[45] Slach, O., Ježek, J. (2015): Czechia. – disP - The Planning Review 51(1): 28-29.
[46] Spilková, J., Šefrna, L. (2010): Uncoordinated new retail development and its impact on land use and soils: A pilot study on the urban fringe of Prague, Czech Republic. – Landscape and Urban Planning 94: 141-148.
[47] Stoianov, I., Chapra, S., Maksimovic, C. (2000): A framework linking urban park land use with pond water quality. – Urban Water 2(1): 47-62.
[48] Stránský, D., Kabelková, I. (2015): Review of the Implementation Process of Sustainable Stormwater Management in the Czech Republic. – In: Hlavínek, P., Zeleňáková, M. (eds.) Storm Water Management. Examples from Czech Republic, Slovakia and Poland. Cham. Springer, Heidelberg, New York, Dordrecht, London.
[49] Swyngedouw, E. (2009): The Political Economy and Political Ecology of the Hydro-Social Cycle. – Journal of Contemporary Water Research & Education 142: 56-60.
[50] Teurlincx, S., Kuiper, J. J., Hoevenaar, E. C., Lurling, M., Brederveld, R. J., Veraart, A. J., Janssen, A. B., Mooij, W. M., de Senerpont Domis, L. N. (2019): Towards restoring urban waters: understanding the main pressures. – Current Opinion in Environmental Sustainability 36: 49-58.
[51] ÚKRMP (2016): Územní plán Plzeň (Master Plan of the City of Pilsen). – The City of Pilsen Urban Planning Institute, Pilsen.
[52] USEPA (2009): Stormwater wet pond and wetland management guidebook. – United States Environmental Protection Agency, Center for Watershed Protection Protection Agency, Ellicott City.
[53] Van Timmeren, A., Kuzniecow Bacchin, T., Aires, C. (2015): Green Blue Infrastructures: Overview of Smart Spatial Strategies: implications for future innovation in design processes. – Delft University of Technology, Delft.
[54] Vítek, J., Stránský, D., Kabelková, I., Bareš, V., Vítek, R. (2015): Hospodaření s dešťovou vodou v ČR (Rainwater management in the Czech Republic). – ZO ČSOP Koniklec, Prague.
[55] Voskamp, I. M., Van de Ven, F. H. M. (2015): Planning support system for climate adaptation: composing effective sets of blue-green measures to reduce urban vulnerability to extreme weather events. – Build. Environ. 83: 159-167.
[56] Wagner, I., Krauze, K., Zalewski, M. (2013): Blue aspects of green infrastructure. – Sustainable Development Applications 4: 145-155.
[57] WEF (2014): Green infrastructure implementation. – Water Environment Federation, Alexandria.
[58] Wong, T. H. F. (2013): Blueprint 2013. Stormwater Management in a Water Sensitive City. – Cooperative Research Centre for Water Sensitive Cities, Clayton.
[59] Wong, T., Breen, P., Somes, N. L. G., Sara, D. L. (1998): Managing Urban Stormwater Using Constructed Wetlands. – Cooperative Research Centre for Catchment Hydrology, Clayton.
[60] Woods Ballard, B., Wilson, S., Udale-Clarke, H., Illman, S., Scott, T., Ashley, R., Kellagher, R. (2015): The SUDS manual (C753). – CIRIA, London.
[61] Yang, J.-Y., Zhang, B., Wu, Y.-F., Feng, Y.-R., Zheng, Y., Shi, B.-X. (2019): Balance between construction and conservation: strategy in water sensitive area planning. – Applied Ecology and Environmental Research 17(4): 7283-7299.

http://www.aloki.hu ● ISSN 1589 1623 (Print) ● ISSN 1785 0037 (Online)
DOI: http://dx.doi.org/10.15666/aeer/1706_1505515072

EFFECTS OF EXOGENOUS *RSRHA2B* GENE ON KEY ENZYME ACTIVITIES AND EXPRESSION OF RELATED GENES IN THE GRAIN FILLING STAGE OF WHEAT (*TRITICUM AESTIVUM* L.)

LI, D. B.[#] – LYU, G. Z.[#] – JIANG, Y. M. – NIU, H. B. – WANG, X. – YIN, J.[*]

National Engineering Research Center for Wheat, State Key Laboratory of Wheat and Maize Crop Science, Collaborative Innovation Center of Henan Grain Crop, Henan Agricultural University, Zhengzhou 450002, China

**Corresponding author*
e-mail: xmzxyj@126.com; phone: +86-371-6355-8203

[#]These authors contributed equally to this work.

(Received 26th Jun 2019; accepted 10th Sep 2019)

Abstract. The influence of pure transgenic wheat strain 1477 and Zhengmai 9023 were used to explore the effect of exogenous *RsRHA2b* gene introduction on the activity of key enzymes for starch synthesis and protein synthesis and the expression of related genes in transgenic wheat during filling period. The results showed that the introduction of exogenous *RsRHA2b* increased the activity of adenosine diphosphate glucose pyrophosphorylase (AGPP), granular starch synthase (GBSS), starch branching enzyme (SBE), soluble starch synthase (SSS) and glutamate synthase (GOGAT), and decreased the activity of glutamyl ammonia synthase (GS). Exogenous *RsRHA2b* promoted the expression of *YTH311, YTH611, YTH1065, YTH2437, YTH2438, YTH2456, YTH2496* and *YTH3049*, and inhibited the expression of *YTH2433*. These results indicated that the change in carbon and nitrogen metabolic key enzyme activity and the effect on related gene expression caused by the introduction of exogenous *RsRHA2b* gene may be the main cause of the increased resistance to ear germination of *RsRHA2b* transgenic wheat.

Keywords: *starch synthase, protein synthase, interacting proteins, gene expression, pre-harvest sprouting*

Introduction

Pre-harvest sprouting (PHS), a problem caused by environmental and genetic factors, affected wheat (*Triticum aestivum* L.*)* production in mature stage. About 85% of the wheat producing areas in China are susceptible to ear germination. After sprouting, the yield and quality of wheat will be reduced, and even food value and processing will be negativly affected, and the number of usable seeds will decrease. Grain traits, including grain maturity and size, seed coat color and thickness, can affect spike germination of wheat to varying degrees.

The main component of wheat grain yield is endosperm starch, followed by endosperm protein. The formation of wheat grain yield is essentially a process of starch and protein synthesis and accumulation in endosperm. Therefore, carbon metabolism and nitrogen metabolism are two main metabolic pathways in wheat grain development. Both of them are interrelated to each other to complete the material accumulation of grains, which determines the quality of grains.

There are many enzymes involved in starch synthesis. It is generally believed that sucrose synthase (SS), ADPG pyrophosphatase (AGPase), starch synthase (SSS and GBSS) and amylopectin branching enzyme (SBE) are key enzymes in the process of starch synthesis and metabolism, and play an important regulatory role in the synthesis

http://www.aloki.hu ● ISSN 1589 1623 (Print) ● ISSN 1785 0037 (Online)
DOI: http://dx.doi.org/10.15666/aeer/1706_1507315086

and accumulation of starch in wheat grains (Yang et al., 2004; Baroja-Fernández et al., 2003; Emes et al., 2003). ADPG-PPase and SSS were positively correlated with total starch and amylopectin accumulation rate (Zhao et al., 2004), while GBSS was positively correlated with amylose accumulation rate (Wang et al., 2003; Li et al., 2001). Protein quality of wheat grain is one of the important indexes for evaluating wheat quality (Wang et al., 2001; Pan and Yu, 2002). The main pathway of nitrogen assimilation in plants is directly involved in the synthesis and transformation of amino acids after nitrate reduction to ammonium. Nitrate reductase (NR), glutamine synthase (GS), glutamine synthase (GOGAT), asparagine transaminase (AspAT) and other key enzymes are involved in catalysis and regulation. This study focused on GS and GOGAT enzymes.

AtRHA2b gene of *Arabidopsis thaliana* encodes E3 ubiquitination ligase, which plays an important role in ABA signal transmission and stress. Cloning and characterization of a wheat RING finger gene *TaRHA2b* whose expression is up-regulated (Li et al., 2019). Overexpression of *AtRHA2b* leads to ABA-related phenotypes, such as seed germination and seedling sensitivity to ABA. The genetic distance between radish and *Arabidopsis* is very close, so *RsRHA2b* gene in radish was used for genetic improvement in wheat to avoid the phenomenon of cohomology inhibition in transgenic plants. The transgenic *RsRHA2b* wheat was successfully created by agrobacterium-mediated method at the early stage of seed germination. Compared with the Zhengmai 9023, the resistance of transgenic strains to PHS was significantly enhanced. The proteins interacting with RHA2b were selected by yeast two-hybrid assay. The information of candidate interacting proteins is shown in *Table 1,* including SBE, nitrite reductase, CBL, DDT domain protein, auxin effector factor 1, E3 UFM1 protein ligase 1 homologue, small G protein, AP2/EREBP protein and AGAP. The study of RHA2b interacting proteins is conducive to the study of the mechanism of the *RHA2b* gene.

Table 1. *Summary of related genes at the grain filling period (from NCBI database)*

Gene	Accession number (Barley)	Accession number (Wheat)	Function
YTH311	FN179383.1	BT008928.1	*SBE starch branching enzyme*
YTH611	AK363669.1	AK331993.1	*Nitrite reductase*
YTH1065	AK252590.1	AK332453.1	*CBL*
YTH2433	AK372028	HX078550.1	*DDT domain protein*
YTH2437	AK358361.18	CK206694.1	*Auxin effector factor 1*
YTH2438	AK364219.1	AK332649.1	*E3 UFM1 protein ligase 1 homologue*
YTH2456	AK251632.1	GU452718.1	*Small G protein*
YTH2496	HQ647352.1	FJ560496.1	*AP2/EREBP protein*
YTH3039	AK372413.1	AK331446.1	*AGAP gene*

In order to reveal the regulatory effect and mechanism of RsRHA2b gene on starch and protein formation in wheat grains, the key enzymes and gene expression of starch synthesis, key enzymes of protein synthesis and gene expression in transgenic and control wheat grains at grain filling stage were analyzed. The aim of this study was to provide a basis for further application of genetically modified wheat (GM) resistant to PHS in production.

http://www.aloki.hu ● ISSN 1589 1623 (Print) ● ISSN 1785 0037 (Online)
DOI: http://dx.doi.org/10.15666/aeer/1706_1507315086

Materials and methods

The elite Chinese bread wheat cultivar Zhengmai 9023, ahexaploid wheat cultivar with weak resistance to PHS, is widely cultivated in Henan Province. Exogenous *RsRHA2b* gene was introduced into wheat "zhengmai 9023" by agrobacterium-mediated method in the early germination stage. After six successive generations of planting, and combined with basta resistance screening, PCR, RT-PCR and southern-blot analysis, the transgenic strain 1477 with stable inheritance of exogenous *RsRHA2b* gene and strong resistance to ear germination was screened. Transgenic lines and non-transgenic control variety Zhengmai 9023 were planted in the Science and Education Demonstration Park of Henan Agricultural University during the growth season from 2013 to 2014.

Determination of enzyme activity in wheat starch synthesis

The single spike with the same flowering date and the same panicle size was selected. Starting from the 5th day after flowering, samples were taken every 5 d for a total of 6 times. Two grains labeled at the base of spikelet from 4th to 10th spikes were selected. every time take 200 grain, put into liquid nitrogen frozen 30 min, buy –80 °C refrigerator, used for determination of enzyme activity and gene expression. Key enzymes for starch synthesis include ADPG, SSS, GBSS and SBE. Cheng Fangmin's method of extracting crude enzymes from wheat grains was used as reference (Cheng et al., 2001). The activity changes of AGPP, SSS and GBSS were determined by Nakamura's method (Nakamura et al., 1989). The activity of SBE was determined by Li Taigui's method (Li et al., 1997). The steps of these methods are optimized as follows.

Determination of ADPG

Take 20 μL enzyme crude extract, 110 μL reaction solution was added (the final concentration of the reaction solution was 100 mM Hepes-NaOH (pH 7.4), 1.2 mM ADPG, 3 mM PPi, 5 mM MgCl2 and 4 mM DTT); 30 °C, reaction for 20 min, 30 s termination reaction in the boiling water; 10000 × g, 10 min, take 100 μL supernatant, add 5.2 μL supernatant to colorimetric solution (5.76 mM NADP, 0.08 unit P-glucomutase (phosphoglucose mutase), 0.07 unit G6p-dehydrogenase); 30 °C reaction for 10 min, determination $OD_{340\ nm}$ value; The activity of ADPG pyrophosphorylase was calculated based on the increase of $OD_{340\ nm}$ value, and the unit was nmol/1000seeds min.

Determination of SSS and GBSS

Weigh the wheat seeds in the mortar, add liquid nitrogen and grind to powder; transfer to the centrifugal tube, and add appropriate amount of extract, containing 100 mM Tris-HCl (pH 7.5),8 mM MgCl2, 2 mM EDTA, 12.5% (V/V) glycerin, 1% (W/V) PVP-40, 50 mM d-mercapto ethanol; 10000 × g, 4 °C centrifugal 30 min, then collect the clear liquid in an ice bath, as crude enzyme liquid for later use; the precipitate was washed twice with 1 mL extract and then suspended in 2 mL extraction medium for GBSS activity measurement; the 20 μL enzyme crude extract was added to 36 μL reaction solution I (the final concentration of the reaction solution was 50 mM Hepes-NaOH (pH 7.4), 1.6 mM ADPG, 0.7 mg amylopectin, 15 mM DTT); 30 °C, reaction for 20 min, 30 s termination reaction in the boiling water, cooled in the ice bath; add 20 μL reaction solution II, containing 50 mM HEPES-NaOH (pH 7.4), 4 mM PEP, 200 mM

http://www.aloki.hu ● ISSN 1589 1623 (Print) ● ISSN 1785 0037 (Online)
DOI: http://dx.doi.org/10.15666/aeer/1706_1507315086

KCl, 10 mM MgCl2, 1.2 unit pyruvate kinase; reaction after 20 min 30 °C, boiling water termination reaction in the 30 s; 10000 × g, 4 °C centrifugal 30 min, the supernatant (60 μL) and 43 μL reaction solution (III), 50 mM HEPES-NaOH (pH 7.4), 10 mM glucose, 20 mM $MgCl_2$, 2 mM NADP, 1.4 unit hexokinase, 0.35 unit G6p-dehydrogenase; 30 °C reaction after 10 min, measuring OD_{340nm} value changes, the unit is nmol 1000 seeds min. The crude enzyme solution boiled at 20 μL was used as the control.

Determination of SBE

The wheat seeds were placed in a mortar, add liquid nitrogen and grind to powder, transfer to centrifugal tube; add 0.05 M citric acid buffer (PH 7.0) (diluted with 0.2 M citric acid buffer by 4 times); 4 °C, 23203 × g under centrifugal 20 min, supernatant is the thick enzyme fluid; take 1 mL crude enzyme solution, add 0.2 M citric acid buffer 1 mL (pH 7.0), 0.1 M EDTA 0.5 mL, 0.75% soluble starch 0.5 mL, according to the same procedure to prepare another as the control; experimental group 40 min in 37 °C water bath heating, control placed on ice, add 4 mL 10% TCA termination reaction; the color was developed with 0.35 mL of iodinated solution (here calculated by adding 0.5 mL of iodinated solution to 10 mL of reaction solution), and the optical density value was measured at $OD_{660\ nm}$ after 10 min, with the non-water bath heating as the control. SBE enzyme activity was expressed as the percentage of decreased $OD_{660\ nm}$.

Determination of the activity of key enzymes for protein synthesis in wheat grains

Key enzymes for protein synthesis include glutamyl ammonia synthase (GS) and glutamate synthase (NADH-GOGAT). Determination of glutamine synthase GS activity by reference to Wang Yuefu's method (Wang et al., 2002). The determination of activity of NADH-GOGAT refers to Wang Xiaochun's method (Wang et al., 2005). The steps of these methods are optimized as follows.

Determination of GS

The wheat seeds were placed in a mortar, liquid nitrogen grinding to powder grinding; transferred to the centrifugal tube, add right amount extraction buffer, 15000 r/min under 4 °C centrifugal 20 min, supernatant fluid is the thick enzyme fluid; in 1.6 mL reaction mixture B, 0.7 mL crude enzyme solution and 0.7 mL ATP solution were added and mixed; 37 °C under thermal insulation 0.5 h, adding chromogenic agent (0.2 M TCA, 0.37 M FeCl3 and 0.6 M HCl mixture) 1 mL, shake and placed after a while; the supernatant was centrifuged at 5000 r/min for 15 min, and the absorbance value at $OD_{540\ nm}$ was determined. 1.6 mL reaction mixture A was added as the control.

Determination of NADH-GOGAT

The wheat seeds were placed in a mortar, ground with liquid nitrogen until the powder, transferred to a centrifuge tube, and an appropriate amount of extract (10 mM Tris-HCl buffer, pH 7.6, containing 1 mM MgCl2, 1 mM EDTA and β-mercaptoethanol l mM); 4 °C under 15000 × g centrifugal 30 min, on a clear night is the enzyme liquid; the total volume of the reaction mixture was 3 mL (containing 0.4 mL 20 mM L-glutamine, 0.05 mL 0.1 mM ketoglutaric acid, 0.1 mL 10 mM KCI, 0.2 mL 3 mM NADH and 0.5 mL enzyme solution, the insufficient volume was supplemented by

http://www.aloki.hu ● ISSN 1589 1623 (Print) ● ISSN 1785 0037 (Online)
DOI: http://dx.doi.org/10.15666/aeer/1706_1507315086

1.75 mL 25 mM pH7.6 Tris-HCl buffer; the reaction was initiated by L-glutamine and the extinction value was measured at $OD_{340\ nm}$. 1 min decreased extinction value was as an enzyme activity unit.

Quantitative real time RT-PCR (RT-qPCR)

15 to 20 seeds of uniform size were frozen and extracted from the seeds using Tiangen plus total plant RNA extraction kit. The total RNA was extracted, the quality of RNA was identified by agarose gel electrophoresis, and the RNA concentration and purity were determined at 260 nm/280 nm. Total RNA is used for the synthesis of the first strand of cDNA. The first strand of cDNA was synthesized by FastQuant RT Kit (With gDNase) and ReverTra Ace qPCR RT Master Mix With gDNA Remover (TIANGEN Biotech (Beijing) Co., Ltd., Beijing, China). The above cDNA was detected by wheat internal reference actin gene primers. Specific Primer 5.0 software was used to design the primers for the experiment (*Table 2*).

Table 2. *The primers for qPCR of related genes (with Primer 5.0 software)*

The name of the primer	The sequence of the primers (from 5'-3')
ACTINF1	CCAAGGCGGAGTACGATGAGTCT
ACTINR1	TTCATACAGCAGGCAAGCACCAT
RsRHA2bF1	TCCGCTCTTTCTTCCTCCG
RsRHA2bR1	CCTCCACGACCAACCAACG
YTH311F1	GCCTTAGACTCCGACGATGC
YTH311R1	CGGATGTTCGGTTGTGAAGTAG
YTH611F1	CGAGTGGAGCATGTGGATC
YTH611R1	CGAGAATAGAAATACGGAAGGT
YTH1065F1	CAAGGAACAAGGAGCAAAGAAG
YTH1065R1	CGAAGCCGAGTTGGTGGAT
YTH2433F1	GATCCGTGCTGCAACCG
YTH2433R1	GCCAGTGATTTCTCCTCCC
YTH2437F1	ATCGGTTAAGGTTGGTTGGG
YTH2437R1	TGACGGATACATAGGGAAGGTTG
YTH2438F1	CTGAGCACTACTGACCGCACTT
YTH2438R1	AAGCCACTTTCCTCTGCTGTATCTC
YTH2456F1	GCTTGATCTGCGGGATGACC
YTH2456R1	TGAGCTGCACTCGATGTAGGC
YTH2496F1	AGGATGCTGCCCGTGCTTAT
YTH2496R1	CAGGATGCACAGGGAAGTTGG
YTH3039F1	ACGACGATAGTGCTTGGGATG
YTH3039R1	CTGGACCTTACTTTCTACTGGCTTA

Statistical analysis

The GraphPad Prism 8 was used for statistical analysis and drawing. For comparing results of different treatments, Variance analysis is followed by a post-hoc test in order to determine pairwise differences. Differences were considered significant for $P < 0.05$.

http://www.aloki.hu ● ISSN 1589 1623 (Print) ● ISSN 1785 0037 (Online)
DOI: http://dx.doi.org/10.15666/aeer/1706_1507315086

Results

Effect of exogenous RsRHA2b gene on the activity of key enzymes in starch synthesis in the mature stage

ADPG-PPase is an enzyme that catalyzes the conversion of G-1-P into ADPG (adenosine diphosphate glucose), and ADPG is the direct precondition of starch synthesis. ADPG-PPase is a rate-limiting enzyme for starch synthesis, which plays an important role in regulating starch synthesis and accumulation in grains. The effect of exogenous *RsRHA2b* gene on the key enzyme ADPG of starch synthesis in mature wheat was shown in *Figure 1A,* after 10 d of wheat grouting, the activity of ADPG enzyme in transgenic lines was significantly higher than Zhengmai 9023; within 10-20 d after anthesis, the enzyme activity of ADPG in transgenic lines decreased sharply, but compared with Zhengmai 9023, the enzyme activity of transgenic lines was still higher (10 d, 0.3044/0.0049); from 20 to 30 d after flowering, the trend of transgenic lines and non-transgenic lines was basically the same; in particular, from 25 to 30 d after anthesis, both showed an upward trend, but their activity was very low.

The granule bound starch synthase (GBSS) is directly related with amylose synthesis enzyme. Endosperm lacking GBSS enzyme activity contains only amylopectin. As can be seen from *Figure 1B,* both the transgenic strain wheat and the control group showed only certain activity of GBSS 10 d after flowering. GBSS activity of transgenic lines gradually increased within the range of 10-25 d after anthesis, reached the highest level at 25 d after anthesis, and then gradually decreased. The GBSS activity of Zhengmai 9023 increased gradually from 10 to 20 d after anthesis, and reached the highest level at 20 d after anthesis. Within 10-25 d after anthesis, GBSS activity of transgenic lines was higher than that of Zhengmai 9023 (25 d, 0.05/0.004). At 30 d after anthesis, the GBSS activity of transgenic lines was lower than that of Zhengmai 9023. The GBSS activity of transgenic lines 30 days after anthesis and control group was very low. However, the GBSS activity of Zhengmai 9023 was slightly higher than that of the transgenic lines.

Soluble starch synthetase (SSS) exists in free state in endosperm cells of wheat seeds and mainly catalyzes the synthesis of amylopectin. The results (*Fig. 1C*) showed that the change trend of transgenic lines was basically consistent with that of the control group, and the SSS enzyme activity of transgenic lines was always higher than that of the control group. At 10 d after anthesis, SSS enzyme activity was the highest in transgenic strains, which was about 3 times of that in control group. Within 10-20 d after anthesis, SSS enzyme activity in transgenic lines and the control group decreased sharply (10 d, 0.03/0.009). At 20 d after anthesis, SSS enzyme activity in both transgenic lines and the control group was at the lowest level. In the range of 20-30 d, the SSS enzyme activity in the control group gradually increased, while the SSS enzyme activity in the transgenic lines first increased 20-25 d after anthesis (25 d, 0.02/0.008), and then decreased in the range of 25-30 d.

During the whole grouting process, the SBE enzyme activity of transgenic strains was always higher than that of the control group (*Fig. 1D*). The activity of SBE enzyme in transgenic lines showed a trend of "up-down-up". At 20 d after anthesis, the activity of SBE enzyme in transgenic lines reached the highest peak (20 d, 1.29/0.338), and then showed a "declining-rising" trend, but the range of declining-rising was small (30 d, 1.25/0.265). The SBE enzyme activity in the control group reached the highest peak at 25 d after anthesis (25 d, 1.212/0.748), and then showed a significant decline.

http://www.aloki.hu ● ISSN 1589 1623 (Print) ● ISSN 1785 0037 (Online)
DOI: http://dx.doi.org/10.15666/aeer/1706_1507315086

To sum up, the introduction of exogenous *RsRHA2b* gene in the mature stage can regulate the activities of key enzymes of starch synthesis, such as ADPG, SSS, GBSS and SBE.

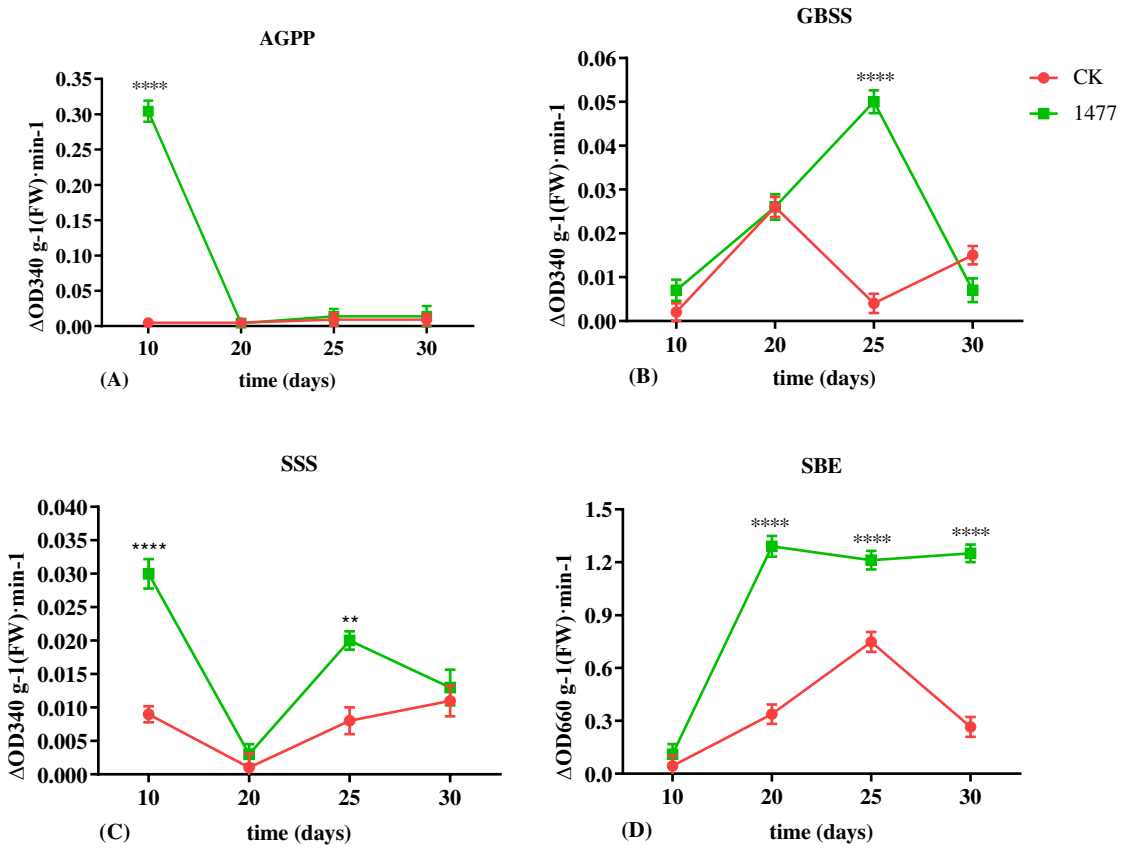

Figure 1. *Activity determination of key enzymes of starch synthesis during grain filling stage. CK, Zhengmai9023; 1477, transgenic wheat lines. (A) AGPP, ADPG-Ppase; (B) GBSS, granule-bound starch synthase; (C) SSS, Soluble starch synthase; (D) SBE: starch branching enzyme. Data are expressed as mean values ± standard errors from three replicates and error bars represent standard errors. The symbol '*' indicates statistically differences P < 0.05, the symbol '**' indicates statistically differences P < 0.01, the symbol '***' indicates statistically differences P < 0.001, the symbol '****' indicates statistically differences P < 0.0001 (two-way ANOVA, Sidak's multiple comparisons test)*

Effect of exogenous RsRHA2b gene introduction on the activity of key enzymes in protein synthesis in wheat maturity stage

The assimilation of ammonia in plants is mainly through GS/GOGAT pathway. GS is a multi-functional enzyme at the center of nitrogen metabolism, which is involved in a variety of nitrogen metabolism regulation. The improvement of GS activity can enhance the operation ability of nitrogen metabolism and promote the synthesis and transformation of amino acids.

The determination result of GS activity in wheat grain was shown in *Figure 2A*. The variation trend of GS content in transgenic lines and the control group was similar, both of which showed a gradually increasing trend with the progress of grouting. However, the activity of GS enzyme in transgenic lines was always lower

http://www.aloki.hu ● ISSN 1589 1623 (Print) ● ISSN 1785 0037 (Online)
DOI: http://dx.doi.org/10.15666/aeer/1706_1507315086

than that in the control group within the range of 10-30 d after flowering (30 d, 2.719/3.691).

The determination of GOGAT enzyme activity was shown in *Figure 2B*. The change trend of GOGAT enzyme activity in transgenic lines was similar to that in the control group, and showed a gradually declining trend throughout the grouting period. At 10-25 d after anthesis, the GOGAT enzyme activity of transgenic lines was significantly higher than that of the control group (10 d, 0.2717/0.1574; 20 d, 0.1887/0.0287), while at 30 d after anthesis, the enzyme activity value of both transgenic lines and the control group decreased to a very low level. To sum up, the introduction of exogenous *RsRHA2b* in the mature stage can regulate the activities of GS and NADH-GOGAT, the key enzymes for protein synthesis in wheat grains.

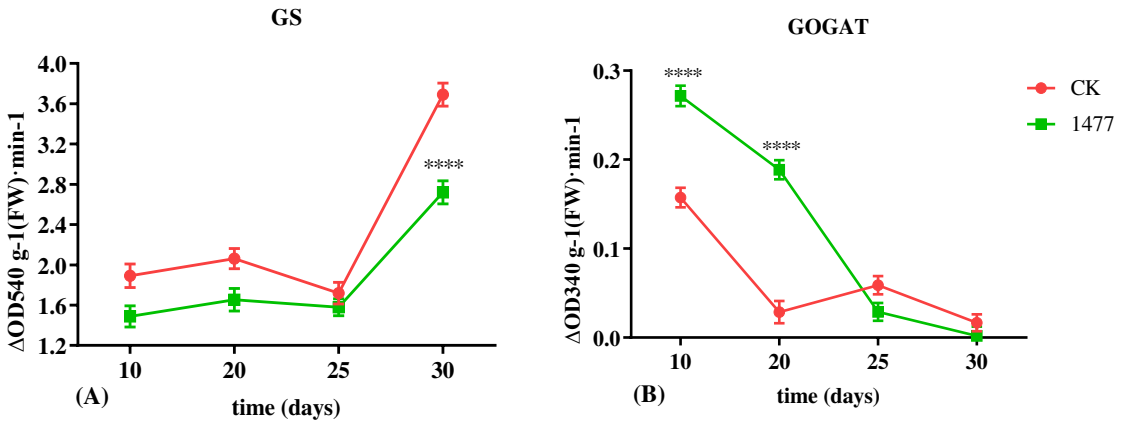

Figure 2. *Activity determination of key enzymes of protein synthesis during grain filling stage. CK, Zhengmai 9023; 1477, Transgenic wheat lines; (A) GS, Glutamine synthase; (B) GOGAT, Glutamate synthetase. Data are expressed as mean values ± standard errors from three replicates and error bars represent standard errors. The symbol '*' indicates statistically differences P < 0.05, the symbol '**' indicates statistically differences P < 0.01, the symbol '***' indicates statistically differences P < 0.001, the symbol '****' indicates statistically differences P < 0.0001 (two-way ANOVA, Sidak's multiple comparisons test)*

Effect of exogenous RsRHA2b gene introduction on the expression of related genes in the mature stage

In order to further study the regulatory mechanism of *RsRHA2b* gene in wheat grain starch synthesis and protein synthesis, the exogenous radish gene *RsRHA2b* was introduced into the transgenic lines for experiment in *Figure 3*. As can be seen from *Figure 3, RsRHA2b* was almost not expressed in the control group during the whole grain-filling period, since there was no *RsRHA2b* gene in the control group. In transgenic lines, the relative expression of *RsRHA2b* showed a trend of first increasing and then decreasing, and reached the maximum at 10 d after anthurium (10 d, 19.361/1), and then decreased, but was always significantly higher than that of the control group.

The proteins encoded by the 9 genes in this study interacted with RHA2b. The effect of exogenous *RHA2b* gene introduction on the expression of RHA2b interacting protein was studied by using transgenic lines.

http://www.aloki.hu ● ISSN 1589 1623 (Print) ● ISSN 1785 0037 (Online)
DOI: http://dx.doi.org/10.15666/aeer/1706_1507315086

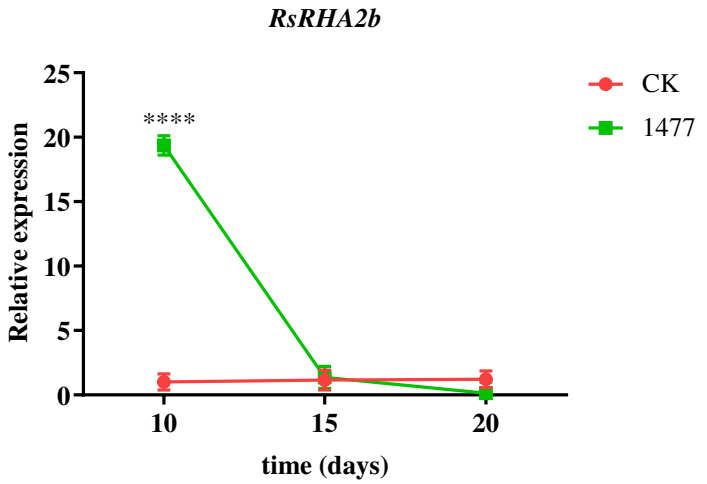

Figure 3. *Expression analysis of RsRHA2b gene during grain filling stage. CK, Zhengmai 9023; 1477, transgenic wheat lines. Data are expressed as mean values ± standard errors from three replicates and error bars represent standard errors. The symbol '*' indicates statistically differences P < 0.05, the symbol '**' indicates statistically differences P < 0.01, the symbol '***' indicates statistically differences P < 0.001, the symbol '****' indicates statistically differences P < 0.0001 (Two-way ANOVA, Sidak's multiple comparisons test)*

YTH311, YTH611 and YTH1065 genes

As can be seen from *Figure 4,* in the process of grain formation, the relative expressions of *YTH311*, *YTH611* and *YTH1065* in the transgenic lines and the control group all showed a trend of increasing first and then decreasing. The relative expression levels of these three genes in transgenic lines were always higher than those in the control group. From 10 to 15 d after anthesis, the relative expressions of these three genes in transgenic lines and the control group showed an increasing trend. At 15 d after anthesis, the relative expression levels of the three genes in the transgenic lines and the control group reached the highest. The highest relative expression of *YTH311* gene (*Fig. 4A*) in transgenic and control groups was 1.2/0.7 (15 d), the highest relative expression of *YTH611* gene (*Fig. 4B*) was 7.5/2.5 (15 d), and the highest relative expression of *YTH1065* gene (*Fig. 4C*) was 10/3 (15 d), respectively. The relative expression levels of the three genes in the transgenic lines decreased about 15-20 d after flowering. The results showed that the introduction of exogenous *RsRHA2b* in the mature stage affected the expression of *YTH311*, *YTH611* and YTH*1065*.

YTH2433 gene

As can be seen from *Figure 4D,* the relative expression of *YTH2433* gene in transgenic lines and the control group both decreased first and then increased during the whole grain filling period (10 d, 1.5/4.46). At 15 d after anthesis, there was no significance between the relative expression level of *YTH2433* gene in both control group and transgenic lines. At 20 d after anthesis, the relative expression level of *YTH2433* gene in the control group was lower than that in the transgenic lines (20 d, 1.07/3.35). The introduction of exogenous *RsRHA2b* in the mature stage affected the expression of *YTH2433*.

http://www.aloki.hu ● ISSN 1589 1623 (Print) ● ISSN 1785 0037 (Online)
DOI: http://dx.doi.org/10.15666/aeer/1706_1507315086

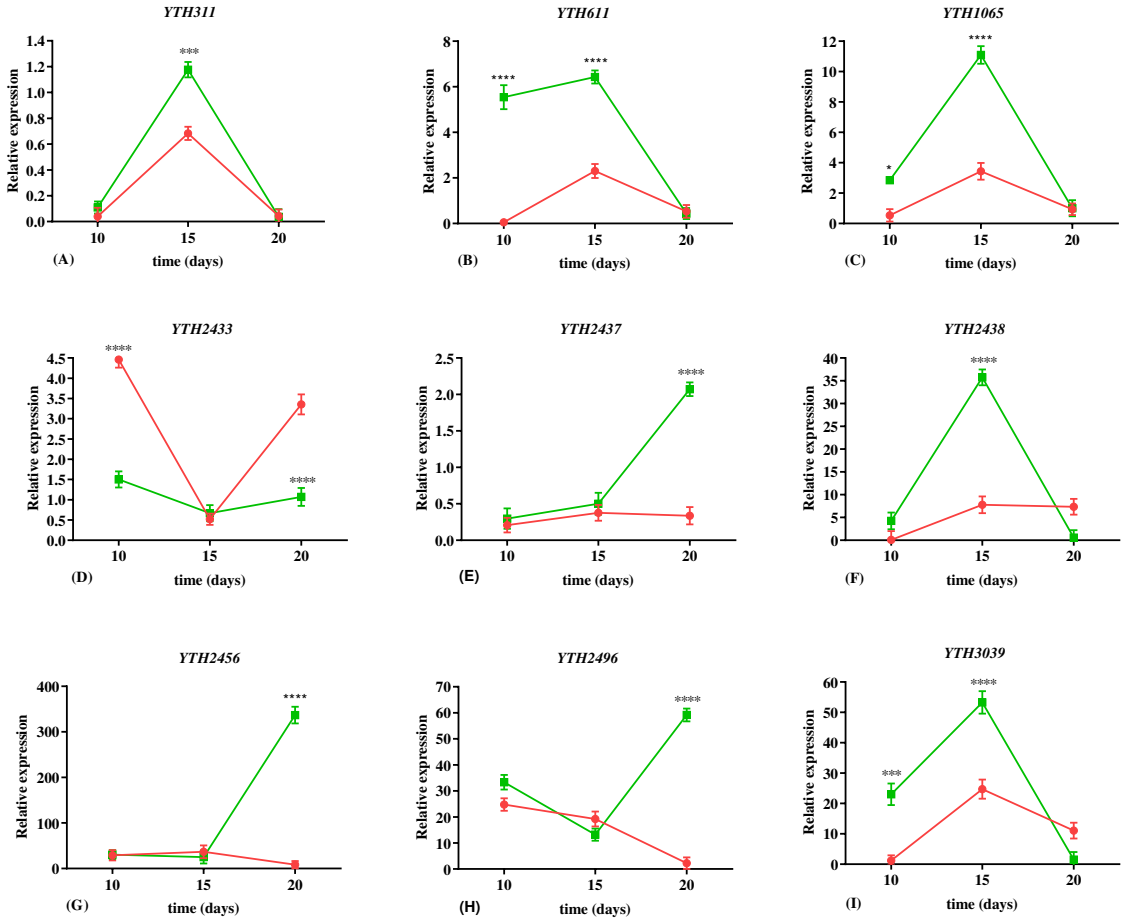

Figure 4. *Expression analysis of candidate genes during grain filling stage. CK, Zhengmai 9023; 1477, transgenic wheat lines. (A) YTH311; (B) YTH611; (C) YTH1065; (D) YTH2433; (E) YTH2437; (F) YTH2438; (G) YTH2456; (H) YTH2496, (I) YTH3039. Data are expressed as mean values ± standard errors from three replicates and error bars represent standard errors. The symbol '*' indicates statistically differences P < 0.05, the symbol '**' indicates statistically differences P < 0.01, the symbol '***' indicates statistically differences P < 0.001, the symbol '****' indicates statistically differences P < 0.0001 (two-way ANOVA, Sidak's multiple comparisons test)*

YTH2437 gene

The relative expression of *YTH2437* gene in transgenic lines and the control group showed an increasing trend during the whole grain filling period (*Fig. 4E*). The expression of *YTH2437* gene in transgenic lines was higher than that in control lines, and reached a significant level at 20 d after anthesis (25 d, 2.071/0.337). The introduction of exogenous *RsRHA2b* in the mature stage affected the expression of *YTH2437*.

YTH2456 and YTH2496 genes

The relative expression levels of *YTH2456* (*Fig. 4G*) and *YTH2496 (Fig. 4H)* in transgenic lines both decreased first and then increased in the process of grain formation, while the relative expression levels of these two genes in the control group

http://www.aloki.hu ● ISSN 1589 1623 (Print) ● ISSN 1785 0037 (Online)
DOI: http://dx.doi.org/10.15666/aeer/1706_1507315086

both showed a trend of continuous decrease. However, there was no significance between the relative expression of these two genes in the control group and the transgenic lines at 10 and 15 days after flowering. At 20 d after anthesis, the relative expression levels of these two genes in transgenic lines were higher than those in the control group (20 d, 336.695/8.619, *YTH2456*; 20 d, 59.171/2.217, *YTH2496*). The results showed that the introduction of exogenous *RsRHA2b* in the mature stage affected the expression of *YTH2456* and *YTH2496* genes.

YTH2438 and YTH3039 genes

The relative expressions of *YTH2438* (*Fig. 4F*) and *YTH3039* (*Fig. 4I*) in transgenic lines showed a trend of first rising and then falling in the process of grain formation. However, at 10 d and 15 d after anthesis, the relative expression levels of these two genes in transgenic lines were significantly higher than those in the control group (10 d, 23.022/1.245, *YTH3039*; 15 d, 37.742/7.799, *YTH2438*; 15 d, 53.284/24.743, *YTH3039*). However, there was no significance between the relative expressions of these two genes in the control group and the transgenic lines at 20 d after flowering. The introduction of exogenous *RsRHA2b* in the mature stage affected the expression of *YTH2438* and *YTH3039.*

Discussion

The regulatory network of a series of proteins interacting with RHA2b involves the processes of protein ubiquitination, cell protein metabolism, low temperature tolerance, and response to water loss, ABA, acidic compounds, oxygen-containing compounds and abiotic stress (Jiang et al., 2009; Kurkela and Franck, 1990; Li et al., 2011; Usadel et al., 2008; Nelson et al., 2010; Stone, 2014; Cho et al., 2011; Zheng et al., 2012; Robinson et al., 2010; Sajan et al., 2007; Haynes et al., 2002).

A series of RHA2b interacting proteins were selected by yeast two hybridization. In screening these proteins, the library is ABA treated, so the focus of the study will be on the ABA signaling pathway, or the signaling pathway indirectly mediated by ABA. Bioinformatics analysis showed that the protein encoded by *YTH311* gene may belong to SBE amylase, which is important for starch synthesis in the late endosperm development (Morell et al., 1995). The protein encoded by *YTH2456* gene may belong to RACD protein and participate in different signal transduction pathways through RAC/ROP (Schultheiss et al., 2003). The protein encoded by *YTH2496* gene may belong to AP2/EREBP protein, which is involved in development and abiotic stress (Jofuku et al., 1994; Ohmetakagi and Shinshi, 1995). The properties of these genes confirm the diversity of protein action.

Considering from the view that wheat with exogenous *RsRHA2b* gene can enhance the ability of ear germination, and the ability of ear germination is mainly affected by dormancy. Should be Does this focus on increased seed dormancy in transgenic wheat? How to enhance?

Dormancy of wheat seeds includes two types: embryo dormancy and seed (fruit) skin dormancy. The author speculated that seed coat dormancy caused by exogenous *RsRHA2b* gene can be easily reflected by seed size, maturity and internal restraining substance. If the dormancy is caused by the embryo, it will be affected by the expression of specific genes, as well as the metabolism and activity of specific nutrients. Because embryo dormancy can also be regulated by hormones. Decreased ABA content

http://www.aloki.hu ● ISSN 1589 1623 (Print) ● ISSN 1785 0037 (Online)
DOI: http://dx.doi.org/10.15666/aeer/1706_1507315086

promoted germination (King, 1976). Therefore, if the introduction of exogenous genes affects the metabolic pathway of specific hormones, it can also change the ability to resist ear germination.

A large number of studies have shown that the key enzymes in the starch anabolism process, such as AGPP, GBSS, SSS and SBE, play a key role in the synthesis and accumulation of wheat starch (Okita, 1992; Keeling et al., 1988; Nakamura et al., 1993). Protein content, protein components content and proportion not only affect the nutritional quality of wheat, but also have a great influence on the processing quality of wheat (Zhu and Khan, 2001). In addition to ensuring the integration and inheritance of exogenous genes, it is better not to change the biological environment and genetic background of recipient materials in the application of transgenic technology in the improvement of crop varieties. It was found that transgenic materials could not only improve the target traits, but also induce some non-target traits.

In the present study, it was found that the introduction of exogenous *RsRHA2b* could positively regulate the activities of the key enzyme for wheat starch synthesis AGPP, GBSS, SSS, SBE and the key enzyme of protein synthesis NADH-GOGAT in the process of grain filling, and only inhibited the activities of the key enzyme of protein synthesis GS. This indicated that the synthesis of wheat protein was greatly affected by the activity of GOGAT enzyme in the grain, but less by the activity of GS enzyme. This indicates that the complex formed by RHA2b and candidate protein may mediate some important regulatory pathways in the metabolism of carbon and nitrogen, change the metabolism of specific nutrients, and thus improve the resistance to ear germination of transgenic materials.

The results of this experiment showed that the introduction of exogenous RsRHA2b gene did affect the influence of related genes. The introduction of exogenous *RsRHA2b* promoted the expression of *YTH311, YTH611, YTH1065, YTH2437, YTH2438, YTH2456, YTH2496* and *YTH3049,* and inhibited the expression of *YTH2433*. This indicates that the complex formed by RHA and candidate protein may mediate some important regulatory networks of hormone response, play a role on specific pathway sites, and then affect the spike germination characteristics of transgenic materials.

Conclusion

The present research revealed that the introduction of exogenous *RsRHA2b* increased the activity of AGPP, GBSS, SSS, SBE and GOGAT, and decreased the activity of GS. Exogenous *RsRHA2b* promoted the expression of *YTH311, YTH611, YTH1065, YTH2437, YTH2438, YTH2456, YTH2496* and *YTH3049*, and inhibited the expression of *YTH2433*. More work is needed to explore the regulation of *RsRHA2b* gene on transgenic wheat grain quality and its mechanism as follows: (1) α-amylase activity, amylopectin activity and starch content of transgenic lines; (2) sulfhydryl content of stored proteins; (3) determination and analysis of quality related indicators, such as gelatinization properties of starch, flour farinograms and tensile parameters.

Acknowledgements. This work was supported by the "Twelfth Five-Year" National Science and Technology Projects in Rural Areas (2013BADD04B01-02) and Henan Science and Technology Project (162102110007).

Conflict of interests. The authors state no conflict of interests.

http://www.aloki.hu ● ISSN 1589 1623 (Print) ● ISSN 1785 0037 (Online)
DOI: http://dx.doi.org/10.15666/aeer/1706_1507315086

REFERENCES

[1] Baroja-Fernández, E., Muñoz, F. J., Saikusa, T., Rodríguez-López, M., Akazawa, T., Pozueta-Romero, J. (2003): Sucrose synthase catalyzes the de novo production of ADPglucose linked to starch biosynthesis in heterotrophic tissues of plants. – Plant and Cell Physiology 44: 500-509.

[2] Cheng, F., Jiang, D., Wu, P., Shi, C. (2001): The dynamic change of starch synthesis enzymes during the grain filling stage and effects of temperature upon it. – Acta Agronomica Sinica 27: 201-206.

[3] Cho, S. K., Ryu, M. Y., Seo, D. H., Kang, B. G., Kim, W. T. (2011): The arabidopsis RING E3 ubiquitin ligase AtAIRP2 plays combinatory roles with AtAIRP1 in abscisic acid-mediated drought stress responses. – Plant Physiology 157: 2240-2257.

[4] Emes, M. J., Bowsher, C. G., Hedley, C., Burrell, M. M., Scrase-Field, E. S. F., Tetlow, I. J. (2003): Starch synthesis and carbon partitioning in developing endosperm. – Journal of Experimental Botany 54: 569-575.

[5] Haynes, C. M., Caldwell, S. R., Cooper, A. A. (2002): An HRD/DER-independent ER quality control mechanism involves Rsp5p-dependent ubiquitination and ER-Golgi transport. – Journal of Cell Biology 158: 91-102.

[6] Jiang, H., Li, H., Bu, Q., Li, C. (2009): The RHA2a-interacting proteins ANAC019 and ANAC055 may play a dual role in regulating ABA response and jasmonate response. – Plant Signaling & Behavior 4: 464-466.

[7] Jofuku, K. D., Den Boer, B. G. W., Van Montagu, M., Okamuro, J. K. (1994): Control of Arabidopsis flower and seed development by the homeotic gene APETALA2. – The Plant Cell 6: 1211-1225.

[8] Keeling, P. L., Wood, J. R., Tyson, R. H., Bridges, I. G. (1988): Starch biosynthesis in developing wheat grain evidence against the direct involvement of triose phosphates in the metabolic pathway. – Plant Physiology 87: 311-319.

[9] King, R. (1976): Abscisic acid in developing wheat grains and its relationship to grain growth and maturation. – Planta 132: 43-51.

[10] Kurkela, S., Franck, M. (1990): Cloning and characterization of a cold-and ABA-inducible Arabidopsis gene. – Plant Molecular Biology 15: 137-144.

[11] Li, D., Lyu, G., Lyu, J., Niu, H., Wang, X., Jun, Y. (2019): Cloning and characterization of a wheat RING finger gene TaRHA2b whose expression is up-regulated by ABA treatment. – Applied Ecology and Environmental Research 17: 7495-7510.

[12] Li, H., Jiang, H., Bu, Q., Zhao, Q., Sun, J., Xie, Q., Li, C. (2011): The arabidopsis RING finger E3 ligase RHA2b acts additively with RHA2a in regulating abscisic acid signaling and drought response. – Plant Physiology 156: 550-563.

[13] Li, T., Shen, B., Chen, N., Luo, Y. (1997): Effect of Q-enzyme on the chalkiness formation of rice grain. – Acta Agronomica Sinica 23: 338-344.

[14] Li, Y., Yu, Z., Jiang, D., Yu, S. (2001): Studies on the dynamic changes of the synthesis of sucrose in the flag leaf and starch in the grain and related enzymes of high-yielding wheat. – Acta Agronomica Sinica 27: 658-664.

[15] Morell, M. K., Rahman, S., Abrahams, S., Appels, R. (1995): The biochemistry and molecular biology of starch synthesis in cereals. – Australian Journal of Plant Physiology 22: 647-660.

[16] Nakamura, T., Yamamori, M., Hirano, H., Hidaka, S. (1993): Decrease of waxy (Wx) protein in two common wheat cultivars with low amylose content. – Plant Breeding 111: 99-105.

[17] Nakamura, Y., Yuki, K., Park, S.-Y., Ohya, T. (1989): Carbohydrate metabolism in the developing endosperm of rice grains. – Plant and Cell Physiology 30: 833-839.

[18] Nelson, D. C., Flematti, G. R., Riseborough, J., Ghisalberti, E. L., Dixon, K. W., Smith, S. M. (2010): Karrikins enhance light responses during germination and seedling

http://www.aloki.hu ● ISSN 1589 1623 (Print) ● ISSN 1785 0037 (Online)
DOI: http://dx.doi.org/10.15666/aeer/1706_1507315086

development in Arabidopsis thaliana. – Proceedings of the National Academy of Sciences of the United States of America 107: 7095-7100.
[19] Ohmetakagi, M., Shinshi, H. (1995): Ethylene-inducible DNA binding proteins that interact with an ethylene-responsive element. – The Plant Cell 7: 173-182.
[20] Okita, T. W. (1992): Is there an alternative pathway for starch synthesis. – Plant Physiology 100: 560-564.
[21] Pan, Q., Yu, Z. (2002): Effects of nitrogen topdressing stage on grain quality and yield of winter wheat. – Journal of Triticeae Crops 22: 65-69.
[22] Robinson, T. J., Dinan, M. A., Dewhirst, M. W., Garciablanco, M. A., Pearson, J. L. (2010): SplicerAV: a tool for mining microarray expression data for changes in RNA processing. – BMC Bioinformatics 11: 108-108.
[23] Sajan, S. A., Warchol, M. E., Lovett, M. (2007): Toward a systems biology of mouse inner ear organogenesis: gene expression pathways, patterns and network analysis. – Genetics 177: 631-653.
[24] Schultheiss, H., Dechert, C., Kogel, K.-H., Hückelhoven, R. (2003): Functional analysis of barley RAC/ROP G-protein family members in susceptibility to the powdery mildew fungus. – The Plant Journal 36: 589-601.
[25] Stone, S. L. (2014): The role of ubiquitin and the 26S proteasome in plant abiotic stress signaling. – Frontiers in Plant Science 5: 135-135.
[26] Usadel, B., Blaesing, O. E., Gibon, Y., Retzlaff, K., Hoehne, M., Guenther, M., Stitt, M. (2008): Global transcript levels respond to small changes of the carbon status during progressive exhaustion of carbohydrates in arabidopsis rosettes. – Plant Physiology 146: 1834-1861.
[27] Wang, H., Ma, C., Xu, F., Andong, W. (2001): Effect of heat-treatment on endersperm protein components of wheat. – Journal of Triticeae Crops 21: 64-66.
[28] Wang, X., Xiong, S., Ma, X., Zhang, J., Wang, Z. (2005): Effects of different nitrogen forms on key enzyme activity involved in nitrogen metabolism and grain protein content in speciality wheat cultivars. – Acta Ecologica Sinica 25: 802-807.
[29] Wang, Y., Yu, Z., Li, S., Yu, S. (2002): Effect of nitrogen nutrition on the change of key enzyme activity during the nitrogen metabolism and kernel protein content in winter wheat. – Acta Agronomica Sinica 28: 743-748.
[30] Wang, Y., Yu, Z., Li, S., Yu, S. (2003): Activity of enzymes related to starch synthesis and their effect during the filling of winter wheat. – Acta Agronomica Sinica 29: 75-81.
[31] Yang, J., Zhang, J., Wang, Z., Xu, G., Zhu, Q. (2004): Activities of key enzymes in sucrose-to-starch conversion in wheat grains subjected to water deficit during grain filling. – Plant physiology 135: 1621-1629.
[32] Zhao, J., Yu, Z., Huimin;, S., Xinghua;, M., Qiang, S. (2004): Differences in starch components and related enzymes activity in the grains of different wheat cultivars. – Acta Agronomica Sinica 30: 525-530.
[33] Zheng, Y., Schumaker, K. S., Guo, Y. (2012): Sumoylation of transcription factor MYB30 by the small ubiquitin-like modifier E3 ligase SIZ1 mediates abscisic acid response in Arabidopsis thaliana. – Proceedings of the National Academy of Sciences of the United States of America 109: 12822-12827.
[34] Zhu, J., Khan, K. (2001): Effects of genotype and environment on glutenin polymers and breadmaking quality. – Cereal Chemistry 78: 125-130.

http://www.aloki.hu ● ISSN 1589 1623 (Print) ● ISSN 1785 0037 (Online)
DOI: http://dx.doi.org/10.15666/aeer/1706_1507315086

AGRARIAN AND WETLAND AREAS UNDER METROPOLITAN THREATS: LEARNING FROM THE CASE OF INCIRALTI, IZMIR (TURKEY)

KARA, B.

Department of Landscape Architecture, Faculty of Agriculture, Aydin Adnan Menderes University, 09970 Cakmar, Aydin, Turkey
(e-mail: bkara@adu.edu.tr; phone: +90-256-772-7022/1401; fax: +90-256-772-7233)

(Received 27th Jun 2019; accepted 25th Oct 2019)

Abstract. The aim of the study is to determine the Land use/land cover (LULC) changes and conversions in Inciralti İzmir (Turkey), and the fragmentation of these land uses between 1996 and 2018. Aerial photographs and Quickbird satellite imagery were used to obtain data. Aerial photographs were georectified using 1: 25,000 scaled topographic maps. The feature (vector) boundary of the study area was used to subset aerial photographs and Quickbird satellite image. LULC classes were defined according to Coordination of Information on the Environment (CORINE) LULC classes. The defined LULCs were digitized. Between 1996 and 2018, the highest conversion rate among agricultural areas occurred in permanently irrigated land with 41.43%, and the highest conversion among wetlands were in inland marshes with 65.19%. Between 1996 and 2018, the LULC with the highest increase in the number of patches was coastal lagoons with 300%. Research data shows that there has been a great change, conversion and fragmentation process in construction sites, wetlands and agricultural areas in Inciralti between 1996 and 2018. Change, conversion, and fragmentation of LULCs have damaged the natural and cultural structure of Inciralti. In order to stop this damage, filling of wetlands and the construction on agricultural areas in Inciralti should be prevented.
Keywords: *agricultural and wetland loss, Cakalburnu Lagoon, CORINE, LULC (land use/land cover) change, landscape fragmentation*

Introduction

Human activities all over the world have been the dominant factor shaping most of the agricultural landscapes (Goudie and Viles, 1997) and wetlands (Moulton and Jacob, 2000). The most important reasons for the loss of agricultural areas and wetlands are population growth (Turner II, 1989; Hobbs et al., 1991) and rapid and unplanned urbanization (Lopez et al., 2001).

Urbanization directly affects fertile agricultural areas by transforming them into residential, commercial areas (Sanders, 2006), and it affects wetlands by transforming them into agricultural (Zhang et al., 2010), industrial and recreational areas and through filling works (Maynard and Wilcox, 1997). This conversion is called as Land use/land cover (LULC) change. One of the most important effects of rapid urbanization is fragmentation, which has a profound impact on urban ecosystems (Fan and Myint, 2014).

Land monitoring enables better using of land. It provides valuable information about the environment (Balado et al., 2018). Analyzing the change characteristics of LULC, revealing the evolution of different time scales are helpful to reveal the process under the influence of human society (Li et al., 2019). There are many ways to monitor or detect LULC change over time (Fonji and Taff, 2014). One of them is LULC mapping. Mapping LULC of large cities is a main component of detecting rapid changes (Rujoiu-Mare and Mihai, 2016; Nuthammachot and Stratoulias, 2019).

http://www.aloki.hu ● ISSN 1589 1623 (Print) ● ISSN 1785 0037 (Online)
DOI: http://dx.doi.org/10.15666/aeer/1706_1508715102

Coordination of Information on the Environment (CORINE) is widely used in LULC mapping. CORINE is the longest available land cover and land cover change database with a consistent class labeling system (Cole et al., 2018). CORINE data sets are useful for describing long term structural changes of ecological complexes (Petrişor et al., 2014). CORINE database is a key for integrated environmental assessment (Dzieszko, 2014).

Urbanization, which has been encouraged by remarkable economic development, has progressed increasingly rapidly in Turkey in the last fifty years. In the industrialization and urbanization processes, it is clearly documented that large agricultural areas have been lost due to non-agricultural uses (Esbah, 2004). Metropolitan areas now cover an important part of Turkey's agriculture. Wetlands are among the most threatened ecosystems of Turkey.

Several studies using Remote Sensing (RS) and Geographical Information Systems (GIS) techniques in Turkey have been conducted to examine the intense pressure of the urbanization on agricultural lands and wetlands and to determine LULC changes.

In a study conducted in Antakya, the Amik plain, one of the most fertile plains of Turkey, was determined to be under the intense pressure of the expansion of urban and industrial areas (Kilic et al., 2005).

LULC changes in the coastal region of the Çandarlı Bay between 1990 and 2005 were examined in terms of the conversion of agricultural areas, olive groves and coastal wetlands into urban areas (Kesgin and Nurlu, 2009).

In the study on the LULC changes in the urban settlement of Kuşadası district between the years 1993 and 2006, it was determined that agricultural areas decreased and were converted into industrial, commercial and residential areas (Kara et al., 2013).

The study area is Inciralti located in the metropolitan area of Izmir, the third largest city of Turkey. The reason for choosing Inciralti as the study area is that it is home to two important ecosystems such as fertile agricultural land and wetlands at the same time in the center of the metropolitan area of Izmir.

The aim of a study is to monitor the changes/conversions and fragmentations in agricultural areas and wetlands in Inciralti in the period of 22 years between 1996 and 2018 by using aerial photographs, satellite image, RS and GIS techniques.

Materials and methods

Study area

Inciralti, which is the study area, is located on the west coast of Turkey, in the Aegean region, in the south of the Izmir bay, and in the metropolitan area of Izmir, the third largest city, within the boundaries of Balcova district (*Fig. 1*). Coordinates of Inciralti are 38°24'42.28"N 27°1'58.47"E and 38°23'55.76"N 27°3'46.64"E. Its surface area is 378.04 ha. Within the boundaries of the study area, there are the Balcova plain and Cakalburnu lagoon, which are among the most fertile agricultural areas and wetlands of the city (*Fig. 2*).

Inciralti is the only area that has been able to maintain its agricultural character despite the intensive urbanization in the metropolitan area of Izmir. In the Balcova plain, there is a very intensive production in greenhouses, open fields, flower, vegetable, citrus gardens and various orchards.

Cakalburnu lagoon, which is one of the most important natural areas of Izmir, is a wetland area integrated with the city, unlike other wetlands. Cakalburnu lagoon is one

http://www.aloki.hu ● ISSN 1589 1623 (Print) ● ISSN 1785 0037 (Online)
DOI: http://dx.doi.org/10.15666/aeer/1706_1508715102

of the important wetlands in Izmir with 103 bird species (Sevil, 2010). The world-wide endangered *Pelecanus crispus* (Dalmatian Pelican) and *Hoplopterus spinosus* (Spur-winged Lapwing) that breeds only in Greece also breed only in Cakalburnu lagoon in Turkey. Cakalburnu lagoon is one of the areas where *Tapes decussatus* (Grooved carpet Shell), a mussel species of economic value, is commercially collected in Turkey (Serdar et al., 2010). The predominant vegetation of Cakalburnu lagoon is composed of *Salicornia europaea* L. (Common glasswort).

In addition to its agricultural potential and ecological value, Inciralti is the only green area in Izmir as the "last coast with accessible recreational potential for all.

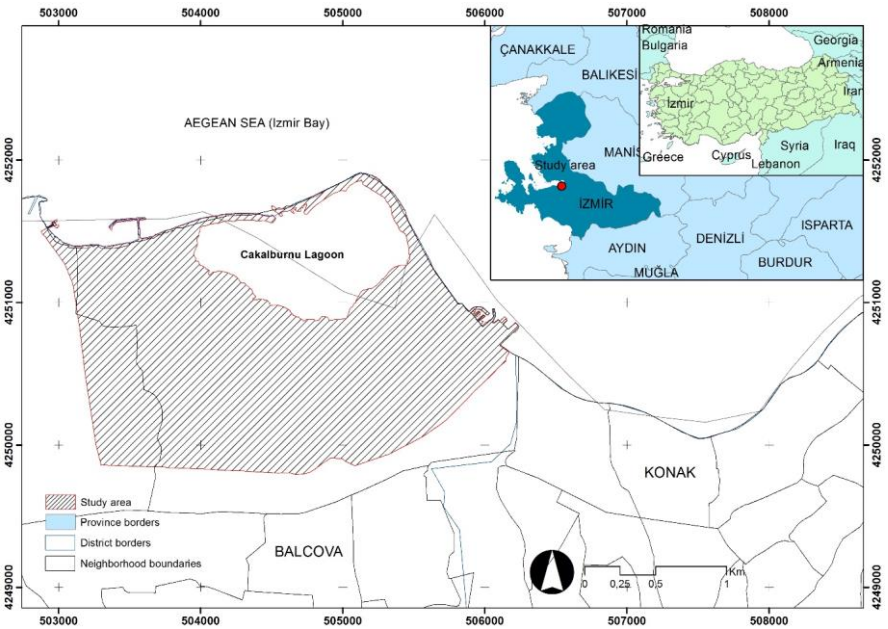

Figure 1. *Location of the study area*

Figure 2. *Inciralti with fertile agricultural areas and wetland lies on the north of Balcova urban area*

http://www.aloki.hu ● ISSN 1589 1623 (Print) ● ISSN 1785 0037 (Online)
DOI: http://dx.doi.org/10.15666/aeer/1706_1508715102

Data collection

The main material of the study consists of aerial photographs and satellite image. Aerial photographs and QuickBird satellite image were used to obtain LULC data for the previous years in the study area. The aerial photographs are monochrome monoscopic/stereoscopic with a 1/35.000 scale belonging to the year 1996. High-resolution QuicBird satellite image has a spatial resolution of 0.6-m dated June 25, 2018. ERDAS IMAGINE® 9.2 and Esri® ArcMap 9.3 software were used to process digital data. RS and GIS techniques were used to detect the LULC changes and conversions.

Image pre-processing

The geometric rectification of the aerial photographs was made according to the topographic map with a 1:25,000 scale. Satellite image and digitized aerial photographs were georectified in the Universal Transverse Mercator (UTM) (Zone 35) coordinate system using first-order polynomial transformation and subsetted according to the feature (vector) boundary of the study area.

Interpretation of aerial photographs and satellite image

Visual interpretation and on-screen digitizing method were used to detect the LULC changes and conversions between 1996 and 2018. Aerial photographs and satellite image were visually interpreted on the screen using direct (tone, texture, shape, and pattern) and indirect (location and relationship) identification elements.

Image classification

LULC changes and conversions were detected by using remotely sensed data. The bi-temporal change detection technique (Royer and Charbonneau, 1988) was used to determine LULC changes and conversions from 1996 to 2018. CORINE Land Cover nomenclature was used in change detection.

The cross-tabulation method was used to determine LULC changes. In this way, a change matrix was produced (Wang et al., 2006).

In the study area, 16 CORINE LULC classes were determined at Level 3 (*Table 1*).

Data processing

A comparison between 1996 and 2018 of the field data were generated. Then, the quantitative data of changes, increases, and losses in the LULC of each category were compiled. Thus, the expansion of urban sprawl on agricultural areas and wetlands was determined.

The digitization process not only provided an analysis of the changes in the total area of LULCs but also produced quantitative information on the rate of fragmentation of the parcels and changes in the average parcel size.

Results

Between 1996 and 2018, there were serious changes in LULC in Inciralti (*Figs. 3* and *4; Table 2*). In 1996, coastal lagoons, covering the 19.04% of the area, constituted the largest LULC of Inciralti. In 2018, coastal lagoons became the third largest LULC with a ratio of 13.32%.

http://www.aloki.hu ● ISSN 1589 1623 (Print) ● ISSN 1785 0037 (Online)
DOI: http://dx.doi.org/10.15666/aeer/1706_1508715102

Table 1. *CORINE LULC classes used in the study*

No.	CORINE classes	LULC	Description
1	112	Discontinuous urban fabric	Urban fabric
2	121	Industrial or commercial units	Industrial, commercial and transport units
3	122	Road and rail networks and associated land	
4	123	Port areas	
5	132	Dump sites	Mine, dump and construction sites
6	133	Construction sites	
7	141	Green urban areas	Artificial, non-agricultural vegetated areas
8	142	Sport and leisure facilities	
9	211	Non-irrigated arable land	Arable land
10	212	Permanently irrigated land	
11	222	Fruit trees and berry plantations	Permanent crops
12	323	Sclerophyllous vegetation	Scrub and/or herbaceous vegetation associations
13	333	Sparsely vegetated areas	Open spaces with little or no vegetation
14	411	Inland marshes	Inland wetlands
15	511	Water courses	Inland waters
16	521	Coastal lagoons	Marine waters

CORINE = coordination of information on the environment, LULC = land use and land cove

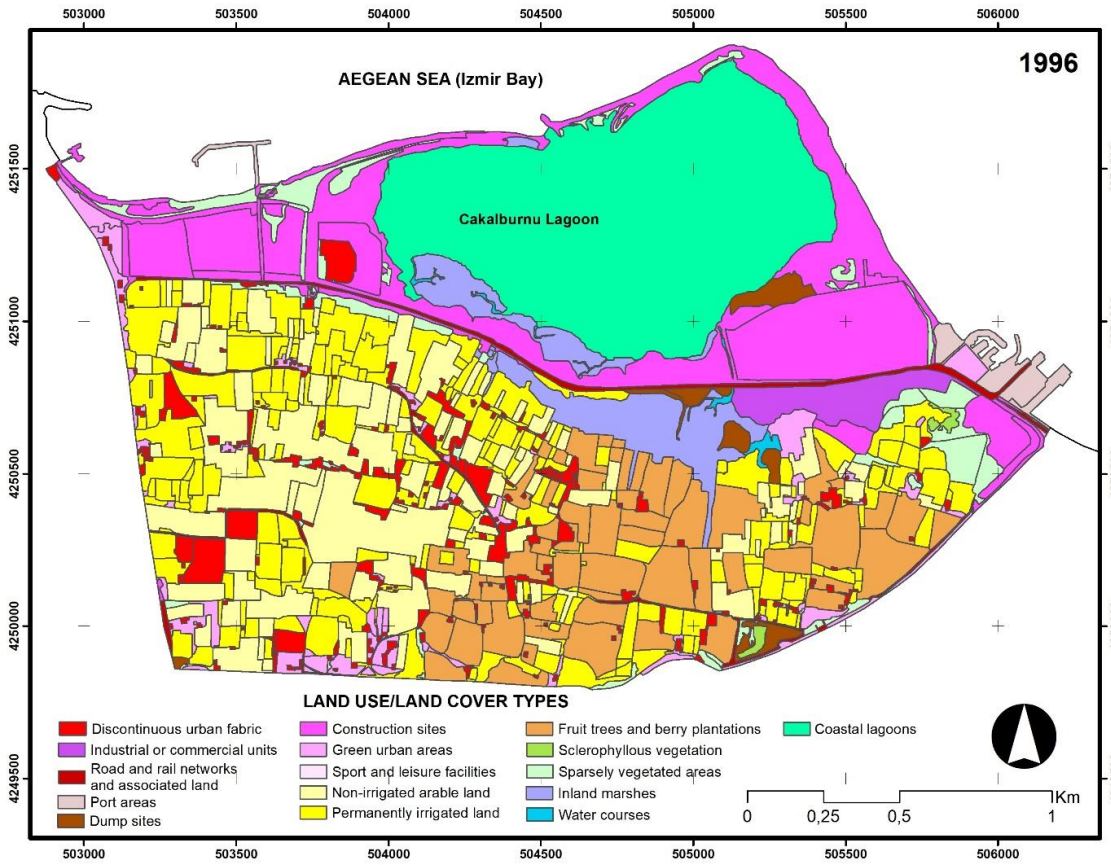

Figure 3. *LULC sizes in 1996*

http://www.aloki.hu ● ISSN 1589 1623 (Print) ● ISSN 1785 0037 (Online)
DOI: http://dx.doi.org/10.15666/aeer/1706_1508715102

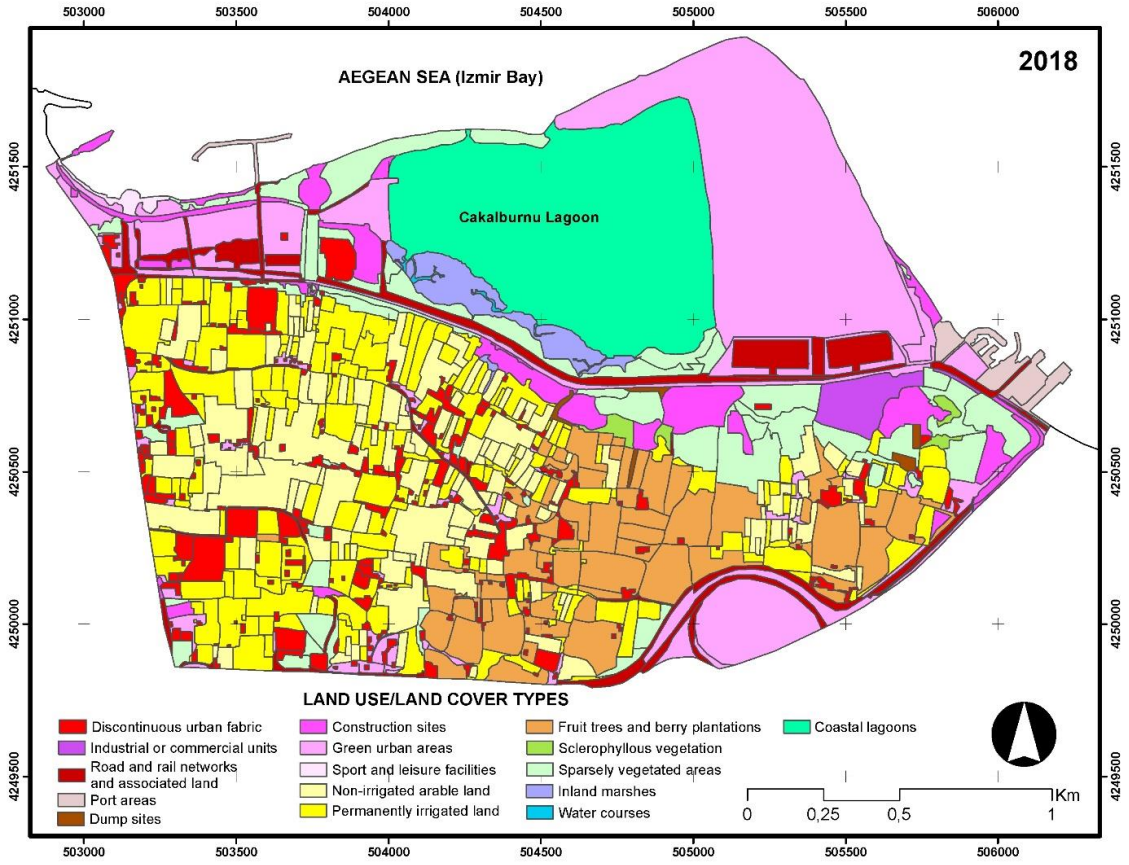

Figure 4. *LULC sizes in 2018*

Table 2. *LULC Changes in Inciralti between 1996 and 2018*

No.	Area					
	1996		2018		Image difference	
	ha	%	ha	%	ha	%
1	19.30	4.13	25.78	5.52	6.47	25.11
2	7.39	1.58	4.55	0.97	-2.83	-62.25
3	6.29	1.35	21.38	4.57	15.09	70.58
4	5.23	1.12	5.23	1.12	0.00	0.00
5	5.24	1.12	1.12	0.24	-4.13	-369.01
6	72.13	15.44	19.20	4.11	-52.93	-275.67
7	14.45	3.09	89.88	19.24	75.43	83.92
8	0.00	0.00	0.87	0.19	0.87	100.00
9	68.58	14.68	58.70	12.56	-9.88	-16.84
10	82.61	17.68	73.63	15.76	-8.98	-12.19
11	58.25	12.47	50.75	10.86	-7.50	-14.78
12	0.87	0.19	1.82	0.39	0.95	52.26
13	16.48	3.53	44.07	9.43	27.59	62.61
14	20.15	4.31	7.54	1.61	-12.62	-167.41
15	1.31	0.28	0.52	0.11	-0.79	-151.45
16	88.97	19.04	62.22	13.32	-26.75	-42.99
Total	467.25	100.00	467.25	100.00		

http://www.aloki.hu ● ISSN 1589 1623 (Print) ● ISSN 1785 0037 (Online)
DOI: http://dx.doi.org/10.15666/aeer/1706_1508715102

The second largest area among LULCs in 1996 (17.68% of the total) was the permanently irrigated land, which is the western part of the study area. The majority of permanently irrigated land consists of the areas where vegetables are cultivated. In 2018, the permanently irrigated land occupied less area compared to 1996 but was the second largest area (15.76% of the total).

The LULC with the third largest area in 1996 (15.44%) was the construction sites. A large part of the construction sites consists of fillings (rubble dumping) made in the northern part of the area on Izmir Bay coast and Cakalburnu lagoon. In 2018, the construction sites accounted for 4.11% of the total area and ranked ninth in terms of area size.

The discontinuous urban fabric ranked seventh in terms of area size among LULCs (4.13%) in 1996. The discontinuous urban fabric consists of agricultural enterprises and luxury villas in the central and western part of the area. The area covered by the discontinuous urban fabric increased to 5.52% but remained in the seventh place in 2018.

Between 1996 and 2018, the most significant increase in the LULC in terms of area size was in sport and leisure facilities (100%), green urban areas (83.92%), road and rail networks and associated land (70.58%). The most significant decrease was in dump sites (369.01%), construction sites (275.67%), and inland marshes (167.41%).

Tables 3 and *4* show the changes and conversions between LULCs. The discontinuous urban fabric increased by 25.11% (6.47 ha). Between 1996 and 2018, the city developed on the 8.22% (1.19 ha) of green urban areas, 5.99% (4.95 ha) of permanently irrigated land, 3.16% (2.17 ha) of non-irrigated arable land and 1.07% (0.62 ha) of fruit trees and berry plantations (*Fig. 5*).

Figure 5. *The spread of the discontinuous urban fabric to the non-irrigated arable land and permanently irrigated land*

Green urban areas increased by 83.92% (75.43 ha). The most important reason for the increase in green urban areas is the conversion of 54.32% (2.85 ha) of the dump sites, 50.69% (36.56 ha) of construction sites and 29.14% (25.92 ha) of coastal lagoons into green urban areas.

The non-irrigated arable land (greenhouse cultivation) showed a decrease of -16.84% (9.88 ha). 26.30% (18.04 ha) of the non-irrigated arable land was converted into permanently irrigated land, 3.16% (2.17 ha) into the discontinuous urban fabric, and 1.86% (1.28 ha) into green urban areas.

http://www.aloki.hu ● ISSN 1589 1623 (Print) ● ISSN 1785 0037 (Online)
DOI: http://dx.doi.org/10.15666/aeer/1706_1508715102

Table 3. *The conversion matrix of LULC change from 1996 to 2018 (%)*

LULC in 2018	LULC class changes (%)															
	LULC in 1996															
	1	**2**	**3**	**4**	**5**	**6**	**7**	**8**	**9**	**10**	**11**	**12**	**13**	**14**	**15**	**16**
1	**85.49**	1.27	0.00	0.00	0.00	0.18	8.22	0.00	3.16	5.99	1.07	0.00	0.74	0.00	0.00	0.00
2	0.00	**54.64**	0.00	0.00	0.00	0.72	0.00	0.00	0.00	0.00	0.00	0.00	0.00	0.00	0.00	0.00
3	1.36	0.00	**50.82**	0.00	0.00	17.72	3.29	0.00	0.25	2.79	2.82	0.00	3.03	0.25	0.00	0.00
4	0.00	0.00	0.00	**100.00**	0.00	0.00	0.00	0.00	0.00	0.00	0.00	0.00	0.00	0.00	0.00	0.00
5	0.00	0.00	0.00	0.00	**3.75**	0.00	0.00	0.00	0.00	0.60	0.00	0.00	0.00	2.12	0.00	0.00
6	0.00	2.04	0.00	0.00	21.64	**9.86**	0.75	0.00	0.51	2.05	0.45	0.00	15.31	27.23	22.69	0.10
7	4.54	1.90	48.17	0.00	54.32	50.69	**60.11**	0.00	1.86	4.91	4.57	46.38	20.16	0.00	7.41	29.14
8	0.00	0.00	0.00	0.00	0.00	1.04	0.00	**0.00**	0.00	0.00	0.00	0.00	0.69	0.00	0.00	0.00
9	2.28	0.00	0.00	0.00	0.00	0.00	1.81	0.00	**66.39**	14.28	1.01	0.00	0.47	0.00	0.00	0.00
10	2.70	0.00	0.48	0.00	0.00	0.00	9.11	0.00	26.30	**58.57**	7.07	0.00	2.24	4.23	0.00	0.00
11	1.98	0.00	0.00	0.00	0.00	0.00	0.00	0.00	0.23	2.73	**81.77**	0.00	0.00	1.59	0.00	0.00
12	0.00	0.00	0.00	0.00	0.00	0.00	0.00	0.00	0.00	0.00	0.00	**25.63**	3.19	5.34	0.00	0.00
13	1.65	40.15	0.53	0.00	20.29	19.37	16.70	0.00	1.30	8.08	1.24	27.99	**53.60**	24.43	35.44	0.62
14	0.00	0.00	0.00	0.00	0.00	0.00	0.00	0.00	0.00	0.00	0.00	0.00	0.29	**34.81**	0.00	0.53
15	0.00	0.00	0.00	0.00	0.00	0.00	0.00	0.00	0.00	0.00	0.00	0.00	0.00	0.00	**34.46**	0.08
16	0.00	0.00	0.00	0.00	0.00	0.43	0.00	0.00	0.00	0.00	0.00	0.00	0.31	0.00	0.00	**69.53**
1996 total	100.00	100.00	100.00	100.00	100.00	100.00	100.00	0.00	100.00	100.00	100.00	100.00	100.00	100.00	100.00	100.00
Class changes	14.51	45.36	49.18	0.00	96.25	90.14	39.89	0.00	33.61	41.43	18.23	74.37	46.40	65.19	65.54	30.47
Image difference	25.11	-62.25	70.58	0.00	-369.01	-275.67	83.92	100.00	-16.84	-12.19	-14.78	52.26	62.61	-167.41	-151.45	-42.99

LULC = land use and land cover. 1. discontinuous urban fabric; 2. industrial or commercial units; 3. road and rail networks and associated land; 4. port areas; 5. dump sites; 6. construction sites; 7. green urban areas; 8. sport and leisure facilities; 9. non-irrigated arable land; 10. permanently irrigated land; 11. fruit trees and berry plantations; 12. sclerophyllous vegetation; 13. sparsely vegetated areas; 14. inland marshes; 15. water courses; 16. coastal lagoons

http://www.aloki.hu ● ISSN 1589 1623 (Print) ● ISSN 1785 0037 (Online)
DOI: http://dx.doi.org/10.15666/aeer/1706_1508715102

Table 4. *The conversion matrix of LULC change from 1996 to 2018 (ha)*

LULC in 2018	**LULC class changes (ha)**																
	LULC in 1996																
	1	**2**	**3**	**4**	**5**	**6**	**7**	**8**	**9**	**10**	**11**	**12**	**13**	**14**	**15**	**16**	**2018 total**
1	**16.50**	0.09	0.00	0.00	0.00	0.13	1.19	0.00	2.17	4.95	0.62	0.00	0.12	0.00	0.00	0.00	25.78
2	0.00	**4.04**	0.00	0.00	0.00	0.52	0.00	0.00	0.00	0.00	0.00	0.00	0.00	0.00	0.00	0.00	4.55
3	0.26	0.00	**3.20**	0.00	0.00	12.78	0.48	0.00	0.17	2.30	1.64	0.00	0.50	0.05	0.00	0.00	21.38
4	0.00	0.00	0.00	**5.23**	0.00	0.00	0.00	0.00	0.00	0.00	0.00	0.00	0.00	0.00	0.00	0.00	5.23
5	0.00	0.00	0.00	0.00	**0.20**	0.00	0.00	0.00	0.00	0.49	0.00	0.00	0.00	0.43	0.00	0.00	1.12
6	0.00	0.15	0.00	0.00	1.13	**7.11**	0.11	0.00	0.35	1.69	0.26	0.00	2.52	5.49	0.30	0.09	19.20
7	0.88	0.14	3.03	0.00	2.85	36.56	**8.69**	0.00	1.28	4.05	2.66	0.40	3.32	0.00	0.10	25.92	89.88
8	0.00	0.00	0.00	0.00	0.00	0.75	0.00	**0.00**	0.00	0.00	0.00	0.00	0.11	0.00	0.00	0.00	0.87
9	0.44	0.00	0.00	0.00	0.00	0.00	0.26	0.00	**45.53**	11.80	0.59	0.00	0.08	0.00	0.00	0.00	58.70
10	0.52	0.00	0.03	0.00	0.00	0.00	1.32	0.00	18.04	**48.38**	4.12	0.00	0.37	0.85	0.00	0.00	73.63
11	0.38	0.00	0.00	0.00	0.00	0.00	0.00	0.00	0.15	2.26	**47.63**	0.00	0.00	0.32	0.00	0.00	50.75
12	0.00	0.00	0.00	0.00	0.00	0.00	0.00	0.00	0.00	0.00	0.00	**0.22**	0.52	1.08	0.00	0.00	1.82
13	0.32	2.97	0.03	0.00	1.06	13.97	2.41	0.00	0.89	6.67	0.72	0.24	**8.83**	4.92	0.46	0.55	44.07
14	0.00	0.00	0.00	0.00	0.00	0.00	0.00	0.00	0.00	0.00	0.00	0.00	0.05	**7.01**	0.00	0.47	7.54
15	0.00	0.00	0.00	0.00	0.00	0.00	0.00	0.00	0.00	0.00	0.00	0.00	0.00	0.00	**0.45**	0.07	0.52
16	0.00	0.00	0.00	0.00	0.00	0.31	0.00	0.00	0.00	0.00	0.00	0.00	0.05	0.00	0.00	**61.86**	62.22
1996 total	19.30	7.39	6.29	5.23	5.24	72.13	14.45	0.00	68.58	82.61	58.25	0.87	16.48	20.15	1.31	88.97	**467.25**
Class changes	2.80	3.35	3.09	0.00	5.05	65.02	5.76	0.00	23.05	34.22	10.62	0.65	7.65	13.14	0.86	27.11	
Image difference	6.47	-2.83	15.09	0.00	-4.13	-52.93	75.43	0.87	-9.88	-8.98	-7.50	0.95	27.59	-12.62	-0.79	-26.75	

LULC = land use and land cover. 1. discontinuous urban fabric; 2. industrial or commercial units; 3. road and rail networks and associated land; 4. port areas; 5. dump sites; 6. construction sites; 7. green urban areas; 8. sport and leisure facilities; 9. non-irrigated arable land; 10. permanently irrigated land; 11. fruit trees and berry plantations; 12. sclerophyllous vegetation; 13. sparsely vegetated areas; 14. inland marshes; 15. water courses; 16. coastal lagoons

http://www.aloki.hu ● ISSN 1589 1623 (Print) ● ISSN 1785 0037 (Online)
DOI: http://dx.doi.org/10.15666/aeer/1706_1508715102

Inland marshes showed a significant decrease of -167.41% (12.62 ha). Upon looking at the conversion matrix, the main reason for the change in these areas is the conversion of 27.23% (5.49 ha) into construction sites, 24.43% (4.92 ha) into sparsely vegetated areas and 5.34% (1.08 ha) into sclerophyllous vegetation.

Coastal lagoons showed a decrease of -42.99% (26.75 ha). 29.14% (25.92 ha) of coastal lagoons were converted into green urban areas (*Fig. 6*).

Between 1996 and 2018, there were significant changes in the patch numbers and patch areas of the LULC categories (*Table 5*). Between these years, the total patch number of the discontinuous urban fabric increased by 24.12% (from 199 to 247). The highest increase in the patch number was in the area with a 0-0.9 ha patch size (23.86%/from 197 to 244). There was no change in the average patch area size of the discontinuous urban fabric (0.1 ha).

The total patch number of green urban areas increased from 65 to 76 (an increase of 16.92%). The highest increase (300%/from 3 to 9) was observed in the patches of 1-4.9 ha. The average patch area increased by 536.36% from 0.22 ha 1.18 ha.

The total patch number of the non-irrigated arable land increased by 30.77% from 104 to 136. The highest increase in the patch number was in the patch group of 0-0.9 ha with 44.19% (from 86 to 124). The average patch area size of the non-irrigated arable land decreased by 34.85% (from 0.66 to 0.43 ha).

The total patch number of inland marshes decreased by 58.33% from 12 to 5. The highest decrease in the patch number was in the areas with a patch size of 0-0.9 ha (60%/from 10 to 4). The average patch area decreased by 10.12% from 1.68 ha to 1.51 ha.

The total patch number of coastal lagoons increased by 300% (from 1 to 3). The highest increase in the patch number was in the areas with a patch size of 0-0.9 (200%/from 0 to 2). The average patch area decreased by 76.69% (from 88.97 ha to 20.74 ha).

Discussion

The effects of urbanization in Inciralti are observed with the conversion of different LULCs into urban areas. The conversion of agricultural areas (permanently irrigated land, non-irrigated arable land, and fruit trees and berry plantations) into urban areas (discontinuous urban fabric) shows that urbanization in Inciralti creates great pressure on agricultural areas. This result is line with results of a previous survey in Nanping city, China, where the pressure of urban expansion on agricultural areas can be seen as decreases in cultivated land (Fan and Zhao, 2019). An indirect indicator of the continuation of a process leading to the construction of Inciralti is that agricultural areas were left unused. The decrease in the importance given to agriculture has led to the large abandonment of agricultural areas (Price et al., 2015).

Although the impact of human activities is for all natural ecosystems, it particularly affects coastal wetlands (Valdez et al., 2016). The reason for the conversion of wetlands into urban and agricultural areas in Inciralti is the filling of the area with rubble and garbage. As a result of filling Cakalburnu lagoon with rubble, Inciralti has been losing its wetlands characteristics. The reason for such losses in coastal wetlands is tremendous demand for land (Jiang et al., 2015; Kingsford et al., 2016). The major threat to coastal wetlands is the transformation of coastal ecosystems, which is the result of urbanization, which leads to significant loss and change of habitat (Gallant, 2015; Xu et al., 2016). Wetland loss is an important problem in local communities as well as for many wetland species that depend on wetlands (Orimoloye et al., 2018).

http://www.aloki.hu ● ISSN 1589 1623 (Print) ● ISSN 1785 0037 (Online)
DOI: http://dx.doi.org/10.15666/aeer/1706_1508715102

Table 5. *Patch numbers of LULC categories according to patch area coverages*

		Years													
		1996							**2018**						
		Patch size category (ha)													
		0-0.9	**1-4.9**	**5-9.9**	**10-49.9**	**50 or more**	**No. of patch (total)**	**Av. patch area (ha)**	**0-0.9**	**1-4.9**	**5-9.9**	**10-49.9**	**50 or more**	**No. of patch (total)**	**Av. patch area (ha)**
1	No. of patch	197	2	-	-	-	199		244	3	-	-	-	247	
	Patch area (ha)	16.31	2.99	-	-	-		0.10	21.51	4.27	-	-	-		0.10
2	No. of patch	-	-	1	-	-	1		1	1	-	-	-	2	
	Patch area (ha)	-	-	7.39	-	-		7.39	0.18	4.37	-	-	-		2.28
3	No. of patch	15	1	-	-	-	16		27	8	-	-	-	35	
	Patch area (ha)	3.18	3.11	-	-	-		0.39	7.63	13.75	-	-	-		0.61
4	No. of patch	3	2	-	-	-	5		3	2	-	-	-	5	
	Patch area (ha)	2.16	3.07	-	-	-		1.05	2.21	3.02	-	-	-		1.05
5	No. of patch	8	2	-	-	-	10		5	-	-	-	-	5	
	Patch area (ha)	2.42	2.82	-	-	-		0.52	1.12	-	-	-	-		0.22
6	No. of patch	21	8	-	3	-	32		20	8	-	-	-	28	
	Patch area (ha)	7.14	19.29	-	45.70	-		2.25	6.20	13.00	-	-	-		0.69
7	No. of patch	62	3	-	-	-	65		65	9	1	-	1	76	
	Patch area (ha)	10.88	3.57	-	-	-		0.22	12.70	17.38	7.83	-	51.97		1.18
8	No. of patch	-	-	-	-	-	-		-	1	-	-	-	1	
	Patch area (ha)	-	-	-	-	-		-	-	0.87	-	-	-		0.87

http://www.aloki.hu ● ISSN 1589 1623 (Print) ● ISSN 1785 0037 (Online)
DOI: http://dx.doi.org/10.15666/aeer/1706_1508715102

Table 5. cont. *Patch numbers of LULC categories according to patch area coverages*

		Years													
		1996							2018						
		Patch size category (ha)													
		0-0.9	1-4.9	5-9.9	10-49.9	50 or more	No. of patch (total)	Av. patch area (ha)	0-0.9	1-4.9	5-9.9	10-49.9	50 or more	No. of patch (total)	Av. patch area (ha)
9	No. of patch	86	16	2	-	-	104		124	12	-	-	-	136	
	Patch area (ha)	28.39	26.40	13.79	-	-		0.66	33.22	25.48	-	-	-		0.43
10	No. of patch	228	18	-	-	-	246		209	13	-	-	-	222	
	Patch area (ha)	57.64	24.97	-	-	-		0.34	55.99	17.64	-	-	-		0.33
11	No. of patch	39	23	-	-	-	62		53	18	-	-	-	71	
	Patch area (ha)	19.78	38.47	-	-	-		0.94	19.71	31.04	-	-	-		0.71
12	No. of patch	2	-	-	-	-	2		4	-	-	-	-	4	
	Patch area (ha)	0.87	-	-	-	-		0.44	1.82	-	-	-	-		0.46
13	No. of patch	44	3	-	-	-	47		39	14	-	-	-	53	
	Patch area (ha)	11.59	4.89	-	-	-		0.35	15.44	28.63	-	-	-		0.83
14	No. of patch	10	-	1	1	-	12		4	-	1	-	-	5	
	Patch area (ha)	1.47	-	6.37	12.31	-		1.68	0.74	-	6.80	-	-		1.51
15	No. of patch	8	-	-	-	-	8		5	-	-	-	-	5	
	Patch area (ha)	1.31	-	-	-	-		0.16	0.52	-	-	-	-		0.10
16	No. of patch	-	-	-	-	1	1		2	-	-	-	1	3	
	Patch area (ha)	-	-	-	-	88.97		88.97	0.22	-	-	-	62		20.74

LULC = land use and land cover. 1. discontinuous urban fabric; 2. industrial or commercial units; 3. road and rail networks and associated land; 4. port areas; 5. dump sites; 6. construction sites; 7. green urban areas; 8. sport and leisure facilities; 9. non-irrigated arable land; 10. permanently irrigated land; 11. fruit trees and berry plantations; 12. sclerophyllous vegetation; 13. sparsely vegetated areas; 14. inland marshes; 15. water courses; 16. coastal lagoons

http://www.aloki.hu ● ISSN 1589 1623 (Print) ● ISSN 1785 0037 (Online)
DOI: http://dx.doi.org/10.15666/aeer/1706_1508715102

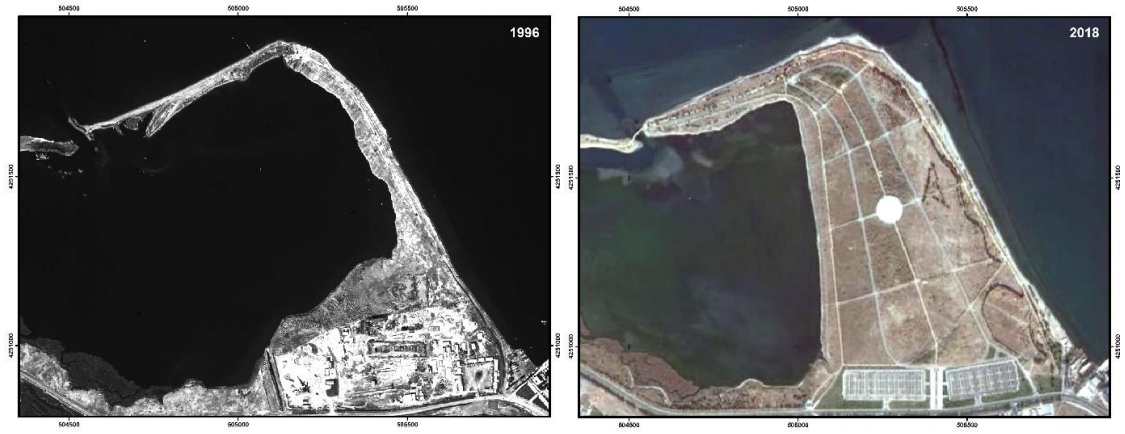

Figure 6. *Conversion of coastal lagoons in Inciralti*

In addition to the change/conversion of the LULC classes, patch numbers and patch area sizes reveal the state of agricultural areas and wetlands in Inciralti. The increase in the patch number with the smallest area size (0-0.9 ha) indicates that the discontinuous urban fabric spread throughout Inciralti (as agricultural enterprises and villas). This result is supported by the view that if the number of small patches increases, fragmentation also increases (Lasanta et al., 2015)

The extension of the discontinuous urban fabric to the west caused fragmentation of the agricultural areas particularly by creating pressure on these areas. The result of this study coincides with the view that the spreading construction areas occupy agricultural areas and divide large agricultural patches into small ones (Liang et al., 2015). A study assessing LULC changes in Romania found that serious fragmentation of agricultural land caused significantly decreasing in the quality and quantity of land use (Popovici et al., 2013).

When the changes in the total patch number, the number of patches with small sizes, the average patch area and total area size of the agricultural areas together, it is observed that these areas were subjected to conversion by severe fragmentation.

The changes in the total area size, total patch number and average patch area and the number of patches with small sizes of wetlands indicates severe fragmentation and rapid conversion. Similarly, on the analysis of LULC changes; it is stated that the total class area, the number of patches, the average patch size and the largest patch size provide information about the fragmentation of the landscape (Grecchi et al., 2014).

The results of the study are important in terms of revealing the LULC changes, conversions and fragmentations in Inciralti in detailed. The results of the study are important to reveal the LULC changes, conversions, and fragmentations in Inciralti in detailed. The results of the study are also important in terms of understanding the agricultural potential and ecological value of the area and contribute to the development of social awareness for the preservation of the agricultural and wetland character of Inciralti.

Conclusion

Changes, conversions, and fragmentations of LULCs in the study area over the years have caused changes in the existing natural and cultural structure of Inciralti. For this

http://www.aloki.hu ● ISSN 1589 1623 (Print) ● ISSN 1785 0037 (Online)
DOI: http://dx.doi.org/10.15666/aeer/1706_1508715102

reason, ecological importance of coastal areas should be prioritized (Rahman et al., 2017). The wetland characteristics of Inciralti can be protected by preventing the filling works for obtaining green urban areas and making wetland restoration.

Small patches of agricultural areas should be combined in order to reduce the severity of fragmentation.

Planning and management studies for Inciralti should focus on the protection of agricultural lands and wetlands as well as physical and economic development. An ecosystem-based conservation approach can be supported in areas accommodating different uses that meet the needs of multiple bird species/communities (Ma, et al., 2010). Appropriate land management is a way to avoid the negative effects of unplanned development (Rahman et al., 2017). To achieve this, planning and management studies should take into account landscape dynamics and LULC changes/conversions.

In future studies, the effects of temporal changes, conversions and fragmentations of the LULC on the agricultural product model, flora and fauna diversity, and people's mental health can be examined. Future studies provide quantified metrics for their study areas such as percent impervious surfaces, road density, and human population density. The effects of the intense demands of landowners for the development of agricultural land, the most important problem threatening Inciralti, on LULC changes can be analyzed. The pressure of green space demands on agricultural areas and wetlands can also be evaluated.

REFERENCES

[1] Balado, J., Arias, P., Diaz-Vilarino, L., Gonzalez de Santos, L. M. (2018): Automatic CORINE land cover classification from airborne LIDAR data. – Procedia Comput Sci 126: 186-194.

[2] Cole, B., Smith, G., Balzter, H. (2018): Acceleration and fragmentation of CORINE land cover changes in the United Kingdom from 2006-2012 detected by Copernicus IMAGE2012 satellite data. – International Journal of Applied Earth Observation and Geoinformation 73: 107-122.

[3] Dzieszko, P. (2014): Land-cover modelling using CORINE land cover data and multi-layer perceptron. – Quaestiones Geographicae 33(1): 5-22.

[4] Esbah, H. (2004): Agricultural land loss due to urbanization. – Proceedings of Agro-Environs, October 20-24, Udine, Italy, pp. 231-238.

[5] Fan, C., Myint, S. (2014): A comparison of spatial auto correlation indices and landscape metrics in measuring urban landscape fragmentation. – Landscape and Urban Planning 121: 117-128.

[6] Fan, X. C., Zhao, L. L. (2019): Land use changes and its driving factors: a case study in Nanping City, China. – Applied Ecology and Environmental Research 17(2): 3709-3721.

[7] Fonji, S. F., Taff, G. N. (2014): Using satellite data to monitor land-use land-cover change in North-eastern Latvia. – SpringerPlus 3: 61.

[8] Gallant, A. L. (2015): The Challenges of remote monitoring of wetlands. – Remote Sensing 7(8): 10938-10950.

[9] Goudie, A., Viles, H. (1997): The Earth Transformed: An Introduction to Human Impacts on the Environment. – Wiley-Blackwell, Oxford.

[10] Grecchi, R. C., Gwyn, Q. H. J., Bénié, G. B., Formaggio, A. R., Fahl, F. C. (2014): Land use and land cover changes in the Brazilian Cerrado: a multidisciplinary approach to assess the impacts of agricultural expansion. – Applied Geography 55: 300-312.

http://www.aloki.hu ● ISSN 1589 1623 (Print) ● ISSN 1785 0037 (Online)
DOI: http://dx.doi.org/10.15666/aeer/1706_1508715102

[11] Hobbs, N. T., Schimel, D. S., Owensby, C. E., Ojima, D. S. (1991): Fire and grazing in the tallgrass prairie: contingent effects on nitrogen budgets. – Ecology 72(4): 1374-1382.
[12] Jiang, T. T., Pan, J. F., Pu, X. M., Wang, B., Pan, J. J. (2015): Current status of coastal wetlands in China: degradation, restoration, and future management. – Estuarine, Coastal and Shelf Science 164: 265-275.
[13] Kingsford, R. T., Basset, A., Jackson, L. (2016): Wetlands: conservation's poor cousins. – Aquatic Conservation 26(5): 892-916.
[14] Li, S. H., Peng, S. Y., Jin, B. X., Zhou, J. S., Li, Y. X. (2019): Scenario simulation of land use/cover change in Fuxian Lake basin based on conversion of land use and its effects at small region extent model, Yunnan province, China. – Applied Ecology and Environmental Research 17(4): 8895-8914.
[15] Kara, B., Esbah, H., Deniz, B. (2013): Monitoring and analyzing land use/land cover changes in a developing coastal town: a case study of Kusadasi, Turkey. – Journal of Coastal Research 29(6): 1361-1372.
[16] Kesgin, B., Nurlu, E. (2009): Land cover changes on the coastal zone of Candarli Bay, Turkey using remotely sensed data. – Environmental Monitoring and Assessment 157(1-4): 89-96.
[17] Kilic, S., Evrendilek, F., Senol, S., Celik, I. (2005): Developing a suitability index for land uses and agricultural land covers: a case study in Turkey. – Environmental Monitoring and Assessment 102(1-3): 323-335.
[18] Lasanta, T., Nadal-Romero, E., Arnáez, J. (2015): Managing abandoned farmland to control the impact of re-vegetation on the environment. The state of the art in Europe. – Environmental Science & Policy 52: 99-109.
[19] Liang, C., Penghui, J., Chen, W., Li, M., Wang, L., Gong, Y., Pian, Y., Xia, N., Duan, Y., Huang, Q. (2015): Farmland protection policies and rapid urbanization in China: a case study for Changzhou City. – Land Use Policy 48: 552-566.
[20] Lopez E., Bocco, G., Mendoza, M., Duhau, E. (2001): Predicting land cover and land use change in the urban fringe: a case in Morelia city, Mexico. – Landscape and Urban Planning 55(4): 271-285.
[21] Ma, Z., Cai, Y., Li, B., Chen, J. (2010): Managing wetland habitats for waterbirds: an international perspective. – Wetlands 30(1): 15-27.
[22] Maynard, L., Wilcox, D. A. (1997): Coastal Wetlands: State of the Lakes Ecosystem Conference 1996 (SOLEC 96) – Background Paper, Ontario.
[23] Moulton, D. W., Jacob, J. S. (2000): Texas Coastal Wetland Guidebook. – Texas Sea Grant Publication, Texas.
[24] Nuthammachot, N., Stratoulias, D. (2019): Fusion of Sentinel-1A and Landsat-8 images for improving land use/land cover classification in Songkla province, Thailand. – Applied Ecology and Environmental Research 17(2): 3123-3135.
[25] Orimoloye, I. R., Kalumba, A. M., Mazinyo, S. P., Nel, W. (2018): Geospatial analysis of wetland dynamics: wetland depletion and biodiversity conservation of Isimangaliso Wetland, South Africa. – Journal of King Saud University–Science. https://doi.org/10.1016/j.jksus.2018.03.004.
[26] Petrişor, A. I., Grigorovschi, M., Meiţă, V., Simion-Melinte, C. P. (2014): Long-term environmental changes analysis using CORINE data. – Environmental Engineering and Management Journal 13(4): 847-860.
[27] Popovici, E. A., Balteanu, D., Kucsicsa, G. (2013): Assessment of changes in land-use and land-cover pattern in Romania using CORINE land cover database. – Carpathian Journal of Earth and Environmental Sciences 8(4): 195-208.
[28] Price, B., Kienast, F., Seidl, I., Ginzler, C., Verburg, P. H., Bolliger, J. (2015): Future landscapes of Switzerland: risk areas for urbanisation and land abandonment. – Applied Geography 57: 32-41.
[29] Rahman, M. T. U., Tabassum, F., Rasheduzzaman, M. D., Saba, H., Sarkar, L., Ferdous, J., Uddin, S. Z., Zahedul Islam, A. Z. M. (2017): Temporal dynamics of land use/land

http://www.aloki.hu ● ISSN 1589 1623 (Print) ● ISSN 1785 0037 (Online)
DOI: http://dx.doi.org/10.15666/aeer/1706_1508715102

cover change and its prediction using CA-ANN model for southwestern coastal Bangladesh. – Environmental Monitoring and Assessment 189: 565.

[30] Royer, A., Charbonneau, L., Bonn, F. (1988): Urbanization and Landsat MSS albedo change in the Windsor–Quebec corridor since 1972. – International Journal of Remote Sensing 9(3): 555-566.

[31] Rujoiu-Mare, M. R., Mihai, B. A. (2016): Mapping land cover using remote sensing data and GIS techniques: a case study of Prahova Subcarpathians. – Procedia Environmental Sciences 32: 244-255.

[32] Sanders, R. (2006): Protection of Agricultural Land from Urban Development - State Planning Policy 1/92. – Natural Resources and Water, Integrated Resource Management, Queensland Government, Australia.

[33] Serdar, S., Lök, A., Kırtık, A., Acarlı, S., Küçükdermenci, A., Güler, M., Yiğitkurt, S. (2010): Comparison of gonadal development of carpet shell clam (Tapes decussatus, Linnaeus 1758) in inside and outside of Çakalburnu lagoon, Izmir bay – Turkish Journal of Fisheries and Aquatic Sciences 10: 395-401.

[34] Sevil, Ş. (2010): Çakalburnu dalyanı (Cakalbunu lagoon) – Ekoloji Magazin 27.

[35] Turner II, B. L. (1989): The Human Causes of Global Environmental Change. – In: DeFries, R. S., Malone, T. (eds.) Global Change and Our Common Future: Papers from a Forum. National Academy Press, Washington, DC, pp. 90-99.

[36] Valdez, V. C., Ruiz-Luna, A., Berlanga-Robles, C. A. (2016): Effects of land use changes on ecosystem services value provided by coastal wetlands: recent and future landscape scenarios. – Journal of Coastal Zone Management 19(1): 418.

[37] Wang, Z., Zhang, B., Zhang, S., Li, X., Liu, D., Song, K., Li, J., Li, F., Duan, H. (2006): Changes of land use and of ecosystem service values in Sanjiang plain Northeast China. – Environmental Monitoring and Assessment 112(1-3): 69-91.

[38] Xu, C., Pu, L., Zhu, M., Li, J., Chen, X., Wang, X., Xie, X. (2016): Ecological security and ecosystem services in response to land use change in the coastal area of Jiangsu, China. – Sustainability 8(8): 1-24.

[39] Zhang, J., Ma, K., Fu, B. (2010): Wetland loss under the impact of agricultural development in the Sanjiang Plain, NE China. – Environmental Monitoring and Assessment 166(1-4): 139-148.

http://www.aloki.hu ● ISSN 1589 1623 (Print) ● ISSN 1785 0037 (Online)
DOI: http://dx.doi.org/10.15666/aeer/1706_1508715102

ALLELOPATHIC EFFECT OF *CASTANOPSIS KAWAKAMII* FOREST LITTER ON SEED GERMINATION OF SMALL PHILIPPINE ACACIA (*ACACIA CONFUSA)*

JIN, M. R.[1,2,3#] – WANG, Z. [1,2,3#] – HE, Z. S.[1,2,3*] – JIANG, L.[1,2,3] – LIU, J. F.[1,2,3*] – LAN, Y. Q.[1,2,3] – SHI, Y. W.[4] – SHEN, C. X.[4]

[1]*College of Forestry, Fujian Agriculture and Forestry University, Fuzhou 350002, China*

[2]*Cross-Strait Nature Reserve Research Center, Fujian Agriculture and Forestry University, Fuzhou 350002, China*

[3]*Key Laboratory of Fujian Universities for Ecology and Resource Statistics, Fuzhou 350002, China*

[4]*Administration Station of Castanopsis kawakamii Nature Reserve in Xinkou of Sanming, Sanming 365000, China*

[#]*These authors contributed equally to this work*

*****Corresponding authors*
e-mails: fjljf@126.com; jxhzs85@fafu.edu.cn

(Received 28th Jun 2019; accepted 16th Oct 2019)

Abstract. Nutrient limitation constrains the regeneration of *Castanopsis kawakamii* seedlings in subtropical forests. Small Philippine acacia (*Acacia confusa*), a common tree species in mixed forests, is known for its nitrogen fixation capabilities. Therefore, we attempted to intercrop *A. confusa* in a *C. kawakamii* natural forest. However, this forest contained abundant litter, harboring ample tannins and total phenols. Whether the allelopathy of litter could constrain the seed germination of *A. confusa* seed was unknown. Therefore, we aimed to explore the influence of forest litter extracts on the seed germination and radicle growth of *A. confusa*. The results indicate that low concentration litter extracts promote whereas high concentrations inhibit *A. confusa* seeds. The stock solution produced the strongest inhibition, whereas the 1:160 litter extract concentration had promoted the germination rate and radicle growth. The *A. confusa* radicle increase was remarkable in the first eight days, and tended to decrease from day 9 to 15. Overall, the allelopathic effect of litter is not a factor limiting the mixing of *C. kawakamii* and *A. confusa*. This could provide an alternative method to improving soil nutrition, thus promoting the regeneration of *C. kawakamii* seedlings.
Keywords: *germination rate, germination potential, germination index, radicle length, mixed forest*

Introduction

Castanopsis kawakamii is a unique subtropical evergreen broad-leaved species. It has survived as an endangered tertiary relict plant, only found in Fujian, Taiwan, Jiangxi, Guangdong, and Guangxi provinces in China (Buanjan et al., 2018). Currently, natural *C. kawakamii* forests are characterized by limited seed germination and seedling growth due to the low total nitrogen and total phosphorus in the soil (Su et al., 2012). As crucial aspects of a forest ecosystem, the physical and chemical properties and nutrients in the soil are significant to seedling development (Hou et al., 2011). However, previous studies mainly focused on community ecology (He et al., 2019); forest gap regeneration (He et al., 2018); natural forest, its plantation litter, and soil biochemistry cycle (Ma et al., 2015); soil microbes, biochemical characteristics (Ma et al., 2014); and soil-litter

http://www.aloki.hu ● ISSN 1589 1623 (Print) ● ISSN 1785 0037 (Online)
DOI: http://dx.doi.org/10.15666/aeer/1706_1510315116

stoichiometry to protect this rare species (Feng et al., 2017). Little research has focused on improving soil nutrition to promote species regeneration in this forest. Thus, in this study, we aimed to replenish soil nutrients to accelerate the regeneration of *C. kawakamii* seedlings.

Consistent with the importance of rhizobia-mediated N partitioning, inclusion of legumes is instrumental for generating positive diversity–productivity relationships (Wang et al., 2019a). With the existence of legumes and rich nitrogen in the litter layers, *Acacia confusa* has powerful fixation ability. Previous reports showed that one hectare of *A. confusa* forest can provide 3500 kg of litter per year, which is equivalent to 500 kg of carbamide after litter decomposition (Hu et al., 2015; Tung et al., 2015; Liu, 2011). As a common tree species in mixed forests, *A. confusa* is cultivated in tropical and subtropical regions in southwestern and southeastern provinces in China. It has a fast growth rate, wide adaptability, high biomass, and good water retention. Mixed with *Castanopsis* plants, such as *C. hainanensis*, *C. carlesii,* and *C. hystrix*, *A. confusa* could help *Castanopsis* plants to grow better. *A. confusa* also does not cause damage to *Castanopsis* plants (Liu, 2011), providing an alternative method for managing *A. confusa* in natural *C. kawakamii* forest to replenish and enrich the nutrient contents and to improve the establishment and regeneration of the target seedlings.

The amount of litter and the contents of tannin and total phenol in the *C. kawakamii* natural forest are relatively high (Feng et al., 2017; Yang et al., 2003). The seed germination and radicle growth of *C. kawakamii* are significantly inhibited under the action of a stock solution of litter (Wang et al., 2019b). The allelochemicals produced by the litter may also affect the germination of *A. confusa* seeds. Therefore, we hypothesized that: (1) different concentrations of litter extracts have different effects on *A. confusa* seeds, and high concentration of litter extracts inhibit the seed germination and radicle growth; (2) under the treatment of litter, *A. confusa* radicles grow considerably in the early period and growth decreases later; and (3) if the litter extract promotes the germination of *A. confusa* seeds, soil N content may be increased to improve the regeneration of *C. kawakamii*'s seedlings; if the litter extract inhibits germination, it indicates that *A. confusa* may not suitable as a mixed tree species in *C. kawakamii* natural forest. Finding other methods to improve the soil N content in this forest is necessary. Therefore, in this study, the extracts of *C. kawakamii* natural forest litter were used as allelopathic substances to explore the allelopathic effects of litter extracts on the germination of *A. confusa* seeds. The objective of our study was to provide a scientific basis for intercropping *A. confusa* species to improve soil nutrition, thereby accelerating the regeneration of *C. kawakamii* seedlings in this forest.

Materials and methods

Study sites and natural history

The *C. kawakamii* Nature Reserve is located in Sanming, Fujian Province, China, at 26°07'–26°12' N and 117°24'–117°29' E. The elevation varies between 180 and 604 m. The climate is medium subtropical monsoon, with an annual average temperature of 19.5 °C, annual precipitation around 1500 mm, and annual relative humidity of 79%. The soil type in this forest is mainly ferric acrisols with abundant humus. The research area has 700 ha of *C. kawakamii*, in which the average age of the population is about 130 years. The arbor layer is dominated by *C. kawakamii, Pinus massoniana,* and *Schima superba*. Accordingly, the population density, average tree height, diameter at

http://www.aloki.hu ● ISSN 1589 1623 (Print) ● ISSN 1785 0037 (Online)
DOI: http://dx.doi.org/10.15666/aeer/1706_1510315116

breast height, and canopy density are estimated to be 100 individuals/hm^2, 21.5 m, 32.4 cm, and 0.8, respectively. The shrub layer is mainly composed of *Litsea subcoriacea, Vaccinium carlesii*, and *Syzygium buxifolium*; and the herbaceous layers are represented by *Dicranopteris pedata*, *Gahnia tristis*, and *Alpinia oblongifolia* (Liu et al., 2011; Ma et al., 2015).

Experiment design

The litter baskets were arranged in the east, south, west, north, and middle of the fixed plots in the *C. kawakamii* natural forest, and were collected monthly from Sept. 2016 to Sept. 2017. We set up a total of 10 plots and the size of each plot was designed to be about 100 m^2 and the litter baskets were 1.0 ×1.0 m. The litter basket arrangement is shown in *Figure 1*. The collected litter was divided into four types: leaves, nutshells, branches, and bark. Then, we mixed the litter of each of the four types in accordance with their proportion. In the next step, we weighed 1 kg of each type. We collected 5 kg of *A. confusa* seeds from the same family for experimental materials.

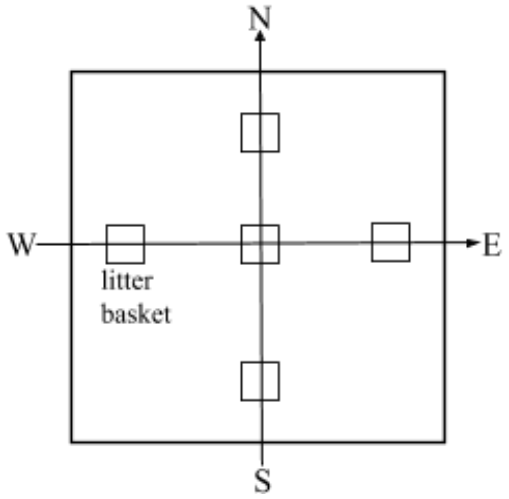

Figure 1. *The location of litter baskets in each plot. The small square box represents the location of the litter basket*

Preparation of litter extracts

Each kilogram of collected litter sample was washed three times with distilled water to remove surface-attached soil and humus. Next, the samples were crushed and sieved after drying in an oven. After sieving, 10 g of litter were placed into a 50 mL centrifuge tube and 15 mL of 70% ethanol was added. The mixture was leached twice at 80 °C for 1 h in a water bath. After free cooling, the samples were placed into a centrifuge at 4 °C for 5 min at a rotation speed at 8000 rpm. To obtain a stock solution (with three replicates), we filtered the extracts twice and then diluted the extracts to 50 mL with distilled water. As the extraction of litter in nature is repetitive and diverse, the range of extract types and contents is relatively wide. Ethanol was applied as an effective extraction agent to ensure polarized allelochemicals could be maximally extracted out of the litter.

The stock solution was then placed on a rotary evaporator to evaporate the ethanol. The average litter quality and annual precipitation of the *C. kawakamii* natural forest

http://www.aloki.hu ● ISSN 1589 1623 (Print) ● ISSN 1785 0037 (Online)
DOI: http://dx.doi.org/10.15666/aeer/1706_1510315116

fixed plot from 2010 to 2017 were 11,010 kg/hm^2 and 1500 mm/year. Referring to the litter conversion (Yuan et al., 2010), 1:160 is the natural leaching concentration of the litter of natural *C. kawakamii* forest. Considering the rain leaching process, repeated extraction, and microbial decomposition, five concentrations were set as treatments: 1:20, 1:40, 1:80, 1:160, and 1:320. Therefore, the stock solution was diluted again with distilled water with five different concentrations. The dilution rates are listed as follows: 1:20 litter extracts (stock solution was diluted 4 times with distilled water), 1:40 litter extracts (stock solution was diluted 8 times with distilled water), 1:80 litter extracts (stock solution was diluted 16 times with distilled water), 1:160 litter extracts (stock solution was diluted 32 times with distilled water), and 1:320 litter extracts (stock solution was diluted 64 times with distilled water), and then we stored the extracts in a 4 °C refrigerator until use. During the extraction, the ethanol evaporation was incomplete. As a consequence, we also created a blank control group as a contrast that was exempted from the treatment: the same procedure was repeated but without the litter.

Seed germination experiment

The selected and same-sized *A. confusa* seeds were disinfected with 0.5% potassium permanganate for 30 min, then washed with distilled water 3 times before arranging them evenly in a petri dish with *C. kawakamii* forest soil. The *C. kawakamii* forest soil was sterilized in a high temperature sterilization pot at 120 °C for 20 min. The different concentrations of litter extracts were added into each petri dish, with 100 seeds placed uniformly in each petri dish. We set up a total of 6 treatments including stock solution, 1:20 litter extract, 1:40 litter extract, 1:80 litter extract, 1:160 litter extract, and 1:320 litter extract with 3 replications each with distilled water, and a blank control group as the control. The experiment conditions were cultured with a 12 h photoperiod at 25 °C, 12 h dark cycle at 15 °C, light intensity 50 nmol/cm^2/s, and relative humidity 75–80% in the incubators. We added 5 mL litter extract daily into the filter paper of the petri dish to maintain moisture.

We recorded the seed germination 3 days after the experiment. A 2 mm seed radicle was defined as seed germination, and the number of germinated seeds was recorded every day (Aldo et al., 2018). We finished the experiment when no further seed germination occurred for 3 continuous days. The radicle length measurements were recorded when the seed germination reached the peak (Wang et al., 2019b). We measured the radicle length of 20 seeds with a similar radicle length in different petri dishes after recording the seed germination for three days when the seed germination reached the peak. The length of the radicle was also measured daily with an electronic digital caliper with a resolution of 0.01 mm. The radicle daily growth amount was simultaneously calculated by the difference in the value of the radicle length between the current day and the previous day. On the 15th day, we finished the radicle experiment when the radicle growth was generally stable. Finally, the germination rate, germination potential, germination index, allelopathic effect index, and the radicle length of seeds were thereby calculated (Bruce et al., 1988). The formulas are listed below (He et al., 2012; Gabriel et al., 2017).

$$\text{Germination rate} = \frac{\text{number of seeds germinated}}{\text{total number of seeds}} \times 100\% \quad \text{(Eq.1)}$$

http://www.aloki.hu ● ISSN 1589 1623 (Print) ● ISSN 1785 0037 (Online)
DOI: http://dx.doi.org/10.15666/aeer/1706_1510315116

$$\text{Germination potential} = \frac{\text{number of seeds that were normally germinated to the highest}}{\text{total number of seeds}} \times 100\% \quad \text{(Eq.2)}$$

$$\text{Germination index} = \Sigma \frac{Gt}{Dt} \quad \text{(Eq.3)}$$

where *Dt* refers to the number of germination days, and *Gt* refers to the number of germinated seeds in that *Dt* day.

Allelopathy index:

$$\begin{aligned} I &= 1 - \frac{C}{T} \quad (\text{when } T \geq C) \\ I &= \frac{T}{C} - 1 \quad (\text{when } T < C) \end{aligned} \quad \text{(Eq.4)}$$

where C refers to the control value, T refers to the treatment value, while $I < 0$ represents the inhibition effect, $I > 0$ represents the promotion effect, and $I = 0$ represents the neutral effect.

Data analysis

The experimental data were calculated and plotted using Excel 2016 (Microsoft, Redmond, Washington, USA). The statistical ANOVA was analyzed using SPSS 21.0 (IBM, Almonk, New York, USA). We first calculated the effect of different concentrations of litter extracts on the germination indices, radicle length, radicle growth, and allelopathy index of *A. confusa* seeds. Then, the variance analysis of these data was performed, and Tukey's test was applied in multiple comparisons to determine the significant difference among various treatments. The data were considered to be significantly different at $P < 0.05$.

Results

Effects of different extract concentrations on germination of A. confusa seeds

The effects of various concentrations of litter extracts on seed germination of *A. confusa* is shown in *Tables 1* and *2*. *A. confusa* seeds demonstrated different sensitivities to different concentrations of litter extract, which generally promoted seed germination at low concentrations and inhibited it at high concentrations. We found a negative correlation between litter extract concentration and germination potential, germination rate, and germination index. The germination rate was highest with a litter concentration of 1:160, which promoted the seed germination rate. The seed germination rate was significantly lower than those of the other treatments at a concentration of 1:20, demonstrating the most inhibition of the seed germination rate. The seed germination rates under high concentration treatments (including stock solution, 1:20, and 1:40) were significantly lower than under low concentration treatments (1:160 and 1:320). High concentrations of litter extract inhibited the seed germination rate, whereas low concentrations had a promotion effect. The germination potentials for high concentration (including stock solution and 1:20) flitter extract treatments were significantly lower than for low concentration (1:80 and 1:160) treatments. The germination potential and index were the lowest for the stock solution, which revealed negative effects on the seed germination potential and index. The

http://www.aloki.hu ● ISSN 1589 1623 (Print) ● ISSN 1785 0037 (Online)
DOI: http://dx.doi.org/10.15666/aeer/1706_1510315116

germination indexes for the high concentration (including stock solution and 1:20) treatments were significantly lower than for the low concentration litter extract treatments (including 1:80, 1:160, and 1:320). No significant differences in germination rate, potential, or index were found between distilled water and the control group. We found that when the concentration of litter extracts exceeded the dilution ratio of 1:40, the seed germination was restrained. The 1:80 dilution rate was considered the turning point for seed germination; the optimum dilution for seed germination was found to be 1:160. The 1:160 litter extract was the most appropriate concentration for the germination of *A. confusa* seeds.

Table 1. *Effects of different concentrations of litter extracts on seed germination of A. confusa*

Leaching solution	Germination rate/%	Allelopathy index	Germination potential/%	Allelopathy index	Germination index	Allelopathy index
Distilled water	63.00±1bcd	0.00	50.00±3a	0.00	81.32±2bc	0.00
Control group	61.60±1.44bcd	0.03	47.50±3abc	-0.05	79.16±2.07cd	-0.05
Stock solution	60.00±1cd	-0.05	13.50±4.5d	-0.73	56.06±2.36f	-0.33
1:20	57.00±0e	-0.10	46.00±0c	-0.08	73.77±0e	-0.12
1:40	60.50±1.5cd	-0.07	46.50±2.5bc	-0.07	75.98±1.5cd	-0.09
1:80	63.50±0.5abc	0.05	52.50±0.5ab	0.05	84.26±0abc	0.01
1:160	66.00±2a	0.09	54.50±3a	0.09	88.61±1.28a	0.06
1:320	64.00±1ab	0.02	51.00±0abc	0.02	81.46±1.76bc	-0.02

The purpose of the control group is to test whether the ethanol solution added to the litter extracts affect the seed germination of *A. confusa*. Data (mean ± SD) marked with different letters in plots were significantly different under p level as 0.05 in the same column. The same below

Table 2. *Effects of treatments on seed germination of A. confusa were tested using one-way ANOVA*

		df	F	P
Germination rate	Between groups	7	15.815	<0.001***
	Within groups	16		
	Total	23		
Germination potential	Between groups	7	98.107	<0.001***
	Within groups	16		
	Total	23		
Germination index	Between groups	7	122.883	<0.001***
	Within groups	16		
	Total	23		

Effects of different concentrations of extracts on radicles of A. confusa seeds

Difference in radicle length between different concentrations of extracts

Figure 2 and *Table 3* show the effects of various concentrations of litter extract on the radicle length of *A. confusa* seeds. Similar to seed germination, the different concentrations of litter extracts tended to promote radicle growth at low concentration and inhibit radicle growth at high concentration. The inhibition effect was aggravated with increasing concentration, among which the most notable effect was observed with the

http://www.aloki.hu ● ISSN 1589 1623 (Print) ● ISSN 1785 0037 (Online)
DOI: http://dx.doi.org/10.15666/aeer/1706_1510315116

stock solution. The 1:40 to 1:160 litter extracts demonstrated a promotion effect, that was the strongest at 1:160, whereas the facilitation effect gradually weakened when the concentration was 1:320. The growth in radicle length in the early stage was not obvious for the different concentrations of litter extracts. The difference in radicle length between various concentration of litter extracts and distilled water increased with time. Significant differences in radicle length were detected among the stock solution, distilled water, and 1:160 concentration litter extract. At the end of the experiment, the average radicle lengths for 1:160 litter extract, distilled water, and stock solution were 36.09, 30.06, and 19.59 mm, respectively. No significant differences in radicle length were found between the distilled water and control groups.

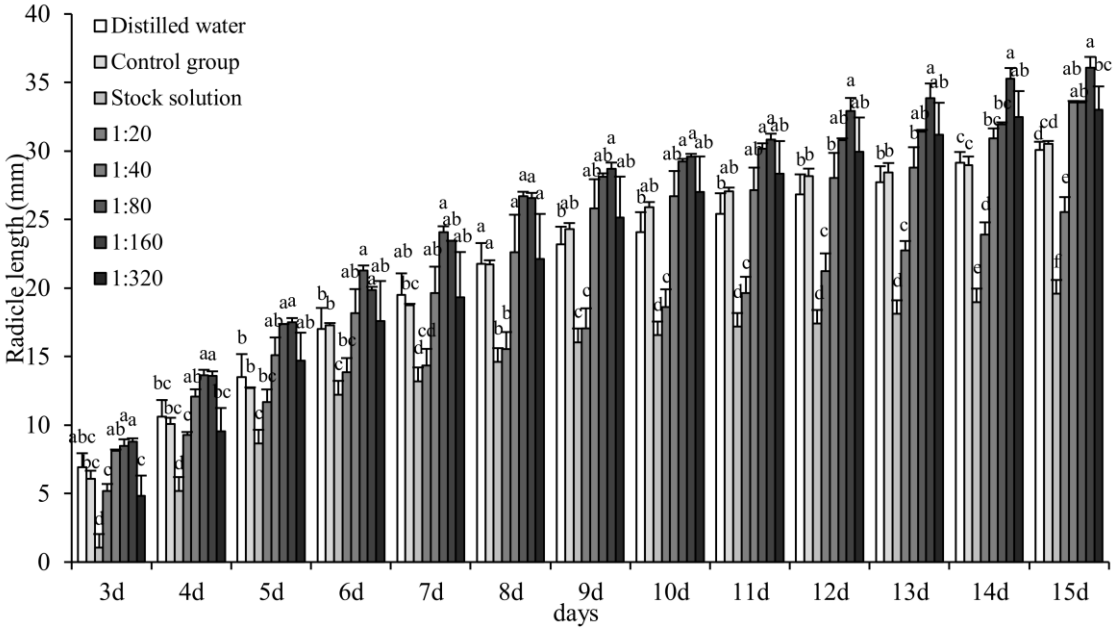

Figure 2. *Effects of different concentrations of litter extracts over time on the radicle length of A. confusa seeds. The different letters (from a to d) represent the difference in radicle length among the different concentrations of the same day. Data (mean ± SD) marked with different letters in plots were significantly different under p level as 0.05 in the same column. Compared with the control group, the treatment group were larger than the control group indicates that the radicle growth is promoted, and vice versa.*

We found that *A. confusa* radicle elongation was inhibited under the stock solution and 1:20 litter extract; at 1:40, 1:80, and 1:160 litter extracts, we observed promotion effects, although it was not conspicuous at the concentration of 1:320 (*Table 3*). The stock solution had the strongest inhibiting effects on seed radicle growth. The best promotion effect was detected for the 1:160 litter extract which showed a relative high promotion effect in the early period, then later decreased. Consequently, the 1:160 litter extract remained the optimum concentration for the growth of *A. confusa* radicle length.

The results of the two-way ANOVA analysis of variance were presented in *Table 4*. There was a significant difference in the length of *A. confusa* radicle treated with time or different concentrations of litter extracts. But the difference in interaction between time and different treatments is not significant.

http://www.aloki.hu ● ISSN 1589 1623 (Print) ● ISSN 1785 0037 (Online)
DOI: http://dx.doi.org/10.15666/aeer/1706_1510315116

Table 3. *Allelopathic index of A. confusa radicle length in different concentrations of litter extracts*

Day	D3	D4	D5	D6	D7	D8	D9	D10	D11	D12	D13	D14	D15
Distilled water	0	0	0	0	0	0	0	0	0	0	0	0	0
Control group	-0.12	-0.05	-0.06	0.02	-0.04	0.00	0.05	0.07	0.06	0.05	0.03	-0.01	0.02
Stock solution	-0.85	-0.51	-0.36	-0.28	-0.32	-0.33	-0.31	-0.31	-0.32	-0.35	-0.35	-0.35	-0.35
1:20	-0.25	-0.13	-0.13	-0.19	-0.26	-0.29	-0.26	-0.23	-0.23	-0.21	-0.18	-0.18	-0.15
1:40	0.15	0.12	0.10	0.06	0.01	0.04	0.10	0.10	0.06	0.04	0.04	0.06	0.10
1:80	0.19	0.22	0.22	0.20	0.19	0.18	0.18	0.18	0.16	0.13	0.12	0.09	0.10
1:160	0.21	0.22	0.23	0.14	0.17	0.18	0.19	0.19	0.18	0.19	0.18	0.17	0.17
1:320	-0.30	-0.10	0.08	0.03	-0.01	0.02	0.08	0.11	0.10	0.10	0.11	0.10	0.09

Table 4. *The two-way ANOVA analysis of two treatments on the radicle length of A. confusa*

	df	F	p
Day	12	274.867	<0.001***
Leaching solution	7	134.259	<0.001***
Day : Leaching solution	84	1.244	0.108
Residuals	208		

Differences in radicle growth of A. confusa seeds in different time periods

The effects of litter extracts on the seed radicle growth is shown in *Figure 3*. It shows that the seed radicle growth of *A. confusa* decreased with time, and the growth trends of various concentrations were different. The growth of the seed radicle was greater in the distilled water group at the period from day 4 to 9, and the growth was stable after the 10th day. The radicle growth increased the most on the fifth day and the least on the 11th day. For the stock solution of litter extracts, the seed radicle growth during day 5 to 7 was significantly higher than on other days; the seed radicle grew the most on the fifth day and the least on the 13th day. The 1:20 litter extract group demonstrated the most seed radicle growth on the fifth day and the least on the eighth day; the seed radicle growth during the first eight days was relatively high compared to that on the following days. At the 1:40 concentration, the radicle growth was relatively high during day 4 to 10 (except for the eighth day); the maximum growth occurred on the fourth day, with the least growth on day 11 to 14, and the radicle growth gradually increased in the later stage. At 1:80 and 1:160 concentrations, the seed radicle growth showed a general downward trend, reaching the maximum on the fourth day, and stabilized after decreasing sharply on day 10 to 15. The seed radicle growth at the 1:320 concentration reached a maximum on the sixth day, then declined from day 7 to 16, and the least growth was observed on the 16th day. The different concentrations of litter extracts inhibited the seed radicle growth less in the early period, where the radicle growth was relatively fast, whereas the various concentrations of litter extract had different effects on seed radicle growth in the later stages. Compared with the distilled water group and the control group, the high litter extract concentrations inhibited the radicle growth of *A. confusa*, which was promoted at low concentrations.

http://www.aloki.hu ● ISSN 1589 1623 (Print) ● ISSN 1785 0037 (Online)
DOI: http://dx.doi.org/10.15666/aeer/1706_1510315116

The *A. confusa* seed radicle growth was inhibited on day 7 to 9 and day 12 to 15, and promoted on day 5 to 6 and 10 to 11 in general (*Table 5*). The inhibition effect was obvious in the stock solution and the 1:20 concentration litter extract. The promotion effect appeared in the 1:80, 1:160, and 1:320 litter extract concentrations. The different days and treatments, along with their interaction, significantly affected the radicle growth of *A. confusa* (*Table 6*). Overall, the 1:160 litter extract concentration was the optimum for the increase in *A. confusa* radicle length.

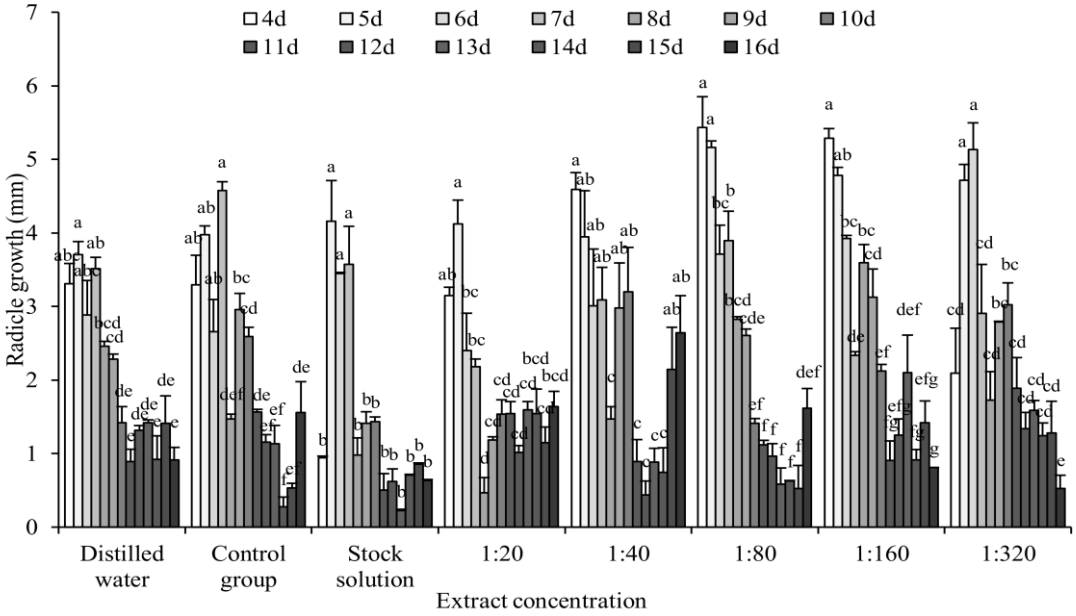

Figure 3. *The seed radicle growth of A. confusa in different time periods. the different letters (from a to g) indicate the difference in radicle growth among different days under the same concentration.The amount of radicle growth refers to the length of the radicle from the next day minus the length of the radicle of the previous day. Data (mean ± SD) marked with different letters in plots were significantly different under p level as 0.05 in the same column*

Table 5. *Allelopathic index of the seed radicle growth of A. confusa in different concentrations of litter extracts*

Day	D4	D5	D6	D7	D8	D9	D10	D11	D12	D13	D14	D15	D16
Distilled water	0	0	0	0	0	0	0	0	0	0	0	0	0
Control group	-0.01	0.07	-0.08	0.23	-0.40	0.23	0.45	0.43	-0.12	-0.20	-0.70	-0.62	0.41
Stock solution	-0.72	0.11	0.16	0.02	-0.60	-0.38	0.01	0.44	-0.53	-0.84	-0.23	-0.39	-0.31
1:20	-0.05	0.10	-0.17	-0.38	-0.81	-0.48	0.08	0.42	-0.23	0.11	0.40	-0.19	0.44
1:40	0.28	0.06	0.04	-0.12	-0.40	0.23	0.56	0.00	-0.67	-0.38	-0.19	0.34	0.65
1:80	0.39	0.28	0.22	0.10	0.13	0.12	-0.01	0.20	-0.27	-0.59	-0.32	-0.63	0.44
1:160	0.37	0.23	0.26	-0.34	0.32	0.27	0.33	0.01	-0.05	0.33	0.00	0.01	-0.11
1:320	-0.37	0.22	0.44	-0.17	-0.30	0.18	0.53	0.53	0.02	0.11	0.26	-0.09	-0.43

Day 4 represents the allelopathy index of the radicle growth amount obtained on the fourth day minus the third day, the same as Day 5 to Day 16.

http://www.aloki.hu ● ISSN 1589 1623 (Print) ● ISSN 1785 0037 (Online)
DOI: http://dx.doi.org/10.15666/aeer/1706_1510315116

Table 6. *The two-way ANOVA analysis of two treatments on the radicle growth of A. confusa*

	df	F	p
Day	12	94.677	<0.001***
Leaching solution	7	12.662	<0.001***
Day: Leaching solution	84	4.759	<0.001***
Residuals	208		

Discussion

With increasing litter extract concentration, the germination potential, germination rate, and germination index of *A. confusa* decreased. The stock solution and the 1:20 litter extracts concentrations had strongest inhibitory effect on seed germination. The germination potential and germination index of the seeds in the stock solution were the lowest, primarily due to the restraining effect of the allelochemicals in the stock solution on the speed of seed germination. The germination rate in the 1:20 litter extraction concentration group was the lowest and the negative effect of allelochemicals on the seeds were most pronounced. This may be caused by the amount of harmful ingredients in the allelochemicals, which were much more than the amount of beneficial components. Under normal circumstances, the production and elimination of free radicles in plant cells maintains a dynamic equilibrium; under stress conditions, this balance is affected and readily destroyed. When free radicals accumulate to a certain extent, membrane lipid peroxidation occurs, which inhibits seed germination (Shibaeva et al., 2018; Marusa and Ishii-Iwamoto., 2011). At the 1:160 concentration, the three seed germination indices were the highest, and the promotion effect was the most obvious. We speculate that this concentration is the optimum concentration of seed germination, and the beneficial components in the allelochemicals accumulate the most. Within this concentration range, the ion transporters in the cell and various ion channel proteins are involved in cell ion homeostasis, increasing seed germination rate and germination speed (Steven et al., 2003; Zhang et al., 2016; Bachleda et al., 2017; Kilic et al., 2016). The 1:320 litter extract concentration also promoted the germination of seeds, but the overall effect was not significant. The reason for this may be that the concentration was lower and similar to distilled water, and the allelochemicals content was relatively low; thus, the promoting effect was not obvious. In general, compared with the distilled water group, no germination index was significant for the low-concentration litter extracts, whereas high-concentration litter extracts significantly inhibited the germination indices of *A. confusa* seeds. When the allelochemicals content is limited, the plant itself produces stress-resistant immunity. At this time, allelopathic chemicals have little effect on the plant. When the residual allelochemicals increase, accumulate, and increase to a certain amount or exceed the critical content, they are harmful to the plant and thus delay seed germination (Liu et al., 2016; Wei et al., 2018).

With the increase in litter extract concentration, the seed radicle growth of *A. confusa* showed an obvious hysteresis effect. The litter extracts had a significant inhibiting effect on seed radicle growth compared with distilled water, mainly because the seed radicle growth was inhibited by the stock solution and the 1:20 concentration. High litter extract concentrations may have physiologically disturbed the plant, inducing intensive anaerobic respiration, which would therefore weaken the plant's ability to scavenge free radicals, resulting in a decrease in its physiological index (Steven et al., 2003; Zhang et al., 2016; Bachleda et al., 2017; Kilic et al., 2016). The hormone content

http://www.aloki.hu ● ISSN 1589 1623 (Print) ● ISSN 1785 0037 (Online)
DOI: http://dx.doi.org/10.15666/aeer/1706_1510315116

and enzyme activity in the seeds of *A. confusa* may have led to the inhibitory effect of litter extracts on seed germination and radicle growth within a certain concentration range (Hunter et al., 2013). When the litter extract concentration was 1:160, the promotion of radicle growth was the most obvious, and the content of beneficial allelochemicals was the highest. We speculate that the concentration of nutrients in this treatment was high, the breathing was strong, the high energy bond in ATP was active, the mitochondria inner membrane activity was strong, the rates of electron transfers and oxidative phosphorylation were fast, and the cell division speed of the apical meristem was accelerated, which effectively promote radicle elongation (Steven et al., 2003; Zhang et al., 2016; Bachleda et al., 2017; Kilic et al., 2016). The 1:320 litter extract also promoted the growth of seed radicle length, but the effect was weakened, which may be due to the litter extract dilution containing less effective allelochemicals. Previous studies have reported low allelopathic effect at low concentration and inhibition at high concentration with: water extracts from corn leaves on the seeds of *Scutellaria baicalensis*, litter extracts on seed germination and seedling growth of *Cunninghamia lanceolate*, and litter leaves and soil extracts on the seed germination and seedling growth of *P. koraiensis* (Chen et al., 2016; Peng et al., 2012; Zhuang et al., 2017). These results are consistent with our findings.

By analyzing the growth in the radicle over time, we discovered that the radicle growth of *A. confusa* treated with litter extract was relatively high in the early stage, and the growth the middle and late stages tended to decline. The reason for this may be that a certain amount of allelopathic substances accumulated in the litter, hindering the water absorption of the seed; inhibiting the respiration, enzyme activity, and radicle growth; and changing the osmotic pressure, thereby constraining the elongation of the radicle (Wei et al., 2018). When the litter extract concentrations were 1:40 and 1:80, the seed radicle growth of *A. confusa* increased gradually in the later stage, which may be due to the increase in peroxidation products in the plant after the stress due to allelopathic substances. When these allelopathic substances reach a certain amount and the stress mechanism is constrained by the plant, its own protective enzyme system could thereby scavenge the free radicals generated. However, this adaptive response is effective, as the degree of damage was relatively low and reversable, whereas the radicle increase was limited at any higher concentration of litter extract (Marusa and Ishii-Iwamoto, 2011).

The low litter extract concentration in nature can promote the germination and radicle growth of *A. confusa* to some extent. So, it is feasible to mix *A. confusa* in *C. kawakamii* forests. However, when mixing *A. confusa*, we should try to select a location where the amount of litter is low and the topography is relatively flat to mitigate the adverse effects of allelopathy. To afforest a successful mixed forest, further studies are required. Firstly, the effects of extracts from *C. kawakamii* natural forest on *A. confusa* should be studied from the perspective of the physiological activity of the radicle. Secondly, the different effects of various types and contents of litter allelochemicals at different forest ages and stages on seeds should be thoroughly considered during the afforestation of mixed forests (Hunter et al., 2013). Allelopathic effect on the plant are complex, having important impacts on the growth of plant seedlings (Kimura et al., 2015; Anne et al., 2019; Chu et al., 2014), thus affecting the colonization and renewal of the population. In the future, research should be continued on the growth response of *C. kawakamii* and *A. confusa* seedlings to litter extract.

http://www.aloki.hu ● ISSN 1589 1623 (Print) ● ISSN 1785 0037 (Online)
DOI: http://dx.doi.org/10.15666/aeer/1706_1510315116

Conclusions

In this study, we examined the effects of different concentrations of *C. kawakamii* litter extract on the germination rate, germination potential, germination rate index, and radicle growth of *A. confusa.* Low concentrations promoted growth, whereas higher concentrations inhibited growth. The stock solution had the most obvious inhibiting effect on seed germination and radicle growth, whereas the 1:160 litter extract concentration displayed the strongest promotion. The natural leaching concentration of litter in the wild is about 1:160, which could actually promote the seed germination and radicle growth of *A. confusa*. Therefore, the allelopathic effect of forest litter is not a limiting factor when mixing *C. kawakamii* and *A. confusa* in a forest, providing an alternative method to improve soil nutrition in this forest, and finally promote the regeneration of *C. kawakamii* seedlings in this forest. Further study is needed of the physiological response of *A. confusa* radicle and growth to litter extracts to provide a practical basis to promote *C. kawakamii* regeneration in this forest.

Acknowledgements. The authors wish to thank Cong Xing, Chensi Wei, Xuelin Wang, Jing Zhu and Yaoshun Lu for assistance in the field and experiment. At the same time, the authors would like to thank Dr. Zhu Dehuang for the constructive comments and suggestions of the manuscript. This research was funded by the National Natural Science Foundation of China (NSFC), grant number 31700550 and 31770678; Nature Science Fund of Fujian Province Science and Technology of China, grant number 2019J01367; Science and Technology Promotion of Project Forestry Bureau of Fujian Province, grant number 2018TG14-2; and Innovation and Technology Fund of Fujian Agriculture and Forestry University, grant number CXZX2016075 and CXZX2018125. The authors also record sincere appreciation for helpful and constructive comments made by reviewers of the manuscript.

REFERENCES

[1] Aldo, B. F., Shovonlal, R., Vitor, M. V. (2018): Allelopathy prevents competitive exclusion and promotes phytoplankton biodiversity. – Oikos 127(1): 85-98.

[2] Anne, L., Leena, L. (2019): Responses of a native plant species from invaded and uninvaded areas to allelopathic effects of an invader. – Ecology and Evolution 9(10): 6116-6123.

[3] Bachleda, N., Timothy, L. G., Zeng, L. L. (2017): Effects of high oleic acid soybean on seed yield, protein and oil contents, and seed germination revealed by near-isogeneic lines. – Plant Breeding 136(4): 231-74.

[4] Bruce, W. G., Richardson, D. (1988): Bioassays for allelopathy: measuring treatment responses with independent controls. – Journal of Chemical Ecology 14(1): 181-187.

[5] Buanjan, S., Liu, J. F., He, Z. S., Feng, X. P. (2018): Effect of gap sizes on specific leaf area and chlorophyll contents at the *Castanopsis kawakamii* natural reserve forest, China. – Forests 9(682): 1-14.

[6] Chen, L. X., Li, S. B., Qiao, L., Bu, F., Duan, W. B. (2016): Effects of leaf litter and leaching liquor on seed germination and seedling growth of *Pinus koraiensis*. – Journal of Nanjing Forestry University 40(2): 81-87.

[7] Chu, C. J., Mortimer, P. E., Wang, H. C., Wang, Y. F., Liu, X. B., Yu, S. Y. (2014): Allelopathic effects of *Eucalyptus* on native and introduced tree species. – Forest Ecology and Management 32(3): 79-84.

[8] Feng, X. P., Liu, J. F., Buanjan, S. J., He, Z. S., Jiang, L., Hong, W., Shi, Y. W. (2017): Ecological stoichiometric characteristics of litter-soil in gap of *Castanopsis kawakamii* in Sanming of Fujian. – Journal of Plant Resources and Environment 26(4): 18-24.

http://www.aloki.hu ● ISSN 1589 1623 (Print) ● ISSN 1785 0037 (Online)
DOI: http://dx.doi.org/10.15666/aeer/1706_1510315116

[9] Gabriel, M. M., Lourens, P., Pauline, B., Godefridus, M. M. (2017): Unleached prosopis litter inhibits germination but leached stimulates seedling growth of dry woodland species. – Journal of Arid Environments 138(1): 44-50.
[10] He, Z. S., Liu, J. F., Hong, W., Zheng, S. Q., Wu, C. Z., Wu, Z. Y., Lin, Y. J., Su, S. J. (2012): Effects of different treatments on seed germination of *Castanopsis kawakamii*. – Journal of Beijing Forestry University 34(2): 66-70.
[11] He, Z. S., Liu, J. F., Zheng, S. Q., Hong, W., Wu, C. Z., Li, J. (2018): Diurnal variation of photosynthetic rates of *Castanopsis kawakamii* seedlings and their relationships with meteorological factors in forest gaps and non-gaps. – Pakistan Journal of Botany 50(4): 1361-1368.
[12] He, Z. S., Wang, L. J., Jiang, L., Wang, Z., Liu, J. F., Xu, D. W., Hong, W. (2019): Effect of microenvironment on species distribution patterns in the regeneration layer of forest gaps and non-gaps in a Subtropical Natural Forest, China. – Forests 10(2): 90-103.
[13] Hou, Y. P., Peng, S. L., Chen, B. M., Ni, G. Y. (2011): Inhibition of an invasive plant (Mikania micrantha H. B. K.) by soils of three different forests in lower subtropical China. – Biological Invasions 13(2): 381-391.
[14] Hu, F., Shi, Q., Huang, L. J. (2015): Induction of adventitious roots during tissue culture of *Acacia mangium* and *A. auriculiformis* elite trees. – Journal of Nanjing Forestry University (Natural Sciences Edition)39(2): 57-62.
[15] Hunter, M. E., Menges, E. S. (2013): Allelopathic effects of litter *Axonopus compressus* against two weedy species and its persistence in soil. – American Journal of Botany 23(1): 69-54.
[16] Kilic, K., Kara, Y., Vaizogullar, H. E. (2016): Allelopathic effects of *Lyophyllum platypum* mushroom extracts on seed germination of *Cynanchum acutum* subspecies acutum weed. – Journal of Biotechnology 231: S23.
[17] Kimura, F., Sato, M., Kato-Noguchi, H. (2015): Allelopathy of pine litter: delivery of allelopathic substances into forest floor. – Journal of Plant Biology 58(1): 61-67.
[18] Liu, G. X., Wan, L. Q., He, F. (2016): Effects of litter, seed position, and water availability on establishment of seedlings for two semiarid grass species. – Plant Ecology 217(3): 277-287.
[19] Liu, J. F., He, Z. S., Hong, W., Zheng, S. Q., Wang, Z. J. (2011): Conservation ecology of endangered plant *Castanopsis kawakamii.* – Journal of Beijing Forestry University 33(5): 136-143.
[20] Liu, X. L. (2011): Close to Nature Forest Management Model on Tropical Coast *Casuarina equisetifolia* Plantation. – Chinese Academy of Forestry, Beijing.
[21] Ma, R. F., Liu, J. F., Wu, Z. Y., Zhang, G. S., Chen, Z. F., Hong, W., He, Z. S. (2014): Soil microbial community structure diversity in *Castanopsis kawakamii* forest. – Journal of Southwest Forestry University 34: 14-19.
[22] Ma, R. F., Liu, J. F., Zhang, G. S., Wu, Z. Y., Hong, W., He, Z. S. (2015): Effects of forest gaps on soil properties in *Castanopsis kawakamii* nature forest. – Journal of Plant Resources and Environment 10(10): 19-27.
[23] Marusa, P., Ishii-Iwamoto, E. L. (2011): Changes in energy metabolism and antioxidant defense systems during seed germination of the weed species *Ipomoea triloba L.* and the responses to allelochemicals. – Journal of Chemical Ecology 37(5): 500-513.
[24] Peng, X. B., Zhang, S. X. (2012): Allelopathic effects of aqueous extract of maize leaf on *Scutellaria baicalensis* seeds. – Pratacultural Science 29(2): 255-262.
[25] Shibaeva, T. G., Sherudilo, E. G., Titov, A. F. (2018): Response of *Cucumber* (*Cucumis sativus L.*) response of *Cucumber* (*Cucumis sativus L.*) plants to prolonged permanent and short-term daily exposures to chilling temperature. – Russian Journal of Plant Physiology 65(2): 286-294.
[26] Steven, M. D., Malthus, T. J., Frédéric, B., Xu, H., Chopping, M. J. (2003): Intercalibration of vegetation indices from different sensor systems. – Remote Sensing of Environmen 88(4): 412-422.

http://www.aloki.hu ● ISSN 1589 1623 (Print) ● ISSN 1785 0037 (Online)
DOI: http://dx.doi.org/10.15666/aeer/1706_1510315116

[27] Su, S. J., Liu, J. F., He, Z. S., Hong, W., Zhang, J. B. (2012): The spatial heterogeneity of soil nutrients in a mid-subtropical *Castanopsis kawakamii* natural forest. – Acta Ecologica Sinica 32(18): 5673-5682.
[28] Tung, Y. T., Chang, W. C., Chen, P. S., Chang, C. T., Chang, S. T. (2015): Ultrasound-assisted extraction of phenolic antioxidants from *Acacia confusa* flowers and buds. – Journal of Separation Science 34(7): 844-851.
[29] Wang, G. Z., Peggy, S., Alice, T., Zhang, J. L., Zhang, F. S., James, D. B. (2019a): Soil microbiome mediates positive plant diversity-productivity relationships in late successional grassland species. – Ecology Letters. https://doi.org/10.1111/ele.13273.
[30] Wang, Z., Lan, Y. Q., He, Z. S., Liu, J. F., Xing, C., Zhu, J., Wang, X. L., Shi, Y. W., Shen, C. X. (2019b): Effects of *Castanopsis kawakamii* forest litter extract on its seed germination and radicle growth. – Journal of Fujian Agriculture and Forestry University (in press).
[31] Wei, Y. L., Mao, M. Q., Zhao, Y., Ma, M. D. (2018): Effects of aqueous extracts from *Paris polyphylla* seeds on seed germination and seedling growth of three kinds of plants. – Plant Science Journal 36(1): 94-102.
[32] Yang, S. Y., Lin, P., Gou, J. Y., Lin, R. Y., Chen, G. S., He, Z. M., Xie, J. S. (2003): Litter production, nutrient return and leaf-litter decomposition in natural and monoculture plantation forests of *Castanopsis kawakamii* in subtropical China. – Acta Ecologica Sinica 23(7): 1278-1289.
[33] Yuan, H., Hou, F. J. (2010): The allelopathy effect of litter from three dominant species on alfalfa seedlings growth in the Loess Plateau. – Pratacultural Science 27(06): 20-24.
[34] Zhang, F. Y., Du, Z. Z., He, J. W., Yang, L. Y. (2016): Effects of *Eupatorium adenophorumii* litter aqueous extract on its seed germination and seedling growth. – Research of Soil and Water Conservation 23(3): 291-296+303.
[35] Zhuang, Z., Li, Y. J., Liu, Q. Q., Yang, Z., Liu, B., Liu, A. Q. (2017): Effects of Chinese fir litter extracts on the seed germination and seedling. – Journal of Forests and Environment 37(1): 29-33.

http://www.aloki.hu ● ISSN 1589 1623 (Print) ● ISSN 1785 0037 (Online)
DOI: http://dx.doi.org/10.15666/aeer/1706_1510315116

DETERMINATION OF REFERENCE ET_O BY USING DIFFERENT K_P EQUATIONS BASED ON CLASS A PAN EVAPORATION IN SOUTHEASTERN ANATOLIA PROJECT (GAP) REGION

AYDIN, Y.

Department of Biosystem Engineering, Faculty of Agriculture, Siirt University, Siirt, Turkey
(e-mail: yusufaydin@siirt.edu.tr; phone: +90-484-212-1111; fax: +90-484-223-1998)

(Received 28th Jun 2019; accepted 11th Oct 2019)

Abstract. An accurate estimation of ET is very important and the ET estimation method that is suited to the region should be used. Evapotranspiration (ET) is calculated by multiplying reference ET_o with the crop coefficient for the studied plant (K_c) or its pan evaporation coefficient (K_p). The purpose of this study was to use the K_p equations developed based on the Pan evaporation principle for estimating ET_o values and determining the best K_p equation for the GAP region by making comparisons via the standard method. $K_{p\text{-}Pere}$ method (RMSE: 0.48, MAE: 0.30, MR: 0.64 and PE: 3.19) displayed a better performance than $K_{p\text{-}Sny}$ (RMSE: 1.08, MAE: 0.70, MR: 0.80 and PE: 29.35) in the semi-arid climate conditions of the GAP region. It was determined according to the regression analysis results that the $K_{p\text{-}Sny}$ equation is better than $K_{p\text{-}Pere}$ by a margin of 2.1%. Accordingly, $K_{p\text{-}Pere}$ equation based on Pan evaporation can be used as an alternative to the standard method for determining reference ET_o in the semi-arid conditions of the GAP region. Similarly, $K_{p\text{-}Sny}$ equation together with $K_{p\text{-}Pere}$ can be used as substitutes for the standard $ET_{o\text{-}PM}$ method since it requires less climate data.
Keywords: *evapotranspiration, reference ET_o, methods comparisons, FAO-PM equation, pan evaporation coefficient, Snyder and Pereira equations*

Introduction

Evapotranspiration (ET) is a synchronous process during which the water is transferred to the atmosphere by way of transpiration and evaporation from the soil-plant system. Hence, ET is a critical parameter for irrigation planning and operation as well as for climatologic and hydrologic studies. Agricultural yield per unit area should be at a maximum level in order to meet the food demand that is increasing due to rapid urbanization and population increase, industrialization as well as decrease in agricultural areas over time and global warming. This can be accomplished best by applying the amount of irrigation water required by the irrigated plants in order to obtain maximum yield from the agricultural activity while eliminating excessive water use (Ertek, 2011). There are many factors that have an impact on evapotranspiration and these factors should be calculated at different regions for each plant species since they are more closely related to the land and climate conditions. Actual evapotranspiration (ET_c) is generally calculated by multiplying the reference evapotranspiration (ET_o) with a coefficient specific to the plant that can be calculated based on many factors encompassing the water regime and operation. Reference evapotranspiration (ET_o) is the amount of evapotranspiration (FAO-24) from the grass plant covering the soil surface at a height of 8-15 cm under full irrigation conditions and is calculated via mathematical methods based on the evapotranspiration ET_o of other plants (Çobaner et al., 2016). The FAO-56 Penman-Monteith (PMF-56) equation developed by Allen et al. (1998) which is also known as the combination method based on mass transfer is widely used as the standard method for determining the reference evapotranspiration. In addition to the standard method, various other techniques have also been developed for calculations based on climate data such as

http://www.aloki.hu ● ISSN 1589 1623 (Print) ● ISSN 1785 0037 (Online)
DOI: http://dx.doi.org/10.15666/aeer/1706_1511715129

temperature (Thorntwaite, 1948; Doorenbos and Pruitt, 1977), solar radiation (Doorenbos and Pruitt, 1977; Hargreaveas and Samani, 1985; Djaman et al., 2015). Direct and indirect measurement methods used in ET_o estimation vary subject to the region, climate, plant species, current data and the purpose of the calculation (Kanber, 2006). Lysimeter method is generally used for the direct estimation of ET_o. However, the evapotranspiration values acquired using this method are not suited for making comparisons with values calculated from meteorological data. The use of lysimeters in ET_o measurement is not a proper method due not only to its cost and complex operation but also the facts that it is used for measurements at limited areas, does not have sufficient surface area and the acquired data are not sufficiently significant. ET_o estimation in application can be calculated from meteorological data as well as by multiplying the evaporation values obtained from the Pan evaporation cup by a transformation factor (K_{pan}) (Tabari et al., 2013). Trajkovic and Kolakovic (2009) reported that the ET_o estimation method based on Pan evaporation principle can be used successfully as an alternative to the standard method of PMF-56 under Serbia conditions. Similarly, Tabari et al. (2013) carried out a study under the humid climate conditions of Iran comparing the PMF-56 model with a total of 31 reference evapotranspiration calculation models with 8 based on Class A Pan, 7 on temperature, 10 on mass transfer, 4 on radiation and 2 again on radiation. According to the comparisons carried out, the methods based on evaporation and temperature and the K_p equation based on evaporation developed by Snyder (1992) displayed the best performance for ET_o estimation. Castaneda and Rao (2005) used the FAO-56 PM method as standard for comparing the Thorntwaite, Blaney-Criddle, Turc and Makkink methods used for estimating reference ET_o in Southern California conditions. Djaman et al. (2015) compared the 16 ET_o estimation method with the ASCE-PM equation for developing an equation that can be used for ET_o estimation under Senegal conditions with less data. Similarly, Shahidian et al. (2012) compared models based on temperature and radiation with the PMF-56 model developed by Allen et al. (1998) published in FAO Irrigation and Drainage Paper, No: 56 which can be operated based on 4 basic data such as temperature, wind speed, radiation and relative humidity. Aydınşakir et al. (2003) indicate that Class A Pan evaporation method is the best ET_o estimation method for use in estimating grass reference evapotranspiration via empirical models.

The purpose of this study was to compare the reference ET_o values estimated via different methods with the standard PMF-56 standard method and determine the performance of the K_p equations based on pan evaporation method in the GAP region with arid and semi-arid climate conditions. For this purpose, 4 year climate data for the Gaziantep province in Southeastern Anatolia Region acquired from Turkish State Meteorological Service (TSMS) records for the years 1999-2002 were used. The ET_o values calculated using the standard reference evapotranspiration method of FAO-PM and the pan coefficients (K_p) developed by Snyder and Pereira calculated based on Class A Pan were compared. The $ET_{o\text{-}PM}$ values calculated at a daily level under Gaziantep climate conditions by Aydın (2004) and Ünlü (2005) were used as the standard FAO-PM method. The same climate data were used for calculating the compared K_p equations.

Materials and method

Description of study area and weather data

Southeastern Anatolia Region, one of the 7 geographical regions of Turkey is known as the GAP region due to the project comprised of 13 project packages on the Fırat-Dicle

http://www.aloki.hu ● ISSN 1589 1623 (Print) ● ISSN 1785 0037 (Online)
DOI: http://dx.doi.org/10.15666/aeer/1706_1511715129

basin for improving soil and water resources and covers a total of 9 provinces including Gaziantep, Kilis, Şanlıurfa, Adıyaman, Diyarbakır, Batman, Mardin, Siirt and Şırnak (*Fig. 1*) (Anonymous, 2019). The GAP region displays continental climate characteristics. Summers are quite hot, whereas winters are rarely cold. Annual average temperatures are 16.4 °C with July averages of 29.8 °C. Annual average rainfall in the region is 565 mm and majority of the rainfall takes place during the winter and spring due to the irregularity in the rain regime. The intensity of aridness increases during the summer months since the annual relative humidity value reaches 53.6% on average. The province of Gaziantep where the study has been carried out is located between eastern longitudes of 36° 28' and 38° 0' and between the northern latitudes of 36° 38' and 37° 32'. It has a climate structure with transition characteristics between the Mediterranean and continental climates. Summers are quite hot and arid, whereas winters are cold and rainy. Average annual temperature is 14.9 °C, with a maximum temperature of 44 °C and minimum temperature of -17.5 °C. The hottest month is July with 27.7 and the coldest month is January with 3.4 whereas the average annual rainfall amount is 544.3 mm. Rains generally take place during the winter months and rarely during the summer months when crops need water and when evapotranspiration is high (Aydın, 2004).

Figure 1. *Locational view of study area*

ET_o estimation methods

Food and Agriculture Organization (FAO), together with the International Commission on Irrigation and Drainage and the World Meteorological Organization (WMO) put forth in 1990 that the FAO-PM (Allen et al., 1998) method can be taken as reference since it yields more consistent and reliable results in comparison with other methods (Castaneda and Rao, 2005; Çobaner et al., 2016). Therefore, FAO-56-PM method was taken as reference in this study for comparing the other methods. Different methods that can be operated with less data have been developed for the difficulties experienced while using the standard method for reference ET_o estimation as well as conditions when sufficient amount of data cannot be acquired. The ET_o estimation

http://www.aloki.hu ● ISSN 1589 1623 (Print) ● ISSN 1785 0037 (Online)
DOI: http://dx.doi.org/10.15666/aeer/1706_1511715129

developed by Snyder (1992) and Pereira et al. (1995) via K_p equations is one of the widely used methods. Hence, various empirical equations used for determining reference evapotranspiration have been evaluated comparatively. However, since these methods are equations operated based on Class A Pan evaporation values and since evaporation is not measured in Turkey during the winter season, ET_o calculations were made only for the April-November period when evaporation measurement is made. In graphical representations, it is shown only as DOY in order to make the number of days between the mentioned periods high and the graphs easy to understand The climate data used for this purpose have been obtained from the Turkish State Meteorological Service (TSMS) (Anonymous, 2018).

FAO-56 Penman Monteith method

The FAO-56 Penman Monteith method used for determining reference evapotranspiration can be used with daily meteorological data such as temperature, wind speed, evaporation, relative humidity. This equation can be expressed as below (Fisher et al., 2013).

$$ET_o = \frac{0.408x(R_n - G) + \gamma \frac{900}{T+278} u_2 (e_s - e_a)}{\Delta + \gamma\ 1 + 0.34u_2} \quad \text{(Eq.1)}$$

where ET_o: reference evapotranspiration (mm/day); R_n: net radiation (MJ m^{-2}), G: soil heat flux (MJ m^{-2}), T_{mean}: average air temperature (°C), U_2: wind speed at 2 m height ($m.s^{-1}$), e_s: saturation vapor pressure (kPa), e_a: actual vapor pressure (kPa), Δ: slope of vapor pressure curve (kPa $°C^{-1}$), γ: psycrometric constant (kPa $°C^{-1}$).

The ET_o software developed by FAO-56 was used for determining reference evapotranspiration. All parameters used in this software are data measured daily and acquired from the meteorological station.

Snyder equation

The equation developed by Snyder (1992) was used for calculating the K_p values based on Class A Pan. This equation can be expressed as follows:

$$K_p = 0.482 + 0.0424xLn(F) - 0.000376xW_s + 0.0045xRH \quad \text{(Eq.2)}$$

where F: fetch distance (meter) has been assumed as 1 m. W_s: daily average wind speed (m sec^{-1} day^{-1}) and RH: daily relative humidity (%).

Pereira equation

The equation developed by Pereira et al. (1995) for calculating reference ET_o based on Class A Pan which is the second method used for comparisons can be expressed as follows (Tabari et al., 2013).

$$K_p = \frac{0.85x(\Delta + \gamma)}{[\Delta + \gamma x(1 + 0.33x U_2)]} \quad \text{(Eq.3)}$$

$$\Delta = \frac{4098\,[0.6108 \exp\,(\frac{17.27T}{T+237.3})]}{(T+237.3)^2} \quad \text{(Eq.4)}$$

http://www.aloki.hu ● ISSN 1589 1623 (Print) ● ISSN 1785 0037 (Online)
DOI: http://dx.doi.org/10.15666/aeer/1706_1511715129

where Δ: slope of the saturated vapour pressure versus temperature curve (kPa °C $^{-1}$) and γ: the psicrometric coefficient (kPa °C $^{-1}$), T: mean air temperature (°C), exp (…) 2.7183 base of natural logarithm) raised to the power (…).

$$T_{mean} = \frac{T_{max} + T_{min}}{2}; \quad \gamma = 0.665.10^{-3} x\ P; \quad P = 101.3\left(\frac{293 - 0.0065z}{293}\right)^{5.26} \qquad \text{(Eq.5)}$$

Parameters such as slope (Δ), average temperature (T), psychrometric constant (γ), elevation above sea level (z) and pressure (P) included in the above equations were calculated in accordance with FAO-56.

The K_p coefficients obtained from the equations were used in reference ET_o calculation, (Doorenbos et al., 1977) and the following equation suggested by Tabari et al. (2013).

$$ET_o = E_{pan} x K_{pan} \qquad \text{(Eq.6)}$$

ET_o: Reference evapotranspiration, mm day^{-1}; K_{pan}: Coefficient based on Class A Pan evaporation cup, E_{pan}: Class A Pan evaporation value, mm day^{-1}

The ET_o values for the studied years related with the FAO-56 PM method taken as the standard method were first calculated in the study. Climate parameters such as temperature, relative humidity, wind speed, solar radiation, rain and evaporation for the years between 1999 and 2002 were acquired from meteorological records after which reference ET_o values were estimated using both the standard method for ET_o estimation and the compared K_p equations. Since the climatic data used in the estimation of ET_o for the last years could not be obtained from the meteorological records, the data of 1999-2002 were used in FAO-56 PM calculations. Fetch distance was taken as 1 m while calculating the $K_{p\text{-}Sny}$ equation since the meteorological station is covered with irrigated green plants. The calculations were made separately for each study year, after which 4 year averages were calculated for the ET_o values of the same day thereby obtaining the long term averages for the daily ET_o values. Annual average ET_o values were calculated using the average daily ET_o values. However, since evaporation measurements are not made during the rainy winter months at the meteorological station, ET_o estimation was made by calculating the K_p values with the E_{pan} values for the months during which measurements were made (April-November).

Statistical analysis

$ET_{o\text{-}Sny}$ and $ET_{o\text{-}Pere}$ obtained by using the standard FAO-PM ET_o values calculated daily and the K_p values calculated using Snyder (1992) and Pereira et al. (1995) equations were compared statistically. Paired comparisons were made between R^2 values and ET_o values which were then subject to linear regression analysis and the R^2 equation was determined for the obtained curve. The equations in *Table 1* suggested by Djaman (2015) and Diouf (2016) were used for a more advanced evaluation of the compared equations.

Result and discussion

Figure 2 shows monthly average and cumulative ET_o values. The reference ET_o values calculated via the pre-determined methods. While the references ET_o values

http://www.aloki.hu ● ISSN 1589 1623 (Print) ● ISSN 1785 0037 (Online)
DOI: http://dx.doi.org/10.15666/aeer/1706_1511715129

calculated using K_p equations based on Pan evaporation were determined to be higher in comparison with the values obtained using the standard method for the months of May-October (overestimated), $ET_{o\text{-}Pere}$ value for the months of April and November were calculated as below the values obtained using the standard method (underestimated).

Table 1. *Statistical analysis equations*

Source	Equation	
Root mean square error (RMSE)	$RMSE = \sqrt{\sum_{k=0}^{n} \frac{(P_i - O_i)^2}{n}}$	(Eq.7)
Mean absolute error (MAE)	$MAE = n^{-1}\sum_{1}^{n}(P_i - O_i)$	(Eq.8)
Percentage error (PE)	$PE = \left\lvert \frac{P_{ave} - O_{ave}}{O_{ave}} \right\rvert 100\%$	(Eq.9)
Mean ratio (MR)	$MR = n^{-1}\sum_{1}^{n} \frac{P_i}{O_i}$	(Eq.10)
Determination coefficient (R^2) (Todorovic et al., 2013)	$R^2 = \left\{ \frac{\sum_{i=1}^{n}(O_i - \bar{O}).(P_i - \bar{P})}{\sqrt{\sum_{i=1}^{n}(O_i - \bar{O})^2}.\sqrt{\sum_{i=1}^{n}(P_i - \bar{P})^2}} \right\}^2$	(Eq.11)

RMSE: root mean square error; MAE: mean absolute error; MR: mean ratio; PE: percentage error of estimate; n: number of observations, P_i: estimated ET_o by other equations, O_i: PM-estimated ET_o (actual), P_{ave}: mean of the estimated ET_o, O_{ave}: mean of the O_i. In order to determine R^2 the pair wise comparisons were made by using linear regression

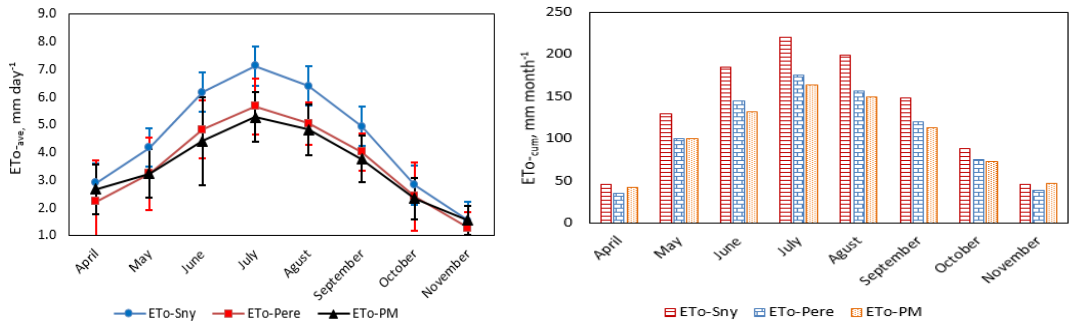

Figure 2. *Temporal variation of four years monthly average and cumulative ET_o values (vertical bars show the standard errors)*

The ET_o values calculated via K_p equations were subject to comparisons between themselves as well as with the standard method. It was observed when the study years were evaluated separately (*Fig. 3*) that the $ET_{o\text{-}Sny}$/$ET_{o\text{-}Pere}$ values calculated via K_p equations and the standard $ET_{o\text{-}PM}$ values put forth tendencies similar to the changes in the monthly averages. The values closest to the standard $ET_{o\text{-}PM}$ method were calculated using the ET_o values obtained by $K_{p\text{-}Pere}$ equation which displayed a better performance than the $ET_{o\text{-}Sny}$ values. This relationship was observed for all study years.

http://www.aloki.hu ● ISSN 1589 1623 (Print) ● ISSN 1785 0037 (Online)
DOI: http://dx.doi.org/10.15666/aeer/1706_1511715129

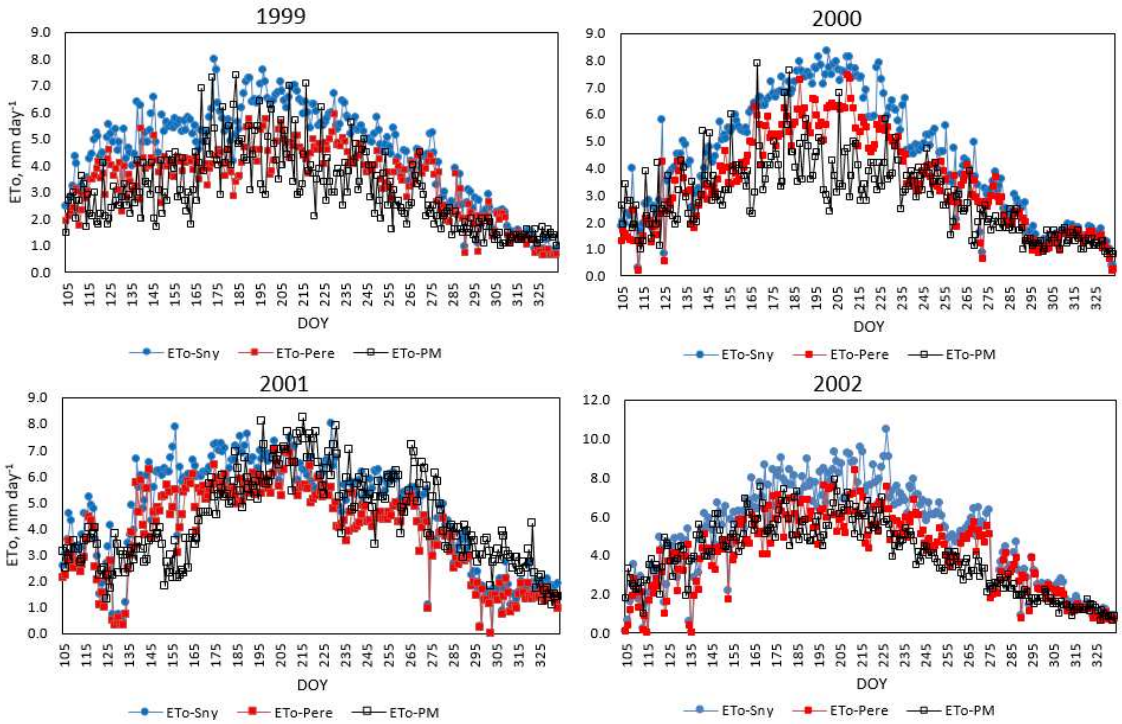

Figure 3. *Comparison of daily average ET_o values obtained from equations and standard method during study years*

Long term daily average ET_o values calculated daily during the study years via K_p equations were subject to paired comparisons separately with the standard FAO-56 PM method (*Fig. 4*). As can be seen from the figure, the ET_o values calculated via the $K_{p\text{-}Pere}$ equation were determined to be closer to the values calculated with the standard method with lower rate of change and change % for the comparison. When compared with the standard method, the $K_{p\text{-}Pere}$ equation displayed a better performance in comparison with the $K_{p\text{-}Sny}$ equation. While both equations yielded overestimated values compared with the standard method, the performances vary with regard to the rates of change and change %. When the changes of the curves in *Figure 2* and the rates of change and change percentage (%) in *Table 2* are evaluated, it can be observed that the $K_{p\text{-}Pere}$ equation put forth a better performance in comparison with $K_{p\text{-}Sny}$ at both the monthly averages level and the hottest months and long term averages levels.

The regression analysis carried out for determining the relationship between the ET_o values obtained via the equations and the standard method along with the R^2 values have been given in *Figure 5* and *Table 3*.

http://www.aloki.hu ● ISSN 1589 1623 (Print) ● ISSN 1785 0037 (Online)
DOI: http://dx.doi.org/10.15666/aeer/1706_1511715129

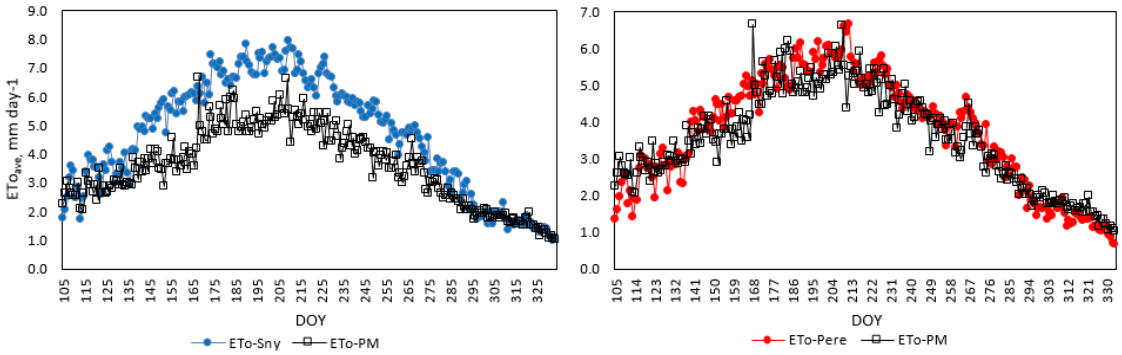

Figure 4. *Comparison of long term daily average ET_o values obtained by K_p equations with standard method*

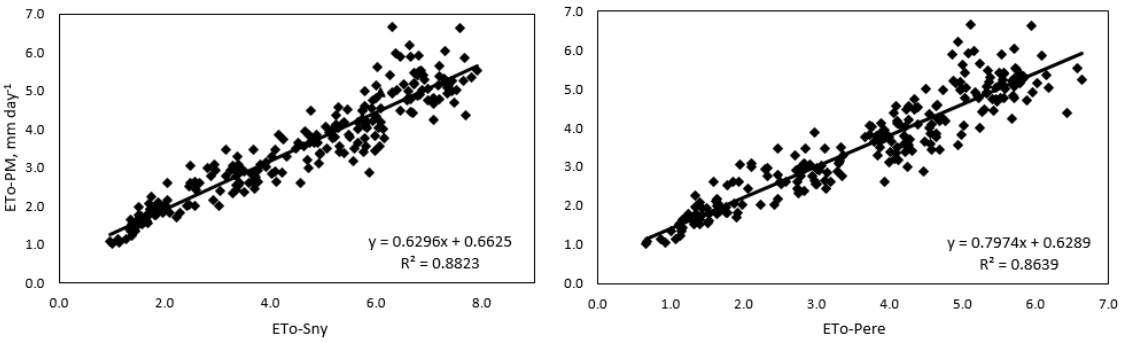

Figure 5. *Determination of regression coefficients between long term daily average $ET_{o\text{-}equations}$ values and standard $ET_{o\text{-}PM}$ method*

The ET_o values calculated via $K_{p\text{-}Sny}$ and $K_{p\text{-}Pere}$ equations used for calculating reference ET_o value were subject to comparisons among themselves for determining their performances and changes throughout the study years (*Fig. 6*). As can be seen from the figure, long term average $ET_{o\text{-}Pere}$ values were lower than $ET_{o\text{-}Sny}$ which can be observed more clearly during the evaporation period, especially during the hot summer months. This distinction can be seen in *Figure 4* where the ET_o values calculated via equations are compared with the standard method. It was observed as a result of the comparison made between ET_o values calculated via equations and the standard method that the $ET_{o\text{-}Pere}$ values provided results that are closer to the standard method than $ET_{o\text{-}Sny}$ thereby displaying a better performance and that the rate of change and change % between the $ET_{o\text{-}Sny}$ and $ET_{o\text{-}PM}$ values are higher in comparison with $ET_{o\text{-}Pere}$.

As can be seen from the comparison between the K_p equations (in *Fig. 6; Table 2*), the $ET_{o\text{-}Sny}/ET_{o\text{-}Pere}$ rate of change varied between 1.30 and 1.17 throughout the calculation period with an average of 1.25 which was calculated as 1.27 for the month of August. The similarities or differences in the rates of change of the equations can also be monitored here when the change %'s are examined. The highest rate of change % was calculated for the month of April (30.3%) while the lowest rate of change was calculated for the month of October and the long term average rate of change was calculated as 24.82%.

http://www.aloki.hu ● ISSN 1589 1623 (Print) ● ISSN 1785 0037 (Online)
DOI: http://dx.doi.org/10.15666/aeer/1706_1511715129

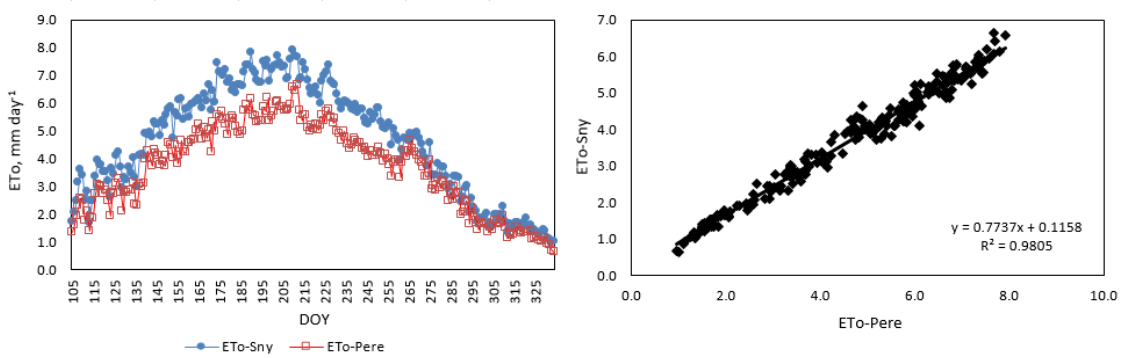

Figure 6. *Comparison of ET_o values obtained by K_p equations with each other and regression coefficient*

Table 2 summarizes the comparisons made between the ET_o values obtained from K_p equations based on Pan evaporation principle used for reference ET_o estimation and Standard FAO-56 PM method. Long term monthly averages were calculated for the ET_o values calculated via the equations and FAO-56 PM values. Afterwards, paired comparisons were carried out for both these values with each other and with the standard method and the relations between the ET_o values and their rates of changes were calculated on a monthly basis.

Table 2. *Monthly average ET_o values obtained from equations and comparison by standard methods*

Methods	Monthly average ET_o values of methods								
	Apr.	**May**	**June**	**July**	**Aug.**	**Sep.**	**Oct.**	**Nov.**	**Mean**
$ET_{o\text{-}Sny}$	2.9	4.2	6.2	7.1	6.4	4.9	2.8	1.5	4.5
$ET_{o\text{-}Pere}$	2.2	3.3	4.8	5.7	5.1	4.0	2.4	1.3	3.6
$ET_{o\text{-}PM}$	2.7	3.3	4.4	5.3	4.8	3.8	2.4	1.6	3.5
Comparisons of equations between them and the standard method as change percentage (%)									
$ET_{o\text{-}Sny}/ET_{o\text{-}PM}$	1.09	1.29	1.40	1.35	1.33	1.31	1.21	0.99	1.24
$ET_{o\text{-}Pere}/ET_{o\text{-}PM}$	0.83	1.00	1.09	1.07	1.05	1.07	1.03	0.83	1.00
$ET_{o\text{-}Sny}/ET_{o\text{-}Pere}$	1.30	1.29	1.28	1.26	1.27	1.23	1.17	1.19	1.25
Variation rates of ET_o values obtained by equations according to standard method (%)									
$ET_{o\text{-}Sny}/ET_{o\text{-}PM}$	8.7	28.8	39.8	35.0	32.8	31.0	20.5	-1.2	24.42
$ET_{o\text{-}Pere}/ET_{o\text{-}PM}$	-16.6	0.1	9.3	7.4	4.9	6.6	2.9	-17.2	-0.33
$ET_{o\text{-}Sny}/ET_{o\text{-}Pere}$	30.3	28.7	27.9	25.8	26.6	22.9	17.2	19.3	24.82

As can be seen from the table, the change in $ET_{o\text{-}Pere}$ values was observed to be lower (underestimated) ($0.83 < 1.09$ and $0.83 < 0.99$) in comparison with $ET_{o\text{-}Sny}$ as a result of the comparison between the ET_o values obtained from equations and the standard method during the months when the evaporation measurement started and ended and the rate of change was calculated as -16.6 and -17.2. The same values were determined as 8.7 and -1.2 respectively for the $ET_{o\text{-}Sny}$ equation. When the compared long term averages are examined, the rate of change for $ET_{o\text{-}Pere}$-$ET_{o\text{-}PM}$ was determined as 1.00 whereas, the rate of change for $ET_{o\text{-}Sny}/ET_{o\text{-}PM}$ was calculated as 1.24. The

http://www.aloki.hu ● ISSN 1589 1623 (Print) ● ISSN 1785 0037 (Online)
DOI: http://dx.doi.org/10.15666/aeer/1706_1511715129

underestimated values observed for $ET_{o\text{-}Pere}$ were at about the same level throughout al the months and were lower than $ET_{o\text{-}Sny}$ during the hottest month of July with a value of 1.07. Similarly, it was also observed as a result of the comparison between $ET_{o\text{-}Pere}$ and $ET_{o\text{-}Sny}$ values with the standard method of $ET_{o\text{-}PM}$ that $ET_{o\text{-}Pere}$ displayed a better performance with regard to the comparison between each other as well as the % rate of change. Trajkovic and Stojnic (2008) carried out a study on reference ET_o determination methods during which Cristiansen and FAO-24 Pan evaporation methods were compared with the standard FAO-PM method. It was reported in the study that the Cristiansen method put forth a better performance in comparison with the standard FAO-PM and the FAO-24 Pan method which is due to the fact that the Cristiansen method makes use of more climate parameters than FAO-24 Pan. Moreover, it was also indicated that the Pan evaporation values can be used as a substitute for the FAO-56 PM method.

Statistical evaluations were carried out in order to define the relationships between the compared K_p equations and the standard FAO-56 PM methods accurately and to determine the levels of relationships (*Table 3*).

Table 3. *Result of statistical analysis among ET_o methods*

	RMSE (mm/day)	**MAE (mm)**	**MR**	**PE (%)**	**R^2**
$ET_{o\text{-}Sny}$-$ET_{o\text{-}PM}$	1.08	0.70	0.80	29.35	0.8823
$ET_{o\text{-}Pere}$-$ET_{o\text{-}PM}$	0.48	0.30	0.64	3.19	0.8639
$K_{p\text{-}Sny}$-$K_{p\text{-}Pere}$	---	---	---	---	0.9805

As can be seen from the table, the ET_o values calculated via $K_{p\text{-}Pere}$ equation yielded values closer to the standard method during the comparisons of the ET_o values obtained using K_p equations with the standard method. The root mean square error (RMSE) values for the $ET_{o\text{-}Pere}$-$ET_{o\text{-}PM}$ comparison were observed to be lower than $ET_{o\text{-}Sny}$ with regard to error statistics (0.48 < 1.08). Similarly, $ET_{o\text{-}Pere}$ put forth values lower in comparison with those of $ET_{o\text{-}Sny}$ with regard to the other error statistics of mean absolute error, mean ratio and percentage error values thereby displaying a higher accordance with the standard method. Contrary to the aforementioned comparisons, a smaller difference is observed only between the R^2 values with $ET_{o\text{-}Sny}$ having an R^2 value of 2.1 times higher than that of $ET_{o\text{-}Pere}$. The K_p equations used in the study were subject to regression analyses as a result of which the R^2 value was calculated as 0.9805 (*Table 3; Fig. 6*). This is an indication that both methods can be used together for ET_o prediction. Tabari et al.(2013) carried out a study during which a total of 31 different models used for determining reference ET_o under the humid climate conditions of northern Iran. A total of 8 methods based on Pan evaporation were evaluated and while the $K_{p\text{-}Sny}$ method was ranked number 4 under humid region conditions (R^2: 0.86, RMSE: 0.53, PE: 4.91), the $K_{p\text{-}Pere}$ method (R^2:0.88, RMSE:0.82, PE:30.16) was ranked number 6. Another study with similar results under conditions of Brazil was carried out by Conceiçâo (2002) regarding the usability of Class A Pan evaporation based equations for determining reference ET_o. In this study, Pan evaporation based $K_{p\text{-}Sny}$, $K_{p\text{-}Pere}$ equations were compared with the standard FAO-PM methods. As a result of the study, the best estimation was obtained with the $K_{p\text{-}Sny}$ equation. It is considered that the better performance of $K_{p\text{-}Pere}$ equation is due to the climate conditions of the region. The consistency and reliability of the method should be re-evaluated for methods based on

http://www.aloki.hu ● ISSN 1589 1623 (Print) ● ISSN 1785 0037 (Online)
DOI: http://dx.doi.org/10.15666/aeer/1706_1511715129

Pan evaporation in case they are used for different regions and climate conditions since they yield reliable results for the environmental conditions for which they have been developed (Kaya et al., 2016). Sentelhas and Folegatti (2003) carried out a study under Brazil-Sao Paulo conditions for the determination of K_p coefficients while determining daily reference ET_o. It was determined in this study during which six equations based on Class A Pan were tested that the $K_{p\text{-}Pere}$ (Pereira et al., 1995) and Cuenca (1989) equations displayed the best performance for ET_o estimation. However, the researcher suggested the calibration of the equations used for different climates and regions.

Conclusion

Even though the standard ET_o estimation method suggested in FAO-56 and developed by Allen et al. (1998) is widely used, its usage is still limited due to its complex structure and its requirement of climate data such as temperature, relative humidity, wind speed, soil heat flux and radiation. It is not always possible to obtain these data in many developing countries due to the required technological infrastructure and the high costs involved. Hence, equations that can be operated with less climate data which can easily be obtained have been developed for use in ET_o estimation. The K_p equations based on Pan evaporation principle for ET_o estimation developed by Snyder (1992) and Pereira (1995) have been used in the present study which were compared with the standard method.

In conclusion, it was determined that methods based on evaporation can be used as alternative or substitute methods to the standard methods for reference evapotranspiration estimation under the hot and semi-arid conditions of the GAP region and that the $K_{p\text{-}Pere}$ equation displayed a better performance under these conditions in comparison with $K_{p\text{-}Sny}$. However, it is expected that changes will take place in the climate of the region over time due to the developing structure of the region, the expansion of drainage basins as well as the increase in evaporation surface areas. Hence, reference evapotranspiration studies should be evaluated in detail for the region including the standard methods as well and further studies should be carried out for determining high performance methods which can adapt to the continental climate conditions of the region. Accurate estimation of reference evapotranspirations will enable the effective use of the irrigation sources for the ongoing projects in the GAP region in addition to the execution of the correct irrigation programs, thereby paving the way for obtaining maximum yield as well as water savings with the efficient use of irrigation water.

REFERENCES

[1] Allen, R. G., Pereira, L. S., Raes, D., Smith, M. (1998): Crop Evapotranspiration (Guidelines for Computing Crop Water Requirements). – Irrigation and Drainage Paper No: 56. FAO, Rome.

[2] Anonymous (2018): General Directorate of State Meteorological Affairs (DMİGM). – https://www.mgm.gov.tr/veridegerlendirme/il-ve-ilceler-istatistik.aspx?k=A&m=SIIRT (date of access, Dec 06, 2018).

[3] Anonymous (2019): Republic of Turkey, Ministry of Industry and Technology, Regional Development Administration of Southeast Anatolian Project (GAP). – http://www.gap.gov.tr/gap-illeri-sayfa-13.html (date of access: April 16, 2019).

http://www.aloki.hu ● ISSN 1589 1623 (Print) ● ISSN 1785 0037 (Online)
DOI: http://dx.doi.org/10.15666/aeer/1706_1511715129

[4] Aydın, Y. (2004): The effect of different irrigation water and Nitrogen Levels on Yield and Alternate Bearing in Pistachio. – Çukurova Uni. Institute of Natural and Applied Science. Department of Agriculture Structure and Irrigation. Ph.D. Thesis (in Turkish).
[5] Aydınşakir, K., Baştuğ, R., Büyüktaş, D. (2003): A research on calibration of some amprical equations for grass reference evapotranspiration under field and small lysimeter conditions in Antalya Region. – Akdeniz Uni. Journal of Agriculture Faculty 16(1): 107-119 (in Turkish).
[6] Castañeda, L., Rao, P. (2005): Comparison of methods for estimating reference evapotranspiration in southern California. – Journal of Environmental Hydrology 13(14).
[7] Cuenca, R. H. (1989): Irrigation System Design: An Engineering Approach. – Prentice-Hall, Englewood Cliffs, NJ.
[8] Çobaner, M., Çıtakoğlu, H., Haktanır, T., Yelkara, F. (2016): Determination of optimal Hargreaves-Samani equation for the Mediterranean region. – Dicle University, Faculty of Engineering, Journal of Engineering 7(2): 181-190 (special issue, in Turkish).
[9] Conceiçâo, M. A. F. (2002): Reference evapotranspiration based on class A pan evaporation. – Scientia Agricola 59(3): 417-420.
[10] Diouf, O. C., Weihermüller, L., Ba, K., Faye, S. C., Faye, S., Vereecken, H. (2016): Estimation of Turc reference evapotranspiration with limited data against the Penman-Monteith formula in Senegal. – Journal of Agriculture and Environment for International Development - JAEID 110(1): 117-137. DOI: 10.12895/jaeid.20161.417.
[11] Djaman, K., Balde, A. B., Sow, A., Muller, B., Irmak, S., N'Diaye, M. K., Manneh, B., Moukoumbi, Y. D., Futakuchic, K., Kazuki Saito, S. (2015): Evaluation of sixteen reference evapotranspiration methods under Sahelian conditions in the Senegal River Valley. – Journal of Hydrology: Regional Studies 3: 139-159.
[12] Doorenbos, J., Pruitt, W. O. (1977): Guidelines to Crop Water Requirements. – Irrigation and Drainage Paper No: 24 (revised). FAO, Rome.
[13] Ertek, A. (2011). Importance of pan evaporation for irrigation scheduling and proper use of crop-pan coefficient (K_{cp}), crop coefficient (K_c) and pan coefficient (K_p). Full length research paper. – African Journal of Agricultural Research 6(32): 6706-6718. DOI: 10.5897/AJAR11.1522.
[14] Fisher, D. K., Pringle III, H. C. (2013). Evaluation of alternative methods for estimating reference evapotranspiration. – Agricultural Science 4(8A): 51-60. http://dx.doi.org/10.4236/as.2013.48A008.
[15] Hargreaves, G. H., Samani, Z. A. (1985): Reference crop evapotranspiration from ambient air temperature. – American Society of Agricultural Engineers, Hyatt Regency, Chicago IL, 1985 Winter Meeting December 17-20, Paper No: 85-2517.
[16] Kanber, R. (2006): Irrigation. – ÇU. Agriculture Faculty, General Publication Number: 174, Textbook Publication Number: A-52: 530 (in Turkish).
[17] Kaya, S., Evren, S., Daşcı, E. (2016): Comparison of various equations for prediction of class A pan evaporation in semi-arid climatic conditions. – Uludağ Uni. Journal of Agriculture Faculty 30(2): 1-9. Bursa (in Turkish).
[18] Pereira, A. R., Nilson, A. V. N., Pereira, A. S., Barbieri, V. (1995): A model for the class A pan coefficient. – Agricultural and Forest Meteorology 76: 75-82.
[19] Sentelhas, P. C., Folegatti, M. V. (2003): Class A pan coefficients (K_p) to estimate daily reference evapotranspiration (ET_o). – Revista Brasileira de Engenharia Agricola e Ambiental 7(1): 111-115. http://www.agriambi.com.br.
[20] Shahidian, S., Serralheiro, R., Serrano, J., Teixeira, J., Haie, N., Santos, F. (2012): Hargreaves and Other Reduced-Set Methods for Calculating Evapotranspiration. – In: Irmak, A. (ed.) Evapotranspiration—Remote Sensing and Modeling. InTech, Morn Hill, pp. 59-80. DOI: 10.5772/725.
[21] Snyder, R. L. (1992): Equation for evaporation pan to evapotranspiration conversions. – J. Irrig. Drain Eng. 118(6): 977-980.

http://www.aloki.hu ● ISSN 1589 1623 (Print) ● ISSN 1785 0037 (Online)
DOI: http://dx.doi.org/10.15666/aeer/1706_1511715129

[22] Tabari, H., Grismer, M. E., Trajkovic, S. (2013): Comparative analysis of 31 reference evapotranspiration methods under humid conditions. – Irrigation Science 31: 107-117.
[23] Thornthwaite, C. V. (1948): An approach toward a rational classification of climate. – Geograph Rev. 38: 55-94.
[24] Todorovic, M., Karic, B., Pereira, L. S. (2013): Reference evapotranspiration estimate with limited weather data across a range of Mediterranean climates. – Journal of Hydrology 481: 166-176.
[25] Trajkovic, S., Kolakovic, S. (2009): Evaluation of reference evapotranspiration equations under humid conditions. – Water Resour. Manage. 23: 3057-3067. http://dx.doi.org/10.1007/s11269-009-9423-4.
[26] Trajković, S., Stojnić, V. (2008): Simple daily ET_o estimation techniques. – Facta Universitatis Series: Architecture and Civil Engineering 6(2): 187-192. DOI: 10.2298/FUACE0802187T.
[27] Ünlü, M., Kanber, R., Steduto, P., Aydın, Y., Diker, K. (2005): Effects of different water and nitrogen levels on the yield and periodicity of pistachio (Pistachia vera L) – Turkish Journal of Agriculture and Forestry Sciences, 29(2005) 39-49.

http://www.aloki.hu ● ISSN 1589 1623 (Print) ● ISSN 1785 0037 (Online)
DOI: http://dx.doi.org/10.15666/aeer/1706_1511715129

EMERGY-BASED URBAN ECOSYSTEM HEALTH EVALUATION FOR A TYPICAL RESOURCE-BASED CITY: A CASE STUDY OF TAIYUAN, CHINA

GUO, X. J.[1,2] – DONG, S. C.[2,3] – WANG, G. K.[4] – LU, C. P.[5*]

[1]*College of Geographical Science, Shanxi Normal University, Linfen 030024, China*

[2]*Institute of Geographic Sciences and Natural Resources Research, Chinese Academy of Sciences, Beijing 100101, China*

[3]*University of Chinese Academy of Sciences, Beijing 100101, China*

[4]*College of Tourism, Xinyang Normal University, Xinyang 464000, China*

[5]*Institute of County Economy Developments & Rural Revitalization Strategy, Lanzhou University, Lanzhou 730000, China*

[*]*Corresponding author*
e-mail: lcp@lzu.edu.cn 2575

(Received 28th Jun 2019; accepted 25th Oct 2019)

Abstract. Urban ecosystem health assessment helps ensure sustainable urban development. As the provincial capital of Shanxi in China, Taiyuan's development also affects Shanxi, an area rich in coal resources, and its urbanization is closely related to the coal energy structure, which has led to ecological deterioration. This study aims to apply emergy synthesis and information entropy to estimate the urban ecosystem health of Taiyuan during the 2001-2017 period, to provide insight into the policy implications. The results indicated that the urban ecological health of Taiyuan has ameliorated during the 17-year period, mainly due to the resilience and ecological service capacity of Taiyuan urban ecosystem improved over the past 17 years. The continuous reduction of industrial waste emissions leads to ecosystem, which have resilience improving. However, we should be cautious since there are still a lot of problems with the organizational structure. And Taiyuan government still needs to adjust the current energy structure, optimize industrial structure, and reduce the dependence on the resources.

Keywords: *city ecosystem, health evaluation, emergy analysis, information entropy, coal-based city*

Introduction

"*For better or For Worse, For Richer or For Poorer*", the words are often part of a traditional Western wedding ceremony, but they also seem to define dilemma city development may bring. Cities always play an important role in local region economic and population agglomerations, politics, social services, and human culture (Pan et al., 2019), and make human life productive and colorful. Consider our polluted environment

http://www.aloki.hu ● ISSN 1589 1623 (Print) ● ISSN 1785 0037 (Online)
DOI: http://dx.doi.org/10.15666/aeer/1706_1513115149

and our increased greenhouse gas emissions and municipal solid wastes along with urban expansion and economic development. It is no doubt that without control, urbanization will not only affect living standard and region social economic development, but also result in the collapse of urban ecosystem itself (Liu et al., 2009a). Since the middle of the 20th century, countries all over the world have experienced tremendous changes from rural to urban areas, especially in developing countries, like China which is the largest developing country in the world (Pan et al., 2019). The urbanization of China was 17.92% in 1978, surge to 59.58% in 2018, at the same time, the volume of wastewater discharge has surged more than two times, the final energy consumption has surged about six times, and SO_2 emission has increased almost two times, compared with the values in 1985 (Zhang et al., 2016). In view of these increasing serious environmental problems, the Chinese government has formulated many policies and regulations aimed at achieving sustainable development (Chen et al., 2018). Therefore, it makes sense to evaluate the urban ecosystem health, and offer a better understanding of energy and materials metabolism, which is essential for future decision makers at various levels to address urban ecosystem equilibrium and sustainable economic and social development.

Urban ecosystems exist in the form of open, thermodynamic and far-from equilibrium (Odum, 1979), which rely on the continual input of high quality, low-entropy energy and waste emission to the ecosystem (Liu et al., 2009b). Given that a healthy urban natural ecosystem is equally important for economic and social sustainability (Liu et al., 2009b), subsequently, increasing efforts have been made to protect ecosystem health as a new goal in the environmental management processes. Particularly, urban ecosystem, as a network of multiple interactive relationships (Xiao et al., 2019), and it is usually evaluated by building assessment model. To date, Material Flow Analysis (MFA) (Huang et al., 2006; Barles, 2009; Kovanda et al., 2009; Browne et al., 2011), Ecological Footprint (Bagliani et al., 2008; Graymore et al., 2008; Zhou and Imura, 2011), Life Cycle Assessment(Perkins et al., 2009; Zhang et al., 2010b) are widely used methods for accounting for inputs, outputs, throughputs and storages in urban area (Ricardo et al., 2013). Exergy (Xu, 1997; Gommans and Dobbelsteen, 2007), and Emergy synthesis (Zhang et al., 2011; Viglia et al., 2018) have been proposed and applied to evaluate urban ecosystem health. However, material flow analysis and ecological footprint methods cannot fairly reveal the characteristics of environmental integrity and resource utilization of socio-economic systems (Chen et al., 2018). Also, those methods can hardly accurately judge the real contribution of local ecosystem to local economic development (Chen et al., 2018). Compare to other methods, emergy promotes the environmental support for resource flows and related support for ecosystem services maintaining the economy of the region under study, rather than other aspects, such as thermodynamic and utilization efficiencies (Ricardo et al., 2013). The emergy theory put forward by Odom in the late 1980s provides a method to combine environment and social and economic flows (such as energy, material,

http://www.aloki.hu ● ISSN 1589 1623 (Print) ● ISSN 1785 0037 (Online)
DOI: http://dx.doi.org/10.15666/aeer/1706_1513115149

information, currency, resources and labor), measured by a common unit (the solar emergy joule abbreviated to sej). Besides, taking into account the 'free of charge' of environmental work and the quality of the resources (Ricardo et al., 2013). Emergy synthesis has been widely used to assess the sustainability of countries, regions and cities (Zhang et al., 2011; Yu et al., 2016; Chen et al., 2018; Viglia et al., 2018). The remarkable advantage of emergy synthesis is that it can reveal the quantity and quality of the input flow and track the interactions among the components of the urban ecosystem (Liu et al., 2019).

China is rich in coal resources which account for 13% of the global recoverable reserves (Xu et al., 2015). Given this reason, the rapid urbanization of China is highly correlated with its coal energy structure. And Shanxi Province, the most important energy bases in China, only cover 1/60 territory but its coal production accounts for over 1/4 of the entire quantity in China (Guo et al., 2018). Taiyuan, as the capital city of Shanxi, its development is also a microcosm of Shanxi, that coal related industry contributed to more than half of its GDP in the past decades. It is no doubt that the key to the problem lies in the metabolic imbalance of resource-based cities and the high proportion of urban heavy industry, so it is necessary to adjust the industry. Local government try to support the tertiary industry and new environmental protection non-resource industries from the aspects of government policy, science and technology, funds, talents and so on. At the same time, the government push on the heavy industry enterprises and resource enterprises upgrade the technology, increase the added value of products, and reduce product pollution. The scientific basis of all this is to find out the existing state of urban ecosystem, the health evaluation of ecosystem and the main problems. Only in this way can the government take targeted measures. In this study, we take the typical coal-based Taiyuan City as the research target, aims to construct a framework and propose the index system for evaluating the health status of urban ecosystem based on emergy theory. Particularly, this research provides an empirical evidence for the evolution of the characteristics of urban ecosystem and ecological efficiency based on emergy synthesis of Taiyuan over the period 2001–2017.

Materials and Methods

The process of emergy analysis is based on the energy symbol language, and this research builds a framework to emergy diagram of social, economic and environmental interactions in a given urban ecosystems (*Fig. 1*). With a view to the dynamic simulation, emergy synthesis was propitious to assesses the input/output flows, and calculate efficiency and environmental loading (Liu et al., 2009b). The emergy system diagram of each renewable and unrenewable resource can be figured out by multiplying its energy with its transformity (Wang et al., 2019). The renewable resource emergy (R) of the urban ecosystem was obtained by taking the sum of the solar, geothermal inputs, the secondary and tertiary inputs (such as wind, rain, runoff). Besides, Non-renewable

http://www.aloki.hu ● ISSN 1589 1623 (Print) ● ISSN 1785 0037 (Online)
DOI: http://dx.doi.org/10.15666/aeer/1706_1513115149

resource emergy (N) is also one of the basic inputs to the urban ecosystem. At the same time, the urban ecosystem receives the input of capital, material and manpower flow, and finally through economic activities exports products and services, also produce waste (W).

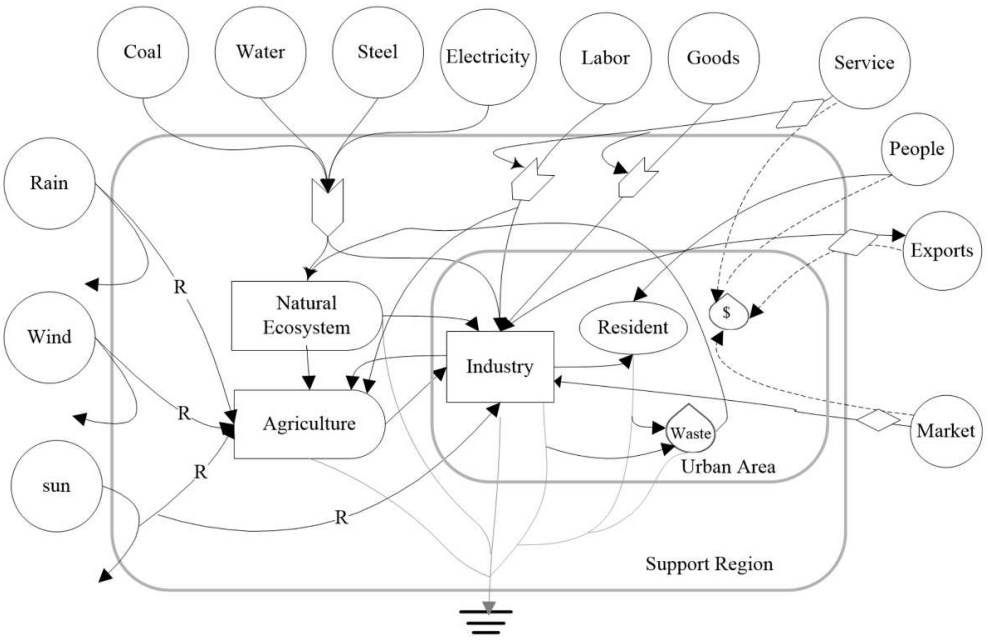

Figure 1. *Emergy system diagram of Taiyuan urban ecosystems*

In this paper, derived from emergy synthesis theory, the comprehensive indicator system of emergy value (*Table 1*) is built to synthetically analyze the material flow, energy flow, money flow and population flow, a set of index and ratios appropriate to policymaking were calculated, and make a unified quantitative analysis of urban ecosystems, finally reveals the evolution trend and characteristics of urban ecosystem.

• Emdollaratio (EDR) = U / GDP. It means that how much emergy would be put into generating an average unit of money in a given year (Viglia et al., 2018). Generally, this ratio is higher in less developed regions because most of the environmental resources are used free of charge. On the contrary, this ratio is usually lower in developed countries because of rapid currency repayments and the huge import of resources.

• Emergy self-sufficiency rate (ESR) = (R + N - Em_O)/U, this rate means that renewable and nonrenewable use of research area to the total emergy use of the research area, was used to evaluate the contribution of local ecosystem to Taiyuan urban ecosystem. The higher the value of ESR, the less reliance on imported resources and the higher economic security (Chen et al., 2018).

http://www.aloki.hu ● ISSN 1589 1623 (Print) ● ISSN 1785 0037 (Online)
DOI: http://dx.doi.org/10.15666/aeer/1706_1513115149

• Emergy exchange rate (EER) = Em_I/Em_O. This rate explains the emergy exchanged in a trade or purchase, equal to the ratio of emergy imput to emergy export) (Lei et al., 2010).

• Emergy density (ED) = U/Area, this index reflects resource available for economic utilization intensity per unit territory, equal to the ratio of total used natural resources to the total regional area (Yu et al., 2016).

Table 1. *The index system of the urban ecosystem health assessment*

Factor	Indicator	Expression	unit
Emergy Flow	Renewable resource emergy	R	sej/yr
	Non-renewable resource emergy	N	sej/yr
	Input emergy	Em_I	sej/yr
	Output emergy	Em_O	sej/yr
	Waste emergy	W	sej/yr
	Total emergy	$U=R+N+Em_I$	sej/yr
	Population	–	–
	GDP	–	$
Vigor (w_i NEYR +w_j ED +w_k REE+w_l EIR)	Net emergy yield ratio (NEYR)	$(N+R+Em_I)/Em_I$	–
	Emergy density (ED)	ED=U/Area	sej/m^2
	ratio of electricity emergy used (REE)	elec/U	–
	emergy investment ratio (EIR)	Em_I / (R + N)	–
organization (w_i NER +w_j EPC +w_k EER)	Non-renewable emergy ratio (NER)	N/U	–
	Emergy per capita (EPC)	U/Population	sej/person
	Emergy exchange rate (EER)	Em_I / Em_O	–
Resilience (w_i ELR +w_j WPR)	Environmental load rate (ELR)	(U-R) / R	–
	Waste produce ratio (WPR)	W/U	–
Ecosystem service (w_i EDR +w_j ESR +w_k ESI)	emdollaratio (EDR)	U/GDP	sej/US $
	Emergy self-sufficiency rate (ESR)	$(N + R - Em_O)/ U$	–
	Emergy Sustainability Index (ESI)	NEYR/ELR	–

• Emergy investment ratio (EIR) = Em_I / (R + N). It mainly measures the energy input required from the local resources of the development unit. In order to make the production process more economical, the rate of stakeholder should be similar to the other competitors. The size of the index is often constrained by political or socio-economic factors.

• Net emergy yield ratio (NEYR) = $(R+N+ Em_I)/Em_I$. This index represents the satisfaction of economic processes in providing basic emergy for economic activity. By comparing the net emergy yield ratio, we can better understand whether a resource is competitive or not, and the economic benefit large or small. If NYER is small, it shows

http://www.aloki.hu ● ISSN 1589 1623 (Print) ● ISSN 1785 0037 (Online)
DOI: http://dx.doi.org/10.15666/aeer/1706_1513115149

that the competitiveness of the resources is weak and the return benefit is lower. On the contrary, the competitiveness is stronger and the development benefit is higher.

• Environmental load rate (ELR) = (U - R) / R. This index is equal to the ratio between the purchased and non-updated local energy values and the free environmental energy values (renewable resource energy values). Odum claims that this ratio is similar to the load on the circuit. A large ratio value indicates that the higher intensity of energy utilization in the social economic system, which leads to the greater pressure on the urban environmental system (Dong et al., 2011). ELR is a warning to the social economic system, once the urban social economic system is always in a high ELR, will result in irreversible degradation or loss of ecological service function. From the perspective of emergy analysis, a large amount of energy derived from outside world and over-exploitation of local non-renewable resources are the mainspring of the environmental deterioration.

• Emergy Sustainability Index (ESI) = NEYR / ELR, this index was often used to evaluate the sustainable development status of local ecosystem combining both environmental impaction and social economic yield (Liu et al., 2009a). It is obvious that if the economic system of a country or region has a high energy output rate and with a relatively low environmental load rate, the local economic system is sustainable and, conversely, unsustainable. However, it is not absolutely that a higher ESI value represents a higher sustainability. In general, the ESI value between 1 and 10 indicates the vitality and development potential of economic system, and ESI > 10 is a symbol of economic underdevelopment. Viglia et al. (2018) believes that when ESI < 1, it is a consumer economic system.

• ratio of electricity emergy used (REE) = elec / U, this index was often used to evaluate the vigor of the urban ecosystem, because electricity can reflect the extent of development in the area and further measure the efficiency, competitiveness and viability of the system.

• Non-renewable emergy ratio (NER) = N / U, this indicator reflects the structure of energy use, especially the proportion of non-renewable resources used. The larger the specific value, the greater the system relies on fossil energy, and the unsustainable risk is high.

• Emergy per capita (EPC) = U / Population, usually reflected economic influence to environment and the people life level.

• Waste produce ratio (WPR) = W/U, this indicator implys the impact of economic development model on the environment.

Based on Vigor-Organization-Resilience model (VOR) proposed by Costanza, was a widely used Ecosystem health Assessment model, and then complementing an important ecosystem service index, therefore the improved VOR model termed the VORS model (Yan et al., 2016). Based on the systematic understanding of urban ecosystem healthy and its feature (Liu et al., 2009a; Jiang et al., 2009; Yan et al., 2016) and combining the emergy based indicators (Huang et al., 2007; Su et al., 2009, 2010),

http://www.aloki.hu ● ISSN 1589 1623 (Print) ● ISSN 1785 0037 (Online)
DOI: http://dx.doi.org/10.15666/aeer/1706_1513115149

thereby the framework of emergy-based urban ecosystem health index is built including vigor (V), organization (O), Resilience (R) and ecosystem service (S) four factors (Su et al., 2009), and reveal the biophysical foundation of environmental impaction to the urban ecosystem health (*Table 1*). Finally, the index system is represented by 14 emergy based indicators expressing different aspects of the urban ecosystem health.

Vigor manifests the ecosystem activities, including material and energy metabolism, as well as primary productivity (Yan et al., 2016). Efficiency and flux of the urban ecosystem states, reflect the vigor of the urban ecosystem (Liu et al., 2009a). This research selected the Net Emergy Yield Raito (NEYR) index, because it directly reflected the satisfaction of economic processes and provided a basic emergy for economic activities (Yan et al., 2016). The ratio of electricity emergy used (REE) was chosen, because electricity can reflect the extent of development in the area and further measure the efficiency, competitiveness and viability of the system (Huang, 2004; Su et al., 2010). The emergy investment ratio reflected the energy input required from the local resources of the development unit. The Emergy density (ED) reflecting resource gradient available for economic utilization (Su et al., 2009, 2010).

Organization demonstrates the composition and diversity of ecosystems (Yan et al., 2016), which refers to the interconnection relationship between the components, and which is proportional to the number and interaction of components of the ecosystem. The more complicated the organization structure, the much healthier the ecosystem. The present research chooses Non-renewable emergy ratio (NER), Emergy per capita (EPC), and Emergy exchange rate (EER) to present the composition and diversity of ecosystems.

The ability of the ecosystem to resist stress, that is, when the external stress has been eliminated that the ability of the ecosystems to return to their original state, is termed as resilience (Yan et al., 2016). The resilience of ecosystem depends on its own condition in a certain region and period, without changes of the composition of ecosystem, and correspondingly the type of the complex ecosystem and ecosystem elasticity also remained stable without change. Due to some emergy-based index, such as renewable resource emergy ratio and environmental load rate (ELR), are relevant (Liu et al., 2009a), we choose Waste produce ratio (WPR) and Environmental load rate (ELR) to express the resilience factor (Liu et al., 2009a; Su et al., 2009). It is true that critical ecosystem services at different scales are different, but for the regional ecosystem health assessment, the indicators should be selected based on regional characteristics and spatial scales to effectively represent the fundamental ecosystem services (Yan et al., 2016). The focus of urban ecosystem health is sustainable ecosystem services that supports the human with material, goods and services (Liu et al., 2009a). Therefore, the maintenance of urban ecosystem services determines the possible supply of the urban ecosystem resource for urban residents, which can be expressed by the Emdollaratio (EDR) (Liu et al., 2009b), Emergy self-sufficiency rate (ESR) and the Emergy Sustainability Index (ESI).

http://www.aloki.hu ● ISSN 1589 1623 (Print) ● ISSN 1785 0037 (Online)
DOI: http://dx.doi.org/10.15666/aeer/1706_1513115149

Based on the built framework, the assessment method of ecosystem health in the study area is divided into three steps.

(1) Calculating the emergy flow and related emergy indicator. The calculation equation is organized on the basis of emergy concept in order to aggregate input flows according to their characteristics and to convert traditional units (such as J, g, $) into emergy units (sej) (Yu et al., 2016). The *equation (1)* represents the solar emergy of all input flows as showed:

$$U = \sum (T_{r_i} E_i) \;\; i = 1,2,3,\cdots,n \tag{Eq.1}$$

Here, U is the total emergy of input flows, with a unit of *sej* (Yu et al., 2016); E_i is *i*th input flow of material or energy; and *Tri* is the unit emergy value (UEV) of the *i*th input flow.

(2) Standardizing the emergy index, and calculating the weight of index on the basis of information entropy. Because these indicators that vary greatly with different evaluating objectives have more significant impaction on the final evaluation results. Therefore, information entropy is applied to calculated the weights of each index of the EHI (Su et al., 2009). In this paper, $M=\{m_r\}$ is indicator set, usually with different types, here M_1 is positive and M_2 is negative (ratio of electricity emergy used, Waste produce ratio and emdollaratio are negative, the other are positive).

$$\mathrm{W}_r = \frac{(1+\frac{1}{lnp}\sum_{k=1}^{p}\frac{q_{kr}}{q_r}ln\frac{q_{kr}}{q_r})}{(n+\frac{1}{lnp}\sum_{r=1}^{n}\sum_{k=1}^{p}\frac{q_{kr}}{q_r}ln\frac{q_{kr}}{q_r})} \quad (\sum_{r=1}^{n}\mathrm{W}_r = 1, 0 \le \mathrm{W}_r \le 1) \tag{Eq.2}$$

$$\mathrm{q}_r = \sum_{k=1}^{p}\mathrm{q}_{kr} \tag{Eq.3}$$

$$\mathrm{q}_{kr} = \begin{cases} \frac{I_{kr}}{I^*_{kr}}, & I^*_{kr} = \max(I_{kr}), m_r \in M_1 \\ \frac{I^*_{kr}}{I_{kr}}, & I^*_{kr} = \min(I_{kr}), m_r \in M_2 \end{cases} \tag{Eq.4}$$

Here W_r is the weight of the index m_r, and q_r is the integrated value of the indicator m_r, and q_{kr} is the standardized value which derived from the raw data of indicator m_r.

http://www.aloki.hu ● ISSN 1589 1623 (Print) ● ISSN 1785 0037 (Online)
DOI: http://dx.doi.org/10.15666/aeer/1706_1513115149

(3) The formula for calculating urban ecosystem health index (EHI):

$$EHI = \sum(W_i\, m_i)\ \ i = 1,2,3,\cdots,n \qquad \text{(Eq.5)}$$

EHI presents ecosystem health score, m_i is the *i*th standardized emergy indicator, W_i is weight of *i*th ecosystem emergy indicator, and *n* is the number of ecosystems emergy indicators.

Taiyuan City, the capital of China's Shanxi Province with the 3 million population, is universally acknowledged as one of the most polluted cities in the world (Mestl et al., 2005). Located at the eastern margin of the Loess Plateau, in the central part of Shanxi, and in the north part of Jinzhong Basin (Zhang et al., 2010a), between the east longitudes 111° 30′ –113° 09′, and north latitudes 37° 27′ – 38° 25′ (see *Figure 2*).

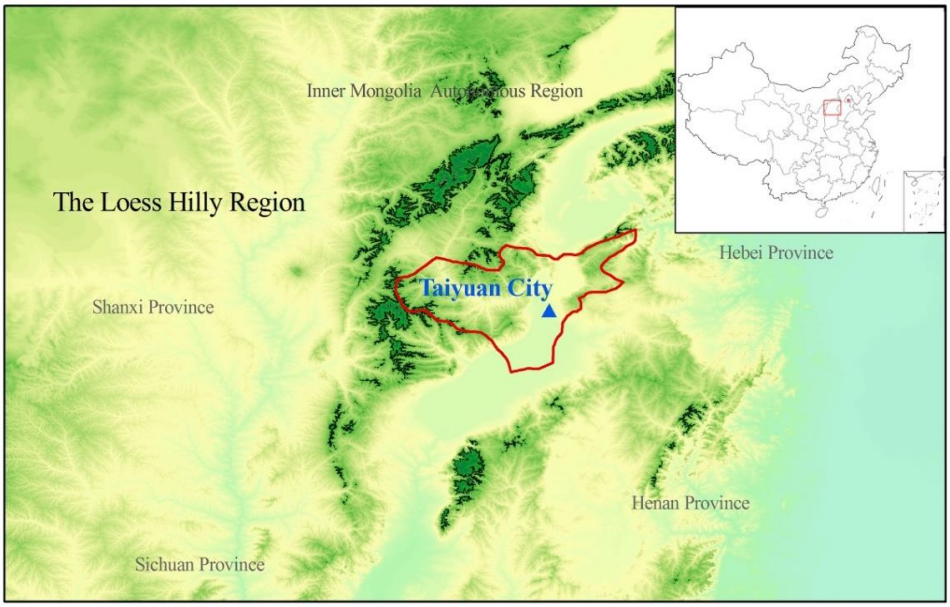

Figure 2. *Location of the study area*

As the important energy and heavy chemical industry bases of China, Taiyuan's economy high relies on the heavy industry, which contributed to more than 75% of its GDP. The urbanization rate in Taiyuan has increased from 54.38% to 84.70% from 2001 to 2017, far higher than the national average of 58.52%. Rapid urban sprawl has promoted the social and economic development, but meanwhile have caused a series of environmental issues, such as the shortage of water resources, serious environmental pollution, fragile ecological environment and so on. Owing to special topography, which surrounded by hills and mountains, thus results in periods of countercurrent and stagnant air masses in the winter, accordingly strengthening the concentration of air

http://www.aloki.hu ● ISSN 1589 1623 (Print) ● ISSN 1785 0037 (Online)
DOI: http://dx.doi.org/10.15666/aeer/1706_1513115149

pollutants (Zhang et al., 2010a). In summary, Taiyuan was chosen as a suitable case study for evaluating the ecosystem health.

The data used in this paper are derived from Shanxi Statistical Yearbook 2002–2018, Taiyuan Statistical Yearbook 2002–2018, and the achievement of the 30-years "Reform and Opening-up" of Shanxi (Shanxi Province Statistical Bureau, 1983-2015, 2009). And, unit emergy value (UEV) of materials and energy flows were drawled on the experience of related references (Jiang et al., 2009; Su et al., 2010; Pan et al., 2019).

Results

The dynamic emergy flow information on Taiyuan urban ecosystem during the 17-years period was calculated using the *equation (1)*. Using information entropy, in light of the expression of indicator system (*Table 1*) and the *equations (2) ~ (5)*, we can calculate the emergy efficiency index and the weight of each indexes, with weight we can finally obtain the Vigor, Organization, Resilience, Ecosystem service and EHI. Using this method, we obtained the urban ecosystem health evaluation table of Taiyuan (*Table 2*).

Table 2. *The urban ecosystem health evaluation table of Taiyuan (2001–2017)*

	Vigor				**Organization**			**Resilience**		**Ecosystem service**			**EHI**
	NEYR	**ED**	**REE**	**EIR**	**NER**	**EPC**	**EER**	**ELR**	**WPR**	**EDR**	**ESR**	**ESI**	
2001	4.358	1.54E+11	0.133	0.217	0.602	9.44E+15	0.320	3.555	0.026	4.71E+12	0.822	1.226	0.332
2002	4.366	1.75E+11	0.132	0.212	0.577	1.06E+16	0.340	3.023	0.023	4.79E+12	0.825	1.444	0.344
2003	4.780	1.78E+11	0.130	0.208	0.558	1.08E+16	0.312	2.699	0.028	4.00E+12	0.828	1.771	0.348
2004	4.350	1.79E+11	0.143	0.231	0.554	1.08E+16	0.336	2.868	0.024	3.23E+12	0.812	1.517	0.369
2005	4.463	1.83E+11	0.150	0.244	0.540	1.10E+16	0.320	2.798	0.022	2.82E+12	0.804	1.595	0.388
2006	5.042	1.92E+11	0.194	0.309	0.513	1.15E+16	0.251	2.987	0.019	2.61E+12	0.764	1.688	0.414
2007	4.784	2.07E+11	0.203	0.330	0.473	1.23E+16	0.273	2.590	0.017	2.28E+12	0.752	1.847	0.445
2008	4.251	1.89E+11	0.210	0.388	0.519	1.12E+16	0.284	3.946	0.010	1.71E+12	0.721	1.077	0.564
2009	5.434	2.03E+11	0.173	0.289	0.483	1.14E+16	0.242	2.413	0.006	1.81E+12	0.776	2.252	0.689
2010	4.090	1.93E+11	0.211	0.406	0.505	9.47E+15	0.296	3.853	0.006	1.50E+12	0.711	1.061	0.717
2011	4.106	2.13E+11	0.233	0.450	0.458	1.04E+16	0.298	3.315	0.005	1.41E+12	0.689	1.238	0.756
2012	4.360	2.06E+11	0.212	0.422	0.474	9.96E+15	0.279	3.365	0.005	1.23E+12	0.703	1.296	0.772
2013	4.325	1.94E+11	0.218	0.472	0.429	9.33E+15	0.282	2.989	0.006	1.11E+12	0.680	1.447	0.753
2014	4.191	1.92E+11	0.225	0.509	0.434	9.18E+15	0.285	3.365	0.007	1.04E+12	0.663	1.246	0.755
2015	3.470	1.89E+11	0.241	0.518	0.438	9.03E+15	0.354	3.530	0.006	9.39E+11	0.659	0.983	0.801
2016	4.018	1.95E+11	0.238	0.446	0.426	9.25E+15	0.317	2.769	0.005	8.96E+11	0.691	1.451	0.920
2017	4.071	1.94E+11	0.256	0.436	0.429	9.14E+15	0.313	2.740	0.005	7.93E+11	0.696	1.486	0.938
Weights	0.011	0.006	0.063	0.104	0.014	0.010	0.011	0.022	0.388	0.312	0.007	0.052	--

http://www.aloki.hu ● ISSN 1589 1623 (Print) ● ISSN 1785 0037 (Online)
DOI: http://dx.doi.org/10.15666/aeer/1706_1513115149

The vigor of Taiyuan City changed little, first slowly climbed up and began to decline in recent years, and its trend line like an elongated *S* curve (*Fig. 3*). Among the vigor's indicates, the environmental investment ratio (EIR) accounted for the largest contribution, with a trend trajectory similar to that of vigor changes during the period 2001-2017. During 2001-2009, although EIS increased slowly, the value was always less than 0.3, probably because the economic system is mainly dependent on local coal resource, more coal is obtained from the environment free of charge than other competitors. However, too low the rate of emergy investment will not be conducive to attracting extra-territorial funds, which in turn will affect the development of local resources. From 2010 to 2015, this ratio become large fast, that means inputs are need to pay, prices are rising, and the system is more competitive than past. But in recent years, the index has also declined, possibly due to the government optimizing industrial structure, and the dependence on the resources has not been as serious as past. For example, the industrial added value of the traditional heavy industries accounts for more than 80% of total industrial added value in 2001, but this proportion has decreased to 39.3% in 2017.

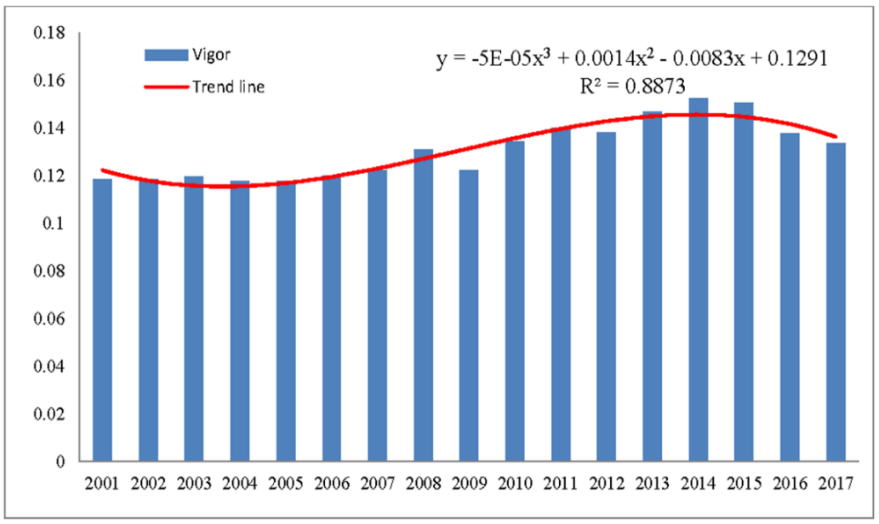

Figure 3. *The vigor and its trend of Taiyuan urban ecosystem*

According to *Figure 4*, we can find that the organization of Taiyuan has fluctuating declined during the 2001-2017 period. The trend line obeys polynomial regression, the equation is y = 2E-05x2 - 0.0007x + 0.034 (R^2 = 0.8406), which reflects the trend line fit the organization well. The contribution of non-renewable emergy ratio (NER), emergy exchange rate (EER) and emergy per capita (EPC) to organization is almost the same level, which is 0.014, 0.010 and 0.011, respectively. But in the recent two years, emergy exchange rate (EER) has slightly picked up.

http://www.aloki.hu ● ISSN 1589 1623 (Print) ● ISSN 1785 0037 (Online)
DOI: http://dx.doi.org/10.15666/aeer/1706_1513115149

The resilience of Taiyuan urban ecosystem fluctuates greatly during the past 17-year period, but overall express rise trend (*Fig. 5*). Here, waste produce ratio (WPR) and Environmental load rate (ELR) were chosen to express the resilience factor. The contribution of waste produce ratio (WPR) and Environmental load rate (ELR)to resilience is 0.388 and 0.022, respectively. Obviously, the continuous reduction of industrial waste emissions leads to ecosystem resilience improving.

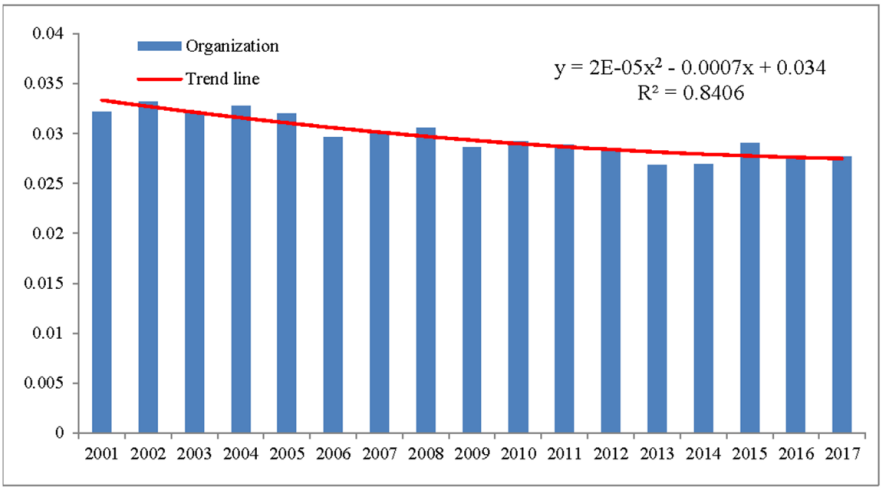

Figure 4. *The organization and its trend of Taiyuan urban ecosystem*

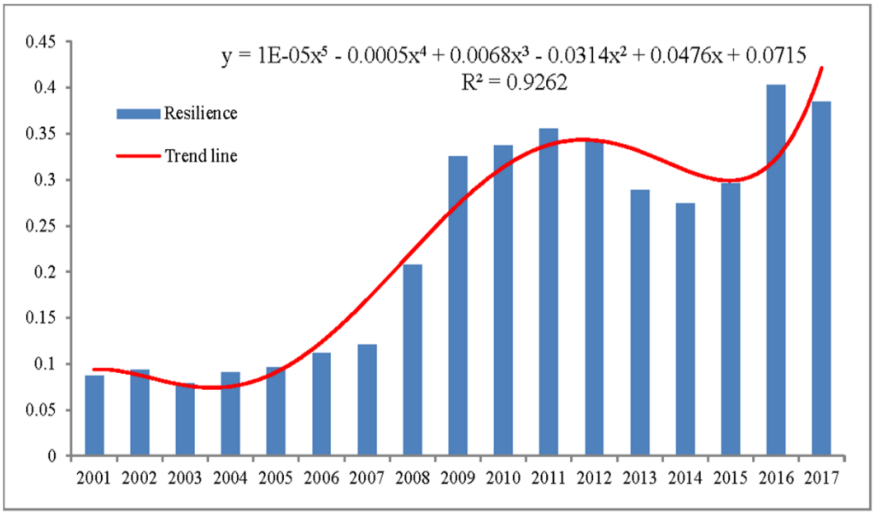

Figure 5. *The resilience and its trend of Taiyuan urban ecosystem*

Figure 6 shows that the urban ecosystem service of Taiyuan was exponential growth during the past 17-years period. The trend line obeys exponential regression, the equation is $y = 0.0899e^{0.088x}$ ($R^2 = 0.9921$), which reflects the trend line better fit the ecosystem service. The contribution of emdollaratio (EDR), emergy self-sufficiency

http://www.aloki.hu ● ISSN 1589 1623 (Print) ● ISSN 1785 0037 (Online)
DOI: http://dx.doi.org/10.15666/aeer/1706_1513115149

rate (ESR) and emergy sustainability index (ESI) to ecosystem service is 0.312, 0.007 and 0.052, respectively. To a great extent, the ecosystem service keeps climbing result from continuous decline of emdollaratio (EDR). In General, this rate is higher in the less developed regions, because natural resources are basis for its economic development and GDP growth (Yu et al., 2016), and most of the environmental resources are used free of charge. On the contrary, this ratio become lower means that the local economy developed because of rapid currency repayments, a large GDP base and the huge import of resources.

As showed in *Figure 7*, the trend of ecological health index and resilience of Taiyuan is very similar during the 2011-2017 period, but it is a little smoother. From the previous analysis, we know that this is mainly due to the resilience and ecological service capacity of Taiyuan urban ecosystem improved over the past 17 years.

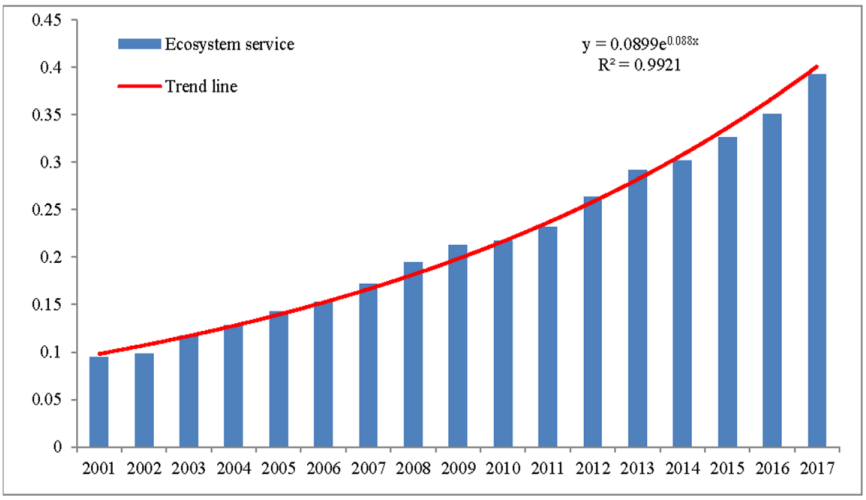

Figure 6. *The urban eco-system service and its trend of Taiyuan*

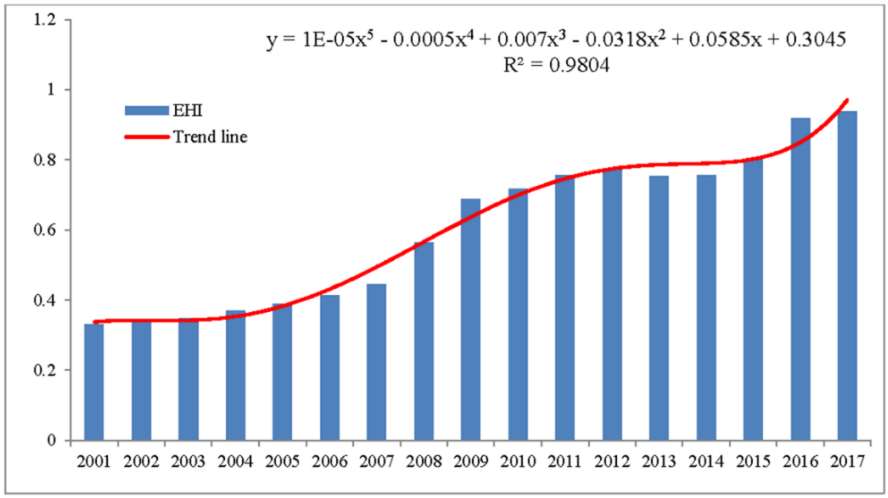

Figure 7. *The EHI and its trend of Taiyuan urban ecosystem*

http://www.aloki.hu ● ISSN 1589 1623 (Print) ● ISSN 1785 0037 (Online)
DOI: http://dx.doi.org/10.15666/aeer/1706_1513115149

However, the vigor of Taiyuan urban ecosystem changed little, and even more cautiously since that there are still a lot of problems with the organizational structure. From *Figure 8*, we can also find that correlation coefficient of the ecological health index and were significant positive except for organization. Mostly because the organization of Taiyuan has fluctuating declined during the 17-years period.

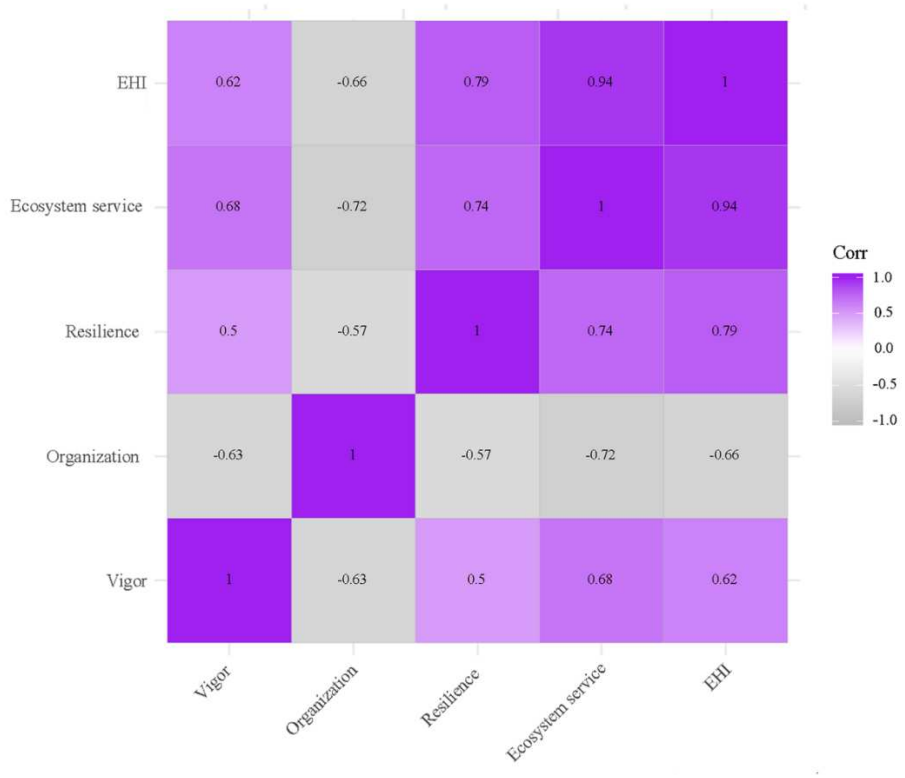

Figure 8. *The correlation coefficient of EHI and VORS4. Discussion*

Discussion

Recently, the relationship between economic growth and environmental performance is worth studying. As Silvio affirmed, cities are the engine of economic development and human wellbeing, however, their dynamics need to be supported by the convergence of a large number of material and energy resources (Viglia et al, 2018). Due to the contradiction between urban economic expansion and environmental protection becomes more and more serious, it is worth investigating the relationship between economic growth and environmental performance (Liu et al., 2009). Basically, the framework definition and application of metrics and models capable of accounting for natural capital value are much needed (Vassallo, 2017). It is necessary to formulate methods and indicators of ecosystem health and apply them to typical coal regional ecosystems (Jiang et al., 2009). This paper tries to construct a framework of assessment model and choose relevant index based on emergy, finally, combining information

http://www.aloki.hu ● ISSN 1589 1623 (Print) ● ISSN 1785 0037 (Online)
DOI: http://dx.doi.org/10.15666/aeer/1706_1513115149

entropy method to evaluate the urban ecosystem health status from the perspective of the energy and materials metabolism. Nevertheless, there are still many problems that need to be studied in depth. What are the most key factors affecting the health of urban ecosystems, whether there is a causal relationship between them, whether they are short-term or long-term impaction, and so on.

As the provincial capital of Shanxi, Taiyuan's development is also a microcosm of Shanxi. Shanxi Province's coal yield accounts for 1/4 of the total coal production in the whole country, whilst coke production accounts for 2/5 (Guo et al., 2018). The energy intensity of Shanxi province is the highest all over the whole country, 2.4 times compared to the national average in 2006 (Tang et al., 2014). Although air pollution has improved since the early 1990s, the air pollution in the city is still very serious compared to other cities in the country. It is possible because the energy structure of Shanxi Province is mainly dependent on coal for a long time. That's also why the organization of Taiyuan has fluctuating declined. In order to reduce the coal consumption, Taiyuan municipal government intends to improve the current energy structure (Guo et al., 2018), optimize industrial structure, and the dependence on the resources has not been as serious as past. For example, Taiyuan municipal government invested 1.5 billion Yuan (180 million USD) to implement its cleaner production program for the purpose of improving the environmental condition, and in 1999 Taiyuan became China's first cleaner production pilot city (Mestl et al., 2005). According to relevant government reports, 12 industrial pollution sources were closed in 2005, and a total of 121 were shut down by 2012 (Tang et al., 2014). But considering the structure of the coal industry lasting almost 100 years, there is still a long way to go. It is necessary to find clean renewable resources to Offset the consumption of coal resources. The empower that is derived from solar, geothermal and tidal sources drives the productive processes, and make it possible to come true (Brown et al., 2016). Under such circumstances, government should take strong actions to reduce coal consumption and related emissions. In particular, the local government should play a leading role in promoting technological innovation among enterprises through carefully designed policies to improve product sustainability, and to regulate public behavior (such as green public transport travel, garbage classification, purchase of energy-saving products, etc.), thereby achieving a 'win-win' environment and economy.

Conclusions

This study applies emergy synthesis and information entropy to assess the urban ecosystem health of Taiyuan during the period 2001–2017, to provide suggestions for local government formulating the policy and regulation. Result shows that the ecological health of Taiyuan has improved during the 2011-2017 period, mainly due to the resilience and ecological service capacity of Taiyuan urban ecosystem improved over the past 17 years. The continuous reduction of industrial waste emissions leads to

http://www.aloki.hu ● ISSN 1589 1623 (Print) ● ISSN 1785 0037 (Online)
DOI: http://dx.doi.org/10.15666/aeer/1706_1513115149

ecosystem resilience improving. However, we should be cautious since that there are still a lot of problems with the organizational structure. And in order to reduce the dependence on the resources, Taiyuan government still needs to improve the current energy structure and optimize industrial structure. In the future study, how to take into account the space-time dimension, compare and analyze the resource-based cities' ecological health in China and predict the trend of ecological health development will be the core work of the next step. At the same time, how to improve the accuracy of its measurement, and then identify the key factors that affect the health of urban ecosystem, and provide a clearer basis for urban development, is also the important research direction.

Acknowledgments. We thank Rong Zhou for her great assistance in this study. We would also like to thank the Science and Technology Basic Resources Survey Project of China (2017FY101304), Major R&D Project of Chinese Academy of Sciences (ZDRW-ZS-2016-6-5), National Natural Science Foundation of China (41701062,41471116,41701142), Shanxi Scholarship Council of China (2016–078), Shanxi Normal University Natural Science Foundation (ZR1714), and the Youth Innovation Promotion Association CAS (2016181). We are also grateful to the anonymous reviewers and all the editors in the process of revision.

REFERENCES

[1] Bagliani, M., Galli, A., Niccolucci, V., Marchettini, N. (2008): Ecological footprint analysis applied to a sub-national area: the case of the Province of Siena (Italy). – J. Environ. Manag 86(2): 354-364.

[2] Barles, S. (2009): Urban Metabolism of Paris and Its Region. – Journal of Industrial Ecology 13(6): 898-913.

[3] Brown, M. T., Ulgiati, S. (2016): Emergy assessment of global renewable sources. – Ecological modelling 339: 148-156.

[4] Browne, D., Bernadette, O. R., Moles, R. (2011): Material flow accounting in an irish city-region 1992–2002. – Journal of Cleaner Production 19(9-10): 967-976.

[5] Chen, W., Geng, Y., Dong, H., Tian, X., Zhong, S., Wu, Q., Xu, Y., Zhang, Q., Li, S. (2018): An emergy accounting based regional sustainability evaluation: A case of Qinghai in China. – Ecological indicators 88: 152-160.

[6] Dong, X., Zhang, Y., Cui, W., Xun, B., Yu, B., Ulgiati, S., Zhang, X. (2011): Emergy-based adjustment of the agricultural structure in a low-carbon economy in Manas County of China. – Energies 4(9): 1428-1442.

[7] Gommans, L., Dobbelsteen, V. D. A. (2007): Synergy between exergy and regional planning. – WIT Transactions on Ecology and the Environment 105: 103-112.

[8] Graymore, M. L., Sipe, N. G., Rickson, R. E. (2008): Regional sustainability: how useful are current tools of sustainability assessment at the regional scale? – Ecol. Econ 67(3): 362-372.

http://www.aloki.hu ● ISSN 1589 1623 (Print) ● ISSN 1785 0037 (Online)
DOI: http://dx.doi.org/10.15666/aeer/1706_1513115149

[9] Guo, X., Zhang, Z., Zhao, R., Wang, G., Xi, J. (2018): Association between coal consumption and urbanization in a coal-based region: a multivariate path analysis. – Environmental Science and Pollution Research 25(1): 533-540.

[10] Huang, S. L. (2004): Energy basis for urban ecological economic system. – Chans Bookstore 147-151. (in Chinese).

[11] Huang, S. L., Lee, C. L., Chen, C. W. (2006): Socioeconomic metabolism in Taiwan: emergy synthesis versus material flow analysis. – Resour. Conserv. Recycl 48(2): 166-196.

[12] Huang, S. L., Kao, W. C., Lee, C. L. (2007): Energetic mechanisms and development of an urban landscape system. – Ecological Modelling 201(3-4): 495-506.

[13] Jiang, M. M., Chen, B., Zhou, J. B., Yang, Z. F., Ji, X., Zhang, L. X., Chen, G. Q. (2009): An ecological evaluation of Beijing ecosystem based on emergy indices. – Communications in Nonlinear Science and Numerical Simulation 14(5): 2482-2494.

[14] Kovanda, J., Weinzettel, J., Hak, T. (2009): Analysis of regional material flows: the case of the Czech Republic. – Resour. Conserv. Recycl 53(5): 243-254.

[15] Lei, K., Zhou, S., Hu, D., Yu, Y. (2010): Ecological energy accounting for the gambling sector: A case study in Macao. – Ecological Complexity 7(2): 149-155.

[16] Liu, G. Y., Yang, Z. F., Chen, B., Ulgiati, S. (2009a): Emergy-based urban health evaluation and development pattern analysis. – Ecological Modelling 220(18): 2291-2301.

[17] Liu, G. Y., Yang, Z. F., Chen, B., Zhang, Y., Zhang, L. X., Zhao, Y. W., Jiang, M. M. (2009b): Emergy-based urban ecosystem health assessment: A case study of Baotou, China. – Communications in Nonlinear Science and Numerical Simulation 14(3): 972-981.

[18] Liu, X., Guo, P., Guo, S. (2019): Assessing the eco-efficiency of a circular economy system in China's coal mining areas: Emergy and data envelopment analysis. – J. Clean. Prod 206: 1101-1109.

[19] Mestl, H. S., Aunan, K., Fang, J., Seip, H. M., Skjelvik, J. M., Vennemo, H. (2005): Cleaner production as climate investment-integrated assessment in Taiyuan City, China. – J. Clean. Prod 13(1): 57-70.

[20] Odum, E. P. (1979): Perturbation theory and the subsidy-stress gradient. – BioScience 29(6): 349-352.

[21] Pan, H. Y., Zhuang, M. F., Geng, Y., Wu, F., Dong, H. J. (2019): Emergy-based ecological footprint analysis for a mega-city: The dynamic changes of Shanghai. – Journal of Cleaner Production 210: 552-562.

[22] Perkins, A., Hamnett, S., Pullen, S., Zito, R., Trebilcock, D. (2009): Transport, housingand urban form: The life cycle energy consumption and emissions of city centre apartments compared with suburban dwellings. – Urban Policy and Research 27(4): 377-396.

[23] Ricardo, E. V. A., Mathias, G., Robert, H., Norma, A. O. G., Rabindranarth, R. L. (2013): An emergy analysis for urban environmental sustainability assessment, the Island of Montreal, Canada. – Landscape and Urban Planning 118: 18-28.

[24] Shanxi Statistical Bureau. (2001-2018): Shanxi Statistical Yearbook. – China Statistics Press: Beijing. (in Chinese).

http://www.aloki.hu ● ISSN 1589 1623 (Print) ● ISSN 1785 0037 (Online)
DOI: http://dx.doi.org/10.15666/aeer/1706_1513115149

[25] Shanxi Statistical Bureau. (2009): Province Bureau of statistics of Shanxi. Exhibition of the achievement on 30-year "Reform and Opening-up" of Shanxi. – China Statistics Press: Beijing. (in Chinese).

[26] Su, M. R., Yang, Z. F., Chen, B., Ulgiati, S. (2009): Urban ecosystem health assessment based on emergy and set pair analysis-A comparative study of typical Chinese cities. – Ecological modelling 220(18): 2341-2348.

[27] Su, M., Yang, Z., Chen, B. (2010): Relative urban ecosystem health assessment: A method integrating comprehensive evaluation and detailed analysis. – Eco. health 7(4): 459-472.

[28] Taiyuan Statistical Bureau. (2002-2018): Taiyuan Statistical Yearbook (2001–2018). – China Statistics Press: Beijing. (in Chinese).

[29] Tang, D. L., Wang, C. C., Nie, J. S., Chen, R. J., Niu, Q., Kan, H. D., Chen, B. H., Perera, F., Taiyuan, C. D. C. (2014): Health benefits of improving air quality in Taiyuan, China. – Environment international 73: 235-242.

[30] Viglia, S., Civitillo, D. F., Cacciapuoti, G., Ulgiati, S. (2018): Indicators of environmental loading and sustainability of urban systems. An emergy-based environmental footprint. – Ecological indicators 94: 82-99.

[31] Wang, X., Liu, G., Coscieme, L., Giannetti, B. F., Hao, Y., Zhang, Y., Brown, M. T. (2019): Study on the emergy-based thermodynamic geography of the Jing-Jin-Ji region: Combined multivariate statistical data with DMSP-OLS nighttime lights data. – Ecological Modelling 397: 1-15.

[32] Xiao, R., Liu, Y., Fei, X., Yu, W., Zhang, Z., Meng, Q. (2019): Ecosystem health assessment: A comprehensive and detailed analysis of the case study in coastal metropolitan region, eastern China. – Ecological Indicators 98: 363-376.

[33] Xu, F. L. (1997): Exergy & structural exergy as ecological indicators for the development state of Lake Chao ecosystems. – Ecol. Model 99(1): 41-49.

[34] Xu, X., Xu, X., Chen, Q., Che, Y. (2015): The impact on regional "resource curse" by coal resource tax reform in China—A dynamic CGE appraisal. – Resources Policy 45: 277-289.

[35] Yan, Y., Zhao, C., Wang, C., Shan, P., Zhang, Y., Wu, G. (2016): Ecosystem health assessment of the Liao River Basin upstream region based on ecosystem services. – Acta Ecologica Sinica 36(4): 294-300.

[36] Yu, X. M., Geng, Y., Dong, H. B., Fujita, T., Liu, Z. (2016): Emergy-based sustainability assessment on natural resource utilization in 30 Chinese provinces. – J. Clean. Prod 133: 18-27.

[37] Zhang, D., Aunan, K., Martin, S. H., Larssen, S., Liu, J., Zhang, D. (2010a): The assessment of health damage caused by air pollution and its implication for policy making in Taiyuan, Shanxi, China. – Energy Policy 38(1): 491-502.

[38] Zhang, Y., Singh, S., Bakshi, B. R. (2010b): Accounting for ecosystem services in life cycle assessment, Part I: A critical review. – Environmental Science and Technology 44(7): 2232-2242.

[39] Zhang, Y., Yang, Z., Liu, G., Yu, X. (2011): Emergy analysis of the urban metabolismof Beijing. – Ecological Modelling 222(14): 2377-2384.

http://www.aloki.hu ● ISSN 1589 1623 (Print) ● ISSN 1785 0037 (Online)
DOI: http://dx.doi.org/10.15666/aeer/1706_1513115149

[40] Zhang, Z., Xue, B., Pang, J., Chen, X. (2016): The decoupling of resource consumption and environmental impact from economic growth in china: Spatial pattern and temporal trend. – Sustainability 8(3): 222.

[41] Zhou, X., Imura, H. (2011): How does consumer behavior influence regional ecological footprints? An empirical analysis for Chinese regions based on the multi-region inputeoutput model. – Ecol. Econ 71: 171-179.

http://www.aloki.hu ● ISSN 1589 1623 (Print) ● ISSN 1785 0037 (Online)
DOI: http://dx.doi.org/10.15666/aeer/1706_1513115149

ENERGETIC POTENTIAL AND ENVIRONMENTAL ASSESSMENT OF SOLID WASTES AS ALTERNATIVE FUEL FOR CEMENT PLANTS

HANNOUN, G.[1] – JAOUAD, A.[2] – SCHEBEK, L.[3] – BELKZIZ, J.[4] – OUAZZANI, N.[1*]

[1]Laboratory of Hydrobiology, Ecotoxicology and Sanitation (LHEA, URAC 33), Department of Biology, Faculty of Sciences Semlalia, Cadi Ayyad University, BP2390 Marrakesh, Morocco (e-mail: hannoun.ghizlane05@gmail.com)

[2]Laboratory of Innovation, Green Chemistry, Expertise and Sustainable Development LICVEDDE, Department of Chemistry, Faculty of Sciences Semlalia, Cadi Ayyad University, BP2390 Marrakesh, Morocco (e-mail: jaouad@uca.ac.ma)

[3]FG Material Flow Management and Resource Management, Technical University of Darmstadt, Darmstadt, Germany (e-mail: L.Schebek@iwar.tu-darmstadt.de)

[4]Ciment du Maroc Industry, Marrakesh, Morocco (e-mail: j.belkziz@cimar.co.ma)

**Corresponding author e-mail: ouazzani@uca.ac.ma; phone: +212-666-720-368*

(Received 28th Jun 2019; accepted 16th Oct 2019)

Abstract. The main objective of this paper is to evaluate the energetic potential and the environmental impacts of different kinds of wastes derived from different sources, namely olive Kernels (OK), sewage sludge (SS), chicken residues (CR), animal meal (AM) and fluffy RDF (F-RDF) and to figure out their feasibility as alternative fuels for cement plants. Decisive parameters promoting the use of wastes as secondary fuels such as: Calorific value, moisture, volatile matter, ash, chlorine, sulfur contents and trace elements were determined. A brief comparison of these fuels has been summarized. A model of fossil fuel savings is estimated using different scenarios with several substitution rates. The results show that chicken residues, fluffy RDF and olive kernels have the highest caloric values, which are 25.02 MJ/kg, 24.79 MJ/kg and 21.68 MJ/kg respectively. Moreover, fluffy RDF can help mitigate carbon dioxide (CO_2) emissions due to its lower carbon content than coal, and its similar caloric power. In addition to their favorable calorific values, chicken residues and olive kernels allow for a significant reduction of fossil-derived CO_2 due to their biogenic origin. Generally nitrogen oxide (NOx), sulfur dioxide (SO_2) emissions decrease while Co-firing waste with coal.
Keywords: *co-processing, organic waste, calorific value, pollutants emissions, fossil fuel saving*

Introduction

Developing countries face a huge challenge in the management and treatment of solid waste (Abdel-Shaf and Mansour, 2018): growing population and urbanization cause rising amounts of waste, landfill capacities are lacking. However, in the case of non-hazardous municipal solid waste, another option has shown its feasibility: Co-processing of pretreated waste as an alternative fuel in cement production is widely applied in industrialized countries. It helps to reduce the volume of waste, conserve natural resources of primary energy, it contributes to reducing landfill emissions and has a positive effect on energy costs for the cement industry.

http://www.aloki.hu ● ISSN 1589 1623 (Print) ● ISSN 1785 0037 (Online)
DOI: http://dx.doi.org/10.15666/aeer/1706_1515115168

Several studies analysed the feasibility of using waste in cement plants: Materials like waste oils (Kääntee et al., 2004), plastics (Feng et al., 1996), waste tires (Karell and Blumenthal, 2001; Hashem et al., 2019) and sewage sludge (Ninomiya et al., 2004) are often used as alternative fuels (AF) in the cement industry. Furthermore animal meal produced from the slaughterhouse residues can also be used as alternative fuel for cement co-combustion (Denafas et al., 2004; Bhatty, 2006). Apart from this, industrial waste such as non-recycled plastics and paper waste studied by Bourtsalas et al. (2018) and wood wastes investigated by Hossain et al. (2019), agricultural biomass and spent pot linings (Lechtenberg, 2009; Al-Salem et al., 2010; Ghenai et al., 2019) have been also used as alternative fuels in the cement industry for many years. Advances and challenges for the co-processing of waste were also studied by Stafford et al. (2015) in Latin American cement industry. The robustness of the co-processing as waste disposal technique was also revealed by the economic and environmental statistical analysis (Rahul et al., 2016).

Consequently, the use of non-hazardous solid waste could be an option to tackle waste management for developing countries, providing the double benefit of environmental protection and energy recovery. However, in developing countries there is generally a lack of data about the characteristics and quantities of non-hazardous municipal solid waste, the real calorific potential of wastes is little known. In addition no accurate data exists about the real environmental benefit that could be gained when using agricultural or biogenic wastes and their environmental impact as well. On real scale we can notice some modest experiences of co-processing of alternative fuels by local and international groups of cement companies which have been using tire chips and olive kernels as alternative fuels (GIZ, 2013) since a couple of years.

Cement is one of the most significant manufactured materials in the world. Global 2015 cement production is estimated at 4.6 billion tons (CEMBUREAU, 2015). Cement is the most important constituent of concrete, and every year, approximately 1 t of concrete is expected to be produced for each human being in the world (Lippiatt and Ahmad, 2004) due to current developmental trends. Cement is a fine powder obtained from grinding clinker together with gypsum. Other additions like limestone, ashes, blast furnace slugs, and chemical additives may be added according to pertinent standards, (EN 197 2000). The most important ingredient of cement is clinker which is obtained by sintering a mixture of limestone, clay and iron ore at approximately 1450 °C by using flame temperatures of around 2000 °C.

The main environmental impacts of cement production are associated with energy intensive processes (Madlool et al., 2011) and air emissions (Davidovits, 1994) where carbon dioxide (CO_2) is relevant because it accounts for approximately 6% of the total stationary source emissions worldwide (Metz, 2005). Emission in term of CO, NO_X and SO_2 generated from cement process contributes to greenhouse and acid rain effects (Zhang et al., 2011).

The cement industry is considered energy-intensive, because it needs to achieve high temperatures. Traditionally, it used fossil fuels such as coal, fuel oil, and petroleum coke. Their co-combustion in cement kilns is contributing to a rapid increase in the average temperature of the planet through the pollutants emitted to air (Harjanne and Korhonen, 2019).

In recent years utilization of alternative fuels in cement manufacturing has gained a wide attention due to its effectiveness in substituting the thermal energy requirement from fossil fuels and reducing the pollutant emission. Alkaline environment, high temperature and long residence time allow rotary kiln to burn a wide range of waste and

http://www.aloki.hu ● ISSN 1589 1623 (Print) ● ISSN 1785 0037 (Online)
DOI: http://dx.doi.org/10.15666/aeer/1706_1515115168

hazardous material via co-processing (Rahman et al., 2015). In this process, waste is added to raw materials by replacing, in part, fuels or virgin raw material itself (Porto and Fernandes, 2006).

Studies on the impact of alternative fuels on environmental emission with regard to CO, NOx, SO_2 and CO_2 emissions have also been discussed (Rahman et al., 2015). The effect of various MBM parameters on the process of co-processing with coal, was determined through many experiments with different MBM/coal ratios carried by Gulyurtlu et al. (2005), these experiments demonstrate when the ratio of MBM is increased a minor impacts on emissions of CO and sulphur dioxide (SO_2) were noticed. Moreover, it was found while increasing MBM portion that NOx emissions decreases despite its high nitrogen content.

In addition to the studies that investigate the environmental impact of using waste in the cement industry, another research line focuses on the practical substitution rate for each type of alternative fuels.

This paper investigates chemical and physical characteristics of a diversity of alternative fuels, to evaluate their energetic potential and their environmental impact according to cement plants requirements. We highlight the potentials of a range of alternative fuels regarding the question of how much coal could be substituted and what impact on emissions one can expect. A calculation model of fossil fuels quantity that can be saved while using such waste is also estimated.

Materials and methods

Samples description

The present study was performed in Cadi Ayyad University, Marrakesh-Morocco in collaboration with Technical university of Darmstadt-Germany.

Different kinds of wastes were taken from different sources (*Table 1*). The target samples undergo a series of pretreatment including drying cutting and grinding to produce a fine powder in order to make their structure homogenous enough for the following analysis:

- Proximate analysis parameters: moisture, volatile, ash, and calorific value
- Ultimate analysis parameters: chlorine, sulphur as well as trace elements

The values obtained are results of three replicates. The results regarding moisture and calorific values could change over time, since the moisture affects the CV of the studied AF a continuous control of such parameters need to be performed before their use.

Analytical method

Moisture content: according to DIN51718

The working principle consists of drying samples at 105 °C for 90 min in a Memmert oven**.** The sample (1 g) is spread evenly on a drying bowl crucible, weighed with 0,1 g accuracy and dried in an oven at 105 ± 2 °C until mass constancy.

Volatiles according to DIN 51720

The working principle consists of treating the samples at 900 °C for 7 min using a Nabertherm oven. Approximately 1.0 g of the pre-dried and ground sample is weighed

http://www.aloki.hu ● ISSN 1589 1623 (Print) ● ISSN 1785 0037 (Online)
DOI: http://dx.doi.org/10.15666/aeer/1706_1515115168

into a crucible which is placed in the oven preheated at 900 ± 5 °C. After 7 min (±5 s), the crucible is removed and reweighed after cooling in a vacuum desiccator. The volatile matter content is calculated from the mass loss of the sample.

Table 1. *Overview of solid waste tested and their origin*

Samples	Description	Sources
Olive mill wastewaters "continuous system" (water-solid mixture) (OMWC)	Since olive production is done by many processes (traditional and continuous), different kinds of OK were collected and other by-product (OMW = water + solid waste mixture)	Olive Oil Factory, Marrakesh, Morocco
Olive kernel "continuous system" (OKC)		Olive Oil Factory, Marrakesh, Morocco
Olive kernel "traditional system" (OKT)		Olive Oil Factory, Marrakesh, Morocco
Olive kernel "canning industry" (OKCa)	OK generated from the process that preserves olives in cans or jars for future uses	Canning Industry, Marrakesh, Morocco
Sewage sludge "M"	The residual, semi-solid material that is produced as a by-product during sewage treatment of industrial or municipal wastewater	Wastewater Treatment Plant, Marrakesh, Morocco
Sewage sludge "G"		Wastewater Treatment Plant, Ennigerloh, Germany (Heidelberg Cement)
Chicken waste	Mixture of chicken heads, intestines, feather and wings	Dajajji Factory, Marrakesh, Morocco
Animal meal	Waste derived from the slaughtering of animals	MVW Lechtenberg and Partner, Duisburg, Germany
Fluffy RDF	Shredded plastic and small parts of paper	MVW Lechtenberg and Partner, Duisburg, Germany

Ash on the basis of DIN 51719

The working principle consists of treating the samples at 815 °C for 5 h.

The ash content is determined by rising the temperature from 550 °C with 5 K/min to 815 °C and holding until constant weight (mass difference ±0.05%) is reached. The ash content is calculated from the mass loss of the sample.

Chlorine and sulphur

Sulphur and chlorine according to DIN51724-3/DIN 51727: The pre-dried and crushed sample is weighted in a porcelain crucible which contains a small quantity of $FePO_4$ powder to help burning. With the aid of a catalyst layer of quartz powder and at high temperatures (>1300 °C) the sulphur/chlorine is oxidized in an oxygen stream. In the resulting solutions, chlorine and sulphur are detected by means of volumetric analysis.

Sulfur titration: Metrohm titrator; standard solution $Ba(ClO_4)_2$, (0.005 mol/l)

The entire solution from the combustion step is transferred into a 250 ml volumetric flask. 50 ml are pipeted off and added with same volume of acetone (for better

http://www.aloki.hu ● ISSN 1589 1623 (Print) ● ISSN 1785 0037 (Online)
DOI: http://dx.doi.org/10.15666/aeer/1706_1515115168

precipitation of $BaSO_4$). A few drops of indicator sulfonazo III are added. Under constant stirring barium perchlorate $Ba(ClO_4)_2$ solution is added until the color changes from violet to blue.

Chlorine titration: with $AgNO_3$ (0.02 M)

The remaining 200 ml of the solution above is transferred into a 400 ml beaker. 10 ml of HNO_3 are added, the titration is done by means of silver nitrate $AgNO_3$.

Calorific value according to DIN 51900

For the determination of the calorific values a bomb calorimeter (IKA calorimeter C 7000 duo IKA C 5000) is used. Around 0.3 to 0.8 g of pre-dried and ground sample is weighed into a combustion capsule. The sample is mounted in the combustion bomb with an ignition. The bomb is placed into the calorimeter after been filled with 30 bar of oxygen.

The ignition and the measurement are done automatically. After the combustion the bomb must be checked for signs of incomplete combustion. Only gross calorific values (GCV) have been determined.

Trace elements on the basis of DIN EN 13657:2003-01

About 3 g of pre-dried and crushed sample is weighed into the reaction vessel. 21 ml of HCl and 7 ml of HNO_3 are added. The digestion vessel is sealed and placed in the heating system. The samples can oxidize slowly with acids to ovoid explosion by the direct heating. It is recommended to increase the temperatures of the digestion mixture from 60 °C in modest steps each 20 min to an end temperature of 160 °C (60 - 80- 120 - 160 °C), the digestion lasts for 2 h. After complete cooling, the reaction vessels are opened and the digestion solution is transferred into a 50 ml plastic volumetric flask and filled with deionized water, then adjusted with HNO_3.

The measurements were performed using Inductively Coupled Plasma ICP and Atomic Absorption Spectrometry. To determine mercury a cold vapor AAS (DIN EN 1483) was used.

Elemental analysis (C, N, O, P, Fe)

The elemental analyses were done by means of, a scanning electron microscope (SEM) (TESCAN VEGA3 Centre d'Analyse et de Caractérisation CAC- Cadi ayyad University).

CO_2 and SO_2 emission calculation

CO_2 and SO_2 emissions prevision are calculated by the following formulas (Madlool et al., 2011; Lechtenberg and Diller, 2012):

$$CO_{2\,[m^3/kg\ fuel]} = \frac{1.854 * C_{[\%]}}{100} \quad \text{(Eq.1)}$$

$$SO_{2\,[m^3/kg\ fuel]} = \frac{0.68 * S_{[\%]}}{100} \quad \text{(Eq.2)}$$

Note: [m³kg-1 fuel] are referred to STP.

http://www.aloki.hu ● ISSN 1589 1623 (Print) ● ISSN 1785 0037 (Online)
DOI: http://dx.doi.org/10.15666/aeer/1706_1515115168

Net CO_2 mitigation calculation

The CO_2 mitigation calculation is done through the following equations: first we calculate the equivalent amount of coal (W) that could substitute 1 t of AF used based on their corresponding calorific values (CV) according to *Equation 3,* then we estimate its corresponding CO_2 emitted amount (X) based on *Equation 4:*

$$W_{[t]}\ of\ coal\ =\ \frac{CV\ (AF)\ (kcal/kg)}{CV\ (Coal)\ (kcal/kg)} \quad \text{(Eq.3)}$$

$$X_{[t]}\ CO_{2\ (coal)} = W * 2.45_{[t]}\ CO_2 \quad \text{(Eq.4)}$$

The calculation of CO_2 emissions from 1 t of alternative fuels (Y) is done by using the carbon content (%C) determined by analysis (*Table 5*) and the molar mass (M) of CO_2 according to *Equation 5*.

$$Y_{[t]}\ CO_2(AF)\ =\ \frac{(C_{[\%]} * (M(C)+2M(O))/M(C))}{100} \quad \text{(Eq.5)}$$

The amount of CO_2 (Z) that could be saved by using AF instead of the equivalent amount of coal is calculated based on *Equation 6:*

$$Z_{[t]}\ CO_2\ =\ 2.45_{[t]}\ -\ Y_{[t]} \quad \text{(Eq.6)}$$

W, X, Y and Z are variables.

Results and discussion

Energetic potential

Proximate and ultimate analysis of the studied alternative fuels: The results regarding calorific value (CV), moisture content, ash, volatiles, carbon, oxygen, nitrogen, sulphur and chlorine of different kinds of waste and of coal as fossil fuel reference are summarized in *Table 2*.

Substitution rate calculation: *Table 3* shows the substitution factor of each alternative fuel referring to calorific value of 1 t of coal or petcoke commonly used in cement facilities.

Olive residues sampled from different industrial units have lower heating values than coal between 18 and 21 MJ kg^{-1}, with carbon content above 50%. The moisture content ranges from 0.33 to 17%, and ash content is between 2 and 30%. The results show that olive kernels produced by means of traditional olive mills systems have the highest calorific value which is close to that of coal due to their higher oily as well as low ash contents compared to OK originated from continuous system (*Table 2*). Hence even that olive kernels are commonly used as alternative fuel it seems very interesting to compare OK from different sources and to highlight the impact of the source on their CV.

As mentioned in *Table 3*, olive residues have calorific values ranging between 4000 and 5000 kcal kg^{-1} (16.75 – 20.93 MJ kg^{-1}); therefore, 1.17 t and 1.58 t are needed to substitute 1 t of coal or 1 t of petcoke respectively, with olive kernels produced by means of traditional system. To maintain a good quality of the final product and

http://www.aloki.hu ● ISSN 1589 1623 (Print) ● ISSN 1785 0037 (Online)
DOI: http://dx.doi.org/10.15666/aeer/1706_1515115168

convenient conditions of the combustion process while using agricultural biomass as alternative fuels, a substitution rate of 20% is recommended. In comparison to other wastes, the capital investment for their pretreatment is considered to be low (Demirbaş, 2003; Murray and Price, 2008). Some limitations of using biomass are their unavailability all around the year (Al-Hamamrea et al., 2017) and the high fluctuation of their heating value (Chinyama, 2011).

Table 2. *Proximate and ultimate analysis of alternative fuels tested, and coal*

Description	Olive kernels (dm)			Dried olive-mill wastewater (dm)	Sewage sludge "M" (dm)	Sewage sludge "G" (dm)	Chicken residues (dm)	Animal meal (ar)	Fluffy RDF (ar)	Coal
	Continuous system	Traditional system	Canning							
Proximate analysis										
Gross calorific value (MJ kg^{-1})	18.67	21.68	21.23	18.08	17.718	14.938	24.794	17.584	25.016	25.5
Moisture (%)	2.79	2.28	1.79	2.06	2.46	1.37	1.05	5.75	1.14	3
Ash (%)	9.61	4.58	2.41	30.46	28.34	34.61	10.46	25.12	8.3	11.1
Volatile matter (%)	68.59	75.09	73.04	57.73	61.62	56.13	80.44	74.88	91.7	35.9
Ultimate analysis										
Carbon (%)	53.80	50.91	58.42	58.04	44.97	33.03	77.89	47	53	70.6
Oxygen (%)	38.47	41.02	33.16	23.33%	36.25	43.06	18.05	n.a	n.a	n.a
Nitrogen (%)	n.a	6.17	3.63	2.75	8.29	10.06	n.a	10	n.a	1.2
Phosphorus (%)	0.15	0.04	0.05	0.04%	1.14	3.45	0.80	3.4-5,9*	n.a	n.a
Iron (%)	n.a	n.a	n.a	0.79	0.22	1.57	n.a	n.a	n.a	n.a
Sulfur (%)	0.14	0.08	0.06	0.13	1.05	1.30	0.52	0.7	0.2	1.3
Chlorine (%)	0.63	0.8	1.99	1.98	0.18	0.49	0.46	1.7	1.4	0.07

*According to ICON IC Consultants (2001). n.a = not available, dm = dry matter, ar = as received

Table 3. *Fuel substitution calculation*

Fuel substitution calculation				
	Gross calorific value (kcal kg^{-1})	Substitution factor CV coal (ton)	Substitution factor CV petcoke (ton)	Saved fossil-derived CO_2 (ton)
Olive mill wastewaters	4319	1.41	1.89	1.73
Olive kernels continuous system	4459	1.36	1.83	1.80
Olive kernels traditional system	5179	1.17	1.58	2.09
Olive kernels canning	5071	1.20	1.61	2.04
Sewage sludge M	4232	1.44	1.93	1.70
Sewage sludge G	3568	1.70	2.29	1.44
Chicken residues	5922	1.03	1.38	2.38
Animal meal	4200	1.45	1.95	1.69
Fluffy RDF	5975	1.02	1.37	-
Coal	6100	1	-	-
Petcoke	8200	-	1	-

For sewage sludge the results show that the calorific value of sewage sludge "M" is 17.718 MJ kg^{-1}, the moisture content is 2.46%, and the ash content is 28.34%, and

http://www.aloki.hu ● ISSN 1589 1623 (Print) ● ISSN 1785 0037 (Online)
DOI: http://dx.doi.org/10.15666/aeer/1706_1515115168

carbon level of 44.97%. For sewage sludge "G" the calorific value, moisture, ash, carbon, and sulphur are 14.938 MJ/kg, 1.37%, 34.61%, 33.03%, and 1.30%, respectively (*Table 2*). The ranges of different contents of elements and calorific values depend on the characteristics of the source and the treatment process of the sewage sludges. We can conclude that the sewage sludge "M" has the highest caloric value along with carbon content of 44.97% and ash content higher than 11.1%. Sewage sludge "M" and sewage sludge "G" have calorific values of 4232 and 3568 kcal kg^{-1} (17.71 – 14.94 MJ kg^{-1}), respectively. To replace 1 t of coal/petcoke with sewage sludge "M", 1.44 t/1.93 t are needed respectively (*Table 3*). To ovoid the possibility of an increased infeed of trace elements, Werther and Ogada (1999) suggested a maximum sewage sludge feeding rate of 5% of the clinker production capacity.

Compared to animal meal, chicken residues have the highest calorific value which is about 24.79 MJ kg^{-1} due to its oily texture and low moisture content of 1.05%. Animal meal has a calorific value of 17.58 MJ kg^{-1} and moisture content of 5.75% (*Table 2*). Therefore 1.03 t and 1.38 t are needed to substitute 1 t of coal or 1 t of petcoke with chicken residues. Around 1.45 t and 1.95 t are needed to replace 1 t of coal or 1 t of petcoke with animal meal (*Table 3*). Animal meal is considered to be available compared to other alternative fuels and their feeding rate is variable from country to another, it is about 15% of the energy needed in Spain cement kilns (Conesa et al., 2005), 40% for Australia (Rahman et al., 2015) and there is no limit in Switzerland.

Owing to its high calorific value of 25.01 MJ kg^{-1} which is similar to that of coal (*Table 2*), and with a low moisture of 1.14% and low ash content, fluffy RDF represents a very suitable alternative fuel for clinker burning. Fluffy RDF represents a perfect candidate for energetic recovery in these industries (Lechtenberg and Diller, 2012). In addition, only1.02 t to 1.37 t of fluffy can substitute 1 t of coal and 1 t of petcoke, respectively. Among all tested alternative fuels**,** chicken residues and fluffy RDF as well as olive kernels produced by means of traditional olive mill system have the highest caloric power along with most favourable substitution factors for the replacement of 1 t of coal/petcoke.

Emissions

CO_2 emissions

CO_2 emitted during co-processing such fuels in cement plant does not exceed the emission resulted from coal [1.30 CO_2 m^3 kg^{-1} fuel] (*Table 4*). However the emitted quantity of CO_2 in case of chicken residues co-firing is higher due to its high carbon level [1.44 CO_2 m^3 kg^{-1} fuel]**.**

The studied products account for pure biogenic material and therefore the co-incineration of such materials contributes to global fossil-derived carbon dioxide mitigation. The extent of the mitigation can be appraised by the following simple calculation: Taking into account the IPCC default emission factor for coal 96 kg CO_2/GJ (IPCC, 1996), 1 t of coal emits approximately 2.45 t of CO_2. Hence, for each ton of coal substituted by 1.45 t of MBM around 2.45 t of fossil-derived carbon dioxide is saved. Or, vice versa, 1 t of MBM can save around 1.69 t of fossil-derived CO_2 from coal (*Table 3*).

Plastics in general cannot be taken into account for fossil CO_2 reduction calculation, this is owing to the fact that their origin is crude oil. Only bio-plastics made of renewable feedstocks (e.g. starch from cereals, corn, sugar cane) can be valuable for

http://www.aloki.hu ● ISSN 1589 1623 (Print) ● ISSN 1785 0037 (Online)
DOI: http://dx.doi.org/10.15666/aeer/1706_1515115168

this. Mathematical modeling revealed a significant reduction of CO_2 emissions, which is approximately 1.0 t of CO_2 per ton of coal replacement in case of the use of pure polyethylene and polystyrene plastics as alternative fuel (Murray and Price, 2008; Ariyaratne et al., 2011).

We can presume that 1 t of chicken residues can save 2.38 t of fossil-derived CO_2 from coal, which allows a significant reduction in terms of fossil-derived CO_2 emissions (*Table 3*). The saving of fossil-derived CO_2 is not only a matter of biogenic carbon. If a fuel material has lower carbon than coal, but similar caloric power, as it is the case of fluffy RDF, then some net CO_2 mitigation could be obtained.

Based on the *Equations 3, 4, 5* and *6,* 1 t of Fluffy RDF can substitute 0.96 t of coal, this quantity emits 2.4 t of CO_2 compared to 1.94 t CO_2 emitted while using 1 t of fluffy RDF which means 0.51 t CO_2 could be saved by using 1 t of fluffy RDF instead of the equivalent amount of coal.

SO_2, NOx emission

As evident in *Table 2* the sulphur content in olive residues is lower than the one in coal and therefore, co-firing biomass fuels with coal show a significant reduction of SO_2 levels (Demirbaş, 2003; Sami et al., 2001) however, the nitrogen content is higher than 1.2%. Experiments show, that using biomass implies low SO_2 and NOx emissions due to lower sulphur and nitrogen contents compared to traditional fuels. Moreover, taking into account that the most of the nitrogen in biomass is converted to ammonia, which promotes the conversion of NOx to gaseous nitrogen, the emissions of NOx are also reduced (Demirbaş, 2003).

The sulfur content in sewage sludge varies between 1.05 and 1.3%. It is similar to coal, which means that SO_2 emissions will be the same in case of sewage sludge co-processing together with coal. High nitrogen levels have been detected (*Table 2*). However, a study by the U.S. Environmental Agency (2008) showed that the use of sewage sludge reduces NOx emissions.

In animal meal the sulphur content is lower than that in coal (*Table 2*), therefore co-processing such alternative fuels with coal has the capability of reducing SO_2 levels. Chinyama (2011) showed that SO_2 reduction depends mainly to the Ca content in MBM which has the capability to capture sulphur in solid phase. It was observed that NO_X decreases with increasing MBM content in a coal-MBM blend, even if the nitrogen content in animal meal is 8 times higher than that in coal (Gulyurtlu et al., 2005; Ferreira et al., 2018). In contrast, a study launched by Denafas et al. (2004) mentioned that during incineration of MBM using heavy fuel oil, the emission of nitrogen oxides increases.

In fluffy RDF the sulphur content is about 0.2% (*Table 2*) which can decrease the level of SO_2 emitted to air. The nitrogen content of the plastic, and the kiln operating conditions such as the flame temperature, air quantity, and oxygen level in the kiln are the main reasons for NOx emissions (Al-Salem et al., 2010).

Theoretically, all tested fuels can generate SO_2, owing to their sulphur contents. The calculated specific SO_2 quantities are displayed in *Table 4*. However, as explained by other studies, the specific conditions in clinker rotary kilns are very suitable to capture SO_2 from fuels, which ultimately ends up in the clinker minerals (Torsten, 2005; Prakash et al., nd).

All samples present high content of nitrogen in comparison with coal, one would expect that NOx emissions would increase. However, the prediction of NOx emission from nitrogen content is not possible because its generation depends on the combustion

http://www.aloki.hu ● ISSN 1589 1623 (Print) ● ISSN 1785 0037 (Online)
DOI: http://dx.doi.org/10.15666/aeer/1706_1515115168

temperature, although the fuel nitrogen contributes to some extent to the formation of NOx. NOx emissions from cement kilns mainly arise from oxidation of fuel-bound nitrogen and nitrogen in the combustion air. Clinker production is a high temperature process with flame temperatures up to some 2.000 °C in the sinter zone and material temperatures up to some 1.450 °C. Due to the quality of the product the process must be operated with excess oxygen. Under these process conditions NOx is inevitably formed from the chemical reaction of the air components, i.e. nitrogen and oxygen. This NOx is called "thermal NOx" (BAT, 2010).

Table 4. *CO_2 and SO_2 emissions calculation according to Equations 1 and 2*

Description	OKC	OKT	OKCa	OMWC	SS "M"	SS "G"	CR	AM	F-RDF	Coal
Carbon (%)	53.80	50.91	58.42	58.04	44.97	33.03	77.89	47	53	70.6
CO_2 (m^3 kg^{-1} fuel)	0.9975	0.9438	1.0831	1.0831	0.8337	0.6123	1.4440	0.8713	0.9826	1.3089
Sulphur (%)	0.14%	0.08%	0.06%	0.13%	1.05%	1.30%	0.52%	0.7%	0.2%	1.3%
SO_2 (m^3kg^{-1} fuel)	0.95210^3	0.54410^{-3}	0.40810^{-3}	0.88410^{-3}	0.71410^{-2}	0.88410^{-2}	0.35410^{-2}	0.47610^{-2}	0.13610^{-2}	0.88410^{-2}

Chlorine

Compared with coal, olive, animal residues, sewage sludge and fluffy RDF have higher chlorine levels (*Table 2*), thus increasing inner salt circulation of volatile elements inside the kiln. These give rise to increased coatings, build-ups and blockages in the colder parts of the preheater (Sami et al., 2001), hence reducing the efficiency of the plant.

A study revealed that biomass can contain considerable alkali and alkaline earth elements and chlorine, which, when mixed with other gas components derived from coal such as sulfur compounds, promotes a different array of vapor and fine particulate deposition in coal fired boilers (Lippiatt and Ahmad, 2004).

Chlorine may have an influence on clinker quality and therefore needs to be limited, as mentioned in the report from U.S. Environmental Protection Agency (2008), which refers to information from US-based Lehigh Cement. However, limitation of chlorine infeed to the kiln in general is advised (according to a rule of thumb, less than 300 g of total chlorine by raw materials and fuels per ton of clinker, which is valid for preheater kilns without bypass (Reference Guide, 2004). Chlorine-based salts are highly volatile under the kiln conditions, thus being the major driver for formation off coatings and cloggings in the preheater. Emission of HCl, dioxins and furans can be increased by the presence of chlorine under specific conditions (Karstensen, 2008; BAT, 2010).

Trace elements

Table 5 shows a detailed characterization of different trace elements as well as a comparison between the hole results obtained regarding ultimate, proximate and chemical analysis with the guideline of requirement of cement plants (average, maximum).

With regard to trace elements like Sb, As, Pb, Cd, Cu, Ni… the results revealed that for olive residues and chicken residues the majority of the elements metals are below the limits mentioned in the Guideline for the Energetic Recovery of Waste in Cement (GERWC) - Lime and Power plants in North Rhine Westphalia (GERWC, 2005; *Table 5*).

http://www.aloki.hu ● ISSN 1589 1623 (Print) ● ISSN 1785 0037 (Online)
DOI: http://dx.doi.org/10.15666/aeer/1706_1515115168

Table 5. *Physico-chemical analyses results and the guideline of requirement of alternative fuels in cement plants (average, maximum) and requirements from Heidelberg Cement Ennigerloh*

	Unit	Requirements of cement plants for the main burner and requirements from Heidelberg cement Ennigerloh										
		From	To	Olive mill waste water	Olive kernels continuous	Olive kernels traditional	Olive cannery	Sewage sludge M	Sewage sludge G	Chicken residues	MBM	Fluffy RDF
Water content	M.-%		< 15	2.06	2.79	2.28	1.79	2.46	1.37	1.05	5.75	1.14
Ash content	M.-%	10	20	30.46	9.61	4.58	2.41	28.34	34.61	10.46	25.12	8.3
Calorific value	MJ kg^{-1}	> 20		18.07	18.66	21.68	21.22	17.71	14.93	24.78	17.58	25.01
Volatile constituents	M.-%	n.a	n.a	57.73	68.59	75.09	73.04	61.62	56.13	80.44	74.88	91.7
Chlorine	M.-%	0.6	1	1.98	0.63	0.81	1.99	0.18	0.49	0.46	0.7	0.8
Sulfur	M.-%		2	0.13	0.14	0.08	0.06	1.05	1.30	0.52	1.7	0.2
Trace elements												
		Average	Max									
Antimony	mg kg^{-1}	50	120	0.66	0.62	0.67	0.64	3.34	3.2	0.67	0.1	15.79
Arsenic	mg kg^{-1}	5	13	4.67	0.85	0.92	0.79	6.01	7.68	0.68	0.20	0.48
Beryllium	mg kg^{-1}	0.5	n.a	0.30	0.17	0.17	0.16	0.26	0.22	0.17	5.19	0.17
Lead	mg kg^{-1}	70-190	200-500	13.35	2.01	2.63	1.92	90.28	43.24	0.71	1.08	4.30
Cadmium	mg kg^{-1}	4	9	0.26	0.03	0.033	0.03	0.9	1.6	0.35	5	0.03
Chrome	mg kg^{-1}	40-125	120-250	63.43	4.02	6.07	2.22	2751.43	193.82	1.03	11.18	5.16
Cobalt	mg kg^{-1}	6	12	4.67	0.30	0.34	0.31	4.67	17.29	0.33	1.68	0.34
Copper	mg kg^{-1}	120-350	300-700	33.38	8.01	10.12	4.2	128.71	341.23	71.87	16.18	10.39
Manganese	mg kg^{-1}	50-250	100-500	273.5	10	15.35	5.33	168.83	302.78	16.71	9.105	6.20
Nickel	mg kg^{-1}	50	100	36.72	2.05	3.13	1.07	17.55	41.65	1.20	1.25	0.69
Mercury	mg kg^{-1}	0.6	1.2	0.03	0.03	0.03	0.03	0.86	0.84	0.03	0.45	0.03
Selenium	mg kg^{-1}	3	n.a	0.78	0.65	0.67	0.64	3.29	3.2	2.19	0.323	0.69
Tellurium	mg kg^{-1}	3	n.a	1.75	1.67	1.68	1.62	1.91	4.80	1.67	7.17	1.73
Thallium	mg kg^{-1}	1	2	0.33	0.33	0.33	0.31	0.33	0.31	0.33	1.85	0.34
Vanadium	mg kg^{-1}	10	25	16.35	1.05	1.26	0.31	25.90	12.65	0.53	0.35	0.37
Zinc	mg kg^{-1}	n.a	n.a	43.39	9.54	13.74	8.25	578.35	2665.78	90.25	108.18	12.06
Tin	mg kg^{-1}	30	70	1.37	0.47	0.53	0.40	9.69	26.75	0.54	21.78	0.44

MBM contains some 3.4-5.9% P (Lechtenberg and Diller, 2012). Phosphorus is the most limiting factor for MBM firing, because it affects setting time and compressive strength development of cement as well.

The same considerations apply when dried sewage sludge is co-fired. As a rule, sewage sludge contains plenty of phosphorus, as it could be also shown by the examined sample "G" in particular, but also by sample "M".

P is absorbed by the clinker minerals to form C3P-C2S mixed crystals which decrease the C3S content, whilst increasing free lime. Altogether, the early strength of cement would be reduced when level of P_2O_5 in clinker is above 0.8% (Lechtenberg and Diller, 2012).

http://www.aloki.hu ● ISSN 1589 1623 (Print) ● ISSN 1785 0037 (Online)
DOI: http://dx.doi.org/10.15666/aeer/1706_1515115168

Heavy metals are also present in sludge and are the major problem in terms of sludge management. However, positive results have been achieved in the case of SS additions in cement manufacturing.

As shown in *Table 5* sewage sludge "M" contains higher levels of Cr and V, while sewage sludge "G" contains high level of Co. The level of mercury (Hg) is high in both sewage sludge samples when compared to the other materials (*Table 5*) which comes from the cleaning process at the sewage plant and from the source of the wastewater (ICON IC Consultants Ltd, 2001). To use sewage sludge in cement industry, the suggested maximum mercury content is 0.5 mg kg^{-1} (Karstensen, 2008; Ninomiya et al., 2004). Conesa et al. (2005) affirmed that there was no correlation between sewage sludge feeding rate and heavy metal emissions. But Cartmell et al. (2006) reported earlier that sewage sludge causes an increase in heavy metal emissions compared to fossil fuels.

It were demonstrated that the content of some heavy metals such as Cr, Zn, and Ni have no influence on the formation of the clinker phases, the final compressive strength, and the initial setting time or hydration level when their concentrations are below 0.1% in the raw mixture. The concentrations of heavy metals in the clinker are related to their volatility during the burning process. More studies are needed to establish the reliability of these findings (Chen et al., 2010).

As it is the case of natural materials, also waste-derived fuels contain environmentally relevant elements. Our examinations show that the samples contain fairly low amounts of heavy metals and metalloids. When co-processed, most of the elements are captured by the clinker minerals. But mercury in particular, and also thallium are volatile elements, which are hardly bound in the clinker. Thus, such elements leave the kiln system via the stack. Sewage sludge may have the potential of containing increased amounts of mercury. This tendency has also been observed in our examinations, for sewage sludge M and G contain around 0.8 mg kg^{-1} of Hg (*Table 5*). Mercury emissions of clinker kilns can be mitigated by an array of specific measures, e.g. dust shuttling, the use of activated carbon as sorbent, or wet scrubbers (CSI, 2016).

When using alternative fuels, a thorough sampling and analysis regime should be implemented for monitoring environmentally relevant elements in those materials.

Saving fuels estimation

Based of the calculation models used by MVW Lechtenberg and partners which is one of the world's leading consulting firms for the implementation of alternative fuels from biomass and useable wastes in the cement industry, we were able to calculate the quantity of coal that can be saved using different substitution rate 5%, 10% and 20% respectively of the studied alternative fuels with coal (*Table 7*).

The Kiln operation (hours and days), clinker production rate, specific heat consumption, heat consumption and the calorific value of each fuel (Fossil or AF) are the most important data that allow the calculation of the saved fossil fuel quantity (*Table 6*):

Scenario 1: 100% coal

The dosage of coal is obtained according to its corresponding calorific value and the heat consumption mentioned in *Table 6*.

http://www.aloki.hu ● ISSN 1589 1623 (Print) ● ISSN 1785 0037 (Online)
DOI: http://dx.doi.org/10.15666/aeer/1706_1515115168

Scenario 2: co-processing of coal and AF

First we defined the substitution rate which is the ratio between heat portion and heat consumption, the heat portion of AF is calculated according to its calorific value and its dosed value which is the added quantity of AF that satisfy the choosing substitution rate. While the heat portion of the remaining coal is the subtraction between the heat consumption and the heat portion of AF, the dosed quantity of the remaining coal in this scenario is the ratio between its CV and its heat portion. Savings of fossil fuels value is the ration of subtraction between the dosed remaining coal quantity in scenario 2 and the dosed quantity of coal in scenario 1.

Table 6. *Kiln data*

Kiln operation hours	[h d^{-1}]	24
Kiln operation days	[d a^{-1}]	330
Current clinker production rate	[t d^{-1}]	65 000
	[t h^{-1}]	2 708
	[t a^{-1}]	21 450 000
Specific heat consumption	[kJ kg^{-1} clinker]	3500
Heat consumption	[kJ h^{-1}]	9 479 166 667

We can notice that the quantity of fossil fuels that can be saved is related directly to the substitution rate, calorific value and the dosing quantity of AF used for each scenario.

For a substitution rate of 5% and 10%, we presume that SS with a calorific value of 17 706 kj kg^{-1} and dosing quantity of 27 t h^{-1} and 53.8 t h^{-1} revealed the highest saving quantity of coal which is about 148 352 t a^{-1} and 295 606 t a^{-1} respectively (*Table 7*).

For the substitution rate of 20% versus 80% of coal, chicken residues revealed the highest saving fuels of 592 038 t a^{-1}.

Table 7. *The saved quantity of coal using different substitution rate of 5%, 10% and 20% respectively of the studied alternative fuels*

	100% Coal	**95% Coal + 5% AF**				
	Coal	**CR**	**AM**	**F-RDF**	**SS**	**OK**
Net caloric value (kj Kg^{-1})	25 522	24 777	17 572	25 000	17 706	21 668
Substitution rate (%)	0	$95_{coal}/5_{CR}$	$95_{coal}/5_{AM}$	$95_{coal}/59_{F\text{-}Rdf}$	$95_{coal}/5_{SS}$	$95_{coal}/5_{OK}$
Dosage fuels (t h^{-1})	371.4	$353_{coal}/19_{CR}$	$352.8_{coal}/27_{AM}$	$352.8_{coal}/19_{F\text{-}Rdf}$	$352.7_{coal}/27_{SS}$	$352.7_{coal}/22_{OK}$
Saving fuels (t a^{-1})	-	146 087	147 230	147 402	148 352	147 929
	100% Coal	**90% Coal + 10% AF**				
	Coal	**CR**	**AM**	**F-RDF**	**SS**	**OK**
Net caloric value (kj Kg^{-1})	25 522	24 777	17 572	25 000	17 706	21 668
Substitution rate (%)	0	$90_{coal}/10_{CR}$	$90_{coal}/10_{AM}$	$90_{coal}/10_{F\text{-}Rdf}$	$90_{coal}/10_{SS}$	$90_{coal}/10_{OK}$
Dosage fuels (t h^{-1})	371.4	$334.1_{coal}/38.4_{CR}$	$334.2_{coal}/54_{AM}$	$334.2_{coal}/38_{F\text{-}Rdf}$	$334.1_{coal}/53.8_{SS}$	$334.4_{coal}/43.6_{OK}$
Saving fuels (t a^{-1})	-	295 250	294 459	294 804	295 606	295 185
	100% Coal	**80% Coal + 20% AF**				
	Coal	**CR**	**AM**	**F-RDF**	**SS**	**OK**
Net caloric value (kj Kg^{-1})	25 522	24 777	17 572	25 000	17 706	21 668
Substitution rate (%)	0	$80_{coal}/20_{CR}$	$80_{coal}/20_{AM}$	$80_{coal}/20_{F\text{-}Rdf}$	$80_{coal}/20_{SS}$	$80_{coal}/20_{OK}$
Dosage fuels (t h^{-1})	371.4	$297_{coal}/76.7_{CR}$	$297.1_{coal}/108_{AM}$	$297_{coal}/76_{F\text{-}Rdf}$	$297.2_{coal}/107_{SS}$	$297_{coal}/87.7_{OK}$
Saving fuels (t a^{-1})	-	589 732	588 919	589 609	587 915	589 697

http://www.aloki.hu ● ISSN 1589 1623 (Print) ● ISSN 1785 0037 (Online)
DOI: http://dx.doi.org/10.15666/aeer/1706_1515115168

The amount of fossil fuels that can be saved is directly influenced by the calorific value and the dosing quantity of the alternative fuel used. Higher substitution rate demands higher dosing quantity of alternative fuels and allow higher saving quantities of fossil fuels. The result connected with sewage sludge and olive kernels are based on the averages of the different sewage and olive kernel sources since the calorific value is not the same.

In this paper several alternative fuels that are being currently used in cement manufacturing, have been tested. These fuels have been critically analysed with regard to their gross calorific values, their levels of chlorine, sulphur, nitrogen and trace elements. Greenhouse gas emissions and environmental impact have been discussed as well.

In regards to calorific values fluffy RDF is the best option. It contributes to some net CO_2 mitigation due to its lower carbon content than coal, while the calorific value is on a similar level. Nowadays the use of plastics as alternative fuel is standard in numerous cement plants. Depending on the feeding point, kiln or calciner burners, plastics have to be crushed into appropriate grain size, furthermore chlorine always comes along with mixed plastics. The depletion of chlorine in the treatment process of plastics is of utmost importance.

Chicken residues followed by olive kernels (traditional olive mill system, canning) also have high calorific value and it reduces the green house gas emission due to their biogenic origin. From the emission point of view agricultural biomass could be the best option but due to the unavailability of a particular agricultural biomass all around the year restrict their usage.

Despite the low calorific value of animal meal it can replace coal to some extent and it offers the advantage of fossil derived CO_2 reduction. The environmental impacts are comparatively low. Still the processing costs are very high in the case of MBM.

Among the studied alternative fuel sewage sludge presents the lowest calorific value but the ash derived from the sludge can substitute raw material which is an additional advantage. In case of sewage sludge co-processing with coal a special attention need to be paid for trace elements, especially Cr, Co, V and Hg.

The generation of nitrogen oxides is inherent to the high-temperature process of clinker production. It is normally not influenced by the use of alternative materials. Moreover, depending on the respective locations, the raw material situation can effect the emissions of sulfur dioxide, the content of heavy metal compounds in the exhaust gas is additionally determined by the input situation in the kiln (VDZ CONGRESS, 2002).

In spite of numerous researches to identify the potential benefits and barriers of using different alternative fuel, none of those studies indicate which fuel is better than the others. This is only because there are lots of criteria which need to be considered from different perspectives. *Table 5* shows various criteria of the alternative fuels that have been discussed in this paper.

Conclusion

Based on the results obtained regarding the energetic potential and the environmental assessment: among all studied alternative fuels chicken residues, fluffy RDF and olive residues could be the best option as alternative fuels. The main advantages of using such fuels in cement industry are economic and environmental:

http://www.aloki.hu ● ISSN 1589 1623 (Print) ● ISSN 1785 0037 (Online)
DOI: http://dx.doi.org/10.15666/aeer/1706_1515115168

These fuels could reduce the carbon footprint and the main atmospheric pollutants (NOx, SO_2…) that result from using fossil fuels and therefore the overall environmental impact of cement manufacturing operations. We presume also from our results that the replacement of coal with such fuels extends the supply of fossil fuels and is a safe way of absorbing waste which otherwise would present disposal problem especially in developing countries. In economic point of view and based on the estimated quantity of coal that can be saved we notice, the use of these waste as fuels saved huge amounts of fossil fuels which is considered to be economically viable.

Heavy metal emissions from the cement industry are a significant environmental concern and need to be controlled through appropriate measures, hence it is necessary that future studies consider the environmental impact from heavy metal emitted after adaptation and implementation of any alternative fuel, through an assessment of these metals released into the environment surrounding (air, soil water and plant from) the cement kilns co-burning waste. A life cycle assessment (LCA) methodology is recommended as well to quantify the potential environmental impacts of each scenario and to figure out the most environmentally friendly ones.

Acknowledgements. This work was supported by the German Academic Exchange Service "DAAD" and MVW Lechtenberg Projektentwicklungs- und Beteiligungsgesellschaft mbH, in Duisburg, Germany: I would like to acknowledge, with grateful thanks, all individuals, companies and associations who have contributed in this work namely: Mrs Joanna Korneluk-Bruns, Dr Hansjoerg Diller, Mr Dirk Lechtenberg, and Heidelberg Cement Ennigerloh Germany.

REFERENCES

[1] Abdel-Shafy, H. I., Mansour, M. S. M. (2018): Solid waste issue: sources, composition, disposal, recycling, and valorization. – Egyptian Journal of Petroleum 27(4): 1275-1290.

[2] Al-Hamamrea, Z., Saidan, M., Rawajfeh, K., Alkhasawneh, H. E., Al-Shannag, M. (2017): Wastes and biomass materials as sustainable-renewable energy resources for Jordan. – Renewable and Sustainable Energy Reviews 67: 295-314.

[3] Al-Salem, S. M., Lettieri, P., Baeyens, J. (2010): The valorization of plastic solid waste (PSW) by primary to quaternary routes: from re-use to energy and chemicals. – Progress in Energy and Combustion Science 36(1): 103-29.

[4] Ariyaratne, W. K. H., Melaaen, M. C., Eine, K., Tokheim, L. A. (2011): Meat and bone meal as a renewable energy source in cement kilns: investigation of optimum feeding rate. – Renewable Energy and Power Quality Journal 2011(May): 1244-49.

[5] BAT Reference Document (2010): Best Available Techniques (BAT) Reference Document for the Production of Cement, Lime and Magnesium Oxide Industrial Emissions Directive 2010/75/EU. – Integrated Pollution Prevention and Control Joint Research Centre Institute for Prospective Technological Studies Sustainable Production and Consumption Unit European IPPC Bureau 2013.

[6] Bhatty, J. I. (2006): Effect of Minor Elements on clinker and Cement Performance: A Laboratory Analysis. – Portland Cement Association, Skokie, IL, pp. 31-34.

[7] Bourtsalas, A. C., Zhang, J., Castaldi, M. J., Themelis, N. J. (2018): Use of non-recycled plastics and paper as alternative fuel in cement production. – Journal of Cleaner Production 181: 8-16.

[8] Cartmell, E., Gostelow, P., Riddell-Black, D., Simms, N., Oakey, J., Morris, J., Jeffrey, P., Howsam, P., Pollard, S. J. (2006): Biosolids - a fuel or a waste? An integrated appraisal of five co-combustion scenarios with policy analysis. – Environ Sci Technol 40: 649-658.

http://www.aloki.hu ● ISSN 1589 1623 (Print) ● ISSN 1785 0037 (Online)
DOI: http://dx.doi.org/10.15666/aeer/1706_1515115168

[9] CEMBUREAU (2015): The European Cement Association. – Activity Report, Brussels, Belgique.
[10] Chen, H., Ma, X., Dai, H. (2010): Reuse of water purification sludge as raw material in cement production. – Cement and Concrete Composites 32(6): 436-439.
[11] Chinyama, M. P. M. (2011): Alternative Fuels in Cement Manufacturing. – In: Manzanera, M. (ed.) Alternative Fuel. InTech, Rijeka.
[12] Conesa, J. A., Fullana, A., Font, R. (2005): Dioxin production during the thermal treatment of meat and bone meal residues. – Chemosphere 59(1): 85-90.
[13] CSI (2016): Guidance for Reducing and Controlling Emissions of Mercury Compounds in the Cement Industry. – Cement Sustainability Initiative (CSI), World Business Council for Sustainable Development, Geneva.
[14] Davidovits, J. (1994): Global warming impact on the cement and aggregates industries. – World Resource Review 6: 263-278.
[15] Demirbas, A. (2003): Sustainable cofiring of biomass with coal. – Energy Conversion and Management 44(9): 1465-79.
[16] Denafas, G., Buinevicius, K., Urniezaite, I., Puškorius, R., Rekašius, J. (2004): Meat and bone meal incineration in terms of industrial and energetic infrastructure in Lithuania. – Energetic and Environmental Aspects 4: 36-48.
[17] EN 197 2000: European Standard EN 197-1: Cement. Part 1: Composition, Specifications and Conformity Criteria for Common Cements.
[18] Feng, Z., Zhao, J., Rockwell, J., Bailey, D., Huffman, G. (1996): Direct liquefaction of waste plastics and coliquefaction of coal-plastic mixtures. – Fuel Processing Technology 49(1-3): 17-30.
[19] Ferreira, L. R. A., Otto, R. B., Silva, F. P., De Souza, S. N. M., Ando Junior, O. H. (2018): Review of the energy potential of the residual biomass for the distributed generation in Brazil. – Renewable and Sustainable Energy Reviews 94: 440-455.
[20] GERWC (2005): Guideline for the Energetic Recovery of Waste in Cement (GERWC) - Lime and Power Plants in North Rhine Westphalia (Leitfaden zur Energetischen Verwertung von Abfällen in Zement-, Kalk- Und Kraftwerken in Nordrhein-Westfalen). 2. Ed. – Ministerium Für Umwelt Und Naturschutz, Landwirtschaft und Verbraucherschutz des Landes Nordrhein-Westfalen, Düsseldorf (in German).
[21] Ghenai, C., Inayat, A., Shanableh, A., Al-Sarairah, E., Janajreh, I. (2019): Combustion and emissions analysis of spent pot lining (SPL) as alternative fuel in cement industry. – Science of the Total Environment 684: 519-526.
[22] GIZ (2013): Diagnostic de l'état de Gestion Des Déchets Non Dangereux et Évaluation Du Gisement Pouvant Être Valorisés En Tant Que Combustibles Secondaires de Substitution. – http://www.gd-maroc.info/fileadmin/user_files/pdf/Etudes/SMQ-AF_EvaluationduGisement-min.pdf.
[23] Gulyurtlu, I., Boavida, D., Abelha, P., Lopes, M. H., Cabrita, I. (2005): Co-combustion of coal and meat and bone meal. – Fuel 84: 2137-48.
[24] Harjannea, A., Korhonenc, J. M. (2019): Abandoning the concept of renewable energy. – Energy Policy 127: 330-340.
[25] Hashem, F. S., Rasek, T. A., Mashout, H. A. (2019): Rubber and plastic wastes as alternative refused fuel in cement industry. – Construction and Building Materials 212: 275-282.
[26] Hossain, M. U., Poon, C. H., Wong, M. Y. K., Khine, A. (2019): Techno-environmental feasibility of wood waste derived fuel for cement production. – Journal of Cleaner Production 230: 663-671.
[27] ICON IC Consultants (2001): Pollutants in Urban Waste Water and Sewage Sludge Final Report. Chap. 2: Potentially Toxic Elements: Sources, Pathways, And Fate Through Urban Wastewater Treatment Systems. – ICON IC Consultants Ltd, London.

http://www.aloki.hu ● ISSN 1589 1623 (Print) ● ISSN 1785 0037 (Online)
DOI: http://dx.doi.org/10.15666/aeer/1706_1515115168

[28] Kääntee, U., Zevenhoven, R., Backman, R., Hupa, M. (2004): Cement manufacturing using alternative fuels and the advantages of process modelling. – Fuel Processing Technology 85(4): 293-301.
[29] Karell, M. A., Blumenthal, M. H. (2001): Air regulatory impacts of the use of tire-derived fuel. – Environmental Progress 20(2): 80-86.
[30] Karstensen, K. H. (2008): Formation, release and control of dioxins in cement kilns. – Chemosphere 70(4): 543-60.
[31] Lechtenberg, D. (2009): Spent cell linings from the aluminium smelting process as an alternative fuel and raw material for cement production. – Global Cement Magazine 2009(Jan): 36-37.
[32] Lechtenberg, D., Diller, H. (2012): Alternative Fuels and Raw Materials Handbook for the Cement and Lime Industry. Vols. 1 and 2. – Verlag Bau + Technik, Düsseldorf.
[33] Lippiatt, B., Ahmad, S. (2004): Measuring the life-cycle environmental and economic performance of concrete: the BEES approach. – International Workshop on Sustainable Development and Concrete Technology, Beijing.
[34] Madlool, N. A., Saidur, R., Hossain, M. S., Rahim, N. A. (2011): A critical review on energy use and savings in the cement industries. – Renewable and Sustainable Energy Reviews 15(4): 2042-60.
[35] Metz, B. (2005): Intergovernmental Panel on Climate Change IPCC Special Report on Carbon Dioxide Capture and Storage. – Cambridge University Press, for the Intergovernmental Panel on Climate Change, Cambridge.
[36] Murray, A., Price, L. (2008): Use of Alternative Fuels in Cement Manufacture: Analysis of Fuel Characteristics and Feasibility for Use in the Chinese Cement Sector. – National Laboratory, Berkeley.
[37] Ninomiya, Y., Zhang, L., Sakano, T., Kanaoka, C., Masui, M. (2004): Transformation of mineral and emission of particulate matters during co-combustion of coal with sewage sludge. – Fuel 83(6): 751-64.
[38] Porto, M. F. S., Fernandes, L. O. (2006): Understanding risks in socially vulnerable contexts: the case of waste burning in cement kilns in Brazil. – Safety Science 44(3): 241-57.
[39] Prakash, S., Chandrasekhar, P., Rajasekar, L. (nd): UltraTech Cement Ltd. Using High Sulphur Raw Materials Fuels Cement Plant. – In: Cement Plant Environmental Handbook, Cemnet, India, pp. 140-142.
[40] Rahman, A., Rasul, M. G., Khan, M. M. K., Sharma, S. (2015): Recent development on the uses of alternative fuels in cement manufacturing process. – Fuel 145(April): 84-99.
[41] Rahul, B., Sadhan, K. G., Ulhas, V. P. (2016): Co-processing of industrial waste in cement kiln: a robust system for material and energy recovery. – Procedia Environmental Sciences 31: 309-317.
[42] Reference Guide (2004): Reference Guide for Process Performance Engineers. 1st Ed. – Holcim Group Support Ltd., Corportate Technical Services, Rapperswil-Jona.
[43] Sami, M., Annamalai, K., Wooldridge, M. (2001): Co-firing of coal and biomass fuel blends. – Progress in Energy and Combustion Science 27(2): 171-214.
[44] Stafford, F. N., Viquez, M. D., Labrincha, J., Hotza, D. (2015): Advances and challenges for the co-processing in Latin American cement industry. – Procedia Materials Science 9: 571-577.
[45] Torsten, S. (2005): Minderung Rohmaterialbedingter SO_2 Emissionen in der Zementindustrie. – Verl. Bau und Technik, Düsseldorf.
[46] US Environmental Protection Agency (2008): Trends in Beneficial Use of Alternative Fuels and Raw Materials Cement Sector. – http://Www.Epa.Gov/Sectors/ Pdf/Cement-Sector-Report.Pdf.
[47] VDZ (2002): Effects of the Use of Secondary Materials on Emissions in Clinker Production. – Dr.-Ing. Martin Oerter, Cement Industry Research Institute, Düsseldorf.

http://www.aloki.hu ● ISSN 1589 1623 (Print) ● ISSN 1785 0037 (Online)
DOI: http://dx.doi.org/10.15666/aeer/1706_1515115168

[48] Werther, J., Ogada, T. (1999): Sewage sludge combustion. – Progress in Energy and Combustion Science 25(1): 55-116.
[49] Zhang, Y., Xue, S. C., Shao, S., Chen, Y., Liu, S.-L., Zhang, S.-S. (2011): Aspen Plus-based simulation of a cement calciner and optimization analysis of air pollutants emission. – Clean Technologies and Environmental Policy 13(3).

http://www.aloki.hu ● ISSN 1589 1623 (Print) ● ISSN 1785 0037 (Online)
DOI: http://dx.doi.org/10.15666/aeer/1706_1515115168

THE SPATIAL QUANTITATIVE EVALUATION AND COUPLING COORDINATION DEGREE OF URBAN ECOSYSTEM CARRYING CAPACITY: A CASE STUDY OF THE URBAN AGGLOMERATION IN THE MIDDLE REACHES OF THE YANGTZE RIVER, CHINA

SHEN, W.[1] – LU, F. X.[1*] – QIN, Y. C.[1*] – ZHOU, Y. S.[2] – XIE, Z. X.[1]

[1]*College of Environment and Planning, Key Laboratory of Geospatial Technology for Middle and Lower Yellow River Region, Henan University, Kaifeng 475004, China*
(e-mail: shenwei@henu.edu.cn)

[2]*School of Surveying & Land Information Engineering, Henan Polytechnic University Jiaozuo 454000, China*

[*]*Corresponding authors*
e-mail: qinyc@henu.edu.cn; lfxhenu@126.com

(Received 30th Jun 2019; accepted 16th Oct 2019)

Abstract. The urban agglomeration in the middle reaches of the Yangtze River is within a typical ecologically sensitive area as well as it is a key development area in China. Scientific assessment of urban ecosystem carrying capacity has important scientific value and practical significance. In this study, we established a new assessment framework for urban ecosystem carrying capacity, and then based on the components and structural characteristics of urban ecosystems, we constructed an extended evaluation index system for urban ecosystem carrying capacity. Spatial analysis and a coupling coordination degree model were used to analyze spatial patterns and coupling coordination degree of urban ecosystem carrying capacity in urban agglomeration in the middle reaches of the Yangtze River in 2015. The results indicated that: (1) The urban ecosystem carrying capacity of the study area was spatially differentiated and clearly clustered. (2) Comprehensive coupling coordination in spatial distribution had a significant north-south differentiation pattern of study area. Highly coordinated cities were mainly distributed in the Poyang Lake urban agglomeration and the area around the Dongting Lake, while the less coordinated cities were mainly distributed in the Wuhan urban agglomeration and south of the urban agglomeration around Changsha-Zhuzhou-Xiangtan. (3) In the surrounding area of Wuhan City and southwest of the urban agglomeration around Changsha-Zhuzhou-Xiangtan of coupling coordination degree is low, mainly due to the backward industrial foundation, low economic development efficiency, and heavy load on resource consumption and the environment.
Keywords: *urban ecosystem carrying capacity, moderate indicator, state-space model, coupling coordination degree model*

Introduction

Since the 1990s, continuous promotion of reform and open policy and the gradual improvement of the market economy system have ushered, China's economy into a period of rapid growth (Qi et al., 2015). However, due to the rapid growth of urban population and built-up area, the overexploitation of natural resources, and environmental pollution had significant negative impacts on land cover, biodiversity, the hydrological system, and local climate at different regional scales. In turn, the natural environment has limited regional social and economic development, causing people to gradually realize that regional sustainable development is closely related to regional ecosystem health (Pei et al., 2019). Therefore, to guide the regional

http://www.aloki.hu ● ISSN 1589 1623 (Print) ●ISSN1785 0037 (Online)
DOI: http://dx.doi.org/10.15666/aeer/1706_1516915190

sustainable development, it is necessary to evaluate the urban ecosystem carrying capacity according to development status. Ecological carrying capacity is an important indicator, which is used for measuring the utilization degree of natural resources and interference intensity of ecological environment caused by human activities. Meanwhile, it is also an important tool for evaluating the level of regional sustainable development (Xiong et al., 2013). In recent years, it has attracted the attention of global scholars and has been widely used to evaluate urban ecosystem carrying capacity and sustainable development (Wackernagel and Galli, 2007; Zhang et al., 2016; Rudolph and Figge, 2017).

In 1922, Hawden and Palmerzai first proposed the concept of ecological carrying capacity when studying the impact of reindeer population on regional ecosystems. The concept was subsequently developed and improved, transforming from research focused on a single ecological element, to the early stage carrying capacity of an ecosystem (Cui and Yang, 1997; Hudak, 1999; Zhu et al., 2005), and finally to the carrying capacity of a composite ecosystem composed of integrated ecological elements such as nature, society and the economy (Wang et al., 2000; Yang and Sui, 2005; Xiong et al., 2014). The study of ecological carrying capacity based on comprehensive ecological factors has gradually enriched the theory and connotations of ecological carrying capacity, enhancing people's understanding of complex ecosystems. Evaluation methods and index systems for ecological carrying capacity, with the continuous development of the concept and connotation of ecological carrying capacity has also gradually improved with applications in different issues and research focuses. The main methods include human appropriation of net primary production (HANPP) (O'Neill et al., 2007; Sjafrie et al., 2018;), ecological footprint method (Jiao et al., 2011; Xiang et al., 2016; Peng et al., 2019), state-space method (Xiong et al., 2014; Ji et al., 2017), system model (Lein, 2010; He et al., 2011; Mondino et al., 2014; Ge et al., 2016), comprehensive evaluation method (Jin et al., 2015; Wang et al., 2017), ecosystem service consumption evaluation method (Rong et al., 2019), and more. Evaluation methods have the characteristics of diversification and synthesis (Ji et al., 2017).

Current research still has the following problems: in terms of the research on the evaluation index system of ecological carrying capacity, the selection of evaluation indicators has primarily focused on natural elements, and seldom considers the impacts of social development and progress, resource consumption, treatments for environmental pollution and other factors on the overall carrying capacity of a complex urban ecosystem, and the selection scope of indicators needs to be further expanded. From the perspective of the application of the state-space method, its calculation formula can be divided into two types: the first is represented by Xiong et al. (2014), Peng et al. (2016), Ji et al. (2017) and Pei et al. (2019), in which the state-space formula is used to calculate the urban ecosystem carrying capacity index a year or a time series. The advantages of this formula are well known and widely used, but it is unable to evaluate the state of the urban ecosystem carrying. The second type is represented by Li and Ma (2013) and Song and Yu (2014), and is used to calculate current and ideal values for urban ecosystem carrying capacity in a cross-section of a year, and then evaluates carrying status of urban ecosystem based on the difference between current and ideal values. The advantage of this formula is that it can quantitatively evaluate the carrying status of an urban ecosystem. In summary, two issues remain in the application of the state-space method: first, moderate indices are

http://www.aloki.hu ● ISSN 1589 1623 (Print) ●ISSN1785 0037 (Online)
DOI: http://dx.doi.org/10.15666/aeer/1706_1516915190

seldom mentioned and the forward processing formulas for them have not been clearly described; Secondly, selecting ideal values for each index need to update. In addition, research on urban ecosystem carrying capacity based on the state space method has focused more on the analysis of spatial and temporal patterns, and less on an in-depth analysis of the coupling and coordination among the dimensions of the state-space axis and their causes.

The middle reaches of china's Yangtze River is an ecologically sensitive region that shoulders the important responsibility of ecological protection in the Yangtze river basin of China. At the same time, it is also one of the regions with the densest population, the highest intensity of water and soil resources development and utilization, and the most severe environmental pollution problems in China. At present, there has not been in-depth research on spatial pattern of the carrying state of the urban ecosystem and the level of coupling coordination between dimensions of urban agglomeration in the middle reaches of the Yangtze River. In light of deficiencies in the current research on the evaluation index system for urban ecosystem carrying capacity and applications of state-space method, firstly, our research established a new assessment framework for urban ecosystem carrying capacity and used multi-source data to construct a comprehensive evaluation index system composed by 25 key indicators. Meanwhile, these indicators are selected to depict urban ecosystem carrying capacity in terms of three aspects: the social-economic coordination force, resource-environment supporting force, and ecological resilience. Secondly, we improved the forward processing formula of moderate indicators and determined the ideal value of all indicators. Thirdly, we used the state-space method and coupling coordination degree model to analysis the spital pattern and coupling coordination of urban ecosystem carrying capacity in urban agglomeration in the middle reaches of the Yangtze River in 2015. This study complemented the theoretical and methodological studies of urban ecological carrying capacity, and this paper also has important practical significance and scientific value in guiding the sustainable development of the urban agglomerations in the middle reaches of the Yangtze river.

Study area and data source

Study area

The Urban agglomeration in the middle reach of the Yangtze River is a super urban agglomeration formed by the Wuhan urban agglomeration, the Poyang lake urban agglomeration, and the Changsha-Zhuzhou-Xiangtan urban agglomeration. It is located in the middle of China’s Yangtze River basin, including a total of 31 prefecture-level cities and some counties (districts) in Hubei, Hunan, and Jiangxi Provinces. Lying at 26°03'~ 32°38' N, 110°45 '~ 118°21'E and with a total area of about 326000 square kilometers, the region has a subtropical monsoon climate with annual average rainfall of about 800-1943 mm. The Urban agglomeration in the middle reaches of the Yangtze river is dominated by plains (*Fig. 1*), with fertile soil and abundant water resources. It is home to Poyang and Dongting Lake, the Han and Qingjiang Rivers, and many other rivers and lakes, with a good combination of water, temperature, and abundant agricultural resources that makes it one of the major grain-producing areas in China. However, the urban agglomeration in the middle reaches of the Yangtze river in this densely populated area and important development zone for Jiangxi, Hubei, and Hunan Provinces has been experienced

http://www.aloki.hu ● ISSN 1589 1623 (Print) ●ISSN1785 0037 (Online)
DOI: http://dx.doi.org/10.15666/aeer/1706_1516915190

prominent problems in recent years, such as carrying pressure of water resource, ecological security, and land pollution (Li et al., 2017; Chen et al., 2018).

Data source

The socio-economic statistical data used in this paper were obtained from 《China urban statistical yearbook of 2016》, 《Jiangxi statistical yearbook of 2016》, 《Hubei statistical yearbook of 2016》, 《Hunan statistical yearbook of 2016》, and 《China urban construction statistical yearbook of 2016》. Land use/cover data (for Jiangxi, Hubei, and Hunan provinces) were downloaded from the national science and technology infrastructure platform -- national earth system science data sharing platform (http://www.geodata.cn). A Python script was used for batch segmentation, transformation and extraction of 2015 land use/cover data, and then the forest and wetland data from each research unit was subdivided and counted (land cover data was available in five year intervals, the year 2015 with relatively complete data was selected as the study period). In addition, data on missing indicators such as total water resources were obtained from the water resources bulletin, total arable land area and urban and rural residential income were obtained from the statistics bulletin of prefecture-level cities.

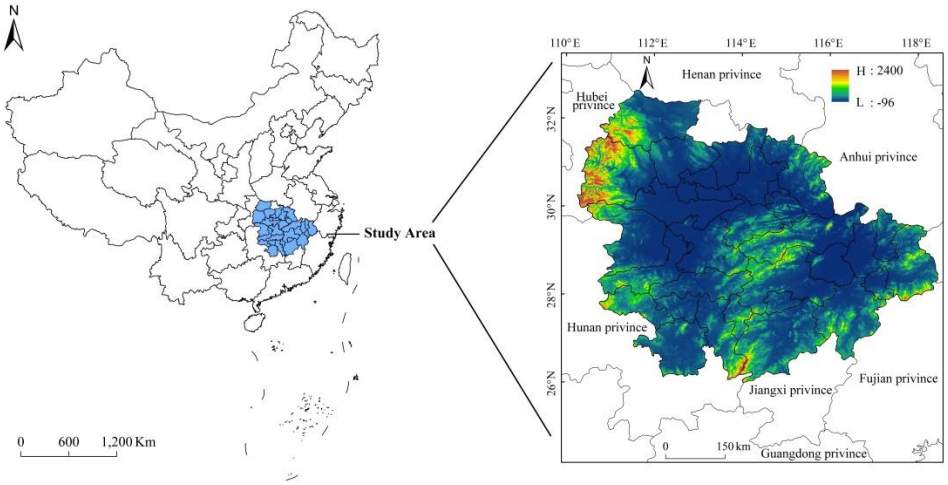

Figure 1. *Location of the study area*

Methodology

Framework of urban ecosystem carrying capacity assessment

There is no uniform concept of urban ecosystem carrying capacity, but by integrating existing research in this paper (Yin et al., 2011; Xiong et al., 2016; Wang et al., 2017; Pan et al., 2017), the concept was defined as: In a certain period and under a certain level of pressure, the urban ecosystem can maintain its own healthy and coordinated development carrying capacity. It is mainly manifested in three parts: the coordination ability generated by the socio-economic subsystem, the supporting ability provided by the resource-environment subsystem to maintain the healthy operation of the system, and the regulating ability and development potential of the ecological resilience subsystem to achieve an appropriate goal.

http://www.aloki.hu ● ISSN 1589 1623 (Print) ●ISSN1785 0037 (Online)
DOI: http://dx.doi.org/10.15666/aeer/1706_1516915190

We referred to existing studies on urban ecosystem carrying capacity and established a new framework for urban ecosystem carrying capacity assessment, we call it "pressure and driving force - supporting force - regulating force" model. As indicated in *Fig. 2*, the framework of urban ecosystem carrying capacity assessment includes the state plane (plane XY) and development potential axis (axis Z), which together constitute the overall development state of urban ecosystem carrying capacity. The evaluation framework also includes three dimensions: social-economic coordination force, resource-environment support force, and ecological resilience. These take into account the pressure and driving forces behind the social and economic subsystem, the supporting forces of resources and environment subsystem, and the regulating forces and development potential of the ecological subsystem.

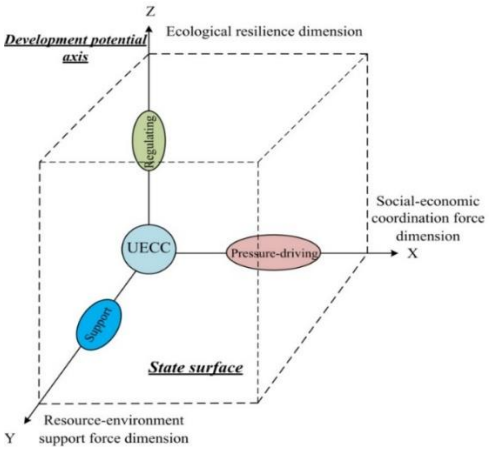

Figure 2. *Framework of urban ecosystem carrying capacity (UECC) assessment*

The composition and functions of the three dimensions of urban ecosystem carrying capacity can be further explained as follows: (1) Social-economic coordination force is the "pressure-driving" part of urban ecosystem carrying capacity. Social and economic coordination force not only reflects unbalanced social development pressure, population bearing pressure, and economic development pressure faced by urban ecosystem, but also reflects driving forces behind social progress, economic improvement, and industrial structure optimization for the overall development of urban ecosystem. (2) Resource-environment supporting force is the supporting and guaranteeing part of urban ecosystem, which reflects the degree of coordination between the supply of regional resource-environment and the demand of social-economic development. (3) Ecological resilience is the regulating part of urban ecosystem, which reflects the regulating power of regional ecological environment, and the development potential generated by human factors acting on the ecological environment.

Index system for urban ecosystem carrying capacity assessment

The purpose of establishing a comprehensive evaluation index system of urban ecosystem carrying capacity is to represent the degree of coordination between the regional socio-economic system and resource-environmental system, and to reflect the carrying capacity of urban complex ecosystem. This paper first considers the component and the structure characteristics of urban ecosystem, takes the impact of human activities as the context, on the

http://www.aloki.hu ● ISSN 1589 1623 (Print) ●ISSN1785 0037 (Online)
DOI: http://dx.doi.org/10.15666/aeer/1706_1516915190

basis of fully considering the characteristics of the study area, the comprehensive evaluation index system of urban ecosystem carrying capacity is established (*Table 1*). An extensive literature review was instrumental in selecting evaluation indicators. On the one hand, we selected indicators that are generally recognized and widely used by scholars in related fields (Xiong et al., 2013; Jin et al., 2015; Rudolph and Figge, 2017; Ji et al., 2017; Wang et al., 2017; Pei et al., 2019; Rong et al., 2019). On the other hand, we fully considered the impacts of social development and progress, resource consumption and environmental pollution control on urban ecosystem carrying capacity, making this paper somewhat innovative in the construction of index system.

Table 1. *Indicators for urban ecosystem carrying capacity assessment*

System layer	Subsystem layer	Criterion layer	Basic index layer	Properties of index
Urban ecosystem carrying capacity	Social-economic coordination force	Social progress factor	X1: Ratio of annual disposable urban household income to rural household income	Negative
			X2: Ratio of annual urban household comsumption to rural household comsumption	Negative
			X3: Highway passenger volume per capita	Positive
			X4: Hospital beds amount of every 10^4 people	Positive
			X5: Buses and trams amount of every 10^4 people	Positive
		Population development factor	X6: Population density	Moderate
			X7: Natural rate of population growth	Moderate
			X8: Population urbanization rate	Moderate
		Economic development factor	X9: Growth rate of per capita GDP	Moderate
			X10: Energy consumption per 10^4 GDP	Negative
			X11: Per capita GDP	Positive
		Industrial structure factor	X12: The percentage of the primary industry output value	Moderate
			X13: The percentage of the tertiary industry output value	Positive
	Resource-environment supporting force	Resource support factor	X14: Water resources per capita	Positive
			X15: Cultivated area per capita	Positive
		Environmental management factor	X16: Comprehensive utilization rate of industrial solid waste	Positive
			X17: Treatment rate of industrial smoke (powder) dust	Positive
			X18: Standard discharge rate of industrial wastewater	Positive
			X19: Domestic sewage treatment rate	Positive
			X20: Domestic waste treatment rate	Positive
	Ecological resilience	Ecological resilience factor	X21: Forest coverage rate	Positive
			X22: The percentage of wetland area to total area	Positive
			X23: Green coverage rate in built-up area	Positive
			X24: Per capita public green area	Positive
		Ecological potential factor	X25: Per capita investment in science and technology	Positive

Note: data of indicators X3 ~ X13 and X23 ~ X25 are from Jiangxi statistical yearbook of 2016, Hubei statistical yearbook of 2016, and Hunan statistical yearbook of 2016. Data of indicators X16 ~ X20 are from China urban statistical yearbook of 2016 and China urban construction statistical yearbook of 2016. Data of indicators X21 ~ X22 are derived from the data of land use/cover in 2015. Data of indicators X1, X2 , and X15 data are from the prefecture level statistical bulletin. Data of indicator X14 is from the prefecture level water resources bulletin

http://www.aloki.hu ● ISSN 1589 1623 (Print) ●ISSN1785 0037 (Online)
DOI: http://dx.doi.org/10.15666/aeer/1706_1516915190

Preprocessing of index data and weight determination

In the process of index data processing, in order to eliminate the possible differences in dimension and magnitude between indices, it was necessary to carry out forward processing and standardized processing of the index data. First, we selected negative indicator for forward processing, referenced the relevant research (Hu et al., 1992), and improved the existing formula, make the value compression after forward processing as $(0,1]$, there will be no height anomalies of $x_{ij}^z = 0$ and avoided the subsequent difficulty of logarithmic operations. The forward processing formula for the negative indicator is:

$$x_{ij}^z = \frac{MAX(x_{ij}) - x_{ij}}{MAX(x_{ij}) - MIN(x_{ij})} + 0.001 \quad \text{(Eq.1)}$$

The forward processing formula for the moderate indicator had not been derived out by existing studies. This study attempts to derive the formula, after verifying several different types of sample data, and found that the dimensionality of the data after the forward calculation by this formula was eliminated. The forward processing formula is as follows:

$$x_{ij}^z = \begin{cases} \frac{1}{\left(1+\left|1-\frac{x_{ij}}{A_i}\right|\right)} & , x_{ij} < A_i \\ \frac{1}{\left(1+\left|\frac{x_{ij}}{A_i}-1\right|\right)} & , \ x_{ij} \geq A_i \end{cases} \quad \text{(Eq.2)}$$

In the above equation (1) and (2): x_{ij} is the original index value, x_{ij}^z is the forward value of the original index, $MAX(x_{ij})$ is the maximum value of the j year and the ith index, $MIN(x_{ij})$ is the minimum value of the j year and the ith index, and A_i is the optimal threshold of the moderate index. By referring to relevant literature (Zhou and Zhao, 2012; Xiao et al., 2013) and consulting experts in relevant fields, the optimal thresholds for GDP growth rate index and the proportion of primary industry in GDP indices were set as 7% and 12.4%, respectively. GDP growth rate and the proportion of the primary industry in GDP were defined as moderate indicators based on the following considerations: (1) Zhou and Zhao (2012) have shown that the GDP growth rate is 7% or lower, which will lead to employment pressure, inflation, and other problems. Therefore, there is an optimal threshold for GDP growth rate. (2) The primary industry usually includes agriculture, forestry, animal husbandry, fishery and other agricultural industries, which provide the basic energy supply for the urban ecosystem. A low proportion of the primary industry affects urban ecosystem stability, while a high proportion is not conducive to the improvement of social and economic coordination. Xiao et al. (2013) pointed out that there is an optimal proportion in the primary industry. In addition, the optimal thresholds for population density, natural population growth rate, and population urbanization rate were set as 600 people /km^2, 5‰ and 60%, respectively, based to relevant research (Li and Li, 2014; Su et al., 2019).

After the forward processing of the negative and moderate indicator, the positive and moderate indicator values were standardized after the forward processing are standardized. In this paper, the maximum and minimum value standardization method was adopted to standardize the data. Considering that the index data in this paper were resources, environment and socio-economic indicators based on the statistics of

http://www.aloki.hu ● ISSN 1589 1623 (Print) ●ISSN1785 0037 (Online)
DOI: http://dx.doi.org/10.15666/aeer/1706_1516915190

administrative units, the weights of evaluation indicators were determined by the entropy weight method (Ji et al., 2017; Wang et al., 2017). The entropy weight method is an objective weighting method, it can avoid the interference of human subjective factors and make the result have objectivity and higher credibility (Shen et al., 2017).

State-space method

The state space method is an effective method for quantitative describing system state in Euclidean geometry space. It is usually composed of three-dimensional state space axes representing the state vectors of each element of the system. In the three dimensional state space, each point represents the spatial combination of resource-environment and human social-economic activities over a certain period of time, and a specific carrying state of the system can be judged by the position of the points (Ji et al., 2017). The formula for calculating the ideal value (ECC) and the current value (ECS) of urban ecosystem carrying capacity are as follows:

$$ECC = \sqrt{\sum_{i=1}^{n} {w_i}^2} \quad \text{(Eq.3)}$$

$$ECS = \sqrt{\sum_{i=1}^{n} (w_i * x_{ij}^b)^2} \quad \text{(Eq.4)}$$

In *Equations (3) and (4)*, w_i is the index weight, and x_{ij}^b is the ratio coefficient between the original value of each city index and its ideal value (*Table 2*) based on the ratio method according to the differences in the three types of indices. The specific calculation process is shown in *Equation (5)*. The main considerations for determining ideal value of all indices are the sustainability and internal coordination of the urban ecosystem, and experts in related fields were consulted for revision.

$$\begin{cases} x_{ij}^b = \frac{x_{ij}}{I_i}, & \text{Positive indicator} \\ x_{ij}^b = \frac{I_i}{x_{ij}}, & \text{Negative indicator} \\ x_{ij}^b = \begin{cases} \frac{x_{ij}}{A_i}, & x_{ij} \le A_i \\ \frac{A_i}{x_{ij}}, & x_{ij} > A_i \end{cases}, & \text{Moderate indicator} \end{cases} \quad \text{(Eq.5)}$$

Coupling coordination degree model

Referring to the coupling model for capacity in physics, the coupling model for two systems (*Equation (6)*) and three systems (*Equation (7)*) were generalized to explore the coupling coordination relationship between the three dimensions: "social-economy, resource-environment, and ecological resilience" (Xing et al., 2019). The model formula is as follows:

$$C = \left\{ \frac{f(x) \cdot g(y)}{\left[\frac{f(x) + g(y)}{2} \right]^2} \right\}^{\frac{1}{2}} \quad \text{(Eq.6)}$$

http://www.aloki.hu ● ISSN 1589 1623 (Print) ●ISSN1785 0037 (Online)
DOI: http://dx.doi.org/10.15666/aeer/1706_1516915190

$$C = \left\{ \frac{f(x) \cdot g(y) \cdot h(z)}{\left[\frac{f(x) + g(y) + h(z)}{3} \right]^3} \right\}^{\frac{1}{3}} \quad \text{(Eq.7)}$$

In the formula, *f(x)*, *g(y)* and *h(z)* are respective standardized values of carrying capacity for the three dimensions. *C* is the coupling degree, which ranges from 0-1. Since the coupling degree can only measure the degree of correlation among dimensions, but cannot reflect the coordination level among dimensions, this paper further introduced a coupling coordination degree model, so as to better measure the coupling coordination level among dimensions. The formula is as follows:

$$D = \sqrt{C \cdot T} \quad \text{(Eq.8)}$$

$$T = \alpha f(x) + \beta g(y) + \gamma h(z) \quad \text{(Eq.9)}$$

In *Equations (8) and (9)*, D is the coupling coordination degree ranging from 0-1 and *T* is used to measure the overall synergy between dimensions. α, β, γ are undetermined coefficients representing the contribution of each dimension. We assumed that the three dimensions were equally important to urban ecosystem carrying capacity, so $\alpha = \beta = \gamma = ⅓$.

Results

Evaluation of the urban ecosystem carrying capacity in urban agglomeration in the middle reaches of the Yangtze River

According to the state-space method, the ideal value for urban ecosystem carrying capacity was ECC=0.216, and the ideal value of social-economic coordination force dimension, resource-environment support force dimension and ecological elastic force are 0.154, 0.133 and 0.07, respectively. In order to judge the carrying state of urban ecosystem, the carrying state index is introduced as CSI. According to the principle of state-space method, CSI= ECS-ECC, and when CSI > 0, the system is in a loadable state. When CSI=0, the system is in a fully loaded state. When CSI < 0, the system is overloaded. Based on urban ecosystem carrying capacity, the ideal value of the three dimensions, and the CSI, 28 cities were divided into six state types8: highly loadable area (CSI > 0.05), moderately loadable area (0.02<CSI≤0.05), mildly loadable area (0<CSI≤0.02), fully loaded area (CSI= 0), mildly overloaded area (-0.02≤CSI <0), moderately overloaded area (-0.05< CSI≤ -0.02).

By virtue of the spatial visualization function of ArcGIS10.3 software was used to visualize, the CSI of the urban ecosystem and three dimensions in 2015 was visualized in accordance with the carrying state classification criteria above (*Fig. 3*).

The social-economic coordination force dimension is the "pressure-driven" part of urban ecological carrying capacity. It not only reflects unbalanced social development pressure, population pressure and economic development pressures faced by an urban ecosystem, but also the development ability provided by social progress, economic strength, and industrial optimization. From the perspective of spatial distribution characteristics (*Fig. 3a*), the dimension had a circling spatial structure extending outward from the provincial capitals of Hubei, Hunan, and Jiangxi Provinces.

http://www.aloki.hu ● ISSN 1589 1623 (Print) ●ISSN1785 0037 (Online)
DOI: http://dx.doi.org/10.15666/aeer/1706_1516915190

Table 2. *Ideal values and sources for each indicator*

Basic index layer	Ideal value	Source of the ideal value
X1: Ratio of annual disposable urban household income to rural household income	1.7	Su et al., 2019
X2: Ratio of annual urban household consumption to rural household consumption	2.0	Chen and Wu, 2017
X3: Highway passenger volume per capita	17	Expert consultation method
X4: Hospital beds amount of per 10^4 people	40	China habitat award standards of 2016
X5: Buses and trams amount of per 10^4 people	15	"China's 13th five-year" plan for urban public transport development targets
X6: Population density	600	China habitat award standards of 2016
X7: Natural population growth rate	5	Zhou and Yin, 2012
X8: Population urbanization rate	60.0	Su et al., 2019
X9: Growth rate of per capita GDP	7	Zhou et al., 2012
X10: Energy consumption per 10^4 GDP	0.68	China habitat award standards of 2016
X11: Per capita GDP	50000	Peng et al., 2016
X12: The percentage of the primary industry output value	12.4	Xiao et al., 2013
X13: The percentage of the tertiary industry output value	50.00	China habitat award standards of 2016
X14: Water resources per capita	1700	Comprehensive report on China's water resources strategy for sustainable development
X15: Cultivated area per capita	533	UN food and agriculture organization, per capita arable land area warning line
X16: Comprehensive utilization rate of industrial solid waste	90	National model city standard for environmental protection
X17: Treatment rate of industrial smoke (powder) dust	95.00	National model city standard for environmental protection
X18: Standard discharge rate of industrial wastewater	80.00	Li and Ma, 2013
X19: Domestic sewage treatment rate	80.00	National garden city series standards of 2015 national garden city series standards
X20: Domestic waste treatment rate	100	China habitat award standards of 2016
X21: Forest coverage rate	47.00	Su et al., 2019
X22: The percentage of the wetland area to the total area	6.00	Xiong et al., 2014
X23: Green coverage rate in built-up area	45	China habitat award standards of 2016
X24: Per capita public green area	15.0	Su et al., 2019
X25: Per capita investment in science and technology	200	Expert consultation method

As shown in *Figure 3*, the proportion of each carrying state grade in the social-economic coordination force dimension is relatively balanced, but the spatial differentiation was obvious. In detail, light and moderately overload areas were mainly distributed around provincial capitals in Hubei, Hunan and Jiangxi Provinces. This is because the surrounding areas of provincial capitals are in a stage of rapid urbanization, social infrastructure is not perfect, and the urban-rural dual structure is still prominent. In addition, due to poor industrial foundation and undertake capital of core city "three highs" (high pollution, high energy consumption, high emissions) industrial transfer and other reasons, led to a higher proportion of the primary and secondary industries and low economic development efficiency. Low loadable areas were scattered in the central and southeastern parts of the urban agglomeration. Moderately loadable and highly loadable areas were mainly distributed in Xiangyang-Jingmen-Yichang urban belt and

http://www.aloki.hu ● ISSN 1589 1623 (Print) ●ISSN1785 0037 (Online)
DOI: http://dx.doi.org/10.15666/aeer/1706_1516915190

the provincial capital city. The high carrying capacity of provincial capital city has benefited from good infrastructure, strong economic power, and reasonable industrial structure, which resulted in strong ability of coordination. To some extent, this has also limited the negative impacts due to the large urban population.

The resource-environment supporting force dimension is the supporting and guaranteeing component of urban ecosystem carrying capacity, which reflects the degree of coordination between the supply of regional resource and the demands of social-economic development. From the perspective of spatial distribution characteristics (*Fig. 3b*), the resource-environment support force dimension presents a pattern of north-south differentiation, and it had obvious spatial characteristics of homogeneous agglomeration.

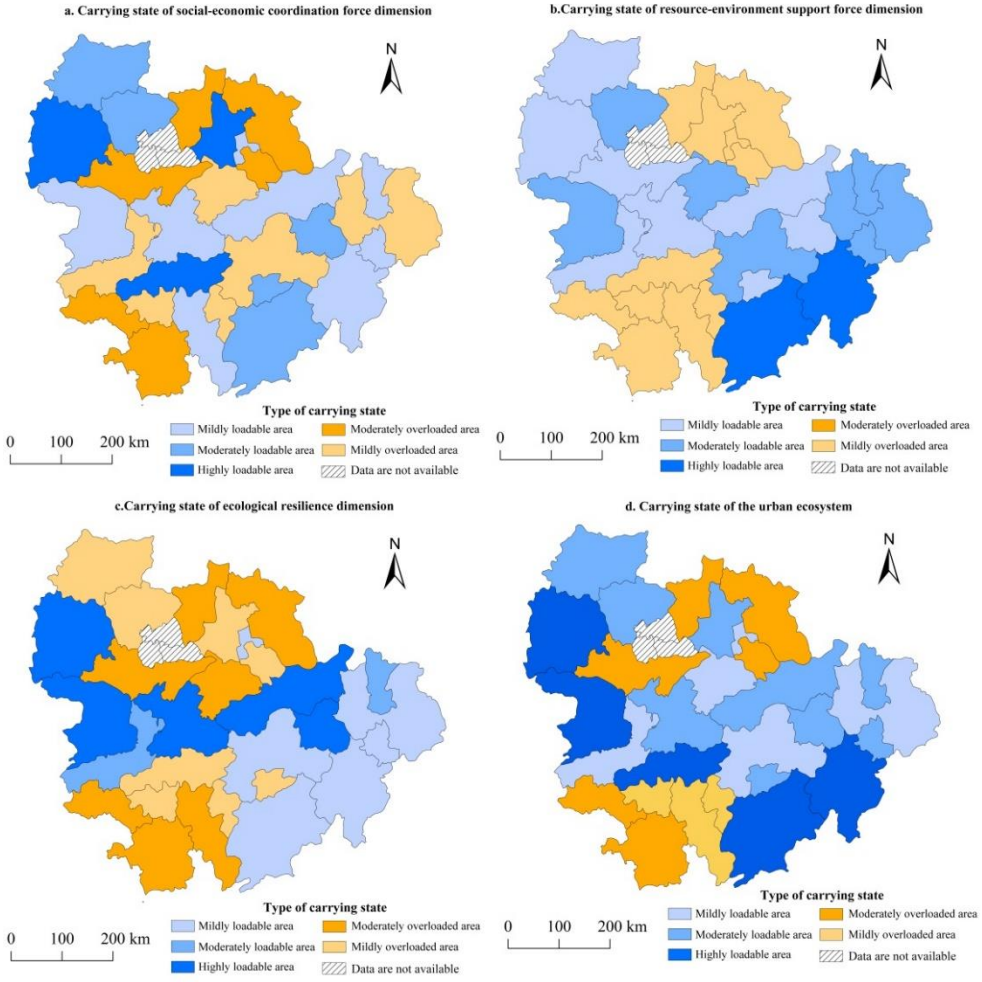

Figure 3. *The spatial pattern of urban ecosystem carrying capacity in the middle reaches of the Yangtze River in 2015*

As shown in *Figure 3*, the proportion of each carrying state grade in the resource-environment supporting force dimension is extremely unequal, and low, medium, and high loadable areas accounted for nearly 65% of the total. In detail, the mildly overload area was mainly distributed in the core area of Wuhan urban agglomeration, and the urban agglomeration around Changsha-Zhuzhou-Xiangtan. The reasons for this are as follows: On

http://www.aloki.hu ● ISSN 1589 1623 (Print) ●ISSN1785 0037 (Online)
DOI: http://dx.doi.org/10.15666/aeer/1706_1516915190

the one hand, population clustering and industrial development in these two areas created great resource supply pressure. On the other hand, regional environmental pollution has not attracted enough attention, resulting in serious environmental pollution. The conflicts between accelerated industrialization and resource-environment constraints were prominent. Light and moderately loadable areas were mainly distributed in the Xiangyang-Jingmen-Yichang urban belt, Poyang Lake urban agglomeration, and the area around Dongting Lake. Poyang Lake urban agglomeration and the area around Dongting Lake are rich in natural resources, so the regional resource supply pressure is small. In addition, recent implementation of ecological and environmental protection policies in the region (《Dongting Lake ecological economic zone planning》, 《Poyang Lake ecological urban agglomeration planning (2015-2030)》, and 《Yangtze River economic zone ecological environmental protection planning》) has further improved the control of regional environmental pollution. Xiangyang and Yichang cities have also recently made efforts to build themselves into two major sub-central cities in Hubei Province. The resource and environmental protection in Xiangyang-Jingmen-Yichang urban belt has received great attention, and the regional resource and environmental support level has been continuously improved.

The ecological resilience dimension is the regulating part of urban ecosystem carrying capacity, which reflects the regulating ability of the regional environment and the ecological potential of human acting on the ecological environment. From the perspective of spatial distribution characteristics (*Fig. 3c*), this dimension had a spatial the pattern of north-south differentiation, and it had obvious spatial characteristics of homogeneous agglomeration. As shown in *Figure 3*, the proportion of each carrying status grade was relatively balanced. In detail, light and moderately overload areas were mainly distributed in the core areas of the Wuhan urban agglomeration and the urban agglomeration around Changsha-Zhuzhou-Xiangtan. Light, moderately, and highly loadable areas were mainly distributed around Dongting and Poyang Lakes, and Yichang city in Hubei province. Investigate its reason, the ecological environment conditions of the core region of the Wuhan urban agglomeration and the urban agglomeration around Changsha-Zhuzhou-Xiangtan were worse than the region of Dongting Lake and Poyang Lake, and in recent years, the Wuhan urban agglomeration and the urban agglomeration around Changsha-Zhuzhou-Xiangtan of the rapid advance of urbanization are in the stage of rapid urbanization. The rapid expansion of urban construction area has gradually nibbled away natural elements such as vegetation and wetlands, lowering ecological resilience. Yichang City on the Yangtze River is a national garden, health, and forest city, and the only national model city for environmental protection in Hubei Province. It therefore has great environment background conditions. In addition, Yichang city's economic strength and scientific-technological level are among the highest in Hubei Province with great ecological potential.

Urban ecosystem carrying capacity is a functional status formed by the structural action of the three dimensions, which reflects the comprehensive carrying capacity of urban ecosystem. From the perspective of spatial distribution characteristics (*Fig. 3d*), the carrying capacity of urban ecosystem presents a significant north-south spatial differentiation pattern, and it had obvious spatial characteristics of homogeneous agglomeration. As shown in *Figure 4*, the proportion of each urban ecosystem carrying status grade was extremely unequal, the types of low, moderately and highly loadable areas accounted for nearly 70% of the total, so the overall carrying state of the urban ecosystem in study area was relatively good. In detail, the light and moderately overloaded areas were mainly distributed in the surrounding areas of Wuhan and Changsha. Light, moderately and highly loadable areas

http://www.aloki.hu ● ISSN 1589 1623 (Print) ●ISSN1785 0037 (Online)
DOI: http://dx.doi.org/10.15666/aeer/1706_1516915190

were mainly distributed in the Xiangyang-Jingmen-Yichang urban belt, and around Dongting and Poyang Lakes. Investigate its reason, although the resource-environment and ecological resilience dimensions in Wuhan and Changsha were slightly overloaded, the overall urban ecosystem were in a loadable state due to their strong social-economic coordination. In their surrounding areas, all dimensions were mostly in the overload state. Low efficiency economic development, urban-rural dual development structure, ecological destruction, and environmental pollution caused by urban population growth and industrial development are the main causes. Rings of Dongting and Poyang Lakes region, as well as the Xiangyang-Jingmen-Yichang urban belt, benefited from strong resources-environment support force and ecological resilience dimensions. In the future, on the premise of maintaining green economic development and protecting environment, we should focus on optimizing regional social infrastructure, improving economic development efficiency and optimizing industrial structure, so as to improve social-economic coordination force in the region.

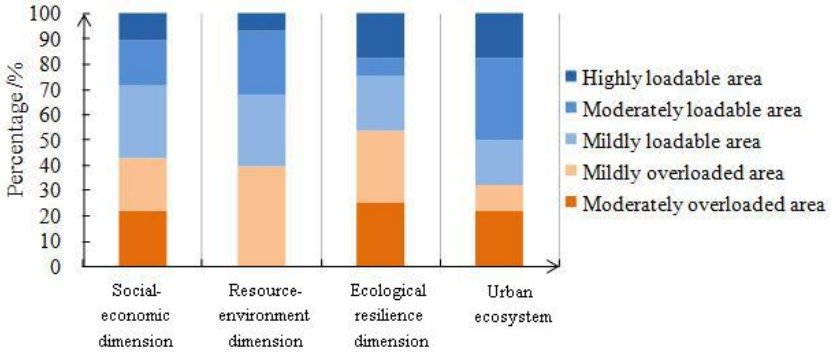

Figure 4. *The percentage of each carrying status in each dimension*

Analysis of coupling coordination among dimensions of urban ecosystem

Evaluating the coupling coordination level between dimensions can reveal the advantages and disadvantages of urban ecological carrying capacity in different regions, and to clarify the direction of development, which are of great significance for regional sustainable development. Because there has been less research on coupling coordination between dimensions, this study adopted a two system model and a three system model to assess coordination between the various dimension, which was visualized using ArcGIS10.3 software (*Fig. 5*).

From the perspective of coupling coordination between socio-economic dimension and resource-environment dimension (*Fig. 5a*), cities with high coupling coordination between socio-economic and resource-environment dimensions were mainly distributed in Xiangyang-Jingmen-Yichang urban belt, southern Jiangxi Province, Wuhan and Changsha. Xiangyang and Yichang in central Hubei Province had strong social development and economic coordination. In addition, as a national garden, health, and ecologically livable city, the area is rich in natural resources and fine environment, so the level of coupling coordination between these two dimensions was relatively high. Wuhan and Changsha, the provincial capitals faced higher population pressure, but had higher society development level, economic strength, and high economic development efficiency. In 2015, for example, tertiary industry proportions in Wuhan, Changsha, and

http://www.aloki.hu ● ISSN 1589 1623 (Print) ●ISSN1785 0037 (Online)
DOI: http://dx.doi.org/10.15666/aeer/1706_1516915190

Nanchang were as high as 51.02%, 45.06%, 41.22%, but average proportions in their surrounding areas were only 33.09%, 35.66%, and 35.77%, so the green economy was prominent. Therefore, the level of coupling coordination between dimensions is high. Low coupling coordination was mainly distributed in the surrounding areas of Wuhan City and southwest of the urban agglomeration around Changsha-Zhuzhou-Xiangtan. The region's social development level and economic strength has largely improved in recent years, but due to poor industrial foundation and undertake "three highs" (high pollution, high energy consumption, high emissions) industrial transfer and so on, it have led to a higher proportion of secondary industries, low economic development efficiency, and weak natural resources and environmental support. Therefore, the level of coupling coordination between dimensions was low. In 2015, for example, the average of primary and secondary industry proportions in the low-value areas around Wuhan and Changsha were as high as 66.91% and 64.34%, respectively.

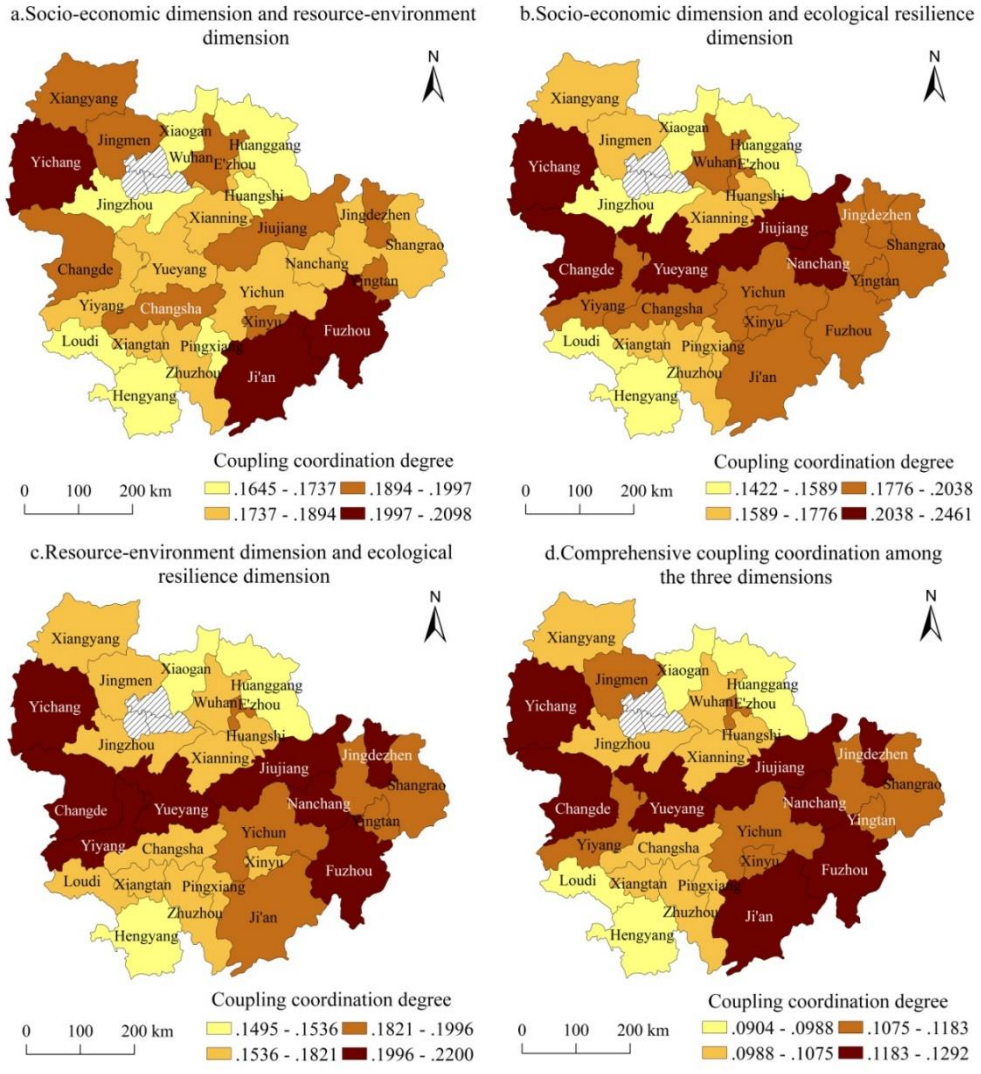

Figure 5. *Spatial distribution of coupling coordination between dimensions in the urban agglomeration in the middle reaches of the Yangtze River in 2015*

http://www.aloki.hu ● ISSN 1589 1623 (Print) ●ISSN1785 0037 (Online)
DOI: http://dx.doi.org/10.15666/aeer/1706_1516915190

Cities with high coupling coordination between social-economic dimension and ecological resilience dimensions were mainly distributed in the Poyang Lake urban agglomeration, the area around Dongting Lake, and Yichang City (*Fig. 5b*). In recent years, the implementation of environmental protection policies around Poyang and Dongting Lake (《planning of Dongting Lake ecological economic zone》, 《planning of Poyang Lake ecological urban agglomeration (2015-2030)》, 《eco-environmental protection planning of Yangtze River economic zone》), and under the promotion of the new urbanization development planning(《National new urbanization plan of China (2014-2020)》), the region gradually transitioned from previous extensive economic development mode to sustainable development with comprehensive attention to environmental protection and social security. Therefore, coupling coordination between the dimensions of social-economy and ecological resilience dimensions in this region was relatively high. As a sub-central city of Hubei Province, Yichang had strong social-economic coordination force. In addition, as a national garden and ecologically livable city, it also had a high ecological resilience, so there was high coupling coordination between socio-economic and ecological resilience dimensions. Cities with Low coupling coordination were mainly distributed in the surrounding area of Wuhan and southwest of the urban agglomeration around Changsha-Zhuzhou-Xiangtan. The loss of natural elements and environmental pollution caused by human activities in such areas are prominent. In the future, social security, social services, and economic development efficiency should be further improved on the basis of improving the regional ecological resilience and ecological potential, so as to improve urban ecosystem carrying capacity.

Cities with high coupling coordination between resource-environment and ecological resilience dimensions were mainly distributed in the Poyang Lake urban agglomeration and around Dongting Lake (*Fig. 5c*). These regions have strong resource and environmental supporting force. On the other hand, as important ecological protection areas in the Yangtze River Basin, Dongting and Poyang Lake areas have abundant forests, wetlands, and other natural elements, and the region has strong ecological regulating force when facing the interference of external natural and human factors. Therefore, the coupling coordination level between resources-environment and ecological resilience dimensions was relatively high. Areas with low coupling coordination levels were mainly distributed in the Wuhan urban agglomeration and southwest of the urban agglomeration around Changsha-Zhuzhou-Xiangtan. This was because rapid urbanization and extensive economic development in this region had significant impact on land use/cover, biodiversity, the hydrological system, local climate, and other factors at different regional scales that resulted in lower resource-environmental support and ecological resilience than other regions.

From the perspective of comprehensive coupling coordination among the three dimensions (*Fig. 5d*), the level of comprehensive coupling coordination between the three dimensions was generally lower than between any two dimensions. Cities with high coupling coordination were mainly distributed around Dongting Lake and the urban agglomeration around Poyang Lake, while cities with lower levels were mainly distributed in the Wuhan urban agglomeration and southwest of the urban agglomeration around Changsha-Zhuzhou-Xiangtan. Their spatial distributions were similar to the patterns observed between the social-economic and ecological elasticity, and between the social-economic and ecological resilience dimensions, and the resources- environment and ecological resilience dimensions. Investigate its reason, the

http://www.aloki.hu ● ISSN 1589 1623 (Print) ●ISSN1785 0037 (Online)
DOI: http://dx.doi.org/10.15666/aeer/1706_1516915190

three-dimensional carrying capacity levels in the area around Dongting Lake, the urban agglomeration around Poyang Lake, and Yichang City were higher than elsewhere and these areas also had the highest coordination levels. Areas around Wuhan and the southern cities of the urban agglomeration around Changsha-Zhuzhou-Xiangtan have undergone recent improves in the resources-environment dimension, but unbalanced development between urban and rural areas, extensive economic development mode, and the loss of natural elements caused by broad problems, such as low social-economic coordination and ecological resilience, still is the most important reason to resulted in a low level of overall coupling coordination.

Discussion

Index system for urban ecosystem carrying capacity assessment

Urban ecosystem is an on-limits, comprehensive "natural - social - economic" compound ecosystem. On the basis of a deep understanding of the concept and connotation of urban ecosystem carrying capacity, we have established a new assessment framework for urban ecosystem carrying capacity, and constructed a multi-dimensional, multi-index and expanded comprehensive index system of urban ecosystem carrying capacity from macro-scale based on multi-metadata such as earth observation data and socio-economic statistics, it makes up for the lack of comprehensiveness of evaluation system in medium and micro scale research. However, the use of various indicators to represent the urban ecosystem carrying capacity has certain limitations due to the accessibility, representativeness and objectivity of data. For example, urban ecosystem is always in a state of dynamic positive and negative feedback, within the system, system and external environment are continuously carrying on the material flow, energy flow, information flow, and population flow. But in the process of calculating urban ecosystem carrying capacity without considering the interaction of elements and the flow of elements between spatial units, also ignores the transmission effect of urban ecosystem structure, process, and function on urban ecosystem carrying capacity, which is a deficiency in the research (Ji et al., 2017). In future research, we should include more data sources and indicators to improve the accuracy of urban ecosystem carrying capacity assessment. Undoubtedly, although the index system in this paper is not ideal, but it can be easily applied to the rapid urbanization areas of developing countries such as China.

Methodology

The most important step before the evaluation of urban ecosystem carrying capacity is the preprocessing of index data, including forward processing and standardized processing of the index data. Existing studies mainly divided the types of indicators into forward indicator and reverse indicator (Song et al., 2014; Xiong et al., 2016; Ji et al., 2017), but rarely mentioned the moderate type indicator, and the positive treatment formula of the moderate type indicator has not been clearly explained. The contribution of this study is to attempt to deduce a forward processing formula for the moderate type index and scientifically determined the ideal value for each index, which was helpful in using the state-space method to quantitatively evaluate urban ecosystem carrying capacity. However, the forward processing formula for the moderate-type index still needs further improvement in future studies. Determining the ideal value for the

http://www.aloki.hu ● ISSN 1589 1623 (Print) ●ISSN1785 0037 (Online)
DOI: http://dx.doi.org/10.15666/aeer/1706_1516915190

individual index requires further discussion. In addition, the ideal indicator value was the standard set in a specific year. As time goes by, the ideal value standard will change and should therefore be constantly updated in subsequent research.

In addition to the preprocessing of index data, the determination of index weight is also an important part in the evaluation of urban ecosystem carrying capacity. In the PDSR model of this paper, the determination of multiple index weights is involved. There is no doubt that the weight of indicators will have an important impact on the final results, so its setting is extremely important. Existing studies (Xiong et al., 2016; Peng et al., 2019) mostly adopt objective weighting methods such as entropy weight method, which eliminates the interference of human factors and makes the determination of index weight objective. Therefore, entropy weight method is selected to determine the index weight in this study. In addition, existing studies have shown that spatial interaction between adjacent research units (Shen et al., 2017) should be considered in studies of large regions or urban agglomerations, but some studies pay less attention to spatial effect in the determination of index weight, which needs to be improved in future studies.

Study scale

Spatial extent and spatial resolution are collectively described as the spatial scale (Turner et al., 1989; Xiao et al., 2019). In the study of urban ecological carrying capacity, some research areas are administrative districts and some are natural borders. However, with urban ecosystem carrying capacity plays a more and more importance part in macro ecological decision-making, administrative districts as research unit has become the mainstream (Zeng et al., 2016; Xiao et al., 2019; Su et al., 2019).

In terms of spatial resolution, some researches take remote sensing image pixel as the basic research unit, and then carry out micro-scale researches with the help of remote sensing data. Some studies take county-level or prefecture-level administrative districts as basic research units, and then carry out macro-scale studies with the help of statistical data or multivariate data such as statistical data and remote sensing data. Dialectically, studies at different scales all have their own emphases. Macroscopic scale studies based on macroscopic data or multivariate data are suitable for assessing the carrying capacity of composite urban ecosystem, which is helpful for macro ecological decision-making, but accompanied by the loss of micro-information. The micro-scale research based on remote sensing data is suitable for the assessment of the carrying capacity of a single ecosystem. It can perfectly display the detailed information inside the research area and contribute to the detailed planning of the region. However, the type of ecosystem studied is limited. Therefore, there is no perfect scale for the selection of spatial resolution of ecological carrying capacity, only the most suitable scale. According to the research trend, with the continuous development of the concept and connotation of urban ecosystem carrying capacity, the evaluation index of urban ecosystem carrying capacity has been involved in many fields, such as society, economy, ecological environment, pollution control, environmental protection idea, etc., and the single remote sensing data has long been unable to meet the needs of the latest research. Therefore, it has become the choice of more and more scholars to combine statistical data and remote sensing data to carry out research on urban ecosystem carrying capacity at macro scale.

http://www.aloki.hu ● ISSN 1589 1623 (Print) ●ISSN1785 0037 (Online)
DOI: http://dx.doi.org/10.15666/aeer/1706_1516915190

Future research direction

At present, the research on ecological carrying capacity has been relatively mature, but the research on urban ecosystem carrying capacity based on complex urban ecosystem is still weak, and many problems need to be further discussed. For example, in this study, the evaluation of urban ecosystem carrying capacity based on state-space method only evaluates the carrying state of urban ecosystem in cross-sectional years. This is because it is very difficult to determine the ideal value of each index in all years, it is unscientific to determine the carrying state of urban ecosystem in all years only by the ideal value of each index in a single year. At present, the evaluation of urban ecological carrying capacity is divided into two categories. Some scholars (Xiong et al., 2014; Ji et al., 2017; Pei et al., 2019) adopted a more flexible method, that is, to compare the change trend of ecological carrying capacity in the same area, in different years or in different regions and in different years through the study of long time series. This method does not determine the carrying state. Another part of scholars (Li and Ma, 2013; Song and Yu, 2014) analyzed the bearing state of urban ecosystem in cross-section years according to the second formula of state-space method. In recent years, many scholars have emphasized that it is of great practical significance to carry out spatio-temporal dynamic analysis and simulation prediction of urban ecosystem carrying capacity from long time series (Zeng et al., 2016; Xiao et al., 2019). Based on this, in future research, we should find a suitable method to determine the ideal value of each index in all years, so as to analyze the changing trend of urban ecosystem carrying state in long time series years, so that we may find more interesting and valuable discoveries.

This study is limited by space and fails to make further analysis on the influencing factors of urban ecosystem carrying capacity, but the research on the influencing factors of urban ecosystem carrying capacity is extremely important, and the results play an important role in guiding the improvement of urban ecosystem carrying capacity in different regions by classification. From the existing research results, future research on the influencing factors of urban ecosystem carrying capacity should focus on the following two aspects. First, in the selection of influencing factors, we should expand the scope of influencing factors and quantify regional policies, environmental protection idea and other factors by questionnaire. Secondly, the interaction between influencing factors and the mechanism of influencing factors should be analyzed in detail.

Conclusion

Multi-source data was used to construct a comprehensive evaluation index system for urban ecosystem carrying capacity. The entropy weight method and state-space method were used to quantitatively evaluate urban ecosystem carrying capacity in the urban agglomeration in the middle reaches of the Yangtze River in 2015. A coupling coordination degree model was then used to analyze the spatial distribution characteristics of coupling coordination degree between dimensions and the reasons for spatial heterogeneity. The conclusions are as follows:

(1) Urban ecosystem carrying capacity in the urban agglomeration in the middle reaches of the Yangtze river presents a significant north-south spatial differentiation pattern, and it had obvious spatial characteristics of homogeneous agglomeration. The social-economic coordination force dimension had a circling spatial structure extending outward from the provincial capitals of Hubei, Hunan, and Jiangxi Provinces. The

http://www.aloki.hu ● ISSN 1589 1623 (Print) ●ISSN1785 0037 (Online)
DOI: http://dx.doi.org/10.15666/aeer/1706_1516915190

resource-environment supporting force and ecological resilience dimensions had similar spatial patterns. Overloaded area was mainly distributed in core area of the Wuhan urban agglomeration and the urban agglomeration around Changsha-Zhuzhou-Xiangtan, which was mainly caused by large resource supply pressures and environmental loads, as well as the massive loss of natural elements.

(2) Wuhan and Changsha have greater population pressure, but thanks to a higher level of social development, economic strength, and economic development efficiency, so the coupling coordination between the socio-economic and resource-environment dimensions was high. In the surrounding area of Wuhan City and southwest of the urban agglomeration around Changsha-Zhuzhou-Xiangtan had low coupling coordination due to the poor industrial foundation, low economic development efficiency, and heavy resource consumption and environmental load. The spatial distribution characteristics of the coupling coordination between the socio-economic and ecological resilience dimensions were similar to those of the resource-environment and ecological resilience dimensions. The area around Dongting Lake, the urban agglomeration around Poyang lake, and Yichang City all had high levels of coupling coordination.

(3) The cities with higher coordination levels were mainly distributed around Dongting Lake and the urban agglomeration around Poyang Lake, while the cities with lower coordination levels were mainly distributed in the Wuhan urban agglomeration and southwest of the urban agglomeration around Changsha-Zhuzhou-Xiangtan. In these areas, weak social-economic coordination and ecological resilience were caused by the imbalance between urban and rural development, extensive economic development, and the loss of natural elements, which need to be paid more attention in the future.

Acknowledgements. We are very grateful to Yushi Zhou for his great assistance in data processing. We are also very grateful to professor Yaochen Qin and professor Fengxian Lu for their professional advice in this study, Zhixiang Xie for his help in research methods. We would also like to thank the National Natural Science Foundation of China (No. 41671536; No. 41501588) for providing the funding for this research.

REFERENCES

[1] Chen, Z. S., Wu, Z. Q. (2017): The change trend of the average consumption tendency between urban and rural areas in China -- based on the perspective of the difference of the average consumption tendency between urban and rural areas. – Economic Perspectives (8): 18-30.

[2] Chen, D. L., Lu, X. H., Kuang, B. (2018): Dynamic evolution and spatial convergence of urban land use efficiency in the middle reaches of the Yangtze River. – China Population, Resources and Environment 28(12): 106-114.

[3] Cui, F. J., Yang, Y. S. (1997): A study on the time-space distribution features and utility intensity of the TEBC resource of MT. TAI. – Geographical Research 16(4): 48-56.

[4] Ge, L. Q., Li, S. M., Xie, G. D., Cheng, Y. P., Ni, Z. S. (2016): The population carrying capacity of waters ecosystem in China. – Journal of Resources and Ecology 7(1): 21-27.

[5] Hadwen, P. (1922): Reindeer in Alaska. – US Dept of Agric 1089: 18-24.

[6] He, R. W., Liu, S. Q., Liu, Y. W. (2011): Application of SD model in analyzing the cultivated land carrying capacity: A case study in Bijie Prefecture, Guizhou Province, China. – Procedia Environmental Sciences 10: 1985-1991.

http://www.aloki.hu ● ISSN 1589 1623 (Print) ●ISSN1785 0037 (Online)
DOI: http://dx.doi.org/10.15666/aeer/1706_1516915190

[7] Hu, B. M., Wang, Z. S., Wu, J. J., Li, W. G. (1992): Structural index system of agroecosystem and their quantitative methods. – Chinese Journal of Applied Ecology 3(2): 144-148.
[8] Hudak, A. T. (1999): Rangeland mismanagement in South Africa: failure to apply ecological knowledge. – Human Ecology 27(1): 55-78.
[9] Ji, X. P., Bai, Y. P., Du, H. B., Wang, J. B., Zhou, L. (2017): Research on the spatial quantitative evaluation and coupling coordination degree of ecological carrying capacity in Gansu Province. – Acta Ecologica Sinica 37(17): 5861-5870.
[10] Jiao, W. J., Min, Q. W., Cheng, S. K., Zhang, D., Sun, Y. H. (2011): The emergy-based ecological footprint (EEF) of traditional agricultural areas in China: A case study of Congjiang County,Guizhou Province. – Journal of Resources and Ecology 2(1): 56-65.
[11] Jin, Y., Lu, Z. H., Tan, F. F., Zhang, M., Zhang, H. Y. (2015): Assessment of ecological carrying capacity on the typical resources-based cities: a case study of Tangshan City. – Acta Geographica Sinica 35(14): 4852-4859.
[12] Lein, J. K. (2010): Mapping environmental carrying capacity using an artificial neural network: A first experiment. – Land Degradation&Development 6(1): 17-28.
[13] Li, N., Ma, Y. J. (2013): Analysis of spatial difference of ecological carrying capacity and its influencing factors in Liaoning Province. – Journal of Arid Land Resources and Environment 17(3): 8-13.
[14] Li, Y. F., Li, D. (2014): Assessment and forecast of Beijing and Shanghai's urban ecosystem health. – Science of the Total Environment 487: 154-163.
[15] Li, H., Huang, X. J., Jin, Y. Z., Zhang, X. (2017): Population Carrying Capacity of Water Resources in the Yangtze River Economic Belt. – Economic Geography 37(1): 181-186.
[16] Mondino, E. B., Fabrizio, E., Chiabrando, R. (2014): A GIS Tool for e Land Carrying the Capacity of Large Solar Plants. – Energy Procedia 48: 1576-1585.
[17] O'Neill, D. W., Tyedmers, P. H., Beazley, K. F. (2007): Human appropriation of net primary production(HANPP) in Nova Scotia, Canada. – Regional Environmental Chang 7(1): 1-14.
[18] Pan, H. Y., Zhu, W. Q., Cui, L. Y., Feng, M. Q., Zhu, F. (2017): Spatial differences in per capita ecological footprint and per capita ecological carrying capacity in Chengdu. – Acta Ecologica Sinica 37(19): 6335-6345.
[19] Pei, Y., Yang, J., Li, B. X., Li, X. M., Ge, Y. T. (2019): Study on spatial-temporal differentiation of eological carrying capacity in urban fringe areas at community scale: A case study of Ganjingzi District in Dalian. – Acta Ecologica Sinica 39(5): 1715-1724.
[20] Peng, J., Du, Y. Y., Liu, Y. X., Hu, X. X. (2016): How to assess urban development potential in mountain areas? An approach of ecological carrying capacity in the view of coupled human and natural systems. – Ecological Indicators 60: 1017-1030.
[21] Peng, B. H., Li, Y., Elahi, E., Guo, W. (2019): Dynamic evolution of ecological carrying capacity based on the ecological footprint theory: A case study of Jiangsu province. – Ecological Indicators 99: 19-26.
[22] Qi, H. Q., Xi, X. W., Gao, Q. Y. (2015): Measurement on the development level of China's urbanization and the time—varying characteristics of the effects of economic growth. – Economist 17(11): 26-34.
[23] Rong, Y. J., Guo, X. Y., Du, S. X., Li, X., Ning. T., Zhang, M. Y. (2019): Study of Ecological Carrying Capacity Using PSR Model Based on Ecosystem Services and Ecological Sensitivit. – Research of Soil and Water Conservation 26(1): 323-329.
[24] Rudolph, A., Figge, L. (2017): Determinants of ecological footprints: What is the role of globalization. – Ecological Indicators 81: 348-361.
[25] Shen, W., Du, Q. Y., Li, Y. H., Zhao, W., Lu, F. X., Zhou, Y. S., Shen, Z. F. (2017): Study on the spatial-temporal pattern evolution and influencing factors of the new urbanization in the Yangtze River Economic Belt. – Journal of Central China Normal University (Natural Sciences) 51(4): 534-541.

http://www.aloki.hu ● ISSN 1589 1623 (Print) ●ISSN1785 0037 (Online)
DOI: http://dx.doi.org/10.15666/aeer/1706_1516915190

[26] Sjafrie, N. D. M., Adrianto, L., Damar, A., Boer, M. (2018): Human appropriation of net primary production (HANPP) in seagrass ecosystem: an example from the east coast of Bintan Regency, Kepulauan Riau Province,Indonesia. – Environment, Development and Sustainability 20(2): 865-881.
[27] Song, Y. C., Yu, D. (2014): Evaluation of comprehensive capacity of resources and environments in Poyang Lake Eco-economic Zone. – Chinese Journal of Applied Ecology 25(10): 2975-2984.
[28] Su, M. R., Xie, H., Yue, W. C., Zhang, L. X., Yang, Z. F., Chen, S. H. (2019): Urban ecosystem health evaluation for typical Chinese cities along the Belt and Road. – Ecological Indicators 101: 572-582.
[29] Turner, M. G. (1989): Landscape ecology: the effect of pattern on process. – Annual Review of Ecology and Systematics 20(20): 171-197.
[30] Wackernagel, M., Galli, A. (2007): An overview on ecological footprint and sustainable development: A chat with Mathis Wackernage. – International Journal of Ecodynamics 2(1): 1-9.
[31] Wang, J. J., Yao, X. H., Li, J. R., Chang, H., Wang, Y. G. (2000): Assessment for Ecological Carrying Capacity of Heihe River Basin. – Research of Environmental Sciences 21(2): 44-48.
[32] Wang, W., Zhang, T., Wang, X. W., Wen, C. H. (2017): Spatial and temporal pattern of urban ecological carrying capacity in Yangtze river economic zone. – Resources and Environment in the Yangtze Basin 26(12): 1963-1971.
[33] Wang, Y. J., Xie, B. G., Li, X. Q., Zhao, W. Q., Wang, J. Y., Luo, H. B. (2017): Ecosystem carrying capacity balance of the Karst region in China, based on the supply and demand of cultivated land. – Acta Ecologica Sinica 37(21): 7030-7038.
[34] Xiang, X. R., Pan, T., Wu, S. H., Liu, W. D., Ma, L., Wang, X. F., Yin, Y. H., Li, J. (2016): Assessment and prediction of ecological carrying capacity for the Northern Slope Economic Belt of Tianshan Mountains. – Geographical Research 35(5): 875-884.
[35] Xiao, Z. X., Peng, Y. Z., Li, S. L. (2013): Chinas optimal industrial structure: The theoretical model and quantitative calculation. – China Economic Quarterly 12(1): 135-162.
[36] Xiao, R., Liu, Y., Fei, X. F., Yu, W. X., Zhang, Z. H., Meng, Q. X. (2019): Ecosystem health assessment: A comprehensive and detailed analysis of the case study in coastal metropolitan region, eastern China. – Ecological Indicators 98: 363-376.
[37] Xing, L., Xue, M. J., Hu, M. S. (2019): Dynamic simulation and assessment of the coupling coordination degree of the economy–resource–environment system: Case of Wuhan City in China. – Journal of Environmental Management 230: 474-487.
[38] Xiong, J. X., Peng, B. F., Chen, D. L., Wang, Y. L., Zhang, M. (2013): Temporal and spatial evolutionary feature of ecological carrying capacity in Dongting Lake region. – Geographical Research 32(11): 2031-2040.
[39] Xiong, J. X., Chen, R. L., Peng, B. F., Deng, S. T., Xie, X. M. (2014): Spatio-temporal Difference of Coupling Coordinative Degree of Ecological Carrying Capacity in the Dongting Lake Region. – Scientia Geographica Sinica 34(9): 1108-1116.
[40] Xiong, J. X., Chen, L. D., Peng, B. F., You, X. J. (2016): Temporal and Spatial Difference of Dynamic Simulation of Ecological Carrying Capacity in Dongting Lake Region. – Economic Geography 36(4): 164-172.
[41] Yang, Z. F., Sui, X. (2005): Assessment of the ecological carrying capacity based on the ecosystem health. – Acta Scientiae Circumstantiae 25(5): 586-594.
[42] Yin, P. J., Du, S. Y., Bai, Z. P. (2011): Analysis and evaluation of the ecological carrying capacity of 17 cities in Shandong Province in 2008. – Acta Scientiae Circumstantiae 31(9): 2048-2057.
[43] Zeng, C., Deng, X. Z., Xu, S., Wang, Y, T., Cui, J. X. (2016): An integrated approach for assessing the urban ecosystem health of megacities in China. – Cities 53: 110-119.

http://www.aloki.hu ● ISSN 1589 1623 (Print) ●ISSN1785 0037 (Online)
DOI: http://dx.doi.org/10.15666/aeer/1706_1516915190

[44] Zhang, Y., Yang, Q. Y., Min, J. (2016): An analysis of coupling between the bearing capacity of the ecological environment and the quality of new urbanization in Chongqing. – Acta Geographica Sinica 71(5): 817-828.
[45] Zhou, T., Yin, Q. (2012): The Urban Land Ecosystem Health Evaluation in Chengdu City. – Earth Science Research 1: 297-302.
[46] Zhou, W., Zhao, G. Q. (2012): China's GDP Growth and CPI: Relationship, Equilibrium and Target Control for the 12th Five-Year Plan. – Economic Research Journal 47(5): 4-17.
[47] Zhu, Y. Z., Xia, J., Wang, G. S. (2005): Assessment of water resources carrying-capacity with multi-criteria scenario analysis method: a case study in Zhangye region. – Geographical Research 24(5): 732-740.

http://www.aloki.hu ● ISSN 1589 1623 (Print) ●ISSN1785 0037 (Online)
DOI: http://dx.doi.org/10.15666/aeer/1706_1516915190

EVALUATION OF ORGANIC ACID PRODUCTION POTENTIAL OF PHOSPHATE SOLUBILIZING FUNGI ISOLATED FROM SOILS IN OKINAWA, JAPAN

ISLAM, M. K.[1,2,4] – SANO, A.[1,2] – MAJUMDER, M. S. I.[1,2] – SAKAGAMI, J-I.[1,5] – GIMA, S.[3]– HOSSAIN, M. A.[1,2*]

[1]*The United Graduate School of Agricultural Sciences, Kagoshima University, Kagoshima 890-0065, Japan*

[2]*Faculty of Agriculture, University of the Ryukyus, Okinawa 903-0213, Japan*

[3]*IRC, University of the Ryukyus, Okinawa 903-0213, Japan*

[4]*Department of Soil Science, Patuakhali Science and Technology University, Patuakhali, Bangladesh*

[5]*Faculty of Agriculture, Kagoshima University, Kagoshima 890-0065, Japan*

[*]*Corresponding author*
e-mail: amzad@agr.u-ryukyu.ac.jp; phone: +81-98-895-8824; fax: +81-98-895-8741

(Received 30th Jun 2019; accepted 25th Oct 2019)

Abstract. Deficiency of available phosphorous (P) in soil is one of the major factors that limit plant growth and yield. Microorganisms play an important role to improving available P status in soil by solubilization. Although phosphate solubilizing mechanism is not clearly understood, organic acid production seems to be the main mechanism of P solubilizing. Therefore, present study evaluated the organic acid production potentials of 16 P solubilizing fungal strains (2 *Aspergillus floccosus,* 3 *Aspergillus niger,* 2 *Aspergillus niveus*, 2 *Penicillium oxalicum*, 5 *Penicillium* spp. and 2 *Talaromyces pinophilus* isolates) isolated from soils in Okinawa, Japan to select outstanding strains that could facilitate the P solubilization process. Results revealed that both type and quantity of microbial organic acids production depend on the P sources and fungal strains. The highest quantity of organic acids was found when $Ca_3(PO_4)_2$ was used as substrate followed by $FePO_4$ and $AlPO_4$. Based on the organic acids production potential, *A. niger* (SI-12URAgr) considered as outstanding P solubilizing fungi regardless of substrates followed *P. oxalicum* (SI-6URAgr, SI-16URAgr) and *A. niger* (SI-10URAgr). These strains could have great potential as promising bioresource for efficient P utilization in agricultural production.
Keywords: *phosphorous, organic acids, Aspergillus niger, Penicillium oxalicum, agricultaral production*

Introduction

Phosphorous is the second major nutrient after nitrogen that limits plant growth and yield (Gyaneshwar et al., 2002). This nutrient exists in nature in a variety of organic and inorganic forms. The majority of soils contain insoluble inorganic phosphates, which are of no use to plants unless they are solubilized (Singh et al., 2011). Acidic environment can enhance the solubility of P minerals significantly (Zhen, 2016). This is a feasible pathway to improve the P release from phosphate minerals. Although phosphate solubilizing mechanism is still now not fully understood, the production of organic acids seems to be the main mechanism of P solubilizing (Alam et al., 2002; Siddique and Robinson, 2003). Organic acids also have multiple industrial applications as food additives, pharmaceutical and cosmetic excipients (Sauer et al., 2008). They are fully

http://www.aloki.hu ● ISSN 1589 1623 (Print) ● ISSN 1785 0037 (Online)
DOI: http://dx.doi.org/10.15666/aeer/1706_1519115201

degradable molecules and can be used as chemical intermediates or as for the production of biodegradable polymers replacing synthetic chemicals (Sauer et al., 2008).

Many phosphate solubilizing microbes (PSM), including bacteria and fungi have the ability to produce organic acids (Kavanagh, 2011) and they contributes to dissolving insoluble P through the process of acidification, chelation and exchange reaction, thus promotes plant growth (Gerresten, 1948; Singh et al., 2011). Compared to bacteria, phosphate solubilizing fungi (PSF) have ten times higher ability to secrete organic acid (Kavanagh, 2011). Among these, *Aspergillus* spp., *Penicilium* spp., *Talaromyces* spp. and *Eupenicilium* spp. are considered "key organisms" in the P cycle (Jose et al., 2010).

The ability of organic acids production by fungi is basically determined by genes, but it can also be affected by environmental condition (Zhen, 2016). For example, type of phosphate compounds could affect both phosphate solubilization and organic acid production. Previously we isolated phosphate solubilizing fungi from subtropical soils in Okinawa, Japan and studied their potentiality to solubilize different insoluble phosphate compounds. However, organic acid production ability of the fungal strains for different P sources were not documented. Therefore the study evaluated the organic acid production potential of 16 phosphate solubilizing fungal strains isolated from soils in subtropical Okinawa, Japan to select outstanding strains that could facilitate the P solubilization process.

Materials and Methods

Description of the Soil sampling area

The sampling area located at 26.5000°N and 128.0000°E. Its climate is subtropical, temperatures range from 10 to 32°C. Low temperature (10 to 26°C) exists in winter season and higher temperature (27 to 32°C) exists in summer with a humidity level near 100%. The major soil types are dark-red, red and grey soils in this area.

Isolation of phosphate solubilizing fungi

This study was carried out in the Mycology Laboratory, Faculty of Agriculture, University of the Ryukyus, Okinawa, during 2017–2018 under a class II biohazard cabinet (BHC-1306IIA/3B, AIRTECH, Tokyo, Japan) followed to the biosafety classification by National Institute of Infectious Disease of Japan, because of possibilities of including toxic fungal species treated as BSL2 during the isolation. Zero to fifty cm depth soil samples were collected from ten different locations of each soil type in Okinawa using sterile auger. One-hundred-gram soil was taken from each sampling point and it makes a total of 500 g composite sample (five points from each location make one composite sample). The samples were transferred to laboratory in sterile sealed polythene bag under aseptic condition and isolation was done by serial dilution method (Rao, 1982).

Identification of phosphate solubilizing fungi

Morphological identification

The genera of phosphate solubilizing fungal isolates were identified based on the taxonomic keys based on morphologies (Watanabe, 2010). The keys were the colour and tint in colony overs and revers, presence of aerial hyphae, colony surface texture, colony margin and pattern of pigment exudations. Wet mounts prepared from micro culture were mounted in lacto phenol and lacto phenol cotton blue. Microscopic examination and

http://www.aloki.hu ● ISSN 1589 1623 (Print) ● ISSN 1785 0037 (Online)
DOI: http://dx.doi.org/10.15666/aeer/1706_1519115201

photomicrography were performed with an OLYMPUS BX50 microscopy equipped with image Analysis system (Olympus Corporation, Tokyo, Japan).

Molecular identification

DNA was extracted from one piece of fungal mycelia from a culture incubated at 25°C for 48 h on Sabrouraud medium containing 2% glucose and 1% peptone using a DEXPAT kit (TaKaRa, Japan) to identify the isolates at genetic level (Yamaguchi et al., 2014). Beta- tubulin gene sequences amplified with primers bt2a and bt2b and calmodulin genes amplified with primers CMD5 and CMD6 were determined (Samson et al., 2014). Sequences were analysed by the NCBI BLAST tool to classify and identify closely related fungal sequences. We identified the isolates to the certain species if the BLAST results showed similarity values of 98% or higher. Nucleotide sequences were deposited into DNA data bank of Japan under accession number (*Table 1*).

Table 1. *List of fungal strains with gene bank accession number isolated from different soils in Okinawa, Japan used in this study*

Isolates	Strain in gene bank	Soil types	Sampling places	Organisms	Accession number	
					Beta tubulin gene	Calmodulin gene
1	SI-1URAgr	Dark red soil	Nishihara, Okinawa	*Penicillium sp.*	LC425316	Not done
2	SI-2URAgr	Dark red soil	Nishihara, Okinawa	*Aspergillus floccosus*	LC425317	Not done
3	SI-3URAgr	Dark red soil	Nishihara, Okinawa	*Aspergillus niveus*	LC425318	LC425334
4	SI-4URAgr	Grey soil	Nishihara, Okinawa	*Talaromyces pinophilus*	LC425319	LC425335
5	SI-5URAgr	Grey soil	Nishihara, Okinawa	*Aspergillus niveus*	LC425320	LC425336
6	SI-6URAgr	Grey soil	Nishihara, Okinawa	*Penicillium oxalicum*	LC425321	Not done
7	SI-7URAgr	Red soils	Kunigami, Okinawa	*Penicillium sp.*	LC425322	Not done
8	SI-8URAgr	Red soils	Kunigami, Okinawa	*Penicillium sp.*	LC425323	Not done
9	SI-9URAgr	Red soils	Kunigami, Okinawa	*Penicillium sp.*	LC425324	Not done
10	SI-10URAgr	Red soils	Kunigami, Okinawa	*Aspergillus niger*	LC425325	LC425337
11	SI-11URAgr	Red soils	Yanbaru forest, Okinawa	*Aspergillus niger*	LC425326	LC425338
12	SI-12URAgr	Red soils	Yanbaru forest, Okinawa	*Aspergillus niger*	LC425327	LC425339
13	SI-13URAgr	Dark red soil	Nishihara, Okinawa	*Penicillium sp.*	LC425328	LC425340
14	SI-14URAgr	Dark red soil	Nishihara, Okinawa	*Aspergillus floccosus*	LC425329	Not done
15	SI-15URAgr	Grey soil	Nishihara, Okinawa	*Talaromyces pinophilus*	LC425330	Not done
16	SI-16URAgr	Dark red soil	Nishihara, Okinawa	*Penicillium oxalicum*	LC425331	Not done

Medium preparation for organic acid production study

Pikoveskaya's (PKV) broth medium consisted of 10.0 g glucose, 5.0 g $Ca_3(PO_4)_2$, 0.5 g $(NH_4)_2SO_4$,0.1 g $MgSO_4 \cdot 7H_2O$, 0.02 g NaCl, 0.02 g KCl, 0.003 g $FeSO_4 \cdot 7H_2O$, 0.003 g $MnSO_4 \cdot H_2O$ 0.5 g yeast extract and 1000 mL distilled water (Pikovskaya, 1948). In this medium $Ca_3(PO_4)_2$ was used as source of insoluble phosphate that was replaced by insoluble $FePO_4$ and $AlPO_4$. The medium was autoclaved at 121^0C for 15 minutes.

http://www.aloki.hu ● ISSN 1589 1623 (Print) ● ISSN 1785 0037 (Online)
DOI: http://dx.doi.org/10.15666/aeer/1706_1519115201

Chloramphenicol (Wako Pure Chemical Corporation, Osaka, Japan) was also used to avoid bacterial growth.

Culturing and preparation of spore suspension

For conducting organic acid production experiment, fungal cultures were made from the re-slanting of pure culture slants that preserved at 4^0C. Sporulated culture slants were selected for preparation of spore suspension. A total volume of 5 ml sterile water with tween 80 (Wako Pure Chemical Corporation, Osaka, Japan) was added in culture slants and the fungal colony surface was lightly scraped by a sterile inoculation loop (Thermo Scientific™, Nunc™ Disposable Loops and Needles, Thermo Scientific™ 251586, Fisher Scientific, Tokyo, Japan).Then cultures were passing through a syringe with a 4×4 cm sheet of a sterile absorbant cotton (Kyualet, Kawamoto Sangyo, Osaka,Japan). Spore count was done by a hemocytometer and the suspension was adjusted to approximately10^6 spores mL^{-1}.

Incubation

The experiments were carried out using Erlenmeyer flask containing 40 ml Pikoveskaya's (PKV) broth medium supplemented with 0.5% tricalcium phosphate [$Ca_3(PO_4)_2$], aluminium phosphate ($AlPO_4$) and iron phosphate ($FePO_4$). After sterilization, the medium of each flask was inoculated with the 5% (v/v) spore suspension of a particular fungal strain containing 10^6 spore mL^{-1}. Sterile distilled water inoculated flaks was treated as control (*Fig. 1.*).

Figure 1. *Farmented Pikovskaya broth culture for organic acid determination by HPLC inoculated with 16 phosphate solubilizing fungal strains*

Three replicates were maintained for each test isolate. Incubation was done at 25^0C in an incubator shaker at 120 rpm up to 7 days. The samples were autoclaved and centrifuged at 5000 rpm for 25 minutes to remove any suspended solids and mycelial parts. The culture supernatants were filtered through 0.22 µm pore size syringe filter unit (Merck KGaA, Darmstadt, Germany).

Detection and quantification of organic acids

Detection and quantification of organic acids were done by High Performance Liquid chromatography (Prominence HPLC system, Shimadzu-CBM-20A, Japan) equipped with diode array detector (SPD-M20A), refractive index detector (RID-10A), column ICE-ION-300 (300 mmX7.8 mm), auto sampler (LC-20AD) and fraction collector (FRC-10A). The injection volume, temperature and flow rate was 50 µl, 50°C and 0.5 ml/min, respectively. Sulfuric acid of 0.01N was used as solvent of mobile phase. Peaks were identified against a set of standards from known organic acids (oxalic, citric, tartaric, malic, lactic, formic and acetic acid).

http://www.aloki.hu ● ISSN 1589 1623 (Print) ● ISSN 1785 0037 (Online)
DOI: http://dx.doi.org/10.15666/aeer/1706_1519115201

Statistical analysis

All experiments were conducted in triplicate and data were analyzed using Microsoft Excel program (version 2016). The mean values were compared by Dancan`s Multiple Range Test and significant differences were detected at $p<0.05$ level.

Results

We detected and quantified seven different organic acids from medium containing insoluble tricalcium phosphate (TCP), aluminium phosphate (Al-P) and iron phosphate (Fe-P). Acids were oxalic, citric, tartaric, malic, lactic, formic and acetic acid. Fungal strains showed significant variation to organic acid production based on phosphate substrates. Detail results presented below under specific headlines.

Organic acid production by fungal strains in TCP [$Ca_3(PO_4)_2$] supplemented medium

All the strains produced oxalic acids and lactic acids. The amount ranged from 2.3-342.0 and 26.3-320.7 µg/ml, respectively. Except SI-3URAgr and SI-5URAgr, other strains produced malic acid ranged from 22.7-139.7 µg/ml, whereas both citric acid and tartaric acid were released by the strains SI-6URAgr, SI-7URAgr, SI-8URAgr, SI-9URAgr, SI-10URAgr, SI-11URAgr, SI-12URAgr, SI-14URAgr and SI-16URAgr. The produced citric acid ranged from 3.0-566.7 and tartaric acid was 1.7-27.3 µg/ml. SI-5URAgr produced citric acid and SI-2URAgr, SI-3URAgr and SI-13URAgr produced tartaric acids. Most of the strains produced formic acid except SI-4URAgr, SI-7URAgr, SI-8URAgr, SI-9URAgr, SI-15URAgr, and most of the strains produced acetic acid except SI-2URAgr, SI-3URAgr, SI-5URAgr and SI-8URAgr. It was ranged from 16.7-1102.7 µg/ml and 9.7-2812.3 µg/ml, respectively. The highest amount of oxalic (342.0 µg/ml), citric (566.7 µg/ml), tartaric (173.3 µg/ml), malic (139.7 µg/ml), lactic (320.7 µg/ml), formic (1102.7 µg/ml) and acetic (2812.3 µg/ml) acids were produced from TCP containing broth by the strain SI-11URAgr, SI-7URAgr, SI-16URAgr, SI-2URAgr, SI-12URAgr, SI-13URAgr and SI-12URAgr, respectively (*Table 2*).

Organic acid production by fungal strains in Al-P ($AlPO_4$) supplimented medium

In aluminium phosphate (Al-P) supplimented medium, most of the strains produced oxalic acid, tartaric acid, malic acid and lactic acid ranged from 3.0-461.3 µg/ml, 3.0-461.3 µg/ml, 16.0-198.0 µg/ml and 5.7-119.0 µg/ml, respectively. The strain SI-2URAgr and SI-8URAgr could not produce oxalic acid and SI-2URAgr, SI-4URAgr and SI-15URAgr could not produce tartaric acids. Only SI-5URAgr could not produce both tartaric and malic acids. The citric acid was produced by most of the fungal strain ranged from 3.7-367.7 µg/ml except the strains SI-2URAgr, SI-3URAgr, SI-4URAgr, SI-5URAgr, SI-14URAgr and SI-15URAgr. Both formic and acetic acids were not detected from the culture filtrate of SI-2URAgr, SI-4URAgr, SI-8URAgr and SI-9URAgr. SI-7URAgr. SI-15URAgr could not produce formic acid. The highest amount of oxalic (461.3 µg/ml), citric (367.7 µg/ml), tartaric (61.0 µg/ml), malic (198.0 µg/ml), lactic (119.0 µg/ml), formic (1313.7 µg/ml) and acetic (1556.0 µg/ml) acids were produced from Al-P containing broth by the strain SI-12URAgr, SI-9URAgr, SI-12URAgr, SI-7URAgr, SI-11URAgr, SI-13 URAgr and SI-6URAgr, respectively (*Table 3*).

http://www.aloki.hu ● ISSN 1589 1623 (Print) ● ISSN 1785 0037 (Online)
DOI: http://dx.doi.org/10.15666/aeer/1706_1519115201

Table 2. *Types and quantities of produced organic acids in the Pikoveskaya's medium supplemented with insoluble $Ca_3(PO_4)_2$ by 16 phosphate solubilizing fungal strains*

Strains	Type of fungi	Organic acid (µg/ml)						
		Oxalic	Citric	Tartaric	Malic	Lactic	Formic	Acetic
SI-1URAgr	*Penicillium sp.*	3.0±1.0^{ef}	N.D.	N.D.	34.7±2.1^{def}	48.7±9.3^{efgh}	567.0±33.9^{c}	1148.0±111.0^{c}
SI-2URAgr	*A. floccosus*	46.3±4.7^{d}	N.D.	6.0±1.0^{de}	139.7±7.5^{a}	170.7±13.5^{c}	183.3±18.2^{e}	N.D.
SI-3URAgr	*A. niveus*	23.0±2.6^{e}	N.D.	7.3±0.6^{cd}	N.D.	77.7±6.0^{de}	162.3±29.7^{e}	N.D.
SI-4URAgr	*T. pinophilus*	3.7±1.2^{ef}	N.D.	N.D.	43.0±3.0^{def}	26.3±2.1^{h}	N.D.	29.0±2.0^{e}
SI-5URAgr	*A. niveus*	4.0±1.0^{ef}	426.3±22.7^{b}	N.D.	N.D.	90.3±13.0^{d}	16.7±4.0^{f}	N.D.
SI-6URAgr	*P. oxalicum*	77.0±10.8^{b}	52.0±2.6^{d}	13.7±2.5^{bc}	22.7±3.1^{f}	74.3±6.1^{def}	749.7±42.1^{b}	1503.0±42.0^{b}
SI-7URAgr	*Penicillium sp.*	2.7±0.6^{ef}	566.7±32.1^{a}	17.3±3.1^{b}	114.3±16.3^{b}	50.7±7.8^{efgh}	N.D.	36.3±8.0^{e}
SI-8URAgr	*Penicillium sp.*	5.3±1.5^{ef}	3.0±1.0^{e}	18.7±3.5^{b}	42.0±5.6^{def}	41.7±4.0^{gh}	N.D.	N.D.
SI-9URAgr	*Penicillium sp.*	5.0±1.0^{ef}	53.0±8.2^{d}	5.3±1.5^{de}	31.0±6.6^{ef}	37.7±5.7^{gh}	N.D.	9.7±0.7^{e}
SI-10URAgr	*A. niger*	69.0±4.0^{bc}	10.3±1.5^{e}	6.0±1.0^{de}	79.7±6.0^{c}	154.3±5.0^{c}	172.7±31.6^{e}	28.7±4.2^{e}
SI-11URAgr	*A. niger*	342.0±20.4^{a}	8.0±1.0^{e}	16.3±2.5^{b}	82.7±6.7^{c}	272.3±26.6^{b}	311.0±22.3^{d}	628.0±16.1^{d}
SI-12URAgr	*A. niger*	49.0±10.5^{cd}	13.7±2.5^{e}	16.0±4.4^{b}	78.7±9.5^{c}	320.7±13.8^{a}	340.3±52.6^{d}	2812.3±76.6^{a}
SI-13URAgr	*Penicillium sp.*	5.7±0.6^{ef}	N.D.	1.7±0.6^{de}	54.0±5.6^{d}	84.7±7.4^{d}	1102.7±80.3^{a}	15.3±2.1^{e}
SI-14URAgr	*A. floccosus*	52.3±5.9^{cd}	10.3±2.1^{e}	26.7±2.5^{a}	35.7±6.4^{def}	94.0±4.6^{d}	54.3±12.7^{f}	20.0±4.6e
SI-15URAgr	*T. pinophilus*	2.3±0.6^{f}	N.D.	N.D.	43.7±4.0^{de}	44.3±5.9^{fgh}	N.D.	31.0±4.6^{e}
SI-16URAgr	*P. oxalicum*	12.3±1.5^{ef}	100.7±6.5^{c}	27.3±3.1^{a}	39.7±4.0^{def}	68.3±6.0^{defg}	696.3±54.8^{b}	1402.0±46.0^{b}

Values given are the mean of three replicates ± standard deviation of the mean. Values with common letters in each column do not differ statistically according to Duncan's Multiple Range Test (DMRT) at $p<0.05$
N.D.: Not detected
Organic acid calculated as micrograms per milliliter

Organic acid production by fungal strains in Fe-P ($FePO_4$) supplemented medium

In iron phosphate (Fe-P) supplimented medium, all strains showed the production of tartaric acid (11.3-408.3 µg/ml), malic acid (12.0-383.0 µg/ml), lactic acid (2.7-88 µg/ml) and formic acid (8.3-1082.0 µg/ml), whereas SI-5URAgr did not produce lactic acid. The oxalic acid was produced (1.5-811.0 µg/ml) by the strain SI-4URAgr, SI-9URAgr, SI-11URAgr and SI-12URAgr. Strains SI-3URAgr, SI-5URAgr, SI-7URAgr, SI-10URAgr, SI-11URAgr, SI-12URAgr SI-15URAgr and SI-16URAgr produced both citric and acetic acids, whereas SI-2URAgr, SI-13URAgr produced citric acid, SI-9URAgr and SI-14URAgr produced acetic acid. The highest amount of oxalic (811.0 µg/ml), citric (955.7 µg/ml), tartaric (408.3 µg/ml), malic (383.3.0 µg/ml), lactic (88.0 µg/ml), formic (1082.7 µg/ml) and acetic (342.3 µg/ml) acids were produced from Fe-P containing medium by the strain SI-10URAgr, SI-12URAgr, SI-13URAgr, SI-10URAgr, SI-4URAgr, SI-13 and SI-12URAgr, respectively (*Table 4*).

Comparison of quantities of organic acids produced by 16 fungal strains in different P substrates

In this study, the strongest organic acid production ability of fungal strains was found in medium containing tri-calcium phosphate (TCP) followed by iron phosphate (Fe-P) and aluminium phosphate (Al-P). The produced organic acid ranged between

http://www.aloki.hu ● ISSN 1589 1623 (Print) ● ISSN 1785 0037 (Online)
DOI: http://dx.doi.org/10.15666/aeer/1706_1519115201

102.0-3630.0 µg/ml, 22.3-2486.9 µg/ml and 118.7-1803.3 µg/ml in the medium supplemented with TCP, Al-P and Fe-P, respectively. Among the fungal strains, the highest amount of organic acids was produced by *Aspergillus niger* strain SI-12URAgr (3630.7 µg/ml) in the medium supplemented with TCP followed by *Penicillium oxalicum* strain SI-6URAgr (2492.3 µg/ml) and SI-16URAgr (2346.7 µg/ml) in Al-P medium and *Aspergillus niger* strain SI-10URAgr (1803.0 µg/ml) in Fe-P medium. These strains were considered as outstanding because this quantity of organic acids was higher than sum of the mean and standard deviation of the total quantities of organic acids produced by 16 fungal strains in this study (*Table 5*). HPLC chromatograms of outstanding fungal strains shown in (*Fig. 2*).

Table 3. *Types and quantities of produced organic acids in the Pikoveskaya's medium supplemented with insoluble $AlPO_4$ by 16 phosphate solubilizing fungal strains*

Strains	Type of fungi	Organic acid (µg/ml)						
		Oxalic	Citric	Tartaric	Malic	Lactic	Formic	Acetic
SI-1URAgr	*Penicillium sp.*	18.7±3.5^{bcd}	3.7±0.6^{ef}	44.0±3.6^{b}	36.3±2.1^{e}	11.3±1.5^{h}	443.3±14.2^{d}	787.0±27.1^{c}
SI-2URAgr	*A. floccosus*	N.D.	N.D.	10.3±1.5^{f}	N.D.	12.0±2.0^{h}	N.D.	N.D.
SI-3URAgr	*A. niveus*	3.0±1.0^{h}	N.D.	6.0±1.0^{g}	16.0±2.6^{g}	21.7±0.6^{g}	23.0±3.0^{h}	34.0±3.6^{f}
SI-4URAgr	*T. pinophilus*	13.3±1.5^{bcdef}	N.D.	N.D.	46.0±4.0cd^{e}	16.0±2.6^{h}	N.D.	N.D.
SI-5URAgr	*A. niveus*	13.7±3.5^{bcdef}	N. D	N.D.	N.D.	25.0±4.0f^{g}	21.0±1.0^{h}	74.0±12.2^{e}
SI-6URAgr	*P. oxalicum*	7.0±1.0^{cdef}	11.0±1.0^{def}	6.5±0.5^{fg}	39.0±3.0^{de}	50.7±5.9^{c}	816.7±10.5^{b}	1556.0±27.2^{a}
SI-7URAgr	*Penicillium sp.*	12.0±1.0^{fg}	356.7±16.8^{a}	8.3±0.6^{fg}	198.0±8.5^{a}	5.7±1.2^{i}	N.D.	32.7±4.5^{f}
SI-8URAgr	*Penicillium sp.*	N.D.	7.3±1.2^{ef}	7.5±0.5^{fg}	54.3±11.6^{c}	5.7±0.6^{i}	N.D.	N.D.
SI-9URAgr	*Penicillium sp.*	N.D.	367.7±25.8^{a}	4.7±0.6^{g}	151.3±11.4^{b}	30.0±3.0^{ef}	N.D.	N.D.
SI-10URAgr	*A. niger*	20.0±1.0^{bc}	13.3±2.1^{def}	20.3±2.1^{d}	27.0±2.6^{f}	6.0±1.0^{i}	315.7±6.7^{e}	96.7±6.8^{e}
SI-11URAgr	*A. niger*	22.3±3.2^{b}	31.0±3.6^{c}	7.0±1.0^{fg}	45.0±5.3^{cde}	119.0±5.6^{a}	268.0±22.9^{f}	12.0±1.0^{fg}
SI-12URAgr	*A. niger*	461.3±13.9^{a}	22.7±4.0^{cd}	61.0±6.6^{a}	24.0±3.6^{fg}	108.7±5.7^{b}	299.3±12.2^{e}	578.0±40^{d}
SI-13URAgr	*Penicillium sp.*	23.7±2.5^{b}	18.0±2.6^{cde}	16.0±2.6^{e}	40.0±2.0^{de}	41.7±6.5^{d}	1313.7±33.6^{a}	567.0±19.7^{d}
SI-14URAgr	*A. floccosus*	20.0±3.0^{bc}	N.D.	24.7±2.1^{c}	36.3±2.5^{e}	31.0±3.6^{e}	136.7±3.1^{g}	37.0±4.6^{f}
SI-15URAgr	*T. pinophilus*	11.0±1.0^{ef}	N.D.	N.D.	48.0±7.0^{cd}	26.3±3.2^{efg}	N.D.	21.7±2.9^{fg}
SI-16URAgr	*P. oxalicum*	16.3±1.5^{bcde}	70.0±6.6^{b}	19.7±1.5^{d}	37.3±2.1^{e}	42.3±7.0^{d}	643.7±10.0^{c}	1196.7±36.9^{b}

Values given are the mean of three replicates ± standard deviation of the mean. Values with common letters in each column do not differ statistically according to Duncan's Multiple Range Test (DMRT) at $p<0.05$
N.D.: Not detected
Organic acid calculated as micrograms per milliliter

Discussion

The sixteen P solubilizing fungal strains used in this study were isolated from different soils in Okinawa, Japan under subtropical environment. The isolates were identified as the genera of *Aspergillus, Penicilium* and *Talaromyces* (Islam et al., 2019). Both type and the quantity of organic acids produced by fugal strains varied with the nature of phosphate substrates and fungal strains. In this study, acetic, lactic and formic acids were the major acids in TCP medium, oxalic, citric, malic, tartaric and acetic acids in Fe-P medium, and formic, lactic, malic and citric acids in Al-P medium. Fungal strains produced the highest amount of organic acids in TCP supplimented medium

http://www.aloki.hu ● ISSN 1589 1623 (Print) ● ISSN 1785 0037 (Online)
DOI: http://dx.doi.org/10.15666/aeer/1706_1519115201

followed by Fe-P and Al-P. It might be the result of interaction between fungal strains and the P sources. Zang et al. (2018) and Scervino et al. (2013) reported that the quantity of organic acid produce by fungi differed with the nature of phosphate substrates. Another point is that organic acid production by microorganism depends on their genetic variation and each strain has specific ability of producing organic acid during the P solubilization (Protiva et al., 2009).

Table 4. *Types and quantities of produced organic acids in the Pikoveskaya's medium supplemented with insoluble $FePO_4$ by 16 phosphate solubilizing fungal strains*

Strains	Type of fungi	Organic acid (µg/ml)						
		Oxalic	Citric	Tartaric	Malic	Lactic	Formic	Acetic
SI-1URAgr	*Penicillium sp.*	214.7±10.5^{d}	N. D	271.7±2.1^{b}	51.3±1.5^{fgh}	2.7±0.6^{jk}	56.0±1.0^{h}	N.D.
SI-2URAgr	*A. floccosus*	2.7±0.6^{f}	6.3±1.5^{gh}	26±1.0^{l}	12±1.0^{k}	7.3±0.6^{i}	566.3±3.5^{d}	N.D.
SI-3URAgr	*A. niveus*	15±1.0^{f}	40.7±1.5^{f}	70.7±1.5^{g}	44.3±3.8^{hi}	20.3±2.1^{g}	325.7±1.5^{e}	32.7±1.5^{f}
SI-4URAgr	*T. pinophilus*	N.D.	N.D.	17±1.0^{m}	47.7±4.0^{gh}	88.0±2.0^{a}	8.3±0.6^{k}	47.0±2.0^{e}
SI-5URAgr	*A. niveus*	1.7±0.6^{f}	432±6.0^{c}	115.7±0.6^{e}	29.3±2.5^{j}	N.D.	791.3±3.5^{c}	69.0±3.6^{d}
SI-6URAgr	*P. oxalicum*	14.0±1.0^{f}	N. D	16.7±1.2^{m}	27±2.6^{j}	72.7±2.5^{c}	225±9.5^{f}	258.7±4.2^{b}
SI-7URAgr	*Penicillium sp.*	3.0±0.6^{f}	349.3±7.5^{d}	127±2.0^{d}	17.3±0.6^{k}	26.7±3.5^{f}	17.3±1.5^{j}	37.3±3.5^{f}
SI-8URAgr	*Penicillium sp.*	2.0±0.0^{f}	N.D.	30±1.0^{k}	60.3±2.5^{e}	48.3±3.2^{d}	12.0±1.0^{jk}	N.D.
SI-9URAgr	*Penicillium sp.*	N.D.	N. D	14.7±1.5^{m}	43.7±1.5^{hi}	30.7±3.2^{f}	5.3±0.6^{k}	22.0±1.7^{g}
SI-10URAgr	*A. niger*	811.0±66.8^{a}	268.7±0.6^{e}	43±1.0^{i}	383.3±4.5^{a}	40±2.6^{e}	48.7±2.5^{hi}	208.3±6.0^{c}
SI-11URAgr	*A. niger*	N.D.	466±12.3^{b}	56.3±2.1^{h}	348±10.8^{b}	4.7±0.6^{ij}	93.0±2.0^{g}	18.0±2.0^{gh}
SI-12URAgr	*A. niger*	N.D.	955.7±9.5^{a}	78±1.0^{f}	218.7±2.1^{c}	14.7±1.5^{h}	46.0±2.0^{i}	342.3±8.5^{a}
SI-13URAgr	*Penicillium sp.*	104.7±4.5^{e}	7.7±0.6^{gh}	408.3±3.5^{a}	38.7±2.1^{i}	78.7±1.5^{b}	1082.7±4.7^{a}	N.D.
SI-14URAgr	*A. floccosus*	459±14^{b}	N. D	34±1.0^{j}	57.3±1.5^{ef}	41±2.0^{e}	871.7±14.0^{b}	43.3±4.9^{e}
SI-15URAgr	*T. pinophilus*	2.7±0.6^{f}	10.7±2.5^{g}	11.3±0.6^{n}	103.7±8.4^{d}	30.3±4.5^{f}	10.0±1.0^{jk}	17.7±2.1^{gh}
SI-16URAgr	*P. oxalicum*	270.7±6.5^{c}	4.3±0.6^{gh}	153±1.7^{c}	54.3±4.0^{efg}	28.7±1.5^{f}	45.7±0.6^{i}	15.0±1.0^{h}

Values given are the mean of three replicates ± standard deviation of the mean. Values with common letters in each column do not differ statistically according to Duncan's Multiple Range Test (DMRT) at $p<0.05$
N.D.: Not detected
Organic acid calculated as micrograms per milliliter

Present study showed that *A. niger,* strain SI-12URAgr have the strongest organic acid production ability regardless of P substrates. Isolates *P. oxalicum* (SI-6URAgr and SI-16URAgr) produced higher amount of organic acids in the medium supplemented with TCP and Al-P. Whereas, *A. niger* SI-10URAgr and *A. flucossus* SI-14URAgr were capable to produce organic acids in the medium supplemented with Fe-P. In our previous study *A. niger* (strain SI-10URAgr, SI-11URAgr and SI-12URAgr) considered as the outstanding P solubilizing fungi due to their high capabilities to solubilized three insoluble phosphate compounds by decreasing pH of the culture medium (Islam et al., 2019). It suggested that higher amount of microbial organic acids were produced during P solubilization that accelarate the solubilization process by providing protons and complexing anions, or ligand exchange reactions or complexion of metal ions release to solution (Zang et al., 2018). The solubilization of P mostly depended on the amount of organic acids production by fungi (Bo et al., 2011). They also reported that tricarboxylic acids such as citric acid, oxalic acid, malic acid, formic acids and other lower molecular

http://www.aloki.hu ● ISSN 1589 1623 (Print) ● ISSN 1785 0037 (Online)
DOI: http://dx.doi.org/10.15666/aeer/1706_1519115201

weight organic acids are the main contributors to solubilization of phosphate and decrease pH in the medium.

Among the filamentous fungi, *Aspergillus* are prominent for higher concentrations of a variety of organic acid production (Liaud, 2014). The fungi of genus *Aspergillus* are widely used for the industrial production of bio-based products, including enzymes and organic acids (Yang et al., 2017). In fact, *A. niger* has been regarded as the workhorse microorganism for the industrial production of organic acids (Show et al., 2015). These acids contributed to P solubilization (Silva et al., 2014; Li et al., 2016). Besides *A. niger* species, *P. oxalicum* also showed an excellent organic acid production ability in the medium supplemented with TCP and Al-P. This fungal species is important in food and drug production (https://en.wikipedia.org/wiki/Penicillium_ oxalicum). Some members of the genus produce penicillin (https://en.wikipedia.org/ wiki/Penicillium). The molecule penicilin is used as an antibiotic.

Table 5. *Comparison of organic acid production form different P sources (TCP, Al-P and Fe-P) by 16 phosphate solubilizing fungal strains*

Strains	Type of fungi	Organic acid (µg/ml) from		
		TCP	Al-P	Fe-P
SI-1URAgr	*Penicillium sp.*	1801.3	1344.3	596.3
SI-2URAgr	*A. floccosus*	546.0	22.3	620.7
SI-3URAgr	*A. niveus*	270.3	103.7	549.3
SI-4URAgr	*T. pinophilus*	102.0	75.3	208.0
SI-5URAgr	*A. niveus*	537.3	133.7	1439.0*
SI-6URAgr	*P. oxalicum*	2492.3*	2486.9*	614.0
SI-7URAgr	*Penicillium sp.*	788.0	613.3	578.0
SI-8URAgr	*Penicillium sp.*	110.7	74.8	152.7
SI-9URAgr	*Penicillium sp.*	141.7	553.7	118.7
SI-10URAgr	*A. niger*	520.7	499.0	1803.0*
SI-11URAgr	*A. niger*	1660.3	504.3	986.0
SI-12URAgr	*A. niger*	3630.7*	1555.0*	1655.3*
SI-13URAgr	*Penicillium sp.*	1264.0	2020	1720.7
SI-14URAgr	*A. floccosus*	293.3	285.7	1506.3*
SI-15URAgr	*T. pinophilus*	121.3	107.0	186.3
SI-16URAgr	*P. oxalicum*	2346.7*	2026.0*	571.7
	Mean ± S	1039.1±1061.9*	775.3±828.5	831.6±599.6

TCP: tricalcium phosphate; Al-P: aluminium phosphate and Fe-P: iron phosphate.
An asterisk (*) indicated outstanding values of produced organic acid. It was higher than sum of the mean and standard deviation of organic acid produced by 16 fungal strains. It also indicated the best substrate for organic acid production

Conclusions

From the above discussion it can be concluded that both type and quantity of microbial organic acid production depended on the P sources and fungal species/strains. All the fungi produced more organic acids in TCP medium compared to $FePO_4$ and $AlPO_4$ supplemented medium, which contributed to P solubilization. Among the isolates, *A. niger* (SI-12URAgr) considered as outstanding P solubilizer based on

http://www.aloki.hu ● ISSN 1589 1623 (Print) ● ISSN 1785 0037 (Online)
DOI: http://dx.doi.org/10.15666/aeer/1706_1519115201

organic acids production potential regardless of substrates followed *P. oxalicum* (SI-6URAgr, SI-16URAgr) and *A. niger* (SI-10URAgr). These strains could have great potential as promising bioresource for efficient P utilization in agricultural production. Future experiment is necessary to evaluate the performance of the outstanding strains on growth and yield of plant in the soils contain insoluble phosphates.

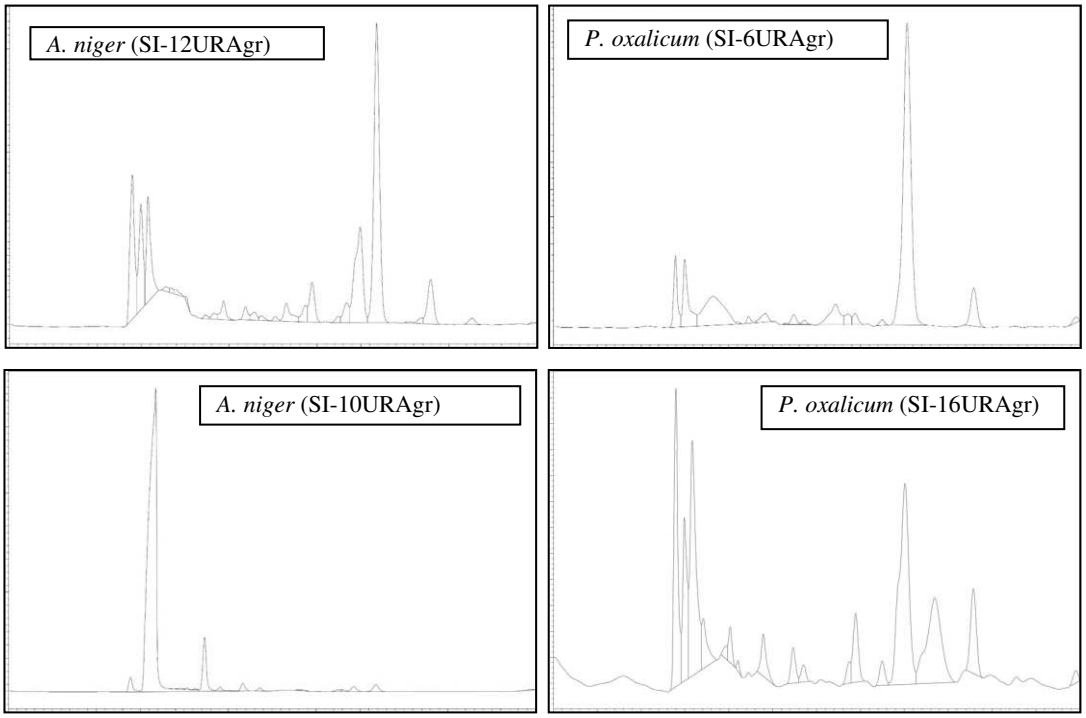

Figure 2. *Chromatograms of organic acids analyzed by HPLC. The acids were produced by outstanding P solubilizing fungal strains [A. niger (SI-12URAgr), P. oxalicum (SI-6URAgr, SI-16URAgr) and A. niger (SI-10URAgr)]*

Acknowledgement. This manuscript has been considered as the requirement of doctoral degree for the first author.

REFERENCES

[1] Alam, S., Khalil, S., Ayub, N., Rashid, M. (2002): In vitro solubilization of inorganic phosphate by phosphate solubilizing microorganisms (PSM) from maize rhizosphere. – Int J Agric Biol 4: 454-458.
[2] Bo, C., Yan, W., Pengming, L., Biao, L., Meiying, G. (2011): Isolation and phosphate solubilizing ability of a fungus, *Penicillium* sp. from soil of alum mine. – JBM 51: 5-14.
[3] Gyaneshwar, P., Kumar, G. N., Parekh, L. J., Poole, P. S. (2002): Role of microorganisms in improving P nutrient of plants. – Plant Soil 245: 83-93.
[4] https://en.wikipedia.org/wiki/Penicillium.
[5] https://en.wikipedia.org/wiki/Penicillium_oxalicum.
[6] Islam, M. K., Sano, A., Majumder, M. S. I., Hossain, M. A., Sakagami, J.-I. (2019): Isolation and molecular characterization of phosphate solubilizing filamentous fungi from subtropical soils in Okinawa. – Applied Ecology and Environmental Research 17(4): 9145-9157.

http://www.aloki.hu ● ISSN 1589 1623 (Print) ● ISSN 1785 0037 (Online)
DOI: http://dx.doi.org/10.15666/aeer/1706_1519115201

[7] Jain, R., Saxena, J., Sharma, V. (2017): The ability of two fungi to dissolve hardly soluble phosphates in solution. – Mycology 8(2): 104-110.
[8] Jose, M. S., Milton, P. M., Ivana, D. M., Marina, R., Nubia, S. M., Alicia, G. (2010): Soil fungal isolates produce different organic acid patterns involved in phosphate salts solubilization. – Biol Fertil Soils 46: 755-763.
[9] Kavanagh, K. (2011): Fungal fermentation systems and products in Fungi: biology and applications. – Wiley.
[10] Liaud, N. (2014): Exploring fungal biodiversity: organic acid production by 66 strains of filamentous fungi. – Fungal Biology and Biotechnology 1: 1.
[11] Pikovskaya, R. I. (1948): Mobilization of Phosphorus in Soil Connection with the Vital Activity of Some Microbial Species. – Microbiology 17: 362-370.
[12] Pratibha, V., Arvind, G. (2009): Organic acid production in vitro and plant growth promotion in maize under controlled environment by phosphate solubilizing fluorescent Pseudomonas. – BMC Microbiology 9: 174.
[13] Rao, N. S. S. (1982): Phosphate Solubilization by Soil Microorganisms. – In: Rao, N. S. S. (ed.) Advances in Agricultural Microbiology. Butterworth-Heinemann, Oxford.
[14] Samson, R. A., Visagie, C. M., Houbraken, J., Hong, S. B., Hubka, V., Klaassen, C. H. W., Perrone, G., Seifert, K. A., Suska, A., Tanney, J. B., Kocsube, S., Szigeti, G., Yaguchi, T., Frisvad, J. C. (2014): Phylogeny, identification and nomenclature of the genus *Aspergillus*. – Studies in Mycology 78: 141-173.
[15] Sauer, M., Porro, D., Mattanovich, D., Branduardi, P. (2008): Microbial production of organic acids; expanding the markets. – Trends Biotechnol 26: 100-80.
[16] Scervino, J. M., Mesa, M. P., Mónica, I. D., Recchi, M., Moreno, S., Godeas, A. (2013): Soil fungal isolates produce different organic acid patterns involved in phosphate salts solubilization. – Biol Fertil Soils 49(6): 779-779.
[17] Show, P. L., Oladele, K. O., Siew, Q. Y., Zakry, F. A. A., Lan, J. C. W., Ling, T. C. (2015): Overview of citric acid production from *Aspergillus niger*. – Front. Life Sci. 8(3): 271-283.
[18] Silva, U. D. C., Mendes, G. D. O., Silva, N. M. R. M., Duarty, J. L., Silva, I. R. (2014): Fluoride Tolerant Mutants of *Aspergillus niger* Show Enhanced Phosphate Solubilization Capacity. – PLOS ONE 9: 10.
[19] Singh, M. S., Yadav, L. S., Singh, S. K., Singh, P., Singh, P. N., Ravindra, R. (2011): Phosphate solubilizing ability of two Arctic Aspergillus niger strains. – Polar Research 30: 72-83.
[20] Watanabe, T. (2010): Pictorial atlas of soil and seed fungi morphologies of cultured fungi and Key to species. – 3rd. CRC press, Florida.
[21] Yamaguchi, S., Sano, A., Hiruw, A. M., Murata, M., Kaneshima, T., Murata, Y., Takahashi, H., Takahashi, S., Takahashi, Y., Chibana, H., Touyama, H., Nguyen, H. T. T., Nakazato, Y., Uhera, Y., Hirakawa, M., Imura, Y., Tereshima, Y., Kawamoto, Y., Takahashi, K., Sugiyama, K., Hiruma, M., Murakami, M., Hosokawa. A., Uezata, H. (2014): Isolation of dermatophytes and domestic fowl (Gallus domesticus). – Mycopathologia 178: 135-143.
[22] Yang, L., Lubeck, M., Lubeck, P. S. (2017): *Aspergillus* as a versatile cell factory for organic acid production. – Fungal Biol. Rev. 31(1): 33-49.
[23] Zhang, Y., Chen, F-S., Wu, X-Q., Luan, F-G., Zang, L-P., Fang, X-M., Wan, S-Z., Hu, X-F., Ye, J-R. (2018): Isolation and characterization of two phosphate solubilizing fungi from rhizosphere soils of moso bamboo and their functional capacities when exposed to different phosphorus sources and pH environment. – PLOS ONE 13: 7.
[24] Zhen, L., Tongshuo, B., Letian, D., Fuwei, W., Jinjin, T., Shiting, M., Yunxiao, H., Shimei, W., Shuijin, H. (2016): A study of organic acid production in contrasts between two phosphate solubilizing fungi: *Penicillium oxalicum* and *Aspergillus niger*. – Sci Rep. 6: 25313.

http://www.aloki.hu ● ISSN 1589 1623 (Print) ● ISSN 1785 0037 (Online)
DOI: http://dx.doi.org/10.15666/aeer/1706_1519115201

EVALUATION OF YIELD AND YIELD COMPONENTS OF COMMON VETCH (*VICIA SATIVA* L.) GENOTYPES GROWN IN DIFFERENT LOCATIONS OF TURKEY BY GGE BIPLOT ANALYSIS

AYDEMIR, S. K.[1] – KARAKOY, T.[2*] – KOKTEN, K.[3] – NADEEM, M. A.[4]

[1]*Department of Field Crops, Faculty of Agriculture and Natural Science, Seyh Edebali University, Bilecik, Turkey*

[2]*Faculty of Agricultural Sciences and Technologies, Sivas University of Science and Technology, Sivas, Turkey*

[3]*Faculty of Agriculture, Bingol University, Bingol, Turkey*

[4]*Department of Field Crops, Faculty of Agricultural and Natural Science, Bolu Abant Izzet Baysal University, Bolu 14030, Turkey*

**Corresponding author*
e-mail: tolgakarakoy73@hotmail.com

(Received 1st Jul 2019; accepted 25th Oct 2019)

Abstract. This study was carried out under the ecological conditions of three locations in Turkey (Bilecik, Sivas and Bingol) during 2016 aiming to investigate the variations in yield and yield components of common vetch and to evaluate in different environmental conditions the best performing genotypes using the GGE Biplot analysis. 5 lines and 8 commercial cultivars were used as plant material. GGE biplot analysis concluded that plant height, forage yield, biological yield and straw yield were included in component 1. Dicle genotype was found superior in terms of forage yield and dry matter yield, while Kralkizi genotype reflected its potential for biological and straw yield. Findings of this study are suggesting that the common vetch, plant height, forage yield, biologic yield, straw yield are important traits and can be used as selection criteria for the evaluation of best performing common vetch genotypes.
Keywords: *common vetch, Vicia sativa, genotype, yields, environment, genotype x environment interactions*

Introduction

Turkey is one of the world's biodiversity centre and considered origin and domestication center for various crops, thanks to its geographic (Arystanbekkyzy et al., 2019; Nadeem et al., 2018), containing 20.5 million hectares of processed agricultural land and forage crops are cultivated on an area of 1.8 million ha (TUIK, 2013). Among the various cultivated forage crops in Turkey, common vetch is considered to be the 2nd most cultivated forage crop after clovers covering 499 thousand ha of (629 thousand ha) plantation area. However, it is observed that this increase in the area of forage crops is not sufficient to meet the demands for roughage of Turkish farm animals (Acar et al., 2015). Besides this, low average meat and milk yields and quality of animal products is low here in Turkey (Yucel et al., 2008). However, according to Gokkus and Koc (1996), field residues are not enough to meet with roughage needs for the whole country. In order to reduce feed gap and decrease fallow fields, it is necessary to increase the cultivation area of forage crops.

In order to feed our animals with high quality feed, and to prevent excessive and early grazing of meadows and pastures, the production of forage crops should be given

http://www.aloki.hu ● ISSN 1589 1623 (Print) ● ISSN 1785 0037 (Online)
DOI: http://dx.doi.org/10.15666/aeer/1706_1520315217

great importance. Therefore, it is necessary to increase the cultivation area of forage crops, to explain the benefits and importance of these crops, to encourage cultivation, initiate breeding activities for these crops to develop new improved varieties superior in quality and yield (Ozkose and Ekiz, 2005; Ayasan, 2010).

Common vetch (*Vicia sativa* L.), which is one of the most important forage crops and serving a source of feed for animals all around the world, is an important species of *Vicia* genus containing a total of 150 species (Tosun, 1974). According to Elci and Acikgoz (1993), Turkey is rich with the flora of this genus and a total of 59 *Vicia* species can be found in Turkey. However, less efforts has been done for the breeding of this important forage crop and only 14 commercial cultivars have been released in Turkey. One of the most important goals in agriculture is to obtain more products or yield from the unit area. In order to achieve this, it is necessary to develop new lines or varieties with superior efficiency or to determine the performance of those developed in other regions in the region (Kokten, 2011).

Vetch plant, which can be used in both grass and grain, has a short period of vegetation, can grow in almost all types of soils and climatic conditions. Vetch grains with protein content of more than 20% are broken into animals as concentrated feed. In addition, the remaining straw from the harvested plants for grain yield is a good animal feed (Acikgoz, 2001).

Genotype x environment interactions (GEI) is considered one of the main area of study for the plant breeders working on for many years. A variety of methods have been developed to characterize the behaviour of varieties under different environmental conditions. Yield trials under different environments give information about the GEI when analyzed by traditional methods, while they do not give any information about the stability measurements of genotypes. Therefore, various methods have been developed to determine the performance of the genotypes under these environments. The most important of these methods is to determine the stable genotype by stability analysis (Kilic et al., 2003).

Yield is a complex trait that depends on many other features and is largely influenced by environmental factors. However, farming community demands stable varieties with higher yield, but a little fluctuation in the performance of such varieties have been also observed when they grow in various environments. Therefore information resulted by GEI can be very beneficial in the introduction of new plant varieties in plant breeding programs (Sayar et al., 2013; Kendal and Dogan, 2015).

Understanding the relationship between plant performance and environment has been an important topic for plant breeders and geneticists (Yan, 2001). Product performance is a function of genotype (G), environment (E) and an interaction of both, which occur when different phenotypes, different varieties or genotypes react differently to different environments. However, the main effect of environment is not related to the evaluation of varieties. Only genotypes and GEI are important and therefore environmental impacts should be removed from data and focused on genotypes and GEI (Gauch and Zobel, 1996). GGE is the contraction of genotype + GE; The GGE of a MET dataset can be displayed in a GGE pair that allows the researcher to concentrate on the part of the MET data most useful in the evaluation of varieties. Various statistical methods have been proposed to investigate the impact of GE interaction and to use the positive part of the variety development process (Flores et al., 1998). However, not all of these methods are always effective in the analysis of GEI of multi environment/years data sets in plant breeding programs (Sabaghnia et al., 2006). This procedure enables plant

http://www.aloki.hu ● ISSN 1589 1623 (Print) ● ISSN 1785 0037 (Online)
DOI: http://dx.doi.org/10.15666/aeer/1706_1520315217

breeders to investigate the performance of genotypes under different environments and helped to evaluate the most stable genotypes as well.

The aim of this study is to evaluate the yield and yield components of common vetch genotypes in Bilecik, Sivas and Bingol ecological conditions by using GGE Biplot analysis method and to determine the performance of these common vetch genotypes in different environments.

Materials and methods

This study was conducted in three different ecological conditions of Turkey: Bilecik, Sivas and Bingol during 2016. The GPS coordinates of these locations are Bilecik: 40° 0' 57.7728" and 30° 10' 52.6692", Sivas: 39° 42' 20.9592" and 37° 1' 56.1108", Bingol: 38° 53' 47.5620" and 40° 29' 25.9836". The research was established in randomized complete blocks design combined over location with three replications. In this study, locations were random factor and genotype were considered as fixed factor. During this study 5 lines named Hat-1, Hat-7, Hat-8, Hat-13, and Hat-17 developed by Bingol University Faculty of Agriculture Field Crops Department and 8 commercial cultivary mainly used in Turkey named Kralkizi, Dicle, Gorkem, Ozveren, Cumhuriyet-99, Yucel, Alinoglu, and Kubilay common vetch cultivar were used as plant materials. Simultaneous field experiments were conducted at the Bingol University Faculty of Agriculture, Research and Application Department, Cumhuriyet University, Sivas Vocational High School Herbal and Animal Program Research Area and Bilecik Şeyh Edebali University Agricultural and Natural Sciences Research and Application Field in October. In the experiment, the parcel dimensions were set as 3 replications according to the randomized block trial design with a row length of 5 m, row between 30 cm row and 4-5 cm. Fertilized with 3 kg N da^{-1} and 5 kg P_2O_5 da^{-1} with sowing.

The soil properties of the environments where the research was conducted are given in *Table 1*.

Table 1. *Some physical and chemical properties of soils*

Environment 1 (Bilecik)													
Sand (%)	**Silt (%)**	**Clay (%)**	**Structure**	**pH**	**Salt (%)**	**P_2O_5 ($kgda^{-1}$)**	**K_2O ($kgda^{-1}$)**	**Org. matter (%)**	**Lime (%)**	**Fe ($mgkg^{-1}$)**	**Zn ($mgkg^{-1}$)**	**Mn ($mgkg^{-1}$)**	**Cu ($mgkg^{-1}$)**
		Sandy-loamy		8.11	0.26	3.5	1.1	1.5	7.3	7.94	1.79	6.73	3.83
Environment 2 (Sivas)													
Sand (%)	**Silt (%)**	**Clay (%)**	**Structure**	**pH**	**Salt (%)**	**P_2O_5 ($kgda^{-1}$)**	**K_2O ($kgda^{-1}$)**	**Org. matter (%)**	**Lime (%)**	**Fe ($mgkg^{-1}$)**	**Zn ($mgkg^{-1}$)**	**Mn ($mgkg^{-1}$)**	**Cu ($mgkg^{-1}$)**
14.6	48.3	37.1	SiCL	7.28	0.33	3.40	93.59	1.7	19.6	3.99	0.42	4.68	1.23
Environment 3 (Bingol)													
Sand (%)	**Silt (%)**	**Clay (%)**	**Structure**	**pH**	**Salt (%)**	**P_2O_5 ($kgda^{-1}$)**	**K_2O ($kgda^{-1}$)**	**Org. matter (%)**	**Lime (%)**	**Fe ($mgkg^{-1}$)**	**Zn ($mgkg^{-1}$)**	**Mn ($mgkg^{-1}$)**	**Cu ($mgkg^{-1}$)**
		Loamy		6.37	0.0006	7.9	24.45	1.26	0.15				

When *Table 1* is examined, the trial area of Bilecik location is sandy, loamy, moderate alkaline (8.11) and medium salted (0.26%). Moreover, the amount of lime (7.3%) and the amount of organic matter (1.5%) is moderate and the amount of phosphorus (3.5 kg da^{-1}) and potassium (1.1 kg da^{-1}) is low and the micro element content is sufficient. The soil of the trial site of the Sivas location is low phosphorus (3.4 kg da^{-1}), slightly

http://www.aloki.hu ● ISSN 1589 1623 (Print) ● ISSN 1785 0037 (Online)
DOI: http://dx.doi.org/10.15666/aeer/1706_1520315217

alkaline (7.28), low in organic matter content (1.7%), salty (19.6%) and silty (19.6%). The contents of potassium (K_2O) are high (93.59 kg da^{-1}), micro element contents are generally sufficient. The soil of the trial area of Bingol location is slightly acidic (6.37) without salt (0.0006%), organic matter is less (1.26%), less calcareous, potassium is less (24.45 kg da^{-1}) phosphorus medium (7.9 kg da^{-1}) level is seen.

The climate data of the environments in which the experiment was conducted are given in *Figures 1, 2* and *3*. When the figures are analyzed, it is seen that the average temperature, total precipitation and relative humidity are quite different from each other.

When the sub-fruits of the plants began to mature (about 120-150 days after sowing), the morphological and phenological observations of the plant were taken and the half of the parcel was cut to calculate the green grass yield (according to the Technical Instructions established on the basis of UPOV criteria of the Seed Registration and Certification Directorate). During the harvesting of green grass, 500 g samples of each parcel were taken and dried in a drying oven at 70 °C for 48 h at a constant weight and weighed and dry matter weight was calculated.

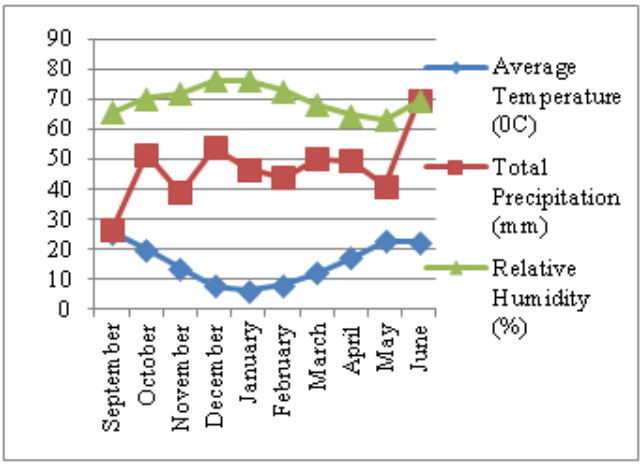

Figure 1. *Climate data of 2016-17 period for the first environment (Bilecik) where the experiment was conducted*

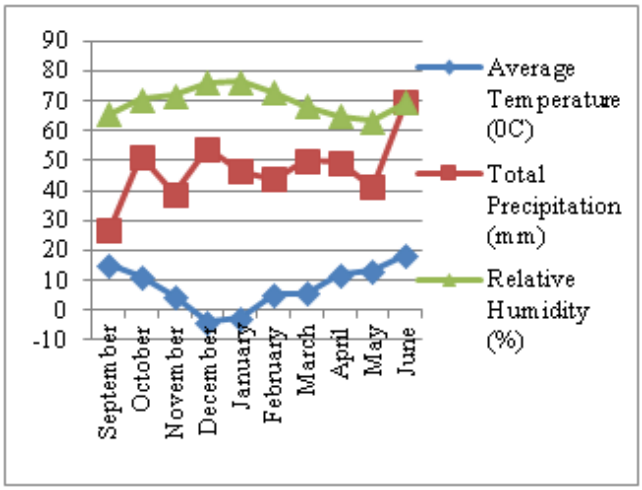

Figure 2. *Climate data of 2016-17 period for the second environment (Sivas) where the experiment was conducted*

http://www.aloki.hu ● ISSN 1589 1623 (Print) ● ISSN 1785 0037 (Online)
DOI: http://dx.doi.org/10.15666/aeer/1706_1520315217

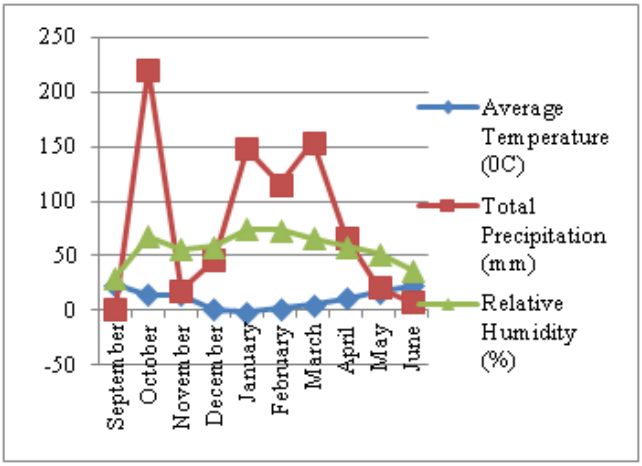

Figure 3. *Climate data of 2016-17 period for the 3 rd environment (Bingöl) where the experiment was conducted*

Seed yield and yield components were made during the period when the plants were completely yellow (about 180-200 days after sowing). The number of pods per plant (pieces/plant), the number of pods in this plant, the seeds of these beans were divided and counted, and the number of seeds (pieces) in pods was found. Then the whole of the parcels was weighed and the biological yield (kg da^{-1}) was calculated, the grains were blended and weighed and the seed yield (kg da^{-1}) was found. Straw yield (kg da-1) was calculated by removing seed yield from biological yield. However, harvest index (%): seed yield × 100/biological yield as calculated. By multiplying the weights of 100 seeds taken from each repetition 4 by 10, the seeds of each species were determined with a weight of 1000 grains.

Data processing

The findings obtained from the study were subjected to variance analysis by using MstatC program. Duncan test was used to determine whether the difference between the averages is significant. Biplot (Genotype + GxE interaction) model analysis was performed using SPSS-16 packet program.

Results and discussion

In this study; values for various observed traits are presented in *Table 2* and statistically significant differences between the lines and varieties in terms of natural plant height in all three locations were observed. Maximum plant height at Bilecik location was obtained from Kralkizi genotype with a value of 49.10 cm, and the shortest plant height was obtained from Kubilay genotype with a value of 22.67 cm. At the Bingol and Sivas locations, maximum plant height was resulted by Dicle genotype with the values of 52.47 and 54.13 cm, respectively, while the minimum plant height was obtained from the Hat-7 genotype with 38.33 and 39.77 cm respectively. In Sivas, high rainfall (154.8 mm) and high relative humidity (66.0%), especially in May, increased the plant height, so the plant height in Sivas was higher than other locations. The average plant height of the common vetch lines and varieties were not found to be statistically significant. Mean plant height ranged between 35.46 and 50.42 cm during

http://www.aloki.hu ● ISSN 1589 1623 (Print) ● ISSN 1785 0037 (Online)
DOI: http://dx.doi.org/10.15666/aeer/1706_1520315217

this study. The study conducted by Kokten (2011) in Bingol dry conditions showed that the average plant height of the common vetch lines and varieties was 22.4 cm. Although these results are different from our study, however results of this study made a strong agreement with the findings of Seydosoglu (2014) using the vetch genotypes and conducted experiment in same province and resulted plant height 33.9-62.6 cm.

Table 2. *Bilecik, Sivas and Bingol ecological conditions obtained from different common vetch genotypes, environment, and those interactions of average number of the height of the natural plant, pod numbers of per plant and seed numbers per pod*

Genotypes	Natural plant height (cm)				Pod numbers of per plant				Seed numbers per pod			
	Bilecik	Bingol	Sivas	Avg.	Bilecik	Bingol	Sivas	Avg.	Bilecik	Bingol	Sivas	Avg.
Kralkizi	49.10 a	27.87 d	29.40 e	35.46	13.37d-f	10.47d	7.60de	10.48 d	6.30	4.73 ab	4.07	5.03
Dicle	44.67a-c	52.47 a	54.13 a	50.42	20.43bc	18.00bc	14.33c	17.72 bc	6.43	4.87 ab	5.20	5.50
Gorkem	30.57b-d	46.73a-c	47.97 a-d	41.76	15.50c-f	12.43d	9.80c-e	12.58 d	6.00	4.30a-c	5.53	5.28
Ozveren	34.53a-d	44.93a-c	46.03 a-d	41.83	16.20c-e	11.67d	6.67e	11.51 d	6.00	4.27a-c	5.93	5.40
Cumh.-99	35.10a-d	45.27a-c	46.87 a-d	42.41	18.70b-d	14.40b-d	12.80c-e	15.30 b-d	4.53	2.97 d	3.33	3.61
Alinoglu	40.70a-c	42.00 bc	43.53 c-d	42.08	17.87c-e	13.37cd	12.40c-e	14.54 cd	6.20	4.57a-c	4.47	5.08
Selcuk	27.27cd	45.33a-c	46.93 a-d	39.84	17.13c-e	12.70d	11.00c-e	13.61 d	6.77	5.37 a	5.33	5.82
Kubilay	22.67d	49.67 ab	51.40 a-c	41.24	23.37 b	18.70b	24.30b	22.12 b	5.97	4.43a-c	6.40	5.60
Hat-1	31.73a-d	39.67 c	41.10 d	37.50	16.73c-e	12.47d	9.00c-e	12.73 d	5.30	3.70b-d	3.20	4.07
Hat-7	31.23a-d	38.33 c	39.77 d	36.44	34.30 a	29.73a	35.00a	33.01 a	4.73	3.37 cd	4.73	4.28
Hat-8	44.30a-c	41.07 bc	44.30 bc	43.22	15.93c-f	15.33b-d	14.00c	15.09 b-d	5.30	3.47 cd	5.33	4.70
Hat-13	47.80ab	40.27 c	43.87 cd	43.98	12.27ef	13.97b-d	10.13c-e	12.12 b-d	5.40	4.03b-d	5.47	4.97
Hat-17	44.07a-c	49.87 ab	53.23 ab	49.06	10.53 f	12.47d	13.30cd	12.10 d	5.13	3.93b-d	4.47	4.51
Average	37.21	43.34	45.27		17.87 A	15.05 AB	13.90 B		5.70 A	4.15 B	4.88AB	
LSD	15.60	7.879	7.959		5.009	4.553	5.348	4.553		1.062		
LSD (lok)						1.223				1.223		
CV (%)	25.36	11.01	10.64	15.99	16.96	18.30	23.27	19.31	13.04	15.47	17.97	15.48

In the same column, the averages indicated by similar group of letters are not different from Duncan (5%)

In terms of the numbers of pods per plant, statistically significant differences were observed between the lines and varieties at all three locations. In Bilecik, Bingol and Sivas locations, the highest numbers of pods per plant was obtained from Hat-7 genotype with 34.30, 29.73 and 35.00 values respectively, while the lowest numbers of pods per plant was found at Bilecik location; 10.53 value byHat-17 genotype, Bingol location; It was obtained from the Kralkizi genotype with 10.47 and the Ozveren genotype with 6.67 in Sivas location. The average of numbers of pods per plant by common vetch lines and varieties was found to be statistically significant, while the numbers of pods per plant was obtained from the genus Hat-7 with a value of 33.01, while the lowest numbers of pods per plant was obtained from Ozveren genotype with a value of 11.51. In addition, the interaction of locations and location x genotype was found to be statistically significant. The highest numbers of pods per plant in Bilecik (17.87 units) was obtained, followed by Bingol location (15.05 units) and the lowest numbers of pods per plant were obtained from Sivas (13.90 units).

Statistically significant differences for number of seed per pod between the lines and varieties were observed in Bingol location. However, there were no statistically significant differences between the lines and varieties in the locations of Bilecik and Sivas. In the location of Bilecik; number of seed per pod ranged from 4.53 to 6.43. In Sivas, number of seed per pod varied between 3.33 and 6.40. In Bingol location, the

http://www.aloki.hu ● ISSN 1589 1623 (Print) ● ISSN 1785 0037 (Online)
DOI: http://dx.doi.org/10.15666/aeer/1706_1520315217

highest number of seed per pod was obtained from Selcuk genotype with a value of 5.37, while the number of seed per pod was obtained from the Cumhuriyet-99 genotype with a value of 2.97. In addition, while the averages of the locations were statistically insignificant, the interaction of locations and location x genotype was found to be statistically significant. The highest number of seed per pod was obtained in Bilecik (5.70), followed by Sivas (4.88) and the lowest seed number per pod were obtained from Bingol (4.15).

Higher temperature with greater relative humidity at the Bilecik location during the period of study resulted in maximum number of pods and the number of seeds in the pods to be higher than the other locations. In addition, as Fehr (1987) stated, it is natural for the study to be different because of the opinion that the environment can have different effects on the same species and variety and differences in their performances can be observed.

Albayrak et al. (2004) used various vetch varieties and lines by conducting multi location experiments and resulted number of seeds per pod for varieties 6.11-8.44 and 5.44 to 7.22 for lines. Seydosoglu, in his study in 2014 founded seed number per pod in a range of 13.5-21.2, the seed number per pod varies between 4.7-5.6 units (Seydosoglu, 2014). These studies seem to be in harmony with our work.

The average value of forage yield and dry matter yield obtained from common vetch lines and varieties used in Bilecik, Bingol and Sivas locations are presented in *Table 3*.

Table 3. *Bilecik, Sivas and Bingol ecological conditions obtained from different common vetch genotypes, environment, and those interactions of average values of forage yield and dry matter yield*

Genotypes	Forage yield (kg da^{-1})				Dry matter yield (kg da^{-1})			
	Bilecik	**Bingol**	**Sivas**	**Average**	**Bilecik**	**Bingol**	**Sivas**	**Average**
Kralkizi	3733.30a	412.67g	653.10g	1599.69	964.47ab	92.70f	230.37f	429.18
Dicle	3400.00a-d	932.53a	1172.87a	1835.14	1107.13a	217.83a	355.57a	560.18
Gorkem	2866.67de	841.13b	1081.77b	1596.52	596.33ab	196.07a-c	314.07b	368.82
Ozveren	3066.67a-e	766.90b-d	1007.50b-d	1613.69	880.57ab	176.37b-d	284.93b-d	444.29
Cumh.-99	3025.33b-e	823.77bc	1064.17bc	1637.76	727.70ab	201.70ab	310.30bc	413.23
Alinoglu	3711.10ab	701.23de	941.83de	1784.72	984.57ab	162.97de	271.63de	473.06
Selcuk	2900.00c-e	739.43cd	979.63cd	1539.69	596.67ab	172.63b-d	281.27b-e	350.19
Kubilay	2630.00e	795.57b-d	1036.27b-d	1487.28	528.77b	169.03c-e	277.74c-e	325.18
Hat-1	3585.50a-c	644.33ef	884.90ef	1700.47	1003.50ab	182.57b-d	291.10b-d	492.39
Hat-7	3140.80a-e	610.10ef	850.67ef	1533.86	698.70ab	159.73de	268.23de	375.56
Hat-8	3418.57a-d	631.57ef	872.33ef	1640.82	821.87ab	176.17b-d	284.40b-d	427.48
Hat-13	3100.00a-e	579.90f	820.50f	1500.13	921.17ab	142.37e	250.57ef	438.03
Hat-17	3025.43b-e	802.80bc	1043.53bc	1623.92	834.53ab	202.60ab	310.83bc	449.32
Average	3200.26A	714.00B	953.51B		820.50A	173.29B	286.30B	
LSD	595.8	87.54	87.47		433.5	27.29	29.62	
LSD(lok)		355.0				247.2		
CV (%)	11.26	7.42	5.54	13.13	31.97	9.53	6.24	35.67

In the same column, the averages indicated by similar group of letters are not different from Duncan (5%)

As seen in *Table 3,* there are statistically significant differences between genotypes in all three locations in terms of forage yield, and it is also observable that there are no statistical differences in the averages where the locations are combined. In addition, the

http://www.aloki.hu ● ISSN 1589 1623 (Print) ● ISSN 1785 0037 (Online)
DOI: http://dx.doi.org/10.15666/aeer/1706_1520315217

interaction of locations and GEI was found to be statistically significant. The highest forage yield was obtained from the Kralkizi genotype with a value of 3733.30 kg da^{-1}, while the lowest forage yield was obtained from the Kubilay genotype with a value of 2630.00 kg da^{-1}. In Bingol and Sivas, respectively, it was obtained from Dicle genotype with 932.53 and 1172.87 kg da^{-1} values, and the lowest forage yield was obtained from Kralkizi genotype with 412.67 and 653.10 kg da^{-1} values. On average, the forage yield varied between 1487.28 and 1835.14 kg da^{-1}. In addition, the highest forage yield was obtained from Bilecik (3200.26 kg da^{-1}), while the lowest forage yield was obtained from Bingol location (714.00 kg da^{-1}).

High temperature with greater relative humidity during the study periods at Bilecik location resulted in higher forage yield as compared to rest of locations. It can be seen that environmental differences such as temperature, relative humidity and precipitation have caused the efficiency of common vetch genotypes to be different in the locations where the study was conducted. According to Gramsh (1982), performance of vetch varieties for forage yield is largely dependent upon the region and its climatic conditions.

In terms of dry matter yield; statistically significant differences between genotypes in all three locations were observed, and it was found that there were no statistical differences in the averages of all the locations when combined. In addition, genotypes and GEI was found to be statistically significant. The highest dry matter yield was obtained from the Dicle genotype with the values of 1107.13, 217.83 and 355.57 kg da^{-1} in Bilecik, Bingol and Sivas locations, respectively, the lowest dry matter yield in the Bilecik location, the Kubilay genotype with 528.77 kg da^{-1} value, Bingol and Sivas and 92.32 and 230.37 kg da^{-1} respectively. On average, the dry matter yields varied between 325.18 and 560.18 kg da^{-1}. In addition, the highest dry matter yield was obtained from the Bilecik location (820.50 kg da^{-1}), while the lowest dry matter yield was obtained from Bingol location (173.29 kg da^{-1}). Similarly to this study, Seydosoglu, in his study in 2014 in the Diyarbakır; stated that forage yield can be vary between 1522.0-3232.3 kg da^{-1} and dry matter yield between 308.0-919.5 kg da^{-1}. Mikic et al. (2014) found 8.8 t ha^{-1} as 2 years averaged DM yield which varied between 8.0 t DM ha^{-1} (cvs. Armantes and Labari) and 10.2 t ha^{-1} (cv. Slavej). These findings are consistent with our findings.

The average value of biological yield and straw yield obtained from common vetch lines and varieties used in Bilecik, Bingol and Sivas locations are presented in *Table 4*.

As it can be seen in *Table 4,* there are statistically significant differences between genotypes in all three locations where the study is conducted and there is no statistically significant difference between the averages where the locations are combined. In addition, the interaction of locations and location x genotype was found to be statistically significant. The highest biological yield was obtained from Kralkizi genotype with 1288.67 kg da^{-1} value at Bilecik location, while the lowest biological yield was obtained from Kubilay genotype with 335.67 kg da^{-1} value. At the Bingol and Sivas locations, the highest biological yield was obtained from the Cumhuriyet-99 genotype with the values of 335.60 and 356.13 kg da^{-1} respectively, while the lowest biological yield was obtained from the Kralkizi genotype with 153.63 and 174.50 kg da^{-1} values respectively. Biological yields ranged between 320.30 and 538.93 kg da^{-1} in the averages of locations. In addition, the highest biological yield was obtained from the Bilecik location (706.95 kg da^{-1}), while the lowest biological yield was obtained from the Bingol location (268.51 kg da^{-1}).

http://www.aloki.hu ● ISSN 1589 1623 (Print) ● ISSN 1785 0037 (Online)
DOI: http://dx.doi.org/10.15666/aeer/1706_1520315217

In terms of straw yield efficiency, statistically significant differences between genotypes in all three locations were observed, and it was also observed that there were no statistical differences in the averages where the locations were combined. Additionally, genotypes and GEI was also found to be statistically significant. Maximum straw yield was obtained from Kralkizi genotype (1154.00 kg da^{-1}) at Bilecik location, the lowest straw yield was obtained from Kubilay genotype with 204.00 kg da^{-1} values. In Bingol and Sivas locations, respectively, it is obtained from Gorkem genotype with 271.87 and 348.73 kg da^{-1} values, the lowest straw yield is in Bingol location, with 106-180 kg da^{-1} Kralkizi genotype and in Sivas location with 198.87 kg da^{-1} values genotype. The straw yields for all locations combined ranged from 255.27 to 486.84 kg da^{-1}. In addition, the maximum straw yield was obtained from Bilecik location (552.33 kg da^{-1}), while the lowest straw yield was obtained from Bingol location (211.84 kg da^{-1}).

Table 4. *Bilecik, Sivas and Bingol ecological conditions obtained from different common vetch genotypes, environment, and those interactions of average values of biological yield and straw yield*

Genotypes	Biological yield (kg da^{-1})				Straw yield (kg da^{-1})			
	Bilecik	Bingol	Sivas	Average	Bilecik	Bingol	Sivas	Average
Kralkizi	1288.67a	153.63h	174.50h	538.93	1154.00a	106.80g	199.73f	486.84
Dicle	666.70cd	287.87cd	308.67cd	421.07	529.67c	241.37bc	334.07ab	368.37
Gorkem	377.70e	327.03ab	347.50ab	350.73	236.33de	271.87a	348.73a	285.64
Ozveren	822.33bc	272.10de	292.47de	462.30	632.67bc	211.10de	257.87de	367.21
Cumh.-99	977.67b	335.60a	356.13a	556.47	836.00b	271.43a	317.77bc	467.30
Alinoglu	733.33cd	306.17bc	326.53bc	455.34	580.67bc	232.00cd	278.53d	363.73
Selcuk	789.00bc	302.33c	323.23c	471.52	625.67bc	257.67ab	304.40c	384.80
Kubilay	335.67e	302.33c	322.90c	320.30	204.00e	257.67ab	304.13c	255.27
Hat-1	644.67cd	228.83f	249.33f	374.28	493.33cd	161.33f	207.83f	287.50
Hat-7	622.00cd	253.57e	273.97e	383.38	459.67c-e	197.57e	244.20e	300.48
Hat-8	533.00de	263.23e	284.03e	360.10	397.33c-e	198.90e	245.40e	280.54
Hat-13	722.00cd	193.63g	214.13g	376.60	518.33c	152.13f	198.87f	289.78
Hat-17	677.67cd	264.27e	284.90e	408.94	546.00c	194.10e	240.77e	326.96
Average	706.95A	268.51B	289.14B		552.33A	211.84B	266.07B	
LSD	219.8	22.12	22.30		240.6	20.93	23.70	
LSD(lok)		127.9				134.6		
CV	18.81	4.98	4.67	18.39	26.23	5.98	5.35	23.84

In the same column, the averages indicated by similar group of letters are not different from Duncan (5%)

According to Unal et al. (2016) differences in the performance of genotypes at different locations may be due to abiotic (climatic features, soil properties and topography) and biotic factors (weed, pest and diseases) at the specific location. During this study, temperature and precipitation were found highly variable over all three locations and highly influenced the plant growth, yield and production potentials of vetch plant. Results of this study made a strong agreement with the findings of Albayrak et al. (2004) resulting biological yield between 584 to 729 kg da^{-1} under multilocations.

http://www.aloki.hu ● ISSN 1589 1623 (Print) ● ISSN 1785 0037 (Online)
DOI: http://dx.doi.org/10.15666/aeer/1706_1520315217

The average value of seed yield, thousand seed weight and harvest index obtained from common vetch lines and varieties used in Bilecik, Bingol and Sivas locations are given in *Table 5*.

Table 5. *Bilecik, Sivas and Bingol ecological conditions obtained from different common vetch genotypes, environment, and those interactions of average values of seed yield, thousand seed weight and harvest index*

Genotypes	Seed yield (kg da^{-1})				Thousand seed weight (gr)				Harvest ındex (%)			
	Bilecik	Bingol	Sivas	Average	Bilecik	Bingol	Sivas	Average	Bilecik	Bingol	Sivas	Average
Kralkizi	134.67	46.83e	55.57e	79.02	64.13bc	46.43cd	62.20b	57.59	34.67	30.53a	48.73cd	29.98
Dicle	137.00	46.50e	55.17e	79.56	56.33f	46.07c-e	61.57bc	54.66	20.50	16.13f	35.00f	23.88
Gorkem	141.33	55.17d	63.43d	86.64	50.60g	42.10e	57.33b-d	50.01	40.07	16.90ef	35.40f	30.79
Ozveren	189.67	61.00cd	69.40cd	106.69	69.87a	53.80a	69.13a	64.27	24.47	22.57c	41.03e	29.36
Cumh.-99	141.67	64.17bc	72.60bc	92.81	61.80cd	52.37ab	68.00a	60.72	15.23	19.17de	37.37f	23.92
Alinoglu	152.67	74.17a	82.67a	103.17	58.27ef	53.67a	68.93a	60.29	21.13	24.23bc	42.80e	29.39
Selcuk	196.67	44.67e	53.23e	98.19	58.60d-f	42.50de	58.13bc	53.08	25.90	14.73f	41.13e	27.26
Kubilay	131.67	44.67e	52.97e	76.43	58.33ef	49.80a-c	59.97bc	56.03	39.13	14.73f	41.17e	31.68
Hat-1	151.33	67.50a-c	76.10a-c	98.31	64.07bc	48.87bc	56.70cd	56.21	23.43	29.57a	56.30a	36.43
Hat-7	162.33	56.00d	64.73d	94.36	65.53b	45.80c-e	53.27d	54.87	26.53	22.07cd	48.50cd	32.37
Hat-8	135.67	64.33bc	73.13bc	91.04	65.80b	53.70a	61.10bc	60.20	25.43	24.47bc	51.00bc	33.63
Hat-13	203.67	41.50e	50.00e	98.39	61.23c-e	37.63f	44.87e	47.91	29.13	21.47cd	47.73d	32.78
Hat-17	131.67	70.17ab	78.60ab	93.48	59.60d-f	53.60a	61.00bc	58.07	19.07	26.57b	53.10b	32.91
Average	154.62A	56.67B	65.20B		61.01A	48.18B	60.17A		24.67B	21.78B	44.56A	
LSD		6.958	6.963		3.062	3.826	4.449			2.770	2.928	
LSD (lok)		32.08				3.88				6.521		
CV	21.67	7.43	6.46	21.32	3.03	4.80	4.47	4.11	13.29	7.69	3.97	13.44

In the same column, the averages indicated by similar group of letters are not different from Duncan (5%)

As seen in *Table 5,* there are statistically significant differences between genotypes in terms of seed yield in Bingol and Sivas locations, but there are no statistically significant differences between genotypes in Bilecik location. The seed yields of the genotypes at the location of Bilecik ranged between 131.67 and 203.67 kg da^{-1}. In the Bingol and Sivas locations, maximum seed yield was obtained from Alinoglu genotype with values of 74.17 and 82.67 kg da^{-1}, respectively, while the lowest seed yield was obtained from the genotype Hat-13 with the values of 41.50 and 50.00 kg da^{-1}. The differences between the common vetch lines were caused by variations in their genetic makeup. The averages of the common vetch genotypes were not found statistically significant and the seed yields varied between 76.43 and 106.69 kg da^{-1}. In addition, the location and genotype interaction were found to be statistically significant. However, the highest seed yield was obtained from Bilecik location (154.62 kg da^{-1}) while the lowest seed yield was obtained from Bingol location (56.67 kg da^{1}). In the Bilecik location, numbers of pods per plant and numbers of seeds per pod were higher than those of Bingol and Sivas locations. Albayrak et al. (2004) conducted multi locations experiments and stated that seed yield of common vetch can be varied between 98-160 kg da^{-1} and the one thousand grains weight ranged from 57.7 to 63.4 g and these results were found in line with the findings of this study. Similarly, our results were further supported by the findings of Gurmani et al. (2006) resulting seed yields in a range of 643.0 to 1620.0 kg ha^{-1}. In terms of one thousand seed weight, statistically significant differences between genotypes in all three locations were observed, and it is

http://www.aloki.hu ● ISSN 1589 1623 (Print) ● ISSN 1785 0037 (Online)
DOI: http://dx.doi.org/10.15666/aeer/1706_1520315217

seen that there are no statistical differences in the averages where the locations are combined. In addition, the interaction of locations and location x genotype was found to be statistically significant. In Bilecik, Bingol and Sivas locations, the maximum thousand seed weight was obtained from Ozveren genotype with 69.87, 53.80 and 69.13 g, respectively, while the lowest thousand seed weight was at Bilecik location; it was obtained from the Gorkem genotype with 50.60 g and from the Hat-13 genotype with 37.63 and 44.87 g values in Bingol and Sivas locations, respectively. In terms of one thousand seed weight, the average of the locations of common vetch genotypes ranged from 47.91 to 64.27 g. In addition, a maximum of thousand seed weight was obtained from Bilecik location (61.01 g), followed by Sivas location (60.17 g), the lowest thousand seed weight from Bingol location (48.18 g). Possible reason behind these variations may be due to differences in the ecological conditions of studied locations. Orak and Nizam (2004) measured data of TSW were between 31.92 and 63.52 g and their findings clearly supported the results of this study.

There are statistically significant differences between genotypes in Bingol and Sivas locations in terms of harvest index, but there are no statistically significant differences between genotypes in Bilecik location. Harvest index of the genotypes at Bilecik location varied between 15.23% and 39.13%. Maximum harvest index was obtained from the Kralkizi genotype with a value of 30.53%, while the lowest harvest index was obtained from Selcuk and Kubilay genotypes with a value of 14.73% at the Bilecik location. In Sivas, the highest harvest index was obtained from Hat-1 genotype with a value of 56.30%, while the lowest harvest index was obtained from the Dicle genotype with a value of 35.00%. The average of the locations where common vetch genotypes were combined was not statistically significant, and the harvest index changed between 27.26% and 36.43%. In addition, the location and genotype interactions were found to be statistically significant in terms of harvest index. However, the highest harvest index was obtained from Sivas location (44.56%) while the lowest harvest index was obtained from Bingol location (21.78%). Hereby, the high seed yield naturally results in greater HI. Unal et al. (2016) found that the harvest index for common vetch can vary between 39.23 and 42.54% and their findings made strong agreement with the results of this study.

Determination of ideal properties with biplot method in Bilecik, Bingol and Sivas locations are given in *Figure 4.*

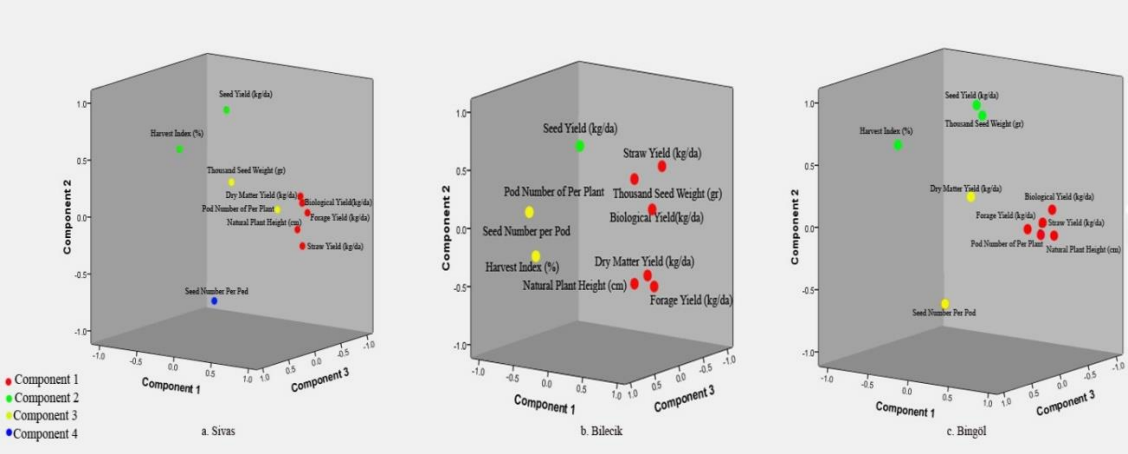

Figure 4. *Determination of ideal properties with biplot method in different locations*

http://www.aloki.hu ● ISSN 1589 1623 (Print) ● ISSN 1785 0037 (Online)
DOI: http://dx.doi.org/10.15666/aeer/1706_1520315217

Biplot analysis is considered one of the most easiest and effective way to select genotypes reflecting superior performance for various traits of interest under multi environments/locations. In this study, biplot analysis was evaluated for each location to evaluate differences for studied traits. It was observable that biological yield, forage yield and straw yield were found main variations contributing factors in component 1 at all three studied locations. However, some differences were present in each location for component two and three for few traits. It is observable that harvest index, seed number per pod and thousand seed weight are changing among the location. Therefore, it can be suggested that good understanding about the behaviour of these traits under multi environmental condition will be helpful in breeding activities. Seed yield is most important trait for any crop and can be used as selection criteria to evaluate genotypes having superior performance. Seed yield was found main contributor in component two in all three locations. Therefore, this trait can be suggested for the selection of genotypes.

Principal component analysis (PCA) was performed to understand the level of variations and importance was given to 1st four components because they accounted maximum variations at the first location (*Fig. 4a*). In the first component, 5 important variables are Forage Yield (0.963), Straw Yield (0.949), Biological Yield (0.909), Dry Matter Yield (0.836) and Natural Plant Height (0.818), respectively, and the second component is Seed Yield (0.934) and Harvest Index (0.454). The third component included Thousand Seed Weight (0.627) and Seed Number per Pod (0.592) and the fourth component included Pod Number of Per Plant (0.651).

Three components were identified at the second location (*Fig. 4b*). In the first component, Dry Matter Yield (0.802), Biological Yield (0.787), Straw Yield (0.771), Forage Yield (0.768), Natural Plant Height (0.692) and Thousand Seed Weight (0.451), respectively were found main variation contributor. In 2nd component Seed Yield (0.738) and number of pods per Plant (0.060) were chief variations contributor. In the third component, maximum variations were due to Seed Number per Pod (0.527) and Harvest Index (0.415).

The third location (*Fig. 4c*) consists of three components. In the first component, Forage Yield (0.958), Straw Yield (0.953), Biological Yield (0.929), Natural Plant Height (0.909) and Pod Number of Per Plant (0.114), respectively. In the second component, Seed Yield (0.935), Thousand Seed Weight (0.868), Harvest Index (0.555), and Seed Number per Pod (0.622) and Dry Matter Yield (0.452) were found.

Analysis of genetic and phenotypic correlations may provide additional benefits to the fundamental analysis of economically important features, as it is used to make indirect choices and predict genetic gain in various annual breeding programs, including soybeans and other annual legumes (Burton, 2011). The cluster analysis of the common vetch inputs tested also confirms that groups may sometimes involve initiatives with close geographical origins, in particular local land areas or varieties used to develop (Potokina et al., 2002).

In this study, biological yield, straw yield, forage yield and natural plant height were included in component 1 at three locations. For this reason, the selection of the genotypes used in the study in the future can be better if the selection is done with these properties. Similar to this study, Mikic et al. (2014) stated that significant differences in the number of common vetch participation and results on the varieties with different geographical origin, feed yield components and related characteristics. Here, information on the relationship between the economically important properties of the

http://www.aloki.hu ● ISSN 1589 1623 (Print) ● ISSN 1785 0037 (Online)
DOI: http://dx.doi.org/10.15666/aeer/1706_1520315217

individual feed yield components, together with the results of the cluster analysis, can help in future reproductive efforts and the selection of parental components for hybridization.

Conclusions

This study was carried out simultaneously at three (Bilecik, Sivas and Bingol) ecological conditions of Turkey during 2016. It can be concluded that various yield components like biological yield, straw yield, forage yield and natural plant height resulted highly significant variations and can be effectively utilized as selection criteria to start the breeding activities for the common vetch. Average plant height of the genotypes in the locations are between 35.46 and 50.42 cm, the pod numbers of per plant is between 11.51 and 33.01, the seed numbers per pod is between 3.61 and 5.60, the seed yield is between 1487.28 and 1835.14 kg da^{-1}, the dry matter yield between 325.18- 560.18 kg da^{-1}, biological yield between 320.30 and 538.93 kg da^{-1}, straw yield between 255.27 and 486.84 kg da^{-1}, seed yield between 76.43 and 106.69 kg da^{-1}, thousand seed weight between 47.91 and 64.27 gr, harvested index was between 27.26% and 36.43%.

Among the common vetch genotypes in the locations, the highest forage yield and dry matter yield were obtained from the Dicle common vetch genotype, the biological and straw yield were from Kralkizi genotype, and the seed yield was from Ozveren genotype. These results suggested that some previously selected genotypes and superior cultivars can be successfully grown and make a significantly positive contribution. Their introduction into crop-rotation will greatly increase dry matter yield and seed yield and overall sustainability by acting as a disease break and contributing immensely to soil fertility.

Acknowledgements. The authors are thankful to Dr. Ferzat TURAN from Department of Animal Science, Faculty of Agriculture, Ondokuz Mayıs University, for making statistical analysis. Authors are also grateful to Bilecik Seyh Edebali University Scientific Research Projects Department for supporting the experiment through Project no: 2015-02. BSEÜ.14-01 at Bilecik location.

REFERENCES

[1] Acar, Z., Sabancı, C. O., Tan, M., Sancak, C., Kizilsimsek, M., Bilgili, U., Ayan, I., Karagoz, A., Mut, H., Asci, O. O., Basaran, U., Kir, B., Temel, S., Yavuzer, G. B., Kirbas, R., Pelen, M. A. (2015): Changes in the production of forage crops and new searches. – Turkey Agricultural Engineering VIII. Technical Congress, pp. 508-547.

[2] Acikgoz, E. (2001): Forage Crops. – Uludağ University Strengthening Foundation, No: 182, Bursa.

[3] Albayrak, S., Töngel, Ö., Güler, M. (2004): Stability analysis and determination of seed yield and yield components of candidate vetch (*Vicia sativa* L.) varieties in middle Black Sea Region. – Journal of Faculty of Agriculture OMU 20(1): 50-55.

[4] Arystanbekkyzy, M., Nadeem, M. A., Aktas, H., Yeken, M. Z., Zencirci, N., Nawaz, M. A., Ali, F., Haider, M. S., Tunc, K., Chung, G., Baloch, F. S. (2019): Phylogenetic and taxonomic relationship of turkish wild and cultivated emmer (triticum turgidum ssp. dicoccoides) revealed by iPBSretrotransposons markers. International Journal of Agriculture and Biology 21: 155–163.

http://www.aloki.hu ● ISSN 1589 1623 (Print) ● ISSN 1785 0037 (Online)
DOI: http://dx.doi.org/10.15666/aeer/1706_1520315217

[5] Ayasan, T. (2010): The use of bitter vetch (*Vicia ervilia* L.) in animal feeding. – Journal of Kafkas Veterinary Faculty 16(1): p.167-171.
[6] Burton, J. W. (2011): Quantitative Genetic: Results in Soybean Breeding. – In: Miladinovic, J., Hrustic, M., Vidic, M. (eds.) Soybean. Institute of Field and Vegetable Crops and Soja Protein, Becej, Serbia, pp. 137–183.
[7] Elci, S., Açıkgöz, E. (1993): Guide to Introducing Legumes and Wheat Forage Crops. – TİGEM, Avsaroğlu Printing House, Ankara.
[8] Fehr, W. R. (1987): Genotype x Environment Interaction. – In: Fehr, W. R. (ed.) Principles of Cultivar Development. Vol. I.: Theory and Technique. Macmillan Publishing Company, New York, pp. 247-260.
[9] Flores, F., Moreno, M. T., Cubero, J. I. (1998): A Comparison of univariate and multivariate methods to analyze G× E interaction. – Field Crops Research 56: 271-286.
[10] Gauch, H. G., R. W. Zobel. (1996): AMMI Analysis of Yield Trials. – In: Kang, M. S., Gauch, H. G. (eds.) Genotype-by-Environment Interaction. CRC Press, Boca Raton, Florida, pp. 85-122.
[11] Gokkus, A., Koc, A. (1996): Agricultural structure in eastern Anatolia region. – Pasture- and Meadow Forage Crops Congress, 17-19 June 1996, Erzurum, pp. 22-31.
[12] Gramsh, E. S. (1982): Variation in the quantitative characters of *Vicia sativa* L. – Plant Breeding Abs. 52(5).
[13] Gurmani, Z. A., Zahid, M. S. and Bashir, M. (2006): Performance of vetch, Vicia sativa cultivars for fodder production under rainfed conditions of Pothwar region [Pakistan]. – Journal of Agricultural Research (Pakistan) 44: 291-297.
[14] Kendal, E., Doğan, Y. (2015): Stability of a candidate and cultivars (Hordeum vulgare L) by GGE biplot analysis of multi-environment yield trial in spring barley. – Agriculture & Forestry/Poljoprivreda i Sumarstvo 61: 307-318.
[15] Kilic, H., Yagbasanlar, T., Tur, Z. (2003): Genotypic environment interaction of some agricultural properties in durum wheat, stability analysis with heritability estimates. – Field Crops Congress of Turkey 1: 52-57.
[16] Kokten, K. (2011): Determination of seed yield and some agricultural characteristics of some common vetch (*Vicia sativa* L.) lines in Bingol ecological conditions. – Bingol University Journal of Science 2011(1).
[17] Mikic, A., Mihailovic, B., Cupina, D., Milic, D., Katic, S., Karagic, D., Pataki, I., Ottavio, P. D., Kralijevic-Balalic, M. (2014): Forage yield components and classification of common vetch (*Vicia sativa* L.) cultivars of diverse geographic origin. – Grass and Forage Science 69: 315-322.
[18] Nadeem, M. A., Habyarimana, E., Çiftçi, V., Nawaz, M. A., Karaköy, T., Comertpay, G., Shahid, M. Q., Hatipoğlu, R., Yeken, M. Z., Ali, F., Ercişli, S., Chung, G., Baloch, F. S. (2018): Characterization of genetic diversity in Turkish common bean gene pool using phenotypic and whole-genome DArTseq-generated silico DArT marker information. – PloS One 13: e0205363.
[19] Orak, A., Nizam, I. (2004): Agronomic and morphological characters of some common vetch (Vicia sativa L.) genotypes under Trakya Region conditions. – Journal of Agronomy 3: 72-75.
[20] Ozkose, A., Ekiz, H. (2005): Effect of sowing time on yield and yield components in Bitter Vetch (*Vicia ervilia* (L.) Willd). – Selçuk University Faculty of Agriculture Journal 19: 13-20.
[21] Potokina E., Blattner F. R., Alexandrova T., Bachmann, K. (2002): AFLP diversity in the common vetch (*Vicia sativa* L.) on the world scale. – Theoretical and Applied Genetics 105: 58-67.
[22] Sabaghnia, N., Dehghani, H., Sabaghpour, S. H. (2006): Nonparametric methods for interpreting genotype× environment interaction of lentil genotypes. – Crop Science 46: 1100-1106.

http://www.aloki.hu ● ISSN 1589 1623 (Print) ● ISSN 1785 0037 (Online)
DOI: http://dx.doi.org/10.15666/aeer/1706_1520315217

[23] Sayar M. S., Anlarsal, A. E., Basbag, M. (2013): Genotype-environment interactions and stability analysis for dry-matter yield and seed yield in Hungarian vetch (*Vicia pannonica* CRANTZ.). – Turkish Journal of Field Crops 18: 238-246.
[24] Seydosoglu, S. (2014): Researches on determination yield and yield components of some common vetch (*Vicia sativa* L.) genotypes in ecological conditions of Diyarbakır. – Turkish Journal of Field Crops 1: 117-127.
[25] Tosun, F. (1974): Leguminous and Cereal Forage Crop Culture. – Atatürk University Faculty of Agriculture Publications, No: 242, Textbook Series No: 8, Erzurum.
[26] TUIK (2013): T. C. Prime Minister Turkey Statistical Institute. – http://www.turkstat.gov.tr and crop production statistics (accessed: 02/12/2017).
[27] Unal, S., Fırıncıoğlu, H. K., Mutlu, Z. (2016): Improvement of winter hardiness in common vetch lines for semi-arid conditions. – Bulgarian Journal of Agricultural Science 22: 756-766.
[28] Yan, W. (2001): GGE Biplot-a windows application for graphical analysis of multi-environment trial data and other types of two-way data. – Agron. J. 93: 1111-1118.
[29] Yucel, C., Gultekin, R., Inal, I., Avci, M. (2008): Determination of yield and yield characters of some common vetch (*Vicia sativa* L.) lines in Çukurova conditions. – Anadolu J. of AARI 18: 38-54.

http://www.aloki.hu ● ISSN 1589 1623 (Print) ● ISSN 1785 0037 (Online)
DOI: http://dx.doi.org/10.15666/aeer/1706_1520315217

COMPARATIVE ANALYSIS OF SOIL HEAVY METAL POLLUTION ON DIFFERENT ROADS: A CASE STUDY IN A TYPICAL INDUSTRIAL CITY OF CHINA

ZHANG, J.[1,2*] – YAO, D.[1]

[1]*School of Earth and Environment, Anhui University of Science and Technology, Huainan, Anhui 232001, P. R. China*

[2]*Wanjiang University of Technology, Ma'anshan, Anhui 243031, P. R. China*

**Corresponding author:Zhang, J.*
e-mail: szxyzj@sina.cn; phone: +86-555-522-6142; fax: +86-555-522-2777

(Received 2nd Jul 2019; accepted 16th Oct 2019)

Abstract. A total of 22 surface soil samples beside three different types of roads (trunk road, sub-trunk road and branch road) collected in Ma'anshan City, Anhui Province, China, were analyzed by inductively coupled plasma-atomic emission spectrometry (ICP-AES) and multivariate statistics. Besides, spatial distribution characteristics analysis was employed to identify the possible sources. The results indicate that the average concentrations of heavy metals following in the order of Mn > Pb > Co > Cr > As > Cd, and Cr content in the sub-trunk road are much lower than that in the trunk road and branch road. Geo-accumulation index shows that heavy metal pollution exists beside urban roads. Moreover, Cd pollution is the most serious, while Co and Pb are at a high pollution level. Potential ecological risk index shows that Cd poses a severe ecological risk; Pb and Co reach the medium ecological risk degree. Furthermore, two principal components (PC1 and PC2) of the heavy metal elements have been extracted by factor analysis, and the cluster analysis was consistent with the factor analysis. Based on spatial distribution characteristics, two sources have been identified: PC1 (Pb, Mn, Co) are contributed mainly by industrial pollution, and PC2 (Cd, As, Cr) are primarily influenced by traffic pollution.
Keywords: *trunk road, sub-trunk road, branch road, pollution assessment, spatial distribution characteristics, multivariate statistical*

Introduction

With the development of the automobile industry and transportation in China, the motorized travel mode of the public has experienced transformation from motorcycle to automobile, and the transportation structure has also undergone fundamental changes, making urban life increasingly convenient. According to statistics from the traffic management bureau of China's ministry of public security, by the end of the 2015 year, there were 279 million vehicles in the country, including 172 million automobiles. In 2015, the number of newly registered cars reached 23.85 million, and the net increase possessions was 17.81 million. However, the rapid development of roads and traffic also brings about a series of environmental pollution problems. For example, particulate matter containing heavy metals discharged by motor vehicles directly deposited in the road dust, or through wet and dry sedimentation deposited in the soil on both sides of the road, resulting in the accumulation of heavy metals in the soil and dust on both sides of the road. Especially in the current situation of poor vehicle emission performance and poor maintenance, heavy metal pollution problem is more prominent (Guo et al., 2008). Moreover, heavy metal is highly toxic and easy to accumulate in the soil, yet challenging to migrate and degrade. If the concentrations exceed a certain level, there will be higher biological toxicity. Once the soil is contaminated by heavy metals, it is

http://www.aloki.hu ● ISSN 1589 1623 (Print) ● ISSN 1785 0037 (Online)
DOI: http://dx.doi.org/10.15666/aeer/1706_1521915232

challenging to recover, causing serious damage to human body, environment, and even the whole food chain (Reza, et al., 2015; Hafeez, et al., 2019).

It is significant to clean the environment so as to avoid their entrance into the food chain because it is essential for protecting the health of animals and human beings. However, it is more realistic to understand the pollution status first, and then the sources of heavy metals, because not all of the heavy metals are released by anthropogenic activities, but they can also be produced by natural weathering processes of crust materials (Hashim, et al., 2011).

Pollution of soil in the current world is a major concern of the government and environment scientists, because of the importance of the soil for the survival and development of human society. Therefore, it is of great significance to analyze the pollution status of heavy metal elements in the soil along the traffic lines. Previous studies on heavy metals in soils on both sides of urban roads mainly focused on elements content, distribution characteristics, pollution status and ecological risk assessment (Afanasyeva, et al., 2019; Komendova, et al., 2018; Billah, et al., 2018; Sun, et al., 2015). However, there are few reports on the comparative study of soil heavy metal pollution besides different urban roads, especially in industrial cities. In this investigation, we selected trunk roads, sub-trunk roads and branch roads for systematic sampling and testing analysis in Ma'anshan city, a typical industrial city. In order to provide a scientific basis for the prevention and treatment of heavy metal pollution caused by highway traffic.

Materials and methods

Study area

Ma'anshan City is a steel industrial city that has risen since the late 1950s. It is located on the south bank of the lower Yangtze River and in the eastern part of Anhui Province, China. The longitude is from 118°21′38″ to 118°52′44″, and the latitude is from 31°46′42″ to 31°17′26″. Influenced by the humid climate of the northern subtropical monsoon, the city has an annual average precipitation of 1100 mm, and an annual average temperature of 15.7 degrees (centigrade). In 2015, the city's registered population was 2.277 million, and the urban resident population was 880,000. Ma'anshan City is located in the middle and lower reaches of the Yangtze River polymetallic metallogenic belt. This area is rich in mineral resources, and the main metal minerals are iron, vanadium, copper, gold, cobalt, which provide guarantee the development of local steel industry. The local manufacturers are mainly dominated iron and steel, special-purpose vehicles, high-grade cardboard, new process carbon black, electronic materials, biomedical, textile clothing, green food. Ma'anshan Iron & Steel Group is a large-scale steel joint enterprise and an important steel production base, as well as one of the largest industrial enterprises in Anhui Province. Geographical location of the study area is shown in *Figure 1*.

Sampling sites and sample collection

According to the urban road planning of the study area, the vehicle design speed of the trunk roads is 60 km/h, the number of vehicle lanes is 5~8, and the width of the road is 45~55 m. The design speed of motor vehicles on the sub-trunk roads is 40 km/h, the number of motor vehicle lanes is 4~6, and the width of the road is 40~50 m. As for the

http://www.aloki.hu ● ISSN 1589 1623 (Print) ● ISSN 1785 0037 (Online)
DOI: http://dx.doi.org/10.15666/aeer/1706_1521915232

branch roads, the design speed of motor vehicles is 30 km/h, the number of motor vehicle lanes is 3~4, and the width of the road is 15~30 m. Before sampling, the trunk roads, sub-trunk roads and branch roads in Ma'anshan city are divided according to the geographical location and the flow of motor vehicles. The trunk road is the main road connecting the main urban districts, mainly including Huolishan Avenue, Jiangdong Avenue, Cihuher Road, Jiuhua Road, Yinshan Road, Yushan Road and the railway line crossing the city. The sub-trunk road is a large number of general traffic roads in the city, which coordinates with the trunk road to form the urban trunk roads network, and plays the role of connecting various parts and distributing traffic, mainly including Hongqi Road, Jiashan Road, Huayu Road, Pingshan Road, Kangle Road. The branch road is an important part of the road system, mainly undertaking short-distance traffic, including Hunan West Road, Jiuhua West Road, Park Road, Xiyuan Road, Pinghu Road, Yucai Road and so on.

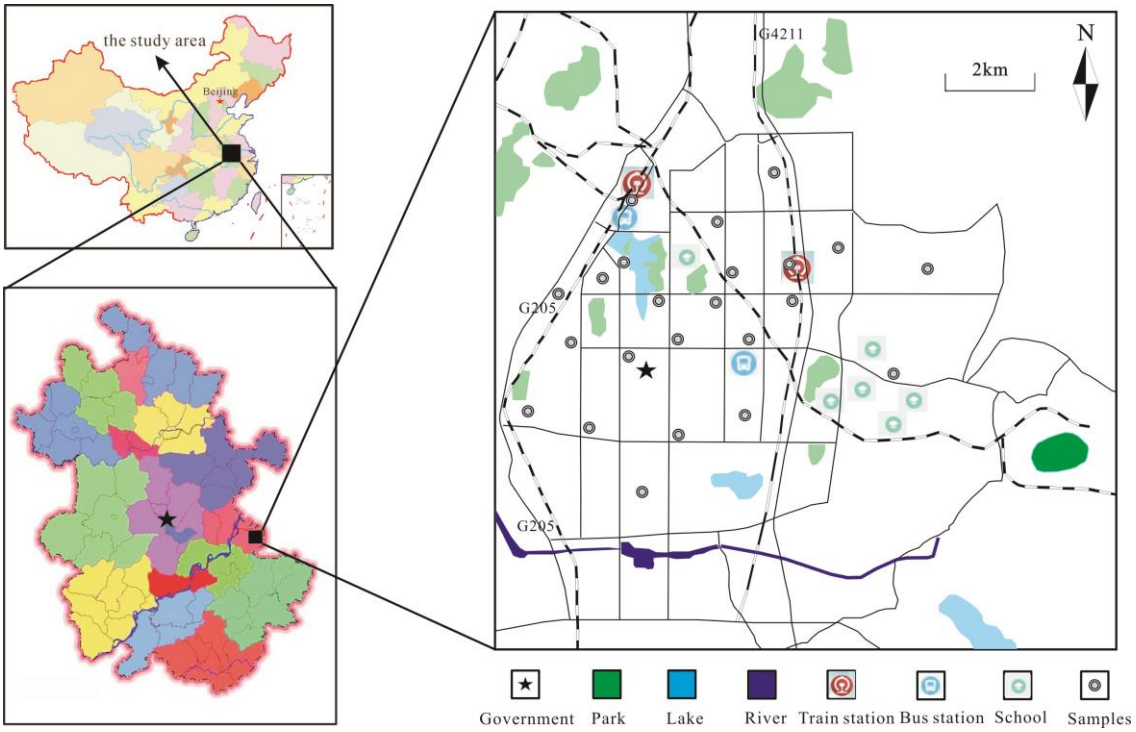

Figure 1. *Geographical location and sampling distribution of the study area*

In this study, samples collection was performed in December, 2015. Plant mulch and topsoil were removed before sample collection, and the sampling depth is 15 cm. For each soil sample, five sub-samples were collected from different cells within a grid of approximately 5 m^2 to form a composite sample to enhance the representativeness of the sample for each sampling site. The samples were stored in polyethylene packages that were transported back to the lab for chemical analysis. The samples were numbered sequentially on the bag. At the same time, GPS was used to determine the location of each sample point. A total of 22 surface soil samples were collected, including 11 trunk roads, 6 sub-trunk roads and 5 branch roads. Soil samples were firstly air-dried in the natural condition, sifted to remove stone and plant root debris, then ground to pass through a 200-mesh sieve.

http://www.aloki.hu ● ISSN 1589 1623 (Print) ● ISSN 1785 0037 (Online)
DOI: http://dx.doi.org/10.15666/aeer/1706_1521915232

Experimental method

(1) The authors weighed 0.1 g soil powder by electronic balance scale and put the soil into a tetrafluoroethylene digestion tank. Besides, 1 mL concentrated nitric acid, and 1 mL hydrofluoric acid is subsequently added. The authors put the sealed digestion tank in the steel sleeve, tightened the lid, and put it into the oven (190 °C) to heat for 20 h. Then take the steel sleeve out of the oven for cooling, take out the digestion tank, heat it on a hot plate (140 °C) to near dry, add 4 mL concentrated nitric acid and 4 mL of deionized water. Then put the digestion tank into the steel sleeve, tighten the lid, put it in the oven at 150 °C for 2 h, take out the steel can for cooling. After cooling, remove the digestion tank, transfer the liquid from the digestion tank into a 100 mL volumetric bottle, and wash the polytetrafluoroethylene with a certain amount of deionized water for 2 to 3 times. All the washing liquid is poured into the volumetric flask. Finally, the nitric acid solution was prepared, in which concentrated nitric acid 2 mL and deionized water 98 mL were used to titrate the volumetric flask.

(2) Using ICP-AES to determine the volume of solution in a volumetric flask, the internal standard of the element was selected, and the calibration curve was drawn. The concentration in the sample solution was calculated by regression equation to determine the heavy metal element content of the soil.

The above analysis and test were carried out at the Engineering Research Center of Coal Exploration, Anhui Province, China.

Analysis methods

Geoaccumulation index

The geoaccumulation index, also known as the Muller index, was proposed by German scientist Muller and developed in Europe as a quantitative index to study heavy metal pollution in sediments and other substances. The index of geoaccumulation (I_{geo}) ensures the assessment of contamination degrees by comparing the current and pre-industrial concentrations (Muller, 1969), and is calculated as follows.

$$I = log_2[C_n/KB_n] \quad \text{(Eq.1)}$$

In *Equation 1,* C_n means the measured content of the element in the sediment; B_n represents the geochemical background value; and K is the coefficient obtained by considering the variation of the background value that may be caused by the rocks differences in different places (in general, the K value is 1.5). Moreover, the geoaccumulation index is classified as *Table 1*. This method takes into account not only human-made pollution factors and environmental geochemical background values but also takes into account the factors that may change background values due to natural diagenesis, which makes up for the shortcomings of other evaluation methods effectively (Jia, et al., 2009; Chai, et al., 2006)

Potential ecological risk index

Potential ecological risk index is a method for evaluating the pollution degree of heavy metals in soil or sediments and their potential ecological hazards. The potential ecological risk index can calculate as follows.

http://www.aloki.hu ● ISSN 1589 1623 (Print) ● ISSN 1785 0037 (Online)
DOI: http://dx.doi.org/10.15666/aeer/1706_1521915232

$$C_f^i = C_s^i / C_n^i \quad \text{(Eq.2)}$$

$$E_r^i = T_r^i \times C_f^i \quad \text{(Eq.3)}$$

$$RI = \sum_{i=1}^{n} E_r^i \quad \text{(Eq.4)}$$

In *Equation 2,* C_f^i means the enrichment coefficient of heavy metal; C_s^i means the concentration of heavy metal in the sample; C_n^i means the reference value, generally taking the national or local environmental standard value in soil as the reference value (Fan et al., 2010); In *Equation 3,* E_r^i means the potential ecological hazard coefficient of individual; T_r^i means the toxicity response coefficient of heavy metal, the toxicity response coefficients were Cd = 30 > As = 10 > Pb = Co = 5 > Cr = 2 > Mn = 1 (Aiuppa, et al., 2003; Armagan, et al., 2008), respectively; In *Equation 4,* RI means the potential of ecological risk of multiple metals. The classification criteria of heavy metals potential ecological risk index are listed in *Table 2*.

Table 1. *Classification of index of geoaccumulation*

I_{geo}	Classification	Degree of pollution
$5 < I_{geo} \leq 10$	6	Extremely serious pollution
$4 < I_{geo} \leq 5$	5	Strong-extreme pollution
$3 < I_{geo} \leq 4$	4	Strong pollution
$2 < I_{geo} \leq 3$	3	Medium-strong pollution
$1 < I_{geo} \leq 2$	2	Medium pollution
$0 < I_{geo} \leq 1$	1	Light pollution
$I_{geo} \leq 0$	0	No pollution

Table 2. *Ranking standard of potential ecological risk hazards*

E_r^i	Single ecological hazard	RI	Overall ecological hazard
< 40	Low	<150	Low
40~80	Moderate	150~300	Moderate
80~160	Heavier	300~600	Heavy
160~320	Heavy	>600	Serious
> 320	Serious		

This method not only considers the content of heavy metals in soil, but also considers the migration rule of toxicity of heavy metals in soil, the sensitivity to heavy metal pollution, and the difference of background value of heavy metals, eliminating the influence of regional differences. The degree of potential ecological risk of heavy metals classified reflects the characteristics of bioavailability, relative contribution, spatial differences and so on. Generally, potential ecological risk index is a comprehensive indicator reflecting the potential impact of heavy metals on the ecological environment (Fan et al., 2010).

http://www.aloki.hu ● ISSN 1589 1623 (Print) ● ISSN 1785 0037 (Online)
DOI: http://dx.doi.org/10.15666/aeer/1706_1521915232

Multivariate statistical analysis

Multivariate statistical analysis is a method of using mathematical statistics to study multivariate problems. It includes regression analysis, discriminant analysis, cluster analysis, principal component analysis, factor analysis, correspondence analysis and so on. It has been widely applied in education, medicine, economics, environmental science and other disciplines. Multivariable statistical analysis provides an alternative method to identify pollution sources, and many scholars use this method to identify the pollution sources of soil or sediment (Aiuppa, et al., 2003; Armagan, et al., 2008; Reisenhofer, et al., 1996; Sun, et al., 2012).

Factor analysis uses a few factors to describe the relationship between multiple indicators, several same-class variables with relatively close correlations with each type of variable becoming a factor, and fewer factors reflecting most of the original information (Zhang, 2004). The general steps are summarized as follows: (1) standardizing raw data, which does not change the correlation coefficients between variables, and eliminate the influence of different variables dimension; which not change the correlation coefficient between variables, on the contrary, it can eliminate the influence of the dimension of different variables. (2) calculating the correlation coefficient matrix of the normalized data and its corresponding eigenvalues and eigenvectors; (3) using the maximum variance method for orthogonal rotation. This process can make the factor load polarized, which easy to find the information represented by the factor; (4) determining the number of factors, calculating the score of factors, and making corresponding statistical analysis.

Cluster analysis is a simple multivariate analysis method that classifies the research objects according to their characteristics (Zhang, 2004). The basic idea of cluster analysis is to use quantitative statistical analysis method to find some statistics that can measure the degree of affinity between samples or variables. Subsequently, based on these statistics, some samples (or variables) with greater similarity are aggregated into one group and others (or variables) are aggregated into another group.

The multivariate statistical analysis methods mentioned above are all completed by International Business Machines Corporation (IBM) SPSS software. IBM SPSS is a software product and related service program developed by IBM for statistical analysis, data mining, predictive analysis, and decision support tasks. It has been applied to various fields of natural science, technological science, and social science.

Visualization analysis

SigmaPlot is an advanced statistical analysis and scientific drawing software developed by Systat Software Company. The software integrates graphics drawing and data analysis. It has been applied to medicine, life sciences, engineering and environmental sciences due to its simple operation and high efficiency. In this study, SigmaPlot software (version 12.5) was used to construct a three-dimensional model of the spatial distribution of heavy metals in the soil of Ma'anshan city of Anhui Province, China.

Results

Content characteristics of heavy metals

The statistical analysis results of heavy metals in both sides along the road in Ma'anshan city of China are shown in *Table 3,* and the statistical analysis of the data was performed by

http://www.aloki.hu ● ISSN 1589 1623 (Print) ● ISSN 1785 0037 (Online)
DOI: http://dx.doi.org/10.15666/aeer/1706_1521915232

IBM SPSS statistic software (version 19). According to *Table 1,* the contents of soil heavy metals in this area varied in a certain range. Among them, Pb content ranged from 193 to 711 ug/g (average 463 ug/g); Cd content ranged from 6.8 to 22.25 ug/g (average 12.55 ug/g); Co content ranged from 284 to 395 ug/g (average 349 ug/g); As content ranged from 2.25 to 63.85 ug/g (average 49.21 ug/g); Mn content ranged from 298 to 717 ug/g (average 467 ug/g); and Cr content ranged from 3.05 to 253 ug/g (average 85.19 ug/g), respectively. The contents following the order of Mn > Pb > Co > Cr > As > Cd.

Table 3. *Statistical analysis of heavy metals in soils (ug/g)*

	Pb	**Cd**	**Co**	**As**	**Mn**	**Cr**
Minimum value	193	6.8	284	2.25	298	3.05
Maximum value	711	22.25	395	63.85	717	253
Mean value	463	12.55	349	49.21	467	85.19
Standard deviation	168	4.94	34.11	15.55	119	84.31
Variance	28285	24.44	1164	241.75	14126	7108
Coefficient of variation (CV)	0.36	0.39	0.1	0.32	0.25	0.99
Skewness	-0.013	0.986	-0.615	-2.189	1.141	0.825
Kurtosis	-1.266	1.13	-0.593	5.77	0.413	0.433
Soil background value Ma'anshan (Liu, 2012)	24.43	0.264	—	10.553	—	86.4
Soil background value in Anhui (Environmental Monitoring of China, 1990)	26.6	0.07	16.3	9	530	66.5
Nationals soil background value (Environmental Monitoring of China, 1990)	26	0.08	12.7	11.2	583	61

Coefficient of variation (CV, represents the ratio of the standard deviation to the mean) is an index that can be used for identifying the anthropogenic contribution degree for pollution in environmental studies (Sarkar, et al., 2010; Sun, et al., 2017), previous studies revealed that when CV < 0.10 and > 0.90 mean low and high anthropogenic contributions, respectively. In this study, the CV of the elements in the study area are following in the turn: Cr > Cd > Pb > As > Mn > Co, and Cr reached 0.99, which was a strong variation, while Mn, Pb, Co, Cr, As and Cd were relatively low (<0.40). The results indicate that anthropogenic activities have probably influenced the soil to a certain degree.

Figure 2 shows the distribution of heavy metal elements in different types of road. The contents of Pb, Co and Mn in the soils on both sides of trunk roads, sub-trunk roads and branch roads are higher and its differences are smaller, while the contents of Cd, As and Cr are relatively lower. The contents of Cr in sub-trunks road are much lower than those in trunks road and branch road.

Pollution assessment

In this study, Ma'anshan City soil background value, Anhui Province soil background value and Chinese national soil background value were selected value for reference (*Table 3*). Geo-accumulation index analysis on both sides of different roads in Ma'anshan urban area was conducted, and the results show in *Table 4* and *Figure 3,* I_{geo-1}, I_{geo-2} and I_{geo-3} represent the geoaccumulation indexes calculated by the soil background values of Ma'anshan city, Anhui Province and Chinese, respectively.

http://www.aloki.hu ● ISSN 1589 1623 (Print) ● ISSN 1785 0037 (Online)
DOI: http://dx.doi.org/10.15666/aeer/1706_1521915232

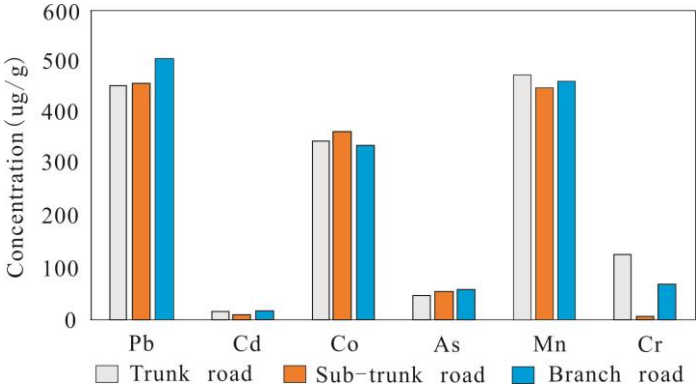

Figure 2. *Distribution of heavy metal elements in different types of road*

Table 4. *Soil heavy metals in different roads on both sides of the geo-accumulation index*

	Trunk roads	**Sub-trunk roads**	**Branch roads**	**Trunk roads**	**Sub-trunk roads**	**Branch roads**	**Trunk roads**	**Sub-trunk roads**	**Branch roads**
	I_{geo-1}			I_{geo-2}			I_{geo-3}		
Pb	3.63	3.64	3.78	3.51	3.52	3.66	3.54	3.55	3.69
Cd	5.23	4.45	5.23	7.15	6.36	7.14	6.96	6.17	6.95
Co	-	-	-	3.82	3.90	3.79	4.18	4.26	4.15
As	1.53	1.76	1.81	1.76	1.99	2.04	1.45	1.67	1.72
Mn	-	-	-	-0.74	-0.83	-0.79	-0.88	-0.96	-0.92
Cr	-0.06	-4.54	-0.97	0.32	-4.16	-0.59	0.45	-4.04	-0.47

According to *Table 4,* no matter which soil background value is taken as reference, soil heavy metals on both sides of urban trunk roads, sub-trunk roads and branch roads have a certain degree of pollution. The Cr and Mn element are non-polluting in the branch roads and the secondary trunk roads. For the trunk roads, if we refer to the soil background value of Ma'anshan City, Cr is non-polluting, if we compare with Anhui Province soil background value and the national soil background value, Cr belongs to mildly polluted. It indicates that the Mn element has not been polluted, Cr element has not been polluted or intensively polluted, and the overall condition is good. Co and Pb were strong pollutions, and Cd was a strong-extremely pollution level in the soil samples on both sides of the urban road in Ma'anshan City.

Risk assessment

The potential ecological risk index of heavy metals pollution in soils on both sides of different roads in Ma'anshan urban area is shown in *Table 5*. According to *Table 5,* the potential ecological hazard coefficients of each element follow the order of Cd > Co > Pb > As > Cr > Mn, which is consistent with the results of the geo-accumulation index method. Among them, Cd reached a severe degree of ecological risk, Pb, Co was a relatively severe degree of ecological risk, As was a moderate degree of ecological risk, Mn, Cr was a low degree of ecological risk. Besides, for the overall potential ecological hazard index (RI), the ecological risk of the sub-trunk road is lower than that of the trunk road and the branch road, but they also have reached the level of potential severe ecological risk. Therefore, the soil heavy metal pollution on both sides

http://www.aloki.hu ● ISSN 1589 1623 (Print) ● ISSN 1785 0037 (Online)
DOI: http://dx.doi.org/10.15666/aeer/1706_1521915232

of the road in Ma'anshan city is a potential severe ecological hazard, and even Pb, Co has reached a relatively severe ecological risk. Therefore, in the process of soil environmental treatment in the future, we should strengthen the management of Cd, Pb and Co.

Table 5. *Potential ecological risk index of heavy metals on both sides of the road*

	E_r^i						RI
	Pb	**Cd**	**Co**	**As**	**Mn**	**Cr**	
Trunk roads	87.51	5592	136	40.94	0.82	4.09	5861
Sub-trunk roads	88.02	3238	143.4	47.87	0.77	0.18	3518
Branch roads	97.11	5569	133.3	49.53	0.79	2.17	5852

Discussion

From the previous analysis, we can find that there is an interesting phenomenon here, that is, in the soil on both sides of the road in the study area, the concentration of heavy metals in the branch road is higher than that in the sub-trunk road, or even similar to that in the trunk road. The main reason we consider is that the traffic conditions of the branch roads are not as good as those of the main and secondary roads. According to China Urban Road Engineering Design Code (Ministry of Housing and Urban-Rural Construction of the People's Republic of China, 2016), the width of branches is generally 15-20 m, while the width of sub-trunk and trunk roads can reach 40-55 m, which directly determines the speed of motor vehicles on the road. Generally speaking, the speed of branches is lower than 30 km/h or even lower. However, the sub-trunk road can reach 30-50 km/h and the trunk road can reach 60 km/h. Therefore, in the process of driving on the branch road, automobiles are bound to brake frequently and even start their cars. Brake, brake and tire wear will inevitably lead to the increase of heavy metal content, which makes the heavy metal content of branch road higher than that of sub-trunk road.

In addition, soil heavy metals are not only related to the background value of bedrock (or parent material), but also influenced by the mode and intensity of human activities. According to the analysis above, soil heavy metals in this area are polluted to some extent. In order to identify pollution sources effectively, factor analysis was carried out for heavy metals. According to the eigenvalue and cumulative variance contribution rate, two factors were extracted (*Table 6*). The explanations of variance were 49.512%, 36.764%, respectively, and the complete explanations of cumulative variance were 86.277%. For the sake of understanding the information represented by each principal component, the factors are rotated using the maximum variance method (*Table 6*). According to *Table 6* and *Figure 3,* PC1 is controlled by Cd, As, and Cr, and PC2 is controlled by Co, Mn and Pb.

Xie (2010) holds that Cd mainly originates from industrial activities, such as smelting, electroplating, batteries, metal processing and so on. The sources of Cd in soil are mainly attributed to natural and human activities. The former mainly comes from the background values of rocks and soils, while the latter mainly comes from industrial "three wastes" (waste water, waste gas, and waste residue) and large amounts of Cd-containing fertilizers. Industrial waste gas is the main source of air Cd pollution. The content of Cd in the air of remote areas is generally lower than 1.0 pg/mL, but the

http://www.aloki.hu ● ISSN 1589 1623 (Print) ● ISSN 1785 0037 (Online)
DOI: http://dx.doi.org/10.15666/aeer/1706_1521915232

concentration of Cd in the atmosphere around industrial areas is higher (Zeng, et al., 2005). Dry and wet deposition of Cd contaminants in the atmosphere is also a significant import cause of soil Cd pollution. Higher concentrations of Cd can enter the soil through rainfall or sedimentation. Plants absorb some of Cd and cause pollution, and the remained Cd accumulates in the soil. Combining the actual situation of iron and steel industry in Ma'anshan city and the spatial characteristics of Cd, As and Cr (*Fig. 4*), it can be concluded that factor 1 is affected by industry. Lead is a tracer element of automobile exhaust emissions (Lv, et al., 2013). In general, The background value of a lead in the environment is very low, and lead is mainly derived from tetraethyl lead anti-explosive agent in gasoline. However, the gasoline combustion process can be decomposed to produce inorganic lead and lead-containing oxides. After being discharged from the vehicle exhaust, it settles in the soil on both sides of roads through the atmosphere. According to this, PC2 can be expressed as the impact of road traffic. So far, it can be concluded that the primary sources of Cd, As and Cr in soils on both sides of urban roads are industrial "three wastes", while the emission of urban traffic exhaust and the wear of urban tires are the essential sources of Pb, Mn and Co pollution in soil samples.

Table 6. *Total variance explained and component matrices for heavy metal contents*

Components	**Initial Eigenvalues**			**Extracting sums of squares**			**Extraction sums of squared loadings**		
	Total	% of variance	Cumulative %	Total	% of variance	Cumulative %	Total	% of variance	Cumulative %
1	3.007	50.112	50.112	3.007	50.112	50.112	2.971	49.512	49.512
2	2.17	36.165	86.277	2.17	36.165	86.277	2.206	36.764	86.277
	Component matrix					Rotated component matrix			
		PC1	PC2				PC1	PC2	
	Pb	-0.313	-0.84			Pb	-0.133	-0.887	
	Cd	0.979	0.067			Cd	0.944	0.268	
	Co	-0.329	0.924			Co	-0.513	0.835	
	As	0.865	-0.257			As	0.9	-0.072	
	Mn	0.447	0.723			Mn	0.288	0.8	
	Cr	0.945	-0.133			Cr	0.952	0.066	

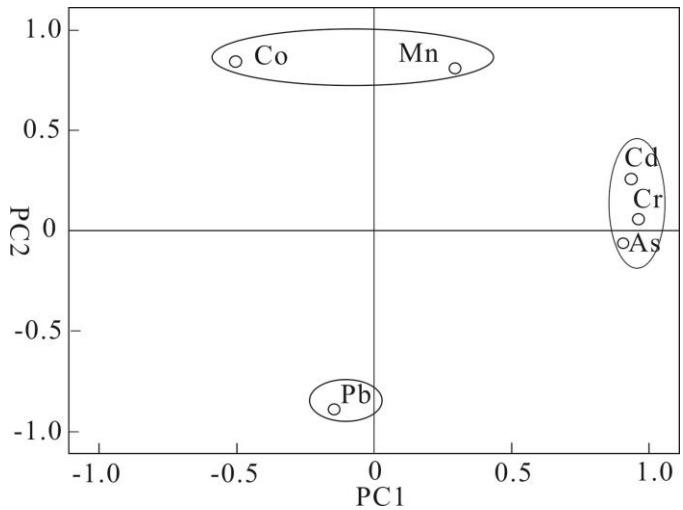

Figure 3. *Factor loading of soil heavy metal sources*

http://www.aloki.hu ● ISSN 1589 1623 (Print) ● ISSN 1785 0037 (Online)
DOI: http://dx.doi.org/10.15666/aeer/1706_1521915232

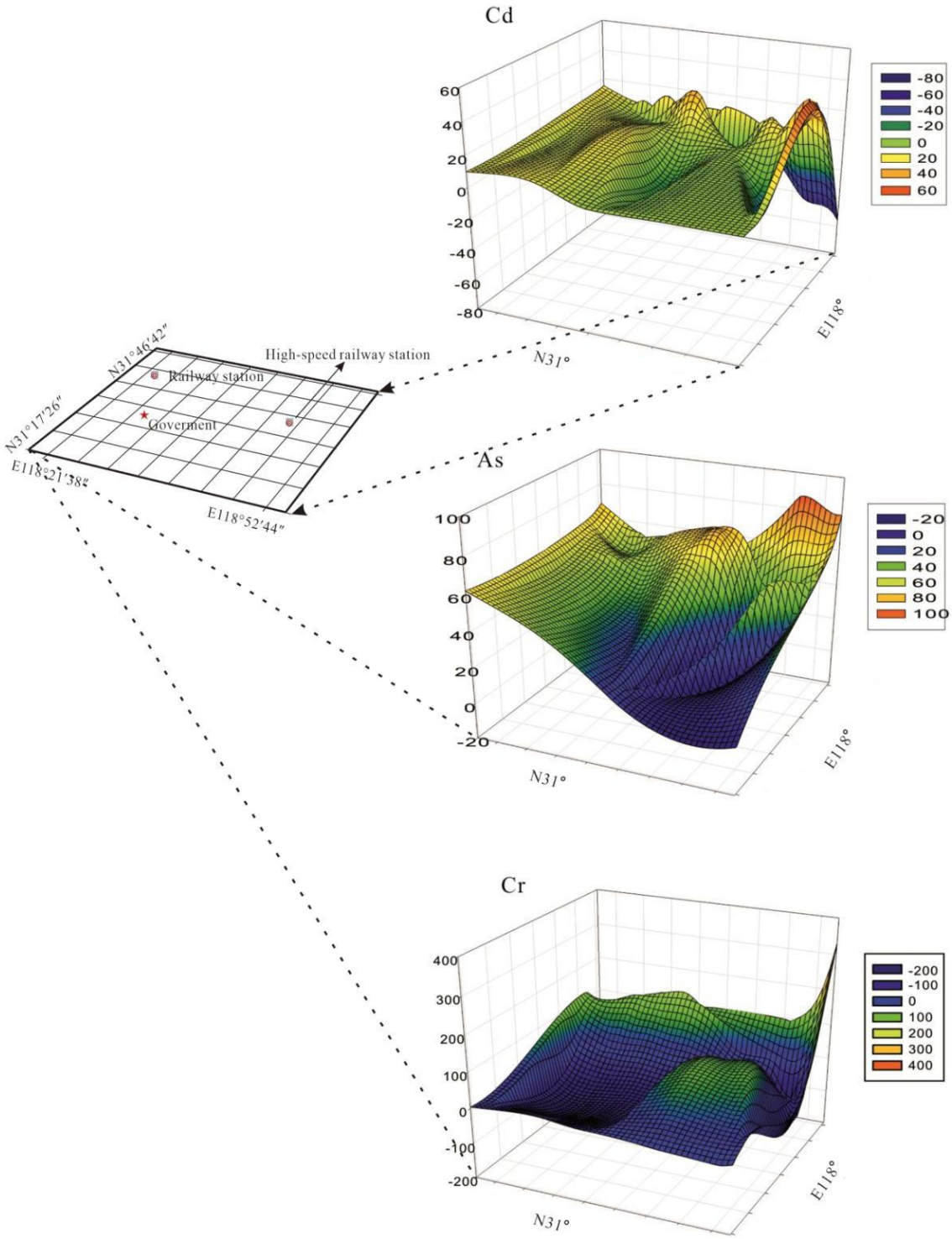

Figure 4. *Spatial distribution characteristics of Cd, As and Cr*

In order to verify the accuracy of the factor analysis method, the soil heavy metal elements were clustered (*Fig. 5*). Clustering results are ideal, and can be divided into three categories: Cd-Cr-As, Co-Mn, Pb clustered into a single group, consistent with the results of factor analysis.

http://www.aloki.hu ● ISSN 1589 1623 (Print) ● ISSN 1785 0037 (Online)
DOI: http://dx.doi.org/10.15666/aeer/1706_1521915232

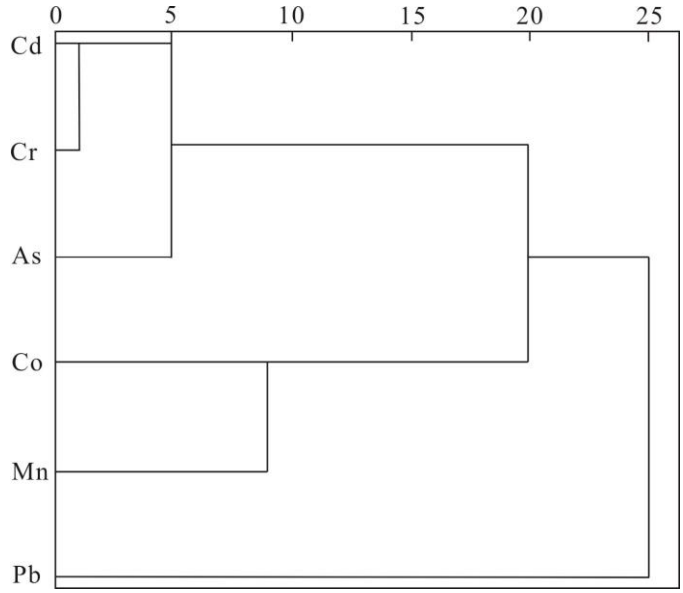

Figure 5. *Cluster analysis of soil heavy metals*

Conclusion

The contents of heavy metals in soils on both sides of roads in Ma'anshan city changed within a certain range, and the average contents were following in the order of Mn > Pb > Co > Cr > As > Cd from large to small. For the soils on both sides of different types of roads, the content of Pb, Co and Mn is higher than that of Cd, As and Cr, and the concentrations of Cr in sub-trunk roads is lower than that of trunk roads and branch roads.

Pollution assessment showed that heavy metals in the soil on both sides of urban trunk roads, sub-trunk roads and branch roads were polluted to a certain extent. Mn is no pollution; Cr element had not been polluted or intensity pollution, the overall situation was good; Co, Pb belonged to strong pollution level; Cd belonged to the severe pollution level.

The risk assessment showed that Cd was a severe ecological risk, Pb and Co was a severe ecological risk, As was a moderate ecological risk, Mn and Cr was a low ecological risk. According to the total potential ecological hazard index, the ecological risk of the sub-trunk road is lower than that of the main road and the sub-trunk road, which has reached a severe potential ecological risk degree. In the future soil quality management process, it is particularly necessary to strengthen the management of cadmium, lead and cobalt pollution.

Two principal components of the six heavy metal elements have been extracted by factor analysis. Combining with the spatial distribution characteristics of heavy metals, two sources have been identified, PC1 (Pb, Mn, Co) and PC2 (Cd, As, Cr). The former are contributed mainly by industrial pollution, while the latter are primarily influenced by traffic pollution.

Recommendations

Taking Ma'anshan City, Anhui Province as an example, this paper discussed the pollution status and sources of heavy metals in soil along the trunk roads, sub-trunk

http://www.aloki.hu ● ISSN 1589 1623 (Print) ● ISSN 1785 0037 (Online)
DOI: http://dx.doi.org/10.15666/aeer/1706_1521915232

roads and branch roads of the city, which has a certain practical significance for the prevention and control of heavy metals pollution in urban soil. In the future research, we need to pay more attention to the study of heavy metal pollution level and occurrence in road ash layer, rainfall and other media. We can even make a comparative study of the heavy metal pollution in the soil on both sides of different roads in industrial and non-industrial cities, so as to explore the impact of different types of cities and different specifications of road traffic activities on the distribution of heavy metals, and evaluate their pollution, so as to provide theoretical support for the prevention and control of heavy metal pollution.

Acknowledgments. This work was financially supported by National Natural Science Foundation of China (No. 51474008), Excellent top talent cultivation project in higher education institutions in Anhui Province (No. gxyq2019151), Key Natural Science Research Projects of Universities in Anhui Province (No. KJ2019A1281), Research Project of Wanjiang University of Technology (No. WG18026).

REFERENCES

[1] Afanasyeva, L. V., Ayushina, T. A.. (2019): Accumulation of heavy metals and biochemical responses in Siberian larch needles in urban area. – Ecotoxicology 28(5): 578-588.
[2] Aiuppa, A., Bellomo, S., Brusca, L., D'Alessandro, W., Federico, C. (2003): Natural and anthropogenic factors affecting groundwater quality of an active volcano (Mt. Etna, Italy). – Applied Geochemistry 18(6): 863-882.
[3] Armagan, G., Turgut, C. (2008): Analysis of environmental pollution with multivariate statistical techniques. – Fresenius Environmental Bulletin 17(8): 978-984.
[4] Billah, M. M., Kokushi, E., Uno, S. (2019): Distribution, geochemical speciation, and bioavailable potencies of cadmium, copper, lead, and zinc in sediments from urban coastal environment in Osaka Bay, Japan. – Water Air Soil Pollut 230: 157. doi.org/10.1007/s11270-019-4196-8.
[5] Chai, S. W., Wen, Y. M., Zhang, Y. L., Zhao, J. F. (2006): Application of index of geoaccumulation to pollution evaluation of heavy metals in soil. – Journal of Tongji University (Natural Science) 34(12): 1657-1661.
[6] Environmental Monitoring of China (1990): Background Values of Soil Elements in China. – China Environmental Science Press, Beijing.
[7] Fan, S. X., Gan, Z. T., Li, M. J., Zhang, Z. Q., Zhou, Q. (2010): Progress of assessment methods of heavy metal pollution in soil. – Chinese Agricultural Science Bulletin 26(17): 310-315.
[8] Guo, G. H., Lei, M., Chen, T. B., Song, B., Li, X. Y. (2008): Effect of road traffic on heavy metals in road dusts and roadside soils. – Acta Scientiae Circumstantiae 28(10): 1937-1945.
[9] Hafeez, F., Zafar, N., Nazir, R., Javeed, H. M. R., Rizwan, M., Faridullah, et al. (2019): Assessment of flood-induced changes in soil heavy metal and nutrient status in Rajanpur, Pakistan. – Environmental Monitoring and Assessment 191(4).
[10] Hashim, M. A., Mukhopadhyay, S., Sahu, J. N. (2011): Remediation technologies for heavy metal contaminated groundwater. – Journal of Environmental Management 92(10): 2355-2388.
[11] Jia, Z., Zhou, H., Zhao, Z., Tao, S., Zhang, B., Zhao, L. (2000): The application of the index of geoaccumulation to evaluate heavy metal pollution in sediments in the Benxi section of the Taizi River. – Acta Scientiarum Naturalium Universitatis Pekinensis 36(4): 525-530.

http://www.aloki.hu ● ISSN 1589 1623 (Print) ● ISSN 1785 0037 (Online)
DOI: http://dx.doi.org/10.15666/aeer/1706_1521915232

[12] Komendova, R., Jezek, S.. (2018): The distribution of platinum in the environment in large cities: a model study from Brno, Czech Republic. – International Journal of Environmental Science and Technology 16(7): 3109-3116.
[13] Liu, H. (2012): Research on Assessment of Heavy Metal Pollution in the Soil in Ma' Anshan Key Mining Area. – Hefei University of Technology, Hefei.
[14] Lv, J. S., Liu, Y., Zhang, Z. L. (2013): Factorial kriging and stepwise regression approach to identify environmental factors influencing spatial multi-scale variability of heavy metals in soils. – Journal of Hazardous Materials 261: 387-397.
[15] Ministry of Housing and Urban-Rural Construction of the People's Republic of China (2016): Code for Urban Road Engineering Design. – Ministry of Housing and Urban-Rural Construction, China, pp. 1-93.
[16] Muller, G. (1969): Index of geoaccumulation in sediments of the Rhine River. – Journal of Geology 2(3): 109-118.
[17] Reisenhofer, E., Adami, G., Favretto, A. (1996): Heavy metals and nutrients in coastal, surface seawaters (Gulf of Trieste, northern Adriatic Sea): an environmental study by factor analysis. – Fresenius Journal of Analytical Chemistry 354(5-6): 729-734.
[18] Reza, S. K., Baruah, U., Singh, S. K., Das, T. H. (2015): Geostatistical and multivariate analysis of soil heavy metal contamination near coal mining area, northeastern India. – Environmental Earth Sciences 73(9): 5425-5433.
[19] Sarkar, D., Datta, R., Hannigan, R. (2007): Concepts and Applications in Environmental Geochemistry. – Elsevier, Amsterdam.
[20] Sun, L. H., Gui, H. R., Xu, D. S., Huang, S. L. (2012): Heavy metal pollution in rural area of china: a case study of pond sediments from Sixian County, Northern Anhui Province. – Fresenius Environmental Bulletin 21(2): 263-268.
[21] Sun, L. H., Cheng, B. X., Chen, S. H. (2017): Trace metal concentrations in the river water near the urban area, a case study in Suzhou, northern Anhui province, China. – Fresenius Environmental Bulletin 26(6): 4017.
[22] Sun, Z. B., Liu, B. J., Zhou, J., Hu, B. B., Meng, W. Q., Wang, Z. L. (2015): Heavy metals pollution and ecological risk assessment on urban street dust of Tianjin. – Environmental Science & Technology 38(8): 244-250.
[23] Xie, H. F., Fang, F., M., Wang, H. D. (2010): Research progress on heavy metal pollution in urban street dust. – Environmental Pollution and Control 32(5): 78-81.
[24] Zeng, Y. M., Mao, K. M., Li, Y. M. (2005): Damage of the cadmium (Cd) pollution in soil and its control. – Journal of Yunnan Agricultural University 20(3): 360-365.
[25] Zhang, W. T. (2004): SPSS Advanced Statistical Analysis Tutorial. – Higher Education Press, Beijing.

http://www.aloki.hu ● ISSN 1589 1623 (Print) ● ISSN 1785 0037 (Online)
DOI: http://dx.doi.org/10.15666/aeer/1706_1521915232

IMPACT OF DIFFERENT FERTILIZATION REGIMES ON THE BIOMASS PRODUCTION OF PERENNIAL GRASS *MISCANTHUS* × *GIGANTEUS* IN SLOVAKIA

KOTRLA, M.* – PAUKOVÁ, Ž. – PRČIK, M.

Faculty of European Studies and Regional Development, Slovak University of Agriculture in Nitra, Tr. A. Hlinku 2, 949 76 Nitra, Slovakia
(phone: +421-37-641-5613; fax: +421-37-641-5730)

**Corresponding author*
e-mail: marian.kotrla@uniag.sk; phone: +421-37-641-5613

(Received 2nd Jul 2019; accepted 16th Oct 2019)

Abstract. *Miscanthus* energy grass, being one of the renewable energy sources, has suitable soil-climatic conditions for growth in the regions of Slovakia. The lifespan of a *Miscanthus* plantation is 15-20 years. In the specific conditions of southwestern Slovakia, the plantation productivity was studied under the application of NPK fertilizer after one third of the plantation's lifespan. The measurement interval was 14 days throughout the growing period of the monitored years (2016-2018). Morphometric and selected ecophysiological and production parameters were analysed under three fertilization variants (C – control, V1 – variant with the application of 50 g NPK per individual and V2 – variant with the application of 100 g NPK per individual). Variant V2 had the highest values of the studied parameters in all monitored years and out of all fertilization variants. The statistical significance of differences in growth indicators between the years of cultivation and total biomass production between variants and years was confirmed. Dynamics of stomatal density per mm^2 were determined by microrelief method in three randomly selected clumps of *Miscanthus* × *giganteus* in control and in each variant of fertilization in 2016. There are significant differences in the density stomatal density and width between the control and variants of fertilization in 2016.
Keywords: *NPK fertilizer, energy grass, growth parameters, production, stomata*

Introduction

The use of biomass as a renewable energy source is rapidly increasing worldwide. Further increases in the use of these resources can be achieved through technological development, long-term planning, implementation of integration strategies and appropriate investment. Biomass as an energy source is an easily accessible that is both technologically and ecologically acceptable. The focus on biofuels is increasing due to the reduction of dependence on fossil fuels and the stimulation of rural development and agriculture.

Miscanthus × *giganteus* is a perennial, warm-season Asian grass with the C_4 photosynthetic pathway. In the search for ideal bioenergy crops following the oil crisis of the 1970s, evaluations to determine the biomass yield potential of giant miscanthus began across Europe. *Miscanthus* × *giganteus* grows to a height of 4 m, produces shoots with a length of up to 4 m and a diameter of approx. 10 mm, and can be grown in one location for up to 15–20 years (Dubis et al., 2017).

Miscanthus plantations have several environmental benefits compared to annual crops. These plantations can use water and nutrients more efficiently, they are resistant to pests and diseases and do not require annual soil cultivation (Cadoux et al., 2012). *Miscanthus* × *giganteus* grows very rapidly and produces a high yield of aboveground biomass at relatively low input costs (Clifton-Brown et al., 2015; Roncucci et al., 2015).

http://www.aloki.hu ● ISSN 1589 1623 (Print) ●ISSN1785 0037 (Online)
DOI: http://dx.doi.org/10.15666/aeer/1706_1523315244

The cultivation and high yield of *Miscanthus* × *giganteus* are characterized in various climatic and environmental conditions. Higher productivity has also been identified on less productive and marginal soils (Stavridou et al., 2017). *Miscanthus* × *giganteus* has low soil fertility requirements, tolerates cultivation on light soils and has no high nitrogen requirements (Kołodziej et al., 2016).

Several authors have observed the impact of *Miscanthus* plantation fertilization on its production (Maughan et al., 2012; Dierking et al., 2016). Larsen et al. (2014) reported that fertilization of the *Miscanthus* × *giganteus* did not increase the yield. Other authors suggest that yields can be increased by applying annual fertilizers to older stands (Arundale et al., 2014).

To predict the production potential of energy plant species in a particular region, it is necessary to identify the basic morphometric and ecophysiological parameters and their changes due to environmental factors. The shape of organs, especially leaves, often shows the ability to adapt to environmental conditions. These include irradiation density, drought, and extreme temperatures, change anatomy and leaf morphology, skin thickness, stomata density, size, and degree of stomata openness. The stomata density is a relatively plastic feature that is potentially adaptable to environmental changes (Killi et al., 2018; Mwendia et al., 2019).

This article presents the results of the influence of various fertilization variants applied after the sixth growing period of the stand on the morphometric, selected ecophysiological and production parameters of the *Miscanthus* × *giganteus* plantation in the conditions of southwestern Slovakia.

Materials and Methods

Plant materials

Perennial grass *Miscanthus* × *giganteus* is a vital triploid hybrid (57 chromosomes) often used in the field trials. The planting material consisted of rhizomes from Hannes Stelzhammer Austria. The fresh weight of the rhizomes was different (on average 2.61 g), the length of the rhizomes was on average 67.5 mm.

Model locality of the research area

The model area of experimental research of growing fast-growing plants on agricultural soils is located in Slovakia in Nitra region in the cadastral area of Kolíňany (48°21'21" N 18°12'25" E). The area has an altitude of 80 m above sea level. The soil is moderate (loam), pH values range from 7.18 to 7.35, humus content is 1.16 to 2.50% (Demo et al., 2013). In terms of exposure, it is a plane without manifestation of areal erosion. According to climatic conditions the research area belongs to the warm, very dry, lowland climate region. The basic climatic parameters (*Table 1*) were evaluated based on the measurements of the Meteorological station located near the research area. The values were compared with the long-term average values of the 50-year period of 1951-2000 in the Nitra region, according to Slovak Hydrometeorological Institute (*Fig. 1*). The average annual air temperature for the period 2015 to 2018 was 10.99°C (the deviation from the long-term average was higher by 1.13°C) and the average annual precipitation was 483.67 mm (the deviation from the long-term annual total was lower by 63.93 mm). The average length of the main growing period during the monitored years in the research area is 186 days.

http://www.aloki.hu ● ISSN 1589 1623 (Print) ●ISSN1785 0037 (Online)
DOI: http://dx.doi.org/10.15666/aeer/1706_1523315244

The research plot was established in 2010. The plant material was planted in a 1 m × 1 m planting distance on an area of 100 m^2. The optimum *Miscanthus* stand density is 10,000 plants per hectare, depending on the abiotic conditions of the habitat – temperature and water. In the research area, *Miscanthus* × *giganteus* rhizomes were planted in wet soil at the beginning of the growing period at a depth of up to 10 cm.

Table 1. *Average monthly precipitation and course of average monthly temperatures in 2015-2018 in the research area in Kolíňany, southwestern Slovakia*

4 year average / month	I	II	III	IV	V	VI	VII	VIII	IX	X	XI	XII
mm	40.20	50.10	45.34	35.20	53.50	46.65	54.75	22.90	27.48	23.35	43.95	40.25
°C	-1.02	1.95	6.05	11.42	16.27	20.17	21.77	21.81	16.39	10.48	5.55	1.05

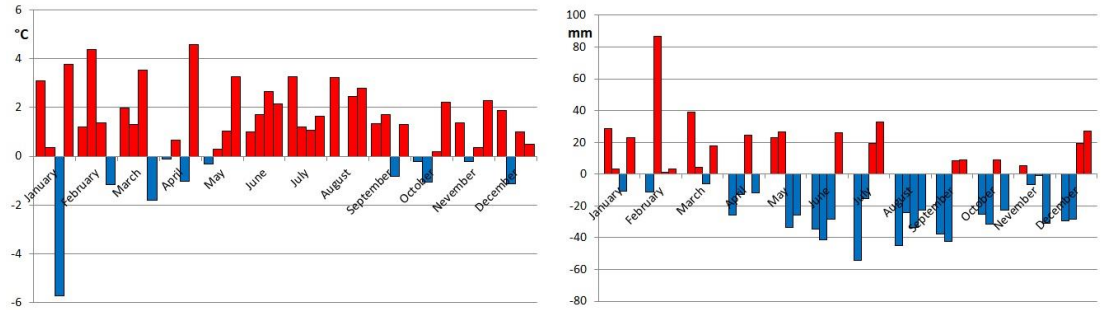

Figure 1. *Average monthly deviations of temperature and average monthly deviations of total precipitation in 2015-2018 from the long-term average in research area in Kolíňany*

Application of different fertilization regimes

The mineral granular fertilizer N P K (15-10-10), type designation B.1, was applied before to the beginning of the growing period (beginning of April in 2016 – after the sixth growing year since the plantation was established). The fertilizer contained 15% of total nitrogen [N], 10% of total phosphorus [P_2O_5] and 10% of water-soluble potassium [K_2O]. The fertilizer was applied at the centre of the tillering circle of each individual before the growth of new shoots (*Fig. 2*).

In the V1 variant, 50 g of fertilizer per individual (500 kg per hectare of which 75 kg of nitrogen, 50 kg of phosphorus and 50 kg of potassium per ha) was applied. In the V2 variant, 100 g per individual (1000 kg per hectare of which 150 kg of nitrogen, 100 kg of phosphorus and 100 kg of potassium per ha) was applied and variant C (control) remained without fertilization. A schematic representation of the research area with variants of fertilization is shown in *Fig. 3*.

Monitored the growth parameters and production yield

Basic morphometric characteristics of *Miscanthus* × *giganteus* were studied for all three variants. The interval of measurement of morphometric parameters was every 14 days during the whole growing period of the monitored years (2016–2018) at 14 selected individuals. The height of the individuals was determined as the distance from the soil surface to the top of the longest shoot. The number of shoots on individual plants

http://www.aloki.hu ● ISSN 1589 1623 (Print) ●ISSN1785 0037 (Online)
DOI: http://dx.doi.org/10.15666/aeer/1706_1523315244

was determined by counting the shoots in the clump. The shoot thickness was measured on the selected shoot of the studied individuals. The number of leaves on the shoot and the number of leaves in the clump were monitored. Accordingly, the senescence of the leaves on the shoot was determined. In the case of energy plants, a destructive determination of the biomass weight is carried out outside the growing period. After cutting, the total weight of the selected individuals (seven clumps from each variant) was determined. The biomass sample was oven-dried at 105°C and the dry weight was determined. The moisture content of *Miscanthus* × *giganteus* ranges from 19 to 22%. The total weight of the above-ground biomass was calculated (t/ha).

Figure 2. *The tillering circle of Miscanthus × giganteus before the application of the fertilizer in the beginning of the seventh growing period*

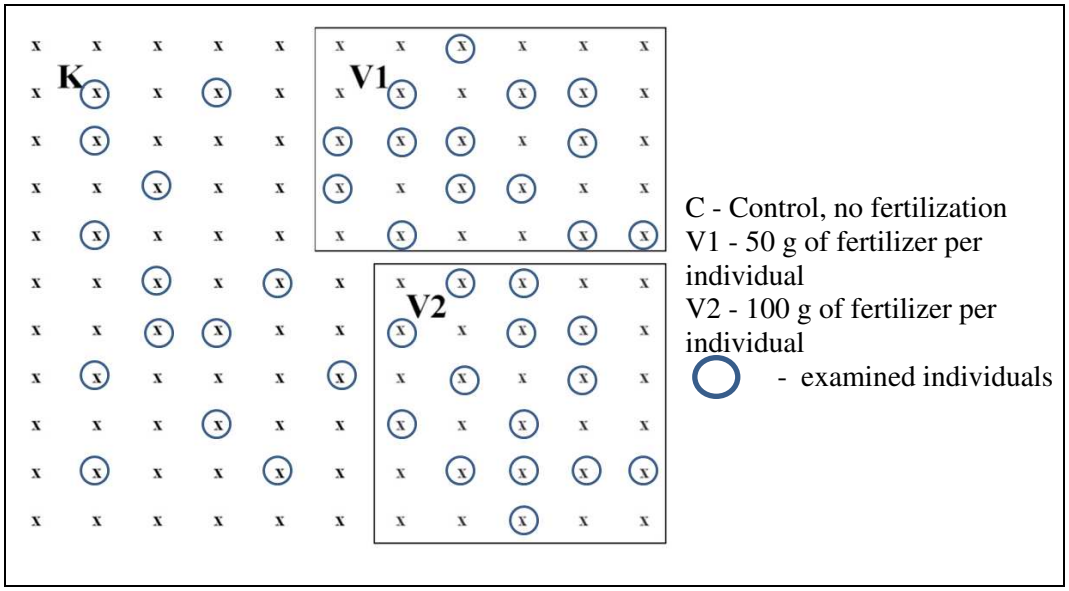

Figure 3. *The schema of application of different fertilization regimes in the research area of Miscanthus × giganteus*

The stomatal density per mm^2 in the leaves was determined non-destructively in three selected clumps in each fertilization variant in 2016. The indicated number of the stomata refers to one treatment. The analysis was performed on the designated stem on the senescence leaf located in the middle of the stand (approximately fifth leaf from the

http://www.aloki.hu ● ISSN 1589 1623 (Print) ●ISSN1785 0037 (Online)
DOI: http://dx.doi.org/10.15666/aeer/1706_1523315244

bottom) exposed to western direction by a micro-relief method. Samples were collected in the middle part of the leaf outside the main vein on the adaxial (top) and abaxial (bottom) skin surface in August 2016. The evaluation of preparations was carried out by optical microscope Axiostar plus, Carl Zeiss lens, CP-Achromat 40 × / 0.65, 10 × eyepiece PI / 18, Canon Utilities software Zoom Browser EX 4.6 and hardware Acer Travel Mate 4600, Canon Power Shot A 95. In total, 144 microscopic view-fields were considered in the counting. Stomata length and width were measured on 162 randomly selected stomata.

Statistical analysis of morphometric and production data was performed using STATISTICA 12 by StatSoft. Inc. ANOVA analysis was used to analyse the statistical significance of morphometric and production indicators between years and variants. The result is statistically significant if $p < 0.05$ or statistically highly significant if $p < 0.001$. Statistical significance of stomatal differences was evaluated by LSD-test.

Results and Discussion

The basic prerequisite for the efficiency of growing plants for energy purposes is the ability of the species to adapt to the region's climate. Without fertilization, *Miscanthus × giganteus* has produced an economically efficient above-ground biomass every year since planting in 2010 (Kotrla et al., 2017; Kotrla and Prčík, 2018). In 2016, fertilization was applied to identify the need for fertilization in relation to the growth and production of biomass of the energy grass.

Morphometric analysis of Miscanthus × giganteus

Production of usable biomass for energy use is realized through the formation of above-ground organs. The growth of above-ground organs is limited by the length of the growing period. In 2016 and 2017, the growing period was 176 days and in 2018 it was 219 days. In 2018, average daily temperatures above 10°C began at the beginning of April and ended at the beginning of November compared to previous years.

Fig. 4 represents the course of growth of selected parameters between 2016 and 2018 in the different fertilization variants. The V2 variant had the highest values of the growth parameters in all studied years and fertilization variants. The comparison of the monitored growth parameter values at the end of the growing period 2016 to 2018 is shown in *Table 2*.

The number of shoots in the clump increases at the beginning of the growing season culminates in the second half of June and subsequently decreases (*Fig. 4a*). The shoots continue with intense growth and higher production of green leaves in June, resulting in the drying of shoots in the middle of the clump. The reason for reducing the number of shoots is the competitive struggle of shoots for space, especially light.

In each year, V2 variant has reached the highest height of the clump. When comparing the variants, V1 variant was on average lower by 3.5% and the C variant was on average lower by 6.5% than V2 variant at the end of the growing period. Based on the analysis of the shoot thickness, it can be stated that the shoots in the V1 and C variants were on average thinner by 1.8% and 2.7%, respectively compared to the variant V2. The number of leaves is closely related to the height of the shoots. The dynamics of the number of green leaves on the shoots is shown in *Fig. 4d and e*. Senescence of the leaves (yellowing and drying) begins in the second half of June and continues until the end of the growing period. The ratio of green and dry leaves on the shoot intensely changes in early October

http://www.aloki.hu ● ISSN 1589 1623 (Print) ●ISSN1785 0037 (Online)
DOI: http://dx.doi.org/10.15666/aeer/1706_1523315244

in favour of dry leaves. This trend continues until the end of the growing period when the photosynthetic activity of the leaves ends. The average number of leaves in the variant V2 was 3.3% higher than in the variant V1 and 15.2% higher compared to the variant C. Drazić et al. (2017) examined the impact of fertilization on *Miscanthus* stand in Serbia. They confirmed the increase in morphometric characteristics of fertilized variants. Pogrzeba et al. (2017) also monitored plant growth parameters for fertilized and non-fertilized varieties in Poland. They found no significant differences between these variants.

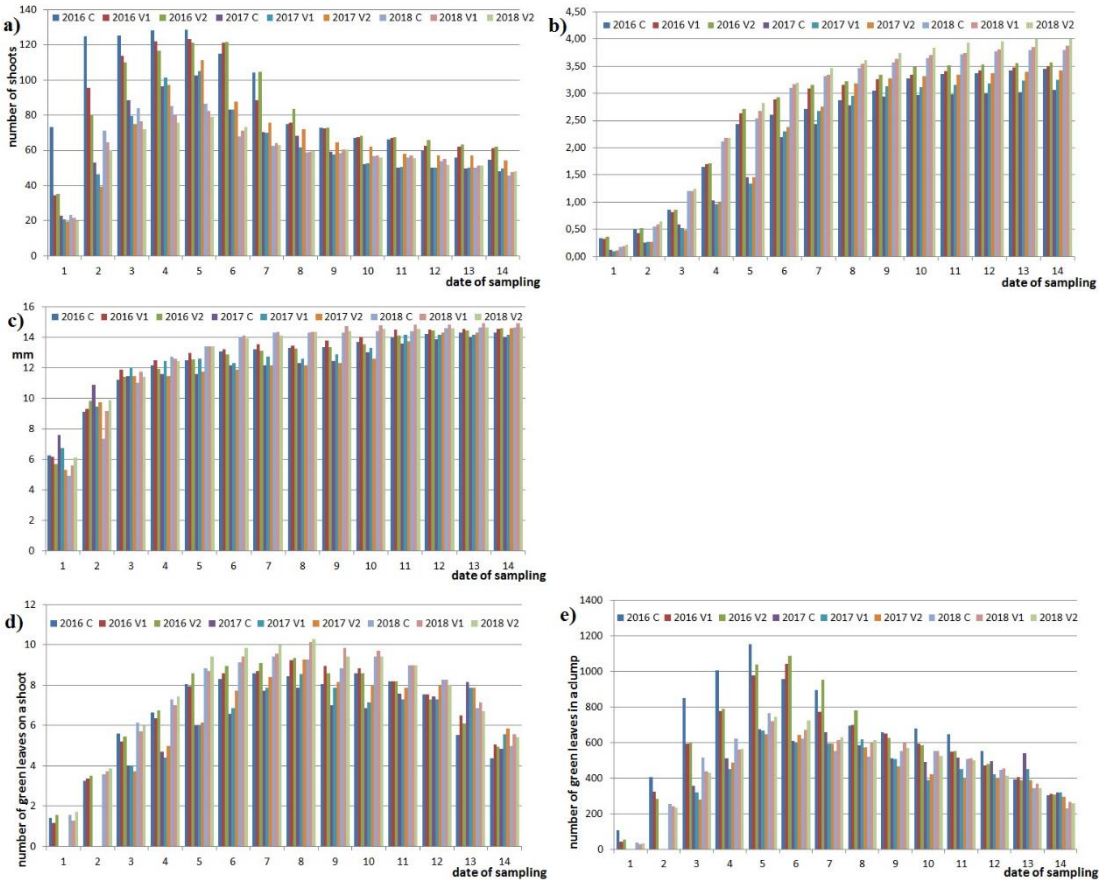

Figure 4. *Morphometric analysis of Miscanthus × giganteus stand in monitored years and fertilization variants [a) number of shoots in a clump, b) height of shoots in a clump, c) shoot diameter, d) number of green leaves on a shoot, e) number of green leaves in a clump]*

The analysis confirmed the statistical significance of the growth parameters between the variants and years. The statistical significance of the growth rate values over the growing period is statistically highly significant only between the monitored years. The reason is the different climatic conditions during the growing period of these years. In each year, the values of the growth parameter between variants C, V1 and V2 are statistically non-significant (*Table 3*).

Production potential of Miscanthus × giganteus

Annual production of the shoots of *Miscanthus × giganteus* represents an amount of biomass usable as an alternative energy source. *Fig. 5* shows the variability of the biomass

http://www.aloki.hu ● ISSN 1589 1623 (Print) ●ISSN1785 0037 (Online)
DOI: http://dx.doi.org/10.15666/aeer/1706_1523315244

samples collected at the end of February in the following year. Differences in the above-ground biomass weight between years and variants are statistically highly significant (*Fig. 6*). The statistical significance between years (p = 0.00029) and also between variants (p = 0.00019) was confirmed at the significance level of 0.001.

Table 2. *Comparison of growth parameter values at the end of the growing period 2016 to 2018 in different fertilization variants*

Year	2016			2017			2018		
Variant / growth parameter	**C**	**V1**	**V2**	**C**	**V1**	**V2**	**C**	**V1**	**V2**
number of shoots in a clump	54.64	61.29	62.29	48.05	49.71	54.29	45.71	47.57	48.14
height of shoots [m]	3.44	3.50	3.57	3.06	3.25	3.42	3.80	3.87	4.00
shoot diameter in a clump [mm]	14.31	14.54	14.60	14.00	14.14	14.57	14.62	14.63	14.93
number of green leaves on a shoot	4.37	4.94	5.07	4.86	5.57	5.86	5.00	5.43	5.57
number of green leaves in a clump	238.67	302.75	315.79	233.39	276.98	317.96	228.57	258.24	268.22

Table 3. *Statistical significance of selected growth and production parameters of Miscanthus × giganteus organs in the studied years and fertilization variants*

Parameter	Years		Variants	
	p-value	**S**	**p-value**	**S**
number of shoots	0.00001	***	0.85937	n
height of shoots	0.04148	*	0.79439	n
shoot diameter	0.03071	*	0.09866	n
number of green leaves on a shoot	0.01412	*	0.80012	n
number of green leaves in a clump	0.00032	***	0.73284	n
weight of an individual	0.00029	***	0.00019	***

S - Level of significance is defined as: n: non-significant impact, *: significant impact in P ≤ 0.05, **: P ≤ 0.01 and ***: P ≤ 0.001

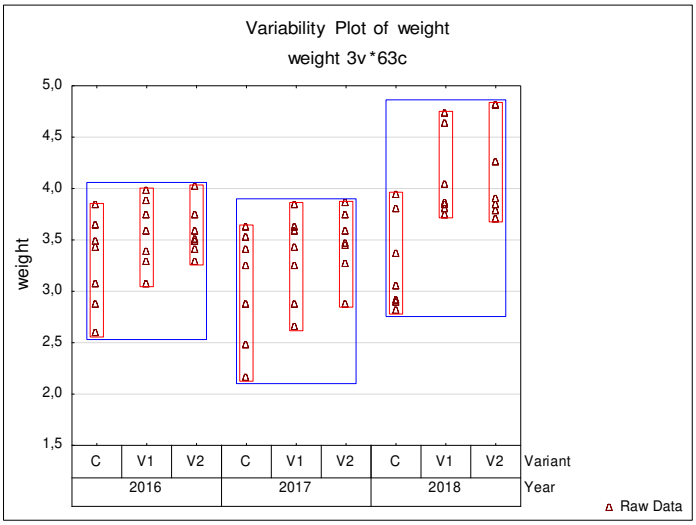

Figure 5. *Variability of biomass samples of the above-ground organs of Miscanthus × giganteus in the studied years and variants of fertilization*

http://www.aloki.hu ● ISSN 1589 1623 (Print) ●ISSN1785 0037 (Online)
DOI: http://dx.doi.org/10.15666/aeer/1706_1523315244

Biomass production increased every year in the research area. Since 2015, slight fluctuations in total biomass production have been monitored (*Table 4*). In 2015, the summer was characterized by low precipitation compared to the long-term average. After the application of fertilizer at the beginning of the 2016 growing period, an increase in biomass was observed in fertilized variants compared to the control variant. The variant without fertilization also produced 8.5% more biomass than in the previous year (2015). The difference between the yield in 2015 and biomass yield without fertilization in 2016 is statistically significant ($p = 0.01560$). When comparing the produced biomass between the non-fertilized and fertilized variants, it is possible to state the average increase in fertilized variants by 7.6% in 2016, 10.1% in 2017 and 13.5% in 2018.

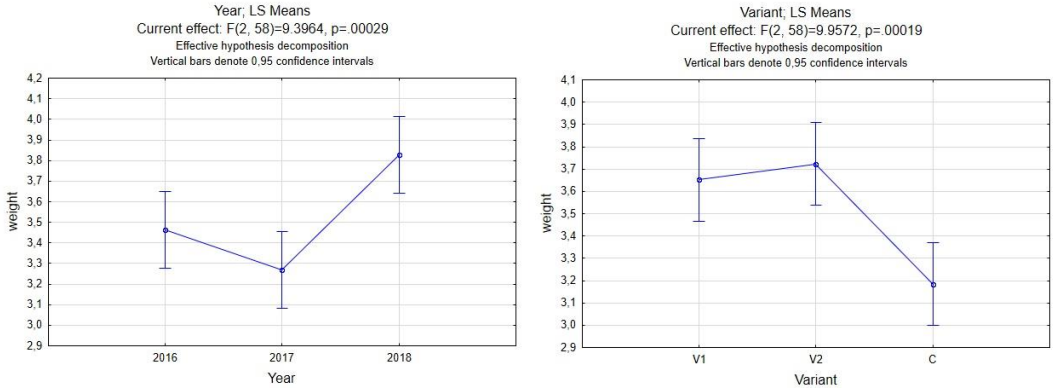

Figure 6. *Statistical analysis of the above-ground biomass weights in the studied years and fertilization variants*

Table 4. *The production of biomass of Miscanthus × giganteus in the fertilization variants since 2016 and compared with 2015 in the research plot in Kolíňany*

Year /Variant	2015	2016	2017	2018
Variant C (without fertilization)	30.1	32.69	30.39	32.97
Variant V1		35.03	33.13	37.17
Variant V2		35.74	34.51	39.1

Lower levels of the biomass produced in 2017 are the result of the climatic situation, especially low temperatures at the beginning of the growing period and spring frosts in late April and early May. The night frost, as a negative phenomenon in 2017, was recorded in the first decade of May (the minimum temperature of -0.196°C was on the 10th of May). These spring frosts negatively affected the growth of the shoots in 2017.

Iqbal et al. (2015) analyzed the stands of energy grasses in a period of ten years. They confirmed that the application of fertilizers did not significantly increase the yield of *Miscanthus*. On the contrary, Dubis et al. (2017) monitored the effect of different fertilization methods on *Miscanthus* productivity. The application of NPK fertilizer increased the biomass yield by 7.7% compared to the non-fertilized variant. Arundale et al. (2014) applied fertilization to older energy grass stand in Illinois, USA. They confirmed an increase in the yield of the fertilized variant compared to the non-fertilized variant by 25%. In the Midwest of the USA, Lee et al. (2017) confirmed a statistically highly significant increase in *Miscanthus* yield compared to the non-fertilized variant, but they did not confirm the differences in the total production between higher and lower

http://www.aloki.hu ● ISSN 1589 1623 (Print) ●ISSN1785 0037 (Online)
DOI: http://dx.doi.org/10.15666/aeer/1706_1523315244

fertilizer doses. Several authors have done fertilization experiments in the first years after planting. However, in the conditions of southwestern Slovakia, it was not necessary to apply fertilizer in the first years, as the energy grass had been reaching an economically profitable yield. The *Miscanthus* stand had shown the culmination of the yield after the sixth year since the establishment, so the fertilization was applied at the beginning of the seventh growing period (which is about a third of the plant's lifespan). Maksimović et al. (2018) observed the effect of fertilization in the first years of the establishment of the *Miscanthus* plantation in Serbia, but they did not find significant differences in biomass production. They confirmed that the profitability of the plantation is affected also by climatic conditions in individual years.

Analysis of the stomata of Miscanthus × giganteus leaves

Photosynthetic performance of *Miscanthus* leaves and their production ability is also influenced by the anatomical structure of assimilation organs. The density and the size of stomata are critical. The stomata play an irreplaceable role in venting the gases between the plant and the atmosphere and they are the place of regulated water discharge in the transpiration process. Their development and movements are indicated by environmental factors.

The number of stomata in leaves was statistically highly significantly affected by adaxial and abaxial leaf surface of the epidermis of *Miscanthus* × *giganteus* (LSD0,05 test ± 12.87). The ratio of stomata was 32:68 on the adaxial and abaxial leaf surface, respectively. The number of stomata per mm^2 of area varied from 97.8 ± 15.0 to 223.6 ± 28.2. Between control and variants of fertilization are significant differences in the density of stomata (LSD $_{0,05\ test}$ ± 7.19 on the adaxial skin, 11.24 on the abaxial skin) (*Fig. 7a*). On the contrary, Weng and Hsu (2001) found that the N treatment could increase the stomatal frequency on the adaxial surface in most tested *Miscanthus* clones in Taiwan, however, no significant effect was observed on that of the abaxial surface.

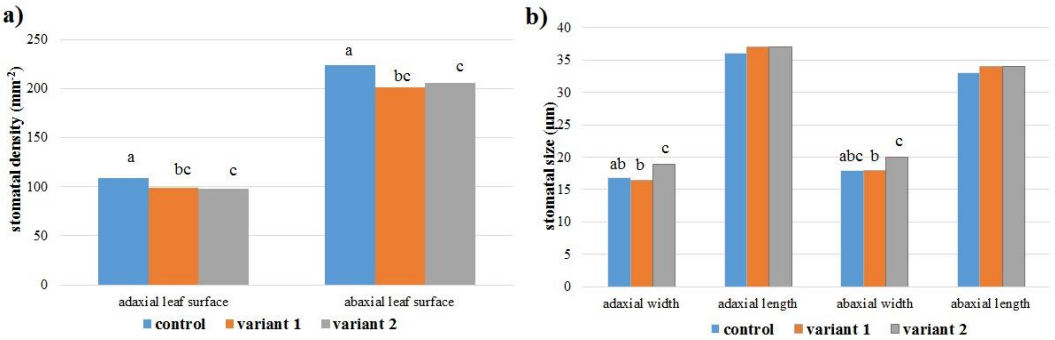

Figure 7. *a) The number of stomata per mm^2 of the adaxial and abaxial surface depending on the variants of fertilization. b) Statistical evaluation of significant differences in the size of stomata (µm) depending on fertilization. Values with different letters (a, b, c) in columns indicate statistically significant difference according to LSD test (P <0.05)*

The stomatal length ranged from 33.5 ± 2.1 µm to 37.4 ± 4.0 µm, and stomatal width from 16.6 ± 1.8 µm to 19.8 ± 2.6 µm (*Fig. 7b*). Rayburn et al. (2009) also compared the size of stomata of two *Miscanthus* genotypes in the USA and confirmed genotypic conditionality of the monitored indicator expressed by the average length of stomata of

http://www.aloki.hu ● ISSN 1589 1623 (Print) ●ISSN1785 0037 (Online)
DOI: http://dx.doi.org/10.15666/aeer/1706_1523315244

Miscanthus × *giganteus* 24.4 μm. Moon et al. (2018) recorded the average length of stomata of *Miscanthus* × *giganteus* ranging from 21 to 28.5 μm. In our observations, the average length of stomata of *Miscanthus* × *giganteus* was higher 35.6 μm.

Differences in stomatal width of leaves between control and variants of fertilization on the adaxial surface and between variants V of fertilization on the abaxial surface and V2 were highly significant (LSD 0,05 test ± 1.07 on the adaxial skin, 1.49 on the abaxial skin), while no significant differences were observed in stomatal lengths (*Fig. 7b*).

Conclusion

The plantation of *Miscanthus* × *giganteus* grown in soil-climatic conditions in south-western Slovakia produced an effective yield (more than 30 t/ha) of the above-ground biomass every year. At the beginning of the seventh growing period, NPK mineral granular fertilizer was applied in order to determine the effect of fertilization on crop yield after the first third of the plantation lifespan. The *Miscanthus* stand was divided into three variants, two with different fertilizer doses and one without fertilization. In the growing periods of 2016-2018, morphometric, selected ecophysiological and production parameters were measured. The morphometric analysis confirmed higher growth performance of the fertilized variants. The statistical analysis of the growth parameters is highly statistically significant only between the monitored years. In each year, the values of the growth parameters between the variants C, V1 and V2 were statistically non-significant. Differences between variants and years were statistically highly significant in total biomass production. Statistical significance between the years ($p = 0.00029$) and also between the variants ($p = 0.00019$) in the biomass production was confirmed at the significance level of 0.001.

As a factor affecting the production ability of the *Miscanthus* plantation, the density and size stomata of the *Miscanthus* leaves were analysed. Significant differences in the density of stomata (LSD 0,05 test ± 7.19, 11.24) and stomatal width (LSD 0,05 test ± 1.07, 1.49) were found between the control and variants of fertilization.

Miscanthus cultivated in southwestern Slovakia produced economically efficient yield despite fertilization. The difference in fertilized and non-fertilized variations ranges from 7.6 to 13.5%. The positive effect of fertilization on above-ground biomass production has been demonstrated. A possible negative phenomenon for the *Miscanthus* plantations production is the climatic conditions in each year of cultivation. However, fertilization at certain stages of the energy grass lifespan can maintain plantation production performance even in the later years of cultivation. The aim of further studies will be to find out the period of culmination and decrease in biomass production of *Miscanthus* × *giganteus* in the conditions of southwestern Slovakia and subsequently to apply another dose of fertilization.

Acknowledgements. This work was supported by the Grant Agency FESRD as projects no. 3/2017 and no. 2/2017, and by the AgroBioTech ITMS 26220220180.

http://www.aloki.hu ● ISSN 1589 1623 (Print) ●ISSN1785 0037 (Online)
DOI: http://dx.doi.org/10.15666/aeer/1706_1523315244

REFERENCES

[1] Arundale, R. A., Dohleman, F. G., Voigt, T. B., Long, S. P. (2014): Nitrogen fertilization does significantly increase yields of stands of *Miscanthus* × *giganteus* and *Panicum virgatum* in multiyear trials in Illinois. – Bioenergy Res. 7: 408-416.

[2] Cadoux, S., Riche, A. B., Yates, N. E., Machet, J. M. (2012): Nutrient requirements of *Miscanthus* × *giganteus*: conclusions from a review of published studies. – Biomass and Bioenergy 38: 14-22.

[3] Clifton-Brown, J., Schwarz, K. U., Hastings, A. (2015): History of the development of Miscanthus as a bioenergy crop: from small beginnings to potential realisation. – Biology and Environment: Proceedings of the Royal Irish Academy 115(1): 45-57.

[4] Demo, M., Bako, A., Húska, D., Hauptvogl, M. (2013): Biomass production potential of different willow varieties (*Salix* spp.) grown in soil-climatic conditions of South-Western Slovakia. – Wood research 58(4): 651-662.

[5] Dierking, R. M., Allen, D. J., Brouder, S. M., Volenec, J. J. (2016): Yield, biomass composition, and N use efficiency during establishment of four *Miscanthus* × *giganteus* genotypes as influenced by N management. – Biomass and bioenergy 91: 98-107.

[6] Drazić, G., Milovanović, J., Ikanović, J., Petrić, I. (2017): Influence of fertilization on *Miscanthus* × *giganteus* (Greef et Deu) yield and biomass traits in three experiments in Serbia. – Plant, Soil and Environment 63(4): 189-193.

[7] Dubis, B., Bułkowska, K., Lewandowska, M., Szempliński, W., Jankowski, K. J., Idźkowski, J., Kordala, N., Szymańska, K. (2017): Effect of different nitrogen fertilizer treatments on the conversion of *Miscanthus* × *giganteus* to ethanol. – Bioresource technology 243: 731-737.

[8] Iqbal, Y., Gauder, M., Claupein, W., Graeff-Hönninger, S., Lewandowski, I. (2015): Yield and quality development comparison between miscanthus and switchgrass over a period of 10 years. – Energy 89: 268-276.

[9] Killi, D., Bussotti, F., Gottardini, E., Pollastrini, M., Mori, J., Tani, C., Papini, A., Ferrini, F., Fini, A., Richardson, A. D., Ashton, P. M. S., Berlyn, G. P., McGrody, M. E., Cameron, I. R. (2018): Photosynthetic and morphological responses of oak species to temperature and [CO_2] increased to levels predicted for 2050. – Urban forestry & urban greening 31: 26-37.

[10] Kołodziej, B., Antonkiewicz, J., Sugier, D. (2016): *Miscanthus* × *giganteus* as a biomass feedstock grown on municipal sewage sludge. – Industrial Crops and Products 81: 72-82.

[11] Kotrla, M., Mandalová, K., Prčík, M. (2017): Regional disparities in Slovakia and the Czech Republic in the context of sustainable growing of energy plants. – European Journal of Sustainable Development 6(2): 165-180.

[12] Kotrla, M., Prčík, M. (2018): Assessment of climatic parameters during the vegetation period in terms of efficiency of growing of energy plants in Slovakia regions. – Scientific papers series management, economic engineering in agriculture and rural development 18(1): 203-209.

[13] Larsen, S. U., Jørgensen, U., Kjeldsen, J. B., Lærke, P. E. (2014): Long-term *Miscanthus* yields influenced by location, genotype, row distance, fertilization and harvest season. – BioEnergy Research 7(2): 620-635.

[14] Lee, M. S., Wycislo, A., Guo, J., Lee, D., Voigt, T. (2017): Nitrogen fertilization effects on biomass production and yield components of *Miscanthus* × *giganteus*. – Frontiers in plant science 8: 544.

[15] Maksimović, J., Dželetović, Ž., Dinić, Z., Stanojković-Sebić, A., Cvetković, O., Pivić, R. (2018): Assessment of the main agro-ecological parameters effects on the cultivation of *Miscanthus* × *giganteus* grown on marginal soils in the Republic of Serbia. – Agriculturae Conspectus Scientificus 83(1): 113-117.

[16] Maughan, M., Bollero, G., Lee, D. K., Darmody, R., Bons, S., Cortese, L., Murphy, J., Gaussoin, R., Sousek, M., Williams, D., Williams, L., Miguez, F., Voigt, T. (2012):

http://www.aloki.hu ● ISSN 1589 1623 (Print) ●ISSN1785 0037 (Online)
DOI: http://dx.doi.org/10.15666/aeer/1706_1523315244

Miscanthus × *giganteus* productivity: the effects of management in different environments. – GCB Bioenergy 4: 253-265.

[17] Moon, Y. H., Lee, J. E., Yu, G. D., Song, Y. S., Lee, Y. H., Kim, K. S., Lee, K. B., Cha, Y. L. (2018): Ploidy level and reproductive organ abnormality in interspecific hybrids between tetraploid *Miscanthus sacchariflorus* and diploid *M. sinensis* bred from a single cross. – Industrial Crops and Products 116: 182-190.

[18] Mwendia, S., Yunusa, I., Sindel, B., Whalley, R., Bruhl, J. (2019): Osmotic adjustment, stomata morphology and function show contrasting responses to water stress in mesic and hydric grasses under elevated CO_2 concentration. – Photosynthetica 51(1): 121-131.

[19] Pogrzeba, M., Rusinowski, S., Sitko, K., Krzyżak, J., Skalska, A., Małkowski, E., Ciszek, D., Werle, S., McCalmont, J. P., Mos, M., Kalaji, H. M. (2017): Relationships between soil parameters and physiological status of *Miscanthus* × *giganteus* cultivated on soil contaminated with trace elements under NPK fertilisation vs. microbial inoculation. – Environmental Pollution 225: 163-174.

[20] Rayburn, A. L., Crawford, J., Rayburn, C. M., Juvik, J. A. (2009): Genome size of three *Miscanthus* species. – Plant Molecular Biology Reporter 27(2): 184-188.

[21] Roncucci, N., Nassi O Di Nasso, N., Tozzini, C., Bonari, E., Ragaglini, G. (2015): *Miscanthus* × *giganteus* nutrient concentrations and uptakes in autumn and winter harvests as influenced by soil texture, irrigation and nitrogen fertilization in the Mediterranean. – Gcb Bioenergy 7(5): 1009-1018.

[22] Stavridou, E., Hastings, A., Webster, R. J., Robson, P. R. (2017): The impact of soil salinity on the yield, composition and physiology of the bioenergy grass *Miscanthus* × *giganteus*. – GCB Bioenergy 9(1): 92-104.

[23] Weng, J. H., Hsu, F. H. (2001): Gas exchange and epidermal characteristics of *Miscanthus* populations in Taiwan varying with habitats and nitrogen application. – Photosynthetica 39(1): 35-41.

http://www.aloki.hu ● ISSN 1589 1623 (Print) ●ISSN1785 0037 (Online)
DOI: http://dx.doi.org/10.15666/aeer/1706_1523315244

EFFECTS OF GROWING LOCATION AND COLD STORAGE ON NUTRITIONAL VALUES OF PURPLE CARROT (*DAUCUS CAROTA* SSP. *SATIVUS* VAR. *ATRORUBENS* ALEF) GENOTYPES

CEBECI, E.[1*] – HANCI, F.[2]

[1]*Bati Akdeniz Agricultural Research Institute, Muratpasa, Antalya, Turkey*

[2]*Department of Horticulture, Faculty of Agriculture, Erciyes University, Kayseri, Turkey*

**Corresponding author*
e-mail: esrac3@hotmail.com; phone: +90-532-583-3701

(Received 4th Jul 2019; accepted 16th Oct 2019)

Abstract. Purple carrots (*Daucus carota* ssp. *Sativus* var. *Atrorubens* Alef) have received much attention as a natural source of antioxidants, which is confirmed to reduce risk of cancer when consumed frequently. In this study, six purple carrot genotypes (DC17, DC28, DC33, DC34, DC36, and DC37) collected from Anatolia, produced under two distant and very different ecological conditions. Field trials have been planned according to the randomized complete blocks design with three replications. After the harvest, antioxidant activity, total phenolic, total flavonoid, anthocyanin, total soluble solid, titratable acidity and invert sugar values of stored and non-stored roots were assessed. Anthocyanin, total flavonoid and total phenolic content of the six genotypes ranked between 11.3-1,692.4 mg/l. 412.7-3,242.4 mg KE/100 g and 491.4-5,772.3 mg GAE/100 g respectively. Antioxidant activity was determined to be between 9,848.46-3,274.62 µmol TE 100 g^{-1}, 4,676.9-235.6 µmol TE 100 g^{-1} according to 1.1-diphenyl-2-picrylhydrazyl (DPPH) and ferric reducing ability of plasma (FRAP) assays respectively. According to the results, the studied parameters of the genotypes were significantly affected. Different ecological conditions affected the phytochemical composition of the purple carrot roots. The effect of storage on all parameters except total flavonoid content was found significant.
Keywords: *anthocyanin, antioxidant activity, flavonoids, phenolic, titratable acidity*

Introduction

Carrot (*Daucus carota* L.) is a biennial, cool-season vegetable, belonging to *Apiaceae* family. In terms of both production areas and market value, it is amongst the top-ten most important vegetable crop in the world (Simon et al., 2008). Cultivated carrot is divided into two main varieties; the western carrot with orange, yellow or white roots and the oriental carrot with black, purple, red or rarely yellowish roots (Esatbeyoglu et al., 2016).

Production of orange carrot has increased initially in large areas and this led to the gradual disappearance of the other colored varieties, today a new trend is being noticed which is named conservation of biodiversity. In addition to this, improved understanding of the importance of healthy nutrition in human dietary and preventive medicine increased the consumption of vitamin-rich vegetables such as carrot. Obviously, different colors are caused by different chemical compositions namely anthocyanin in purple or black ones (Arscott and Tanumihardjo, 2010). Nowadays, consumption of black or purple carrots is increasing steadily due to their definition as an important source of natural antioxidants (Sharma et al., 2012). Purple or black carrot is useful source of minerals and vitamins and it contains high amount of anthocyanin, which is known as natural dye used in the food industry. Because of their healthful

http://www.aloki.hu ● ISSN 1589 1623 (Print) ● ISSN 1785 0037 (Online)
DOI: http://dx.doi.org/10.15666/aeer/1706_1524515254

properties, the development of food colorants from the natural sources has increased interest as alternatives to synthetic dyes (Smeriglio et al., 2018).

Additionally, purple carrot roots have 9 times more phenolic than roots of other colored carrots also they have high antiradical activity which is caused from high anthocyanin content (Leja et al., 2013). As well as the availability of common antioxidants such as vitamins C and E, purple carrots have much more interest with their phenolic (Alasalvar et al., 2001; Kırca et al., 2006; Singh et al., 2011), which contributed to the antioxidant capacity positively (Algarra et al., 2014). In particular, purple carrots have higher antioxidant capacity in comparison with other colors (Sun et al., 2009). Nicolle et al. (2004) tried to understand the influences of genetic variability on carotenoid, vitamin, phenolic and mineral content of the different carrot roots to assist the breeding programs. Purple carrots are often consumed processed (Alasalvar et al., 2001). Limited fresh consumption of them has been maintained in Turkey for years. Mostly it has been used to produce of local drink called 'salgam'. In recent years, production has been increasing dramatically due to the use for anthocyanin extraction by the pigment industry; more than 90% of the purple carrots produced in Turkey are being used by this industry (Ipek et al., 2016).

Because of favorable climate and soil conditions, purple carrot production is mostly spread in Turkey's Konya province. It is considered that quality of the purple carrot roots harvested from this area higher than the other production areas. This makes Konya's purple carrot locally called "Black Carrot" to be well known by the world and makes it an important export product. In this study, the effects of different ecologies on root quality were compared. It is thought that at the end of the project, obtained results could be contributed to spread the production out of the certain growth areas thus; production of purple carrot, also consumption of the vegetable with obvious benefits could be increased. Purple carrot roots, generally consumed by processing, before fabricated they may have to be stored for several months. During the storage, some visible deteriorations occur in the carrot roots and the effects of storage on root quality are not clear. With this study the effects of storage on the quality of the purple carrot roots was determined. Briefly, this study aims to compare the effects of different ecological conditions and long-term cooled storage on the quality characteristics of six local purple carrot genotypes. In this research "quality characteristics" means, determination of antioxidant activity (AA), contents of anthocyanin (AC), total phenolic (TP), total flavonoids (TF), titratable acidity (TA), total soluble solids (TSS), invert sugar (IS) values of the purple carrot root samples.

Materials and methods

Plant material

In the current study, six black carrot genotypes (DC17, DC28, DC33, DC34, DC36, and DC37) collected from the general production areas of Konya province were used as a plant material. These genotypes have been maintained in a limited area (nearly 20 000 da in Eregli and Karapınar regions) by local farmers who act as a seed saver for many years. Before this study, root samples were collected by visits to the local carrot growing fields in Kuzukuyu, Pınarozu, Akoren villages and Basin plateau in Ereğli District within another project. Collected roots brought to the institutes which are located in Yalova (40° 39′N, 29° 17′E) and Konya (Karapinar region; 37° 42' N, 33° 33' E) for planting and selfing. Selfed purple carrot seeds were planted separately when

http://www.aloki.hu ● ISSN 1589 1623 (Print) ● ISSN 1785 0037 (Online)
DOI: http://dx.doi.org/10.15666/aeer/1706_1524515254

the season was appropriate. After a successful vegetation period harvested root samples were divided in two parts and non-stored roots were directly taken to the laboratory. The other part was stored for two months in the cold storage, temperature ranged from 2 to 3 °C and relative humidity (RH) was 85 to 90%. Followed to the storing stage, these samples were taken to the laboratory likewise. Extraction and the laboratory analyzes were done three times at the Ataturk Central Horticultural Research Institute, Yalova.

Field trials

Field trials planned according to the randomized complete blocks design with three replications. Each trial areas' soil conditions are listed in *Table 1.* Because of the climatic conditions (*Table 2*) seed sowing was done on May 15 in Konya and on August 15 in Yalova, harvest was started November 15 in Konya and February 15 in Yalova between the years of 2016-2017.

Table 1. *Pedological properties of the tested soils*

Location	WHC (%)	pH	OM (%)	$CaCO_3$ (%)	P_2O_5 mg kg^{-1}	K_2O (me100g^{-1})	EC (mmhos cm^{-1})	Class
Konya	37.40	8.39	0.99	56.11	9.64	103.33	220	Loamy
Yalova	68.00	7.68	2.09	0.60	5.70	0.53	191	Clay loam

WHC: water holding capacity, OM: organic matter

Table 2. *Weather conditions of Yalova and Konya province during 2016 (Anonymous, 2018)*

Months	Temperature (°C)						Average humidity (%)		Total rainfall (mm)	
	Minimum		Maximum		Average					
	Yalova	Konya	Yalova	Konya	Yalova	Konya	Yalova	Konya	Yalova	Konya
Jan.	4.5	-4.6	10.2	5.5	6.9	0.0	73.5	75.4	136.4	40.8
Feb.	8.1	-0.2	14.8	13.8	11.0	6.5	76.3	65.1	74.4	7.2
Mar.	7.6	0.2	15.0	15.5	10.9	7.7	73.2	54.7	91.9	34.4
Apr.	11.2	4.9	21.3	22.9	15.7	14.2	69.1	42.1	32.2	4.8
May	14.0	8.8	29.0	23.8	18.1	16.0	73.4	55.6	56.1	44.4
June	18.3	13.8	22.9	29.4	23.4	21.8	69.3	44.7	29.4	33.8
July	19.9	14.8	30.8	31.8	25.0	24.0	70.3	36.7	4.6	0.0
Aug.	25.6	15.5	30.3	32.9	25.4	24.4	76.2	38.5	52.9	20.2
Sept.	16.8	8.9	26.3	25.8	21.1	17.5	73.4	48.3	39.6	24.4
Oct.	12.5	4.4	20.0	22.1	15.9	13.1	78.9	48.5	34.1	0.6
Nov.	8.8	-3.3	15.8	14.3	11.9	5.0	75.3	57.4	97.7	10.2
Dec.	2.8	-8.1	7.6	2.3	4.9	-2.3	80.7	82.6	153.4	97.8

Physicochemical analysis

After sowing, cultural practices have been done properly throughout the season in two trial areas. Following the harvest, AA, TP, TF, AC, TSS, TA, and IS values of stored and non-stored roots were investigated in 2017. The amount of TF in extracts was determined spectrophotometrically according to the Folin-Ciocalteu method (Thaipong et al., 2006). Total flavonoid content of extracts was measured according to

http://www.aloki.hu ● ISSN 1589 1623 (Print) ● ISSN 1785 0037 (Online)
DOI: http://dx.doi.org/10.15666/aeer/1706_1524515254

the modified method of Zhisnen et al. (1999). Anthocyanin quantitation was performed by the pH differential method (Moyer et al., 2002). Antioxidant activity was determined by two methods which were 1,1-diphenyl-2-picrylhydrazyl (DPPH) (Thaipong et al., 2006) and ferric reducing ability of plasma (FRAP) (Benzie and Strain, 1996) because of no single method represents AA well. TSS values, were determined by the Abbe refractometer, TA and IS values determined according to Cemeroglu (2007).

Statistical analysis

Study was completed between the years of 2015-2017. Field trials planned according to the randomized complete blocks design with three replications and laboratory tests were done 3 times. All data were analysed using analysis of variance (ANOVA). Analysis of variance was employed to compare the means of genotypes, location, storage and their interactions. The significance of differences between results was determined by DUNCAN multiple comparison technique. The statistical significance is indicated within the *Table 3* ($p < 1\%$).

Results and discussion

Trial areas' soil conditions are listed in *Table 1.* According to the analyzes, Konya's soil is loamy and poor in organic matter, Yalova's soil is clay-loam and richer in organic matter compared to the Konya. According to *Table 2,* climatic conditions of the trial sites are quite different from each other, such as while Yalova was temperate and rainy Konya was arid and hot throughout the growing period. Because of this, different periods of the year were selected for root production. After the harvest it was observed that, the differences between the areas weather and soil conditions affect the roots visible quality, which means harvested roots from Konya looked smoother and marketable compared to the Yalova's mostly shapeless and rough roots. It is thought that, Yalova's different day and night temperature regimes and high air and soil humidity could lead to, undesired lateral root branching and woody root growth. In addition to this it was understood from the researchers' previous studies that, production of purple carrot during spring and summer time cause the undesired early flowering in Yalova conditions. Therefore, cultivation was started in late August for Yalova. Seljasen et al. (2013) reported that quality characteristics of carrots are very sensitive to the influences of biotic and abiotic stresses.

The results of variance analyses for the investigated characters were showed in *Table 3*. All characters were significant for the interaction of three factors (genotype, location and storage) except TF content and TA values ($P < 0.01$). The content of TF and TA were significant for interaction of genotype × storage, and genotype × location (*Table 3*).

According to variance analysis, there was not individual effect of each factor on the content of IS, so all the results about IS, TSS, AC, TP, FRAP and DPPH were compared to each other (totally 24 values) and all the results were summarized in *Table 4*. The lowest IS content measured in genotype-DC28 harvested from Yalova (YL) location, and in non-storage (NS) treatment (3.00 g 100 ml^{-1}), while the highest value obtained from genotype-DC33 harvested from same location and storage (S) treatment (69.25 g 100 ml^{-1}). In a study conducted by Ersus and Yurdagel (2007) IS determined as 3.80 g 100 g^{-1} that was very similar to our non-stored genotype-DC28 harvested from Yalova.

http://www.aloki.hu ● ISSN 1589 1623 (Print) ● ISSN 1785 0037 (Online)
DOI: http://dx.doi.org/10.15666/aeer/1706_1524515254

Table 3. *The results of variance analysis*

	C. Total	Error	F values						
			Genotype	Location	Storage	Genotype × location	Genotype × storage	Location × storage	Genotype × location × storage
DF	71	48	5	1	1	5	5	1	5
DPPH			610.19*	30.41*	10.64*	147.54*	42.94*	1.28^{ns}	29.8*
FRAP			130.25*	66.46*	1.48^{ns}	74.54*	199.22*	21.89*	60.98*
TP			1,087.28*	0.01^{ns}	7.91*	24.33*	21.21*	2.12^{ns}	16.71*
TF			178.89*	1.67^{ns}	0.88^{ns}	2.46*	6.72*	0.03^{ns}	2.27^{ns}
AC			461.11*	60.04*	5.06*	17.85*	5.02*	2.49^{ns}	9.59*
TSS			2,117.25*	7,007.11*	6.53*	892.96*	762.54*	549.16*	339.22*
TA			152.04*	344.10*	660.01*	14.03*	161.18*	0.05^{ns}	0.05^{ns}
IS			439.11*	196.16*	1,946.74*	130.32*	105.77*	4.51*	27.26*

*Significant ($p < 0.01$), ns: non significant F: freedom, DF: degree of freedom, C. Total: corrected total, Dpph: 1,1-diphenyl-2-picrylhydrazyl, frap: ferric reducing ability of plasma, TP: total phenol, TF: total flavonoid, AC: antocyanin, TSS: total soluble solids, TA: titratable acidity, IS: invert sugar

Table 4. *The effects of storage and location on some parameters of purple carrot genotypes*

Tre.	Location	Genotype	IS	TSS	AC	TP	FRAP	DPPH
Stored	Konya	DC17	30.97 h	11.60 b	420.81 e	2,521.90 c	1,380.05 e	4,816.92 gh
		DC28	27.30 ij	9.20 f	27.97 g	2,015.24 de	984.93 h	7,951.79 c
		DC33	61.68 b	11.73 b	40.91 g	491.42 i	284.94 n	6,044.10 f
		DC34	57.72 c	7.03 j	31.73 g	1,479.04 g	667.14 k	4,415.64 hı
		DC36	43.07 f	10.13 d	1,306.69 b	5,300.95 b	3,756.25 d	**9,818.46 a**
		DC37	64.93 b	6.83 k	26.30 g	562.85 i	412.74 m	6,510.77 de
	Yalova	DC17	51.03 d	10.23 d	251.00 f	2,263.56 cd	1,213.90 f	4,839.45 gh
		DC28	24.87 j	6.35 l	17.13 g	1,501.74 g	820.37 ij	6,020.80 f
		DC33	**69.25 a***	7.93 h	60.99 g	538.86 i	260.56 n	4,659.62 gh
		DC34	63.37 b	7.48 i	26.50 g	1,673.31 fg	747.26 j	6,006.39 f
		DC36	57.84 c	9.64 e	1,004.87 c	5,394.27 b	4,217.13 c	**9,781.66 a**
		DC37	55.95 c	5.13 m	32.44 g	636.55 i	452.32 lm	6,600.44 de
Non-stored	Konya	DC17	11.61 m	7.90 h	140.97 fg	600.95 i	414.42 m	6,180.00 ef
		DC28	4.94 n	10.53 c	20.43 g	2,291.43 cd	1,109.13 g	8,597.95 b
		DC33	19.73 k	10.20 d	11.34 g	621.90 i	310.57 n	3,404.10 k
		DC34	26.89 ij	8.93 g	27.97 g	993.33 h	512.50 l	3,973.33 j
		DC36	42.51 f	**12.36 a**	**1,692.43 a**	**5,772.38 a**	4,519.47 b	**9,733.84 a**
		DC37	37.43 g	10.53 c	37.85 g	948.57 h	237.26 n	6,867.18 d
	Yalova	DC17	42.37 f	8.80 g	575.28 d	2,005.24 de	1,047.75 gh	4,861.79 g
		DC28	3.00 n	5.10 m	55.11 g	988.57 h	656.73 k	4,090.00 ıj
		DC33	29.32 hi	6.76 k	12.76 g	586.19 i	235.65 n	3,274.62 k
		DC34	55.15 c	7.96 h	35.48 g	1,867.62 ef	827.08 i	7,592.82 c
		DC36	47.30 e	10.43 c	1,123.00 c	**5,486.67 ab**	**4,676.92 a**	**9,744.10 a**
		DC37	15.69 l	4.56 n	28.81 g	710.47 hi	492.07 l	6,690.26 d

*Means within a column that have a different small letter are significantly different from each other ($P < 0.01$). Lettering was made according to results of variance analyses. Abbrevations as in *Table 3*

http://www.aloki.hu ● ISSN 1589 1623 (Print) ● ISSN 1785 0037 (Online)
DOI: http://dx.doi.org/10.15666/aeer/1706_1524515254

According to *Table 4,* AC content of the six purple carrot genotypes ranked between 1,692.43 - 11.34 mg l^{-1}, obtained from non-stored roots of genotype DC36 and genotype DC33 respectively, grown in Konya location. With respect to the results, AC content of genotype DC36 found higher than the other genotypes in all locations whether stored or not. Leja et al. (2013) compared the contents of carrots in different colours and reported that purple or black carrots contain more AC than the other coloured varieties.

In a study conducted in Spain, researchers found that two commercial varieties (Antonina, Purple haze) have AC 93-126 mg/100 g in fresh weight respectively (Algarra et al., 2014). In another study, researchers stated that analyses of TP and AC showed significant genotype × environment interactions also in blueberry cultivars (Connor et al., 2002). Recently, newly developed carrot varieties with an extremely high content of anthocyanin (nearly 1,750.00 mg/kg in fresh weight) is cultivated in the fields (Mazza and Miniati, 1993).

The difference between the TP contents of genotypes was found statistically significant ($p < 0.01$). The fresh roots of genotype DC36 cultivated in Konya and Yalova received the highest value (5.772,38 - 5.486,67 mg GAE 100 g^{-1}). In this study, the lowest TP values obtained from stored roots of genotype DC33 harvested from Yalova and Konya (538.86- 491.42 mg GAE 100 g^{-1}). When the results considered location and location × storage interactions were non-significant on TP content. Kramer et al. (2012) reported that total phenolic content varied in a wide range among different coloured carrot roots but purple cultivars significantly exceeded other coloured roots and also influence of growing location was found to be weak in that study. In a trial, 35 carrot accessions, 15 of them orange, 8 yellow, 5 white, 5 red and 2 purple roots were investigated and purple and red ones were determined as rich in phenols (19.8 to 342.2 mg 100 g^{-1} in fresh weight). Also researchers stated that, carrots developing purple roots possessed on average 9 times more phenolic than roots of other colours (Leja et al., 2013). Obtained results showed that used genotypes of the current study, have higher TP content than the previous results. In addition to this, in a research on Guava fruit, TP contents of four genotypes were found 170-344 mg 100 g^{-1} in fresh weight (Thaipong et al., 2006). It can be understood that studied carrot roots have much TP content even from the guava genotypes.

It is evident from the *Table 4* that used genotypes were significantly influenced all of the studied parameters. So the genotypes were grown in Konya or Yalova even if they stored or not, when the studied parameters considered, the differences between the used purple carrot genotypes found significant. Like these findings, Nicolle et al. (2004) and Kramer et al. (2012) found significant differences on mineral compound and total phenolic content of the different carrot cultivars used in their study even if they were in same color.

With the current experiment, functional properties of the selected six genotypes were identified, so it is possible to choose the appropriate genotype before start the any study. Such as, it was clear from the experiment, genotype DC36 was found superior to the other genotypes in all applications for all parameters except IS. On the other hand, when the results of genotype DC33 considered, according to AC, TF, TP content and AA values, it was ranked last on the list but its TSS and IS values ranked top compared to the other genotypes.

In the present work used two (Konya, Yalova) locations did not find significant in terms of the total phenolic and flavonoid content of the purple carrot roots (*Table 5*). However, the other examined parameters like those of AC, AA, TSS and TA were

http://www.aloki.hu ● ISSN 1589 1623 (Print) ● ISSN 1785 0037 (Online)
DOI: http://dx.doi.org/10.15666/aeer/1706_1524515254

affected from the different environmental conditions. When the TSS values were examined, it was determined that the effect of the location was significant and the genotypes DC36, DC33, DC17, DC28 and DC37 from the carrots grown in Konya were higher TSS values than the ones in Yalova. It has been found that genotype DC34 received 8.9 TSS from the fresh roots of Konya and the other DC34 numbered applications were below this value. It is possible to have different TSS contents because of the effects of different climate conditions (Ersus and Yurdagel, 2007). In a study researchers deal with the detect of the AC profile and AA features of two different black carrots cultivars. While material collecting, researchers took into account growing region and they picked roots from the same location of Southern Spain. As could be understood that, the field conditions could be affect the characteristic of the roots (Algarra, 2014).

The contents of TF was significant for interaction of genotype × storage, and genotype × location (*Table 5*). According to this study, although the genotypes differ in their TF content, chill storage for two months did not affect the TF content of carrot roots (*Table 5*). Moreover, chill storage did not affect the AA according to FRAP values but with respect to DPPH results, storage effect was found statistically important on AA. Alasalvar et al. (2005) studied chill storage effects on AA, AC and TP contents. While total AA remained comparatively constant in orange ones, there was significant decrease was observed in purples. In addition, the content of AC in purples decreased slightly but TP increased at a much higher rate during storage than orange carrots. In our research the effect of chill storage for two months found statistically important when the other applications considered. Klaiber et al. (2005) reported that the content of TP increased throughout the storage of carrots under aerobic conditions.

Table 5. *The effects of location and storage on flavonoid and titratable acid contents of purple carrot genotypes*

Location	Genotype	TF	TA	Storage	Genotype	TF	TA
Konya	DC17	1,208.46 b	0.14 e	Stored	DC17	1,505.18 c	0.20 cd
	DC28	1,232.38 b	0.14 e		DC28	1,046.33 d	0.21 c
	DC33	417.58 f	0.14 e		DC33	476.20 gh	0.18 de
	DC34	628.16 def	0.27 b		DC34	777.72 def	0.43 a
	DC36	**3,101.31 a***	0.26 b		DC36	2,832.26 b	0.36 b
	DC37	600.64 def	0.14 e		DC37	489.36 gh	0.17 ef
Yalova	DC17	1,088.80 bc	0.22 c	Non-stored	DC17	792.08 def	0.16 gh
	DC28	803.44 cde	0.26 b		DC28	989.49 de	0.19 de
	DC33	471.42 f	0.20 cd		DC33	412.79 h	0.16 gh
	DC34	878.22 cd	0.31 a		DC34	728.67 efg	0.14 h
	DC36	**2,973.45 a**	0.30 a		DC36	**3,242.49 a**	**0.20 cd**
	DC37	520.46 ef	0.19 d		DC37	631.75 fgh	0.15 fg

*Means within a column that have a different small letter are significantly different from each other ($P < 0.01$). Lettering was made according to results of variance analyses

Conclusion

Because of its nutritional features, purple carrot is a valuable product and it is exported to the many countries around the world from Turkey. With this study, the

http://www.aloki.hu ● ISSN 1589 1623 (Print) ● ISSN 1785 0037 (Online)
DOI: http://dx.doi.org/10.15666/aeer/1706_1524515254

effects of different environmental conditions and storage on the characteristics of the purple carrot roots were determined. The studies were carried out under natural environmental conditions. It has been understood that the used purple carrot genotypes could be grown outside the current cultivation area. However, with the effect of ecological conditions, the differences in both quality characteristics and external appearance of the roots have been detected. It was observed that the roots harvested from Yalova unsuitable for the fresh market. Moreover, the effect of storage on all applications except total flavonoid content was found significant. These results should be taken into consideration by the producers, plant breeders and processing industry members. In future studies, detailed physiological analysis under fully controlled conditions (such as growth chamber) can be great benefit to plant breeders and food scientists. Furthermore, associations between dietary patterns and gene expression profiles of healthy men and women and additionally investigating the relationship between nutritional values and gene expression profiles of genotypes can be great benefit to plant breeders. With the further studies, the production and consumption of purple carrot, a beneficial, highly nutritional and inexpensive food, can be expanded.

Acknowledgements. The authors would like to thank to Dr. S. Secil Erdogan for the technical advices in laboratory studies and Necati Simsekli for the field experiments in Konya location. This study supported by the General Directorate of Agricultural Research and Policies of Ministry of Agriculture and Forestry of Turkey Republic between the years of 2013-2017.

REFERENCES

[1] Alasalvar, C. J., Grigor, M., Zhang, D., Quantick, P. C. Shahidi, F. (2001): Comparison of volatiles, phenolics, sugars, antioxidant vitamins, and sensory quality of different coloured carrot varieties. – Journal of Agriculture and Food Chemistry 49: 1410-1416. https://doi.org/10.1016/j.foodchem.2005.07.042.

[2] Alasalvar, C. J., Al-Farsi, M., Quantick, P. C., Shahidi, F., Wiktorowicz, R. (2005): Effect of chill storage and modified atmosphere packaging (MAP) on antioxidant activity, anthocyanins, carotenoids, phenolics and sensory quality of ready to eat shredded orange and purple carrots. – Food Chemistry 89(1): 69-76. https://doi.org/10.1016/j.foodchem.2004.02.013.

[3] Algarra, M., Fernandes, A., Mateus, N., Freitas, V., Esteves da Silva, J. C. G., Casado, J. (2014): Anthocyanin profile and antioxidant capacity of black carrots from Cuevas Bajas, Spain. – Journal of Food Composition Analysis 33: 71-76. https://doi.org/10.1016/j.jfca.2013.11.005.

[4] Anonymous (2018): Turkish State Meteorological Service. – https://mgm.gov.tr/eng/forecast-cities.aspx.

[5] Arscott, S. A., Tanumihardjo, S. A. (2010): Carrots of many colors provide basic nutrition and bioavailable phytochemicals acting as a functional food. – Comprehensive Reviews in Food Science and Food Safety (9): 223-239. https://doi.org/10.1111/j.1541-4337.2009.00103.x.

[6] Benzie, I. F., Strain, J. J. (1996): The FRAP as a measure of "antioxidant power": the FRAP assay. – Analytical Biochemistry 239: 70-76. https://doi.org/10.1006/abio.1996.0292.

[7] Cemeroglu, B. (2007): Food analysis. – Food Technology Association Publication 34: 70-75.

[8] Connor, A. M., Luby, J. J., Tong, C. B. S., Finn, C. E., Hancock, J. F. (2002): Genotyping and environmental variation in antioxidant activity, total phenolic content, anthocyanin

http://www.aloki.hu ● ISSN 1589 1623 (Print) ● ISSN 1785 0037 (Online)
DOI: http://dx.doi.org/10.15666/aeer/1706_1524515254

content among blueberry cultivars. – Journal of American Society for Horticultural Science 127(1): 89-97.

[9] Ersus, S., Yurdagel, U. (2007): Microencapsulation of anthocyanin pigments of black carrot by spray drier. – Journal of Food Engineering 80: 805-812. https://doi.org/10.1016/j.jfoodeng.2006.07.009.

[10] Esatbeyoglu, T., Rodríguez-Werner, M., Schlösser Liehr, A. M., Ipharraguerre, I., Winterhalter, P., Rimbach, G. (2016): Fractionation of plant bioactives from black carrots by adsorptive membrane chromatography and analysis of their potential anti-diabetic activity. – Journal of Agriculture and Food Chemistry 64: 5901-5908. DOI: 10.1021/acs.jafc.6b02292.

[11] Ipek, A., Turkmen, O., Fidan, S., Ipek, M., Karcı, H. (2016): Genetic variation within the purple carrot population grown in Ereğli District in Turkey. – Turkish Journal of Agriculture and Forestry 40: 570-576. DOI: 10.3906/tar-1512-90.

[12] Kırca, A., Özkan, M., Cemeroglu, B. (2006): Stability of black carrot anthocyanins in various fruit juices and nectars. – Food Chemistry 97: 598-605. https://doi.org/10.1016/j.foodchem.2005.05.036.

[13] Klaiber, R. G., Baur, S., Koblo, A., Carle, R. (2005): Influence of washing treatment and storage atmosphere on phenyl alanine ammonialyase activity and phenolic acid content of minimally processed carrot sticks. – Journal of Agriculture and Food Chemistry 53: 1065-1072. DOI: 10.1021/jf049084b.

[14] Kramer, M., Maksylewicz-Kau, A., Baranski, R., Nothnagel, T., Carle, R., Kammerer, D. R. (2013): Effects of cultivation year and growing location on the phenolic profile of differently coloured carrot cultivars. – Journal of Applied Botany and Food Quality 85(2): 235.

[15] Leja, M., Kamińska, I., Kramer, M., Maksylewicz-Kaul, A., Kammerer, D., Carle, R., Baranski, R. (2013): The content of phenolic compounds and radical scavenging activity varies with carrot origin and root color. – Plant Food and Human Nutrition 68: 163-170. doi.org/10.1007/s11130-013-0351-3.

[16] Mazza, G., Miniati, E. (1993): Anthocyanins in fruits, vegetables, and grains. – CRC Press, Boca Raton, FL.

[17] Moyer, R. A., Hummer, K. E., Fınn, C. E., Frei, B., Wrolstad, R. E. (2002): Anthocyanins, phenolics, and antioxidant capacity in diverse small fruits: vaccinium, rubus, and ribes. – Journal of Agriculture and Food Chemistry 50: 519-525. DOI: 10.1021/jf011062r.

[18] Nicolle, C., Simon, G., Rock, E., Amoroux, P., Remesy, C. (2004): Genetic variability influences carotenoid, vitamin, phenolic and mineral content in white, yellow, purple, orange, dark orange carrot cultivars. – Journal of American Society for Horticultural Science 129(4): 523-529.

[19] Seljasen, R., Kristensen, H. L., Lauridsen, C., Wyss, G. S., Kretzschmar, U., Birlouez-Aragone, I., Kahl, J. (2013): Quality of carrots as affected by pre-and postharvest factors and processing. – Journal of the Science of Food and Agriculture 93(11): 2611-2626.

[20] Sharma, K. D., Karki, S., Thakur, N. S., Attri, S. (2012): Chemical composition, functional properties and processing of carrot. A review. – Journal of Food Science and Technology 49: 22. https://doi.org/10.1007/s13197-011-0310-7.

[21] Simon, P. W., Freeman, R. E., Vieira, J. V., Boiteux, L. S., Briard, M., Nothnagel, T., Michalik, B., Kwon, Y. S. (2008): Carrot. – In: Prohens, J., Nuez, F. (eds.) Vegetables II. Handbook of Plant Breeding. Vol. 2. Springer, New York, pp: 327-357.

[22] Smeriglio, A., Denaro, M., Barreca, D., D'Angelo, V., Germanò, M. P., Trombetta, D. (2018): Polyphenolic profile and biological activities of black carrot crude extract. – Fitoterapia 124: 49-57. https://doi.org/10.1016/j.fitote.2017.10.006.

[23] Singh, D. P., Beloy, J., Mclnerney, J. K., Day, L. (2011): Impact of boron, calcium and genetic factors on vitamin C, carotenoids, phenolic acids, anthocyanins and antioxidant

http://www.aloki.hu ● ISSN 1589 1623 (Print) ● ISSN 1785 0037 (Online)
DOI: http://dx.doi.org/10.15666/aeer/1706_1524515254

capacity of carrots. – Food Chemistry 132: 1161-1170. https://doi.org/10.1016/j.foodchem.2011.11.045.

[24] Sun, T., Simon, P. W., Tanumihardjo, S. A. (2009): Antioxidant phytochemicals and antioxidant capacity of biofortified carrots (Daucus carota L.) of various colors. – Journal of Agricultural and Food Chemistry 57(10): 4142-4147.

[25] Thaipong, K., Unaroj, B., Crosbyb, K., Cisneros-Zevallosc, L., Byrne, D. H. (2006): Comparison of ABTS, DPPH, FRAP, and ORAC assays for estimating antioxidant activity from guava fruit extracts. – Journal of Food Composition Analysis 19: 669-675. https://doi.org/10.1016/j.jfca.2006.01.003.

[26] Zhishen, J., Mengcheng, T., Jianming, W. (1999): The determination of flavonoid contents in mulberry and their scavenging effects on superoxide radicals. – Food Chemistry 64(4): 555-559.

http://www.aloki.hu ● ISSN 1589 1623 (Print) ● ISSN 1785 0037 (Online)
DOI: http://dx.doi.org/10.15666/aeer/1706_1524515254

NATURAL, ENVIRONMENTAL AND PRACTICAL BIOLOGICAL CONTROL OPTIONS FOR FUSARIUM WILT DISEASE OF CARNATION (*FUSARIUM OXYSPORUM* F. SP. *DIANTHI*)

ARICI, S. E.[1*] – ERDOĞAN, O.[2] – TUNCEL, Z. N.[1]

[1]*Isparta University of Applied Sciences, Agricultural Faculty, Department of Plant Protection, 32260 Isparta, Turkey*

[2]*Pamukkale University, School of Applied Sciences, Department of Organic Farming Business Management, 20600 Çivril-Denizli, Turkey*

**Corresponding author*
e-mail: evrimarici@isparta.edu.tr

(Received 4th Jul 2019; accepted 25th Oct 2019)

Abstract. Carnation (*Dianthus caryophyllus* L.) is one of the most important cut flowers in the world. Some fungi, bacteria and viruses lead to diseases that affect carnation plants, and most of these severe diseases are caused by Fungi. It is considered that *Fusarium oxysporum f. sp. dianthi (Fod)* has induced one of the most serious and detrimental diseases that impair carnation. In this study, the effect of some biological preparations [*Trichoderma harzianum Pseudomonas fluorescens; Bacillus subtilis* QST 713 (SERENADE), *Mycorrhiza* spp., *Trichoderma* spp., *Bacillus* spp. (PANORAMIX), *Lactobacillus acidophilus* + *Lactobacillus paracasei* (VITANAL), tea tree oil extract (TIMOREX GOLD), orange oil extract (PREV-AM), plant extracts of Reynoutria spp. (REGALIA) against *Fod* were investigated. Experiments were performed using a randomized plots design with five replications (five pots and one plant per pot) in a growth chamber. After 30 days, carnation plants were evaluated with a scale of 0-5 values. The effect of biological preparations was calculated based on root size, root number, plant height and number of nodes, then the acquired data were evaluated. The best results were obtained with *T. harzianum* (96%), SERENADE (96%) and PANORAMIX (88%) against *Fusarium oxysporum* f. sp. *dianthi*. All of the control plants (+) were completely dead due to the disease. In conclusion, the biological control improves the Fusarium wilt suppression capabilities of carnation.
Keywords: *Pseudomonas fluorescens, Bacillus subtilis, Trichoderma harzianum, plant extract, orange oil extract*

Introduction

Carnation (*Dianthus caryophyllus* L.) belongs to the Caryophyllaceae family and has been extremely popular amongst cut flowers since the 18th century. Carnation is one of the most demanded cut flower in the world. Netherlands is a leading country which has the biggest market share of carnations in 2015 with around 47% of all imports in the European Union followed by The United Kingdom, Spain, Poland, Bulgaria, Slovenia, Romania and the Baltic states (https://www.cbi.eu/market-information). Turkey also has a substantial place among producers of carnation plant, which is the major horticultural product of that country. Turkey has introduced a variety of popular standards and spray for carnations to marketplace for a long time. Sixty percent of the cut flower production has comprised of carnation plant in Turkey..In addition, most of the grown cut flowers are chrysanthemums, gerberas, solidange, gladiolus and freesia. The lion's share of ornamental plant production in Turkey has been churning out between the cities of Antalya, İzmir and Yalova, and Isparta (TSI, 2016).

http://www.aloki.hu ● ISSN 1589 1623 (Print) ● ISSN 1785 0037 (Online)
DOI: http://dx.doi.org/10.15666/aeer/1706_1525515265

Some diseases and pests lead to economic damage during the process of carnation cultivation. The most important disease is Fusarium wilt, caused by *Fusarium oxysporum* Schlechtend: Fr. f. sp. *dianthi* (Prill & Delacr.) W. C. Snyd. & H. N. Hans., which is a soil-borne fungus disease. Fusarium wilt disease is common in 79% of carnation production areas and affects 45% of total production (Anonymous, 2006). The most important phytopathological problem affecting carnation in most areas of the world is Fusarium wilt, caused by *Fusarium oxysporum* f. sp. *dianthi*. (*Fod*). Fusarium wilt is prevalent in 79% of the national production areas of carnation and affects 45% of its total production (Anonymous, 2006). The symptom of *Fod* is characterised by wilting of shoots, discolouration of leaves, and brown streaks on vascular tissue in stem. The infected leaves turn out chlorotic and finally wilt (Sohi, 1992). *F. oxysporum* f. sp. *dianthi* has various biological races and occurs in different carnation cultivars due to their selective virulence. Race 2 of *Fod* is the most prevalent in carnation cultivars (Denmik et al., 1989; Sarrocco et al., 2007). Fusarium wilting disease is controlled by systemic fungicides. This situation has a negative impact on human health, causes pollution and toxicity and also reduces the population of beneficial microorganisms in the soil. Therefore, alternative methods must be found to reduce the use of chemical fungicides. For this reason, biological control studies are of great importance. Mahalakshmi et al. (2015) investigated the effect of different organic inputs viz., neem cake, mauha cake, coipith and vermicompost against the wilt disease in carnation. As a result, Neemcake (10%) effectively prevented the growth of Fod. Hanudin et al. (2017) reported that *Bacillus subtilis* and *Pseudomonas fluorescens* suspended in the vermicompost extract and molases on the concentration level of 0.5% were consistenly effective in suppressing Fusarium wilt on carnation. In addition, fungicides adversely affect human and environmental health. Hence, alternative control methods as biological control which are more environmentally friendly are necessary.

The aim of this study was to evaluate the effectiveness of some biological methods against Fusarium carnation wilt disease using a randomized plots design with five replications over a 30 day period, in order to find the best biological practice to combat the disease.

Material and methods

Fusarium oxysporum f. sp. *dianthi* (*Fod*) was used as a pathogen. *Fod* was isolated from Isparta carnation greenhouses in Turkey and tested for pathogenicity). Some biological organisms and plant extracts were utilised as a biological control. Microorganisms and plant extracts used in the experiment are given in *Table 1*. All treatments were applied on the carnation cuttings by root-dipping.

Isolation and identification of Fusarium oxysporum f. sp. dianthi

Samples exhibiting wilt disease of carnation were collected from the 5 different greenhouses of Isparta, Turkey during 2017-2018 and brought to the laboratory. From these samples five isolates of *Fod* were isolated and identified (Nelson et al., 1983; Burgess et al., 1994). Pathogenicity of isolates was assessed. As a result of the pathogenicity test, ISP-3 isolate, which caused the most diseases in commercial carnation cultivar was used in the experiments.

http://www.aloki.hu ● ISSN 1589 1623 (Print) ● ISSN 1785 0037 (Online)
DOI: http://dx.doi.org/10.15666/aeer/1706_1525515265

Table 1. *The biological microorganisms and plant extracts used in the experiment*

Treatments	Number of plant
Trichoderma harzianum	5
Pseudomonas fluorescens	5
Bacillus subtilis QST 713 (SERENADE)	5
Mycorrhiza spp., *Trichoderma* spp., *Bacillus* spp (PANORAMIX)	5
Lactobacillus acidophilus + *Lactobacillus paracasei* (VITANAL)	5
Tea tree oil extract (TIMOREX GOLD)	5
Orange oil extract (PREV-AM)	5
Plant extracts of *Reynoutria* spp. (REGALIA)	5

Isolation of Trichoderma harzianum, Pseudomonas fluorescens

Trichoderma harzianum and *Pseudomonas fluorescens* were isolated by dilution plate technique from the soil samples collected from Isparta and Aydın, in Turkey (Johanson, 1957). The fungal isolate was grown on PDA plates, the bacteria isolate was grown on Nutrient Agar (HIMEDIA, 13 g/L) media at 25 °C. The isolated species were identified by Rhodes (1959), Whipps (2001) and Chin et al. (2003). The isolates of *T. harzianum* and *Pseudomonas fluorescens* were kept on the PDA/NA medium in the Biotechnology and Plant Pathology Research Laboratory, Isparta University of Applied Sciences, Isparta.

Plant material

The commercial carnation cultivar of Picasso was used for its potential antagonistic capacity to Fusarium carnation wilt disease reaction in a growth chamber condition.

Treatment and assessment

Pseudomonas fluorescens were grown in Nutrient Agar (HIMEDIA, 13 g/L) medium and placed at 90 rpm on a rotary shaker for 48 h at room temperature. The cells were harvested by centrifugation for 15 min at 5000 rpm and the pellet was suspended in distilled water. Suspension of bacteria was adjusted to 1×10^7 cfu/ml. The isolates of *T. harzianum* and *F. oxysporum* f. sp. *dianthii* were cultured in PDA plates and incubated at 25 °C for 10 days. Sterile distilled water was poured on the mycelium of fungi and mycelia were collected with a scalpel and the liquid was taken out. Suspensions were then filtered through sterilized cotton filters to obtain pure conidial suspensions and the spores were counted by using a hemocytometer. The spore suspensions of both fungi were adjusted to 1×10^6 conida/mL concentration with sterile distilled water. When plants had 6-8 true-leaf stages, all treatments (REGULAR-200 ml/100 L, TIMOREX-200 ml/100 L, PREW-AM 200 ml/100 L, VITANOL-300 ml/100 L, PANORAMIX-600 ml/100 L, SERENADE-1000 ml/100 L, *T. harzianum*-1×10^6 conida/mL), *P. fluorescens* -1×10^7 cfu/ml.) were applied on the carnation cuttings by root-dipping for 30 min using 20 mL per plant. Treated plants were separately planted in pots with 2 torf:1 perlit: substrate and the remainder suspensions were added to the pots. After 48 h, inoculum suspension of *F. oxysporum* f. sp. *dianthii* were added using 20 ml per plant. The plants were transferred to growth chambers at 24 °C and 12-h day/12-h night for 30 days (*Fig. 1*). Experiments were performed using a randomized plots design with five

http://www.aloki.hu ● ISSN 1589 1623 (Print) ● ISSN 1785 0037 (Online)
DOI: http://dx.doi.org/10.15666/aeer/1706_1525515265

replications (five pots and one plant per pot) in a growth chamber. The experiment was repeated twice. Diseases severity was evaluated 30 days after inoculation with a 0-5 scale values as follows: 0 = no symptoms (0% disease); 1 = weakly affected plant (5%); 2 = local base-stem symptoms (20%); 3 = one-sided and well-developed symptoms (50%); 4 = severe disease symptoms throughout the plant (80%); 5 = dead plant (100%) (Baayen and van der Plas, 1992).

Figure 1. *Different treatment against Fod on carnation cv Picasso in a growth chamber*

The disease severity was monitored every week throughout experimental procedure. The disease severity was evaluated using Townsend-Heuberger's formula (Towsend and Heuberger, 1943). The percentage effect of the applications was calculated using the Abbott formula (Abbott, 1925). The effect of biological preparations (%) was calculated, root size (cm), root number, plant height (cm), number of nodes were measured. Control plant groups were used in the experiment, and control positive plants groups were applied only to Fod and control negative plants only water was applied.

All data were analyzed by analysis of variance (ANOVA) to detect differences between treatments. Mean comparisons were made by using Duncan's tests; all statistical tests were conducted at a probability level of $P \leq 0.05$. All analyses were performed using the SPSS 21 software.

Results

Trichoderma harzianum, *P. fluorescens*, *B. subtilis* QST 713 (SERENADE), *Bacillus* spp + *Trichoderma* spp. + *Endomycorrhiza* (PANORAMIX), *L. acidophilus* + *L. paracasei* (VITANAL), and plant extracts of Tea tree oil extract (TIMOREX GOLD), Orange oil extract (PREV-AM), *Reynoutria* spp. (REGALIA) were applied to carnation wilt disease caused by *F. oxysporum* f. sp. *dianthi*. All applications reduce disease symptoms significantly (*Fig. 2*).

The lowest disease severity (%) was obtained from *P. fluorescens* (4%), SERENADE (6%), and *T. harzianum* (10%) to Fod. Disease severity (%) was determined in the application of PANORAMIX (12%). The percentage of disease severity in control plants was observed as 96% (*Fig. 3*). In the experiment, it was determined that the highest percentage of efficacy values of the biological preparations were for *P. fluorescens* (96%), SERENADE (94%), and *T. harzianum* (90%) to Fod.

http://www.aloki.hu ● ISSN 1589 1623 (Print) ● ISSN 1785 0037 (Online)
DOI: http://dx.doi.org/10.15666/aeer/1706_1525515265

Control plant groups (+) were completely dead due to the disease. The lowest percentage of efficacy values of the biological preparations were determined with the application of TIMOREX (76%), VİTANAL and REGALIA (72%). In conclusion, the biological control method improves the suppressive capacity against Fusarium wilt disease in carnation (*Table 2*).

Figure 2. *Effects of different treatments on Fod incidence on pot assay in a growth chamber*

Figure 3. *Effects of SERENADE, TIMOREX GOLD and T. harzianum on plant growth*

The effect of different treatments on plant parameters of carnation was presented in *Table 3.* Statistical analysis of figure showed significant differences in treatments at $P \leq 0.05$ levels. Application of different treatments have improved carnation growth statistically. Plant height was showed significant variation with TIMOREX GOLD application. The longest plant height was found in TIMOREX GOLD application (31.60 cm) followed by PANORAMIX (26.46 cm), REGALIA (26.44 cm) and SERENADE (25.98 cm)) applications. The shortest plant height were in *P. Fluorescens*

http://www.aloki.hu ● ISSN 1589 1623 (Print) ● ISSN 1785 0037 (Online)
DOI: http://dx.doi.org/10.15666/aeer/1706_1525515265

(21.25 cm) application. Significant variation was observed in the case of the number of roots with different treatments. The maximum root number was in TIMOREX GOLD application with 23.20, the minimum number of root was determined in PREV-AM with 11.60. The root length was showed significant variation with different treatments. The maximum root length was determined on REGALIA application (4.28 cm). Significant variation was determined in the case of the number of nodes. It was indicated that the maximum number of node (9.00) was found VITANAL and REGALIA, the minimum number of node (5.60) was in *P. fluorescens*. Results showed that TIMOREX GOLD, REGALIA and SERENADE in generally were found effective to enhance the plant growth percentage compared to control.

Table 2. *Effectiveness of different treatments against F. oxysporum f. sp. dianthi on carnation*

Treatments	DS*	E*
Orange oil extract (PREV-AM)	20.0	80.0 ab
T. harzianum	10.0	**90.0 a**
B. subtilis QST 713 (SERENADE)	6.0	**94.0 a**
L. acidophilus + *L. paracasei* (VITANAL)	28.0	72.0 bc
P. fluorescens	4.0	**96.0 a**
Mycorrhiza spp., *Trichoderma* spp., *Bacillus* spp (PANORAMIX)	12.0	88.0 ab
Tea tree oil extract (TIMOREX GOLD)	24.0	76.0 b
Plant extracts of *Reynoutria* spp. (REGALIA)	28.0	72.0 bc
Control (+)	96.0	

*Mean values with the same letter within a column are not significantly different at the $P \leq 0.05$ probability level by Duncan, DS: Disease severity (%), E: Effect (%)

Table 3. *Effectiveness of different treatments on root length (cm), number of root, plant height (cm) and node number on carnation*

Treatments	RL*	NR*	PH*	NN*
Orange oil extract (PREV-AM)	2.40 bc	11.60 e	22.30 b	7.20 ab
T. harzianum	2.40 bc	17.20 bcd	22.56 b	8.40 a
B. subtilis QST 713 (SERENADE)	**2.82 b**	14.60 bcd	**25.38 ab**	8.20 ab
L. acidophilus + *L. paracasei* (VITANAL)	2.14 bc	18.00 abc	21.30 b	9.00 a
P. fluorescens	1.66 c	14.00 bcd	21.25 b	5.60 b
Mycorrhiza spp., *Trichoderma* spp., *Bacillus* spp (PANORAMIX)	2.54 bc	14.20 bcd	24.46 ab	8.20 ab
Tea tree oil extract (TIMOREX GOLD)	**2.82 b**	**23.20 a**	**31.60 a**	8.20 ab
Plant extracts of *Reynoutria* spp. (REGALIA)	**4.28 a**	15.66 bcd	**26.44 ab**	9.00 a
Control (-)	1.59 c	19.60 ab	22.00 b	8.00 ab

**Mean values with the same letter within a column are not significantly different at the $P \leq 0.05$ probability level by Duncan, RL: Root length (cm), NR: Number of root, PH: Plant height (cm), NN: Node number

Discussion

In this study, *F. oxysporum* f. sp. *dianthi* was significantly reduced by several microorganisms and plant extracts. In the experiment, it was determined that the highest percentage of efficacy values of the biological preparations were for *P. fluorescens*, SERENADE and *T. harzianum* to Fod. In addition, the application of SERENADE, TIMOREX GOLD and REGALIA increased plant height. SERENADE, *T. harzianum* and *P. fluorescens* are very common biocontrol agents against the pathogen. Biocontrol

http://www.aloki.hu ● ISSN 1589 1623 (Print) ● ISSN 1785 0037 (Online)
DOI: http://dx.doi.org/10.15666/aeer/1706_1525515265

bacteria and fungi produce multiple antibiotics that eliminate plant pathogen bacteria and fungi (Strange, 2007; Wang et al., 2016). *Trichoderma* spp. produce various antibiotics, such as viridin, gliotoxin, polyketides and pyrones, against fungal phytopathogens (Howell, 2003; Harman et al., 2004; Naher et al., 2014). *Bacillus* spp. include bacitracin, mycosubtilin polymyxin, bacillomycins and gramicidin and they inhibit fungal germination, suppress of some plant pathogen. One of the most important antibiotics compound produced by *P. fluorescens* is pyrollnitrin, which inhibited growth of some plant fungal pathogens (Karimi et al., 2012; Santoya et al., 2012; Chapelle et al., 2016).

Competition for nutrients and plant surface is another mechanism for plant pathogens. Competitive exception of pathogens as the result of fast colonization of the rhizosphere or plant surface by biological fungus and bacteria may also be an important factor in the control of plant pathogens. Biocontrol species have a higher affinity for nutrients especially iron, phosphorus, nitrogen and can stimulate plant growth directly by or indirectly. They can suppress a broad spectrum of bacterial, fungal and nematode diseases (Jan et al., 2011).

Many biocontrol bacteria and fungi induced systemic resistance which is characterised by a broad spectrum of resistance against pathogens (Conrath et al., 2006; Pieterse et al., 2014; O'Brien, 2017). Beneficial microbes elicite the signalling pathways, and stimulate the host's immune system. Biocontrol bacteria and fungus induced systemic resistance (ISR), may also contribute to disease suppressiveness (Beredsen et al., 2018).

Plant extracts and essential oils appeared to be efficient to control *F. oxysporum* f. sp. *dianthi*. Some research studies reported the efficacy of REGALIA in controlling bacterial spot of tomatoes and peppers (*Botrytis* spp. of grapes and strawberries, powdery mildew of cucurbits, downy mildew of lettuce (*Bremia lactucae*), Cercospora on soybeans (*Cercospora kikuchii*), *Cercospora zeae-maydis; Podospheria leucotricha*, *Venturia inaequalis,* bacterial canker on citrus (*Xanthomonas axonopodis* pv. *citri*), *Xanthomonas campestris* pv. *vesicatoria* and *Xanthomonas euvesicatoria* (Su, 2012; Worthington et al., 2012; Harbou and Jaksen Ziems, 2015; Delong et al., 2018). Many beneficial bacteria and fungi have a general plant growth promoting effect, and produce analogues of plant growth regulatory hormones, volatile compounds to stimulate plant growth. (Harman et al., 2004; Taghavi et al., 2009; Hermosa et al., 2012; Rashid et al., 2012; Truyens et al., 2014). Some beneficial microorganism is able to establish a symbiotic relationship with plants and they increase the availability of these nutrients to plants (Gutiérrez-Luna et al., 2010; Saharan and Nehra, 2011). Its beneficial effects of *Trichoderma* sp. on beside abiotic stress have been well documented (Donoso et al., 2008; Mastouri et al., 2010, Roatti et al., 2013).

In our experiment, the application of TIMOREX GOLD significantly reduced the Fod. TIMOREX GOLD components include cineole cymene, linalool and terpinen-4-ol (Carson et al., 2006; Goni et al., 2014; Wei et al., 2018). The plant oil and plant extracts include secondary chemical compounds such as terpenes, alcohols, aldehydes and phenols, and these materials exhibit fungicidal potential (Zanellato et al., 2009). Essential oil from tea tree oil extract has shown promising results in reducing disease occurrence and severity induced by *Cercospore beticola* in sugar beets, and *Alternari solani* in potato (Caolotanski et al., 2002). It was also reported that tea tree oil was effective against Fusarium head blight in wheat, barley and oats, barley leaf stripe and powdery mildew Terzi et al., 2007). The application of tea tree oil at 2.0% inhibited the

http://www.aloki.hu ● ISSN 1589 1623 (Print) ● ISSN 1785 0037 (Online)
DOI: http://dx.doi.org/10.15666/aeer/1706_1525515265

mycelium growth of *Botrytis oryzae, Alternaria brassicicola, Fusarium moniliforme, Aspergillus flavus, Fusarium proliferatum* (Thobunluepop et al., 2009).

Conclusion

It has been observed that the treatments had a positive effect against the *F. oxysporum* f. sp. *dianthi* and the plant growth of carnation. Biological control method seems to be safe and environmentally friendly and an alternative method with respect to fungicides. Utilization of beneficial microorganisms could be a common agricultural practice in the near future. In addition, biological control methods might be combined with other control methods, but additional research is needed to develop methods of incorporation of biological organisms into other control strategies for the carnation wilt disease management. It is helpful to conduct an extended study that identifies the microorganisms and plant extracts used in the experiment under greenhouse conditions against Fod and carnation plant growth.

Acknowledgements. We would like to thank Assoc. Prof. Dr. Özgür KOŞKAN for his helps in statistical analysis.

Conflict of interests. The authors declare that they have no conflict of interests.

Funding. This study was not supported by any Research Fund.

Ethical approval. For this type of study formal consent is not required.

Informed consent. Informed consent was obtained from all individual participants included in the study.

Author contributions. The research was conducted by S. Evrim ARICI and Oktay ERDOĞAN. The experiment was carried out by Evrim ARICI, Oktay ERDOĞAN and Zinnet Nurcin TUNCEL. The article was written by Evrim ARICI.

REFERENCES

[1] Abbott, W. S. (1925): A method of computing the effectiveness of an insecticide. – J Econ Entom 18: 265-267.
[2] Anonymous (2006): Anuario De Estadística Agroalimentaria (Cap.). – Ministerio de Agricultura Pescay Alimentación, Spain 12: 1-13.
[3] Baayen, R. P., Van der Plas, C. H. (1992): Localization ability, latent period and wilting rate in eleven carnation cultiva rs with partial resistance to Fusarium Wilt. – Euphytica 59: 165-174.
[4] Berendsen. R. L., Vismans, G., Yu, K., Song, Y., de Jonge, R., Burgman, W. P., Burmølle, M., Herschend, J., Bakker, P. A. H. M., Pieterse, C. M. J. (2018): Disease-induced assemblage of a plant-beneficial bacterial consortium. – ISME J. https://doi.org/10.1038/s41396-018-0093-1.
[5] Burgess, L. W., Summerell, B. A., Bullock, S., Got, K. P., Backhouse, D. (1994): Laboratory Manual for Fusarium Research. 3rd Ed. – Univ. of Sydney, Sydney.
[6] Caolotanski, J. M., Hanson, L. E., Hill, A. L., Hill, J. P. (2002): Use of *Melaleuca alternifolia* oil for plant disease control. – Phytopathology 92(6): S12.
[7] Carson, C. F., Hammer, A., Riley, T. V. (2006): *Melaleuca alternifolia* (tea tree) oil: a review of antimicrobial and other medicinal properties. – Clinical Microbiology Reviews 2006(1): 50-62.
[8] Chapelle, E., Mendes, R., Bakker, P. (2016): Fungal invasion of the rhizosphere microbiome. – ISME J 10: 265–268.

http://www.aloki.hu ● ISSN 1589 1623 (Print) ● ISSN 1785 0037 (Online)
DOI: http://dx.doi.org/10.15666/aeer/1706_1525515265

[9] Chin-A-Woeng, T. F., Bloemberg, G. V., Lugtenberg, B. J. (2003): Phenazines and their role in biocontrol by *Pseudomonas* Bacteria. – New Phytology 157: 503-523.
[10] Conrath, U., Beckers, G. J. M., Flors, V., Garcia-Agustin, P., Jakab, G., Mauch, F., Newman, M. A., Pieterse, C. M. J., Poinssot, B., Pozo, M. J., Pugin, A., Schaffrath U., Ton J., Wendehenne D., Zimmerli L., Mauch-Mani B. (2006): Prime APG priming: getting ready for battle. – Molecular Plant-Microbe Interactions 19: 1062-1071.
[11] DeLong, C. N., Yoder, K. S., Cochran, A. E., Kilmer, S. W., Royston, W. S., Combs, l. D. (2018): Apple disease control and bloom-thinning effects by lime sulfur, regalia, and JMS stylet-oil. – Plant Health Programme Jan 19(2): 143-52.
[12] Denmik, J. F., Baayen, R. P. and Sparnaaij, L. D. (1989): Evaluation of the virulence of race 1, 2 and 4 of *Fusarium oxysporum,* f. sp. *dianthi* in carnation. – Euphytica 42: 55-63.
[13] Donoso, E. P., Bustamante, R. O., Caru, M., Niemeyer, H. M. (2008): Water deficit as a driver of the mutualistic relationship between the fungus *Trichoderma harzianum* and two wheat genotypes. – Applied and Environmental Microbiology 74: 1412-1417.
[14] Goñi, M. G., Tomadoni, B., Roura, S. I., Moreira, M. R. (2014): Effect of preharvest application of chitosan and tea tree essential oil on postharvest evolution of lettuce native microflora and exogenous *Escherichia coli* O157:H7. – Journal of Food Safety 34: 353-360.
[15] Gutiérrez-Luna, F., López-Bucio, J., Altamirano-Hernández, J., Valencia-Cantero, E., Cruz, H., Macías-Rodríguez, L. (2010): Plant growth-promoting rhizobacteria modulate root-system architecture in *Arabidopsis Thaliana* through volatile organic compound emission. – Symbiosis 51: 75-83.
[16] Hanudin Nuryani, W., Silvia Yusuf, E., Djatnika, I., Soedarjo, M. (2011): Comparison of inoculation techniques and selection of antagonist bacteria to control white rust disease on chrysanthemum. – The Journal of Horticultural Science 21(2): 173-184.
[17] Harbour, J. D., Jackson-Ziems, T. A. (2015): The effects of fungicides and regalia tank mixtures on fray leaf spot in Nebraska Field Corn. – Papers in Plant Pathology 499. http://digitalcommons.unl.edu/plantpathpapers/499.
[18] Harman, G. E., Howell, C. H., Viterbo, A., Chet, I., Lorito, M. (2004): Trichoderma species - opportunistic, avirulent plant symbionts. – Nature Reviews Microbiology 2: 43-56.
[19] Hermosa, R., Viterbo, R., Chet, I., Monte, R. (2012): Plant-beneficial effects of trichoderma and of its genes. – Microbiology 158: 17-25.
[20] Howell, C. R. (2003): Mechanisms employed by *Trichoderma* species in the biological control of plant diseases: the history and evolution of current concepts. – Plant Disease 87: 4-10.
[21] Jan, A. T., Azam, M., Ali, A., Haq, Q. M. R. (2011): Novel approaches of beneficial pseudomonas in mitigation of plant diseases-an appraisal. – Journal of Plant Interactions 6: 195-205. DOI: 10.1080/17429145.2010.541944.
[22] Johnson, L. A. (1957): Effect of antibodies on the number of bacteria and fungi isolated from soil by dilution plate method. – Phytopathology 47: 21-22.
[23] Karimi, K., Amini, J., Harighi, B., Bahramnejad, B. (2012): Evaluation of biocontrol potential of Pseudomonas and Bacillus spp. against Fusarium Wilt of chickpea. – Australian Journal of Crop Science 6: 695-703.
[24] Mahalakshmi, P., Mohan, S., Theradimani, M. (2015): Evaluation of tree borne oil cakes for the management of Fusarium wilt of carnation (*Dianthus caryophllus* L.) caused by *Fusarium oxysporum* f. sp. *Dianthi* P. – Advances in Tree Seed Science and Silviculture, 164-171.
[25] Mastouri, F., Bjorkman, T., Harman, G. E. (2010): Seed Treatment with *Trichoderma harzianum* alleviates biotic, abiotic, and physiological stresses in germinating seeds and seedlings. – Phytopathology 100: 1213-1221.

http://www.aloki.hu ● ISSN 1589 1623 (Print) ● ISSN 1785 0037 (Online)
DOI: http://dx.doi.org/10.15666/aeer/1706_1525515265

[26] Naher, L., Yusuf, U., Ismail, A., Hossain, K. (2014): *Trichoderma* spp.: a biocontrol agent for sustainable management of plant diseases. – Pakistan Journal of Botany 46(4): 1489-1493.
[27] Nelson, P. E., Toussoun, T. A., Marasas, W. F. O. (1983): *Fusarium* Species. An Illustrated Manual for Identification. – The Penn State University Press, University Park, Pennsylvania.
[28] O'Brien, P. A. (2017): Biological control of plant diseases. – Australasian Plant Pathology 44: 1-12. DOI: 10.1007/s13313-017-0466-3.
[29] Pieterse, C. M. J., Zamioudis, C., Berendsen, R. L., Weller, D. M., Van Wees, S. C. M., Bakker, P. (2014): Induced systemic resistance by beneficial microbes. – Annual Review of Phytopathology 52: 347-375. DOI: 10.1146/annurevphyto-082712-102340.
[30] Rashid, S., Charles, T. C., Glick, B. R. (2012): Isolation and characterization of new plant growth-promoting bacterial endophytes. – Applied Soil Ecology 61: 217-224.
[31] Rhodes, M. E. (1959): The characterization of *Pseudomonas Jluorescens*. – Journal of General Microbiology 21: 221.
[32] Roatti, B., Perazzolli, M., Gessler, C., Pertot, I. (2013): Abiotic stresses affect *Trichoderma harzianum* t39-induced resistance to downy mildew in grapevine. – Phytopathology 103(12): 1227-1234.
[33] Saharan, B., Nehra, V. (2011): Plant growth promoting rhizobacteria: a critical review. – Life Sciences Med Research 21: 1-30.
[34] Santoyo, G., Orozoco-Mosqueda, M. C., Govindappa, M. (2012): Mechanisms of biocontrol and plant growth-promoting activity on soil bacterial species of bacillus and pseudomonas: a review. – Biocontrol Science and Technology 22: 855-872.
[35] Sarrocco, S., Falaschi, N., Vergara, M., Nicoletti, F., Vannacci, G. (2007): Use of *Fusarium oxysporum* f. sp. *dianthi* transformed with marker genes to follow colonization of carnation roots. – Journal of Plant Pathology 89: 61-68.
[36] Sohi, H. S. (1992): Diseases of Ornamental Plants in India. – Publication and Information Division, Indian Council of Agricultural Research, Krishi Anusandhan Bhavan, New Delhi.
[37] Strange, R. N. (2007): Phytotoxins produced by microbial plant pathogens. – Natural Product Reports 24: 127-144. DOI: 10.1039/b513232k.
[38] Su, H. (2012): REGALIA® bioprotectant in plant disease management. – Outlooks on Pest Management 23(1): 30-34.
[39] Taghavi, S., Garafola, C., Monchy, S., Newman, L., Hoffman, A., Weyens, N., Barac, T., Vangronsveld, J., Vander Lelie, D. (2009): Genome survey and characterization of endophytic bacteria exhibiting a beneficial effect on growth and development of poplar trees. – Applied and Environmental Microbiology 75: 748-757.
[40] Terzi, V., Morcia, M., Faccioli, P., Valè, G., Tacconi, G., Malnati, M. (2007): *In vitro* antifungal activity of the tea tree (*Melaleuca alternifolia*) essential oil and its major components against plant pathogens. – Letters in Applied Microbiology 44(6): 613-618.
[41] Thobunluepop, P., Udomsilp, J., Piyo, A., Khaengkhan, P. (2009): Screening for the antifungal activity of essential oils from bergamot oil (Citrus hystrix DC.) and tea tree oil (*Melaleuca alternifolia*) against economically rice pathogenic fungi: a driving force of organic rice Cv. KDML 105 production. – Asian Journal of Food & Agro-Industry Special Issue: S374-S380.
[42] Townsend, G. K., Heuberger, W. (1943): Methods for estimating losses caused by diseases in fungicide experiments. – Plant Disease Report 27: 340-343.
[43] Truyens, S., Weyens, N., Cuypers, A., Vangronsveld, J. (2014): Bacterial seed endophytes: genera, vertical transmission and interaction with plants. – Environmental Microbiology Reports 7: 40-50.
[44] TSI (2016): Türkiye İstatistik Kurumu (TÜİK). – http://www.tuik.gov.tr/PreTablo.do?alt_id=1001 Erişim tarihi: 23.08.2017A.

http://www.aloki.hu ● ISSN 1589 1623 (Print) ● ISSN 1785 0037 (Online)
DOI: http://dx.doi.org/10.15666/aeer/1706_1525515265

[45] Wang, M. C., Tachibana, S., Murai, Y., Li, L., Lau, S. Y. L., Cao, M. C., Zhu, G. N., Hashimoto, M., Hashidoko, Y. (2016): Indole-3-acetic acid produced by *Burkholderia heleia* acts as a phenylacetic acid antagonist to disrupt tropolone biosynthesis in *Burkholderia plantarii*. – Scientific Reports 6: 22596-22596.

[46] Wei, Y., Shao, X., Wei, Y., Xu, F., Wang, H. (2018): Effect of preharvest application of tea tree oil on strawberry fruit quality parameters and possible disease resistance mechanisms. – Scientia Horticulturae 241: 18-28.

[47] Whipps, J. M. (2001): Microbial interactions and biocontrol in the rhizosphere. – Journal of Experimental Botany 52: 487-511.

[48] Worthington, R. J., Rogers, S. A., Huigens, R. W., Melander, C., Ritchie, D. F. (2012): Foliar-applied small molecule that suppresses biofilm formation and enhances control of copper-resistant Xanthomonas euvesicatoria on pepper. – Plant Disease 96(11): 1638-44. DOI: 10.1094/PDIS-02-12-0190-RE.

[49] Zanellato, M., Masciarelli, E., Casorri, L., Boccia, P., Sturchio, E., Pezzella, M., Cavalieri, A., Caporali, F. (2009): The essential oils in agriculture as an alternative strategy to herbicides: a case study. – International Journal of Environment and Health 3(2): 198-213.

http://www.aloki.hu ● ISSN 1589 1623 (Print) ● ISSN 1785 0037 (Online)
DOI: http://dx.doi.org/10.15666/aeer/1706_1525515265

ANALYSIS OF EFFECTS OF COVER CROP AND TILLAGE METHOD COMBINATIONS ON THE PHENOTYPIC TRAITS OF SPRING WHEAT (*TRITICUM AESTIVUM* L.) USING MULTIVARIATE METHODS

BOCIANOWSKI, J.[1*] – MAJCHRZAK, L.[2]

[1]*Department of Mathematical and Statistical Methods, Poznań University of Life Sciences*
Wojska Polskiego 28, 60-637 Poznań, Poland
(ORCID: 0000-0002-0102-0084; phone: +48-61-848-7143; fax: +48-61-848-7140)

[2]*Department of Agronomy, Poznań University of Life Sciences*
Dojazd 11, 60-632 Poznań, Poland
(ORCID: 0000-0002-1593-491X; phone: +48-61-848-7574; fax: +48-61-848-7397)

[*]*Corresponding author*
e-mail: jan.bocianowski@up.poznan.pl; phone: +48-61-848-7143; fax: +48-61-848-7140

(Received 5th Jul 2019; accepted 16th Oct 2019)

Abstract. The paper presents the results of multivariate analysis assessing variation in quantitative traits after the application of various cover crops and tillage methods in cultivation of spring wheat in three years of study. The purpose of this study was to assess the multivariate phenotypic variation of spring wheat under 27 different combinations of three cover crops, three tillage methods and three years of study. 13 quantitative traits were monitored through the course of three years (2011-2013) in Poland. The result was statistically analyzed using the multivariate methods. Analysis of canonical variables proved to be a reliable tool providing a comprehensive assessment of variation in the effect of cover crop and method of tillage combinations on many traits simultaneously. The most diverse treatments were Z-A-1 (cover crop: zero, method of tillage: aggregate, in 2011) and N-P-2 (cover crop: no tillage, method of tillage: plowing, in 2012). The most similar treatments (in terms of 13 traits assessed) included Z-A-1 (cover crop: zero, method of tillage: aggregate, in 2011) and N-A-1 (cover crop: N – no tillage, method of tillage: aggregate, in 2011).
Keywords: *canonical variate analysis, grain yield, biomass of spring wheat, white mustard, Mahalanobis' distances, quantitative traits*

Introduction

In the area of integrated production, it seems necessary to develop a technology for the production of spring wheat, while also taking into account the inclusion of stubble. Crop rotation with a large share of cereals, will improve soil efficiency and create better phytosanitary conditions for the development of spring wheat (Majchrzak, 2015). Catch crops deliver environmental benefits, and they are widely recommended by programs which promote environmentally friendly agricultural practices (Wanic et al., 2019). Simplification of the tillage system can cause an increase in weeds and consequently, a decrease the yield of cultivated plants. Changes in weeds can affect also stubble catch crops and fertilization used as regeneration factors. Regenerating and yielding effect of catch crops cultivation depends, among from habitat conditions, as well as on the type of catch crop and species of the cultivated plant.

Numerous authors have proposed statistical methods for estimation the manner of factors reaction to diverse environmental condition (Wricke and Weber, 1986). Multivariate analysis tools, such as principal component analysis, canonical variables

http://www.aloki.hu ● ISSN 1589 1623 (Print) ●ISSN1785 0037 (Online)
DOI: http://dx.doi.org/10.15666/aeer/1706_1526715276

analysis, canonical correlation analysis, additive main effects and multiplicative interaction and multiple regression, are powerful in dealing with intercorrelated data, such as agroclimatic and other factors limiting crop yields (Qian et al., 2009; Hussain et al., 2014; Nowosad et al., 2017; Nowosad et al., 2018; Bocianowski et al., 2018).

The aim of this study was to conduct a multivariate characteristic of phenotypic variability in 27 treatments being combinations of cover crop, method of tillage and years. The canonical variables analysis was applied, based on the model of multivariate analysis of variance (MANOVA), for observations of 13 quantitative traits in an experiment established in the split-plot design.

Material and methods

Experimental field

The field experiment was performed at the Brody Research and Education Station of the Poznań University of Life Sciences, Poland (52° 26' N; 16° 17' E) on soil classified (WRB 2007) as *Albic Luvisols* develop on loamy sands overlying loamy material (12% clay, 19% silt and 69% sand) in the years 2011-2013 (*Figure 1*).

Figure 1. *The experimental design of spring wheat (Triticum aestivum L.) at the Brody Research and Education Station of the Poznań University of Life Sciences, Poland (52° 26' N; 16° 17' E)*

They were performed in the random block (split-plot) design with three experimental factors in four field replications resulting in a total of 9 plots. The experiment was designed to analyses the effect of cover crop (white mustard cultivar Nakielska) sowing: (control: zero – Z, no sowing of cover crop, sowing of cover crop following skiming – S and no tillage – N direct sowing of cover crop), three tillage methods for spring cultivation (direct sowing – D, simplified tillage (cultivation aggregate to a depth of 12-15 cm) – A, spring ploughing to a depth of 25 cm – P) on 13 quantitative traits (grain

http://www.aloki.hu ● ISSN 1589 1623 (Print) ●ISSN1785 0037 (Online)
DOI: http://dx.doi.org/10.15666/aeer/1706_1526715276

yield, [t ha^{-1}], protein grain yield of spring wheat [kg ha^{-1}], test weight of spring wheat grain [kg ha^{-1}], plants number of spring wheat after emergence [no m^{-2}], leaf greenness index SPAD, height plants [cm], leaf area index [LAI], biomass yield of spring wheat in BBCH 23 [t ha^{-1} DM], biomass yield of spring wheat in BBCH 32 [t ha^{-1} DM], biomass yield of spring wheat in BBCH 55 [t ha^{-1} DM], biomass yield of spring wheat in BBCH 75 [t ha^{-1} DM], number of weeds [no m^{-2}] and the fresh weight of weeds [g m^{-2}]).

Spring wheat cultivar, Vinjett, was sown at the rate of 400 seeds per 1 m^2 across all tillage systems. The size of each tillage plots was 10 m long and 4.5 m wide (45 m^2).

Sowing dates of spring depended of soil water conditions and occurred between 23rd of March 2012 and 17th of April 2013 and sowing depth in all tillage systems were 3-4 cm.

Fertilization was uniform for all tillage systems and each experimental year (90 kg N ha^{-1}, 26 kg P ha^{-1}, 50 kg K ha^{-1}). The herbicide program for tillage systems consisted of pre-plant and post-emergence applications. Before sowing 1.5 L ha^{-1} of Gliphosate herbicide + 1.5 L ha^{-1} adjuvant As 500 SL was applied to all plots with no-tillage to control perennial weed and volunteer plants. For weed control, during the growing season post-emergence BBCH 22 Lintur 70 WG (dicamba 65.9%+triasulfuron 4.1%)+Chwastox Extra 300 SL (MCPA 300 g L^{-1}) herbicide were applied at the rate of 150 g ha^{-1}+1.0 L ha^{-1}. For disease control, Falcon 460 EC fungicide (spiroksamine 250 g L^{-1}+tebuconazole 167 g L^{-1}+triadimenol 43 g L^{-1}) at the rate of 0.6 L ha^{-1} was applied in all plots at BBCH 32 growth stage and Fury 100 EW insecticide (zeta-cypermetryne 100 g L^{-1}) at the rate of 0.1 L ha^{-1} and at last year Karate Zeon 050 CS (lambda – cyhalotryne) at the rate 0.1 L ha^{-1} at BBCH 61 growth stage.

Sampling and Measurements

Plants number of spring wheat after emergence [no m^{-2}] – frame method (2 × 0.25 m^{-2}). Biomass yield of spring wheat in BBCH 23, BBCH 32, BBCH 55, BBCH 75 [t ha^{-1} DM] (2 × 0.25 m^{-2}). Mesurements of leaf area index [LAI] was made in BBCH 51-53 phase, using SunScan Canopy Analysis System type SSI – Delta-T Devices Ltd. Great Britain. Chlopchlorophyll content indicator (SPAD) was determined in BBCH 39 phase using Chlorophyll Hydro N-Tester. Number [no m^{-2}] and the fresh weight of weeds [g m^{-2}] were carried out annually on randomly determined parts of experimental plots covered with foil covers during the application of herbicides. In the development phase (BBCH 31–32) spring wheat was determined on an area of 1 m^2.

Meteorological conditions

In the first year of research, only in July the amount of precipitation exceeded by 86.4 mm the precipitation needs of spring wheat (*Table 1*). For optimal wheat development this year there was no rain: in April 31.1 mm. in May 32.0 mm and June 67.6 mm. Such water shortages adversely affected the emergence, development of plants, tillering and the formation of ears. In year 2012, rainfall deficiencies occurred in April (22.1 mm) and in June (13.2 mm), May precipitation exceeded the demand for water by 11.2 mm, and in July by as much as 108.6 mm. In the last year of research, water was lacking in April (deficit by 29.6 mm), which was partly complemented by May (excess in relation to optimum 97 mm) and June (42.3 above optimal). The rainfall deficit also occurred in July (21.7 mm below needs) for this period. Comparing the multiannual average with precipitation needs, it should be stated that the sums of precipitation occurring in the analyzed region are usually lower than the demand for

http://www.aloki.hu ● ISSN 1589 1623 (Print) ●ISSN1785 0037 (Online)
DOI: http://dx.doi.org/10.15666/aeer/1706_1526715276

water necessary for the optimal development of spring wheat. To sum up the course of weather conditions, it can be said that the first year of research was the least favorable for the growth and development of spring wheat, while the most favorable was year 2013.

Table 1. *Rainfall sums and rainfall requirements (Dzieżyc, 1989)*

Years	Rainfall sums [mm]			
	April	May	June	July
2011	13.9	34.0	15.4	175.4
2012	22.9	77.2	69.8	197.6
2013	15.4	163.0	125.3	67.3
Means 1961-2010	38.0	57.4	61.8	77.5
Demand volume in month [mm]				
Rainfall requirements	45	66	83	89

Statistical analysis

Firstly, the normality of the distributions of the studied traits were tested using Shapiro-Wilk's normality test (Shapiro and Wilk, 1965). Multivariate analysis of variance (MANOVA) was performed on the basis of following model using a procedure MANOVA in GenStat 18th edition: **Y=XT+E**, where: **Y** is ($n\times p$)-dimensional matrix of observations, n is number of all observations, p is number of traits (in this study p=13), **X** is ($n\times k$)-dimensional matrix of design, **T** is ($k\times p$)-dimensional matrix of unknown effects, **E** – ($n\times p$)-dimensional matrix of residuals. Nextly, the effects of the main factors under study (cover crop, method of tillage and years), as well as the all interactions between them were estimated using a linear model for three-way analysis of variance (ANOVA) for particular traits. The relationships between observed traits were assessed on the basis of Pearson's correlation coefficients and tested by the t-test. Results were also analysed using multivariate methods. The canonical variate analysis was applied in order to present multitrait assessment of similarity of the investigated treatments in a lower number of dimensions with the least possible loss of information (Rencher, 1992). This makes it possible to illustrate variation in investigated treatments in terms of all observed traits in the graphic form. Mahalanobis' distance was suggested as a measure of "polytrait" treatments similarity (Seidler-Łożykowska and Bocianowski, 2012), whose significance was verified by means of critical value D_α called "the least significant distance" (Mahalanobis, 1936). Mahalanobis' distances were calculated for investigated treatments. In order to determine the relative share of each original trait in the multivariate variation of analysed treatments Pearson's simple correlation coefficients were estimated between values of the first two canonical variables and values of individual original traits. All the analyses were conducted using the GenStat v. 18 statistical software package.

Results and Discussion

All studied quantitative traits have a normal distribution as well as a multivariate normality. Results of MANOVA indicate that the all factors (years: Wilk's λ=0.00127, $F_{2;81}$=143.60, P<0.0001; cover crop: Wilk's λ=0.16470, $F_{2;81}$=7.77, P<0.0001; method of tillage for spring wheat: Wilk's λ=0.07879, $F_{2;81}$=13.60, P<0.0001) and their

http://www.aloki.hu ● ISSN 1589 1623 (Print) ●ISSN1785 0037 (Online)
DOI: http://dx.doi.org/10.15666/aeer/1706_1526715276

interactions (years × cover crop: Wilk's λ=0.06601, $F_{4;81}$=5.27, P<0.0001; year × method of tillage for spring wheat: Wilk's λ=0.07601, $F_{4;81}$=4.90, P<0.0001; cover crop × method of tillage for spring wheat: Wilk's λ=0.15555, $F_{4;81}$=3.19, P<0.0001; years × cover crop × method of tillage for spring wheat: Wilk's λ=0.07820, $F_{8;81}$=2.09, P<0.0001) were significant different for all 13 traits. The ANOVA indicated statistically significant influence of years for all observed traits (*Table 2*). Cover crop was significant for all traits except leaf greenness index, biomass yield in BBCH 23, biomass yield in BBCH 32, biomass yield in BBCH 75 and number of weeds, however method of tillage for all traits except leaf greenness index, height plants, LAI and weight of weeds. In research by Kulig et al. (2010) there was not significant correlation between SPAD values and grain yield but a strong link with the protein content and with the values of grain yield. Lepiarczyk et al. (2005) showed that the method of cultivation and use of fore crop significantly influenced the size of leaf surface. They showed that the value of LAI and the conopy of wheat grain yield is significant and has a high correlation. The year × cover crop × method of tillage for spring wheat interaction was significant for plants number after emergence, biomass yield in BBCH 55 and weight of weeds (*Table 2*).

Table 2. *F-statistic from three-way analysis of variance for observed traits*

Source of variation	Year (Y)	Cover crop (Cc)	Method of tillage (Mt)	Y×Cc	Y×Mt	Cc×Mt	Y×Cc×Mt
d.f.	2	2	2	4	4	4	8
GY	58.2***	20.84***	6.49**	2.91*	0.47	0.7	0.68
PGY	29.67***	16.17***	6.04**	2.63*	0.21	0.48	0.77
TW	54.33***	4.5*	7.41**	0.88	2.45	0.27	1.84
PNE	700.38***	12.92***	74.62***	14.27***	14.57***	6.24***	3.35**
SPAD	42.51***	1.74	1.34	1.2	2.18	0.54	0.24
HP	378.92***	8.98***	0.41	0.17	1.67	2.34	0.64
LAI	18.9***	26.38***	1.65	0.98	0.11	2.96*	0.72
BY23	90.63***	2.14	125.58***	5.75***	20.62***	2.14	1.63
BY32	18.39***	1.38	13.95***	1.46	6.71***	1.01	1.03
BY55	203.25***	6.36**	12.78***	8.59***	5.23***	3.54*	2.32*
BY75	56.14***	1.31	4.91*	4.25**	1.29	1.04	0.99
NW	8.72***	0.99	21.24***	2.12	4.42**	7.32***	1.63
WW	25.91***	27.64***	2.52	20.15***	7.41***	8.63***	7.32***

*p<0.05; ** P<0.01; *** P<0.001; d.f. – degrees of freedom.
GY - grain yield, PGY - protein grain yield, TW - test weight, PNE - plants number after emergence, SPAD - leaf greenness index, HP - height plants, LAI - leaf area index, BY23 - biomass yield in BBCH 23, BY32 - biomass yield in BBCH 32, BY55 - biomass yield in BBCH 55, BY75 - biomass yield in BBCH 75, NW - number of weeds, WW - weight of weeds

Kraska (2012) found that with regard to the yield, more reliable were undersown catch crops, compared with stubble crops. Kwiatkowski (2009) think that degree to which catch crops affect regulation of weed infestation is diversified and depends on habitat conditions, cereal species, type of catch crop and plant selection as well as method of its management. According to Wozniak (2011) compared to plough tillage ploughless tillage significantly increased air-dry weight of weeds in the spring wheat crop. The tillage system under comparison did not differentiate the number of weeds per 1 m^2.

http://www.aloki.hu ● ISSN 1589 1623 (Print) ●ISSN1785 0037 (Online)
DOI: http://dx.doi.org/10.15666/aeer/1706_1526715276

Testing of Pearson's correlation coefficients made it possible to observe several statistically significant interdependencies between observed traits of spring wheat. Grain yield was significantly positively correlated with protein grain yield, test weight of spring wheat grain, plants number after emergence, LAI, biomass yield in BBCH 23, biomass yield in BBCH 55 and biomass yield in BBCH 75 (*Table 3*). Faber and Nieróbca (1999) found a strong correlation between the maximum LAI and above ground dry mass and slightly less with the grain yield. Lepiarczyk et al. (2005) showed that the values of LAI and the conopy of wheat grain yield is significant and has a high correlation. In our research generally, was observed 42 pairs of significant correlation coefficient: 36 positive and six negative (*Table 3*).

Table 3. *Correlation coefficients between observed quantitative traits of spring wheat*

Trait	GY	PGY	TW	PNE	SPAD	HP	LAI	BY23	BY32	BY55	BY75	NW
PGY	0.86***											
TW	0.70***	0.33										
PNE	0.59**	0.15	0.78***									
SPAD	-0.28	0.17	-0.58**	-0.70***								
HP	0.34	-0.13	0.74***	0.79***	-0.84***							
LAI	0.83***	0.86***	0.30	0.30	0.02	0.07						
BY23	0.65***	0.56**	0.62***	0.50**	-0.10	0.13	0.43*					
BY32	0.30	0.02	0.43*	0.64***	-0.47*	0.55**	0.19	0.41*				
BY55	0.58**	0.18	0.69***	0.81***	-0.77***	0.75***	0.36	0.50**	0.69***			
BY75	0.75***	0.47*	0.63***	0.72***	-0.59**	0.46*	0.51**	0.61***	0.36	0.80***		
NW	0.33	0.20	0.36	0.48*	-0.16	0.25	0.16	0.51**	0.58**	0.42*	0.31	
WW	0.09	0.06	-0.07	0.13	-0.07	-0.06	-0.07	-0.04	-0.08	0.07	0.14	0.48*

* P<0.05; ** P<0.01; *** P<0.001.
GY - grain yield, PGY - protein grain yield, TW - test weight, PNE - plants number after emergence, SPAD - leaf greenness index, HP - height plants, LAI - leaf area index, BY23 - biomass yield in BBCH 23, BY32 - biomass yield in BBCH 32, BY55 - biomass yield in BBCH 55, BY75 - biomass yield in BBCH 75, NW - number of weeds, WW - weight of weeds

Individual traits are of different importance and have a different share in the joint multivariate variation. A study on the multivariate variation for treatments includes also identification of the most important traits in the multivariate variation of treatments. Canonical variables analysis (CVA) is a statistical tool making it possible to solve this problem (Bocianowski et al., 2016; Lahuta et al., 2018). Results of the CVA for investigated treatments are presented in *Table 4*. The first two canonical variables explained jointly 87.03% total variation between treatments (*Table 4*, *Figure 2*). *Figure 2* presents variation in traits of investigated treatments in the system of the first two canonical variables. In the graph the coordinates of a point of a given treatment are values of the first and second canonical variables, respectively. The greatest, significant linear relationship with the first canonical variables was found for the grain yield, test weight of spring wheat grain, plants number after emergence, height plants, biomass yield in BBCH 32, biomass yield in BBCH 55, and biomass yield in BBCH 75 (positive dependencies), and SPAD (negative) (*Table 4*). The second canonical variable was significantly positively correlated with grain yield, protein grain yield, LAI, biomass yield in BBCH 23, biomass yield in BBCH 75 and number of weeds (*Table 4*). The greatest diverse in terms of all the 13 traits jointly (measured Mahalanobis distances) was found for treatments denoted with symbols Z-A-1 (cover crop: zero, method of tillage: aggregate, in 2011) and N-P-2 (cover crop: no tillage, method of tillage:

http://www.aloki.hu ● ISSN 1589 1623 (Print) ●ISSN1785 0037 (Online)
DOI: http://dx.doi.org/10.15666/aeer/1706_1526715276

plowing, in 2012) (the Mahalanobis distance between them amounted to 24.49). The greatest similarity was found for treatments Z-A-1 (cover crop: zero, method of tillage: aggregate, in 2011) and N-A-1 (cover crop: N – no tillage, method of tillage: aggregate, in 2011) (2.27). Values of Mahalanobis distances for all pairs of treatments are presented in *Table 5*.

Table 4. *Correlation coefficients between the first two canonical variables and original traits*

Trait	First canonical variable	Second canonical variable
GY	0.552**	0.542**
PGY	0.057	0.653***
TW	0.842***	0.24
PNE	0.913***	0.274
SPAD	-0.845***	0.248
HP	0.919***	-0.273
LAI	0.221	0.501**
BY23	0.373	0.861***
BY32	0.576**	0.243
BY55	0.877***	0.188
BY75	0.704***	0.457*
NW	0.331	0.453*
WW	0.049	0.054

* P<0.05; ** P<0.01; *** P<0.001.
GY - grain yield, PGY - protein grain yield, TW - test weight, PNE - plants number after emergence, SPAD - leaf greenness index, HP - height plants, LAI - leaf area index, BY23 - biomass yield in BBCH 23, BY32 - biomass yield in BBCH 32, BY55 - biomass yield in BBCH 55, BY75 - biomass yield in BBCH 75, NW - number of weeds, WW - weight of weeds

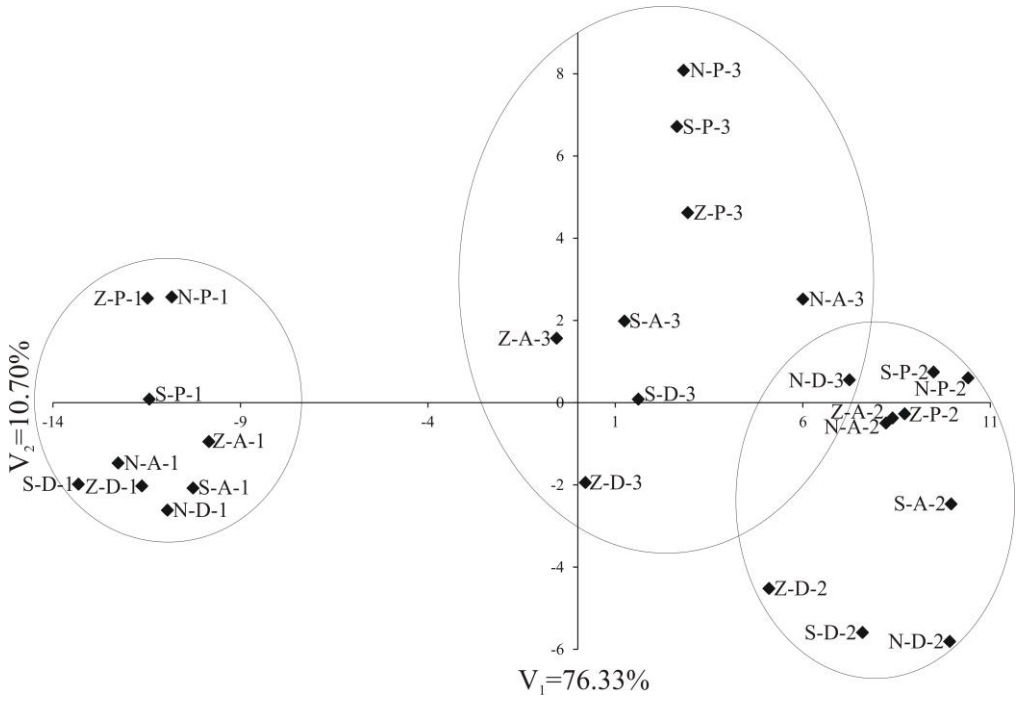

Figure 2. *Distribution of spring wheat treatments in the two first canonical variables (cover crop: Z – zero, S – skiming, N – no tillage; method of tillage for spring wheat: D – direct sowing, A – simplified tillage, P – spring ploughing; years: 1 – 2011, 2 – 2012, 3 – 2013)*

http://www.aloki.hu ● ISSN 1589 1623 (Print) ●ISSN1785 0037 (Online)
DOI: http://dx.doi.org/10.15666/aeer/1706_1526715276

Table 5. *Mahalanobis distances between analyzed treatments of spring wheat*

Treatments	No	1	2	3	4	5	6	7	8	9	10	11	12	13
Z-A-11	**2**	2.57												
Z-P-11	**3**	5.33	4.88											
S-D-11	**4**	4.41	4.84	7.15										
S-A-11	**5**	4.48	3.32	7.12	3.38									
S-P-11	**6**	4.91	4.07	5.56	3.9	3.55								
N-D-11	**7**	4.03	3.74	7.22	3.31	2.3	3.27							
N-A-11	**8**	4.49	4.47	6.8	**2.27**	3.27	2.44	2.72						
N-P-11	**9**	5.63	4.87	2.99	7.34	7.02	5.07	6.82	6.58					
Z-D-12	**10**	17.35	15.73	18.6	18.88	15.95	17.45	16.6	17.88	17.89				
Z-A-12	**11**	20.4	18.68	20.55	22.23	19.47	20.4	20.03	21.08	20.06	7.14			
Z-P-12	**12**	20.69	18.76	20.59	22.41	19.37	20.5	20.21	21.42	20.23	6.86	4.49		
S-D-12	**13**	20.01	18.38	21.38	21.3	18.38	20.06	19.01	20.38	20.74	3.53	7	6.9	
S-A-12	**14**	21.82	20.06	22.51	23.37	20.4	21.7	21.05	22.3	21.83	5.89	4.19	4.52	4.53
S-P-12	**15**	21.95	20.2	21.57	24.14	21.31	21.94	21.72	22.96	21.11	10.38	5.34	5.74	10.31
N-D-12	**16**	22.29	20.65	23.49	23.85	20.82	22.37	21.3	22.91	22.63	5.94	8.26	7.47	4.03
N-A-12	**17**	20.25	18.4	20.26	21.86	18.95	19.88	19.55	20.75	19.77	6.41	3.58	3.3	6.22
N-P-12	**18**	22.57	20.66	22.28	**24.49**	21.39	22.4	22.13	23.53	21.79	9.12	7.03	3.8	9.06
Z-D-13	**19**	14.33	13.23	15.84	16.43	14.04	15.36	14.4	15.66	15.4	11.24	11.73	12.82	12.83
Z-A-13	**20**	12.69	11.05	12.65	14.65	12.19	12.73	12.68	13.58	11.94	10.38	10.53	11.43	12.6
Z-P-13	**21**	16.66	14.43	15.67	17.64	14.94	15.49	16.04	16.66	15.06	9.86	9.23	8.6	11.44
S-D-13	**22**	13.91	11.89	14.11	15.46	12.52	13.58	13.19	14.53	13.11	6.97	8.73	8.44	9.05
S-A-13	**23**	13.83	11.74	13.36	15.53	12.75	13.26	13.34	14.38	12.41	8.54	8.59	8.89	10.56
S-P-13	**24**	17.21	15.09	15.63	18.41	15.98	15.92	16.87	17.21	15.15	11.87	10.06	10.08	13.51
N-D-13	**25**	20.09	17.99	20.29	21.17	18.12	19.35	18.89	20.28	19.28	8.02	8.06	6.92	7.86
N-A-13	**26**	18.91	16.78	18.79	20.09	17.18	18.1	18.04	19.04	17.81	8.34	7.15	7.01	9.01
N-P-13	**27**	18.3	16.11	16.48	19.21	16.82	16.56	17.6	18.01	15.53	13.16	11.5	11.5	14.66

Treatments	No	14	15	16	17	18	19	20	21	22	23	24	25	26
S-P-12	**15**	7.35												
N-D-12	**16**	5.02	10.05											
N-A-12	**17**	4.14	5.89	7.14										
N-P-12	**18**	6.35	6.41	8.04	5.55									
Z-D-13	**19**	13.11	13.99	14.53	12.99	14.37								
Z-A-13	**20**	12.54	12.65	14.37	11.32	13.13	5.61							
Z-P-13	**21**	10.44	11.49	13.21	8.68	10.14	11.69	7.9						
S-D-13	**22**	9.44	10.56	10.45	8.17	10.02	9.44	6.27	6.17					
S-A-13	**23**	10.24	10.01	12.04	8.42	10.66	9.67	5.52	5.65	3.02				
S-P-13	**24**	12	11.8	15.19	9.79	11.38	12.76	8.67	3.58	8.44	6.83			
N-D-13	**25**	6.69	9.81	7.9	6.79	7.44	12.92	11.09	7.6	6.62	7.81	10.06		
N-A-13	**26**	7.2	9.5	9.99	6.96	8.36	11.72	9.23	5.17	6.03	6.09	7.23	3.82	
N-P-13	**27**	13.03	12.94	15.82	10.96	12.36	14.22	9.72	4.78	8.75	7.25	4.08	9.52	7.05

cover crop: Z – zero, S – skiming, N – no tillage.
method of tillage for spring wheat: D – direct sowing, A – simplified tillage, P – spring ploughing; years: 11 – 2011, 12 – 2012, 13 – 2013

Conclusion

The presented multivariate characteristic of the behaviour of analysed treatments is a convincing illustration of this aspect. In this way efficiency of the canonical variables analysis was shown. This results from the fact that these variables explained a considerable part of total variation (87.03%). Additionally, we obtained three groups of treatments, classified by the years of study (*Figure 2*). Thus this is a reliable method, which may be confirmed by its extensive application by breeders and geneticists

http://www.aloki.hu ● ISSN 1589 1623 (Print) ●ISSN1785 0037 (Online)
DOI: http://dx.doi.org/10.15666/aeer/1706_1526715276

(Shamsuddin, 1985; Seidler-Łożykowska et al., 2013; Nowosad et al., 2016; Bocianowski et al., 2018, 2019; Wrońska-Pilarek et al., 2018). In our study, the greatest diverse in terms of all the 13 traits jointly (measured Mahalanobis distances) was found for cover crop: zero, method of tillage: aggregate (in 2011) and cover crop: no tillage, method of tillage: plowing (in 2012). However, the greatest similarity was found for cover crop: zero, method of tillage: aggregate (in 2011) and cover crop: N – no tillage, method of tillage: aggregate (in 2011).

Acknowledgements. The publication was co-financed within the framework of Ministry of Science and Higher Education programme as "Regional Initiative Excellence" in years 2019-2022, Project No. 005/RID/2018/19.

REFERENCES

[1] Bocianowski, J., Szulc, P., Nowosad, K. (2016): Analysis of effects of nitrogen and magnesium fertilization combinations of phenotypic traits of two maize (*Zea mays* L.) cultivars using multivariate methods. – Polish Journal of Agronomy 26: 3-8.

[2] Bocianowski, J., Szulc, P., Nowosad, K. (2018): Soil tillage methods by years interaction for dry matter of plant yield of maize (*Zea mays* L.) using additive main effects and multiplicative interaction model. – Journal of Integrative Agriculture 17(12): 2836-2839.

[3] Bocianowski, J., Nowosad, K., Szulc, P. (2019): Soil tillage methods by years interaction for harvest index of maize (*Zea mays* L.) using additive main effects and multiplicative interaction model. – Acta Agriculturae Scandinavica Section B-Soil and Plant Science 69(1): 75-81.

[4] Dzieżyc, J. (1989): Water requirement of the cultivated plants. – PWN Warszawa: 418 p. (in Polish).

[5] Faber, A., Nieróbca, A. (1999): Winter wheat field forecasting using leaf area index. – Fragmenta Agronomica 1(61): 59-68. (in Polish).

[6] Hussain, S. B., Wahid, M. A., Zubair, M., Babar, M., Wahid, K. (2014): Assessment of germplasm using multivariate analysis for grain yield and quality traits in spring wheat. – Pakistan Journal of Botany 46(3): 989-994.

[7] Kraska, P. (2012): Effect of tillage system and catch crop on weed infestation and spring wheat stands (*Triticum aestivum* L.). – Acta Scientiarum Polonorum seria Agricultura 11(2): 27-43.

[8] Kulig, B., Lepiarczyk, A., Oleksy, A., Kołodziejczyk, M. (2010): The effect of tillage system and forecrop on the yield and values of LAI and SPAD indices of spring wheat. – European Journal of Agronomy 33: 43-51.

[9] Kwiatkowski, C. (2009): Studies on the Fielding of naked and husked spring barley In crop rotation and monoculture. – Rozprawy Naukowe UP Lublin (in Polish).

[10] Lahuta, L. B., Ciak, M., Rybiński, W., Bocianowski, J., Börner, A. (2018): Diversity of the composition and content of soluble carbohydrates in seeds of the genus *Vicia* (Leguminosae). – Genetic Resources and Crop Evolution 65(2): 541-554.

[11] Lepiarczyk, A., Kulig, B., Stępnik, K. (2005): The influence of simplified soil cultivation and forecrop on the development LAI of selected cultivars of winter wheat in cereal crop rotation. – Fragmenta Agronomica 24(2): 98-105. (in Polish).

[12] Mahalanobis, P. C. (1936): On the generalized distance in statistics. – Proceedings of the National Academy of Sciences India 12: 49-55.

[13] Majchrzak, L. (2015): Influence of white mustard cover crop and method of tillage on soil properties, growth and field of spring wheat. – Monograph 480, pp. 113. Poznań University of Life Sciences (in Polish).

http://www.aloki.hu ● ISSN 1589 1623 (Print) ●ISSN1785 0037 (Online)
DOI: http://dx.doi.org/10.15666/aeer/1706_1526715276

[14] Nowosad, K., Liersch, A., Popławska, W., Bocianowski, J. (2016): Genotype by environment interaction for seed yield in rapeseed (*Brassica napus* L.) using additive main effects and multiplicative interaction model. – Euphytica 208: 187-194.
[15] Nowosad, K., Liersch, A., Poplawska, W., Bocianowski, J. (2017): Genotype by environment interaction for oil content in winter oilseed rape (*Brassica napus* L.) using additive main effects and multiplicative interaction model. – Indian Journal of Genetics and Plant Breeding 77(2): 293-297.
[16] Nowosad, K., Tratwal, A., Bocianowski, J. (2018): Genotype by environment interaction for grain yield in spring barley using additive main effects and multiplicative interaction model. – Cereal Research Communications 46(4): 729-738.
[17] Qian, B., De Jong, R., Gameda, S. (2009): Multivariate analysis of water-related agroclimatic factors limiting spring wheat yields on the Canadian prairies. – European Journal of Agronomy 30: 140-150.
[18] Rencher, A. C. (1992): Interpretation of canonical discriminant functions, canonical variates, and principal components. – American Statistics 46: 217-225.
[19] Seidler-Łożykowska, K., Bocianowski, J. (2012): Evaluation of variability of morphological traits of selected caraway (*Carum carvi* L.) genotypes. – Industrial Crops and Products 35: 140-145.
[20] Seidler-Łożykowska, K., Bocianowski, J., Król, D. (2013): The evaluation of the variability of morphological and chemical traits of the selected lemon balm (*Melissa officinalis* L.) genotypes. – Industrial Crops and Products 49: 515-520.
[21] Shamsuddin, A. K. M. (1985): Genetic diversity in relation to heterosis and combining ability in spring wheat. – Theoretical and Applied Genetics 70: 306-308.
[22] Shapiro, S. S., Wilk, M. B. (1965): An analysis of variance test for normality (complete samples). – Biometrika 52: 591-611.
[23] Wanic, M., Żuk-Gołaszewska, K., Orzech, K. (2019): Catch crops and soil environment – a review of the literature. – Journal of Elementology 24(1): 31-45.
[24] Wozniak, A. (2011): Weed infestation of a spring wheat (*Triticum aestivum* L.) crop under the conditions of plough and ploughless tillage. – Acta Agrobotanica 64(3): 133-140.
[25] Wricke, G., Weber, W. E. (1986): Quantitative Genetics and Selection in Plant Breeding. – Walter de Gruyter, Berlin, New York.
[26] Wrońska-Pilarek, D., Szkudlarz, P., Bocianowski, J. (2018): Systematic importance of morphological features of pollen grains of species from *Erica* (Ericaceae) genus. – PLoS ONE 13(10), e0204557.

http://www.aloki.hu ● ISSN 1589 1623 (Print) ●ISSN1785 0037 (Online)
DOI: http://dx.doi.org/10.15666/aeer/1706_1526715276

EFFECT OF TESTOSTERONE ENANTHATE HORMONES ON SOME PRODUCTION, PHYSIOLOGICAL TRAITS AND THEIR RESIDUE IN THE MEAT OF LOCAL RABBITS IN SULAYMANIYAH, IRAQ

REBAZ, R. A.[1*] – CHOWMAN, A. O.[2*] – BAHZAD, H. M.[2]

[1]*Research center, Qrga Street University of Sulaimani Polytechnic, Sulaimaniah, Iraq*

[2]*College of Agricultural Engineering Sciences, Bakrajo Street, University of Sulaimani, Sulaimaniah, Iraq*

[*]*Corresponding authors*

e-mail: rebaz.ramazan@spu.edu.iq; phone: +96-477-1950-2597

e-mail: choman.omer@univsul.edu.iq; phone: +96-477-0157-0015

(e-mail: bahzad.mustafa@univsul.edu.iq; phone: +96-477-0152-2076)

(Received 6th Jul 2019; accepted 25th Oct 2019)

Abstract. A total of 48 weaned male rabbits were randomly arrangement to evaluate the effects of the Testosterone Enanthate (TE) for four treatments: negative control-without injection, positive control-Phosphate-buffered saline PBS, (TE) 4 IU and 8 IU injected intramuscularly (B1 and B2, respectively). Body weight traits measured by weekly weighing for 72 days (slaughter weight) their body weight and average daily gains (ADG) were calculated, and were then slaughtered to assess the TE residues of meat. Blood samples were collected for measuring phosphate-buffered saline (CBC) count, ALT, AST, ALP, Growth Hormone (GH) and Testosterone concentration The present study observed a significant increase in total BW gain for group B2 (8 IU), compared to negative control, positive control, and B1 group. The blood Testosterone concentration in the B2 group, significantly increased were higher than other treatment groups, at 2.73±0.26 ng/dL. The TE residue in meat there was no significant difference after 30 days end of treatment. In conclusion, TE injection improves BW traits in male growing rabbits when injected with a double dose of TE, with the exception of some CBC counts and has a significant mitigating effect on stress parameters, and increasing effect on serum GH and Testosterone concentration, with no significant changes in the TE residue in the meat.

Keywords: *buck rabbits, TE injection, body weight gain, CBC, testosterone concentration, TE residues*

Introduction

Domestic rabbits, in recent years, have been identified as economy livestock of meat shortage in high human population developing countries. Animals Meat, including rabbit's meat, supply a valuable and palatable source of protein. Rabbit meat has a very good nutritive value, being comparatively high in protein, low in fat, calories and sodium, and so could bridge the wide gap in dietary protein intake (Adeyinka et al., 2007). Anabolic androgenic steroids (AAS) are synthetic derivatives of testosterone hormone in the male that have been adjusting to improve their anabolic rather than androgenic activity (Shahidi, 2001). The AAS effects promote protein synthesis, muscle growth and erythropoiesis (Mottram and George, 2000). Anabolic steroids are a class of steroid hormones based on the androgen testosterone and are recognized for their effects on building up muscle and are used as an enhancing drug (Thienpont et al., 1998). Anabolic steroids increase muscle size by the promotion of positive nitrogen balance by stimulating protein production and decreasing destruction (Guan et al., 2010). However, there is

http://www.aloki.hu ● ISSN 1589 1623 (Print) ● ISSN 1785 0037 (Online)
DOI: http://dx.doi.org/10.15666/aeer/1706_1527715287

insufficient available information for their use in these animals. Recently, boldenone undecylenate (androgenic steroid) has been used in the growth improvement and conversion of food in food-producing animals. It is also well known for increasing vascularity in preparation for bodybuilding contests. It might also play an important role not only in controlling normal testicular development, but also in maintaining spermatogenesis and normal testicular function (Tousson et al., 2012). The use of the anabolic steroid (BOL) resulted in obvious improvement in the growth rate (Tousson et al., 2012). This effect could be attributed to the promotion of the body tissue building process by protein synthesis indirectly via stimulation of growth hormone, insulin-like growth factor secretion, and animal appetite (Ferreira et al., 1998) or reduction of glucocorticoid receptor levels and sensitivity to endogenous glucocorticoids; therefore, the strong growth promoting potency is based not only on its anabolic activity as an antiglucocorticoid (Melloni et al., 1997; Thienpont et al., 1998). However, there were some reports reviewed that the rabbits' growth performance was not affected by testosterone injection (Tawfeek et al., 1994). Administration of BOL to male rabbits at a dose of (5 mg/kg body weight) had a positive and significant benefit on growth performance (feed efficiency, total and daily weight gain) and a significant increase in dressing percent (Mohammed et al., 2016). Nahed et al. (2010) reported that using of BOL in rabbit was not sufficient to confirm its use in rabbits although a considerable improvement of total weight gain, feed efficiency and feed conversion ratio were attained after application of BOL in the male rabbit. However, there is no reported in detail study on the effect of BOL on all carcass traits and blood parameters (Abdel-Hamid and Farahat, 2015). The double and the normal recommended dose positively increase serum total protein and globulin, while normal recommended dose apparently increases serum cholesterol and decrease plasma corticosterone level. The European Economic Community (EEC) banned the use of anabolic compounds as growth accelerators in food animals. While the United States Food and Drug Administration (USFDA) permitted the limited use of some hormones with natural origins (such as estradiol and testosterone) and some synthetic hormones (such as Zeranol and trenbolone) in animal husbandry (MacVinish and Galbraith, 1988; Sadek et al., 1998). Little work has been conducted in Iraq regarding the use of testosterone enanthate TE injection as a growth promoter and their residue in edible tissue. A report of Omar (2012), there were no significant differences among the three experimental groups in the TE residue of the cooked meat at 8 months of age, but their values were significantly lower than the fresh meat of Karadi lambs at the same period. A number of authors and official international committees proved that residues of natural steroidal hormones are not dangerous on the health of the consumer (JECFA, 1988; Lone and Van Ginkel, 1997; Galbraith, 2002). Testosterone is usually given in an injection vehicle with oestradiol, and as same with other steroid hormones, the testosterone injection do not differ than the natural hormone inside the body of the organism, and this hormone focused in the liver tissue and kidney, but in fat are the highest concentration of this hormone, When comparing the residues in treated animals and the natural ratios in animals without treatment, they have to be equal or close to it (Omar, 2012). As well as the content of the natural hormone and the testosterone in male sheep and goats is higher than females, although the consumer is preferred the meat of males on other meats. Hence, this study was performed to determine the effects of Two-doses administration of TE on body weight (BW), some blood biochemical parameters and testosterone residual effect of mature local male rabbits.

http://www.aloki.hu ● ISSN 1589 1623 (Print) ● ISSN 1785 0037 (Online)
DOI: http://dx.doi.org/10.15666/aeer/1706_1527715287

Materials and Methods

Location and duration of the study: The present study was carried out at the Experimental farm of the University of Sulaimani Polytechnic, Halabja Technical Agriculture College, Halabja-Iraq, during spring (April to June) of 2017. A total of (48 bucks) weaned male rabbits (14 weeks old) of Local breed were randomly assigned to a completely randomized design arrangement of treatments (Four treat 12 bucks /treat: negative control-without injection, positive control injected intramuscularly by Phosphate-buffered saline PBS, Testosterone Enanthate (4 IU) injected intramuscularly (B1) and Testosterone Enanthate (8 IU) injected intramuscularly (B2). All rabbits were injected after 14 days of adaptation and repeated once after 30 days of the first injection. Bucks were housed in a semi-closed rabbitry housing system with does and kept in batteries of individual cages (60 x 50 x 35 cm) supplied with feeding hoppers made of galvanized steel sheet and nipples for an automatic drinker. A commercial concentrate pellets ration is introduced to bucks throughout the experiment (*Table 1*), containing (16.91%) crude protein and (2703 Kcal/Kg DM) ration metabolizable energy (ME) (NRC, 1977). Fresh and clean drinking water was supplied *ad-libitum*. The feed and the water were offered *ad-libitum*. All the bucks were grown under identical environmental and feeding conditions as well as the same stocking density. A photoperiod (12L:12D) from 0900 to 2100 h was used throughout the experimental period. The temperature was maintained at a range of 28-32ºC inside the house.

Table 1. *Ingredient Composition Of The Diet During The Experiment Period*

Ingredient	%
Maize	35
Wheat Grain	25
Soybean Meal	10
Sesame Oil	15
Wheat Bran	14
Common Salt	0.6
Premix	0.25
Dl. Methionine	0.15
Total	100
Crud Protein (%)	16.91
Metabolizable Energy Kcal/Kg Dm	2703

Traits Measurements: Traits measured were; body weights: fryer rabbits were weighed weekly until 72 (slaughter weight) days and weights were recorded in grams. Body weight gain: calculated as differences between two successive different weights. Average daily gains ADG: calculated as the differences between two successive different weights at two different periods divided by the number of days between the two weights.

Blood parameters: Blood samples were collected twice in the experiment, before treatment and after one month after the first injection. The samples were taken in two test tubes, one with an anticoagulant for measuring CBC count levels and the other one without using anticoagulant to separate the serum for measuring ALT, AST, ALP, Growth Hormone (GH) and Testosterone concentration. Plasma and serum samples were stored at -20ºC until assayed. ALT, AST, ALP, Growth Hormone (GH) and Testosterone concentration were measured using commercial kits. For CBC levels we used Hematology analyzer (URIT 2900z, Vet Z plus, China), and for enzymes activity, we

http://www.aloki.hu ● ISSN 1589 1623 (Print) ● ISSN 1785 0037 (Online)
DOI: http://dx.doi.org/10.15666/aeer/1706_1527715287

used Biochemical Analyser (Floxer pro. S, China), and Hormone concentration by (MINI VIDAS®, France). For each treatment, five samples were assayed.

TE residue in meat: After slaughtering the bucks, 30 days after the last injection of the experiment. 500 gm of muscle were taken and placed in polyethylene bags and stored at -18ºC. Semimembranosus (SM) from pelvic limb leg was dissected according to the procedure of Butterfield et al. (1983). The surfaces of the muscles were cleaned from all fat and connective tissue. Quantitative determination of testosterone concentration (µg/kg = ng/mL) was carried out by using Radioimmunoassay (RIA) by using (cobas e 411 analyzer, made in Germany). The analytic sensitivity of the assay was 0.025 ng/mL.

Statistical analysis: Complete Randomized Design (CRD) procedures of XLstat. (7.5.2, 2010) in one-way ANOVA were used to determine the effects of Testosterone Enanthate TE and injection effect on the body weight characteristics, blood parameters, and TE residue. Group differences were determined using Duncan's multiple range tests at ($p \leq 0.05$) (Duncan, 1955).

Results

The effect of Testosterone Enanthate-TE hormone on growth performance parameters of local male rabbits was showed in *Table 2*. The results revealed that TE injection in male rabbits resulted not significant ($p>0.05$) different among groups, in initial BW, final BW gain, average daily gain ADG, and the high weight record were seen in B2 group for final BW and ADG (1593.3±41.5 and 6.292±0.384) gm, respectively. But there were a significant ($p<0.05$) different in total BW gain for group B2 (8 IU), which recorded (377.5±23.0) gm compared to negative control, positive control and B1 group, which were recorded (281.2± 60.8) gm, (271.2± 32.5) gm and (284.1± 37.1) gm, respectively. The best results were for the group (B2) in total BW and ADG increased in the ADG for groups (B1) and (B2) compared with the control.

Table 2. *Effect of te hormone on growth performance parameters of male rabbits*

Parameters	TREATMENT GROUPS			
	NEGATIVE CONTROL	POSITIVE CONTROL	B1	B2
Initial Bw (gm)	1225.0±58.2[a]	1260.8± 37.0[a]	1246.6±30.8[a]	1194.1±26.1[a]
Final Bw (gm)	1521.6±44.8[a]	1556.6±25.4[a]	1516.6± 36.8[a]	1593.3±41.5[a]
Total Bw Gain (gm)	281.2± 60.8[b]	271.2± 32.5[b]	284.1± 37.1[b]	377.5±23.0[a]
ADG (gm)	4.688±1.013[a]	4.521±0.543[a]	4.736±0.620[a]	6.292±0.384[a]

-Negative Control: Without Injection
-Positive Control: Injected Intramuscularly With Bps (0.25 Ml)
-B1: Received (4 Iu) Intramuscular Injections Of T.E
-B2: Received (8 Iu) Intramuscular Injections Of T.E
-Bw: Body Weight; ADG: Average Daily Gain
-[abc] Means In The Same Row With Different Superscripts Are Significantly Different At ($P<0.05$)

Effects of dose of TE and the injection effect on complete blood picture levels parameters were summarized in *Table 3*. Statistically, no significant differences ($p>0.05$) were recorded before treatment for complete blood picture levels parameters. While, there were significant differences ($p<0.05$) were observed for control groups (negative and positive) compared to TE hormone injection groups after treatment for Hb (g/dL), RBC (10^6xUL) and HCT (%). The hormone injection groups (TE injection) significantly

http://www.aloki.hu ● ISSN 1589 1623 (Print) ● ISSN 1785 0037 (Online)
DOI: http://dx.doi.org/10.15666/aeer/1706_1527715287

($p<0.05$) decrease the Hb concentration, which was (13.0±0.4 g/dL and 13.0±0.4 g/dL) for B1 and B2 respectively, compared to positive control (14.8±0.8 g/dL). Furthermore, the B2 group (8 IU) significantly ($p<0.05$) decrease in RBC and HCT, when compared to positive control (6.97±0.34)10^6xUL and (46.1±2.4) %, respectively. While MCV of the negative control was significant ($p<0.05$) overpowered (69.4±0.1) µL on other injection groups. But, there was no significant ($p>0.05$) difference between control and all injected groups for platelet count PLT (10^3x cells/mcL) count.

Table 3. *Changes in the complete blood picture levels in different groups under study*

Items	TREATMENT GROUPS			
	Negative Control	Positive Control	B1	B2
Before treatment				
Hb (g/dl)	13.6±0.6^a	13.1±1.4a	13.8±0.2^a	13.1±0.3^a
RBC (10^6xul)	6.02±0.33^a	6.23±0.75a	6.59±0.35^a	6.12±0.22^a
HCT (%)	42.7±2.4^a	41.3±4.5a	42.9±0.9^a	39.8±1.2^a
MCV (µl)	70.8±0.5^a	61.0±5.2a	65.4±2.1^a	65.2±0.9^a
MCH (%)	22.6 ±0.1^a	19.4±1.5^a	21.1±0.6^a	21.4±0.3^a
MCHC (%)	32.0±0.2^a	29.1 ±2.5^a	32.2±0.3^a	32.9±0.1^a
PLT (10^3x Cells/Mcl)	213.3 ±6.3^a	216.2±41.2^a	220.5±19.5^a	177.0±45.2^a
RDW (%)	15.1±0.4^a	13.4±1.3^a	15.6±0.58^a	14.3±0.1^a
After treatment				
Hb (g/dl)	14.1±0.5^{ab}	14.8±0.8^a	13.0±0.4^b	13.0±0.4^b
RBC (10^6xul)	6.45±0.14^{ab}	6.97±0.34^a	6.48±0.17^{ab}	6.02±0.13^b
HCT (%)	44.8±1.1^{ab}	46.1±2.4^a	42.3±0.5^{ab}	40.4±1.1^b
MCV (µl)	69.4±0.1^a	66.1±0.8^b	65.4±0.9^b	67.0±0.3^b
MCH (%)	21.8 ±0.3^a	21.2 ±0.1^a	20.1±0.4^b	21.6±0.3^a
MCHC (%)	31.4±0.4^{ab}	32.2±0.2^a	30.7±0.3^b	32.2±0.2^a
PLT (10^3x Cells/Mcl)	233.0±4.0^a	276.3±31.6^a	303.0±17.9^a	258.0±60.4^a
RDW (%)	15.9±0.3^{ab}	15.6±0.5^{ab}	14.6±0.1^b	17.3 ±1.1^a

-Negative Control: Without injection.
-Positive Control: injected intramuscularly with BPS (0.25 ml).
-B1: received (4 IU) intramuscular injections of T.E.
-B2: received (8 IU) intramuscular injections of T.E.
-Hb: hemoglobin; RBC: red blood cell; HCT: hematocrit; MCV: mean corpuscular volume; MCH: mean corpuscular hemoglobin; MCHC: mean corpuscular hemoglobin concentration; PLT: platelet count; RDW: red cell distribution width.
-^{abc} Means in the same row with different superscripts are significantly different at ($p<0.05$).

The results of *Table 4* demonstrated that changes in Leukocytes levels changed significantly ($p<0.05$) after TE hormone treated. Before treatment there were no significant differences ($p>0.05$) in the leukocytes levels, on the other hand, we recorded significant differences ($p<0.05$) in WBC count, Lymphocyte %, Monocytes %, Neutrophil%, Mean platelet volume (MPV%) and platelet distribution width (PDW). The TE injection increased the WBC count significantly ($p<0.05$), which high count recorded in B1 (4 IU, TE), and the highly significant value for lymphocyte and monocyte percent were recorded in B2 (8 IU) (61.0±1.0 % and 0.75±0.02 %, respectively). Conversely, the neutrophils count significantly ($p<0.05$) higher in BPS injection (Positive Control) (59.6±3.0 %). Also, the significant level was seen in MPV and PDW for B2 injection, which was 6.05±0.02 % and 9.10 ±0.44 %, respectively. As well, B1 injection significantly differenced too in PDW (8.60±0.01 %), when they compared to negative and positive control (7.50 ±0.01 and 7.63 ±0.02, respectively).

http://www.aloki.hu ● ISSN 1589 1623 (Print) ● ISSN 1785 0037 (Online)
DOI: http://dx.doi.org/10.15666/aeer/1706_1527715287

The comparison between the injection groups and negative control in the concentration of ALT, AST, ALP, Growth Hormone GH and Testosterone levels in the local rabbit are summarized in *Table 5*. Indeed, no significant differences were seen before treatment in all parameters, except in B1 treatment for AST and ALP levels. The AST recorded high level in B1 (39.0±1.6 IU/L). And ALP recorded less level in B1 (79.0±1.2 IU/L) when they compared to other treatments. After treatment, the parameters level change, the significant record seen in ALT, GH and testosterone concentration for B2 (8 IU) TE injection. The significant level for ALT recorded (69.5±9.4 IU/L), as compared to negative control, positive control and B1 injection. The GH concentration recorded significantly ($p<0.05$) higher level (0.32±0.01 ng/dL) at B2 (8 IU) TE injection when it compared to negative control and positive control (0.24±0.01 and 0.28±0.01 ng/dL, respectively). As well as, the Testosterone concentration in the B2 group, significantly ($p<0.05$) increased and higher than other treatments groups, which recorded (2.73±0.26 ng/dL). And the other groups recorded significant differences for negative control, positive control and B1(4 IU) TE injection, which were (0.60±0.06, 0.83±0.10 and 1.28±0.15 ng/dL).

Table 4. *Changes in the leukocyte levels in different groups under study*

Items	TREATMENT GROUPS			
	Negative Control	Positive Control	B1	B2
Before treatment				
WBC (10^6xul)	3.33±0.63^a	2.76±0.49^a	4.50±1.07^a	4.75±0.85^a
Lym. (%)	75.5±1.8^a	56.4±9.2^a	57.6±11.9^a	64.3±4.5^a
Mon. (%)	7.86±3.02^a	0.87±0.67^a	0.27±0.08^a	0.50±0.14^a
Neu. (%)	16.0±1.1^a	32.2±9.8^a	47.9±11.3^a	34.0±4.41^a
MPV (%)	6.26±0.06^a	6.05±0.71^a	6.35±0.05^a	6.47±0.31^a
PCT	0.133±0.003^a	0.144±0.030^a	0.331± 0.142^a	0.111±0.026^a
PDW	9.50±0.10^a	9.85±1.11^a	10.48±0.15^a	10.62±0.70^a
After treatment				
WBC (10^6xul)	4.65±0.26^b	5.16±0.63^{ab}	6.15±0.10^a	4.65±0.42^b
Lym. (%)	55.2±2.0^a	33.3±1.1^b	55.4±7.7^a	61.0±1.0^a
Mon. (%)	0.45±0.10^b	0.33±0.08^b	0.30±0.04^b	0.75±0.02^a
Neu. (%)	42.1±1.8^b	59.6±3.0^a	39.8±6.2^b	34.0±1.2^b
MPV (%)	5.75±0.02^b	5.56±0.02^c	5.70±0.04^b	6.05±0.02^a
PCT	0.134±0.002^a	0.153±0.018^a	0.173± 0.011^a	0.155±0.037^a
PDW	7.50 ±0.01^b	7.63 ±0.02^b	8.60±0.01^a	9.10 ±0.44^a

-Negative Control: Without injection.
-Positive Control: injected intramuscularly with BPS (0.25 ml).
-B1: received (4 IU) intramuscular injections of T.E.
-B2: received (8 IU) intramuscular injections of T.E.
-WBC: white blood cell; Lym.: lymphocyte; Mon.: monocyte; New.: neutrophil; MPV: Mean platelet volume; PCT: procalcitonin test; PDW: platelet distribution width.
-^{abc} Means in the same row with different superscripts are significantly different at ($p<0.05$).

The results of TE residues in bucks' meat after 30 days of treatment are presented in *Figure 1*. Significant differences were not seen in the testosterone residue of the fresh meat, while there was no significant ($P> 0.05$) increase in the TE residue in the fresh meat of B1 and B2 group intramuscular injections of TE with 4IU and 8IU (0.093 and 0.134 μg/kg) and as compared to the negative and positive groups which were 0.086 and 0.061 μg/kg, respectively *Figure 1*.

http://www.aloki.hu ● ISSN 1589 1623 (Print) ● ISSN 1785 0037 (Online)
DOI: http://dx.doi.org/10.15666/aeer/1706_1527715287

Table 5. *Changes in the concentrations of alt, ast, alp, growth hormone and testosterone levels in different groups under study*

Items	TREATMENT GROUPS			
	Negative Control	Positive Control	B1	B2
Before treatment				
ALT (IU /l)	59.0±1.6^{a}	55.0±10.2^{a}	56.0±1.2^{a}	54.6±1.2^{a}
AST (IU /l)	34.0±4.4^{ab}	29.0±2.4^{b}	39.0±1.6^{a}	35.9±1.4^{ab}
ALP (IU /l)	158.3±3.8^{a}	112.3±22.2^{a}	79.0±1.2^{b}	174.4±34.3^{a}
GH (ng/dl)	0.26±0.02^{a}	0.32±0.02^{a}	0.15±0.02^{a}	0.27±0.01^{a}
Testosterone (ng/dl)	0.45±0.02^{a}	0.86±0.12^{a}	0.60±0.12^{a}	0.70±0.14^{a}
After treatment				
ALT (IU /l)	41.0±2.7^{b}	39.9±1.1^{b}	50.8±3.0^{b}	69.5±9.4^{a}
AST (IU /l)	25.6±0.9^{a}	25.5±0.7^{a}	25.1±2.1^{a}	28.7±3.0^{a}
ALP (IU /l)	108.6±4.0^{a}	117.0±16.1^{a}	107.7±13.9^{a}	111.5±12.0^{a}
GH (ng/dl)	0.24±0.01^{c}	0.28±0.01^{b}	0.29±0.01^{ab}	0.32±0.01^{a}
Testosterone (ng/dl)	0.60±0.06^{c}	0.83±0.10^{bc}	1.28±0.15^{b}	2.73±0.26^{a}

-Negative Control: Without injection.
-Positive Control: injected intramuscularly with BPS (0.25 ml).
-B1: received (4 IU) intramuscular injections of T.E.
-B2: received (8 IU) intramuscular injections of T.E.
-ALT: alanine aminotransferase; AST: aspartate aminotransferase; ALP: alkaline phosphatase level; GH: growth hormone.
-^{abc} Means in the same row with different superscripts are significantly different at ($p<0.05$).

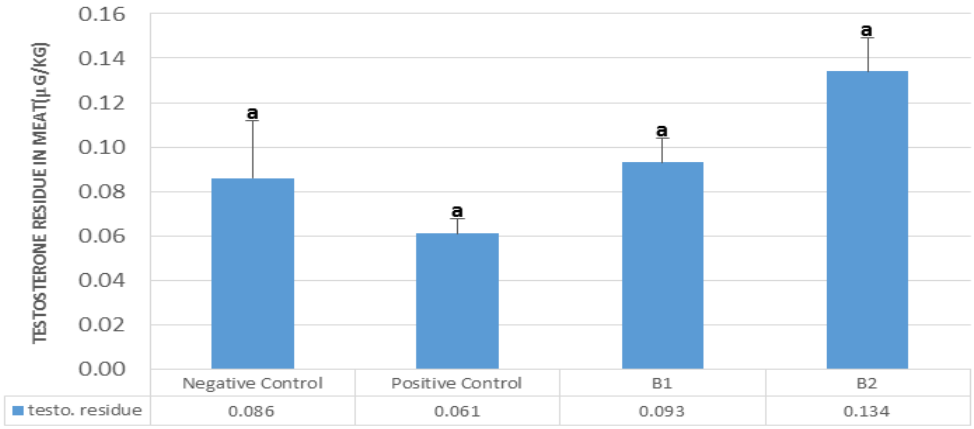

Figure 1. *Concentration residue of Testosterone Enanthate in meat of local rabbit bucks (Negative Control: Without injection; Positive Control: injected intramuscularly with BPS (0.25 ml); B1: received (4 IU) intramuscular injections of T.E.B2: received (8 IU) intramuscular injections of T.E.^{a}Means in the same row with different superscripts are significantly different at ($p<0.05$))*

Discussions

The growth performance improved in treated groups (B1 and B2) proportional to the control groups (*Table 2*), which is consistent with antecedent reports (Thabet et al., 2010). The same observation was described by Tousson et al. (2012) and Mohammed et al. (2016) when they use anabolic steroid (BOL, boldenone undecylenate), who stated that the use of the (BOL) give rise to an obvious improvement in the growth rate. This effect could be imputed to the promotion of the body tissue building process by protein synthesis

http://www.aloki.hu ● ISSN 1589 1623 (Print) ● ISSN 1785 0037 (Online)
DOI: http://dx.doi.org/10.15666/aeer/1706_1527715287

indirectly via stimulation of growth hormone, insulin-like growth factor secretion, and animal appetite (Ferreira et al., 1998) or reduction of glucocorticoid receptor levels and sensitivity to endogenous glucocorticoids; therefore, the strong growth promoting potency is based not only on its anabolic activity as an antiglucocorticoid (Melloni et al., 1997; Thienpont et al., 1998). However, Tawfeek et al. (1994) reported that the rabbits' growth performance was not affected by testosterone injection.

The obtained findings in *Table 3* agree with the results of Battista et al. (2003) and Liewellyn (2006) who founded that, testosterone dosage and its entrance to the body caused an increase in hematocrit %. Moreover, Gagnon et al. (1994) founded that, the raised hematocrit and hemoglobin persist for extended periods after the cessation of androgenic steroids use. Similarly, Ahmed (2014) recorded significant increase RBCs, Hb, and PCV in boldenone administered groups as compared to the control one. These results may be imputed to that; anabolic steroids could stimulate erythropoiesis (Gabr et al., 2009) through the direct positive effect of androgenic steroids on erythropoietin production in renal tissues (Liewellyn, 2006). This reaction is mainly driven by the androgen receptor stimulation in renal tissue, leading to the stimulation of erythropoietin production directly. Androgens may also influence the stem cells directly, perhaps by enhancing the stem cell's responsiveness to erythropoietin (Snyder, 2008).

Anabolic steroids could spur erythropoiesis, a mechanism that may occur by stimulating erythropoietic-stimulating factor (Gabr et al., 2009). These results (*Table 4*) are in agreement with Urhausen et al. (2003) and Gabr et al. (2009) who adduced that the liver and kidney functions increased significantly after intramuscular BOL undecylenate injection on weaned male lambs. Similarly, current results are in conformity with Dickerman et al. (1999) and Tousson et al. (2011a, 2011b) who noticed that the anabolic steroid-induced hepatotoxicity. Following the same opinions, Istasse et al. (1988) reported that 17b-estradiol increased nitrogen retention and decreased blood urea nitrogen concentrations. Injection of the anabolic steroid BOL induced changes in oxidative stress biomarker levels and antioxidant defense systems in rabbit liver and kidney (El-Moghazy et al., 2012).

In agreement with our findings (*Table 5*), in treated groups with anabolic androgenic steroid, the serum testosterone levels were significantly higher than that in the control group (Urhausen et al., 2003; Takahashi et al., 2004; Gabr and Shaker, 2006; Gabr et al., 2009; Ishak and Omer, 2014). Simontacchi et al. (2004) reported that administration of testosterone derivatives alone did not induce plasma testosterone levels. Also, Shimomura et al. (2005) showed that the treatment of rats with ethinyloestradiol alone the testosterone levels decreased significantly in serum and the testis. Our results are in agreement with Omar (2012) who studied the effects of Testosterone Enanthate injection on testis function, live weight gain and carcass traits of Karadi lamb rams. The significant increase in testosterone observed in (B1 and B2) of mature rabbits treated by boldenone may be in accordance with the findings of Urhausen et al. (2003), Takahashi et al. (2004) and Gabr and Shaker (2006) who founded that, serum testosterone levels in treated groups with androgenic steroids were significantly higher than that in the control group. These results shore up former reports (Gabr et al., 2009; Tousson et al., 2012) who mentioned that an increase of testosterone may be attributed to the synthesis of a substrate related to the primary male sex hormone.

In the present study, results of TE residue in the fresh meat after 30 days stopped injection, showed no significant difference between the groups (*Figure 1*), these results are in contrast with the finding of Paris et al. (2006), when they found a significant

http://www.aloki.hu ● ISSN 1589 1623 (Print) ● ISSN 1785 0037 (Online)
DOI: http://dx.doi.org/10.15666/aeer/1706_1527715287

difference between the treated and non-treated lambs of the same age group, for example, the anabolic steroids in the muscle, liver, kidneys and adipose tissue. While there was an increase of TE residue in the fresh meat of the male rabbit treated with 4IU TE and those treated with 8IU TE as compared to control groups. The main possible mechanism for these results could be the testicular hormone especially testosterone which let the male be superior in TE residue than the control groups (Omar, 2012). The exogenous testosterone has also been considered as the other reason for elevating TE residue in fresh meat of the intact animal as compared to the castrated. To our knowledge detained from available literature, no other previous study dealt with TE injection on rabbit male and their residue in meat. These differences may be related to exogenous testosterone in addition to testicular hormone especially testosterone which produce mainly by leydig cells. As well as increasing TE residue in fresh meat, which could be reduced in the cooking process (Omar, 2012).

Conclusion

From the obtained results it could be concluded that, although intramuscular injection of Testosterone Enanthate espesioly B2 (8IU) to male local rabbits enhances body gain and increased some hematological parameters, it increased oxidative stresses biomarkers levels, pro-inflammatory cytokines and creatinine indicating side effects on the liver and kidneys. And a no significant deferences in TE residue was seen in the fresh meat after 30 days of injection.

Acknowledgments. The authors gratefully thank the University of Sulaimani Polytechnic, Halabja Technical Agriculture College, for performing a place to conduct research in the Experimental farm of the Halabja Technical Agriculture College.

REFERENCES

[1] Abdel-Hamid, T. M., Farahat, M. H. (2015): Carcass traits and some blood stress parameters of summer stressed growing male rabbits of different breeds in response to boldenone undecylenate. – J. Adv. Vet. Anim. Res. 2: 263-270.
[2] Adeyinka, I. A., Akanwa, C. L., Iyeghe-Erakpotobor, G. T., Adeyinka, F. D., Orunmuyi, M. (2007): Factors affecting some traits of economic importance in rabbit in a tropical environment of Northern Nigeria. – J. Biol. Sci. 7: 425-428.
[3] Ahmed, N. F. N. (2014): Effect of Boldenone Undecylenate on Hematological and Biochemical Parameters in Veal Calves. – Global Veterinaria 13(6): 1092-1096.
[4] Battista, V., Combs, J., Warne, W. J. (2003): Asynchronous bilateral Achilles tendon ruptures and androstenediol use. – Am. J. Sports Med. 31: 1007-1009.
[5] Butterfield, R. M., Griffiths, D. A., Thompson, J. M., Zamora, J., James, A. M. (1983): Changes in body composition relative to weight and maturity in large and small strains of Australian Merino rams. 1. Muscle, bone and fat. – Animal production 36: 29-37.
[6] Dickerman, R. D., Pertusi, R. M., Zachariah, N. Y., Dufour, D. R., McConathy, W. J. (1999): Anabolic steroidinduced hepatotoxicity: is it overstated? – Clinical J. Sport Med. 9: 34-39.
[7] Duncan, D. B. (1955): Multiple range and multiple f-test. – Biometrix 11: 1-24.
[8] El-Moghazy, M., Tousson, E., Sakeran, M. (2012): Changes in the hepatic and renal structure and function after a growth promoter Boldenone injection in Rabbits. – Animal Biology 62: 171-180.

http://www.aloki.hu ● ISSN 1589 1623 (Print) ● ISSN 1785 0037 (Online)
DOI: http://dx.doi.org/10.15666/aeer/1706_1527715287

[9] Ferreira, I. M., Verreschi, I. T., Nery, L. E., Goldstein, R. S., Zamel, N., Brooks, D. (1998): The influence of 6 months of oral anabolic steroids on body mass and respiratory muscles in undernourished COPD patients. – Chest 114: 19-28.
[10] Gabr, F. I., Shaker, M. H. (2006): Effect of anabolic steroids (Boldenone Undecylenate) on metabolic, hormones and reproductive performance of mature rams. – Journal of Egyptian Veterinary Medical Association 66: 235-248.
[11] Gabr, F., Abo El-Maaty, T., Amal, M., Aotifa, A. M. (2009): Effects of growth promoter boldenone undecylenate on weaned male lambs. – Nature and Science 7(3): 61-69.
[12] Gagnon, D. R., Zhang, T. J., Brand, F. N., Kannel, W. B. (1994): Hematocrit and Risk of Cardiovascular Disease – the Framingham Study: a 34-Year Follow Up. – Am. Heart J. 127: 674-682.
[13] Galbraith, H. (2002): Hormones in international meat production: biological, sociological and consumer issues. – Nut. Res. Rev. 15: 293-314.
[14] Guan, F., Ubon, C., Soma, R., Yu, Y., Liu, Y., Li, X. (2010): High-throughput UHPLC-MS/MS method for the detection, quantification and identification of fifty-five anabolic and androgenic steroids in equine plasma. – J Mass Spectrometry 45: 1270-1279.
[15] Ishak, M. A., Omar, C. A. (2014): Effect of Testosterone Enanthate Injection and Castration on some Productive Traits of Karadi Lambs. – Journal of Zankoy Sulaimani 16 - Special Issue: 219-230.
[16] Istasse, L., Evrard, P., Van Eenaeme, C., Gielen, M., Maghuin-Rogister, G., Bienfait, J. M. (1988): Trenbolone acetate in combination with 17 beta-estradiol: influence of implant supports and dose levels on animal performance and plasma metabolites. – J. Anim. Sci. 66(5): 1212-1222.
[17] Joint, FAO/WHO; Expert Committee on Food Additives, JECFA (1988): Evaluation of certain veterinary drugs residues in food. Thirty-second Report of the Joint FAO/WHO Expert Commitee on Food Additives. – WHO Technical Report Series 763, World Health Organization, Geneva.
[18] Liewellyn, W. (2006): Anabolic 2007. 6th ed. – Molecular Nutrition, Jupiter.
[19] Lone, K. P., Van Ginkel, D. A. (1997): Natural sex steroids and their xenobiotic analogs in animal production; Growth, carcass quality, pharmacokinetics, metabolism, mode of action, residues, methods, and epidemiology. – Critical reviews in food science and nutrition 37(2): 93-209.
[20] MacVinish, L. J., Galbraith, H. (1988): The effect of implantation of trenbolone acetate and oestradiol-17β in wether lambs at two initial live weights on concentrations of steroidal residues and blood glucose, urea and thyroid hormones. – Anim. Prod. 47: 75-85.
[21] Melloni, R. H., Conner, D. F., Hang, P. T., Harrison, R. J., Ferris, C. F. (1997): Anabolic androgenic steroid exposure during adolescence and aggressive behavior in golden hamsters. – Physiol Behav 61: 359-364.
[22] Mohammed, H. H., Badawi, M. E., El-Tarabany, M. S., Rania, M. (2016): Effects of boldenone undecylenate on growth performance, maintenance behaviour, reproductive hormones and carcass traits of growing rabbits. – Polish journal of veterinary sciences 19(2): 245-251.
[23] Mottram, D. R., George, A. J. (2000): Anabolic steroids. – Best Pract. Res. Clin. Endocrinol. Metab. 14: 55-69.
[24] Nahed, S. T., Emad, M. A., Emad, W. G., Salah, S. E. (2010): Effect of anabolic steroids, boldenone undecylenate on reproductive performance of male rabbits. – Journal of Reproduction and Infertility 1: 08-17.
[25] National Research Council, NRC (1977): Nutrient Requirements of Rabbits. – Second Revised Washington, DC Edition. The National Academies Press. doi: 10.17226/35.
[26] Omar, C. A. (2012): Effect of Testosterone Enanthate Injection on Some Productive, Physiological Traits and Their Residue in The Tissues of Karadi Lambs. – Doctoral Dissertation, University of Sulaimani.

http://www.aloki.hu ● ISSN 1589 1623 (Print) ● ISSN 1785 0037 (Online)
DOI: http://dx.doi.org/10.15666/aeer/1706_1527715287

[27] Paris, A., Andre, F., Antignac, J. P., Le Bizec, B., Bonneau, M., Briant, C., Caraty, A., Chillard, Y., Cognie, Y., Combarnous, Y., Cravedi, J. P., Fabre-Nys, C., Fernandez-Suarez, A., Fostier, A., Humblot, P., Laudet, V., Leboeuf, B., Louveau, I., Malpaux, B., Martinat-Botte, F., Maurel, M. C., Pelicier-Rubio, M. T., Picard-Hagen, N., Pinault, L., Pinel, G., Ponsard, C., Popot, M. A., Schmidely, P., Toutain, P. L., Zalko, D. (2006): Hormones and growth promoters: from physiologic to risk assessment. – INRA. Prod. Anim. 19: 149-240.
[28] Sadek, A. I., Ismail, H. M., Sallam, H. N., Salem, M. (1998): Survey of hormonal levels in meat and poultry sold in Alexandria, Egypt. – Etern. Mediterranean Health 4(2): 234-239.
[29] Shahidi, N. T. (2001): A review of the chemistry, biological action, and clinical applications of anabolic-androgenic steroids. – Clin. Ther. 23: 1355-1390.
[30] Shimomura, K., Shimada, M., Hagiwara, M., Harada, S., Kato, M., Furuhama, K. (2005): Insights into testicular damage induced by ethinylestradiol in rats. – Reproductive Toxicology 20: 157-163.
[31] Simontacchi, C., Perez de Altamirano, T., Marinelli, L., Angeletti, R., Gabai, G. (2004): Plasma steroid variations in bull calves repeatedly treated with testosterone, nor testosterone and oestradiol administered alone or in combination. – Veterinary Research Communications 28: 467-477.
[32] Snyder, P. J. (2008): Use of Androgens and Other Drugs by Athletes. – Up To Date, October 2008.
[33] Takahashi, M., Tatsugi, Y., Kohno, T. (2004): Endocrinological and pathological effects of anabolic-androgenic steroid in male rats. – Endocrine Journal 51: 425-434.
[34] Tawfeek, M. I., El-Gaafary, M. N., Abdel-Hamid, M. Y. (1994): Effect of testosterone injection on pre and post- sexual maturity in male rabbits. – Options Mediterraneennes, International Conference of rabbit production in hot climates, Cairo (Egypt): 367-373.
[35] Thabet, N. S., Abdelrazek, E. M., Ghazy, E. W., Elballal, S. S. (2010): Effect of the anabolic steroid, boldenone undecylenate on reproductive performance of male rabbits. – J Reprod Infertility 1: 8-17.
[36] Thienpont, L., Verhseghe, P., Brussel, K. V., De-Leenheer, A. (1998): Efforts by industry toward standardization of serum estradiol-17 f measurements. – Clin Chem. 44: 671-674.
[37] Tousson, E., Alm-Eldeen, A., El-Moghazy, M. (2011a): p53 and Bcl-2 expression in response to boldenone induced liver cells injury. – Toxicology and Industrial Health 27: 711-718.
[38] Tousson, E., El-Gerbed, M. S. A., Shaleby, S. (2011b): Effects of maturity on histopathological alteration after a growth promoter boldenone injection in rabbits. – Journal of American Science 7: 1074-1080.
[39] Tousson, E., El-Moghazy, M., Massoud, A., Akel, A. (2012): Histopathological and immunohistochemical changes in the testes of rabbits after injection with the growth promoter boldenone. – Reprod. Sci. 19: 253-259.
[40] Urhausen, A., Torsten, A., Wilfried, K. (2003): Reversibility of the effects on blood cells, lipids, liver function and hormones in former anabolic-androgenic steroid abusers. – Journal of Steroid Biochemistry and Molecular Biology 84: 369-375.
[41] XLstat, 752 (2010).

http://www.aloki.hu ● ISSN 1589 1623 (Print) ● ISSN 1785 0037 (Online)
DOI: http://dx.doi.org/10.15666/aeer/1706_1527715287

ROOT-ENDOPHYTIC FUNGI DIVERSITY OF FUZI (*ACONITUM CARMICHAELII*) AND THEIR ANTI-FUNGAL ACTIVITY

LV, Y.[1,2,3#] – SHEN, Y.[5#] – SHI, Y.[6] – SHEN, F.[4] – CHEN, Y.[4] – ZI, S.[5] – ZHU, Z.[2*] – KENNELLY, E. J.[7,8*] – ZHAO, D.[1,2,3*#]

[1]*Laboratory of Ecology and Evolutionary Biology, State Key Laboratory for Conservation and Utilization of Bio-Resources in Yunnan University, Kunming 650091, China*

[2]*Yunnan Institute of Materia Medica, Yunnan Baiyao Group Company Limited, Kunming 650111, China*

[3]*Key Laboratory of Tropical Plant Resources and Sustainable Use, Xishuangbanna Tropical Botanical Garden, Chinese Academy of Sciences, Kunming 650000, China*

[4]*School of Agriculture, Yunnan University, Kunming 650504, China*

[5]*College of Agriculture and Biotechnology, Yunnan Agricultural University, Kunming, China*

[6]*Institute of Medicine Plants, Yunnan Academy of Agricultural Sciences, Kunming 650201, People's Republic of China*

[7]*Department of Biological Sciences, Lehman College, City University of New York, New York 10468, United States of America*

[8]*Ph.D. Programs in Biochemistry, Biology, and Chemistry, The Graduate Center, City University of New York, New York 10468, United States of America*

[#]*These authors contributed equally to this work.*

**Corresponding authors*
e-mail: zzy1370@163.com (Z. Zhu), Edward.kennelly@lehman.cuny.edu (E. J. Kennelly), zhaodk2012@ynu.edu.cn (D. Zhao)

(Received 8th Jul 2019; accepted 16th Oct 2019)

Abstract. Endophytic fungi (EFs) are one of the important and quantifiable components of fungal biodiversity. In the study, 171 endophytic fungi were isolated from the roots of *Aconitum carmichaelii*, a traditional Chinese medicine, collected from six production sites of Yunnan Province in southwestern China. These EFs were categorized to belong to 28 taxa by molecular identification, and *Chaetomium* and *Fusarium* were the dominant genera with a relative frequency of 16.96% and 16.37% respectively. *Cladosporium* and *Pochonia* were found to be unique dominant genera from the roots of *A. carmichaelii* in Huize and Yulong counties, respectively. The Shannon index ranged from 1.68 to 2.05 and the Simpson's diversity index ranged from 0.81 to 0.92 for the EFs of *A. carmichaeli*, indicating the rich diversity of EFs in *A. carmichaelii*. Preliminary screening of the growth inhibition of three severe fungal pathogens by the isolated EFs was conducted and 17 genera of EFs were found to inhibit the growth of the tested pathogens. For example, *Acrostalagmus luteoalbus, Phoma* sp., and *Thielavia* sp. each displayed good anti-fungal activity against *Alternaria alternate*, *Fusarium oxysporum* f. sp. *cucumerinum,* and *Phytophthora drechleri.* The investigation of the root-EFs diversity of *A. carmichaelii* provides additional fungal resources with the potential to biologically control pathogenic fungi.
Keywords: *traditional Chinese medicine, fungal biodiversity, community composition, ITS sequence, antagonism against fungal pathogens*

http://www.aloki.hu ● ISSN 1589 1623 (Print) ● ISSN 1785 0037 (Online)
DOI: http://dx.doi.org/10.15666/aeer/1706_1528915300

Introduction

Endophytic fungi (EFs), well-studied to be potential resources for producing bioactive natural products (Aly et al., 2008), asymptomatically infect healthy plant tissues for all, or at least a significant part of their life cycles (Hyde and Soytong, 2008). The diversity of endophytes has been fully investigated in the case of many plant taxa (Sun et al., 2011; Silva et al., 2012; Kohout et al., 2013; Fernandes et al., 2015; Nascimento et al., 2015), and endophytes were shown to increase ecological adaption by protecting plants against biotic and abiotic stresses (Liu et al., 2009; Morsy et al., 2010; Bittleston et al., 2011).

Nowadays, drug-resistance among bacteria and fungi is spreading significantly, and therefore further search is urgently needed for new and effective antimicrobial agents. Endophytes have the potential to produce bioactive compounds, such as alkaloids, resulting in the improvement of the evolutionary fitness of their host by providing resistance against micro-pathogens (Strobel et al., 2004; Kusari and Spiteller, 2012; Newman, 2015). EFs can produce the antimicrobial compounds with inhibitory activity toward pathogenic fungi (Li et al., 2005), and therefore can be helpful in fungal biocontrol in agricultural production (Mishra et al., 2012).

Aconitum L. is a large genus of more than 400 species, mainly distributed in the temperate regions of the northern hemisphere (Xiao et al., 2006). *Aconitum carmichaelii,* a perennial plant of the Ranunculaceae family, is one of the famous traditional Chinese medicines (TCM) fuzi (附子). As one of the most important TCMs, it has been used extensively by humans as a cardiotonic, to protect cardiomyocytes, as an analgesic and to treat arrhythmia (Zhou et al., 2015). However, there has been only one preliminary study about the EFs in *Aconitum* (Li et al., 2009). We aimed to isolate and identify naturally-occurring EFs in *A. carmichaelii* roots collected from the main production area of Yunnan Province, China, and explore their potential inhibitory activity against three primary fungal pathogens, *Alternaria alternate, Fusarium oxysporum* f. sp. *cucumerinum*, and *Phytophthora drechsleri.*

Materials and methods

Plant materials

The roots of *A. carmichaelii* were sampled in September 2014 across six selected counties including Heqing, Huize, Luquan, Malong, Panlong, and Yulong in Yunnan Province, southwestern China (*Fig. 1*), in order to maximize the endophytic fungal diversity. These *A. carmichaelii* were cultivated by local people. Five plants were randomly selected from each site, from which 3-5 lateral roots were collected. The roots and associated soil were packaged separately in sealable plastic bags, immediately transported to the laboratory, and then stored at 4 °C for isolating of endophytic fungi.

Endophyte isolation and primary classification based on morphological traits

The collected roots were washed under running tap water for 5 min, sterilized in 75% ethanol for 1 min, rinsed once in sterile water, 2% NaOCl for 5 min, and then rinsed three times in sterile water. After drying the roots on sterile paper, they were cut into segments, each about 1cm long. From each of the six collections, we randomly selected 45 segments, and divided into them into three groups with 15 segments each to comprise a replicate sample. The samples were placed in Petri dish containing potato

http://www.aloki.hu ● ISSN 1589 1623 (Print) ● ISSN 1785 0037 (Online)
DOI: http://dx.doi.org/10.15666/aeer/1706_1528915300

dextrose agar (PDA) medium amended with 0.5 g/L streptomycin sulfate, with one segment per plate. The plates were incubated at 28 °C and checked every other day for 3 weeks; and the fungi growing out of the roots were transferred to fresh PDA plates. Primary classification was carried out based on mycelia and colony morphological traits and secretion. After that, at least 50% isolates in each group were randomly selected for the molecular identification.

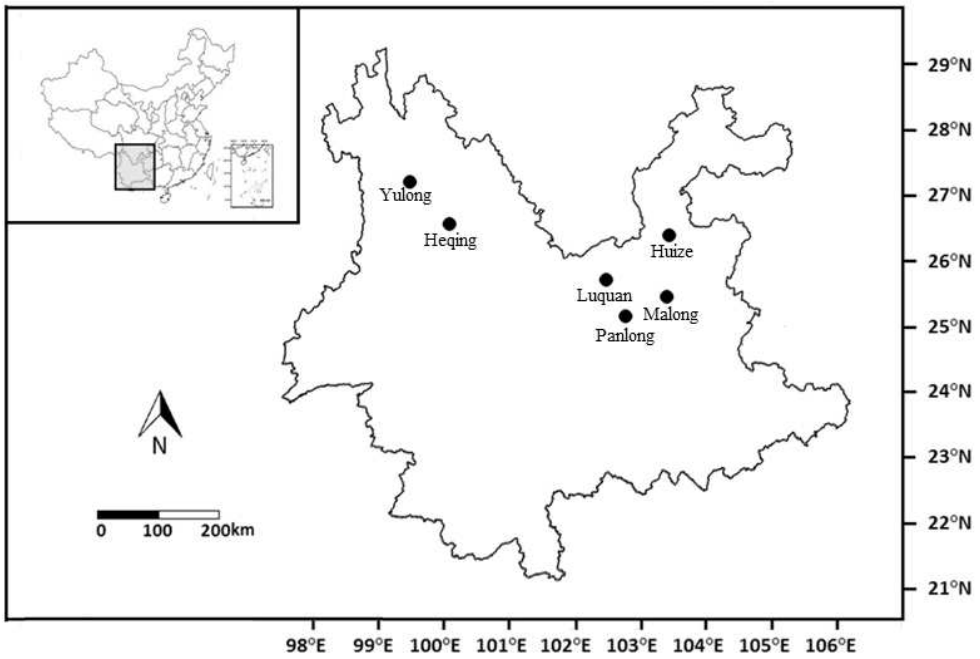

Figure 1. *The geographical locations from left to right represent Yulong, Heqing, Luquan, Panlong, Malong, and Huize counties*

Fungal identification by DNA analysis

Fungal DNA was extracted from pure culture mycelia using a 1 × cetyltrimethylammonium bromide (CTAB) method (Niu et al., 2010). The internal transcribed spacer (ITS) region of nuclear rDNA was amplified with the universal eukaryotic primer pair ITS1 (5'-CTTGGTCATTTAGAGGAAGTAA-3') and ITS4 (5'-TCCTCCGCTTATTGATATGC-3'). PCR amplifications were performed in a reaction mixture containing 2 × PCR EasyTaq PCR SuperMix, DNA extracts, and the primer pair. Thermocycler settings were 5 min initial denaturation at 94 °C, followed by 35 cycles of 30 s at 94 °C, 50 s at 53 °C, 1 min at 72 °C, with a 10 min final extension at 72 °C. Sequences were manually inspected and edited using Chromas 2.4.1. Putative identification of sequences was carried out by comparing consensus sequences to the National Center for Biotechnology Information (NCBI) DNA database using the Basic Alignment Search Tool (BLAST). The following parameters were used to determine significance of BLAST results: alignment score > 500, E < 0.0001, and over 97 % sequence similarity were identified as the same species. The ITS sequences of those isolates were deposited in NCBI (MF962929-MF963015). Through sequences analysis in comparison with each other, phylogenetic tree figure of the isolated EFs was constructed using neighbor-joining (NJ) methods with 1000 boot-strap replications using MEGA 6.0.

http://www.aloki.hu ● ISSN 1589 1623 (Print) ● ISSN 1785 0037 (Online)
DOI: http://dx.doi.org/10.15666/aeer/1706_1528915300

Analyses of relative frequency and diversity index

The colonization rate was calculated as follows (*Eq. 1*) (Su et al., 2010), where N_i is the total number of segments colonized by endophytes, and N_t is the total number of segments.

$$\text{colonization rate } (\%) = \frac{N_i}{N_t} \times 100 \quad \text{(Eq.1)}$$

The relative frequency (RF %) (Yuan et al., 2010) was calculated according to the following formula (*Eq. 2*), where n_i is the number of isolates of one species divided, and the N is the total number of isolates.

$$RF(\%) = \frac{n_i}{N} \times 100 \quad \text{(Eq.2)}$$

The Shannon index (H') (Shannon and Weiner, 1963) was calculated according to the following formula (*Eq. 3*), where k is the total species number of one plot and P_i is the relative abundance of endophytic fungal species in the community.

$$H' = -\sum_{i=1}^{k} (P_i \times \ln P_i) \quad \text{(Eq.3)}$$

The fungal dominance was determined by Camargo's index (*Eq. 4*) (Hunter and Gaston, 1988), where S was species richness = the number of species present in any given sample. A species was defined as dominant if $P_i >$ Camargo's index.

$$\text{Camargo's index} = \frac{1}{S} \quad \text{(Eq.4)}$$

Simpson's index (D) and Simpson's diversity index (1-D) (Camargo, 1993), where D was calculated as (*Eq. 5*). D could range between 0 (infinite diversity) and 1 (no diversity).

$$D = \sum_{i=1}^{k} \left(\frac{n_i \times (n_i - 1)}{N \times (N - 1)} \right) \quad \text{(Eq.5)}$$

Anti-fungal activity assays

The anti-fungal activity of the EFs was evaluated against three fungal pathogens: *Alternaria alternate*, *Fusarium oxysporum* f. sp. *cucumerinum*, and *Phytophthora drechsleri* (all provided by Professor Zhiwei Zhao of the State Key Laboratory for Conservation and Utilization of Bio-Resources, Yunnan University). A dual-culture technique was modified to study antagonism (Gao et al., 2002). The pathogen was inoculated on PDA medium center and four different isolated fungi were inoculated around pathogen, incubated at 28 °C for a week, and the anti-fungal zone were measured by ruler (mm).

http://www.aloki.hu ● ISSN 1589 1623 (Print) ● ISSN 1785 0037 (Online)
DOI: http://dx.doi.org/10.15666/aeer/1706_1528915300

Results

Colonization rates and diversity of EFs

Colonization rate is an indication of the number of EFs in host plants and varies with the altitude, humidity, precipitation, temperature and plant community (Hashizume et al., 2010). In the present study, the colonization rate of the EFs from six sites ranged from 46.7% to 73.3%, and the highest colonization rate appeared in Malong, while the lowest was appeared in Panlong (*Table 1*). To further investigate the biodiversity of the EFs, we calculated the Shannon diversity index (H'), Simpson's index (D) and Simpson's diversity index (1-D). The Shannon diversity indexes (H') of the endophytic community in the six different sites were 1.98, 1.88, 1.82, 1.76, 2.05 and 1.68, respectively. The Simpson's diversity index is between 1 and 0, with 1 representing infinite variety of diversity, and 0 representing no diversity. The Simpson's diversity index showed a similar pattern for the six sites, which were 0.92, 0.85, 0.88, 0.89, 0.88 and 0.81, respectively.

Table 1. *Number, colonization rate, Shannon-Weiner index (H') and Simpson's diversity index (1-D) of the root- endophytic fungi (EF) of A. carmichaelii from the six regions of Yunnan, China*

Collection site	No. of EFs isolated	Colonization rate (%)	H′	1-D
Heqing	26	48.9	1.98	0.92
Huize	44	60.0	1.88	0.85
Luquan	38	64.4	1.82	0.88
Malong	38	73.3	1.76	0.89
Panlong	26	46.7	2.05	0.88
Yulong	39	53.3	1.68	0.81
Total	171	57.8		

Community composition of EFs

A total of 171 isolates were obtained from collected roots, and identified into 28 taxa by molecular identification based on rDNA ITS sequence analysis (*Table 2*). A total of 10 endophytic taxa from Heqing; 12 taxa were identified from Huize; 10 taxa from Luquan; 12 taxa from Malong; 11 taxa from Panlong; and 10 taxa from Yulong (*Table 2*). The dominant taxa determined by the Camargo's index and P_i were *Chaetomidium arxii*, *Chaetomium* sp., and *Phoma* sp. in Heqing; *Chaetomium* sp., *Cladosporium* sp., and *Fusarium* sp. in Huize; *Chaetomidium arxii*, *Plectosphaerella* sp., and *Pochonia* sp. in Luquan; *Chaetomium* sp. and *Plectosphaerella* sp. in Malong; *Chaetomidium arxii*, *Chaetomium globosum, Ilyonectria* sp., *Phoma* sp., and *Plectosphaerella* sp. in Panlong; and *Fusarium oxysporum* and *Ilyonectria* sp. in Yulong. Only *Chaetomidium arxii* and *Plectosphaerella* sp. were identified in all six sites (*Table 2*). The rates of colonization for *Chaetomium* sp. in Huize and *Fusarium oxysporum* in Yulong were higher than in other sites (*Table 2*). Endemic endogenous fungi were isolated from five habitats of *A. carmichaelii*, including: Huize (*Cladosporium* sp., *Cylindrocarpon* sp., *Mucor racemosus*, and *Verticillium tricorpus*,); Luquan (*Bjerkandera* sp., *Pochonia* sp., and *Thielavia* sp.); Malong (*Acrostalagmus luteoalbus* and *Trametes versicolor*); Panlong (*Daldiniafissa* sp.); and Yulong (*Clonostachys rosea* and *Paraphaeosphaeria sporulosa*). The phylogenetic tree indicated that *Chaetomium* sp., *Fusarium* sp. and *Plectosphaerella* sp. were the

http://www.aloki.hu ● ISSN 1589 1623 (Print) ● ISSN 1785 0037 (Online)
DOI: http://dx.doi.org/10.15666/aeer/1706_1528915300

dominant EFs in this medicinal plant. In this study, phylogenetic analysis revealed that all sequences clustered in at least 18 discrete sequence groups (*Fig. 2*). The majority of clones (73.08%) fell into the G 1 (Group 1), G 2 (Group 2) and G 4 (Group 4), which were distributed across most root samples.

Anti-fungal activity assays

The diversity and antimicrobial potential of EFs from a number of medicinal plants have been studied (Qin et al., 2009; Egamberdieva et al., 2017; Xiang et al., 2017). Our screening of anti-fungal activity of the isolated EFs identified 17 genera which are resistant to the three fungal pathogens (*Alternaria alternate, Fusarium oxysporum* f. sp. *cucumerinum*, and *Phytophthora drechsleri*) in agricultural production (*Table 3*). A*crostalagmus luteoalbus* (LD34), *Phoma* sp. (MC6), and *Thielavia* sp. (LQ14) displayed good anti-fungal effects, and the anti-fungal zone for *Alternaria alternate*, *Fusarium oxysporum* f. sp. *cucumerinum*, and *Phytophthora drechsleri* were 4, 3, and 2 mm; 5, 3, and 3 mm; and 4, 3, and 3 mm, respectively, although they accounted for the small proportion of the colonization (*Table 3*). In addition, *Chaetomium* sp. and *Fusarium* sp., two dominant strains obtained in this experiment, also showed some anti-fungal activity (*Table 3*).

Table 2. *Number, taxa and relative frequency (RF) of the root-EFs of A. carmichaelii collected from six regions of Yunnan, China*

Taxa	No. of strains isolated from each regions (RF %)						
	Heqing	**Huize**	**Luquan**	**Malong**	**Panlong**	**Yulong**	**Total (RF %)**
Acrostalagmus luteoalbus				1(2.63)			1(0.58)
Alternaria sp.			1(2.63)		1(3.85)		2(1.17)
Bjerkandera sp.			1(2.63)				1(0.58)
Chaetomidium arxii	3(11.54)	2(4.55)	6(15.79)	1(2.63)	3(11.54)	1(2.56)	16(9.36)
Chaetomium globosum		2(4.55)			3(11.54)		5(2.92)
Chaetomium sp.	3(11.54)	12(27.27)		6(15.79)	1(3.85)	2(5.13)	24(14.04)
Cladosporium sp.		6(13.64)					6(3.51)
Clonostachys rosea						2(5.13)	2(1.17)
Cryptococcus sp.	1(3.85)		1(2.63)				2(1.17)
Cylindrocarpon sp.		1(2.27)					1(0.58)
Daldinia fissa					1(3.85)		1(0.58)
Fusarium oxysporum	1(3.85)	2(4.55)		3(7.89)		11(28.21)	17(9.94)
Fusarium sp.	2(7.69)	4(9.09)		2(5.26)	1(3.85)	2(5.13)	11(6.43)
Geomyces sp.				1(2.63)	1(3.85)		2(1.17)
Ilyonectria sp.	4(15.38)		2(5.26)	1(2.63)	1(3.85)	9(23.08)	17(9.94)
Irpex lacteus				1(2.63)		1(2.56)	2(1.17)
Mortierella sp.		1(2.27)		1(2.63)			2(1.17)
Mucor racemosus		1(2.27)					1(0.58)
Paraphaeosphaeria sporulosa						1(2.56)	1(0.58)
Penicillium sp.	1(3.85)	1(2.27)	2(5.26)				4(2.34)
Phoma sp.	3(11.54)				6(23.08)	2(5.13)	11(6.43)
Plectosphaerella sp.	2(7.69)	3(6.81)	5(13.16)	6(15.79)	6(23.08)	1(2.56)	23(13.45)
Pleosporales sp.				1(2.63)	1(3.85)		2(1.17)
Pochonia sp.			7(18.42)				7(4.09)
Thielavia sp.			3(7.89)				3(1.75)
Trametes versicolor				2(5.26)			2(1.17)
Trichocladium sp.	2(7.69)		2(5.26)				4(2.34)
Verticillium tricorpus		1(2.27)					1(0.58)
Total taxa recovered	10	12	10	12	11	10	28

http://www.aloki.hu ● ISSN 1589 1623 (Print) ● ISSN 1785 0037 (Online)
DOI: http://dx.doi.org/10.15666/aeer/1706_1528915300

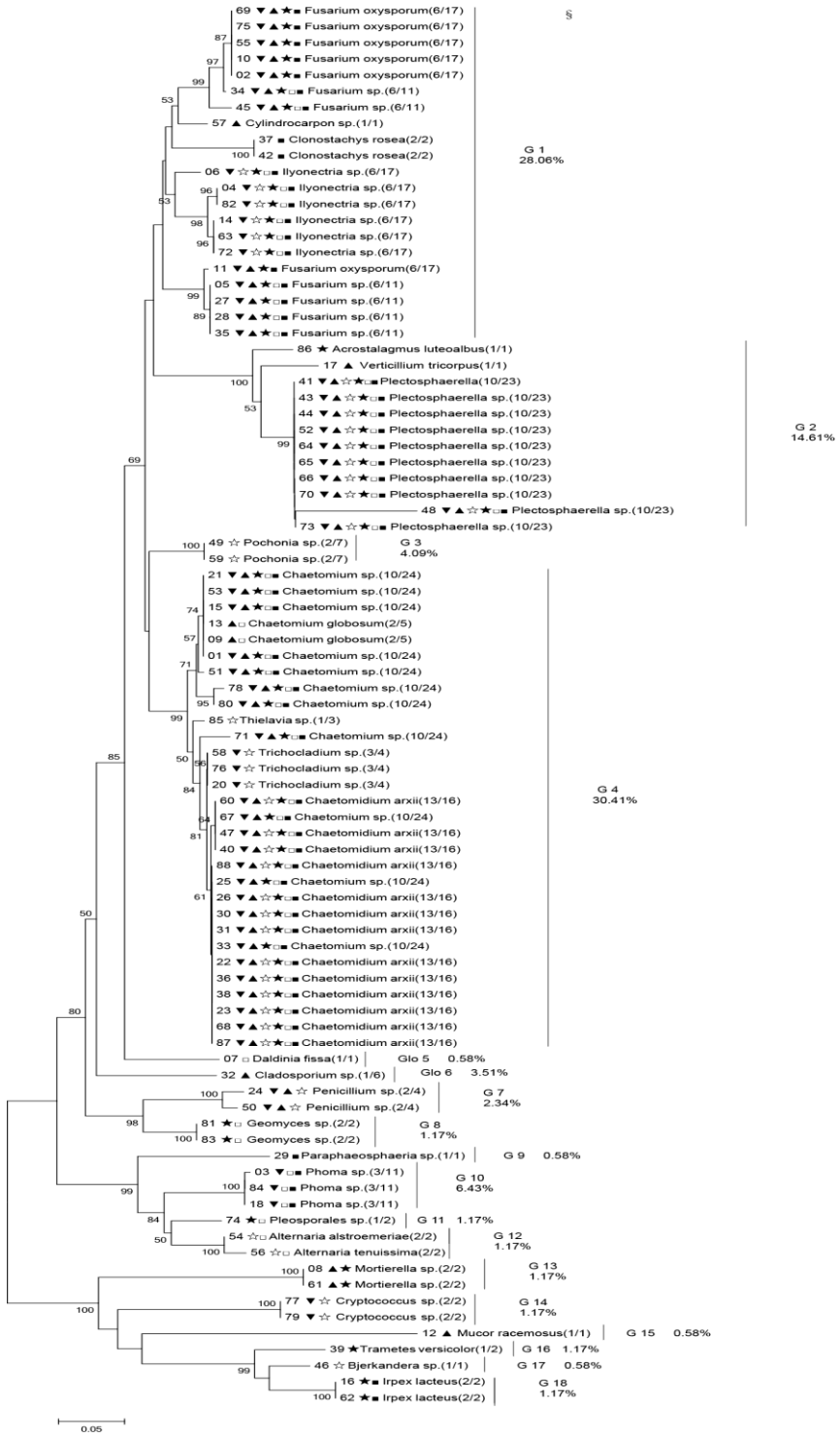

Figure 2. *Neighbor-joining tree of ITS sequence of endophytic fungi associated with Aconitum carmichaelii constructed with a 1000 boot-strap replications. Bar: 0.5% sequence divergence. Numbers above the nodes indicate bootstrap support in neighbor-joining analysis. Representative sequences with Anti-black triangles (▼), black triangles (▲), white pentagram (☆), black pentagram (★), white square (□), black square (■) represent EFs originating from Heqing, Huize, Luquan, Malong, Panlong, Yulong. Arabic numbers in parentheses indicate the number of sequences (above slash) and the number of sequenced clones (below slash). §: represents the ratio of the numbers of sequences in a given clade to the total sequenced clones*

http://www.aloki.hu ● ISSN 1589 1623 (Print) ● ISSN 1785 0037 (Online)
DOI: http://dx.doi.org/10.15666/aeer/1706_1528915300

Table 3. *The anti-fungal activity of EF collected from A. carmichaelii*

Taxa	No.	Pathogen fungi (mm)		
		Alternaria alternate	***Fusarium oxysporum* f. sp. *Cucumerinum***	***Phytophthora drechsleri***
Acrostalagmus luteoalbus	ML20	3	3	3
Alternaria sp.	PL16	1	1	2
Chaetomidium arxii	LQ30	1	1	2
Chaetomidium arxii	PL1	1	2	1
Chaetomidium arxii	PL18	1	1	1
Chaetomidium arxii	YL15	1		2
Chaetomium sp.	HZ34	1	1	1
Chaetomium sp.	HZ35	2		
Chaetomium sp.	HZ36	1	1	1
Chaetomium sp.	ML7	2		2
Chaetomium sp.	ML11	1	1	2
Clonostachys rosea	YL32	1		1
Cylindrocarpon sp.	HZ15	1		1
Fusarium oxysporum	YL17		2	1
Fusarium sp.	HQ1			2
Fusarium sp.	HZ11	1		1
Ilyonectria sp.	ML4	2	1	1
Ilyonectria sp.	PL13	2		2
Ilyonectria sp.	YL34	3	3	4
Mortierella sp.	HZ39	1	1	1
Paraphaeosphaeria sporulosa	YL30	2		1
Phoma sp.	HQ6	3	3	5
Plectosphaerella sp.	HZ43	1	1	1
Plectosphaerella sp.	PL17	1	2	2
Pleosporales sp.	PL20		2	1
Thielavia sp.	LQ14	2	3	4
Trichocladium sp.	HQ24	1	1	
Trichocladium sp.	LQ22	2	2	
Verticillium tricorpus	HZ41		1	2

The values of the anti-fungal zone in the table are the average of the three experiments. HQ, HZ, LQ, ML, PL, and YL are indicative of Heqing, Huize, Luquan, Malong, Panlong, and Yulong, respectively and the number after abbreviations showed the isolation order of the endophytic fungi

Discussion

Endophytic fungi were isolated from *Aconitum carmichaelii*, one of the most important TCMs, which laid the foundation for future biological control research. In this study, roots of *A. carmichaelii* were collected from six sites in Yunnan Province, the People's Republic of China for the isolation, identification and antibacterial analysis of EFs. Colonization rate and Shannon diversity index (H') of the EFs in different areas (*Table 1*) indicated that there were rich root-fungal endophytes existing in *A. carmichaelii* in Yunnan. In all isolates, only *Chaetomidium arxii* and *Plectosphaerella* sp. were identified in all six sites (*Table 2*), suggesting that these two endophytic fungi

http://www.aloki.hu ● ISSN 1589 1623 (Print) ● ISSN 1785 0037 (Online)
DOI: http://dx.doi.org/10.15666/aeer/1706_1528915300

are host-generalists. The rates of colonization for *Chaetomium* sp. in Huize and *Fusarium oxysporum* in Yulong were higher than in other sites (*Table 2*). This may be due to the fact that the roots are persistent, and can form unique endophytic fungal community. In addition, Huize has been documented heavy metal contamination (Lu et al., 2014), and *Chaetomium* sp. is known as a soil and contaminant fungi (Abdel-Lateff, 2008). Endemic EFs were isolated from five habitats, and the population structure of endophytic fungi normally represents a certain degree of regional specificity (Jia et al., 2016). In contrast to the endemic EFs, dominate endophytic fungi lived in a wide variety of plants such as *Phoma* sp. (Nisa et al., 2015), which was also isolated from *A. carmichaelii* with a RF as 6.43%.

Screening of anti-fungal activity of the isolated EFs identified 29 isolates, such as *Chaetomium* sp. (*Table 3*), with wide-spectrum antibacterial activity (Li et al., 2009). Previous research showed that *Chaetomium* sp. suppressed the growth of bacteria and fungi through direct competition, mycoparasitism, and antibiosis (Rodríguez et al., 2002). Two antibacterial furano-polyenes, (-) - musanahol and 3-epi-aureonitol, were isolated from cultures of *Chaetomium* sp. (Marwah et al., 2007). Dutch elm disease, caused by the fungal pathogen *Ceratocystis ulmi*, can be controlled by the endophytic fungus *Phomopsis oblonga* (Webber, 1981). Leutou et al. (2016) concluded that the microbial transformation of anthranilic acid by the marine-mudflat-derived fungus *Thielavia* sp. produced an antibacterial polycyclic quinazoline alkaloid, thielaviazoline. *Fusarium oxysporum* is well represented in the rhizosphere microflora (Lecomte et al., 2016). Some isolates can induce wilt or root rots while others are considered as nonpathogenic taxa. For example, nonpathogenic *F. oxysporum* in soil can suppress *Fusarium* wilts (Fravel et al., 2003), and the strain has also attracted interest for soil bioremediation and water purification due to its capability to detoxify and colonize polluted environments (Steinberg et al., 2016). Ratnaweera et al. (2015) found that equisetin, isolated from endophytic *Fusarium* sp., exhibited antibacterial activities against the Gram-positive bacteria.

Some recent studies have shown that *Lentzea* sp., *Nigrospora* sp. and *Streptomyces* sp. isolated from *A. carmichaelii* have antibiotic activity (Qiu et al., 2015; Zhang et al., 2016). EFs isolated from medicinal plants sometimes produce similar compounds as their hosts (Newman, 2015). Diterpene alkaloids are the dominant secondary metabolites of *Aconitum* species (Zhou et al., 2015), and other diterpene alkaloids have been reported to be produced by endophytic fungi of the genus *Epichloë* in perennial ryegrass (Philippe, 2016). Based on the anti-fungi activity of diterpene alkaloids (Kobayashi et al., 1998), we hypothesize that certain EFs from *A. carmichaelii* could produce aconitum alkaloids that inhibit these three fungal pathogens. We plan to examine the chemistry of these EFs in the future.

In this study, 171 strains of EFs were isolated and identified from six parts of *A. carmichaelii* roots, of which 29 isolates in 17 genera showed some level of anti-fungal activity. This study helps to lay a foundation for the potential association of EFs and disease resistance in *A. carmichaelii*.

Conclusion

Isolated from the roots of *A. carmichaelii* from six different production sites in Yunnan province, China, the root-endophytic fungi are assigned to 28 taxa. Among these identified taxa, *Chaetomium* and *Fusarium* were the dominant genera in all six

http://www.aloki.hu ● ISSN 1589 1623 (Print) ● ISSN 1785 0037 (Online)
DOI: http://dx.doi.org/10.15666/aeer/1706_1528915300

sites while *Cladosporium* and *Pochonia* were unique dominant genera in Huize and Yulong counties. *Acrostalagmus luteoalbus*, *Phoma* sp., and *Thielavia* sp. displayed good anti-fungal activity against *Alternaria alternate*, *Fusarium oxysporum* f. sp. *cucumerinum* and *Phytophthora drechsleri*, providing new biological control clues for these pathogenic fungi. In subsequent experiments, further investigation on whether the endophytic fungi have the same fungal pathogen resistance *in vivo* was necessary. In addition, exploring the chemical composition against these fungal pathogens of endophytic fungi would be helpful for identifying the active leading chemical compounds for fungal disease control.

Acknowledgements. This work was supported by the National Natural Science Foundation of China (No. 81560622; No. 31960082) and Science and Technology Office, Yunnan Province (2016RA046).

REFERENCES

[1] Abdel-Lateff, A. (2008): Chaetominedione, a new tyrosine kinase inhibitor isolated from the algicolous marine fungus *Chaetomium* sp. – Tetrahedron Letters 49: 6398-6400.

[2] Aly, A. H., Edrada-Ebel, R., Wray, V., Müller, W. E., Kozytska, S., Hentschel, U., Proksch, P., Ebel, R. (2008): Bioactive metabolites from the endophytic fungus *Ampelomyces* sp. isolated from the medicinal plant *Urospermum picroides*. – Phytochemistry 69: 716-1725.

[3] Bittleston, L. S., Brockmann, F., Wcislo, W., Bael, S. A. V. (2011): Endophytic fungi reduce leaf-cutting ant damage to seedlings. – Biology Letters 7: 30-32.

[4] Camargo, J. A. (1993): Must dominance increase with the number of subordinate species in competitive interactions. – Journal of Theoretical Biology 161: 537-542.

[5] Egamberdieva, D., Wirth, S., Behrendt, U., Ahmad, P., Berg, G. (2017): Antimicrobial activity of medicinal plants correlates with the proportion of antagonistic endophytes. – Frontiers in Microbiology 8: 99.

[6] Fernandes, E. G., Pereira, O. L., da Silva, C. C., Bento, C. B. P., de Queiroz, M. V. (2015): Diversity of endophytic fungi in *Glycine max*. – Microbiological Research 181: 84-92.

[7] Fravel, D., Olivain, C., Alabouvette, C. (2003): *Fusarium oxysporum* and its biocontrol. – New Phytologist 157: 493-502.

[8] Gao, K., Liu, X., Liu, Y., Zhu, T., Wang, S. (2002): Potential of *Trichoderma harzianum* and *T. atroviride* to control *Botryosphaeria berengeriana* f. sp. *Piricola*, the cause of apple ring rot. – Journal of Phytopathology 150: 271-276.

[9] Hashizume, Y., Fukuda, K., Sahashi, N. (2010): Effects of summer temperature on fungal endophyte assemblages in Japanese beech *(Fagus crenata*) leaves in pure beech stands. – Botany 88: 266-274.

[10] Hunter, P. R., Gaston, M. A. (1988): Numerical index of the discriminatory ability of typing systems: an application of Simpson's index of diversity. – Journal of Clinical Microbiology 26: 2465-2466.

[11] Hyde, K. D., Soytong, K. (2008): The fungal endophyte dilemma. – Fungal Diversity 33: 163-173.

[12] Jia, M., Chen, L., Xin, H. L., Zheng, C. J., Rahman, K., Han, T., Qin, L. P. (2016): A friendly relationship between endophytic fungi and medicinal plants: a systematic review. – Frontiers in Microbiology 7: 906.

[13] Kobayashi, M., Mori, K., Kobayashi, H., Pollard, R. B., Suzuki, F. (1998): The regulation of burn-associated infections with herpes simplex virus type 1 or *Candida albicans* by a

http://www.aloki.hu ● ISSN 1589 1623 (Print) ● ISSN 1785 0037 (Online)
DOI: http://dx.doi.org/10.15666/aeer/1706_1528915300

non-toxic aconitine-hydrolysate, benzoylmesaconine. Part 1: Antiviral and anti-fungal activities in thermally injured mice. – Immunology and Cell Biology 76: 202-208.

[14] Kohout, P., Těšitelová, T., Roy, M., Vohník, M., Jersáková, J. (2013): A diverse fungal community associated with *Pseudorchis albida* (Orchidaceae) roots. – Fungal Ecology 6: 50-64.

[15] Kusari, S., Spiteller, M. (2012): Metabolomics of Endophytic Fungi Producing Associated Plant Secondary Metabolites: Progress, Challenges and Opportunities. – In: Prasain, J. (ed.) Metabolomics. InTech, London, pp. 241-266.

[16] Lecomte, C., Alabouvette, C., Edel-Hermann, V., Robert, F., Steinberg, C. (2016): Biological control of ornamental plant diseases caused by *Fusarium oxysporum*: a review. – Biological Control 101: 17-30.

[17] Leutou, A. S., Yun, K., Son, B. W. (2016): New production of antibacterial polycyclic quinazoline alkaloid, Thielaviazoline, from anthranilic acid by the Marine-Mudflat-derived fungus *Thielavia* sp. – Natural Product Sciences 22: 216-219.

[18] Li, Y., Song, Y., Liu, J., Ma, Y., Tan, R. (2005): Anti-*Helicobacter pylori* substances from endophytic fungal cultures. – World Journal of Microbiology and Biotechnology 21: 553-558.

[19] Li, Z. Y., Chen, Y. W., Yang, L. Y., Li, S. L., Wu, S. H. (2009): Antipathogenic activity of endophytic fungi in *Radix aconiti* plant. – Natural Product Research and Development 21: 676-678.

[20] Liu, L., Li, Y., Liu, S., Zheng, Z., Chen, X., Zhang, H., Guo, L., Che, Y. (2009): Chloropestolide A, an antitumor metabolite with an unprecedented spiroketal skeleton from *Pestalotiopsis fici*. – Organic Letters 11: 2836-2839.

[21] Lu, S. J., Wang, Y. Y., He, L. H. (2014): Heavy metal pollution and ecological risk assessment of paddy soils around a Pb-Zn mine in Huize country. – Ecology and Environmental Sciences 23: 1832-1838.

[22] Marwah, R. G., Fatope, M. O., Deadman, M. L., Al-Maqbali, Y. M., Husband, J. (2007): Musanahol: a new aureonitol-related metabolite from a *Chaetomium* sp. – Tetrahedron 63: 8174-8180.

[23] Mishra, A., Gond, S. K., Kumar, A., Sharma, V. K., Verma, S. K., Kharwar, R. (2012): Sourcing the Fungal Endophytes: A Beneficial Transaction of Biodiversity, Bioactive natural Products, Plant Protection and Nanotechnology. – In: Satyanarayana, T. et al. (eds.) Microorganisms in Sustainable Agriculture and Biotechnology. Springer, New Delhi, pp. 581-612.

[24] Morsy, M. R., Oswald, J., He, J., Tang, Y., Roossinck, M. J. (2010): Teasing apart a three-way symbiosis: transcriptome analyses of *Curvularia protuberata* in response to viral infection and heat stress. – Biochemical and Biophysical Research Communications 401: 225-230.

[25] Nascimento, T., Oki, Y., Lima, D., Almeida-Cortez, J., Fernandes, G. W., Souza-Motta, C. (2015): Biodiversity of endophytic fungi in different leaf ages of *Calotropis procera* and their antimicrobial activity. – Fungal Ecology 14: 79-86.

[26] Newman, D. (2015): Hot topics in Pharmacognosy: belated recognition of old friends? – The ASP Newsletter 51: 16-18.

[27] Nisa, H., Kamili, A. N., Nawchoo, I. A., Shafi, S., Shameem, N., Bandh, S. A. (2015): Fungal endophytes as prolific source of phytochemicals and other bioactive natural products: a review. – Microbial Pathogenesis 82: 50-59.

[28] Niu, C., Kebede, H., Auld, D. L., Woodward, J. E., Burow, G., Wright, R. J. (2010): A safe inexpensive method to isolate high quality plant and fungal DNA in an open laboratory environment. – African Journal of Biotechnology 7: 2818-2822.

[29] Philippe, G. (2016): Lolitrem B and indole diterpene alkaloids produced by endophytic fungi of the genus *Epichloë* and their toxic effects in livestock. – Toxins 8: 47.

[30] Qin, S., Li, J., Chen, H. H., Zhao, G. Z., Zhu, W. Y., Jiang, C. L., Xu, L. H., Li, W. J. (2009): Isolation, diversity, and antimicrobial activity of rare actinobacteria from

http://www.aloki.hu ● ISSN 1589 1623 (Print) ● ISSN 1785 0037 (Online)
DOI: http://dx.doi.org/10.15666/aeer/1706_1528915300

medicinal plants of tropical rain forests in Xishuangbanna, China. – Applied and Environmental Microbiology 75: 6176-6186.

[31] Qiu, P., Feng, Z. X., Tian, J. W., Lei, Z. C., Wang, L., Zeng, Z. G., Chu, Y. W., Tian, Y. Q. (2015): Diversity, bioactivities, and metabolic potentials of endophytic actinomycetes isolated from traditional medicinal plants in Sichuan, China. – Chinese Journal of Natural Medicines 13: 942-953.

[32] Ratnaweera, P. B., de Silva, E. D., Williams, D. E., Andersen, R. J. (2015): Antimicrobial activities of endophytic fungi obtained from the arid zone invasive plant *Opuntia dillenii* and the isolation of equisetin, from endophytic *Fusarium* sp. – BMC Complementary and Alternative Medicine 15: 220.

[33] Rodríguez, K., Stchigel, A., Guarro, J. (2002): Three new species of *Chaetomium* from soil. – Mycologia 94: 116-126.

[34] Shannon, C. E., Wiener, W. (1963): The Mathematical Theory of Communication. – University of Illinois Press, Urbana.

[35] Silva, H. S., Tozzi, J. P., Terrasan, C. R., Bettiol, W. (2012): Endophytic microorganisms from coffee tissues as plant growth promoters and biocontrol agents of coffee leaf rust. – Biological Control 63: 62-67.

[36] Steinberg, C., Lecomte, C., Alabouvette, C., Edel-Hermann, V. (2016): Root Interactions with Nonpathogenic Fusarium Oxysporum. – In: Vos, C., Kazan, K. (eds.) Belowground Defence Strategies in Plants. Springer, Switzerland, pp. 281-299.

[37] Strobel, G., Daisy, B., Castillo, U., Harper, J. (2004): Naturalproducts from endophytic microorganisms. – Journal of Natural Products 67: 257-268.

[38] Su, Y. Y., Guo, L. D., Hyde, K. D. (2010): Response of endophytic fungi of Stipa grandis to experimental plant function group removal in Inner Mongolia steppe, China. – Fungal Diversity 43: 93-101.

[39] Sun, X., Guo, L. D., Hyde, K. (2011): Community composition of endophytic fungi in *Acer truncatum* and their role in decomposition. – Fungal Diversity 47: 85-95.

[40] Webber, J. (1981): A natural biological control of Dutch elm disease. – Nature 292: 449-451.

[41] Xiang, L., Gong, S., Yang, L., Hao, J., Xue, M. F., Zeng, F. S., Zhang, X. J., Shi, W. Q., Wang, H., Yu, D. (2016): Biocontrol potential of endophytic fungi in medicinal plants from Wuhan Botanical Garden in China. – Biological Control 94: 47-55.

[42] Xiao, P., Wang, F., Gao, F., Yan, L., Chen, D., Liu, Y. (2006): A pharmacophylogenetic study of *Aconitum* L. (Ranunculaceae) from China. – Acta Phytotaxonomica Sinica 44: 1-46.

[43] Yuan, Z. L., Zhang, C. L., Lin, F. C., Kubicek, C. P. (2010): Identity, diversity, and molecular phylogeny of the endophytic mycobiota in the roots of rare wild rice (*Oryza granulate*) from a nature reserve in Yunnan, China. – Applied and Environmental Microbiology 76: 1642-1652.

[44] Zhang, S. P., Huang, R., Li, F. F., Wei, H. X., Fang, X. W., Xie, X. S., Lin, D. G., Wu, S. H., He, J. (2016): Antiviral anthraquinones and azaphilones produced by an endophytic fungus *Nigrospora* sp. from *Aconitum carmichaeli*. – Fitoterapia 112: 85-89.

[45] Zhou, G., Tang, L., Zhou, X., Wang, T., Kou, Z., Wang, Z. (2015): A review on phytochemistry and pharmacological activities of the processed lateral root of *Aconitum carmichaeli* Debeaux. – Journal of Ethnopharmacology 160: 173-193.

http://www.aloki.hu ● ISSN 1589 1623 (Print) ● ISSN 1785 0037 (Online)
DOI: http://dx.doi.org/10.15666/aeer/1706_1528915300

MONITORING AND ANALYSIS OF TEA ROOT PARAMETERS BASED ON CI600 IN SITU ROOT IMAGER

SUN, D. Z.[1,2,3,4] – WANG, W. X.[1,3,4*] – HUANG, Y.[5*] – SONG, SH. R.[1,2,3,4] – XIE, J. X.[1,2,3,4] – LAI, J. G.[1] – PENG, G.[1]

[1]*School of Electronic Engineering, South China Agricultural University Guangzhou 510642, China*

[2]*Guangdong Citrus Mango Technology System Machinery Research Laboratory Guangzhou 510642, China*

[3]*Guangdong Agricultural Information Monitoring Engineering Technology Research Center Guangzhou 5106424, China*

[4]*Guangzhou Key Laboratory of Agricultural Information Acquisition and Application Guangzhou 510642, China*

[5]*Liuzhou Railway Vocational Technical College, Liuzhou Guangxi 545616, China*

[*]*Corresponding authors*
e-mail: weixing@scau.edu.cn (Wang, W. X.); huangying800816@163.com (Huang, Y.)

(Received 8th Jul 2019; accepted 16th Oct 2019)

Abstract. Four groups of one-year-old Yinghong No. 9 tea plants were studied under with different gradients of water. The correlation test and analysis of soil moisture and tea root coefficient, root length, root area and root volume were carried out. The number, length, area and the volume of tea roots were collected by CI600 plant root growth monitoring equipment, and the correlation between the parameters and water was analyzed to determine the suitable range of soil moisture for tea plant growth. The results showed that the soil moisture suitable for tea tree growth in the case of red loam soil was 35%. During the 90-day test period, 13 young roots were newly born for tea trees with 35% soil moisture, the root length increased by 299.02 mm, the root area increased by 1285.207 mm^2, and the volume increased by 1169.063 mm^3. The number, length, area and volume of roots were positively correlated with the growth time at soil moisture of 35%, and the R^2 values were 0.9887, 0.9907, 0.9801 and 0.9919, which were higher than those under difference soil moisture. At the end of the experiment, the root coefficient of tea roots under 35% soil moisture increased by 2.16 times; the length of roots increased by 1.0068 times; the area increased by 0.515 times and the volume increased by 0.64 times. The performance of each index of tea planted under 25% soil moisture was slightly worse than for those tea planted under 35% soil moisture. The performance of each index of tea planted under 15% and 45% soil moisture was average. So the number, length, area and volume of tea roots are positively correlated with growth time at soil moisture of 35%. The tea tree under other moisture conditions does not exhibit this relationship.
Keywords: *CI600, tea tree, root monitoring, soil moisture, situ root measurements*

Introduction

Root system is an important way of material exchange between plants and their environment, and the primary means of water intake. Root system can absorb a large amount of water from soil and provide life activities (Hu, 2013; Guo, 2018). The growth and development of plants are reflected by root growth state, which is mainly concentrated in the development and distribution of roots and physiological characteristics (Wang, 2007; Wang, 2015; Niu, 2017).

http://www.aloki.hu ● ISSN 1589 1623 (Print) ●ISSN1785 0037 (Online)
DOI: http://dx.doi.org/10.15666/aeer/1706_1530115309

Different morphology of root growth is showed under different water stress conditions. Studies have shown that plants subjected to water stress will adapt to water deficit by changing root structure and morphology, which had higher plasticity (Zhanyang, 2017). Zhu (2012) and Lai (2018) presented that the morphological structure and root biomass of the root system may change accordingly to the change of soil moisture, which affected the physiological characteristics of root system and the growth and development of the whole plant. Zhou (2008) pointed out that the root growth index of citrus increased with the increase of water, and Liu (2014) pointed out that the activity and osmotic adjustment ability of various enzymes in roots of drought-resistant peanut varieties were higher than those of weak drought-resistant varieties. Wei (2011) concluded that there is a significant correlation between root volume and water in jujube trees in horizontal and vertical directions. Meng et al. (2017) said that the development of root hair is regulated by a variety of nutrient elements.

The analysis and research methods of root system have made great progress and development from the initial soil-removing research to the later digital analysis, but there are still some limitations, such as inconvenience monitoring methods and complexity of real-time analysis (Liu, 2013; Qin, 2019). The root growth state under water stress was monitored by CI600 plant root growth. The number, length, area and volume of tea roots were collected. The data were analyzed by least squares method to obtain the correlation between root related parameters and soil moisture. Relationships provide a reference for the scientific planting of tea trees.

The article aimed to use CI600 plant root growth monitoring equipment to analyze the roots of four years old Yinghong No. 9 tea plants under varying soil moisture, in order to find the optimal value.

Materials and Method

Test environment

Experiment location: The experimental site is located in the campus of South China Agricultural University, Guangzhou City, Guangdong Province (113°34'N, 23°14'E). The region is warm and rainy, with humid climate and abundant sunshine. It belongs to the subtropical monsoon climate. The annual average temperature is around 20 to 22°C; the annual rainfall is 1720 mm, and the annual relative humidity is 77%. Good climatic conditions are suitable for most plants. The experiment lasted from Feb.10 to May 11, 2019; the daily average maximum temperature was 25°C; the daily average minimum temperature was 17°C, and the daily average relative humidity was 53%, which is suitable for plant growth and control of experimental variables.

Plant culture

Four groups of one-year-old Yinghong No. 9 tea trees with the same growth potential and smaller root differences were selected for experiment. The tea roots need to be properly trimmed to make the whole suitable for the test requirements, and the treated tea trees are planted in a soil box containing red loam for 20 days. Only 2 one-year-old tea trees are planted for each of soil moisture content.

http://www.aloki.hu ● ISSN 1589 1623 (Print) ●ISSN1785 0037 (Online)
DOI: http://dx.doi.org/10.15666/aeer/1706_1530115309

Experiment equipment

(1) DECAGON Em50 Data Logger (DECAGON, USA), including sensors and collectors, is used to collect soil moisture.

(2) CI600 root parameters monitoring system (CID-Bioscience, USA), includes CI600 Root Scanne (Hardware Scanner), CI600 In-Situ Root Imager (Scanning Software) and CI690 Root Snap (Image Analysis Software).

(3) SHT11 air temperature and humidity sensor is used to measure the temperature and humidity of the air.

Experimental design

Four kinds of soil moisture were designed, which were 15%, 25%, 35% and 45%. The red loam soil was mixed, stirred evenly, and sand and gravel were removed before being packed. The weight was evenly distributed into four soil tanks and compacted. The average weight of red loam in each soil box was 20 kg. The experimental tea tree is shown in *Figure 1*.

Figure 1. *The experimental tea tree*

Experiment results and analysis

The root coefficient, root length, root area and root volume of the tea tree roots are measured by CI600 Root Scanne and CI600 In-Situ Root Imager. Date will be automatically calculated by CI690 RootSnap. Resultes is processed by averaging its data.

The root coefficient is defined as the number of tea roots that grow during the test period.

Root coefficient, root length, root area and root volume of tea trees will be tested to find out the effect and relationship of soil water content between them.

http://www.aloki.hu ● ISSN 1589 1623 (Print) ●ISSN1785 0037 (Online)
DOI: http://dx.doi.org/10.15666/aeer/1706_1530115309

The growth rate is defined as the ratio of the current root coefficient to the previous root coefficient.

The growth rate is given by *Equation (1)*.

$$\text{Growth rate} = \frac{N_2 - N_1}{N_1} * 100\% \quad \text{(Eq.1)}$$

where N_2 represents the parameter measured at the moment, and N_1 represents the parameter measured at the previous moment. These parameters can be root coefficient, root length, root area and root volume of tea trees.

Effect of Soil Moisture on Root Coefficient of Tea Trees

The variation of the root coefficient of tea tree under different soil moisture is shown by CI600 Root Scanne and CI600 In-Situ Root Imager, and the corresponding curve is shown in *Figure 2*.

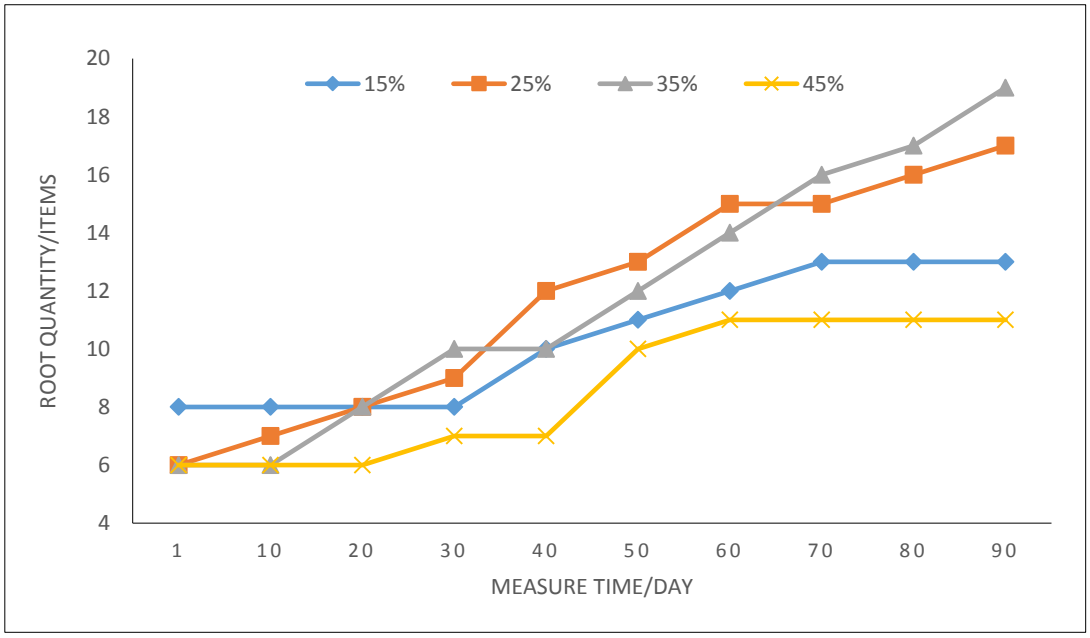

Figure 2. *Curve of the variation of tea root coefficient under different soil moisture*

Experiments show that the coefficient of tea root system under four soil moisture conditions increased by 5, 11, 13 and 5, and increased by 0.625, 1.83, 2.16 and 0.83 times. *Figure 2* shows that the rate of increase of root coefficient of tea tree planted under 35% soil moisture was relatively stable, and had a good performance but slowed in the later stage under 25% soil moisture. Compared with 35% soil moisture, root coefficient growth rate fluctuates too much throughout during the experiment period. However, the root coefficient of tea trees planted under 15% and 45% soil moisture has almost no change. It can be speculated that this humidity is not suitable for tea tree growth. The relationship between the four root coefficient quantities and the growth time was curve-fitted, and the determination coefficients R^2 were 0.9108, 0.9773, 0.9887 and 0.8685.

http://www.aloki.hu ● ISSN 1589 1623 (Print) ●ISSN1785 0037 (Online)
DOI: http://dx.doi.org/10.15666/aeer/1706_1530115309

Effects of Soil Moisture on Root Length of Tea Trees

The root length of tea tree under different soil moisture is measured by CI600 Root Scanne and CI600 In-Situ Root Imager., and the corresponding curve is shown in *Figure 3*.

Experiments show that the initial root length of tea planted with 15% soil moisture is significantly longer than that of the other three groups. It can be seen from *Figure 3* that the root lengths of tea trees planted under 15% and 45% soil moisture have similar trends, while the root lengths of tea trees planted under 25% and 35% soil moisture are similar, but the growth rate of root length is significantly larger than that. 15% and 45% soil moisture in two groups of tea trees. Compared with the beginning of the experiment, the root length of tea planted under four soil moisture conditions increased by 31%, 83.5%, 100.68% and 37.75% at the end of the experiment. It can be speculated that it is more suitable for tea tree root growth under the 35% soil moisture. The relationship between the four root coefficient quantities and the growth time was curve-fitted, and the determination coefficients R^2 were 0.9711, 0.9938, 0.9907 and 0.9763.

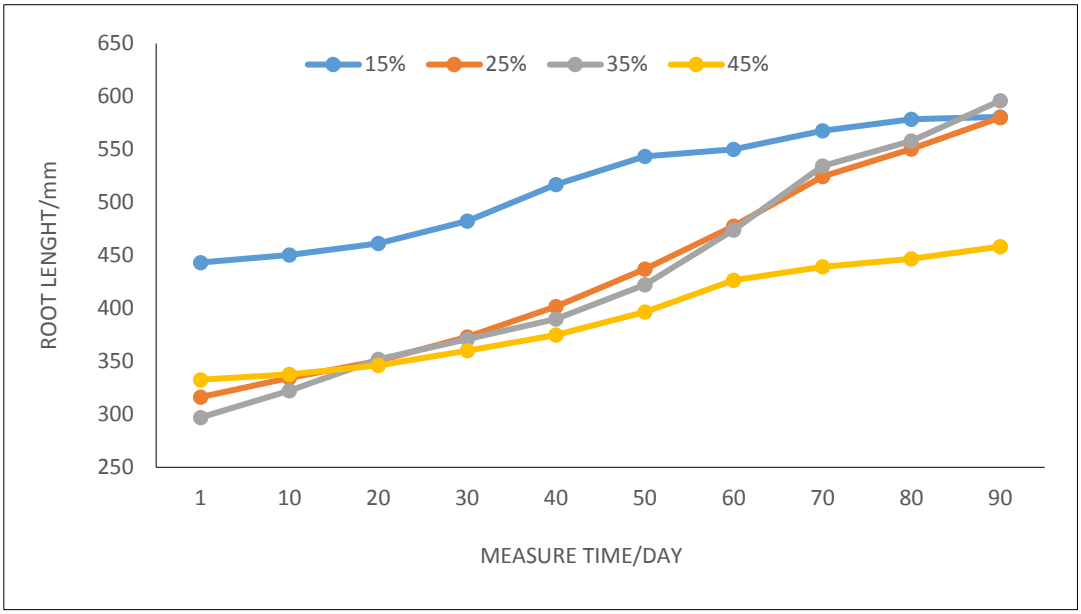

Figure 3. *Curve of the variation of tea root length under different soil moisture*

Effect of Soil Moisture on Root Area of Tea Trees

The changes of root area of tea planted under different soil moisture were obtained from experimental calculations and the corresponding curves were shown in *Figure 4*.

Experiments show that the root area of tea tree planted under four soil moisture conditions increased by 259.509 mm2, 879.491 mm2, 1285.207 mm2 and 369.107 mm2, with corresponding growth rates of 7.56%, 33.4%, 51.5% and 13.6%. *Figure 4* shows that the root area of tea trees planted under 15% and 45% soil moisture is relatively flat, which may be caused by more serious water stress. The root area of tea trees planted under 25% soil moisture increased rapidly, and the tea trees planted at 35% soil moisture increased fastest, indicating that root growth was the fastest. The determination coefficients R^2 were 0.9867, 0.9938, 0.9801 and 0.9946.

http://www.aloki.hu ● ISSN 1589 1623 (Print) ●ISSN1785 0037 (Online)
DOI: http://dx.doi.org/10.15666/aeer/1706_1530115309

Effects of Soil Moisture on Root Volume of Tea Trees

The change of tea root area under different soil moisture was obtained from experimental calculations and the corresponding curve was shown in *Figure 5*.

Experiments show that the initial value of root volume of tea tree planted under 15% soil moisture is larger. During the experimental period, the root area of tea planted under 4 kinds of soil moisture increased by 214.458 mm^3, 766.661 mm^3, 1169.063 mm^3 and 316.605 mm^3, with corresponding growth rates of 8.8%, 40.2%, 64.0% and 15.8%. *Figure 5* shows that the root volume of tea trees planted under 15% and 45% soil moisture increased more slowly, while the root volume of tea planted under 25% and 35% soil moisture increased more rapidly. The tea tree planted under 35% soil moisture increased the fastest, reaching 64%, indicating that the root growth was the fastest. The determination coefficients R^2 were 0.9957, 0.9957, 0.9919 and 0.9869, respectively.

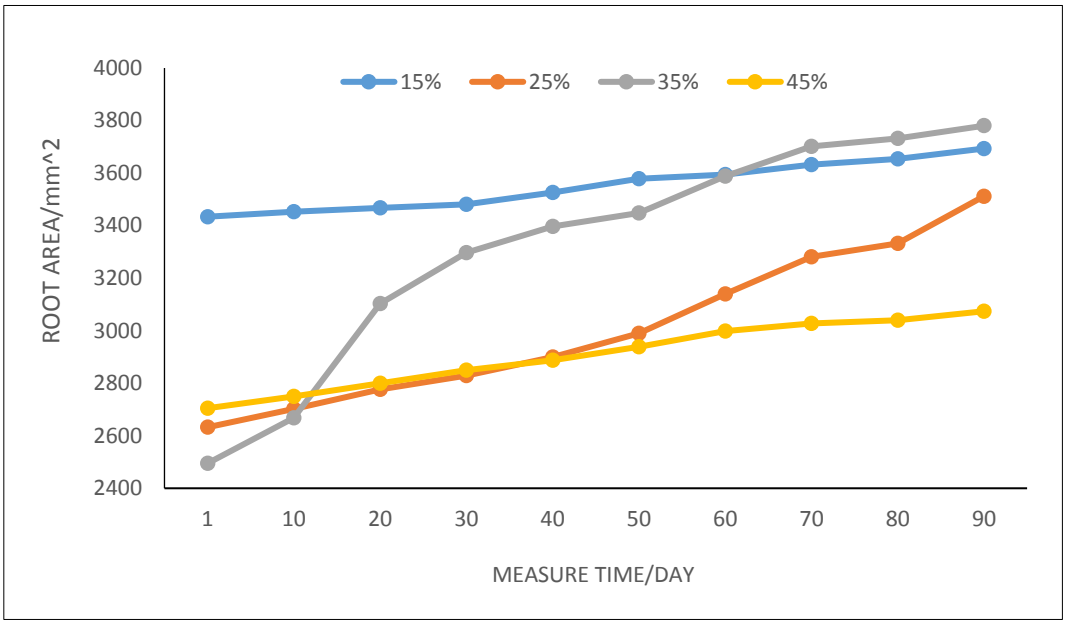

Figure 4. *Curve of the variation of tea root area under different soil moisture*

The comparison of various indicators of tea roots planted under four kinds of soil moisture is shown in *Figure 6*.

Figure 6 shows that the growth rate of various roots of tea trees planted under the condition of soil moisture of 35% is higher than that of other tea trees, and the growth rate of 25% is slightly worse. Soil moisture of 15% and 45% soil moisture is not conducive to the roots growth of tea trees.

Conclusions

First, the relationship between the root development of tea plants and soil moisture was studied. The changes of the number, length, area and volume of tea roots under different soil moisture were studied. Experiments were studied out with 4 groups of one-year-old Yinghong 9 tea trees. The soil moisture was collected by DECAGON

http://www.aloki.hu ● ISSN 1589 1623 (Print) ●ISSN1785 0037 (Online)
DOI: http://dx.doi.org/10.15666/aeer/1706_1530115309

Em50 Data Logger, and the related indicators of tea roots were monitored by CI600 root growth monitoring system.

Second, the results show that the growth rate of various roots of tea trees planted under the condition of soil moisture of 35% is higher than that of other tea trees, and the growth rate of 25% is slightly worse. Soil moisture of 15% and 45% soil moisture is not conducive to the roots growth of tea trees. The number, length, area and volume of tea roots are positively correlated with growth time at soil moisture of 35%. The tea tree under other moisture conditions does not exhibit this relationship. This conclusion can be seen in the experiment and analysis in the second chapter of the paper.

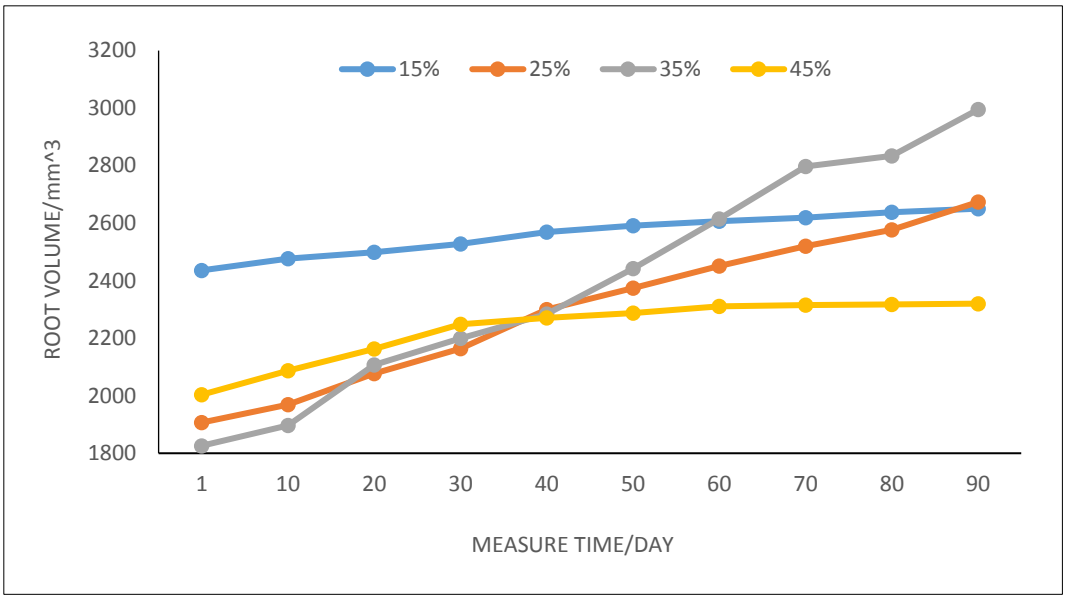

Figure 5. *Curve of the variation of tea root volume under different soil moisture*

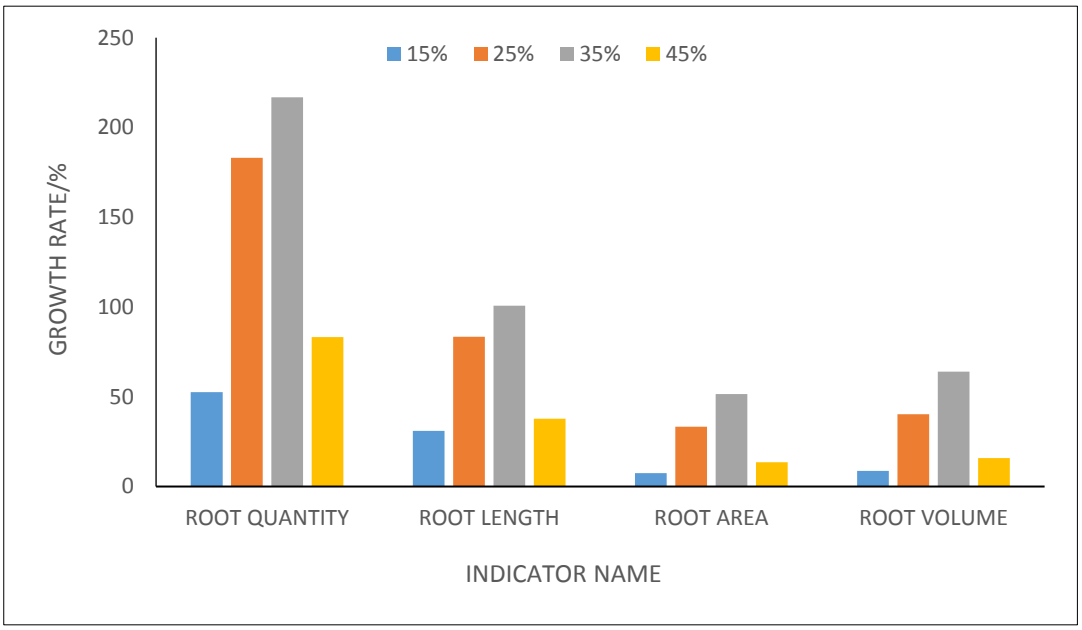

Figure 6. *Contrast of the growth rate of each index of tea root system*

http://www.aloki.hu ● ISSN 1589 1623 (Print) ●ISSN1785 0037 (Online)
DOI: http://dx.doi.org/10.15666/aeer/1706_1530115309

Discussion

The root surface and root volume are derived measures therefore analysing both of those is needed further discussion. The preliminary tests were not considered adequately, and subsequent tests will focus on the parameters that the instrument can directly measure.

The container capacity has been taken into account during the test. The roots of adult tea trees are more developed, and the 20 L container obviously does not meet the requirements. However, the root system of one-year old tea tree is relatively small. According to the experimental observation, the 20 L container does not affect the root development. In the later experiments, the tea tree has been transplanted to cuboid container with a length, width and height of 60 cm * 60 cm * 55 cm.

The test period is only 90 days, and it is carried out in the spring. The growth period is too short and the weather conditions are relatively simple. Subsequent repeated tests will prolong the test time and improve the credibility of the measured data.

The red loam soil was mixed, stirred evenly, and sand and gravel were removed before being packed. However, the nutrient and porosity characteristics of the soil were not analyzed. The experiment only considered the influence of soil moisture on root development. The factors such as nutrient, illumination, air temperature and humidity were not taken into consideration, and subsequent multi-factor tests were carried out. The analysis had significant effects on the root development.

Only four kinds of soil moisture were designed. It was roughly concluded that tea root system developed better when soil moisture was 35%. However, but no further subdivision and tracking test were carried out. The subsequent research will be carried out between soil moisture of 25%-35%.

Acknowledgements. The paper is funded by Liuzhou Science and Technology Plan Project (under No. 2017BE10303), Guangxi Science and Technology Key Research and Development Project (under No. Guike AB16380286), Guangdong Province Key Area R&D Program (under No. 2019B020214003), Guangdong Science and Technology Plan Project (under No. 2017A020208049), 2018 Provincial Agricultural Science and Technology Innovation and Extension Project (under No. 2018LM2163), South China Agricultural University Science and Technology Achievement Transformation and Incubation Project (under No. CGZHT2018004), Guangdong Universities and Universities Characteristic Innovation Project (2018KTS)CX020, 2018 Provincial College Students Innovation and Entrepreneurship Project (under No. 201810564197), Guangdong Science and Technology Project (under No. 2017A020208049), Modern Agricultural Industry Technology System Construction Project (under No. CARS-27), Guangxi High School Innovation Team and Excellence Scholar Program.

REFERENCES

[1] Guo, B., Dai, Y., Song, L. (2018): Research progress of plant hormones affecting crop root development under drought. – Biotechnology Bulletin 34(7): 48-56.
[2] Hu, H. (2013): Effect of water on germination, seedling growth and natural distribution of Bermudagrass. – Jiangxi: Jiangxi Normal University.
[3] Lai, J., Li, X., Xue, L. (2018): Advances in plant drought resistance. – Jiangsu Agricultural Science 46(17): 23-27.
[4] Liu, X., Liu, L. (2013): An overview of root research methods. – Agricultural Science and Technology Newsletter 3: 147-148.

http://www.aloki.hu ● ISSN 1589 1623 (Print) ●ISSN1785 0037 (Online)
DOI: http://dx.doi.org/10.15666/aeer/1706_1530115309

[5] Liu, Y. (2014): Study on the relationship between drought resistance of peanut varieties and root morphology, distribution and physiological characteristics. – Shandong: Shandong Agricultural University.
[6] Meng, H., Feng, J., Hu, D. (2017): Root system development and nutrient uptake. – Shanxi Agricultural Science 45(6): 1048-1052.
[7] Niu, X., Nanbiao (2017): Progress in the study of fine roots of grassland plants by microroot canal technique. – Journal of Grassland Science 26(11): 205-215.
[8] Qin, T., Sun, C., Bi, Z. (2019): Advances in plant root imaging technology and application prospects of potato root research. – Journal of Nuclear Agriculture 33(2): 0412-0419.
[9] Wang, C., Sun, X., Ma, J. (2007): Study on water uptake by plant roots. – Shanxi Water Conservancy 1: 85-88.
[10] Wang, Q., Rong, L. (2015): Research progress on the growth and distribution characteristics of plant roots under environmental impact. – Journal of Guiyang University 10(4): 61-66.
[11] Wei, G. (2011): Root distribution of jujube trees on sloping land and its relationship with soil moisture and nutrients. – Shaanxi: Northwest University of Agriculture and Forestry Science and Technology.
[12] Zhou, J. (2008): Study on the effect of red soil water condition on Citrus physiological and ecological factors and its mechanism. – Nanjing: Nanjing Agricultural University.
[13] Zhu, Y. (2012): Progress in plant root growth and research methods. – Northern Horticulture 20: 176-179.

http://www.aloki.hu ● ISSN 1589 1623 (Print) ●ISSN1785 0037 (Online)
DOI: http://dx.doi.org/10.15666/aeer/1706_1530115309

HEXAVALENT CHROMIUM ADSORPTION REMOVAL FROM AQUEOUS SOLUTION BY FE-MODIFIED BIOCHAR DERIVED FROM RICE STRAW

FAN, L. Q.[1,2*] – LIU, Q.[1,2] – WAN, Y.[1,2] – WANG, X. D.[1,2] – MIAO, J. X.[1,2] – CAI, J.[3] – CHEN, W.[1,2] – CHEN, F. H.[1,2] – CHENG, L.[1,2] – JI, L.[1,2] – LUO, H. B.[1,2]

[1]*College of Civil Engineering, Sichuan Agricultural University, Dujiangyan 611830, China*

[2]*Sichuan Higher Education Engineering Research Center for Disaster Prevention and Mitigation of Village Construction, Sichuan Agricultural University, Dujiangyan 611830, China*

[3]*Department of Physical and Chemical Analysis, Dujiangyan Center for Disease Control and Prevention, Dujiangyan 611830, China*

[*]*Corresponding author*
e-mail: flqjacky@163.com

(Received 8th Jul 2019; accepted 15th Nov 2019)

Abstract. In this study, Fe-modified biochar (Fe-R-BC) was made from rice straw by modified with $FeCl_3$ through pyrolysis, and used to adsorb Cr(VI) from aqueous solution. The properties of Fe-R-BC and rice straw biochar (R-BC) were characterized by Fe content, Brunauer-Emmett-Teller (BET) analysis, Boehm titration, and Fourier-transform infrared (FT-IR) spectroscopy. The Cr(VI) adsorption removal mechanism and regenerative property of Fe-R-BC were explored with batch adsorption experiment. Compared to those of R-BC, the Fe content, specific surface area (BET), total pore volume, and amount of hydroxyl group of Fe-R-BC increased, while the average pore size and amount of methenyl group decreased. For Fe-R-BC, the maximum Cr(VI) adsorption removal capacity was 94.95 $mg \cdot g^{-1}$ at 313 K. The Cr(VI) adsorption kinetics and isotherms can be well described by the pseudo second order model and the Langmuir-Freundlich model, respectively. The Cr(VI) adsorption removal was spontaneous and endothermic. Low pH was beneficial for the Cr(VI) adsorption removal. SO_4^{2-} showed the largest influence on the Cr(VI) adsorption removal, followed by NO_3^- and Cl^-. After 4 sorption-desorption cycles, the regenerated Fe-R-BC still maintained 76.27% of adsorption removal ability compared to that of Fe-R-BC in the initial use. Overall, Fe-R-BC can be applied to treat wastewater containing Cr(VI).
Keywords: *rice straw biochar, modification, property, hexavalent chromium, adsorption removal mechanism*

Introduction

Chromium and its alloys are widely used in daily life and industrial production. With the development of economy, the demanded quantity of chromium and its alloys grows with each passing day. As a result, a large amount of wastewater containing chromium (Cr) was produced in recent decades. Two valence states, i.e., Cr(III) (trivalent chromium) and Cr(VI) (hexavalent chromium), were the main occurrence forms of Cr in these wastewaters. Compared with Cr(III), Cr(VI) has higher carcinogenicity and mutagenicity (Liu et al., 2010). In view of this, many countries and organizations listed Cr(VI) as one of the strictly controlled heavy metals in industrial wastewater (Ma et al., 2014). That is to say, before discharging the industrial wastewater containing Cr(VI), its concentration should be strictly controlled.

There are various methods to remove heavy metals from wastewater such as electrochemical treatment (Golder et al., 2011; Mella et al., 2015), ionic exchange (Rafati et al., 2010), membrane filtration (Soylak et al., 2007), adsorption (Liu et al.,

http://www.aloki.hu ● ISSN 1589 1623 (Print) ●ISSN1785 0037 (Online)
DOI: http://dx.doi.org/10.15666/aeer/1706_1531115327

2010). Among these methods, adsorption was regarded as a valid and dependable method to remove heavy metals, which could avoid some disadvantages of other methods, such as the high cost of equipment, production of toxic sludge and other wastes (Baran et al., 2007; Liu et al., 2010). For adsorption method, the treatment effectiveness depends primarily on the adsorbent used (Gu et al., 2005). At present, activated carbon (Kaveeshwar et al., 2018), bioadsorbents (Gupta et al., 2015), zeolite (Wang and Peng, 2010), clay minerals (Uddin, 2017), biochar (Dong et al., 2011; Xu et al., 2013; Inyang et al., 2016), etc. are commonly used as adsorbents. Among these adsorbents, biochar was considered as an emerging and promising adsorbent in view of its low cost and sustainability (Chun et al., 2004; Ahmad et al., 2014; Park et al., 2016a). However, the original biochar has a low adsorption capacity for heavy metals (Zhou et al., 2013; Ma et al., 2014). In recent years, many physical and chemical modification methods have been used to improve the adsorption capacity of biochar (Rajapaksha et al., 2016). For example, Park et al. (2016b) reported that steam activation significantly enhanced the adsorption capacity of red macroalga *Porphyra tenera* biochar for Cu. Ding et al. (2016) found alkali modification promoted the adsorption capacity of hickory wood biochar for Pb, Cu, Cd, Zn, and Ni. Zhou et al. (2017) indicated that introduction of nano-MnO_2 on corn stalk biochar improved its adsorption capacity for Cu.

Rice straw is a kind of common agricultural waste. In China, about 201.0-301.5 million tons of rice straw was generated per year (Jiang et al., 2015). To realize the sustainable development of agriculture, the Chinese government has been sparing no effort to encourage and promote resource utilization technology of rice straw in recent years. Converting rice straw to biochar not only can achieve reutilization of rice straw, but also can benefit carbon-emission reduction. Thus, biochar technology was considered as an effective resource technology for rice straw. At present, rice straw biochar (R-BC) was successfully applied to remove different heavy metals from wastewater (Han et al., 2013; Pan et al., 2013; Xu et al., 2014; Park et al., 2017; Dong et al., 2018). Nevertheless, modification of R-BC could further enhance its utilization efficiency considering the advantage of modification technology for heavy metal adsorption. In the previous studies, Fe oxides were found to have the good selectivity and affinity to Cr(VI) (Tzou et al., 2003). In recent years, Agrafioti et al. (2014) also found that the sewage sludge biochar with high Fe content had higher adsorption rate of Cr(VI) compared with the other two biomass-based biochars. Thus, the Cr(VI) adsorption capacity of R-BC is expected to be promoted by introducing Fe/Fe oxides onto it.

In this study, R-BC and Fe-modified R-BC (Fe-R-BC) were prepared firstly. Then, the properties of R-BC and Fe-R-BC (i.e., the yield, Fe content, specific surface area (BET), total pore volume, average pore size, number of acidic and basic surface functional groups, and category of surface functional group) were compared. After that, a series of batch experiments including adsorption kinetic, adsorption isotherms, initial solution pH, and coexisting ions influence were performed. Moreover, the regenerative property of Fe-R-BC was evaluated by several cycles of adsorption-desorption experiment. The purposes of this study are to (1) characterize the properties of Fe-R-BC, (2) explore the Cr(VI) adsorption removal mechanism of Fe-R-BC, and (3) evaluate the regenerative performance of Fe-R-BC.

http://www.aloki.hu ● ISSN 1589 1623 (Print) ●ISSN1785 0037 (Online)
DOI: http://dx.doi.org/10.15666/aeer/1706_1531115327

Materials and methods

Preparation of R-BC and Fe-R-BC

Rice straw was gathered from Shuangliu County, Sichuan province, China. The gathered rice straw was washed several times with tap water and dried in the air. Then the rice straw was smashed and sieved through a screen (10-mesh). The sieved rice straw was divided into two parts. One part was soaked in the $FeCl_3$ solution (1 M, m/v (g/mL)=1/10) for 48 h at room temperature. After that, the Fe-soaked rice straw was separated by filtration and dried at 333 K to constant weight. The Fe-soaked rice straw and the other part of pristine rice straw were respectively putted into the different crucibles with covers and pyrolyzed for 2 h in a muffle furnace (SX2-4-10, Shenyang Energy Saving Electric Furnace Factory, Shenyang, China) at 673 K. After pyrolyzed, the carbonized pristine rice straw was smashed again and sieved through a screen (60-mesh). The sieved carbon material was R-BC. For the carbonized Fe-soaked rice straw, it was rinsed several times with 3 M HCl to remove excessive iron. And then, the carbonized Fe-soaked rice straw was washed several times with deionized water (18.25 MΩ). After that, the carbonized Fe-soaked rice straw was dried at 333 K to constant weight. At last, the carbonized Fe-soaked rice straw was ground and sieved through a screen (60-mesh). The sieved powder was Fe-R-BC.

Property detection

The yield was determined by the following *Equation 1*:

$$\text{Yield}(\%)=\left(\frac{m_a}{m_b}\right)\times 100\% \quad \text{(Eq.1)}$$

where m_a refers to the acquired R-BC or Fe-R-BC mass (g), m_b denotes the rice straw mass (g).

The specific surface area (BET), total pore volume, and average pore size were measured using a specific surface area analyzer (NOVA-1200, Quantachrome Corp., Boynton Beach, Florida, USA) with N_2 adsorption method (Dong et al., 2011). The quantities of acidic and basic surface functional groups were quantified using Boehm titration (Giannakoudakis et al., 2016). The category of surface functional group was determined by FT-IR spectrometer (Spectrum II, Perkin-Elmer Crop., Norwalk, OH, USA). For the Fe content in R-BC or Fe-R-BC, 0.10 g R-BC or Fe-R-BC was digested with HNO_3 using microwave digestion method, and the Fe concentration in the digestion solutions was detected using a flame atomic absorption spectrometer (PinAAcle 900T, PerkinElmer Management (Shanghai) Co., Ltd., Shanghai, China) to calculate its content. Furthermore, the zeta potential of Fe-R-BC was determined using a zeta potentiometer (JS94H2M, Shanghai Zhongcheng Digital Technology Equipment Co., Ltd., Shanghai, China) to explain the influence of initial solution pH on Cr(VI) adsorption removal.

Batch adsorption experiments

Adsorption kinetics: 0.10 g R-BC or Fe-R-BC was added into 50 mL Cr(VI) solution (100 $mg \cdot L^{-1}$, prepared with $K_2Cr_2O_7$). Then, the initial pH value of the mixed solution was adjusted to 2.0. After that, the mixed solution was placed in a constant temperature oscillation box (TS-2012C, Shanghai Xiren Scientific Instruments Co., Ltd., Shanghai,

http://www.aloki.hu ● ISSN 1589 1623 (Print) ●ISSN1785 0037 (Online)
DOI: http://dx.doi.org/10.15666/aeer/1706_1531115327

China) to experience a predefined time period (0.5, 1, 2, 4, 6, 8, 10, 12, 16, 20, and 24 h, respectively) at 120 rpm and 298 K.

Adsorption isotherms: 0.10 g Fe-R-BC was added into 50 mL Cr(VI) solution with a certain concentration (75, 100, 200, 300, 400, 500, 600, and 800 $mg \cdot L^{-1}$, respectively). Then, the initial pH value of the mixed solution was adjusted to 2.0. After that, the mixed solution was placed in the constant temperature oscillation box for 24 h at 120 rpm and a fixed temperature (283 K, 298 K, and 313 K, respectively).

Initial solution pH: 0.10 g Fe-R-BC was added into 50 mL Cr(VI) solution (100 $mg \cdot L^{-1}$). Then, the initial pH value of the mixture solution was adjusted to a predesigned value (2.0, 3.0, 4.0, 5.0, 6.0, 7.0, and 8.0, respectively). After that, the mixed solution was placed in the constant temperature oscillation box for 24 h at 120 rpm and 298 K.

Coexisting ions influence: 0.10 g Fe-R-BC was added into 50 mL Cr(VI) solution (100 $mg \cdot L^{-1}$). Then, the coexisting ion concentration (Cl^- or NO_3^- or SO_4^{2-}) in the mixture was adjusted to a predetermined value (0.005, 0.01, 0.02, 0.05, 0.10, 0.20, 0.50, 1.0, and 2.0 M, respectively). After that, the initial pH value of the mixed solution was adjusted to 2.0. At last, the mixed solution was placed in the constant temperature oscillation box for 24 h at 120 rpm and 298 K.

Adsorption-desorption experiment: Four cycles of adsorption-desorption were conducted in this experiment to evaluate the regenerative property of Fe-R-BC. A cycle of adsorption-desorption was described as follows: 0.10 g Fe-R-BC was added into 50 mL Cr(VI) solution (100 $mg \cdot L^{-1}$). Then, the initial pH value of the mixed solution was adjusted to 2.0. After that, the mixed solution was placed in the constant temperature oscillation box for 24 h at 120 rpm and 298 K. Afterwards the mixture was separated by filtering. The separated adsorbent was added into 50 mL NaOH solution (0.1 M), and shaken at 298 K for 24 h. After that was done, the adsorbent was separated and washed several times with deionized water. The washed adsorbent was used to the next cycle of adsorption-desorption.

After each treatment was completed, the residual Cr(VI) concentration in the solution was analyzed using a UV-vis spectrophotometer (UV-1800, Shanghai Mapada Instruments Co., Ltd., Shanghai, China) with 1,5-diphenylcarbohydrazide spectrophotometric method. The Cr(VI) adsorption removal rate (AR, %) and the Cr(VI) adsorption removal amount at equilibrium (q_e, $mg \cdot g^{-1}$) were calculated by the following *Equations 2-3*, respectively.

$$AR=\left(\frac{C_0-C_i}{C_0}\right)\times 100\% \quad \text{(Eq.2)}$$

$$q_e=\frac{(C_0-C_i)\times 0.05}{0.10} \quad \text{(Eq.3)}$$

where C_0 and C_i denotes the initial and residual Cr(VI) concentration in each treatment, respectively.

Modeling

In this study, the pseudo first order model, the pseudo second order model, and the intraparticle diffusion model were used to fit the adsorption kinetics data. The following

http://www.aloki.hu ● ISSN 1589 1623 (Print) ●ISSN1785 0037 (Online)
DOI: http://dx.doi.org/10.15666/aeer/1706_1531115327

Equations 4-6 gives the function expression of the above three models, respectively (Wu et al., 2017).

The pseudo first order model:

$$q_t=q_e\left(1-\exp^{-k_1,t}\right) \quad \text{(Eq.4)}$$

The pseudo second order model:

$$q_t=\frac{tq_e^2k_2}{1+tq_ek_2} \quad \text{(Eq.5)}$$

The intraparticle diffusion model:

$$q_t=k_3t^{0.5}+C \quad \text{(Eq.6)}$$

where q_t represents the Cr(VI) adsorption removal amount at time t ($mg\cdot g^{-1}$). k_1 (h^{-1}), k_2 ($g\cdot mg^{-1}\cdot h^{-1}$), and k_3 ($mg\cdot g^{-1}\cdot h^{-1/2}$) are the reaction rate constants. C is a constant ($mg\cdot g^{-1}$).

The Freundlich isotherm model, the Langmuir isotherm model, and the Langmuir-Freundlich isotherm model were used to simulate adsorption isotherms. The following *Equations 7-9* gives the function expression of the above three models, respectively (Jung et al., 2015).

The Freundlich isotherm model:

$$q_e=K_F\times C_e^{1/n} \quad \text{(Eq.7)}$$

The Langmuir isotherm model:

$$q_e=\frac{q_mK_LC_e}{1+K_LC_e} \quad \text{(Eq.8)}$$

The Langmuir-Freundlich isotherm model:

$$q_e=\frac{q_mKC_e^{1/n}}{1+KC_e^{1/n}} \quad \text{(Eq.9)}$$

where q_m represents the Cr(VI) maximum adsorption removal capacity ($mg\cdot g^{-1}$), C_e is the equilibrium concentration ($mg\cdot L^{-1}$), K_F ($(mg\cdot g^{-1})\cdot(L\cdot mg^{-1})^{1/n}$), K_L ($L\cdot mg^{-1}$) and K ($L\cdot mg^{-1}$) are the constants, and 1/n is the heterogeneity factor.

The thermodynamics of the adsorption processes were estimated by three important thermodynamic parameters (i.e., ΔG^0 (Gibbs free energy, $kJ\cdot mol^{-1}$), ΔH^0 (enthalpy, $kJ\cdot mol^{-1}$), and ΔS^0 (entropy, $kJ\cdot mol^{-1}\cdot K^{-1}$)). And they were calculated based on the results of adsorption isotherms by using the following *Equations 10,11*.

$$\ln K_c=-\frac{\Delta H^0}{RT}+\frac{\Delta S^0}{R} \quad \text{(Eq.10)}$$

http://www.aloki.hu ● ISSN 1589 1623 (Print) ●ISSN1785 0037 (Online)
DOI: http://dx.doi.org/10.15666/aeer/1706_1531115327

$$\Delta G^0 = -RT\ln K_c \quad \text{(Eq.11)}$$

where K_c denotes the adsorption equilibrium constant ($L \cdot g^{-1}$), which can be acquired by plotting $\ln(q_e/C_e)$ vs. C_e (Gan et al., 2015). T is the absolute temperature (K). R represents the universal gas constant.

Data processing

All treatments were conducted in triplicate, and the average value of three replicates was taken as the experimental result. Excel 2007 and Origin 2018 were used for data management, processing, and drawing. Moreover, one-way ANOVA analysis was used to analyze the significant differences of the experimental data with IBM SPSS Statistics 22.

Results and discussion

Properties of R-BC and Fe-R-BC

Table 1 shows the yield, Fe content, specific surface area (BET), total pore volume, average pore size, and numbers of acidic and basic surface functional groups of R-BC and Fe-R-BC. The yield of R-BC and Fe-R-BC was 40.30% and 36.20%, respectively ($p<0.05$). As a result of modification with $FeCl_3$, Fe-R-BC had a higher Fe content than R-BC ($p<0.05$). Compared to those of R-BC, the specific surface area (BET) and total pore volume of Fe-R-BC increased by 24.16 $m^2 \cdot g^{-1}$ and 0.91 $cm^3 \cdot g^{-1}$, respectively, while the average pore size decreased by 2.63 nm. The number of basic groups of Fe-R-BC was 0.23 $mmol \cdot g^{-1}$, which significantly lower than that of R-BC (0.62 $mmol \cdot g^{-1}$) ($p<0.05$). On the contrary, the number of acid groups of Fe-R-BC (0.56 $mmol \cdot g^{-1}$) increased compared to that of R-BC (0.53 $mmol \cdot g^{-1}$) ($p<0.05$).

Table 1. *Yield, Fe content, specific surface area (BET), total pore volume, average pore size, and numbers of acidic and basic surface functional groups of R-BC and Fe-R-BC*

Designation	Yield (%)	Fe ($mg \cdot g^{-1}$)	SSA ($m^2 \cdot g^{-1}$)	TPV ($cm^3 \cdot g^{-1}$)	APS (nm)	BG ($mmol \cdot g^{-1}$)	AG ($mmol \cdot g^{-1}$)
Fe-R- BC	36.20±2.96	17.61±0.69	27.92	1.10	8.54	0.23±0.03	0.56±0.13
R-BC	40.30±1.55	1.31±0.08	3.76	0.19	11.17	0.62±0.10	0.53±0.13

SSA represents specific surface area (BET), TPV denotes total pore volume, APS refers to average pore size, BG is basic groups, and AG is acidic groups

Figure 1 shows the FT-IR spectra of R-BC and Fe-R-BC. The peaks around 3409 cm^{-1} and 3430 cm^{-1} were caused by the -OH (Dong et al., 2011; Samsuri et al., 2013; Xu et al., 2013; Zhang et al., 2015). The peaks at 2922 cm^{-1} to 2928 cm^{-1} can be attributed to the stretching vibration of –CH (Dong et al., 2011; Samsuri et al., 2013; Zhang et al., 2015). The peaks at 1612 cm^{-1} to 1616 cm^{-1} were caused by the C=O (Garg et al., 2007; Yang et al., 2009; Tang et al., 2014; Zhang et al., 2015). The peaks at 1103 cm^{-1} to 1107 cm^{-1} were related to C-O (Dong et al., 2011; Samsuri et al., 2013; Zhang et al., 2015). The absorption peaks at 800 cm^{-1} to 809 cm^{-1} can be assigned to the aromatic compounds =C-H (Pan et al., 2013; Samsuri et al., 2013). Compared the spectra of Fe-R-BC with that of R-BC, it can be found that the peaks of the two materials were roughly the same. The results

http://www.aloki.hu ● ISSN 1589 1623 (Print) ●ISSN1785 0037 (Online)
DOI: http://dx.doi.org/10.15666/aeer/1706_1531115327

indicated that the category of surface functional group of Fe-R-BC did not change. For Fe-R-BC, although the category of surface functional groups did not change, the intensity of the peak around 3409 cm^{-1} to 3430 cm^{-1} obviously increased, and the intensity of peak around 2922 cm^{-1} to 2928 cm^{-1} decreased (*Figure 1*). The results indicated that the hydroxyl group and methenyl group respectively increased and decreased for Fe-R-BC. The results were consistent with the changes of the number of basic and acid groups (*Table 1*).

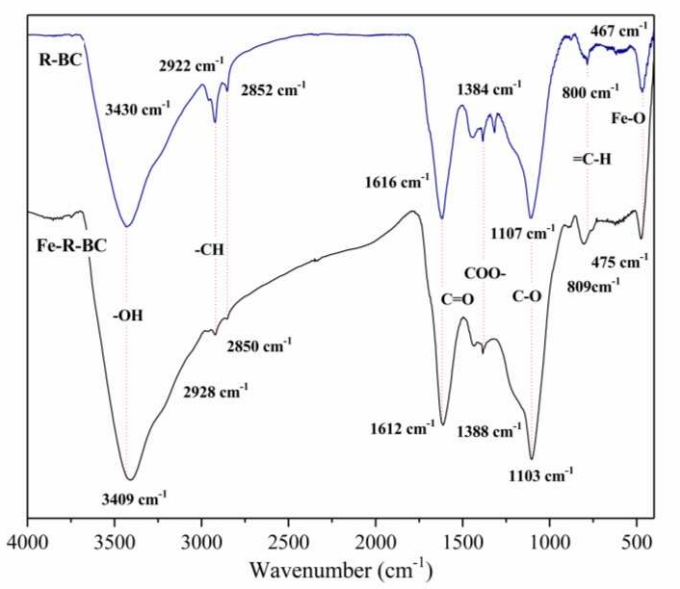

Figure 1. *FT-IR spectra of R-BC and Fe-R-BC*

In summary, some physicochemical properties of R-BC (i.e., specific surface area (BET), total pore volume, average pore size, and numbers of surface functional groups) were changed after modification with $FeCl_3$. The attachment of Fe-oxides particles on the surface of R-BC and the increase of the pore structure of R-BC by the Fe-oxide particles entered the original pores of R-BC led to the changes of basic physical properties (i.e., specific surface area and total pore volume increased, and average pore size decreased) (Wang et al., 2017). The decrease of basic groups and the increase of acidic groups indicate the acidity was increased for Fe-R-BC, which may be due to the protonation-deprotonation reaction on the surface of Fe (hydro) oxide (Sun et al., 2019). In general, the above changes of physicochemical properties of R-BC are beneficial for the Cr(VI) adsorption.

Comparation of the Cr(VI) adsorption removal capacity between R-BC and Fe-R-BC

Figure 2 shows the Cr(VI) adsorption removal rates of R-BC and Fe-R-BC with increasing contact time. For R-BC, the Cr(VI) adsorption removal rate gradually increased and tended to equilibrium after 20 h ($p<0.05$). For Fe-R-BC, the Cr(VI) adsorption removal rate rapidly increased to 93.59% at 6 h ($p<0.05$), and then slowly increased ($p<0.05$) to a stable value ($p>0.05$). The maximum Cr(VI) adsorption removal rate of Fe-R-BC (97.13%, at 24 h) was 1.73 times than that of R-BC (56.01% at 24 h). In general, the results indicated that the Cr(VI) adsorption removal capacity of Fe-R-BC was

http://www.aloki.hu ● ISSN 1589 1623 (Print) ●ISSN1785 0037 (Online)
DOI: http://dx.doi.org/10.15666/aeer/1706_1531115327

higher than that of R-BC. The results can be attributed to the following reasons: (1) Fe-R-BC had higher specific surface area (BET) and total pore volume. (2) The surface of Fe-R-BC had the more adsorption sites for Cr(VI), owing to the more acidic groups on the surface of Fe-R-BC (Liu et al., 2010). (3) The Fe oxides formed on the surface of Fe-R-BC had the good selectivity and affinity to Cr(VI) (Tzou et al., 2003).

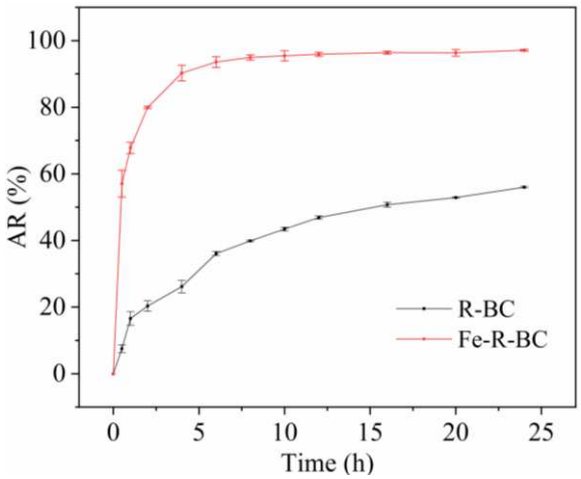

Figure 2. *Cr(VI) adsorption removal rates of R-BC and Fe-R-BC with increasing contact time*

Adsorption kinetics

Figure 3 displays the Cr(VI) adsorption kinetics data of Fe-R-BC. There were three different adsorption removal stages in *Figure 3*, i.e., the rapid increasing stage (0-6 h) ($p<0.05$), the slow increasing stage (6-16 h) ($p<0.05$), and the equilibrium stage (16-24 h) ($p>0.05$). The rapid increasing stage was due to the abundant adsorption sites on the surface of Fe-R-BC in the beginning of experiment, and the slow increasing stage was owing to the decrease of the available surface adsorption sites with the prolongation of experimental time, while the equilibrium stage was related to the adsorption saturation of the surface adsorption sites (Deveci and Kar, 2013; Kaveeshwar et al., 2018).

The fitting results of the adsorption kinetic data by the pseudo first order model, the pseudo second order model, and the intraparticle diffusion model are also displayed in *Figure 3*. The corresponding fitting parameters are listed in *Table 2*. *Figure 3* shows that the pseudo first order model and intraparticle diffusion model could not fit the Cr(VI) adsorption kinetics data of Fe-R-BC very well. The results were also verified by the R^2 values (square of correlation coefficient) in *Table 2*. Compared with the above two models, the pseudo second order model acquired a higher R^2 value (0.997). Moreover, the q_e value (adsorption removal amount at equilibrium) acquired by fitting with the pseudo second order model was 49.46 $mg \cdot g^{-1}$ (*Table 2*), which was consistent with the experimental result (48.57 $mg \cdot g^{-1}$) (*Figure 3)*. The results indicated that the Cr(VI) adsorption kinetics process of Fe-R-BC can be well described by the pseudo second order model. For the pseudo second order model, adsorption process is controlled by chemical adsorption (Mohan et al., 2011). Thus, the rate-limiting step of Cr(VI) adsorption removal by Fe-R-BC was the chemical adsorption process. For the Cr(VI) adsorption removal, the most dominant mechanism is the reduction of Cr(VI) to Cr(III) on the surface of adsorbent (Saha et al., 2010). *Figure 3* also gives the Cr(III) concentration in the experiment. It can be found that the Cr(III) concentration gradually increased ($p<0.05$) and finally

http://www.aloki.hu ● ISSN 1589 1623 (Print) ●ISSN1785 0037 (Online)
DOI: http://dx.doi.org/10.15666/aeer/1706_1531115327

maintained equilibrium after 6 h ($p>0.05$), and the change trend of Cr(III) concentration was consistent with that of Cr(VI) adsorption removal amount (q_t). The results verified that the reduction of Cr(VI) to Cr(III) did happened during the Cr(VI) adsorption removal process. According to the results, it can be deduced that the reduction of Cr(VI) to Cr(III) is maybe a main chemical reaction which controlled the Cr(VI) adsorption removal process of Fe-R-BC.

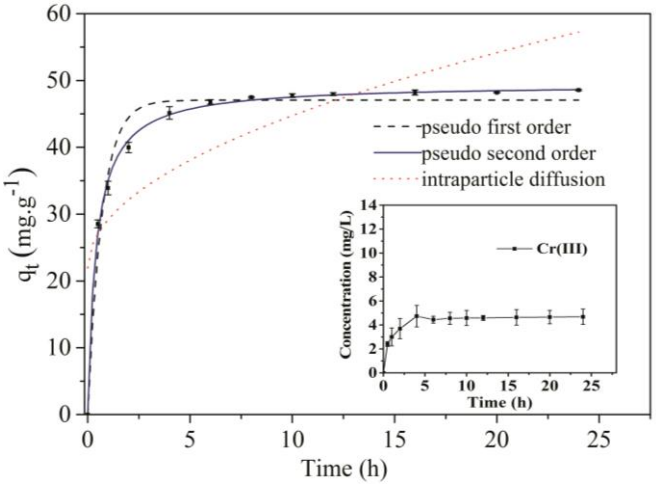

Figure 3. *Kinetics data, fitted models and Cr(III) concentration of Cr(VI) adsorption removal by Fe-R-BC*

Table 2. *Fitting parameters for the pseudo first order model, the pseudo second order model and intraparticle diffusion model*

Pseudo first order			**Pseudo second order**			**Intraparticle diffusion model**		
q_e (mg·g^{-1})	k_1 (h^{-1})	R^2	q_e (mg·g^{-1})	k_2 (g·mg^{-1}·h^{-1})	R^2	C (mg·g^{-1})	k_3 (mg·g^{-1}·h$^{-1/2}$)	R^2
47.05	1.29	0.948	49.46	0.049	0.997	21.95	7.20	0.579

Adsorption isotherms

The Cr(VI) adsorption isotherms of Fe-R-BC at three different temperatures (283 K, 298 K, and 313 K) are displayed in *Figure 4*. Generally speaking, for the all three adsorption isotherms, the Cr(VI) equilibrium adsorption removal amount (q_e) rapidly increased at first ($p<0.05$), and then gradually approached to the maximum equilibrium adsorption removal amount ($p>0.05$) with the increase of equilibrium concentration (C_e).

The fitted results of adsorption isotherms by the Freundlich isotherm model, the Langmuir isotherm model, and the Langmuir-Freundlich isotherm model are presented in *Figure 4*. *Table 3* lists the corresponding model parameters. At all temperatures, the adsorption isotherms fitted with the Langmuir-Freundlich isotherm model were closer to the experimental data (*Figure 4*). Furthermore, compared to those of other two isotherm models, the R^2 values (square of correlation coefficient) of Langmuir-Freundlich isotherm model (R^2=0.998, 0.999, and 0.990 at 283 K, 298 K, and 313 K, respectively) (*Table 3*) were the largest. The results illuminated that the Cr(VI) adsorption isotherms of Fe-R-BC can be better explained by the Langmuir-Freundlich isotherm model. The

http://www.aloki.hu ● ISSN 1589 1623 (Print) ●ISSN1785 0037 (Online)
DOI: http://dx.doi.org/10.15666/aeer/1706_1531115327

conclusion means that the Cr(VI) adsorption removal by Fe-R-BC belongs to the multi-molecular layer adsorption, which is regulated by multiple processes due to the heterogeneity of Fe-R-BC (Liu et al., 2010; Jung et al., 2015).

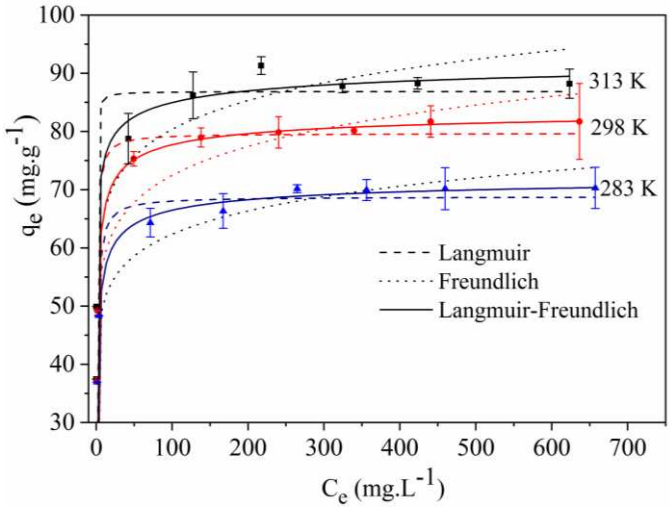

Figure 4. *Isotherms and fitted models of Cr(VI) adsorption removal by Fe-R-BC at three different temperatures*

Table 3. *Fitting parameters for the Freundlich isotherm model, the Langmuir isotherm model and the Langmuir-Freundlich isotherm model*

T (K)	Langmuir model			Freundlich model			Langmuir-Freundlich model			
	q_m (mg·g^{-1})	K_L (L·mg^{-1})	R^2	K_F (mg·g^{-1})·(L·mg^{-1})$^{1/n}$	1/n	R^2	q_m (mg·g^{-1})	K (L·mg^{-1})	1/n	R^2
283	68.81	0.86	0.991	41.25	0.090	0.983	73.04	0.99	0.505	0.998
298	79.68	1.41	0.986	46.60	0.095	0.975	84.68	1.12	0.498	0.999
313	86.88	6.51	0.988	53.89	0.089	0.976	94.95	1.64	0.358	0.990

According to the previous report (Tseng and Wu, 2008), the favorable degree of an adsorption reaction can be divided to five levels based on the value of heterogeneity factor (1/n), namely, 1/n < 0.01: the pseudo-irreversible level, 0.01 < 1/n <0.1: the strong favorable level, 0.1 < 1/n <0.5: the favorable level, 0.5 < 1/n <1: the pseudo-linear level, and 1/n >1: the unfavorable level. According to the values of 1/n (*Table 3*), the favorable degree of Cr(VI) adsorption removal by Fe-R-BC at 283 K belonged to the pseudo-linear level, whereas the favorable degree of Cr(VI) adsorption removal by Fe-R-BC at 298 K and 313 K can be classified as the favorable level. For the constant K (*Table 3*), the value was positively correlated with temperature, which indicated that the adsorption removal capacity of Fe-R-BC for Cr(VI) is enhanced with increasing temperature (Jung et al., 2015). For q_m (*Table 3*), the value calculated from the Langmuir-Freundlich model was respectively 73.04 mg·g^{-1}, 84.68 mg·g^{-1}, and 94.95 mg·g^{-1} at 283 K, 298 K, and 313 K, which was unanimous with our experiment results (71.29 mg·g^{-1}, 81.73 mg·g^{-1}, 88.19 mg·g^{-1} at 283 K, 298 K, and 313 K, respectively).

http://www.aloki.hu ● ISSN 1589 1623 (Print) ●ISSN1785 0037 (Online)
DOI: http://dx.doi.org/10.15666/aeer/1706_1531115327

Compared with some previous reported carbon materials for the Cr(VI) adsorption removal (*Table 4*), Fe-R-BC had a relatively high Cr(VI) adsorption removal capacity. Furthermore, as the raw materials (i.e., rice straw and $FeCl_3$) have the properties of low cost and extensive sources, Fe-R-BC is economical. Moreover, the pyrolysis temperature was 673 K, which was much lower than that of activated carbon (Giri et al., 2012; Nethaji et al., 2013). Therefore the preparation of Fe-R-BC had low energy consumption advantage. In addition, for the modification, only one-time immersion is used. Thereform, the preparation process was relatively simple. In view of the above advantages, Fe-R-BC has the great potential of application for Cr(VI) adsorption removal.

Table 4. *Comparison of the maximum Cr(VI) adsorption removal capacity with those of some previous reported carbon materials*

Adsorbents	q_m ($mg \cdot g^{-1}$)	Temperature (K)
Fe-modified activated carbon prepared from *Trapanatans* husk (Liu et al., 2010)	18.66	313
Polyethylenimine modified biochar (Ma et al., 2014)	435.7	/
Chitosan modification of magnetic biochar produced from Eichhorniacrassipes (Zhang et al., 2015)	167.31	313
Biochar from the blends of oily seeds of *P. terebinthus L.* with alumina (Deveci and Kar, 2013)	6.08	/
Activated carbon derived from *Eichhorniacrassipes* root biomass (Giri et al., 2012)	36.34	298
Mycelial pellets impregnated with powdered biochar (Xu et al., 2015)	28.00	301
corn cob activated carbon coated with nano-sized magnetite particles (Nethaji et al., 2013)	57.37	300
Fe-R-BC	94.95	313

Thermodynamic analysis

To better understand the Cr(VI) adsorption removal process of Fe-R-BC, the thermodynamic analysis was performed. *Table 5* lists the calculated values of ΔG^0, ΔH^0, and ΔS^0 for the Cr(VI) adsorption removal by Fe-R-BC. The value of ΔG^0 was -2.05 $kJ \cdot mol^{-1}$, -2.76 $kJ \cdot mol^{-1}$, -3.54 $kJ \cdot mol^{-1}$ at 283 K, 298 K, 313 K, respectively. On the one hand, the values of ΔG^0 were always negative at different temperatures, which manifested that the Cr(VI) adsorption removal process of Fe-R-BC was spontaneous (Tan et al., 2015). On the other hand, the value of ΔG^0 presented a negative correlation with temperature (i.e., the ΔG^0 value decreased as the temperature increased), which indicated that high temperature is favorable for Cr(VI) adsorption removal by Fe-R-BC. The ΔH^0 and ΔS^0 value was 0.0058 $kJ \cdot mol^{-1}$ and 0.034 $kJ \cdot mol^{-1} \cdot K^{-1}$, respectively. The positive value of ΔH^0 and ΔS^0 implied that the Cr(VI) adsorption removal by Fe-R-BC is an endothermic process and the randomness at Fe-R-BC-solution interface has the increasing trend during the adsorption process (Siddiqui et al., 2016).

Effect of initial solution pH on the Cr(VI) adsorption removal

The effect of initial solution pH on the Cr(VI) adsorption removal by Fe-R-BC is shown in *Figure 5*. It can be found that the initial solution pH obviously influenced the Cr(VI) adsorption removal by Fe-R-BC ($p<0.05$). The maximum and minimum Cr(VI) adsorption removal rate was 97.13% and 7.81%, respectively. With decreasing pH, the

http://www.aloki.hu ● ISSN 1589 1623 (Print) ●ISSN1785 0037 (Online)
DOI: http://dx.doi.org/10.15666/aeer/1706_1531115327

Cr(VI) adsorption removal rate presented an increasing tendency in *Figure 5*. The result was in accordance with the previous studies (Liu et al., 2010; Ma et al., 2014; Wu et al., 2017). For Cr(VI), it can present as the forms of $HCrO_4^-$, CrO_4^{2-} and $Cr_2O_7^{2-}$ in aqueous solutions. At low pH (2<pH< 3), $HCrO_4^-$ is the primary form of Cr(VI). However, the primary form gradually shifts to CrO_4^{2-} and $Cr_2O_7^{2-}$ as pH increases. Compared with CrO_4^{2-} and $Cr_2O_7^{2-}$, the adsorption of $HCrO_4^-$ is easier and more rapid due to its requirement of only one adsorption site (Kuppusamy et al., 2016). Thus, the Cr(VI) adsorption removal efficiency of Fe-R-BC increased as pH decreased. Furthermore, the surface charge of adsorbent significantly influences the Cr(VI) adsorption removal efficiency (Zhao et al., 2017). For Fe-R-BC, *Figure 5* also displays the change of zeta potential with the variation of pH. The point of zero charge (pH_{zpc}) of Fe-R-BC was obtained from the change of zeta potential. For Fe-R-BC, the pH_{zpc} was 2.79. That is to say, the surface charge of Fe-R-BC was positive when the solution pH < 2.79, whereas the surface charge of Fe-R-BC was negative when the solution pH > 2.79. The positive surface charge of Fe-R-BC in the solution pH < 2.79 could promote the positive-negative charge attraction, thus it is beneficial for the Cr(VI) adsorption (Zhao et al., 2017). This may be the other reason for the high Cr(VI) adsorption efficiency of Fe-R-BC under the low pH conditions, especially at pH=2.

Table 5. *Values of Gibbs free energy, enthalpy, and entropy*

ΔG^0 (kJ·mol^{-1})			ΔH^0 (kJ·mol^{-1})	ΔS^0 (kJ·mol^{-1}·K^{-1})
283 K	298 K	313 K	0.0058	0.034
-2.05	-2.76	-3.54		

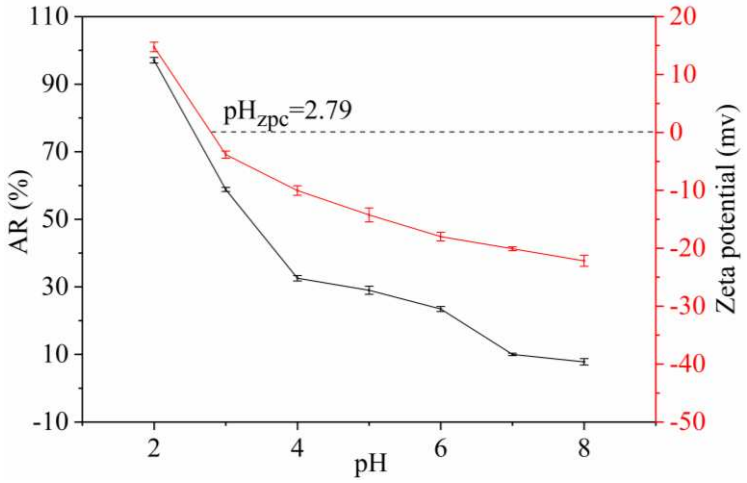

Figure 5. *Effect of initial solution pH on the Cr(VI) adsorption removal by Fe-R-BC and Zeta potentials of Fe-R-BC at different pH*

Effect of coexisting ions on Cr(VI) adsorption removal

Figure 6 shows the effects of three coexisting ions (i.e., Cl^-, NO_3^-, and SO_4^{2-}) on the Cr(VI) adsorption removal by Fe-R-BC. The Cr(VI) adsorption removal rate of Fe-R-BC decreased with increasing the concentrations of three coexisting ions ($p<0.05$). Cl^-, NO_3^- and SO_4^{2-} respectively resulted in 20.65%, 28.82%, and 35.89% reduction of the Cr(VI)

http://www.aloki.hu ● ISSN 1589 1623 (Print) ●ISSN1785 0037 (Online)
DOI: http://dx.doi.org/10.15666/aeer/1706_1531115327

adsorption removal rate with the increase of their concentrations from 0 M to 2.0 M. The results showed that the three coexisting ions can affect the Cr(VI) adsorption removal by Fe-R-BC, but the influence degrees of the three coexisting ions were different. Under the same condition of ion concentration, SO_4^{2-} had the strongest effect on the Cr(VI) adsorption removal by Fe-R-BC, followed by NO_3^- and Cl^-. For the three coexisting ions, the reduction of Cr(VI) adsorption removal rate with the increase of ion concentration could be attribute to the decreasing activity of Cr(VI) in solution with increasing the ion concentration (Zhang et al., 2013). However, the different influence degrees on the Cr(VI) adsorption removal might be related to the different adsorption competitiveness of the three coexisting ions with Cr(VI). For SO_4^{2-}, it was a polyvalent anion with semblable structure and size to $HCrO_4^-$, CrO_7^{2-}, and CrO_4^{2-}, thus it had the strong adsorption competitiveness with $HCrO_4^-$, CrO_7^{2-}, and CrO_4^{2-} compared with NO_3^- and Cl^- (Wang et al., 2017). The strong adsorption competitiveness of SO_4^{2-} led to its greatest influence on the Cr(VI) adsorption removal. Based on the above results, for the practical application of Fe-R-BC to remove Cr(VI) from high salt wastewater (especially sulfate and nitrate wastewater), the wastewater should be desalinated firstly.

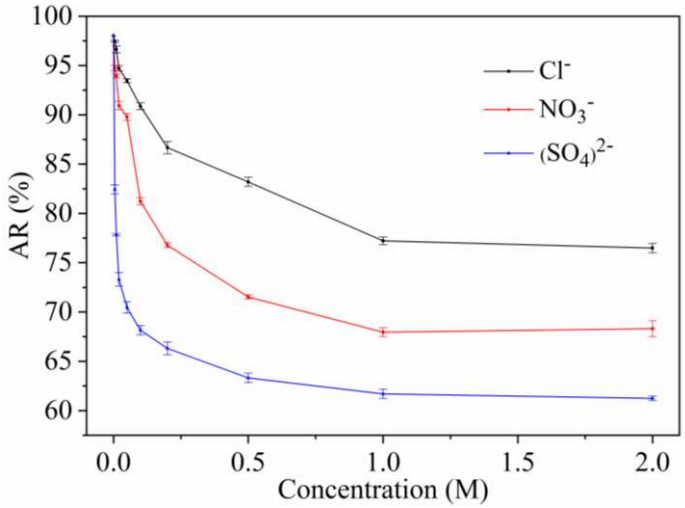

Figure 6. *Influence of coexisting ions on Cr(VI) adsorption removal by Fe-R-BC*

Regeneration of Fe-R-BC

For the application of an adsorbent, the regenerative property of adsorbent should be considered because it determines the economic efficiency of an adsorbent. In this study, the regenerative property of Fe-R-BC was evaluated through 4 cycles of adsorption-desorption experiment. *Figure 7* shows the Cr(VI) adsorption removal rates of Fe-R-BC after experiencing different cycles of adsorption-desorption. With increasing the cycle, the Cr(VI) adsorption removal rate gradually decreased ($p<0.05$). This is a common problem for adsorbents in the cyclic utilization process. It might be owing to the quantity loss of adsorbent and the continuous damage of adsorbent structure during regeneration (Salvador et al., 2015). However, in the fourth cycle, the Cr(VI) adsorption removal rate was 75.12%, which was equal to 76.27% of that of the pristine Fe-R-BC (0 cycle). The results indicated that Fe-R-BC had the good regenerative property, and 0.1 M NaOH solution can be used as an eluent for its regeneration. Generally speaking, the good regenerative property of Fe-R-BC is beneficial to decrease the cost of use.

http://www.aloki.hu ● ISSN 1589 1623 (Print) ●ISSN1785 0037 (Online)
DOI: http://dx.doi.org/10.15666/aeer/1706_1531115327

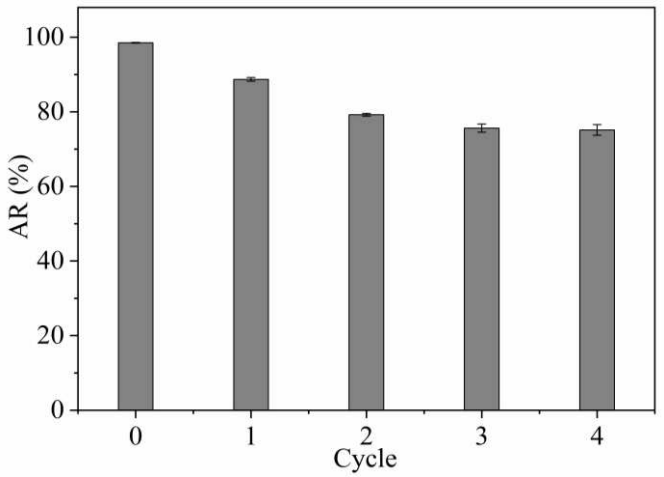

Figure 7. *Cr(VI) adsorption removal rates of Fe-R-BC after experiencing different cycles of adsorption-desorption*

Conclusions

Fe-R-BC was prepared from rice straw with $FeCl_3$ modification by pyrolyzing in this study. Compared to those of R-BC, the Fe content, specific surface area (BET), total pore volume, and number of hydroxyl group of Fe-R-BC increased, while the average pore size and number of methenyl group decreased. For the Cr(VI) adsorption removal by Fe-R-BC, the adsorption kinetics data can be well described by the pseudo second order model, while the adsorption isotherms data can be well described by the Langmuir-Freundlich isotherm model. For Fe-R-BC, the maximum Cr(VI) adsorption removal capacity was 94.95 $mg \cdot g^{-1}$, which exceed those of some previous reported carbon materials. The initial solution pH had a significant effect on the Cr(VI) adsorption removal capacity of Fe-R-BC, which increased with decreasing the initial solution pH. The Cr(VI) adsorption removal by Fe-R-BC was a spontaneous and endothermic process. The Cr(VI) adsorption removal capacity of Fe-R-BC decreased with increasing coexistence ion (Cl^-, NO_3^-, and SO_4^{2-}) concentration in solution. In addition, the influence degree of Cl^-, NO_3^-, and SO_4^{2-} was ordered as follows: $SO_4^{2-} > NO_3^- > Cl^-$. Fe-R-BC had the good regenerative property, and 0.1 M NaOH solution can be used as an eluent for the regeneration. Overall, Fe-R-BC can be applied to the treatment of wastewater containing Cr(VI). In the future, the treatment effect of Fe-R-BC for other anions needs to be further explored.

Acknowledgements. This work was supported by the Scientific Research Innovation Team Project of Sichuan Provincial Department of Education (No. 16TD0006) and the Undergraduate Training Program for Innovation and Entrepreneurship of Sichuan Agricultural University (No. 201610626042).

REFERENCES

[1] Agrafioti, E., Kalderis, D., Diamadopoulos, E. (2014): Arsenic and chromium removal from water using biochars derived from rice husk, organic solid wastes and sewage sludge. – J. Environ. Manage. 133: 309-314.

http://www.aloki.hu ● ISSN 1589 1623 (Print) ●ISSN1785 0037 (Online)
DOI: http://dx.doi.org/10.15666/aeer/1706_1531115327

[2] Ahmad, M., Rajapaksha, A. U., Lim, J. E., Zhang, M., Bolan, N., Mohan, D., Vithanage, M., Lee, S. S., Ok, Y. S. (2014): Biochar as a sorbent for contaminant management in soil and water: A review. – Chemosphere 99: 19-33.
[3] Baran, A., Bıçak, E., Baysal, Ş. H., Önal, S. (2007): Comparative studies on the adsorption of Cr(VI) ions on to various sorbents. – Bioresour. Technol. 98: 661-665.
[4] Chun, Y., Sheng, G., Chiou, C. T., Xing, B. (2004): Compositions and sorptive properties of crop residue-derived chars. – Environ. Sci. Technol. 38: 4649-4655.
[5] Deveci, H., Kar, Y. (2013): Adsorption of hexavalent chromium from aqueous solutions by bio-chars obtained during biomass pyrolysis. – J. Ind. Eng. Chem. 19: 190-196.
[6] Ding, Z., Hu, X., Wan, Y., Wang, S., Gao, B. (2016): Removal of lead, copper, cadmium, zinc, nickel from aqueous solutions by alkali-modified biochar: Batch and column tests. – J. Ind. Eng. Chem. 33: 239-245.
[7] Dong, X., Ma, L. Q., Li, Y. (2011): Characteristics and mechanisms of hexavalent chromium removal by biochar from sugar beet tailing. – J. Hazard. Mater. 190: 909-915.
[8] Dong, L., Chang, K., Wang, L., Linghu, W., Zhao, D., Asiri, A. M., Alamry, K. A., Alsaedi, A., Hayat, T., Li, X., Wu, X. (2018): Application of biochar derived from rice straw for the removal of Th(IV) from aqueous solution. – Sep. Sci. Technol. 53: 1511-1521.
[9] Gan, C., Liu, Y., Tan, X., Wang, S., Zeng, G., Zheng, B., Li, T., Jiang, Z., Liu, W. (2015): Effect of porous Zinc–biochar nanocomposites on Cr(VI) adsorption from aqueous solution. – RSC Adv. 5: 35107-35115.
[10] Garg, U. K., Kaur, M. P., Garg, V. K., Sud, D. (2007): Removal of hexavalent chromium from aqueous solution by agricultural waste biomass. – J. Hazard. Mater. 140: 60-68.
[11] Giannakoudakis, D. A., Kyzas, G. Z., Avranas, A., Lazaridis, N. K. (2016): Multi-parametric adsorption effects of the reactive dye removal with commercial activated carbons. – J. Mol. Liq. 213: 381-389.
[12] Giri, A. K., Patel, R., Mandal, S. (2012): Removal of Cr (VI) from aqueous solution by Eichhornia crassipes root biomass-derived activated carbon. – Chem. Eng. J. 185-186: 71-81.
[13] Golder, A. K., Chanda, A. K., Samanta, A. N., Ray, S. (2011): Removal of hexavalent chromium by electrochemical reduction and ash precipitation: Investigation of process performance and reaction stoichiometry. – Sep. Purif. Technol. 76: 345-350.
[14] Gu, Z., Fang, J., Deng, B. (2005): Preparation and evaluation of GAC-based iron-containing adsorbents for arsenic removal. – Environ. Sci. Technol. 39: 3833-3843.
[15] Gupta, V. K., Nayak, A., Agarwal, S. (2015): Bioadsorbents for remediation of heavy metals: Current status and their future prospects. – Environ. Eng. Res. 20: 1-18.
[16] Han, X., Liang, C., Li, T., Wang, K., Huang, H., Yang, X. (2013): Simultaneous removal of cadmium and sulfamethoxazole from aqueous solution by rice straw biochar. – J. Zhejiang Univ.-SCI. B. 14: 640-649.
[17] Inyang, M. I., Gao, B., Yao, Y., Xue, Y., Zimmerman, A., Mosa, A., Pullammanappallil, P., Ok, Y. S., Cao, X. (2016): A review of biochar as a low-cost adsorbent for aqueous heavy metal removal. – Crit. Rev. Environ. Sci. Technol. 46: 406-433.
[18] Jiang, J., Peng, Y., Yuan, M., Hong, Z., Wang, D., Xu, R. (2015): Rice straw-derived biochar properties and functions as Cu(II) and cyromazine sorbents as influenced by pyrolysis temperature. – Pedosphere 25: 781-789.
[19] Jung, K. W., Hwang, M. J., Jeong, T. U., Ahn, K. H. (2015): A novel approach for preparation of modified-biochar derived from marine macroalgae: Dual purpose electro-modification for improvement of surface area and metal impregnation. – Bioresour. Technol. 191: 342-345.
[20] Kaveeshwar, A. R., Ponnusamy, S. K., Revellame, E. D., Gang, D. D., Zappi1, M. E., Subramaniam, R. (2018): Pecan shell based activated carbon for removal of iron(II) from fracking wastewater: Adsorption kinetics, isotherm and thermodynamic studies. – Process Saf. Environ. Prot. 114: 107-122.

http://www.aloki.hu ● ISSN 1589 1623 (Print) ●ISSN1785 0037 (Online)
DOI: http://dx.doi.org/10.15666/aeer/1706_1531115327

[21] Kuppusamy, S., Thavamani, P., Megharaj, M., Venkateswarlu, K., Lee, Y. B., Naidu, R. (2016): Oak (Quercus robur) Acorn Peel as a low-cost adsorbent for hexavalent chromium removal from aquatic ecosystems and industrial effluents. – Water Air Soil Pollut. 227: 62.
[22] Liu, W., Zhang, J., Zhang, C., Wang, Y., Li, Y. (2010): Adsorptive removal of Cr (VI) by Fe-modified activated carbon prepared from trapa natans husk. – Chem. Eng. J. 162: 677-684.
[23] Ma, Y., Liu, W. J., Zhang, N., Li, Y. S., Jiang, H., Sheng, G. P. (2014): Polyethylenimine modified biochar adsorbent for hexavalent chromium removal from the aqueous solution. – Bioresour. Technol. 169: 403-408.
[24] Mella, B., Glanert, A. C., Gutterres, M. (2015): Removal of chromium from tanning wastewater and its reuse. – Process Saf. Environ. 95: 195-201.
[25] Mohan, D., Rajput, S., Singh, V. K., Steele, P. H., Pittman, C. U. (2011): Modeling and evaluation of chromium remediation from water using low cost bio-char, a green adsorbent. – J. Hazard. Mater. 188: 319-333.
[26] Nethaji, S., Sivasamy, A., Mandal, A. B. (2013): Preparation and characterization of corn cob activated carbon coated with nano-sized magnetite particles for the removal of Cr(VI). – Bioresour. Technol. 134: 94-100.
[27] Pan, J., Jiang, J., Xu, R. (2013): Adsorption of Cr(III) from acidic solutions by crop straw derived biochars. – J. Environ. Sci. 25: 1957-1965.
[28] Park, J. H., Ok, Y. S., Kim, S. H., Cho, J. S., Heo, J. S., Delaune, R. D., Seo, D. C. (2016a): Competitive adsorption of heavy metals onto sesame straw biochar in aqueous solutions. – Chemosphere 142: 77-83.
[29] Park, S. H., Cho, H. J., Ryu, C., Park, Y. K. (2016b): Removal of copper(II) in aqueous solution using pyrolytic biochars derived from red macroalga *Porphyra tenera*. – J. Ind. Eng. Chem. 36: 314-319.
[30] Park, J. H., Wang, J. J., Kim, S. H., Cho, J. S., Kang, S. W., Delaune, R. D., Han, K. J., Seo, D. C. (2017): Recycling of rice straw through pyrolysis and its adsorption behaviors for Cu and Zn ions in aqueous solution. – Colloid Surf. A-Physicochem. Eng. Asp. 533: 330-337.
[31] Rafati, L., Mahvi, A. H., Asgari, A. R., Hosseini, S. S. (2010): Removal of chromium (VI) from aqueous solutions using Lewatit FO 36 nano ion exchange resin. – Int. J. Environ. Sci. Technol. 7: 147-156.
[32] Rajapaksha, A. U., Chen, S. S., Tsang, D. C. W., Zhang, M., Vithanage, M., Mandal, S., Gao, B., Bolan, N. S., Ok, Y. S. (2016): Engineered/designer biochar for contaminant removal/immobilization from soil and water: Potential and implication of biochar modification. – Chemosphere 148: 276-291.
[33] Saha, B., Orvig, C. (2010): Biosorbents for hexavalent chromium elimination for industrial and municipal effluents. – Coord. Chem. Rev. 254: 2959-2972.
[34] Salvador, F., Martin-Sanchez, N., Sanchez-Hernandez, R., Sanchez-Montero, M. J., Izquierdo, C. (2015): Regeneration of carbonaceous adsorbents. Part I: Thermal Regeneration. – Microporous Mesoporous Mat. 202: 259-276.
[35] Samsuri, A. W., Sadegh-Zadeh, F., Seh-Bardan, B. J. (2013): Adsorption of As(III) and As(V) by Fe coated biochars and biochars produced from empty fruit bunch and rice husk. – J. Environ. Chem. Eng. 1: 981-988.
[36] Siddiqui, S. H., Ahmad, R. (2017): Pistachio Shell Carbon (PSC) - an agricultural adsorbent for the removal of Pb(II) from aqueous solution. – Groundw. Sustain. Dev. 4: 42-48.
[37] Soylak, M., Divrikli, U., Saracoglu, S., Elci, L. (2007): Membrane filtration-atomic absorption spectrometry combination for copper, cobalt, cadmium, lead and chromium in environmental samples. – Environ. Monit. Assess. 127: 169-176.
[38] Sun, Y., Yu, I. K. M., Tsang, D. C. W., Cao, X., Lin, D., Wang, L., Graham, N. J. D., Alessi, D. S., Komárek, M., Ok, Y. S., Feng, Y., Li, X. D. (2019): Multifunctional iron-biochar composites for the removal of potentially toxic elements, inherent cations, and hetero-chloride from hydraulic fracturing wastewater. – Environ. Int. 124: 521-532.

http://www.aloki.hu ● ISSN 1589 1623 (Print) ●ISSN1785 0037 (Online)
DOI: http://dx.doi.org/10.15666/aeer/1706_1531115327

[39] Tan, X., Liu, Y., Zeng, G., Wang, X., Hu, X., Gu, Y., Yang, Z. (2015): Application of biochar for the removal of pollutants from aqueous solutions. – Chemosphere 125: 70-85.
[40] Tang, L., Yang, G. D., Zeng, G. M., Cai, Y., Li, S. S., Zhou, Y. Y., Pang, Y., Liu, Y. Y., Zhang, Y., Luna, B. (2014): Synergistic effect of iron doped ordered mesoporous carbon on adsorption-coupled reduction of hexavalent chromium and the relative mechanism study. – Chem. Eng. J. 239: 114-122.
[41] Tseng, R. L., Wu, F. C. (2008): Inferring the favorable adsorption level and the concurrent multi-stage process with the Freundlich constant. – J. Hazard. Mater. 155: 277-287.
[42] Tzou, Y. M., Wang, M. K., Loeppert, R. H. (2003): Sorption of phosphate and Cr(VI) by Fe(III) and Cr(III) hydroxides. – Arch. Environ. Contam. Toxicol. 44: 445-453.
[43] Uddin, M. K. (2017): A review on the adsorption of heavy metals by clay minerals, with special focus on the past decade. – Chem. Eng. J. 308: 438-462.
[44] Wang, S., Peng, Y. (2010): Natural zeolites as effective adsorbents in water and wastewater treatment. – Chem. Eng. J. 156: 11-24.
[45] Wang, P., Tang, L., Wei, X., Zeng, G., Zhou, Y., Deng, Y., Wang, J., Xie, Z., Fang, W. (2017): Synthesis and application of iron and zinc doped biochar for removal of p-nitrophenol in wastewater and assessment of the influence of co-existed Pb(II). – Appl. Surf. Sci. 392: 391-401.
[46] Wu, C., Huang, L., Xue, S. G., Huang, Y. Y., Hartley, W., Cui, M. Q., Wong, M. H. (2017): Arsenic sorption by red mud-modified biochar produced from rice straw. – Environ. Sci. Pollut. Res. 24: 18168-18178.
[47] Xu, X., Cao, X., Zhao, L., Wang, H., Yu, H., Gao, B. (2013): Removal of Cu, Zn, Cd from aqueous solutions by the dairy manure-derived biochar. – Environ. Sci. Pollut. Res. 20: 358-368.
[48] Xu, X., Cao, X., Zhao, L., Zhou, H., Luo, Q. (2014): Interaction of organic and inorganic fractions of biochar with Pb(II) ion: Further elucidation of mechanisms for Pb(II) removal by biochar. – RSC Adv. 4: 44930-44937.
[49] Xu, W., Jian, H., Liu, Y., Zeng, G., Li, X., Gu, Y., Tan, X. (2015): Removal of Chromium (VI) from aqueous solution using mycelial pellets of penicillium simplicissimum impregnated with powdered biochar. – Biorem. J. 19: 259-268.
[50] Yang, Z. H., Wang, B., Chai, L. Y., Wang, Y. Y., Wang, H. Y., Su, C. Q. (2009): Removal of Cr(III) and Cr(VI) from aqueous solution by adsorption on sugarcane pulp residue. – J. Cent. South Univ. Technol. 16: 101-107.
[51] Zhang, Z. B., Cao, X. H., Liang, P., Liu, Y. H. (2013): Adsorption of uranium from aqueous solution using biochar produced by hydrothermal carbonization. – J. Radioanal. Nucl. Chem. 295: 1201-1208.
[52] Zhang, M., Liu, Y., Li, T., Xu, W., Zheng, B., Tan, X., Wang, H., Guo, Y., Guo, F., Wang, S. (2015): Chitosan modification of magnetic biochar produced from Eichhornia crassipes for enhanced sorption of Cr(VI) from aqueous solution. – RSC Adv. 5: 46955-46964.
[53] Zhao, Z., Wei, J., Li, F., Qu, X., Liang, S., Zhang, H., Yu, Q. (2017): Synthesis, characterization and hexavalent chromium adsorption characteristics of Aluminum- and sucrose-incorporated tobermorite. – Materials. 10: 597.
[54] Zhou, Y., Gao, B., Zimmerman, A. R., Fang, J., Sun, Y., Cao, X. (2013): Sorption of heavy metals on chitosan-modified biochars and its biological effects. – Chem. Eng. J. 231: 512-518.
[55] Zhou, L., Huang, Y., Qiu, W., Sun, Z., Liu, Z., Song, Z. (2017): Adsorption properties of nano-MnO_2–biochar composites for copper in aqueous solution. – Molecules 22: 173.

http://www.aloki.hu ● ISSN 1589 1623 (Print) ●ISSN1785 0037 (Online)
DOI: http://dx.doi.org/10.15666/aeer/1706_1531115327

EFFECTS OF TWO NATURAL DIETS ON THE RESPONSE OF THE PREDATOR *ARMA CHINENSIS* (HEMIPTERA: PENTATOMIDAE: ASOPINAE) TO COLD STORAGE

LI, X. P.[1,2] – SONG, L. W.[2] – COUDRON, T. A.[3] – ZUO, T. T.[2] – CHEN, Y. Q.[2] – ZHANG, Y.[2] – WU, S. A.[1*]

[1]*Key Laboratory for Silviculture and Conservation of Ministry of Education, Beijing Forestry University, Beijing, China*

[2]*Jilin Provincial Academy of Forestry Sciences, Changchun 130033, China*

[3]*Biological Control of Insects Research Laboratory, USDA Agricultural Research Service, Columbia, Missouri 65203, USA*

**Corresponding author*
e-mail: lxpjsx@126.com; sananwu@bjfu.edu.cn; phone: +86-010-6233-7731

(Received 10th Jul 2019; accepted 15th Nov 2019)

Abstract. The preservation and rearing of insect natural enemies is the key for biological control. The biological (survival, longevity and the fecundity) and biochemical (low-molecular-weight carbohydrates, glycerol and fatty acids contents) indexes of *Arma chinensis* fed by *Antherea pernyi* (diet AP) or *Tenebrio molitor* (diet TM) were measured after cold storage treatments. The results showed that the diet affected several biological and biochemical parameters, but varied with the length of cold storage. The survival rate and longevity after 30-day cold storage, and the fecundity after 40-day cold storage were significantly higher for adults reared on TM compared to AP. The super-cooling points and the freezing points were significantly lower for adults reared on TM than AP. Low-molecular-weight carbohydrates, glycerol and unsaturated fatty acids were significantly higher for TM than for AP. The structural equation model showed that diet influenced survival, fertility and SCPs of *A. chinensis* indirectly through the enzyme activity, and the content of carbohydrates, glycerol and unsaturated fatty acids. These results suggested that the nutrient content of diets affects the accumulation of cold-resistant substances, metabolism level and activities of related enzymes in *A. chinensis* in a manner that enhances tolerance to cold storage.
Keywords: *natural enemies, cold tolerance, rearing, development, low-molecular-weight carbohydrates, fatty acids*

Introduction

The preservation and transportation of living insects and the rearing of these insects in sufficient numbers and quality for fluctuating markets is one of the obstacles to the use of insect natural enemies for biological control (Coudron et al., 2007). According to the principle of insect cryogenics, cold storage (cryopreservation technology) may be a useful technique to store and ship insects for extended periods, and accumulate sufficient numbers of insects for the undulating and unpredictable demands, and provide the protection of some endangered insect species (Coudron et al., 2007; Leopold, 2007). Cold storage tolerance in insects has significant plasticity (Gotthard and Nylin, 1995), which can be affected by multiple endogenous and exogenous factors. The effect of temperature, photoperiod, age/stadium on the cold tolerance of insects have been researched extensively (Hodkova and Socha, 1995), whereas the effects of the nutrient quality (diet) are less known (Tzanakakis et al., 1992; Ruberson et al., 1998). Previous studies showed that cold storage tolerance of predators improved by selecting

http://www.aloki.hu ● ISSN 1589 1623 (Print) ● ISSN 1785 0037 (Online)
DOI: http://dx.doi.org/10.15666/aeer/1706_1532915347

appropriate developmental stages, temperatures and feeding parameters (Coudron et al., 2007). For example, the survival rate and the reproductive rate of *Podisus Maculiventris* and *Chrysopa Carnea* enhanced by the nutrient quality of diets after the cold storage and pre-processed in cold storage (Chang et al., 1995; Thorpe and Aldrich, 2004). The low temperature survival of *Nasonia vitripennis* significantly improved when parasitism occurred in a host that of those contained more cryoprotectants (glycerol and alanine) (Rivers et al., 2000). The cold storage capacity of *Cotesia marginiventris* adults enhanced with feeding honey or sucrose (Ergin and Uckan, 2003). Egg viability of the *P. maculiventris* adults fed artificial diets was significantly higher than that fed by natural prey (Coudron et al., 2009), which may result from the high protein content and low lipid content contained in the artificial diets (Coudron et al., 2007). Those studies focused on the effect of diet on growth and fecundity indexes after cold storage. However, we know less about how diet influences biochemical indexes of insects after cold storage. Consequently, the physiological mechanisms linking dietary nutrition and cold storage tolerance of a predatory insect are still not known.

Arma chinensis is a predatory insect that is widely distributed in more than 10 provinces in northern China. They prey on several lepidopteran, coleopteran and hemipteran insect pests of agricultural and forestry ecosystems (Chai et al., 2000; Chen et al., 2007; Wang et al., 2012; Zou, 2012), and can use to control the density of pest populations with artificial releases. Since *A. chinensis* plays a vital role in the biocontrol of pests, researchers have investigated environmental (Song et al., 2010) and dietary (Zou et al., 2015; Li et al., 2016, 2018) conditions to optimize the mass production of *A. chinensis*. Some researchers found no distinct difference in developmental duration, survival rate, fecundity, and egg viability of *A. chinensis* reared on diets with different nutrient composition (Li et al., 2016). However, many insect herbivores have evolved counter-adaptations to overcome the plant defence. These adaptations include host plant choice, non-disruptive feeding guilds and various physiological adaptations as well as metabolic enzymatic strategies of the insect's digestive system (Pentzold et al., 2014). There may be an adaptation to the cold tolerance for the various food to the polyphagous *A. chinensis*.

Unlike rearing at normal temperature, consequences of cold storage may result from a combination of both chill-injuries and exhaustion of energy reserves (Colinet et al., 2006). Substances such as glycogen, lipids, glycerol and cell membrane construction maybe activated in response to cold exposure as a method to help insects survive in the adverse environments (Feng et al., 2014). Therefore, the accumulation and the metabolic rate of these substances in insects affect their cold storage tolerance. In this study, we focus on the effects of different diets on the response of *A. chinensis* to cold storage treatments, including its physiological and biochemical responses. We hope to advance diet formulation as a way to improve the use of cold storage for mass production of *A. chinensis*.

Materials and methods

Experimental insects and diet

Rearing A. chinensis

A. chinensis used for these studies originated from over-wintering adults collected from *Ulmus pumila* plantation (farmland shelterbelts) located in Linzi Town, Qian'an

http://www.aloki.hu ● ISSN 1589 1623 (Print) ● ISSN 1785 0037 (Online)
DOI: http://dx.doi.org/10.15666/aeer/1706_1532915347

County, Jilin Province, China (N123°22'16"-124°22′E, 44°38'47"N) in April 2016. After diapause termination, colonies *A. chinensis* were continuously fed (*ad libitum*) either pupae of *Antherea pernyi* (diet AP) or pupae of *Tenebrio molitor* (diet TM) for 12 generations in insect rearing cages at the ambient temperature of 25 ± 1 °C, humidity of 65 ± 5%, and lighting of 16L: 8D (*Figs. 1* and *2*). For these studies, 3- to 7-day-old adults were collected after 12 generations of rearing on either *A. pernyi* (diet AP; 2,154 adults collected) or on *T. molitor* (diet TM; 2,436 adults collected).

Figure 1. *Morphological of A. chinensis (Fallou). a, Egg mass; b, First instar Nymph; c, third instar Nymph; d, Female adult*

Figure 2. *The nymph of A. chinensis feeding Antherea pernyi (a) and Tenebrio molitor (b)*

Nutrient component and content of two natural diets

The pupae of *A. pernyi* (diet AP) and *T. molitor* (diet TM) were collected from the rearing factory. After rinsing the pupae of *A. pernyi* (9) and *T. molitor* (120) were dried of any extraneous moisture using the filter paper, then labeled and weighted individually. The pupae were frozen dried at -40 °C for 72 h, weighted again for calculating the water content, then grounded and analyzed the nutrient component using the method described by Jiang et al. (2016). The nutrients of pupae of *A. pernyi* and *T. molitor* were showed in *Table 1*.

Design of cold storage treatment

20 adults for each treatment were placed in a culture dish (11 cm in diameter) with filter paper at the bottom, then were placed into a low temperature incubator without illumination at the temperature of 4 ± 1 °C and the humidity of 65 ± 5% RH. The preliminary test showed no significant difference in biological indexes for male and female adults fed either AP or TM and subjected to 3 weeks of cold treatment. Therefore, the minimum cold storage period was set as 30 days without considering the sex, followed by 10-day extensions in cold storage period until all adults in the treatment dead. Five cold storage periods were established with a control group held at 25 ± 1 °C and humidity of 65 ± 5% RH. All the *A. chinensis* were provided with

http://www.aloki.hu ● ISSN 1589 1623 (Print) ● ISSN 1785 0037 (Online)
DOI: http://dx.doi.org/10.15666/aeer/1706_1532915347

sufficient water but no food during the cold storage, and were discarded after measuring biological indexes (Coudron et al., 2007).

At each cold storage time point, 400 adults were collected for survival rate measurement from each diet treatment after holding at 25 ± 1 °C and 65 ± 5% RH for 24 h. Then 20 pairs of survivors (one male and one female per pair) were placed in paper cups (7 cm in diameter and 8 cm in height) for each diet treatment. Fresh diet (1 silkworm pupa or 4 mealworm pupae) and water via a wet cotton ball was provided every day in each cup. The quantity of eggs laid, the time of egg oviposition, and time of death were recorded for two weeks. Egg viability was determined using 15 to 20 eggs from each cup.

Table 1. *Main ingredients and amounts of Antherea pernyi (AP) and Tenebrio molitor (TM)*

Ingredient		**Amount**	
		AP*	**TM***
Water (%)		75.10	62.50
Protein (%)		12.90	16.80
Carbohydrates (%)		1.90	10.00
Lipids (%)		7.80	8.60
Fatty acid (percentage of total fat) (%)	< $C^0$16	1.20	1.50
	$C^0$16	18.10	23.60
	$C^0$18	6.70	1.40
	< $C^1$18	5.60	4.50
	$C^1$18	54.00	44.70
	$C^2$18	10.70	24.10
	$C^3$18	2.00	1.50
Mineral (mg/100 g)	K	272.00	1420.00
	Na	140.20	63.20
	Ca	81.00	125.00
	Mg	103.00	185.00
	Fe	2.60	6.40
	Mn	0.64	1.50
	Zn	6.17	11.90
	Cu	0.53	4.30
	P	207.00	691.00
	Se (μg)	11.10	47.50
Vitamins (mg/100 g)	B1	0.11	0.07
	B2	6.39	0.52
	A (μg)	0.25	1.90
	E	5.34	1.90
	D (μg)	-	10.45

Influences of different diets on biochemical indexes of A. chinensis

The physiological and biochemical indexes related to cold resistance of adult of *A. chinensis* were measured after 30-days cold storing period, including super-cooling points, low-molecular carbohydrates, fatty acids and glycerol, nutrient absorption and enzyme activities.

http://www.aloki.hu ● ISSN 1589 1623 (Print) ● ISSN 1785 0037 (Online)
DOI: http://dx.doi.org/10.15666/aeer/1706_1532915347

Super-cooling points (SCPs) and freezing points (FPs)

Super-cooling and freezing points were determined for 40 adults from each diet after 30-day cold storage treatment. Individual adult was dried of any extraneous moisture, placed in a centrifuge tube and fixed to a thermocouple attached to an automatic recorder (UR100, Model 4152, Yokogawa Electric Co., Seoul, Korea) via a bridge. The thermocouple with the adult was lowered into a freezing chamber (VM04/100, Heraeus Co., Germany) at 0 °C for 20 min, and then was cooled to -40 °C at a rate of 1 °C/min, and the decreasing body temperatures were measured. The SCPs was taken as the lowest temperature before the increase in temperature caused by the latent heat of crystallization (Mohammadzadeh and Izadi, 2016).

Low-molecular-weight carbohydrates in the insect body

The content of low-molecular-weight carbohydrates were measured in 300 adults for each diet after 30-day cold storage treatment, freeze-dried for 48 h (2.5L FreeZone, LabconcoInc., USA), ground, and then measured by the method as described by Heydari and Izadi (2014). Briefly, 1 g of dried powder of *A. chinensis* was extracted with 20 ml of 80% ethanol, and heated at 75 °C for 20 min in a water bath, and then centrifuged for 3 min at 10000 rpm. The supernatant was analyzed with the Agilent 1200 liquid chromatograph (Agilent Technologies Inc., USA) for determining contents of trehalose, glucose, mannitol, sorbitol, and fructose. The other portion of freeze-dried powder of *A. chinensis* were used to the measurement of glycerol content and fatty acid content.

Glycerol content in the insect body

Briefly, 1 g of freeze-dried powder of *A. chinensis* was extracted with 1 ml of distilled water using a glass hand homogenizer placed in an ice bath and centrifuged at 4 °C and 5000 rpm for 15 min. The supernatant was analyzed with the Glycerol Assay Kit (Catalog Number MAK117, Storage Temperature -20 °C, Sigma-Aldrich, St. Louis, USA). The procedure followed the instruction of the test kit (Jehrke et al., 2018).

Fatty acids contents in the insect body

Briefly, 0.5 g of freeze-dried powder of *A. chinensis* was extracted with a 2:1 v:v solution of chloroform-methanol (Gołębiowski et al., 2008). Fatty acids in the organic phase were methyl esterified, and quantified by gas chromatography (Agilent 7890A, Agilent Technologies Inc., USA; adopting fused-silica capillary column as chromatographic column, 100 m × 0.25 mm × 0.2 μm, CP-Sil 88, Chrompack; Agilent Technologies Inc., USA).

Enzyme activities related to the transformation of cold-resistant substances

For each enzyme activity analysis, 20 adults were pooled for each diet after 30-day cold storage treatment. The insects were grounded with the liquid nitrogen freezing grinder (JXFSTPRP-II-01 Shanghai Jingxin Co., LD, China). Briefly, 0.1 g of powder of *A. chinensis* was extracted with 0.9 ml extracting solution using a glass hand homogenizer placed in an ice bath. Then centrifuged at 4 °C for 10 min with the speed 2500 rpm for Catalase (CAT), Peroxidase (POD), total superoxide dismutase (T-SOD), 8000 rpm for trehalase (THL) and Glyceraldehyde-3-phosphate dehydrogenase

http://www.aloki.hu ● ISSN 1589 1623 (Print) ● ISSN 1785 0037 (Online)
DOI: http://dx.doi.org/10.15666/aeer/1706_1532915347

(GAPDH), 10000 rpm for Trypsin, and 2000 rpm for Adenosine triphosphatase (ATP) (Na^+K^+-ATP, $Ca^{2+}Mg^{2+}$-ATP), respectively. The extracted solution centrifuged at 4 °C and 16000 rpm for 40 min for fatty acid synthetase (FAS). Then the supernatants were taken to prepare the samples for analyses enzyme activity analysis.

Trypsin activity, GAPDH activity, THL activity, and FAS activity were determined with a kit (Suzhou Keying Biotechnology Co., Ltd., Suzhou, China) according to the instruction; CAT, T-SOD, ATP, and POD activities were determined with a kit produced by Nanjing Jiancheng Bioengineering Institute (Nanjing, China) according to instruction.

Data analysis

Prior to analysis, data for survival rate, longevity, fertility, the time of egg oviposition, fecundity, egg viability were ln (x + 1) transformed to achieve normality. The effect of diet and length of cold storage on cold tolerance of *A. chinensis* were analyzed using general linear models with LSD significant difference test ($P < 0.05$). The effect of the length of cold storage was analyzed with non-parametric tests (Cruskal-Wallis rank-sum test) of multiple independent samples ($P < 0.05$). The effect of diet on biological indexes (survival rate, longevity, fertility, egg oviposition time, fecundity, and egg viability), and biochemical indexes (super-cooling point, the content of micro-molecule carbohydrates, glycerol, and fatty acids) and enzyme activity were tested by the Independent sample T test ($P < 0.05$). The analysis were performed using SPSS statistical software (SPSS 17.0 for windows, SPSS Inc., Chicago, USA).

Structural equation modeling (SEM) was used to evaluate the general hypothesis that carbohydrate, glycerol, saturated fatty acid (SFA), and unsaturated fatty acid (UFA) content of adult affect survival rate, longevity, fertility, fecundity, egg viability of *A. chinensis*. We hypothesized that the adaptations of metabolic enzymatic strategies of the *A. chinensis* induced by diet and cold treatments influenced the content of energy reserves, which then altered the cold tolerance of *A. chinensis*. We constructed an a priori model including possible causal relationships among predictors, i.e. the enzymatic activity was the main factor influencing the content of carbohydrates, glycerol and fatty acids induced by diet and cold treatments, which then influenced fertility, survival rate, egg viability, fecundity and changed super-cooling points (SCPs). All of the predicators were treated as observed variables. Finally our results only showed the significant biochemical pathways. Mardia's test was used to estimate the multivariate normality of the dataset. The model fitness was assessed using the $\chi 2$-test, comparative fit index (CFI), and root mean square error of approximation (RMSEA). The analysis was performed with SPSS AMOS 21.0 software (SPSS Inc., Hong Kong) using the "robust" maximum likelihood estimation procedures.

Results

Effect of diet on the biological indexes after cold storage treatment

The effect of diet and cold storage time on the survival rate, longevity, and female fertility, egg oviposition time, fecundity, and egg viability varied with the length of time in cold storage (*Table 2*).

http://www.aloki.hu ● ISSN 1589 1623 (Print) ● ISSN 1785 0037 (Online)
DOI: http://dx.doi.org/10.15666/aeer/1706_1532915347

Survival rate

The length of time in cold storage significantly affected the survival rate of adults from colonies reared on either TM or AP (*Table 2*). The survival rate decreased significantly with increased time in cold storage (AP, H = 32.125, df = 5, P < 0.001; TM, H = 32.224, df = 5, P < 0.001). The effect of diet on survival rate varied with the length of time in cold storage (*Fig. 3*). The survival rate for TM was significantly higher than for AP (30-day, F = 0.225, T = -2.573, df = 10, P = 0.028; 40-day, F = 1.084, T = -2.349, df = 10, P = 0.041) at the 30-day and 40-day cold storage periods (*Fig. 3*). In addition, the survival rate for AP (90.83%) was significantly lower than for the control group (P < 0.05), but the survival rate for TM (96.67%) and the control group was not significantly different (P > 0.05) at the 30-day cold storage period. The survival rates for both AP and TM dropped to 12% at 70-day cold storage period.

Table 2. *Two-way ANOVA analysis of the biological indicators after cold storage*

Source of variation	Survival (%)			Longevity (days)			Fertility (%)		
	df	**F**	**P**	**df**	**F**	**P**	**df**	**F**	**P**
D	1	0.793	0.377	1	8.459	**0.004**	1	163.416	**< 0.001**
S	5	107.164	**< 0.001**	4	81.820	**< 0.001**	4	706.635	**< 0.001**
D×S	5	0.223	0.951	4	1.437	0.254	4	9.442	**< 0.001**
Error	60			190			50		
	Egg oviposition time			**Total fecundity**			**Egg viability (%)**		
	df	**F**	**P**	**df**	**F**	**P**	**df**	**F**	**P**
D	1	0.560	0.456	1	2.530	0.115	1	14.371	**< 0.001**
S	4	32.740	**< 0.001**	4	285.966	**< 0.001**	4	131.935	**< 0.001**
D×S	4	0.410	0.841	4	1.189	0.320	4	0.969	0.433
Error	100			100			50		

D: diet; S: storage period

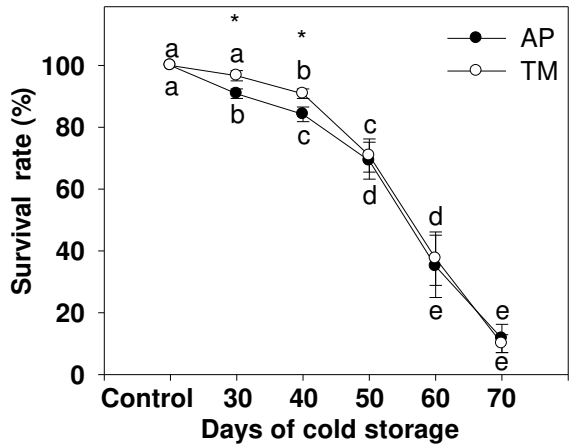

Figure 3. *Survival of A. chinensis adults from colonies reared on diets Antherea pernyi (AP) and Tenebrio molitor (TM) after cold storage for different lengths of time at 4 °C. The same colonies of A. chinensis reared at 25 °C is shown as the control. The different letters represent significant difference among the different cold storage periods at P < 0.05 level (Cruskal-Wallis Rank Sum Test). * represents a significant difference among the two diet treatments (T-test, P < 0.05)*

http://www.aloki.hu ● ISSN 1589 1623 (Print) ● ISSN 1785 0037 (Online)
DOI: http://dx.doi.org/10.15666/aeer/1706_1532915347

Longevity

Both diet and length of cold storage showed a significant effect on the longevity of adults (*Table 2*). The longevity of adults for both diets significantly decreased with the increasing length of time in cold storage (AP, $H = 109.548$, $df = 5$, $P < 0.001$; TM, $H = 107.922$, $df = 5$, $P < 0.001$), which was lower than 3 days at 60-day cold storage period (*Fig. 4*). Overall, the longevity of the adult for TM was higher than for AP at all the cold storage time periods and the control group (*Fig. 4*). Moreover the differences in the longevity of adults for both diets were significant at 30-day and 50-day cold storage periods, respectively (30-day, $F = 11.350$, $T = -2.439$, $df = 38$, $P = 0.019$; 50-day, $F = 0.417$, $T = -4.09$, $df = 38$, $P < 0.001$) (as shown in *Fig. 4*).

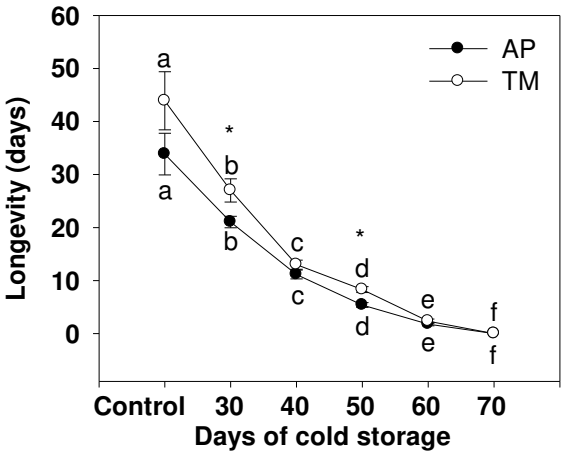

Figure 4. *Longevity of A. chinensis adults from colonies reared on diets Antherea pernyi (AP) and Tenebrio molitor (TM) after cold storage for different lengths of time at 4 °C. The different letters represent significant difference among the different cold storage periods at $P < 0.05$ level (Cruskal-Wallis Rank Sum Test). * represents a significant difference among the two diet treatments (T-test, $P < 0.05$)*

Fertility

Both diet and cold storage time showed a significant effect on fertility (*Table 2*). The fertility declined with the increasing cold storage time for both diets compared to the control group reared on 25 °C (the fertility was 70.19% and 79.93% for AP and TM, respectively) (*Fig. 5*). After 60 days of cold storage, fertility had dropped to below 10% for both diet treatments (AP, $H = 34.208$, $df = 5$, $P < 0.001$; TM, $H = 33.388$, $df = 5$, $P < 0.001$). The fertilities for TM were significantly higher than those for AP before cold storage (control, $F = 0.243$, $T = -6.247$, $df = 10$, $P < 0.001$), and from the 30-day to 50-day cold storage period (30-day, $F = 1.546$, $T = -6.043$, $df = 10$, $P < 0.001$; 40-day, $F = 1.091$, $T = -5.975$, $df = 10$, $P < 0.001$; 50-day, $F = 0.069$, $T = -8.344$, $df = 10$, $P < 0.001$) (*Fig. 5*).

http://www.aloki.hu ● ISSN 1589 1623 (Print) ● ISSN 1785 0037 (Online)
DOI: http://dx.doi.org/10.15666/aeer/1706_1532915347

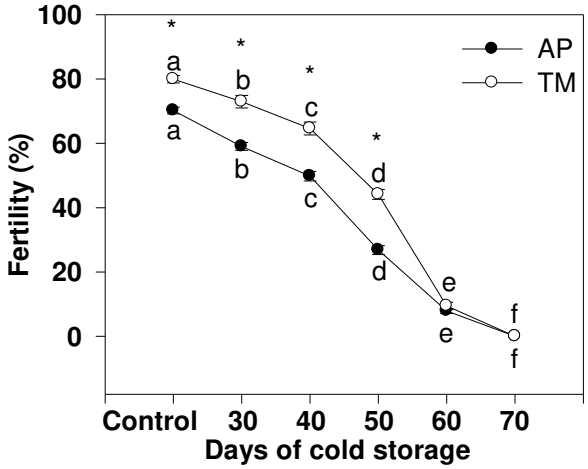

Figure 5. *Fertility of A. chinensis adult from colonies reared on Antherea pernyi (AP) and Tenebrio molitor (TM) after cold storage for different lengths of time at 4 °C. The different letters represent significant difference among the different cold storage periods at P < 0.05 level (Cruskal-Wallis Rank Sum Test). * represents a significant difference among the two diet treatments (T-test, P < 0.05)*

Egg oviposition time

The cold storage period had a significant effect on the time of egg oviposition (*Table 2*), which decreased with the increasing of the cold storage time for both diets (AP, H = 46.692, df = 5, P < 0.001; TM, H = 42.356, df = 5, P < 0.001) (*Fig. 6*). There was no significant effect of diet on the time of egg oviposition at all cold storage periods (P > 0.05) (*Table 2; Fig. 6*).

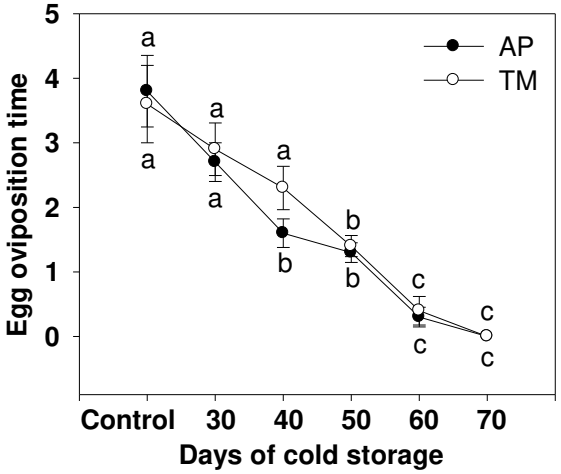

Figure 6. *Egg oviposition time of A. chinensis adults from colonies reared on Antherea pernyi (AP) and Tenebrio molitor (TM) after cold storage for different lengths of time at 4 °C. The different letters represent significant difference among the different cold storage periods at P < 0.05 level (Cruskal-Wallis Rank Sum Test)*

http://www.aloki.hu ● ISSN 1589 1623 (Print) ● ISSN 1785 0037 (Online)
DOI: http://dx.doi.org/10.15666/aeer/1706_1532915347

Fecundity

Length of cold storage had a significant effect on the fecundity of *A. chinensis* reared on either diets (*Table 2*). Overall, fecundity decreased with the increasing length of time in cold storage (AP, H = 56.991, df = 5, P < 0.001; TM, H = 55.013, df = 5, P < 0.001) (*Fig. 7*). There was no significant difference in the fecundity for AP and TM (*Table 2*), but the average fecundity for TM was significant higher (by 30%) than that for AP at 40-day cold storage (F = 0.752, T = -3.018, df = 18, P = 0.008) (*Fig. 7*).

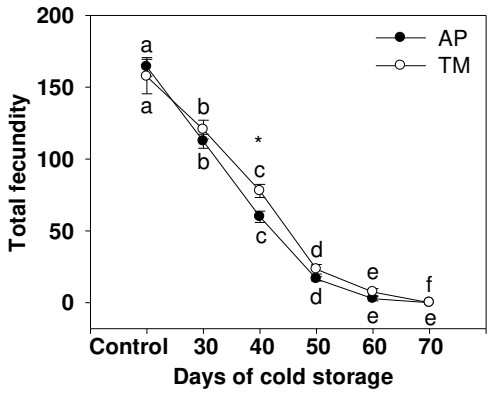

Figure 7. *Fecundity of A. chinensis adults from colonies reared on Antherea pernyi (AP) and Tenebrio molitor (TM) after cold storage for different lengths of time at 4 °C. The different letters represent significant difference among the different cold storage periods at P < 0.05 level (Cruskal-Wallis Rank Sum Test). * represents a significant difference among the two diet treatments (T-test, P < 0.05)*

Egg viability

Both diet and length of time in cold storage had a significant effect on egg viability for *A. chinensis* (*Table 2*). Egg viability declined for both diet treatments with the increasing length of time in cold storage (AP, H = 33.379, df = 5, P < 0.001; TM, H = 33.292, df = 5, P < 0.001) (*Fig. 8*). Egg viability for TM was higher than for AP, but the significant difference only occurred at 40-day cold storage period (F = 0.222, T = -4.592, df = 10, P = 0.001) (*Fig. 8*).

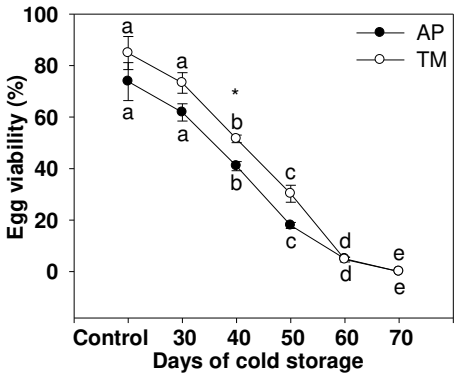

Figure 8. *Egg viability of A. chinensis adults from colonies reared on Antherea pernyi (AP) and Tenebrio molitor (TM) after cold different lengths of time in cold storage at 4 °C. The different letters represent significant difference among the different cold storage periods at P < 0.05 level (Cruskal-Wallis Rank Sum Test). * represents a significant difference among the two diet treatments (T-test, P < 0.05)*

http://www.aloki.hu ● ISSN 1589 1623 (Print) ● ISSN 1785 0037 (Online)
DOI: http://dx.doi.org/10.15666/aeer/1706_1532915347

Effect of diet and lengths of time in cold storage on physiological indexes

Super-cooling and freezing points

Diet treatments had a significant effect on the super-cooling and freezing points (SCPs, $F = 0.399$, $T = 19.294$, $df = 18$, $P < 0.001$; FPs, $F = 0.336$, $T = 16.512$, $df = 18$, $P < 0.001$). The super-cooling and freezing points for TM were 20% lower than for AP (*Fig. 9*).

Low-molecular-weight sugars and glycerol

Low-molecular-weight sugars (trehalose, mannitol, sorbitol) and glycerol were significantly higher for TM than AP, by 31%, 228%, 211% and 56%, respectively (*Fig. 10*, Trehalose, $F = 0.238$, $T = -3.153$, $df = 8$, $P = 0.014$; Mannitol, $F = 38.515$, $T = -3.157$, $df = 8$, $P = 0.013$; Sorbitol, $F = 0.436$, $T = -9.711$, $df = 8$, $P < 0.001$; Glycerol, $F = 2.860$, $T = -133.056$, $df = 8$, $P < 0.001$).

Fatty acids

There was no significant difference in the total content of fatty acids for AP and TM ($F = 6.51$, $T = 0.51$, $df = 6.06$, $P = 0.63$). However, the content of saturated fatty acids for AP was significantly higher by 129% than for TM ($F = 21.65$, $T = 12.95$, $df = 4.72$, $P < 0.001$), but the content of unsaturated fatty acids were significantly lower by 28% than for TM ($F = 1.97$, $T = 6.5$, $df = 8$, $P < 0.001$) (*Table 3*).

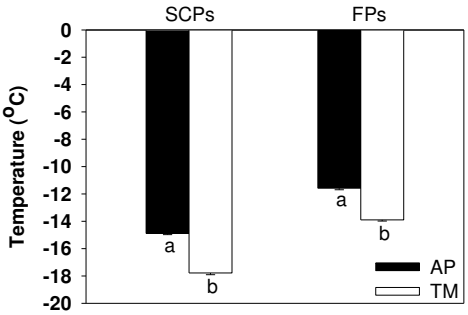

Figure 9. *Super-cooling and freezing points of A. chinensis adults from colonies reared Antherea pernyi (AP) and Tenebrio molitor (TM) after cold storage for 30 days at 4 °C. Different letters indicate significant differences between diet treatments at P < 0.05 level (T-test)*

Table 3. *Fatty acid content in A. chinensis adults from colonies reared on Antherea pernyi (AP) and Tenebrio molitor (TM) after cold storage for 30 days at 4 °C (means ± standard error)*

Fatty acids	**Contents (mg/g)**	
	***Antherea pernyi* (AP)**	***Tenebrio molitor* (TM)**
Σ Fatty acid	77.66 ± 3.53a	75.63 ± 1.86a
Σ Saturated fatty acids	34.08 ± 1.42a	14.89 ± 0.43b
Σ Unsaturated fatty acids	43.58 ± 2.15a	60.74 ± 1.54b
Σ Monounsaturated fatty acids	6.34 ± 0.29a	20.59 ± 0.95b
Σ Polyunsaturated fatty acids	37.23 ± 1.86a	40.15 ± 0.78a

Different letters indicate significantly statistical difference at the same row at $P < 0.05$ (T-test)

http://www.aloki.hu ● ISSN 1589 1623 (Print) ● ISSN 1785 0037 (Online)
DOI: http://dx.doi.org/10.15666/aeer/1706_1532915347

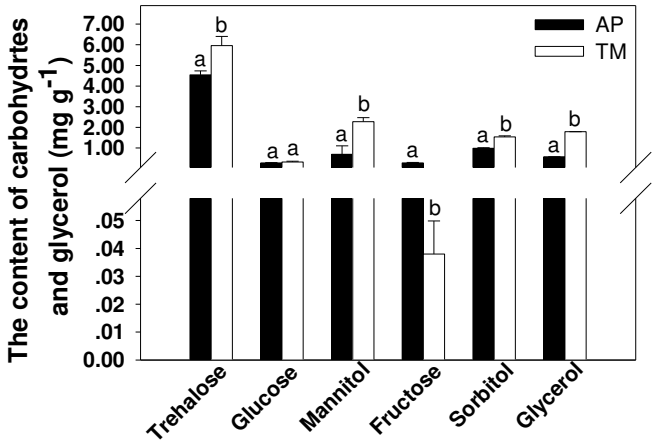

Figure 10. *Low-molecular-weight sugars and glycerol content of A. chinensis adults from colonies reared on Antherea pernyi (AP) and Tenebrio molitor (TM) after cold storage for 30 days at 4 °C. Different letters indicate significant differences between diet treatments at P < 0.05 level (T-test)*

Enzyme activities

The effect of diet on the enzyme activities in adults varied among the different enzymes (*Fig. 11*). Activities of GAPDH, Na^+K^+-ATPase, and $Ca^{2+}Mg^{2+}$-ATPase for TM were greatly higher, by 2.53 times, 2.00 times and 3.10 times, respectively, than for AP (GAPDH, F = 0.029, T = 40.782, df = 10, P < 0.001; Na^+K^+-ATPase, F = 0.309, T = 7.741, df = 10, P < 0.001; $Ca^{2+}Mg^{2+}$-ATPase, F = 4.774, T = 14.35, df = 10, P < 0.001). The FAS activity for AP was significantly lower, by 37%, than for TM (F = 1.285, T = -5.410, df = 10, P < 0.001).

The relationships between diets induced factors and cold tolerance

The SEM revealed that the predictors explained 50% of the variation in diet effect (*Fig. 12*). The content of glycerol, SFA and UFA directly contributed to the survival rate of *A. chinensis*. Activities of GAPDH and FAS were associated with the survival rate through the content of SFA and UFA, respectively. It was worth noting that diet influenced the survival rate of *A. chinensis* indirectly through the activity of GAPDH and the content of glycerol. The content of fructose directly contributed to the fertility, and the activity of $Ca^{2+}Mg^{2+}$-ATPase was associated with the fertility through the content of fructose. Diet influenced the fertility of *A. chinensis* indirectly through the activity of $Ca^{2+}Mg^{2+}$-ATPase. The content of glycerol, fructose, sorbitol, SFA and UFA directly contributed to SCPs. And the activity of $Ca^{2+}Mg^{2+}$-ATPase was associated with SCPs through the content of fructose, the activities of GAPDH and FAS was associated with SCPs through the content of SFA and UFA, respectively. Diet influenced SCPs of *A. chinensis* indirectly through the activities of $Ca^{2+}Mg^{2+}$-ATPase and GAPDH, and the content of glycerol, sorbitol and UFA (*Fig. 12*).

Discussion

Response to cold storage can be a combination of adaptation to low temperatures and to starvation (Renault, 2003). As part of the adaptation, insects require a large amount

http://www.aloki.hu ● ISSN 1589 1623 (Print) ● ISSN 1785 0037 (Online)
DOI: http://dx.doi.org/10.15666/aeer/1706_1532915347

of energy, which is derived solely from metabolic stores (lipids, proteins and eventually glycogen), and, therefore, body tissues are depleted because of catabolic activities (Hervant et al., 1999; Wang et al., 2017). With the depletion of energy reserves, starvation periods will have dramatic consequences on reproduction in adults (Leather, 1984).

Developmental and reproductive indexes used during cold storage can be affected by the diet consumed prior to the cold treatment. Previous studies demonstrated that species, diet, temperature and length-of-time affected the result of cold storage for insects (Colinet and Boivin, 2011; Koštál et al., 2016). We found that storage at 4 °C for less than 30 days had no significant effect on most biological indexes that we measured. However, survival rate, longevity, female fertility rate, fecundity, egg viability and time of oviposition for adults from colonies reared on the two diets we tested were affected when cold storage was extended beyond 30 days. Survival rate and longevity for TM were higher than for AP beyond 30-day cold storage. In contrast, the fecundity was significantly higher for AP than TM at 40-day cold storage.

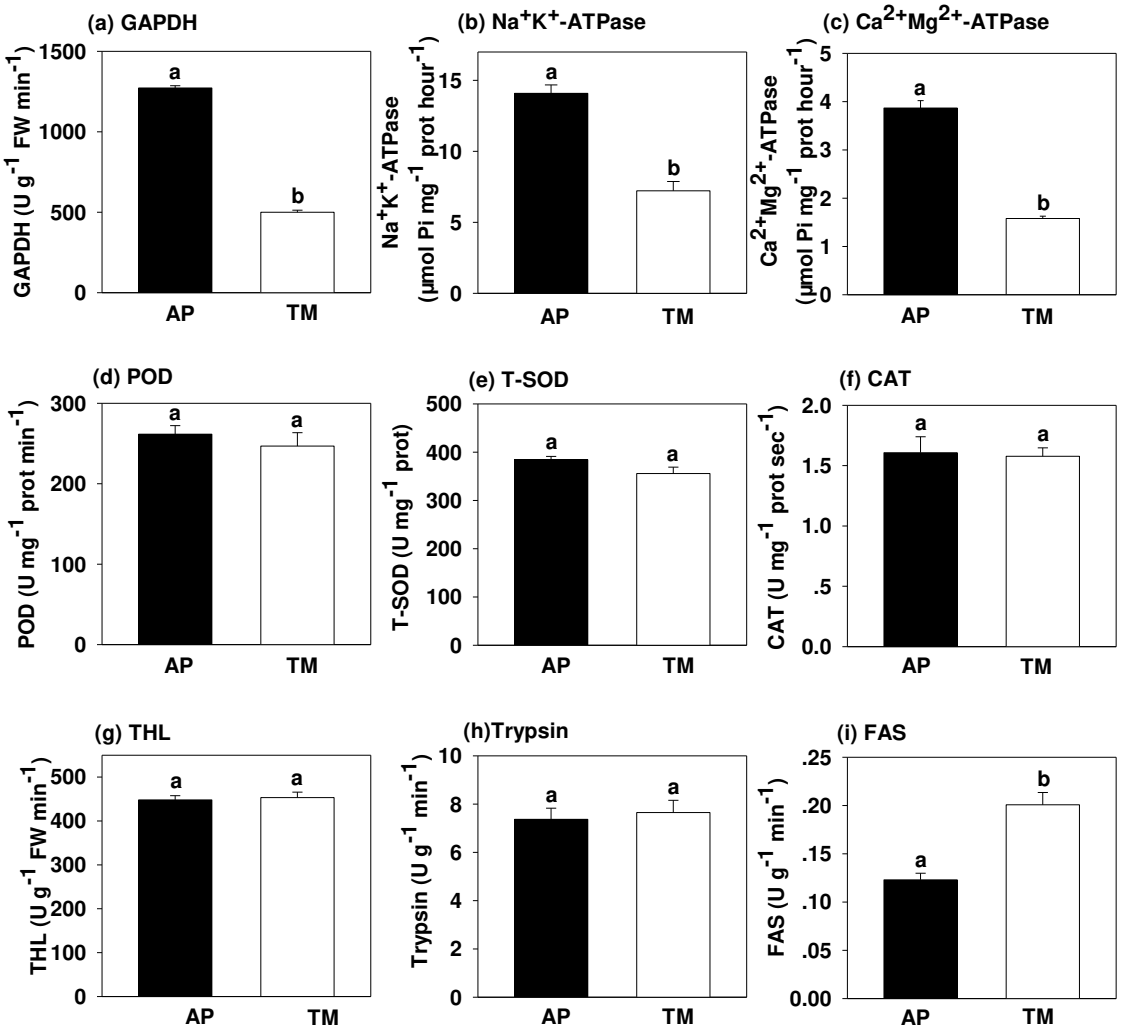

Figure 11. *Enzymatic activity of A. chinensis adult fed on Antherea pernyi (AP) and Tenebrio molitor (TM) after cold storage 30 days at 4 °C. (a) GAPDH; (b) Na^+K^+ATPase; (c) $Ca^{2+}Mg^{2+}$ATPase; (d) POD; (e) T-SOD; (f) CAT; (g) THL; (h) Trysin; (i) FAS. Different letters indicate significant differences between diet treatments at $P < 0.05$ level (T-test)*

http://www.aloki.hu ● ISSN 1589 1623 (Print) ● ISSN 1785 0037 (Online)
DOI: http://dx.doi.org/10.15666/aeer/1706_1532915347

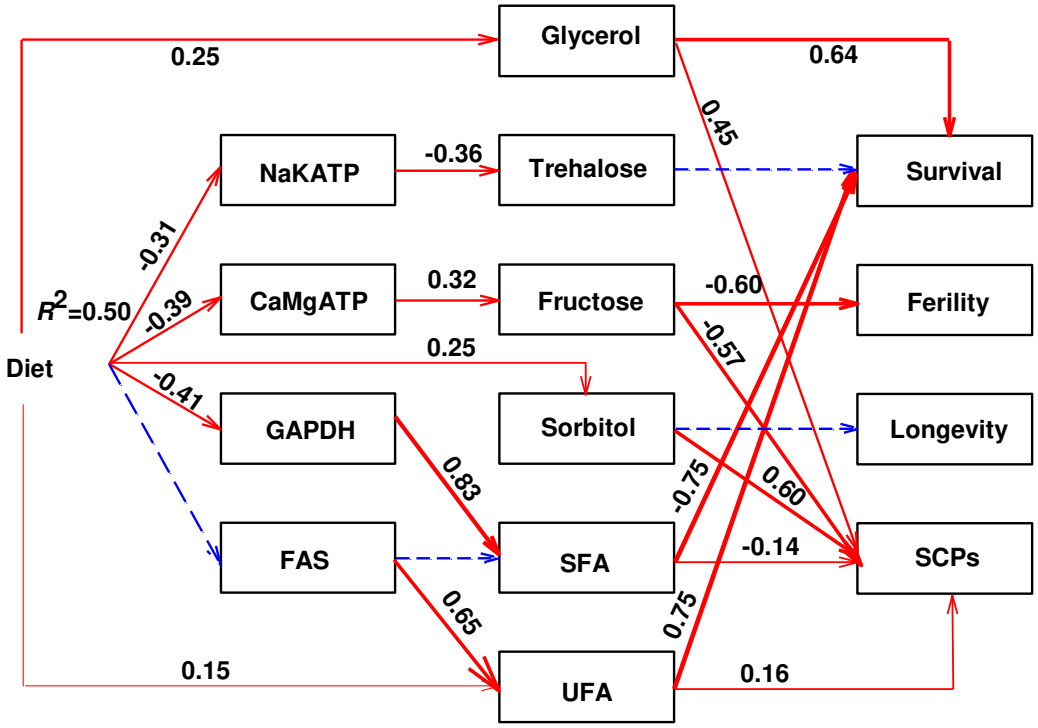

Figure 12. *Structural equation model showing the potential mechanism of diet effects on the cold tolerance of A. chinensis (χ^2 = 73.416; df = 72; P = 0.654; CFI = 1.000; RMSEA = 0.000). Arrow thickness represents the magnitude of the path coefficient, red solid line arrows represent significant paths (P < 0.05), and blue dotted lines represent non-significant paths. SFA: saturated fatty acid, UFA: unsaturated fatty acid, SCPs: super-cooling points*

The quality of food consumed prior to cold storage was an important endogenous factor affecting the cold storage tolerance of insects (Ayrinhac et al., 2004; Coudron et al., 2009; Li et al., 2014). The nutrient content of food not only influence the storage of energy-related substances (such as low-molecule-weight hydrocarbons, glycerol, and lipids, etc.) before cold storage (Liu et al., 2009; Mohammadzadeh and Izadi, 2018), but also the metabolic processes related to energy for insects during the cold storage (Han and Bauce, 1998; Naya et al., 2007; Teets and Denlinger, 2014). Those changes in the physiological and metabolic processes have been credited with cold tolerance in a polyphagous insect herbivore (Hunter and McNeil, 1997). In our research, the contents of proteins, fats, and carbohydrates in TM are higher than those in AP (*Table 1*). The different nutrients in food may influence the production and accumulation of low-molecular-weight cryoprotectants in insects under cold stress (Storey and Storey, 1991; Liu et al., 2007). The trehalose, glucose, mannitol, sorbitol and glycerol are proved to be cryoprotectants for many insects (Renault et al., 2006; Clark and Worland, 2008; Teets and Denlinger, 2013). Increased energy reserves, including glycogen, glycerol and total proteins were correlated with cold tolerance in Drosophila melanogaster (Chen and Walker, 1993). The SEM revealed that the content of glycerol and fructose directly contributed to the survival rate and the fertility of *A. chinensis*. In addition, diet influenced the survival rate and SCPs of *A. chinensis* indirectly through the content of glycerol and sorbitol (*Fig. 12*). The higher contents of trehalose, mannitol, sorbitol and

http://www.aloki.hu ● ISSN 1589 1623 (Print) ● ISSN 1785 0037 (Online)
DOI: http://dx.doi.org/10.15666/aeer/1706_1532915347

glycerol in *A. chinensis* adults from a colony reared on TM after cold storage may be one of the reason that greater cold tolerance of *A. chinensis* fed on TM.

There were no significant differences in the total amount of fatty acids in adults from colonies reared on either of the two diets and subsequently exposed to the cold storage treatment. However, the content of unsaturated fatty acid in adults from colonies reared on TM was higher by 39% than for AP. This difference, may account, in part, to the 20% lower super-cooling and freezing points of adults from colonies reared on TM and AP, and the SEM results showed that diet influenced SCPs of *A. chinensis* indirectly through the content of UFA (*Fig. 12*). Fatty acids are not only one of the substrates for synthesizing fats, but also one of the basic substances of cell membranes which are important for growth and fertility of insects (Chang and Vargas, 2007). More unsaturated fatty acids in the cell membrane of insects can accelerate the movement of energy substances such as glycerol, lipids and carbohydrates into the cells (Matsuo et al., 2019); and decrease the phase transition temperature of the cell membrane, which ensure that bio-membranes are stable at low temperatures to overcome adverse conditions (Kasamo et al., 1992; Worland, 2005). Therefore, the different contents of fatty acids in *A. chinensis* induced by the different diets may contribute to the survival effects manifested during cold storage, especially the content of unsaturated fatty acids that is positively related to the survival of *A. chinensis*, but the saturated fatty acids were negatively related to the survival of *A. chinensis* (*Fig. 12*). However, it remains to be determined if types and contents of fatty acids in insect are an adaptive advantage in surviving exposure to low temperatures.

When diets with high carbohydrates were fed to *Drosophila melanogaster*, the expression of multiple enzymes such as glucosidase used for glycolysis and fatty acid synthase for fatty acid synthesis increased significantly (Baker and Thummel, 2007; Matsuda et al., 2014), while the expression of many carbohydrases and lipases were repressed (Chng et al., 2014). Similarly, the contents of nutrients in the diet also impacted the activity of enzymes related to glycometabolism, fat metabolism, and vitellogenin formation in insects (Chang et al., 2010; Chng et al., 2016). In our research, the GAPDH (related to gluconeogenesis), Na^+K^+-ATPase and $Ca^{2+}Mg^{2+}$-ATPase enzymes (related to energy release and transmembrane transportation) and glycolytic-related enzymes (energy source) in adults from colonies reared on AP were higher than those for TM, but the FAS activity was lower (*Fig. 11*).

In order to explain the effect diet type on the biological and biochemical parameters of *A. chinensis*, and explore the adaptations of *A. chinensis* to cold storage, we develop a conceptual model of the metabolic enzymatic strategies of the *A. chinensis* pathways that diet influence cold storage tolerance of insects. The SEM revealed that the diet influenced the survival rate, the fertility and SCPs of *A. chinensis* indirectly through the activities of GAPDH, FAS and $Ca^{2+}Mg^{2+}$-ATPase (*Fig. 12*). Those metabolic enzymatic activity (GAPDH, FAS and $Ca^{2+}Mg^{2+}$-ATPase) were related to energy reserves, the higher content of glycerol and sorbitol directly contributed to SCPs, which induced the greater cold tolerance of *A. chinensis* reared on TM.

Conclusion

The present study demonstrated a dietary effect on the response of adult *A. chinensis* to cold temperatures. The content of glycerol, trehalose, sorbitol and fatty acids (unsaturated and saturated) in the adults were identified as possibly contributing to cold

http://www.aloki.hu ● ISSN 1589 1623 (Print) ● ISSN 1785 0037 (Online)
DOI: http://dx.doi.org/10.15666/aeer/1706_1532915347

tolerance and dietary content was shown as affecting the level of those substances in the adults, thus providing an explanation for the observed differences in responses to cold storage treatments. Those results suggest that the diet with higher content of carbohydrates and mineral in *T. moliter* (TM) could enhance the cold tolerance of *A. chinensis* by increasing energy reserves (glycerol, trehalose, sorbitol and unsaturated fatty acids) and decreasing super-cooling points. Our results are helpful for the selection of natural diet and the optimization of artificial diet for *A. chinensis* and other predatory insects. Using modern molecular biology technology such as nutrigenomics and metabonomics to analyze the influence of specific nutrients of diet on the synthesis and metabolism of cold resistant substances of insects, which would be beneficial to optimize the formula of insect artificial diet.

Acknowledgements. The project was financially supported by National Key R & D Program of China (2018YFC1200400) and the National Natural Science Foundation of China (31300552).

Conflict of interests. The authors declare that there is no conflict of interests.

REFERENCES

[1] Ayrinhac, A., Debat, V., Gibert, P., Legout, H., Moreteau, B., Vergilino, R., David, J. R. (2004): Cold adaptation in geographical populations of *Drosophila melanogaster*: Phenotypic plasticity is more important than genetic variability. – Functional Ecology 18: 700-706.

[2] Baker, K. D., Thummel, C. S. (2007): Diabetic larvae and obese flies - emerging studies of metabolism in Drosophila. – Cell Metabolism 6: 257-266.

[3] Chai, X. M., He, Z. H., Jiang, P. (2000): Studies on natural enemies of *Dendrolimus* punctatus in Zhejiang Province. – Journal of Zhejiang Forestry Science & Technology 20(4): 56-61 (in Chinese).

[4] Chang, C. L., Vargas, R. I. (2007): Wheat germ oil and its effects on a liquid larval rearing diet for oriental fruit flies (Diptera: Tephritidae). – Journal of Economic Entomology 100(2): 322-326.

[5] Chang, C. L., Coudron, T. A., Goodman, C., Stanley, D., An, S. H., Song, Q. S. (2010): Wheat germ oil in larval diet influences gene expression in adult oriental fruit fly. – Journal of Insect Physiology 56(4): 356-365.

[6] Chang, Y. F., Tauber, M. J., Tauber, C. A. (1995): Storage of the mass-produced predator *Chrysoperla carnea* (Neuroptera: Chrysopidae): Influence of photoperiod, temperature, and diet. – Environmental Entomology 24: 1365-1374.

[7] Chen, C. P., Walker, V. K. (1993): Increase in cold-shock tolerance by selection of cold resistant lines in *Drosophila melanogaster*. – Ecological Entomology 18(3): 184-190.

[8] Chen, J., Zhang, J. P., Zhang, J. H., Tian, Y. H., Chao, X. Z., Li. G. W. (2007): Study on functional response of *Arma chinensis* to the adults of *Monolepta hieroglyphica*. – Natural Enemies of Insects 29(4): 149-154 (in Chinese).

[9] Chng, W. B. A., BouSleiman, M. S., Schüpfer, F., Lemaitre, B. (2014): Transforming growth factor β/activin signaling functions as a sugar-sensing feedback loop to regulate digestive enzyme expression. – Cell Reports 9: 336-348.

[10] Chng, W. B. A., Hietakangas, V., Lemaitre, B. (2016): Physiological Adaptations to Sugar Intake: New Paradigms from Drosophila melanogaster. – Trends in Endocrinology and Metabolism 28(2): 131-142.

[11] Clark, M. S., Worland, M. R. (2008): How insects survive the cold: molecular mechanisms - a review. – Journal of Comparative Physiology B 178(8): 917-933.

http://www.aloki.hu ● ISSN 1589 1623 (Print) ● ISSN 1785 0037 (Online)
DOI: http://dx.doi.org/10.15666/aeer/1706_1532915347

[12] Colinet, H., Hance, T. (2010): Interspecific variation in the response to low temperature storage in different aphid parasitoids. – Annals of Applied Biology 156: 147-156.
[13] Colinet, H., Hance, T., Vernon, P. (2006): Water relations, fat reserves, survival, and longevity of a cold-exposed parasitic wasp *Aphidius colemani* (Hymenoptera: Aphidiinae). – Environmental Entomology 35(2): 228-236.
[14] Coudron, T. A., Ellersieck, M. R., Shelby, K. S. (2007): Influence of diet on long-term cold storage of the predator *Podisus maculiventris* (Say) (Heteroptera: Pentatomidae). – Biological Control 42: 186-195.
[15] Coudron, T. A., Popham, H. J. R., Ellersieck, M. R. (2009): Influence of diet on cold storage of the predator *Perillus bioculatus* (F.). – BioControl 54: 773-783.
[16] Ergin, E., Uckan, F. (2003): Temperature and food source effects on adult longevity of *Apanteles galleriae* Wilkinson (Hymenoptera: Braconidae). – Environmental Entomology 32(3): 441-446.
[17] Feng, Y., Wang, J., Zong, S. (2014): Review of Insects overwintering stages and cold-resistance strategies. – Chinese Agricultural Science Bulletin 30(9): 22-25 (in Chinese).
[18] Gołębiowski, M., Maliński, E., Boguś, M. I., Kumirska, J., Stepnowski, P. (2008): The cuticular fatty acids of *Calliphora vicina*, *Dendrolimus pini* and *Galleria mellonella* larvae and their role in resistance to fungal infection. – Insect Biochemistry and Molecular Biology 38: 619-627.
[19] Gotthard, K., Nylin, S. (1995): Adaptive plasticity and plasticity as an adaptation: a selective review of plasticity in animal morphology and life history. – Oikos 74: 3-17.
[20] Han, E., Bauce, E. (1998): Timing of diapause induction, metabolic changes and overwintering survival of the spruce budworm, *Choristoneura fumiferana*. – Ecological Entomology 23: 160-167.
[21] Hervant, F., Mathieu, J., Barre, H. (1999): Comparative study on the metabolic responses of subterranean and surface-dwelling amphipods to long-term starvation and subsequent refeeding. – Journal of Experimental Biology 202(24): 3587-3595.
[22] Heydari, M., Izadi, H. (2014): Effects of seasonal acclimation on cold tolerance and biochemical status of the carob moth, *Ectomyelois ceratoniae* (Zeller), last instar larvae. – Bulletin of Entomological Research 104(5): 592-600.
[23] Hodkova, M., Socha, R. (1995): Effect of temperature on photoperiodic response in a selected 'non-dapause' strain of *Pyrrhocoris apterus* (Heteroptera). – Physiological Entomology 20: 303-308.
[24] Hunter, M. D., Mcneil, J. N. (1997): Host-plant quality influences diapause and voltinism in a polyphagous insect herbivore. – Ecology 78: 977-986.
[25] Jehrke, L., Stewart, F. A., Droste, A., Beller, M. (2018): The impact of genome variation and diet on the metabolic phenotype and microbiome composition of Drosophila melanogaster. – Scientific Reports 8: 6215.
[26] Jiang, X. J., Chen, T. H., Huang, Y., Luo, J. (2016): Analysis and evaluation of nutritional component of *Galleria mellonella*. – Guangxi Forestry Science 45(4): 452-454 (in Chinese).
[27] Kasamo, K., Kagita, F., Yamanishi, H., Sakaki, T. (1992): Low temperature-Induced changes in the thermotropic properties and fatty acid composition of the plasma membrane and tonoplast of cultured rice (*Oryza sativa* L.) Cells. – Plant and Cell Physiology 33: 609-616.
[28] Koštál, V., Korbelová, J., Poupardin, R., Moos, M., Šimek, P. (2016): Arginine and proline applied as food additives stimulate high freeze tolerance in larvae of Drosophila melanogaster. – The Journal of Experimental Biology 219(15): 2358-2367.
[29] Leather, S. R. (1984): Factors affecting pupal survival and eclosion in the pine beauty moth, *Panolis flammea* (D&S). – Oecologia 63(1): 75-79.
[30] Leopold, R. A. (2007): Colony Maintenance and Mass-Rearing: Using Cold Storage Technology for Extending the Shelf-Life of Insects. – In: Vreysen, M. J. B., Robinson, A.

http://www.aloki.hu ● ISSN 1589 1623 (Print) ● ISSN 1785 0037 (Online)
DOI: http://dx.doi.org/10.15666/aeer/1706_1532915347

S., Hendrichs, J. (eds.) Area-Wide Control of Insect Pests: From Research to Field Implementation. Springer, Heidelberg, pp. 149-162.

[31] Li, J. J., Zhang, C. H., Yi, Z. J., Ran, X. C., Zhang, L. S., Liu, C. X., Wang, M. Q., Chen, H. Y. (2016): Effects of three prey species on development and fecundity of the predaceous Stinkbug *Arma chinensis* (Hemiptera: Pentatomidae). – Chinese Journal of Biological Control 32(5): 553-561 (in Chinese).

[32] Li, X. P., Song, L. W., Chen, Y. Q., Li, Y. N., Zuo, T. T., Wu, S. A. (2018): Influence of different fatty acids in artificial diets on growth, development and fecundity of *Arma chinensis*. – Scientia Silvae Sinicae 54(6): 85-93 (in Chinese).

[33] Li, Y. Y., Zhang, L. S., Zhang, Q. R., Chen, H. Y., Denlinger, D. L. (2014): Host diapause status and host diets augmented with cryoprotectants enhance cold hardiness in the parasitoid Nasonia vitripennis. – Journal of Insect Physiology 70: 8-14.

[34] Liu, Z. D., Gong, P. Y., Wu, K. J., Wei, W., Sun, J. H., Li, D. M. (2007): Effects of larval host plants on over-wintering preparedness and survival of the cotton bollworm, *Helicoverpa armigera* (Hübner) (lepidoptera: noctuidae). – Journal of Insect Physiology 53: 1016-1026.

[35] Liu, Z. D., Gong, P. Y., Heckel, D. G., Wei, W., Sun, J. H., Li, D. M. (2009): Effects of larval host plants on over-wintering physiological dynamics and survival of the cotton bollworm, *Helicoverpa armigera* (Hübner) (Lepidoptera: Noctuidae). – Journal of Insect Physiology 55: 1-9.

[36] Matsuda, H., Yamada, T., Yoshida, M., Nishimura, T. (2015): Flies without trehalose. – Journal of Biological Chemistry 290: 1244-1255.

[37] Matsuo, N., Nagao, K., Suito, T., Juni, N., Kato, U., Hara, Y., Umeda, M. (2019): Different mechanisms for selective transport of fatty acids using a single class of lipoprotein in Drosophila. – Journal of Lipid Research 60(7): 1199-1211.

[38] Mohammadzadeh, M., Izadi, H. (2016): Enzyme activity, cold hardiness, and supercooling point in developmental stages of *Acrosternum arabicum* (Hemiptera: Pentatomidae). – Journal of Insect Science 16: 1-6.

[39] Mohammadzadeh, M., Izadi, H. (2018): Different diets affecting biology, physiology and cold tolerance of *Trogoderma granarium* (Everts) (Coleoptera: Dermestidae). – Journal of Stored Products Research 76: 58-65.

[40] Naya, D. E., Lardies, M. A., Bozinovic, F. (2007): The effect of diet quality on physiological and life-history traits in the harvestman *Pachylus paessleri*. – Journal of Insect Physiology 53: 132-138.

[41] Pentzold, S., Zagrobelny, M., Rook, F., Bak, S. (2014): How insects overcome two-component plant chemical defence: plant β-glucosidases as the main target for herbivore adaptation. – Biological Reviews 89(3): 531-551.

[42] Renault, D., Hance, T., Vannier, G., Vernon, P. (2003): Is body size an influential parameter in determining the duration of survival at low temperatures in *Alphitobius diaperinus* (Panzer) (Coleoptera: Tenebrionidae). – Journal of Zoology 259: 381-388.

[43] Renault, D., Bouchereau, A., Delettre, Y. R., Hervant, F., Vernon, P. (2006): Changes in free amino acids in *Alphitobius diaperinus* (Coleoptera: Tenebrionidae) during thermal and food stress. – Comparative Biochemistry and Physiology-Part A: Molecular & Integrative Physiology 143(3): 279-285.

[44] Rivers, D. B., Lee, R. E. L., Denlinger, D. L. (2000): Cold hardiness of the fly pupal parasitoid Nasonia vitripennis is enhanced by its host Sarcophaga crassipalpis. – Journal of Insect Physiology 46: 99-106.

[45] Ruberson, J. R., Kring, T. J., Elkassabany, N. (1998): Overwintering and the Diapause Syndrome of Predatory Heteropter. – In: Coll, M., Ruberson, J. R. (eds.) Proceedings, Symposium: Predatory Heteroptera: Their Ecology and Use in Biological Control. Annual Meeting of the Entomological Society of America, Indianapolis, IN, 1993. Thomas Say Publications in Entomology. Entomological Society of America, Lanham, MD, pp. 49-69.

http://www.aloki.hu ● ISSN 1589 1623 (Print) ● ISSN 1785 0037 (Online)
DOI: http://dx.doi.org/10.15666/aeer/1706_1532915347

[46] Song, L. W., Tao, W. Q., Ling, L., Li, X. P., Chen, Y. Q. (2010): Influence of host plants and rearing density on growth, development and fecundity of *Arma chinensis*. – Scientia Silvae Sinicae 46: 105-110 (in Chinese).
[47] Storey, K. B., Storey, J. M. (1991): Biochemistry of Cryoprotectants. – In: Lee, R. E., Denlinger, D. L. (eds.) Insects at Low Temperature. Chapman and Hall, New York, pp. 64-93.
[48] Teets, N. M., Denlinger, D. L. (2013): Physiological mechanisms of seasonal and rapid cold-hardening in insects. – Physiological Entomology 38(2): 105-116.
[49] Teets, N. M., Denlinger, D. L. (2014): Surviving in a frozen desert: environmental stress physiology of terrestrial Antarctic arthropods. – Journal of Experimental Biology 217(1): 84-93.
[50] Thorpe, K. W., Aldrich, J. R. (2004): Conditions for short-term storage of field-collected spined soldier bug, *Podisus maculiventris* (Say) (Heteroptera: Pentatomidae), adults prior to augmentative release. – Journal of Entomological Science 39: 483-489.
[51] Tzanakakis, M. E., Veenendaal, R. L., Veerman, A. (1992): Effects of photoperiod and temperature on the termination of diapause in the univoltine seed wasp Eurytoma plotnikovi. – Physiological Entomology 17: 176-182.
[52] Wang, J., Guo, G. Q., Zhang, R. R., Dai, L. L., Chen, H. (2017): Metabolism and cold tolerance of Chinese white pine beetle *Dendroctonus armandi* (Coleoptera: Curculionidae: Scolytinae) during the overwintering period. – Agriculture and Forest Entomology 19(1): 10-22.
[53] Wang, W., Qin, L., Yan, J. H., Zhi, K., Lin, Z. Q., Zhang, X. H., Yang, Q. M., Wang, J., Ma, J., Sun, Y. L. (2012): Preliminary observation of preyed ability of *Arma chinensis* (Fallou), a new natural enemy of *Hyphantria cunea* (Drury). – Journal of Shandong Forestry Science and Technology 42(1): 11-14 (in Chinese).
[54] Worland, M. R. (2005): Factors that influence freezing in the sub-Antarctic springtail *Tullbergia antarctica*. – Journal of Insect Physiology 51: 881-894.
[55] Zou, D. Y., Wang, M. Q., Zhang, L. S., Zhang, Y., Zhang, X. J., Chen, H. Y. (2012): Taxonomic and bionomic notes on *Arma chinensis* (Fallou) (Hemiptera: Pentatomidae: Asopinae). – Zootaxa 3382: 41-52.
[56] Zou, D. Y., Coudron, T. A., Wu, H. H., Gu, X. S., Xu, W. H., Zhang, L. S., Chen, H. Y. (2015): Performance and cost comparisons for continuous rearing of *Arma chinensis* (Hemiptera: Pentatomidae: Asopinae) on a zoophytogenous artificial diet and a secondary prey. – Journal of Economic Entomology 108: 454-461.

http://www.aloki.hu ● ISSN 1589 1623 (Print) ● ISSN 1785 0037 (Online)
DOI: http://dx.doi.org/10.15666/aeer/1706_1532915347

DETERMINATION OF PHYTOCHEMICALS, ANTIOXIDANT ACTIVITY AND BIOCHEMICAL COMPOSITION OF CHINESE MUGWORT (*ARTEMISIA ARGYI* L.) LEAF EXTRACT FROM NORTHEAST CHINA

AHMED, M.[1] – JI, M.[1*] – QIN, P.[1] – GU, Z.[1] – LIU, Y.[1] – SIKANDAR, A.[1] – IQBAL, M. F.[2] – JAVEED, A.[2] – SHAFI, J.[3] – DU, Y.[1]

[1]*College of Plant Protection, Shenyang Agricultural University*
No. 120 Dongling Road, Shenyang, 110866 Liaoning, China

[2]*College of Biosciences and Biotechnology, Shenyang Agricultural University*
No. 120 Dongling Road, Shenyang, 110866 Liaoning, China

[3]*Department of Plant Pathology, University of Agriculture, 38040 Faisalabad, Pakistan*

[*]*Corresponding author*
e-mail: jimingshan@163.com; phone: +86-24-8848-7148; fax: +86-24-8834-2315

(Received 8th Jul 2019; accepted 15th Nov 2019)

Abstract. Present study aimed to investigate phytoconstituents, total phenolic and flavonoids content, antioxidant activity and biochemical composition of the leaf extract of *Artemisia argyi* L. Qualitative analysis was conducted using standard methods however, total phenolic, flavonoids content and antioxidant activity was assessed by Folin-Ciocalteu, aluminium chloride colourimetric method and 1, 1-Diphenyl-2-picrylhydrazyl (DPPH) assay, respectively. Compositional analysis was carried out by Gas chromatography-mass spectrometry (GC-MS). The outcome of the qualitative analysis suggested the presence of flavonoids, phenols, terpenoids, steroids, saponins, tannins and flavones except for alkaloids and glycosides. However, total phenols recorded were 16.89, 7.45 and 3.63 mg gallic acid equivalent GAE/g; flavonoids 20.80, 7.13 and 2.42 mg quercetin equivalent QE/g and DPPH inhibition percent was 81.48, 65.62 and 57.78% from 1st, 2nd and 3rd extraction, respectively. GC-MS analysis exposed the existence of ten biological compounds corresponding to 99.91% of the total extract. However, erucylamide (33.42%), 1-decene, 4-methyl- (12.63%), *myo*-Inositol, (10.42%), α-Cadinol (9.13%) and 2-pyrrolidinone (8.68%) were the major compounds with five minor compounds. It was concluded that the leaves of *A. argyi* contain biological constituents responsible for antioxidant properties which can be introduced as a natural antioxidant pharmacologically and as botanical alternative of synthetic chemicals. However further studies are required on identification of specific components responsible for such activities.
Keywords: *Chemical analysis, Artemisia argyi, total phenols, total flavonoids, DPPH, GC-MS*

Introduction

Free radicals are highly reactive species that can be produced either endogenously in the body or exogenously through ingestion of pollutants or chemicals. These free radicals are beneficial in the process of signaling, regulation of molecules and destruction of bacteria and viruses at physiological levels. However, excessiveness of free radicals in the body causes oxidative stress that negatively amend the cell structures by interacting with DNA, proteins and lipids, may ultimately lead to certain diseases like cancer, atherosclerosis, Parkinson's, stroke, diabetes, rheumatoid arthritis and senile dementia hence, antioxidants perform their function as reducing agents for neutralization of these free radicals (Fang et al., 2002; Lobo et al., 2010; Liu et al., 2011; Wong et al., 2012). Moreover, secondary metabolites, phenolic and flavonoids

http://www.aloki.hu ● ISSN 1589 1623 (Print) ●ISSN1785 0037 (Online)
DOI: http://dx.doi.org/10.15666/aeer/1706_1534915362

content are beneficial for human health as well as animals and their usefulness is linked to their antioxidant properties (Meot-Duros and Magne, 2009). However, richness of phytoconstituents in plants food which are non-nutritive agents that protect from disease exploitation and interplays with nutrients, dietary material and also contain several properties like antioxidants, anti-microbial and physiological activities (Adesuyi et al., 2012).

Extensive studies have been conducted on antioxidants as preventative or illness curative associated with oxidative stress. They are also used in the food stuff business to protect from food deterioration, and skin aging in the cosmetic industry. Antioxidants also obstruct with the oxidation process because of their activity as scavenging free radicals (Büyükokuroğlu et al., 2001). Although, synthetically prepared antioxidants, such as *tert*-butyl hydroxytoluene (BHT), *tert*-butyl hydroxyanisole (BHA) and antibacterial peptides are available for therapeutic and food industry but, they are carcinogenic so, interest in searching for natural antioxidants from natural resources is increasing gradually (Ling et al., 2011). Natural compounds may have great commercial value in the food industry, but their use is limited due to their high cost. Hence, an effective and cost effective preparation of natural antioxidant is the need of time. The selection of an appropriate extraction method for natural antioxidants concerning extraction effectiveness and economic feasibility aspects to non-conventional extraction methods. Solvent extraction is helpful because of ease to conduct, take less time for extraction as well as higher extraction yields to recuperate maximum antioxidant compounds from medicinal plants (Xu et al., 2017).

Artemisia belongs to family Asteraceae is largest and widely found genus throughout the world, is important from medicinal view point and have got increased attention due to phytochemical activities, chemical and biological diversification (Tan et al., 1998). *Artemisia* species are well known in Chinese traditional herbal medicines and commonly used in the treatments of cancer, inflammation, hepatitis, menstrual disorders, malaria, metabolism disorders, circulatory system and some infectious diseases caused by viruses, bacteria and fungi (Reynold, 1996; Lis-Balchin and Deans, 1997; Adams et al., 2012; Zhang et al., 2014). It comprises of or more than 500 species (Abad et al., 2012) among which, *A. argyi* is a prevailing species, mostly found in North America, Asia and Europe (Bora and Sharma, 2011). Historically, *A. argyi* was first recorded in the Liang Dynasty in ‘‘Ming Yi Bie Lu’’(Zhou et al., 2000) however, the true region is considered to be Hubei Province in Qizhou County (Li, 2002). Several compounds were reported containing anti-inflammatory properties from *A. argyi* (Choi et al., 2013; Jeong et al., 2014; Zeng et al., 2014; Park et al., 2015). Essential oil extracted from this plant contains antioxidant properties, anti-melanogenic and insecticidal behavior (Lee and Vairappan, 2011; Huang et al., 2012; Zhang et al., 2014). It is also an imperative plant for nutritional concerns contain essential amino acids, vitamin C, polyunsaturated fatty acids, phenolic contents and possess good DPPH scavenging activity (Kim et al., 2015).

Several protocols have been used for the analysis of chemical compounds among which Gas chromatography-mass spectrometry (GC-MS) is a useful methodology to find out different biological compounds. However, biochemical composition of *A. argyi* oil from flowers and leaves possess major components such as sesquiterpenes, monoterpenes, ketones, alcohols, aromatic components and ethers, etc. (Hu et al., 2013). Moreover, due to its aromatic properties, essential oil of *A. argyi* could play a prominent function in food preservation and safety (Wang et al., 2006).

http://www.aloki.hu ● ISSN 1589 1623 (Print) ●ISSN1785 0037 (Online)
DOI: http://dx.doi.org/10.15666/aeer/1706_1534915362

Although, some studies have been conducted on *A. argyi* but data on quantitative analysis, antioxidant activity and biologically active compounds of *A. argyi* is not well described. Therefore, the present research work was planned to evaluate phytochemicals, total phenolic contents, flavonoids content, antioxidant potential and investigations on biochemical compounds by GC-MS analysis from crude solvent extract of *A. argyi* for their appliances as a purposeful food and antioxidants source. The study was conducted at the Biopesticides lab at Shenyang Agricultural University Shenyang, Liaoning China during the year 2019.

Materials and methods

Collection and plant materials preparation

As aerial parts of the plants tend to have more interesting compounds and most of the photosynthesis/ respiration take place in the aerial parts. Also, most of the secondary metabolites from plants can be produced in leaves. Thus, young leaves of one month old plants were collected from surrounding locations of Shenyang Agricultural University Shenyang, Liaoning China in April 2019 (*Fig. 1a and 1b*).

a b

Figure 1 a and b. *Photographic views of A. argyi plant*

Ten samples of the same species were collected and mixed together and were washed out beneath tap water to remove impurities and allowed to dry under shade at room temperature. Then, dried leaves were ground to fine powder by electric blender and subjected to successive extraction three times for 72 h using methanol as solvent (6 ml/g) of plant sample. Contents were filtered and concentrated on rotary evaporator (Buchi Switzerland R-210) to remove solvent from extract. Extract yield was calculated using following *Equation 1* and stored at 4°C for further use.

http://www.aloki.hu ● ISSN 1589 1623 (Print) ●ISSN1785 0037 (Online)
DOI: http://dx.doi.org/10.15666/aeer/1706_1534915362

$$Extract\ yield\ (\%) = \frac{Weight\ of extract\ (g)}{Weight\ of\ the\ sample} \times 100 \qquad \text{(Eq.1)}$$

Qualitative phytochemical screening

Methanolic extract of *A. argyi* leaves was subjected to screening tests for the investigation of phytoconstituents using standard methods.

Test for alkaloids

Half ml of extract solution was permitted to dry in test tubes and in the consequent reside, 2 ml of 2% hydrochloric acid (HCl) was added and positioned in water bath at 100°C for 15 min. Then, the mixture was filtered on cooling and divided equally into two portions. Addition of few drops of Mayer's reagent into one portion and Dragendoff's to the other portion resulted in turbidity or yellow precipitate confirm alkaloids (Siddiqui and Ali, 1997).

Test for glycosides

Into 2 ml of extract solution, ferric chloride ($FeCl_3$) 5% and 2 ml distilled water was added and resultant mixture was placed on water bath for 15 min and then on cooling 1 ml of benzene was added, shacked and allowed to settle for 1 min. Next, addition of few drops of concentrated ammonia (NH_3) resulted in appearance of pink or red color which confirm glycosides (Siddiqui et al., 2009).

Test for terpenoids and steroids

Briefly, dried extract 0.5 g was added in to 2 ml of trichloromethane, shacked to dissolve the extract, filtered and placed on ice; following that 2 ml of glacial acetic acid was added. Next, addition of few drops of concentrated sulfuric acid (H_2SO_4) resulted in emergence of a pink or pinkish brown and, or blue/bluish green color indicate terpenoids and steroids respectively (Siddiqui and Ali, 1997).

Test for flavonoids and flavones

Into 3 ml extract solution 2 ml of diluted sodium hydroxide (NaOH) was added resulting in yellow colored solution. Solution become colorless on addition of 1 ml of 5 N hydrochloric acid (HCl) which is the indication of flavonoids however, the appearance of orange color confirms flavones (Sofowora, 1993; Siddiqui et al., 2009).

Test for tannins

To estimate tannins, 1 ml distilled water and few drops of ferric chloride ($FeCl_3$) were added to 0.5 ml extract. From the resulting mixture gallic tannins were confirmed by the appearance of blue color and catecholic tannin by green/black color (Iyengar, 1995).

Test for phenols

For the detection of phenols, 0.5 g of extract was added into distilled water and shacked until dissolve and then, 3 ml of 10% lead acetate ($Pb(C_2H_3O_2)_2$ was added to

http://www.aloki.hu ● ISSN 1589 1623 (Print) ●ISSN1785 0037 (Online)
DOI: http://dx.doi.org/10.15666/aeer/1706_1534915362

the solution resulted in appearance of white precipitation confirms phenols (Trease et al., 2003).

Test for saponins

To confirm saponins, addition of 1 g of extract into 20 ml of distilled water then, shacked strongly resulting in appearance of a foam layer confirms saponins (Siddiqui and Ali, 1997).

Quantitative phytochemical screening

Total phenolic content (TPC)

Folin-Ciocalteu reagent assay was employed for assessing the total phenolic stuffing in *A. argyi* leaves extract. Briefly, mixed 2.5 ml of 10% Folin-Ciocalteu reagent into 1 ml plant extract equivalent to (1 $mgml^{-1}$ of methanol) followed by addition of 2 ml of 2% sodium carbonate (Na_2CO_3). Then, incubation of substantial mixture was carried out for 15 min in the absence of light at 28°C. The mixture's absorbance was determined in ELISA 96-well plate at 765 nm using an absorbance microplate reader (SpectraMax 190, manufactured in China; designed in USA). Gallic acid (1 $mgml^{-1}$) was used with different concentrations (1, 0.50, 0.25, 0.10, 0.05, 0.02, 0.01 and 0 $mgml^{-1}$) for standard calibration curve construction and is shown as GAE (gallic acid equivalent) mgg^{-1} of extract (Aiyegoro and Okoh, 2010). Experiment was replicated three times.

Total flavonoid contents (TFC)

Total flavonoids contents in the *A. argyi* leaves extract were determined through aluminium chloride colourimetric method. Briefly, 1 ml of extract equivalent to (1 $mgml^{-1}$ of methanol) was added in to 3 ml methanol, 0.2 ml 1 M potassium acetate (CH_3COOK), 0.2 ml 10% aluminium chloride ($AlCl_3$) and distilled water 5.6 ml. Then, incubated the resulting mixture for half an hour at 28°C in the dark. After that, absorbance was calculated in ELISA 96-well plates at 420 nm on absorbance microplate reader (SpectraMax 190, manufactured in China; designed in USA). Quercetin was used as the standard (1 $mgml^{-1}$) to obtain standard curve at different concentrations (1, 0.50, 0.25, 0.10, 0.05, 0.02, 0.01 and 0 $mgml^{-1}$). Results were expressed as quercetin equivalent (QE) mgg^{-1} of extract (Aiyegoro and Okoh, 2010). Experiment was replicated three times.

DPPH radical scavenging activity

The antioxidant properties of the extract of *A. argyi* was measured with stable 1,1-diphenyl-2-picrylhydrazyl 'DPPH' (Yu et al., 2003). In brief, extract solution 0.5 ml ($1mgml^{-1}$) was added to 3.5 ml of freshly made solution of DPPH (0.002 g 50 ml^{-1} methanol) and incubated for half an hour in the dark at room temperature to measure absorbance in ELISA 96-wellplates at 517 nm on absorbance microplate reader (SpectraMax 190, manufactured in China; designed in USA). The inhibition percent of DPPH was calculated from the decrease of absorbance by using *Equation* 2. A lower absorbance value represents elevated scavenging activity of free radical. (Zhao et al., 2008).

$$Inhibition(\%) = \frac{A_{blank} - A_{sample}}{A_{blank}} \times 100 \qquad \text{(Eq.2)}$$

http://www.aloki.hu ● ISSN 1589 1623 (Print) ●ISSN1785 0037 (Online)
DOI: http://dx.doi.org/10.15666/aeer/1706_1534915362

whereas; A_{blank}=(absorbance of control); A_{sample}=(absorbance of samples).

Biochemical analysis by Gas chromatography-mass spectrophotometry (GC-MS)

Gas chromatography-mass spectrophotometry analysis of crude extract of *A. argyi* leaves was assessed by using (Agilent 6890-5973N USA), and gas chromatograph (GC) which was equipped with capillary column HP1 model number (TG-5MS) polydimethylsiloxane (30 m × 250 µm × 0.25 µm) interfaced with Hewlett Packard mass selective detector 5973. Gas chromatographic parameters were;

- Temperature fixed for 2 min at 110°C primarily and finally raised to 200 and 280°C with increase rate of 10°C/min and 5°C/min, respectively.
- Inlet temperature was 250°C and 10:1 split ratio.
- MS temperature 230°C.
- MS Quadruple temperature 150°C.
- Thermal Aux temperature 285°C.
- Ionization current 60 µA.
- MS Scan ranges 40-450 units.
- Ionization energy 70 eV and Helium was selected as carrier gas with flow rate: 1.0 ml/min.

Compounds were recognized by elucidation on gas chromatography mass spectrum by literature data or database at Wiley/NIST.98.1 (Joulain and König, 1998; Sparkman, 2005). The comparative yield of each compound was assessed which was based on raw data areas of gas chromatography (GC) with no response factor correction of FID.

Statistical analysis

Recorded data for total phenols, flavonoids and DPPH inhibition (%) was analyzed through ANOVA (one-way analysis of variance) and mean values were calculated for significance test by Tukey's HSD at P=0.05 level. All statistical processes were administered by different statistical packages with IBM-SPSS statistics 25.0 version.

Results

Extract yield (%)

Extraction from natural plants material is depends upon polarity based solvents and type of the material used. Methanol is a high polarity solvent which is considered as the solvent of choice for higher extract yield, phenolic and flavonoids content. So, for extraction purposes in the current experiment, methanol was selected as solvent. However, according to our findings methanol produced prominent yield in each successive extraction which was 9.91, 2.58 and 1.45% for 1st, 2nd and 3rd extraction, respectively (*Fig. 2*).

Qualitative phytochemical screening

Preliminary evaluation tests are helpful in bioactive component determination which consequently leads towards discovery and development of drugs and also for agricultural prospects. Tests were conducted for screening of phytochemical like alkaloids, glycosides, terpenoids, flavonoids, flavones, steroids, tannins, phenols and

http://www.aloki.hu ● ISSN 1589 1623 (Print) ●ISSN1785 0037 (Online)
DOI: http://dx.doi.org/10.15666/aeer/1706_1534915362

saponins from *A. argyi* leaves. These screening tests led to the identification of bioactive compounds which are important form pharmacological and agricultural point of view. However, the confirmation of a bioactive compound during screening tests was referred as presence (+) and absence (-). Terpenoids were confirmed by pink or pinkish brown color of the solution. Flavonoids and flavones were observed by the conversion of the reaction mixture from yellow to colorless for flavonoids and orange for flavones. Appearance of a blue and green/black color confirms gallic tannin and catecholic tannin respectively. Phenols were confirmed by the appearance of blue or green color in the reaction mixture while, foaming character in extract solution confirms saponins. Phytochemical tests confirmed the existence of tannins, terpenoids, flavonoids, steroids, flavones, phenols and saponins except for alkaloids and glycosides from crude extract of *A. argyi* leaves (*Table 1*).

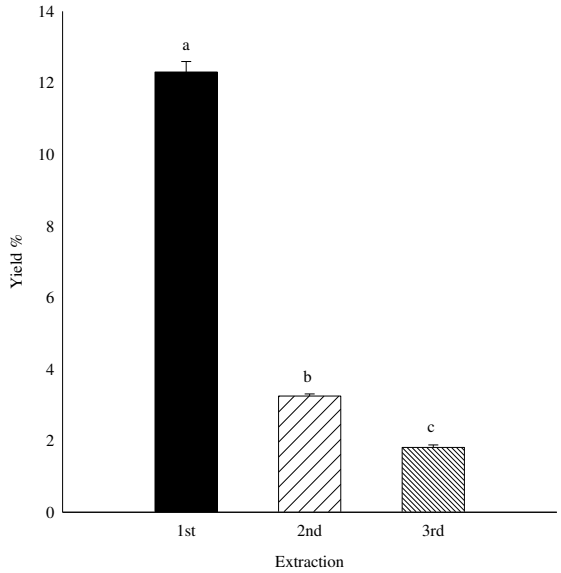

Figure 2. *Extract yield produced by methanol by three successive extractions. Values are offered as mean ± standard error. Same superscripts on the bars designate that values for mean are not significantly different referred to Tukey's HSD test (P > 0.05).*

Table 1. *Qualitative phytochemical screening of A. argyi leaf extract*

Phytochemical constituents	Extraction		
	1st	2nd	3rd
Alkaloids	--	--	--
G. Tannins	+	+	+
C. tannins	+	+	+
Steroids	+	+	+
Glycosides	--	--	--
Terpenoids	+	+	+
Flavonoids	+	+	+
Flavones	+	+	+
Phenols	+	+	+
Saponins	+	+	+

Whereas; + presence, -- absence

http://www.aloki.hu ● ISSN 1589 1623 (Print) ●ISSN1785 0037 (Online)
DOI: http://dx.doi.org/10.15666/aeer/1706_1534915362

Quantitative phytochemical evaluation of total phenolic and flavonoids contents

The total phenolic content and flavonoid content for three successive extractions are presented in *Table 2*. Obtained results demonstrated that phenolic content in total were 16.89, 7.45 and 3.63 mg gallic acid equivalent GAE/g for 1st, 2nd and 3rd extraction respectively while, total flavonoids for 1st, 2nd and 3rd extraction were 20.80, 7.13 and 2.42 mg quercetin equivalent QE/g, respectively. Results also revealed that extract afforded phenol and flavonoids in each extraction however, their quantity decreased gradually for each consequential extraction.

DPPH radical scavenging activity

1,1-Diphenyl-2-picrylhydrazyl (DPPH) is a constant and stable free radical that can easily dissolved in methanol. It showed prominent color absorption on spectrophotometer at 517 nm. The free radical antioxidant molecules were scavenged through contribution of hydrogen molecules and thus the DPPH assay solution's color changed to light yellow resulted in reduction of absorbance. Data obtained by the 1,1-Diphenyl-2-picrylhydrazyl of free radical scavenging commotion is given in *Table 2*. Results showed that inhibition recorded was 81.48, 65.62 and 57.78% for 1st, 2nd and 3rd extraction respectively which clearly demonstrate that inhibition percent did not more influenced by successive extraction from the same sample.

Table 2. *Total phenolic content (TPC), Total flavonoids contents (TFC) and DPPH inhibition percent of A. argyi leaf extract*

Solvent extract	Extraction	Total phenolic content mg (GAE/g)	Total flavonoid content mg (QE/g)	DPPH Inhibition (%)
Methanol	1st	16.89±0.07[a]	20.80±0.18[a]	81.48±0.41[a]
	2nd	7.45±0.09[b]	7.13±0.08[b]	65.62±0.24[b]
	3rd	3.63±0.11[c]	2.42±0.07[c]	57.78±1.00[c]
Statistics Summary		*F*=5137.75, *P*= 0.000, DF=2	*F*=6122.23, *P*= 0.000, DF=2	*F*=144.34, *P*= 0.000, DF=2

Values are presented as the mean ± standard error. Same letters within a column specify that mean values are not significantly different according to Tukey's HSD at ($P > 0.05$)

Biochemical analysis

GC-MS analysis was performed to find out the occurrence of biochemical components in the crude extract of *A. argyi* leaves. Active compounds with their peak area (%) along with their molecular formula (M.F), molecular weight (M.W) and retention time (R.T) are presented in *Table 3*.

Table 3. *Biochemical composition of A. argyi leaf extract*

Peak #	R.T	Area%	Compounds	M.F	M.W (g/Mol)
1	3.485	8.68	2-Pyrrolidinone	C_4H_7NO	85.11
2	9.016	4.39	3-Ethylthiolane	$C_6H_{12}S$	116.22
3	10.210	12.65	1-Decene, 4-methyl-	$C_{11}H_{22}$	154.29
4	10.519	9.13	α-Cadinol	$C_{15}H_{26}O$	222.37
5	10.714	10.42	Myo-Inositol, 2-C-methyl-	$C_7H_{14}O_6$	194.18
6	16.449	5.31	Phenylephrine	$C_9H_{13}NO_2$	167.21
7	16.791	6.04	3-Chloro-N,N-diethyl-4 nitroanilin	$C_{10}H_{13}ClN_2O_2$	228.67

http://www.aloki.hu ● ISSN 1589 1623 (Print) ●ISSN1785 0037 (Online)
DOI: http://dx.doi.org/10.15666/aeer/1706_1534915362

8	22.902	6.60	Demecolcine	$C_{21}H_{25}NO_5$	371.43
9	23.335	3.27	2-Ethylacridine	$C_{15}H_{13}N$	207.27
10	25.727	33.42	Erucylamide	$C_{22}H_{43}NO$	337.58

R.T (retention time); M.F (Molecular formula); M.W (Molecular Weight)

The analysis of compounds from GC-MS, resulted in the detection of several biologically active compounds from methanol extract. Results showed the presence of ten biochemical components corresponding to 99.91% of total extract. Among the identified compounds erucylamide (33.42%), 1-decene, 4-methyl- (12.65%), *myo*-Inositol, 2-C-methyl- (10.42%), α-Cadinol (9.13%) and 2-pyrrolidinone (8.68%) were the main compounds while, other five compounds were considered as minor compounds because of their low abundance from 3.27-6.60%. The GC-MS chromatogram showing different peaks of major and minor compounds is presented in *Fig. 3*.

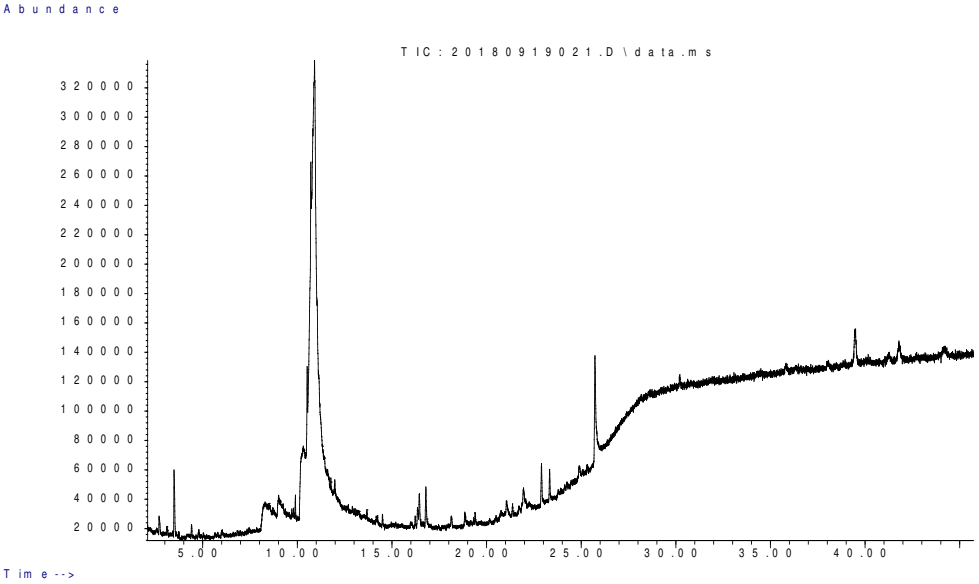

Figure 3. *Chromatogram obtained from crude extract of A. argyi leaf*

Discussion

The extraction process of bioactive components is immensely related to the method of extraction, used solvent and the biological and chemical properties of the extracted compounds. According to our findings methanol being a high polarity solvent produced higher extract yield in each successive extraction. However, similar results were documented by Ahmed et al. (2019) that methanol produced elevated extract yield from *C. colocynthis* and *C. sativa* leaves. Moreover, the result indicated the existence of flavonoids, flavones, saponins, steroid, terpenoids, phenols and tannin with exception of alkaloids and glycosides. The existence of secondary metabolites and a variety of phytoconstituents in natural plant resources could be beneficial for humans in multitude of ways. The phenolic and flavonoids contents exhibited the ability to scavenge free radicals, anti-inflammatory properties, anti-carcinogenic potential, depressurization, immunoregulation, analgesia and anti-lipid peroxidation. However, tannins are well known because of their anti-fungal, anti-tumor, anti-allergic and anti-aging while,

http://www.aloki.hu ● ISSN 1589 1623 (Print) ●ISSN1785 0037 (Online)
DOI: http://dx.doi.org/10.15666/aeer/1706_1534915362

saponins as well as steroids possess anticancer, anti-inflammatory, antioxidant and have potential for cholesterol reduction and also responsible for insecticidal properties (Prabuseenivasan et al., 2006; Thamaraiselvi and Jayanthi, 2012; Mei et al., 2013; Zhang et al., 2014). Moreover, the existence of phytoconstituents like flavonoid, saponins, tannins, essential oil and steroid of *A. argyi* lead the plant toward increasing potential with nutritional or pharmacological values. However, similar finding were reported by Dhanapal et al. (2016) that dry matter of *A. argyi* contain maximum phenolic and flavonoid contents 234.52±0.99 and 737.72±25.55 mgg^{-1}, respectively, Extract also demonstrated EC_{50} values of DPPH 63.34±1.10 μgmL^{-1}.

Mostly flavonoids and phenolic contents were corresponded to antioxidant activities of the extracts. Some studies reported that flavonoids and phenol from plant extracts not only related with antioxidant activities but, some other phytoconstituents such as peptides and polysaccharides may also influenced antioxidant potential of plants (Borkataky et al., 2014). However, our results showed higher phenolic and flavonoids content and high inhibition percent of DPPH radical.

GC-MS analysis of crude extract of *A. argyi* leaves showed the existence of ten chemical compounds responsible for antioxidant activities. Our findings were supported by Chen et al. (2017) who reported 17 chemical compounds by GC-MS analysis including cineole, camphor, borneol and thujone from essential oil of *A. argyi* were found to contain anti-inflammatory activities. Moreover, 33 chemicals constituents were reported from essential oil of *A. argyi* leaves were ether, alcohols, sesquiterpenes, esters, monoterpenes, ketones and aromatic compounds 23.66, 16.72, 15.21, 11.78, 11.63, 6.09 and 5.01% respectively which account for 90.10% of its chemical composition and all these compounds contribute to antioxidant activities except for alcohols. Similar findings were documented by Rather et al. (2012) who reported 25 phytoconstituents from *Artemisia amygdalina* leaf essential oil which was dominated by monoterpenes oxygenated monoterpenes, hydrocarbons and other compounds constituting 43.8, 38.2 and 82.0% respectively, of whole oil composition. Additionally, essential oil extracted from stem, reported to be contain 32 compounds including monoterpenes, and sesquiterpenes hydrocarbons, oxygenated monoterpenes with ratio 66.1:11.2:12.8% respectively were responsible for antioxidant profile.

Chemical compounds occupied by *A. argyi* contain curative values against diseases and other humans related issues, such as erucylamide is a monounsaturated fatty acid omega-9 which is necessary for adults with an average of around 500 $mgday^{-1}$ for normal body functioning, accordingly for Food Standards Australia (Zealand, 2003). Demecolcine also called as colcemidis closely related to natural alkaloid known as colchicine is a type of drug which is used in chemotherapy. Phenylephrine is used as a decongestant and available in the market as solid form, an oral medicine and as nasal spray. It can also be used for the prevention of hemorrhoids. Phenylephrine is used as an eye drop to dilate the pupil to facilitate visualization of the retina (Demopulos et al., 2016) and to control blood pressure effects (Shih and Chen, 2004). Another compound Inositol also called as *myo*-inositol is a carbocyclic sugar which is considered as efficient for the treatment of polycystic ovary syndrome (Monastra et al., 2017), effective in restoration of normal ovary functioning and metabolic stability in patients (Monastra et al., 2017), effectual in restoring FSH/LH ratio and of regularization menstrual cycle (Unfer et al., 2012). α-Cadinol is a famous chemical compound contained by *A. argyi* possess anti-fungal properties (Ho et al., 2011) and also used as hepatoprotective (Tung et al., 2011). Various pharmaceutical drugs derived from 2-

http://www.aloki.hu ● ISSN 1589 1623 (Print) ●ISSN1785 0037 (Online)
DOI: http://dx.doi.org/10.15666/aeer/1706_1534915362

pyrrolidone including Cotinine, Piracetam, Ethosuximide, Doxapram and Povidone are effective medicines while, 2-pyrrolidone also used in ink cartridges (Borase et al., 2014).

However, limited studies have been conducted on quantification of total phenols and flavonoids contents and antioxidant activities from *A. argyi* as pharmacological and alternative of synthetic chemicals and recognition of biologically active components from biomass of crude extract of *A. argyi*. This study fulfills the present research gap and provides comprehensive findings concerning with phytochemicals, phenol and flavonoids contents and antioxidant properties of *A. argyi* leaves.

Conclusion

Results suggested the presence of important phytoconstituents like flavones, terpenoids, steroids, saponins and tannins, phenols and flavonoids responsible for antioxidant activities which are sources of pharmacological and agricultural applications. Moreover, GC-MS profile presents ten chemical compounds which are linked with antioxidant potential. Therefore, *A. argyi* might be introduced as an alternative of synthetic antioxidant. However, comprehensive study is required on separation, purification and identification of specific compounds exibit antioxidant activities and their evaluation against insect pest as safer alternative of synthetic chemicals.

Acknowledgment. The financial support provided by National Key Research & Development Programme of China (2016YFD0200500) is greatly acknowledged.

Conflicts of interests. The authors declare no conflict of interests.

REFERENCES

[1] Abad, M. J., Bedoya, L. M., Apaza, L., Bermejo, P. (2012): The *Artemisia* L. genus: a review of bioactive essential oils. – Molecules 17: 2542-2566.

[2] Adams, J. D., Garcia, C., Garg, G. (2012): Mugwort (*Artemisia vulgaris*, *Artemisia douglasiana*, *Artemisia argyi*) in the treatment of menopause, premenstrual syndrome, dysmenorrhea and attention deficit hyperactivity disorder. – Chinese medicine 3: 116.

[3] Adesuyi, A., Elumm, I., Adaramola, F., Nwokocha, A. (2012): Nutritional and phytochemical screening of *Garcinia kola*. – Advance Journal of Food Science and Technology 4: 9-14.

[4] Ahmed, M., Ji, M., Qin, P., Gu, Z., Liu, Y., Sikandar, A., Iqbal, M. F., Javeed, A. (2019): Phytochemical screening, total phenolic and flavonoids contents and antioxidant activities of *Citrullus colocynthis* L. and *Cannabis sativa* L. – Applied Ecology and Environmental Research 17(3): 6961-6979.

[5] Aiyegoro, O. A., Okoh, A. I. (2010): Preliminary phytochemical screening and in vitro antioxidant activities of the aqueous extract of *Helichrysum longifolium* DC. – BMC complementary and alternative medicine 10: 21.

[6] Bora, K. S., Sharma, A. (2011): The genus *Artemisia*: a comprehensive review. – Pharmaceutical Biology 49: 101-109.

[7] Borase, H. P., Patil, C. D., Salunkhe, R. B., Suryawanshi, R. K., Salunke, B. K., Patil, S. V. (2014): Transformation of aromatic dyes using green synthesized silver nanoparticles. – Bioprocess and biosystems engineering 37: 1695-1705.

http://www.aloki.hu ● ISSN 1589 1623 (Print) ●ISSN1785 0037 (Online)
DOI: http://dx.doi.org/10.15666/aeer/1706_1534915362

[8] Borkataky, M., Kakoti, B., Saikia, L. (2014): Influence of total phenolic content and total flavonoid content on the DPPH radical scavenging activity of *Costus speciosus* (Koen ex. Retz.) Sm. – South Asian Journal of Experimental Biology 4: 261-266.
[9] Büyükokuroğlu, M., Gülçin, I., Oktay, M., Küfrevioğlu, O. (2001): In vitro antioxidant properties of dantrolene sodium. – Pharmacological Research 44: 491-494.
[10] Chen, L.-L., Zhang, H.-J., Chao, J., Liu, J.-F. (2017): Essential oil of *Artemisia argyi* suppresses inflammatory responses by inhibiting JAK/STATs activation. – Journal of Ethnopharmacology 204: 107-117.
[11] Choi, E., Park, H., Lee, J., Kim, G. (2013): Anticancer, antiobesity, and anti-inflammatory activity of *Artemisia* species in vitro. – Journal of traditional Chinese medicine 33: 92-97.
[12] Demopulos, G. A., Shen, H.-R.,Tedford, C. E. (2016): Stable preservative-free mydriatic and anti-inflammatory solutions for injection. – Google Patents.
[13] Dhanapal, A., Ming, T. W., Aung, H. P., Hao, S. J. (2016): Preliminary screening of *Artemisia argyi* for antioxidant potentials. – Int. J. Pharmacog. Phytochem. Res 8: 347-355.
[14] Dong-Ping, X., Ya, Li., Xiao, M., Tong, Z., Yue, Z., Jie, Z., Jiao-Jiao, Z., Hua-Bin, Li. (2017): Natural Antioxidants in Foods and Medicinal Plants: Extraction, Assessment and Resources. – International Journal of Molecular Sciences 18: 96.
[15] Fang, Y.-Z., Yang, S., Wu, G. (2002): Free radicals, antioxidants, and nutrition. – Nutrition 18: 872-879.
[16] Ho, C.-L., Liao, P.-C., Wang, E. I.-C., Su, Y.-C. (2011): Composition and antifungal activities of the leaf essential oil of *Neolitsea parvigemma* from Taiwan. – Natural product communications 6: 1934578X1100600935.
[17] Hu, Y., Yang, Y., Ning, Y., Wang, C., Tong, Z. (2013): Facile preparation of *Artemisia argyi* oil-loaded antibacterial microcapsules by hydroxyapatite-stabilized Pickering emulsion templating. – Colloids and Surfaces B: Biointerfaces 112: 96-102.
[18] Huang, H.-C., Wang, H.-F., Yih, K.-H., Chang, L.-Z., Chang, T.-M. (2012): Dual bioactivities of essential oil extracted from the leaves of *Artemisia argyi* as an antimelanogenic versus antioxidant agent and chemical composition analysis by GC/MS. – International journal of molecular sciences 13: 14679-14697.
[19] Iyengar, M. (1995): Study of Crude Drugs. – 8th. Manipal. India: Power Press.
[20] Jeong, D., Yi, Y.-S., Sung, G.-H., Yang, W. S., Park, J. G., Yoon, K., Yoon, D. H., Song, C., Lee, Y., Rhee, M. H. (2014): Anti-inflammatory activities and mechanisms of *Artemisia asiatica* ethanol extract. – Journal of Ethnopharmacology 152: 487-496.
[21] Joulain, D., König, W. A. (1998): The atlas of spectral data of sesquiterpene hydrocarbons. – EB-Verlag.
[22] Kim, J. K., Shin, E.-C., Lim, H.-J., Choi, S. J., Kim, C. R., Suh, S. H., Kim, C.-J., Park, G. G., Park, C.-S., Kim, H. K. (2015): Characterization of nutritional composition, antioxidative capacity, and sensory attributes of seomae mugwort, a native Korean variety of *Artemisia argyi* H. Lev. & Vaniot. – Journal of analytical methods in chemistry, Volume 2015, Article ID: 916346.
[23] Lee, T. K., Vairappan, C. S. (2011): Antioxidant, antibacterial and cytotoxic activities of essential oils and ethanol extracts of selected South East Asian herbs. – Journal of Medicinal Plants Research 5: 5284-5290.
[24] Li, H. (2002): Research medicinal function of argy wormwood leaf and their development and utilization. – Pri J Chin Materia Med 16: 51-3.
[25] Ling, M., Yili, A., Aisa, H., Bo, Z., Veshkurova, O., Salikhov, S. I. (2011): Isolation of a new peptide from seeds of *Apium graveolens* indigenous to China. – Chemistry of Natural Compounds 46: 932-934.
[26] Lis-Balchin, M., Deans, S. (1997): Bioactivity of selected plant essential oils against *Listeria monocytogenes*. – Journal of applied microbiology 82: 759-762.

http://www.aloki.hu ● ISSN 1589 1623 (Print) ●ISSN1785 0037 (Online)
DOI: http://dx.doi.org/10.15666/aeer/1706_1534915362

[27] Liu, Y.-h., Lv, J.-l., Yuan, K., Yang, P. (2011): Antioxidant Activities of The Extracts of *Carya cathayensis* Sarg. – Asian Journal of Chemistry 23: 676.
[28] Lobo, V., Patil, A., Phatak, A., Chandra, N. (2010): Free radicals, antioxidants and functional foods: Impact on human health. – Pharmacognosy reviews 4: 118.
[29] Mei, Q., Gao, Y., Tian, S., Dai, W. (2013): The Research and Application of Folium *Artemisiae Argyi*. – China Press of Traditional Chinese Medicine, Beijing.
[30] Meot-Duros, L., Magne, C. (2009): Antioxidant activity and phenol content of *Crithmum maritimum* L. leaves. – Plant Physiology and Biochemistry 47: 37-41.
[31] Monastra, G., Unfer, V., Harrath, A. H., Bizzarri, M. (2017): Combining treatment with myo-inositol and D-chiro-inositol (40: 1) is effective in restoring ovary function and metabolic balance in PCOS patients. – Gynecological Endocrinology 33: 1-9.
[32] Park, J.-M., Han, Y.-M., Lee, J.-S., Ko, K. H., Hong, S.-P., Kim, E.-H., Hahm, K.-B. (2015): Nrf2-mediated mucoprotective and anti-inflammatory actions of *Artemisia* extracts led to attenuate stress related mucosal damages. – Journal of clinical biochemistry and nutrition 56: 132-142.
[33] Prabuseenivasan, S., Jayakumar, M., Ignacimuthu, S. (2006): In vitro antibacterial activity of some plant essential oils. – BMC complementary and alternative medicine 6: 39.
[34] Rather, M. A., Ganai, B. A., Kamili, A. N., Qayoom, M., Akbar, S., Masood, A., Rasool, R., Wani, S. H., Qurishi, M. A. (2012): Comparative GC–FID and GC–MS analysis of the mono and sesquiterpene secondary metabolites produced by the field grown and micropropagated plants of *Artemisia amygdalina* Decne. – Acta Physiologiae Plantarum 34: 885-890.
[35] Reynold, J. E. (1996): Martindale–The Extra Pharmacopoeia. – London: The 3.
[36] Shih, J., Chen, K. (2004): Regulation of MAO-A and MAO-B gene expression. – Current medicinal chemistry 11: 1995-2005.
[37] Siddiqui, A. A., Ali, M. (1997): Practical pharmaceutical chemistry. – CBS Publishers & Distributors.
[38] Siddiqui, S., Verma, A., Rather, A. A., Jabeen, F., Meghvansi, M. K. (2009): Preliminary phytochemicals analysis of some important medicinal and aromatic plants. – Advances in biological research 3: 188-195.
[39] Sofowora, A. (1993): Medicinal plants and traditional medicine in Africa. Ibadan. – Nigeria: Spectrum Books Ltd.
[40] Sparkman, O. D. (2005): Identification of essential oil components by gas chromatography/quadrupole mass spectroscopy Robert P. Adams. – Journal of the American Society for Mass Spectrometry 16(11): 1902-1903.
[41] Tan, R. X., Zheng, W., Tang, H. (1998): Biologically active substances from the genus *Artemisia*. – Planta medica 64: 295-302.
[42] Thamaraiselvi, P., Jayanthi, P. (2012): Preliminary studies on phytochemicals and antimicrobial activity of solvent extracts of *Eichhornia crassipes* (Mart.) Solms. – Asian Journal of Plant Science and Research 2: 115-122.
[43] Trease, G. E., Evans, W., Pharmacognosy, E. (2003): Baillier Tindall. – ELBS: 479-480.
[44] Tung, Y.-T., Huang, C.-C., Ho, S.-T., Kuo, Y.-H., Lin, C.-C., Lin, C.-T., Wu, J.-H. (2011): Bioactive phytochemicals of leaf essential oils of *Cinnamomum osmophloeum* prevent lipopolysaccharide/D-galactosamine (LPS/D-GalN)-induced acute hepatitis in mice. – Journal of agricultural and food chemistry 59: 8117-8123.
[45] Unfer, V., Carlomagno, G., Dante, G., Facchinetti, F. (2012): Effects of myo-inositol in women with PCOS: a systematic review of randomized controlled trials. – Gynecological Endocrinology 28: 509-515.
[46] Wang, W., Zhang, X.-k., Wu, N., Fu, Y.-j., Zu, Y.-g. (2006): Antimicrobial activities of essential oil from *Artemisiae argyi* leaves. – Journal of Forestry Research 17: 332.

http://www.aloki.hu ● ISSN 1589 1623 (Print) ●ISSN1785 0037 (Online)
DOI: http://dx.doi.org/10.15666/aeer/1706_1534915362

[47] Wong, F.-C., Chai, T.-T., Hoo, Y.-W. (2012): Antioxidation and cytotoxic activities of selected medicinal herbs used in Malaysia. – Journal of Medicinal Plants Research 6: 3169-3175.
[48] Yu, L., Perret, J., Harris, M., Wilson, J., Haley, S. (2003): Antioxidant properties of bran extracts from "Akron" wheat grown at different locations. – Journal of Agricultural and Food Chemistry 51: 1566-1570.
[49] Zealand, F. (2003): Erucic acid in food: a toxicological review and risk assessment. – Canberra Food Stand Aust Newzeal: 17-23.
[50] Zeng, K.-W., Wang, S., Dong, X., Jiang, Y., Tu, P.-F. (2014): Sesquiterpene dimer (DSF-52) from *Artemisia argyi* inhibits microglia-mediated neuroinflammation via suppression of NF-κB, JNK/p38 MAPKs and Jak2/Stat3 signaling pathways. – Phytomedicine 21: 298-306.
[51] Zhang, W.-J., You, C.-X., Yang, K., Chen, R., Wang, Y., Wu, Y., Geng, Z.-F., Chen, H.-P., Jiang, H.-Y., Su, Y. (2014): Bioactivity of essential oil of *Artemisia argyi* Lévl. et Van. and its main compounds against Lasioderma serricorne. – Journal of oleo science 63: 829-837.
[52] Zhao, H., Fan, W., Dong, J., Lu, J., Chen, J., Shan, L., Lin, Y., Kong, W. (2008): Evaluation of antioxidant activities and total phenolic contents of typical malting barley varieties. – Food Chemistry 107: 296-304.
[53] Zhou, F., Qin, L., Lian, J., Zhen, Q. (2000): Chemical constituents, biological activities and plant resources of Folium *Artemisia argyi*. – J Pharm Pract 2: 96-98.

http://www.aloki.hu ● ISSN 1589 1623 (Print) ●ISSN1785 0037 (Online)
DOI: http://dx.doi.org/10.15666/aeer/1706_1534915362

RELATIONSHIP OF DOMINANT HERBACEOUS PLANT SPECIES AND GROUNDWATER DEPTH IN TONGLIAO PLAIN, NORTHWESTERN CHINA

ZHU, Y. H.[1,2] – ZHANG, S.[2*] – SUN, B.[2] – YAN, L.[3] – WANG, Y.[3]

[1]*College of Architectural Engineering, Yan'an University, Yan'an 716000, China*

[2]*College of Water Conservancy and Earth Building Engineering, Inner Mongolia Agricultural University, Hohhot 001018, China*

[3]*China Institute of Water Resources and Hydropower Research, Beijing 100076, China*

**Corresponding author*
e-mail: szimau@163.com

(Received 11th Jul 2019; accepted 16th Oct 2019)

Abstract. Diversification of vegetation communities could be associated with the change of groundwater depth (GD). To get a better understanding of this relationship, a field survey assessing GD, and herbaceous plants etc. was carried in Tongliao plain (TP), northwestern China, where GD has declined significantly mainly due to pumping for agricultural irrigation. The photos data method was used to identify vegetation characteristics including coverage, biomass, height, ecological type, and name etc. Some diversity indexes were applied to identify the relationship between the groundwater table and the plant features. Growth and composition of vegetation were affected by the depth of groundwater and the degree of utilization of herbaceous vegetation on water resources. Different depth of groundwater had different influence on vegetation. The ecotype distribution of vegetation following depth based on survey data demonstrated that mesophytes, mesoxerophytes and xerophytes were found over groundwater depths between 1.38 and 3.43 m, 1.4 and 3.4 m and 2.4 and > 4.0 m respectively. This study proved that the depth of 3.4 m may be the transition range for the evolution of vegetation in TP.
Keywords: *vegetation characteristic, diversity, ecotype, transition range, water resources*

Introduction

Semi-arid regions cover ~22% of the land surface and supports 6% of the population in China. The ecosystems in such regions are fragile and sensitive (Fu and Burgher, 2015). Herbaceous vegetation is an important part of ecosystem, which could be very sensitive to a series of environmental factors (Boyd et al., 2017; Hedl et al., 2017; Singh et al., 2017). Especially in arid and semiarid regions, growth status and distributions of herbaceous plants could extremely associate with buried depths of groundwater table. The effects of groundwater utilization to the vegetations have become increasingly interested in eco-environment protection and restoration (McLendon et al., 2008; O'Grady et al., 2006). Plant communities (Liu et al., 2016), morphological characteristics and vegetation (Galassi, 2001) respond to soil and groundwater quality and vegetation productivity, vegetation and other factors between groundwater. For the Tongliao plain (TP), the researches concentrate on the ecological level, suitable water level, ecological warning level and the relationship between research and critical depth saline vegetation (Liu et al., 2013; Qian et al., 2017; Yang and Chui, 2017), etc. Many studies also focused on the relationship between trees, shrubs and groundwater (Monteleone et al., 2018; Nolan et al., 2017); the trees and shrubs include poplar, elm, and microphyll etc. However, our knowledge on the relationships between the dominant

http://www.aloki.hu ● ISSN 1589 1623 (Print) ● ISSN 1785 0037 (Online)
DOI: http://dx.doi.org/10.15666/aeer/1706_1536315374

herbaceous vegetation of the large watershed and groundwater depth (GD) is still limited. Some models (Liu et al., 2006; Zhu et al., 2010) were often qualitatively considered with the lower boundary of the bottom of the root, and it should be further clarified.

To obtain a comprehensive understanding of grassland degradation requires a combination of change detection by remote sensing, field investigation and literature review. The purpose of this study is to enhance the understanding of grassland degradation and to find the role of GD in changes in vegetation diversity for the study area of TP using such a portfolio of methods. The novelty of this paper lies in linking grassland degradation and perceived change to GD and providing lower boundary of the bottom of the root for hydrological mathematical model. On the basis of the dominant herbaceous vegetation species in TP area, the observed data was used to analyze the relationship between ecotype plants, species diversity, importance value and GD. This research will not only provide data for the scientific research model, but also provide scientific support for the management of local environment.

Within this paper, the specific aims of this study are to (1) investigate the spatial patterns and trends of vegetation diversity and cover change; (2) link grassland degradation with the GD; and (3) explore the role of changes of GD in grassland.

Materials and methods

Study area

The study area is located in a typical ecotone in North of China, which is a climate transition zone from sub-humid to semi-arid with an annual rainfall of 350-450 mm and evaporation of 1817 mm (20 cm pan). The root layer soil is mainly meadow, Aeolian sandy, and sandy chestnut etc. The plain is mainly formed by dunes, sandlot, lowland, and pasture land etc. Spatial distribution of vegetation is strong heterogeneity with dominant plant species of *Salsolacollina, Setariaviridis, Artemisiafrigida, Cleistogenessquarrosa, Poapretensis, and Artemisia campbellii Hook etc*.

From July to August, 2015, based on grassland type distribution under remote sensing images in study areas, 32 investigation sites (100 m × 100 m) centered on herbaceous plant communities were investigated (*Table 1*). Typical points were selected within each investigation site. Three random sampling plots were surveyed with a diameter of 1 × 1 m, including plant height, ecological style, name, wet weight, and biomass etc. The vegetation coverage was analyzed by ENVI 5.3 software through the supervised classification method. Meanwhile, soil sampler (specification: L is 4 m, Φ is 10 cm) was used to measure the corresponding GD data in each sample plot. Kriging interpolation and draw contour lines of depth were worked out based on the groundwater table data (*Fig. 1*). To detect the soil type of each survey plot, spatial distribution data of soil types in China were used that were got from Chinese Academy of Science (http://www.resdc.cn) at a scale of 1:1,000,000.

Methods

Vegetation importance value (Ma et al., 2009), niche breadth (Feinsinger, 1981), richness index (Li et al., 2008), community species diversity index (Hejda and Pyšek, 2006), evenness index (Ma, 2005), and dominance index (Wood et al., 2005) were applied to identify the change of species diversity.

http://www.aloki.hu ● ISSN 1589 1623 (Print) ● ISSN 1785 0037 (Online)
DOI: http://dx.doi.org/10.15666/aeer/1706_1536315374

Important value:

$$IV = (RD + RF + RC)/3 \quad \text{(Eq.1)}$$

Niche breadth:

$$Bi = (1/r)\sum_{j=1}^{r} P_{ij}^2 \quad \text{(Eq.2)}$$

Margalef richness index:

$$D = (S-1)/InN \quad \text{(Eq.3)}$$

Shannon community species diversity index:

$$D = -\sum_{i=1}^{S}(p_i Inp_i) \quad \text{(Eq.4)}$$

Alatalo evenness index:

$$D = \left[1/\sum_{i=1}^{S}(\frac{N_i}{N})^2 - 1\right] / \left[e^{(-\sum_{i=1}^{S}\frac{N_i}{N}In\frac{N_i}{N})} - 1\right] \quad \text{(Eq.5)}$$

Simpson dominance index:

$$D = 1 - In\sum_{i=1}^{S}\left(\frac{N_i}{N}\right)^2 \quad \text{(Eq.6)}$$

where: *IV* is the important value, *Bi* is the niche breadth, *RD, RF, RC* are the relative density, relative frequency, and relative coverage of vegetation, *D* is the diversity index, *S* is the total number of species, *N* is the number of trees of all species, *P* is the vegetation density, *i* is the i^{th} vegetation.

Results

Vegetation composition

41 species of herbaceous vegetation were identified, which belonged to 2 classes, 12 families and 24 genuses. Perennial and annual herbaceous vegetations presented 58%, and 48% respectively. They were classified as mesophytes, mesoxerophytes, xerophytes, psammophyte, ultra-xerophytes, and halophytes that presented for 38%, 8%, 38%, 15%, 3%, and 5% respectively. The most important is that 11 species of the dominant herbaceous species were recognized. They belonged to 2 classes, 3 families and 7 genuses, among which perennial and annual herbaceous vegetation accounted for 45% and 55% respectively.

http://www.aloki.hu ● ISSN 1589 1623 (Print) ● ISSN 1785 0037 (Online)
DOI: http://dx.doi.org/10.15666/aeer/1706_1536315374

Table 1. *Sampling point information*

ID	X	Y	GD (m)	ST	Species	GE	LF	ET
1	120.37	43.64	> 4	Ca	*Poa annua*	*World*	*Th*	*M*
2	120.51	43.54	> 4	Ca	*Artemisia campbellii*	*North temperate zone*	*Pn*	*X*
3	120.28	43.47	> 4	Ca	*Poa annua*	*World*	*Th*	*M*
4	120.63	43.63	> 4	Ca	*Artemisia pubescens*	*North temperate zone*	*Pn*	*X*
5	121.83	44.10	2.25	Ca	*Chloris virgata*	*Pantropic*	*Th*	*M*
6	121.57	44.25	1.4	Ae	*Corispermum hyssopifolium*	-	*Pn*	*X*
7	121.28	44.42	3.1	Ca	*Artemisia pubescens*	*North temperate zone*	*Pn*	*X*
8	121.10	44.48	1.8	Ca	*Suaeda glauca*	*Central Asia - Mongolia*	*Th*	*Mx*
9	121.57	44.24	1.5	Fl	*Carex duriuscula*	*World*	*Pn*	*Mx*
10	121.59	43.54	3.3	Fl	*Artemisia pubescens*	*North temperate zone*	*Pn*	*X*
11	121.57	43.65	3.7	Ca	*Corispermum hyssopifolium*	-	*Pn*	*X*
12	121.25	43.65	3.4	Ca	*Suaeda glauca*	*Central Asia - Mongolia*	*Th*	*Mx*
13	121.87	43.35	2.8	Ae	*Suaeda glauca*	*Central Asia - Mongolia*	*Th*	*Mx*
14	120.43	42.79	> 4	Ae	*Setaria viridis*	*Pantropic*	*Th*	*M*
15	120.76	43.02	3.8	Ae	*Corispermum hyssopifolium*	-	*Pn*	*X*
16	120.97	43.26	> 4	Ae	*Echinochloa crusgalli*	*Pantropic*	*Th*	*M*
17	121.38	43.24	3.3	Ae	*Echinochloa crusgalli*	*Pantropic*	*Th*	*M*
18	121.66	43.34	3.1	Fl	*Setaria viridis*	*Pantropic*	*Th*	*M*
19	121.76	43.08	2.8	Ae	*Setaria viridis*	*Pantropic*	*Th*	*M*
20	121.35	43.07	3.3	Ae	*Echinochloa crusgalli*	*Pantropic*	*Th*	*M*
21	121.06	42.98	3.7	Ae	*Setaria viridis*	*Pantropic*	*Th*	*M*
22	121.84	43.32	2.8	Ae	*Echinochloa crusgalli*	*Pantropic*	*Th*	*M*
23	121.62	42.91	3	Ae	*Poa annua*	*World*	*Th*	*M*
24	121.73	42.92	2.9	Ae	*Leymus chinensis*	*World*	*Pn*	*M*
25	122.38	43.09	1.8	Ae	*Carex duriuscula*	*World*	*Pn*	*Mx*
26	122.66	43.37	2.4	Ae	*Carex duriuscula*	*World*	*Pn*	*Mx*
27	122.55	43.45	2.65	Ae	*Setaria viridis*	*Pantropic*	*Th*	*M*
28	122.72	43.59	2.2	Ae	*Corispermum hyssopifolium*	-	*Pn*	*X*
29	122.99	43.52	1.6	Ae	*Setaria viridis*	*Pantropic*	*Th*	*M*
30	123.18	43.80	1.38	Ae	*Setaria viridis*	*Pantropic*	*Th*	*M*
31	121.32	43.58	3.4	Fl	*Setaria viridis*	*Pantropic*	*Th*	*M*
32	120.77	43.64	> 4	Ca	*Artemisia frigida Willd*	*North temperate zone*	*Pn*	*X*

GD: groundwater (unit: m); ST: soil type; Ca: castanozems; Fl: fluvo-aquic soils; Ae: aeolian soil; -: not available; Th: Therophyte; Pn: Perennial; M: Mcsophyte; Mx: Mcso-xerophyte; X: Xerophyte

Geographical elements of herbaceous plant

Based on the previous studies and the vegetation survey results, the geographical elements of the dominant herbaceous plants were World, Eastern Asia and variations, Central Asia - Mongolia, Pantropic, Old World and North Temperate in the study area (*Table 1*).

Relationship between GD and herbaceous plant

Ecological niche is a concept in ecology that describes how a species responds to the distribution of resources and competitors. Niche breadth represents the sum of a variety of different resources utilized by a species. Through field investigation and laboratory data collation, important value proportion and niche breadth of each survey point dominant species were analyzed corresponding to the different groundwater tables.

http://www.aloki.hu ● ISSN 1589 1623 (Print) ● ISSN 1785 0037 (Online)
DOI: http://dx.doi.org/10.15666/aeer/1706_1536315374

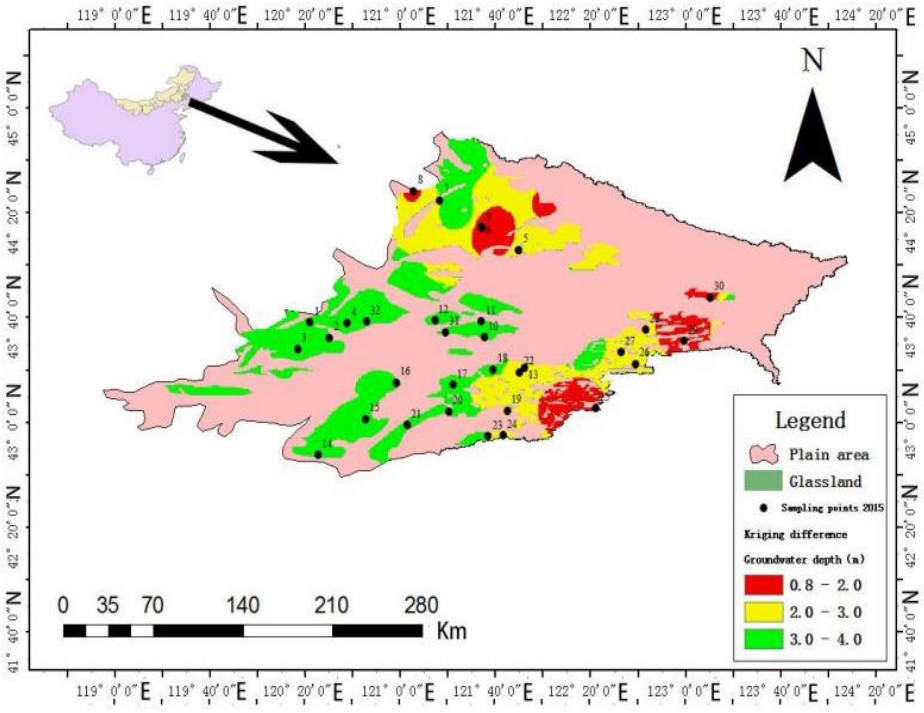

Figure 1. *Field survey sites and groundwater depth contour*

The data in *Table 2* shows that, in the direction of increasing depth gradient, corresponding vegetation types changed with slight difference. There are five dominant vegetation species at the depth of 1~2 m. Their importance value ratio and niche breadth were lower, indicating that the depth range is not suitable for the growth of these species; eight types of vegetation were found at about 2~3 m and > 4 m respectively. *Chloris virgata. Leymus chinensis and Artemisia frigida Willd* appear concentrated with the higher value of the proportion and niche breadth. At the depth of 2~3 m, vegetation species decreased, but the proportion of importance value and niche breadth increased.

Table 2*. Proportion and niche breadth of each species corresponded to TP*

Species	Groundwater depth (m)			
	1~2	2~3	3~4	> 4
Poa annua	0 (0)	0 (0)	0.47 (0.04)	0.53 (0.06)
Artemisia campbellii	0 (0)	0.18 (0.006)	0.26 (0.01)	0.56 (0.06)
Artemisia pubescens	0.09 (0.002)	0.06 (0.0007)	0.6 (0.07)	0.25 (0.01)
Chloris virgata	0 (0)	1 (0.2)	0 (0)	0 (0)
Corispermum hyssopifolium	0.25 (0.01)	0.15 (0.005)	0.45 (0.04)	0.15 (0.005)
Suaeda glauca	0.23 (0.01)	0.27 (0.01)	0.23 (0.01)	0.27 (0.01)
Carex duriuscula	0.5 (0.05)	0.5 (0.05)	0 (0)	0 (0)
Setaira Viridis	0.22 (0.01)	0.21 (0.009)	0.36 (0.03)	0.21 (0.009)
Echinochloa crusgalli	0 (0)	0.23 (0.01)	0.4 (0.03)	0.37 (0.03)
Leymus chinensis	0 (0)	1 (0.2)	0 (0)	0 (0)
Artemisia frigida Willd.	0 (0)	0 (0)	0 (0)	1 (0.2)

(): niche breadth

http://www.aloki.hu ● ISSN 1589 1623 (Print) ● ISSN 1785 0037 (Online)
DOI: http://dx.doi.org/10.15666/aeer/1706_1536315374

The value of the *Artemisia campbellii*, *Artemisia pubescens*, *Corispermum hyssopifolium*, *Setaira Viridis* and *Echinochloa crusgalli* significantly increased, indicating that they were the main vegetation community composition in this depth. *Softwood Artemisia*, *Corispermum hyssopifolium* and *Suaeda glauca* were widely distributed ranging from 1~4 m, the proportion of importance value and niche breadth were relatively balance.

The same dominant vegetation at the different GD, the proportion and niche breadth are different, which indicates that the growth and distribution of vegetation are affected by groundwater. The proportion and niche breadth of different dominant vegetation at the different GD were different too, which suggests there are differences in the utilization degree of water resources by different species. However, under the same groundwater level, some dominant species vegetation with the same characteristics had similar proportion and niche, which indicated that the same species had similar adaptation strategies to groundwater or have a similar competition on demand for groundwater.

Variation of herbaceous vegetation cover and biomass

Through correlation analysis, the correlation coefficients between GD and vegetation characteristics below 0.5 only very weak. However, the correlation coefficients between GD and biomass and vegetation coverage were significant at the 0.05 level (2-tailed), which meant that the GD has the most significant effects on the plant communities.

To further understand the relationship between them, we analyzed vegetation characteristics of survey sites to different depth gradient. Wet weight, biomass and vegetation coverage of survey sites increased first, and then decreased with the rising of GD; It shows that the groundwater has a certain influence on them (*Fig. 2*). Ranging from 1.4~2.4 m, these indexes that highlight rising trends with the coefficient of variation were 0.24, 0.45 and 0.32. There was a rapid decrease in these indexes at the depth of 2.65~3.4 m. In addition, the maximum value of the coefficient of variation of the three were 0.62, 0.75 and 0.44. At the same time, the dominant species vegetation, *Leymuschinensi* and *Artemisiapubescens*, which have lower value of each index was mostly the perennial at the depth of 2.9 m and 3.3 m. However, the dominant species vegetation, *Chloris virgata* and *Echinochloa crusgalli*, which have higher value of each index is mostly the annual at the depth of 2.8 m and 3.0 m. Every index continues the downward trend at the depth of 3.4~ > 4 m with the value of 0.62, 0.59 and 0.31. The trend line shows that the depth of about 3.4 m was the evolution of vegetation transition zone, which became elevated by the reduced. With the increase of depth gradient, the dominant species of survey sites evolved from the mesophytes to the xerophytes. Although each index declines overall, the individual differences in levels of groundwater, it suggests that different depth of groundwater has different influence on vegetation.

Herbaceous vegetation ecological variation

Based on the average GD data of field survey of 32 points and dominant species vegetation ecological values of survey sites, the correlation coefficient calculated. The results showed that the plant ecotypes and GD were significantly correlated. To a certain extent, GD determines the type of plant ecological distribution (*Fig. 3*). By superimposing dominant species vegetation and the corresponding GD of each survey

http://www.aloki.hu ● ISSN 1589 1623 (Print) ● ISSN 1785 0037 (Online)
DOI: http://dx.doi.org/10.15666/aeer/1706_1536315374

point, the quantitative relationship was revealed. The ecotype of dominant vegetation, such as mesophytes, meso-xerophytes and xerophytes correspond to a depth range, namely 1.38~3.43 m, 1.4~3.45 m and 2.40~ > 4.00 m. Only the planting of mesophytes and meso-xerophytes dominant species exist in the GD of 1~2 m; they have significant depth transition phase. Only the dominant species planting of xerophytes coexist in the GD of more than 3.5 m. In the 2.65~3.43 m, mesophytes appeared more concentrated. Meso-xerophytes rooted in uniform distribution ranging from 1.4~3.45 m. Because the distribution of dominant species vegetation was increasing, the depth at about 3.4 m would be the evolution of vegetation transition zone.

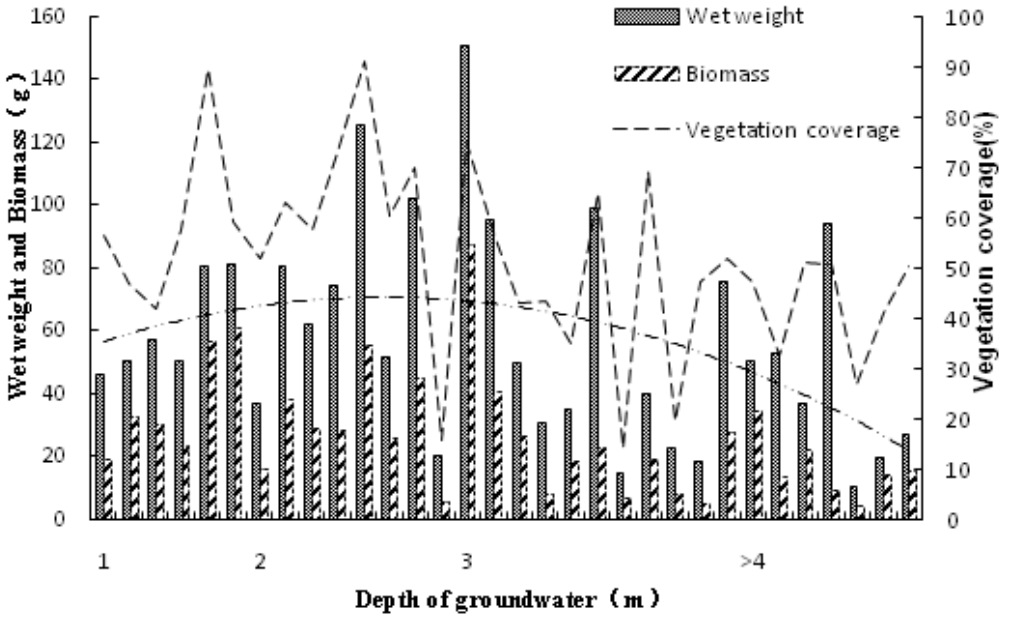

Figure 2. *Vegetation characteristics of survey sites to different depth gradient*

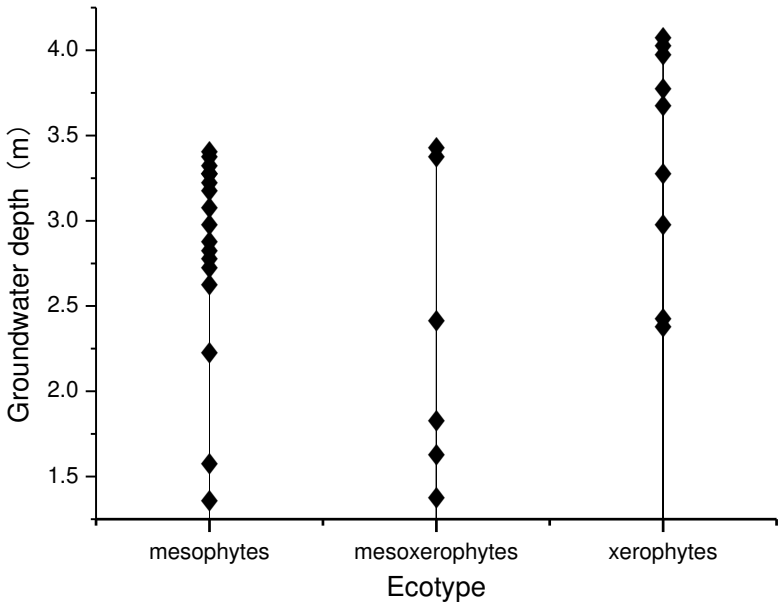

Figure 3*. Dominant species pattern distribution with groundwater level*

http://www.aloki.hu ● ISSN 1589 1623 (Print) ● ISSN 1785 0037 (Online)
DOI: http://dx.doi.org/10.15666/aeer/1706_1536315374

Variation of species diversity index

Through field investigation and laboratory data collation, the distributions of each diversity index were analyzed following the direction of depth gradient, in order to study the internal correlation between GD and herbaceous vegetation species diversity (*Fig. 4*).

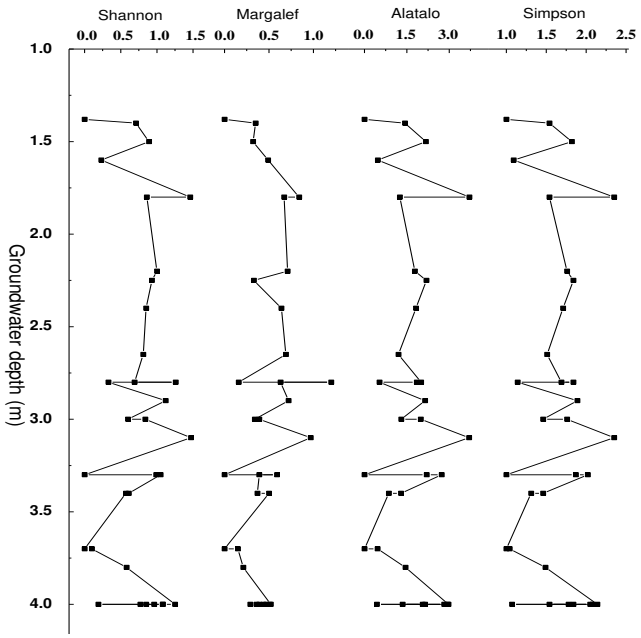

Figure 4. *The result of diversity ordination to different depth gradient*

At depth ranging 1.8~2.4 m, species diversity was relatively stable, means were 0.91, 0.59, 1.76 and 1.71, expressed as per survey quadrate vegetation types ranged from 2-6 species. As the depth gradient increases, at depth ranging about 2.65~3.4 m, the diversity index fluctuated frequently, the various diversity index means were 0.82, 0.54, 1.74 and 1.67; at depth ranging 3.4~ > 4 m, diversity index showed slight fluctuations, means were 0.67, 0.35, 1.59 and 1.58, expressed as per survey quadrats vegetation types ranging from 1-5 species. With the increase of depth, the diversity index value of vegetation species fluctuated, about 1.8~2.4 m > 2.65~3.4 m > 3.4~4 m > 1.4~1.8 m. With the increase of depth, all index increased firstly, then decreased, generally in the 1.8~2.4 m up to the maximum. The values of Margalef, Shannon-Wiener and Simpson index at the 1.8~2.4 m were slightly higher than the values at other depths, while the Alatalo index value is 2.56 ~3.4 m below the value of 1.8~2.4 m. The smallest variation is the Magalef index, and the maximum variation range is Alatolo index. The result suggests that the most suitable depth of groundwater for plant growth in the region is 1.8~3.4 m, after as the underground water level decline gradually, the diversity of the species evenness and abundance emerged decline trend. The relationships between species diversity index and groundwater revealed that with the increase of depth gradient, the diversity index value of vegetation species fluctuated, closely related with each other.

Based on the four indexes, most scholars have studied the relationship between them and vegetation, climate, groundwater, soil water and so on. Most predecessors considered that, as the depth increases, the diversity of vegetation shows an obvious

http://www.aloki.hu ● ISSN 1589 1623 (Print) ● ISSN 1785 0037 (Online)
DOI: http://dx.doi.org/10.15666/aeer/1706_1536315374

decreasing trend. However, because of the complexity of the natural ecosystem and the actual situation of the local pastoral transitional zone, the diversity of vegetation at the depth of the transition zone was deeply influenced.

Discussion

In arid and semiarid regions, herbaceous vegetation is among the most important ecosystem components. Each vegetation is also very sensitive to environmental factors, so it is necessary to reveal the basis (Chauhan and Johnson, 2008) for the evolution of groundwater on vegetation. In arid and semiarid regions, the evolution of herbaceous vegetation will be affected in addition to precipitation and temperature, may also be affected by other environmental factors (Tao et al., 2017). TP is a typical semi-arid region where the ecological environment is fragile. Between groundwater and the characteristics of herbaceous vegetation, there obviously will be some intrinsic link.

Groundwater-Dependent Ecological systems (GDEs) refers to the survival and development of vegetation ecosystem which depends on groundwater systems. GDEs belongs to interdisciplinary. For now, it is not very clear on the relationship between the groundwater system and vegetation ecosystem; there are full of challenges and opportunities in this area. Deeper GDEs (Kløve et al., 2011; Zhu et al., 2012) have been divided into three categories according to the exposed conditions. On the basis of previous studies, domestic scholars also have made a lot of research and field investigation on the relationship between vegetation ecosystems in large areas and groundwater systems.

This paper will determine GD at about 3.4 m to divide completely dependent and semi-dependent GDEs basis: Completely dependent GDEs is at 2.65~3.4 m of the GD, mainly refers to the vegetation ecosystem which relies on capillary action to recharge in semi-arid zones; semi-dependent GDEs is at 1.4~2.4 m of the GD, mainly refers to the vegetation ecosystem which not only relies on irrigation, precipitation or river bank to recharge but also relies on groundwater; completely independent GDEs is at 3.4~ > 4 m of the GD, mainly refers to the vegetation ecosystem which does not rely on groundwater. According to available data, with the increase of depth, vegetation coverage, wet weight and biomass, their segmentation coefficient of variation have a significant difference; they have fluctuated downward trend, which reveals: (1) the dominant vegetation evolved from the annual shallow-rooted vegetation to the perennial deep rooted vegetation; (2) Differences in surface characteristics of completely dependent, semi-dependent and completely independent GDEs vegetation are significant, which also shows that in addition to the impact of groundwater, the herbaceous vegetation is also affected by the multiple effects of precipitation (Sneva,1982), topography (Hardin and Wistendahl, 1983), man-made and other factors; within the range of groundwater, importance value proportion of the value and diversity index shows the trend of different frequency fluctuations, namely the increasing direction along the depth gradient, showing Mesozoic - in xerophytic - xerophytic vegetation types, quantity and life - form evolution trend. This article was also based on the frequency of appearance and niche theory of dominant species survey sites, using niche breadth and other indicators, analyzed the degree of utilization of herbaceous vegetation on water resources in the study area, obtained niche breadth of a variety of dominant species at different depth gradient. It shows that *Artemisia*, *Echinochloa crusgalli* and *Setairaviridis* constitute a more dominant community of survey sites, and

http://www.aloki.hu ● ISSN 1589 1623 (Print) ● ISSN 1785 0037 (Online)
DOI: http://dx.doi.org/10.15666/aeer/1706_1536315374

can be widely distributed. The overall survey sites niche breadth of dominant species was small, and it also shows that the degree of utilization of water resources is not high; they may be affected by other factors. The evolution of the transition range of herbaceous vegetation in the study area is at about 3.4 m. In this range of more than 3.4 m, a variety of species diversity indexes decreased significantly, proportion and niche breadth were obviously shrunk, vegetation coverage wet weight and biomass firstly decreased.

Conclusions

This paper has attempted to recognize the groundwater as the key factors affecting the activity and distribution of vegetation. The topic is perhaps too obvious, but born under the perspective to explore the pattern of vegetation characteristics under groundwater change conditions in TP. Through correlation analysis, there is a certain relationship between them groundwater and characteristics of vegetation. Following the change of GD, the trend of vegetation characteristics is increasing first, and then decreasing. Different ecotype of dominant vegetation corresponds to different depth of groundwater. Mesophytes, meso-xerophytes and xerophytes have their own depth transition zone which are 1.38~3.43 m, 1.4~3.45 m and 2.4~ > 4 m. The important value proportion, niche breadth and each species diversity index of dominant herbaceous vegetation in each survey point have apparent indication. There is obvious intrinsic link between them and GD. When the groundwater is too shallow, the growth of the height, crown and so on of the herbaceous plants will be inhibited, because the surface due to evaporation and the accumulation of much salt limits the growth of herbs. Our results also suggest that the evolution of the transition range of herbaceous vegetation in TP is at about 3.4 m.

It is well known that groundwater has a significant effect on regional vegetation growth and distribution. Scarcity of water resources, great changes of the groundwater extraction volume and depth are some of the main factors in the evolution of natural vegetation in TP. Because vegetation growth and distribution are affected by many factors, such as climate, grazing and soil, how to determine the impact of groundwater change on vegetation growth and distribution is very important. However, we lack more adequate information and method on the relationship between grassland community characteristics and GD. The depth of groundwater in this study is less than 4.0 m, and whether it still has a good correlation still needs to be further studied under the condition of more than 4.0 m? Moreover, how to determine the water source of natural herbaceous vegetation in agropastoral ecotone in semi-arid region?

Further work needs to be done to determination of critical area of groundwater and water source for different vegetation evolution. Additionally, relationships between GD and vegetation characteristics need to be investigated at high spatial and temporal resolutions.

Acknowledgment. The authors would like to thank the Editors and the anonymous reviewers for their crucial comments, which improved the quality of this paper. This research project is financed by ministry of Water Resources Public welfare special scientific research project—semi-arid zone water cycle and water ecological security key technology research—with number 201501031. This study was supported by the National Natural Science Foundation of China (51779118, 51669021), Natural Science Foundation of Inner Mongolia (2017BS0510).

http://www.aloki.hu ● ISSN 1589 1623 (Print) ● ISSN 1785 0037 (Online)
DOI: http://dx.doi.org/10.15666/aeer/1706_1536315374

REFERENCES

[1] Boyd, C. S., Davies, K. W., Collins, G. H. (2017): Impacts of feral horse use on herbaceous riparian vegetation within a sagebrush steppe ecosystem. – Rangeland Ecology & Management 70: 411-417.
[2] Chauhan, B. S., Johnson, D. E. (2008): Seed germination and seedling emergence of giant sensitiveplant (Mimosa invisa). – Weed Science 56: 244-248.
[3] Feinsinger, P. (1981): A simple measure of niche breadth. – Ecology 62(1): 27-32.
[4] Fu, B., Burgher, I. (2015): Riparian vegetation NDVI dynamics and its relationship with climate, surface water and groundwater. – Journal of Arid Environments 113: 59-68.
[5] Galassi, D. M. P. (2001): Groundwater copepods: diversity patterns over ecological and evolutionary scales. – Hydrobiologia 453/454: 227-253.
[6] Hardin, E. D., Wistendahl, W. A. (1983): The effects of floodplain trees on herbaceous vegetation patterns, microtopography and litter. – Bulletin of the Torrey Botanical Club 110: 23-30.
[7] Hedl, R., Sipos, J., Chudomelova, M., Utinek, D. (2017): Dynamics of herbaceous vegetation during four years of experimental coppice introduction. – Folia Geobotanica 52: 83-99.
[8] Hejda, M., Pyšek, P. (2006): What is the impact of Impatiens glandulifera on species diversity of invaded riparian vegetation? – Biological Conservation 132(2): 143-152.
[9] Kløve, B., Ala-Aho, P., Bertrand, G., Boukalova, Z., Ertürk, A., Goldscheider, N., Ilmonen, J., Karakaya, N., Kupfersberger, H., Kvœrner, J. (2011): Groundwater dependent ecosystems. Part I: Hydroecological status and trends. – Environmental Science & Policy 14: 770-781.
[10] Li, E. H., Liu, G. H., Wei, L., Yuan, L. Y., Li, S. C. (2008): The seed-bank of a lakeshore wetland in lake honghu: implications for restoration. – Plant Ecology 195(1): 69-76.
[11] Liu, G., Wan, L., He, F., Tong, Z., Liu, Z., Li, X. (2016): Effects of litter, seed position, and water availability on establishment of seedlings for two semiarid grass species. – Plant Ecology 217: 277-287.
[12] Liu, R. T., Zhao, H. L., Zhao, X. Y. (2013): Changes in soil macrofaunal community composition under selective; afforestation in shifting sand lands in Horqin of Inner Mongolia, northern China. – Ecological Research 28: 1-8.
[13] Liu, Y., Pereira, L. S., Fernando, R. M. (2006): Fluxes through the bottom boundary of the root zone in silty soils: parametric approaches to estimate groundwater contribution and percolation. – Agricultural Water Management 84: 27-40.
[14] Ma, M. (2005): Species richness vs evenness: independent relationship and different responses to edaphic factors. – Oikos 111(1): 192-198.
[15] Ma, Q., Wang, J., Li, X., Zhu, S., Liu, H., Zhan, K. (2009): Long-term changes oftamarix-vegetation in the oasis-desert ecotone and its driving factors: implication for dryland management. – Environmental Earth Sciences 59(4): 765-774.
[16] McLendon, T., Hubbard, P. J., Martin, D. W. (2008): Partitioning the use of precipitation- and groundwater-derived moisture by vegetation in an arid ecosystem in California. – Journal of Arid Environments 72: 986-1001.
[17] Monteleone, A., Skousen, J., Shuler, J., Mcdonald, L., Williams, R., Holaskova, I. (2018): Survival and growth of 20 species of trees and shrubs on Appalachian surface mines. – Land Degradation & Development 29. https://doi.org/10.1002/ldr.2962.
[18] Nolan, R. H., Fairweather, K. A., Tarin, T., Santini, N. S., Cleverly, J., Faux, R., Eamus, D. (2017): Divergence in plant water-use strategies in semiarid woody species. – Functional Plant Biology 44: 1134-1146.
[19] O'Grady, A. P., Eamus, D., Cook, P. G., Lamontagne, S. (2006): Groundwater use by riparian vegetation in the wet–dry tropics of northern Australia. – Australian Journal of Botany 54: 145.

http://www.aloki.hu ● ISSN 1589 1623 (Print) ● ISSN 1785 0037 (Online)
DOI: http://dx.doi.org/10.15666/aeer/1706_1536315374

[20] Qian, J., Wang, Z., Liu, Z., Busso, C. A. (2017): Belowground bud bank responses to grazing intensity in the Inner-Mongolia Steppe, China. – Land Degradation & Development 28: 822-832.
[21] Singh, R., Sagar, R., Srivastava, P., Singh, P., Singh, J. S. (2017): Herbaceous species diversity and soil attributes along a forest-savanna-grassland continuum in a dry tropical region. – Ecological Engineering 103: 226-235.
[22] Sneva, F. A. (1982): Relation of precipitation and temperature with yield of herbaceous plants in eastern Oregon. – International Journal of Biometeorology 26: 263-276.
[23] Tao, Y., Wu, G. L., Zhang, Y. M. (2017): Dune-scale distribution pattern of herbaceous plants and their relationship with environmental factors in a saline-alkali desert in Central Asia. – Science of the Total Environment 576: 473-480.
[24] Wood, P. J., Gunn, J., Smith, H., Abaskutty, A. (2005): Flow permanence and macroinvertebrate community diversity within groundwater dominated headwater streams and springs. – Hydrobiologia 545(1): 55-64.
[25] Yang, Y., Chui, T. F. M. (2017): Aquatic environmental changes and ecological implications from the combined effects of sea-level rise and land reclamation in Deep Bay, Pearl River Estuary, China. – Ecological Engineering 108: 30-39.
[26] Zhu, J. T., Li, X. Y., Zhang, X. M., Yu, Q., Lin, L. S. (2012): Leaf nitrogen allocation and partitioning in three groundwater-dependent herbaceous species in a hyper-arid desert region of north-western China. – Australian Journal of Botany 60: 61.
[27] Zhu, Y., Ren, L., Skaggs, T. H., Lü, H., Yu, Z., Wu, Y., Fang, X. (2010): Simulation of Populus euphratica root uptake of groundwater in an arid woodland of the Ejina Basin, China. – Hydrological Processes 23: 2460-2469.

http://www.aloki.hu ● ISSN 1589 1623 (Print) ● ISSN 1785 0037 (Online)
DOI: http://dx.doi.org/10.15666/aeer/1706_1536315374

EFFECT OF VARIOUS LEVELS OF BIOCHAR INCORPORATION ON SOYBEAN YIELDS, PHYSICAL QUALITY AND NITRIFYING BACTERIA OF BLACK SOIL IN NORTHEAST CHINA

JIN, L.[1,2#] – WEI, D.[1*] – YIN, D.[3#] – ZHOU, B.[2] – LI, Y.[2] – WANG, W.[2] – ZHANG, J.[2] – YU, S.[4] – JIANG, Y.[5] – LI, Y.[6] – CAI, S.[2,7]

[1]*Plant Nutriention and Resources Institute, Beijing Academy of Agriculture and Forestry Sciences, Beijing 100097, China*

[2]*Soil Fertilizer and Environment Resource Institute, Heilongjiang Academy of Agriculture and Science, The Key Laboratory of Soil Environment and Plant Nutrition of Heilongjiang Province, Harbin 150086, China*

[3]*College of Agricultural Science and Technology, Heilongjiang Bayi Agricultural University, Daqing, Heilongjiang 163319, China*

[4]*Institute of Crop Cultivation and Tillage, Heilongjiang Academy of Agricultural Sciences, Harbin 150027, China*

[5]*Heihe Branch of Heilongjiang Academy of Agriculture and Sciences, Heihe 164300, China*

[6]*College of Resources and Environment, Northeast Agricultural University, Harbin 150030, China*

[7]*College of Land and Environment, Shenyang Agricultural University, Shenyang 110866, China*

[#]*These authors contributed equally to this research and should be considered as co-first authors*

**Corresponding author*
e-mail: jinliang19762003@aliyun.com

(Received 12th Jul 2019; accepted 30th Sep 2019)

Abstract. Maize-straw biochar (BC) was applied in a black soil area in Northeast China for investigating its effects on crop yield, soil physical properties and nitrifying bacteria. In this study, BC forms BC1, BC2 and BC3 were incorporated at levels of 15.75, 31.50 and 47.25 t ha^{-1}, respectively, from 2013 to 2014. The control soil was treated with chemical fertilizer (NPK). The results showed that yields of soybean were significantly improved overall due to BC applications, compared with the control. Meanwhile, average soil compaction values of 0 – 20 cm deep soil were decreased from 17.9% to 47.4%. Biochar supplementation decreased the soil wilting coefficients, but increased saturated water content. The available soil water content increased from 0.211 to 0.329 cm^3 cm^{-3} ($R^2 = 0.97$), whereas the bulk density decreased from 1.42 to 1.40 g cm^{-3} ($R^2 = 0.97$) in response to BC supplementation. Unexpectedly, soybean yields began to decline at 31.50 and 47.25 t ha^{-1} of BC application. as well as soil aggregate stability, available water content, and capillary pores, mainly. Moreover, the BC supplementation significantly affected soil ammonia-oxidizing archaea (AOA) abundance. These results demonstrate that BC has positive potential for enhancing crop and soil properties performances in black soil at the level of 15.75 t ha^{-1} under continuous soybean system.

Keywords: *maize-derived biochar, application levels, physical properties, field experiment, black soil*

http://www.aloki.hu ● ISSN 1589 1623 (Print) ● ISSN 1785 0037 (Online)
DOI: http://dx.doi.org/10.15666/aeer/1706_1537515391

Introduction

Given the growth rates since 1960, the global population is expected to reach 9.7 billion by 2050 (Gonzalo et al., 2016). The consequences of human population growth have great impacts on the environment, and also on social and economic development. China accounts for approximately 22% of the world's population which is expected to increase to 14.53 billion by 2030 (Yin and Guo, 2015). Consequently, the additional food required to feed future generations would challenge the production capacity of arable land in the years to come (Golley and Zheng, 2015). The agricultural sustenance of a growing population in the black soil area of Northeast China is threatened by excessive exploitation of soil resources, leading inevitably to soil degradation. In the long run, the current production capacity of the soil may not sustain the long-term needs of a growing population under the current agricultural management level. Thus, control of soil erosion and prevention of organic matter loss have been proposed as critical strategies for sustained agriculture in this area (Luo et al., 2017; Lenka et al., 2017). In Northeast China, manure and corn straw have been used to improve soil fertility and crop yields (Hui et al., 2017; Tong et al., 2017; Liang et al., 2016). Moreover, carbon sequestration and bacterial soil contents have been improved using corn straw and manure (Yang et al., 2017; Ding et al., 2016). However, in contrast to these substrates, biochar (BC) is highly recalcitrant and unavailable to soil microorganisms (Sizmur et al., 2016).

Biochar, being a carbonaceous compound, has been used as a soil additive to counter the degradation of arable land (Luo et al., 2017). Several studies have been carried out on the effects of BC supplementation on soil aggregate formation and the physical properties of a variety of soils (Obia et al., 2016; Pratiwi and Shinogi, 2016; Lim et al., 2016; Guo, 2016). Indeed, Burrell et al. (2016) have reported that BC from straw improved the stability of soil aggregates in Planosol and Cambisol soils, and also improved the water availability to plants in Planosol soil by 38%. A soil study in the Huang-Huai-Hai Plain, China revealed that treatment with BC significantly decreased the bulk density, but increased its total porosity (Du et al., 2016). Moreover, studies have been carried out on the effect of BC supplementation level on the physical and hydraulic properties of soil. In these studies, Igalavithana et al. (2017) applied corn residue BC at levels of 2.5, 5.0, 7.5 and 10% ($w \cdot w^{-1}$) in sandy loamy soil, and after equilibration for 30 days, there were highly significant exponential reductions in Ksat as a result of incorporation of BC500 at levels of up to 7.5%, with Ksat approaching an asymptote at 10% BC500. In another study, it was shown that incubation of soil for 36 days with BC at levels of 1, 2, 5 and 10% (by wt.) reduced the water losses through evaporation and stabilized the activities of some extracellular enzymes (Elzobair et al., 2016). In field experiments, Ippolito et al. (2016) reported that graded applications of BC (1, 2, and 10% by wt.) improved the water content of calcareous soil. Supplementation of podzolic soil with BC at levels of 10, 20 and 30 t ha^{-1}) for 3 years produced significant and positive effects on the yield of winter rye (Kraska et al., 2016) However, most recent studies focused on low-fertility soils or under-leached, acidic saline soils. Thus, not much is known about the effect of levels of application of BC on crop yield and physical conditions of soil in degraded soils containing higher organic matter. The objective of the present study was to investigate the influence of different levels of maize straw-derived BC on continuous soybean production and soil properties such as physical environment and soil nitrifying bacteria. It was hypothesized that higher BC levels should exert positive and negative effects on soybean yield, as well as

http://www.aloki.hu ● ISSN 1589 1623 (Print) ● ISSN 1785 0037 (Online)
DOI: http://dx.doi.org/10.15666/aeer/1706_1537515391

the physical properties of black soil. Three levels of BC supplementation (15.75, 31.5 and 47.25 t ha^{-1}), each mixed with a chemical fertilizer (NPK) separately in a selected field of black soil (Mollisols), were used. Crop yield and physical and hydraulic properties of soil such as compaction, aggregation stability, bulk density, hydraulic parameters and soil surface area were analyzed. The nitrifying bacteria in the BC-supplementaed soils were also evaluated.

Materials and methods

Site, soil and biochar

A long-term BC field experiment was initiated in Minzhu town, Daowai district in Haerbin city, China (E126°51'05", N45°50'3", *Fig. 1*). Climatological data, soil properties of surface layer and biochar properties can be seen in *Tables 1, 2,* and *3* respectively. Biochar applied in this study was derived from maize straw and manufactured by Liaoning Biochar Engineering Technology Center.

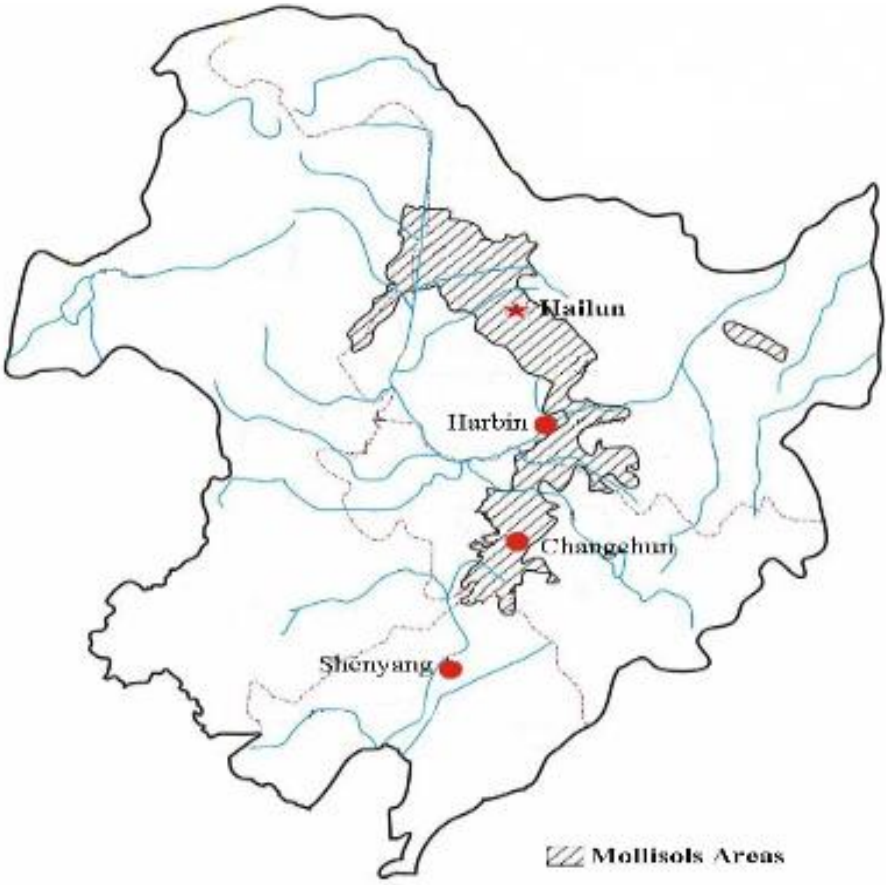

Figure 1. *Map of study area*

Table 1. *Climatological data of experiment station*

Average annual rainfall (mm)	Mean annual wind speed ($m.s^{-1}$)	Maximum wind speed ($m.s^{-1}$)	Sea level (m)	Ground water table depth (m)
514	4.1	18.9	138	80

http://www.aloki.hu ● ISSN 1589 1623 (Print) ● ISSN 1785 0037 (Online)
DOI: http://dx.doi.org/10.15666/aeer/1706_1537515391

Table 2. *Basic chemical and physical properties in soil top layer in experiment plots*

Depth	Mechanical composition (% America)			Texture	Available N	Available P	Available K	SOM*	pH	BD**
cm	Sand	Silt	Clay		mg.kg^{-1}	mg.kg^{-1}	mg.kg^{-1}	g.kg^{-1}		g.cm^{-3}
0-30	21.8	56.3	21.9	Silty clay loam	163.3	20.61	187.92	29.87	6.74	1.31

*SOM: soil organic matter; **BD: bulk density

Table 3. *Biochar components*

Particle components %											
SOC* g.kg^{-1}	O g.kg^{-1}	N g.kg^{-1}	P g.kg^{-1}	K g.kg^{-1}	Si g.kg^{-1}	Mg g.kg^{-1}	Ca g.kg^{-1}	pH	< 0.1 mm	0.1-2 mm	> 2 mm
598	166	7.85	1.327	17.0	60	2	3	8.69	15.0	60.2	24.8

*SOC: soil organic carbon

Treatments

A field experiment with soybean was carried out in 2013 and 2014. The treatments consisted of 3 levels of BC supplementation viz: NPK only, NPK + BC at level of 15.75 t.ha^{-1} (BC1), NPK + BC at level of 31.50 t.ha^{-1} (BC2), and NPK + BC at level of 47.25 t.ha^{-1} (BC3). Each treatment was replicated thrice. In order to guarantee soil and plant samling, every experiment plot was set up by covering an area of 39 m^2 (6 ridges×0.65 m width× 10 m ridge length). The sowing density of soybean was 300,000 plants per hectare. Soybean received sub-surface fertilizer application of 47 kg N ha^{-1}, 78 kg P_2O_5 ha^{-1} and 68 kg K_2O ha^{-1}, with which insecticide were applied of 0.13 to 0.2 kg chlorpyrifos granules ha^{-1} for controlling grubs. Spring soybean cultivar Heinong 58 was planted in May 2013 and harvested in October 2013, while the one planted on May 10, 2014 was harvested on October 5 in 2014. Prior to planting, the chemical fertilizer (NPK) for soybean was applied. In the 2013 period, the BC was spread over the furrow by the ridges. It was thoroughly mixed with soil using a ploughing machine (a tractor with a rototiller, *Fig. 2*), and then plowed to a depth of over 20 cm and then mainary ranked for a leveling. Herbicide applied over the ridges just after soybean sowing (*Table 4*).

Table 4. *Basic physical and chemical properties of soil after harvest in 2014*

Treatment	N (%)	H (%)	O (%)	C (%)	BD* g.cm^{-3}	CEC** cmol.kg^{-1}	SSA*** m^2.g^{-1}	C/N	O/C	H/C
NPK	0.094 ± 0.01d	0.666 ± 0.01a	2.290 ± 0.09b	0.915 ± 0.01c	1.40 ± 0.05a	22.77 ± 0.23c	29.35 ± 0.43d	9.76	2.50	0.73
BC1****	0.179 ± 0.02c	0.624 ± 0.03a	2.344 ± 0.13a	1.800 ± 0.02a	1.28 ± 0.03b	23.08 ± 0.41b	32.74 ± 0.61a	10.05	1.30	0.35
BC2	0.186 ± 0.01b	0.660 ± 0.02a	2.211 ± 0.21b	1.150 ± 0.03b	1.18 ± 0.02d	24.72 ± 0.53a	31.62 ± 0.21b	6.17	1.92	0.57
BC3	0.203 ± 0.02a	0.647 ± 0.01a	1.944 ± 0.11c	0.885 ± 0.02d	1.22 ± 0.02c	24.10 ± 0.20a	30.19 ± 0.20c	4.37	2.20	0.73

BD*: bulk density; CEC**: cation exchange capacity; SSA***: specific surface area; BC****: biochar

http://www.aloki.hu ● ISSN 1589 1623 (Print) ● ISSN 1785 0037 (Online)
DOI: http://dx.doi.org/10.15666/aeer/1706_1537515391

Figure 2. *Ploughing machine working in the biochar-additive field plots*

Measurements

Particle size distribution of BC

The particle size distribution of BC was determined by dry-sieving the samples using a sieve shaker (Endecott Test Sieve Shaker, Watson Victor Ltd.). Seven different fractions were obtained using 2.00, 1.00, 0.50, 0.25 and 0.106 mm sieves. Three consecutive shakings were conducted, and it was observed that the weights of different fractions remained unchanged. The first shaking was continued for 3 min, and the other two shakings were done for only 2 min. Measurements of N_2 gas adsorption for the determination of BET (Brunauer-Emmett-Teller) surface area of BC were carried out using a Micromeritics ASAP 2020 volumetric adsorption system.

Soil compaction

In the field, the soil compaction values were measured with in 2014 after the harvest of soybean with a soil compaction meter (SC-900, *Fig. 3*). The data for the top layer (0-20 cm) were automatically recorded once every 2.5 cm as the soil compaction meter descended from the surface.

Figure 3. *Soil compaction meter (SC-900)*

Soil aggregates and their stability parameters

The size distribution of wet-sieving aggregates was determined with a rototap machine containing a nest of eight 100-mm diameter sieves with screen openings of 10, 7, 5, 2, 1, 0.5 and 0.25 mm. The weight of soil retained on each sieve was measured after dry-sieving 0.5 kg of soil for 2 min. Moreover, 50 g of soil aggregates retained on 100 mm sieve was used for the analysis of wet-sieving which was carried out mechanically using Yoder's apparatus.

The nest of sieves used had mesh sizes of 2, 1, 0.5, 0.25 and 0.106 mm. Wet sieving was continued for 20 min with 40 oscillations per min. The aggregates retained on each sieve were transferred to a set of pre-weighed beakers, oven-dried at 105 °C for 24 h,

http://www.aloki.hu ● ISSN 1589 1623 (Print) ● ISSN 1785 0037 (Online)
DOI: http://dx.doi.org/10.15666/aeer/1706_1537515391

and weighed. The mean weight diameter (MWD) and geometric mean diameter (GMD) were calculated as indices of aggregation as shown in *Equations 1* and *2:*

$$MWD = \frac{\sum_{i=1}^{n}(\bar{d}_i W_i)}{\sum_{i=1}^{n} W_i} \quad \text{(Eq.1)}$$

$$GWD = \text{EXP}\left[\frac{\sum_{i=1}^{n} W_i \ln(\bar{d}_i)}{\sum_{i=1}^{n} W_i}\right] \quad \text{(Eq.2)}$$

where $\bar{d}_i$ is the mean diameter of the class (mm), and W_i is the proportion of aggregate retained on the sieves. The fractal dimension was determined in line with method of Yang et al. (1993), as shown in *Equation 3:*

$$\frac{M(r< \bar{X}_i)}{M_T} = \left(\frac{\bar{X}_i}{X_{max}}\right)^{3-D} \quad \text{(Eq.3)}$$

where $M(r < \bar{X}_i)$ is the cumulative mass of objects or fragments of the i^{th} size, $r < \bar{X}_i$; M_T is the total mass of particles; $\bar{X}_i$ is the mean particle diameter (mm) of the i^{th} size class; and X_{max} is the mean diameter of the largest particle.

Hydraulic parameters

The water retention curve θ (h) of soil was determined using the pressure plate method. Saturated hydraulic conductivity (Ks) was determined using a fixed-head permeameter instrument, and the parameters of θ (h) and unsaturated hydraulic conductivity K (h) were obtained using the van Genuchten–Mulem model (*Eq. 4*).

$$\theta(h) = \theta_r + \frac{\theta_s - \theta_r}{[1+|\alpha h|^n]^m} \quad \text{(Eq.4)}$$

This equation was fitted on the moisture retention data of soil, and the parameters i.e. saturated water content (θs), residual water content (θr), inverse of suction at the inflexion point of the moisture curve (α), and shape parameters (*m* and *n*) were estimated through a non-linear least-squares optimization using RETC (RETention Curve) software.

Pore size distribution

The soil pore size distribution (PSD) was determined using mercury intrusion porosimetry (MIP) (Autopore IV 9500, Micromeritics Inc. USA). In the MIP method, the mercury pressure was increased stepwise, and the intruded volume of mercury was monitored for each pressure in the range of 0.0036–310 MPa. The MIP test indicates the volume of cumulative mercury intruded as a function of equivalent pore radius (EPR). The results obtained were plotted in two graphical forms: cumulative pore volume versus logarithmic EPR, and differential PSD versus logarithmic differentiation (dV/dlog r). The values of pore radii on the cumulative curve and differential curve were 0.003 μm and 360 μm, respectively. This wide range allowed for the detection of diverse soil pore classes along the PSD curve. The pores were classified according to their equivalent pore diameter (EPD) into five classes of sizes: macropores (>75 μm),

http://www.aloki.hu ● ISSN 1589 1623 (Print) ● ISSN 1785 0037 (Online)
DOI: http://dx.doi.org/10.15666/aeer/1706_1537515391

mesopores (30–75 μm), micropores (5–30 μm), ultramicropores (0.1–5 μm), and crytopores (0.1–0.007 μm) according to the method of Camerson and Buchan (2006).

Soil ammonia bacteria [ammonia-oxidizing archaea (AOA) and ammonia-oxidizing bacteria (AOB)]

Total DNA was extracted from frozen soil samples (0.5 g wet weight) using a FastDNA® SPIN Kit For Soil (MP Biomedicals, LLC) in line with the manufacturer's instructions. The concentration and quality of the extracts were determined using UV spectrophotometer (Implen, München, Germany), and the extracts were kept at -20 °C prior to further molecular analysis. Real-time PCR assays (total reaction volume = 20 μL) were carried out using SYBR®Premix Ex TaqTM Perfect Real Time (Takara, Dalian, China), and multicolor real-time PCR detection system (Bio-Rad Laboratories Inc., Hercules, CA, USA). The primer sets (AOA: Arch-amoAF/Arch-amoAR; AOB: amoA-1F/amoA-2R) and thermal profiles used to amplify each target gene with real-time PCR are listed in *Table 1*. The abundance (copy number) of bacterial AOA and AOB genes were calculated using a regression equation to convert the cycle threshold (Ct) values to the known number of copies in the standard curves.

Statistical analysis

All data were analyzed using Microsoft Excel (2003). The significance of differences among different treatments and sampling dates were tested with ANOVA using SPSS software package (SPSS Inc., 2003). Differences between values were considered statistically significant at $p < 0.05$. The coefficient of determination (R^2) of non-linear regression was used to determine the best fit of the water retention model of soil.

Results

Site, soil and BC

The effect of BC application on soybean yields (2013 and 2014) is shown in *Figure 4*. Soybean yields were significantly influenced by BC over two years, when compared with the control (NPK). In the first year, BC1, BC2 and BC3 increased soybean yields by 18.5, 12.5 and 9.7%, respectively, when compared with NPK. Similarly, in the next year, increases in the soybean yield ranged from 15.4% (for BC1) to 4.6% (for BC3). The predominant yield for each year was produced by BC1.

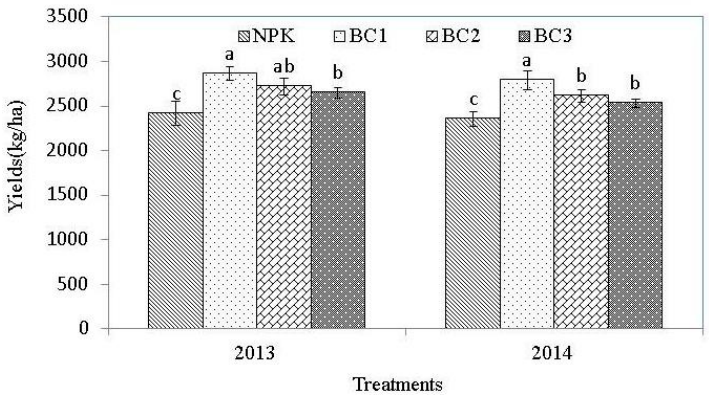

Figure 4. *Effect of BC application on soybean yields from 2013 to 2014*

http://www.aloki.hu ● ISSN 1589 1623 (Print) ● ISSN 1785 0037 (Online)
DOI: http://dx.doi.org/10.15666/aeer/1706_1537515391

Effect of field application of BC on the distribution of soil compaction in the top layer (0-20 cm)

Soil compaction reflects the conditions of pores in the soil and the strength of the junction force in the soil particles. After two years of field application of BC, there was an 'S' trend in the distribution of soil compaction values from the top of the soil (0–20 cm layer) for all treatments, and the compactability increased with increase in soil depth (*Fig. 5A*).

Compared with NPK treatment, BC1, BC2 and BC3 decreased average values of soil compactability distribution within 0-20 cm of soil by 47.4, 38.4 and 17.9%, respectively. The order of average soil compaction values was NPK > BC3 > BC2 > BC1. Except for NPK treatment, the strength of soil compaction was positively related to the supplementation level of BC i.e. BC3 > BC2 > BC1.

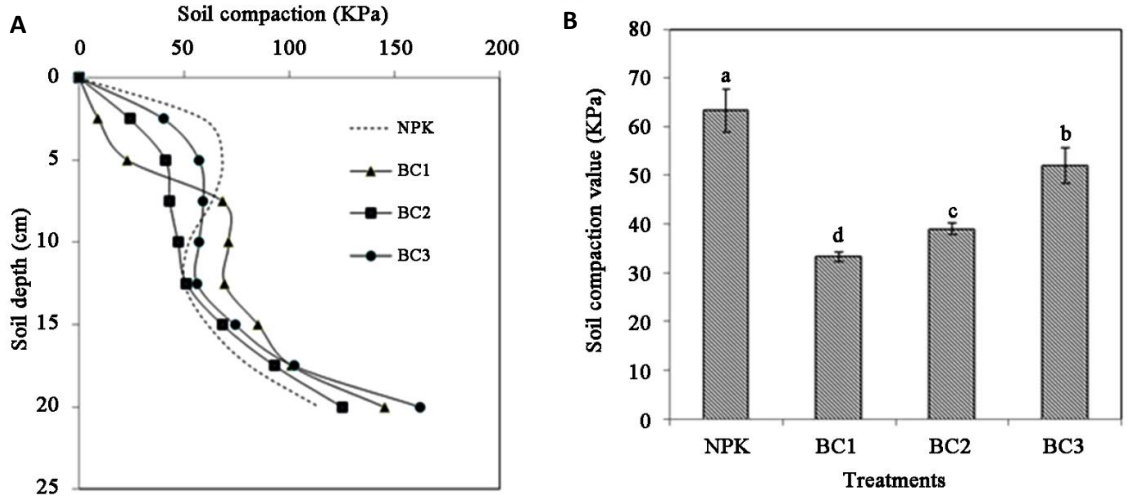

Figure 5. *Effect of BC on the distribution of soil compaction in the top soil layer (0-20 cm, (A); average soil compaction values at 0-20 cm (B)*

Effect of field application levels of BC on the water-stable aggregates

The details are presented in *Table 5.*

Table 5. *Effect of level of supplementation of BC on the composition and stability indices of water-stable aggregates for two years*

Treatments	Aggregate size composition (%)				> 0.25 mm Aggregates (%)	MWD* (mm)	GWD** (mm)
	> 2 mm	2-0.25 mm	0.25-0.106 mm	< 0.106 mm			
NPK	4.54 ± 0.21c	57.94 ± 1.17c	21.92 ± 1.35b	15.60 ± 0.61b	62.48 ± 2.61c	0.26 ± 0.05c	0.27 ± 0.01a
BC1	7.60 ± 0.41a	62.68 ± 1.05a	19.22 ± 1.89c	10.50 ± 0.25d	70.28 ± 1.43a	0.33 ± 0.02a	0.27 ± 0.01a
BC2	6.40 ± 0.11b	60.76 ± 2.06b	19.72 ± 0.94c	13.12 ± 1.54c	67.16 ± 1.51b	0.30 ± 0.01b	0.28 ± 0.02a
BC3	6.19 ± 0.18d	49.01 ± 1.03d	26.02 ± 0.61a	18.78 ± 0.92a	55.20 ± 0.85d	0.27 ± 0.04c	0.28 ± 0.01a

*MWD = mean weight diameter; **GWD = geometric mean diameter

http://www.aloki.hu ● ISSN 1589 1623 (Print) ● ISSN 1785 0037 (Online)
DOI: http://dx.doi.org/10.15666/aeer/1706_1537515391

Aggregate and its stability

The results from wet-sieving (*Table 5*) showed that the addition of BC significantly affected the amounts of macroaggregates (> 0.25 mm), which were increased by 12.5, 7.5 and -11.7% for BC1, BC2 and BC3, respectively, when compared to control (NPK). The changes in the aggregate sizes of 2-0.25 mm showed a positive relationship with MWD values with a correlation coefficient of 0.64 ($P < 0.05$). The mean weight diameter (MWD), geometric mean diameter (GMD) can be used for amended-soil aggregates in the evaluation of the aggregation stability of soil. Higher values of these indices indicate the predominance of the more stable aggregates over the smaller, less stable fractions (Nath and Rattan, 2017; Rabot et al., 2018). From *Table 5*, after two years of the field application of BC in 2014, the MWDs of the of soil aggregate of the three treatments (BC1, BC2 and BC3) were enhanced by 26.6, 15.4 and 3.8%, respectively over the control. No significant differences in GMD were found among the four treatments.

Effect of BC on the hydraulic characteristics of soil

Hydraulic parameters were significantly influenced by the level of BC incorporation, except in a few items in this study such as θs (for BC1, BC2 and BC3) and total porosity (for BC2 and BC3) compared with the control (*Table 6*). Compared to NPK, the incorporation of maize BC at levels of 15.75, 31.5 and 47.25 t.ha^{-1} increased field capacity to 0.379, 0.381 and 0.326 cm.cm^{-1}, respectively, from initial value of 0.291 cm. cm^{-1}. As shown in *Table 6,* wilting coefficient (θ_r) values were significantly reduced, while saturated water content (θ_s) values were not significantly increased at all levels of BC treatments ($p < 0.05$). Smaller particle fraction in BC increased water holding space in black soil more significantly than larger particles (*Tables 2* and *5*). The results showed clearly that incorporation of BC at the level of 15.75 t.ha^{-1} increased the soil k_s, θ_s and available water content by 50.14, 17.94 and 55.92%, respectively, when compared to NPK control ($p < 0.05$). The available water content refers to the difference between field capacity and wilting point; it is the quantity of soil water available for the usage of plants. The highest available water content was 0.332 cm.cm^{-1} for the soil containing BC at the level of 15.75 t.ha^{-1}, while BC at levels of 31.5 and 47.25 t.ha^{-1} decreased available water content to 0.316 and 0.266 cm.cm^{-1}, respectively. The regression equation for the available water capacity of soil as a function of level of incorporation of BC is shown in *Equation 5:*

$$\text{Available water content} = -0.0002(\text{t ha}^{-1}\text{biochar})^2 + 0.0126(\text{t ha}^{-1}\text{biochar}) + 0.2684 \quad \text{(Eq.5)}$$

It is clear from the quadratic equation that the addition of BC at the level of 15.75 t.ha^{-1} increased available water content in the soil, but decreased it at levels of 30.5 and 47.25 t.ha^{-1} ($R^2 = 0.9355$). Field capacity was enhanced by BC incorporation, reaching the highest value of 0.382 cm.cm^{-1}), but wilting point was significantly lower with BC3 than BC2. Thus, the difference (available water content) determined by the two coefficients for BC level of 15.75 t.ha^{-1} was lower (0.329) than that for BC level of 31.5 t.ha^{-1} (0.328).

Figure 6 shows the regression models developed from the results on *Table 6*, which indicates the positive effect of BC on bulk density and available water content. The lower bulk density of the biochar-supplemented soil resulted directly from the

http://www.aloki.hu ● ISSN 1589 1623 (Print) ● ISSN 1785 0037 (Online)
DOI: http://dx.doi.org/10.15666/aeer/1706_1537515391

contribution of pores of BC, since the bulk density of BC-excluded treatment was significantly lower than that of the unamended NPK control. This may be due to changes in total porosity. The results of hydraulic conductivity revealed an initial increase at BC level of 15.75 t.ha^{-1}, which was followed by decreases at BC supplementation levels of 31.5 and 45.25 t.ha^{-1}. This may be due to the hydrophobic nature of organic matter in BC.

Table 6. *Effect of BC on hydraulic parameters of soil samples*

Treatment (0-30 cm)	Θr*	Θs**	α***	n***	k_s**** (mm.min^{-1})	Field capacity (cm.cm^{-1})	Available water content (cm.cm^{-1})	Total porosity %
NPK	0.080 ± 0.005a	0.340 ± 0.03a	0.078 ± 0.01a	1.96 ± 0.17b	10.71 ± 0.56d	0.291 ± 0.02d	0.211 ± 0.02d	47.16 ± 2.61d
BC1	0.050 ± 0.003b	0.401 ± 0.01b	0.017 ± 0.01d	1.71 ± 0.09c	16.08 ± 0.42a	0.379 ± 0.03b	0.329 ± 0.03c	55.47 ± 1.51a
BC2	0.056 ± 0.002c	0.397 ± 0.02b	0.035 ± 0.01b	2.28 ± 0.15a	15.48 ± 0.23b	0.381 ± 0.01a	0.325 ± 0.02a	53.96 ± 0.49b
BC3	0.060 ± 0.005d	0.389 ± 0.02b	0.023 ± 0.02c	1.05 ± 0.3d	11.90 ± 1.05c	0.326 ± 0.03c	0.266 ± 0.02b	51.70 ± 0.84b

*θ_r = soil residual water content/wilting coefficient (cm^3·cm^{-3}); **θ_s = soil saturated water content (cm^3·cm^{-3}); ***α and n = parameters related to the shape of the soil water characteristics curve; ****k_s = hydraulic conductivity

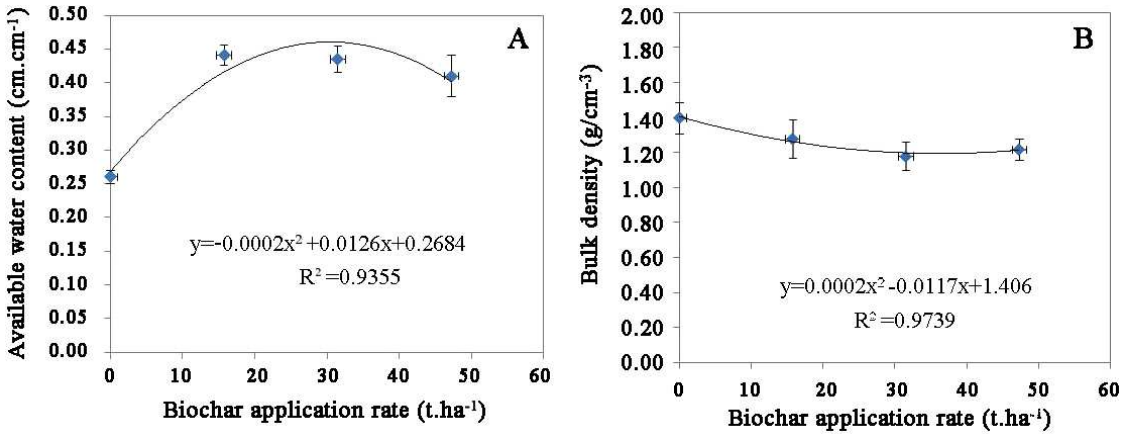

Figure 6. *Regression models for the physical properties and the level of incorporation of BC. A: model for available water content and level of BC supplementation; B: model for bulk density and level of incorporation of BC*

Effect of BC on the pore distribution of soil

The results of pore analysis porosity and pore size distribution of BC-amended soils are shown in *Table 7*. Total pore volume and porosity of soils were higher ($p < 0.05$) in BC-treated soils than in NPK control soil. The degree to which the total porosity values increased with the BC incorporation level varied among the treated soils. The relative increases in total porosity due to BC1, BC2 and BC3 were 17.6, 14.4, and 9.6%, respectively, relative to NPK control. The BC treatment caused significant changes in

http://www.aloki.hu ● ISSN 1589 1623 (Print) ● ISSN 1785 0037 (Online)
DOI: http://dx.doi.org/10.15666/aeer/1706_1537515391

the pore in the ranges of > 75, 30-75, 5-30, and 0.1-5 μm, which indicates that it indeed altered the macro-, meso-, and micropores. However, BC did not significantly affect the crytopores (< 0.1 μm). In SB-amended soil, approximately 32% of the total porosity was in > 75 μm pores, followed by 0.1-5 μm class (approximately 25%), 5-30 μm class (approximately 14%), and 0.01-0.1 μm class (approximately 8%). The changes in pore size distribution brought about by BC treatments could possibly reflect the particle size distribution of BC. Compared with BC1, BC at the higher level of 31.5 $t.ha^{-1}$ increased the total volume, but decreased the macropores and mesopores by 53.54 and 16.50%, respectively, indicating that BC2 produced more unavailable pores leading to less available water in the soil. Compared with BC2, the 78.76% increase in 5-30 μm micropores, and 74.42% decrease in 30-75 μm mesopores are in agreement with the hypothesis that direct changes in capillary pores are caused by the occupation of finer BC particles, leading to decreased available water content at BC levels of 31.5 and 47.5 $t.ha^{-1}$.

Table 7. *Total porosity and pore-size distribution of BC-amended soils*

Treatment	Total volume ($cm^3 g^{-1}$)	Pore size distribution ($cm^3 g^{-1}$)						
		Total porosity (%)	> 75 μm	30-75 μm	5-30 μm	0.1-5 μm	0.1-0.01 μm	< 0.01 μm
NPK	0.2559 ± 0.01d	47.16 ± 1.52d	0.0975± 0.03b	0.0234 ± 0.01c	0.0365 ± 0.0028c	0.0600 ± 0.0041c	0.0261 ± 0.0017c	0.0124 ± 0.0005b
BC1	0.4115 ± 0.02b	55.47 ± 0.97a	0.1892± 0.05a	0.0988 ± 0.03a	0.0224 ± 0.0019d	0.0598 ± 0.0057c	0.0288 ± 0.0011b	0.0125 ± 0.0002b
BC2	0.4201 ± 0.01a	53.96 ± 1.12b	0.0879± 0.04d	0.0825 ± 0.01b	0.053 ± 0.0049b	0.1389 ± 0.0093a	0.0455 ± 0.0035a	0.0123 ± 0.0004b
BC3	0.3197 ± 0.01c	51.70 ± 2.51c	0.0910± 0.01c	0.0211 ± 0.02d	0.0771 ± 0.0065a	0.0902 ± 0.065b	0.0271 ± 0.0012bc	0.0132 ± 0.0003a

Effect of BC incorporation level on the soil nitrifying oxidizers

Changes in soil nitrifying bacteria [soil ammonia-oxidizing archaea (AOA) and soil ammonia-oxidizing bacteria (AOB)] of BC-treated soils are presented in *Table 8*. Values of AOA and AOB ranged from 0.91 to 1.16×10^8 $cfu.g^{-1}$, and from 0.65 to 0.76×10^7 $cfu.g^{-1}$, respectively.

Table 8. *The abundance of soil nitrifying bacteria of biochar-amended soils during harvest in 2014*

Treatment	AOA (10^8)	AOB (10^7)	pH
	$Cfu.g^{-1}$	$Cfu.g^{-1}$	
NPK	1.09 ± 0.03b	0.65 ± 0.03b	6.80 ± 0.23a
BC1	1.16 ± 0.02a	0.81 ± 0.02a	7.13 ± 0.51b
BC2	0.97 ± 0.04c	0.73 ± 0.02b	7.29 ± 0.34c
BC3	0.91 ± 0.05cd	0.76 ± 0.04ab	7.65 ± 0.13b

Similar to pH, AOA abundance was significantly enhanced by the addition of BC, when compared to NPK, but AOB was not significantly increased. The ratio of AOB to

http://www.aloki.hu ● ISSN 1589 1623 (Print) ● ISSN 1785 0037 (Online)
DOI: http://dx.doi.org/10.15666/aeer/1706_1537515391

AOA increases with increasing pH gradient in the rhizosphere (Yu et al., 2019). Biochar at the level in BC1 enhanced AOA and AOB copies, but decreased them in BC2 and BC3.

Discussion

The application of BC enhances crop yields as well as a range of physical properties of soil (Laird et al., 2017; Agegnehu et al., 2016; Burrell et al., 2016; Du et al., 2016). In addition, BC influences soil nitrifying bacteria (Pan et al., 2017; Radwan et al., 2018; Azerang et al., 2018). The application of BC significantly increased the yield of soybean due to soil structure and improvement in moisture content as a result of changes in soil nitrifying bacteria. This can be attributed to the enhanced specific surface area and higher porosity as seen in the present study, which have been shown to enhance microbial activity and increase SOM (Chen et al., 2017; Ren et al., 2018; Sripreechasak et al., 2018; Sangdee et al., 2017). When BC is applied under the influence of tillage and cultivation operations, the distribution of soil compaction in the top layer of soil could be due to a dilution effect for the lighter fraction at the top layer (0-20 cm) (Soane, 1990). It has been reported that microaggregate formation and aggregate stability are significantly improved by the addition of BC (Kaiser et al., 2017; Hartley et al., 2016). The macroaggregates of black soil were significantly increased by incorporation of maize straw-derived BC at the levels of 15.75 and 31.5 $t.ha^{-1}$, and the stability of BC1 (15.75 $t.ha^{-1}$) was enhanced in the additive treatments. On the other hand, BC at levels of 31.5 and 47.25 $t.ha^{-1}$ produced negative effects on aggregate formation, leading to decreases in percentage of macroaggregates and lower MWD values, relative to BC1. This may be partially due to the fine particles with excessive biochar occupying the exist capillary under the external forces of mechanical cultivation and rainfall (Busscher et al., 2010) and then the restrict of microbial activity and nitrogen mineralization (Dempster et al., 2012) leading to less soil cement existed in unit soil mass. Another reason could be the effect of excessive BC which effectively decreased the risk of surface sealing in the BC-amended soils, relative to BC1 (Sun and Lu, 2014). Moreover, the C:N ratio of BC1 was the highest (10.05, *Table* 4), whereas the O:C and H:C ratios were the lowest (1.32 and 0.35, respectively, *Table* 4) among the four treatments (*Table 4*). Generally, a critical C:N ratio of < 25 is important because it indicates the probability of net mineralization of nitrogen (Chapin et al., 2002). The stability of BC-amended soil with a dominant level of BC could also be reflected in O:C and H:C ratios, the correlation coefficient of which was positive 0.97. The lower values of the two ratios resulted in a more stable BC-amended soil (Spokas, 2010; Budai et al., 2013), which could be a major factor that influences the formation of soil aggregates.

The effect of application of BC on water retention capacity is linked to the improvement of soil aggregation or structure (Ibrahim et al., 2017). The available water content in the soil was increased by BC addition at the level of 15.75 t.ha-1, but was decreased at BC levels of 31.5 and 47.25 $t.ha^{-1}$ mainly due to the changes in the capillary pores of the BC-amended soil. The negative effect of these changes could be due to the partial replacement of the clay particles by the finer particles in the BC, followed by a decrease in wilting point. Studies by Nadeem et al. (2017) showed that BC enhanced field capacity, which is consistent with the outcomes of this study. In a series of well constrained laboratory experiments, Liu et al. (2017a) showed that BC particle sizes affected soil water content by changing the pore spaces between particles

http://www.aloki.hu ● ISSN 1589 1623 (Print) ● ISSN 1785 0037 (Online)
DOI: http://dx.doi.org/10.15666/aeer/1706_1537515391

(interpores), and by adding pores that are part of the biochar (intrapores). Moreover, it has been reported that BC treatment either decreases (clogs) or increases pore spaces in the mixture, based on the quantity of fine BC fraction, which in turn could decrease or increase the hydraulic conductivity of the mixture (Trifunovic et al., 2018).

The addition of excess amount of BC (15.75 $t.ha^{-1}$) probably led to filling up of some of the capillary pores existing in the BC-amended soil by the additional dust (< 0.1 mm) that accompanied BC. Thus, the water holding capacity of the soil was reduced at higher BC levels. It has been reported that fine particles of excessive BC fill the soil pores, thereby reducing the permeability while increasing the water retention of BC-amended soil (Uzoma et al., 2011; Busscher et al., 2010). This provides the physical environment in response to changes in soil nitrifying bacteria. Similar to the available water content of soil, bulk density is a parameter which is useful for measuring the relative mass of a solid relative to the bulk volume that the solid occupies, including void spaces. For the non-amended soil, the bulk density was 1.40 $cm.cm^{-1}$, and was decreased to 1.28, 1.18, and 1.22 $g.cm^{-3}$ by BC1, BC2 and BC3, respectively. Bulk density also showed a quadratic regression relationship with increasing level of BC ($R^2 = 0.97$). Recent studies on the negative effect of high BC application on soil-plant system revealed that addition of BC at levels of 10, 20 and 30 t ha^{-1} produced positive influence on grain yield of winter rye, with 20 t ha^{-1} resulting in the highest grain yields (Kraska et al., 2016). Pot experiments revealed that *S. salsa* yield increased from 11.7 to 115% with WS application in the range of 5–10 g kg^{-1}, when compared with control (Sun et al., 2016). However, as BC level increased to 20 g kg^{-1}, the yield decreased to 102%. Usowicz et al. (2016) have reported that incorporation of BC under the fallow led to reduction of soil bulk density and particle density from 1.18–1.20 mg m^{-3} and 2.48–2.55 mg m^{-3} from 0 $t.ha^{-1}$ and 10 t ha^{-1} to 1.00 Mg m^{-3} and 2.20 Mg m^{-3} under 30 t ha^{-1}, respectively. In a field experiment conducted by Liu et al. (2017b), it was found that BC supplementation at levels of 10 and 20 g kg^{-1} soil increased peanut nitrogen fixation by 15.52 and 14.11%, respectively, in an intercropping system where maize (*Zea mays* L.) was intercropped with either soybean (*Glycine max* L.) or peanut (*Arachis hypogaea* L.).

The results obtained in this study reveal that BC exerts both positive and negative effects on the physical environment of black soil, and provide a real growth condition for crop yield, depending on the level of application. Higher concentrations of AOA and AOB improve the conversion of other forms of nitrogen to available nitrogen fertilizer so as to enhance the fertility of soil and promote plant growth (Luo and Lin, 2013). The bacterial indices AOA and AOB are the real driving forces, with AOA being more sensitive to changes in soil rhizosphere environment, especially pH. Indeed, AOA may be regarded as a factor for direct assessment of the benefits of BC, which is in agreement with the results observed in a hydroagric Stagnic Anthrosol and an entic Halpudept (Lin et al., 2017). In this study, increases in pH occurred along with increases in AOB: AOA ratio, leading to increased nitrogen mineralization by stimulating mircrobial activity (Teutscherova et al., 2017). On the other hand, AOA was reduced at higher BC levels mainly due to adverse physical condition of soil, especially decreased availability of water and capillary pores, which negatively affected rhizosphere soil nutrient supply required for crop growth.

http://www.aloki.hu ● ISSN 1589 1623 (Print) ● ISSN 1785 0037 (Online)
DOI: http://dx.doi.org/10.15666/aeer/1706_1537515391

Conclusion

Maize-derived BC incorporation increased the yields of soybean, and improved the physical properties of black soil such as aggregation stability, water holding capacity and pore size distribution. It is evident that as the level of application of BC increased to 37.5 and 47.25 t ha^{-1}, soil aggregation became less stable, possibly due to the negative effect on microbial habitat, leading to decreased stability of soil aggregates and lower levels of binding agents per unit of soil volume. Similarly, available water holding capacity started to decreases at BC level of 37.5 t ha^{-1}, due mainly to the filling of the capillary pore space of BC-soil mixture with finer ashes in excess BC. Moreover, AOA and AOB were enhanced by the lowest BC level (BC1), but inhibited at higher levels (BC2 and BC3), which resulted in direct reduction of crop yield by affecting the nitrogen supply capacity of rhizosphere soil. It is necessary that these results are verified in long-time field observations. Therefore, it can be concluded from these results that the maize straw-derived BC can be applied to black soils as a strategy for optimization of sustainable agricultural production.

Acknowledgements. This research was funded by national Natural Science Foundation of China (41977095; 31901479; 41771284), the Special Fund for National Key R&D Program of China (2018YFD0201000; 2017YFD0200803), Heilongjiang Natural Science Foundation (No. ZD2017008), and we thank the reviewers and issue editor of the journal for the valuable comments and suggestions that led to significant improvements of this manuscript.

REFERENCES

[1] Agegnehu, G., Bass, A. M., Nelson, P. N., Bird, M. I. (2016): Benefits of biochar, compost and biochar-compost for soil quality, maize yield and greenhouse gas emissions in a tropical agricultural soil. – Science of the Total Environment 543: 295-306.

[2] Azerang, P., Sardari, S., Kobarfard, F., Owlia, P., Farahani, Y. F. (2018): Isolation of membrane-active fraction of Streptomyces spp. from soil. – Tropical Journal of Pharmaceutical Research 17(5): 849-855.

[3] Budai, A., Zimmerman, A. R., Cowie, A. L., Webber, J. B. W., Singh, B. P., Glaser, B., Joseph, S. (2013): Biochar carbon stability test method: an assessment of methods to determine biochar carbon stability. – Carbon Methodology, IBI Document, 20 September.

[4] Burrell, L. D., Zehetner, F., Rampazzo, N., Wimmer, B., Soja, G. (2016): Long-term effects of biochar on soil physical properties. – Geoderma 282: 96-102.

[5] Busscher, W. J., Novak, J. M., Evans, D. E., Watts, D. W., Niandou, M. A. S., Ahmedna, M. (2010): Influence of pecan biochar on physical properties of a Norfolk loamy sand. – Soil Science 175(1): 10-14.

[6] Cameron, K. C., Buchan, G. D. (2006): Porosity and Pore-Size Distribution. – In: Lal, R. (ed.) Encyclopedia of Soil Science, CRC, Boca Raton, pp. 1350-1353.

[7] Chapin III, F. S., Matson, P. A., Mooney, H. A. (2002): Terrestrial Nutrient Cycling. – In: Chapin, F. S. I., Matson, P. A., Mooney, H. A. (eds.) Principles of Terrestrial Ecosystem Ecology. Springer-Verlag, New York.

[8] Chen, J., Li, S., Liang, C., Xu, Q., Li, Y., Qin, H., Fuhrmann, J. J. (2017): Response of microbial community structure and function to short-term biochar amendment in an intensively managed bamboo (Phyllostachys praecox) plantation soil: effect of particle size and addition rate. – Science of the Total Environment 574: 24-33.

[9] Dempster, D. N., Gleeson, D. B., Solaiman, Z. I., Jones, D. L., Murphy, D. V. (2012): Decreased soil microbial biomass and nitrogen mineralisation with Eucalyptus biochar addition to a coarse textured soil. – Plant and Soil 354(1-2): 311-324.

http://www.aloki.hu ● ISSN 1589 1623 (Print) ● ISSN 1785 0037 (Online)
DOI: http://dx.doi.org/10.15666/aeer/1706_1537515391

[10] Ding, J., Jiang, X., Ma, M., Zhou, B., Guan, D., Zhao, B., Zhou, J., Cao, F., Li, L., Li, J. (2016): Effect of 35 years inorganic fertilizer and manure amendment on structure of bacterial and archaeal communities in black soil of northeast China. – Applied Soil Ecology 105: 187-195.
[11] Du, Z., Chen, X., Qi, X., Li, Z., Nan, J., Deng, J. (2016): The effects of biochar and hoggery biogas slurry on fluvo-aquic soil physical and hydraulic properties: a field study of four consecutive wheat–maize rotations. – Journal of Soils and Sediments 16(8): 2050-2058.
[12] Elzobair, K. A., Stromberger, M. E., Ippolito, J. A. (2016): Stabilizing effect of biochar on soil extracellular enzymes after a denaturing stress. – Chemosphere 142: 114-119.
[13] Golley, J., Wei, Z. (2015): Population dynamics and economic growth in China. – China Economic Review 35: 15-32.
[14] Gonzalo, J. A., Alfonseca, M., Munoz, F. F. (2016): World Population: Past, Present and Future. Chap. 4: World Population Growth. – World Scientific Publishing, Singapore.
[15] Guo, M. (2016): Application of biochar for soil physical improvement. – Agricultural and Environmental Applications of Biochar: Advances and Barriers, SSSA Special Publication 63: 101-122.
[16] Hartley, W., Riby, P., Waterson, J. (2016): Effects of three different biochars on aggregate stability, organic carbon mobility and micronutrient bioavailability. – Journal of Environmental Management 181: 770-778.
[17] Hui, L. I., Feng, W. T., He, X. H., Ping, Z. H. U., Gao, H. J., Nan, S. U. N., Xu, M. G. (2017): Chemical fertilizers could be completely replaced by manure to maintain high maize yield and soil organic carbon (SOC) when SOC reaches a threshold in the Northeast China Plain. – Journal of Integrative Agriculture 16(4): 937-946.
[18] Ibrahim, A., Usman, A. R. A., Al-Wabel, M. I., Nadeem, M., Ok, Y. S., Al-Omran, A. (2017): Effects of conocarpus biochar on hydraulic properties of calcareous sandy soil: influence of particle size and application depth. – Archives of Agronomy and Soil Science 63(2): 185-197.
[19] Igalavithana, A., Ok, Y., Niazi, N., Rizwan, M., Al-Wabel, M., Usman, A., Lee, S. (2017): Effect of corn residue biochar on the hydraulic properties of sandy loam soil. – Sustainability 9(2): 266.
[20] Ippolito, J. A., Stromberger, M. E., Lentz, R. D., Dungan, R. S. (2016): Hardwood biochar and manure co-application to a calcareous soil. – Chemosphere 142: 84-91.
[21] Kaiser, M., Grunwald, D., Koch, H. J., Rauber, R., Ludwig, B. (2017): Influence of the individual or combined application of biochar and slurry on soil macro-aggregate formation under varying moisture conditions. – EGU General Assembly Conference Abstracts. Vol. 19, EGU2017-6581.
[22] Kraska, P., Oleszczuk, P., Andruszczak, S., Kwiecińska-Poppe, E., Różyło, K., Pałys, E., Gierasimiuk, P., Michałojć, Z. (2016): Effect of various biochar rates on winter rye yield and the concentration of available nutrients in the soil. – Plant, Soil and Environment 62(11): 483-489.
[23] Laird, D. A., Novak, J. M., Collins, H. P., Ippolito, J. A., Karlen, D. L., Lentz, R. D., Sistani, K. R., Spokas, K., Van Pelt, R. S. (2017): Multi-year and multi-location soil quality and crop biomass yield responses to hardwood fast pyrolysis biochar. – Geoderma 289: 46-53.
[24] Lenka, N. K., Satapathy, K. K., Lal, R., Singh, R. K., Singh, N. A. K., Agrawal, P. K., Choudhury, P., Rathore, A. (2017): Weed strip management for minimizing soil erosion and enhancing productivity in the sloping lands of north-eastern India. – Soil and Tillage Research 170: 104-113.
[25] Liang, W., Yuan, J. C., Zhang, H. X. (2016): Research progress on mechanism and related technology of corn straw returning in Northeast China. – Journal of Northeast Agricultural Sciences 41(2): 44-49.

http://www.aloki.hu ● ISSN 1589 1623 (Print) ● ISSN 1785 0037 (Online)
DOI: http://dx.doi.org/10.15666/aeer/1706_1537515391

[26] Lim, T. J., Spokas, K. A., Feyereisen, G., Novak, J. M. (2016): Predicting the impact of biochar additions on soil hydraulic properties. – Chemosphere 142: 136-144.
[27] Lin, Y., Ding, W., Liu, D., He, T., Yoo, G., Yuan, J., Fan, J. (2017): Wheat straw-derived biochar amendment stimulated N_2O emissions from rice paddy soils by regulating the amoA genes of ammonia-oxidizing bacteria. – Soil Biology and Biochemistry 113: 89-98.
[28] Liu, L., Wang, Y., Yan, X., Li, J., Jiao, N., Hu, S. (2017a): Biochar amendments increase the yield advantage of legume-based intercropping systems over monoculture. – Agriculture, Ecosystems & Environment 237: 16-23.
[29] Liu, Z., Dugan, B., Masiello, C. A., Gonnermann, H. M. (2017b): Biochar particle size, shape, and porosity act together to influence soil water properties. – PloS One 12(6): 0179079.
[30] Luo, J., Lin, W. T. (2013): Research progress of ammonia-oxidizing archaea. – Journal of South China University of Technology 41(12): 107-114.
[31] Luo, X., Liu, G., Xia, Y., Chen, L., Jiang, Z., Zheng, H., Wang, Z. (2017): Use of biochar-compost to improve properties and productivity of the degraded coastal soil in the Yellow River Delta, China. – Journal of Soils and Sediments 17(3): 780-789.
[32] Nadeem, S. M., Imran, M., Naveed, M., Khan, M. Y., Ahmad, M., Zahir, Z. A., Crowley, D. E. (2017): Synergistic use of biochar, compost and plant growth-promoting rhizobacteria for enhancing cucumber growth under water deficit conditions. – Journal of the Science of Food and Agriculture 97(15): 5139-5145.
[33] Nath, A. J., Rattan, L. A. L. (2017): Effects of tillage practices and land use management on soil aggregates and soil organic carbon in the north Appalachian region, USA. – Pedosphere 27(1): 172-176.
[34] Obia, A., Mulder, J., Martinsen, V., Cornelissen, G., Børresen, T. (2016): In situ effects of biochar on aggregation, water retention and porosity in light-textured tropical soils. – Soil and Tillage Research 155: 35-44.
[35] Pan, F., Chapman, S. J., Li, Y., Yao, H. (2017): Straw amendment to paddy soil stimulates denitrification but biochar amendment promotes anaerobic ammonia oxidation. – Journal of Soils and Sediments 17(10): 2428-2437.
[36] Pratiwi, E. P. A., Shinogi, Y. (2016): Rice husk biochar application to paddy soil and its effects on soil physical properties, plant growth, and methane emission. – Paddy and Water Environment 14(4): 521-532.
[37] Rabot, E., Wiesmeier, M., Schlüter, S., Vogel, H. J. (2018): Soil structure as an indicator of soil functions: a review. – Geoderma 314: 122-137.
[38] Radwan, A. M., Reyad, N. F., Donia, A. E. R. M., Ganaie, M. A. (2018): Comparative studies on the effect of environmental pollution on secondary metabolite contents and genotoxicity of two plants in Asir area, Saudi Arabia. – Tropical Journal of Pharmaceutical Research 17(8): 1599-1605.
[39] Ren, X., Zeng, G., Tang, L., Wang, J., Wan, J., Liu, Y., Yu, J., Yi, H., Ye, S., Deng, R. (2018): Sorption, transport and biodegradation–an insight into bioavailability of persistent organic pollutants in soil. – Science of the Total Environment 610: 1154-1163.
[40] Sangdee, K., Buranrat, B., Seephonkai, P., Surapong, N., Sangdee, A. (2017): Investigation of antibacterial and anti-cancer activities of Streptomyces sp SRF1 culture filtrate. – Tropical Journal of Pharmaceutical Research 16(11): 2727-2734.
[41] Sizmur, T., Quilliam, R., Puga, A. P., Moreno-Jiménez, E., Beesley, L., Gomez-Eyles, J. L. (2016): Application of biochar for soil remediation. – Agricultural and Environmental Applications of Biochar: Advances and Barriers, SSSA Special Publication 63: 295-324.
[42] Soane, B. D. (1990): The role of organic matter in soil compactibility: a review of some practical aspects. – Soil and Tillage Research 16(1-2): 179-201.
[43] Spokas, K. A. (2010): Review of the stability of biochar in soils: predictability of O:C molar ratios. – Carbon Management 1(2): 289-303.

http://www.aloki.hu ● ISSN 1589 1623 (Print) ● ISSN 1785 0037 (Online)
DOI: http://dx.doi.org/10.15666/aeer/1706_1537515391

[44] Sripreechasak, P., Phongsopitanun, W., Supong, K., Tanasupawat, S. (2018): Lipolytic and antimicrobial activities of Pseudomonas strains isolated from soils in Phetchaburi Province, Thailand. – Tropical Journal of Pharmaceutical Research 17(3): 499-505.
[45] Sun, F., Lu, S. (2014): Biochars improve aggregate stability, water retention, and pore-space properties of clayey soil. – Journal of Plant Nutrition and Soil Science 177(1): 26-33.
[46] Sun, J., He, F., Shao, H., Zhang, Z., Xu, G. (2016): Effects of biochar application on Suaeda salsa growth and saline soil properties. – Environmental Earth Sciences 75(8): 1-6.
[47] Teutscherova, N., Vazquez, E., Masaguer, A., Navas, M., Scow, K. M., Schmidt, R., Benito, M. (2017): Comparison of lime-and biochar-mediated pH changes in nitrification and ammonia oxidizers in degraded acid soil. – Biology and Fertility of Soils 53(7): 811-821.
[48] Tong, Y., Liu, J., Li, X., Sun, J., Herzberger, A., Wei, D., Zhang, W., Dou, Z., Zhang, F. (2017): Cropping system conversion led to organic carbon change in China's Mollisols Regions. – Scientific Reports 7(1): 18064.
[49] Trifunovic, B., Gonzales, H. B., Ravi, S., Sharratt, B. S., Mohanty, S. K. (2018): Dynamic effects of biochar concentration and particle size on hydraulic properties of sand. – Land Degradation & Development 29(4): 884-893.
[50] Usowicz, B., Lipiec, J., Łukowski, M., Marczewski, W., Usowicz, J. (2016): The effect of biochar application on thermal properties and albedo of loess soil under grassland and fallow. – Soil and Tillage Research 164: 45-51.
[51] Uzoma, K. C., Inoue, M., Andry, H., Zahoor, A., Nishihara, E. (2011): Influence of biochar application on sandy soil hydraulic properties and nutrient retention. – Journal of Food Agriculture and Environment 9: 1137-1143.
[52] Yang, P. L., Luo, Y. P., Shi, Y. C. (1993): Soil fractal characteristics measured by mass of particle-size distribution. – Chinese Science Bulletin 38(20): 1896-1899.
[53] Yang, X., Meng, J., Lan, Y., Chen, W., Yang, T., Yuan, J., Liu, S., Han, J. (2017): Effects of maize stover and its biochar on soil CO2 emissions and labile organic carbon fractions in Northeast China. – Agriculture, Ecosystems & Environment 240: 24-31.
[54] Yin, G., Guo, G. (2015): Analysis on China's mid- and long-term food supply and demand trend. – Journal of South China Agricultural University 2: 76-83.
[55] Yu, M., Meng, J., Yu, L., Su, W., Afzal, M., Li, Y., Xu, J. (2019): Changes in nitrogen related functional genes along soil pH, C and nutrient gradients in the charosphere. – Science of the Total Environment 650: 626-632.

http://www.aloki.hu ● ISSN 1589 1623 (Print) ● ISSN 1785 0037 (Online)
DOI: http://dx.doi.org/10.15666/aeer/1706_1537515391

EFFECTS OF THE COUPLING OF WATER AND NITROGEN ON THE YIELD AND QUALITY OF KING GRASS (*PONNISETUM PURPUREUM SCHUMACHER* × *P. GLAUCUM* (LINNAEUS) R. BROWN)

FENG, H. D.[1] – WU, X. C.[2] – ZHONG, C. B.[3] – WANG, H.[1] – WANG, D. F.[1*]

[1]*Tropical Crops Genetic Resources Institute, CATAS, Haikou, Hainan 570211, China*

[2]*Hainan Research Academy of Environmental Sciences, Haikou, Hainan 570206, China*

[3]*Hainan soil and fertilizer station, Haikou, Hainan 570203, China*

[*]*Corresponding author*
e-mail: dfwang@vip.163.com; phone: +86-182-8967-7079

(Received 12th Jul 2019; accepted 14th Nov 2019)

Abstract. Using the method of pot culture, the effect of different water and nitrogen conditions on the growth of King grass [*Ponnisetum purpureum* Schumacher × *P. Glaucum* (Linnaeus) R. Brown] and its physiological response mechanisms were examined. The results showed that under the soil moisture conditions designated as W1 (35%-45%), W2 (55%-65%) and W3 (75%-85%), the application rate of nitrogen corresponded to maximum yields of 271.78, 355.05 and 329.06 kg hm^{-2}, and protein contents of 361.54, 505.44 and 647.88 kg hm^{-2}. With the increase of water stress, the proline content of King grass increased, while the CAT enzyme significantly decreased, and the CAT enzyme increased significantly with the nitrogen content under the same moisture condition. Soil moisture conditions had a greater effect on the yield and quality of King grass than the application rate of nitrogen, but there was a synergistic effect between them. Therefore, if water and nitrogen are properly matched, higher yield and quality can be obtained. The best conditions for water and nitrogen were found to be a soil moisture content of 75%-85% of field capacity and an application rate of 329.06 kg hm^{-2} for nitrogen.
Keywords: *nitrogen, filed capacity, proline, catalase activity, Hainan*

Introduction

King grass [*Ponnisetum purpureum* Schumacher × *P. Glaucum* (Linnaeus) R. Brown] is a perennial grass, also called Napier, in Colombia or Pennisetum and elephant grass or Africa Pennisetum (Xu et al., 2006). King grass has a short growing season, high yield, more tillers, regeneration capacity and other characteristics (Zhao et al., 2015). Under moderate water and fertilizer conditions, King grass can grow for up to 9 months each year (Xie et al., 2012), fresh yield of 2.25×10^5 kg hm^{-2}, stump tiller 50 to 80, the second year of high fresh yield $(3.0\text{-}3.75)\times10^5$ kg hm^{-2}. King grass not only provides high yield, but nutritious protein, the per hectare of which can reach that of 8-10 hm^2 corn. In addition, King grass is soft and juicy, highly palatability, and is one of the best feeds for herbivorous livestock and fish (Li et al., 2015).

Irrigation and application of chemical fertilizer are two major factors for agricultural production, and they are two important technical measures that also offer productivity control. In crop production, irrational use of water and chemical fertilizer resources can waste water and fertilizer and pose a serious threat to the environment (Zhou et al., 2016). Therefore, a study of rational application of water and chemical fertilizer aspect cannot be ignored. For the purpose of detect the effects of the coupling of water and nitrogen on the yield and quality of King grass, soil moisture and nitrogen fertilizer

http://www.aloki.hu ● ISSN 1589 1623 (Print) ●ISSN1785 0037 (Online)
DOI: http://dx.doi.org/10.15666/aeer/1706_1539315401

were used as dependant variables in trial pot experiments to determine the impact of water and nitrogen coupling on King grass growth traits. In addition, the response of proline and catalase (CAT) and other physiological traits under different water and nitrogen conditions was also examined (Meng et al., 2019).

Material and methods

Materials

The *P. purpureum* × *P. Glaucum* CV. Reyan No. 4 was selected as test materials. The latsol granite was applied for pot culture of King grass. Soil texture is sandy loam soil, and the main physical and chemical properties shown in *Table 1*.

Table 1. *Soil physical and chemical characteristics*

pH	Organic matter g kg^{-1}	Alkaline hydrolysis N mg kg^{-1}	Available P mg kg^{-1}	Available K mg kg^{-1}
6.12	6.9	101.5	7.2	47.1

Experimental design

The soil was air-dried and passed through 2 mm mesh. Each pot, which was 31 cm × 29 cm (D × H), fitted 20 kg soil.

Set three soil moisture levels, namely: W1: saturation field capacity of 35%-45%; W2: saturation field capacity of 55%-65%; W3: saturation field capacity of 75%-85%. Soil moisture of each pot was measured using a moisture meter (DELMHORST) at 4:30pm each day, and water was added to maintain the preset moisture level in each pot. To the pots containing these three soil moisture conditions, four nitrogen contents were applied as follows: N0: 0 g kg^{-1}; N1: 0.0675 g kg^{-1}; N2: 0.135 g kg^{-1}; N3: 0.2025 g kg^{-1}. These applications were equivalent to the following amount of nitrogen fertilizer per hectacre 0 kg hm^{-2}, 151.875 kg hm^{-2}, 303.75 kg hm^{-2}, 455.625 kg hm^{-2}. All the treatments were conducted with completely randomized block design and three replicates. In addition, each pot was treated with 0.0668 g P_2O_5 kg^{-1} and 0.0668 g K_2O kg^{-1}. Phosphate fertilizer was applied as basic fertilizer. Potassium fertilizer was applied in two batches, 50% as basic fertilizer and 50% used as additional fertilizer after 60 days of planting. Nirtrogen fertilizer dissolved in water and was applied in three batches, which were after planting 30, 60 and 90 days. Fertilizer types were: urea nitrogen, phosphate with calcium magnesium phosphate and potassium chloride.

These tests were conducted in August 10th to 20th December, in 2017 at greenhouse of Danzhou County (Hainan, China), Hainan University, College of Agriculture campus bases.

Analytical methods

Fresh yields and dried yields above ground were weighted after planting 130 days (Bao, 2000). The field capacity was determined by Wilcox method (Jiang et al., 2006). All crude fiber contents of King grass were determined with acid elimination decomposition method. The crude grass protein contents were converted from total

http://www.aloki.hu ● ISSN 1589 1623 (Print) ●ISSN1785 0037 (Online)
DOI: http://dx.doi.org/10.15666/aeer/1706_1539315401

nitrogen contents, which was determined by semi-micro Kjeldahl method (He, 1983). Proline content was measured using ninhydrin colorimetric method (Wang, 2011). Catalase activity was determined by potassium permanganate titration method (Wang, 2011).

Statistical analysis

Description statistics, Anova test were performed by SAS 9.0 on Windows. And the none linear regression model was applied to estimate the optimized soil moisture and application rate of nitrogen in King grass. The figures were conducted by Sigmaplot 10.0 on Windows.

Results

Effects of different water and nitrogen treatments on King grass yield

As shown in *Figure 1*, at a constant level of nitrogen fertilizer, the yield of grass was directly related to the soil water content. This is confirmed by the fact that the W1, W2, W3 moisture conditions, resulted in yields of 37.33%-62.41%, 56.69%-76.42%. At W3 each fertilization yields are the highest and significantly higher than other water treatment levels, indicating that W3 is optimum moisture content of the soil for growing King grass. As can be seen from the figure at the W1, W2 and W3 water level, the correlation coefficient of nitrogen fertilizer rates and yield were: 0.998, 0.994 and 0.998 (n=12, P<0.001). According to nitrogen contents at different water levels, it can be seen that the corresponding moisture conditions Nitrogen yield the highest point of the King grass were 2.42 g pot^{-1}, 3.16 g pot^{-1}, 2.92 g pot^{-1}, equivalent hectare fertilizer were: 271.78 kg hm^{-2}, 355.05 kg hm^{-2} and 329.06 kg hm^{-2}.

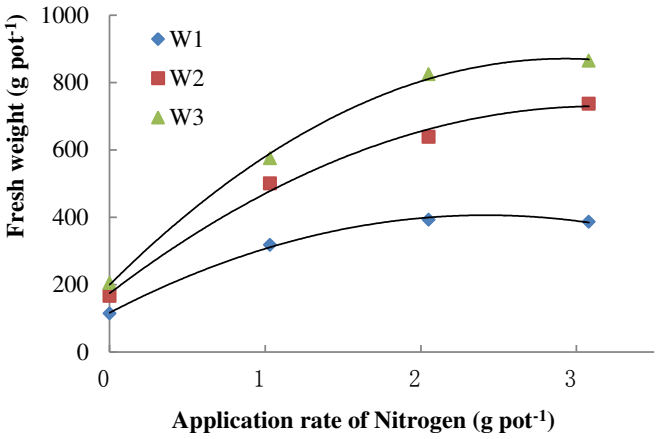

Figure 1. *Effect of application rate of N on the production of King grass in different moisture conditions*

Effects of different water and nitrogen treatments on the crude protein content

The contents of crude protein in King grass with decreasing soil moisture content at a fixed nitrogen level (*Fig. 2*). At a fixed nitrogen content, the King grass crude protein content under moderate water (W1) treatment was significantly higher than the other

http://www.aloki.hu ● ISSN 1589 1623 (Print) ●ISSN1785 0037 (Online)
DOI: http://dx.doi.org/10.15666/aeer/1706_1539315401

two soil moisture content levels and the mild water treatment (W2) is slightly higher than the appropriate water treatment (W3). Within a range, the Nitrogen content can result in higher protein yields form King Grass. In the W1, W2 and W3 water levels, the correlation coefficient between nitrogen fertilizer rates and crude protein were: 0.937, 0.868 and 0.939 (n=12, P<0.001). At different soil water contents the crude protein content of the highest levels of nitrogen were 3.21 g pot^{-1}, 4.49 g pot^{-1} and 5.76 g pot^{-1}, equivalent hectares of 361.54 kg hm^{-2}, 505.44 kg hm^{-2} and 647.88 kg hm^{-2}.

Effects of different water and nitrogen treatments on crude fiber content

Figure 3 shows that at a constant moisture content, the crude fiber content of King grass increased as the with nitrogen soil content decreased. Beyond a minimum nitrogen content the grass crude fiber content increased, but there is an optimum soil nitrogen content as the data show. When nitrogen levels were in the range of N1-N2, the crude fiber content of the King grass was in the range of 28.06%-30.93%. Therefore, the optimum application rate of nitrogen is between 28.17%-34.08%.

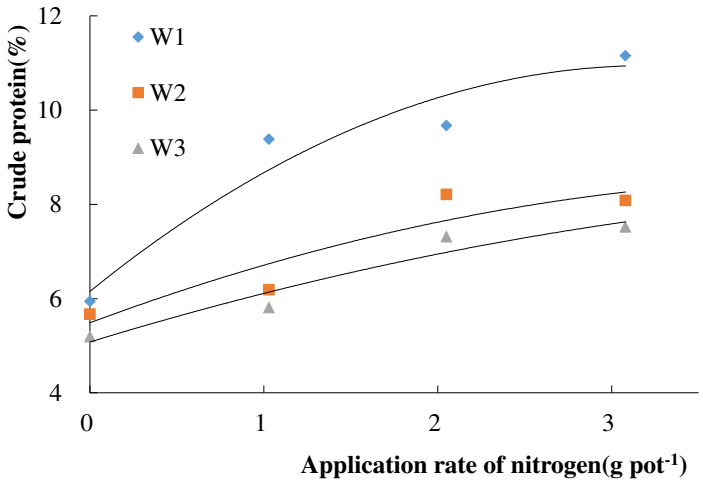

Figure 2. *Effect of application rate of N on the crude protein of King grass in different moisture conditions*

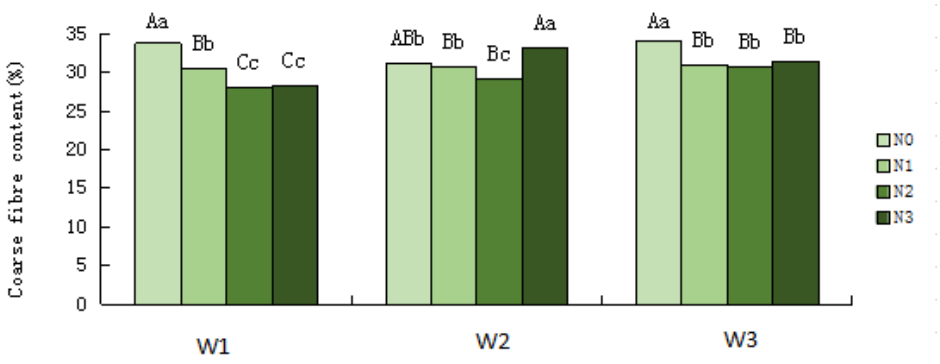

Figure 3. *Effects of water and nitrogen coupling on the crude fibre content of King grass*[†]
[†]*Among columns followed by different miniscule (capital) letters are significantly different at P <0.05 (P<0.01)*

http://www.aloki.hu ● ISSN 1589 1623 (Print) ●ISSN1785 0037 (Online)
DOI: http://dx.doi.org/10.15666/aeer/1706_1539315401

Effects of different water and nitrogen treatments on Proline content

As the water stress on the grass increased, there was a significant increase in the accumulation of proline in the King grass (*Fig. 4*). Under moderate water deficit level W1, proline content was between 109.02-215.91 ug g^{-1}. Conditions W2 and W3 led to average increase of 54.64% and 135.73%, The water level in W1 caused the King grass proline content to increase with increasing nitrogen rate. As can be seen, compared with N0, N1, N2, N3, resulted in, an increase of 6.38%, 60.63%, 98.04% of proline content. Moisture levels in W2 caused, the King grass proline content to be in the range of 75.22-125.61 ug g^{-1} also exhibiting increases with the amount of nitrogen fertilizer. This increase for N, N1, N2, N3, respectively, was 23.91%, 38.70%, 67.00% proline content. Proline accumulation was lowest in the W3 water treatment condition, its content was between 50.76-81.73 ug g^{-1}, significantly lower than the other two under each N treatments moisture levels.

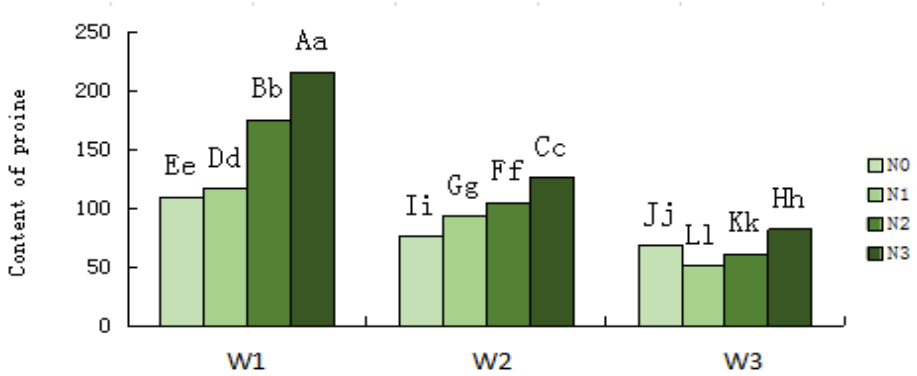

Figure 4. *Effects of different water and nitrogen on the proline of King grass*[†]
[†]*Among columns followed by different miniscule (capital) letters are significantly different at P <0.05 (P<0.01)*

Effects of different water and nitrogen treatments on catalase activity

The effect of water and nitrogen on CAT enzyme activity in the King grass is shown in *Figure 5*. As water stress increased, CAT activity in the King grass decreased, while at constant soil moisture content CAT activity increased gradually with increasing amounts of nitrogen. CAT activity was the highest at the highest level of nitrogen, N2. Under moderate water deficit situation W1, the CAT activity was the lowest, between 1.76-1.99 mg g^{-1} min^{-1}. At the W3 water treatment, the CAT activity exhibited the highest performance, between 1.98-2.12 mg g^{-1} min^{-1}, but at the N2, N3 levels it was 2.12 mg g^{-1} min^{-1}, significantly higher than the other treatments.

King grass yield and fertilizer coupling model building

With the King grass yields as the dependent variable, the relative soil moisture content, and nitrogen rate as the independent variables, regression analysis, yields the following regression model:

$$Y=-48.3549+203.1436X_1+0.1547X_2+0.3259X_1X_2-142.6219X_1^2-0.000545X_2^2 \quad \text{(Eq.1)}$$

http://www.aloki.hu ● ISSN 1589 1623 (Print) ●ISSN1785 0037 (Online)
DOI: http://dx.doi.org/10.15666/aeer/1706_1539315401

where: X_1 for soil moisture (%), X_2 is nitrogen rate (kg hm^{-2}), Y is yield of King grass (t hm^{-2}). Upon examination, the F value is 130.25, the coefficient of determination R^2 is 0.99 ($P<0.001$), indicating that the regression equation was highly significant. Factor levels are the dimensionless linear encoder substitution, standardized partial regression coefficient, it can affect the primary and secondary status on yield trial judge according to their size factors, factors which characterize the role of sign direction. Considering the partial regression coefficient 1, 2 times the item, we can see the level of soil moisture (X_1) the degree of influence on the King grass yield is higher than the amount of nitrogen fertilizer (X_2) the degree of influence.

A term X_1 (soil moisture), X_2 (nitrogen) coefficients 203.1436, 0.1547 are positive, indicating increased soil moisture and nitrogen fertilizer applied were significantly increased yield, soil moisture coefficient is higher than nitrogen rate coefficient, indicating that the soil water is the more important factor affecting the King grass production; independent variables X_1, X_2 interaction term coefficient of 0.3259 is greater than zero, indicating that there are obvious synergies between soil moisture and nitrogen fertilizer application, so a reasonable match between the two, the King grass can obtain a higher yield; since squared variable coefficients are negative, indicating that the King grass yield and moisture content and the amount of nitrogen fertilizer as a function of diminishing returns, that is, when the moisture content and the amount of excess nitrogen can lead to lower yields.

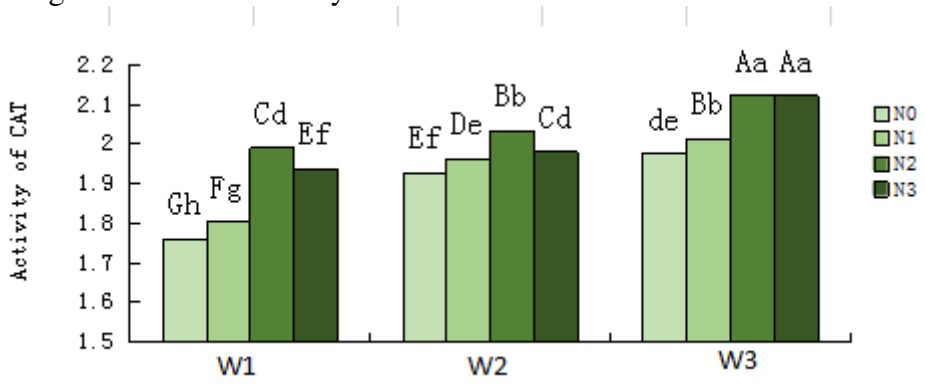

Figure 5. *The effect of different water and nitrogen treatments on activity of CAT of king grass*[†]
[†]*Among columns followed by different miniscule (capital) letters are significantly different at P <0.05 (P<0.01)*

Discussion

Water and Nitrogen Conditions relationship with King grass yield and nutrition

This study shows that under different moisture conditions, although King grass yields increase with increasing nitrogen, the increase in production gradually reduced, showing a decreasing rate fertilizer law (Si et al., 2017). Under this condition, the moisture content is a major factor limiting the growth of the King grass. The soil moisture at a mild deficit (W2) condition, results in an inadequate supply of water so that increases in nitrogen are needed to compensate (Luo et al., 2019). This weakens the degree of production caused by inadequate water supply; while under appropriate moisture (W3) condition, an insufficient supply of nitrogen fertilizer can compensate for low soil moisture content demonstrating the synergistic effect required to achieve the

http://www.aloki.hu ● ISSN 1589 1623 (Print) ●ISSN1785 0037 (Online)
DOI: http://dx.doi.org/10.15666/aeer/1706_1539315401

"water promote fat" effect, reducing the King grass yield caused by the lack of nitrogen to reduce hazards (Wang et al., 2019).

At various levels of soil moisture content, the highest crude protein content of King grass required fertilizer inputs that were higher than the required amount of nitrogen to maintain the highest yield. So simply increasing nitrogen to increase the proportion of crude protein in the grass, will reduce yield, but will also lead to reduction in the utilization of nitrogen and eventual nitrogen leaching which will present environmental risks (Liu et al., 2012). Soil moisture levels and nitrogen inputs are the main limiting factor affecting crop yield and quality (Huang, 2003), and are the two factors that offer significant synergies (Hajaji et al., 2013). Therefore, the King grass yield can be based on the actual production to adjust the ratio of water and nitrogen.

Physiological response to different water and nitrogen conditions

Osmotic adjustment is an important physiological mechanism of plant adaptation to drought stress. Increasing the intracellular concentration of solute plants through metabolic activity, lowers osmotic potential and maintains turgor pressure, so a variety of physiological processes are related normal turgor (Xu et al., 2016). Currently crop drought resistance is closely related to the penetration of regulating substances of which there are three, namely, proline (Pro), betaine and soluble sugars. Often in the free state of proline widespread in plants, when the plants are exposed to environmental stress, free proline increasingly accumulates in plants (Li et al., 2017), the largest accumulation of proline results from drought stress. For the King grass, under moderate water deficit (W1) cases, the highest accumulation of proline, is when nitrogen increases, which is consistent with findings Nadzariah et al. (2018). The moisture deficit (W2) condition, causes proline accumulation which is secondary only to the W1 condition, but also exhibited an increase with nitrogen rate rise phenomenon. As shown under water stress, proline accumulation is closely related to the ability of King grass to react to water stress. But on the other hand, studies have shown that nitrogen levels can improve the ability of the plant to adjust to osmotic changes while strengthening the crop's sensitivity to drought, this aspect needs further study (Zhang, 2008; Li et al., 2014).

Conclusions

Within the scope of this study, under W1, W2 and W3 water level, the highest yield of the corresponding amount of nitrogen fertilizer were 271.78 kg hm^{-2}, 355.05 kg hm^{-2} and 329.06 kg hm^{-2}. The impact of soil moisture on grass yield is higher than the influence of the King grass amount of nitrogen, and there are significant synergies between the two facots, both with a reasonable, King grass can get a higher yield, to meet the needs of herbivorous livestock in order to maintain the balance of ecological environment. Under the experimental conditions, when soil moisture is W3 (75%-85%), nitrogen rate was 329.06 kg hm^{-2}, the King grass can significantly increase yields and improve its quality. The nitrogen can be applied by water solution, the concentrations and application volumes should be studied in future.

Acknowledgements. Anonymous reviewers are appreciated for their comments on this study. The National Key Research and Development Program of China (2017YFD0202100); Key Research and Development Program of Hainan Province Hainan Province (ZDYF2018065); Central Public-interest Scientific Institution Basal Research Fund for Chinese Academy of Tropical Agricultural Sciences (1630032017042).

http://www.aloki.hu ● ISSN 1589 1623 (Print) ●ISSN1785 0037 (Online)
DOI: http://dx.doi.org/10.15666/aeer/1706_1539315401

REFFERENCES

[1] Bao, S. D. (2000): Agricultural soil analysis. – China Agriculture Press, Beijing.
[2] Hajaji, A. N., Donia, B., Raghda, H., Houda, G., Karine, P., Haouari, C. C. (2013): The Role of Nitrogen Availability for the Salt-Tolerance of Two Different Varieties of Durum Wheat. – Bulletin of Environmental Contamination and Toxicology 91: 711-717.
[3] He, Z. Y. (1983): Oils and grain quality analysis techniques. – Agricultural Press, Beijing.
[4] Huang, J. G. (2003): Plant Nutrition. – China Forestry Press, Beijing.
[5] Jiang, P. F., Lei, T. W., Liu, X. H., Wu, Y., Li, X. (2006): Principles and experimental verification of capillary suction method for fast measurement of field capacity. – Transactions of the CSAE 22: 1-5.
[6] Li, S. T., Han, J. G., Mao, P. S., Qian, J. L. (2014): Effect of osmotic stress and phosphorus on growth of kentucky bluegrass under hydroponic culture and mowing conditions. – Acta Agriculturae boreali-occidentalis sinica 23: 138-144.
[7] Li, M., Zi, X. J., Bai, C. J., Zhou, H. L., Liu, G. D. (2015): Rumen degradation characteristics of kinggrass at different plant heights. – Acta Veterinaria et Zootechnica sinica 46: 1806-1815.
[8] Li, T. L., Hu, X. T., Wang, W. E., Du, B., Ma, W. G. (2017): Effects of Water Stress on Proline and Malonadialdehyde Content in Leaves of Spring Maize. – Water Saving Irrigation 34-37.
[9] Liu, Y., Shen, C. Y., Xiao, X. Y., Liu, X. P., Liao, Z. H., Zhong, Y. D., Qiu, R. J., Li, Z. Y. (2012): Effects of Water and Fertilizer Coupling on Growth, Yield, Quality and Fertilizer Utilization Rate of Tobacco in Dry Land. – Acta Agriculturae Jiangxi 24: 100-102.
[10] Luo, Y. J., Song, B., Liu, J. P., Meng, Y. L., Zhou, X. (2019): Effect of water and fertilizer coupling at seedling stage on agronomic traits，yield and yield traits of maize. – Journal of Mountain Agriculture and Biology 38: 79-83.
[11] Meng, F. X., Duan, Y. J., Yang, Y. J., Yang, G. H., Hai, H. G. (2019): Effects of mixed saline Stress on photosynthetic characteristics and antioxidant enzymes activity of cassava seedlings. – Chinese Agricultural Science Bulletin 35: 34-39.
[12] Nadzariah, K. Z., Mohd, Y. A., Sariam, O., Nadzirah, K. Z. (2018): Growth and Physiological Performance of Aerobic and Lowland Rice as Affected by Water Stress at Selected Growth Stages. – Rice Science 25: 82-93.
[13] Si, Z. Y., Gao, Y., Shen, X. J., Liu, H., Gong, X. W., Duan, A. W. (2017): Effects of nitrogen and irrigation water application on yield, water and nitrogen utilization and soil nitrate nitrogen accumulation in summer cotton. – Journal of Applied Ecology 28(12): 3945-3954.
[14] Wang, X. K. (2011): Principle and Technology of Plant Physiological and Biochemical Experiments. – Higher Education Press, Beijing.
[15] Wang, H. D., Li, J., Cheng, M. H., Zhang, F. C., Wang, X. K., Fan, J. L., Wu, L. F. Fang, D. P., Zou, H. Y., Xiang, Y. Z. (2019): Optimal drip fertigation management improves yield, quality, water and nitrogen use efficiency of greenhouse cucumber. – Scientia Horticulturae 357-366.
[16] Xie, Y., Wu, P. B., Qi, Z. P., Wu, W. D. (2012): Responses of imperatoria yield and quality to biochar of different concentration gradient. – Guangdong Agricultural Sciences 11: 133-135, 144.
[17] Xu, M. Y., Xie, F., Guo, M. (2006): Cultivation and Utilization of Hybrid Giant Napier. – Heilongjiang Animal Science and Veterinary Medicine 3: 53-55.
[18] Xu, L. X., Yi, H. L., Guo, E. H., Zhang, A. Y. (2016): Influence of drought stress on physiology characteristics and agronomic traits at heading stage of setaria italica L. – Journal of shanxi university (Nat. Sci. Ed): 672-678.

http://www.aloki.hu ● ISSN 1589 1623 (Print) ●ISSN1785 0037 (Online)
DOI: http://dx.doi.org/10.15666/aeer/1706_1539315401

[19] Zhang, W. W. (2008): Yield and utilization of water and nitrogen for winter wheat/summer maize affected by nitrogen and phosphorus on day-land. – Northwest A&F University.
[20] Zhao, Y. H., Lu, Y. H., Chen, W., Jiang, W. (2015): Research on the comprehensive exploitation and utilization of hybrid giant napier. – Journal of Yichun College 37: 89-91.
[21] Zhou, M. Y., Zhao, R. L., Gu, Y. F., Zhang, F. X., Xu, H. P. (2016): Effects of water and nitrogen coupling on growth and physiological characteristics of overground part of rice. – Transactions of the CSAE 22: 38-43.

http://www.aloki.hu ● ISSN 1589 1623 (Print) ●ISSN1785 0037 (Online)
DOI: http://dx.doi.org/10.15666/aeer/1706_1539315401

AN APPROACH TO GROWTH AND YIELD MODELS FOR INDIVIDUAL CHINA-FIR (*CUNNINGHAMIA LANCEOLATA*) TREES IN SOUTHEAST CHINA

XU, H.[1] – SUN, Y. J.[2*] – WU, X. D.[3] – WANG, Z. J.[3] – HE, J. L.[3] – YU, H. Q.[3]

[1]*School of Economics and Management, Ningxia University*
No. 489 Helanshan West Road, Yinchuan 750021, PR China
(phone: +86-952-509-3001)

[2]*College of Forestry, Beijing Forestry University*
No. 35 Qinghua East Road, Haidian District, Beijing 100083, PR China

[3]*Research Institute of Desertification Control, Ningxia Academy of Agriculture and Forestry Science, No. 590 Huanghe East Road, Yinchuan 750002, PR China*

[*]*Corresponding author*
e-mail: sunyj@bjfu.edu.cn; phone: +86-10-6233-8197

(Received 12th Jul 2019; accepted 14th Nov 2019)

Abstract. As the most commonly grown afforestation species in southeast China, China-fir (*Cunninghamia lanceolata*) shows a huge ecological service function. Generalized individual-tree growth models were developed for *C. lanceolata*. Data was obtained from 61 plantation-grown China-fir trees in 17 single-species plots located in four sites by stem analysis. The best base models were chosen from five theoretical growth equations for modeling increases in diameter at breast high, tree, height and stem volume using ordinary nonlinear least squares regression; selection criteria were the smallest absolute mean residual, root mean square error and the largest adjusted coefficient of determination. To account for autocorrelation in the data with repeated measures, we developed a nested multi-level nonlinear mixed-effects (NLME) model, constructed on the selected base model; the NLME models incorporated random effect for tree, plot and site. The best random-effects combinations for the NLME models were identified by Akaike's information criterion, Bayesian information criterion and -2 logarithm likelihood. Heteroscedasticity was reduced and autocorrelation was also addressed. For diameter and height growth, the NLME models including the exponential function and ARMA(1,1) performed best, and the NLME models including the power function and ARMA(1,1) performed best for stem growth. The NLME models were considered to be the best approach to analyze the variation of tree growth and yield.
Keywords: *individual-tree model, autocorrelation, heteroscedasticity, nonlinear mixed-effects models, Cunninghamia lanceolata*

Introduction

China-fir (*Cunninghamia lanceolata* (Lamb.) Hook.) is the most commonly grown afforestation species in southeast China. According to the National Continuous Forest Inventory, about 10.96 million ha and 726.09 million m^3 of China-fir is distributed in more than ten provinces in China in 2015, making it the number one species in terms of harvest volume. As a result, a sustainable forest management plan for the species needs to be established.

The availability of growth information, such as growth models for individual tree characteristics including diameter at breast height (d), total tree height (h) and stem volume (v), enables a more detailed description than stand-level models (Burkhart, 2003; Vanclay, 2003). This important asset in sustainable forest management allows the selection of tree species for estimation of cutting cycles as well as for logging or

http://www.aloki.hu ● ISSN 1589 1623 (Print) ●ISSN1785 0037 (Online)
DOI: http://dx.doi.org/10.15666/aeer/1706_1540315418

protection (Adame et al., 2008). These basic growth models simplify the study of the variability of individual-tree increments and the estimation of yields directly; they also serve as the main tool used to estimate dynamic variability of biomass and carbon storage indirectly. In addition, they allow silvicultural treatments to be simulated and enable comparison of alternative thinning regimes (Mabvurira and Miina, 2002).

Individual-tree growth models are established based on tree growth increments as the dependent variable and the comparable factors, such as age, as the independent variables. They can simulate growth for individual trees (Sharma et al., 2016) and provide an invaluable tool for forest management planning at any level (Uzoh and Oliver, 2008).

The ordinary non-linear least squares (ONLS) regression, is the most commonly used statistical method in forest modeling (Grégoire et al., 1995). Individual-tree growth models have been fitted to growth increment data collected repeatedly over time on the same tree. The hierarchical nature of the data results in spatial and temporal correlation among observations made in the same sampling unit (i.e., site, plot and tree). However, the stochastic structure is often ignored and independence of observations is assumed (Gutzwiller and Riffell, 2007; Hao et al., 2015). Furthermore, when data are autocorrelated they cannot be considered to be independent samples of the basic tree population (Fox et al., 2001). Therefore, a violation of the ONLS regression assumption of independent residuals exists and results in biased estimates of the standard error of parameter estimation (Dumont et al., 2018).

Nonlinear mixed-effects (NLME) models incorporate both fixed and random effects. Fixed effects are parameters associated with an entire population or with certain repeatable levels of experimental factors, while random effects are associated with individual experimental units drawn at random from a population (Zhu et al., 2019). Random effects account for spatial and temporal correlation by defining the covariance structure of the model's random components and by using this structure during parameter estimation. Therefore, the evolution of NLME models provides an efficient statistical method for explicitly modeling hierarchical stochastic structure (Sharma et al., 2016; Abiyu et al., 2018; Huff et al., 2018). Because of their flexibility, NLME models have become increasingly used to forest growth and yield modeling (Fu et al., 2013; Matos et al., 2013; Xu et al., 2014; Huff et al., 2018).

The main objective of this study was to develop individual-tree growth models for *C. lanceolata* in Fujian Province, southeast China. The data were derived from 61 trees in 17 sample plots located in four sites. A multi-level nonlinear mixed modeling approach that included both fixed and random components was applied to the hierarchical structure of the data. This diminished the level of variance among the sampling units, which were included as covariates. In developing the growth models, we considered the use of nested three-level models. The first, second, and third levels are the site, the plots nested within the site, and the tree, nested within the plot within site, respectively. Our preliminary analysis showed that the NLME models with random effects effectively removed the heteroscedasticity and autocorrelations in repeated-measure data, and therefore could be important tools for sustainable management of the China-fir species within the study area. The predictive ability of the model developed here and the applicability of the NLME model were demonstrated using separate validation data.

http://www.aloki.hu ● ISSN 1589 1623 (Print) ●ISSN1785 0037 (Online)
DOI: http://dx.doi.org/10.15666/aeer/1706_1540315418

Materials and methods

Data

Pure China-fir stands located in Jiangle County (26°26′–27°04′N, 117°05′–117°40′E), Fujian Province, in southeast China with a red soil type were used in this study. Average mean precipitation, frost-free length, and temperature were about 1699 mm, 287 days, and 18.7°C, respectively.

The sampling period took place over 2016-2017 during the summer. The data were obtained from 61 trees in 17 single-species plots of plantation-grown China-fir that located in four sites, identified as the Qiantan, Shuinan, Yuhua and Yuandang areas, which were numbered I, II, III and IV, respectively (*Fig. 1*).

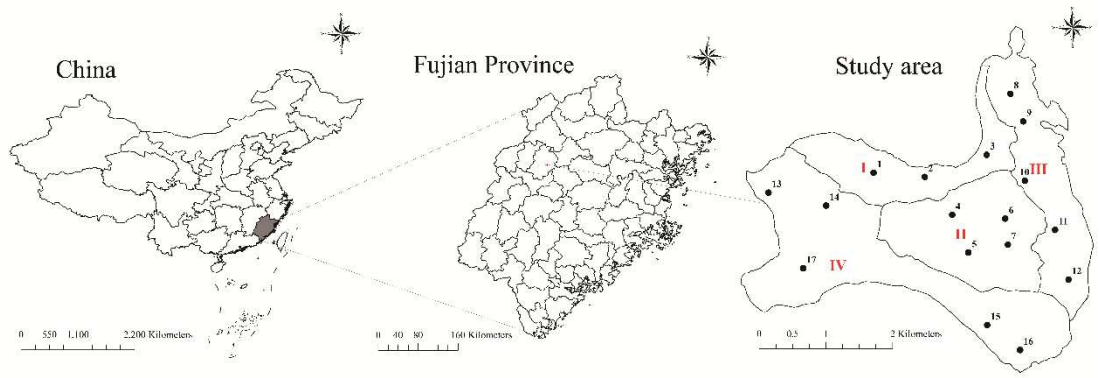

Figure 1. *Seventeen sample plots located in four regions in Fujian Province, southeast China*

Sample plots were square and varied in size from 400 to 600 m^2. The increments of *d*, *h* and *v* per year were measured or calculated, using the stem analysis approach. The data were randomly divided into two groups; 75% of the points were used for model fitting, and 25% were used for model validation. The fitting data and the validation data included 23 trees from eight plots, and eight trees from four plots, respectively. To achieve more confidence in the results, the fitting and validation data were chosen three times and the model estimation and prediction procedures were also iterated. However, the procedures and results were listed only once in this paper, including summary statistics for both fitting and validation data (*Table 1*). The increments data of *d*, *h* and *v* are graphically depicted in *Fig. 2*.

Methods

Individual-tree growth equations

Five theoretical nonlinear growth equations (NLs), the Richards, Weibull, Korf, Logistic and Schumacher equations, were selected as candidates for modeling individual-tree growth. These equations are widely used for the simulation of individual-tree growth, particularly the Richards and Korf equations (Zhang et al., 2011; Xu et al., 2014). *Table 2* shows the mathematical expressions of the equations.

The five equations mentioned above are all S-shaped growth equations with inflection points and asymptotes. One characteristic of the Richards, Weilbull and Korf equations is that the coordinates of inflection points are variable multiples of asymptotic values; in contrast, the equivalent of the Logistic and Schumacher equations are fixed

http://www.aloki.hu ● ISSN 1589 1623 (Print) ●ISSN1785 0037 (Online)
DOI: http://dx.doi.org/10.15666/aeer/1706_1540315418

multiples. The five equations were initially fit by ONLS regression without considering random parameters. Different initial values for the parameters were tried to ensure that a global minimum was achieved. The best performing function was selected as the base model by applying three statistical criteria; absolute mean residual (AMR), root mean square error (RMSE), and adjusted coefficient of determination (adj-R^2) (Zhang et al., 2011). The function with the smallest AMR and RMSE and the largest adj-R^2 provides the best fit. Similarly, the adjusted coefficient of determination is used as an unbiased estimator in both multiple regression and canonical redundancy analysis. The formulas of the fit statistics are:

$$\text{AMR} = \sum_{i=1}^{M}\sum_{j=1}^{M_i}\sum_{k=1}^{n_{ij}}\frac{\left|y_{ijk}-\hat{y}_{ijk}\right|}{n_{ij}} \quad \text{(Eq.1)}$$

$$\textbf{RMSE} = \sqrt{\sum_{i=1}^{M}\sum_{j=1}^{M_i}\sum_{k=1}^{M_{ij}}\sum_{l=1}^{n_{ijk}}\frac{\left(y_{ijkl}-\hat{y}_{ijkl}\right)^2}{n_{ijk}-r}} \quad \text{(Eq.2)}$$

$$\textbf{adj-R}^2 = 1-\left(n_{ijk}-1\right)\left[\frac{\sum_{i=1}^{M}\sum_{j=1}^{M_i}\sum_{k=1}^{M_{ij}}\sum_{l=1}^{n_{ijk}}\frac{\left(y_{ijkl}-\hat{y}_{ijkl}\right)^2}{n_{ijk}-r}}{\sum_{i=1}^{M}\sum_{j=1}^{M_i}\sum_{k=1}^{M_{ij}}\sum_{l=1}^{n_{ijk}}\left(y_{ijkl}-\bar{y}\right)^2}\right] \quad \text{(Eq.3)}$$

where M is the number of sites, M_i is the number of plots within the i^{th} site, M_{ij} is the number of trees within the j^{th} plot of the i^{th} site, n_{ijk} is the number of observations (increments), r is the number of parameters in the model, y_{ijkl} is the value of increments of k^{th} tree taken from the j^{th} plot in the i^{th} site, $\hat{y}_{ijkl}$ is the increment prediction, and $\bar{y}$ is the average of observations. The accuracy of the models was tested against the modeling data and against independent data from the same site and plot (Adame et al., 2008).

Table 1. *Summary statistics for increment data for Cunninghamia lanceolata in Fujian Province, in southeast China*

Site	1	2	3	4
Plot	3	4	5	5
Tree	10	14	21	16
d (cm)	13.4–27.7 (18.9)	15.8-22.4 (19.5)	7.3-26.6(15.0)	5.1-10.1 (7.3)
SD	4.4	2.7	6.6	1.8
h (m)	11.5-22.3 (18.0)	15.0-25.0 (19.8)	7.0-24.0 (14.8)	4.1-7.6 (5.9)
SD	3.9	3.6	5.4	1.4
Age (years)	25-38 (30)	23-32 (28)	15-35 (25)	6-8 (7)
SD	4	4	6	1
Elevation (m)	192-242 (226)	227-332 (293)	219-286 (249)	210-276 (243)
SD	21	51	24	36
Slope (°)	15-45(30)	30-41(37)	22-44(29)	34-37(36)
SD	13	5	6	2

Note: *d,* diameter at breast height; *h*, total tree height; SD, standard deviation

http://www.aloki.hu ● ISSN 1589 1623 (Print) ●ISSN1785 0037 (Online)
DOI: http://dx.doi.org/10.15666/aeer/1706_1540315418

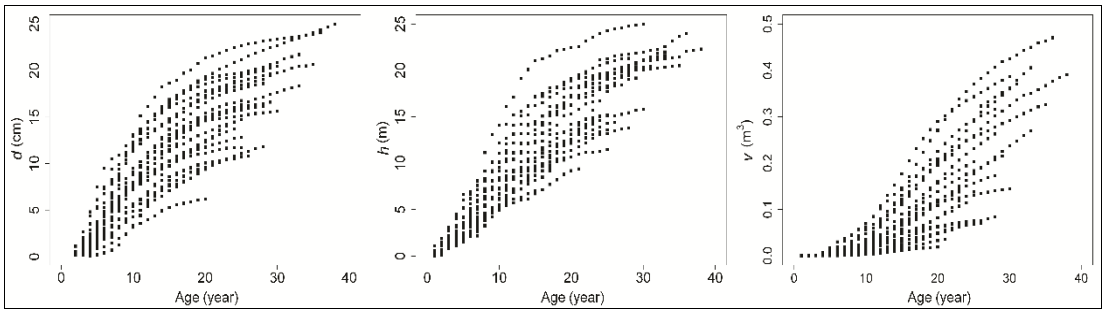

Figure 2. *Plots of increments against age for China-fir*

Table 2. *Mathematical expressions for the five theoretical growth equations*

Equation	Expression	Inflection point		Parameter
		Abscissa	Ordinate	
Richards	$y=a\left(1-\exp\left(-bx\right)\right)^{c}$	$1/\left(b\ln c\right)$	$a\left(1-1/c\right)^{c}$	a, b>0
Weibull	$y=a\left(1-\exp\left(-bx^{c}\right)\right)$	$\left((c-1)/bc\right)^{1/c}$	$a\left(1-\exp\left(1-c\right)/c\right)$	a, b, c>0
Korf	$y=a\exp\left(-b/x^{c}\right)$	$\left((c+1)/bc\right)^{-1/c}$	$a\exp\left((c-1)/c\right)$	a, b, c>0
Logistic	$y=a/\left(1+\exp\left(b-cx\right)\right)$	b/c	$a/2$	a, c>0
Schumacher	$y=a\exp\left(-b/x\right)$	$b/2$	ae^{-2}	a, b>0

Source of equations: Duan et al., 2003; Zhang et al., 2011

Multi-level NLME models

Available data were based on the measured annual increment of the sample plots located at different sites. The nested sampling structure created a high degree of correlation among observations taken from the same tree, plot and site. To alleviate this, a mixed-effects model approach has been proposed by other authors (Laird and Ware, 1982; Palmer et al., 1991; Grégoire et al., 1995). A general expression for a NLME model can be defined as (Lindstrom and Bates, 1990; Vonesh and Chinchilli, 1997):

$$y_{ijkl}=f\left(\phi_{ijkl},x_{ijkl}\right)+\varepsilon_{ijkl}\ i=1,...,M,\ j=1,...,M_i,\ \ k=1,...,M_{ij},\ l=1,...,n_{ijk} \quad \text{(Eq.4a)}$$

where x_{ijkl} is the age, ϕ_{ijkl} is a parameter vector, $r\times 1$, f is a nonlinear function of the predictor variables and the parameter vector, and ε_{ijkl} is the within-group error including the within-group variance and correlation (Davidian and Giltinan, 1995) which is assumed to be normally distributed with zero expectation and a positive-definite variance-covariance structure R_{ijkl} (Meng and Huang, 2009):

$$\varepsilon_{ijkl}\sim \mathrm{N}\left(0,R_{ijkl}\right) \quad \text{(Eq.4b)}$$

http://www.aloki.hu ● ISSN 1589 1623 (Print) ●ISSN1785 0037 (Online)
DOI: http://dx.doi.org/10.15666/aeer/1706_1540315418

Moreover, ϕ_{ijkl} can be expressed as:

$$\phi_{ijkl} = A_{ijkl}\lambda + B_{i,jkl}\mu_i + B_{ij,kl}\mu_{ij} + B_{ijkl}\mu_{ijk} \quad \text{(Eq.4c)}$$

$$\mu_i \sim \mathrm{N}(0,\psi_i),\ \mu_{ij} \sim \mathrm{N}(0,\psi_{ij}),\ \mu_{ijk} \sim \mathrm{N}(0,\psi_{ijk}) \quad \text{(Eq.4d)}$$

where λ is the $p \times 1$ vector of fixed population parameters (where p is the number of fixed parameters in the model). μ_i, μ_{ij} and μ_{ijk} are the $q_1 \times 1$, $q_2 \times 1$ and $q_3 \times 1$ vectors of random effects associated with the first, the second and the third levels, respectively (where q_1, q_2, q_3 are the numbers of random parameters of different levels in the model). μ_i, μ_{ij} and μ_{ijk} are assumed to be normal (or Gaussian) with a mean of 0 and have the variance-covariance matrices ψ_i, ψ_{ij} and ψ_{ijk}, which are the $q_1 \times q_1$, $q_2 \times q_2$ and $q_3 \times q_3$ variance-covariance matrices of random effects in three levels, respectively. A_{ijkl}, $B_{i,jkl}$, $B_{ij,kl}$ and B_{ijkl} are design matrices of size $r \times p$, $r \times q_1$, $r \times q_2$ and $r \times q_3$ for the fixed and random effects of different levels specific to each sampling unit, respectively.

Determining the variance-covariance structure

The variance-covariance matrices Ψ_i, Ψ_{ij} and Ψ_{ijk} are positive-definite and symmetric, which is to say that all their eigenvalues must be strictly positive (Pinheiro and Bates, 2000). A hypothetical 2×2 variance-covariance matrix is shown as follows (Calama and Montero, 2004; Fu et al., 2013):

$$\begin{bmatrix} \sigma_u^2 & \sigma_{uw} \\ \sigma_{wu} & \sigma_w^2 \end{bmatrix} \quad \text{(Eq.5)}$$

where σ_u^2 and σ_w^2 are the variances for the random effects u and w, respectively, and $\sigma_{uw} = \sigma_{wu}$ is the covariance among random effects u and w.

Determining the structure of R

The matrix R_{ijkl} can be proposed to include both correlation effects and weighting factors to account for within-tree heteroscedasticity and autocorrelation (Davidian and Giltinan, 1995; Calama and Montero, 2004; Meng and Huang, 2009). In this study, a general expression for the matrix is given by (Calama and Montero, 2004; Crecente-Campo et al., 2010):

$$R_{ijkl} = \sigma^2 G_{ijk}^{0.5} I_{ijk} G_{ijk}^{0.5} \quad \text{(Eq.6)}$$

where G_{ijk} is an $n_{ijk} \times n_{ijk}$ diagonal matrix within-tree heteroscedasticity variances and I_{ijk} is an $n_{ijk} \times n_{ijk}$ matrix showing the within-tree autocorrelation structure of errors, and σ^2 is a scaling factor for the error dispersion (Calama and Montero, 2004; Crecente-Campo et al., 2010).

http://www.aloki.hu ● ISSN 1589 1623 (Print) ●ISSN1785 0037 (Online)
DOI: http://dx.doi.org/10.15666/aeer/1706_1540315418

In individual-tree growth models, the variance is often found to be dependent of the means, and the variance will generally increase with increasing mean tree diameter. To remove this effect, we modeled the variance as an exponential function or power function (Pinheiro and Bates, 2000). Autocorrelation structures were used to address the within-tree correlations observed in the data. A method was selected from among three commonly used approaches: first-order autoregressive structure [AR (1)], a combination of first-order autoregressive and moving average structures [ARMA (1,1)], and the compound symmetry structure (CS) (Pinheiro and Bates, 2000).

$$V\left(\varepsilon_{ijkl}\right)=\sigma^2\exp\left(2\delta x_{ijkl}\right) \quad \text{(Eq.7)}$$

$$V\left(\varepsilon_{ijkl}\right)=\sigma^2 x_{ijkl}^{2\delta} \quad \text{(Eq.8)}$$

$$\mathbf{AR}(1)=\sigma^2\begin{bmatrix}1 & \rho & \rho^2\\ \rho & 1 & \rho\\ \rho^2 & \rho & 1\end{bmatrix} \quad \text{(Eq.9)}$$

$$\mathbf{ARMA}(1,1)=\sigma^2\begin{bmatrix}1 & \gamma & \gamma\rho\\ \gamma & 1 & \gamma\\ \gamma\rho & \gamma & 1\end{bmatrix} \quad \text{(Eq.10)}$$

$$\mathbf{CS}=\begin{bmatrix}\sigma^2+\sigma_1 & \sigma_1 & \sigma_1\\ \sigma_1 & \sigma^2+\sigma_1 & \sigma_1\\ \sigma_1 & \sigma_1 & \sigma^2+\sigma_1\end{bmatrix} \quad \text{(Eq.11)}$$

where δ is an estimated parameter, ρ is the autoregressive parameter, γ is a moving average component, σ^2 is the residual variance, and σ_1 is the residual covariance (Leak, 1996).

Mixed parameter evaluation

A crucial issue in fitting mixed-effects models is deciding which parameters should be considered random effects and which can be treated as fixed effects. A common approach is to start with random effects for all parameters and then to examine the fitted object to decide which, if any, of the random effects can be eliminated from the model (Pinheiro and Bates, 2000). Therefore, different combinations of model parameters were tested to ascertain their contribution to predictions of individual-tree growth (Adame et al., 2008).

Parameter estimation

The parameters in the equation were estimated by maximum likelihood (ML) using the Lindstrom and Bates (LB) algorithm implemented in the R nlme function (Lindstrom and Bates, 1990; Pinheiro and Bates, 2000). Several articles provide details related to the LB algorithm and nlme function (Lindstrom and Bates, 1990; Pinheiro and Bates, 2000).

http://www.aloki.hu ● ISSN 1589 1623 (Print) ●ISSN1785 0037 (Online)
DOI: http://dx.doi.org/10.15666/aeer/1706_1540315418

Predicting the random effects parameters is more problematic during model application and prediction than during the fitting process. In this case, they were estimated by the EBLUPs (Vonesh and Chinchilli, 1997), using the increment data.

$$\hat{b}_{ijk} \approx \mathrm{D}\mathrm{Z}_{ijk}^{\mathrm{T}}\left(\mathrm{R}_{ijk}+\mathrm{Z}_{ijk}\mathrm{D}\mathrm{Z}_{ijk}^{\mathrm{T}}\right)^{-1}\hat{e}_{ijk} \quad \text{(Eq.12)}$$

where D is the estimated variance-covariance matrix for the random effects $\hat{b}_{ijk}$, R_{ijk} is the estimated variance-covariance matrix for the error term, Z_{ijk} is the estimated partial derivatives matrix, which contains the values of partial derivatives with respect to random effects parameters for the new observation.

Model evaluation

To compare the candidate models and to determine the fixed- versus random-effects parameters for each candidate model, Akaike's information criterion, Bayesian information criterion and -2 logarithm likelihood (Zhao et al., 2012) were used. AIC is the log-likelihood penalized by the number of parameters. BIC is similar but penalizes more for models with more parameters. Based on the AIC, BIC and -2 LL statistics, one or more candidate models were selected for further evaluation (Yang et al., 2009; Hao et al., 2015). The appropriate variance function and autoregressive structure for the NLME models were determined by the likelihood ratio test (LRT) (Pinheiro and Bates, 2000; Fang and Bailey, 2001). The predictions were calculated by *Equation 4* based on the fixed- and random-effects parameters. All models presented in this paper were calibrated using the nlme function in the R statistical environment (Ihaka and Gentleman, 2004; Pinheiro et al., 2005).

Results

Function selection

The R nls function was used to evaluate the parameter estimates and model fit statistics of the five equations (*Table 2*). For *d* and *h* growth models, the Korf equation has slightly better predictive ability than the others do. For *v* growth models, the Richard's equation performs better than the others perform. Therefore, the Korf equation was selected as the basic nonlinear model for estimating *d* and *h* growth models and the Richards equation was selected as the *v* growth model. The final base models are given by:

$$d_{ijkl} = a\exp\left(-b/x_{ijkl}{}^{c}\right)+\varepsilon_{ijkl} \quad \text{(Eq.13)}$$

$$h_{ijkl} = a\exp\left(-b/x_{ijkl}{}^{c}\right)+\varepsilon_{ijkl} \quad \text{(Eq.14)}$$

$$v_{ijkl} = a\left(1-\exp\left(-bx_{ijkl}\right)\right)^{c}+\varepsilon_{ijkl} \quad \text{(Eq.15)}$$

where *a*, *b* and *c* are fixed effects parameters, and ε_{ijk} is the residual noise term.

http://www.aloki.hu ● ISSN 1589 1623 (Print) ●ISSN1785 0037 (Online)
DOI: http://dx.doi.org/10.15666/aeer/1706_1540315418

Construction of NLME models

AIC, BIC and −2 LL fit statistics were compared among different combinations of random effects parameters (*Table 3*). The models represented by *Eqs. 16–17* based on the Korf equation and incorporating the nested effects of site as well as plot and tree on *a* and *b*, yielded the smallest AIC, BIC and −2 LL. Meanwhile, the model represented by *Eq. 18* based on the Richards equation with the nested effects of site, plot and tree on *a* and *b* performed better.

$$d_{ijkl} = \left(\alpha + u_i + u_{ij} + u_{ijk}\right)\exp\left(-\left(\beta + w_i + w_{ij} + w_{ijk}\right)\Big/ x_{ijkl}^{\ \gamma}\right) + \varepsilon_{ijkl} \quad \text{(Eq.16)}$$

$$h_{ijkl} = \left(\alpha + u_i + u_{ij} + u_{ijk}\right)\exp\left(-\left(\beta + w_i + w_{ij} + w_{ijk}\right)\Big/ x_{ijkl}^{\ \gamma}\right) + \varepsilon_{ijkl} \quad \text{(Eq.17)}$$

$$v_{ijkl} = \left(\alpha + u_i + u_{ij} + u_{ijk}\right)\left(1 - \exp\left(-\beta x_{ijkl}\right)\right)^{\left(\gamma + w_i + w_{ij} + w_{ijk}\right)} + \varepsilon_{ijkl} \quad \text{(Eq.18)}$$

where α, β and γ are fixed-effects parameters, u_i and w_i are random-effects parameters generated by site, u_{ij} and w_{ij} are random-effects parameters generated by plot, and u_{ijk} and w_{ijk} are random-effects parameters generated by interaction by tree.

Table 3. *Evaluation indices of each NLME model*

Mixed parameters	*d*			*h*			*v*		
	AIC	BIC	-2 LL	AIC	BIC	-2 LL	AIC	BIC	-2 LL
a	1370.53	1400.00	1356.53	1648.74	1678.78	1634.74	-3364.98	-3334.92	-3378.98
b	1461.37	1490.85	1447.37	1661.18	1691.22	1647.18	-3284.45	-3254.40	-3298.45
c	1336.96	1366.43	1322.96	1619.78	1649.82	1605.78	not converge		
a, *b*	768.90	823.64	742.90	1307.83	1363.62	1281.83	-3951.46	-3895.64	-3977.46
a, *c*	not converge			not converge			-3956.04	-3900.23	-3982.04
b, *c*	864.86	919.60	838.86	1330.43	1386.22	1304.43	-3743.03	-3687.22	-3769.03
a, *b*, *c*	not converge			not converge			not converge		

Note: *a*, *b*, and *c* are fixed parameters; *d*, *h*, and *v* are growth models; AIC, Akaike's information criterion; BIC, Bayesian information criterion; -2 LL, -2 logarithm likelihood

NLME models with heteroscedasticity and autocorrelation

The power function or the exponential function were used as the variance functions and the AR(1), ARMA(1,1) or CS were used as the autocorrelation structures to fit growth models incorporating different random effects (*Table 4*). The selected models had the smallest AIC, BIC and -2 LL. Thus, the final models of the three nested effects of site, plot and tree for *d*, *h*, *v* growth are, respectively:

Eq.16+Eq.7+Eq.10 (Eq.19)

Eq.17+Eq.7+Eq.10 (Eq.20)

Eq.18+Eq.8+Eq.10 (Eq.21)

http://www.aloki.hu ● ISSN 1589 1623 (Print) ●ISSN1785 0037 (Online)
DOI: http://dx.doi.org/10.15666/aeer/1706_1540315418

Parameter estimates

We can conclude the general growth models for China-fir individual-tree in southeast China become:

$$d_{ijkl} = \left(21.1384 + u_i + u_{ij} + u_{ijk}\right)\exp\left(-\left(12.4464 + w_i + w_{ij} + w_{ijk}\right)\Big/ x_{ijkl}^{1.0994}\right) + \varepsilon_{ijkl} \quad \text{(Eq.22)}$$

$$h_{ijkl} = \left(32.7823 + u_i + u_{ij} + u_{ijk}\right)\exp\left(-\left(7.5768 + w_i + w_{ij} + w_{ijk}\right)\Big/ x_{ijkl}^{0.7240}\right) + \varepsilon_{ijkl} \quad \text{(Eq.23)}$$

$$v_{ijkl} = \left(0.2527 + u_i + u_{ij} + u_{ijk}\right)\left(1 - \exp\left(-0.0982 x_{ijkl}\right)\right)^{\left(5.3620 + w_i + w_{ij} + w_{ijk}\right)} + \varepsilon_{ijkl} \quad \text{(Eq.24)}$$

where *Table 5* lists the random effect matrix, residual error, heteroscedasticity and autocorrelation of *d*, *h* and *v* growth NLME models.

Table 4. *Performance criteria for the best NLME models*

Factors	Variance function	Correlation structure	AIC	BIC	-2 LL	LRT	*P* value
d	None	None	768.90	823.64	742.90		
	Exponent	None	768.73	827.67	740.73	2.1744	0.1403
	None	ARMA(1, 1)	10.58	73.74	-19.42	760.1422	<0.0001
	Exponent	ARMA(1, 1)	-183.20	-115.83	-215.20	195.7787	<0.0001
h	None	None	1307.83	1363.62	1281.83		
	Exponent	None	1301.75	1361.83	1273.75	8.0797	0.0045
	None	ARMA(1, 1)	703.78	768.15	673.78	604.9958	<0.0001
	Exponent	ARMA(1, 1)	699.32	767.99	667.32	15.2631	0.0001
v	None	None	-3956.04	-3900.23	-3982.04		
	Power	None	-4811.76	-4751.66	-4839.76	857.7244	<0.0001
	None	ARMA(1, 1)	-4644.57	-4580.17	-4674.57	165.1945	<0.0001
	Power	ARMA(1, 1)	-5694.74	-5626.05	-5726.74	1052.2020	<0.0001

Note: *d*, *h*, and *v* are growth models; AIC, Akaike's information criterion; BIC, Bayesian information criterion; -2 LL, -2 logarithm likelihood; LRT, likelihood ratio test; ARMA, Auto-Regressive and Moving Average

Model prediction

The predictive ability of *Eqs. 13–15* was evaluated using prediction procedures and *Eqs. 1–3* on both fitting and validation data. The performance of the NLME models was evaluated using cross-validation procedures for both fitting and validation data; the random effects were predicted with EBLUPs (*Eq. 12*), using the measurement data.

Table 6 lists the three fit statistics for *Eqs. 13–15* and *22–24*. *Eqs. 22–24* were the best predictors, with increases in adj-R^2 and decreases in RMSE for both fitting and validation data. In *Fig. 3*, the residuals of *Eqs. 13–15* and *22–24* are plotted against the fitted values; the fitted values are plotted against the observed values (*Fig. 4*). Based on the above analysis, we can conclude that the NLME models, such as *Eqs. 22–24*, incorporating nested multi-level effects of site, plot and tree, have sufficiently high predictive power. Therefore, the NLME models incorporating the random effects of site, plot and tree were the best model for predicting *d*, *h* and *v* growth of individual China-fir trees in the single-species plantations of the study area.

http://www.aloki.hu ● ISSN 1589 1623 (Print) ●ISSN1785 0037 (Online)
DOI: http://dx.doi.org/10.15666/aeer/1706_1540315418

Table 5. *The factors of d, h and v growth NLME models*

Factors	*d*	*h*	*v*
Random effect matrix	$\mu_i = \begin{bmatrix} u_i \\ w_i \end{bmatrix} \sim \mathrm{N}\left\{\begin{bmatrix} 0 \\ 0 \end{bmatrix}, \psi_i = \begin{pmatrix} 2.82\text{E-}08 & -0.9936 \\ -0.9936 & 1.3291 \end{pmatrix}\right\}$ $\mu_{ij} = \begin{bmatrix} u_{ij} \\ w_{ij} \end{bmatrix} \sim \mathrm{N}\left\{\begin{bmatrix} 0 \\ 0 \end{bmatrix}, \psi_{ij} = \begin{pmatrix} 2.9163 & -0.7655 \\ -0.7655 & 2.2948 \end{pmatrix}\right\}$ $\mu_{ijk} = \begin{bmatrix} u_{ijk} \\ w_{ijk} \end{bmatrix} \sim \mathrm{N}\left\{\begin{bmatrix} 0 \\ 0 \end{bmatrix}, \psi_{ijk} = \begin{pmatrix} 3.8666 & 0.6956 \\ 0.6956 & 2.1672 \end{pmatrix}\right\}$	$\mu_i = \begin{bmatrix} u_i \\ w_i \end{bmatrix} \sim \mathrm{N}\left\{\begin{bmatrix} 0 \\ 0 \end{bmatrix}, \psi_i = \begin{pmatrix} 6.95\text{E-}04 & -0.0008 \\ -0.0008 & 1.47\text{E-}04 \end{pmatrix}\right\}$ $\mu_{ij} = \begin{bmatrix} u_{ij} \\ w_{ij} \end{bmatrix} \sim \mathrm{N}\left\{\begin{bmatrix} 0 \\ 0 \end{bmatrix}, \psi_{ij} = \begin{pmatrix} 9.4242 & 0.8010 \\ 0.8010 & 1.6542 \end{pmatrix}\right\}$ $\mu_{ijk} = \begin{bmatrix} u_{ijk} \\ w_{ijk} \end{bmatrix} \sim \mathrm{N}\left\{\begin{bmatrix} 0 \\ 0 \end{bmatrix}, \psi_{ijk} = \begin{pmatrix} 2.1015 & 0.0876 \\ 0.0876 & 0.4544 \end{pmatrix}\right\}$	$\mu_i = \begin{bmatrix} u_i \\ w_i \end{bmatrix} \sim \mathrm{N}\left\{\begin{bmatrix} 0 \\ 0 \end{bmatrix}, \psi_i = \begin{pmatrix} 3.71\text{E-}05 & 0.0009 \\ -0.0009 & 1.21\text{E-}05 \end{pmatrix}\right\}$ $\mu_{ij} = \begin{bmatrix} u_{ij} \\ w_{ij} \end{bmatrix} \sim \mathrm{N}\left\{\begin{bmatrix} 0 \\ 0 \end{bmatrix}, \psi_{ij} = \begin{pmatrix} 2.14\text{E-}15 & 0.0012 \\ 0.0012 & 0.9670 \end{pmatrix}\right\}$ $\mu_{ijk} = \begin{bmatrix} u_{ijk} \\ w_{ijk} \end{bmatrix} \sim \mathrm{N}\left\{\begin{bmatrix} 0 \\ 0 \end{bmatrix}, \psi_{ijk} = \begin{pmatrix} 0.1432 & 0.0704 \\ 0.0704 & 0.0005 \end{pmatrix}\right\}$
Residual error	$\varepsilon_{ijkl} \sim N\left(0, R_{ijkl} = 1.4817 G_{ijk}^{0.5} I_{ijk} G_{ijk}^{0.5}\right)$	$\varepsilon_{ijkl} \sim N\left(0, R_{ijkl} = 1.1042 G_{ijk}^{0.5} I_{ijk} G_{ijk}^{0.5}\right)$	$\varepsilon_{ijkl} \sim N\left(0, R_{ijkl} = 0.0302 G_{ijk}^{0.5} I_{ijk} G_{ijk}^{0.5}\right)$
Heterosced-asticity	$V\left(e_{ijkl}\right) = 1.4817 \exp\left(-0.172 x_{ijkl}\right)$	$V\left(e_{ijkl}\right) = 1.1042 \exp\left(-0.0512 x_{ijkl}\right)$	$V\left(e_{ijkl}\right) = 0.0302 x_{ijkl}^{0.9746}$
Correlation structure	$\mathbf{ARMA}(1,1) = 1.4817 \times \begin{bmatrix} 1 & 0.9157 & 0.5409 \\ 0.9157 & 1 & 0.9157 \\ 0.5409 & 0.9157 & 1 \end{bmatrix}$	$\mathbf{ARMA}(1,1) = 1.1042 \times \begin{bmatrix} 1 & 1.0406 & -0.1795 \\ 1.0406 & 1 & 1.0406 \\ -0.1795 & 1.0406 & 1 \end{bmatrix}$	$\mathbf{ARMA}(1,1) = 0.0302 \times \begin{bmatrix} 1 & 1.3387 & -0.4140 \\ 1.3387 & 1 & 1.3387 \\ -0.4140 & 1.3387 & 1 \end{bmatrix}$

Note: *d*, *h*, and *v* are growth models

Table 6. *Performance criteria for each model*

Factor	Model	Fitting data			Validation data		
		AMR	RMSE	adj-R^2	AMR	RMSE	adj-R^2
d	Eq.13	2.3513	2.9111	0.7886	2.5415	3.2828	0.7682
	Eq.22	0.3782	0.5336	0.9929	0.6273	1.3551	0.9601
h	Eq.14	1.7484	2.2899	0.8846	1.8974	3.5255	0.7711
	Eq.23	0.5436	0.7402	0.9869	0.6589	1.5179	0.9576
v	Eq.15	0.0308	0.0482	0.7934	0.0581	0.0704	0.6992
	Eq.24	0.0039	0.0068	0.9956	0.0121	0.0162	0.9841

Note: *d*, *h*, and *v* are growth models

http://www.aloki.hu ● ISSN 1589 1623 (Print) ●ISSN1785 0037 (Online)
DOI: http://dx.doi.org/10.15666/aeer/1706_1540315418

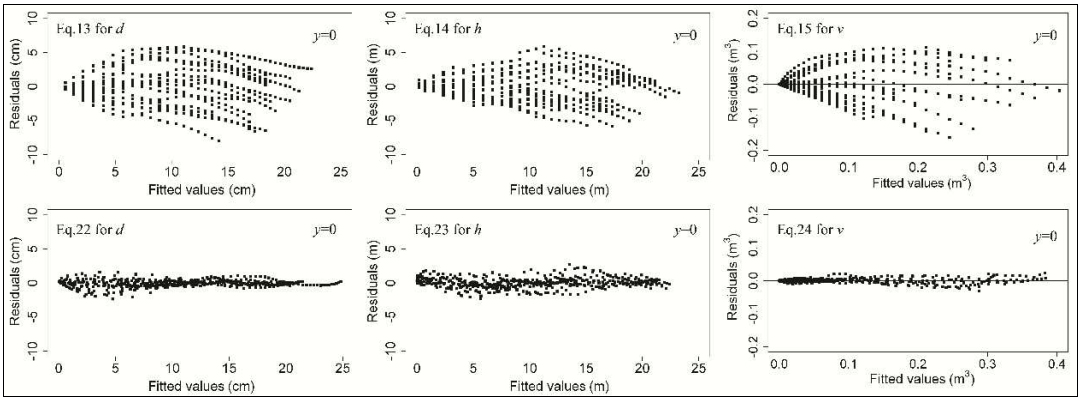

Figure 3. *Distribution of residuals for six equations predicting d, h and v growth of China-fir trees in southeast China*

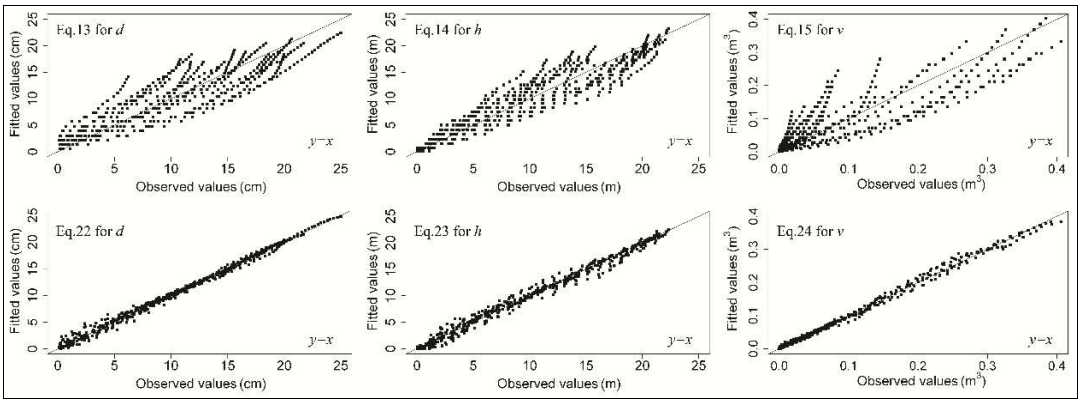

Figure 4. *Fitted values of six equations for d, h and v growth of China-fir trees in southeast China against observed values*

Discussion

Of the five theoretical growth equations tested, the Korf equation provided the best fit for *d* and *h* growth data of China-fir when evaluated based on AMR, RMSE and adj-R^2, while the Richards equation showed the best performance for *v* growth. The results were consistent with the ones of the other two groups of data (*Table 7*). In general, the Korf and Richards equations have been widely used for forest growth and yield simulation models (Birch, 1999; Li et al., 2000; Malik et al., 2005; Gea-Izquierdo et al., 2008; Rugmini and Jayaraman, 2009; Bontemps and Duplat, 2012; Xu et al., 2014). ONLS regression is commonly used to build forest growth and yield models, but its usefulness is limited because tree data typically violate the assumption of independence and identically distributed errors (West et al., 1984; Grégoire et al., 1995). NLME models are useful tools for analyzing repeated measures data and spatially correlated data (Pinheiro and Bates, 2000; Fang and Bailey, 2001). A model can be constructed with a unique variance-covariance structure that eliminates the influence of random effects (site, plot and tree effects in this study) (Zhu et al., 2019). The two primary challenges in fitting NLME models are determining the mixed parameter and calculating the random effects (Uzoh and Oliver, 2008; Yang et al., 2009; Dumont et al., 2018; Huff et al., 2018).

http://www.aloki.hu ● ISSN 1589 1623 (Print) ●ISSN1785 0037 (Online)
DOI: http://dx.doi.org/10.15666/aeer/1706_1540315418

The Richards and Korf equations have been widely used as the base NLME model for modeling forest growth and yield. For example, Fang and Bailey (2001) successfully used a modified Richards equation with an NLME model to build a slash pine (*Pinus elliottii* Engelm.) dominant height growth model. In their study, the Korf equation was chosen as the base model of the NLME model to fit loblolly pine (*Pinus taeda* Linn) *d*-age relationships (Cheng and Gordon, 2012); in that case, the nested three-level individual-tree NLME models (*Eqs. 22–24*) provided the best fit. Parameters *a*, *b*, *c* are the asymptotic values, the values associated with the growth rate of the tree and the values associated with the curve shape of both the Richards and Korf equations, respectively (Zhang and Sun, 2010). Therefore, the random effects (site, plot and tree) mainly influence the growth rate and the maximum value of the tree for *d* and *h* growth, and the maximum value and curve shape for *v* growth.

Table 7. *Performance criteria of each model for the other two groups of data*

Factor	Model	Fitting data			Validation data			Fitting data			Validation data		
		AMR	RMSE	adj-R^2	AMR	RMSE	adj-R^2	AMR	RMSE	adj-R^2	AMR	RMSE	adj-R^2
d	NL	2.4651	3.1384	0.7864	2.6182	2.5714	0.7239	2.3921	2.9307	0.8011	2.4138	3.0136	0.7115
	NLME	0.4103	0.5602	0.9932	0.5048	1.0890	0.9505	0.2978	0.4462	0.9954	0.6421	1.4126	0.9366
h	NL	1.8253	2.6288	0.8634	1.9182	2.3799	0.8291	2.1056	2.6702	0.8541	2.3251	2.6509	0.8179
	NLME	0.5814	0.8215	0.9865	0.7082	1.4060	0.9403	0.6631	0.9141	0.9829	0.7980	1.4794	0.9388
v	NL	0.0508	0.0573	0.7739	0.0604	0.0340	0.6756	0.0827	0.0561	0.7583	0.0904	0.0572	0.7263
	NLME	0.0055	0.0178	0.9782	0.0095	0.0129	0.9535	0.0049	0.0170	0.9778	0.0084	0.0217	0.9438

Note: *d*, *h*, and *v* are growth models

Sometimes, no prior information is available from which the random parameters can be predicted. In this case, the mixed-effects model with the random parameters set to 0 is not the same as the population average model and will give biased predictions. Instead, the population average model, fit without random effects, should be used.

Conclusions

China-fir trees play an important role in ecological service functions in Fujian Province of southeastern China. In order to estimate accurately the ecological values, five theoretical growth equations were evaluated for estimating the *d*, *h* and *v* growth for China-fir trees grown in monospecific plantations. The equations can be evaluated for both a biological perspective and for statistical meaning. All five equations and the Korf and Richards equations in particular have commonly and successfully been used to model individual-tree growth. A multi-level NLME models based on the Korf and Richards equations, with variance functions and correlation structures, were used to estimate *d*, *h* and *v* growth of individual trees; this approach was necessitated by the hierarchical structure of the experimental design and the autocorrelated increment data. The results showed that the NLME models (*Eqs. 22–24*) with random effects provided a better fit than the other models (*Eqs. 13–15*) (*Table 6*, *Figs. 3 and 4*). For the other two groups of data, the adj-R^2 of the NLME models were more than 0.9 and better than the results of the NLMs (*Table 7*). Therefore, we recommend using a nonlinear mixed-effects model to estimate individual-tree growth and yield models.

http://www.aloki.hu ● ISSN 1589 1623 (Print) ●ISSN1785 0037 (Online)
DOI: http://dx.doi.org/10.15666/aeer/1706_1540315418

Acknowledgements. This work was supported by World Bank Loan Project for Sand Prevention and Control on East Coast of the yellow river in Ningxia [grant numbers P121289]; the Independent Subject of Ningxia Academy of Agriculture and Forestry Sciences "Study of Carbon Sequestration Ability and Potential of Planted-forest in the arid aeolian sand region, Ningxia Province"; the National Natural Science Foundation of China [grant numbers 71663041]; and the Theoretical Economics First-class Discipline of Ningxia University [grant numbers NXYLXK2017B04].

REFERENCES

[1] Abiyu, A., Mokria, M., Gebrekirstos, A., Bräuning, A. (2018): Tree-ring record in Ethiopian church forests reveals successive generation differences in growth rates and disturbance events. – Forest Ecology and Management 409: 835-844.

[2] Adame, P., Hynynen, J., Canellas, I., Del Rio, M. (2008): Individual-tree diameter growth model for rebollo oak (*Quercus pyrenaica* Willd.) coppices. – Forest Ecology and Management 255(3-4): 1011-1022.

[3] Birch, C. P. (1999): A new generalized logistic sigmoid growth equation compared with the Richards growth equation. – Annals of Botany 83(6): 713-723.

[4] Bontemps, J., Duplat, P. (2012): A non-asymptotic sigmoid growth curve for top height growth in forest stands. – Forestry 85(3): 353-367.

[5] Burkhart, H. E. (2003): Suggestions for Choosing an Appropriate Level for Modeling Forest Stands. – In: Modeling Forest Systems. Wallingford, UK: CAB International: 3-10.

[6] Calama, R., Montero, G. (2004): Interregional nonlinear height-diameter model with random coefficients for stone pine in Spain. – Canadian Journal of Forest Research 34(1): 150-163.

[7] Cheng, C., Gordon, D. N. (2012): An analysis and comparison of predictors of random parameters demonstrated on planted loblolly pine diameter growth prediction. – Forestry 85(2): 271-280.

[8] Crecente-Campo, F., Tome, M., Soares, P., Dieguez-Aranda, U. (2010): A generalized nonlinear mixed-effects height-diameter model for *Eucalyptus globulus* L. in northwestern Spain. – Forest Ecology and Management 259(5): 943-952.

[9] Davidian, M., Giltinan, D. M. (1995): Nonlinear Models for Repeated Measurement Data. – New York: Chapman& Hall.

[10] Dumont, C., Lestini, G., Le Nagard, H., Mentre, F., Comets, E., Nguyen, T. T. (2018): PFIM 4.0, an extended R program for design evaluation and optimization in nonlinear mixed-effect models. – Comput Methods Programs Biomed 156: 217-229.

[11] Fang, Z., Bailey, R. L. (2001): Nonlinear mixed effects modeling for slash pine dominant height growth following intensive silvicultural treatments. – Forest Science 47(3): 287-300.

[12] Fox, J. C., Ades, P. K., Bi, H. (2001): Stochastic structure and individual-tree growth models. – Forest Ecology and Management 154(1): 261-276.

[13] Fu, L., Sun, H., Sharma, R. P., Lei, Y., Zhang, H., Tang, S. (2013): Nonlinear mixed-effects crown width models for individual trees of Chinese fir (*Cunninghamia lanceolata*) in south-central China. – Forest Ecology and Management 302: 210-220.

[14] Gea-Izquierdo, G., Canellas, I., Montero, G. (2008): Site index in agroforestry systems: age-dependent and age-independent dynamic diameter growth models for *Quercus ilex* in Iberian open oak woodlands. – Canadian Journal of Forest Research 38(1): 101-113.

[15] Grégoire, T. G., Schabenberger, O., Barrett, J. P. (1995): Linear modelling of irregularly spaced, unbalanced, longitudinal data from permanent-plot measurements. – Canadian Journal of Forest Research 1(25): 137-156.

[16] Gutzwiller, K. J., Riffell, S. K. (2007): Using statistical models to study temporal dynamics of animal-landscape relations. – In: Bissonette, J. A., Storch, I. (eds.) Temporal

http://www.aloki.hu ● ISSN 1589 1623 (Print) ●ISSN1785 0037 (Online)
DOI: http://dx.doi.org/10.15666/aeer/1706_1540315418

Dimensions of Landscape Ecology: Wildlife Responses to Variable Resources. New York: Spinger-Verlag.

[17] Hao, X., Yujun, S., Xinjie, W., Jin, W., Yao, F. (2015): Linear Mixed-Effects Models to Describe Individual Tree Crown Width for China-Fir in Fujian Province, Southeast China. – PLoS One 10(4): e122257.

[18] Huff, S., Poudel, K. P., Ritchie, M., Temesgen, H., (2018): Quantifying aboveground biomass for common shrubs in northeastern California using nonlinear mixed effect models. – Forest Ecology and Management 424: 154-163.

[19] Ihaka, R., Gentleman, R. (2004): R: a language and environment for statistical computing. – Vienna, Austria: R Foundation for Statistical Computing.

[20] Laird, N. M., Ware, J. H. (1982): Random-effects models for longitudinal data. – Biometrics 38: 963-974.

[21] Leak, W. (1996): Analysis of multiple systematic remeasurement. – Forest Science 1(12): 69-73.

[22] Li, F., Zhao, B., Su, G. (2000): A deriavtion of the generalized Korf growth equation and its application. – Journal of Forestry Research 11(2): 81-88.

[23] Lindstrom, M. J., Bates, D. M. (1990): Nonlinear mixed effects models for repeated measures data. – Biometrics 46: 673-687.

[24] Mabvurira, D., Miina, J. (2002): Individual-tree growth and mortality models for *Eucalyptus grandis*(Hill) Maiden plantations in Zimbabwe. – Forest Ecology and Management 161(1): 231-245.

[25] Malik, M. S., Surendran, C., Kailasham, K. (2005): Predicting growth of *Eucalyptus globulus* under agroforestry plantation. – Indian Journal of Agroforestry 7(1): 57-61.

[26] Matos, L. A., Lachos, V. H., Balakrishnan, N., Labra, F. V. (2013): Influence diagnostics in linear and nonlinear mixed-effects models with censored data. – Computational Statistics & Data Analysis 57: 450-464.

[27] Meng, S. X., Huang, S. (2009): Improved calibration of nonlinear mixed-effects models demonstrated on a height growth function. – Forest Science 55(3): 238-248.

[28] Palmer, M. J., Phillips, B. F., Smith, G. T. (1991): Application of nonlinear models with random coefficients to growth data. – Biometrics 47: 623-635.

[29] Pinheiro, J. C., Bates, D. M. (2000): Mixed Effects Models in S and S-Plus. – New York: Spring-Verlag.

[30] Pinheiro, J., Bates, D., DebRoy, S., Sarkar, D. (2005): NLME: linear and nonlinear mixed effects models. – Vienna, Austria: R Foundation for Statistical Computing.

[31] Rugmini, P., Jayaraman, K. (2009): Intrinsic units of growth for teak trees. – Tree-Structure and Function 23(1): 51-58.

[32] Sharma, R. P., Vacek, Z., Vacek, S. (2016): Individual tree crown width models for Norway spruce and European beech in Czech Republic. – Forest Ecology and Management 366: 208-220.

[33] Uzoh, F. C. C., Oliver, W. W. (2008): Individual tree diameter increment model for managed even-aged stands of ponderosa pine throughout the western United States using a multilevel linear mixed effects model. – Forest Ecology and Management 256(3): 438-445.

[34] Vanclay, K. (2003): Modelling forest growth and yield-application to mixed tropical forests. – In: Modelling Forest Development. UK: CAB international, Kluwer Academic Publishers.

[35] Vonesh, E., Chinchilli, V. M. (1997): Linear and Nonlinear Models for the Analysis of Repeated Measurements. – New York: Marcel Dekker.

[36] West, P. W., Ratkowsky, D. A., Davis, A. W. (1984): Problems of hypothesis testing of regressions with multiple measurements from individual sampling units. – Forest Ecology and Management 7(3): 207-224.

http://www.aloki.hu ● ISSN 1589 1623 (Print) ●ISSN1785 0037 (Online)
DOI: http://dx.doi.org/10.15666/aeer/1706_1540315418

[37] Xu, H., Sun, Y., Wang, X., Fu, Y., Dong, Y., Li, Y. (2014): Nonlinear mixed-effects (NLME) diameter growth models for individual China-Fir (*Cunninghamia lanceolata*) trees in Southeast China. – PLoS One 9(8): e104012.
[38] Yang, Y. Q., Huang, S. M., Trincado, G., Meng, S. X. (2009): Nonlinear mixed-effects modeling of variable-exponent taper equations for lodgepole pine in Alberta, Canada. – European Journal of Forest Research 128(4): 415-429.
[39] Zhang, J. G., Sun, H. G. (2010): Basal Area Growth and Modeling of Chinese fir Plantations. – Beijing: Science Press.
[40] Zhang, J., Duan, A., Sun, H., Fu, L. (2011): Self-thinning and growth modelling for even-aged Chinese fir (*Cunninghamia lanceolata* (lamb.) hook.) stands. – Beijing: Science Press.
[41] Zhao, L., Li, C., Tang, S. (2012): Individual-tree diameter growth model for fir plantations based on multi-level linear mixed effects models across southeast China. – Journal of Forest Research 18(4): 305-315.
[42] Zhu, G., Hu, S., Chin, S., Zhang, X., He, P. (2019): Modelling site index of Chinese fir plantations using a random effects model across regional site types in Hunan province, China. – Forest Ecology and Management 446: 143-150.

http://www.aloki.hu ● ISSN 1589 1623 (Print) ●ISSN1785 0037 (Online)
DOI: http://dx.doi.org/10.15666/aeer/1706_1540315418

THE EFFECT OF LANDSCAPE PATTERN IN RESPONSE TO ECOLOGICAL ENVIRONMENT AND CLIMATE CHANGE IN XIAOXING'ANLING, HEILONGJIANG PROVINCE, CHINA

GAO, W.[1,2] – WAN, L. H.[1,2*] – DU, Y. X.[1,2] – ZHU, D. Y.[1,2]

[1]*Heilongjiang Province Key Laboratory of Geographical Environment Monitoring and Spatial Information Service in Cold Regions, Harbin Normal University, Harbin 150025, China*

[2]*College of Geographical Science, Harbin Normal University, Harbin 150025, China*
(e-mail: 834655281@qq.com, wanluhe@163.com, 78862668@qq.com, zhudy0717@163.com)

[*]*Corresponding author*
e-mail: wanluhe@163.com

(Received 12th Jul 2019; accepted 14th Nov 2019)

Abstract. Wetlands play an important role in conserving water sources, regulating climate, and protecting biodiversity and have extremely high ecological value. However, global natural wetlands are rapidly degrading. Therefore, protecting wetlands is of strategic importance for ensuring ecological and environmental security. Based on the Landsat remote sensing images from 1975 to 2015 and the monthly meteorological data during the same periods, this study analyzed the landscape pattern change and explored the relationship with climate change and wetland change in Xiaoxing'anling, using the methods of landscape ecology and mathematical statistics. The results showed that the degree of landscape fragmentation was unused land < water area < forest land < urban land < cultivated land < wetland and the number of patches had increasing trend. The wetlands were mainly converted into cultivated land and the wetland areas have significantly degraded in the past 40 years in Xiaoxing'anling. The change of landscape diversity had a close correlation with annual precipitation and average summer precipitation. This study provides a theoretical basis for regional wetland protection.
Keywords: *wetland, cumulative anomaly analysis, canonical correlation analysis, Landsat, transfer matrix*

Introduction

Wetlands have a role in regulating water sources, regulating climate, purifying water quality, protecting species and regional ecological security (Zhu and Li, 1996), and significantly affect on economic development, human living environment, and climate change of regionally, and even globally (Liu, 2005). There are many wetlands in Northeast China, but the wetland areas were rapidly declining due to global warming and human activity (Gong et al., 2016). Using remote sensing measures to study wetlands has the advantages of low cost and easy access (Dogan et al., 2009; Lane et al., 2014). The classification methods of wetland include supervised classification, unsupervised classification, object-oriented classification and machine learning classification. Dronova et al. (2011) analyzed wetland classification accuracy by object-oriented and supervised classification methods. Sadeghi et al. (2012) used the support vector machine (SVM) to predict the distribution of invasive water ferns in the Anzhali wetland of Iran.

Wetland landscape has become closely related to many factors such as regional and resource distribution, anti-interference ability, self-recovery and biodiversity, and has become an important research field of landscape ecology (Li and Zeng, 2002). The quantitative method is the main method to study the change of wetland landscape pattern, for example, Fan et al. (2014) analyzed the change characteristics of wetland landscape

http://www.aloki.hu ● ISSN 1589 1623 (Print) ● ISSN 1785 0037 (Online)
DOI: http://dx.doi.org/10.15666/aeer/1706_1541915429

patterns in Nansi Lake of Shandong Province from 1982 to 2012 by landscape pattern index. Wang et al. (2012) compared the wetland landscape pattern changes in different time and space scales in the Yellow River Delta in 2000 and 2009 year from the aspects of landscape area change, landscape patch characteristics and overall landscape pattern. Chen et al. (2006) applied the landscape gradient model to analyze the landscape pattern characteristics of the Xianghai Nature Reserve in different periods. Luo et al. (2015) studied the temporal and spatial change of the landscape pattern of the Kazakhstan Delta through cellular automaton (CA)-Markov model.

In the study, using the Landsat remote sensing data with a 30-m resolution of 1975, 1985, 1995, 2005 and 2015 year and the monthly meteorological data, by the landscape ecology and mathematical statistics methods, we analyzed the landscape pattern change in Xiaoxing'anling. Our aim was to find the correlation between landscape pattern change and climate change in Xiaoxing'anling, and reveal the relationship between landscape pattern change and climate change. The study provides scientific theoretical basis and important guiding significance for landscape protection of Xiaoxing'anling wetland.

Materials and Methods

Study area

Xiaoxing'anling lies in the northern part of Heilongjiang Province, where the north and northeast are bounded by the Heilongjiang River, the northwest, the Aihui District of Heihe city and Nenjiang County are connected to Daxinganling, the east is adjacent to the Sanjiang Plain, the southeast is separated from the Zhangguangcai Mountains by the Songhua River Valley, and the southwest is connected to the Nenjiang Plain (*Fig. 1*).

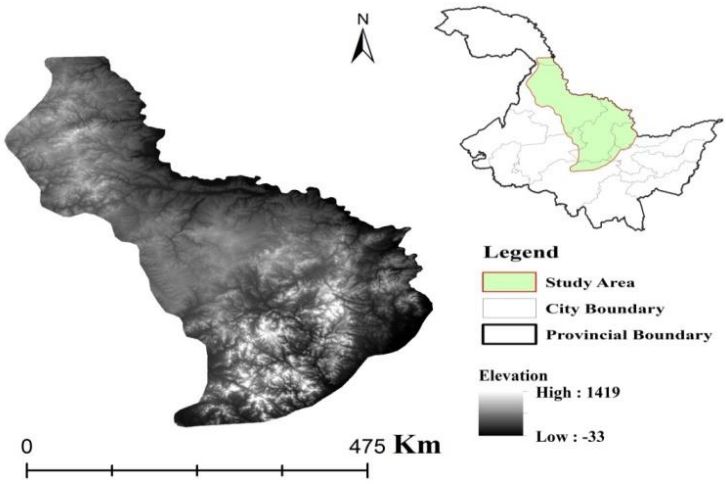

Figure 1. *Location and elevation of the study area*

The geographical coordinates are 45 50' - 51 10'N, 125 20' - 131 20'E (Liu, 2012). The altitude of the mountain range is approximately 500~800 meters, and the individual peaks are above 1000 meters. The average annual precipitation in the study area is approximately 550~700 mm. This area is one of the most concentrated areas of wetland, with abundant wetland types such as forest swamps, shrub swamps, and herb swamps et al. (Liu, 2012).

http://www.aloki.hu ● ISSN 1589 1623 (Print) ● ISSN 1785 0037 (Online)
DOI: http://dx.doi.org/10.15666/aeer/1706_1541915429

Dataset

The Landsat remote sensing data with a 30-m resolution of the study were downloaded from https://glovis.usgs.gov/. The images with less 5% cloud cover from June to August in 1975, 1985, 1995, 2005 and 2015 year were select. Band combination, geometric correction, image mosaic and cropping for every period were completed using ENVI5.1 software. Based on the land use classification standard in China, we collected 1011 training samples from field data (collected using GPS) and classified the land use types as wetland, cultivated land, forest, urban, waters, and unused land using the support vector machine method.

The meteorological data used in the study came from the National Meteorological Information Center (http://www.cma.gov.cn/2011qxfw/2011qsjgx/). We collected the monthly and annual average minimum temperature, average maximum temperature, average temperature, average relative humidity, and precipitation from 1975 to 2015 for in Huma, Aihui, Sunwu, Yichun, Tieli, Hegang, Jiamusi and Yilan eight meteorological stations in Xiaoxing'anling and its surrounding areas.

Methods

Landscape pattern index

The landscape pattern index can quantify the complex landscape pattern and its changing process, condensing its information and reflecting its structure and configuration (Peng, 2006). The landscape pattern index that included the number of plaques (NP), percentage of landscape types (PLAND), aggregation index (AI), largest patch index (LPI), plaque density (PD), perimeter area fractal (PAFRAC), Shannon diversity index (SHDI) and Shannon evenness index (SHEI) were used to reflect the size of patches, the fragmentation, and the diversity of landscapes in the study area (Wang et al., 2017; Du et al., 2018; Wu and Li, 2018). The literature described the above eight landscape pattern indices in detail (Li et al., 2016; Ma et al., 2018).

Moving average method

The moving average method could visually reflect the trend of changes in meteorological sequences and eliminated the effects of sequence fluctuations. In general, a new sequence y_1 was obtained by calculating 2k or 2k+1 continuous averaging in the meteorological sequence $x_1, x_2 \ldots\ldots x_n$. The specific equation was as follows (Xu et al., 2015).

$$y_1 = \frac{1}{2k+1} \sum_{-k}^{k} x_{i+1} \quad \text{(Eq.1)}$$

The trend analysis of the meteorological sequence was calculated using a 5-year moving average in our study (k=2).

Canonical correlation analysis

The canonical correlation analysis was used to analyze the correlation between the two groups of variables. The core idea was that the correlations between (the independent variable group and the standard variable group) were indicated by selecting several representative comprehensive indicators from the two sets of random variables. In the study of landscape pattern change, because different landscape types interact and restrict

http://www.aloki.hu ● ISSN 1589 1623 (Print) ● ISSN 1785 0037 (Online)
DOI: http://dx.doi.org/10.15666/aeer/1706_1541915429

each other, the canonical correlation analysis was often used to analyze the relationship between landscape patterns and various natural and socio-economic drivers (Huang, 2010).

Results

Land use transfer matrix

The land use transfer matrix (*Table 1*) from 1975 to 2015 was obtained using the SVM classification method to classify the remote sensing images in the study area in1975, 1985, 1995, 2005 and 2015 year.

From the perspective of transfer, the land use transfer in the study area was that the forest with the area of 10430.13 km^2 was converted into wetland and cultivated land; the wetland with the area of 24706.11 km^2 was converted into forest and cultivated land; the cultivated land with the area of 3175.67 km^2 was converted into forest and wetland from 1975 to 2015. From the perspective of transition, the changes mainly occurred that the water was mainly converted from forest and wetlands with the area of 302.9 km^2; the unused land was mainly converted from wetland, forest and cultivated land with the area of 628.82 km^2; urban was mainly converted from wetland, cultivated land and forest with the area of 1022.02 km^2. In short, the landscape type transfer in Xiaoxing'anling mainly occurred between cultivated land, forest and wetland.

Table 1. *Land use transfer matrix in the study area from 1975 to 2015 (km^2)*

1975 - 2015	water	forest	unused land	urban	wetland	cultivated land
water	395.30	146.05	3.68	25.23	156.40	58.67
forest	72.48	44261.30	53.00	83.76	13713.55	2164.02
unused land	13.78	139.10	6.58	14.70	388.56	101.16
urban	27.02	296.31	10.37	138.20	417.00	309.02
wetland	59.67	5478.66	25.30	65.74	9121.86	1011.65
cultivated land	74.23	4951.47	83.12	270.72	10992.56	4030.91

Landscape pattern change analysis

The Landscape pattern index at plaque type level (*Table 2*) and Landscape pattern index on landscape level (*Table 3*) in Xiaoxing'anling from 1975 to 2015 year were calculated by Fragstats software.

The number of plaques (NP) increasing and the aggregation index (AI) decreasing from 90.53% to 84.13% indicated that the number of plaques increased continuously, and the landscape became more and more fragmented in Xiaoxing'anling from1975 to 2015. At the landscape level, the largest plaque index (LPI) in Xiaoxing'anling decreased from 48.94% to 16.79% from 1975 to 2015, indicating that the maximum plaque area was declined, and the landscape dominance decreases with the decrease of the total area of the landscape. The diversity index in the study area has increased year by year, and the growth trend of uniformity index is consistent with the decreasing trend of landscape dominance difference, indicating that the distribution of landscape elements tends to be balanced. The perimeter area fractal (PAFRAC) first increased and then decreased and

http://www.aloki.hu ● ISSN 1589 1623 (Print) ● ISSN 1785 0037 (Online)
DOI: http://dx.doi.org/10.15666/aeer/1706_1541915429

the fractal dimension was the largest in 1985 year, indicating that the shape of the plaque in the study area was closer to the square since 1985. It could be inferred that the study area had been disturbed by humans, and was still moving in the direction of increased interference.

Table 2. *The landscape pattern index at plaque type level in study area from 1975 to 2015*

year	Land use type	Plaque type level landscape pattern index				
		NP	PLAND%	AI%	LPI%	PD
1975	cultivated land	46605	3.04	80.63	1.17	0.47
	forest	38232	67.33	92.67	25.73	0.39
	water	2527	0.42	78.25	0.22	0.03
	wetland	96416	28.41	81.54	10.86	0.98
	urban	70856	0.71	80.17	0.25	0.72
	unused land	1983	0.09	52.34	0.05	0.20
1985	cultivated land	143089	3.44	82.5	1.28	1.44
	forest	40909	66.66	87.29	27.96	0.11
	water	20992	0.79	72.72	0.22	0.21
	wetland	140658	28.06	80.08	10.62	1.42
	urban	76590	0.76	79.66	0.28	0.77
	unused land	6839	0.29	74.97	0.10	0.37
1995	cultivated land	264385	13.90	87.53	5.59	1.58
	forest	53471	57.29	80.55	21.35	0.42
	water	35851	0.86	76.35	0.31	0.34
	wetland	357435	26.09	77.24	10.94	3.14
	urban	79853	1.33	82.54	0.55	0.65
	unused land	8951	0.52	82.61	0.23	0.58
2005	cultivated land	407235	17.06	92.32	7.22	1.42
	forest	59782	56.03	76.23	21.10	0.48
	water	41352	0.87	76.37	0.65	0.41
	wetland	482152	23.61	76.12	8.74	4.57
	urban	83425	1.20	85.02	0.47	0.62
	unused land	11225	1.23	90.35	0.50	0.46
2015	cultivated land	557832	13.31	95.26	4.30	1.37
	forest	65065	71.02	71.33	27.66	0.66
	water	49884	0.88	76.19	0.33	0.50
	wetland	638265	12.84	72.69	4.80	6.44
	urban	85065	1.08	84.85	0.45	0.57
	unused land	13614	0.84	95.26	0.32	0.47

http://www.aloki.hu ● ISSN 1589 1623 (Print) ● ISSN 1785 0037 (Online)
DOI: http://dx.doi.org/10.15666/aeer/1706_1541915429

Table 3. *The landscape pattern index of the landscape level in study area from 1975 to 2015*

year	landscape pattern index at landscape level					
	NP	**LPI%**	**AI%**	**PAFRAC**	**SHDI**	**SHEI**
1975	274469	48.94	90.53	1.40	0.97	0.54
1985	399077	38.20	87.51	1.47	0.95	0.53
1995	753562	33.48	88.73	1.38	0.98	0.55
2005	1052345	20.56	86.54	1.32	1.02	0.57
2015	1464177	16.79	84.13	1.34	1.05	0.58

Note: The meanings of the abbreviation of the captions in the *Table 3* are as follows: PAFRAC - perimeter area fractal, SHDI – Shannon's diversity index, SHEI – Shannon's evenness index

Climate change analysis

The climatic characteristics were represented by the annual climatic data of the eight meteorological stations for 40 years. The climate change trend was shown in *Fig. 2*. The annual relative humidity in Xiaoxing'anling was decreasing and annual decrease rate was 0.0174%. The annual precipitation in Xiaoxing'anling showed an increase trend with the rate 1.59 mm and passed 0.1. significance level test ($p < 0.1$).

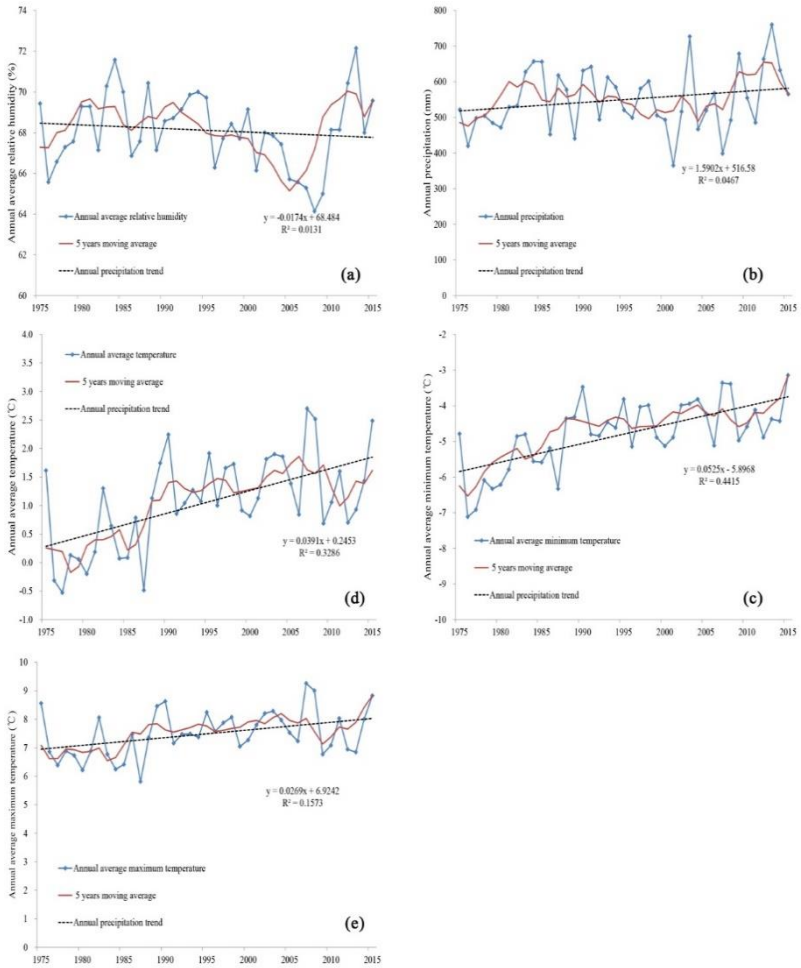

Figure 2. *Climate trend analyzing in Xiaoxing'anling from 1975 to 2015*

http://www.aloki.hu ● ISSN 1589 1623 (Print) ● ISSN 1785 0037 (Online)
DOI: http://dx.doi.org/10.15666/aeer/1706_1541915429

The trends of annual average temperature, annual average minimum temperature and annual average maximum temperature in Xiaoxing'anling had increased, and the increasing rates were 0.39℃/10a, 0.525℃/10a and 0.27℃/10a, respectively, which passed 0.05 significance level test ($p < 0.05$). The annual warming trend of the study area was synchronized with the background of continuous warming since the 1950s in the Northeast, and the growth rate of the annual average minimum temperature was higher than the annual average maximum temperature and the annual average temperature, so the temperature was more affected by the increase in the annual average minimum temperature.

By monthly data, the average temperature and precipitation data of spring (March-May), summer (June-August), autumn (September-November) and winter (December-February) are counted. 5 years moving average seasonal and annual climatic factors were obtained in *Fig. 3*.

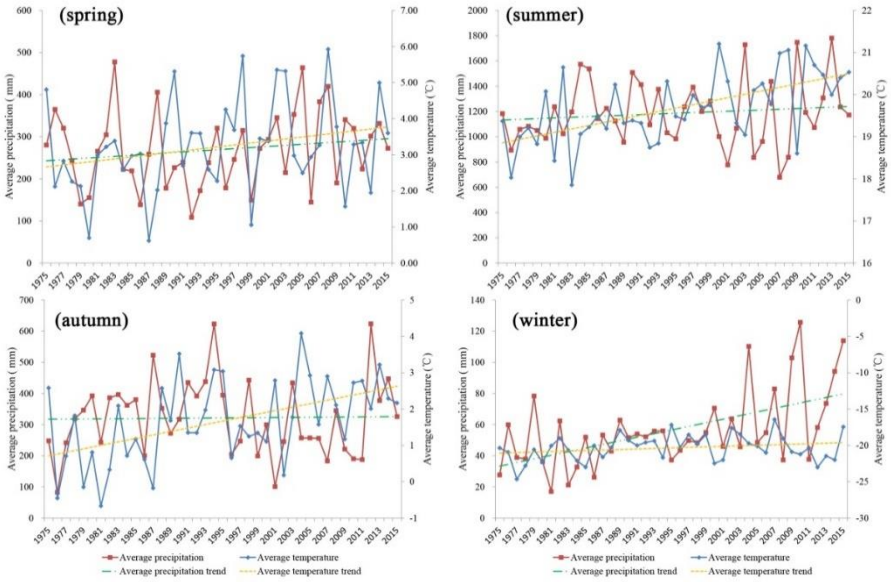

Figure 3. *Climatic trend in each quarter from 1975 to 2015*

From 1975 to 2015, the temperature and precipitation in the Xiaoxing'anling showed an upward trend, and the increase rates of the temperature from spring to winter were 0.28/10a, 0.41℃/10a, 0.48℃/10a and 0.35℃/10a, respectively. In addition, the average temperature in summer and autumn passed the 0.05 significance level test ($p < 0.05$). The change rates of precipitation from spring to winter were 13.09 mm/10a, 26.45 mm/10a, 18.9 mm/10a and 15.96 mm/10a, respectively. Although the seasonal precipitation was on the rise, only the precipitation trend passed the 0.05 significance level ($p < 0.05$) in winter.

Response relationship between climate change and wetland landscape pattern change

According to the basic data and our research purpose, the analysis results with confidence greater than 95% ($p < 0.05$) were used for all correlation coefficients. The canonical correlation analysis result of wetlands was shown in *Table 4*. There was a typical correlation coefficient of 0.881, and the statistical test reached a significant level,

http://www.aloki.hu ● ISSN 1589 1623 (Print) ● ISSN 1785 0037 (Online)
DOI: http://dx.doi.org/10.15666/aeer/1706_1541915429

so the first pair of typical variables was selected for analysis. According to *Fig. 4*, the first linear combination (canonical) of the climatic factor variables was x2 (annual precipitation) and x9 (summer average precipitation), and canonical variables for maximum correlation were y1 (NP) and y5 (PD). There was a close correlation between the annual precipitation and the average summer precipitation and the wetland landscape fragmentation index. From 1975 to 1985 year, the annual precipitation decreased first and then increased, the wetland areas decreased and the change was the smallest in the five periods. However, from 1995 to 2005 year, the annual precipitation decreased continuously, the wetland areas decreased and the landscape fragmentation increased sharply. It was concluded that due to the change of annual precipitation, it was likely to cause changes in the wetland areas at the same time and thus the change of landscape fragmentation.

Table 4. *Canonical correlation coefficient*

Typical variables	Canonical Correlations	Chi-SQ	DF	Sig
1	0.881	111.088	65.000	0.000
2	0.791	65.337	48.000	0.249
3	0.709	35.326	33.000	0.359
4	0.527	13.979	20.000	0.832
5	0.353	4.062	9.000	0.907

Note: Chi-SQ refers to chi square statistic, DF is degree of freedom and Sig is significant level

Standardized Canonical Coefficients for Set-1

	1	2	3	4	5
x1	-.356	-.260	.119	-.414	.220
x2	-188.953	700.335	-89.851	-25.183	-511.394
x3	-.519	-1.829	-.281	-2.094	-1.245
x4	-2.358	-2.567	-1.812	-2.065	-1.707
x5	4.523	-5.759	-1.264	6.089	14.396
x6	-.320	4.124	1.472	-.925	-4.360
x7	58.344	-216.219	26.979	7.674	157.090
x8	-.004	2.461	.389	-1.010	-2.733
x9	166.389	-616.998	78.626	22.358	449.481
x10	-.549	3.309	1.650	-.123	-3.876
x11	77.654	-288.622	37.282	10.177	210.078
x12	-.882	5.523	2.006	-1.955	-6.587
x13	15.991	-59.187	7.465	2.175	42.582

Standardized Canonical Coefficients for Set-2

	1	2	3	4	5
y1	7.160	17.056	-35.295	-23.315	42.949
y2	1.592	4.765	-2.979	4.217	.013
y3	.724	1.425	-3.081	-2.717	-.048
y4	-1.996	-5.490	10.572	.261	-8.711
y5	-5.834	-16.517	39.037	24.883	-50.664

Figure 4. *Standardized canonical coefficients*

Note: x1- annual relative humidity; x2- annual precipitation; x3- annual minimum temperature; x4- annual maximum temperature; x5- annual average temperature; x6- average spring temperature; x7- average spring precipitation; x8- average summer temperature; x9- average summer precipitation; x10- average autumn temperature; x11- average autumn precipitation; x12- average winter temperature; x13- average winter precipitation; y1- NP; y2- PLAND; y3- AI; y4- LPI; y5- PD

Discussion

Previous studies showed that climate change and the human activities played a key role in the fragmentation of wetland landscapes (Xiao et al., 2010; Hu et al., 2015; Cong et al., 2019). Our findings are similar to the above studies. From 1975 to 2015, the areas of forest and wetland accounted for the largest proportion and they were the type of

http://www.aloki.hu ● ISSN 1589 1623 (Print) ● ISSN 1785 0037 (Online)
DOI: http://dx.doi.org/10.15666/aeer/1706_1541915429

substrate landscape in Xiaoxing'anling. However, the proportion of cultivated land and urban was gradually increasing, indicating that the wetland degradation trend in Xiaoxing'anling was obvious. The wetland change in Xiaoxing'anling was consistent with the shrinking trend of wetland in Northeast China (Gao et al., 2018; Yu et al., 2018). The landscape type transfer in Xiaoxing'anling mainly occurred between cultivated land, forest and wetland. At the plaque level, the wetland landscape dominance continued to decline significantly from 1975 to 2015, the dominant degree of forest land decreased first and then increased, and the dominance of cultivated land gradually increased. The overall dominance trend of each landscape type tended to balance development; the landscape fragmentation degree of Xiaoxing'anling was ranked as unused land < water area < forest land < urban land < cultivated land < wetland.

At the landscape level, the NP value had increased year by year from 1975 to 2015, and the number of patches in Xiaoxing'anling has been increasing, indicating the landscape of the whole study area has become more and more fragmented. The AI and the largest plaque index (LPI) decreased from 90.53 % to 84.13% and from 48.94% to 16.79% during 1975 - 2015 year respectively, indicating the diversity index increasing. The fractal dimension was the largest in 1985, indicating that the study area was interfered with human activities and the interference had been larger and stronger since 1985.

In the past 40 years, the annual minimum temperature, annual maximum temperature and annual average temperature in Xiaoxing'anling had increased significantly. The wetlands in the study area were significantly correlated with annual precipitation and average summer precipitation. The landscape level had the greatest correlation with climate change factors. Typical variables were PAFRAC and SHEI. The change of landscape diversity of Xiaoxing'anling wetland had a close correlation with annual precipitation and average summer precipitation.

Conclusions

Based on Landsat images and meteorological data, using landscape ecology and mathematical statistics methods, the changes of landscape pattern of wetland and response of climate change on landscape pattern change in Xiaoxing'anling were analyzed. The results showed that substrate landscapes in Xiaoxing'anling were forest and wetland, but the proportion of cultivated and urban was gradually increasing; the landscape type transfer in Xiaoxing'anling mainly occurred between cultivated land, forest and wetland; and the wetland degradation trend was obvious. The landscape fragmentation ranking was unused land < water area < forest land < urban land < cultivated land < wetland. At the landscapelevel, the number of patches and diversity index in Xiaoxing'anling were increasing year by year. The wetlands in the study area were significantly correlated with annual precipitation and average summer precipitation. The landscape level had the greatest correlation with climate change factors. The canonical variables were PAFRAC and SHEI. The change of landscape diversity of Xiaoxing'anling had a close correlation with annual precipitation and average summer precipitation. This paper revealed the response of landscape pattern change to climate change macroscopically from 1975 to 2015 in Xiaoxing'anling. We will furtherly research the driving mechanism of landscape pattern change in the future, and provide scientific basis for wetland planning and protection.

http://www.aloki.hu ● ISSN 1589 1623 (Print) ● ISSN 1785 0037 (Online)
DOI: http://dx.doi.org/10.15666/aeer/1706_1541915429

Acknowledgments. The study was supported by The National Natural Science Foundation of China (No.41671100).

REFERENCES

[1] Chen, M., Wang, Z. M., Zhang, S. Q., Zhang, B., Li, X. F., Ren, C. Y. (2006): Study on the variation of landscape pattern and the gradient distribution of wetland in the Xianghai Nature Reserve. – Arid Land Geography 05: 694-699. [in Chinese].
[2] Cong, P., Chen, K., Qu, L., Han, J. (2019): Dynamic Changes in the Wetland Landscape Pattern of the Yellow River Delta from 1976 to 2016 Based on Satellite Data. – Chinese Geographical Science 29(3): 372-381.
[3] Dogan, O. K., Akyurek, Z., Beklioglu, M. (2009): Identification and mapping of submerged plants in a shallow lake using quickbird satellite data. – Journal of Environmental Management 90(7): 2138-2143.
[4] Dronova, I., Peng, G., Wang, L. (2011): Object-based analysis and change detection of major wetland cover types and their classification uncertainty during the low water period at Poyang Lake, China. – Remote Sensing of Environment 115(12): 3220-3236.
[5] Du, J. L., Zhu, J. W., Xie, J. C., Ma, Z. H. (2018): Changes of land use and landscape pattern in the Guanzhong area in recent 25 years. – Arid Zone Research 35(01): 217-226. [in Chinese].
[6] Fan, Q., Du, T., Yang, J., Xi, J. C., Li, X. M., Chen, P. (2014): Landscape pattern changes for Nansihu wetland from 1982 to 2012. – Resources Science 36(4): 865-873. [in Chinese].
[7] Gao, C. Y., Zhang, S. Q., Liu, H. X., Cong, J. X., Li, Y. H., Wang, G. P. (2018): The impacts of land reclamation on the accumulation of key elements in wetland ecosystems in the Sanjiang Plain, northeast China. – Environmental Pollution 237.
[8] Gong, N., Niu, Z. G., Qi, W., Zhang, H. Y. (2016): Driving forces of wetland change in China. – Journal of Remote Sensing 20(2): 172-183. [in Chinese].
[9] Hu, Y., Huang, J., Du, Y., Han, P., Huang, W. (2015): Monitoring spatial and temporal dynamics of flood regimes and their relation to wetland landscape patterns in Dongting Lake from MODIS time-series imagery. – Remote Sensing 38(6): 7494-7520.
[10] Huang, C. (2010): Analysis of the relationship between landscape pattern change and climate factors in Karamay Plantation area. – Xinjiang University. [in Chinese].
[11] Lan, Y. C., Liu, G. S., La, C. F., Zhu, Y. T., Ma, Q. J., Shi, M. X. (2017): Study on the characteristics and trend of runoff change in the source region of the Yellow River and its regional difference. – Journal of Mountain Science 35(03): 257-265. [in Chinese].
[12] Lane, C. R., Anenkhonov, O., Liu, H., Autrey, B. C., Chepinoga, V. (2014): Classification and inventory of freshwater wetlands and aquatic habitats in the Selenga river delta of lake Baikal, Russia, using high-resolution satellite imagery. – Wetlands Ecology & Management 23(2): 1-20.
[13] Li, S. J., Zeng, H. (2002): The utilities of remote sensing technique in landscape study. – Journal of Remote Sensing 6(3): 233-240. [in Chinese].
[14] Li, M. Y., Xing, Y. Q., Wang, Z., Liu, M. S., Yao, S. T., Xie, J., Zeng, X. J. (2016): Changes of land coverage and land use in the Wangqing County based on RS and GIS. – Journal of Northwest Forestry University 31(06): 257-263. [in Chinese].
[15] Liu, H. Y. (2005): Characteristics of wetland resources and ecological safety in China. – Resources Science (03): 54-60. [in Chinese].
[16] Liu, L. X. (2012): Study on the plant biodiversity and ecosystem service functions evaluation of forest ecosystem in Xiaoxing'an Mountains. – Northeast Forestry University 9-13. [in Chinese].
[17] Luo, G., Amuti, T., Zhu, L., Mambetov, B. T., Maisupova, B., Zhang, C. (2015): Dynamics of landscape patterns in an inland river delta of eentral asia based on a cellular automata-Markov model. – Regional Environmental Change 15(2): 277-289.

http://www.aloki.hu ● ISSN 1589 1623 (Print) ● ISSN 1785 0037 (Online)
DOI: http://dx.doi.org/10.15666/aeer/1706_1541915429

[18] Ma, B. R., Ma, A. Q., Yu, X. X., Hu, J., Xing, R. R. (2018): Analysis on dynamic characteristics in the wetlands of Ziya river basin. – Periodical of Ocean University of China 48(09): 108-117. [in Chinese].
[19] Peng, W. C. (2006): Study of EUO-tourism developing strategy in Hei Longjiang province. – Northeast Normal University. [in Chinese].
[20] Sadeghi, R., Zarkami, R., Sabetraftar, K., Damme, P. V. (2012): Use of support vector machines (SVMs) to predict distribution of an invasive water fern Azolla filiculoides (Lam.) in Anzali wetland, southern Caspian Sea, Iran. – Ecological Modelling 244: 117-126.
[21] Wang, Y. L., Yu, J. B., Dong, H. F., Li, Y. Z., Zhou, D., Fu, Y. Q., Han, G. X., Mao, P. L. (2012): Spatial evolution of landscape pattern of coastal wetlands in Yellow river delta. – Scientia Geographica Sinica 32(6): 717-724. [in Chinese].
[22] Wang, Y., Liu, C. L., He, P. (2017): Landscape pattern analysis based on GIS and landscape index in Huanghua city. – Journal of Anhui Agricultural Sciences 45(16): 63-67. [in Chinese].
[23] Wu, H. Y., Li, K. G. (2018): Changes of Land Use and Landscape Pattern in Beidaihe District of Qinhuangdao City. – Geospatial Information 16(01): 91-93+106+9. [in Chinese].
[24] Xiao, D. R., Tian, B., Tian, K., Yang, Y. (2010): Landscape patterns and their changes in Sichuan Ruoergai wetland national nature reserve. – Acta Ecologica Sinica 30(1): 27-32.
[25] Xu, T., Shao, H., Zhang, C. (2015): Temporal pattern analysis of air temperature change in Central Asia during 1980-2011. – Arid Land Geography 38(01): 25-35. [in Chinese].
[26] Yu, X. F., Ding, S. S., Zou, Y. C., Xue, Z. S., Lyu, X. G., Wang, G. P. (2018): Review of rapid transformation of floodplain wetlands in northeast China: roles of human development and global environmental change. – Chinese Geographical Science 28(4): 654-664.
[27] Zhu, J. G., Li, Y. Z. (1996): Review of research on wetland in China. – Journal of China Agricultural Resources and Regional Planning (2): 21-24. [in Chinese].

http://www.aloki.hu ● ISSN 1589 1623 (Print) ● ISSN 1785 0037 (Online)
DOI: http://dx.doi.org/10.15666/aeer/1706_1541915429

EFFECT OF CANOPY MICROCLIMATE ON MERLOT (*VITIS VINIFERA* L.) GRAPE COMPOSITION

CANDAR, S.[1*] – KORKUTAL, I.[2] – BAHAR, E.[2]

[1]*Tekirdağ Viticulture Research Institute, 59100 Tekirdağ, Turkey*

[2]*Department of Horticulture, Agricultural Faculty, Namik Kemal University, 59030 Tekirdag, Turkey*

**Corresponding author*
e-mail: serkan.candar@tarimorman.gov.tr

(Received 14th Jul 2019; accepted 15th Nov 2019)

Abstract. The objective of this work was to evaluate the effect of different canopy management practices on canopy microclimate and consequently berry quality components of the Merlot (*Vitis vinifera* L.) grape variety. Different microclimate effects were created by the limitations of 1 m, 1.25 m and 1.5 m main shoot lengths and full lateral shoots (FLS), half lateral shoots (HLS) and no lateral shoots (NLS). Microclimatic data was gathered by the sensors placed in the canopies of FLS, HLS and NLS vines located under the 1.25 m main shoot length parcel. In the study, total soluble solids content, titratable acidity, pH, total phenolic content, total anthocyanin content, total tannin content, tartaric and malic acid content and potassium content in the juice were evaluated as the biochemical quality properties. The results of two years indicated that canopy microclimate arrangements may provide some manipulation on grape berry quality according to the vegetation period's climate characteristics and the desired target quality within limits of macro-meso climate effects.
Keywords: *canopy management, summer pruning, phenolic content, anthocyanins, must quality*

Introduction

Canopy management applications may have some adverse affects on the physiological properties of the vine as a result of the isolation of vine-canopy microclimate from environmental factors, such as temperature, light exposure, atmospheric humidity and air flow when they are not considered as serious cultivation practices. As the green pruning is not performed according to a methodology, appropriate to the characteristics of the vegetation period, the production/consumption balance may deteriorate in the physiological sense. Exposure of clusters to direct sunlight can also cause physical damage and deterioration of the chemical structure of the berries under high temperatures.

There is an important amount of knowledge about the relationship between microclimate parameters and quality components. Temperature is the main factor controlling growth and quality. Improvements in criteria such as total phenolic, anthocyanin content, main components of sensory characteristics of wines, aroma, color and taste can be seen at certain stress levels (Matthews et al., 1990). Similarly, the positive effects of polyphenol components and antioxidant activity on human health can be increased (German and Walzem, 2000; Dixon et al., 2005). However, high evaporative demand during high temperature periods and growing period may play a role in limiting yield, berry wine quality (Escalona et al., 1999; Chaves et al., 2007). This can lead to wine acidity problems by reducing the coloration and sugar accumulation of the berry (Medrano et al., 2003; Romero et al., 2010). In addition, under the total intertwined impact of environmental stress factors, instant

http://www.aloki.hu ● ISSN 1589 1623 (Print) ● ISSN 1785 0037 (Online)
DOI: http://dx.doi.org/10.15666/aeer/1706_1543115446

photosynthesis reduction and risky losses in total carbon assimilation and even total canopy area may occur (Flexas et al., 1998, 2002; Maroco et al., 2002; Santos et al., 2007). The effect of light exposure on the vine (often not easily separated from temperature) is observed in physiological activities, shoot development and wooding, berry formation, fall, ripening processes and quality (Reynolds et al., 1986; Crippen and Morrison, 1986; Rojas-Lara and Morrison, 1989; Schubert et al., 1996; Haselgrove et al., 2000; Bertamini and Nedunchezhian, 2003; Spayd et al., 2011; Profio et al., 2011).

The effects of the climate crisis that are going on beyond the traditional interaction between viticulture and climate are also discussed by researchers in a multi-dimensional context (Schultz, 2000; Nemani et al., 2001; Jones, 2007; Webb et al., 2008; Fraga et al., 2012; Vrsic and Vodovnik, 2012; Donat et al., 2013). As climate change is inevitable (Carbonneau and Bahar, 2009), different canopy management practices are an important tool for managing and adapting this process (This et al., 2006; Olsen et al., 2011). Canopy microclimate arrangements may provide some manipulation on grape berry and wine quality within limits of macro-meso climate affects and climate crisis.

There is a close relationship between the quality of grapes and wine and the composition of the berries. Therefore, quality depends on many components such as grape varieties, total soluble solids (TSS), organic acids, pH, phenolic substances, the thickness of the berry skin, the berry skin area, the ratio of the skin area/berry volume, the effect of ecological conditions, maturity time, the effect of diseases, rootstock and canopy management (Ribéreau-Gayon et al., 2000; Blouin and Guimberteau, 2000; Keller, 2010; Treutter, 2010).

The aim of the present study was to provide a better understanding of the effect of different canopy management practices on canopy microclimate and consequently berry quality components.

Materials and methods

Location, plant material and trial design

The two-year study (2014 and 2015) was conducted at the Tekirdağ Viticulture Research Institute, located in Northwest of Turkey (in Thrace), within the coordinates 40.969184°N-40.973562°N latitudes and 27.461911°E-27.477504°E. longitudes. The climate of Tekirdağ, is defined as a transitional climate among the Continental climate, the Black Sea climate and the Mediterranean climate with an average annual temperature of 14 °C, annual precipitation of 581.80 mm and 1887.00 growing day-degree Winkler Index for the years of 1939-2017 period. The altitude of vineyard was approximately 36 m and was approximately 4 km away from the sea. Merlot/5BB grafting combination 12-13 years old vines were oriented North-South on a high groundwater and clay-loam soil. Vines were arranged in a between-row and within-row spacing of 2.5 × 1.5 m respectively. Double Guyot training vines pruned 16-18 bud per vine.

Different microclimate effects were created by the limitations of 1 m, 1.25 m and 1.5 m main shoot lengths while they reached 170-180 cm (EL 31-33) shoot lengths for main parcels. Lateral shoot applications were sub-parcels which created by full lateral shoots (6-7 leaves), half lateral shoots (3-4 leaves) and no lateral shoots (no leaf) performed in verasion (EL 35) according to Lorenz et al. (1995). Both applications were kept at the same length until the harvest period.

http://www.aloki.hu ● ISSN 1589 1623 (Print) ● ISSN 1785 0037 (Online)
DOI: http://dx.doi.org/10.15666/aeer/1706_1543115446

Data was gathered from meteorological stations located in Tekirdag Viticulture Research Institute in order to determine mesoclimatic and microclimatic conditions. A climate station which located 2 m high from ground was used to collect mesoclimatic data reflecting the general climatic characteristics of the vineyard. Mesoclimatic measurements; temperature, relative humidity, light intensity, wind speed, total precipitation and microclimatic measurements from the insides of the vine canopies which were the descriptive features such as temperature, relative humidity, light intensity, wind speed and leaf wetness were monitored during the years 2014 and 2015.

Microclimatic data sensors were placed in the canopies of full lateral shoot (FLS, 6-7 leaves), half lateral shoot (HLS, 3-4 leaves) and no lateral shoot (NLS) sub-parcel vines that located under 1.25 m main shoot length main parcel, from the beginning of the vegetation period and measurements were continued until the end of harvest by SHT11 Temperature, humidity and leaf wetness sensor module (Sensirion AG, Switzerland) for temperature, humidity and leaf wetness. TEMT 6000 light sensor (Vishay Intertechnology, Inc., Germany) and WGR800 wind sensor (Oregon scientific, USA) readings were gathered by a cloud based datalogger (Mrme AR-GE Bilişim, Turkey). The 5 min averages of two-second readings from each sensor derived as the station's hourly value.

The inside of the three canopies were equipped with one temperature, humidity, leaf wetness, wind and four light intensity sensors (*Fig. 1*). Also light intensity sensors positioned two each around cluster zone and center canopy. The wind sensor in the canopy is enclosed in a suitably sized wireframe that does not stop the wind flow to prevent contact with leaves and shoots. Maintenance and control of the sensors placed inside vines were done regularly to avoid any data loses after cultivation practices such as spraying, green pruning etc.

Figure 1. *Placing of different sensors and loggers in vineyard (a) main electric and GSM unity, (b) cloud based datalogger, (c) wind sensor, (d) temperature, humidity, leaf wetness, (e) light sensor*

Although the data received from all of the above sensors for all growing process, only outputs of temperature and light intensity effects between verasion-harvest period are evaluated in this publication due to the important effects on must composition.

http://www.aloki.hu ● ISSN 1589 1623 (Print) ● ISSN 1785 0037 (Online)
DOI: http://dx.doi.org/10.15666/aeer/1706_1543115446

Despite the equal number of (16) buds left in the winter pruning, the plants that disrupt homogeneity in the number of shoots and bunches were balanced when the shoots reached an average length of 30-40 cm (EL 15-17) or excluded from the trial. Standard cultural practices in the region were applied to all treatments during research. The vines data taken were selected from the same development period and with the approximate charge and those without spaces.

Must composition

The total soluble solids (%), pH, total acidity (g/L of tartaric acid), and the concentration of tartaric acid (g/L), malic acid (g/L) and potassium (mg/L) in must from grapes collected from each experimental replication at the harvest date was determined using the official methods of the Organisation Internationale de la Vigne et du Vin (OIV) (OIV, 2012). Also, total phenolic content (mg/kg), total anthocyanin content (mg/kg) and total tannin content (g/kg) were found out as biochemical analysis (AOAC, 1998; Waterhouse, 2002).

Statistical analysis

The experiment consisted with combination of 3 different main shoot length and 3 different lateral shoot length applications. A randomized block design was used with 3 replications of a total of 108 vines under 27 parcels. JMP 13.2.0 statistical program was used for determining of differences in applications and years. In order to determine differences in findings, LSD test was used at 5% significance level.

Results and discussion

Phenological development stages

As a result of the phenological observations made throughout the trial, the day green shoot tips seen clearly in the buds was 02.04.2014 (91st calendar day) for the year 2014, for 2015 it was observed as 12.04.2015 (101st calendar day) (*Table 1*).

Table 1. *Phenological development stages of Merlot variety during the experiment years*

Budburst (EL 04-07)	Flowering (EL 23-25)	Verasion (EL 35)	Harvest (EL 38)
02.04.2014	29.05.2014	30.07.2014	16.09.2014
12.04.2015	28.05.2015	01.08.2015	05.10.2015

Climatic conditions

General climatic conditions of 2014-2015 years'

While the average temperature was recorded as 16.08 °C in 2014 and 16.00 °C in 2015, the average temperature in Tekirdağ province for long years (1939-2017) was 14 °C. 2014 was an extraordinary year in terms of precipitation. The annual total precipitation was 770.50 mm, which is significantly higher than the average of 589.10 mm for long years. Vegetation period precipitation was also remarkable with 475.20 mm which is also above 139.00 mm average of long years. In 2015, the total annual precipitation was 507.90 mm and 187.40 mm precipitation in the vegetation

http://www.aloki.hu ● ISSN 1589 1623 (Print) ● ISSN 1785 0037 (Online)
DOI: http://dx.doi.org/10.15666/aeer/1706_1543115446

period is around the average for long years. Due to the general characteristics of 2014, light exposure (PFD) and wind speed were lower than 2015 in 2014 both during the year and vegetation period. Average proportional humidity was also higher for year and vegetation period in 2014.

In 2014, the maximum temperature was measured as 33.50 °C, while the lowest temperature was recorded as 16.10 °C. Also verasion-harvest periot average temperature ranged from 22.00 to 27.60 °C. The light intensity (PFD) ranged between 62.53 µmol m²/s and 1976.27 µmol m²/sec, with an average of 1134.53 µmol m²/s in 2014.

In 2015, the highest temperature was recorded as 39.70 °C and the lowest temperature was 12.30 °C and the average temperature was between 14.30 and 29.00 °C. In the same period, while PFD measurements ranged from 44.37 µmol m²/s to 1894.88 µmol m²/sec, the average period was recorded as 1042.43 µmol m²/s (*Fig. 2*).

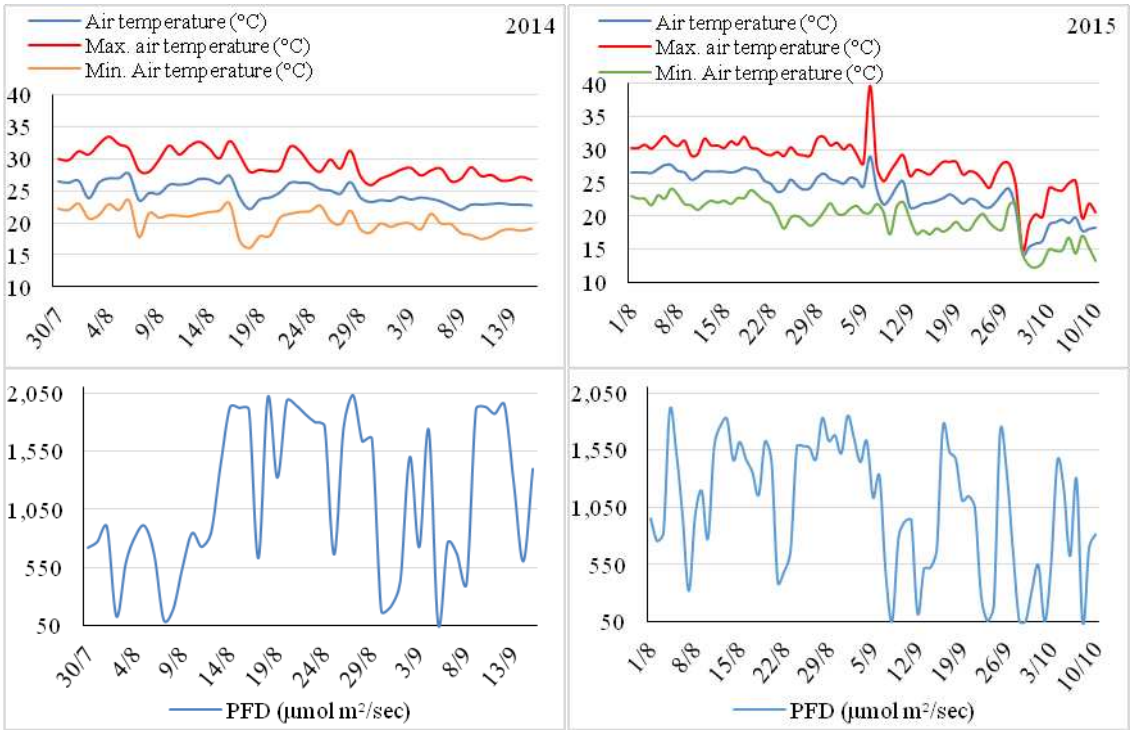

Figure 2. *General temperature and light intensity data of verasion-harvest period in year 2014 and 2015*

Microclimatic conditions inside canopies between verasion and harvest period

Temperature related microclimatic assessments were made for 5 critical intervals per hours/day in terms of the duration of exposure for lateral shoot applications. In addition, the average, lowest and highest temperatures in the related phenological periods were determined.

All lateral shoot leaf removal applications were completed in the first week of August in both years and targeted canopy architectures were created. The most remarkable issue in terms of temperatures for 2014, while the highest temperature in the whole of the vineyard was recorded as 30.10 °C in August and 27.70 °C in August-September mean, the temperature of the canopy was exposed to temperatures in the

http://www.aloki.hu ● ISSN 1589 1623 (Print) ● ISSN 1785 0037 (Online)
DOI: http://dx.doi.org/10.15666/aeer/1706_1543115446

range of 30-35 °C and over 35 °C in all lateral shoot applications. It is noteworthy that temperatures below 20 °C in 2015 are 3-4 times more than in 2014. In both years; temperatures above 35 °C were observed in the NLS application for the longest period, while the temperature above 30 °C was measured at the maximum HLS application. It was observed that in the period between verasion and harvest; most seen temperature range was between 20 and 25 °C in 2014 and 2015. Another remarkable point is that the FLS application remains the longest at temperatures below 20 °C. Temperatures above 35 °C were observed for longer periods with the removal of the lateral leaves (*Table 2*). The positive and negative aspects of this phenomenon will be mentioned in the headings on must analytical analysis.

Table 2. *Verasion-harvest period temperature intervals in canopy (hours/day)*

Verasion-harvest period	≤20 °C		20-25 °C		25-30 °C		30-35 °C		≥35 °C	
	2014	2015	2014	2015	2014	2015	2014	2015	2014	2015
NLS	2.45	6.18	9.34	8.14	3.44	3.19	4.34	3.43	3.23	2.25
HLS	2.36	5.49	8.55	6.49	3.53	4.20	8.1	5.51	0.27	1.11
FLS	2.53	8.29	7.41	6.15	4.47	5.11	6.39	3.20	0.16	0.43

NLS, HLS, and FLS represent no lateral shoots (no leaf), half lateral shoots (3-4 leaves) full lateral shoots (6-7 leaves)

While the mean temperature in the canopy ranged between 26.16 and 26.92 °C in of 2014 verasion-harvest period, the average outside canopy temperature at 2 m was recorded as 23.02 °C. In 2015 verasion-harvest period in canopy mean temperature was changed between 23.36 and 25.26 °C and average temperature at 2 m outside canopy was recorded as 24.40 °C.

During the same period in 2014, the highest average temperature was 27.70 °C at 2 m, while the maximum high temperature was 46.06 °C (NLS) and the lowest high temperature was 37.80 °C (HLS). The highest average temperature was 35.90 °C at 2 m and in canopy measurement was found 49.77 °C for NLS application and 42.77 °C for HLS application in 2015.

In canopy low temperature averages range between 14.46 °C and 15.70 °C and 2 m was recorded as 18.70 °C in year of 2014. Two meters low temperature averages were also recorded as 15.40 °C in 2015, and ranged between 5.12 °C (NLS) and 11.18 °C (FLS) in canopy (*Table 3*).

In both years, outside canopy low temperatures are higher than in canopy low temperatures. Cold weather is trapped inside the canopy at night. In summary, there are no significant differences between the inside and outside of the canopy in terms of average temperatures, but dramatic differences can be observed at low and high temperatures. In the case of high temperatures, it is observed that in canopy temperatures have increased by 18.36 °C for 2014 and 13.87 °C in 2015 for the NLS application due to loss of shade effect created by lateral shoot leaves.

Light intensity averages based on phenological periods

The light intensity measurements were evaluated by calculating the mean data from the canopy microclimates and the data mean obtained from the overall vineyard according to phenological periods.

http://www.aloki.hu ● ISSN 1589 1623 (Print) ● ISSN 1785 0037 (Online)
DOI: http://dx.doi.org/10.15666/aeer/1706_1543115446

In 2014 Verasion-harvest period NLS, HLS and FLS applications were measured as 51.29 µmol m²/sec, 45.75 µmol m²/s and 30.30 µmol m²/sec, respectively and the outside canopy light at 2 m level was recorded as 1155.14 µmol m²/s (*Table 4*). In this period, it was seen that the total light intensity that reached to the whole of the vineyard could only reach the canopy center and clusters in 4.44% NLS application, 3.96% in HLS application and 2.62% in FLS application (*Fig. 3*).

Table 3. *In and outside canopy temperature averages according to the applications between the periods of verasion-harvest in 2014 and 2015 (°C)*

Verasion-harvest period	Max. temperature (°C)		Mean temperature (°C)		Min. temperature (°C)	
	2014	2015	2014	2015	2014	2015
NLS	46.06	49.77	26.92	24.83	15.70	5.12
HLS	37.80	42.77	26.42	25.26	15.58	10.36
FLS	41.91	43.33	26.16	23.36	14.46	11.18
Outside canopy 2 m.	27.70	35.90	23.02	24.40	18.70	15.40

NLS, HLS, and FLS represent no lateral shoots (no leaf), half lateral shoots (3-4 leaves) full lateral shoots (6-7 leaves)

Table 4. *In and outside canopy light intensity averages according to the applications between the periods of verasion-harvest in 2014 and 2015 (µmol m²/s)*

Verasion-harvest period	2014	2015
NLS	51.29	28.71
HLS	45.75	21.43
FLS	30.30	23.05
Outside canopy 2 m.	1155.14	1068.69

NLS, HLS, and FLS represent no lateral shoots (no leaf), half lateral shoots (3-4 leaves) full lateral shoots (6-7 leaves)

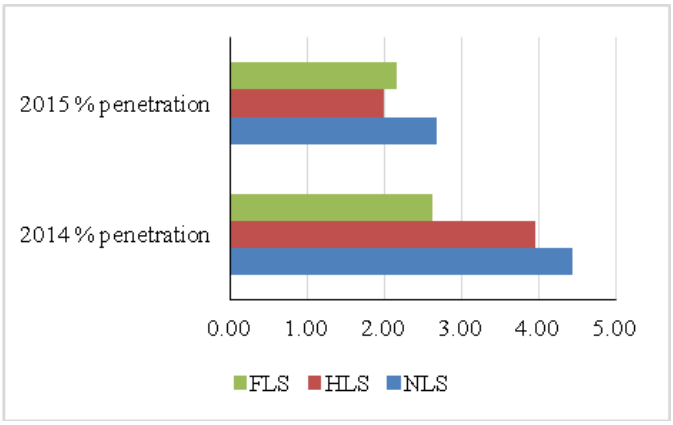

Figure 3. *Penetration percentage of light into the canopy from outside in version-harvest period in years' 2014 and 2015*

Although 2015 was a year with a higher number of cloudless skies compared to the previous year, the late harvest date led to a decrease in the overall average light

http://www.aloki.hu ● ISSN 1589 1623 (Print) ● ISSN 1785 0037 (Online)
DOI: http://dx.doi.org/10.15666/aeer/1706_1543115446

intensity across the vineyard. Thus, the average light intensity of the outside canopy at 2 m was measured as 1068.69 µmol m²/s while the application of NLS was 28.71 µmol m²/s, HLS application was 21.43 µmol m²/s and FLS application was 23.05 µmol m²/s. The penetration rates into the canopy were calculated as 2.19% for NLS application, 2.01% for HLS application and 2.16% for FLS application (*Fig. 3*). In addition, the damage to the leaves and the relative reduction in total leaf area due to the severe *Plasmopara viticola* outbreak in 2014 may have resulted in higher light penetration into the canopy this year. Although not statistically significant, this phenomenon is supported by the decrease in yield and the increase in anthocyanin amounts this year.

Although these values appear to be very low, Smart et al. (1990) stated that approximately only 6% of the intense light from the sun is absorbed by the leaf, and that when the intense canopy formation is seen in the grapevine, the light penetration into the canopy is very low and only 1% of the upper leaves are able to be illuminated. Escalona et al. (2003) also have obtained similar results in double-cordon trained Monte Negro grapes from measurements of outer and inner surfaces of canopies. On the other hand, in Taiz and Zeiger (2010), indicated that only 5% of the total energy presence was used in carbohydrate production while explaining the process of converting solar energy into leaves by carbohydrates.

Must analytical analyzes

Yield (kg per vine)

As stated before, in both years, 16 buds per vine were left in winter prunings, and shoots and clusters were equalized when the shoots reached 30-40 cm in length. Thus, the differences between the yield values were not statistically significant. Yield values were seen the lowest for NLS application with 4.60 kg/vine and highest for FLS application with 5.00 kg/vine.

Total soluble solids (%)

As known, the amount of sugar in the berry is one of the most important components of industrial maturity. While the effects of lateral shoot applications were found to be statistically significant in both years, differences in main shoot practices were found to be insignificant in terms of TSS values. In the average of two years, 1.25 m main shoot length application reached 21.88% highest TSS quantity while FLS application remained at 21.67%. Differences in years averages were insignificant (*Table 5*).

It is observed that the application of NLS in water-soluble dry matter gives different results in both years. In 2014, the extreme rainfall and high proportional moisture occurring during the vegetation period affected the physiological activity positively in the application of full-fledged seat shoot and accelerated the availability of photosynthesis and hence the accumulation of dry matter throughout the vine. Under the relatively hot and dry conditions of 2015, the microclimate, in which the NLS application was affected, in particular in terms of high temperatures, slowed down the accumulation of TSS.

Therefore, it can be seen that the manipulations made at the right time and in the right way on the canopies provide options for the struggle against the negativity caused by the general climate characteristics.

http://www.aloki.hu ● ISSN 1589 1623 (Print) ● ISSN 1785 0037 (Online)
DOI: http://dx.doi.org/10.15666/aeer/1706_1543115446

Total acidity (g/L)

The effects of different main and lateral shoot applications on total acidity were found to be statistically significant in 2014 and for the mean of two years in terms of lateral shoot applications, whereas in 2015 the differences were not significant. At the two-year average, the HLS and FLS applications were in the same statistical class with higher values, while the NLS application created another statistical class with lower total acidity (*Table 5*).

Table 5. *Effects of main shoot and lateral shoot treatments on total soluble solids, total acidity and pH*

Treatments	2014			2015			Mean of years		
	TSS (%)	Total acidity (g/L)	pH	TSS (%)	Total acidity (g/L)	pH	TSS (%)	Total acidity (g/L)	pH
1 m	20.97	7.45	3.54	22.42	5.85	3.75	21.70	6.65	3.65
1.25 m	20.97	7.53	3.54	22.80	5.83	3.73	21.88	6.68	3.63
1.5 m	20.86	7.56	3.53	22.75	5.90	3.77	21.81	6.73	3.65
NLS	21.31^{a}	7.13^{b}	3.58^{a}	22.42^{b}	5.78	3.75	21.86	6.45^{b}	3.66^{a}
HLS	20.84^{b}	7.61^{a}	3.54^{b}	22.86^{a}	5.86	3.75	21.85	6.74^{a}	3.65^{ab}
FLS	20.66^{b}	7.80^{a}	3.50^{c}	22.68^{ab}	5.93	3.75	21.67	6.86^{a}	3.62^{b}
YME	20.94^{B}	7.51^{A}	3.54^{B}	22.65^{A}	5.86^{B}	3.75^{A}			
MSME $LSD_{0.05}$	n.s.	n.s.	n.s.	n.s.	n.s.	n.s.	n.s.	n.s.	n.s.
LSME $LSD_{0.05}$	0.383	0.273	0.034	0.343	n.s.	n.s.	n.s.	0.219	0.023
YME $LSD_{0.05}$	0.234	0.180	0.019	0.234	0.180	0.019			

NLS, HLS, and FLS represent no lateral shoots (no leaf), half lateral shoots (3-4 leaves) full lateral shoots (6-7 leaves). MSME means main shoot main effect, LSME means lateral shoot main effect and YME means year main effect. Different lowercase superscript letters in same column and uppercase letters in same line represent statistically significant differences between means at $p < 0.05$ according to least significant difference test. n.s. means not significant

The most significant relationship between temperature and berry quality appears by reduction of organic acid concentration in berry with high temperatures (Kliewer, 1973).

Tartaric and malic acids are the predominant organic acids which are effective in all stages of berry development and cause significant effects on acidity and pH (Morris et al., 1983). In particular, the malate is stored in berries until the verasion period as a potential source for the carbon demand in the maturation process (Ruffner, 1982). In this period, the decrease in malic acid decreases the total acidity and balances the sugar and acid ratios (Kliewer, 1965). The decrease in titratable acid levels for 2014 and 2015 was directly proportional to the daily exposure time at temperatures between 20-25 °C. At temperatures near 30 °C, seems to reduce the consumption of malic acid by inhibiting photosynthesis. Sweetman et al. (2014) states that enzymes and metabolic pathways that are effective in regulating organic acids during berry growth and development should be further investigated, especially in temperature rise and day/night temperature changes. On the other hand, the increase in the main shoot length caused an increase in titratable acid in years. According to a different study in the same location; Although it is not statistically significant, the main shoot length increase leads to a decrease in total acidity (Yasasin et al., 2018).

http://www.aloki.hu ● ISSN 1589 1623 (Print) ● ISSN 1785 0037 (Online)
DOI: http://dx.doi.org/10.15666/aeer/1706_1543115446

pH

Ph values were found to be very close among the applications in 2015. In 2014 and the average of years, the NLS application reached the highest values and created a different statistical class. Thus, it can be said that in the years of unusual precipitation in vegetation period such as 2014, lateral shoot applications made a difference (*Table 5*).

Total anthocyanin (mg/kg)

When total anthocyanin contents of grape varieties were examined, it was determined that the highest mean of total anthocyanin content was obtained from NLS application in 2014 (*Table 6*). The amount of high anthocyanin in the lateral shoot applications in both years between verasion harvest period was observed to be proportional to the time spent in 20-25 °C temperature range. But similar relationships were not determined at temperatures above 30 °C as found by Kliewer (1970), Kataoka et al. (1984), Mori et al. (2004), Tomana et al. (1979) or in Yamane et al. (2006) for the night temperatures below 20 °C. Maybe, the lower number of berries in cluster, lower berry fresh weights and lower leaves of pH and factors like higher skin/flesh ratio and acidity in 2014 (data not shown) may have appeared as more important factors than temperature and rainfall.

In our study, it is seen that the increasing stress tendency caused higher anthocyanin levels in mean of years with increasing main shoot lengths, but not statistically. According to Yasasin et al. (2018), although it is not statistically significant, the total amount of anthocyanin in the main shoot length of 1.5 m is higher than the 1 m main shoot length.

Observing the direct effects of canopy management practices on the total amount of anthocyanins is quite difficult, as the mechanisms affecting the synthesis, deposition and degradation of anthocyanin are related to a number of factors. However, it is possible to influence the amount of anthocyanins by specific applications selected according to the prescribed climatic characteristics.

Total tannin (g/kg)

In terms of tannins, there was no significant relationship between lateral and main shoot length applications and total tannin amount except for the different climatic characteristics of the two years (*Table 6*).

Total phenolic (mg/kg)

The statistical significance differences between the applications for phenolic substances were only seen in 2014. The highest phenolic substance content was found in the application of NLS (*Table 6*). Roby et al. (2004) and Chacon et al. (2009) reported that increased water stress increases the total phenolic content. In our study, it is seen that the relationship with the increased main shoot length did not significantly affect the total phenolic substance on the basis of years or years. However, it should be kept in mind that water stress did not occur at the levels that can be considered significant in the years when the trial was conducted. The increase in light intensity level and the relative increase in photosynthesis rates due to the removal of all lateral leaves under the effect of the climate conditions of 2014 is thought to have led to this increase.

http://www.aloki.hu ● ISSN 1589 1623 (Print) ● ISSN 1785 0037 (Online)
DOI: http://dx.doi.org/10.15666/aeer/1706_1543115446

Table 6. *Effects of main shoot and lateral shoot treatments on total anthocyanin, total tannins and total phenolics*

Treatments	2014			2015			Mean of years		
	Total anthocyanin (mg/kg)	Total tannins (g/kg)	Total phenolics (mg/kg)	Total anthocyanin (mg/kg)	Total tannins (g/kg)	Total phenolics (mg/kg)	Total anthocyanin (mg/kg)	Total tannins (g/kg)	Total phenolics (mg/kg)
1 m	624.51	2.48	1810.27	472.64	4.22	2900.00	548.57	3.35	2355.14
1.25 m	628.62	2.68	1822.50	562.97	4.37	2985.83	595.79	3.52	2404.17
1.5 m	666.51	2.61	1966.38	572.29	4.39	3037.91	619.40	3.50	2502.15
NLS	719.68^{a}	2.75	2069.44^{a}	574.57	4.35	3098.33	647.13^{a}	3.55	2583.88^{a}
HLS	621.28^{ab}	2.53	1742.77^{b}	521.70	4.37	2909.44	571.49^{b}	3.45	2326.45^{b}
FLS	578.68^{b}	2.49	1786.94^{b}	511.63	4.26	2915.97	545.16^{b}	3.38	2351.45^{b}
YME	639.88^{A}	2.59^{B}	1866.38^{B}	535.97^{B}	4.32^{A}	2974.58^{A}			
MSME $LSD_{0.05}$	n.s.	n.s.	n.s.	n.s.	n.s.	n.s.	n.s.	n.s.	n.s.
LSME $LSD_{0.05}$	101.184	n.s.	230.276	n.s.	n.s.	n.s.	61.893	N.S.	183.857
YME $LSD_{0.05}$	50.404	0.115	150.129	50.404	0.115	150.129			

NLS, HLS, and FLS represent no lateral shoots (no leaf), half lateral shoots (3-4 leaves) full lateral shoots (6-7 leaves). MSME means main shoot main effect, LSME means lateral shoot main effect and YME means year main effect. Different lowercase superscript letters in same column and uppercase letters in same line represent statistically significant differences between means at $p < 0.05$ according to least significant difference test. n.s. means not significant

Tartaric acid (g/L)

It was observed that different lateral shoot length and main shoot length applications did not significantly affect the amount of tartaric acid in grape berries in 2014 and 2015. However, in the rainy 2014 year, the year main effect of tartaric acid was found to be 6.28 g/L, whereas in it was found lower and statistically significant with 4.28 g/L. the drier and warmer 2015 (*Table 7*).

Table 7. *Effects of main shoot and lateral shoot treatments on tartaric acid, malic acid and potassium*

Treatments	2014			2015			Mean of years		
	Tartaric acid (g/L)	Malic acid (g/L)	Potassium (mg/L)	Tartaric acid (g/L)	Malic acid (g/L)	Potassium (mg/L)	Tartaric acid (g/L)	Malic acid (g/L)	Potassium (mg/L)
1 m	6.10	1.68	2496.28	3.56	1.20	1084.77	4.83^{b}	1.44	1790.53
1.25 m	6.23	1.65	2332.11	5.34	1.05	1065.66	5.79^{a}	1.35	1698.89
1.5 m	6.53	1.89	2485.08	3.92	0.88	935.99	5.22^{b}	1.39	1710.34
NLS	6.27	1.53	2475.53	4.53	1.01^{b}	963.26	5.40	1.27^{b}	1719.40
HLS	6.25	1.93	2478.49	4.45	1.30^{a}	1091.68	5.35	1.62^{a}	1785.09
FLS	6.33	1.76	2359345	3.86	0.82^{b}	1031.09	5.09	1.29^{b}	1695.27
YME	6.28^{A}	1.74^{A}	2437.82^{A}	4.28^{B}	1.05^{B}	1028.67^{B}			
MSME $LSD_{0.05}$	n.s.	n.s.	n.s.	n.s.	n.s.	n.s.	0.482	n.s.	n.s.
LSME $LSD_{0.05}$	n.s.	n.s.	n.s.	n.s.	0.238	n.s.	n.s.	0.179	n.s.
YME $LSD_{0.05}$	0.453	0.138	123.45	0.453	0.138	123.45			

NLS, HLS, and FLS represent no lateral shoots (no leaf), half lateral shoots (3-4 leaves) full lateral shoots (6-7 leaves). MSME means main shoot main effect, LSME means lateral shoot main effect and YME means year main effect. Different lowercase superscript letters in same column and uppercase letters in same line represent statistically significant differences between means at $p < 0.05$ according to least significant difference test. n.s. means not significant

Malic acid (g/L)

Significant differences were found in malic acid amount in lateral shoot practices in 2015. While HLS application reached the highest amount of malic acid with 1.30 g/L,

http://www.aloki.hu ● ISSN 1589 1623 (Print) ● ISSN 1785 0037 (Online)
DOI: http://dx.doi.org/10.15666/aeer/1706_1543115446

NLS application was measured as 1.01 g/L and FLS application was measured as 0.82 g/L and they produced different statistic classes. In 2014, no significant differences were found between the practices. As the main effect of the year, in 2015, as in tartaric acid, lower amounts of malic acid were detected (*Table 7*).

Potassium (mg/L)

One of the prominent features in the determination of maturity is the accumulation of potassium in the skin in parallel with the accumulation of sugar in berry flesh. Although it is one of the most important mineral substances in berry composition, very high potassium levels may decrease quality and may have a negative effect on wine quality especially in red wines (Davies et al., 2006).

It also plays an important role in the rapid phase of the cell division during the first stage of berry development due to the potent role in osmotic regulation. Potassium levels during berry development can be affected by many external factors such as soil, grape variety and cultivation practices (Mpelasoka et al., 2003).

However, although potassium levels were not significantly affected by different main shoot and lateral shoot applications, it was observed that higher potassium accumulation occurred in berries in 2014, when precipitation occurred above normal conditions. However, potassium levels were within the expected values in both years (*Table 7*).

Conclusion

As a result, Merlot/5BB combination vines are affected positively in terms of physiological activities and quality criteria when the lateral shoots are kept with 3-4 leaves from the verasion to the harvest in hot years like 2015 (187.40 mm precipitation, 73.43% relative humidity, 1243.56 µmol m²/s light intensity) when rainfall and proportional humidity are relatively low in vegetation period. It is recommended that the lateral shoots should be completely removed during verasion to harvest period, in cool years like 2014 (475.20 mm precipitation, 77.53% relative humidity, 790.31 µmol m²/s light intensity) when vegetation period has high rainfall and proportional humidity and low light intensity.

In terms of main shoot lengths, as the shoot length increases, stress and some quality criteria tend to increase, but these effects are generally not statistically significant. Even when the main shoot length is kept at 1 m, leaf area can reach a sufficient level in terms of yield and quality.

It is considered that future studies should be carried out with modeling studies related to clustermicroclimate, especially with regard to lighting and wind movements within the canopy. In addition, it is considered necessary to transfer green pruning applications to mechanization in practical terms.

Acknowledgements. This study is based on a part of the doctoral thesis of the corresponding author and supported by Republic of Turkey Ministry of Agriculture and Forestry General Directorate of Agricultural Research and Policies with the project number TAGEM/BBAD/2013/A08/P04-08.

REFERENCES

[1] AOAC (1998): Official Methods of Analysis. – Method 952-03. 16th Ed. Revision.

http://www.aloki.hu ● ISSN 1589 1623 (Print) ● ISSN 1785 0037 (Online)
DOI: http://dx.doi.org/10.15666/aeer/1706_1543115446

[2] Bertamini, M. Nedunchezhian, N. (2003): Photoinhibition of photosynthesis in mature and young leaves of grapevine (*Vitis vinifera* L.). – Plant Science 164(4): 635-644. doi.org/10.1016/S0168-9452(03)00018-9.
[3] Blouin, J., Guimberteau, G. (2000): Maturation et Maturite des Raisins. – Feret, Bordeaux.
[4] Carbonneau, A., Bahar, E. (2009): Vine and berry responses to contrasted water fluxes in ecotron around 'veraison'. Manipulation of berry shrivelling and consequences on berry growth, sugar loading and maturation. – Proceedings of the 16th International G*i*ESCO Symposium, July 12-15, University of California, Davis, pp. 145-155.
[5] Chacón, J. L., García, E., Martínez, J., Romero, R., Gómez, S. (2009): Impact of the vine water status on the berry and seed phenolic composition of Merlot (*Vitis vinifera* L.) cultivated in a warm climate: consequence for the style of wine. – Vitis 48(1): 7-9.
[6] Chaves, M. M., Santos, T. P., Souza, C. (2007): Deficit irrigation in grapevine improves water-use efficiency while controlling vigour and production quality. – Annals of Applied Biology 150: 237-252. doi.org/10.1111/j.1744-7348.2006.00123.x.
[7] Crippen, J. R., Morrison, J. C. (1986): The effects of sun exposure on the compositional development of Cabernet Sauvignon berries. – American Journal of Enology and Viticulture 37: 235-242.
[8] Davies, C., Shin, R., Liu, W., Thomas, M. R., Schactman, D. P. (2006): Transporters expressed during grape berry (*Vitis vinifera* L.) development are associated with an increase in berry size and potassium accumulation. – Journal of Experimental Botany 57: 3209-3216. DOI: 10.1093/jxb/erl091.
[9] Dixon, R. A., Xie, D. Y., Sharma, S. B. (2005): Proanthocyanidins: a final frontier in flavonoid research? – New Phytologist 165: 9-28. DOI: 10.1111/j.1469-8137.2004.01217.x.
[10] Donat, M. G., Alexander, L. V., Yang, H., Durre, I., Vose, R., Caesar, J. (2013): Global land-based datasets for monitoring climatic extremes. – Bulletin of the American Meteorological Society 94: 997-1006. doi.org/10.1175/BAMS-D-12-00109.1.
[11] Escalona, J., Flexas, J., Medrano, H. (1999): Stomatal and nonstomatal limitations of photosynthesis under water stress in fieldgrown grapevines. – Australian Journal of Plant Physiology 26: 421-433. DOI: 10.1071/PP99019_CO.
[12] Escalona, J., Flexas, J., Bota, J., Medrano, H. (2003): Distribution of leaf photosynthesis and transpiration within grapevine canopies under different drought conditions. – Vitis 42(2): 57-64.
[13] Flexas, J., Escalona, J. M., Medrano, H. (1998): Down-regulation of photosynthesis by drought under field conditions in grapevine leaves. – Australian Journal of Plant Physiology 25: 893-900. DOI: 10.1071/PP98054.
[14] Flexas, J., Medrano, H., Escalona, J. M., Bota, J., Gulias, J. (2002): Regulation of photosynthesis of C3 plants in response to progressive drought: stomatal conductance as a reference parameter. – Annals of Botany 89: 895-905. DOI: 10.1093/aob/mcf079.
[15] Fraga, H., Malheiro, A. C., Moutinho-Pereira, J., Santos, J. A. (2012): An overview of climate change impacts on European viticulture. – Food and Energy Security 1(2): 94-110. doi.org/10.1002/fes3.14.
[16] German, J. B., Walzem, R. L. (2000): The health benefits of wine. – Annual Review of Nutrition 20: 561-593. doi.org/10.1146/annurev.nutr.20.1.561.
[17] Haselgrove, L., Botting, D., van Heeswijck, R., Hoj, P. B., Dry, P. R., Ford, C., Iland, P. G. (2000): Canopy microclimate and berry composition: the effect of bunch exposure on the phenolic composition of *Vitis vinifera* L. cv. Shiraz grape berries. – Australian Journal of Grape and Wine Research 6: 141-149. doi.org/10.1111/j.1755-0238.2000.tb00173.x.
[18] Jones, G. V. (2007): Climate change: observations, projections, and general implications for viticulture and wine production. – OIV Climate and Viticulture Congress, April 10-14, Spain.

http://www.aloki.hu ● ISSN 1589 1623 (Print) ● ISSN 1785 0037 (Online)
DOI: http://dx.doi.org/10.15666/aeer/1706_1543115446

[19] Kataoka, I., Kubo, Y., Sugiura, A., Tomana, T. (1984): Effects of temperature, cluster shading and some growth regulators on l-phenylalanine ammonia-lyase activity and anthocyanin accumulation in black grapes. – Memoirs of the College of Agriculture/Agronomy and Horticultural Science Series 124: 35-44.
[20] Keller, M. (2010): The Science of Grapevines, Anatomy and Physiology. 1st Ed. – Academic Press, Cambridge, MA.
[21] Kliewer, W. M. (1965): Changes in the concentration of malates, tartrates, and total free acids in flowers and berries of *Vitis Vinifera*. – American Journal of Enology and Viticulture 16: 92-100.
[22] Kliewer, W. M. (1970): Effect of day temperature and light intensity on coloration of *Vitis vinifera* grapes. – Journal of the American Society for Horticultural Science 95: 693-697.
[23] Kliewer, W. M. (1973): Berry composition of *Vitis vinifera* cultivars as influenced by photo temperatures and nycto-temperatures during maturation. – Journal of the American Society for Horticultural Science 98: 153-159.
[24] Lorenz, D., Eichhorn, K., Bleiholder, H., Klose, R., Meier, U., Weber, E. (1995): Phenological growth stages of the grapevine (*Vitis vinifera* L. *ssp. vinifera*)-codes and descriptions according to the extended BBCH scale. – Australian Journal of Grape and Wine Research 1: 100-110. doi.org/10.1111/j.1755-0238.1995.tb00085.x.
[25] Matthews, M., Ishii, R., Anderson, M., O'mahony, M. (1990): Dependence of wine sensory attributes on vine water status. –Journal of Science, Food and Agriculture 51: 321-335. doi.org/10.1002/jsfa.2740510305.
[26] Maroco, J. P., Rodrigues, M. L., Lopes, C., Chaves, M. M. (2002): Limitations to leaf photosynthesis in field-grown grapevine under drought. Metabolic and modelling approaches. – Functional Plant Biology 29: 451-459. DOI: 10.1071/PP01040.
[27] Medrano, H., Escalona, J. M., Cifre, J., Bota, J., Flexas, J. (2003): A ten-year study on the physiology of two spanish grapevine cultivars under field conditions: effects of water availability from leaf photosynthesis to grape yield and quality. – Functional Plant Biology 30(6): 607-619. doi.org/10.1071/FP02110.
[28] Mori, K., Sugaya, S., Gemma, H. (2004): Regulatory mechanism of anthocyanin biosynthesis in 'Kyoho' grape berries grown under different temperature conditions. – Environmental Control in Biology 42: 21-30. DOI: 10.2525/ecb1963.42.21.
[29] Morris, J. R., Sims, C. A., Cawthon, D. L. (1983): Effects of excessive potassium levels on ph, acidity and color of fresh and stored grape juice. – American Journal of Enology and Viticulture 34: 35-39.
[30] Mpelasoka, B. S., Schachtman, D. P., Treeby, M. T., Thomas, M. R. (2003): A review of potassium nutrition in grapevines with special emphasis on berry accumulation. – Australian Journal of Grape and Wine Research 9: 154-168. DOI: 10.1111/J.1755-0238.2003.Tb00265.x.
[31] Nemani, R. R., White, M. A., Cayan, D. R., Jones, G. V., Runnin, S. W., Coughlan, J. C. (2001): Asymmetric climatic warming improves California vintages. – Climate Research 19(1): 25-34.
[32] OIV (2012): Compendium of International Methods of Wine and Musts. Vol. 1-2. – OIV, Paris.
[33] Olsen, J. L., Olesen, A., Breuning-Madsen, H., Balstrom, T. (2011): A method to identify potential cold-climate vine growing sites. A case study from Rosnaes in Denmark. – Danish Journal of Geography 111: 73-84.
[34] Profio, F. D., Reynolds, A. G., Kasimos, A. (2011): Canopy management and enzyme impacts on Merlot, Cabernet Franc and Cabernet Sauvignon. II. Yield and berry composition. – American Journal of Enology and Viticulture 62(2): 152-168. DOI: 10.5344/ajev.2010.10024.
[35] Reynolds, A. G., Pool, R. M., Mattick, L. R. (1986): Influence of cluster exposure on fruit composition and wine quality of Seyyal Blanc grapes. – Vitis 25: 85-95.

http://www.aloki.hu ● ISSN 1589 1623 (Print) ● ISSN 1785 0037 (Online)
DOI: http://dx.doi.org/10.15666/aeer/1706_1543115446

[36] Ribéreau-Gayon, P., Glories, Y., Maujean, A., Dubourdieau, D. (2000): Handbook of Enology. Vol. 2: The Chemistry of Wine and Stabilization and Treatments. – John Wiley and Sons Ltd, Chichester.
[37] Roby, G., James, F., Douglas, A., Adams, A., Mark, A. (2004): Berry size and vine water deficits as factors in winegrape composition: anthocyanins and tannins. – Australian Journal of Grape and Wine Research 10: 100-107. doi.org/10.1111/j.1755-0238.2004.tb00012.x.
[38] Rojas-Lara, B. A., Morrison, J. C. (1989): Differential effects of shading fruit or foliage on the development and composition of grape berries. – Vitis 28(4): 199-208.
[39] Romero, P., Fernández-Fernández, J. I., Cutillas, A. (2010): Physiological thresholds for efficient regulated deficit-irrigation management in winegrapes grown under semiarid conditions. – American Journal of Enology and Viticulture 61: 300-312.
[40] Ruffner, H. P. (1982): Metabolism of tartaric and malic acids in *Vitis.* A review. – Vitis 21: 346-358.
[41] Santos, T., Lopes, C. M., Rodrigues, M. L., Souza, C. R., Maroco, J., Pereira, J. S., Silva, J. R., Chaves, M. M. (2007): Partial rootzone drying irrigation affects cluster microclimate improving fruit composition of 'Moscatel' field-grown grapevines. – Scientia Horticulturae 112: 321-330. DOI: 10.1071/FP02180.
[42] Schubert, A., Restagno, M., Lovisolo, C. (1996): Net photosynthesis of grapevine leaves of different age exposed to high or low light intensities. – Advances in Horticultural Science 10(3): 163-166.
[43] Schultz, H. R. (2000): Climate change and viticulture: a European perspective on climatology, carbon dioxide and UV-B effects. – Australian Journal of Grape and Wine Research 6: 2-12. doi.org/10.1111/j.1755-0238.2000.tb00156.x.
[44] Smart, R. E., Dick, J. K., Gravett, I. M., Fisher, B. M. (1990): Canopy management to improve grape yield and wine quality-principles and practices. – South African Enology and Viticulture 11(1): 3-17. doi.org/10.21548/11-1-2232.
[45] Spayd, S. E., Tarara, J. M., Mee, D. L., Ferguson, J. C. (2011): Separation of sunlight and temperature effects on the composition of *Vitis vinifera* cv. Merlot berries. – American Journal of Enology and Viticulture 53: 171-182.
[46] Sweetman, C. V., Sadras, O., Hancock, R. D., Soole, K. L., Ford, C. M. (2014): Metabolic effects of elevated temperature on organic acid degradation in ripening *Vitis vinifera.* – Fruit Journal of Experimental Botany 65(20): 5975-5988. DOI: 10.1093/jxb/eru343.
[47] Taiz, L., Zeiger, E. (2010): Plant Physiology. 5th Ed. – Sinauer Associates, Sunderland, MA.
[48] This, P., Lacombe, T., Thoma, M. R. (2006): Historical origins and genetic diversity of wine grapes. – Trends in Genetics 22: 511-519. DOI: 10.1016/j.tig. 2006.07.008.
[49] Tomana, T., Utsunomiya, N., Kataoka, I. (1979): The effect of environmental temperature on fruit ripening on the tree. II. The effect of temperatures around whole vines and clusters on the coloration of 'Kyoho' grapes. – Journal of the Japanese Society for Horticultural Science 48: 261-266.
[50] Treutter, D. (2010): Managing phenol contents in crop plants by phytochemical farming and breeding-visions and constraints. – International Journal of Molecular Sciences 11(3): 807-857. dx.doi.org/10.3390/ijms11030807.
[51] Vrsic, S., Vodovnik, T. (2012): Reactions of grape varieties to climate changes in North East Slovenia. – Plant Soil and Environment 58: 34-41. DOI: 10.17221/352/2011-PSE.
[52] Waterhouse, A. L. (2002): Determination of total phenolics. – Current Protocols in Food Analytical Chemistry. https://doi.org/10.1002/0471142913.fai0101s06.
[53] Webb, L. B., Whetton, P. H., Barlown, E. W. R. (2008): Climate change and wine grape quality in Australia. – Climate Research 36: 99-111.
[54] Yasasin, A. S., Bahar, E., Boz, Y., Kiraci, M. A., Gündüz, A., Avcı, G. G., Gülcü, M. (2018): Different soil tillage and shoot length effects on vegetative growth, water stress

http://www.aloki.hu ● ISSN 1589 1623 (Print) ● ISSN 1785 0037 (Online)
DOI: http://dx.doi.org/10.15666/aeer/1706_1543115446

and yield in cv. Cabernet Sauvignon (*Vitis vinifera* L.). – I. International Agricultural Science Congress. 9-12 May 2018, Van, Turkey.

[55] Yamane, T., Shibayama, K. (2006): Effects of changes in the sensitivity to temperature on skin coloration in 'Aki Queen' grape berries. – Journal of the Japanese Society for Horticultural Science 75: 458-462.

http://www.aloki.hu ● ISSN 1589 1623 (Print) ● ISSN 1785 0037 (Online)
DOI: http://dx.doi.org/10.15666/aeer/1706_1543115446

EFFECT OF DIFFERENT SOWING DATES ON SOME COTTON (*Gossypium hirsutum* L.) VARIETIES UNDER THE SECOND CROP GROWING CONDITIONS

COPUR, O.[1*] – POLAT, D.[2] – ODABASIOĞLU, C.[1] – HALILOGLU, H.[1]

[1]*Department of Field Crops, Faculty of Agriculture, Harran University, 63190 Sanliurfa, Turkey*

[2]*Department of Field Crops, Graduate School of Natural and Applied Sciences, Harran University, 63190 Sanliurfa, Turkey*

**Corresponding author*
e-mail: ocopur@harran.edu.tr; phone: +90-414-318-3690

(Received 16th Jul 2019; accepted 15th Nov 2019)

Abstract. Determining the genotypic effect on yield and fiber quality of cotton grown especially as a second crop is an important production strategy in some regions. The aim of this study was to determine the effects of different planting dates on cotton grown as second crop under the ecological conditions of the Harran Plain in Sanliurfa Turkey. The experiment was conducted on the experimental area of Agricultural Faculty of Harran University at Eyyubiye Campus in 2014 and 2015 growing seasons. Seeds of cotton cultivars were sown at different sowing dates with the randomized complete block design using split plot experimental design with three replications. Sowing dates (1th of June, 10th of June and 20th of June) were arranged as main plots and four cotton (Stoneville 468, BA 119, DP 499 and PG 2018) varieties were distributed to sub plots size of 2.8 m x 10 m and row spacing and intra-row spacing of 70 cm and 15 cm, respectively. Results indicated that seed cotton yields varied between 1440 kg ha^{-1} and 4560 kg ha^{-1} in this study and that the most suitable planting date was June 1st to June 10th. As the planting dates delayed, seed cotton yield, number of bolls per plant and seed cotton weight per boll decreased while number of days from sowing to first boll opening, plant height and fiber fineness increased. Sowing dates were not significantly different concerning number of sympodia, seed index, ginning outturn, fiber length, fiber strength and fiber uniformity. Cultivars Stoneville 468, BA 119, DP 499 and PG 2018 had preferable seed cotton yields compared to the other ones.
Keywords: *cotton, planting time, cultivars, yield, fiber quality*

Introduction and literature review

Among the industrial crops, cotton has the highest planting area and production value and has an important place in Turkish exports. Cotton is a plant that requires more input usage than many agricultural products. Low prices due to inadequate support policies and high production costs in cotton farming have negatively affected cotton cultivation in recent years and cultivation areas have decreased. Cotton was planted in an area of 518 000 hectares from which 976 000 tons of cotton fiber was produced in 2018 in Turkey (Anonymous, 2019). Turkey had been characterized as an exporter country of cotton in past years. However, depending on the developments in the textile and confection sector, especially after the 1990s, it started to import a significant amount of cotton and today it has become the fifth country with 680 000 tons after Bangladesh, China, Indonesia and Pakistan. In other words, the amount of cotton production in our country cannot fully meet the demands of the textile and confection sector and the increasing demand is met through imports.

http://www.aloki.hu ● ISSN 1589 1623 (Print) ● ISSN 1785 0037 (Online)
DOI: http://dx.doi.org/10.15666/aeer/1706_1544715462

Aegean, Mediterranean (Cukurova and Antalya) and Southeastern Anatolia Regions were the main cotton production places in Turkey although 56% of the cotton produced in Southeastern Anatolia Region, especially 40% is produced in the province of Sanliurfa (Anonymous, 2019). Therefore Sanliurfa province has an important role in cotton production in Turkey. This ratio is expected to increase with the completion of SAP (Southeastern Anatolian Project) irrigation and energy project.

Producing the amount of fiber cotton needed in Turkey by using our own resources will reduce our dependence on foreign sources and prevent foreign exchange losses for imports. The way to increase cotton production is by expanding plantation areas, using available resources economically or by increasing productivity per unit area. In the fields where wheat-cotton alternation is applied in Turkey, the fields remain empty for about 10 months until the cotton or another main product is sown after the wheat harvest. Especially in areas where irrigation is possible, plants such as corn, soybean and peanut can be sown as second crop. In these areas, spreading the cultivation of early cotton cultivars like a second crop can be an economic cultivation aimed at increasing production since cotton can yield in a shorter period. In Sanliurfa province, first crop was cultivated in approximately 210 000 ha area and second crop was cultivated in 20 000 ha area (Anonymous, 2019).

All of the cotton varieties cultivated in Turkey belong to *Gossypium hirsutum* L. species. Cotton production is a form of production depending on environmental conditions. In addition to the ecological differences, the differences in the cotton production techniques applied as well as genetic structure of the varieties grown in cotton production regions can lead to the formation of the yield and quality quite differently from each other (Killi, 2005). Nowadays, the main purpose of cotton production is to improve the technological properties of fiber as well as high yield, to increase earliness, ginning efficiency, resistance to diseases and pests and to reduce production costs.

In recent years, especially in the studies conducted for cotton production after barley and wheat in Turkey, early cultivation of varieties can be done successfully but yield is reduced and fiber technology features are partially adversely affected respect to the main product planting (Killi, 2005; Killi and Bolek, 2006). There is a need to search the effect of different sowing times on yield and fiber technological properties of mid-early cotton cultivars that grow as second crop conditions especially considering lentil, barley and wheat production. In the second crop conditions, it is possible to tolerate the decrease in yields in cotton production by determining the varieties of cotton which are efficient in sowing time, having grater fiber-technological features, earlier, resistant to diseases and pests. As a matter of fact, in the study carried out with the varieties belonging to different mature groups under the second crop conditions, it is stated that cotton production can be made with early or middle early varieties (Copur and Yuka, 2016).

In the Sanliurfa Harran and Viransehir Plains, producers have recently turned to second crop cotton after lentil, barley and wheat. Producers have problems in choosing the cultivar and the date of planting.

This study was carried out in order to determine yield and fiber properties of some cotton cultivars at different sowing times in the second crop conditions of Sanliurfa Harran Plain and to give practical information to the producers about the second crop cotton cultivation and to shed light on the studies to be done on this subject.

http://www.aloki.hu ● ISSN 1589 1623 (Print) ● ISSN 1785 0037 (Online)
DOI: http://dx.doi.org/10.15666/aeer/1706_1544715462

Materials and methods

Field trials were carried out on a clay textured soil (vertic calciorthid aridisol) during the 2014 and 2015 double crop cotton-growing seasons at Faculty of Agriculture Research and Application Centre of Harran University located in Sanliurfa, Turkey. The experimental site is located in Harran Plain (altitude: 465 m; 37° 08' North and 38° 46' East), near to the Turkish-Syrian border (*Figs. 1* and *2*). The soil texture was of clay loam-type (Anonymous, 2006). Average field capacity, permanent wilting point, dry bulk density and pH of the site at 90 cm soil depth were 32%, 22%, 1.41 g cm^{-3} and 7.2, respectively (*Table 1*).

Figure 1. *The map of the experimental area*

Figure 2. *Photography from the experimental field*

http://www.aloki.hu ● ISSN 1589 1623 (Print) ● ISSN 1785 0037 (Online)
DOI: http://dx.doi.org/10.15666/aeer/1706_1544715462

Table 1. *Some soil properties of the study area (Harran University Research Station, Sanliurfa, Turkey)*

Depth (cm)	BD (g cm^{-3})	OM (%)	Soil particle distribution (%)			pH	N (kg ha^{-1})	P_2O_5 (kg ha^{-1})	K_2O (kg ha^{-1})	FC (%)	PWP (%)
			Sand	Silt	Clay						
0-30	1.37	1.2	7	34	59	7.3	25	27	1280	31.5	22.2
30-60	1.40	0.8	17	25	58	7.2	12	20	900	31.8	22.6
60-90	1.43	0.6	20	21	59	7.2	6	17	810	32.3	21.5
90-120	1.43	0.5	19	20	62	7.2	-	-	-	32.5	21.5

BD: bulk density, OM: organic matter, FC: field capacity, PWP: permanent wilting point

The average air temperatures were in 12 °C-32.5 °C range during the double crop cotton growing season, while relative humidity was below 50% in June, July and August for the both treatment years (*Table 2;* Anonymous, 2016). After the wheat had been harvested, the tillage was done in the trial area and the seeds of the cotton were drilled and then the trial area was irrigated by sprinkler system according to sowing times. In the scope of the study, seeds of cotton cultivars were sown according to sowing dates with the randomized complete block with split plot experimental design with three replications. Sowing dates (June 1st, June 10th and June 20th) were kept in main plot and cultivars (Stoneville 468, BA 119, DP 499 and PG 2018) were in sub plot and cultivars are widely cultivated in southeast of Turkey. The plots consisted of four rows, 10 m in length with inter-row spacing of 70 cm and intra-row spacing of 15 cm; oriented in south-north direction; and hand-thinned to 6 to 7 plants per meter row when the seedlings had approximately three true leaves. The cotton was sown in each plot at 4-5 cm depth by an experimental driller on June 1st, June 10th, and June 20th, 2014 and 2015. Pre-plant fertilizer was applied at a rate of 70 kg N ha^{-1} and 70 kg P ha^{-1} as 20-20-0 compose fertilizer and followed by 90 kg ha^{-1} N as 46% urea applied at the initiation of flowering. K_2O was not applied due to its abundance in the soil. A total of 900, 860 and 800 mm of water were applied in respect to sowing times from cotton sowing to harvest. The first irrigation was applied 4 weeks after each sowing time and the other irrigation was done 9, 8 and 7 times in 10-day intervals respectively. Last irrigation was done when 10% of the bolls in the plots opened.

During the cultivation season in the trial years, the plots were hoed twice by hand and three times by tractor hoe. 1500 g ha^{-1} *fluazifop-p-butyl* herbicide was used against narrow-leaved weeds. 1500 ml ha^{-1} dose of *lambda cyhalothrin* and 200 ml ha^{-1} *thiamethoxam* insecticide were used against the cotton boll worm and aphid pest. No fungicides were used for the diseases.

A 2-m border spacing was left between blocks to reduce edge effects. Also before harvesting, 0.5 m was left in each plot's top and bottom, and 1 row was left as side effect from each side of every plot. Seed cotton samples were hand harvested from all plants, from 9-m sections of the two middle rows in each four row plot. The first hand-picking was done on October 23rd, 2014 and October 15th, 2015, and the second hand-picking was done on November 6th, 2014 and November 4th, 2015.

Seed cotton yield, number of days from sowing to first boll opening, plant height, number of sympodia, number of bolls per plant, seed cotton weight per boll, ginning outturn and seed index were determined according to Worley et al. (1976).

http://www.aloki.hu ● ISSN 1589 1623 (Print) ● ISSN 1785 0037 (Online)
DOI: http://dx.doi.org/10.15666/aeer/1706_1544715462

Approximately a 300-g seed cotton sample collected from each plot was ginned to determine fiber length, fiber fineness, fiber strength and fiber uniformity. Fiber tests were conducted at a relative humidity of 65 ± 2% and a temperature of 20 ± 1 °C to determine fiber characters were measured by High Volume Instrument (HVI-1000) test device (Anonymous, 1997). Statistical analysis was performed using the MSTATC statistical program (Anonymous, 1989). Means were separated using Fisher's protected least significant differences (LSD) test and $P < 0.05$ denotes the level of significance.

Table 2. *Climatic data of the experimental area during cotton crop growing season for the years 2014 and 2015*

Climatic parameters	June	July	August	September	October	November
2014						
Min. air temp. (°C)	15.3	20.3	20.2	14.5	9.5	4.8
Max. air temp. (°C)	40.1	43.4	43.5	40.6	31.9	22.8
Average air temp. (°C)	28.4	32.5	32.4	26.2	20.3	12.1
Relative humidity (%)	43.8	35.2	38.8	41.0	49.5	53.9
Wind speed (ms^{-1})	1.9	1.9	1.5	1.5	1.0	1.6
Soil temperature (°C)	30.4	34.4	35.6	27.8	20.6	11.3
Rainfall (mm)	20.6	------	1.0	28.8	25.7	78.6
2015						
Min. air temp. (°C)	16.7	21.4	22.1	18.7	12.7	6.8
Max. air temp. (°C)	38.4	42.8	43.1	40.4	33.0	24.3
Average air temp. (°C)	27.7	33.2	31.5	29.8	21.6	14.0
Relative humidity (%)	40.1	37.9	37.4	42.7	50.5	51.2
Wind speed (ms^{-1})	1.9	1.7	1.6	1.3	1.4	1.5
Soil temperature (°C)	29.0	32.3	32.9	30.7	24.6	13.8
Rainfall (mm)	0.7	0.2	---	---	58.8	7.9
Average temperatures for 46 years period (1970-2016)						
Min. air temp. (°C)	10.0	16.00	16.0	11.2	2.5	-2.7
Max. air temp. (°C)	44.0	46.8	44.8	42.0	36.4	29.4
Average air temp. (°C)	28.2	32.0	31.2	26.8	20.3	7.5
Relative humidity (%)	34.9	32.2	35.3	37.9	47.5	69.9
Wind speed (ms^{-1})	2.4	2.4	2.2	1.9	1.4	1.4
Soil temperature (°C)	33.2	37.4	36.3	31.0	22.6	13.4
Rainfall (mm)	3.6	0.7	1.1	3.2	25.3	46.0

Results and discussion

Seed cotton yield (kg ha^{-1})

The averaged seed cotton yield (SCY) in terms of cultivars changed between 2579.36 kg ha^{-1} and 3374.97 kg ha^{-1} in both years and the average was 2961.30 kg ha^{-1} and 3019.30 kg ha^{-1} in 2014 and 2015, respectively (*Table 3*). The highest averaged SCY was obtained from Stoneville 468 and the lowest SCY was obtained from PG 2018 cultivar (*Table 3*). In terms of sowing times, SCY varied from 1932.93 kg ha^{-1} to 4154.64 kg ha^{-1} (*Table 3*). According to LSD (Least Significant Difference) test, different cotton yield groups were formed in terms of sowing times and cultivars and

http://www.aloki.hu ● ISSN 1589 1623 (Print) ● ISSN 1785 0037 (Online)
DOI: http://dx.doi.org/10.15666/aeer/1706_1544715462

that SCY decreases with delay of sowing time. This may be due to the lack of sufficient photosynthesis and the reduction of dry matter accumulation, since there was not enough temperature for the development of plants with the delay of sowing time. Therefore, plantings at June 10th and 20th requires a longer period of time for the development and opening of the bolls with the cooling during boll opening period (Gormus and Yucel, 2002). Sowing date x cultivar interaction was statistically significant meaning that SCY was affected by both sowing time and cultivars (*Table 3*). SCY is the result of interaction of genotypes with the environment. Therefore, the highest SCY was obtained from June 1st sowing in addition to cultivars Stoneville 468 and BA 119. This may be due to the similar adaptability of these cultivars to ecological conditions. These varieties have high adaptability and are medium-early varieties, thus opening earlier bolls and higher seed cotton yield. Therefore, Stoneville 468 and BA 119 varieties can be recommended under second crop conditions. Our findings are in agreement with the findings of Copur (1999), Copur et al. (2001), Dong et al. (2006), Barradas and Bellido (2009), Braunack et al. (2012), Baran (2013), Karademir et al. (2013), Copur and Yuka (2016), Wumbei (2014) and Du et al. (2015).

Number of days from sowing to first boll opening (days)

The average number of days from sowing to first boll opening (DTB) ranged from 98 days to 116 days; the mean was 107.25 days in 2014 and 108.53 days in 2015. In terms of cultivars, the highest averaged DTB belonged to PG 2018 while Stoneville 458 was the earliest (*Table 3*). In terms of sowing times, DTB varied between 104.25 and 111.33 days. As a result of the variability analysis there was a significant (0.01) difference between sowing dates and cultivars in both years in terms of DTB (*Table 3*). According to the LSD test, different groupings formed for DTB that increases with the delay of sowing time. It can be observed that plants open bolls with a delay of approximately 5 days compared to June 1st and June 20th. Stoneville 468 and BA 119 varieties are middle early varieties, thus forming bolls earlier than other varieties. As a matter of fact, these varieties also produced higher cotton yields than other varieties. Our findings are consistent with the findings of Copur (1999) that the number of days has increased with the delay of sowing date. It is seen that there is a 4-5 day difference between cultivars in terms of DTB. This difference may be due to the genotype effect, as well as the different response of the varieties to climate and soil conditions. Our findings have similarities of Soyler and Temel (2007), Ozbek et al. (2009), Baran (2013) and Iqbal et al. (2018).

Plant height (cm)

The plant height (PH) values of the cultivars varied between 96.44 cm and 120.96 cm in 2014 and the average was 106.16 cm while the values ranged from 98.91 cm to 118.73 cm and the average was 106.71 cm in 2015. In terms of cultivars, the highest PH was obtained from DP-499 and the lowest was obtained from Stoneville 458 variety (*Table 3*). In terms of sowing times, the averaged PH in 2014 was between 100.8 cm and 112.78 cm and between 103.69 and 110.32 cm in 2015 (*Table 3*). As a result of the variability analysis, sowing dates, cultivars and sowing date x cultivar interaction were significantly (0.05 and 0.01) different regarding to PH (*Table 3*). According to the LSD test, different PH groups were formed in terms of sowing dates and that it increases on the 10th of June and with the delay of sowing time it decreased

http://www.aloki.hu ● ISSN 1589 1623 (Print) ● ISSN 1785 0037 (Online)
DOI: http://dx.doi.org/10.15666/aeer/1706_1544715462

on June 20th. This is due to the shorter vegetation period in late sowing and the limitation of the growth of plants due to the difference in day and night temperature (Usman et al., 2016). Sowing date x cultivar interaction was also important in both years. The highest plants were obtained from June 10th and DP-499 cultivars and the shortest plants were obtained from June 20th and Stoneville-468 cultivars. Specifically, DP-499 was taller than other varieties and thus plants were more vegetatively developed. The lower yield values of the DP-499 cultivar compared to the Stoneville 468 and BA-119 cultivars support our findings. This may be due to the effects of the growth and development cycles of cotton cultivars on different environmental conditions planted in different sowing dates. Our findings are in line with the findings of Copur (1999), Soyler and Temel (2007), Ozbek et al. (2009), Baran (2013) and Copur and Yuka (2016) that plant height increases with delay of sowing date.

Table 3. *Seed cotton yield, number of days from sowing to first boll opening, plant height and their contributions in response to different sowing date and cultivars in 2014 and 2015*

Sowing date (SD)	Seed cotton yield (kg ha^{-1})		Number of days from sowing to first boll opening (days)		Plant height (cm)	
	2014	**2015**	**2014**	**2015**	**2014**	**2015**
1-1th June	4154.64 a	4118.53 a	104.25 b	105.58 c	100.08 c	103.69 b
2-10th June	2796.33 b	2886.80 b	108.25 a	108.67 b	112.78 a	110.32 a
3-20th June	1932.93 c	2052.58 c	109.25 a	111.33 a	105.62 b	106.11 b
Cultivars						
1-Stoneville 468	3374.97 a*	3314.74 a	101.67 d*	98.00 d	96.44 c*	98.91 c
2-BA 119	3222.58 a	3276.73 a	105.00 c	107.78 c	99.54 c	100.16 c
3-DP 499	2668.28 b	2795.84 b	109.00 b	111.78 b	120.96 a	118.78 a
4- PG 2018	2579.36 b	2689.90 b	113.33 a	116.56 a	107.69 b	109.02 c
Interaction						
SD1xC1	4560.53 a	4483.47	98.00	94.00	83.53 g	93.33 d
SD1xC2	4520.30 a	4420.00	102.00	104.67	93.30 f	97.10 cd
SD1xC3	3973.83 b	3903.55	107.00	110.33	115.17 bc	116.93 ab
SD1xC4	3563.90 c	3667.11	110.00	113.33	108.33 cd	107.40 bc
SD2xC1	2957.31 d	3016.84	103.00	97.67	103.60 de	100.73 cd
SD2xC2	2963.74 d	3110.20	107.00	109.67	105.33 de	102.30 cd
SD2xC3	2530.49 e	2753.45	110.00	111.67	127.57 a	117.30 ab
SD2xC4	2733.75 de	2666.71	113.00	115.67	114.60 bc	120.93 a
SD3xC1	2607.07 e	2443.91	104.00	102.33	102.20 de	102.67 cd
SD3xC2	2183.72 f	2300.00	106.00	109.00	100.00 ef	101.08 cd
SD3xC3	1500.50 g	1730.51	110.00	113.33	120.13 ab	121.97 a
SD3xC4	1440.43 g	1735.89	117.00	120.67	100.13 ef	98.73 cd
Grand mean	2961.30	3019.30	107.25	108.53	106.16	106.71
LSD (SD)	85.21	137.40	1.60	1.00	3.98	3.31
LSD (C)	196.00	157.30	3.09	1.93	4.39	6.47
SDxC interaction	339.50	ns	ns	ns	7.60	11.21
C.V. %	6.68	5.26	1.97	1.79	4.17	6.12

*Means in each column followed by the same letter are not significantly different ($p < 0.05$). SD: sowing date, C: cultivar

http://www.aloki.hu ● ISSN 1589 1623 (Print) ● ISSN 1785 0037 (Online)
DOI: http://dx.doi.org/10.15666/aeer/1706_1544715462

Number of bolls per plant (no. plant^{-1})

The number of bolls per plant (BPP) is one of the most important characteristics affecting the cotton yield. The genotypic structure and cultivation techniques of the varieties may affect the number of bolls (Usman et al., 2016). With increasing BBP, cotton yield increases. Variance analysis showed that the BBP was affected by different sowing dates and different cultivars in both years. Although different BBP groups were formed, but the sowing date x cultivar interaction was not significant (*Table 4*). BPP decreased with the delay of sowing time. On the other hand, the BPP obtained in June 1st sowing has led to 40% more bolls compared to June 20th sowing. Decreasing BPP because of late sowing is due to short vegetation time led to decrease number of flowers formed on the plant and insufficient carbohydrate production effecting flowers not to develop into bolls thus shed off the plant. As a matter of fact, the decrease in cotton yield with delayed sowing supports our findings. The average BPP was between 7.96 plant^{-1} and 11.89 plant^{-1} in 2014, with an average of 9.98 plant^{-1} and similar results occurred in 2015. In terms of cultivars, the highest BPP was obtained from Stoneville 468 and the lowest BPP was obtained from PG 2018 (*Table 4*). There were also differences in terms of BPP among the cultivars and that the cultivars yielding the least seed cotton constitute the least BPP (*Table 4*). This may be due to the different reactions of the cultivars to different genotypic structure and environmental conditions. Stoneville 468 variety constitutes the highest number of bolls, thus producing the highest seed cotton yield. Copur (1999), Arshad et al. (2007), Soyler and Temel (2007), Ali et al. (2009), Ozbek et al. (2009), Baran (2013), Copur and Yuka (2016) and Usman et al. (2016) reported that the number of bolls decreased with delay in planting and there were significant differences between cotton varieties.

Number of sympodia (no. plant^{-1})

The number of sympodia (SYM) affects the number of bolls per plant and hence the cotton yield. Number of fruit branches was affected by different sowing dates and varieties according to statistical analysis, but sowing date x cultivar interaction was insignificant in 2014 and significant in 2015 (*Table 4*). Thus SYM decreased with the delay of sowing time. Similar findings were found by Copur (1999), Gur et al. (2001) and Soyler and Durmus (2007) and Baran (2013). The average SYM of cotton cultivars ranged from 11.58 to 13.80 number plant^{-1} averaging 12.57 number plant^{-1} in 2014 while it was between 9.62 and 11.93 number plant^{-1} averaging 11.05 number plant^{-1} in 2015. DP 499 and Stoneville 458 had the highest SYM in 2014 and 2015, respectively while PG-2018 had the lowest SYM in both years (*Table 4*). Different groups were formed in terms of SYM in cotton cultivars. Although the cotton cultivars used in the experiment are in the same maturation group, they can form different SYM due to differences in genotype structure in adaptation to different environmental conditions (Copur, 2006; Soyler and Temel, 2007; Ozbek et al., 2009; Baran, 2013; Copur and Yuka, 2016 and Iqbal et al., 2018).

Seed cotton weight per boll (g boll^{-1})

Seed cotton weight (SCW) was significantly influenced by different sowing dates and cultivars. According to the LSD test, different SCW groups were formed in terms of sowing dates and the SCW decreases with delay of sowing time. The highest SCW was obtained from June 1st sowing and DP 499 cultivars while the lowest SCW was

http://www.aloki.hu ● ISSN 1589 1623 (Print) ● ISSN 1785 0037 (Online)
DOI: http://dx.doi.org/10.15666/aeer/1706_1544715462

obtained from June 20th and BA 119 cultivars in both years. The average SCW was 4.75 g in 2014 and 4.67 g in 2015. The decrease in SCW compared to sowing date shows that plants cannot produce enough carbohydrates for boll development due to low night temperature during the boll development period (Copur, 1999; Ali et al., 2009; Usman et al., 2016 and Iqbal et al., 2018). Therefore, a higher yield of cotton was obtained in June 1st sowing. In addition, there were differences in terms of SCW (*Table 4*). The highest SCW was obtained from DPL 499 variety but it did not produce the highest yield of cotton per hectare. This may be due to the fact that the number of bolls in the mentioned variety was low compared to other productive cultivars and the resulting carbohydrates were used in a less number of bolls (Pettigrew, 2002; Dong et al., 2006; Baran, 2013 and Copur and Yuka, 2016). For this purpose, DPL 499 variety can be selected as a parent in breeding studies that will be carried out for the seed cotton weight.

Table 4. *Number of bolls, number of sympodia, seed cotton weight and their contributions in response to different sowing date and cultivars in 2014 and 2015*

Sowing date (SD)	Number of bolls (no. plant^{-1})		Number of sympodia (no. plant^{-1})		Seed cotton weight (g boll^{-1})	
	2014	2015	2014	2015	2014	2015
1-1th June	11.88 a	11.72 a	13.52	11.93 a	4.96 a	4.97 a
2-10th June	10.13 b	9.59 b	12.63	11.61 a	4.79 a	4.87 b
3-20th June	7.92 c	7.59 c	11.52	9.62 b	4.50 b	4.20 c
Cultivars (C)						
1-Stoneville 468	11.89 a*	11.33 a	12.89 ab*	11.99 a	4.66 b*	4.62 c
2-BA 119	11.11 a	9.74 b	11.96 bc	11.07 a	4.65 b	4.53 c
3-DP 499	8.94 b	9.12 bc	13.80 a	11.10 a	5.22 a	5.00 a
4- PG 2018	7.96 c	8.33 c	11.58 c	10.04 b	4.47 b	4.71 b
Interaction						
SD1xC1	14.37	14.13	13.20	11.47 bc	4.76	4.62 c
SD1xC2	12.43	11.33	12.67	11.50 abc	4.92	4.71 c
SD1xC3	11.10	11.13	15.03	12.00 ab	5.28	5.72 a
SD1xC4	9.63	10.27	13.17	12.73 ab	4.87	4.82 bc
SD2xC1	11.57	11.37	13.10	13.20 a	4.71	4.68 c
SD2xC2	12.50	10.00	11.77	12.23 ab	4.57	4.67 c
SD2xC3	8.07	8.33	13.70	11.47 bc	5.41	5.06 b
SD2xC4	8.37	8.67	11.97	9.53 de	4.48	5.08 b
SD3xC1	9.73	8.50	12.37	11.30 bc	4.51	4.09 d
SD3xC2	8.40	7.90	11.43	9.47 de	4.56	4.22 d
SD3xC3	7.67	7.90	12.67	9.83 cd	4.97	4.23 d
SD3xC4	5.87	6.07	9.60	7.87 e	4.06	4.24 d
Grand mean	9.98	9.63	12.57	11.05	4.75	4.67
LSD (SD)	0.75	1.07	ns	1.43	0.18	0.04
LSD (C)	0.97	0.94	0.96	0.99	0.26	0.17
SDxC interaction	ns	ns	ns	1.72	ns	0.29
C.V. %	9.81	9.89	7.73	9.07	5.59	3.64

*Means in each column followed by the same letter are not significantly different ($p < 0.05$). SD: sowing date, C: cultivar

http://www.aloki.hu ● ISSN 1589 1623 (Print) ● ISSN 1785 0037 (Online)
DOI: http://dx.doi.org/10.15666/aeer/1706_1544715462

Seed index (g)

One of the characteristics affecting the cotton yield is seed index. Seed index (SI) was not affected by sowing time in 2014, but there were significant differences between cultivars, and in 2015, both sowing date and cultivars were significantly different (*Table 5*). The sowing date x cultivar interaction was significant in 2014 and insignificant in 2015. The highest SI was obtained from a June 1st planting and SI decreased in both years with the delay of sowing time (*Table 5*). In terms of cultivars, the highest SI was obtained from DP 499 and the lowest was obtained from PG 2018 variety in both years. Since the number of bolls was low in DP 499, all of the carbohydrates were used in a few bolls. Therefore, the seed weight of DP 499 variety was higher than other varieties. Also, the differences between the cultivars may be due to the genotypic structure as well as the adaptability of the cultivars to environmental conditions. Our findings were parallel with the reports of Arshad et al. (2007), Ali et al. (2009), Barradas and Bellido (2009), Baran (2013) and Copur and Yuka (2016), and are partially consistent with the findings of Copur (1999). This may be due to the fact that the trials were conducted in different years and places and the cultivars used in the trials were different.

Ginning outturn (%)

Ginning outturn (GO) was not affected by different sowing times in both years, but there were significant (0.01) differences between cultivars and sowing date x cultivar interaction was not significant (*Table 5*). In terms of cultivars, the highest GO was determined in PG 2018 and the lowest GO was determined in Stoneville 468 (*Table 5*). Average GO was 41.05% in 2014 and 41.58% in 2015. According to LSD test, different GO groups were formed in terms of cultivars and GO partially decreased with delay of sowing time but it was not statistically significant. The partial reduction in GO with the delay of planting is may be due to weak boll development and consequently the fibres in the seeds did not grow well. In addition, there were differences between the cultivars in terms of GO. PG 2018 variety produced higher gin turnout value compared to other varieties. This may be due to the fact that the cultivars have different genotypic structure in terms of GO. Similar findings are found in Copur (1999), Pettigrew (2002), Arshad et al. (2007), Ali et al. (2009) and Copur and Yuka (2016), Usman et al. (2016), and partially contradicts the findings of Barradas and Bellido (2009) and Baran (2013). This may be due to the fact that the experiments were carried out under different ecological conditions and that the cultivars used in the trials were different.

Fiber length (mm)

Although fiber length (FL) is an inherited property, it may partially be affected by environmental conditions (Bradow and Davidonis, 2000). FL was not affected by different sowing dates and different cotton cultivars, but the sowing date x cultivar interactions were insignificant in 2014 and statistically significant in 2015 (*Table 5*). In 2015, fiber length was affected by variety and environmental interaction. According to the sowing dates and cultivars, the average FL was between 28-29 mm in both years. When the FL values were examined, all of the cultivars are in the medium-length fiber group (Anonymous, 1997) and all of the fiber values obtained can be used in the textile industry. Bauer et al. (2000), Gormus and Yucel (2002),

http://www.aloki.hu ● ISSN 1589 1623 (Print) ● ISSN 1785 0037 (Online)
DOI: http://dx.doi.org/10.15666/aeer/1706_1544715462

Dong et al. (2006), Killi and Bolek (2006), Ali et al. (2009), Barrdas and Bellido (2009), Saeed et al. (2014) and Saleem et al. (2014) stated that FL was not affected by sowing time, while Copur et al. (2001) stated that FL increases with delay of sowing. This may be due to differences in environmental conditions and genotypic differences.

Table 5. *Seed index, ginning outturn, fiber length and their contributions in response to different sowing date and cultivars in 2014 and 2015*

Sowing date (SD)	Seed index (g)		Ginning outturn (g)		Fiber length (mm)	
	2014	**2015**	**2014**	**2015**	**2014**	**2015**
1- 1th June	9.33	9.95 a	41.41	41.58	28.50	28.57
2- 10th June	9.32	9.00 b	41.00	41.28	30.22	28.56
3- 20th June	9.12	8.42 b	40.74	42.12	29.59	29.38
Cultivars (C)						
1-Stoneville 468	9.49 b*	9.07 b	40.59 b*	41.07 b	29.51	29.22
2-BA 119	9.09 c	9.00 b	40.79 b	40.91 b	29.58	29.57
3-DP 499	10.01 a	9.66 a	40.89 b	41.49 b	28.96	28.14
4- PG 2018	8.43 d	8.77 b	41.93 a	42.87 a	29.69	28.42
Interaction						
SD1xC1	9.45 cd	10.04	41.40	40.93	28.15	28.68 abcd
SD1xC2	9.40 cd	9.91	41.11	41.13	28.50	29.68 a
SD1xC3	9.89 abc	10.47	40.86	40.42	28.04	28.12 bcde
SD1xC4	8.57 e	9.38	42.29	43.88	29.30	27.81 de
SD2xC1	9.66 bcd	8.75	40.61	41.48	30.30	29.15 ab
SD2xC2	9.52 bcd	8.72	40.78	41.34	30.03	29.07 abc
SD2xC3	9.99 ab	9.69	40.64	41.89	30.58	27.95 cde
SD2xC4	8.13 e	8.81	41.98	42.27	29.95	28.06 bcde
SD3xC1	9.37 d	8.41	39.77	40.82	30.08	28.81abcd
SD3xC2	8.36 e	8.36	40.50	40.24	30.23	28.97 abc
SD3xC3	10.16 a	8.81	41.17	42.16	28.26	27.35 e
SD3xC4	8.59 e	8.12	41.51	42.47	29.80	28.37 bcde
Grand mean	9.26	9.12	41.05	41.58	29.44	28.50
LSD (SD)	ns	0.65	ns	ns	ns	ns
LSD (C)	0.29	0.43	0.76	0.87	ns	ns
SDxC interaction	0.50	ns	ns	ns	ns	1.15
C.V. %	3.13	4.79	1.86	2.11	3.83	2.36

*Means in each column followed by the same letter are not significantly different ($p < 0.05$). SD: sowing date, C: cultivar

Fiber fineness (micronaire)

There were statistically significant (0.05) differences at sowing date and cultivars in terms of fiber fineness (FF) in 2014 and 2015 but the sowing date x cultivar interaction were not significant (*Table 6*). According to LSD test, different FF groups were determined in terms of sowing date and cultivars. According to the same table, the average FF obtained for cultivars was 3.83-4.80 micronaire (mic) in 2014 and the average was 4.21 mic and changed between 3.45-4.43 mic in 2015 the average was

http://www.aloki.hu ● ISSN 1589 1623 (Print) ● ISSN 1785 0037 (Online)
DOI: http://dx.doi.org/10.15666/aeer/1706_1544715462

3.94 mic. The coarser fibres were obtained from DP 499 variety in both years and the finest fibres were obtained from PG 2018 and BA-119 cultivars in 2014 and 2015, respectively. In terms of sowing dates, the average FF in 2014 varied between 3.99-4.52 mic and the average was 4.21 mic, in 2015, it was 3.45-4.43 mic and the average was 3.94 mic (*Table 6*). The FF value increased by 20% from June 1st to June 20. It can be seen that FF increases with delay of sowing time. FF is an inherited property, but it is influenced by many factors (Jost and Cothren, 2000). In particular, temperature and the consequent accumulation of carbohydrates associated with photosynthesis can affect FF. Moreover, the FF (3.99-4.52 mic) values that occurred with sowing time were positively affected due to temperature change (*Table 6*). In addition, there were differences in FF between cultivars. This is due to the fact that the cultivars have different genotypic structure. In the obtained values, except DP 499 variety, other cultivars are in the middle and fine fiber group (Anonymous, 1997). Fibres are thin with delay of sowing (Dong et al., 2006; Ali et al., 2009, Braunack et al., 2012 and Baran, 2013) but Gormus and Yucel (2002), Pettigrew (2002), Barradas and Bellido (2009) and Saleem et al. (2014) reported that fiber fineness is not affected by different sowing times. This may have been due to the different locations and years of the trials and the diversity of the cultivars used.

Fiber strength (g tex^{-1})

Fiber strength (FS) was not significantly affected by sowing date in 2014 but it was significant in 2015 (*Table 6*). With the delay of sowing, FS was partially increased in 2014 but it was not statistically significant while FS was decreased in 2015 but it was not stable. This may be due to the differences in temperature during the day and night and the change in temperature towards the end of the vegetation period (Bradow and Davidonis, 2000; Killi and Bolek, 2006; Braunack et al., 2012). Significant differences between cultivars occurred in both years; sowing date x cultivar interaction was insignificant in 2014 but significant in 2015 (*Table 6*). The average FS was 37.19 g tex^{-1} in 2014 and 36.12 g tex^{-1} in 2015. In terms of cultivars, the highest FS was obtained from DP 499 and the lowest one was obtained from PG 2018 variety. This may be due to the fact that the cultivars have different genotypic structure in terms of fiber strength (Copur and Yuka, 2016; Usman et al., 2016).

Fiber uniformity

Fiber uniformity (FU) ratio was not affected by different sowing dates and different cotton cultivars and sowing date x cultivar were found to be insignificant in both years (*Table 6*). It can be seen from the same table that the FU ratio was 86.35% in 2014 and 86.25% in 2016. In addition, all cultivars (85-87%) were ranked as high or good when FU values were examined (Anonymous, 1997). All of the fiber values obtained can be evaluated in the textile industry. Our results indicate that FU rate is not affected by sowing time, whereas it is similar to the findings of Killi and Bolek (2006), Barradas and Bellido (2009) and Saleem et al. (2014) while Usman et al. (2016) reported that FU is affected by different sowing dates and there were differences between the cultivars used in the experiment. This may be due to the fact that the cultivars used in the experiments have different genotypic structure, the application of different cultural processes and different climatic conditions.

http://www.aloki.hu ● ISSN 1589 1623 (Print) ● ISSN 1785 0037 (Online)
DOI: http://dx.doi.org/10.15666/aeer/1706_1544715462

Table 6. *Fiber fineness, fiber strength, fiber uniformity and their contributions in response to different sowing date and cultivars in 2014 and 2015*

Sowing date (SD)	Fiber fineness (mic)		Fiber strength (g/tex)		Fiber uniformity (%)	
	2014	2015	2014	2015	2014	2015
1- 1th June	4.52 a	4.43 a	36.48	37.25 a	85.59	86.20
2- 10th June	4.11 b	3.95 b	37.27	34.88 b	86.63	86.40
3- 20th June	3.99 b	3.45 c	37.83	36.22 ab	86.83	86.14
Cultivars (C)						
1-Stoneville 468	4.24 b*	3.81 b	36.98 b*	36.48 ab	86.10	86.34
2-BA 119	3.96 bc	3.52 c	36.44 b	35.69 bc	86.91	86.18
3-DP 499	4.80 a	4.28 a	39.16 a	37.80 a	86.44	86.48
4- PG 2018	3.83 c	4.17 a	36.19 b	34.57 c	85.94	85.99
Interaction						
SD1xC1	4.58	4.25	36.67	36.53 bc	85.47	86.37
SD1xC2	4.30	3.69	35.53	36.57 bc	85.87	86.17
SD1xC3	4.96	4.88	38.50	41.47 a	85.33	86.93
SD1xC4	4.23	4.92	35.23	34.43 c	85.70	85.33
SD2xC1	4.01	3.85	37.63	36.53 bc	86.10	86.20
SD2xC2	4.16	3.78	36.27	34.63 c	88.00	86.87
SD2xC3	4.67	4.16	40.30	33.87 c	86.37	86.30
SD2xC4	3.61	4.03	34.87	34.50 c	86.07	86.23
SD3xC1	4.13	3.32	36.63	36.37 bc	86.73	86.47
SD3xC2	3.41	3.11	37.53	35.67 bc	86.87	85.50
SD3xC3	4.77	3.80	38.67	38.07 b	87.63	86.20
SD3xC4	3.65	3.55	38.47	34.77 c	86.07	86.40
Grand mean	4.21	3.94	37.19	36.12	86.35	86.25
LSD (SD)	0.34	0.24	ns	1.48	ns	ns
LSD (C)	0.32	0.28	1.74	1.56	ns	ns
SDxC interaction	ns	ns	ns	2.71	ns	ns
C.V. %	7.59	7.12	4.73	4.37	1.43	1.83

*Means in each column followed by the same letter are not significantly different ($p < 0.05$). SD: sowing date, C: cultivar

Conclusion

As a result of the research, seed cotton yield, plant height, number of bolls per plant, seed cotton weight and seed index decreased with delayed sowing while the number of days from sowing to boll opening and fiber fineness values increased. The number of fruiting branches per plant, ginning outturn, fiber length, fiber strength and fiber uniformity ratio were not affected by different sowing dates.

When the cultivars were investigated according to sowing dates, Stoneville 468 for seed cotton yield and number of days to open bolls; Stoneville 468 and BA 119 for number of bolls; DP-499 for plant height, number of fruiting branches, seed cotton weight, seed index and fiber strength; PG 2018 for ginning outturn and fiber fineness were promising. In addition, there was no significant difference between the cultivars in terms of fiber length and fiber uniformity ratio.

http://www.aloki.hu ● ISSN 1589 1623 (Print) ● ISSN 1785 0037 (Online)
DOI: http://dx.doi.org/10.15666/aeer/1706_1544715462

The most important issue that cotton producers have focused on in cotton production is the seed cotton yield. In this study; cotton yield was found to be varied between 1440 kg ha^{-1} and 4560 kg ha^{-1}. Autumn rainfall was early in the 2014 and 2015 cotton growing season. It is a major disadvantage for the trial years. Four cotton varieties used in the experiment; Stoneville 468 and BA 119 are medium early and have high adaptability. In addition, it was found that these varieties were not statistically different in terms of cotton yield. For this purpose, after wheat production under Harran Plain ecological conditions, Stoneville 468 and BA 119 cultivars may be preferred for second crop conditions.

Fiber properties were generally not affected by late sowing. However, a general decrease in fiber fineness values was observed. This is expected for late sowing. Therefore, for the development of cotton fibres and high seed cotton yield, sowing of cotton seeds must be completed immediately after the main crop harvest. For this purpose, stubble cultivation applications should be emphasized, early cultivars should be preferred and early cotton cultivars should be improvement for second crop cotton farming. In addition, since the vegetation period is short in the second crop cotton cultivation, studies on plant growth regulators should be carried out for the development of cotton plants.

REFERENCES

[1] Ali, H., Afzal, M. N., Ahmad, S., Muhammad, D. (2009): Effect of cultivars and sowing dates on yield and quality of *Gossypium hirsutum* L. Crop. – Journal of Food, Agriculture and Environment 7(3-4): 244-247.

[2] Anonymous (1989): User's Guide to MSTATC. An Analysis of Agronomic Research Experiments. – Michigan State University, USA.

[3] Anonymous (1997): High Volume Instruments (HVI) Catalog. – Costumer Information Service, No: 40, Volume: May, Sweden.

[4] Anonymous (2006): GAP Agricultural Research Institute, Soil Analysis Laboratory Results. – Sanliurfa, Turkey.

[5] Anonymous (2016): Official Record of Meteorology Directory. – Sanliurfa, Turkey.

[6] Anonymous (2019): Official record of Turkish Statistical Institute. – http://www.tuik.gov.tr/bitkiselapp/bitkisel.zul (20 April 2019).

[7] Arshad, M., Wajid, A., Maqsood, M., Hussain, K., Aslam, M., Ibrahim, M. (2007): Response of growth, yield and quality of different cotton cultivars to sowing dates. – Pakistan Journal of Agricultural Sciences 42(2): 208-212.

[8] Baran, F. O. (2013): The effects of different planting date on agronomical and technological properties in cotton (*Gossypium hirsutum* L.) under short season production conditions. – Adnan Menderes University, Graduate School of Natural and Applied Sciences, MSc Thesis, Aydın, Turkey (in Turkish).

[9] Barradas, G., Bellido, R. L. (2009): Genotype and planting date effects on cotton growth and production under South Portugal conditions, III. boll set percentage, boll location, yield and lint quality. – Journal of Food and Environment 7(2): 322-328.

[10] Bauer, P. J., Frederick, J. R., Bradow, J. M., Sadler, E. J., Evans, D. E. (2000): Canopy photosynthesis and fiber properties of normal and late planted cotton. – Agronomy Journal 92: 518-523.

[11] Bradow, J. M., Davidonis, G. H. (2000): Quantitation of fiber quality and the cotton production-processing interface: a physiologist's perspective. – The Journal of Cotton Science 4: 34-64.

http://www.aloki.hu ● ISSN 1589 1623 (Print) ● ISSN 1785 0037 (Online)
DOI: http://dx.doi.org/10.15666/aeer/1706_1544715462

[12] Braunack, M., Bange, M., Johnston, D. (2012): Can planting date and cultivar selection improve resource use efficiency of cotton systems? – Field Crops Research 137: 1-11.
[13] Copur, O. (1999): A research on the effects of different planting dates on flowering, yield, yield components and earliness criteria of cotton (*Gossypium hirsutum* L.) at the Harran Plain conditions. – Harran University, Graduate School of Natural and Applied Sciences, PhD Thesis, Sanlıurfa, Turkey (in Turkish).
[14] Copur, O. (2006): Determination of yield and yield components of some cotton cultivars in semi arid conditions. – Pakistan Journal of Biological Science 9(14): 2572-2578.
[15] Copur, O., Yuka, A. (2016): Determination of yield and yield components of cotton varieties (*Gossypium hirsutum* L.) grown as second crop after the wheat. – Yuzuncu Yil University, Journal of Agriculture Science 26(2): 245-253 (in Turkish).
[16] Copur, O., Gur, A., Özel, A., Oglakci, M. (2001): A research on the effects of different planting dates on the boll and fiber technological characteristics of cotton (*Gossypium hirsutum* L.) plant in the Harran Plain conditions-II. – Trakya University, Tekirdag Faculty of Agriculture, 4th National Field Crops Congress, 17-21 September 2001, Tekirdag, Turkey, pp. 181-186 (in Turkish).
[17] Dong, H., Li, W., Tang, W., Li, Z., Zhang, D., Niu, Y. (2006): Yield quality and leaf senescence of cotton grown at varying planting dates and plant densities in the Yellow River Valley of China. – Field Crops Research 98: 106-115.
[18] Du, X., Chen, B., Shen, T., Zhang, Y., Zhou, Z. (2015): Effect of cropping system on radiation use efficiency in double-cropped wheat–cotton. – Field Crop Research 170: 21-31.
[19] Gormus, O., Yucel, C. (2002): Different planting date and potassium fertility effects on cotton yield and fiber properties in the Cukurova Region, Turkey. – Field Crops Research 98: 106-115.
[20] Gur, A., Copur, O., Ozel, A., Oglakci, M. (2001): A research on the effects of different planting dates on the yield, agronomic characteristics and earliness criteria of cotton (G*ossypium hirsutum* L.) plant in the Harran Plain conditions-I. – Trakya University Tekirdag, Faculty of Agriculture, 4th National Field Crops Congress, 17-21 September 2001, Tekirdag, Turkey, pp. 175-180 (in Turkish).
[21] Iqbal, M., Ul-allah, S., Naeem, M., Hussain, M., Ijaz, M., Wasaya, A., Ahmad, M. Q. (2018): Reproductive development and seed cotton yield of *Gossypium hirsutum* L. affected by genotype and planting time. – Int. J. Aric. Biol. 20(7): 1591-1596.
[22] Jost, P. H., Cothren, J. T. (2000): Growth and yield comparisons of cotton in conventional and ultra narrow row spacing. – Crop Science 40: 430-435.
[23] Karademir, E., Karademir, C., Sezener, V. (2013): Adaptation of some cotton varieties for Diyarbakır Province conditions. – Selcuk University, Faculty of Agriculture, Proceeding of 10th National Field Crops Congress, Vol. 2, 10-13 September 2013, Konya, Turkey, pp. 198-202 (in Turkish).
[24] Killi, F. (2005): Effect of early, normal and late planting dates on yield components of two cotton cultivars under irrigated conditions of Turkey. – Innovative Scientific Information & Services Network Bioscience Research 2(1): 38-42.
[25] Killi, F., Bolek, Y. (2006): Timing of planting is crucial for cotton yield. – Acta Agriculturae Scandinavica Section B. Soil and Plant Science 56: 155-160.
[26] Ozbek, N., Eksi, İ., Erdogan, H. (2009): Improvement of early cotton cultivars by hybridization breeding method. – Mustafa Kemal University, 8th National Field Crops Congress, 19-22 October 2009, Hatay, Turkey, pp. 747-751 (in Turkish).
[27] Pettigrew, W. T. (2002): Improved yield potential with an early planting cotton production system. – Agronomy Journal 94: 997-1003.
[28] Saeed, F., Kang, S. A., Amin, M. (2014): Performance of genotypes at different sowing dates on yield and quality traits in *Gossypium hirsutum* L. – Int. J. of Agric. and Crop Sci. 7(5): 274-278.

http://www.aloki.hu ● ISSN 1589 1623 (Print) ● ISSN 1785 0037 (Online)
DOI: http://dx.doi.org/10.15666/aeer/1706_1544715462

[29] Saleem, M. F., Bilal, M. F., Anjum, S. A., Khan, H. Z., Sarwar, M., Farhad, W. (2014): Planting time and nutrition on cell membrane thermostability, bolls' retention and fibre traits in cotton. – The Journal of Animal & Plant Sciences 24(3): 829-837.

[30] Soyler, D., Temel, N. (2007): Determination of suitable cotton (*Gossypium hirsitum* L.) varieties for growing as second crop after wheat in Hatay Province. – Ataturk University Faculty of Agriculture, 7th National Field Crops Congress, Vol. 2, 25-27 June 2007, Erzurum, Turkey, pp. 736-739 (in Turkish).

[31] Usman, K., Ayatullah, K., Khan, N., Khan, S. (2016): Genotype-by-sowing date interaction effects on cotton yield and quality in irrigated condition of Dera Ismail Khan, Pakistan. – Pak. J. Bot. 1933-1944.

[32] Worley, S. Jr., Harmon, H. R., Harrel, D. C., Culp, T. W. (1976): Ontogenetic model of cotton yield. – Crop Science 16: 30-34.

[33] Wumbei, A. (2014): The effect of date of planting on the performance of promising cotton varieties. – Journal of Environment and Earth Science 4(4): 1-9.

http://www.aloki.hu ● ISSN 1589 1623 (Print) ● ISSN 1785 0037 (Online)
DOI: http://dx.doi.org/10.15666/aeer/1706_1544715462

COMBINATION OF BIOAUGMENTATION AND BIOSTIMULATION AS AN OIL-DRILLING MUD CONTAMINATED SOIL BIOREMEDIATION TREATMENT

HAMOUDI-BELARBI, L.[1*] – DEMDOUM, S.[2] – MEDJRAS, S.[2] – HAMOUDI, S.[3]

[1]*Laboratory of Valorisation and Bio-Engineering of Natural Resources, Department of Nature and Life Sciences, Faculty of Sciences, University of Algiers, 16000 Algiers, Algeria*

[2]*Department of Biology, Faculty of Sciences, University of M'Hamed Bougara, 35000 Boumerdes, Algeria*

[3]*Department of Soil Sciences and Agri-Food Engineering, Centre in Green Chemistry and Catalysis (CGCC), Université Laval, Quebec, QC G1V 0A6, Canada (phone: +1-418-656-2131 ext. 408460; fax: +1-418-656-3723)*

**Corresponding author*
e-mail: l.hamoudi@univ-alger.dz; phone/fax: +213-24-911-116

(Received 19th Jul 2019; accepted 15th Nov 2019)

Abstract. The removal of oil-drilling mud contaminated soil generated from oilfields in the Algerian Sahara by bioaugmentation with *Yarrowia lipolytica* and biostimulation with carrot peel waste amendment during 45 days was investigated. Initially, the evaluation of growth and gasoil degrading ability of *Yarrowia lipolytica* in carrot peel waste, and carob kibbles media were compared. Afterwards, the effect of bioaugmentation and organic amendment on oil-drilling mud contaminated soil was studied for 45 days of study period. Total petroleum hydrocarbon (TPH) was measured by distillation using distiller mud. The results indicated that, higher augmentation in growth was observed in carrot peel waste medium and when the concentration of gasoil was increased from 15% to 30%. TPH decreased to 35 ± 1.66% and 30.60 ± 1.50% the first 15 days, 33 ± 2.30% and 26.8 ± 1.66%, respectively at the end of study. TPH rate did not undergo any significant change from its initial value in the control for the entire period of incubation. This study demonstrated the effectiveness of co-application of bioaugmentation with *Yarrowia lipolytica* and biostimulation with carrot peel waste amendment for bioremediation of oil-drilling mud contaminated sites.
Keywords: *bioremediation, carrot peel waste, Yarrowia lipolytica, soil remediation, oil-drilling mud*

Introduction

The mud generated from oil-drilling, causes considerable ecological and health problems like toxicity and carcinogenicity (Singh and Chandra, 2014). About 20% of generated waste drilling mud is treated by thermal treatment, solidification, solvent washing, landfilling of contaminated soils, stabilization and transport which are some of the available techniques that are highly expensive, ineffective, rarely neutral, and environmentally destructive (Lu et al., 2010; Minai-Tehrani et al., 2009; Dadrasnia et al., 2014). While the rest is temporarily deposited in so-called mud pits. Bioremediation of mud pits has proven to be an effective, non-invasive, eco-friendly and clean-up technology (Cerqueira et al., 2014; Silva-Castro et al., 2015). Bioremediation is utilization of specific microorganisms to reduce or transform petroleum products into less toxic forms (Esmaeil and Akbar, 2015). Biostimulation and bioaugmentation are bioremediation methods that have been successfully used earlier (Esmaeil and Akbar, 2015). Bioaugmentation involves introducing allochthonous degrading microorganisms to detoxify petroleum contaminated soils (Taccari et al., 2012; Ceci et al.,

http://www.aloki.hu ● ISSN 1589 1623 (Print) ● ISSN 1785 0037 (Online)
DOI: http://dx.doi.org/10.15666/aeer/1706_1546315475

2019). Biostimulation is based on stimulation of the catabolic activity of degrading microorganisms by adding nutrient-rich organic and inorganic materials to avoid metabolic limitations (Taccari et al., 2012). Bioaugmentation studies using *Yarrowia lipolytica* were reported by Sekova et al. (2015) to degrade hydrocarbons and triglycerides. The yeast *Candida maltosa* was used to degrade phenyl alkanes, which constitute refined gasoline fuel oil, by Awe et al. (2008). In arid areas, addition of nutrients may be necessary to stimulate the growth of biodegrading microbiota in contaminated soils poor in organic matter (Nyman, 1999). Addition of pure nutrients and organic waste material as biostimulants has been well documented, to support microbial activity in the contaminated soils (Decesaro et al., 2016). Compared to pure nutrients, organic waste material supplementation is a cost-effective method (Andreolli et al., 2015). Organic biostimulants, containing enzymes, enhance substantially the growth of microbial activity (Shahi et al., 2016). Besides, biostimulants release biosurfactants that increase the bioavailability of poorly soluble hydrocarbon petroleum compounds (Yi and Crowley, 2007; Yoshitomi and Shann, 2001). In the few last years, few studies have shown the efficiency of co-application of bioaugmentation by yeast with addition of organic amendment for biodegradation of petroleum contaminated soils (Zhang et al., 2011; Qin et al., 2013). Zhang et al. (2011) used bioaugmentation in combination with biostimulation to treat hydrocarbons contaminated soils by incubating *Fusarium* sp. with a mixture of leaves, branches, and biowastes. Qin et al. (2013) used biochar produced from rice straw in bioremediation of hydrocarbons. These authors demonstrated that application of amendment and yeasts simultaneously, gave promising results compared to bioaugmentation only. The aim of this study was to examine the efficiency of this combination strategy for biodegrading of oil-drilling from contaminated soil using carrot peel waste as organic amendment. However, review of the literature shows that there is no information on the application of this organic matter and *Y. lipolytica* for bioremediation of crude oil contaminated soil.

Materials and methods

The oil-drilling mud contaminated soil origin

The oil-drilling mud was collected in the Hassi Messaoud field (Algeria), located at 30° 25.006' N and 5° 23.637' E (*Fig. 1*).

Samples were collected at 0-50 cm depth using a stainless steel sampler, placed in appropriate containers thoroughly mixed therein. The oil-drilling mud contaminated soil was sterilized by heating at 180 °C for 2 h in a closed stainless container which prevents loss of volatile fractions, then cooled down overnight before use. The significant characteristics of the oil-drilling mud contaminated soil are listed in *Table 1*.

Physico-chemical characterization of oil-drilling mud contaminated soil

Preparation of the lixiviate

10 g of oil-drilling mud contaminated soil was placed in the beaker containing 100 mL of distilled water. After agitation during 1 h and filtration (Whatman 125 mm), lixiviate obtained was then diluted at 1/100 and used for analysis.

http://www.aloki.hu ● ISSN 1589 1623 (Print) ● ISSN 1785 0037 (Online)
DOI: http://dx.doi.org/10.15666/aeer/1706_1546315475

Determination of the indicating organic pollution parameters

HACH DR900 Colorimeter was used for the determination of dissolved oxygen, chemical oxygen demand (COD), nitrate, nitrite, phosphorus, sulphates, and ammonia nitrogen content in the oil-drilling mud contaminated soil. Analytical methods were used to determine alkalinity, and chloride by volumetry. Calcium, magnesium were measured by complexometric titration with standard solution of EDTA. Total iron and potassium were measured by an atomic absorption spectrophotometer (PerkinElmer A-Analyst 200).

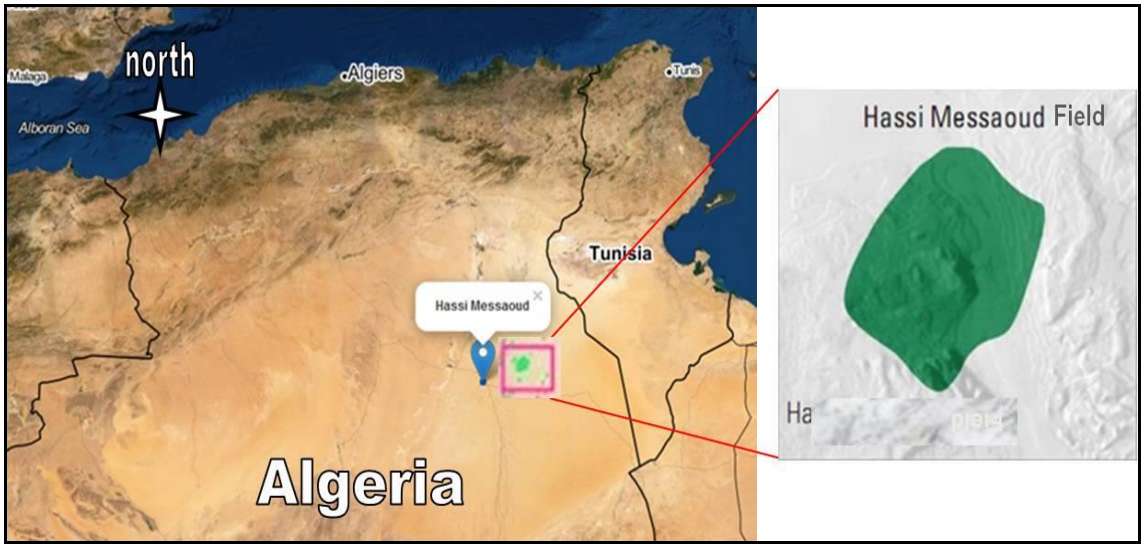

Figure 1. *Location map of the study area*

Biochemical oxygen demand after 5 days (BOD_5)

The Biochemical Oxygen Demand measured for 5 days (BOD_5), was carried out by respirometry (Khodja, 2008).

Evaluation of growth and gasoil degrading ability of Yarrowia lipolytica in carrot peel waste, and carob kibbles media

Carrots were purchased from a local vegetable market and dry pods of carob were obtained from locality of Ighil-Ali (Bejaïa, Algeria). Carrot peels and carob kibbles were macerated separately at a ratio of 1 kg in 2.5 L of distilled water at 85 °C for 45 min with continuous stirring (Acourene and Tama, 2001). After filtration and decantation, media were autoclaved at 120 °C for 20 min and stored at 4 °C before use as biostimulating media.

The yeast *Yarrowia lipolytica* used in this study was isolated and identified earlier in our previous work (published results by Hamoudi-Belarbi et al., 2016). *Y. lipolytica* was grown in 500 mL Erlenmeyer flasks containing 100 mL of Yeast Extract Glucose (YEG broth) prepared using: 10 g/L yeast extract (Himedia, Mumbay, India), 20 g/L glucose (Sigma, Switzerland) in an orbital shaker cabinet maintained at 25 °C under an agitation rate of 80 rpm for 24 h. This 1st culture was then used to inoculate (3% v/v) a carrot peels waste, and carob kibbles media which were incubated at 25 °C for 48 h in an orbital shaker (80 rpm). Gasoil (15% or 30%) was added to the 500 mL Erlenmeyer

http://www.aloki.hu ● ISSN 1589 1623 (Print) ● ISSN 1785 0037 (Online)
DOI: http://dx.doi.org/10.15666/aeer/1706_1546315475

flasks containing 100 mL of sterilized carrot peels waste or carob kibbles media and then incubated at 25 °C in an orbital shaker (80 rpm) for 12 days. At four days regular intervals, turbidity was measured at 600 nm. A volume of 1 mL of each Erlenmeyer flask containing carrot peel waste or carob kibbles media was diluted in 9.9 mL of peptone water solution (Difco, Detroit, USA). After serial dilutions, 1 mL aliquots of suitable dilutions were pour plated in potato dextrose agar medium (Difco). The number of viable cells was counted after 48 h of incubation at room temperature (25 °C).

Bioaugmentation using Yarrowia lipolytica in combination with biostimulation using a selected medium

Experimental design

200 g of sterilized oil-drilling mud in the slurry was used for bioremediation studies and conducted by the following: (i) addition of only yeast (3% v/v); (ii) addition of both the organic amendment and yeast; (iii) sterilized oil-drilling mud in the slurry without yeast and organic amendment (control). Each slurry mixture was placed in circular cell, run in the open air and mixed thoroughly every 3 days to ensure homogenous distribution during 45 days of remediation studies. Each treatment was carried out in duplicate (*Fig. 2*).

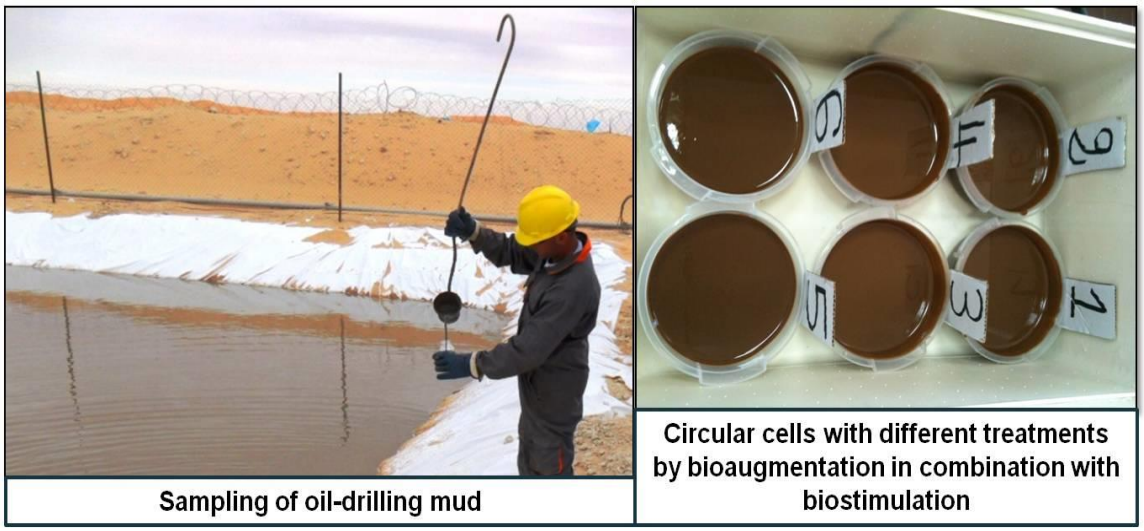

Figure 2. *Experimental design of oil-drilling mud remediation under laboratory scale*

Physico-chemical characterization

Temperature, pH and residual moisture measurements

The temperature and pH were determined using thermometer (MRC 201, France) and, pH meter (Accumet AE150 instrument; Fisher Scientific, France), respectively. The residual moisture (RM) of oil-drilling mud contaminated soil samples was determined (in duplicate) by the difference in weight before and after drying in a vacuum oven at 105 °C for 3 h in the presence of P_2O_5.

http://www.aloki.hu ● ISSN 1589 1623 (Print) ● ISSN 1785 0037 (Online)
DOI: http://dx.doi.org/10.15666/aeer/1706_1546315475

Total petroleum hydrocarbon (TPH) measurement by distillation

TPH percentage of oil-drilling mud samples was measured by distillation using Fann distiller and by determination of the percentage of water/oil in the mud. 20 mL of each soil sample is placed in a distiller, then heated up to 800 °C. The vapors of water and oil are then condensed back into liquid form and collected (distillate). After about 30 to 60 min of decantation, the volumes of water and oil are read directly. After distillation, the remaining mass of mud is weighed. The percentages of water and oil are directly determined. Two replications were conducted for all measurements.

Microbiological analysis

Two replicate samples from each oil-drilling mud (i) with yeast only; (ii) with both the organic amendment and yeast; (iii) without yeast and organic amendment (control) were withdrawn at the end of the second, fourth and sixth week of study for the enumeration of yeast. A volume of 1 mL of each sample was diluted in 9.9 mL of peptone water solution (Difco, Detroit, USA). After serial dilutions, 1 mL of aliquots from suitable dilutions was pour-plated in potato dextrose agar (PDA) medium (Difco). The PDA agar was acidified to pH 3.5 using 100 g/L of tartaric acid solution.

Statistical analysis

Data were analyzed by Data Analysis Tool pack of Microsoft Office Excel 2007 (Microsoft, New York, NY, USA).

Results and discussion

Physicochemical properties of oil-drilling mud contaminated soil

Table 1 lists the physico-chemical properties of oil-drilling mud contaminated soil. The temperature of oil-drilling mud was approximately 21.8 °C ± 0.28; the effect of temperature on the physical nature and chemical composition of the oil, rate of hydrocarbon metabolism by microorganisms and composition of the microbial community, influences oil biodegradation (Atlas, 1981). Moisture content of oil-drilling mud was 51.0 ± 2.12%; according to Kumari et al. (2016), moisture is a limiting factor during biodegradation. As shown in the table, dissolved oxygen is low (7.6 mg/mL). Indeed, a high chemical oxygen demand (COD) (1362 mg O_2/L), that is a measure of the oxygen required to degrade the organic matter present in oil-drilling mud, is an indicator of strong pollution at the site studied (Damo and Icka, 2015). Total organic carbon (TOC) is considered as the most relevant parameter for quantifying organic pollution in soil (Wang et al., 2013). The highest value observed in this study (17.94%) confirmed that the soil studied was polluted by hydrocarbons present in the oil-drilling mud contaminated soil. pH value of oil-drilling contaminated soil used in this study was basic (8.5 ± 0.26). In arid areas, soils tend to be alkaline (Ma et al., 2015), mainly due to the dry environmental conditions. According to Khodja (2008), alkalinity of oil-drilling contaminated soil is maintained between 9.5 and 10.5 in order to prevent corrosion and control the solubility of calcium and magnesium salts. Oil-drilling contaminated soil was mineralized with predominance of ions such as Cl^-, Ca^{+2}, SO_4^{-2}, and Mg^{+2}. However, nitrites (HNO_2^-), nitrates ($N\text{-}HNO_3^-$), phosphorus (PO_4^{-3}), and Fe^{+2} were negligible. According to Abd-Alla et al. (2014), alkaline soils are characterized by poor

http://www.aloki.hu ● ISSN 1589 1623 (Print) ● ISSN 1785 0037 (Online)
DOI: http://dx.doi.org/10.15666/aeer/1706_1546315475

availability of phosphorus and micronutrient transition metals. Analysis of carrot peel waste showed that it contains 25.10 ± 1.20 mg/L phosphorus, and 1.4 mg/L nitrogen (Hamoudi-Belarbi et al., 2018). Therefore this waste can compensate for the nutrient deficiencies in the oil-drilling mud contaminated soil.

Table 1. *Physicochemical properties of oil-drilling mud contaminated soil*

Parameters	Values
Temperature	21.7
Residual moisture %	51.0 ± 2.12
pH	8.5 ± 0.26
COT (%)	17.94
$N\text{-}HNO_3^-$	0.152
HNO_2^-	1.3
PO_4^{-3}	0.23
COD (mg/L)	1362
BOD_5 (mg/L)	56.5
Dissolved O_2 (mg/L)	7.60
CO_3^-	-
HCO_3^-	51.85
SO_4^{2-}	80
Cl^-	4627.13
Ca^{++}	841.68
Mg^{++}	60.8
Na^+	1454.4
K^+	28.67
Fe^{++}	21.45

Evaluation of growth and gasoil degrading ability of Yarrowia lipolytica in carrot peel waste, and carob kibbles media

Figure 3 shows the growth of *Yarrowia lipolytica* after incubation using biostimulating media (carrot peel waste, and carob kibbles) with adding gasoil at 15%, and 30% concentration as sole source of carbon, in comparison with a control without adding gasoil, during 12 days. The nature of biostimulating media and concentration of gasoil affected the growth of *Y. lipolytica*. Higher augmentation in growth was observed in carrot peel waste medium and when the concentration of gasoil was increased from 15% to 30%, indicating that phosphorus and nitrogen nutrients present in carrot peel waste played a major role in growing the cultures. As an example, at 4 days of incubation at 15% concentration, log (CFU/mL) was 11.93 (*Fig. 3A* and *B*). At 8 days of incubation, log (CFU/mL) decreased to 9.00 for 15% and 7.97 for 30%. After 8 days of incubation, log (CFU/mL) increased to reach 11.27 for all 15% and 30% concentration at 12 days of incubation. Carob kibbles are widely used as biostimulating medium during bioremediation of petroleum (Hamoudi-Belarbi et al., 2017, 2018). Carob kibbles did not provide a good biostimulating medium to *Y. lipolytica*, with log (CFU/mL) of 10.38 for 15% and 30% concentration simultaneously at 4 days of incubation. Log (CFU/mL) increased then decreased to 11.16, and 10.41 for 15% and 30%, respectively at 8 days of incubation. A drastic decreasing was observed at 12 days

http://www.aloki.hu ● ISSN 1589 1623 (Print) ● ISSN 1785 0037 (Online)
DOI: http://dx.doi.org/10.15666/aeer/1706_1546315475

of incubation with log [CFU/mL] of 8.34 for 15% and 30% concentration simultaneously. This better growth using carrot peel waste than carob kibbles can be explained by the fact that phosphorus and nitrogen nutrients present in carrot peel waste played a major role in growing the cultures of *Y. lipolytica*. Vidali (2001) demonstrated that the additional nutrient nitrogen and phosphorus contained in the carrot peel waste stimulated microbial growth and led to synthesized enzymes required to degrade hydrocarbon compounds. On the other hand, carrots are known to release linoleic acid, which can increase the bioavailability of poorly soluble hydrocarbon compounds (Yi and Crowley, 2007; Yoshitomi and Shann, 2001; Kosaric, 2001).

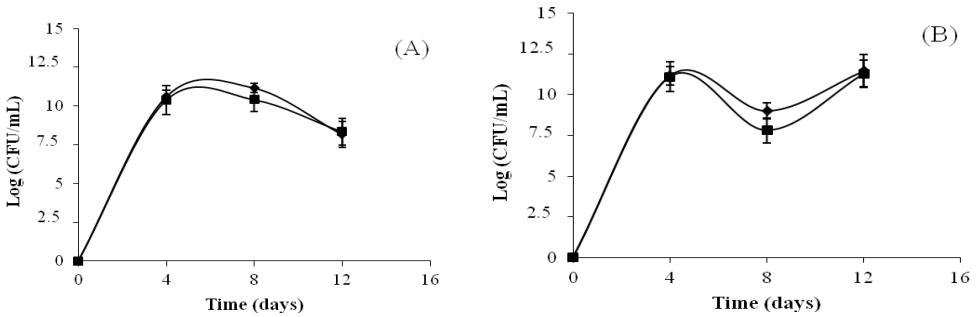

Figure 3. *Growth and gasoil degradation by Yarrowia lipolytica during 12 days at concentrations (♦) 15% and (■) 30% v/v. Y. lipolytica was grown in (A) carob kibbles medium; (B) carrot peel waste medium. Error bars represent the standard error of replicates*

Effect of bioaugmentation and organic amendment on oil-drilling mud contaminated soil

Figure 4A, B, and *C* illustrate variation of temperature, moisture content and pH of oil-drilling mud contaminated soil using bioaugmentation by *Y. lipolytica* and biostimulation with carrot peel waste for one week intervals and during 45 days of study period. *Figure 4A* shows the evolution of temperature as a function of time throughout the study. The effect of temperature on the chemical composition and physical nature of the oil, metabolism of hydrocarbon by microorganisms, influences oil-petroleum biodegradation (Atlas, 1981). At the beginning of the study, the temperature of oil-drilling mud with both the organic amendment and yeast, and without yeast and organic amendment (control) was approximately 21.8 °C ± 0.28.

At the beginning of study, the temperature of crude oil unamended and amended soil was approximately 21.8 °C ± 0.34. An increase in soil temperature was obtained for all samples after 15 days followed by gradual decreasing then stabilisation at 21.3 °C ± 1.5 for unamended soil control at the end of the study, while temperature values of amended samples continue their progression. After 15 days of treatment, an increase in oil-drilling mud temperature was obtained for all samples, followed by gradual decreasing then stabilization at 21.3 °C ± 0.42 for control at the end of the study, while temperature values continue their progression followed by gradual decreasing then stabilization at 22.85 °C ± 0.42 for oil-drilling mud with yeast only at the end of the study, while temperature values of amended samples continue their progression. These results may be due to the intensity of the metabolic activity of *Y. lipolytica* present in carrot peel waste amended oil-drilling mud soil. According to Insam et al. (2010), during microbial

http://www.aloki.hu ● ISSN 1589 1623 (Print) ● ISSN 1785 0037 (Online)
DOI: http://dx.doi.org/10.15666/aeer/1706_1546315475

activities, fragmentation of complexes molecules liberates energy; some of this energy is used for anabolism and the rest is dissipated as heating. At the laboratory scale, the metabolism of hydrocarbons occurs in the temperature range from 4 to 30 °C (Aislabie et al., 2006).

Moisture content of the oil-drilling mud with both the organic amendment and yeast ranged between 51.0 ± 2.12% and 56.50 ± 2.32% at the end of the treatment while that of oil-drilling mud amended with yeast only ranged from 51.0 ± 2.12% and 53.11 ± 2.63% at the end of treatment, respectively (*Fig. 4B*). However, the moisture content of control stabilized at 51.01 ± 1.11% at the end of treatment. According to Kumari et al. (2016), moisture is a limiting factor during biodegradation; further more during microbial catabolism, energy and water are produced.

pH value of all oil-drilling mud contaminated soil with yeast only, with both the organic amendment-yeast, without yeast and organic amendment (control) was basic at the beginning of study (8.5 ± 0.26) (*Fig. 4C*). pH value of organic amended samples with yeast decreased gradually then increased to reach, at the end of study, 8.08 ± 0.10 for carrot peel waste amended oil-drilling mud and yeast and 7.61 ± 0.11 for yeast only. According to Vero et al. (2019), solubilization and formation of ammonia by organic nitrogen ammonification by *Y. lipolytica* results in increased pH. It has also been reported that alkaline condition enhances hydrocarbon degradation in contaminated soil (Morgan and Atlas, 1989).

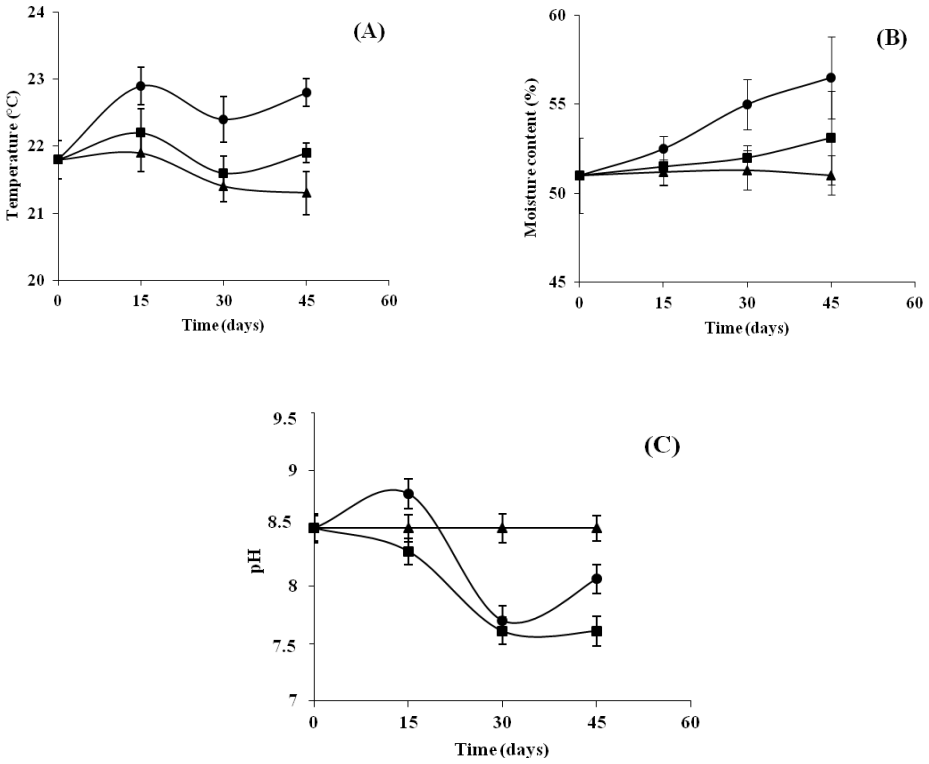

Figure 4. *Evolution of temperature (A), moisture (B), and pH (C) during 45 days of treatment. Mud + Carrot + Yeast (•); Mud + Yeast (■); Mud (▲). Error bars represent the standard error of replicates*

http://www.aloki.hu ● ISSN 1589 1623 (Print) ● ISSN 1785 0037 (Online)
DOI: http://dx.doi.org/10.15666/aeer/1706_1546315475

Figure 5 shows the degradation of total petroleum hydrocarbons (TPH) of the oil-drilling mud contaminated soil using the various bioremediation strategies and during 45 days. At the beginning of study, initial concentration of TPH was about 38 ± 1.4% (corresponding to 3.60 g/kg) for all samples (*Fig. 5*). When oil-drilling contaminated soil was incubated with only *Y. lipolytica* (6 mL, 3×10^7 CFU/mL) and both *Y. lipolytica* (6 mL, 3×10^7 CFU/mL) and carrot peel waste amendment (4 mL), TPH decreased to 35 ± 1.66% and 30.60 ± 1.50% the first 15 days, 33 ± 2.30% and 26.8 ± 1.66% respectively at the end of study. TPH rate did not undergo any significant change from its initial value in the control for all the period of incubation. These results indicate that combining application of *Y. lipolytica* with carrot peel waste has a positive effect on TPH biodegradation in oil-drilling contaminated soil. Without organic amendment, *Y. lipolytica* activity was slow due to low organic matter content in the oil-drilling mud contaminated soil. This low TPH removal was attributed to nutrition deficiency in the soil. Mancera-López et al. (2008) found that *Rhizopus* sp., *Penicillium funiculosum* and *Aspergillus sydowii* fungi removed, respectively, 36%, 30% and 17% more polycyclic aromatic hydrocarbon (PAH) from crude oil in comparison with biostimulation alone. Besides, Ataikiru et al. (2018) demonstrated that yeasts have great potentials to degrade hydrocarbons, and their use is one of the cheaper solutions to remediation in comparison to highly expensive physical and chemical techniques.

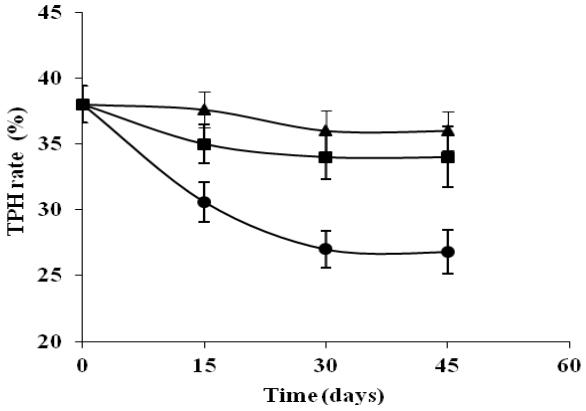

Figure 5. *The rate of TPH during 45 days of treatment. Mud + Carrot + Yeast (•); Mud + Yeast (■); Mud (▲). Error bars represent the standard error of replicates*

The growth and evolution of *Y. lipolytica* cells in the oil-drilling mud contaminated soil, as function of incubation time, is represented in *Figure 6*. At the end of the second week, the log (CFU/g) reached a value of 7.47 ± 0.53 for both *Y. lipolytica* and carrot peel waste amendment and 7.50 ± 0.77 for yeast only. At 30 days of incubation, log (CFU/g) of oil-drilling mud contaminated soil reached a value of 8.20 ± 0.55 for both *Y. lipolytica* and carrot peel waste amendment and 7.60 ± 0.51 for yeast only. At 45 days of incubation, log (CFU/g) increased to reach a value of 8.90 ± 0.54 for both *Y. lipolytica* and carrot peel waste amendment and 7.80 ± 0.60 for yeast only. The log (CFU/g) of oil-drilling mud soil (control) did not change from its initial value. Without organic amendment, the activity of *Y. lipolytica* was slow due to the low organic matter content in the oil-drilling mud contaminated soil. Li et al. (2015) and Borowik et al.

http://www.aloki.hu ● ISSN 1589 1623 (Print) ● ISSN 1785 0037 (Online)
DOI: http://dx.doi.org/10.15666/aeer/1706_1546315475

(2017) had also reported increase of biomass on bioaugmentation with microorganisms and organic amendment. Presence of considerable quantities of P in carrot peel waste (25.10 ± 1.20 mg/L), which is a necessary nutrient for microbial biodegradative activities (Hamoudi-Belarbi et al., 2018). In addition, production of linoleic acid biosurfactant by carrot increases the solubility and availability of hydrocarbons to biodegrading microorganisms (Marinescu et al., 2017) and contributes to the biodegradation of petroleum hydrocarbons. Desert soils have been previously shown to be nutrients-limited (Al-Saleh and Hassan, 2016).

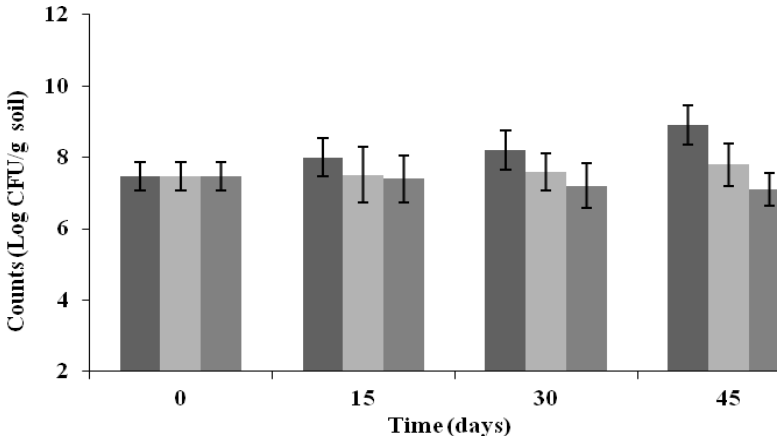

Figure 6. *Evolution of cell count during 45 days of treatment. Mud+ Carrot + Yeast (■); Mud + Yeast (■); Mud (■). Error bars represent the standard error of replicates*

Conclusion

This study demonstrated that combination of bioaugmentation by the isolate *Yarrowia lipolytica* and biostimulation with carrot peel waste as an organic amendment is a good strategy for bioremediation of oil-drilling mud contaminated soil. The TPH degradation in the oil-drilling mud contaminated soil was enhanced by biostimulation with nutrients present in the carrot peel waste and bioaugmentation by *Y. lipolytica* in comparison to *Y. lipolytica* only and control. Carrot peel waste, containing high amounts of phosphorus, enhanced bioremediation of oil-drilling mud contaminated soil by increasing activities of yeast *Y. lipolytica*. Besides, linoleic acid produced by carrot peel waste, increased the solubility and availability of hydrocarbons to biodegrading yeast. For future research, the selection of other bioproducts as biostimulants in combination with consortium of yeasts and bacteria for bioremediation should be recommended. It will be interesting to select the efficient combination for the better results.

Acknowledgements. The Algerian Ministry of High Education and Scientific Research is gratefully acknowledged for financial support.

http://www.aloki.hu ● ISSN 1589 1623 (Print) ● ISSN 1785 0037 (Online)
DOI: http://dx.doi.org/10.15666/aeer/1706_1546315475

REFERENCES

[1] Abd-Alla, M. H., El-Enany, A. W. E., Nafady, N. A., Khalaf, D. M., Morsy, F. M. (2014): Synergistic interaction of *Rhizobium leguminosarum* bv. *viciae* and *arbuscular* mycorrhizal fungi as a plant growth promoting biofertilizers for faba bean (*Vicia faba* L.) in alkaline soil. – Microbiological Research 169(1): 49-58.

[2] Acourene, S., Tama, M. (2001): Utilisation des dattes de faible valeur marchande (rebuts de Deglet-Nour, Tinissine et Tantboucht) comme substrat pour la fabrication de la levure boulangère. – Revue des Energies Renouvelable 1-10. http://www.cder.dz/download/bio_1.pdf.

[3] Aislabie, J., Saul, D. J., Foght, J. M. (2006): Bioremediation of hydrocarbon-contaminated polar soils. – Extremophiles 10: 171-179.

[4] Al-Saleh, E., Hassan, A. (2016): Enhanced crude oil biodegradation in soil via biostimulation. – International Journal of Phytoremediation 18(8): 822-831.

[5] Andreolli, M., Lampis, S., Brignoli, P., Vallini, G. (2015): Bioaugmentation and biostimulation as strategies for the bioremediation of a burned woodland soil contaminated by toxic hydrocarbons: a comparative study. – Journal of Environmental Management 153: 121-131.

[6] Ataikiru, T. L., Okerentugba, P. O., Iheanacho, C. C. (2018): Bioremediation of bonny light crude oil polluted soil by bioaugmentation using yeast isolates (*Candida adriatica* ZIM 2468 and *Candida taoyuanica* MYA-4700). – International Journal of Environmental Research and Public Health 5(4): 52-61.

[7] Atlas, R. M. (1981): Microbial degradation of petroleum hydrocarbons: an environmental perspective. – Microbiological Reviews 45(1): 180-209.

[8] Awe, S., Mikolasch, A., Hammer, E., Schauer, F. (2008): Degradation of phenylalkanes and characterization of aromatic intermediates acting as growth inhibiting substances in hydrocarbon utilizing yeast *Candida maltosa*. – International Biodeterioration and Biodegradation 62(4): 408-414.

[9] Borowik, A., Wyszkowska, J., Oszust, K. (2017): Functional diversity of fungal communities in soil contaminated with diesel oil. – Frontiers in Microbiology 8: 1862.

[10] Ceci, A., Pinzari, F., Russo, F., Persiani, A. M., Gadd, G. M. (2019): Roles of saprotrophic fungi in biodegradation or transformation of organic and inorganic pollutants in co-contaminated sites. – Applied Microbiology and Biotechnology 103(1): 53-68.

[11] Cerqueira, V. S., Maria do Carmo, R. P., Camargo, F. A., Bento, F. M. (2014): Comparison of bioremediation strategies for soil impacted with petrochemical oily sludge. – International Biodeterioration and Biodegradation 95: 338-345.

[12] Dadrasnia, A., Salmah, I., Emenike, C. U., Shahsavari, N. (2015): Remediation of oil contaminated media Using organic material supplementation. – Petroleum Science and Technology 33: 1030-1037.

[13] Damo, R., Icka, P. (2015): Environmental impact assessment generated by albanian petroleum industry into Gjanica rIVeR. – Romanian Biotechnological Letters 20(1): 10151.

[14] Decesaro, A., Rampel, A., Machado, T. S., Thomé, A., Reddy, K., Margarites, A. C., Colla, L. M. (2016): Bioremediation of soil contaminated with diesel and biodiesel fuel using biostimulation with microalgae biomass. – Journal of Environmental Engineering 143(4): 04016091.

[15] Esmaeil, A. S., Akbar, A. (2015): Occurrence of *Pseudomonas aeruginosa* in Kuwait soil. – Chemosphere 120: 100-107.

[16] Hamoudi-Belarbi, L., Nouri, L. H., Belkacemi, K. (2016): Effectiveness of convective drying to conserve indigenous yeasts with high volatile profile isolated from algerian fermented raw bovine milk (Rayeb). – Food Sciences and Technology 36(3): 476-484.

http://www.aloki.hu ● ISSN 1589 1623 (Print) ● ISSN 1785 0037 (Online)
DOI: http://dx.doi.org/10.15666/aeer/1706_1546315475

[17] Hamoudi-Belarbi, L., Bendifallah, L., Hamoudi, S., Belkacemi, K. (2017): Biostimulation of Microbial Community by Carob (*Ceratonia siliqua*) to Degrade Total Petroleum Hydrocarbon (TPH) in Contaminated Soil. – In: Kallel, A., Ksibi, M., Dhia, H. B., Khélifi, N. (eds.) Euro-Mediterranean Conference for Environmental Integration. Springer, Cham.
[18] Hamoudi-Belarbi, L., Hamoudi, S., Belkacemi, K., Nouri, L. H., Bendifallah, L., Khodja, M. (2018): Bioremediation of polluted soil sites with crude oil hydrocarbons using carrot peel waste. – Environments 5(11): 124.
[19] Insam, H., Franke-Whittle, I., Goberna, M. (2010): Microbes in Aerobic and Anaerobic Waste Treatment. – In: Insam, H., Franke-Whittle, I., Goberna, M. (eds.) Microbes at Work. Springer, Berlin.
[20] Khodja, M. (2008): Drilling fluid: performance study and environmental considerations. – PhD Thesis, Institut National Polytechnique, Toulouse, France.
[21] Kosaric, N. (2001): Biosurfactants and their application for soil bioremediation. – Food Technology and Biotechnology 39(4): 295-304.
[22] Kumari, B., Singh, S. N., Singh, D. P. (2016): Induced degradation of crude oil mediated by microbial augmentation and bulking agents. – International Journal of Environmental Science and Technology 13(4): 1029-1042.
[23] Li, H., Tan, L., Ning, S., He, M. (2015): Reactor performance and microbial community dynamics during aerobic degradation and detoxification of Acid Red B with activated sludge bioaugmented by a yeast *Candida tropicalis* TL-F1 in MBR. – International Biodeterioration and Biodegradation 104: 149-156.
[24] Lu, M., Zhang, Z., Sun, S., Wei, X., Wang, Q., Su, Y. (2010): The use of goosegrass (*Eleusine indica*) to remediate soil contaminated with petroleum. – Water, Air, and Soil Pollution 209: 181-189.
[25] Ma, H., Yang, H., Lü, X., Pan, Y., Wu, H., Liang, Z., Ooi, M. K. (2015): Does high pH give a reliable assessment of the effect of alkaline soil on seed germination? A case study with *Leymus chinensis* (Poaceae). – Plant Soil 394(1-2): 35-43.
[26] Mancera-López, M. E., Esparza-García, F., Chávez-Gómez, B., Rodríguez-Vázquez, R., Saucedo-Castaneda, G., Barrera-Cortés, J. (2008): Bioremediation of an aged hydrocarbon-contaminated soil by a combined system of biostimulation–bioaugmentation with filamentous fungi. – International Biodeterioration and Biodegradation 61(2): 151-160.
[27] Marinescu, M., Lacatusu, A., Gament, E., Plopeanu, G., Carabulea, V., Marinescu, M. (2017): A review of biological methods to remediate crude oil polluted soil. – Annals of the University of Craiova-Agriculture, Montanology, Cadastre Series 46(1): 35-340.
[28] Minai-Tehrani, D., Minoui, S., Herfatmanesh, A. (2009): Effect of salinity on biodegradation of polycyclic aromatic hydrocarbons (PAHs) of heavy crude oil in soil. – Bulletin of Environmental Contamination and Toxicology 82: 179-184.
[29] Morgan, P., Atlas, R. M. (1989): Hydrocarbon degradation in soils and methods for soil biotreatment. – Critical Reviews in Biotechnology 8(4): 305-333.
[30] Nyman, J. A. (1999): Effect of crude oil and chemical additives on metabolic activity of mixed microbial populations in fresh marsh soils. – Microbial Ecology 37(2): 152-162.
[31] Qin, G., Gong, D., Fan, M. Y. (2013): Bioremediation of petroleum-contaminated soil by biostimulation amended with biochar. – International Biodeterioration and Biodegradation 85: 150-155.
[32] Sekova, V. Y., Isakova, E. P., Deryabina, Y. I. (2015): Biotechnological applications of the extremophilic yeast *Yarrowia lipolytica*. – Applied Biochemistry and Microbiology 51(3): 278-291.
[33] Shahi, A., Aydin, S., Ince, B., Ince, O. (2016): Reconstruction of bacterial community structure and variation for enhanced petroleum hydrocarbons degradation through biostimulation of oil contaminated soil. – Chemical Engineering Journal 306: 60-66.

http://www.aloki.hu ● ISSN 1589 1623 (Print) ● ISSN 1785 0037 (Online)
DOI: http://dx.doi.org/10.15666/aeer/1706_1546315475

[34] Silva-Castro, G. A., Uad, I., Rodríguez-Calvo, A., González-López, J., Calvo, C. (2015): Response of autochthonous microbiota of diesel polluted soils to land-farming treatments. – Environmental Research 137: 49-58.
[35] Singh, K., Chandra, S. (2014): Treatment of petroleum hydrocarbon polluted environment through bioremediation: a review. – Pakistan Journal of Biological Sciences 17(1): 1-8.
[36] Taccari, M., Milanovic, V., Comitini, F., Casucci, C., Ciani, M. (2012): Effects of biostimulation and bioaugmentation on diesel removal and bacterial community. – International Biodeterioration and Biodegradation 66(1): 39-46.
[37] Vero, S., Garmendia, G., Martínez-Silveira, A., Cavello, I., Wisniewski, M. (2019): Yeast Activities Involved in Carbon and Nitrogen Cycles in Antarctica. – In: Castro-Sowinski, S. (ed.) The Ecological Role of Micro-organisms in the Antarctic Environment. Springer, Cham.
[38] Vidali, M. (2001): Bioremediation. An overview. – Pure and Applied Chemistry 73(7): 1163-1172.
[39] Wang, M., Liu, X., Pan, B., Zhang, S. (2013): Photodegradation of acid orange 7 in a UV/acetylacetone process. – Chemosphere 93(11): 2877-2882.
[40] Yi, H., Crowley, D. E. (2007): Biostimulation of PAH degradation with plants containing high concentrations of linoleic acid. – Environmental Science and Technology 41(12): 4382-4388.
[41] Yoshitomi, K. J., Shann, J. R. (2001): Corn (*Zea mays* L.) root exudates and their impact on 14C-pyrene mineralization. – Soil Biology and Biochemistry 33(12-13): 1769-1776.
[42] Zhang, Y., Zhu, Y. G., Houot, S., Qiao, M., Nunan, N., Garnier, P. (2011): Remediation of polycyclic aromatic hydrocarbon (PAH) contaminated soil through composting with fresh organic wastes. – Environmental Science and Pollution Research 18(9): 1574-1584.

http://www.aloki.hu ● ISSN 1589 1623 (Print) ● ISSN 1785 0037 (Online)
DOI: http://dx.doi.org/10.15666/aeer/1706_1546315475

A FIRST EVER DETAILED ECOLOGICAL EXPLORATION OF THE WESTERN HIMALAYAN FORESTS OF SUDHAN GALI AND GANGA SUMMIT, AZAD JAMMU AND KASHMIR, PAKISTAN

KHAN, A. M.[1,2*] – QURESHI, R.[2] – SAQIB, Z.[3] – MUNIR, M.[4] – SHAHEEN, H.[5] – HABIB, T.[5] – DAR, M. E. U. I.[5] – FATIMAH, H.[6] – AFZA, R.[7] – HUSSAIN, M. A.[8]

[1]*Department of Botany, Govt. Hashmat Ali Islamia Degree College, Rawalpindi, Pakistan*

[2]*Department of Botany, Pir Mehr Ali Shah Arid Agriculture University, Rawalpindi, Pakistan*

[3]*Department of Environmental Science, International Islamic University, Islamabad, Pakistan*

[4]*Department of Botany, University of Animal & Plant Sciences, Ravi Campus, Pattoki, Punjab, Pakistan*

[5]*Department of Botany, University of Azad Jammu & Kashmir, Muzaffarabad, Pakistan*

[6]*Department of Biology & Environmental Science, Allama Iqbal Open University, H-8 Islamabad, Pakistan*

[7]*Department of Botany, Hazara University Mansehra, Khyber Pakhtunkhwa, Pakistan*

[8]*Department of Biotechnology, Mirpur University of Science & Technology, 10250 Mirpur, AJK, Pakistan*

**Corresponding author*
e-mail: arshadbotanist@gmail.com; phone: +92-33-3521-7235

(Received 22nd Jul 2019; accepted 16th Oct 2019)

Abstract. The baseline ecological exploratory studies of floristically rich areas like the western Himalaya are very important to determine the diversity variations. Based on research gaps detected in ecological literature of the western Himalayan forests of Sudhan Gali and Ganga summit, the study area is revisited. Plots data was collected during 2016, and advanced multivariate statistical tools were used to analyze it. Some of multivariate tools including permutation test, indicator species analysis and variation partitioning (partial CCA) were used for the first time in the area. The results of hierarchical clustering and permutation test revealed that there were four ecologically meaningful vegetation groups (1. *Berberis-Micromeria-Desmodium* (BMD), 2. *Pinus-Rubus-Persicaria* (PRP), 3. *Viburnum-Abies-Dryopteris* (VAD) and 4. *Sibbaldia-Thymus-Bistorta* (STB) associations) in the area. A significant ($p \leq 0.05$) pairwise compositional difference of all the detected plant communities was observed. The results of canonical correspondence analysis (net effect) depicted that all the studied environmental variables were significantly important, and explains about 73.1% variations in the species data. The higher ($r > 0.9$) species-environment pseudo-canonical correlations values for the first four CCA-axes revealed that the selected explanatory variables were determinants of the response (species) data variations, and the high values for the CCA axes 2 to 4 indicated that there was no single dominant environmental gradient in this part of the western Himalaya. The highest β diversity value of Himalayan alpine scrubland at the Ganga summit depicted that even a minor variation in environment affects the high altitude vegetation more rapidly than the vegetation of low elevation areas. The vegetation of the study area is under continuous deterioration, and this exploratory work can be used as a baseline study for the future management, sustainable use, and conservation programs in the area.

Keywords: *canonical correspondence analysis, biodiversity, indicator species analysis, Monte Carlo permutation test, variation partitioning, vegetation types, phytosociology*

http://www.aloki.hu ● ISSN 1589 1623 (Print) ● ISSN 1785 0037 (Online)
DOI: http://dx.doi.org/10.15666/aeer/1706_1547715505

Introduction

The ecological studies of the forests are necessary to determine the state of biodiversity pattern, vegetation structure, and species compositional dynamics over time and space. These baseline ecological studies further help in development of forest management, sustainable use of forest resources, and conservation strategies. Therefore, identification of environmental requirements of especially vulnerable plant species of any region is important and can be further used to model and identify suitable habitats. Being placed at the bottom of trophic level, plants not only serve as baseline resources for the biotic components of the higher levels, but also effectively remained engaged in maintaining the biodiversity of an area and mitigate the adverse impacts of the threatening climate changes (Khan et al., 2018a, 2019). The interactions of the various environmental factors like climate, soil, topography and anthropogenic activities strongly influence and control the vegetation structure, types, species composition and their distribution patterns (Salama et al., 2016). Therefore, the impacts of these changes on the vegetation of a given area should be studied on regular basis including species-environment relationships, both on temporal and spatial scale (Akhlaq et al., 2018; Ilyas et al., 2018). The Himalayan ecosystem in general and the western Himalayan area in particular is a floristically rich area. The western Himalayan region of Pakistan is also the most fragile, comprised of about 67% of total forest cover of the country, and under serious threat of climate changes amplified by overpopulation (Qamer et al., 2016; Tewari et al., 2017). Therefore, the area need immediate attention of the ecologists to understand the biodiversity and its distribution pattern (Rahman et al., 2017; Haq, 2018; Saima et al., 2018; Kamran et al., 2019).

Community ecology deals with the documentation of number and composition of plant species/assemblages within a geographic unit. Ecologists record multivariate field data of plots, releves or quadrats, and perform multivariate analyses to test their hypotheses. Classification of vegetation types, structure and composition of any area can be evaluated more easily and efficiently by using the tools of computer modelling and multivariate statistics (viz. hierarchical clustering, indicator species analysis, ordination etc.) for the last 04 decade (Legendre and Legendre, 1998; Khan et al., 2015; Abdel Khalik et al., 2017; Bürzle et al., 2017; Devetter et al., 2017; Chandra et al., 2018; Salama et al., 2018; Zakaria et al., 2019). Constrained ordination models or direct gradient analyses techniques including unimodal model like canonical correspondence analysis (CCA) and linear model like redundancy analysis (RDA) are the most popular ones in this regard. CCA was developed by Ter Braak (1986) by arranging a marriage between multiple regression and correspondence analysis (CA). It can be used to assess the species-environment relationships and its strength. In CCA, statistical significance can be evaluated by using the permutation test for overall the model, CCA axes, and explanatory variables. The CCA ordination diagram can be interpreted by following the centroid rule; species/response points are located at the centroid (weighted average) of the samples points where it is distributed. Similarly, all the samples having a set of particular species are scattered around the same species. The other information in such ordination biplot/triplot includes the importance of explanatory variables (arrow lengths), correlation of the variables to the CCA axes (direction of the arrows), correlation amongst the variables (angle amongst the arrows), ranking of the species response (optimum) and samples values for the environmental variable (perpendiculars drawn from species/samples points to environmental arrows). CCA calculates species-environment correlation which is actually a correlation between two types of site scores i.e. linear

http://www.aloki.hu ● ISSN 1589 1623 (Print) ● ISSN 1785 0037 (Online)
DOI: http://dx.doi.org/10.15666/aeer/1706_1547715505

combinations of the environmental variables (LC's) and the weighted averages of the species scores (WA's) (Ter Braak, 1986; Legendre and Legendre, 1998).

Sudhan Gali and Ganga hills remained the focal site for vegetation analyses in the past (*Table 6*) due to its complex pattern of topography, extended elevation range, thick woody vegetation cover, species richness and scenic beauty of the area. However the complex interactions between the local vegetation and its environment, classification and ordination by using the multivariate tools are not documented. First ecological exploration (vegetation structure, composition and phenology) in the study area was conducted by Khan (2001), but environmental influence was not tested by using any multivariate statistical analysis. The same is true about the subsequent study conducted by Malik et al. (2007). The use of multivariate statistical methods to vegetation data of the area was started by Siddiqui et al. (2010a, b) followed by Siddiqui et al. (2014) and Shaheen et al. (2016, 2017, 2018). An unconstrained linear ordination model (PCA) was used in all of these earlier studies, therefore the real contribution of the studied predictors was missing. A total of two separate studies conducted by Shaheen et al. (2011c, 2012) attempted to use constrained unimodal ordination (CCA) to determine the species-environment relationship, but error like model overfitting was detected. The assessment of edaphic predictor's contribution was also missing in all of these earlier studies. In Pakistan, the major issue was the modest understanding about the use of advanced multivariate statistical methods in ecology, which is now improving over time. By considering this, many geographical areas of Pakistan need revisit and attention of ecological workers. It was hypothesized in every earlier vegetation study that the local environment is significantly controlling the species distribution pattern in the area but until this study, the following un-answered questions were thoroughly investigated for the first time to achieve the set objectives. (1) What are the number of biological meaningful vegetation groups, their composition and indicator species? (2) What about the species-environment relationships and contribution of the studied environment? (3) How diversity and richness in the area is related to the studied environment? (4) How the groups of the studied variables are important (partial CCA/variations partitioning) in the area? Therefore, the findings of this study will serve as the first detailed document and help in future biodiversity conservation and management projects in the region.

Materials and methods

Study area

Sudhan Gali and Ganga hills are part of the western Himalayan mountainous area in the district Bagh, Azad Jammu and Kashmir, Pakistan. It is located toward the north and about 20 km road distance from the Bagh city. It lies between 34°02' to 34°04'N latitude and 73°44' to 73°45'E longitude, and elevation ranges from 1195 to 3004 m above sea level (m.). It is bounded by the Hattian Bala and Muzaffarabad districts in the north, Haveli district towards the east, Poonch in the south, and Murree and Hazara hills in the west. The total land area is 770 km^2, and human population of 0.434 million in 2013 with an annual growth rate of 2% (Shaheen et al., 2011a; Anonymous, 2015) (*Fig. 1*).

Climate, soil, and natural vegetation

The climate of the study area is humid, sub-continental highland type, and during the last ten years (2007-2016), the mean monthly maximum temperature in June varied from

http://www.aloki.hu ● ISSN 1589 1623 (Print) ● ISSN 1785 0037 (Online)
DOI: http://dx.doi.org/10.15666/aeer/1706_1547715505

20-26 °C, whereas the winter temperature mostly drops to or below freezing point. Similarly, the mean annual minimum temperature varied from 6.31-13.19 °C, and the mean maximum temperature varied from 20.36-27 °C. The mean annual rainfall of the same period varied from 463 mm in the year 2009 to 2242 mm in the year 2015, whereas only two months including July and August received the maximum (> 50%) during monsoon showers. During the year 2016, the mean annual minimum temperature, maximum temperature, and precipitation remained 7.91 °C, 22.45 °C, and 1798 mm respectively (PMD, 2018). Snowfall frequently occurs from December to February and mountains remain covered with snow until the end of April each year (Waseem et al., 2006; Saeeda and Zakir, 2012). Temperature and precipitation data (2007-2016 = 10 years) of the study area was acquired from the United States National Centers for Environmental Prediction (US-NCEP) Climate Forecast System Reanalysis (CFSR) by using the climate engine (https://app.climateengine.org/). The temperature data source was CFSv2 19200 m (1/5-deg) daily reanalysis dataset (NOAA). The wind blows from west to east during the day time, and from south-east to north during the night. The wind velocity was higher in the afternoon as compared to morning time. There is no river in the study area, although a big seasonal stream "*Nala Mahl*" flows through the area.

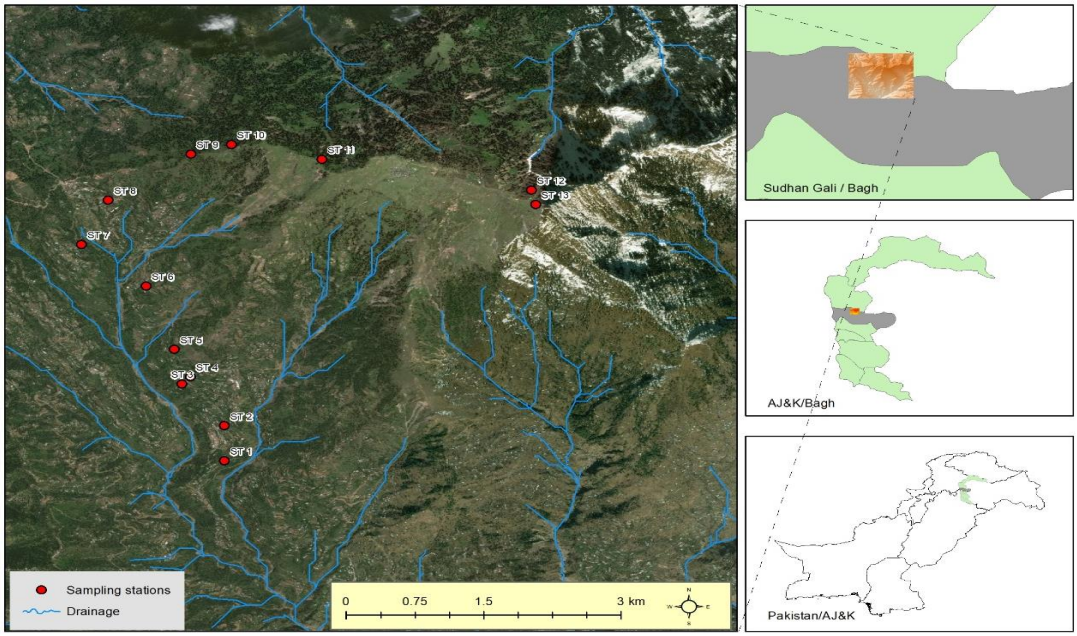

Figure 1. *A GIS map of the Sudhan Gali and Ganga hills showing the distribution of 13 sampled stations in the study area*

The soil of the study area is varied from clay loam to sandy loam in texture, and from yellowish brown to dark brown or to black in color. The bedrock is comprised of two types of rocks; light grey to black coloured Dogra slates of early Cambrian area (comprised of slates with quartz and feldspar, phyllites, and trilobites) and sedimentary Murree formations of the Miocene (shale and red clastic sand or sandstone) (Khan, 2001).

The natural vegetation of the area is mainly comprised of three eco-zones. These include humid sub-tropical Chir-pine, moist temperate blue-pine, and Himalayan sub-alpine coniferous zones. The important tree element of the natural vegetation includes

http://www.aloki.hu ● ISSN 1589 1623 (Print) ● ISSN 1785 0037 (Online)
DOI: http://dx.doi.org/10.15666/aeer/1706_1547715505

Pinus roxburghii, P. wallichiana, and *Abies pindrow*. Similarly, the shrub layer is comprised of *Berberis lycium, Rubus niveus, Rosa moschata, Indigofera heterantha,* and *Viburnum grandiflorum*. The important herbaceous elements includes *Micromeria biflora, Galium elegans, Veronica laxa, Oenothera rosea, Rumex nepalensis, R. dentatus, G. wallichianum, Achillea millefolium, Trifolium repens, Sibbaldia procumbens, Thymus linearis,* and *Persicaria amplexicaulis*.

Vegetation (plot) data collection

A stratified random method of vegetation sampling by using plots was adopted to study the vegetation types and intensity of anthropogenic disturbance in the area. The study area was surveyed during the growing season (Monsoon) of the years 2016. A total of 13 sampling stations were randomly selected along the altitudinal gradient. At each station, three sub-stations were again randomly selected, and based on minimal area method, at each of 39 sub-station, 3 plots were randomly laid and studied to record the data of tree layer (size: 30×30 m^2). Nested plots for shrub layer (size: 5 × 5 m^2) and herb layers (size: 1×1 m^2) were also studied. The absolute values of density, frequency and cover of each plant species were recorded, averaged, relative values were calculated, followed by calculation of importance values index (IVI) of each species (Curtis and McIntosh, 1950; Cox, 1967; Khan et al., 2018b, 2019). First three alphabets of each of generic and specific binomials separated by a dot of each plant species were created and used in all multivariate analyses.

Geographic coordinates (locations) of each studied plot were recorded by using Garmin, 76CSx handheld GPS device and topographic variables say altitude, slope, and slope aspect were calculated by using 30 m digital elevation model (URL: https://asterweb.jpl.nasa.gov/gdem.asp) of the study area. The ArcGIS (ver. 10.3) was used to extract the values. Cos-transformation of the slope aspect (CTA) values was performed prior to use in the multivariate analysis. The number of stumps and herbivore dungs were also counted to measure and test the deforestation and grazing pressure respectively in each plot (Khan et al., 2019).

The collected plant specimens were pressed, dried and mounted on standard sized herbarium sheets and identified by using the available local and regional taxonomic literature (Stewart, 1972; Nasir and Ali, 1971-1995; Ali and Qaiser, 1995-2009; Nakaike and Malik, 1992; EFLORAS, 2012; TROPICOS, 2012; Khan et al., 2016), cross-matched with herbaria collections at the University of Azad Jammu and Kashmir, Muzaffarabad and deposited in the same herbarium for future references and record.

For edaphic contribution, soil samples (about 500 g) were collected from each plot and topsoil layer (about 30 cm depth), and a composite mixture (about 1.5 kg) was prepared for each sub-station. A total of six physicochemical parameters of the soil samples were studied at the Soil and Water testing Laboratory Rawalpindi, Pakistan. The soil samples were dried at room temperature followed by sieving (2 mm sieve) and storage. The soil pH was assessed by using 1:5 soil-water suspension and pH meter (Schofield and Taylor, 1955), whereas electrical conductance (mS cm^{-1}) ability of the soil samples was tested as conveyed by Richards (1954). Soil organic matter (%) was calculated by using the standardized solutions of $FeSO_4$ and $K_2Cr_2O_7$ as communicated by Nelson and Sommer (1982). Available phosphorus (ppm) in soil was determined by using $NaHCO_3$ solution as extracting agent (Olsen et al., 1954). Similarly, available potassium (ppm) in soil was calculated by using the standardized solutions of CH_3COONH_4 and KCl (Richards, 1954). The nitrate-N (mg/kg) of soil samples was

http://www.aloki.hu ● ISSN 1589 1623 (Print) ● ISSN 1785 0037 (Online)
DOI: http://dx.doi.org/10.15666/aeer/1706_1547715505

measured by using 1:5 soil-water suspension, and LAQUA twin Nitrate Ion meter (Othman et al., 2014).

Statistical analyses

The decision about the number of biologically meaningful plant associations in the areas was made on the basis of Monte Carlo permutation test results. A total of two to six (2-6) possible groups were tested, and the mean p-value and the number of significant indicator species were observed. A criterion of minimized p-value and/or maximized significant species was used to decide the number of plant association (Khan et al., 2018b, 2019). For ecological classification of the studied samples, two-way agglomerative hierarchical clustering (distance "Euclidean"; linkage "Ward") dendrogram of the studied vegetation samples (sub-stations) and their allied plant species was developed. Multi-response permutation procedure (MRPP) test was used to identify the pairwise compositional difference of the identified vegetation groups. Indicator species analysis (Dufrêne and Legendre, 1997) was used to identify the indicators of each group. The different diversity measure including species richness (Margalef, 1958), Shannon's diversity (Shannon and Weaver, 1949), Simpson's reciprocal diversity index (1/D; Magurran, 1988), and evenness (Pielou, 1975) were calculated for each plant association. Unimodal ordination models including detrended correspondence analysis (DCA) and canonical correspondence analysis (CCA) were used to seek the beta-diversity variations and species-environment relationships respectively. The significance of the studied variables was tested by using both simple (marginal) and conditional (net) terms effects via permutation test available in Canoco software (Ter Braak and Smilauer, 2012). Similarly, the significance of the constrained axes and pairwise comparasion of the three groups of variables (viz. topographic, edaphic and anthropogenic) was tested by using variation partitioning (partial CCA) method to seek their contribution towards the species distribution pattern in the study area (Khan et al., 2019).

Results

Taxonomic and life form classification

A total of 90 plant species of the vascular plants were recorded in the studied samples (39 sub-stations × 9 plots at each sub-station = 351 total plots studied), and were allied to 78 genera and 41 families. The majority of plant species (81, 90.01%) were belonged to the angiosperms and found distributed in 71 genera and 38 families. The gymnosperms were represented by a single Pinaceae family, further comprising of 3 genera and 4 coniferous species (4.45%) in the area. Pteridophytes were represented by 2 families, 4 genera and 5 species (*Table 1*).

Life form classification of the same 90 plant species depicted that there were 14 (15.56%) megaphanerophytes, 9 (10%) nanophanerophytes, 30 (33.3%) hemicryptophytes, 21 (23.3%) therophytes, 5 (5.56%) chamaephytes, 10 (11.1%) geophytes and 1 (1.1%) liana species in the area (*Table 4*).

Biologically meaningful vegetation associations in the area

The first-ever results of Monte Carlo permutation testing from the area for two to six (2-6) possible vegetation groups depicted that the minimum mean p-value of 0.098, and

http://www.aloki.hu ● ISSN 1589 1623 (Print) ● ISSN 1785 0037 (Online)
DOI: http://dx.doi.org/10.15666/aeer/1706_1547715505

maximum number of significant indicator species of 59 were recorded at the 4th level of division. Therefore, this study recognized a total of four (4) biologically meaningful (significant) vegetation clusters in the study area (*Fig. 2*). The two-way agglomerative hierarchical clustering dendrogram of the vegetation associations (grouping pattern of the 39 studied samples) and their allied plant species (90) is presented in *Figure 3*. A pairwise comparasion of the detected plant association was made by using MRPP test for further confirmation. The results showed that all the 6 pairwise comparisons of the 4 groups were statistically significant ($p < 0.001$), therefore depicting a reasonable species compositional differences amongst the detected groups. The higher negative T-values were observed for all the pairwise comparisons, and we know that a more negative T-value represent stronger separation of the compared plant communities. On the basis of three leading diagnostic plant species of each group (detected by using indicator species analysis, ISA), the vegetation associations were renamed as BMD (group 1), PRP (group 2), VAD (group 3) and STB (group 4). The maximum compositional separation (T-value: -17.26; p-value < 0.01) was observed between BMD and VAD associations because the former one belong to sub-tropical and the latter one to sub-alpine zone in the area. This analysis also gave A-values (within-group agreement) in the range of 0.2 to 0.37 for overall and all the 6 pairwise comparisons of the plant communities. This proves that within groups heterogeneity equals expectation by chance. The maximum A-value can be $A_{max} = 1$, which means that all items/samples within the group are identical. Conversely, A = 0 mean that within groups heterogeneity equals expectation by chance and if the A-value is < 0, it mean that within groups heterogeneity is higher than expected by chance (*Table 2*).

Table 1. *A table showing the summary of taxonomic classification of the plant species*

Phyto-taxa	Families (%)	Genera (%)	Species (%)
Pteridophytes	2 (4.88%)	4 (5.13%)	5 (5.56%)
Gymnosperms	1 (2.44%)	3 (3.85%)	4 (4.45%)
Monocots	3 (7.32%)	11 (14.11%)	12 (13.34%)
Dicots	35 (85.37%)	60 (76.93%)	69 (76.67%)
Total	41 (100%)	78 (100%)	90 (100%)

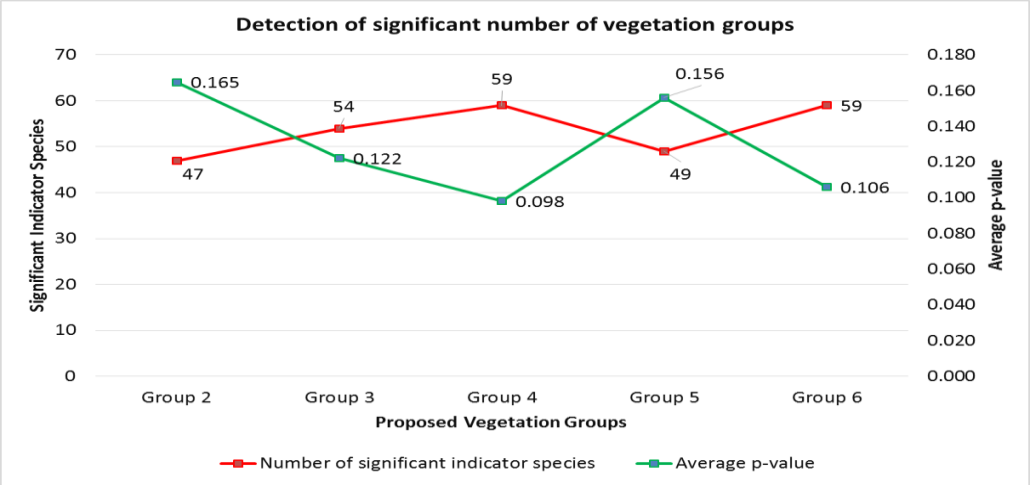

Figure 2. *A graph showing the results of Monte Carlo test statistics used to decide the number of biologically significant vegetation groups in the study area*

http://www.aloki.hu ● ISSN 1589 1623 (Print) ● ISSN 1785 0037 (Online)
DOI: http://dx.doi.org/10.15666/aeer/1706_1547715505

Table 2. *A table showing the results of pairwise comparisons (MRPP) of four (4) plant associations of the Sudhan Gali & Ganga Hills*

Plant communities compared			T-statistic	A-value	p-value
1.BMD-18	vs.	2.PRP-6	-13.63082095	0.20444995	0.00000015
1.BMD-18	vs.	3.VAD-9	-17.26453215	0.30257625	0.00000005
1.BMD-18	vs.	4.STB-6	-13.77931008	0.19771649	0.00000008
2.PRP-6	vs.	3.VAD-9	-9.15073886	0.37825685	0.00007066
2.PRP-6	vs.	4.STB-6	-6.65738026	0.30063123	0.00043338
3.VAD-9	vs.	4.STB-6	-7.99291567	0.26328556	0.00009218
Overall			-21.590644	0.36049829	0.00000001

For abbreviations see *Table 4*

Vegetation types, composition and their key factors

A total of three leading significant indicator species of each vegetation group were used to rename the vegetation groups as; 1. *Berberis-Micromeria-Desmodium* (BMD) association, 2. *Pinus-Rubus-Persicaria* (PRP) association, 3. *Viburnum-Abies-Dryopteris* (VAD) association and 4. *Sibbaldia-Thymus-Bistorta* (STB) association (*Table 4*). The details of each association is presented below:

Berberis-Micromeria-Desmodium (BMD) community (sub-tropical chir-pine forest)

This plant community was recorded at and around the Birpani town at an elevation range of 1700-2100 m (a), longitude (in dd) varied from 73.749-73.756 E, latitude from 34.046-34.066 N, and comprised of 18 samples/sub-stations (*Fig. 3*). This association was mostly located at the western faces (solar aspect) with moderate slope inclination ($22.49 \pm 5.73°$). A total of 63 plant species were recorded in this association out of which 41 appeared as indicator species (IS) and 20 as significant indicator species (SIS) of this community. The average species count per sample was 22.89 ± 4.13, and the absolute value varied from 14-30 in the studied samples. The leading ones were *Berberis lycium*, *Micromeria biflora* and *Desmodium multiflorum*. The least indicator value was recorded for *Avena barbata* and *Solanum pseudocapsicum* species. The Shannon's diversity index value was 2.87 ± 0.18, whereas Simpson's diversity index (0.94 ± 0.02), Inverse Simpson's/Fischer's diversity (14.47 ± 2.52), Pielou's evenness (0.93 ± 0.03), Margalef's richness (5.05 ± 0.68), and β-diversity (mean Euclidean distance: 67.3) were also recorded. The mean soil pH of this group was 7.22 ± 0.61, whereas soil EC (mS/cm), nitrate-N (mg/kg), phosphorus (ppm), potassium (ppm), and organic matter (%) values were 28 ± 0.111, 14 ± 1.11, 1.44 ± 1.04, 82.67 ± 21.51, and 2.25 ± 0.61 respectively. Some of the key factors of this association includes the highest values of mean soil pH (basic soils), species, richness, α-diversities, and household density as compared to other associations. Similarly, the least values of altitude, nitrate-nitrogen, phosphorus, potassium, and organic matter, fuelwood collection (deforestation) and grazing pressure were other important factors (*Tables 3* and *4*). This scrubland association represents the remnants of stable Chir-pine forest, and extreme anthropogenic pressure in the past might be responsible of takeover of *Berberis*, *Micromeria* and *Desmodium* species.

http://www.aloki.hu ● ISSN 1589 1623 (Print) ● ISSN 1785 0037 (Online)
DOI: http://dx.doi.org/10.15666/aeer/1706_1547715505

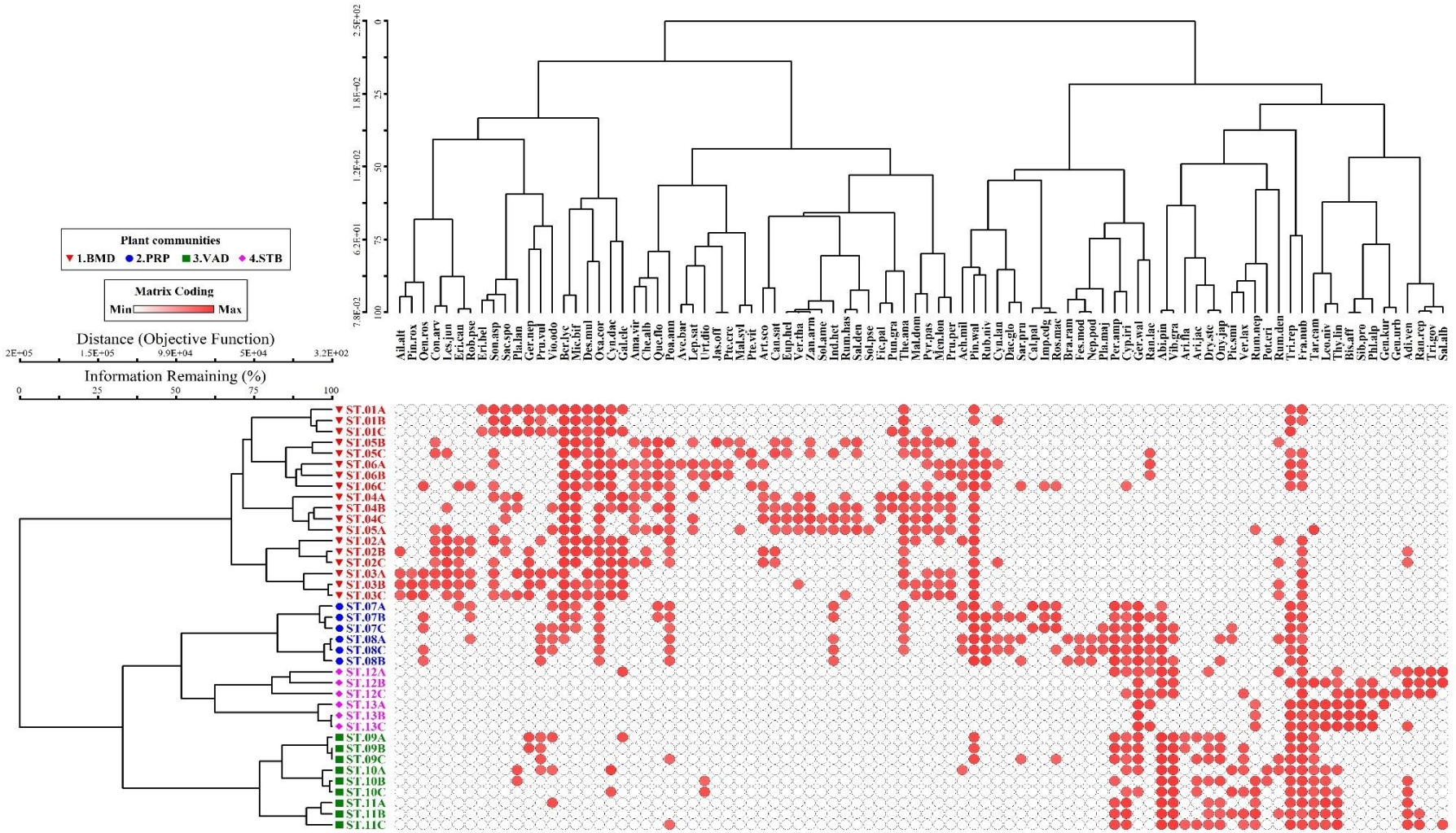

Figure 3. *A clustering dendrogram showing the vegetation types, and their allied plant species of the western Himalayan forests of Sudhan Gali AJ&K, Pakistan. (For species codes see Table 4)*

http://www.aloki.hu ● ISSN 1589 1623 (Print) ● ISSN 1785 0037 (Online)
DOI: http://dx.doi.org/10.15666/aeer/1706_1547715505

Table 3. *A table showing the values (mean ± SD (min-max)) of studied factors of plant communities of the western Himalayan forests of Sudhan Gali, Azad Jammu and Kashmir, Pakistan*

Variables		1. BMD Association	2. PRP Association	3. VAD Association	4. STB Association	All plots
Locality/ Samples/Plots		Birpani/18/162	Sudhan Gali/6/54	Upper Sudhan/9/81	Ganga Top/6/54	Study Area/39/351
Topographic variables						
1	Altitude (m)	1834.95 ± 100.72 (1700-2000)	2151.67 ± 53.72 (2100-2500)	2601.34 ± 86.48 (2500-2800)	2950.67 ± 53.69 (2900-3000)	2232.17 ± 437.47 (1700-3000)
2	Slope (°)	22.49 ± 5.73 (12.0491-29.1633)	34.13 ± 6.49 (28.2045-40.0466)	29.54 ± 10.62 (21.9847-43.6736)	20.6 ± 8.23 (13.088-28.0975)	25.61 ± 8.63 (12.04-43.67)
3	Slope aspect (°)	227.9 ± 48.38 (129.753-271.975)	133.08 ± 64.17 (74.505-191.646)	197.54 ± 139.28 (12.588-304.479)	158.34 ± 157.73 (14.349-302.32)	195.59 ± 100.06 (12.58-304.47)
4	Longitude (E)	73.753 ± 0.003 (73.749-73.756)	73.744 ± 0.002 (73.742-73.745)	73.759 ± 0.006 (73.753-73.766)	73.787 ± 0.001 (73.787-73.787)	73.75 ± 0.01 (73.74-73.78)
5	Latitude (N)	34.055 ± 0.007 (34.046-34.066)	34.074 ± 0.003 (34.071-34.076)	34.082 ± 0.001 (34.081-34.083)	34.077 ± 0.001 (34.076-34.078)	34.06 ± 0.01 (34.04-34.08)
Diversity variables						
6	Shannon's	2.87 ± 0.18 (2.4-3.12)	2.83 ± 0.17 (2.57-3.06)	2.47 ± 0.11 (2.29-2.9)	2.48 ± 0.17 (2.24-2.69)	2.7 ± 0.24 (2.24-3.12)
7	Simpson's	0.94 ± 0.02 (0.9-0.95)	0.93 ± 0.02 (0.9-0.94)	0.89 ± 0.02 (0.85-0.93)	0.91 ± 0.02 (0.89-0.93)	0.91 ± 0.02 (0.85-0.95)
8	Inverse Simpson's	14.47 ± 2.52 (9.19-19.46)	12.47 ± 2.16 (9.41-15.66)	8.44 ± 1.27 (6.54-14.07)	10.51 ± 1.65 (8.48-12.58)	12.15 ± 3.18 (6.54-19.46)
9	Pielou's	0.93 ± 0.03 (0.88-0.97)	0.9 ± 0.02 (0.86-0.91)	0.88 ± 0.03 (0.83-0.91)	0.95 ± 0.04 (0.88-0.97)	0.91 ± 0.03 (0.83-0.97)
10	Margalef's	5.05 ± 0.68 (3.92-6.28)	4.88 ± 0.6 (4.12-5.84)	3.49 ± 0.38 (2.82-5.1)	2.87 ± 0.55 (2.21-3.47)	4.32 ± 1.04 (2.21-6.28)
11	Average species	22.89 ± 4.13 (14-30)	23.50 ± 3.08 (20-29)	17.11 ± 1.62 (14-19)	14.17 ± 2.56 (11-17)	20.3 ± 4.77 (11-30)
12	Total species	63	36	34	26	90
13	Indicator species (IS)	41	21	14	14	90
14	Significant indicator species (SIS)	20	17	10	12	59

http://www.aloki.hu ● ISSN 1589 1623 (Print) ● ISSN 1785 0037 (Online)
DOI: http://dx.doi.org/10.15666/aeer/1706_1547715505

	Variables	1. BMD Association	2. PRP Association	3. VAD Association	4. STB Association	All plots
15	SIS to IS ratio	48.78	80.95	71.42	85.71	65.55
16	β-diversity (mean Euclidean distance)	67.3	47.88	54.81	78.65	62.16
	Edaphic variables					
17	Soil pH.	7.22 ± 0.61 (5.96-7.7)	7.63 ± 0.04 (7.6-7.66)	6.16 ± 0.49 (5.52-7.66)	5.33 ± 0.2 (5.15-5.5)	6.74 ± 0.9 (5.15-7.7)
18	Soil EC	0.28 ± 0.11 (0.17-0.45)	0.24 ± 0.04 (0.21-0.27)	0.29 ± 0.1 (0.17-0.39)	0.28 ± 0.24 (0.07-0.49)	0.27 ± 0.11 (0.07-0.49)
19	Nitrate-N (mg/kg)	1.14 ± 1.11 (0.43-3.5)	0.84 ± 0.08 (0.77-0.9)	4.76 ± 1.68 (2.75-6.62)	4.3 ± 2.8 (1.75-6.85)	2.41 ± 2.25 (0.43-6.85)
20	Phosphorus (ppm)	1.44 ± 1.04 (0.16-2.8)	1.16 ± 0.08 (1.09-1.22)	4.05 ± 2.02 (1.79-6.43)	1.61 ± 1.32 (0.41-2.81)	2.01 ± 1.66 (0.16-6.43)
21	Potassium (ppm)	82.67 ± 21.51 (56-118)	108 ± 52.59 (60-156)	183.34 ± 86.75 (80-280)	67 ± 3.29 (64-70)	107.38 ± 62.96 (56-280)
22	Organic matter (%)	2.25 ± 0.61 (1.1-2.9)	2.2 ± 0.22 (2-2.4)	3.47 ± 1.39 (2.4-5.3)	2.65 ± 0.06 (2.6-2.7)	2.58 ± 0.9 (1.1-5.3)
	Anthropogenic variables					
23	Grazing pressure (dungs/ha)	3.17 ± 1.3 (1-6)	17.17 ± 1.17 (16-19)	13.12 ± 8.33 (2-23)	0.17 ± 0.41 (0-1)	7.15 ± 7.32 (0-23)
24	Deforestation pressure (stumps/ha)	5.23 ± 2.19 (1-9)	4.34 ± 2.07 (2-6)	14.78 ± 2.54 (11-19)	0.5 ± 0.84 (0-2)	6.56 ± 5.18 (0-19)
25	Forest types (Champion et al.,1965)	Sub-Tropical Chir-Pine Forest	West Himalayan Moist Temperate Blue-Pine Forest	West Himalayan Sub-Alpine Fir Forest	West Himalayan Alpine Scrubland Forest	West Himalayan Forest of Sudhan Gali and Ganga Summit
26	Key factors	Higher number of species, richness, diversities, soil pH (basic) & human population; moderate grazing and deforestation pressure; and least elevation	Higher average species count in the plot, and proportion of significant indicators to indicators, grazing pressure, slope, soil pH (basic); mid-elevation; and least deforestation pressure	Higher soil fertility (NPK), organic matter, deforestation, grazing, proportion of significant indicators to indicators (2^{nd}); and least richness, diversities, and soil pH (acidic)	Highest elevation, β-diversity, proportion of significant indicators to indicators; moderate NPK & organic matter; and least slope, alpha-diversities, richness, soil pH (acidic)	The vegetation of the study area is found under strong influence of the local environment

http://www.aloki.hu ● ISSN 1589 1623 (Print) ● ISSN 1785 0037 (Online)
DOI: http://dx.doi.org/10.15666/aeer/1706_1547715505

Table 4. *A table showing the detailed results of indicator species analysis (ISA), vegetation types, species composition, and their significance*

#	Latin Binomial/Common Name (English)	Codes	GF	Groups (samples)				Max. Grp	Obs. IV	Mean	SD	p-value
				1(18)	2(6)	3(9)	4(6)					
				Indicator value (IV)								
1	***Berberis lycium* Royle/Indian Barberry**	***Ber.lyc***	**Np**	**86**	**9**	**0**	**0**	**1**	**86**	**25.7**	**6.6**	**0.0002**
2	***Micromeria biflora* (Buch.-Ham. ex D.Don) Benth./ Indian Wild Thyme**	***Mic.bif***	**Th**	**81**	**4**	**0**	**0**	**1**	**81**	**24.4**	**7.2**	**0.0002**
3	***Desmodium multiflorum* DC./Hawaiian Tick-trefoil**	***Des.mul***	**Np**	**72**	**0**	**0**	**0**	**1**	**72**	**20.9**	**8**	**0.0004**
4	*Sonchus asper* (L.) Hill/Spiny Sow Thistle	*Son.asp*	H	72	0	0	0	1	72.2	21.5	8.4	0.0002
5	*Oxalis corniculata* L./Creeping Woodsorrel	*Oxa.cor*	H	67	29	0	0	1	67.2	26.9	6.94	0.0002
6	*Pyrus pashia* Buch.-Ham. ex D.Don/Indian Wild Pear	*Pyr.pas*	Mp	67	0	0	0	1	66.7	20.2	8.12	0.0006
7	*Cynodon dactylon* (L.) Pers./Bermuda Grass	*Cyn.dac*	H	66	0	5	0	1	65.9	22.9	7.2	0.0004
8	*Themeda anathera* (Nees ex Steud.) Hack./Kangaroo Grass	*The.ana*	H	57	27	0	0	1	56.8	25.4	7.48	0.0016
9	*Mentha longifolia* (L.) L./Wild Horse Mint	*Men.lon*	H	56	0	0	0	1	55.6	18.6	8	0.0018
10	*Prunus persica* (L.) Batsch./Common Peach	*Pru.per*	Mp	56	0	0	0	1	55.6	18.5	7.9	0.0028
11	*Saccharum spontaneum* L./Wild Sugarcane	*Sac.spo*	G	50	0	0	0	1	50	18.9	8.73	0.0082
12	*Lespedeza juncea* (L.f.) Pers./ Chinese Lespedeza, Silky Bush-Clover	*Les.jun*	H	50	0	0	0	1	50	18.1	8.16	0.0038
13	*Chenopodium album* L./Lamb's Quarters, Fat Hen	*Che.alb*	Th	50	0	0	0	1	50	17.8	8.02	0.0036
14	*Amaranthus viridis* L./Green Amaranth, Slender Amaranth	*Ama.vir*	Th	50	0	0	0	1	50	17.6	7.93	0.0054
15	*Malus domestica* Borkh./Apple	*Mal.dom*	Mp	50	0	0	0	1	50	17.6	7.83	0.0036
16	*Galium elegans* Wall. ex Roxb./Elegant Goose Grass	*Gal.ele*	Th	48	0	1	2	1	48.3	20.5	7.65	0.008
17	*Convolvulus arvensis* L./Field Bindweed	*Con.arv*	L	44	0	0	0	1	44.4	17.3	8.07	0.0118
18	*Cannabis sativa* L./Marijuana	*Can.sat*	Th	44	0	0	0	1	44.4	17	7.92	0.011
19	*Artemisia scoparia* Waldst. & Kitam./Red-stem Wormwood	*Art.sco*	H	39	0	0	0	1	38.9	16.1	8.04	0.0182
20	*Zanthoxylum armatum* DC./Winged Prickly Ash	*Zan.arm*	Np	33	0	0	0	1	33.3	15.7	8.25	0.0478
21	*Lepidium sativum* L./Common Garden Cress	*Lep.sat*	Th	33	0	0	0	1	33.3	15.2	7.89	0.0452
22	*Rumex hastatus* D. Don/Arrow-Leaf Dock	*Rum.has*	H	33	0	0	0	1	33.3	15.2	8.04	0.0502

http://www.aloki.hu ● ISSN 1589 1623 (Print) ● ISSN 1785 0037 (Online)
DOI: http://dx.doi.org/10.15666/aeer/1706_1547715505

#	Latin Binomial/Common Name (English)	Codes	GF	Groups (samples)				Max. Grp	Obs. IV	Mean	SD	p-value
				1(18)	2(6)	3(9)	4(6)					
				Indicator value (IV)								
23	*Erigeron canadensis* L./Canadian Horseweed	*Eri.can*	Th	31	3	0	0	1	31.1	16.9	7.6	0.0528
24	*Geranium nepalense* Sweet/Nepalese Crane's Bill	*Ger.nep*	H	30	0	7	0	1	30.3	18.1	7.86	0.075
25	*Verbascum thapsus* L./Great Mullein	*Ver.tha*	Th	28	0	0	0	1	27.8	14.8	8.15	0.0692
26	*Euphorbia helioscopia* L./Sun Spurge	*Eup.hel*	Th	28	0	0	0	1	27.8	14.5	8.01	0.0604
27	*Salix denticulata* Andersson/Elegant Willow	*Sal.den*	Mp	28	0	0	0	1	27.8	14.5	8.07	0.0616
28	*Quercus floribunda* Lindl. ex A.Camus/Moru Oak, Green Oak	*Que.flo*	Mp	27	10	0	0	1	27.2	17.6	7.82	0.118
29	*Plantago lanceolata* L./Ribwort Plantain	*Pla.lan*	H	24	0	6	0	1	23.8	17	7.91	0.1814
30	*Ailanthus altissima* (Mill.) Swingle/Tree of Heaven	*Ail.alt*	Mp	22	0	0	0	1	22.2	13.3	7.66	0.1772
31	*Pinus roxburghii* Sarg./Chir Pine, Roxburgh's Pine	*Pin.rox*	Mp	17	0	0	0	1	16.7	13.2	6.8	0.2436
32	*Malva sylvestris* L./Common Mallow	*Mal.syl*	Ch	17	0	0	0	1	16.7	12.5	7.2	0.2745
33	*Jasminum officinale* L./Common Jasmine	*Jas.off*	Np	17	0	0	0	1	16.7	12.4	7.02	0.2509
34	*Pteris vittata* L./Chinese Laddar Brake	*Pte.vit*	G	17	0	0	0	1	16.7	12.3	6.93	0.2577
35	*Punica granatum* L./Pomegranate	*Pun.gra*	Mp	17	0	0	0	1	16.7	12.3	7.08	0.2851
36	*Ficus palmata* Forssk./Wild Fig	*Fic.pal*	Mp	17	0	0	0	1	16.7	12.2	7.06	0.2629
37	*Pteris cretica* L./Cretan Brake	*Pte.cre*	G	17	0	0	0	1	16.7	12.1	7.03	0.2851
38	*Solanum americanum* Mill./Black Nightshade	*Sol.ame*	Th	11	0	0	0	1	11.1	11.8	5.42	0.5227
39	*Erigeron bellidioides* (Buch.-Ham. ex D.Don) Benth. ex C.B.Clarke/Daisy Fleabane	*Eri.bel*	H	11	0	0	0	1	11.1	11.7	5.62	0.5065
40	*Avena barbata* Pott ex Link/Wild Oat	*Ave.bar*	Th	6	0	0	0	1	5.6	10.1	4.77	1
41	*Solanum pseudocapsicum* L./Jerusalem Cherry	*Sol.pse*	Th	6	0	0	0	1	5.6	10.1	4.77	1
42	***Pinus wallichiana* A.B.Jacks./ Blue Pine, Himalayan White Pine**	***Pin.wal***	**Mp**	**22**	**72**	**2**	**0**	**2**	**72**	**28.3**	**6.4**	**0.0002**
43	***Rubus niveus* Thunb./Ceylon Raspberry**	***Rub.niv***	**Np**	**3**	**71**	**0**	**0**	**2**	**71**	**17.6**	**7.6**	**0.0002**
44	***Persicaria amplexicaulis* (D.Don) Ronse Decr./ Mountain's Fleece**	***Per.amp***	**H**	**0**	**64**	**23**	**1**	**2**	**64**	**21.6**	**8.1**	**0.0016**
45	*Rosa moschata* Herrm./Musk Rose	*Ros.mos*	Np	0	63	0	0	2	63.3	16.2	8.47	0.0012

http://www.aloki.hu ● ISSN 1589 1623 (Print) ● ISSN 1785 0037 (Online)
DOI: http://dx.doi.org/10.15666/aeer/1706_1547715505

#	Latin Binomial/Common Name (English)	Codes	GF	Groups (samples)				Max. Grp	Obs. IV	Mean	SD	p-value
				1(18)	2(6)	3(9)	4(6)					
				Indicator value (IV)								
46	*Indigofera heterantha* Brandis/Himalayan Indigo	*Ind.het*	Np	6	60	0	0	2	60	17.8	8.04	0.0012
47	*Cynoglossum lanceolatum* Forssk./ Chinese Forget-Me-Not, Hound's Tongue	*Cyn.lan*	Th	4	53	0	0	2	52.6	16.1	8.07	0.004
48	*Geranium wallichianum* D.Don ex Sweet/Buxton's Blue	*Ger.wal*	H	0	52	6	37	2	51.8	23.1	7.47	0.0042
49	*Nepeta podostachys* Benth./Long Stalked Catmint	*Nep.pod*	Ch	0	50	0	0	2	50	12.6	7.17	0.0048
50	*Festuca modesta* Steud./Fescue	*Fes.mod*	H	0	50	0	0	2	50	12.4	7.13	0.0048
51	*Dactylis glomerata* L./Cock's Foot, Orchard Grass	*Dac.glo*	H	0	50	0	0	2	50	12	6.9	0.0048
52	*Plantago major* L./Broad-Leaved Plantain, White-Man's Foot	*Pla.maj*	H	0	50	0	0	2	50	12	6.93	0.0038
53	*Impatiens edgeworthii* Hook.f./Edgeworth's Balsam	*Imp.edg*	Th	0	49	0	0	2	48.9	13.8	7.82	0.003
54	*Achillea millefolium* L./Common Yarrow	*Ach.mil*	H	6	47	0	0	2	46.9	17.7	7.82	0.0064
55	*Sarcococca pruniformis* Lindl./Christmas Box, Sweet Box	*Sar.pru*	Np	0	43	1	0	2	42.9	14.4	7.8	0.0066
56	*Oenothera rosea* L'Hér. ex Aiton/Evening Primrose	*Oen.ros*	Ch	9	40	0	0	2	40.2	17	7.77	0.0178
57	*Brachiaria ramosa* (L.) Stapf./Brown-top Millet	*Bra.ram*	Th	0	33	0	0	2	33.3	12	5.67	0.0452
58	*Caltha palustris* L./Yellow Marsh Marigold	*Cal.pal*	Th	0	33	0	0	2	33.3	12	5.68	0.044
59	*Prunella vulgaris* L./Carpenter's Weed, Common Heal-All	*Pru.vul*	Th	10	31	10	0	2	31.4	21.3	7.85	0.1086
60	*Viola odorata* L./Sweet Violet, English Violet	*Vio.odo*	H	11	27	9	0	2	27.2	20.4	7.67	0.1718
61	*Picea smithiana* (Wall.) Boiss./ West Himalayan Spruce, Morinda Spruce	*Pic.smi*	Mp	0	24	11	0	2	24.3	14.3	7.88	0.1028
62	*Robinia pseudoacacia* L./Black Locust	*Rob.pse*	Mp	17	20	0	0	2	19.7	17	7.95	0.2523
63	***Viburnum grandiflorum* Wall. ex DC./Cranberry Bush**	***Vib.gra***	**Np**	**0**	**4**	**75**	**8**	**3**	**75**	**22.3**	**7.8**	**0.0002**
64	***Abies pindrow* (Royle ex D.Don) Royle/West Himalayan Fir**	***Abi.pin***	**Mp**	**0**	**15**	**74**	**6**	**3**	**74**	**24.3**	**7.7**	**0.0002**
65	***Dryopteris stewartii* Fraser-Jenk./Stewart's Wood Fern**	***Dry.ste***	**G**	**0**	**0**	**68**	**2**	**3**	**68**	**17.2**	**8**	**0.0004**
66	*Onychium japonicum* (Thunb.) Kunze/Carrot Fern	*Ony.jap*	G	0	8	60	0	3	60.2	18	8.07	0.0016
67	*Arisaema jacquemontii* Blume/Cobra Lily	*Ari.jac*	G	0	0	56	0	3	55.6	14	7.84	0.0008
68	*Veronica laxa* Benth./Lax Speedwell	*Ver.lax*	Th	0	0	54	3	3	53.6	16.3	8.03	0.0026
69	*Cyperus iria* L./Rice Flat-Sedge	*Cyp.iri*	G	0	34	50	3	3	50	24.4	8.4	0.0136

http://www.aloki.hu ● ISSN 1589 1623 (Print) ● ISSN 1785 0037 (Online)
DOI: http://dx.doi.org/10.15666/aeer/1706_1547715505

#	Latin Binomial/Common Name (English)	Codes	GF	Groups (samples)				Max. Grp	Obs. IV	Mean	SD	p-value
				1(18)	2(6)	3(9)	4(6)					
				Indicator value (IV)								
70	*Rumex nepalensis* Spreng./Nepal Dock	*Rum.nep*	Ch	0	0	40	13	3	39.8	18.4	8.59	0.0274
71	*Taraxacum campylodes* G.E.Haglund/Blow-Ball, Lion's Tooth	*Tar.cam*	H	0	0	39	37	3	39.3	21.4	7.69	0.0298
72	*Arisaema flavum* (Forssk.) Schott/Yellow Cobra Lily	*Ari.fla*	G	0	0	33	0	3	33.3	12.1	7.18	0.016
73	*Trifolium repens* L./White Clover	*Tri.rep*	H	4	29	33	18	3	33	26.9	5.45	0.1438
74	*Potentilla eriocarpa* Wall. ex Lehm./Woolly-Fruit Cinquefoil	*Pot.eri*	Th	0	0	22	0	3	22.2	11.9	5.45	0.0888
75	*Urtica dioica* L./Stinging Nettle	*Urt.dio*	H	7	0	13	0	3	12.7	14.5	7.99	0.4693
76	*Rumex dentatus* L./Toothed Dock, Aegean Dock	*Rum.den*	Ch	6	3	12	4	3	11.5	18.6	8.22	0.831
77	***Sibbaldia procumbens* L./Creeping Sibbaldia**	***Sib.pro***	**H**	**0**	**0**	**0**	**83**	**4**	**83**	**14.5**	**7.9**	**0.0002**
78	***Thymus linearis* Benth./Himalayan Thyme**	***Thy.lin***	**H**	**0**	**0**	**18**	**67**	**4**	**67**	**19.8**	**8.4**	**0.0002**
79	***Bistorta affinis* (D.Don) Greene/Himalayan Fleece Flower**	***Bis.aff***	**H**	**0**	**0**	**0**	**67**	**4**	**67**	**12.9**	**7.4**	**0.0002**
80	*Phleum alpinum* L./Alpine Cat's-Tail, Alpine Timothy	*Phl.alp*	G	0	0	0	67	4	66.7	13.3	7.78	0.001
81	*Poa annua* L./Annual Meadow Grass, Annual Blue-Grass	*Poa.ann*	H	5	9	22	58	4	58.4	30.8	5.82	0.0002
82	*Trillium govanianum* Wall. ex D.Don/Himalayan Trillium	*Tri.gov*	Th	0	0	0	50	4	50	12.2	7.37	0.0062
83	*Ranunculus repens* L./Creeping Buttercup	*Ran.rep*	H	0	0	5	40	4	39.7	14.2	8.03	0.0176
84	*Leontopodium nivale* subsp. *alpinum* (Cass.) Greuter/Edelweiss	*Leo.niv*	H	0	0	28	39	4	39	18.9	8.25	0.0322
85	*Adiantum venustum* D. Don/Himalayan Maiden-Hair Fern	*Adi.ven*	G	0	0	23	37	4	37.2	19.6	8.07	0.0402
86	*Fragaria nubicola* (Lindl. ex Hook.f.) Lacaita/ Wild Himalayan Strawberry	*Fra.nub*	H	8	22	32	35	4	34.6	29.3	3.9	0.1016
87	*Ranunculus laetus* Wall. ex Hook. f. & J.W. Thomson/ Cheerful Buttercup	*Ran.lae*	H	2	26	0	34	4	34	19.5	8.12	0.0648
88	*Gentiana kurroo* Royle/Himalayan Gentian	*Gen.kur*	Th	0	0	0	33	4	33.3	11.8	5.39	0.0392
89	*Geum urbanum* L./Herb Bennet, Wood Avens	*Geu.urb*	H	0	0	0	33	4	33.3	11.8	6.14	0.0412
90	*Salix alba* L./White Willow	*Sal.alb*	Mp	0	0	1	31	4	31.4	13	6.94	0.0456

Three leading plant species of each plant community are in bold
GF: Growth Form; Mp: Megaphanerophyte; Np: Nanophanerophyte; Ch: Chamaephyte; Th: Therophyte; H: Hemicryptophyte; G: Geophyte; L: Lianas/Climbers; Max. Grp: Maximum group; IV: Indicator value

http://www.aloki.hu ● ISSN 1589 1623 (Print) ● ISSN 1785 0037 (Online)
DOI: http://dx.doi.org/10.15666/aeer/1706_1547715505

Pinus-Rubus-Persicaria (PRP) community (Himalayan moist temperate forest)

This community was studied at the Sudhan Gali at an elevation range of 2100-2500 m (a.), and comprised of 6 samples. It was located at 73.742-73.745 E longitude, and 34.071-34.076 N latitude (*Fig. 3*). This community was recorded at the south-eastern faces having maximum mean slope (34.13 ± 6.49; range: 28.2-40.05) value. A total of 36 species with 21 IS and 17 SIS species were recorded in this group. The average species count was 23.50 ± 3.08 (20-29) for this association, and was highest as compared to all other associations but least β-diversity (mean Euclidean distance: 47.8) value depicting the homogeneity and least compositional dissimilarity amongst the studied samples (*Table 3*). It was dominated by *Pinus wallichiana*, *Rubus niveus* and *Persicaria amplexicaulis*, whereas the least IV was observed for *Picea smithiana* and *Robinia pseudoacacia* (*Table 4*). Total species (richness) and α-diversities were lower than the BMD association but higher than the other two (VAD and STB) associations of the higher elevation areas. The mean values of edaphic variables including soil pH, soil EC, nitrate-N (mg/kg), phosphorus (ppm), potassium (ppm), and organic matter (%) were 7.63 ± 0.04, 0.24 ± 0.04, 0.84 ± 0.08, 1.16 ± 0.08, 108 ± 52.59, and 2.2 ± 0.22, respectively. Some key factors of this association includes the highest values of slope, average species count in the plots, proportion of significant indicators to indicators (2nd), basic soil, and grazing pressure (17.17 ± 1.17 dungs/ha), and the least values of β-diversity, soil EC, nitrogen, phosphorus, and organic matter as compared to other associations (*Tables 3* and *4*).

Viburnum-Abies-Dryopteris (VAD) community (Himalayan sub-alpine forest)

This association was studied at upper Sudhan Gali areas and an elevation range of 2500-2800 m (a.), comprised of 9 samples (81 plots). It was located at 73.753-73.766 E longitude, and 34.081-34.083 N latitude (*Fig. 3*). It was studied at north western faces with mean slope value of 29.54 ± 10.62° (range: 21.98-43.67°). It was comprised of 34 species, 14 indicator species and 10 significant indicator species. The leading significant ones were *Viburnum grandiflorum*, *Abies pindrow*, and *Dryopteris stewartii*. The species with minimum IV were *Urtica dioica* and *Rumex dentatus* (*Tables 3* and *4*). Total species (richness) and α-diversities were further decreased as compared to both BMD and PRP associations of low elevation areas, and were almost alike to STB association of the higher elevation areas of the Ganga summit. The mean values of edaphic variables including soil pH, soil EC, nitrate-N (mg/kg), phosphorus (ppm), potassium (ppm), and organic matter (%) were 6.16 ± 0.49, 0.29 ± 0.1, 4.76 ± 1.68, 4.05 ± 2.02, 183.34 ± 86.75, and 3.47 ± 1.39 respectively. The grazing (dungs/ha) and deforestation (stumps/ha) pressure values were 13.12 ± 8.33 (2-23), and 14.78 ± 2.54 (11-19) respectively. Key factors of this association includes the highest values of soil EC, soil fertility (NPK), organic matter, vegetation cover, deforestation and higher grazing pressure (2nd), and proportion of significant indicators to indicators species. Similarly, least values of indicator species, SIS, α-diversities, evenness, and relatively lower soil pH (acidic) values were other important factors (*Tables 3* and *4*). The interactions of the least values of soil pH, higher soil fertility in term of NPK and thickest vegetation cover variables are all very important and correlated. The core areas of this association

http://www.aloki.hu ● ISSN 1589 1623 (Print) ● ISSN 1785 0037 (Online)
DOI: http://dx.doi.org/10.15666/aeer/1706_1547715505

were least diverse with conifer dominancy, and no human settlements, therefore recorded under severe deforestation pressure and activities of the timber mafia.

Sibbaldia-Thymus-Bistorta (STB) community (Himalayan alpine scrubland forest)

This plant association was recorded at and around Ganga summit areas, elevation ranged from 2900 to 3000 m (a.), and comprised of 6 samples. It was located at 73.787 E longitude, and 34.076-34.078 N latitude (*Fig. 3*). This vegetation cluster was comprised of a total of 26 species, 14 indicator species, and 12 significant indicator species (*Tables 3* and *4*). The proportion of significant indicators to indicators was highest in this community, therefore, representing the uniqueness of this microhabitat in the area, and the important determining factors includes high altitude and associated least mean minimum temperatures. Three leading significant indicator species of this community were *Sibbaldia procumbens*, *Thymus linearis,* and *Bistorta affinis*, whereas the least IV was recorded for *Gentiana kurroo, Geum urbanum* and *Salix alba* species. During the ecological surveys, it was also observed that local inhabitants visit the areas of this association frequently during the growing season for collection of variety of medicinal plant species. Similarly, except Margalef's richness (2.87 ± 0.55), all other diversity values (viz. Shannon's diversity 2.48 ± 0.17; Simpson's diversity 0.91 ± 0.02; Simpson's reciprocal diversity 10.51 ± 1.65; Pielou's evenness 0.95 ± 0.04; and β-diversity 78.65) were higher than the previous sub-alpine VAD vegetation type, and lower than the first two (viz. BMD and PRP) vegetation types of low elevation area (*Tables 3* and *4*). This might be due to increase of anthropogenic activities (other than deforestation) above the timberline in the area. The mean values of edaphic variables including soil pH, soil EC, nitrate-N (mg/kg), phosphorus (ppm), potassium (ppm), and organic matter (%) were 5.33 ± 0.2, 0.28 ± 0.24, 4.3 ± 2.8, 1.61 ± 1.32, 67 ± 3.29, and 2.65 ± 0.06 respectively.

The key factors controlling this association were the highest values of altitude, evenness, β-diversity, and proportion of significant indicator to indicator species, and the least values of slope, total species (richness), average species, IS, SIS, soil pH, and potassium contents of the soil (*Tables 3* and *4*).

Ordination analyses

Detrended correspondence analysis

The gradient length in the compositional response data was above 4 SD (standard deviations of species turnover) units, therefore, unimodal ordination models like DCA and CCA were analyzed. DCA was used to confirm the results of hierarchical clustering of the vegetation samples collected from the western Himalayan forests of Sudhan Gali, Pakistan. Total variations in the species response data were 2.84, whereas the first four axes cumulatively represents 37.3% variations. The gradient length of the first four DCA-axes was 4.4, 2.09, 2.49, and 1.25 respectively. DCA biplot of the plant species and studied samples allied to four vegetation types showed that both species and samples are reasonably separated in the ordination space (*Fig. 4*). Along the DCA axis-1, the plant species of the low elevation areas are distributed in the left half and species of higher elevation areas in the right hand side of the biplot. This species distribution pattern depicted the prominent role of altitude in the area. Secondly, this biplot is also depicting the pattern of diversity

http://www.aloki.hu ● ISSN 1589 1623 (Print) ● ISSN 1785 0037 (Online)
DOI: http://dx.doi.org/10.15666/aeer/1706_1547715505

variations along the DCA axis-1 (or altitude), which continuously decreased up to VAD association and then again increased for the alpine STB association (*Fig. 4*).

Canonical correspondence analysis (CCA) and variation partitioning

The contribution of five topographic (altitude, Cos-trans aspect, slope, latitude, and longitude), six edaphic (soil pH, organic matter, EC, N, P, and K), and two anthropogenic (grazing pressure, and deforestation) variables toward explaining the variations in the response data were tested by using CCA. All the richness, evenness, and diversity variables were not included in this test. The CCA model (overall) was detected as significant (Pseudo F-value = 4.61; p-value = 0.001). Therefore, all the 13 constrained axes and variables were further tested by using permutation test. The results showed that first seven (7) CCA axes were significant (p-value ≤ 0.003) (*Fig. 5*). Out of total inertia of 2.84 of the response data, all the explanatory variables explained 73.1% variations, whereas the adjusted explained variations were 59.2%. First four CCA axes cumulatively explained 50.15% and 68.57% of variations and fitted variations respectively. A very high values of species-environment pseudo-canonical correlations of the first four CCA axes were observed (viz. r 0.99, 0.98, 0.97 and 0.92). This showed that the selected explanatory variables were determinants of the response (species) data variations. Similarly, the high values of species-environment correlation for the CCA axes 2-4 indicated that there was no single dominant environmental gradient in this part of the western Himalaya. By using permutation test, both simple (marginal) and conditional (net) term effects were tested for all the 13 explanatory variables. The results of simple term effect testing revealed that only the soil EC was not much important towards explaining variations in the species data, whereas the net effect testing made the same as significant as well (*Table 5*). The ranking (order of importance) results of the studied variables depicted that altitude is the leading factor followed by grazing pressure, deforestation, nitrate-N, soil pH, potassium, slope, longitude, phosphorus, cos-trans aspect, organic matter, latitude, and soil EC in the area (*Table 5*).

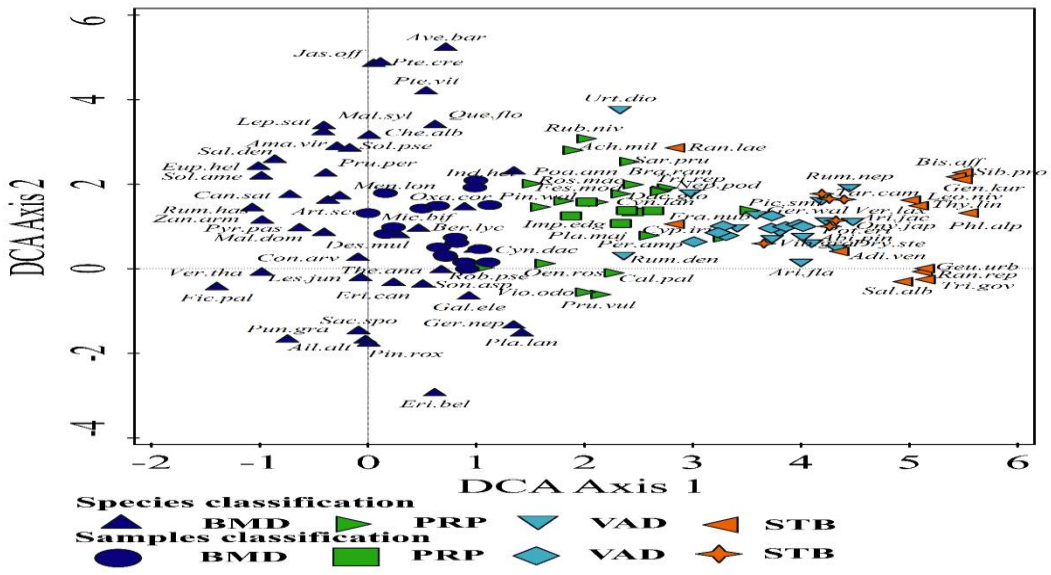

Figure 4. *A DCA biplot showing distribution pattern of 39 samples and 90 plant species in four vegetation groups of western Himalayan forests of Sudhan Gali*

http://www.aloki.hu ● ISSN 1589 1623 (Print) ● ISSN 1785 0037 (Online)
DOI: http://dx.doi.org/10.15666/aeer/1706_1547715505

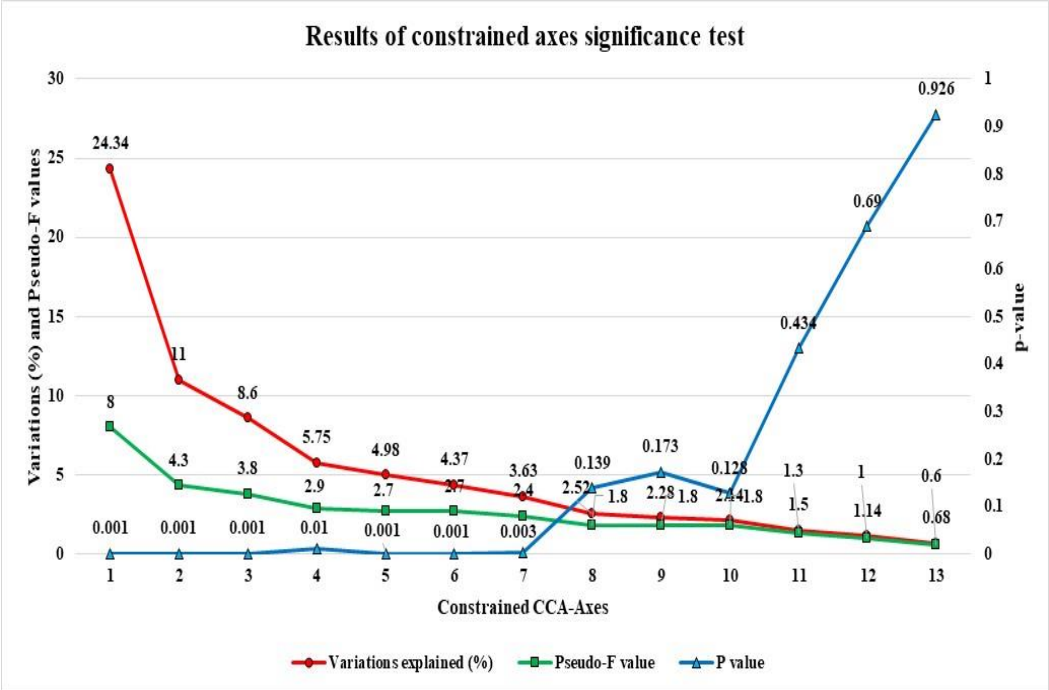

Figure 5. *A plot showing the results of significance testing of 13 constrained axes*

Table 5. *A table showing the contribution and ranking of the studied environmental variables (p-values were corrected by false discovery rate method)*

Simple term effects:					Conditional term effects:				
Variable	**Explains %**	**Pseudo-F**	**P-value**	**P(adj)**	**Variable**	**Explains %**	**Pseudo-F**	**P-value**	**P(adj)**
Altitude	23.2	11.2	0.001	0.0028	Altitude	23.2	11.2	0.001	0.0014
Nitrate-N	15.3	6.7	0.001	0.0028	Grazing pressure	9	4.8	0.001	0.0014
Soil pH	12.6	5.4	0.001	0.0028	Deforestation	6.4	3.7	0.001	0.0014
Cos-trans Aspect	9.4	3.9	0.001	0.0028	Nitrate-N	4	2.4	0.002	0.00233
Grazing pressure	9.1	3.7	0.001	0.0028	Soil pH	3.9	2.4	0.003	0.003
Deforestation	8.5	3.4	0.004	0.007	Potassium	3.5	2.2	0.003	0.003
Potassium	7.2	2.9	0.002	0.00467	Slope	4.7	3.3	0.001	0.0014
Phosphorus	6.9	2.7	0.004	0.007	Longitude	4.2	3.1	0.001	0.0014
Organic matter	6	2.4	0.012	0.01527	Phosphorus	3.8	2.9	0.001	0.0014
Latitude	6	2.3	0.008	0.01244	Cos-trans Aspect	3	2.5	0.001	0.0014
Slope	5.9	2.3	0.009	0.0126	Organic matter	2.9	2.5	0.001	0.0014
Longitude	5.9	2.3	0.014	0.01633	Latitude	2.7	2.4	0.002	0.00233
Soil EC	4	1.5	0.092	0.092	Soil EC	2.7	2.9	0.001	0.0014

The graphical results of the CCA (first three CCA axes) are presented in *Figure 6*. These CCA biplots revealed that the species distribution of the four detected associations are controlled by the studied environment. The species of STB community got the maximum score along CCA axis 1, and the species of BMD community got the least, therefore primarily controlled by altitude, followed by N, P, K, grazing and organic matter. Similarly, BMD and PRP associations are found separated along CCA axis-2, and controlled by deforestation, soil pH, longitude and slope variables (*Fig. 6*).

http://www.aloki.hu ● ISSN 1589 1623 (Print) ● ISSN 1785 0037 (Online)
DOI: http://dx.doi.org/10.15666/aeer/1706_1547715505

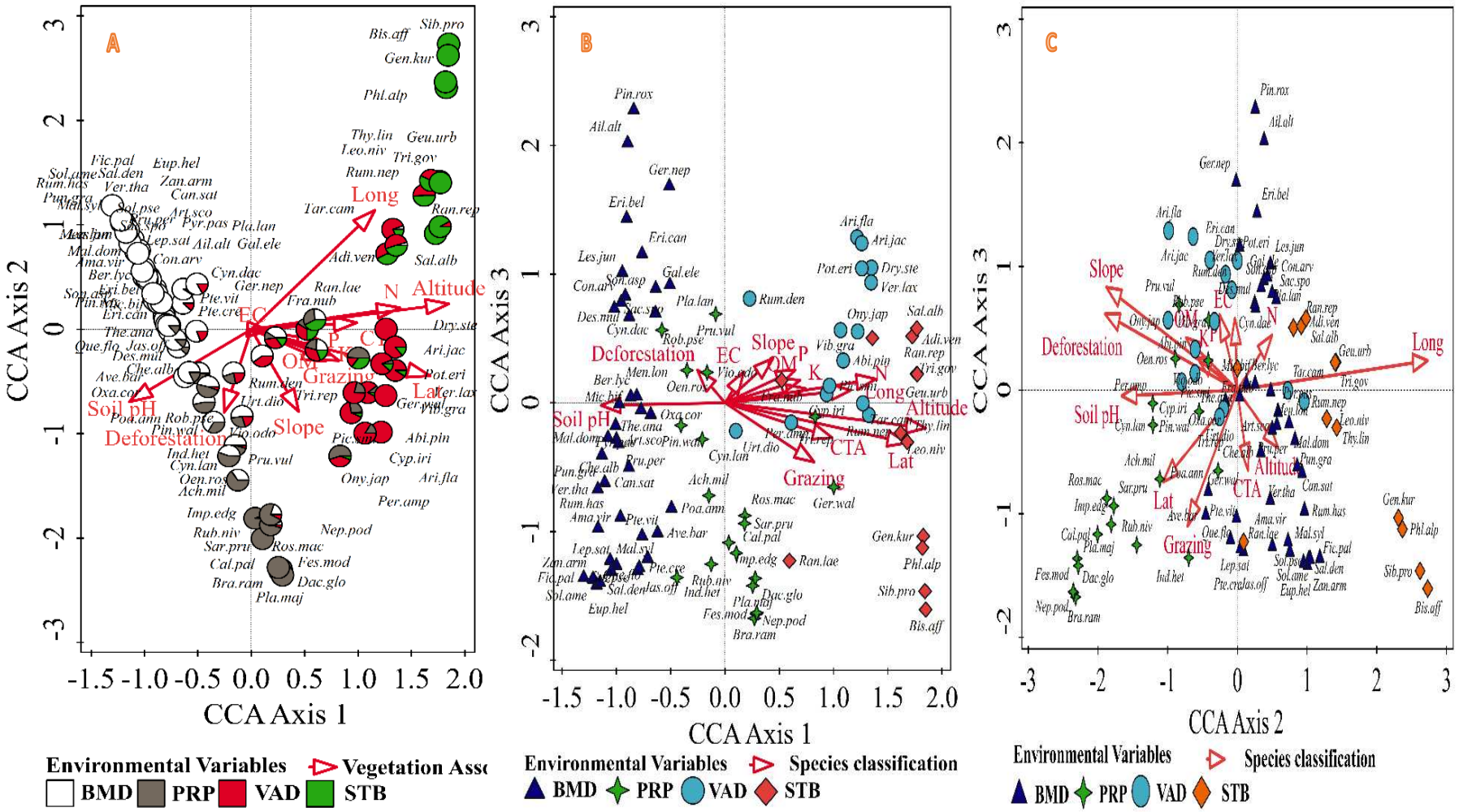

Figure 6. *A group of CCA biplots depicting the species-environment relationships of the four vegetation types of the western Himalayan forests of Sudhan Gali, AJ&K, Pakistan (CCA axes: A = 1&2; B = 1&3; C = 2&3)*

APPLIED ECOLOGY AND ENVIRONMENTAL RESEARCH 17(6):15477-15505.
http://www.aloki.hu ● ISSN 1589 1623 (Print) ● ISSN 1785 0037 (Online)
DOI: http://dx.doi.org/10.15666/aeer/1706_1547715505

A total of two leading factors of each of topographic (altitude and slope), edaphic (nitrate-N and soil pH), and anthropogenic (grazing pressure and deforestation) class were used to perform variation partitioning (partial CCA) to seek the contribution of each class and their interactions. Like CCA, permutation test was performed for net effects of each class. This analysis results depicted that topography was the leading (explained variations 32.6%) class, followed by anthropogenic (25.8%), and topographic vs. edaphic interaction (25.5%). Similarly, least variations were explained by the interactions of all classes (-5.5%). This negative value of the adjusted explained variations can be interpreted as zero, and linked to the samples where the explanatory variables explain less variations than what the random normal variables do (*Fig. 7*). However, at this moment, higher contribution of anthropogenic than the edaphic class is a major concern in the study area.

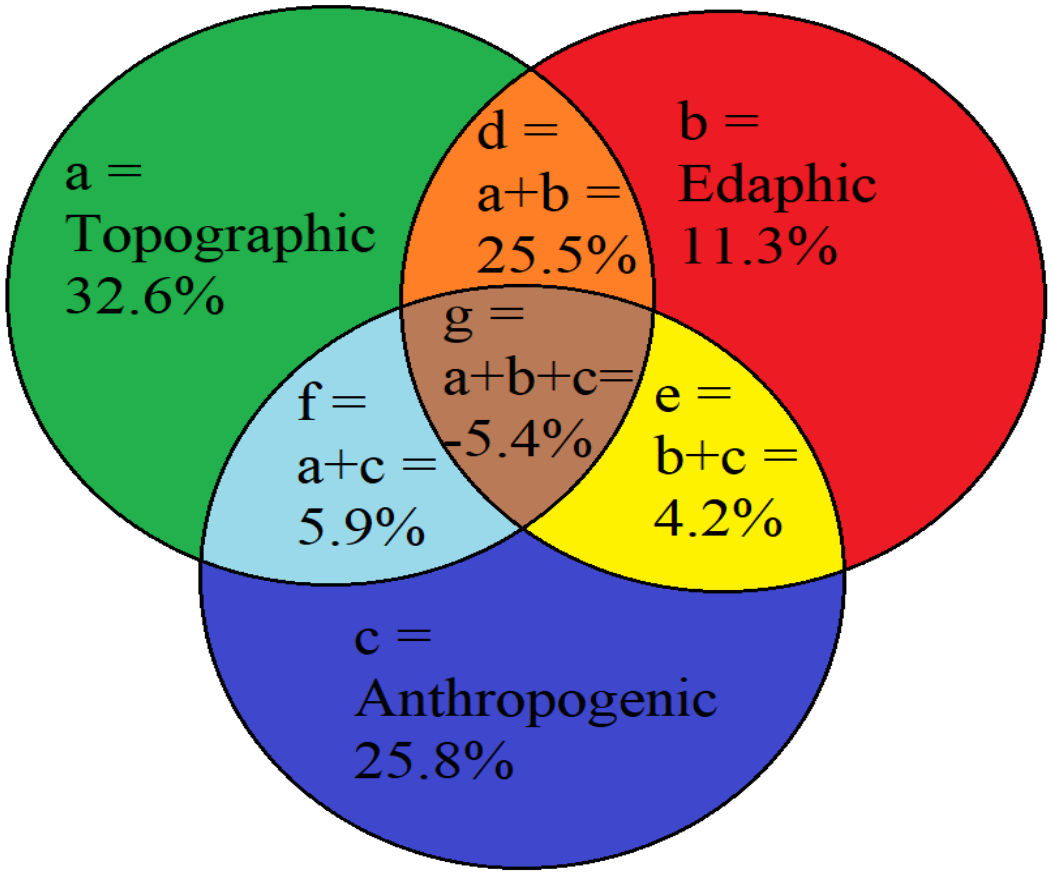

Figure 7. *A Venn diagram showing the amount of explained variations (%) in the species data by the three groups of explanatory variables*

Discussion

A detailed ecological exploration of the western Himalayan forests is necessary for future biodiversity management, sustainable utilization and conservation (Shaheen et al., 2012; Khan et al., 2019). This study thoroughly and comparatively reviewed the history of forest ecological work conducted at the Sudhan Gali and Ganga summit of Bagh, AJ&K, Pakistan, and identified few research gaps that needed to be explored. Prior to this study, a total of 14 different ecological studies were conducted from 2007 to 2018, but a lot

http://www.aloki.hu ● ISSN 1589 1623 (Print) ● ISSN 1785 0037 (Online)
DOI: http://dx.doi.org/10.15666/aeer/1706_1547715505

of questions remained un-answered (*Table 6*). Therefore, this study represents the first ever detailed ecological exploration of the area. Majority of earlier studies rarely used agglomerative hierarchical clustering for classification, and mostly used a linear un-constrained model (PCA) for arranging the species along the environmental gradients. The drawback of using PCA include the Horseshoe Effect (an artifact of the ordination diagram similar to the Arch Effect), therefore, PCA axis-2 did not truly represent the secondary gradient. A study close to this one was conducted by Shaheen et al. (2012) in the study area, however, Monte Carlo permutation test to decide the ecological meaningful number of vegetation types, significant indicator species of each type by using indicator species analysis, pairwise compositional significance of the plant associations, contribution of edaphic variables, order of importance of studied environment, and variation partitioning were performed for the first time from the study area.

A total of four plant associations (1. *Berberis-Micromeria-Desmodium* (BMD), 2. *Pinus-Rubus-Persicaria* (PRP), 3. *Viburnum-Abies-Dryopteris* (VAD) and 4. *Sibbaldia-Thymus-Bistorta* (STB) associations) were recorded in this study, and confirmed by using different multivariate statistics. Sher et al. (2013) studied the vegetation at 13 different stations along the altitudinal gradient from the Sudhan Gali and Ganga area like this study, but communicated the composition of each station as a plant community and further place them in the higher hierarchy of four plant associations. Secondly, the elevation gradient of their studied stations was ranged from 2200 to 2500 m (a.) unlike this study which ranges from 1700 to 3000 m (a.). Malik and Malik (2012) also recorded four plant associations from the same area. Both these earlier studies did not employ any multivariate analysis tool. Therefore, a sufficient compositional differences were observed while comparing this with both prior studies. Unlike this study, both prior studies also communicated that there is no significant correlation between species turnover and altitudinal variations. However, the status of overall dominant species (especially *Pinus wallichiana* and *Abies pindrow*) in the area are same. The composition of alpine meadow (Ganga) matches with the results of Shaheen et al. (2011c), who also reported the similar community composition and leading dominants in the other areas of district Bagh. We recorded low indicator values of *Pinus roxburghii* and *Pinus wallichiana* (Blue Pine) at the lower elevation in the BMD vegetation type. Khan et al. (2019) reported the dominancy of Chir pine at the low elevation areas of adjacent Muzaffarabad district, whereas this study detected the dominancy of *Berberis lycium* and *Micromeria biflora* at the similar elevation areas. This might be due to higher rate of fuelwood collection and consumption than regeneration as compared to other related adjacent areas (Shaheen et al., 2011b). The other contributing factor might include the findings of Saeeda and Zakir (2012), which communicated the highest correlation between forest deterioration and poor socioeconomic status of the inhabitants of the Bagh area. The mid-elevation areas (2100-2500 m) of PRP vegetation type is relatively more stable than the other three types, but higher grazing pressure needs immediate attention. The shrub species of *Viburnum grandiflorum* has taken over the *Abies pindrow* and *Picea smithiana* in the sub-alpine VAD type (elevation: 2500-2800 m). This type was recorded under sever deforestation pressure, possibly because located far from the human settlements, therefore a relatively easy target for timber mafia. Secondly, the local government has completed a new metallic road up to 2700 m elevation, and this provide an easy transportation tool for illegally obtained forest resources. The study area (especially STB type: 2900-3000 m is receiving a huge number of tourist's visits especially during the growing season which sometime get involved in uprooting of rare medicinal species.

http://www.aloki.hu ● ISSN 1589 1623 (Print) ● ISSN 1785 0037 (Online)
DOI: http://dx.doi.org/10.15666/aeer/1706_1547715505

Table 6. *A table showing the comparative history of vegetation explorations of the western Himalayan forests of Sudhan Gali & Ganga summit, AJ&K, Pakistan*

No	Reference	Major research objective	Environment studied			HC	ISA	ORD	Remarks/research gap
			T	S	D				
1	Malik et al., 2007	Raunkiaer's life forms and leaf spectra classification	×	×	×	×	×	×	Environmental influence is missing.
2	Siddiqui et al., 2010a	Vegetation classification	✓	×	×	×	×	PCA	Environmental influence is missing. *Cedrus deodara* is recorded as dominant, presently it is not recorded in any sample
3	Siddiqui et al., 2010b	Vegetation-environment interactions	✓	✓	×	✓	×	DCA	Recorded environmental variables were not included in DCA as supplementary variables
4	Shaheen et al., 2011c	Vegetation classification, diversity & distribution	✓	×	✓	×	×	CCA	Contribution of edaphic variations is missing
5	Siddiqui et al., 2011	Vegetation classification & description	✓	×	×	×	×	×	Environmental influence is missing
6	Shaheen et al., 2012	Vegetation classification, diversity & regeneration	✓	×	✓	✓	×	CCA	Overall, CCA model was non-significant possibly because all the 13 studied sites instead of plots were treated as samples with 6 explanatory variables, & therefore, CCA did not remain as a constrained model
7	Malik and Malik, 2012	Vegetation classification and diversity	×	×	×	×	×	×	Environmental influence is missing
8	Siddiqui et al., 2013	Vegetation classification & description	✓	×	×	×	×	×	Environmental influence is missing
9	Sher et al., 2013	Vegetation classification & description	×	×	×	×	×	×	Environmental influence is missing
10	Siddiqui et al., 2014	Vegetation classification & contribution of topography & soil	✓	✓	×	✓	×	PCA	A linear un-constrained multivariate model (PCA) with studied environment as supplementary variables is used. Therefore, the question that how environment variations are influencing species distribution is still un-answered
11	Malik and Malik, 2014	Vegetation and species phenology	×	×	×	×	×	×	Environmental influence is missing
12	Shaheen et al., 2016	Vegetation attributes and fuelwood pressure	×	×	×	✓	×	PCA	Environmental influence is missing
13	Shaheen et al., 2017	Regeneration pattern of the tree species	×	×	×	✓	×	PCA	Environmental influence is missing
14	Shaheen et al., 2018	Vegetation & anthropogenic disturbance	×	×	✓	✓	×	PCA	Environmental influence is missing
15	This study	Vegetation classification, indicators significance, variation partitioning, diversity & distribution	✓	✓	✓	✓	✓	DCA & CCA	Attempted to fill the gaps. Additionally, detection of ecologically meaningful vegetation types, MRPP, and variation partitioning were also performed. Ordination models were selected on the basis of gradient length in the response data

T: topography; S: Soil; D: disturbance; HC: hierarchical classification; ISA: indicator species analysis; ORD: ordination
×: No; ✓: Yes

The study area is diverse and the mean Shannon's diversity values of the four plant communities varied from 2.47-2.87, Simpson's diversity index from 0.89-0.94, reciprocal Simpson's diversity from 8.44-14.47, Pielou's evenness from 0.88-0.95, and Margalef's richness from 2.87-5.05. These values are comparable with the earlier work of Shaheen et al. (2011c), Malik and Malik (2012) and Sher et al. (2013) conducted in the same area. These diversity variations are also comparable with the other vegetation surveys in the Himalayas (Roy and Behera, 2005; Kharkwal, 2009). The β-diversity (amongst studied samples) in the study area varied from 47.88-78.65. It was observed

http://www.aloki.hu ● ISSN 1589 1623 (Print) ● ISSN 1785 0037 (Online)
DOI: http://dx.doi.org/10.15666/aeer/1706_1547715505

that the number of species, indicator and significant indicator species of groups continuously decreased along the increasing elevation, whereas diversity values also showed the similar pattern except it again started to increase at the Ganga summit. However, the proportion of significant indicator species to indicators continuously increased along the elevation gradient, therefore depict the uniqueness of sub-alpine to alpine microhabitats in the Himalayas. The results of this study also suggested that the forests edges of the Sudhan Gali are more diverse than the forest interiors, and the similar results are also reported by Khan et al. (2019).

The role of topography and especially altitude is well documented (Shaheen et al., 2011c; Khan et al., 2019) in the Himalayas, however, CCA net effect testing proved that anthropogenic influences has come very close to topography and taken over the edaphic contribution in this regard. The order of importance of the studied environment is presented in *Table 5* and *Figure 7*. All these disturbances and the rarest plant species are presented in *Figure 8*. Therefore, the study area need development and implementation of management plans for the restoration of important and valuable forest resources in this part of the western Himalaya.

Conclusion and recommendations

The species composition and vegetation structure of the observed four vegetation groups of the study area was significantly different. Therefore, these groups are supporting some rarest plant species and unique composition. The topography is detected as the leading driver of species distribution pattern variation followed by grazing and deforestation pressures. The highest correlation was observed between deforestation and thick coniferous forest patches, and grazing intensity and temperate grassland pastures in the area. Therefore, this study concluded that vegetation composition of the sub-alpine to alpine areas is changing at faster rates than the low elevation areas. The results of CCA (net effect) depicted that all the studied environmental variables (thirteen in total) were significantly important, and explains 73.1% variations. This study also concluded that the selected explanatory variables were determinants of the response (species) data variations and there was no single dominant environmental gradient in this part of the western Himalaya. Similarly, the highest β-diversity value of west Himalayan alpine scrubland association as compared to others, is representative of variety of microhabitats with unique flora. This also mean that even a minor variation in environment affects the high altitude vegetation more rapidly than the vegetation of low elevation areas.

An effective management plan for the restoration of vegetation in area are required including provision of fuel alternatives for the local masses. This study recommend that the importance of local biodiversity and consequences of its depletion should be regularly addressed and communicated to local masses. The launching of afforestation and reforestation programs, and their continuous monitoring will prove effective. Similarly, stimulus of medicinal species cultivation can help a lot in this regard. The provision of free seedlings of valuable native species, strict enforcement of biodiversity protection law, periodic monitoring of endangered species populations are some other effective tools. All this is necessary because these wild relatives can serve as an important germplasm for the future drugs, and different stress and disease tolerance characteristics which can be used for the improvement of masses health, and existing valuable agricultural species respectively.

http://www.aloki.hu ● ISSN 1589 1623 (Print) ● ISSN 1785 0037 (Online)
DOI: http://dx.doi.org/10.15666/aeer/1706_1547715505

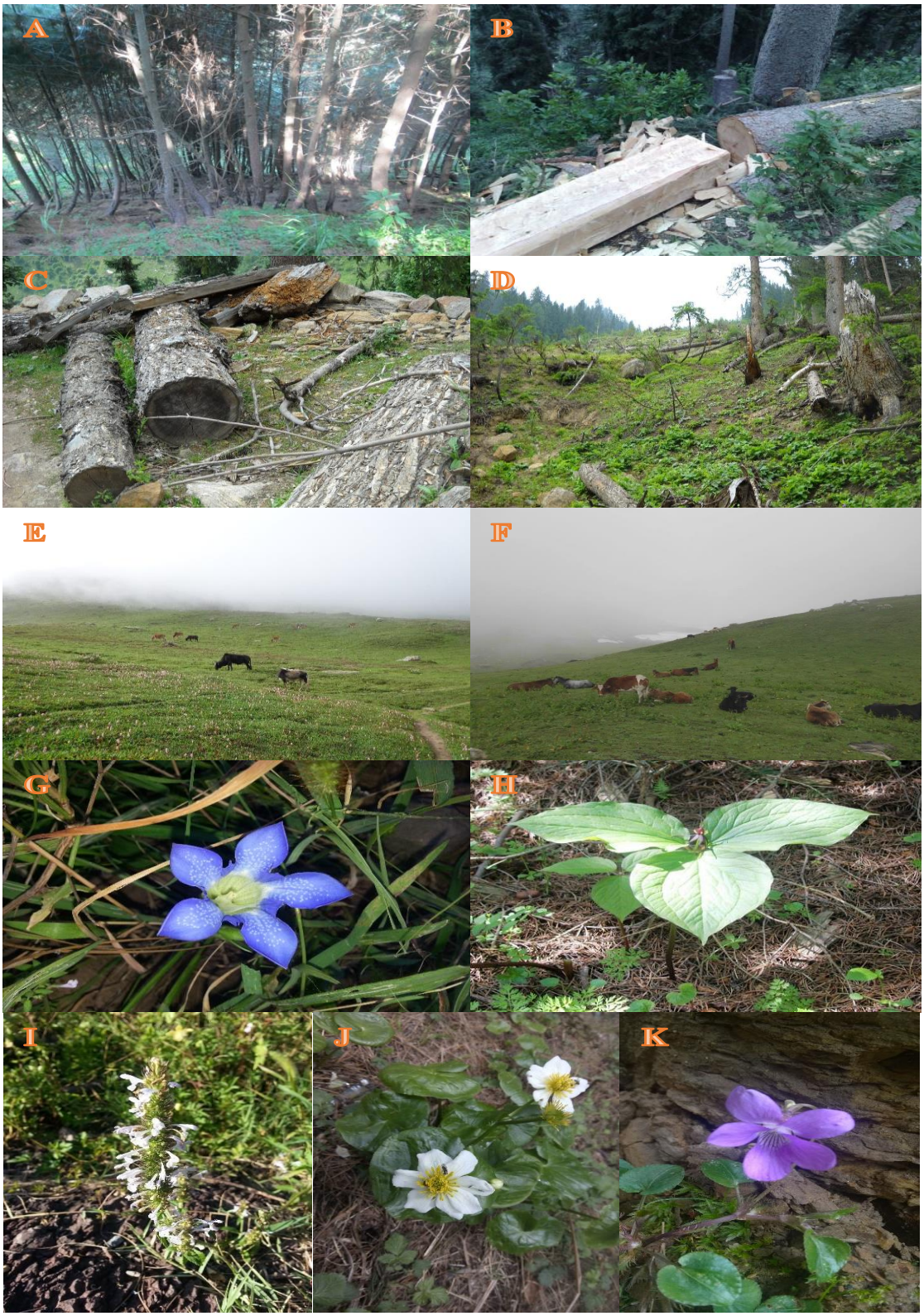

Figure 8. *Some visuals depicting the influential anthropogenic factors (A: forest fire; B-D: deforestation; E-F: grazing), and extremely rare plant species (G: Gentiana kurroo; H: Trillium govanianum; I: Nepeta podostachys; J: Caltha palustris var. alba; K: Viola odorata) of the western Himalayan forests of AJ&K, Pakistan*

http://www.aloki.hu ● ISSN 1589 1623 (Print) ● ISSN 1785 0037 (Online)
DOI: http://dx.doi.org/10.15666/aeer/1706_1547715505

We concluded that overall vegetation of the area is under heavy anthropogenic pressure and sustainable use of these natural resources is recommended. Various concerned departments like wildlife, forest, environment, tourisms and local government should play their role in launching of awareness campaigns, conservation/management plan development, execution and implementation to save this wealth of the area.

This study observed that over-exploitation of medicinal plant species especially from the Ganga summit and adjacent alpine area is resulted in least population size of *Geum urbanum*, *Gentiana kurroo, Nepeta podostachys, Caltha palustris var. alba, Viola odorata* and *Trillium govanianum*. According to literature, species like *Saussurea costus* and *Rheum australe* were once surviving and now become extinct in the area. Therefore, future studies like documentation of rate of population fluctuation, potential habitat mapping under present, past and future climate scenarios should be conducted immediately to ensure their sustainable use, forest management and conservation.

REFERENCES

[1] Abdel Khalik, K., Al-Gohary, I., Al-Sodany, Y. (2017): Floristic composition and vegetation: environmental relationships of Wadi Fatimah, Mecca, Saudi Arabia. – Arid Land Research and Management 31: 316-334.

[2] Akhlaq, R., Amjad, M. S., Qaseem, M. F., Fatima, S., Chaudhari, S. K., Khan, A. M., Khan, S., Malik, N. Z., Gardazi, S. M. H., Bibi, A., Sabaoon (2018): Species diversity and vegetation structure from different climatic zones of Tehsil Harighel, Bagh, Azad Kasmir, Pakistan analysed through multivariate techniques. – Applied Ecology and Environmental Research 16(4): 5193-5211.

[3] Ali, S. I., Qaiser, M. (1995-2009): Flora of West Pakistan. – Department of Botany, University of Karachi, Karachi, Pakistan.

[4] Anonymous. (2015): AJK at Glance. – http://pndajk.gov.pk (accessed: 4/2/2017).

[5] Bürzle, B., Schickhoff, U., Schwab, N., Oldeland, J., Müller, M., Böhner, J., Chaudhary, R. P., Scholten, T., Dickoré, W. B. (2017): Phytosociology and ecology of treeline ecotone vegetation in Rolwaling Himal, Nepal. – Phytocoenologia 47: 197-220.

[6] Champion, S. H., Seth, S. K., Khattak, G. M. (1965): Forest Types of Pakistan. – Pakistan Forest Institute, Peshawar.

[7] Chandra, S., Singh, A., Singh, C. P., Nautiyal, M. C., Rawat, L. S. (2018): Vascular plants distribution in relation to topography and environmental variables in alpine zone of Kedarnath Wild Life Sanctuary, West Himalaya. – Journal of Mountain Science 15: 1936-1949.

[8] Cox, G. W. (1967): Laboratory Manual of General Ecology. – William C Brown, Dubuque.

[9] Curtis, J. T., McIntosh, R. P. (1950): The interrelations of certain analytic and synthetic phytosociological characters. – Ecology 31: 434-455.

[10] Devetter, M., Háněl, L., Řeháková, K., Doležal, J. (2017): Diversity and feeding strategies of soil microfauna along elevation gradients in Himalayan cold deserts. – PloS One 12: e0187646. https://doi.org/10.1371/journal.pone.0187646.

[11] Dufrêne, M., Legendre, P. (1997): Species assemblages and indicator species: the need for a flexible asymmetrical approach. – Ecol. Monogr. 67(3): 345-366.

[12] EFLORAS (2012): Flora of Pakistan @ eflorasrg. – http://www.efloras.org/flora_page.aspx?flora_id=5 (accessed 16/9/2018).

[13] Haq, F. (2018): Vegetation mapping above tree line in Nandiar Valley, western Himalayas. A multivariate approach. – Acta Ecologica Sinica 38: 15-20.

http://www.aloki.hu ● ISSN 1589 1623 (Print) ● ISSN 1785 0037 (Online)
DOI: http://dx.doi.org/10.15666/aeer/1706_1547715505

[14] Ilyas, M., Qureshi, R., Akhtar, N., Ziaul-Haq, Khan, A. M. (2018): Floristic diversity and vegetation structure of the remnant subtropical broad leaved forests from Kabal Valley, Swat, Pakistan. – Pak. J. Bot. 50(1): 217-230.

[15] Kamran, S., Khan, S. M., Ahmad, Z., Rahman, A. U., Iqbal, M., Manan, F., Haq, Z. U., Ullah, S. (2019): The role of graveyards in species conservation and beta diversity: a vegetation appraisal of sacred habitats from Bannu, Pakistan. – Journal of Forestry Research. https://doi.org/10.1007/s11676-019-00893-1.

[16] Khan, A. M. (2001): Phytosociology, floristic composition & phenological studies with special reference to rangeland at Sudhan Gali and Ganga Chotti hills (District Bagh AK) during, 2000. – MSc. Thesis (unpublished), Department of Botany, AJ&K University, Muzaffarabad, Pakistan.

[17] Khan, A. M., Qureshi, R., Qaseem, M. F., Munir, M., Ilyas, M., Saqib, Z. (2015): Floristic checklist of district Kotli, Azad Jammu & Kashmir. – Pak. J. Bot. 47(5): 1957-1968.

[18] Khan, A. M., Qureshi, R., Qaseem, M. F., Ahmad, W., Saqib, Z., Habib, T. (2016): Status of basic taxonomic skills in botanical articles related to Azad Jammu and Kashmir, Pakistan: A Review. – J. Bioresource Manage. 3(3): 22-54.

[19] Khan, A. M., Qureshi, R., Arshad, M., Mirza, S. N. (2018a): Climatic and flowering phenological relationships of Western Himalayan Flora of Muzaffarabad District, Azad Jammu and Kashmir, Pakistan. – Pak. J. Bot. 50(3): 1093-1112.

[20] Khan, A. M., Qureshi, R., Saqib, Z., Habib, T., Ilyas, M., Maqsood, M., Kosar, R., Akram, M., Rahim, B. Z. (2018b): A novel study of the interrelationship of seasonality, satellite data and weed compositional changes of the agro-ecological system of Gujrat, Pakistan. – Applied Ecology and Environmental Research 16(3): 2995-3018. http://dx.doi.org/10.15666/aeer/1603_29953018.

[21] Khan, A. M., Qureshi, R., Saqib, Z. (2019): Multivariate analyses of the vegetation of the western Himalayan forests of Muzaffarabad district, Azad Jammu and Kashmir, Pakistan. – Ecological Indicators 104: 723-736. https://doi.org/10.1016/j.ecolind.2019.05.048.

[22] Kharkwal, G. (2009): Qualitative analysis of tree species in evergreen forests of Kumaun Himalaya, Uttarakhand, India. – African Journal of Plant Science 3(3): 49-52.

[23] Legendre, P., Legendre, L. (1998): Numerical ecology. 2nd ed. – Elsevier B., Amsterdam.

[24] Magurran, A. E. (1988): Ecological Diversity and Its Measurement. Chap. 1: Why Diversity? – Springer, Dordrecht, pp. 1-5.

[25] Malik, Z. H., Malik, N. Z. (2012): High altitude forest composition diversity and its component in a part of Ganga chotti and Bedori hills district Bagh. Azad Jammu and Kashmir, Pakistan. – Acta Geographica Debrecina Landscape & Environment 6(1): 31-40.

[26] Malik, Z. H., Malik, N. Z. (2014): Phenological patterns among the vegetation of Ganga Chotti and Bedori Hills in a moist temperate to alpine forests. – International Journal of Biodiversity and Conservation 6(6): 444-451.

[27] Malik, Z. H., Hussain, F., Malik, N. Z. (2007): Life form and leaf size spectra of plant communities Harbouring Ganga Chotti and Bedori Hills during 1999-2000. – Int. J. Agric. Biol. 9(6): 833-838.

[28] Margalef, R. (1958): Temporal Succession and Spatial Heterogeneity in Phytoplankton. – In: Buzzati-Traverso, A. A. (ed.) Perspectives in Marine Biology. University of California Press, Berkeley, CA.

[29] Nakaike, T., Malik, S. (1992): Cryptogamic Flora of Pakistan. – National Science Museum, Tokyo.

[30] Nasir, E., Ali, S. I. (1971-1995): Flora of West Pakistan. – Department of Botany, University of Karachi, Karachi.

[31] Nelson, D. W., Sommer, L. E. (1982): Total Carbon, Organic Carbon, and Organic Matter 1. – In: Page, A. L. (ed.) Methods of Soil Analysis. Part 2. Agronomy Series No. 9. ASA, Madison, WI, pp. 539-579.

http://www.aloki.hu ● ISSN 1589 1623 (Print) ● ISSN 1785 0037 (Online)
DOI: http://dx.doi.org/10.15666/aeer/1706_1547715505

[32] Olsen, S. R., Cole, C. V., Watanabe, F. S., Dean, L. A. (1954): Estimation of available phosphorus in soils by extraction with sodium bicarbonate. – USDA Circ. 939: 1-19.
[33] Othman, F., Chowdhury, M. S. U., Sakai, N., Shaaban, M. G., Shimizu, Y. (2014): Identification of pollution loading in a tropical river basin: a case study of Selangor River, Malaysia. – WIT Trans Built Environ 156. DOI: 10.2495/ESBE140121.
[34] Pielou, E. C. (1975): Ecological Diversity. – Wiley, New York.
[35] PMD (2018): Pakistan Meteorological Department. – National Agromet Centre, Islamabad, Pakistan.
[36] Qamer, F., Shehzad, K., Abbas, S., Murthy, M. S. R., Xi, C., Gilani, H., Bajracharya, B. (2016): Mapping deforestation and forest degradation patterns in western Himalaya, Pakistan. – Remote Sensing 8(5): 385.
[37] Rahman, I. U., Khan, N., Ali, K. (2017): Classification and ordination of understory vegetation using multivariate techniques in the Pinus wallichiana forests of Swat Valley, northern Pakistan. – The Science of Nature 104: 24. DOI: 10.1007/s00114-017-1431-2.
[38] Richards, L. A. (1954): Diagnosis and Improvement of Saline and Alkali Soils. – In: Richards, L. A. (ed.) Agriculture Handbook No. 60. United States Salinity Laboratory, Riverside, CA.
[39] Roy, P. S., Behera, M. D. (2005): Assessment of biological richness in different altitudinal zones in the Eastern Himalayas, Arunachal Pradesh, India. – Curr. Sci. India 88(2): 321-330.
[40] Saeeda, S., Zakir, S. (2012): Environmental awareness as a tool to promote the wise practices of wild plant resources in the Himalayas (Sudhangali-Kashmir, Pakistan). – PUTAJ Sciences 19: 139-154.
[41] Saima, S., Altaf, A., Faiz, M. H., Shahnaz, F., Wu, G. (2018): Vegetation patterns and composition of mixed coniferous forests along an altitudinal gradient in the Western Himalayas of Pakistan. – Austrian Journal of Forest Science 135: 159-180.
[42] Salama, F., El-Ghani, M. A., Gadallah, M., El-Naggar, S., Amro, A. (2016): Characteristics of desert vegetation along four transects in the arid environment of southern Egypt. – Turkish Journal of Botany 40: 59-73.
[43] Salama, F., El-Ghani, M. A., Gadalla, M., Ramadan, T., Galal, H., Gaafar, A. (2018): Vegetation patterns and floristic composition along elevation gradient on Jabal Musa, South Sinai, Egypt. – Catrina-The International Journal of Environmental Sciences 16: 41-57.
[44] Schofield, R. K., Taylor, A. W. (1955): The measurement of soil pH. – Soil Sci. Soc. Am. J. 19: 164-167.
[45] Shaheen, H., Qureshi, R. A., Shinwari, Z. K. (2011a): Structural diversity, vegetation dynamics and anthropogenic impact on lesser Himalayan sub-tropical forests of Bagh district, Kashmir. – Pak. J. Bot. 43(4): 1861-1866.
[46] Shaheen, H., Qureshi, R. A., Ullah, Z., Ahmad, T. (2011b): Anthropogenic pressure on the western Himalayan moist temperate forests of Bagh, Azad Jammu & Kashmir. – Pak. J. Bot. 43(1): 695-703.
[47] Shaheen, H., Khan, S. M., Harper, D. M., Ullah, Z., Qureshi, R. A. (2011c): Species diversity, community structure, and distribution patterns in western Himalayan alpine pastures of Kashmir, Pakistan. – Mt. Res. Dev. 31(2): 153-159.
[48] Shaheen, H., Ullah, Z., Khan, S. M., Harper, D. M. (2012): Species composition and community structure of western Himalayan moist temperate forests in Kashmir. – Forest Ecology and Management 278: 138-145.
[49] Shaheen, H., Azad, B., Mushtaq, A., Khan, R. W. A. (2016): Fuelwood consumption pattern and its impact on forest structure in Kashmir Himalayas. – Bosque 37(2): 419-424.
[50] Shaheen, H., Nasar, S., Aziz, S. Mumtaz, N., Aziz, S. (2017): Regeneration pattern in subtropical and moist temperate forest stands of Kashmir Himalayas. – Environment and Ecology Research 5(5): 340-346. DOI: 10.13189/eer.2017.050503.

http://www.aloki.hu ● ISSN 1589 1623 (Print) ● ISSN 1785 0037 (Online)
DOI: http://dx.doi.org/10.15666/aeer/1706_1547715505

[51] Shaheen, H., Riffat, A., Salika, M., Firdous, S. S. (2018): Impacts of roads and trails on floral diversity and structure of Ganga-Choti forest in Kashmir Himalayas. – Bosque 39(1): 71-79.
[52] Shannon, C. E., Weaver, W. (1949): The Mathematical Theory of Communication. – University of Illinois Press, Urbana, IL.
[53] Sher, Z., Hussain, F., Badshah, L. (2013): Phytosociology of summer vegetation of Sudan Galli Hills, District Bagh, Azad Kashmir, Pakistan. – Pak. J. Bot. 45(1): 1-9.
[54] Siddiqui, M. F., Ahmed, M. Khan, N., Khan, I. A. (2010a): A quantitative description of moist temperate conifer forests of Himalayan region of Pakistan and Azad Kashmir. – International Journal of Biology and Biotechnology 7(3): 175-185.
[55] Siddiqui, M. F., Ahmed, M., Shaukat, S. S., Khan, N. (2010b): Advanced multivariate techniques to investigate vegetation-environmental complex of pine forests of moist temperate areas of Pakistan. – Pak. J. Bot. 42(SI): 267-293.
[56] Siddiqui, M. F., Ahmed, M., Hussain, S. S., Shaukat, S. S., Khan, N. (2011): Vegetation description and current status of moist temperate coniferous forests of Himalayan and Hindukush region of Pakistan. – FUUAST J. Biol. 1(2): 99-114.
[57] Siddiqui, M. F., Shaukat, S. S., Ahmed, M., Khan, N., Khan, I. A. (2013): Vegetation-Environment relationship of conifer dominating forests of moist temperate belt of Himalayan and Hindukush regions of Pakistan. – Pak. J. Bot. 45(2): 577-592.
[58] Siddiqui, M. F., Shaukat, S. S., Ahmed, M. (2014): Topographic and edaphic control of arboreal vegetation and the distribution and growth of tree species in moist temperate areas of Himalayan and Hindukush regions of Pakistan. – Pakistan J. Bot. 46(4): 1187-1196.
[59] Stewart, R. R. (1972): An Annotated Catalogue of the Vascular Plants of West Pakistan and Kashmir. – Fakhri Printing Press, Karachi.
[60] Ter Braak, C. J. F. (1986): Canonical correspondence analysis: a new eigenvector technique for multivariate direct gradient analysis. – Ecology 67(5): 1167-1179.
[61] Ter Braak, C. J. F., Smilauer, P. (2012): Canoco 5. Windows Release (5.00). Software for Canonical Community Ordination. – Microcomputer Power, Ithaca.
[62] Tewari, V. P., Verma, R. Kn Gadow, K. (2017): Climate change effects in the Western Himalayan ecosystems of India: evidence and strategies. – Forest Ecosystems 4(1): 13.
[63] TROPICOS (2012): Flora of Pakistan. – http://www.tropicos.org/NameSearch.aspx?projectid=32 (accessed 22/9/2018).
[64] Waseem, M., Shah, M. A. U., Qureshi, R. A., Muhammad, I., Afza, R., Yousaf, S. (2006): Ethnopharmacological survey of plants used for the treatment of stomach, diabetes, and ophthalmic diseases in Sudhan Gali, Kashmir, Pakistan. – Acta Botanica Yunnanica 28(5): 535-542.
[65] Zakaria, R., Nizam, M. S., Faridah-Hanum, I. (2019): Association of tree communities with soil properties in a semi deciduous forest of Perlis, Peninsular Malaysia. – Biotropia - The Southeast Asian Journal of Tropical Biology 27: 8. DOI: 10.11598/btb.2020.27.1.1122.

http://www.aloki.hu ● ISSN 1589 1623 (Print) ● ISSN 1785 0037 (Online)
DOI: http://dx.doi.org/10.15666/aeer/1706_1547715505

COMPARISON OF DIFFERENT LACTATION CURVE MODELS TO DESCRIBE LACTATION CURVE IN AWASSI SHEEP RAISED IN TURKEY

TEKEL, N.[1] – ŞIRELI, H. D.[1] – KARATAŞ, A.[2] – VURAL, M. E.[2] – KONCAGÜL, S.[3] – TUTKUN, M.[1*]

[1]*University of Dicle, Faculty of Agriculture, Department of Animal Science, Diyarbakır, Turkey*

[2]*GAP International Agricultural Research and Training Center, Diyarbakır, Turkey*

[3]*Ankara University, Faculty of Agriculture, Department of Animal Science, Ankara, Turkey*

[*]*Corresponding author*
e-mail: tutkunmuhittin@yahoo.com; phone: +90-532-668-7313; fax: +90-412-248-5381

(Received 23rd Jul 2019; accepted 15th Nov 2019)

Abstract. The study was carried out in the International GAP Agricultural Research and Training Centre (GATEA) between the years 2010-2014 in Diyarbakır, Turkey. The aims of this study were 1) to compare 8 different models (MG, Dhanoa, Nelder, Wood, CLD, and 2nd-, 3rd- and 4th-degree polynomial) used to describe the lactation curve for Awassi sheep by using 557 completed lactation milk yield records, and 2) to identify the suitable model. In addition, the most effects of birth season, parity, and birth type on the lactation milk yield and parameters on the identified model were investigated. As a result of this study, it was determined that the 4th-degree polynomial (POL4) model is the most suitable. In addition, it was found that all the factors, excluding birth type, have significant effects on the model parameters and lactation milk yield ($P < 0.05$).
Keywords: *sheep, milk yield, lactation curve,mathematical model, curve fitting*

Introduction

In Turkey, seventeen percent of the total sheep population is raised in the Southeastern Anatolia Region of Turkey (Anonymous, 2017). The Awassi sheep is the prevalent in the region due to high milk yield. However, the milk yield of Awassi shows wide variation depending on the level of breeding in milk yield, age and weight at birth, lambing month, birth type, production system, and lactation period. Average lactation milk yield of the sheep raised in Southeastern Anatolia is about 80-100 kg/lac (Kaymakçı, 2006), and some breeding studies must be performed in that region in order to benefit from the higher milk yield potential of the Awassi sheep.

In the case of milk production, the appropriate description of the lactation curve is a useful tool in management decision making and in design genetic improvement strategies for the group of animals evaluated (Vázquez-Peláez et al., 2014). A lactation curve is defined as the variation of milk yield depending on time, representing of the milk yield with respect to time using a figure, or the milk yield shown in a figure after lambing (Keskin, 2006; Koncagül et al., 2012). Lactation curves can be beneficial in terms of biological and economic efficiency, selection, monitoring of animal health, ration formulation, and determination of type of care and feeding methods (Wood, 1967; Ruiz et al., 2000; Dağ et al., 2005; Koncagül et al., 2012). Moreover, it is possible to use lactation curve models to estimate the total lactation milk yield from partial lactations and to use the peak yield and persistency values as selection criteria in developing a model for the improvement of milk yield (Wiggans and Gangler, 1999;

http://www.aloki.hu ● ISSN 1589 1623 (Print) ●ISSN1785 0037 (Online)
DOI: http://dx.doi.org/10.15666/aeer/1706_1550715517

Takma et al., 2009). The shape of the lactation curve and environmental factors that affect the curve can be used to determine the biological affectivity (Grossman and Koops, 1988). The environmental factors that affect the milk yield and lactation curve have been determined by many researchers, and different mathematical models have been proposed for determining the lactation milk yield in dairy cattle (Koncagül and Yazgan, 2011). Most of these models developed for dairy cattle can also be used to identify the lactation curves of sheep and goats (Fernandez et al., 2002; Koncagül et al., 2012; Angeles-Hernandez et al., 2013). Among them, Wood's model (1967) has been the most widely used (Nezamidoust et al., 2013; Angeles-Hernandez et al., 2013)

Lactation curve studies have conducted rarely in Awassi sheep. The aims of this study were to compare 8 different models (MG, Dhanoa, Nelder, Wood, CLD, POL2, POL3, and POL4) used to define the lactation curve for the Awassi breed and to identify the suitable models. In addition, the effects of birth season, parity, and birth types on lactation milk yield and model parameters were investigated.

Material and Methods

Data

The experiment was conducted in the International GAP Agricultural Research and Training Centre (GATEA) between the years 2010-2014 in Diyarbakır, Turkey (37°57'41 N and 40°13'54 E, 650 m asl) (*Fig. 1*). Study area has a semi-arid climate and is very hot during the summer months. The temperature rises above 40°C in summer. Rainfall is almost non-existent during the summer months. Winters are cool and wet. Spring and automn are warm and wet as well.

Figure 1. *Study location map (https://www.express.co.uk)*

The animal material consisted of 557 Awassi sheep raised in training center above mentioned. Semi-intensive care and feeding was applied in addition to 10 hours of pasture time each day, and supplementary feeding was provided following pasture. The milk controls were started 15 days after the first lambing occurred in the herd, and the amount of milk was measured on a scale with 50 g of precision and repeated every 14 days interval until the end of lactation. The test day of the milking were made at 14 days intervals (Gürsu and Aygün, 2014). Lactation milk yield (LMY) was calculated using the Fleischmann method (Barillet et al., 1992).

http://www.aloki.hu ● ISSN 1589 1623 (Print) ●ISSN1785 0037 (Online)
DOI: http://dx.doi.org/10.15666/aeer/1706_1550715517

Data Analysis

The models used in this study were chosen from among the models applied previously to describe lactation curves of sheep. For the analyses of the lactation, the following models were used.

MG model (Morant and Gnanasakthy, 1989):

$$y_t = e^{(a - bt_1 - ct_1^2 - d/t)} \quad \text{(Eq.1)}$$

Nel model (Nelder, 1966):

$$y_t = t/a + bt + ct^2 \quad \text{(Eq.2)}$$

Wood model (Wood, 1967):

$$y_t = at^b e^{-ct} \quad \text{(Eq.3)}$$

CLD model (Cobby and Le Du, 1978):

$$y_t = a - bt - ae^{-ct} \quad \text{(Eq.4)}$$

Dhanoa model (1981):

$$y_t = at^{bc} e^{-ct} \quad \text{(Eq.5)}$$

Three polynomials: the second degree (POL2):

$$y_t = a + bt + ct^2 \quad \text{(Eq.6)}$$

The third degree (POL3):

$$y_t = a + bt + ct^2 + dt^3 \quad \text{(Eq.7)}$$

The fourth degree (POL4):

$$y_t = a + bt + ct^2 + dt^3 + et^4 \quad \text{(Eq.8)}$$

The parameters of the models defined above were as follows: yt is the milk yield on the tth day after lambing; a, b, c, d and e are the model parameters; t is the tth day after lambing; and t1 = (t –lactation period / 2) / 100. Starting values for the parameters of the models mentioned in "a, b, c d and e" were taken from various analyses conducted by many researcher such as Dağ et al. (2005).

Analyses were performed using the Proc Nlin procedure in the SAS program (SAS, 2000). For the comparison of the models, the coefficient of determination (R^2), mean square error (RMSE), and correlation coefficient (r) between observed and estimated

http://www.aloki.hu ● ISSN 1589 1623 (Print) ●ISSN1785 0037 (Online)
DOI: http://dx.doi.org/10.15666/aeer/1706_1550715517

lactation curves were considered as the comparison criteria. After identifying the best mathematical model description of the lactation curve, the estimated lactation milk yield (ELMY) for each sheep was calculated using the parameters of the identified model. Then, the ELMY was compared with the LMY calculated by the Fleischmann method (Barillet et al., 1992) described below:

$$LSV = S_1 x A_1 + \sum_{i=2}^{n} \frac{S_i + S_{i-1}}{2} A_i + S_n x15 \quad \text{(Eq.9)}$$

where LMY is lactation milk yield, Ai is the number of days between lambing and first milk control day, A_I is the number of days between the ith and (i-1)th control milking, Si is the amount of milk in the ith control milking day, and 15 is the number of days assumed to have passed between the last day of control milking and the end of the lactation. The values of LMY and ELMY were adjusted to 180 days of lactation length.

The correlation coefficients between LMY and ELMY were calculated by the Proc Corr procedure in SAS (2000).

In order to examine the effects of environmental factors on the model parameters, LMY and ELMY, the linear model given below was used in the Proc Glm procedure in SAS (2000):

$$Yijkl = \mu + Pi + LSj + BTk + eijkl \quad \text{(Eq.10)}$$

where Yijklm is the model parameters, LMY or ELMY, μ refers to the average value for the trait being analyzed, Pi is the effect of the ith parity, LSj is the effect of the jth lambing season, BTk is the effect of the kth birth type, and eijkl refers to the random residual. Differences among the means of the environmental factors were tested using the Tukey-Cramer test option.

Results

Model Selection

Fit statistics of the mathematical model are given in *Table 1*. In terms of mean square error (MSE), the highest value was observed in the Dhanoa model, followed by the Wood, CLD, MG, and Nelder models, respectively. It has also been determined that MSEs obtained from polynomial models were not different from zero. The best performance in terms of determination coefficient (R^2) belonged to the polynomial and Nelder models. POL4 has the highest R^2 value (0.99), followed by the POL3, POL2, and Nelder models (0.98, 0.97, and 0.93, respectively). R^2 values of the other models were below 0.85. A similar situation was also observed in terms of the correlation coefficient (r) between observed and estimated lactation curves. POL4 (0.90) had the highest value in terms of correlation coefficient, followed by the POL3, POL2, and CLD models (0.84, 0.74, and 0.69, respectively). The correlation coefficients obtained from the other models were found to have lower values.

Considering the MSE, R^2, and r parameters all together, it was concluded that the best model to properly identify the lactation curves of the Awassi sheep breed was POL4. Therefore, the characteristics of lactation curve and environmental factors affecting the LMY were investigated by taking into account the POL4 model.

http://www.aloki.hu ● ISSN 1589 1623 (Print) ●ISSN1785 0037 (Online)
DOI: http://dx.doi.org/10.15666/aeer/1706_1550715517

Table 1. *Comparison criteriaof models used fordescibing lactation curves of Awassi sheep*

Model	MSE	R^2	r
MG	150±9.333	0.06±0.126	0.12±0.022
Dhanoa	532.37±9.996	0.35±0.019	0.12±0.025
Nelder	39.68±5.197	0.93±0.003	0.51±0.018
Wood	530.52±9.969	0.35±0.019	0.13±0.026
CLD	151.76±6.584	0.84±0.009	0.69±0.011
POL2	0.00±3.192	0.97±0.001	0.74±0.009
POL3	0.00±2.574	0.98±0.001	0.84±0.007
POL4	0.00±1.989	0.99±0.001	0.90±0.005

R^2: coefficient of determination, MSE: Mean square eroor, r: correlation coefficient between observed and estimated lactaion curve, MG: Morantand Gnanasakthy model, Dhanoa: Dhanoa model, Nelder: Nelder model, Wood: Wood model, CLD: Cobby and Le Du model, POL2: 2nd degree polynomial model, POL3: 3rd degree polynomial model, POL4: 4rd degree polynomial model

Model Parameters

The model parameters, standard deviations and correlations between model parameters are given in *Table 2*. Accordingly, parameter (a) refers to the milk yield when standardized time was equal to zero. Standardized time is in the range between -1 and +1; when time is at 0, it has been accepted as the middle of lactation (midpoint). Therefore, parameter (a) represents the estimated milk yield in the middle of lactation. Parameters (b) and (c) refer to the increases and decreases in milk yield until the midpoint of lactation, and parameters (d) and (e) refer to the increases and decreases in milk yield after the midpoint of lactation.

Table 2. *Parameters (±SE) of POL4 function, LMY means (±SE) (kg), and correlation coefficients between model parameters*

Factors	N	a	b	c	d	e	LMY
Parity							
1	141	628±139.6^{a}	-470±168.5	326±87.4^{a}	-49±18.6^{a}	1.0±1.35^{a}	109±5.4^{a}
2	132	936±137.0^{ab}	-554±165.4	363±85.8^{a}	-58±18.2^{a}	1.6±1.32^{a}	129±5.3^{b}
3	103	1059±139.4^{b}	-218±168.2	96±87.2^{b}	-6±18.6^{b}	-3.1±1.35^{b}	139±5.4^{b}
4	94	1221±140.2^{b}	-606±169.2	311±87.7^{ab}	-41±18.7^{ab}	0.2±1.35^{ab}	132±5.4^{b}
5	51	846±170.5^{ab}	-510±205.8	298±106.7^{ab}	-39±22.7^{ab}	0.1±1.65^{ab}	108±6.6^{a}
6≤	36	986±191.2^{ab}	-691±230.8	426±119.7^{ab}	-73±25.5^{a}	2.9±1.85^{a}	105±7.4^{a}
Lambing Season							
December-January	481	916±125.2	-464±151.1	265±78.4	-32±16.7	-0.3±1.21	126±4.9^{a}
February-March	76	976±119.7	-552±144.4	342±74.9	-53±15.9	1.2±1.16	115±4.6^{b}
Birth Type							
Single	283	923±106.3	-446±128.3	271±66.5	-37±14.2	0.1±1.03	120±4.1
Twin	274	969±148.3	-570±178.9	336±92.8	-48±19.7	0.8±1.43	121±5.8
Correlation							
A			-0.732**	0.414**	-0.224**	0.125**	0.235**
B				-0.895**	0.751**	-0.637**	0.065
C					-0.962**	0.893**	-0.051
D						-0.980**	0.040
E							-0.035

a, b, c, d, e: model parameters of POL4; LMY: lactation milk yield corrected for lactation length

http://www.aloki.hu ● ISSN 1589 1623 (Print) ●ISSN1785 0037 (Online)
DOI: http://dx.doi.org/10.15666/aeer/1706_1550715517

Relationship Among Parameters

The correlation coefficients among model parameters are given in *Table 2*. As expected from polynomial functions, the correlations between sequential parameters (a-b, b-c, c-d, and d-e) have taken negative and increasing values, whereas the correlations between other parameters (a-c, b-d, and c-e) have taken positive and increasing values, respectively. Because linear interpolation is the basis of determination of LMY using the Fleischmann method, the possibility of errors for estimating milk production between two consecutive control days would increase as the interval between two consecutive milk control days increases. However, there were 14 days between the two milk control days in our study; therefore, LMY was assumed to be estimated closer to the actual amount of milk production.

Effects of Environmental Factors

The mean and standard errors of LMY and model parameters based on environmental factors are given in *Table 3*. All factors except birth type had significant effects with varying degrees on the model parameters and LMY. The differences between average values of 1st, 5th and 6th lactations and 2nd, 3rd and 4th lactations have been found significant ($P < 0.05$). The difference between milk yield of the sheep lambing in the December-January season and the February-March season was found significant ($P < 0.05$). The type of birth did not have any significant effect on the LMY.

Table 3. *Descriptive statistics of LL, LMY, ADMY and LMY180 day*

	N	Mean	Std.Err.	Min	Max.	CV%
LL	1077	150.3	0.77	100.0	213.0	16.9
LMY	1077	123.9	1.23	40.9	268.8	32.6
ADMY	1077	819.7	6.60	361.7	1551.6	26.4
LMY180	1077	147.6	1.19	65.1	279.3	26.4

N: Number of observation, Std.Err.: Standard error, Min: minimum, Max: maximum, CV%: coefficient of variation, LL: Lactation length, LMY: Lactation milk yield, ADMY: Avarege Daily milk yield

In this study, all factors except type of birth had significant effects with varying degrees on the model parameters and LMY (*Table 2*). The differences between average values of 1st, 5th, and 6th lactations and 2nd, 3rd, and 4th lactations were found statistically significant ($P < 0.05$). As indicated by Mavrogenis (1996), this situation was to be expected because the milk yield of the Awassi sheep increases in the first 4 parities and has a tendency of decreasing in the following parities. The difference between milk yield of the sheep lambing in December-January season and February-March season was found statistically significant ($P < 0.05$). This can be explained by the fact that the pasture conditions in the December-January season are better than those of other seasons, and thus sheep can benefit from pastures more than others lambing in other seasons. These pastures lose their efficiency after April due to the rapid warming of the weather in the area where this study was conducted.

The differences between means of 1st lactation and 3rd and 4th lactations have been found statistically significant ($P < 0.05$). This shows that the peak yield values of 1st lactation sheep were lower than the peak yield values of 3rd and 4th lactation sheep in terms of parameter (a). The effect of lambing month on parameter (a) was found insignificant, which shows that the peak yield is not affected by the lambing month. The

http://www.aloki.hu ● ISSN 1589 1623 (Print) ●ISSN1785 0037 (Online)
DOI: http://dx.doi.org/10.15666/aeer/1706_1550715517

differences between levels of birth types in terms of parameter (a), when the time is equal to zero, were found insignificant.

Descriptive statistics of the research data set in lactation milk yield has shown in *Table 3*.

The effect of parity on the parameter (a) was insignificant, whereas its effect on parameters c, d, and e was found to be statistically significant ($P < 0.05$). The differences between 1st, 2nd, and 3rd lactations in terms of upward oscillation speed (parameter c) before the peak yield were found statistically significant ($P < 0.05$). In addition, the differences between 1st, 2nd, and 6th and 3rd lactations in terms of upward and downward oscillation speeds after the peak yield were found statistically significant ($P < 0.05$) (*Fig. 2*).

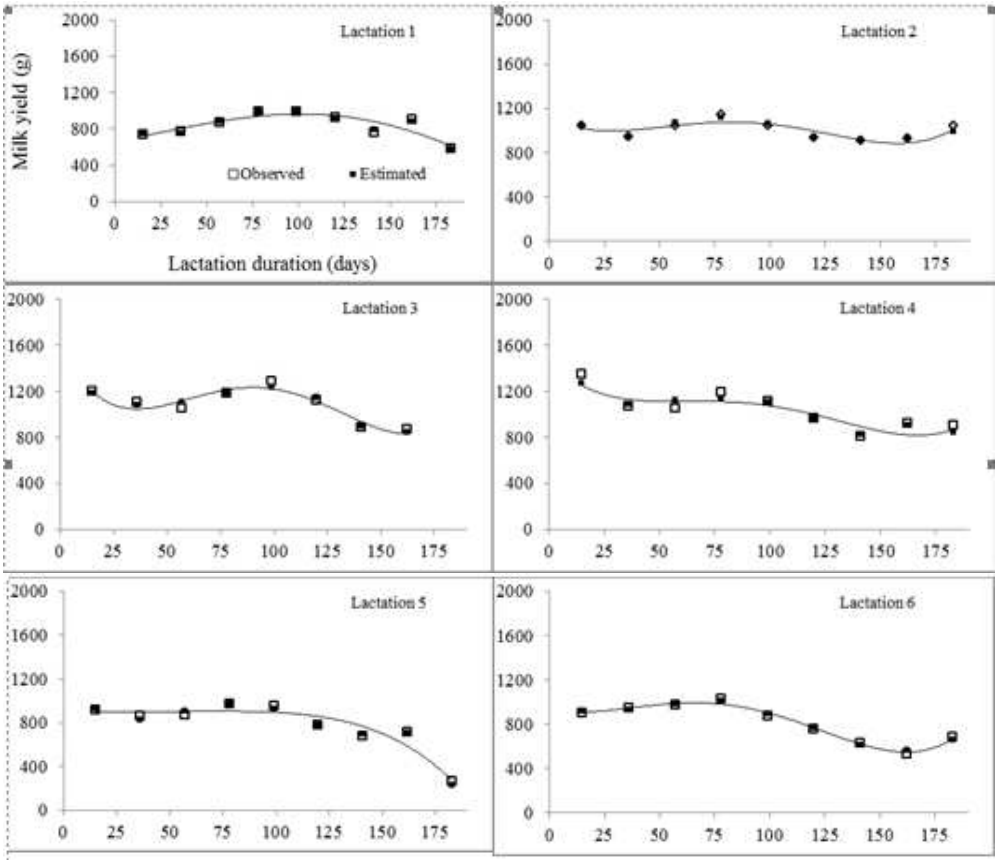

Figure 2. *Milk yield vs. lactation duration in different lactation stages*

It was found in this study that the best fit model identifying the lactation curve is the POL4 model. Ruiz et al. (2000) reported that in the case of a higher positive correlation between parameters of the mathematical model identifying the lactation curve, the lactation curve model cannot be identified properly. However, in this study, as can be seen in *Table 2*, because there is a negative correlation between 4th-degree polynomial model parameters in general, this model sufficiently identified the lactation curve of the Awassi sheep breed. Moreover, the highest correlation between LMY and ELMY (0.90) was obtained when the POL4 model was applied, and this indicates that the POL4 model can be used for LMY estimations of the Awassi breed.

http://www.aloki.hu ● ISSN 1589 1623 (Print) ●ISSN1785 0037 (Online)
DOI: http://dx.doi.org/10.15666/aeer/1706_1550715517

Discussion

The lactation milk yields found in this research are consistent with the values reported by Dağ et al. (2005), Şeker et al. (2000), and Tekel et al. (2007). In addition, the lactation curve *(Fig. 3)* shows consistency with the lactation curve given by Kaymakçı (2006). As can be seen in *Fig. 3*, there was an increase in the first 2 months of lactation, and the peak value was reached; then, a gradual decline was observed. As shown in *Fig. 3*, the decrease in milk yield accelerates after the first 100th day of lactation approximetly. These changes in ambient temperature and pasture conditions are thought to have an effect on this situation. As a matter of fact, the climatic and pasture conditions in the first 3 months of lactation constitute a suitable environment for milk production of Awassi ewes. However, in the later stages of lactation, the air temperature increases and the pasture conditions decrease significantly due to the temperature increase.

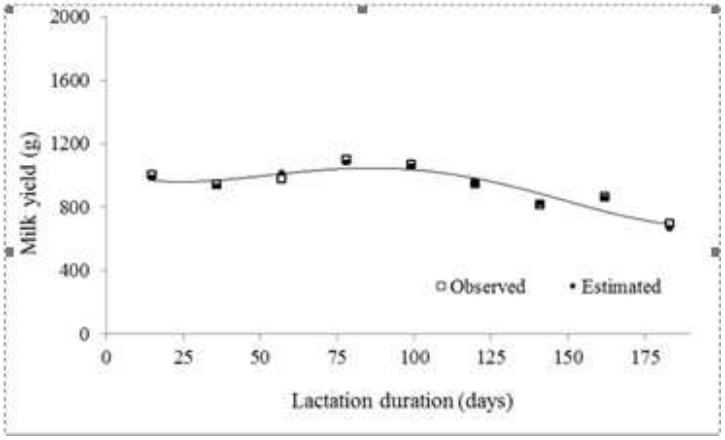

Figure 3. *An overall view of the lactation course in Awassi sheep*

All of the factors considered in this study, except for the type of birth, had significant effects on model parameters or LMY at various degrees. These results were similar to other studies on the milk yield characteristics of Awassi sheep (Özbey and Akcan, 2000; Reiad et al., 2010; Üstüner and Ogan, 2013). Differences between 1th, 5th, 6th lactations and 2nd, 3rd, 4th lactations were statistically significant ($P < 0.05$) in terms of LMY. As Mavrogenis (1996) states this sitiuation is expected due to an increase in milk yield in the first 4th lactation and later tendency to decrease in Awassi sheep. The difference between the milk yield of sheep gave birth in December-January and February-March season were statistically significant ($P < 0.05$). This can be explained by the fact that those who give birth in December-January season have the opportunity to benefit from the pasture for a longer period when the pasture conditions are good. Because the pastures in the region lose their qualities after April due to the rapid heating of the weather.

It has been reported that if there is a high correlation between the parameters of a mathematical model defining the lactation curve, the model used will not define the lactation exactly (Ruiz et al., 2000). When polynomial functions are used in this research, the correlations between sequential parameters (a-b, b-c, c-d, and d-e) have negative and increasing values, whereas the correlations between other parameters (a-c, b-d, and c-e) have positive and increasing values respectively. Because linear

http://www.aloki.hu ● ISSN 1589 1623 (Print) ●ISSN1785 0037 (Online)
DOI: http://dx.doi.org/10.15666/aeer/1706_1550715517

interpolation is the basis of determination of LMY using the Fleischmann method, the possibility of errors for estimating milk production between two consecutive control days would increase as the interval between two consecutive milk control days increases. However, the POL4 model showed the best performance in terms of comparison criteria due to high correlation between LMY and ELMY (0.90) was obtained. This indicates that the POL4 model can be used for LMY estimations of the Awassi breed.

Lactation milk yield is determined by genotype and environmental conditions in addition to other quantitative properties. Therefore, the suitability of lactation curve models used by researchers may vary depending on the breed and species. Accordingly, the most appropriate model defining the lactation curve differ from breeds to breeds in different environmental conditions (Ünal et al., 2007). It has been reported that the Pollott Additive and Fractional Polynomial models are the best ones for Lacaune breed (Elvira et al., 2013). In addition, the Wilmink model is the most suitable one, followed by Wood and Dhanoa models, for studies conducted in Akkaraman, Kıvırcık-Akkaraman, and Sakız-Akkaraman crossbred sheep (Ünal et al., 2007). It has been determined that Wood, Wilmink, POL2 and POL3 models can be used to estimate milk yield in F_1 cross-breeds (Angeles-Hernandez et al., 2013). It has been determined that the Wood model can be used to estimate lactation milk yield in organically raised sheep such as East Friesian, Pelibuey, Suffolk and Black Belly (Angeles-Hernandez et al., 2014). On the other hand, in a study conducted on Awassi sheep, the most suitable model was found to be the Cubic model (Dağ et al., 2005), whereas the Wood model was found to be the best one in another study (Yıldız, 1997). Furthermore Wood, Cobby and Le Du, Dhanoa, and Wilmink models have been found equally suitable for studies conducted on the Awassi sheep breed.

Conclusions

Using of the best suitable lactation model will affect the efficiency and profitability of production. In addition, suitable model provide increasing of the genotypic gain in breeding program. The POL4 model used in the study give better results compared to the other 7 models. The value of ELMY calculated by POL4 was very close to the value of LMY calculated by using the Fleischmann method ($r = 0.90$). This result shows that the POL4 model can be used for LMY estimations of the Awassi sheep breed.

Further researchers are needed to understand different predictive power of models. It is important that different models must be tested by different researchers due to Awassi breed raised in various countries and under different envoirmental conditions.

REFERENCES

[1] Angeles-Hernandez, J. C., Albarran-Portillo, B., Gomez Gonzalez, A. V., Pescador Salas, N., Gonzalez-Ronquillo, M. (2013): Comparision of Mathemathical models applied to F1 dairy sheep lactations in organic farm and envoirmental factors affecting lactation curve parameter. – Asian Australas. J. Anim. Sci. 26(8): 1119-1126.

[2] Angeles-Hernandez, J. C., Ortega, O. C., Albarran-Portillo, B., Moltaldo, H. H., Gonzalez-Ronquillo, M. (2014): Application of the Wood model to analyse lactation curves of organic dairy sheep farming. – Animal Pruduction Science 54: 1609-1614.

http://www.aloki.hu ● ISSN 1589 1623 (Print) ●ISSN1785 0037 (Online)
DOI: http://dx.doi.org/10.15666/aeer/1706_1550715517

[3] Anonymous (2017): Livestock Data. – Statistical Institution of Turkey. Available on10.12.2018 www.tuik.gov.tr. (in Turkish).
[4] Barillet, F., Astruc, J. M., de Brauwer, P., Casu, S., Fabbri, G., Feddersen, E., Frangos, K., Gabina, D., Gama, T. J., Sanna, S. R. (1992): Int. Committee for animal recording guidelines. – International regulations for milk recording in sheep. pp.15, Ins, de Elevage, Paris, France.
[5] Cobby, J. N., Ledu, Y. L. P. (1978): On fitting lactation data. – Anim. Prod. 26: 127-133.
[6] Dağ, B., Keskin, I., Mikailsoy, F. (2005): Application of different model to the lactation curves of unimproved Awassi Ewes in Turkey. – South African Journal of Animal Science 35(4): 238-243.
[7] Dhanoa, M. S. (1981): A note on an alternative form of the lactation model of Wood. – Animal Production 32: 349.
[8] Elvira, L., Hernandez, F., Cuesta, P., Cano, S., Gonzalez-Martin, J. V., Astiz, S. (2012): Accurate Mathematical models to describe the lactation curve of Lacune dairy sheep under intensive management. – Animal 7(6): 1044-1052.
[9] Elvira, L., Hernandez, F., Cuesta, P., Cano, S., Gonzalez-Martin, J. V., Astiz, S. (2013): Factors affecting the lactation curves of intensive lymanaged sheep based on a clustering approach. – Journal of Dairy Research 80: 439-447.
[10] Fernandez, C., Sanchez, A., Garces, C. (2002): Modeling the lactation curve for test-day milk yield in Murciano-Granadina goats. – Small Rum Res 46: 29-41.
[11] Grossman, M., Koops, W. J. (1988): Multiphasic analysis of lactation curves in dairy cattle. – J. Dairy Sci 71: 1598-1608.
[12] Gürsu, G., Aygün, T. (2014): Some characteristics of milk yield in Awassi ewes maintained at village conditions. – Journal of Advanced Agricultural Technologies 1:19-23.
[13] Kaymakçı, M. (2006): Sheep Breeding. – 2. Press, Meta Pressing, Bornova-İzmir, Turkey. (in Turkish).
[14] Keskin, I., Dağ, B. (2006): Comparison of different mathematical models for describing the complete lactation of Akkaraman ewes in Turkey. – Asian-Aust. J. Anim. Sci. 19: 1551-1555.
[15] Koncagül, S., Yazgan, K. (2011): Comparison of spline and legendre polynomial functions with conventional methods for describing lactation curves of holstein dairy cows. – Hay. Üret. Derg 52(1): 17-23.
[16] Koncagül, S., Daşkıran, İ., Bingöl, M. (2012): Factors affecting lactation milk yield and lactation curve of norduz sheep in farmer condition. – Kafkas Univ. Vet. Fak. Derg. 18(4): 677-684.
[17] Mavrogenis, A. P. (1996): Estimates of environmental and genetic parameters influencing milk and growth traits of Awassi Sheep in Cyprus. – Small Rum. Res. 20: 141-146.
[18] Morant, S. V., Gnanasakthy, A. (1989): A new approach to the mathematical formulation of lactation curves. – Anim. Prod. 49: 151-162.
[19] Nelder, J. A. (1966): Inverse polynomials, a useful group of multi-factor response functions. – Biometrics 22: 128-141.
[20] Nezamidoust, M., Kominakis, A., Safari, A. (2013): Use of Wood's Model to analyse the effects of milking methods on lactation curve in sheep. – Small Rum. Research 113: 195-204.
[21] Özbey, O., Akcan, A. (2000): Production performance of Akkaraman, Morkaman and Awasi sheep under semi-intensive conditions I. Fertility and milk production characteristics. – Vet. Bil. Derg. 16(1): 109-120.
[22] Reiad, K., Al-Azzawi, W., Al-Najjar, K., Masri, Y., Salhab, S., Abdo, Z., El-Herek, İ., Omed, H., Saatçı, M. (2010): Factorin fluencing the milk production of Awassi sheep in a flockwiththe ve selectedlines at the Agricultural Scientific Research Center in Salamieh/Syria. – Kafkas Univ. Vet. Fak. Derg. 16(3): 425-430.

http://www.aloki.hu ● ISSN 1589 1623 (Print) ●ISSN1785 0037 (Online)
DOI: http://dx.doi.org/10.15666/aeer/1706_1550715517

[23] Ruiz, R., Oregui, L. M., Herrerot, M. (2000): Comparison of models for describing the lactation curve of latxa sheep and an analysis of factors affecting milk yield. – Journal of Dairy Science 83(11): 2709-2719.
[24] SAS. (2000): SAS/STAT SAS Inst. Inc. – Cary, NC, USA.
[25] Şeker, İ., Kul, S., Bayraktar, M. (2000): Linear udder traits and relationshiphs between these and milk yield in Awassi and East-Friesian x Awassi crossbreed (F1) ewes. – Lalahan Hay. Araşt. Enst. Derg. 40(2): 45-55.
[26] Takma, Ç., Akbaş, Y., Taşkın, T. (2009): Modeling lactation curves of Saanen and Bornova Goats. – Asian Journal of Veterinary Advances 4(3): 122-129.
[27] Tekel, N., Şireli, H. D., Eliçin, M. (2007): A research on the repeatability of milk yield in Awassi sheep. – Harran. Üniversitesi Ziraat Fakültesi Dergisi 11(1/2): 49-53.
[28] Ünal, N., Orman, M. N., Çolak, C., Atasoy, F., Mundan, D., Aytaç, M. (2007): Comparison of various models for lactation curves of Akkaraman sheep and its crossbreed (Chios x Akkaraman F1 and Kıvırcık x Akkaraman F1) ewes. – Lalahan Hay. Arast. Enst. Der. 47(2): 7-13.
[29] Üstüner, H., Ogan, M. M. (2013): Main productive performance of Awassi sheep in the Central Anatolian Region of Turkey. – Turkish Journal of Veterinary and Animal Science 37(3): 271-276.
[30] Vázquez-Peláez, C. G., García-Muñiz, J. G., Lopez-Villalobos, N. (2014): Empirical models used for lactation curve analysis in the Chiapas sheep breed using random regression models. – International Journal of Livestock Production 5(3): 55-64.
[31] Wiggans, G. R., Gangler, N. (1999): Strategies for combing test-day evaluation into on index for lactation performance. – J. Dairy Sci 82: 102.
[32] Wood, P. D. P. (1967): Algebraic model of the lactation curve in cattle. – Nature (tond.) 216: 164-165.
[33] Yıldız, A. (1997): Lactation curve of Awassi sheep and affecting factors in the State of Ceylanpınar Farm. – PhD Thesis, Fırat Üniv. Sağlık Bil. Enst., Elazığ, Turkey. (in Turkish).

http://www.aloki.hu ● ISSN 1589 1623 (Print) ●ISSN1785 0037 (Online)
DOI: http://dx.doi.org/10.15666/aeer/1706_1550715517

THE EFFECTS OF EXOGENOUS AMINO ACID ON GROWTH, IONIC HOMEOSTASIS, BIOCHEMICAL COMPOSITION AND ANTIOXIDATIVE ACTIVITY OF GUAR (*CYAMOPSIS TETRAGONOLOBA* (L.) TAUB.) SEEDLINGS

KUSVURAN, A.[1*] – KAYTEZ, I. A.[2] – YILMAZ, U.[3] – KUSVURAN, S.[1]

[1]*Cankiri Karatekin University, Kizilirmak Vocational High Scholl, Cankiri, Turkey (phone: +90-376-324-1018; fax: +90-376-324-1048)*

[2]*Cankiri Karatekin University, Institute of Natural and Applied Science, Cankiri, Turkey (phone: +90-376-324-1018; fax: +90-376-324-1048)*

[3]*Cankiri Karatekin University, Faculty of Forestry, Cankiri, Turkey (phone: +90-376-212-2757; fax: +90-376-213-6983)*

[*]*Corresponding author*
e-mail: akusvuran@gmail.com; phone: +90-376-324-1018; fax: +90-376-324-1048

(Received 1st Aug 2019; accepted 31st Oct 2019)

Abstract. Amino acids, being the primary products of inorganic assimilation and precursors of proteins, play an essential role in plant metabolism. The objective of this study was to compare guar plants which were grown under salt-stress conditions (150 mM NaCl), in terms of the effect of different amino acid treatments (300, 600, 1200, and 1800 mg L^{-1} amino acid) on physiological, morphological, and enzymatic activity. Amino acid (AA) applications significantly increased fresh and dry weight, relative water content, photosynthetic pigments, total phenolic, flavonoid and free amino acid contents, K^+ and Ca^{++} ion concentration, ascorbate peroxidase (APX), catalase (CAT), glutathione reductase (GR), and superoxide dismutase (SOD) activity of guar plants compared to the salt stress treatment the ones under no AA treatment. According to the results, the malondialdehyde (MDA) content, Na^+ and Cl^- ion contents were significantly decreased. Hence, the results support the application of the amino acid in 600 mg L^{-1} doses in order to increase the defense system of the guar plant, enabling it to tolerate the negative effects induced by salinity.
Keywords: *biostimulant, cluster bean, enzyme activity, ion regulation, oxidative stress, seconder metabolite*

Introduction

Salinity is a significant abiotic stress factor that threatens agriculture in both arid and semiarid environments, affecting over 20% of the world's irrigated land (Wu et al., 2017). Salt stress induces changes in a plant's biochemical, physiological, and morphological responses resulting in reduced growth, yield, biomass, and quality of crop plants.

Salinity in growth mediums have an unfavorable impact on the growth of plants and their development, which could presumably be the result of the presence of salt in the soil, thus reducing the plant's water uptake (low osmotic potential), resulting in high levels of salt entering the plant via transpiration, which causes damage to the transpiring leaf cells (specific ion toxity) (Parihar et al., 2015; Rady et al., 2018).

Salt stress, like other environmental stresses, induces the accumulation of reactive oxygen species (ROS) such as hydrogen peroxide (H_2O_2), superoxide (O_2^-), and hydroxyl radicals (OH-) (Sekmen et al., 2013). Increased ROS concentration causes

http://www.aloki.hu ● ISSN 1589 1623 (Print) ● ISSN 1785 0037 (Online)
DOI: http://dx.doi.org/10.15666/aeer/1706_1551915530

oxidative damage for plant tissues in various ways (e.g., decrease in chlorophyll content, damage to cell membrane, protein oxidation, strand breaks in nucleic acids, etc.), leading finally to cell death. The degree of stress injuries to plants is reflected by membrane permeability. Furthermore, ROS levels above threshold cause lipid peroxidation (LPO) in both cellular and organelle membranes, which not only directly affects cellular functioning, but also aggravates the oxidation stress through the production of lipid-derived radicals (Patel et al., 2013). In response to salinity, plants have developed a series of enzymatic (e.g., super oxide dismutase (SOD), catalase (CAT), ascorbate peroksidase (APX), glutathione reductase (GR) and several peroxidases) and non-enzymatic (ascorbate, carotenoids, flavonoids and other phenolic compounds etc.) detoxification systems to counteract reactive oxygen species, and protect cells from oxidative damage (Taibi et al., 2016). SOD converts O_2^- to H_2O_2, which is detoxified to water and oxygen by CAT, POX, and APX. SOD is localized in almost all cellular compartments and the water–water cycle in chloroplasts. The components of the ascorbate–glutathione cycle are localized in chloroplasts, cytosol, mitochondria, and apoplast, while both glutathione peroxidase (GPX) and CAT are localized in peroxisomes (Sekmen et al*.,* 2013).

Plants have developed various approaches to reduce the negative effects resulting from abiotic stressors, several of which have been related to the metabolism of amino acids (Batista Silva et al., 2019). They have improved the ability to physiologically and/or behaviorally respond and adapt to environmental stressors through organic solute accumulation or ion movement control, which enables the increase of solute concentrations at the intracellular level. Osmotic adjustment involves the accumulation of low molecular weight compounds in the cytosol, compatible osmolytes, which do not interfere with normal biochemical reactions (De Freitas et al., 2018) and these osmolytes that do not interfere with plant metabolism even at high concentrations and may also act as ROS scavengers (Batista Silva et al., 2019). Amino acids are organic nitrogenous compounds that are the building blocks in the synthesis of proteins (Sarojnee et al., 2009). El-Din et al. (2005) reported that, in higher plants, amino acids have the ability to behave like growth factors, because they are protein synthesis building blocks, and may be enzymes significant for metabolic activity. These components are particularly important for cell growth stimulation, because they behave like buffers that aid in maintaining an appropriate pH value in plant cells. Moreover, because they comprise both acidic and basic groups, they are able to aid in ammonia removal within the cell (Nahed et al., 2010). Furthermore, amino acids assist in the synthesis of various organic compounds, including alkaloids, amines, enzymes, terpenoids, proteins, purines and pyrimidines, vitamins, etc. (Talaat et al., 2014).

Cluster bean, or Guar, has gained an important commercial status as a result of its gum and is now the most significant product exported in the farming sector, due to it being a cash crop that is highly-valued in both arid and semi-arid areas because of its tolerance to drought and vast array of uses (Pathak, 2015).

It has been reported that amino acids that were applied exogenously to plants exposed to abiotic stressors brought about a preventive or recovery effect. Therefore the following two hypotheses were tested: 1) the effect of AA concentrations on the growth, and 2) how AA reveal a change in biochemical composition, ion regulation and oxidative status in guar seedlings.

http://www.aloki.hu ● ISSN 1589 1623 (Print) ● ISSN 1785 0037 (Online)
DOI: http://dx.doi.org/10.15666/aeer/1706_1551915530

Materials and methods

The study was conducted at an experimental site of Cankiri Karatekin University in Turkey. For this experiment, a mixture of peat:perlite substrate (2:1) was used to germinate the guar seeds, which were then housed in a greenhouse kept at day/night temperatures of 26 ± 2°C and 18 ± 2°C, and a relative humidity of 65% ± 5. Growth chamber and nutrient solution (following that of Dasgan and Koc, 2009) irrigation was used to grow the plants. Each pot contained 5 plants and each of the 3 replications also every treatment included 5 pots (total 90 pots). According to our previous studies were determined NaCl doses (data not shown). Starting from 39 days of after sowing (DAS), the saline treatment began with 50 mM NaCl on the first day and was increased by 50 mM NaCl each day until the 2th day, where it reached 150 mM NaCl. For this experiment, the amount of water applied was calculated based on the ratio of water drained: water applied (Schubert and Lauchli, 1990). In the control plant were not exposed to saline stress. Amino acid treatments were added in the irrigation water with salinity treatments. The commercial product "Amino gold" was used as a source of amino acids and it contains 29% free L. amino acids, 70% total organic matter, 14% organic carbon, 3% organic nitrogen, 20% humidity and 2.5-4.5 pH. The experiment involved the following treatments; 1) control (nutrient solution irrigation void of NaCl) (C), 2) Salts treatments (salinity at 150 mM NaCl) (S), 3) Salinity+300 mg L^{-1} amino acid (AA1), 4) Salinity+600 mg L^{-1} amino acid (AA2), 5) Salinity+1200 mg L^{-1} amino acid (AA3), 6) Salinity+1800 mg L^{-1} amino acid (AA4).

The end of the experiment (61 DAS), plants were evaluated using some plant physiological (shoot fresh and dry weights, shoot diameter, shoot length, and number of leaves and leaf area per plant, relative water content (RWC), photosynthetic pigments (Chl-a, Chl-b, total carotenoid), Na^+, K^+, Ca^{2+}, and Cl^- ions content) and biochemical parameters such as total phenolic content (TPC), flavonoids, total free amino acid, and lipid peroxide content (malondialdehyde, MDA); ascorbat peroxidase (APX), catalase (CAT), glutathione reductase (GR), superoxide dismutase (SOD), and antioxidative enzyme activities.

For ion determination, the plants were harvested and dried at 65°C for 48 h. The leaves of were burned at 550°C, and dissolved in 1% (v/v) hydrochloric acid, and then analyzed for Na^+, K^+, and Ca^{2+} using an atomic absorption spectrometer (Varian Spectra AA 220 FS). The Cl concentration was determined using the Mohr method (Dasgan and Koc, 2009).

Determination of the chlorophyll (Chl) a and b and contents were done according to the method of Arnon (1949). Extraction of the leaf pigment was done using 80% (v/v) acetone and the extraction absorbance was measured with a spectrophotometer (Shimadzu UVmini-1240; Shimadzu Corporation, Kyoto, Japan) at 663, 645, and 470 nm. The total phenolic content was determined using a Folin-Ciocalteu reagent. The phenolic content of leaves and stems was expressed in milligrams. Gallic acid was used as a standard (Singleton et al., 1999). The colorimetric assay was used to establish the flavonoid content (Molina-Quijada et al., 2010; Medina-Juárez et al., 2012). Total flavonoids were expressed on a fresh weight (fw) basis as milligrams of quercetin equivalents per gram. Total free amino acid content was determined with the ninhydrin reagent method (Yemm and Cocking, 1955).

A mortar and pestle, along with an extraction buffer (5 mL) comprised of a potassium-phosphate buffer (50 mM, pH 7.6) and disodium ethylene diamine tetra acetate (0.1 mM) was used to extract the enzymes from 0.5 g of leaf tissue. After centrifugation of the

http://www.aloki.hu ● ISSN 1589 1623 (Print) ● ISSN 1785 0037 (Online)
DOI: http://dx.doi.org/10.15666/aeer/1706_1551915530

homogenate at 15.000 × g for 15 min, the supernatant fraction was then used for the enzyme assay. All of the enzyme extraction preparation operations were carried out at 4°C. Nitro blue tetrazolium (NBT) was used to reduce the superoxide radical, which was monitored at 560 nm to essay the SOD, according to the method of Karanlik (2001). Monitoring the disappearance of HO was used to determine the CAT activity, while measuring the ascorbate consumption from its absorbance at 290 nm was used to determine the APX activity. One unit of APX activity was determined as the amount of enzyme necessary to consume 1 µMol of ascorbate min^{-1} (Cakmak and Marschner, 1992). Determination of the GR activity was performed via measurement of NADPH enzyme-dependent oxidation based on its absorbance at 340 nm. One unit of GR activity was determined as the amount of enzyme necessary to oxidize 1 µMol of NADPH min^{-1}.

The amount of MDA ascertained via the thiobarbituric acid reaction was used to measure the lipid peroxidation (Heath and Packer, 1968). The calculation of the MDA content was based on the MDA molar extinction coefficient; 155 mM^{-1} cm^{-1}.

The experimental plot design was randomized, comprising 3 replications. A comparison of the parameter mean values was performed via the least significant difference test. Statistical significance was determined as $p<0.05$ using JMP statistical software, ver. 5.1 (SAS Institute Inc., USA). Data are presented as the mean ± standard deviation. and in all figures error bars are representing standard errors of the means.

Results

An improvement value in growth parameters of the guar plants which were grown under saline conditions by using amino acids is shown in *Table 1*. Guar plants were treated with NaCl and these values were reduced by 41-87%, respectively, compared to the control. However, amino acid applications under salt stress significantly enhanced the growth components such as shoot fresh and dry weight, shoot length, shoot diameter, number of leaves per plant, leaf area per plant, compared to the salt-stressed groups. These reactions changed between 16-67% ratios. When compared to S, S+AA enhanced the amelioration for growth by 39-392%. Among to these applications the highest effect was determined in AA2 and the improvement was identified by 76-883%.

Table 1. *Effects of AA applications on growth parameters of guar plants under saline condition (C: control; S: salt stress (150 mM NaCl); AA1: 150 mM NaCl+300 mg L^{-1} amino acid; AA2: 150 mM NaCl+600 mg L^{-1} amino acid; AA3: 150 mM NaCl+1200 mg L^{-1} amino acid; AA4: 150 mM NaCl+1800 mg L^{-1} amino acid*

	Shoot fresh weight (g $plant^{-1}$)	Shoot dry weight (g $plant^{-1}$)	Shoot length (cm $plant^{-1}$)	Shoot diameter (mm $plant^{-1}$)	Steam Number (num. $plant^{-1}$)	Leaf Area (cm^2 $plant^{-1}$)
C	65.10±2.26^{b}	24.74±2.42^{b}	24.00±2.00^{b}	5.08±0.72^{a}	9.67±1.53^{ab}	663.44±25.98^{a}
S	9.05±3.27^{d}	3.35±1.21^{e}	13.00±2.65^{c}	2.33±0.28^{c}	5.67±1.15^{b}	108.36±13.10^{d}
AA1	27.62±3.65^{c}	17.80±1.00^{c}	14.67±2.52^{c}	3.32±0.48^{bc}	8.67±1.51^{ab}	165.47±19.14^{cd}
AA2	82.33±5.53^{a}	32.95±2.22^{a}	27.33±1.15^{a}	5.70±0.57^{a}	10.00±2.00^{a}	420.91±37.88^{b}
AA3	21.72±3.66^{c}	8.25±1.39^{d}	15.00±1.00^{c}	2.69±0.39^{bc}	8.33±2.08^{ab}	221.53±12.34^{c}
AA4	19.48±4.98^{c}	7.02±1.79^{d}	15.33±0.58^{c}	3.37±0.83^{b}	7.67±1.06^{ab}	145.72±15.01^{cd}

* Each value represents the mean of three replicates. For each parameter of each different letters are significantly different at $p< 0.05$ according to LSD test

http://www.aloki.hu ● ISSN 1589 1623 (Print) ● ISSN 1785 0037 (Online)
DOI: http://dx.doi.org/10.15666/aeer/1706_1551915530

Guar seedling treated with salt stress demonstrated a decrease in RWC at 44% ration, compared to control (*Table 2*). However, a significant improvement in the RWC of AA-treated plants was observed an increase 48, 60, 34, and 25% in AA1, AA2, AA3, and AA4, respectively, compared to the plant that was treated with 150 mM NaCl solely ($p<0.05$). Under salt (150 mM) stress, photosynthetic pigments such as total Chl-a, Chl-b, and total carotenoid were reduced by 43, 47, and 61%, in guar plants, respectively (*Table 2*). Auxiliary addition of amino acids to the salt-stressed guar plants induced a significant increase in photosynthetic pigments by 8-46%, 37-96%, and 54-143%, compared to salinity conditions, respectively.

Table 2. *Effects of AA applications on relative water content (RWC) and photosynthetic pigments of guar under saline condition (C: control; S: salt stress (150 mM NaCl); AA1: 150 mM NaCl+300 mg L^{-1} amino acid; AA2: 150 mM NaCl+600 mg L^{-1} amino acid; AA3: 150 mM NaCl+1200 mg L^{-1} amino acid; AA4: 150 mM NaCl+1800 mg L^{-1} amino acid)*

	RWC (%)	**Chl a (mg g^{-1} FW)**	**Chl b (mg g^{-1} FW)**	**Total carotenoids (mg g^{-1} FW)**
C	97.36±2.00^{a}	2.26±0.10^{a}	1.61±0.15^{a}	1.14±0.08^{a}
S	54.35±1.99^{e}	1.28±0.16^{d}	0.89±0.06^{d}	0.44±0.07^{c}
AA1	80.46±2.93^{bc}	1.87±0.10^{b}	1.43±0.05^{b}	0.67±0.03^{b}
AA2	87.31±2.14^{b}	2.17±0.08^{a}	1.69±0.09^{a}	1.07±0.08^{a}
AA3	72.57±2.11^{cd}	1.61±0.16^{c}	1.57±0.05^{ab}	0.74±0.12^{b}
AA4	68.32±1.41^{d}	1.39±0.06^{d}	1.18±0.07^{c}	0.68±0.04^{b}

* Each value represents the mean of three replicates. For each parameter of each different letters are significantly different at $p<0.05$ according to LSD test

To confirm the salinity-induced oxidative stress conditions, intercellular levels of stress biomarker MDA were evaluated (*Table 3*). The MDA content was the lowest in control plants and increased significantly in 150 mM NaCl conditions. When compared to the control groups, the MDA levels increased by 189% (6.72 µmol g^{-1} FW).

Table 3. *Effects of AA applications on MDA content, total phenolic, flavonoid and free amino acid contents of guar under saline condition (C: control; S: salt stress (150 mM NaCl); AA1: 150 mM NaCl+300 mg L^{-1} amino acid; AA2: 150 mM NaCl+600 mg L^{-1} amino acid; AA3: 150 mM NaCl+1200 mg L^{-1} amino acid; AA4: 150 mM NaCl+1800 mg L^{-1} amino acid)*

	MDA (µmol g^{-1} FW)	**Total phenolic (µg GAE ml^{-1})**	**Total flavonoid (mgQE $100g^{-1}$)**	**Total free amino acids (mg g^{-1} DW)**
C	2.32±0.24^{d}	21.20±0.39^{d}	8.68±0.52^{d}	7.42±1.23^{c}
S	6.72±0.26^{a}	16.99±0.43^{e}	11.68±1.41^{c}	9.90±0.65^{bc}
AA1	4.19±0.17^{c}	22.76±1.34^{cd}	13.56±1.13^{b}	11.42±1.02^{b}
AA2	3.46±0.18^{c}	30.09±1.19^{a}	16.88±1.03^{a}	15.42±1.01^{a}
AA3	5.42±0.15^{b}	25.43±1.81^{bc}	16.31±0.89^{a}	16.76±1.06^{a}
AA4	5.22±0.19^{b}	26.71±1.68^{b}	13.83±0.67^{b}	19.05±2.33^{a}

* Each value represents the mean of three replicates. For each parameter of each different letters are significantly different at $p<0.05$ according to LSD test

http://www.aloki.hu ● ISSN 1589 1623 (Print) ● ISSN 1785 0037 (Online)
DOI: http://dx.doi.org/10.15666/aeer/1706_1551915530

However, AA mitigated the stress effects on plants and further decreased the contents of MDA. In point of fact, through AA treatments, MDA content was decreased by 19-48% ratios. In addition to this, the lowest values were recorded at AA1 and AA2 treatments compared to with corresponding salinity.

Under salt stress, total phenolic and flavonoid contents decreased in guar (19 and 11% decreases, respectively) compared to the control group (*Table 3*). Contrarily, AA treatments proved to result in a significant increase in the mean values of total phenolic and flavonoid contents, compared to both control group (23-74% increase) and 150 mM NaCl (54-97% increase) individually. The maximum mean values were obtained in the AA2 application (30.09 µgGAE mL^{-1} of total phenolic; 16.88 mgQE 100 g^{-1}) and with AA2 treatment in guar total phenolic and flavonoid contents demonstrated an increase between 77% and 45%, compared to salinity conditions.

Total free amino acid content slightly increased with AAs applications, there after a constant increment in this content was recorded at AA1 (48%), AA2 (108%), AA3 (126%), and AA4 (157%) compared with untreated control (*Table 3*).

Compared to the control groups, salt stress increased the Na and Cl contents of all applications (320-545% increase in Na and 571-890% in Cl) (*Table 4*). However, these values were clearer in without AA application under salt stress condition (Na: 3.10%; Cl: 3.17%). With AA application, salt-stressed plants accumulated less Na and Cl, and these ion accumulations decreased by 16-18% compared to the salt application only. On the contrary of toxic Na and Cl ions, K and Ca ion accumulation decreased in salt conditions. These reactions were determined as 52% and 53% under salt stress conditions, respectively. The AA applications alleviated the stress effects on these parameters and significantly increased the K and Ca contents, compared to NaCl contents. According to results, AA applications ensured an increase of the K content by 11-53 % and Ca content by 23-70%. Under salt stress, the best effect was determined in AA2 applications and in this treatment, K and Ca values increased by 53 and 70% compared to salt stress.

Table 4. *Effects of AA applications on Na, K, Ca and Cl contents of guar under saline condition (C: control; S: salt stress (150 mM NaCl); AA1: 150 mM NaCl+300 mg L^{-1} amino acid; AA2: 150 mM NaCl+600 mg L^{-1} amino acid; AA3: 150 mM NaCl+1200 mg L^{-1} amino acid; AA4: 150 mM NaCl+1800 mg L^{-1} amino acid)*

	Na (%)	K (%)	Ca (%)	Cl (%)
C	0.48±0.04^{d}	4.07±0.18^{a}	5.17±0.16^{a}	0.32±0.03^{e}
S	3.10±0.19^{a}	1.95±0.17^{d}	2.45±0.13^{f}	3.17±0.09^{a}
AA1	2.71±0.16^{b}	2.18±0.04^{c}	3.03±0.12^{e}	2.90±0.11^{b}
AA2	2.02±0.13^{c}	3.00±0.18^{b}	4.17±0.18^{b}	2.15±0.07^{d}
AA3	2.66±0.09^{b}	2.43±0.17^{c}	3.72±0.21^{c}	2.70±0.08^{c}
AA4	2.78±0.07^{b}	2.23±0.10^{c}	3.34±0.20^{d}	2.86±0.05^{b}

* Each value represents the mean of three replicates. For each parameter of each different letters are significantly different at $p<0.05$ according to LSD test

Antioxidative enzyme activity (SOD, CAT, GR, and APX) levels were evaluated in C, S, and S+AA treatments (*Table 5*). Salt stress caused an increase in SOD, CAT, GR and APX activities at different levels. It is evident from the figure that AA treatments had

http://www.aloki.hu ● ISSN 1589 1623 (Print) ● ISSN 1785 0037 (Online)
DOI: http://dx.doi.org/10.15666/aeer/1706_1551915530

a serious effect on antioxidative enzyme activities such as SOD, CAT, GR, and APX of the guar seedlings under salt stress. In S+AA applications, enzyme activities (SOD, CAT, GR, and APX) increased by 9-48, 12-51, 14-112, and 14-129%, compared to the 150 mM treatment. In addition to these results, the highest enzyme activities were noted at AA2 treatment (SOD: 510.46 U min^{-1} mg^{-1} FW; CAT: 637.26 μmol min^{-1} mg^{-1} FW; GR: 229.62 μmol min^{-1} mg^{-1} FW, APX: 220.19 μmol min^{-1} mg^{-1} FW) compared with control and salinity.

Table 5. *Effects of AA applications on SOD, CAT, GR, and APX enzyme activities of guar under saline condition (C: control; S: salt stress (150 mM NaCl); AA1: 150 mM NaCl+300 mg L^{-1} amino acid; AA2: 150 mM NaCl+600 mg L^{-1} amino acid; AA3: 150 mM NaCl+1200 mg L^{-1} amino acid; AA4: 150 mM NaCl+1800 mg L^{-1} amino acid) (SOD U min^{-1} mg^{-1} FW; CAT, GR, APX: μmol min^{-1} mg^{-1} FW)*

	SOD	CAT	GR	APX
C	68.74±10.96^{e}	122.67±18.75^{d}	29.44±5.29^{d}	18.62±2.80^{d}
S	342.90±54.92^{d}	419.63±23.32^{c}	45.63±2.43^{c}	25.95±4.29^{c}
AA1	424.18±19.57^{bc}	469.23±22.26^{bc}	59.82±6.95^{b}	49.52±2.26^{b}
AA2	510.46±34.84^{a}	637.26±15.23^{a}	97.04±4.45^{a}	59.62±1.68^{a}
AA3	446.38±29.93^{b}	525.93±23.41^{b}	62.00±2.67^{b}	29.59±2.25^{c}
AA4	374.40±25.79^{cd}	479.72±34.32^{bc}	52.44±3.45^{bc}	30.60±2.30^{c}

* Each value represents the mean of three replicates. For each parameter of each different letters are significantly different at $p \leq 0.05$ according to LSD test

Discussion

Salt stress is a major environmental factor which prevents crop plants from attaining their full genetic potential; therefore, salt stress in plants induces several growth limitations. The increase in fresh weight of shoots by 205.1% (AA1), 809.7% (AA2), 140% (AA3), and 115.2% (AA4) compared with salt treated plants, as well as dry weight of shoot by 431.3% (AA1), 883.5% (AA2), 146.3% (AA3), and 109.6% (AA4) (*Table 1*). Generally, all growth parameters effected positively with AA treatment under salt stress condition. Goss (1973) reported the positive effect that amino acids have on growth and indicated that they can be used as an energy and carbon source, when there is a carbohydrate deficiency and the plants amino acids have been determined, via the release of the organic acid and ammonia that originally formed the amino acid. Nahed et al. (2010) reported that it was possible to indirectly explain amino acid regulatory effects, as some amino acids had been observed to affect the development of plants via the influence they had on the biosynthesis of gibberellins. In plant cells, amino acids are a source of nitrogen that is instantly available and can usually be more rapidly used than inorganic nitrogen. Additionally, amino acid conversion into some plant growth regulators may be the result of growth promotion in plants (Afifipour and Khosh-Khui, 2015). Amino acids can directly or indirectly influence the physiological activities in plant growth and development such as exogenous application of amino acids have been reported to modulate the growth, production and quality of tomato in plastic greenhouse (Boras et al., 2011). Also, Sadak et al. (2015) reported that also, amino acids are commonly known as a biostimulant that positively effects plant growth and yield, and significantly reduces

http://www.aloki.hu ● ISSN 1589 1623 (Print) ● ISSN 1785 0037 (Online)
DOI: http://dx.doi.org/10.15666/aeer/1706_1551915530

damage as a result of abiotic stressors, and amino total, as an amino acid source, may have a significant part in the metabolism of plants and assimilation of protein, which is very important in the formation of cells and thus, results in a fresh and dry matter increase.

It is well known that, when transpiration exceeds water absorption, cell turgor falls as relative water content and cell volume decreased and low turgor and RWC slow plant growth and decrease of stomatal conductance (Hammad and Ali, 2014). In this study, concerning the effect of treatment guar plants with amino acids, data in *Table 2* showed clearly significant increments in RWC compared to untreated plants at 150 mM NaCl. While RWC values decreased under salt stress between 44% in salty plants, with the AA applications to RWC demonstrated an increase by 25-60% in the same conditions. The accumulation of osmolytes in cells aids in the preservation of turgor pressure in the cell and provides protection for cell membranes, metabolic machinery, protein against cell dehydration (Krishnan et al., 2013). Amino acids contribute to osmotic adjustment by acting as osmolytes (Cuin and Shabala, 2007).

Salt stress results in significantly reduced photosynthesis, which is related to the photosynthesizing tissue (i.e. the leaf area) and photosynthetic pigments (Sadak et al., 2015). The pigments declined in plants when salt stress was introduced. In here, the favorable effects of the AA treatments were identified on the chlorophyll components and increased between 8-46 and 37-66%, compared to salinity (*Table 2*). The other component carotenoid content increased in guar plants that were treated with AA under salt stress (52-143% increase). In plants, pigments like carotenoids have various roles, in addition to the specific role they play in photosynthesis, one of which is their involvement in defense mechanisms against oxidative stress (Taibi et al., 2016). It is possible that the increased photosynthetic pigments were the result of the effect of amino acids on metabolism instigation and metabolically processes to increases plant efficiency (Starck, 2005). It seems that the mentioned amino acids were able to enhance the tolerant ability of the wheat against salt stress by increment the photosynthetic pigments (Bahari et al., 2013). Amino acids play a role in increasing the concentration of chlorophyll in plants, resulting in more efficient photosynthesis. Any influence that results in increased photosynthetic pigment levels will subsequently result in increased carbohydrate content. As a significant photosynthetic energy repository, carbohydrates encompass the plant's structural polysaccharides, specifically cellulose, hemicelluloses, lignin, and pectin, which have been deemed as significant structural compounds (El-Ghamry et al., 2009). Additionally, the effect that amino acids have on the total carbohydrate content could be the result of their vital involvement in chlorophyll molecule biosynthesis, which also affects the metabolism of carbohydrates (Talat et al., 2014).

In plants, phenolic and flavonoid compounds also perform many other roles, such as in cell wall structural components, taking part in the developmental process and growth regulation, in addition to defense mechanisms against abiotic and biotic stressors (Taibi et al., 2016). Talat et al. (2014) reported that compounds are some of the most widespread molecules among plant secondary metabolites, and are of great significance in plant development. Flavonoids represent the main and most complex subgroup of polyphenols with a wide array of biological functions including lipid peroxidation inhibition (Taibi et al., 2016). Our results indicated that the utilization of amino acid maintained an important increase in total phenolic, total flavonoid contents and total free amino acid content compared to untreated plants under salt stress (33-77, 16-44, and 53-156% increase). These results clearly indicate that the amino acid play a stimulatory influence in phenolic accumulation in guar (*Table 3*). The metabolism of AA has a significant regulatory affect,

http://www.aloki.hu ● ISSN 1589 1623 (Print) ● ISSN 1785 0037 (Online)
DOI: http://dx.doi.org/10.15666/aeer/1706_1551915530

not merely due to AAs as protein constituents, but also due to the potential of free AAs as regulatory and signaling molecules, and energy-associated metabolite precursors, in addition to various secondary metabolites that play a role in the growth of plants and their ability to adaptively respond to numerous stresses (Planchet et al., 2015). Sadiq et al. (2016) explained that abiotic stress causes hydrolysis of proteins into free amino acids, and foliar treatment of antioxidants enhances the biosynthesis of free amino acids and their utilization into protein. As lipid peroxidation is the mostly ascribed symptom to oxidative damage, it is often used as a marker of oxidative stress (Taibi et al., 2016). In this study, lipid peroxidation of guar seedlings increased with salt stress (189.7% increases). The results showed that AA treatments reduced the MDA levels, presenting a favorable effect in reducing the oxidative stress emerging from salt stress.

Ion toxicity in plant cells is the result of the salt-stress caused by a significant Na^+ and Cl^- cell influx, as well as the reality that the majority of plants amasses a high concentration of Na^+ and Cl^- ion in their shoots when cultivated under salt stress, which is a significant cause of decreased growth (Parihar et al., 2015; Liang et al., 2018). The uptake of K^+ and Ca^{2+} was reduced by Na^+ in guar under salinity conditions. Sodium concentration increased in plants grown under salinity; however amino acid application significantly reduced Na^+ concentration in guar leaves. Application of AA resulted in improvement uptake K^+ and Ca^{2+} ions. Thereby AA applications counteracted partially or completely the adverse effect of salinity as it increased the accumulation of K^+ and Ca^{2+}, in the same time it decreased the absorption of Na^+ and Cl^- in guar leaves compared with the corresponding salinity (*Table 4*). Increased K^+ concentration and reduced Na^+ in leaves may be one of the possible mechanisms of increased salinity tolerance by amino acid application in guar plants. Calcium is considered as an important factor for the maintenance of cell membrane integrity and the regulation of ion-transport. Ca^{2+} is essential for K^+ vs Na^+ ion selectivity and membrane integrity (Rady, 2012). Increasing potassium uptake is also a known strategy to counteract the entry of sodium. Rai (2002) indicated that amino acids promoting stomatal opening promoted K^+ influx into the guard cells while amino acids inhibiting stomatal opening inhibited K^+ flux into the guard cells. According to these results exogenous amino acid can modulate membrane permeability and ion uptake and apparently this is the major component by which amino acids help in mitigating salt stress effects (Rai, 2002). Sadak et al. (2015) indicated that amino acid has a chelating effect on micronutrient when applied, that make the absorption and transportation of micronutrients inside the plant easier due to its effect on cell membrane permeability. Similarity, exogenous amino acids have been shown to promote K^+ uptake by 15% in radish and Ca^{++} uptake by 20-60% in bean (Rai, 2002).

ROS in plant cells are generated via normal cellular metabolism or stressful environmental conditions such as drought, heavy metals, herbicides, nutrient deficiency, radiation, or salinity. A direct consequence of salinity is the induction of stress and antioxidant enzymes by exposed plants to minimize the damage caused by reactive oxygen species (Amar and Nourredine, 2016). Enzymatic antioxidant defense systems, such as APX, CAT, DHAR, GR, MDHAR, POX, SOD; and non-enzymatic antioxidant defense systems, such as ascorbate, carotenoids, glutathione, glycine betaine, phenolic compounds, polyamines, proline, and sugar (Sen, 2012). In here, responses to AA applications in the salt-stressed medium were examined and researchers reported an increase in antioxidative enzyme activities such as SOD, CAT, GR, and APX. These increases were statistically significant and determined by average 27-48% ratios (*Table 5*). Amino acids are important components of antioxidant systems in plants. The

http://www.aloki.hu ● ISSN 1589 1623 (Print) ● ISSN 1785 0037 (Online)
DOI: http://dx.doi.org/10.15666/aeer/1706_1551915530

action of these molecules involves the reduction of free radicals and osmoprotection. Our results showed that, treatment of amino acid had a stimulating effect on antioxidative enzyme activities. Thus, Darwesh (2013) reported that CAT and POD enzymes activity increased with salt treatment, same to be found at amino acid applications, all levels significant were enhanced activity of CAT and POD particular the highest levels of 6.0 ml L^{-1} of amino acids treatment.

Conclusion

Salinity stress led to significant reductions in growth parameters, photosynthetic pigments, seconder metabolites such as total phenolic compounds and flavonoid contents, potassium and calcium concentrations of guar seedlings while induced higher contents of sodium, chlorine, and malondialdehyde. The application of amino acid to salinity condition appeared to be favorable to growth and development, in addition to biochemical and physiological processes of the guar. Therefore, amino acid application has been achieved to be helpful strategy for enhancing the tolerance of the guar plants when grown under salinity conditions. Moreover, 600 mg L^{-1} amino acid treatment was the stronger effect in alleviating the harmful effect of salt stress compared to the other amino acid applications. The effects of 600 mg L^{-1} amino acid administration on yield under salt stress conditions can be examined in future studies.

REFERENCES

[1] Afifipour, Z., Khosh-Khui, M. (2015): Efficacy of spraying a mixture of amino acids on the physiological and morphological characteristics of tuberose (*Polianthes tuberosa* L.). – International Journal of Horticultural Science and Technology 2(2): 199-204.

[2] Amar, T., Nourredine, Y. (2016): Morphometric variability and biochemical analysis of growth seedlings under salt stress in tomato (*Lycopersicon esculentum* Mill.) cultivars. – Molecular Plant Breeding 7(4): 1-9.

[3] Arnon, D. I. (1949): Copper enzymes ın isolated chloroplast: polyphenoloxidase ın *Beta vulgaris*. – Plant Physiology 14: 1-15.

[4] Bahari, A., Pirdashti, H., Yaghubi, M. (2013): The effects of amino acid fertilizers spraying on photosynthetic pigments and antioxidant enzymes of wheat (*Triticum aestivum* L.) under salinity stress. – International Journal of Agronomy and Plant Production 4(4): 787-793.

[5] Batista-Silva, W., Heinemann, B., Rugen, N., Nunes-Nesi, A., Araújo, W. L., Braun, H. P., Hildebrandt, T. M. (2019): The role of amino acid metabolism during abiotic stress release. – Plant, Cell and Environment 42(5): 1630-1644.

[6] Boras, M., Zidan, R., Halloum, W. (2011): Effect of amino acids on growth, production and quality of tomato in plastic greenhouse. – Biological Sciences Series 33(5): 229-238.

[7] Cakmak, I., Marschner, H. (1992): Magnesium defficiency and highlight intensity enhance activities of superoxide dismutase,ascorbate peroxidase and glutathione reductase in bean leaves. – Plant Physiology 98: 1222-1226.

[8] Cuin, T. A., Shabala, S. (2007): Amino acids regulate salinity-induced potassium efflux in barley root epidermis. – Planta 225(3): 753.

[9] Darwesh, R. S. (2013): Improving growth of date palm plantlets grown under salt stress with yeast and amino acids applications. – Annals of Agricultural Sciences 58(2): 247-256.

[10] Dasgan, H. Y., Koc, S. (2009): Evaluation of salt tolerance in common bean genotypes by ion regulation and searching for screening parameters. – Journal of Food, Agriculture and Environment 7(2): 363-372.

http://www.aloki.hu ● ISSN 1589 1623 (Print) ● ISSN 1785 0037 (Online)
DOI: http://dx.doi.org/10.15666/aeer/1706_1551915530

[11] De Freitas, P. A. F., De Souza Miranda, R., Marques, E. C., Prisco, J. T., Gomes-Filho, E. (2018): Salt tolerance induced by exogenous proline in maize is related to low oxidative damage and favorable ionic homeostasis. – Journal of Plant Growth Regulation 37(3): 911-924.
[12] El-Din, K. M. G., El-Wahed, M. A. (2005): Effect of some amino acids on growth and essential oil content of chamomile plant. – International Journal of Agriculture and Biology 7: 376-380.
[13] El-Ghamry, A. M., El-Hai, K. A., Ghoneem, K. M. (2009): Amino and humic acids promote growth, yield and disease resistance of faba bean cultivated in clayey soil. – Australian Journal of Basic and Applied Sciences 3(2): 731-739.
[14] Goss, J. A. (1973): Amino acid synthesis and metabolism. – Physiology of plants and their cells. Pergamon Press, Inc., New York.
[15] Hammad, S. A., Ali, O. A. (2014): Physiological and biochemical studies on drought tolerance of wheat plants by application of amino acids and yeast extract. – Annals of Agricultural Sciences 59(1): 133-145.
[16] Heath, R. L., Packer, L. (1968): Photoperoxidation in isolated chloroplasts. I. Kinetics and stoichiometry of fatty acid peroxidation. – Archives of Biochemistry and Biophysics 125: 189-198.
[17] Karanlik, S. (2001): Resistance to salinity in different wheat genotypes and physiological mechanisms involved in salt resistance. – Institute of Natural and Applied Sciences, University of Cukurova, Turkey.
[18] Krishnan, S., Laskowski, K., Shukla, V., Merewitz, E. B. (2013): Mitigation of drought stress damage by exogenous application of a non-protein amino acid γ–aminobutyric acid on perennial ryegrass. – Journal of the American Society for Horticultural Science 138(5): 358-366.
[19] Liang, W., Ma, X., Wan, P., Liu, L. (2018): Plant salt-tolerance mechanism. – Biochemical and Biophysical Research Communications 495(1): 286-291.
[20] Medina-Juárez, L. Á., Molina-Quijada, D., Del Toro Sánchez, C. L., González-Aguilar, G. A., Gámez-Meza, N. (2012): Antioxidant activity of peppers (*Capsicum annuum* L.) extracts and characterization of their phenolic constituents. – Interciencia 37(8): 588-592.
[21] Molina-Quijada, D. M. A., Medina-Juárez, L. A., González-Aguilar, G. A., Robles-Sánchez, R. M., Gámez-Meza, N. (2010): Phenolic compounds and antioxidant activity of table grape (*Vitis vinifera* L.) skin from northwest Mexico. – CyTA-Journal of Food 8: 57-63.
[22] Nahed, G., Abdel Aziz, A. A., Mazher, M., Farahat, M. M. (2010): Response of vegetative growth and chemical constituents of Thuja orientalis L. plant to foliar application of different amino acids at Nubaria. – Journal of American Science 6(3): 295-301.
[23] Parihar, P., Singh, S., Singh, R., Singh, V. P., Prasad, S. M. (2015): Effect of salinity stress on plants and its tolerance strategies. – Environmental Science and Pollution Research 22(6): 4056-4075.
[24] Patel, A. D., Lalcheta, K., Gill, S. S., Tuteja, N. (2013): Salinity Tolerance of *Avicennia officinalis* L. (*Acanthaceae*) from Gujarat Coasts of India. – In: Tuteja, N., Gill, S. (eds.) Climate Change and Plant Abiotic Stress Tolerance. Wiley-VCH Verlag GmbH & Co. KGaA.
[25] Pathak, R. (2015): Clusterbean: Physiology, Genetics and Cultivation. – Springer.
[26] Planchet, E., Limami, A. M., D'mello, J. P. (2015): Amino acid synthesis under abiotic stress. – In: D'Mello, J. P. H. (ed.) Amino acids in higher plants CAB International.
[27] Rady, M. M. (2012): A novel organo-mineral fertilizer can mitigate salinity stress effects for tomato production on reclaimed saline soil. – South African Journal of Botany 81: 8-14.
[28] Rady, M. M., Taha, S. S., Kusvuran, S. (2018): Integrative application of cyanobacteria and antioxidants improves common bean performance under saline conditions. – Scientia Horticulturae 233: 61-69.

http://www.aloki.hu ● ISSN 1589 1623 (Print) ● ISSN 1785 0037 (Online)
DOI: http://dx.doi.org/10.15666/aeer/1706_1551915530

[29] Rai, V. K. (2002): Role of amino acids in plant responses to stresses. – Biologia Plantarum 45(4): 481-487.
[30] Sadak, M. S., Abdelhamid, M. T. (2015): Influence of amino acids mixture application on some biochemical aspects, antioxidant enzymes and endogenous polyamines of Vicia faba plant grown under seawater salinity stress. – Gesunde Pflanzen 67(3): 119-129.
[31] Sadiq, M., Akram, N. A., Javed, M. T. (2016): Alpha-tocopherol alters endogenous oxidative defense system in mung bean plants under water-deficit conditions. – Pakistan Journal of Botany 48(6): 2177-2182.
[32] Sarojnee, D. Y., Navindra, B., Chandrabose, S. (2009): Effect of naturally occurring amino acid stimulants on the growth and yield of hot peppers. – Journal of Animal Plant Sciences 5(1): 414-424.
[33] Schubert, S., Läuchli, A. (1990): Sodium exclusion mechanisms at the root surface of two maize cultivars. – In Genetic Aspects of Plant Mineral Nutrition: 183-187.
[34] Sekmen, A. H., Bor, M., Ozdemir, F., Turkan, I. (2013): Current concepts about salinity and salinity tolerance in plants. – In: Tuteja, N., Gill, S. (eds.) Climate Change and Plant Abiotic Stress Tolerance. Wiley-VCH Verlag GmbH & Co. KGaA.
[35] Sen, A. (2012): Oxidative stress studies in plant tissue culture. – Antioxidant Enzyme 3: 59-88.
[36] Singleton, V. L., Orthofer, R., Lamuela-Raventós, R. M. (1999): Analysis of total phenols and other oxidation substrates and antioxidants by means of folin-ciocalteu reagent. – Methods in Enzymolog 299: 152-178.
[37] Starck, Z. (2005): Growing assistant: Application of growth regulators and biostimulators in modern plant cultivation. – Rolnik Dzierawca 2: 74-76.
[38] Taibi, K., Taibi, F., Abderrahim, L. A., Ennajah, A., Belkhodja, M., Mulet, J. M. (2016): Effect of salt stress on growth, chlorophyll content, lipid peroxidation and antioxidant defence systems in *Phaseolus vulgaris* L. – South African Journal of Botany 105: 306-312.
[39] Talaat, I. M., Khattab, H. I., Ahmed, A. M. (2014): Changes in growth, hormones levels and essential oil content of *Ammi visnaga* L. plants treated with some bioregulators. – Saudi Journal of Biological Sciences 21(4): 355-365.
[40] Wu, G. Q., Feng, R. J., Li, S. J., Du, Y. Y. (2017): Exogenous application of proline alleviates salt-induced toxicity in sainfoin seedlings. – The Journal of Animal and Plant Sciences 27(1): 246-251.
[41] Yemm, E. W., Cocking, E. C. (1955): The determination of amino acids with ninhydrin. – Analyst 80: 209-214.

http://www.aloki.hu ● ISSN 1589 1623 (Print) ● ISSN 1785 0037 (Online)
DOI: http://dx.doi.org/10.15666/aeer/1706_1551915530

DETERMINATION OF VEGETATION AND SOIL PROPERTIES OF THE FLOODPLAIN RANGELAND IN THE CONTINENTAL CLIMATE ZONE OF TURKEY

DEMIRHAN, E. – ÖZYAZICI, M. A.*

Department of Field Crops, Faculty of Agriculture, Siirt University, Siirt, Turkey

**Corresponding author*
e-mail: arifozyazici@siirt.edu.tr; phone: +90-532-633-4592

(Received 2nd Aug 2019; accepted 14th Nov 2019)

Abstract. This study was conducted in May 2017 to investigate vegetation and soil properties of a floodplain rangeland, which is located in the continental climate zone of Turkey. In the study, vegetation surveys were performed in the rangeland areas with two different slope degrees (0-1% and 2-5%), and the Modified Wheel Point method with loop was used in vegetation measurements. A total of 23 different species belonging to 20 genera from 9 families, were identified in the rangeland where vegetation surveys were conducted. It was determined that 2 of the identified species were decreaser, 2 of them were increaser, and 19 of them were invasive species. The plant cover ratio of the studied rangeland area where the study was conducted covered with the plant was 76.87%. In general, the ratio of the Poaceae in the botanical composition of the examined rangeland was 35.32%, the ratio of legumes was 28.60%, and the ratio of other families was 36.08%. The examined rangeland soils had medium structure, mild alkaline character, and no salinity problem. It was determined that organic matter, available phosphorus and potassium content of the rangeland's moderately calcareous soils were higher in the base areas than in the slightly inclined areas.
Keywords: *rangeland, botanical composition, plant cover percentage, Fabaceae, soil properties*

Introduction

Meadows and rangelands covering approximately 25% of the Earth's land area (Alkemade et al., 2013), in addition to providing important ecosystem products and services to many people (Sala et al., 2017), being the most important source of roughage for livestock (Seydoşoğlu et al., 2019) and hosting wildlife, are also known as important areas in terms of having rich biodiversity and storing about 10-30% of the world's terrestrial carbon (Derner et al., 2006; Booker et al., 2013). While in Turkey these areas covered about 44 million hectares in the 1940s, nowadays they have been decreased to 14.6 million ha, and they constitute 38% of the total agricultural area (Anonymous, 2019a). In Turkey, available meadow and rangeland areas can meet about 20% of the roughage need of existing animals (~16 million animal unit) (Çaçan and Yüksel, 2016; Demiroğlu Topçu and Özkan, 2017). Meadows and rangelands, which provide the cheapest input for animal production, seem to be far from meeting the need for feed, and the reason for this is undoubtedly them having low feed production and/or yield. The free grazing system is effective on low amount of feed obtained from rangelands around the World as well as in Turkey. However, the full implementation of sustainable rangeland management can be achieved by following the principles of correct use and management.

According to the results of many studies conducted on rangelands in Turkey, it is reported that dry herbage yield of rangelands range between 640-2920 kg ha^{-1} according to the differences in ecology, vegetation and application and they have lost their yield

http://www.aloki.hu ● ISSN 1589 1623 (Print) ● ISSN 1785 0037 (Online)
DOI: http://dx.doi.org/10.15666/aeer/1706_1553115546

ability (Terzioğlu and Yalvaç, 2004; Polat et al., 2018; Sürmen and Kara, 2018), that in many rangeland vegetations, the ratios of plant species with high feed yield and quality were found to be low, while the ratios of invasive species were found to be high (Gür and Altın, 2015; İspirli et al., 2016; Seydoşoğlu et al., 2019; Seydoşoğlu and Kökten, 2018, 2019; Tutar and Kökten, 2019), in other words, that rangelands are away from climax vegetation and produce feed below their potential (Aydın and Uzun, 2005, 2008), and that there is an urgent improvement need in Turkey's rangelands (Yavuz et al., 2011, 2012; Alay et al., 2016).

In order to achieve success in rangeland improvement, which aims to create better vegetation and bring the rangeland to a position so that it can produce high-quality feed with high yield, knowing the vegetation structure of the rangeland to be improved. (Çınar et al., 2019) and listing the species from which the vegetation is composed, i.e. the plant species composing it, are important. Determination of the botanical composition, which is the main character of plant communities, constitutes the first and primary step of investigating meadow and rangeland vegetations (Gençkan, 1985).

Together with the biotic factors constituting the living environment, abiotic factors such as climate, soil, and topography are effective in the formation, development, and extinction of meadow and rangeland vegetations. For this reason, it is extremely important to know and/or reveal some physical and chemical properties of rangeland soils, especially in order to shed light on rangeland improvement studies. On the other hand, slope differences in rangeland areas affect soil fertility, the ratio of plant-covered areas, and ultimately, the meadow and rangeland crop significantly (Sürmen and Kara, 2018). This study aimed to determine vegetation and soil properties of a floodplain rangeland, which is located in the continental climate zone of Turkey.

Materials and methods

General description and some geographical features of the study area

The study was conducted in 2017 in the floodplain rangeland of Gözpınar village in Kurtalan district of Siirt province, which is located in the Southeastern Anatolia Region of Turkey (*Fig. 1*). Kurtalan district is located between 37° 55' 36" north latitude and 41° 42' 9" east longitudes, and Gözpınar village, where the study was conducted, is located between 37° 58' 35.0328" north latitude and 41° 27' 24.5304" east longitudes (Anonymous, 2019b).

Siirt province is located within the borders of the Dicle Region of Turkey's Southeastern Anatolia Region, and it is surrounded by Şırnak and Van provinces to the east, Batman and Bitlis provinces to the north, Batman province to the West, and Şırnak and Mardin provinces to the south. Siirt province consists of mountains and hills topographically, and the western part of the province including Kurtalan district is composed of plains that are mainly flat and close to flat. Some flatlands extend from Kurtalan district center to Batman province border and are severed from each other. The average elevation of the plain, which displays a rough structure and spreads over an area that is not very wide, is between 550-850 m (Anonymous, 1997). Areas with low slope values, lands entering in the "no or little erosion" class, and deep and medium-deep soils are also located in the western part of the province. The dominant large soil group in the study area is brown soils (Özyazıcı et al., 2014). The examined rangeland has a homogeneous area in terms of the drought index, aspect, and altitude (Avağ et al., 2012).

http://www.aloki.hu ● ISSN 1589 1623 (Print) ● ISSN 1785 0037 (Online)
DOI: http://dx.doi.org/10.15666/aeer/1706_1553115546

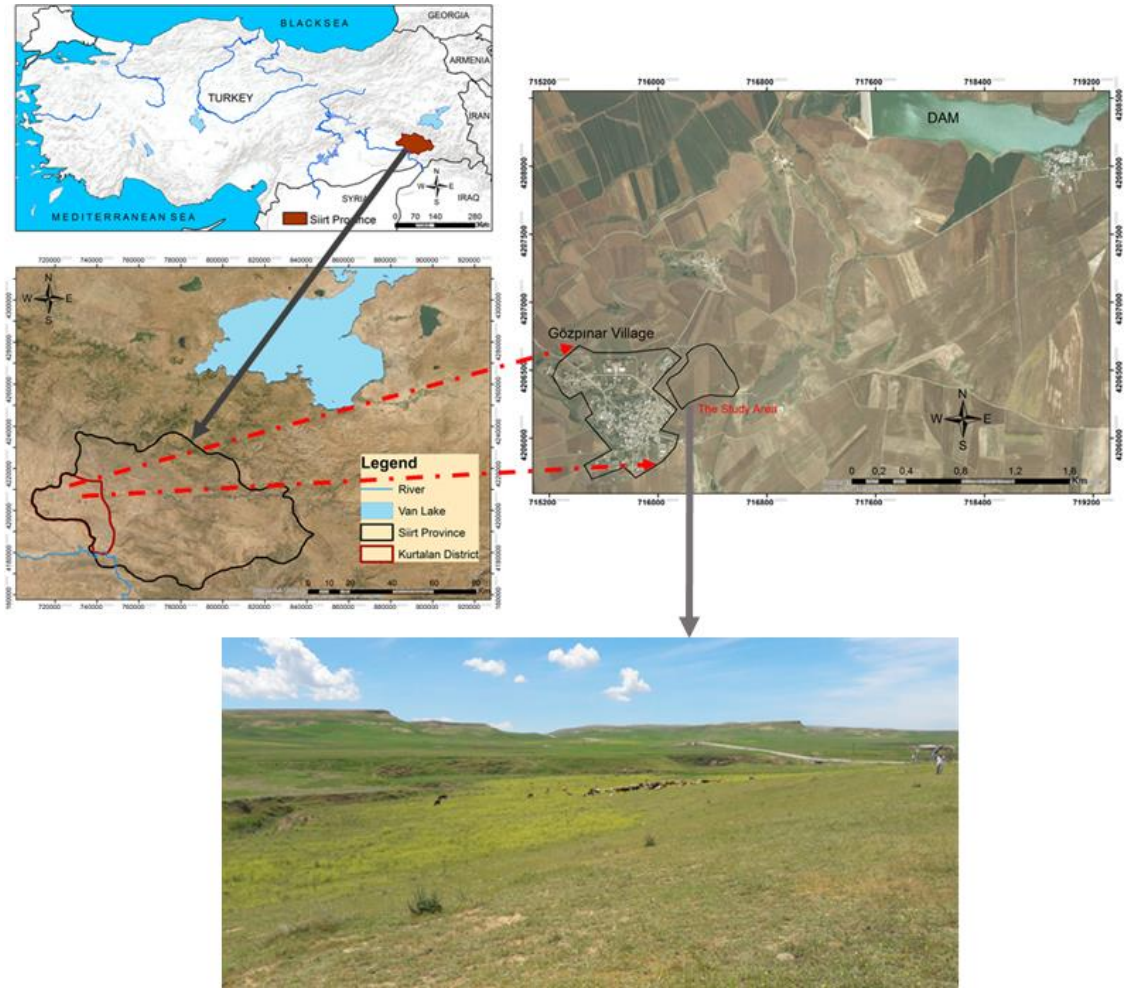

Figure 1. *Location of the study area*

A continental climate generally dominates Siirt province. Summers are hot and dry. Not much rainfall is observed between June and October. According to the long-term climatic data (1980-2017), the average annual temperature of the study area was 16.4 °C, and the average of annual rainfall was 700.3 mm. The average annual temperature in 2017, when the study was conducted, was recorded to be 17.2 °C and the total annual rainfall amount was recorded to be 547.9 mm (*Fig. 2*).

Vegetation measurement methods

In the study, vegetation surveys were performed in May 2017 in the Gözpınar village rangeland, in the regions with two different slope degrees (0-1% and 2-5%). The Modified Wheel Point method with loop was used in vegetation measurements (Koç and Çakal, 2004). The measurements were carried out in the Gözpınar village rangeland, in the part with two different slope degrees, during the flowering period of dominant plants in the rangeland, in 3 different part (in the block) which were very homogeneous in terms of vegetation and soil, and along four 20-m long lines, which extended from a point considered as the center towards 4 main directions (east, west, north, and south) in each part (in the block). Plant reading was performed to be 100 in total on each 20-m line and 400 in each block (Gökkuş et al., 2000).

http://www.aloki.hu ● ISSN 1589 1623 (Print) ● ISSN 1785 0037 (Online)
DOI: http://dx.doi.org/10.15666/aeer/1706_1553115546

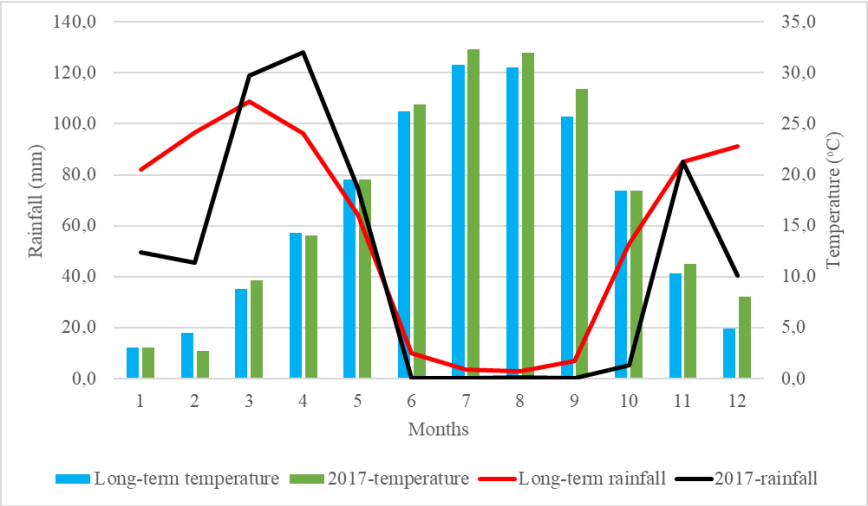

Figure 2. *Long-term (1980-2017) and 2017 climate diagram for Siirt province*

Identification of plants found in vegetation surveys was performed by benefiting from the studies carried out by Edgecombe (1964), Garms et al. (1968), Davis (1969), Polunin and Huxley (1974), Huxley and Taylor (1977), Weymer (1981), Demiri (1983), and Öztan and Okatan (1985).

The lifespan and families of the species and the degree of effect which expresses the plant species' palatability and response to grazing (decreaser, increaser, and invasive species) were determined according to Anonymous (2008).

In the rangeland, the plant coverage ratio (PCR) was determined by proportioning the number of points, where a plant was observed during the vegetation survey, to the total number of measured points, and it was expressed as a percentage (%) according to Gökkuş et al. (2000). By proportioning the values of each plant species to the total number of plants, the botanical composition ratio (BCR) was determined (Gökkuş et al., 2000). The BCR were calculated by separating the plant species observed in each loop line in the studied rangeland into three different plant groups, such as the Poaceae, Fabaceae, and other families.

Soil analysis methods

In the rangeland area, in each block where vegetation measurement was made, soil samples were taken from 0-20 cm soil depth with a stainless steel shovel following the general rules (Jackson, 1958). Soil samples were laid on clean packaging paper under laboratory conditions, stone and plant particles were picked over, and they were allowed to air dry. All dried soils were ground with wooden mallets, passed through a 2 mm steel sieve, and made ready for analysis.

The particle size distribution of soil was performed with the Bouyoucus hydrometer method; soil reaction (pH) was determined in the prepared saturated soil paste using a pH meter with a glass electrode; total salt was determined with the extract obtained from saturated soil paste using a conductivity device; lime was determined using a Scheibler calcimeter; organic matter was determined by the modified Walkley Black method; the available phosphorus was determined according to the Olsen method; the available potassium was determined with the extraction method by using 1 N ammonium acetate (pH = 7.0) (Anonymous, 1982, 1986).

http://www.aloki.hu ● ISSN 1589 1623 (Print) ● ISSN 1785 0037 (Online)
DOI: http://dx.doi.org/10.15666/aeer/1706_1553115546

Results and discussion

Vegetation characteristics

The species detected at different slope degrees in the Gözpınar village rangeland during the study and vegetation characteristics of these species were presented in *Table 1*. As it can be observed from *Table 1*, in the rangeland of Gözpınar village, 23 species belonging to 20 different plant genera from 9 different families were detected in the region which has 0-1% slope degree, 21 species belonging to 19 different plant genera from 8 different families were detected in the region which has 2-5% slope degree, and in general, a total of 23 different species belonging to 20 genera from 9 families were detected in the Gözpınar village rangeland.

In similar studies conducted in natural rangelands of Turkey, the number of species was reported to be 207 in the rangelands of Samsun by Yavuz et al. (2011), 186 in Amasya rangelands by Yavuz et al. (2012), 53 in a rangeland in Derik district of Mardin province by Aydın et al. (2014), 41 in the floodplain rangelands of Kırıkhan district of Hatay province by Çınar et al. (2014), 122 in the Zengi rangeland of Isparta province by Babalık and Sarıkaya (2015), 206 in the rangelands of Karahisar village of Tekirdağ province by Gür and Altın (2015), 90 in Çanakkale rangelands by Özaslan Parlak et al. (2015), 43 in the floodplain rangelands of Silvan district of Diyarbakır province by Seydoşoğlu et al. (2015a), 35 in the steppe rangelands of Eğil district of Diyarbakır province by Seydoşoğlu et al. (2015b), 103 in the rangelands of Taşköprü district of Kastamonu province by İspirli et al. (2016), 176 in the rangelands of Antalya province by Öten et al. (2016), 89 in the Karaören village rangeland within the boundaries of Seyitgazi district of Eskişehir province by Babalık and Ercan (2018), 117 in the rangelands of Beşiri district of Batman province by Seydoşoğlu and Kökten (2018), 202 in Batman province rangelands by Seydoşoğlu and Kökten (2019), and 53 in the Ormanardı village rangeland of Bingöl city center by Tutar and Kökten (2019). The difference in terms of the number of species between the data reported in the literature and the results of our study could be explained by the differences in grazing pressure, climate, soil structure, and topographic structure between the rangelands.

The family with the highest number of species in the examined rangeland area is the Poaceae, and this family was followed by the Fabaceae, and by the Brassicaceae, Asteraceae, and Umbelliferae families with two plant species in each of them (*Table 1*).

The lifespan that expresses a meaning within the "Life Form," which constitutes one of the qualitative characteristics of meadow and rangeland vegetation, is important in terms of plant sociology and ecology, and it is an important feature that needs to be emphasized in the subject of culture, management, and rehabilitation of meadows and rangelands (Gençkan, 1985). In this study, according to the life spans, in the rangeland section with a slope degree of 0-1%, 15 of the plant species were detected to be annual and 8 of them to be perennial; in the region section with a slope degree of 2-5%, 13 of the plant species were detected to be annual and 8 of them to be perennial (*Table 1*). In vegetation studies carried out in similar ecologies, for example, in the studies carried out in the rangelands of Derik district of Mardin province (Aydın et al., 2014), in the floodplain rangelands of Silvan district of Diyarbakır province (Seydoşoğlu et al., 2015a) and in steppe rangelands of Eğil district of Diyarbakır province (Seydoşoğlu et al., 2015b), as in the results of our study, annual species were reported to be present more in vegetation. The fact that annual species constitute the majority means that the rangeland loses its natural vegetation characteristics.

http://www.aloki.hu ● ISSN 1589 1623 (Print) ● ISSN 1785 0037 (Online)
DOI: http://dx.doi.org/10.15666/aeer/1706_1553115546

Table 1. *The species detected at two different slope degrees of the Gözpınar village rangeland, families of the species, their lifespans, responses to grazing (effect), plant coverage ratio (PCR), and botanical composition ratio (BCR)*

Species	Family	Lifespan	Effect	PCR (%)	BCR (%)
0-1%					
Avena sterilis	Poaceae	Annual	Invasive	5.00	6.03
Bromus tectorum	Poaceae	Annual	Invasive	1.00	1.20
Dactylis glomerata	Poaceae	Perennial	Decreaser	1.00	1.20
Hordeum murinum	Poaceae	Annual	Invasive	11.75	14.15
Hordeum spontaneum	Poaceae	Annual	Invasive	5.50	6.63
Lolium perenne	Poaceae	Perennial	Decreaser	2.75	3.31
Poa bulbosa	Poaceae	Perennial	Increaser	2.00	2.42
Astragalus hamosus	Fabaceae	Annual	Invasive	7.00	8.44
Medicago rigidula	Fabaceae	Annual	Invasive	4.75	5.72
Trifolium campestre	Fabaceae	Annual	Invasive	5.00	6.03
Trifolium subterraneum	Fabaceae	Annual	Invasive	3.75	4.52
Trigonella monantha	Fabaceae	Annual	Invasive	2.50	3.01
Trigonella monspeliaca	Fabaceae	Annual	Invasive	1.00	1.20
Aristolochia bodamae	Aristolochiaceae	Perennial	Invasive	2.50	3.01
Capsella bursa-pastoris	Brassicaceae	Annual	Invasive	1.50	1.81
Cardaria draba	Brassicaceae	Perennial	Invasive	1.25	1.51
Chardinia orientalis	Asteraceae	Annual	Invasive	3.00	3.60
Taraxacum aleppicum	Asteraceae	Perennial	Invasive	5.50	6.63
Parentucellia latifolia	Scrophulariaceae	Annual	Invasive	2.00	2.42
Scandix stellata	Umbelliferae	Annual	Invasive	6.25	7.52
Torilis leptophylla	Umbelliferae	Perennial	Invasive	5.00	6.03
Teucrium polium	Lamiaceae	Perennial	Increaser	2.50	3.01
Valerianella vesicaria	Valerianaceae	Annual	Invasive	0.50	0.60
Total				**83.00**	**100.00**
2-5%					
Avena sterilis	Poaceae	Annual	Invasive	3.75	5.30
Bromus tectorum	Poaceae	Annual	Invasive	1.00	1.41
Dactylis glomerata	Poaceae	Perennial	Decreaser	1.00	1.41
Hordeum murinum	Poaceae	Annual	Invasive	9.50	13.43
Hordeum spontaneum	Poaceae	Annual	Invasive	5.00	7.07
Lolium perenne	Poaceae	Perennial	Decreaser	2.00	2.83
Poa bulbosa	Poaceae	Perennial	Increaser	3.00	4.24
Astragalus hamosus	Fabaceae	Annual	Invasive	9.50	13.43
Medicago rigidula	Fabaceae	Annual	Invasive	2.25	3.18
Trifolium campestre	Fabaceae	Annual	Invasive	3.75	5.30
Trifolium subterraneum	Fabaceae	Annual	Invasive	2.50	3.53
Trigonella monantha	Fabaceae	Annual	Invasive	2.00	2.83
Aristolochia bodamae	Aristolochiaceae	Perennial	Invasive	2.00	2.83
Capsella bursa-pastoris	Brassicaceae	Annual	Invasive	1.75	2.47
Cardaria draba	Brassicaceae	Perennial	Invasive	1.50	2.12
Chardinia orientalis	Asteraceae	Annual	Invasive	2.50	3.53
Taraxacum aleppicum	Asteraceae	Perennial	Invasive	5.00	7.07
Parentucellia latifolia	Scrophulariaceae	Annual	Invasive	2.25	3.18
Scandix stellata	Umbelliferae	Annual	Invasive	3.75	5.30
Torilis leptophylla	Umbelliferae	Perennial	Invasive	4.50	6.36
Teucrium polium	Lamiaceae	Perennial	Increaser	2.25	3.18
Total				**70.75**	**100.00**

http://www.aloki.hu ● ISSN 1589 1623 (Print) ● ISSN 1785 0037 (Online)
DOI: http://dx.doi.org/10.15666/aeer/1706_1553115546

As a matter of fact, Wester (1981) reported that the perennial Poaceae are more common in rangelands with natural vegetation characteristics, and Gökkuş (1994) reported that annuals are commonly found in re-created areas where natural vegetation is degraded.

According to the responses of the species to grazing, in other words, when the distribution of the species according to their quality degrees was examined, of the species determined in the rangeland section with a slope degree of 0-1%, 2 were decreaser, 2 were increaser, and 19 were invasive; and in the rangeland section with a slope degree of 2-5%, 2 of the species were decreaser, 2 were increaser, and 17 were invasive. In the rangeland section with a slope degree of 0-1%, the ratio of decreaser species in the botanical composition of the examined rangeland was 4.51%, the ratio of increaser species was 5.43%, and the ratio of invasive species was 90.06%; and the ratios of the same species were 4.24%, 7.42%, and 88.34%, respectively, in the rangeland section with a slope degree of 2-5% (*Table 1; Fig. 3*). The invasive species were observed to be more proportionately in the base parts, which have flat or close to the flat slope, of the examined rangeland than the slightly inclined parts of the rangeland. This situation may be explained by the fact that animals prefer flat areas instead of slightly sloping areas and as a result of overgrazing of these areas, plant species with a low feed value replace plant species with a high feed value constituting the vegetation.

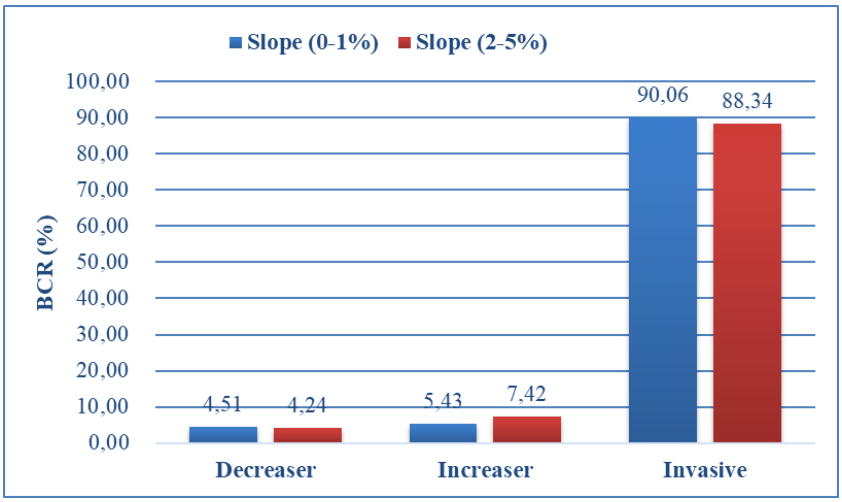

Figure 3. *The ratios of species with a different quality degree in the botanical composition in the Gözpınar village rangeland (%)*

Furthermore, in the study, invasive plants had the highest value with 68.63% in terms of the soil covering ratio, invasive plants were followed by increaser and decreaser plant species with the ratios of 4.87% and 3.37%, respectively (*Table 1*).

Studies conducted in different regions of Turkey reported that invasive species form the majority of rangeland vegetation (Uzun et al., 2010; Ünal et al., 2013, 2014; Yavuz et al., 2012; Çınar et al., 2014, 2019; Seydoşoğlu et al., 2015a, b; Alay et al., 2016; İspirli et al., 2016; Öten et al., 2016; Seydoşoğlu and Kökten, 2019; Tutar and Kökten, 2019).

Decreaser species, which symbolize dominant and most valuable forage plants of climax vegetation, are species that are grazed by rangeland animals firstly due to the superiority of their palatability (Gençkan, 1985). *Lolium perene* (3.31% and 2.83%) and

http://www.aloki.hu ● ISSN 1589 1623 (Print) ● ISSN 1785 0037 (Online)
DOI: http://dx.doi.org/10.15666/aeer/1706_1553115546

Dactylis glomerata (1.20% and 1.41%) were determined as the decreaser species in terms of their ratios in the botanical composition at both slope degrees of the examined rangeland (*Table 1*).

At both slope degrees, *Poa bulbosa* (2.42% and 4.24%) and *Teucrium polium* (3.01% and 3.18%) were found to be increaser species, of which feed values and palatability were lower than those of decreaser species and which are grazed less by rangeland animals (Gençkan, 1985) (*Table 1*).

In rangeland vegetations, there are foreign plant species, which are not the leading members of climax vegetation, but which are found in the climax rangeland vegetation even at a small ratio, which are not grazed or grazed to a small extent by animals, which are tasteless, which have a low feed value, and which are expressed as invasive species (Gençkan, 1985). In our study, in the rangeland, where vegetation surveys were performed, in both regions having different slope degrees (0-1% and 2-5%), according to the ratio in the botanical composition, *Hordeum murinum* (14.15% and 13.43%), *Astragalus hamosus* (8.44% and 13.43%), *Hordeum spontaneum* (6.63% and 7.07%) and *Taraxacum aleppicum* (6.63% and 7.07%) were determined as prominent invasive species (*Table 1*).

In the Gözpınar village rangeland where vegetation survey was carried out, the plant covered area ratio (PCR) in the parts of the rangeland having different slope degrees were presented in *Table 2*. Upon examining *Table 2*, while the plant covered area value was detected to be 83.00% in the region of the rangeland having 0-1% slope degree, it was detected to be 70.75% in the region having 2-5% slope degree. In other words, it was found out that the total plant cover decreased with increasing slope degree. The vegetation surveys carried out by İspirli et al. (2016) in 12 different village rangelands which are located in Taşköprü district of Kastamonu province and of which altitudes vary between 612 m and 1414 m reported that in parallel with the increase in slope degree, the total plant cover generally decreased. Similarly, Öten et al. (2016) stated that the total plant cover was low in rangeland areas with a high slope degree.

Table 2. *PCR values for families according to different slope degrees of the Gözpınar village rangeland compared to BCR*

Slope degree	Family	PCR (%)	Total (%)
0-1%	Poaceae	29.00	83.00
	Fabaceae	24.00	
	Other families	30.00	
	Empty space	17.00	17.00
	Total (BCR)	100.00	100.00
2-5%	Poaceae	25.25	70.75
	Fabaceae	20.00	
	Other families	25.50	
	Empty space	29.25	29.25
	Total (BCR)	100.00	100.00
Average	Poaceae	27.13	76.87
	Fabaceae	22.00	
	Other families	27.74	
	Empty space	23.13	23.13
	Total (BCR)	100.00	100.00

http://www.aloki.hu ● ISSN 1589 1623 (Print) ● ISSN 1785 0037 (Online)
DOI: http://dx.doi.org/10.15666/aeer/1706_1553115546

The average PCR of the Gözpınar village floodplain rangeland of Kurtalan district of Siirt province was detected to be 76.87% (*Table 2*). When the vegetation survey studies conducted in different rangeland areas of Turkey were examined, the PCR was determined to vary between 46.2%-72.0% in the floodplain rangelands of Silvan district of Diyarbakır province (Seydoşoğlu et al., 2015a), between 26.60-60.36% in the steppe rangelands of Eğil district of Diyarbakır province (Seydoşoğlu et al., 2015b), between 75.00%-98.25% in the rangelands of Antalya province (Öten et al., 2016), between 74.00%-91.25% in the rangelands of Beşiri district of Batman province (Seydoşoğlu and Kökten, 2018), between 90.3%-97.9% in the rangelands of Tufanbeyli district of Adana province (Çınar et al., 2019), and between 47.50%-93.00% in the rangelands of Batman province (Seydoşoğlu and Kökten, 2019). In addition, the average TPC was reported to be 21.75% in the Zengi rangeland of Isparta province (Babalık and Sarıkaya, 2015), 88.2% in the natural rangelands of Sinop province (Alay et al., 2016), 83.34% in the natural rangelands of Taşköprü district of Kastamonu province (İspirli et al., 2016), 71.35% in the rangelands of Mardin province (Seydoşoğlu et al., 2018), and 85.8% in the Ormanardı village rangeland of Bingöl city center (Tutar and Kökten, 2019).

As a result of the study, our findings obtained in terms of the PCR were observed to display similarities and differences with the studies carried out under many ecological conditions. As these differences may be caused by the method differences used in vegetation measurements, it is thought that differences in climate, soil structure, and rangeland management (grazing capacity, animal species, grazing period) applications may also cause this result.

In the Gözpınar village rangeland, in the rangeland region with a slope degree of 0-1%, 29.00% of the PCR was constituted by the Poaceae, 24.00% by the Fabaceae, and 30.00% by plants from other families. In the study, in the region with a slope degree of 2-5%, the PCR ratios of the Poaceae, Fabaceae, and other family plants were detected to be 25.25%, 20.00%, and 25.50%, respectively. When the Gözpınar village rangeland was examined in general, 27.13% of the PCR was observed to be the Poaceae, 22.00% were observed to be the Fabaceae, and 27.74% were observed to be the plants from other families (*Table 2; Fig. 4*).

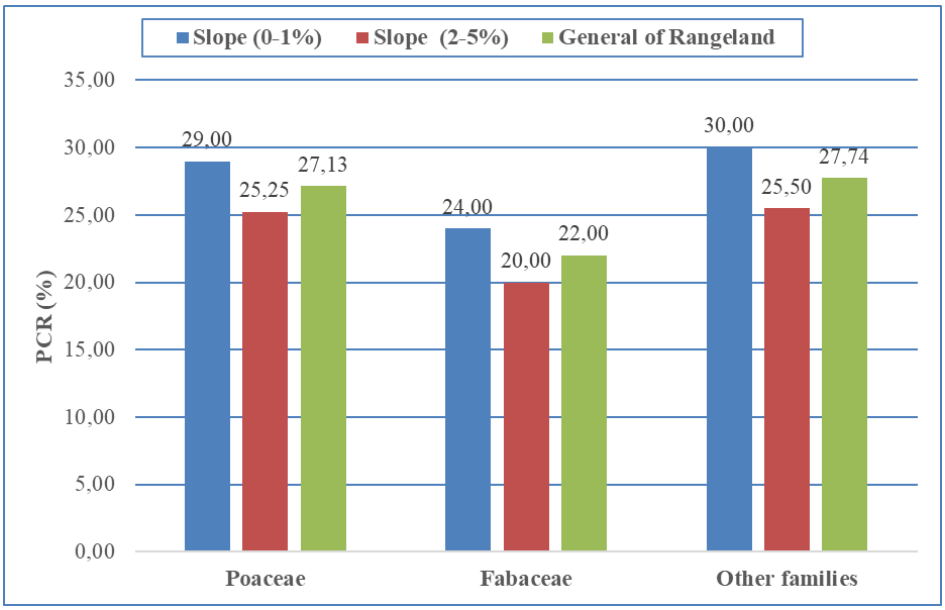

Figure 4. *Distribution of the PCR according to families (%)*

http://www.aloki.hu ● ISSN 1589 1623 (Print) ● ISSN 1785 0037 (Online)
DOI: http://dx.doi.org/10.15666/aeer/1706_1553115546

Plant species in the rangeland area were examined by being gathered in three groups as plants from the Poaceae family, Fabaceae family, and other families, and their ratios in the botanical composition were determined according to the PCR (*Table 3*).

In the Gözpınar village floodplain rangeland, where vegetation surveys were performed, in the rangeland region having 0-1% slope degree, of the identified species, 7 (34.94%) were the Poaceae, 6 (28.92%) were the Fabaceae, and 10 (36.14%) were species belonging to other families. In the examined rangeland, in the region having a slope degree of 2-5%, of the identified species, 7 (35.69%) were the Poaceae, 5 (28.27%) were the Fabaceae, and 9 (36.04%) were species belonging to other families. In general, the botanical composition of the examined rangeland was composed of the Poaceae with a ratio of 35.32%, the Fabaceae with a ratio of 28.60%, and other families with a ratio of 36.08% (*Table 3; Fig. 5*). In this case, it is possible to say that plants belonging to other families constitute the dominant plant group in vegetation. Similar results were also reported by Aydın et al. (2014), Seydoşoğlu et al. (2015b), Alay et al. (2016), İspirli et al. (2016), Öten et al. (2016), Seydoşoğlu and Kökten (2018, 2019), Sürmen and Kara (2018) and Çınar et al. (2019).

Table 3. *Ratios of families in the botanical composition ratio*

Families	Botanical composition ratio (%)		
	0-1%	2-5%	Average
Poaceae	34.94	35.69	35.32
Fabaceae	28.92	28.27	28.60
Other families	36.14	36.04	36.08
Total	100.00	100.00	100.00

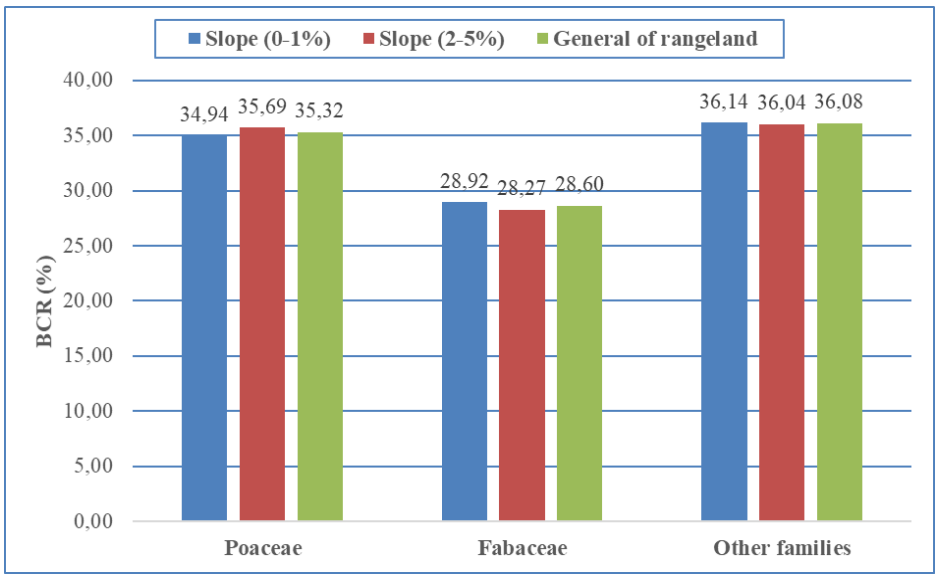

Figure 5. *Botanical composition ratios grouped by families*

While the most common Fabaceae in the vegetation were *Astragalus hamosus* (8.44%, 13.43%), *Trifolium campestre* (6.03%, 5.30%), *Medicago rigidula* (5.72%, 3.18%), and *T. subterraneum* (4.52%, 3.53%); *Hordeum murinum* (14.15%, 13.43%),

http://www.aloki.hu ● ISSN 1589 1623 (Print) ● ISSN 1785 0037 (Online)
DOI: http://dx.doi.org/10.15666/aeer/1706_1553115546

H. spontaneum (6.63%, 7.07%) and *Avena sterilis* (6.03%, 5.30%) were the most commonly observed Poaceae. In vegetation, the most common species belonging to other families were detected to be *Scandix stellata* (7.52%, 5.30%), *Taraxacum aleppicum* (6.63%, 7.07%), and *Torilis leptophylla* (6.03%, 6.36%) (*Table 1*).

Some physical and chemical properties of rangeland soils

Some physical and chemical analysis results of the soil samples taken from the regions of the Gözpınar village rangeland with different slope degrees were presented in *Table 4*. The sand content of the soils belonging to the flat and close to flat (0-1%) and slightly sloping (2-5%) rangeland regions was determined to be high. As a result of the classification made according to Anonymous (1951), the texture class was determined to be sandy-loam in the slightly sloping rangeland region and sandy-clayey-loam in the flat rangeland region. According to the general grouping, rangeland soils are loamy soils. Bilgin and Özalp (2016) reported that in the soils belonging to the rangeland vegetation, the texture class did not differ at low elevations (1900, 2000, and 2200 m), but the sand content of the soils was high. Özaslan Parlak et al. (2015) reported in the study they conducted in different rangeland regions that sand, silt, and clay contents of rangeland soils significantly differ from each other and that coastal rangeland has sandy loam, lowland shrubland has clayey loam, reseeded rangeland has clayey, protected and overgrazed rangeland has sandy loam structure. Some other studies reported that rangeland soils were loamy or clayey-loamy (Ağın and Kökten, 2013; Çaçan and Kökten, 2014; Taşdemir, 2015).

Table 4. *Some physical and chemical properties of soils of the Gözpınar village rangeland according to slope degrees*

Soil properties	Slope degree		Average
	0-1%	2-5%	
Sand, %	47.32	55.36	51.34
Clay, %	27.44	18.98	23.21
Silt, %	25.24	25.66	25.45
pH	8.25	8.25	8.25
Total salt, %	0.054	0.080	0.067
Lime ($CaCO_3$), %	4.1	5.4	4.8
Organic matter, %	1.88	1.25	1.57
Available phosphorus (P), kg P_2O_5/da	29.2	5.4	17.3
Available potassium (K), ppm	6233	5116	5675

In terms of soil reaction and salinity, no difference was determined between the examined rangeland regions, and the rangeland soil was detected to have slightly alkaline character and be salt-free (*Table 4*). In the studies conducted in different regions of Turkey, rangeland soils had slightly acid (Şengönül et al., 2009; Bilgin and Özalp, 2016; Çaçan and Kökten, 2014), slightly alkaline (Babalık and Sarıkaya, 2015; Babalık and Ercan, 2018), and neutral character (Ağın and Kökten, 2013; Özaslan Parlak et al., 2015; Taşdemir, 2015), and it was reported that there was no problem in terms of salinity in rangelands.

http://www.aloki.hu ● ISSN 1589 1623 (Print) ● ISSN 1785 0037 (Online)
DOI: http://dx.doi.org/10.15666/aeer/1706_1553115546

While the lime content of the soil was 4.1% in the regions of the Gözpınar rangeland that were flat or close to flat, this amount was detected to be 5.4% in the slightly sloping rangeland region (*Table 4*). According to the classification reported by Ülgen and Yurtsever (1995), the rangeland soils examined were found to be "calcareous" and/or "medium calcareous." The amount of lime varying under the effect of climate and main material was reported to vary at non-calcareous, low calcareous, high calcareous levels in the rangelands of different ecology areas (Bolat, 2007; Sengönül et al., 2009; Ağın and Kökten, 2013; Çaçan and Kökten, 2014; Taşdemir, 2015; Babalık and Sarıkaya, 2015; Özaslan Parlak et al., 2015; Babalık and Ercan, 2018).

The organic matter content of the soil was detected to be 1.88% in the regions of the Gözpınar village rangeland that were flat or close to flat, and 1.25% in the slightly sloping rangeland region, and the average organic matter content of the mentioned rangeland was 1.57% (*Table 4*). The high organic matter content in the flat region of the rangeland can be explained by the accumulation of nutrients in these areas depending on both soil and water transport towards the base of the rangeland by erosion. However, the organic matter content in both regions was found to be low according to the classification based on the study by Ülgen and Yurtsever (1995). It is thought that the total plant cover and the ratio of the Fabaceae in the botanical composition were effective in the low level of the organic matter content of rangeland soils. In the studies carried out in rangeland areas with different elevation and slope degrees, soil organic matter was generally reported to be at good levels (Babalık and Sarıkaya, 2015; Bilgin and Özalp, 2016; Özaslan Parlak et al., 2015). On the other hand, Birhan (1999) noted that there was no excessive difference between topographic positions in terms of organic matter content and that there was no significant relationship between organic matter content and topographic factors. In the study carried out by Kadıoğlu and Canbolat (2014) in order to reveal the change in soil quality index parameters in agricultural and rangeland areas located in different topographic positions, it was determined that from the topographic positions, the structure was thinned and the organic matter content increased from the peak position to the skirt position.

When rangeland soils were examined in terms of the P and K content available to plants, the base regions were found to contain higher amounts of P and K compared to slightly sloped regions (*Table 4*). According to the classification reported by Ülgen and Yurtsever (1995), while the available P level of the soil is "very high" in the rangeland regions where the slope degree is flat or close to flat, it is "low" in the slightly sloped regions of the rangeland. According to the classification made by Pizer (1967), the K content of the soil is very high in both rangeland regions. Our findings on the available P and K contents of the rangeland soils were found to be compatible with the findings of Ağın and Kökten (2013), Çaçan and Kökten (2014) and Özaslan Parlak et al. (2015).

Conclusion

There were 23 species in the examined rangeland, and the majority of these species (19 sp.) were found to be invasive. Although the ratio of plant covered area (76.87%) was high, the determined ratio of plants belonging to fabaceae, which is important in terms of feeding of animals, was very low. According to these results, it was concluded that in the floodplain rangelands with continental climate, grazing of animals in accordance with the management rules, and improvement of rangeland with fertilization will have a positive effect on the botanical composition of the rangeland.

http://www.aloki.hu ● ISSN 1589 1623 (Print) ● ISSN 1785 0037 (Online)
DOI: http://dx.doi.org/10.15666/aeer/1706_1553115546

Acknowledgements. This study was produced from the first author's master's thesis accepted by the Graduate School of Natural and Applied Science of Siirt University.

REFERENCES

[1] Ağın, Ö., Kökten, K. (2013): Research on the botanical composition of a range in Karapolat village, Yedisu-Bingöl. – Tr. J. Nature Sci. 2(1): 41-45 (in Turkish).
[2] Alay, F., İspirli, K., Uzun, F., Çınar, S., Aydın, İ., Çankaya, N. (2016): Effects of long-term free grazing on natural rangelands. – Journal of Agricultural Faculty of Gaziosmanpasa University 33(1): 116-124 (in Turkish).
[3] Alkemade, R., Reid, R. S., Van Den Berg, M., De Leeuw, J., Jeuken, M. (2013): Assessing the impacts of livestock production on biodiversity in rangeland ecosystems. – Proc. Natl. Acad. Sci. PNAS 110(52): 20900-20905.
[4] Anonymous (1951): Soli Survey Staff, Soil Survey Manuel. – Agricultural Research Administration U. S. Dept. of Agriculture Handbook. No.18, Gount Point Office, Washington, pp. 340-377.
[5] Anonymous (1982): Methods of Soil Analysis. Part II: Chemical and Microbiological Properties. – Agronomy Monograph No: 9. ASA-SSSA, Madison, WI, pp. 323-336.
[6] Anonymous (1986): Methods of Soil Analysis. Part I: Physical and Mineralogical Properties. 2nd Ed. – Agronomy Nomograph No: 9. ASA-SSSA, Madison, WI.
[7] Anonymous (1997): Siirt Province Land Presence. – Publications of General Directorate of Rural Services, Ankara (in Turkish).
[8] Anonymous (2008): Turkey's Meadow and Rangeland Crops. – T. C. Ministry of Agriculture and Rural Affairs, Ankara (in Turkish).
[9] Anonymous (2019a): Basic Statistics, Agriculture. – Turkish Statistical Institute. http://www. tuik.gov.tr/UstMenu.do?metod=temelist (date of access: 15.04.2019; in Turkish).
[10] Anonymous (2019b): Map TR, Map of Gozpinar Village. – https://www.haritatr.com/gozpinar-koyu-haritasi-m96ba (date of access: 16.06.2019; in Turkish).
[11] Avağ, A., Mermer, A., Yıldız, H., Ünal, E., Urla, Ö., Aydoğdu, M., Dedeoğlu, F., Aydoğmuş, O., Torunlar, H., Tuğaç, M. G., Ünal, S., Mutlu, Z., Özaydın, K. A., Özgöz, M. M., Aksakal, E., Kara, A., Uzun, M., Çakal, S., Yıldırım, T., Aksoyak, S., Tezel, M., Aygün, C., Kara, İ., Erdoğdu, İ., Sever, L., Atalay, A., Yavuz, T., Avcı, M., Çınar, S., İnal, İ., Yücel, C., Cebel, H., Keçeci, M., Başkan, O., Depel, G., Palta, Ç., Çarkacı, A., Karadavut, U., Şimşek, U., Sürmen, M., Odabaşı, G., Gül, D., Koç, A., Erkovan, H. İ., Güllapoğlu, K., Kendir, H., Şahin, N. (2012): National Pasture Use and Management Project Final Report. – TUBİTAK-106G017, Ankara.
[12] Aydın, A., Çaçan, E., Başbağ, M. (2014): Determination of the botanical composition of a pasture in the Derik district of Mardin. – Turkish Journal of Agricultural and Natural Sciences 2(Special Issue): 1625-1630 (in Turkish).
[13] Aydın, İ., Uzun, F. (2005): Nitrogen and phosphorus fertilization of rangelands affects yield, forage quality and the botanical composition. – European Journal of Agronomy 23(1): 8-14.
[14] Aydın, İ., Uzun, F. (2008): Potential decrease of grass tetany risk in rangelands combining N and K fertilization with MgO treatments. – European Journal of Agronomy 29(1): 33-37.
[15] Babalık, A. A., Ercan, A. (2018): Determination of vegetation properties of the Karaören village rangeland in Eskişehir province. – Turkish Journal of Forestry 19(3): 246-251.
[16] Babalık, A. A., Sarıkaya, H. (2015): A research on the hay yield and botanical composition of the Zengi Rangeland in Isparta. – Turkish Journal of Forestry 16(2): 96-101.

http://www.aloki.hu ● ISSN 1589 1623 (Print) ● ISSN 1785 0037 (Online)
DOI: http://dx.doi.org/10.15666/aeer/1706_1553115546

[17] Bilgin, F., Özalp, M. (2016): Investigating the effects of elevation changes on vegetation structure and soil properties for the pasturelands above forest line. – Artvin Coruh University Journal of Forestry Faculty 17(2): 135-147.
[18] Birhan, H. (1999): Comparison of different topographic positions in terms of yield and some soil properties. – Atatürk University, Institute of Natural and Applied Science, M.Sc. Thesis (in Turkish).
[19] Bolat, İ. (2007): The effect of different land uses on the soil microbial biomass carbon (C_{mic}) and nitrogen (N_{mic}). – Zonguldak Karaelmas University, Institute of Natural and Applied Science, M.Sc. Thesis (in Turkish).
[20] Booker, K., Huntsinger, L., Bartolome, J. W., Sayre, N. F., Stewart, W. (2013): What can ecological science tell us about opportunities for carbon sequestration on arid rangelands in the United States? – Glob. Environ. Chang. 23: 240-251.
[21] Çaçan, E., Kökten, K. (2014): Research on the yield herbage and grazing capacity of a range in Çiçekyayla village, central district Bingöl. – Turkish Journal of Agricultural and Natural Sciences 2: 1727-1733 (in Turkish).
[22] Çaçan, E., Yüksel, A. (2016): Influence of meadows and pastures on regional development. – UNIDAP International Regional Development Conference, Mus, Turkey, pp. 521-531 (in Turkish).
[23] Çınar, S., Hatipoğlu, R., Avcı, M., İnal, İ., Yücel, C., Avağ, A. (2014): A research on the vegetation structures of the pastures in district Kırıkhan, Hatay. – Journal of Agricultural Faculty of Gaziosmanpasa University 31(2): 52-60 (in Turkish).
[24] Çınar, S., Hatipoğlu, R., Avcı, M., Yücel, C., İnal, İ. (2019): A research on the vegetation structures of the rangelands of district Tufanbeyli, Adana. – KSU J. Agric Nat 22(1): 143-152 (in Turkish).
[25] Davis, P. H. (1969): Flora of Turkey and the Eastaege an Islands. Vols. 1-3. – University of Edinburgh Press, Edinburgh.
[26] Demiri, M. (1983): Flora Ekskursioniste e Shqiperise. – Shtepia Botuese e Librit Shkollor, Tirana.
[27] Demiroğlu Topçu, G., Özkan, Ş. S. (2017): General view to meadow-rangelands and forage crops cultivation of Aegean region and Turkey. – COMU J. Agric. Fac. 5(1): 21-28 (in Turkish).
[28] Derner, J. D., Boutton, T. W., Briske, D. D. (2006): Grazing and ecosystem carbon storage in the North American Great Plains. – Plant and Soil 280: 77-90.
[29] Edgecombe, W. (1964): Weeds of Lebanon. – Publication No: 24. Faculty of Agriculture Sciences, American University of Beirut, Lebanon.
[30] Garms, H., Eigener, W., Melderis, A., Pope, T., Durrell, G. (1968): The Natural History of Europe. – Paol Hamilyn Limited, London.
[31] Gençkan, M. S. (1985): Breeding and Management of Meadow-Rangeland Culture. – Publication ID: 483. Ege University, Faculty of Agriculture, Publisher of Ege University, Bornova-İzmir (in Turkish).
[32] Gökkuş, A. (1994): Secondary Succession in Abandoned Areas. – Atatürk University Publication ID: 787, Publication Number of Agricultural Faculty: 321, Research Series ID: 197, Erzurum (in Turkish).
[33] Gökkuş, A., Koç, A., Çomaklı, B. (2000): Meadow Pasture Application Guide. Extended 3rd Ed. – Atatürk University Faculty of Agriculture Publications No: 142 (in Turkish).
[34] Gür, M., Altın, M. (2015): Some features of floristic composition of different using history of natural pastures in Thrace Region. – Anadolu Journal of Agricultural Sciences 30: 60-67 (in Turkish).
[35] Huxley, A., Taylor, W. (1977): Flowers of Greece and the Aegean. – Chatto and Windus, London.
[36] İspirli, K., Alay, F., Uzun, F., Çankaya, N. (2016): Impacts of livestock grazing and topography on vegetation cover and structure in natural rangelands. – Turk J Agric Res 3(1): 14-22 (in Turkish).

http://www.aloki.hu ● ISSN 1589 1623 (Print) ● ISSN 1785 0037 (Online)
DOI: http://dx.doi.org/10.15666/aeer/1706_1553115546

[37] Jackson, M. L. (1958): Soil Chemical Analysis. – Prentice-Hall, Inc. Englewood Cliffs, NJ.
[38] Kadıoğlu, B., Canbolat, M. Y. (2014): Change of soil quality index parameters depending on topographic positions in different agricultural and grazing lands. – Alınteri, 26(B): 1-8 (in Turkish).
[39] Koç, A., Çakal, Ş. (2004): Comparison of some range land canopy coverage methods. – Int. Soil Cong. on Natural Resource Manage. For Sust. Develp. June 7-10, Erzurum-Turkey, pp. 41-45.
[40] Öten, M., Kiremitci, S., Erdurmuş, C., Soysal, M., Kabaş, Ö., Avcı, M. (2016): Determination of botanical composition of some pastures in Antalya province. – Journal of Atatürk University, Faculty of Agriculture 47(1): 23-30 (in Turkish).
[41] Özaslan Parlak, A., Parlak, M., Gökkuş, A., Demiray, H. C. (2015): Forage yield and quality, botanical composition and some soil characteristics of Mediterranean (Çanakkale) rangelands. – COMU J. Agric. Fac. 3(1): 99-108 (in Turkish).
[42] Öztan, Y., Okatan, A. (1985): Meadow Rangeland, Legume and Grasses Forage Plants Introductory Guide. – Black Sea Technical University Faculty of Forestry, General Publication ID: 95, Faculty Publication ID: 8, Trabzon (in Turkish).
[43] Özyazıcı, M. A., Dengiz, O., İmamoğlu, A. (2014): Determination of some land and soil characteristics of Siirt province with geographic information system analysis. – Turk J Agric Res 1(2): 128-137 (in Turkish).
[44] Pizer, N. H. (1967): Some advisory aspect. Soil potassium and magnesium. – Tech. Bull. 14: 184.
[45] Polat, T., Budak, S., Akkaya, G. (2018): A research on the hay yield, quality and botanical composition of natural grassland of Adıyaman Kuyulu village. – Harran Journal of Agricultural and Food Science 22(3): 348-354 (in Turkish).
[46] Polunin, O., Huxley, A. (1974): Flowers of the Mediterranean. – Chatto and Windus, London.
[47] Sala, O. E., Yahdjian, L., Havstad, K., Aguiar, M. R. (2017): Rangeland Ecosystem Services: Nature's Supply and Humans' Demand. – In: Briske, D. D. (ed.) Rangeland Systems: Processes, Management and Challenges. Series on Environmental Management. Springer, Switzerland, pp. 467-489.
[48] Seydoşoğlu, S., Kökten, K. (2018): Some characters of rangeland vegetation in Batman province of Beşiri district. – Journal of Agriculture Faculty of Ege University 55(4): 491-497 (in Turkish).
[49] Seydoşoğlu, S., Kökten, K. (2019): Some characters of rangeland vegetation in Batman province. – Harran Journal of Agricultural and Food Science 23(1): 60-68 (in Turkish).
[50] Seydoşoğlu, S., Saruhan, V., Mermer, A. (2015a): Research on the vegetation structure of the pastures in Silvan district, Diyarbakır. – Turk J Agric Res 2(1): 1-7 (in Turkish).
[51] Seydoşoğlu, S., Saruhan, V., Mermer, A. (2015b): Determination of the botanical composition of the arid pasture in district Eğil, Diyarbakır. – Turk J Agric Res 2(2): 76-82 (in Turkish).
[52] Seydoşoğlu, S., Kökten, K., Sevilmiş, U. (2018): Basic vegetation characteristics of village pastures connected to Mardin province and its provinces. – Turkish Journal of Agricultural and Natural Sciences 5(4): 406-413.
[53] Seydoşoğlu, S., Çaçan, E., Sevilmiş, U. (2019): Determination of botanical composition, yield and pasture quality ratings of infertile pastures in Kozluk district of Batman province of Turkey. – Fresenius Environmental Bulletin 28(4A/2019): 3388-3394.
[54] Sürmen, M., Kara, E. (2018): Yield and quality characteristics of rangelands which have different slopes in Aydın ecological conditions. – Derim 35(1): 67-72 (in Turkish).
[55] Şengönül, K., Kara, Ö., Palta, Ş., Şensoy, H. (2009): Determination of some quantitative properties of range vegetation and ecological conditions in Bartın Uluyayla. – Journal of Bartin Faculty of Forestry 11(16): 81-94 (in Turkish).

http://www.aloki.hu ● ISSN 1589 1623 (Print) ● ISSN 1785 0037 (Online)
DOI: http://dx.doi.org/10.15666/aeer/1706_1553115546

[56] Taşdemir, V. (2015): Research on the hay yield and botanical composition of a range in Bahcecik village, Karakocan-Elazıg. – Bingöl University, Institute of Natural and Applied Science, M.Sc. Thesis (in Turkish).
[57] Terzioğlu, Ö., Yalvaç, N. (2004): A research on determination of grazing starting time hay yield and botanical composition of natural rangelands in Van region. – J. Agric. Sci. 14(1): 23-26 (in Turkish).
[58] Tutar, H., Kökten, K. (2019): Determination of botanical composition of Ormanardı village rangeland in Bingöl province center. – Turkish Journal of Agricultural and Natural Sciences 6(1): 16-23 (in Turkish).
[59] Ülgen, N., Yurtsever, N. (1995): Turkey Fertilizer and Fertilization Guide. 4. Press. – Publications of Soil and Fertilizer Research Institute, General Publication No: 209, Technical Publication No: T.66. General Directorate of Rural Services, Ankara (in Turkish).
[60] Ünal, S., Mutlu, Z., Urla, Ö., Yıldız, H., Şahin, B. (2013): Evaluation and determination of rangeland vegetation in Kayseri province. – Journal of Central Research Institute for Field Crops 22(2): 86-95.
[61] Ünal, S., Mutlu, Z., Urla, Ö., Yıldız, H., Aydoğdu, M., Şahin, B., Aslan, S. (2014): Improvement possibilities and effects of vegetation subjected to long-term heavy grazing in the stepe rangelands of Sivas. – Journal of Central Research Institute for Field Crops 23(1): 22-30.
[62] Uzun, F., Garipoğlu, A. V., Algan, D. (2010): Plant characteristics and control of yellow starhistle (*Centaurea solstitialis* L.) appeared at our rangelands. – Anadolu J. Agric. Sci. 25(3): 213-222 (in Turkish).
[63] Wester, L. (1981): Composition of native grasslands in the San Joaquin Valley, California. – Madroño 28: 231-241.
[64] Weymer, H. (1981): Lernt Pflanzen Kennen. – Ferdinand Enke Verlag, Stuttgart.
[65] Yavuz, T., Sürmen, M., Töngel, M. Ö., Avağ, A., Özaydın, A. K., Yıldız, H. (2011): Vegetation characteristics of pastures in Samsun province. – 9. Field Crops Congress of Turkey, 12-15 September, Bursa, pp. 1773-1778 (in Turkish).
[66] Yavuz, T., Sürmen, M., Töngel, M. Ö., Avağ, A., Özaydın, K., Yıldız, H. (2012): Some characters of pasture vegetation in Amasya province. – TABAD 5(1): 181-185 (in Turkish).

http://www.aloki.hu ● ISSN 1589 1623 (Print) ● ISSN 1785 0037 (Online)
DOI: http://dx.doi.org/10.15666/aeer/1706_1553115546

SPRING LEAF PHENOLOGICAL CHARACTERISTICS OF COMMON LANDSCAPE TREE SPECIES IN NYINGCHI PREFECTURE, TIBET, CHINA

LIU, Z. N. – XU, J.*

Resources & Environment College, Tibet Agriculture & Animal Husbandry University
Tibet, Nyingchi 860000, China
(e-mail: 799748121@qq.com; phone:+86-136-2894-7896)

**Corresponding author*
e-mail: 872395595@qq.com; phone: +86-136-5894-2629

(Received 3rd Aug 2019; accepted 14th Nov 2019)

Abstract. Studying the phenological characteristics of landscape trees can determine the optimal afforestation time for local landscaping, while also providing a theoretical basis for garden design, plant configuration and garden phenology prediction. In order to grasp the leaf pheniological rhythm of common landscape tree species in Nyingchi Prefecture, optimize the garden plant configuration of Nyingchi Prefecture, 53 kinds of landscape tree species were selected as the object for continuous 5a parallel observation and analysis of their leaf phenology. The results showed that: the budding period lasts from early March to mid-April, and that of 20 species concentrates in late March. It is recommended that afforestation be completed before mid-April. The leaf expansion period lasts from early March to mid-June, and the peak period is from mid-April to early May. It is recommended to arrange the seasonal landscape according to the leaf expansion characteristics of the tree species. The 53 tree species were classified into 5 types based on leaf phenological characteristics. Finally, corresponding measures and suggestions were proposed for local garden afforestation and tree arrangement.
Keywords: *Tibet, phenological phase, budding, leaf expansion, leaf phenology classification*

Introduction

The phenology of plants refers to their cyclical changes with the climate during annual growth, including budding, branching, leaf expansion, flowering, fruiting, defoliation and dormancy. The external features exhibited by plant organs in different phenological stages are known as phenophase (Zhao et al., 2016). Phenology is often used to study the natural seasonal variation of plants, which has long been valued by biologists (Zhao, 1983). The data for phenological changes can not only provide guidance on afforestation (Wang, 2006; Chang et al., 2011), but also offer certain reference value for optimal configuration of plant landscapes (Yang and Chen, 2000; Xu et al., 2004; Chen et al., 2011), so that the matching relationship of landscapes between different time periods is coordinated, thus exhibiting the temporal and special beauty of the landscape (Hu et al., 2006; Zhang et al., 2008; Gu and Zhang, 2011).

The dynamic landscape of a region's gardens is, to a large extent, a result of phenological seasonal variations of garden plants. The phenological phases differ for different regions. Studying the phenological changes of local garden plants can provide certain basis and reference for local plant community construction and seasonal landscape, garden plant landscaping. So far, there have been garden phenology related researches mainly in Beijing (Zhang et al., 2018), Shanghai (Zhao et al., 2016), Nanjing (Zhang et al., 2016), Xi'an (Bai et al., 2016), Changchun (Chen et al., 2015), Hengshui (Liu et al., 2013) and Hohhot (Gu and Zhang, 2015), while phenological studies on

http://www.aloki.hu ● ISSN 1589 1623 (Print) ●ISSN1785 0037 (Online)
DOI: http://dx.doi.org/10.15666/aeer/1706_1554715558

Nyingchi in Tibet Autonomous Region are few. Only a few scholars such as Liu et al. (2015), Xue et al. (2014), Ma et al. (2010), and Wang et al. (2019) have done research from different perspectives of forestry. Study on garden phenology of Nyingchi is extremely scarce. In view of this, with 53 kinds of common landscape trees in Nyingchi as testing pieces, this study researched and analyzed the characteristics of budding and leaf expansion phenology, with a view to providing a useful reference for optimizing the garden plant configuration of Nyingchi Prefecture and upgrading the connotation and quality of garden landscape.

Research method

Overview of the study area

The study area is located in Fujian Park and Wetland Park in Nyingchi Prefecture, Tibet (*Fig. 1*), which is at the densely populated commercial and cultural center of Nyingchi Prefecture. It is located in the lower reaches of the Yarlung Zangbo River in southeastern Tibet (E93°25', N29 °50'), with an elevation of 2,960 m, an average annual temperature of 8.7°C, an average annual rainfall of 650 mm, an average relative humidity of 71%, annual sunshine hours of 2,022.2 h, a sunshine percentage of 46% and a frost-free period of 180 d (Ran et al., 2013).

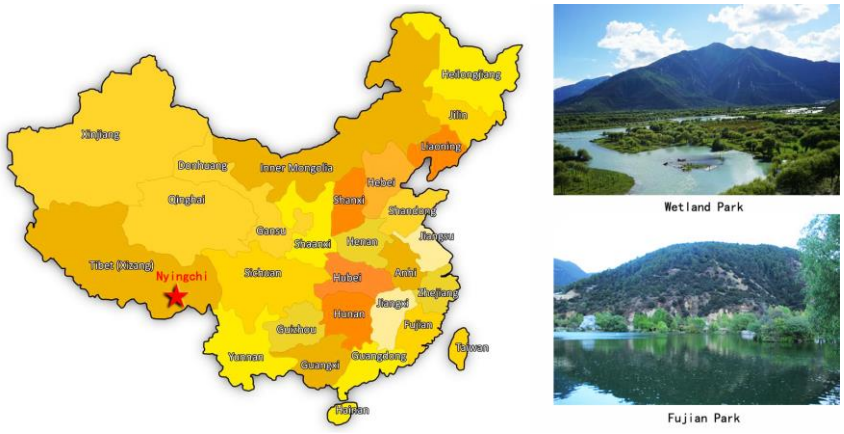

Figure 1. *Sample area location and habitat status map*

The humid climate belongs to the warm and humid climate zone in southeastern Tibet. Known as the “Snowy Regions South of the Yangtze River”, it boasts rich and varied garden plants. The park's greening is mainly native tree species like local wild ornamental seedlings, together with sporadic and small-scale landscape trees introduced from the interior areas. Fujian Park covers an area of 12.4 hm^2. 59 species of woody garden plants were introduced and cultivated from the interior area at its construction (Liu et al., 2015). With the continuous construction of the park, there are 72 species of arbors and 46 species of shrubs in general overall growth. The wetland park covers an area of 35.1 hm^2. Mainly composed of native plants, the near natural urban forest has 68 species of arbors and 56 species of shrubs in good overall growth. These two parks serve as key city-level parks in Nyingchi Prefecture, which play an important role in improved ecological balance, citizens' recreation and enhanced physical and mental health.

http://www.aloki.hu ● ISSN 1589 1623 (Print) ●ISSN1785 0037 (Online)
DOI: http://dx.doi.org/10.15666/aeer/1706_1554715558

During the study period (2014-2019), the average annual temperature of the study area is 8.9°C, the average annual rainfall is 648 mm and the average relative humidity is 71%. The annual average temperature is slightly higher than previous years, the rainfall and the relative humidity are almost the same as previous years. The climate change has a certain impact on the observation results (Nyingchi, 2014-2019).

Sample selection

In this study, 53 species of deciduous trees with large planting area, large number and strong group representation were selected as observation objects (*Table 1*), including 31 species of arbors, 20 species of shrubs and 2 species of vines (which were omitted in this study due to the relatively simple phonological ornamental function of coniferous evergreen species). Three strains of representative plants (middle-aged trees in an open area, enjoying healthy growth without plant disease or insect pests, and with flowering and fruiting for 3a) were selected from each plant type, and the community and soil type, elevation, slope data were recorded.

Observation methods

According to the "Chinese Phenology Observation Method", the selected 53 species of trees were subject to fixed-strain (marked by tag), fixed-person, regular observation for budding and leaf expansion phenology from March to June of 2014~2019. The observation period was 1 time every 2 d in the early stage and 1 time every week in the late stage, which lasted for 122 d. To reduce the error, fixed personnel made observations mainly based on visual inspection using combination of tools like telescope, magnifying glass, etc. (Wan et al., 1978; Zhang, 1985). Phenology data were recorded at 14:00-17:00 on the observation day. To facilitate observation and comparison, south side of all samples was selected for observation. To facilitate comparison between different years, all data are preprocessed first, then Julian Day conversion was applied for phenological date, which was to calculate the period from March 1 to the date as Julian Day (Zhu and Wan, 1980).

Phenological observation criteria: the budding period refers to the period when buds of the plants display green leaf opex (in the case of scales, the time shall prevail when scales are cracked to reveal bright colors at the bud top). The leaf expansion period is divided into initial stage of leaf expansion, peak period of leaf expansion and end of leaf expansion. Initial leaf expansion means the buds of individual branches of the observed object show the first batch of flat leaves; peak period of leaf expansion means leaflets on half of the branches of the observed object are completely flattened; end of leaf expansion means over 90% of the leaflets of the observed object are completely flattened. The duration of leaf expansion refers to the interval between the initial and end of leaf expansion (Wan and Liu, 1979).

Data processing

Correlation analysis on different parameters in this study was conducted by Pearson correlation coefficient test, and phenological phase load analysis was performed by principal component analysis. Data processing was completed by Excell 2007 and SPSS25.0. In order to facilitate the query and distinguish the phenological phases, the results took 10 d as the unit in which month was divided into three segments: first, middle and last ten days.

http://www.aloki.hu ● ISSN 1589 1623 (Print) ●ISSN1785 0037 (Online)
DOI: http://dx.doi.org/10.15666/aeer/1706_1554715558

Table 1. *Leaf phenology of common landscape trees in Nyingchi Prefecture*

Serial No.	Scientific name	Budding period *	Initial stage of leaf expansion *	Peak period of leaf expansion*	End of leaf expansion*	Duration of leaf expansion/d
1	*Larix griffithiana*	3.16	3.20	4.3	4.13	24
2	*Metasequoia glyptostroboides*	3.29	4.11	4.25	5.1	20
3	*Betula utilis*	3.31	4.4	4.20	5.2	28
4	*Ginkgo biloba*	4.11	4.16	4.25	5.12	26
5	*Michelia alba*	3.23	3.29	4.10	4.25	27
6	*Juglans regia*	4.11	4.17	4.30	5.10	23
7	*Platanus acerifolia*	4.11	4.16	4.30	5.13	27
8	*Populus szechuanica* var. *tibetica*	4.5	4.5	4.20	5.2	27
9	*Malus halliana*	3.20	3.20	4.13	4.24	35
10	*Salix alba*	3.5	3.5	3.17	3.26	21
11	*Salix cheilophila*	4.4	4.4	4.18	4.28	24
12	*Myricaria elegans*	4.9	4.18	5.9	5.26	34
13	*Ulmus pumila* 'jinye'	3.27	4.8	4.23	4.31	23
14	*Morus mongolica* var. *diabolica*	4.16	4.19	5.5	5.19	30
15	*Rosa xanthina*	4.24	4.30	5.10	5.19	19
16	*Rosa omeiensis*	3.31	4.4	4.22	5.7	33
17	*Amygdalus mira*	3.30	3.30	4.14	4.25	26
18	*Amygdalus triloba*	3.11	3.11	3.25	4.9	29
19	*Prunus cerasifera* f. *atropurpurea*	3.25	4.1	4.13	4.22	21
20	*Pyrus bretschneideri*	3.22	4.3	4.18	5.1	28
21	*Armeniaca mume* var. *bungo*	3.20	4.9	4.20	4.28	19
22	*Cerasus serrulata* var. *lannesiana*	3.16	4.4	4.17	5.1	27
23	*Malus pumila*	3.20	4.7	4.26	5.3	26
24	*Malus halliana*	3.2	3.2	3.22	3.29	28
25	*Malus baccata*	3.23	4.4	4.19	5.1	27
26	*Crataegus pinnatifida*	4.26	5.2	5.18	5.30	28
27	*Sorbus rehderiana*	4.4	4.8	4.23	5.4	26
28	*Spiraea canescens*	3.29	4.3	4.24	5.8	35
29	*Sorbaria arborea*	3.29	4.4	4.23	5.12	38
30	*Rubus biflorus* var. *biflorus*	4.11	4.16	4.29	5.9	23
31	*Sophora japonica* var. *japonica* f. *pendula*	4.16	4.25	5.11	5.20	25
32	*Robinia pseudoacacia*	4.8	4.20	5.3	5.19	29
33	*Cercis chinensis*	4.21	5.6	5.28	6.18	42
34	*Wisteria sinensis*	4.25	4.25	5.12	5.26	31
35	*Caragana bicolor*	5.6	5.11	5.28	6.18	30
36	*Desmodium callianthum*	4.9	4.14	4.26	5.6	22
37	*Piptanthus nepalensis*	3.5	3.13	3.22	3.29	16
38	*Syringa oblata*	3.14	3.20	4.1	4.9	20
39	*Fraxinus chinensis*	4.11	4.26	5.5	5.13	17
40	*Chionanthus retusus*	4.18	4.25	5.5	5.13	18
41	*Forsythia suspensa*	3.26	4.15	4.30	5.13	28
42	*Chimonanthus praecox*	4.3	4.3	4.17	5.2	29
43	*Swida alba*	3.22	3.29	4.13	4.24	26
44	*Paeonia ludlowii*	3.31	4.5	4.20	5.1	26
45	*Hippophae rhamnoides* subsp. *gyantsensis*	3.10	3.20	4.15	5.6	47
46	*Berberis thunbergii* var. *atropurpurea*	3.13	3.13	3.29	4.10	28
47	*Acer caudatum*	4.8	4.17	5.1	5.13	22
48	*Acer palmatum* cv.*atropurpureum*	4.11	4.20	5.3	5.12	26
49	*Celastrus stylosus*	3.28	4.12	4.28	5.10	28
50	*Hypericum choisianum*	3.2	3.30	4.15	4.27	28
51	*Zanthoxylum motuoense*	4.22	4.28	5.12	5.21	23
52	*Lagerstroemia indica*	5.6	5.17	6.2	6.16	30
53	*Punica granatum*	4.30	5.4	5.20	6.2	28

Note: *: Phenological time is represented by the number of days from March 1 (Julian Day)

http://www.aloki.hu ● ISSN 1589 1623 (Print) ●ISSN1785 0037 (Online)
DOI: http://dx.doi.org/10.15666/aeer/1706_1554715558

Results and analysis

Phenological phase observation on budding and leaf expansion

It can be seen from *Table 1* and *Fig. 2* that the budding period of the 53 common landscape tree species in Nyingchi Prefecture lasts from the beginning of March to the beginning of May, and the concentration period is mid-to-late March (26 species, 49.06%). The budding characteristics of different plant species vary greatly, with the earliest budding in *Salix alba*, *Piptanthus nepalensis* (March 5), while *Caragana bicolor*, *Lagerstroemia indica* have the latest budding (May 6), with a discrepancy of 62d between the two.

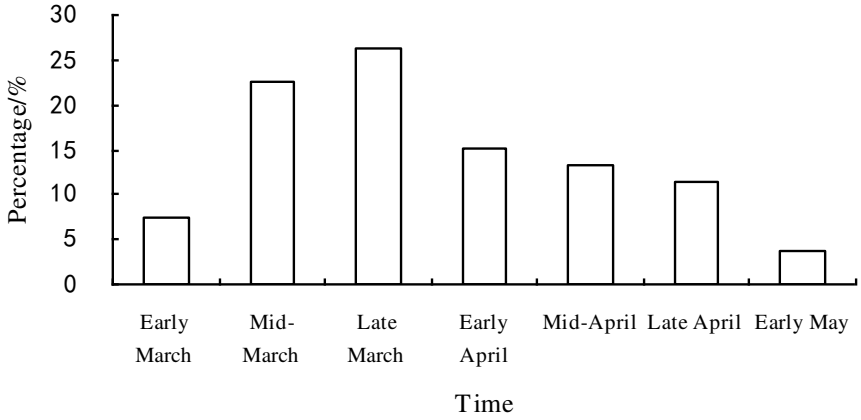

Figure 2. *Budding characteristics of 53 landscape trees*

Phenological characteristics of leaf expansion

It can be seen from *Table 1* and *Fig. 3* that the leaf expansion period of the 53 common landscape tree species lasts from the beginning of March to the middle of June. Initial stage of leaf expansion lasts from early March to mid-May. Where, *Salix alba* has the earliest initial leaf expansion (March 5), *lagerstroemia indica* has the latest initial leaf expansion (May 17), with a discrepancy of 73 d between the two. Peak period of leaf expansion lasts from mid-March to late May. Where, *Salix alba* is the earliest in peak leaf expansion (March 17), *Caragana bicolor* is the latest in peak leaf expansion (May 28), with a discrepancy of 72 d between the two. End of leaf expansion lasts from late March to mid-June. Where, *Salix alba* has the earliest end of leaf expansion (March 26), *Caragana bicolor* has the latest end of leaf expansion (June 18), with a discrepancy of 84 d between the two. The average duration of leaf expansion is 26.81 d, which is relatively long. In terms of the duration of leaf expansion, the longest is *Hippophae rhamnoides* subsp. *gyantsensis* (47 d), the shortest is *Piptanthus nepalensis* (16 d), with a discrepancy of 31 d between the two.

The initial stage of leaf expansion is mainly concentrated in early April (14 species, 26.41%) and mid-April (12 species, 22.64%), the peak period of leaf expansion is mainly concentrated in mid-April (15 species, 28.30%) and late April (14 species, 26.41%), and the end of leaf expansion is mainly concentrated in mid-May (18 species, 33.96%) and late May (12 species, 22.64%). It provides a theoretical basis for the construction time to local landscape.

http://www.aloki.hu ● ISSN 1589 1623 (Print) ●ISSN1785 0037 (Online)
DOI: http://dx.doi.org/10.15666/aeer/1706_1554715558

The analysis shows that there exists a significant correlation between the initial stage of leaf expansion and budding period, the peak period of leaf expansion and the budding period, the end of leaf expansion and the budding period (*Table 2*). It indicates close correlation between leaf expansion time and budding time. Tree species with earlier budding period have earlier leaf expansion stage，the result is consistent with Zhao et al. (2016). The average interval between budding period and initial stage of leaf expansion is 7.11 d. The result showed that: Some species had no budding period and they are mainly Salicaceae, such as *Populus szechuanica* var. *Tibetica*,*Malus hallian*, *Salix alba* et al. On the other hand, the longest interval between budding period and initial stage of leaf expansion was *Hypericum choisianu* (28 d). In addition, the duration of leaf expansion is significantly correlated with the end of leaf expansion, but not with other parameters of leaf phenology.

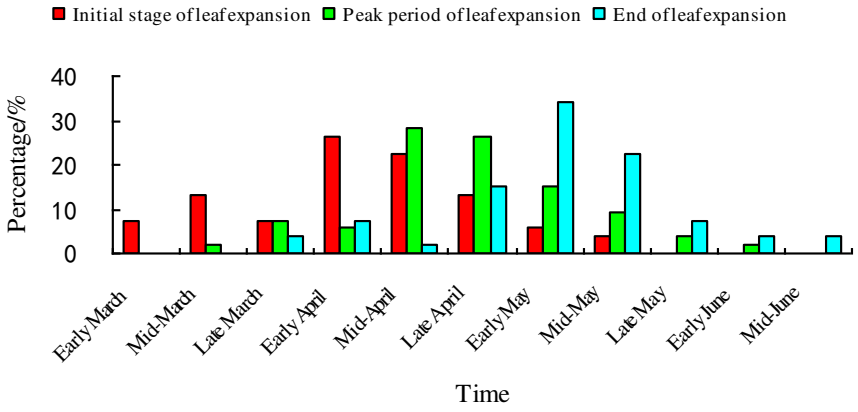

Figure 3. *Leaf expansion characteristics of 53 landscape trees*

Table 2. *Total variance of the original variables explained in leaf phenology PCA of each tree species*

	Budding period	**Initial stage of leaf expansion**	**Peak period of leaf expansion**	**End of leaf expansion**	**Leaf extension duration**
Budding period	1	0.943**	0.921**	0.897**	0.032
Initial stage of leaf expansion	0.943**	1	0.973**	0.943**	0.010
Peak period of leaf expansion	0.921**	0.973**	1	0.982**	0.203
End of leaf expansion	0.897**	0.943**	0.982**	1	0.342*
Leaf extension duration	0.032	0.010	0.203	0.342*	1

Note: $^{**}P<0.01$, $^{*}P<0.05$

Leaf phenology classification of 53 tree species

According to the classification of phenological differences between tree species, to more clearly study the occurrence and duration of phenology of different tree species, this study conducted principal component analysis on budding and leaf expansion phenology of 53 tree species (*Table 3*). The analysis shows that the two main components of budding period and initial stage of leaf expansion play a significant role, with a contribution rate of 77.203% and 20.908%, respectively, and the cumulative variance is 98.111%. At the same time, it can be seen from *Table 4* that the budding and leaf expansion parameters of the first principal component have high factor loading,

http://www.aloki.hu ● ISSN 1589 1623 (Print) ●ISSN1785 0037 (Online)
DOI: http://dx.doi.org/10.15666/aeer/1706_1554715558

which can represent the budding period, the initial stage, the peak and the end of leaf expansion respectively. Duration of leaf expansion in the second principal component has a higher factor loading, which can represent the duration of leaf expansion. The results are consistent with the correlation analysis (*Table 2*) between the various phenological parameters.

From the results of the above correlation analysis combined with *Fig. 4*, the leaf phenology of the 53 tree species can be divided into five categories. First, according to leaf budding time, there are three types of early, middle and late budding, each of which can be further divided into two categories according to the duration of leaf expansion.

Category 1: Early budding - short-medium duration of leaf expansion. The budding time is concentrated on March 5 and 6, and the leaf duration is 16～28 d. The tree species include *Salix alba*, *Piptanthus nepalensis*, and *Malus halliana* (5.66%). Where, *Piptanthus nepalensis* has the shortest duration of leaf expansion among the 53 species (16 d).

Table 3. *Correlation coefficients matrix for phenological parameters*

Component	Initial eigenvalue			Extraction sum of squared load		
	Total	Variance %	Cumulative %	Total	Variance %	Cumulative %
1	3.860	77.203	77.203	3.860	77.203	77.203
2	1.045	20.908	98.111	1.045	20.908	98.111
3	0.084	1.678	99.789			
4	0.011	0.211	100.000			
5	0.005	0.110	100.000			

Table 4. *Statistics of the first 2 PCs of leaf phenology for each tree species*

	PC1	PC2
Budding period	0.953	-0.174
Initial stage of leaf expansion	0.977	-0.189
Peak period of leaf expansion	0.992	0.006
End of leaf expansion	0.986	0.148
Duration of leaf expansion	0.202	0.979

Category 2: Early budding-long duration of leaf expansion. There is only one species (1.89%), i.e. *Hippophae gyantsensis*, whose budding time is March 10, and the duration of leaf expansion is the longest (47 d) among the 53 tree species.

Category 3: Medium budding –medium-short duration of leaf expansion. The budding time is concentrated between March 11 to April 16, and the duration of leaf expansion is 17~38 d. There are 40 tree species (75.47%), including *Larix griffithii*, *Populusszechuanicavar.tibetica*, *Hypericum choisianum*, *Prunus mira*, *Desmodium callianthum Franch*, *Morus mongolica var. Diabolica*, *Celastrus stylosus*, *Sorbus rehderiana*, *Acer caudatum*, *Sorbaria arborea*, *Myricaria elegans Royle*, *Salixaureo-pendula*, *Cerasus yedoensis*, *Syringa oblata*, etc.

Category 4: Late budding – medium-short duration of leaf expansion. The budding time is concentrated on April 18-May 6, and the duration of leaf expansion is 18～31 d. There are 8 tree species (15.09%), including *Chionanthus retusus*, *Rosa xanthina*, *Zanthoxylum motuoense*, *Fructus Crataegi*, *Chinese wisteria*, *Caragana bicolor*,

http://www.aloki.hu ● ISSN 1589 1623 (Print) ●ISSN1785 0037 (Online)
DOI: http://dx.doi.org/10.15666/aeer/1706_1554715558

Lagerstroemia indica. Where, *Lagerstroemia indica* has the latest end of leaf expansion among the 53 tree species (June 16).

Category 5: Late budding- long duration of leaf expansion. There is only one species (1.89%), i.e. *Cercis chinensis*, whose budding time is April 21, and the duration of leaf expansion is 42 d.

It can be seen from the above that the spring leaf phenology of the landscape tree species in the prefecture mainly features "medium budding-medium-short duration of leaf expansion". The type accounts for 75.47% of the investigated tree species.

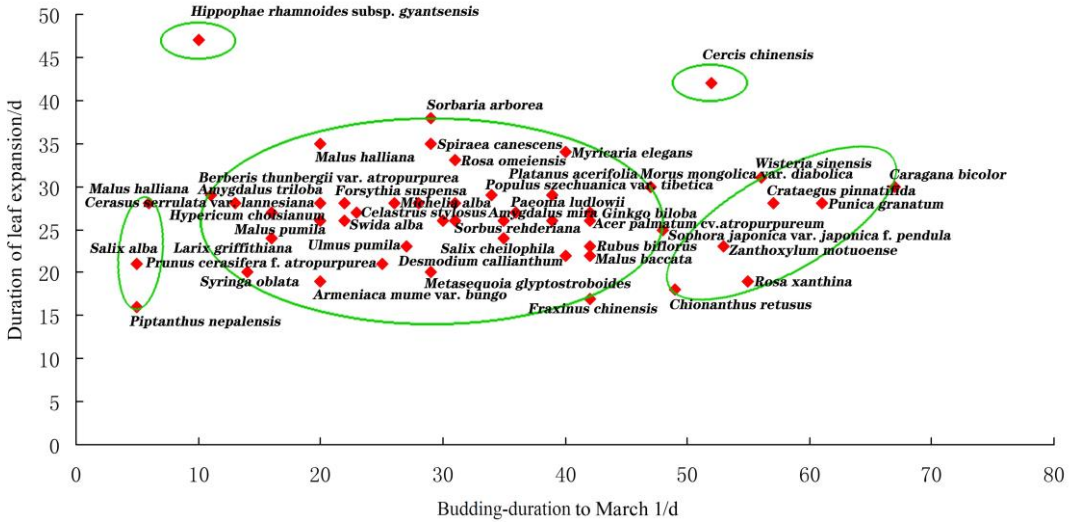

Figure 4. *Scatter plot of budding-duration of leaf expansion*

Discussion

Sequential correlation of budding phenology

Zhao et al. (1979) proposed sequential correlation law of phenology through correlation analysis on tree phenology, who believed that phenological phenomena were related to the emergence of another phenological phenomenon. Cao and Liu (1999) conducted clustering analysis on 16 broad-leaved trees in Nanchang Arboretum for the management of forest culture time, while phenological combination of urban landscape trees was not much studied. The phenological studies in Europe show that the phenology of plants in the mid-latitudes such as budding and leaf expansion depends mainly on temperature (Sparks et al., 2000; Kramer et al., 2000; Chmielewski and Rotzer, 2001; Fitter et al., 2002; Broadhead et al., 2003), which is consistent with the conclusion of phenological study by Zhang et al. (1995) on Beijing. Nyingchi Prefecture located in the western part of China has relatively cold winter and spring. Temperature is the dominant factor affecting the budding and leaf expansion of trees. The various trees have concentrated budding and leaf expansion, with difference weakened by the dominant environmental factors, which is consistent with phenological study by Hu et al. (2016) on Shenyang.

With the recent increase of temperature, the plant growth season is prolonged and the spring phenology is advanced (Ahas et al., 2000; Anderson et al., 2005). At present, phenological research focuses on the relationship between phenology and climate

http://www.aloki.hu ● ISSN 1589 1623 (Print) ●ISSN1785 0037 (Online)
DOI: http://dx.doi.org/10.15666/aeer/1706_1554715558

change (Zhao et al., 1983; Menzel and Fabian, 1999; Schwartz and Reiter, 2000; Walther et al., 2000), phenology response to the environment (Snyder et al., 2001; Augspurger, 2008; Ahas, 2009). Constructing different predictive models (Li et al., 2000) for corresponding studies on communities and above is an important aspect of future phenological research.

Budding phenology and afforestation

Due to its special natural environmental conditions, Tibet has difficulty in afforestation, and the budding period of different tree species varies greatly. “Not high survival rate of afforestation, frequent phenomenon of repeated replanting”, “no tree despite years of afforestation” are prominent problems in most areas for a long time (Liu et al., 2015; Zhang et al., 2016). Afforestation faces easy damage and difficult recovery, further increasing the pressure on Tibet's ecological environment.

Practice has proved that planting before leaf budding can significantly improve the afforestation survival rate of local landscape tree species. Examples of planting failures are frequent in Nyingchi Prefecture due to improper planting seasons (especially old tree transplants). According to the leaf phenological characteristics of the landscape trees in the Prefecture, the first and second types of tree species with earlier budding are recommended to be planted in late February. The third type of tree with moderate budding time is suitable for planting in March. Where, *Larix griffithii*, *Prunus triloba*, *Syringa oblate*, etc. with relatively early budding are suitable for planting in early March, while *Morus mongolica Schneid*, *Chinese pagoda tree*, *Fraxinus chinensis*, etc. with relatively late budding are suitable for planting in late March. The 4th and 5th category of tree species with the latest budding time are suitable for planting before mid-April. Recent years have witnessed vigorous development of ecological construction projects in the Prefecture. Under the premise of respecting nature, adapting to local conditions and planting at the right time can effectively improve survival rate of landscape tree planting, enhance the water source conservation function, effectively curb sandstorm hazard, especially the “air drying phenomenon” prevalent in the Prefecture (Liu et al., 2015), and improve the green looking ratio and the ornamental and ecological effects, greatly promote the gradual transition of the Prefecture's green space from “single-layer structure” to “multi-layer ecological structure”, thus creating unique plateau urban garden landscape in Tibet.

Leaf expansion phenology and landscape construction

Studies have shown concentrated phenology in Nyingchi Prefecture. There are few tree species with early budding and late budding. Medium budding time is the main case, which is mainly concentrated in mid-March to mid-April. This is not conducive to seasonal aspect and continuous landscape construction. Garden landscaping should consider the influence of plant budding period, seasonal distribution and duration of leaf expansion on landscaping. The landscape trees with early leaf expansion and late leaf expansion should be rationally combined in planting to optimize plant collocation, which can enrich seasonal scenery in spring, extend the viewing time, enhance ecological benefits and also provide biological basis for the local garden planning and design, cultivation management and plant configuration to form rich urban landscape. It is suggested that 5 types of leaf phenological species be combined with each other to better construct local characteristic garden landscapes and enrich the community levels.

http://www.aloki.hu ● ISSN 1589 1623 (Print) ●ISSN1785 0037 (Online)
DOI: http://dx.doi.org/10.15666/aeer/1706_1554715558

Garden phenology forecast

With the development of local tourism, Nyingchi Prefecture has become an international tourism city with increasingly developed relevant tourism industry. Affected by natural factors such as climate fluctuations, phenology of local landscape plants varies from year to year. Studies on garden phenology to accumulate relevant phenological data is conducive to the accurate implementation of relevant garden phenology prediction work, thus providing guidance for the annual "Peach Blossom Festival", garden visit, travel and tourists' sightseeing.

Conclusion

1). Budding and leaf expansion phenology features long duration. The budding period of the 53 common landscape tree species in Nyingchi Prefecture is concentrated in the middle and late March, with a total duration of 62 d and an average duration of 7.56 d. The entire leaf expansion period lasts from early March to mid-June, with a total duration of 108 d and an average duration of 26.81 d. The total duration and average duration of budding and leaf expansion periods are longer than those of Shanghai (Zhao et al., 2016), which may be related to the local cold climate and the difference between seed selection objects. Therefore, it is recommended the afforestation should be completed before mid-April according to the leaf phenological characteristics of Nyingchi Prefecture.

2) There is a significant correlation between the initial stage of leaf expansion and budding period, the peak period of leaf expansion and the budding period, and the end of leaf expansion and budding period. The duration of leaf expansion is significantly correlated with the end of leaf expansion, but not with other parameters of leaf phenology. It is recommended to arrange the seasonal landscape according to the leaf expansion characteristics of the tree species.

3) The leaf phenological type is mainly "medium budding – medium-short duration of leaf expansion". Corresponding suitable planting time was proposed based on tree species with different phenological types in Nyingchi Prefecture.

Acknowledgements. The project was funded by the National Natural Science Foundation of China (51568059).

REFERENCES

[1] Ahas, R., Jaagus, J., Aasa, A. (2000): The phenological calendar of Estonia and its correlation with mean air temperature. – Int. J. Biometeorol 44(4): 159-166.

[2] Ahas, R. (2009): Long term phyto-， ornitho- and ichthyo phenological time series analyses in Estonia. – International Journal of Biometeorology 42: 119-127.

[3] Anderson, D. P., Nordheim, E. V., Moermond, T. C., Gone, B. Z. (2005): Factors influencing tree phenology in TaÏ National Park, Côte d'lvoire. – Biotropica. Côte d'lvoire 37: 631-640.

[4] Augspurger, C. K. (2008): Early spring leaf out enhances growth and survival of sapling in a temperate deciduous forest. – Oecologia 156: 281-286.

[5] Bai, J., Ge, Q. S., Dai, J. H., Wang, Y. (2016): Relationship between woody plants phenology and climate factors in Xi'an, China. – Chinese Journal of Plant Ecology 34(11): 1274-1282.

http://www.aloki.hu ● ISSN 1589 1623 (Print) ●ISSN1785 0037 (Online)
DOI: http://dx.doi.org/10.15666/aeer/1706_1554715558

[6] Broadhead, J. S., Ong, C. K., Black, C. R. (2003): Tree phenology and water availability in semi-arid agroforestry systems. – Forest Ecology and Management 180: 61-73.
[7] Cao, Z. B., Liu, G. Z. (1999): Study on phenological characteristics of 16 fine broad-leaved tree species. – Jiangxi Forestry Science and Technology 4: 1-3.
[8] Chen, S. P., Dai, X. Z., Guo, T. J., Zhuang, Q. Q. (2015): Phenophase of landscape trees and its application in disposition of plants in Changchun City. – Journal of Jilin Agricultural University 33(2): 189-194.
[9] Chmielewski, F. M., Rotzer, T. (2001): Response of tree phenology to climate change across Europe. – Agric. For. Meteorol 108(2): 101-112.
[10] Fitter, A. H., Fitter, R. S. (2002): Rapid changes in flowering time in British plants. – Science 296: 1687-1691.
[11] Gu, A. Z., Zhang, H. L. (2015): The phenological characteristics of twenty major tree species of flower in the spring in Hohhot. – Northern Horticulture 12: 78-80.
[12] Hu, J. B., Xu, W. D., Chen, W., He, X. Y., Wen, H. (2016): Phenological analysis of main tree species in Shenyang urban forest. – Chinese Journal of Ecology 25(12): 1455-1459.
[13] Kramer, K., Leinonen, I., Loustau, D. (2000): The importance of phenology for the evaluation of impact of climate change on growth of boreal, temperate and Mediterranean forests ecosys-tems: An overview. – Int. J. Biometeorol 44(2): 67-75.
[14] Li, R. P., Zhou, G. S., Yan, Q. L. (2015): Study on plants phonological model. – Chinese Journal of Agrometeorology 26(4): 210-214.
[15] Liu, G. R. (2013): Phenological observation on common garden plants in Hengshui City. – Hubei Agricultural Sciences 52(16): 3884-3888.
[16] Liu, Z. N., Zhou, P., Pan, G., Fang, J. P., Wang, W., Zhang, H. F. (2015): Investigation and application research of landscape plants in Tibet of Shigatse City. – Northern Horticulture 20(29): 74-80.
[17] Liu, Z. N., Zhou, P., Yao, X. Z., Bao, L. Y. (2015): Research about the woody landscape plants' introduction in Linzhi Preferecture of Tibet. – Journal of Sichuan Agricultural University 23(29): 208-213.
[18] Liu, Z. N., Zhang, H. F., Wang, W., Zhou, P., Hao, W. Y., Xu, J. (2017): Resources of Colored-leaf Trees and Their Phenological Ornamental Characteristics in Linzhi City. – Journal of Northwest Forestry University 32(4): 266-273.
[19] Ma, H. P., Zhu, X. L., Yang, X. L., Pan, G., Jin, Z. T. (2010): Study on the phenology characteristics of Juglans regia L. in Linzhi area of Tibet. – Journal of Anhui Agricultural Sciences 38(33): 18960-18962.
[20] Menzel, A., Fabian, P. (1999): Growing season extended in Europe. – Nature 397(6721): 659.
[21] Nyingchi, S. B. (2014-2019): Nyingchi statistical yearbook. – China Statistics Press, Beijing.
[22] Ran, G. H., He, Q. Y., Fan, S. H., Wang, D. (2013): Analysis of precipitation agricultural climate resources in Linzhi area. – Agriculture and Technology 1: 142-144.
[23] Schwartz, M. D., Reiter, B. E. (2000): Changes in North American spring. – Int. J. Climatol 20(8): 929-932.
[24] Snyder, R. L., Spano, D., Duce, P. (2001): Temperature data for phenological models. – Int. J. Biometeorol 45(4): 178-183.
[25] Sparks, T. H., Jeffree, E. P., Jeffree, C. E. (2000): An examination of the relationship between flowering times and temperature at the national scale using long-term phenological records from the UK. – Int J Biometeorol 44: 82-87.
[26] Walther, G. R., Post, E., Convey, P. (2002): Ecological responses to recent climate changes. – Nature 416: 389-395.
[27] Wan, M. W., Liu, X. Z. (1979): Phenological observation method in China. – Science Press, Beijing.

http://www.aloki.hu ● ISSN 1589 1623 (Print) ●ISSN1785 0037 (Online)
DOI: http://dx.doi.org/10.15666/aeer/1706_1554715558

[28] Xue, L. S., Luo, D. Q. (2014): Relationship analysis on phenological characteristics of Paeonia ludlowii with its main meteorological factors. – Guangdong Agricultural Sciences 7: 43-47.
[29] Zhang, F. C. (1985): Phenology. – China Meteorological Press, Beijing.
[30] Zhang, F. C. (1995): Effects of global warming on plants phenological everts in China. – Acta Geographica Sinica 50(5): 402-409.
[31] Zhang, C. Y. (2016): Afforestation in Lasha river basin. – Forestry Construction 6: 29-32.
[32] Zhang, Z. X., Huang, Y. H., Wang, Y. X., Ye, J. Z., Li, X. L., Jiang, A. G. (2016): Investigation and application of flowering phenology of landscape plants in Nanjing. – Guizhou Agricultural Sciences 42(12): 195-198.
[33] Zhang, M. Q., Yang, G. D., Zhang, L. (2018): Study on season aspect characteristics in Beijing City. – Journal of Capital Normal University (Natural Science Edition) 29(5): 62-65.
[34] Zhao, F. C. (1983): Effects of global worming on plant phenological everts in China. – Acta geographica sinica 50(5): 402-410.
[35] Zhao, X. L., Shi, C. Y., He, B., Ran, W. R., Cai, Y. L. (2016): Spring phenological characteristics and phenophase classification of landscape greening tree species in Changming Island of Shanghai. – Chinese Journal of Ecology 32(9): 2275-2280.
[36] Zhu, K. Z., Wan, M. W. (1980): Phenology (Enlarged edition). – Science Press, Beijing.

http://www.aloki.hu ● ISSN 1589 1623 (Print) ●ISSN1785 0037 (Online)
DOI: http://dx.doi.org/10.15666/aeer/1706_1554715558

SALINIZATION PROCESS AND INFLUENCING FACTORS IN WESTERN JILIN PROVINCE, CHINA

BAO, S. C.[1*] – QIU, Y.Y.[1] – WANG, Q.[2] – WANG, Z. J.[3]

[1]*School of Civil Engineering, Jilin Jianzhu University*
No.5088 Xincheng Street, Changchun, Jilin, China
(phone: +86-135-9647-1419; fax: +86-0431-8456-6417)

[2]*College of Construction Engineering, Jilin University*
No.6 Ximinzhu Street, Changchun, Jilin, China

[3]*Jilin Team of Geological Survey Center of China Building Materials Industry*
No.6 Ximinzhu Street, Changchun, Jilin, China

[*]*Corresponding author*
e-mail: baoshuochao@126.com

(Received 3rd Aug 2019; accepted 14th Nov 2019)

Abstract. Saline soil is widely distributed in western Jilin province, China, agriculture and engineering are affected by the saline soil. Its formation and development process are influenced the most by factors of the natural geological environment. For the purpose of investigating the salinization process and influence factors in western Jilin, this study analyzes the saline soil of Nong'an in western Jilin Province, which was sampled during a field investigation. Thereafter, the characteristics of the water and salt migration in the soil have been investigated in the laboratory, the environmental factors of the study area, and the influence of the ecological environment on salinization have also been discussed. The results show that the water and salt migrate with seasonal changes in soil. The water content is low in autumn, and high in spring and summer. The salt content of the soil near the ground surface is low in autumn, and high in spring and summer, meanwhile, the salt content in the deep soil layers is low in spring and autumn, and high in summer. During both the unfrozen period and the frost-thawing periods, the soil salinization continues to enhance, and salinization eventually causes land desertification. This study can provide the theoretical basis for the protection of fragile ecological environments.
Keywords: *saline soil, soil enviroment, salinization process, secological environment, desertification*

Introduction

Saline soil is widely distributed in western Jilin province, China, which has caused decline in soil fertility and reduction in grain production (Wang, 1993). Further, the saline soil has also caused several engineering problems, such as road sinking, salt heaving and corrosion. In western Jilin, agricultural and engineering works are affected by saline soil. Western Jilin is located in a seasonally frozen ground area, in which the formation and process of development are influenced by the especial natural geological environment of the area.

According to earlier studies, the formation of saline soil in western Jilin is caused by the natural conditions and aggravated by the human activities (Wang et al., 2011; Zhang et al., 2013; Xu and Dou, 2013). Zhang and Li (2000) considered Songnen plian salinization development was exacerbated by the unreasonable land exploitation by humans, which caused secondary salinization. Yang and Luo (1999) studied the dynamic characteristics relationship between Songnen plain soil salinization and the underground water characteristics. He concluded that the salty underground water was a major

http://www.aloki.hu ● ISSN 1589 1623 (Print) ●ISSN1785 0037 (Online)
DOI: http://dx.doi.org/10.15666/aeer/1706_1555915572

contributor to the formation of the saline soil on the Songnen plain. Liu (2001) monitored the water and salt content movements of the saline soil in the Hongqi irrigation area in Songnen plain, China. Zheng (2005) discussed the driving force for the water and salt accumulation in winter. Wang et al. (2011) named the saline soil in western Jilin as dispersive soil and analyzed the influence factors of dispersibility and frost heaving characteristics. Bao et al. (2018) took laboratory test of salin soil in west Jilin to find out t the frost-heaving rate of soil.

This study aims to investigate the saline soil in Nong'an area of western Jilin, China. In this study, laboratory tests have been carried out to determine the characteristics of the soil samples. The environmental factors of the study area have also been analyzed, and the salinization process in western Jilin has been discussed. The results of this study can be used as a theoretical foundation of salinization treatment in western Jilin and the whole Songnen plain.

Material and Methods

The soil samples were collected from Nong'an area in western Jilin province, China. The study area is located in north of Song'nen plain in China, which is a typical temperate continental semiarid and arid monsoon climate area. This region has severe cold winters and torrid summers, with low annual precipitation. Based on the local salinizated distribution characteristics, two representative sampling locations have been chosen, which have been named as Location I (N: 44°22'43.02", E: 124°58'4.20") and Location II (N: 44°22'26.88", E: 125° 0'52.56"). The sampling locations are shown in *Fig. 1*.

Figure 1. *Sampling locations*

The ground surface of Location I was dry ang barely grass covered (*Fig. 2)*. The ground surface of Location II was grassland which is mostly covered by green grass in summer (*Fig. 3*). For the purpose of comparing the salinization processs, the soil samples were collected in May, June, September and November in 2015. The collected samples were at the depths of 0 cm, 20 cm, 30 cm, 40 cm from the ground surface.

The natural water content, salt content were tested in laboratory of soil samples to investigate the water and salt migration law of saline soil of western Jilin, then the

http://www.aloki.hu ● ISSN 1589 1623 (Print) ●ISSN1785 0037 (Online)
DOI: http://dx.doi.org/10.15666/aeer/1706_1555915572

environmental factors of the study area have also been investigated to analysis the salinization process. According to earlier studies, the salinization of western Jilin was due to the strong evaporation effect of the earth's surface (Chen, 2013; Kusmiyati, 2014; Wang et al., 2015). The evaporation effect is influenced by natural facotors such as temperture and rainfall, so this study choose 3 environment factors as temperture, precipitation and evaporation to discusse the salinaztion process. The enviroment data was investaged and processed from Chinameteorological Data Sharing Service System of China (CDSSSC).

Figure 2. *Location I*

Figure 3. *Location II*

Results

Water content seasonal variations

The soil samples were first weighed at the sampling location, and then dried in the laboratory in order to gain the natural water content. Water content was caluted by *Formula 1*.

$$W = \left(\frac{m_0}{m_d} - 1\right) \times 100\% \quad \text{(Eq.1)}$$

where
W - water content of soil, %.
m_d - mass of dry soil, kg.
m_0 - mass of wet (natural) soil, kg.

The water content variations with depths are shown as *Fig. 4*.

As shown in *Fig. 4*, natural water contens of soil water are between 5.0%~34.1%, water migrates with depth, but the migration laws are quite different in diffent seasons. For the purpose of studing the water seasonal migration law, water content seasonal variations of the soil samples at two locations are shown as *Fig. 5*.

As shown in *Fig. 4* and *Fig. 5*, for the soil samples at the two locations, the water contents are high in spring and summer, and low in autumn. For the soil samples near the ground surface, the water contents are low in spring, highest in summer, and then fall in autumn. For the soil samples at 20-30 cm depth, the water contents are highest in spring, and fall in summer. The gradients of the water seasonal variation curves are large in this range, and the water contents fall in autumn. For the soil samples at 40 cm depth, the water contents are relatively constant, which means that the water contents of these

http://www.aloki.hu ● ISSN 1589 1623 (Print) ●ISSN1785 0037 (Online)
DOI: http://dx.doi.org/10.15666/aeer/1706_1555915572

samples are about the same in spring and summer, but they are lower in autumn. Hence, it can be concluded that seasonal rainfall affect the soil near the ground surface more than that deep underground. Further, the surface soil always shows the variation of being dry in spring and autumn, and wet in summer as influenced by the short-term rainfall.

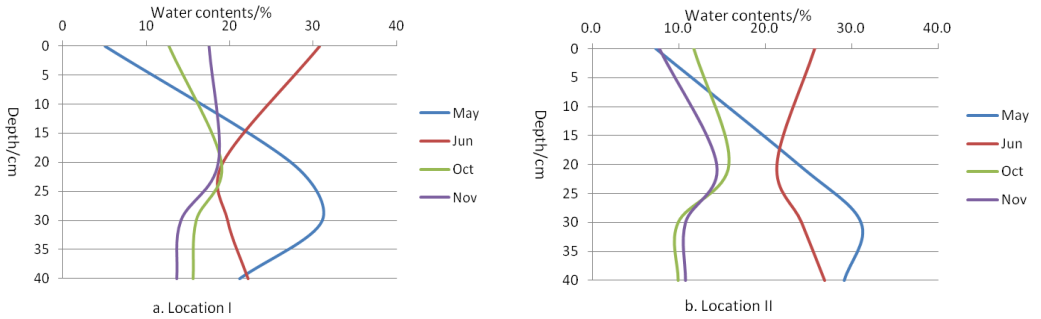

Figure 4. *Water content of soil samples at two locations*

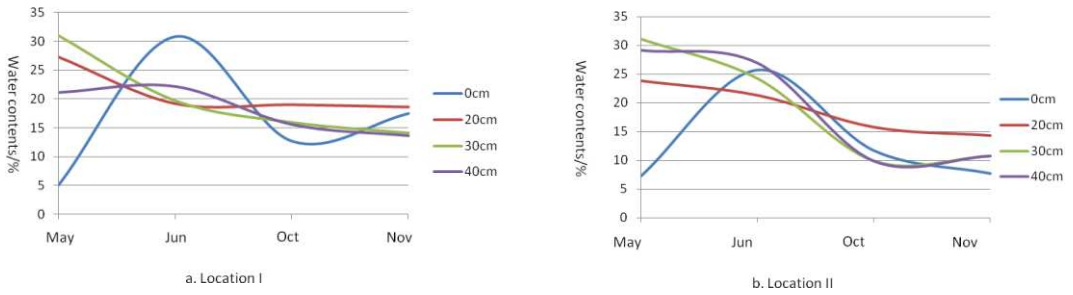

Figure 5. *Water content seasonal variations of soil samples at two locations*

Salt content seasonal variations

The salt contents of the soil samples have been tested by the distillation method, salt content variations with depths are shown as *Fig. 6*.

As shown in *Fig. 6*, salt migrates with depth in general. But the migration law are not only different between 2 locations, but also different in different seasons. For the purpose of studing the salt seasonal migration law, the salt content seasonal variations of the soil samples at two locations and at different depths are shown in *Fig 7*.

As shown in *Fig. 6* and *Fig. 7*, except for the soil samples near the ground surface, the salt contents of the soil samples at the other depth are all higher in summer, and lower in spring and autumn. Thus, for these soil samples, the salt content seasonal variations show a "n" shape. However, the salt content seasonal variations of the soil samples near the ground surface show an inverse "n" shape, i.e., "u" shape. The salt content of a soil obviously changes with season, and weather affects the salt accumulation in the soil, which varies with season and soil depth.

Meanwhile, the composition of salt in soil were tested by titration and flame photometry methods. The test results are shown as *Table 1*.

As shown in *Table 1*, the Na^+ contents are high and other positive ion are relatively low of soil samples. The salinization types can be determined by calculating the Cl^-/SO_4^{2}

http://www.aloki.hu ● ISSN 1589 1623 (Print) ●ISSN1785 0037 (Online)
DOI: http://dx.doi.org/10.15666/aeer/1706_1555915572

or $(CO_3^{2-}+HCO_3^-)/(Cl^-+SO_4^{2-})$. When meet the *Formula 2* or *Formula 3*, the soil can be named as carbonate saline soil.

$$A= Cl^-/SO_4^{2-} < 0.3 \quad \text{(Eq.2)}$$

$$B=(CO_3^{2-}+HCO_3^-)/(Cl^-+SO_4^{2-}) > 0.3 \quad \text{(Eq.3)}$$

According to *Table 1*, since the SO_4^{2-} of all samples are 0, it can only be calculated as B value using *Formula 2*. After calculating the datas from *Table 1*, the B values of soil samples are between 0.31-1.67, soil samples of study area are *carbonate saline soil*.

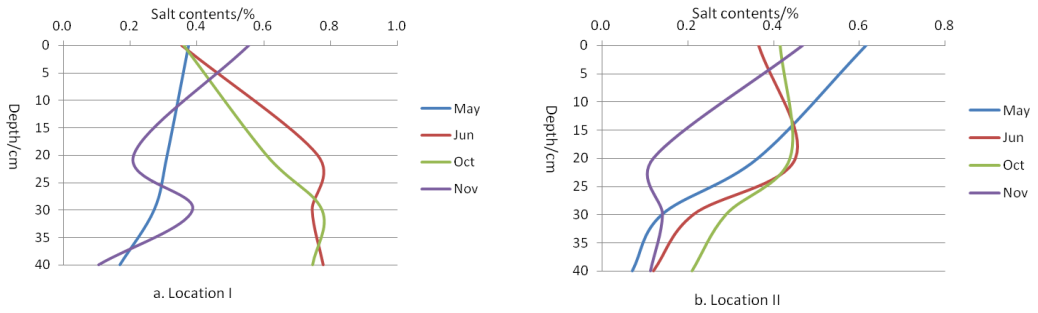

Figure 6. *Salt content of soil samples at two locations*

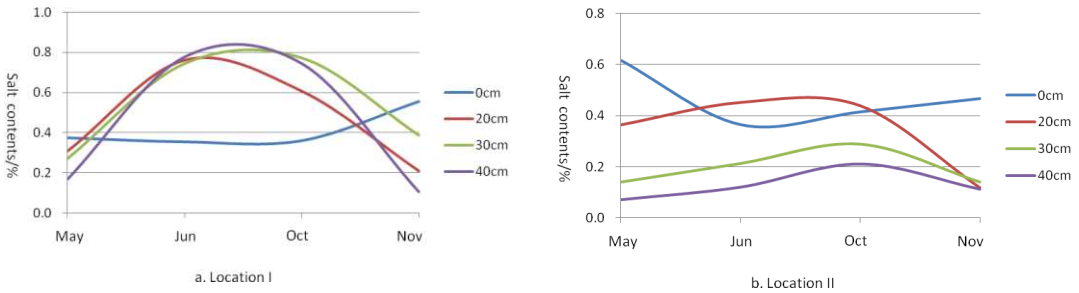

Figure 7. *Salt content seasonal variations of soil samples at two locations*

The salinization progress and salinization types are relevant to local environment. Therefore, it is necessary to research both the environmental and climatic factors in the investigation of the salinization progress of soil in western Jilin.

The changes in seasonal climate and environment affect evaporation, eluviations and frost-thawing. These changes produce different driving force in moving the water in soil in different directions, i.e. water migration. Further, as salt is dissolved in water, it also migrates with the water in the soil. Different environmental processes cause the migration in different directions and the accumulation of salt in different amounts.

Weather environment has an important influence on the migration of water and salt, accumulation and transportation of saline soil in western Jilin. It is the driving force of saline soil's formation.

http://www.aloki.hu ● ISSN 1589 1623 (Print) ●ISSN1785 0037 (Online)
DOI: http://dx.doi.org/10.15666/aeer/1706_1555915572

Table 1. *Ion contents of soil samples*

Locations	Time	Depth/cm	Ion contents/(mmol/100g)							
			K^+	Na^+	Ca^{2+}	Mg^{2+}	CO_3^{2-}	HCO_3^-	Cl^-	SO_4^{2-}
I	May	0	0.02	3.62	0.01	0	0	0.07	0.05	0
		20	0.02	3.01	0.01	0.01	0	0.01	0.03	0
		30	0.01	2.63	0	0.01	0	0.01	0.02	0
		40	0.02	1.72	0.01	0.01	0	0.01	0.02	0
	June	0	0.01	4.36	0.02	0.01	0	0.01	0.03	0
		20	0.01	6.89	0.01	0.01	0	0.01	0.03	0
		30	0.02	6.35	0.01	0	0.03	0.01	0.03	0.03
		40	0.01	6.22	0.01	0	0	0.01	0.02	0
	October	0	0.02	4.52	0.01	0.01	0	0.01	0.02	0
		20	0.01	5.68	0.01	0.01	0	0.02	0.01	0
		30	0.01	6.74	0.01	0.01	0	0.01	0.04	0
		40	0.01	6.13	0.01	0	0	0.01	0.06	0
	November	0	0.02	5.46	0.02	0.02	0	0.01	0.02	0
		20	0.01	2.38	0.01	0.01	0	0.01	0.03	0
		30	0.02	3.36	0.01	0	0	0.01	0.03	0
		40	0.02	1.17	0.01	0	0	0.01	0.04	0
II	May	0	0.01	6.03	0	0	0.01	0	0.04	0.01
		20	0.02	3.49	0.02	0	0	0.01	0.01	0
		30	0.02	1.28	0	0.01	0	0	0.01	0
		40	0.01	1.03	0.01	0.01	0	0.01	0.01	0
	June	0	0.02	3.72	0.01	0.01	0.01	0.01	0.02	0.01
		20	0.02	4.29	0.01	0.01	0	0.01	0.01	0
		30	0.02	2.05	0.01	0	0	0.01	0.01	0
		40	0.01	1.16	0.01	0	0	0	0	0
	October	0	0.02	4.09	0.02	0	0	0.02	0.03	0
		20	0.01	4.1	0	0.01	0	0.03	0.09	0
		30	0.01	2.73	0.01	0	0	0.02	0.06	0
		40	0.02	1.97	0.01	0	0	0.02	0.05	0
	November	0	0.02	4.48	0.01	0.01	0.01	0.01	0.01	0.01
		20	0.02	1.15	0.01	0.01	0.01	0.01	0.04	0.01
		30	0.01	1.24	0.01	0	0.01	0.01	0.04	0.01
		40	0.01	1.02	0.01	0.01	0.01	0.01	0.03	0.01

Temperature factors in wester Jilin

The daily temperature of Nong'an during 2003-2013 ten years has been analyzed (CDSSSC). These data have been organized into average monthly temperature, as shown in *Fig. 8*.

As shown in *Fig. 8*, western Jilin has four distinctive seasons. The monthly average temperature varies between 19.55℃ and 23.06℃. The monthly average temperature in January is the lowest, and in July is the highest. From January to December, the temperature varies in a parabola shape. The four seasons in western Jilin can be concluded

http://www.aloki.hu ● ISSN 1589 1623 (Print) ●ISSN1785 0037 (Online)
DOI: http://dx.doi.org/10.15666/aeer/1706_1555915572

by the variations in the temperature, i.e. April to May is spring, June to August is summer which has the highest temperature, September to October is autumn, and winter is from November to next March, which is the longest season in western Jilin. The average temperatures for the four months in winter are always below 0℃. As a conclusion, western Jilin has hot summer, frigid and long winter, which causes the soil to freeze in winter and thaw in spring. The frost and thawing processes cause the water and salt to migrate with a temperature gradient. Further, during an unfrozen season, the evaporation and elucidation in spring, summer and winter affect the soil salinization process. So, these two factors should also be investigated.

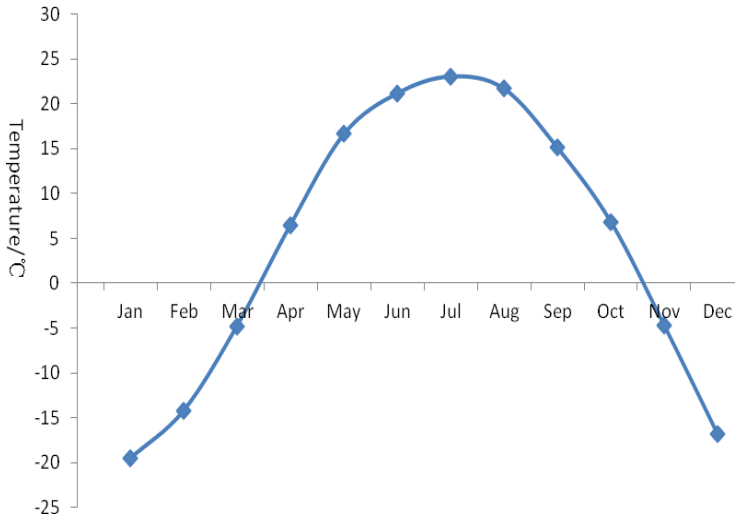

Figure 8. *Average monthly temperature of Nong'an*

Precipitation factors in wester Jilin

The daily rainfall precipitation of Nong'an during 2003-2013 has been analyzed (CDSSSC). These data have been organized into average monthly precipitation, as shown in *Fig. 9*.

As shown in *Fig. 9*, in the last ten years, the average annual precipitation is 523.07 mm. The main rainfall months are May to August, which receive 73.74% of the precipitation for whole year. The highest precipitation is in July, which is 27.11% of the precipitation for the whole year. The rainfall is low in January to March, especially in January. These data show that summer is short in western Jilin, but the elucidation caused by rainfall cannot be ignored in a salinization study.

Evaporation factors in wester Jilin

In order to compare the effects of precipitation and evaporation, the evaporation during 2003-2013 has also been analyzed (CDSSSC). *Fig. 10* shows the average monthly precipitation and evaporation.

As shown in *Fig. 10*, the average annual evaporation is 1104 mm, which is much higher than the average annual precipitation. The evaporation amount is quite different from the precipitation amount, which is high in March to October. Evaporation is highest in April, which is 16.53% of the evaporation for the whole year. The evaporation effect is influenced by the especial climatic characteristics in western Jilin as windy springtime.

http://www.aloki.hu ● ISSN 1589 1623 (Print) ●ISSN1785 0037 (Online)
DOI: http://dx.doi.org/10.15666/aeer/1706_1555915572

As shown in *Fig. 10*, the precipitation and evaporation differ significantly in spring and autumn. Evaporation has a major effect on the water in the soil. In summer, precipitation and evaporation are about the same. Only in July, the precipitation amount is higher than the evaporation amount.

In conclusion, western Jilin has an arid and semi-arid monsoon climate, which has high temperature and rainy in summer, windy spring and autumn, cold and long winter, and the annual evaporation amount is much higher than the precipitation amount. This especial climate characteristic provides the condition for salt accumulation on the ground surface. The soluble salt produced by rock wreathing during the soil formation period migrates and accumulates with water at different directions with frost effect in winter, evaporation effect in spring and autumn, and precipitation effect in summer. Eventually, the soil is salinized.

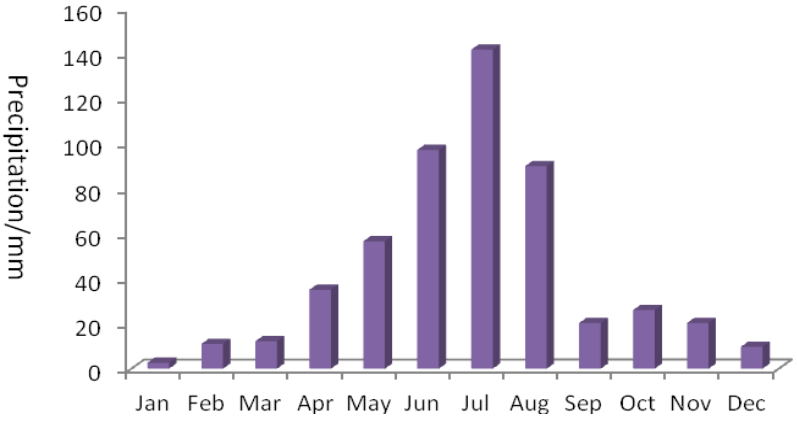

Figure 9. *Average monthly precipitation of Nong'an*

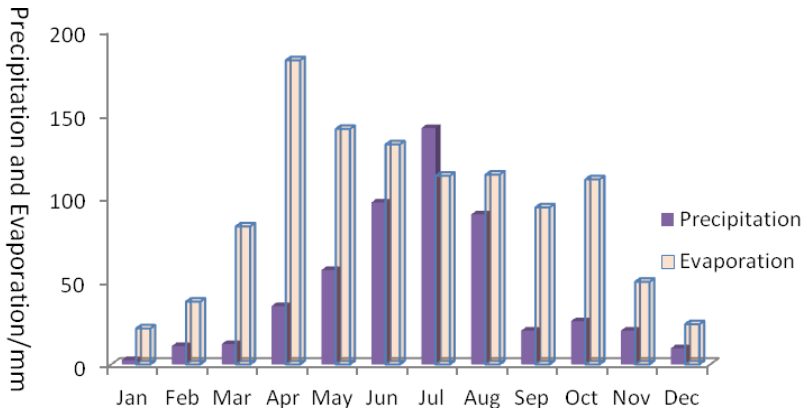

Figure 10. *Average monthly precipitation and evaporation of Nong'an*

Discussions

According to the analyses in Section 3, different seasons have different climatic conditions, which cause the water and salt in the soil to have different movements. The salinization process during unfrozen period and frost-thawing period is discussed in this section.

http://www.aloki.hu ● ISSN 1589 1623 (Print) ●ISSN1785 0037 (Online)
DOI: http://dx.doi.org/10.15666/aeer/1706_1555915572

Water and salt migration in unfrozen period

According to the water and salt migration curves (*Fig. 5* and *Fig. 7*), the salt accumulation in western Jilin is uncontinuous, which is influenced by the seasons, i.e. spring and autumn are the salification period, and summer is the desalination period.

Accoding to *Fig. 4* and *Fig. 6,* firstly, the initial salt in soil comes from soluble salt produced by parent rock wreathing effect, this salt dissolves into water during rainy season and migrates from high terrain areas to low terrain areas. This is why most saline soil is distributed in the low terrain areas. However, during a rainy season, little salt is accumulated on the ground surface as it migrates with direct surface runoff (*Fig. 7*), in which most of the salt is leached with water to the soil deep underground. So, the salt and water migrate downward during this period, and there is little salt accumulated on the ground surface.

By the end of rainy seasons, dry seasons begin, and the evaporation effect comes in during this period. The evaporation effect provides the driving force for the water to flow from the ground surface the deep soil (*Fig. 4*), in which salt migrates with soil upwards. The surface water evaporates into air, causing the salt to stay in the soil. Hence, salt accumulates near the ground surface as *Fig. 6* shown. As time passes, soil becomes salinized.

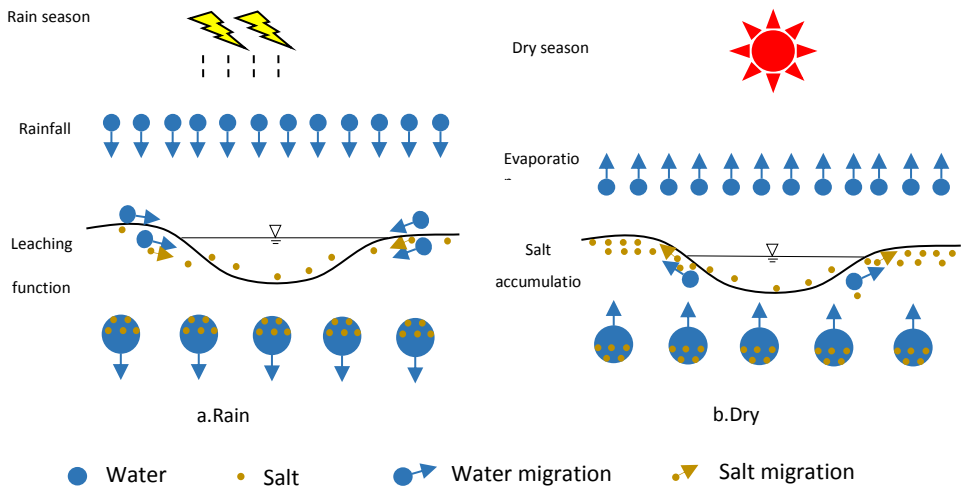

Figure 11. *Salt migration during unfrozen periods*

In conclusion, although salt accumulates in dry season and desalinizes in rainy season during unfrozen period which makes the soil salinization process discontinuous. However, according to the former discussions, the salification effect is much stronger than desalination effect. Therefore, salt is still accumulated in long term and the soil in western Jilin is still saline. Gradually over time, the soil becomes more saline.

Water and salt migration in frost-thawing period

Based on the *Fig. 8*, western Jilin has long winters. So, the soil goes through long freezing periods, and then thaws at spring. During the freezing period, according to the temperature gradient, frost is formed on the soil surface (Jozef and Katarina, 2014). So, the freezing depth increases gradually. In the frozen soil, free water freezes into ice.

http://www.aloki.hu ● ISSN 1589 1623 (Print) ●ISSN1785 0037 (Online)
DOI: http://dx.doi.org/10.15666/aeer/1706_1555915572

Hence, it cannot migrate freely in the soil. But some unfrozen water becomes bound water. The freezing point of this strong bound water is -78℃ (Bouyoucos, 1920). The freezing point of the loose bound water is between -20℃ and -30℃ (*Fig. 12*). This bound water in western Jilin cannot be freezed. The bound water can still migrate due to the temperature gradient effect, which is from high temperature to low temperature. Therefore, during the frost period, the direction of water migration is upwards. Salt that is dissolved in the bound water can also migrate upwards with it.

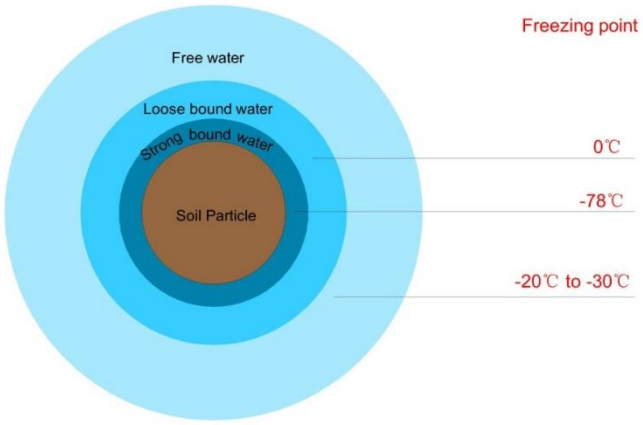

Figure 12. *Freezing points of free and bound water*

Salt migration requires a supply source. During the freezing process in winter, the frozen frontal moves downwards continually. Hence, the distance between the unfrozen soil layer and the underground water level becomes smaller and smaller. Finally, the distance becomes less than maximum that the underground water can rise to. The salt in the underground water therefore migrates into the frozen soil layer. Under this circumstance, the salt comes from the underground water that migrates towards the frozen frontal surface, which makes the salty underground water stays in the pores of soil as ice. Meanwhile, some salt in the soil dissolves into water during the underground water movement. Besides, salt migrates also requires a driving force. Salt in the frozen soil layer crystallizes during the freezing process, causing the solution concentration in the soil's pores to change. Since the extents of freezing of whole soil freezing profile are different, as well as the degrees of salt crystallization are different, which results in a potential gradient in the pore solution. Salt migrates with unfrozen water upwards driven by the temperature gradient and solution potential gradient.

When spring comes, soil starts to melt from frozen top layer and bottom layer at the same time. During the melting process, some soluble salt comes from the melting snow water, rainfall water and irrigation water migrates into the soil. Further, between the frozen layer and the unfrozen layer, there is a potential gradient in the solution. Moreover, the ground surface temperature is getting higher during this period, the solubility of water in the top soil layer is getting greater, which is the condition for carrying more salt. That's why *Fig. 7* shows the law that salt contents are high in spring. Based on the climatic characteristics of western Jilin, the rainfall is low in February to April. During spring in western Jilin, the evaporation capacity is much higher than precipitation. This causes the migration rate in spring to be higher and water evaporates faster, which enhances the soil salinization process.

http://www.aloki.hu ● ISSN 1589 1623 (Print) ●ISSN1785 0037 (Online)
DOI: http://dx.doi.org/10.15666/aeer/1706_1555915572

Ecological environment influnces of salinization in western Jilin province

According to the analyses in *Section 4.2* and *4.3*, salinization process enhanced during forzen and unfrozen periods effected with seasonal environmental conditions. Salinization function can cause land dererioration and ecological system gets fragile, which can harm the agriculture, engineering and ecological enviroment. In recnt years, annually financial loss reached up to 8.9 million RMB caused by salination in northeast China (Lin, 2016).

Western Jilin is locted in south Songnen plain, which is the crucial agriculture production area in China. Soil salinization deduced productivity of land, according to Lin (2016), since the 1950s, 22% land turned into salinization and desertification of Songnen plain, the ecological deterioration rates in western Jilin are shown as *Fig. 13*. As those rates, the 1/2 land will turn to desert of western Jilin.

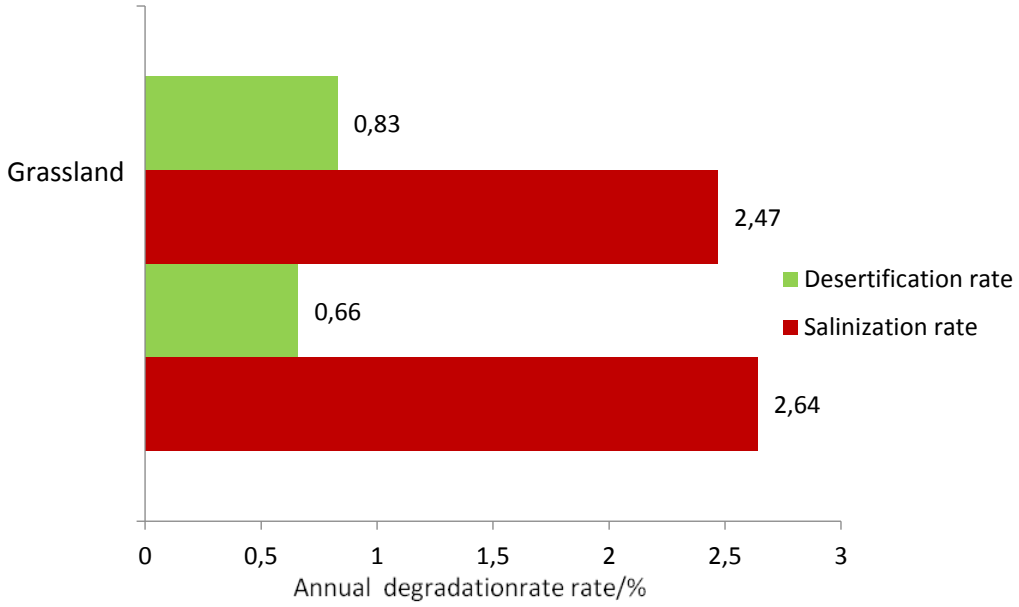

Figure 13. *Ecological deterioration rates of wester Jilin*

Based the analyses above, *Fig. 14* shows the salinization process in western Jilin. Soil salinization destroys ecological system, changes physical behavior and chemical component of soil, deduces nurient of soil, causes the productivity decline, as the result, land turns desertification eventually.

According to earlier studies, saline soil was caused by weather conditions. Zhou and Zhao (1979) considered the harmful climatic conditions that aggravate the salinization progress are spring drought and summer waterlogging. Xu and Dou (2013) considered flooding tillage method causing underground water level to rise increased the degree of salinization. Most of the earlier studies discussed salinization progress in the unfrozen period. In this study, water migration and salt migration have been tested to provide the basic data to show the migration process in soil, and the salinization progress has been discussed particularly during the unfrozen period and the frost-thawing period. Discussion of the salization fuction and process of Jilin province in this sudy can provide the theoretical basis of fragile ecological enviroment protection.

http://www.aloki.hu ● ISSN 1589 1623 (Print) ●ISSN1785 0037 (Online)
DOI: http://dx.doi.org/10.15666/aeer/1706_1555915572

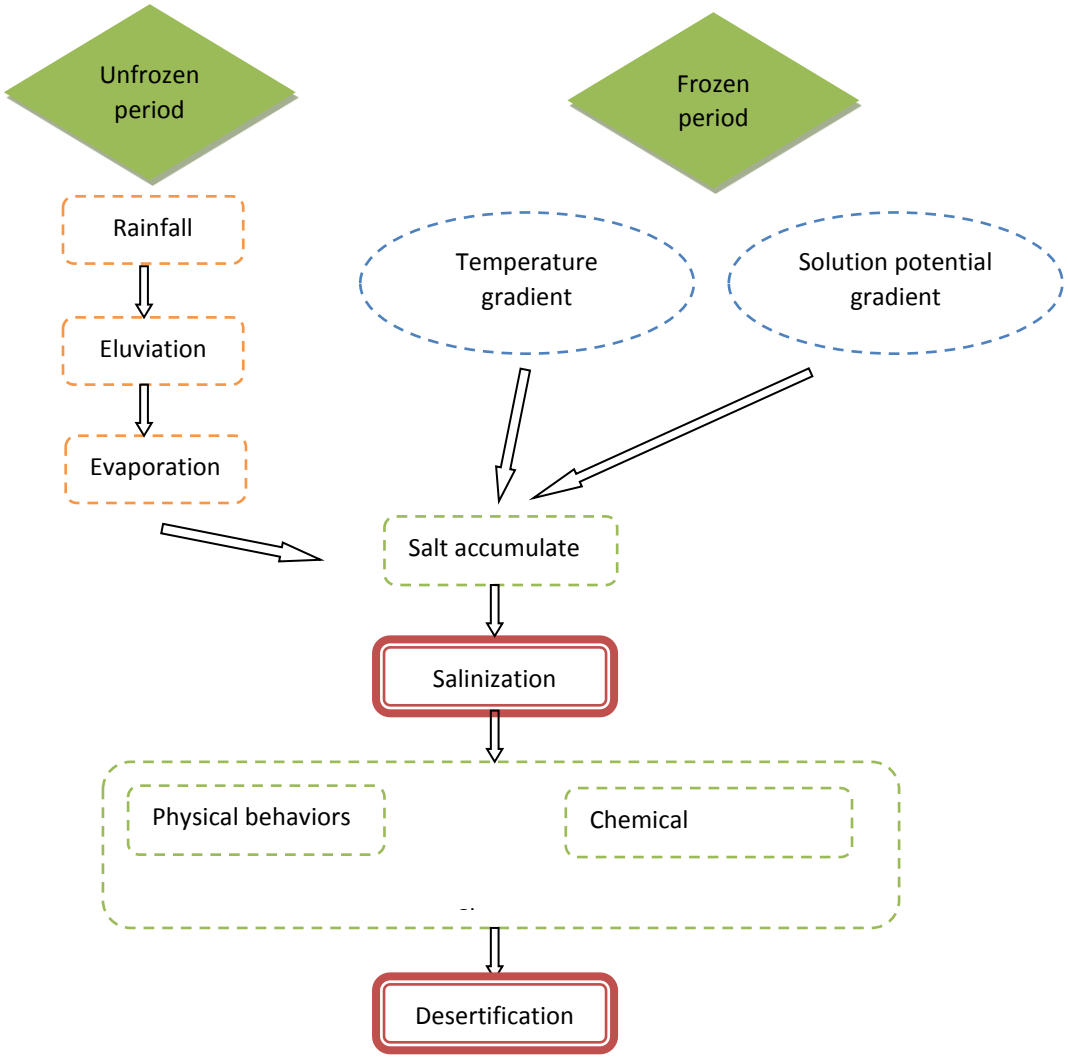

Figure 14. *Salinization process in western Jilin*

Conclusions

In this study, the saline soil water and salt migration characteristics and the environmental characteristics in western Jilin in relation to the salinization progress have been investigated. The conclusions are:

a. Water in soil migrates with seasonal changes, the water content is high in spring and summer, and low in autumn. Salt in soil also migrates with seasonal changes. The salt content of the soil near the ground surface is high in spring and summer, and low in autumn. However, the salt content of deep soil layer is low in spring and autumn, and low in summer.

b. Soil salinization continues to develop both in unfrozen period and frost-thawing period. During the unfrozen period, the process is: rainfall→direct surface runoff movements→salt goes into soil with eluviation function→evaporation→salt migrates upwards and accumulates.

c. During the unfrozen period, underground water supplies soil‘s water and salt. Salt migrates upwards driven by the temperature gradient and solution potential gradient, which enhances soil salinization progress in western Jilin.

http://www.aloki.hu ● ISSN 1589 1623 (Print) ●ISSN1785 0037 (Online)
DOI: http://dx.doi.org/10.15666/aeer/1706_1555915572

d. The salinization progress is related to the environmental characteristics of western Jilin. Therefore, the salinization prevention in western Jilin should focus on ecological environment management, and the engineering should focus on frost-heaving prevention in western Jilin. This conclusion has great significance for the agriculture and engineering developments in western Jilin province, China.

e. There are other environmental variables such as the groundwater level, soil parameters furthermore the irrigation strategy could influence the salt concentration, which should be tested in further study. So it will be draw more comprehensive conclusion due to further study.

Acknowledgements. This work was supported by Jilin Province Science and Technology Development Projects (grant number: No. 20180520063JH), Scientific Research project of Jilin Province Department of Education (grant number: JJKH20190867KJ), Research and Development Project of the Ministry of Housing and Urban-rural Development (2018-K9-009).

REFERENCES

[1] Bao, S. C., Wang, Q., Bian, J. M., Li, M., Wang, Z. J. (2018): Characteristics and laboratory freeze-thaw test of saline soil in west Jilin, China. – Applied Ecology an Environmental Reserch 16(1): 511-520.

[2] Bouyoucos, G. (1920): Degree of temperature to which soils can be cooledwithout freezing. – Monthly Weather Review 48(12): 718-718.

[3] Chen, Y. (2013): Study on irrigation and discharge schedules for ameliorating saline-sodic soils in paddies on irrigation districts of the Songnen Plain. – University of Chinese Academy of Sciences, Beijing.

[4] Chinameteorological data sharing service system of China. – http: //cdc.cma.gov.cn/.

[5] Jozef, K., Katarina, G. (2014): Soil monitoring system as a basic tool for protection of soils and sustainable land use in Slovakia. – Jornal of Agricultural Science and Technology 4(6): 504-513.

[6] Kusmiyati, F. (2014): Effect of mulch and mixed cropping grass- legume at saline soil on growth, forage yield and nutritional quality of guinea grass. – Journal of the Indonesian Tropical Animal Agriculture 10: 72-78.

[7] Lin, N. F. (2016): Biology-Soil system comprehensive development and utilization. – Jilin University Press, Changchun.

[8] Liu, J. (2001): Studies on the principles of water and salt movement and secondary salinization in Songnen plain. – Northeast Agricultural University 3: 22-25.

[9] Wang, Z. Q. (1993): Saline soil in China. – Science Press, Beijing.

[10] Wang, W. H., Wang, Q., Zhang, J. (2011): An experiment study of the fundamental property of the carbonate-saline soil in sest of Jilin province. – Journal of Beijing University of Technology 37(2): 217-224.

[11] Wang, Z. L., Fu, Q., Meng, J., Wang, X. H., Wang, X. W. (2015): Analysis on variations of black soil water in Songnen plain during ice and snow thaqing periods. – South-to-north water transfers and water science & technology 13(1): 173-175.

[12] Xu, B. Y., Dou, S. (2013): Problems and Suggestions in land consolidation in songyuan city. – China Agriculture Information 7: 200-201.

[13] Yang, J. X., Luo, X. X. (1999): Study on the relationship between soil salinization and groundwater dynamics. – Water and Soil Conservation Bulletin 7(6): 1-11.

[14] Zhang, D. F., Li, F. Q. (2000): Mechanism of formation of fragile eco-geo-environment of agro-pastoral zigzag zone in northern China. – Rural Eco-environment 16(4): 58-62.

http://www.aloki.hu ● ISSN 1589 1623 (Print) ●ISSN1785 0037 (Online)
DOI: http://dx.doi.org/10.15666/aeer/1706_1555915572

[15] Zhang, H. Q., Wang, L. X., Sun, G. Y. (2013): Evaluation of saline-alkali land resource and development potential in low Songnen plains. – Chinese Journal of Agricultural Resources and Regional Planning 34(2): 7-11.
[16] Zheng, D. M. (2005): Study on the temporal rhythm of water and salt transference of alkalization soil in Songnen Plain. – Northeast Normal University, Changchun.
[17] Zhou, Y. C., Zhao, H. S. (1979): Study on soil moisture dynamics in songnen plain. – Journal of Soil 3: 302-305.

http://www.aloki.hu ● ISSN 1589 1623 (Print) ●ISSN1785 0037 (Online)
DOI: http://dx.doi.org/10.15666/aeer/1706_1555915572

WINTER HOME RANGE OF THE MANCHURIAN WAPITI (*CERVUS CANADENSIS XANTHOPYGUS*) BASED ON NONINVASIVE SAMPLING

TIAN, X. M.[1,2] – WANG, X. L.[1] – ZHANG, M. H.[1*]

[1]*College of Wildlife and Protected Area, Northeast Forestry University, Harbin 150040, China*

[2]*College of Life Science and Technology, Mudanjiang Normal University, Mudanjiang 157011, China*

**Corresponding author*
e-mail: zhangminghai2004@126.com; phone: +86-139-3639-6197

(Received 5th Aug 2019; accepted 15th Nov 2019)

Abstract. The noninvasive sampling was applied to analyze the winter home range of the Manchurian wapiti (*Cervus canadensis xanthopygus*) in the east of the Wanda Mountains, north-eastern China's Heilongjiang Province. A total of 210 feces samples of the animal were collected from the study area during two consecutive winters. The DNAs were successfully extracted from 167 samples, and all genotypes of 7 microsatellite loci were obtained. Individual identification shows that the 167 samples belonged to 66 individuals. Through gender identification by the SRY gene, it was learned that the 66 individuals were 22 females and 44 males. Then, the winter home ranges of seven individuals (5 males and 2 females) were determined by Minimum Convex Polygons estimation. The results show that the winter home ranges of male individuals varied from 169.26 to 1,085.61 hm^2 (mean: 557.62 ± 411.83 hm^2), while those of female individuals were 43.72 hm^2 and 14.71 hm^2 (mean: 29.21 ± 20.51 hm^2). Finally, it is concluded that the noninvasive sampling is a feasible way to study the home range of endangered animals. This technique can be applied in the future to acquire more comprehensive information about the home range of animals.
Keywords: *home range, noninvasive sampling, gender identification, minimum convex polygon method, animal movement, spatial distribution, Cervus canadensis xanthopygus*

Introduction

The home range is the area in which animals perform daily activities such as feeding, mating, and breeding, and guarantees the normal survival and reproduction of animals (Burt, 1943). Home range research is very important for us to understand ungulate society organizations, improve the quality of their habitats, determine the optimal carrying capacity of their habitats, protect and reintroduce endangered species, and other projects (Howell, 1954; Dunbar and Dunbar, 1974; Inglis et al., 1979; Green, 1986; Cederlund and Okarma, 1988; Arcese, 1999; Woolnough and Toit, 2001). For large ungulates, traditional home range research methods are mainly radio telemetry and GPS collar tracking, the premise of which is to capture the wild animals, the capture process may cause injury to the individuals, and the collars worn by the animals may produce certain effects on their behaviors (Ensing et al., 2014; Kropil et al., 2015). The noninvasive sampling method can extract the DNA from the feces, hairs and urine left by the animals without disturbing them, and then through molecular marker individual identification and gender identification, and analysis of repeated sampling positions, the home range information could be obtained (Taberlet et al., 1997; Kohn et al., 1999; Smith et al., 2006). The combination of noninvasive sampling and GIS analysis overcomes the interference of traditional research methods on animals, and it receives

http://www.aloki.hu ● ISSN 1589 1623 (Print) ● ISSN 1785 0037 (Online)
DOI: http://dx.doi.org/10.15666/aeer/1706_1557315583

wide attention from endangered wild animal researches as an auxiliary method for home range research.

The number of Manchurian wapiti (*Cervus canadensis xanthopygus* Milne-Edwards, 1867) within Chinese territory has continued to decline due to illegal hunting and habitat loss (Ohtaishi and Sheng, 1993). At the beginning of the 19th century, the Manchurian wapitis in Shanxi and Hebei provinces were extinct (Jiang et al., 2007). The current distribution of Manchurian wapiti is mainly limited to some parts of Northeast China (Heilongjiang, Inner Mongolia, and Jilin Provinces), Ningxia, Xinjiang, Gansu, Qinghai, Sichuan, and Tibet (Xu et al., 2000), and it has been listed as a secondary national protected wild animal (Wang, 1998).

The body size of the Manchurian wapitis distributed in northeastern China is big. The body weight of male individuals is 200-250 kg and that of female ones is about 150 kg (*Fig. 1*). Female individuals are mature sexually at 2 years old and usually give birth to one cub each time (Chen et al., 1997). The Manchurian wapitis are the main prey for the extremely endangered species Amur tiger (*Panthera tigris altaica*) and Amur leopard (*Panthera pardus orientalis*) (Li et al., 2001; Qi et al., 2015). In recent years, there has been a significant decline and retreat in the population and distribution of Manchurian wapitis in Northeast China (Xu et al., 2000). The Wanda Mountains area in northeastern China was once the largest population density distribution area of Manchurian wapiti in Heilongjiang Province (Chen et al., 1997). Habitat fragmentation and illegal hunting have led to a sharp decline in the number of Manchurian wapitis in the region (Zhang and Zhang, 2011; Zhou et al., 2015). The survey found that the population density of Manchurian wapiti in Wanda Mountains area was 1.05 individuals per km^2 in 1989, and 0.20 individuals per km^2 in 2002, with a annual decline rate of 13.48% between 1989 and 2002 (Zhang and Zhang, 2011); while between 2004 and 2010, the annual average decline rate of relative population abundance was 37.30% (Zhou et al., 2015); and the survey in 2015 showed that the Manchurian wapitis in Wanda Mountains were on the verge of extinction (Zhou, 2019, personal communication).

Therefore, this study analyzes the home range size of Manchurian wapiti in east Wanda Mountains area based on noninvasive sampling method, in the hopes of providing references for formulating restoration and protection strategies for Manchurian wapitis, and meanwhile discussing the feasibility of applying noninvasive sampling to the study of home range of endangered animals.

Figure 1. *A male Manchurian wapiti monitored by an infrared camera in the study area*

http://www.aloki.hu ● ISSN 1589 1623 (Print) ● ISSN 1785 0037 (Online)
DOI: http://dx.doi.org/10.15666/aeer/1706_1557315583

Materials and methods

Research area overview

The research area is located in the Wupao Forest Farm of Yingchun Forestry Bureau in the eastern part of Wanda Mountains in Heilongjiang Province. The geographical coordinates are 46°27′ - 46°38′N, 133°04′ - 133°16′E, and the total area of the forest farm is 155.6 km^2 (*Fig. 2*). The area is in the cold temperate zone, and the weather condition is continental monsoon climate, with long winter and a frost-free period of about 120 days. The freezing period is relatively long and generally freezes in October and unfreezes in late April. The annual average temperature is 2.5-3.0 °C, the annual rainfall is 500-600 mm, and 60-70% rainfall is concentrated between June and August. The terrain of the area is low hills with an altitude of 300-500 m, and the forest area accounts for more than 80% of the total area. The large mammals distributed in this area include Siberian tiger (*Panthera tigris altaica*), Manchurian wapiti (*Cervus elaphus xanthopygus*), lynx (*Lynx lynx*), black bear (*Ursus thibetanus*), wild boar (*Sus scrofa*), roe deer (*Capreolus capreolus*), and sable (*Martes zibellina*), etc.

Sample collection and DNA extraction

During the winter of 2006 and 2007, samples were collected in the whole area of Wupao forest farm. Along the fresh footprint chains on the snow, feces of Manchurian wapiti were found, several feces were taken and put into the sealed bags, and the positions of the samples were located with GPS. Then other fresh footprint chains were followed and samples were collected as well. A total of 210 samples (120 in 2006 and 90 in 2007) were collected and stored and frozen at -20 °C (*Fig. 2*). Four pieces of muscle samples of culled Manchurian wapitis were obtained from the Harbin Changcheng Deer Farm (Heilongjiang, China). DNA extraction of the feces was performed using the QIAamp DNA Stool Mini Kit (Qiagen, Germany) according to the manual; and muscle DNAs were extracted by phenol/chloroform; all extracted DNAs were stored at -20 °C.

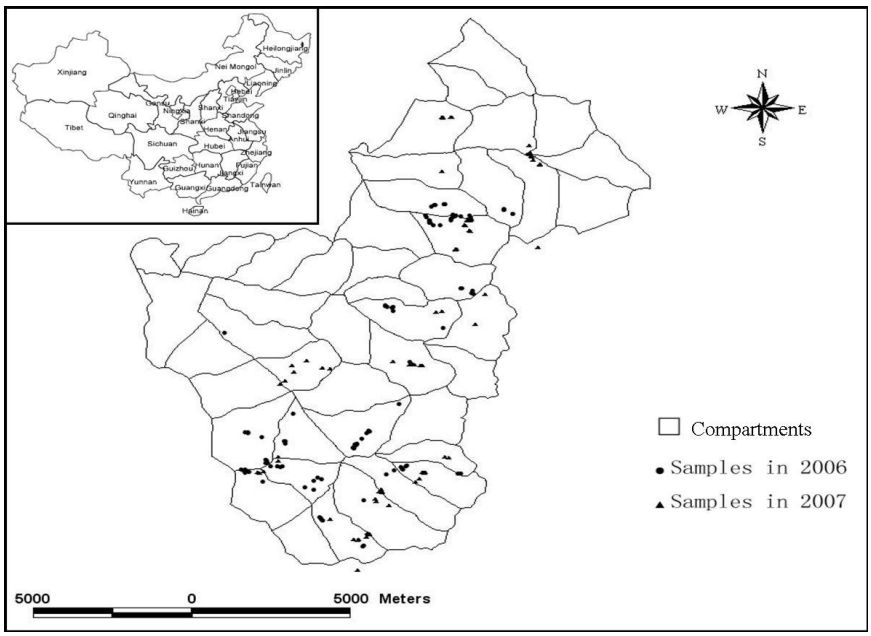

Figure 2. *Sampling locations in the study area*

http://www.aloki.hu ● ISSN 1589 1623 (Print) ● ISSN 1785 0037 (Online)
DOI: http://dx.doi.org/10.15666/aeer/1706_1557315583

Individual identification

Seven microsatellite loci (T507, CSSM19, T530, T501, C143, T123, T156) with high polymorphism were selected, and the 5' ends of the upstream primers of all microsatellite loci were fluorescently labeled (FAM, HEX, TAMARA). Primer information, PCR amplification and genotype identification procedures are described in the literature (Tian et al., 2010). Genotyping was performed using multi-tube PCR amplification method (Bellemain et al., 2005), for each locus, positive amplification was performed for 3-4 times to determine the final genotype (Tian and Zhang, 2010). Then the software Excel Mircosatellite Tool kit (Park, 2001) was adopted to find matching genotypes in the data. For different samples, if the genotype of all loci was the same or there's difference in only one allele in one locus, then the samples were judged to be from the same individual (Bellemain et al., 2005; Tian and Zhang, 2010). And then software Cervus 3.0 (Kalinowski et al., 2007) was used to calculate the joint P_{ID} value and P_{sib} value of the 7 loci.

Gender identification

SRY12 and BMC1009 2 were used to carry out gender identification on the prime multiplex amplification, SRY12 was used to amplify the SRY12 segment of the Y chromosome, and BMC1009 2 was used as a positive control to amplify the autosomal microsatellite loci (Huber et al., 2002). Each sample had bee amplified for 3 times, if double bands appeared at least 2 times, then the sample was judged to be a female; if single band (300 bp BMC1009) appeared at least 2 times, then it is judged to be a male; for other situations, the PCR was performed again for the identification. The prime information and PCR amplification conditions are available in the literature (Tian and Zhang, 2010).

Home range analysis

According to the individual identification results, individuals that had been sampled 4 times, or more than 4 times had been selected, and home range analysis was performed according to each GPS position of the same individual. And the size of the home range was calculated by the Minimum Convex Polygons (MCP) using the ArcView 3.3a's amplification module Home Range Analysis (ESRI Inc.).

Results

In the 210 samples of extracted fecal DNA, some of the DNAs were yellow, no amplification product could be obtained, and these samples were subject to the second-time DNA extraction. At last, 90 samples from 2006 and 77 samples from 2007 were used, and a total of 167 DNA samples were subject to subsequent analysis.

In the individual recognition, the combined discrimination rate of the 7 microsatellite loci was very high ($P_{ID} = 1.3\times10^{-7}$ and $P_{sib} = 0.19\%$), which means that for unrelated individuals, the probability of having the same genotype is 1.3×10^{-7}. Even in the case of twins, the probability of misjudgment is only 0.19%. Individual identification results: there are 39 individuals in the 90 samples of 2006, 36 individuals in the 77 samples of 2007, the 167 samples of the two years belonged to 66 individuals. Out of the individuals of 2006, 9 individuals appeared repeatedly in 2007.

http://www.aloki.hu ● ISSN 1589 1623 (Print) ● ISSN 1785 0037 (Online)
DOI: http://dx.doi.org/10.15666/aeer/1706_1557315583

To verify the accuracy of gender identification, 4 muscle samples (2 Male, 2 Female) and 4 fecal samples (2 Male, 2 Female) of known gender Manchurian wapitis in Harbin Changcheng Deer Farm (Heilongjiang, China) were analyzed. At the same time, 8 fecal samples (6 Male, 2 Female) whose gender was determined by the urinary positions of wild Manchurian wapitis' lying trace had been analyzed as well, and correct results were obtained (*Fig. 3*). Gender identification results: there are 28 male and 11 female individuals in the 39 individuals of 2006; there are 21 male and 15 female individuals in the 36 individuals of 2007; in the 66 individuals of the two years, there are 44 male and 22 female individuals.

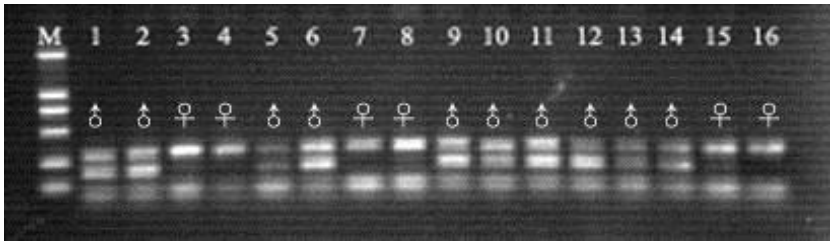

Figure 3. *Amplification results of SRY12 and BMC1009 loci of samples with known gender; M: Marker DL-2000; 1-16: samples with known gender*

In different years, there are fewer individuals that appeared repeatedly, so the home range analysis was performed for different years. Among the 66 individuals, 10 individuals with ≥ 4 repeated samples were selected. As for the No. 1, No. 4 and No. 8 individuals, since the sampling time interval is too short, the range of activity is smaller, so these 3 individuals' home range values were removed as abnormal values. Finally, the winter home range size of 7 individuals was analyzed. The number of repeated samples of the 7 individuals was 4-9 times, with an average of 6.43 times (see *Table 1*). Based on MCP, the size of home range was calculated, the home range size area of male individuals was 169.26-1085.61 ha with an average of 557.62 ± 411.83 ha; the home range areas of the 2 female individuals were 43.72 ha and 14.71 ha, with an average of 29.21 ± 20.51 ha. Compared with male individuals, female Manchurian wapiti's home range area is smaller (see *Table 1; Fig. 4*). There is a certain overlap in the range of activity between male individuals and between female and male individuals (see *Fig. 4*). Manchurian wapitis are gregarious animals. Since we cannot determine whether these 7 individuals are from the same group, the overlap of the Manchurian wapitis' home ranges had not been analyzed further.

Discussion

The size of the home range is the result of animal individual movement and spatial distribution of the population. Various factors such as age, gender, population density, season, food richness, predation risk, landscape spatial heterogeneity and human disturbance can affect the size of home range (Anderson et al., 2005; Reinecke et al., 2014; Kropil et al., 2015). According to the noninvasive sampling analysis, this study determined that the average size of winter home range of male wapiti individuals was 557.62 ha, this number for female individuals was 29.21 ha, and the male/female HRS ratio was 19.09. Compared with female wapitis, the male wapitis are larger in body size

http://www.aloki.hu ● ISSN 1589 1623 (Print) ● ISSN 1785 0037 (Online)
DOI: http://dx.doi.org/10.15666/aeer/1706_1557315583

(Clutton-Brook et al., 1982; Chen et al., 1997), so they need to enlarge the home range to meet their physiological needs (Jetz et al., 2004), therefore, the home range size of most male wapitis is larger than that of the female ones (see *Table 2*). The study of Kamler et al. (2008) on wapiti home range shows that the male/female HRS ratios vary from 1.58 to 4.29, and the home ranges of female individuals (IDs 9 and 10, 43.72 ha and 14.71 ha) and male individuals (IDs 2 and 5, 169.26 ha and 205.23 ha) are quite small (see *Table 1*), and these results are closer to the winter home range of wapitis in related researches of Germany (female: 14 ± 2.4 ha, male: 12 ± 2.5 ha), Denmark (12-February: 33.8 ± 23.4 ha, March: 53.3 ± 19.2 ha) and Poland (female: 106 ± 12 ha, male: 112 ± 17 ha) (Georgii, 1980; Georgii and Schröder, 1983; Jeppesen, 1987; Kamler et al., 2007). The home range sizes of male individuals (IDs 3, 6 and 7) were 438.13 ha, 1085.61 ha and 889.85 ha, respectively, which is closer to the winter home size of wapitis in Europe and North America (see *Table 2*). We believe that the home ranges of female and male individuals (IDs 2 and 5) were smaller, the male/female HRS ratio is too high, insufficient sampling had resulted in deviations in these results, and the home range size of these individuals can only represent the range of activity of wapitis on a certain day or a few certain days in winter.

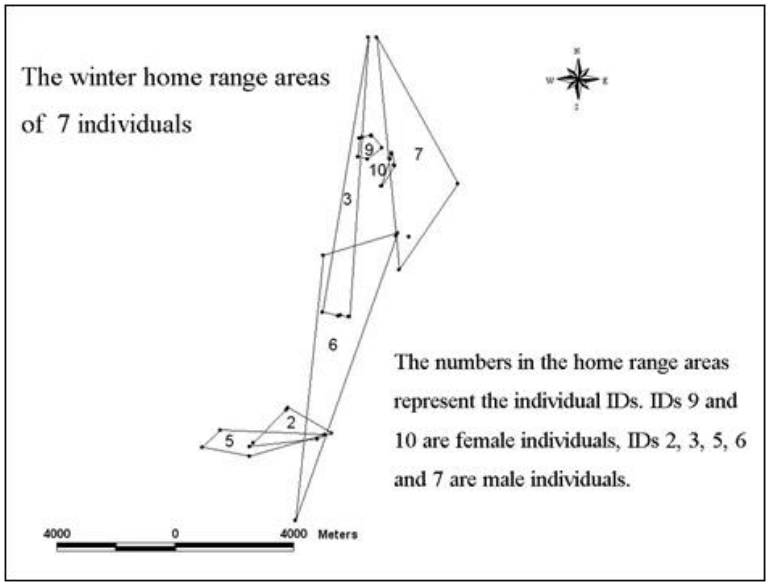

Figure 4. *Winter home range sizes of wapitis calculated by MCP*

Table 1. *Analysis of winter home range sizes of wapitis*

Individual ID	Gender	Repeated sampling number	GPS coordinates	Year of sampling	Home range size (ha)
2	Male	5	46°29′40.4138″N, 133°10′50.1412″E 46°29′33.5416″N, 133°10′27.2930″E 46°30′04.7822″N, 133°09′38.1336″E 46°30′07.2392″N, 133°09′39.8799″E 46°29′23.9251″N, 133°08′40.8985″E	2006	169.26

http://www.aloki.hu ● ISSN 1589 1623 (Print) ● ISSN 1785 0037 (Online)
DOI: http://dx.doi.org/10.15666/aeer/1706_1557315583

3	Male	8	46°36′56.1911″N, 133°11′34.5398″E 46°31′49.4170″N, 133°10′56.8140″E 46°31′49.2191″N, 133°10′56.5859″E 46°31′49.2185″N, 133°11′12.8690″E 46°31′49.2166″N, 133°11′14.7930″E 46°31′49.0715″N, 133°11′13.8124″E 46°31′52.7444″N, 133°10′31.8791″E 46°31′50.2182″N, 133°11′00.3536″E	2007	438.13
5	Male	5	46°29′27.8412″N, 133°08′46.7205″E 46°29′38.7495″N, 133°10′39.1767″E 46°29′40.7186″N, 133°07′54.2299″E 46°29′21.4747″N, 133°07′26.1455″E 46°29′12.7009″N, 133°08′41.7491″E	2006	205.23
6	Male	4	46°33′22.1126″N, 133°12′27.5197″E 46°32′55.1068″N, 133°10′31.0565″E 46°28′03.6527″N, 133°09′55.9965″E 46°33′18.7175″N, 133°12′25.8006″E	2006	1085.61
7	Male	6	46°33′17.9203″N, 133°12′45.2157″E 46°34′43.7355″N, 133°12′11.6790″E 46°36′56.0080″N, 133°11′47.5645″E 46°32′41.4994″N, 133°12′31.5793″E 46°33′24.7041″N, 133°12′11.0494″E 46°34′17.3325″N, 133°14′01.3121″E	2007	889.85
9	Female	8	46°34′54.7801″N, 133°11′59.3837″E 46°35′06.4236″N, 133°11′27.6206″E 46°35′08.5082″N, 133°11′42.7235″E 46°35′08.1101″N, 133°11′42.1260″E 46°34′42.0893″N, 133°11′37.0720″E 46°35′04.8008″N, 133°11′23.3062″E 46°35′07.7722″N, 133°11′42.1859″E 46°34′44.7024″N, 133°11′22.0966″E	2006	43.72

http://www.aloki.hu ● ISSN 1589 1623 (Print) ● ISSN 1785 0037 (Online)
DOI: http://dx.doi.org/10.15666/aeer/1706_1557315583

10	Female	9	46°34′42.6564″N, 133°12′13.0767″E 46°34′49.2009″N, 133°12′15.3028″E 46°34′48.8132″N, 133°12′15.3626″E 46°34′36.2776″N, 133°12′19.3459″E 46°34′35.4839″N, 133°12′20.3584″E 46°34′49.2009″N, 133°12′15.3028″E 46°34′12.8702″N, 133°11′59.2212″E 46°34′13.0977″N, 133°12′01.3269″E 46°34′48.6146″N, 133°12′15.0873″E	2007	14.71

Table 2. *Summary of winter home range of wapitis calculated by minimum convex polygon method*

Country	Region	No. of animals	HRS (km^2)	Comments	Author
Germany	Bavarian Alps	10♀	0.65♀		Georgii, 1980
Germany	Bavarian Alps	9♂	1.13♂		Georgii and Schröder, 1983
Germany	Grafenwöhr; Kellerwald-Edersee NP; Schleswig-Holstein	37 (♂ + ♀)	10-33♂ 2.8-11♀		Reinecke et al., 2014
Czech Republic	Jeseniky Mts.	3♂ + 5♀	0.84♂ 0.35♀	Monthly ranges	Koubek and Hrabe, 1996
Slovakis	Kremnica Mts.	20♂	6.01: 8.26♂	Resident: Migrant	Kropil et al., 2015
America	Idaho	4♂ + 12♀	2.1 average		Irwin and Peek, 1983
America; Canada	Wisconsin; Yellowstone; Alberta	44♀	14.15-439.73♀	95% kernel	Anderson et al., 2005
China	Heilongjiang	5♂ + 2♀	1.69-10.86♂ 0.15-0.44♀		Tian et al. (this study)

Mts: mountains; NP: national park; HRS: home range size

This study suggests that it is feasible to study the home range of animals using noninvasive sampling method. Although traditional home research methods are still the mainstream methods of animal home range research, the noninvasive sampling method does not require animals to be captured, so it could obtain a large amount of genetic information without causing any interference to animals. Especially for rare and endangered wild animals with high alertness and complex distribution terrain, the noninvasive sampling method is more feasible for home range research of these animal species (Taberlet et al., 1997; Kohn et al., 1999; Smith et al., 2006). The analysis results

http://www.aloki.hu ● ISSN 1589 1623 (Print) ● ISSN 1785 0037 (Online)
DOI: http://dx.doi.org/10.15666/aeer/1706_1557315583

suggest that using noninvasive sampling method to study animal home range requires larger sampling intensity, and it should be combined with the footprints, lying traces, feeding marks, and other location information to obtain more distribution points of a same individual so as to obtain the accurate size of home range. At the same time, the multi-tube approach should be performed strictly so as to eliminate allele dropouts and false alleles during fecal DNA microsatellite genotyping, and avoid false individual identification (Taberlet et al., 1996; Bellemain et al., 2005; Pérez-Espona et al., 2008). Moreover, by applying noninvasive sampling method for future studies we could obtain more comprehensive information of animal home range, such as individual daily home range, winter home range size, home range overlapping, core area, sub-herd home range, kinship, and diffusion, etc. At the same time, combining with factors such as population density, food richness, snow density, predation risk and human disturbance, the influencing factors of home range changes could be revealed.

Conclusion

Based on noninvasive sampling, the winter home ranges of male individuals of the Manchurian wapiti varied from 169.26 to 1,085.61 hm^2 (mean: 557.62 ± 411.83 hm^2), while those of female individuals were 43.72 hm^2 and 14.71 hm^2 (mean: 29.21 ± 20.51 hm^2). The winter home ranges of both females and several males were too small, due to the limited sample size.

Our analysis revealed that the noninvasive sampling is a feasible way to study the home range of endangered animals. It requires larger sampling intensity to obtain more accurate size of home range. The footprints, lying traces, feeding marks, and other location information should be considered to obtain more distribution points of the same individual. This study suggests that the noninvasive sampling method and traditional home range research method should be combined to reveal individual daily home range, winter home range size, home range overlapping, core area, sub-herd home range, kinship, diffusion and the influencing factors of home range changes. It proposes speeding up the construction of the reserve in Wanda Mountains to reduce the disturbance of human activities on the survival of the Manchurian wapiti.

Acknowledgements. Our study was funded by the Heilongjiang Provincial Basic Research Business Support Project, China (1353ZD006); National Science Foundation of China (30870309); Mudanjiang Normal College National Cultivation Project (Study on Population Spatial Genetic Structure and Dispersal Model of Manchurian Wapiti in Northeast China) and Excellent Youth Key Teacher Training Plan Project of Mudanjiang Normal College (MQP201405). We thank Y. Li and L. F. Wang for help given throughout this project. We appreciate help from the staff of Heilongjiang Provincial Forest Department, especially H. Y. Dong. We acknowledge the professional staff, guides, and drivers of Heilongjiang Provincial Yingchun Forest Bureau.

REFERENCES

[1] Anderson, D. P., Forester, J. D., Turner, M. G., Frair, J. L., Merrill, E. H., Fortin, D., Mao, J. S., Boyce, M. S. (2005): Factors influencing female home range sizes in elk (Cervus elaphus) in North American landscapes. – Landscape Ecology 20(3): 257-271.

[2] Arcese, P. (1999): Effect of auxiliary males on territory ownership in the Oribi and the attributes of multimale groups. – Animal Behaviour 57(1): 61-71.

http://www.aloki.hu ● ISSN 1589 1623 (Print) ● ISSN 1785 0037 (Online)
DOI: http://dx.doi.org/10.15666/aeer/1706_1557315583

[3] Bellemain, E., Swenson, J. E., Tallmon, D., Brunberg, S., Taberlet, P. (2005): Estimating population size of elusive animals with DNA from hunter-collected feces: four methods for brown bears. – Conservation Biology 19(1): 150-161.
[4] Burt, W. H. (1943): Territoriality and home range concepts as applied to mammals. – Journal of Mammalogy 24(3): 346-352.
[5] Cederlund, G., Okarma, H. (1988): Home range and habitat use of adult female moose – Journal of Wildlife Management 52(2): 336-343.
[6] Chen, H. P., Wu, J. P., Zhang, M. H. (1997): Heilongjiang Provincial Red Deer. – Northeast Forestry University Press, Harbin.
[7] Clutton-Brock, T. H., Guinness, F. E., Albon, S. D. (1982): Red Deer: Behavior and Ecology of Two Sexes. – Edinburgh University Press, Edinburgh.
[8] Dunbar, R. I. M., Dunbar, E. P. (1974): Social organization and ecology of the Klipspringer (Oreotragus oreotragus) in Ethiopia. – Ethology 35(5): 481-493.
[9] Ensing, E. P., Ciuti, S., de Wijs, F. A., Lentferink, D. H., Ten Hoedt, A., Boyce, M. S., Hut, R. A. (2014): GPS based daily activity patterns in European red deer and North American elk (Cervus elaphus): indication for a weak circadian clock in ungulates. – PloS One 9(9): e106997.
[10] Georgii, B. (1980): Home range patterns of female red deer (Cervus elaphus L.) in the Alps. – Oecologia 47(2): 278-285.
[11] Georgii, B., Schröder, W. (1983): Home range and activity patterns of male red deer (Cervus elaphus L.) in the Alps. – Oecologia 58(2): 238-248.
[12] Green, M. J. B. (1986): The distribution, status and conservation of the Himalayan mask deer (Moschus chrysogaster). – Biological Conservation 35(4): 347-375.
[13] Howell, J. C. (1954): Populations and home ranges of small mammals on an overgrown field. – Journal of Mammalogy 35(2): 177-186.
[14] Huber, S., Bruns, U., Arnold, W. (2002): Sex determination of red deer using polymerase chain reaction of DNA from feces. – Wildlife Society Bulletin 30(1): 208-212.
[15] Inglis, J. M., Hood, R. E., Brown, B. A., DeYoung, C. A. (1979): Home range of white-tailed deer in Texas Coastal Prairie Brushland. – Journal of Mammalogy 60(2): 377-389.
[16] Irwin, L. L., Peek, J. M. (1983): Elk habitat use relative to forest succession in Idaho. – The Journal of Wildlife Management 47(3): 664-672.
[17] Jeppesen, J. L. (1987): Impact of human disturbance on home range, movements and activity of red deer (Cervus elaphus) in a Danish environment. – Danish Review of Game Biology 13(2): 1-38.
[18] Jetz, W., Carbone, C., Fulford, J., Brown, J. H. (2004): The scaling of animal space use. – Science 306(5694): 266-268.
[19] Jiang, G. S., Zhang, M. H., Ma, J. Z. (2007): Effects of human disturbance on movement, foraging and bed selection in red deer Cervus elaphus xanthopygus from the Wandashan Mountains, northeastern China. – Acta Theriologica 52(4): 435-446.
[20] Kalinowski, S. T., Taper, M. L., Marshall, T. C. (2007): Revising how the computer program CERVUS accommodates genotyping error increases success in paternity assignment. – Molecular Ecology 16(5): 1099-1106.
[21] Kamler, J. F., Jędrzejewska, B., Jędrzejewski, W. (2007): Factors affecting daily ranges of red deer Cervus elaphus in Białowieża Primeval Forest, Poland. – Acta Theriologica 52(2): 113-118.
[22] Kamler, J. F., Jędrzejewski, W., Jędrzejewska, B. (2008): Home ranges of red deer in a European old-growth forest. – American Midland Naturalist 159(1): 75-82.
[23] Kohn, M. H., York, E. C., Kamradt, D. A., Haught, G., Sauvajot, R. M., Wayne, R. K. (1999): Estimating population size by genotyping faeces. – Proceedings of the Royal Society B: Biological Sciences 266(1420): 657-663.
[24] Koubek, P., Hrabe, V. (1996): Home range dynamics in the red deer (Cervus elaphus) in a mountain forest in central Europe. – Folia Zoologica 45(3): 219-222.

http://www.aloki.hu ● ISSN 1589 1623 (Print) ● ISSN 1785 0037 (Online)
DOI: http://dx.doi.org/10.15666/aeer/1706_1557315583

[25] Kropil, R., Smolko, P., Garaj, P. (2015): Home range and migration patterns of male red deer Cervus elaphus in Western Carpathians. – European Journal of Wildlife Research 61(1): 63-72.
[26] Li, T., Jiang, J. S., Wu, Z. G., Han, X. D., Wu, J. C., Yang, X. J. (2001): Survey on Amur tiger in Jilin Province. – Acta Theriologica Sinica 21(1): 1-6.
[27] Ohtaishi, N., Sheng, H. L. (1993): Deer of China: Biology and Management. – Elsevier Science Publishers B.V., Amsterdam.
[28] Park, S. D. E. (2001): Trypanotolerance in West African Cattle and the Population Genetic Effects of Selection. – University of Dublin, Dublin.
[29] Pérez-Espona, S., Pérez-Barbería, F. J., Mcleod, J. E., Jiggins, C. D., Gordon, I. J., Pemberton, J. M. (2008): Landscape features affect gene flow of Scottish Highland red deer (Cervus elaphus). – Molecular ecology 17(4): 981-996.
[30] Qi, J. Z., Shi, Q. H., Wang, G. M., Li, Z. L., Sun, Q., Hua, Y., Jiang, G. S. (2015): Spatial distribution drivers of Amur leopard density in northeast China. – Biological Conservation 191: 258-265.
[31] Reinecke, H., Leinen, L., Thißen, I., Meißner, M., Herzog, S., Schütz, S., Kiffner, C. (2014): Home range size estimates of red deer in Germany: environmental, individual and methodological correlates. – European Journal of Wildlife Research 60(2): 237-247.
[32] Smith, D. A., Ralls, K., Hurt, A., Adams, B., Parker, M., Maldonado, J. E. (2006): Assessing reliability of microsatellite genotypes from kit fox faecal samples using genetic and GIS analyses. – Molecular Ecology 15(2): 387-406.
[33] Taberlet, P., Griffin, S., Goossens, B., Questiau, S., Manceau, V., Escaravage, N., Waits, L. P., Bouvet, J. (1996): Reliable genotyping of samples with very low DNA quantities using PCR. – Nucleic Acids Research 24(16): 3189-3194.
[34] Taberlet, P., Camarra, J. J., Griffin, S., Uhrès, E., Hanotte, O., Waits, L. P., Dubois-Paganon, C., Burke, T., Bouvet, J. (1997): Noninvasive genetic tracking of the endangered Pyrenean brown bear population. – Molecular Ecology 6(9): 869-876.
[35] Tian, X. M., Zhang, M. H. (2010): Population size and sex ratio of wapiti (Cervus elephus xanthopygus) as revealed by fecal DNA. – Acta Ecologica Sinica 30(22): 6249-6254.
[36] Tian, X. M., Zhang, M. H., Zhang, H., Yang, C. W., Jin, Z. M. (2010): Genetic diversity of wapiti population in eastern Wandashan Mountains of Heilongjiang Province, China based on microsatellite analysis. – Chinese Journal of Ecology 29(3): 543-548.
[37] Wang, S. (1998): China red data book of endangered animals. – Beijing: Science Press.
[38] Woolnough, A., Toit, J. D. (2001): Vertical zonation of browse quality in tree canopies exposed to a size-structured guild of African browsing ungulates. – Oecologia 129(4): 585-590.
[39] Xu, Q. X., Zhang, M. H., Lu, B. X. (2000): Study on the status of red deer population in Heilongjiang Province. – Journal of Economic Animal 4(1): 57-62.
[40] Zhang, C. Z., Zhang, M. H. (2011): Population status and dynamic trends of Amur tiger's prey in eastern Wandashan Mountains, Heilongjiang Province. – Acta Ecologica Sinica 31(21): 6481-6487.
[41] Zhou, S. C., Sun, H. Y., Yang, J., Huang, H. J. (2015): Study on population dynamic trends of Amur tiger's prey and impact factors in eastern Wandashan Mountains. – Forestry Science & Technology 40(3): 37-40.

http://www.aloki.hu ● ISSN 1589 1623 (Print) ● ISSN 1785 0037 (Online)
DOI: http://dx.doi.org/10.15666/aeer/1706_1557315583

EFFECTS OF IRRIGATION FREQUENCY AND LEVEL ON YIELD AND STOMATAL RESISTANCE OF EGGPLANT (*SOLANUM MELONGENA* L.) GROWN IN OPEN FIELD IRRIGATED WITH SURFACE AND SUBSURFACE DRIP METHODS

BOZKURT ÇOLAK, Y.

Soil and Water Resources Research Unit, Alata Horticultural Research Institute
33400 Mersin, Turkey
(e-mail: yesimcolak@ymail.com; phone: +90-324-644-6478)

(Received 6th Aug 2019; accepted 15th Nov 2019)

Abstract. A two-year field experiment was conducted to evaluate the physiological response of eggplant stomatal resistance (r_s) and yield to different deficit irrigation levels using surface and subsurface drip methods under Mediterranean climatic conditions. Treatments consisted of surface (SDI) and subsurface drip (SSDI); 3-day and 6-day irrigation frequencies (IF_3, IF_6); and full irrigation (FI), deficit irrigations (DI_{50}, DI_{75}) and partial root-zone drying (PRD_{50}). Irrigation systems, frequencies and levels produced significantly different eggplant yields. IF_3FI treatment produced the greatest yield in the experimental years and followed by IF_3DI_{75}. The results revealed that 3-day interval resulted in significantly greater yields than 6-day frequency. Water deficit in the root-zone decreased fresh eggplant yield drastically and IF_6PRD_{50} produced the lowest yield. Smaller r_s values were observed in FI treatment in SDI and SSDI systems under 3-day frequency than deficit irrigated and 6-day frequency plots. Significant relationships among r_s and yield, dry matter yield, SWC, ET, and LAI were obtained. A value of 60 s m^{-1} could be considered as the threshold to regulate rs for high eggplant yield. Therefore rs could be utilized for scheduling irrigations. The r_s response to water stress can be used for sustainable crop production in water scarce regions.
Keywords: *deficit irrigation, partial root-zone drying, water use efficiency, irrigation scheduling*

Introduction

Vegetable production in many countries relies on irrigation. Optimizing irrigation amount and frequency is thus essential to ensure yield increase without compromising quality. All over the world, the reduction in the amount of water which is used for irrigation and environmental concerns make obtaining the most benefit from a unit of water necessary. Therefore micro irrigation systems such as surface drip (SDI) and subsurface drip systems (SSDI) are necessary for efficient use of scarce water resources in irrigated agriculture for increasing yield and saving water. A number of field studies indicated relevant benefits of managing SSDI for production of vegetables (Lamm and Camp, 2007; Kong et al., 2012; Bozkurt and Sayilikan Mansuroğlu, 2018).

Deficit irrigation (DI) is an important water-saving practice in irrigated agriculture (English et al., 2002). DI could decrease vegetative growth, while having little effect on fruit growth and development through balancing the relationship between reproductive and vegetative growth (Goodwin and Boland, 2002). Moreover, DI significantly reduces irrigation amount (Pérez-Pérez et al., 2008).

Several field trials on eggplant irrigation have been conducted in various locations around the world (Chartzoulakis and Drosos, 1995; Gaveh et al., 2011; Diaz-Perez and Eaton, 2015; Mohawesh, 2016; Müller et al., 2016; Bozkurt Çolak et al., 2017) indicating that eggplant production can be realized at moderate water stress levels without major reduction in crop yield.

http://www.aloki.hu ● ISSN 1589 1623 (Print) ● ISSN 1785 0037 (Online)
DOI: http://dx.doi.org/10.15666/aeer/1706_1558515604

Irrigation scheduling methods is usually categorized on soil, plant, and meteorological basis. Plant-based irrigation scheduling techniques are more advantageous since plants respond to both the soil and aerial environmental conditions (Yazar et al., 1999). For that reason, crop based irrigation scheduling is used more and more in recent years. The irrigation time can be determined by detecting the water stress status of the plant. Among the possible measures of some aspect of plant water status include direct measuring stomatal resistance or conductance (Yao et al., 2001; Agele et al., 2006; Lianga et al., 2011) that is known to respond sensitively to water stress.

Stomatal have an important task in regulating water losses through transpiration and CO_2 uptake for photosynthesis and plant growth (Gerosa et al., 2012). Also, stomatal control is a major physiological way for optimizing water use under drought condition (Makbul et al., 2011). Crop water use estimation based on scaling up from leaf stomatal conductance to canopy conductance is of paramount importance for improving efficient use of limited water resources in agriculture (Zhang et al., 2011).

It is believed that virtually most of the plants' first reaction to severe water stress is the stomatal closure to prevent the water losses by transpiration (Berry et al., 2010; Brodribb and McAdam, 2011; Nemeskeri et al., 2015). Stomatal closure occurs due to from direct evaporation of water from the guard cells without any metabolic action. When available soil water content is decreased, the stomata open little or even remain closed in response to severity of water deficiency. The crop prevents dehydration by maintaining stomata closed under drought conditions (Anjum et al., 2011; Osakabe et al., 2014; Clauw et al., 2015). Behboudian (1977) reported that eggplants have greater resistance to water stress than the other vegetable crops.

For sustainable eggplant production and making decision on the best irrigation practice, a comprehensive assessment of the yield and physiological response of the crop to a specific soil type, production method and irrigation strategy is required. Therefore, determination of the critical threshold values (beyond which yield loss or reduction is inevitable) of stomatal resistance (r_s) is important for a specific crop growing under different climatic and soil conditions so that they can be utilized effectively for irrigation scheduling purposes. The main objectives of this research were to evaluate the physiological response of eggplant such as stomatal resistance (r_s) to different deficit irrigation strategies under subsurface and surface drip systems; and to establish threshold levels for stomatal resistance for irrigation scheduling of eggplant for high and good quality yield under the semi-arid climatic environment in the Mediterranean region.

Materials and methods

Experimental site description

Field experiments were conducted during 2013 and 2014 growing seasons on the experimental farm at the Alata Horticultural Research Institute in Tarsus in Mediterranean region of Turkey. The experimental site is located between latitude 36°53' N and longitude 34°57' E with an elevation of 60 m. Mediterranean climate prevails in the experimental site. Monthly mean climatic data for the study years along with long-term means are depicted in *Figure 1*. The mean annual rainfall, temperature, evaporation and relative humidity are 616 mm, 17.8°C, 1487 mm, 70.5%, respectively. The amount of rainfall recorded during the eggplant growing season (May through August) was 163.0 mm in 2013, and 126.0 mm in the 2014 growing season.

http://www.aloki.hu ● ISSN 1589 1623 (Print) ● ISSN 1785 0037 (Online)
DOI: http://dx.doi.org/10.15666/aeer/1706_1558515604

The experimental soil has a clayey-silt texture with volumetric water content at field capacity 29.6% and wilting point 19.2% and mean bulk density of 1.39 g cm^{-3}. Plant available water in the effective root depth of 60.0 cm was estimated as 88 mm.

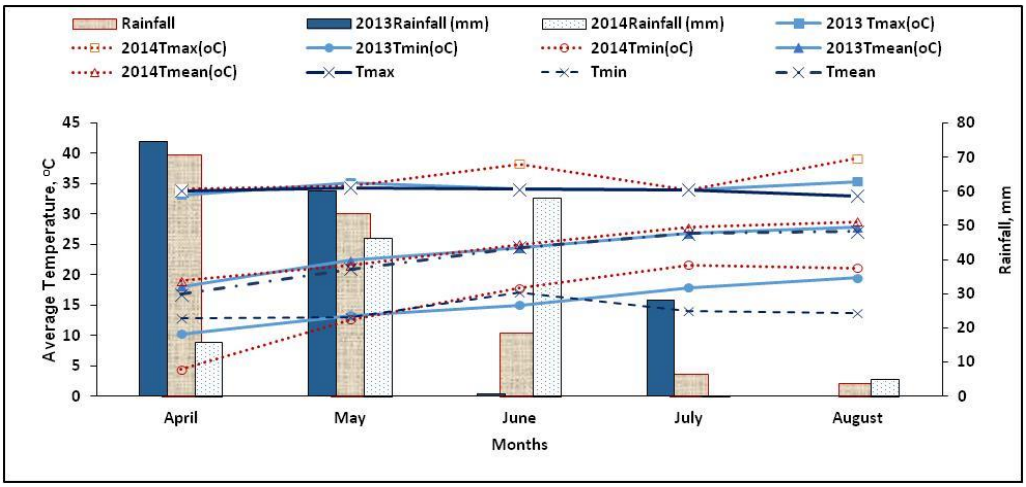

Figure 1. *Mean monthly climatic data in the experimental years along with long-term means*

Agronomic practices

Four weeks old eggplant seedlings of *Solanum Melongena* L. (cv. Anamur Karası) were transplanted into the experimental plots in 90 cm row spacing and with 70 cm plant spacing on May 6 and April 14 in 2013 and 2014, respectively.

Compound fertilizers were incorporated into the plant beds at a rate of 50 N; 50 P_2O_5; and 50 kg ha^{-1} K_2O prior to transplanting. About 21 days after transplantation, plots received Nitrogen via fertigation every 6 days (160.0 kg ha^{-1} N) during the eggplant growth period.

Agronomic and plant protection practices carried out during the growing seasons are summarized in *Table 1*.

Design of the experiment and treatments

The experiment was designed split-split plots with four replicates. Experimental treatments consisted of surface drip (SDI) and subsurface drip systems (SSDI); 3-day 6-day (IF_3; IF_6) irrigation frequencies; and Full irrigation (FI); deficit irrigations, DI_{50} and DI_{75}; and Partial Root-zone drying (PRD_{50}). Irrigation was launched when 25% of available water in the root-zone depth of 60 cm was depleted and replenished to field capacity in all treatments. Then treatment irrigations were scheduled based on replenishment of soil water deficit in effective root-zone depth of 60 cm to field capacity in fully irrigated treatments (FI) in the two irrigation frequencies considered. In the deficit irrigation plots of DI_{50} and DI_{75}, respectively received 50 and 75% of water applied to full irrigation plots. PRD_{50} plots were irrigated alternately from the two laterals on both side of the crop row and received 50% of water applied to full irrigation plots. In the experiment, subplots were 10 m long and 5.4 m (6 plant rows) wide. A general view of the experimental plots is shown in *Figure 2*.

In the surface drip system plots (SDI), drip lateral pipes were placed in every plant row for FI and DI_{50}, and DI_{75} treatments. Drip tapes had inline emitters with discharge

http://www.aloki.hu ● ISSN 1589 1623 (Print) ● ISSN 1785 0037 (Online)
DOI: http://dx.doi.org/10.15666/aeer/1706_1558515604

rate of 1.6 l h^{-1} spaced at 0.20 m. In the PRD_{50} treatment, two drip laterals were laid on each side of the plant row 25 cm away from the eggplant rows. In the subsurface drip irrigation plots (SSDI), laterals were buried at 25 cm depth in the soil under the plant rows. Lateral with in-line emitters spaced at 0.20 m intervals and with flow rate of 2.3 l h^{-1} were used (Geoflow Corte Madera, CA, USA). Since the same flow rate and emitter interval surface and subsurface drip systems were not available in the local market, we used the abovementioned systems in the study. The irrigation amount in each plot was measured by a flow meter.

Table 1. *Some agronomic and management practices carried out during the experiments in 2013 and 2014*

Agronomic Practices	**2013**	**2014**
Transplanting date	May 6	April 14
Cultivar	Anamur Karası	Anamur Karası
Planting spacing	90 cm x70 cm	90 cm x70 cm
Plant density	155 556 plants ha^{-1}	155 556 plants ha^{-1}
Fertilization	50 N; 50 P_2O_5; and 50 kg ha^{-1} K compound fertilizer at transplanting plots stated to receive N through fertigation at every 6-day irrigation interval (160 kg ha^{-1} N) three weeks after transplanting	50 N; 50 P_2O_5; and 50 kg ha^{-1} K compound fertilizer at transplanting plots stated to receive N through fertigation at every 6-day irrigation interval (160 kg ha^{-1} N) three weeks after transplanting
Irrigation system	Inline surface and inline subsurface drip irrigation	Inline surface and inline subsurface drip irrigation
Effective cultivated area	3456 (80 m lenght x 43.2 m width)	3456 (80m lenght x 43.2 m width)
First picking	June 27	June 16
Hoeing and weeding	23 May, 10, 17 June; 2 July	22 and 29 May, 17 June and 1 July
Plant Protection	On 20.06.2013, insecticide applied against green worms, leaf galleria fly, red spider, white fly various insecticides and on 01.08.2013 fungicide against Fusarium oxysporum fungus was sprayed.	Various insecticides against green worms, aphids, leaf galleria fly, red spider, white fly on 25 April, 7 May, 14 May and 23 May; On 25 April, 14 May and 23 May, fungicide was applied against lead mold and powdery mildew and Fusarium oxysporum.
First picking	June 27	June 16
Last picking	Agust 5	July 25

Figure 2. *A general view of the experimental plots*

http://www.aloki.hu ● ISSN 1589 1623 (Print) ● ISSN 1785 0037 (Online)
DOI: http://dx.doi.org/10.15666/aeer/1706_1558515604

Measurements

Soil water content

A neutron moisture meter was used to measure the soil water content (SWC) with (Model 503 DR, Martinez, CA) at 0.2 m depth intervals down to 0.80 m prior to irrigation applications with 3- and 6-day frequencies during the eggplant growing seasons. Access tubes were placed in the mid plant rows between two plants in the experimental subplots. Average of four replications was taken as mean soil water content for each depth to reduce spatial variability. Gravimetrical sampling method was used to measure SWC in the upper soil layer of 20 cm during the growing seasons.

Eggplant evapotranspiration and water use efficiency

Seasonal evapotranspiration (ET) or crop water use was estimated using the water budget equation *Eq. (1)*.

$$ET = R + I \mp \Delta W - Dp - Roff \quad \text{(Eq.1)}$$

In this equation, ET is seasonal crop water use or evapotranspiration (mm), R is rainfall (mm), I is seasonal total irrigation water applied (mm), ΔW is change in soil water storage in the root zone depth (mm), Dp is downward soil water movement or deep percolation below the root-zone depth (mm), and Roff is surface runoff (mm). Dp and Roff were neglected since the amount of irrigation water applied via drip systems was precisely controlled and rainfalls received during the growing season was less than soil storage capacity in 60 cm profile depth.

Water use efficiency (WUE) values were estimated as the ratio of fresh eggplant yield over seasonal crop water use or evapotranspiration (Gong et al., 2017).

Leaf area index

Leaf areas for experimental treatment plots were estimated using LAI-2000 Plant Canopy Analyzer equipment (Li-Cor 2000, Lincoln, NE) at weekly interval throughout the growing season. In this method of LAI measurement, four measurements below the plant canopy and one measurement above the canopy were taken for each treatment plots to account for the canopy light interception in crop canopy at five different angles, from which LAI was estimated employing radiative transfer model.

Dry matter yield

Variation of dry matter yields with time in each experimental sub-plot was determined at two-week intervals until harvest by cutting the plants in 2.10 m of a row section in each subplot at the ground level. The plant samples taken were dried in an oven at 65°C for several days until constant dry weight reached.

Stomatal resistance

A diffusion porometer (AP4 Leaf Porometer, Delta–T Devices, Cambridge, England) was used to determine the stomatal resistance of eggplant leaves (*Figure 3*).

Measurements were taken at 6-day intervals prior to irrigations until harvest between 12:00 and 14:00 O'clock on the fully developed upper two leaves and under clear sky conditions. Soil water contents were also measured on the same day with porometer

http://www.aloki.hu ● ISSN 1589 1623 (Print) ● ISSN 1785 0037 (Online)
DOI: http://dx.doi.org/10.15666/aeer/1706_1558515604

readings. The porometer was calibrated before making each reading. Using the calibration values, the lower and upper surface resistances of the leaf were calculated with the *Equation 2* given by Clawson and Blad (1982).

$$r_S = \frac{r_u + r_l}{r_u \cdot r_l} \quad \text{(Eq.2)}$$

where r_s is the average stomatal resistance s m^{-1}; r_u and r_l are stomatal resistance of the upper and the lower surface of the leaf, respectively.

Diurnal variations of stomatal resistance were also measured in mid-growth stage once each year before an irrigation application.

Figure 3. *Measurement of stomatal resitance in eggplant with porometer*

Statistical analysis

Statistical analysis of the data was carried out using the JMP Statistical software (SAS Institute, Inc., Cary, NC, USA). Two-way variance analyses (ANOVA) were conducted, and to determine the differences among treatment means Least Significant Difference (LSD) at a 5% probability level was made (Steel and Torrie, 1980).

Results

Irrigation and crop water use results

The data on total irrigation water applied, seasonal evapotranspiration, yield and water use efficiency for the treatments in the experimental years were presented in *Table 2*. Seasonal irrigation amounts differed between the treatment plots in the growing seasons due to prevailing weather conditions and distribution and quantity of rainfall received during each season. The rainfall received during the growing season in the experimental years was 163 and 126 mm, respectively, which wre greater than long-term mean of 86 mm. Mean maximum temperatures in 2014 in June was 38.2°C was higher than 2013 and long-term mean. Mean minimum temperatures in June through August in 2014 were greater than those in 2013 and long-term mean. The data revealed that the seasonal irrigation amount varied between 243 mm in IF_6DI_{50} and IF_6PRD_{50} and 495 mm in IF_3FI plots in the SDI plots, and ranged from 228 mm IF_6DI_{50} and IF_6PRD_{50} to 450 mm in IF_3FI

http://www.aloki.hu ● ISSN 1589 1623 (Print) ● ISSN 1785 0037 (Online)
DOI: http://dx.doi.org/10.15666/aeer/1706_1558515604

plots the SSDI in 2013 (*Table 2*). The total irrigation water changed between 229 mm in IF_6DI_{50} and IF_6PRD_{50} to 444 mm in IF_3FI in SDI plots; and varied from 216 mm IF_6DI_{50} and IF_6PRD_{50} to 418 mm in IF_3FI in the SSDI treatment plots in 2014. PRD_{50} and DI_{50} plots received the same quantity of irrigation water.

Table 2. *Eggplant yield, seasonal irrigation, ET, WUE and LAI values under the different treatments in the experimental years*

Years	Irrigation systems	Treatments	Seasonal irrigation mm	ET mm	Yield t ha^{-1}	WUE kg m^{-3}	LAI
2013	Surface Drip (SDI)	IF_3FI	495	543	78.7	14.5 h*	4.13
		IF_3DI_{75}	382	441	75.3	17.1 def	3.8
		IF_3DI_{50}	268	339	70.4	20.8 b	3.47
		IF_3PRD_{50}	268	346	58.1	16.8 f	2.95
	SDI	IF_6FI	446	517	69.8	13.5 ı	3.56
		IF_6DI_{75}	344	425	63.4	14.9 g	3.2
		IF_6DI_{50}	243	349	60.8	17.4 d	3.07
		IF_6PRD_{50}	243	356	48.7	13.7 ı	2.65
	Subsurface Drip (SSDI)	IF_3FI	450	495	71.9	14.5 h	4.02
		IF_3DI_{75}	348	403	69.3	17.2 de	3.73
		IF_3DI_{50}	245	306	66.9	21.9 a	3.25
		IF_3PRD_{50}	245	318	53.9	17.0 ef	2.75
	SSDI	IF_6FI	414	479	60.7	12.7 j	3.45
		IF_6DI_{75}	321	398	58.1	14.6 gh	3.15
		IF_6DI_{50}	228	317	56.8	17.9 c	2.91
		IF_6PRD_{50}	228	335	40.9	12.2 k	2.6
2014	Surface Drip (SDI)	IF_3FI	444	527	92.2	17.5 g	4.30
		IF_3DI_{75}	349	441	87.6	19.9 de	3.85
		IF_3DI_{50}	253	367	83.0	22.6 b	3.55
		IF_3PRD_{50}	253	375	68.3	18.2 f	3.03
	SDI	IF_6FI	396	508	87.7	17.3 g	3.99
		IF_6DI_{75}	312	433	84.6	19.5 e	3.65
		IF_6DI_{50}	229	363	77.2	21.3 c	3.30
		IF_6PRD_{50}	229	369	64.3	17.4 g	2.80
	Subsurface Drip (SSDI)	IF_3FI	418	494	92.7	18.8 f	4.18
		IF_3DI_{75}	329	419	88.6	21.2 c	3.79
		IF_3DI_{50}	240	350	85.7	24.5 a	3.34
		IF_3PRD_{50}	240	353	68.9	19.5 e	2.97
	SSDI	IF_6FI	369	473	86.2	18.2 f	3.95
		IF_6DI_{75}	292	411	83.4	20.3 d	3.47
		IF_6DI_{50}	216	349	75.5	21.7 c	3.10
		IF_6PRD_{50}	216	354	58.8	16.6 h	2.64

* LSD grouping at 5 % level; each year was analyzed separately

Soil water content variation in different treatments with time in the experimental years are characterized by a gradual decrease in SWC in response to deficit irrigated treatments towards the end of the season as compared with full irrigation plots. In the two drip systems with 3-day frequency plots, plant available water in FI and DI_{75} treatments were greater than 50% during the growing seasons. On the other hand, in DI_{50} and PRD_{50} treatments SWC values were below the 50% available soil water level (soil water data not presented). The detailed information on soil water content variations in the experimental treatments and years can be found in previous publication by Bozkurt Çolak et al. (2017).

http://www.aloki.hu ● ISSN 1589 1623 (Print) ● ISSN 1785 0037 (Online)
DOI: http://dx.doi.org/10.15666/aeer/1706_1558515604

Irrigation systems and irrigation levels resulted in significantly different ET values in the first experimental year, but only irrigation levels had significantly different effect in the second year (*Table 3*). Seasonal evapotranspiration changed between 339 mm in DI_{50} with 3-day frequency treatment and 543 mm in IF_3 FI under the SDI in the first experimental year, and 363 mm in IF_6 DI_{50} and 527 mm in IF_3 FI in the second year. In SSDI treatment plots, ET values changed between 306 mm in IF_3 DI_{50} to 495 mm in IF_3 FI plots in 2013; and 349 mm in IF_6 DI_{50} to 494 mm in IF_3 FI in 2014 (*Table 2*). In the second growing season slightly lower ET values were determined compared with ET values in 2013 probably due to occurrence of the lower monthly minimum temperatures in April 2014, and prevailing high maximum air temperatures in June and August in the second season. Prevaling considerably lower air temperatures in April (4.4°C) in the second year hampered the plant establishment and growth. The results revealed that DI_{50} plots in both drip systems resulted in an average of 3% less crop water use values than PRD_{50} plots despite of receiving the same quantity of irrigation water.

Table 3. *Statistical analysis results on yield of eggplant under different treatments in the experimental years*

Years	Irrigation Treatments	Yield (kg ha^{-1})	WUE (kg m^{-3})	ET (mm)	LAI
2013	Irrigation systems	LSD=1541 P=0.0012**	ns	LSD=5.051 P=0.0001**	LSD=0.117 P=0.0457*
	Irrigation frequency	LSD=1245 P=0.0001**	LSD=0.12 P=0.0001**	ns	LSD=0.045 P=0.0001**
	Irrigation levels	LSD=1886 P=0.0001**	LSD=0.17 P=0.0001**	LSD= 15.64 P=0.0001**	LSD=0.058 P=0.0001**
	Int. of irr. syst. and irr fre.	ns	LSD=0.17 P=0.0001**	ns	ns
	Int. of irr. sys.and irr. lev.	ns	LSD=0.24 P=0.0001**	ns	ns
	Int. of irr. fre. and irr. lev.	ns	LSD=0.24 P=0.0001**	ns	LSD=0.083 P=0.0001**
	Int. of irr. syst. and irr. fre. and irr. lev.	ns	LSD=0.34 P=0.0061**	ns	ns
2014	Irrigation systems	ns	LSD=0.44 P=0.0080**	ns	LSD=0.049 P=0.0054**
	Irrigation frequency	LSD=1749 P=0.0001**	LSD=0.19 P=0.0001**	ns	LSD=0.019 P=0.0001**
	Irrigation levels	LSD=2844 P=0.0001**	LSD=0.30 P=0.0001**	LSD= 15.69 P=0.0001**	LSD=0.049 P=0.0001**
	Int. of irr. syst. and irr fre.	LSD=2473 P=0.0425*	LSD=0.27 P=0.0004**	ns	ns
	Int. of irr. sys.and irr. lev.	ns	LSD=0.42 P=0.0122*	ns	LSD=0.069 P=0.0486*
	Int. of irr. fre. and irr. lev.	ns	LSD=0.42 P=0.0001**	ns	ns
	Int. of irr. syst. and irr. fre. and irr. lev.	ns	LSD=0.6 P=0.0115*	ns	ns

** LSD grouping at 1% level, * LSD grouping at 5 % level

Eggplant yield

The fresh eggplant yields obtained from the experimental treatment plots in the study years are given in *Table 2*. *Table 3* presents statistical analysis on the mean eggplant yields. The effects of various treatments on eggplant yield differed in the experimental

http://www.aloki.hu ● ISSN 1589 1623 (Print) ● ISSN 1785 0037 (Online)
DOI: http://dx.doi.org/10.15666/aeer/1706_1558515604

years. Since the years were statistically different in combined variance analysis, we analyzed the data for each experimental year separately. The results indicated that irrigation systems, frequencies and levels resulted in significantly different eggplant yield values ($P < 0.01$). SDI system performed better than the SSDI in the first year, however they performed similarly in the second growing season.

Eggplant yields varied from a minimum of 40.90 t ha^{-1} in subsurface drip irrigated IF_6 PRD_{50} treatment plots to greatest 78.7 t ha^{-1} in the surface drip irrigated IF_3 FI in 2013, and changed between 58.8 t ha^{-1} in IF_6 PRD_{50} in SSDI and 92.7 t ha^{-1} in the IF_3 FI in SSDI 2014 growing season. PRD_{50} treatments produced the least yields in the experimental years. The second growing season resulted in significantly higher yields than in the first season because of prevailing favourable climatic conditions in the 2014.

Water use efficiency

Water use efficiency values were significantly affected by drip irrigation systems, irrigation frequencies and levels in the experimental years (*Table 3*). WUE values varied between 12.2 kg m^{-3} in IF_6 PRD_{50} under SSDI and 21.9 kg m^{-3} in the IF_3 DI_{50} in SSDI in 2013 and ranged from 16.6 kg m^{-3} in the IF_6 PRD_{50} treatment under SDI to 24.5 kg m^{-3} in the IF_3 DI_{50} under SSDI in 2014. The results revealed that WUE increased with decreasing irrigation water amounts except in the PRD_{50} treatment which resulted in minimum WUE values in both growing seasons.

Dry matter yield and leaf area index

The evolution of the dry matter yield with time for different treatments under the surface and subsurface drip systems in the experimental is depicted in *Fig. 4a-d*. The IF_3FI under the SDI system resulted in the maximum dry matter yield of 6329 and 6400 kg ha^{-1} in 2013 and 2014 growing seasons, respectively; and the least dry matter yields were observed in the IF_6 PRD_{50} treatment under the SSDI.

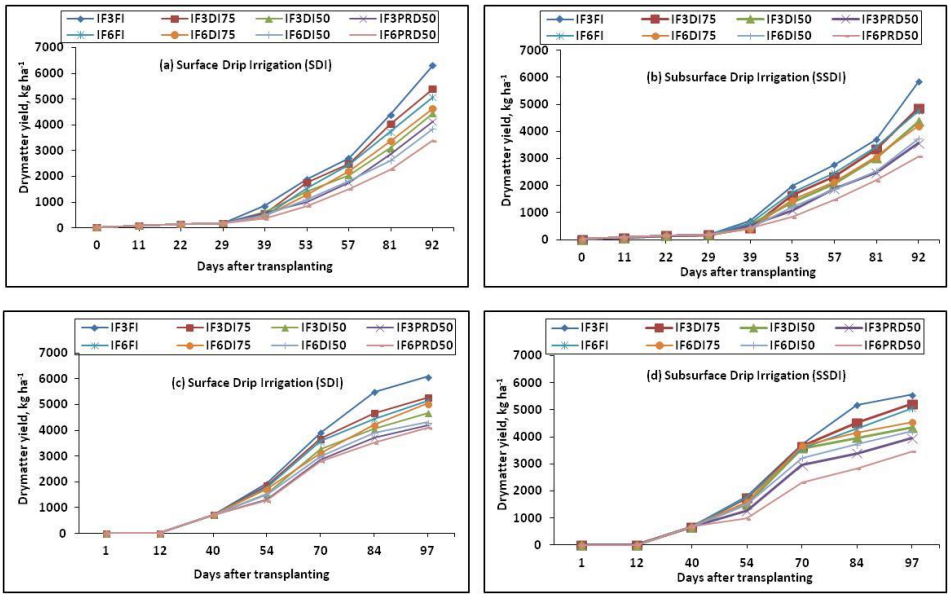

Figure 4. *Dry matter yield variation during the 2013 and 2014 eggplant growing season in all treatments under surface and subsurface drip irrigation. (a) SDI, 2013; (b) SSDI, 2013; (c) SDI, 2014; (d) SSDI, 2014*

http://www.aloki.hu ● ISSN 1589 1623 (Print) ● ISSN 1785 0037 (Online)
DOI: http://dx.doi.org/10.15666/aeer/1706_1558515604

The maximum leaf area index (LAI) values for the different treatments under both drip systems in the experimental years are presented in *Table 2*. Irrigation systems, frequency and level resulted in significantly different LAI values (*Table 3*). The IF_3 FI treatment under SDI produced the maximum LAI of 4.13 and 4.30 in the first and second growing seasons, respectively; the minimum LAI values of 2.6 and 2.1 were observed in the IF_6 PRD_{50} treatment under SSDI in 2013 and 2014, respectively.

Stomatal resistance

Stomatal resistance (r_s) evolution with time in the experimental years for different treatments under SDI and SSDI systems are depicted in *Fig. 5a-d*, respectively. The stomatal resistances showed tendency to increase with increasing water stress. Smaller r_s values were observed in FI plots under the two drip systems with 3-day irrigation frequency than DI_{50} and PRD_{50} treatments with 6-day irrigation frequency. Generally, the lower r_s value was measured in the beginning of the growing season, and the r_s rises towards the end of the growing season. In the SDI treatments, stomatal resistance values ranged between 40 s m^{-1} in IF_3FI and 132 s m^{-1} in IF_6PRD_{50} in 2013, and varied between 36 s m^{-1} IF_3FI and 136 s m^{-1} IF_6PRD_{50} in the 2014. In SSDI plots, r_s values varied between 34 s m^{-1} IF_3FI plots and 121 s m^{-1} IF_6PRD_{50} in 2013, and varied from 30 s m^{-1} IF_3FI to 132 s m^{-1} IF_6PRD_{50} in the 2014. Higher stomatal resistance values were observed in the PRD_{50} than those in the DI_{50} plots under both drip irrigation systems. We also observed that the values of stomatal resistance (r_s) in SSDI plots were slightly lower than those of SDI plots in general.

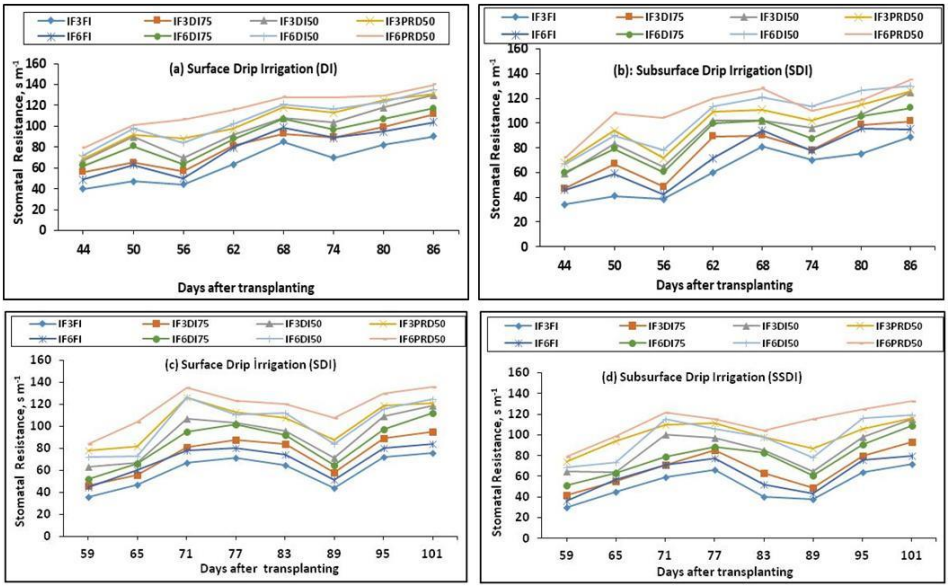

Figure 5. *Stomatal resistance variation during the experimental years in all treatments. (a) Surface drip irrigation (2013); (b) Subsurface drip irrigation (2013); (c) Surface drip irrigation (2014); (d) Subsurface drip irrigation (2014)*

Diurnal variation of stomatal resistance values for the different treatments in the study years are presented in *Figure 6a-d*, respectively. As shown in these figures rs values were lower in the morning hours and gradually increased with time and reached their maximum at solar noon time (13:00-14:00). Then r_s values started to decrease towards the sunset

http://www.aloki.hu ● ISSN 1589 1623 (Print) ● ISSN 1785 0037 (Online)
DOI: http://dx.doi.org/10.15666/aeer/1706_1558515604

time in all treatments due to lower air temperatures. The lowest rs values were observed in the IF_3FI plot in both study years; maximum r_s values were measured in IF_6PRD_{50} and IF_6DI_{50} treatments.

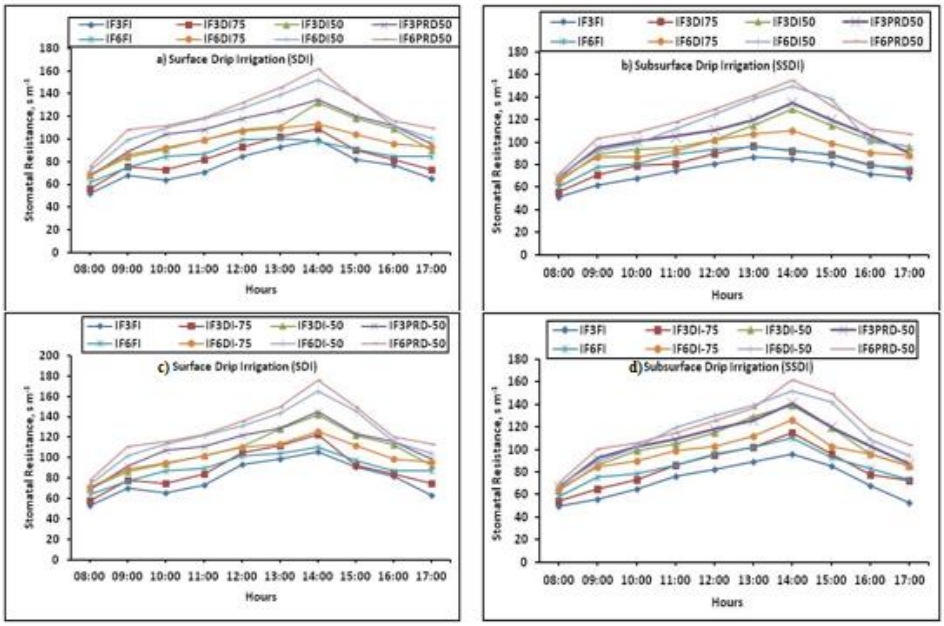

Figure 6. *Diurnal variation of stomatal resistance values in all treatments. (a) Surface drip irrigation (2013); (b) Subsurface drip irrigation (2013); (c) Surface drip irrigation (2014); (d) Subsurface drip irrigation (2014)*

Relations between soil water content, yield, dry matter, evapotranspiration, water use efficiency and stomatal resistance

The relationships between soil water content and stomatal resistance (r_s) prior to irrigations in treatments in the 2013 and 2014 growing seasons for surface and subsurface drip systems are depicted in *Fig. 7a-d*, respectively. Mean stomatal resistance was calculated by taking average of the readings taken before irrigation throughout the growing season.

Significant second order polynomial relations were obtained between soil water content in the effective root-zone depth and stomatal resistance in the experimental years. Stomatal resistance values decreased as the soil water content increased towards the field capacity (245 mm) under both drip systems.

The relationships between mean stomatal resistance and total eggplant yield values for SDI and SSDI treatments in the experimental years are presented in *Fig. 8*. Significant relations were found between fresh eggplant yield and stomatal resistance. The relationship between yield and stomatal resistance was expressed with a second order polynomial in the first year (R^2=0.66), and strong linear equation in the second year (R^2=0.83). Sezen et al. (2019) also expressed significant relationships among the stomatal resistance, evapotranspiration and red pepper yield in the Mediterranean region.

The relationship between stomatal resistance and dry matter yield for SDI and SSDI treatment plots were presented in *Fig. 9*. We found significant linear relations between

http://www.aloki.hu ● ISSN 1589 1623 (Print) ● ISSN 1785 0037 (Online)
DOI: http://dx.doi.org/10.15666/aeer/1706_1558515604

dry matter yield and stomatal resistance for eggplant with the coefficient of determination (R^2) for the stomatal resistance was 0.84 and 0.85 in 2013 and 2014, respectively.

The relationships between stomatal resistance and evapotranspiration for SDI and SSDI treatments were shown in *Fig. 10*. We found significant linear equations between evapotranspiration and stomatal resistance for eggplant with the coefficient of determination (R^2) for the stomatal resistance was 0.68 and 0.74 in 2013 and 2014, respectively. Liu et al. (2016) reported that transpiration rate linearly increased with increasing stomatal conductance. It was observed that plants experiencing water deficit generally increase r_s, thereby decreasing transpiration rate, increasing leaf temperatures (Ballester et al., 2013).

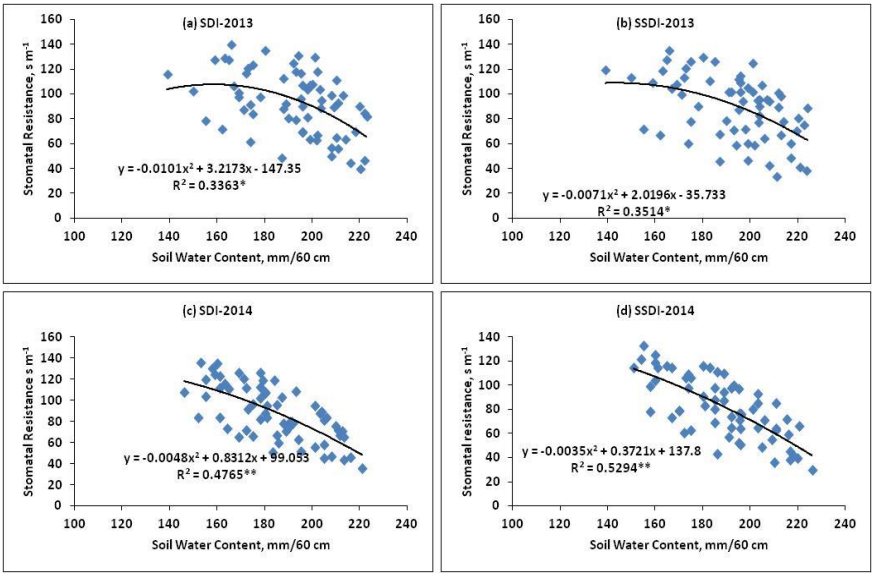

Figure 7. *The relationship between soil water content and stomatal resistance (rs) in treatments in the experimental years (a) SDI-2013; (b) SSDI-2013; (c) SDI-2014; (d) SSDI-2014*

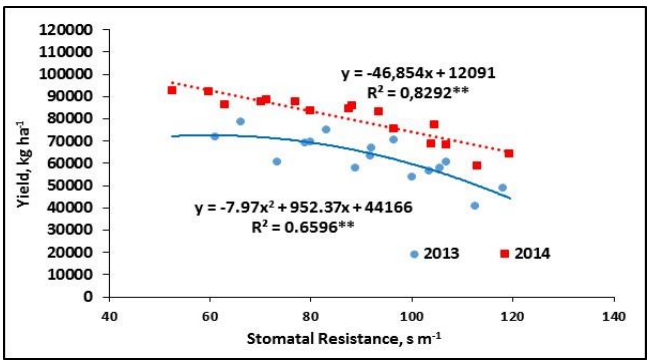

Figure 8. *The relationship between total yield and stomatal resistance in the 2013 and 2014 growing seasons*

The relationships between stomatal resistance and water use efficiency values for SDI and SSDI treatment plots were depicted in *Fig. 11*. We found significant second order equations between WUE and stomatal resistance for eggplant with the coefficient of determination (R^2) for the rs was 0.27 and 0.42 in 2013 and 2014, respectively. The

http://www.aloki.hu ● ISSN 1589 1623 (Print) ● ISSN 1785 0037 (Online)
DOI: http://dx.doi.org/10.15666/aeer/1706_1558515604

relationship between LAI and stomatal resistance for the different treatments were depicted in *Figure 12*. Significant linear relation was obtained between LAI and rs for the 2013 and 2014 growing seasons with high coefficient of determination (R^2) values as 0.90 and 0.84, respectively.

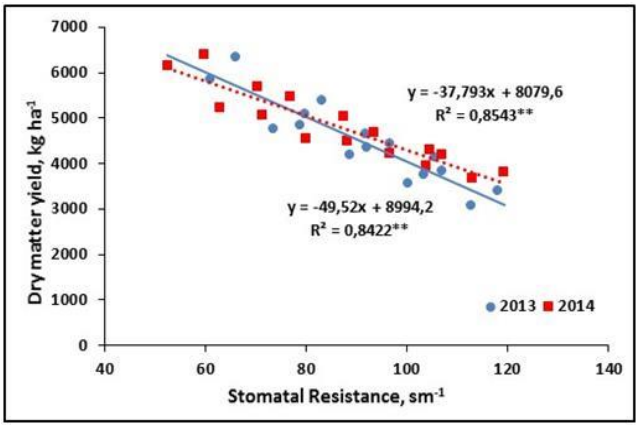

Figure 9. *The relationship between dry matter yield and stomatal resistance (rs) in the 2013 and 2014 growing seasons in all treatments*

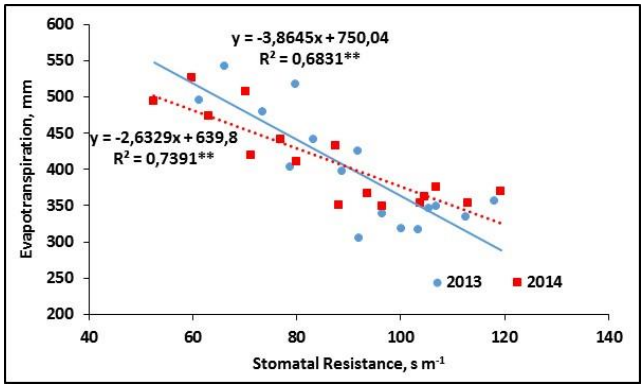

Figure 10. *The relationship between ET and stomatal resistance in the 2013 and 2014 growing seasons*

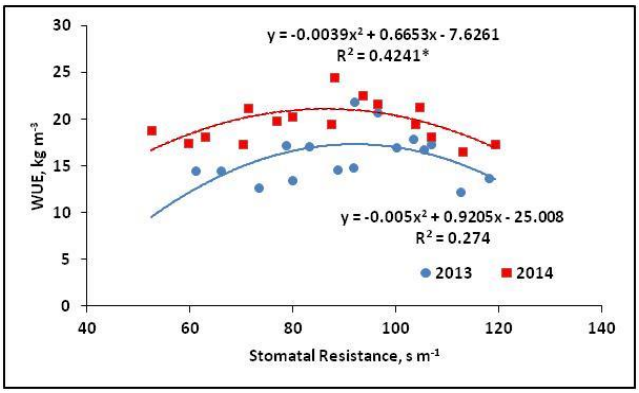

Figure 11. *The relationship between WUE and stomatal resistance in the 2013 and 2014 growing seasons*

http://www.aloki.hu ● ISSN 1589 1623 (Print) ● ISSN 1785 0037 (Online)
DOI: http://dx.doi.org/10.15666/aeer/1706_1558515604

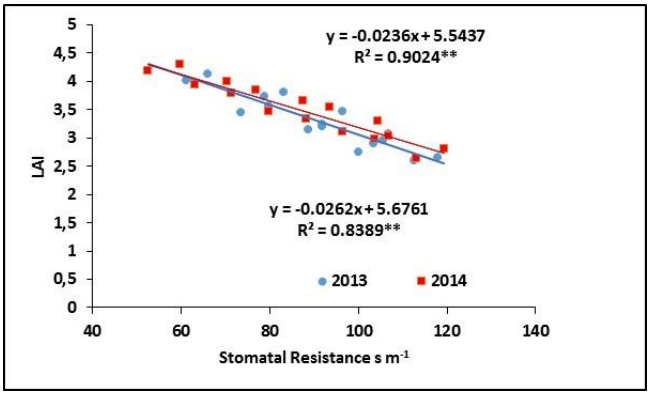

Figure 12. *The relationship between LAI and stomatal resistance in the 2013 and 2014 growing seasons*

Discussions

Studies were made to see whether physiological responses of SDI and SSDI irrigated eggplant to full and various deficit irrigation regimes and frequencies could be utilized for irrigation scheduling.

The research results revealed that the effects of SDI and SSDI systems, irrigation frequencies and levels were found to be significant on total yield and evapotranspiration of eggplant for obtaining greater yield in the Mediterranean environment.

The full irrigation with more frequent irrigation frequency (3-day) under the two drip systems produced significantly greater eggplant yields, followed by DI_{75} treatment which produced slightly lower yield (about 5%) than FI in both experimental years but resulted in water saving of 22.5%. The improved yield under high irrigation frequency as observed in our experiment might be due to the enhanced nutrients uptake (Silber et al., 2003; Ta et al., 2012), consistent with studies on tomato (Pires et al., 2011; Rodriguez-Ortega et al., 2017) and other crops such as bell pepper (Sezen et al., 2006) and melon (Sensoy et al., 2007).

The results revealed that water stress occurring in DI_{50} and PRD_{50} treatments under both drip systems resulted in decreased eggplant yield significantly. These reductions for 6-day irrigation frequency were much greater than those in 3-day frequency. Our findings are in agreement with those found by Kırnak et al. (2002) who reported that deficit irrigations caused a decrease in yield and fruit size of eggplant. The most sensitive growth periods of eggplant to water stress are during flowering and fruit formation. Therefore, occurrence of any water stress in these growth stages might lead to the development of blossom end rot and malformed fruits. Kemble et al. (1998) reported that fruit size and yield as well as dry matter yield (Sarker et al., 2005) are decreased by water stress. Aujla et al. (2007) obtained eggplant yields changing between 43.10 and 103.10 t ha^{-1} in India; Kuşcu et al. (2009) reported maximum marketable eggplant yield of 46.40 t ha^{-1} when irrigations were scheduled at 80% replenishment of the evaporation form Class A pan in Turkey. Karam et al. (2011) determined fresh eggplant yields changing from 13.40 to 33.80 t ha^{-1} for full and deficit irrigations under Lebanease conditions. Douh and Boujelben (2010) investigated the effects of subsurface and surface drip systems on eggplant yield Tunisia and they concluded that SSDI had better performance than SDI. Rakhymzhanov et al. (2015) reported that drip irrigation produced 41% greater yield than

http://www.aloki.hu ● ISSN 1589 1623 (Print) ● ISSN 1785 0037 (Online)
DOI: http://dx.doi.org/10.15666/aeer/1706_1558515604

furrow method and resulted in water saving of 29% as compared to furrow irrigation in Kazakhstan.

Three-day irrigation frequency (IF_3) produced significantly higher yields than six-day (IF_6) frequency for the corresponding treatments. The reason for greater yield under the more frequent irrigations is that plants can uptake water more easily without experiencing any stress effect compared with longer irrigation frequency treatments. There was no significant difference between the SDI and SSDI systems with regard to eggplant yields although SDI performed slightly better than the SSDI in the first year but they performed similarly in the second year. The results indicated that both SDI and SSDI full irrigation with 3-day irrigation frequency (IF_3 FI) treatment can be recommended. Deficit irrigation DI_{50} and PRD_{50} produced lowest eggplant yields. Although the DI_{75} received approximately 22.5% less water as compared to the FI, yield was reduced only by an average of 4.3%. Therefore, considering water deficiency in dry years DI_{75} irrigation practices can be a good alternative for high yields. The physiological response of eggplant to different water stress levels can be used for optimization and sustainability of crop production in areas where water sources are limited or expensive.

The 3-day irrigation frequency produced higher dry matter yields than the 6-day frequency treatments in both drip methods. The significantly greater reduction in dry matter yields for plants under water stress in DI_{50} and PRD_{50} treatments during fruit ripening stage might be due to decrease in fruit dry-matter yields, as reported by Chaves et al. (2003), and Lovelli et al. (2007). Passioura and Angus (2010) indicated that decreases in plant growth in semi-arid agriculture might be the results of reductions in assimilate transfer from leaves to fruits due to increasingly unfavourable water supply conditions. This observation is apparently pertinent to eggplant produced under water stress conditions.

Water stress resulted in lower leaf area index values under both SDI and SSDI treatments in the experimental years. Madramootoo and Rigby (1991) indicated that water stress reduced the leaf areas of eggplants. Karam et al. (2011) observed the highest LAI in the full irrigation plots, while 44 and 10% reductions were reported for deficit irrigations. Mohawesh (2016) found that water deficit resulted in reduction in growth of eggplant which in turn reduced LAI. The main reason for the decreased vegetative growth of vegetable crops under water stress might be acceleration of leaf senescense, as pointed out by Kırnak et al. (2002) on eggplant and Karam et al. (2009) on bell pepper plants. Passioura and Angus (2010) demonstrated that under water stress, the life cycles of annual plants are shortened and leaf senescense accelerated due to reduced water uptake by the roots. These findings are similar with our results obtained in the present study.

Our finding indicated that the highest WUE was not associated with the least irrigation quantity is because increasing water stress hindered plant growth and consequently reduced the final yield, consistent with previous studies on tomato, and eggplant (Kang et al., 2004; Cantore et al., 2016). Similarly, the minimum WUE was not associated with the highest irrigation amount because it enhanced non-productive transpiration, alluding that increasing irrigation amount benefited yield but not WUE (Du et al., 2017). It is suggested that high WUE should be associated with high (or acceptable) yields, particularly in water scarce areas. Karam et al. (2011) reported the maximum WUE in the deficit irrigated plots as 5.6 kg m^{-3} in Lebanon, while Lovelli et al. (2007) observed the greatest WUE value of 10.3 kg m^{-3} in full irrigation in Italy. Other researchers reported increased WUE in deficit irrigation treatments for red pepper (Sezen et al., 2014), eggplant (Kırnak et al., 2002). The reason for greater WUE in crops under water stress is

http://www.aloki.hu ● ISSN 1589 1623 (Print) ● ISSN 1785 0037 (Online)
DOI: http://dx.doi.org/10.15666/aeer/1706_1558515604

because stressed plants wilt far more than unstressed plants and wilting invariably occurs in times when the vapour pressure deficit of the atmosphere is large (Bloch et al., 2006).

It was observed that slightly lower rs values were recorded for SSDI plots than the SDI treatments in general. Stomatal resistance values influenced by changing weather conditions especially they were sensitive to changes in vapour pressure deficit, wind speed, and air temperature as well as soil water content variation at measurement times. Thus, this parameter fluctuates significantly with changing soil water and weather conditions. Therefore, utilizing rs values for irrigation scheduling requires considerable attention for reliable and practical applications.

Weng et al. (2011) stated that stomata play a significant role in determining the carbon and water cycle between the plants and the atmosphere. One of the first physiological responses of plants exposed to water restriction is to control the stomatal opening and closing movements in order to decrease water loss via transpiration. However, since CO_2 entry is also inhibited, the photosynthesis activity of the plant is directly affected by these movements (Arve et al., 2011). It is noted that water stress decrease stomatal conductance (gs) and transpiration rate (Tr), and the photosynthesis rate primarily decreased in response to reduced stomatal conductance (Ma et al., 2015). It is also mentioned that lower stomatal conductance would decrease CO_2 assimilation very slightly, however would significantly reduce Tr, since transpiration rises linearly with stomatal conductance, due to constant difference in water vapor concentration between leaves and the air (Liu et al., 2016).

In this study, the evapotranspiration rates of the eggplant reduced with decreasing amount of applied irrigation water, resulting in increased stomatal resistance and subsequent reduction in yield and plant growth. These results confirm many earlier studies on different crops (Ma et al., 2015; Liu et al., 2016). Thus, our findings demonstrated that the stomatal resistance is a good indicator for describing the plant water status.

Water shortage resulted in greater stomatal resistance values. The current study results demonstrated that there were strong linear relations among the yield, dry matter yield and stomatal resistance (rs). In addition, we found strong significant linear relations between crop water use (ET) and stomatal resistance. Significant curvilinear relationships were obtained between the soil water content and WUE and rs. All these relations indicated that an average value of 60 s m^{-1} stomatal resistance value prior to irrigation is the threshold value for irrigation scheduling of eggplants. Since rs values were lower in the early season and increased towards the end of season as shown in *Figs. 5 and 6*, rs value range of 30-40 s m^{-1} in the vegetative stage until flowering; 40-60 s m^{-1} during flowering and yield formation stage, and 60-80 s m^{-1} during late growth stage can be used for irrigation scheduling purpose.

Conclusions

Studies were made to see whether physiological responses such as stomatal resistance of SDI and SSDI irrigated eggplant to full and various deficit irrigation regimes and frequencies could be utilized for irrigation scheduling. Water shortage resulted in greater stomatal resistance values. The current study results demonstrated that there were strong linear relations among the yield, dry matter yield and stomatal resistance (rs). In addition, we found strong significant linear relations between crop water use (ET) and stomatal resistance. Curvilinear relationships were obtained between the WUE and rs.

http://www.aloki.hu ● ISSN 1589 1623 (Print) ● ISSN 1785 0037 (Online)
DOI: http://dx.doi.org/10.15666/aeer/1706_1558515604

Stomatal resistance values in subsurface drip irrigated eggplant were generally lower than those in the surface drip irrigated plots. Frequent irrigations also resulted in lower stomatal resistance values when compared with 6-day irrigation frequency in this study. Lower rs values were observed in FI plots under two drip systems with 3-day frequency than DI_{50} and PRD_{50} plots and 6-day frequency. The results indicated that threshold value of stomatal resistance was approximately 60 s m^{-1} for eggplant for irrigation scheduling. Therefore, it is proved that rs can be used for irrigation scheduling. The predicting the yield response to stomatal resistance is important for developing strategies and making decisions for use by farmers as well as researchers for managing irrigation under scarce water resources conditions.

The research results also revealed that the effects of SDI and SSDI systems, irrigation frequencies and levels were found to be significant on total yield and evapotranspiration of eggplant for obtaining greater yield in the Mediterranean environment. The results indicated that both SDI and SSDI full irrigation with 3-day irrigation frequency (IF_3 FI) treatment can be recommended. Deficit irrigation DI_{50} and PRD_{50} produced lowest eggplant yields. Although the DI_{75} received approximately 22.5% less water as compared to the FI, yield was reduced only by an average of 4.3%. Therefore, considering water deficiency in dry years DI_{75} irrigation practices can be a good alternative for high yields. The physiological response of eggplant to different water stress levels can be used for optimization and sustainability of crop production in areas where water sources are limited or expensive.

Acknowledgement. The authors would like to thank the Turkish Scientific and Technical Research Council (TUBITAK) for its financial support for the project TOVAG-112O870.

REFERENCES

[1] Agele, S., Shabtai Cohen, S., Assouline, S. (2006): Hydraulic characteristics and water relations of net house-grown bell pepper as affected by irrigation regimes in a Mediterranean climate. – Environ. Exp. Bot. 57: 226-235.

[2] Anjum, S. A., Xie, X. Y., Wang, L. C., Saleem, M. F., Man, C., Lei, W. (2011): Morphological, physiological and biochemical responses of plants to drought stress. – Afr. J. Agric. Res. 6: 2026-2032.

[3] Arve, L. E., Torre, S., Olsen, J. E., Tanino, K. K. (2011): Stomatal Responses to Drought Stress and Air Humidity, Abiotic Stress in Plants. – In: Shanker, A. (ed.) Mechanisms and Adaptations. ISBN: 978-953-307-394-1, InTech, p 428.

[4] Aujla, M. S., Thind, H. S., Buttar, G. S. (2007): Fruit yield and water use efficiency of eggplant (*Solanum Melongema* L.) as influenced by different quantities of nitrogen and water applied through drip and furrow irrigation. – Scientia Horticulturae 112: 142-148.

[5] Ballester, C., Jimenez-Bello, M. A. Castel, J. R., Intrigliolo, D. S. (2013): Usefulness of thermography for plant water stress detection in citrus and persimmon trees. – Agric. For. Meteorol. 168: 120-129.

[6] Behboudian, M. H. (1977): Responses of eggplant to drought. I. Plant water balance. – Scientia Horticulturae 7(4): 303-31.

[7] Berry, J. A., Beerling, D. J., Franks, P. J. (2010): Stomata: key players in the earth system, past and present. – Curr. Opinion Plant Biol. 13: 233-240.

[8] Bloch, D., Hoffmann, C. M., Marlander, B. (2006): Impact of water supply on photosynthesis, water use and carbon isotope discrimination of sugar beet genotypes. – Eur. J. Agron. 24: 218-225.

http://www.aloki.hu ● ISSN 1589 1623 (Print) ● ISSN 1785 0037 (Online)
DOI: http://dx.doi.org/10.15666/aeer/1706_1558515604

[9] Bozkurt Çolak, Y., Yazar, A., Sesveren, S., Colak, I. (2017): Evaluation of yield and leaf water potantial (LWP) for eggplant under varying irrigation regimes using surface and subsurface drip systems. – Scientia Horticulturae 219: 10-21.
[10] Bozkurt, S., Sayilikan Mansuroğlu, G. (2018): Response of unheated greenhouse grown green bean to buried drip tape placement depth and watering levels. – Agricultural Water Management 197: 1-8.
[11] Brodribb, T. J., McAdam, S. A. (2011): Passive origins of stomatal control in vascular plants. – Sci. 331: 582-585.
[12] Cantore. V., Lechkar, O., Karabulut, E., Sellami, M. H., Albrizio, R., Boari, F., Stellacci, A. M., Todorovic, M. (2016): Combined effect of deficit irrigation and strobilurin application on yield, fruit quality and water use efficiency of "cherry" tomato (*Solanum lycopersicum* L.). – Agricultural Water Management 167: 53-61.
[13] Chartzoulakis, K., Drosos, N. (1995): Water use and yield of greenhouse grown eggplant under drip irrigation. – Agricultural Water Management 28: 113-120.
[14] Chaves, M. M., Maroco, J, P., Pereira, J. S. (2003): Understanding plant responses to drought from genes to whole plant. – Funct. Plant Biol. 30: 239-264.
[15] Clauw, P., Coppens, F., De Beuf, K., Dhondt, S., Van Daele, T., Maleux, K., Inze, D. (2015): Leaf responses to mild drought stress in natural variants of Arabidopsis thaliana. – Plant Physiol doi: 10.1104/pp.114.
[16] Clawson, K. L., Blad, B. L. (1982): Infrared thermometry for scheduling irrigation of corn. – Agronomy Journal 74(2): 311-316.
[17] Diaz-Perez, J. C., Eaton, T. E. (2015): Eggplant (Solanum melongena L.) plant growth and fruit yield as affected by drip irrigation rate. – Hortscience 50(11): 1709-1714.
[18] Douh, B., Boujelben, A. (2010): Water saving and eggplant response to subsurface drip irrigation. – Agricultural Segment: 1(2) AGS/1525.
[19] Du, Y., Cao H., Liu, S., Gu, X., Cao, Y. (2017): Response of yield, quality, water and nitrogen use efficiency of tomato to different levels of water and nitrogen under drip irrigation in Northwestern China. – Journal of Integrative Agriculture 16: 1153-1161.
[20] English, M. J., Salomon, K. H., Hoffman, G. J. (2002): A paradigm shift in irrigation management. – J. Irrigation and Drainage Engineering 128(5): 267-277.
[21] Gaveh, E. A., Timpo, G. M., Agodzo, S. K., Shin, D. H. (2011): Effect of irrigation, transplant age and season on growth, yield and irrigation water use efficiency of the African eggplant. – J. Hort. Environ. Biotechnol. 52: 13-28.
[22] Gerosa, G., Mereu, S., Finco, A., Marzuoli, R. (2012): Stomatal conductance modeling to estimate the evapotranspiration of natural and agricultural ecosystems. – In: Irmak, A. (ed.) Evapotranspiration-Remote Sensing and Modeling. Intech. 403-420.
[23] Gong, D., Mei, X., Hao, W., Wang, H., Caylor, K. K. (2017): Comparison of multi-level water use efficiency between plastic film partially mulched and non- mulched croplands at eastern Loess Plateau of China. – Agric. Water Manage. 179: 215-226.
[24] Goodwin, I., Boland, A. M. (2002): Scheduling deficit irrigation of fruit trees for optimizing water use efficiency. – In: Deficit Irrigation Practices, Water Reports, FAO.
[25] Kang, Y., Wang, F. X., Liu, H. J., Yuan, B. Z. (2004): Potato evapotranspiration and yield under different drip irrigation regimes. – Irrigation Science 23: 133-143.
[26] Karam, F., Masaad, R., Bachour, R., Rhayem, C., Rouphael, Y. (2009): Water and radiation use efficiencies in drip irrigated pepper (*Capsicum annuum* L.): response to full and deficit irrigation regimes. – Eur. J. Hortic. Sci. 74: 79-85.
[27] Karam, F., Sabiha, R., Skaf, S., Breidy, J., Rouphael, Y., Balendonck, J. (2011): Yield and water use of eggplants (Solanum Melongena L.) under full and deficit irrigation regimes. – Agricultural Water Management 98: 1307-1316.
[28] Kemble, J. M., Sikora, E. J., Simonne, E. H., Zehnder, G. W., Patterson, M. G. (1998): Guide to Commercial Eggplant Production. – Agronomy and Soils, all at Auburn Univ. ANR-1098.

http://www.aloki.hu ● ISSN 1589 1623 (Print) ● ISSN 1785 0037 (Online)
DOI: http://dx.doi.org/10.15666/aeer/1706_1558515604

[29] Kırnak, H., Taş, İ., Kaya, C., Higgs, D. (2002): Effects of deficit irrigation on growth, yield and fruit quality of eggplant under semi-arid conditions. – Aust. J. Agric. Res. 53: 1367-1373.
[30] Kong, Q., Li, G., Wang, Y., Hua, H. (2012): Bell pepper response to surface and subsurface drip irrigation under different fertigation levels. – Irrig Sci. 30: 233-245.
[31] Kuşçu, H., Çetin, B., Turhan, A. (2009): Yield and economic return of drip-irrigated vegetable production in Turkey. – New Zealand Journal of Crop and Horticultural Science 37: 51-59.
[32] Lamm, F. R., Camp, C. R. (2007): Design, Operation, and Management, Subsurface Drip Irrigation. – In: Lamm, F. R., Ayars, J. E., Nakayama, F. S. (eds.) Microirrigation for Crop Production. Elsevier, Amsterdam, The Netherlands, pp 473-551.
[33] Lianga, Y. L., Wu, X., Zhu, J. J., Zhou, M. J., Peng, Q. (2011): Response of hot pepper (Capsicum annuum L.) to mulching practices under planted greenhouse condition. – Agric. Water Manage. 99: 111-120.
[34] Liu, E. K., Mei, X. R., Yan, C. R., Gong, D. Z., Zhang, Y. Q. (2016): Effects of water stress on photosynthetic characteristics, dry matter translocation and WUE in two winter wheat genotypes. – Agric. Water Manage. 167: 75-85.
[35] Lovelli, S., Perniola, M., Ferrara, A., Di Tommaso, T. (2007): Yield response factor to water (Ky) and water use efficiency of Carthamus tinctorius L. and Solanum melongena L. – Agric. Water Manage. 92: 73-80.
[36] Ma, S. C., Duan, A. W., Wang, R., Guan, Z. M., Yang, S. J., Ma, S. T., Shao, Y. (2015): Root-sourced signal and photosynthetic traits dry matter accumulation and remobilization, and yield stability in winter wheat as affected by regulated deficit irrigation. – Agric. Water Manage. 148: 123-129.
[37] Madramootoo, C. A., Rigby, M. (1991): Effects of trickle irrigation on the growth and sunscald of bell peppers (*Capsicum annuum L.*) in southern Quebec. – Agric. Water Manage. 19: 181-189.
[38] Makbul, S., Saruhan-Guler, N., Durmus, N., Guven, S. (2011): Changes in anatomical and physiological parameters of soybean under drought stress. – Turk. J. Bot. 35: 369-377.
[39] Mohawesh, O. (2016): Utilizing deficit irrigation to enhance growth performance and water-use efficiency of eggplant in arid environments. – Journal of Agricultural Science and Technology 18(1): 265-276.
[40] Müller, T., Ranquet Bouleau, C., Perona, P. (2016): Optimazing drip irrigation for eggplant crops in semi-arid zones using evolving thresholds. – Agric. Water Mange. 177: 54-65.
[41] Nemeskeri, E., Molnar, K., Vigh, R., Nagy, J., Dobos, A. (2015): Relationships between stomatal behaviour, spectral traits and water use and productivity of green peas (Pisum sativum L.) in dry seasons. – Acta Physiol Plant 37: 1-16.
[42] Osakabe, Y., Osakabe, K., Shinozaki, K., Tran, L. S. P. (2014): Response of plants to water stress. – Frontiers Plant Sci. 5: 1-8.
[43] Passioura, J. B., Angus, J. F. (2010): Improving productivity of crops in water-limited environments. – In: Sparks, D. L. (ed.) Advances in Agronomy 106: 37-75.
[44] Pérez-Pérez, J. G., Romero, P., Navarro, J. M., Botía, P. (2008): Response of sweet orange cv 'lane late' to deficit irrigation in two rootstocks. I: water relations, leaf gas exchange and vegetative growth. – Irrig. Sci. 26(5): 415-425.
[45] Pires, R. C. M., Furlani, P. R., Ribeiro, R. V., Bodine Junior, D., Sakai, E., Lourenção, A. L., Neto, A. T. (2011): Irrigation frequency and substrate volume effects in the growth and yield of tomato plants under greenhouse conditions. – Scientia Agricola 68: 400-405.
[46] Rakhymzhanov, B. S., Aitbaev, T. E., Tazhibaev, T. S., Cholacov, T. L. (2015): Cultivation of egg plant (Solanum melongena L.) using drip ırrigation with the use of mineral fertilizers in the conditions of the South-east Kazakhstan. – Biosciences Biotechnology Research Asia 12(1): 101-109.
[47] Rodriguez-Ortega, W. M., Martinez, V., Rivero, R. M., Camara-Zapata, J. M., Mestre, T., Garcia-Sanchez, F. (2017): Use of a smart irrigation system to study the effects of irrigation

http://www.aloki.hu ● ISSN 1589 1623 (Print) ● ISSN 1785 0037 (Online)
DOI: http://dx.doi.org/10.15666/aeer/1706_1558515604

management on the agronomic and physiological responses of tomato plants grown under different temperatures regimes. – Agricultural Water Management 183: 158-168.

[48] Sarker, B. C., Hara, M., Uemura, M. (2005): Proline synthesis, physiological responses and biomass yield of eggplants during and after repetitive soil moisture stress. – Sci. Hortic. 103: 387-402.

[49] Sensoy, S., Ertek, A., Gedik, I., Kucukyumuk, C. (2007): Irrigation frequency and amount affect yield and quality of field-grown melon (Cucumis melo L.). – Agricultural Water Management 88: 269-274.

[50] Sezen, S. M., Yazar, A., Eker, S. (2006): Effect of drip irrigation regimes on yield and quality of field grown bell pepper. – Agricultural Water Management 81: 115-131.

[51] Sezen, S. M., Yazar, A., Daşgan, Y., Yücel, S., Akyıldız, A., Tekin, S., Akhoundnejad, Y. (2014): Evaluation of crop water stress index (CWSI) for red pepper with drip and furrow irrigation under varying irrigation regimes. – Agric. Water Manage. 143: 59-70.

[52] Sezen, S. M., Yazar, A., Tekin, S. (2019): Physiological response of red pepper to different irrigation regimes under drip irrigation in the Mediterranean region of Turkey. – Scientia Horticulturae 245: 280-288.

[53] Silber, A., Xu, G., Levkovitch, I., Soriano, S., Bilu, A., Wallach, R. (2003): High fertigation frequency: the effects on uptake of nutrients, water and plant growth. – Plant and soil 253: 467-477.

[54] Steel, R. G. D., Torrie, J. H. (1980): Principles and Procedures of Statistics. – 2nd ed. McGraw-Hill, New York.

[55] Ta, T. H., Shin, J. H., Noh, E. H., Son, J. E. (2012): Transpiration, growth, and water use efficiency of paprika plants (*Capsicum annuum* L.) as affected by irrigation frequency. – Horticulture, Environment, and Biotechnology 53: 129-134.

[56] Weng, J. H., Chien, C. T., Chen, C. W., Lai, X. M. (2011): Effects of osmotic- and high-light stresses on PSII efficiency of attached and detached leaves of three tree species adapted to different water regimes. – Photosynthetica 49: 555-563.

[57] Yao, C., Moreshet, S., Aloni, B. (2001): Water relations and hydraulic control of stomatal behaviour in bell pepper plant in partial soil drying. – Plant Cell Environ. 24(2): 227-235.

[58] Yazar, A., Howell, A. T., Dusek, D. A., Copeland, K. S. (1999): Evaluation of crop water stress index for LEPA Irrigated Corn. – Irrig. Sci. 18: 171-180.

[59] Zhang, B., Liu, Y., Xu, D., Cai, J., Li, F. (2011): Evapotranspiration estimation based on scaling up from leaf stomatal conductance to canopy conductance. – Agricultural and Forest Meteorology 151: 1086-1095.

http://www.aloki.hu ● ISSN 1589 1623 (Print) ● ISSN 1785 0037 (Online)
DOI: http://dx.doi.org/10.15666/aeer/1706_1558515604

BASE ON MODEL EXPERIMENT TO STUDY THE EFFECTS OF VERTICAL SPACE ON THE TEMPERATURE OF SOIL MICROHABITATS IN THE PROCESS OF KARST ROCK DESERTIFICATION

YAN, L. B.[1] – ZHANG, J. L.[2] – ZHU, S. Y.[1] – GAO, F.[1] – YANG, Y. Z.[1] – HUANG, Z. S.[3] – YU, L. F.[1*]

[1]Research Center of Karst Ecological Environment, The Key Laboratory of Plant Resources Conservation and Germplasm Innovation in Mountainous Region (Ministry of Education)/Collaborative Innovation Center for Mountain Ecology and Agro-Bioengineering (CICEAB), College of Life Sciences/Institute of Agro-Bioengineering, Guizhou University, Guiyang 550025, Guizhou, People's Republic of China

[2]College of Eco-Environmental Engineering (The Institute of Karst Wetland Ecology), Guizhou Minzu University, Guiyang 550025, Guizhou, People's Republic of China

[3]College of Architecture and Urban Planning, Guizhou University, Guiyang 550025, Guizhou, People's Republic of China

**Corresponding author*
e-mail: lfyu@gzu.edu.cn

(Received 6th Aug 2019; accepted 31st Oct 2019)

Abstract. Heterogeneity, the most prominent feature of karst ecological conditions, makes the restoration of areas experiencing Karst Rock Desertification (KRD) difficult. Soil temperature is one of the most important ecological factors creating KRD, but little research on this topic has been conducted. The present study was causing to understand whether the exposure of bedrock during the process of KRD changes the soil temperature of karst microhabitats. Thus, a simulated soil temperature of KRD microhabitat in different time periods and with varied soil thickness was quantified. The results showed that bedrock exposure can change soil temperature. The trend varied with soil depth. In the high temperature period, the exposure of bedrock resulted in heating of soil, but in the low temperature period the exposure of bedrock resulted in cooling of soil. Both soil depth and bedrock exposure have a significant effect on soil temperature. However, the influence of bedrock exposure on soil temperature changed dramatically during different periods.
Keywords: *limestone, lime soil, soil thickness, exposed bedrock, soil physical properties*

Introduction

Human activities and interference can easily degrade a fragile karst ecosystem that normally degenerates into an area of karst rock desertification (KRD). Ecosystem restoration has proved difficult in areas of KRD (Peng et al., 2008). Also, one main feature of karst areas is that they have shallow soil with a limited total amount, a phenomenon that is exacerbated by KRD. Therefore, KRD results in discontinuous soil cover, a change in the composition of energy conducting media, and enhanced heterogeneity. The smallest classification unit of habitat heterogeneity is the microhabitat level. The earliest classification of karst divided karst microhabitat into six categories: stony surface, stony gully, stony crevice, stony trough, stony cave, and soil surface (Zhu, 1993). Other scholars have proposed more categories or new classification methods (Li, 2002; Yang et al., 2008), but the most widely used classification methods identify six types of microhabitats. Early scholars paid attention to the distribution of

http://www.aloki.hu ● ISSN 1589 1623 (Print) ● ISSN 1785 0037 (Online)
DOI: http://dx.doi.org/10.15666/aeer/1706_1560515614

karst microhabitats as well as their morphological and spatial characteristics of microhabitats by comparing soil temperature, soil moisture, and the light environment of microhabitats (Zhang et al., 1996; Zhu, 2003). Later, scholars paid attention to the relationship between complex microhabitats and biodiversity (Yu, 2006; Yu et al., 2007), physical and chemical properties of soil (Tang et al., 2016; Liao et al., 2010, 2012a, b; Liu et al., 2008), and soil ecosystem processes (Hu et al., 2016a, b; Du et al., 2011; Liao et al., 2013).

Almost no research has been conducted on soil temperatures in karst areas because of its need for long-term observations and high temporal resolution; this is complicated by the fact that field conditions are impossible to reproduce, measuring tools are expensive, and older analytical methods were employed in previous studies (Yu et al., 2011; Yuan, 2015a). However, soil temperature is one of the most important ecological factors; it has important effects on the soil microbial community, respiration, and enzyme activity (Yuan et al., 2015b); it will also affect plant metabolic activity. The present study was established to imitate the characteristics of KRD microhabitat which occur on bare bedrock with the goals of filling the gap in research related to soil temperatures in the areas of KRD and discover the effects of KRD on changing ecological factors. The present study compared areas of the soil surface with KRD on bedrock that was not bare by conducting research on the features and regular daily changes in soil temperature under varied meteorological conditions.

Materials and methods

The typical karst microhabitats soil is shallow (Li et al., 2016). According to the field investigation, it is found that the soil thickness is about 30 cm. To simulate KRD microhabitat, the present study used man-made devices filled with lime soil and limestone having a soil thickness of 5, 25, 35, and 45 cm (The sensor of 15 cm was damaged by water invasion), it was carried out in Guizhou, China. Plants of *Pueraria lobata* var. *thomsonii* were planted in each type of soil, and button thermometers (DS1923, Wdsen Electronic Technology Co., Ltd.) were buried in these devices (*Fig. 1*).

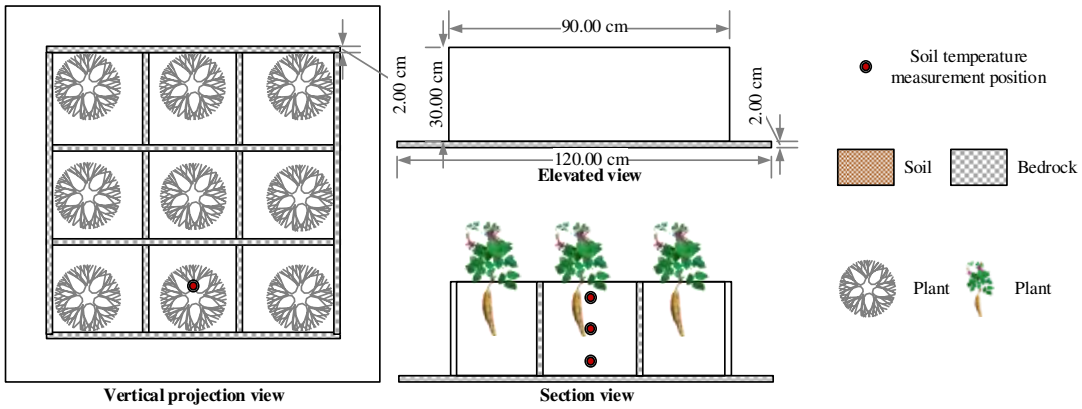

Figure 1. *Experimental device, take the soil thickness of 30 cm as an example*

Under natural precipitation conditions, soil temperature at different depths was measured record once per hour. The resulting data that were compared with a natural

http://www.aloki.hu ● ISSN 1589 1623 (Print) ● ISSN 1785 0037 (Online)
DOI: http://dx.doi.org/10.15666/aeer/1706_1560515614

habitat having deep soil and unexposed bedrock. Valid data for 3680 groups data point collections were recorded from 00:00 on July 13 to 23:00 on December 14, 2017. These devices and data were represented by codes representing each type of treatment (*Table 1*). Data were analyzed and figures were draw using software packages known as change-point (Killick and Eckley, 2015) and ggplot2 (Wickham, 2016) in R software (Team, 2019).

The effects of different sites and layers on soil temperature were analyzed by the method of analysis of variance, and the mean value was tested by *t*-test. Difference markers are marked by Tukey's method.

Table 1. *Comparison of the meanings of experimental design codes*

Code	Mean	Code	Mean
CK	Experimental control habitat, unexposed bedrock, soil thickness > 1 m	T	Air temperature at 1.4 m high
O1	KRD habitat, soil thickness is 10 cm	A	Depth range is 0-10 cm
O3	KRD habitat, soil thickness is 30 cm	B	Depth range is 10-20 cm
O4	KRD habitat, soil thickness is 40 cm	C	Depth range is 20-30 cm
O5	KRD habitat, soil thickness is 50 cm	D	Depth range is 30-40 cm
		E	Depth range is 40-50 cm

Results

Time series segmentation

The image (*Fig. 2*) of air and soil temperature time series shows that during the period from 13 July to 14 December air and soil temperature exhibited a stepwise decline with different amplitudes of fluctuations. Based on the mean and variance of change point analysis the change points were obtained for the critical time points of falling temperatures and the amplitude of the change.

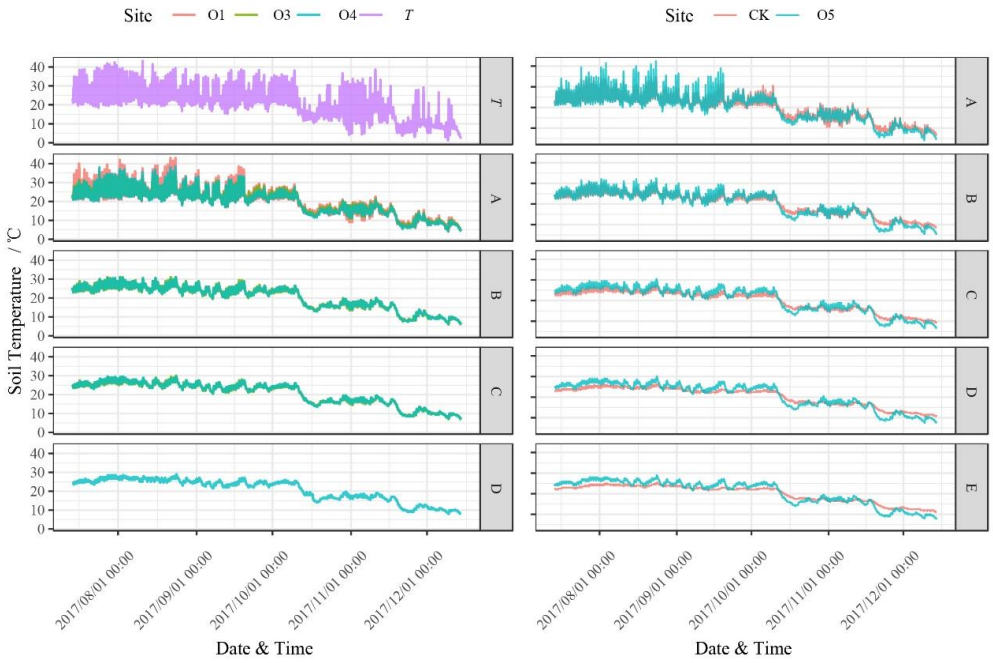

Figure 2. *Time series of air and soil temperatures for sites T, CK, O1, O3, O4, and O5. A, B, C, D and E are the soil layer, all abbreviations have the same meaning as listed in Table 1*

http://www.aloki.hu ● ISSN 1589 1623 (Print) ● ISSN 1785 0037 (Online)
DOI: http://dx.doi.org/10.15666/aeer/1706_1560515614

The results show that the critical time point was 11 October when the temperature fell and 18 November when the amplitude changes. The two time points were used to divide the air and soil temperature time series to three periods; these were named based on the meteorological characteristics of each period (*Table 2*). The three periods were the high temperature period (13 July to 11 October), mid-range temperature period (12 October to 18 November), and low temperature period (19 November to 14 December).

Table 2. *Meteorological characteristics of three periods*

Period	Precipitation mm/d	Evaporation mm/d	T °C	RH %	Soil temperature °C				
					A	B	C	D	E
High	2.4±5.1	3.4±1.2	25.4±0.1	74.8±0.4	24.3±0.1	24.2±0.0	23.6±0.0	23.7±0.0	23.2±0.0
Mid-range	1.9±4	1.8±0.9	16.2±0.2	77.3±0.6	15.7±0.0	16.4±0.0	16.5±0.0	17.4±0.0	17.4±0.0
Low	0.6±1.1	0.8±0.5	8.9±0.2	80.5±0.6	9.8±0.1	10.8±0.0	11.3±0.0	12.4±0.0	12.8±0.0

T: air temperature; RH: relative humidity; high, mid-range, and low temperature periods were 13 July to 11 October, 12 October to 18 November, and 19 November to 14 December, respectively. The codes for soil depth are provided in *Table 1*

Each of the three time periods exhibited different climatic conditions. The high temperature period featured more precipitation and higher evaporation rates. The mid-range temperature period featured average precipitation, evaporation, and relative humidity (RH). The low temperature period featured less precipitation, low evaporation rates, and high humidity. In the entire soil layer from to top to a depth of 40-50 cm, the soil temperature declined in the high temperature period, and rose in the mid-range and low temperature periods. The temperature differences between the upper and lower soil layers was 1.0 °C in high, 1.5 °C in mid-range, and 3.0 °C in the low temperature periods.

The analysis of variance results (*Table 3*) showed that temperature of air and every soil layer were extremely significantly ($P < 0.001$) different in the three time periods. Based on the F value of layers and sites in different periods, the soil layers caused a wide variation in temperatures. However, in the high temperature period, the difference caused by the site (devices with different soil thicknesses) were variable. It was higher than the effects of soil layers in the high (Judging from the F value) temperature period, relatively small in the mid-range temperature period and generally high but lower the lower layers during the low temperature period.

High temperature period

For find the temperature pattern the soil layer and site, and also based on multiple comparisons using Tukey's honestly significant difference test ($P < 0.05$), means of temperature were drawn (*Fig. 3*) and compared. The trend of soil temperature rose in the KRD microhabitat experiment but the CK treatment had reduced temperatures during the high temperature period. In addition, the mean soil temperatures in the O1, O3, O4, and O5 treatments designed to imitate KRD microhabitats were higher than in the CK treatment.

Differences in air and soil temperature were compared for different soil thicknesses in the same habitat. For the O1 treatment, the temperature difference between air (T, 25.4 ± 0.12) and soil layer A (25.05 ± 0.1) was insignificant. For the O3 treatment, T and temperatures of soil layer C (25.1 ± 0.04) > soil layer A (24.75 ± 0.07), while the

http://www.aloki.hu ● ISSN 1589 1623 (Print) ● ISSN 1785 0037 (Online)
DOI: http://dx.doi.org/10.15666/aeer/1706_1560515614

temperature differences between soil layer B (25.07 ± 0.05) and T, soil layers C and A were insignificant. For the O4 treatment, T, temperatures of soil layers D (25.23 ± 0.03), C (25.23 ± 0.04), and B (25.11 ± 0.05) > A (24.35 ± 0.08). For the O5 treatment, temperatures of T and soil layers D (25.6 ± 0.04), C (25.28 ± 0.04) > B (24.84 ± 0.05), A (24.84 ± 0.09), the temperature differences of soil layers E (25.17 ± 0.03) with C and B were insignificant. However, the soil temperature of soil layer E was significantly lower than D; for the CK treatment, T > temperatures of B (24.23 ± 0.04) and A (24.32 ± 0.06) > C (23.62 ± 0.03) and D (23.77 ± 0.02) > E (23.18 ± 0.02).

Table 3. *Analysis of variance of soil layer and sites at the three periods: high, mid-range, and low temperature periods were 13 July to 11 October, 12 October to 18 November, and 19 November to 14 December, respectively*

		Df	Sum sq.	Mean sq.	F value	P
High temperature	Layer	5	10563	2112.66	189.69	<0.001***
	Site	5	12292	2458.49	220.75	<0.001***
	Residuals	45559	507400	11.14		
	Total	45569	530256			
Mid-range temperature	Layer	5	7697	1539.31	232.294	<0.001***
	Site	5	454	90.82	13.706	<0.001***
	Residuals	18847	124891	6.63		
	Total	18857	133041			
Low temperature	Layer	5	10219	2043.84	484.45	<0.001***
	Site	5	6267	1253.48	297.11	<0.001***
	Residuals	12316	51959	4.22		
	Total	12326	68446			

Differences in air and soil temperatures in different habitats were compared with the same soil thickness. For soil layer A, T (25.4 ± 0.12) > O5 (24.84 ± 0.09) and O3 (24.75 ± 0.07) > O4 (24.35 ± 0.08) and CK (24.32 ± 0.06). The temperature difference between habitat O1 (25.05 ± 0.1) with T, O5, and O3 were insignificant. Soil temperature of O1 treatment was higher than O4 and CK. For soil layer B, T > O5 (24.84 ± 0.05) > CK (24.23 ± 0.04), the temperature differences between O4 (25.11 ± 0.05) and O3 (25.07 ± 0.05) with T and O5 were insignificant. The soil temperatures for the O4 and O3 treatments were higher than those of the CK treatment. For soil layer C, T, O5 (25.28 ± 0.04), O4 (25.23 ± 0.04) and O3 (25.1 ± 0.04) > CK (23.62 ± 0.03). For soil layer D, O5 (25.6 ± 0.04) and T > O4 (25.23 ± 0.03) > CK (23.77 ± 0.02). For soil layer E, T and O5 (25.17 ± 0.03) > CK (23.18 ± 0.02).

Mid-range temperature period

Soil temperature rose consistently in the experimental KRD microhabitats and in the CK treatment during the mid-range temperature period.

Air and soil temperatures were compared in treatments with different soil thicknesses in the same habitat. For the O1 treatment, T (16.16 ± 0.19) > A (15.23 ± 0.08). For the O3 treatment, C (16.52 ± 0.04), T and B (16.14 ± 0.05) > A(15.4 ± 0.06). For the O4 treatment, D (17.05 ± 0.04) and C (16.63 ± 0.05) > T > A (15.02 ± 0.06). The temperatures were significantly different between layer B (16.23 ± 0.05) when

http://www.aloki.hu ● ISSN 1589 1623 (Print) ● ISSN 1785 0037 (Online)
DOI: http://dx.doi.org/10.15666/aeer/1706_1560515614

compared with C and T. The temperature of layer B was lower than that of D and higher than A. For the O5 treatment, the temperature differences were D (17.02 ± 0.05) > C (16.46 ± 0.05) > B (15.77 ± 0.06) and A (15.42 ± 0.06), but temperature differences between layer E (16.85 ± 0.04) with D and C were insignificant; The temperature differences between T with C and B were insignificant, The temperature of layer E was higher than that of B. The air temperature (T) was lower than that of D and higher than that of A. For the CK treatment, E (17.38 ± 0.04) and D (17.36 ± 0.04) > C (16.48 ± 0.03) and B (16.36 ± 0.04) > A (15.72 ± 0.07). The temperature differences of air T with C, B, and A were insignificant, and air temperature was lower than layer E and D.

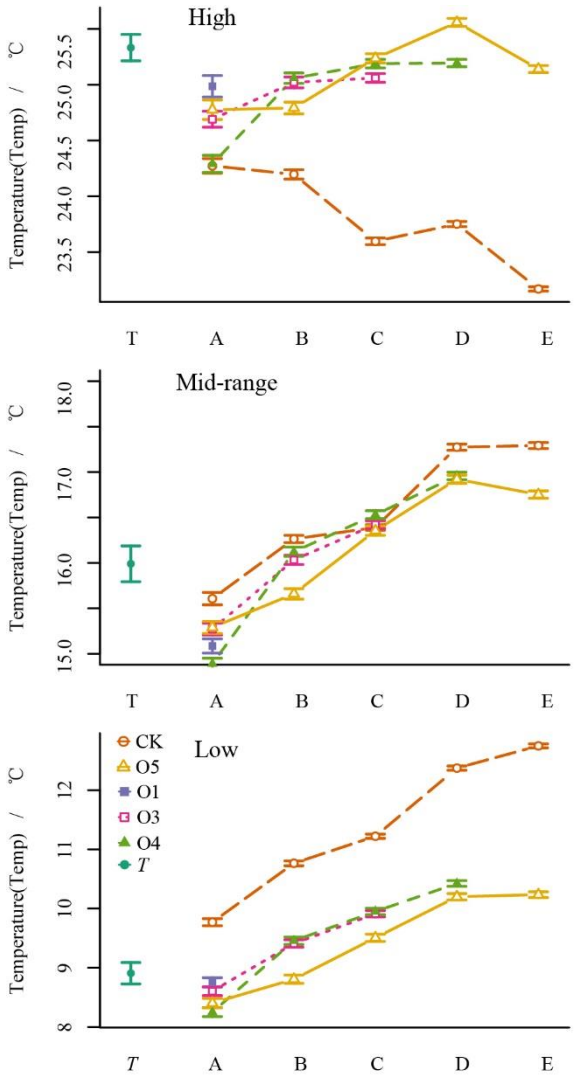

Figure 3. *Temperature features of air and soil in the high, mid-range, and low temperature periods: 13 July to 11 October, 12 October to 18 November, and 19 November to 14 December, respectively. T, CK, O1, O3, O4, and O5 are the sites. A, B, C, D and E are the soil layer, all abbreviations have the same meaning as listed in Table 1*

Air and soil temperatures were compared in different habitats with the same soil thickness. For the layer A treatment, T (16.16 ± 0.19) and CK (15.72 ± 0.07) > O3

http://www.aloki.hu ● ISSN 1589 1623 (Print) ● ISSN 1785 0037 (Online)
DOI: http://dx.doi.org/10.15666/aeer/1706_1560515614

(15.4 ± 0.06) and O5 (15.42 ± 0.06) > O1 (15.23 ± 0.08) > O4 (15.02 ± 0.06). For the layer B treatment, CK (16.36 ± 0.04), T and O4 (16.23 ± 0.05) > O5 (15.77 ± 0.06), but the temperature differences of O3 with other habitats were insignificant. For the layer C treatment, O4 (16.63 ± 0.05) > T, and the temperature differences of O3 (16.52 ± 0.04), CK (16.48 ± 0.03) and O5 (16.46 ± 0.05) with O4 and T were insignificant. For the layer D treatment, CK (17.36 ± 0.04), O4 (17.05 ± 0.04) and O5 (17.02 ± 0.05) > T. For the layer E treatment, CK (17.38 ± 0.04) > O5 (16.85 ± 0.04) > T.

Low temperature period

The soil temperatures tended to increase in the experimental KRD microhabitats and increased in the CK treatment during the low temperature period. The difference between the low and mid-range temperature periods was that soil temperature in the experimental KRD microhabitats were lower than the CK treatment in the same layer.

Differences in air and soil temperature with different soil thicknesses were compared in the same habitat. For the O1 treatment, the temperature difference of layer A (8.76 ± 0.08) with T (8.87 ± 0.18) was insignificant. For the O3 treatment, C (9.96 ± 0.05) > B (9.44 ± 0.06) > T and A (8.62 ± 0.07). For the O4 treatment, D (10.49 ± 0.05) > C (10.01 ± 0.06) > B (9.49 ± 0.06) > T > A (8.26 ± 0.07). For the O5 treatment, E (10.31 ± 0.05) and D (10.26 ± 0.06) > C (9.55 ± 0.06) > B (8.83 ± 0.07) and A (8.41 ± 0.08), and the difference in T with layer B was insignificant, while T was lower than layer C and higher than A. For the CK treatment, E (12.82 ± 0.04) and D (12.44 ± 0.04) > C (11.28 ± 0.04) > B (10.81 ± 0.04) > A (9.8 ± 0.06) > T.

Differences in air and soil temperature with different habitats were compared with the same soil thickness. For the layer A treatment, CK (9.8 ± 0.06) > O1 (8.76 ± 0.08) > O4 (8.26 ± 0.07), and differences between O3 (8.62 ± 0.07) and O5 (8.41 ± 0.08) with O1 and O4 were insignificant, the temperatures of O3 and O5 were lower than CK, differences of T (8.87 ± 0.18) with O1 and O3 were insignificant, and the temperature of T (8.87 ± 0.18) was lower than CK and higher than O5. For the layer B treatment, CK (10.81 ± 0.04) > O4 (9.49 ± 0.06) and O3 (9.44 ± 0.06) > T and O5 (8.83 ± 0.07). For the layer C treatment, CK (11.28 ± 0.04) > O4 (10.01 ± 0.06) and O3 (9.96 ± 0.05) > O5 (9.55 ± 0.06) > T. For the layer D treatment, CK (12.44 ± 0.04) > O4 (10.49 ± 0.05) > O5 (10.26 ± 0.06) > T. For the layer E treatment, CK (12.82 ± 0.04) > O5 (10.31 ± 0.05) > T.

Discussion

The changes in the vertical space feature of soil microhabitats may be caused by differences in the thermo-physical properties of soil and bedrock that could make a difference under the same heat release and absorption conditions. In karst areas, the bedrock was mainly limestone and dolomite which develop into a lime soil type. Here, we reviewed their thermo-physical properties based on a review of the literature (*Table 4*).

Specific heat of soil was calculated according to the formula of Hanks (1992): where $c_v=\rho_b(0.8374+4.187\theta_m)$ $kJ\cdot m^{-3}\cdot ℃^{-1}$ is specific heat of soil, ρ_b is soil density, θ_m is volumetric soil water content. The reference range for soil density is 2.21-2.81 $g\cdot cm^{-3}$ (Lu, 2006). Soil volumetric water content was based on long-term monitoring data (0-25%).

http://www.aloki.hu ● ISSN 1589 1623 (Print) ● ISSN 1785 0037 (Online)
DOI: http://dx.doi.org/10.15666/aeer/1706_1560515614

When comparing the thermo-physical properties of soil and bedrock, soil has a greater amount of specific heat, lower thermal conductivity, and slower thermal diffusivity than bedrock. When the same amount of heat is input to soil and exposed bedrock, these features would be make the temperature of bedrock increase more quickly and the thermal energy of bedrock is then transmitted to the bottom more effectively and faster than in soil. This will cause the soil temperature of KRD microhabitats to be higher than soil surface, something that does not occur in KRD microhabitat, unexposed bedrock, and deep soil.

Table 4. *Thermo-physical properties of major bedrock and soil types*

	Specific heat $MJ \cdot m^{-3} \cdot ℃^{-1}$		**Thermal conductivity** $W \cdot m^{-1} \cdot K^{-1}$		**Thermal diffusivity** $\times 10^{-6} m^2 \cdot s^{-1}$	
	Range	**Mean**	**Range**	**Mean**	**Range**	**Mean**
Limestone (Lei et al., 2018)	1.298-2.396	1.861	2.648-5.273	3.742	0.886-3.442	2.031
Dolomite (Lei et al., 2018)	1.497-2.385	1.798	1.664-6.327	4.330	0.886-3.442	2.481
Lime soil (Zhang, 2007)	1.85-5.29	-	0.2-1.5	-	0.2-0.5	-

A higher base soil temperature during the high temperature period in the bare bedrock microhabitats would result in stronger air transfer to roots for plants growing in these areas. These high temperatures will cost more energy to be used by plants and to expend more water to maintain their increased metabolic activity. As a result, the higher temperatures must exacerbate related problems for the plant that limit its ability to survive. Also, to circumvent this restriction, the plant root may find lower temperature soil and deeper underground water by increasing the length of the root system, resulting in a lower root-crown ratio and higher costs.

Conclusions

When bedrock becomes exposed this can change the soil temperature of karst microhabitat. Bedrock serves for heating karst in summer with high temperature and relatively greater amounts of precipitation and for cooling in winter with relatively low temperature and high humidity. Variations in karst microhabitats has a greater influence during the high temperature period (summer) than the effects of soil depth in the range of 0 to 50 cm. Variations in karst microhabitats have a significant but smaller than the effects of soil depth on soil temperature during the mid-range temperature period (autumn). During the low temperature period, variations in karst microhabitats have a significant and greater effect but the effect is also lower than the effect of soil depth. Furthermore, soil temperatures of KRD microhabitats were significantly different in different seasons.

In the high temperature period, the soil temperatures at the same depth in different KRD microhabitats were higher than at the soil surface microhabitat. The trends of soil temperature changing with soil depth were different for different habitats. For soil surface microhabitat the temperature fell with increasing soil depth, but for the KRD microhabitats, from 0 to 40 cm, temperatures increased with increasing depth. In natural soil surface habitat, soil temperature of any depth was lower than air temperature. But in the KRD microhabitat, the mean difference of soil temperature at a depth of 40 cm with

http://www.aloki.hu ● ISSN 1589 1623 (Print) ● ISSN 1785 0037 (Online)
DOI: http://dx.doi.org/10.15666/aeer/1706_1560515614

air temperature was insignificant. Soil temperature at a depth of 40 cm or so in KRD microhabitat may have been at the turning point in the trend of soil temperature changing with depth.

In the mid-range temperature period, the trends of soil temperature changing with depth were same between the soil surface microhabitat and KRD microhabitat, with increasing temperature as the depth of soil increased. At the surface (0-10 cm), soil temperatures of KRD microhabitats were uncommonly lower than air temperature. But the difference between surface temperature at the soil surface microhabitat with air temperature was insignificant.

In the low temperature period, the soil temperature at the same depth of different KRD microhabitats were lower than that of soil surface microhabitat. The trends of soil temperature changing with soil depth were the same, because temperature increased with an increase in the depth of soil. At the surface (0-10 cm), soil temperature of KRD microhabitats was lower than air temperature but soil temperature at the surface was higher than air temperature.

This study employed a quantifiable and repeatable experimental device and resulted in an increased level of soil temperature. Future research could also be conducted that is more in-depth. Such research could be designed to consider factors such as rock volume, exposed bedrock area, soil water content, and soil water-holding capacity with a dependent variable of soil temperature to verify the relationships between them. One could also study characteristics of variation over time and the effects of change.

Acknowledgements. This research was funded by the Project of National Key Research and Development Program of China (Grant No. 2016YFC0502604), the National Natural Science Foundation of China (Grant No. 31560187, 51868008), the Construction Program of Biology First-class Discipline in Guizhou (Grant No. GNYL[2017]009), and the Project of Promoted Innovation for Colleges and Universities of Guizhou Province (Grant No. Qian Jiao He Collaborative Innovation [2014]01).

REFERENCES

[1] Du, X., Wang, S., Rong, L. (2011): Characteristics of foliar δ13C values of common shrub species in various microhabitats with different karst rocky desertification degrees. – Chinese Journal of Applied Ecology 22: 3094-3100.

[2] Hanks, R. J. (1992): Applied Soil Physics: Soil Water and Temperature Applications. – Springer Science & Business Media, New York.

[3] Hu, N., Li, H., Tang, Z., Li, Z. F., Li, G. C., Jiang, Y., Hu, X. M., Lou, Y. L. (2016a): Community size, activity and C:N stoichiometry of soil microorganisms following reforestation in a Karst region. – European Journal of Soil Biology 73: 77-83.

[4] Hu, N., Li, H., Tang, Z., Li, Z. F., Tian, J., Lou, Y. L., Li, J. W., Li, G. C., Hu, X. M. (2016b): Community diversity, structure and carbon footprint of nematode food web following reforestation on degraded karst soil. – Scientific Reports 6: 28138.

[5] Killick, R., Eckley, I. A. (2015): changepoint: An R package for changepoint analysis. – Journal of Statistical Software 58: 1-19.

[6] Lei, X., Hu, S., Li, J., Yang, Q., Han, Y., Jiang, G., Zheng, J. (2018): Thermal properties analysis of bedrock in Beijing. – Progress in Geophysics 33: 1814-1823.

[7] Li, J. X., Xiong, G. M., Xu, W. T., Xie, Z. Q. (2016): Distribution of shrublands in relation to soil and climate in mid-subtropical China. – Journal of Plant Ecology 9: 393-401.

http://www.aloki.hu ● ISSN 1589 1623 (Print) ● ISSN 1785 0037 (Online)
DOI: http://dx.doi.org/10.15666/aeer/1706_1560515614

[8] Li, Y. (2002): Morphological types and their features of Shilin Karst in Yunnan, China. – Carsologica Sinica 21: 14-21.
[9] Liao, H., Long, J., Li, J., Yang, J., Feng, Y. (2010): Preliminary study on spatial heterogeneity of soil mineral composition and organic carbon content at different micro-habitats that under different vegetation types in karst region. – Carsologica Sinica 29: 434-439.
[10] Liao, H., Long, J., Li, J. (2012a): Effect of different micro-habitats types on organic carbon and labile organic carbon distribution in surface soil aggregates in Chinese prickly ash orchard of karst mountain area. – Journal of Soil and Water Conservation 26: 156-160.
[11] Liao, H., Long, J., Li, J., Yang, J., Feng, Y. (2012b) Distribution characteristics of soil carbon and nitrogen under different vegetation types in micro-habitats of karst dry-hot valley region of South Western China. – Soils 44: 421-428.
[12] Liao, H., Li, J., Long, J. (2013): Effect of vegetation type and micro-habitat on soil active organic carbon and basal respiration in karst dry and hot valley region of Guizhou Province, China. – Chinese Journal of Soil Science 44: 580-586.
[13] Liu, F., Wang, S., Luo, H., Liu, Y., Liu, H. (2008): Micro-habitats in karst forest ecosystem and variability of soils. – Acta Pedologica Sinica 45: 1055-1062.
[14] Lu, H. (2006): Soil Biogeochemical Characteristics in the Process of Karst Rocky Desertification—A Case of Chaeryan Catchment in Guizhou Huajiang Area. – Institute of Geochemi, Chinese Academy of Sciences, Guiyang.
[15] Peng, W., Wang, K., Song, T., Zeng, F., Wang, J. (2008): Controlling and restoration models of complex degradation of vulnerable karst ecosystem. – Acta Ecologica Sinica 28: 811-820.
[16] Tang, F. K., Cui, M., Lu, Q., Liu, Y. G., Guo, H. Y., Zhou, J. X. (2016): Effects of vegetation restoration on the aggregate stability and distribution of aggregate-associated organic carbon in a typical karst gorge region. – Solid Earth 7: 141-151.
[17] Team, R. C. (2019): R: A Language and Environment for Statistical Computing. – https://www.R-project.org/. Vienna, Austria.
[18] Wickham, H. (2016): ggplot2: Elegant Graphics for Data Analysis. – Springer-Verlag, New York.
[19] Yang, R., Yu, L., An, M. (2008): Analysis on microhabitat characteristic in karst region—taking Maolan nature reserve as an example. – Guizhou Agricultural Sciences 36: 168-169.
[20] Yu, G., Wang, S., Rong, L. (2011): Microclimate characteristics of different microhabitats in successional stages of Maolan karst forest. – Earth and Environment 39: 469-477.
[21] Yu, X. (2006): The Study on the Role of Karst Microhabitats in Karst Vegetation Restoration—An Example of the Shilin National Geopark. – Yunnan Normal University, Kunming.
[22] Yu, X., Li, Y., Ma, Z. (2007): A preliminary study on flora diversity of karst microhabitat in Shilin Park, Yunnan, China. – Journal of Mountain Science 25: 438-447.
[23] Yuan, M. (2015a): Study on Soil Temperature and Water Characteristics in Karst Area. – Yunnan Normal University, Kunming.
[24] Yuan, M., Li, H., Wang, D. (2015b); Research progress of forest soil temperature in China. – Hubei Forestry Science and Technology 44: 37-41.
[25] Zhang, B., Wei, X., Zeng, X. (1996): A study of microclimate characters of different microhabitats on karst landform forest. – Journal of Guizhou Agric. Coll. 11: 7-10.
[26] Zhang, L. (2007): Theoretical and Experimental Study on Heat and Moisture Transfer in Soil and Ground-Source Heat Pump. – Zhejiang University, Hangzhou.
[27] Zhu, S. (1993): Ecological Research on Karst Forest (I). – Guizhou Science and Technology Press, Guiyang.
[28] Zhu, S. (2003): Ecological Research on Karst Forest (III). – Guizhou Science and Technology Press, Guiyang.

http://www.aloki.hu ● ISSN 1589 1623 (Print) ● ISSN 1785 0037 (Online)
DOI: http://dx.doi.org/10.15666/aeer/1706_1560515614

YIELD AND QUALITY PERFORMANCES OF ALFALFA (*MEDICAGO SATIVA*) CULTIVARS SOWN AT VARIOUS DATES UNDER SUB-MEDITERRANEAN ECOLOGICAL CONDITIONS

TURAN, N.

Department of Field Crops, Faculty of Agriculture, Siirt University, Siirt, Turkey
(e-mail: nturan49@siirt.edu.tr)

(Received 8th Aug 2019; accepted 15th Nov 2019)

Abstract. In this study it was aimed to determine the best sowing date and cultivar for the cultivation of alfalfa (*Medicago sativa* L.) in the Southeastern Anatolian Region of Turkey, using a randomized split-block design with three replicates. The study was conducted from 2015 to 2017 using alfalfa cultivars of Kayseri, Magnum V, Gea, and Nimet and these cultivars sowed at three different sowing dates March 10, April 5, and April 30, 2015. The mean plant height of the cultivars was 66.04 cm, mean number of main stems was 10.77 number/plant, mean fresh herbage yield was 50020.1 kg ha^{-1}, mean hay yield was 13509.2 kg ha^{-1}, mean crude protein yield was 2464.0 kg ha^{-1}, mean crude protein rate was 17.88%, mean acid detergent fiber (ADF) rate was 34.01%, and mean neutral detergent fiber (NDF) rate was 39.49%. The highest mean plant height, fresh herbage yield, hay yield, and crude protein yield were observed at first and second sowing times. The results clearly indicate that the first and second sowing dates were the most suitable periods for alfalfa planting in the region studied. Additionally, Magnum V cultivar was the highest cultivator for fresh herbage and hay yield.
Keywords: *alfalfa, sowing dates, varieties, yield, forage quality*

Introduction

Among forage crops, alfalfa (*Medicago sativa*) has the highest forage yield. Alfalfa's herbage is rich in vitamins and high in protein. Because its herbage and hay are quite beneficial and nutritious for farm animals, alfalfa is known as "the queen of forage crops" (Demiroglu et al., 2008).

The seed-sowing dates for alfalfa planting change from region to region. In coastal regions dominated by a Mediterranean climate, winter sowing is common. On the other hand, in regions having a terrestrial climate such as the Central Anatolian and Eastern Anatolian Regions, sowing are generally performed in spring periods. Some regions in which alfalfa is sown in spring might not produce yield in that first year. Nevertheless, the Southeastern Anatolian Region has the ecological conditions that are suitable for harvesting a considerable yield during the sowing year; however, according to Lowe et al. (1972), the main limiting factors affecting cultivar spreading and growth are precipitation and temperature. Thus, temperate and semitropical regions such as the Mediterranean regions alfalfa can harvest up to eight or nine times per year; however, this yield of alfalfa reduce up to two to three times in colder regions. In another study (Eginlioglu et al., 1996) it was reported that the number of sowings, soil fertility, and climate factors also have an effect on alfalfa yield. In that study, it stated that number of harvest for alfalfa can range from 2 to 4 for Eastern Anatolian and Central Anatolian Region, whereas in the coastal regions harvesting of 7 or 8 can be foreseen.

Saruhan and Kusvuran (2011) have reported for several alfalfa cultivars in the Southeastern Anatolian region that the highest fresh herbage yield (48960 kg ha^{-1}) and hay yield (12660 kg ha^{-1}) was produced by the Elci cultivar, while the highest crude

http://www.aloki.hu ● ISSN 1589 1623 (Print) ● ISSN 1785 0037 (Online)
DOI: http://dx.doi.org/10.15666/aeer/1706_1561515631

protein rate (22.67%) was obtained from Bilensoy cultivar. Aka and Avcioglu (2003), who investigated the adaptation of seven alfalfa cultivars to the conditions within the Aegean Region, indicated that the height of the main stem varied between 61.56 and 67.50 cm, and that the highest hay yield was obtained from Pioneer-5715 (15730 kg ha^{-1}), whereas it was the lowest for Elci (11780 kg ha^{-1}). In Similar studies on alfalfa cultivars it showed that hay yield of alfalfa was 11020 - 12660 of kg ha^{-1}, 9820 - 17970 of kg ha^{-1} and 12910 - 17810 of kg ha^{-1} (Sengul and Tahtacioglu, 1996).

Moreover, Yılmaz and Albayrak (2016) sowing the some cultivars such as Bilensoy, Verko, Gea, Prosementi or candidate alfalfa cultivars under Isparta conditions found that the highest crude protein rate was produced by candidate cultivars (17.3 7%). In that study it was detected that acid detergent fiber (ADF) and neutral detergent fiber (NDF) rates in Bilensoy cultivar were the lowest (34.50 and 42.20%, respectively). Engin and Mut (2017) conducted at to identify some quality parameters in alfalfa fodder and determine hay yield under Yozgat conditions using alfalfa cultivars of Bilensoy, Kayseri, Verko, Gea, Plato, Victoria, Emiliano, Sunter, Nimet and Basbag during the 2013 and 2015. The mean plant height was the highest in Emiliano cultivar (86.90 cm), whereas it was lowest in Kayseri cultivar (57.50 cm). Authors detected that total hay yield for two year was 21070.0 and 43305.0 kg ha^{-1} for Bilensoy and Sunter, respectively. Again, in that study, the crude protein rate was between 24.20% and 26.10% of percent, and the total protein yield was the highest for Sunter (5906.0 kg ha^{-1}), whereas it was the lowest for Gea (3251.0 kg ha^{-1}).

Alfalfa can be effectively grown for both silage and grain production in Southeastern region of Turkey and thus increasing forage shortage currently encountered will considerably be decreased. The aim of this study was to determine the optimum sowing date for alfalfa under the Southeastern conditions of Turkey, and identify the alfalfa cultivars with the highest quality and yield.

Materials and methods

This research was conducted in researching and application fields of Siirt University Faculty from 2015 through 2017 (*Fig. 1*). As plant material we used four cultivars of alfalfa cultivars such as Gea, Magnum V, Kayseri, Nimet obtained from different research institutes and private seed companies in Turkey. These cultivars sown three different sowing dates (March 10, April 05, and April 30, 2015) are more plant height and more resistant to lodging, and the characters of growing is upright. These cultivars in Turkey have been also recommended for the Southern Marmara, Aegean, Thrace, Black Sea, Southeastern and Eastern Anatolia, Central Anatolia, and Mediterranean regions.

According to the randomized split-block trial design with three replications, the whole plot was divided according to the alfalfa cultivars, and subplot parcels were determined by sowing date. There were eight rows in each parcel with 25 cm between them, and the seeds were sown to a depth of 1 - 1.5 cm. Three kilograms of seeds were sown over each 0.1 hectare and fertilized with 150 kg ha^{-1} diammonium phosphate. The parcel was 2 m wide and 5 m long. There were 2 m of distance between each block and 1 m between each parcel. The entire experimental field was 19 m wide and 35 m long, encompassing a total area of 0.0665 ha.

http://www.aloki.hu ● ISSN 1589 1623 (Print) ● ISSN 1785 0037 (Online)
DOI: http://dx.doi.org/10.15666/aeer/1706_1561515631

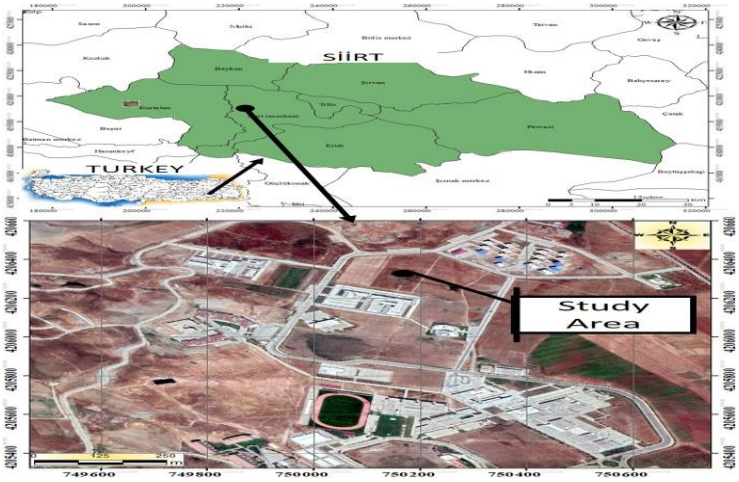

Figure 1. *The location of study area*

Seeds sown in three different sowing dates (March 10, April 05, and April 30, 2015) had the high performance and harvested during 10 - 15% of blooming. 6 rows of plants in the middle of the parcels were harvested after removing one row from the beginning and end of each plot. The processes for pre and post-harvesting were conducted on trial site. Because alfalfa is grown under wet conditions in 2015, five cutting were conducted in the first and second sowing periods, while four cutting were conducted in the third sowing date. In 2016 and 2017, 5 cutting were performed from each sowing period. From each parcel, 0.5 kg samples were randomly collected, air dried under shadow, placed in an oven set to 78 °C for 24 h, and dried until there were no further changes in the sample. At this point, the samples were ground and prepared for analyses.

The characteristics measured in the study were plant height (cm), number of main stems (number/plant), fresh herbage yield (kg ha^{-1}), and hay yield (kg ha^{-1}). In addition, crude protein rate, ADF, and NDF were determined by near infrared analysis using the Near Infrared Reflectance Spectroscopy (NIRS) instrument (Hoy et al., 2002).

The 3-year mean values obtained from the study were used for the analysis of variance with JUMP at 0.05 and 0.01 significance levels (SAS, 1998). The differences among the mean values were compared using Fisher's Least Significant Difference multiple comparison test (Gulumser et al., 2006).

Climate characteristics of the research area

Climate characteristics of the research area are presented in *Table 1*. The Siirt climate has a long-term precipitation (713.10 mm/year), their relative humidity and temperature are 44.73%, and is 16.03 °C, respectively. During this study, the relative humidity was highest in January, and the temperature was generally low. The highest precipitation in 2015 was at 188.00 mm in October 2015, at 162.40 mm in January 2016, and at 126.60 mm in March 2017 (*Table 1*).

As shown in *Table 1,* in the time periods of research, temperatures and relative humidity had higher than the long-term mean climate values. In 2015 and 2017, the total precipitation was 668.00 and 540.80 mm, respectively, which were lower than the long-term average of 713.10 mm; however, in 2016, total precipitation at 731.20 mm, which was higher than the long-term average (*Table 1*). Because region performed in this study are hot and dry, the field was irrigated after each sowing.

http://www.aloki.hu ● ISSN 1589 1623 (Print) ● ISSN 1785 0037 (Online)
DOI: http://dx.doi.org/10.15666/aeer/1706_1561515631

Table 1. *Temperature, precipitation and relative humidity values of the research area (Meteorology Regional Directorate, Siirt)*

Months	Temperature (°C)				Precipitation (mm)				Relative humidity (%)			
	LYA	2015	2016	2017	LYA	2015	2016	2017	LYA	2015	2016	2017
January	2.60	3.86	1.69	2.95	96.80	60.80	162.40	48.80	73.30	73.98	76.04	66.11
February	4.20	6.04	8.06	2.74	97.50	92.00	63.80	26.60	68.50	70.72	68.39	64.49
March	8.30	9.14	10.07	9.54	111.10	125.00	135.60	126.60	60.4	63.19	62.35	64.16
April	13.70	13.72	16.70	14.00	104.70	53.20	66.80	124.60	50.40	55.48	47.45	59.18
May	19.30	20.42	19.90	19.55	62.00	26.80	64.60	74.60	41.50	42.99	48.92	51.62
June	26.00	26.87	26.52	26.94	8.70	3.60	20.40	0.0	24.10	27.79	32.63	29.44
July	30.60	32.09	31.37	32.28	1.60	0.00	2.40	0.0	18.10	19.56	24.48	18.99
August	30.10	31.37	32.28	31.94	0.90	2.40	0.20	0.40	17.20	22.55	20.55	18.99
September	25.10	28.13	24.86	28.31	4.90	1.60	18.80	0.0	24.00	23.14	29.82	19.22
October	17.90	18.54	19.49	18.35	49.10	188.00	40.20	18.40	45.30	59.23	37.10	35.15
November	10.40	10.56	10.33	11.13	81.40	56.80	51.80	73.40	57.10	64.76	49.82	64.44
December	4.80	5.00	3.35	7.95	94.40	57.80	104.2	47.40	56.9	61.75	72.92	65.29
Total/Average	16.08	17.15	17.05	17.14	713.10	668.00	731.20	540.80	44.73	48.76	47.54	46.42

LYA: Long years' average (1960-2017)

Soil properties in the research area

The results of the soil analysis of research area performed by Siirt University Science and Technology Application and Research Center Laboratory are presented in *Table 2*.

The soil analysis showed that the soil of research field had a neutral pH, was highly calcareous, non saline, had low organic matter and plant-available phosphorus, and had sufficient potassium, copper and iron but was low in zinc and manganese concentrate (*Table 2*).

Table 2. *Soil analysis results of the research area*

pH	Salt ds/m	Lime ($CaCO_3$) (%)	Organic matter (%)	P (P_2O_5) kg ha^{-1}	K (K_2O) ppm	Fe ppm	Cu ppm	Zn ppm	Mn ppm	Soil (%)		
										Sand	Clay	Silt
7.21	1.47	16.30	1.96	24.4	620	14.07	5.89	1.13	22.71	36	44	20

Soil analyses were conducted at the Siirt University Science and Technology Application and Research Center Directorate (2015).

Results and discussion

Plant height

The plant height of the alfalfa cultivars sown at different dates under Siirt conditions and the results of their multiple comparison are presented in *Table 3*. The results of the effect of cultivar, sowing date, and sowing date x year interaction for the mean plant height of the alfalfa were significant at $p < 0.05$, while those of year and cultivar x year interaction were significant at $p < 0.01$. Effects of interactions of cultivar x sowing date and the cultivar x sowing date x year were not significant.

http://www.aloki.hu ● ISSN 1589 1623 (Print) ● ISSN 1785 0037 (Online)
DOI: http://dx.doi.org/10.15666/aeer/1706_1561515631

When the findings were examined (*Table 3*), the mean plant height of the cultivars in the study ranged from 62.62 to 67.91 cm. The mean plant height were the highest for cultivars of Kayseri (67.91 cm), Gea (67.35 cm), and Magnum V (66.28 cm), whereas Nimet cultivar was the lowest for this characteristics (62.62 cm). The mean plant height according to sowing dates was 66.04 cm. In the first and second sowing dates, plant height was the highest (67.81 and 67.76 cm, respectively). However, it was 62.55 cm in plants from the third sowing date. The mean plant heights in different years were 52.39, 71.96, and 73.77 cm for years of 2015, 2016, and 2017, respectively.

In the current study, varieties investigated were significantly affected form interaction of sowing date x year, showing that there are differences based on sowing dates. Through the years, the height of plants was the lowest at first planting period, but there were a ongoing increase in the following years. Thus, the height of plant was affected form variety x year interaction. For example, Magnum V was the lowest for plant height at first year of trial, but there was a significant increase for plant height in the following years compared with the other cultivars.

Table 3. *Effect of cultivar and sowing date on plant height (cm)*

Years	Sowing dates	Varieties				
		Kayseri	**Magnum V**	**Gea**	**Nimet**	**Variety mean**
2015	1st sowing date	60.93	53.03	60.17	60.37	58.63 ^{B}
	2nd sowing date	48.67	55.23	55.17	55.67	53.69 ^{B}
	3rd sowing date	44.70	42.40	49.27	43.17	44.88 ^{C}
	Mean	51.43 ^{E}	50.22 ^{E}	54.87 ^{E}	53.07 ^{E}	52.40 ^{B}
2016	1st sowing date	74.27	69.13	70.93	66.40	70.18 ^{A}
	2nd sowing date	73.93	71.00	72.60	75.47	73.25 ^{A}
	3rd sowing date	76.60	72.06	70.80	70.33	72.44 ^{A}
	Mean	74.93 $^{A\text{-}C}$	70.73 ^{C}	71.44 ^{BC}	70.73 ^{C}	71.95 ^{A}
2017	1st sowing date	79.43	75.87	79.30	63.93	74.63 ^{A}
	2nd sowing date	73.03	87.13	80.20	65.00	76.34 ^{A}
	3rd sowing date	79.67	70.70	67.73	63.23	70.33 ^{A}
	Mean	77.37 ^{AB}	77.90 ^{A}	75.74 $^{A\text{-}C}$	64.05 ^{D}	73.76 ^{A}
Mean years	1st sowing date	71.54	66.01	70.13	63.56	67.81 ^{A}
	2nd sowing date	65.21	71.12	69.32	65.38	67.76 ^{A}
	3rd sowing date	66.99	61.72	62.60	58.91	62.55 ^{B}
	Mean of mean	67.91 ^{A}	66.28 ^{A}	67.35 ^{A}	62.62 ^{B}	66.04
CV (%)		9.50				
$LSD_{variety}$		3.40*				
$LSD_{sowing\ date}$		3.81*				
LSD_{year}		3.81**				
$LSD_{variety\ x\ year}$		5.92**				
$LSD_{sowing\ date\ x\ year}$		6.62*				
$LSD_{variety\ x\ sowing\ date}$		ns				
$LSD_{variety\ x\ sowing\ date\ x\ year}$		ns				

The difference between the averages indicated by the same letter in the same group is not statistically significant. *:Significant difference at $P < 0.05$ level, **:Significant difference at $P < 0.01$ level, CV: variation coefficient, LSD: least significant difference, NS: non-significant.

http://www.aloki.hu ● ISSN 1589 1623 (Print) ● ISSN 1785 0037 (Online)
DOI: http://dx.doi.org/10.15666/aeer/1706_1561515631

The results obtained in this study are similar those of plant height taken from another study done in Izmir and Selcuk regions in Turkey (61.56 - 67.50 cm) (Aka and Avcioglu, 1999); however, the plant heights in our study were higher than those observed in the studies done in the Eastern Anatolian Region (54.7) (Cacan et al., 2018), Southeastern Anatolian Region (40.1 - 49.7) (Saruhan and Kusvuran, 2011), Kirşehir (53.91 - 63.47 cm) (Inal, 2015). But our findings for plant height were lower than those from the studies in the Aegean region (Kavut et al., 2014) and Yozgat (Engin and Mut, 2017) at 73.97 - 81.50 and 57.50 - 86.90 cm, respectively.

Number of main stems

According to the mean number of main stems in the alfalfa cultivars sown at different dates and their multiple comparisons (*Table 4*), effect of cultivar, sowing date, and cultivar x sowing date x year on the number of main stems were significant at $p < 0.05$; again, year and cultivar x year were significant at $p < 0.01$. Nonetheless, effect of sowing date x year and cultivar x sowing date were not statistically significant. When these results were examined, we observed that the mean number of main stems in the cultivars ranged between 10.33 and 11.05 number/plant, and the differences in the mean number of main stems in the cultivars were not statistically significant, except for Nimet cultivar (*Table 4*).

Table 4. *Effect of cultivar and sowing date on number of main stem (number/plant)*

Years	Sowing dates	Varieties				
		Kayseri	**Magnum V**	**Gea**	**Nimet**	**Variety mean**
2015	1st sowing date	7.73 ^{mn}	6.97 ^{n}	9.33 $^{j-l}$	8.83 $^{k-m}$	8.21
	2nd sowing date	10.36 $^{h-j}$	7.83 ^{mn}	9.83 $^{ı-k}$	8.63 $^{k-m}$	9.16
	3rd sowing date	6.83 ^{n}	7.10 ^{n}	8.16 $^{l-n}$	8.1 $^{l-n}$	7.55
	Mean	8.31 ^{d}	7.30 ^{e}	9.11 ^{d}	8.52 ^{d}	8.31 ^{B}
2016	1st sowing date	11.86 $^{c-g}$	12.53 $^{a-f}$	11.33 $^{d-h}$	11.46 $^{d-h}$	11.80
	2nd sowing date	12.26 $^{b-f}$	12.73 $^{a-d}$	12.06 $^{b-g}$	10.73 $^{g-j}$	11.95
	3rd sowing date	11.73 $^{d-h}$	11.60 $^{d-h}$	11.60 $^{d-h}$	11.66 $^{d-h}$	11.65
	Mean	11.95 $^{a-c}$	12.28 ^{ab}	11.66 ^{bc}	11.28 ^{c}	11.80 ^{A}
2017	1st sowing date	12.63 $^{a-e}$	12.53 $^{a-f}$	12.50 $^{a-f}$	11.20 $^{e-ı}$	12.21
	2nd sowing date	11.76 $^{d-h}$	13.93 ^{a}	13.36 ^{ab}	11.16 $^{f-ı}$	12.55
	3rd sowing date	13.30 $^{a-c}$	11.83 $^{d-g}$	11.26 $^{e-ı}$	11.20 $^{e-ı}$	11.90
	Mean	12.56 ^{a}	12.76 ^{a}	12.37 ^{ab}	11.18 ^{c}	12.22 ^{A}
Mean years	1st sowing date	10.74	10.68	11.05	10.50	10.74 ^{AB}
	2nd sowing date	11.46	11.50	11.75	10.17	11.22 ^{A}
	3rd sowing date	10.62	10.18	10.34	10.32	10.36 ^{B}
	Mean of mean	10.94 ^{A}	10.78 ^{AB}	11.05 ^{A}	10.33 ^{B}	10.78
CV (%)		8.30				
$LSD_{variety}$		0.48*				
$LSD_{sowing\ date}$		0.60*				
LSD_{year}		0.60**				
$LSD_{variety\ x\ year}$		0.84**				
$LSD_{sowing\ date\ x\ year}$		ns				
$LSD_{variety\ x\ sowing\ date}$		ns				
$LSD_{variety\ x\ sowing\ date\ x\ year}$		1.46*				

The difference between the averages indicated by the same letter in the same group is not statistically significant, *:Significant difference at $P < 0.05$ level, **:Significant difference at $P < 0.01$ level, CV: variation coefficient, LSD: least significant difference, NS: non-significant.

http://www.aloki.hu ● ISSN 1589 1623 (Print) ● ISSN 1785 0037 (Online)
DOI: http://dx.doi.org/10.15666/aeer/1706_1561515631

There were no differences between the first and second sowing dates for number of main stems, except for third sowing date. The highest mean number of main stems was 11.22 number/plant from the second sowing date, and the lowest was 10.36 number/plant observed from the third sowing date. The mean number of main stem in different sowing years was 8.31, 11.80, and 12.22 number/plant, respectively, for years of 2015, 2016, and 2017. The differences in the mean number of main stems in the alfalfa cultivars changed throughout the years, and cultivar x year interaction was significant as statistical. Magnum V cultivar had an increase for numbers of main stems over the years and it was the highest compared to the other cultivars at the end of the year.

The values obtained for the number of main stems were lower than those obtained in the studies performed by Turan et al. (2017), Demiroglu et al. (2008), Kavut et al. (2014), Petkova et al. (2003) and Seker et al. (2003), but higher than those from obtained in the study performed by Inal (2015).

Fresh herbage yield

The difference in mean fresh herbage yield from the alfalfa cultivars sown at different dates and their multiple comparisons indicated that effect of sowing date x year were statistically significant at $p < 0.05$, and sowing date and years were significant at $p < 0.01$. On the other hand, the differences in mean fresh herbage yields for cultivar, cultivar x year, cultivar x sowing date, and cultivar x sowing date x year were not statistically significant (*Table 5*).

Mean fresh herbage yields in different sowing dates ranged between 42948.0 and 54893.3 kg ha^{-1}. There were no differences between the first and second sowing dates whereas, there was a difference in the third sowing date. The mean fresh herbage yield according to year was 36549.1, 55548.0, and 57963.3 kg ha^{-1}, respectively, for 2015, 2016, and 2017. Cultivars had different fresh herbage yields according to different sowing dates, and the ones with lower fresh herbage yields had increasingly higher yields in the following years; however, among the sowing dates used, the second had the highest fresh herbage yield. There were statistically significant differences for year x sowing date (*Table 5*).

The fresh herbage yields detected in this study were lower than the results reported by Demiroglu et al. (2008), Kavut et al. (2014), Avci et al. (2013), Petkova et al. (2003), Aka and Avcioglu (1999), and Seker et al. (2003). However, our findings for fresh herbage yield were higher than the values reported by Turan et al. (2017), Cacan et al. (2018) and Inal (2015), and it was in accordance with findings Saruhan and Kusvuran (2011).

Hay yield

Table 6 illustrates the values for mean hay yield of alfalfa cultivars sown on different dates. These values clearly show that effect of cultivar x sowing date on mean hay yield is statistically significant at $p < 0.05$, and that sowing date and years are statistically significant at $p < 0.01$.

In the present study, the effect of the cultivars, cultivar x year, sowing date x year, and cultivar x sowing date x year on mean hay yield was not statistically significant. While the fresh herbage and hay yield of the cultivars examined in the study (Kayseri, Magnum V and Gea) were higher than the second year; the values of the second year was higher than values of the third year.

http://www.aloki.hu ● ISSN 1589 1623 (Print) ● ISSN 1785 0037 (Online)
DOI: http://dx.doi.org/10.15666/aeer/1706_1561515631

Table 5. *Effect of cultivar and sowing date on fresh herbage yield (kg ha^{-1})*

Years	Sowing dates	Varieties				
		Kayseri	**Magnum V**	**Gea**	**Nimet**	**Variety mean**
2015	1st sowing date	46280.0	33360.0	47136.7	44886.7	42915.8 ^{B}
	2nd sowing date	40853.3	39040.0	50166.7	49756.7	44954.1 ^{B}
	3rd sowing date	21386.7	25353.3	23613.3	16756.7	21777.5 ^{C}
	Mean	36173.3	32584.4	40305.5	37133.3	36549.1 ^{B}
2016	1st sowing date	51860.0	57033.3	57976.7	55910.0	55695.0 ^{A}
	2nd sowing date	54503.3	62783.3	60710.0	60086.7	59520.8 ^{A}
	3rd sowing date	55320.0	46850.0	50496.7	53046.7	51428.3 ^{AB}
	Mean	53894.4	55555.5	56394.4	56347.8	55548.0 ^{A}
2017	1st sowing date	59473.3	57813.3	60683.3	54216.7	58046.7 ^{A}
	2nd sowing date	55960.0	67713.3	62176.7	54970.0	60205.0 ^{A}
	3rd sowing date	60366.7	52770.0	53670.0	55746.7	55638.3 ^{A}
	Mean	58600.0	59432.2	58843.3	54977.8	57963.3 ^{A}
Mean years	1st sowing date	52537.8	49402.2	55265.6	51671.1	52219.1 ^{A}
	2nd sowing date	50438.9	56512.2	57684.5	54937.8	54893.3 ^{A}
	3rd sowing date	45691.1	41657.8	42593.3	41850.0	42948.0 ^{B}
	Mean of mean	49555.9	49190.7	51847.8	49486.3	50020.1
CV (%)		14.00				
$LSD_{variety}$		ns				
$LSD_{sowing\ date}$		ns				
LSD_{year}		562.29**				
$LSD_{variety\ x\ year}$		ns				
$LSD_{sowing\ date\ x\ year}$		973.74*				
$LSD_{variety\ x\ sowing\ date}$		ns				
$LSD_{variety\ x\ sowing\ date\ x\ year}$		ns				

The difference between the averages indicated by the same letter in the same group is not statistically significant, *:Significant difference at $P < 0.05$ level, **:Significant difference at $P < 0.01$ level, CV: variation coefficient, LSD: least significant difference, NS: non-significant.

The fresh herbage and hay yield were 37133.3 - 9139.5 kg ha^{-1} in the first year, in the second year increased to 56347.7 - 15946.0 kg ha^{-1}, then decreased to 54977.7 - 15534.6 kg ha^{-1} in the final year. This situation is believed to be related to the characteristic differences in cultivars and their different responses to varying ecological conditions.

The mean hay yields of the groups from the different sowing dates ranged from 11932.7 to 14589.1 kg ha^{-1}, with the highest hay yield observed from the second sowing date and the lowest from the third sowing date. Mean hay yields were 8 635.7, 15 557.4, and 16334.7 kg ha^{-1}, respectively, for years of 2015, 2016, and 2017. Considering the three-year values together with the year of the sowing, fresh herbage and hay yield values had an similar increase. However, the hay yield in second sowing date was the highest, indicating that cultivar x sowing date interaction lead to these differences (*Table 6*).

In the present study, the hay yield were higher than that of values reported in the Eastern Anatolian Region (13154.0 and 12270.0 kg ha^{-1}) (Turan et al., 2017; Cacan et

http://www.aloki.hu ● ISSN 1589 1623 (Print) ● ISSN 1785 0037 (Online)
DOI: http://dx.doi.org/10.15666/aeer/1706_1561515631

al., 2018) and in Europe, North Africa, and the United States (14200.0 kg ha^{-1}) (Pecetti et al., 2008). However, our findings for hay yield were lower than those observed in the study done in Bornova and Odemiş in Turkey (Demiroglu et al., 2008), with yields ranging from 18920.0 to 24740.0 kg ha^{-1}.

Table 6. *Effect of cultivar and sowing date on dry herbage yield (kg ha^{-1})*

Years	Sowing dates	Varieties				
		Kayseri	**Magnum V**	**Gea**	**Nimet**	**Variety mean**
2015	1st sowing date	10689.8	8006.5	10614.0	11063.8	10093.5
	2nd sowing date	8469.3	9273.5	11891.7	12081.7	10429.0
	3rd sowing date	5323.1	5991.9	5950.3	4272.9	5384.5
	Mean	8160.7	7757.3	9485.3	9139.5	8635.7^{B}
2016	1st sowing date	14536.3	15613.5	15696.1	15173.1	15254.7
	2nd sowing date	15155.2	17522.5	17006.4	17240.2	16731.1
	3rd sowing date	15512.2	13401.3	14407.0	15424.7	14686.3
	Mean	15067.9	15512.4	15703.2	15946.0	15557.4^{A}
2017	1st sowing date	17050.9	15975.5	18058.5	15593.5	16669.6
	2nd sowing date	14471.3	19060.9	17890.5	15005.9	16607.1
	3rd sowing date	16819.0	13232.9	16852.8	16004.4	15727.3
	Mean	16113.7	16089.8	17600.6	15534.6	16334.7^{A}
Mean years	1st sowing date	14092.3^{A-C}	13198.5^{B-D}	14789.5^{AB}	13943.5^{A-C}	14006.0^{A}
	2nd sowing date	12698.6^{CD}	15285.6^{A}	15596.2^{A}	14776.0^{AB}	14589.1^{A}
	3rd sowing date	12551.4^{C-E}	10875.3^{E}	12403.4^{C-E}	11900.7^{DE}	11932.7^{B}
	Mean of mean	13114.1	13119.8	14263.0	13540.0	13509.2
CV (%)		13.99				
$LSD_{variety}$		ns				
$LSD_{sowing\ date}$		141.12**				
LSD_{year}		141.12**				
$LSD_{variety\ x\ year}$		ns				
$LSD_{sowing\ date\ x\ year}$		ns				
$LSD_{variety\ x\ sowing\ date}$		178.32*				
$LSD_{variety\ x\ sowing\ date\ x\ year}$		ns				

The difference between the averages indicated by the same letter in the same group is not statistically significant, *:Significant difference at P < 0.05 level, **:Significant difference at P < 0.01 level, CV: variation coefficient, LSD: least significant difference, NS: non-significant.

Moreover, the hay yields in our study were in accordance with findings of Aka and Avcioglu (2003), in which the adaptations of alfalfa to Aegean Region conditions were examined with hay yield values for seven different alfalfa cultivars ranging from 11780.0 to 15730.0 kg ha^{-1} with those observed in another study done under Erzurum conditions with different alfalfa cultivars (Seker, 2003), which showed the highest hay yield of 13335.0 kg ha^{-1}. Because of that the development of root and storing of spare nutrients in the root region. Thus, it is understood that the development of subsoil parts is given more importance rather than above ground ones. Despite this five cutting were performed in second year of trial and an increase was observed an increase over years (*Tables 3–8*).

http://www.aloki.hu ● ISSN 1589 1623 (Print) ● ISSN 1785 0037 (Online)
DOI: http://dx.doi.org/10.15666/aeer/1706_1561515631

Crude protein content

The effect of cultivar x year, cultivar x sowing date, and cultivar x sowing date x year on the mean crude protein rates in the alfalfa cultivars sown at different dates were statistically significant at $p < 0.05$, and also the effect of cultivars and years were significant at $p < 0.01$. On the other hand, the impacts of sowing date and sowing date x year were not statistically significant. Cultivars had a mean crude protein rate of 17.88% with a high value of Magnum V (18.54%) and a low value of Nimet (17.40%).

The mean values for the different years were 16.18, 16.60, and 20.87%, respectively. Mean crude protein rate was the highest for all cultivars in 2017 (*Table 7*). Cultivar x year interaction was statistically significant at $p < 0.05$. In the cultivar x sowing date, the highest mean crude protein rate was 18.57% in first Magnum V sowing date, and the lowest rate one was observed from the third Nimet sowing date at 17.03%.

Table 7. *Effect of cultivar and sowing date on crude protein ratio (%)*

Years	Sowing dates	Varieties				
		Kayseri	**Magnum V**	**Gea**	**Nimet**	**Variety mean**
2015	1st sowing date	15.86 f-j	17.17 b-e	16.47 d-h	17.10 b-e	16.65
	2nd sowing date	16.57 c-g	16.40 d-i	15.00 j	15.23 ij	15.80
	3rd sowing date	16.43 d-h	16.53 d-h	16.57 c-g	14.87 j	16.10
	Mean	16.28 CD	16.70 C	16.01 CD	15.73 D	16.18 B
2016	1st sowing date	16.90 c-f	17.54 b-d	17.55 b-d	15.55 g-j	16.89
	2nd sowing date	16.06 e-j	18.21 b	15.39 g-j	16.43 d-h	16.52
	3rd sowing date	16.58 c-g	17.73 bc	15.88 f-j	15.34 h-j	16.39
	Mean	16.51 C	17.83 B	16.27 CD	15.77 D	16.60 B
2017	1st sowing date	20.54 a	21.00 a	20.96 a	20.87 a	20.85
	2nd sowing date	20.96 a	20.89 a	20.80 a	20.32 a	20.74
	3rd sowing date	21.07 a	21.38 a	20.73 a	20.88 a	21.01
	Mean	20.86 A	21.09 A	20.83 A	20.69 A	20.87 A
Mean years	1st sowing date	17.77 DE	18.57 A	18.33 A-D	17.84 C-E	18.13
	2nd sowing date	17.86 B-E	18.50 A-C	17.06 FG	17.33 E-G	17.69
	3rd sowing date	18.03 A-D	18.55 AB	17.73 D-F	17.03 G	17.83
	Mean of mean	17.88 B	18.54 A	17.70 BC	17.40 C	17.88
CV (%)		4.08				
$LSD_{variety}$		0.38**				
$LSD_{sowing\ date}$		ns				
LSD_{year}		0.47**				
$LSD_{variety\ x\ year}$		0.68*				
$LSD_{sowing\ date\ x\ year}$		ns				
$LSD_{variety\ x\ sowing\ date}$		0.68*				
$LSD_{variety\ x\ sowing\ date\ x\ year}$		1.18*				

The difference between the averages indicated by the same letter in the same group is not statistically significant, *:Significant difference at $P < 0.05$ level, **:Significant difference at $P < 0.01$ level, CV: variation coefficient, LSD: least significant difference, NS: non-significant.

http://www.aloki.hu ● ISSN 1589 1623 (Print) ● ISSN 1785 0037 (Online)
DOI: http://dx.doi.org/10.15666/aeer/1706_1561515631

Under different environmental conditions, different crude protein rates were observed in many studies. The values reported in the literature were from Awad and Bakri (2009) at 19.99 - 26.96%, Geleti et al. (2014) at 18.15 - 19.56%, Katic et al. (2009) at 17.3 - 19.7%, Saruhan and Kusvuran (2011) at 22.67%, Yilmaz and Albayrak (2016) at 17.37%, Zeinab et al. (2013) at 18.5 - 23.0%, Engin and Mut (2017) at 24.2 - 26.1%, Kir and Soya (2008) at 17.86 - 20.26%, Kir (2010) at 22.21 - 23.31%, Saruhan and Kusvuran (2011) at 17.94 - 22.67%, Kavut and Avcioglu (2015) at 19.83 - 20.11%, Inal (2015) at 18.38 - 20.45%, Yuksel et al. (2016) at 15.14 - 19.13%, Cinar and Hatipoglu (2015) at 20.6%, Yilmaz and Albayrak (2016) at 16.23 - 17.53%, Avci et al. (2013) at 18.5 - 19.4%, Turan et al. (2017) at 16.55 - 17.55%, Strbanovic et al. (2017) at 20.00%, Oten et al. (2018) at 18.39%, Walie et al. (2016) at 18.06%, Holman et al. (2016) at 19.50 - 26.50%, Titei et al. (2018) at 23.00%, Mazza et al. (2001) at 19.99 - 21.70%, Toricelli et al. (2001) at 19.99 - 21.70%, Stanacev et al. (2010) at 19.70%, and Scholtz et al. (2009) at 13.90 - 27.80%.

When the values obtained in this study are compared with those above, we see that they are in accordance with some higher and some lower. The differences in crude protein rates were considered to be related to the differences among soil, cultivar, sowing date, and other environmental conditions.

Crude protein yield

Table 8 presents the statistically significant results in mean crude protein yield of the different groups. According to these results, the effect of sowing date x year and cultivar x sowing date on mean crude protein yield were statistically significant at $p < 0.05$, and also the effect of sowing date and year were statistically significant at $p < 0.01$. On the other hand, the effect of cultivar, cultivar x year, and cultivar x sowing date x year were not statistically significant for crude protein yield.

The effect of sowing time on crude protein yield was statistically divided into two groups, first and second sowing time was the highest group, while the third sowing time was the lowest group. When the crude protein yield of the years is examined (*Table 8*). The highest crude protein yield with 3409.7 kg ha^{-1} was obtained in 2017, while the lowest crude protein yield with 1385.7 kg ha^{-1} was obtained in 2015.

Nimet and Magnum V were in the same statistically significant groups and had the highest mean crude protein yield from their second sowing date and the lowest from the third sowing date, while Gea had the highest crude protein yield from its first and second sowing dates. These results were statistically significant at $p < 0.05$ for cultivar x sowing date.

In current study, year x sowing date interaction was statistically significant and was between 1385.7 and 3409.7 kg ha^{-1}. These values obtained for crude protein yield were higher than those from Inal (2015) at 881.9 - 1129.3 kg ha^{-1}, Turan et al. (2017) at 1348.0 - 2827.0 kg ha^{-1}, Cacan et al. (2018) at 3010.0 kg ha^{-1}, and Kir and Soya (2008) at 372.5 - 522.3 kg ha^{-1} and also these values were lower than those from Hansen and Krueger (1973) at 2700.0 - 3250.0 kg ha^{-1}, Avci et al. (2013) at 4020.0 - 4220.0 kg ha^{-1}, Yilmaz and Albayrak (2016) at 3173.6 - 3837.9 kg ha^{-1}, and Engin and Mut (2017) at 3251.0 - 5906.0 kg ha^{-1}.

Even though the differences in the mean crude protein rate were not statistically significant, there were statistically significant differences in crude protein yields, which can be explained by the differences in hay yields from the cultivars and sowing years (*Table 8*). The correlation between increasing hay yield and crude protein content is also indicated by other researchers (Kir and Soya, 2008).

http://www.aloki.hu ● ISSN 1589 1623 (Print) ● ISSN 1785 0037 (Online)
DOI: http://dx.doi.org/10.15666/aeer/1706_1561515631

Table 8. *Effect of cultivar and sowing date on crude protein yield (kg ha^{-1})*

Years	Sowing dates	Varieties				
		Kayseri	Magnum V	Gea	Nimet	Variety mean
2015	1st sowing date	1690.4	1371.9	1740.0	1873.8	1669.0 ^{D}
	2nd sowing date	1396.8	1507.5	1772.8	1798.2	1619.0 ^{D}
	3rd sowing date	871.3	983.0	983.6	638.5	869.1 ^{E}
	Mean	1319.5	1287.5	1498.8	1436.8	1385.7 ^{C}
2016	1st sowing date	2443.0	2730.3	2801.9	2381.6	2589.2 ^{BC}
	2nd sowing date	2437.1	3219.1	2574.7	2864.7	2773.9 ^{B}
	3rd sowing date	2604.1	2386.8	2358.0	2356.5	2426.3 ^{C}
	Mean	2494.7	2778.7	2578.2	2534.3	2596.5 ^{B}
2017	1st sowing date	3502.9	3379.0	3787.6	3253.8	3480.8 ^{A}
	2nd sowing date	3027.9	3984.4	3714.2	3050.5	3444.3 ^{A}
	3rd sowing date	3542.7	2830.9	3500.5	3341.4	3303.9 ^{A}
	Mean	3358.0	3398.1	3667.4	3215.2	3409.7 ^{A}
Mean years	1st sowing date	2545.4 ^{BC}	2494.0 ^{BC}	2776.5 ^{AB}	2503.1 ^{BC}	2579.7 ^{A}
	2nd sowing date	2281.0 ^{CD}	2904.0 ^{A}	2687.2 ^{AB}	2571.1 $^{A-C}$	2610.8 ^{A}
	3rd sowing date	2339.3 ^{CD}	2067.0 ^{D}	2281.0 ^{CD}	2112.2 ^{D}	2200.0 ^{B}
	Mean of mean	2388.6	2488.3	2581.6	2395.5	2464.0
CV (%)		14.60				
$LSD_{variety}$		ns				
$LSD_{sowing\ date}$		18.79**				
LSD_{year}		18.79**				
$LSD_{variety\ x\ year}$		ns				
$LSD_{sowing\ date\ x\ year}$		32.57*				
$LSD_{variety\ x\ sowing\ date}$		33.92*				
$LSD_{variety\ x\ sowing\ date\ x\ year}$		ns				

The difference between the averages indicated by the same letter in the same group is not statistically significant, *:Significant difference at P < 0.05 level, **:Significant difference at P < 0.01 level, CV: variation coefficient, LSD: least significant difference, NS: non-significant.

Acid detergent fiber (ADF) rates

According to the ADF rates in this study (*Table 9*), the effect of sowing date, cultivar, year, and cultivar x sowing date on ADF rate were statistically significant at $p < 0.05$, while cultivar x year and sowing date x year were statistically significant at $p < 0.01$; nevertheless, the effect of cultivar x sowing date x year were not statistically significant.

The lowest ADF rate at 31.99% was observed in Magnum V cultivar and the highest was observed in Kayseri cultivar (34.78%). When examined in terms of sowing date, the first and second sowing dates were once again in the same statistically significant group and had lower ADF rates compared with third sowing date.

Magnum V had always the lowest ADF rates, although Gea cultivar had the lowest ADF rate in 2017. For this reason cultivar x year interaction was significant ($p < 0.05$). The effect of cultivar x sowing date indicated that Magnum V's lowest ADF rate was in the second sowing date at 30.58%, and that Kayseri cultivar (35.90%) and Nimet cultivar (36.82) were the highest for ADF rate in the second sowing date and third sowing date, respectively (*Table 9*).

http://www.aloki.hu ● ISSN 1589 1623 (Print) ● ISSN 1785 0037 (Online)
DOI: http://dx.doi.org/10.15666/aeer/1706_1561515631

Table 9. *Effect of cultivar and sowing date on ADF (%)*

Years	Sowing dates	Varieties				
		Kayseri	**Magnum V**	**Gea**	**Nimet**	**Variety mean**
2015	1st sowing date	33.81	33.69	31.66	36.78	33.98 ^{BC}
	2nd sowing date	37.24	29.71	35.64	34.60	34.30 ^{B}
	3rd sowing date	36.71	32.78	35.14	38.82	35.86 ^{A}
	Mean	35.92 ^{A}	32.06 ^{DE}	34.15 ^{BC}	36.73 ^{A}	34.71 ^{A}
2016	1st sowing date	33.07	33.40	30.60	35.27	33.08 $^{B-D}$
	2nd sowing date	37.30	30.00	34.83	34.27	34.10 ^{B}
	3rd sowing date	36.10	32.53	35.00	38.67	35.57 ^{A}
	Mean	35.49 ^{AB}	31.98 ^{E}	33.48 ^{CD}	36.07 ^{A}	34.25 ^{A}
2017	1st sowing date	33.53	32.46	31.53	32.80	32.58 ^{D}
	2nd sowing date	33.17	32.04	32.51	33.28	32.75 ^{CD}
	3rd sowing date	32.13	31.26	33.59	32.97	32.49 ^{D}
	Mean	32.94 $^{C-E}$	31.92 ^{E}	32.54 ^{DE}	33.02 $^{C-E}$	32.61 ^{B}
Mean years	1st sowing date	33.47 ^{DE}	33.18 ^{FG}	31.26 ^{FG}	34.95 ^{BC}	33.21 ^{B}
	2nd sowing date	35.90 ^{AB}	30.58 ^{G}	34.33 ^{CD}	34.05 ^{CD}	33.72 ^{B}
	3rd sowing date	34.98 ^{BC}	32.19 ^{EF}	34.58 $^{B-D}$	36.82 ^{A}	34.64 ^{A}
	Mean of mean	34.78 ^{A}	31.98 ^{C}	33.39 ^{B}	35.27 ^{A}	33.86
CV (%)	4.49					
$LSD_{variety}$	0.82^{**}					
$LSD_{sowing\ date}$	0.72^{**}					
LSD_{year}	0.72^{**}					
$LSD_{variety\ x\ year}$	1.43^{*}					
$LSD_{sowing\ date\ x\ year}$	1.23^{*}					
$LSD_{variety\ x\ sowing\ date}$	1.43^{**}					
$LSD_{variety\ x\ sowing\ date\ x\ year}$	ns					

The difference between the averages indicated by the same letter in the same group is not statistically significant, *:Significant difference at $P < 0.05$ level, **:Significant difference at $P < 0.01$ level, CV: variation coefficient, LSD: least significant difference, NS: non-significant.

The ADF values obtained in this study were higher than those of Geleti et al. (2014) at 21.49 - 26.19%, Engin and Mut (2017) at 27.5 - 29.7%, Toricelli et al. (2001) at 28.89 - 32.29%, Markovic et al. (2008) at 16.3%, and Kanani et al. (2006) at 26.50%. In several similar studies, the ADF rates ranged from 35.16 to 36.03% (Kir, 2010) and from 31.97 to 41.5% (Gungor et al., 2008), which were higher than those from our study; however, the results of our study were in accordance with values reported by Cacan et al. (2015) at 31.86% and Yilmaz and Albayrak (2016) at 34.50%.

Neutral detergent fiber (NDF) rates

When the NDF rates were examined by cultivars and sowing dates, the effect of cultivar, year, and cultivar x sowing date were statistically significant at $p < 0.01$; whereas it were not statistically significant for sowing date, sowing date x year, cultivar x year, and cultivar x sowing date x year for NDF rates (*Table 10*).

http://www.aloki.hu ● ISSN 1589 1623 (Print) ● ISSN 1785 0037 (Online)
DOI: http://dx.doi.org/10.15666/aeer/1706_1561515631

Table 10. *Effect of cultivar and sowing date on NDF (%)*

Years	Sowing dates	Varieties				
		Kayseri	Magnum V	Gea	Nimet	Variety mean
2015	1st sowing date	40.47	39.23	38.14	42.05	39.97
	2nd sowing date	43.27	37.57	42.06	41.22	41.03
	3rd sowing date	39.23	39.63	42.91	44.40	41.54
	Mean	40.99	38.81	41.04	42.55	40.85 ^{A}
2016	1st sowing date	38.58	38.33	39.50	42.27	39.67
	2nd sowing date	41.33	37.03	43.33	41.63	40.83
	3rd sowing date	37.57	38.87	41.13	43.77	40.33
	Mean	39.16	38.08	41.32	42.56	40.28 ^{A}
2017	1st sowing date	37.38	36.00	36.37	37.57	36.83
	2nd sowing date	36.87	35.79	36.51	37.60	36.69
	3rd sowing date	36.04	35.09	38.48	37.62	36.81
	Mean	36.76	35.63	37.12	37.59	36.78 ^{B}
Mean years	1st sowing date	38.81 ^{CD}	37.85 ^{DE}	38.00 ^{DE}	40.63 ^{AB}	38.82
	2nd sowing date	40.49 ^{B}	36.80 ^{E}	40.63 ^{AB}	40.15 ^{BC}	39.52
	3rd sowing date	37.61 ^{DE}	37.86 ^{DE}	40.84 ^{AB}	41.93 ^{A}	39.56
	Mean of mean	38.97 ^{C}	37.50 ^{D}	39.82 ^{B}	40.9 ^{A}	39.30
CV (%)	3.84					
$LSD_{variety}$	0.82**					
$LSD_{sowing\ date}$	ns					
LSD_{year}	0.70**					
$LSD_{variety\ x\ year}$	ns					
$LSD_{sowing\ date\ x\ year}$	ns					
$LSD_{variety\ x\ sowing\ date}$	1.41**					
$LSD_{variety\ x\ sowing\ date\ x\ year}$	ns					

The difference between the averages indicated by the same letter in the same group is not statistically significant, *:Significant difference at P < 0.05 level, **:Significant difference at P < 0.01 level, CV: variation coefficient, LSD: least significant difference, NS: non-significant.

Considering the different NDF rates in different cultivars, Magnum V had the lowest at 37.51%, while Nimet had the highest at 40.90%. In terms of sowing dates, there are two different statistically significant groups, and the lowest NDF rate was in the first sowing date group, while other sowing dates are in another group together. The NDF rates were 40.85, 40.28, and 36.78%, respectively, for years of 2015, 2016, and 2017. The cultivar x sowing date group values ranged between 36.80 and 42.93%. The NDF values obtained in this study were higher than those of Kanani et al. (2006) at 34.20%, lower than those of Kir (2010) at 42.68 - 44.13% and Yilmaz and Albayrak (2016) at 42.20%, and comparable to those of Engin and Mut (2017) at 40.0 - 42.9% and Geleti et al. (2014) at 36.86 - 43.53%.

The ADF and NDF rates can be altered by environmental conditions, soil, sowing date, and cultivar.

http://www.aloki.hu ● ISSN 1589 1623 (Print) ● ISSN 1785 0037 (Online)
DOI: http://dx.doi.org/10.15666/aeer/1706_1561515631

Conclusion

Throughout this study, domestic and foreign alfalfa cultivars obtained from various sources were sown in Siirt city of Turkey and the effect of sowing date and type of the cultivar over yield and other properties related to its agricultural value were investigated. Our results showed that the highest crude protein rate and yield, and the lowest ADF and NDF rates were founded in Magnum V cultivar. According to the sowing date mean values, the plant height, number of main stems, fresh herbage, and hay yields were higher from the first and second sowing dates on 10 March 2015 and 5 April 2015, respectively. Taken together, the most suitable dates to sow alfalfa in Siirt city of Turkey were the dates of 10 March and 5 April. Our results also showed that the Magnum V alfalfa cultivar is the best option for the production of herbage and high-quality hay.

Acknowledgements. The study was supported by the Scientific Research Projects Coordinatorship of Siirt University with the project code 2014-SİUZİR-01.

REFERENCES

[1] Aka, M. A., Avcioglu, R. (1999): Research on yield and some other yield properties of seven different alfalfa varieties in Selcuk conditions. – MSc Thesis, unpublished. Ege University, Institute of Science, Department of Field Crops.

[2] Aka, M. A., Avcioglu, R. (2003): Investigation on the yield and some other yield characteristics of seven different alfalfa varieties under Selcuk conditions. – Turkey 5th Field Crops Congress 13-17 Oct. 2003, pp. 533-536.

[3] Avci, M. A., Ozkose, A., Tamkoc, A. (2013): Determination of yield and quality characteristics of alfalfa (*Medicago sativa* L.) varieties grown in different locations. – Journal of Animal and Veterinary Advances 12: 487-490.

[4] Awad, O. A., Bakri, E. (2009): Effect of water quality and weeding on yield and quality of three alfalfa (*Medicago sativa* L.) cultivars. – Australian Journal of Crop Science 3(6): 315-321.

[5] Cacan, E., Kokten, K., Kaplan, M. (2018): Determination of yield and quality characteristics of some alfalfa (*Medicago sativa* L.) cultivars in the East Anatolia Region of Turkey and correlation analysis between these properties. – Applied Ecology and Environmental Research 16: 1185-1198.

[6] Cinar, S., Hatipoglu, R. (2015): Quality characteristics of the mixtures of some warm season perennial grasses with aifalfa (*Medicago sativa* L.) under irrigated conditions of Cukurova. – Turkish Journal of Field Crops 20: 31-37.

[7] Demiroglu, G., Geren, H., Avcioglu, R. (2008): Adaptation of different alfalfa (*Medicago sativa* L.) genotypes under Aegean Region conditions. – Journal of Agriculture Faculty of Ege University 45: 1-10.

[8] Eginlioglu, G., Sabanci, C. O., Bugdaycigil, M., Ozpinar, H. (1996): A study on the adaptation of some alfalfa (*Medicago sativa* L.) varieties to Menemen conditions. – Turkey 3 rd Pasture and Forage Plants Congress, 17-19 June, Erzurum, pp. 321-327 (in Turkish).

[9] Engin, B., Mut, H. (2017): Determination of herbage yield and some quality characteristics of different alfalfa varieties. – YYU J Agr. Sci. 27: 212-219.

[10] Geleti, D., Hailemariam, M., Mengistu, A., Tolera, A. (2014): Biomass yield potential and nutritive value of selected Alfalfa (*Medicago sativa* L.) cultivars grown under tepid

http://www.aloki.hu ● ISSN 1589 1623 (Print) ● ISSN 1785 0037 (Online)
DOI: http://dx.doi.org/10.15666/aeer/1706_1561515631

to cool sub-moist agro-ecology of Ethiopia. – E3 Journal of Agricultural Research and Development 4: 007-014.

[11] Gulumser, A., Bozoglu, H., Peksen, E. (2006): Research and Testing Methods. – Ondokuz Mayıs University, Faculty of Agriculture, Text Book (2. Press) No: 48, Samsun.

[12] Gungor, T., Basalan, M., Aydogan, I. (2008): Determination of nutrient content and metabolized energy levels in some roughages produced in Kirikkale region. – Journal of Veterinary Faculty of Ankara University 55: 111-115.

[13] Hansen, L. H., Krueger, C. R. (1973): Effect of establishment method, variety, and seeding rate on the production and quality of alfalfa under dryland and irrigation. – Agron. J. 65: 755-759.

[14] Holman, J., Min, D., Klocke, N., Kisekka, I., Currie, R. (2016): Effects of irrigation amount and timing on alfalfa nutritive value. – Transactions of the ASABE 59(4): 849-860.

[15] Hoy, M. D., Moore, K. J., George, J. R., Brummer, E. C. (2002): Alfalfa yield and quality as influenced by establishment method. – Agronomy Journal 94: 65-71.

[16] Inal, N. (2015): Determination of yield and quality characteristics of some alfalfa varieties under Kirsehir conditions. – MSc Thesis, Kirsehir Ahi Evran University, Institute of Science.

[17] Kanani, J., Lukefahr, S. D., Stanko, R. L. (2006): Evaluation of tropical forage legumes (*Medicago sativa*, *Dolichos lablab*, *Leucaena leucocephala* and *Desmanthus bicornutus*) for growing goats. – Small Ruminant Research 65: 1-7.

[18] Katic, S., Milić, D., Karagić, D., Vasiljević, S., Glamočić, D., Jajić, I. (2009): Variation of protein, cellulose and mineral contents of lucerne as influenced by cultivar and cut. – Biotechnology in Animal Husbandry 25(5-6): 1189-1195.

[19] Kavut, Y. T., Avcioglu, R. (2015): Yield and quality performances of various alfalfa (*Medicago sativa* L.) cultivars in different Mediterranean environments. – Turkish Journal of Field Crops 20: 65-71.

[20] Kavut, Y. T., Celen, A. E., Demiroglu Topcu, G., Kir, B. (2014): A research on the yield and yield characteristics of some alfalfa (*Medicago sativa* L.) genotypes at different locations. – Journal of Agriculture Faculty of Ege University 51: 23-29.

[21] Kir, H. (2010): Determination of performance of some alfalfa varieties in Tokat-Kazova conditions. – MSc Thesis, Gaziosmanpasa University, Graduate School of Natural and Applied Sciences Department of Agronomy, Turkey.

[22] Kir, B., Soya, H. (2008): The investigation on some yield and quality characteristics of some pasture type alfalfa cultivars. – Ege University, Faculty of Agriculture, Electronic Journal 45: 11-19.

[23] Lowe, C. C., Marble, W. L., Rumbaugh, M. D. (1972): Alfalfa Adaptation, Varieties and Usage. – Amer. Soc. Agron. Inc., Madison, WI.

[24] Markovic, J., Radovic, J., Lugic, Z., Sokolovic, D. (2008): Nutritive value in leaves and stems of lucerne with advanced maturity and a comparison of methods for determination of lignin content. Proceedings of the 22nd General Meeting of the European Grassland Federation, Upsala, Sweeden. – Grassland Science in Europe 13: 480-482.

[25] Mazza, L., Schiatti, F., Torricelli, R., Veronesi, F. (2001): Quality Evaluation of *Medicago Sativa* Materials Belonging to the Italian Ecotype "Romagnola". – In: Delgado, I., Lloveras, J. (eds.) Quality in Lucerne and Medics for Animal Production. CIHEAM Options Méditerranéennes 45, Zaragoza, pp. 67-71.

[26] Oten, M., Kiremitci, S., Albayrak, S., Turk, M. (2018): New source populations development studies in the alfalfa (*Medicago sativa* L.) breeding. – Fresenius Environmental Bulletin 27: 7520-7526.

[27] Pecetti, L., Carroni, A. M., Annicchiarico, P., Manunza, P., Longu, A., Congiu, G. (2008): Adaptation, summer survival and autumn dormancy of lucerne cultivars in a south European Mediterranean region (Sardinia). – CIHEAM/FAO/ENMP/SPPF 79: 471-474.

http://www.aloki.hu ● ISSN 1589 1623 (Print) ● ISSN 1785 0037 (Online)
DOI: http://dx.doi.org/10.15666/aeer/1706_1561515631

[28] Petkova, D., Vlahova, M., Marinova, D., Atanasov, A. (2003): Breeding evaluation of transgenic lucerne (*Medicago sativa* L.) lines. – Optimal Forage Systems for Animal Production and the Environment, 26-28 May, Pleven, Bulgaria.
[29] Saruhan, V., Kusvuran, A. (2011): Determination of yield performances of some lucerne cultivars and genotypes under the Southeastern Anatolia region conditions. – Ege University, Faculty of Agriculture Journal 48: 133-140.
[30] SAS Institute. (1998): INC SAS/STAT Users' Guide Release 7.0. – SAS, Cary, NC.
[31] Scholtz, G. D. J., Van Der Merwe, H. J., Tylutki, T. P. (2009): The nutritive value of South African *Medicago sativa* L. hay. – South African Society for Animal Science 39(1): 179-182.
[32] Seker, H. (2003): The distribution of green grass and hay yields and hay grass yields according to Kayseri and Bilensoy-80 varieties of the lines obtained from the East alfalfa. – Journal of Agriculture Faculty of Ataturk University 34: 1-7.
[33] Sengul, S., Tahtacioglu, L. (1996): Determining of hay yield and crude protein content of different alfalfa lines and cultivars under Erzurum ecological conditions. – Turkey 3rd Grassland and Forage Crops Congress, 17-19 June 1996, pp. 608-614, Erzurum, Turkey.
[34] Stanacev, V., Dukic, D., Kovcin, S., Drinic, M., Puvaca, N., Stanacev, V. (2010): Nutritive value of the genetically divergent genotypes of lucerne (*Medicago sativa* L.). – African Journal of Agricultural Research 5 (11): 1284-1287.
[35] Strbanovic, R., Stanisavljevic, R., Dukanovic, L., Postic, D., Markovic, J., Gavrilovic, V., Dolovac, N. (2017): Variability and correlation of yield and forage quality in alfalfa varieties of different origin. – Journal of Agricultural Sciences 23 (2017): 128-137.
[36] Titei, V., Teleuta, A. (2018): Introduction and economical value of some species of the *Malvaceae* family in the republic of Moldova. – Science 1 (1): 126-133.
[37] Toricelli, R., Mazza, L., Schiatti, F., Veronesi, F. (2001): Quality evaluation of Medicago sativa materials belonging to the Italian ecotype 'Romagnola'. – Centre International de Hautes Etudes Agronomiques Mediterraneennes, Zaragoza.
[38] Turan, N., Celen, A. E., Ozyazici, M. A. (2017): Yield and quality characterıstics of some alfalfa (*Medicago sativa* L.) varieties grown in the eastern Turkey. – Turkish Journal of Field Crops 22(2): 160-165.
[39] Walie, M., Eshetie, T., Mekonnen, W., Hunegnaw, B., Kebede, A. (2016): Dry Matter Yield, Chemical Composition and *In Vitro* Dry Matter Digestibility of Selected Alfalfa (*Medicago sativa* L.) Accessions in North Western, Ethiopia. – J. Life Sci. Biomed. 6 (3): 60-65.
[40] Yilmaz, M., Albayrak, S. (2016): Determination of herbage yield and quality of some alfalfa (*Medicago sativa* L.) varieties in İsparta ecological conditions. – Journal of Central Research Institute For Field Crops 25: 42-47.
[41] Yuksel, O., Albayrak, S., Turk, M., Sevimay, C. S. (2016): Dry matter yields and some quality features of alfalfa (*Medicago sativa* L.) cultivars under two different locations of Turkey. – Suleyman Demirel University Journal of Natural and Applied Sciences 20: 155-160.
[42] Zeinab, A. E. M., Sallam, A. M., Mohamed, N. A. (2013): Evaluating yield and quality of three alfalfa cultivars using laboratory and saline affected soil. – Journal of American Science 9(12): 5-14.

http://www.aloki.hu ● ISSN 1589 1623 (Print) ● ISSN 1785 0037 (Online)
DOI: http://dx.doi.org/10.15666/aeer/1706_1561515631

DAMAGE CAUSED BY THE EUROPEAN BEAVER (*CASTOR FIBER* L.) IN AGRICULTURAL AND FOREST FARMS IN VIEW OF SELECTED ATMOSPHERIC FACTORS AND ANIMAL BEHAVIOR

JANISZEWSKI, P.* – HERMANOWSKA, Z.

Department of Fur-Bearing Animal Breeding and Game Management, Faculty of Animal Bioengineering, University of Warmia and Mazury in Olsztyn, Oczapowskiego 5, 10-719 Olsztyn, Poland

**Corresponding author*
e-mail: janisz@uwm.edu.pl; Tel.: +48-89-523-4442, ORCID: 0000-0003-4654-7805

(Received 20th Aug 2019; accepted 14th Nov 2019)

Abstract. The aim of this study was to track and characterize damage caused by the European beaver in private farms in the Region of Warmia and Mazury (NE Poland) in 2009-2016. The influence of selected atmospheric factors and beaver behaviour aspects on the number of compensation claims was also analyzed. The majority of damages resulting from beavers' negative impact on the human economy were related to the flooding of grasslands. The second and third most prevalent types of damage were tree cutting and flooding of tree stands, respectively. Most losses were reported in spring and summer months, which suggest that preventive measures should be undertaken mainly during that period. There were no significant relationships between the number of filed claims, temperature and precipitation levels in the analyzed years.
Keywords: *Castor fiber, population increasing, beaver damage, forests, arable areas, flooding*

Introduction

Beavers exert a positive influence on their occupied ecosystems, reflected in increasing biodiversity. However, beaver activity can also have negative implications for private agricultural and forest farms (Derwich and Mróz, 2008; Janiszewski et al., 2014). Beavers can substantially modify the structure of forests by foraging on the preferred tree species, which can lead to the devastation of valuable tree stands (Ciechanowski, 2010; Janiszewski and Hanzal, 2015; Tajchman et al., 2018). Beaver activity can directly or indirectly contribute to landslides and local floods. Rational management of local beaver populations poses a challenge due to the animals' unique lifestyle as well as the fact that beavers often inhabit hard-to-reach biotopes. The prevalence of active family groups is difficult to determine, and attempts to control the beaver population through harvest or hunting may be impossible or ineffective (Janiszewski et al., 2007; Janiszewski and Misiukiewicz, 2012; Januszewicz et al., 2018). Estimates of the damage caused by beavers in private farms based on the filed damage claims provide reliable information on beaver activity.

The aim of this study was to track and characterize the damage caused by the European beaver *Castor fiber* in private farms in the North-Eastern Poland (Region of Warmia and Mazury) in 2009-2016 in view of selected atmospheric factors and animal behavior.

Materials and methods

The study relied on data from the estimation of losses sustained due to the activity of the European beaver *Castor fiber* in the Region of Warmia and Mazury (NE Poland) in

http://www.aloki.hu ● ISSN 1589 1623 (Print) ● ISSN 1785 0037 (Online)
DOI: http://dx.doi.org/10.15666/aeer/1706_1563315642

2009-2016 (*Fig. 1*). The relevant data was obtained from the Regional Directorate for Environmental Protection in Olsztyn (20°30'E; 53°47'N). Damage claims contained the following information:

- Date of loss
- Type of damage

The effects of the following atmospheric factors on the number of damage claims were analyzed:

- Total annual precipitation
- Mean annual temperature
- Mean temperature between March and November

Data on total annual precipitation were obtained from the Regional Inspectorate of Environmental Protection (2018), and temperature data were acquired from Statistics Poland (Statistics of Poland, 2010-2017).

In view of the legal regulations in force (Journal of Laws 2017, item 142, as amended), losses caused by beavers on private land constitute the liability of the State Treasury represented by the Regional Director of Environmental Protection.

The Region of Warmia and Mazury spans an area of 24,173.47 km^2, and it accounts for 7.7% of Poland's territory. Forest cover in the region was estimated at 3.12% at the end of 2015 (Statistics of Poland, 2017).

The results were processed in Microsoft Excel 2013 and presented in tabular and graphic forms with an indication of absolute values and percentages. The coefficients of linear correlation between the total number of damage claims, flood damage claims and the analyzed atmospheric factors were calculated in Statistica 12 PL.

Figure 1. *Research area localization*

http://www.aloki.hu ● ISSN 1589 1623 (Print) ● ISSN 1785 0037 (Online)
DOI: http://dx.doi.org/10.15666/aeer/1706_1563315642

Results

The number and type of beaver damage reported each year during the analyzed period were evaluated. The results are presented in *Table 1*.

Table 1. *Number of complaints describing various types of beaver damage in each year of the study [number/%]*

Type of damage		Year							
		2009	**2010**	**2011**	**2012**	**2013**	**2014**	**2015**	**2016**
Grasslands - flooding	[number]	425	549	660	775	863	855	755	738
	[%]	66.41	61.96	51.68	50.85	47.76	55.74	51.54	48.49
Crops - flooding	[number]	6	17	23	28	31	53	37	77
	[%]	0.93	1.92	1.80	1.84	1.72	3.45	2.53	5.06
Tree stands - flooding	[number]	9	46	160	349	442	64	74	206
	[%]	1.41	5.19	12.53	22.90	24.46	4.17	5.05	13.54
Tree stands - cutting	[number]	180	253	406	350	430	503	509	396
	[%]	28.12	28.57	31.79	22.97	23.80	32.79	34.74	26.02
Garden crops - cutting	[number]	5	8	9	5	12	20	18	39
	[%]	0.78	0.90	0.70	0.33	0.66	1.30	1.23	2.56
Crops - foraging	[number]	1	1	0	0	0	0	0	1
	[%]	0.16	0.11	0	0	0	0	0	0.06
Fish ponds - weir damage	[number]	11	8	8	4	8	22	46	14
	[%]	1.72	0.90	0.64	0.26	0.44	1.43	3.14	0.92
Hydraulic structures	[number]	0	0	1	8	9	1	0	0
	[%]	0	0	0.08	0.52	0.50	0.07	0	0
Livestock	[number]	0	0	1	0	0	3	0	0
	[%]	0	0	0.08	0	0	0.20	0	0
Apiaries	[number]	0	0	0	0	0	1	2	1
	[%]	0	0	0	0	0	0.07	0.14	0.06
Other	[number]	3	4	9	5	12	12	24	50
	[%]	0.47	0.45	0.70	0.33	0.66	0.78	1.63	3.29
Total	**[number]**	**640**	**886**	**1277**	**1524**	**1807**	**1534**	**1465**	**1522**
	[%]	**100**	**100**	**100**	**100**	**100**	**100**	**100**	**100**

The number of beaver damage complaints continued to increase in the first years of the analyzed period from 640 in 2009 to 1807 in 2013. These observations could point to a higher prevalence of beaver damage in the evaluated region (due to migration and/or population growth) or growing levels of awareness about financial compensation options among land owners. A minor decrease in the number of claims was noted in the following two years of the examined period (2014-2016), which could testify to the effectiveness of the implemented protective measures (such as the construction of overflow channels in beaver dams). However, the total number of compensation claims was considerably higher than in the first years of the studied period.

An analysis of the proportions of various types of damage during the studied period indicates that nearly 53% of the submitted compensation claims involved flooding and inundation of grasslands (meadows and pastures) (*Fig. 2*). More than 40% of the reported losses were sustained in private forests and coppices, including tree cutting (28.41%) and flooding of tree stands (12.67%). The relevant losses were least

http://www.aloki.hu ● ISSN 1589 1623 (Print) ● ISSN 1785 0037 (Online)
DOI: http://dx.doi.org/10.15666/aeer/1706_1563315642

frequently sustained in crops (0.03%). However, damage due to floods in grasslands, arable land and private forests accounted for 68% of all damages caused by beavers in the studied region.

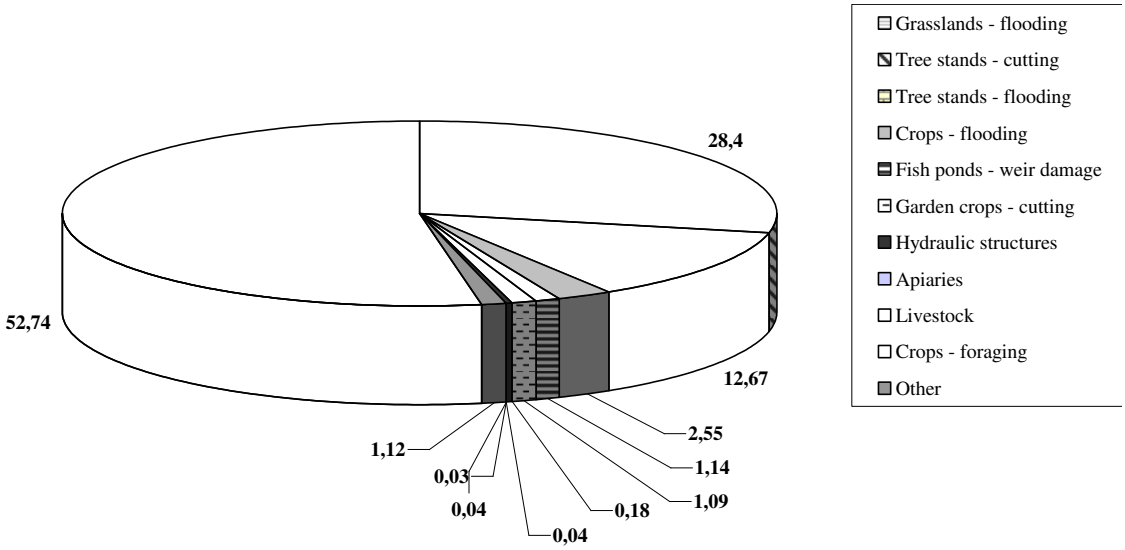

Figure 2. *Different types of damage caused by beavers in 2009-2016*

The number of compensation claims differed across months. The distribution (%) of beaver damage in each month of the year is presented in *Figure 3.*

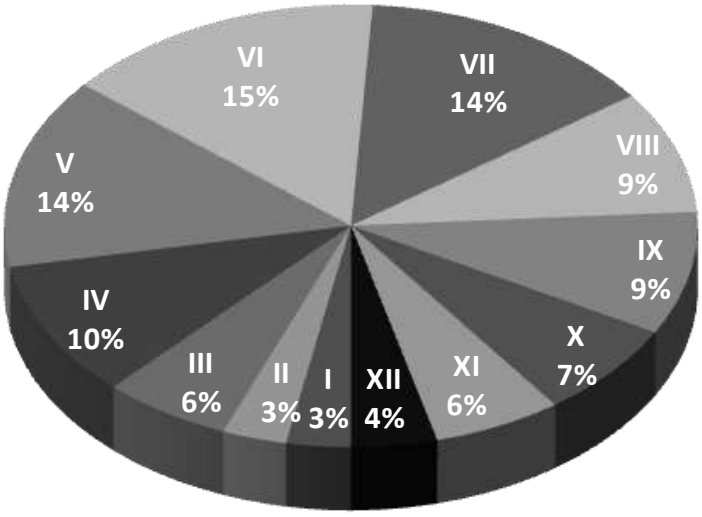

Figure 3. *Distribution (%) of reported damage caused by beavers in each month of the year*

The highest number of damage claims was noted in late spring and in summer: May (14%), June (15%) and July (14%), followed by April (10%), August (9%) and September (9%).

Precipitation and temperature data (*Table 2*) and the correlations between selected atmospheric factors that could potentially influence the severity of beaver damage and the number of compensation claims in each year were analyzed (*Table 3; Fig. 4*).

http://www.aloki.hu ● ISSN 1589 1623 (Print) ● ISSN 1785 0037 (Online)
DOI: http://dx.doi.org/10.15666/aeer/1706_1563315642

Table 2. *Total annual precipitation [mm], mean air temperature [°C] and the number of damage claims [number] in the analyzed area*

Specification	Year							
	2009	**2010**	**2011**	**2012**	**2013**	**2014**	**2015**	**2016**
Total annual precipitation	614.8	750.0	588.4	685.3	616.8	493.3	550.2	727.6
Mean annual temperature	7.7	6.7	8.2	7.5	7.8	8.9	9	8.6
Temperature (March-November)	11	11	11.5	11.4	10.8	12.2	11.5	11.4
Total number of damage claims	640	886	1277	1524	1807	1534	1465	1522
Number of flood damage claims	440	312	843	1152	1336	972	866	1021

Table 3. *Coefficients of correlation between the number of damage claims and selected atmospheric factors*

Parameter	Total precipitation	Annual temperature	Temperature March-November	Total number of damage claims
Total precipitation				
Annual temperature	-0.684			
Temperature – March-November	-0.584	0.683		
Total number of damage claims	-0.236	0.482	0.290	
Number of flood damage claims	-0.230	0.423	0.185	0.941*

* $P \leq 0.05$

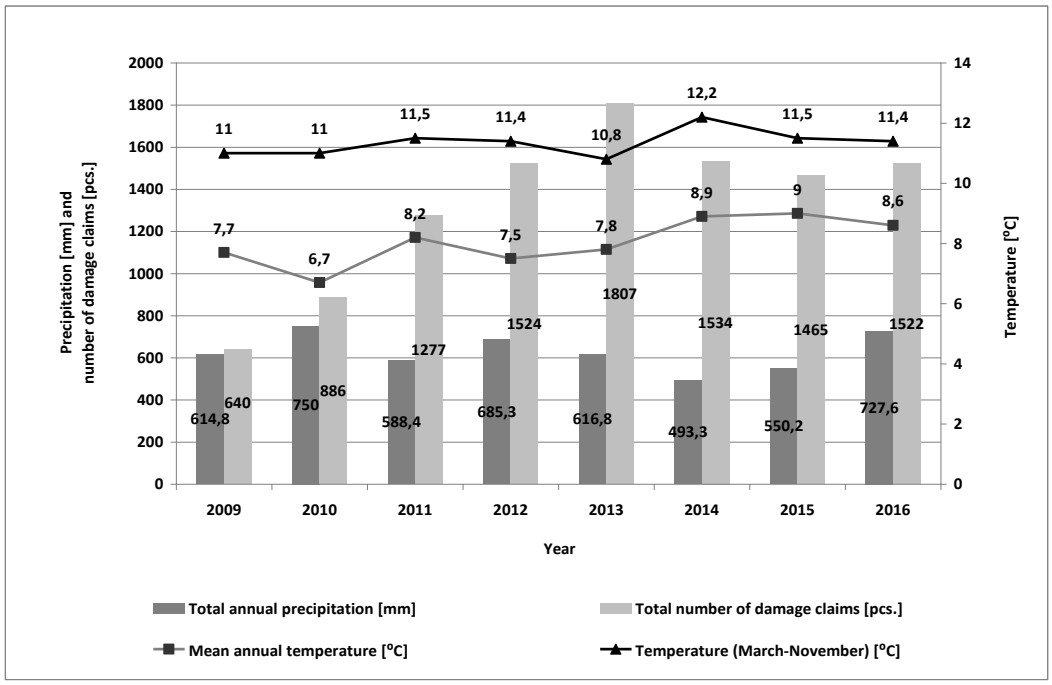

Figure 4. *Number of damage claims vs. temperature and precipitation in the analyzed period*

http://www.aloki.hu ● ISSN 1589 1623 (Print) ● ISSN 1785 0037 (Online)
DOI: http://dx.doi.org/10.15666/aeer/1706_1563315642

The coefficients of correlation between the total number of damage claims, the number of flood damage claims and selected atmospheric factors were calculated. The results are presented in *Table 3*.

An analysis of the above data (*Tables 2* and *3; Fig. 4*) indicates that special attention should be paid to the correlations between annual temperature, the total number of damage claims and the number of flood damage claims. These relationships were not statistically significant, but the above variables were bound by positive correlations, and the correlation coefficient exceeded 0.4. The above implies that higher temperature intensifies beaver activity and prompts these animals to build more dams which raise water levels in rivers and increase the risk of flooding on arable land and in forests. Total precipitation and the number of compensation claims were bound by a negative correlation (-0.23), which suggests that higher precipitation discourages beavers from building dams and minimizes flooding in areas directly adjacent to watercourses.

Discussion

The severity of damage caused by beavers has not been analyzed in detail often in relevant literature (Reynolds, 2000). Various types of beaver damage were evaluated by Brzuski and Kulczycka (1999) based on the compensation claims filed in 1995-1997 in the former Polish voivodeships (before the reform of Poland's administrative division system). A total of 790 claims describing different types of damage caused by beavers had been filed in Poland in the analyzed period. The total amount of compensation payments for damage caused by beavers reached the equivalent of USD 141,000. According to the cited authors (Brzuski and Kulczycka, 1999), field and grassland floods accounted for 30% of all reported damages. In our study, flooding was the most common cause of the reported losses, but the prevalence of flood-related damage in the Region of Warmia and Mazury was higher at around 50% (from 47.76% to 66.41%) (*Table 1; Fig. 2*). A comparison of our findings with the cited results points to a rapid increase in the population size of beavers in north-eastern Poland, which is associated with a higher incidence of damage caused by beavers and, consequently, an increase in the amount of compensation payments.

Various types and extent of damage caused by beavers were also investigated in 2002-2003 by Czech (2010). In his study, the destruction of flood embankments and pond levees by burrowing beavers was the most prevalent type of damage, followed by farm flooding. In a study by Derwich et al. (2007), the most severe losses associated with beaver activity in the region of Podkarpacie (South-Eastern Poland) also included damage to flood embankments and tree stands.

Different results were noted by Wajdzik et al. (2013) who reported a total of 262 beaver damage, complaints totaling PLN 150,000 in the Region of Małopolska (South Poland). In their study, the most extensive losses (120 compensation claims) were observed in forests where beavers felled more than 14,000 of trees with a combined volume of 752 m^3. The most affected tree species were willows (5850), poplars (3550), alders (2100) and oaks (1500). Beavers had a preference for trees whose diameter at breast height did not exceed 11 cm. A total of 116 damage claims were filed by farms where beavers damaged mostly root and tuber crops (beets, carrots, parsnips) and cereals (maize, wheat). Flooding and seasonal inundation of meadows and pastures were also prevalent on agricultural land. The predominant types of losses in fish ponds included burrowing and weakening of levees, blockage of culverts, and restricted water

http://www.aloki.hu ● ISSN 1589 1623 (Print) ● ISSN 1785 0037 (Online)
DOI: http://dx.doi.org/10.15666/aeer/1706_1563315642

flow in ditches. Kłoskowski (2011) conducted a detailed analysis of damage caused by beavers in fish farms. Severe losses were reported in 21.2% and moderate losses – in 46% of the 110 surveyed fish farms in eastern Poland. Fish ponds were not affected by beaver activity in 32.8% of the examined cases.

The expansion of the existing and potential beaver populations after reintroduction can have serious financial consequences if beaver colonies private forest and agricultural area. The relevant risks can be minimized through monitoring, which is not easily accomplished with regard to beavers, partly because of difficulties in determining the exact number of beaver colonies (Januszewicz et al., 2018). Campbell-Palmer et al. (2015) estimated the costs associated with the payment of compensation for damages caused by beavers. In Denmark, where the first beaver reintroduction scheme was introduced only in 1999, equipment costs range from EUR 1000 to 3000 per year, the cost of field staff dealing with beaver conflicts was estimated at EUR 50,000 per year, whereas EUR 40,000 is additionally spent on monitoring. In the Czech Republic which has a stable beaver population, more than EUR 2.8 million has been paid in state compensation for damages to crops and forestry in the last 15 years (average of EUR 187,000 per year). In Bavaria, voluntary state compensation for beaver damage is estimated at EUR 450,000 per year, and around 1000 beavers are now culled annually. However, while the costs associated with the mitigation of human-beaver conflicts and the payment of compensations can be estimated, the potential benefits of beavers are much more difficult to determine.

Road damages caused by beaver (*Castor canadensis*) were a costly problem for transportation department in the U.S. Population control and dam destruction were the most widely used methods to reduce conflicts but benefits of such measures in some situations were often very short-term (Boyles and Savitsky, 2008). To determine the potential benefits of using flow devices were installed 40 devices in 21 sites. It was important, that the costs to install and maintain the devices were significantly lower than preventative road maintenance, damage repairs, and/or population control costs.

Similar results were obtained in the territory of Alberta, Canada (Hood et al., 2018). There were 12 pond levelers devices installed to prevent flooding by *Castor nanadensis* and the Authors developed a cost-benefit analysis for these areas. It was found that one of the devices required constant maintenance and modification during 3 years, while the other devices required almost no maintenance. Based on a "willingness-to-pay" (WTP) of 0$ and discount rate of 3% was found that installing pond levelers resulted in a present value net benefit of 81 519$ over 3 years and 179 440$ over 7 years. Scenarios incorporating discount rates of 3% and 7%, horizons of either 3 or 7 years, and varying WTPs resulted in significant net benefits. Hood et al. (2018) also found that provincially, municipalities employed up to seven different methods to control damages caused by beavers, but the most commonly were: lethal control and dam removal. Total annual costs provided by 48 municipalities and 4 provincial parks districts were 3,139,223 $.

Czyżowski et al. (2009) compared the extent of damage to tree stands caused by beavers based on the species' foraging preferences in urban and protected areas. They found that unlike in protected areas, beavers did not have clear preferences regarding tree species and tree diameter in urban areas.

Janiszewski and Misiukiewicz (2012) analyzed the compensation claims submitted to Regional Directorates for Environmental Protection across Poland in 2009. The incidence of beaver damage was highest in the Region of Podlasie and the Region of

http://www.aloki.hu ● ISSN 1589 1623 (Print) ● ISSN 1785 0037 (Online)
DOI: http://dx.doi.org/10.15666/aeer/1706_1563315642

Warmia and Mazury, and it was lowest in the Region of Silesia. Grassland flooding was the most prevalent type of beaver damage which was reported in 69.72% of the examined cases. The number of approved compensation claims was twice lower in the Region of Warmia and Mazury than in the Region of Podlasie, but the amount of paid compensation was highly similar in both regions. In the cited study, the following types of damage were most prevalent: flooding of meadows and pastures (30.4%), damage to embankments and levees in fish ponds (20.12%), tree damage (19.28%) and losses sustained in horticulture (18.04%).

The distribution of beaver-induced losses in different months of the year can be influenced by the biological characteristics of the species as well as the annual cycle of agricultural and forestry operations. The number of damage claims was highest in the months when many field operations are performed, in particular on grasslands which are most susceptible to beaver damage (*Table 1*). The summer months are also a season of beaver migration (Janiszewski et al., 2014). Offsprings are typically born in May and June which is also a period during which other members of beaver family groups temporarily leave their habitats, and individuals who attain sexual maturity (at around 3 years of age) migrate in search of mating partners and new habitats (Hartman 1997). Annual migration patterns and behaviors can also contribute to the severity of damage because migrating beavers build dams in new locations and cause floods in areas adjacent to rivers and water bodies (Gorshkov and Gorshkov, 2011).

The number of damage claims was lower in October and November (*Fig. 2*), which is not correlated with beaver activity, but could be linked with a small number of field operations (mainly in grasslands). However, tree cutting and felling can be intensified in autumn when beavers attempt to harvest sufficient amounts of material for reinforcing dams or accumulate food reserves before winter (Hartman, 1997; Janiszewski and Hanzal, 2015).

Janiszewski and Misiukiewicz (2012) analyzed the factors that affect the extent and type of damage caused by beavers. In addition to the size and density of beaver populations, the type and severity of the inflicted losses were directly associated with the proportion of arable land and private forests in the studied area. The area of agricultural land intersected by large rivers is one of the key factors that determine the type and extent of beaver damage. These areas are readily colonized by migrating beavers.

Tajchman et al. (2018) reported interesting findings in a study evaluating beaver damage to tree stands. The number of damaged trees was bound by a negative and non-significant correlation with the hardness of the analyzed tree species. A similar relationship was noted between the diameter of damaged trees and their distance from beaver lodges: the diameter of trees cut by beavers decreased with an increase in distance from beaver habitats.

The increasing Canadian beaver population has caused forest damage in Finland (Härkönen, 1999). The most important type of damage was flooding (50%) caused by the damming activity of beavers, according to own results. The trees were dead or dying in 18% of the damage areas. Prevention of beaver damage has been carried out in 80%of the damage area. In the study area (Härkönen, 1999) beaver numbers have steadily increasing, although the number of beavers taken by hunting have sharply increased too. It can suggest that the methods used to prevent beaver damages should be improved.

http://www.aloki.hu ● ISSN 1589 1623 (Print) ● ISSN 1785 0037 (Online)
DOI: http://dx.doi.org/10.15666/aeer/1706_1563315642

In the light of legal regulations, land owners and tenants are entitled to compensation in virtue of damage caused by beavers (Art. 126, section 1, point 5 of the Nature Conservation Act of 16 April 2004; Journal of Laws 2017, item 142, as amended). However, land owners and tenants are not compensated for lost profits. It should be noted that until 2013, the State Treasury (represented by the Regional Director for Environmental Protection in the relevant matters) was liable only for losses sustained in agricultural, forest and fish farms. The above regulation was repealed on 26 July 2013 pursuant to a decision of the Constitutional Tribunal of 3 July 2013 (Journal of Laws 2013, item 842). The Constitutional Tribunal ruled that Art. 126, section 1, point 5 of the Nature Conservation Act violates the provisions of Art. 32, section 1 and Art. 64, section 2 of the Constitution in the part limiting the State Treasury's liability for beaver damage to agricultural, forest and fish farms. As a result, land owners and tenants became able to claim compensation for damage to agricultural equipment, vehicles, residential buildings, farm buildings and fencing caused by the collapse of trees cut by beavers or floods provoked by burrowing animals.

The consequences of this legal amendment are reflected in the results of this study. Beginning from 2014, the number of compensation claims for losses in hydraulic structures, livestock farms and apiaries, and the value of claims in the 'other' category increased dramatically (*Table 1*).

Conclusions

The analysis of the losses sustained due to the activity of the European beaver (*Castor fiber*) in the Region of Warmia and Mazury in North-Eastern Poland in 2009-2016 revealed a gradual increase in the number of damage compensation claims until 2014. The number of compensation claims relating to beaver damage decreased and stabilized after 2014. These findings could indicate that the implemented protective measures are effective. The majority of damages resulting from beavers' negative impact on the human economy were related to the flooding of grasslands, and they accounted for 50% of all beaver-induced losses. The second and third most prevalent types of damage were tree cutting and flooding of tree stands, respectively. Most claims were made in spring and summer months, which suggests that preventive measures should be undertaken mainly during that period, in particular in years characterized by low precipitation.

REFERENCES

[1] Boules, S. L., Savitzky, B. A. (2008): An Analysis of the Efficacy and Comparative Costs of Using Flow Devices to Resolve Conflicts with North American Beavers Along Roadways in the Coastal Plain of Virginia. – Timm, R. M., Madon, M. B. (eds.) Proc. 23rd Vertebr. Pest Conf. University of California, Davis, pp. 47-52.

[2] Brzuski, P., Kulczycka, A. (1999): Beaver - Symbol of a Return to Nature. – PZŁ Publisher, Warszawa.

[3] Campbell-Palmer, R., Schwab, G., Girling, S., Lisle, S., Gow, D. (2015): Managing Wild Eurasian Beavers: a Review of European Management Practices with Consideration for Scottish Application. – Scottish Natural Heritage Commissioned Report No. 812, Inverness, UK.

http://www.aloki.hu ● ISSN 1589 1623 (Print) ● ISSN 1785 0037 (Online)
DOI: http://dx.doi.org/10.15666/aeer/1706_1563315642

[4] Ciechanowski, M. (2010): Beaver - Environmental Engineer. How One Animal Can Affect the Ecological Diversity of the Ecosystem. – In: Frąckiel, K. (ed.) Beaver, Symbol of Return to Nature - Problems or Benefits? Osowiec Twierdza, pp. 62-79 (in Polish).
[5] Czech, A. (2010): Beaver - a Builder and an Engineer. – Fundacja Wspierania Inicjatyw Ekologicznych, Kraków (in Polish).
[6] Czyżowski, P., Karpiński, M., Drozd, L. (2009): Forage preferences of the European Beaver (Castor fiber L.) on urban and protected areas. – Sylwan 153(6): 425-432 (in Polish).
[7] Derwich, A., Brzuski, P., Hędrzak, M. (2007): Bóbr w biotopach Bieszczadów Wysokich. – Akademia Rolnicza, Zespół Metod i Organizacji Hodowli Zwierząt Gospodarczych i Wolno Żyjących, Kraków.
[8] Derwich, A., Mróz, I. (2008): The European beaver Castor fiber L. 1758 as a factor supporting the restoration of habitats on the Upper San River. – Studia i Materiały Centrum Edukacji Przyrodniczo-Leśnej 10: 173-183 (in Polish).
[9] Gorshkov, Y., Gorshkov, D. (2011): Radiotelemetry of the Reintroduced Beavers in Volga-Kama National Nature Preserve. – In: Sjoberg, G. and Ball, J. P. (ed.) (2011): Restoring the European Beaver: 50 Years of Experience. Pensoft, Sofia-Moscow.
[10] Hartman, G. (1997): Notes on age at dispersal of beaver (*Castor fiber*) in an expanding population. – Canadian Journal of Zoology 75: 959-962.
[11] Härkönen, S. (1999): Forest damage caused by Canadian beaver (*Castor canadensis*) in South Savo, Finland. – Silva Fennica 33(4): 247-259.
[12] Hood, G. A., Manaloor, V., Dzioba, B. (2018): Mitigating infrastructure loss from beaver flooding: a cost–benefit analysis. – Human Dimensions of Wildlife Research 23(2): 146-159.
[13] Janiszewski, P., Weigle, A., Gugołek, A. (2007): Stan i rozmieszczenie bobra europejskiego (*Castor fiber* L.) w województwie mazowieckim. – Roczniki Naukowe PTZ III 4: 367-374.
[14] Janiszewski, P., Hanzal, V. (2015): European Beaver *Castor fiber* - Biology and Ecology of the Species. – UWM, Olsztyn (in Polish).
[15] Janiszewski, P., Hanzal, V., Misiukiewicz, W. (2014): The European Beaver (*Castor fiber*) as a Keystone Species - a Literature Review. – Baltic Forestry 20(2): 277-286.
[16] Janiszewski, P., Misiukiewicz, W. (2012): European Beaver *Castor fiber*. – BTL Works, Warszawa (in Polish).
[17] Januszewicz, M., Misiukiewicz, W., Janiszewski, P., Folborski, J. (2018): Methodological requirements for identifying sites colonized by European beaver *Castor fiber* L. with the use of thermal imaging technology. – Polish Journal of Natural Science 33(1): 7-16.
[18] Kłoskowski, J. (2011): Human–wildlife conflicts at pond fisheries in eastern Poland: perceptions and management of wildlife damage. – European Journal of Wildlife Research 57: 295-304.
[19] Reynolds, P. (2000): European beaver in woodland habitats: a review. – Scottish Natural Heritage Review No 126.
[20] Statistic of Poland (2010-2017): Statistical Yearbook of the Republic of Poland. – GUS, Warszawa.
[21] Tajchman, T., Czyżowski, P., Drozd, L. (2018): Food selectivity of European beaver (*Castor fiber* L.) occurring in the area Lubaczów and Chotyłów forest districts. – Polish Journal of Natural Science 33(4): 533-543.
[22] Wajdzik, M., Kubacki, T., Tomek, A. (2013): Damage caused by the European beaver *Castor fiber* in agriculture, forestry and fisheries in Malopolska area. – Studia i Materiały CEPL w Rogowie 36(3): 131-137 (in Polish).

http://www.aloki.hu ● ISSN 1589 1623 (Print) ● ISSN 1785 0037 (Online)
DOI: http://dx.doi.org/10.15666/aeer/1706_1563315642

INCREASING GRAIN YIELD OF SUBMERGENCE-TOLERANT RICE (*ORYZA SATIVA* L.) THROUGH APPROPRIATE NUTRIENT MANAGEMENT

HTWE, T.[1] – TECHATO, K.[1,2] – CHOTIKARN, P.[3,4] – SINUTOK, S.[1,3*]

[1]*Faculty of Environmental Management, Prince of Songkla University, 90110 Songkhla, Thailand*

[2]*Environmental Assessment and Technology for Hazardous Waste Management Research Center, Prince of Songkla University, 90110 Songkhla, Thailand*

[3]*Coastal Oceanography and Climate Change Research Center, Prince of Songkla University, Songkhla, 90110 Thailand*

[4]*Marine and Coastal Resources Institute, Prince of Songkla University, 90110 Songkhla, Thailand*

**Corresponding author*
e-mail: ssutinee@gmail.com; phone: + 66-74-286-847; fax: +66-74-429-758

(Received 21st Aug 2019; accepted 15th Nov 2019)

Abstract. Flooding is one of the environmental stresses that cause a reduction in rice yield and the effect varies between rice varieties. This study aimed to investigate the response of different rice varieties (Hnan Gar, Swarna-Sub1, Bio-6, and Bio-8) to the application of various combinations of nutrient doses (110:0:75, 110:50:0, 110:50:75, 110:80:75 and 110:50:110 of $N:P_2O_5:K_2O$ kg ha^{-1}) under natural submergence conditions in Myanmar. The survival percentages of the different rice genotypes were found not to be significantly varied after 20 days of submergence. Swarna-Sub1 and Bio-8 produced lower underwater shoot elongation, which tended to save energy to be used for later growth, and this resiliency contributed to higher grain yield. Varying the fertilizer application rates produced no significant effect on the percentage of shoot elongation. The Swarna-Sub1 and Bio-8 varieties produced much higher yields compared to Hnan Gar and Bio-6 as a result of a higher filled grain percentage and panicle number m^{-2}. In addition, fertilizing with a dosage of 110:50:110 kg ha^{-1} ($N:P_2O_5:K_2O$) provided better crop performance and higher yield. These results demonstrate that appropriate nutrient management by combining tolerant varieties is able to help in the mitigation of the adverse effect of submergence stress.
Keywords: *survival, shoot elongation, nutrient, submergence, Myanmar*

Introduction

Flooding is one of the abiotic stresses that cause severe rice yield reduction in Southeast Asia and threaten global food security (FAO, 2016; Yin et al., 2017). Flooding can be categorized into water logging and submergence. Water logging is a condition in which excess water is in the root zone, and water covers on the soil surface while it covers partial or whole plant in submergence condition (Nishiuchi et al., 2012; Sasidhran et al., 2017). The most common and damaging type of submergence which can occur during the vegetative growth of rice is short-term complete inundation (generally less than 2 weeks), also referred to as a flash flood. Grain yield in rainfed lowland rice is constantly challenged by this type of flooding (Iftekharuddaula et al., 2016; Pradhan et al., 2019; Gautam et al., 2019), and can result in severe damage and plant mortality if sustained for more than a week. More than 22 million ha of rainfed lowland rice are affected by submergence in Asia (Gautam et al., 2014a). The FAO (2015) estimated that USD 7.8 billion worth of crops were damaged by major floods

http://www.aloki.hu ● ISSN 1589 1623 (Print) ● ISSN 1785 0037 (Online)
DOI: http://dx.doi.org/10.15666/aeer/1706_1564315655

around the world between 2003 and 2013. Further, in the so-called rice bowl of Myanmar, the Ayeyarwaddy delta, in which the research reported in this paper was conducted, which covers a total of 2.89 million ha each year, as much as 371990 ha are inundated because of seasonal heavy rainfall and the low lying topography (FAO/WFP, 2016). The extent of damage to rice crops caused by complete submergence during their vegetative stage depends on environmental conditions, such as higher temperatures, greater water turbidity, and lower solar radiation, which worsen the severity of the stress (Das et al., 2009; Ye et al., 2018a, b).

Energy shortage caused by anoxia may lead to reduced nutrient uptake by plants, resulting in the cessation of root elongation, leading to pronounced root injury and death of the tips (Bui et al., 2019; Liu et al., 2015; Singh et al., 2014). Moreover, the plant hormone, ethylene accumulates under submergence conditions because its diffusive escape is slower than the synthesis induced by flooding. Several researchers have reported that ethylene promotes internode elongation, chlorophyll degradation and leaf senescence, causing a reduction in photosynthetic carbon fixation during and after submergence (Ella et al., 2003; Jackson, 2008; Yin et al., 2017). Both the excessive use of energy for shoot elongation and the reduction in carbon fixation during submergence accelerate the depletion of carbohydrate. This leads to the increased mortality of submerged plants (Das et al., 2005; Bui et al., 2019; Ye et al., 2018b). In addition, chlorophyll and non-structural carbohydrate retention after submergence has been found to be positively correlated with plant survival (Gautam et al., 2014a).

The mechanism of plant adaptation to flooding depends on the water regime. In deep water areas, internode elongation is necessary to maintain portions of foliage above the water surface for photosynthesis and oxygen transport. On the other hand, reduced elongation is desirable during flash floods since stem or internode elongation may compete with the plant's maintenance processes for energy, and as a result, reduce the chances of survival during flash floods (Bui et al., 2019; Ram et al., 2002). Das et al. (2005) also reported that the survival of seedlings is negatively correlated with stem elongation.

Although traditional cultivars are moderately tolerant to complete submergence, their yield potential is lower (Singh et al., 2014). Gribaldi et al. (2017) stated that fertilizing with half dose of N and the remaining half at 42 days after planting gave better crop performance and higher yield. Additional potassium and nitrogen application post-submergence has been noted to increase their survival and yield (Dwivedi et al., 2018). However, farmers in flood-prone area usually use only nitrogenous fertilizer and small amount of phosphorus and potassium sources (FAO/WFP, 2016; Soni and Soe, 2016). In view of this, proper nutrient management is vital for achieving better performance from submergence-tolerant rice varieties, and there is limited information available regarding the appropriate application rate of nutrients in specific areas under natural conditions. Thus, the aim of the research reported herein was to establish the most suitable fertilizer application rate to increase the grain yield of rice in flash flood-prone areas along with the most tolerant genotypes.

Materials and methods

This research was conducted between June and October 2015 at Thayaungchaung Seed Farm in the Ayeyarwaddy Region, in lower Myanmar (GPS coordinate: 16° 45' 41.2" N, 94° 44' 54.1"E, *Fig. 1*). The research employed a split plot design with three

http://www.aloki.hu ● ISSN 1589 1623 (Print) ● ISSN 1785 0037 (Online)
DOI: http://dx.doi.org/10.15666/aeer/1706_1564315655

replications. The main factor tested was the nutrient application rate, as follows (all figures $N:P_2O_5:K_2O$, kg ha^{-1}): N_1 = control (no fertilizer application), N_2 = 110:0:75, N_3 = 110:50:0, N_4 = 110:50:75, N_5 = 110:80:75 and N_6 = 110:50:110, and the sub-factor investigated was the rice variety, as follows: V_1 = Hnan Gar, V_2 = Swarna-Sub1 (local name Yemyoke Khan 1), V_3 = Bio-6, V_4 = Bio-8. The seeds were soaked for 24 h on 27th June, 2015 and incubated for 24 h. Then, the pre-germinated seeds were carefully sown on raised bed. Care and management of seed beds were done as per standard method. Twenty seven-day old seedlings were transplanted to the main field. The spacing was 20 cm x 15 cm with 2-3 seedlings per hill. Main plots (fertilizer treatments) were separated by bunds of 0.30 m width and 0.30 m height, and there was a 1 m wide alley between the bunds (Pimratch et al., 2015; Atapattu et al., 2018). The plots were subdivided into four unbunded subplots for variety treatments. Each subplot occupied 7.35 m^2. The seed source of the Swarna-Sub1 and Hnan Gar was Thayaungchaung Seed Farm and that of Bio-8 and Bio-6 was Aung Myay Ya Seed Farm. *Table 1* shows the soil properties of the experimental site. All the doses of triple super phosphate ($Ca(H_2PO_4)_2$; source of P) and potassium chloride (KCL; source of K), and 25% of the dose of urea ($CO(NH_2)_2$; source of N) were applied during final land preparation of the main field. Of the remaining N dose, 50% was added at the maximum tillering stage and 25% at the panicle ignition stage.

Table 1. *Mean values of soil characteristics from experimental field (n = 20)*

Characteristics	Mean
Soil pH	4.69
Total N (%)	0.24
Available P (ppm)(Bray)	0.90
Extractable K (meq/100 g soil)	0.45
Soil texture	Silty clay

Meteorological data during the experiment were recorded in Thayaungchaung Seed Farm. Mean daily temperature was from 20 to 37 °C during the experiment. As a result of successive heavy rain and overflow of river, accumulated water in upstream brought to flood the experimental field from 7 to 27 days after transplanting the seedlings (see *Fig. 2*) and flooding occurred for 20 days to a depth of between 35 and 60 cm (*Fig. 3*). After that, complete submergence was not occurred although it rained fairly.

The plant height was measured from the base of the plant to the longest leaf tip before and after submergence at vegetative stage. It was measured from the base of the plant to the tip of longest panicle at harvesting stage. In order to calculate the underwater shoot elongation, the height before submergence was subtracted from the height after submergence and expressed as a percentage of the plant height before submergence. Surviving plants with at least one new leaf were recorded 10 days after the recession of water and the survival was expressed as a percentage of the number of plants before flooding.

Twelve hills from each sub-plot were randomly selected at harvest time for the determination of the plant height and yield components such as filled grain percentage, 1000-grain weight, and spikelets per panicle. The whole sub-plot except two border rows was harvested, threshed, dried (to a 14% moisture content), and the grain yield was recorded and converted to yield of kg per hectare.

http://www.aloki.hu ● ISSN 1589 1623 (Print) ● ISSN 1785 0037 (Online)
DOI: http://dx.doi.org/10.15666/aeer/1706_1564315655

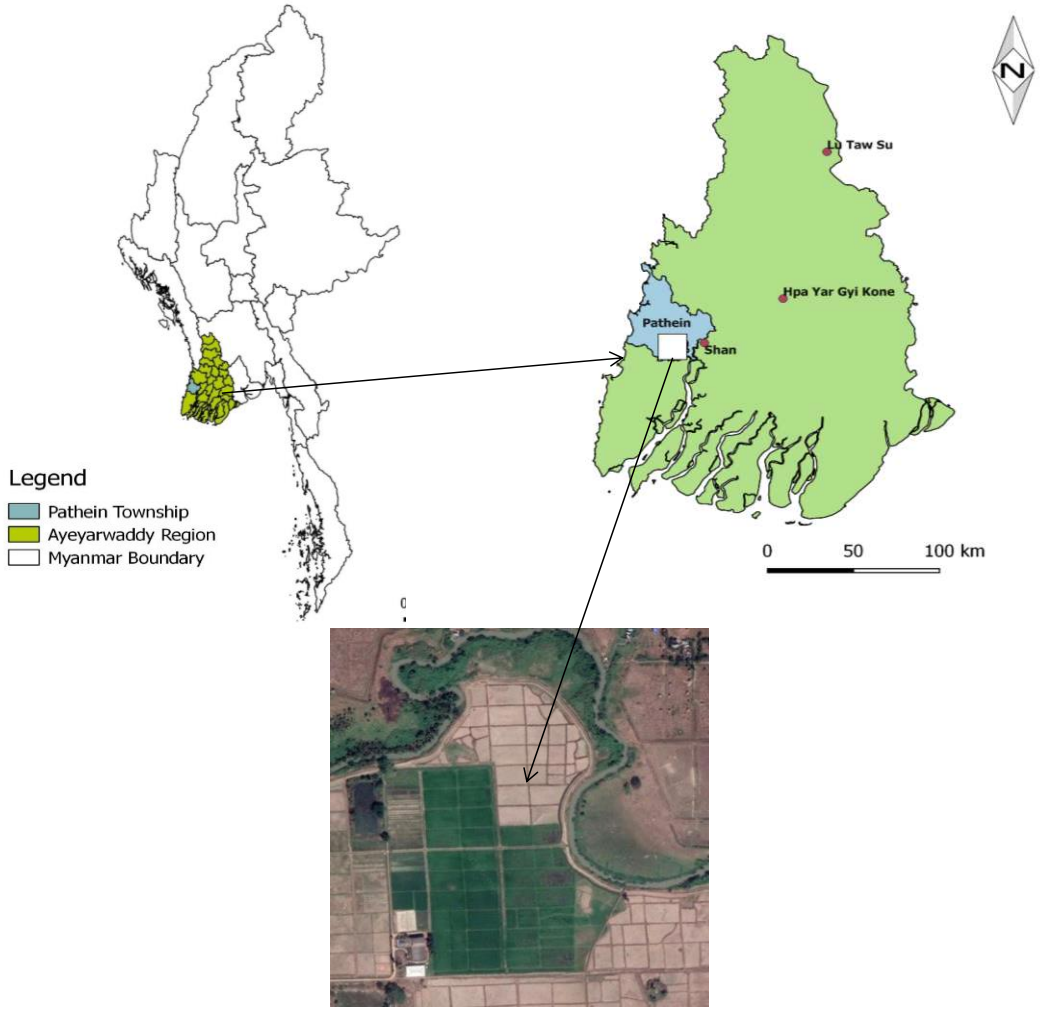

Figure 1. *Map showing experimental site in Myanmar*

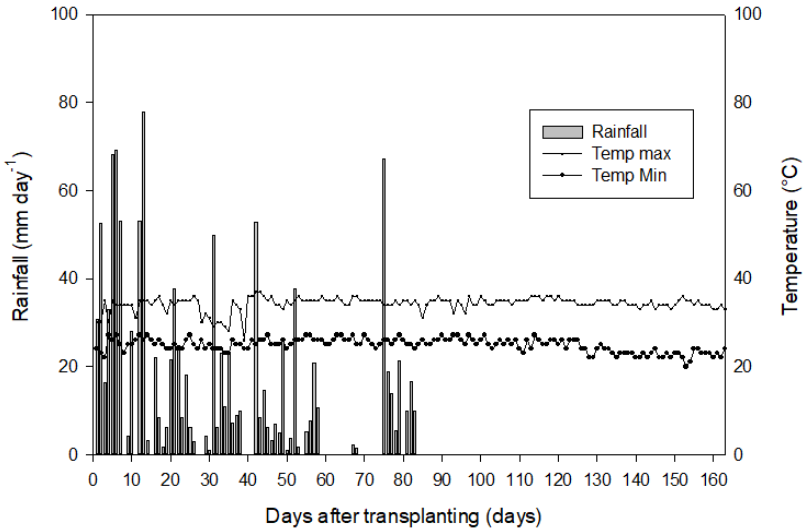

Figure 2. *Mean daily maximum and minimum temperature (°C) and rainfall (mm) during experiment*

http://www.aloki.hu ● ISSN 1589 1623 (Print) ● ISSN 1785 0037 (Online)
DOI: http://dx.doi.org/10.15666/aeer/1706_1564315655

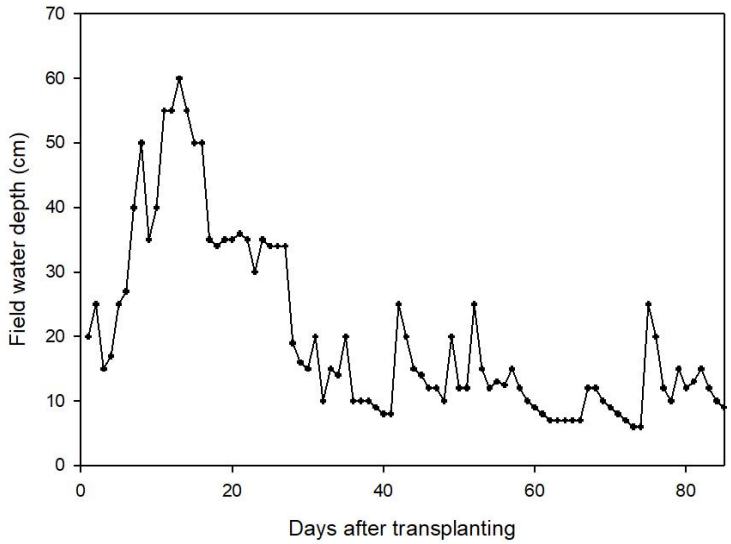

Figure 3. *Field water depth during heavy rain at the experimental site, Myanmar*

Statistical analysis

To test for significant differences in rice growth parameters among the different fertilizer treatments and rice varieties, two-way analysis of variance (ANOVA) was employed using the SPSS statistical package (SPSS Statistics Bass 17.0 for Windows EDU). All tests were performed with a significant level of 95%, and Tukey's honestly significant difference post-hoc test was used to identify the statistically distinct groups.

Results

Effect of submergence and nutrient application on survival and under-water shoot elongation

The Hnan Gar variety showed higher plant survival than the other varieties; however, the differences were not significant ($P > 0.05$). Applying fertilizer at different rates also had no significant effect on survival when the rice experienced flooding to a depth of 35-60 cm starting from 7 days after transplanting for 20 days (*Table 2*). The Hnan Gar variety was taller than the other three varieties tested before submergence ($P < 0.001$). The shortest plant height was observed in Bio-8 although this was not significantly different from the heights of Swarna-Sub1 and Bio-6. The individual effect of fertilizer application and its interaction with the rice variety variable was not significant ($P > 0.05$). A similar trend was noted at desubmergence. All the varieties revealed submergence-induced shoot elongation. However, the Hnan Gar variety showed a significantly higher elongation percentage under water than those of Swarna-Sub1 and Bio-8 ($P < 0.001$). There were no significant differences ($P > 0.05$) in the percentage shoot elongation during submergence based on the various rates of fertilizer application (*Fig. 4*).

Effect of submergence and nutrient application rates on plant height at harvesting time and days to maturity of Hnan Gar, Swarna-Sub1, Bio-6 and Bio-8

Local variety was significantly taller than those of other tested varieties ($P < 0.001$) while the heights of Swarna-Sub1, Bio-6 and Bio-8 were statistically similar. The effect

http://www.aloki.hu ● ISSN 1589 1623 (Print) ● ISSN 1785 0037 (Online)
DOI: http://dx.doi.org/10.15666/aeer/1706_1564315655

of fertilizer application rates on plant height can be seen only between the control and the fertilizer applied treatments. The crop duration of Hnan Gar variety was significantly longer than those of other three varieties ($P < 0.001$). The shortest crop duration was occurred in Bio-6, followed by Swarna-Sub1, Bio-8 and Hnan Gar variety (*Table 3*).

Table 2. *Survival % of different rice genotypes (Mean ± SE) under varying fertilizer application rates after 20 days of submergence*

T	N_1	N_2	N_3	N_4	N_5	N_6
V_1	66.11 ± 0.36	82.5 ± 5.53	69.58 ± 3.6	59.03 ± 4.93	69.58 ± 6.26	73.75 ± 7.81
V_2	57.64 ± 1.44	76.11 ± 5.54	56.39 ± 3.6	52.22 ± 3.73	58.33 ± 4.57	63.47 ± 2.41
V_3	61.94 ± 0.24	79.03 ± 5.77	66.67 ± 5.24	55.28 ± 5.41	64.17 ± 2.76	69.44 ± 5.77
V_4	50.42 ± 2.16	70.39 ± 4.5	51.81 ± 6.25	63.61 ± 2.52	58.89 ± 1.32	63.47 ± 6.13

T = Treatment, V_1 = Hnan Gar, V_2 = Swarna-Sub1, V_3 = Bio-6, V_4 = Bio-8. N_1 = control, N_2 = 110:0:75, N_3 = 110:50:0, N_4 = 110:50:75, N_5 = 110:80:75, N_6 = 110:50:110, $N:P_2O_5:K_2O$ $kgha^{-1}$)

Table 3*. Effect of different nutrient application rates on plant height at harvesting time and days to maturity of Hnan Gar, Swarna-Sub1, Bio-6 and Bio-8 after being submerged for 20 days*

Treatments	Plant height (cm)	Days to maturity
Variety (V)		
Hnan Gar (local variety)	160.00 a	172.22 a
Swarna-Sub1	112.92 b	160.44 b
Bio-6	112.78 b	128.00 c
Bio-8	113.47 b	162.17 b
Nutrient Application (N) kg ha^{-1} ($N:P_2O_5:K_2O$)		
N_1(0:0:0, control)	121.04 b	156.00
N_2 (110:0:75)	126.45 a	154.75
N_3(110:50:0)	125.00 a	155.92
N_4(110:50:75)	125.20 a	155.67
N_5(110:80:75)	125.20 a	155.42
N_6(110:50:110)	125.83 a	156.60
V	**	**
N	**	ns
VxN	ns	ns

Mean values followed by a different letter are significantly different at Tukey's test ($P \leq 0.05$). ** = significant difference at $P \leq 0.01$, ns = not significant difference at $P > 0.05$

Effect of submergence and fertilizer application rates on grain yield and yield attributes of Hnan Gar, Swarna-Sub1, Bio-6 and Bio-8

Number of spikelets per panicle

Under submergence condition, the highest number of spikelets per panicle was observed in Swarna-Sub1, followed by Bio-8, Hnan Gar and Bio-6 ($P < 0.001$). In the case of fertilizer application, there was no significant difference among the treatments (*Table 4*).

http://www.aloki.hu ● ISSN 1589 1623 (Print) ● ISSN 1785 0037 (Online)
DOI: http://dx.doi.org/10.15666/aeer/1706_1564315655

Table 4. *Effect of different nutrient application rates on yield and its components of Hnan Gar, Swarna-Sub1, Bio-6 and Bio-8 after being submerged for 20 days*

Treatments	Filled grain (%)	1000-grain weight (g)	Spikelets panicle^{-1}	Panicles m^{-2}	Yield (t ha^{-1})
Variety (V)					
Hnan Gar (local variety)	80.70 b	20.28 b	121.17 b	170.61 c	2.35 b
Swarna-Sub1	88.37 a	20.06 b	170.00 a	255.92 ab	4.22 a
Bio-6	70.07 c	25.82 a	108.50 b	232.32 b	2.20 b
Bio-8	86.65 a	20.36 b	168.67 a	266.81 a	4.27 a
Nutrient Application (N) kg ha^{-1} (N:P_2O_5:K_2O)					
N_1(0:0:0, control)	79.58 bc	21.36 b	140.33	228.69	2.87 c
N_2 (110:0:75)	83.16 ab	21.72 ab	134.50	234.14	3.45 ab
N_3(110:50:0)	78.71 c	21.46 b	147.08	228.69	3.08 bc
N_4(110:50:75)	81.24 abc	21.61 ab	141.33	228.69	3.31 abc
N_5(110:80:75)	82.06 abc	21.67 ab	136.67	245.14	3.31 abc
N_6(110:50:110)	83.93 a	21.97 a	152.58	223.24	3.51 a
V	**	**	**	**	**
N	*	*	ns	ns	**
VxN	**	**	ns	ns	ns

Mean values followed by a different letter are significantly different at Tukey's test ($P \leq 0.05$). ** = significant difference at $P \leq 0.01$, * = significant difference at $P \leq 0.05$, ns = not significant difference at $P > 0.05$

Number of panicles per m^2

The local variety, Hnan Gar produced the lowest number of panicles per m^2, which was significantly different from Swarna-Sub1, Bio-6 and Bio-8 ($P < 0.001$). The highest number of panicles per m^2 was observed in Swarna-Sub1, followed by Bio-8, and Bio-6. The effect of different fertilizer application rates on the number of panicles was not significantly different among the treatments.

1000-grain weight

Genotype Bio-6 produced the heaviest thousand-grain weight among the varieties tested ($P < 0.001$). Hnan Gar, Bio-8 and Swarna-Sub1 had similar thousand-grain weights. In the case of the effect of the fertilizer application rate, N_6 produced the heaviest seeds and the difference from other potassium omitting treatments (N_1 and N_3) was significant $P < 0.05$). There were no significant differences in seed weight among treatments N_1, N_2, N_4 and N_5. The interaction effect of fertilizer application and variety produced significant differences, showing that the Bio-8 and Hnan Gar varieties were more responsive and produced heavier grain under the N_6 treatment.

Filled grain percentage

The highest filled grain % was observed in Swarna-Sub1 which was not significantly different from that of Bio-8. On the other hand, the Bio-6 genotype showed the lowest filled grain percentage after submergence ($P < 0.001$). In the case of the fertilizer effect, N_6 produced significantly higher filled grain percentage than those of the potassium

http://www.aloki.hu ● ISSN 1589 1623 (Print) ● ISSN 1785 0037 (Online)
DOI: http://dx.doi.org/10.15666/aeer/1706_1564315655

omitting treatments (N_1 and N_3; $P < 0.05$). The filled grain percentages for the N_2, N_4 and N_5 treatments were not significantly different.

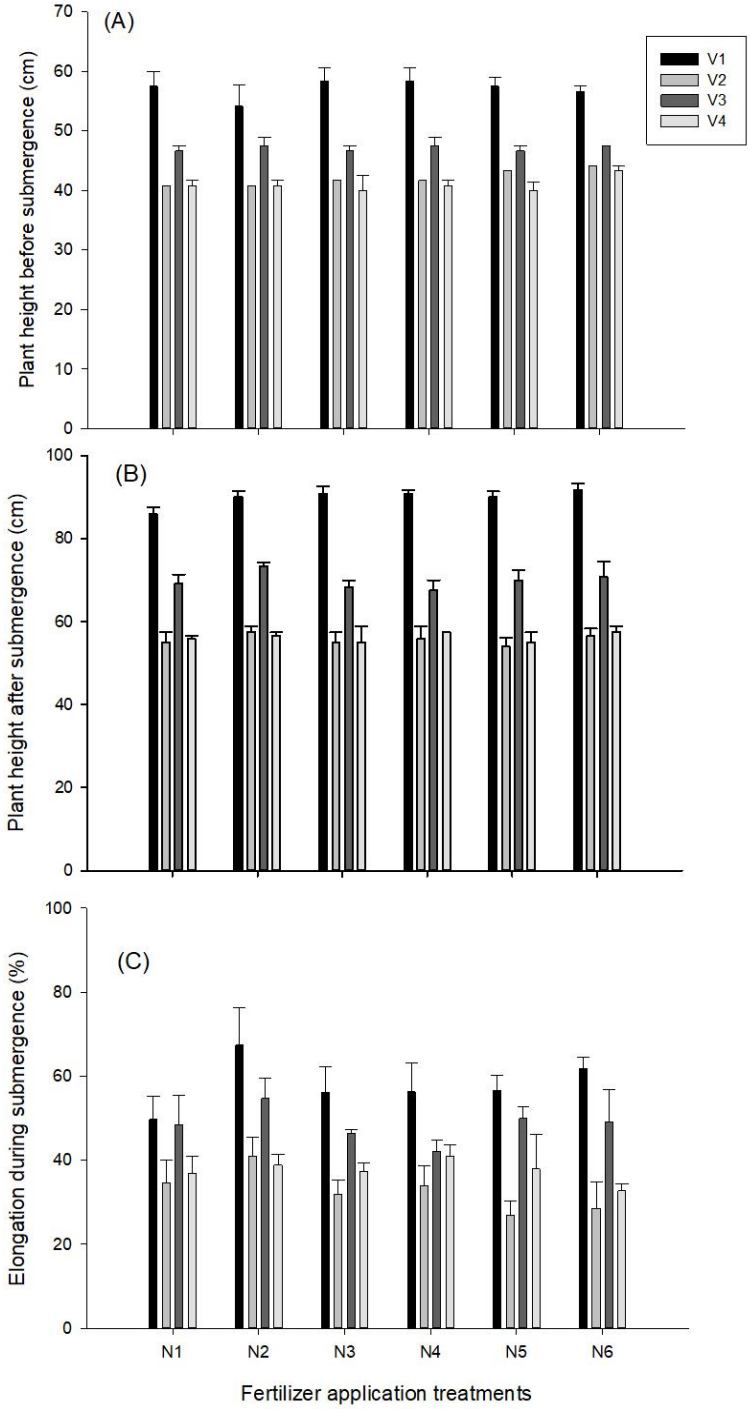

Figure 4. *Responses of combination of nutrient application rates and varieties to plant height (A) before submergence (B) after submergence and (C) elongation percentage during submergence. Data are means ± standard error (SE). Error bars indicate SE. V_1 = Hnan Gar, V_2 = Swarna-Sub1, V_3 = Bio-6, V_4 = Bio-8. N_1 = control, N_2 = 110:0:75, N_3 = 110:50:0, N_4 = 110:50:75, N_5 = 110:80:75, N_6 = 110:50:110; N:P_2O_5:K_2O kg ha^{-1})*

http://www.aloki.hu ● ISSN 1589 1623 (Print) ● ISSN 1785 0037 (Online)
DOI: http://dx.doi.org/10.15666/aeer/1706_1564315655

Grain yield (t ha^{-1})

The grain yield was higher in Swarna-Sub1 (4.22 t ha^{-1}) and Bio-8 (4.27 t ha^{-1}) than those of Bio-6 and Hnan Gar (2.20 and 2.35 t ha^{-1}, respectively; $P < 0.001$) which were almost half those of the two higher yielding varieties. The maximum grain yield was observed in the N_6 fertilizer treatment, followed by the N_2, N_5 and N_4 treatments. N_3 There were no significant differences in grain yield among the control (N_1) and N_3, N_4 and N_5 treatments. The interaction effect of fertilizer application and variety was not significantly different.

Discussion

The soil test results before the experiment revealed an acid soil with low to moderate content of nitrogen, phosphorus and potassium, suggesting that the optimal application of nutrients could increase performance and yield of the rice plants (*Table 1*). Flash flood or submergence of rice frequently occurs in monsoon rice production and adversely affects crop establishment and grain yield. In combination with varietal development, submergence tolerance of rice could be manipulated through crop management practices (Sarkar et al., 2014). In the present study, the local variety, Hnan Gar and other three varieties: Swarna-Sub1, Bio-8 and Bio-6 were tested to depict their tolerance capacity of inundation under natural condition.

There were no significant differences observed in the plant survival percentages among the different genotypes under varying fertilizer application rates. Minimizing shoot elongation during complete submergence is a desirable characteristic of rice plants, which can save energy for the regeneration of plant growth after the recession of flood water (Bailey-Serres et al., 2010). On the other hand, varieties which produce greater shoot elongation under flooding have poorer ability to recover quickly after inundation (Jackson and Ram, 2003). In this study, Swarna-Sub1 and Bio-8 exhibited lower shoot elongation percentages in comparison with a local variety, demonstrating a quiescence strategy (*Fig. 4*). However, no significant differences in shoot elongation percentages were observed based on the different nutrient application treatments. In a previous study, applying post-submergence N and basal P was found to decrease the extent of shoot elongation and increase plant survival while the application of N, 2 days prior to submergence increased elongation (Gautam et al., 2014b).

Local variety was the tallest among the tested varieties. The response of plant height to fertilizer application was occurred only between the fertilizers applied treatments and no applied one. Regarding with crop duration, submergence tolerant variety that has shorter days to maturity is a desirable character for increasing cropping intensity in rainfed lowland areas (Iftekharuddaula et al., 2016). In the present study, Bio-6 variety can be harvested about one month earlier than Swarna-Sub1 and Bio-8, while the crop duration of Bio-6 was about 45 days shorter than that of local variety (*Table 3*).

The differential performance of cultivars regarding with yield and yield components was observed in this study (*Table 4*). The grain yields of the Swarna-Sub1 and Bio-8 varieties were close to double those of the Bio-6 and Hnan Gar varieties and this resulted from their higher filled grain percentage and grain number per panicle following exposure to inundation. It was observed that Swarna-Sub1 and Bio-8 recovered quickly after the recession of the flood water and they also demonstrated higher tillering capacity even after being submerged for 20 days starting from 7 days after transplanting. The early-developed tillers resulted in a higher filled grain

http://www.aloki.hu ● ISSN 1589 1623 (Print) ● ISSN 1785 0037 (Online)
DOI: http://dx.doi.org/10.15666/aeer/1706_1564315655

percentage. According to Gribaldi et al. (2017), submergence-tolerant rice not only survives but also grows quickly after submergence. On the other hand, genotypes without *SUB1* have revealed a delay in tiller emergence during the recovery period (Singh et al., 2014).

Appropriate crop and nutrient management increased the grain yield of rice under stagnant flooded condition (Sarangi et al., 2015). In the current experiment, applying fertilizer at the rate of 110:50:110, $N{:}P_2O_5{:}K_2O$ (kg ha^{-1}) produced a higher filled grain percentage and 1000-grain weight leading to a higher grain yield. Similar finding was occurred in the report of Bhowmick et al. (2014), in which, higher seed setting rate contributed to higher grain yield of submergence rice. In addition, filled grain percentage was affected by increase water depth and flooding duration (Zhang et al., 2015). In the present study, the treatments in which no potassium was applied (N_1 and N_3) adversely affected the yield and its components. This result was supported by the finding of Gautam et al. (2016) which stated that adding sufficient K can alleviate the impairment of rice due to submergence stress. Potassium has been found to be involved in many abiotic stress toleration processes and contributes to sustainable crop growth, yield and quality, and also influences plant health and reduces environmental risks (Wang et al., 2013). Potassium was sensitive to water logged condition and it affect negatively to the plant growth in flood-prone area. Application of higher dose of potassium to the rice field increased the survival of rice after submergence (Dwivedi et al., 2017). Furthermore, in a previous study, the basal application of P enhanced for the development of effective tillers (Gautam et al., 2015). Therefore, application of proper nutrient management helps in alleviation of damage caused by submergence.

Conclusions

Higher grain yield was produced by the Swarna-Sub1 and Bio-8 varieties after 20 days of natural flooding, showing their better performance and yield potential. In addition, application of fertilizer at the optimal rate of 110:50:110, $N{:}P_2O_5{:}K_2O$ kg ha^{-1} aided the plants' ability to recover quickly from inundation. The results of this study will be useful in mitigating the adverse effects of inundation on rice grown on low land during the rainy season and increase the potential of submergence-tolerant rice varieties.

It can be concluded that Bio-6 variety can be a good candidate in term of crop duration for promoting cropping intensity while Swarna-Sub1 and Bio-8 varieties are good for offering higher grain output toward global food security. Further studies in different location and rainfall conditions and more seasons of study might be needed.

Acknowledgements. This project was financially supported by Interdisciplinary Graduate School of Energy System (IGS-Energy) scholarship, Faculty of Environmental Management and Graduate School of Prince of Songkla University (PSU). Authors would like to thank to for Michael Guy Currie for English proof. Ms. Than would like to give sincere thanks to the Department of Agriculture, Myanmar for their permission to conduct the experiment and providing for the seed.

REFERENCES

[1] Atapattu, A. J., Prasantha, B. D. R., Amaratunga, K. S. P., Marambe, B. (2018): Increased rate of potassium fertilizer at the time of heading enhances the quality of direct seeded

http://www.aloki.hu ● ISSN 1589 1623 (Print) ● ISSN 1785 0037 (Online)
DOI: http://dx.doi.org/10.15666/aeer/1706_1564315655

rice. – Chemical and Biological Technologies in Agriculture 5. DOI: 10.1186/s40538-018-0136-x.

[2] Bailey-Serres, J., Fukao, T., Ronald, P., Ismail, A., Heuer, S., Mackill, D. (2010): Submergence tolerant rice: *SUB1*'s journey from landrace to modern cultivar. – Rice 31: 138-147.

[3] Bhowmick, M. K., Dhara, M. C., Singh, S., Dar, M. H., Singh, U. S. (2014): Improved management options for submergence-tolerance (sub1) rice genotype in flood-prone rainfed lowlands of West Bengal. – American Journal of Plant Sciences 5: 14-23.

[4] Bui, L. T., Ella, E. S., Dionisio-Sese, M. L., Ismail, A. M. (2019): Morpho-physiological changes in roots of rice seedling upon submergence. – Rice Science 26: 167-177.

[5] Das, K. K., Sarkar, R. K., Ismail, A. M. (2005): Elongation ability and non-structural carbohydrate levels in relation to submergence tolerance in rice. – Plant Science 168: 131-136.

[6] Das, K. K., Panda D., Sarkar, R. K., Reddy, J. N., Ismail, A. M. (2009): Submergence tolerance in relation to variable floodwater conditions in rice. – Environmental and Experimental Botany 66: 425-434.

[7] Dwivedi, S. K., Kumar, S., Bhakta, N., Singh, S. K., Rao, K. K., Mishra, J. S., Singh, A. K. (2017): Improvement of submergence tolerance in rice through efficient applicaton of potassium under submergence-prone rainfed ecology of Indo-Gangetic Plain. – Functional Plant Biology 44: 907-916.

[8] Dwivedi, S. K., Kumar, S., Bhakta, N., Srivastava, A. K., Mishra, J. S., Kumar, V., Kumara, B. H., Bhatt, B. P., Singh, S. (2018): Physiological mechanism and nutriment management strategies for flood tolerance in rice grown in lowland flood prone ecosystem. – Journal of Crop Science and Biotechnology 21: 321-333.

[9] Ella, E. S., Kawano, N., Yamauchi, Y., Tanaka, K., Ismail, A. M. (2003): Blocking ethylene perception enhances flooding tolerance in rice seedlings. – Functional Plant Biology 30: 813-819.

[10] FAO (2015): The impact of Natural Hazards and Disasters on Agriculture and Food Security and Nutrition. – FAO, Rome.

[11] FAO (2016): Global Information and Early Warning System on Food and Agriculture. – FAO, Rome

[12] FAO/WFP (2016): Special Report by Food and Agriculture Organization of the United Nations, World Food Programmme. – Crop and food security assessment mission to Myanmar. FAO, Rome.

[13] Gautam, P., Nayak, A. K., Lal, B., Bhattacharyya, P., Tripathi, R., Shahid, M., Mohanty, S., Raja, R., Panda, B. B. (2014a): Submergence tolerance in relation to application time of nitrogen and phosphorus in rice (*Oryza sativa* L.). – Environmental and Experimental Botany 99: 159-166.

[14] Gautam, P., Lal, b., Raja, R., Baig, M. J., Haldar, D., Rath, L., Shahid, M., Tripathi, R., Mohanty, S., Bhattacharyya, P., Nayak, A. K. (2014b): Post-flood nitrogen and basal phosphorus management affects survival, metabolic changes and anti-oxidant enzyme activities of submerged rice (Orzo sativa). – Functional Plant Biology 41: 1284-1294.

[15] Gautam, P., Lal, B., Raja, R., Tripathi, R., Shahid, M., Baig, M. J., Puree, C., Mohanty, S., Nayak, A. K. (2015): Effect of simulated flash flooding on rice and its recovery after flooding with nutrient management strategies. – Ecological Engineering 77: 250-256.

[16] Gautam, P., Lal, B., Tripathi, R., Shahid, M., Baig, M. J., Maharana, S., Puree, C., Nayak, A. K. (2016): Beneficial effects of potassium application in improving submergence tolerance of rice (*Oryza sativa* L.). – Environmental and Experimental Botany 128: 18-30.

[17] Gautam, P., Lal, B., Nayak, A. K., Tripathi, R., Shahid, M., Meena, B. P., Singh S., Srivastava, A. K. (2019): Nutient management and submergence-tolerant varieties antecedently enhances the productivity and profitability of rice in flood-prone regions. – Journal of Plant Nutrition 42: 1913-1927.

http://www.aloki.hu ● ISSN 1589 1623 (Print) ● ISSN 1785 0037 (Online)
DOI: http://dx.doi.org/10.15666/aeer/1706_1564315655

[18] Gribaldi, G., Nurlaili, N., Dewi, N., Danial, E., Sakalena, F., Suwignyo, R. A. (2017): Modified application of nitrogen fertilizer for increasing rice variety tolerance toward submergence stress. – International Journal of Agronomy DOI: 10.1155/2017/9734036.

[19] Iftekharuddaula, K. M., Ahmed, H. U., Ghosal, S., Amin, A., Moni, Z. R., Ray, B. P., Barman, H. N., Siddique, M. A., Collard, B. C. Y., Septiningsih, E. M. (2016): Development of early maturing submergence-tolerant rice varieties for Bangladesh. – Field Crops Research 190: 44-53.

[20] Jackson, M. B. (2008): Ethylene-promoted elongation: an adaptation to submergence stress. – Annals of Botany 101: 229-248.

[21] Jackson, M. B., Ram P. C. (2003): Physiological and molecular basis of susceptibility and tolerance of rice plants to complete submergence. – Annals of Botany 91: 227-241.

[22] Liu, G., Li, Y., Fu, X. (2015): Practices to minimize flooding damage to commercial vegetable production. – http://ufdc.ufl.edu/IR00007329/00001.

[23] Nishiuchi, S., Yamauchi, T., Takahashi, H., Kotula, L., Nakazono, M. (2012): Mechanisms for coping with submergence and waterlogging in rice. – Rice 5. DOI: 10.1186/1939-8433-5-2.

[24] Pimratch, S., Butsat, S., Kesmala, T. (2015): Application of blue-green algae and mineral fertilizers to direct seeding lowland rice**.** – Science Asia 41: 305-314.

[25] Pradhan, S. K., Pandit, E., Pawar, S., Baksh, S. Y., Mukherjee, A. K., Mohanty, S. P. (2019): Development of flash-flood tolerant and durable bacterial blight resistant versions of mega rice variety 'Swarna' through marker-assisted backcross breeding. – Scientific Reports 9: 12810.

[26] Ram, P. C., Singh, B. B., Singh, A. K., Ram, P., Singh, P. N., Singh, H. P., Boamfa, I., Harren, F., Santosa, E., Jackson, M. B., Stter, T. L., Reuss, J., Wade, I. J., Singh, V. P., Singh, R. K. (2002): Submergence tolerance in rainfed lowland rice: physiological basis and prospects for cultivar improvement through marker-aided breeding. – Field Crops Research 76: 131-152.

[27] Sarangi, S. K., Maji, B., Singh, S., Sharma, D. K., Burman, D., Singh, U. S., Ismail, A. M., Haefele, S. M. (2015): Using improved variety and management enhances rice productivity in stagnant flood-affected tropical coastal zones. – Field Crops Research 190: 70-81.

[28] Sarkar, R. K., Das K. K., Panda, D., Reddy, J. N., Patnaik, S. S. C., Patra, B. C., Singh, D. P. (2014): Submergence Tolerance in Rice: Biophysical Constraints, Physiological Basis and Identification of Donors. – Central Rice Research Institute (Indian Council of Agricultural Research), Cuttack.

[29] Sasidharan, R., Bailey-Serres, J., Ashikari, M., Atwell, B. J., Colmer, T. D., Fagerstedt, K., Fukao, T., Geigenberger, P., Hebelstrup, K. H., Hill, R. D., Holdsworth, M. J., Ismail, A. M., Licausi, F., Mustroph, A., Nakazono, M., Pedersen, O., Perata, P., Sauter, M., Shih, M-C., Sorrell, B. K., Striker, G. G., Dongen, J. T. V., Whelan, J., Xiao, S., Visser, E. J. W., Voesenek, L. A. C. J. (2017): Community recommendations on terminology and procedures used in flooding and low oxygen stress research. – New Phytologist 214: 1403-1407.

[30] Singh, S., Mackil, D. J., Ismail, A. M. (2014): Physiological basis of tolerance to complete submergence in rice involves genetic factors in addition to the *SUB1* gene. – AoB Plants 6: plu060. DOI: 10.1093/aobpla/plu060.

[31] Soni, P., Soe, M. N. (2016): Energy balance and energy economic analyses of rice production system in Ayeyarwaddy Region of Myanmar. – Energy Efficiency 9: 223-237.

[32] Wang, M., Zheng, Q., Shen, Q., Guo, S**.** (2013**):** The critical role of potassium in plant stress response**.** – International Journal of Molecular Sciences 14*:* 7370-7390.

[33] Ye, X. Q., Zeng, B., Meng, J. L., Wu, M., Zhang, X. P. (2018a): Responses in shoot elongation, carbohydrate utilization and growth recovery of an invasive species to submergence at different water temperatures. – Scientific Reports 8: 306.

http://www.aloki.hu ● ISSN 1589 1623 (Print) ● ISSN 1785 0037 (Online)
DOI: http://dx.doi.org/10.15666/aeer/1706_1564315655

[34] Ye, X. Q., Meng, J. L., Zeng, B., Wu, M. (2018b): Improved flooding tolerance and carbohydrate status of flood-tolerant plant *Arundinella anomala* at lower water temperature. – PloS One 13. https://doi.org/10.1371/journal.pone.0192608.
[35] Yin, C-C., Zhao, H., Ma, B., Chen, S-Y., Zhang, J-S. (2017): Diverse roles of ethylene in regulating agronomic traits in rice. – Frontiers in Plant Science 8: 1676.
[36] Zhang, Y., Wang, Z., Li, L., Zhou, Q., Xiao, Y., Wei, X., Zhou, M. (2015): Short-term complete submergence of rice at the tillering stage increases yield. – PLoS One. DOI: 10.1371/journal.pone.0127982.

APPENDIX

Appendix 1. *Submergence condition of experimental field after heavy rain*

Appendix 2. *Experimental field showing different in plant height and maturity time among the treatments*

http://www.aloki.hu ● ISSN 1589 1623 (Print) ● ISSN 1785 0037 (Online)
DOI: http://dx.doi.org/10.15666/aeer/1706_1564315655

RESTORATION OF AQUATIC PLANTS AFTER EXTREME FLOODING AND DROUGHT: A CASE STUDY FROM POYANG LAKE NATIONAL NATURE RESERVE

ZHANG, X. K.[1,2] – LIU, X. Q.[1*] – YANG, Z. D.[1] – WANG, H. Z.[1]

[1]*Institute of Hydrobiology, Chinese Academy of Sciences, Wuhan 430072, China*

[2]*Research Center of Aquatic Organism Conservation and Water Ecosystem Restoration in University of Anhui Province, Anqing Normal University, Anqing 246133, China*

[*]*Corresponding author*
e-mail: xqliu@ihb.ac.cn

(Received 21st Aug 2019; accepted 31st Oct 2019)

Abstract. Poyang Lake is the largest freshwater lake in China. Extreme flooding and drought occurred in 1998 and 2011, respectively, resulting in a massive loss of aquatic plants. To compare the effects of flooding and drought on aquatic plants and the subsequent recovery process, field investigations were conducted in Poyang Lake National Nature Reserve (PLN) in 2012 and 2014. Historical data from 1984, 1999, and 2001 were also used for comparison. The results revealed that the species composition of aquatic plants after extreme flooding differed from that after extreme drought. After flooding, the species composition was basically the same as the historical records from 1984 under normal hydrological conditions; however, after drought, *Najas marina* and *N. minor* disappeared. Moreover, the resilience ability of aquatic plants was higher after extreme flooding than following extreme drought. The dominant species also differed after the two hydrological events. *Vallisneria* spp. and *Hydrilla verticillata* were first to recover after flooding, while *Vallisneria* spp. and *Nymphoides peltata* recovered fastest after drought. Since extreme drought is more damaging to aquatic vegetation than extreme flooding, we suggest that lakes in the Yangtze River basin aim to maintain a minimum water level through rational regulation of water resources.
Keywords: *macrophytes, extreme hydrological events, ecological restoration, resilience ability, regulation*

Introduction

Natural interference is an essential component of most intact ecosystems (Lytle and Poff, 2004). Flooding and drought, as the main disturbances affecting freshwater ecosystems, play important roles in regulating aquatic plant diversity and population size across a range of spatial and temporal scales (Jentsch et al., 2007; Lake, 2007). Under natural conditions, aquatic plants have adapted to periodic flooding and drought through morphological or life-history strategical changes (Lytle and Poff, 2004). However, anthropogenic disturbances (such as overuse of water resources, and building of sluices and dams) and climate change are severely affecting the periodic rhythms of flooding and drought, increasing the occurrence frequency and magnitude in many freshwater ecosystems (Meehl et al., 2007; Miao et al., 2009). Non-periodic high-intensity extreme hydrological events can severely destroy the ecosystem structure of wetland environments, altering the natural habitat conditions required by aquatic plants (Li et al., 2004; Lake, 2007). However, studies on aquatic plants in freshwater lakes tend to focus on the effects of water depth, rates of water level change, fluctuation amplitude, and fluctuation duration, with little known about the impact of extreme hydrological events such as flooding and drought, and subsequent restoration and succession.

http://www.aloki.hu ● ISSN 1589 1623 (Print) ● ISSN 1785 0037 (Online)
DOI: http://dx.doi.org/10.15666/aeer/1706_1565715668

Poyang Lake (N: 28°22′-29°45′, E: 115°47′-116°45′) is the largest freshwater lake in China, located on the south bank of the Yangtze River in Jiangxi Province. It is an internationally important wetland, and one of three river-connected lakes in the middle and lower Yangtze River. Poyang Lake mainly collects water from five rivers, the Ganjiang, Xiushui, Raohe, Fuhe and Xinjiang River, flowing into the Yangtze River in Hukou County (*Figure 1*). In the flooding season, when the water level in the Yangtze River is higher than that of Poyang Lake, water flows back into the lake. The perennial average water level of Poyang Lake is 12.86 m above mean sea level (amsl), but the annual variation can exceed 10 m (Li et al., 2008). The surface area also differs significantly between flooding and drought periods, from 2933 km^2 at a flood water level of 21.69 m amsl to only 146 km^2 at a water level of 10.20 m amsl (Wang and Dou, 1998). Because of this unique hydrological rhythm, Poyang Lake consists of diverse habitats with high species diversity, and enormous ecological and service functions. However, due to the impact of climate change and the Three Gorges Reservoir, extreme hydrological events have occurred frequently during the past few decades (Xu et al., 2014), the most serious of which were the extreme floods of 1998 and extreme drought of 2011.

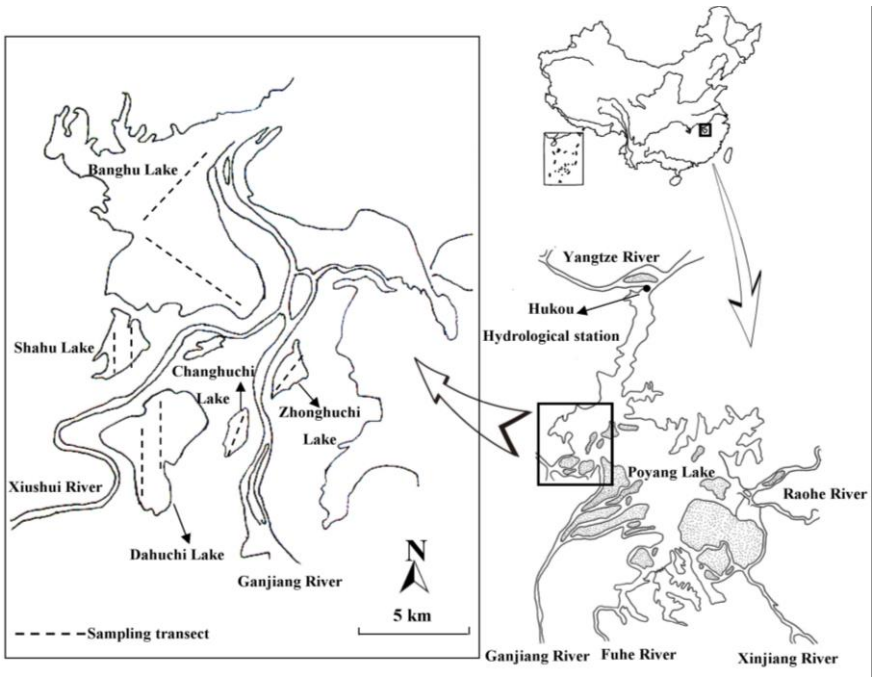

Figure 1. *Sampling transects in PLN*

Poyang Lake National Nature Reserve (PLN) is located northwest of Poyang Lake, and is mainly composed of sub-lakes with differing mean lake bottom elevations. In this study, we selected five sub-lakes (*Figure 1*) in PLN and, combined with historical data, determined the following: 1) The difference in community structure and resilience ability of aquatic plants in PLN following extreme flooding and extreme drought; and 2) Differences in the resilience ability of aquatic plants in the five sub-lakes with increasing mean lake bottom elevation. Since flooding and drought have differing effects on aquatic plants, the former largely affecting aboveground parts and the latter acting both aboveground and underground, we hypothesized that the community

http://www.aloki.hu ● ISSN 1589 1623 (Print) ● ISSN 1785 0037 (Online)
DOI: http://dx.doi.org/10.15666/aeer/1706_1565715668

structure would also differ after each hydrological event, with greater resilience after flooding. In addition, since under normal circumstances, increasing distribution elevation gradually weakens the impact of flooding, while increasing that of drought, we further hypothesized that aquatic plants in sub-lakes with a higher mean lake bottom elevation would show stronger resilience ability after flooding than drought. The results of this study not only enrich our understanding of extreme hydrological events, but also have significant implications for the restoration of aquatic plants in other lakes with similar situations.

Materials and methods

Research area

PLN (N: 28°22′-29°45′, E: 115°47′-116°45′) was established in 1983 and listed in the International List of Wetlands in 1992, forming the main habitat for a number of rare animals and plants (Ji et al., 2007). It has a subtropical monsoon climate with an average annual temperature of 17.1°C and average annual rainfall of 1426.4 mm. The protected area of PLN covers 224 km^2, and is mainly composed of nine sub-lakes with differing mean lake bottom elevations (*Figure 1*, *Table 1*). When the water level in the main area of Poyang Lake is higher than 16.0 m amsl, all these sub-lakes merge into Poyang; however, when the water level is less than 12.92 m amsl, these sub-lakes gradually emerge and become independent lakes (Li et al., 2004).

Table 1. *Area, bottom elevation and sampling transects in the five sub-lakes in PLN. Bottom elevation data was obtained from Lu and Cheng (2003). All other data were from Zhang (2013)*

Item	Banghu	Zhonghuchi	Changhuchi	Dahuchi	Shahu
Area (km^2)	73	6	7	30	14
Maximum length (km)	10.08	3.84	3.70	7.43	4.46
Maximum width (km)	8.04	1.82	2.22	4.36	3.48
Mean water depth (m)	0.46	1.07	0.50	0.70	0.45
Bottom elevation (m)	12.6	13.5	14.5	14.7	15.1
Total nitrogen content of the substrate (mg/g)	0.68	1.08	1.17	0.68	1.33
Total phosphorus content of the substrate (mg/g)	0.68	0.66	0.74	0.62	0.92
Organic matter content of the substrate (%)	20.88	28.93	28.94	19.88	33.93
Number of sampling transects (sites)	2 (12)	1 (10)	1 (4)	2 (11)	2 (11)

In 1998 and 2011, Poyang Lake experienced the most serious flooding (Min et al., 2006) and drought (Li et al., 2019) events in nearly 60 years, respectively (*Figure 2*). In the summer of 1998, the water level of Poyang Lake reached a maximum of 22.54 m, and remained higher than warning level for 58 consecutive days. Following this extreme hydrological event, almost all aquatic plants in the nine sub-lakes were reported extinct (Li et al., 2004). Subsequently, in the spring of 2011, Poyang Lake remained at a consistently low level, causing all nine sub-lakes (except Banghu Lake) to dry up, seriously damaging the aquatic plant populations.

http://www.aloki.hu ● ISSN 1589 1623 (Print) ● ISSN 1785 0037 (Online)
DOI: http://dx.doi.org/10.15666/aeer/1706_1565715668

Sampling method and data analyses

In July 2012 and June 2014, following the extreme drought of 2011, analysis of the aquatic vegetation in five sub-lakes was carried out; namely, Banghu, Dahuchi, Zhonghuchi, Changhuchi and Shahu lakes. According to differences in lake area (*Table 1*), 1-2 sampling transects were set in each sub-lake, and in each sampling transect, 4-10 sampling sites were established (*Figure 1*). Aquatic plant populations were quantitatively sampled using a scythe three times in each site. Samples were then cleaned and superfluous water removed before weighing using an electronic balance to determine wet biomass. In this study, aquatic plants only included submerged and floating macrophytes, not hygrophytes and emergent macrophytes.

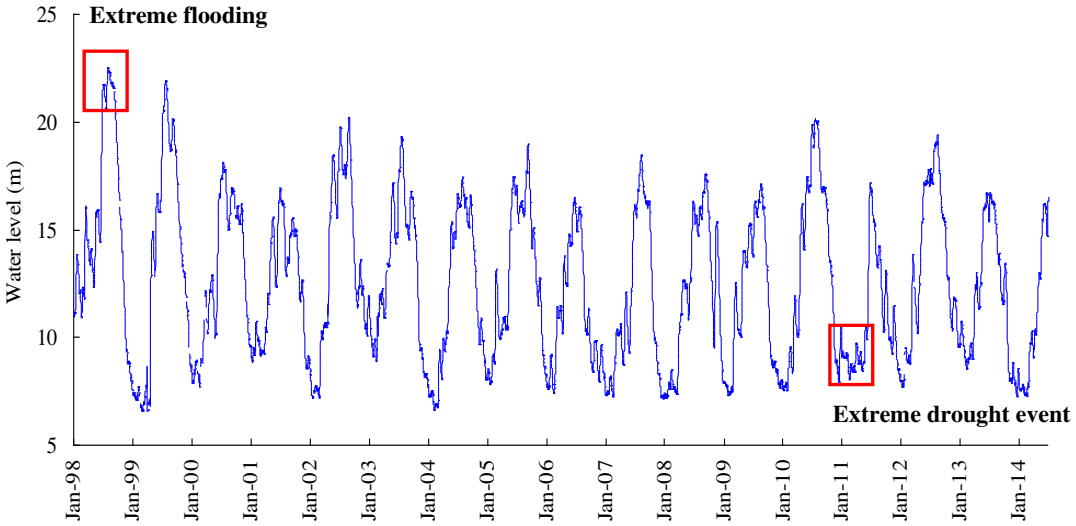

Figure 2. *Water level fluctuations in Poyang Lake from 1998 to 2014*

Hydrological data for 1998 to 2014 were obtained from Hukou Hydrological Station of Poyang Lake and from the Hubei Province Water and Rain Information Inquiry System (http://219.140.162.169:8800/rw4/report/fa02.asp). Aquatic vegetation data for PLN in 1984 (normal hydrological year), 1999 and 2001 (after flooding), and 2012 and 2014 (after drought) were used for comparative analyses. Data for 1984 were obtained from Guan et al. (1987) and, since the scope of his investigation covered entire Poyang Lake, were corrected to represent PLN area. Data for 1999 and 2001 were derived from Li et al. (2004), and corrected by removing the hygrophyte and emergent plant data. All the five field investigations were conducted during summer to early autumn, and the sampling methods were similar. Therefore, the results of different investigations are comparable and can reflect the actual situation of aquatic plants in PLN in different periods. One-way analysis of variance (ANOVA) was used to analyze the difference of species number and biomass among 1999, 2001, 2012, and 2014. Before conducting the ANOVA, the normality and homogeneity of the variances were tested, and transformed if necessary to meet the assumption of ANOVA. Post-hoc multiple comparisons were conducted to examine the differences between groups using Tukey's HSD (Honestly Significant Difference) multiple comparisions. Due to the lack of occurrence frequency data for each aquatic plant in PLN at different times, this study used relative biomass to

http://www.aloki.hu ● ISSN 1589 1623 (Print) ● ISSN 1785 0037 (Online)
DOI: http://dx.doi.org/10.15666/aeer/1706_1565715668

calculate the dominance of each species. The resilience ability of each aquatic plant in different years following each extreme hydrological event was determined using the following formula (*Eq.1*):

$$R_i = \frac{B_i}{B_h} \times \frac{N_i}{N_h} \quad \text{(Eq.1)}$$

where R_i indicates the resilience ability in the i-th year, B_i indicates the aquatic plant biomass in the *i*-th year, B_h indicates historical data of aquatic plant biomass in a normal hydrological year, N_i indicates the species number of aquatic plants in the *i*-th year, and N_h indicates historical data of species number in a normal hydrological year. Both B_h and N_h values in this study represent historical data from 1984. All data analyses were carried out using SPSS version 13.0.

Results

Species composition

In 2012 and 2014, the species composition in PNL was the same, with eight genera and eight species (*Table 2*). However, in 2012, all species, except *Vallisneria* spp. were only sporadically found. Meanwhile, in 2014, the occurrence frequency of *Nymphoides peltata* and *Trapa* spp. markedly increased. Compared to the normal hydrological year of 1984 (*Table 2*), the species composition was notably different after the droughts of 2012 and 2014, with the disappearance of *Najas marina* and *N. minor*, and emergence of *Charaphyte*. Meanwhile, the species composition following the flood in 2001 was basically the same as that in 1984, with the emergence of only one species, *Charaphyte*.

Table 2. *Species composition and biomass (g/m^2) in PLN*

Species	1984	1999	2001	2012	2014
Charaphyte		0.1	43.9	0.1	0.2
Vallisneria spp.	840.3	159.8	944.5	58.9	100.8
Hydrilla verticillata	514.7	139.3	742.7	8.4	38.6
Potamogeton malaianus	796.3	0.5	25.26	2.4	2.3
Potamogeton pectinatus		8.2			
Najas minor	119.7	0.1	12.4		
Najas marina	11.3		1.0		
Nymphoides peltata	134.7	1.0	0.7	39.5	119.8
Trapa spp.	93	18.0	31.7	9.3	100.1
Ceratophyllum demersum	307.7		0.8	0.8	34.8
Myriophyllum pectinatus	84.3		34.8	0.1	2.5

In 1999, after the flood in 1998, the number of aquatic plant species in Banghu, Zhonghuchi, Changhuchi, Dahuchi and Shahu lakes was 3, 5, 3, 3 and 4, respectively (*Figure 3*). In 2001, the species number in all sub-lakes, except Zhonghuchi, and the entire PLN region increased significantly. In 2012, after the drought of 2011, the number of aquatic plant species in the five sub-lakes was 7, 1, 3, 2 and 3, respectively.

http://www.aloki.hu ● ISSN 1589 1623 (Print) ● ISSN 1785 0037 (Online)
DOI: http://dx.doi.org/10.15666/aeer/1706_1565715668

Meanwhile, in 2014, an obvious increase in species number was observed in Zhonghuchi, Changhuchi, and Shahuchi Lakes only (*Figure 3*). However, ANOVA analysis showed that the species number did not have significant difference among the four years ($F = 1.327$, $P = 0.300$).

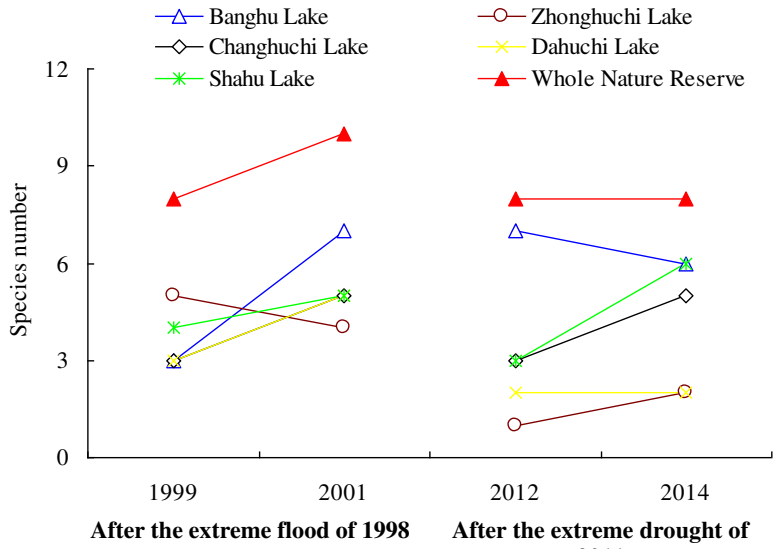

Figure 3. *Changes in species numbers after extreme flooding (1998) and drought (2011) in five sub-lakes in PLN*

Biomass

The biomass of aquatic plants in PLN was low in 1999 and 2012 at 327 and 120 g/m^2, respectively, while in 2001 and 2014, biomass was restored to 1838 and 391 g/m^2, respectively, although both values were obviously lower than that in 1984 (2902 g/m^2) (*Figure 4*). ANOVA analysis indicated that the biomass has significant difference among the four years ($F = 8.545$, $P = 0.001$), and the biomass in 2001 was significantly higher than in the other three years. Of the five sub-lakes, Banghu and Zhonghuchi lakes recovered fastest after flooding, reaching a biomass of 2454 and 2534 g/m^2 in 2001, respectively. In 2014, following drought, the biomass of aquatic plants in each sub-lake was low, with a maximum value of 782 g/m^2 in Zhonghuchi Lake (*Figure 5*).

Vallisneria spp. and *Hydrilla verticillata* recovered fastest after flooding, and in 2001, their biomass exceeded historical levels (*Table 2*). Meanwhile, *Vallisneria* spp. and *Nymphoides peltata* recovered fastest after drought, but their biomass remained lower than historical levels (*Table 2*). *Potomageon malaianus* had the highest historical biomass, but recovered slowly after both drought and flooding, and had a very low biomass.

Dominant species

Differences in the dominant species in PLN were observed between years (*Figure 6*). In 1984, the main dominant species were *Vallisneria* spp. and *P. malaianus*, while in 1999 and 2001 *Vallisneria* spp. and *H. verticillata* were dominant. In 2012, the dominant species were *Vallisneria* spp. and *N. peltata*, while in 2014, *Trapa* spp. as well as *Vallisneria* spp. and *N. peltata* dominated.

http://www.aloki.hu ● ISSN 1589 1623 (Print) ● ISSN 1785 0037 (Online)
DOI: http://dx.doi.org/10.15666/aeer/1706_1565715668

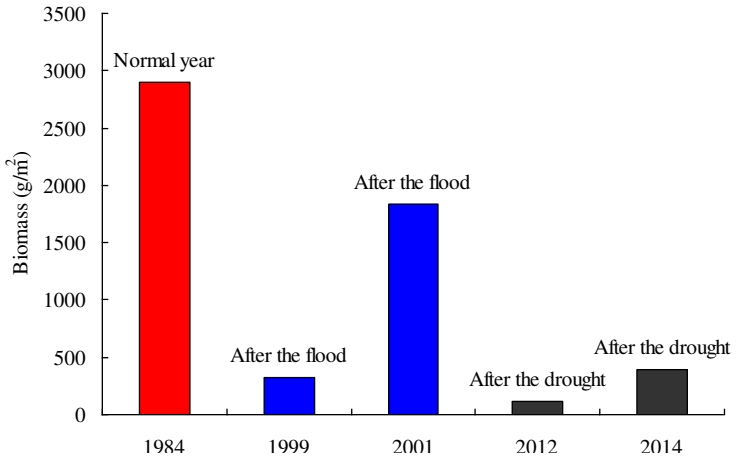

Figure 4. *Comparisons of macrophyte biomass after extreme flooding and drought in PLN*

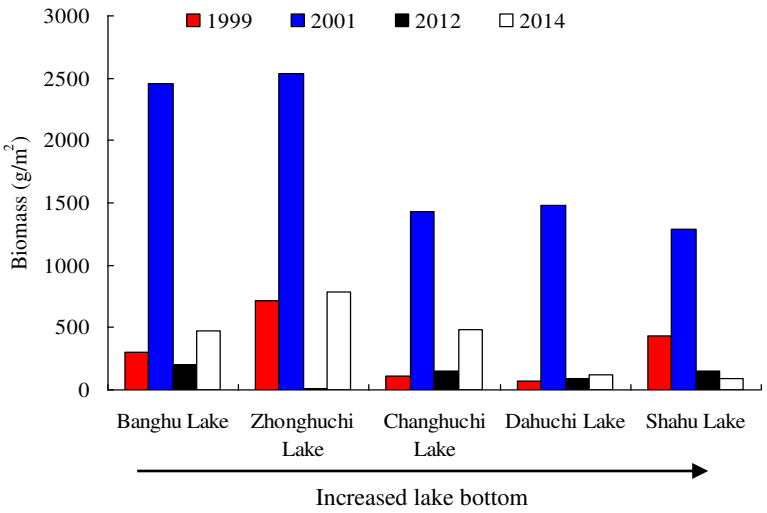

Figure 5. *Comparisons of macrophyte biomass in five sub-lakes in PLN*

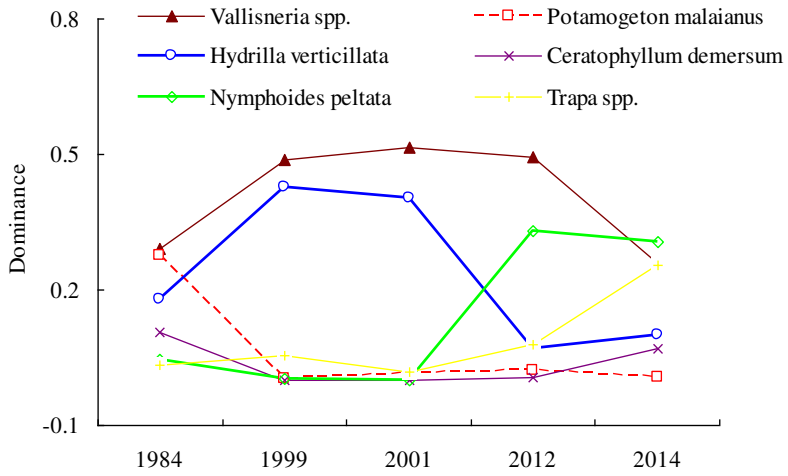

Figure 6. *Changes in the dominance of different species in PLN. Only species with a dominance > 0.1 in one of the five study years are shown*

http://www.aloki.hu ● ISSN 1589 1623 (Print) ● ISSN 1785 0037 (Online)
DOI: http://dx.doi.org/10.15666/aeer/1706_1565715668

Resilience ability

In 1999, 2001, 2012 and 2014, the resilience ability of aquatic plants in PLN was 0.10, 0.70, 0.04 and 0.12, respectively. Aquatic plants apparently showed greater resilience ability after flooding than drought. No obvious differences in resilience ability were observed with increasing bottom elevation of the sub-lakes (*Figure 7*). The largest resilience ability was observed in Zhonghuchi (0.14) and Banghu lakes (0.66) in 1999 and 2001, respectively. Meanwhile, in 2012 and 2014, Banghu Lake showed the largest resilience ability at 0.05 and 0.11, respectively.

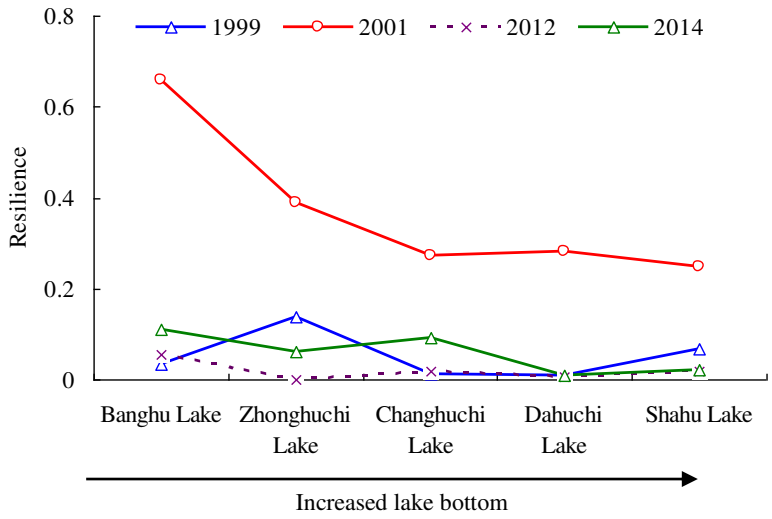

Figure 7. *Resilience ability of aquatic plants in each sub-lake in PLN*

Discussion

The increasing frequency and magnitude of extreme hydrological events are highlighting the negative effects on freshwater ecosystems (Jentsch et al., 2007). The results of this study suggest that drought has a greater impact than flooding on the species composition of aquatic plants. In PLN, the species composition after flooding was basically the same as that in 1984, while after drought, *N. marina* and *N. minor* disappeared. Both species are annuals, germinating in March-April, flowering and fruiting in July and August, and mainly propagated by seed. The aboveground stems are fragile and easily broken in turbulent water (Chen, 1984). Moreover, their roots are largely fibrous, and grow poorly in soil with high viscosity (Handley and Davy, 2005; Hoffmann et al., 2013). The sediment is mainly composed of clay in PLN (Ding et al., 2014), and the water level fluctuations are extremely large. These two species therefore tend to have only limited distribution. Before the summer flood in 1998, a small number of *Najas* plants may have completed flowering and fruiting, thereby supplementing the seed bank, aiding survival after the flood, despite the reduction in biomass. However, following the drought in spring 2011, most *Najas* seedlings were probably killed, preventing replenishment of the seed bank and resulting in extinction.

The changes in species number in the five sub-lakes may also suggest that drought has a more damaging effect on aquatic plants. After the flood in 1999, the species number in all sub-lakes, except Banghu, was higher than after the drought in 2012

http://www.aloki.hu ● ISSN 1589 1623 (Print) ● ISSN 1785 0037 (Online)
DOI: http://dx.doi.org/10.15666/aeer/1706_1565715668

(*Figure 3*). Banghu Lake did not completely dry up during the drought of 2011; therefore, the species number remained high in 2012. Meanwhile, *Charaphyte* emerged after both flooding and drought, although its dominance was very low. Studies in a number of temperate lakes suggest that *Charaphyte* is not only a pioneer species in the restoration of aquatic plants, but one of the main dominant species (Blindow, 1992; van den Berg et al., 1999). These findings suggest that the recovery process of aquatic plants in subtropical lakes is different from that in temperate lakes. Although *Charaphyte* can be a pioneer species under low light conditions, it has no real roots and is easily uprooted by wind and waves (Havens et al., 2004). Thus, since the water level fluctuations are frequent and extreme in PLN, it is thought to be difficult for *Charaphyte* to establish in large numbers.

The results of this study also suggest that the resilience ability of aquatic plants is higher after flooding than drought. The resilience ability was 0.10 and 0.70 in 1999 and 2001, and 0.04 and 0.12 in 2012 and 2014, respectively. This is thought to be related to the differing effects of flooding and drought. Although flooding destroys the aerial parts of aquatic plants, most underground parts remain; however, drought can have adverse effects both aboveground and underground. Nevertheless, compared with 1984 (Guan et al., 1987), the biomass after both events was much lower than the historical level of 2902 g/m^2, suggesting that full recovery is difficult in the short term. However, no obvious differences in the restoration of aquatic plants were observed with increasing mean lake bottom elevation of the five sub-lakes. Although lake bottom elevation can significantly affect infiltration between sub-lakes and adjacent water bodies, the sediment type and distance from adjacent water also play important roles (Van Geest et al., 2005). In general, sub-lakes with sandy sediment and close to the main area of Poyang Lake experience larger water level fluctuations. Moreover, human disturbances, such as fishing during the flooding season, also affect the restoration of aquatic plants in different sub-lakes.

Obvious differences in the recovery rate of different species after flooding and drought were observed. *Vallisneria* spp. and *H. verticillata* were fastest to recover after flooding. Li et al. (2004) suggested that this is largely related to asexual reproduction. That is, although flooding caused the disappearance of aboveground parts, it had little effect on asexual propagules in the lake sediment; therefore, species possessing specialized propagules or underground rhizomes recovered rapidly. Of the nine aquatic plants that existed in the normal hydrological year of 1984, *Vallisneria* spp., *H. verticillata* and *P. malaianus* were not only rich in biomass, but also possess specialized vegetative propagules or underground stems, aiding recovery after flooding. However, in the 1999 and 2001 field surveys, the *P. malaianus* biomass was extremely low after flooding, possibly due to its small population size before flooding (Cui et al., 2000). The first species to recover after drought were *Vallisneria* spp. and *N. peltata*, but the biomass of both species was lower than historical levels. This was possibly due to the effect of drought on underground parts, which is also related to their burial depth. *Vallisneria* spp. and *N. peltata* could therefore be considered pioneer species, with recovery aided by the deep burial depth of their underground parts. In line with this, studies suggest that the burial depth of *Vallisneria* spp. winter buds can reach 30 cm, while that of *P. malaianus* underground stems is only 10 cm (Li et al., 2005). In addition, *N. peltata* is an amphibious species that is more resistant to drought than submerged plants (Brock and Casanova, 1997), providing further advantages for the establishment of its dominant position.

http://www.aloki.hu ● ISSN 1589 1623 (Print) ● ISSN 1785 0037 (Online)
DOI: http://dx.doi.org/10.15666/aeer/1706_1565715668

The analyses of dominant species further suggest that extreme hydrological events also have a significant impact on succession. As part of Poyang Lake, PLN experiences large water level fluctuations, and therefore, the species composition and dominant species are relatively simple. In 1984, the dominant species were *Vallisneria* spp. and *P. malaianus* (Guan et al., 1987), both of which have flexible aboveground parts that allow them to adapt to fluctuating water levels and strong wave disturbances. After flooding, *H. verticillata* replaced *P. malaianus* as one of the main dominant species; however, due to the lower burial depth of its asexual propagules, its dominance status was replaced by *N. peltata*.

The results of this study also suggest that the resilience ability of aquatic plants is higher after flooding than drought. Nevertheless, compared with 1984 (Guan et al., 1987), the biomass after both events was much lower than the historical level of 2902 g/m^2, suggesting that full recovery is difficult in the short term. As one of the most important wetlands in the world, Poyang Lake plays important roles in biodiversity conservation. With the increasing occurrence frequency and magnitude of extreme hydrological events in Poyang Lake basin (Ye et al., 2014), it is therefore necessary to implement effective measures to prevent further degradation of aquatic vegetation. In the future, experiments should be carried out to determine the tolerance thresholds of dominant aquatic plants such as *Vallisneria* spp. and *P. malaianus* in response to drought and flooding to provide a quantitative basis for the recovery of aquatic plants. Besides, compared with flooding, drought had more destructive effects; however, it is relatively easier to control. Strengthening the regulation of water resources should be considered to reduce the adverse effects of drought on dominant aquatic plants (such as *Vallisneria* spp.). At present, there are a number of small water conservation projects in the Poyang Lake basin, with plans to build Poyang Lake dam in the foreseeable future, which will further help regulate water levels in PLN. This study also suggests that aquatic plants are generally slow to recover after extreme hydrological events, highlighting the need for artificial methods aimed at supplementing seed banks or propagules to promote recovery.

Conclusion

The species composition and subsequent recovery process of lake plants after extreme flooding and drought are obviously different in the PLN. In general, extreme drought is more damaging to lake plants than extreme flooding. Therefore, the lakes should maintain a minimum water level in dry year through rational regulation of water resources to prevent the degradation of lake plants. Besides, the resilience ability of aquatic plants was higher after extreme flooding than following extreme drought; however, artificial methods aimed at supplementing seed banks or propagules are also needed to promote the recovery of aquatic plants in a short time. Finally, it is highly recommened that future researches carry out more studies to determine the tolerance thresholds of dominant aquatic plants (such as *Vallisneria* spp. and *P. Malaianus* in this study) in response to drought and flooding, thus providing a quantitative basis for the recovery of aquatic plants.

Acknowledgements. This work was supported by the National Natural Science Foundation of China (grant numbers 41501028, 51579234, and 41371054).

http://www.aloki.hu ● ISSN 1589 1623 (Print) ● ISSN 1785 0037 (Online)
DOI: http://dx.doi.org/10.15666/aeer/1706_1565715668

REFERENCES

[1] Blindow, I. (1992): Long and short term dynamics of submerged macrophytes in two shallow lakes. – Freshwater Biology 28: 15-27.
[2] Brock, M. A., Casanova, M. T. (1997): Plant Life at the Edge of Wetlands: Ecological Responses to Wetting and Drying Patterns. – In: Klomp, N., Lunt, I. (eds.) Frontiers in Ecology: Building the Links. Elsevier, Oxford.
[3] Chen, H. D. (1984): Study on *Najas major* All. community of Lake Donghu, Wuhan. – Acta Hydrobiologica Sinica 8: 331-340.
[4] Cui, X. H., Zhong, Y., Li, W., Chen, J. K. (2000): The effect of catastrophic flood on biomass and density of three dominant aquatic plant species in the Poyang Lake. – Acta Hydrobiologica Sinica 24: 322-325.
[5] Ding, Q. Z., Liu, X. Q., Zhang, X. K. (2014): Impacts of water level fluctuations on substrate environments of lakeshore zone of the lakes in the middle and lower reaches of the Yangtze River. – Journal of Lake Science 26: 340-348.
[6] Guan, S. F., Lang, Q., Zhang, B. (1987): Biomass of macrophytes of the Poyang Lake with suggestions of its rational exploitation. – Acta Hydrobiologica Sinica 11: 219-227.
[7] Handley, R. J., Davy, A. (2005): Temperature effects on seed maturity and dormancy cycles in an aquatic annual, *Najas marina*, at the edge of its range. – Journal of Ecology 93: 1185-1193.
[8] Havens, K. E., Sharfstein, B., Brady, M. A., East, T. L., Harwell, M. C., Maki, R. P., Rodusky, A. J. (2004): Recovery of submerged plants from high water stress in a large subtropical lake in Florida, USA. – Aquatic Botany 78: 67-82.
[9] Hoffmann, M., Sacher, M., Lehner, S., Raeder, U., Melzer, A. (2013): Influence of sediment on the growth of the invasive macrophyte *Najas marina* ssp. *intermedia* in lakes. – Limnologica 43: 265-271.
[10] Jentsch, A., Kreyling, J., Berierkuhnlein, C. (2007): A new generation of climate change experiments: events, not trends. – Frontiers in Ecology and the Environment 5: 315-324.
[11] Ji, W., Zeng, N., Wang, Y., Gong, P., Xu, B., Bao, S. (2007): Analysis on the waterbirds community survey of Poyang Lake in winter. – Geographic Information Sciences 13: 51-64.
[12] Lake, P. S. (2007): Flow-generated Disturbances and Ecological Responses: Floods and Droughts. – In: Wood, P. J., Hannah, D. M., Sadler, J. P. (eds.) Hydroecology and Ecohydrology: Past, Present and Future. John Wiley & Sons Ltd, Chichester.
[13] Li, W., Liu, G. H., Xiong, B. H., Pu, Y. H. (2004): The restoration of aquatic vegetation in lakes of Poyang Lake Nature Reserve after catastrophic flooding in 1998. – Journal of Wuhan Botanical Research 22: 301-306.
[14] Li, W., Cheng, Y., Liu, G. H. (2005): Resource and Environmental Characteristics of the Poyang Lake, a Large Lake Interconnected with the Changjiang River-Aquatic macrophytes. – In: Cui, Y. B., Li, Z. J. (eds.) Fishery Resources and Conservation of Environment in Lakes of the Changjiang River Basin. Science Press, Beijing.
[15] Li, H., Li, C. A., Zhang, L. H., Tian, L. Q. (2008): Relationship between water level and water area in Poyang Lake based on MODIS image. – Quaternary Sciences 28: 332-337.
[16] Li, M., Chai, X., Wang, G., Hu, W., Zhang, L. (2019): Research on meteorological drought in the middle and lower reaches of the Yangtze Rive. – Journal of Natural Resources 34(2): 374-384.
[17] Lu, B., Cheng, S. C. (2003): An analysis of the ecological environment of the Poyang Lake Nature Preservation Zone. – Transactions of Oceanology and Limnology 3: 35-42.
[18] Lytle, D. A., Poff, N. L. (2004): Adaption to natural flow regimes. – Trends in Ecology and Evolution 19: 94-100.
[19] Meehl, G. A., Stocker, T. F., Collins, W., Friedlingstein, P., Gaye, A., Gregory, J. (2007): Global Climate Projections. – In: Solomon, S., Qin, D., Manning, M., Chen, Z., Marquis, M., Averyt, K. B., Tignor, M. M. B., Miller, H. L. Jr. (eds.) Climate Change 2007: the

http://www.aloki.hu ● ISSN 1589 1623 (Print) ● ISSN 1785 0037 (Online)
DOI: http://dx.doi.org/10.15666/aeer/1706_1565715668

Physical Science Basis. Contribution of Working Group I to the Fourth Assessment Report of the Intergovernmental Panelon Climate Change. Cambridge University Press, Cambridge and New York.

[20] Miao, S. L., Zou, C. B., Breshears, D. D. (2009): Vegetation responses to extreme hydrological events: sequence matters. – The American Naturalist 173: 113-118.

[21] Min, Q., Liu, Y., Ma, D. (2006): Impact of restoring lake by stopping cultivation on flood control capacity of Poyang Lake. – Resources and Environment in the Yangtze Basin 15(5): 574-578.

[22] Van den Berg, M. S., Scheffer, M., van Nes, E., Coops, H. (1999): Dynamics and stability of *Chara* sp. and *Potamogeton pecutinatus* in a shallow lake changing in eutrophication level. – Hydrobiologia 408/409: 335-342.

[23] Van Geest, G. J., Coops, H., Roijackers, R. M. M., Buijse, A. D., Scheffer, M. (2005): Succession of aquatic vegetation driven by reduced water-level fluctuations in floodplain lakes. – Journal of Applied Ecology 42: 251-260.

[24] Wang, S. M., Dou, H. S. (1998): Lakes of China. Science Press, Beijing.

[25] Xu, Z. M., Hu, W. Z., You, Z. Q. (2014): Analysis of low flow situation of Poyang Lake area after operation of Three Gorges Reservoir and its causes. – Yangtze River 45(7): 18-22.

[26] Ye, C., Wu, G. P., Zhao, X. S., Wang, X. L., Liu, Y. B. (2014): Responses of wetland vegetation to droughts and its impact factors in Poyang Lake National Nature Reserve. – Journal of Lake Science 26(2): 253-259.

[27] Zhang, L., Du, H., Jun, X., Xu, X. (2011): Progress in the study of extreme hydrologic events under climate change. – Progress in Geography 30(11): 1370-1379.

[28] Zhang, X. (2013): Water level fluctuation requirements of plants in the Yangtze floodplain lakes. – Ph.D. Thesis of University of Chinese Academy of Science, Beijing, China.

http://www.aloki.hu ● ISSN 1589 1623 (Print) ● ISSN 1785 0037 (Online)
DOI: http://dx.doi.org/10.15666/aeer/1706_1565715668

RUNOFF AND SEDIMENT YIELD VARIATIONS UNDER DIFFERENT PRECIPITATION CONDITION AND LAND-USE TYPE: A CASE STUDY OF FANGXI WATERSHED IN THE POYANG LAKE BASIN, CHINA

TONG, X. X.[1,2] – ZHOU, Y. C.[1*] – XU, W. S.[1,2] – DONG, L. Y.[1,2]

[1]*Changjiang River Scientific Research Institute of Changjiang Water Resources Commission, Wuhan, Hubei 430010, China*

[2]*Research Center on Mountain Torrents and Geological Disaster Prevention, Ministry of Water Resources, Wuhan, Hubei 430010, China*
(phone: +86-027-8292-6559; fax: +86-027-8292-6357)

**Corresponding author*
e-mail: zhouyc_omg@126.com; phone: +86-027-8292-7551; fax: +86-027-8292-6357

(Received 23rd Aug 2019; accepted 15th Nov 2019)

Abstract. A research was conducted on runoff and sediment yield variations under different precipitation and land-use conditions was performed based on the Soil and Water Assessment Too1 (SWAT) model using China Meteorological Assimilation Driving Datasets (CMADS). The observation data was collected in the Fangxi Lake Watershed, a typical irrigation district in the Poyang Lake basin of China. The results indicated a positive correlation between annual runoff and precipitation, as well as between annual sediment yield and precipitation. The correlation coefficient of annual runoff yield and precipitation was 0.94, whereas that of annual sediment yield and precipitation was 0.85. The monthly yield of runoff and sediment of a typical year (2004) was simulated. The runoff and sediment yields had the same tendency of changes with precipitation variations. Differences were found among the per unit area yield of total runoff from different land-use types in 2004. The order from highest to lowest was paddy land > rural residential land > dry land > water area. For the per unit area yield of total sediment from different land-use types, the order from highest to lowest was rural residential land > dry land > water area > paddy land. The results of this study might provide guidance for soil erosion control in irrigation districts.
Keywords: *land-use, precipitation, runoff and sediment yield, SWAT model, CMADS*

Introduction

The Soil and Water Assessment Too1 (SWAT) model is one of the distributed hydrological models. It is a physically based model developed by the Blackland Research and Extension Center and the United States Department of Agriculture – Agricultural Research Service to predict the effect of land management practices on water, sediment, and agricultural chemical yields in large, complex basins with varying soil types, land use, and management conditions over long periods of time (Gassman et al., 2007). The SWAT model can respond to the changes in land use, weather, topography, and soil data. The effectiveness and applicability of this model has been validated by numerous studies worldwide (Binh et al., 2011; Daggupati et al., 2018; Hao and Cheng, 2006; Himanshu et al., 2017; Koua et al., 2013; Lam et al., 2010; Loliyana and Patel, 2018; Santhi et al., 2006; Zettam et al., 2017).

Runoff and sediment simulation is one of the most basic and important functions of SWAT model. The SWAT model has been improved by numerous investigators by combining it with the local watershed. Some researchers demonstrated the applicability

http://www.aloki.hu ● ISSN 1589 1623 (Print) ● ISSN 1785 0037 (Online)
DOI: http://dx.doi.org/10.15666/aeer/1706_1566915685

of SWAT model for runoff and sediment simulation under different temporal and spatial scales and different hydrogeological conditions in the Mississippi River basin and other river basins in the United States (Arnold et al., 1999; Green and Griensven, 2008). Several studies analyzed different aspects of SWAT model simulation, such as the correlation between runoff and precipitation and the impact of land use on sediment and non-point source pollution in other countries and districts (Bärlund and Kirkkala, 2008; Di Luzio et al., 2005; Lee and Kim, 2017; Min and Shibata, 2016; Panagopoulos et al., 2011; Weber et al., 2001).

Most of the studies were based on a natural watershed. However, huge differences were found between irrigation district and natural watershed on account of intensive human activities on land cover and hydrological cycle system in irrigation districts. The SWAT model has been improved with the practical situation of irrigation district to enhance the simulation accuracy. Some researchers (Dai and Cui, 2009a, b; Dechmi et al., 2012; Li et al., 2014) improved the SWAT model based on specific irrigated watershed considering the water cycle in paddy land, irrigation, and drainage management, and other irrigation channel management actions. The results indicated that the improved SWAT model could show more accurate and better simulation performance than the original SWAT model.

Although the SWAT model has been widely used across the world, it is difficult to apply in areas where meteorological data are scarce (Meng et al., 2018). Therefore, the meteorological data is needed for runoff and sediment simulation in a watershed with scarce data (Meng et al., 2016). The China Meteorological Assimilation Driving Datasets for the SWAT model was developed by Meng from the China Institute of Water Resources and Hydropower Research (IWHR). It covers the entire East Asian region between 2008 and 2014 (Meng and Wang, 2017). Some studies demonstrated that the SWAT model yielded better results for runoff simulation with CMADS (Liu et al., 2017, 2018). Meng et al. also used three different datasets to simulate runoff in the Heihe basin, and the results indicated that the simulation accuracy of the CMADS was higher than that of other datasets (Meng et al., 2016).

The SWAT model and CMADS data were used in the present study to simulate the runoff and sediment yield under different precipitation and land-use conditions in the study area, a small irrigated plain district of Poyang Lake region. The correlation between runoff and precipitation, as well as between sediment and precipitation, was investigated. In addition, the diversities of runoff yield and sediment yield from different land-use types were simulated and analyzed. The results obtained in this study might provide guidance for soil and water conservation and land-use management of the study area as well as other irrigation districts of Poyang Lake region.

Materials and methods

Study area

The Fangxi Lake Watershed is located in the southwestern region of Poyang Lake basin, which is in the southeastern of China, between 116°0’E and 116°5’E and between 28°29’N and 28°33’N, covering an area of 3080.20 ha (*Fig. 1*). The Fangxi Lake Watershed features a subtropical monsoon climate and has four distinct seasons, where summers are warm with abundant precipitation whereas winters are cold and dry with little precipitation. The multi-year average precipitation is 1624.4 mm per year, and the annual rainy days are about 147.3 days. The annual average temperature is 17.6 °C.

http://www.aloki.hu ● ISSN 1589 1623 (Print) ● ISSN 1785 0037 (Online)
DOI: http://dx.doi.org/10.15666/aeer/1706_1566915685

The main soil type in this watershed is paddy clayey soil, which occupies 90.69% of the total area. It includes three subclasses: yellow clayey soil (76.52%), lake clayey soil (12.38%), and sand clayey soil (1.79%). The main land-use types in the study area are paddy land (79.27%), water area (12.63%), rural residential land (6.11%), dry land (1.71%), forest and grass land (0.24%), and bare land (0.04%). The main crop is rice and the double-cropping paddy area occupies approximately 95% of the total cultivated area. Other crops include watermelon, muskmelon, garlic, and fragrant-flowered garlic.

The area has 17,404 permanent residents, and the main types of livestock and poultry industry are ducks, chickens, pigs, cattle, and sheep. Aquaculture is highly developed because of its abundant water resources in this area. The aquaculture area occupies 30% of the water area.

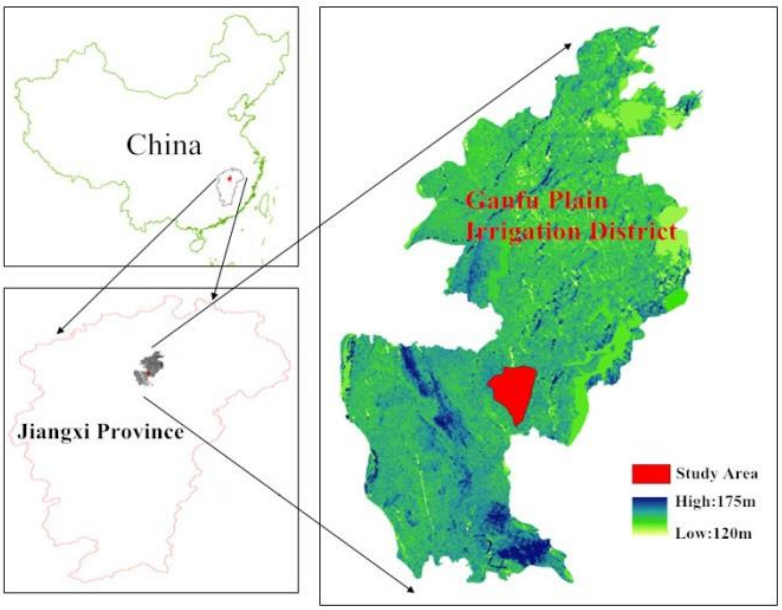

Figure 1. *Location of the study area*

Data collection

The distributed model based on the SWAT model requires spatial and attribute data. Furthermore, the spatial data includes digital elevation model (DEM), water distribution map, and land-use and soil maps. The attribute data includes the physical and chemical properties of soil, meteorological and hydrological information (including rainfall, temperature, wind speed, relative humidity, and net solar radiation.), observed runoff, and farmland management measures. The sources and main types of data collected are shown in *Table 1*. The DEM, land-use map, and soil maps are shown in *Figure 2a-c.*

The simulation accuracy of SWAT model depends largely on the description of the watershed characteristics of the input data. For runoff and sediment simulation, high-precision meteorological data can accurately describe the meteorological characteristics of the watershed and lead to better simulation results (Chen et al., 2016). Only one precipitation station exists near the study area. The China Meteorological Assimilation Driving Datasets for the SWAT model version 1.1 (CMADS V1.1) was introduced in this study to get the entire meteorological data for the study area. The climate data used in this study were downloaded from the official website (http://www.cmads.org).

http://www.aloki.hu ● ISSN 1589 1623 (Print) ● ISSN 1785 0037 (Online)
DOI: http://dx.doi.org/10.15666/aeer/1706_1566915685

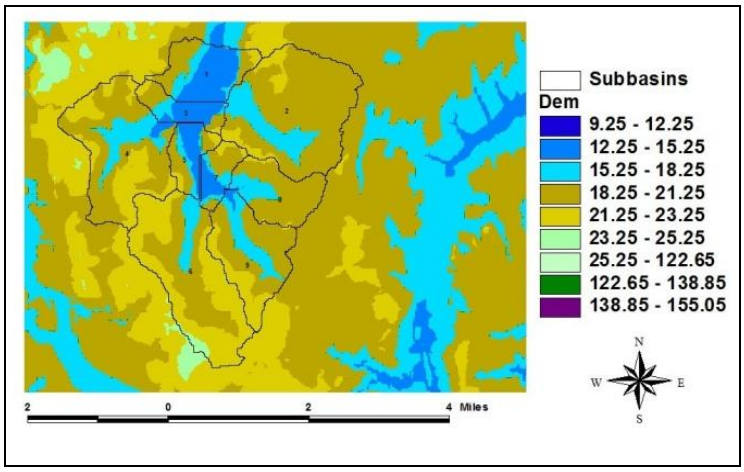

Figure 2a. *DEM of the study area*

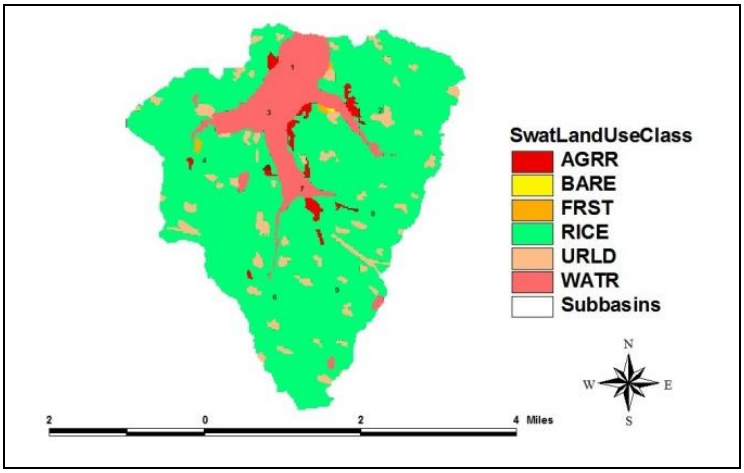

Figure 2b. *Land-use map of the study area (AGRR is dry land, BARE is bare land, FRST is forest and grass land, RICE is paddy land, URLD is rural residential land, and WATR is water area)*

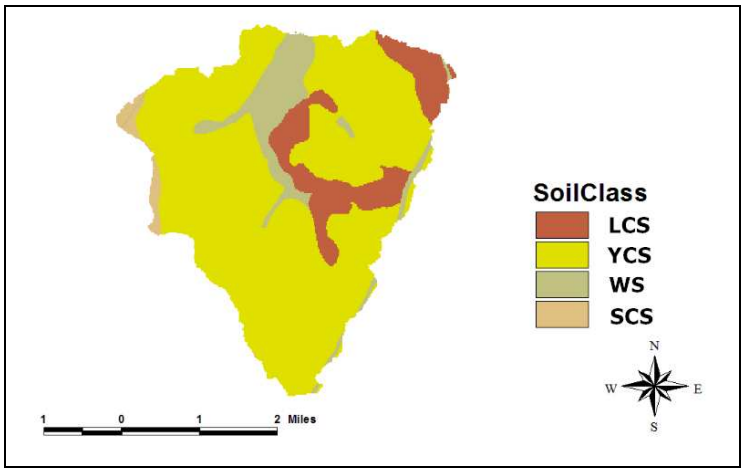

Figure 2c. *Soil map of the study area (LCS is lake clayey soil, YCS is yellow clayey soil, WS is water surface, and SCS is sand clayey soil)*

http://www.aloki.hu ● ISSN 1589 1623 (Print) ● ISSN 1785 0037 (Online)
DOI: http://dx.doi.org/10.15666/aeer/1706_1566915685

Table 1. *Sources and types of data collected for the SWAT model*

No.	Data type		Temporal/spatial resolution	Source
1	Spatial data	Digital elevation model (DEM), 25 m	Grid format, 30 m/grid	Geospatial Data Cloud of China (http://www.gscloud.cn/)
2		Water distribution map	Shape format	Drawn by the authors of this manuscript based on the water distribution of the study area
3		Soil map	At the scale of 1:100,000, compiled in 2009	Nanchang County Agricultural Bureau
4		Land-use map	At the scale of 1:100,000, compiled in 2009	Computer Network Information Center of Chinese Academy of Science (http://www.cnic.cas.cn)
5	Attribute data	Meteorological data, daily	Daily data	China Meteorological Assimilation Driving Datasets for the SWAT Model (CMADS) (calculated temperature, solar, wind data between 2008 and 2014), Jiangxi Irrigation Experimental Center (observed precipitation data between January 1, 1978 and November 30, 2011)
6		Hydrological data	Daily runoff yield	Jiangxi Irrigation Experimental Center (observed data between May to October in 2011)
7		Farmland management measures	Daily data during crop growth period	Field investigation based on the study area (observed data in 2011)

The farmland management measures are also important information for runoff and sediment yield research in the study area. Double-cropping rice is cultivated in most of the study area. The growing period of early rice is April to July and that of late rice is July to October. Irrigation and drainage measures of double-cropping rice are gained by farm surveys. The surveyed data are shown in *Table 2*.

Table 2. *Irrigation and drainage measures*

	Date	Measures
Early rice	April 14	Irrigation, 50 mm
	April 23	Irrigation, 50 mm
	May 18	Drainage
	May 22	Irrigation, 50 mm
	July 6	Drainage
Late rice	July 18	Irrigation, 50 mm
	July 26	Irrigation, 50 mm
	July 31	Irrigation, 50 mm
	August 7	Irrigation, 50 mm
	August 19	Drainage
	September 3	Irrigation, 50 mm
	September 21	Irrigation, 50 mm
	October 31	Drainage

All data were prepared for the model setup

http://www.aloki.hu ● ISSN 1589 1623 (Print) ● ISSN 1785 0037 (Online)
DOI: http://dx.doi.org/10.15666/aeer/1706_1566915685

SWAT model setup

Model construction

In this study, the spatial data in *Table 1* were loaded into the SWAT model, and the distributed hydrological model based on the study area was constructed. Nine sub-basins were calculated based on the DEM and river network distribution of the study area, and then 51 hydrological response units (HRUs) were subdivided based on the spatial distribution of the land-use type, soil type, and slope. The results are shown in *Figure 3* and *Table 3*.

The meteorological data were loaded into the SWAT model after HRU subdivision. Then, a distributed hydrological model based on the SWAT model was constructed in the study area.

Table 3. *Area of sub-basins and HRUs in the study area*

Sub-basins	Number of HRUs	Area (ha)	Area percentage (%)
1	4	253.59	8.23
2	8	685.23	22.25
3	6	122.63	3.98
4	6	571.78	18.56
5	7	127.43	4.14
6	2	623.55	20.24
7	10	105.14	3.41
8	5	232.73	7.56
9	3	358.12	11.63
Total	**51**	**3080.20**	**100**

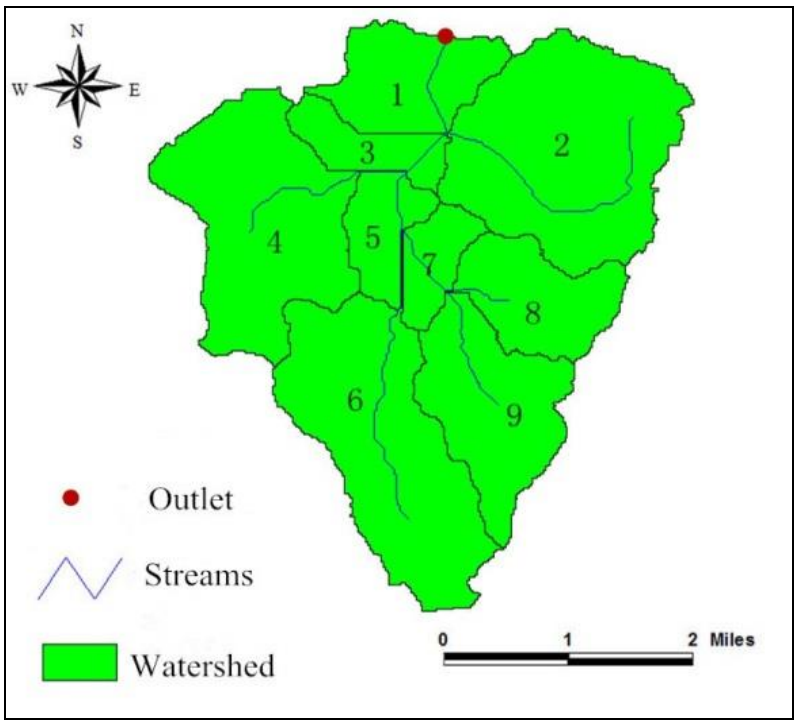

Figure 3. *Sub-basins of the study area*

http://www.aloki.hu ● ISSN 1589 1623 (Print) ● ISSN 1785 0037 (Online)
DOI: http://dx.doi.org/10.15666/aeer/1706_1566915685

Model calibration and evaluation

Model calibration was based on the optimization of the parameter values by adjusting the simulated runoff and sediment yield data at the outlet of the basin with observed data. That is to say, the parameters of runoff and sediment yield in the SWAT model were adjusted to a reasonable range to get accurate simulation results in this study.

Some parameters called sensitive parameters can have an evident impact on the results of model simulation. These parameters were adjusted to a reasonable value for better simulation results. On the basis of some studies on the sensitivity analysis of SWAT model (Me et al., 2015; Yang et al., 2013), the main sensitive parameters of runoff and sediment yield adjusted in this study are shown in *Table 4*.

Table 4. *Main parameters of runoff and sediment yield in the SWAT model*

	Parameter	Description
Runoff parameter	CN_2	SCS runoff curve calculating parameter
	ESCO	Soil evaporation compensation coefficient
	EPCO	Crop transpiration compensation coefficient
	SOL-AWC	Soil available water capacity
	REVAPMN	Water table threshold for shallow groundwater re-evaporation
	GW-REVAP	Groundwater re-evaporation coefficient
	GWQMN	Runoff coefficient of shallow groundwater
Sediment parameter	USLE_C	Minimum value of vegetation coverage factor
	USLE_P	Soil and water conservation factor of USLE equation
	USLE_K	Soil erosion coefficient of USLE equation
	CH_EROD	Channel scour coefficient
	CH_COV	Channel coverage coefficient
	SPCON	Linear coefficient of sediment transport
	SPEXP	Index coefficient of sediment transport

The relative error (R_e), correlation coefficient (R^2), and Nash–Sutcliffe efficiency (Ens) were used to evaluate the model performance. The formulas used for calculating these indexes are as follows:

$$R_e = \frac{Q_p - Q_0}{Q_0} \times 100\% \quad \text{(Eq.1)}$$

$$R^2 = \left[\frac{\sum_{i=1}^{n}(Q_0 - \overline{Q_0})(Q_P - \overline{Q_P})}{\sqrt{\sum_{i=1}^{n}(Q_0 - \overline{Q_0})^2 \sum_{i=1}^{n}(Q_P - \overline{Q_P})^2}} \right]^2 \quad \text{(Eq.2)}$$

$$Ens = 1 - \frac{\sum_{i=1}^{n}(Q_0 - Q_P)^2}{\sum_{i=1}^{n}(Q_0 - \overline{Q_0})^2} \quad \text{(Eq.3)}$$

where Q_p is the simulation value, $\overline{Q_P}$ is the average simulation value, Q_0 is the observed value, $\overline{Q_0}$ is the average observed value, and n is the number of observed data. The

http://www.aloki.hu ● ISSN 1589 1623 (Print) ● ISSN 1785 0037 (Online)
DOI: http://dx.doi.org/10.15666/aeer/1706_1566915685

evaluation standard indexes of model simulation efficiency are shown in *Table 5*. Generally, the model performances are identified to be good enough to apply in actual numerical simulation if R_e < 10%, R^2 > 0.79, and Ens > 0.59.

Table 5. *Evaluation standard of model simulation efficiency*

Standard	Relative error (R_e, %)	Correlation coefficient (R^2)	Nash–Sutcliffe efficiency (*Ens*)
Excellent	–5 to + 5	1.00–0.95	1.00–0.80
Good	± 5 to ± 10	0.94–0.80	0.79–0.60
Medium	± 10 to ± 20	0.79–0.70	0.59–0.40
Awful	> 20 or < –20	< 0.70	< 0.40

For runoff parameters, the observed runoff data at the outlet of the study area from May to October 2011 were used for model calibration and evaluation. Especially, the meteorological data of CMADS were used for model simulation to increase the accuracy of model simulation. In addition, the daily runoff data during the period 2008–2011 were simulated, choosing 2008–2010 as the warm-up period of SWAT model simulation. Some studies showed that the warm-up could make better simulation results for SWAT model simulation (Li et al., 2013; Nyeko, 2015; Wang et al., 2017, 2015). *Figure 4* shows the comparisons between the observed and simulated runoff yield of the study area outlet during the model calibration and validation period. *Table 6* shows the performance of SWAT model during the calibration and validation periods. The optimum values of the calibrated runoff parameters are shown in *Table 7*.

Table 6. *Evaluation standard of model simulation efficiency*

	Re (%)	***R^2***	***Ens***
Calibration period	15.5	0.88	0.74
Validation period	12.4	0.90	0.78

Table 7. *Optimum value of calibrated runoff parameters for the SWAT model*

Name	Paddy land	Dry land	Rural residential land	Bare land	Grass land
CN2	70	85	86	90	78
ESCO	0.3	0.6	0.7	0.5	0.5
EPCO	0.7	0.8	0.5	0.5	0.8
SOL-AWC	0.18	0.13	0.14	0.16	0.18
REVAPMN	450	450	450	450	450
GW-REVAP	0.2	0.2	0.2	0.2	0.2
GWQMN	1	1	1	1	1

For sediment parameters, the model was calibrated by experience according to the related studies due to the lack of observed data (Qiu et al., 2012; Wang and Cui, 2011; Xu et al., 2008; Zhang et al., 2003). The optimum value of the calibrated sediment parameters is shown in *Table 8*.

http://www.aloki.hu ● ISSN 1589 1623 (Print) ● ISSN 1785 0037 (Online)
DOI: http://dx.doi.org/10.15666/aeer/1706_1566915685

Table 8. *Optimum value of calibrated sediment parameters for the SWAT model*

Name	USLE_C	USLE_P	USLE_K	CH_EROD	CH_COV	SPCON	SPEXP
Value	0.5	0.2	0.15	0.15	0.6	0.005	1.2

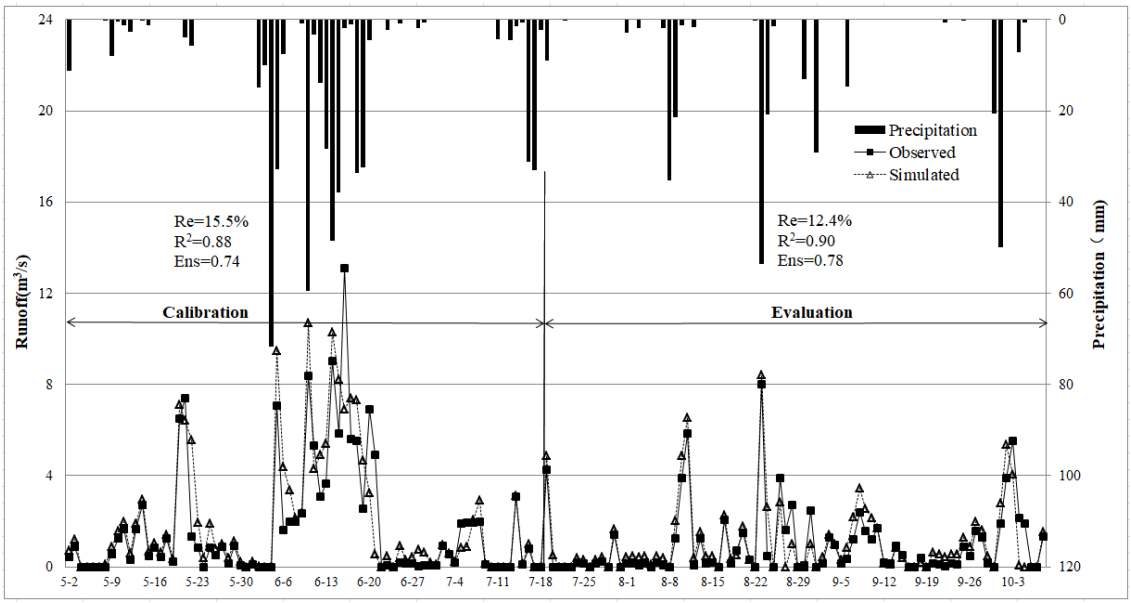

Figure 4. *Comparisons between the observed and simulated daily runoff during the calibration and validation period*

The SWAT model simulated value reflected the actual changes in the runoff yield, and the SWAT model could be used for runoff simulation in the study area. Hence, the distributed hydrological model of the study area based on the SWAT model was successfully constructed.

Results

Runoff and sediment yield variations in response to precipitation

Statistical analysis of precipitation data

In this study, the annual precipitation data of the study area during 1978–2010 were used for frequency calculation and the characteristic hydrological years were identified. The empirical frequency is calculated using the equation as follows:

$$P = \frac{m}{n+1} \quad \text{(Eq.4)}$$

where P is the empirical frequency of the annual precipitation of a particular year, m is the number in order from largest to smallest of the precipitation (*Table 9*), n is the total number of annual precipitation data.

Table 9 shows the precipitation and the result of empirical frequency calculation. As shown in *Table 9*, the multi-year average precipitation was 1523.19 mm.

http://www.aloki.hu ● ISSN 1589 1623 (Print) ● ISSN 1785 0037 (Online)
DOI: http://dx.doi.org/10.15666/aeer/1706_1566915685

Table 9. *Precipitation and the result of frequency calculation*

Year	Precipitation (mm)	No.	Frequency (P, %)	Year	Precipitation (mm)	No.	Frequency (P, %)
2010	2317	1	2.94	1997	1468.2	18	52.94
1995	2296	2	5.88	2001	1459.9	19	55.88
2002	2120.1	3	8.82	1992	1404.8	20	58.82
2005	2063.5	4	11.76	1989	1400.3	21	61.76
1999	1884.4	5	14.71	1987	1376.6	22	64.71
2006	1856.4	6	17.65	2008	1362.9	23	67.65
1993	1784.3	7	20.59	1996	1342.4	24	70.59
1998	1748.1	8	23.53	1979	1295.3	25	73.53
2003	1720.6	9	26.47	1985	1241.2	26	76.47
2000	1680.1	10	29.41	1990	1228.2	27	79.41
1983	1670.7	11	32.35	1988	1221.9	28	82.35
1980	1583.7	12	35.29	1986	1211.8	29	85.29
1994	1517.2	13	38.24	2009	1086.1	30	88.24
1984	1501.2	14	41.18	2007	1045.3	31	91.18
2004	1485	15	44.12	1978	986.9	32	94.12
1981	1483.4	16	47.06	1991	940.9	33	97.06
1982	1481	17	50.00	Average	1523.19	Cv	0.23

The variation coefficient and ocular estimation method was used to draw theoretical frequency curve of the annual precipitation data, the best-fitted theoretical frequency curve was drawn when the coefficient of variation (Cv) was 0.23, as shown in *Figure 5*. The characteristic hydrological years were chosen with the frequency of 5%, 20%, 50%, 70%, and 95% according to the theoretical frequency curve. According to *Table 1*, the soil map and land-use map were compiled in 2009, so 2002 (8.82%), 2006 (17.65%), 2004 (44.12%), 2008 (67.65%), and 2009 (88.24%) were chosen as the corresponding years, which are close to 2009 and will decrease the impact of land-use and soil change on simulation results in SWAT model.

Analysis of runoff and sediment variation response to precipitation change

At first, the annual yield of runoff and sediment of characteristic hydrological years was analyzed. The results are shown in *Table 10* and *Figure 6.* The runoff and sediment yields increased with an increase in precipitation. The correlation coefficient of runoff yield and precipitation was 0.94, whereas that of the sediment yield and precipitation was 0.85. Hence, a strong positive correlation was observed between the runoff yield and precipitation, as well as between sediment yield and precipitation.

Table 10. *Precipitation and the result of frequency calculation*

Year	2002	2006	2004	2008	2009
P (%)	5	20	50	70	95
Precipitation (mm)	2120.1	1856.4	1485	1362.9	1086.1
Runoff ($m^3 s^{-1}$)	1.90	1.76	1.22	1.28	1.09
Sediment (ta^{-1})	438.02	490.47	291.04	267.93	207.93

http://www.aloki.hu ● ISSN 1589 1623 (Print) ● ISSN 1785 0037 (Online)
DOI: http://dx.doi.org/10.15666/aeer/1706_1566915685

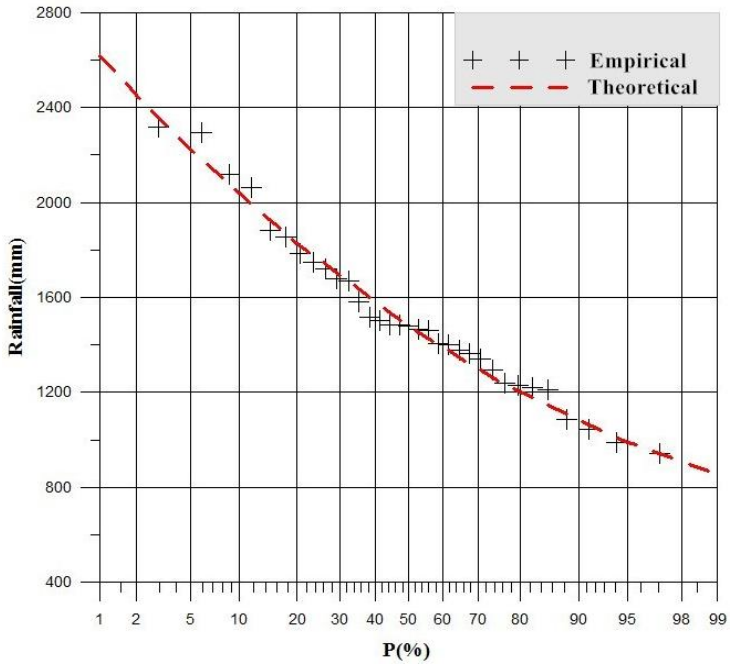

Figure 5. *Theoretical frequency curve of precipitation*

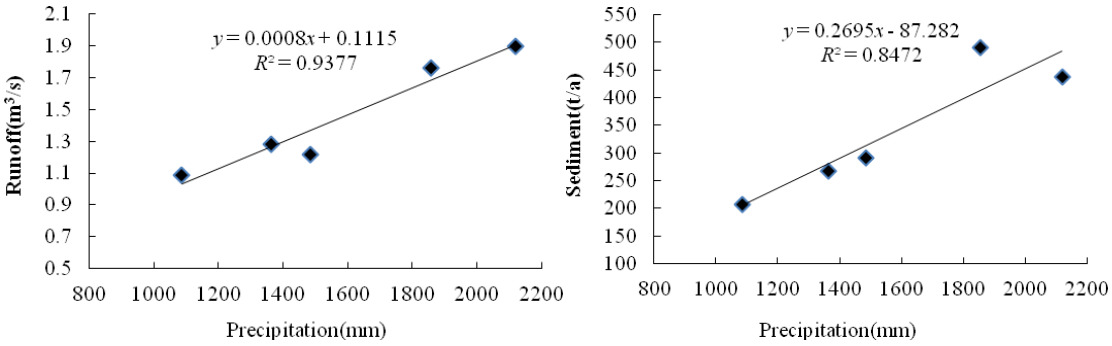

Figure 6. *Correlation diagram of runoff and precipitation, as well as sediment and precipitation*

Then, 2004 was chosen as the typical year (P = 50%), and the monthly yield of runoff and sediment were simulated. The results are shown in *Figure 7*. The runoff and sediment had the same tendency of changes with precipitation variation.

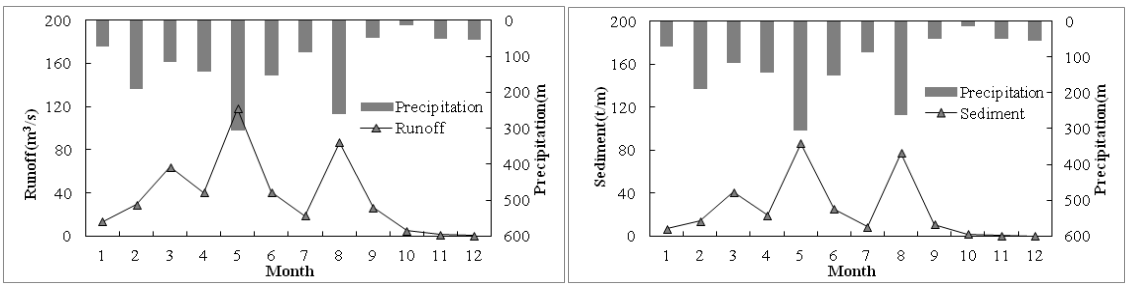

(a) (b)

Figure 7. *Monthly runoff and sediment variation response to precipitation changes*

http://www.aloki.hu ● ISSN 1589 1623 (Print) ● ISSN 1785 0037 (Online)
DOI: http://dx.doi.org/10.15666/aeer/1706_1566915685

Runoff and sediment yield under different land use type

During sub-basin calculation, the land-use area threshold setting method was used to reduce the calculation amount of SWAT model and the HRU amount of the study area. Therefore, the land-use type was readjusted to another type if the area percentage was less than the area threshold. In this study, 1% was used as the land-use area threshold. The changes in the land-use area before and after HRU calculation are shown in *Table 11*.

Table 11. *Land-use area changes before and after HRU calculation*

Type	Before		After	
	Area (ha)	Percentage (%)	Area (ha)	Percentage (%)
AGRR (dry land)	52.67	1.71	73.30	2.38
RICE (paddy land)	2441.67	79.27	2442.60	79.30
URLD (rural residential land)	188.20	6.11	186.40	6.05
WATR (water area)	389.03	12.63	377.90	12.27
FRST (forest and grass land)	7.39	0.24	0	0
BARE (bare land)	1.23	0.04	0	0
Total	3080.20	100	3080.20	100

Then, the per unit area yield of runoff and sediment of different land-use types in 2004 was calculated. The results are shown in *Figure 8*.

As illustrated in *Figure 8a*, the order of per unit area yield of total runoff from high to low was paddy land, rural residential land, dry land, and water area. Specially, the total yield from paddy land was much more than that from other land-use types in the study area. Likewise, the ground water runoff from paddy land was also much more than that from other land-use types in the study area. Further, the surface runoff yields from different land-use types were almost the same.

As illustrated in *Figure 8b,* the order of sediment yield from high to low was rural residential land, dry land, water area, and paddy land.

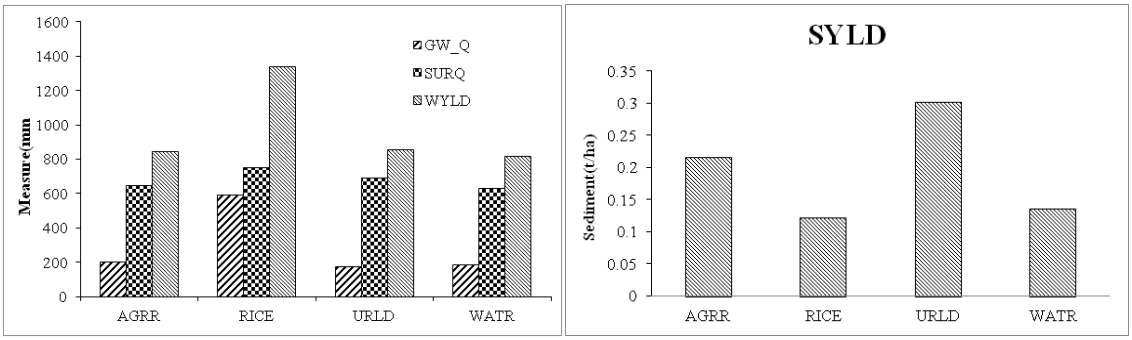

(a) (b)

Figure 8. *Runoff and sediment yield of per unit area from different land-use types in 2004.* ***a*** *Per unit area yield of runoff (GW_Q is groundwater, SURQ is surface runoff, WYLD is total runoff).* ***b*** *Per unit area yield of sediment (SYLD is total yield of sediment)*

http://www.aloki.hu ● ISSN 1589 1623 (Print) ● ISSN 1785 0037 (Online)
DOI: http://dx.doi.org/10.15666/aeer/1706_1566915685

Discussion

Based on the SWAT model with CMADS data, observed data from Jiangxi Irrigation Experimental Center, and field observation, the distributed hydrological model of the study area was constructed and the runoff and sediment yield variations under different precipitation and land-use conditions were simulated and analyzed.

For model calibration and evaluation, the observed runoff yield data were used to finish runoff parameter calibration. The sediment yield parameters were calibrated based on the results of other studies in different study areas due to the lack of observed data. For further study, the sediment simulation would be more accurate if the observed sediment data in the study area are used for model calibration.

At first, the observed annual precipitation data from 1978 to 2011 were used to finish frequency calculation and characteristic hydrological year identification. The runoff yield and sediment yield of characteristic hydrological years were simulated. A strong positive correlation was observed between the annual runoff yield and annual precipitation, as well as between sediment yield and precipitation, such results are also available from other studies (Li and Gao, 2015; Ruan et al., 2017; Zhu et al., 2015).

Then, 2004 was chosen as the typical year (50%), and the monthly yield of runoff and sediment was simulated. Runoff and sediment had the same tendency of changes with precipitation variation. Specifically, a small spike for runoff, as well as for sediment, was observed in March with the decrease in precipitation, while a sharp decrease appeared in April with a relatively high increase in precipitation. That is to say, precipitation variation was not the only influencing factor for runoff and sediment changes. Several studies explored the influencing factors for runoff and sediment yield in different watersheds around the world (Jiang et al., 2008; Nguyen et al., 2017; Perry, 2015; Tong et al., 2018; Xiang et al., 2012; Alibuyog et al., 2009). Some other studies also indicated that the land-use type was one of the most important influencing factors for runoff and sediment yield variation (Gyamfi et al., 2016; Huang and Lo, 2015; Zhang et al., 2010).

In this study, the per unit area yields of runoff and sediment in 2004 of different land-use types were calculated.

The total runoff, surface runoff, and ground water runoff yield of different land-use types were analyzed. No significant difference was found in surface runoff yields from different land-use types. However, the underground runoff yields from different land-use types varied greatly. The ground water runoff from paddy land was also much more than that from other land-use types in the study area. This might be attributed to the fact that the paddy land is irrigated during the growing period of double-cropping rice, and the underground water maintains a relatively high level for a long time. Therefore, it is not comprehensive to only consider the surface runoff in the simulation of watershed runoff. The difference between surface runoff and subsurface runoff may increase, and hence the change and difference in runoff can be assessed from the time and space scale in the future studies.

The order of per unit area yield of total sediment from high to low was rural residential land, dry land, water area, and paddy land. The sediment yields from the rural residential land and dry land were much more than that from paddy land and water area. Thus, the rural residential land and dry land should be the major focus of soil erosion control and soil conservation.

http://www.aloki.hu ● ISSN 1589 1623 (Print) ● ISSN 1785 0037 (Online)
DOI: http://dx.doi.org/10.15666/aeer/1706_1566915685

Conclusions

A distributed hydrological model was constructed in this study based on the SWAT model with CMADS data in the Fangxi Lake Watershed, a typical irrigation district in the Poyang Lake basin. The SWAT model was calibrated with observed runoff data. The results showed that the model was accurate enough for runoff and sediment yield simulation in the study area.

The runoff and sediment yield variations under different precipitation and land-use conditions were analyzed. The correlation coefficient of annual runoff yield and precipitation was 0.94, whereas that of annual sediment yield and precipitation was 0.85. Therefore, a positive correlation was observed between the annual runoff yield and precipitation, as well as between annual sediment yield and precipitation. When the monthly yield of runoff and sediment of typical year (2004) was simulated, the runoff and sediment yields had the same tendency of changes with precipitation variations. Then, the per unit area yield of runoff and sediment of different land-use types in 2004 was calculated. The order of per unit area yield of total runoff from high to low was paddy land, rural residential land, dry land, and water area. The order of per unit area yield of total sediment from high to low was rural residential land, dry land, water area, and paddy land. These findings figured out that the rural residential land and dry land are the main source of soil erosion.

However, several limitations in this study merit further research and investigation. The space distribution law of runoff and sediment should be taken into consideration in further studies. In addition, the transfer law of underground runoff and sediment in underground water under different rainfall and land-use conditions should be the focus of these studies.

Acknowledgments. The authors would like to express their sincere thanks to the State Key Laboratory of Water Resources and Hydropower Engineering Science, Wuhan University; the Nanchang County Agricultural Bureau Computer Network Information Center of Chinese Academy of Science; the China Meteorological Assimilation Driving Datasets for the SWAT Model; and the Jiangxi Irrigation Experimental Center for providing spatial and attribute data on Fangxi Lake Watershed. The authors also acknowledge the guidance from Professor Cui Yuanlai. They also thank the journal editors and anonymous reviewers for their useful comments and suggestions. This study was funded by the National Key R&D Program of China (2017YFC150250304), the National Natural Science Foundation of China (51609009), the Fundamental Research Funds for Central Public Welfare Research Institutes (CKSF2016040/TB) and the Fundamental Research Funds for Central Public Welfare Research Institutes (CKSF2019410/TB).

Conflict of interests. The authors declare no conflict of interests.

REFERENCES

[1] Alibuyog, N. R., Ella, V. B., Reyes, M. R., Srinivasan, R., Heatwole, C., Dillaha, T., Gassman, P. W. (2009): Predicting the effects of land use change on runoff and sediment yield in Manupali River subwatersheds using the SWAT model. – International Agricultural Engineering Journal 18: 15-25.

[2] Arnold, J. G., Srinivasan, R., Muttiah, R. S., Allen, P. M. (1999): Continental scale simulation of the hydrologic balance 1. – JAWRA Journal of the American Water Resources Association 35: 1037-1051.

http://www.aloki.hu ● ISSN 1589 1623 (Print) ● ISSN 1785 0037 (Online)
DOI: http://dx.doi.org/10.15666/aeer/1706_1566915685

[3] Bärlund, I., Kirkkala, T. (2008): Examining a model and assessing its performance in describing nutrient and sediment transport dynamics in a catchment in southwestern Finland. – Boreal Environ Res. 13: 195-207.
[4] Binh, P. D., Wu, C.-C., Hsieh, S.-C. (2011): Land use change effects on discharge and sediment yield of song cau catchment in northern Vietnam. – Journal of Environmental Science & Engineering 5: 92-101.
[5] Chen, X., Xiao, W., Huang, Z., Zeng, L. (2016): Impact of spatial data on the accuracy of watershed hydrological simulation of SWAT model. – Science of Soil & Water Conservation 2: 138-143.
[6] Daggupati, P., Shukla, R., Mekonnen, B., Rudra, R., Biswas, A., Goel, P. K., Prasher, S., Yang, W. (2018): Hydrological responses to various land use, soil and weather inputs in northern Lake Erie basin in Canada. – Water 10: 222.
[7] Dai, J. F., Cui, Y. L. (2009a): Distributed hydrological model for irrigation area based on SWAT I. Principle and method. – Journal of Hydraulic Engineering 40: 145-152.
[8] Dai, J. F., Cui, Y. L. (2009b): Distributed hydrological model for irrigation area based on SWAT II. Model application. – Journal of Hydraulic Engineering 40: 311-318.
[9] Dechmi, F., Burguete, J., Skhiri, A. (2012): SWAT application in intensive irrigation systems: model modification, calibration and validation. – Journal of Hydrology 470: 227-238.
[10] Di Luzio, M., Arnold, J. G., Srinivasan, R. (2005): Effect of GIS data quality on small watershed stream flow and sediment simulations. – Hydrological Processes: An International Journal 19: 629-650.
[11] Gassman, P. W., Reyes, M. R., Green, C. H., Arnold, J. G. (2007): The soil and water assessment tool: historical development, applications, and future research directions. – Transactions of the ASABE 50(4): 1211-1250.
[12] Green, C. H., Griensven, A. V. (2008): Autocalibration in hydrologic modeling: Using SWAT2005 in small-scale watersheds. – Environmental Modelling & Software 23: 422-434.
[13] Gyamfi, C., Ndambuki, J. M., Salim, R. W. (2016): Simulation of sediment yield in a semi-arid river basin under changing land use: an integrated approach of hydrologic modelling and principal component analysis. – Sustainability 8: 1133.
[14] Hao, F. H., Cheng, H. G. (2006): Theory and application of non-point source pollution model. – China Environmental Science Press, Beijing.
[15] Himanshu, S. K., Pandey, A., Shrestha, P. (2017): Application of SWAT in an Indian river basin for modeling runoff, sediment and water balance. – Environmental Earth Sciences 76: 3.
[16] Huang, T. C., Lo, K. F. A. (2015): Effects of land use change on sediment and water yields in Yang Ming Shan National Park, Taiwan. – Environments 2: 32-42.
[17] Jiang, X., Huang, C., Ruan, F. (2008): Impacts of land cover changes on runoff and sediment in the Cedar Creek Watershed, St. Joseph River, Indiana, United States. – Journal of Mountain Science 5: 113-121.
[18] Koua, T. J., Jourda, J. P., Kouame, K. J., Anoh, K. A. (2013): Assessment of sediment and pollutants in Buyo Lake, Ivory Coast, using SWAT (soil and water assessment tool) model. – Journal of Chemistry and Chemical Engineering 7: 1054.
[19] Lam, Q. D., Schmalz, B., Fohrer, N. (2010): Modelling point and diffuse source pollution of nitrate in a rural lowland catchment using the SWAT model. – Agricultural Water Management 97: 317-325.
[20] Lee, S., Kim, S. U. (2017): Quantification of hydrological responses due to climate change and human activities over various time scales in South Korea. – Water 9: 34.
[21] Li, T., Gao, Y. (2015): Runoff and sediment yield variations in response to precipitation changes: a case study of Xichuan watershed in the Loess Plateau, China. – Water 7: 5638-5656.

http://www.aloki.hu ● ISSN 1589 1623 (Print) ● ISSN 1785 0037 (Online)
DOI: http://dx.doi.org/10.15666/aeer/1706_1566915685

[22] Li, Y., Wang, K., Zhou, Z. (2014): Simulation of drainage and agricultural non-point source pollutions transport processes in paddy irrigation district in North-East China using SWAT. – Transactions of the Chinese Society of Agricultural Engineering 30: 42-53.
[23] Li, Z., Sun, W., Wang, Z., Zhao, W., Sang, Y. (2013): Simulation of drainage and agricultural non-point source pollutions transportprocesses in paddy irrigation district in North-East China using SWAT. – J Hydroelectr Eng 77-82.
[24] Liu, J., Liu, S., Shangguan, D., Jingdong, X. U. (2017): Applicability evaluation of precipitation datasets from CMADS, ITPCAS and TRMM 3B42 in Yurungkax River basin. – Journal of North China University of Water Resources & Electric Power 38: 28-37.
[25] Liu, J., Shanguan, D., Liu, S., Ding, Y. (2018): Evaluation and hydrological simulation of CMADS and CFSR reanalysis datasets in the Qinghai-Tibet Plateau. – Water 10: 513.
[26] Loliyana, V. D., Patel, P. L. (2018): Performance evaluation and parameters sensitivity of a distributed hydrological model for a semi-arid catchment in India. – Journal of Earth System Science 127: 117.
[27] Me, W., Abell, J. M., Hamilton, D. P. (2015): Effects of hydrologic conditions on SWAT model performance and parameter sensitivity for a small, mixed land use catchment in New Zealand. – Hydrology and Earth System Sciences 19: 4127-4147.
[28] Meng, X., Wang, H. (2017): Significance of the China meteorological assimilation driving datasets for the SWAT Model (CMADS) of East Asia. – Water.
[29] Meng, X., Shi, C., Liu, S., Wang, H., Lei, X., Liu, Z., Xiaonan, J. I., Cai, S., Zhao, Q. (2016): CMADS datasets and its application in watershed hydrological simulation: a case study of the Heihe River basin. – Pearl River 37: 1-19.
[30] Meng, X., Long, A., Wu, Y., Yin, G., Wang, H., Ji, X. (2018): Simulation and spatiotemporal pattern of air temperature and precipitation in Eastern Central Asia using RegCM. – Scientific Reports 8: 3639.
[31] Min, F., Shibata, H. (2016): Water yield, nitrogen and sediment retentions in Northern Japan (Teshio river watershed): land use change scenario analysis. – Mitigation & Adaptation Strategies for Global Change 21: 119-133.
[32] Nguyen, H. H., Recknagel, F., Meyer, W., Frizenschaf, J. (2017): Analysing the effects of forest cover and irrigation farm dams on streamflows of water-scarce catchments in South Australia through the SWAT model. – Water 9: 33.
[33] Nyeko, M. (2015): Hydrologic modelling of data scarce basin with SWAT model: capabilities and limitations. – Water Resources Management 29: 81-94.
[34] Panagopoulos, Y., Makropoulos, C., Baltas, E., Mimikou, M. (2011): SWAT parameterization for the identification of critical diffuse pollution source areas under data limitations. – Ecological Modelling 222: 3500-3512.
[35] Perry, K. A. (2015): Application of the SWAT hydrological model in a small, mountainous catchment in South Africa. – Mini-dissertation (MSc), University of Pretoria.
[36] Qiu, L., Zheng, F., Yin, R. (2012): SWAT-based runoff and sediment simulation in a small watershed, the loessial hilly-gullied region of China: capabilities and challenges. – International Journal of Sediment Research 27: 226-234.
[37] Ruan, H., Zou, S., Yang, D., Wang, Y., Yin, Z., Lu, Z., Li, F., Xu, B. (2017): Runoff simulation by SWAT model using high-resolution gridded precipitation in the upper Heihe River Basin, Northeastern Tibetan Plateau. – Water 9: 866.
[38] Santhi, C., Srinivasan, R., Arnold, J. G., Williams, J. R. (2006): A modeling approach to evaluate the impacts of water quality management plans implemented in a watershed in Texas. – Environmental Modelling & Software 21: 1141-1157.
[39] Tong, X. X., Cui, Y. L., Chen, M. Y., Hu, B., Xu, W. S. (2018): Simulation on change law of runoff, sediment and non-point source nitrogen and phosphorus discharge under

http://www.aloki.hu ● ISSN 1589 1623 (Print) ● ISSN 1785 0037 (Online)
DOI: http://dx.doi.org/10.15666/aeer/1706_1566915685

different land uses based on SWAT model: a case study of Er hai Lake small watershed. – IOP Conference Series: Earth and Environmental Science 153(5): 062062.

[40] Wang, H., Han, L., Wang, X., Zhu, Z. (2017): Research of runoff simulation in Xihe basin using SWAT model. – Journal of Liaoning Normal University 4: 558-562.

[41] Wang, J., Cui, Y. (2011): Modified SWAT for rice-based irrigation system and its assessment. – Transactions of the Chinese Society of Agricultural Engineering 27: 22-28.

[42] Wang, S., Xu, H. M., Gao, C. (2015): Water balance response of the climate change based on SWAT model in the Upper-Middle Reach of Huaihe River Basin. – Advances in Climate Change Research 11: 402-411.

[43] Weber, A., Fohrer, N., Möller, D. (2001): Long-term land use changes in a mesoscale watershed due to socio-economic factors—effects on landscape structures and functions. – Ecological modelling 140: 125-140.

[44] Xiang, L., Niu, J. Z., Xie, B. Y., Han, Y. N., Tan, J. P., Zhang, Y. H. (2012): Characteristics of runoff and sediment generation of forest vegetation on a hill slope by use of artificial rainfall apparatus. – Journal of Forestry Research 23: 419-424.

[45] Xu, Q. G., Xi, B. D., He, L. S., Wei, Z. M., Yao, B., Huo, S. L. (2008): Research on non-point pollution sources in Daning River watershed of the Three Georges Reservoir. – Journal of Environmental Engineering 2: 299-303.

[46] Yang, J. J., Gao, X. H., Qi-Jiang, L. I., Chen, Q., Feng, S. C. (2013): SWAT model construction and uncertainty analysis on its parameters for the Huangshui River basin. – Research of Soil & Water Conservation 2: 82-93.

[47] Zettam, A., Taleb, A., Sauvage, S., Boithias, L., Belaidi, N., Sánchez-Pérez, J. M. (2017): Modelling hydrology and sediment transport in a semi-arid and anthropized catchment using the SWAT model: the case of the Tafna river (northwest Algeria). – Water 9: 216.

[48] Zhang, X. S., Hao, F. H., Yang, Z. F., Cheng, H. G., Beijing (2003): Runoff and sediment yield modeling in meso-scale watershed based on SWAT model. – Research of Soil & Water Conservation 10: 38-42.

[49] Zhang, X., Wenhong, C., Qingchao, G., Sihong, W. (2010): Effects of landuse change on surface runoff and sediment yield at different watershed scales on the Loess Plateau. – International Journal of Sediment Research 25: 283-293.

[50] Zhu, Q. D., Sun, J. H., Hua, G. F., Wang, J. H., Wang, H. (2015): Runoff characteristics and non-point source pollution analysis in the Taihu Lake Basin: a case study of the town of Xueyan, China. – Environmental Science and Pollution Research 22: 15029-15036.

http://www.aloki.hu ● ISSN 1589 1623 (Print) ● ISSN 1785 0037 (Online)
DOI: http://dx.doi.org/10.15666/aeer/1706_1566915685

EFFECT OF *CONIOTHYRIUM MINITANS* AND *TRICHODERMA HARZIANUM* IN THE BIOLOGICAL CONTROL OF WHITE MOLD DISEASE (*SCLEROTINIA SCLEROTIORUM*) IN LETTUCE (*LACTUCA SATIVA* L.)

ÇOLAK ATEŞ, A.

Biological Control Research Institute, Department of Phytopathology, Adana, Turkey
e-mail: aysegulcolak@hotmail.com; phone: +90-322-344-1784

(Received 29th Aug 2019; accepted 15th Nov 2019)

Abstract. *Sclerotinia sclerotiorum* (SC) is one of the most destructive soil-borne diseases in lettuce cultivation. In the present study, the effectiveness of single and combined use of *Coniothyrium minitans* (C) and *Trichoderma harzianum* (TH) as biological alternative to chemical SC control was investigated in two lettuce fields in the 2018-2019 production seasons in the province of Mersin/Turkey. In both lettuce trial plots, it was determined that the SC disease rates under single and combined use of *C* and TH were significantly reduced when compared to both the control and application of chemical fungicide that contained active substances Fluopyram + Pyrimethanil (Luna Tranquility). In all parcels where the biological preparations were applied alone and in combination, the obtained results suggest that these treatments may be a viable alternative to chemical methods. Thus, the highest impact on SC in both lettuce trial fields was 80-86.05% in C (4 kg/ha) + TH combination, while the lowest effect was obtained of only TH application with 54-60.47%. Analysis of the lettuce plant yield demonstrated that the application led to a significant increase in the yield in all lettuce cultivation fields when compared to control. The increase in yield ranged between 13-34% and 16-27% in the experimental fields and the highest increase was obtained with *Coniothyrium minitans* (4 kg/ha) + *Trichoderma harzianum* co-administration.
Keywords: *Biological control agent, Lactuca sativa L., Sclerotinia sclerotiorum, Trichoderma harzianum, yield*

Introduction

Lettuce (*Lactuca sativa* L.), which is a popular agricultural produce worldwide, is a cool climate vegetable that plays an important role in human nutrition. China is the leader in lettuce production followed by the USA, India and Spain, respectively. Different varieties are produced in different regions in Turkey with open field and greenhouse cultivation of this vegetable varieties with edible leaves. Turkey is the eighth largest lettuce producer in the world with 419 066 tons according to FAO statistics (Anonymous, 2017). In Turkey, lettuce farming is most popular in the Mediterranean, Marmara and Aegean regions.

The fungal diseases reduce the market value in the cultivation of lettuce, which has a rich nutritive value. *Sclerotinia sclerotiorum* is the most important and most common cause of fungal diseases that lead to major problems in lettuce cultivation fields. *S. sclerotiorum*, a soil-borne pathogen, is a member of *Sclerotiniaceae* family of the *Helotiales* group of the Discomycetes class. The host sequence of the disease agent is quite extensive and it leads to root, trunk and fruit rot in about 400 plant species (Purdy, 1979; Elshestawi et al., 2017; Smolinska and Kowalska, 2018). The disease agent spends the winter as sclerotium in the soil or in plant residues. The *S. sclerotiorum* sclerotia, which are prevalent in temperate regions, were recorded to survive in the soil for more than 10 years (Adams and Ayers, 1979; Clarkson et al., 2004). It was reported

http://www.aloki.hu ● ISSN 1589 1623 (Print) ● ISSN 1785 0037 (Online)
DOI: http://dx.doi.org/10.15666/aeer/1706_1568715701

that the product losses due to white mold disease caused by *Sclerotinia sclerotiorum* agent were up to 95% worldwide and in Turkey (Purdy, 1979; Young et al., 2001; Hao and Subbarao, 2005; Chitrampalam et al., 2010). It was reported that the crops are completely lost in completely infected fields and loses its market value due to losses in crop size and weight in partially infected fields (Clarkson et al., 2014).

In several studies conducted on the control of *Sclerotinia sclerotiorum* disease agent, it was reported that fungicide use harms the environment, as well as the reliability of the products consumed fresh, and increased the tolerance of the diseases against fungicides. In several studies, it was reported that mycoparasite fungi were effective against *Sclerotinia* diseases. Among these, *Coniothyrium minitans* and *Trichoderma* spp. are the most commonly used species (Turner and Tribe, 1976; Whipps and Budge, 1990; Budge and Whipps, 1991, 2001; Jones and Whipps, 2002). In the control of sclerotia diseases, it was emphasized that biological preparations were extremely important, since their action paths are not similar to fungicides and they directly destroy the sclerotia in the soil (Porter et al., 2002; Villalta et al., 2012). *C. minitans* produces secondary metabolites such as macrosphelide A, benzo furanones and chromans, which increase the colonization and degradation of *S. sclerotiorum* sclerotia and a wide range of cell wall degrading enzymes such as chitinases and glucans (Giczey et al., 2001; Tomprefa et al., 2011). Trichoderma fungi are highly competitive when compared to other soil-borne microorganisms due to its rapid growth and abundant spore production. The ability to secrete active compounds differs significantly among *Trichoderma* species and isolates. Thus, the mechanisms used by *Trichoderma* spp. in biological control vary based on the species, the pathogen and the host plant. In the case of antifungal activity against *S. sclerotiorum*, Trichoderma's mycoparasite properties play an important role. Trichoderma enzymes that break down the cellular wall of the pathogens were identified as chitinases, glucans, proteases and cellulases (Qualhato et al., 2013; Lopez-Mondejar et al., 2011; Naher et al., 2018). It was reported that Trichoderma species may be an important factor in the induction of plant growth and yield, as well as the control of plant phytopathogenic fungi in various plant species (Vinale et al., 2008; Bal and Altıntaş, 2008; Çolak, 2007; Çolak and Biçici, 2013; Elias et al., 2016).

Several studies were conducted globally that aimed to discover alternatives to fungicides in sclerotia diseases. Porter et al. (2002) preferred control with biological preparations in the control of *Sclerotinia* diseases and utilized *Coniothyrium minitans* and *Trichoderma* spp. species. Their findings were more successful when compared to fungicidal and Metham sodium applications. Villata et al. (2012), in a study conducted with biological preparations of *T. hamatum* 6sr4, *C. minitans* A69 and *C. minitans* in lettuce, reported that biocontrol agents could be used as an effective management tool against S. minor, the factor for white mold disease, in lettuce cultivation. Matheron and Porchas (2003) used Boscalid and Iprodion in lettuce cultivation fields against *S. sclerotiorum* and *S. minor*, which lead to white rot disease, while *Coniothyrium minitans* (Contans) was used as biological control agent. It was reported that their effectiveness was 33-38% and 52%, respectively in lettuce fields contaminated with *S. sclerotiorum*, and 53-35-32%, respectively in *S. minor* infected fields. Chitrapalam et al. (2008) conducted a two-year field study at Yuma County to investigate the effects of several biological agents against the disease induced by Sclerotinia species. Commercial formulations of biological preparations such as *Trichoderma harzianum* (Plantshield, Supersivit), *Gliocladium virens* (Soilgard), *Coniothyrium minitans* (Contans) and

http://www.aloki.hu ● ISSN 1589 1623 (Print) ● ISSN 1785 0037 (Online)
DOI: http://dx.doi.org/10.15666/aeer/1706_1568715701

Bacillus subtilis (Companion), and a chemical fungicide, Iprodione (Rovral) were evaluated and compared against *Sclerotinia sclerotiorum* and *S. minor*. In the study, it was found that using the preparations once was not sufficient, however it was determined that the severity of the disease decreased when the administrations were conducted twice. At the end of the study, *Coniothyrium minitans* (Contans) biological preparation provided the most effective control against *Sclerotinia sclerotiorum.*

The preparation that contains *Coniothyrium minitans* isolate is a mycoparasite fungus species that was not certified in Turkey, however used successfully in the control of white mold disease in the USA and G8 countries with the commercial brand of Contans WG in greenhouses and fields. However, in Turkey, no studies were conducted to assess the success criteria for these biological preparations in the control of white mold disease induced by *Sclerotinia sclerotiorum* in lettuce fields (Anonymous, 2017). In Turkey, several studies were conducted on the prevalence of *S. Sclerotiorum* disease agents, which determined the mycelial fitness groups (MFG), and in-vivo and in-vitro biological control opportunities (Çarkacı and Maden, 1986; Aksay et al., 1991; Mert-Turk and Mermer, 2004; Çolak, 2007; Çoşkun and Yildiz, 2017; Soylu et al., 2017). In studies on the prevalence of disease factor in lettuce conducted in Turkey, the prevalence was determined as 82.5% in Çanakkale (Mert-Türk and Mermer, 2004), 25-57.1% in Hatay province and districts (Soylu et al., 2017), 3.3% in Adana province Karataş district, 10.6% in Tarsus district and 4.6% in Osmaniye province (Çolak and Fidan, 2018). However, the studies on the control of the disease agent with biological control agents in the field are rather recent, and the effectiveness of the *Coniothyrium minitans* biological preparation on *Sclerotinia sclerotiorum* was investigated for the first time in the present study. Studies on the parasite effect on sclerotia and reduction of apothecia density of *Trichoderma harzianum* that we tested in control of *S. sclerotiorum* were mostly conducted in greenhouse and laboratory conditions (Bal and Altintaş, 2008; Geraldine et al., 2013; Smolinska et al., 2016). The number of studies on the antagonistic activity of *Trichoderma* in the field is very limited (Knudsen et al., 1991; Zeng et al., 2012a; Geraldine et al., 2013).

S. sclerotiorum is a disease agent difficult to control due to the resistant structures created by the disease agent in the soil. Currently, the losses due to the rapid degradation of the fungicides in the soil range between 5% and 40% in the control of the disease (Chitrampalan et al., 2011). The majority of the chemicals used in control aim to protect the parts of the host plant that are above the ground, especially the flowers, from ascospore infection. Thus, the application time should be carefully selected and the green parts should be covered with medication for an effective chemical control. In this context, due to the residual risks caused by the use of chemicals in control, the research on possibilities of biological control became popular in recent years. In biological control studies, it was observed that the studies mostly focused on the parasite infection of sclerotia mainly by mycoparasite fungi. The present study investigated the effectiveness of single and combined applications of *Coniothyrium minitans* and *Trichoderma harzianum,* which are biological agents alternative to chemical control, in the control of white mold disease (*Sclerotinia sclerotiorum*) that causes economic damages in lettuce cultivation.

http://www.aloki.hu ● ISSN 1589 1623 (Print) ● ISSN 1785 0037 (Online)
DOI: http://dx.doi.org/10.15666/aeer/1706_1568715701

Materials and methods

The study area

Control experiments were set up under producer conditions in the study lettuce fields to determine the effectiveness of *Coniothyrium minitans* (strain CON/M/91-08, 1 x 10^{12} CFU/kg, Contans, Bayer) and *Trichoderma hazianum* (*Trichoderma harzianum* Rifai race KRL-AG2 (TH, T-22 Planter Box, 1x10^{7} CFU/g, Bioglobal) biological preparations against white mold disease. Yonca 80 lettuce variety was used as material. For this purpose, field experiments were set up in two lettuce fields in Mersin province Kazanlı (KA) and Demirhisar (DE) regions that are naturally inoculated and in which the disease was prevalent in the previous cultivation season in the 2018-2019 cultivation season. However, for homogenous distribution of the disease agent in all experiment plots, artificial inoculation (25 g/m^2) was conducted with *Sclerotinia sclerotiorum* (SC) after the soil was plowed and ready for seeding. For this purpose, SC region isolate obtained from lettuce plant was used in field trials. The SC isolate was incubated in PDA for 10 days at 25 °C and the disks obtained from the SC isolate were inoculated to humidified and sterilized wheat medium (1000 g wheat + 800 ml water) in Erlenmeyer flasks and allowed to incubate another 10 days at 25 °C. The inoculum developed in the incubation was broken down and 25 g was applied per 1 square meter experimental soil. Then the soil was processed with a rotovator at a depth of 5-10 cm to allow homogenous distribution of the inoculum in the soil (Chitrampalam et al., 2008; Elshestawi et al., 2017). Lettuce seedlings were planted in the fields of sandy loam soil structure in a distance of 40 cm on the row and between rows. The experiment was designed in 4 replicates for each application and 20 lettuce plants per replicate (total 80 plants) based on randomized blocks experimental design.

Biological preparation and fungicide application

Coniothyrium minitans and *Trichoderma harzianum* biological preparations were applied to the soil via absorption immediately after the lettuce seedlings planted. Biological preparations were applied to the plant for the second time as recommended in the thinning period after the initial single and combined applications. For this purpose, *Coniothyrium minitans* (C) biological preparation was applied in recommended three doses (C2: 2 kg/ha, C3: 3 kg/ha; C4: 4 kg/ha), while *Trichoderma harzianum* (TH) biological preparation was applied in the recommended (50 g/100 lt/T-22) dose. In the study, Luna Tranquility SC (125 g/L Fluopyram + 375 g/L Pyrimethanil/SC, Bayer) was used as a chemical fungicide which was used extensively in *Sclerotinia sclerotiorum* control in lettuce fields. Luna Tranquility SC was applied once in the thinning period on green sections in a single dose of 100 lt/da as recommended in manufacturer's instructions (*Table 1*). A row of safety lanes was left between the application plots. The control plot plants were applied only water (without biological preparat and fungicide) (Elsheshtaewi et al., 2017). In the harvest, the plants were evaluated as sick and healthy.

At the end of the count, percentage of infected and non-infected plants were determined among the plants divided as sick and healthy and the percentage of the impact of the treatments were evaluated with Abbott's formula (% effect = [control (%) – application (%) / control (%)] × 100) and statistical analyzes were conducted (Karman, 1971). The analyses of variance and mean values were compared with the LSD test (P: 0.05).

http://www.aloki.hu ● ISSN 1589 1623 (Print) ● ISSN 1785 0037 (Online)
DOI: http://dx.doi.org/10.15666/aeer/1706_1568715701

Determination of the effect of applications on the yield and certain physical properties

In the study, when the lettuce in the experimental fields were ready for harvest, 10 plants were removed from each replicate to represent the average in all application plots and mean marketable head weight (kg/plant), root weight (g), root length and crown diameter (mm) were measured. After the weights of the plants harvested from each plot were determined, the mean plant weight (kg/plant) and parcel yield (kg/da) were calculated. For this purpose, marketable head weight (kg/plant) was determined after poor quality leaves and the roots were removed using precision scales. Crown diameter (mm) was measured by a digital caliper (SC Mitutoyo, Japan), which was sensitive to 0.02 mm, using the plants harvested from inoculated fields. Mean root length (cm) and weight (g) were determined by measuring from the crown (cm) and by weighing with a precision scale (g) after the plants were harvested and washed without damaging the roots (Tüzel et al., 2011).

Table 1. *Information on products tested against white mold disease in lettuce*

Active ıngredient	Product name	Formulation type	Application rate
Coniothyrium minitans (strain CON/M/91-08, 1 x 10^{12} CFU/kg)	Contans	Wettable granule-WG	2-4 kg/ha
125 g/L Fluopyram + 375 g/L Pyrimethanil	Luna Tranquility	Suspension concentrate-SC	100 ml/da
Trichoderma harzianum Rifai race KRL-*AG2*, 1×10^7 CFU/g	T-22 Planter Box	Wettable powder-WP	50 g/100 lt

Results and discussion

The effects of biological preparation applications on White mold disease

The data obtained in the studies conducted to demonstrate the efficiency of single and combined use of biological agents *Coniothyrium minitans* and *Trichoderma harzianum* that are alternatives to chemical control of white mold disease (*Sclerotinia sclerotiorum*) that causes significant economic damages in the cultivation of lettuce, which is an edible vegetable are presented in *Table 1*. *Table 1* demonstrated that the differences between the applications in both trial fields were statistically significant ($P < 0.05$). The disease infection rates in control plots in both lettuce trials were 62.50% and 53.75%. It was observed that the rate of disease rate significantly decreased in both single and combined use of *Coniothyrium minitans* and *Trichoderma harzianum* when compared to both the control and chemical fungicide use. In this context, the lowest infected plant rate was 12.5% in C4 + TH applied plots among the biological preparation applications in SC control when compared to control and pesticide applications and that was followed by C3 (3 kg/da) + TH and C4 (4 kg/da) applications (*Table 1*). Certain studies also reported that a combination of certain antagonists could lead to a higher level of protection, however improved control could not be observed in all cases (Spadaro and Gullino, 2005). The success of biological preparations could differ based on the soil type, type of biological agent, plant interactions and disease pathogen (Celar, 2002; Smolinska and Kowalska, 2018). It was reported that high soil moisture is important in degradation of the sclerotia in the soil by *C. minitans* (Trutmann et al., 1980). Budge et al. (1995) successfully integrated *C. minitans* and

http://www.aloki.hu ● ISSN 1589 1623 (Print) ● ISSN 1785 0037 (Online)
DOI: http://dx.doi.org/10.15666/aeer/1706_1568715701

Trichoderma virens combinations in *S. sclerotiorum* control in greenhouse studies. The greatest decrease in the number and viability of sclerotia was obtained with the combination of *C. minitans* and *Trichoderma virens* in the second harvest, while in the third harvest the only significant reduction was achieved with *C. minitans* applications. In another study, *T. harzianum* T-22 isolate (PlantShield) protected the soybean against S. sclerotiorum and reduced the disease severity index by 38.5% in the field crops (Zeng et al., 2012a). Gerlagh et al. (1999) reported that mycoparasite *C. minitans* had the potential to keep soil contamination at low levels in crop rotations in various sclerotiorum-sensitive crops.

In the present study, the statistical analyzes conducted on the data obtained in KA plot trials demonstrated that the lowest infected plant rate was obtained with Luna (11.25%), C4 + TH (12.50%) and C3 + TH (15%) applications, while the highest infected plant rate was obtained with TH application (28.75%). In DE plot, the lowest infected plant rate was obtained with Luna (6.25%), C4 + TH (7.50%) and C3 + TH (8.75%), while the highest infected plant rate was obtained with TH application (21.25%). The most successful alternative to chemical applications was obtained with C4 + TH application (86.5%) in DE plots, followed by C3 + TH and single C4 application with 83.72% (*Fig. 1*). Chitrampalan et al. (2008) investigated the action of *Trichoderma harzianum* (Plantshield), *Gliocladium virens* (Soilgard), *Coniothyrium minitans* (Contans), *Bacillus subtilis* (Companion) biological preparations and the fungicide with Iprodione (Rovral) active agent in control of *Sclerotinia sclerotiorum* and *S. minor* disease agents that are destructive in lettuce cultivation. It was reported in the study that single applications of biological preparations and fungicide were not effective in the control of disease agents. It was reported that twice *Coniothyrium minitans* application during the planting and post-thinning periods reduced *Sclerotinia sclerotiorum* incidence and improved the yield. There was no significant decrease in disease rates in other biocontrol products. The study findings demonstrated that *Coniothyrium minitans* (Contans) was the most effective application in control of *S. sclerotiorum* induced white mold disease in lettuce. These findings were consistent with the present study. Similar to the current study, it was reported that successful results were achieved with twice application of biologic preparations in disease control in several studies (Chitrampalam et al., 2010). The effects of single application of Contans (*Coniothyrium minitans*) and in combination with Radix (*Trichoderma asperellum* and *Trichoderma gamsii*), Kraft pine lignin and Rovral were compared in disease control in naturally S. Sclerotiorum-infected lettuce greenhouses. Single application of 4 kg/ha Contans had a negative effect on sclerotia viability, however did not reduce the disease incidence in lettuce. In the study, the highest impact on disease rate in different harvest periods was obtained in the third harvest and the lowest disease rate was obtained with Contans + lignin application (4.7%). In the study, this was followed by Contans + lignin + Radix application with a 6.7% rate among biological applications when compared to chemical combinations. In the study, it was reported that the significant decrease in sclerotia viability that was observed in the soil treated with Contans could be due to the long incubation time, repeated application, different climatic conditions and the use of different varieties (Van Bendeneden et al., 2010).

Commercial Luna was successful as a standard fungicide in the control of Sc in lettuce trial fields. However, significant losses in lettuce due to white mold despite excessive fungicide applications continue today. Chitrampalam et al. (2011) investigated the effectiveness of *C. minitans* (Contans) application in different doses

http://www.aloki.hu ● ISSN 1589 1623 (Print) ● ISSN 1785 0037 (Online)
DOI: http://dx.doi.org/10.15666/aeer/1706_1568715701

and times on white mold in lettuce in 2011. In field experiments, lower sclerotia was detected in all Contans applications when compared to Endura chemical fungicide and control applications. It was found that the disease rate was low in other applications similar to Endura fungicide application plots. As a result of the study, it was reported that Contans use to lower the sclerotia count in the soil was the key to long-term success in white mold disease control and Endura fungicide application was also useful to protect the plant from disease infection. The findings of the study were consistent with our findings.

Figure 1. *Sclerotinia sclerotiorum which causes white mold disease in lettuce, black sclerotia, white mycelium and brown, soft, watery decays in lettuce leaf in control plant*

In our study, the impact rates of the applications in disease control demonstrated that the highest effect was obtained with Luna chemical application in the field experiments (*Table 2*). In both field experiments where the biological preparations were applied alone and in combination, hopeful results that may be an alternative to the success of the chemical applications were obtained. Thus, the highest effect was obtained with C4 + TH application (80-86.05%), while the lowest effect was obtained with TH application (54-60.47%). The low variation among the effects of biological agents on the disease in both experiment fields was due to the fact that, as stated by Howel (2003), the biological control factor was dependent on the pathogen and host plant interaction and the presence of other microorganisms in soil microflora. The studies on parasite infection of Trichoderma isolates and S. sclerotiorum induced sclerotia and on reduction of apothecia concentration were mostly conducted in greenhouse and laboratory conditions (Inbar et al., 1996; Matroudi et al., 2009; Smolinska et al., 2016). In a study conducted in greenhouse, Inbar et al. (1996) determined that *Trichoderma harzianum* applications reduced white mold disease by 46-72% in lettuce when compared to control plants. However, the number of studies on antagonistic activity of Trichoderma in field conditions is quite limited (Knudsen et al., 1991; Zeng et al., 2012a; Geraldine et al., 2013). The effects of biological control agents *Coniothyrium minitans* CON/M/91-08, *Trichoderma harzianum* T-22, *Bacillus subtilis* QST 713 and *Streptomyces lydicus* WYEC 108 on Sclerotinia sclerotiorum production and sclerotia survival were investigated under controlled conditions. In the study, it was determined that *C. minitans* decreased apothecia and sclerotia by 81.2% and 50%, respectively, while *Trichoderma harzianum* decreased apothecia and sclerotia by 80.5% and 31.7%, respectively (Zeng et al., 2012b). Budge and Whipps (1991) investigated the effects of *Coniothyrium minitans*, *Trichoderma harzianum* (HH3) and *Trichoderma* sp (Bl) in Sclerotinia sclerotiorum induced disease control in two lettuce greenhouses and in a celery greenhouse. It was found that single C. Minitas applications reduced white mold

http://www.aloki.hu ● ISSN 1589 1623 (Print) ● ISSN 1785 0037 (Online)
DOI: http://dx.doi.org/10.15666/aeer/1706_1568715701

disease in lettuce and improved marketable yield. In the study, it was found that the tested Trichoderma species had no significant effect on the disease and had virtually no effect on the survival of sclerotia. In the study, the lowest S. sclerotiorum disease rate in lettuce was obtained with C. minitas application (48.2-50.3%) in the first and second harvest when compared to control (90.3-58.5%), and it was followed by *T. harzianum* Rifai (HH3) isolate application (62.8-56.2%). These findings were similar to the present study findings. In the study, the significant gradual reduction of sclerotia count in time, especially in the second lettuce crop, led to the idea that sclerotes caused an attack by natural microflora and micro-fauna. Huang et al. (2000) reported that *C. minitans* spore suspension spray during bean plant flowering reduced white mold disease rate by 56%. In the study conducted by application of *C. minitans* on the upper soil before soybean seeding, it was determined that the application reduced the *S. sclerotiorum* disease severity index by 68% and the sclerotia count in the soil by 95.3% (Zeng et al., 2012a).

In the present study, it was concluded that combined use of Contans (4 kg/da) + *Trichoderma harzianum* (50 g/100 lt, T-22) that included *Coniothyrium minitans* biological agent could an alternative to chemical applications in control of the white mold disease that leads to losses in market value of the lettuce crop, as well as significant yield losses (*Fig. 2*).

Figure 2. *An image from the most effective C. minitas and TH applications to control white mold disease in lettuce parcel*

Determination of the effect of the applications on the yield and certain physical properties

The data on the effects of the single and combined use of *Coniothyrium minitans* and *Trichoderma harzianum* biological preparations in control of SC disease agent that causes significant yield losses in lettuce cultivation on marketable mean head weight (kg/plant), yield (kg/da), root weight (g), root length (cm) and crown diameter (mm) of Iceberg lettuce cultivar are presented in *Table 3.*

Analysis of the lettuce plant yield demonstrated that KA and DE resulted in significant yield increases in lettuce cultivation. The increase in yield ranged between 13-34% and 16-27% in the experimental fields and the highest increase was obtained with 7560-6701 kg/da C4 + TH application and the lowest was obtained with control with 5640-5240 kg/da. An important parameter in yield and quality in lettuce cultivation is marketable head weight. The effects of biological preparation applications on marketable head weight were found to be statistically significant. In the study, an increase was observed in marketable head weight with all combined *Coniothyrium minitans* and *Trichoderma harzianum* applications. The highest marketable head weight

http://www.aloki.hu ● ISSN 1589 1623 (Print) ● ISSN 1785 0037 (Online)
DOI: http://dx.doi.org/10.15666/aeer/1706_1568715701

was obtained with combined C4 + TH (1.260-1.117 kg/plant) application in both experimental plots, followed by Luna chemical application (1.257-1.107 kg/plant). Chitrampalam et al. (2008) did not report statistically significant differences between the lettuce head weigh and yield with *Trichoderma harzianum* (Plantshield), *Gliocladium virens* (Soilgard), *Coniothyrium minitans* (Contans) and *Bacillus subtilis* (Companion) biological preparation applications used to control *S. sclerotiorum* in lettuce. However, in both lettuce locations, it was found that the twice *Coniothyrium minitans* application in planting and thinning periods effectively suppressed S. sclerotiorum, thus indirectly increasing the lettuce head weight. These findings were followed by *Gliocladium virens*, *Trichoderma harzianum* and *Bacillus subtilis* applications. These findings were consistent with the findings of our study.

Under field conditions, Knudsen et al. (1991) found that Trichoderma isolates contributed to an increase in lettuce head weight by releasing Trichoderma isolates to the soil for *S. sclerotiorum* sclerotia infection, and the experiments reduced the infection by 100%. In a study, Bal and Altıntaş (2008) investigated the effects of *Trichoderma harzianum* on lettuce plant development. It was determined that *T. harzianum* applications did not lead to a significant increase in lettuce yield and root growth. Rabeendran et al. (2000) reported that two *Trichoderma harzianum* isolates applied to the lettuce plant in the field increased the yield significantly. It was reported in several studies that various Trichoderma species increased the growth, development and plant yields at different rates in studies conducted with different plants. *Trichoderma* species are not only found on plant root surfaces, but also in various parts of the plant endophytically. It was also reported that these endophytic species promoted plant growth and protected the plant against biotic and abiotic factors (Bae et al., 2009 Poldma et al., 2002; Altıntaş and Bal, 2005; Elad et al., 2006; Druzhinina et al., 2011).

In the present study, the effects of single and combined *Coniothyrium minitans* and *Trichoderma harzianum* biological agent application in lettuce cultivation were statistically significant on lettuce root weight, root length and root diameter. When compared to the control application, the root weight increased in all applications in both experimental plots. The highest root weight was obtained in the KA plot with C4 + TH and Luna applications (45.59 g – 44.87 g) and in the DE plot, with C3 + TH and TH 3 + TH and C4 + TH applications (48.47 g – 46.59 g).

When compared to the control application, the highest increase in the root length in all applications in both experimental plots was 32-31%. The highest root length measurements were 18.82 cm with Luna and 18.61cm with C4 + TH applications. In DE parcel, the highest root length of 18.80 cm was obtained with combined C4 + TH biological preparation application, followed by C3 + TH application with 18.21 cm. Yedidia et al. (2001) reported that *Trichoderma harzianum* increased the root length in cucumber plant by 75% and root area by 95% in a study they conducted. In another study on the effects of *Trichoderma harzianum* on the development of lettuce plant, it was determined that TH application did not significantly increase the root growth in lettuce (Bal and Altintas, 2008).

The effects of the single and combined use of biological preparations compared to the control and chemical application (*Table 2*) demonstrated that the application led to an increase in crown diameter of the lettuce in KA and DE plots by 18% to 36%, respectively. The increase in crown diameter in both experimental plots was obtained in all plots where *Coniothyrium minitans* and *Trichoderma harzianum* were applied in combination. The highest increase in KA plot in crown diameter was obtained with C4

http://www.aloki.hu ● ISSN 1589 1623 (Print) ● ISSN 1785 0037 (Online)
DOI: http://dx.doi.org/10.15666/aeer/1706_1568715701

+ TH and C3 + TH applications (31.44 mm – 31.35 mm), while it was obtained with C4 + TH application (37.30 mm) in DE plot, followed by combined C3 + TH application (35.48 mm). The crown diameter was determined as 26.54-27.29 mm in the two experimental plots, respectively.

Table 2. *Lettuce white mold disease of applications in the control against the disease incidence and effect*

Treatments	Experiment area KA		Experiment area DE	
	Disease incidence (%)	% Effect	Disease incidence (%)	% Effect
C2	26.25 cd	58.00	20.00 b	62.79
C3	17.50 abc	72.00	10.00 a	81.40
C4	16.25 abc	74.00	8.75 a	83.72
TH	28.75 d	54.00	21.25 b	60.47
C2 + TH	25.0 bcd	56.00	11.25a	79.07
C3 + TH	15.00 ab	76.00	8.75 a	83.72
C4 + TH	12.50 a	80.00	7.50 a	86.05
Luna	11.25 a	82.00	6.25 a	88.37
Control	62.50 e	-	53.75 e	-
Lsd 0.05	9.703		7.463	

C2: Contans application of 2 kg/ha; C3: Contans application of 3 kg/ha; C4: Contans application of 4 kg/ha; TH: *Trichoderma harzianum* application of 50 g/100 lt; Luna application of 100 ml/da; Control: only water (without biological preparat and fungicide)

Table 3. *Effect of applications and some plant physical properties*

Treatments	Marketable mean head weight (kg/plant)		Yield (kg/da)		Root weight (g)		Root length (cm)		Root collar diameter (mm)	
	KA	DE	KA	DE	KA	DE	KA	DE	KA	DE
C2	1.063c	1.013b	6375c	6075ab	36.13de	37.79d	18.43abc	15.04e	28.84de	32.10e
C3	1.117bc	1.043ab	6702bc	6260ab	39.20c	40.60c	18.14abc	16.32cd	29.47cd	33.08d
C4	1.120bc	1.027ab	6720bc	6160ab	36.52c	40.73c	18.57ab	17.41b	29.60c	34.72c
TH	1.167b	1.073ab	7002b	6435ab	40.93b	36.95d	17.83abc	17.34b	30.52b	31.27f
C2 + TH	1.153b	1.050ab	6920b	6300ab	35.24de	38.52cd	17.46c	16.08d	27.69f	33.32d
C3 + TH	1.113bc	1.057ab	6678bc	6340ab	40.29bc	48.47a	17.53bc	18.21a	31.35a	35.48b
C4 + TH	1.260a	1.117a	7560a	6701a	45.59a	46.59ab	18.61a	18.80a	31.44a	37.30a
LUNA	1.257a	1.107ab	7542 a	6640ab	44.87a	44.20b	18.82a	17.03bc	28.58e	36.09b
Control	0.940 d	0.873c	5640 d	5240c	34.53e	36.04d	14.17d	14.31e	26.54g	27.29g
Lsd 0.05	0.057	0.084	341.984	508.269	1.641	2.670	0.959	0.754	0.704	0.729

C2: Contans application of 2 kg/ha; C3: Contans application of 3 kg/ha; C4: Contans application of 4 kg/ha; TH: *Trichoderma harzianum* application of 50 g/100 lt; Luna application of 100 ml/da; Control: only water (without biological preparat and fungicide)

http://www.aloki.hu ● ISSN 1589 1623 (Print) ● ISSN 1785 0037 (Online)
DOI: http://dx.doi.org/10.15666/aeer/1706_1568715701

Discussion

Although certified chemical fungicides are available in Turkey, especially in control of white mold disease in lettuce, the number of disinfestations or doses are increased due to the severity of the disease. This does not improve the control success, as well as causing environmental pollution and residual product threatens human health and disrupts the balance of nature. The emergence of plant resistance to agents used in these products is one of the most important problems induced by chemical control. The best way to limit the application of pesticides used in *Sclerotinia sclerotiorum* control in lettuce is cultivation of resistant varieties. However, due to the specific character of the disease induced by this pathogen, breeding programs had a limited success (Uloth et al., 2014). Today, in the absence of disease-resistant varieties, the research on environment-friendly methods such as biological methods have intensified for long-term destruction of *Sclerotinia sclerotiorum* in the soil.

In this context, the present study findings suggested that the use of Contans that contains *Coniothyrium minitans* biological agent (4 kg/da) + *Trichoderma harzianum* (50 g/100 lt/T-22) combination could be an alternative to chemicals in control of white mold disease that leads to market value losses and significant losses in the yield, especially in highly infected fields in lettuce cultivation. It was observed that several studies were conducted worldwide on biological control of white mold disease induced by *Sclerotinia sclerotiorum* disease agent. In both field and greenhouse experiments conducted to determine the impact of *Coniothyrium minitans* as a biological control agent against white mold disease, it was determined that single use of the biological preparations were not sufficient, however twice application of the agent significantly to reduces the severity of the disease (Chitrampalam et al., 2008).

The application of biological methods to control plant pathogens is known to be safer for the environment when compared to the use of pesticides. Chemical control of *Sclerotinia sclerotiorum* is quite difficult since ascospores can infect any part of the lettuce head. Also, it is more difficult to prevent after the presence of apothecia in the plant (Patterson and Grogan, 1985). Biological control methods may be partially sufficient to completely reduce the populations of plant disease pathogens. The complete destruction of the disease in the soil can only be possible if the pathogen concentration is already low in the soil. The most successful method, thus, is the combined application of antagonistic fungi with strong parasitic properties such as *C. minitas* and *Trichoderma* genus fungi (Smolinska and Kowalska, 2018).

However, in order to ensure a long-term and effective biological control in soil-borne diseases such as plant pathogens, especially *Sclerotinia sclerotiorum*, crop rotation, the use of resistant varieties, solarization (soil disinfection) and taking all cultural measures in combination are important (Subbarao, 1998; Villata et al., 2012; Çolak Ates et al., 2019). Therefore, an integrated approach that adopts multiple control measures could provide sustainable control against sclerotia. In the success of such a strategy, selection of agricultural and crop management practices that reduces the accumulation of pathogen inoculum and the risk of disease propagation is important (Koike et al., 2003).

http://www.aloki.hu ● ISSN 1589 1623 (Print) ● ISSN 1785 0037 (Online)
DOI: http://dx.doi.org/10.15666/aeer/1706_1568715701

Conclusion

In this study, it was concluded that Contans containing *Coniothyrium minitans* biological agent (4 kg/da) + *Trichoderma harzianum* (50 g/100 lt/T-22) could be an effective alternative to chemicals in the control against white mold disease by *Sclerotinia sclerotiorum.* Furthermore, *S. sclerotiorum* in areas where the risk of disease is very high, in order to prevent high *S. sclerotiorum* levels, very detailed control studies with biological preparations and existing fungicide applications and at different application doses are required.

Acknowledgements. The authors are so grateful to General Directorate of Agricultural Research and Policies (project number TAGEM-BS-15/09-10/02-08 (04)) for financial support.

REFERENCES

[1] Adams, P. B., Ayers, W. A. (1979): Ecology of Sclerotinia species. – Phytopathology 69: 896-899.
[2] Aksay, A., Biçici, M., Çınar, Ö. (1991): Beyaz çürüklük etmeni *Sclerotinia sclerotiorum* (Lib) de Bary'a karşı antagonistlerin belirlenmesi. – Çukurova Üniv. Ziraat Fak., Derg. 6(2): 55-62.
[3] Altıntas, S., Bal, U. (2005): Application of *Trichoderma harzianum* increases yield in cucumber (*Cucumis sativus*) grown in an unheated glasshouse. – J. Appl. Horticulture 7: 25-28.
[4] Anonymous (2017): FAOSTAT. – www.fao.org.
[5] Bae, H., Sicher, R. C., Kim, M. S., Kim, S. H., Strem, M. D., MeInice, R. L., Bailey, B. A. (2009): The beneficial endophyte *Trichoderma hamatum* isolate DS 219b promotes growth and delays the onset of the drought response in Theobroma cacao. – Journal of Experimental Botany 60: 3279-3295.
[6] Bal, U., Altintas, S. (2008): Effects Of *Trichoderma harzianum* on lettuce in protected cultivation. – Journal of Central European Agriculture 9(1): 63-70.
[7] Budge, S. P., Whipps, J. M. (1991): Glasshouse trials of Coniothyrium minitans and Trichoderma species for the biological control of *Sclerotinia sclerotiorum* in celery and lettuce. – Plant Pathol 40: 59-66.
[8] Budge, S. P., Whipps, J. M. (2001): Potential for integrated control of *Sclerotinia sclerotiorum* in glasshouse lettuce using *Coniothyrium minitans* and reduced fungicide application. – Phytopathology 91: 221-227.
[9] Budge, S. P., McQuilken, M. P., Fenion, J. S., Whipps, J. M. (1995): Use of *Coniothyrium minitans* and *Gliocladium virens* for biological control of *Sclerotinia sclerotiorum* in glasshouse lettuce. – Biol Control 5: 513-522.
[10] Çarkacı, N., Maden, S. (1986): Host speciation, antagonists and parasites of Sclerotinia sclerotiorum (Lib.) de Bary. – J. Turk. Phytopath. 15: 113-122.
[11] Celar, F. (2002): Influence of root exudates of different plant seedlings on mycelial growth of antagonistic fungi *Trichoderma* spp. and *Gliocladium roseum*. Zb. – Biotech. Fak. Univ. Ljublj. Kmet. 79-2: 343-348.
[12] Chitrampalam, P., Figuli, P. J., Matheron, M. E., Subbarao, K. V., Pryor, B. M. (2008): Biocontrol of lettuce drop caused by *Sclerotinia sclerotiorum* and *S. minor* in desert agroecosystems. – Plant. Dis. 92: 1625-1634.
[13] Chitrampalam, P., Cox, C. A., Turini, T. A., Pryor, B. M. (2010): Efficacy of *Coniothyrium minitans* on lettuce drop caused by *S. minor* in desert agroecosystem. – Biological Control 55: 92-96.

http://www.aloki.hu ● ISSN 1589 1623 (Print) ● ISSN 1785 0037 (Online)
DOI: http://dx.doi.org/10.15666/aeer/1706_1568715701

[14] Chitrampalam, P., Wu, B. M., Koike, S. T., Subbarao, K. V. (2011): Interactions between *Coniothyrium minitans* and *Sclerotinia minor* affect biocontrol efficacy of *C. Minitans.* – Phytopathology 101(3): 358-366.
[15] Clarkson, J. P., Phelps, K., Whipps, J. M., Young, C. S., Smith, J. A., Watling, M. (2004): Forecasting Sclerotinia disease on lettuce: toward developing a prediction model for carpogenic germination of sclerotia. – Phytopathology 94: 268-279.
[16] Clarkson, J. P., Fawcett, L., Anthony, S. G., Young, C. (2014): A model for *Sclerotinia sclerotiorum* infection and disease development in lettuce, based on the effects of temperature, relative humidity and ascospore density. – PLoS One 9(4): e94049.
[17] Çolak, A. (2007): Biocontrol products for use against tomato diseases. – II. International Symposium on Tomato Diseases, 8-12 October, Kuşadası/İzmir, Turkey.
[18] Çolak, A., Biçici, M. (2013): Integrated disease management of fusarium crown and root rot of greenhouse-grown tomato in eastern Mediterranean region of Turkey. – Journal of Agricultural Sciences 19: 89-100.
[19] Çolak, A. A., Fidan, H. (2018): Identification of white rot and the most common virus diseases in lettuce growing in eastern Mediterranean region. – 1st Internatıonal Gap Agriculture and Livestock Congress, 25-27 April 2018, Şanlıurfa, Turkey
[20] Çolak Ates, A., Fidan, A., Karacaoğlu, M., Dasgan, H. Y. (2019): The identification of the resistance levels of *Fusarium oxysporum* f. sp. *radicis-lycopersici* and *Tomato yellow leaf curl viruses* in different tomato genotypes through traditional and molecular methods. – Applied Ecology and Environmental Research 17(2): 2203-2218.
[21] Çoşkun, B. Ç., Yıldız, F. (2017): Biological control of white mold disease (*Sclerotinia sclerotiorum*) on lettuce by using fungal antagonists. – J. Turk. Phytopath. 46(1): 1-14.
[22] Druzhinina, I. S., Seidl-Seiboth, V., Herrera-Estrella, A., Horwitz, B. A., Kenerley, C. M., Monte, E., Mukherjee, P. K., Zeilinger, S., Grigoriev, I., Kubicek, C. P. (2011): *Trichoderma* - the genomics of opportunistic success. – Nature Reviews Microbiology 9: 749-759.
[23] Elad, Y., Chet, I., Henis, Y. (2006): Biological control of Rhizoctonia solani in strawberry fields by Trichoderma harzianum. – Plant and Soil 60: 245-254.
[24] Elias, L. M., Domingues, M. V. P. F., Moura, K. E., Salomão, D., Harakava, R., Patricio, F. R. A. (2016): Selection of Trichoderma isolates for biological control of Sclerotinia minor and S. sclerotiorum in lettuce. – Summa Phytopathologica 42(3): 216-221.
[25] Elsheshtawi, M., Maged, T. E., Shaban, R. S., Ali, H. B., Arif, A. M., Dikshit, G., Aref, S. M., Elgorban, A. M. (2017): Integrated control of white rot disease on beans caused by Sclerotinia sclerotiorum using Contans and reduced fungicides application. – Saudi Journal of Biological Sciences 24: 405-409.
[26] Geraldine, A. M., Lopes, F. A. C., Carvalho, D. D. C., Barbosa, E. T., Rodrigues, A. F., Brandao, R. S., Ulhoa, C. J., Junior, M. L. (2013): Cell wall-degrading enzymes and parasitism of sclerotia are key factors on field biocontrol of white mold by *Trichoderma* spp. – Biol Control 67: 308-316.
[27] Gerlagh, M., Goossen-van de Geijn, H. M., Fokkema, N. J., Vereijken, P. F. G. (1999): Long-term biosanitation by application of *Coniothyrium minitans* on *Sclerotinia sclerotiorum* infected crops. – Phytopathology 89: 141-147.
[28] Giczey, G., Kerenyi, Z., Fulop, L., Hornok, L. (2001): Expression of cmg1, and exo-beta-1,3-glucanase gene from *Coniothyrium minitans*, increases during sclerotial parasitism. – Appl. Environ. Microbiol. 67: 865-871.
[29] Hao, J. J., Subbarao, K. S. (2005): Comparative analyses of lettuce drop epidemics caused by *Sclerotinia minor* and *S. sclerotiorum*. – Plant Dis. 89: 717-725.
[30] Howell, C. R. (2003): Mechanisms employed by *Trichoderma* species in the biological control of plant diseases: the history and evolution of current concepts. – Plant Disease 87: 4-10.

http://www.aloki.hu ● ISSN 1589 1623 (Print) ● ISSN 1785 0037 (Online)
DOI: http://dx.doi.org/10.15666/aeer/1706_1568715701

[31] Huang, H. C., Patterson, C. L., Grogan, R. G. (1985): Differences in epidemiology and control of lettuce drop caused by *Sclerotinia minor* and *S. sclerotiorum.* – Plant Disease St. Paul 69: 766-770.
[32] Inbar, J., Menendez, A., Chet, I. (1996): Hyphal interaction between *Trichoderma harzianum* and *Sclerotinia sclerotiorum* and its role in biological control. – Soil Biol. Biochem. 28: 757-763.
[33] Jones, E. E., Whipps, J. M. (2002): Effect of inoculums rates and sources of *Coniothyrium minitans* on control of *Sclerotinia sclerotiorum* disease in glasshouse lettuce. – Eur J Plant Pathol 108: 527-538.
[34] Karman, M. (1971): Bitki Koruma Araştırmalarında Genel Bilgiler Kitabı. – T. C. Tarım Bakanlığı Zirai Mücadele ve Zirai Karantina Genel Müdürlüğü Yayınları. Bornova/ İzmir. Ağustos 1971.
[35] Knudsen, G. R., Eschen, D. J., Dandurand, L. M. (1991): Potential for biocontrol of *S. sclerotiorum* through colonization of sclerotia by *T. harzianum.* – The American Phythopathological Society. Plant Dis. 75(5): 466-470.
[36] Koike, S. T., Subbarao, K. V., Davis, R. M., Turini, T. A. (2003): Vegetable Disease Caused by Soil Borne Pathogens. – University of California, Division of Agriculture and Natural Resources, Commercial Greenhouse Vegetable Handbook, Publication 21575, pp. 1-13.
[37] Lopez-Mondejar, R., Ros, M., Pascual, J. A. (2011): Mycoparasitism-related genes expression of *Trichoderma harzianum* isolates to evaluate their efficiency as biological control agents. – Biol Control 56: 59-66.
[38] Matheron, M. E., Porchas, M. (2003): Vegetable Crops 1997-2003. – The University of Arizona Cooperative Extension Search Reports, Tucson, AZ.
[39] Matroudi, S., Zamani, M. R., Motallebi, M. (2009): Antagonistic effects of three species of Trichoderma sp. on *Sclerotinia sclerotiorum*, the causal agent of canola stem rot. – Egypt J Biol 11: 37-44.
[40] Mert-Türk, F., Mermer, D. (2004): Çanakkale'de Örtüaltında Yetiştirilen Marullarda *Sclerotinia sclerotiorum'*un Yaygınlığının ve Misel Uyum Gruplarının Saptanması. MKU. – Ziraat Fakültesi Dergisi 9(1-2): 1-8.
[41] Naher, L., Yusuf, U. K., Habib, S. H., Ky, H., Siddiquee, S. (2018): Mycoparasitsm activity of Trichoderma harzianum associated with chitinase expression against Ganoderma boninense. – Pak. J. Bot. 50(3): 1241-1245.
[42] Poldma, P., Albrecht, A., Merivee, A. (2002): Influence of fungus *Trichoderma viride* on the yield of cucumber in greenhouse conditions. – Proc. Conference on Scientific Aspects of Organic Farming. Jelgava, Latvia 21-22 March 2002, pp. 176-180.
[43] Porter, I., Pung, H., Villalta, O., Crnov, R., Stewart, A. (2002): Development of biological controls for Sclerotinia diseases of horticultural crops in Australasia. – 2nd Australasian Lettuce Industry Conference, 5-8 May 2002, University of Queensland, Gatton Campus.
[44] Purdy, L. H. (1979): *Sclerotinia sclerotiorum* - history, diseases and symptomatology, host range, geographic distribution, and impact. – Phytopathology 69: 875-880.
[45] Qualhato, F. T., Cardoso, L. A. F., Steindorft, S. A., Brandao, S. R., Jesuino, A. S. R., Ulhoa, J. C. (2013): Mycoparasitism studies of Trichoderma species against three phytopathogenic fungi: evaluation of antagonism and hydrolytic enzyme production. – Biotechnol. Letter 35: 1461-1468.
[46] Rabeendran, N., Moot, D. J., Jones, E. E., Stewart, A. (2000): Inconsistent growth promotion of cabbage and lettuce from Trichoderma isolates. – N. Z. Plant Prot. 53: 143-146.
[47] Patterson, C. L., Grogan, R. G. (1985): Differences in epidemiology and control of lettuce drop caused by *Sclerotinia minor* and *S. Sclerotiorum.* – Plant Disease 69: 766-770.
[48] Smolinska, U., Kowalska, B. (2018): Biological control of the soil-borne fungal pathogen *Sclerotinia sclerotiorum*, a review. – Journal of Plant Pathology 100: 1-12.

http://www.aloki.hu ● ISSN 1589 1623 (Print) ● ISSN 1785 0037 (Online)
DOI: http://dx.doi.org/10.15666/aeer/1706_1568715701

[49] Smolinska, U., Kowalska, B., Kowalczyk, W., Szczech, M., Murgrabia, A. (2016): Eradication of *Sclerotinia sclerotiorum* sclerotia from soil using organic waste materials as Trichoderma fungi carriers. – J Horticultural Res 24: 101-110

[50] Soylu, S., Sertkaya, E., Üremiş, I., Bozkurt, A., Kurt., Ş. (2017): Prevalence and incidence of important disease agents, insects and weed species in lettuce (*Lactuca sativa* L.) growing fields in Hatay Province. – Journal of Agricultural Faculty of Mustafa Kemal University 22(1): 23-33.

[51] Subbaro, K. V. (1998): Progress toward integrated management of lettuce drop. – Plant Dis. 82: 1068-1078.

[52] Spadaro, D., Gullino, M. L. (2005): Improving the efficacy of biocontrol agents against soilborne pathogens. – Crop Prot. 24: 601-613.

[53] Subbarao, K. V. (1998): Progress toward integrated management of lettuce drop. – Plant Dis. 82: 1068-1078.

[54] Tomprefa, N., Hill, R., Whipps, J., McQuilken, M. (2011): Some environmental factors affect growth and antibiotic production by mycoparasite *Coniothyrium minitans*. – Biocontrol Sci Tech 21: 721-731.

[55] Trutmann, P., Keane, P. J., Merriman, P. R. (1980): Reduction of sclerotial inoculums of *Sclerotinia sclerotiorum* with *Coniothyrium minitans*. – Soil Biol Biochem 12: 461-465

[56] Turner, G. J., Tribe, H. T. (1976): On *Coniothyrium minitans* and its parasitism of *Sclerotinia* species. – Transactions of the British Mycological Society 66: 97-105.

[57] Tüzel, Y., Oztekin, G. B., Duyar, H., Eşiyok, D., Kılıç, G. O., Anaç, D., Kayıkçıoğlu, H. H. (2011): Effects of some organic fertilizers and agryl cover on yield, quality and leaf nutrient content and soil productivity in organic lettuce growing. – Journal of Agricultural Sciences 17: 190-203.

[58] Uloth, M., You, M. P., Finnegan, P. M., Banga, S. S., Yi, H., Barbetti, M. J. (2014): Seedling resistance to *Sclerotinia sclerotiorum* as expressed across diverse cruciferous species. – Plant Dis 98: 184-190.

[59] Van Beneden, S., Leenknegt, I., Franca, S. C. and Hofte, M. (2010): Improved control of lettuce drop caused by *Sclerotinia sclerotiorum* using Contans combined with lignin or a reduced fungicide application. – Crop Prot. 29(2): 7.

[60] Villalta, O. N., Wite, D., Hunt, J., Stewart, A., Porter, I. J. (2012): Biological control of *Sclerotinia minor* on lettuce using *Trichoderma* and *Coniothyrium* species. – Acta Horticulturae 944: 51-58.

[61] Vinale, F., Sivasithamparam, K., Ghisalberti, E. L., Marra, R., Woo, S. L., Lorito, M. (2008): Trichoderma-plant-pathogen interactions. – Soil Biol Biochem 40: 1-10

[62] Whipps, J. M., Budge, S. P. (1990): Screening for sclerotial mycoparasites of *Sclerotinia sclerotiorum*. – Mycological Res. 94: 607-661.

[63] Yedidia, I., Srivastava, A. K., Kapulnik, Y., Chet, I. (2001): Effect of *Trichoderma harzianum* on microelement concentrations and increased growth of cucumber plants. – Plant Soil 235: 235-242.

[64] Young, C. S., Smith, J. A., Watling, M., Clarkson, J. P., Whipps, J. M. (2001): Environmental Conditions Influencing Apothecial Production and Lettuce Infection by *Sclerotinia sclerotiorum* in Field Conditions. – In Young, C., Hughes, K. (eds.) Proceedings of the 6th International Sclerotinia Workshop. York, pp. 181-182.

[65] Zeng, W., Kırk, W., Hao, J. (2012a): Field management of Sclerotinia stem rot of soybean using biological control agents. – Biol Control 60: 141-147.

[66] Zeng, W., Wang, D., Kırk, W., Hao, J. (2012b): Use of *Coniothyrium minitans* and other microorganisms for reducing *Sclerotinia sclerotiorum*. – Biol Control 60: 225-232.

http://www.aloki.hu ● ISSN 1589 1623 (Print) ● ISSN 1785 0037 (Online)
DOI: http://dx.doi.org/10.15666/aeer/1706_1568715701

PHYSIOLOGICAL CHANGES OF CULTIVATED EGGPLANT (*SOLANUM MELONGENA* L.) IN RESPONSE TO WATER DEFICIT

AL-MUWAYHI, M. A.

Department of Physics and Chemistry, Faculty of Science, Shaqra University
P.O. Box 33, Shaqra, 11961, Kingdom of Saudi Arabia
(e-mail: malmuwayhi@su.edu.sa; phone: +966-11-6224-4118)

(Received 5th Sep 2019; accepted 15th Nov 2019)

Abstract. The effects of drought on the physiology of eggplants (*Solanum melongena* L. cv., Madona) were studied. Drought stress treatment had been done by irrigating the plants with 80%, 60% and 40% of water needed to reach soil pot capacity, plus normal irrigation (control treatment). The objective of this research was to reveal physiological response of eggplant to different levels of drought stress, as well as, its nutrient. The obtained results showed that, nutrients concentrations of the studied eggplants grown in pots under different irrigation treatments decrease according to water stress levels. Drought stress significantly reduced the ammount of total chlorophyll, chlorophyll a, chlorophyll b and total carotenoids resulting in damaged leaves. Carotenoids decreased in response to water stress from 8.65 mg/g FW under control in comparison to 5.84 mg/g FW the fourth water deficit treatment. All water stress treatments increased the accumulation of proline content in plant. Lack of water in plant modified anti-oxidative enzyme activities in order to alleviate the water stress. The results indicate that irrigation treatment with 80% of pot capacity have more efficient water use than 60% and 40%, which reduces drought stress and improves ionic balance of the plants.
Keywords: *eggplant, water stress, nutrients, antioxidant enzymes, pigments, proline*

Introduction

Eggplant (*Solanum melongena* L.) is a popular nightshade crop plant commonly cultivated in tropical and subtropical farmland. The stunted growth, lack of yield and poor quality of plant product caused by water stress has been well studied by researchers and agriculturists, and many physiological processes involved for this reduction in variable crop plants. Many studies has been carried out in Asia, Africa, Europe and different region on eggplant irrigation (Gaveh et al., 2011; Karam et al., 2011) showing that eggplant can be produced at moderate levels of water stress without severe effect on fruit yield. There is a complex relationship between yield, physiological responses and vegetative growth to different level of water stress, especially in eggplant under semi-arid conditions (Kirnak et al., 2001). Plants experience water stress during intense transpiration rate or when there is limited water supply around their roots. Plants attempt to eleviate the negative effect of drought stress using a set of biochemical and physiological mechanisms.

Concerning water scarcity, Saudi Arabia is an arid high temperature zone and faced with increased competitions for water resources between different sectors (agriculture, industry or domestic consumption). So economic and effective irrigation regimes is an important matter to solve.

High yield of crop production and water savings are some of the benefits in optimizing irrigation water management. Appropriate strategies in agriculture practices are need to be found to get efficient use of limited water in semi arid zones. Abd El-Ghany et al. (2004) stated that the identified varieties that had high and/or moderate

http://www.aloki.hu ● ISSN 1589 1623 (Print) ● ISSN 1785 0037 (Online)
DOI: http://dx.doi.org/10.15666/aeer/1706_1570315711

yield potential besides desirable specific adaptation traits are useful for drought stress and could be combined to achieve optimum performance. One important strategy is to better manage water and increase its productivity (Molden, 1997; Molden et al., 2001; Gupta et al., 2016; Tani et al., 2018). Effective irrigation scheduling needs to be designed to ensure the optimal use of limited water. Díaz-Pérez and Eaton (2015) indicated that eggplant may tolerate moderate drought stress, since plants watered at 67% Evapotranspiration level (Etc). A comprehensive knowledge of drought stress effect on plants is critical to enhanced management practices and crops breeding efforts in agriculture under semi arid condition. Many works in this field were developed over the past twenty years, covering topics from plant approaches to control water status under drought, to the physiological and biochemical processes underlying plant response to water deficits (Chaves, 1991; Cornic and Massacci, 1996; Kurniawati, 2014; Buhtz et al., 2017). Kurniawati (2014) found that during the drought treatment, plant growth, biomass, media water content, relative water content, chlorophyll content concentration were reduced while proline and polyamines were increased and reached the high levels on 14 to 21 days after the treatment.

The present research was carried out to study the effect of drought stress on physiological characters of studied eggplants, i.e., leaf chlorophyll, carotenoids, proline and enzyme activity, as well as, some nutrients (K, P, C and N) uptake.

Materials and Methods

Within the experimental researches to evaluate many of solanaceae plants at the Agricultural Experimental and Research Station (24°42'N 44°46'E, 600 Alt.) in Dirab region, Saudi Arabia, during the spring growing season (March to June), it is worth mentioning like research Almohisen (2015). Seeds had been planted at nursery in greenhouse until seedlings have three foliage leaves and reached 15 cm shoot height, then were transported to 30 cm pots size (30 cm top dimeter, 25 cm base dimeter and 30 cm pot height) after filled with sandy loam (1:1) media in the outfield. Irrigating treatment started on 1st of March and the harvest were done on 1st of June. All agronomy practices and plant protection had been done according to the agricultural region. Randomized complex block design with three replications were used. Soil physical and chemical properties measured according to Cassel and Nielsen (1986), Klute et al. (1986) and Rhoades (1982). Also, chemical properties of irrigation water were estimated according to Bock (1984) as shown in *Table 1*.

Irrigation treatments

Irrigation treatments depended on measuring the deficit of soil moisture contents from the pot capacity, the potential evaporation was calculated using the Pan evaporation as described by Richards (1969). Irrigation treatments included 4 levels of water deficit stress that were control T1 (100% pot capacity), T2 (80% pot capacity), T3 (60% pot capacity) and T4 (40% pot capacity).

Physiological parameters

Elements were estimated according to Doorenbos (1975). Regarding to Chlorophyll and carotenoid content, the extraction of leaf pigments was performed with 80% acetone, and the absorbance at 663 and 645 nm was measured with an Ultrospec 2100

http://www.aloki.hu ● ISSN 1589 1623 (Print) ● ISSN 1785 0037 (Online)
DOI: http://dx.doi.org/10.15666/aeer/1706_1570315711

pro spectrophotometer (Amersham Biosciences). Total carotenoid content, chlorophyll a, chlorophyll b, and total chlorophyll quantities were calculated according to the method of Arnon (1949) using the following formula:

$$A_{663} = 82.04\ Chl_a + 9.27\ Chl_b \quad \text{(Eq.1)}$$

$$A_{645} = 16.75\ Chl_a + 45.6\ Chl_b \quad \text{(Eq.2)}$$

where A is the density values at the respective wavelengths as obtained on the spectrophotometer and Chl_a, Chl_b are grams per liter of chlorophyll a and b, respectively. From the solving previous equations we will obtain the following:

$$\text{Chl a (mg/l)} = 12.7\ (A_{663}) - 2.69\ (A_{645}) \quad \text{(Eq.3)}$$

$$\text{Chl b (mg/l)} = 22.9\ (A_{645}) - 4.68\ (A_{663}) \quad \text{(Eq.4)}$$

$$\text{Total Chl (a and b) (mg/l)} = 20.2\ (A_{645}) + 8.02\ (A_{663}) \quad \text{(Eq.5)}$$

Then carotenoid content can be calculated as following:

$$\text{Car (mg/l)} = A_{480} \text{ x } 200 \quad \text{(Eq.6)}$$

The pigment concentration was calculated in mg/g FW of samples.

Table 1. *Physical and chemical properties of soil and irrigation water*

		Irrigation water	Soil
PH		7.1	8.40
EC(dS/m)		7.0	9.1
Soluble	Ca^{2+}	3.6	35.0
Cations	Mg^{2+}	0.5	19.5
meq/L	Na^{+}	3.2	34.3
	K^{+}	0.114	2.0
Soluble	CO_3^{-2}	0	0.125
Anions	HCO_3^{-}	1.0	3.5
meq/L	Cl^{-}	4.7	56.3
	SO_4^{-2}	1.71	21.9
	Saturation point %		27.3
	Pot capacity (at 1 bar)		13.6
	Wilting point (at 15 bar)		6.8

Extraction and determination of proline were directed according to the techniques described by Bates et al. (1973). Plant tissues (0.5 g) were homogenized with 5 ml of 3% sulfosalicylic acid and the homogenates were centrifuged at 3000×g for 20 min. One ml of the supernatant was mixed with 1 ml acid ninhydrin reagent and 1 ml of glacial acetic acid in a test tube and incubated in 100°C in water bath for 1 h, and then the absorbance value at 520 nm was noted. Free proline content in sample is determined by referring to a proline standard curve of known concentrations and the results were expressed as μmol proline g^{-1} FW (fresh weight).

http://www.aloki.hu ● ISSN 1589 1623 (Print) ● ISSN 1785 0037 (Online)
DOI: http://dx.doi.org/10.15666/aeer/1706_1570315711

For extraction and analysis of antioxidant enzymes, leaf samples (0.5 g fresh weight, FW) were homogenized in 3 ml extraction buffer (0.1 M pH 7.0 potassium phosphate buffer, 1 mM EDTA, 0.05% Triton X-100) in a pre-chilled pestle and mortar, centrifuged at 15,000 g for 20 min at 4°C. The supernatant was used for the estimation antioxidant enzyme activities. Superoxide dismutase activity (SOD EC 1.15.1.1) activity was estimated by the ability of this enzyme to impede the photochemical decrease of nitrobluetetrazolium salt (NBT). The SOD activity was measured at 560 nm according to the technique of Beyer and Fridovich (1987) and the assays were carried out at 25°C. The final assay volume of 3 ml contained 50 mM Tris-HCl buffer (pH 7.8), 33 µM NBT, 10 mM L- methionine, 0.66 mM disodium EDTA, 0.0033 mM riboflavin and 50 µl of supernatant. Reaction was underway under fluorescent light for 15 minutes by adding 10 µl of riboflavin solution. One unit of antioxydant SOD was defined as the amount of enzyme activity that inhibited the photo reduction of NBT to blue formazan by 50%. The SOD activity of each extract was expressed as Ug^{-1} FW. Peroxidase (POX) activity was estimated by the method of Sakharov and Ardila (1999). Peroxidase enzyme activity was determined by the oxidation of guaiacol in the presence of H_2O_2. The increase in absorbance was recorded at 470 nm for 1 min with a spectrophotometer. The reaction mixture contained 50 µl of 28 mM guaiacol, 900 µl of 50 mM potassium phosphate buffer (pH 6.0), 50 µl of 5 mM H_2O_2, and 10 µl of crude extract. POX activity of the extract was expressed as the POX Ug^{-1} FW. Catalase (CAT EC 1.11.1.6) activity was measured spectrophotometrically according to the method of Aebi (1974). The disappearance of H_2O_2 were determined at 240 nm wavelength in a mixture containing 50 mM sodium phosphate buffer (pH 7.0), 20 mM H_2O_2 and 5 µl of supernatant. The decrease in the absorption was followed for 1 min at 240 nm, and 1 mmol H_2O_2 oxidized ml^{-1} min^{-1} was defined as 1 U of CAT activity. Ascorbate peroxidase (APX EC 1.11.1.11) content was determined according to the means of Wang et al. (1991). The mixture contained in a test tube, 50 mM pH 7.0 potassium phosphate buffer, 0.5 mM ascorbic acid, 0.1 mM hydrogen peroxide, and 20 µl of enzyme extract were added in a total volume of 1 ml. The concentration of oxidized ascorbate was calculated by the decrease in absorbance at 290 nm. The absorption coefficient was 2.8 mM^{-1} cm^{-1}. One unit of APX was counted as 1 mmol ml^{-1} ascorbate oxidized min^{-1}.

Statistical procedures

Data obtained were subjected to statistical Analysis Of Variance (ANOVA), according to Gomez and Gomez (1984). Averages of the main effects of stress water irrigation were associated using the revised Least Significant Difference test (LSD) method at 0.05 probability level. Computations and statistical analysis were done using Statistical Analysis System computerized package program (SAS).

Results and discussion

The statistical analysis of variance for the resulting data showed that, the four water stress levels had significant differences on the all physiological studied traits except nitrogen percentage in regard to the examined genotype eggplant (*Table 2*). Studied plants content of Potassium (K), Phosphorous (P), Carbon (C) and Nitrogen (N) were measured. Results show that highest average of potassium (14.30 mg/g DW) was obtained from irrigation treatment with 80% of pot capacity (T2), while the lowest

http://www.aloki.hu ● ISSN 1589 1623 (Print) ● ISSN 1785 0037 (Online)
DOI: http://dx.doi.org/10.15666/aeer/1706_1570315711

(6.13 mg/g DW) was recorded by the irrigation treatment with 60% of pot capacity (T3) without any significant differences with (T4) 40% of pot capacity (6.23 mg/g DW). There was significant difference in Phosphorous content between treatments, highest was in T2 by (54.9 mg/g DW), while the lowest was (19.53 mg/g DW). Similar trend was obtained with carbon content, where the highest value (37.61 mg/g DW) was obtained by (T2) and the lowest value (31.54 mg/g DW) was obtained by (T4). The water stress treatments resulted in no significant (at $P<0.05$) regarding to nitrogen percentage in all treatments. Eggplant total yield affected by leaf N and decreased at the lowest irrigation rate 33% Etc (Díaz-Pérez and Eaton, 2015). In general, T2 shows the highest values of mineral content NPK. Farghali and El-Sharkawl (1988) found that total K^+ content in Cotton seedlings roots and aerial parts increased progressively with decreasing water stress, particularly under light condition. Data are agree with Kirnak et al. (2001) whose, found that nutrient concentrations in mature leaves of eggplants grown in pots under different irrigation treatments decrease according to water stress levels. In addition, Almohisen (2015) found that similar trend with Carbon, Potassium, Phosphorous content and Nitrogen percentage in tomato.

The effect of water stress treatments on total chlorophyll, chlorophyll a, chlorophyll b and total carotenoids resulted in significant decrease (at $P<0.05$) in accumulation of pigments. Total chlorophyll was (1.17, 0.70, 0.92, and 0.76 mg/g FW) in T1, T2, T3 and T4 of water stress, respectively. Kirnak et al. (2001) found that total chlorophyll content in water stress treatment was lowered by 55% compared to control treatment. Regarding to chlorophyll a data obtained was (0.80, 0.36, 0.36 and 0.30 mg/g FW) for the four water deficit treatments; T1, T2, T3 and T4, respectively. The highest value of chlorophyll b was 0.38 mg/g FW in both T1 and T4, on the other side, T3 gave the lowest value (0.38 mg/g FW). Chlorophyll indexes have been used as subsidiary estimators of chlorophyll content and leaf nitrogen concentrations (Liu et al., 2006). Carotenoids decreased dramatically in response to water stress from 8.65 mg/g FW in T1 (control treatment) to 5.84 mg/g FW in the fourth treatment (the most stress).

Regarding the proline content, as mentioned in the first paragraph of results and discussion, the analysis of variance data showed that, the three water stress treatments (40, 60, 80%) had significant effect on increasing proline accumulation compared to control. Data showed that proline was 3.63, 6.24, 5.42 and 5.42 μmol g^{-1} FW in T1, T2, T3 and T4, respectively. In response to water stress, proline accumulation usually occurs in the cytosol which plays a significant role in adjustment of cytoplasmic osmotic (Anjum et al., 2012; Almohisen, 2015). In this study, the higher levels of proline accumulation in T4 followed by T3 then T2 enabled the water-stressed plants to maintain low water potentials. Data in *Table 2* show the effect of four water stress treatment on four enzymes content in eggplants. Peroxidase was 15.77 Ug^{-1} FW in control treatment (T1, 0% water deficit), in treatment number two (T2, 20% water deficit) Peroxidase was 2.64 Ug^{-1} FW, while it was 36.76 and 12.45 Ug^{-1} FW in (T3, 40% water deficit) and (T4, 60% water deficit), respectively. Ascorbate peroxidase and Catalase decreased significantly with water stress from 1.76 and 430.15 Ug^{-1} FW in control treatment (T1) to 0.54 and 109.45 Ug^{-1} FW in T4 (the high level from water scarcity), respectively. On the other hand, superoxide dismutase values varied significantly, where the accumulation of superoxide dismutase was 21.66, 28.49, 14.56 and 27.37 Ug^{-1} FW in T1, T2, T3 and T4, respectively. On the other hand, superoxide dismutase values varied significantly, where the accumulation of superoxide dismutase was 21.66, 28.49, 14.56 and 27.37 Ug^{-1} FW in T1, T2, T3 and T4, respectively.

http://www.aloki.hu ● ISSN 1589 1623 (Print) ● ISSN 1785 0037 (Online)
DOI: http://dx.doi.org/10.15666/aeer/1706_1570315711

Table 2. *Some physiological characters of studied genotype eggplant in response to water deficit*

Chapter	**K**	**P**	**C**	**N%**	**Total Chlorophyll (mg/g FW)**	**Chlorophyll a (mg/g FW)**	**Chlorophyll b (mg/g FW)**	**Carotenoids (mg/g FW)**	**Proline (µmol g^{-1} FW)**	**Peroxidase (Ug^{-1} FW)**	**Ascorpate peroxidase (Ug^{-1} FW)**	**Catalase (Ug^{-1} FW)**	**Superoxide dismutase (Ug^{-1} FW)**
Treatments	**(mg/g DW)**												
T1	6.90	23.70	36.71	1.68	1.17	0.80	0.38	8.65	3.63	15.77	1.76	430.15	21.66
T2	14.30	54.90	37.61	1.75	0.70	0.36	0.33	8.76	6.24	2.64	1.13	383.46	28.49
T3	6.13	29.33	35.71	1.73	0.92	0.63	0.28	6.85	5.42	36.76	0.63	239.26	14.56
T4	6.23	19.53	31.54	1.32	0.76	0.30	0.38	5.84	8.11	12.45	0.54	109.45	27.37
F test	*	*	*	ns	*	*	*	*	*	*	*	*	*
L.S.D at 0.5%	0.353	0.602	1.858	--	0.127	0.005	0.024	0.118	0.152	0.359	0.107	1.696	0.650

T1: 100%, T2: 80%, T3: 60%, T4: 40%, of pot capacity *: significant at 5% level of probability and ns: not significant

http://www.aloki.hu ● ISSN 1589 1623 (Print) ● ISSN 1785 0037 (Online)
DOI: http://dx.doi.org/10.15666/aeer/1706_1570315711

Drought stress brought different variations in the anti-oxidative enzymes activities (Anjum et al., 2012). Moreover, it has been reported that peroxidase, and catalase activities showed an increased or stabled in the early level of drought and then decreased with progression of water stress. It is conspicuous that, higher levels of antioxidants are interrelated to tolerance of plant toward water stress (Tahi et al., 2008). Superoxide dismutase is considered to form the first line of protection against reactive oxygen species (ROS), which catalyzed the superoxide radical (O_2-) to O_2 and H_2O_2 which are further quenched by diverse antioxidant enzymes.

These significant differences between all values for leaf chlorophyll, carotenoids, proline, enzyme activity and nutrients elements as impact to water stress treatments that may be reflecting the role of these components as a biological regulator in plant (El-Saidy et al., 2011; Ahanger et al., 2016), and may be due to the roll of each one in metabolism system in plant, plus the partial inhibition co-with vitamins of a few interaction in reactive oxygen species production (Ratnakar and Rai, 2013; Ahanger et al., 2017).

Conclusion

In Considering the previous results as a whole and in regard to the examined genotype, it can be concluded that, there are different physiological changes for all studied tratis exeptonly one (N contant) in response to drought stress treatments. The results indicate that irrigation treatment with 80% of pot capacity (T2) more effectively than 60% of pot capacity (T3) and 40% of pot capacity (T4) from the standpoint of more efficient water use. Which would help to diminish drought injury, retain healthy plants to achieve optimum performance and adaptation under drought stress and saving irrigation water usage by 20%.

Change history: The online version of this paper was modified on 27th April 2020. In the following sentence of the Abstract the last percentage data was mistyped (it was corrected from 20% to 40%): "Drought stress treatment had been done by irrigating the plants with 80%, 60% and 40% of water needed to reach soil pot capacity, plus normal irrigation (control treatment)."

REFERENCES

[1] Abd El-Ghany, H. M., Nawar, A. A., Ibrahim, M. E., El-Shamarka, Sh. A., Selim, M. M., Fahmi, A. I. (2004): Using tissue culture to select for drought tolerance in bread wheat. – http://www.cropscience.org.au/icsc2004/poster/3/4/2/563_hatam.htm#TopOfPage.

[2] Aebi, H. (1974): Catalase. – Methods of Enzymatic Analysis. – Elsevier.

[3] Ahanger, M. A., Akram, N. A., Ashraf, M., Alyemeni, M. N., Wijaya, L., Ahmad, P. (2016): Signal transduction and biotechnology in response to environmental stresses. – Biologia Plantarum 61: 401-416.

[4] Ahanger, M. A., Akram, N. A., Ashraf, M., Alyemeni, M. N., Wijaya, L., Ahmad, P. (2017): Plant responses to environmental stresses—from gene to biotechnology. – AoB Plants 9(4):plx025.

[5] Almohisen, I. A. A. (2015): Effect of Water Stress on Growth and Physiology of Tomato (Lycopersicon esculentum Mill.). – Hortscience Journal of Suez Canal University 4: 1-5.

[6] Anjum, S. A., Saleem, M. F., Wang, L.-C., Bilal, M. F., Saeed, A. (2012): Protective role of glycinebetaine in maize against drought-induced lipid peroxidation by enhancing capacity of antioxidative system. – Australian Journal of Crop Science 6: 576.

http://www.aloki.hu ● ISSN 1589 1623 (Print) ● ISSN 1785 0037 (Online)
DOI: http://dx.doi.org/10.15666/aeer/1706_1570315711

[7] Arnon, D. I. (1949): Copper enzymes in isolated chloroplasts. Polyphenoloxidase in Beta vulgaris. – Plant physiology 24: 1-15.
[8] Bates, L. S., Waldren, R. P., Teare, I. D. (1973): Rapid determination of free proline for water-stress studies. – Plant and Soil 39: 205-207.
[9] Beyer, W. F., Fridovich, I. (1987): Assaying for superoxide dismutase activity: Some large consequences of minor changes in conditions. – Analytical Biochemistry 161: 559-566.
[10] Bock, R. (1984): A handbook of decomposition methods in analytical chemistry. – International Textbook Co, 444p.
[11] Buhtz, A., Hohe, A., Schwarz, D., Grosch, R. (2017): Effects of *Verticillium dahliae* on tomato root morphology considering plant growth response and defense. – Plant Pathol. 66: 667-676.
[12] Cassel, D., Nielsen, D. (1986): Field capacity and available water capacity. – In: Klute, A. (ed.) Methods of Soil Analysis: Part 1-Physical and Mineralogical Methods, SSA Book Series 5.1: 901-926.
[13] Chaves, M. M. (1991): Effects of Water Deficits on Carbon Assimilation. – Journal of Experimental Botany 42: 1-16.
[14] Cornic, G., Massacci, A. (1996): Leaf photosynthesis under drought stress. – Photosynthesis and the Environment. Springer.
[15] Díaz-Pérez, J. C., Eaton, T. E. (2015): Eggplant (*Solanum melongena* L.) plant growth and fruit yield as affected by drip irrigation rate. – HortScience 50: 1709-1714.
[16] Doorenbos, J. (1975): Guidelines for predicting crop water requirements. – Food and Agriculture organization, Rome. FAO Irrig. Drainage paper 24.
[17] El-Saidy, A. E. A., Farouk, S., Abd El-Ghany, H. M. A. (2011): Evaluation of Different Seed Priming on Seedling Growth, Yield and Quality Components in Two Sunflower (*Helianthus annuus* L.) Cultivars. – Trends in Applied Sciences Research 6: 977-991.
[18] Farghali, K., El-Sharkawl, H. (1988): Interactive Effects of NPK Nutrients, Water Potential and Irradiance on Contents of Potassium and Phosphate in Cotton Seedlings. – Phyton 28: 171-181.
[19] Gaveh, E. A., Timpo, G. M., Agodzo, S. K., Shin, D. H. (2011): Effect of irrigation, transplant age and season on growth, yield and irrigation water use efficiency of the African eggplant. – Horticulture, Environment, and Biotechnology 52: 13-28.
[20] Gomez, K. A., Gomez, A. A. (1984): Statistical procedures for agricultural research. – John Wiley & Sons.
[21] Gupta, A., Dixit, S. K., Senthil-Kumar, M. (2016): Drought stress predominantly endures *Arabidopsis thaliana* to *Pseudomonas syringae* infection. – Front. Plant Sci. 7: 808-819.
[22] Karam, F., Saliba, R., Skaf, S., Breidy, J., Rouphael, Y., Balendonck, J. (2011): Yield and water use of eggplants (Solanum melongena L.) under full and deficit irrigation regimes. – Agricultural Water Management 98: 1307-1316.
[23] Kirnak, H., Kaya, C., Tas, I., Higgs, D. (2001): The influence of water deficit on vegetative growth, physiology, fruit yield and quality in eggplants. – Bulg. J. Plant Physiol 27: 34-46.
[24] Klute, A., Gee, G. W., Bauder, J. W. (1986): Particle-size Analysis. – SSSA Book Series. Soil Science Society of America, American Society of Agronomy.
[25] Kurniawati, S. (2014): Drought Stress Tolerance Mechanisms of Eggplant (Solanum spp.): Physiology and Molecular. – Institut Pertanian Bogor, Scientific Repository.
[26] Liu, Y. J., Tong, Y. P., Zhu, Y. G., Ding, H., Smith, E. A. (2006): Leaf Chlorophyll Readings as an Indicator for Spinach Yield and Nutritional Quality with Different Nitrogen Fertilizer Applications. – Journal of Plant Nutrition 29: 1207-1217.
[27] Molden, D. (1997): Accounting for water use and productivity, SWIM Paper 1, system-wide initiative for water management. – International Water Management Institute, Colombo, Sri Lanka, 16.

http://www.aloki.hu ● ISSN 1589 1623 (Print) ● ISSN 1785 0037 (Online)
DOI: http://dx.doi.org/10.15666/aeer/1706_1570315711

[28] Molden, D., Sakthivadivel, R., Habib, Z. (2001): Basin-level use and productivity of water: Examples from South Asia. – IWMI.
[29] Ratnakar, A., Rai, A. (2013): Influence of NaCl salinity on β-carotene, thiamine, riboflavin and ascorbic acid contents in the leaves of Atriplex hortensis L. var. Pusa Bathua No. 1. – Journal of Stress Physiology & Biochemistry 9: 187-192.
[30] Rhoades, J. (1982): Soluble salts. – In: Page, A. L., Miller, R. H., Keeney, D. R. (eds.) Methods of soil analysis. Part 2: 167-178.
[31] Richards, L. A. (1969): Diagnosis and improvement of saline and alkali soils. – United States Department Of Agriculture; Washington.
[32] Sakharov, I. Y., Ardila, G. B. (1999): Variations of peroxidase activity in cocoa (Theobroma cacao L.) beans during their ripening, fermentation and drying. – Food Chemistry 65: 51-54.
[33] Tahi, H., Wahbi, S., El Modafar, C., Aganchich, A., Serraj, R. (2008): Changes in antioxidant activities and phenol content in tomato plants subjected to partial root drying and regulated deficit irrigation. – Plant Biosystems - An International Journal Dealing with all Aspects of Plant Biology 142: 550-562.
[34] Tani, E., Kizis, D., Markellou, E., Papadakis, I., Tsamadia, D., Leventis, G., Makrogianni, D., Karapanos, I. (2018): Cultivar-Dependent Responses of Eggplant (*Solanum melongena* L.) to Simultaneous *Verticillium dahliae* Infection and Drought. – Front Plant Sci. 9: 1181-1192
[35] Wang, S. Y., Jiao, M., Faust, M. (1991): Changes in ascorbate, glutathione, and related enzyme activities during thidiazuron-induced bud break of apple. – Physiologia Plantarum 82: 231-236.

http://www.aloki.hu ● ISSN 1589 1623 (Print) ● ISSN 1785 0037 (Online)
DOI: http://dx.doi.org/10.15666/aeer/1706_1570315711

BACTERIAL DIVERSITY OF THE PANJIN RED BEACH BASED ON HIGH-THROUGHPUT AND CULTURE-DEPENDENT METHODS

WEI, C. Y.[1] – GAO, T.[1] – YUAN, Y.[1] – LI, Y. Y.[1] – WANG, L. L.[1]– LI, X. M.[1] – YU, C. M.[2*] – MA, L. J.[1*]

[1]*College of Life Science, Shenyang Normal University, No. 253 Huanghe North Street, Shenyang, Liaoning 110034, China*

[2]*College of Agronomy, Shenyang Agricultural University, Shenyang 110161, China*

**Corresponding authors*
e-mail: yucuimei@163.com, malianju@163.com

(Received 6th Sep 2019; accepted 15th Nov 2019)

Abstract. There are in plenty of microbial resources in Panjin Red Beach, which is a unique wetland in Liaoning province. In this experiment, we investigated bacterial diversity and community in order to understand internal soil microbial community characteristics composition of the soil. Soil samples were collected in five different areas. The bacterial diversity and community were investigated using combined culture-dependent and culture-independent approaches (high-throughput sequencing technology). Through the high-throughput sequencing of the Panjin Red Beach soil, bacterial community turned out to be mainly composed of 13 phyla in the samples collected from the five studied areas, which were Tenericutes, Spirochaetae, Latescibacteria, Verrucomicrobia, Planctomycetes, Cyanobacteria, Actinobacteria, Gemmationadetes, Chloroflexi, Acidobacteria, Firmicutes, Bacteroidetes and Proteobacteria. By cultivable methods, 80 halophilic and alkalophilic bacteria were isolated, and 42 bacteria were selected to be identified by 16S rDNA, and were determined to belong to nine genus and four phyla. *Bacillus* and *Planococcus* was the dominant genus. Accordingly, the bacterial diversity was rich in Panjin Red Beach. Moreover, the data gathered using high-throughput technology is far more accessible than culture-dependant methods.
Keywords: *microbial resources, extreme environment, culture-independent, culture-dependent, bacterial diversity*

Introduction

Extreme environmental microbes are groups of microbes which can grow and reproduce in the extreme regions. For example, thermophilic microbes growing in environments such as hot springs and craters (Stetter et al., 1990), cold-loving microbes growing in extreme cold regions such as the Antarctic, snowy mountains and deep oceans (Liu et al., 2001), acidophilic microorganisms growing in metal deposits, saline soils and sulfur-bearing hot springs (Olson et al., 2003; Zettler et al., 2002), halophilic bacteria growing saline-alkali soil, alkaline lake and ocean environment (Horikoshi, 1999; Margesin and Schinner, 2001; Shi et al., 2012). A broad-spectrum of salt- and alkali-tolerant, and even drought-resistant microbial species resources were found in saline-alkaline soil (Shi et al., 2012). Panjin Red Beach is a very rare shallow shoal, in which soil belongs to saline-alkaline type. Though the microorganisms in extreme environments of saline-alkaline soil has been reported in former researches (Rietz and Haynes, 2003; Zahran, 1997), an in-depth study on the microbial resources in Panjin Red Beach extreme saline-alkaline soils is particularly rare. Therefore, we investigated structure and diversity of soil microbial communities in Panjin Red Beach region.

http://www.aloki.hu ● ISSN 1589 1623 (Print) ● ISSN 1785 0037 (Online)
DOI: http://dx.doi.org/10.15666/aeer/1706_1571315720

Not only the survival status of the microbes was understood in a given habitat under certain culture conditions, but also the new species resources were obtained with potential application value by the traditional cultivable method (Bever et al., 2012). However, diversity of microbial communities is affected by culture-dependent methods in laboratory due to some uncertain factors. Moreover, 0.001-15% of the microbes in the environment can be cultured by culture-dependent methods. For the microorganisms existing in extreme environments, a large number of them are not allowed to be cultured. The microbial information obtained by culture-dependent methods is greatly limited. Some researchers explored methods and techniques by DGGE, clone library and T-RFLP for microbial community structure, but not explain the composition, diversity and function of microbial communities (Theron et al., 2000; Vanwonterghem et al., 2014). High-throughput sequencing technology provides an efficient method for analyzing species composition and relative abundance of microbial communities in complex environments, which can directly sequencing 16S rRNA gene PCR products and simultaneously analyze hundreds of different samples (Chistoserdova, 2010; Rinke et al., 2013). At present, it has been widely used in studies on the structural diversity of microbial communities in ocean, soil, human intestinal tract and other samples (Herlemann et al., 2011; Xia et al., 2011; Passalacqua et al., 2009). Therefore, traditional culture methods combining with High-throughput sequencing technology can comprehensively reflect the diversity of soil microbial. At present, the study on the diversity of microbial resources in Panjin Red Beach mainly focused on the soil microbes in *Suaeda salsa* the roots and endophyte (Zhao et al., 2015; Tian et al., 2016). In the present study, we used traditional culture methods combining with High-throughput sequencing technology to study the diversity of soil microbial in Panjin Red Beach.

Materials and methods

Samples collection and analysis

Soil samples were collected from Panjin Red Beach in Panjin city of Liaoning province, China in July and September, 2016. Samples collected from 0-15 cm depth soil by five dot collection methods were homogeneously mixed and placed in sterile PVC bag, respectively, at five representative plots selected in the test area. All treatments were conducted in triplicate at each plot. Soil samples were put into ice box and brought lab. Some of them were kept in -80 °C and sent to Shanghai Majorbio Corporation (Shanghai, China) to analyze bacteria community structure by high-throughput sequencing. The microbial species richness was represented by the number of unique OTUs (16S rDNA). Chao and Shannon's diversity index were also calculated based on 16S rDNA for comparison of alpha-diversity.

The others were used to determine soil character and analyzed bacterial diversity by culture-dependent methods.

Determination of soil pH and electric conductivity

Soil samples were put into clean paper and dried in shade place at temperature. The dried samples screened by 1 mm net. Samples (10 g) were put into 50 mL bottle. After adding 25 mL distilled water, samples were violently vibrated 5 min on magnetic

http://www.aloki.hu ● ISSN 1589 1623 (Print) ● ISSN 1785 0037 (Online)
DOI: http://dx.doi.org/10.15666/aeer/1706_1571315720

agitator and let stand for 1 h. Then, pH was determined by pH meter. All samples were conducted in triplicate. All samples were conducted in triplicate.

Samples (20 g) adding 100 mL water (1:5 m/V) were vibrated 5 min at 20 ± 1 °C. The 30 mL extraction buffer was used to determine electric conductivity at 25 ± 1 °C by conductivity meter.

Solid medium

Beef extract 0.3%, peptone 1%, NaCl 1.5%, agar 2%, pH 9.0, 121 °C autoclave steam sterilization 30 min (Shen et al., 2006).

Isolation and purification of microorganisms

Five studied areas samples (10 g) were gradient diluted with sterile saline, respectively. Different gradient bacterial suspension (10^{-3}, 10^{-4}, 10^{-5}) were uniformly spread on the surface of solid isolation medium plate. Each dilution was conducted in triplicate. Aseptic water was used as control. All treatments were cultured 2 days at 37 °C in incubator. According to clone morphology, different single clone was purified and inoculated in solid slope media for other treatments.

Molecular identification of cultured bacteria

The total genomic DNA of the cultured bacteria strain was extracted and purified using Bacterial DNA Isolation Kit (Sangon Biotech Co., Ltd, China) according to manufacturer's instructions. The 16S rDNA of the isolate was amplified through PCR reaction using the universal primers 27f (5'-AGAGTTTGATCATCCTGGCTCAG-3') and 1492r (5'-TACGGTTACCTTGTTACGACTT-3') synthesized by Sangon Biotech Co., Ltd (Shanghai, China). PCR reactions were performed in 50 μL mixture PCR reaction system containing 27f (10 μM) and 1492r (10 μM) primer 1 μL, respectively, DNA template 2 μL, 2×Premix Taq (5.0 U/μL) 25 μL, ddH_2O 21 μL. PCR reaction condition was 95 °C 5 min, 95 °C 1 min, 55 °C 1 min, 72 °C 2 min, 35 cycles, 72 °C 10 min. PCR products were sent to Shanghai Sangon Biotech Co. Ltd to sequence. Homology comparison was conducted online in EzBioCloud database (https://www.ezbiocloud.net/).

Results and discussion

Soil electric conductivity and pH value

Soil electric conductivity and pH value reflected degree of soil saline-alkali. In five geographical regions studied, the highest pH value is 8.66, and the lowest pH value is 8.09. The highest electric conductivity is 10.6 mS/cm, and the lowest value is 3.65 mS/cm (*Table 1*). These data showed that the soil of five geographical regions studied is saline-alkali soil.

Table 1. *Soil electric conductivity and pH value in five checked plots*

	HHT-1	HHT-2	HHT-3	HHT-4	HHT-5
pH	8.57	8.66	8.46	8.36	8.09
Electric conductivity	6.05	4.92	10.6	5.21	3.65

http://www.aloki.hu ● ISSN 1589 1623 (Print) ● ISSN 1785 0037 (Online)
DOI: http://dx.doi.org/10.15666/aeer/1706_1571315720

Diversity of cultured bacteria by culture-dependent

Cultured bacteria of five studied areas samples were isolated and purified in solid medium by culture-dependent methods, respectively. A total of 80 strains were isolated and purified from the plates that could grow steadily and fast in solid medium. Forty-two strains were selected as the representative strains according to the morphological characteristics of the colonies and the Gram stains. However, Tian et al. (2016) isolated and purified 22 strains in *Suaeda* rhizosphere soil in Panjin delta. This circumstance may be partly due to the difference in sampling time and location, and may also be due to the different media used. In the present study, the selected 42 selected isolates were identified by 16S rDNA sequence analysis (*Table 2*), which belonged to four phyla containing Actinobacteria 14.29%, Bacteroidetes 4.76%, Firmicutes 50%, Proteobacteria 30.95%. Forty-two isolates were divided into nine genera respectively, for example *Agromyces*, *Arthrobacter*, *Kocuria*, *Pseudarthrobacter*, *Zhihengliuella, Cellulosimicrobium*, *Pontibacter*, *Myroides* and *Bacillus.* Among nine genera, *Bacillus* and *Pseudomonas* were dominant genus.

Diversity of uncultured bacteria by high-throughput sequencing

Rarefaction curves of five samples were gradually towards flatness, and index reached saturation, which indicated that amount of sequencing data was reasonable and covered composition of flora in five samples (*Fig. 1*). Sequencing data represented microbe level of five samples, respectively. The number of unique operational taxonomic units (OTUs) (16S rRNA gene) represented the microbial species richness (Li et al., 2018). In this study, there were 184079 reads and 10154 OTUs at a cutoff of 97% sequence similarity across all soil samples. The observed bacterial OTU numbers varied between 1854 and 2322 in samples of five studied areas (*Table 3*). The coverage frequency was 99.26%, 99.44%, 99.53%, 99.6% and 99.57%, respectively. These showed that the information of microbial species in each region studied is basically fully reflected.

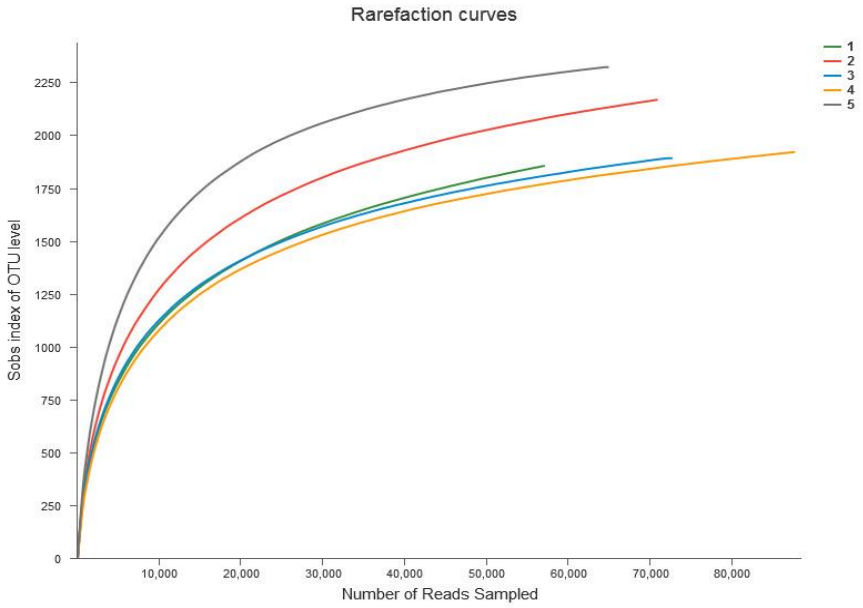

Figure 1. *Rarefaction curves of five studied areas samples*

http://www.aloki.hu ● ISSN 1589 1623 (Print) ● ISSN 1785 0037 (Online)
DOI: http://dx.doi.org/10.15666/aeer/1706_1571315720

Table 2. *Halophilic alkali bacteria cultured in five studied areas samples*

Name	Top-hit taxon	Accession No.	Similarity (%)
YJ1	*Bacillus siamensis*	KCTC 13613	99.79
YJ2	*Bacillus megaterium*	NBRC 15308	99.93
YJ3	*Cellulosimicrobium cellulans*	LMG 16121	99.86
YJ4	*Bacillus altitudinis*	41KF2b	100
YJ5	*Bacillus wiedmannii*	FSL W8-0169	99.93
YJ7	*Bacillus paramycoides*	NH24A2(T)	99.67
YJ10	*Arthrobacter endophyticus*	EGI 6500322	99.5
YJ14	*Bacillus aryabhattai*	B8W22	100
YJ24	*Brevibacterium frigoritolerans*	DSM 8801	99.37
YJ25	*Paenibacillus lautus*	NRRL NRS-666	99.42
YJ26	*Acinetobacter johnsonii*	CIP 64.6	98.89
YJ27	*Bacillus velezensis*	CR-502	99.43
YJ29	*Sphingorhabdus marina*	DSM 22363	98.37
YJ30	*Pseudomonas songnenensis*	NEAU-ST5-5	99.5
YJ31	*Exiguobacterium marinum*	DSM 16307	99.93
YJ33	*Bacillus aquimaris*	KCTC 3903	98.83
YJ34	*Nitratireductor aquimarinus*	CL-SC21	99.7
YJ35	*Sphingorhabdus marina*	DSM 22363	97.4
YJ38	*Bacillus flexus*	NBRC 15715	99.17
YJ39	*Myroides marinus*	JS-08	99.42
YJ40	*Planococcus rifietoensis*	M8	99.38
YJ42	*Bacillus crassostreae*	JSM100118	100
YJ43	*Bacillus cereus*	ATCC 14579	100
YJ44	*Photobacterium halotolerans*	MACL01	99.25
YJ45	*Bacillus safensis*	FO-36b	100
YJ46	*Agromyces arachidis*	AK-1	99.27
YJ48	*Halomonas heilongjiangensis*	9-2	99.27
YJ49	*Bacillus litoralis*	SW-211	99.31
YJ51	*Zhihengliuella halotolerans*	YIM 70185	99.56
YJ52	*Bacillus idriensis*	SMC 4352-2	99.43
YJ54	*Planococcus salinarum*	DSM 23820	99.29
YJ55	*Arthrobacter subterraneus*	CH7	99.21
YJ56	*Pontibacter odishensis*	JC130	98.27
YJ61	*Erythrobacter citreus*	RE35F/1	98.41
YJ63	*Pseudomonas linyingensis*	LYBRD3-7	99.03
YJ64	*Pseudomonas kunmingensis*	HL22-2	98.75
YJ65	*Pseudomonas zhaodongensis*	NEAU-ST5-21	99.5
YJ66	*Kocuria polaris*	CMS 76	98.74
YJ67	*Pseudarthrobacter oxydans*	KCTC 3383	99.71
YJ68	*Bacillus zhangzhouensis*	DW5-4	99.86
YJ71	*Exiguobacterium profundum*	10C	99.93
YJ77	*Pseudomonas guineae*	LMG 24016	99.07
YJ78	*Bacillus alkalisediminis*	K1-25	99.36

http://www.aloki.hu ● ISSN 1589 1623 (Print) ● ISSN 1785 0037 (Online)
DOI: http://dx.doi.org/10.15666/aeer/1706_1571315720

Table 3. *Community indices of five samples*

Sample	reads	OTUs	Chao index	Shannon index	Coverage (%)
HHT1	32030	1854	2181	5.72	99.26
HHT 2	40125	2167	2256	5.64	99.44
HHT 3	36007	1891	2413	5.76	99.53
HHT 4	38580	1920	2267	5.01	99.61
HHT 5	37337	2322	2497	5.87	99.57

The Chao and Shannon diversity index are the indicator of the abundance and an assessment of the diversity of bacteria in the biological environment, respectively (Chao, 1984; Shannon, 1948; Smalla, 2001). The index Chao across all soil samples was very high (*Table 3*). The index Chao of the HHT5 sample was the highest among them. However, the value of the HHT1 samples was the lowest, which indicated that the abundance was the lowest. The index Shannon of the HHT5 sample was the largest among them, which indicated that the diversity of bacteria was the most abundance.

There were mainly 13 phyla in five samples, which were Tenericutes, Spirochaetae, Latescibacteria, Verrucomicrobia, Planctomycetes, Cyanobacteria, Actinobacteria, Gemmationadetes, Chloroflexi, Acidobacteria, Firmicutes, Bacteroidetes and Proteobacteria. The relative abundance of each category varied across the five samples. The relative abundance of Proteobacteria of HHT1 sample was the highest among five samples, which reached 48.03%. Firmicutes was also the widely distributed bacterial phylum in the other four studied samples, but it was completely missing in the HHT5 sample (*Fig. 2A*). The dominant phyla across soil samples were Proteobacteria (from 33.54 to 48.03% in five studied samples) and Bacteroidets (from 16.6 to 32.3% in five studied samples), which were consistent with the observation of Tian et al. (2016). The *Aliifodinibius* was the most abundant genus in all the samples accounting for 41.06%, 44.57%, 37.78%, 31.06% and 36.9%, respectively, followed by *Gillisia* and *Bacillus*. And, there were many bacteria unidentified in genus level in five samples (*Fig. 2B*).

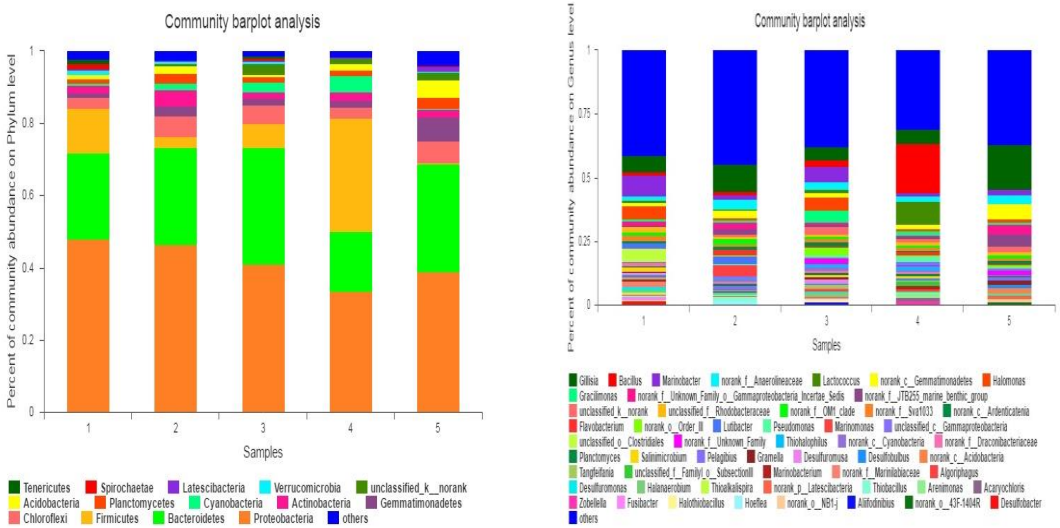

A B

Figure 2. *Bacterial relative abundance of five studied areas samples in phylum (A) and genus (B) level*

http://www.aloki.hu ● ISSN 1589 1623 (Print) ● ISSN 1785 0037 (Online)
DOI: http://dx.doi.org/10.15666/aeer/1706_1571315720

In comparison with the culture-dependent methods, more bacteria were observed by high-throughput sequencing in phylum. Only four phyla bacteria were isolated by culture-dependent methods. However, there were 13 phyla, and more Chloroflexi bacteria of five studied areas samples and Gemmationadetes bacteria of HHT5 sample were observed by high-throughput sequencing (*Fig. 2A*), but these bacteria were not isolated by the culture-dependent methods (*Table 2*). Maybe, a special medium is needed to thrive for those bacteria. Therefore, the media suitable for saline-alkali environment should be developed to isolate species or strains that are best adapted to grow in saline-alkali soil.

Conclusion

The soil of five geographical regions studied is saline-alkali soil. By cultivable methods, 42 bacteria selected to identify by 16S rDNA belonged to nine genus and four phyla. *Bacillus* and *Planococcus* was the dominant genus. Through the high-throughput sequencing in five studied areas samples, bacterial community was mainly composed of 13 phyla, which were Tenericutes, Spirochaetae, Latescibacteria, Verrucomicrobia, Planctomycetes, Cyanobacteria, Actinobacteria, Gemmationadetes, Chloroflexi, Acidobacteria, Firmicutes, Bacteroidetes and Proteobacteria. Therefore, the bacterial diversity was very rich in Panjin Red Beach. The bacteria strains should further be explored for agricultural and industrial use.

Acknowledgments. This work was supported by the National Natural Science Foundation of China (31600314), the Education Department of Liaoning Province fundamental project (LJC201912, LZD201901), Major incubating project of Shenyang Normal University (ZD201705) and Liaoning Province Science and Technology Plan Project (No.2017208001).

REFERENCES

[1] Bever, J. D., Platt, T. G., Morton, E. R. (2012): Microbial population and community dynamics on plant roots and their feedbacks on plant communities. – Annu Rev Microbiol 66: 265-283.

[2] Chao, A. (1984): Nonparametric estimation of the number of classes in a population. – Scand J Stat 11: 265-270.

[3] Chistoserdova, L. (2010): Recent progress and new challenges in metagenomics for biotechnology. – Biotechnol Lett 32(10): 1351-1359.

[4] Herlemann, D. P., Labrenz, M., Jürgens, K., Bertilsson, S., Waniek, J. J., Andersson, A. F. (2011): Transitions in bacterial communities along the 2000 km salinity gradient of the Baltic Sea. – ISME J 5(10): 1571-1579.

[5] Horikoshi, K. (1999): Alkaliphiles: some applications of their products for biotechnology. – Microbiol Mol Biol Rev 63(4): 735-750.

[6] Li, H., Xu, Z. W., Yan, Q. Y., Yang, S., Van Nostrand, J. D., Wang, Z. R., He, Z. L., Zhou, J. Z., Jiang, Y., Deng, Y. (2018): Soil microbial beta-diversity is linked with compositional variation in aboveground plant biomass in a semi-arid grassland. – Plant Soil 423: 465-480.

[7] Liu, G. X., Hu, C. Q., Zhang, J. B., Shen, Y. P. (2001): Microbial communities in permafrost of the Tibetan Plateau and their significance. – J Glaciol Geocryol 23(4): 419-422 (in Chinese).

http://www.aloki.hu ● ISSN 1589 1623 (Print) ● ISSN 1785 0037 (Online)
DOI: http://dx.doi.org/10.15666/aeer/1706_1571315720

[8] Margesin, R., Schinner, F. (2001): Potential of halotolerant and halophilic microorganisms for biotechnology. – Extremophiles 5(2): 73-83.
[9] Olson, G. J., Brierley, J. A., Brierley, C. L. (2003): Bioleaching review part B: progress in bioleaching: applications of microbial processes by the minerals industries. – Appl Microbiol Biotech 63(3): 249-257.
[10] Passalacqua, K. D., Varadarajan, A., Ondov, B. D., Okou, D. T., Zwick, M. E., Bergman, N. H. (2009): Structure and complexity of a bacterial transcriptome. – J Bacteriol 191(10): 3203-3211.
[11] Rietz, D. N., Haynes, R. J. (2003): Effects of irrigation-induced salinity and sodicity on soil microbial activity. – Soil Biol Biochem 35(6): 845-854.
[12] Rinke, C., Schwientek, P., Sczyrba, A., Ivanova, N. N., Anderson, I. J., Cheng, J. F., Darling, A., Malfatti, S., Swan, B. K., Gies, E. A., Dodsworth, J. A., Hedlund, B. P., Tsiamis, G., Sievert, S. M., Liu, W. T., Eisen, J. A., Hallam, S. J., Kyrpides, N. C., Stepanauskas, R., Rubin, E. M., Hugenholtz, P., Woyke, T. (2013): Insights into the phylogeny and coding potential of microbial dark matter. – Nature 499(7459): 431-437.
[13] Shannon, C. E. (1948): A mathematical theory of communication. – Bell Syst Tech J 27: 379-423 and 623-656.
[14] Shen, P., Fan, X. R., Li, G. W. (2006): Microbiology Experiment. – Higher Education Press, Beijing, pp. 50-54 (in Chinese).
[15] Shi, W., Takano, T., Liu, S. K. (2012): Isolation and characterization of novel bacterial taxa from extreme alkali-saline soil. – World J Microbiol Biotechnol 28: 2147-2157.
[16] Smalla, K., Wieland, G., Buchner, A., Zock, A., Parzy, J., Kaiser, S., Roskot, N., Heuer, H., Berg, G. (2001): Bulk and rhizosphere soil bacterial communities studied by denaturing gradient gel electrophoresis: plant-dependent enrichment and seasonal shifts revealed. – Appl Environ Microbial 67(10): 4742-4751.
[17] Stetter, K. O., Fiah, G., Huber, G., Huber, R., Segerer, A. (1990): Hyperthermophilic microorganisms. – FEMS Microbiol Rev 75: 117-124.
[18] Theron, J., Cloete, T. E. (2000): Molecular techniques for determining microbial diversity and community structure in natural environments. – Crit Rev Microbiol 26(1): 37-57.
[19] Tian, R., Yu, Z. C., Li, Z. Y., Wang, X. L., Wang, B. (2016): Diversity of endophytic and rhizospheric bacteria of *Suaeda heteroptera* Kitag from Panjin Delta in Liaoning Province. – Microbiol China 43(07): 1462-1472 (in Chinese).
[20] Vanwonterghem, I., Jensen, P. D., Ho, D. P., Batstone, D. J., Tyson, G. W. (2014): Linking microbial community structure, interactions and function in anaerobic digesters using new molecular techniques. – Curr Opin Biotech 27: 55-64.
[21] Xia, W. W., Zhang, C. X., Zeng, X. W., Feng, Y. Z., Weng, J. H., Lin, X. G., Zhu, J. G., Xiong, Z. Q., Xu, J., Cai, Z. C., Jia, Z. J. (2011): Autotrophic growth of nitrifying community in an agricultural soil. – ISME J 5(7): 1226-1236.
[22] Zahran, H. H. (1997): Diversity, adaptation and activity of the bacterial flora in saline environments. – Biol Fertil Soils 25(3): 211-223.
[23] Zettler, L. A. A., Gómez, F., Zettler, E., Keenan, B. G., Amils, R., Sogin, M. L. (2002): Eukaryotic diversity in Spain's River of Fire. – Nature 417: 137.
[24] Zhao, Y., Yu, F., Guo, M. M., Bu, N. (2015): Isolation, identification and growth-promoting effect of *Suaeda salsa* endophyte fungus JP3. – J Shenyang Norm Univ 33: 116-120 (in Chinese).

http://www.aloki.hu ● ISSN 1589 1623 (Print) ● ISSN 1785 0037 (Online)
DOI: http://dx.doi.org/10.15666/aeer/1706_1571315720

EFFICACY OF MASS TRAPPING OF TOMATO LEAFMINER (*TUTA ABSOLUTA*) WITH DIFFERENT TYPES AND COLOURS OF TRAPS IN OPEN- FIELD TOMATO

POLAT, B.

Çanakkale Onsekiz Mart University, Faculty of Agriculture, Department of Plant Protection
17020 Çanakkale, Turkey
(e-mail: brkpolat@gmail.com; phone: +90-286-218-0018; fax: +90-286-218-0545)

(Received 6th Sep 2019; accepted 15th Nov 2019)

Abstract. As a limiting factor on tomato production, tomato leafminer *Tuta absoluta* (Meyrick, 1917) (Lepidoptera: Gelechiidae) has recently been considered as the main tomato pest. Different control methods should be considered for integrated pest management. This study was carried out to control *T. absoluta* by using pheromones and traps of five different colours (red, yellow, blue, white, black) and three different types (ferolite, water pan, roll) in combination at trial plots in Dardanos and Dumrek and Cıplak villages in Çanakkale province, Turkey. A randomized plot experimental design was implemented and traps were controlled and counted twice a week. Ferolite traps were determined to have the most success in capturing adults, followed by water and roll traps. The highest number of adults was captured with the colours black and white regardless of trap type, whereas the lowest number of adults was captured with yellow traps. It was observed upon comparing the capture rates of T. absoluta adults subject to trap type that 49% of the adults were counted in the ferolite traps. Water pans and roll traps followed the ferolite trap with 38% and 13%, respectively. Results indicate that mass trapping is effective in reducing the pest population in open-field tomato cultivars.
Keywords: *Çanakkale, light trap, water pan trap, roll trap, pest management*

Introduction

The tomato leafminer *Tuta absoluta* (Meyrick, 1917) (Lepidoptera: Gelechiidae) of South American origin was first encountered in Europe in 2006 in tomatoes cultivated under greenhouse conditions. The pest had spread rapidly causing significant damage in countries located in the Mediterranean basin (Urbaneja et al., 2007; Zappalà et al., 2013). It was first discovered in Turkey in open-field tomatoes in 2009 (Kılıc, 2010; Kasap et al., 2011). *Tuta absoluta* is a multivoltine and oligophagous pest and may damage many solanaceous crops (Torres et al., 2001; Desneux et al., 2010; Portakaldalı et al., 2013; Gozel and Kasap, 2015; Uzun et al., 2015). The larvae of this invasive pest feed on all above-ground parts of the tomato plant and cause 100% damage in the plant when not taken under control (EPPO, 2005). Male longevity was observed by Polat et al. (2016) as 3.37-6.14 days while female longevity was 7.7-9.75 days. The total number of eggs per female for each generation varied between 31 and 186. The females laid 68-72% of their eggs in the first five days, while data indicated that 81-83% of the eggs were laid on the 6th day (Polat et al., 2016).

The tomato is grown in many countries but is one of the most important vegetables produced in Turkey where it was ranked fourth in the world in 2016 with 12.600.000 tons of tomato production and a total plantation area of 180.670 ha (TUIK, 2017). As a major pest, similarly to its global prominence, the tomato leafminer poses a significant threat to tomato cultivation in the province of Çanakkale. It has been determined that 88% of all tomato growing areas in Çanakkale province are infested with *T. absoluta* (Polat et al., 2015).

http://www.aloki.hu ● ISSN 1589 1623 (Print) ● ISSN 1785 0037 (Online)
DOI: http://dx.doi.org/10.15666/aeer/1706_1572115730

Comprehensive and alternative control methods should be investigated for use in integrated pest management programs (IPM), especially in terms of issues related to resistance and extensive insecticide use (Polat and Tiryaki, 2019). Among the alternative methods, pheromones are used to monitor the population of insects to identify the correct timing to apply various control strategies, such as the introduction of natural enemies, intensification of mass trapping and application of insecticides (Megido et al., 2013; Braham, 2014). Different types of traps such as water pans and coloured traps also interfere in the attraction of the adults of *T. absoluta*. This pest has been controlled in many countries in the world by way of IPM programs, based on the use of pheromones and mass trapping applications (Gonzales-Cabrera et al., 2011; Cherif and Lebdi-Grissa, 2014; Aksoy and Kovancı, 2016; Bayram et al., 2017). On the other hand, light traps have also been used as part of the mass trapping method for pest control (Stol et al., 2009; Cocco et al., 2012; Ozkan et al., 2017). In other research, roll traps were designed to reduce the *T. absoluta* population for tomato growing in greenhouses (Hassan and Alzaidi, 2010). However, these studies were performed with a limited number of traps of different colour and type. In addition, roll traps with pheromones have not been used yet to determine *T. absoluta* in open-field tomato production.

Therefore, the purpose of the present research was to define the efficacy of mass trapping *T. absoluta* with five different colours (red, yellow, blue, white, black) and three different types of trap (ferolite, water pan, roll) in open-field tomato cultivation.

Materials and methods

Experimental area

The mass trapping experiments were carried out in 2017 on open-field tomato crops at the villages of Dumrek and Cıplak in the province of Çanakkale located in northwest Turkey (*Figure 1*, *Table 1*).

Figure 1. *Location of 3 trial areas in study*

Tomato was cultivated at Faculty of Agriculture Application Area in Dardanos. In addition, producer-controlled trial parcels were also established in the villages of Dumrek and Cıplak near the site of ancient Troy. Each experimental area was four da in size. The tomatoes were transplanted on 12.05.2017 at Dumrek, on 14.05.2017 at Cıplak, and on 24.05.2017 at Dardanos and the traps were placed on the same days.

http://www.aloki.hu ● ISSN 1589 1623 (Print) ● ISSN 1785 0037 (Online)
DOI: http://dx.doi.org/10.15666/aeer/1706_1572115730

The pest population did not reach an intensity which could result in economic damage and hence no insecticide was applied during the study. Fungicides (Penconazole, Copper oxychloride) were used to ensure the healthy growth of the tomatoes and drip irrigation applied to fulfil their water requirement. Furthermore, the parcels were fertilized according to soil analysis that was carried out at the beginning of the season.

Table 1. *Study areas and parcel data*

Study Area	Tomato variety	GPS Coordinates
Dardanos	*Lycopersicum esculentum* Mill. cv. Troy F1	40°4'29.67" N 26°21'51.13" E
Dumrek	*Lycopersicum esculentum* Mill. cv. Troy F1	39°58'17.05" N 26°18'4.10" E
Cıplak	*Lycopersicum esculentum* Mill. cv. Troy F1	39°56'24.42" N 26°15'19.48" E

Agricultural applications

Five different colours (red, blue, yellow, white, black) and three different types of trap (ferolite, water pan, roll) were used for the mass trapping applications. To obtain data on the colour of the traps, a Minolta CR-400 Chroma meter (Konica, Minolta, Japan) was used in the study (*Table 2*).

Table 2. *Colour data used in traps*

Colour of trap	L	a	b	c	Hue
White	65.23	0.17	-3.36	3.6	272.99
Black	17.67	-0.24	4.03	4.04	93.41
Blue	32.12	11.07	-40.83	42.51	285.17
Yellow	76.44	-6.56	79.97	80.24	94.69
Red	37.49	40.73	39.26	50.15	38.92

The water pan traps (Tutasan, Turkey) and ferolite (with light source, Russell IPM Ltd., UK) used in this study contain pheromone lures (E3, Z8, Z11-Tetradecatrienil). Roll traps (Russell IPM Ltd., UK and Tutasan, Turkey) which make use of high attraction pheromone film were also used. The dimensions of the traps were as follows. The height of the water pan traps from bottom to top was 7 cm and the diameter was 36 cm. For ferolite traps the lamp height was 30 cm, base length 26 cm, and the diameter 40 cm. To prepare the roll traps, the film was glued on a pipe with a diameter and length of 7.5 cm and 150 cm, respectively, thereby covering the whole pipe. Traps were placed in the field with four traps per day (Aksoy and Kovancı, 2016; Cherif et al., 2018). The traps used in the trial were placed in the parcels in the pattern indicated below (*Figures 2 and 3*).

Adults in the traps were counted twice per week; after that they were removed and the traps were cleaned for the new count. The water level was checked during inspection and the traps were refilled when necessary. Pheromone lures were replaced every four weeks. However, the roll traps were replaced every three weeks due to dryness of the sticky film.

http://www.aloki.hu ● ISSN 1589 1623 (Print) ● ISSN 1785 0037 (Online)
DOI: http://dx.doi.org/10.15666/aeer/1706_1572115730

Statistical analysis

The data were analyzed by Minitab R18 (StatSoft, Inc. Tulsa OK, USA) statistical software. Differences between the data were evaluated by means of variance analysis (ANOVA) using GLM. Tukey's method was applied as a group comparison test.

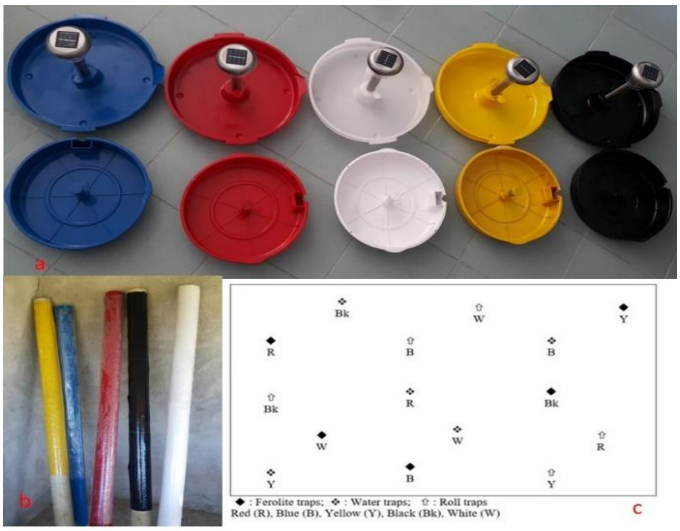

Figure 2. *Three different traps used in ferolite and water traps (a), roll traps (b) and their placement pattern (c)*

Figure 3. *Different traps and colours placed in trial plots*

Results and discussion

The first adult *Tuta absoluta* at the Dardanos experimental site were trapped on 25.05.2017 when the average temperature was 11.1°C. The highest number of captured adults in the season was 267 on 24.08.2017 in the white ferolite traps. The proportional average humidity was measured in this 4-day interval (21-24.08.2017) as 75.2%, while the average temperature was 22.1°C. The highest total number of adults captured was 3.864 in the white ferolite traps. This was followed by the black ferolite traps with 3.678 and blue ferolite traps with 2.955 adults (*Figure 4*).

http://www.aloki.hu ● ISSN 1589 1623 (Print) ● ISSN 1785 0037 (Online)
DOI: http://dx.doi.org/10.15666/aeer/1706_1572115730

The first adult at the Dumrek trial area were captured on 18.05.2017 when the average temperature was 17.1°C. The highest number of captured adults during the season was 401 on 24.08.2017 in the black ferolite traps. The proportional average humidity was measured in this time interval (21-24.08.2017) as 70.5%, while the temperature average was 24.6°C. Overall, the highest total number of adults captured was 4.645 in the white ferolite traps. This was followed by the black ferolite traps with 4.599 and the black water pan traps with 4.520 adults (*Figure 5*).

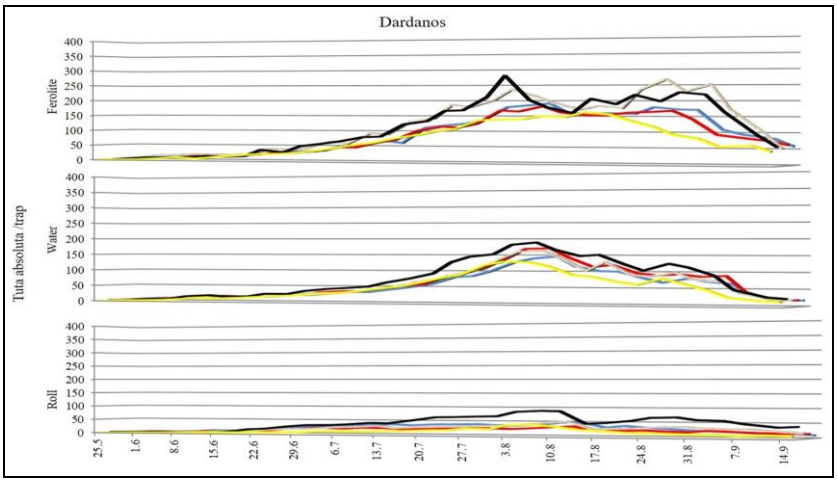

Figure 4. *Tuta absoluta captured at Dardanos by type and colour of trap*

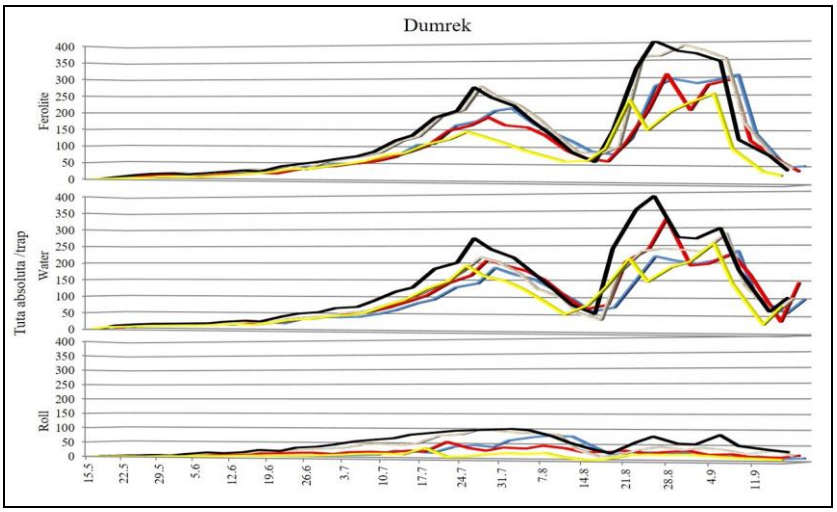

Figure 5. *Tuta absoluta captured at Dumrek by type and colour of trap*

The first leafminer adults at the Cıplak trial area were captured on 18.05.2017 when the average temperature was 17.1°C. The highest number of captured adults throughout the season was 282 on 27.07.2017 in the black ferolite traps. The proportional average humidity was measured in this time interval (24-27.07.2017) as 61.2%, while the temperature average was 22.6°C. The highest total number of adults captured was 4.028 in the white ferolite traps. This was followed by the black ferolite traps with 3.969 and blue ferolite traps with 3.518 adults (*Figure 6*).

http://www.aloki.hu ● ISSN 1589 1623 (Print) ● ISSN 1785 0037 (Online)
DOI: http://dx.doi.org/10.15666/aeer/1706_1572115730

A statistically significant difference was determined between the traps based on the adult count (P<0.05; F=91.54). As can be seen in *Figure 7*, a difference was observed between the trap types. In all study areas, ferolite traps were the most successful in catching adults and this was followed by the water pan traps and roll traps. The effectiveness of trap types does not change between different locations. A total of 108.043 *T. absoluta* adults were captured in the traps. The proportional distribution is given in *Figure 8*.

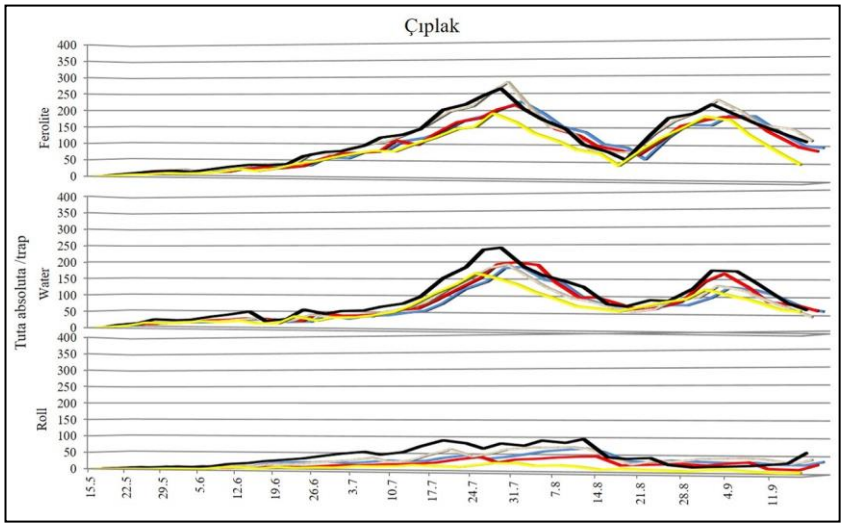

Figure 6. *Tuta absoluta captured at Cıplak by type and colour of trap*

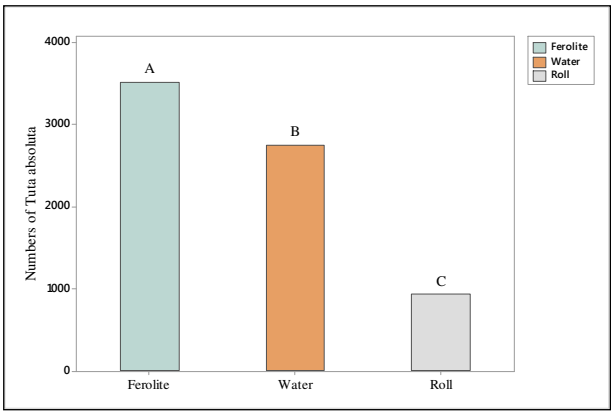

Figure 7. *Tuta absoluta captured by different trap type.*
**Different letters indicate statistical significance (P<0.05) for in-column comparisons*

The highest number of adults was captured in ferolite traps with a total of 52.748 (49%), followed by water pan traps and roll traps with 41.257 (38%) and 14.038 (13%) captured adults, respectively. As can be seen in *Figure 9*, while the highest number of adults among the ferolite traps was captured in white traps (12.537), a statistically significant difference was not determined with those captured in black traps (12.246). The lowest number of tomato leafminer adults was captured in yellow ferolite traps with 8.029. Stol et al. (2009) stated that light traps in greenhouses attract both females and

http://www.aloki.hu ● ISSN 1589 1623 (Print) ● ISSN 1785 0037 (Online)
DOI: http://dx.doi.org/10.15666/aeer/1706_1572115730

males in the struggle against *T. absoluta*, whereas pheromones attract only males, leading to minimum damage in greenhouses. Similar results were found in studies by Matos et al. (2012) and Özkan et al. (2017) in which it was shown that a greater number of adults were captured with light traps. However, Aksoy and Kovancı (2016) carried out a study in which the damage rates were compared for ferolite and water pan traps; as a result of which it was found there is no difference except for the fact that the ferolite trap is not economically feasible since it has a higher unit cost in comparison with the other trap.

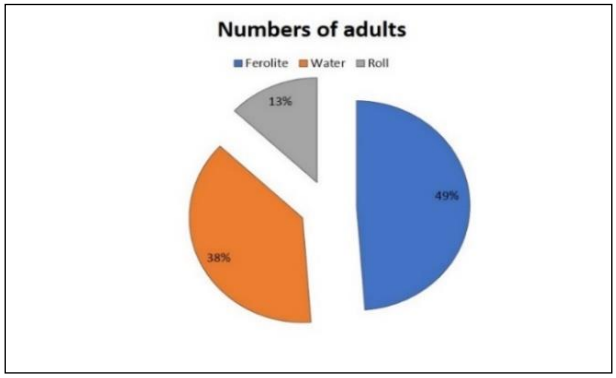

Figure 8. *Total number of Tuta absoluta captured by type of traps (%)*

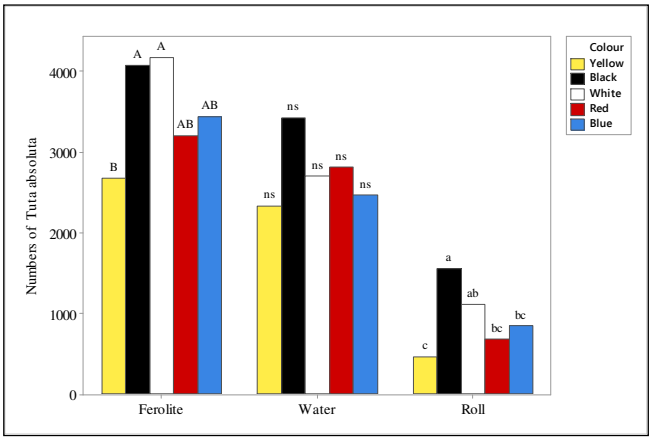

Figure 9. *Tuta absoluta captured by type and colour of traps.*
**Different letters indicate statistical significance (P<0.05) for in-column comparisons.*
ns = no significant difference

Despite the lack of a statistically significant difference between the water pan traps, the highest number of adults was captured in black traps with 10.299; this was followed by red, white, blue and yellow traps with 8.441, 8.106, 7.395 and 7.016, respectively. Taha et al. (2012) carried out a study with red, blue, green and yellow traps in which it was found that the highest number of *T. absoluta* adults was captured in the red water pan traps, and sequentially by blue, green and yellow traps, respectively. Similar to the results of Taha et al. (2012), in our study the yellow water pan traps were found the least attractive for adults of *T. absoluta*, whereas red traps were found the most attractive.

http://www.aloki.hu ● ISSN 1589 1623 (Print) ● ISSN 1785 0037 (Online)
DOI: http://dx.doi.org/10.15666/aeer/1706_1572115730

It was observed as a result of analysis carried out based on the colour, independent of trap type, that black and white attracted the highest number of adults whereas yellow attracted the least number of adults ($P<0.05$; $F = 6.57$). Mahmoud et al. (2014) found that white and yellow were more attractive, while Shiberu and Getu (2017) reported that the highest number of adults was captured in white and blue sticky traps, whereas the lowest number of adults was captured in green and red traps. These studies show that the white traps have the highest potential to attract *T. absoluta*. A statistically significant difference was observed between the roll traps with the highest number of adults captured in the black trap (4.690). This was followed by white, blue, red and yellow traps with 3.353, 2.550, 2.036 and 1.409, respectively.

Hassan and Alzaidi (2010) reported that yellow rolls can be used to catch *T. absoluta* but their use is not recommended in greenhouses because yellow traps could also attract beneficial insects. However, yellow was found to have the lowest efficiency for capturing tomato leafminer in all trap types in the current research. Therefore, yellow-coloured traps are not recommended for use in open-field tomato cultivation to capture *T. absoluta*. On the other hand, more adults were captured in all traps that were black and white. Therefore, black and white traps are highly recommended for attracting *T. absoluta* in open-field tomato production.

Conclusion

As a result, the mass trapping method is effective with low pest populations. Even though it is not directly effective in reducing *T. absoluta* in high pest populations, when it is used together with other control methods, the tomato leafminer population can be kept below harmful economic levels. Consequently, it can also be useful to increase the producer's profits by decreasing the use of insecticides. In addition to its impact on reducing costs, this aspect of the mass trapping method is also important due to the adverse impact that insecticides have on human health and the balance of nature. Also, studying different hues of black and white colours, which were the most effective colours in further researches, would be beneficial to increase the effectiveness of the traps.

Acknowledgements. Financial support from the Scientific Research Projects Committee (Project: FBA 2017/1260) of Çanakkale Onsekiz Mart University, Turkey is gratefully acknowledged.

REFERENCES

[1] Aksoy, E., Kovanci, O. (2016): Mass trapping low-density populations of *Tuta absoluta* with various types of traps in field-grown tomatoes. – Jour. of Plant Dis. and Prot. 123: 51-57.

[2] Bayram, Y., Duman, M., Buyuk, M., Mutlu, C. (2017): Effciency of pheromone water traps and life cycle of *Tuta absoluta* (Lepidoptera: Gelechiidae) in Diyarbakır province, Turkey. – Fresen. Environ. Bull. 26: 531-538.

[3] Braham, M. (2014): Role of trap colours and exposure time of pheromone on trapping efficacy of males of the tomato leaf miner, *Tuta absoluta* (Meyrick) (Lepidoptera: Gelechiidae). – African Journal of Agricultural Res. 29: 2263-2271.

[4] Cherif, A., Harbaoui, K., Zappalà, L., Grissa-Lebdi, K. (2018): Efficacy of mass trapping and insecticides to control *T. absoluta* in Tunisia. – J. Plant. Dis. Prot. 125: 51-61.

http://www.aloki.hu ● ISSN 1589 1623 (Print) ● ISSN 1785 0037 (Online)
DOI: http://dx.doi.org/10.15666/aeer/1706_1572115730

[5] Cocco, A., Deliperi, S., Delrio, G. (2012): Potential of mass trapping for *Tuta absoluta* management in greenhouse tomato crops using light and pheromone traps. – IOBC WPRS Bull. 80: 319-324.
[6] Desneux, N., Wajnberg, E., Wyckhuys, K. A. G., Burgio, G., Arpaia S., Narváez-Vasquez, C. A., González-Cabrera, J., Ruescas, D. C., Tabone, E., Frandon, J., Pizzol, J., Poncet, C. (2010): Biological invasion of European tomato crops by *Tuta absoluta*: ecology, geographic expansion and prospects for biological control. – Journal of Pest Science 83: 197-215.
[7] EPPO (2005): Data sheets on quarantine pests, *Tuta absoluta*. – EPPO Bulletin 35: 434-435.
[8] Gonza´lez-Cabrera, J., Molla´, O., Monto´n, H., Urbaneja, A. (2011): Efficacy of *Bacillus thuringiensis* (Berliner) in controlling the tomato borer, *Tuta absoluta* (Meyrick) (Lepidoptera: Gelechiidae). – Biocontrol 56: 71-80.
[9] Gozel, C., Kasap, I. (2015): Efficacy of entomopathogenic nematodes against the Tomato leafminer *Tuta absoluta* (Meyrick) (Lepidoptera: Gelechiidae) in tomato field. – Turk J. Entomology 39: 229-237.
[10] Hassan, N., Al-Zaidi, S. (2010): Tutaroll – an innovative solution for *Tuta absoluta*. – Int. Pest Control 52: 262-264.
[11] Kasap, İ., Gözel, U., Özpınar, A. (2011): A new pest in tomatoes; the tomato borer, *Tuta absoluta* (Meyrick) (Lepidoptera: Gelechiidae). – Çanakkale Agriculture Symposium Past, Present, Future, 10-11 Jan 2011, Çanakkale: 284-288. (In Turkish).
[12] Kılıç, T. (2010): First record of *Tuta absoluta* in Turkey. – Phytoparasitica 38: 243-244.
[13] Mahmoud, Y. A., Ebadah, I. M. A., Abd-Elrazik, A. S., Tabd-Elwahab, E., Deif, S. H. (2014): Efficiency of different colored traps baited with pheromone in capturing tomato adult moth, *Tuta absoluta* (meyrick) (Lepidoptera: Gelechiidae) during summer plantation. – World Applied Sciences Journal 30(4): 406-412.
[14] Matos, T., Figueiredo, E., Mexia, A. (2012): Sexual pheromone traps with light for mass trapping of *Tuta absoluta* (Meyrick), yes or no? – Rev Cienc Agrar 35: 282-286.
[15] Megido, R. C., Haubruge, E., Verheggen, F. J. (2013): Pheromone-based management strategies to control the tomato leafminer, *Tuta absoluta* (Lepidoptera: Gelechiidae). A review. – Biotechnology, Agronomy, Society and Environment 17: 475-482.
[16] Özkan, Z., Ünlü, L., Ögür, E. (2017): Örtü altı domates yetiştiriciliğinde domates güvesi (*Tuta absoluta* Meyrick)'ne karşı kullanılan feromon ve ferolite tuzaklarının etkinliğinin karşılaştırılması. – Harran Tarım ve Gıda Bilimleri Dergisi 21(4): 394-403. (In Turkish).
[17] Polat, B., Özpinar, A., Şahin, A. K. (2015): Çanakkale ilinde Domates güvesi (*Tuta absoluta* (Meyrick 1917), (Lepidoptera: Gelechiidae))'nin konukçularının belirlenmesi. – Bitki Koruma Bülteni 55: 331-339. (In Turkish).
[18] Polat, B., Özpinar, A., Şahin, A. K. (2016): Studies of selected biological parameters of tomato leafminer Tuta absoluta (Meyrick), (Lepidoptera: Gelechiidae) under natural conditions. – Phytoparasitica 44: 192-202.
[19] Polat, B., Tiryaki, O. (2019): Determination of some pesticide residues in conventional grown and IPM- grown tomato by using QuEChERS method. – J. of Envir. Science and Health Part B-Pesticides Food Contaminants and Agricultural Wastes 54(2): 112-117.
[20] Portakaldalı, M., Öztemiz, S., Kütük, H., Büyüköztürk, D., Çolakateş, A. (2013): Distribution of *Tuta absoluta* (Meyrick) (Lepidoptera: Gelechiidae) in the Eastern Mediterranean and Southeastern Anatolia Regions. – Turkish Bulletin of Entomology 3(3): 133-139.
[21] Shiberu, T., Getu, E. (2017): Evaluation of colored sticky traps for the monitoring of *Tuta absoluta* Meyrick (Lepidoptera: Gelechiidae) in tomato under glasshouse in Ethiopia. – Agri. Res. Tech. 9(3): 555762.
[22] Stol, W., Griepink, F. C., Deventer, P. V. (2009): *Tuta absoluta*: A new pest for tomato growing in Europe. – 2nd. Conference on Pheromones, Food Lure, Traps and Bıologıcal Control: Alternatıves for The 21st Century Murcıa, 18.

http://www.aloki.hu ● ISSN 1589 1623 (Print) ● ISSN 1785 0037 (Online)
DOI: http://dx.doi.org/10.15666/aeer/1706_1572115730

[23] Taha, M., Homam, H., Afsah, E., EL-Sharkawy, M. (2012): Effect of trap color on captures of Tuta absoluta moths (Lepidoptera: Gelechiidae). – Int. J. Environ. Sci. Eng 3: 43-48.
[24] Torres, J. B., Faria, C. A., Evangelista, W. S., Pratissoli, D. (2001): Within-plant distribution of the leaf miner *Tuta absoluta* (Meyrick) immatures in processing tomatoes, with notes on plant phenology. – International Journal of Pest Management 47: 173-178.
[25] TUİK (2017): Turkish Statistical Institute. – http://www.tuik.gov.tr, Accessed: January 2018.
[26] Urbaneja, A., Vercher, R., Navarro, V., García Marí, F., Porcuna, J. L. (2007): La Polilla del Tomate, *Tuta absoluta*. – Phytoma España 194: 16-23.
[27] Uzun, F., Birgücü, A. K., Karaca, İ. (2015): Determination of oviposition preference of *Tuta absoluta* to tomato, pepper and eggplant. – Asian Journal of Agriculture and Food Science 3(5): 569-578.
[28] Zappalà, L., Biondi, A., Alma, A., Al-Jboory, I., Arno, J., Bayram, A., Chailleux, A., El-Arnaouty, A., Gerling, D., Guenaoui, Y., Shaltiel-Harpaz, L., Siscaro, G., Stavrinides, M., Tavella, L., Vercher Aznar, R., Urbaneja, A., Desneux, N. (2013): Natural enemies of the South American moth, *Tuta absoluta*, in Europe, North Africa and Middle East, and their potential use in pest control strategies. – Journal of Pest Science 86: 635-647

http://www.aloki.hu ● ISSN 1589 1623 (Print) ● ISSN 1785 0037 (Online)
DOI: http://dx.doi.org/10.15666/aeer/1706_1572115730

FRACTAL FEATURES OF SOIL PARTICLES UNDER DIFFERENT PLANT COMMUNITIES IN THE YIMENG MOUNTAIN OF CHINA

LI, H.[1] – ZHAN, H. X.[2] – XU, H.[1*]

[1]*Department of Landscape Architecture, School of Geography, Geomatics and Planning, Jiangsu Normal University, Xuzhou 221116, China*

[2]*Forestry College, Shandong Agricultural University, Tai'an 271018, China*

[*]*Corresponding author*
e-mail: yiduohuanle@163.com

(Received 8th Sep 2019; accepted 15th Nov 2019)

Abstract. The vegetation in fragile ecological areas easily degrades and the original ecosystem is hard to preserve. This paper attempts to disclose the effects of different plant communities on the physical properties of the soil in the Yimeng Mountains of eastern China. For this purpose, the relative weight of soil particles in varied sizes was measured by the mechanical sieving method firstly. Next, the fractal dimensions of soil particles were computed based on their mass. After that, the uniformity and curvature were calculated for soil particles in varied sizes, under the cumulative percentage contents of 10%, 30%, and 60%. The results show that the local soil is predominately coarse sandy soil and the soil structure of forests is way better than that of slope wasteland; by fractal dimension, the coverage types were ranked in descending order as mixed forest > pure forest > economic forest > farmland > slope wasteland; the fractal dimension has a significant positive correlation with the particle size of fine sandy soil and coarse powder. The research findings shed new light on how to select tree species and design vegetation types to recover and reconstruct the vegetation in mountainous regions of eastern China.
Keywords: *fractal dimension, soil structure, uniformity, plant diversity, ecological protection*

Introduction

More than 60% of China is covered by fragile ecological areas, where vegetation easily degrades and the ecology is hard to preserve. The vegetation growth largely depends on the soil properties. In return, the soil properties are directly and indirectly affected by the overlying vegetation. The plant communities provide above- and belowground litterfall, release and recycle nutrients, modify the microclimate, regulate the water cycle, and alter the composition of fauna and flora in soil (Jose, 2009; Li et al., 2016). However, the soil structure is extremely complex. Some soil properties are too irregular and stochastic to describe by traditional statistical methods (Turcotte, 1986; Xiao et al., 2014; Luo et al., 2015).

The above problem can be solved effectively by fractal theory, powerful tool to tackle complex phenomena. The fractal theory has been widely adopted in numerous fields (Li and Wei, 2014). Since the 1980s, fractal theory has been applied to soil science (Turcotte, 1986; Gao et al., 2014; Sun et al., 2019). In the following decade, many scholars explored the feasibility of characterizing particle size distribution with fractal theory (Tyler and Wheatcraft, 1992; Su et al., 2004; Wei et al., 2016). The particle size distribution is an important physical attribute of soil that changes with the soil conditions (Xu et al., 2013; Lyu et al., 2015). The variation of the soil particle size distribution helps to identify the structure, dynamics and physical processes of soil (Ghorbani et al., 2012; Peng et al., 2014).

http://www.aloki.hu ● ISSN 1589 1623 (Print) ● ISSN 1785 0037 (Online)
DOI: http://dx.doi.org/10.15666/aeer/1706_1573115743

The fractal dimension is a useful metric to quantify various soil properties, namely, structure, erodibility (Perfect, 1997; Xia et al., 2015; Deng et al., 2018) and water permeability (Yu et al., 2015; Zhao et al., 2016; Zhao et al., 2017). The fractal information facilitates the design of soil conservation measures and selection of vegetation types in plateaus and mountainous regions (Liu et al., 2009; Wei et al., 2016). However, the fractal theory has not been extensively applied to analyze the soil particle size distribution in the Yimeng Mountain of central Shandong, China. In addition, the impacts of plant communities on the composition and distribution of soil particles remain unclear.

To make up for the gaps, this paper analyses the fractal features of soil particles under 11 plant communities in the Yimeng Mountains of eastern China. The analysis results shed new light on how to select tree species and design vegetation types to recover and reconstruct the vegetation in mountainous regions of eastern China, laying the technical basis for erosion control in fragile ecological areas.

The remainder of this paper is organized as follows: Section 2 describes the test materials and methods; Section 3 analyzes the composition, fractal dimension and size distribution of soil particles under 11 plant communities, and discusses the impacts of fractal dimension on the composition and uniformity of soil particles; Section 4 puts forward the research conclusions. This study attempts to disclose the effects of different plant communities on the physical properties of the soil in the Yimeng Mountains of eastern China. For this purpose, 11 local plant communities were selected, and the fractal theory was employed to examine their effects on the composition and size distribution of soil particles.

Materials and Methods

Study area

As shown in *Figure 1*, the study area lies in the upstream of the Taihe Reservoir, a large water conservancy project on the Zihe River. Located in the southeast of Zichuan District, Zibo Prefecture, Shandong Province, the northern part of the Yimeng Mountain of eastern China (117.9°E-118.2°E, 36.3°N-36.7°N), this area spans across several counties and towns, covering a total area of 278.02 km^2.

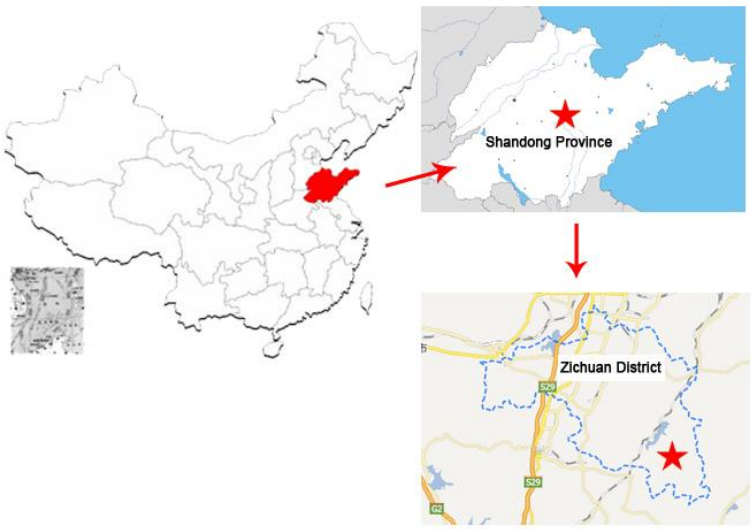

Figure 1. *Location and satellite map of the study area*

http://www.aloki.hu ● ISSN 1589 1623 (Print) ● ISSN 1785 0037 (Online)
DOI: http://dx.doi.org/10.15666/aeer/1706_1573115743

The maximum south-to-north distance is 18.2 km and the maximum east-to-west distance is 26 km. The region is a warm-temperature and semi-arid continental monsoon climate, with annual average temperature of 12.9°C. Annual average precipitation is 664 mm with 70% occurring between June and August. Annual average sunshine time is 2364 h, and the frostfree period is 189 days.

The soil type in the project area is mainly brown soil, and there are three subclasses: the brown soil subclasses, the leaching brown soil subclasses and the brown soil subclasses. The vegetation type has three types of natural vegetation, artificial vegetation and cultivated crops, among which, the natural vegetation is mainly grass and wild shrubs, and the natural vegetation is mainly of grass and wild shrubs, and the main tree species of the artificial vegetation are *pinus thunbergii*, *pinus densifla*, *Quercus acutissima*, *Robinia pseudoacaca* and *Castanea mollissima*, etc. The cultivated crops are sweet potato, *scutellaria baicalensis*, and the rest are wheat, corn and soybean. Typical plant communities and soil types in the Yimeng Mountain can be found in the study area (*Figure 2*).

Figure 2. *Photos of the study area*

Test materials

As shown in *Table 1*, eleven typical plant communities were selected from the study area to identify the size distribution of soil particles, and disclose the effects of vegetation types on the fractal dimension of soil particles (*Figure 3*). The eleven plant communities belong to five vegetation types, namely, pure forest (*Pinus thunbergii* and *Robinia pseudoacacia*), mixed forest (*Robinia pseudoacacia- Quercus acutissima* and *Pinus densiflora- Pinus thunbergii*), economic forest (*Castanea mollissima* and apple), farmland (*Scutellaria baicalensis*, sweet potato, other crops) and slope wasteland (wild grass 1 and wild grass 2). Three test plots were set up in each land use type, and the test sample points were determined according to the diagonal 3-point sampling method in each sample plot, repeat three samples (average analysis) at each test sample point.

http://www.aloki.hu ● ISSN 1589 1623 (Print) ● ISSN 1785 0037 (Online)
DOI: http://dx.doi.org/10.15666/aeer/1706_1573115743

Table 1. *Selected vegetation types and plant communities*

Vegetation types	Plant communities	Abbreviations	Serial number	GPS coordinates
Pure forest	*Pinus thunbergii*	PT	1	118.17E, 36.46N
	Robinia pseudoacacia	RP	2	118.19E, 36.47N
Mixed forest	*Robinia pseudoacacia- Quercus acutissima*	RQ	3	118.20E, 36.50N
	Pinus densiflora- Pinus thunbergii	PP	4	118.14E, 36.48N
Economic forest	*Castanea mollissima*	CM	5	118.17E, 36.48N
	Apple	A	6	118.16E, 36.50N
Farmland	*Scutellaria baicalensis*	SB	7	118.12E, 36.44N
	Other crops	OC	8	118.11E, 36.46N
	Sweet potato	SP	9	118.17E, 36.53N
Slope wasteland	Wild grass 1	WG1	10	118.18E, 36.54N
	Wild grass 2	WG2	11	118.17E, 36.51N

Figure 3. *Photos of the sampling site*

Test methods

Composition of soil particles

The size and weight distributions of soil particles were tested by the mechanical sieving method (dry sieving). Firstly, soil samples (particle size: 0~40cm) of each plant community from five points, dried and then mixed. The gravels with diameter greater than 2 mm were filtered out. Next, the relative weight contents of soil particles in varied sizes were measured by a ZBSX-92A standard electric sieve shaker (sieve swaying times: 221 times/min; shaking times: 147 times/min; shaking amplitude: 25 mm; motor power: 0.37 kW) with sieve sizes of 1.00, 0.50, 0.25, 0.10 and 0.05 mm.

Fractal dimension of soil particles

After the soil samples were dry-sieved, the weights and percentage contents of soil particles in varied sizes were measured and calculated. On this basis, the fractal dimensions of soil particles were computed based on their mass weight, assuming that

http://www.aloki.hu ● ISSN 1589 1623 (Print) ● ISSN 1785 0037 (Online)
DOI: http://dx.doi.org/10.15666/aeer/1706_1573115743

soil particles in varied sizes have the same density. The quantitative distribution of soil particles was represented by weight distribution (Yang et al., 1993). Then, the fractal dimension (D) can be derived by the method of limits.

$$D = 3 - \lg\left(\frac{w_i}{w_o}\right) / \lg\left(\frac{d_i^*}{d_{max}^*}\right) \quad \text{(Eq.1)}$$

where w_i is the cumulative mass of soil particles smaller than d_i*; w_0 is the total weight of all soil particles; d_i^* is the mean particle diameter (mm) between d_i and d_{i+1} of two adjacent particle size; d_{max}^* is the mean diameter of the largest soil particle. The mean particle diameter is the arithmetic mean of the upper and lower sieve sizes.

Size distribution of soil particles

Based on the weights of soil particles in varied sizes, the size distribution of soil particles was described by the tabular method and the cumulative curve method. The particle sizes corresponding to the cumulative percentage contents of 10%, 30% and 60% were denoted as d_{10}, d_{30}, and d_{60}, respectively. The index d_{10} means the particles smaller than this size account for 10% of the total soil mass. The meanings of d_{30} and d_{60} can be derived by analogy. The size distribution was measured by two coefficients, namely, uniformity (C_u) and curvature (C_c):

$$C_u = d_{60}/d_{10} \quad \text{(Eq.2)}$$

$$C_c = d_{30}^2/ (d_{60} \times d_{10}) \quad \text{(Eq.3)}$$

where d_{10} is the effective particle size, i.e. the pore diameter of the sieve; d_{60} is the control particle size. The uniformity is a key evaluation index of particle size distribution. A high uniformity means a wide distribution of particle sizes (If $C_u < 5$, the soil is uniform but poorly graded; if $Cu > 10$, the soil is well graded), but an excessively high uniformity may cause discontinuous grading, i.e. the absence of medium particle size. Thus, the curvature index was introduced to measure the overall shape of the cumulative curve.

Results and Analysis

Composition of soil particles

Size distribution of soil particles

Most soil particles were irregular, some varied greatly in three-dimensional (3D) size, and coarse and fine soil particles differed markedly in properties. For simplicity, the soil particles were viewed as smooth solid spheres, and divided into several groups based on diameter according to a standard for soil size fraction in China (*Table 2*) (Huang, 2000).

Composition of soil particles

The relative contents of dry-sieved soil particles in varied sizes are displayed in *Table 3* below. As shown in *Tables 2 and 3*, the soil particle sizes ranged between 0.25 and 1.0 mm under different plant communities, indicating that the local soil is predominately coarse sandy soil. This soil structure is a typical pattern in rocky hills of

http://www.aloki.hu ● ISSN 1589 1623 (Print) ● ISSN 1785 0037 (Online)
DOI: http://dx.doi.org/10.15666/aeer/1706_1573115743

northern China. The lack of fine particles (e.g. powder and clay particles), coupled with the high content of sandy soil, makes the soil structure extremely weak, loose and permeable, which is unfavorable to soil conservation (Deng et al., 2008).

By plant communities, the sampling sites of PT, RP and RQ were all rich in clay and powder particles; the sampling sites of A, WG1 and WG2 had high contents of fine sandy soils; the sampling sites of SP, SB and OC were dominated by sandy soils. The results show that both mixed and pure forests have a much better soil structure than slope wasteland, and mixed forest has more rational soil structure than pure forest. Therefore, needle-broad leaved or broad-leaved mixed forest can increase the contents of fine particles (e.g. clay and powder particles) in soil, and reduce the content of sandy soils. This is conducive to the soil structure and soil conservation. By contrast, the farmland witnesses a gradual reduction of fine sandy soils, which undermines the soil texture. This calls for prompt improvement of cultivation and irrigation methods.

Table 2. *The standard for soil size fraction*

Name of particle		Size (mm)
Gravel	Gravel	2~1
Sand	Coarse sand	1~0.5 0.5~0.25
	Fine sand	0.25~0.2 0.2~0.1 0. 1~0.05
Powder	Coarse powder	≤ 0.05

Table 3. *Composition of soil particles under different plant communities*

Plant communities	Percentage contents of soil particles in varied sizes (%)					
	1~2	0.5~1	0.25~0.5	0.1~0.25	0.05~0.1	≤ 0.05
PT	21.34	28.18	14.92	19.15	6.2	10.21
RP	16.51	24.05	15.48	22.02	7.45	14.48
RQ	22.73	27.34	13.08	16.68	6.59	13.59
PP	19.12	28.09	14.56	17.34	5.7	15.18
CM	21.57	32.54	16.87	17.94	4.49	6.59
A	18.65	27.04	14.89	20.98	7.32	11.12
SB	20.7	32.51	18.12	18.56	4.52	5.6
OC	17.5	40.2	22.55	14.05	2.19	3.51
SP	20.51	31.53	18.11	19.32	4.38	6.15
WG1	25.88	34.19	14.92	16.71	3.42	2.99
WG2	36.69	35.08	12.1	9.35	2.26	4.52

* Abbreviations of plant communities please refer to table 1 in detail

Fractal features of soil particles

Fractal dimension of soil particles under different plant communities

The fractal dimensions of soil particles were calculated by linear regression with *Equation 1*. The results are recorded in *Table 4*. Based on the data in *Table 4*, a graph (*Figure 4*) was plotted with fractal dimension as the y-coordinate and plant community as the x-coordinate.

As shown in *Table 4*, the calculated fractal dimensions fell within a small interval: 2.0044~2.4925. The results are basically within the range of sandy soil in China

http://www.aloki.hu ● ISSN 1589 1623 (Print) ● ISSN 1785 0037 (Online)
DOI: http://dx.doi.org/10.15666/aeer/1706_1573115743

(1.834~2.641) (Hu et al., 2003). This conclusion agrees with the data in *Table 3*. It can be seen from *Figure 4* that RQ corresponded to the highest fractal dimension, followed by PP, RP, A, PT, CM, SB, OC, WG2, WG1 and SP in succession.

Table 4. *D-value of soil particles under different plant communities*

Types	Code	Sample plot	Slope	D
Pure forest	PT	1	0.98	2.3574
	RP	2	0.97	2.4542
Mixed forest	RQ	3	0.99	2.4925
	PP	4	0.99	2.4618
Economic forest	CM	5	0.98	2.2908
	A	6	0.97	2.3845
Farmland	SB	7	0.97	2.2002
	OC	8	0.97	2.1798
	SP	9	0.97	2.0044
Slope wasteland	WG1	10	0.99	2.1152
	WG2	11	0.97	2.1367

* Abbreviations of Code please refer to table 1 in detail

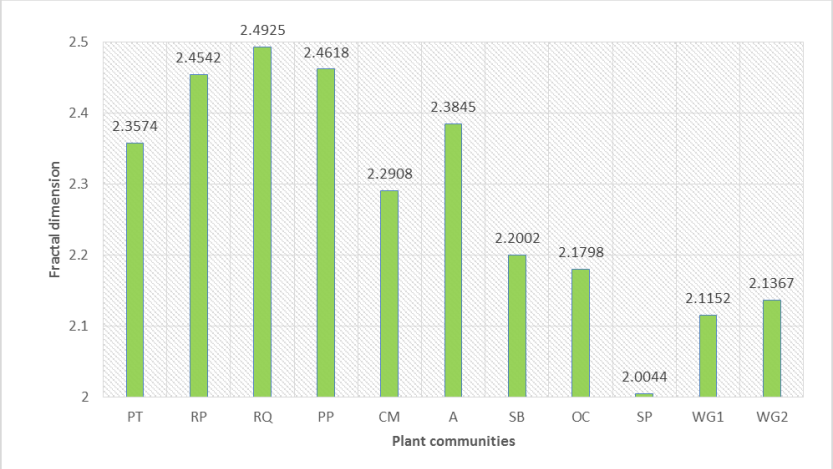

Figure 4. *The fractal dimensions of soil particles under different plant communities*

Effects of coverage type on fractal dimension

The effects of coverage type on fractal dimension are manifested as soil improvement and protection of plant communities. In *Table 4* and *Figure 4*, the fractal dimensions of the 11 plant communities fell between 2.0044 and 2.4925. Thus, all types of plant communities have a major impact on fractal dimension.

By fractal dimension, the coverage types were ranked in descending order as mixed forest > pure forest > economic forest > farmland > slope wasteland.

The forests had higher dimensional values than the other vegetation types, revealing that forest species can greatly enhance soil structure. Among forest lands, mixed forest (RQ > PP) is the most effective vegetation type to ameliorate soil structure, followed by pure forest and economic forest. The advantage of forests is attributable to the importance of forest species in soil development. The soil beneath forests often features small particle

http://www.aloki.hu ● ISSN 1589 1623 (Print) ● ISSN 1785 0037 (Online)
DOI: http://dx.doi.org/10.15666/aeer/1706_1573115743

size, good air permeability and coexistence of large and small pores. This type of soil is easy to conserve.

By contrast, farmland and slope wasteland showed similarly small fractal dimensions. This means the coarse soil texture under crops can slightly improve the soil structure. The soil texture is coarsen by the erosion of gravel surface.

Relationship between content and fractal dimension

Based on *Tables 3 and 4*, the relationship between content and fractal dimension of soil particle in each size was plotted (*Figure 5*). It can be seen that the percentage contents of soil particles in varied sizes differed in their impacts on fractal dimension. Overall, fractal dimension has a linear correlation with the content of soil particles in each size. The linear correlation was significantly positive for fine sandy soil and coarse powder, as evidenced by the correlation coefficients (R^2): 0.2888 and 0.901. By contrast, the linear correlation was significantly negative for coarse sandy soil, with the R^2 being 0.7342; the linear correlation was not evident for gravel. The results show that the percentage contents of soil particles in varied sizes have different correlations with fractal dimension. This finding may be related to the high percentage contents of soil particles in other sizes within the study area. The fractal dimension failed to reflect the non-uniformity of soil texture in the study area correctly, implying that it cannot clearly measure the content variation of soil in each particle size.

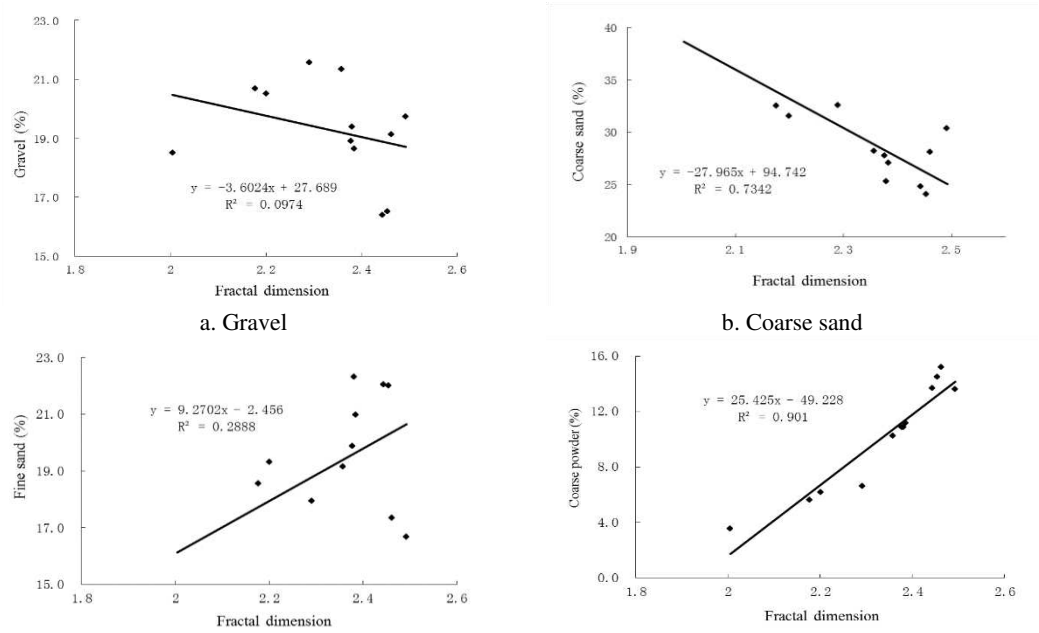

Figure 5. *The relationship between percentage content and fractal dimension of soil particle in each size*

Combining with existing research results, the author found that fractal dimension is closely related to the size, quantity, and distribution uniformity of soil particles. The fractal dimension changed evidently with soil particle size. The above results show that the fractal dimension is an important index to evaluate soil texture. Small soil particles tend to have a high fractal dimension, because of their fine texture and high content of

http://www.aloki.hu ● ISSN 1589 1623 (Print) ● ISSN 1785 0037 (Online)
DOI: http://dx.doi.org/10.15666/aeer/1706_1573115743

fine particles, while large soil particles usually have a low fractal dimension. In other word, the fractal dimension increases with the size of soil particles. The fractal dimension of sandy soil was significantly lower than that of loam and clay soils. High fractal dimensions mean good soil texture but poor air permeability, which contribute to soil conservation. The inverse is also true. Furthermore, since water and wind erosions mainly induce losses of superficial clay and powder particles, a low content of fine particles indicates serious soil erosion. Therefore, the prediction of fractal dimension is critical to the evaluation of the degree of soil erosion.

Uniformity and curvature of soil under different vegetation types

The uniformity and curvature of soil under each plant community were computed by *Equations 2 and 3*, respectively. The computed results (*Table 5*) show that PT led to the highest uniformity, followed in descending order by RQ, RP, PP, A, CM, SB, OC, SP, WG1 and WG2. By uniformity, the five vegetation types were ranked in ascending order as of slope wasteland < farmland < economic forest < mixed forest < pure forest.

Table 5. *The uniformity and curvature of soil under each plant community*

Plant community	d_{60}	d_{30}	d_{10}	C_u	C_c
PT	0.56	0.18	0.02	28.00	2.89
RP	0.65	0.19	0.03	21.67	1.85
RQ	0.72	0.22	0.03	24.00	2.24
PP	0.66	0.25	0.04	16.50	2.37
CM	0.95	0.29	0.09	11.88	1.11
A	0.65	0.23	0.04	16.25	2.03
SB	0.90	0.37	0.08	11.25	1.90
OC	0.96	0.30	0.12	8.00	0.78
SP	0.58	0.25	0.09	6.44	1.08
WG1	0.80	0.32	0.15	5.33	0.85
WG2	0.95	0.55	0.20	4.75	1.59

* Abbreviations of plant communities please refer to table 1 in detail

Specifically, slope wasteland and farmland possessed a relatively uniform soil texture, showing a small difference of content between coarse and fine soil particles. The curvatures of these two vegetation types fell between 0.78 and 1.90, indicating that their soil particles are poorly graded.

For economic and mixed forests, the uniformities ranged from 11.88 to 24, and the curvatures varied between 1.11 and 2.37. Thus, these two vegetation types have well graded soil particles. For pure forest, the uniformity was 21.67~28 and the curvature was 1.85~2.89, a signal of good grading.

Discussion

The soil texture can be evaluated by the contents and uniformities of soil particles in varied sizes. Being a porous medium, soil has a self-similar structure and certain fractal features. The fractal dimension is the main index of fractal features. Therefore, the relationship between uniformity and fractal dimension is conducive to the analysis on soil structure and texture. The relationship curves between the two factors were plotted

http://www.aloki.hu ● ISSN 1589 1623 (Print) ● ISSN 1785 0037 (Online)
DOI: http://dx.doi.org/10.15666/aeer/1706_1573115743

(*Figure 6*) based on *Tables 4 and 5*, with fractal dimension as the x-coordinate and uniformity as the y-coordinate.

The linear fitting results were Y = 40.94X − 79.325 and R^2 = 0.7039, indicating a significantly positive linear correlation between fractal dimension and uniformity, that is, the fractal dimension increases with uniformity. The complexity of soil texture depends on the quantitative distribution of soil particles in varied sizes (texture uniformity) and the soil aggregates (excluding small particles). It is found that the fractal dimension has a good linear correlation with the two feature parameters of soil texture, namely, the content of clay and powder particles and the uniformity. Hence, fractal dimension is a good index to quantify the soil structure and texture.

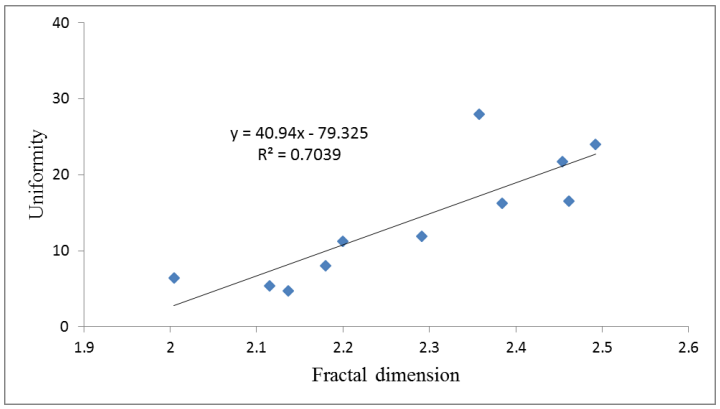

Figure 6. *Correlation between fractal dimension and uniformity*

In the aspect of soil fractal dimension used to quantitatively describe soil texture, physical properties and fertility characteristics, the existing studies show that when the soil texture changes from coarse to fine, the fractal dimension of soil particle composition changes from small to large (Yang et al., 1993; Zhao et al., 2016). The fractal dimension of soil with good texture structure and fertility is about 2.60 ~ 2.80 (Zhao et al., 2016), while the soil fractal dimension of different plant communities in this study area is between 2.0044 and 2.4925 (average 2.2798, *Fig. 4*), which is smaller than the fractal dimension of well-structured soil and belongs to the range of sandy soil (1.834 ~ 2.641) (Lyu et al., 2015; Wei et al., 2016). Obviously, the higher the fractal dimension of soil, the stronger the function of improving soil structure.

The effect of the forest community on the soil physical structure is related to the nature of the fractal dimension of the soil particles, because the fractal dimension of the soil is used as the parameter to describe the soil structure geometry, and the filling capacity of the soil particle to the space is essentially reflected (Luo et al., 2015; Zhao et al., 2017). That is, the smaller the diameter of the soil particles, the higher the content of the fine-grained material (the particles, the powder, the organic matter, etc.), the stronger the filling capacity of the space, the larger the fractal dimension of the soil, the better the formation of the better texture and the pore structure, and vice versa. This relationship is particularly evident in relatively coarse soil, such as sandy soil. It can also be said that in the mountainous area of coarse bone soil, forest community can increase the fractal dimension of soil by increasing the content of fine matter in soil, which is the fractal mechanism to improve the physical structure of soil and give full play to the function of soil and water conservation.

http://www.aloki.hu ● ISSN 1589 1623 (Print) ● ISSN 1785 0037 (Online)
DOI: http://dx.doi.org/10.15666/aeer/1706_1573115743

Conclusions

The vegetation in fragile ecological areas easily degrades and the ecology is hard to preserve. This paper explores the effects of different plant communities on the physical properties of soil in the Yimeng Mountains of eastern China. Firstly, the composition, fractal features and size distribution indices (uniformity and continuity) of soil particles under 11 plant communities were discussed based on fractal theory. Next, the relationships between fractal dimension, particle size composition and uniformity were analyzed in details. The main conclusions were drawn as follows:

(1) The soil composition shows that the soil particle sizes ranged between 0.25 and 1.0 mm under different plant communities, indicating that the local soil is predominately coarse sandy soil. Both pure and mixed forests have high contents of clay and powder particles; the slope wasteland possesses high contents of fine sandy soils; the farmland witnesses a high content of sandy soils. The soil structure of forests is way better than that of slope wasteland, and the soil structure of mixed forest is markedly better than that of pure forest.

(2) The fractal dimensions of the 11 plant communities fell within a small interval: 2.0044~2.4925. RQ corresponded to the highest fractal dimension, followed by PP, RP, A, PT, CM, SB, OC, WG2, WG1 and SP in succession. The forests had higher dimensional values than the other vegetation types, revealing that forest species can greatly enhance soil structure. Among forest lands, mixed forest is the most effective vegetation type to ameliorate soil structure, followed by pure forest and economic forest.

(3) Fractal dimension has a linear correlation with the content of soil particles in each size. The linear correlation was significantly positive for fine sandy soil and coarse powder, as evidenced by R^2: 0.2888 and 0.901. By contrast, the linear correlation was significantly negative for coarse sandy soil, with the R^2 being 0.7342; the linear correlation was not evident for gravel.

(4) PT led to the highest uniformity, followed in descending order by RQ, RP, PP, A, CM, SB, OC, SP, WG1 and WG2. By uniformity, the five vegetation types were ranked in ascending order as of slope wasteland < farmland < economic forest < mixed forest < pure forest. Thus, economic forest and mixed forest can significantly improve soil texture. Moreover, a positive linear correlation was observed between the uniformity and fractal dimension of each plant community ($R^2 = 0.7039$).

The above results shed new light on how to select tree species and design vegetation types to recover and reconstruct the vegetation in mountainous regions of eastern China, laying the technical basis for erosion control in fragile ecological areas. Further research will combine fractal analysis with the correlation analysis between fractal dimension and infiltration features in the study area.

Acknowledgements. This study was supported by the National Natural Science Foundation of China (No. 31500575) and a Project Funded by the Priority Academic Program Development of Jiangsu Higher Education Institutions (PAPD).

REFERENCES

[1] Deng, L. J., Lin, Z. Y., Gao, X. S., Zhang, S. R. (2008): Fractal feature of soil particles in the Chengdu plain. – Chinese Journal of Soil Science 39(1): 38-42.

http://www.aloki.hu ● ISSN 1589 1623 (Print) ● ISSN 1785 0037 (Online)
DOI: http://dx.doi.org/10.15666/aeer/1706_1573115743

[2] Deng, J., Ma, C., Yu, H. (2018): Different soil particle-size classification systems for calculating volume fractal dimension-a case study of pinus sylvestris var. mongolica in mu us sandy land, China. – Appl Sci-Basel 8(10): 1872.
[3] Gao, G. L., Ding, G. D., Zhao, Y. Y., Wu, B., Zhang, Y. Q., Qin, S. G., Bao, T. F., Yu, M. H., Liu, Y. D. (2014): Fractal approach to estimating changes in soil properties following the establishment of Caragana Korshinskii, shelterbelts in Ningxia, NW China. – Ecol Indic 43: 236-243.
[4] Ghorbani, N., Raiesi, F., Ghorbani, S. (2012): Bulk soil and particle size-associated c and n under grazed and ungrazed regimes in mountainous arid and semi-arid rangelands. – Nutr Cycl Agroecosys 93(1): 15-34.
[5] Hu, Y. F., Liu, J. Y., Zhuang, D. F. (2003): Progress in Wind Erosion Research. – Progress in Geography 22(3): 288-295.
[6] Huang, C. Y. (2000): Soil Science. – 1st ed., China Agriculture Press: Beijing, China 71-72.
[7] Jose, S. (2009): Agroforestry for ecosystem services and environmental benefits: an overview. – Agroforest Syst 76(1): 1-10.
[8] Li, X., Wei, X. (2014): Analysis of the relationship between soil erosion risk and surplus floodwater during flood season. – J Hydrol Eng 19(7): 1294-1311.
[9] Li, T., He, B., Zhang, Y., Tian, J. L., He, X. R., Yao, Y., Chen, X. Y. (2016): Fractal analysis of soil physical and chemical properties in five tree-cropping systems in Southwestern China. – Agroforest Syst 90(3): 457-468.
[10] Liu, X., Zhang, G. C., Heathman, G. C., Wang, Y. Q., Huang, C. H. (2009): Fractal features of soil particle-size distribution as affected by plant communities in the forested region of Mountain Yimeng, China. – Geoderma 154(1): 123-130.
[11] Luo, B. L., Chen, X. Y., Ding, L. Q., Huang, Y. H., Zhou, J., Yang, T. T. (2015): Response characteristics of soil fractal features to different land uses in typical purple soil watershed. – Plos One 10(4): e0122842: 1-19.
[12] Lyu, X., Yu, J., Zhou, M., Ma. B., Wang, G. M., Zhan, C., Han, G. X., Guan, B., Wu, H. F., Li, Y. Z., Wang, D. (2015): Changes of soil particle size distribution in tidal flats in the yellow river delta. – Plos One 10(3): e0121368: 1-12.
[13] Peng, G., Xiang, N., Lv, S. Q., Zhang, G. C. (2014): Fractal characterization of soil particle-size distribution under different land-use patterns in the yellow river delta wetland in China. – J Soil Sediment 14(6): 1116-1122.
[14] Perfect, E. (1997): Fractal models for the fragmentation of rocks and soils: a review. – Eng Geol 48(48): 185-198.
[15] Su, Y. Z., Zhao, H. L., Zhao, W. Z., Zhang, T. H. (2004): Fractal features of soil particle size distribution and the implication for indicating desertification. – Geoderma 122(1): 43-49.
[16] Sun, J., Huang, C. H., Han, G., Wang, Y. (2019): Effects of cover on soil particle and associated soil nutrient redistribution on slopes under rainfall simulation. – J Soil Sediment 19(2): 729-740.
[17] Turcotte, D. L. (1986): Fractals and fragmentation. – J Geophys Res Solid Earth 91(B2): 1921-1926.
[18] Tyler, S. W., Wheatcraft, S. W. (1992): Fractal scaling of soil particle-size distributions: analysis and limitations. – Soil Sci Soc Am J 56(2): 362-369.
[19] Wei, X., Li, X., Wei, N. (2016): Fractal features of soil particle size distribution in layered sediments behind two check dams: implications for the Loess Plateau, China. – Geomorphology 266: 133-145.
[20] Xia, D., Deng, Y. S., Wang, S. L., Ding, S. W., Cai, C. F. (2015): Fractal features of soil particle-size distribution of different weathering profiles of the collapsing gullies in the hilly granitic region, South China. – Nat Hazards 79(1): 455-478.
[21] Xiao, L., Xue, S., Liu, G. B., Zhang, C. (2014): Fractal features of soil profiles under different land use patterns on the loess plateau, China. – J Arid Land 6(5): 550-560.

http://www.aloki.hu ● ISSN 1589 1623 (Print) ● ISSN 1785 0037 (Online)
DOI: http://dx.doi.org/10.15666/aeer/1706_1573115743

[22] Xu, G., Li, Z., Li, P. (2013): Fractal features of soil particle-size distribution and total soil nitrogen distribution in a typical watershed in the source area of the middle dan river, China. – Catena 101(2): 17-23.
[23] Yang, P. L., Luo, Y. P., Shi, Y. C. (1993): Fractal characteristics of soil by weight distribution of particle size. – Chinese Sci Bull 38(20): 1896-1899.
[24] Yu, J., Lv, X., Bin, M., Wu, H. F., Du, S. Y., Zhou, M., Yang, Y. M., Han, G. X. (2015): Fractal features of soil particle size distribution in newly formed wetlands in the yellow river delta. – Sci Rep-UK 5: 10540.
[25] Zhao, Q., Lu, X., Tang, Q., Zhang, W., Liu, P. (2016): Fractal dimension characteristic of soil particle size in the riparian buffer zone of the middle and lower reaches of the yellow river. – Science of Soil and Water Conservation 14(5): 37-45.
[26] Zhao, Y., Feng, Q., Yang, H. (2016): Soil salinity distribution and its relationship with soil particle size in the lower reaches of Heihe River, Northwestern China. – Environ Earth Sci 75(9): 1-18.
[27] Zhao, W. J., Cui, Z., Ma, H. (2017): Fractal features of soil particle-size distributions and their relationships with soil properties in gravel-mulched fields. – Arab J Geosci 10(9): 211.

http://www.aloki.hu ● ISSN 1589 1623 (Print) ● ISSN 1785 0037 (Online)
DOI: http://dx.doi.org/10.15666/aeer/1706_1573115743

DETERMINATION OF THE BACTERIAL COMPOSITION OF A FULL-SCALE MULTI-LAYER BIOFILTER SYSTEM BASED ON 454 PYROSEQUENCING

WANG, X. M. – LI, X. D. – QIU, J. P. – LI, Y.S.*

School of Agriculture and biology, Shanghai Jiao Tong University, Shanghai 200240, China

**Corresponding author*
e-mail: yinshengli@sjtu.edu.cn

(Received 8th Sep 2019; accepted 15th Nov 2019)

Abstract. The multi-layer biofilter (MBF) is a promising tool for low-strength wastewater treatment. This paper investigates the microbial composition of a full-scale MBF system in the suburb of Shanghai, China, and analyzes the structure of the bacterial community with 454-pyrosequencing. The results show that different parts of the MBF, namely, the second, fourth and sixth layers (L2, L4 and L6) differed in bacteria composition. A total of 7,385, 7,042 and 5,974 sequences with high-quality 16S rRNA genes were recovered from L2, L4 and L6, respectively, and subjected to community analysis. The libraries of L2, L4 and L6 consist of 1,457, 1,310 and 1,197 operational taxonomic units (OTUs), respectively. In addition, L2, L4 and L6, had 89, 87 and 80 classes of bacteria, respectively. However, 73 classes of L2, 70 classes of L4 and 62 classes of L6 had an abundance lower than 1%. Besides, Thermus was only found in L2. This research is the first one ever to study the microbial communities in the biofilm of full-scale MBF systems in wastewater treatment. The research findings shed new light on the biological mechanism of contaminant removal in the MBF, and promote the application of the MBF in wastewater treatment.
Keywords: *biofilter, 454 pyrosequencing, bacterial composition, community richness, wastewater*

Introduction

Extended from conventional trickling filters, multi-layer biofilter (MBF) is a new wastewater treatment tool that effectively eliminates organic and nutrient contaminants, using a mixture of microorganisms (Ou et al., 2009).

Previously, the bacterial community in wastewater treatment plants has often been identified by culture-dependent methods. However, these methods can only cultivate and characterize less than 1% of the microorganisms in different habitats (Torsvik et al., 2002). In recent years, pyrosequencing has emerged as a popular method to examine the structure of bacterial communities. This approach can obtain varied genetic information on the microbes in the environment. For example, 454 Life Sciences (Branford, US) designed the 454 pyrosequencing, a high-throughput analytical method that utilizes a single strand of DNA with a length of 400~500bp. With the aid of 454 pyrosequencing, Wen et al. (2017) found that the population of ammonia oxidizing bacteria (AOB) shrank with the decline of ammonia concentration, but failed to observe a dramatic drop in the percentage of anammox bacteria. Lautenschlager (2014) applied 454 pyrosequencing to three biofilters with similar microbial composition, yet the results go against the actual situation. As an emerging microbial research method Roche 454-high throughput pyrosequecing have been used widely to analyze the microbial community in WWTPs (Ye et al., 2011; Zhang et al., 2012; Hu et al., 2012; Ye and Zhang, 2013; Pervin et al., 2013; Zheng et al., 2017; Liu et al., 2017).

Despite the above studies, there is little report that fully discloses the variation in microbial composition in wastewater treatment plants, especially in biofilters. Yang et al.

http://www.aloki.hu ● ISSN 1589 1623 (Print) ● ISSN 1785 0037 (Online)
DOI: http://dx.doi.org/10.15666/aeer/1706_1574515753

(2013) compared vermifilter and the conventional biofilter, and drew the following conclusions: the biofilm of vermifilter has two types of bacterial strains (firmicutes and γ - proteobacteria), while that of conventional biofilter has four types (firmicutes, γ- proteobacteria, β-proteobacteria and actinobacteria).

This paper attempts to characterize and compare the bacteria community at different positions along the MBF. For this purpose, the author probed deep into the microbial composition of a full-scale MBF system in the suburb of Shanghai, China, and analyzed the structure of the bacterial community with 454-pyrosequencing.

Materials and Methods

Research object

Located in the suburb of Shanghai, China, our research object, i.e. a full-scale MBF system, has been operating stably for nearly 7 years (GPS, 31.587,121.656). The system consists of multiple modules of the same size (L×W×H: 675 cm×485 cm×400 cm). A vertical gap of 15 cm is maintained between adjacent modules. The biofilm on the filler surface is in full contact with the air, allowing the microorganisms to get enough oxygen. From top to bottom, the biofilter chamber can be divided into seven layers. The upper four layers are filled with ceramists, and the lower three layers, volcanic rocks. The treatment efficiency is 500 m^3 per day.

The technological process involves an equalization tank, a lifting pump, a MBF, an intermediate tank, and a constructed wetland. After being collected by the pipe network, the wastewater from the equalization tank is pumped by the lifting pump to the MBF, and be dispersed to all places through the water channel. From top to bottom, the sewage flows through MBF, and then converges from the bottom to the sedimentation tank at the rear. and comes into full contact with the biofilm on the filler. The spilled part flows back to the middle pool. Then, the contaminants are absorbed and degraded by the microorganisms on the biofilm.

Sample collection and processing

The biofilm samples were collected from the second, fourth and sixth layers, and denoted as L2, L4 and L6, respectively. In order to ensure the reliability and uniformity of the samples, five-point sampling method is adopted, that is, sampling from five different positions of the same level, and mixing. Each sample was obtained from the filler by 5 min ultrasonic treatment, and then flushed with deionized water. Then, the sample was relocated to a 50 mL tube, and centrifuged at 8,000×g for 10 min. The sediments were stored at -80°C until DNA extraction.

DNA extraction and polymerase chain reactions (PCRs)

The total genomic DNA was extracted by E.Z.N.A.® Soil DNA Kit (Omega Bio-tek, US). To construct the clone library, the primer set 341F (5'-CCTACGGGAGGCAGCAG-3') and 907R (5'- CCGTCAATTCMTTTRAGT-3') was used to amplify the hypervariable V3~V5 region (about 560bp) of bacterial 16S rRNA gene. The fused forward primer includes a10-base long barcode inserted between the 454 adapter and the 341F primer, aiming to distinguish each sample in the mixed reaction.

http://www.aloki.hu ● ISSN 1589 1623 (Print) ● ISSN 1785 0037 (Online)
DOI: http://dx.doi.org/10.15666/aeer/1706_1574515753

The PCRs were performed in a 25 μL volume containing 2.5 μL 10×buffer , 2 μL dNTP, 1 μL of each primer (10 μM), 2 μL of DNA (20 ng/μL) and 0.125 μL pyrobest polymerase (5 U/μL, Takara, China). The thermocycling was carried out in the following steps: 94℃ for 4 min, followed by 27 cycles at 95℃ for 30 s, 55℃ for 45 s, 72℃ for 1 min and a final extension at 72℃ for 7 min. In this study, the number of PCR cycles is reduced to ensure the accuracy and reliability of the subsequent analysis. The PCR products were run on a 0.8% agarose gel, with the amplicon size of 500bp.

Pyrosequencing

The PCR products were purified using the AMPure XP beads, quantified by Quant-iT PicoGreen dsDNA Assay Kit (Thermo Fisher Scientific, US), and pyro-sequenced on 454 Gs Flx Titanium Platform (Roche, US) in Shanghai Personalbio Co., Ltd.

Sequence analysis

Following pyrosequencing, the genetic sequences were analyzed on QIIME, an open-source bioinformatics pipeline for performing microbiome analysis from raw DNA sequencing data. Firstly, the ineffective sequences were filtered out, leaving only sequences satisfying the following requirements: the length falls within 200~1,000bp, fewer than 6 consecutive bases are identical, no ambiguous base is included, and the quality score is above 25.

The uchime_denovo command was called to remove chimera, which would otherwise affect sequence quality. Then, sequences with similarities of greater than 97% were clustered into one operational taxonomic unit (OTU), using the QIIME program. Community richness and diversity indices (i.e. Chao1 estimator, ACE estimator and Simpson's diversity) and rarefaction curves were obtained with mothur. The larger the Chao / ACE index is, the higher the community richness is. The larger the Simpson index is, the lower the community diversity is.

Results and Discussion

MBF performance

The water quality of MBF obtained by measuring three parallel water samples at different positions is as follows. The project has been in stable operation for several years, and the effluent quality has reached the national water quality discharge standard of China (GB 8978-1996).

Table 1 lists several water quality indices before and after the water treatment. During the treatment, the mean chemical oxygen demand (COD) of influent was 306 mg/L, while the mean COD of effluent was 232, 215 and 227 mg/L for L2, L4 and L6, respectively. Thus, the COD removal rate of the MBF was 25.8%.

The mean ammonia nitrogen (NH_3-N) was 19 mg/L before the treatment. After the treatment, the mean NH_3-N of effluent was 15.33, 10.83 and 9.54 mg/L, for L2, L4 and L6, respectively. Thus, the MBF removed 50% of the NH_3-N from the wastewater.

The mean total nitrogen (TN) was 31.82 mg/L in the influent. After the treatment, the mean TN of effluent was 20.94, 29.48 and 27.76 mg/L, for L2, L4 and L6, respectively. Therefore, the TN removal rate of the MBF was 12.8%, lower than that of NH_3-N.

http://www.aloki.hu ● ISSN 1589 1623 (Print) ● ISSN 1785 0037 (Online)
DOI: http://dx.doi.org/10.15666/aeer/1706_1574515753

The mean total phosphorus (TP) was 3.89 mg/L in the influent. After the treatment, the mean TP of effluent was 3.75, 3.8 and 3.7 mg/L, for L2, L4 and L6, respectively. Hence, the MBF removed 4% of the TP from the influent.

Table 1. *Water quality indices (temperature: 19.45±0.49°C)*

	pH	DO	COD (mg/L)	NH_3-N (mg/L)	TN (mg/L)	TP (mg/L)
Influent	7.544	1.42	306	19	31.82	3.89
L2	7.806	5.43	232	15.33	20.94	3.75
L4	7.643	5.65	215	10.83	29.48	3.8
L6	7.739	3.29	227	9.54	27.76	3.7

Bacteria diversity

As shown in *Table 2*, a total of 7,385, 7,042 and 5,974 sequences with high-quality 16S rRNA genes were recovered from L2, L4 and L6, respectively, and subjected to community analysis. The libraries with L2, L4 and L6 consist of 1,457, 1,310 and 1,197 OTUs, respectively.

Table 2. *Community richness and diversity indices*

Sample number	Number of effective sequences	Number of high-quality sequences	OTUs	ACE estimator	Chao1 estimator	Simpson's diversity	Coverage
L2	11,239	7,385	1,457	3,164.202	2,791.603	0.002979	0.907651
L4	10,840	7,042	1,310	2,905.24	2,476.287	0.004794	0.912099
L6	9,611	5,974	1,197	2,446.65	2,164.788	0.004775	0.907934

The rarefaction curves were plotted (*Figure 1*) based on the OTUs at 3% cutoff to compare the community richness of the three samples. As shown in *Figure 1*, none of the curves approached a plateau, suggesting that further sequencing will continue to increase the number of OTUs in each sample. However, the coverage of all three samples had already reached 90%. Pyrosequencing analysis output numerous OTUs, providing the genetic information needed to find scarce species (Zhang, 2011).

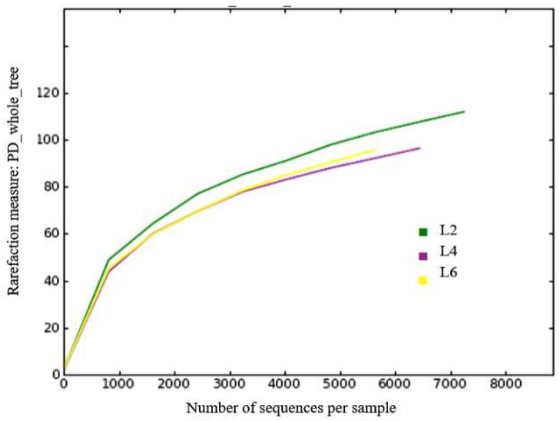

Figure 1. *Rarefaction curves of OTUs in L2, L4 and L6*

http://www.aloki.hu ● ISSN 1589 1623 (Print) ● ISSN 1785 0037 (Online)
DOI: http://dx.doi.org/10.15666/aeer/1706_1574515753

It can also be seen from *Table 2* that L2 contained richer species than any other sample. Besides, the values of ACE estimator, Chao1 estimator, and Simpson's diversity show that L2 had the highest bacterial diversity, followed by L4 and then L6. The ranking of bacterial diversity agrees with the positions of the three layers in the MBF: the wastewater first flows through L2 first, then through L4, and finally through L6. In other words, the bacteria diversity decreases along the MBF. This conclusion echoes with the number of OTUs in these layers.

Next, the samples were sorted in descending order of OTU abundance, and the distribution curves of OTU abundance were plotted (*Figure 2*), taking log2 of abundance. In *Figure 2*, the horizontal length of each curve reflects the community richness of the corresponding sample, while the curve shape demonstrates species evenness. Obviously, the three samples were ranked as L2>L4>L6 in abundance, that is, the abundance also decreased along the MBF. It means that the more abundant the species are, the higher the evenness is reflected by the curve shape. By contrast, there was no significant difference among the samples in species evenness.

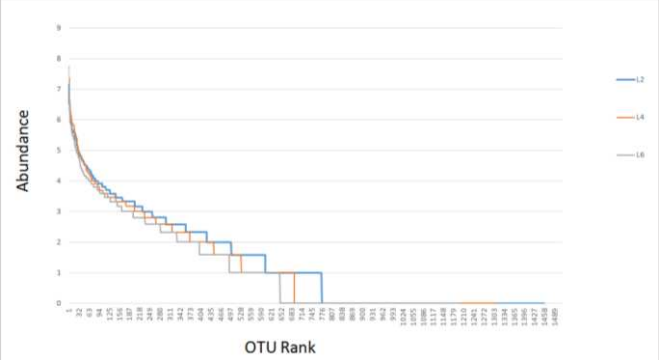

Figure 2. *Distribution curves of OTU abundance*

The Venn diagram of OTUs (*Figure 3*) was drawn by Venny 2.1.0 (http://bioinfogp.cnb.csic.es/tools/venny/index.html). An evident difference could be observed along the MBF at the genus-level. The difference between L4 and L6 was particularly obvious, revealing the function division in the filter. This result is confirmed by the subsequent analysis on bacterial composition.

Bacteria composition

The total number of phyla identified in L2, L4 and L6 was 34, 32 and 29, respectively, which, as previously discovered, decreases along the MBF. Here, a phylum with no less than 0.5% relative abundance is called a major phylum. *Figure 4* shows the proportion of sequences in each phylum in the total number of sequences in each sample. The sequences that do not belong to any known phylum were categorized as unclassified bacteria.

As shown in *Figure 5*, L2 mainly contains proteobacteria (54.18%), Bacteroidetes (14.07%), actinobacteria (9.13%) and nitrospirae (5.06%). The bacteria in L4 mostly belong to proteobacteria (52.47%), acidobacteria (15.04%) and bacteroidetes (11.87%). The major bacterial groups in L6 include proteobacteria (54.18%), acidobacteria (12.45%), bacteroidetes (12.29%) and nitrospirae (6.58%). To sum up, the three samples differed slightly in major bacterial groups.

http://www.aloki.hu ● ISSN 1589 1623 (Print) ● ISSN 1785 0037 (Online)
DOI: http://dx.doi.org/10.15666/aeer/1706_1574515753

According to the comparison between the vermifilter and the conventional biofilter (Yang, 2013), the bacteria composition of the MBF is distinct from that of these two filters.

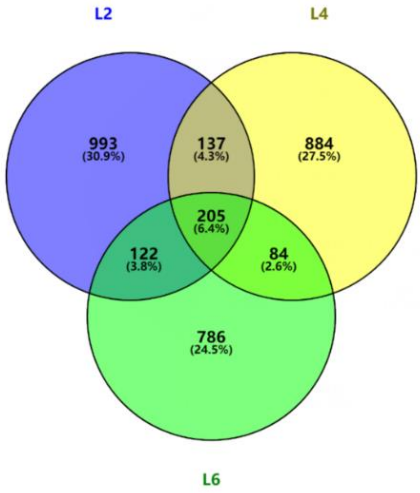

Figure 3. *The Venn diagram of OTUs*

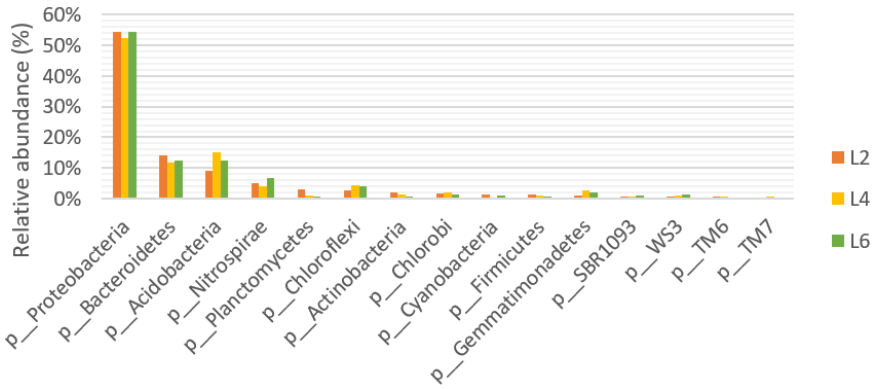

Figure 4. *Proportion of sequences in each phylum*

However, the three samples had marked differences in the class level of taxonomic classifications. As shown in *Table 3*, α-proteobacteria, β-proteobacteria, δ-proteobacteria and γ-proteobacteria and TA18 were found in all three samples, but the content of each component varied greatly from sample to sample. Along the MBF, the content of α-proteobacteria increased first and then decreased; the content of β-proteobacteria declined all the way; the contents of γ-proteobacteria and δ-proteobacteria reduced first and then rebounded. Meanwhile, zetaproteobacteria, exclusively belonging to L6, was rare and represented by a single described species, *Mariprofundus ferrooxydans*. It is an iron-oxidizing neutrophilic chemolithoautotroph first discovered in 1996, at the hydrothermal vents at Loihi Seamount, Hawaii (Emerson, 2002, 2007). Then, the dominant classes were δ-proteobacteria, clostridia and γ-proteobacteria.

http://www.aloki.hu ● ISSN 1589 1623 (Print) ● ISSN 1785 0037 (Online)
DOI: http://dx.doi.org/10.15666/aeer/1706_1574515753

The differences in bacteria content are attributable to various factors, such as climate zone, wastewater composition and weather condition. Most bacteria in the biofilter are not involved in the key processes of the wastewater treatment.

In total, a total of 89, 87 and 80 classes of bacteria were identified for L2, L4 and L6, respectively. However, 73 classes of L2, 70 classes of L4 and 62 classes of L6 had an abundance less than 1%. In addition, Thermus was only found in L2.

The research of MBF mainly focuses on the improvement of structure and the selection of filler (Cui, 2014), but there is no research on microorganism.

Most of the biofilters with stratification, such as tower biofilters, are mostly anaerobic, and most of the microorganisms are anaerobic, which is far from the MBF in this paper (Malakar, 2017).

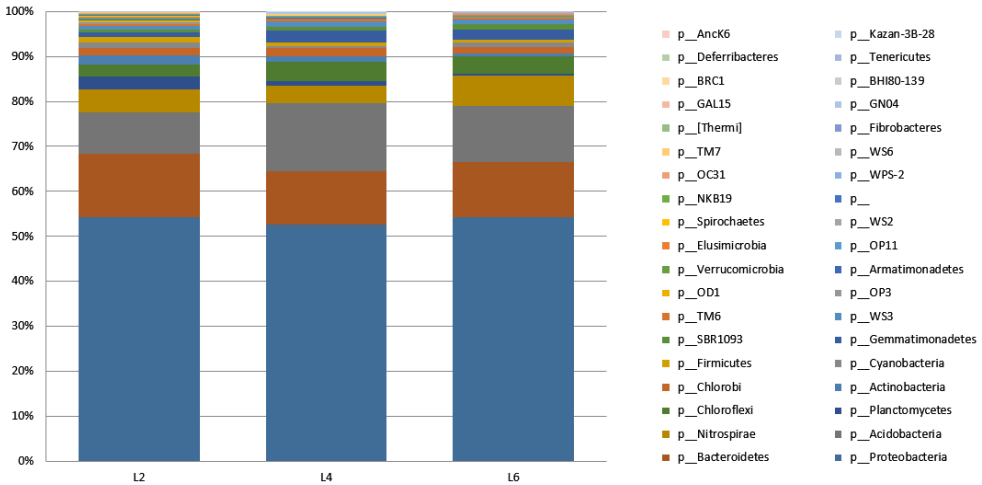

Figure 5. *The proportions of sequences in different classes*

Table 3. *The class level of proteobacteria*

L2	(%)	L4	(%)	L6	(%)	
1,112	27.79%	1436	38.86%	988	30.52%	α-proteobacteria
1,063	26.57%	866	23.44%	1,015	31.36%	γ-proteobacteria
954	23.84%	890	24.09%	656	20.27%	β-proteobacteria
833	20.82%	461	12.48%	563	17.39%	δ-proteobacteria
29	0.72%	19	0.51%	12	0.37%	TA18
10	0.25%	23	0.62%	2	0.06%	No blast hit
0	0.00%	0	0.00%	1	0.03%	Zetaproteobacteria

Conclusions

To our knowledge, this is the first time to investigate microbial communities in the biofilm of the full-scale MBF system for wastewater treatment. Through the analysis on MBF performance, bacteria diversity and bacteria composition, it is concluded that different parts of the MBF system vary greatly in bacteria composition. The bacteria of L2, L4 and L6 belong to 89, 87 and 80 classes, respectively. However, 73 classes of L2, 70 classes of L4 and 62 classes of L6 had an abundance less than 1%. In addition,

http://www.aloki.hu ● ISSN 1589 1623 (Print) ● ISSN 1785 0037 (Online)
DOI: http://dx.doi.org/10.15666/aeer/1706_1574515753

Thermus was only found in L2. The research findings provide new insights into the biological mechanism of contaminant removal in the MBF system.

Suggestions for future improvement are as follows. In engineering, the ventilation performance is increased while the aesthetics is ensured, for example, more louvers are used. Microorganisms need certain temperature conditions. It is suggested that heat preservation and dissipation should be considered when using this process in other places. Improving the efficiency of biological treatment can increase the porosity and specific surface area of the material. The particle size of the material has a certain influence on the good sample condition and sludge removal, which can be further studied. The roughness of the material surface also has a positive effect on the formation of biofilm. If the cost allows, increasing the number of layers within a certain range can improve the diversity of microorganisms. The nitrification of the lower layer is stronger than that of the upper layer. It is suggested that the materials should also be studied from the environment suitable for the growth of nitrifying bacteria.

REFERENCES

[1] Cui, T. T., He, X. J., Ling, R., Sun, X., Li, X. D. (2014): Nitrogen and phosphorus removal performance in the novel multi-layered biological tricking filter. – Journal of Agricultural Resources & Environment.

[2] Emerson, D., Moyer, C. L. (2002): Neutrophilic fe-oxidizing bacteria are abundant at the loihi seamount hydrothermal vents and play a major role in Fe oxide deposition. – Applied and Environmental Microbiology 68(6): 3085-3093.

[3] Emerson, D., Rentz, J. A., Lilburn, T. G., Davis, R. E., Aldrich, H., Chan, C., Moyer, C. L. (2007): A novel lineage of proteobacteria involved in formation of marine fe-oxidizing microbial mat communities. – PLOS ONE 2.

[4] Hu, M., Wang, X., Wen, X., Xia, Y. (2012): Microbial community structures in different wastewater treatment plants as revealed by 454-pyrosequencing analysis. – Bioresour Technol 117: 72-79.

[5] Lautenschlager, K., Hwang, C., Ling, F., Liu, W. T., Boon, N., KoSter, O., Egli, T., Hammes, F. (2014): Abundance and composition of indigenous bacterial communities in a multi-step biofiltration-based drinking water treatment plant. – Water Research 62(Complete): 40-52.

[6] Liu, T., Mao, Y. J., Shi, Y. P., Quan, X. (2017): Start-up and bacterial community compositions of partial nitrification in moving bed biofilm reactor. – Appl Microbiol Biotechnol 101(6): 2563-2574.

[7] Malakar, S., Saha, P. D., Baskaran, D., Rajamanickam, R. (2017): Microbial biofilter for toluene removal: performance evaluation, transient operation and theoretical prediction of elimination capacity. – Sustainable Environment Research 28(3): 121-127.

[8] Ou, W. T., Li, X. D., Pang, H. R., Dai, Y. Q., Qiu, J. P. (2009): Treatment of Rural Sewage by Using Combined Processes of Multi-Layered Biological Filter and Constructed Wetland. – Water Purification Technology.

[9] Torsvik, V., Ovreas, L. (2002): Microbial diversity and function in soil: from genes to ecosystems. – Current Opinion in Microbiology 5(3): 240-245.

[10] Wen, X., Gong, B., Zhou, J., He, Q., Qing, X. (2017): Efficient simultaneous partial nitrification, anammox and denitrification (snad) system equipped with a real-time dissolved oxygen (do) intelligent control system and microbial community shifts of different substrate concentrations. – Water Research 119: 201-211.

[11] Yang, J., Liu, J., Xing, M., Lu, Z., Yan, Q. (2013): Effect of earthworms on the biochemical characterization of biofilms in vermifiltration treatment of excess sludge. – Bioresource Technology 143(Complete): 10-17.

http://www.aloki.hu ● ISSN 1589 1623 (Print) ● ISSN 1785 0037 (Online)
DOI: http://dx.doi.org/10.15666/aeer/1706_1574515753

[12] Ye, L., Shao, M. F., Zhang, T., Tong, A. H., Lok, S. (2011): Analysis of the bacterial community in a laboratory-scale nitrification reactor and a wastewater treatment plant by 454-pyrosequencing. – Water Res 45(15): 4390-4398.
[13] Ye, L., Zhang, T. (2013): Bacterial communities in different sections of a municipal wastewater treatment plant revealed by 16S rDNA 454 pyrosequencing. – Appl Microbiol Biotechnol 97(6): 2681-2690.
[14] Zhang, X., Yue, S., Zhong, H., Hua, W., Chen, R., Cao, Y. (2011): A diverse bacterial community in an anoxic quinoline-degrading bioreactor determined by using pyrosequencing and clone library analysis. – Applied Microbiology & Biotechnology 91(2): 425-434.
[15] Zhang, T., Shao, M. F., Ye, L. (2012): 454 pyrosequencing reveals bacterial diversity of activated sludge from 14 sewage treatment plants. – ISME J 6(6): 1137-1147.
[16] Zheng, M., Zuo, Z. Q., Zhang, Y. Z., Cui, Y. J., Dong, Q., Liu, Y. C. (2017): Nitrite production from urine for sulfide control in sewers. – Water Res 122: 447-454.

http://www.aloki.hu ● ISSN 1589 1623 (Print) ● ISSN 1785 0037 (Online)
DOI: http://dx.doi.org/10.15666/aeer/1706_1574515753

DETERMINATION OF THE SILAGE QUALITY CHARACTERISTICS OF DIFFERENT SWITCHGRASS (*PANICUM VIRGATUM* L.) CULTIVARS

ELİŞ, S. – ÖZYAZICI, M. A.*

Department of Field Crops, Faculty of Agriculture, Siirt University, Siirt, Turkey

**Corresponding author*
e-mail: arifozyazici@siirt.edu.tr; phone: +90-532-633-4592

(Received 10th Sep 2019; accepted 14th Nov 2019)

Abstract. This study was carried out to determine the silage quality characteristics of some switchgrass (*Panicum virgatum* L.) cultivars. Kanlow, Shelter, Shawnee, BoMaster, Alamo, Trailblazer, Cave in Rock and Long Island cultivars of switchgrass constituted the plant material of the study. For silage purposes, the plants were harvested 10-15 days after reaching the flowering period. The harvested plants were allowed to ferment for 70 days. According to the results, the silage of switchgrass cultivars was statistically significantly at $p<0.01$ level for both physical and chemical properties. In the study, pH content, the dry matter, lactic acid, butyric acid, acetic acid, crude protein, acid detergent fiber, and neutral detergent fiber ratios of the silage of switchgrass cultivars varied between 3.84-4.86, 39.0-51.0%, 1.78-2.35%, 0.05-0.33%, 0.35-1.55%, 3.76-5.57%, 39.30-41.73%, and 70.96-75.41%, respectively. In terms of the Fleig score, it was determined that the quality of the silage obtained from switchgrass cultivars could be classified as "very good". According to result, it was determined that BoMaster, Alamo, and Trailblazer cultivars, especially Long Island and Cave in Rock cultivars of switchgrass that came to the forefront in terms of silage quality, could be successfully used in silage production.
Keywords: *switchgrass, physical properties, acetic acid, lactic acid, butyric acid*

Introduction

Switchgrass (*Panicum virgatum* L.) is a perennial warm-season C4 plant, which is one of the grass species specific to North American meadows (McLaughlin and Kszos, 2005; Missaoui et al., 2006; Jiang et al., 2019). It is used as an energy plant in the United States, Canada, and some European countries (Elbersen et al., 2001; Casler and Boe, 2003; Belanger et al., 2012). Furthermore, it is also an important species used for many purposes such as soil and water conservation, grazing and forage (Sanderson et al., 1999; Muir et al., 2001; Vogel et al., 2002; Vogel, 2004; Lee et al., 2007; Sanderson and Burns, 2010; Belanger et al., 2012; Jiang et al., 2019). In the studies carried out, it were reported that high yield and high-quality feed was obtained from some genotypes of switchgrass, and it had the potential to be used as an animal feed (Ameen et al., 2018; Davis et al., 2018; Milenković et al., 2018; Sena et al., 2018).

Few studies were conducted on switchgrass, which is a new plant for Turkey. In this sense, the first basic information about the growing techniques of switchgrass was produced within the scope of the TUBITAK project developed by Soylu et al. (2010). Within the scope of that project, adaptation studies were conducted on switchgrass cultivars as an introductory material in the Central Anatolia Region with an arid and/or semi-arid climate in Turkey, and the cultivars suitable for Turkey were determined. Within the scope of the same study, the necessary information about the growing techniques of high-performance switchgrass cultivars from planting to harvest in Turkey, and their potential to be utilized as a bio-fuel was obtained (Soylu, 2012). As a

http://www.aloki.hu ● ISSN 1589 1623 (Print) ● ISSN 1785 0037 (Online)
DOI: http://dx.doi.org/10.15666/aeer/1706_1575515773

result of these studies carried out by Soylu et al. (2010), it was emphasized that the facts that the switchgrass cultivars examined yielded a green biomass in quantities ranging 60-70 tons/ha, that dry matter ratios ranged between 31.84-40.97% during the flowering period, the protein ratio in green biomass increased up to 9-10% in many cultivars, and acid detergent fiber (ADF) and neutral detergent fiber (NDF) values revealed positive results regarding the consumption and digestibility of the feed to be obtained from this plant were the indications that the silage quality of switchgrass plant would also be high, and it was reported that switchgrass plant had a high economic growing potential especially for silage purposes.

The studies carried out around the world mostly focused on the bioenergy value (Brodowska et al., 2018; Kimura et al., 2018), adaptation (Ma et al., 2011), morphological and biological properties (Brunken and Estes, 1975), forage yield (Wolf and Fiske, 1995; Kimura et al., 2018) and biomass yield (Sanderson et al., 1999; Piscioneri et al., 2001; Lemus et al., 2002; Kimura et al., 2018), genetics and genetic variation (Quinn, 1969; Hopkins et al., 1995, 1996; Quinn and Wetherington, 2002) of switchgrass. There are very few studies on the silage and silage quality of switchgrass.

On the other hand, in silage plant production, it is possible to obtain high quality and high yield by the cultivation of varieties suitable for ecologies. In this sense, the selection of variety is also an important cultural practice to achieve a sustainable yield from plant production (Ileri et al., 2018). Undoubtfully, the difference of cultivars, as well as the factors such as climate and soil factors, cultural practices, and harvesting period, significantly affects the silage quality. This study was carried out to determine the silage quality of some switchgrass (*Panicum virgatum* L.) cultivars.

Materials and methods

Silage material and growing conditions

The plant material of the study consisted of Kanlow, Shelter, Shawnee, BoMaster, Alamo, Trailblazer, Cave in Rock, and Long Island cultivars of switchgrass. In the study, the plant materials of the second year (2017) of switchgrass cultivars established on July 10, 2015, under the conditions of Siirt province (*Figure 1*), which is located in the Southeastern Anatolia Region of Turkey with a semi-arid climate, were used for silage purposes.

According to long-term (1960-2017) meteorological data (Anonymous, 2017) of the Siirt province, the current climate in the region is semi-arid. Summers are warmer than winters (the average temperature in July is 30.6 and in January is 2.8°C). The mean annual temperature, rainfall, and evapotranspiration are 16.2ºC, 691.4 mm, and 937.5 mm, respectively. According to the soil climate regime of the Newhall simulation model (Van Wambeke, 2000), it was determined that the study site has a thermic soil temperature regime and xeric (dry xeric in the subgroup) soil moisture regime (*Figure 2*).

Some physical and chemical properties of the soils where the switchgrass is grown are given in *Table 1*. Organic matter content of soil was determined according to Nelson and Sommers (1982) and other parameters were determined according to Anonymous (1992). The soils where switchgrass is grown are clayey textured, salt-free, slightly alkaline and have moderate lime content, less organic matter and available phosphorus (P) coverage, and high available potassium (K) content (*Table 1*).

http://www.aloki.hu ● ISSN 1589 1623 (Print) ● ISSN 1785 0037 (Online)
DOI: http://dx.doi.org/10.15666/aeer/1706_1575515773

In the study, the field experiment was established according to the randomized block experimental design with 4 replications. In sowing, row spacing was 20 cm, and the number of rows in a parcel was 10. Sowing was performed so that there would be 400 live seeds per square meter. Before sowing, diammonium phosphate (18-46-0%, N-P-K) fertilizer was applied equally to each parcel with the calculation of 100 kg/ha pure P_2O_5 according to the soil analysis results. A drip irrigation system was established immediately after sowing, and irrigation was performed. When plants were 10-15 cm, ammonium nitrate (33% N) fertilizer was given equally to each parcel with the calculation of 60 kg/ha pure nitrogen (N) (*Figure 3*).

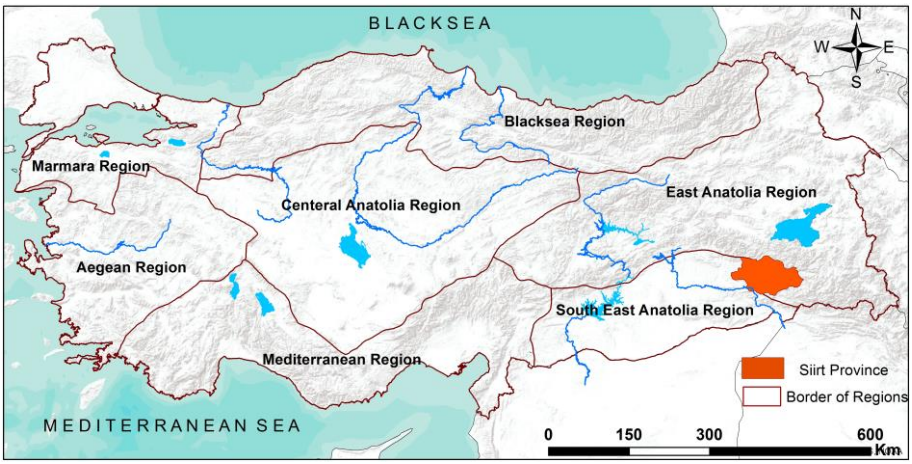

Figure 1. *The location where silaged switchgrass cultivars are grown*

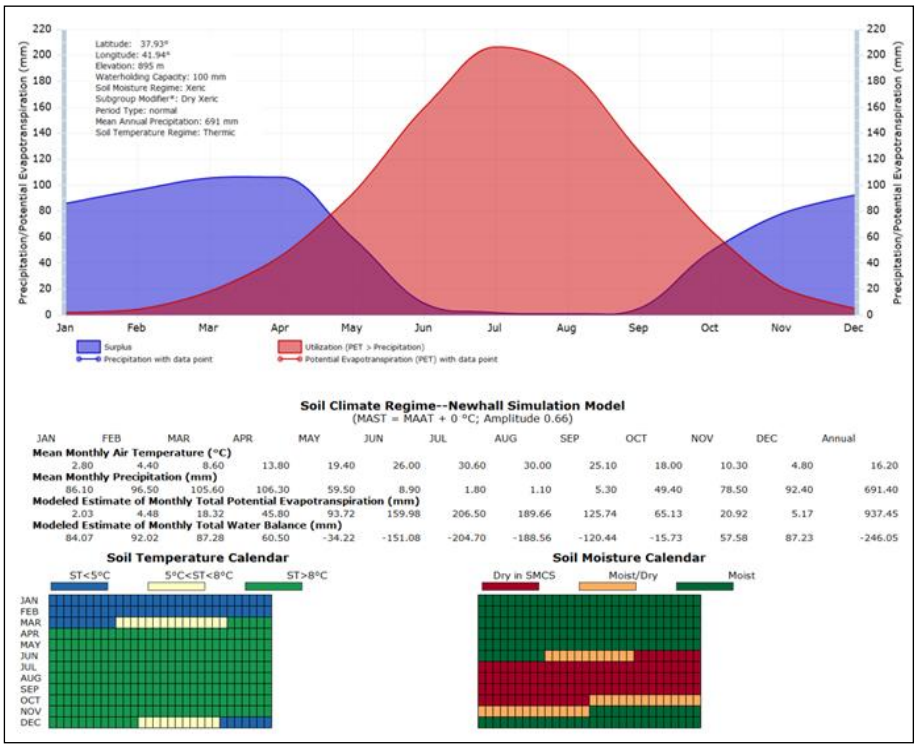

Figure 2. *Soil moisture and temperature regime diagrams according to the Newhall simulation model*

http://www.aloki.hu ● ISSN 1589 1623 (Print) ● ISSN 1785 0037 (Online)
DOI: http://dx.doi.org/10.15666/aeer/1706_1575515773

Table 1. *Some physical and chemical properties of the soils where switchgrass is grown (0-20 cm)*[*]

Parameters	Value
Clay, %	55.84
Sand, %	36.26
Silt, %	7.90
pH	7.98
Electrical conductivity (EC), mS cm^{-1}	0.363
Calcareous ($CaCO_3$), %	13.0
Organic matter, %	1.31
Available P, kg P_2O_5 ha^{-1}	43
Available K, kg K_2O ha^{-1}	1150

*: The analyzes were carried out in the laboratory of Black Sea Agricultural Research Institute

Figure 3. *Switchgrass experimental site and harvest*

Silage making technique

For silage purposes, switchgrass cultivars were harvested separately for each parcel 10-15 days after reaching the flowering period (Soylu, 2012). The harvested plants were brought to the laboratory environment, and all green plant materials were manually chopped into 0.5-1 cm sizes with a knife. The chopped plant particles were mixed with 0.5% table salt (NaCl) for protection purposes (Kılıç, 1986; Geren et al., 2011). Then, the material of each parcel was filled in 3-liter glass jars by pressing well in accordance with the sequential filling technique (Petterson, 1988), and the lid borders of the jars tightly closed with silicone plastic lids were wrapped with thick packaging tape for 3-4 rounds for airtightness. The silage jars prepared in this way were allowed to ferment for 70 days at room temperature in a dark environment.

Physical and chemical analysis methods of silage samples

After the fermentation process was completed, the matured silage was opened, a 3-4 cm portion was discarded from the cap opening, and then physical and chemical analyses were performed in the remaining silage samples.

In the samples taken to represent the mass in the opened silage jars, physical examinations such as odor, structure, and color were subjectively performed by three subject matter experts. The evaluation of physical analyses was based on the scoring

http://www.aloki.hu ● ISSN 1589 1623 (Print) ● ISSN 1785 0037 (Online)
DOI: http://dx.doi.org/10.15666/aeer/1706_1575515773

method developed by Anonymous (1987). The silage quality class according to the physical properties of the silage was determined by the DLG (Deutsche Landwirtschafts-Gesellschaft) score (*Table 2*). The DLG score is the total physical score (0-20 points) obtained from the sum of odor, structure, and color scores (Akyıldız, 1984; Anonymous, 1987; Ergün et al., 2013).

Table 2. *Physical examination key developed by DLG and silage quality class*

Physical examination key	
1. Odor	**Score**
No butter acid odor, slightly sour, fruity and aromatic odor	14
A small amount of butter acid, strong sour odor, and slight escalation	8
Moderate butter acid odor, strong escalation-musty odor	4
Strong butter acid or ammonia odor, very slight sour odor	2
Strong decomposition, ammonia or musty odor	0
2. Structure	
Intact leaves and stems	4
A slightly deteriorated structure of leaves	2
A deteriorated structure of leaves and stems, musty and dirty	1
Rotten Leaf and Stalk	0
3. Color	
Preserved its color at the moment it was silaged (brown in withered silage)	2
Slightly changed color (yellow to brown)	1
Completely changed color (reseda green)	0
Quality class according to the physical properties of silage	
Quality class	**DLG score**
I- Very good	20-18
II- Good	17-14
III- Medium	13-10
IV- Low (low value)	9-5
V- Corrupted (useless)	4-0

Some silage material was taken from each silage jar to represent the jar and mixed homogeneously, and 25 g of the wet silage sample of this mixture was weighed on the precision balance and placed in the mixer. 250 ml of distilled water was added to the sample, and it was mixed for 10 minutes, then filtered through filter paper (Whatman™ No. 1441-125, GE Healthcare Life Sciences, Marlborough, MA, USA), and pH was determined by means of a pH meter in a 200 ml strainer taken into glass beakers (Anonymous, 1993). Lactic acid (LA), acetic acid (AA), and butyric acid (BA) were determined using high-performance liquid chromatography (HPLC) as per the methods of Canale et al. (1984). 300 g of the wet sample was taken from matured silage separately in each silage jar, and it was dried in an oven at 70°C for 48 hours. Dried silage samples were weighed on the precision balance, and their weights were determined, and the dry matter (DM) ratio was determined by proportioning to wet weight (Bulgurlu and Ergül, 1978).

The dried silage samples were ground separately for each jar. The ADF, NDF, and crude protein (CP) ratios in the ground samples were determined by NIRS (Near Infrared Reflectance Spectroscopy) and #IC-0904FE calibration set (Anonymous, 2018) in the laboratory of Ondokuz Mayıs University Faculty of Agriculture Department of Field Crops (Brogna et al., 2009).

http://www.aloki.hu ● ISSN 1589 1623 (Print) ● ISSN 1785 0037 (Online)
DOI: http://dx.doi.org/10.15666/aeer/1706_1575515773

Quality of silage according to the Fleig score

One of the most common methods used to determine the silage quality practically is the Fleig score (FS), which is determined by using the relationship between the DM content and pH value of silage. FS was calculated using *Equation 1* created by DLG (Anonymous, 1987).

$$FS= [220 + (2 \times \text{silage DM ratio} - 15)] - 40 \times \text{silage pH value} \quad \text{(Eq.1)}$$

Considering the FS values obtained from the above-mentioned equation, the silage quality class was evaluated according to the score criteria presented in *Table 3*.

Table 3. *Quality classes of silo feeds according to FS (Anonymous, 1987)*

Calculated FS	Silage quality class
100-81	I- Very good
80-61	II- Good
60-41	III- Satisfactory (Medium)
40-21	IV- Low (low value)
20-0	V- Bad

Statistical analyses

The data obtained from the study were subjected to the analysis of variance according to the randomized block experimental design. The differences between the groups according to the F-test results were determined by Tukey's multiple comparison test (Açıkgöz and Açıkgöz, 2001).

Results and discussion

Silage dry matter ratio of switchgrass cultivars and some chemical properties of silage

Silage dry matter ratio

The DM ratio has great importance in the full realization of chemical events during silage formation, and this ratio is the most important quality criterion used in the determination of silage quality (Geren, 2001; Çakmak et al., 2013). In the study, the highest DM ratio was found in the Alamo, BoMaster, Kanlow, Trailblazer, and Cave in Rock switchgrass cultivars that statistically constituted the first group. The DM ratios of these cultivars varied between 47.3-51.0%. The lowest DM ratio was found in the silage of Shawnee and Long Island cultivars by 39.0% and 39.7%, respectively. This difference between the cultivars in terms of the silage DM ratio was found to be statistically significant at $p<0.01$ level (*Table 4*). The reason for this difference between the cultivars can be explained by different amounts of DM they can produce by their genetic capacity. Furthermore, it is considered that the difference in the silage DM ratio between the cultivars was also affected by the difference in DM losses, caused by chemical events in the fermentation process, according to cultivars. While Luginbuhl et al. (2000) reported that the silage DM ratio was 27.2% in Kanlow switchgrass cultivar, Cassida et al. (2005) reported that the DM ratio in switchgrass varied between 39.4-45.1%, and Zhao et al. (2017) reported that the DM ratio varied between 24.68-26.43%. It is considered that the fact that the DM ratios determined in our study

http://www.aloki.hu ● ISSN 1589 1623 (Print) ● ISSN 1785 0037 (Online)
DOI: http://dx.doi.org/10.15666/aeer/1706_1575515773

were different from those reported in the literature was affected by different genotype, harvest time, and growing conditions.

On the other hand, in the adaptation study carried out by Soylu et al. (2010) with 9 switchgrass cultivars (Alamo, Forestburg, Cave in Rock, Carthage, Shelter, Dacotah, Blackwell, Shawnee, and Kanlow) under irrigated conditions in the Central Anatolia Region of Turkey, they reported that the DM ratios of cultivars varied between 31.84%-40.97% and that the DM ratio of above 30% in switchgrass cultivars was extremely important in terms of use both for silage and directly in animal feeding. Accordingly, although the DM ratio among cultivars varies, a high DM ratio is important for silage quality. Indeed, while Çayıroğlu et al. (2016) reported that the DM content of silage material was an important factor affecting aerobic stability, Filya et al. (2000) reported that the aerobic stability of silage made with the material with a low DM content decreased, and Barnes et al. (1995) and Mohd-Setapar et al. (2012) reported that the DM contents of the material to be silaged for good quality silage and/or successful fermentation should be between 28-42% and 25-40%, respectively. In view of these values reported by the researchers, it was observed that all switchgrass cultivars contained quite sufficient DM.

Table 4. *Values of the DM ratio and some chemical properties of silage obtained from switchgrass cultivars*[*]

Cultivars	DM (%)	LA (%)	BA (%)	AA (%)	pH	CP (%)	ADF (%)	NDF (%)
Kanlow	48.0 a	1.78 b	0.33 a	1.29 ab	4.73 a	4.35 bc	41.20	75.41 a
Shelter	44.7 ab	1.96 ab	0.29 a	1.02 ab	4.72 a	3.76 c	41.73	73.56 abc
Shawnee	39.0 b	1.99 ab	0.21 ab	1.55 a	4.86 a	4.72 abc	39.30	70.96 c
BoMaster	48.7 a	2.22 a	0.08 b	0.45 b	3.94 bcd	4.53 abc	40.33	75.25 a
Alamo	51.0 a	1.94 ab	0.12 b	1.33 ab	4.32 b	4.23 bc	40.77	73.71 ab
Trailblazer	47.7 a	2.01 ab	0.13 b	0.65 ab	4.24 bc	5.33 ab	40.57	71.54 bc
Cave in Rock	47.3 a	2.05 ab	0.08 b	0.62 ab	3.88 cd	5.23 ab	40.72	72.86 abc
Long Island	39.7 b	2.35 a	0.05 b	0.35 b	3.84 d	5.57 a	40.59	73.17 abc
$F_{cultivar}$	9.698[**]	4.524[**]	10.365[**]	4.931[**]	27.695[**]	7.210[**]	0.831	9.054[**]
CV (%)	5.26	6.98	34.38	38.79	3.13	8.49	3.25	1.24

[*]: The difference between the means indicated by the same letter in the same column is not significant,
[**]: $p<0.01$ is significant within error limits, CV: Coefficient variation

No study was found on the silage characteristics of cultivars in switchgrass plant. Therefore, in view of the silage studies carried out with corn plant which is a physiologically C4 plant such as switchgrass, it was reported that there were significant differences between the cultivars in terms of DM, similarly to the results of our study, and that the DM ratio according to cultivars in corn silage varied between 18.35%-30.72% (Özdüven et al., 2009), 25.30%-31.58% (Güney et al., 2010), 20.3%-28.1% (Seydoşoğlu, 2017), 20.57%-23.35% (Ileri et al., 2018).

Lactic acid (LA) content of silage

The amount and composition of organic acids such as LA formed during silage fermentation determine the quality of fermentation, and LA is one of the main preservative organic acids in the silage (Filya, 2001). According to the results of statistical analysis, it was determined that the LA contents of the silage obtained from switchgrass cultivars showed significant differences ($p<0.01$). The most distinctive

http://www.aloki.hu ● ISSN 1589 1623 (Print) ● ISSN 1785 0037 (Online)
DOI: http://dx.doi.org/10.15666/aeer/1706_1575515773

difference was between Kanlow and all other cultivars. The highest LA ratio was found in the Long Island (2.35%) and BoMaster (2.22%) cultivars that were statistically included in the first group (*Table 4*).

It was reported that the LA ratio should be above 2.00% in high-quality silage feeds (Kılıç, 1986; McDonald et al., 1991; Alçiçek and Özkan, 1997; Weinberg and Ashbell, 2003) and that a high LA ratio was the assurance of a healthy fermentation (Johnson and Harrison, 2001). According to the results of our study (*Table 4*), it was found out that the LA values found in the Long Island, BoMaster, Cave in Rock, and Trailblazer silage of switchgrass cultivars were above the reference value and included in the high-quality silage group. In the silage made with corn and sorghum cultivars, it was reported that the LA ratio varied between 1.58%-8.57% by Reeves et al. (1989), 2.6%-3.1% by Hart (1990), 0.67%-2.35% by Geren and Kavut (2009), and 7.64%-12.33% by Seydoşoğlu (2017) depending on the maturity period.

Butyric acid (BA) content of silage

An important parameter in the determination of silage quality by analytical methods is the BA, which negatively affects silage quality (Geren and Kavut, 2009). In a quality silage feed obtained as a result of a good fermentation, the fact that BA was generally between 0.1-0.7% was considered to be normal although it was undesirable (Woolfort, 1984; Weinberg and Ashbell, 2003). On the other hand, Catchpoole and Henzell (1971) reported that the BA concentration in quality silage was less than 0.2%. When the data of our study were examined, it was observed that the BA content of the silage of switchgrass cultivars varied between 0.05-0.33% and that the BA content of all silaged switchgrass cultivars was within acceptable limits. Nevertheless, the difference between the cultivars in terms of BA was found to be statistically significant at $p<0.01$ level, and the BA ratios of Kanlow (0.33%), Shelter (0.29%), and Shawnee (0.21%) silage were higher than other cultivars (*Table 4*). It can be explained by the limited propagation and activity of LA bacteria during fermentation and/or the degradation of LA into BA, as it was indicated by Bolsen et al. (1996). Indeed, as it is seen in *Table 4*, the low LA values of the cultivars with a high BA ratio confirm this situation.

In the studies carried out with corn silage, the BA ratio was determined to be 0.07% (Phillip and Hidalgo, 1989) and 0.08% (Deswysen et al., 1993). On the contrary, while Geren and Kavut (2009) and Arslan et al. (2017) reported that the BA value was not measured in sorghum and corn silage and sorghum silage, respectively; Hart (1990) reported that the BA value varied between 0.006% and 0.037% in the sorghum silage, and Reeves et al. (1989) reported that the BA value varied between 0.06% and 0.43% in the corn silage. In our study, it is possible to say that the BA values determined in the silage of switchgrass cultivars were compatible with these values in the literature determined in corn and sorghum silage, which are C4 plants like switchgrass.

Acetic acid (AA) content of silage

When the AA ratios of the silage obtained from switchgrass cultivars were examined, the highest AA ratio was found to be 1.55% in Shawnee cultivar, and the difference in terms of AA between Shawnee cultivar and Kanlow, Shelter, Alamo, Trailblazer, and Cave in Rock cultivars was found to be insignificant. The lowest AA content was determined in Long Island (0.35%) and BoMaster (0.45%) cultivars. This difference between the cultivars was statistically significant at $p<0.01$ level (*Table 4*). While Weinberg and Ashbell (2003) reported that the AA ratio should be less than 0.8% in the

http://www.aloki.hu ● ISSN 1589 1623 (Print) ● ISSN 1785 0037 (Online)
DOI: http://dx.doi.org/10.15666/aeer/1706_1575515773

silage feed as a result of a good fermentation, McDonald et al. (1991) and Alçiçek and Özkan (1997) reported that the AA ratio should be between 0.3-0.7%. When these values reported in the literature are taken into consideration, it is possible to say that the AA ratios of the silage of BoMaster, Trailblazer, Cave in Rock, and Long Island switchgrass cultivars were below the critical value.

It was reported that the AA ratio varied between 0.6-1.42% in the sorghum silage (Hart, 1990; Arslan and Çakmakçı, 2011; Arslan et al., 2017) and between 0.2-3.71% in the corn silage (Phillip and Hidalgo, 1989; Reeves et al., 1989; Deswysen et al., 1993; Sucu and Filya, 2006). These results obtained from sorghum and corn silage, which are physiologically included in the C4 group such as switchgrass, were similar to the results of our study.

pH of silage

pH formed during silage fermentation is one of the most important parameters determining the quality of fermentation (Kiermeier and Renner, 1963; Filya, 2001). In our study, a statistically significant difference at $p<0.01$ level was found in terms of the pH of silage between switchgrass cultivars. The lowest silage pH value was found to be 3.84 in the Long Island switchgrass cultivar. The highest silage pH value was found in the Shawnee (4.86), Kanlow (4.73), and Shelter (4.72) cultivars that were statistically included in the same group (*Table 4*). The difference in terms of pH between cultivars can be explained by the fact that LA production varies by cultivars. In other words, as it is seen in *Table 4*, the silage pH was found to be low in the cultivars with a high LA ratio. This decrease in pH was due to the accumulation of LA. Indeed, Ohmomo et al. (1995) reported that it was important that pH was less than 4.2 in silage fermentation, which was possible with the efficient production of LA from sugar in a silo.

The way to remove odors, prevent spoilage, and protect nutrients in silage feeds is to make silage protected by good fermentation. Protection is based on high acidity depending on LA formation (Isnandar et al., 2010). Furthermore, low pH may also prevent the growth of parasites and some pathogenic microorganisms (Göhl, 1981). Church (1986) and Ergün et al. (2013) reported that the optimum pH range for the growth of milk acid bacteria growing in the acid medium was 3.8-4.2 and that bacteria causing spoilage and decomposition did not live in the silage with a value in this pH range. Some other researchers (Danley et al., 1973; Comberg, 1974; Kılıç, 1986; Roth, 2001; Açıkgöz et al., 2002; Kılıç, 2006) reported that the pH value of very good silage was between 3.5 and 4.5. It can be said that Long Island, Cave in Rock, BoMaster, Alamo, and Trailblazer from switchgrass cultivars were within the appropriate limits in terms of silage pH. Therefore, a successful fermentation process took place in the silage formation process, especially with respect to these cultivars. While Belanger et al. (2012) reported that pH varied between 4.0-4.3 in the switchgrass silage, Zhao et al. (2017) reported that the pH value was 5.4 in the 30-day silaged switchgrass material.

In the studies carried out on corn and sorghum cultivars that are C4 plant such as switchgrass, it was reported that the silage pH value was different between the cultivars and the pH value ranged between 3.03-5.20 (Hart, 1990; Deswysen et al., 1993; Geren, 2000, 2001; Kavut and Soya, 2012; Canbolat et al., 2016; Seydoşoğlu, 2017; Ileri et al., 2018).

http://www.aloki.hu ● ISSN 1589 1623 (Print) ● ISSN 1785 0037 (Online)
DOI: http://dx.doi.org/10.15666/aeer/1706_1575515773

Crude protein (CP) ratio in silage

A statistically significant difference at $p<0.01$ level was found between switchgrass cultivars in terms of the CP ratio. While the highest CP ratio was found to be 5.57% in the Long Island silage, the difference between the Long Island, Shawnee, BoMaster, Trailblazer, and Cave in Rock cultivars in terms of the CP ratio was found to be statistically insignificant. The lowest silage CP ratio was found in the Shelter cultivar by 3.76% (*Table 4*). The CP ratio emerges a result of the genetic and morphological characteristics of plants (Güney et al., 2010). Therefore, it is possible to say that it is an expected result that there are significant differences between the cultivars with different properties. Indeed, in some studies carried out with the corn plant (Seydoşoğlu, 2017; Ileri et al., 2018), it was also reported that cultivars had a significant effect on the silage CP content.

It was observed that the CP ratio values determined in the silage of switchgrass cultivars were consistent with the results of Sanderson et al. (1999) and Mantino et al. (2017), slightly higher than the data of Cassida et al. (2005), and lower than the values obtained by Anderson et al. (1988), Soylu et al. (2010), Çiçek (2017), and Mohammed and Desta (2017). Milenković et al. (2018) reported that the CP ratio of switchgrass cultivars varied between 5.62% (Alamo) and 8.74% (Kanlov). The difference between the values obtained in our study and the literature in terms of the CP ratio can be explained by different ecologies, cultural processes, and genotypic structures of plants.

In the silage made with the corn plant which is a C4 plant like switchgrass, CP values varied between 5.01%-10.63% (Filya, 2001; Polat et al., 2005; Güney et al., 2010; Çakmak et al., 2013; Rafiuddin et al., 2016).

Silage acid detergent fiber (ADF) and neutral detergent fiber (NDF) ratio

The difference between switchgrass cultivars in terms of the ADF ratio was found to be statistically insignificant. However, the NDF ratio showed a statistically significant difference at the level of $p<0.01$ between the cultivars. The ADF ratio of silage varied between 39.30-41.73%. The lowest NDF ratio was found in the Shawnee cultivar by 70.96%. The highest NDF ratio was found in the Kanlow (75.41%) and BoMaster (75.25%) cultivars that statistically constituted the first group. Nevertheless, a statistically significant difference in terms of the NDF ratio was between the Shawnee and Trailblazer cultivars and other cultivars (*Table 4*). This difference between the cultivars in terms of NDF can be explained by different temperature, moisture, and fertilizer utilization during the period from sowing-time to harvest.

The ADF and NDF ratios, which are the plant cell wall components, are a good indicator of total digestible nutrients, and the ADF and NDF ratios are desired to be low in roughage (Van Soest, 1994; Gürsoy and Macit, 2014). When the roughage quality standard for farm animals (<31%= top quality, 31-35%= very good, 36-40%= good, 41-42%= medium, 43-45%= bad and >45%= unacceptable for ADF; <40%= top quality, 40-46%= very good, 47-53%= good, 54-60%= medium, 61-65%= bad and >65%= unacceptable for NDF) reported by Rohweder et al. (1978) is considered, it can be said that the silage of switchgrass cultivars was of good and/or medium quality in terms of the ADF ratio and unacceptable in terms of the NDF ratio. The fact that the NDF ratio, which expresses the whole fiber including hemicellulose, cellulose, and fiber in the plant, was high in the silage of switchgrass cultivars is considered to be due to the slowdown of the degradability of cell wall agents such as NDF as a result of the low

http://www.aloki.hu ● ISSN 1589 1623 (Print) ● ISSN 1785 0037 (Online)
DOI: http://dx.doi.org/10.15666/aeer/1706_1575515773

number of LA bacteria in the silage medium although some cultivars were slightly more than 2% (*Table 4*), as it was also indicated by Filya (2001).

In the studies conducted for different purposes with switchgrass cultivars, it was reported that the ADF and NDF ratios varied between 21.3%-66.9% and 57.6%-86.5%, respectively (Madakadze et al., 1999; Sanderson et al., 1999; Soylu et al., 2010; Mantino et al., 2017; Mohammed and Desta, 2017).

Fleig score (FS)

One of the most important criteria used in the determination of the quality of silage feed is the FS, which is calculated based on the regression equation between DM and pH of the silage (Woolfort, 1984; Kılıç, 1986; Geren, 2001). In terms of the FS, the difference between the silage of the switchgrass cultivars examined in the study was found to be statistically significant at $p<0.01$ level. Although the highest FS was determined in the BoMaster (144.7 points) cultivar, the difference between the Alamo, Trailblazer, Cave in Rock, and Long Island cultivars was found to be statistically insignificant. The lowest FS was found in the Shawnee cultivar by 88.6 (*Table 5*).

Table 5. *Fleig scores of the silage obtained from switchgrass cultivars*[*]

Cultivars	FS
Kanlow	111.9 b
Shelter	105.5 bc
Shawnee	88.6 c
BoMaster	144.7 a
Alamo	134.2 a
Trailblazer	130.9 a
Cave in Rock	144.3 a
Long Island	130.6 a
$F_{cultivar}$	30.658[**]
CV (%)	5.00

[*]: The difference between the means indicated by the same letter is not significant, [**]: $p<0.01$ is significant within error limits, CV: Coefficient variation

In the study, when the FS of the silage of switchgrass cultivars ranging from 88.6-144.7 were evaluated according to *Table 3*, the quality of silage obtained from switchgrass cultivars was found to be "very good". When the FS calculated by considering the DM and pH contents of silo feeds is compared with the studies carried out in corn (Geren, 2000, 2001; Demirel et al., 2001; Kavut and Soya, 2012), it can be said that similar results have been achieved.

When the desired pH and DM ratio is ensured in the silo feed, the FS is also high. In our study, it was observed that the FS of all switchgrass cultivars other than the Shawnee cultivar was above 100 (*Table 5*). Similar results were also achieved in corn (150.5 points) and sorghum (123.3 points) silage by Öten et al. (2016) and in corn (104.2 points) silage by Seydoşoğlu (2017).

Physical properties of the silage of switchgrass cultivars

The scores of the physical properties (odor, structure, and color) of the silage obtained from switchgrass cultivars, the DLG score, and the silage quality class according to physical properties are presented in *Table 6*.

http://www.aloki.hu ● ISSN 1589 1623 (Print) ● ISSN 1785 0037 (Online)
DOI: http://dx.doi.org/10.15666/aeer/1706_1575515773

While the difference between the cultivars in terms of odor and structure was found to be statistically significant at p<0.01 level, the difference between the cultivars in terms of color was found to be insignificant. The Long Island cultivar had the highest score in terms of all three physical properties. Nevertheless, the difference between the Long Island cultivar and the Cave in Rock cultivar in terms of odor and the difference between the Cave in Rock, Alamo, BoMaster, and Shelter cultivars in terms of the structure were found to be statistically insignificant (*Table 6*). In the silage made with switchgrass, the fact that the physical appearance was largely preserved, especially in terms of the above-mentioned cultivars producing high scores, indicates that successful silage can be achieved with switchgrass plant. On the other hand, silage quality also varies depending on the fermentation process (Geren, 2001). Therefore, as it was also indicated by Comberg (1974) and Akyıldız (1984), the silage feed of an ideal quality may have a pleasant acidic, slightly sour and aromatic odor resulting from the odor of the products produced by LA bacteria. Furthermore, it was reported that the physical structure of the feed (Geren, 2001) and the color of the silage (Woolfort, 1984) could be largely preserved if the silage was made well.

Table 6. *Mean scores of the physical properties of the silage obtained from switchgrass cultivars, and the quality class*[*]

Cultivars	Odor	Structure	Color	DLG score	Quality class
Kanlow	8.0 e	2.0 b	1.3	11.3 d	Medium
Shelter	8.7 de	3.3 ab	1.3	13.3 cd	Medium
Shawnee	9.3 cde	2.0 b	1.3	12.7 d	Medium
BoMaster	11.3 bc	3.3 ab	1.3	16.0 bc	Good
Alamo	10.7 bcd	4.0 a	1.7	16.3 b	Good
Trailblazer	10.3 bcd	2.0 b	1.0	13.3 cd	Medium
Cave in Rock	12.0 ab	4.0 a	1.7	17.7 ab	Very good
Long Island	13.7 a	4.0 a	2.0	19.7 a	Very good
$F_{cultivar}$	18.58[**]	7.40[**]	1.06	24.78[**]	
CV (%)	7.09	12.85	6.08	6.55	

[*]: The difference between the means indicated by the same letter in the same column is not significant,
[**]: p<0.01 is significant within error limits, CV: Coefficient variation

When the DLG scores were considered, the highest value was determined in the silage of the Long Island cultivar by 19.7 points, followed by the Cave in Rock cultivar by 17.7 points. The lowest DLG score was found in the Kanlow (11.3 points) and Shawnee (12.7) cultivars. This difference between the cultivars in terms of DLG was found to be statistically significant at p<0.01 level. According to the classification of the DLG score obtained by adding the odor, structure, and color scores of the silage (Anonymous, 1987) in the evaluation of the physical properties of silage feed, it was observed that "good" quality silage was obtained from the BoMaster and Alamo cultivars and "very good" quality silage was obtained from the Long Island and Cave in Rock cultivars (*Table 6*).

The harvest time (10-15 days after the beginning of flowering) was effective in obtaining high-quality silage from switchgrass cultivars in terms of physical properties. In the silage study carried out with corn and sorghum plants in a different flowering period (Rafiuddin et al., 2016), it was reported that the color, odor, structure, and total physical score values of the silage increased from early flowering to the full flowering period (as the developmental stage progresses), and the silage quality class became

http://www.aloki.hu ● ISSN 1589 1623 (Print) ● ISSN 1785 0037 (Online)
DOI: http://dx.doi.org/10.15666/aeer/1706_1575515773

"very good" from a physical aspect. The improvement in the physical properties of silage as the harvest period progressed was also indicated by Khan et al. (2011) and Khan et al. (2012). Moreover, it is considered that the high score in physical properties was affected by low pH, high DM, and high LA values, as it was also indicated by Rafiuddin et al. (2016).

With respect to the switchgrass plant, there was no study on the physical characteristics of silage. However, when compared to the properties of silage made with plants such as corn, sorghum, sorghum x sudangrass hybrid which are physiologically C4 plants such as switchgrass plant, it was observed that the results similar to the results of our study were achieved. In the silage studies carried out with these C4 plants (Geren, 2000; Güney et al., 2010; Öten et al., 2016; Rafiuddin et al., 2016; Seydoşoğlu, 2017), it was reported that the physical score of silage odor varied between 8-14, the silage structure varied between 2-4 points, and the silage color varied between 1-2, and good and/or very good quality silage was obtained according to the DLG score, as in the switchgrass cultivars in the results of our study. Furthermore, our results indicating that cultivars had no significant effects on silage color were found to be consistent with the results obtained by Geren (2000), Güney et al. (2010), Kavut and Soya (2012), and Seydoşoğlu (2017).

Conclusions

According to the study results, it was determined that the Long Island and Cave in Rock cultivars came to the forefront in terms of silage quality and that the BoMaster, Alamo, and Trailblazer cultivars could also be used successfully in silage production. In this study carried out with switchgrass which is used as an alternative plant for the production of bioethanol and forage plants in the world but is a new plant for Turkey, it was concluded that promising results were achieved in terms of silage quality and it could be an alternative source of roughage for livestock businesses. Since switchgrass is a perennial plant with 10 to 15 years lifespan, it would be a longterm resource for silage production.

Acknowledgements. This study was produced from the first author's master's thesis accepted by the Graduate School of Natural and Applied Science of Siirt University. The study was supported by the Scientific Research Projects Coordinatorship of Siirt University with the project code 2017-SİÜFEB-85.

REFERENCES

[1] Açıkgöz, N., Açıkgöz, N. (2001): Common mistakes in the statistical analyzes of agricultural experiments I. Single factorials. – Anadolu 11(1): 135-147. (In Turkish).
[2] Açıkgöz, E., Turgut, İ., Filya, İ. (2002): Silage Plants Growing and Silage Making. – Hasat Yayınları, İstanbul, Turkey. (In Turkish).
[3] Akyıldız, A. R. (1984): Foods Information Laboratory Guide. – University of Ankara, Faculty of Agriculture, Publication No: 893, Application Guide: 213, Ankara, Turkey. (In Turkish).
[4] Alçiçek, A., Özkan, K. (1997): Determination of silage quality by physical and chemical methods in silo feeds. – Turkey I. Silage Congress, Bursa, Turkey, pp. 241-247. (In Turkish).

http://www.aloki.hu ● ISSN 1589 1623 (Print) ● ISSN 1785 0037 (Online)
DOI: http://dx.doi.org/10.15666/aeer/1706_1575515773

[5] Ameen, A., Tang, C., Liu, J., Han, L., Xie, G. H. (2018): Switchgrass as forage and biofuel feedstock: Effect of nitrogen fertilization rate on the quality of biomass harvested in late summer and early fall. – Field Crops Research 235: 154-162.
[6] Anderson, B., Ward, J. K., Vogel, K. P., Ward, M. G., Gorz, H. J., Haskins, F. A. (1988): Forage quality and performance of yearlings grazing switchgrass strains selected for differing digestibility. – University of Nebraska-Lincoln, Agronomy-Faculty Publications, 308p.
[7] Anonymous (1987): Bewertung von Grünfutter, Silage und Heu. – Deutsche Landwirtschafts-Gesellschaft (DLG), DLG Merkblatt 224, Frankfurt.
[8] Anonymous (1992): Procedures For Collecting Soil Samples and Methods of Analysis For Soil Survey. – Soil Survey Staff, Soil Survey Investigations Report No. 42, Washington DC, USA.
[9] Anonymous (1993): Bestimmung des pH-Wertes. – In: Die chemischen Untersuchungen von Futtermitteln. Teil 18 Silage. Abschnit 18.1 Bestimmung des pH-Wertes., Methodenbuch Bd. III., VDLUFAVerlag, Darmstadt.
[10] Anonymous (2017): Siirt Province Climate Data. – T.C. Ministry of Agriculture and Forestry, General Directorate of Meteorology, Turkey.
[11] Anonymous (2018): WinISI 4 Calibration Software: Ground, Expandable Equation Packages. – (http://www.winisi.com/product_calibrations.htm) (Date of Access: 20.05.2018).
[12] Arslan, M., Çakmakçı, S. (2011): Comparison of corn (*Zea mays*) and sorghum (*Sorghum bicolor*) silages mixed with different plants. – Mediterranean Agricultural Sciences 24(1): 47-53. (In Turkish).
[13] Arslan, M., Erdurmuş, C., Öten, M., Aydınoğlu, B., Çakmakçı, S. (2017): Quality charecteristics of sorghum and some plants silages mixed at different rates. – Journal of Tekirdag Agricultural Faculty 14(02): 34-41. (In Turkish).
[14] Barnes, R. F., Miller, D. A., Nelson, C. J. (1995): Forages, Volume II: The science of grassland agriculture. – 5th Ed. Iowa State Univ. Press. Ames., 357p.
[15] Belanger, G., Savoie, P., Parent, G., Claessens, A., Bertrand, A., Tremblay, G. F., Masse, D., Gilbert, Y., Babineau, D. (2012): Switchgrass silage for methane production as affected by date of harvest. – Canadian Journal of Plant Science 92: 1187-1197.
[16] Bolsen, K. K., Ashbell, G., Weinberg, Z. G. (1996): Silage fermentation and silage additives. – Ajas 9(5): 483-493.
[17] Brodowska, M. S., Muszyński, P., Haliniarz, M., Brodowski, R., Kowalczyk-Juśko, A., Sekutowski, T., Kurzyna-Szklarek, M. (2018): Agronomic aspects of switchgrass cultivation and use for energy purposes. – Applied Ecology and Environmental Research 16(5): 5715-5743.
[18] Brogna, N., Pacchioli, M. T., Immovilli, A., Ruozzi, F., Ward, R., Formigoni, A. (2009): The use of near-infrared reflectance spectroscopy (NIRS) in the prediction of chemical composition and in vitro neutral detergent fiber (NDF) digestibility of Italian alfalfa hay. – Italian Journal of Animal Science 8(Suppl. 2): 271-273.
[19] Brunken, J. N., Estes, J. R. (1975): Cytological and morphological variation in *Panicum virgatum* L. – The Southwestern Naturalist 19(4): 379-385.
[20] Bulgurlu, Ş., Ergül, M. (1978): Physical, Chemical and Biological Analysis Methods of Feed. – University of Ege, Faculty of Agriculture, Publication No: 127, Ege University Printing House, Bornova-İzmir, Turkey, pp. 58-76. (In Turkish).
[21] Canale, A., Valente, M. E., Ciotti, A. (1984): Determination of volatile carboxylic acids (C_1-C_{5i}) and lactic acid in aqueous acid extracts of silage by high performance liquid chromatography. – Journal of the Science of Food and Agriculture 35: 1178-1182.
[22] Canbolat, Ö., Karasu, A., Bayram, G., Filya, İ., Kamalak, A. (2016): The effect of sowing density on the nutritive value, silage quality characteristics and nutrient yields of non stover sweet corn (*Zea mays* L. *saccharata* Sturt.). – Journal of Agricultural Faculty of Uludag University 30(1): 101-112. (In Turkish).

http://www.aloki.hu ● ISSN 1589 1623 (Print) ● ISSN 1785 0037 (Online)
DOI: http://dx.doi.org/10.15666/aeer/1706_1575515773

[23] Casler, M. D., Boe, A. R. (2003): Cultivar x environment interactions in switchgrass. – Crop Sci. 43: 2226-2233.
[24] Cassida, K. A., Muir, J. P., Hussey, M. A., Read, J. C., Venuto, B. C., Ocumpaugh, W. R. (2005): Biofuel component concentrations and yields of switchgrass in South Central U.S. environmental. – Crop Sci. 45: 682-692.
[25] Catchpoole, V. R., Henzell, E. F. (1971): Silage and silage-making from Tropical Herbage species. – Herbage Abstracts 41(3): 213-221.
[26] Church, D. C. (1986): Feed and Feeding. – Prentice Hill A Division of Simon and Schuster., Inc. Englewood Cliffs, NY, United Stated of America.
[27] Comberg, G. (1974): Gärfutter: Betriebswirtschaft, Erzeugung, Verfütterung. – Verlag Eugen Ulmer Stuttgart, Gerokstraße 19, Printed in Germany, ISBN: 3-8001-4321-6, 260p.
[28] Çakmak, B., Yalçın, H., Bilgen, H. (2013): The effect of packing pressure and storage duration on the crude nutrient content and the quality of silages made from green and fermented corn. – Journal of Agricultural Sciences 19: 22-32. (In Turkish).
[29] Çayıroğlu, H., Coşkun, İ., Şahin, A. (2016): Factors affecting the aerobic stability of silage and improvement strategies. – Alınteri 31(B): 91-97. (In Turkish).
[30] Çiçek, F. (2017): The determination of G.D.D. for different morphological stages and physiological characteristics of cutting times of switchgrass varieties (*Panicum virgatium* L.). – Ms Thesis, The Graduate School of Natural and Applied Science of Selçuk University, Konya, Turkey, 73p. (In Turkish).
[31] Danley, M. M., Vetter, R. L., Wedin, W. F. (1973): Modified laboratory silo unit for studying the fermentation of corn (*Zea mays* L.) grain. – Agronomy Journal 65: 621-624.
[32] Davis, D., Pas, G. A., Liewellyn, D. A., Lea, K., Smith, S. R. (2018): Case study: Intake and apparent digestibility by beef calves of Alamo and Cave-in-Rock switchgrass cultivars harvested as hay at 3 different maturities. – The Professional Animal Scientist 34(5): 469-473.
[33] Demirel, M., Cengiz, F., Çelik, S., Erdoğan, S. (2001): A study on degradability in rumen and silage quality of mixture of corn and hungarian vetch grown in Van ecological conditions. – J. Agric. Sci. 11(1): 69-78. (In Turkish).
[34] Deswysen, A. G., Dutilleud, P., Godfrin, J. P., Ellis, W. C. (1993): Nycterohemeral eating and ruminating patterns in heifers fed grass or corn silage: analysis by finite fourier transform. – J. Anim. Sci. 71: 2739-2747.
[35] Elbersen, H. W., Christian, D. G., El Bassen, N., Bacher, W., Sauerbeck, G., Aleopoulou, E., Sharma, N., Piscioneri, I., De Visser, P., Van Den Berg, D. (2001): Switchgrass variety choice in Europe. – Aspects of Applied Biology 65: 21-28.
[36] Ergün, A., Tuncer, Ş. D., Çolpan, İ., Yalçın, S., Yıldız, G., Küçükersan, M. K., Küçükersan, S., Şehu, A., Saçaklı, P. (2013): Feed, Feed Hygiene and Technology. – Ankara University, Faculty of Veterinary Medicine, Extended 5th Edition, Ankara, Turkey, 448p. (In Turkish).
[37] Filya, İ., Ashbell, G., Hen, Y., Weinberg, Z. G. (2000): The effect of bacterial inoculants on the fermentation and aerobic stability of whole crop wheat silage. – Animal Feed Science and Technology 88(1-2): 39-46.
[38] Filya, İ. (2001): Silage Technology. – Uludağ University, Faculty of Agriculture, Department of Animal Science, Bursa, Turkey. (In Turkish).
[39] Geren, H. (2000): Investigations on the effect of sowing dates on the forage yields and agronomical characteristics related to silage of different maize (*Zea mays* L.) cultivars grown as main and second crops. – PhD Thesis, The Graduate School of Natural and Applied Science of Ege University, İzmir, Turkey, 251p. (In Turkish).
[40] Geren, H. (2001): Effect of sowing dates on silage characteristics of different maize cultivars grown as second crop under Bornova conditions. – Journal of Agriculture Faculty of Ege University 38(2-3): 47-54. (In Turkish).

http://www.aloki.hu ● ISSN 1589 1623 (Print) ● ISSN 1785 0037 (Online)
DOI: http://dx.doi.org/10.15666/aeer/1706_1575515773

[41] Geren, H., Kavut, Y. T. (2009): An investigation on comparison of Sorghum (*Sorghum* sp.) species with corn (*Zea mays* L.) grown under second crop production. – Journal of Agriculture Faculty of Ege University 46(1): 9-16. (In Turkish).
[42] Geren, H., Kavut, Y. T., Avcıoğlu, R. (2011): A preliminary study on ensilability characteristics and yield and other related traits of elephant grass (*Miscanthus* x *giganteus*) under Mediterranean climatic conditions. – Journal of Agriculture Faculty of Ege University 48(3): 203-209. (In Turkish).
[43] Göhl, B. (1981): Tropical Feeds: Feeds Information Summaries and Nutritive Values. – Food and Agriculture Organization of the United Nations, Rome, 529p.
[44] Güney, E., Tan, M., Dumlu Gül, Z., Gül, İ. (2010): Determination of yield and silage quality of some maize cultivars in Erzurum conditions. – Journal of Agricultural Faculty of Atatürk University 41(2): 105-111. (In Turkish).
[45] Gürsoy, E., Macit, M. (2014): Determination of *in vitro* gas production parameters of some grass forages grown as naturally in the pastures of Erzurum. – YYU J Agr Sci 24(3): 218-227. (In Turkish).
[46] Hart, S. P. (1990): Effects of altering the grain content of sorghum silage on its nutritive value. – J. Anim. Sci. 68: 3832-3842.
[47] Hopkins, A. A., Vogel, K. P., Moore, K. J., Johnson, K. D., Carlson, I. T. (1995): Genotypic variability and genotype ×environment interactions among switchgrass accessions from the Midwestern USA. – Crop Sci. 35: 565-571.
[48] Hopkins, A. A., Taliaferro, C. M., Murphy, C. D., Christian, D. (1996): Chromosome number and nuclear DNA content of several switchgrass populations. – Crop Sci. 36: 1192-1195.
[49] Ileri, O., Budaklı Carpıcı, E., Erbeyi, B., Avcı, S., Koc, A. (2018): Effect of sowing methods on silage yield and quality of some corn cultivars grown in second crop season under irrigated condition of Central Anatolia, Turkey. – Turk J Field Crops 23(1): 72-79. DOI: 10.17557/tjfc.424379.
[50] Isnandar, U. R., Chuzaemi, S., Sutariningsih, E., Yusiati, L. M. (2010): The role of lactic acid bacteria on silage duration process and rumen content silage quality. – The 5th International Seminar on Tropical Animal Production, Community Empowerment and Tropical Animal Industry, October 19-22, Yogyakarta, Indonesia, pp. 243-249.
[51] Jiang, Q., Webb, S. L., Bhandari, H. S., Bouton, J. H., Saha, M. C. (2019): Ecotypic and genotypic effects on regrowth and heading date in switchgrass (*Panicum virgatum*). – Plant Direct 3: 1-9.
[52] Johnson, L. M., Harrison, J. H. (2001): Scientific aspects of silage making. – Proceedings, 31st California Alfalfa & Forage Symposium, 12-13 December, Modesto, CA, UC Cooperative Extension, University of California, Davis.
[53] Kavut, Y. T., Soya, H. (2012): An investigation on the silage quality characteristics of some maize (*Zea mays* L.) cultivars under Aegean region conditions. – Journal of Agriculture Faculty of Ege University 49(3): 223-227. (In Turkish).
[54] Khan, S. H., Azim, A., Sarwar, M., Khan, A. G. (2011): Effect of maturity on comparative nutritive value and Fermentation characteristic of maize, sorghum and millet silages. – Pak. J. Bot. 43(6): 2967-2970.
[55] Khan, N. A., Tewoldebrhan, T. A., Zom, R. L. G., Cone, J. W., Hendriks, W. H. (2012): Effect of corn silage harvest maturity and concentrate type on milk fatty acid composition of dairy cows. – J. Dairy Sci. 95: 1472-1483.
[56] Kılıç, A. (1986): Silo Feed (Teaching, Learning and Application Suggestions). – Ege University, Faculty of Agriculture, Department of Animal Science, Bilgehan Printing House, İzmir, Turkey, 327p. (In Turkish).
[57] Kılıç, A. (2006): Determination of Quality in Roughage. – Hasat Publishing, İstanbul, Turkey. (In Turkish).
[58] Kiermeier, F., Renner, E. (1963): Der pH- Wert Ais Kriterium der Verwendbarkeit von Silage für die Milchvieh Fütterung. – Das Wirtschaftseiq, Futterq: 106-113.

http://www.aloki.hu ● ISSN 1589 1623 (Print) ● ISSN 1785 0037 (Online)
DOI: http://dx.doi.org/10.15666/aeer/1706_1575515773

[59] Kimura, E., Fransen, S. C., Collins, H. P., Stanton, B. J., Himes, A., Smith, J., Guy, S. O., Johnston, W. J. (2018): Effect of intercropping hybrid poplar and switchgrass on biomass yield, forage quality, and land use efficiency for bioenergy production. – Biomass and Bioenergy 111: 31-38.
[60] Lee, D. K., Owens, V. N., Doolittle, J. J. (2007): Switchgrass and soil carbon sequestration response to ammonium nitrate, manure, and harvest frequency on Conservation Reserve Program land. – Agron J 99(2): 462-468.
[61] Lemus, R., Brummer, E. C., Moore, K. J., Molstad, N. E., Burras, C. L., Barker, M. F. (2002): Biomass yield and quality of 20 switchgrass populations in southern Iowa, USA. – Biomass and Bioenergy 23: 433-442.
[62] Luginbuhl, J. M., Pond, K. R., Burns, J. C., Fisher, D. S. (2000): Intake and chewing behavior of steers consuming switchgrass preserved as hay or silage. – American Society of Animal Science 78: 1983-1989.
[63] Ma, Y., An, Y., Shui, J., Sun, Z. (2011): Adaptability evaluation of switchgrass (*Panicum virgatum* L.) cultivars on the Loess Plateau of China. – Plant Science 181: 638-643.
[64] Madakadze, I. C., Stewart, K. A., Peterson, P. R., Bruce, E., Coulman, E., Smith, D. L. (1999): Switchgrass biomass and chemical composition for biofuel in Eastern Canada. – Agronomy Journal 91: 696-701.
[65] Mantino, A., Ragaglini, G., Nassi o di Nasso, N., Cappucci, A., Mele, M., Bonari, E. (2017): Suitability of switchgrass (*Panicum virgatum* L.) as a forage crop in the Mediterranean area. – Grassland Science in Europe 22: 194-196.
[66] McDonald, P., Henderson, A. R., Heron, S. J. E. (1991): The Biochemistry of Silage. – 2nd Edition, Chalcombe Publications, Printed in Great Britain by Cambrian Printers Ltd, Aberystwyth, ISBN: 0-948617-22-5, 327p.
[67] McLaughlin, S. B., Kszos, L. A. (2005): Development of switchgrass (*Panicum* virgatum) as a bioenergy feedstock in the United States. – Biomass Bioenergy 28: 515-535.
[68] Milenković, J., Stanisavljević, R., Marković, J., Petrović, M., Vasić, T., Anđelković, S., Terzić, D. (2018): Biomass quality of different genotypes of switchgrass (*Panicum virgatum* L.) for animal feed. – Journal on Processing and Energy in Agriculture 22(3): 122-124.
[69] Missaoui, A. M., Bouton, J. H., Paterson, A. H. (2006): Molecular markers for the classification of switchgrass (*Panicum virgatum* L.) germplasm and to assess genetic diversity in three synthetic switchgrass populations. – Gen. Res. Crop Evol. 53: 1291-1302.
[70] Mohammed, Y. A., Desta, K. G. (2017): Nutrient source affected quality biomass production of early harvest switchgrass for animal feed. – International Journal of Agriculture and Environmental Research 3(2): 2546-2555.
[71] Mohd-Setapar, S. H., Abd-Talib, N., Aziz, R. (2012): Review on crucial parameters of silage quality. – APCBEE Procedia 3: 99-103.
[72] Muir, J. P., Sanderson, M. A., Ocumpaugh, W. R., Jones, R. M., Reed, R. L. (2001): Biomass production of 'Alamo' switchgrass in response to nitrogen, phosphorus, and row spacing. – Agron J 93(4): 896-901.
[73] Nelson, D. W., Sommers, L. E. (1982): Total Carbon, Organic Carbon and Organic Matter. – In: Page, L. A., Miller, R. H., Keeney, D. R. (eds.) Methods of Soil Analysis, Part 2. Chemical and Microbiological Methods (2nd ed.) American Society of Agronomy, Madison, pp. 539-579.
[74] Ohmomo, S., Katayama, N., Potacharoen, W., Tanaka, O., Sırıanuntapıboon, S., Atthasampunna, P. (1995): Screening of lactic acid bacteria suitable for silage-making in tropical regions. – JARQ 29: 251-256.
[75] Öten, M., Kiremitci, S., Çınar, O. (2016): Determination of silage quality of some forage crops and mixtures by different methods. – J. of AARI 26(2): 33-43. (In Turkish).

http://www.aloki.hu ● ISSN 1589 1623 (Print) ● ISSN 1785 0037 (Online)
DOI: http://dx.doi.org/10.15666/aeer/1706_1575515773

[76] Özdüven, M. L., Koç, F., Polat, P., Coşkuntuna, L., Başkavak, S., Şamlı, H. E. (2009): Effects of fermentation characteristics and feed value of some maize cultivars ensiled at different stages of maturity. – Journal of Tekirdag Agricultural Faculty 6(2): 121-129. (In Turkish).
[77] Petterson, K. (1988): Ensiling of forages: Factors affecting silage fermentation and quality. – Swedish University of Agricultural Sciences, Department of Animal Nutrition and Management, Uppsala, 46p.
[78] Phillip, L. E., Hidalgo, V. (1989): Voluntary feed intake, acıd-base balance and partitioning of urinary nitrogen in lambs fed corn silage with added sodium bicarbonate or sodium sesquicarbonate. – J. Anim. Sci. 67: 2116-2122.
[79] Piscioneri, I., Pignatelli, V., Palazzo, S., Sharma, N. (2001): Switchgrass production and establishment in the Southern Italy climatic conditions. – Energy Conversion and Management 42(18): 2071-2082.
[80] Polat, C., Koç, F., Özdüven, M. L. (2005): The effects of lactic acid bacteria and lactic acid bacteria+enzyme mixture silage inoculants on maize silage fermentation and nutrient digestibility in lambs. – Journal of Tekirdag Agricultural Faculty 2(1): 13-22. (In Turkish).
[81] Quinn, J. A. (1969): Variability among high plains populations of *Panicum virgatum*. – Bulletin of the Torrey Botanical Club 96(1): 20-41.
[82] Quinn, J. A., Wetherington, J. D. (2002): Genetic variability and phenotypic plasticity in flowering phenology in populations of two grasses. – The Journal of the Torrey Botanical Society 129(2): 96-106.
[83] Rafiuddin, Abdullah, M., Javed, K., Jabbar, M. A., Shahid, M. Q., Jan, P. S., Khan, M. A., Ramzan, M., Hamdullah. (2016): Impact of flowering stage on nutritive value, physical quality and digestibility of silages made from cereal fodders. – Applied Ecology And Environmental Research 14(5): 149-157.
[84] Reeves, J. B., Blosser, T. H., Colenbrander, V. F. (1989): Near infrared reflectance spectroscopy for analyzing undried silage. – J. Dairy Sci. 72: 79-88.
[85] Rohweder, D. A., Barnes, R. F., Jorgensen, N. (1978): Proposed hay grading standards based on laboratory analyses for evaluating quality. – Journal of Animal Science 47(3): 747-759.
[86] Roth, G. W. (2001): Corn Silage Productionand Management. – College of Agricultural Sciences. Agricultural Research and Coop. Extension, Agronomy Facts 18.
[87] Sanderson, M. A., Read, J. C., Reed, R. L. (1999): Harvest management of switchgrass for biomass feedstock and forage production. – Argon. J. 91: 5-10.
[88] Sanderson, M. A., Burns, J. C. (2010): Digestibility and intake of hays from upland switchgrass cultivars. – Crop Science 50: 2641-2648.
[89] Sena, K. L., Goff, B., Davis, D., Smith, S. R. (2018): Switchgrass growth and forage quality trends provide insight for management. – Crop, Forage & Turfgrass Management 4(1): 170053. doi:10.2134/cftm2017.08.0053.
[90] Seydoşoğlu, S. (2017): Investigation of the effects of different sowing times of different varieties on second crop maize silage yield and quality. – PhD Thesis, Institute of Natural and Applied Sciences University of Dicle, Diyarbakır, Turkey, 201p. (In Turkish).
[91] Soylu, S., Sade, B., Öğüt, H., Akınerdem, F., Babaoğlu, M., Ada, R., Eryılmaz, T., Öztürk, Ö., Oğuz, H. (2010): Investigation of the possibilities of growing switchgrass (*Panicum virgatum* L.) as an alternative biofuel and silage plant for Turkey. – TÜBİTAK Project Finally Report, Project No: TOVAG-107 O 161, Konya, Turkey. (In Turkish).
[92] Soylu, S. (2012): Investigation of agronomic techniques of switchgrass (*Panicum virgatum* L.) as an alternative biofuel plant in Turkey. – Journal of Agricultural Machinery Science 8(3): 257-263. (In Turkish).
[93] Sucu, E., Filya, İ. (2006): Effects of homofermentative lactic acid bacterial ınoculants on the fermentation and aerobic stability characteristics of low dry matter corn silages. – Turkish Journal of Veterinary and Animal Sciences 30: 83-88.

http://www.aloki.hu ● ISSN 1589 1623 (Print) ● ISSN 1785 0037 (Online)
DOI: http://dx.doi.org/10.15666/aeer/1706_1575515773

[94] Van Soest, P. J. (1994): Nutritional Ecology of the Ruminant (2nd Ed.). – Ithaca, N.Y. Cornell University Press.
[95] Van Wambeke, A. R. (2000): The Newhall Simulation Model for Estimating Soil Moisture and Temperature Regimes. – Department of Crop and Soil Sciences, Cornell University, Ithaca, NY.
[96] Vogel, K. P., Brejda, J. J., Walters, D. T., Buxton, D. R. (2002): Switchgrass biomass production in the midwest USA: harvest and nitrogen management. – Agron J 94(3): 413-420.
[97] Vogel, K. P. (2004): Switchgrass. – In: Moser, L. E., Sollenberger, L., Burson, B. (eds.) Warm-season (C4) grasses. Madison, WI: ASA, CSSA, and SSSA, pp. 561-588.
[98] Weinberg, Z. G., Ashbell, G. (2003): Engineering aspects of ensiling. – Biochemical Engineering Journal 13: 181-188.
[99] Wolf, D. D., Fiske, D. A. (1995): Planting and Managing Switchgrass for Forage, Wildlife, and Conservation. – Virginia Polytechnic Institute and State University, Virginia Cooperative Extension Publication, Blacksburg, VA, pp. 418-513.
[100] Woolfort, M. K. (1984): The Silage Ferment. – Grassland Research Inst, Hurley, England, 350p.
[101] Zhao, X., Liu, J., Liu, J., Yang, F., Zhu, W., Yuan, X., Hua, Y., Cui, Z., Wang, X. (2017): Effect of ensiling and silage additives on biogas production and microbial community dynamics during anaerobic digestion of switchgrass. – Bioresource Technology 241: 349-359.

http://www.aloki.hu ● ISSN 1589 1623 (Print) ● ISSN 1785 0037 (Online)
DOI: http://dx.doi.org/10.15666/aeer/1706_1575515773

COMMUNITY STRUCTURE AND CONSERVATION OF RARE AND ENDANGERED PLANTS OF GEOMANTIC FOREST IN SOUTHERN CHINA

ZOU, Z. Y.[1#] – HUANG, R. R.[2#] – FAN, Y. M.[3] – ZHANG, Q. M.[4*] – LIU, S. Z.[4] – CHU, G. W.[4]

[1]*College of Life Sciences, South China Agricultural University, Guangzhou, China*

[2]*School of Architecture and Civil Engineering, Xiamen University, Xiamen, China*

[3]*School of Physics and Optoelectronic Engineering, Foshan Institute of Science and Technology, Foshan, China*

[4]*South China Botanical Garden, Chinese Academy of Sciences, Guangzhou, China*

[#]*These authors contributed equally to this work*

**Corresponding author*
e-mail: zqm@scib.ac.cn

(Received 15th Sep 2019; accepted 15th Nov 2019)

Abstract. Exploring the effects of urbanization on the conservation status of geomantic forest containing rare and endangered plants is very important for the ecological development of southern China. We studied the community structure and habitat characteristics of geomantic forest in Guangzhou City, southern China, as well as the population characteristics of the rare and endangered plant *Aquilaria sinensis* that resides there. The results showed that, within geomantic forest, there were 23 species vascular plants belonging to 23 genera and 14 families. This community was dominated by tropical and subtropical species. This community was mainly composed with mesophanerophytes, miphanerophytes and mesophyll. The community was less diverse than natural forests in the same region and contained one adult and eight seedling individuals of *Aquilaria sinensis*. This geomantic forest is a secondary evergreen broad-leaved forest with poor soil. In order to protect rare and endangered plants, as well as native species in this region, we suggest that all geomantic forests with rare and endangered plants in Guangzhou be set as small natural reserves that can be strictly managed. This kind of small natural reserve can facilitate the conservation of regional plant diversity and provide more ecosystem service.
Keywords: *floristic composition, Shuixi Village, Aquilaria sinensis, soil property, urbanization*

Introduction

Geomantic forest is purposely preserved to maintain the ecological environment in Southern China, Japan, and Korea, and is also shaped by both religion and the traditional culture of geomancy (Kim, 2014, 2017; Fan et al., 2019). The geomantic forest refers to the evergreen broad-leaved forest that has grown on edge of the villages for many years. The geomantic forest not only protects local plant resources but also contains rare and endangered species. In addition to protecting the environment, the geomantic forest also serves as a gene bank for the development and utilization of biological resources in the future (Cheng, 2011; Ye et al., 2013). Monsoon evergreen broad-leaved forests, with their complex community structure and rich biodiversity, are the typical zonal vegetation in southern China. They are an important part of the subtropical terrestrial ecosystem and play an important role in ecosystem services (Ren et al., 1996; Song et al., 2005). The monsoon evergreen broad-leaved forests in Southern China are mainly preserved in the form of nature reserves. Most of the geomantic forests in Guangzhou are inhabited by the

http://www.aloki.hu ● ISSN 1589 1623 (Print) ● ISSN 1785 0037 (Online)
DOI: http://dx.doi.org/10.15666/aeer/1706_1577515785

rare, endangered *Aquilaria sinensis* plant, but the forests are scattered and have been seriously damaged by deforestation and related human activities (Ye et al., 2013).

Aquilaria sinensis is a perennial tropical and subtropical evergreen tree that belongs to the Thymelaeaceae family. It is listed as a national second-class protected plant and an internationally protected tree. *Aquilaria sinensis* is a valuable resource in Chinese herbal medicine and is listed as one of the top ten broad-spectrum drugs (Mao et al., 2017; Wang et al., 2012). Due to over-harvesting, few *Aquilaria sinensis* individuals remain in the wild.

As a typical Chinese traditional forest, geomantic forest has mainly been studied in China, where research has been conducted to analyze their classification and conservation value (Hu et al., 2011; Luo et al., 2011; Tang et al., 2012; Deng, 2013; Gao et al., 2013), species composition and diversity (Liu et al., 2005; Mo et al., 2011; Lee et al., 2017; Lü et al., 2009c), community structure characteristics (Cai et al., 1998; Yang et al., 2012; Kong et al., 2013; Chen, 2017; Zhu et al., 2011; Lü et al., 2009a, b), biomass and carbon storage (Lu, 2017), spatial form and distribution (Lin et al., 2013), plant resources and utilization (Li et al., 2013), landscape reconstruction and planning, related human settlements and environmental culture (Cheng, 2011; Ye et al., 2013). The community characteristics and protection of *Aquilaria sinensis* in Guangzhou were also analyzed by several scholars (Zhu et al., 2011). In general, however, there are few studies on rare and endangered plants and their habitats in geomantic forest. The geomantic forest, home to many local native species, endemic species, and rare and endangered plants, is a local source of species diversity and provides shelter for rare and endangered plants (Ye et al., 2013). Within the Luogang District in Guangzhou City there are 15 geomantic forests, all with similar species composition and community structure (Ye et al., 2013).

For this analysis, we focused our research on the geomantic forest in Shuixi Village, which is representative of the geomantic forest in Guangzhou and is inhabited by *Aquilaria sinensis*. Shuixi Village is located in the eastern suburbs of Guangzhou. After relocation to the Huangpu District in 2014, it has become an important area for development and transformation. Shuixi Village was listed as one of the old village reconstruction projects in Guangzhou in 2016. With the growing population and increased economic development of the village, the forest faces the negative effects of human interference and climate change caused by urbanization. In this study, we examined the community structure of the geomantic forest in Shuixi Village, as well as the structure and community habitat of the *Aquilaria sinensis* population within this forest. Specifically, we addressed the following three topics: (1) the community structure and habitat of the geomantic forest, (2) the population status of *Aquilaria sinensis* in the geomantic forest and (3) the strategies to protect the geomantic forest, as well as its rare and endangered plants.

Materials and methods

Research site

The geomantic forest (*Fig. 1*), with an area of approximately 6 hectares, is located at the rear of Shuixi Village, in northeast Guangzhou, Guangdong Province, China, 113°28’41.6”N, 23°11’49.2”E. The forest is located about 50 m above sea level, and has an eastern slope of 15°. It belongs to the lower subtropical monsoon climate, and has an average annual temperature of 23 °C. The lowest temperature occurs in January and is 13 °C, and the highest temperature is 28 °C and occurs in August (Mao et al., 2017). The annual average humidity is about 79%, the annual average rainfall is about 1700 mm, and the rainy season is from April to October (Zhu et al., 2011; Yi et al., 2012). The zonal

http://www.aloki.hu ● ISSN 1589 1623 (Print) ● ISSN 1785 0037 (Online)
DOI: http://dx.doi.org/10.15666/aeer/1706_1577515785

vegetation in this area is the lower subtropical monsoon evergreen broad-leaved forest, and the zonal soil is laterite. Shuixi Village covers a significant area with a large population. It is surrounded by artificially planted *Acacia mangium*, *Cinnamomum burmanni*, and *Manglietia glauca*. In the geomantic forest, *Acacia mangium* covers the most area, and native species only cover about 900 m^2. There are some signs of deforestation and we find that human activities have affected the geomantic forest, as there are traces of raising chickens, stacking garbage and walking around the forest.

Figure 1. *The community structure and habitat of the geomantic forest*

Investigation and analysis methods

The typical community sampling method was used to investigate the vegetation of the geomantic forest in Shuixi Village in November 2017. Samples of soil and leaf litter were also taken for analysis. As mentioned above, the area of the geomantic forest where native species remain is about 900 m^2. Only eight 10 m × 10 m quadrates were established in the area containing native species. We investigated the crown density, species, plant height, and diameter at breast height (DBH) in the arbor layer, where the DBH is ≥ 1 cm. A 5 m × 5 m shrub quadrate was randomly selected from each 10 m × 10 m quadrate, and a 1 m × 1 m herb layer was randomly set in the shrub quadrate (Ren et al., 1996). The species name, height, and coverage of each individual in the shrub and herb quadrates were recorded. Three 1 m×1 m litter layers were randomly collected from each 10 m × 10 m square to measure the litter standing crop in the ground layer (Ren et al., 1998).

Five 10 m × 10 m quadrates were selected for soil property analysis. In each of the five quadrates chosen, six soil samples (0-20 cm) were randomly collected using drilling tools and mixed. Soil samples were brought back to the laboratory. Samples were air-dried and sieved for analysis of soil organic matter, pH, N, P, and K contents. The analysis method followed Peng (1996) and Ren et al. (1996). There were five replicates per site (i.e. one replicate per quadrat). In addition, the leaf area index and extinction coefficient were analyzed using the LAI-2000 plant canopy analyzer (Ren et al., 1996).

http://www.aloki.hu ● ISSN 1589 1623 (Print) ● ISSN 1785 0037 (Online)
DOI: http://dx.doi.org/10.15666/aeer/1706_1577515785

Data analysis

Based on the standards of Raunkiaer's Life-form Spectrum and the Flora of China and Guangdong Flora (Cai et al., 1998), various life forms of plants were comprehensively determined. Field observations and survey data were used to determine the leaf type. The basal area, frequency, relative frequency, relative density, relative significance, importance value, diversity index, ecological dominance and uniformity index were calculated (Ren et al., 1996). The species composition of the shrub layer in the community, the spatial structure, the species structure of *Aquilaria sinensis* and the soil chemical properties were determined. The relevant equations are as follows:

$$\text{Important value } IV = 100 \times (\text{relative degree} + \text{relative frequency} + \text{relative significance}) / 3 \quad \text{(Eq.1)}$$

$$\text{Shannon} - \text{Wiener index } HP = -\sum (Pi \times \ln Pi) = -\sum |(Ni / N) \times \ln(Ni / N)| \quad \text{(Eq.2)}$$

$$\text{Ecological dominance } C = Ni\ (Ni - 1) / [N\ (N - 1)] \quad \text{(Eq.3)}$$

$$\text{Pielou evenness index } JSW = -\sum (Pi \ln Pi) / \ln S \quad \text{(Eq.4)}$$

where Pi is the relative abundance of the i-th species, Ni is the number of plants of the i-th species, N is the total number of plants, and S is the total number of species (Peng, 1996; Luo et al., 2011).

The data were processed using Office Excel.

Results and analysis

Community structure

Geomantic forests are evergreen all year round, with an overall height of about 10 m and a canopy closure of about 70%. The leaf area index (LAI) of the community is 4.98 and the extinction coefficient, K, is 0.325. The canopy layer is discontinuous, and there is a notable vertical stratification of tree layer, shrub layer and herb layer.

In the 800 m^2 area, there are 167 individuals, some of which are monoecious, bringing the total to 178 individuals in the arbor layer. These individuals belong to 14 families and 23 genera, and have an average DBH of 6.8 cm and an average height of 5.5 m. Among 178 individuals, there are three genera and three species in each family of Euphorbiaceae, Rubiaceae and Polygonaceae. The arbor layer is dominated by families and genera of tropical and subtropical plants. There are 115 individuals shorter than 5 m, making up 65% of the total; 43 individuals between 5-10 m tall, accounting for 24% of the total and 20 individuals taller than 10 m occupying 11% of the total. There are 124 individuals with a DBH within 5 cm, accounting for 70% of the total, 33 individuals with a DBH between 5 and 10 cm, making up 18% of the total, and 21 individuals with a DBH greater than 10 cm, occupying 12% of the total. In general, the community is relatively short, with the majority of trees being small in size.

The geomantic forest community is made up of a diverse array of species. In the arbor layer, four species, including *Engelhardia roxburghiana* Wall., *Acacia mangium* Willd., *Psychotria rubra* (Lour.) Poir., and *Aporosa dioica* (Roxb.) Muell. Arg., account

http://www.aloki.hu ● ISSN 1589 1623 (Print) ● ISSN 1785 0037 (Online)
DOI: http://dx.doi.org/10.15666/aeer/1706_1577515785

for about 65% of the importance value (*Table 1*). There are only seven large *Acacia mangium* individuals, which have the largest height and DBH within the community. This species has no young individuals. As the pioneer species, it will gradually withdraw from the community. *Astragalus membranaceus*, which is the most dominant species in the arbor layer, has 31 individuals. *Psychotria rubra* and *Aporosa dioica* have the largest number of individuals, all of which are short, small trees. There are 13 species of shrubs, 10 of which are also present in the arbor layer, and one of which is also present in the herb layer (*Table 2*). There are seven species within the herbaceous layer, four of which also in the arbor layer, one of which is present in the shrub layer, and two of which are ferns (*Tables 1-3*).

According to the Raunkiaer's Life-form Spectrum, among the 23 species in the arbor layer, only five species are middle phanerophytes, and the other 18 species are small phanerophytes. Moreover, two species have large-sized leaves and five species have small-sized leaves. The other 16 species have medium-sized leaves. In the wild, plants in this community predominantly have leathery, single medium-sized leaves. The Shannon-Wiener biodiversity index of the arbor layer is 2.458, which is significantly lower than the diversity index of 4.01 in the Dinghu Mountain zonal vegetation–monsoon evergreen broad leaved forest in 1992. The indexes of ecological dominance and uniformity have little difference, as they are 0.13 and 0.784, respectively (Ren et al., 1996).

Population structure of the rare species Aquilaria sinensis

There is one *Aquilaria sinensis* individual in the arbor layer, with a DBH of 8 cm and a height of 6.5 m in the geomantic forest. There are six *Aquilaria sinensis* individuals in the shrub layer, one with a basal diameter of 1.3 cm and a height of 1.7 m, four with a basal diameter of 0.7 cm and a height of 0.7 m, and one with a basal diameter of 0.4 cm and a height of 0.6 m. Two *Aquilaria sinensis* individuals occupy the herbaceous layer, with a height of 0.2 m. The importance value of *Aquilaria sinensis* is 0.72, accounting for 0.7% of the community. *Aquilaria sinensis* is a mesophanerophyte, a group which makes up a small portion of the community. *Aquilaria sinensis* is also a species with medium-sized leaves, and these types of species occupy a large portion of the community.

Soil properties of the community

The soil in the sample plot consists of a thick layer of fertile laterite. The average weight of the litter layer is 530 ± 50.99 g m^{-2}, and the litter layer is rich in humus. The A layer of soil, with a thickness of 0-20 cm, has a pH of 4.46, making it acidic. The organic content is 30.48 g kg^{-1}, and the total nitrogen content is 1.18 g kg^{-1}. The main chemical properties of the soils are shown in *Table 4*. The soil of this community is similar to that of nearby Changlong Village in Longgang District and Zhongling Village in Zengcheng District, but there are some differences. Overall, the soil fertility of the sample plot is not as high as that of the zonal climax vegetation in Dinghu Mountain. This indicates that the soil fertility of the small-size geomantic forest has been influenced by human activities and needs to be improved to be on par with that of the natural soil in a large-size nature reserve. The content of organic matter and available potassium in this plot is particularly high, which may be related to activities of local villagers, such as raising chickens and stacking garbage.

http://www.aloki.hu ● ISSN 1589 1623 (Print) ● ISSN 1785 0037 (Online)
DOI: http://dx.doi.org/10.15666/aeer/1706_1577515785

Table 1. *Species and its important value in arbor layer*

No.	Species	Families	Genera	Lifestyle	Number of trees	Average DBH /cm	Average H /m	Importance values
1	*Engelhardia roxburghiana* Wall.	Juglandaceae	Engelhardia	Mesophanerophyte	31	15.5	9.6	26.54
2	*Acacia mangium* Willd.	Fabaceae	Acacia	Mesophanerophyte	7	41.5	21.0	16.78
3	*Psychotria rubra* (Lour.) Poir.	Psychotria	Psychotria	Microphanerophyte	45	2.5	2.8	12.04
4	*Aporusa dioica* (Roxb.) Müll. Arg.	Euphorbiaceae	Aporusa	Microphanerophyte	26	3.6	3.8	9.10
5	*Endospermum chinense* Benth	Euphorbiaceae	Endospermum	Mesophanerophyte	9	8.1	9.0	4.94
6	*Castanopsis chinensis* Hance	Fagaceae	Castanopsis	Mesophanerophyte	8	4.9	5.0	4.09
7	*Garcinia multiflora Champ.* Ex Benth.	Clusiaceae	Garcinia	Microphanerophyte	8	2.8	3.6	3.91
8	*Litsea rotundifoliaHemsl.* Var. oblongifolia (Nees) Allen	Lauraceae	Litsea	Microphanerophyte	7	1.9	3.0	3.19
9	*Acronychia pedunculata* (L.) Miq.	Rutaceae	Acronychia	Microphanerophyte	6	5.2	5.8	3.19
10	*Ardisia quinquegona* Bl.	Myrsinaceae	Ardisia	Microphanerophyte	7	1.5	2.9	3.18
11	*Ilex asprella* (Hook. et Arn.) Champ. ex Benth.	Aquifoliaceae	Ilex	Microphanerophyte	4	1.4	2.4	2.15
12	*Cinnamomum burmanni* (Nees et T. Nees) Blume	Lauraceae	Cinnamomum	Microphanerophyte	3	1.5	2.8	1.50
13	*Glochidion eriocarpum* Champ. ex Benth.	Euphorbiaceae	Glochidion	Microphanerophyte	3	1.4	2.6	1.50
14	*Archidendron lucidum* Benth.	Fabaceae	Archidendron	Microphanerophyte	2	1.2	2.4	1.30
15	*Manglietie glauca* Blume	Magnoliaceae	Manglietie	Microphanerophyte	2	4.1	5.1	0.88
16	*Aidia pycnantha* (Drake) Tirveng.	Psychotria	Aidia	Microphanerophyte	2	3.4	4.1	0.86
17	*Schefflera octophylla* (Lour.) Harms	Araliaceae	Schefflera	Mesophanerophyte	2	1.3	2.2	0.84
18	*Aquilaria sinensis* (Lour.) Spreng.	Thymelaeaceae	Aquilaria	Mesophanerophyte	1	8.0	6.5	0.72
19	*Cratoxylum cochinchinense* (Lour.) Bl.	Clusiaceae	Cratoxylum	Microphanerophyte	1	4.3	4.5	0.67
20	*Adina pilulifera* (Lam.) Franch. ex Drake	Psychotria	Adina	Microphanerophyte	1	2.2	3.5	0.66
21	*Viburnum sempervrens* K. Koch	Caprifoliaceae	Viburnum	Microphanerophyte	1	1.4	2.2	0.65
22	*Machilus chekiangensis* S. Lee	Lauraceae	Machilus	Mesophanerophyte	1	1.3	2.7	0.65
23	*Melicope pteleifolia* (Champ. ex Benth.) T. Hartley	Rutaceae	Melicope	Microphanerophyte	1	1.0	2.2	0.65
	Total				**178**	**6.8**	**5.5**	**100**

http://www.aloki.hu ● ISSN 1589 1623 (Print) ● ISSN 1785 0037 (Online)
DOI: http://dx.doi.org/10.15666/aeer/1706_1577515785

Table 2. *Species composition in shrub layer*

No.	Species	Families	Genera	Lifestyle	Number of trees	Average H /cm	Average base diameter /cm
1	*Litsea rotundifoliaHemsl.* Var. oblongifolia (Nees) Allen	Lauraceae	Litsea	Microphanerophyte	5	93.3	0.6
2	*Garcinia multiflora Champ.* Ex Benth.	Clusiaceae	Garcinia	Microphanerophyte	2	80.0	0.9
3	*Alchornea trewioides* (Benth.) Muell. Arg.	Euphorbiaceae	Alchornea	Nanophanerophytes	2	100.0	0.5
4	*Acronychia pedunculata* (L.) Miq.	Rutaceae	Acronychia	Microphanerophyte	3	80.0	0.6
5	*Psychotria rubra* (Lour.) Poir.	Psychotria	Psychotria	Microphanerophyte	20	93.3	0.9
6	*Archidendron lucidum* Benth.	Fabaceae	Archidendron	Microphanerophyte	1	100.0	0.5
7	*Ixora chinensis* Lam.	Psychotria	Ixora	Nanophanerophytes	2	60.0	0.4
8	*Ardisia quinquegona* Bl.	Araliaceae	Ardisia	Microphanerophyte	6	140.0	1.1
9	*Glochidion eriocarpum* Champ. Ex Benth.	Euphorbiaceae	Glochidion	Microphanerophyte	4	95.0	0.8
10	*Aquilaria sinensis* (Lour.) Spreng.	Thymelaeaceae	Aquilaria	Mesophanerophyte	6	100.0	0.8
11	*Gardenia jasminoides* Ellis	Psychotria	Gardenia	Nanophanerophytes	1	21	0.7
12	*Cinnamomum burmanni* (Nees et T. Nees) Blume	Lauraceae	Cinnamomum	Microphanerophyte	1	120.0	1.0
13	*Aporusa dioica (Roxb.)* Müll. Arg.	Euphorbiaceae	Aporusa	Microphanerophyte	10	103.3	0.9
	Total				**63**	**91.2**	**0.8**

Table 3. *Species composition in grass layer*

No.	Species	Families	Genera	Lifestyle*	No. of trees	Average H/cm	Coverage /%
1	*Pteris semipinnata* Linn	Pteridaceae	Pteris	Fern	5	45.0	6.0
2	*Litsea rotundifoliaHemsl.* Var. oblongifolia (Nees) Allen	Lauraceae	Litsea	Microphanerophyte	3	10.0	1.0
3	*Psychotria rubra* (Lour.) Poir.	Psychotria	Psychotria	Microphanerophyte	4	17.5	3.5
4	*Ixora chinensis* Lam.	Psychotria	Ixora	Nanophanerophytes	3	25.0	2.0
5	*Ardisia quinquegona* Bl.	Myrsinaceae	Ardisia	Microphanerophyte	2	35.0	4.0
6	*Adiantum flabellulatum* Linn.	Adiantaceae	Adiantum	Fern	4	15.0	3.0
7	*Aquilaria sinensis* (Lour.) Spreng.	Thymelaeaceae	Aquilaria	Mesophanerophyte	2	20.0	4.0
	Total				**23**	**24.5**	**23.5**

Table 4. *Chemical properties of the soils*

Location	pH value	Organic matter /(g*kg-1)	Total N /(g*kg-1)	Total P /(g*kg-1)	Effective P /ppm	Total K /%	Available K /ppm
Shuixi Village *	4.46 ± 0.06	30.48 ± 2.38	1.18 ± 0.06	0.252 ± 0.03	3.95 ± 2.67	3.19 ± 0.15	52.32 ± 12.09
Zhongling Village**	4.42	15.06	0.70	0.15	1.53	1.41	20.11
Changlong Village 1**	3.84	14.70	8.20	0.31		1.80	
Changlong Village 2**	3.76	37.60	1.97				
Mount Dinghu**	4.10	24.80	2.00	0.80	4.60	3.70	14.20

*The data measured in Shuixi Village include standard deviation. **The data measured in Zhongling Village are from our investigation. The data measured in Changlong Village 1 are cited from Zhu Baozhu (2011). The data measured in Changlong Village 2 are cited from Cai Xi'an (1998). The data measured in Mount Dinghu are cited from Peng Shaolin (1996)

http://www.aloki.hu ● ISSN 1589 1623 (Print) ● ISSN 1785 0037 (Online)
DOI: http://dx.doi.org/10.15666/aeer/1706_1577515785

Discussion

The community structure indicates that the geomantic forest is a secondary monsoon evergreen broad-leaved forest. There are artificially planted *Acacia mangium* individuals outside the native species community. The community species are somewhat similar to those seen in the monsoon evergreen broad-leaved forest at Dinghu Mountain, despite the presence of *Acacia mangium*. However, the geomantic forest in Shuixi Village also shows tropical and subtropical properties in its floristic composition, community life type and leaf type spectrum. However, there are no plate-like roots, cladanthy, drip-tip plants, or woody vines that are typically observed in natural vegetation. Compared with natural forests, the number of species in the geomantic forest in Shuixi Village is smaller, the population density is lower, the overall height of the vegetation is shorter and the DBH of the vegetation is smaller. There are only three layers in this community, arbor, shrub and herb, meaning that the liana layer, three sub-layers of the arbor and five sub-layers of shrub and herb that are present in natural forests are missing in the Shuixi village forest. Although the community is mainly composed of species with medium-sized leaves, it is different from the structure of natural forests, which have reasonable proportions of species with various types of leaves. The mesophanerophytes and miphanerophytes are the main components of the community, and there are no phaenerophytes. This is mainly due to the fact that the community is not mature enough. In addition, the community's diversity index is significantly lower than that of Dinghu Mountain (Ren et al., 1996). Therefore, this geomantic forest is a lower subtropical monsoon evergreen broad-leaved forest displaying secondary growth after human disturbances. However, the species coefficient of this forest is 100%, indicating that it still has a large development trend with its species richness (Cai et al., 1998).

In terms of the soil chemical properties, the fertile lateritic soil of this geomantic forest is the same as that of the monsoon evergreen broad-leaved forest in Dinghu Mountain. However, aside from the organic matter and available potassium levels, other indicators of the soil health in the geomantic forest are lower than those for the soil in the Dinghu Mountain forest. Moreover, soil indicators in the geomantic forest in Shuixi Village are also different from those of the other nearby geomantic forests (Fan et al., 2019). There are two possible reasons for the increased soil fertility in this geomantic forest. First, the geomantic forest is close to the village where there are chickens and garbage, which may contaminate the soil. Second, the vegetation is inferior to what is observed in natural forests, which is the result of various types of disturbances. Despite this, the geomantic forest in Shuixi Village still has high soil fertility and can ensure the growth of the native vegetation.

There are nine *Aquilaria sinensis* individuals in the geomantic forest in Shuixi Village. These individuals have a certain age structure, indicating that they are still capable of self-renewal, and the habitat of this community is suitable for the regeneration and growth of *Aquilaria sinensis*. In particular, the acidic soil (pH 4.46) of the geomantic forest in Shuixi Village makes it suitable for *Aquilaria sinensis* growth. The nutrient content of the soil in the Shuixi Village geomantic forest is generally lower than that of the forest in Dinghu Mountain, however, *Aquilaria sinensis* can adapt to nutrient-poor environments (Wang et al., 2012). The poor soil affects the secretion of the resin from *Aquilaria sinensis*, and in terms of resin quality, growth in barren soil may be better than growth in fertile soil (Luo et al., 2011).

http://www.aloki.hu ● ISSN 1589 1623 (Print) ● ISSN 1785 0037 (Online)
DOI: http://dx.doi.org/10.15666/aeer/1706_1577515785

With the rapid development of society and the acceleration of urbanization in Southern China, the disturbance of the monsoon evergreen broad-leaved forest in Shuixi Village is becoming more serious. Both the distribution and area of the forest are shrinking. Meanwhile, the forest quality is decreasing, leading to a simplified community structure, decreased function, invasion of exotic species, and the disappearance of a large number of rare species. In this area, the ability of the forest to positively influence climate regulation and water conservation will be weakened to some extent, and the soil will be degraded. The geomantic forest in Shuixi Village is a natural secondary forest but it is also part of the urban landscape. The geomantic forest is well-preserved compared to other types of forests, but it also reveals the influence of urbanization and human disturbance on natural forest (Chen et al., 2018). This forest is a local species bank and the provenance of rare and endangered plants in the region. It is also part of a unique environmental and cultural tradition in Southern China, making it an important resource for studying zonal forest communities, local culture and history. Furthermore, the forest provides certain ecological services, as well as landscape cultural value. Overall, the geomantic forest is an important element in the construction of rural landscapes and it needs to be actively preserved (Lin et al., 2013).

Conclusion

Shuixi Village in Guangzhou is representative of the other villages located in the center of the Guangdong-Hong Kong-Macao Greater Bay Area and its geomantic forest is characteristic of those seen in urban cities. The geomantic forest in the region can help preserve and recover the monsoon evergreen broad-leafed forest in the region, and maintain the harmony between humans and nature, thus promoting sustainable ecological development in the Greater Bay Area. The nature reserves were effectively protected by regulations and laws. However, there are no such regulations or laws in place to protect geomantic forests. Therefore, setting environmental regulations for geomantic forests, where most rare and endangered plants grow, will provide ecological support for sustainable development and will improve the ecological civilization in the Greater Bay Area. In addition, the dynamic monitoring and ecosystem service on geomantic forest is needed in future.

Acknowledgements. This work is supported by Guangdong Forestry Ecology Positioning Monitoring Network Platform Construction Project (2019KJCX021); Dinghushan Forest Ecosystem Research Station, the Chinese Academy of Sciences; and Dinghushan Forest Ecosystem National Field Scientific Observation and Research Station, the Ministry of Science and Technology, China.

REFERENCES

[1] Cai, X. A., Peng, S. L., Cao, H. L., Yu, Z. Y. (1998): Community analysis of a secondary evergreen broadleaved forest at Luogang, Guangzhou, China. – Journal of Applied and Environmental Biology 4(2): 107-114.

[2] Chen, B. X., Chris, C., Jesse, M., Zhang, Y. (2018): Fengshui forests and village landscapes in China: Geographic extent, socioecological significance, and conservation prospects. – Urban Forestry & Urban Greening 31: 79-92.

[3] Chen, W. F. (2017): Study on community structure of Fengshui Forest in Dongguan. – Agriculture and the Ecological Environment 26: 101-103.

http://www.aloki.hu ● ISSN 1589 1623 (Print) ● ISSN 1785 0037 (Online)
DOI: http://dx.doi.org/10.15666/aeer/1706_1577515785

[4] Cheng, J. (2011): Survey and Research of Village Geomantic Wood in Pearl River Delta. – Beijing Forestry University, Beijing.
[5] Deng, J. (2013): Discussion on the ecological characteristics and conservation value of Fengshui Forest. – Journal of Heilongjiang Vocational Institute of Ecological Engineering 26(5): 9-10.
[6] Fan, Y. M., Zhang, Q. M., Zou, Z. Y., Liu, S. Z., Chu, G. W. (2019): The community structure and its rare and endangered plants conservation status of geomantic forest at Zhongling village in Guangzhou. – Ecological Science 38(2): 162-167.
[7] Gao, H., Ouyang, Z., Chen, S. (2013): Role of culturally protected forests in biodiversity conservation in Southeast China. – Biodiversity and Conservation 22: 531-544.
[8] Hu, L., Li, Z., Liao, W. B., Fan, Q. (2011): Values of village Fengshui Forest patches in biodiversity conservation in the Pearl River Delta, China. – Biological Conservation 144: 1553-1559.
[9] Kim, Y. S. (2014): A study on Kimon evasion in Japanese Fengshui. – Journal of East Aisan Cultures 56: 161-187.
[10] Kim, Y. S. (2017): A theoretical review on the planting and management of coastal forests in Korea. – Korean Journal of Plant Resources 30: 110-123.
[11] Kong, B., Cao, H. L., Ma, L., Wu, L. F., Chen, C., L, H. Z. (2013): Community characteristics of the Fengshui-wood of Erythrophleum fordii in Guangzhou. – Tropical Geography 33(3): 307-313.
[12] Lee, E., Krasny, M. E. (2017): Adaptive capacity in community forest management: a systematic review of studies in East Asia. – Environmental Management 59: 34-49.
[13] Li, S. Y., Ye, Y. S., Wang, F. G., Zeng, F. Y., Xu, Z. C. (2013): Analyses on species composition and areal-type of "Fengshui woods" in Guangzhou City. – Journal of Plant Resources and Environment 22(1): 102-109.
[14] Lin, G. J., Ma, L., Wu, L. F., Huang, M. C., Cao, H. L., Ye, H. G. (2013): Community heterogeneity of Fengshui Woods in Guangzhou and its contribution to regional species diversity. – Journal of Tropical and Subtropical Botany 21(2): 168-174.
[15] Liu, S. S., Ye, Y. C., Zhang, Z. S., Li, N. S., Zhu, J. Y., Cao, H. L. (2005): The species composition of secondary forest at Dalinshan in Dongguan City and its contribution to the species pool. – Guangdong Forestry Technology 21(4): 18-22.
[16] Lü, H. R., Liu, S. S., Ye, Y. C., Zhu, J. Y., Mo, L. J., Chen, H. Y. (2009a): The characteristics of Fungshui woods Pygeum to Pengii Endospermum chinense community in Fenggang Town, Dongguan City. – Journal of Tropical and Subtropical Botany 17(2): 613-619.
[17] Lü, H. R., Liu, S. S., Ye, Y. C., Zhu, J. Y., Mo, L. J., Chen, H. Y. (2009b): Impacts of anthropogenic disturbance on tree species composition and diversity of Fungshui Forest community in Dongguan City of Guandong Province. – Chinese Journal of Ecology 28(4): 613-619.
[18] Lü, H. R., Liu, S. S., Zhu, J. Y., Ye, Y. C., Chen, H. Y., Mo, L. J. (2009c): Effects of human disturbance on understory woody species composition and diversity in Fengshui Forests. – Biodiversity Science 17(5): 458-467.
[19] Lu, Z. B. (2017): Distribution of Fengshui Forest biomass and carbon reserves in Dongguan Forest by product and speciality in China. – Forest by Product and Speciality in China 150(5): 43-45.
[20] Luo, S. Q., Tang, G. D., Zheng, M. X., Qiu, J. L., Ma, H. Y., Hou, B. Q., Xu, Z. C. (2011): Classification and conservation strategy of geomantic forests in Conghua Municipality, Guangdong Province. – Journal of Southwest Forestry University 6: 25-30.
[21] Mao, Y. T., Wang, C., Sun, C. H., Chen, X. Y., Li, Y. Z., Wen, X. J. (2017): Study on resistance of Aquilaria sinensis against Heortia vitessoides. – Journal of South China Agricultural University 38(6): 89-96.

http://www.aloki.hu ● ISSN 1589 1623 (Print) ● ISSN 1785 0037 (Online)
DOI: http://dx.doi.org/10.15666/aeer/1706_1577515785

[22] Mo, H. Z., Zhang, X. Y., Huang, C. T., Xu, R. J., Zhou, X. G., Wei, Y. N., Tang, X. Q. (2011): Conservation and utilization of the floristic diversity of Xijing village Fengshui Wood in Zengcheng City. – Guangdong Agricultural Sciences 24: 144-148.
[23] Peng, S. L. (1996): Dynamics of Plant Communities in the Subtropical. – Science Press, Beijing.
[24] Ren, H., Peng, S. L., Zhang, Z. P., Zhang, W. Q. (1996): Study on canopy structure and canopy radiation of monsoon evergreen broad leaf forest in Dinghushan Biosphere Reserve, Guangdong. – Acta Ecologica Sinica 16(2): 174-179.
[25] Ren, H., Peng, S. L., Liu, H. X., Yu, Z. Y., Fang, D. Y. (1998): Litter fall and its ecological effects at Xiaoliang tropical artificial mixed plantation. – Chinese Journal of Applied Ecology 9(5): 458-462.
[26] Song, Y. C., Chen, X. Y., Wang, X. H. (2005): Studies on evergreen broad-leaved forests of China: a retrospect and prospect. – Journal of East China Normal University (Natural Science) 1: 1-8.
[27] Tang, G. D., Chen, D. P., Luo, S. Q., Zheng, M. X., Hou, B. Q., Xu, Z. C. (2012): Plant community diversity of geomantic woods in Jiangpu, Conghua, Guangzhou, Guangdong. – Guangdong Forestry Technology 28(1): 1-6.
[28] Wang, R., He, Q., Ding, X. G., Li, J. Y., Zhang, F. Q., Pan, W. (2012): Analysis on soil characters of the growing environment and nutrition characteristic of Aquilaria sinensis. – Ecology and Environmental Sciences 21(4): 666-672.
[29] Yang, Q. H., Chen, M. F., Lai, W. N., Yang, H. S., Kuang, W. (2012): Community characteristics investigation of Fengshui Woods in Eastern Guangdong Province. – Journal of Southern Agriculture 43(12): 2040-2044.
[30] Ye, H. G., Xu, Z. C., Wu, M., Cao, H. L. (2013): Guangzhou Fengshui Forest. – Huazhong University of Science and Technology University Press. Wuhan.
[31] Yi, Q. F., Wang, F. G., Liu, D. M., Chen, H. F., Xing, F. W. (2012): Analyses on species composition and community structure of "Fengshui woods" in Luogang District in Guangzhou City. – Journal of Plant Resources and Environment 21(1): 104-110.
[32] Zhu, B. Z., Zhang, F. Q., Li, Z. K., Wang, R., Pan, W., Wang, Y. X. (2011): The community characteristics and conservation of geomantic forest including Aquilaria sinensis in Guangzhou. – Guangdong Forestry Technology 27(2): 15-21.

http://www.aloki.hu ● ISSN 1589 1623 (Print) ● ISSN 1785 0037 (Online)
DOI: http://dx.doi.org/10.15666/aeer/1706_1577515785

THE EFFECT OF ILLICIT DRUGS ON ARTERIAL STIFFNESS IN YOUNG AND MIDDLE-AGED ILLICIT DRUG USERS: A POPULATION-BASED STUDY IN CHINA

PENG, X.[1] – ZHENG, L.[1*] – ZHOU, Z.[3] – TANG, C.[1] – JIAN, X.[1] – CHEN, Z.[1] – TAN, J.[1] – GUO, Y.[1] – LU, C.[1] – ZHU, P.[3] – LI, J.[1] – CHENG, D.[1] – JIANG, Y.[1] – WANG, W.[1] – PENG, W.[1] – SU, T.[1] – WANG, J.[1] – LI, H.[1] – LIU, Y.[1] – LUO, J.[1] – WAN, S.[2*] – ZHANG, J.[2*]

[1]*Key Laboratory of Physical Fitness and Exercise Rehabilitation of Hunan Province, Hunan Normal University, Chang Sha 410012, Hunan, China*

[2]*Hunan Judicial Police Vocational College, Chang Sha 410126, Hunan, China*

[3]*Guangdong Cardiovascular Institute, Guangdong General Hospital, Guangdong Academy of Medical Sciences, Guangzhou 510100, Guangdong, China*

**Corresponding authors*
e-mail: Lanzheng@hunnu.edu.cn; wsp506@163.com; zhangju888aaa@163.com

(Received 25th Sep 2019; accepted 11th Nov 2019)

Abstract. Many illicit drugs have been linked to cardiovascular diseases, but large epidemiological studies are still needed to unveil the full effect of their use on the cardiovascular system. The aim of this study was to explore the relationship between illicit drug use and the prevalence of abnormal arterial stiffness in young and middle-aged illicit drug users. In total, 1247 illicit drug users and 107 non-illicit drug users were recruited for the Cardiovascular Damage Study, and 731 illicit drug users and 55 non-illicit drug users completed the cross-sectional analysis. Data was collected using questionnaires and a noninvasive vascular screening device. The value of brachial-ankle pulse wave velocity (baPWV) varied in a statistically significant manner depending on the type and duration of illicit drug use. The prevalence of abnormal baPWV varied significantly among different illicit drug user groups ($\chi^2 = 10.69$, $p < 0.01$). Multivariate logistic regression analysis revealed that age, sex, and the type of illicit drug used were crucial risk factors for abnormal baPWV. Older male narcotic drug users were associated with a significantly higher prevalence of abnormal baPWV. The main risk factors of arterial stiffness in young and middle-aged drug users were age, sex, and the type of illicit drug used.
Keywords: *vascular elasticity, brachial-ankle pulse wave velocity, cardiovascular disease, narcotic drug, psychotropic drug, risk factor*

Introduction

Abuse of illicit drugs results in a variety of pathophysiological changes to the cardiovascular system, such as the constriction of coronary vessels, dysfunction of the vascular endothelium, and decreased aortic elasticity. The cardiovascular impact of illicit drug use can lead to death, which is a growing public concern as the consumption of illicit drugs is increasing annually (Devlin and Henry, 2008; Maceira et al., 2014; Akkina et al., 2012). For example, cocaine abuse affects the elastic properties of the aorta and leads to increased systolic blood pressure and aortic stiffness (Bigi et al., 2008; Zhu et al., 2018). Other illicit drugs, including cannabis, amphetamines, and 3-4 methylenedioxymethamphetamine (MDMA), are also reported to be associated with hypertension, arrhythmia, and sudden death (Kaye et al., 2008; Heal et al., 2013; Singla et al., 2012; Wolff et al., 2011; Satoh et al., 2009).

http://www.aloki.hu ● ISSN 1589 1623 (Print) ● ISSN 1785 0037 (Online)
DOI: http://dx.doi.org/10.15666/aeer/1706_1578715797

A means of early detection of cardiovascular system damage in illicit drug users would be significantly helpful for clinical and emergency treatment. Currently, an easily obtained, reproducible, and non-invasive parameter, known as brachial-ankle pulse wave velocity (baPWV), is considered to be a useful tool for the management of cardiovascular disease and its risk factors in illicit drug users. BaPWV mainly reflects segmental arterial elasticity (Kim et al., 2015). Since an increase in arterial stiffness will increase the propagation speed of a pulse wave in the artery (Tomiyama et al., 2016), baPWV can serve as a marker of arterial stiffness. A baPWV more than or equal to 1400 cm/s indicates severe arterial stiffness (Yamashina et al., 2003; Wang et al., 2014) and a strong and independent association with coronary artery calcium (CAC), which is a powerful marker of coronary atherosclerosis (Cainzos-Achirica et al., 2015).

The cardiotoxic properties of illicit drugs have been studied for decades. Reports of the actual effects of illicit drugs on the cardiovascular systems of illicit drug users have not been well documented. Furthermore, the relationship between the abuse of various illicit drugs and arterial stiffness has not been reported.

According to the Illicit Drug Classification of United Nations Convention, illicit drugs were divided into two categories based on their pharmacological properties: narcotic and psychotropic. In this study, users of illicit narcotic drugs (opium, heroin, morphine, dolantin, marijuana, and cocaine) and illicit psychotropic drugs (methamphetamine, ketamine, and MDMA) were enrolled in the analysis. Users were divided into three groups: illicit narcotic drug users, illicit psychotropic drug users and users of both narcotic and psychotropic drugs (poly drug users). The possible relationships between the type, duration, and method of illicit drug abuse and arterial stiffness were evaluated using baPWV. The results of this study may provide new clues for the prediction and prevention of illicit drug abuse-related cardiovascular disease.

Materials and methods

Subjects

The illicit drug users were recruited from the drug rehabilitation centers of Hunan, Yunnan, Guangxi, Shanxi, and Guizhou provinces of China. The duration of survey was eight months which is from August 2017 to March 2018. A total of 1247 illicit drug users agreed to participate in the Cardiovascular Damage Study and signed the informed consent forms approved by the Institutional Ethics Committee of Hunan Normal University describing the procedures and assessments of the study. Subsequently, 878 cases completed the data collection. According to the results of the physical examination that participants completed when entering the drug rehabilitation center, 147 users did not meet the following selection criteria: (1) no history of metabolic diseases and organic diseases; (2) no cardiovascular drug treatment in the past five years; and (3) ≤ 45 years of age. As such, 731 cases were enrolled in the final analysis. Non-illicit drug users were recruited from the local communities of Hunan, Yunnan, Guangxi, Shanxi, and Guizhou provinces of China. 107 non-illicit drug users agreed to participate and signed the informed consent forms of Cardiovascular Damage Study. After screening, 55 non-illicit drug users met the above mentioned selection criteria and were enrolled in the final analysis.

http://www.aloki.hu ● ISSN 1589 1623 (Print) ● ISSN 1785 0037 (Online)
DOI: http://dx.doi.org/10.15666/aeer/1706_1578715797

Questionnaires and quality control

The questionnaires assessed demographic data and illicit drug abuse history including the type, duration, and method of illicit drug abuse. Participants were interviewed face-to-face by investigators trained to complete the questionnaire. All responses were reviewed by other trained investigators at the time of the interview.

Measurements

Blood pressure, baPWV and ankle-brachial index were measured using a BP-203 RPE III networked noninvasive vascular screening device produced by OMRON according to the manufacturer's instructions. The examination process was the same as previously descried (Wang et al., 2016). The subject was asked to sit for at least 5 min in an air-conditioned room (22-25 °C). Participants wore light clothing and were instructed to lay in a supine position. Cuffs were placed on both arms and ankles and participants were asked to keep quiet during the examination process. All technicians were well-trained and familiar with the device. The measurements were performed by a single technician and were monitored by another researcher throughout the duration of the study.

Statistical methods

Statistical analysis was performed using R software, version 3.3.1 (R Core Team, 2016), and SPSS 20 (SPSS, Chicago, IL, USA). Continuous variables were presented as means±standard deviations (SD) and categorical variables were presented as percentages (%). For multiple comparisons of means, a pairwise t-test was used and p values were adjusted by false discovery rate (FDR) using the Benjaminni-Hochberg (BH) method. ANOVA was used to compare non-paired samples of normally distributed parameters. Pearson's chi-square test was used to compare prevalence differences. The aforementioned functions we used for data analysis were included in the R base package (R Core Team, 2016R Foundation, Australia). baPWV multivariate unconditional logistic regression analysis was analysed by both R base package and SPSS 20. A p value less than 0.05 was considered statistically significant.

Results

General characteristics of study illicit drug users

In the end, 731 illicit drug users with complete personal information who fulfilled the selection criteria were included in the final analysis. The general characteristics of the subjects are presented in *Table 1*. Among the 731 illicit drug users, 535 (73.2%) were male and 196 (26.8%) were female. The mean age was 36.06±4.52 years (range 23–45 years old). A total of 374 cases (51.2%), 283 cases (38.7%), and 74 cases (10.1%) were narcotic drug users, psychotropic drug users, and ploy drug users, respectively. Age, height, blood pressure, baPWV, and other indicators were significantly different among different illicit drug users (*Table 1*).

Statistical analysis revealed that baPWV exhibited significant differences based on the type and the duration of illicit drug used (*Tables 1* and *2*). No significant difference was observed in baPWV value based on the method of illicit drug abuse (*Table A1* in the *Appendix*).

http://www.aloki.hu ● ISSN 1589 1623 (Print) ● ISSN 1785 0037 (Online)
DOI: http://dx.doi.org/10.15666/aeer/1706_1578715797

Table 1. *Baseline characteristics of the study subjects*

	Narcotic (n = 374)	Psychotropic (n = 283)	Poly (n = 74)
Age, years	37.45 ± 4.11	34.41 ± 4.54 [a]	35.36 ± 3.96 [a]
Height, cm	163.19 ± 7.73	166.93 ± 7.63 [a]	163.81 ± 7.78 [b]
Weight, Kg	61.01 ± 9.88	64.56 ± 10.19 [a]	60.71 ± 11.04 [b]
BMI, Kg/m^2	22.90 ± 3.30	23.17 ± 3.24	22.56 ± 3.10
Vital capacity, ml	2674.70 ± 692.28	2881.44 ± 747.41 [a]	2669.22 ± 697.39 [b]
Heart rate, b/min	78.52 ± 13.22	75.04 ± 11.70 [a]	75.74 ± 10.72
SBP, mmHg	119.51 ± 15.86	118.84 ± 29.22	116.81 ± 15.44
DBP, mmHg	75.88 ± 11.35	71.98 ± 11.70 [a]	75.74 ± 10.72 [a]
RbaPWV	1226.82 ± 186.09	1178.67 ± 126.18 [a]	1176.74 ± 155.33 [a]
LbaPWV	1227.59 ± 178.66	1186.52 ± 122.04 [a]	1184.35 ± 153.33
Rabi	1.07 ± 0.10	1.07 ± 0.10	1.05 ± 0.08
Labi	1.06 ± 0.10	1.07 ± 0.10	1.06 ± 0.08
IAD, mmHg	3.63 ± 3.22	3.62 ± 3.24	2.81 ± 2.50
Duration, months	71.32 ± 80.76	50.47 ± 47.47 [a]	94.68 ± 70.51 [ab]

BMI: body mass index; SBP: systolic blood pressure; DBP: diastolic blood pressure; Rabi: right ankle-brachial index; Labi: left ankle-brachial index; RbaPWV: right brachial-ankle pulse wave velocity; LbaPWV: left brachial-ankle pulse wave velocity; IAD: inter-arm blood pressure difference. The *p* values were adjusted by false discovery rate (FDR) using the Benjamini-Hochberg (BH) method. [a]$p < 0.05$ versus the narcotic drug users; [b]$p < 0.05$ versus the psychotropic drug users

Table 2. *Comparison of the baPWV value among the different illicit drug abuse duration groups*

Duration, months	RbaPWV	LbaPWV
12	1241.13 ± 209.38	1246.89 ± 197.42
36	1202.73 ± 165.19	1206.44 ± 152.74
72	1186.49 ± 167.59	1196.92 ± 158.71
144	1183.97 ± 166.19	1187.82 ± 159.04
> 144	1181.63 ± 146.48	1175.40 ± 156.52
p value	0.04	< 0.01

RbaPWV: right brachial-ankle pulse wave velocity. One-way ANOVA was used to analyze the difference among different drug abuse duration groups

Analysis of the prevalence of abnormal baPWV in different sex, age, and drug user groups

The total detection rates of abnormal baPWV in illicit drug users (14.4%) were significantly greater than those of non-illicit drug users (3.6%) ($\chi^2 = 4.13$, $p < 0.05$) (*Table 3*). To investigate the risk factors for abnormal baPWV in illicit drug users, the prevalence of abnormal baPWV in different sex, age, and drug user groups were analyzed. The results showed that the prevalence of abnormal baPWV was not significantly different between male and female illicit drug users ($\chi^2 = 3.76$, $p > 0.05$) (*Table A2* in the *Appendix*). It has been reported that peripheral vascular resistance increases and arterial elasticity decreases with age, which results in a higher prevalence of abnormal baPWV in the elderly population (Ishida et al., 2018). Therefore, according

http://www.aloki.hu ● ISSN 1589 1623 (Print) ● ISSN 1785 0037 (Online)
DOI: http://dx.doi.org/10.15666/aeer/1706_1578715797

to the age composition of the illicit drug users, the cases were divided into three groups. The detection rate of abnormal baPWV in illicit drug users between the ages of 21–30, 31–40, and over 40 was 8.0%, 14.3%, and 19.3%, respectively. There was no significant difference in the prevalence of abnormal baPWV among different age groups ($\chi^2 = 5.32$, $p > 0.05$) (*Table A3*).

Table 3. *Comparison of abnormal baPWV prevalence rates between illicit drug users and non-illicit drug users*

	baPWV ≥ 1400	**baPWV < 1400**	**Total**
Illicit drug users	626 (85.6%)	105 (14.4%)	731
Non-illicit drug users	2 (3.6%)	53 (96.4%)	55

baPWV: brachial-ankle pulse wave velocity. The difference between each group was analyzed by Pearson's chi-square test $\chi^2 = 4.13$, $p < 0.05$

Since the value of baPWV showed significant differences among different illicit drug abuse duration groups, the prevalence of abnormal baPWV differences among them was further analyzed. The detection rate of abnormal baPWV in different illicit drug abuse duration groups of 0–12, 13–36, 37–72, 73–144 and over 144 months was 20.1%, 14.4%, 13.0%, 11.3%, and 9.4%, respectively, but no significant difference was found among these groups ($\chi^2 = 7.90$, $p > 0.05$) (*Table A4*). Nevertheless, our further investigation of cardiovascular damage in illicit drug users based on baPWV revealed that the prevalence of abnormal baPWV showed a significant difference between the different illicit drug user groups: 18.4% in the narcotic drug user group, 10.6% in the psychotropic drug user group, and 8.1% in the poly drug user group ($\chi^2 = 10.69$, $p < 0.01$) (*Table 4*).

Table 4. *Comparison of abnormal baPWV prevalence rates of different type illicit drug users*

	baPWV ≥ 1400	**baPWV < 1400**	**Total**
Narcotic	69 (18.4%)	305 (81.6%)	374 (51.2%)
Psychotropic	30 (10.6%)	253 (89.4%)	283 (38.7%)
Poly	6 (8.1%)	68 (91.9%)	74 (10.1%)
Total	105 (14.4%)	626 (85.6%)	731

baPWV: brachial-ankle pulse wave velocity. The difference between each group was analyzed by Pearson's chi-square test $\chi^2 = 10.69$, $p < 0.01$

Analysis of the relevant risk factors for abnormal baPWV in illicit drug users

To avoid possible interactions between each risk factor, multivariate logistic regression analysis was used to evaluate the effect of illicit drug abuse on arterial stiffness. The result showed that significant predictors of abnormal baPWV were age, sex, and the type of illicit drug used. In males, the risk of abnormal baPWV was 1.97-fold higher (OR = 1.97, 95% CI = 1.11–3.47) than that in females. The risk of developing abnormal baPWV increased by 1.10-fold per year of age (OR = 1.10, 95% CI = 1.04–1.17). Compared with narcotic drug users (OR = 1), the risk of abnormal baPWV in psychotropic drug users (OR = 0.49, 95% CI = 0.28–0.84) and poly drug users (OR = 0.63, 95% CI = 0.23–1.72) was lower (*Table 5*).

http://www.aloki.hu ● ISSN 1589 1623 (Print) ● ISSN 1785 0037 (Online)
DOI: http://dx.doi.org/10.15666/aeer/1706_1578715797

Table 5. *Multivariate unconditional logistic regression analysis of risk factors for abnormal baPWV in illicit drug users*

	B	S. E.	Wald	df	*p* value	OR	95% CI
Sex	0.68	0.29	5.42	1	0.02	1.97	1.11-3.47
Age	0.10	0.03	3.52	1	< 0.01	1.10	1.04-1.17
BMI			1.71	3	0.64		
normal						1	
Slim	0.43	0.68	0.39	1	0.53	1.53	0.40-5.82
Overweight	0.11	0.27	0.16	1	0.69	1.12	0.65-1.90
Obesity	0.59	0.50	1.36	1	0.24	1.80	0.67-4.82
Drug type			6.91	2	0.03		
narcotic						1	
Psychotropic	−0.72	0.28	6.65	1	0.01	0.49	0.28-0.84
Poly	−0.46	0.51	0.81	1	0.37	0.63	0.23-1.72
Duration			5.66	4	0.23		
0-12 m						1	
13-36 m	−0.21	0.30	0.51	1	0.48	0.81	0.45-1.45
37-72 m	−0.39	0.35	1.23	1	0.27	0.68	0.34-1.35
73-144 m	−0.64	0.39	2.72	1	0.10	0.53	0.25-1.13
>144 m	−0.85	0.42	4.11	1	0.04	0.43	0.19-0.97
Method			1.73	6	0.94		
sucking						1	
P.O	−0.17	0.53	0.11	1	0.74	0.84	0.30-2.36
Snorting	−15.04	686.82	0.00	1	1.00	0.00	0.00
IV	−0.29	0.34	0.72	1	0.40	0.75	0.39-1.46
Smoking	−0.44	0.47	0.87	1	0.35	0.65	0.26-1.62
mixture	0.22	0.61	0.13	1	0.72	1.24	0.38-4.09
others	−0.24	1.11	0.05	1	0.83	0.79	0.09-6.91
Constant	−5.26	1.16	20.56	1	0.00	0.01	

P.O: *per os*, IV: intravenous injection

A predictive model of the risk of arterial stiffness of illicit drug users (ASIDU) was developed based on multivariate logistic regression analysis according to the value of baPWV collected in this study. This ASIDU model contains six factors, including sex, age, Body Mass Index (BMI), the type of illicit drug used, the duration of illicit drug used and the method of taking illicit drugs. To evaluate the predictive performance of the ASIDU model, Receiver Operating Characteristic (ROC) analysis was used. The ASIDU model exhibited an area under the ROC curve (AUC) of 0.70 (95% CI = 0.64–0.75). The cut-off point (male, 29 years old, overweight, narcotic drug users and 12–36 months of illicit drug abuse) showed 60% sensitivity and 72% specificity in predicting arterial stiffness of illicit drug users according to the value of baPWV (*Fig. 1*).

Discussion

The present study indicates that cardiovascular damage in illicit drug users is significantly associated with age, sex, and the type of illicit drug used. Among the 731

http://www.aloki.hu ● ISSN 1589 1623 (Print) ● ISSN 1785 0037 (Online)
DOI: http://dx.doi.org/10.15666/aeer/1706_1578715797

young and middle-aged illicit drug users in our study, 105 cases (14.4%) exhibited various degrees of abnormal arterial stiffness. It is significantly higher than the detection rate of that in the young and middle-aged normal population (3.6%). This indicates that abnormal arterial stiffness occurs in illicit drug users at a relatively young age. The incidence of cardiovascular disease and cerebral infarction induced by arterial stiffness is increasing year by year (Mikael et al., 2017; Hatanaka et al., 2011). Thus, detection of the changes in arterial stiffness in high-risk drug users can effectively predict the occurrence and development of cardiovascular and cerebrovascular diseases, which may reduce mortality among illicit drug users.

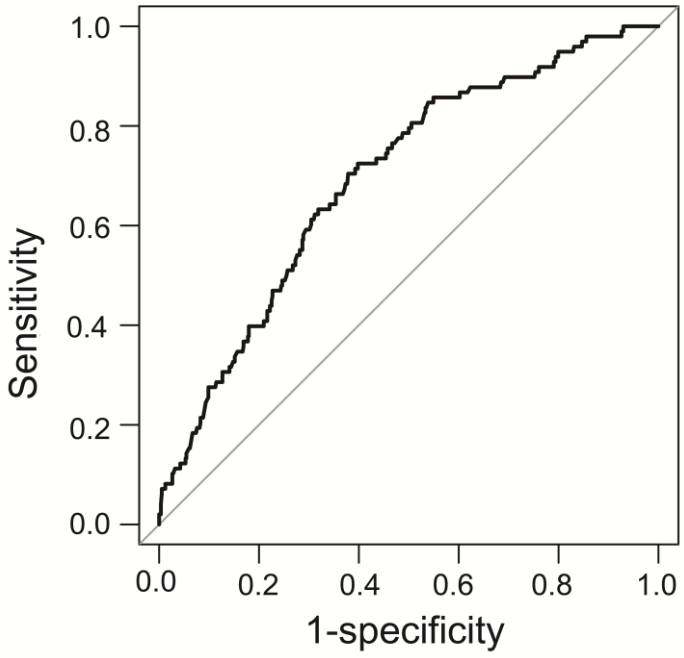

Figure 1. *ROC curve analysis of the predictive performance of the ASIDU model. AUC = 0.70, 95% CI = 0.64–0.75. (ROC: Receiver operating characteristic; ASIDU: arterial stiffness of illicit drug users; AUC: area under curve)*

Previous reports demonstrated that age is a major determinant of arterial stiffness (Lee and Oh, 2010). During the aging process, the vessel wall undergoes a variety of changes, including increased calcium deposition, quantitative and qualitative changes in medial layer collagen, and arterial wall hypertrophy. These results in disorganized microarchitecture, decreased vessel wall compliance and elasticity, and increased arterial stiffness (Tomiyama et al., 2003). Individuals more than 45 years old are more susceptible to arterial stiffness (Ishida et al., 2018). In addition, metabolic problems and a sedentary lifestyle also are critical factors affecting the arterial stiffness process (Satoh et al., 2009; Garcia-Hermoso et al., 2015). Thus, individuals less than 45 years old without metabolic and organic diseases were recruited to better evaluate the effect of illicit drugs on the cardiovascular system.

Some illicit drugs have been found to be associated with cardiovascular problems, such as arrhythmia, hypertension, myocardial infarction (MI), and atherosclerosis. In the United States, cocaine is the cause of 25% of MIs in people under 45 years of age (Qureshi et al., 2001). Up to 83% of asymptomatic cocaine users suffer from silent

http://www.aloki.hu ● ISSN 1589 1623 (Print) ● ISSN 1785 0037 (Online)
DOI: http://dx.doi.org/10.15666/aeer/1706_1578715797

myocardial injuries such as myocardial edema and myocardial fibrosis (Aquaro et al., 2011). Cardiovascular pathology, typically atherosclerosis, has been detected in 58% of MDMA users. This detection rate is higher than that expected among similarly aged members of the general population (Kaye et al., 2009). Amphetamine and cannabis are also thought to be linked to various cardiovascular problems, such as hypertension, cardiac arrhythmia and increased heart rate (Vitiello, 2008). Although the cardiotoxic properties of some of these illicit drugs have been well documented theoretically, the exact effect of different types of illicit drugs on humans has not been fully investigated. Our study revealed that illicit narcotic drug users have a higher detection rate of abnormal baPWV than illicit psychotropic drug users, which indicates that illicit narcotic drugs have a stronger effect on cardiovascular damage than that of illicit psychotropic drugs.

In a study of 121 intravenous drug abusers, 95 had systolic murmurs and 44 had extra-cardiac infections (Hecht and Berger, 1992). Vitiello et al. found that the effect of illicit abuse via intravenous injection is more pronounced that that associated with other methods of illicit drug abuse (Vitiello, 2008). However, in this study, we did not find a significant difference between different methods of drug abuse. This discrepancy may be a result of differences in the characteristics of the studied populations. Equal sample selection criteria are required to make a parallel comparison between the results.

Conclusion

In summary, age, sex and type of illicit drug used were crucial risk factors for abnormal arterial stiffness in young and middle-aged illicit drug users. The effects of different durations of illicit drug abuse on the cardiovascular system were compared, but no significant difference was found after multivariate logistic regression analysis. This may be due to the fact that the effect of illicit drug abuse is generated by the accumulation of cardiotoxicity, which is not only determined by the duration of drug abuse but is also related to the frequency of drug abuse and the average amount of illicit drug used in each time. Therefore, in order to further explore the cardiovascular impact illicit drug use, the duration and frequency of drug abuse and the average amount of illicit drug used should be taken into consideration.

Acknowledgments. This research was supported by grants from National Natural Science Foundation of China (31671243, 81801392, 81570279), National Key Research and Development Program of China (2016YFC0800908, 2018YFA0108700), and China Postdoctoral Science Foundation (2018M630903).

REFERENCES

[1] Akkina, S. K., Ricardo, A. C., Patel, A., Das, A., Bazzano, L. A., Brecklin, C., Fischer, M. J., Lash, J. P. (2012): Illicit drug use, hypertension, and chronic kidney disease in the US adult population. – Translational Research: The Journal of Laboratory and Clinical Medicine 160(6): 391-398.

[2] Aquaro, G. D., Gabutti, A., Meini, M., Prontera, C., Pasanisi, E., Passino, C., Emdin, M., Lombardi, M. (2011): Silent myocardial damage in cocaine addicts. – Heart 97(24): 2056-2062.

[3] Bigi, M. A., Aslani, A., Mehrpour, M. (2008): Effect of chronic cocaine abuse on the elastic properties of aorta. – Echocardiography 25(3): 308-311.

http://www.aloki.hu ● ISSN 1589 1623 (Print) ● ISSN 1785 0037 (Online)
DOI: http://dx.doi.org/10.15666/aeer/1706_1578715797

[4] Cainzos-Achirica, M., Rampal, S., Chang, Y., Ryu, S., Zhang, Y., Zhao, D., Cho, J., Choi, Y., Pastor-Barriuso, R., Lim, S. Y., Bruguera, J., Elosua, R., Lima, J. A., Shin, H., Guallar, E. (2015): Brachial-ankle pulse wave velocity is associated with coronary calcium in young and middle-aged asymptomatic adults: the Kangbuk Samsung Health Study. – Atherosclerosis 241(2): 350-356.

[5] Devlin, R. J., Henry, J. A. (2008): Clinical review: major consequences of illicit drug consumption. – Critical Care 12(1): 202.

[6] Garcia-Hermoso, A., Notario-Pacheco, B., Recio-Rodriguez, J. I., Martinez-Vizcaino, V., Rodrigo de Pablo, E., Magdalena Belio, J. F., Gomez-Marcos, M. A., Garcia-Ortiz, L., Group, E. (2015): Sedentary behaviour patterns and arterial stiffness in a Spanish adult population - the EVIDENT trial. – Atherosclerosis 243(2): 516-522.

[7] Hatanaka, R., Obara, T., Watabe, D., Ishikawa, T., Kondo, T., Ishikura, K., Aikawa, T., Aono, Y., Hara, A., Metoki, H., Asayama, K., Kikuya, M., Mano, N., Ohkubo, T., Izumi, S., Imai, Y. (2011): Association of arterial stiffness with silent cerebrovascular lesions: the Ohasama study. – Cerebrovascular Diseases 31(4): 329-337.

[8] Heal, D. J., Smith, S. L., Gosden, J., Nutt, D. J. (2013): Amphetamine, past and present - a pharmacological and clinical perspective. – Journal of Psychopharmacology 27(6): 479-496.

[9] Hecht, S. R., Berger, M. (1992): Right-sided endocarditis in intravenous drug users. Prognostic features in 102 episodes. – Annals of Internal Medicine 117(7): 560-566.

[10] Ishida, A., Fujisawa, M., Del Saz, E. G., Okumiya, K., Kimura, Y., Manuaba, I. I. B., Kareth, M. F., Rantetampang, A. L., Ohya, Y., Matsubayashi, K. (2018): Arterial stiffness, not systolic blood pressure, increases with age in native Papuan populations. – Hypertension Research: Official Journal of the Japanese Society of Hypertension 41(7): 539-546.

[11] Kaye, S., Darke, S., Duflou, J., McKetin, R. (2008): Methamphetamine-related fatalities in Australia: demographics, circumstances, toxicology and major organ pathology. – Addiction 103(8): 1353-1360.

[12] Kaye, S., Darke, S., Duflou, J. (2009): Methylenedioxymethamphetamine (MDMA)-related fatalities in Australia: demographics, circumstances, toxicology and major organ pathology. – Drug and Alcohol Dependence 104(3): 254-261.

[13] Kim, E. K., Chang, S. A., Jang, S. Y., Choi, K. H., Huh, E. H., Kim, J. H., Kim, S. M., Choe, Y. H., Kim, D. K. (2015): Brachial-ankle pulse wave velocity as a screen for arterial stiffness: a comparison with cardiac magnetic resonance. – Yonsei Medical Journal 56(3): 617-624.

[14] Lee, H. Y., Oh, B. H. (2010): Aging and arterial stiffness. – Circulation Journal: Official Journal of the Japanese Circulation Society 74(11): 2257-2262.

[15] Maceira, A. M., Ripoll, C., Cosin-Sales, J., Igual, B., Gavilan, M., Salazar, J., Belloch, V., Pennell, D. J. (2014): Long term effects of cocaine on the heart assessed by cardiovascular magnetic resonance at 3T. – Journal of Cardiovascular Magnetic Resonance: Official Journal of the Society for Cardiovascular Magnetic Resonance 16: 26.

[16] Mikael, L. R., Paiva, A. M. G., Gomes, M. M., Sousa, A. L. L., Jardim, P., Vitorino, P. V. O., Euzebio, M. B., Sousa, W. M., Barroso, W. K. S. (2017): Vascular aging and arterial stiffness. – Arquivos Brasileiros de Cardiologia 109(3): 253-258.

[17] Qureshi, A. I., Suri, M. F., Guterman, L. R., Hopkins, L. N. (2001): Cocaine use and the likelihood of nonfatal myocardial infarction and stroke: data from the Third National Health and Nutrition Examination Survey. – Circulation 103(4): 502-506.

[18] R Core Team (2016): R: A Language and Environment for Statistical Computing. – R Foundation for Statistical Computing, Vienna, Austria.

[19] Satoh, H., Kishi, R., Tsutsui, H. (2009): Metabolic syndrome is a significant and independent risk factor for increased arterial stiffness in Japanese subjects. – Hypertension Research: Official Journal of the Japanese Society of Hypertension 32(12): 1067-1071.

http://www.aloki.hu ● ISSN 1589 1623 (Print) ● ISSN 1785 0037 (Online)
DOI: http://dx.doi.org/10.15666/aeer/1706_1578715797

[20] Singla, S., Sachdeva, R., Mehta, J. L. (2012): Cannabinoids and atherosclerotic coronary heart disease. – Clinical Cardiology 35(6): 329-335.
[21] Tomiyama, H., Yamashina, A., Arai, T., Hirose, K., Koji, Y., Chikamori, T., Hori, S., Yamamoto, Y., Doba, N., Hinohara, S. (2003): Influences of age and gender on results of noninvasive brachial-ankle pulse wave velocity measurement - a survey of 12517 subjects. – Atherosclerosis 166(2): 303-309.
[22] Tomiyama, H., Matsumoto, C., Shiina, K., Yamashina, A. (2016): Brachial-ankle PWV: current status and future directions as a useful marker in the management of cardiovascular disease and/or cardiovascular risk factors. – Journal of Atherosclerosis and Thrombosis 23(2): 128-146.
[23] Vitiello, B. (2008): Understanding the risk of using medications for attention deficit hyperactivity disorder with respect to physical growth and cardiovascular function. – Child and Adolescent Psychiatric Clinics of North America 17(2): 459-474.
[24] Wang, A., Tao, J., Guo, X., Liu, X., Luo, Y., Liu, X., Huang, Z., Chen, S., Zhao, X., Jonas, J. B., Wu, S. (2014): The product of resting heart rate times blood pressure is associated with high brachial-ankle pulse wave velocity. – PloS One 9(9): 107852.
[25] Wang, Y., Yang, Y., Wang, A., An, S., Li, Z., Zhang, W., Liu, X., Ruan, C., Liu, X., Guo, X., Zhao X., Wu, S. (2016): Association of long-term blood pressure variability and brachial-ankle pulse wave velocity: a retrospective study from the APAC cohort. – Scientific Reports 6: 21303.
[26] Wolff, V., Lauer, V., Rouyer, O., Sellal, F., Meyer, N., Raul, J. S., Sabourdy, C., Boujan, F., Jahn, C., Beaujeux, R., Marescaux, C. (2011): Cannabis use, ischemic stroke, and multifocal intracranial vasoconstriction: a prospective study in 48 consecutive young patients. – Stroke 42(6): 1778-1780.
[27] Yamashina, A., Tomiyama, H., Arai, T., Hirose, K., Koji, Y., Hirayama, Y., Yamamoto, Y., Hori, S. (2003): Brachial-ankle pulse wave velocity as a marker of atherosclerotic vascular damage and cardiovascular risk. – Hypertension Research: Official Journal of the Japanese Society of Hypertension 26(8): 615-622.
[28] Zhu, W., Wang, H., Wei, J., Sartor, G. C., Bao, M. M., Pierce, C. T., Wahlestedt, C. R., Dykxhoorn, D. M., Dong, C. (2018): Cocaine exposure increases blood pressure and aortic stiffness via the miR-30c-5p-malic enzyme 1-reactive oxygen species pathway. – Hypertension 71(4): 752-760.

APPENDIX

Table A1. *Comparison of the baPWV value among different drug abuse method groups*

Methods	RbaPWV	LbaPWV
Sucking	1200.61 ± 179.05	1209.56 ± 173.91
P.O	1231.21 ± 140.65	1234.88 ± 132.89
Snorting	1183.18 ± 173.7	1172.09 ± 152.04
IV	1210.49 ± 187.06	1203.13 ± 170.34
Smoking	1206.02 ± 144.25	1207.06 ± 142.14
Mixture	1259.86 ± 221.81	1253.33 ± 187.26
others	1150.00 ± 170.59	1156.00 ± 175.33
p value	0.63	0.65

RbaPWV: right brachial-ankle pulse wave velocity; LbaPWV: left brachial-ankle pulse wave velocity; P.O: per os; IV: intravenous injection. One-way ANOVA was used to analyze the difference among different drug abuse method groups

http://www.aloki.hu ● ISSN 1589 1623 (Print) ● ISSN 1785 0037 (Online)
DOI: http://dx.doi.org/10.15666/aeer/1706_1578715797

Table A2. *Comparison of abnormal baPWV prevalence rates between males and females*

	baPWV ≥ 1400	**baPWV < 1400**	**Total**
Male	85 (16.9%)	450 (83.1%)	535 (73.2%)
Female	20 (10.2%)	176 (89.8%)	196 (26.8%)
Total	105 (14.4%)	626 (85.6%)	731

baPWV: brachial-ankle pulse wave velocity. The difference between each group was analyzed by Pearson's chi-square test $\chi^2 = 3.76$, $p > 0.05$

Table A3. *Comparison of abnormal baPWV prevalence rates among different age groups*

Age, years	**baPWV ≥ 1400**	**baPWV < 1400**	**Total**
21–30	7 (8.0%)	81 (92.0%)	88 (12.0%)
31–40	75 (14.3%)	449 (85.7%)	524 (71.7%)
>40	23 (19.3%)	96 (80.7%)	119 (16.3%)
Total	105 (14.4%)	626 (85.6%)	731

baPWV: brachial-ankle pulse wave velocity. The difference between each group was analyzed by Pearson's chi-square test $\chi^2 = 5.32$, $p > 0.05$

Table A4. *Comparison of abnormal baPWV prevalence rates of different type illicit drug abuse durations*

Duration, months	**baPWV ≥ 1400**	**baPWV < 1400**	**Total**
0–12	36 (20.1%)	143 (79.9%)	179 (24.5%)
13–36	28 (14.4%)	166 (85.6%)	194 (26.5%)
37–72	18 (13.0%)	120 (87.0%)	138 (18.9%)
73–144	14 (11.3%)	110 (88.7%)	124 (17.0%)
>144	9 (9.4%)	87 (80.6%)	96 (13.1%)
Total	105 (14.4%)	626 (85.6%)	731

baPWV: brachial-ankle pulse wave velocity. The difference between each group was analyzed by Pearson's chi-square test $\chi^2 = 7.90$, $p > 0.05$

http://www.aloki.hu ● ISSN 1589 1623 (Print) ● ISSN 1785 0037 (Online)
DOI: http://dx.doi.org/10.15666/aeer/1706_1578715797